ACTA CHEMICA SCANDINAVICA 16 (1962) 1–19

X-Ray Investigations of the Ternary System Fe-P-B. Some Features of the Systems Cr-P-B, Mn-P-B, Co-P-B and Ni-P-B

STIG RUNDQVIST

Institute of Chemistry, University of Uppsala, Uppsala, Sweden

The solid region of the Fe–P–B system has been investigated in the range Fe–FeP_2–BP–FeB–Fe by means of X-ray and chemical analyses. The main features of an isothermal section at 1 000°C have been determined. Boron substitutes for phosphorus to a large extent in Fe_3P and to a smaller extent in Fe_2P and FeP. Two ternary phases exist, *viz.* Fe_5PB_2, homogeneous in a relatively narrow composition range, and $Fe_3P_{1-x}B_x$ (denoted ε_1), homogeneous in the approximate range $0.48 < x < 1$ at 1 000°C.

Solid solubility of boron is appreciable in Cr_3P and Mn_3P, but is very restricted in Ni_3P. The ternary phase Mn_5PB_2 is isostructural with Fe_5PB_2. In the Co–P–B system, three ternary phases have been found, *viz.* $Co_3P_{1-x}B_x$, homogeneous in a narrow range near $x = 0.7$ and isostructural with the ε_1 phase in the Fe–P–B system, $Co_3P_{1-y}B_y$, homogeneous in a narrow range near $y = 0.5$ and isostructural with Fe_3P, and finally Co_5PB_2, isostructural with Fe_5PB_2 and Mn_5PB_2.

The crystal structures of Fe_3P, ε_1 (with the composition $Fe_3P_{0.37}B_{0.63}$), and Fe_5PB_2 have been determined and refined using single-crystal methods. The space-group of the ε_1 structure is $P\,4_2/n$ with 24 iron atoms in three sets of eightfold positions. The boron and phosphorus atoms are randomly distributed in one eightfold position. The structure is very closely related to that of Fe_3P. Fe_5PB_2 has the Cr_5B_3 ($D\,8_l$)-type structure. The distribution of the boron and phosphorus atoms is essentially ordered.

During investigations of borides, silicides and phosphides of the Group VII and VIII transition metals made at this Institute, some attention has been devoted to ternary systems containing one transition metal and two non-metals [1,2]. The present paper deals with X-ray investigations of the ternary system Fe–P–B and the closely related systems Cr–P–B, Mn–P–B, Co–P–B and Ni–P–B. As far as the author is aware, no earlier investigations of these systems have been published. The results will be presented in two main parts, the first dealing with the phase analyses and the second with the crystal structure determinations.

I. PHASE-ANALYTICAL INVESTIGATIONS

The preparation of pure Fe—P—B alloys in equilibrium proved difficult. Heat treatments must be made in closed containers to avoid phosphorus losses at high temperatures. Since the alloys sometimes react with silica, the simple method of heating the elements together in evacuated and sealed silica tubes leads to contamination, mostly by oxygen and also to some extent by silicon. Nevertheless, preliminary investigations of the Fe—P—B system were made on a large number of alloys of purities about 97 %, prepared by heating iron powder (98 %), red phosphorus (99 %) and boron (97 %) in silica tubes. The data obtained from these alloys were quite consistent and provided a rough general picture of the system. In order to substantiate the results, efforts were made to prepare a smaller number of pure alloys in selected parts of the system.

Experimental

Preparation

The starting materials were iron powder or iron rods (both *ex* Johnson, Matthey & Co. Ltd., London, spectrographically standardized, the former containing about 5 % oxygen, the latter only very small amounts of gaseous impurities), red phosphorus (purity higher than 99 %) and boron, (Borax Consolidated Ltd., London, purity higher than 99 %).

Master alloys of iron borides were made by sintering iron powder and boron in a high-frequency vacuum furnace as follows. The mixed powders were pressed into pellets and heated in crucibles of pure aluminium oxide (Degussit Al 23 from Degussa, Frankfurt) lined with boron nitride (Norton Company, Massachusetts). The boron oxide formed by reduction was separated magnetically, and the process of sintering and magnetic separation was repeated until no more boron oxide could be eliminated. The final products had a purity higher than 99.7 %, the remaining impurities being mainly oxygen.

Master alloys of iron phosphides were made by dropping pellets of red phosphorus into molten iron, contained in a Degussit Al 23 crucible. The melting was done by induction heating in a closed chamber filled with argon, previously purified over hot calcium chips and over hot turnings of a 1:1 titanium-zirconium alloy. On analysis, phosphides prepared in this way gave totals for iron and phosphorus between 99.94 % and 100.02 %.

Ternary Fe—P—B alloys were prepared as follows. Appropriate mixtures of the master alloys were melted rapidly in an argon-filled arc furnace using the lowest possible temperature to avoid excessive phosphorus losses. Equilibrium was attained only after prolonged heat treatment. For this purpose the alloys, contained in small alumina crucibles, were sealed under vacuum in silica tubes. The annealing time (after which no further changes were noticed on the powder photographs of the alloys) was generally 1—2 weeks, and the alloys were quenched in oil or water. Small amounts of oxygen unavoidably entered the alloys during the final heat-treatments, but the total amount of impurities in the final products could generally be kept below 1 %.

The ternary alloys containing chromium, manganese, cobalt or nickel were prepared by heating the elements directly in silica tubes. No chemical analyses were made, but from the appearance of the silica tube walls it was estimated that the impurity content of these alloys is no higher than that of the iron alloys made in the same way.

Chemical analysis

The chemical analyses were performed by the Analytical Department of this Institute.

Determination of iron and phosphorus. The sample was dissolved in *aqua regia* and iron and phosphorus were determined in separate aliquots of this solution.

For the determination of iron, the solution was evaporated with nitric acid, which was afterwards removed by evaporation with sulphuric acid. The diluted solution was passed through a cadmium reductor, and then titrated with 0.1 N cerium sulphate, previously standardized against a solution prepared from spectrographically pure iron rods (Johnson, Matthey & Co, London).

Phosphorus was determined as follows. The solution was evaporated twice with nitric acid to remove the hydrochloric acid, and the residue dissolved in perchloric acid. Oxidation to orthophosphoric acid was completed by boiling the solution for a few minutes. Phosphorus was determined by precipitating ammonium molybdophosphate and weighing as $P_2O_5 \cdot 24MoO_3$ according to Nydahl [3].

Determination of boron. The sample was dissolved by refluxing with dilute sulphuric acid, hydrogen peroxide and a few drops of hydrochloric acid. The boric acid was separated as methyl borate by distillation, and titrated potentiometrically with sodium hydroxide in the presence of mannitol.

X-Ray methods

X-Ray powder photographs were taken with Guinier-type focussing cameras using Cr*Ka* radiation and with calcium fluoride (a = 5.4630 Å) or silicon (a = 5.4305 Å) as internal calibration standards. Although the accuracy of a single lattice parameter determination is not claimed to be higher than 0.04 %, lattice parameter differences larger than 0.02 % for a given phase, measured in different alloys, are considered significant.

The binary boundary systems

Fe—P. The system has been investigated by several methods, and previous work is summarized in Ref.[4]. The existence of the intermediate phases Fe_3P, Fe_2P, FeP and FeP_2 has been demonstrated. The existence of phosphides with a phosphorus content higher than FeP_2 has also been claimed [5].

Fe—B. The system has been investigated in the range 0—50 atom % boron (for references, see Ref.[4]). Two intermediate phases exist, *viz.* Fe_2B and FeB. It has been claimed that FeB has two modifications [6]. In the present work only the normal *B* 27 structure for FeB was observed.

B—P. This system is still incompletely known. The existence of the compound BP, first reported by Besson [7] and Moissan [8,9], has been confirmed by several investigations [10–12]. The existence of B_5P_3, claimed by Moissan [9], has not been confirmed, but a boron phosphide of the approximate composition $B_{13}P_2$ has been prepared by Matkovich [13].

During the present investigation, the author observed the appearance of BP in ternary Fe—P—B alloys. BP was sometimes obtained as orange-red, octahedral crystals of remarkable hardness. Weissenberg photographs of these crystals confirmed the proposed zincblende structure. Heating boron and phosphorus in evacuated and sealed silica tubes yielded BP as the only identifiable reaction product. However, when BP was heated strongly in an argon-filled arc furnace, some phosphorus volatilized, leaving a very hard, grey-black residue. The powder photographs of this substance showed the presence of boron together with another phase, which gave diffraction data in close agreement with those quoted by Matkovich [13] for $B_{13}P_2$. No traces of $B_{13}P_2$ were, however, found in Fe—B—P alloys. This phase is presumably formed only at temperatures higher than 1 100°C.

Table 1. Crystallographic data for the binary phases. (Unit cell dimensions (Å) determined in the present investigation).

Compound	*Space group*	*Structure type*	*a*	*b*	*c*
Fe_3P	$I\,\bar{4}$	$D\,0_c$	9.107	—	4.460
Fe_2P	$P\,\bar{6}2m$	C 22 *	5.865	—	3.456
FeP	$Pnma$	B 31	5.191	3.099	5.792
FeP_2	$Pnnm$	C 18	4.971	5.654	2.719
Fe_3B	$I\,4/mcm$	C 16	5.109	—	4.249
FeB	$Pnma$	B 27	5.502	2.948	4.057
BP	$F\,\bar{4}3m$	B 3	4.538	—	—

* revised structure type [22].

The ternary system Fe—P—B

Since the author was primarily interested in the crystal structure data of the Fe—P—B system, only X-ray and chemical analyses were used in this investigation. Although in general, accurate determinations of phase-boundaries and tie-lines were not attempted, the main three-phase equilibria were determined. In addition, lattice parameters were determined for the binary phases (see Table 1) and for all phases appearing in the various three-phase triangles (see Table 2). The isothermal section of the Fe—P—B system given in Figs. 1 and 2 was constructed using results from the phase-analyses of alloys annealed at 1 000° for 7—14 days and quenched. The investigation was restricted to the range Fe—FeP_2—BP—FeB—Fe. Alloys with a non-metal content less than 10 atom % were not studied.

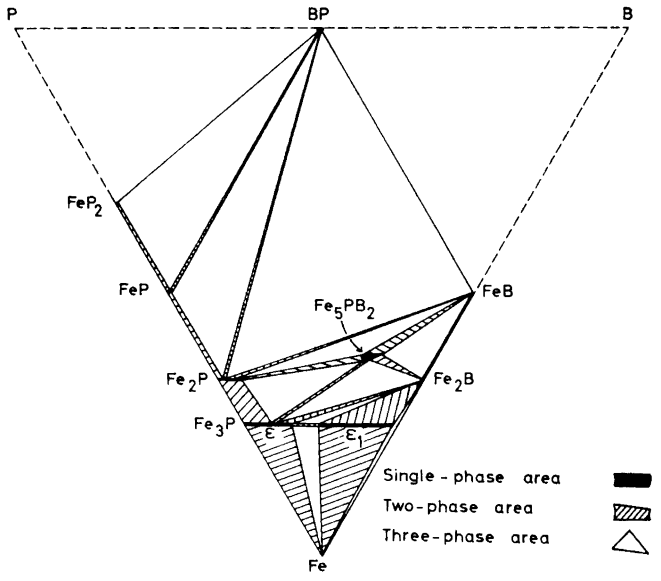

Fig. 1. Isothermal section at 1 000°C of the Fe—P—B system. (Some of the areas are enlarged for clarity).

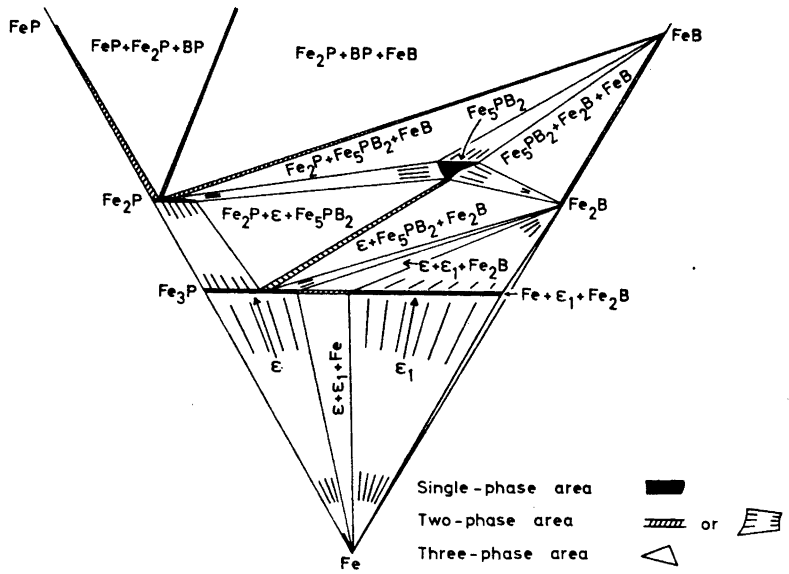

Fig. 2. Isothermal section at 1 000°C of the Fe—P—B system. (Some of the areas are enlarged for clarity. The two-phase area Fe + Fe_2B is not indicated).

The data obtained for the pure binary phases were in agreement with earlier investigations. Phase transformations were not detected in binary and ternary alloys quenched from different temperatures up to the melting point or, for high-melting alloys, up to 1 100°C.

No unit cell variations were found for Fe_2B, FeB and BP in different parts of the system. In ternary alloys, the unit cell of α-iron appeared to be slightly

Table 2. Unit cell dimensions (Å) of Fe_2P, Fe_5PB_2, ε and ε_1 in the various three-phase equilibria. Measurements are made on alloys annealed at 1 000°C for 7—14 days and quenched. The unit cell dimensions of FeP_2, FeP, FeB, Fe_2B and BP are not significantly different from the values quoted in Table 1.

Three-phase equilibrium	Fe_2P		Fe_5PB_2		ε		ε_1	
	a	*c*	*a*	*c*	*a*	*c*	*a*	*c*
FeP + Fe_2P + BP	5.872	3.442						
Fe_2P + BP + FeB	5.872	3.442						
Fe_2P + Fe_5PB_2 + FeB	5.900	3.404	5.493	10.370				
Fe_2P + Fe_5PB_2 + ε	5.923	3.350	5.485	10.349	9.025	4.435		
ε + Fe_5PB_2 + Fe_2B			5.483	10.345	9.013	4.428		
Fe_5PB_2 + FeB + Fe_2B			5.473	10.316				
ε + ε_1 + Fe_2B					8.968	4.414	8.888	4.401
ε + ε_1 + α-Fe					8.968	4.414	8.888	4.401

Table 3. X-Ray and chemical analytical data for $Fe_3P_{1-x}B_x$ alloys.

Alloy	Chemical analysis(weight %)				Phases observed in powder photographs	Calculated composition of ε and ε_1	Lattice parameter		Unit cell volume (Å^3)
	Fe	P	B	Σ			a(Å)	c(Å)	
$Fe_{2.990}P$	84.37	15.65	—	100.02	ε	Fe_3P	ε : 9.107	4.460	369.9
$Fe_{3.092}P$	84.74	15.20	—	99.94	ε + α-Fe	Fe_3P	ε : 9.107	4.460	369.9
$Fe_{3.19}P_{0.92}B_{0.08}$	84.90	13.52	0.43	98.85	ε + α-Fe	$Fe_3P_{0.92}B_{0.08}$	ε : 9.068	4.447	365.7
$Fe_{3.03}P_{0.81}B_{0.19}$	85.88	12.72	1.04	99.54	ε	$Fe_3P_{0.81}B_{0.19}$	ε : 9.022	4.431	360.7
$Fe_{3.17}P_{0.71}B_{0.29}$	87.07	10.85	1.54	99.46	ε + α-Fe	$Fe_3P_{0.71}B_{0.29}$	ε : 8.975	4.415	355.6
$Fe_3P_{0.6}B_{0.4}$	—	—	—	—	ε + ε_1	—	ε : 8.968 ε_1: 8.888	4.414 4.401	355.0 347.7
$Fe_{3.10}P_{0.45}B_{0.55}$	88.78	7.21	3.03	99.02	ε_1 + α-Fe	$Fe_3P_{0.45}B_{0.55}$	ε_1: 8.848	4.387	343.4
$Fe_{3.01}P_{0.35}B_{0.65}$	89.92	5.84	3.75	99.51	ε_1	$Fe_3P_{0.35}B_{0.65}$	ε_1: 8.801	4 370	338 5
$Fe_{3.06}P_{0.24}B_{0.76}$	91.19	4.04	4.37	99.60	ε_1	$Fe_3P_{0.24}B_{0.76}$	ε_1: 8.752	4.353	333.4
$Fe_{2.93}P_{0.16}B_{0.84}$	90.67	2.68	5.06	98.41	ε_1 + Fe_2B	$Fe_3P_{0.17}B_{0.83}$	ε_1: 8.707	4.336	328.7
$Fe_{2.85}P_{0.05}B_{0.95}$	92.32	0.89	5.91	99.12	ε_1 + Fe_2B	$Fe_3P_{0.06}B_{0.94}$	ε_1: 8.649	4.316	322.9

smaller than that of pure iron, but the difference was near the limit of experimental error. This observation is, however, in qualitative agreement with the data obtained by Gale [14] for solid solutions of phosphorus in iron. The pure binary phosphides showed no lattice parameter variation, but in ternary alloys, small variations (detected only at temperatures above 1 100°C) were observed for FeP, larger variations for Fe_2P and very large variations for Fe_3P.

The system contains two new ternary phases in addition to the binary phases already reported. One ternary phase has a crystal structure (see below) corresponding to the formula Fe_5PB_2, but small variations in the unit cell dimensions (see Table 2) indicate deviations from the ideal composition. The other ternary phase has a variable composition corresponding to the formula $Fe_3P_{1-x}B_x$. This phase has a striking structural similarity to Fe_3P (see below). In his investigation of the Fe—P system, Hägg [15] has denoted the Fe_3P phase by the symbol ε. For convenience, this notation is used in the following text for phases with the Fe_3P structure, while the symbol ε_1 is used for phases with the closely similar structure.

Phase-analytical data and unit cell dimensions for a series of alloys with compositions near the line Fe_3P—Fe_3B are collected in Table 3. ε and ε_1 are both tetragonal with similar unit cell dimensions. While the alloys do not contain ε or ε_1 alone, the compositions of these phases can be calculated from the figures in Table 3 assuming:

1) a metal/non-metal atomic ratio equal to 3,
2) a small solid solubility of boron and phosphorus in α-Fe,
3) a small solid solubility of phosphorus in Fe_2B,
4) a negligible effect of the impurities.

The first assumption is supported by the appearance of α-Fe in the alloys with a metal/non-metal atomic ratio larger than 3 and of Fe_2B in the alloys with a ratio smaller than 3. The solubilities of phosphorus and boron in α-Fe are small [4], and judging from the previously mentioned lattice parameter values

for α-Fe in ternary alloys, the simultaneous solubility of the non-metals in α-Fe is also very restricted. Within the limits of experimental error, the lattice parameters of Fe_2B are unchanged in ternary alloys, and this together with crystal-chemical considerations is taken as support of the third assumption. As regards contamination, the main impurities are oxygen and silicon, and the errors in the fourth assumption arise from the extrapolation of results from the quinary system Fe—P—B—O—Si to the ternary system Fe—P—B.

Some information on the influence of impurities was collected from a phase analysis of carefully annealed $Fe_3P_{1-x}B_x$ alloys containing 2—3.5 % oxygen and 0.1—0.2 % silicon. The powder photographs of these alloys contained only lines from the phases in the ternary Fe—P—B system. The absence of diffraction lines belonging to oxygen- or silicon-containing impurity phases may be explained as follows: the impurities are dissolved in the ε, ε_1 or α-Fe lattices, alternatively the impurity phases have a small scattering power, or else they are present in a finely divided state. A microscopic examination revealed the presence in several alloys of small, white globules of boron oxide. This phase was not detected in the powder photographs owing to its small scattering power. However, in the boron-poor alloys at least, boron oxide cannot be the only oxygen-containing phase. As an example, data are quoted for an alloy with the following analysis: iron 86.8 %, phosphorus 8.68 %, boron 0.94 %, silicon $\sim$ 0.2 % and oxygen (by difference) 3.4 %. The powder photograph of this alloy contained lines from α-Fe and ε. The lattice parameters of ε (a = 9.023 Å; c = 4.432 Å) indicate that part of the boron is dissolved in this phase. Even if all the boron were combined with oxygen as B_2O_3, 1.3 % oxygen remains to be accounted for. The possibility of solid solubility of oxygen in ε hardly seems probable. In ternary Fe—P—O alloys, no lattice parameter variations for Fe_3P were observed. The remaining oxygen may therefore be present as an iron oxide or an iron phosphate.

A substantial expansion of the Fe_3P unit cell observed in Fe—P—Si alloys indicates that silicon can substitute for phosphorus in the ε phase. However, if silicon is dissolved in ε or ε_1, the limited amount (0.1—0.2 %) has no serious effect on the lattice parameter determinations.

From the above mentioned observations it is evident that the compositions of ε and ε_1 cannot be corrected for impurities in a simple and accurate way. The compositions of ε and ε_1 given in Table 3 are calculated by disregarding the impurities. A comparison of the data in Table 3 with those obtained for

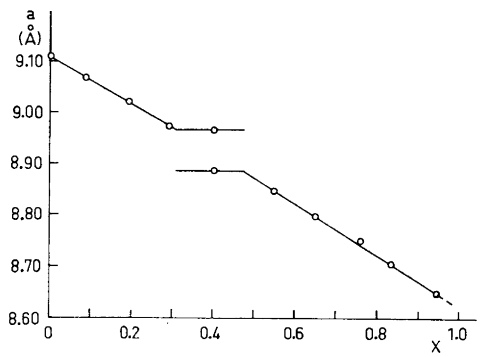

Fig. 3. Variation of the a axis with the boron content in $Fe_3P_{1-x}B_x$.

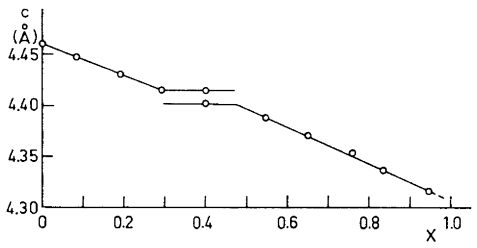

Fig. 4. Variation of the c axis with the boron content in $Fe_3P_{1-x}B_x$.

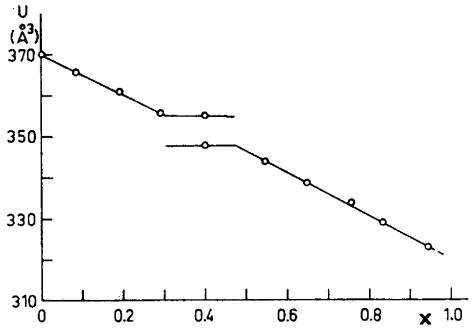

Fig. 5. Variation of the cell volume with the boron content in $Fe_3P_{1-x}B_x$.

the oxygen-rich alloys indicated that the boron/phosphorus atomic ratio in the impurity phases is larger than 1, except possibly in the most phosphorus-rich alloys. This means that the boron/phosphorus ratios for ε and ε_1 given in Table 3, are slightly too high.

In Figs. 3, 4, and 5 curves of lattice parameter *versus* composition are plotted for ε and ε_1. It is seen that at 1 000°C, the boron-rich limit of ε lies close to the composition $Fe_3P_{0.70}B_{0.30}$ and the phosphorus-rich limit of ε_1 close to $Fe_3P_{0.52}B_{0.48}$. The boron-rich limit of ε_1 could not be located with certainty. Since ε_1 does not exist in the binary Fe—B system, a three-phase region α-Fe + ε_1 + Fe_2B should exist in the ternary system. In spite of numerous attempts it was not possible to prepare an alloy containing the three phases in equilibrium. One alloy contained α-Fe and ε_1 for which $a = 8.618$ Å. This value is close to the limiting a-value found by extrapolation of the curve in Fig. 3 to the composition Fe_3B. Unfortunately, the amount of this alloy was too small for accurate chemical analysis. However, it seems highly probable that ε_1 is stable down to a phosphorus/boron atomic ratio less than 0.01. The virtual impossibility of obtaining a three-phase α-Fe + ε_1 + Fe_2B alloy may be attributable both to unfavourable reaction kinetic factors and to the difficulty of detecting very small amounts of a phase by the X-ray technique.

The unit cell variation of Fe_2P in the ternary alloys occurs mainly through phosphorus/boron substitution, but no accurate determination of the single-phase boundaries was attempted. The data indicate a maximum phosphorus/boron substitution of the order of 10 % at 1 000°C. The single-phase area is larger at higher temperatures. The single-phase boundaries of Fe_5PB_2 were not studied in detail. Phase-analytical data for two alloys, one lying in the two-phase region ε + Fe_5PB_2 and the other in the single-phase area close to the region ε + Fe_5PB_2, are given in Table 4. A metal/non-metal atomic ratio larger than 5/3 is indicated. It is felt that small amounts of ε may be present in the apparently single-phase Fe_5PB_2 alloy without being detected in the powder photographs, and that the metal/non-metal atomic ratio may accordingly be smaller than 5.12/3. The boron/phosphorus atomic ratio is, however, definitely larger than 2/1, even assuming the total impurity content to be boron oxide. Small amounts of ε in the alloys would not invalidate this conclusion, since the boron/phosphorous atomic ratio is much smaller in ε than in

Table 4. X-Ray and chemical analytical data for Fe_5PB_2 alloys.

Alloy	Chemical analysis (weight %)				Phases observed in powder photographs	Lattice parameters of Fe_5PB_2	
	Fe	P	B	Σ		a (Å)	c (Å)
$Fe_{5.23}P_{0.95}B_{2.05}$	84.19	8.52	6.38	99.09	$\varepsilon + Fe_5PB_2$	5.485	10.346
$Fe_{5.12}P_{0.92}B_{2.08}$	84.38	8.46	6.63	99.47	Fe_5PB_2	5.485	10.349

Fe_5PB_2. A boron/phosphorus atomic ratio larger than 2/1 is also in accordance with crystal-chemical considerations to be discussed later in this paper.

Some data for the systems Cr—P—B, Mn—P—B, Co—P—B and Ni—P—B

The results from the Fe—P—B system aroused interest in ternary systems containing the transition metal neighbours of iron in the periodic system. Owing to the experimental difficulties, only a very limited number of alloys in selected parts of the systems were investigated.

The Cr—P—B system. To prepare ternary Cr—P—B alloys, temperatures above 1 100°C were found to be necessary, and consequently only limited results were obtained by the silica tube technique. It was found, however, that Cr_3P dissolves boron, as is demonstrated by the measured lattice parameters. For Cr_3P, $a = 9.185$ Å; $c = 4.560$ Å (somewhat different from the values given by Nowotny and Henglein [16], and by Schönberg [17], but in good agreement with those obtained by Lundström [18]), whereas for the ε phase in an alloy with the nominal composition $Cr_3P_{0.8}B_{0.2}$, $a = 9.134$ Å; $c = 4.545$ Å.

The Mn—P—B system. As with Cr_3P and Fe_3P, Mn_3P was also found to dissolve boron. The measured lattice parameters of binary Mn_3P are $a = 9.181$ Å; $c = 4.568$ Å (the c axis differs from the value given by Årstad and Nowotny [19]) whereas for the ε phase in an alloy, quenched from 950°C with the nominal composition $Mn_3P_{0.5}B_{0.5}$ and containing small amounts of Mn_4B, the parameter values are $a = 9.121$ Å; $c = 4.530$ Å. There were no indications that an ε_1 type phase occurs in this system. A ternary phase close to the composition Mn_5PB_2 was found to be isomorphous with Fe_5PB_2. The measured lattice parameters display a similar variation to those of Fe_5PB_2, and are approximately $a = 5.54$ Å; $c = 10.49$ Å.

The Co—P—B system. A phosphide Co_3P of the ε type does not occur in the binary Co—P system [4]. Nevertheless, ternary phases of both the ε and ε_1 types exist in the ternary Co—P—B system. The lattice parameters of ε, measured in alloys quenched from 950°C, ranged from $a = 8.780$ Å; $c = 4.336$ Å (phosphorus-rich) to $a = 8.752$ Å; $c = 4.326$ Å (boron-rich). The corresponding values for the ε_1 phase were $a = 8.686$ Å; $c = 4.303$ Å; and $a = 8.673$; $c = 4.297$ Å. These values suggest that the homogeneity ranges are much smaller than those for the corresponding iron phases. Although compositions were not determined accurately, compositions close to $Co_3P_{0.5}B_{0.5}$ for the ε

phase and to $Co_3P_{0.3}B_{0.7}$ for the ε_1 phase were indicated. Lattice parameter variations of Co_2P and CoP in ternary alloys indicated some boron solubility in these phases. The Co—P—B system also contains a ternary phase of the Fe_5PB_2 type, with small lattice parameter variations. The approximate unit cell dimensions for Co_5PB_2 were found to be $a = 5.42$ Å; $c = 10.20$ Å.

The Ni—P—B system. In contrast to the above-mentioned systems, Ni_3P does not dissolve any appreciable amounts of boron. Within the limits of experimental error the unit cell dimensions of Ni_3P were unchanged in ternary Ni—P—B alloys. The rather complicated Ni—P—B system was not studied in any detail. Changes of the Ni_2P unit cell dimensions were observed which indicated a substantial boron solubility in this phase.

II. THE CRYSTAL STRUCTURES OF Fe_3P, $Fe_3P_{0.37}B_{0.63}$ AND Fe_5PB_2

Among the phases occurring in the ternary Fe—P—B system, the crystal structure types have been determined [10-12,20-25] for Fe_2B, FeB, Fe_3P, Fe_2P, FeP, FeP_2 and BP (see Table 1). Accurate interatomic distances have at present been determined only for Fe_2P and BP.

The subsequent part of this paper contains accounts of the structure determinations of the ε_1 and Fe_5PB_2 phases, and of the refinement of the Fe_3P structure.

Experimental

Single crystal fragments were selected from alloys prepared as described above. Fragments with uniform cross-sections not larger than 0.05 mm were chosen so that absorption effects should be as low as possible.

Unit cell dimensions were determined using Guinier-type powder cameras with Cr$K\alpha$ radiation, giving an estimated accuracy of 0.04 %.

Weissenberg photographs were taken using MoK radiation and the multiple-film technique with thin iron foils between successive films. The intensities were estimated visually. No direct corrections for absorption were made. Corrections for Lorentz and polarisation factors together with Fourier summations, structure factor calculations, and calculations of interatomic distances were made on the electronic digital computer BESK using programmes devised by Westman *et al.*[26], Åsbrink *et al.*[27] and Liminga [28]. Atomic scattering factors were taken from tables given by Thomas and Umeda [29] for iron, by Tomiie and Stam [30] for phosphorus and by Ibers [31] for boron. The real part of the dispersion correction, taken from the table by Dauben and Templeton [32], was included in the structure factor calculations. Standard deviations of the atomic parameters were estimated by Cruickshank's [33] formula. (Lists of observed and calculated structure factors can be obtained from this Institute on request.)

The structure of Fe_3P

Fe_3P is isostructural with Ni_3P, the structure of which was determined by Aronsson [22]. The space group of Ni_3P is $I\,\bar{4}$, with 24 nickel atoms in three sets of eightfold positions and 8 phosphorus atoms in one eightfold position.

The Weissenberg photographs of Fe_3P were taken about the a-axis and the c-axis. The intensity data were consistent with the proposed structure, and the atomic positions were refined starting with the parameter values given by Aronsson for Ni_3P. Successive difference syntheses were made in the ab and ac projections. 138 $F(hk0)$- and 83 $F(h0l)$-values were measured, and after

the final refinements R-values of 0.058 were obtained for both $F(hk0)$ and $F(h0l)$. (The very strong (004) reflexion was omitted because of serious extinction effects.)

Isotropic temperature factors with $B = 0.37_8$ Å^2 for $F(hk0)$ and $B = 0.41_4$ Å^2 for $F(h0l)$ were applied. The differences between the two sets of x and y parameters obtained from the ab and ac projections were smaller than the standard deviations.

The final structural data for Fe_3P are as follows,

Space-group $I\ \bar{4}\ -(S_4^2)$ $a = 9.107$ Å; $c = 4.460$ Å; $U = 369.9$ Å^3; $Z = 8$.

Atoms in 8(g)	x	$\sigma(x)$	y	$\sigma(y)$	z	$\sigma(z)$
Fe_I	0.0793	0.0002	0.1059	0.0002	0.2338	0.0008
Fe_{II}	0.3605	0.0002	0.0310	0.0002	0.9860	0.0008
Fe_{III}	0.1717	0.0002	0.2195	0.0002	0.7548	0.0008
P	0.2921	0.0004	0.0454	0.0004	0.4903	0.0014

Interatomic distances are given in Table 5. A projection of the structure on the basal plane is given in Fig. 6.

The structure of ε_1 with the composition $Fe_3P_{0.37}B_{0.63}$

The powder photographs of the ε_1 phase show strong similarities to those of the ε phase. The diffraction lines can be indexed on the basis of tetragonal unit cells with dimensions similar to those of ε. Reflexions with $h + k + l = 2n + 1$ are present, however, showing that the cell is primitive.

A single crystal of ε_1 suitable for X-ray work was found in an alloy with the nominal composition $Fe_3P_{0.35}B_{0.65}$. The powder photographs of this alloy (powder data are listed in Table 6) gave the following lattice parameter values for ε_1: $a = 8.812$ Å, $c = 4.375$ Å. From Figs. 3 and 4 it is seen that the real composition of the ε_1 sample is close to $Fe_3P_{0.37}B_{0.63}$.

The Weissenberg photographs indicated the Laue symmetry $4/m$. The following extinctions were observed: $(hk0)$ for $h + k = 2n + 1$, and $(00l)$ for $l = 2n + 1$. This points to the space group $P\ 4_2/n$. The $F(hk0)$ values for ε_1

Table 5. Interatomic distances in Fe_3P (Å). Distances shorter than 3.6 Å listed.

	Fe_I	Fe_{II}	Fe_{III}	P
Fe_I	2.41_0, 2.69_3 (2), 2.92_3 (2)	2.71_0, 2.87_1 3.53_6	2.51_8, 2.67_9, 2.77_1, 2.78_7, 2.83_3	2.31_7, 2.38_3, 3.55_5
Fe_{II}	2.71_0, 2.87_1, 3.53_6	2.60_3, 2.79_6 (2), 2.98_9 (2)	2.52_8, 2.58_6, 2.63_9, 3.52_0	2.30_1, 2.33_3, 2.33_8, 2.34_1
Fe_{III}	2.51_8, 2.67_9, 2.77_1, 2.78_7, 2.83_3	2.52_8, 2.58_6, 2.63_9, 3.52_0	2.70_5 (2)	2.26_0, 2.35_4, 2.40_7, 3.59_0
P	2.31_7, 2.38_3, 3.55_5	2.30_1, 2.33_3, 2.33_8, 2.34_1	2.26_0, 2.35_4, 2.40_7, 3.59_0	3.47_2 (2), 3.58_8 (2)

Table 6. Powder data for ε_1 with the composition $Fe_3P_{0.37}B_{0.63}$. (Cr$K\alpha$ radiation, $\lambda = 2.2909$ Å).

hkl	$\sin^2\Theta_{obs} \times 10^4$	$\sin^2\Theta_{calc} \times 10^4$	$p\,F^2_{calc} \times 10^{-3}$	I_{obs}
100	337	338	0.4	v.v.w
200	—	676	0.0	—
101	—	854	0.0	—
111	—	1 023	1.1	—
220	1 352	1 352	10.6	v.w
201	1 362	1 361	20.4	w
211	1 531	1 530	0.0	v.w
121			4.0	
310	1 691	1 690	7.9	v.w
130			0.8	
221	2 036	2 037	9.0	v.w
301	2 206	2 206	36.8	w
311	2 374	2 375	18.1	m+
131			136.2	
400	2 702	2 703	20.9	w
002	2 740	2 741	23.2	w
321	2 881	2 882	349.4	st+
231			176.4	
330	3 043	3 041	155.6	m
112	3 079	3 079	327.4	st
420	3 377	3 379	231.2	m+
240			0.1	
401	3 387	3 389	90.1	m—
202	3 418	3 418	89.5	m—
411	3 556	3 557	75.7	st+
141			365.7	
212	3 588	3 587	0.5	v.w
122			9.9	
331	3 726	3 726	36.9	w
421	4 063	4 064	10.1	m—
241			57.9	
222	4 093	4 093	132.7	m
302	4 264	4 262	16.9	w
510	4 393	4 393	4.3	m
150			148.8	
312	4 431	4 431	210.0	st—
132			0.0	
431	4 910	4 909	14.4	w
341			1.7	
501			4.3	
322	—	4 939	0.0	—
232			0.8	

are remarkably similar to the corresponding values for Fe_3P, and it was concluded that the two structures must look almost identical when viewed in projection on the basal plane. From this argument, and from a consideration of the different symmetry elements operating in the two space groups $I\bar{4}$ and $P4_2/n$, the following model was proposed for the structure of ε_1. The atomic

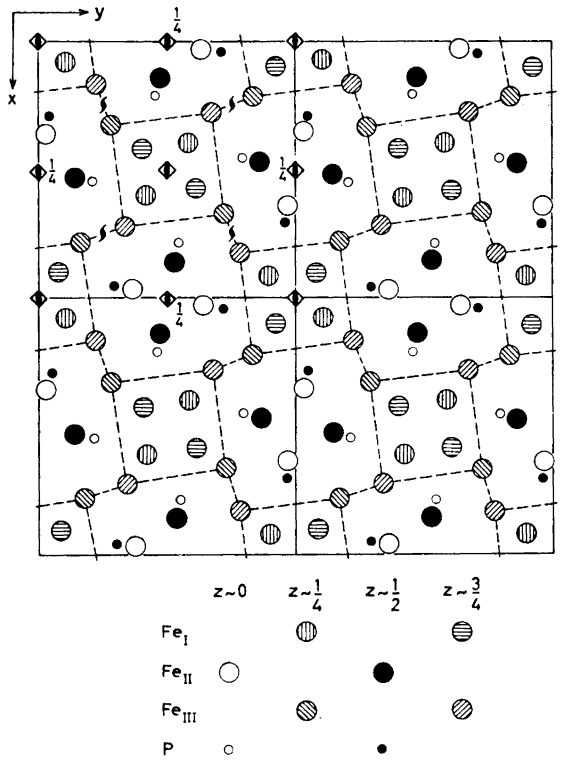

Fig. 6. The structure of Fe_3P projected on the basal plane.

coordinates for the asymmetric part of the Fe_3P structure (referring to the origin at $\bar{4}$ in $I\,\bar{4}$) are related to the corresponding coordinates in ε_1 (referring to $\bar{1}$ as the origin in $P\,4_2/n$) as follows:

$I\,\bar{4}$: atom in $x,\ y,\ z$
$P\,4_2/n$: corresponding atom in $x + \frac{3}{4},\ y + \frac{1}{4},\ z$

The electron density projections $\varrho(xy)$ and $\varrho(xz)$ were calculated for ε_1 on this basis. The signs of the structure factors were taken from the iron contributions only. In addition to the expected iron maxima, other maxima corresponding to an $8(h)$ position were discernible. The heights of these maxima were seen to correspond roughly to 9/26 of the iron maxima. Since no indications of superstructure reflexions could be detected, it was concluded that the boron and phosphorus atoms occupy one $8(h)$ position randomly.

The ε_1 structure was refined by the same methods as those described for Fe_3P. A weighted average of the atomic scattering factors for boron and phosphorus was used in the structure factor calculations. After the final refinements the following R-values were obtained: 59 observed $F(hk0)$ values $R = 0.104$, 41 observed $F(h0l)$ values $R = 0.108$. (The very strong (004) reflexion was

omitted because of extinction effects). Over all temperature factors with $B = 0.70$ Å^2 for $F(hk0)$ and $B = 0.65$ Å^2 for $F(h0l)$ were applied. The corresponding x and y parameters obtained from the ab and ac projections agreed within the limits of the standard deviations.

The satisfactory agreement between observed and calculated structure factors shows that the initial assumptions made for the ε_1 structure are most probably correct.

Structure data obtained for ε_1 with the composition $Fe_3P_{0.37}B_{0.63}$ are as follows:

Space group $P\ 4_2/n$ — (C_{4h}^4) $a = 8.812$ Å; $c = 4.375$ Å; $U = 339.7$ Å^3. (Origin at $\bar{1}$).

Atoms in 8(g)	x	$\sigma(x)$	y	$\sigma(y)$	z	$\sigma(z)$
Fe_I	0.1678	0.0004	0.6422	0.0004	0.731_2	0.0017
Fe_{II}	0.1115	0.0004	0.2813	0.0004	0.518_7	0.0017
Fe_{III}	0.0742	0.0004	0.5317	0.0004	0.242_4	0.0017
(0.37P + 0.63B) randomly	0.045_0	0.0013	0.294_9	0.0013	0.016	0.006

Interatomic distances are listed in Table 7. A projection of the structure on the basal plane is shown in Fig. 7.

Discussion of the ε (Fe_3P) and ε_1 structures

The packing of the atoms in ε and ε_1 is somewhat complicated. In order to illustrate the difference between the two structures more clearly, the following simple description may be convenient.

The Fe_I atoms are arranged in slightly distorted tetrahedra near the $\bar{4}$ axes with inversion at $z = 0$ in ε, and near the 4_2 axes in ε_1. The Fe_I tetrahedra are situated within larger (distorted) tetrahedra of Fe_{III} atoms. The Fe_I and Fe_{III} tetrahedra form a network throughout the structure (indicated in Figs. 6 and 7) leaving large "channels" along the $\bar{4}$ axes with inversion at $z = \frac{1}{4}$. In these "channels", (distorted) tetrahedra of Fe_{II} atoms are situated within

Table 7. Interatomic distances in $Fe_3P_{0.37}B_{0.63}$ (Å). Distances shorter than 3.5 Å listed. (X = non-metal atoms).

	Fe_I	Fe_{II}	Fe_{III}	X
Fe_I	2.39, 2.76 (4)	2.68, 2.78, 3.35	2.49, 2.57, 2.63, 2.72, 2.77	2.25, 2.27, 3.48
Fe_{II}	2.68, 2.78, 3.35	2.50, 2.69 (2) 2.94 (2)	2.50, 2.54, 2.55, 3.36	2.23, 2.24 2.26, 2.28
Fe_{III}	2.49, 2.57, 2.63 2.72, 2.77	2.50, 2.54, 2.55, 3.36	2.55, 2.67	2.17, 2.31 2.32, 3.47
X	2.25, 2.27 3.48	2.23, 2.24 2.26, 2.28	2.17, 2.31 2.32, 3.47	3.32 (2) 3.50 (2)

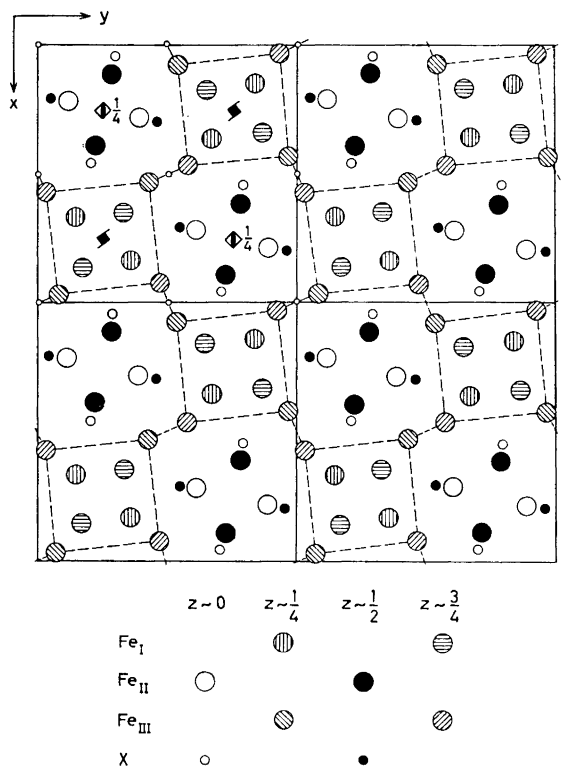

Fig. 7. The structure of ε_1 projected on the basal plane.

larger (distorted) tetrahedra of non-metal atoms. Whereas the network of Fe_I and Fe_{III} tetrahedra is almost identical in the two structures, the arrangement of the Fe_{II} and non-metal tetrahedra is different. In the ε structure the Fe_{II} and non-metal tetrahedra in one "channel" are translated a distance equal to $c/2$ along the tetragonal axis with respect to the tetrahedra with equal orientation in the four adjacent "channels". In the ε_1 structure the Fe_{II} and non-metal tetrahedra at the same c-level have approximately the same orientation in all "channels".

The above description shows that the main difference between the two structures lies in the "long-range" configuration of the atoms. The near environment of corresponding atoms in ε and ε_1 is very similar. One special feature is worth mentioning. There is one very short Fe_I—Fe_I distance in both ε and ε_1. The two Fe_I atoms have six close iron neighbours in common, and the short distance can be explained from geometric considerations as was shown by Frank and Kasper [34]. The Fe_I—Fe_I distance in ε_1 (2.39 Å) is only slightly shorter than that in ε (2.41 Å). In general, however, the Fe—Fe as well as the Fe—X (X = non-metal) distances are 0.07—0.08 Å shorter in ε_1 than in ε, as is shown by the values listed in Table 8.

Table 8. Average Fe—Fe and Fe—X (X = non-metal) distances in ε and ε_1.

Neighbours	Average in Fe_3P (Å)	Average in $Fe_3P_{0.37}B_{0.63}$ (Å)	Difference (Å)
Fe_I — 12Fe	2.73_4	2.67_4	$+ 0.06_0$
Fe_I — 2X	2.35_0	2.25_7	$+ 0.09_3$
Fe_{II} — 10Fe	2.75_1	2.68_0	$+ 0.07_1$
Fe_{II} — 4X	2.32_8	2.25_3	$+ 0.07_5$
Fe_{III} — 10Fe	2.67_5	2.59_8	$+ 0.07_7$
Fe_{III} — 3X	2.34_0	2.27_0	$+ 0.07_0$
X — 9Fe	2.33_7	2.26_0	$+ 0.07_7$

It might be expected, that the morphotropic transition from ε to ε_1 is dependent upon the size-effect of the non-metal atoms. However, from the comments made above, it appears that the near environment of the atoms found in ε_1 could be attained equally well in a structure of the ε type merely by a contraction of the unit cell and small adjustments of the atomic parameters. An explanation of the transition in terms of the size effect is therefore not obvious. Judging from the close similarity between ε and ε_1, the differences in free energy between the two structures must certainly be very small.

The crystal structure of Fe_5PB_2

Excellent single crystals of Fe_5PB_2 were often found in the annealed alloys. They occurred mostly as square plates with the *c* axis perpendicular to the plane and the *a* axes along the diagonals of the square.

Table 9. Powder data for an alloy containing Fe_5PB_2. (Cr*Ka* radiation, $\lambda = 2.2909$ Å).

hkl	$\sin^2\Theta_{obs} \times 10^4$	$\sin^2\Theta_{calc} \times 10^4$	$p\,F^2_{calc} \times 10^{-3}$	I_{obs}
002	—	492	0.0	—
110	872	873	6.0	v.w
112	1 365	1 365	16.3	w
200	1 747	1 746	8.9	v.w
004	1 967	1 966	47.3	w+
202	2 237	2 238	37.4	w+
211	2 306	2 306	278.3	st—
114	2 840	2 840	220.4	m+
—	3 241	—	—	v.w*
213	3 290	3 289	644.1	st +
220	3 493	3 492	136.7	m
204	3 712	3 713	473.0	st
222	—	3 984	3.4	—
310	4 365	4 366	463.6	st
006	4 424	4 424	74.7	w+
312	—	4 858	4.5	—

* The (211) reflexion from Fe_2B.

A single crystal was selected from an alloy, containing Fe_5PB_2 (lattice parameters, $a = 5.482$ Å; $c = 10.332$ Å) together with traces of Fe_2B. The powder data for this alloy are given in Table 9.

The Weissenberg photographs showed that the Laue symmetry is $4/mmm$, and the possible space groups I $4/mcm$, $I\,\bar{4}c2$ and $I\,4cm$ were indicated. From the unit cell dimensions and the general distribution of the intensities it seemed highly probable that Fe_5PB_2 should be isostructural with Cr_5B_3, the structure of which has been determined by Bertaut and Blum [35].

Starting with this assumption the electron density projection $\varrho(xz)$ was evaluated for Fe_5PB_2. The electron density map indicated ordered positions for the boron and phosphorus atoms, in a similar fashion to that found by Aronsson [36] for the boron and silicon atoms in Mo_5SiB_2.

The atomic parameters in Fe_5PB_2 were refined in the usual way. Large discrepancies between F_c and F_o values for the strongest reflexions (especially (004), (006), (008), (204), (400) and (600)) were, however, observed. Another set of intensity data were obtained using a very small crystal with a different habit to that of the first. Although the discrepancies for the strongest reflexions were reduced, they remained noticeable. Since both crystals were so small that the absorption effects could not be very serious, the discrepancies were thought to arise largely through extinction. This is consistent with the extremely perfect external shape of the crystals. In the subsequent refinement, the contributions from the above-mentioned reflexions were neglected. The final R-value for the 64 observed $F(h0l)$-values was 0.13 for the smallest crystal and 0.18 for the larger crystal. With the omission of the six strongest reflexions, the R-value was 0.08 for both crystals. An isotropic temperature factor with $B = 0.20$ Å^2 was applied.

The following structure data were obtained for Fe_5PB_2:

Space-group $I\,4/mcm$ — (D_{4h}^{18}) $a = 5.482$ Å; $c = 10.332$ Å; $U = 310.5$ Å^3; $Z = 4$.

			x	$\sigma(x)$	z	$\sigma(z)$
16	Fe_I	in 16(l)	0.1690	0.0005	0.1400	0.0003
4	Fe_{II}	in 4(c)				
8	B	in 8(h)	0.375	—		
4	P	in 4(a)				

Interatomic distances are listed in Table 10.

On account of the marked extinction effects in the intensity material, no attempt was made to refine the scattering parameters for the different atomic positions. The difference between the scattering parameters of the 8(h) and the 4(a) atoms was so large, however, that the conclusion regarding the ordered distribution of boron and phosphorus atoms must be essentially correct.

Discussion of the Fe_5PB_2 structure

The Cr_5B_3 ($D\,8_l$) type of structure has been thoroughly described and discussed by Parthé *et al.*[37] and by Aronsson [36], among others. Several silicoborides crystallize with this structure. Data given by Aronsson [36,2] show that lattice parameter variations for Mo_5SiB_2 and Fe_5SiB_2 are very similar to those for Fe_5PB_2. The smallest unit cell volume is found in boron-rich alloys,

Table 10. Interatomic distances in Fe_5PB_2 (Å). Distances shorter than 3.0 Å listed.

	Fe_I	Fe_{II}	B	P
Fe_I	2.60, 2.62, 2.88 (4) 2.89, 2.93 (2)	2.50 (2)	2.18, 2.16	2.33 (2)
Fe_{II}	2.50 (8)	—	2.17 (4)	2.58 (2)
B	2.18 (4) 2.16 (2)	2.17 (2)	1.94	—
P	2.33 (8)	2.58 (2)	—	—

which may indicate that boron substitutes for silicon and phosphorus to some extent. This is in accordance with the phase-analytical data quoted above. It must be pointed out, however, that the lattice parameter variations may also depend on simultaneous variations of the metal/non-metal ratio.

Aronsson [36] mentions that there are two types of "hole" in the metal atom lattice of the Cr_5B_3 type, which permit non-metal atoms of two different sizes to be neatly accomodated in the structure. The smaller non-metal atoms are situated in trigonal prismatic holes and the larger non-metal atoms in anti-prismatic holes. If in Mo_5SiB_2, the molybdenum radius is 1.38 Å the "hole" radii are 0.98 Å for the trigonal prismatic and 1.18 Å for the anti-prismatic holes. The corresponding values in Fe_5PB_2 (iron radius 1.26 Å) are 0.93 Å and 1.08 Å. It is seen that the sizes of the holes correspond roughly to the normal tetrahedral radii $r_B = 0.88$ Å; $r_P = 1.10$ Å and $r_{Si} = 1.17$ Å. The size-factor considerations indicate that boron may substitute for silicon and phosphorus, whereas substitution for boron by the larger non-metals is less probable.

General remarks on Me—P—B systems

The metal-rich transition metal borides, silicides and phosphides are known to have many crystal-chemical properties in common, and the present investigation gives further support to this general picture. In this respect the phosphorus/boron substitution in binary phosphide structures is especially noteworthy. Furthermore, the similarities between corresponding Me—P—B and Me—Si—B systems are very marked. Accordingly, a crystal-chemical discussion of transition metal phosphides and their relations to silicides and borides seems warranted, but is deferred to a later paper.

Acknowledgements. This work has been financially supported by the *Swedish State Council of Technical Research* and by the *Air Force Office of Scientific Research of the Air Research and Development Command, United States Air Force,* through its European Office under Contract No. AF 61(052)—40. Facilities for use of the electronic digital computer BESK were given by the *Swedish Board For Computing Machinery.*

The author wishes to thank Prof. G. Hägg for his encouraging interest and valuable comments on the manuscript. The author is indebted to Dr. B. Aronsson for valuable hints and many stimulating discussions during the investigation. Thanks are also due to Dr. L. Gustafsson for her very careful approach to the problems of chemical analysis.

REFERENCES

1. Aronsson, B. and Lundgren, G. *Acta Chem. Scand.* **13** (1959) 433.
2. Aronsson, B. and Engström, I. *Ibid.* **14** (1960) 1403.
3. Nydahl, F. *Lantbrukshögsk. Ann.* **10** (1942) 114.
4. Hansen, M. *Constitution of binary alloys. Mc Graw-Hill, New York-Toronto-London* 1958.
5. Heimbrecht, M. and Biltz, W. *Z. anorg. Chem.* **242** (1939) 233.
6. Fruchart, R. *C.r. Acad. Sci. Paris* **247** (1958) 1464.
7. Besson, M. A. *Ibid.* **113** (1891) 78.
8. Moissan, H. *Ibid.* **113** (1891) 624.
9. Moissan, H. *Ibid.* **113** (1891) 726.
10. Rundqvist, S. *XVI*^{e} *Congr. Int. de Chim. Pure et App., Section de Chim. Min., Sedes Paris* 1957, 539.
11. Popper, P. and Ingles, T. A. *Nature* **179** (1957) 1075.
12. Perri, J. A., La Placa, S. and Post, B. *Acta Cryst.* **11** (1958) 310.
13. Matkovich, V. I. *Ibid.* **14** (1961) 93.
14. Gale, B. *Acta Met.* **7** (1959) 420.
15. Hägg, G. *Nova Acta Regiae Soc. Sci. Upsaliensis,* Ser. IV, **7** (1929) No. 1.
16. Nowotny, H. and Henglein, E. *Z. anorg. Chem.* **239** (1938) 14.
17. Schönberg, N. *Acta Chem. Scand.* **8** (1954) 226.
18. Lundström, T. *Ibid.* **16** (1962). *In press.*
19. Årstad, O. and Nowotny, H. *Z. physik. Chem.* **B 38** (1937) 356.
20. Hägg, G. *Z. physik. Chem.* **B 11** (1930) 152.
21. Bjurström, T. *Arkiv Kemi, Mineral. Geol.* **11 A** (1933) No. 5.
22. Aronsson, B. *Acta Chem. Scand.* **9** (1955) 137.
23. Rundqvist, S. and Jellinek, F. *Ibid.* **13** (1959) 425.
24. Fylking, K.-E. *Arkiv Kemi Mineral Geol.* **11 B** (1935) No. 48.
25. Meisel, K. *Z. anorg. Chem.* **218** (1934) 360.
26. Westman, S., Blomqvist, G. and Åsbrink, S. *Arkiv Kemi* **14** (1959) 535.
27. Åsbrink, S., Blomqvist, G. and Westman, S. *Ibid.* **14** (1959) 545.
28. Liminga, R. Program available at BESK.
29. Thomas, L. H. and Umeda, K. *J. Chem. Phys.* **26** (1957) 293.
30. Tomiie, Y. and Stam, C. H. *Acta Cryst.* **11** (1958) 126.
31. Ibers, J. A. *Ibid.* **10** (1957) 86.
32. Dauben, C. H. and Templeton, D. H. *Ibid.* **8** (1955) 841.
33. Cruickshank, D. W. J. *Ibid.* **2** (1949) 65.
34. Frank, F. C. and Kasper, J. S. *Ibid.* **11** (1958) 184.
35. Bertaut, F. and Blum, P. *C.r. Acad. Sci. Paris* **236** (1953) 1055.
36. Aronsson, B. *Acta Chem. Scand.* **12** (1958) 31.
37. Parthé, E., Lux, B. and Nowotny, H. *Monatsh.* **86** (1955) 859.

Received June 21, 1961.

ACTA CHEMICA SCANDINAVICA 16 (1962) 20–30

Crystal Structure Investigations on the Zr-Al and Hf-Al Systems

LARS-ERIK EDSHAMMAR

Institute of Inorganic and Physical Chemistry, University of Stockholm, Stockholm, Sweden

A review is given of phase analysis and structure studies on the Zr-Al and Hf-Al systems. The structures and properties of the phases are discussed and compared with those of some transition metal borides and silicides and other metal phases.

The atomic parameters of Hf_2Al_3 have been refined.

When the work on the binary systems Zr—Al and Hf—Al was began at this Institute two years ago, the structures of only two phases, *viz.* Zr_3Al and $ZrAl_3$, were known in the zirconium-aluminium system. No investigation at all had been reported on the hafnium-aluminium system. Recently the two systems have been extensively investigated by the present author and independently by various other investigators. The intermetallic compounds that have been crystallographically characterized are listed in Table 1.

In this paper the results of the present phase analysis are given. Some features concerning the structures are discussed and the refinement of the crystal strutucre of Hf_2Al_3 is presented.

I. PHASE ANALYSIS OF THE Zr-Al AND Hf-Al SYSTEMS

Experimental

The alloys were prepared from weighed amounts of hafnium (98.5 % from I.C.I.), zirconium (99.9 % from Foote Mineral Company) and aluminium (99.99 %) by melting in an electric arc furnace under an atmosphere of argon. No chemical analyses have been made since the melting losses were relatively small — not exceeding 1 % up to aluminium contents corresponding to the formulae of $ZrAl_3$ and Hf_2Al_3. This implies that accurate data cannot be given for the actual compositions of various phases. The work has been concentrated on structure determinations and not on the phase diagram.

The specimens were also studied after a period of heating followed by quenching in water. The zirconium alloys were heated at 875°C and the hafnium alloys at 850°C for about 2—4 weeks. The heat treatments were carried out with pieces of the crushed alloys sealed in evacuated silica tubes. Tantalum foils protected the alloys from reacting with the silica.

Table 1. Crystallographic data of phases in the Zr-Al and Hf-Al systems. The unit axes given refer to the first reference in the reference column.

	Structure type	Lattice parameters (in Å)			Refs.
Zr_3Al	$L1_2$	$a = 4.372$			1
Zr_2Al	$D8_3$	$a = 4.894$	$c = 5.928$		2,3
Zr_5Al_3	$D8_m$	$a = 11.049$	$c = 5.396$		4
$Zr_5Al_3O_x$	ternary $D8_8$	$a = 8.177$	$c = 5.674$		4
Zr_3Al_2	tetragonal	$a = 7.630$	$c = 6.998$		5
Zr_4Al_3	hexagonal	$a = 5.433$	$c = 5.390$		6
Zr_2Al_3	orthorhombic	$a = 9.601$	$b = 13.906$	$c = 5.57$	7,3
$ZrAl_2$	$C14$	$a = 5.282$	$c = 8.748$		8
$ZrAl_3$	$D0_{23}$	$a = 4.306$	$c = 16.90$		9
$Hf_5Al_3O_x$	ternary $D8_8$	$a = 8.066$	$c = 5.678$		10,11
Hf_3Al_2	Zr_3Al_2	$a = 7.535$	$c = 6.906$		10,3
Hf_4Al_3	Zr_4Al_3	$a = 5.343$	$c = 5.422$		3,11
HfAl	B_f	$a = 3.253$	$b = 10.831$	$c = 4.282$	12
Hf_2Al_3	Zr_2Al_3	$a = 9.523$	$b = 13.763$	$c = 5.522$	13,3
$HfAl_2$	$C14$	$a = 5.23$	$c = 8.66$		11,3,4
$HfAl_3$	$D0_{23}$	$a = 3.98$	$c = 17.2$		11,3,4,14
$HfAl_3$	$D0_{22}$	$a = 3.93$	$c = 8.89$		11,3

The identification of the samples was performed by means of the X-ray powder patterns obtained in a Guinier focusing camera using monochromatized CuKa_1 radiation and with KCl as internal standard.

Results

The Zr—Al system. The zirconium-aluminium phase diagram was investigated by McPherson *et al.*[15] and the following intermediate phases were reported: Zr_3Al below 975°C, Zr_2Al below 1 250°C, Zr_5Al_3 formed from the melt but breaking down at lower temperatures, Zr_3Al_2 and Zr_4Al_3 both formed from melt, ZrAl formed in the solid state and stable below 1 250°C and Zr_2Al_3, $ZrAl_2$, $ZrAl_3$ all formed from melt.

The present study of the arc-melted alloys confirms the results of McPherson *et al.* However, the powder photograph of Zr_4Al_3 was diffuse depending on incomplete equilibrium. In the tempered region, there is one exception. The existence of the binary phase ZrAl reported by McPherson *et al.* could not be confirmed but it may be that this is a ternary phase containing hafnium since HfAl seems to be very stable. Because of slow reactions, each of the powder patterns of Zr_3Al, Zr_2Al and Zr_3Al_2 contained lines from their neighbouring phases.

The Hf—Al system. The phase diagram of the hafnium-aluminium system has so far not been described except for the aluminium end of the diagram [16]. The present study has revealed the existence of five binary compounds in arc-melted samples at the compositions of Hf_3Al_2, HfAl, Hf_2Al_3, $HfAl_2$ and $HfAl_3$. The same phases,and also a phase Hf_4Al_3, were found in samples heated at 850°C. Compound analogous to the zirconium phases Zr_3Al, Zr_2Al and Zr_5Al_3 have not been observed but the rate of reaction seems to be very low at 850°C in the hafnium-rich part of the system and therefore the phase conditions in this region merit further study.

II. SOME FEATURES CONCERNING THE CRYSTAL CHEMISTRY OF THE INTERMEDIATE PHASES FOUND IN THE Zr-Al AND Hf-Al SYSTEMS

Silicide-like structures: Me_5Al_3, Me_3Al_2 and MeAl.

There are many similarities in the crystal chemistry of some zirconium and hafnium-aluminides and the borides and silicides of the transition metals *. This does not seem to be the case with other transition metal aluminides. This is probably due to the atomic sizes, Zr and Hf being considerably larger than the other transition metals and giving a metal radius ratio with aluminium that is comparable with the ratios present in borides and silicides. This assumption seems to be supported by the fact that another large metal atom, thorium, also forms boride- and silicide-like aluminides, *viz.* Th_3Al_2 of the $D5_a$ type (*e.g.* V_3B_{1-2} and U_3Si_2), ThAl of the B_f type (*e.g.* CrB and CaSi) and Th_2Al of the $C16$ type (*e.g.* Cr_2B and Ta_2Si).

Me_5Al_3. Only one phase has been found with this composition, *viz.* Zr_5Al_3[4]. Zr_5Al_3 is isomorphous with W_5Si_3 of the $D8_m$ type and the structure is built up by a zirconium-aluminium net shown in Fig. 1a. This net is repeated along the *c*-axis by translating it half the diagonal distance of the *ab* plane marked in the figure. The holes between two successive nets are filled with aluminium and zirconium (*cf.* Fig. 1b). The zirconium atoms in the holes are fourteen-coordinated and form compressed chains along the *c*-axis like chains in other $D8_m$ structures. The Zr—Zr distances in these chains are 2.70 Å (normal Zr—Zr = 3.20). Wilson *et al.* described Zr_5Al_3 as belonging to the $D8_8$ structures [18]. In the present author's opinion, this is probably a ternary $D8_8$ phase

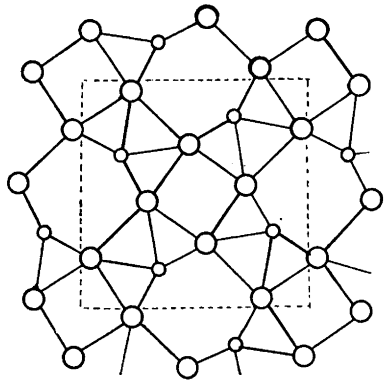

Fig. 1a. The metal atom net of Zr_5Al_3 ($D8_m$). Zr atoms are shown as large circles and Al atoms as small circles. The *ab* plane of the unit cell is indicated with dashed lines.

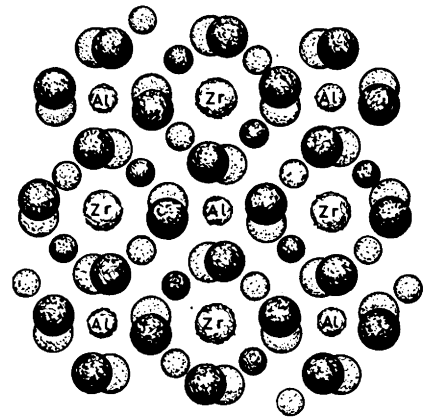

Fig. 1b. The atomic arrangement of Zr_5Al_3 ($D8_m$) seen along the *c*-axis. The lettered atoms are situated at $z = 1/4$ between the main layers at $z = 0$ and $z = 1/2$.

* The borides and silicides of the transition metals have recently been reviewed by Aronsson [17]

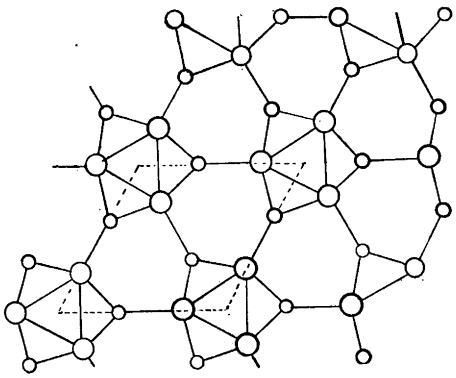

Fig. 2a. The metal atom net of $Zr_5Al_3O_x$ ($D8_8$).

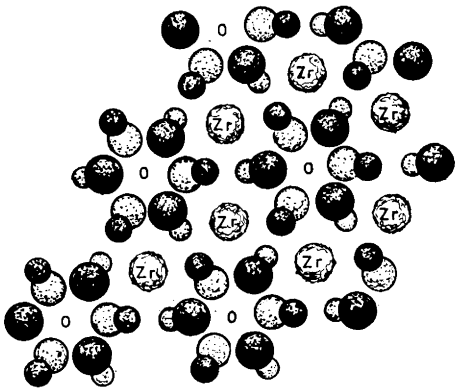

Fig. 2b. The atomic arrangement of $Zr_5Al_3O_x$ ($D8_8$) seen along the *c*-axis. The two main layers are at $z = 1/4$ and $z = 3/4$ and the lattered atoms at $z = 1/2$. The octahedral voids in 000 and 00 ½ are marked with the letter 0.

of the $Me_5Si_3(X)$ type (X = O) since a gradual addition of oxygen to the $D8_m$ phase finally gave pure $D8_8$ [4]. The ternary $D8_8$ phases have been studied particularly by Nowotny. Aronsson has suggested that the interstitial atoms are located in the octahedral voids of the $D8_8$ structure [19]. These voids are formed when the metal net seen in Fig. 2a is repeated along the *c*-axis by a rotation of 60°. The positions of the voids in the hexagonal cell are 000 and 00 ½ and if they are completely filled with oxygen the formula will than be Zr_5Al_3O. However, the oxygen contents have not so far been estimated and the formula is therefore written $Zr_5Al_3O_x$.

Though the $D8_m$ phase is not found in the hafnium-aluminium system, the ternary phase $Hf_5Al_3O_x$ ($D8_8$) is formed when oxygen is added to samples of the approximate composition $HfAl_{0.6}$.[10]

Me_3Al_2. The isotypic compounds Zr_3Al_2 and Hf_3Al_2 are very closely related to silicides belonging to the so-called $CuAl_2$ family. Following Frank and Kasper [20,21], structures of this type are built up by a square-triangle net $3^2.4.3.4$ or, in Black's notation, by an A-layer [22]. In the $D5_a$ type of structure represented by U_3Si_2, these A-layers are placed directly above each other. The cubic holes are filled with uranium atoms and the triangular prismatic holes with silicon. Zr_3Al_2 and Hf_3Al_2 are built up in the same way by two differently deformed A-layers. This arrangement (*cf.* Fig. 3) makes the *c*-axes of these phases twice the length of the *c*-axis of U_3Si_2 and the aluminium atoms are translated from their ideal positions at $z = 0.25$.

The ratio r_{Me}/r_X calculated for the seven U_3Si_2-type structures tabled by Aronsson [17] are between the values 1.31 and 1.67 if the C.N. 12 radii given in the same paper are used. The ratio $r_{Zr}/r_{Al} = r_{Hf}/r_{Al}$ should be about 1.2. The aluminium atom thus seems to be too large to fit into a regular triangular prism formed by hafnium or zirconium in an atomic arrangement of U_3Si_2 type.

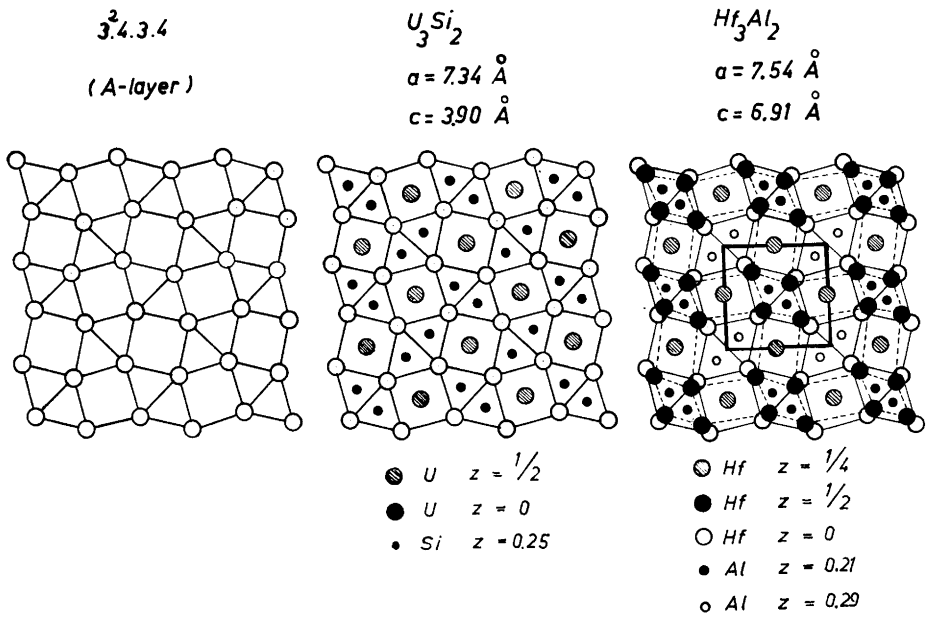

Fig. 3. The relationship between Hf_3Al_2 and U_3Si_2 ($D5_4$).

In this connection the tetragonal phase Zr_3Zn_2 reported by Petersen and Rinn [23] seems to be of considerable interest. A structure for this phase is not proposed by these authors but the X-ray data reported indicate that it is most probably isomorphous with Zr_3Al_2 and Hf_3Al_2. Since the radius of Zn is slightly larger than that of Al, this fact will support the assumption that the size factor is important for the formation of the Zr_3Al_2 type of structure.

MeAl. Only the compound HfAl has been found with this composition. HfAl is isomorphous with CrB. Short Al—Al distances corresponding to the short B—B distances along the zig-zag chains in CrB are not found in HfAl. According to Aronsson [17], the "electronic" requirements on the smaller component may not be crucial for the stability of the B_f-type structures. This assumption is exemplified by the structure of HfAl and even more by the phase CeNi recently reported by Finney and Rosenzweig [24].

The NiAs-family structure Zr_2Al.

The $B8_2$ structure Zr_2Al may also be included among the silicidelike phases. The $B8_2$ structures belong to the NiAs-family. The only silicide reported with a $B8_2$ structure is Ni_2Si but several silicides have the $C22$ and $C23$ type of structure which are also members of the NiAs-family. The occurrence of the $B8_2$ and $D8_8$ type, represented by Zr_2Al and Zr_5Al_3, belonging to the same binary system has been discussed by Wilson *et al.*[2] It may be observed, however that the $D8_8$-phase found in the zirconium-aluminium system is probably ternary.

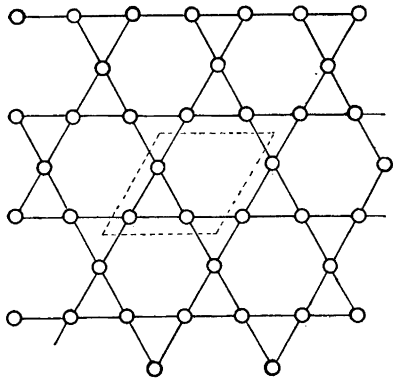

Fig. 4a. The kagomé net of aluminium in Zr_4Al_3.

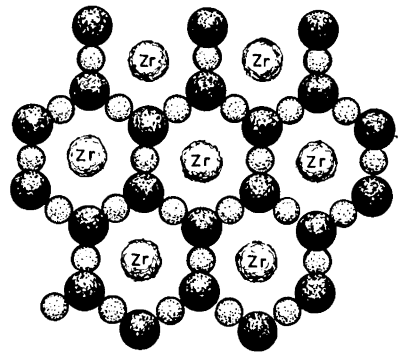

Fig. 4b. The atomic arrangement of Zr_4Al_3 seen along the *c*-axis. The kagomé net of aluminium is situated at $z = 0$, the honeycomb net of zirconium at $z = 1/2$ and lettered atoms at $z = 1/4$ and $z = 3/4$.

The σ-phase-like structure Me_4Al_3

The σ-like structure Me_4Al_3 contains metal chains with very short Me—Me distances (Zr—Zr = 2.70 Å), very much like the chains found in Zr_5Al_3 of the $D8_m$ type of structure (Zr—Zr = 2.70 Å). This is in agreement with the statement by Frank and Kasper [21] that the distances between atoms having this type of environment (Z14 atoms) should be short. It is interesting to note that the structure of Zr_3Al_2 (the composition of which is intermediate between those of the two former) contains Zr—Zr distances of normal length. This also suggests that the close metal-metal approach in Zr_4Al_3 and Zr_5Al_3 depends on the geometrical arrangement rather than on some kind of bonding between the metal atoms.

The similarity between the σ-phase and the Zr_4Al_3-type of structure was pointed out by Wilson *et al.*[6] The existence of σ-phases in the niobium and tantalum-aluminium systems, with the compositions Nb_2Al [25,26] and Ta_2Al [27], are worth noting in this connection. The structures of Zr_4Al_3 and Ta_2Al seen along the *c*-axis are demonstrated in Figs. 4 and 5. The large density of the Z14 atoms is the most striking resemblence between the two structure types. However, the layers that build up the structures differ consideribly. Ta_2Al is built up by a kagomé-tiling net containing both tantalum and aluminium atoms. This net is repeated along half the *c*-axis by the translation $a/2$ and $b/2$ and a rotation of 90°. Zr_4Al_3 on the other hand is built up from kagomé nets of aluminium atoms and hexagonal honeycomb layers of zirconium atoms stacked on each other along the *c*-axis.

As pointed out by Wilson *et al.*, the Zr_4Al_3 type of structure is identical with the hypothetical "split calcium $CaZn_5$ structure" derived by Frank and Kasper [20]. However, it is also interesting to observe the great similarities between Zr_4Al_3 and ε-TaN or also δ-TiO_x studied by Andersson and found to

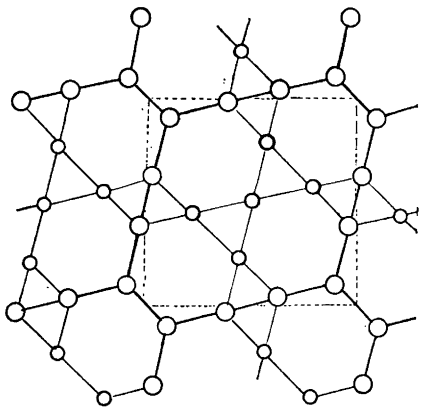

Fig. 5a. The kagomé-tiling net of Ta_2Al (σ-phase). Ta atoms are shown as large circles and Al atoms as small circles.

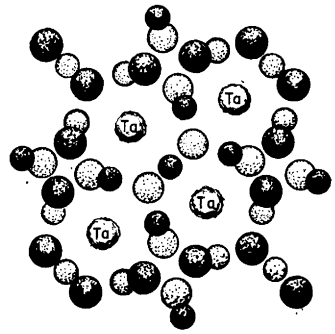

Fig. 5b. The atomic arrangement of Ta_2Al seen along the c-axis. The two kagomé nets are at $z = 0$ and $z = 1/2$ and the lettered Ta atoms at $z = 1/4$ and $3/4$.

show about 50 % vacancies in the nonmetal positions [28]. The latter structure may alternatively be described as an interstitial solution of oxygen in a metal structure of the ω-phase type. The analogies between $CaZn_5$, Zr_4Al_3 and δ-TiO_x are shown in Fig. 6. All these structures may be regarded as being built up by kagomé nets and honeycomb nets. The filling-in of the tunnels formed by the hexagons of the layers is different in the three structures.

Other structures

Zr_3Al ($L1_2$), $ZrAl_2$ ($C14$) and $HfAl_2$ ($C14$) belong to well-known structure families and will not be discussed here. Except for these structures and those described above, there are two other phases occurring in the two systems, *viz.* Me_2Al_3 and $MeAl_3$.

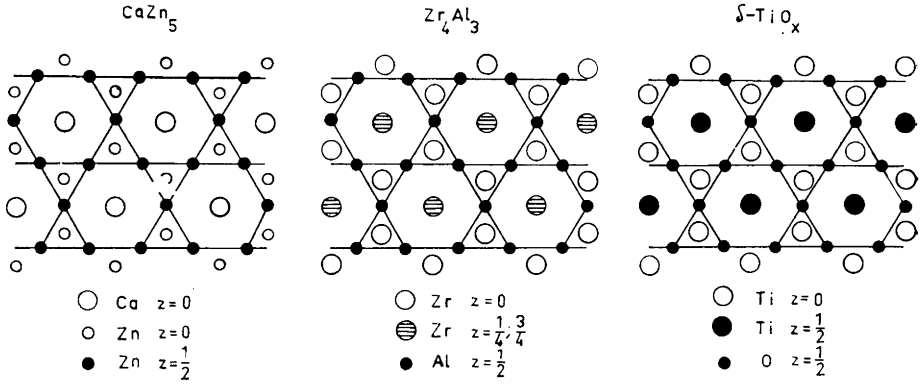

Fig. 6. The relationship between the structures of $CaZn_5$, Zr_4Al_3 and δ-TiO_x.

Me_2Al_3. The crystal structures of the isomorphous Zr_2Al_3 and Hf_2Al_3 have recently been reported [3,7,13]. This type of structure will be discussed in connection with the refinement of Hf_2Al_3 (*v. infra*).

$MeAl_3$. $ZrAl_3$ is of the $D0_{23}$ type whilst $HfAl_3$ crystallizes in both the $D0_{23}$ and $D0_{22}$ forms. These two structure types have been described by Brauer [9] and are formed by ordered substitution of transition metals in the aluminium structure. Ti, V, Nb and Ta give a $MeAl_3$ structure of the $D0_{22}$ type but the larger zirconium atom results in the formation of the $D0_{23}$ type. The fact that $HfAl_3$ crysaltlizes in both the $D0_{23}$ and $D0_{22}$ forms has been independently reported by Schubert *et al.*[3] and Boller *et al.*[11] It is astonishing to find that the very small difference in size ($r_{Zr} = 1.595$ kX and $r_{Hf} = 1.585$ kX at CN 12) between Zr and Hf should cause the formation of only the $D0_{23}$ type in the zirconium-aluminium system but both the structure types in the hafnium-aluminium system.

III. THE CRYSTAL STRUCTURE OF Hf_2Al_3

Experimental

Very small crystals could be found in the crushed melt of Hf_2Al_3. Weissenberg photographs were taken with rotation around the *a*-axis and the *c*-axis using Cu*K* radiation. The multiple film technique was employed and the relative intensities were visually estimated by comparison with an intensity scale.

Two and three dimensional Fourier syntheses and also structure factors were obtained using the digital electronic computer BESK with programs devised by Westman *et al.*[29] and Åsbrink *et al.*[30] No corrections were made for absorption but the real part of the dispersion correction for hafnium (−7) was taken from the table of Dauben and Templeton [31].

Derivation of the structure

The single crystal photographs showed that Hf_2Al_3 is orthorhombic. Accurate cell dimensions were obtained from Guinier powder photographs, giving the axes of the orthorhombic cell:

$$a = 9.52_3, \quad b = 13.76_3, \quad c = 5.52_2 \text{ Å}.$$

The density of the compound was found experimentally to be 8.00 g cm^{-3}. With eight formula units Hf_2Al_3 per unit cell, the theoretical density can be calculated to be 8.04 g cm^{-3}. The powder pattern of Hf_2Al_3 is given in Table 2.

Reflections *hkl* were observed only for $h + k = 2n$ and $k + l = 2n$, $0kl$ only for $k + l = 4n$ and $h0l$ only for $l + h = 4n$. The probable space group is thus *Fdd*2.

The space group contains only positions 16(*b*) and 8(*a*). From space considerations (length of the *c*-axis only 5.5 Å), the 16 hafnium atoms in the unit cell must be placed in position 16(*b*) while the remaining 24 aluminium atoms must be distributed over 16(*b*) and 8(*a*) positions. The Patterson projection along [001] gave approximate *x* and *y* parameters for these positions and the parameters were refined by successive calculations of the electron density projection.

Table 2. The Guinier powder pattern of Hf_2Al_3 ($CuKa_1$ radiation).

hkl	$\sin^2\Theta_{obs}$	$\sin^2\Theta_{calc}$	I_{obs}	I_{calc}	*hkl*	$\sin^2\Theta_{obs}$	$\sin^2\Theta_{calc}$	I_{obs}	I_{calc}
111	0.0291	0.0291	st	18.9	640	0.2858	0.2856	w	2.8
220	0.0387	0.0387	st	19.7	462	—	0.2953	—	0.1
131	0.0541	0.0542	st+	29.4	282	0.3044	0.3044	w	4.1
240	0.0762	0.0763	st	18.1	480	—	0.3051	—	0.1
311	0.0815	0.0815	st+	24.5	004	0.3120	0.3113	w	4.0
022	0.0905	0.0904	st	16.4	353	—	0.3123	—	0.9
202 / 151	0.1042	0.1040 / 0.1043	vst	15.5 / 28.2	602	0.3135	0.3133	m	5.2
					622	0.3260	0.3259	w	3.3
400	—	0.1047	—	0.0	391	0.3319	0.3320	m	6.0
331	0.1064	0.1065	m+	10.0	173	0.3352	0.3351	w	4.0
222	0.1165	0.1165	m+	13.2	571	0.3364	0.3365	m	8.0
420	0.1172	0.1172	m+	12.3	2.10.0	0.3393	0.3394	w	4.1
260	0.1389	0.1389	vw	2.1	513	0.3422	0.3418	m	4.8
242	—	0.1541	—	0.3	711	—	0.3431	—	0.8
440	—	0.1548	—	0.1	660	—	0.3483	—	0.4
351	0.1566	0.1566	w	2.8	224	0.3504	0.3500	w	4.7
171	0.1794	0.1795	m	6.7	642	—	0.3635	—	0.1
113	0.1845	0.1848	vw	2.3	533 / 731	0.3675	0.3669 / 0.3681	m	3.4 / 4.7
511	0.1862	0.1861	m	6.2					
062	0.1907	0.1906	vw	2.1	482	0.3830	0.3829	w	2.9
422	—	0.1950	—	0.2	373 / 244	0.3877	0.3875 / 0.3876	m+	5.7 / 6.9
080	0.2002	0.2004	vw	2.8					
133	0.2099	0.2098	m	6.8	0.10.2	0.3908	0.3910	m	7.8
531	0.2109	0.2112	w	4.4	1.11.1	0.4045	0.4050	vw	3.3
262	0.2167	0.2167	w	3.0	404	—	0.4160	—	0.1
460	0.2174	0.2174	m	5.7	553	—	0.4170	—	2.0
280	0.2266	0.2266	vw	1.0	2.10.2	—	0.4172	—	0.2
371	0.2318	0.2318	m	5.7	4.10.2	—	0.4179	—	0.1
442	0.2326	0.2326	st	16.8	751 / 800	0.4183	0.4183 / 0.4187	m+	7.6 / 4.4
313	0.2375	0.2371	m	4.8					
620	0.2480	0.2480	w	3.6	662	0.4263	0.4261	vw	3.7
153	0.2601	0.2600	m	8.1	424	0.4290	0.4285	m	8.8
551	0.2613	0.2613	vw	1.7					
333	0.2625	0.2622	w	3.0					
191	0.2795	0.2797	vw	1.6					

The Patterson projection along [100] shows that the 16 Hf and 16 Al are all situated in planes perpendicular to the *c*-axis and with a spacing of about 0.25*c*. The *z*-parameter of the aluminium atom in 8(*a*) could also be estimated in this Patterson projection. However, the relatively low scattering power of the aluminium atom makes the accuracy of the aluminium position rather low.

Theresulting parameters are:

16 Hf in 16(*b*) : $x = 0.185$, $y = 0.054$, $z = 0.00$
16 Al in 16(*b*) : $x = 0.185$, $y = 0.129$, $z = 0.50$
8 Al in 8(*a*) : $x = 0$, $y = 0$, $z = 0.63$

Interatomic distances are given in Table 3. The final *R*-values were 10.8 % the *hk*0, 12.1 % for the *hk*1, 14.5 % for the *hk*2, 12.9 % for the *hk*3 and 13.1 % for the 0*kl* reflections. No temperature factor was applied.

Table 3. Interatomic distances in Hf_2Al_3.

Hf	2 Hf	3.37 Å	Al(*a*)	2 Hf	2.80 Å	Al(*b*)	1 Hf	2.81 Å
	2 Hf	3.38		2 Hf	2.85		1 Hf	2.90
	1 Al(*a*)	2.80		2 Hf	3.17		1 Hf	2.90
	1 Al(*a*)	2.85		2 Al(*b*)	2.60		2 Hf	2.95
	1 Al(*a*)	3.17		2 Al(*b*)	2.75		1 Hf	3.00
	1 Al(*b*)	2.81					1 Al(*a*)	2.60
	1 Al(*b*)	2.90					1 Al(*a*)	2.75
	1 Al(*b*)	2.90					2 Al(*b*)	2.75
	2 Al(*b*)	2.95						
	1 Al(*b*)	3.00						

The crystal structure of Zr_2Al_3, which is isomorphous with Hf_2Al_3, has been given by both Renouf and Beevers [7] and Schubert *et al.*[3] The *z*-parameters of the aluminium atoms in 16(*b*) differ in the two investigations, *viz.* 0.500 as reported by Renouf and Beevers and 0.45 by Schubert *et al.* The former value seems to be preferred for packing reasons and is in close agreement with the one found for Hf_2Al_3 in this study ($z = 0.49$ from a three-dimensional Fourier synthesis within a "box" around this position [29]). The aluminium atoms in the special position were found to have the *z* co-ordinate 0.63 by three-dimensional calculations and this is in accordance with the value found in the Patterson projection along [100].

The structure

The structure of Zr_2Al_3 and Hf_2Al_3 has been described by Renouf and Beevers as being built up by puckered triangular nets [7]. These nets, containing as many zirconium atoms as aluminium atoms, are repeated along the *y* axis and leave holes that are filled with aluminium atoms. It is interesting to note that a plane-packing of equal numbers of zirconium or hafnium atoms and aluminium atoms is realized by the square-triangle net of the $3^3.4^2$ type found in HfAl [12] while the triangular packing of the type found in Zr_2Al_3 and Hf_2Al_3 reveals a departure from planarity.

In a preliminary note, the structure was described in terms of Hf_2Al_3 units. Each such unit forms a triangular bipyramid with Hf atoms in the tops and three Al atoms in the corners of the pyramids. This description is a rather formal one since two of the aluminium atoms are not in contact with each other in the pyramid. Similar pyramids with close-packed arrangements of atoms are found in the hexagonal $HfAl_2$ of the *C*14 type.

Attempts to find simple relationships between Hf_2Al_3 and other alloy structures were unsuccesful and it is remarkable that A_2B_3-phases with a ratio r_A/r_B of about 1.2 seem to be very rare.

The author wishes to thank Professor A. Magnéli for his encouraging interest and many valuable comments. Thanks are also due to Dr. S. Andersson who introduced me to this field of chemistry.

REFERENCES

1. Keeler, J. H. and Mallery, J. H. *J. Metals* **7** (1955) 394.
2. Wilson, C. G. and Sams, D. *Acta Cryst.* **14** (1961) 71.
3. Schubert, K., Anantharaman, T. R., Ata, H. O. K., Meissner, H. G., Pötschke, M., Rossteutscher, W. and Stoltz, E. *Naturwiss.* **47** (1960) 512.
4. Edshammar, L.-E. and Andersson, S. *Acta Chem. Scand.* **14** (1960) 223.
5. Wilson, C. G. and Spooner, F. J. *Acta Cryst.* **13** (1960) 358.
6. Wilson, C. G., Thomas, D. K. and Spooner, F. J. *Acta Cryst.* **13** (1960) 56.
7. Renouf, T. J. and Beevers, C. A. *Acta Cryst.* **14** (1961) 469.
8. Wilson, C. G. *Acta Cryst.* **12** (1959) 660.
9. Brauer, G. *Z. anorg. Chem.* **242** (1939) 1.
10. Edshammar, L.-E. *Acta Chem. Scand.* **14** (1960) 1220.
11. Boller, H., Nowotny, H. and Wittman, A. *Monatsh.* **91** (1960) 1174.
12. Edshammar, L.-E. *Acta Chem. Scand.* **15** (1961) 403.
13. Edshammar, L.-E. *Acta Chem. Scand.* **14** (1960) 2244.
14. Dwight, A. E., Downey, J. W. and Conner, Jr., R. A. *Acta Cryst* **14** (1961) 75.
15. McPherson, D. J. and Hansen, M. *Trans. Am. Soc. Metals* **46** (1954) 354.
16. Bhakta, B. R., Ganesh, P. M. and Mondolfo, L. F. *J. Inst. Metals* **89** (1961) 248.
17. Aronsson, B. *Arkiv Kemi* **16** (1960) 379.
18. Wilson, C. G., Sams, D. and Renouf, T. J. *Acta Cryst.* **12** (1959) 947.
19. Aronsson, B. *Acta Chem. Scand.* **12** (1958) 31.
20. Frank, F. C. and Kasper, J. S. *Acta Cryst.* **11** (1958) 184.
21. Frank, F. C. and Kasper, J. S. *Acta Cryst* **12** (1959) 483.
22. Black, P. J. *Acta Met.* **4** (1956) 172.
23. Petersen, D. R. and Rinn, H. W. *Acta Cryst.* **14** (1961) 328.
24. Finney, J. J. and Rosezweig, A. *Acta Cryst.* **14** (1961) 69.
25. McKinsey, C. R. and Faulring, G. M. *Acta Cryst.* **12** (1959) 701.
26. Brown, P. J. and Forsyth, J. B. *Acta Cryst.* **14** (1961) 362.
27. Edshammar, L.-E. and Holmberg, B. *Acta Chem. Scand.* **14** (1960) 1219.
28. Andersson, S. *Acta Chem. Scand.* **13** (1959) 415.
29. Westman, S., Blomqvist, G. and Åsbrink, S. *Arkiv Kemi* **14** (1959) 535.
30. Åsbrink, S., Blomqvist, G. and Westman, S. *Arkiv Kemi* **14** (1959) 545.
31. Dauben, C. H. and Templeton, D. H. *Acta Cryst.* **8** (1955) 841.

Received June 9, 1961.

ACTA CHEMICA SCANDINAVICA 16 (1962) 31–40

Fractionation of Some Plant Estrogens and their Animal Excretion Metabolites on Dextran Gels

ANNA NILSSON

The National Animal Experiment Station, Uppsala 7, Sweden

Some experiments with Sephadex gel filtration in the separation of isoflavones and their animal excretion products are reported and discussed. The fractionation of the compounds is rather a result of different adsorption to the gel matrix than of a molecular sieving.

Gel-filtration has been used for separating substances of different molecular size [1]. Besides the molecular sieve action, the gel material also exerts an adsorptive effect on substances of aromatic and heterocyclic character [2]. This secondary effect was taken advantage of in the present separation of four plant estrogens in a mixture: biochanin A, genistein, formononetin and daidzein. The compounds are all isoflavones. Biochanin A, genistein and formononetin occur in the common forage plant, red clover *(Trifolium pratense)* [3–5]. The substances are also found in other species of the family *Leguminosae* [6]. Biochanin A is on account of its higher concentration responsible for the main estrogenic activity of the red clover [3]. The specific activity of both biochanin A and genistein is about 10^{-5} times that of diethylstilbestrol [7]. As to formononetin its estrogenic activity is negligible [8]. Daidzein never occurs free in nature but is found in soybeans *(Soja hispida)*, bound as a glucoside [9]. Some authors report that the compound is completely inactive as an estrogen by injection [6], others that its estrogenic activity when given orally is even greater than that of genistein [8].

Biochanin A, labelled with tritium, was used in metabolic studies with rats and sheep [10]. In the present study the gel filtration technique was used for separating conjugates and free metabolites of biochanin A from urine and feces extracts of rats, which had been given an intraperitoneal injection of the compound.

EXPERIMENTAL

Materials. Sephadex G-25, coarse, (manufactured by Pharmacia, Ltd, Uppsala), was used in this investigation throughout. This type of gel allows an entry of molecules with a maximum molecular weight of 1 000 – 4 000.

The columns were packed according to directions in the paper of Porath [9]. An account of the size of the columns and the elution performance is given in connection with each experiment described.

The four isoflavones were synthesized according to known methods [11,12].

The tritium labelling of biochanin A was performed by the Wilzbach method [13] at the Pharm. Dept., Kungl. Veterinärhögskolan, Stockholm. By chromatography and recrystallizations, the labelled compound was purified from tritiated by-products and labile tritium [10]. The labelled substance was mixed with carrier biochanin A to give a final specific activity of 0.2—0.5 μC/mg. Adult rats were given biochanin A by intraperitoneal injections. A very fine suspension of the compound in physiological saline was used as the injection medium. Urine and feces were collected from the period 0—48 h following injection.

The urine samples were put on the columns directly or else following a pretreatment described below. An extract of feces was prepared. The details of the extraction procedure are given along with the description of the gel filtration experiment.

Analytical methods. Ultraviolet absorbing zones in the eluates from the columns were recorded at 2537 Å with an Uvicord Ultraviolet Absorptiometer (LKB-products, Stockholm). The isoflavones were identified by paper chromatography in different solvent systems together with reference substances [14]. Glucuronides were determined by the naphthoresorcinol method according to Fischman-Green [15]. Sulphuric esters were determined by the turbidimetric method of Sperber [16]. The occurrence of urea in the eluates was measured by the urease method of Van Slyke and Cohen [17]. The quantity of sodium chloride, as a representative of the inorganic salts, was determined by Volhard-Arnhold titration [18].

Aliquots of the fractions were analyzed for radioactivity in an Ekco 612 liquid scintillation counter at a temperature of −20°C. The samples were counted both with and without an internal standard of a known amount of biochanin A of high activity. The radioactivity in each eluate could therefore be determined quantitatively.

RESULTS AND DISCUSSION

Fractionation of four isoflavones in a model experiment.

The molecular structures of the four compounds are given in Fig. 1. These isoflavones are soluble in alkaline solution but insoluble in diluted acid or water. They are, however, susceptible to even very mild alkaline hydrolysis, which opens the pyrone ring in the molecule. It was therefore convenient to choose the relatively weak base of 0.1 M ammonium hydroxide as the eluant. This eluant also has the advantage of being volatile. A mixture of 5 mg of each of the isoflavones, biochanin A, genistein, formononetin, and daidzein, was filtered through the first column (Fig. 2). It was difficult to dissolve the isoflavone crystals directly in the diluted ammonium hydroxide solution in a sufficiently small volume. They were therefore first dissolved in 5 ml 0.1 N NaOH. This solution was neutralized with diluted HCl. A very fine suspension of the com-

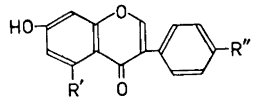

Fig. 1. Molecular structure of genistein, biochanin A, formononetin and daidzein.

Genistein	R′ = OH	R″ = OH	Formononetin	R′ = H	R″ = OCH_3
Biochanin A	R′ = OH	R″ = OCH_3	Daidzein	R′ = H	R″ = OH

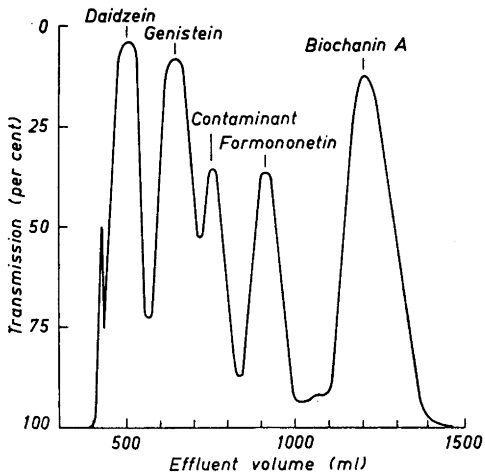

Fig. 2. Filtration diagram of a mixture of genistein, biochanin A, formononetin and daidzein on a gel column of the size 4.5 × 37 cm. Eluant: ammonium hydroxide.

pounds in saline was then obtained. The suspended particles were now readily dissolved when the solution was adjusted to be 0.1 M with regard to NH_4OH in a final volume of 10 ml. The sodium chloride in the solution left the column far ahead of the isoflavones.

The column was of the dimensions 4.5 × 37 cm and had a volume of 500 ml. The rate of the elution was 1 ml per minute. The outer or void volume was experimentally determined as the elution volume for serum albumin from horse, with 0.1 M NH_4OH as the eluant. It was found to be 165 ml. It is not possible to explain the position of the different isoflavones in the Sephadex chromatogram from the differences in their chemical configurations.

The elution volumes are the same if the compounds are put on the column alone or together in a mixture.

Fractionation of urine metabolites

Pretreated urine samples. Each of 35 rats were injected intraperitoneally with 30 mg of biochanin A (specific activity 0.23 μC/mg). The urine, 330 ml, contained about 30 % of the injected radioactivity. By four extractions with 300 ml butanol, 80 % of the radioactivity in the urine was transferred into the butanol phase. The solvent was evaporated under vacuum and the dry residue, 12 g, was dissolved in hot methanol and cooled. To its volume was added three times this volume of ether. The methanol-ether soluble part of the urine contained 56 % of the radioactivity of the untreated urine. The precipitate which was formed when the ether was added to the methanolic solution contained the rest of the butanol extractable substances, 7.5 g, and 24 % of the radioactivity. It contained no free isoflavones.

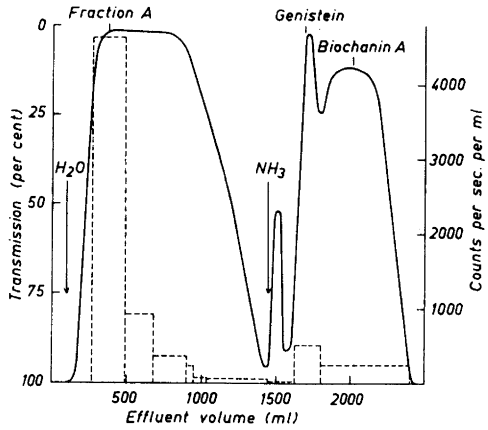

Fig. 3. Diagram showing the fractionation of a methanol-ether extract of 330 ml of urine on a column of the size 4.5 × 26 cm. Eluant: I water and II ammonium hydroxide. Ultraviolet absorption curve ————. Radioactivity of pooled eluates --------. Fraction A contains unknown metabolites.

In Fig. 3 is illustrated the separation of the biochanin A metabolites in the methanol-ether soluble part of the urine. The solvent was evaporated and the dry residue, 4.5 g, was dissolved in 18 ml H_2O. The separation was performed on a Sephadex column, 4.5 × 26 cm, and with a gel volume of 360 ml. 1400 ml distilled water was filtered through the column. When the ultraviolet absorption curves, recorded during the elution, returned to zero, the eluant was changed to 0.1 M NH_4OH. The rate of the elution was 3 ml/min.

The bulk of the labelled compounds left the column without being strongly retarded. The radioactive eluates contained glucuronic acid and organic sulphates. A limited fractionation was achieved but these eluates have to be further purified before identification of labelled metabolites is possible.

A small amount of biochanin A passed the body unchanged. Another part of the compound was demethylated in the liver to genistein [19]. The free isoflavones could not be eluted with pure water, but were easily displaced from the column by the ammonium hydroxide solution and were recovered essentially free from contaminants. The two fractions containing the isoflavones overlap each other, but could be well separated by repeated gel filtration, Figs. 4 and 5. This second fractionation was performed at a later occasion. Samples had been taken for different analysis, and account for the deficit in material used for the second filtration. A Sephadex column was used with the dimensions 4.5 × 37 cm and with a gel volume of 500 ml. The dried eluates from the first separation were dissolved in 15 ml 0.1 M NH_4OH and the column was eluted with the same solvent, at the rate of 3 ml/min. An estimation of the recovered radioactivity gave 2.2 % in the genistein and 5.6 % in the biochanin A fraction of the total radioactivity in the urine sample. There is thus a very small amount of unconjugated isoflavones in the urine.

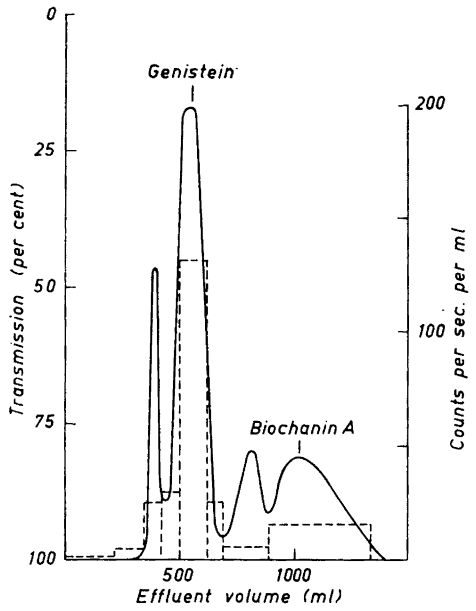

Fig. 4. Second filtration of the fraction "genistein" (Fig. 3) on a column of the size 4.5 × 37 cm. Eluant: ammonium hydroxide. Ultraviolet absorption curve ———. Radioactivity of pooled eluates ------.

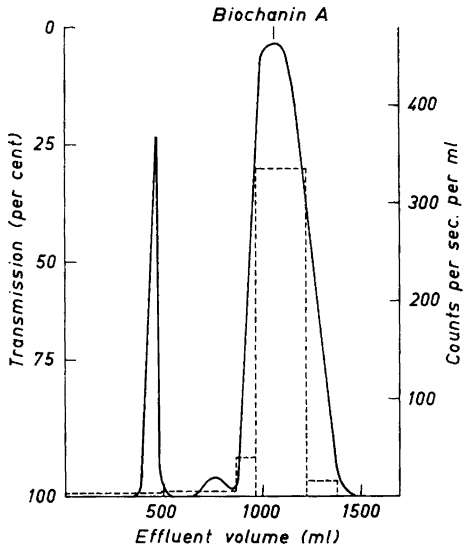

Fig. 5. Second filtration of the fraction "biochanin A" (Fig. 3) on the same column and under the same conditions as in Fig. 4.

Untreated urine. During the extraction procedures described above a large part of the metabolites was lost judging from the recovery of radioactivity in the extracts. It was therefore attempted to put the urine sample directly on the column without any preliminary purification. A total of 70 ml of urine was collected from five rats, each of which had been injected with 25 mg of labelled biochanin A (specific activity 0.5 μC/mg). The urine contained 28 % of the injected radioactivity.

The ultraviolet absorption of the isoflavone fractions from the crude urine would have been rather weak due to the low concentration of these compounds in the sample. Carrier isoflavones were therefore added to mark the ultraviolet absorbing zones of genistein and biochanin A. 10 mg each of unlabelled genistein and biochanin were suspended in 20 ml saline and added to the urine samples. There was no visible precipitate in the diluted urine.

The dimensions of the column were 4.5 × 37 cm with a gel volume of 500 ml. Distilled water was used as the first eluant. The effluent was collected in fractions of 23—25 ml every 20 min. When 1400 ml water had passed through the column the eluting agent was changed to 0.1 M NH_4OH. The distribution of the radioactive metabolites is shown in Fig. 6. Two highly radioactive fractions (Fig. 6 A) eluted with water, contained both glucuronic acid and organic sulfate conjugates (Fig. 7). The labelled compounds amounted to only a minor

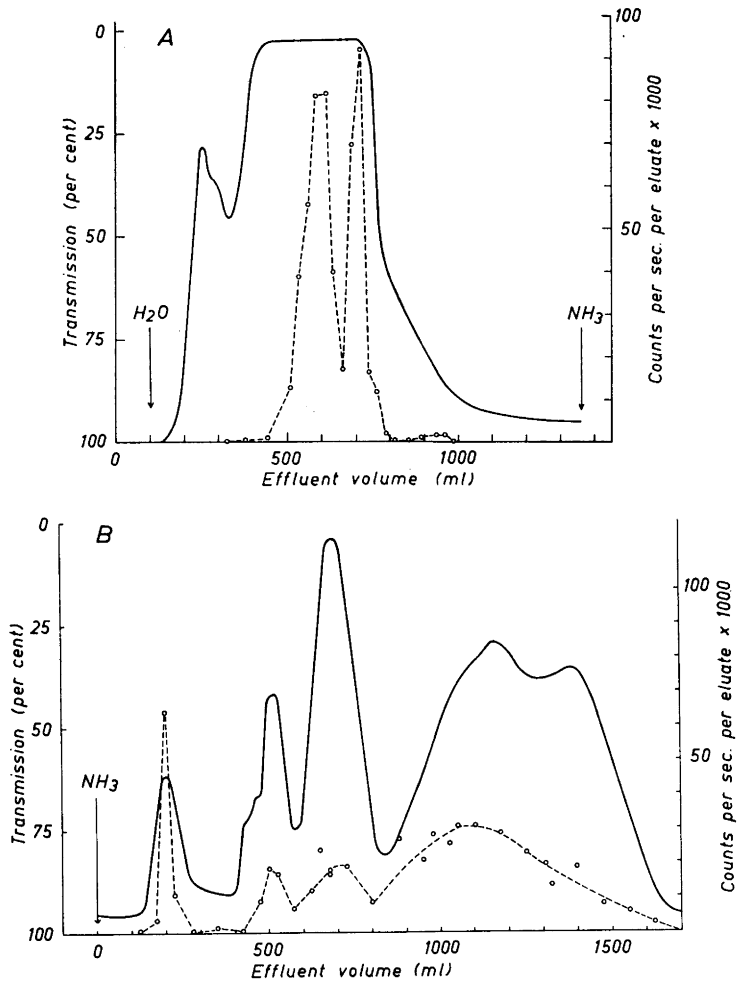

Fig. 6. Gel filtration of an untreated urine sample (70 ml). Column: 4,5 × 37 cm. Eluant: I water (Diagram A) and II ammonium hydroxide (Diagram B). Ultraviolet absorption curve ————. Radioactivity of individual eluates O-----O. Eluate volume 23—25 ml.

part of the substances in these eluates, which contained all the urine conjugates of glucuronic acid and of sulfate. Urea and sodium chloride move a little ahead of the conjugates (Fig. 8). An attempt was also made to separate the crude urine sample with 0.1 M NH_4OH, as the only eluant. However, a better separation of the conjugates was not obtained. The eluates with pure water were used directly for enzymatic hydrolysis with glucuronidase and sulfatase enzymes, while the ammonium hydroxide eluates had to be freed from ammonia before the enzymatic hydrolysis. It is therefore preferable to make the

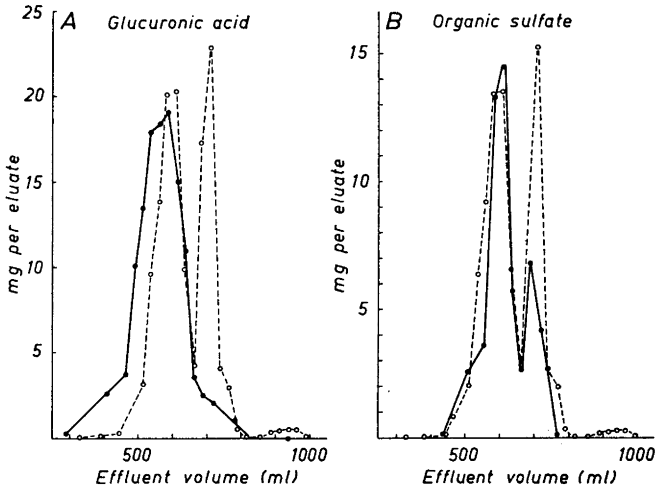

Fig. 7. Diagram showing the distribution of glucuronic acid ●———● (Diagram A) and organic sulfate ●———● (Diagram B) in the eluates of the urine sample from Fig. 6 A. Radioactivity curve O-----O.

elution in two steps: first with water and then with 0.1 M NH_4OH. The results from the analysis of the water soluble metabolites will be published later.

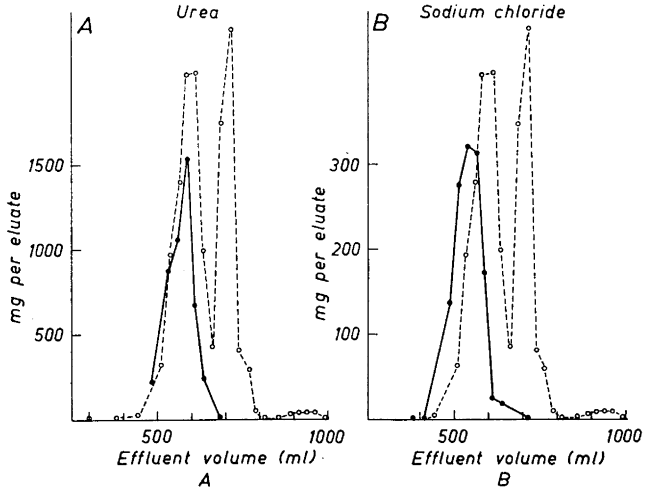

Fig. 8. Diagram showing the distribution of urea ●———● (Diagram A) and sodium chloride ●———● (Diagram B) in the eluates of the urine sample from Fig. 6 A. Radioactivity curve O-----O.

The radioactivity peaks in Fig. 6 B coincide with the peaks of the ultraviolet absorption curves for genistein and biochanin A. Two unknown metabolites of low concentration move ahead of the genistein and biochanin A fractions.

The recovery of the radioactivity was quantitative to the extent that it could be estimated from a summation of the analyzed individual eluates. About 90 % of the labelled compounds were obtained in the purely water soluble fractions. The genistein fraction contained about 1 % and the biochanin A about 8 % of the radioactivity in the urine. This corresponded to 0.34 mg genistein and 2,7 mg biochanin A from the labelled injected compound.

Fractionation of metabolites in feces

Feces samples were collected from 15 rats, each of which had been injected with 25 mg of tritiated biochanin A (specific activity 0.18 μC/mg). The feces sample was repeatedly extracted with hot 95 % alcohol. The alcohol extract contained 60 % of the injected radioactivity. No more radioactivity could be extracted from the feces by additional extractions with other solvents. The alcoholic extract was further purified as illustrated in the following scheme. The radioactivity of the crude alcoholic extract is indicated as 100 %. The recovered radioactivity during the purification steps are given within the parenthesis.

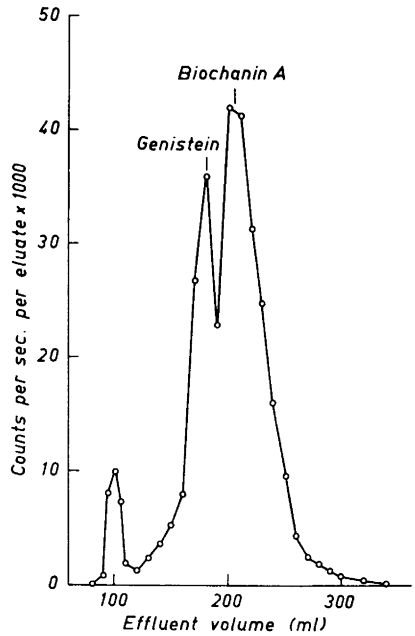

Fig. 9. Gel filtration of an ether extract of feces. Column size: 1.8 × 42 cm. Eluant: ammonium hydroxide. Radioactivity curve O———O.

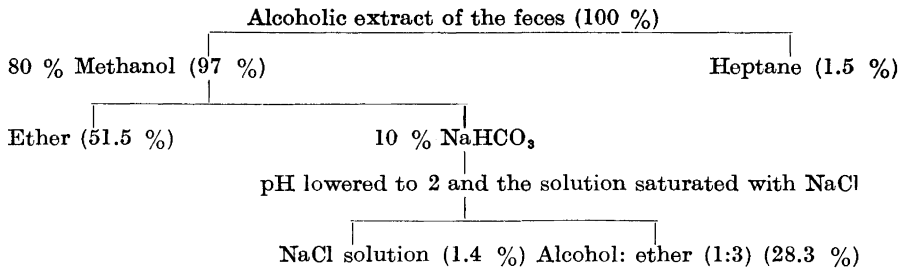

The ether extract was dried and the residue dissolved in 0.1 M NH_4OH and filtered through a Sephadex column 1.8 × 42 cm, with a gel volume of 110 ml. Eluates of 5 ml were collected every 30 min. The distribution of the radioactivity is shown in Fig. 9. The bulk of the radioactive compounds in the ether extract consisted of genistein and biochanin A. As the load of the column, 100 mg, was very large in proportion to its size (100 ml gel volume) it was not possible to get a complete separation of the two isoflavones. A second gel filtration with the genistein and biochanin A fractions on a column of the size 4.5 × 26 cm gave a better separation of the zones (Figs. 10 and 11). It was estimated that the feces contained about 40 % biochanin A and 14 % genistein, which were not conjugated. The alcohol-ether soluble part of the feces was also filtered through a gel column, but no fractionation was obtained in this experiment. The occurrence of such a large amount of free isoflavones in the feces may naturally be the result of hydrolysis of conjugates in the in-

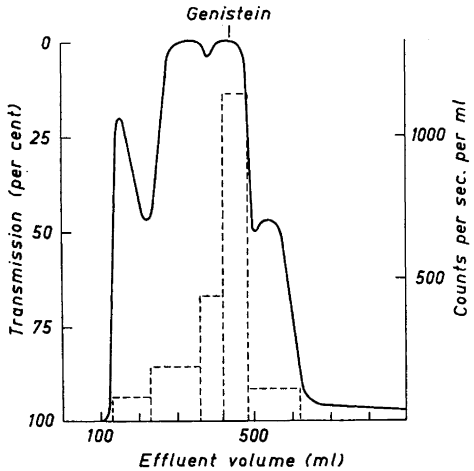

Fig. 10. Second filtration of the fraction "genistein" (Fig. 9) on a column of the size 4.5 × 26 cm. Eluant: ammonium hydroxide. Ultraviolet absorption curve ————. Radioactivity of pooled eluates --------.

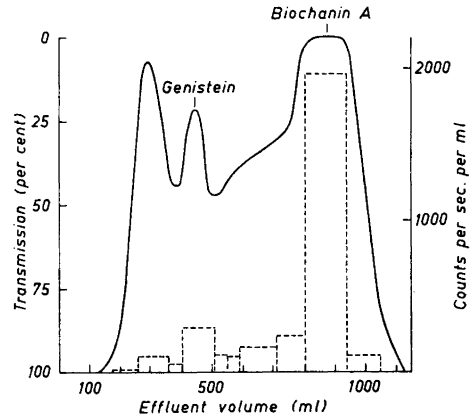

Fig. 11. Second filtration of the fraction "biochanin A" (Fig. 9) on the same column and under the same conditions as in Fig. 10.

testines by the fecal flora. The demethylation to genistein does however not take place in the intestines, but rather in the liver [19]. Incubation of biochanin A with intestine contents gave no genistein.

DISCUSSION

The four isoflavones in the model experiment are of very equal molecular size. The good separation obtained is therefore probably the result of a different adsorption to the gel matrix. The separation procedures were also applicable to biological fluids and extracts of biological material. When water was used as the eluant, the isoflavones were retained in the upper part of the column. They could be eluted with fairly high purity by ammonium hydroxide, when all water soluble components had left the column. The amount of substances and the load volumes, put on the columns, have been very large in these experiments. Nevertheless a good fractionation of the metabolites has been obtained. Work is in progress to study if the new finely ground Sephadex will give an improved separation.

I wish to express my gratitude to Professor P. E. Lindahl for his stimulating interest in this work and for his valuable criticism of the manuscript and to Docent J. Porath for helpful advice and discussion.

REFERENCES

1. Porath, J. and Flodin, P. *Nature* **183** (1959) 1657.
2. Porath, J. *Biochim. Biophys. Acta* **39** (1960) 193.
3. Pope, G. S., Elcoate, P. V., Simpson, S. A. and Andrews, D. G. *Chem. & Ind. London* **1953** 1092.
4. Pope, G. S. and Wright, H. G. *Chem. & Ind. London* **1954** 1019.
5. Bate-Smith, E. C., Swain, T. and Pope, G. S. *Chem. & Ind. London* **1953** 1127.
6. Bradbury, R. B. and White, D. E. *Vit. and Horm.* **12** (1954) 207.
7. Pope, G. S. *Dairy Science Abstracts* **16** (1954) 334.
8. Cheng, E. W., Yoder, L., Story, Ch. D. and Burroughts, W. *Science* **120** (1954) 575.
9. Walz, E. *Ann. Chem.* **489** (1931) 118.
10. Nilsson, A. *To be published.*
11. Yoder, L., Cheng, E. and Burroughs, W. *Proc. Iowa Acad. Sci.* **61** (1954) 271.
12. Baker, W., Chadderton, J. B., Harbone, J. B. and Ollis, W. D. *J. Chem. Soc.* **11** (1953) 1952.
13. Wilzbach, K. E. *J. Am. Chem. Soc.* **79** (1957) 1013.
14. Nilsson, A. *Arkiv Kemi* **17** (1961) 305.
15. Fischman, W. H. and Green, S. J. *J. Biol. Chem.* **215** (1955) 527.
16. Sperber, I. *J. Biol. Chem.* **172** (1948) 441.
17. Hawk, Ph. B., Oser, B. L. and Summerson, W. H. *Practical Physiol. Chem.* p. 883, XIII Ed. New York, 1954.
18. Ibid. p. 955.
19. Nilsson, A. *To be published.*

Received June 14, 1961.

ACTA CHEMICA SCANDINAVICA 16 (1962) 41–45

A Proposed Structure for Crystalline Zinc-Insulin

K. MARCKER and J. GRAAE

Universitetets fysisk-kemiske Institut, Copenhagen, Denmark *

A structure is proposed for crystalline zinc-insulin containing two atoms of zinc per unit cell. It is shown that the proposed structure is in agreement with the available chemical and crystallographic data for crystalline zinc-insulin.

A great deal of speculation has been devoted to the problem of constructing a satisfactory model of the unit cell of crystalline zinc-insulin. The specific information available for this purpose comprises: the complete amino acid sequence of the insulin monomer, the site of binding of the »structural» zinc ions, the amount of the »structural» zinc ions present in the cell, the molecular weight of 36×10^3 which indicates the presence of six monomers in the cell and finally the X-ray diffraction data.

A model based on the α-helix structure and Sanger's formula and constructed in accordance with model-building technique has been suggested by Lindley and Rollet [1]. The model proposed by these authors was constructed on the assumptions that the zinc was responsible for the dimerization and that the amount of zinc which belongs to the structure as an integral part was three atoms per unit cell and finally that the site of binding of the »structural» zinc atoms was the imidazole groups, each zinc atom being bound to two such groups.

It is now known, however, that zinc atoms are not necessary for the formation of the dimer as zinc-free insulin is able to dimerize. In fact the minimum molecular weight of zinc-free insulin at acid reaction has been shown [2] to be 12×10^3. In addition it should be pointed out that the binding of zinc to insulin is impossible at acid reaction where the behaviour of crystalline zinc-insulin is identical with that of zinc-free insulin in having a minimum molecular weight of 12×10^3 as also demonstrated by Gutfreund [3].

The problem about the amount of zinc which belongs to the structure as as integral part seems to be settled by the experiments performed by Schlichtkrull [4] and Cunningham [5]. By repeated crystallizations Schlichtkrull demonstrated that the minimum amount of zinc sufficient for crystallization was two atoms per unit cell. This result is in accordance with the work of Cunningham *et al.* who by equilibrium dialysis experiments showed that two atoms of zinc per unit cell were bound so firmly to insulin that they could not be dialyzed

* Present address: Københavns Tandlægehøjskole, Biokemisk afd., Copenhagen, Denmark.

away. It is generally accepted that the building stone in the hexamer unit is the dimer, primarily because the monomer unit only seems to exist as such in aqueous solution under special conditions such as very dilute basic solutions (pH about 10). It can therefore be concluded that the unit cell of zinc-insulin consists of three dimers linked together by two zinc atoms and not by three zinc atoms as generally believed.

In a previous paper [6] it was demonstrated that the site of binding of the »structural» zinc atoms is the N-terminal amino group of phenylalanine and not the imidazole groups as suggested by Tanford and Epstein [7]. It has been shown previously too that the dimerization of insulin [8] probably proceeds by a disulfide interchange mechanism from which it could be concluded that the two monomers have an antiparallel arrangement in the dimer as shown schematically in Fig. 1.

The dimer thus has two carboxyl groups and two N-terminal amino groups in each end. The proposed structure then consists of three dimers placed in a parallel arrangement and linked together by two zinc atoms by means of coordinative bonds to the three available N-terminal amino groups of phenylalanine present in each end of the rod. The proposed structure is shown schematically in Fig. 2. As a consequence of the proposed structure it is seen that the addition of the calculated amount of zinc (two atoms per unit cell) to a solution of zinc-free insulin under certain circumstances should lead to the displacement of six hydrogen ions per unit of 36×10^3. In order to investigate this point titration curves for insulin with and without the presence of the calculated amount of zinc were determined. The results are shown in Fig. 3 An examination of Fig. 3 will show that in insulin containing two atoms of zinc per unit

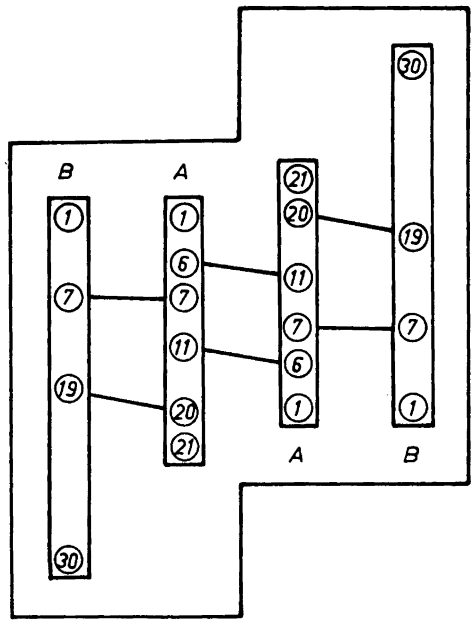

Fig. 1. The proposed model of the insulin dimer, showing the antiparallel arrangement of the monomers. The two longer rods represent the B-chains and the two shorter ones the A-chains. The numbers refer to the amino acids in the "Sanger-unit".

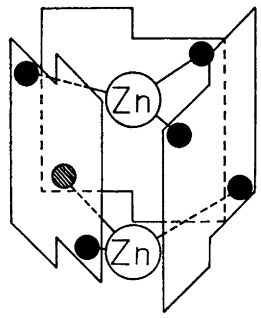

Fig. 2. The proposed model of crystalline zinc-insuiln. The three frames represents three dimers with structures similar to the one proposed proposed in Fig. 1. The black circles refer to the N-terminal amino groups of phenylalanine. The two water molecules probably attached to the two zinc atoms have not been drawn.

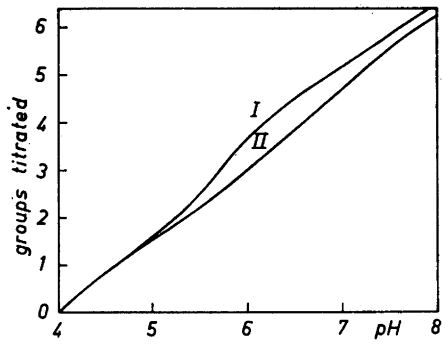

Fig. 3. Titration curves for insulin with and without the presence of two zinc atoms per unit of 36 × 10^3. The ordinate gives the number of groups titrated per unit of 6 000. Abscissa = pH. The titration were performed in 0.2 M KNO_3. I = titration curve for insulin in the presence of the calculated amount of zinc. II = titration curve for zincfree insulin.

of 36 × 10^3 the binding of six hydrogen ions has been shifted from the region about pH 7 towards more acid pH values. The result of this experiment therefore support the validity of the proposed structure.

The result of osmotic pressure measurements shows that crystalline zinc-insulin containing two atoms of zinc per unit of 36 × 10^3 is monodisperse in basic and neutral solution having a molecular weight of 36 × 10^3. This important fact is in accordance with the proposed model, since it is seen that zinc-insulin having this structure is not able to polymerize further by means of the two zinc ions. In the authors' opinion other possible structures would lead to compounds that are able to polymerize in solution depending on the insulin concentration. Such compounds would resemble zinc-free insulin in being heterodisperse in solution but as mentioned this is in diasgreement with experimental facts.

By isotope tracer experiments using ^{65}Zn Schlichtkrull [9] has shown that all the zinc ions present in the insulin crystal are exchanged within one hour, from which it can be concluded that the zinc ions are not captured within steric blockings. In the proposed model one zinc ion is placed in each end of the rod and it is therefore to be expected that zinc ions placed in this way would be easily exchangeable in agreement with the finding of Schlichtkrull.

CRYSTALLOGRAPHY

It is essential that any postulated structure of the hexamer unit of crystalline zinc insulin is in agreement with the available crystallographic data. Of special interest in this connection is the experiments performed by Low and Einstein [10] who by X-ray crystallographic studies showed that the insulin dimer basically has an invariant structure in acid solution, that is, the two insulin monomers in the dimer are related to each other by a twofold rotation axis. In Fig. 1 it is seen that the proposed structure of the dimer is in agree-

ment with this finding. A threefold rotation axis relating three dimer units has previously been found in rhombohedral zinc-insulin [11]. It appears therefore, as also pointed out by Low and Einstein, that the dimer as subunit of the hexamer may well have the point group 2. It is therefore probable that the hexamer has the point group 32 with each single molecule equivalent. If the hexamer unit has the point group 32 then the three twofold rotation axes relating the monomers to each other in the dimer subunit lie in a plane normal to the threefold rotation axis and at angles of 120° to each other. From Fig. 2 it is evident that the proposed structure fulfills all the necessary requirements for configurations belonging to point group 32.

Any postulated structure of the hexamer unit of crystalline zinc-insulin should be able to fit into the unit cell determined for the air-dried protein by Crowfoot [12]. The dimensions of the unit cell are given in Table 1. Calculations based upon the model proposed by Linderstrøm-Lang [13] for the monomer unit yields that the proposed model for the hexamer unit is 84 Å long and 30 Å broad. These dimensions correspond closely to the body diagonals in the unit cell determined by Crowfoot. It can therefore be concluded that the proposed structure is able to fit into the unit cell.

In aqueous solution the tails of the proposed model which are not stabilized by disulfide bonds, is supposed to be unfolded or in a state of equilibrium between the folded and the unfolded form in which the latter predominates. As a consequence of this the length of the proposed model would be considerably greater in aqueous solution than in the wet crystal. In the latter case an increase in the direction of the *a* axis should be seen, whereas the *c* axis should be the same as in the dry crystal since the width of the model is not affected by the unfolding of the tails. This is in exellent agreement with experimental facts since it has been shown, that on drying of the wet crystal the unit cell shrinks but only in the direction of the *a* axis, whereas the *c* axis remains practically constant [11].

Crystal growth studies of insulin crystals have been performed by Schlichtkrull [14]. In these investigations an anisotropic growth was demonstrated as only three faces of the crystal move whereas the other three faces are immobile. This indicates an up and down direction in the unit cell, that is, when the unit cell is turned upside down so as to invert the trigonal axis, it is impossible to obtain the original atomic configuration by rotating about this axis. This is in disagreement with the proposed model as shown in Fig. 2, where no up and down direction is present on account of the highly symmetric arrangement of the dimers.

It should be pointed out, however, that other parallel arrangements of the dimers in the hexamer are possible. In Fig. 4 A is schematically shown the arrangement of the dimers in the structure presented in Fig. 2. An alternate arrangement is shown in Fig. 4 B. As further illustrated in Fig. 5 the

Table 1. Lattice constants for air-dried insulin crystals determined by Crowfoot.

Rhombohedral cell	*Hexagonal cell*
a = 44.4 Å	a = 74.8 Å
α = 114°28'	c = 30.9 Å

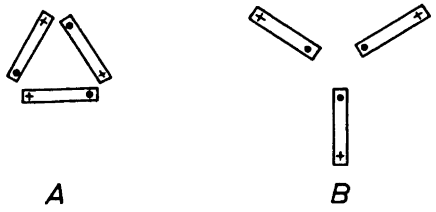

Fig. 4. Schematic illustration of two of the possible arrangements of the dimers. A rectangle illustrates a dimer; ● and + refer to the location of the N-terminal amino groups. ● amino group up and + amino group down. The zinc ions have not been drawn. 4 A refers to the structure proposed in Figs. 2 and 4 B to an alternate possible structure.

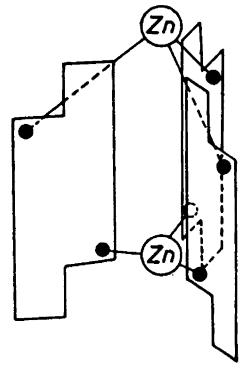

Fig. 5. A more detailed representation of the structure proposed in Fig. 4 B. The slight difference in the binding of the two zinc ions is apparent.

latter arrangement gives rise to a minor difference in the binding of the two zinc ions and consequently to an up and down direction in the unit cell. On account of the very slight difference in the ends of the rod the twofold rotation symmetry is lost.

Which one of these or other possible parallel arrangement of the dimers is the correct one it is at the moment impossible to say, but it seems that the main features of the proposed model are correct, since it is able to account for most of the available chemical and crystallographic data for crystalline zinc-insulin.

Acknowledgements. The authors wish to thank professor, Dr. J. A. Christiansen, professor, Dr. A. Tovborg Jensen, mag.scient. E. Jensen and mag.scient. M. Lassen for their kind interest and many valuable suggestions.

Financial support from *Statens Almindelige Videnskabsfond* and *Købmand i Odense Johann og Hanne Weimann, født Seedorfs Legat is* gratefully acknowledged. The receipt of *Nordisk Forskningsstipendium* from the University of Oslo, Norway, is acknowledged by J. G.

REFERENCES

1. Lindley, H. and Rollett, J. S. *Biochim. et Biophys. Acta* **18** (1955) 183.
2. Marcker, K. *Acta Chem. Scand.* **14** (1960) 194.
3. Gutfreund, H. *Biochem. J.* **50** (1952) 564.
4. Schlichtkrull, J. *Acta Chem. Scand.* **10** (1956) 1455.
5. Cunningham, L. W., Fischer, R. L. and Vestling, C. S. *J. Am. Chem. Soc.* **77** (1955) 5703.
6. Marcker, K. *Acta Chem. Scand.* **14** (1960) 2071.
7. Tanford, C. and Epstein, J. *J. Am. Chem. Soc.* **76** (1954) 2170.
8. Marcker, K. and Graae, J. *Acta Chem. Scand.* **15** (1961) 565.
9. Schlichtkrull, J. *Insulin Crystals* (Diss.) København 1958.
10. Low, B. W. and Einstein, J. R. *Nature* **186** (1960) 470.
11. Crowfoot, D. and Riley, D. *Nature* **144** (1939) 1011.
12. Crowfoot, D. *Proc. Roy. Soc. London* A **164** (1938) 580.
13. Linderstrøm-Lang, K. *Symposium on Peptide Chemistry. The Chemical Society.* London 1955.
14. Schlichtkrull, J. *Acta Chem. Scand.* **11** (1957) 484.

Received June 27, 1961.

ACTA CHEMICA SCANDINAVICA 16 (1962) 46–52

Heats of Combustion of Cyclic Ketones and Alcohols

PETER SELLERS* and STIG SUNNER

Thermochemistry Laboratory **, *University of Lund, Lund, Sweden*

Values are reported for the heats of combustion of *cyclo*pentanone −686.91 ± 0.22 kcal/mole; *cyclo*pentanol −740.47 ± 0.20; *cyclo*hexanone −841.04 ± 0.25; *cyclo*hexanol −890.99 ± 0.26.

Heats of hydrogenation of the cyclic ketones derived from these data are in reasonable agreement with those from direct measurements, and are used in a discussion of the steric strain energies of the five- and six-membered rings.

The heat of hydrogenation of *cyclo*hexanone (−15.4 kcal) determined by Kistiakowsky *et al.*[1] is apparently anomalous since it would be expected to lie near the figures for straight chain ketones, *e.g.* acetone (−13.41) and methyl ethyl ketone (−13.19)[2], if the ring is assumed to be strain free. The value for *cyclo*pentanone (−12.5) has also been under discussion, and it was therefore decided to determine the heats of hydrogenation of the cyclic ketones *via* their heats of combustion and the heats of combustion of the corresponding alcohols.

The only existing literature value for the ketones is that of Roth[3] for *cyclo*pentanone. The heats of combustion of *cyclo*pentanol and *cyclo*hexanol have been determined by Parks and co-workers[4]. *Cyclo*hexanol has also been studied much earlier by Richards and Davis[5].

MATERIALS

Cyclo*pentanone* of purum grade was distilled twice at reduced pressure through a 10-plate column and the main-fraction was distilled through a 32-plate column, the fraction boiling between 130.2 – 130.6°C at 757 mm Hg being kept for further treatment. Most of the water in the sample was removed azeotropically at 94°C but gas-liquid chromatography (LAC-3R-726 as liquid phase) showed that some water was still present, although all organic impurities had been removed. The sample was then shaken with anhydrous potassium carbonate, filtered, and infra red spectra taken of the pure sample and of the sample with known added amounts of water. From the spectra the water content of the sample was calculated to be between 0.02 and 0.03 %.

* Now at University College of North Staffordshire, Keele, England.

** Sponsored by *The Swedish Natural Science Research Council* and *The Swedish Technical Research Council.*

Cyclo*pentanol*. This substance was prepared by hydrogenation of *cyclo*pentanone using the method of Noller and Adams [6], with Adams platinum oxide as catalyst. Similar treatment and analysis to above gave a sample free from organic impurities and water.

Cyclo*hexanone*. A purum grade sample was repeatedly distilled at different pressures. Five distillations were required before all the *cyclo*hexanol was removed. The sample was dried by treating with P_2O_5 and distilling. Infra red spectra and melting curves * showed the absence of all impurities.

Cyclo*hexanol*. The purum grade sample was found to be very hygroscopic and contained a considerable amount of water even after several fractional distillations. By repeated slow freezing and evaporation under vacuum most of the water was removed but it proved impossible to remove all of it. By the use of accurate infra red spectrometry a calibration curve was obtained for water content of the sample, by taking spectra of the pure sample and the sample with known amounts of added water. The water content was found to be 0.10 ± 0.02 %.

Table 1 gives the physical constants of the compounds and amounts of impurities.

Table 1. Physical constants.

Substance	Bp 760 mm corr. °C	m.p. °C **	d_4^{25}	n_D^{25}	% water
*Cyclo*pentanone	130.7	−53.1	0.94368	1.4352	0.03
*Cyclo*pentanol	140.8	−***	0.94229	1.4515	0.00
*Cyclo*hexanone	155.6	−32.1	0.94010	1.4497	0.00
*Cyclo*hexanol	161.2	23.91	0.94506	1.4641	0.10

COMBUSTION CALORIMETRY

The calorimetric system used was that described by Bjellerup [7], with the exception that the rotating mechanism was not used. Since all the compounds were contained in glass ampoules, a platinum baffle and shield were placed over the crucible to avoid splashing of the sample when the ampoule burst on ignition [8]. As an auxiliary fuel to aid combustion paraffin oil of known heat of combustion [9] was used. After each combustion, the amount of nitric acid present was determined by potentiometric titration against standard alkali.

In each combustion experiment the calorimeter can was filled with water until a fixed total weight of calorimeter with mounted bomb was reached. This required the amount of water in the calorimeter to vary with the mass of contents in the bomb, and the energy equivalent of the system consists of: ε° (Calor), the energy equivalent of a standard system consisting of the whole system assembled as normally but with no contents in the bomb *i.e.* no removable matter; $C_p(H_2O)m^i$ (Cont.), the energy equivalent of an amount of water equal in mass to the bomb contents; ε^i (Cont.), the energy equivalent of the contents of the bomb.

Calibration. The calorimetric system was calibrated by the combustion of benzoic acid (NBS sample 39 h), under conditions specified in the accompanying certificate [10]. The results of the calibration experiments are given in Table 2.

* Melting curves were obtained by the use of a glass enclosed platinum resistance thermometer of dimensions 20 by 4 mm, surrounded by a thin layer of sample.

** from melting curves. *** no defined m.p. due to formation of glass.

Table 2. Results of calibration experiments.

t_h = 25.0°C V(Bomb) = 0.2751 litre m^i(Cont.) = 36.26 g*
t_i = 24.1°C $V^i(H_2O$ tot.) = 0.820 ml $-\Delta E_c/M$ (Benzoic Acid) = 6 317.87 ± 0.62 cal/g
P^i(gas) = 30.0 atm m(Pt) = 23.690 g $-\Delta E_c/M$(Fuse) = 3 971 ± 4 cal/g
ε^i(Cont.) = 3.96 cal/deg *

m'	m'''	Δt	$-\Delta E(HNO_3)$	$-\Delta E_{I.B.P.}/\Delta t$
g	g	deg	cal	cal/deg
0.826338	0.004721	0.88827	2.22	5900.95
0.826406	0.004973	0.88864	2.44	5900.36
0.824306	0.004947	0.88647	2.39	5899.66
0.824446	0.005188	0.88652	1.66	5900.58
0.826637	0.004963	0.88942	2.09	5896.42
0.825514	0.004894	0.88736	2.05	5901.75
				Mean = 5899.91

Standard deviation of mean ± 0.76
ε° (Calor) = 5932.21 ± 0.76 cal/deg

* These values are the same for all experiments, so the mean is taken before they are included.

RESULTS

The results of the combustions on the compounds under investigation are given in Tables 3—6. The symbols used are those of Hubbard, Scott, and Waddington [11]. All calorimetric quantities are expressed in terms of the defined calorie, which is equal to 4.1840 absolute joules, and all weighings are reduced to mass. The molecular weight for each compound is based upon the 1954 International Atomic Weights. The uncertainties given are the final overall standard deviations. Washburn corrections were applied as described by Hubbard, Scott, and Waddington [11]. The values have been corrected where necessary for the water contents of the samples.
ΔH_c° values were computed using the relation

$$\Delta H_c^\circ = \Delta E_c^\circ + \Delta nRT$$

where Δn is the change in the number of moles of gas accompanying the combustion reaction. Heats of formation were calculated using the heat of formation values at 25°C [12].

$$CO_2(g): \Delta Hf^\circ = -94.0518 \text{ kcal/mole}$$

$$H_2O(l): \Delta Hf^\circ = -68.3174 \text{ kcal/mole}$$

HEATS OF VAPORISATION

The heats of vaporisation of the four compounds were determined calorimetrically ** in an apparatus which has been previously described [13].

** The co-operation of Dr. and Mrs. Ingemar Wadsö of this laboratory is gratefully acknowledged.

*Table 3. Cyclo*pentanone.

t_h = 25.0°C V(Bomb) = 0.2751 litre ε° (Calor) = 5932.21 ± 0.76 cal/deg
t_i = 24.1°C V^i (H_2O tot.) = 0.820 ml $-\Delta E_c^\circ/M$ (Oil) = 10 986.6 ± 0.6 cal/g
P^i (gas) = 30.0 atm m(Pt) = 23.69 g $-\Delta E_c^\circ/M$ (Fuse) = 3 971 ± 4 cal/g
M = 84.11 ε^i (Cont.) = 3.84 cal/deg
m^i (Cont.) = 36.14 g ΔE_Σ = 2.09 cal

m' g	m'' g	m''' g	Δt deg	$-\Delta E$(HNO_3) cal	$-\Delta E_c^\circ/M$ cal/g
0.422345	0.159776	0.004243	0.88511	1.82	8158.99
0.445034	0.149969	0.004324	0.89710	1.91	8143.15
0.432500	0.137313	0.004261	0.85694	3.08	8150.68
0.454633	0.132005	0.004414	0.87787	2.99	8152.71
0.370645	0.192849	0.004303	0.87521	2.55	8156.48
0.452851	0.133419	0.004842	0.87879	2.46	8159.81
				Mean	8153.63

Standard deviation of mean ± 2.7
$-\Delta E_c^\circ$ = 685.83 ± 0.22 kcal/mole

DISCUSSION

In Tables 7 and 8 the results of the present work are summarized, together with data from the literature. It can be seen that the heats of combustion obtained here lead to heats of hydrogenation of the cyclic ketones which are about 1 kcal/mole lower than those of Kistiakowsky *et al.*

The heats of combustion of the alcohols are in excellent agreement with those obtained by Parks and co-workers.

The heats of hydrogenation of the cyclic ketones may be used in a discussion of the strain energies of these compounds and of their hydrogenation products, the alcohols.

*Table 4. Cyclo*pentanol.

t_h = 25.0°C V(Bomb) = 0.2751 litre ε° (Calor) = 5932.21 ± 0.76 cal/deg
t_i = 24.1°C V^i(H_2O tot.) = 0.820 ml $-\Delta E_c^\circ/M$ (Oil) = 10 986.6 ± 0.6 cal/g
P^i (gas) = 30.0 atm m(Pt) = 23.690 g $-\Delta E_c^\circ/M$(Fuse) = 3971 ± 4 cal/g
M = 86.13 ε^i (Cont.) = 3.63 cal/deg
m^i (Cont.) = 36.12 g ΔE_Σ = 1.78 cal

m' g	m'' g	m''' g	Δt deg	$-\Delta E$(HNO_3) cal	$-\Delta E_c^\circ/M$ cal/g
0.450705	0.116581	0.004168	0.87614	2.95	8579.71
0.458209	0.119113	0.003989	0.89096	2.82	8571.11
0.451100	0.118264	0.004256	0.88011	2.82	8582.66
0.407453	0.147699	0.003999	0.87104	2.52	8580.20
0.433886	0.135402	0.004271	0.88641	3.66	8574.85
0.468391	0.123072	0.004185	0.91426	2.54	8584.37
				Mean:	8578.22

Standard deviation of mean ± 2.4
$-\Delta E_c^\circ$ = 739.15 ± 0.20 kcal/mole

*Table 5. Cyclo*hexanone.

t_h = 25.0°C
t_i = 24.1°C
P^i (gas) = 30.0 atm
V(Bomb) = 0.2751 litre
V^i (H_2O tot.) = 0.820 ml
m(Pt) = 23.692 g
M = 98.14
$\varepsilon°$ (Calor) = 5930.29 ± 0.76 cal/deg *
$-\Delta E_c°/M$ (Oil) = 10 986.6±0.6 cal/g
$-\Delta E_c°/M$(Fuse) = 3971 ± 4 cal/g
ε^i (Cont.) = 3.81 cal/deg
m^i (Cont.) = 36.26 g ΔE_Σ = 2.00 cal.

m' g	m'' g	m''' g	Δt deg	$-\Delta E$ (HNO_3) cal	$-\Delta E_c°/M$ cal/g
0.449731	0.121876	0.004465	0.88308	2.29	8555.18
0.445930	0.125748	0.004651	0.88532	2.62	8558.74
0.445556	0.128251	0.004505	0.88929	2.24	8560.11
0.444189	0.127791	0.004313	0.88566	2.37	8551.16
0.380247	0.178054	0.004769	0.8872:	2.88	8554.96
0.571384	0.097524	0.004268	1.01494	2.95	8563.29
0.571871	0.069726	0.004523	0.96349	1.77	8559.79
				Mean:	8557.46

Standard deviation of mean ± 2.6
$-\Delta E_c°$ = 839.84 ± 0.25 kcal/mole

* Calculated from previous value after a small mechanical change in the bomb.

*Cyclo*pentanone is known to be a puckered non-planar ring [14] and Pitzer [15] has calculated its torsional strain energy to be about 2.8 kcal/mole less than that of *cyclo*pentane. The ketone, however, will have a greater C-C-C bond angular strain due to the double bond of the carbonyl group, and the value for methylene-*cyclo*pentane (0.9 kcal/mole)[15] may be taken. Thus *cyclo*pentanone has about 1.9 kcal/mole less strain energy than *cyclo*pentane.

Since the heat of hydrogenation of *cyclo*pentanone is less than those of straight chain ketones, steric effects in the product *i.e. cyclo*pentanol, must be

*Table 6. Cyclo*hexanol.

t_h = 25.0°C
t_i = 24.1°C
P^i (gas) = 30.0 atm
V (Bomb) = 0.2751 litre
V^i (H_2O tot.) = 0.820 ml
m(Pt) = 23.696 g
M = 100.14
$\varepsilon°$ (Calor) = 5959.23 ± 0.74 cal/deg*
$-\Delta E_c°/M$ (Oil) = 10 986.6±0.6 cal/g
$-\Delta E_c°/M$ (Fuse) = 3971 ± 4 cal/g
ε^i (Cont.) = 3.71 cal/deg
m^i(Cont) = 36.32 g ΔE_Σ = 1.92 cal

m' g	m'' g	m''' g	Δt deg	$-\Delta E$(HNO_3) cal	$-\Delta E_c°/M$ cal/g
0.444036	0.116563	0.004623	0.88472	2.23	8873.80
0.433960	0.122207	0.004490	0.88016	2.01	8876.39
0.437664	0.118886	0.004691	0.87904	1.76	8868.21
0.456876	0.110529	0.004530	0.89642	2.38	8877.99
0.442470	0.119468	0.004722	0.88618	2.11	8874.60
0.441523	0.120471	0.004586	0.88001	2.61	8870.71
				Mean:	8873.61

Standard deviation of mean ± 2.6
$-\Delta E_c°$ = 888.78 ± 0.26 kcal/mole

* Measured after gasket of bomb had been changed.

Table 7. Heats of combustion, vaporisation and formation at 25° C

Substance	$-\Delta H_c°$(l)	$-\Delta H_f°$(l)	ΔH_v	$-\Delta H_f°$(g)	Earlier work $-\Delta H_c°$(l)
*Cyclo*pentanone	686.91 ± 0.22	56.52	10.21	46.31	683.8 [3]
*Cyclo*pentanol	740.47 ± 0.20	71.37	13.74	57.63	740.07 [4]
*Cyclo*hexanone	841.04 ± 0.25	64.86	10.77	54.09	—
*Cyclo*hexanol	890.99 ± 0.26	83.23	14.82	68.41	890.77 [4] 890.0 [5]

Table 8. Heats of hydrogenation.

Substance	This work	Kistiakowsky *et al.*
*Cyclo*pentanone	−11.32	−12.26 [a]
*Cyclo*hexanone	−14.32	−15.23 [a]
Acetone		−13.29 [a]
Methyl ethyl ketone		−13.07 [a]

[a] Corrected from 82°C to 25°C.

Table 9. Heats of formation of cycloparaffins and alcohols.

n	C_nH_{2n}	$C_nH_{2n-1}OH$	Δ(H→OH)
5	−18.46	−57.63	−39.17
6	−29.43	−68.41	−38.98

greater than those in the reactant. In other words, part of the energy occurring during the hydrogenation process is retained by the product molecule as steric energy.

By considering the heats of formation of the five- and six-membered *cyclo*-paraffins [16] and their alcohols, and assuming the six-membered rings to be free from strain (at 25°C), the strain energy of *cyclo*pentanol is seen to be virtually the same as that in *cyclo*pentane (Table 9). Thus, the process

$$\textit{Cyclo}\text{pentanone} \xrightarrow{H_2} \textit{Cyclo}\text{pentanol}$$

results in an increase in strain energy of approximately 1.9 kcal and we would expect the heat of hydrogenation to be less by this amount than those of the straight chain ketones (−13.3).

The experimental figure is almost exactly 1.9 kcal but such good agreement is fortuitous since there is an uncertainty of a few tenths of a kilocalorie. The above discussion on the strain energies of the five-membered rings would, however, seem to be valid.

Disagreement has existed on the question of strain in the *cyclo*hexanone molecule. Brown *et al.*[17] have proposed that strain does exist, the structural explanation being strain associated with the opposed orientation of the double bond relative to the C—H bonds of adjacent ring methylene groups. Allinger [18] has supported this view and gave a value of 1.6 kcal for the strain energy of

*cyclo*hexanone. Pitzer [15] on the other hand has been inclined to the view that the molecule is unstrained, as shown by microwave studies [19] which have the opposed orientation as the stable one.

The thermochemical data given here show that *cyclo*hexanone has a heat of hydrogenation about 1 kcal greater than those of straight chain ketones, and on this basis it will have a strain energy of about 1 kcal if its hydrogenation product, *cyclo*hexanol, is assumed to be free from strain.

Acknowledgements. One of us (Peter Sellers) thanks the University College of North Staffordshire and the Scandinavian Council for Applied Research, through the Growing Points Programme, for financial support.

REFERENCES

1. Conn, J. B., Kistiakowsky, G. B. and Smith, E. A. *J. Am. Chem. Soc.* **61** (1939) 1868.
2. Dolliver, M. A., Gresham, T. L., Kistiakowsky, G. B., Smith, E. A. and Vaughan, W. E. *J. Am. Chem. Soc.* **60** (1938) 440.
3. See Kharasch, M. S. *J. Research Natl. Bur. Standards* **2** (1929) 359.
4. Parks, G. S., Mosley, J. R. and Peterson, P. V. *J. Chem. Phys.* **18** (1950) 152.
5. Davis, H. S. and Richards, T. W. *J. Am. Chem. Soc.* **42** (1920) 1599.
6. Noller, C. R. and Adams, R. *J. Am. Chem. Soc.* **42** (1926) 1084.
7. Bjellerup, L. *Acta Chem. Scand.* **13** (1959) 1511.
8. Sunner, S. *Studies in Combustion Calorimetry Applied to Organo-Sulphur Compounds (Diss.)*, Lund 1949.
9. Sellers, P. *Unpublished measurements.*
10. *Provisional Certificate of Analysis of Standard Sample 39 h, Benzoic Acid*, National Bureau of Standards, 1960.
11. Hubbard, W. N., Scott, D. W. and Waddington, G. *Standard States and Corrections for Combustions in a Bomb at Constant Volume.* Chapter 5 of Rossini, F. D. (Ed.), *Experimental Thermochemistry*, New York 1956.
12. Selected Values of Chemical Thermodynamic Properties, *Circular of Natl. Bur. Standards 500*, Washington D. C. 1952.
13. Wadsö, I. *Acta Chem. Scand.* **14** (1960) 566.
14. Aston, J. G., Schumann, S. C., Fink, H. L. and Doty, P. M. *J. Am. Chem. Soc.* **63** (1941) 2029.
15. Donath, W. E. and Pitzer, K. S. *J. Am. Chem. Soc.* **81** (1959) 3213.
16. Spitzer, R. and Huffman, H. *J. Am. Chem. Soc.* **69** (1947) 211.
17. Brown, H. C., Brewster, J. H. and Schecter, H. *J. Am. Chem. Soc.* **76** (1954) 467.
18. Allinger, N. L. *J. Am. Chem. Soc.* **81** (1959) 572.
19. Kilb, R. W., Lin, C. C. and Wilson, E. B. *J. Chem. Phys.* **26** (1957) 1695.

Received June 21, 1961.

ACTA CHEMICA SCANDINAVICA 16 (1962) 53–62

The Influence of the Solvent on Reaction Velocity

XX. The Reaction of Dinitrobenzenes with Hydroxyl and Alkoxyl Ions

EERO TOMMILA and JUHANI MURTO

Department of Chemistry, University of Helsinki, Finland

The bimolecular rate constants of the reactions of *o*- and *p*-dinitrobenzenes with hydroxyl ion in pure water and those of the reaction of *p*-dinitrobenzene in 50 vol-% dioxan-water have been measured at different temperatures. The velocities of the reactions of *o*- and *p*-dinitrobenzenes with ethoxyl ion have been measured in pure ethanol and the velocity of the reaction of *p*-dinitrobenzene with methoxyl ion in pure methanol. The simultaneous reactions of *o*- and *p*-dinitrobenzenes with hydroxyl ion and ethoxyl ion in alkaline ethanol-water mixtures and the corresponding reactions of *p*-dinitrobenzene in alkaline methanol-water mixtures have been studied. Equations for calculating the rate constants of the concurrent reactions were derived by taking into account the equilibrium between hydroxyl and alkoxyl ions. Except for the rates in dioxan-water, which were measured at four temperatures, the rates were measured at three temperatures. The parameters of the Arrhenius equation were evaluated. The results are discussed.

The dinitrobenzenes undergo the following reactions with alkoxyl and hydroxyl ions:

$$NO_2 \cdot C_6H_4 \cdot NO_2 + AlkO^- \rightarrow NO_2 \cdot C_6H_4 \cdot OAlk + NO_2^- \quad (1)$$

$$NO_2 \cdot C_6H_4 \cdot NO_2 + OH^- \rightarrow NO_2 \cdot C_6H_4 \cdot OH + NO_2^- \quad (2)$$

The nitrophenol formed is converted into the ionic form in the alkaline solution, so that instead of (2) we have the total reaction

$$NO_2 \cdot C_6H_4 \cdot NO_2 + 2OH^- \rightarrow NO_2 \cdot C_6H_4 \cdot O^- + NO_2^- + H_2O \quad (3)$$

These reactions present an interesting object for kinetic study since it is possible to follow the variation of the concentration of each reactant in the reaction mixture, also in aqueous alcohols where the reactions occur simultaneously. The concentration of the phenol in the reaction mixture can be determined colorimetrically and the concentration of the base by titration. The concentration of the unreacted dinitrocompound can be calculated from these two values. If necessary, also the concentration of the nitrite ion can be determined separately. However, only the reactions of the *ortho*- and *para*-compounds are

appropriate for kinetic study because the reactions of *m*-dinitrobenzene are complicated by the formation of *m*-dinitroazoxybenzene.

The kinetics of the reactions were first studied by Lobry de Bruyn and Steger [1]. Steger [2] investigated the reactions of *o*- and *p*-dinitrobenzenes with methoxyl ion and ethoxyl ion in absolute methanol and ethanol at the temperatures 25°, 35° and 45°C, and Lobry de Bruyn and Steger [3] the reactions of *o*-dinitrobenzene in methanol-water and ethanol-water mixtures at 25°C. They found that the *para*-isomeride reacts faster than the *ortho*-isomeride in the absolute alcohols and that the reaction with ethoxyl ion in ethanol is faster than the reaction with methoxyl ion in methanol. In ethanol-water and methanol-water mixtures the over-all reaction velocity is greatly dependent on the composition of the solvent. Lobry de Bruyn and Steger also determined the concentration of the nitrophenol formed and they deduced from their results that the relative concentration of the alcoholate ion in aqueous alcohol is considerable up to a high water content. The reaction between *p*-dinitrobenzene and methoxyl ion in absolute methanol has been studied also by Parijs [4] and by Bolto and Miller [5], but these investigations contribute very little to the results of Lobry de Bruyn and Steger.

The work now described was initiated to obtain more detailed information on the kinetics of the reactions in alcohol-water mixtures than was collected by the early workers, and especially to study the equilibrium

$$\mathrm{AlkO^-} + \mathrm{H_2O} \rightleftharpoons \mathrm{AlkOH} + \mathrm{OH^-} \qquad (4)$$

The results concerning the latter will be published later by one of us (J.M.) and only the kinetic results are reported in the present communication.

CALCULATIONS

If the initial molar concentration of both reactants is a, and if the amount of the dinitrobenzene consumed in the formation of the ether and phenol up to time t are x and y mole/litre, respectively, the total concentration of the unreacted alkali at time t is

$$[\mathrm{OH^-}] + [\mathrm{AlkO^-}] = a-x-2y \qquad (5)$$

According to eqn. (4)

$$[\mathrm{OH^-}] = K'[\mathrm{AlkO^-}] \qquad (6)$$

where

$$K' = K[\mathrm{H_2O}]/[\mathrm{AlkOH}] \qquad (7)$$

is practically invariable at constant temperature.

From eqns. (5) and (6) we obtain

$$[\mathrm{AlkO^-}] = (a-x-2y)/(K' + 1) \qquad (8)$$

and

$$[\mathrm{OH^-}] = K'(a-x-2y)/(K' + 1) \qquad (9)$$

Hence, if the reactions (1) and (2) are related only through the equilibrium (4), the rate equations are

$$\frac{dx}{dt} = k_e^\circ (a-x-y)(a-x-2y)/(K' + 1) \quad (10)$$

$$\frac{dy}{dt} = k_f^\circ (a-x-y)(a-x-2y)K'/(K' + 1) \quad (11)$$

The subscripts e and f refer to the formation of ether and phenol, respectively. Dividing (11) by (10) and taking into account that $dx/dy = x/y$, we find

$$\frac{x}{y} = \frac{k_e^\circ}{k_f^\circ K'} \quad (12)$$

Substituting the expression for y derived from eqn. (12) in eqn. (10), we have

$$dx/(\alpha-\beta x)(\alpha-\gamma x) = p\,dt \quad (13)$$

where

$$\alpha = k_e^\circ a,\ \beta = k_e^\circ + k_f^\circ K',\ \gamma = k_e^\circ + 2k_f^\circ K' \text{ and } p = 1/[k_e^\circ (K' + 1)].$$

Introduction of the expression for y in eqn. (11) gives the same result. Eqn. (13) can be integrated by the method of partial fractions; the following solutions of eqns. (10) and (11) are obtained:

$$\frac{k_e^\circ}{K' + 1} = \frac{x}{y}\frac{1}{at} \ln \frac{(a-x-y)}{(a-x-2y)} \quad (14)$$

$$\frac{k_f^\circ K'}{K' + 1} = \frac{1}{at} \ln \frac{(a-x-y)}{(a-x-2y)} \quad (15)$$

The constants

$$\frac{k_e^\circ}{K' + 1} = k_e \text{ and } \frac{k_f^\circ K'}{K' + 1} = k_f \quad (16-17)$$

can be determined experimentally, for $a-x-2y$, the total alkali concentration, can be measured titrimetrically and y, the concentration of the phenol, can be determined colorimetrically. If we write $a-x-2y = b$, or $a-x-y = b + y$, we obtain from (14) and (16) the expression

$$k_e = \frac{x}{y}\frac{1}{at} \ln (1 + \frac{y}{b}) \quad (18)$$

which is a very convenient one for the practical calculation of k_e from the experiments. If one of the constants k_e and k_f has been determined, the other can be obtained by the equation

$$\frac{k_e}{k_f} = \frac{x}{y} \quad (19)$$

If reaction (1) is much faster than reaction (2), the second order rate constant computed from the total alkali consumptions by the usual formula $dx/dt = k(a-x)^2$ can be taken to be k_e. This formula was used to calculate the rate of reaction of *p*-dinitrobenzene in methanol-water mixtures. Also in this case k_f was computed from formula (19).

EXPERIMENTAL

Materials. The-*o*-dinitrobenzene was a product of "purissimum" grade (Fluka); it was used as received. The *p*-dinitrobenzene was a product of the "purum" grade (Fluka) and was recrystallized twice from 96 % ethanol, after which it melted at 174—175°C.

The ethanol used as solvent in the kinetic experiments was commercial absolute ethanol that had been purified by the method of Walden [6] and finally distilled over anhydrous copper sulphate. The methanol was commercial methanol which was purified by running it through a column of the cation exchange resin Zeo-karb Hl, treating it by the method of Lund and Bjerrum [7] and distilling it over anhydrous copper sulphate. The water was freshly distilled.

Preliminary experiments. All three dinitrobenzenes coloured in solutions containing acetone deep brown. Therefore acetone could not be used as a solvent in the kinetic experiments. *m*-Dinitrobenzene produced brown colour in all solvents used.

The solvolysis of the dinitrobenzenes by alcohols or water is so slow that it can be completely neglected; no detectable ether or phenol formation occurred in the absence of alkali during two weeks at 60°C. The Griess test [8] for nitrite ion was negative. The hydrolysis of the ether produced to phenol is always so slow that it could be neglected [9].

Method. The kinetic experiments were carried out in reaction vessels that have been previously described [10]. In the experiments with *o*-dinitrobenzene in ethanol-water, 5 ml of a 0.08 N sodium hydroxide solution was introduced into the smaller compartment of the vessel and 20 ml of a 0.02 N solution of the nitrocompound into the larger compartment, so that after thermostating and mixing, the concentration of each reactant was 0.016 M. In the experiments with *p*-dinitrobenzene, owing to its poorer solubility, 10 ml of 0.04 N sodium hydroxide and 40 ml of a 0.01 N solution of the dinitrobenzene were used, so that the initial concentrations of the reactants were 0.008 M. In these experiments the reaction vessels were about twice as large as in the experiments with *o*-dinitrobenzene.

The reaction vessels were taken from the thermostat after suitable times, cooled quickly to room temperature by immersion in cold water, and the mixtures were analysed as quickly as possible. The analytical method was essentially the same as that used by Lobry de Bruyn and Steger. The phenol was determined colorimetrically on a small sample, the sample rinsed back into the reaction vessel and the total alkali in the mixture determined by titration. To avoid decomposition of the nitrite, the titration was carried out with 0.05 N acetic acid. Phenolphthalein was used as indicator.

In most experiments a Bausch & Lomb Spectronic 20 colorimeter was used. In the case of *o*-dinitrobenzene the wave lengths were 475 and 488 mμ; identical results were obtained at both wave lengths. Different wave lengths were tried in the analysis of the reaction mixtures in the case of *p*-dinitrobenzene. The best results were obtained with the wave lengths 400 and 413 mμ. The readings were taken against a blank consisting of the same mixture acidified with acetic acid. However, the accuracy of the analyses was somewhat less in the case of *p*-dinitrobenzene than in the case of *o*-dinitrobenzene. In the experiments with *p*-dinitrobenzene in methanol-water mixtures, where the concentration of the phenol formed was very low, a Beckman DU Spectrophotometer was used instead of the Bausch & Lomb instrument, and the measurements were made at reaction percentages exceeding fifty (*cf.* Table 5).

The temperatures of the electrically controlled thermostats were constant within $\pm$ 0.02°. The thermometers were checked against a thermometer calibrated at the U. S. Bureau of Standards.

To study reaction (2) in absence of reaction (1), experiments were performed with pure water as solvent. Owing to the poor solubility, the following method was used. The dinitrocompound was shaken with hot water about half an hour, and the solution was filtered after it had cooled. No phenol formation was observed during this operation. The reaction was carried out in 100-ml glass-stoppered flasks. At suitable times 5-ml samples were taken with a pipette and the phenol contents determined colorimetrically. The wave lengths used were 400 mμ for the *para* and 425 mμ for the *ortho* compound. The initial concentration of sodium hydroxide was 0.016 M. To determine the initial concentration of the dinitrobenzene, a measured quantity of the solution was sealed in an ampoule and kept at 100° until the reaction had gone to completion (about 12 h). The ampoule was

Table 1. *o*-Dinitrobenzene in 100 % EtOH, $a = 0.016$, 50°. Formula $dx/dt = k(a-x)^2$.

t min	Titr. ml	p	10^5k l mole^{-1}s^{-1}
0	(8.00)		
168	5.56	30.5	272
265	4.72	41.0	285
281	4.67	41.6	264
383	4.20	47.5	275
350	4.17	47.9	273
478	3.57	55.4	271
485	3.53	55.9	272
		Mean	273.1

Table 2. *p*-Dinitrobenzene in 100 % MeOH, $a = 0.008$, 40°. Formula $dx/dt = k(a-x)^2$.

t min	Titr. ml	p	10^5k l mole^{-1}s^{-1}
0	(8.00)		
285	6.27	21.6	202
504	5.41	32.4	196
534	5.31	33.6	198
992	4.07	49.1	203
1 203	3.70	53.8	201
1 208	3.68	54.0	202
1 410	3.39	57.6	202
		Mean	200.6

then opened and the phenol determined spectrophotometrically. The rate constant was calculated by the formula

$$\frac{dx}{dt} = k(a-x)(b-2x),$$

which on integration gives

$$k = \frac{2.303}{(2a-b)t} \log \frac{b(a-x)}{a(b-2x)} \qquad (20)$$

The constancy of k was satisfactory in all runs.

With *p*-dinitrobenzene some experiments were made also in dioxan-water that contained 50 ml of water in 100 ml of the mixture. The initial concentrations of the dinitrobenzene and sodium hydroxide were 0.008 M. Two-millilitre samples of the reaction mixtures were sealed in ampoules of Pyrex glass after deaeration with nitrogen and transferred to the thermostat. After suitable times the ampoules were taken from the thermostat and the phenol formed determined spectrophotometrically. The rate constant was calculated by formula (20). In the experiments with dioxan-water mixtures it was difficult to obtain a good constancy for k. In these runs k in general gradually decreased as the reaction proceeded. It seemed that the walls of the ampoules were attacked by the alkali during the long reaction periods.

The results of some runs are recorded in Tables 1—5 (p is the per cent conversion).

Table 3. *o*-Dinitrobenzene in 76.6 wt-% EtOH, $a = 0.016$, 40°. Formula 14.

t min	Titr. ml	p	10^4y	10^4x	x/y	10^5k_e l mole^{-1}s^{-1}
0	(8.00)					
944	5.60	30.0	2.45	43.2	17.6	42.1
1 240	5.11	36.1	2.92	52.0	17.8	42.2
1 254	5.12	36.0	2.93	51.9	17.7	41.8
1 434	4.92	38.5	2.81	56.1	20.0	40.8
2 227	4.01	49.9	3.51	72.9	20.8	41.6
2 236	3.99	50.1	3.54	73.2	20.7	41.9
2 705	3.64	54.5	4.20	19.0	18.8	40.6
					Mean 19.1	41.57

To correct for the thermal expansion of the solvent the above value must be multiplied by 1.020, which gives $k_e = 0.0004241$ l mole^{-1}s^{-1}.

$$k_f = k_e \cdot \frac{x}{y} = 0.0004241/19.1 = 0.0000222 \text{ l mole}^{-1}\text{s}^{-1}.$$

Table 4. *p*-Dinitrobenzene in 88.3 wt.-% EtOH, $a = 0.008$, 40°. Formula 14.

t min	Titr. ml	p	10^4y	10^4x	x/y	$10/k^5$ l mole^{-1}s^{-1}
0	(8.00)					
127	5.46	31.8	0.153	25.1	164	752
132	5.41	32.4	0.156	25.6	164	744
201	4.62	42.3	0.198	33.4	169	746
201	4.60	42.5	0.211	33.5	159	754
258	4.13	48.4	0.239	38.2	160	744
330	3.52	56.0	0.273	44.2	162	789
396	3.24	59.5	0.311	46.9	151	757
					Mean 161	755.3

When corrected for the thermal expansion of the solvent:
$k_e = 1.021 \times 0.007553 = 0.007710$;
$k_f = 0.007710/161 = 0.0000479$.

RESULTS AND DISCUSSION

The results of our kinetic experiments in alcoholic solutions are summarized in Tables 6 and 7. The values of k_e and k_f have been corrected for the thermal expansion of the solvent. The activation energies and frequency factors were calculated from the variation of log k with $1/T$ by the method of least squares. The Arrhenius equation was obeyed within the limits of experimental error in all cases. The entropy of activation was calculated from the equation

$$A = e \frac{kT}{h} e^{\Delta S^*/R}$$

The values of k_e, E and log A for reaction (1) in pure alcohols (Table 6) represent the true bimolecular rate constant, the true activation energy and the true frequency factor for the reaction. If $[H_2O]/[AlkOH]$ is small, also $K' = K[H_2O]/[AlkOH]$ is small. According to the results of Caldin [11], $K \approx 2$ at 25° for ethanol-water mixtures, and according to Koskikallio [12] $K = 0{,}13$ for methanol-water mixtures. On the basis of the value $K = 2$ we can estimate

Table 5. *p*-Dinitrobenzene in 88.0 wt.-% MeOH, $a = 0.008$, 40°.

a. Rate constants.

Formula $\frac{dx}{dt} = k(a-x)^2$

t min	Titr. ml	p	10^5k l mole^{-1}s^{-1}
0	(8.00)		
466	5.14	35.8	249
473	5.12	36.0	251
544	4.87	39.1	246
857	3.92	51.0	253
862	3.90	51.3	254
870	3.92	51.0	249
928	3.77	52.9	252
			Mean 250.6

b. Ratio x/y.

(Different samples)

p	x/y
50.9	2 220
51.1	2 300
51.6	2 160
62.1	2 460
	Mean 2 290

When corrected for the thermal expansion of the solvent:
$k = k_e = 1.023 \times 0.002506 = 0.002563$;
$k_f = 0.002563/2290 = 0.00000112$.

Table 6. The reaction $NO_2 \cdot C_6H_4 \cdot NO_2 + AlkO^- \rightarrow NO_2 \cdot C_6H_4 \cdot OAlk + NO_2^-$ in alcohol-water mixtures.

Isomeride Alcohol	In the solvent			$10^5 k_e$ l mole^{-1}s^{-1}			E cal.	log A	ΔS^* (35°) E.U.
	H_2O ml/l	alcohol wt.-%	$x_{alc.}$	25.00°	40.00°	50.00°			
Ortho EtOH	0	100	1.000	18.5	99.0	283	20 890	11.57	− 7.7
	50	94.2	0.862	13.5	70.2	195	20 450	11.12	− 9.7
	100	88.3	0.743	11.4	57.9	156	20 080	10.77	−11.3
	200	76.6	0.562	9.03	42.4	107	18 960	9.85	−15.5
	300	66.0	0.427	7.12	29.8	74.7	17 980	9.03	−19.2
	400	55.6	0.329	5.51	22.7	53.1	17 370	8.49	−21.8
Para EtOH	0	100	1.000	197 [a]	1 160	3 590	21 960	13.40	+ 0.7
	50	94.2	0.862	171	1 000	2 860	21 600	13.07	− 0.8
	100	88.3	0.743	144	771	2 250	21 060	12.59	− 3.0
	150	82.6	0.645	120					
	200	76.6	0.562	100	498	1 340	19 870	11.56	− 7.7
Para MeOH	0	100	1.000	34.0	206	640	22 450	12.98	− 1.2
	100	88.0	0.804	41.9	256	784	22 430	13.06	− 0.8
	200	76.7	0.650	45.9	280	852	22 370	13.06	− 0.8

[a] 15.00° : 56.2.

that if $[H_2O]/[AlkOH] < 0.1$, $K' < 0.2$ and $1 < k_e^o/k_e < 1.2$. Thus in highly alcoholic solvents the values of k_e, E and log A of Table 6 do not differ much from the true values. By contrast, the values of k_f, E and log A given in Table 7 for reaction (2) in these solvents differ much from the true values; *e.g.*, if $[H_2O]/[AlkOH] = 0.1$, $k_f^o/k_f > 6$. With increasing water content this ratio becomes smaller; thus if $[H_2O]/[AlkOH] = 1$, $k_f^o/k_f \approx 1.5$. In highly aqueous solvents this latter ratio approaches unity. It seems that if specific

Table 7. The reaction $NO_2 \cdot C_6H_4 \cdot NO_2 + OH^- \rightarrow NO_2 \cdot C_6H_4 \cdot OH + NO_2$ in alcohol-water mixtures.

Isomeride Alcohol	Alcohol wt.-%	x/y			$10^5 k_f$ l mole^{-1}s^{-1}			E cal	log A	ΔS^* (35°) E.U.
		25.00°	40.00°	50.00°	25.00°	40.00°	50.00°			
Ortho EtOH	94.2	62.0	35.7	27.2	0.218	1.97	7.18	26 800	14.0	+ 3.5
	88.3	40.5	24.9	18.5	0.280	2.33	8.41	26 100	13.6	+ 1.6
	76.6	28.3	19.1	13.8	0.319	2.22	7.75	24 400	12.4	− 4.0
	66.0	23.3	13.5	10.1	0.306	2.20	7.43	24 400	12.4	− 4.0
	55.6	18.1	11.9	8.35	0.305	1.91	6.36	23 200	11.5	− 8.3
Para EtOH	94.2	503	316	220	0.340	3.16	13.0	28 300	15.2	+ 9.0
	88.3	254	161	119	0.565	4.79	18.9	27 000	14.5	+ 5.8
	76.6	157	86	65	0.641	5.78	20.8	26 800	14.4	+ 5.3
Para MeOH	88.0	3 760	2 290	1 510	0.0111	0.112	0.519	29 500	14.7	+ 6.7
	76.7	1 570	1 010	850	0.0292	0.277	1.00	27 100	13.3	+ 0.3

Table 8. The reaction $NO_2 \cdot C_6H_4 \cdot NO_2 + OH^- \rightarrow NO_2 \cdot C_6H_4 \cdot OH + NO_2^-$ in pure water

Compound	Initial conc.		$10^5 k$ l mole^{-1}s^{-1}				E cal	log A	ΔS^* (35°) E.U.
	[NaOH]	[Dinitrobenzene]	25.00°	40.00°	50.00°	60.00 °			
Ortho	0.016	4.73×10^{-4}	(0.260)	1.68	5.18	15.4	23 010	11.28	−9.0
Para	0.016	1.64×10^{-4}	(0.0968)	0.758	2.70	8.93	25 560	12.72	−2.4

The values for 25° given in brackets were calculated from the Arrhenius equation.

solvent influences are taken into account the values of Table 7 gradually change with increasing water content towards values found for reaction (2) in pure water (Table 8; in this table $k = k_f^0$).

The results obtained for *p*-dinitrobenzene in dioxan-water containing 50 ml of water in 100 ml of the mixture are:

	25.00°	40.00°	50.00°	60.00°
$10^5 k$ l mole^{-1}s^{-1}	1.45	9.20	25.0	67.0

E = 21 600 cal, log A = 11.0.

The rate constants are considerably larger and the activation energy lower than for the reaction in pure water. The frequency factor is of the same order of magnitude as in water. Evidently the addition of dioxan to the water accelerates the reaction by lowering the energy of activation.

Lobry de Bruyn and Steger used for the calculation of the rate constants the formula

$$k = \frac{100\ (T_1 - T_t)}{tT_1T_t\Theta}$$

where t is the time, Θ the normality of the acid used as titrant, T_1 the consumption of the acid at the start of the reaction and T_t the consumption at time t. The volume of the sample does not occur in this formula, and therefore their values of k are twice as great as the true values [13]. The rate constants recalculated from the data of Lobry de Bruyn and Steger for pure alcohols and corrected for the thermal expansion of the solvent and the activation energies,

Table 9. Reaction (1) of dinitrobenzenes in absolute ethanol and methanol. (Based on data of Lobry de Bruyn and Steger.)

	Temperature	Ethanol		Methanol	
		Ortho	*Para*	*Ortho*	*Para*
$10^5 k$ l mole^{-1}s^{-1}	25°	21.8	177	14.3	37.1
	35°	66.6	599	41.1	121
	45°	200	1 890	119	407
E cal		20 800	22 300	20 000	22 600
log A		11.6	13.6	10.8	13.1
ΔS^* (35°), E.U.		−7.5	+1.6	−11.3	−0.6

frequency factors and activation entropies obtained from these values are given in Table 9. The values are in good agreement with the values of Table 6 for the reactions in absolute alcohols.

The rate constants of Lobry de Bruyn and Steger for *o*-dinitrobenzene in aqueous ethanol and methanol at 25° are, when corrected as above:

Alcohol, wt.-%		100	98	96	94	92	90	80	70	60	50
10^5k,	EtOH	21.7	20.0	18.8	17.6	16.5	15.8	12.8	10.3	9.3	8.7
$l\,mole^{-1}s^{-1}$	MeOH	14.1	14.3				15.2	16.3	17.4	18.8	20.8

To compare our results for *o*-dinitrobenzene in ethanol-water with these values the rate constant for the total reaction at 25° was calculated from the simple second-order formula. The following results were obtained:

EtOH, wt.-%	100	94.2	88.3	76.6	66.0	55.6
$10^5k\ l\,mole^{-1}s^{-1}$	18.5	14.4	12.0	9.79	7.84	6.23

It is seen that our values are considerably lower than those of Lobry de Bruyn and Steger.

For the molar ratios of the ether (x) and phenol (y) formed in the reaction of *o*-dinitrobenzene Lobry de Bruyn and Steger obtained the following values:

AlkOH, wt.-%	90	80	70	60	50
EtOH, x/y	51	35	27	24.5	21
MeOH, x/y		209	176	170	146

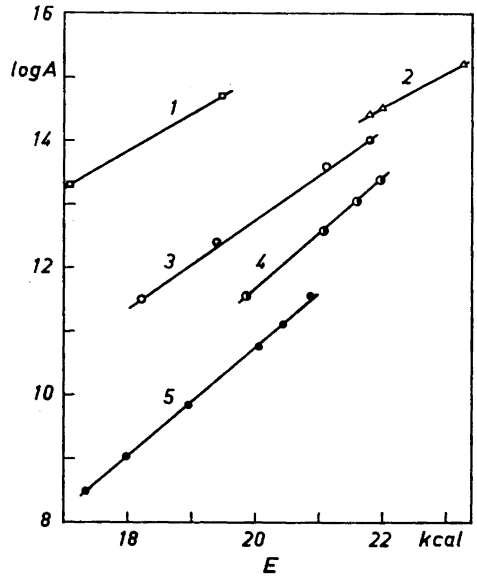

Fig. 1. Plot of log A against E. 1. *p*-dinitro + OH^- (MeOH, E — 10 kcal) 2. *p*-dinitro + OH^- (EtOH, E — 5 kcal), 3. *o*-dinitro + OH^- (EtOH, E — 5 kcal), 4. *p*-dinitro + EtO^-, 5. *o*-dinitro + EtO^-.

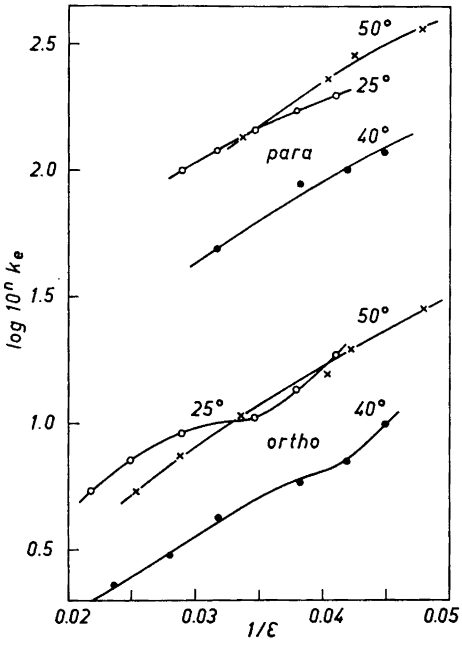

Fig. 2. Plot of log 10^n k against $1/\varepsilon$ in ethanol-water. *o*-dinitro: for 40° and 50° $n = 5$, for 25° $n = 6$. *p*-dinitro: For 40° and 50° $n = 4$, for 25° $n = 5$.

Thus 6—7 times more phenol is formed in ethanol than in methanol. This is in good agreement with our results that were obtained by a more refined technique and more accurate calculations.

Lobry de Bruyn and Steger also stated that the ratio x/y remains constant as the reaction proceeds. This is in accordance with our observations. The derivations of eqns. (14) and (15) are based on the constancy of the ratio x/y.

It is remarkable that k_e and k_f show many regularities. First and foremost they obey the Arrhenius equation. Also is there a simple relation between E and log A when the composition of the binary solvent mixture is varied. From Fig. 1 we see that straight lines are obtained when log A is plotted against E. The linear relationship can, of course, be only incidental and be based on the shift of the equilibrium (4) as the composition of the solvent changes. However, one must bear in mind that a linear relationship between log A and E has often been observed as the composition of a mixed solvent is varied, also in cases where no equilibrium (4) exists. This relationship has been extensively discussed [14,15].

The relation between the rate constant and the dielectric constant ε of the medium has often been considered. According to theory, a roughly linear relationship between log k and $1/\varepsilon$ should be expected. Plots based on the data of the present study are shown in Fig. 2.

On the basis of our experimental results the following general statements can be made. Reaction (1) is about ten times as fast for *p*-dinitrobenzene as for *o*-dinitrobenzene in ethanol and ethanol-water. This reaction is much slower in methanol and methanol-water than in ethanol and ethanol-water. The velocity of reaction (2) is much smaller than that of (1), and, at least in water, for *p*-dinitrobenzene clearly smaller than for *o*-dinitrobenzene. The activation energy of reaction (2) is always much higher than that of reaction (1).

REFERENCES

1. Lobry de Bruyn, C. A. and Steger, A. *Rec. trav. chim.* **18** (1899) 9.
2. Steger, A. *Rec. trav. chim.* **18** (1899) 13; *Z. physik. Chem.* **49** (1904) 329.
3. Lobry de Bruyn, C. A. and Steger, A. *Rec. trav chim.* **18** (1899) 41; *Z. physik. Chem.* **49** (1904) 333.
4. Parijs, H. *Rec. trav. chim.* **48** (1929) 560; *Thesis*, Leyden 1928.
5. Bolto, B. A. and Miller, J. *Austral. J. Chem.* **9** (1956) 74.
6. Walden, P. *Z. physik. Chem.* **114** (1925) 281.
7. Lund, H. and Bjerrum, J. *Ber.* **64** (1931) 210.
8. Treadwell, F. P. *Kurzes Lehrbuch der analytischen Chemie 11. Aufl.* (1927), p. 295.
9. Blom, A. V. *Helv. Chim. Acta* **4** (1921) 510.
10. Tommila, E. and Lindholm, M. *Acta Chem. Scand.* **5** (1951) 647.
11. Caldin, E. F. and Long, G. *J. Chem. Soc.* **1954** 3737.
12. Koskikallio, J. *Suomen Kemistilehti B* **30** (1957) 111.
13. Lorang, H. F. J. *Rec. trav. chim.* **46** (1927) 891.
14. Tommila, E., Koivisto, A., Lyyra, J. P., Antell, K. and Heimo, S. *Ann. Acad. Sci.Fennicae A II* (1952) No. 47.
15. Blackadder, D. A. and Hinshelwood, Sir Cyril, *J. Chem. Soc.* **1958** 2728.

Received June 15, 1961.

ACTA CHEMICA SCANDINAVICA 16 (1962) 63–70

The Influence of the Solvent on Reaction Velocity

XXI. The Reaction of 2,4-Dinitrophenyl Alkyl Ethers with Hydroxyl Ion in Water and in Methanol-Water and Ethanol-Water Mixtures

JUHANI MURTO and EERO TOMMILA

Department of Chemistry, University of Helsinki, Finland

The following reactions have been kinetically investigated: the reaction of 2,4-dinitroanisole with hydroxyl ion in water and in methanol-water mixtures; the reaction of 2,4-dinitrophenetole with hydroxyl ion in water and in ethanol-water mixtures; the reaction of 2,4-dinitrophenyl *n*-propyl ether with hydroxyl ion in water. For the first of these reactions the plot of log k against log $[H_2O]$ of the medium is linear, whereas the plot for the second reaction passes through a maximum. The curves plotting E and log A as functions of the composition of the solvent resemble closely the corresponding curves for the alkaline hydrolysis of esters in methanol-water and ethanol-water mixtures, but run much higher. The results are discussed.

In a preceding investigation [1] of the reactions of dinitrobenzenes with hydroxyl and alkoxyl ions, our attention was drawn to the corresponding reactions of halogenonitrobenzenes. The monohalogenomononitrobenzenes, except the fluoro-derivatives, react considerably slower than the dinitrobenzenes, whereas the 1-halogeno-2,4-dinitrobenzenes react much faster. These reactions have been kinetically investigated in pure methanol and ethanol and also in methanol-water and ethanol-water mixtures [2]. The possible reactions in alcohol-water mixtures are [3] (X = halogen):

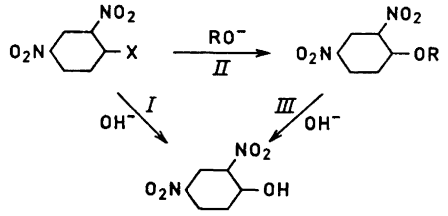

In these previous investigations only the reactions I and II were taken into account. It is, however, possible that phenol is formed by route III, the ether

formed in reaction II reacting with hydroxyl ion. Already the first preliminary experiments showed that under the conditions employed this reaction may proceed at a considerable velocity. The whole process in an alkaline solution is

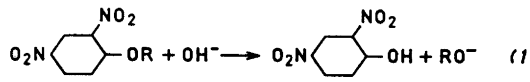

(1)



(2)

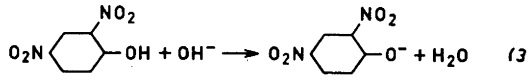

(3)

The over-all reaction is

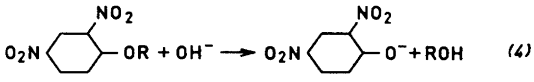

(4)

(R = Me, Et, or *n*-Pr).

The kinetics of reaction (1) which, as far as we are aware, have not been investigated before, formed the subject of the present study. It has been previously known [4] and was also confirmed in our own experiments, that the reactions of *para*- and *ortho*nitroanisole and phenetole with hydroxyl ion is so slow at the temperatures used [1], that they can be completely neglected when studying the reactions of the dinitrobenzenes in alkaline alcohol-water mixtures.

EXPERIMENTAL

Materials. The dinitrophenyl methyl and ethyl ethers were prepared by treating 1-chloro-2,4-dinitrobenzene (purissimum, Fluka) with a solution of sodium hydroxide in the alcohol, and dinitrophenyl propyl ether by treating 1-chloro-2,4-dinitrobenzene with a solution obtained by dissolving sodium metal in propanol. The ethers were crystallized twice from the corresponding alcohol; in the case of the propyl ether the solution was cooled in an ice-salt bath. The melting points were: methyl ether 86.6—87.9°, ethyl ether 84.3—85.5°, *n*-propyl ether 30.7—31.2°C.

Methanol and ethanol were purified as in the previous investigation. The *n*-propanol was purified by the same method as ethanol.

Method. In the kinetic experiments, the progress of the reaction was followed by determining the concentration of the phenol formed colorimetrically with a Bausch & Lomb Spectronic 20 spectrophotometer. The wave length used was 400 mμ. In all experiments the initial concentration of the alkali (NaOH) was 0.016 mole/l, and that of the ether, when its solubility permitted, 0.004 mole/l. The reaction mixture was kept in a 50-ml glass-stoppered flask from which 2 ml-samples were taken after suitable intervals and diluted with an appropriate amount of water (to a 2—20-fold volume) for the colorimetric analyses. Since the extinction of 2,4-dinitrophenol proved to be somewhat dependent upon its concentration the readings were compared with a calibration curve recorded with solutions of known dinitrophenol concentrations. Seven to ten samples were taken in each run.

Table 1. Reaction of 2,4-dinitroanisole with hydroxyl ion in 76.7 wt. % methanol. Temperature 40°C, $a_{base} = 0.016$, $a_{ether} = 0.004$ mole/l. p = percentage of ether that has reacted.

Time min.	$10^4 x$	p	$10^5 k$ l mole^{-1}s^{-1}
699	5.85	15.0	24.6
1383	10.35	26.8	23.9
1960	14.05	36.0	24.8
1980	14.34	36.7	25.3
2854	17.95	46.0	24.0
4949	24.63	63.0	23.0
4953	24.65	63.1	23.0
6000	27.70	70.9	23.9
			Mean 24.06

When corrected for solvent expansion, $k = 1.021 \times 0.0002406 = 0.0002457$ l mole^{-1}s^{-1}.

The rate constants were calculated using the formula

$$k = \frac{2.303}{t(a - b)} \log \frac{b(a - x)}{a(b - x)}$$

where a is the initial concentration of the base and b that of the ether. The reactions were of the second order in all cases. Data from several runs are given in Tables 1—3.

Because the ethers are sparingly soluble in pure water, the experiments in pure water and in solvents of high water content were carried out in the same manner as the determinations of the velocities of hydrolysis of the dinitrobenzenes in water in the earlier investigation [1].

RESULTS AND DISCUSSION

The results of the kinetic measurements are summarized in Tables 4, 5 and 6. The rate constants are corrected for the thermal expansion of the solvent. The Arrhenius equation was obeyed in all cases within the limits of

Table 2. Reaction of 2,4-dinitrophenetole with hydroxyl ion in 36.3 wt. % ethanol. Temperature 25°C, $a_{base} = 0.016$, $a_{ether} = 0.004$ mole/l.

Time min.	$10^4 x$	p	$10^5 x$ l mole^{-1}s^{-1}
759	8.45	21.2	33.6
1228	12.52	31.4	33.4
1402	13.79	34.6	33.1
1454	14.10	35.3	32.8
1734	16.30	40.8	33.5
1961	17.85	47.2	33.7
3044	23.32	58.4	32.9
3044	23.44	58.9	33.2
3499	24.78	62.2	31.9
4338	28.00	70.2	32.6
			Mean 33.07

When corrected for solvent expansion, $k = 1.003 \times 0.0003307 = 0.0003317$ l mole^{-1}s^{-1}.

Table 3. Reaction of 2,4-dinitrophenyl propylether with hydroxyl ion in water. Temperature 40°C, $a_{NaOH} = 0.016$, $a_{ether} = 1.81 \times 10^{-4}$ mole/l.

Time min.	$10^4 x$	p	$10^5 k$ l mole^{-1}s^{-1}
154	0.245	13.5	98.7
251	0.397	21.9	102.9
354	0.536	29.6	103.6
437	0.641	35.4	104.5
479	0.697	38.6	106.0
597	0.821	45.4	105.8
643	0.859	47.5	104.5
1383	1.326	73.4	99.9
∞	1.81		Mean 103.2

When corrected for solvent expansion, $k = 1.006 \times 0.001032 = 0.001038$ l mole^{-1}s^{-1}.

experimental error. The activation energies, frequency factors and activation entropies were calculated as described before.

In pure water the rate constants follow the sequence Me> Et ≈ Pr. Except in highly aqueous media, the specific rates of the reaction of the ethyl ether in ethanol-water mixtures are greater than those of the methyl ether in methanol-water mixtures of equal water content (Fig. 1). The rate constant of the latter reaction increases continuously with the water content of the solvent, whereas the curve plotting k as a function of the solvent composition for the former reaction passes through a pronounced maximum. From Fig. 2 it is seen that the plot of log k against log [H_2O] for 2,4-dinitroanisole is a straight line whose slope approaches the value 1 as the temperature rises. This can be taken to imply that one water molecule participates in the formation of the transition state, for if the rate equation is written in the form

Table 4. The reaction R · OMe + OH^- = R · O^- + MeOH in methanol-water. a_{base} = 0.016 mole/l. (R · OMe = 2,4-dinitroanisole).

In the solvent			a_{ether} mole/l	$10^5 k$ l mole^{-1}s^{-1}				E cal.	log A
H_2O ml/l	MeOH wt. %	x_{MeOH}		25.00°	25.10°	40.00°	50.00°		
1000	0	0	6.60×10^{-4}	34.5	76.6[b]	182	499	20 480	11.55
800	16.2	0.097	4.49×10^{-4}	24.8		142	406	21 430	12.10
600	36.5	0.244	0.004	(16.2)[a]	16.4	94.4	287	22 010	12.34
500	46.1	0.325	»	(12.7)[a]	12.8	76.7	235	22 360	12.49
400	56.0	0.417	»	(9.32)[a]	9.44	59.1	181	22 730	12.63
300	66.1	0.523	»	(6.40)[a]	6.49	40.7	130	23 020	12.68
200	76.7	0.650	»	(3.67)[a]	3.72	24.6	79.6	23 560	12.83
100	88.0	0.804	»	(1.43)[a]	1.45	11.1	36.0	24 760	13.31

a. By the Arrhenius equation.
b. At 32.00°.

Table 5. The reaction R · OEt + OH^- = R · O^- + EtOH in ethanol-water. a_{base} = 0.016 mole/l. (R · OEt = 2,4-dinitrophenetole).

In the solvent			a_{ether} mole/l	$10^5\ k$ l mole^{-1}s^{-1}					E cal	log A
H_2O ml/l	EtOH wt. %	x_{EtOH}		15.00°	25.00°	25.10°	40.00°	50.00°		
1000	0	0	2.66×10^{-4}		20.9	45.7[a]	105	283	19 950	10.95
800	16.2	0.070	3.84×10^{-4}		30.1	63.0[a]	142	376	19 350	10.66
600	36.3	0.182	0.004	[b]	(32.8)[d]	33.2	148	384	18 820	10.31
500	45.6[c]	0.247	»	10.7	(33.0)[d]	33.4	155	402	19 150	10.55
400	55.2[c]	0.326	»	9.80	(33.0)[d]	33.4	164	432	19 990	11.16
300	65.5[c]	0.425	»	9.68	(33.8)[d]	34.2	173	483	20 610	11.62
200	76.6	0.562	»	9.68	(33.6)[d]	34.0	187	506	20 970	11.90
100	88.3	0.743	»	7.78	(27.8)[d]	28.1	157	467	21 620	12.29
50	93.3[c]	0.844	»	5.25	(19.4)[d]	19.7	120	358	22 350	12.70

a. At 32.00°.
b. A part of the ether crystallized from the solution.
c. The ethanol in these experiments was "ethanol for spectroscopy", which contained a little water; hence the values of the mole fractions differ slightly from these given in the previous paper.
d. Calculated from the Arrhenius equation.

$$\frac{dx}{dt} = k' \, [H_2O]^n \, (a - x) \, (b - x) \qquad (5)$$

we see that the experimental bimolecular rate constant $k = k' \, [H_2O]^n$ or $\log k = \log k' + n \log [H_2O]$. A change in the value of n may be connected with the shift of the equilibrium

$$AlkO^- + H_2O \rightleftharpoons AlkOH + OH^- \qquad (6)$$

with temperature. Also the form of the curve in Fig. 1 which plots the rate constant of the reaction between 2,4-dinitrophenetole and hydroxyl ion in ethanol-water can probably be explained, at least partly by a shift of the above equilibrium with varying solvent composition. From Table 7 of the previous paper we see that also the curves plotting the rate constants of the reactions between the dinitrobenzenes and hydroxyl ion in ethanol-water mixtures go through a maximum. This shows that the discussion in the previous paper rests on a sound basis.

Figs. 3 and 4 in which the activation energy and frequency factor are plotted as functions of the composition of the solvent show that both E and A are greater for anisole than for phenetole. Except in pure water and in the highly aqueous solutions where the frequency factor governs the situation,

Table 6. The reaction R · OPr + OH^- = R · O^- + PrOH in water. (R · OPr = 2,4-dinitrophenyl *n*-propylether). a_{NaOH} = 0.016, a_{ether} = 1.81×10^{-4} mole/l.

Temp.	25.00°	40.00°	50.00°	E = 20 480 cal
$10^5\ k$ (l mole^{-1}s^{-1})	20.1	104	293	log A = 11.32

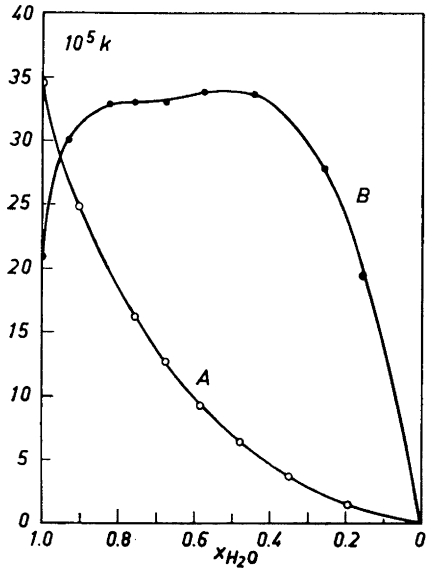

Fig. 1. Plot of k against the mole fraction of water. A the methyl ether in methanol-water, B the ethyl ether in ethanol-water. Temperature 25°C.

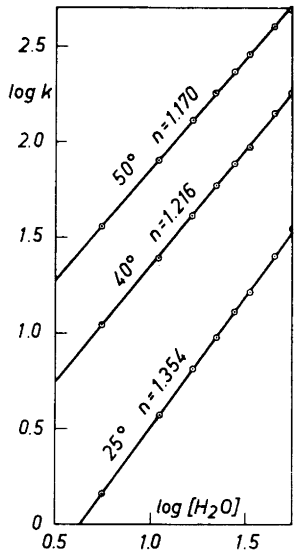

Fig. 2. 2,4-Dinitroanisole, methanol-water. Plot of log k against log [H_2O].

the order of the rate constants of both reactions is due to differences in the activation energies. The plots of E and log A for 2,4-dinitroanisole in methanol-water mixtures rise continuously with decreasing water content, whereas the curves for the reaction of 2,4-dinitrophenetole in ethanol-water pass through a pronounced minimum. It is interesting that E and log A for these reactions vary similarly as E and log A for the alkaline hydrolysis of esters in alcohol-water mixtures. The curves for the reaction of 2,4-dinitroanisole in methanol-water mixtures have the same form as the curves for the hydrolysis of methyl acetate or ethyl acetate in methanol-water mixtures [5,6], and the curves for reaction of 2,4-dinitrophenetole in ethanol-water mixtures have the same form as the curves for the hydrolysis of ethyl acetate or ethyl benzoate in ethanol-water mixtures [6,7]. The reactions are similar in that the reagent which attacks the substrate is the hydroxyl ion and that the hydroxyl ion concentration is determined by equilibrium (6).

According to previous discussions [6], the minima observed for the activation energies and entropies arise because of changes in the solvation of the reaction system, *i.e.* the reactants and the activated complex, the water molecules having a specific attraction for the hydrophilic part and the organic solvent molecules for the alkyl groups. It is interesting that the rules found valid for ester hydrolysis are valid also for the reactions between the dinitrophenyl

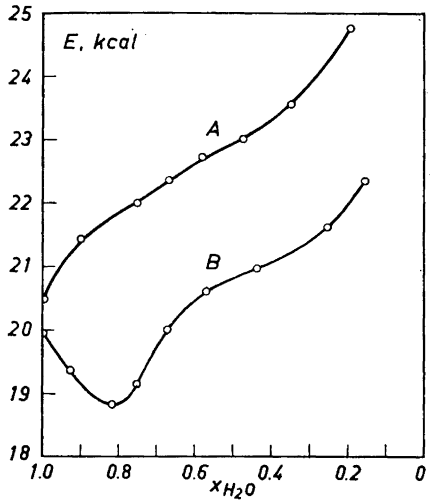

Fig. 3. E as a function of x_{water}. *A* 2,4-dinitroanisole in methanol-water, *B* 2,4-dinitrophenetole in ethanol-water.

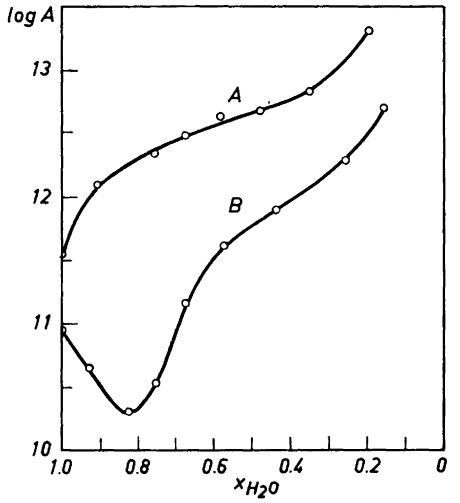

Fig. 4. Log A as a function of x_{water}. *A* 2,4-dinitroanisole in methanol-water, *B* 2,4-dinitrophenetole in ethanol-water.

ethers and the hydroxyl ion. The shift of the equilibrium (6) with varying solvent composition plays a minor part in the formation of the minimum in the plots of E and log A, since the plots for ester hydrolysis have the same form

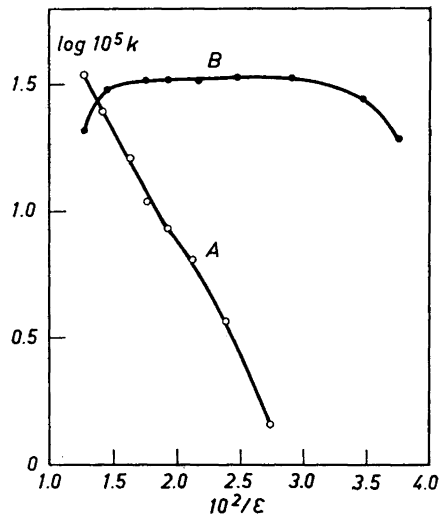

Fig. 5. Plot of log k against $1/\varepsilon$. *A* 2,4-dinitroanisole in methanol-water, *B* 2,4-dinitrophenetole in ethanol-water.

also in other mixed solvents, *e.g.*, in acetone-water and in dioxan-water mixtures [6]. When suitable concentrations of both water and the organic solvent are present, the solvation of the transition complex is greater than in either solvent alone, with the result that E and A go through a minimum. It appears, however, that when methanol is the organic component of the solvent, changes in solvation do not lead to minimum values of E and A. The non-appearance of the minimum is specific for methanol and not for the reactant since the minimum is observed also when the alkaline hydrolysis of methyl acetate is carried out in acetone-water mixtures. Furthermore, it has been found for ester hydrolysis that the minimum is deeper the larger the hydrocarbon part of the solvent alcohol molecule.

The activation energies and frequency factors are much higher for the reactions of the dinitrophenyl ethers than for ester hydrolysis in the same solvents. This and especially the fact that the frequency factor is "normal", *i.e.* log A is about 11—13, for the dinitrophenyl ethers whereas the value of log A for ester hydrolysis is only 7—9, indicate a difference in reaction mechanism.

The relationship between rate constant and dielectric constant of the medium is shown in Fig. 5. The plots of log k against $1/\varepsilon$ are seen to be nearly linear for the reaction of the methyl ether in methanol-water mixtures. For the reaction of the ethyl ether in ethanol-water mixtures log k is practically constant in the solvent range from 20 wt. % to 75 wt. % ethanol.

REFERENCES

1. Tommila, E. and Murto, J. *Acta Chem. Scand.* **16** (1962) 53.
2. Lulofs, P. K. *Rec. trav. chim.* **20** (1901) 292; *Z. physik. Chem.* **49**(1904) 341; Baudet, H. P. *Rec. trav. chim.* **43** (1924) 707; Bevan, C. W. L. and Bye, G. C. *J. Chem. Soc.* **1956** 469.
3. Funakubo, E., Imoto, M. and Imoto, E. *Ber.* **71** B (1938) 950.
4. Blom, A. V. *Helv. Chim. Acta* **4** (1921) 510.
5. Tommila, E. and Maltamo, S. *Suomen Kemistilehti B* **28** (1955) 118.
6. Tommila, E., Koivisto, A., Lyyra, J. P., Antell, K. and Heimo, S. *Ann.Acad.Sci. Fennicae A. II.* **47** (1952).
7. Tommila, E. *Suomen Kemistilehti B* **15** (1942) 9; *A* **17** (1944) 14; *B* **25** (1952) 37.

Received June 29, 1961.

ACTA CHEMICA SCANDINAVICA 16 (1962) 71–77

Isothiocyanates XL *. Glucosisaustricin, a Novel Glucoside Present in Seeds of *Sisymbrium austriacum* Jacq.

ANDERS KJÆR and BO W. CHRISTENSEN

Department of Organic Chemistry, The Royal Veterinary and Agricultural College, Copenhagen, Denmark

Structure determinations of two glucosides in seed extracts of *Sisymbrium austriacum* Jacq. have been described in two preceding papers [1,2]. The present communication reports on the chemical structure of a third glucoside, *glucosisaustricin*, from the same source, characterized by undergoing enzymic hydrolysis to glucose, sulphate and (+)-4-ethyl-2-oxazolidinethione (sisaustricin), the latter arising from cyclization of 1-ethyl-2-hydroxyethyl isothiocyanate, initially formed by the enzymic hydrolysis.

The structure and absolute configuration of sisaustricin, (VI), are established by synthesis and stereochemical correlation with 2-aminobutyric acid. The absolute configuration of optically active 2-amino-1-butanol is determined.

The biosynthetic origin of the isothiocyanate producing glycosides with branched side-chains is discussed and a possible relationship to the metabolism of valine and isoleucine is suggested.

Previous communications of this series dealt with structure elucidations of glucosisymbrin [1] and glucobenzosisymbrin [2], two glucosides occurring in seed extracts of the crucifer *Sisymbrium austriacum* Jacq. Paperchromatographic studies, however, indicated the presence in the same seed material ** of an additional glycoside, previously referred to [1] as glycoside B.*** It is the purpose of the present paper to report on the structure determination of this novel glycoside.

* Presented in abstract before the *1st Scandinavian Symposium on Natural Product Chemistry*, June 1961, Bornholm, Denmark.

Part XXXIX of this series: *Acta Chem. Scand.* **15** (1961) 1477.

** The present investigation was carried out on seed material propagated in 1959–1960 in *The Botanical Garden of the University of Copenhagen* from the authentic stock employed in our previous studies.

*** Only this additional glycoside, (B), was reported in the previous communication [1]. However, more recent investigations have disclosed the presence in the same extracts of minor amounts of a fourth glycoside, with an R_F-value still higher than that of glucobenzosisymbrin [2]. A subsequent paper [4] reports on the structure of this glycoside.

Paper chromatography of a methanolic seed extract of *S. austriacum* Jacq., followed by elution of the appropriate band, furnished a solution of glycoside B which was subjected to acid hydrolysis according to Ettlinger and Lundeen [3]. The presence of glucose and hydroxylamine in the hydrolysate was demonstrated by paper chromatography, and concomitantly liberated sulphate by precipitation as barium sulphate. Hence, glycoside B is a glucoside of the conventional type [3] for which we propose the name *glucosisaustricin*.

For preparative purposes, a methanolic extract of defatted seed material was subjected to enzymic hydrolysis by myrosinase in a citrate buffer. Steam distillation served to remove the volatile ester isothiocyanates, originating from glucobenzosisymbrin [2] and glucobenzsisaustricin [4]. In a previous paper [1], evidence was presented for the probable structure of *sisaustricin* ('THIOX B'), the aglucone of glucosisaustricin, as a substituted 2-oxazolidinethione. Consequently, the unknown compound must be searched for in the steam-distilled residue, together with (+)-4-methyl-2-oxazolidinethione (sisymbrin) (I), the latter originating from glucosisymbrin [1]. A 180-plate counter-current distribution in the solvent system benzene:heptane:water (9:2:9) was utilized to separate the two aglucones, both of which could be isolated in pure form as low-melting, crystalline products. The sisymbrin fraction possessed all the properties previously recorded for a specimen prepared by fractional crystallization [1]. Sisaustricin, m.p. 33—34°, had the elemental composition C_5H_9ONS which together with its ultra-violet and infra-red spectra strongly indicated its character as a higher homologue of sisymbrin. These data, in conjunction with the established optical activity, admitted of only three substitution patterns for sisaustricin, *viz.* 4,5-dimethyl (II), 5-ethyl (III), and 4-ethyl (IV).

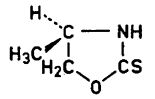

I

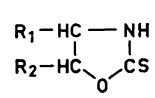

II. $R_1 = R_2 = CH_3$

III. $R_1 = H$; $R_2 = CH_3CH_2$

IV. $R_1 = CH_3CH_2$; $R_2 = H$

A racemic modification of (II), with unknown stereochemistry at C_4 and C_5, was prepared during the present work. Whereas none of the optically active isomers have formerly been described, racemic modifications of (III)[5] and (IV)[6,7] were recorded in the literature and both were synthesized for comparison purposes in this laboratory. Considerable deviations in melting points and solid phase infrared spectra between racemates and enantiomers have frequently been noticed in the present series (*cf. e.g. Ref.*[1]), a fact which makes comparisons of melting points and IR-spectra of limited diagnostic value. However, careful comparative paper-chromatographic studies * indicated that sisaustricin was in all probability the *dextro*rotatory enantiomer of (IV), a surmise for which experimental support was obtained by the following syn-

* In no case have differences in R_F-values been noticed between racemates and enantiomers in the 2-oxazolidinethione series.

thesis of (+)-4-ethyl-2-oxazolidinethione, proceeding by a route which provides full information as to its absolute configuration.

(−)-2-Amino-1-butanol was prepared by resolution of the racemic aminoalcohol with (+)-tartaric acid as described by Radke *et al.*[8] The *levo*rotatory enantiomer was further converted into (+)-4-ethyl-2-oxazolidinethione by the procedure employed by Rosen [6] for the preparation of the corresponding racemic compound. The synthetic specimen proved to be identical with sisaustricin with regard to sign and magnitude of rotation as well as all other physical criteria. Furthermore, its absolute configuration was established on basis of the following chemical correlation: (−)-2-amino-1-butanol was converted into its *levo*rotatory acid oxalate, whereas the 2-amino-1-butanol obtained by lithium aluminium hydride reduction of configurationally known L-2-aminobutyric acid [9] yielded the enantiomeric, *dextro*rotatory acid oxalate, derivable from (+)-2-amino-1-butanol. Consequently, (−)-2-amino-1-butanol has the absolute configuration shown in (V)* whereas the naturally derived (+)-sisaustricin possesses the absolute configuration depicted in (VI)**. It is noteworthy that

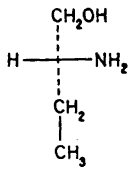

V

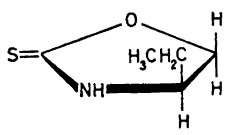

VI

the homologous, *dextro*rotatory, 4-substituted 2-oxazolidinethiones, sisymbrin and sisaustricin, belong to the same configurational series. It has been previously established in this laboratory that in the isomeric (+)-5-ethyl-2-oxazolidinethione the substituent is located below the ring plane in the same depiction [11].

The structure elucidation of sisaustricin furnishes the clue to the structure of glucosisaustricin, the parent glucoside whence it derives. On the likely assumption that the enzymic hydrolysis, as well as the subsequent ring-closure of the initially formed 1-ethyl-2-hydroxyethyl isothiocyanate, proceeds with retention of configuration, the parent glucoside ion possesses the structure (VII), depicted in analogy with the general structure of similar glucosides [3].

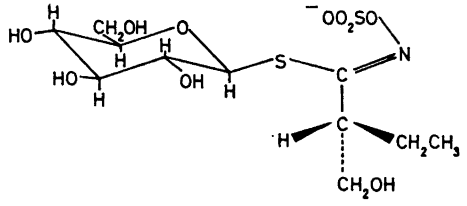

VII

* (*R*)-2-Amino-1-butanol in the specification system of Cahn *et al.*[10]
** (*R*)-4-Methyl-2-oxazolidinethione in the same specification.

The following communication [4] reports on the occurrence of O-benzoylated glucosisaustricin in the same seed material.

Unpublished considerations suggest that energy-rich esters, RCOOX, may function as biogenetic precursors in the *in vivo* synthesis of isothiocyanate glucosides containing the side chains R. In the case of glucosisymbrin and glucosisaustricin, the biosynthesis of such esters of 2-methyl- and 3-methylhydracrylic acid, or their biological equivalents, therefore has to be accounted for.

The catabolism of valine as a possible source of the 2-methyl substitute was discussed previously in this series [1]. In analogy, (X) may conceivably arise from an analogous degradation of isoleucine. It is generally agreed that the metabolic pathways of valine and isoleucine run closely parallel both in animals and various microorganisms, partly catalyzed by the same enzyme systems. The frequently observed, simultaneous appearance in plants of isothiocyanate glucosides containing the isopropyl and sec-butyl side-chains [12], as well as their β-hydroxylated derivatives, therefore lends support to the idea that intermediates on the catabolic pathway of the branched amino acids may function as biogenetic precursors of the isothiocyanate glucosides with branched side-chains *. Thus, glucosisaustricin may originate from the coenzyme A ester of 2-methylbutyric acid (VIII), an accepted intermediate in isoleucine catabolism in mammalian tissue, by the following route:

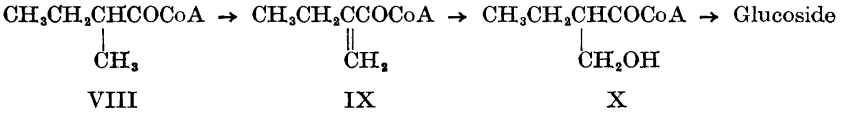

VIII IX X

This highly speculative scheme deviates from the usually accepted pathway in animal tissue by the postulation of the 2-ethylacrylic ester (IX) as an intermediate, furnishing (X) upon hydration, rather than the isomeric tiglyl ester, normally functioning as an intermediate in the further degradation of (VIII) to the coenzyme A esters of acetic and propionic acid [14].

The possibility that the above transformations occur subsequent to incorporation of (VIII) into thioglucosidic linkage should, of course, not be overlooked. It is intended to subject the above biosynthetic schemes to experimental trials.

EXPERIMENTAL

When not otherwise indicated melting points are determined in capillary tubes in an Anschütz-Hershberg apparatus equipped with fully immersed thermometers. Rotations are measured in a 1 dm tube. All infra-red spectra are determined in KBr pellets on an 'Infracord' instrument. Analytical specimens are dried *in vacuo* over calcium chloride at room temperature.

* It is of interest in this connexion that Butler and Butler [13] demonstrated that products from the valine and isoleucine metabolism are involved in the biosynthesis of the cyanogenetic glucosides, lotaustralin and linamarin, derivable from the cyanohydrins of methyl ethyl ketone and acetone, respectively, and occurring together in *Trifolium repens* L.

Acid hydrolysis of glucosisymbrin and 'glycoside B'. A methanolic seed extract of *Sisymbrium austriacum* Jacq. was prepared and chromatographed on paper as previously reported [2]. The bands containing glucosisymbrin and 'glycoside B'[1] were cut out and individually eluted with water. Both solutions were treated with conc. hydrochloric acid for 2 h at 60° to accomplish hydrolytic fission according to Ettlinger and Lundeen [3]. The presence of glucose and hydroxylamine in the hydrolyzed solutions was established on paper chromatography [3], whereas the liberation of sulphate ions was proved by precipitation as barium sulphate. Appropriate blanks were employed to exclude contaminations from the paper.

Consequently, both glucosisymbrin and 'glycoside B'[1] are of the customary type [3], the latter henceforth designated *glucosisaustricin.*

Enzymic production and isolation of sisaustricin. A portion (1 110 g) of dry seeds of *S. austriacum* Jacq. was milled, defatted and extracted with 70 % methanol, exactly as described previously [2]. The extract was concentrated to a syrup which was taken up in water (3 l), and the solution was filtered. The volume was increased to 5.6 l and 1 M sodium citrate (430 ml) was added. The pH-value was then adjusted to 6.8 by addition of solid citric acid, and a cell-free, crude myrosinase solution (120 ml) was added. After having been kept for 18 h at room temperature, at the end of which the pH-value had decreased to 6.1, the enzymically hydrolyzed solution was steam-distilled to remove volatile isothiocyanates. A total of 6 l of distillate was collected.

The steam-distilled residue was concentrated to a brown suspension (800 ml) which was continuously extracted with ether for 48 h. The ether phase, including some solid material, was then extracted with one 1-l and two 0.5-l portions of 0.2 N NaOH. Several hours were required for the emulsions to break. After adjustment of the pH-value to 7 with conc. HCl the aqueous solution was concentrated *in vacuo* to a volume of 0.5 l, and the brown suspension was percolated with ether for 24 h. The procedure of extraction with 0.2 N NaOH, neutralization, and percolation with ether was repeated. The now almost colourless ether solution was dried over calcium chloride and concentrated to a yellowish oil, essentially consisting of a mixture of sisymbrin and sisaustricin.

The oily material was distributed over the first four tubes (each holding 20 ml) of a Craig-apparatus preloaded with the lower phase of the solvent system benzene:heptane: water (9:2:9). After 180 transfers, paperchromatographic analysis indicated that complete separation of the two oxazolidinethiones had been achieved.

On concentration of the contents of tubes Nos. 10-34, a sligthly yellow oil was obtained which crystallized spontaneously (2.84 g). Two recrystallizations from ether afforded pure *sisymbrin,* m.p. 65°, $[\alpha]_D^{17}$ +21° (*c* 0.7,EtOH), indistinguishable from the previously isolated specimen [1] as estimated from infra-red spectra and mixed melting point determination.

The contents of tubes Nos. 42—68 were likewise concentrated to a yellowish oil which crystallized on prolonged cooling (1.34 g). The product was dissolved in ether at 0°, the solution was filtered, one third volume of pentane was added, and the solution cooled to —80°. Colourless prisms separated slowly, and repetition of this recrystallization procedure afforded a pure specimen of *sisaustricin,* (674 mg), m.p. 32—33° (uncorr., water-bath), $[\alpha]_D^{26}$ +46.3° (*c* 1.4, 96 % EtOH). No depression of the m.p. was observed on admixture with the synthetic specimen described in the sequel. Again, the infra-red spectrum was identical with that of the synthetic material and exhibited conspicuous bands at 3 120 vs, 2 930 s, 1 510 vs, 1 455 m, 1 440 w, 1 398 m, 1 375 w, 1 330 s, 1 270 s, 1 255 s, 1 175 vs, 1 115 w, 1 095 w, 1 065 m, 1 018 w, 970 s, and 915 s cm^{-1}.

The ultra-violet spectrum of sisaustricin (in 96 % EtOH) was characteristic of 2-oxazolidinethiones, and exhibited λ_{max} 244 mμ (ε 17 800), λ_{max} 203 mμ (ε 4 000) and λ_{min} 218 mμ (ε 350).

Paper chromatography of sisaustricin and isomerides. Small, but consistent differences were noticed on paper chromatography in two solvent systems of sisaustricin and the two racemic isomerides (II and III), whereas the naturally derived compound was indistinguishable from the racemic 4-ethyl-substitute (IV). In Table 1, the R_{Ph}-values, *i.e.* the ratio of the distances travelled by the said compound and (±)-5-phenyl-2-oxazolidinethione [15], are presented. The compounds were revealed as blue spots on spraying with Grote's reagent.

Table 1.

Substituents	Formula	R_{Ph}-Value	
		System A[a]	System B[b]
4,5-Dimethyl	II	0.56	0.41
(±)-5-Ethyl	III	0.62	0.47
(±)-4-Ethyl	IV	0.66	0.55
Sisaustricin	VI	0.66	0.55

[a] Benzene:heptane:water (9:2:9)
[b] Carbon tetrachloride:30 % acetic acid (1:1) [16].

4,5-Dimethyl-2-oxazolidinethione (II). The 3-amino-2-butanol required for the synthesis of (II) was obtained by reduction of diacetyl monoxime (5 g) with lithium aluminium hydride (5 g) in ether (100 ml). After reaction and hydrolysis of excess hydride with small amounts of water, the solid hydroxides were extracted in a Soxhlet apparatus with ether for 24 h. The amino-alcohol (2.3 g) distilled at 110—125°/15 mm as a colourless liquid. Without further purification, it was converted into 4,5-dimethyl-2-oxazolidinethione by means of thiocarbonyl chloride and triethylamine in chloroform solution by our standard procedure [1]. A low yield (400 mg) of a solid product was thus obtained, which separated from ethyl acetate-pentane mixtures as colourless prisms, m.p. 107° (Found: C 45.92; H 6.96: N 10.51. Calc. for C_5H_9NOS: C 45.77; H 6.92; N 10.68). λ_{max}^{EtOH} 244 mμ (ε 17 000), 203 mμ (ε 3 600), λ_{min}^{EtOH} 218 mμ (ε 700). The infrared spectrum displayed the expected bands.

The sharp melting point suggests that the synthetic specimen is homogeneous but no attempts were made to decide whether it represents the *cis-* or *trans*-isomeride.

(±)-*4-Ethyl-2-oxazolidinethione.* This compound was prepared as a model, essentially as described by Rosen [6]. M.p. 72-3°; lit.values: 74-5° [6], 72.8-73.2° [7]. The considerable difference in melting point between the racemic compound and the (+)-enantiomer (33°) is noteworthy.

(±)-*5-Ethyl-2-oxazolidinethione.* Propionaldehyde cyanohydrin [17] was reduced with $LiAlH_4$ to give a 70 % yield of (±)-1-amino-2-butanol, b.p. 74.5°/9 mm. The amino-alcohol, on reaction with thiocarbonyl chloride and triethylamine in chloroform solution [1], furnished a 25 % yield of (+)-5-ethyl-2-oxazolidinethione, which was recrystallized from ethyl acetate-pentane mixtures, m.p. 86.5°. Clapp and Watjen [5] reported the m.p. 84.6—85.2° for a specimen prepared by a different method.

(−)-*2-Amino-1-butanol and its acid oxalate.* Essentially as described by Radke *et al.*[8], racemic 2-amino-1-butanol was resolved by means of (+)-tartaric acid to give a monohydrated acid tartrate of the *levo*rotatory amino-alcohol, $[\alpha]_D^{24}$ + 10.9° (*c* 5.7, H_2O), m.p. 71—3°, with loss of water, resolidification, and final melting at 103—104°. Lit.data [8]: $[\alpha]_D^{23}$ +10.5° (*c* 5, H_2O), m.p. 103°. The amino-alcohol was set free by means of CaO[8] and distilled, b.p. 76°/8 mm, $[\alpha]_D^{26}$ −9.9° (neat) (reported[8]: $[\alpha]_D^{26}$ −9.92°).

On addition of a solution of the *levo*rotatory amino-alcohol (400 mg) in ethanol (7 ml) to a solution of oxalic acid dihydrate (650 mg) in ethanol (7 ml), the acid oxalate separated as colourless needles, which were recrystallized from ethanol, m.p. 141—142°, $[\alpha]_D^{27}$ −9.0° ± 1° (*c* 3, H_2O). (Found: C 40.14; H 7.33; N 7.79. Calc. for $C_6H_{13}NO_5$: C 40.21; H 7.31; N 7.82).

Synthesis of (+)-4-ethyl-2-oxazolidinethione. The *levo*rotatory amino-alcohol (2.0 g) was converted into the *dextro*rotatory 4-ethyl-2-oxazolidinethione by the method designed by Rosen [6] for the synthesis of the racemic isomeride. On careful recrystallization of the crude, semi-solid reaction product from ether-pentane at −80°, a colourless product (1.20 g) was obtained. Another recrystallization from the same solvent system afforded a

pure specimen as colourless prisms, m.p. 32.5—33.5° (uncorr., water bath), $[\alpha]_D^{26}$ +49.2° (*c* 1.2, 96 % EtOH). (Found: 45.85; H 7.05; N 10.79. Calc. for C_5H_9NOS: C 45.78; H 6.91; N 10.68). No depression of the m.p. was observed on admixture with the naturally derived sisaustricin. Again, ultra-violet and infra-red spectra of the two specimens coincided.

In connexion with the present work it was noticed that a synthetic specimen of (+)-4-ethyl-2-oxazolidinethione, which had been stored at 0° for one year, had undergone some change. This parallels observations made earlier in this laboratory on other substitutes of the same series. A characteristic feature of the change is an increased absorption at 1 640 cm^{-1}, as well as the formation of varying amounts of ether-insoluble material. We attribute this change to the formation of disulphides, arising from oxidation of the ring system in its thio-enolized form. Recrystallization readily removes the secondary products.

Absolute configuration of 2-amino-1-butanol and 4-ethyl-2-oxazolidinethione. Correlation of (−)-2-amino-1-butanol, and hence of sisymbrin, with configurationally known substances was achieved by reduction of L-2-aminobutyric acid * (1.8 g) with lithium aluminium hydride (2.0 g) in tetrahydrofuran (30 ml) by a procedure analogous to that employed by Vogel and Pöhm [18] for reduction of the racemic amino acid. The resulting amino alcohol (390 mg) was distilled, b.p. 80—82°/10 mm, and without further characterization transformed into its acid oxalate as described above for the antipode. Colourless needles were obtained after recrystallization from ethanol, m.p. 141—142°, $[\alpha]_D^{27}$ +8.2° ± 1° (*c* 3, H_2O) (Found: C 40.20; H 7.29; H 7.96. Calc. for $C_6H_{13}NO_5$: C 40.21; H 7.31; N 7.82). The infra-red spectra of the antipodal acid oxalates were identical. By the above transformations, sterical correlation has been achieved between the naturally derived (+)-sisaustricin and D-2-aminobutyric acid.

Microanalyses were performed by Mr. G. Cornali. The assistance of E. Vesterager, M.Sc., in part of the synthetic work is acknowledged. The authors are very grateful to the *Botanical Garden of the University of Copenhagen* for valuable assistance in propagating the employed seed material.

The present work is part of investigations supported by *The Danish State Research Foundation (Statens Almindelige Videnskabsfond), The Carlsberg Foundation (Carlsbergfondet)* and *Kai Hansen's Fond.*

REFERENCES

1. Kjær, A. and Christensen, B. W. *Acta Chem. Scand.* **13** (1959) 1575.
2. Kjær, A. and Christensen, B. W. *Acta Chem. Scand.* **15** (1961) 1477.
3. Ettlinger, M. G. and Lundeen, A. J. *J. Am. Chem. Soc.* **78** (1956) 4172.
4. Kjær, A. and Christensen, B. W. *Acta Chem. Scand.* **16** (1962) 83.
5. Clapp, L. B. and Watjen, J. W. *J. Am. Chem. Soc.* **75** (1953) 1490.
6. Rosen, A. A. *J. Am. Chem. Soc.* **74** (1952) 2994.
7. Sommerville, W. T. and Andersen, C. N. *J. Org. Chem.* **25** (1960) 656.
8. Radke, F. H., Fearing, R. B. and Fox, S. W. *J. Am. Chem. Soc.* **76** (1954) 2801.
9. Greenstein, J. P. and Winitz, M. *Chemistry of the Amino Acids.* Wiley and Sons, New York 1961, vol. 1, p. 86, 116; vol. 3, p. 2401.
10. Cahn, R. S., Ingold, C. K. and Prelog, V. *Experientia* **12** (1956) 81.
11. Kjær, A., Christensen, B. W. and Hansen, S. E. *Acta Chem. Scand.* **13** (1959) 144.
12. Kjær, A. *Fortschr. Chem. org. Naturstoffe* **18** (1960) 122.
13. Butler, G. W. and Butler, B. G. *Nature* **187** (1960) 780.
14. Robinson, W. G., Bachhawat, B. K. and Coon, M. J. *J. Biol. Chem.* **218** (1956) 391.
15. Kjær, A. and Gmelin, R. *Acta Chem. Scand.* **11** (1957) 906.
16. Procházka, Ž., Šanda, V. and Jirousek, L. *Collection Czechoslov. Chem. Communs.* **24** (1959) 3606.
17. Linstead, R. P. and Whalley, M. *J. Chem. Soc.* **1954** 3722.
18. Vogl, O. and Pöhm, M. *Monatsh.* **84** (1953) 1097.

Received July 8, 1961.

* A preparation with $[\alpha]_D$ +20.5° (*c* 4.0, 6 N HCl), purchased from California Corp. for Biochemical Research, Los Angeles 63, was employed.

ACTA CHEMICA SCANDINAVICA 16 (1962) 78–82

The Conversion of Kojic Acid into Comenaldehyde and Comenic Acid

HANS-DIETER BECKER

Institutionen för organisk kemi, Chalmers Tekniska Högskola, Göteborg, Sweden

Oxidation of kojic acid monomethylether (II) by active manganese dioxide yields a γ-pyrone aldehyde (III) that was demethylated by $AlCl_3$ forming comenaldehyde (IV). The structure of comenic acid (VI) was confirmed by its preparation from kojic acid (I).

The structural relationship between kojic acid (I) and comenic acid (VI) has been established by the thorough investigations of Yabuta [1].*

The structure of kojic acid as 2-hydroxymethyl-5-hydroxy-γ-pyrone has been recently confirmed by its conversion into 5-hydroxypicolinic acid by Heyns and Vogelsang [3]. Examination of the correctness of structure I had become necessary since Belonosov [4] had brought forward evidence that favored structure VIb for comenic acid, and the correctness of the structure of kojic acid depended on the correctness of the structure of comenic acid proposed as VIa by Peratoner and co-workers [5,6].

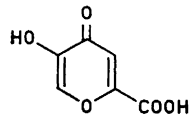

VI a

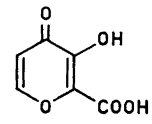

VI b

The purpose of this research was to prepare unknown γ-pyrone aldehydes and to confirm the structure of comenic acid by its preparation from kojic acid. Several attempts had been made to prepare the aldehyde of kojic acid (IV, comenaldehyde) by either reduction of comenic acid derivatives [7] or direct oxidation [8] of kojic acid by mild oxidizing reagents as nitrosodimethylaniline, phenylhydroxylamine sulfonic acid, H_2O_2 and $FeSO_4$, and methyleneblue and sunlight. The unknown comenaldehyde had not been obtained.

* Kojic acid has been reviewed by A. Beélik [2].

Also the conversion of kojic acid or its derivatives into comenic acid had not been successful. By direct catalytic oxidation kojic acid was destroyed and only traces of comenic acid could be detected by paper chromatography [3].

When we used active manganese dioxide for the oxidation of kojic acid in dioxane at room temperature the starting material was recovered unchanged. Oxidation in boiling dioxane only decreased the amount of starting material that could be recovered. Probably ring cleavage and degradation occurred since similar degradation reactions of ketols and glycols in boiling solvents in the presence of manganese dioxide have been described [9].

The methyl ether of kojic acid (II, 2-hydroxymethyl-5-methoxy-γ-pyrone), however, could be oxidized by manganese dioxide forming 2-formyl-5-methoxy-γ-pyrone (III) in good yield [10]. All other attempts to prepare formyl substituted γ-pyrones by oxidation of the hydroxymethyl or methyl side chain have been unsuccessful [11]. The oxidation of II by manganese dioxide was carried out in boiling benzene or dioxane. Acetone otherwise successfully applied as solvent for oxidations with manganese dioxide [12] could not be used in the present case because the reaction product was adsorbed very strongly.

The presence of a formyl group in III was indicated unequivocally by the appearance of a strong C=O band at 1 705 cm^{-1} in the IR spectrum. The region between 6.0 and 6.3 μ is characteristic for the γ-pyrone system [13], and the C=O absorption of the γ-pyrone group in the compounds investigated (I—VI) was never found to be at higher frequencies than 1 670 cm^{-1}.

When III was treated with phenylhydrazine under mild conditions, a phenylhydrazone (m.p. 205—206°C) was formed. The N-analysis of the product indicates that probably no further reactions of the hydrazine group and the γ-pyrone ring as studied by Thomas and Marxer [14] occurred under these conditions.

When III was oxidized in acetone by CrO_3/H_2SO_4, comenic acid methylether (V) was formed immediately. The oxidation by CrO_3/H_2SO_4 in acetone

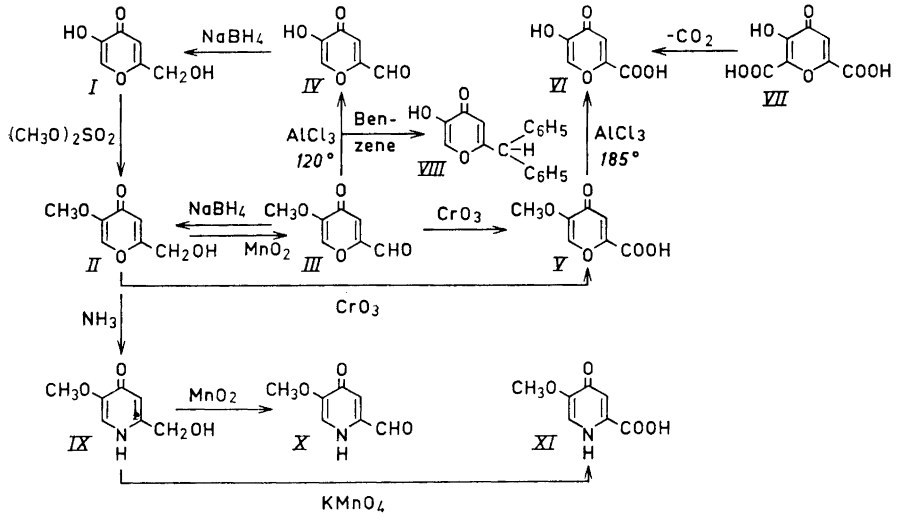

was found to be a very convenient method for the preparation of V directly from kojic acid methylether (II).

The γ-pyrone ring system itself is reduced by $LiAlH_4$[15] but the γ-pyrone aldehyde III was reduced selectively by $NaBH_4$ in ethanol solution, forming 2-hydroxymethyl-5-methoxy-γ-pyrone (II).

While all earlier attempts to prepare comenaldehyde (IV) had been unsuccessful the demethylation of III by $AlCl_3$ without a solvent at 120°C yielded IV [10]. As with the γ-pyrone aldehyde III, the presence of a formyl group in comenaldehyde (IV) was indicated by IR spectroscopy by the appearance of a strong C=O band at 1 718 cm^{-1}. Treatment of IV with $NaBH_4$ in ethanol solution did not affect the γ-pyrone group but yielded kojic acid by selective reduction. The presence of the OH group in IV was shown by absorption in the IR spectrum at 3 230 cm^{-1} and its enolic character was demonstrated by an intense red color reaction with $FeCl_3$ in ethanol.

The UV spectra of the new γ-pyrone aldehydes were very similar to the corresponding alcohols (Table 1) and other 2,5 disubstituted γ-pyrones [16,17].

Demethylation of III with $AlCl_3$ in boiling benzene gave a solid compound that probably has the structure of 2-(diphenylmethyl)-5-hydroxy-γ-pyrone (VIII), since this structure is supported by C,H-analysis, IR-spectrum and its red color reaction with $FeCl_3$. The analogous reaction of benzaldehyde in benzene solution in the presence of $AlCl_3$ to form triphenylmethane has been reported earlier [18].

In an attempt to demethylate comenic acid methylether by heating with pyridinium chloride at 185° for 2 h, only decomposition products were obtained. Attempted demethylation by $AlCl_3$ at 120—140°C for 4 h without a solvent was unsuccessful. The starting material was recovered unchanged (90 %). Finally demethylation was achieved by heating V together with $AlCl_3$ in a sealed tube at 185°C; comenic acid (VI) was obtained in about 50 % yield. The identity was also proved by comparison of the UV and IR spectra of a sample of comenic acid obtained by decarboxylation of meconic acid (VII).

The present investigation was also extended to a γ-pyridone alcohol. Earlier described oxidations of 2-hydroxymethyl-5-methoxy-γ-pyridone (IX) by aqueous $KMnO_4$[19] or nitric acid [20] had resulted in the formation of comenaminic acid methylether (XI) but a γ-pyridone aldehyde had not been obtained. Application of active manganese dioxide in boiling dioxane, however, yielded 2-formyl-5-methoxy-γ-pyridone (X). Formation of the formyl group in X was supported by the appearance of a strong C=O band in the IR spectrum

Table 1. UV-Spectra of γ-pyrones (in Methanol).

γ-Pyrone	λ^1_{max} (in mμ)		λ^2_{max}	
Kojic acid (I)	218;	$\varepsilon = 1.2 \times 10^4$	269;	$\varepsilon = 8 \times 10^3$
Comenaldehyde (IV)	218;	1.3×10^4	272;	7×10^3
2-Hydroxymethyl-5-methoxy-γ-pyrone (II)	216;	1.2×10^4	266;	9×10^3
2-Formyl-5-methoxy-γ-pyrone (III)	216;	1.3×10^4	268;	9×10^3

at 1 708 cm^{-1}. The 2-formyl-5-hydroxy-γ-pyridone (2-formyl-4,5-dihydroxypyridine) that could not be obtained by reduction [21] of comenaminic acid might now be available by demethylation of X.

Added in proof. In a recent publication [*J. Org. Chem.* **26** (1961) 2588] it has been claimed that the oxidation of kojic acid by chloranil in boiling ethanol yields a 6,6′-bipyrone. However, the UV spectrum of this product is identical with that of kojic acid as reported earlier [17] and as found in the present work. Since the IR spectrum is also identical with that of kojic acid no evidence for a 6,6′-bipyrone would be apparent.

EXPERIMENTAL

The IR spectra were taken in KBr pellets on a Perkin Elmer model 21 instrument with the technical assistance of Ing. C. B. Skarstedt. The UV spectra were measured with a Cary Recording Spectrophotometer Model 11 MS. The microanalyses were carried out by Dr. O. Pfundt, Göttingen (Germany).

Kojic acid (I) was purchased from Fa. Th. Schuchardt, München (Germany), *Meconic acid (VII)* from K and K Laboratories, Jamaica, N. Y. (USA).

Kojic acid monomethylether (II) was prepared by the method described by Campbell, Ackerman and Campbell [22]. For the preparation of *2-hydroxymethyl-5-methoxy-γ-pyridone (IX)* the method described by Armit and Nolan [20] was applied. *Comenic acid (VI)* was prepared by decarboxylation of meconic acid (VII) according to Meyer [23].

Active managese dioxide was prepared by the method of Attenburrow *et al.*[24]

2-Formyl-5-methoxy-γ-pyrone (III). 600 mg of 2-hydroxymethyl-5-methoxy-γ-pyrone were dissolved in 1 000 ml of boiling benzene; 6 g of manganese dioxide were added and the mixture was refluxed for one hour. The solution was filtered and the MnO_2 was washed with *ca.* 300 ml of benzene. From the filtered solution most of the benzene was removed by distillation, the rest of benzene (*ca.* 100 ml) was evaporated *in vacuo* at room temperature. Residue, colorless needles of III. Yield 410 mg (70 %), m.p. 202°C (sealed tube). Purification of III by sublimation at 12 mm/120°C. (Found: C 54.75; H 3.91. Calc. for $C_7H_6O_4$: C 54.55; H 3.92).

Reduction of III by $NaBH_4$. 100 mg of III and 70 mg of $NaBH_4$ were dissolved in 50 ml of ethanol (95 %) and shaken for 18 h. Then 30 ml of water were added and the solution was extracted with 100 ml of chloroform. The chloroform solution was dried over Na_2SO_4, filtered and evaporated *in vacuo*. Yield 70 mg of II (70 %), m.p. 161°C, IR spectrum identical with authentic sample of II.

Comenaldehyde (IV). 154 mg of III were mixed with 200 mg of sublimed $AlCl_3$ and heated at 120°C for 3 h. The reaction mixture was decomposed by addition of 5 ml of HCl (10 %), and the aqueous solution was extracted continuously with ether for 14 h. The ether solution was evaporated *in vacuo*, yielding 130 mg (93 %) of yellowish crystals of IV. Recrystallization from boiling $CHCl_3$ with addition of charcoal gave colorless crystals. The substance can be sublimed at 100°C/0.1 mm. M.p. 162–163°C (after drying *in vacuo* at 10^{-2} mm). (Found: C 51.48; H 2.96. Calc. for $C_6H_4O_4$: C 51.44; H 2.88).

Reduction of IV by $NaBH_4$. 15 mg of IV were dissolved in 5 ml of ethanol and 10 mg of $NaBH_4$ in 1 ml of ethanol were added. After 3 h shaking 2 ml of HCl (10 %) were added and the solution was extracted continuously with ether for 15 h. The ether was removed *in vacuo*, and to the aqueous residue 15 ml of abs. ethanol were added. After evaporation *in vacuo* kojic acid (14 mg) crystallized. M.p. 152°C, IR spectrum identical with authentic sample of I.

Comenic acid methyl ether (V), (a) from III. 150 mg of III were suspended in 5 ml of acetone, and 1.3 ml of CrO_3/H_2SO_4 solution prepared according to Bowden *et al.*[25] were added. The colorless solution turned green immediately and V precipitated. After 30 min 150 mg of V were isolated (90 %). M.p. 282°C (after recrystallization from C_2H_5OH/H_2O). (Found: C 49.97; H 3.60. Calc. for $C_7H_6O_5$: C 49.42; H 3.56).

(*b*) *V from II.* 150 mg of II were dissolved in 5 ml of acetone and 3.5 ml of CrO_3/H_2SO_4 solution [25] were added. After 24 h 120 mg (73 %) of V were isolated by filtration. M.p. 282°C, IR spectrum identical with V obtained from III.

Comenic acid (VI). 150 mg of V and 250 mg of sublimed $AlCl_3$ were mixed and heated in a sealed tube at 185°C for 4 1/2 h. The reaction product was decomposed with 5 ml of HCl (10 %) and the precipitate (70 mg) was recrystallized from boiling ethanol in presence of charcoal. M.p. 285°C (decomp.). The identity with comenic acid was proved by comparison with the IR and UV spectra * of an authentic sample obtained by decarboxylation of meconic acid (VII).

2-(Diphenylmethyl)-5-hydroxy-γ-pyrone (VIII). 100 mg of III were dissolved in 200 ml of benzene, 500 mg of $AlCl_3$ (subl.) were added, and the solution was refluxed for 45 h. The yellowish cloudy solution was evaporated, and the oily residue was decomposed by addition of 35 ml of H_2O and 4 ml of HCl (conc). This solution was extracted continuously with ether for 24 h. The ether solution was dried over Na_2SO_4 and evaporated. The yellow oil crystallized (refrigerator) after addition of a few drops of ether. The crystalline product was recrystallized from benzene and decolorized by charcoal. Yield 72 mg of VIII. After sublimation at 0.1 mm/135°C colorless crystals. M.p. 150–152°C. (Found: C 77.24; H 5.17. Calc. for $C_{18}H_{14}O_3$: C 77.68; H 5.07).

2-Formyl-5-methoxy-γ-pyridone (X). 50 mg of IX were dissolved in 50 ml of boiling dioxane, 500 mg of MnO_2 were added and the mixture was refluxed for 90 min. The mixture was filtered and the MnO_2 was washed with 30 ml of warm dioxane. From the filtrate the dioxane was removed *in vacuo* and an almost colorless crystalline residue was obtained (pyridine-like odor). M.p. 176–178°C, after sublimation at 0.1 mm/100°C. (Found: C 54.58; H 4.69. Calc. for $C_7H_7NO_3$. C 54.90; H 4.61).

Acknowledgement. The author is kindly indebted to Professor E. Adler in whose laboratory this work was carried out.

REFERENCES

1. Yabuta, T. *J. Chem. Soc. Japan* **37** (1916) 1185, 1234; *Chem. Abstr.* **17** (1923) 1475.
2. Beélik, A. *Advances in Carbohydrate Chem.* **11** (1956) 145.
3. Heyns, K. and Vogelsang, G. *Chem. Ber.* **87** (1954) 13.
4. Belonosov, I. S. *Zhur. Priklad. Khim.* **22** (1949) 1103; *Chem. Abstr.* **45** (1951) 5650; *Zhur. Priklad. Khim.* **24** (1951) 113; *Chem. Zentr.* **122** (1951) 1583.
5. Peratoner, A. and Leonardi, G. *Gazz. chim. ital.* **30 I** (1900) 539.
6. Peratoner, A. and Palazzo, F. C. *Gazz. chim. ital.* **36 I** (1906) 7.
7. Yabuta, T. *J. Chem. Soc.* **125** (1924) 575.
8. Obata, Y. and Yamanishi, T. *J. Agr. Chem. Soc. Japan* **24** (1951) 334; *Chem. Abstr.* **46** (1952) 11474.
9. Barakat, M. Z., Abdel-Wahab, M. F. and El-Sadr, M. M. *J. Chem. Soc.* **1956** 4685.
10. Becker, H.-D. *Acta Chem. Scand.* **15** (1961) 683.
11. Woods, L. L. and Dix, P. A. *J. Org. Chem.* **26** (1961) 1028.
12. Adler, E. and Becker, H.-D. *Acta Chem. Scand.* **15** (1961) 849.
13. Hurd, C. D. and Trofimenko, S. *J. Am. Chem. Soc.* **81** (1959) 2430.
14. Thomas, A. F. and Marxer, A. *Helv. Chim. Acta* **43** (1960) 469.
15. Mirza, R. and Robinson, R. *Nature* **166** (1950) 997.
16. Tolstikov, G. A. *Zhur. Obschei. Khim.* **29** (1959) 2372.
17. Berson, J. A., Jones, W. M. and O'Callaghan, L. F. *J. Am. Chem. Soc.* **78** (1956) 622.
18. Schaarschmidt, A., Hermann, L. and Szemö, B. *Ber.* **58** (1925) 1914.
19. Yabuta, T. and Kambe, K. *J. Agr. Chem. Soc. Japan* **6** (1930) 516; *Chem. Abstr.* **26** (1932) 1931.
20. Armit, J. W. and Nolan, T. J. *J. Chem. Soc.* **1931** 3023.
21. a) Ost, H. *Ber.* **16** (1883) 1373.
    b) Bellmann, Th. *Ber.* **17** (1884) 106.
22. Campbell, K. N., Ackerman, J. F. and Campbell, B. K. *J. Org. Chem.* **15** (1950) 221.
23. Meyer, H. *Monatsh.* **26** (1905) 1311.
24. Attenburrow, J., Cameron, A. F. B., Chapman, J. H., Evans, R. M., Hems, B. A., Jansen, A. B. A. and Walker, T. *J. Chem. Soc.* **1952** 1094.
25. Bowden, K., Heilbron, I., Jones, E. R. H. and Weedon, B. C. L. *J. Chem. Soc.* **1946** 39.

Received June 9, 1961.

* λ^1_{max} 223 mμ; λ^2_{max} 284 mμ (H_2O). Reported [16], 224; 290 mμ.

ACTA CHEMICA SCANDINAVICA 16 (1962) 83–86

Isothiocyanates XLI *. Glucobenzsisaustricin, a New Glucoside Present in Seeds of *Sisymbrium austriacum* Jacq.

ANDERS KJÆR and BO W. CHRISTENSEN

Department of Organic Chemistry, The Royal Veterinary and Agricultural College, Copenhagen, Denmark

In continuation of previous studies of the isothiocyanate-producing glucosides in seed material of the crucifer *Sisymbrium austriacum* Jacq., a glucoside of the ordinary type, migrating faster on paper chromatography than any of the three formerly identified glucosides [1-3], has been recognized as the benzoic acid ester of glucosisaustricin [3]. The designation *glucobenzsisaustricin* is proposed for the new glucoside.

Enzymic hydrolysis of the glucoside yields a volatile ester isothiocyanate which on alkali treatment is converted into (+)-4-ethyl-2-oxazolidinethione of known absolute configuration [3]. Upon ammonia treatment under controlled conditions, the new isothiocyanate yields a thiourea, which on alkaline fission splits off benzoic acid. These facts establish the relationship of the new glucoside to glucosisaustricin, present in the same seeds.

The production of the O-benzoylated glucosides seems to occur in the seeds during the ripening process.

According to the paperchromatographic pattern, seed extracts of *Sisymbrium austriacum* Jacq. were originally reported to contain two glycosides ('A' and 'B') in the R_B-range 0.3—0.6, besides one glycoside ('C') migrating much faster on the paper ($R_B \sim 1.7$). In addition, faint glycoside spots, tentatively assigned to glucoputranjivin and glucocochlearin, were recorded [1]. Previous communications from this laboratory described the structure identification of 'A', *glucosisymbrin*, containing the 2-hydroxyisopropyl side-chain [1], and *glucobenzosisymbrin*, 'C', the same glucoside esterified with benzoic acid in its side-chain [2]. Glycoside 'B', named *glucosisaustricin*, has since been identified as a glucoside possessing the higher homologous 1-ethyl-2-hydroxyethyl side-chain [3].

Paperchromatographic studies on seed material, propagated in the Botanical Garden of the University of Copenhagen during 1959—1960 from the stock

* Presented in abstract before the *1st Scandinavian Symposium on Natural Product Chemistry*, June 1961, Bornholm, Denmark.

Part XL of this series: *Acta Chem. Scand.* **16** (1962) 71.

used in our previous studies [1], revealed the presence of the three above-mentioned glucosides, and, in addition, a rather faint but distinct glycoside spot with an R_B-value [1] as high as 2.0. (Fig. 1). A desire to complete the glucoside picture of the seed material of *S. austriacum* Jacq. prompted the present investigation. It was established that a paperchromatographically purified solution of the unknown glycoside on treatment with strong hydrochloric acid [4] afforded glucose, hydroxylamine and sulphate ions. Consequently, and in view of its structural relationship to glucosisaustricin outlined in the sequel, the designation *glucobenzsisaustricin* was introduced for the new glucoside.

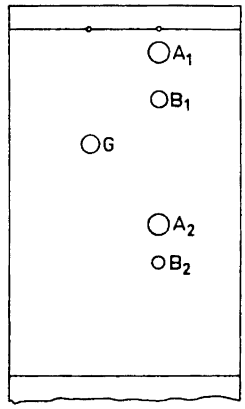

Fig. 1. Paper-chromatographic pattern of the four major isothiocyanate glucosides in ripe seeds of *Sisymbrium austriacum* Jacq.
A_1: glucosisymbrin; A_2: glucobenzosisymbrin;
B_1: glucosisaustricin; B_2: glucobenzsisaustricin.
G: reference sample of glucotropaeolin.
Solvent system: *n*-butanol:ethanol:water (4:1:4)

In analogy with observations made on glucobenzosisymbrin [2], aqueous ammonia effected conversion of the unknown into a much more hydrophilic glucoside, indistinguishable on paper chromatography in two solvent systems from glucosisaustricin, and suggesting a chemical relationship with the latter.

Enzymic hydrolysis of the entire seed glucoside fraction, followed by steam-distillation of the liberated volatile isothiocyanates, gave a mixture of the isothiocyanate, (benzsisaustricin), derivable from the unknown glucoside, and 2-benzoyloxyisopropyl isothiocyanate originating from glucobenzosisymbrin [2].

The limited quantities on hand precluded a fractional distillation of the mixture, in which benzosisymbrin was the predominant constituent, as estimated from paper-chromatography of the corresponding thioureas. The chemical similarity between the two volatile isothiocyanates appeared from their common behaviour towards ammonia. As described in a previous paper of this series [2], non-aqueous conditions are essential to preclude competing ammonolysis of the ester linkage during thiourea formation of benzosisymbrin. A completely analogous behaviour was now noticed in the case of benzsisaustricin and there can be no doubt that the benzosisymbrin-thiourea contamination, referred to

in a previous paper [2] and removable only by counter-current distribution, was, in fact, the thiourea of benzsisaustricin. No attempts were made to isolate a pure specimen of the latter. Proof of its identity was obtained, however, by subjecting the volatile isothiocyanate fraction to treatment with alkali, whereby a mixture of two 2-oxazolidinethiones was produced. One of these was previously established to be (+)-4-methyl-2-oxazolidinethione (sisymbrin), arising from cyclization of a 2-hydroxyisopropyl isothiocyanate which again resulted from alkaline hydrolysis of the benzoate ester linkage in benzosisymbrin [2]. Information as to the second oxazolidinethione was provided by isolation of the compound in pure form from a 180-plate counter current distribution, exactly as described in a previous paper of this series [3]. Critical comparison proved the isolate to be identical with sisaustricin, established in the preceding paper [3] as (+)-4-ethyl-2-oxazolidinethione of known absolute configuration, arising from enzymic fission of glucosisaustricin, present in the same seed material. From the above it appears that glucobenzsisaustricin is an ester of glucosisaustricin.

Information regarding the acid moiety was obtained upon saponification of a paperchromatographic eluate of the thiourea derivative of benzosisaustricin. Chromatography clearly indicated that the esterifying acid is *benzoic acid*, a fact which concludes the structure proof of glucobenzsisaustricin.

In conclusion, the present paper, together with previous communications of this series [1-3], provides complete knowledge as to the structure of the four major isothiocyanate-producing glucosides present in ripe seeds of *Sisymbrium austriacum* Jacq., none of which had formerly been encountered in Nature. No attempts have been made to isolate the glucosides in pure form. As discussed in the preceding communication [3], glucosisymbrin and glucosisaustricin may be biogenetically related to products on the metabolic pathways of the branched chain amino acids valine and isoleucine.

No conclusive evidence is on hand regarding the biosynthetic origin of the two O-benzoylated glucosides. It appears significant, however, that paperchromatographic analysis of a fresh plant of *S. austriacum* Jacq. has shown the roots, flowers and unripe siliques to be entirely devoid of the benzoylated glucosides, but rich in glucosisymbrin and glucosisautricin. The green leaves contain only negligible amounts of glucosides. This observation suggests that enzymic benzoylation of the side-chains of the glucosides occurs during the ripening process. It is hoped that planned experiments will provide further insight into the biosynthesis of this interesting series of related isothiocyanate producing glucosides.

EXPERIMENTAL

Paperchromatographic studies. A methanolic seed extract of ground, mature seeds of *Sisymbrium austriacum* Jacq. (1960 harvest) was chromatographed as previously described [1]. A schematic depiction of the observed pattern is shown in Fig. 1. The present investigation deals with the structure elucidation of glucoside B_2.

An aqueous solution containing only the unknown glycoside was produced by elution of the appropriate zones from four chromatograms, exactly as described for glucobenzosisymbrin [2]. Half of the eluate was left standing for 28 h with conc. ammonia and was then rechromatographed. The unknown glycoside had been quantitatively converted into a new glycoside which on chromatography was indistinguishable from glucosisaustricin [3].

Acid hydrolysis of the unknown glycoside. The remaining half of the above eluate was treated with conc. hydrochloride acid for 2 h at 60°, conditions similar to those employed by Ettlinger and Lundeen [4] in analogous hydrolysis experiments. Paper chromatography indicated the formation during this treatment of hydroxylamine [4] and glucose, whereas liberation of sulphate ions was proved by precipitation as $BaSO_4$. Appropriate blanks were run to preclude contaminations from the chromatography paper. Hence, the new glycoside is of the customary structural type [4] and from here on named *glucobenzsisaustricin.*

Enzymic liberation and chemical characterization of benzsisaustricin. On a preparative scale, the condensate (6 l) from the steam distillation described in the preceding communication [3] was extracted with three 1-l portions of ether. After removal of the solvent through a column, a brown oil remained (3.82 g), which was dissolved in dioxane (120 ml) and treated with 0.2 N NaOH (120 ml) at room temperature for 4 h, at the end of which hydrochloric acid was added to bring the pH to 7. Dioxane and water were removed *in vacuo* and the oily material was dissolved in water (400 ml) to which 1 N NaOH (80 ml) was added. The solution was extracted with ether and the extract discarded. The aqueous solution was readjusted to pH 7 and continuously extracted with ether for 24 h. On removal of the solvent from the dried ether solution, a mixture of two oxazolidinethiones remained as a yellow oil (1.48 g). On comparative paper chromatography in benzene: heptane: water (9:2:9), the two components were indistinguishable from authentic specimens of (+)-4-methyl-2-oxazolidinethione (sisymbrin)[1] and (+)-4-ethyl-2-oxazolidinethione (sisaustricin)[3].

The mixture was dissolved in a total of 40 ml of equal volumes of the upper and lower phase of the above benzene:heptane:water system and introduced into the first two tubes of a Craig counter current apparatus. 180 transfers were made and analysis performed exactly as described in the preceding communication [3]. Again, isolation of the two constituents was achived as previously described [3]. Both sisymbrin (437 mg) and sisaustricin (312 mg) were thus obtained in the pure state. Their identity with (+)-4-methyl-2-oxazolidinethione and (+)-4-ethyl-2-oxazolidinethione, respectively, was secured on critical comparison of the two isolates with authentic specimens [1,3].

Identification of benzoic acid. A mixture of the thioureas of the volatile isothiocyanate fraction was prepared upon treating the latter with anhydrous ammonia under controlled conditions, precisely as previously reported [2]. A solution (240 μl), containing an estimated total of 1.6 mg of the thiourea mixture, was evenly applied to two strips (15 cm broad) of Whatman paper No. 1. Descending chromatography for 3 h in the solvent system: carbon tetrachloride: glacial acetic acid (1:1) resulted in complete separation of the two thioureas. The fastest migrating band was eluted with 96 % ethanol (2 ml), to which 1 N NaOH (2 ml) was added. The solution was kept at 70° for 1 h and then at room temperature overnight. After acidification, the solution was extracted with ether and the ethereal phase assayed by paper chromatography in the solvent system: *n*-butanol: ethanol:water:ammonia (40:40:16:4), along with a blind and a reference sample of benzoic acid [5]. Spraying reagent: 0.2 % ninhydrin in ethanol plus 5 % formic acid [5]. A spot of benzoic acid was noticed in the hydrolyzed sample, indicating the production of this acid during the alkaline hydrolysis of the thiourea. Hence, glucobenzsisaustricin is the O-benzoate of glucosisaustricin [3].

The authors are very grateful to the *Botanical Garden of the University of Copenhagen* for valuable assistance in propagating the employed seed material.

The present work is part of investigations supported by *The Danish State Research Foundation (Statens Almindelige Videnskabsfond), The Carlsberg Foundation (Carlsbergfondet)* and *Kai Hansen's Fond.*

REFERENCES

1. Kjær, A. and Christensen, B. W. *Acta Chem. Scand.* **13** (1959) 1575.
2. Kjær, A. and Christensen, B. W. *Acta Chem. Scand.* **15** (1961) 1477.
3. Kjær, A. and Christensen, B. W. *Acta Chem. Scand.* **16** (1962) 71.
4. Ettlinger, M. G. and Lundeen, A. J. *J. Am. Chem. Soc.* **78** (1956) 4172.
5. Long, A. G., Quayle, J. R. and Stedman, R. J. *J. Chem. Soc.* **1951** 2197.

Received July 8, 1961.

ACTA CHEMICA SCANDINAVICA 16 (1962) 87–93

Versuche zur Darstellung optisch aktiver bororganischer Verbindungen

IV. Darstellung und Spaltung von einem koordinativ vierwertigen Borspiran

KURT TORSSELL

Institut für Organische Chemie und Biochemie der Universität, Stockholm, Schweden

Digrignard- oder Dilithiumverbindungen geben mit Bortrifluorid im Molverhältnis 2:1 Borspirane, die als Ammoniumsalze isoliert worden sind. Das asymmetrische Spiran V ist mit einem optisch aktiven Ammoniumsalz gespalten worden. Einige neue Diarylborsäuren sind auch dargestellt worden.

In den früheren Arbeiten dieser Reihe wurden Methoden für die Darstellung asymmetrischer bororganischer Verbindungen entwickelt[1–3]. Mit dem Ziel, möglichst stabile Verbindungen zu erhalten, wurden die Arbeiten zunächst auf die Anlagerung aromatischer Liganden am Bor eingerichtet. Es hat sich erwiesen, dass im allgemeinen die Arylderivate des Bors stabiler sind als die entsprechenden Alkylderivate. Eine Schwierigkeit, mit der man immer rechnen muss, ist die Neigung des asymmetrischen Bors, sich in symmetrische Derivate zu disproportionieren, ein Befund, den zuerst Krause und Nobbe [4] machten und der später von einer Reihe von Forschern bestätigt worden ist*. Die Diarylborsäureester und gemischten Aryl-alkylborsäureester sind unterhalb etwa 200° gegen Disproportionierung stabil[2,3].

Zunächst wurde versucht, die Alkoxygruppe durch einen dritten aromatischen Rest auszutauschen:

$$\mathrm{ArAr'BOR} \xrightarrow{\mathrm{Ar''MgX\ (Li)}} \mathrm{ArAr'Ar''B} \qquad (1)$$

* Eine Zusammenfassung über bororganische Verbindungen ist von M. F. Lappert in *Chem. Revs.* **56** (1956) 959 veröffentlicht worden.

Die Aufarbeitung ergab aber nur Produkte mit einem Siedepunktsintervall, was auf eine Disproportionierung hindeutete. Auch die Versuche, das Triarylboran über einen Aminkomplex zu isolieren, scheiterten. Es wurde versucht, die Alkoxygruppe mit Chlor zu ersetzen [5,6] und dann zu grignardieren. Auf diesem Wege ist es Mikhailov *et al.*[6] gelungen, eine asymmetrische Borverbindung zu gewinnen. Über Spaltungsversuche sind keine Angaben vorhanden.

$$\mathrm{ArAr'BOR} \xrightarrow{\mathrm{PCl_5}} \mathrm{ArAr'BCl} \xrightarrow{\mathrm{Ar''MgX}} \mathrm{ArAr'Ar''B} \qquad (2)$$

Es stellte sich heraus, dass bei der Chlorierung die Borverbindung sich teilweise zersetzte. Es konnten neben dem erwünschten Chlorid auch kleine Mengen von Arylbordichloriden nachgewiesen werden. Ausserdem traten bei der Destillation des Monochlorids in der Vorlage Schlieren auf, die jedenfalls auf eine partielle Disproportionierung hindeuteten.

$$\mathrm{ArAr'BCl} \longrightarrow \mathrm{Ar_2BCl} + \mathrm{Ar'_2BCl} \qquad (3)$$

Diese Befunde machten es wünschenswert, andere Wege aufzusuchen, um ein koordinativ vierwertiges Bor zu gewinnen. Wittig und Herwig [7] haben über *O,O'*-Dilithiumbiphenyl und Bortrifluorid das Spiran I dargestellt. Wenn man nun von einem asymmetrischen Biphenylderivat ausgeht, sollte man

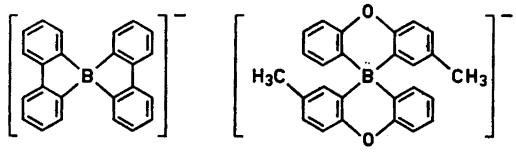

I *II*

Komplexe erhalten, die ein asymmetrisches quaternäres Bor enthalten. 2,2'-Dibrom-4-methyl-diphenyläther [8] war früher in der Literatur beschrieben. Er wurde in die Grignardverbindung übergeführt und mit Bortrifluorid umgesetzt. Das Spiran II konnte leicht über das Tetramethylammoniumsalz isoliert werden.

Jetzt taucht die Frage auf, wie sich eine solche Verbindung spalten lässt. Orientierende Versuche zeigten, dass Alkaloide, z.B. Strychnin, mit II amorphe Niederschläge gaben. Sie erwiesen sich aber als schwerlöslich in den meisten Lösungsmitteln und eigneten sich schlecht zu einer Aufspaltung der Borverbindung. Besser wäre vielleicht gewesen, wenn man ein quaternäres Ammoniumsalz verwendet hätte. Ausserhalb der Naturstoffchemie hatten Pope and Peachey [9] als erste ein optisch aktives Ammoniumsalz dargestellt. Für unseren Zweck haben wir das Methyl-propyl-benzyl-phenylammoniumsalz von α-Brom-[*d*-campher]-π-sulphonsäure verwendet, das nach der Methode von Wedekind und Frölich [10] gespalten wurde. Es ergab mit dem Borion II ein kristallines Salz, das einer fraktionierten Kristallisation aus verschiedenen Lösungsmitteln unterworfen wurde. Eine Änderung des Drehungsvermögens der verschiedenen Fraktionen war nicht zu beobachten. Die Einwirkung des metaständigen Methyls auf das Symmetriecentrum ist wahrscheinlich zu klein. Deswegen wurde mit einem anderen System versucht. Das Diamin III wurde

in das Dijodid IV übergeführt und mit Butyllithium bei −30° behandelt. Die Ausbeute von Dijodid konnte durch Zersetzung des Diazoniumsalzes mit Kaliumjodid in einem Zweiphasensystem (Benzol-Wasser) verbessert werden. Die Dilithiumverbindung schien eine schlechte Ausbeute zu ergeben, die nicht durch Variieren der Bedingungen verbessert werden konnte. Das Dibromid wurde auch dargestellt und in die Digrignardverbindung übergeführt (Ausbeute niedrig). Beide Methoden gaben allerdings dasselbe Produkt. Mit Bortrifluorid erhielt man das Spiran V, das mit dem aktiven Ammoniumsalz einen gelben Niederschlag ergab. Nach mehrmaligem Kristallisieren aus Nitromethan wurde eine weisse kristalline Verbindung von konstanter Drehung $[\alpha]_D = -91°$ erhalten. Sie enthielt Bor, ergab mit Quecksilberchlorid einen weissen amorphen Niederschlag und eine richtige Analyse für V. In Tabelle 1 sind die Dre-

Tabelle 1. Specifische und molekulare Drehungen aktiver Ammoniumsalze und Borspirane in Nitromethan bei Zimmertemperatur gemessen. N^+ = Methyl-propyl-benzyl-phenyl-ammoniumion.

Verbindung	Mol. Gewicht	Konz. M	$[\alpha]_D$	$[M]_D$
N^+ α-Brom [*d*-campher]-π-sulphonat	550,5	0,062	+12°	+66°
NH_4^+ α-Brom-[*d*-campher]-π-sulphonat	328,2	0,024	+100°	+328°*
N^+-Ion				−262°
N^+ Jodid	367,3	0,026	−69°	−253° } −258°
N^+ Borkomplex II	615,6	0,0163	−42°	−259°
N^+ Borkomplex V	655,6	0,0167	−91°	−596°
Borkomplex-ion V				−338°

* 80 % Nitromethan, 20 % Äthylalkohol.

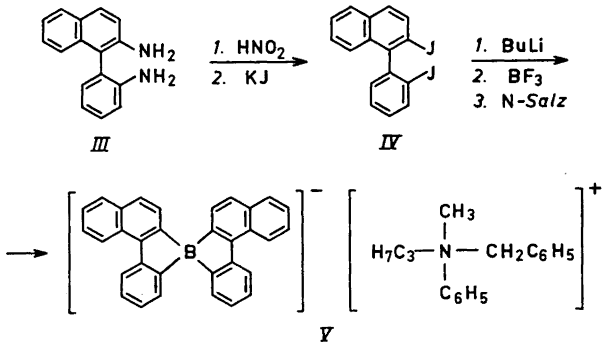

hungsmessungen zusammengestellt. Die molekulare Drehung des Ammoniumions verschiedener Salze ist praktisch konstant und nicht von der Art des Anions beeinflusst, $[M]_D = -258°$ (Mittelwert). Die Drehung des razemischen Ammonium-Borsalzez I, $[M]_D = -259°$ liegt diesem Mittelwert sehr nahe.

Tabelle 2. Ester einiger Diarylborsäuren.

Verbindung	Mol. Gewicht	Schmp. °C oder Kp. °C/ torr	Analysen			
			Gefunden		Berechnet	
			C	H	C	H
R=R′=*p*-Methoxyphenyl	285,2	177–8[a]	67,37	6,71	67,38	7,07
R= Phenyl, R′ = *o*-Biphenyl	301,2	181–2	80,07	7,28	79,74	6,70
R=R′= *m*-Tolyl	253,2	190–1[b]	75,84	8,25	75,90	7,96
R= *m*-Tolyl, R′= *p*-Chlorophenyl	273,6	56–8	65,72	6,74	65,84	6,26
R= Phenyl, R′= *o*-Tolyl	239,1	173–6	74,94	7,30	75,35	7,59
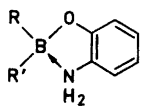						
R=R′= *m*-Tolyl	301,2	181–2	79,93	7,02	79,74	6,70
R=R′= Phenyl	273,1	183–4	78,51	6,14	79,15	5,91
R= Phenyl, R′ = Naphthyl	323,2	187–9	81,42	5,88	81,74	5,61
R=R′ = *p*-Tolyl	301,2	189–90	79,95	6,86	79,74	6,70
m-Tolyl-*p*-chloro-phenylborsäure-*n*-propylester	272,6	172–4/8	Ber. B 3,97; Gef. B 3,85.			

a,b Povlock, T. P. und Lippincott, W. T. *J. Am. Chem. Soc.* **80** (1958) 5409 geben für *a* den Schmp. 173–4° und für *b* den Schmp. 180–1° an.

Die Drehung von Borsalz II ist ausserordentlich gross, $[M]_D = -596°$. Aus dem Unterschied erhält man die Drehung des Borions, $[M]_D = -338°$. Das Salz zeigte nach einjährigem Aufbewahren an der Luft dieselbe Drehung.

Im Laufe der Arbeit wurde eine Reihe symmetrischer und unsymmetrischer Diarylborsäuren dargestellt. Die Diarylborsäuren wurden am einfachsten über ihre Äthanolaminkomplexe isoliert[11]. In der Zwischenzeit sind einige von diesen in anderen Laboratorien dargestellt worden [12].

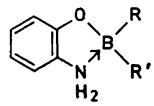

VI

Einige Diarylborsäuren sind auch als *o*-Aminophenoladdukte VI erfasst. Sie bilden gelbbraune kristalline Verbindungen, die aber nicht so stabil sind wie die Äthanolaminkomplexe. In Tabelle 2 sind die physikalischen Daten der Verbindungen zusammengestellt.

EXPERIMENTELLER TEIL

Die Schmelzpunkte sind korrigiert.

1-(2-Bromphenyl)-2-bromnaphthalin. 1-(2-Aminophenyl)-2-napthylamin [13,14] (8,5 g) wurde mit Natriumnitrit (5,1 g) in schwefelsaurer Lösung bei 0° diazotiert. Die Diazoniumlösung wurde unter Rühren zu einer verdünnten wässrigen Lösung von Quecksilbernitrat (40 g) und Kaliumbromid (60 g) gegeben. Der gelbe Niederschlag wurde abgenutscht, auf dem Filter mit Wasser und dann mit Aceton gewaschen. Nach Trocknen (nicht zu scharf!) wurde der Quecksilberkomplex nach Schwechtens Methode [15] zersetzt. Das Rohprodukt wurde in Cyklohexan aufgelöst, von unlöslichem Material befreit und auf einer Aluminiumoxydsäule chromatographiert (filtriert). Mit der Front kam das Dibromid heraus (5 g), das einer Vakuumdestillation in einem Säbelkolben unterworfen wurde. Kp. 203—204°/2 torr. Ausbeute 4,0 g. Die Analyse zeigte einen etwas zu hohen Kohlenstoffwert, was auf eine kleine Menge von Monobromid im Destillat hindeutet. (Gef.: C 54,34; H 3,14; Ber. für $C_{16}H_{10}Br_2$ (362,1): C 53,23; H 2,79).

1-(2-Jodphenyl)-2-jodnaphthalin. Das Diamin [13] (9,5 g) in Wasser (100 ml) und konz. Schwefelsäure (20 ml) wurden mit Natriumnitrit (5,8 g) diazotiert. Die Diazoniumlösung wurde langsam unter kräftigem Rühren auf eine eisgekühlte Mischung von Wasser (400 ml), Kaliumjodid (30g) und Benzol (200 ml) gegossen. Man liess die Lösung unter Rühren Zimmertemperatur erreichen, und nach einer Stunde wurde die organische Phase von der wässrigen getrennt. Es hinterblieb im Reaktionsgefäss eine schmierige Masse, die einmal mit 50 ml Benzol digeriert wurde. Von den vereinigten Benzollösungen wurde das Lösungsmittel abgetrieben und der Rückstand in heissem Cyklohexan (60 ml) aufgenommen, filtriert und auf Aluminiumoxyd chromatographiert (Cyklohexan). Es wurden 8 g rohes Dijodid gewonnen, das aus Methanol einmal umkristallisiert wurde. Ausbeute 6 g vom Schmp. 94—96° (Lit.[14] 99—100°).

Darstellung des Komplexes II. Die Digrignardverbindung aus 2,2′-Dibrom-4-methylbiphenyläther [8] (5,4 g) und Magnesium (0,80 g) in Tetrahydrofuran (50 ml) wurde unter Rühren mit Bortrifluoridätherat (1,0 g) in Äther (5 ml) tropfenweise versetzt und dann 15 Min. auf 40° erhitzt. Das Tetrahydrofuran wurde im Vakuum abgetrieben und durch Äthylalkohol (45 ml) ersetzt. Methyl-propyl-benzyl-phenylammonium-*a*-Brom-[*d*-Campher]-π-sulphonat [10] (2,6 g) in Äthylalkohol (30 ml) wurden zugegeben, wobei sich ein hellgelber Niederschlag bildete (2,9 g). Er wurde in lauwarmem Nitromethan (15 ml) gelöst, filtriert und wieder mit Äthylalkohol (80 ml) gefällt. 1,7 g, $[a]_D = -40°$. Das Filtrat wurde auf 20 ml im Vakuum eingeengt und mit Äthylalkohol gefällt (0,45 g, $[a]_D = -42°$). Die Fällung konnte aus Nitromethan-Äthylalkohol (1:3) umkristallisiert werden, $[\alpha]_D = -42°$. Schmp. 187—91°, (Gef.: C 83,25; H 6,71; Ber.: für $C_{43}H_{42}O_2NB$ (615,6): C 83,87; H 6,88.

In einem anderen Versuch wurde das Borspiran als das Tetramethylammoniumsalz, Schmp. > 300°, und auch als das Trimethylbenzylammoniumsalz, Schmp. 291—292°, ausgefällt. Die Salze wurden aus Nitromethan-Äthanol (1:3) kristallisiert. Analysen für die beiden Verbindungen: Gef.: C 79,86; H 7,06; N 3,38; Ber. für $C_{30}H_{32}O_2NB$ (449,5) C 80,19; H 7,18; N 3,12. Gef.: C 81,98; H 6,73; Ber. für $C_{36}H_{36}O_2NB$ (525,5): C 82,28; H 6,91.

Fraktionierte Kristallisation des aktiven Salzes. z.B. aus Nitromethan oder Äthylacetat, ergab keine Änderung des Drehungsvermögens.

Darstellung des Komplexes V. 1-(2-Jodphenyl)-2-jodnaphthalin (2,0 g) in Äther (15 ml) wurde bei −30 bis −40° mit 1 N Butyllithium (9,0 ml) versetzt. Nach anderthalb Stunden bei −10° wurde Bortrifluoridätherat (0,43 g) in Äther (5 ml) langsam unter Rühren zugetropft. Es wurde 15 Min. unter Rückfluss gekocht. Der Äther wurde abgedampft und Äthylalkohol (30 ml) zugegeben. Beim Zusatz vom aktiven Ammoniumsalz (0,8 g war genügend um alles auszufällen) fiel ein gelber Niederschlag aus, der in 14 ml

50°-igem Nitromethan gelöst wurde. Nach Filtrieren wurde mit Äthanol (40 ml) gefällt. Die hellgelben körnigen Kristalle wurden dreimal aus Nitromethan umkristallisiert (Temperatur < 70°). Es wurden 0,10 g weisse blätterförmige Kristalle vom Schmp. 203–204°, $[\alpha]_D = -91°$, gewonnen. (Gef.: C 88,96; H 6,42; N 2,64; Ber. für $C_{49}H_{42}NB$ (655,6): C 89,76; H 6,46; N 2,14).

Es wurde versucht, die Dilithiumverbindung mit metallischem Lithiumd arzustellen. Dabei fielen aus der Lösung unlösliche Kondensationsprodukte aus und die Lösung färbte sich dunkelblau. Nur ein winziger Niederschlag entstand beim Zugeben vom Ammoniumsalz. Mit der Digrignardverbindung in Tetrahydrafuran konnte in kleiner Ausbeute dasselbe aktive Borspiran wie oben gewonnen werden.

Methyl-propyl-benzyl-phenylammoniumjodid. Aus dem aktiven Ammonium α-Brom-(*d*-campher)-π-sulphonat [10], $[\alpha]_D = +12°$, konnte das Jodid durch Umsetzung mit Lithiumjodid in Aceton erhalten werden. Körnige Kristalle aus Nitromethan. Zersp. ~ 160°. $[\alpha]_D = -69°$. (Gef.: 55,75; H 6,12; N 4,20; Ber. für: $C_{17}H_{22}NJ$ (367,3): C 55,60; H 6,03; N 3,82).

m-*Tolyl*-p-*chlorphenylborsäure*-n-*propylester.* *m*-Tolylborsäure-dipropylester [1] (24 g) in Äther (100 ml) wurde mit *p*-Chlormagnesiumbromid (aus 20 g *p*-Chlor-brombenzol) unter Rühren bei −60° langsam versetzt. Nachdem die Mischung Zimmertemperatur erreicht hatte (etwa 2 Stunden), wurde sie mit verdünnter eisgekühlter Schwefelsäure hydrolysiert. Die wässrige Phase wurde einmal mit Äther (50 ml) ausgeschüttelt, die vereinigten Ätherlösungen einmal mit Wasser ausgewaschen und der Äther in Vakuum abgetrieben. *n*-Propanol (120 ml) wurde zugegeben und die Borsäure azeotropisch verestert [2]. Destillation im Vakuum ergab *m*-Tolyl-*p*-chlorphenylborsäure-*n*-propylester in 71 % Ausbeute. Kp. 172–174°/8 torr. Die Substanz soll unter Stickstoff aufbewahrt werden.

Chlorierung von m-*Tolyl*-p-*chlorphenylborsäure*-n-*propylester.* Der Diarylborsäurepropylester (14,0 g) wurde unter Stickstoff mit Phosphorpentachlorid (11,0 g) gemischt. Beim gelinden Erwärmen ging das Phosphorpentachlorid in Lösung. Gebildetes Propylchlorid und Phosphoroxychlorid wurde beim Atmosphärendruck abdestilliert und dann der Rest im Vakuum. Ein Vorlauf (etwa 1 g) kam bei 72–75°/8 und die Hauptfraktion bei 169–172°/8 torr. Der Vorlauf reagierte heftig mit Wasser und ergab einen weissen Niederschlag, der als m-Tolylborsäure und *p*-Chlorphenylborsäure identifiziert wurde. Die Hauptfraktion wurde nochmals destilliert. In der Vorlage traten leichte Schlieren auf. Der Fraktion 165–166°/8 torr (2,9 g) wurde eine Analysenprobe entnommen. Die Analyse deutete auf eine Disproportionierung hin.

m-*Tolyl*-p-*chlorphenylborsäure-aminoäthylester.* *m*-Tolylborsäuredipropylester (24 g) wurde wie oben grignardiert. Zum Rückstand nach Einengen der ätherischen Lösung wurde erst Äthylalkohol (100 ml) zugegeben, dann Äthanolamin (7 ml). Beim Zusatz von Wasser (300 ml) schied sich eine ölige Masse ab, die bald kristallisierte. Der Ester wurde in heissem Äther-Cyklohexan (3:2) gelöst, schnell filtriert und zum Filtrat wurde dasselbe Volumen Äther zugegeben. Nach Erkalten fiel der Aminoäthylester (17 g) heraus, Schmp. 56–58°.

Umwandlung eines Aminoäthylesters in den entsprechenden o-*Aminophenolester VI.* Diphenylborsäure-aminoäthylester (0,5 g) wurde in Äther (15 ml) aufgeschlämmt und mit 4 N Salzsäure (5 ml) in einem Separiertrichter geschüttelt bis alles in Lösung gegangen war. Man liess die wässrige Phase ab und wusch zweimal mit Wasser nach. Nach Eindampfen des Äthers wurde *o*-Aminophenol (0,26 g) in Äthylalkohol (6 ml) zugegeben. Der Ester wurde mit kaltem Wasser gefällt und aus Wasser-Äthanol (1:1) umkristallisiert. Braungelbe Nadeln vom Schmp. 182–183°. Ausbeute 0,38 g.

Diese Arbeit wurde in Prof. G. Wittigs Laboratorium in Tübingen begonnen. Für die freundliche Überlassung des Arbeitsgebiets danke ich herzlich Prof. Wittig. Diese Arbeit ist vom *Statens Naturvetenskapliga Forskningsråd*, Stockholm, unterstützt worden.

LITERATUR

1. Torssell, K. *Acta Chem. Scand.* **8** (1954) 1779.
2. Torssell, K. *Ibid.* **9** (1955) 239.
3. Torssell, K. *Ibid.* **9** (1955) 242.

4. Krause, E. und Nobbe, P. *Ber.* **64** (1931) 2112.
5. Mikhailov, B. M. und Aronovich, P. M. *Isvest Akad. Nauk SSSR, Otdel Khim. Nauk* **1956** 322.
6. Mikhailov, B. M., Kostroma, T. V. und Fedotova, N. J. *Ibid.* **1957** 589.
7. Wittig, G. und Herwig, W. *Ber.* **88** (1955) 962.
8. Campbell, I. B. M. *J. Chem. Soc.* **1947** 4.
9. Pope, W. J. und Peachey, St. J. *J. Chem. Soc.* **75** (1899) 1127.
10. Wedekind, E. und Frölich, E. *Ber.* **38** (1905) 3438.
11. Letsinger, R. L., Skoog, I. H. und Remes, N. *J. Am. Chem. Soc.* **76** (1954) 4047.
12. Povlock, T. P. und Lippincott, W. T. *J. Am. Chem. Soc.* **80** (1958) 5409.
13. Fuchs, W. und Niszel, F. *Ber.* **60** (1927) 209.
14. Cava, M. P. uns Stucker, J. F. *J. Am. Chem. Soc.* **77** (1955) 6022.
15. Schwechten, H. W. *Ber.* **65** (1932) 1605.

Eingegangen am 3. Juli 1961.

ACTA CHEMICA SCANDINAVICA 16 (1962) 94–104

Studies of Metal Complexes of Radiobiological Interest

I. The Acidity Constants of Croconic Acid

BIRGER CARLQVIST and DAVID DYRSSEN*

The Research Institute of National Defence, Dept. 4 (FOA 4), Stockholm 80, Sweden

Potentiometric and spectrophotometric methods were used for the determination of the dissociation constants of croconic acid at 25°C.

The potentiometric method gave only approximate values of pK_1 0.3–0.5 and pK_2 1.4–1.6 (2 M (H, Na)Cl) and $pK_1 \simeq 0.6$ and $pK_2 \simeq 1.8$ (0.1 M (H, Na) Cl).

The ultraviolet spectra of croconic acid have been determined in mixed solutions of 2 M HCl and 2 M NaCl. The absorption data were treated by two methods:

(*a*) The graphical method for determining the four unknown parameters in eqn. (9) by testing reasonable values of the molar extinction coefficients of H_2A and HA^-. The slope and intercept of the best straight lines corresponded to $pK_1 = 0.2–0.3$ and $pK_2 = 1.3–1.5$.

(*b*) The least squares technique using a high-speed digital computer for determining a set of parameters giving the minimum standard deviation. This minimum was obtained for $pK_1 = 0.32$ and $pK_2 = 1.51$. In addition the spectra for the H_2A and HA^- forms of croconic acid were obtained by this method.

In recent years, the coordination chemistry of the alkaline earth metals has attracted special interest due to the occurrence of strontium and barium among the fission products of heavy atoms. Since soluble calcium or strontium chelates have proved to have little or no effect in eliminating strontium from the living body, attention has been turned to more insoluble complexes.

It has been known for a long time that strontium rhodizonate (SrC_6O_6) is less soluble than the calcium salt (see, *e.g.*, Weiss and Shipman [1]) and this fact has encouraged the use of sodium rhodizonate in biochemical investigations. Rhodizonate solutions (especially acid solutions) are, however, not very stable, thus preventing wider use of this reagent. One of the decomposition products is croconic acid, which is a homologous compound with a 5 membered ring. Croconate solutions seem to be more stable than rhodizonate solutions.

* Present address: Department of Inorganic Chemistry, Royal Institute of Technology, Stockholm 70, Sweden.

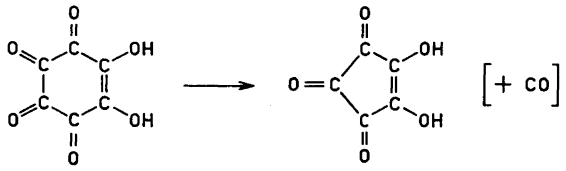

Rhodizonic acid *Croconic acid*

The acidity constants of croconic acid are not accurately known. Carpéni [2] has reported the values of pK_1 and pK_2 to be 2.17 and 4.0 from potentiometric data, but quite different from this, Yamada, Mizuno and Hirata[3] have roughly estimated $pK_1 < 1 < pK_2 < 2$ from spectrophotometric measurements. For a study of the complex chemistry of croconic acid a more accurate determination of these dissociation constants is therefore desirable. Both the potentiometric and the spectroscopic methods have been investigated here and the latter method has proved to give more reliable values of K_1 and K_2.

EXPERIMENTAL

Potassium croconate was prepared by oxidation of sodium rhodizonate in alkaline solution according to the method of Nietzki and Benckiser [4]. Either oxygen was bubbled through the rhodizonate solution in 1 M KOH at 60—70° for a few hours, or sodium rhodizonate was oxidized with MnO_2 in a solution of potassium carbonate (*cf.* Yamada, Mizuno and Hirata [3]). The crystals formed after cooling were filtered off. The filtrate was evaporated and more crystals were obtained. The salt was recrystallized twice from water and dried at 110°. Combustion with V_2O_5 as catalyst gave a carbon content of 27.8 % (no hydrogen). Calculated for $C_5O_5K_2$: 27.5 % C. Yield *ca.* 50 %.

The potentiometric titrations of $[H^+]$ were carried out at 25°C in a thermostated room. The emf was measured with a Radiometer pH Meter 4 using a Radiometer G 202 B glass electrode. The titrations of dipotassium croconate (K_2A) were carried out with 50—150 ml of 2 M or 0.1 M (H, Na)Cl in 2 M or 0.1 M NaCl solutions using a common saturated KCl/Hg_2Cl_2, Hg electrode as a reference. The cells were standardized against solutions of known $-\log [H^+]$ and constant ionic strength (0.1 M and 2 M, respectively).

The light absorption measurements were made with a Zeiss PMQ II spectrophotometer with 1 cm quartz cells. In neutral or alkaline solutions the absorption was fairly stable but it decreased slowly in weakly acid solutions. This decrease was especially rapid in strong $HClO_4$, whereas 89 % of the initial absorption still remained after 7 days in 5 M HCl.

LIST OF SYMBOLS

[ ]	concentrations
$[A]_{tot}$	total concentration of croconic acid (3)
H_2A, HA^-, A^{2-}	croconic acid and croconate ions
D	optical density = extinction (6)
E	electromotive force in mV
I	ionic strength
K_1, K_2	stoichiometric acid dissociation constants (7)
K_{av}	average dissociation constant (5)
m	number of different wave-lengths (14)

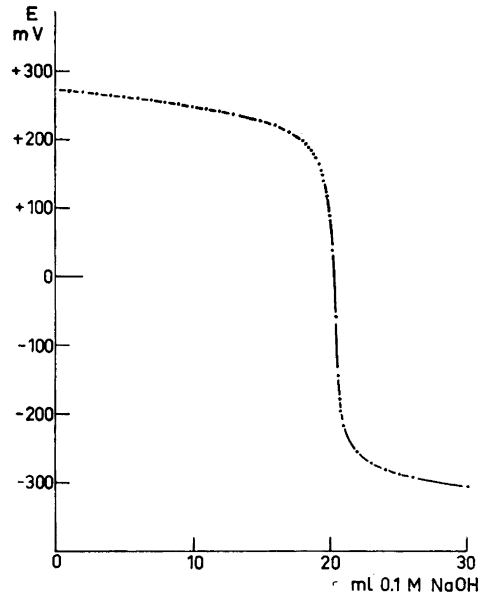

Fig. 1. Potentiometric titration of 1 mmole of croconic acid (obtained by ion-exchange of the dipotassium salt) with 0.1 M NaOH.

n	number of experimental points in least squares calculation (13)
$\bar{n}$	formation function according to Bjerrum [5]
Z	average number of H bound per A (1)
ε	overall molar extinction coefficient (9)
ε_0, ε_1, ε_2	molar extinction coefficients (6)
λ	wave-length in mμ
σ_λ	standard deviation in ε at a certain wavelength (13)
σ_{tot}	standard deviation in ε for nine wave-lengths (14)

RESULTS

The determination of Z function from potentiometric titrations. From the potentiometric titration curve (Fig. 1) it is quite evident that croconic acid is highly dissociated even at very low pH values. The acid is dibasic but the two dissociation steps are so close that they do not appear in Fig. 1. The average number of hydrogen atoms bound to the croconate ion is defined by:

$$Z = \frac{2[H_2A] + [HA^-]}{[A]_{tot}} \qquad (1)$$

The concentration of H_2A and HA^- were computed using the law of electroneutrality (ionic medium not included):

$$[K^+] + [H^+] = [Cl^-] + [HA^-] + 2[A^{2-}] \quad (2)$$

where $[K^+] = 2[A]_{tot}$ and $[Cl^-]$ is the amount of HCl added.

The total concentration of croconic acid in all its forms is

$$[A]_{tot} = [H_2A] + [HA^-] + [A^{2-}] \quad (3)$$

From (1), (2) and (3) it follows that

$$Z = \frac{[Cl^-] - [H^+]}{[A]_{tot}} \quad (4)$$

There is a close relation between the formation function, $\bar{n}$, for the complex formation described by Bjerrum [5] and the Z function for polyvalent acids (*cf.* Sillén [6]). Thus the ligands of a complex correspond to the protons and the central metal atom to the anion of the acid. If $\bar{n}$ is plotted *versus* the logarithm of the ligand concentration curves are obtained with the same form as plots of Z against log $[H^+]$. The "average" constant may be calculated from the midpoint of this curve. Regardless of the number of ligands or the difference between the individual constants, Bjerrum [5] has shown that the average formation constant is equal to the reciprocal ligand concentration at the midpoint provided the formation curve is symmetrical.

In a similar way, one can prove that the average dissociation constant, K_{av}, is equal to the hydrogen ion concentration at the midpoint of the Z function. In the special case of a dibasic acid we thus have

$$pK_{av} = \frac{1}{2}(pK_1 + pK_2) = -\log [H^+]_m \quad (5)$$

where $[H^+]_m$ refers to the midpoint value of $Z = 1$. When the ratio between K_1 and K_2 is large (about 10 000 or more) the two steps are separated and

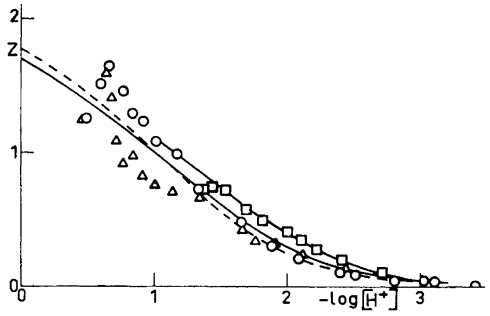

Fig. 2. Z-data (see text) as a function of $-\log [H^+]$ for 2 M (H,Na)Cl: O (5 mmoles of K_2A), △ (1 mmole of K_2A), and 0.1 M (H,Na)Cl: □ (1 mmole of K_2A). The normalized curve $Y = (pv + 2v^2)(1 + pv + v^2)^{-1}$, $X = \log v$ with $p = 4$ (full-drawn curves) and $p = 3$ (dashed curve) are fitted to the data (*cf.* Sillén [6]).

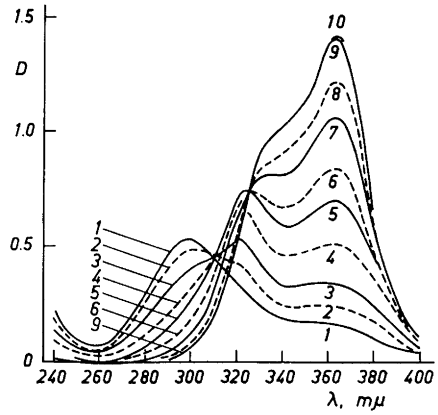

Fig. 3. Spectra of 4×10^{-5} M croconic acid in 2 M (H,Na)Cl. The following numbers refer to curves at different $[H^+]$: 1, 1.98 M; 2, 0.98 M; 3, 0.50 M; 4, 0.22 M; 5, 0.11 M; 6, 0.050 M; 7, 0.022 M; 8, 0.01 M; 9, 0.001 M; 10, 10^{-6} M. Curve 1 has maximum at 299 mμ and curve 9 at 363 mμ.

under these conditions, pK_1 and pK_2 are equal to $-\log [H^+]$ at $Z = 1.5$ and 0.5, respectively. However, if the constants are close to each other two steps cannot be seen in the Z-curve (*cf.* Sillén [6]).

From the titration without croconate, all other conditions being unchanged, the calibration curve of E *versus* $-\log[H^+]$ was obtained. Fig. 2 shows the Z function at 0.1 M and 2 M ionic strength. It was impossible to obtain the complete curves due to the inaccuracy of the Z values in strong acid solutions.

By curve-fitting (*cf.* Sillén [6]) we could estimate: $pK_1 \simeq 0.6$, $pK_2 \simeq 1.8$ in 0.1 M (H,Na)Cl, and $pK_1 = 0.3-0.5$ and $pK_2 = 1.4-1.6$ in 2 M (H,Na)Cl. The latter values agree with the spectrophotometric measurement below.

Spectrophotometric determination of K_1 *and* K_2. In the main series, the $[H^+]$ covered the range from 2 M HCl to 2 M NaOH and the ionic strength was kept constant at 2.0 M with NaCl. In Fig. 3 the spectra are shown for 4×10^{-5} M total croconic acid in 2 M (H,Na)Cl. There is very little change in the spectra below $[H^+] = 0.001$ M, which shows that croconic acid is a rather strong acid.

The two isosbestic points (at *ca.* 310 and *ca.* 325 mμ) are not sharp, and they indicate that there are three different species of croconic acid. In strong acid (5 or 12 M HCl) or alkali solvent effects seem to occur; these spectra are not included in Fig. 3 (*cf.* Fig. 4).

At a certain wave-length the optical density, D, is the sum of the absorption of all forms of croconic acid

$$D = \varepsilon_0[H_2A] + \varepsilon_1[HA^-] + \varepsilon_2[A^{-2}] \qquad (6)$$

where ε_0, ε_1, and ε_2 are the molar extinction coefficients of the forms H_2A, HA^- and A^{2-}, respectively (cell of unit length = 1 cm).

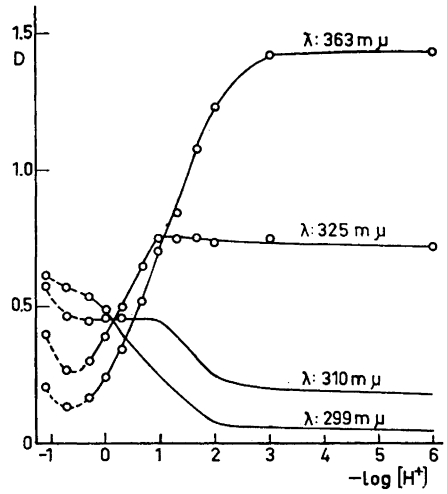

Fig. 4. Variation of optical density, D, for 4×10^{-5} M croconic acid with acidity at four different wave-lengths (the two maxima and the two isosbestic points).

The stoichiometric dissociation constants are

$$K_1 = \frac{[H^+]\,[HA^-]}{[H_2A]} \text{ and } K_2 = \frac{[H^+]\,[A^{2-}]}{[HA^-]} \tag{7}$$

Combining eqns. (3), (6) and (7) one can derive the relation

$$D[A]_{tot}^{-1} = \frac{[H^+]^2\varepsilon_o + K_1[H^+]\varepsilon_1 + K_1K_2\varepsilon_2}{[H^+]^2 + K_1[H^+] + K_1K_2} \tag{8}$$

Eqn. (8) can be rearranged to a form more suitable for numerical calculations

$$\frac{(\varepsilon_o - \varepsilon)}{(\varepsilon - \varepsilon_2)}[H^+]^2 = \frac{(\varepsilon - \varepsilon_1)}{(\varepsilon - \varepsilon_2)}[H^+]K_1 + K_1K_2 \tag{9}$$

where $\varepsilon = D[A]_{tot}^{-1}$ is obtained experimentally. There is no direct way in which ε_1 can be obtained and ε_o is not accurately known since some HA^- still exists in the most acid solution, 2 M HCl (Fig. 4). A graphical method was used for evaluating K_1 and K_2 from eqn. (9) which may be written as linear equation

$$Y = K_1X + K_1K_2 \tag{10}$$

$$\text{where } Y = \frac{\varepsilon_o - \varepsilon}{\varepsilon - \varepsilon_2}[H^+]^2 \text{ and } X = \frac{\varepsilon - \varepsilon_1}{\varepsilon - \varepsilon_2}[H^+].$$

Plots were made of Y *versus* X for combinations of reasonable values of ε_o and ε_1 for the two peaks at 363 mμ and 299 mμ. The best fit with a straight line was obtained for $\varepsilon_o = 1.0 \times 10^3$ and $\varepsilon_1 = (13\text{—}15) \times 10^3$ at 363 mμ and

Table 1. Graphical solutions of eqn. (9)

λ	$\varepsilon_0 \times 10^{-3}$	$\varepsilon_1 \times 10^{-3}$	$\varepsilon_2 \times 10^{-3}$	K_1	K_1K_2	K_2
363	1.0	13.0	35.9	0.64	0.025	0.035
»	»	15.0	»	0.50	0.015	0.03
299	15.0	5.0	1.1	0.49	0.015	0.03
»	»	6.0	»	0.54	0.025	0.04
»	»	7.0	»	0.62	0.035	0.05

$pK_1 = 0.2 - 0.3$
$pK_2 = 1.3 - 1.5$

for $\varepsilon_0 = 15.5 \times 10^3$ and $\varepsilon_1 = (5-7) \times 10^3$ at 299 mμ. The slope of these lines corresponds to K_1. The intercept on the horizontal axis is $-K_2$ and that on the vertical axis is K_1K_2. The results are summarized in Table 1. On the whole this method is rather time-consuming even if a desk-calculator is employed.

Thamer and Voigt [7] have developed a method for determining overlapping dissociation constants for dibasic acids if ε_0 and ε_2 can be obtained by direct measurement at low and high pH values. This method fails, however, in our case since the absorption does not reach a limiting value in the strong acidic region.

In order to obtain more accurate results, the data were treated by the method of least squares. These calculations are very time-consuming unless a high-speed digital computer is employed. In cooperation with Mr. Kurt Eriksson at the FOA division of applied mathematics a program [8] was developed for the FACIT EDB computer to calculate the best values of the 4 constants K_1, K_2, ε_0 and ε_1 from eqn. (8). The input data were the values of $[H^+]$, ε_2 and the "over all" molar extinction coefficient, $\varepsilon = D[A]_{tot}^{-1}$, for 9 different wave-lengths.

In the first place we investigated the possibility of a direct estimation of all four parameters. At certain wavelengths, however, some of the parameters turn out to be negative.

The program was changed so that the values of ε_0 and ε_1 would be calculated by the method of least squares for a series of reasonable values of K_1 and K_2. This approach is in a way closely related to the "error-pit" calculation method by Dyrssen, Ingri and Sillén [9]. Since the dissociation constants are independent of the wave-length they were used as input data. Eqn. (8) can be written in the form

$$D[A]_{tot}^{-1} = \varepsilon = f([H^+]) \qquad (11)$$

where the dependent variable, ε, is subject to random errors; the error in $[H^+]$ can be neglected. The least squares method requires that a set of parameters be determined which minimizes

$$\Delta \varepsilon = [\varepsilon - f([H^+])] \qquad (12)$$

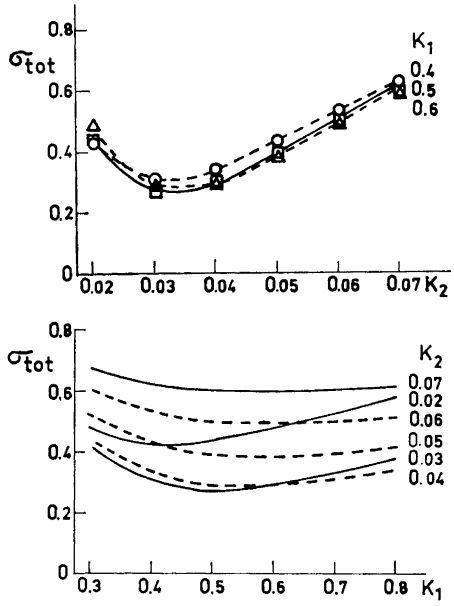

Fig. 5. High-speed computing of ε_0, ε_1, K_1 and K_2. 36 combinations of K_1 (0.3—0.8) and K_2 (0.02—0.07) were tested. The vertical axis is σ_{tot} for nine different wave-lengths.

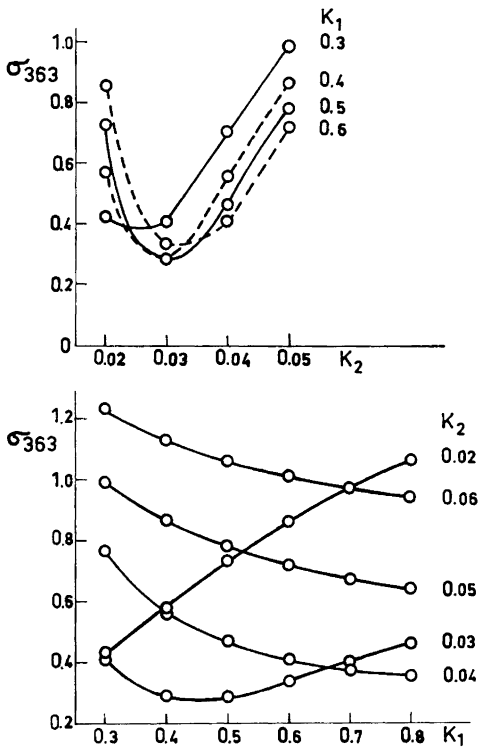

Fig. 6. High-speed computing of ε_0, ε_1, K_1 and K_2. Selected wave-length 363 mμ.

Table 2. Final computation of ε_0 and ε_1 at various wave-lengths. $K_1 = 0.48$ and $K_2 = 0.031$.

λ mμ	$\varepsilon_2 \times 10^{-3}$	$\varepsilon_0 \times 10^{-3}$	$\varepsilon_1 \times 10^{-3}$	σ_λ
280	0.05	9.29	0.73	0.1088
299	1.08	15.31	5.45	0.2250
310	4.30	10.81	12.87	0.2641
320	12.22	5.71	20.95	0.3083
325	17.78	4.01	21.20	0.3214
330	22.75	3.09	17.77	0.2941
340	25.75	2.26	13.72	0.1940
363	35.72	1.19	15.02	0.2763
380	15.45	0.03	12.34	0.3680
				$\sigma_{tot} = 0.2721$

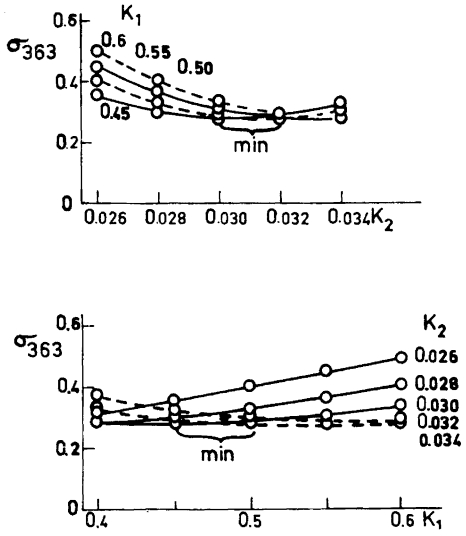

Fig. 7. High-speed computing of ε_0, ε_1, K_1 and K_2. Final step in the successive approximation of K_1 and K_2 (*cf.* Figs. 5 and 6). Selected wave-length 363 mμ.

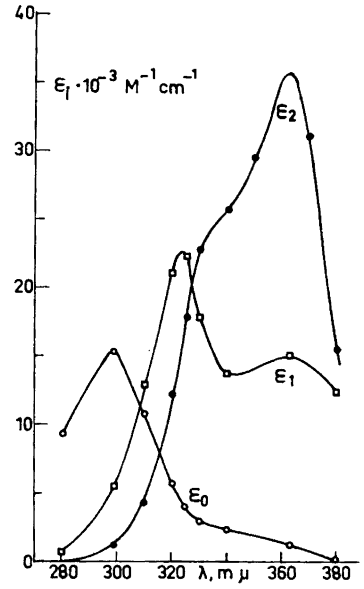

Fig. 8. Croconic acid (H_2A). Spectra of the species H_2A and HA^- calculated by high-speed computing using the values of $K_1 = 0.48$ and $K_2 = 0.031$. It may be seen that the intensity of the peak at 363 mμ is considerably increased for each proton that is removed from H_2A. At the same time the peak at 299 mμ shows a bathochromic shift.

The standard deviation in ε at a certain wave-length for eight different $[H^+]$ (Fig. 3) is

$$\sigma_\lambda = [1/(n-1)]^{1/2} \left[\sum_1^n (\Delta\varepsilon)^2 - \frac{1}{n} \left(\sum_1^n (\Delta\varepsilon) \right)^2 \right]^{1/2} \quad (n=8) \qquad (13)$$

The corresponding standard deviation taken over all wave-lengths is

$$\sigma_{tot} = (1/m)^{1/2} \left[\sum_1^m \sigma_\lambda^2 \right]^{1/2} \quad (m=9) \qquad (14)$$

Input data: $\varepsilon = D[A]_{tot}^{-1}$, $[H^+]$, ε_2, combinations of K_1 and K_2.
Output data: ε_0, ε_1, σ_λ, σ_{tot}.

In the first computation, the values of K_1 were 1, 0.5 and 0.1 and those of K_2 were 0.1, 0.05 and 0.01 (nine combinations). A lowest value of σ_{tot} (nine wave-lengths, *cf.* Table 2) was obtained for the pair $K_1 = 0.5$ and $K_2 = 0.05$.

Table 3. Values of the dissociation constants for croconic acid.

Reference	pK_1	pK_2	Ionic strength M	Method
Carpéni [2]	2.93	4.05	0.1	Potentiometric
	2.17	4.0	0.1	corrected values
Yamada *et al.*[3]	<1	1—2	1	Spectrophotometric
This work	0.3—0.5	1.4—1.6	2	Potentiometric
	~0.6	~1.8	0.1	»
				Spectrophotometric
	0.32	1.51	2	least squares calculation with digital machine.
	0.2—0.3	1.3—1.5	2	graphical evaluation

Three other computations were made with the following K-values:

(II) K_1: 0.3, 0.4, 0.5, 0.6, 0.7 and 0.8
K_2: 0.02, 0.03, 0.04, 0.05, 0.06 and 0.07
36 combinations
(III) (only for $\lambda = 363$ mμ)
K_1: 0.40, 0.45, 0.50, 0.55 and 0.60
K_2: 0.026, 0.028, 0.030, 0.032 and 0.034
25 combinations
(IV) (nine wave-lenghts)
K_1: 0.48
K_2: 0.031.

Fig. 5 shows the relation between σ_{tot} and the various combinations of K_1 and K_2. The minima corresponded to $K_1 \simeq 0.5$ and $K_2 \simeq 0.03$. The plots of the standard deviations for a specific wave-length may give sharper minima, in this case at $\lambda = 363$ mμ (Fig. 6). The results from the computation III with narrow intervals of K_1 and K_2 at $\lambda = 363$ mμ are shown in Fig. 7. The least standard deviation from these curves corresponded to $K_1 = 0.48$ and $K_2 = 0.031$. Finally, the calculations were made with this pair of K values over the whole spectrum in order to get the spectra for the three forms of croconic acid (Table 2 and Fig. 8).

In Table 3 we have collected values of the dissociation constants of croconic acid. Both our work and the investigation of Yamada, Mizuno and Hirata [3] show that the K-values found by Carpéni [2] are probably erroneous.

Acknowledgements. We wish to thank the head of FOA 4, Dr. T. Magnusson, for the permission to publish this work, which is based on a FOA 4 report A 4195—412. We wish also to thank Mr. K. Eriksson and Professor L. G. Sillén for valuable discussions, and Dr. D. Lewis for revision of the English.

REFERENCES

1. Weiss, H. V. and Shipman, W. H. *Anal. Chem.* **29** (1957) 1764.
2. Carpéni, G. *J. chim. phys.* **35** (1938) 193, 233.
3. Yamada, K., Mizuno, N. and Hirata, Y. *Bull. Chem. Soc. Japan* **31** (1958) 543.
4. Nietzki, R. and Benckiser, Th. *Ber.* **18** (1885) 499, 1833; **19** (1886) 293.
5. Bjerrum, J. *Diss.* Copenhagen 1941.
6. Sillén, L. G. *Acta Chem. Scand.* **10** (1956) 186.
7. Thamer, B. J. and Voigt, A. F. *J. Phys. Chem.* **56** (1952) 225.
8. Eriksson, K. and Strahl, M. *FOA 2 report C 2052—2990* (Nov. 1960).
9. Dyrssen, D., Ingri, N. and Sillén, L. G. *Acta Chem. Scand.* **15** (1961) 694

Received June 29, 1961.

ACTA CHEMICA SCANDINAVICA 16 (1962) 105–110

On the Structure of the So-called 3,4-Thiolanedithione

SALO GRONOWITZ and PINCHAS MOSES*

Institute of Chemistry, University of Uppsala, Sweden

3,4-Thiophenedithiol (IV) has been prepared through halogen-metal interconversion between the lithium salt of 4-bromo-3-thiophenethiol and *n*-butyllithium at −70°, followed by reaction with sulphur. IR-, NMR- and UV-spectra show that this compound exists in the dithiol form. The compound obtained as a by-product in the commercial thiophene synthesis from butane and sulphur and described in the literature as 3,4-thiolanedithione (II) (*viz.* the tautomeric dithione form of 3,4-thiophenedithiol) is most probably 5-methyl-1,2-dithiole-3-thione (VI)**.

Pyrolysis of the "thiophene tars" obtained in the commercial synthesis of thiophene from butane and sulphur [1] yields as the main product 3-thiophenethiol, the structure of which has been proved by Caesar and Branton [2] through comparison with an authentic sample, prepared from 3-thiophenemagnesium iodide and sulphur. They [2] also obtained a subsidiary product (I) which they described as a deep-red oil boiling at 120—125°/2 mm Hg, and which they claimed to have the empirical formula $C_4H_4S_3$, although the discrepancy between the calculated and found values for carbon and sulphur were large. They suggested this product to be 3,4-thiolanedithione (II) on the following evidence: Boiling of I with alcoholic alkali resulted in the evolution of approximately one mole equivalent of hydrogen sulphide upon acidifi-

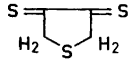

II

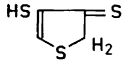

III

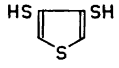

IV

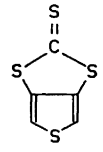

V

* On leave of absence from the Hebrew University of Jerusalem, Israel.

** According to modern nomenclature, *dithiole* means a five-membered ring with two sulphur atoms incorporated in the ring and one double bond. It should not be confounded with *dithiol*, which signifies a compound containing two thiol groups.

cation. Destructive hydrogenation with Raney-nickel yielded *n*-butane. Hartough [3] states as unpublished work by Caesar that I can be reduced to 3-thiophenethiol with zinc dust and hydrochloric acid, though no mention of this occurs in Ref.[2] The IR-spectrum of I showed absorption characteristics neither for the thiophene ring nor for the thiol group. From the UV-spectrum of the product [4] and from mechanistic considerations [2] on the formation of I from butane and sulphur, they chose II as its most probable structure, in preference to the three other isomeric thiolanedithiones. The IR-data eliminate the possibility of I existing as the tautomeric thiolenethiolthione (III) or as the dithiol (IV). As Caesar and Branton [2] admit that their structure assignment is rather speculative, it is unfortunate that in a recent handbook on sulphur compounds, I is described as 3,4-thiophenedithiol [5].

Although it has been found that some 2-hydroxythiophenes exist predominantly as the tautomeric thiolen-2-ones [6], an investigation of the structures of methyl-, methylthio- and bromothiophenethiols [7,8] showed that in these cases the compounds exist as thiols. It seemed to us therefore rather improbable that 3,4-thiophenedithiol should exist in its dithione form II, in which the aromatic character of the thiophene ring has been entirely lost. In view of this, we decided to investigate the true structure of 3,4-thiophenedithiol in greater detail.

3,4-Thiophenedithiol was prepared by treating 4-bromo-3-thiophenethiol [7] with two moles of *n*-butyllithium at −70° followed by one mole of sulphur. We obtained the product as a yellow liquid boiling at 88—93°/1.5 mm Hg, which was soluble in alkali. Though not as unstable as the bromothiophene-

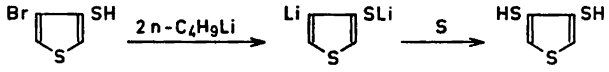

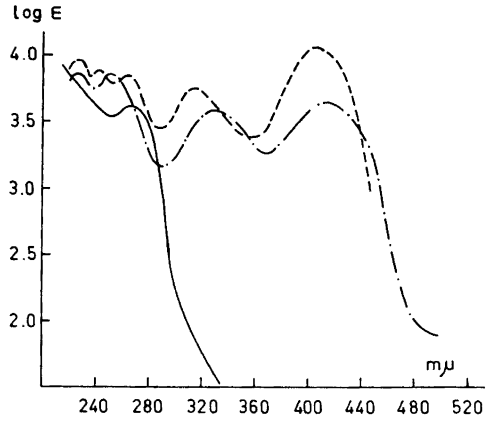

Fig. 1. UV-spectrum of ————3,4-thiophenedithiol in hexane, of ----- 5-methyl-1,2-dithiole-3-thione according to Ref.[20], of -·-·-·- 3,4-thiolanedithione in *iso*octane according to Ref.[4]

thiols [7], it nevertheless decomposes after some time even when stored at −15°. Apart from elementary analyses, the product was further characterized as the trithiocarbonic acid derivative (V) obtained in amber-coloured needles upon reacting IV with carbon disulphide in alkali. We suggest naming V as thieno[3,4-d]-1,3-dithiolane-2-thione. The structure of IV was proved by studying its UV-, IR- and NMR-spectra.

Its UV-spectrum (Fig. 1) in hexane solution is that to be expected for a thiophene derivative [9], having an absorption peak at 269 mμ (log ε = 3.60) and being similar to the UV-spectrum of methyl 3-thienyl sulphide [9].

Its IR-spectrum (Fig. 2) shows a strong peak due to S-H stretching at 3.95 μ (2530 cm^{-1})[10] with additional characteristic peaks at 6.75 μ (1480 cm^{-1}), 7.15 μ (1400 cm^{-1}), 7.52 μ (1330 cm^{-1}) and 8.30 μ (1200 cm^{-1}) which fall in the regions, or almost so, given by Katritzky and Boulton [11] for the characteristic ring stretching frequencies of thiophenes. The presence of the three peaks at 10.80 μ (926 cm^{-1}), 11.60 μ (862 cm^{-1}) and 12.70 μ (787 cm^{-1}) is characteristic for 3,4-disubstituted thiophenes and has been found by the present authors in many 3,4-disubstituted thiophenes (*cf.* IR-spectra in Refs.[7,12]).

Its NMR-spectrum in *cyclo*hexane solution showed two peaks with relative intensities of 1:1 at τ = 2.91 ppm and τ = = 6.69 ppm. The resonances occur in the region characteristic for thiophenic ring hydrogens [8, 13] and thiophenic thiol hydrogens [8] respectively. At higher resolution the bands show some fine-structure due to couplings between the ring and thiol hydrogens [8]. For 3,4-thiolanedithione, only one resonance is expected, while a structure like III contains three types of non-equivalent hydrogens.

The above-mentioned spectroscopic data thus show not only that the compound is a thiophenethiol but also that it is the 3,4-isomer, *i.e.* the rearrangements that are known to occur in some halogen-metal interconversions involving bromothiophenes [14] have not been observed here.

Since the NMR-spectrum of the dithiol in 30 % *cyclo*hexane solution did not undergo any change during a period of several months, it is evident that in the 3,4-thiophenedithiol system the dithiol form is the most stable tautomer,

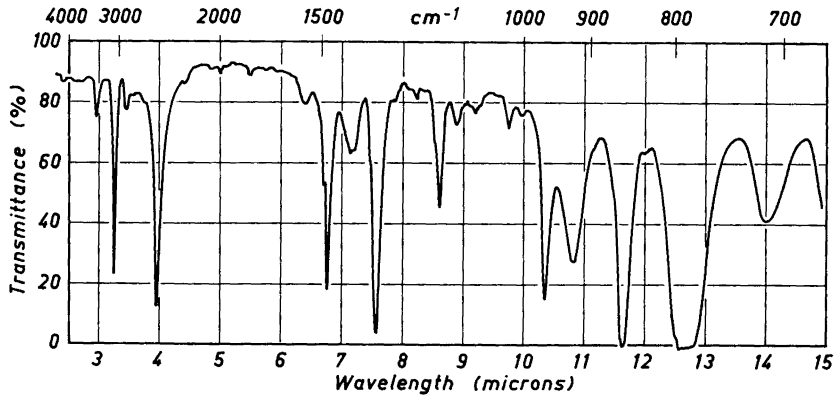

Fig. 2. IR-spectrum of 3,4-thiophenedithiol.

as in this system equilibration can be expected to be rapid and should certainly have been established during this period. It seems therefore very improbable that Caesar and Branton [2] should have obtained the product entirely in its unstable form and that no equilibration should have occurred during their distillation. It is also rather improbable that the product I is a thiolanedithione corresponding to one of the three remaining isomeric thiophenedithiols, since the latter appear to be very unstable compounds with properties differing from I. Pandya and Tilak [15] tried in vain to obtain the 2,5-isomer from 2,5-dilithiumthiophene and sulphur, and we have tried to prepare the 2,4- and 2,3-isomer from 4-bromo-2-thiophenethiol and 3-bromo-2-thiophenethiol according to the same method as used for the 3,4-isomer. The product obtained in the attempted synthesis of 2,4-thiophenedithiol decomposed as soon as the solvent (ether) was removed at room temperature. In the case of the 2,3-isomer, we did manage to obtain an IR-spectrum of the undistilled residue obtained upon removal of the ether before the product decomposed. In this spectrum, the S-H stretching band was present indicating the presence of at least one SH group. It seems thus quite clear that I is certainly not 3,4-thiolanedithione (which exists entirely, or almost so, in its tautomeric dithiol form) and hardly any of the other isomeric thiolanedithiones.

The conditions under which I is formed [1] together with its chemical and physical properties, point instead rather convincingly to the conclusion that this by-product of the thiophene synthesis is not at all a thiophene, but is impure 5-methyl-1,2-dithiole-3-thione (VI) (a trithione).

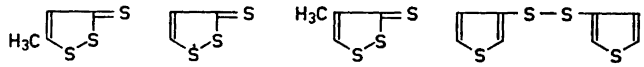

VI VII VIII IX

It is known that treatment of olefins with sulphur at higher temperatures and pressures leads to the 1,2-dithiole-3-thione system [16–18]. Lüttringhaus *et al.*[17] obtained the unsubstituted ring (VII) from propylene and sulphur and Spindt *et al.*[18] obtained 4-methyl-1,2-dithiole-3-thione (VIII) in rather good yield on heating *iso*butylene and sulphur in a bomb. VI is, however, most conveniently prepared through the reaction of ethyl acetoacetate with phosphorus pentasulphide [19] and has also been obtained in the reaction of *n*-butyl sulphide and *n*-butyl disulphide with sulphur [20]. It is characteristic for the 1,2-dithiole-3-thiones that they split off sulphur as sodium sulphide upon treatment with alkali [16,18], as was also observed for I. The boiling-point of I is the same range as that given for VI (which has an m.p. of 33°) and finally, the UV-spectrum of the alleged 3,4-thiolanedithione as given in Ref. [4] is almost identical with that of authentic VI[20] (Fig. 1), showing the characteristic absorption at 410 mμ [18,20] of this ring system. The minor differences are most probably due to impurities in I. If the 3-thiophenethiol obtained through reduction of I with zinc and hydrochloric acid [3] is not due to 3,3'-dithienyl disulphide (IX)[21] possibly present * as an impurity in I, its formation must involve an

* Caesar and Brantons analytical data fit very well for a mixture of 89 % VI and 11 % IX.

interesting rearrangement from the 1,2-dithiole-3-thione system to the thiophene ring system, with the elimination of one sulphur atom.

It seems probable that the present findings are of relevance in connection with the mechanism of the formation of thiophene from butane and sulphur, and it is obvious that Harthough's hypothesis [22] regarding the constitution of the major constituent of the "thiophene-tars" cannot explain the formation of 5-methyl-1,2-dithiole-3-thione.

EXPERIMENTAL

3,4-Thiophenedithiol. Into the usual nitrogen-swept four-necked apparatus was introduced 228 ml of 1.29 N ethereal *n*-butyllithium and the solution cooled to −70°. 25.4 g (0.128 mole) of 3-bromo-4-thiophenethiol [7], freshly prepared from 3,4-dibromothiophene, was dissolved in 50 ml of ether and added with stirring to the *n*-butyllithium. After 10 min, 5.2 g (0.16 mole) of sulphur was added in one portion and the mixture stirred at −70° for a further half hour. It was then poured into water, the aqueous phase was separated, the ether phase extracted with two portion of 2 N sodium hydroxide and the combined aqueous phase acidified with 2 N hydrochloric acid under strong cooling. The acidified mixture was immediately extracted with three portions of ether, dried and fractionated *in vacuo* after removal of the solvent. After a forerun consisting of 5.4 g of impure 3-thiophenethiol, boiling at 52−72°/2 mm Hg, 9.3 g (49 %) of crude 3,4-thiophenedithiol distilled at 80−92°/2 mm Hg. Redistillation yielded the pure product as a yellow oil, b.p. 88−93°/1.5 mm Hg. (Found: C 32.87; H 2.87; S 64.19. Calc. for $C_4H_4S_3$ (148.3): C 32.40; H 2.72; S 64.87).

Thieno [3,4-d] 1,3-dithiolane-2-thione. 5.2 g (0.035 mole) of 3,4-thiophenedithiol was treated with 20 ml of carbon disulphide and 60 ml of 2 N sodium hydroxide and the mixture refluxed for 4 h under nitrogen. The excess carbon disulphide was then allowed to evaporate off. The resulting dark-coloured product was filtered off, washed and dried, giving 3.2 g (48 %) of crude product, m.p. 139−141°. After decolourizing with Norit and recrystallization from 50 ml of acetic acid, 2.3 g of pure product was obtained in amber-coloured needles, m.p. 141−141.5°. (Found: C 31.78; H 1.28; S 67.34. Calc. for $C_5H_2S_4$ (190.3): C 31.55; H 1.06; S 67.38.)

The UV-measurements were carried out with a Beckman model DU-spectrophotometer. The IR-spectra were recorded on a Perkin−Elmer Infracord spectrophotometer. The NMR-spectra were obtained with a Varian Associates model V-4 300-B high resolution spectrometer, operating at 40.00 Mc/s and a flux-stabilized 12 in. magnet equipped with shim-coils from the same company. The magnet sweep was calibrated with the conventional side-band technique using a General Radio 617-C interpolation oscillator and a Hewlett−Packard 524-D frequency counter. The chemical shifts were obtained from *cyclo*hexane solutions containing 2 % of tetramethyl silane and are given as τ-values [23].

Acknowledgements. The authors wish to express their thanks to Prof. Arne Fredga for his interest in this work and for all facilities put at their disposal. Thanks are also due to Mr Bo Gestblom and Mr S. Johansson for recording the NMR- and UV-spectra respectively. The elementary analyses were carried out at the Analytical Department of the Chemical Institute. A grant from the *Swedish Natural Science Research Council* to S. G. is gratefully acknowledged.

REFERENCES

1. Rasmussen, H. E., Hansford, R. C. and Sachanen, A. N. *Ind. Eng. Chem.* **38** (1946) 376.
2. Caesar, P. D. and Branton, P. D. *Ind. Eng. Chem.* **44** (1952) 122.
3. Hartough, H. D. Thiophene and its derivatives, New York 1952, p. 432.
4. Ref.[3], p. 105.
5. Reid, E. E. Organic Chemistry of bivalent sulfur. Volume I. New York 1958, p. 71.
6. Gronowitz, S. and Hoffman, R. A. *Arkiv Kemi* **15** (1960) 499.
7. Gronowitz, S., Moses, P. and Hörnfeldt, A.-B. *Arkiv Kemi* **17** (1961) 273.

8. Hoffman, R. A. and Gronowitz, S. *Arkiv Kemi* **16** (1960) 563.
9. Gronowitz, S. *Arkiv Kemi* **13** (1958) 239.
10. Bellamy, L. J. The infra-red spectra of complex molecules, London 1958, p. 350.
11. Katritzky, A. R. and Boulton, A. J. *J. Chem. Soc.* **1959** 3500.
12. Gronowitz, S., Moses, P. and Håkansson, R. *Arkiv Kemi* **16** (1960) 267.
13. Hoffman, R. A. and Gronowitz, S. *Arkiv Kemi* **16** (1960) 515.
14. Moses, P. and Gronowitz, S. *Arkiv Kemi*, **18** (1961) 119.
15. Pandya, L. J. and Tilak, B. D. *Chem. & Ind. London* **1958** 981.
16. Böttcher, B. and Lüttringhaus, A. *Ann.* **557** (1947) 89.
17. Lüttringhaus, A., König, H. B. and Böttcher, B. *Ann.* **560** (1948) 201.
18. Spindt, R. S., Stevens, D. R. and Baldwin, W. E. *J. Am. Chem. Soc.* **73** (1951) 3693.
19. Legrand, L., Mollier, Y. and Lozac'h, N. *Bull. soc. chim. France* **1953** 327.
20. Wessely, F. and Siegel, A. *Monatsh.* **82** (1951) 607.
21. Gronowitz, S. and Håkansson, R. *Arkiv Kemi* **16** (1960) 309.
22. Ref.[3], p. 433.
23. Tiers, G. V. D. *J. Phys. Chem.* **62** (1958) 1151.

Received June 26, 1961.

ACTA CHEMICA SCANDINAVICA 16 (1962) 111–116

Microwave Discharge Production of Hydrogen Atoms. Control of Hydrogen Atom Quantity Produced

BØRGE BAK and JOHN RASTRUP-ANDERSEN

Chemical Laboratory of the University of Copenhagen, Copenhagen, Denmark

Production of hydrogen (and deuterium) atoms by a microwave discharge is described. Three different methods of estimating the quantity of atoms produced have been tested. A hotwire detector, a thermometric detector, and a 'chemical', luminescent detector. Application of each of the three types of indicator is useful in various phases of experimental work.

As is well-known, hydrogen atoms have very frequently been produced in a so-called Wood's tube [1] (from its inventor) in which a stream of molecular hydrogen passes metallic electrodes. In an electrodic discharge, dissociation occurs to an appreciable extent.

Experience has, however, shown such production to be unreliable, one main reason being that somehow or other metal dust particles are soon scattered in almost every part of the equipment. As this happens, the yield of hydrogen atoms decreases very rapidly because metals catalyze the recombination of hydrogen atoms to molecules. This is why an electrodeless discharge of the type which can be arranged by means of microwaves, is advantageous *a priori*.

Of course, other factors are operative in helping the hydrogen atoms to recombine. While recombination cannot occur in a simple two-body collision (because of energy), the *walls* of the container may assist. Already Wood discovered that he could make the container walls less effective as a recombination catalyst by 'poisoning' them with syrupous phosphoric acid or other compounds. If this precaution is not taken, the walls slowly 'dry out' in the vacuum usually applied. A *dry* glass surface seems rather effective as a hydrogen combiner. Phosphoric acid *etc.* thus serves as a source of loosely bound water. Evidently, constant admixing of water vapor may serve as well in many cases since the inevitable production of the OH radical from H_2O will do no harm in cases where the reaction zone is well separated from the production zone, so that the reaction $H + OH \rightarrow H_2O$ annihilates all OH radicals before the reaction zone has been reached. In all our experiments we have,

therefore, used moist hydrogen or deuterium, produced by letting the gas at atmospheric pressure bubble through water at room temperature, the water vapor content thereby being of the order of 3—4 %. If the temperature of the water, through which H_2 (or D_2) was bubbled, was lowered to 1°C, a marked decrease in hydrogen atom yield was noted.

THE PRODUCTION OF HYDROGEN OR DEUTERIUM ATOMS

Commercial tank hydrogen (free of CO and halogens) or D_2 (produced by electrolysis of D_2O + NaOD) was passed through a commercial De-oxo unit * (for removal of oxygen) and a washbottle with water at atmospheric pressure into a capillary tube (length 10 cm, i.d. 0.18 mm), backed up by the rest of the equipment, consisting of 17 mm i.d. tubing, wider flasks, traps *etc.* and a Leybold D2 vacuum pump (capacity 2 m^3 per hour at the pressure of 0.1—1 mm Hg applied here). The hydrogen pressure was read on a silicon oil manometer.

Quartz tubing was used at the place where molecular hydrogen was passed through a microwave cavity because of its dielectric properties, superior to those of ordinary glass and Pyrexglass, the microwave input through a glass wall being smaller (although by no means negligible). The cylindrically shaped microwave cavity, made of brass, (dimensions: 75 mm of diameter, 75 mm of length, with a central hole at both ends, 25 mm wide) was coupled to a Q.K.62 magnetron (forced-air cooled) by means of a coaxial connexion with two perpendicular tuning stubs (Fig. 1). Forced-air was continuously blown into the cavity through one of the two central openings. Matching of the magnetron-cavity system was ensured by means of the tuning stubs and adjusted to maximum brilliance of the discharge, the starting of which was performed by a Tesla-coil leak detector. Final matching of magnetron and cavity, resulting in maximum production of hydrogen atoms, was obtained by use of a hot-

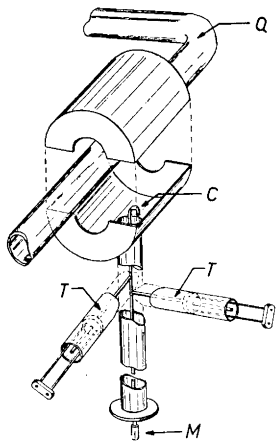

Fig. 1. Microwave discharge arrangement. Q = quartz tube for streaming gas; C = coupling loop; T = tuning stub; M = magnetron connector.

* Engelhard Industries Ltd., Baker Platinum Div., High Holborn, London W.C.I.

wire hydrogen atom detector to be described in a later paragraph. The Q.K.62 Raytheon magnetron was powered by a 1250 V d.c. power-supply, capable of yielding 100 mA. The actual current was 80—90 mA. The magnetron filament current was 3.3 A, the voltage 6.2. V.

CONTROL OF ATOM PRODUCTION

A. Hot-wire detector

Hot-wire detectors for the control of hydrogen atom production have been constructed by numerous investigators [1]. The present construction owes most of its features to T. M. Shaw who has published a most valuable report on studies of microwave gas discharges [2]. The use of some sort of hydrogen atom detector seems indispensable, although often neglected, since probably no equipment can be constructed yielding a constant production of hydrogen atoms because of uncontrollable contamination with dust that may include metal particles. Shaw's three-dimensional hot-wire detector was replaced by us by a simpler two-dimensional construction which seemed equally effective and less difficult to prepare and to handle (Fig. 2). The detector was placed at the location in the equipment where we expected the hydrogen atoms to react, *i.e.* 18 cm from the microwave discharge. Electrically, the detector formed one of four arms of a bridge (Fig. 3), the same arm including an ammeter (1000 mA full scale) for measurement of the detector current I_D. Also, the voltage across the detector wire could be measured (detector voltage V_D), When the bridge is balanced, the resistance of the hot-wire detector attains a reference value (R_1 of Fig. 3). The current across the bridge (and through the detector) is variable by means of R_4 (Fig. 3).

In one experiment, undissociated molecular hydrogen, at the pressure and temperature to be used under hydrogen atom production, passed the detector, suitably heated to a light-read glow (700—800°C) by I_D, in this case denoted by I_D°, the corresponding voltage drop being V_D°. Now, the microwave discharge was started. This caused the temperature of the detector to rise because of the recombining hydrogen atoms. Therefore, the bridge current was lowered, until balance was again obtained at current I_D^x and voltage V_D^x. Obviously, the recombination of hydrogen produced

$$I_D^\circ \, V_D^\circ - I_D^x \, V_D^x \text{ watts.}$$

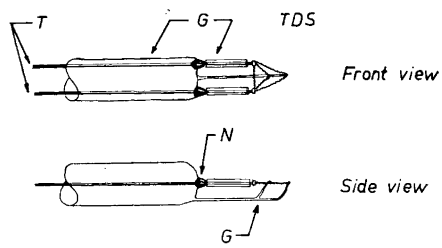

Fig. 2. Hot-wire detector. T = tungsten rod; TDS = tungsten double spirals (filaments from 75 watts electric bulbs (220 V)); G = glass; N = Nonex beads.

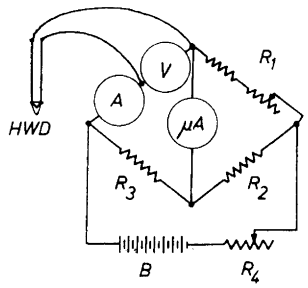

Fig. 3. Balanced bridge A = ammeter (1 A., full scale); V = voltmeter (25 V, full scale); μA = microammeter (−50 to 50 μA); R_1 = 52 Ω plus 10 Ω variable; $R_2 = R_3 = 100\ \Omega$; $R_4 = 50\ \Omega$; HWD = hot-wire detector; B = battery (30 V.).

In a typical example, $I_D^o = 0.362$ A, $V_D^o = 11.0$ V (3.99 watt) and $I_D^x = 0.254$ A, $V_D^x = 7.7$ V (1.95 watt). Difference, 2.04 watt. In this experiment, the molecular hydrogen input ($p = 0.3$ mm Hg) was 0.140 ml/sec, or 5.86×10^{-6} moles/sec. Complete dissociation would produce 11.72×10^{-6} atoms/sec. At their recombination, they would liberate $\frac{1}{2} \times 11.72 \times 10^{-6} \times 1.03 \times 10^5$ cal. or 2.52 watts. This means that at 18 cm from the microwave discharge, 80 % of the hydrogen still existed as atoms. If the above-mentioned 18 cm distance was increased to 25 cm, the yield decreased to 65 %. In view of this it is, therefore, quite probable, that our hot-wire detector gives a fair measure of the quantity of atomic hydrogen. It was inpracticable for us to arrange an experiment with a distance *smaller* than 18 cm because a bend on the quartz tubing had deliberately been introduced in order to prevent the radiation from the microwave zone to reach the point where the quantity of hydrogen atoms is measured and where the atoms are scheduled to react with other compounds.

B. Effect of pressure and temperature changes

Doubling of the molecular hydrogen input and pressure ($p = 0.6$ mm Hg) to 0.280 ml/sec gave $I_D^o\ V_D^o - I_D^x\ V_D^x = 2.35$ watts, the yield now having decreased to 37 %.

Heating of the quartz tube (to 200°C) in a 5 cm zone between the generator and the detector caused a very serious decrease in yield (to about one-half) This may be in disharmony with Shaw's findings [2]. However, while the walls of our tubing were not 'poisoned' (moist hydrogen or deuterium being used instead), Shaw treated his equipment with GE Dri-Film SC77 ($(CH_3)_2SiCl_2 + CH_3SiCl_3$), which might account for the fact that the hydrogen atom yield, obtained by Shaw, was rather independent of heating of the tube following the discharge zone. A film of adsorbed water, 'poisoning' our tubing at 25°C, obviously partly evaporates at higher temperatures. This latter circumstance, on the other hand, gives the possibility of constructing a variable hydrogen atom 'attenuator', permitting the investigator to vary his hydrogen atom production in a very useful way without change of molecular hydrogen input.

C. Thermometric detector

Already Bonhöffer [1] demonstrated the usefulness of a metal-coated thermometer as a detector. We have studied this matter in somewhat greater detail because of the simplicity of the principle. The following procedure for coating the thermometer bulb with a thin layer of silver gave fully reproducable results. The bulb of an ordinary 350°C thermometer (lenght of the bulb 10 mm, diameter 5 mm) was ground by emery cloth. The matt surface thus produced was treated by hot cromic acid-sulphuric acid mixture, washed thouroughly with distilled water, immersed in alcohol for a few seconds and thereafter immersed in 0.1 N aqueous $AgNO_3$. After wetting, the bulb was dried in a stream of hot air, while the thermometer was rotated. It is important that no $AgNO_3$ reaches the thermometer stem. 3—4 times, a fresh droplet of $AgNO_3$ was added and the water evaporated. No further addition of $AgNO_3$ was necessary, as shown by our experiments.

When a thermometer so prepared is placed in the equipment instead of the hot-wire detector, and immersed in a stream of atomic hydrogen, $AgNO_3$ is rapidly reduced to metallic silver, which sticks extremely well to the bulb. In a stream of hydrogen atoms, such as the first one described under paragraph A of this paper, the equilibrium temperature obtained after 10—15 min) is as much as 300°C. Since this detector type is easy to make, easy to place in a side-arm of almost any type of equipment, and easy to insert and withdraw (magnetically) without braking the vacuum or interrupting an experiment, this high thermometer reading deserves attention. We have, for example, found it useful to place a thermometer after the zone of a chemical reaction. The initiation and the termination of a chemical reaction between hydrogen atoms and a reagent was simply indicated by a pronounced drop and rise in temperature. Table 1 shows a series of experiments in which the hot-wire detector and a given thermometric detector were compared.

Table 1. Comparison of hot-wire and thermometric detector.

Moles H_2/sec $\times 10^5$	0.586	0.732	0.878	1.024	1.170
$I_D^o\ V_D^o - I_D^x\ V_D^x$ watts	2.04	2.19	2.25	2.32	2.35
Temperature reading	308°	317°	319°	312°	307°

In these five experiments, approximately a constant quantity of hydrogen atoms is produced (as shown by the wattage) in spite of the increasing molecular hydrogen input. To a fair degree, the thermometer reading is also constant. On several occasions we have observed that inferior atomic output (for example, due to impurities left-over from chemical reactions, or because of incorrect matching of the magnetron) is easily and unequivocally indicated by the thermometer, provided that the thermometer is correctly stored between uses, for example, by withdrawel to a side-arm of the equipment, the bulb being removed 8—10 cm from the zone of the hydrogen atoms.

D. Chemical detection

In a paper by Vance and Bauman [3] it is stated that at a specified concentration of CCl_4 vapor, the reaction between hydrogen atoms and CCl_4 may be used to determine the concentration of hydrogens actually being produced, since all hydrogen atoms are converted to HCl. The conditions necessary for obtaining this are: a pressure of about 0.8 mm Hg, a temperature of 150—200° and a CCl_4:H ratio of about 10:1, that is, in the equipment specified in Ref.[3].

If CCl_4 vapor was introduced by us through a jet in a small heated zone (215°C) where, from previous experiments, we know that a hydrogen atom yield of about 35 % is obtained, the yield of HCl, trapped in 2 successive, liquid nitrogen-cooled traps, turned out to be 7 % with respect to hydrogen. In this experiment, the CCl_4:H ratio was about 9:1, the somewhat undefined pressure of the reaction zone being of the order of 0.4 mm of Hg. Hence, we were unable to reproduce the result of Ref.[3]. Nevertheless, it is of interest to see what happens at the more easily obtainable room temperature. Here, in experiments, where our hot-wire detector indicated the presence of 64 % dissociated hydrogen molecules, an excess of CCl_4 vapor produced only 15 % HCl. The reaction zone was clearly visible, because a light-green radiation was emitted. This result was reproducible. Under many circumstances this radiation and the accompanying HCl-production might be used as an indicator of an existing hydrogen atom production, 8—10 times higher than indicated by the amount of HCl formed. The method of Ref.[3] has not been listed in the appropriate paragraph II, 8 of Ref.[1].

REFERENCES

1. Steacie, E. W. R. *Atomic and Free Radical Reactions*, Reinhold Publishing Co., N.Y. 1954.
2. Shaw, T. M. *General Electric Techn. Inform.* No R 58, ELM 115, G.E. Microwave Laboratory, Palo Alto, California.
3. Vance, J. E. and Bauman, W. C. *J. Chem. Phys.* **6** (1938) 811.

Received July 8, 1961.

ACTA CHEMICA SCANDINAVICA 16 (1952) 117–122

Beiträge zur Chemie α-substituierter Sulfide

VII *. Potentiell fungizide Verbindungen: Trichlormethylarylsulfide

ALEXANDER SENNING und SVEN-OLOV LAWESSON

Laboratorium für Organische Chemie, Chemisches Institut der Universität Uppsala, Uppsala, Schweden

In Fortführung unserer Arbeiten über potentiell fungizide Verbindungen, die die Trichlormethylmerkaptogruppe enthalten [1], wurden siebzehn Methylarylsulfide mit jeweils drei Mol Chlor umgesetzt. Wir erhielten ein bekanntes und elf neue Trichlormethylarylsulfide sowie ein bekanntes und ein neues Chlormethylarylsulfid (in diesen beiden Fällen behinderten *ortho*ständige Substituenten die Chlorierung). Bei der Chlorierung von *o*-Bromthioanisol, *o*-Chlorthioanisol und 2-Methyl-6-*iso*propylthioanisol wurden keine wohldefinierten Produkte erhalten. Als Ausgangsmaterial für die oben genannten Versuche wurden vier neue mono- bzw. dialkylierte Thioanisole durch Methylierung der entsprechenden Thiophenole dargestellt.

Die Tatsache, dass sich das 1952 von Kittleson [2] beschriebene N-Trichlormethylmerkaptotetrahydrophthalimid (I) in der Praxis als Fungizid ausgezeichnet bewährte, hat ein reges Interesse für die vorher wenig untersuchten

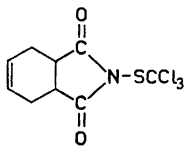

I Handelsname: Captan

Verbindungen, die eine Trichlormethylmerkaptogruppe enthalten, hervorgerufen. Auch die einige Jahre später entdeckte krebshemmende Wirkung einiger N-Trichlormethylmerkaptokarbonsäureimide bzw. -sulfonamide [3–5] dürfte in diesem Zusammenhang eine Rolle spielen. Im Laufe der letzten zehn Jahre wurde Trichlormethansulfenylchlorid (das bei der Darstel-

* VI. Mitteilung siehe Literaturzitat (26). VIII. Mitteilung: Senning, A. und Lawesson, S.-O. *Acta Chem. Scand.* 15 (1961) 1203.

lung des Captans mit Tetrahydrophthalimid umgesetzt wird) systematisch mit H-aziden Verbindungen zur Umsetzung gebracht (z.B. Karbonsäureimide, Sulfonamide, Phenole, N-Hydroxyimide, Arylsulfinsäuren, Merkaptane; vgl. Sosnosvkys Übersichtsartikel [6]), wobei zahlreiche Substanzen erhalten wurden, die eine mehr oder weniger ausgeprägte fungizide Wirkung zeigten.

Von den Verbindungen, bei denen die Trichlormethylmerkaptogruppe an ein Kohlenstoffatom gebunden ist, sind sowohl Trichlormethylalkyl- als auch Trichlormethylarylsulfide bekannt, wenn auch verhältnismässig wenig untersucht. Aliphatische Verbindungen vom Typ II wurden bei der Chlorierung des Dimethylsulfids erhalten [7–10], während die Anlagerung von Trichlormethansulfenylchlorid an Doppelbindungen (katalysiert durch ultraviolettes Licht oder durch organische Peroxyde) zu Verbindungen vom Typ III führt [11–14]. Die letzteren sind als Fungizide und Insektizide patentiert worden.

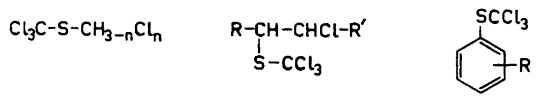

II III IV

Die Trichlormethylarylsulfide (IV), eine Verbindungsklasse, die um 1910 von Zincke und Mitarbeitern entdeckt wurde [15–17], werden in der Literatur nur sporadisch erwähnt [1,10,18–22].

Orwoll [18] postulierte Trichlormethylarylsulfide als Zwischenstufe bei der von ihm gefundenen Darstellung von Thiophosgen aus Trichlormethansulfenylchlorid in Gegenwart von aromatischen Kohlenwasserstoffen und Friedel-Crafts-Katalysatoren. Egen [19], dem die Synthese von Trichlormethylarylsulfiden mit Hilfe von Trichlormethansulfenylchlorid unter den Bedingungen der Friedel-Crafts-Reaktion misslang, untersuchte den Einfluss von Substituenten auf die fungistatische und kontaktinsektizide Wirkung der Trichlormethylarylsulfide (hauptsächlich an *para*substituierten Verbindungen). Böhme und Gran [10] überprüften die allgemein angezweifelte Beschreibung des Trichlormethylphenylsulfids von Sanna und Stefano [20] und wiesen die Unhaltbarkeit dieser Angaben nach. Yagupolsky und Marenets [21,22] erhielten bei der Darstellung von Trifluormethylmerkaptoverbindungen als Zwischenprodukte Trichlormethylarylsulfide. Senning und Lawesson [1] griffen kürzlich den in Egens Arbeit [19] aufgeworfenen Fragenkomplex wieder auf. Der Darstellung der Trichlormethylmerkaptobenzosäuren und -benzoesäureäthylester (IV, R = COOH bzw. $COOC_2H_5$) folgt jetzt die Beschreibung einer Reihe weiterer Trichlormethylarylsulfide, deren biologische Untersuchung (deren Ergebnisse an anderem Ort veröffentlicht werden) den Zusammenhang zwischen Substitution und biologischer Aktivität weiter beleuchten soll.

Die Synthese der Trichlormethylarylsulfide geht, wie erstmals von Zincke beschrieben, von den entsprechenden Methylarylsulfiden aus, die in einem organischen Lösungsmittel (z.B. Tetrachlorkohlenstoff, Chloroform, Eisessig) mit freiem Chlor umgesetzt werden. Der erste Schritt dieser Reaktion ist die

Bildung der polaren Sulfiddichloride (V), die, zum Teil spontan, zum Teil beim Erwärmen, in das α-chlorierte Sulfid und Chlorwasserstoff zerfallen.

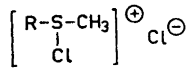

V

*Ortho*ständige Substituenten können in gewissen Fällen die Chlorierung der Methylgruppe behindern oder auch eine Sekundärreaktion mit einem α-Chloratom eingehen. Beim *o*-Nitrothioanisol und beim Pentachlorthioanisol lässt sich bei der Chlorierung in Tetrachlorkohlenstoff (Kp. 76,8°) jeweils nur ein Chloratom in die Methylgruppe einführen. *o*-Bromthioanisol und *o*-Chlorthioanisol ergeben (wie auch *o*-Methylmerkaptobenzoesäureäthylester [1]) auch in Gegenwart eines Überschusses an Chlor Produkte mit einem niedrigeren Chlorgehalt als dem für das Trichlormethylarylsulfid berechneten, aus denen sich keine wohldefinierten Verbindungen isolieren lassen. Bei der Chlorierung der *o*-Methylmerkaptobenzoesäure mit einem Überschuss an Chlor [1] beobachteten wir eine Zyklisierung, die zum 3,3-Dichlor-4-thia*iso*chroman-1-on (VI) führte. Diesem Verbindungstyp haben wir eine nähere Untersuchung gewidmet, deren Ergebnisse an anderem Ort veröffentlicht wurden [23–26].

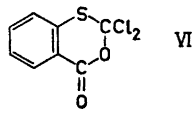

VI

BESCHREIBUNG DER VERSUCHE

Alle Schmelz- und Siedepunkte sind unkorrigiert. Die Infrarotspektrogramme wurden mit einem Spektrographen Perkin-Elmer Modell 137 aufgenommen. Die Analysen wurden im Institut für Analytische Chemie der Universität Uppsala, im Institut für Medizinische Chemie der Universität Uppsala sowie von der Firma Alfred Bernhardt, Mülheim (Ruhr) ausgeführt. Alle chlorhaltigen Substanzen wurden in Schutzgasatmosphäre (N_2) destilliert.

β-Naphthylmethylsulfid und Pentachlorthioanisol wurden nach bekannten Methoden durch Alkylierung der käuflichen Merkaptoverbindungen dargestellt. Ebenfalls nach bekannten Methoden wurden dargestellt: *o*-Nitrothioanisol aus *o*-Chlornitrobenzol, α-Naphthylmethylsulfid, *o*-Tolylmethylsulfid, *m*-Tolylmethylsulfid, *o*-Anisylmethylsulfid und *m*-Anisylmethylsulfid aus den entsprechenden Bromverbindungen sowie *m*-Nitrothioanisol, *o*-Bromthioanisol, *m*-Bromthioanisol, *o*-Chlorthioanisol und *m*-Chlorthioanisol aus den entsprechenden Aminen.

Bei der Darstellung von 4-*t*-Butylthioanisol, 2-Methyl-4-t-butylthioanisol, 2-*Iso*propylthioanisol und 2-Methyl-6-*iso*propylthioanisol gingen wir von den entsprechenden Thiophenolen aus, für deren kostenlose Überlassung wir der Firma Consolidation Coal Company, Library, USA (Dr. Neuworth) hiermit unseren verbindlichsten Dank aussprechen. Die Thiophenole wurden in alkalischer wässriger Lösung unter Rühren eine halbe Stunde mit einem 10 %-igen Überschuss an Dimethylsulfat behandelt. Anschliessend wurde wie üblich aufgearbeitet.

4-t-Butylthioanisol. Ausgangsmaterial: 20,7 g (0,125 Mol) 4-*t*-Butylthiophenol. Zwischen 124°/13 mm und 125°/13 mm gingen 18,3 g Produkt (Rohausbeute 81 %) vom Schmelzpunkt 30°—33° über. Aus Petroläther umkristallisiert schmolz das 4-*t*-Butyl-

thioanisol (farblose Spiesse) zwischen 30° und 33°. (Gef. C 72,98; H 8,61; S 16,88. Ber. für $C_{11}H_{16}S$: C 73,27; H 8,94; S 17,78).

2-Methyl-4-t-butylthioanisol. Ausgangsmaterial: 21,0 g (0,117 Mol) 2-Methyl-4-*t*-butylthiophenol. Zwischen 125°/12 mm und 130°/12 mm gingen 18,2 g Produkt (Rohausbeute 82 %) über (n_D^{20} 1,5459). 2-Methyl-4-*t*-butylthioanisol siedet bei 142°/30 mm und hat n_D^{20} 1,5461. (Gef. C 74,96; H 9,39; S 15,62. Ber. für $C_{11}H_{16}S$: C 74,16; H 9,34; S 16,50).

2-Isopropylthioanisol. Ausgangsmaterial: 22,7 g (0,149 Mol) 2-*Iso*-propylthiophenol. Zwischen 116°/25 mm und 120°/25 mm gingen 21,6 g Produkt (Rohausbeute 87 %) über (n_D^{20} 1,5589). 2-*Iso*propylthioanisol siedet bei 123°/30 mm und hat n_D^{20} 1,5592. (Gef. C 71,64; H 8,32; S 19,52. Ber. für $C_{10}H_{14}S$: C 72,23; H 8,49; S 19,28).

2-Methyl-6-isopropylthioanisol. Ausgangsmaterial: 22,9 g (0,140 Mol) 2-Methyl-6-*iso*propylthiophenol. Zwischen 107°/13 mm und 109°/13 mm gingen 19,8 g Produkt (Rohausbeute 79 %) über (n_D^{20} 1,5453). 2-Methyl-6-*iso*propylthioanisol siedet bei 109°/13 mm und hat n_D^{20} 1,5412. (Gef. C 73,31; H 9,03; S 17,61. Ber. für $C_{11}H_{16}S$: C 73,27; H 8,94; S 17,78).

Chlorierungsversuche

Versuchsanordnung. In einem Dreihalskolben mit Rührer, Rückflusskühler mit aufgesetztem Kalziumchloridrohr und Tropftrichter wurden 0,1 bis 0,2 Mol Methylarylsulfid in 50 bis 100 ml Tetrachlorkohlenstoff gelöst und im Laufe von etwa 1/2 Stunde mit 0,3 bis 0,6 Mol Chlor, gelöst im kleinstmöglichen Volumen Tetrachlorkohlenstoff (für 0,6 Mol Chlor 500 ml), versetzt. Im allgemeinen entwickelte sich nach einigen Minuten unter Selbsterwärmung Chlorwasserstoff. Wenn alles Chlor zugegeben war und die spontane Chlorwasserstoffentwicklung aufhörte, wurde der Kohlbeninhalt auf einem Wasserbad bis zur Beendigung der Chlorwasserstoffentwicklung erwärmt (ca. 3 Stunden). Anschliessend wurde das Lösungsmittel abgezogen, zuletzt im Wasserstrahlvakuum, und das Produkt durch Vakuumdestillation oder Umkristallisieren gereinigt. Die Chlorierungsprodukte waren verhältnismässig stabil und wurden an der Luft und durch kaltes Wasser nur so langsam angegriffen, dass sie sich ohne allzu strenge Vorsichtsmassnahmen handhaben liessen.

Chlormethyl-2-nitrophenylsulfid. Ausgangsmaterial: 23,4 g (0,15 Mol) *o*-Nitrothioanisol und 35,5 g (0,50 Mol) Chlor. Rohausbeute 11,7 g = 38 % der Theorie (F: 89°—94°). Nach Umkristallisieren aus Petroläther und Essigester schmolz das Produkt zwischen 94° und 96°. Literatur[27]: F: 95°. Auch die Elementaranalyse war in Übereinstimmung mit der Zusammensetzung $C_7H_6ClNO_2S$.

Trichlormethyl-3-nitrophenylsulfid. Ausgangsmaterial: 33,8 g (0,2 Mol) *m*-Nitrothioanisol und 46,2 g (0,65 Mol) Chlor. Rohausbeute 29,8 g = 55 % der Theorie (F: 55°—63°). Nach mehrmahligen Umkristallisieren aus Petroläther schmolz die Substanz zwischen 71° und 73°. Literatur[32]: F: 73°—74°.

Trichlormethyl-o-tolylsulfid. Ausgangsmaterial: 27,6 g (0,2 Mol) *o*-Tolylmethylsulfid und 42,6 g (0,6 Mol) Chlor. Zwischen 88°/0,2 mm und 95°/0,2 mm gingen 44,5 g Produkt (92 % der Theorie) über (n_D^{20} 1,5910). Trichlormethyl-*o*-tolylsulfid is teine farblose Flüssigkeit, Kp. 92°/0,1 mm, n_D^{20} 1,5912. (Gef. Cl 43,95; S 13,21. Ber. für $C_8H_7Cl_3S$: Cl 44,03; S 13,27).

Trichlormethyl-m-tolylsulfid. Ausgangsmaterial: 27,6 g (0,2 Mol) *m*-Tolylmethylsulfid und 42,6 g (0,6 Mol) Chlor. Zwischen 99°/0,8 mm und 110°/0,8 mm gingen 35,2 g Produkt (73 % der Theorie) über (n_D^{20} 1,5788). Trichlormethyl-*m*-tolylsulfid ist eine gelbe Flüssigkeit, Kp. 91°/0,2 mm, n_D^{20} 1,5839. (Gef. Cl 44,19; S 12,82. Ber. für $C_8H_7Cl_3S$: Cl 44,03; S 13,27).

Trichlormethyl-4-t-butylphenylsulfid. Ausgangsmaterial: 18,0 g (0,1 Mol) 4-*t*-Butylthioanisol und 21,3 g (0,3 Mol) Chlor. Zwischen 127°/0,4 mm und 132°/0,4 mm gingen 24,2 g (85 % der Theorie) Produkt vom Schmelzpunkt 30°—38° über. Nach mehrmaligem Umkristallisieren aus Petroläther schmolz die Substanz (farblose feine Nadeln) zwischen 41° und 43°. (Gef. Cl 37,33; S 11,20. Ber. für $C_{11}H_{13}Cl_3S$: Cl 37,50; S 11,30).

Trichlormethyl-2-methyl-4-t-butylphenylsulfid. Ausgangsmaterial: 14,9 g (0,077 Mol) 2-Methyl-4-*t*-butylthioanisol und 16,4 g (0,231 Mol) Chlor. Zwischen 123°/0,2 mm und 160°/0,8 mm gingen 17,5 g (71 % der Theorie) Produkt über (n_D^{20} 1,5640). Trichlormethyl-2-methyl-4-t-butylphenylsulfid ist eine gelbe Flüssigkeit, Kp. 160°/0,8 mm. n_D^{20} 1,5632. (Gef. Cl 35,76; S 10,57. Ber. für $C_{12}H_{15}Cl_3S$: Cl 35,73; S 10,77).

*Trichlormethyl-2-*iso*propylphenylsulfid.* Ausgangsmaterial: 18,6 g (0,112 Mol) 2-*Iso*propylthioanisol und 23,9 g (0,336 Mol) Chlor. Zwischen 101°/0,6 mm und 112°/0,8 mm gingen 24,1 g (76 % der Theorie) Produkt über (n_D^{20} 1,5748). Trichlormethyl-2-*iso*propylphenylsulfid ist eine gelbe Flüssigkeit, Kp. 110°/0,8 mm bis 112°/0,8 mm, n_D^{20} 1,5748. (Gef. Cl 40,06; S 11,98. Ber. für $C_{10}H_{11}Cl_3S$: Cl 39,45; S 11,89).

*Chlorierung von 2-Methyl-6-*iso*propylthioanisol.* Aus dem Chlorierungsprodukt, das innerhalb eines grossen Siedeintervalls überging, liess sich keine konstant siedende Fraktion gewinnen, deren Chlorgehalt einer wohldefinierten Zusammensetzung entsprach.

*Trichlormethyl-*o*-anisylsulfid.* Ausgangsmaterial: 30,8 g (0,2 Mol) *o*-Anisylmethylsulfid und 42,6 g (0,6 Mol) Chlor. Zwischen 110°/0,8 mm und 120°/0,8 mm gingen 39,8 g (72 % der Theorie) Produkt über (n_D^{20} 1,5963). Trichlormethyl-*o*-anisylsulfid ist eine gelbe Flüssigkeit, Kp. 115°/1 mm, n_D^{20} 1,5981. (Gef. Cl 40,49; S 12,12. Ber. für $C_8H_7Cl_3OS$: Cl 41,30; S 12,45).

*Trichlormethyl-*m*-anisylsulfid.* Ausgangsmaterial: 30,8 g (0,2 Mol) *m*-Anisylmethylsulfid und 42,6 g (0,6 Mol) Chlor. Zwischen 160°/0,2 mm und 166°/0,2 mm gingen 40,9 g (75 % der Theorie) über. Nach Umkristallisieren aus Äther und Petroläther schmolz das Trichlormethyl-*m*-anisylsulfid (mikrokristalline Agglomerate) zwischen 91° und 92°. (Gef. Cl 41,12; S 12,36. Ber. für $C_8H_7Cl_3OS$: Cl 41,30; S 12,45).

Chlorierung von o*-Chlorthioanisol.* Weder mit 3 Mol noch mit 4 Mol Chlor liess sich *o*-Chlorthioanisol zum Trichlormethyl-2-chlorphenylsulfid chlorieren. Das Chlorierungsprodukt, das sich bei der Destillation einheitlich verhielt, war eine hellgrüne Flüssigkeit, Kp. 144°/13 mm bis 145°/13 mm, n_D^{20} 1,6053. (Gef. Cl 42,52. Ber. für $C_7H_5Cl_3S$: Cl 46,75; für $C_7H_6Cl_2S$: Cl 36,73).

Trichlormethyl-3-chlorphenylsulfid. Ausgangsmaterial: 31,6 g (0,2 Mol) *m*-Chlorthioanisol und 42,6 g (0,6 Mol) Chlor. Zwischen 111°/0,4 mm und 123°/0,4 mm gingen 41,2 g (79 % der Theorie) Produkt über (n_D^{20} 1,5973). Trichlormethyl-3-chlorphenylsulfid ist eine hellgrüne Flüssigkeit, Kp. 104°/0,1 mm, n_D^{20} 1,6013. (Gef. Cl 53,75; S 11,93. Ber. für $C_7H_4Cl_4S$: Cl 54,13; S 12,24).

Chlormethylpentachlorphenylsulfid. Ausgangsmaterial: 29,7 g (0,1 Mol) Pentachlorthioanisol und 21,3 g (0,3 Mol) Chlor. In diesem Fall trat keine spontane Chlorwasserstoffentwicklung auf. Der Kolbeninhalt wurde schon während des Zutropfens der Chlorlösung auf Wasserbadtemperatur gehalten. Rohausbeute 24,6 g = 74 % der Theorie (F: 118°—120°). Nach mehrmaligem Umkristallisieren aus Essigester schmolz das Chlormethylpentachlorphenylsulfid (silberglänzende Blättchen) zwischen 122° und 124°. (Gef. Cl 63,80; S 9,63. Ber. für $C_7H_2Cl_6S$: Cl 64,29; S 9,69).

Chlorierung von o*-Bromthioanisol.* Weder mit 3 Mol noch mit 4 Mol Chlor liess sich *o*-Bromthioanisol zum Trichlormethyl-2-bromphenylsulfid chlorieren. Das Chlorierungsprodukt, das sich bei der Destillation einheitlich verhielt, war eine gelbe Flüssigkeit, Kp. 125°/0,2 mm, n_D^{20} 1,6270. (Gef. Cl 31,84. Ber. für $C_7H_4BrCl_3S$: Cl 34,71; für $C_7H_5BrCl_2S$: Cl 26,07).

Trichlormethyl-3-bromphenylsulfid. Ausgangsmaterial: 40,6 g (0,2 Mol) *m*-Bromthioanisol und 42,6 g (0,6 Mol) Chlor. Zwischen 123°/0,2 mm und 126°/0,2 mm gingen 49,8 g (82 % der Theorie) Produkt über (n_D^{20} 1,6212). Trichlormethyl-3-bromphenylsulfid ist eine hellgrüne Flüssigkeit, Kp. 124°/0,4 mm, n_D^{20} 1,6219. (Gef. Br 26,02; Cl 34,28; S 10,09. Ber. für $C_7H_4BrCl_3S$: Br 26,08; Cl 34,71; S 10,46).

Trichlormethyl-α-naphthylsulfid. Ausgangsmaterial: 34,8 g (0,2 Mol) α-Naphthylmethylsulfid und 46,2 g (0,6 Mol) Chlor. Zwischen 169°/1 mm und 173°/1 mm gingen 47,0 g (85 % der Theorie) Produkt über (n_D^{20} 1,6607). Trichlormethyl-α-naphthylsulfid ist eine gelbe Flüssigkeit, Kp. 151°/0,2 mm, n_D^{20} 1,6624. (Gef. Cl 38,17; S 11,38. Ber. für $C_{11}H_7Cl_3S$: Cl 38,32; S 11,55).

Trichlormethyl-β-naphthylsulfid. Ausgangsmaterial: 34,8 g (0,2 Mol) β-Naphthylmethylsulfid und 42,6 g (0,6 Mol) Chlor. Rohausbeute 31,2 g = 56 % der Theorie (F: 67°—82°). Nach mehrmaligem Umkristallisieren aus Petroläther schmolz das Trichlormethyl-β-naphthylsulfid zwischen 92° und 94° (farblose Nadeln). (Gef. Cl 38,57; S 11,44. Ber. für $C_{11}H_7Cl_3S$: Cl 38,32; S 11,55).

Wir sind dem Institutsvorstand, Herrn Professor A. Fredga, für die Überlassung des Arbeitsplatzes und *Jordbrukets Forskningsråd* sowie der Mathematisch-Naturwissenschaftlichen Fakultät der Universität Uppsala für die finanzielle Unterstützung unserer Arbeit zu Dank verpflichtet.

LITERATUR

1. Senning, A. und Lawesson, S.-O. *Acta Chem. Scand.* **14** (1960) 2230.
2. Kittleson, A. R. *Science* **115** (1952) 84.
3. Aderhold, K. und Fischer, F. *Naturwiss.* **44** (1957) 517.
4. Aderhold, K. *Acta Biol. Med. Germ.* **1** (1958) 455.
5. Fischer, F. und Wacha, O. *J. prakt. Chem.* [4] **12** (1961) 172.
6. Sosnovsky, G. *Chem. Revs.* **58** (1958) 509.
7. Böhme, H. und Gran, H.-J. *Deutsches Patent 875651* (1953); *Chem. Abstr.* **49**, 11862.
8. Truce, W. E., Birum, G. H. und McBee, E. T. *J. Am. Chem. Soc.* **74** (1952) 3594.
9. Richtzenhain, H. und Alfredsson, B. *Ber.* **86** (1953) 142.
10. Böhme, H. und Gran, H.-J. *Ann.* **581** (1953) 133.
11. Kittleson, A. R. und Yowell, H. L. (Standard Oil Development Co.), US Pat. 2553772 (1951); *Chem. Abstr.* **45**, 7292.
12. Ter Horst, W. P. (Olin Mathieson Chemical Corp.), US Pat. 2696502 (1954); *Chem. Abstr.* **49**, 3463.
13. Prey, V. und Gutschik, E. *Monatsh.* **90** (1959) 551.
14. Prey, V. und Gutschik, E. *Monatsh.* **91** (1960) 794.
15. Zincke, T. und Frohneberg, W. *Ber.* **43** (1910) 837.
16. Zincke, T. und Jörg, P. *Ber.* **43** (1910) 3443.
17. Zincke, T. und Müller, J. *Ber.* **46** (1913) 775.
18. Orwoll, E. F. (Sharples Chemicals Inc.), US Pat. 2668853 (1954); *Chem. Abstr.* **49**, 2496.
19. Egen, R. *Diss.* Erlangen 1951; vgl. Pfleger, R. *Angew. Chem.* **65** (1953) 415.
20. Sanna, G. und Stefano, S. *Gazz. chim. ital.* **72** (1942) 305.
21. Yagupolsky, L. M. und Marenets, M. S. *J. Gen. Chem. U.S.S.R.* (Engl. Transl.) **24** (1954) 885.
22. Yagupolsky, L. M. und Marenets, M. S. *J. Gen. Chem. U.S.S.R.* (Engl. Transl.) **26** (1956) 99.
23. Senning, A. und Lawesson, S.-O. *Arkiv Kemi* **17** (1961) 261.
24. Senning, A. und Lawesson, S.-O. *Arkiv Kemi* **17** (1961) 387.
25. Senning, A. und Lawesson, S.-O. *Arkiv Kemi* **17** (1961) 489.
26. Senning, A. und Lawesson, S.-O. *Arkiv Kemi* **18** (1961) 95.
27. Schönberg, A. und Stolpp, T. *Ber.* **63** (1930) 3102.

Eingegangen am 17. Juli 1961.

ACTA CHEMICA SCANDINAVICA 16 (1962) 123–126

Synthesis of Alpha- and Beta Carbon Isotopically Labelled Furan

BØRGE BAK, JØRGEN TORMOD NIELSEN and MARIANNE SCHOTTLÄNDER

Chemical Laboratory of the University of Copenhagen, Copenhagen, Denmark

The preparation of 200 mg quantities of 22 % enriched [α-^{13}C] furan and [β-^{13}C]furan from enriched K^{13}CN is described. The over-all yields are, respectively, 11 and 8 % with respect to K^{13}CN. The first synthesis involves 6 steps, the second 17 steps. The purity, as controlled by the infrared gas-spectrum, was highly satisfactory.

To the best of our knowledge, enriched [α-^{13}C]— and [β-^{13}C]furan have never been synthesized. Their preparation is of interest to the spectroscopist who wants to find the structure of furan by means of the so-called substitution procedure, in which changes in rotational constants, caused by substitution of one atom (^{12}C) by (^{13}C), serve as basis for a calculation of the position of the atom in question.

Also, our procedures worked out may probably serve well in the case of ^{14}C-synthetic work with furan, thus enabling the biologist to follow the role of furan or furan derivatives in the metabolism of living organisms.

[α-^{13}C]FURAN

The sequence of reactions was as follows *:

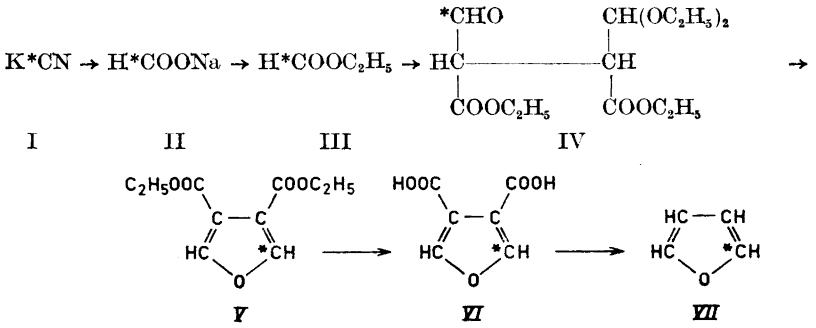

* The asterisk indicates the position which is enriched by ^{13}C.

Essentially following Grant and Turner [1], we converted 6.05 g (0.0929 mole) of commercial, 22 % enriched $K^{13}CN$ (I) to 5.58 g (0.0820 mole) of $H^{13}COONa$ (II). Conversion of this salt to ethyl [^{13}C]formate (III) was carried out according to Burr's procedure [2]. The yield, 6.36 g (0.0857 mole), showed the presence of an impurity, unimportant for the following steps. Formylation [3] of 11.55 g (0.0418 mole) diethyl α-diethoxymethylsuccinate by means of 6.21 g (III) resulted in 6.66 g (0.0219 mole) of diethyl α-[^{13}C]formyl-β-diethoxymethylsuccinate (IV). The infrared spectrum of (IV) showed it to be pure as compared with the spectrum of 'ordinary', highly purified (IV). Conversion [3] of 6.54 g (0.0215 mole) (IV) to diethyl [α-^{13}C]furan-β,β'-dicarboxylate (V) resulted in 3.65 g (0.0172 mole) of (V), the infrared spectrum of which was satisfactory.

3.52 g (0.0166 mole) of (V) was converted to [α-^{13}C]furan-β,β'-dicarboxylic acid (VI) by refluxing with 25 ml 2.5 N NaOH for 2 ½ h, cooling, filtering, addition of 4 ml of water, and subsequent removal of 3 ml solvent by distillation. Addition of 10 ml conc. HCl caused (VI) to precipitate. Filtering and drying for 24 h *in vacuo* over P_2O_5 and NaOH resulted in a yield of 2.20 g (0.0141 mole) of (VI), the infrared spectrum of which was satisfactory.

Only part of (VI) was converted into [α-^{13}C]furan (VII). 750 mg of (VI) mixed with 400 mg Cu, 400 mg CuO, and 5 ml quinoline was heated for 2 h at 180°—190°C in an evacuated, sealed off ampulla. Herafter, the CO_2 produced was removed by distillation *in vacuo* at —80°C. (VII) was collected by subsequent distillation at 0°C *in vacuo*. After 1 h exposure to finely divided NaOH and subsequent distillation, 235 mg (0.0035 mole) of pure (VII) was obtained, its infrared absorption curve being satisfactory. Based on the initial 0.0929 moles of enriched $K^{13}CN$, the over-all yield of this 6-step synthesis was 11 %.

[β-^{13}C]FURAN

The sequence of reactions was as follows:

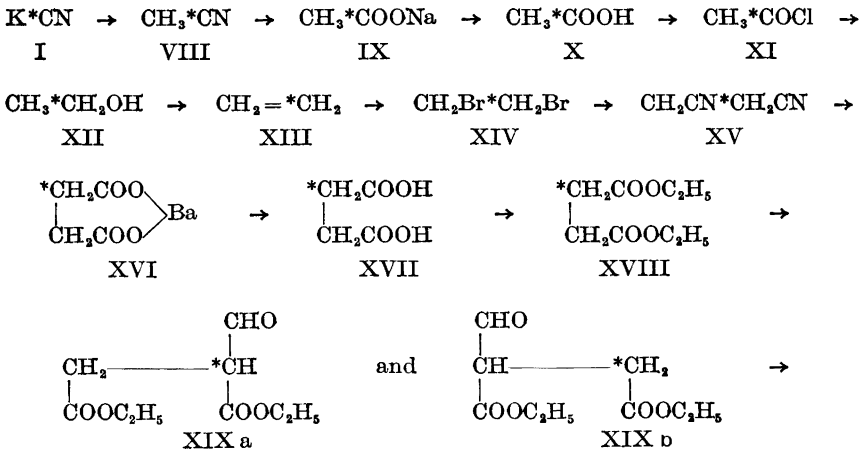

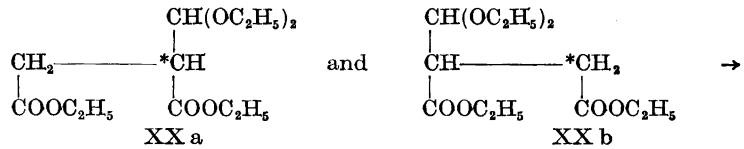

XX a and XX b →

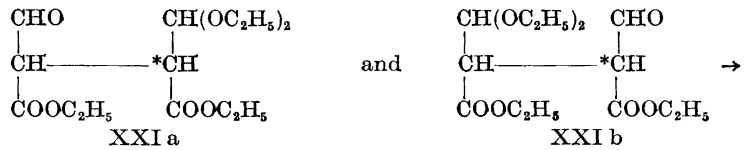

XXI a and XXI b →

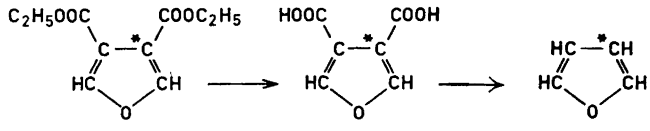

XXII XXIII XXIV

Methyl iodide was converted to $CH_3{}^{13}COONa$ (IX) following Cox *et al.*[4] 1.96 g (0.0301 mole) of commercial 22 % enriched $K^{13}CN$ was used, resulting in 2.24 g (0.0273 mole) of (IX).The procedure, being unsuited for use in larger scale, was repeated 3 times so that eventually 8.79 g (0.1071 mole) of (IX) was obtained. Following Cox and Turner[5], (IX) was converted to 6.15 g (0.1022 mole) of $CH_3{}^{13}COOH$ (X). (X) was transformed into 7.78 g (0.0990 mole) of $CH_3{}^{13}COCl$ (XI). In two separate operations, 4.02 g, respectively 3.76 g of (XI) were reduced to a combined quantity, 4.26 g (0.0923 mole) of $CH_3{}^{13}CH_2OH$ (XII), which in its turn[6], was converted into 14.58 g (0.0775 mole) of (XIV).

This quantity of (XIV) was converted into [α-^{13}C]succinonitrile (XV)[6] and barium [α-^{13}C]succinate (XVI)[6], 16.60 g (0.0655 mole), which was transformed into [α-^{13}C]succinic acid (XVII) by means of 6.50 g (0.0649 mole) conc. H_2SO_4, dissolved in 200 ml of water, stirring the mixture over-night. After filtering and removal of water (XVII) esterification was performed[7], resulting in 10.30 g (0.0592 mole) diethyl [α-^{13}C]succinate (XVIII).

Formylation of 10.10 g (XVIII) with ethyl formate[3] gave 8.45 g (0.0418 mole) of a mixture of diethyl α-formyl-[α-^{13}C]succinate (XIX a) and diethyl β-formyl-[α-^{13}C]succinate (XIX b), 8.34 g of which was converted to 10.16 g (0.0368 mole) of diethyl α-diethoxymethyl-[α-^{13}C]succinate (XX a) and diethyl β-diethoxymethyl-[α-^{13}C]succinate (XX b). Repeated formylation[3] with ethyl formate of 10.06 g of (XX a) and (XX b) gave 6.06 g (0.0199 mole) of diethyl α-diethoxymethyl-β-formyl-[α-^{13}C]succinate (XXI a) and diethyl-β-diethoxymethyl-α-formyl-[α-^{13}C]succinate (XXI b).

Ring closure[3] resulted in 3.36 g (0.0158 mole) of diethyl [β-^{13}C]furan-β,β'-dicarboxylate (XXII) from 5.94 g (XXI a) and (XXI b).

Infrared control of the products XVI → XXII was satisfactory.

Transformation of 3.32 g (0.0157 mole) of (XXII) to 2.15 g (0.0138 mole) of [β-^{13}C]furan-β,β'-dicarboxylic acid (XXIII) and subsequent conversion of part of (XXIII), 750 mg, to 230 mg (0.0034 mole) of [β-^{13}C]furan (XXIV) were carried out as indicated under [α-^{13}C]furan.

Based on the initial 0.1204 moles of enriched K^{13}CN, the over-all yield of this 17-step synthesis was 8 %.

REFERENCES

1. Grant, D. G. and Turner, H. S. *Nature* **165** (1950) 153.
2. Burr, J. G. *J. Am. Chem. Soc.* **73** (1951) 823.
3. Kornfeld, E. C. and Jones, R. G. *J. Org. Chem.* **19** (1954) 1671.
4. Cox, J. D., Turner, H. S. and Warne, R. J. *J. Chem. Soc.* **1950** 3167.
5. Cox, J. D. and Turner, H. S. *J. Chem. Soc.* **1950** 3176.
6. Bak, B., Christiansen, J. and Nielsen, J. T. *Acta Chem. Scand.* **14** (1960) 1865.
7. Thielepape, E. *Ber.* **66** (1933) 1454.

Received July 8, 1961.

ACTA CHEMICA SCANDINAVICA 16 (1962) 127–134

Immunological Studies of Modified and Enzymically Degraded β-Lactoglobulin and α-Lactalbumin

C. BENGTSSON, L. Å. HANSON and B. G. JOHANSSON

Dept. of Bacteriology and Dept. of Medical Biochemistry, University of Gothenburg, Sweden

α-Lactalbumin and β-lactoglobulin were modified by dinitrophenylation, acetylation or esterification. Immune electrophoretic studies of the modified proteins indicated that a modification of amino groups did not necessarily inhibit the immunoprecipitation reaction with antibodies against the native proteins. Esterification of carboxyl groups in the proteins diminished their ability to form immunoprecipitates.

Studies of tryptic hydrolysates of native or acetylated β-lactoglobulin did not reveal any fragment with ability to precipitate with antibodies against the native protein. Similar studies on α-lactalbumin demonstrated several precipitation lines, but only one of them was obviously formed by native α-lactalbumin, whereas the others were due to trace impurities of serum albumin in the preparation.

Several studies have shown that chemical modification and enzymic degradation can be used in the investigations of groupings determining the antigenic properties of proteins, *e.g.* ribonuclease [1], human serum albumin [2–4], bovine serum albumin [5–9], ovalbumin [10], rabbit γ-globulin [11], and human γ-globulin [12–15].

The present report comprises a study of chemically modified and enzymically degraded α-lactalbumin and β-lactoglobulin from bovine milk whey. These proteins were chosen as they can be easily prepared, have low molecular weights and are fairly well-characterized.

MATERIALS AND METHODS

Preparation of proteins. α-Lactalbumin and β-lactoglobulin were prepared according to Aschaffenburg and Drewry [16] and were recrystallized at least five times before use. The two proteins were both found to be pure by immune electrophoresis. Using very high concentrations of the α-lactalbumin preparation, however, a faint serum albumin precipitate was also formed. This impurity of serum albumin could be removed by gel filtration of the α-lactalbumin preparation on Sephadex G-75. The gel filtration procedure was essentially the same as the technique described below for gel filtration of tryptic hydrolysates except using a "Uvicord ultraviolet absorptiometer" (LKB-produkter AB,

Stockholm) for continuous registration in the filtrate of material absorbing ultraviolet light of wave length 253.7 mμ (spectral line obtained from a mercury vapour lamp).

2,4-Dinitrophenylated proteins (DNP-proteins). The proteins were dinitrophenylated according to Sanger [17] by which procedure amino groups are known to react.

Acetylated proteins. Acetylation of amino groups was performed with acetic anhydride as described by Radichevich *et al* [18]. Acetyl determination on the products were performed according to Fraenckel-Conrat *et al.*[19].

Methoxylated proteins. Esterification of the carboxyl groups was performed by treatment of the proteins with dry methanol containing hydrochloric acid at 0° for 24 h [19].

Tryptic degradation of the proteins. The protein (0.5 g) was dissolved in 10 ml 0.01 M tris(hydroxymethyl-)aminomethane-hydrochloric acid (THAM-HCl) buffer, pH 8.0, containing 0.05 M sodium chloride and incubated in a water bath at 37°C. The pH was adjusted to 8.25 and 25 mg of trypsin (2 × crystallized, 50 % w/w $MgSO_4$, obtained from Mann Research Lab., USA) was added. The degradation was followed by recording the amount of 0.05 M NaOH required to keep the pH at 8.25 (TT 1 titrator, Radiometer, Copenhagen). After about 4 h another 25 mg of trypsin was added. After 6 h the reaction was interrupted by freezing the incubation mixture at −20°C, where it was kept until use.

Gel filtration of tryptic hydrolysate of α-lactalbumin. Gel filtration according to Porath and Flodin [20] was performed on Sephadex G-50 (Pharmacia, Uppsala, Sweden) having a water regain of 4.9 per g dry gel. A column of the dimensions 5 × 46 cm was packed as described by Flodin [21] and was equilibrated with the buffer used in the degradation experiments. 200−500 mg of hydrolysate was applied to the column and was filtrated with a flow rate of 40−60 ml/h. The filtrate was collected in 10 ml fractions, and the optical density of each fraction was determined at 280 mμ in a Zeiss spectrophotometer, model PMQ II using 1 cm cells. The filtration was carried out at a temperature of +4°C. The fractions obtained were pooled, desalted by filtration through a column of Sephadex G-25 which was equilibrated with a 0.03 M triethylammonium carbonate buffer pH 8.5 and finally they were lyophilized.

Immunological material and techniques. Rabbit immune sera against bovine milk and colostrum and the isolated proteins were produced by weekly subcutaneous injections on rabbits.

Agar gel electrophoresis and immune electrophoresis were performed according to Grabar and Williams [22] in the modifications of Wadsworth and Hanson [23]. Comparative immune electrophoresis was carried out according to Wadsworth and Hanson [23].

RESULTS

Studies of chemically modified proteins

Modification of amino groups was carried out in two ways, by treatment with Sanger's reagent giving DNP-proteins and by N-acetylation.

DNP-α-lactalbumin was soluble at pH 8.6. The preparation gave no detectable reaction with ninhydrin indicating a practically complete modification of amino groups. By gel electrophoresis it moved as a yellow spot with a much higher mobility than the untreated protein due to the absence of positively charged amino groups, which results by dinitrophenylation (Figs. 1 a and b). No immunoprecipitate was obtained with this derivative. By *acetylation of the α-lactalbumin* a similar change in mobility was observed but this derivative formed a precipitation line with anti-milk sera (Fig. 1 c). The acetyl determination on the acetylated α-lactalbumin indicated the presence of 14.5 acetyl groups per molecule of protein, which is in accordance with 12 lysin residues [24] and one N-terminal residue [25] in the protein. In addition no reaction was obtained with ninhydrin.

DNP-β-lactoglobulin, obtained as a poorly soluble product, moved as a broad zone extending from the starting basin, probably due to adsorption to

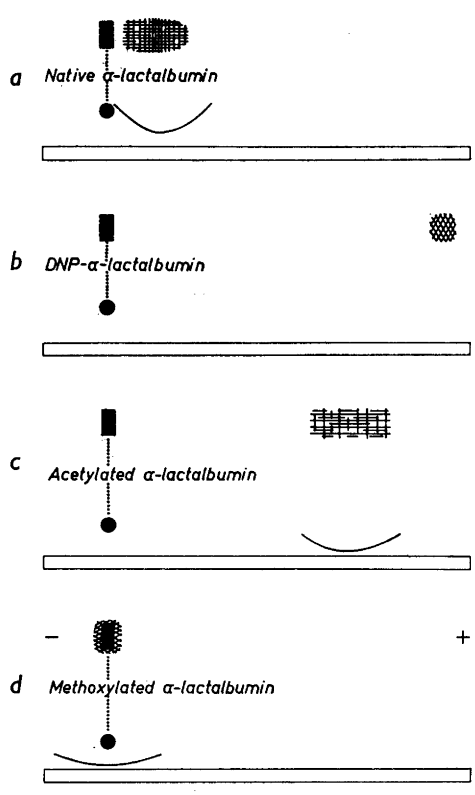

Fig. 1. Agar gel electrophoresis and immune electrophoresis of native (a) and modified (b—d) α-lactalbumin. Antiserum against bovine colostrum was employed.

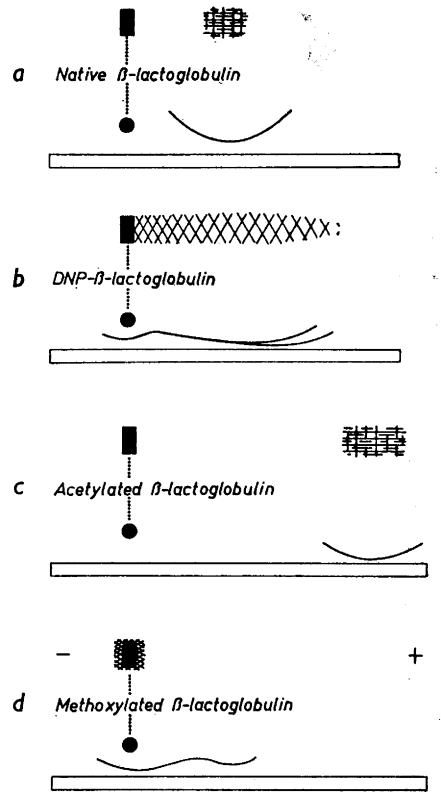

Fig. 2. Agar gel electrophoresis and immune electrophoresis of native (a) and modified (b—d) β-lactoglobulin. Antiserum against bovine colostrum was employed.

the agar gel. In immune electrophoresis a complex pattern of lines was obtained (Fig. 2 b). As occurred with α-lactalbumin *acetylation of β-lactoglobulin* resulted in a fast moving component with ability to precipitate anti-β-lactoglobulin antibodies (Fig. 2c).

Carboxyl groups of the two proteins were modified by esterification. *The methoxylated proteins* did not move from the starting basin in gel electrophoresis. By immune electrophoresis both proteins gave a faint precipitation line at the starting basin. The precipitate obtained with methoxylated β-lactoglobulin had an additional maximum with the same electrophoretic localization as native β-lactoglobulin (Figs. 1 d and 2 d).

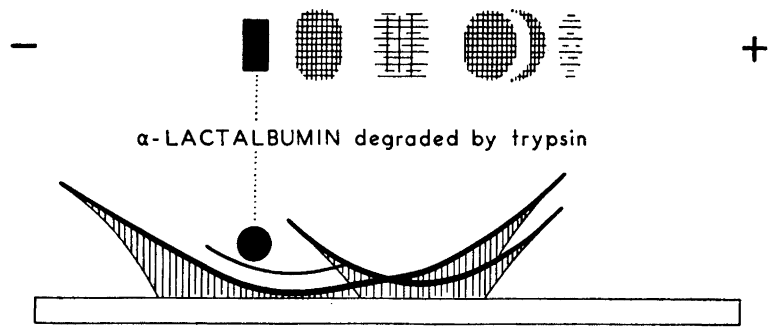

Fig. 3. Agar gel electrophoresis and immune electrophoresis of tryptic hydrolysate of α-lactalbumin.

Studies on proteolytically degraded proteins

Immune electrophoretic analysis of *β-lactoglobulin hydrolysate* after tryptic degradation showed in all experiments only one line situated in the same electrophoretic region as native β-lactoglobulin. A reaction of identity was also obtained with the native protein by comparative immune electrophoresis.

Tryptic *degradation of α-lactalbumin* prepared according to Aschaffenburg and Drewry gave rise to at least three precipitates in immune electrophoresis (Fig. 3). Precipitate A had the same localization as native α-lactalbumin. Precipitate B was found in the same electrophoretic region but localized somewhat farther from the immune serum basin. The latter precipitate showed a reaction of partial identity (or possibly of inhibition) with a precipitate, C,

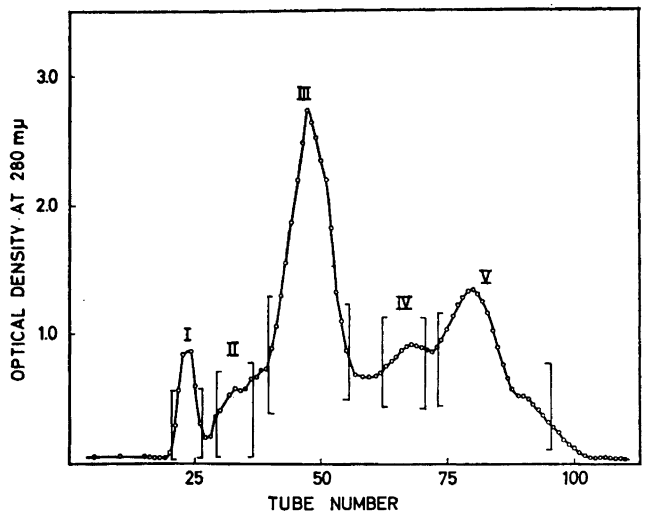

Fig. 4. Gel filtration diagram of tryptic hydrolysate of α-lactalbumin, filtrated through Sephadex G-50. Column dimensions 5 × 46 cm.

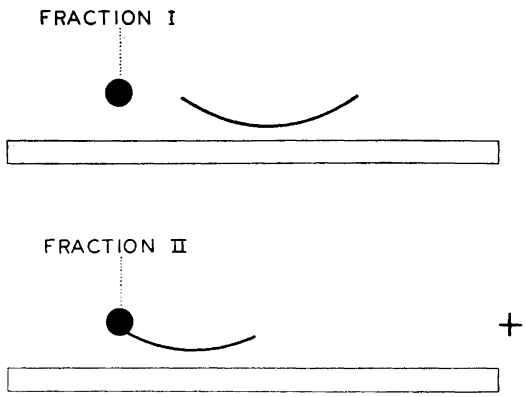

Fig. 5. Immune electrophoresis of fractions I and II of the tryptic hydrolysate of α-lactalbumin obtained by gel filtration. Immune serum employed was anti-bovine colostrum serum.

situated farther towards the anode. Gel filtration of the enzymatic hydrolysate and subsequent lyophilization was performed to obtain concentrated peptide fractions (Fig. 4). Five fractions were obtained and were examined by immune electrophoresis. Fraction I was found to form only one precipitate in the same region as precipitate C, while fraction II formed a faint precipitate in the area of native α-lactalbumin (Fig. 5). With fractiosn III—V no precipitates were observed.

Comparative immune electrophoretic analyses of the α-lactalbumin hydrolysate and of bovine milk was performed and it was then found that the precipitate A identified with the α-lactalbumin line but the precipitate C showed a reaction of identity with the blood serum albumin precipitate. The

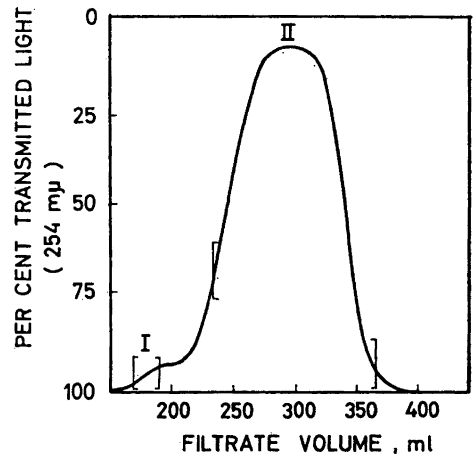

Fig. 6. Gel filtration of α-lactalbumin (5 times crystallized) filtrated through Sephadex G-75. Light transmission at 254 mμ continously recorded by a "Uvicord" ultraviolet absorptiometer.

line B showed a reaction of partial identity with the serum albumin precipitate. The precipitate formed by fraction I (Fig. 5) identified with serum albumin. The precipitate formed by fraction II (Fig. 5) gave a reaction of identity with precipitate A, which identified with native α-lactalbumin.

Gel filtration of the crystalline α-lactalbumin on Sephadex G—75 (Fig. 6) revealed a small but definite impurity (fraction I) which had an electrophoretic mobility of serum albumin. The remaining large fraction (II in Fig. 6) was homogeneous α-lactalbumin in immune electrophoresis. Tryptic hydrolysis of the purified α-lactalbumin formed only a faint precipitate identifying with α-lactalbumin.

Tryptic *degradation of acetylated α-lactalbumin and β-lactoglobulin* gave similar precipitates as the unhydrolyzed protein derivatives.

DISCUSSION

In agreement with other reports [3,4] acetylation of the amino groups in the proteins does not seem to affect the ability to precipitate with antibodies against the native proteins as judged from the immune electrophoretic results. The proteins used seem to have been completely substituted as seen from determination of their ninhydrin colour values and from acetyl determinations of the α-lactalbumin derivative.

The disappearance of the precipitation ability of α-lactalbumin induced by blocking of the amino groups with Sanger's reagent might be due to the introduction of a large number of aromatic residues causing a steric hindrance for the antigen-antibody reaction. DNP-β-lactoglobulin, however, gave a complex precipitation pattern. It has been reported that 1-fluoro-2,4-dinitrobenzene reacts incompletely with the ε-amino groups of lysine in β-lactoglobulin [26] and this might explain these precipitation patterns as the splitting of the precipitate may be caused by various degrees of substitution of the amino groups. Two precipitation lines have been obtained with an antigen extensively or partially diazotized or halogenated [27,28]. The complex precipitation pattern might also be due to protein denaturation accompanying the modification procedure.

The localization of the methoxylated proteins at the starting basin after electrophoresis could be due to either a change in the mobility or to denaturation of the protein molecule by the treatment, causing aggregation of the protein molecules or adsorption to the agar gel. The esterified proteins showed an ability to form immuno-precipitates. No quantitative evaluation of precipitating ability or degree of esterification of the antigen was performed but it was noted that very faint precipitates were obtained with the esterified proteins. Sri Ram and Maurer [7] and Steinbuch *et al.* [4] have reported a diminished precipitating ability with increased degree of esterification of serum albumin.

The immunological studies of the enzymic hydrolysates did not give evidence that any fragments of β-lactoglobulin or α-lactalbumin with immuno-precipitating ability were present. These findings do not exclude, however, that an immunologically inert part of the antigen molecule might have been split off without change of the determinant groups or of the electrophoretic mobility of the antigen. The multiplicity of lines in the α-lactalbumin hydro-

lysates were due to the presence of trace amounts of blood serum albumin in the preparations, not demonstrable by zone electrophoresis or moving boundary electrophoresis. The serum albumin impurity in the α-lactalbumin preparation could be removed by gel filtration. Hydrolysates of this further purified α-lactalbumin only formed a faint α-lactalbumin precipitate.

Tryptic hydrolysates of the acetylated proteins each gave only one immunoprecipitate probably formed by unhydrolyzed proteins. It is known that blocking of the ε-amino groups of lysine inhibits the tryptic hydrolysis of the peptide bonds involving the lysin carboxyl groups [19], thus resulting in hydrolysis only of peptide bonds formed by arginine carboxyl groups. The α-lactalbumin molecule has twelve lysine residues [24] and only one arginine residue [24] and it has been reported that only one peptide bond is split in acetylated α-lactalbumin by trypsin [30]. Thus at least one relatively large peptide might be expected by the hydrolysis. The immunological experiments, however, did not demonstrate any fragment with retained immunoprecipitating ability.

Recently Richard *et al.*[9] have claimed that serum albumin peptides with molecular weights of 3 200 to 6 800 can form immunoprecipitates. The concentration of peptides necessary for a precipitation reaction was about 1 000 times that of the albumin. In judging the results of Richard *et al.* the great sensitivity of the immunological techniques should be considered. Even extremely small impurities not revealed by physico-chemical homogeneity tests can give false results, especially when using very high concentrations. This is illustrated by our findings of albumin impurities in the five times recrystallized α-lactalbumin.

REFERENCES

1. Singer, S. J. and Richards, F. M. *J. Biol. Chem.* **234** (1959) 2911.
2. Lapresle, C. *Ann. Inst. Pasteur* **97** (1959) 626.
3. Houghton, P. B. and Martin, N. H. *Nature* **182** (1958) 329.
4. Steinbuch, M., Fine, J. M. and Battistini, A. *Clin. Chim. Acta* **5** (1960) 345.
5. Porter, R. R. *Biochem. J.* **66** (1957) 677.
6. Maurer, P. H. *Arch. Biochem. Biophys.* **79** (1959) 13.
7. Sri Ram, J. and Maurer, P. H. *Arch. Biochem. Biophys.* **80** (1959) 462.
8. Sri Ram, J. and Maurer, P. H. *Arch. Biochem. Bhiophys.* **83** (1959) 223.
9. Richard, A. J., Beck, S. and Hoch, H. *Arch. Biochem. Biophys.* **90** (1960) 309.
10. Kaminski, M. *Ann. Inst. Pasteur* **98** (1960) 51.
11. Porter, R. R. *Nature* **182** (1958) 670.
12. Augustin, R. and Hayward, B. J. *Nature* **187** (1960) 129.
13. Edelman, G. M., Heremans, J. F., Heremans, M.-Th. and Kunkel, H. G. *J. Exptl. Med.* **112** (1960) 203.
14. Hanson, L. Å. and Johansson, B. G. *Nature* **187** (1960) 599.
15. Burtin, P. *Proc. 8th Colloquium Bruges 1960, Protides of the Biological Fluids.* Elsevier, Amsterdam 1960, p. 119.
16. Aschaffenburg, R. and Drewry, J. *Biochem. J.* **65** (1957) 273.
17. Sanger, F. *Biochem. J.* **39** (1945) 507.
18. Radichevich, I., Becker, M. M., Eitingon, M., Gettler, V. H., Toralballa, G. C. and Galdwell, M. L. *J. Am. Chem. Soc.* **81** (1959) 2845.
19. Fraenkel-Conrat, H., Bean, R. S. and Lineweaver, H. *J. Biol. Chem.* **177** (1949) 385.
20. Porath, J. and Flodin, P. *Nature* **183** (1959) 1657.
21. Flodin, P. *J. Chromatography* **5** (1961) 103.
22. Grabar, P. and Williams, C. A. *Biochim. et Biophys. Acta* **10** (1953) 193.

23. Wadsworth, C. and Hanson, L. Å. *Intern. Arch. Allergy Appl. Immunol.* **17** (1960) 165.
24. Gordon, W. G. and Ziegler, J. *Arch. Biochem. Biophys.* **71** (1957) 473.
25. Yasomoku, K. T. and Wilcox, P. E. *J. Biol. Chem.* **231** (1958) 309.
26. Porter, R. R. *Biochim. et Biophys. Acta* **2** (1948) 105.
27. Augustin, R. *Immunology* **2** (1959) 148.
28. Wilson, M. W. and Pringle, B. H. *J. Immunol.* **77** (1956) 324.
29. Neurath, H. and Schwert, G. *Chem. Revs.* **46** (1950) 69.
30. Weil, L. and Telka, M. *Arch. Biochem. Biophys.* **71** (1957) 473.

Received July 19, 1961.

ACTA CHEMICA SCANDINAVICA 16 (1962) 135–141

The Kinetics and Mechanism of the Decomposition of 2,4-Dihydroxy-1,4-benzoxazin-3-one

J. B-SON BREDENBERG, ERKKI HONKANEN and ARTTURI I. VIRTANEN

Laboratory of the Foundation for Chemical Research, Biochemical Institute, Helsinki, Finland

The kinetics of the decomposition of 2,4-dihydroxy-1,4-benzoxazin-3-one in aqueous buffer solutions has been investigated. The reaction follows first-order kinetics and is dependent on the concentration of the anion of the compound. The reaction rate in pure water and ethanol has been studied and is discussed in relation to earlier results. A mechanism is postulated for the reaction.

The antifungal compound 2,4-dihydroxy-1,4-benzoxazin-3-one (Ia)[1], occurring as the glucoside [2] in rye seedlings, has been found to decompose into 2(3)-benzoxazolinone (V) and formic acid upon heating in aqueous solution [1]. The rather unusual reaction which corresponds to a disproportionation has been studied with labelled carbon and the atom at the position 2 has been found to split off [3]. Based on the stability of related compounds it has been concluded that the presence of a N-hydroxyl group and an easily ruptured O(1)-C(2) bond is a prerequisite for this reaction.

In order to investigate the decomposition more closely the kinetics of the reaction has been studied. Some earlier results [2] seemed to indicate that the relative amount of benzoxazolinone formed from the benzoxazinone decreases when the concentration rises. The results were, however, only preliminary and needed confirmation. The formation of benzoxazolinone in an extraction procedure earlier used [5] also necessitated a renewed investigation.

The reaction was first studied in distilled water. A dilute solution of the compound in water was thermostated and ultraviolet spectra taken from samples withdrawn at intervals. The series of spectra obtained (Fig. 1) gave two isosbestic points at 232 and 221 mμ, thus showing that only the starting material and the reaction product contribute to the spectra. The rate-determining step is dependent on the concentration of the benzoxazinone. The reaction rate, calculated from the absorption intensities at 252 mμ, could not, however, be correlated with any definite order of reaction.

The benzoxazinone (Ia) is an acid with a pK value 7.02 [1]. Since a stronger acid, formic acid ($K = 1.77 \times 10^{-4}$)[6], is formed the difficulties in obtaining

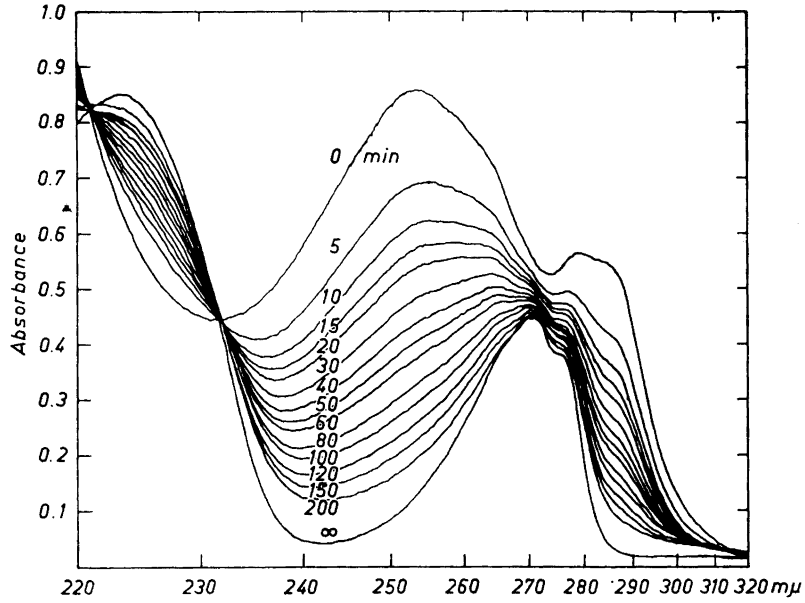

Fig. 1. The decomposition of 2,4-dihydroxy-1,4-benzoxazin-3-one in distilled water, $c_0 = 10^{-4}$ mole/l, temperature 90°. The time is given in minutes.

a definite reaction order could be ascribed to a pH effect. The reaction was therefore performed in buffer solutions at different pH values. The reaction now followed first-order kinetics (Table 1). The order of reaction was further checked by measuring the rates at a tenfold concentration (pH 4.0 and 7.0). The rate constants at the same pH value were identical within the limits of error. The rates depended strongly on the pH but leveled off to a value of about 1.8×10^{-1} min^{-1} (75°) at pH values above 7.

The pH-rate dependence can be explained on the assumption that the benzoxazinone anion (Ib) is the rate-determining entity. The reaction can be pictured as follows:

$$\mathrm{HA} \underset{}{\overset{K_1}{\rightleftharpoons}} \mathrm{A^{\ominus}} + \mathrm{H^{\oplus}}$$

$$\downarrow k_A$$

$$\mathrm{B} + \mathrm{HCOO^{\ominus}}$$

$$\Downarrow K_2$$

$$\mathrm{HCOOH}$$

If the degree of dissociation of HA is α, the observed rate constant k at a constant pH is obtained from

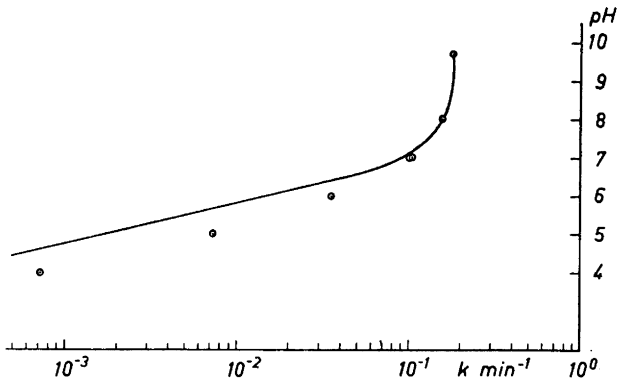

Fig. 2. The observed rate constants at 75° plotted against pH. The solid line is the theoretical curve for $k = k_A a (k_A = 1.8 \times 10^{-1} \text{min}^{-1}, K_1 = 10^{-7})$.

$$\frac{dB}{dt} = k\,[HA] = k_A\,a[HA] \tag{1}$$

$$k = k_A\,a \tag{2}$$

In Fig. 2 the theoretical curve for the values $K_1 = 10^{-7}$ and $k_A = 1.8 \times 10^{-1}$ min^{-1} is given together with the observed rate constants. There is a close agreement between the observed and calculated values. The deviations may be partly ascribed to the uncertainty in the values of K_1 and k_A and partly to the different buffer solutions used.

The energy of activation of the reaction at pH 7.0 was 24.1 kcal/mole. Due to the uncertainty in K_1 the entropy of activation cannot be calculated.

The decomposition rate of the benzoxazinone in pure water can be nicely explained from the reaction scheme. The basic equations are

$$K_1 = \frac{[H^{\oplus}][A^{\ominus}]}{[HA]} \tag{3} \qquad K_2 = \frac{[H^{\oplus}][HCOO^{\ominus}]}{[HCOOH]} \tag{4}$$

$$[H^{\oplus}] = [A^{\ominus}] + [HCOO^{\ominus}] + [OH^{\ominus}] \tag{5}$$

$$[HCOO^{\ominus}] + [HCOOH] = [B] = c_0 - ([HA] + [A^{\ominus}]) \tag{6}$$

were c_0 is the initial concentration. Since $[OH^{\ominus}]$ can be neglected eqn. (7) is obtained.

$$[H^{\oplus}] = \frac{2([HA]\,(K_1 - K_2 + K_2 c_0)}{K_2 + \sqrt{K_2^2 + 4K_2 c_0 + 4[HA](K_1 - K_2)}} \tag{7}$$

The pH of the solution (Fig. 3) drops rapidly in the first part of the reaction which explains the corresponding drop in the apparent first-order rate constants. The pH of the solution decreases when c_0 increases. This explains

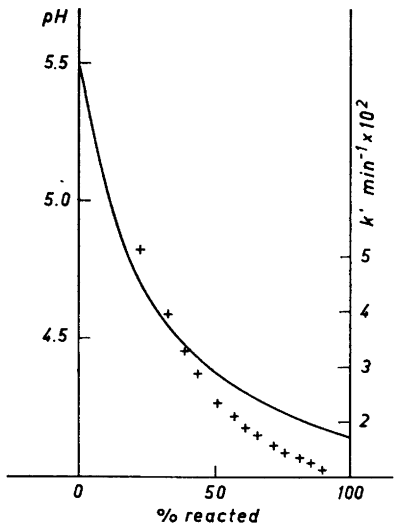

Fig. 3. The change of pH, calculated from eqn. (7), (solid line, left scale) and the apparent first-order rate constants, k', (temperature 90°) (crosses, right scale) in pure water, $c_0 = 10^{-4}$ mole/l.

the earlier results [2] as a result of the more slowly occurring reaction at the higher concentrations with corresponding decrease in benzoxazolinone yield after the same time.

The observation that the benzoxazinone decomposes rather slowly in pure water raised the question as to how benzoxazolinone had been obtained in the earlier isolation procedures [5] where the temperature and pH were kept low throughout the isolation. Since an *iso*propanol-water (8:2) solution had been used in the procedure mentioned, the decomposition rate was measured in 80 % ethanol. (Ethanol was preferred for practical reasons.) The decomposition rate was found to be much higher in ethanol than in water in the first part of the reaction (Fig. 4). Since the isolation procedure involved several vacuum evaporation stages where the formic acid formed was partly removed continuously, the reaction rate probably was rapid during the isolation.

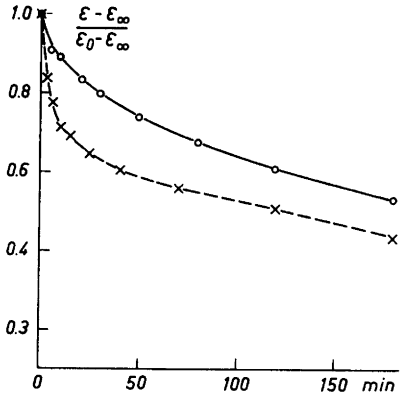

Fig. 4. The decomposition curves for 2,4-dihydroxy-1,4-benzoxazin-3-one in pure water (solid line) and in 80 % ethanol (broken line). Temperature 75°, $c_0 = 10^{-4}$ mole/l.

As already pointed out, the decomposition reaction is of an unusual type of which, so far as the authors are aware, no precedent is known. Difficulties are experienced in postulating a completely satisfactory mechanism. The reaction is difficult to reconcile with a Lossen-type rearrangement. In the mechanism depicted below the major features are accounted for.

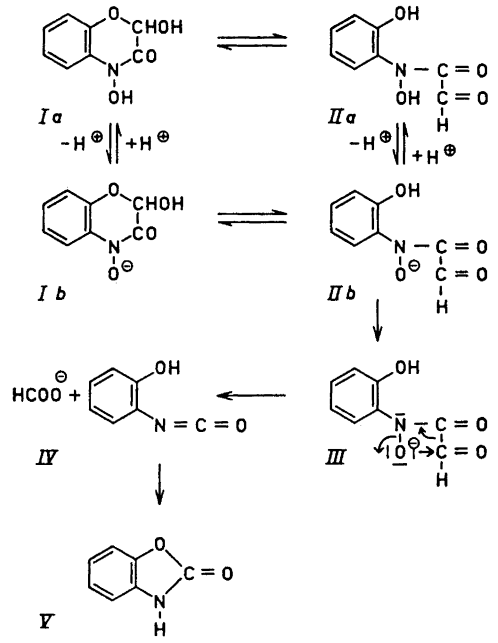

From the kinetic results it is known that no intermediate substance is formed in measurable quantities and that the reaction rate is proportional to the anion (Ib) concentration which in turn is a function of the dissociation constant K_1 only. The step I→II involves a semiacetal-aldehyde equilibrium, the reaction rate of which is known to be acid-base-catalysed and thus pH-dependent [7]. It is necessary to postulate that the I ⇌ II equilibrium which is on the left side is rapidly attained in the pH-range used. The rate-determining step would then be IIb→IV. The intermediate III depicts the concurrent breaking of the N—O and C—C bonds and the formation of the formate ion. The last step IV→V corresponds to the latter part of several benzoxazolinone syntheses methods [8].

The formation of benzoxazolinone is quantitative in the pH-range 4—8. At pH 9.7 there was a slow formation of a small amount of side products exhibiting absorption at 320 mμ. In 0.1 N hydrochloric acid the reaction deviated completely from the normal course. This decomposition has not been investigated further.

It has been found [3,4] that 4-hydroxy-1,4-benzoxazine-2,3-dione (VI) also decomposes with formation of benzoxazolinone when heated in aqueous solution. The rate of decomposition of this compound has been determined

Table 1. The first-order rate constants of the decomposition of 2,4-dihydroxy-1,4-benzoxazin-3-one in buffer solutions.

pH	Temperature °C	Concentration mole/l	k min^{-1}
9.7	75°	10^{-4}	1.81×10^{-1}
8.0	75°	10^{-4}	1.55×10^{-1}
7.0	90°	10^{-4}	4.05×10^{-1}
	82.5°	10^{-4}	2.66×10^{-1}
	75°	10^{-3}	1.00×10^{-1}
	75°	10^{-4}	1.03×10^{-1}
	67.5°	10^{-4}	4.74×10^{-2}
	60°	10^{-4}	2.25×10^{-2}
6.0	75°	10^{-4}	3.57×10^{-2}
5.0	75°	10^{-4}	7.26×10^{-3}
4.0	75°	10^{-3}	7.25×10^{-4}
	75°	10^{-4}	7.20×10^{-4}
3.9	90°	10^{-4}	4.07×10^{-4}

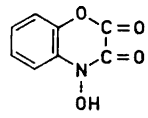

VI

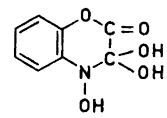

VII

in the same way as for the decomposition of (Ia) at a pH of 6.0 and a temperature of 60° ($c_0 = 2 \times 10^{-4}$ mole/l). The reaction followed first order kinetics. The rate constant, $k = 2.43 \times 10^{-2}$ min^{-1}, is higher than that of the benzoxazinone Ia under the same conditions, as would be expected from the postulated mechanism.

The ultraviolet spectra of the compound VI in absolute ether (λ_{max} 232, 305 mμ, log ε 3.86, 3.86), ethanol (303 mμ, 3.76)[4], and water or buffer solutions (pH 3—7) (279 mμ, 3.51) indicates that it probably occurs as a hydrate, VII, in aqueous solutions. The hydrate formation is rapid.

EXPERIMENTAL

Solvents and starting materials. The benzoxazinone compounds were synthetical[4,9]. They were purified by crystallisation before use. The water was distilled in an all-silica apparatus. The reagents for the buffer solutions were analytical grade. The buffer solutions used were: pH 3.9—5.0 Sörensen citrate buffer, pH 5.4—8.0 Sörensen phosphate buffer, pH 9.7 Clark and Lubs borate buffer. The citrate buffer slowly turned cloudy in the experiments continued for several days.

Apparatus. The temperature of the thermostat was controlled to $\pm 0.°05$. The spectra were measured with a Beckman DK-2 spectrophotometer.

Performance of the measurements. The compound was rapidly dissolved by shaking it with the solution which had been previously warmed to the desired temperature. Samples were withdrawn at intervals, measured from the time of dissolving the compound. The samples were rapidly chilled to room temperature and the spectrum (350—220 mμ) recorded. Spectra of the starting material as well as the end product were recorded by dissolving the compounds at room temperature in the solution used. The spectra were recorded immediately after dissolution.

The spectra of the dihydroxybenzoxazinone series had, in the pH-range 3.9—6.0, isosbestic points at 221 and 232 mμ, at pH 7.0 they were at 224 and 230 mμ, and at pH 9.7 at 231, 254, and 322 mμ. The lines did not intersect at pH 8.0. The spectra in 0.1 N HCl (90°) gave, up to 60 min after the start of the reaction, a series of spectra which had no isosbestic points. After this time isosbestic points were formed at 234 and 269 mμ.

The spectra from 4-hydroxy-1,4-benzoxazine-2,3-dione had isosbestic points at 233, 253, and 278 mμ.

The reaction rates were calculated from the extinction values at 252 mμ (pH 3.9—6.0) or 290 mμ (pH 7.0—9.7) and inserted into the equation

$$k = \frac{1}{t} \ln \frac{\varepsilon_0 - \varepsilon_\infty}{\varepsilon - \varepsilon_\infty}$$

where ε_0 is the extinction value of the starting material and ε_∞ that of the reaction product. For compound VI the values at 270 mμ were used.

The activation energy was calculated by the least-square method.

This investigation belongs to a research project under U.S. Public Law No 480, 83rd Congress.

REFERENCES

1. Virtanen, A. I. and Hietala, P. K. *Acta Chem. Scand.* **14** (1960) 499.
2. Hietala, P. K. and Virtanen, A. I. *Ibid.* **14** (1960) 502.
3. Honkanen, E. and Virtanen, A. I. *Ibid.* **15** (1961) 221.
4. Honkanen, E. and Virtanen, A. I. *Ibid.* **14** (1960) 1214.
5. Virtanen, A. I. and Hietala, P. K. *Ibid.* **9** (1955) 1543.
6. Dippy, J. F. J. *Chem. Revs.* **25** (1939) 151.
7. Brönsted, J. N. and Guggenheim, E. A. *J. Am. Chem. Soc.* **49** (1927) 2554.
8. Müller, E. (Ed) *Methoden der organischen Chemie.* Band VIII. Georg Thieme Verlag, Stuttgart 1952, p. 145.
9. Honkanen, E. and Virtanen, A. I. *Acta Chem. Scand.* **14** (1960) 504.

Received June 30, 1961.

ACTA CHEMICA SCANDINAVICA 16 (1962) 142–148

3-(3-Carboxy-4-hydroxy-phenyl)-L-alanine (*m*-Carboxy-L-tyrosine), a New Amino Acid Isolated from Seeds of *Reseda odorata* L.*

P. OLESEN LARSEN and ANDERS KJÆR

Department of Organic Chemistry, The Royal Veterinary and Agricultural College, Copenhagen, Denmark

A new amino acid, isolated from the free amino acid fraction of seeds of *Reseda odorata* L., is demonstrated to be 3-(3-carboxy-4-hydroxy-phenyl)-L-alanine (*m*-carboxy-L-tyrosine) (I).

The isolation was accomplished by means of strongly acid and weakly basic ion exchange resins and the final purification by recrystallization from water. Elemental analysis, ultra-violet and infra-red absorption spectra, protolytic properties and other data suggested 3-(3-carboxy-4-hydroxy-phenyl)-alanine as a likely structure for the isolate. Authentic material with L-configuration was synthesized by a series of steps departing from 3-nitro-L-tyrosine (II) and proceeding *via* 3-(3-cyano-4-hydroxy-phenyl)-L-alanine (IV). On comparison, the synthetic specimen proved identical with the natural amino acid. The latter represents the third example of *m*-carboxy-substituted aromatic amino acids encountered in higher plants.

During investigations of the contents of free amino acids in certain plants containing isothiocyanate-producing glucosides, attention was directed to species of the family *Resedaceae*. When a seed extract of the popular flower garden subject mignonette (*Reseda odorata* L.) was subjected to paperchromatographic amino acid analysis, a compound, exhibiting a greyish-blue colour with ninhydrin, was noticed next to a strong spot of glutamic acid on two-dimensional chromatograms (Fig. 1). The same compound possessed the notable property of exhibiting a brilliant blue or violet-blue fluorescence on exposure of the paper chromatograms to light of the wave-lengths 254 mμ and 350 mμ, respectively. Paper electrophoresis indicated that the unknown substance was a strongly acid amino acid. Efforts were hence directed towards isolation and characterization of the new amino acid.

On a preparative scale, 1 kg of ground seeds of *Reseda odorata* L. was defatted with carbon tetrachloride and subsequently extracted with aqueous

* Presented in abstract before the *1st Scandinavian Symposium on Natural Product Chemistry*, June 1961, Bornholm, Denmark.

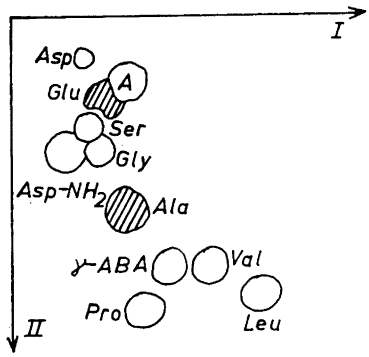

Fig. 1. Two-dimensional paper-chromatogram of the amino acid fraction of *Reseda odorata* L. (1) solvent: butanol:acetic acid:water (12:3:5); (2) solvent: phenol:water: conc. NH_3 (120:30:1). Developed with ninhydrin in acetone. A: 3-(3-Carboxy-4-hydroxy-phenyl)-L-alanine; other abbreviations are those commonly used.

methanol. The total amino acid fraction was separated from the extract by means of a strongly acid ion exchanger. When the amino acid fraction was applied to a weakly basic ion exchanger in the acetate form all acid amino acids including the unknown were retained. Aspartic and glutamic acid were eluted with acetic acid, whereas the new amino acid could be obtained virtually uncontaminated with other amino acids on subsequent elution with hydrochloric acid. The substance crystallized from the concentrated eluate at pH 2.5 in a total amount of 640 mg. It could readily be obtained in pure form as colourless needles on recrystallization from water.

The elemental composition, $C_{10}H_{11}NO_5$, together with the infra-red spectrum (Fig. 2) clearly revealed the aromatic character of the new amino acid. The strong band at 1650 cm^{-1} was tentatively interpreted as the C=O-stretching

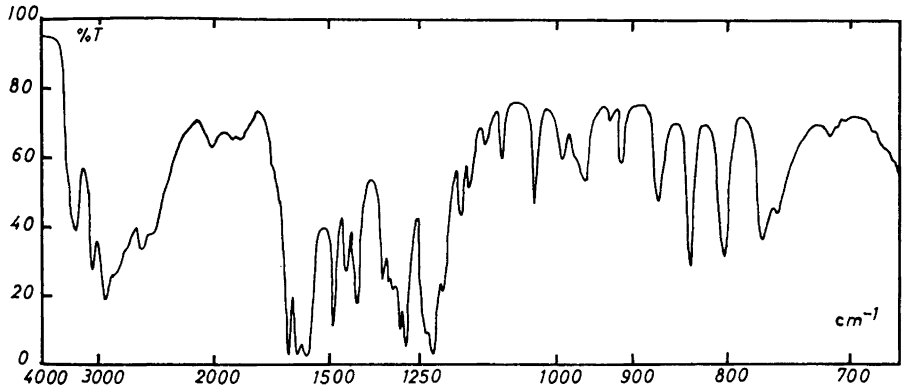

Fig. 2. Infra-red spectrum (in KBr) of 3-(3-carboxy-4-hydroxy-phenyl)-L-alanine.

mode of a highly chelated carboxyl-group whereas the band at 1560 cm^{-1} was suggestive of a carboxylate ion. The two peaks at 870 cm^{-1} and 805 cm^{-1} provided evidence for a 1,2,4-aromatic substitution pattern. Application of the diagnostic assay developed in this laboratory [1] indicated that the unknown was an α-amino acid. With ferric chloride a strong violet colour was produced, indistinguishable from that given by salicylic acid, which also exhibits visible fluorescence in ultra-violet light. The characteristic ultra-violet spectra of the amino acid also provided useful information. The amino acid exhibited bands at 308 mμ, 236 mμ and 212 mμ (Fig. 3) in acid solution, a pattern reminiscent of that of salicylic acid [2]. According to the rule of Doub and Vandelbelt [3] for the absorption patterns of trisubstituted aromatic compounds, the observed UV-spectrum is consistent with a formulation of the new amino acid as 3-(3-carboxy-4-hydroxy-phenyl)-alanine (I); this structure is considered preferable to the isomeric 3-(3-hydroxy-4-carboxy-phenyl)-alanine because of the recent discovery in higher plants of the formally analogous *m*-carboxyphenylglycine [4] and *m*-carboxyphenylalanine [5].

The potentiometric titration curve (Fig. 4), revealing four protolytic functions, is in agreement with the proposed structure. The first dissociation step (pK 2) is due to the aliphatic carboxylic group. The second step (pK 3.4) can be assigned to the aromatic carboxylic group, the third step (pK 9.3) to the ammonium group whereas the last step (pK 12—13) indicates ionization of the phenol function, in agreement with the pK_2-value of 13 reported for sali-

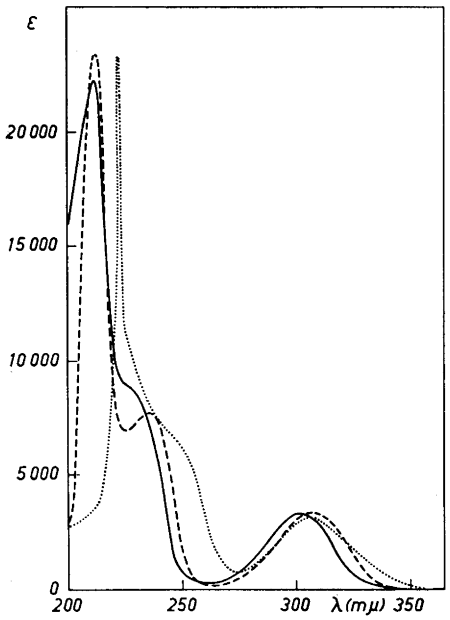

Fig. 3. Ultra-violet spectrum of 3-(3-carboxy-4-hydroxy-phenyl)-L-alanine. — — — —: in 0.5 N HCl, ... : in phosphate buffer, pH 7, ——— :in 0.5 N NaOH.

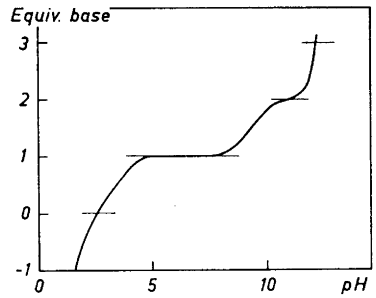

Fig. 4. Potentiometric titration curve of 3-(3-carboxy-4-hydroxy-phenyl)-L-alanine in water. Determined by titration with 1 N NaOH of 19.33 mg of the amino acid in 100 μl 1 N HCl + 1 ml of water. The curve is strongly deformed in the pH-region above 11.5.

cylic acid [6]. The isoelectric point for the amino acid, deducible from the titration curve, is 2.5.

As a first synthetic approach, the O,N-diacetate of *m*-nitro-L-tyrosine was prepared by the method employed by Sealock [7] for preparing O,N-diacetyl-L-tyrosine. Reduction of the diacetate, however, was accompanied by undesired acyl migrations, even under acid conditions. Hence, this approach was abandoned.

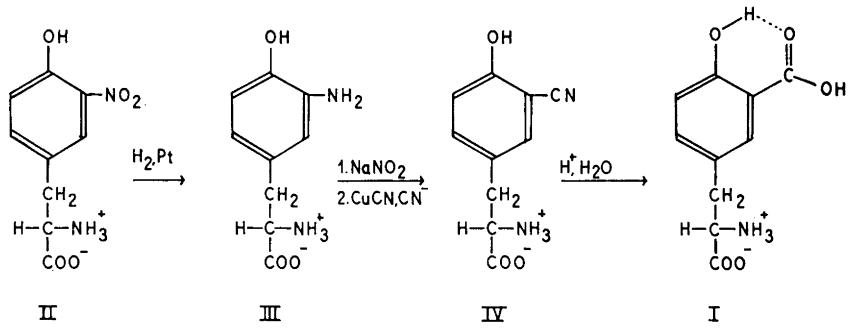

Final corroboration of the deduced structure, including information on the stereochemistry, was, however, obtained by the following unambiguous synthesis of the heretofore unknown 3-(3-carboxy-4-hydroxy-phenyl)-L-alanine (I), by a route analogous to that previously developed for 3,4-dihydroxyphenylalanine [8]. 3-Nitro-L-tyrosine [9] (II) was reduced catalytically to 3-amino-L-tyrosine (III) which was, in turn, diazotized and treated with cuprous cyanide in cyanide to yield 3-(3-cyano-4-hydroxy-phenyl)-L-alanine (IV). Acid hydrolysis converted this compound into the desired 3-(3-carboxy-4-hydroxy-phenyl)-L-alanine which was compared with the amino acid isolated from *Reseda* seeds. The two preparations were identical as judged from paper chromatography, infra-red spectra and optical rotation data.

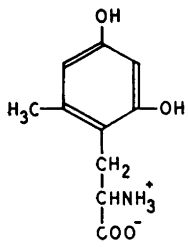

V

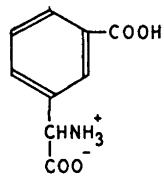

VI

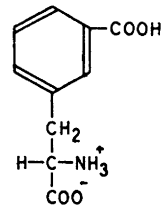

VII

Within the last few years several new aromatic amino acids have been encountered in higher plants. Thus, Schneider [10] identified 2,4-dihydroxy-6-methylphenylalanine (V) as a constituent of seeds of *Agrostemma githago* L., whereas Morris *et al.*[4] made the remarkable discovery of *m*-carboxyphenylglycine (VI) in bulbs of *Iris tingitana* Wedgw. Very recently, the latter group has also reported the isolation of the higher homologue, *m*-carboxy-L-phenylalanine [5] (VII), from the same source. The finding of three *m*-carboxylated aromatic acids, of course, raises the question as to a possible common or related biogenetic pathway of these. In this connexion it is noteworthy that the family *Resedaceae* systematically is very remote from the monocotyledonous family *Iridaceae*, a fact which suggests a much broader distribution of *m*-carboxy substituted aromatic compounds in higher plants than previously assumed.

During the present investigation, the occurrence of 3-(3-carboxy-4-hydroxyphenyl)-L-alanine in seeds of several other species of various genera within the family *Resedaceae* has been noticed. Among various species tested of the phylogenetically allied family *Cruciferae*, the new amino acid seems to be present in seeds of *Lunaria annua* L. and *L. rediviva* L.

EXPERIMENTAL

Microanalyses were performed by Mr. G. Cornali.

Rotations were measured in a 1 dm tube. Infra-red spectra were determined in potassium bromide pellets on a Perkin-Elmer 'Infracord'-instrument. Melting points were determined in capillary tubes in an Anschütz-Hershberg apparatus equipped with fully immersed thermometers. The standard rate of heating was 2° per min.

Isolation of 3-(3-carboxy-4-hydroxy-phenyl)-L-alanine (I) from seeds of Reseda odorata *L.* The seed, *i.e.* garden hybride material designated 'grandiflora', was purchased from I. E. Ohlsen's Enke, Copenhagen. One kilogram was portionwise suspended in carbon tetrachloride and disintegrated in a Waring blendor. After filtration, the residues were refluxed with the same solvent for 30 min, cooled and filtered. The procedure was repeated, whereupon the air-dried powder (680 g) was refluxed for 4 h with methanol:water (4 l, 7:3 (v/v)) and filtered again. The extraction was repeated twice with fresh portions of solvent. The combined filtrates were then evaporated *in vacuo* to a dark-brown syrup (81 g), which was partly dissolved in water (1 l) and centrifuged. The supernatant was divided into two equal parts, and the total amino acid fraction in each half was bound on a strongly acid ion exchange resin (Zeokarb 225, 4 × 50 cm) in the acid form. After washing the column with water (1 l), the amino acids were eluted with NH_3 (1.5 l, 1 N). The combined eluates from the two halves were evaporated to a dark-brown syrup (14 g), which was dissolved in water (200 ml) and fractionated on a weakly basic ion exchange resin (Dowex

3, 3.2 × 40 cm) in the acetate form. After washing with water (900 ml), glutamic and aspartic acid were eluted with acetic acid (3.6 l, 1 N). The unknown amino acid was retained even on washing with formic acid (3.6 l, 1 N) whereas it could be eluted with HCl (2 l, 1 N). The eluate was evaporated to give a tan, crystalline residue (960 mg). Excess HCl was removed on evaporation and the residue was dissolved in water (10 ml), treated with charcoal, and adjusted to pH 2.5 with ammonia. 3-(3-Carboxy-4-hydroxy-phenyl)-L-alanine separated as brownish crystals (540 mg). On concentration of the mother liquor a further crop (100 mg) could be obtained. Two recrystallizations from water afforded a pure specimen, m.p. 263—264° (decomp.), $[\alpha]_D^{25}$ + 1° (*c* 1.2, 1 N HCl), $[\alpha]_D^{25}$ −7.7° (*c* 0.9, 1 N NaOH) (Found: C 53.16; H 5.08; N 6.18. Calc. for $C_{10}H_{11}NO_5$: C 53.33; H 4.92; N 6.22). The infra-red spectrum is shown in Fig. 2. The ultra-violet spectra (Fig. 3) are measured at a concentration of 0.09 μequiv/ml. Extinctions below 240 mμ are highly dependent on the concentration, due to association. λ_{max} in mμ: (*a*) 0.5 N HCl: 308, 236, 212; (*b*) phosphate buffer, pH 7: 302, 211; (*c*) 0.5 N NaOH: 307, 222.

L-*2-Acetamido-3-(3-nitro-4-acetoxy-phenyl)-propionic acid.* *m*-Nitro-L-tyrosine (10 mmoles) was dissolved in NaOH (6 ml, 2 N) and water (3 ml), and the solution was placed in a pH-stat. Acetylation was accomplished in the course of 80 min at 0° with acetic anhydride (30 mmoles). pH was kept at 7.5 by automatic addition of NaOH (2 N). Conc. HCl was then added to pH 1.9, resulting in the separation of an oil which crystallized overnight to give L-2-acetamido-3-(3-nitro-4-acetoxy-phenyl)-propionic acid (2.65 g, 86 %). Three recrystallizations from ethyl acetate gave a pure specimen, m.p. 158—159°, $[\alpha]_D^{28}$ +37.1° (*c* 2.6, 96 % C_2H_5OH) (Found: C 50.26; H 4.56; N 8.87. Calc. for $C_{13}H_{14}N_2O_7$: C 50.32; H 4.55; N 9.03).

3-(3-Cyano-4-hydroxy-phenyl)-L-alanine (IV). 3-Nitro-L-tyrosine (II) (20 mmoles) was dissolved in HCl (20 ml, 1 N) and reduced catalytically with Adam's PtO_2 catalyst (220 mg) and hydrogen (65 mmoles). After filtration, addition of HCl (12.5 ml, 4 N) and cooling to 0°, a solution of $NaNO_2$ (20.3 mmoles) in water (5 ml) was added. Solid Na_2CO_3 (28 mmoles) was added to bring pH to 3—4 and the solution was added in small portions to a second aqueous solution (40 ml), kept at 75° and containing CuCN (40 mmoles), NaCN (120 mmoles) and Na_2CO_3 (53 mmoles). A brisk evolution of nitrogen was observed. After 2 h at 75° and 1.5 h at 95°, the reaction mixture was cooled and adjusted to pH 2—3 with conc. HCl (hood!). CuCN was filtered off and the filtrate was brought to pH 6 with ammonia, whereupon the solution was diluted to a volume of 400 ml and applied to a strongly acid ion exchange resin (Zeokarb 225, 4 × 50 cm) in the acid form. The column was washed with water (500 ml), and the amino acids eluted with ammonia (1.3 l, 1 N). The eluate was evaporated to give a brown semi-crystalline solid (4.75 g), which was dissolved in water (10 ml). pH was adjusted to 6 with HCl, causing the 3-(3-cyano-4-hydroxy-phenyl)-L-alanine (2.3 g, 48 %) to precipitate. Several recrystallizations from water afforded a slightly yellow product retaining 1 3/4 moles of water of crystallization when air-dried, and decomposing above 250°, $[\alpha]_D^{28}$ +5° (*c* 1.5, 1 N HCl). (Found: C 50.27; H 5.82; N 11.49: H_2O (determined as weight loss at 120° over P_2O_5 at 0.01 mm Hg) 13.24. Calc. for $C_{10}H_{11}NO_5$, 1 3/4 H_2O: C 50.52; H 5.73; N 11.79; H_2O 13.26). The anhydrous product was hygroscopic and took up water to the same final weight when exposed to the atmosphere.

The nitrile seems to undergo decomposition in hot water as apparent from the production of a yellow contamination. In consequence hereof, nitrogen analyses tend to be low.

3-(3-Carboxy-4-hydroxy-phenyl)-L-alanine. (I). The nitrile (IV) (0.95 mmoles) was dissolved in conc. HCl (25 ml) and kept at room temperature for 26 h. Water (25 ml) was then added and the solution was refluxed for 27 h. After evaporation to dryness and removal of excess HCl, the residue was dissolved in water (3 ml) and pH was adjusted to 2.5 with ammonia, whereupon the 3-(3-carboxy-4-hydroxy-phenyl)-L-alanine (102 mg) separated. Concentration of the mother liquor gave a second crop (53 mg, total yield 73 %). A sample for analysis was produced by recrystallization from water, m.p. 263—264° (alone or in admixture with the natural compound), $[\alpha]_D^{26}$ −7.5° (*c* 0.9, 1 N NaOH) (Found: 53.39; H 4.88; N 6.11). The infra-red spectrum was indistinguishable from that of the natural product.

Attempts to produce the amino acid in one step from *m*-nitro-L-tyrosine proceeded satisfactorily as estimated from paperchromatographic analysis. However, the isolation of the pure amino acid in this case proved very tedious.

Paper chromatography. In accord with the strongly acid properties of the 3-(3-carboxy-4-hydroxy-phenyl)-alanine, R_F-values proved to be highly dependent on the pH of the applied solution, when solvent systems of low buffering capacity towards acids (*e.g.* butanol:acetic acid:water) were employed. The following R_F-values were determined for the new amino acid by descending chromatography on Whatman paper No. 1 at 25°: butanol:acetic acid:water (12:3:5): 0.31, when applied in neutral solution; 0.48, when applied in acid solution; phenol:water: conc.ammonia (120:30:1 (w/v/v)): 0.24.

The present work is part of investigations supported by *Kai Hansen's Fond.* A research grant to one of us (P.O.L.) from *The Carlsberg Memorial Foundation for Brewer I.C. Jacobsen* is gratefully acknowledged.

REFERENCES

1. Olesen Larsen, P. and Kjær, A. *Biochim. et Biophys. Acta* **38** (1960)148.
2. Doub, L. and Vandenbelt, J. M. *J. Am. Chem. Soc.* **71** (1949) 2414.
3. Doub, L. and Vandenbelt, J. M. *J. Am. Chem. Soc.* **77** (1955) 4535.
4. Morris, C. J., Thompson, J. F., Asen, S. and Irreverre, F. *J. Am. Chem. Soc.* **81** (1959) 6069.
5. Thompson, J. F., Morris, C. J., Asen, S. and Irreverre, F. *J. Biol. Chem.* **236** (1961) 1183.
6. Ågren, A. *Acta Chem. Scand.* **9** (1955) 49.
7. Sealock, R. R. *J. Biol. Chem.* **166** (1946) 1.
8. Waser, E. and Lewandowski, M. *Helv. Chim. Acta* **4** (1921) 657.
9. Bauer, H. and Strauss, E. *Ber.* **68B** (1935) 1108.
10. Schneider, G. *Biochem. Z.* **330** (1958) 428.

Received July 8, 1961.

ACTA CHEMICA SCANDINAVICA 16 (1962) 149–154

A Ternary Sigma Phase in the System Cr-Ni-P

TORSTEN LUNDSTRÖM

Institute of Chemistry, University of Uppsala, Uppsala, Sweden

The metal-rich part of the ternary phase diagram Cr-Ni-P at 1050°C has been described briefly. The l.p. variations for the sigma phase have been studied.

A study has also been made of the possible occurrence of sigma phases in other Cr-Ni-X systems (where X = Al, Si, Ge, Sn, As) and also in the systems Mo-Pd-Si and W-Pt-Si. Only phosphorus has been found to have an effect comparable to silicon in stabilizing sigma phases.

Following the work of Jette and Foote in 1936 [1], several investigators have studied the influence of silicon on the formation of sigma phases [2-4]. The indications are that silicon shows an extensive solid solubility in binary sigma phases of 3*d* elements and that silicon extends the stability range of the sigma phase both as regards the metal-metal ratio and as regards the temperature.

The effect of carbon, nitrogen or boron on the sigma phase formation [5-7] is quite different from that of silicon. These elements do not show any appreciable solubility in the sigma phase. Instead, they form carbides, nitrides and borides with the element having the lower atomic number (in a given transition series)[7]. The effect of aluminium is similar [4], the sigma field in Fe-V-Al and Cr-Co-Al being very limited. On the other hand the formation rate of the sigma phase is accelerated by the addition of small amounts of aluminium (< 0.3 at %) and retarded by somewhat larger amounts [8].

The aim of this investigation has been to study the effect of aluminium, silicon, germanium, tin, phosphorus and arsenic on the sigma phase formation in the Cr-Ni system. Only phosphorus and silicon were found to give a ternary sigma phase. Since Gupta, Rajan and Beck published their results for the Cr-Ni-Si system while the present work was in progress, the detailed study was confined to the Cr-Ni-P system.

EXPERIMENTAL

Chemicals. The samples were prepared from chemicals of the following purity. Chromium (electrolytic) found on analysis to contain 99.97 % Cr.

Nickel powder from Mond Nickel Co., Ltd., claimed purity 99.9 %.
Red phosphorus with purity 99 % or better.
Germanium (zone-melted) better than 99.9 %.
Aluminium (rod), tin (rod) and arsenic (powder) from Johnson, Matthey & Co., London, claimed purity better than 99.9 %.
Silicon from Pechiney, Paris, claimed purity better than 99.9 %.
Platinum and palladium from Hereaus, Hanau, Germany with claimed purity better than 99.9 %.
Vanadium, found on analysis 99.7 %.
Molybdenum 99.7 %.
Tungsten of unknown purity.
Iron powder with approximately 2 % oxygen.

Preparation. Samples in the Cr-Ni-P system were prepared in the following way. Initially a master alloy of Ni_3P was prepared according to a method used by Haughton [10], Hägg [11] and by Rundqvist [12]. By this technique, pellets of red phosphorus are dropped into a melt of nickel under an argon atmosphere.

Samples, low in phosphorus (< 12 at %) were obtained by arc-melting pellets of metal and master alloy powder. They were subsequently heat-treated at 1050°C for 20—30 days in evacuated and sealed silica tubes. The samples with higher phosphorus contents were given this heat-treatment only. For the heat-treatments the alloys were put into small tubes of recrystallized alumina inside the silica tube. Arc-melted alloys were found to reach equilibrium faster than those not arc-melted.

In each of the systems Cr-Ni-X (X = Al, Si, Ge, Sn, As) five samples were prepared with a Cr-Ni ratio of 65:35 and an X-concentration ranging from 2 at % to 20 at %. The samples were heat-treated at 950°C for 10—30 days. In several instances this was preceeded by cold working, since this is known to accelerate the sigma phase formation [1,12,13]. The samples in the Cr-Ni-Ge system were also heat-treated at 750°C and 1150°C.

X-Ray work. The phase analysis was performed with powder photographs taken with a Guinier focussing camera using $CrK\alpha_1$ radiation ($\lambda_{CrK\alpha_1} = 2.2896$ Å) and with silicon ($a = 5.4306$ Å) as internal standard. The precision of an l.p. measurement is estimated to be ± 0.02 %, while the absolute accuracy is probably not better than ± 0.04 %.

Chemical analysis. Some of the Cr-Ni-P samples were chemically analyzed in the Department of Analytical Chemistry at this Institute.

Five samples from, or close to, the sigma phase region were analyzed for phosphorus and silicon. The samples were dissolved in HCl + Br_2, followed by treatment in HNO_3 + $HClO_4$ for complete oxidation of phosphorus and chromium. The residue was treated with HNO_3 + H_2SO_4 and then with $HClO_4$. The phosphorus was weighed as $P_2O_5 \cdot 24MoO_3$ according to Nydahl [14]. The phosphorus content obtained from this chemical analysis deviated very little from the nominal composition (the deviation was in all cases less then 2 % of the total phosphorus content).

For the determination of silicon the samples were dissolved in HCl + Br_2. This treatment was followed by boiling with $HClO_4$ to evaporate chromium as chromylchloride. The amount of silicon dioxide was determined from the weight loss, produced by treating the precipitate with hydrofluoric and sulfuric acids. The analysis of the five samples gave an average value of 0.1 % silicon. The accuracy of this value is a little uncertain, owing to the presence of a very small amount of residue which could be observed after the solution procedure, and because the silicon dioxide content in the precipitate was unusually small. However, not more than 0.2 % silicon was estimated to be present in the samples.

The samples were not analyzed for chromium and nickel, as previous experience has not given any reason to except departure from nominal composition. The concentration values for chromium and nickel given below are nominal.

RESULTS

Cr-Ni-P system at 1050°C. The metal-rich part of this system is outlined in Fig. 1. The diagram is characterized by a ternary sigma phase, the phase boundaries of which have an estimated accuracy of ±0.5 % for each component. One phase (X), coexisting with the sigma phase, has not been identified,

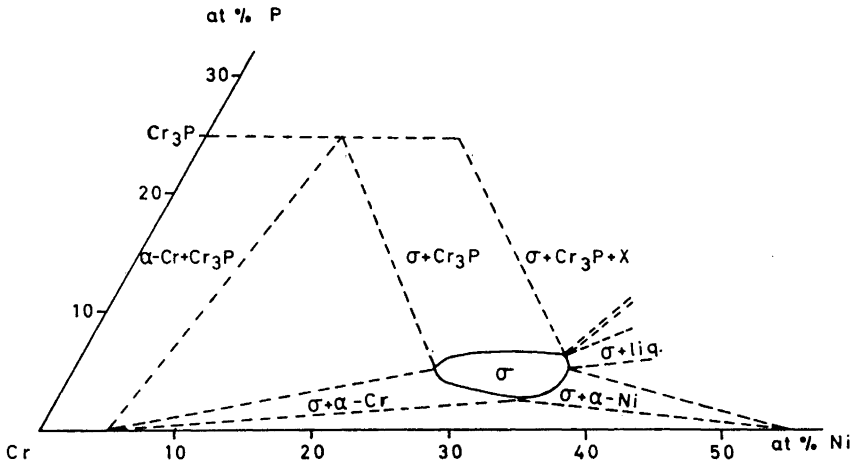

Fig. 1. The sigma field in the Cr-Ni-P system at 1050°C.

but it seems probable that it is a ternary Cr-Ni-P phase. The solid solubility of nickel in Cr_3P has been determined using the l.p. variation method. The binary Cr_3P phase was found to have $a = 9.186$ Å and $c = 4.558$ Å, while the smallest l.p.'s observed were $a = 9.131$ Å and $c = 4.529$ Å for the $(Cr,Ni)_3P$ phase. This corresponds to an interchange of 18.5 % of the chromium atoms with nickel atoms. This value is considerably larger than that given by Nowotny and Henglein [15].

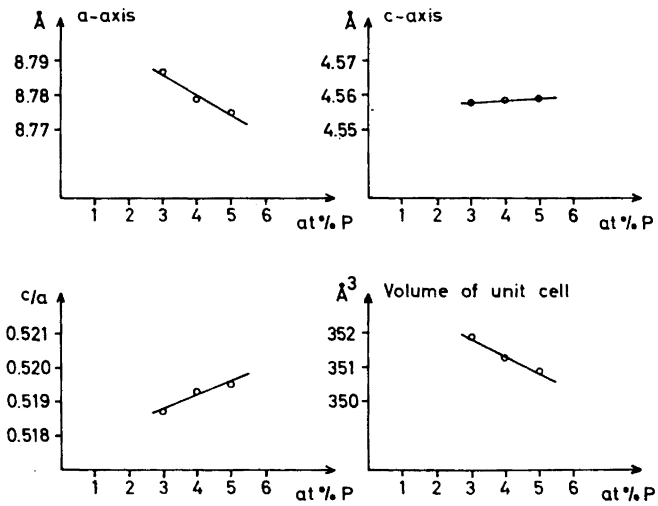

Fig. 2. Lattice parameters of the sigma phase CrNiP as functions of phosphorus content at 1050°C and with Cr/Ni ratio 65/35.

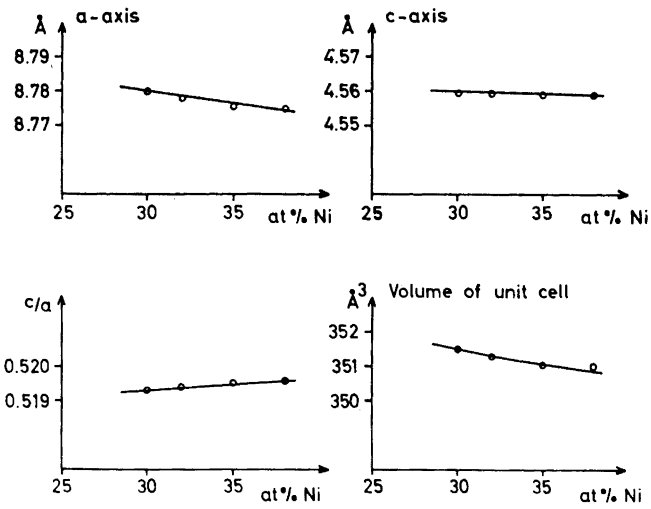

Fig. 3. Lattice parameters of the sigma phase CrNiP with 5 at % P as functions of Ni content at 1050°C.

The measured lattice parameters for the sigma phase in the Cr-Ni-P system are given in Figs. 2 and 3. It is found that for a constant Cr/Ni ratio, an increase in phosphorus content causes a decrease in the *a*-dimension, while within the limits of experimental error, the *c*-dimension is unaltered. As shown earlier [4] the introduction of silicon in the FeCr sigma phase causes a decrease in the *a*-dimension and an increase in the *c*-dimension. In both cases the introduction of phosphorus or silicon causes a contraction of the unit cell. The l.p. and cell volume variations of the Cr-Fe-Si sigma phase are typical of those of a number of Me_1—Me_2—Si systems described by Stüwe [16].

Fig. 3 shows no unexpected features. Both cell dimensions decrease when the larger chromium atom is replaced by the smaller nickel atom.

The Fe-V-P system. In this system the sigma single-phase field has been found to include phosphorus concentrations as high as 4 at % at 1050°C.

The systems Cr-Ni-X (X = Al, Si, Ge, Sn, As). A sigma phase was observed in the system Cr-Ni-Si only, and in this instance the results are in agreement with those of Gupta, Rajan and Beck [4]. The absence of a sigma phase in the Cr-Ni-Al system is in accordance with the ability of Al to suppress sigma phase formation in the related systems V-Fe-Al and Cr-Co-Al [4]. Although the data, presented here, are insufficient to permit any definite conclusion to be drawn, it is quite clear that aluminium, germanium, tin and arsenic do not stabilize the sigma phase as effectively as do silicon and phosphorus.

The systems Mo-Pd-Si and W-Pt-Si. Silicon has a stabilizing influence on sigma phases formed between 3*d* elements. Accordingly it was thought possible that in the systems Mo-Pd and W-Pt in which sigma phases do not occur [17–19], the addition of silicon might promote their formation. Fifteen

samples in each system were therefore prepared with the silicon content ranging from 2 at % to 12 at % and the Mo-Pd (or W-Pt) ratio ranging from 9:1 to 1:1. No sigma phase could be detected after heat-treatment at 1150°C for 30 days.

DISCUSSION

In connection with the ternary sigma phase Cr-Ni-P comment may be made concerning the Cr-Ni system. In an electron-microscopic study, Schüller and Schwab [20] demonstrated the existence of a binary Cr-Ni sigma phase. However, in view of the great stabilizing power of silicon it is not unlikely that the sigma phase observed may be stabilized by silicon impurities. Furthermore, the existence of a phase in a foil sufficiently thin for electron microscopy does not necessarily mean that it is also stable in bulk material.

In discussing the stabilizing of binary sigma phases by a third component, two factors are often considered to be important, namely the size factor and the "electronic" factor. The importance of the first has been particularly stressed by Stüwe [16], who from the assumption of closest packing of the atoms calculated the l.p. variations in binary sigma phases produced by the addition of a third element. These calculations agree fairly well with observed values, (though perhaps not quite convincingly), for sigma phases, where the added third element is a transition element. However, when the third element is silicon the calculations are unsatisfactory, even on a qualitive basis.

The investigation shows that in this respect phosphorus is similar to silicon. The l.p. variations at constant phosphorus content show qualitative agreement with the calculations. Calculated variations in the *a*- and *c*-dimensions of −0.041 Å and −0.021 Å respectively are matched by the measured values of −0.006 Å and −0.001 Å.

On the addition of silicon (and phosphorus) the cell volume and *a*-dimension decrease. This is a surprising result in view of the Goldschmidt radius of 1.34 Å for silicon in twelve coordination [21]. However, results obtained from structure determination of silicides and from the solid solubility of silicon in transition metals (with unfilled *d*-shells), indicate [22] an apparent silicon "radius" of 1.20 Å. Similar experience obtained from studies of phosphides and the solid solubility of phosphorus in iron [23] points to an apparent phosphorus "radius" of less than 1.2 Å. This value is in agreement with the observation that phosphorus has a more pronounced effect on the l.p.'s than silicon. If these revised estimates of atomic radius are used, the cell shrinkage is quite understandable, and the cell volume variation is perhaps the most significant from the point of view of the size factor.

In the Fe-Cr-Si sigma phase it was shown [3] that the silicon atoms prefer the IV (or D) position in the main layers of the sigma structure (not the V (or E) position as was wrongly quoted by Stüwe [16]). If any similar ordering exists in the Cr-Ni-P sigma phase, it may perhaps explain the absence of variation in the *c*-dimension.

Acknowledgements. The author wishes to thank professor G. Hägg for his stimulating interest. Thanks are also due to Dr. B. Aronsson and Dr. S. Rundqvist for valuable advice and interesting discussions.

Financial support is gratefully acknowledged from the *Air Force Office of Scientific Research of the Air Research and Development Command, United States Air Force*, through its European Office under Contract No. AF 61(052)-40 and from the *Swedisch State Council of Technical Research.*

REFERENCES

1. Jette, E. R. and Foote, F. *Metals & Alloys*, **7** (1936) 207.
2. Andersen, A. G. H. and Jette, E. R. *Trans. Am. Soc. Metals* **24** (1936) 375.
3. Aronsson, B. and Lundström, T. *Acta Chem. Scand.* **11** (1957) 365.
4. Gupta, K. P., Rajan, N. S. and Beck, P. A. *Trans. A.I.M.E.* **218** (1960) 617.
5. Shortsleave, F. J. and Nicholson, M. E. *Trans. Am. Soc. Metals* **43** (1951) 142.
6. Tisinai, G. F., Stanley, J. K. and Samans, C. H. *Trans. Am. Inst. Mining Met. Eng.* **200** (1954) 1259.
7. Aronsson, B. and Åselius, J. *Acta Chem. Scand.* **12** (1958) 1476.
8. Tagaya, M., Nenno, S. and Kawamato, M. *Nippon Kinzoku Gakkai-Si* **22** (1958) 387.
9. Haughton, J. L. *J. Iron Steel Inst.* **115** (1927) 417.
10. Hägg, G. *Nova Acta Regaie Soc. Sci. Upsaliensis*, Ser. IV, **7** (1929) No. 1.
11. Rundqvist, S. *Acta Chem. Scand.* **14** (1960) 1961.
12. Dulis, E. J. and Smith, G. V. *Metal Progr.* **53** (1952) 86.
13. Lena, A. J. and Curry, W. E. *Trans. Am. Soc. Metals* **47** (1955) 193.
14. Nydahl, F. *Lantbrukshögskolans Ann.* **10** (1942) 109.
15. Nowotny, H. and Henglein, E. *Monatsh.* **79** (1948) 385.
16. Stüwe, H. P. *Trans. A.I.M.E.* **215** (1959) 408.
17. Jaffee, R. I. and Nielsen, H. P. *Trans. A.I.M.E.* **180** (1949) 603.
18. Raub, E. *Z. Metallkunde* **45** (1954) 23.
19. Greenfield, P. and Beck, P. A. *Trans. A.I.M.E.* **206** (1956) 265.
20. Schüller, H. G. and Schwab, P. *Z. Metallkunde* **51** (1960) 81.
21. Laves, F. p. 124 in Theory of Alloy Phases, Cleveland, Ohio, 1956.
22. Aronsson, B. *Arkiv Kemi* **16** (1960) 379.
23. Gale, B. *Acta Met.* **7** (1959) 420.

Received July 21, 1961.

ACTA CHEMICA SCANDINAVICA 16 (1962) 155–158

On a New Type of Rearrangement during Ring-closure

SALO GRONOWITZ and PINCHAS MOSES*

Chemical Institute, University of Uppsala, Uppsala, Sweden

Rearrangement occurs during the ring-closure of (2-thienylthio) acetic acid with sulphuric acid. The main ketone formed is 2H,3H-[3,2-b]thiophen-3-one (V), which is the only ketone obtained in the ring-closure of (3-thienylthio)acetic acid.

Gronowitz *et al.*[1,2] have shown that a rearrangement occurs during the ring-closure of (2-pyrrolylthio)acetic acid (I) to 2H, 3H-thieno [3,2-b] pyrrole 3-one (II)

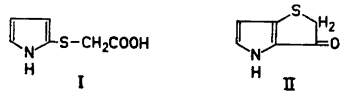

I II

with polyphosphoric acid [3].

One of the mechanisms previously suggested [2] to account for the rearrangement involves electrophilic substitution by the cationoid carbonyl carbon at the α-carbon carrying the sulphur atom, with simultaneous rearrangement of the sulphur to the 3-position, a reaction which, as far as we know, has no precedence in the chemical literature. Granting the above mechanism, one can expect that this type of ring-closure with rearrangement will occur in other compounds having a thioglycolic acid group situated in that position, which is most reactive in electrophilic aromatic substitution, or more precisely, where the reactivity to electrophilic substitution is considerably greater than that of its *ortho* position, as is the case in the α-position of pyrrole relative to its β-position. This is also true in the thiophene series where Melander and Halvarsson [4] have shown that the α-position is about 1000 times as reactive



III IV

* On leave of absence from the Hebrew University, Jerusalem, Israel.

as the β-position in electrophilic hydrogen exchange. We have therefore investigated the ring-closure of the isomeric (thienylthio) acetic acids III and IV.

The ring-closure of IV has been carefully studied by Challenger and Holmes [5] in their work dealing with the structure of the thiophtenes. We could confirm their result that cyclization is best achieved with concentrated sulphuric acid. We did not obtain any defined ring-closed products when III was treated with polyphosphoric acid at 135°, or with anhydrous HF at room temperature. An attempted Friedel-Crafts ring-closure of the acid chloride in benzene, using stannic chloride as catalyst was also unsuccessful. Even in the ring-closure with sulphuric acid, the yields are low, Challenger and Holmes [5] having obtained a yield of 14 % of the ketone * V in the best instance.

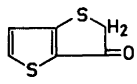

V

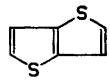

VI

This is most probably due to extensive sulphonation of the starting acid, and possibly also of the product formed. These water-soluble by-products do not, however, interfere in the isolation and purification of the ketones. Tilak *et al.*[6], who have extensively studied the cyclization of various (arylthio)-acetaldehyde acetals, found that in the case of the (thienylthio)acetaldehydes the yields were also low [7,9].

We found that no rearrangement occurred in the cyclization of IV, only one ketone being produced namely 2H,3H-thieno[3,2-b]-thiophene-3-one (V). There is no doubt as to the structure of this compound since Challenger and Holmes [5] reduced it to the solid thiophtene (VI), the structure of which has been determined by X-ray and dipole moment measurements [5,9].

In the ring-closure of III with concentrated sulphuric acid, however, we invariably obtained a mixture of two ketones, the total yields of which ranged from 9—11 %. Through fractional crystallization we managed to separate the two constituents from each other. The major constituent was shown by IR-spectroscopy and mixed m.p. to be identical with V, while the structure of the minor product (VII) analyzing correctly for $C_{10}H_8O_2S_3$ has not yet been determined. Quantitative analysis by means of IR-spectroscopy showed that VII and V are formed approximately in the ratio 1:9 **.

It is excluded that V could have been formed from small amounts of IV possibly present in III. III was prepared through metalation of thiophene with *n*-butyllithium, followed by reaction with sulphur and chloroacetate. Since the metalation of thiophene takes place exclusively in the α-position, it is most improbable that any of the 3-isomer was formed. Furthermore IR-spectro-

* V may to some extent, exist in its tautomeric hydroxythiophtene structure. The strong C=O stretching bond in its IR-spectra indicates, however, that it mainly exists in the ketoform.

** In earlier experiments when the reactions were carried out without stirring total yields were only 3—6 % and the product consisted of a mixture of VII to V in the ratio of 2:1. This procedure is to be preferred if it is desired to prepare VII.

scopy verified that, if the 2-isomer was at all contaminated with 3-isomer, the maximum quantity of the latter present was far below the amount required to account for the experimental results.

It is thus evident that the rearrangement during ring-closure first discovered by Gronowitz *et al.*[1,2] in the pyrrole series is of a more general nature. It is possible that it might also have occurred in the cyclization of (2-thienylthio)-acetaldehyde acetal with phosphorous acid and phosphorus pentoxide where Pandya and Tilak[8] obtained thieno[2,3-b]thiophene in 11 % yield, and might have overlooked smaller amounts of VI during their purification of the crude product. We are continuing our investigations on the scope of this ring-closure with rearrangement and especially on its mechanism.

EXPERIMENTAL

(2-Thienylthio)acetic acid. A solution of 190 g (2.26 moles) of thiophene in 250 ml of dry ether was introduced into the usal nitrogen-swept four-necked apparatus and 1400 ml of 1.35 N *n*-butyllithium was added with stirring. The solution was refluxed for 2 h more, cooled to −70° and treated with 57.6 g (1.80 moles) of sulphur. The mixture was stirred at −70° for 1 h, poured into water, the aqueous layer separated and washed once with water. The aqueous solution containing the lithium salt of 2-thiophenethiol was then poured into a neutral solution made up from 170 g (1.82 moles) of chloroacetic acid and 124 g of potassium carbonate.

The reaction mixture was allowed to stand over-night at room temperature, extracted with ether, the aqueous layer cooled and acidified with dilute hydrochloric acid. The desired product separated out as an oil, which was extracted with ether. The ether layer was washed twice with water, treated with anhydrous sodium sulphate and Norit, filtered and the solvent removed *in vacuo*. The oily residue was cooled in an ice-salt mixture and the resulting crystalline mass was broken up and twice washed with a 1:9 ether-petrol-ether mixture; yielding 250 g (80 %) of light brown (2-thienylthio) acetic acid m.p. 42−46°. Recrystallization by dissolving in ether and massively diluting with petrol-ether raised the m.p. to 47−48°. (Found: C 41.24; H 3.58; S 36.71. Calc for $C_6H_6O_2S_2$ (174.2): C 41.36; H 3.47; S 36.80).

Ring-closure of (2-thienylthio)acetic acid. One part (by weight) of (2-thienylthio)acetic acid was added under stirring to ten parts (by volume) of concentrated sulphuric acid at 100° and the mixture stirred at that temperature for 45 min. It was cooled, poured onto crushed ice and extracted with chloroform. The solution was dried, the chloroform distilled off *in vacuo* (nitrogen atmosphere) and the oily residue cooled in ice. The resulting yellow solid product (9−11 %) was analyzed by IR-spectroscopy.

Through the fractional crystallization from alcohol of 7.5 g of crude product, which was shown by IR-analysis to consist of a mixture of 90 % of V and 10 % of VII we obtained 1.1 g of V m.p. 93−96°, whose IR-spectrum was identical to that of an authentic sample of 2H,3H-thieno[2,3-b]thiophene-3-one melting at 97−98.6°, prepared by ring-closing(3-thienylthio)acetic acid according to Challenger and Holmes[5]. One additional recrystallization raised the m.p. to 96.5−97.5°.

In addition 100 mg of a an unknown ketone, m.p. 111−112.5° was obtained. (Found: C 46.81; H 3.19; S 37.43. Calc. for $C_{10}H_8O_2S_3$: C 46.88; H 3.13; S 37.50). Its IR-spectrum was free from the characteristic peaks of V.

The spectroscopic analyses were carried out utilizing the ratio of the absorption of a characteristic peak of one component to that of the other component (*cf.* Ref.[10]). The peaks at 6.65 μ and at 13.75 μ of VII and those at 6.75 and 13.25 μ of V were used. In three experiments carried out with adequate stirring the cyclization product consisted of 90 % V and 10 % VII. Without adequate stirring, it was found in seven experiments that the cyclization product consisted of 28−42 % of V and 72−58 % of VII. The IR-spectra were recorded on a Perkin-Elmer Infracord spectrophotometer.

Acknowledgements. The authors wish to express their thanks to Professor Arne Fredga for many fruitful suggestions concerning this work and for all facilities put at their disposal. The elementary analyses were carried out at the Analytical Department of the Chemical Institute and by Dr. A. Bernhardt, Mülheim (Ruhr). A grant from the *Swedish Natural Research Council* to S. G. is gratefully acknowledged.

REFERENCES

1. Gronowitz, S., Hörnfeldt, A.-B., Gestblom, B. and Hoffman, R. A. *J. Org. Chem.* **26** (1961) 2615.
2. Gronowitz, S., Hörnfeldt, A.-B., Gestblom, B. and Hoffman, R. A. *Arkiv Kemi* **18** (1961) 133.
3. Matteson, D. S. and Snyder, H. R. *J. Org. Chem.* **22** (1957) 1500.
4. Halvarson, K. and Melander, L. *Arkiv Kemi* **8** (1955) 29.
5. Challenger, F. and Holmes, J. L. *J. Chem. Soc.* **1953** 1837.
6. Tilak, B. D. *Tetrahedron* **9** (1960) 76.
7. Ghaisas, V. V. and Tilak, B. D. *Proc. Indian Acad. Sci.* **39 A** (1954) 14.
8. Pandya, L. J. and Tilak, B. D. *J. Sci. Ind. Res.*, India **18 B** (1959) 371.
9. Cox, E. G., Gillot, R. J. J. H. and Jeffrey, G. A. *Acta Cryst.* **2** (1949) 356.
10. Moses, P. and Gronowitz, S. *Arkiv Kemi* **18** (1961) 119.

Received August 29, 1961.

ACTA CHEMICA SCANDINAVICA 16 (1962) 159–172

High-speed Computers as a Supplement to Graphical Methods

I. Functional Behavior of the Error Square Sum

LARS GUNNAR SILLÉN

Department of Inorganic Chemistry, Royal Institute of Technology, Stockholm 70, Sweden

The paper discusses the principles underlying "LETAGROP", a computer program being used for calculating, from experimental data $(y_i, a_{1i}, a_{2i} \ldots)$, $(i = 1 \ldots n)$, a set of unknown constants k_r $(r = 1 \ldots N)$, assuming a functional relationship $y = f(k_r, a_1, a_2 \ldots)$. The "best" values k_r'' searched for, are those that minimize the error square sum U (eqn. 7). The method may be described as a generalized least-squares method, valid also for non-linear and implicit functions, which are hard to treat by the standard treatment for linear functions or by the Gauss' approximation method.

The functional behavior of U $(k_1 \ldots k_N)$ is discussed for the general linear case, and for $N = 1$ and $N = 2$. The "standard deviations" D_r are interpreted geometrically by means of the extreme values $k_r'' \pm D_r$ of each k_r on the "D boundary", defined by $U - U_0 = \sigma^2$ (47).

A high-speed computer can very easily "map" U $(k_1 \ldots k_N)$, even for non-linear and implicit functions. As an approximation it is assumed that U is a second-degree function of the k_r; then $\frac{1}{2}(N + 1) \cdot (N + 2)$ points suffice to calculate the position of the minimum and the D boundary. Starting from a first, approximate set k_r', the "best" values k_r'' are reached by (usually only two or a few) successive approximations. The need for choosing the k_r as independent as possible is pointed out.

The limitations of the whole "least squares" approach are discussed. At present there seems to be still more need for better chemical work than for better statistical treatment.

The following papers will deal with a number of computer programs that have proved very helpful in our present work on complicated equilibria. One of these programs, called "LETAGROP" was designed to adjust a number of equilibrium constants simultaneously, once the formulas of the complexes and the approximate values of the equilibrium constants had been found by means of graphical methods. It can also be applied to other types of problems where several unknown parameters are to be determined.

As distinguished from the usual "least squares" method, "LETAGROP" ("pit-mapping") can be applied also to cases where the measured quantity cannot be expressed as a linear or even as an explicit function of the unknown parameters.

Since this way of treatment has not been described in any source that the author is aware of, and at any rate may prove useful for many chemical problems, it seems appropriate to describe its principles in brief.

GENERAL PROBLEM

We have n measurements y_i of the variable quantity y and assume that we know the functional relationship.

$$y = f(k_1,\ k_2 \ldots k_r \ldots k_N\ ;\ a_1, a_2 \ldots) \tag{1}$$

Here, a_1 a_2, *etc.* are quantities that can be varied but whose values (a_{1i}, a_{2i}, *etc.*) are assumed to be known accurately in each experiment. From the n sets of data (y_i, a_{1i}, a_{2i} ...), $i = 1, 2 \ldots n$, we want to determine the set of N unknown constants k_r, $r = 1, 2 \ldots N$.

Example I a. Mononuclear complexes A_pB, data (A, B, a, b). We have a series of n solutions in each of which one knows the total concentrations A and B, and the concentrations a and b of free A (ligand) and free B (central group). In the expression

$$y = B/b = 1 + \beta_1 a + \beta_2 a^2 + \beta_3 a^3 + \ldots = 1 + \Sigma\beta_p a^p \tag{2}$$

one wants to determine the unknown stability constants $\beta_1 \ldots \beta_N$ from a number of experimental sets (y, a).

Example I b. Mononuclear complexes A_pB, data (A, B, a). From the data we may calculate the ligand number Z (or $\bar{n}$) $= (A - a)/B$. For calculating $\beta_1 \ldots \beta_N$ we may use the relationship

$$Z = \frac{\Sigma p\beta_p a^p}{1 + \Sigma\beta_p a^p} \tag{3}$$

One may rearrange (3) to give, for instance,

$$y = Z + \Sigma(Z - p)\beta_p a^p = 0 \tag{4}$$

Because of experimental errors, the value found is usually not exactly zero. Other rearrangements can also be made. Again, we want to determine the N unkown β_p from n sets (Z, a).

Example II. Polynuclear complexes A_pB_q, data (B, A, a). If there are several polynuclear complexes in a system, the mass balance and the law of mass action give

$$B = b + \Sigma\Sigma q\beta_{pq} a^p b^q \tag{5a}$$

$$BZ = A - a = \Sigma\Sigma p\beta_{pq} a^p b^q \tag{5b}$$

The unknown constants β_{pq} should be determined from n sets (B, Z, a). Nature in general does not seem anxious to provide such sets of (p, q) as would make it easy to eliminate b from (5a) and (5b). So, in general, no explicit expression for Z can be derived.

Example III. Hydrolysis studies in self-medium. We have the equations (Hietanen and Sillén [1]):

$$B = b + \Sigma\Sigma q\beta_{pq}h^{-p}b^q \tag{6a}$$

$$BZ = h - H - \Delta = \Sigma\Sigma p\beta_{pq}h^{-p}b^q \tag{6b}$$

$$E = E_0 - 59.154 \log h + jh \tag{6c}$$

Here, H is the total (analytical) proton excess, E is the measured emf, E_0 and j are constants, which cannot be determined independently, and Δ is the correction for a possible analytical error in H. The experimental data are (E, H), the unknown constants are the β_{pq}, E_0, j, and Δ, whereas b and h should be eliminated. Even here, it is in general not possible to give an explicit expression $E(H)$.

Of these examples, Ia is easily accessible to the standard "least squares" treatment Refs.[2-6], which can also be applied to I b after some transformation. For finding and refining the constants in examples II and III (and even in I) successive approximations have usually been used.

Error square sum

It is customary to search for that set of constants k_r'': $k_1'' \ldots k_N''$, that will minimize the error-square sum U

$$U = \Sigma w_i[y_i - f(k_1 \ldots k_N ; a_{1i}, a_{2i} \ldots)]^2 \tag{7}$$

where w_i is the "weight" assigned to each measurement y_i. The mathematical condition for our criterion

$$U = \text{minimum} \tag{8}$$

is a set of N "normal equations"

$$(\partial U/\partial k_r) = 0, r = 1 \ldots N \tag{8a}$$

Whether the person using (8) realizes this or not it is a strictly valid criterion for "maximum likelihood" only under the following conditions:

(*a*) The functional relationship (1) is correct; for instance, no important terms have been left out.

(*b*) There are no other errors to be considered than the random experimental error in y. Especially, there are no systematic errors.

(*c*) The random errors in y follow a "normal" (Gaussian) distribution.

(*d*) The weight

$$w_i (y_i, a_{1i}, a_{2i} \ldots) \tag{9}$$

assigned to each measurement is an exact measure of its inherent accuracy as defined by (28).

These conditions call for some comments:

(*a*) The choice of (1) is a matter of judgment. Sometimes, several functions f_{I}, f_{II} *etc.* are compared, and one is in general inclined to prefer the function that gives the lowest value for $U_{\min}$. The judgment comes in especially when one considers the functions that were never tried. With the standard "least squares" treatment one is restricted to functions linear in the k_r.

(*b*) It is usually not difficult to choose the variable y, that should "carry" the experimental error. In the examples above one would probably use Z in

I and II and H or E in III. If there are random errors also in a_1 *etc.* these can usually be accounted for by a corresponding increase in the random error in y. However, if there is a range where the random variation in, say, a would correspond to a variation in y, much greater than any experimental errors, then misleading results will be obtained; this is illustrated in Ref.[3], p. 2031, where the authors have started from eqn. (4) but put the error on the ligand concentration instead of on the ligand number. Thus, some caution is needed.

The most important condition, which is, alas, frequently not fulfilled, is the absence of systematic errors. An especially insidious combination is that of systematic errors and an erroneous function (1) which may sometimes give an agreement between experiment and erroneous theory that seems quite convincing. A wrong conclusion can of course be reached also without the aid of a computer, or statistics.

There is evidently no statistical way of avoiding this risk. One must keep an open mind for the possibilities of systematic errors, apply as many independent experimental approaches as possible, and always strive to prove oneself wrong.

(*c*) There may be shades of opinion among statisticians as to whether a "normal" distribution is a frequent phenomenon or not in this harsh world of reality. At any rate, if the errors in a quantity x are "normally" distributed, then the errors are not "normally" distributed in non-linear functions of x like $\log x$, x^{-1}, or x^2.

If, as is usually the case, nothing is known about the real error distribution, out of all guesses that can be made, the "normal" distribution is the one that gives the simplest calculations.

(*d*) is the second point where judgment (or lack of it) creeps into all calculations founded on (7) and (8).

It is certainly seldom that one can hope that all these assumptions (*a*) — (*d*) are correct. Nevertheless, the "least squares" criterion (8) is often employed because of its simplicity, and this will be done in the present paper also.

The set of constants, k_r'' ($r = 1 \ldots N$) that fulfil (8) we shall call the "best" set of constants. It is "objective" in the sense that with the same set of data, the same theoretical function (1), and the same weight function (9), the condition (8) should give the same "best" set of constants in the hands of different workers. This is an example of how some quantities that are defined exactly (under given conditions) in mathematical statistics, have acquired highly suggestive names, which may lead non-statisticians to over-estimate their significance in the world of reality: "normal" distribution, "maximum likelihood", "probable" error, "significant" result, "standard" deviation, "best" values.

Remembering the limitations of the whole approach, we shall not forget the quotation marks around "best". Some other authors leave them out.

The standard "least squares" treatment

If f in (1) is a linear function of the various k_r, say $f = \Sigma k_r a_r$, then (8a) leads to a system of linear equations which can be solved by elimination methods or, for not too large N values, by means of determinants.

Most of the larger high-speed computers have standard "least squares" programs that can be adapted to this type of problem. Of the examples I—III given above, only I a and (with some transformation and difficulty) I b can be treated in this way. The "least squares" treatment has been applied to equilibria of complex formation by several authors, especially by Sullivan, Rydberg and Miller [3-6]. Earlier work in this direction has been summarized by Rydberg [6].

If f in (1) is not a linear function, the general trend has been to reduce it to a linear one, either by transformation (as was done in example I b), or by Gauss' approximation method, in which one starts with an approximative set k_r', expresses the derivatives of U (8a) around k_r' by means of Taylor series for f and uses only the first terms. Programming a computer for Gauss' method is not always simple, and according to Moore and Ziegler [8] its performance is somewhat unpredictable. It seems hard to apply Gauss' method to cases such as II and III above, where no explicit relationship (1) can be given.

"Pit-mapping"

However, one can make oneself free from the condition that (1) should be linear, or even explicit, if one considers directly the functional behavior of the error-square sum

$$U(k_1 \ldots k_N) \tag{10}$$

as a function of the various k_r. By means of a high-speed computer one may rapidly calculate U for various sets of k_r and it is natural to ask whether one could not use a selected set of points of the function (10) for finding the lowest point:

$$U_{\min} = U_0 = U(k_1'', k_2'' \ldots k_N'') \tag{11}$$

If f is linear, (10) is a second-degree surface, as will be seen below. (Eqn. 40, *cf.* eqn. 39). With $N = 1$ it is a parabola, with $N = 2$ an elliptic paraboloid, and for higher N a generalized elliptic paraboloid in $(N + 1)$-dimensional space. For any value of N we shall refer to the lowest point U_0 and its immediate surroundings as the "pit". The procedure to be proposed, which was indicated in a short note by Dyrssen, Ingri and Sillén [9], we shall call "pit-mapping" since in a way it describes the shape of the pit. We shall see how this map can be used also for estimating the statistical "standard deviation" which may be obtained, for the linear case, as a by-product of the standard computer programs.

LINEAR EQUATIONS

As a starting point we shall study the behavior of U in the linear case. The symbolism will, to a large extent, be the same as is used by Cramér [7]. For a stochastic varable , say x, with the distribution function $F(x)$ (probability that it in a particular case is $\leq x$), the average will be written

$$\bar{x} = E\{x\} = \int_{-\infty}^{\infty} x \, \mathrm{d}F(x) \tag{12}$$

and the standard deviation

$$D\{x\} = \sigma_x \tag{13}$$

will be defined by

$$D^2\{x\} = E\{(x - \bar{x})^2\} \tag{14}$$

(Some other textbooks use D for what is here called D^2). These definitions do not presume any special form of $F(x)$.

We shall carry out the mathematical discussion only insofar as this is necessary to explain our method. We shall set down for future use a result, which is easily seen from the usual treatment, although usually not written this way: the minimum value U_0 is a stochastic variable, for which

$$E(U_0) = \sigma^2 (n - N) \tag{15}$$

$$D^2(U_0) = 2\sigma^4 (n - N) \tag{16}$$

$U_0\sigma^{-2}$ follows a χ^2-distribution with $(n - N)$ degrees of freedom. Here, σ is the "standard deviation" for y_i in a point with the weight $w_i = 1$. In the following, we shall take the "best" experimental value of σ from

$$U_0 = \sigma^2(n - N) \tag{17}$$

f linear, $N = 1$

If $N = 1$ there is only one constant, k_1, to be determined. If (1) is linear, we can always transform it to read

$$(y \approx)\, f = k_1$$

We have n measurements, y_i $(i = 1, 2 \ldots n)$, to each of which we ascribe a weight w_i $(i = 1, 2 \ldots n)$. The error square sum is

$$U = \Sigma w_i(y_i - k_1)^2 = \Sigma(w_i y_i^2 - 2\, w_i y_i k_1 + w_i k_1^2) \tag{19}$$

We introduce the weight sum W, and the weighted average $\bar{y}$, defined by

$$W = \Sigma w_i \,;\; \bar{y}\, W = \Sigma w_i y_i \tag{20}$$

Inserting (20) into (19) gives

$$U = \Sigma w_i y_i^2 - 2\, k_1 \bar{y}\, W + k_1^2 W \tag{21}$$

By differentiation with respect to k_1 we find the condition for a minimum in U:

$$\partial U/\partial k_1 = 2W(k_1 - \bar{y}) = 0 \tag{22}$$

At the minimum point we have, from (22) and (21)

$$k_1'' = \bar{y} \tag{23}$$

$$U_0 = \Sigma w_i y_i^2 - W\, k_1''^2 \tag{24}$$

According to (23) the "best" value is the weighted average. We shall study the behavior of $U(k_1)$ around this point, for simplicity replacing k_1 by its deviation d_1 from the "best" value:

$$k_1 = k_1'' + d_1 \tag{25}$$

Inserting (24) and (25) into (21) gives

$$U = U_0 + Wd_1^2 \tag{26}$$

Hence, the "pit" $U(d_1)$ is a parabola. The squared standard deviation of k_1'' will be, using (23) and (20):

$$D_1^2 = D^2\{k_1''\} = D^2\{\Sigma w_i y_i/W\} = \Sigma(w_i/W)^2 D^2\{y_i\} \tag{27}$$

Up to now, we have made no assumption about the error distribution or weights. Let us assume, however, that we have managed to choose, for each y_i, its weight so that

$$D^2\{y_i\} = \sigma^2/w_i\ ;\ \sigma = \text{constant} \tag{28}$$

Inserting (28) into (27) we find

$$D_1^2 = \sigma^2\ \Sigma w_i/W^2 = \sigma^2/W \tag{29}$$

If we may assume that we have a "normal" distribution, we can apply (17) $U_0 = \sigma^2(n - N)$.

One may ask what value U has for $d_1 = D_1 = D\{k_1''\}$. Inserting this value into (26) and applying (29) we find

$$U(D_1) = U_0 + \sigma^2 \tag{30}$$

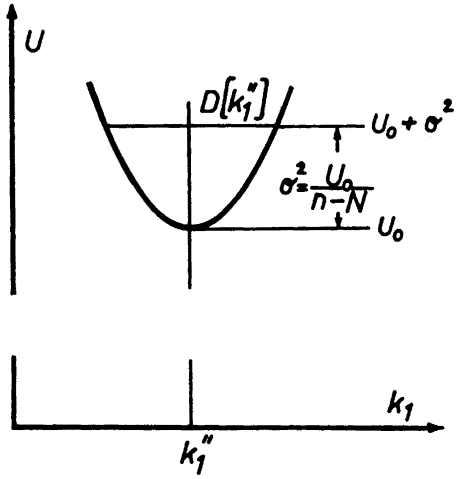

Fig. 1. Direct method for calculating the "best" value k_1'' and its "standard deviation" D_1 provided the functional relationship between the error square sum U and k_1 is known. The "best" value, k_1'', is the one that gives the minimum value, U_0, for U. The points where $U - U_0 = U_0/(n - N)$ are $k_1'' \pm D_1$.

or using (17)

$$U - U_0 = \frac{U_0}{n-N} \text{ for } d_1 = D\{k_1''\} \tag{30a}$$

Thus, if the shape of the "pit" is known, (30a) gives a direct method for finding the "best" value for $D\{k_1''\}$ (Fig. 1).

General linear case

Let us assume that the theoretical function has the general linear form

$$y_i \approx f_i = \sum_r k_r a_r \tag{31}$$

and that we have n measurements y_i ($i = 1, 2 \ldots n$), each of weight w_i, to determine the N unknown constants k_r ($r = 1, 2 \ldots N$) searched for. In the following, r, s and t will be used indiscriminately for the index of k, and sums over them imply "from 1 to N"; sums over i are " from 1 to n".

The error square sum is then

$$U = \sum_i w_i(y_i - \sum_r k_r a_{ri})^2 = \sum_i w_i y_i^2 - 2 \sum_i \sum_r w_i y_i k_r a_{ri} + \sum_i \sum_r \sum_s w_i k_r k_s a_{ri} a_{si} \tag{32}$$

We replace the sums over i by the sets of quantities b_{rs} and c_r defined by

$$W b_{rs} = \sum_i w_i a_{ri} a_{si} \tag{33}$$

$$W c_r = \sum_i w_i y_i a_{ri} \tag{34}$$

As before, $W = \sum_i w_i$. (eqn. 20) Then, (32) takes the form

$$U = \sum_i w_i y_i^2 - 2W \sum_r c_r k_r + W \sum_r \sum_s k_r k_s b_{rs} \tag{35}$$

Differentiation with respect to the k_r gives a set of conditions (the normal equations, 8a) for U to have a minimum:

$$\sum_s k_s'' b_{rs} = c_r \tag{36}$$

The solution of (36) is

$$k_r'' = B^{-1} \sum_s c_s B_{rs} \tag{37}$$

were B is the determinant of the symmetrical matrix $\| b_{rs} \|$ and B_{rs} is the subdeterminant corresponding to b_{rs}. Combining (35) and (36) we find at the minimum point

$$U_0 = \sum_i w_i y_i^2 - W \sum_r k_r'' c_r \tag{38}$$

We replace k_r by the difference d_r from the "best" value

$$k_r = k_r'' + d_r \tag{39}$$

After some arithmetic, (35) can be transformed, using (39), (38), and (36):

$$U - U_0 = W \sum_r \sum_s d_r d_s b_{rs} \tag{40}$$

So, $U - U_0$ is a homogeneous function of second degree in the d_r.

The standard deviations of the "best" values k_r'' are deduced as follows. Using (37) and (34) we have,

$$D_r^2 = D^2\{k_r''\} = D^2\{B^{-1}W^{-1} \sum_i \sum_r w_i a_{si} B_{rs} y_i\} = B^{-2}W^{-2} \sum_i w_i^2 (\sum_s a_{si} B_{rs})^2 D^2\{y_i\}$$

If we assume that the weights have been chosen so that (28) holds, we find, using (33)

$$D_r^2 = \sigma^2 B^{-2} W^{-2} \sum_i \sum_s \sum_t w_i a_{si} a_{ti} B_{rs} B_{rt} = \sigma^2 B^{-2} W^{-1} \sum_s \sum_t b_{st} B_{rs} B_{rt}$$

It follows from the properties of determinants that the double sum equals BB_{rr} so that

$$D_r^2 = D^2\{k_r''\} = \sigma^2 B_{rr}/BW \tag{41}$$

Calculation of k_r'' and D_r from a map of U

Suppose that we start from a set of approximate constants $k_1' \ldots k_N'$ and that we have calculated values of U for a sufficient number of sets in the neighborhood, to determine the coefficients in

$$U = c_0 + 2 \sum_r c_{0r} x_r + \sum_r \sum_s c_{rs} x_r x_s \tag{42}$$

$$x_r = k_r - k_r' \tag{42a}$$

The minimum point is then found from the equation system (differentiating U):

$$\sum_s x_s'' c_{rs} + c_{0r} = 0, \; (r = 1,2 \ldots N) \tag{43}$$

which gives the "best values"

$$x_r'' = -\sum_s c_{0s} C_{rs} C^{-1}; \; k_r'' = k_r' + x_r'' \tag{43a}$$

Here, C is the determinant of the matrix $\| c_{rs} \|$, and C_{rs} the subdeterminant of c_{rs}.

Inserting (43) into (42) gives

$$U_0 = U_{\min} = c_0 + 2 \sum_r c_{0r} x_r'' - \sum_r c_{0r} x_r'' = c_0 + \sum_r c_{0r} x_r'' \tag{44}$$

We may compare (35) or (40) and (42). Since the second-degree terms must be independent of parallel shifts of the coordinates, we have

$$c_{rs} = b_{rs} W; \; C_{rs} = B_{rs} W^{N-1}; \; C = BW^N \tag{45}$$

We may derive an expression for the standard deviations, starting from (41), taking $\sigma^2 = U_0/(n - N)$ from (17), and inserting (45):

$$D_r^2 = D^2\{k_r''\} = U_0 C_{rr}/C(n - N) \tag{46}$$

The procedure would then be as follows. In order to find the constants c_0, c_{0r} and c_{rs} in (42), one determines at least as many, thus $1 + N + \frac{1}{2} N (N + 1) = \frac{1}{2}(N + 1)(N + 2)$ values for U: 3 values for $N = 1$, 6 values

for $N = 2$, 10 for $N = 3$, *etc.* From these one calculates the constants in (42), then the "best" values k_r'' from (43a), U_0 from (44), the "standard deviation" in y, σ, from (17) and the "standard deviations" of the k_r'' from (46). For both (43a) and (46) one should calculate the reciprocal matrix of c_{rs}, with elements $C_{rs}C^{-1}$.

Geometrical interpretation; the D boundary

We may imagine the function $U(k_1 \ldots k_N)$ as an N-dimensional surface in $(N + 1)$-dimensional space. We shall introduce, as a generalization of the result (30), the D *boundary*, characterized by

$$U = U_0 + \sigma^2 \tag{47}$$

From (47) and (40), on the D boundary

$$\sum_r \sum_s d_r d_s b_{rs} = \sigma^2/W \tag{48}$$

If $N = 2$, the U surface (the pit) is an elliptic paraboloid and the D boundary an ellipse; if $N = 3$, the D boundary is an ellipsoid *etc;* in general, the U surface is a generalized elliptic paraboloid and the D boundary a generalized ellipsoid.

Now we propose that for each k_r the standard deviation D_r is equal to the maximum value that d_r can attain on the D boundary. Differentiating (48) gives

$$\sum_r \mathrm{d}d_r \sum_s d_s b_{rs} = 0$$

For d_r to be extreme we must then have

$$\sum_s d_s b_{ts} = 0,\ t \neq r\ ;\ \sum_s d_s b_{rs} = c \neq 0 \tag{49}$$

where c is a constant to be eliminated. The solution of (49) is

$$(d_r)_{\max} = c\, B_{rr}B^{-1}\ ;\ d_s = c\, B_{rs}B^{-1} = (d_r)_{\max} B_{rs}B_{rr}^{-1} \tag{49a}$$

Inserting into (48) first (49), then (49a), we find

$$\sigma^2/W = (d_r)_{\max} \sum_s d_s b_{rs} = (d_r)^2_{\max} \sum_s B_{rs}b_{rs}B_{rr}^{-1} = (d_r)^2_{\max} B B_{rr}^{-1} \tag{50}$$

Comparison of (50) and (41) confirms our proposition:

$$(d_r)_{\max} = D_r = D\{k_r''\} \tag{51}$$

Example, $N = 2$. Let us, for illustration, assume that we measure

$$y \approx f = k_1 + k_2 a \tag{52}$$

Hence in (31), $a_{1i} = 1$, $a_{2i} = a_i$ and, from (33) and (34)
$Wb_{11} = \Sigma w_i = W$; $Wb_{12} = \Sigma w_i a_i = W\bar{a}$ etc., or in brief
$b_{11} = 1$; $b_{12} = \bar{a}$; $b_{22} = \overline{aa}$; $c_1 = \bar{y}$; $c_2 = \overline{ay}$; $B = \overline{aa} - \bar{a}^2$;

The bar stands for average: $\overline{aa}$ is the average of a^2, *etc.* From (37) we find:

$$k_1'' = (\bar{y}\,\overline{aa} - \overline{ay}\,\bar{a})\, B^{-1}\ ;\ k_2'' = (\overline{ay} - \bar{a}\,\bar{y})\, B^{-1} \tag{53}$$

The D boundary (48) is an ellipse:

$$d_1^2 + 2\bar{a}\, d_1 d_2 + \overline{aa}\, d_2^2 = \sigma^2/W \tag{54}$$

The "standard deviations" (41) of the "best" values are:

$$D_1 = \sigma\sqrt{\overline{aa}}\,/\sqrt{BW}\,;\; D_2 = \sigma\,/\sqrt{BW} \tag{55}$$

By a shift of origin we may replace k_1 by k_1^*, and a by a^*, defined by

$$k_1^* = k_1 + k_2\bar{a}\,;\; a^* = a - \bar{a}\,;\; y = k_1^* + k_2 a^* \tag{52a}$$

We then find

$$b_{11}^* = 1, b_{12}^* = 0\,;\; b_{22}^* = \overline{aa} - \bar{a}^2 = B^* = B\,;\; c_1^* = \bar{y}\,;\; c_2^* = \overline{ay} - \bar{a}\,\bar{y}\,;\; k_1^{*\prime\prime} = k_1^{\prime\prime} + k_2^{\prime\prime}\,\bar{a} \tag{53a}$$

The D boundary (48) is now another ellipse:

$$d_1^{*2} + Bd_2^2 = \sigma^2/W \tag{54a}$$

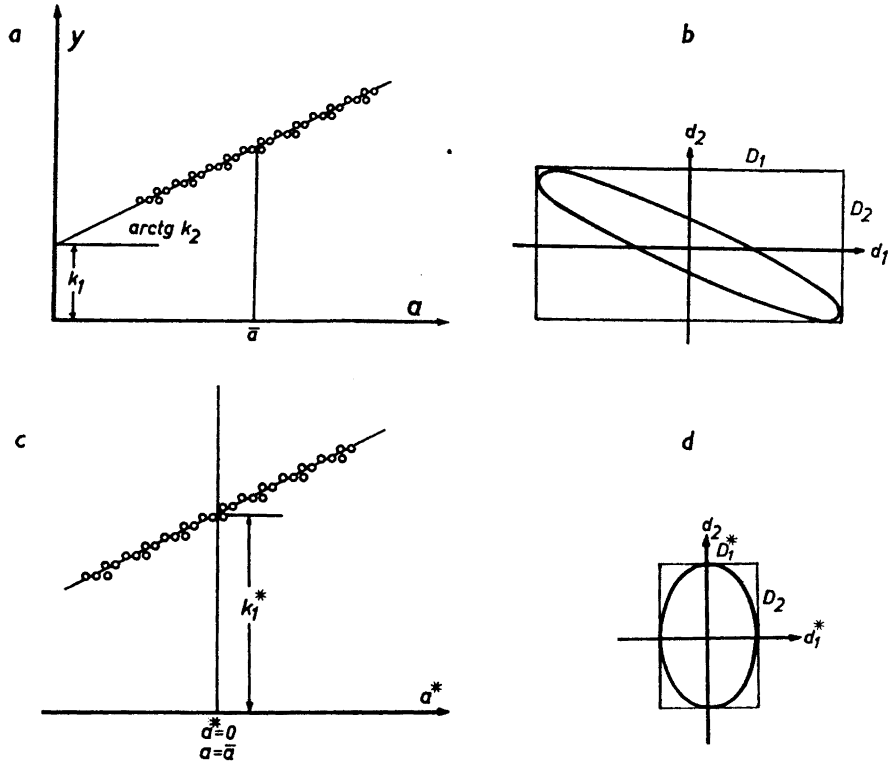

Fig. 2. (Schematic) a) experimental points $y(a)$ and "best" line, $y = k_1 + k_2 a$. b) "D boundary", in this case a skew ellipse. c) = Fig. 2 a, with origin shifted to the average value $\bar{a}$. d) D boundary corresponding to 2 c: now the axes of the ellipse coincide with the coordinate axes. Explanations, see text.

The standard deviations (41) are

$$D_1^* = \sigma / \sqrt{W} \; ; D_2 = \sigma / \sqrt{BW} \tag{55a}$$

The schematic Figs. 2a and 2c indicate the experimental points and "best" line, with the two different choices of origin; Figs. 2b and 2d give the corresponding D boundaries, which indicate the shape of the "pit". The scale of d_1 and d_1^* is magnified in comparison with k_1 and k_1^*. The scale for d_2 is arbitrary.

For a given set of points, the "best" line is independent of the transformation (52a), and so is the standard deviation D_2 of the slope. However, the standard deviation of the constant k_1 is larger than the value D_1^* obtained if the origin is taken at the average $\bar{a}$.

In Figs. 2a—2b the pit is skew: if k_1 is fixed at another value than the "best", say at a higher value, then the minimum for U is obtained at a slope k_2 which is smaller than the "best" one. In Figs. 2c—2d, however, the two unknown constants are independent: the same value for the slope k_2 is obtained whatever value is assumed for k_1^*.

The general non-linear case

Now let us assume that we have a non-linear relationship — perhaps not even explicit — between $y \approx f$ in (1) and the various k_r. Such a case is hard to attack by the standard straight-forward "least squares" method. We shall, however, still adopt as a criterion for the "best" values k_r that they should give a minimum in U (8a).

By means of a high-speed computer it is relatively easy to calculate U for a number of sets of the k_r. In principle one might start with some approximate set of k_r — calculated, estimated or guessed — by trial and error find one's way to regions with lower and lower U values, and finally come as close as desired to the minimum point U_0. With one unknown ($N = 1$) this is easy enough, but some experience has shown us that even with $N = 2$ this may be a lengthy procedure, especially if the "pit" is skew (*cf.* Fig. 2b). A more systematic method of search is therefore needed.

The equation of the "pit" (10) in the general case may be very complicated. However, we may use Taylor's series to develop U as a power series of the coordinates d_r measured from the minimum point k_r''. The constant term is then U_0, and all terms of first degree in the d_r are zero, since U_0 is a minimum value. So, near the bottom of the pit we would have

$$U - U_0 = \sum_r \sum_s c_{rs} d_r d_s \; (+ \sum_r \sum_s \sum_t c_{rst} d_r d_s d_t + \ldots) \tag{56}$$

In the computer program "LETAGROP" to be described in a following paper (Ingri and Sillén [10]) all terms of higher degree than second are neglected in (56). This approximation should be better, the closer one is to the bottom of the pit.

Starting from an approximate set k_r' of the unknown constants, one calculates, by a systematic approach, the appropriate number of U values, $\frac{1}{2}(N + 1)(N + 2)$, and from them the constants in (42). Using the procedure

for the linear case, one then calculates with (43a) the parameters k_r'' of the minimum point.

If f is linear, one would get the correct coordinates of the minimum point, however bad the guessed k_r'. In the general case, because of the presence of terms of higher degree, the minimum point must be found by a series of successive approximations. In our experience hitherto with "LETAGROP" it seems that the procedure is reasonably rapidly convergent: 2—3 approximations suffice, dependent on how good the original guess is. However, there is certainly still much to be learnt about the complications that may arise in special cases.

Again, we shall define the D boundary by the equation

$$U - U_0 = \sigma^2 \tag{47}$$

As a measure of the standard deviations of the various k_r'' we shall use the maximum values D_r of the various d_r on the D boundary.

Once one knows the c_{rs} and hence the approximate shape of the pit, D_r can be calculated using (46). The influence of the terms of higher degree in (56) is minimized, and hence the approximation of D_r and k_r'' is better, if in the final approximation step the estimate k_r' is close to the minimum point, and the other points used are close to the D boundary.

A few additional points may be made in connection with Fig. 2. It is advisable to choose the constants to be determined, in such a way that their influence on the data is independent, thus so that the "pit" is as little skew as possible. For instance, if B/b is studied with mononuclear complexes (Example Ia), $\beta_1 \ldots \beta_N$ may be the best choice, whereas for data $Z(a)$, the step-wise constants K_1, $K_2 \ldots K_N$ are more independent: there are often ranges, where the Z value is only influenced by one or two of the K_r values.

A systematic error may often be thought of as an additional unknown constant (for instance an analytical error, Example III) which one should have included in the calculations, and which gives a skew pit (see Fig. 2b); if it did not, it would do little harm.

The expressions for the standard deviations $D\{k_r''\}$ in (41) contain the standard deviation in the y measurements, σ, and in addition only factors that depend on the arrangement of the experiments (the various a_{si}, see eqn. 33). It might thus be said (provided the general assumptions (*a*) — (*d*), page 161 are valid) that the standard deviation of each constant is determined as soon as the series of experiments has been designed. If the standard deviation for a specific constant is found to be relatively large, this may be because the constant is relatively small, or because the experiments were not particularly well designed for determining this constant.

Methods founded on the principle described may be used, as will be shown in subsequent papers, for a fairly rapid refining of the unknown constants in a number of problems, which have been inaccessible to the standard "least squares" treatment, and may thus save much time. However, ultimately they depend on graphical methods: especially the choice of the function f, and the choice of the first set of constants is preferably made by graphical methods, and the last step will be a graph, to check for systematic deviations.

In a development of the program one might check that the distribution of the deviations $(y_i - f_i)$ is "normal" or at least symmetrical, for instance by studying the various moments $\Sigma w_i(y_i - f_i)^m$, $m = 1, 3, 4...$ and the relation to the sum with $m = 2$ (which is U_0). One might even apply a chi-square test. It may be noted in passing that what Rydberg and Sullivan [4] denote as a χ^2 test (chi-square test) is not what is usually meant by the expression (Ref. [7], chapter 30) but rather a test that the σ^2 calculated from U_0 using (17) agrees reasonably well with the estimated experimental inaccuracy of y.

It would be deplorable if the use of LETAGROP or other, less powerful computer methods should lead to an over-estimate of the significance of "best" values. The main purpose of computer methods is to save time, for with good data the differences in results obtained by graphical and computer refining should not be large enough to be interesting. Most of the errors in chemical literature, unfortunately, would not be reduced by statistical treatment. Sometimes what is wanted is some theoretical understanding, or some imagination concerning the various possible reactions that may take place in a solution. Often, results can be improved, not by mathematical analysis but only bu purifying the reagents, repeating the experiments, varying the factors that may influence the results (range of concentrations *etc.*), and checking with independent experimental methods.

Acknowledgements. Thanks are due to many of my coworkers, and especially to Dr. Nils Ingri, for valuable discussions and never-failing willingness to help me in the practical computer work. After the manuscript was written, Dr. Germund Dahlqvist, Dr. Howard J. Evans Jr, Professor Ulf Grenander and Dr. Arne Håkansson have given helpful comments. Professor Harald Cramér was kind enough to read the manuscript.

This work is part of a program supported by *Statens Naturvetenskapliga Forskningsråd (Swedish Natural Science Research Council)* and *Statens Råd för Atomforskning (Swedish Atomic Energy Research Council)* and also by the *Office of Scientific Research* of the Office of Aerospace Research, USAF through its European office.

REFERENCES

1. Hietanen, S. and Sillén, L. G. *Acta Chem. Scand.* **13** (1959) 533.
2. McMasters, D. L. and Schaap, W. B. *Proc. Indiana Acad. Sci.* **67** (1958) 111.
3. Sullivan, J. C., Rydberg, J. and Miller, W. F. *Acta Chem. Scand.* **13** (1959) 2023.
4. Rydberg, J. and Sullivan, J. C. *Acta Chem. Scand.* **13** (1959) 186, 2057.
5. Rydberg, J. *Acta Chem. Scand.* **14** (1960) 157.
6. Rydberg, J. *Acta Chem. Scand.* **15** (1961) 1723.
7. Cramér, H. *Mathematical methods of statistics*, Uppsala 1945.
8. Moore, R. H. and Ziegler, R. K. *Los Alamos Report* LA-2367, 1960.
9. Dyrssen, D., Ingri, N. and Sillén, L. G. *Acta Chem. Scand.* **15** (1961) 694.
10. Ingri, N. and Sillén, L. G. *Acta Chem. Scand.* **16** (1962) 173.

Received June 21, 1961.

ACTA CHEMICA SCANDINAVICA 16 (1962) 173–191

High-speed Computers as a Supplement to Graphical Methods

II. Some Computer Programs for Studies of Complex Formation Equilibria

NILS INGRI and LARS GUNNAR SILLÉN

Department of Inorganic Chemistry, Royal Institute of Technology, Stockholm 70, Sweden

A series of programs for high-speed electronic computers have proved useful in investigations on equilibria with polynuclear complexes. The programs are so constructed, that, when a new system is to be studied, only a small part (the "SP") needs to be rewritten (and this is easily done) whereas the main part (the "HP") can be used without change. It could also be used for problems from other fields, chemical or not.

The programs KUSKA, PROKAUS, PROKAIS, HALTA and LETAGROP are given in full — written in Ferranti Mercury Autocode — their principles are discussed, and some initial difficulties of a general interest are pointed out. These programs solve the problems indicated in (6), in the text.

LETAGROP may be called a generalized least-squares method for finding a set of unknown constants from experimental data, even with a non-linear and implicit functional relationship. The principles of LETAGROP were indicated in part I [1].

The studies of complicated solution equilibria in this laboratory have required a fair amount of computational work. At first, the primary measurements (emf's, analyses, volumes) are reduced to the type of data, say (Z, a, B), (b, a, B), most suited for mathematical treatment. From these data, and with no previous assumption as to which out of all conceivable complexes A_pB_q are important, it is usually possible by a mainly graphical treatment to deduce the formulas and approximate formation constants of the main products, or at least to exclude all but a few possibilities. This part of the work is relatively simple.

The hard work, however, comes in with the refinement of the equilibrium constants, and the attempts to deduce formulas and stability constants for species present in smaller amounts. For the construction of the graphs it is often necessary to solve a large number of equations of, say, 6th, 7th or 12th

degree; if only desk computers are available, the best but still very time-consuming way is to use auxiliary graphs.

Since electronic high-speed computers were used to a large extent in the crystallographic work in this laboratory, it was natural to apply such computers to the computations of solution chemistry. Indeed, during the last year or so a Ferranti-Mercury computer has been used by workers of this laboratory to calculate projection maps[1] and species distribution diagrams for polynuclear systems, thus saving, for each system studied, weeks of drudgery and making it possible to increase the accuracy of the result.

The time-determining factor, which had earlier been the calculation of the points on the projection maps, now became the plotting of the points from the tables calculated by the computer. Especially for systems with many species, the refinement of the equilibrium constants required a large number of maps, which sometimes became a little difficult to survey. Since the standard "least squares" treatment (see, *e.g.*, Rydberg [2]) cannot be applied in our systems with polynuclear species, the program LETAGROP [3] was worked out in early 1961, which made possible a simultaneous refinement of many constants.

Notes on the teaching of computer programming

In the meantime, many more of the chemists in this laboratory learned how to program a computer by means of seminars and lectures in the department of inorganic chemistry, by learning from others, and by reading for themselves. The Ferranti-Mercury computer, which was used for most of our calculations of solution equilibria, has a very good and easily understandable automatic code [4], the "autocode". It seems possible in 4 hours lectures + 4 hours problem class to teach students how to write simple programs in the autocode, if one applies the same principles as when teaching a new language. One should rather begin by giving simple sentences and making it clear what they mean than by first studying the muscles of the tongue and larynx, or memorizing the grammar, or memorizing a dictionary.

One must only first realize that the computer contains a number of boxes (registers), each of which has a label like A, B, C_4, *etc.*, and contains a number which is zero until changed by order. Some boxes, the "indexes" I, J...S, T can only contain integers between -512 and $+511$ whereas the others can contain numbers between $\approx 10^{-70}$ and 10^{70}.

Practically the only other thing the chemist needs to know about the inside of the machine is that there is a little demon in it, the "computer", who can do simple arithmetical calculations very rapidly and who can place a new number in a given box, read the content of any box, and send letters and numbers to be printed, if he is told to do so in correct computer language.

At first we did not intend to publish our programs in detail since we thought that anybody who can write down a set of mathematical equations can also make a computer program for them. We have, however, come to think that it might be useful to publish some programs in full, and tell about our experiences since this might save time for other chemists, and help them to overcome initial hesitations and start programming for themselves.

The programs will be written in the Ferranti Mercury autocode [4] but should not be hard to translate to other computer codes.

Main parts of the program

The program that we give the computer to read, as a punched tape, in general consists of three parts, which are usually separate tapes, the first two ending with the instruction "→"; which means: "stop and hoot, and you will get more tape to read".

1. HP (huvudprogram) the main program.
2. SP (särprogram) the special program.
3. The data.

The HP has a name, usually derived from Swedish terms: Kuska, Proka, Halta, Letagrop. Each HP has been so devised that it can be applied to a general class of problems whereas everything that is special in a problem is stated in the SP. Thus, when one passes to a new chemical system, or a new hypothesis, only the SP need be rewritten, which is very easy, and there is no need to think through the functioning of the HP.

The data are the equilibrium constants, concentrations, *etc.*, needed in the calculations on a special problem.

Equations for polynuclear complexes

The programs Kuska, Proka and Halta were primarily designed for calculations on equilibria with polynuclear complexes; with a proper SP, however, they can also be applied to very different problems.

If two reagents, A and B, form a series of complexes A_pB_q, the law of mass action gives for each of these complexes

$$c_{pq} = [A_pB_q] = \beta_{pq}a^pb^q \qquad (1)$$

where a and b are the concentrations of free A and B. The mass balance gives [5] for the total (analytical) concentrations A and B, and the average number of A bound per B, Z:

$$B = b + \Sigma\, qc_{pq},\ A - a = BZ = \Sigma\, pc_{pq} \qquad (2)$$

In dealing with hydrolysis reactions, one often counts ($-H^+$) as the ligand [6]; then, a is replaced by h^{-1} in (1) whereas in (2)

$$BZ = h - H = \Sigma\, pc_{pq} \qquad (2a)$$

In eqns. (2) and (2a), the sums are taken over all sets (p, q).

In translation to computer language, it would be helpful to use symbols that are as similar as possible to those used by equilibrium chemists. However, a few changes must be made since the computer does not distinguish between small and big letters (upper and lower case letters), nor can it use double indices:

Chemical	$A(-H)$	B	Z	BZ	$a(h^{-1})$	b	c_{pq}	β_{pq}	$\log \beta_{pq}$
Computer	A	B	Z	C	U	V	c_i	b_i	e_i

The "chemical" symbols in parentheses are for the special ligand ($-H^+$). Although the usual typescript of the program uses only upper case letters, and sets the index on the main line, we have chosen for readability sometimes to use lower case letters and subscripts, even when we render computer language.

There are no special symbols for p and q; their numerical values for each complex follow from the SP.

With the symbols of the computer (but not yet correct computer language) eqns. (1) and (2) would read:

$$b_i = 10^{e_i} = \exp(e_i \ln 10) \; ; \; c_i = b_i U^p V^q \tag{3}$$

$$B = V + \Sigma q c_i \; ; \; BZ = C = \Sigma p c_i \tag{4}$$

In addition we have

$$A - U = BZ \tag{5}$$

or for the special ligand ($-H^+$)

$$A + 1/U = BZ \tag{5a}$$

The problems solved by the various programs are as follows:

Known	Searched for	Program	Table
B, U	V, *etc.*	Kuska	1
Z, V	B, U, *etc.*	Prokais	2
Z, U	B, V, *etc.*	Prokaus	3
A, B	U, V, *etc.*	Halta	4

(6)

The "known" quantities may be read one by one from the data tape on instructions like: "read B;". Preferably they are calculated as members of an arithmetical series with first term (say, a_1) and increment (say, a_2) given; then one uses a cycle instruction of the type: "$K = 0(1)R \; ; \; Z = a_1 + Ka_2$ ..... repeat;". In Tables 1—4 the programs are written for the most common way of giving the "known" quantities in each case. This part is easily rewritten if it should be necessary.

The SP contains the relationships $B(U, V)$ for Kuska, and in addition $C(U, V)$ for Prokais and Prokaus, and $A(U, V)$ for Halta. There is nothing in the main program that restricts the functions $B(U, V)$, *etc.*, to be of the forms given by (3) and (4) above. In fact, the same HP could equally well be adapted to an SP with any other functions of the two variables U and V.

The example below with Prokais and Prokaus will illustrate difficulties that may occur with functions that do not increase regularly with both U and V, and how these difficulties can be remedied.

In Tables 1—5, " ; " stands for "carriage return, line feed", the conventional division between two instructions.

Some practical details — such as the controlling indices used in various places — will not be discussed in the following but will be easily recognized by the reader who follows the program in detail.

Table 1. KUSKA.

HP

Title ; KUSKA ; chapter 0 ; $a \rightarrow 6$; $b \rightarrow 10$; $c \rightarrow 10$; $d \rightarrow 3$; $e \rightarrow 10$; $y \rightarrow 4$; newline ;
$H = \Psi\log(10)$; jump 1 ;
2) read(N) ; print(N)2,0 ; read(a_1) ; print(a_1)2,2 ; read(a_2) ;
print(a_2)2,2 ; read(R) ; print(R)3,0 ; read(E) ; print(E)1,5 ; newline;
$i = 1(1)N$; read(e_i) ; print(e_i)1,3 ; $b_i = \Psi\exp(He_i)$; repeat ; newline ;
7) read(B) ; print(B)1,5 ; $y_1 = EB$; newline ; $M = 0$;
$K = 0(1)R$; $W = a_1 + Ka_2$; $U = \Psi\exp(HW)$; print(W)2,2 ; $D = 1$; $V = D$; $G = 2$; jump 3 ;
4) $y_2 = \Psi\mathrm{mod}(B_0 - B)$; jump 5, $y_1 > y_2$; jump 8, $B > B_0$;
$G = 0.5$; $D = GD$; $V = V - D$; jump 3 ;
8) $D = GD$; $V = V + D$; jump 3 ;
6) repeat ; newline ; jump 7 ; → ;

SP

1) print(1.1)1,1 ; print(1.3)1,1 ; print(2.4)1,1 ; newline ; jump 2 ;
3) $c_1 = b_1UV$; $c_2 = b_2UVVV$; $c_3 = b_3UUVVVV$; $C_0 = c_1 + c_2 + 2c_3$;
$B_0 = V + c_1 + 3c_2 + 4c_3$; jump 4 ;
5) print(C_0/B)1,3 ; $M = M + 1$; jump 6, $2 > M$; newline ; $M = 0$; jump 6 ;
Ψexp ; Ψlog ; close ;

Data

3	−8.0	0.1	40	0.0001	; 5.27	7.31	13.50
N	a_1	a_2	*R*	*E*	e_1	e_2	e_3
0.6	0.4	0.2	0.1	0.05	0.02		
B	*B*	*B*	*B*	*B*	*B*		

KUSKA

Table 1 gives the HP, and an example of an SP for Kuska. Name from *kurvska*ra — family of curves. The specific example is from studies of the reactions of $B = B(OH)_3$ with $A = OH^-$ in 3M NaBr. In the SP given, the three complexes AB, AB_3, A_2B_4 ($B(OH)_4^-$, $B_3O_3(OH)_4^-$, $B_4O_5(OH)_4^{2-}$) were considered. The expressions for the equilibrium concentrations of the various complexes are readily recognized after label **3**) in the SP, and also the expressions for $BZ(C_0)$ and $B(B_0)$, The log β_{pq} are given as e_1 through e_3. The problem is to calculate, for a given B, Z as a function of $\log U = \log[OH^-]$. B is given a series of values, which are taken from the experiments. For each B, one sets $\log U = a_1 + Ka_2$, where K goes from 0 to R.

N is the number of complexes, E is the desired accuracy, B_0 and C_0 are the values for B and C calculated with a tentative value for V.

Already during the input of the HP and SP, the computer gives printing order for the title KUSKA, assigns boxes for $a_0 \rightarrow a_6$, $b_0 \rightarrow b_{10}$, *etc.*, and stores the remainder of the program in its quick memory. At "close" it stops, and when restarted begins to read instructions at "chapter 0". Then it calculates ln 10 for future use, has the values $p.q$ for the various complexes printed as decimal fractions (label **1** in SP), reads and prints a number of quantities from the data strip (label **2** in HP), and calculates the b_i from the logarithms e_i.

The main principle of the program is given in Fig. 1a, and still more abbreviated in Fig. 1b. After B has been read from the tape, the required accuracy $y_1 = EB$ is calculated, the first value of U is set, and V guessed. Then the machine begins to adjust V by means of the two "loops":

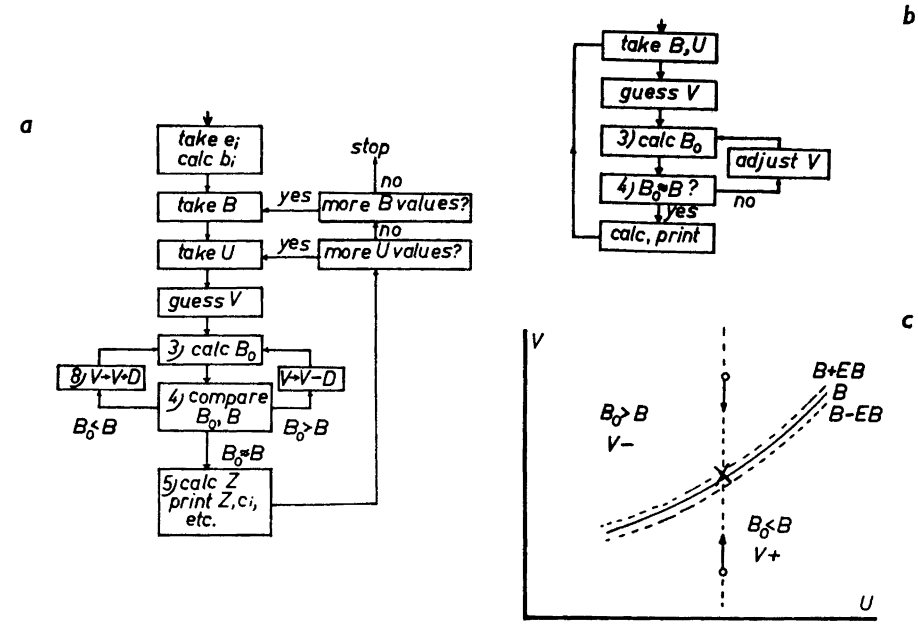

Fig. 1. a) Schematic flow-sheet for central part of program "KUSKA" (Table 1).
b) Same, abbreviated.
c) Adjustment of V for constant U in KUSKA. On the curves $V(U)$ shown, $B_0(U,V) = B$ and $= B \pm EB$.

3) $c_1 = b_1 UV$; $c_2 = b_2 UVVV$; $c_3 = b_3 UUVVVV$; $C_0 = c_1 + c_2 + 2c_3$;
$B_0 = V + c_1 + 3c_2 + 4c_3$; jump 4 ;

4) $y_2 = \Psi \mathrm{mod}(B_0 - B)$; jump 5, $y_1 > y_2$; jump 8, $B > B_0$;
$G = 0.5$; $D = GD$; $V = V - D$; jump 3 ;

8) $D = GD$; $V = V + D$; jump 3 ;

In this part of the program V is systematically varied (adjusted) until $y_2 = |B_0 - B| < EB = y_1$; after that, printing order is given ("jump 5"). D, the correction to V, is doubled (note that at first $G=2$) until V has become too large. After that, D is halved ($G=0.5$) at each turn and is added or subtracted from V depending on whether B_0 is less or larger than B.

To illustrate, if the correct value for V were 59.8, a series of estimated values for V and the following corrections $\pm D$ might be as follows:

1(+2) 3(+4) 7(+8) 15(+16) 31(+32) 63(−16) 47(+8) 55(+4) 59(+2) 61(−1) 60(−0.5) 59.5(+0.25) 59.75(+0.125) *etc.*

When the desired adjustment has been obtained, the values for U, V, all c_i, B and BZ are known so that whatever quantities are needed may be printed. In the special case, only Z was asked for; by using the index M, a more economic use of the paper is achieved. (Six values are printed on the same line).

Table 2. PROKAIS.

```
HP
Title ; PROKAIS ; Chapter 0 ; a→6 ; b→10 ; c→10 ; d→3 ; e→10 ; y→4 ;
   newline ; H=Ψlog(10) ; a5=Ψexp(145) ; a6=Ψexp(−145) ; jump 1 ;
2) read(N) ; print(N)2,0 ; read(a1) ; print(a1)1,3 ; read(a2) ; print(a2)1,3 ; read(R) ;
   print(R)3,0 ; read(a3) ; print(a3)1,2 ; read(a4) ; print(a4)1,2 ; read(S) ; print(S)3,0 ;
   read(E) ; print(E)1,6 ; newline ;
7) i=1(1)N ; read(ei) ; print(ei)1,3 ; bi=Ψexp(Hei) ; repeat ; newline ;
K=0(1)R ; Z=a1+Ka2 ; print(Z)1,3 ; newline ;
M=0 ;
L=0(1)S ; V=Ψexp(LHa4−Ha3) ; D=1 ; U=D ; G=2 ; jump 3 ;
4) jump 6, B0>a5 ; jump 6, a6>B0 ; y1=B0Z−C0 ; y2=Ψmod(y1) ; y3=EB0 ;
   jump 5, y3>y2 ; jump 8,y1>0 ;
G=0.5 ; D=GD ; U=U−D ; jump 3 ;
8) D=GD ; U=U+D ; jump 3 ;
6) repeat ;
newline ; repeat ;
newline ; jump 7 ; → ;

SP
1) print (1.1)1,1 ; print(1.3)1,1 ; print(2.4)1,1 ; newline ; jump 2 ;
3) c1=b1UV ; c2=b2UVVV ; c3=b3UUVVVV ; C0=c1+c2+2c3 ;
   B0=V+c1+3c2+4c3 ; jump 4 ;
5) W=Ψlog(U) ; print(W/H)3,3 ; W=Ψlog(B0) ; print (W/H)1,3 ; M=M+1 ;
   jump 6, 3>M ; newline ; M=0 ; jump 6 ;
   Ψexp ; Ψlog ; close ;

Data
   3    0.1  0.1  6    2    0.2  16   0.0001 ;  0    0    0.9 ;
   N    a1   a2   R    a3   a4   S      E       e1   e2   e3

   0    0    0.6 ; 0    0    0.3 ; 0    0    0 ; 0    0   −0.3  0    0   −1 ;
   e1   e2   e3    e1   e2   e3    e1   e2   e3   e1   e2   e3   e1   e2   e3

   0    0   −1.6 ;
```

After printing, another value of U, and eventually another value of B, is taken.

The procedure is illustrated in Fig. 1c, which gives curves $V(U)_{B_0}$ thus curves with B_0 constant in the coordinate plane (U, V). The adjustment is satisfactory and the calculation ended when B_0 comes within the limits $B \pm EB$.

PROKA

In the names Prokais and Prokaus, "Proka" comes from the Swedish *pro*jektions*kar*ta = projection map and "S" from säkring (safety catch).

Tables 2 and 3 give the HP for Prokais and Prokaus. Table 2 also gives an example of an SP (which is the same for Prokais and Prokaus) and of a data strip.

The SP shown refers to the same system, $OH^- + B(OH)_3$, and the same complexes as in Kuska (**3** and **1**).

The Proka programs can be used for calculating a series of projection maps [1] $\log B(\log U)_Z$ for comparison with the experimental data, and estimation of equilibrium constants. Since a normalized projection map is required, two of the equilibrium constants can arbitrarily be set equal to 1 (thus the

Table 3. PROKAUS.

HP

Title ; PROKAUS ; Chapter 0 ; $a \to 6$; $b \to 10$; $c \to 10$; $d \to 3$; $e \to 10$; $y \to 4$;
newline ; $H = \Psi\log(10)$; $a_5 = \Psi\exp(145)$; $a_6 = \Psi\exp(-145)$; jump 1 ;
2) read(N) ; print(N)2,0 ; read(a_1) ; print(a_1)1,3 ; read(a_2) ;print(a_2)1,3 ; read(R) ;
print (R)3,0 ; read(a_3) ; print(a_3)1,2 ; read(a_4) ; print(a_4)1,2 ; read(S) ;
print(S)3,0 ; read(E) ; print(E)1,5 ; newline ;
7) $i = 1(1)N$; read(e_i) ; print(e_i)1,3 ; $b_i = \Psi\exp(He_i)$; repeat ; newline ;
$K = 0(1)R$; $Z = a_1 + Ka_2$; print(Z)1,3 ; newline ;
$M = 0$;
$L = 0(1)S$; $U = \Psi\exp(LHa_4 - Ha_3)$; $D = 1$; $V = D$; $G = 2$; jump 3 ;
4) jump 6, $B_0 > a_5$; jump 6, $a_6 > B_0$;
$y_1 = B_0Z - C_0$; $y_2 = \Psi\mathrm{mod}(y_1)$; $y_3 = EB_0$; jump 5, $y_3 > y_2$; jump 8, $0 > y_1$;
$G = 0.5$; $D = GD$; $V = V - D$; jump 3 ;
8) $D = GD$; $V = V + D$; jump 3 ;
6) repeat ;
newline ; repeat ;
newline ; jump 7 ; $\to$;

SP

1) print(1.1)1,1 ; print(1.3)1,1 ; print(2.4)1,1 ; newline ; jump 2 ;
3) $c_1 = b_1UV$; $c_2 = b_2UVVV$; $c_3 = b_3UUVVVV$; $C_0 = c_1 + c_2 + 2c_3$;
$B_0 = V + c_1 + 3c_2 + 4c_3$; jump 4 ;
5) $W = \Psi\log(U)$; print(W/H)3,3 ; $W = \Psi\log(B_0)$; print (W/H)1,3 ; $M = M + 1$;
jump 6, $3 > M$; newline ; $M = 0$; jump 6 ;
Ψexp ; Ψlog ; close ;

Data

3	0.55	0.05	9	0.00	0.20	15	0.0001	;	0	0	0.9 ;						
N	a_1	a_2	R	a_3	a_4	S	E		e_1	e_2	e_3						
0	0	0.6 ;	0	0	0.3 ;	0	0	0 ;	0	0	−0.3 ;	0	0	−1 ;			
e_1	e_2	e_3	e_1	e_2	e_3	e_1	e_2	e_4	e_1	e_2	e_3	e_1	e_2	e_3			
0	0	−1.6 ;															

corresponding $e_i = \log \beta_{pq} = 0$). To Z a series of values $Z = a_1 + Ka_2$ are given, where K goes from 0 to R. For each value of Z, log V (in Prokais) or log U (in Prokaus) passes through a series of values $(La_4 - a_3)$ where L goes from 0 to S.

The general principle of Prokais is shown in Fig. 2a, (flowsheet) and Fig. 2b. For each set (Z, V), U is adjusted until the ratio C_0/B_0 is close enough to the Z desired. If $C_0/B_0 < Z$, then U is increased, otherwise decreased. This procedure converges as rapidly as Kuska in case $Z(U)_V$ increases over the whole range, as shown in Fig. 2b.

In some systems, however, $V(U)_Z$ has a maximum (Fig. 2c). This behavior was first met with in the borate system, for $Z > 0.5$. If V is chosen larger than the maximum value, C_0/B_0 is always $< Z$, and the computer goes on increasing U until some number (one of the c_i, B_0 or C_0) becomes larger than the largest allowable number in the computer ($2^{256} \approx 10^{77}$) and the machine stops.

In order to avoid machine stops for this reason, there is a safety exit after label **4**: if B_0 would become larger than $a_5 = e^{145} \approx 10^{63}$ or smaller than $a_6 = e^{-145}$, the machine stops trying to solve the equations and jumps to the next set (V, Z).

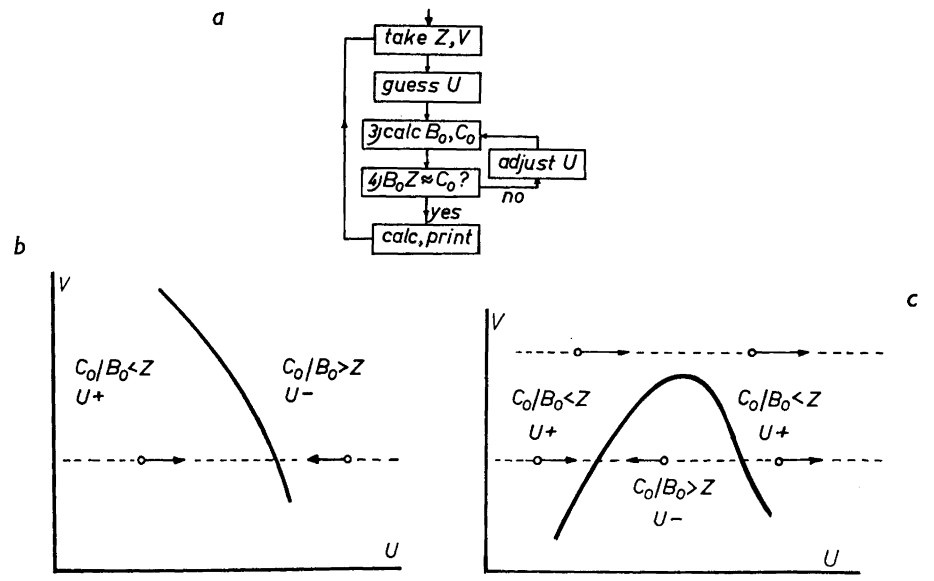

Fig. 2. a) Schematic flow-sheet for central part of "PROKAIS" (Table 2).
b) Adjustment of U for constant V with PROKAIS, to approach desired value Z for C_0/B_0 (thick curve).
c) Behavior of PROKAIS for curve with a maximum.

Even for values smaller than the maximum V, at a given Z Prokais can only find U values that correspond to the left branch of the curve, in Fig. 2c. If one happens to pass beyond the right-hand branch, U will increase till the safety catch is triggered.

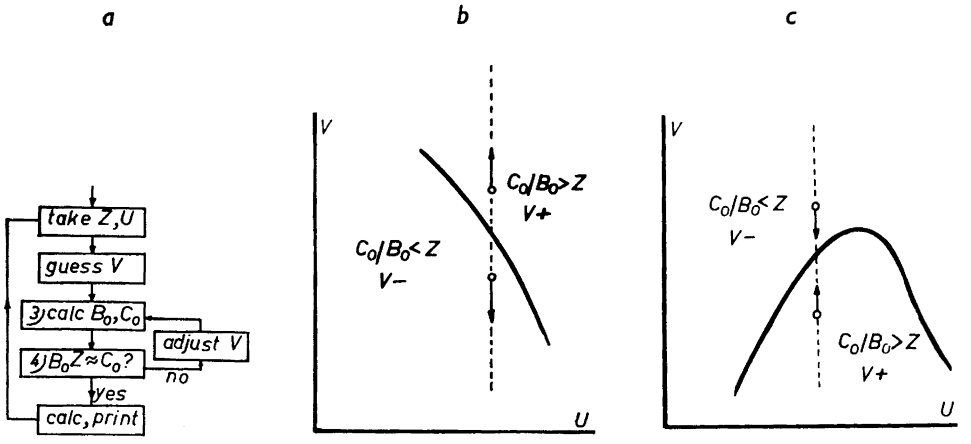

Fig. 3. a) Schematic flow-sheet for central part of "PROKAUS" (Table 3.).
b) Behavior of PROKAUS for curve shown in Fig. 2 b (no adjustment possible).
c) Adjustment of V for constant U with PROKAUS for curve shown in Fig. 2 c.

For systems of this type, the program Prokaus (Table 3, Figs. 3a—c) has been devised: for various sets (Z, U) it adjusts V, increasing V if C_0/B_0 is too high and decreasing V if C_0/B_0 is too low. This program will give the whole of a curve like that in Fig. 3c, but no part of a curve like that in Fig. 3b. For a system where part of the ranges behaves like Figs. 2c—3c, one should apply both Prokais and Prokaus, and so obtains supplementary parts of the projection map, overlapping to some extent.

Table 4. HALTA.

HP

```
Title ; HALTAPIFF ; Chapter 0 ; a→6 ; b→10 ; c→10 ; d→3 ; e→10 ; f→3 ; g→4 ; u→4 ;
   v→4 ; w→4 ; y→4 ; newline ; H=Ψlog(10) ; jump 1 ;
2) read(N) ; print(N)2,0 ; read(E) ; print(E)1,8 ; read(G1) ; print(G1)3,0 ; read(T) ;
   print(T)2,0 ; newline ;
i=1(1)N ; read(ei) ; print(ei)1,3 ; bi=Ψexp(Hei) ; repeat ; newline ;
7) read(B) ; print(B)1,5 ; newline ; y0=EB ; y=y0G1 ;
read(a1) ; print(a1)1,5 ; read(a2) ; print(a2)1,5 ; read(R) ; print(R)2,0 ; newline ;
U=0.1B ; V=0.1B ;
K=0(1)R ; A=a1+a2K ; print(A)1,5 ; Q=0 ;
14) P=0 ; U0=U ; D0=2 ; D2=V ; G=2 ; J=0 ; jump 3 ;
4) y1=B−B0 ; y2=Ψmod(y1) ; y3=A−A0 ; y4=Ψmod(y3) ;
   J=J+1 ; jump 17, J>100 ; jump 10, 1>D0 ; jump 9, y0>y2 ;
15) jump 8, y1>0 ; G=0.5 ; D2=GD2 ; V=V−D2 ; jump 3 ;
8) D2=GD2 ; V=V+D2 ; jump 3 ;
9) jump 5, y>y4 ; P=P+1 ; VP=V ; Q=Q+1 ; D0=0 ; D1=U ; G=2 ; J=0 ;
10) jump 11, y0>y4 ; jump 12, y3>0 ;
G=0.5 ; D1=GD1 ; U=U−D1 ; jump 3 ;
12) D1=GD1 ; U=U+D1 ; jump 3 ;
11) jump 5, y>y2 ; P=P+1 ; UP=U ; Q=Q+1 ;
jump 5, Q>T ; jump 13, P>3 ;
D0=2 ; D2=V ; G=2 ; J=0 ; jump 15 ;
13) F0=2U2−U0−U4 ; U3=U4−U2 ; V2=V3−V1 ; W3=U3/F0 ; U=U4+U3W3 ;
   V=V3+V2W3 ; Q=Q+1 ;
jump 16, 0>U ; jump 16, 0>V ; jump 14 ;
16) print(16)2,0 ; newline ; U=U4 ; V=V3 ; jump 14 ;
17) print(17)2,0 ; newline ; jump 11, 1>D0 ; jump 9 ;
6) repeat ;
newline ; jump 7 ;→ ;
```

SP

```
1) Title ; URAN 14 APRIL 1961 ; print(2.2)1,1 ; print(4.3)1,1 ;
   print(5.3)1,1 ; print(6.4)1,1 ; newline ; jump 2
3) W=UUV ; c1=b1VW ; c2=b2c1W ; c3=b3c1UW ; c4=b4c1c1UU ;
   A0=−1/U+2c1+4c2+5c3+6c4 ; B0=V+2c1+3c3+4c4 ; jump 4
5) W=A0+1/U ; Z=W/B0 ; print(1000Z)3,3 ; W=Ψlog(U) ;
   print(W/H)1,5 ; W=2000c1/B0 ; print(W)3,3 ; W=4000c2/B0 ;
   print(W)3,3 ; W=5000c3/B0 ; print(W)3,3 ; W=6000c4/B0 ;
   print(W)3,3 ; print (Q) 3,0 ; newline ; jump 6
   Ψexp ; Ψlog ; close ;
```

Data

```
4      0.000001   100   33   −6.03   −7.17   −10.52   −7.36  ;  0.100   0.050
N        E        G1    T     e1      e2      e3       e4        B       a1

−0.004   30  ;  0.075  0.040  −0.003  30  ;  0.050  0.030  −0.002  30  ;  0.025
 a2      R        B      a1     a2      R        B      a1     a2      R       B
```

HALTA

Table 4 gives the HP for a member (Haltapiff) of the program family Halta, (*halt-ta*beller = concentration tables) which is intended to calculate U and V, and thus all concentrations c_i, in cases where only A and B are known. The SP and the data are for the hydrolysis of $B = UO_2^{2+}$; $A = -H^+$. (Calorimetric titrations of Dr. Kurt Schlyter).

This program has, among other applications proved useful for calculations of the concentrations of various species in calorimetric titrations with polynuclear equilibria.

The SP and the data refer to the hydrolysis of $B = UO_2^{2+}$, $A = -H^+$. It is assumed that (in the range studied) only the complexes A_2B_2, A_4B_3, A_5B_3, and A_6B_4 need to be considered; (compare list at SP label **1**). In the present case, the variable $W = U^2V$ has been introduced for simplicity. The equilibrium concentrations $c_1 ... c_4$ of the four complexes are easily recognized at label **3** of the SP.

When U and V, and thus the c_i are known, the printing order (SP, label **5**) in this case starts with 1 000 Z, with three decimals. The following numbers are: log U(= $-\log [H^+]$), and $2c_1/B$, $4c_2/B$, *etc.* = the number of A per B bound in the form of A_2B_2, A_4B_3, *etc.*

B has a series of values, which are here given by the experiments. For each B, one uses a series of values, $A = a_1 + Ka_2$, where K goes from 0 to R. The first, and more subordinate, part of the HP can be rewritten to meet special needs, for instance, so that A and B are varied simultaneously, as happens in some titrations.

The flow-sheet of the first edition of Halta is given in Fig. 4a. The procedure is depicted in Fig. 4b, which gives, in the (U, V) plane, the two curves on which the functions A_0 and B_0 have the desired values, $A_0 = A$ and B_0

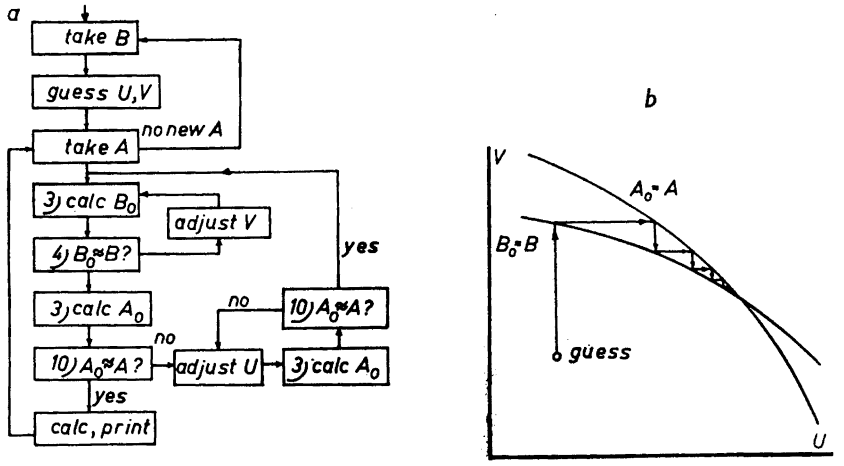

Fig. 4. a) Schematic flow-sheet of original "HALTA" (complete program not given here)
b) Performance of original HALTA in approaching the desired point (intersection point between $B_0(U, V) = B$ and $A_0(U, V) = A$).

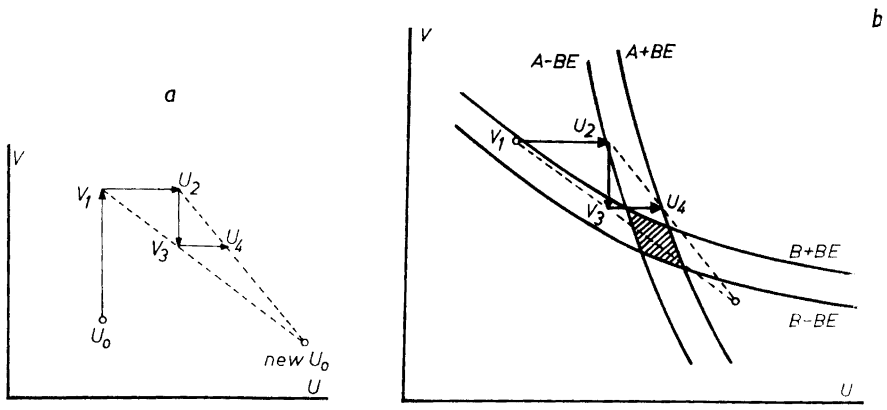

Fig. 5. a) "Shot" for a new point in "HALTAPIFF" (Table 4).
b) "Miss" because of bad aim. The shaded area is the "bull's eye", where both equations $B_0 = B$ and $A_0 = A$ are fulfilled within the desired accuracy.

$= B$. First, U is kept constant and V adjusted to make $B_0 = B$, then V is kept constant and U adjusted to make $A_0 = A$, *etc.* In this way, one approaches the intersection point of the two curves. The convergence was sometimes rather rapid (a matter of a few seconds, thus something like 3—5 turns between the curves). However, in some cases the machine could keep working for several minutes before it found the intersection point; it always did find it, but at a high cost of computer time. The performance was followed in detail, and in one case, where the angle between the two curves was small, 210 attempts were counted before the intersection point was found within the accuracy prescribed; in other cases the number may have been still higher.

In order to save time we let the machine "shoot" its way, (Fig. 5a). After it had found four points, two on each curve, it calculated the point of intersection of two straight lines through them (label **13**, Table 4), and used this point as its next guess. This speeded up the approach considerably, but the computer invented a number of practical jokes. Sometimes the machine stopped because the shot had hit a point with negative U or V; this was easily avoided by adding a new "safety catch" (label **16**).

In a number of cases, the computer was stuck in an infinite loop so that it kept working on a single point for minutes without result (Fig. 5b). The reason was found to be that for each adjustment one does not reach the curve $B_0 = B$ or $A_0 = A$ exactly but is certain only to come within the limits $B_0 = B \pm BE$ and $A_0 = A \pm BE$, thus in a band surrounding the correct curves (in the program, $y_0 = BE$). The closer one is to the intersection point, the larger will be the risk that the small deviations will give a bad aim, so that the "shot" may even take one further away from the intersection point than one was originally. Therefore, the computer was aiming and shooting madly to hit the bull's-eye but the hit-points bounced away.

As a remedy, the requirements on fit were sharpened by decreasing E; on the other hand, the "bull's-eye" was increased by giving printing order at a larger tolerance, $y = G_1BE$, each time one had solved the equation for B_0 and first tried to see if the one for A_0 was satisfied (labels **4→9→5**). The calculations were shortened in most cases, but eventually the computer could again get stuck in a loop. This might probably have been remedied by decreasing E and increasing G_1 further, but instead the calculation was interrupted after a certain number, T, of attempts; this is controlled by a counting index Q. The number of attempts Q, is printed as a check (label **5**).

LETAGROP

Part 1 of this series of papers [3] described a general principle for adjusting a number of unknown constants k_r from measurements of the function y, containing the constants searched for and a number of known quantities a_1, a_2... The principle is that the (weighted) error-square sum is calculated for a number of points, as a function of the unknown constants (which are here considered as variables). The error-square sum is approximated as a second-degree equation and its minimum searched for. By using the "D boundary", one can also derive expressions for the "standard deviation" of the various constants.

Table 5. LETAGROP.

HP
Chapter I ; Title ; LETAGROP ; $a\rightarrow 13$; $b\rightarrow 13$; $c\rightarrow 13$; $d\rightarrow 13$; $e\rightarrow 13$; $F\rightarrow 120$;
$g\rightarrow 13$; $h\rightarrow 13$; $U\rightarrow 120$; $v\rightarrow 13$; $X\rightarrow 2$; $Z\rightarrow 120$;
1) $a'\approx 1$; $x'\approx 101$; $y'\approx 201$; $v'\approx 1001$; $w'\approx 2001$; $b'\approx 3001$; $c'\approx 4001$; $d'\approx 5001$;
jump 7, $L>0$; jump 2, $M=1$; jump 3, $M=2$; $X_0=X$; $j=1(1)R$; read(g_j) ;
read(h_j) ; repeat ; $j = 1$;
5) $M=1$; $s=\Psi$intpt(g_j) ; $e_s=e_s+h_j$; across 3/0 ;
2) $X_1=X$; $e_s=e_s-2h_j$; $M=2$; across 3/0 ;
3) $X_2=X$; $e_s=e_s+h_j$; jump 4, $X_2>X_1$; $h_j=-h_j$; $w=X_1$; $X_1=X_2$; $X_2=w$;
4) $a_j=0.25X_2-0.25X_1$; $d_j=0.25X_1+0.25X_2-0.5X_0$; $j=j+1$; jump 6, $j>R$; jump 5 ;
6) $\Psi_7(1)a_1$, R ; $j=0$;
11) $j=j+1$; jump 12, $j>R$;
$L=1(1)j$; $v_L=0$; repeat ; $v_j=d_j$; jump 10, $j=R$; $s=\Psi$intpt(g_j) ; $e_s=e_s+h_j$;
$L=j+1$;
8) $t=\Psi$intpt(g_L) ; $e_t=e_t+h_L$; across 3/0 ;
7) $v_L=0.5X-0.5X_0+a_j+a_L-d_j-d_L$; $e_t=e_t-h_L$; $L=L+1$; jump 9, $L>R$; jump 8 ;
9) $e_s=e_s-h_j$;
10) $O=R_j-R$; $\Psi_7(1001+O)v_1$, R ; jump 11 ;
12) $a=R$; $w'=\Psi_{16}(1001,a,a)$; $c\approx aa$; $b'=\Psi_{11}(1001,2001,c)$; $c'=\Psi_{17}(4001,a)$;
$c'=\Psi_{28}(3001,R,R)$; $x'=\Psi_{26}(4001,1,a,1,a)$; $y'=\Psi_{26}(101,1,1,1,a)$; $\Psi_6(201)y,1$
$\Psi_6(101)v_1$, R ; $X=X_0-y$; jump 14, $X>0$; $X=-X$; print(-1)1,1 ; newline ;
14) $w=Q-P+1-N$; $y=X/w$; $w=\Psi$sqrt(y) ; print(w)1,4 ; newline ;
$j=1(1)R$; $s=\Psi$intpt(g_j) ; print(s)2,0 ; $e_s=e_s+h_jv_j$; print(e_s)2,3 ;
$O=Rj-R+j$; $\Psi_6(4000+O)w,1$; $X=wy$; jump 13, $0>X$; $w=\Psi$sqrt(X) ; $X=wh$;
print(X) 1,3 ;
13) newline ; repeat ;
newline ; $'c'=\Psi_{15}(5001,c)$; across 14/0 ;
Ψsqrt ; close ;
Chapter 0 ; variables 1 ; $H=\Psi$log(10) ; jump 1 ;
2) read(Q) ; $K=1(1)Q$; read(F_K) ; read(U_K) ; read(Z_K) ; repeat ; *stop* ; jump 14, $R=-2$;
15) read(N) ; $i=1(1)N$; read(e_i) ; repeat ; read(E) ;

14) read(R) ; jump 15, $R=-1$; jump 2, $-1>R$; read(P) ; read(Q) ; $j=0$; $L=0$; $M=0$; $K=P$; jump 3 ;
6) $V=D$; $G=2$; $E_0=EB$; jump 7 ;
8) $D_0=\Psi\mathrm{mod}(B_0-B)$; jump 10, $E_0>D_0$; jump 9, $B>B_0$; $G=0.5$; $D=GD$; $V=V-D$; jump 7 ;
9) $D=GD$; $V=V+D$; jump 7 ;
11) $w=Z_0-Z_K$; $X=X+G_0ww$; jump 12, $R>0$; newline ; print(K) 2,0 ; print(F_K)1,5 print(U_K) 1,3 ; print(Z_K) 1,3 ; print(Z_0-Z_K) 1,4 ;
12) $K=K+1$; jump 13, $K>Q$; jump 5 ;
13) print(10000X) 3,4 ; print($Q+1-P$) 3,0 ; $K=P$; newline ; jump 14 ; $R=0$; across 1/1 ; → ;

SP

1) Title ; borat 3MNaClO$_4$; print(1.1)1,1 ; print(1.3)1,1 ; print(1.5)1,1 ; newline ; jump 2 ;
3) $X=0$; $i=1(1)N$; $b_i=\Psi\exp(He_i)$; print(e_i)1,3 ; jump 4, $i\neq 6$; newline ;
4) repeat ;
5) $B=F_K$; $w=14.22-U_K$; $U=\Psi\exp(Hw)$; $D=0.001$; jump 6 ;
7) $c_1=b_1UV$; $c_2=b_2UVVV$; $c_3=b_3UVVVVV$; $B_0=V+c_1+3c_2+5c_3$; jump 8 ;
10) $C_0=c_1+c_2+c_3$; $Z_0=C_0/B_0$; $G_0=1$; jump 11 ;
Ψexp ; close ; → ;

MD

90	;	0.01	;	6.283	;	0.08	;	0.01	;	6.342	;	0.07	;	;
Q		F_1		U_1		Z_1		F_2		U_2		Z_2		...

DS

3	;	−9.005	;	−6.911	;	−6.620	;	0.0001	;
N		e_1		e_2		e_3		E	

3	;	1	;	90	;	1	;	0.02	;	2	;	0.05	;	3	;	0.05	;
R		P		Q		g_1		h_1		g_2		h_2		g_3		h_3	

0	;	1	;	90	;
R		P		Q	

Table 5 gives an HP, which is applicable under rather general conditions, an SP, devised for a specific case from borate equilibria, and an example of data, which consist of two parts: the experimental data MD (mätdata) and DS ("dagens spaning, = day's orders for searching").

It has been necessary to change the symbols a little from part I, partly to use the language of the computer, partly to use symbols similar to those used in the older programs Kuska, Proka and Halta.

The experimental data are assumed to be given as triplets of numbers (F_K, U_K, Z_K), with K from 1 to Q. The present program provides for at most 120 such triplets thus $Q \leq 120$. (This is ample for most work on mononuclear complexes, but requires some random screening for most of our systems with polynuclear complexes).

The unknown quantities, N in number, are denoted by $e_1 ... e_N$, and one is assumed to know the function

$$Z_0 (F_K, U_K, e_1 ... e_N) \approx Z_K \tag{7}$$

The only error present is assumed to be the random error in Z_K; if a systematic error is suspected, it may be treated as another unknown constant e_i.

To each point measured one can assign a weight G_0, which can be expressed as a function of known quantities; this expression, like everything else that is special for the problem, is given in the SP.

The symbols in part I have been translated as follows to computer language:

Part I	k_r	N	y_i	f	a_{1i}	a_{2i}	n	w_i	U
Computer	e_i	N	Z_k	Z_0	U_K	F_K	Q or $(Q-\mathrm{P}+1)$	G_0	X

Calculating the error square sum

After stopping at "close", the computer begins to read the instructions at "Chapter 0": it calculates $H = \ln 10$, prints the various $p.q$ as before (**1**/0)*, reads the Q triplets of data (label **2**/0) and a set of approximate values for $e_1 \ldots e_N$ — calculated by graphical methods, estimated or guessed — and then it searches for the error square sum. At first (**3**/0 SP), the e_i may be recalculated to quantities (here the b_i) more suitable for the calculations. The following treatment differs depending on whether (7) is given explicitly or not.

Implicit equations. The program is specially designed for cases with two equations:

$$B = B_0(U,V,e_1 \ldots e_N)\,;\; Z_K = Z_0(U,V,e_1 \ldots e_N) \qquad (8,9)$$

Here, B and U are functions of F_K and U_K which are given in the SP, label **5**/0. Note that (9) differs from (7) in that V is unknown and must be eliminated using (8).

In the present case, Z_K is simply the number of OH bound per $B(OH)_3$, $B = F_K$ is the total boron concentration, $U_K = \log [OH^-] = \log U$, so that $U = 10^{U_K}$. The equations (SP, **7**/0) are easily recognized as expressing the law of mass action, and the mass balance.

First, V is calculated from the set (B, U) using a Kuska loop (**8**, **9**/0). Then, Z and the weight G_0 are calculated (SP, **10**/0), the squared error multiplied by the weight, $G_0(Z_0 - Z_K)^2$, is added to the error square sum X(HP, **11**/0), and a new value for K is taken. When all points have been worked through (**13**/0), 10 000 times the error square sum, 10 000 X, is calculated and printed, together with the number of points $(Q + 1 - P)$.

Explicit equations. If, on the other hand, (7) is given explicitly, the expression for Z can be calculated straightforwardly in the SP between (**5**/0) and "jump 11", without any need to go through a Kuska loop. One should, however, set out the labels **7**) and **10**) at some harmless point, if one does not care to delete the Kuska in the HP. (The computer does not accept "jump" instructions, even if void, without a corresponding label).

If the data consist of sets of two values (as for instance in the adjustment of a straight line), $U_K = 0$ may be written everywhere and not used, or the HP may be rewritten for data pairs.

*1/0" means label 1 in chapter 0.

Table 6. Example of results with LETAGROP.

LETAGROP

1.1	1.3	1.5		
−9.005	−6.911	−6.620	4.0083	90
−8.985	−6.911	−6.620	4.8430	90
−9.025	−6.911	−6.620	4.8535	90
−9.005	−6.861	−6.620	6.8642	90
−9.005	−6.961	−6.620	7.8930	90
−9.005	−6.911	−6.570	4.1038	90
−9.005	−6.911	−6.670	4.1076	90
−8.985	−6.861	−6.620	8.7998	90
−8.985	−6.911	−6.570	4.9771	90
−9.005	−6.861	−6.570	7.7148	90

0.0021

1	−9.007	0.005
2	−6.903	0.008
3	−6.648	0.047

−9.007	−6.903	−6.648				
1	0.01000	6.283	0.080	−0.0010		
2	0.01000	6.342	0.070	−0.0004		
3	0.01000	6.434	0.054	0.0027		
4	0.01000	6.521	0.046	0.0018		
5	0.01000	6.659	0.033	0.0015		
6	0.01000	6.808	0.024	0.0007		
—	—	—	—	—		
—	—	—	—	—		
90	0.60000	7.568	0.095	−0.0039	3.9416	90

The first table gives e_1, e_2, e_3, X and Q. Then comes the standard deviation of Z, 0.0021; the "best" values of e_1, e_2 and e_3 with their standard deviations; and a table of the data (B, log U, Z) ending with the deviation in Z.

At last comes the error square sum with these "best" values, and the number of points, Q.

Variation of the e_i

All the operations described hitherto have been made in Chapter 0 of HP + SP. When the error-square sum, X, has been calculated (**13**/0), the computer passes across to **1**/1, thus label **1** in Chapter 1, and begins to vary the constants systematically; for each new set of e_i it goes back to chapter 0 to calculate the error square sum X.

Through DS the computer has been told how many (R) constants it should vary (**14**/0), and after (**1**/1) it is told their indices ($g_1 ... g_R$), and the steps to vary them in ($h_1 ... h_R$).

It may be helpful to compare Table 5 with Table 6, which gives an example of the results, in a special case. The first line in Table 6 gives the first approximate values of the constants (let us call them e_i') and the X value (X_0) obtained with them.

The first constant e_s ($s = g_1$ is here = 1) is first set at $e'_s + h_1$ (**5**/1), the error sum calculated and called X_1 (**2**/1), e_1 set at $e_s' - h_1$, the error sum calculated and called X_2, and e_s reset at e_s' (**3**/1). If the second error-square sum,

X_2 is smaller than the first, e_s' should probably be decreased; then h_1 is replaced by $(-h_1)$, and X_1 and X_2 change places. This is done in order to have the mixed points (see below) as close as possible to the minimum point. — This is repeated for all the e_i to be varied.

For each e_j (**4**/1) the quantities a_j and d_j are calculated, which are related to the constants in the general equation (part I, eqn. 42)

$$U = c_0 + 2\Sigma c_{0r}x_r + \Sigma\Sigma c_{rs}x_r x_s \qquad \text{(I:42)}$$

With our notations we have

$$x_j = e_s - e_s'; \ (s = g_j) \qquad (10)$$

$$X_0 = c_0; \ X_1 = c_0 + 2\,c_{0j}h_j + c_{jj}h_j^2;$$

$$X_2 = c_0 - 2c_{0j}h_j + c_{jj}\,h_j^2 \qquad (11)$$

Comparing eqn. (11) and Table 5 (**4**/1) we see that

$$a_j = 0.25\,X_2 - 0.25\,X_1 = -\,c_{0j}h_j \qquad (12)$$

$$d_j = 0.25\,X_1 + 0.25\,X_2 - 0.5\,X_0 = 0.5\,c_{jj}h_j^2 \qquad (13)$$

When this procedure has been repeated with all the constants e_i to be varied, the R terms a_j are accumulated in the auxiliary store from box No. 1 on (**6**/1).

Now (**11**/1,**7**/1) from box 1001 (v') on, a $R \times R$ matrix is laid out, row by row, which will contain the elements ("v_L")

$$\begin{aligned} v_{Lj} &= 0 \text{ for } L<j \\ v_{Lj} &= d_j = 0.5\,c_{jj}h_j^2 \text{ for } L = j \\ v_{Lj} &= c_{Lj}h_L h_j \text{ for } L<j \end{aligned} \qquad (14)$$

The "mixed" terms are obtained by calculating X for $e_s = e_s' + h_j$, $(x_j = h_j, \ s = g_j)$ and $e_t = e_t' + h_L$, $(x_L = h_L, \ t = g_L)$.

This error-square sum, from (I:42) becomes

$$X = c_0 + 2c_{0j}h_j + 2c_{0L}h_L + c_{jj}h_j^2 + c_{LL}h_L^2 + 2c_{Lj}h_L h_j =$$

$$X_0 - 2a_j - 2a_L + 2d_j + 2d_L + 2c_{Lj}h_L h_j$$

$$c_{Lj}h_L h_j = 0.5\,X - 0.5\,X_0 + a_j + a_L - d_j - d_L \qquad (15)$$

Thanks to the instructions (label **3**/1), the e_i sets with two constants varied will usually be on the same side of e_i' as the minimum of the pit.

Matrix operations

From (**12**/1) on begins a series of matrix operations. The mirror image of the matrix (14) is calculated and stored from box 2001 (w') on. The sum of the two matrices, which means the $R \times R$ quadratic form, $c_{Lj}h_L h_j$, is calculated and stored from box 3001 (b') on. The reciprocal of the latter is calculated and stored from box 4001 (c') on by instruction Ψ_{28}.

Multiplication with the $1 \times R$ matrix a_j gives (eqn. I:43a) the R corrections x_j'' to the e_s' to be varied, in units of h_j. They are stored from box 101

(x') on. In box 201 (y') is stored the sum $-\Sigma c_{0_j} x_j''$, and then X at the minimum point (eqn. I:44), thus U_0, is calculated. For each constant to be varied, the corrected value is calculated by addition of $h_j v_j$, and the standard deviation is calculated and printed (eqn. I:41).

The last operation, $c' = \Psi_{15}$ (5001, c) uses the zeros in the empty boxes from 5001 on to "sweep" c' for the next use.

Some of the more surprising "≈" and "Ψ intpt" instructions in Table 5 have proved necessary since the computer is rather particular on having indexes in some contexts and "variables" in others. Reference is made to the manual [4] for details on matrix operations.

Check. Since there may be many pitfalls in working out a program like this, we have checked the program on some textbook examples of finding the parameters of a straight line. LETAGROP at once found the same answers (parameters and standard deviation) as the textbook, either it started with a bad or a good guess. This is expected, since with a linear equation, the error square sum is exactly a secondary degree function.

Procedure

A treatment with the program Letagrop gives, starting from an approximate set of constants, in general an improved set, and estimates of their standard deviations. If the standard deviation of the data, σ comes out much higher than expected, usually something is wrong with the input of the data, or with the selection of the function (7).

If the function is linear, the minimum in the error squares' sum is found at once, however bad the first guess. On the other hand, for nonlinear functions, the first approximation found may be in error and successive attempts must be made. It is our experience that two or three approximations will in general suffice, if the first guess was reasonably good. The further one is from the minimum the more important become higher-degree terms. The matrix term C_{rr}/C (eqn I:46) that occurs in the standard deviation D_r^2 may sometimes come out as negative. To prevent the machine from stopping, a safety exit has been inserted, so that only an empty space is left, as an indication that the surface misbehaves. This may happen for very bad guesses, or for erroneous functions.

It will be seen from Table 5 how the index R is used for giving new orders. If R is a positive number, it means the number of constants to be varied in a new attempt. For $R = 0$, the computer uses the last "best" set of constants to calculate and print the deviation $Z_0 - Z_K$ for each of the experimental points. As a check of the input of the data, the experimental data (F_K, U_K, Z_K) are again printed (**11**/0).

For $R = -2$ new data are offered instead of the earlier ones (**14—2**/0), whereas the SP and the e_i are retained. With $R = -1$, (**14—15**/0) the data are kept but the constants are changed. With $R = -3$, both data and constants are changed.

By using the instruction "rmp" = "read more program", one may make the computer read a new "chapter 0", thus let it start on a new problem with-

out the necessity for reading chapter 1 again. This may save some time in studying series of problems with different SP.

A program as given in Table 5 is limited to 120 triplets of data, and 13 unknown to be varied. It would not be hard to rewrite the program, using the auxiliary memory, or rearranging the quick memory, in order to increase the number of unknown constants, or data sets.

For some reason, the matrix operations do not seem to work with $R = 1$. So, with only one constant to be varied one would have to add a special program, which we shall do on the day we meet with so simple a problem.

Examples of the results will be given in following papers.

Acknowledgements. We wish to thank Dr. Germund Dahlqvist and Mr. Per Erik Persson, fil.kand., for teaching us the elements of computer programming, and for helping us when we were in trouble. The technical staff of the Ferranti-Mercury computer of AB Atomenergi have always been very helpful. We would specially like to thank Mr. Assar Åkesson. Our friends in the Department of inorganic chemistry have helped us in many ways and provided the right mixture of patience and enthusiasm in the periods when the programs were worked out.

This is part of a program supported by *Statens Naturvetenskapliga Forskningsråd (Swedish National Science Research Council)*, *Statens Råd för Atomforskning (Swedish Atomic Energy Research Council)* and by the *Office of Scientific Research* of the Office of Aerospace Research, USAF, through its European Office on Contract No AF 61–(052)162.

REFERENCES

1. Sillén, L. G. *Acta Chem. Scand.* **10** (1956) 803.
2. Sullivan, J. C., Rydberg, J. and Miller, W. F. *Acta Chem. Scand.* **13** (1959) 2023.
3. Sillén, L. G. *Acta Chem. Scand.* **16** (1962) 159 (Part I).
4. Brooker, R. A., Richards, B., Berg, E. and Kerr, R. H. *The Manchester Mercury Autocode system*, University, Manchester 1959.
5. Sillén, L. G. *Acta Chem. Scand.* **8** (1954) 299.
6. Hietanen, S. and Sillén, L. G. *Acta Chem. Scand.* **8** (1954) 1607.

Received June 21, 1961.

ACTA CHEMICA SCANDINAVICA 16 (1962) 192–204

Studies on Derivatives of Malachite Green. Protolytic Equilibria and Reaction Rate Constants of *o*-Hydroxy Malachite Green

RUNE CIGÉN

Department of Inorganic and Physical Chemistry, Chemical Institute, University of Lund, Lund, Sweden

In aqueous solutions *o*-hydroxy Malachite Green gives seven species, three coloured (R, B, and G) and four colourless (C′, C, S′, and S″) between which the following reversible reactions take place; $R + 2H^+ \rightleftharpoons B + H^+ \rightleftharpoons G$; $C' + 3H^+ \rightleftharpoons C + 2H^+ \rightleftharpoons S' + H^+ \rightleftharpoons S''$; $G + H_2O \rightleftharpoons S''$; $B + H_2O \rightleftharpoons S'$; $R + H_2O \rightleftharpoons C$; $R + OH^- \rightleftharpoons C'$. The equilibria between G, B, and R and between C′, C, S′, and S″ are reached instantaneously whereas the hydration equilibria are reached only after a certain time.

Five dissociation, three hydration, and eight reaction rate constants for the above indicated reactions have been determined by spectrophotometric measurements in aqueous solutions having a constant ionic strength 0.5 M at 20.0°C.

The *ortho*-hydroxy group has a very strong influence on the hydration reactions in the pH-range, 8—10, where the proton of the —OH group is released. The hydration reaction $R + H_2O \rightarrow C$, for example, proceeds 3000 times faster than the corresponding reaction for *para*-hydroxy Malachite Green. The rate constants of the reactions in acid solutions, on the contrary, are 2—4 times smaller for *o*-hydroxy than for *p*-hydroxy Malachite Green.

The reaction scheme which has been proposed and used in the investigations on Malachite Green (MG) and a number of its derivatives [1–4] can not be used without extension for *o*-hydroxy MG, because the *o*-hydroxy-derivative gives, in alkaline solutions, two additional forms, one coloured and one colourless. The reason for this is that the —OH group reacts like an acid and releases its proton at pH 8—9. An *ortho*-quinoid structure then becomes possible giving an additional coloured form. The corresponding *para*-derivative reacts in the same manner and for this dye the dissociation, hydration and some of the reaction rate constants were determined in Ref.[1]. The remaining rate constants will be reported in this paper.

The reaction-equilibrium scheme which was applied to Crystal Violet [5] can also be applied to *o*-hydroxy MG and the same non-approximated equations for equilibria and reaction rates can be used. The differences in magnitude of the corresponding constants in the dyes mentioned requires, however, quite different approximations of the equations.

The changes in colour nuancies and colour intensities that take place when the pH of a water solution of *o*-hydroxy MG is changed depend on a series of reactions according to the following simplified scheme. ($R = C_6H_4NMe_2$).

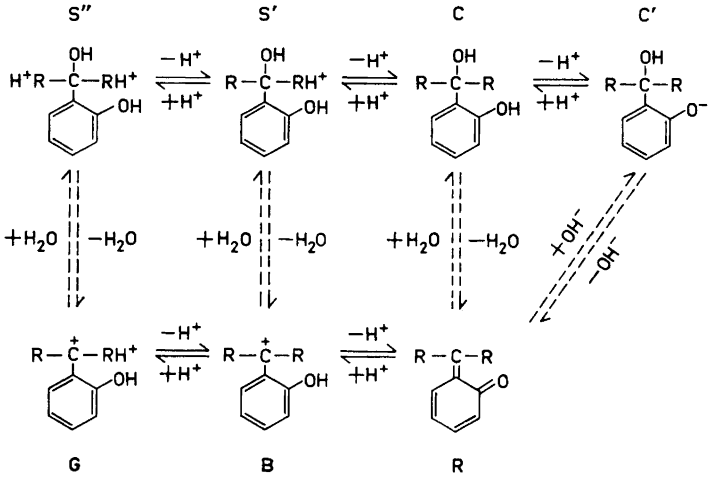

Whole arrows indicate that the reactions proceed with a non-measurable velocity — that is, instantaneously — whereas dashed arrows indicate that the reactions take place with a measurable velocity.

The following definitions and symbols are used *

a) Dissociation constants: $K_1 = \frac{[G]}{[B][H^+]}$; $K_7 = \frac{[R][H^+]}{[B]}$; $K_3 = \frac{[S'][H^+]}{[S'']}$:

$$K_4 = \frac{[C][H^+]}{[S']} \; ; \; K_8 = \frac{[C'][H^+]}{[C]}$$

b) Hydration constants: $K_2 = \frac{[S'']_\infty}{[G]_\infty}$; $K_6 = \frac{[B]_\infty}{[S']_\infty}$; $K_9 = \frac{[R]_\infty}{[C]_\infty}$

c) Rate constants:

k_1 = rate constant for the reaction $G + H_2O \rightarrow S''$
k_2 = » » » » » $S'' \rightarrow G + H_2O$
k_3 = » » » » » $B + H_2O \rightarrow S'$
k_4 = » » » » » $S' \rightarrow B + H_2O$

* The constants $K_1 - K_9$ are defined in the same manner as in Ref.[1] but correspond to the following constants within brackets in Ref.[5]: $K_1(1/K_1)$, $K_2(K_4)$, $K_3(K_1')$, $K_4(K_2')$, $K_6(1/K_5)$, $K_7(K_2)$, $K_8(K_3')$, $K_9(1/K_6)$.

k_5 = » » » » » $R + H_2O \rightarrow C$
k_6 = » » » » » $C \rightarrow R + H_2O$
k_7 = » » » » » $R + OH^- \rightarrow C'$
k_8 = » » » » » $C' \rightarrow R + OH^-$
k = rate constant for the total reaction

d) ε_R, ε_B, ε_G = the molar extinction coefficient of R, B, and G.
e_0, e_t, e_∞ = the absorbance per cm of a solution at the times 0 and t and at equilibrium (thickness of absorbing layer d = 1 cm).
E_0, E_t, E_∞ = the absorbance when $d \neq 1$ cm.
e_R, e_B, e_G = the absorbance per cm of a solution containing only R, B or G.
C_M = the total concentration of dyestuff.
$h = [H^+]$; $oh = [OH^-]$; $K_w = [H^+][OH^-]$.

The constants in the equilibrium scheme can be calculated if the following data are determined for a large number of solutions with varying pH: 1) The absorbance, e_0, at the moment o mixing a dye stock solution with the appropriate buffers. 2) The absorbance, e_∞, when equilibrium is reached. 3) The pH of the solutions. 4) The total rate constant, k, for the reactions that change the intensity of the colour of the solutions either through hydration of the coloured forms (R, B, and G) to the colourless (C', C, S', and S") or *vice versa*.

EQUATIONS

1. The equation for the initial absorbance, e_0

The following equation for e_0 can be derived.

$$e_0 = \frac{K_7 e_R + h e_B + h^2 K_1 e_G}{K_7 + h + h^2 K_1} \tag{1}$$

Eqn. (1) requires that the dyestuff is present only as the coloured forms R, B, and G when it is mixed with the buffer solution. This can be realized in a dye stock solution which is buffered very weakly with an acetate buffer, pH≈4.5. In such a stock solution the dye is present to an extent of about 99.5 % as the coloured ion B.

Determination of K_1. In acid solutions, pH<5, [R] can be omitted in comparison to [B] + [G]. Eqn. (1) is then approximated and transformed to

$$\frac{h}{e_B - e_0} = \frac{h}{e_B - e_G} + \frac{1}{K_1(e_B - e_G)} \tag{2}$$

When h, e_0 and e_B have been determined K_1 and e_G can be obtained from eqn. (2) by a graphical method.

Determination of K_7. In alkaline solutions [G] can be omitted in comparison to [B] + [R]. Eqn. (1) is approximated and transformed to

$$\frac{1}{e_B - e_0} = \frac{1}{e_B - e_R} + \frac{h}{K_7(e_B - e_R)} \tag{3}$$

If e_B and h are known K_7 and e_R can be determined from eqn. (3) by a graphical method.

2. The equation for the equilibrium absorbance, e_∞

The following equation for e_∞ can be derived

$$e_\infty = \frac{K_7 e_R + h e_B + h^2 K_1 e_G}{K_7 + K_7/K_9 + K_7 K_8/h K_9 + h(1 + 1/K_6) + h^2 K_1 (1 + K_2)} \quad (4)$$

Determination of K_2. In acid solutions $[R]_\infty$, $[C]_\infty$, and $[C']_\infty$ can be omitted in comparison to $[B]_\infty + [G]_\infty + [S']_\infty + [S'']_\infty$. Eqn. (4) can be approximated and transformed to

$$K_2 = \frac{e_G}{e_\infty} + \frac{e_B - e_\infty(1 + hK_1 + 1/K_6)}{e_\infty h K_1} \quad (5)$$

The constant K_2 can be calculated from eqn. (5) when K_1 and K_6 are known. The term $1/K_6$ has the character of a correction term since $K_6 \gg 1$.

Determination of K_6. The hydration constant K_6 can not be determined solely through equilibrium measurements. These have to be completed with kinetic measurements.

Determination of K_8 *and* K_9. In alkaline solutions the only species of the dye to be regarded are B, R, S', C, and C'. In view of this and the fact that $K_6 \gg 1$ eqn. (4) is approximated and transformed to

$$K_9 = \frac{e_\infty(1 + K_8/h)}{e_R + h(e_B - e_\infty)/K_7 - e_\infty} \quad (6)$$

when $h \approx K_7$. From eqn. (6) the hydration constant K_9 and the dissociation constant K_8 are calculated by the following method. Different values of K_8 are tried in eqn. (6) until a constant value of K_9 is obtained in a pH-range about pK_8.

Determination of K_3, K_4, *and* K_6. The constants K_3, K_4, and K_6 can be determined only by a combination of equilibrium and kinetic measurements.

3. The equation for the total rate constant k

For dyes of this type the proton equilibria between the coloured species R, B, and G as well as between the colourless species C', C, S', and S'' are reached instantaneously. The hydration equilibria between a coloured and a corresponding colourless form as well as the equilibrium $R + OH^- \rightleftharpoons C'$, on the other hand, are reached with a measurable velocity.

The following equation can be derived for the total rate constant, k (*cf.* Ref.[5]):

$$k = \frac{1}{t} \ln \frac{e_0 - e_\infty}{e_0 - e_t} = \frac{h^3 k_2 + h^2 k_4 K_3 + h k_6 K_3 K_4 + k_8 K_3 K_4 K_8}{h^3 + h^2 K_3 + h K_3 K_4 + K_3 K_4 K_8} + \\ + \frac{h^2 k_1 K_1 + h k_3 + k_5 K_7 + k_7 K_7 h}{h^2 K_1 + h + K_7} \quad (7)$$

Determination of k_1 and k_2. Approximate values of k_1 and k_2 can be obtained by kinetic measurements in strongly acid solutions, pH$\geq$2. Eqn. (7) is then approximated to

$$k = k_1 \frac{\mathrm{h}K_1}{1 + \mathrm{h}K_1} + k_2 \qquad (8)$$

From eqn. (8) the rate constants k_1 and k_2 can be calculated when K_1 and K_2 have been determined since $k_1[\mathrm{G}]_\infty = k_2[\mathrm{B}]_\infty$ at equilibrium and therefore $k_1 = k_2K_2$. More refined values of k_1 and k_2 are calculated later from an equation which is not approximated as much as eqn. (8), when at least approximate values of k_3 and k_4 have been determined.

Determination of k_5, k_6, k_7, and k_8. In strongly alkaline solutions, pH>11, the following approximations of eqn. (7) proved to be applicable

$$k = k_5 + k_7\mathrm{oh} + k_8 \qquad (9)$$

If k is plotted as a function of $[OH^-]$ a straight line is obtained. The slope of this line gives k_7 and the intercept on the y-axis gives $k_5 + k_8$.

An expression for k_8 can be obtained from the following equations: $k_7\mathrm{oh}[\mathrm{R}]_\infty = k_8[\mathrm{C}']_\infty$, $K_9[\mathrm{C}]_\infty = [\mathrm{R}]_\infty$, $\mathrm{h}[\mathrm{C}']_\infty = K_8[\mathrm{C}]_\infty$, and $\mathrm{h} \cdot \mathrm{oh} = K_w$ which give

$$k_8 = k_7K_wK_9/K_8 \qquad (10)$$

However, $k_8 \ll k_5$ and therefore the intercept mentioned above giving $k_5 + k_8$ in reality gives only k_5. Then the rate constant k_6 is obtained from the expressions $k_5[\mathrm{R}]_\infty = k_6[\mathrm{C}]_\infty$ and $K_9[\mathrm{C}]_\infty = [\mathrm{R}]_\infty$ which gives $k_6 = k_5K_9$.

The determination of the remaining constants k_3, k_4, K_3, K_4, and K_6 are performed in a very special way which is described in the "Measurements and Results" part.

EXPERIMENTAL

Chemicals and solutions. o-Hydroxy Malachite Green. The leuco compound was prepared in a nitrogen atmosphere by refluxing a mixture of o-hydroxy-benzaldehyde (0.1 mole), dimethylaniline (0.3 mole), conc. hydrochloric acid (0.3 mole) and urea (0.1 mole) for 18 h. The leuco compound was recrystallized from benzene-ethanol. White needles were obtained, m.p. 132°C. The dyestuff was prepared by oxidizing 3.6 g of the leuco compound dissolved in 5 ml of 5 M hydrochloric acid and diluted with 500 ml of 10 % acetic acid. For an oxidizing agent 3.0 g of lead dioxide was used. From the oxidized product a perchlorate was prepared that was obtained as small shining green balls of needle-like crystals after repeated recrystallizations from 1 % acetic acid. (Found: C 62.0; H 5.96; O 17.91; N 6.39; Cl 8.09. Calc. for $C_{23}H_{25}O_5N_2Cl$: C 62.1; H 5.66; O 17.98; N 6.30; Cl 7.97).

A stock solution of the dye was prepared by weighing and dissolving the perchlorate in acetone which was then diluted with a potassium chloride solution giving a final solution with ionic strength 0.5 M and containing 4 % of acetone. The stock solution, with $C_M = 2 \times 10^{-5}$ M, was buffered very weakly with an acetate buffer, pH $\approx$ 4.5, and was diluted, when necessary, with 0.5 M potassium chloride containing 4 % of acetone. The perchlorate is so slightly soluble in water that it is almost impossible to prepare reproducible stock solutions with a fixed C_M by dissolving the perchlorate directly in 0.5 M potassium chloride.

Hydrochloric acid, sodium acetate, potassium dihydrogen phosphate, disodium hydrogen phosphate, ammonium chloride, ammonia, and *sodium hydroxide,* all of analytical grade,

were used in the buffer solutions. *Potassium chloride* of analytical grade was used to keep the ionic strength constant (0.5 M).

Apparatus. The determinations of $[H^+]$ were carried out titrimetrically ($pH < 2$ and $pH \geq 12$) and potentiometrically ($2 < pH < 12$). For the potentiometric measurements a reference solution ($pH = 2$) having the composition 0.01 M HCl + 0.49 M KCl was used. In this paper pH always means $-\log[H^+]$ and not $-\log a_{H^+}$. For the electrodes quinhydrone and platinum-plate were used for $pH \leq 8$ and platinum-black and hydrogen gas for $pH > 8$. The temperature was kept at 20.0°C.

For the spectrophotometric measurements a Beckman DU quartz spectrophotometer with photomultiplier was used. The spectrophotometer was furnished with arrangements, used for some measurements in alkaline solutions, for rapid kinetic studies according to the principles for a rapid flow apparatus worked out by Hartridge and Roughton [6] and modified by Dalziel [7] for a Beckman DU spectrophotometer. Our arrangement differs from that of Dalziel's in some respects. The two solutions which are to react are fed to the reacting chamber by two synchronously driven 100 ml all-glass syringes. Dalziel used a pressure chamber for this purpose. A carefully selected 8 mm Pyrex-capillary with 2 mm bore is used as an absorption cell. The capillary is placed vertically and a slit, 2 mm high and 0.2 mm wide, is placed close to the capillary in the path of the beam from the spectrophotometer. This slit can be centered, by means of a micrometer screw, before the capillary, thus making the refraction in the curved surfaces of the capillary very small. Further, the optical length of the part of the solution in the capillary through which light is passed can be considered as constant.

MEASUREMENTS AND RESULTS

Preliminary measurements showed that for *o*-hydroxy Malachite Green, as in the previously investigated *p*-hydroxy MG, the equilibrium $B + H_2O \rightleftharpoons S'$ is strongly displaced towards the blue-green ion B. By mixing the dye stock solution with a very small amount of an acetate buffer, giving $pH \approx 4.5$, a stock solution is obtained in which the dyestuff is present to an extent of > 99.5 % as the coloured form B. If such a stock solution is mixed with appropriate buffer solutions the equilibria $B + H^+ \rightleftharpoons G$ and $B \rightleftharpoons R + H^+$ are reached instantaneously and e_0 in eqn. (1) can be determined. The initial absorbance, e_0, is obtained through extrapolation of the absorbance to the time $t = 0$ since the solutions fade owing to the formation of the colourless species by hydration of the coloured species.

In Fig. 1 absorption curves of the three coloured species R, B, and G are seen. The curve B was obtained in acetate buffer, $pH = 4.5$: $\lambda_{Bmax} = 624$

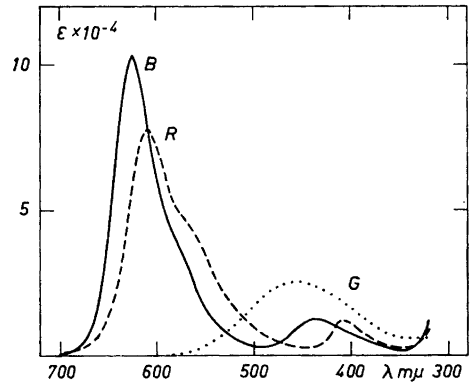

Fig. 1. Absorption curves of *o*-hydroxy Malachite Green. Curve R is the molecule $(Me_2NC_6H_4)_2CC_6H_4O$ in ammonia-ammonium chloride buffer. Curve B is the ion $[(MeNC_6H_4)_2CC_6H_4OH]^+$ in acetate buffer. Curve G is the ion

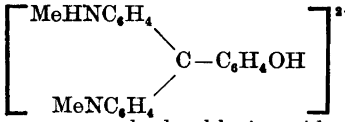

in dilute hydrochloric acid.

mμ and 436 mμ, $\varepsilon_{max} = 1.03 \times 10^5$ and 1.23×10^4. The curve G was obtained in dilute hydrochloric acid: $\lambda_{Gmax} = 455$ mμ, $\varepsilon_{Gmax} = 2.6 \times 10^4$. ε_G was calculated for 20 different wavelengths from eqn. (5) when K_1, K_2, and e_B were determined. The curve R is obtained in an ammonia—ammonium chloride buffer, pH = 10.5, by extrapolation of the absorbance to $t = 0$ at 47 different wavelengths: $\lambda_{Rmax} = 609$ mμ and 408 mμ, $\varepsilon_{Rmax} = 7.8 \times 10^4$ and 1.2×10^4.

Determination of K_1. A series of solutions having the composition x M HCl + $(0.5 - x)$ M KCl were quickly mixed with an equivalent volume of the dye stock solution. The mixing was carried out by injecting the thermostated buffer directly into the thermostated absorption cell in the absorption cell house. The equilibrium $B + H^+ \rightleftharpoons G$ is reached instantaneously during the mixing, where upon the solution fades owing to the reaction $G + H_2O \rightarrow S''$. By determining the fading rate and extrapolating the absorbance to $t = 0$, e_0 was obtained. The measurements were carried out at the wavelength 624 mμ, where the absorption curve for the blue-green ion B has a sharp maximum and $\varepsilon_G \langle\langle \varepsilon_B$. In these acid solutions we need not consider the component R.

In Fig. 2 $[H^+]/(e_B - e_0)$ is plotted against $[H^+]$. According to eqn. (2) a straight line is obtained; the slope, l, and the intercept, y, on the y-axis give $e_B - e_G = 1/l$ and $K_1 = l/y$. From the figure the following values are obtained: $l = 1.003$, $y = 0.0343$ M, which gives ($C_M = 1 \times 10^{-5}$ M, $e_B = 1.015$) $e_G = 0.018$ and $\mathbf{K_1 = 29.2 \pm 0.3\ M^{-1}}$.

Determination of K_7. The dissociation constant K_7 was determined in the same way as K_1. Equivalent volumes of a dye stock solution and ammonia—ammonium chloride buffers were mixed. The equilibrium $B \rightleftharpoons R + H^+$ is reached instantaneously where upon the solution quickly fades owing to the reaction $R + H_2O \rightarrow C$. The concentration of the dye was kept very low, $C_M = 2.5 \times 10^{-6}$ M, since there was a risk of a precipitation of the almost insoluble carbinol, C.

The measurements were carried out at the wavelength 624 mμ where the difference between e_B and e_R is sufficient to permit eqn. (3) to be used. According to eqn. (3) a straight line is obtained when $1/(e_B - e_0)$ is plotted as a function

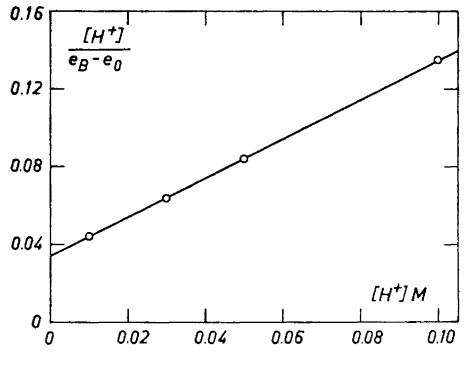

Fig. 2. $[H^+]/(e_B - e_0)$ as a function of $[H^+]$ for the determination of K_1.

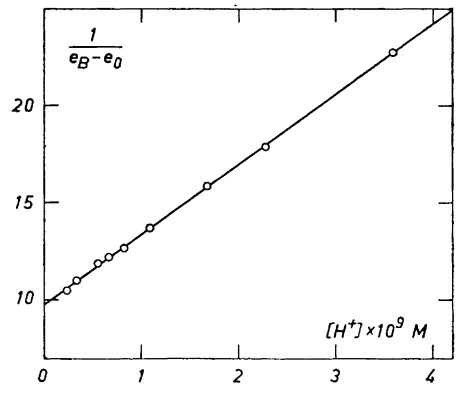

Fig. 3. $1/(e_B - e_0)$ as a function of $[H^+]$ for the determination of $K_4/(K_6 + 1)$.

Table 1. Determination of K_2 and k_1 and e_0-values for the determination of K_1. $\lambda = 624$ mμ; $C_M = 1 \times 10^{-5}$ M; $T = 20.0$°C; $d = 1$ and 5 cm; $e_B = 1.015$.

[H$^+$] M	e_0	$e\infty$	K_2	k min^{-1}	k_1 min^{-1}
0.010	0.789	0.419	3.92	0.0229	0.0435
0.020		0.266	3.89		
0.030	0.546	0.194	3.92	0.0329	0.0440
0.040		0.1526	3.96		
0.050	0.421	0.1268	3.94	0.0383	0.0444
0.060		0.1092	3.89		
0.080	0.311	0.0846	3.92	0.0443	0.0458
0.100	0.273	0.0688	3.97	0.0465	0.0461
Mean			3.93		0.0448

of [H$^+$] (Fig. 3). The solutions fade, however, much more rapidly than the solutions used for the determination of K_1. Therefore, the extrapolated e_0-values (Table 2) are not so reliable. The difference between e_B and e_0 is rather small which also increases the uncertainty. From Fig. 3 the following values are obtained ($C_M = 2.5 \times 10^{-6}$ M, $e_B = 0.250$): $y = 9.80$, $l = 3.60 \times 10^9$ M^{-1} which gives $e_R = 0.148$, $\varepsilon_R = 5.92 \times 10^4$, and $\mathbf{K_7 = (2.72 \pm 0.15) \times 10^{-9}}$ **M.**

Determination of K_2. The dye stock solution was mixed with appropriate HCl + KCl-buffers. The solutions were thermostated and the equilibrium absorbancies, E_∞, were read off after 6 h. $C_M = 1 \times 10^{-5}$ M, $d = 1$ and 5 cm. The hydration constant K_2 was calculated from eqn. (5) ($e_B = 1.015$, $e_G = 0.018$). The results are found in Table 1 from which the mean value $\mathbf{K_2 = 3.93 \pm 0.04}$ is obtained.

Table 2. $e\infty$- and e_0-values for the determination of K_7 and K_9; $T = 20.0$°C.

$\lambda = 624$ mμ	$C_M = 2.5 \times 10^{-6}$ M $d = 1$ cm	$C_M = 5 \times 10^{-6}$ M $d = 5$ cm	$\lambda = 625$ mμ $e_R = 0.275$
[H$^+$] $\times 10^9$ M	e_0	$E\infty = 5\,e\infty$	K_9
3.60	0.206	0.470	0.154
2.28	0.194	0.338	0.152
1.68	0.187	0.275	0.152
1.09	0.177	0.205	0.154
0.824	0.171	0.168	0.154
0.668	0.168	0.144	0.153
0.551	0.166	0.127	0.156
0.332	0.159	0.085	0.153
0.242	0.154	0.065	0.151
Mean			0.153

Determination of K_8 and K_9. The dye stock solution was mixed with ammonia-ammonium chloride buffers and the equilibrium absorbancies, E_∞, were read off after 10—20 min. $C_M = 5 \times 10^{-6}$ M, $d = 5$ cm, $\lambda = 624$ mμ, $e_B = 0.496$, $e_R = 0.274$. The constant K_9 was calculated from eqn. (6) by trying different values for K_8. A reasonable constancy for K_9 is obtained within the rather broad pH-range 8.4—9.6 if the value $K_8 = 6.1 \times 10^{-10}$ M is chosen. The results are found in Table 2. As a mean value $\mathbf{K_9 = 0.153 \pm 0.005}$ was obtained when $\mathbf{K_8 = (6.1 \pm 0.2) \times 10^{-10}}$ **M.**

Note. Borate buffers cannot be used for the determination of K_7, K_8, and K_9 since borate ions react which *o*-hydroxy MG giving complex species. This complex formation has been investigated and the results will be published. The dye also seems to react with ammonia when the concentration of ammonia is high. Therefore $[NH_3]$ was kept ≤ 0.05 M in the ammonia-ammonium chloride buffers.

Kinetic measurements

Determination of k_1 and k_2. The total fading rate, k, was determined in the measurements from which e_0 for the determination of K_1 was obtained. From eqn. (8) an approximate value of k_1 was initially calculated. A refined value for k_1 was obtained from eqn. (7) when k_3 and k_4 were approximately determined. Table 1 contains the k-values and the refined k_1-values. The mean value $\mathbf{k_1 = 0.0448 \pm 0.0010\ min^{-1}}$ was obtained. Then k_2 is obtained from the expression $k_1 = k_2K_2$ which gives $\mathbf{k_2 = 0.0114 \pm 0.0003\ min^{-1}}$.

Determination of k_5, k_6, k_7 and k_8. The kinetic measurements were carried out in strongly alkaline solutions. The dye stock solution was mixed with solutions of the type x M NaOH + $(0.5 - x)$ M KCl where $x = 0.025$, 0.100, 0.150, 0.200, and 0.250. In Fig. 4 k is plotted as a function of $[OH^-]$. According to eqn. (9) a straight line is obtained with the slope, $l = 0.967$ min^{-1} M^{-1} and the intercept on the y-axis, $y = 0.735$ min^{-1}. This gives $\mathbf{k_7 = 0.97 \pm 0.02\ min^{-1}\ M^{-1}}$ and $k_5 + k_8 = 0.735$ min^{-1}. From eqn. (10) $\mathbf{k_8 = (3.0 \pm 0.2) \times 10^{-6}\ min^{-1}}$ is obtained ($K_w = 1.24 \times 10^{-14}$ M^2). Thus $k_8 \ll k_5$, and therefore Fig. 4 gives $\mathbf{k_5 = 0.735 \pm 0.010\ min^{-1}}$. The rate constant k_6 can be calculated from the expression $k_6 = k_5K_9$ which gives $\mathbf{k_6 = 0.113 \pm 0.05\ min^{-1}}$.

The remaining constants k_3, k_4, K_3, K_4, and K_6 were determined by a large number of kinetic measurements in the pH-range 3.9—11. It has been possible to determine the constants from the experimentally obtained connection between k and $[H^+]$ by the following approximation procedure. In the pH-range 4—6 eqn. (7) can be approximated and written as

$$k - A = \frac{hk_4K_3}{h^2 + hK_3 + K_3K_4} + k_3 \qquad (11)$$

where

$$A = \frac{h^2k_2 + k_6K_3K_4}{h^2 + hK_3 + K_3K_4} - hk_1K_1 - \frac{k_5K_7}{h}$$

In the actual pH-range A is a correction term that can be calculated with sufficient accuracy using rather highly approximated values of K_3 and K_4.

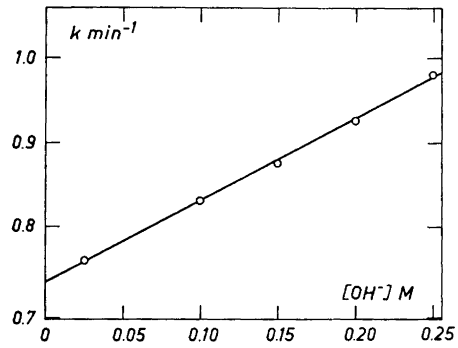

Fig. 4. The total rate constant k plotted against [OH^-] for the determination of k_6 and k_7.

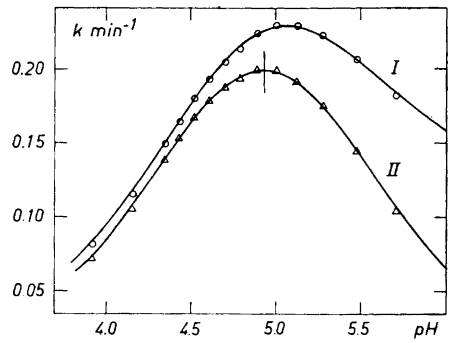

Fig. 5. Curve I. The total rate constant k plotted against pH. The points represented by the symbol O are experimentally obtained; the full-drawn curve is calculated from eqn. (7). Curve II. The total rate constant k minus the term A in eqn. (11) plotted against pH. The full-drawn curve is calculated from eqn. (11).

Previously investigated *para*-hydroxy MG and *para*-methoxy MG (Ref.[1]) and *meta*-hydroxy MG and *meta*-methoxy MG (Ref.[3]) show that there is a comparatively small difference between corresponding constants of *p*-hydroxy MG and *p*-methoxy MG and between corresponding constants of *m*-hydroxy MG and *m*-methoxy MG. Therefore it seems reasonable to assume that K_3 and K_4 for *ortho*-hydroxy MG have about the same values as K_3 and K_4 for *ortho*-methoxy MG. The constants of the latter dye have been determined (Ref.[4]): $K_3 = 2.8 \times 10^{-5}$ M and $K_4 = 3.7 \times 10^{-6}$ M. A comparison between the constants, already determined, for *o*-hydroxy MG and *o*-methoxy MG

	K_1	K_2	k_1	k_2
o-methoxy MG	29.2	3.92	0.0449	0.0114
o-hydroxy MG	30.3	4.65	0.0530	0.0108

gives further support for using the K_3- and K_4-values of *o*-methoxy MG in the correction term A in eqn. (11) as a first approximation. In Fig. 5, curve I, the experimentally obtained k-values (circles) are plotted as a function of pH whereas curve II shows $k - A$ as a function of pH.

If $k - A$ in eqn. (11) is differentiated with respect to [H^+] it is found that $k - A$ has a maximum when $[H^+] = \sqrt{K_3K_4}$. From Fig. 5 $(k - A)_{max} = 0.199$ is obtained when pH = 4.93 which gives $K_3K_4 = 1.40 \times 10^{-10}$ M^2. Eqn. (11) can be transformed to

$$k_3 = \frac{k - A}{\dfrac{hK_3K_6}{h^2 + hK_3 + K_3K_4} + 1} \qquad (12)$$

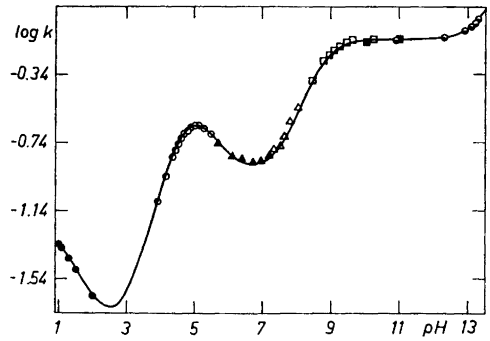

Fig. 6. log k for the total rate constant plotted against pH. The full drawn curve is calculated from eqn. (7). The points represented by the different symbols are experimentally obtained in the following solutions: ●, "fading" in HCl + KCl-buffers; ○ "restoring of colour" in acetate buffers; ▲, "restoring of colour" in primary phosphate buffers; △, "fading" in primary phosphate buffers; □, "fading" in ammonia-ammonium chloride buffers; ■, "fading" in secondary phosphate buffers; ◒, "fading" in NaOH + KCl-buffers.

since $k_4 = k_3K_6$. Different values of K_3 were tried until the best possible constant value of k_3 was obtained from eqn. (12). The term K_6 was obtained from the expression $K_1K_2K_3K_6 = 1$, by definition, when K_3 was fixed and K_1 and K_2 were known.

When $K_3 = 3.3 \times 10^{-5}$ M a constant value of k_3 is obtained; $k_3 = 0.00129$. The remaining constants can now be calculated. The following values were obtained: $\mathbf{K_3 = (3.30 \pm 0.10) \times 10^{-5}\ M}$, $\mathbf{K_4 = (4\,24 \pm 0.15) \times 10^{-6}\ M}$, $\mathbf{K_6 = 263 \pm 10}$, $\mathbf{k_3 = 0.00129 \pm 0.00005\ min^{-1}}$, $\mathbf{k_4 = 0.341 \pm 0\,015\ min^{-1}}$.

By definition $K_1K_2K_3K_6 = 1$ and $K_6K_7/K_4K_9 = 1$. The constant K_6 was determined from the former expression. If this value of K_6 is used in the latter expression, $K_6K_7/K_4K_9 = 1.10$ is obtained. The difference of 10 % must be considered as tolerable if we think of the uncertainty in K_7 and K_9 and the method used to calculate K_6 and K_4.

In Fig. 5 the full drawn curve II is calculated from eqn. (11) using the values of the constants, listed above, also in the correction term A. The symbol, △, represents the experimentally obtained k-values minus A. The full drawn curve I is calculated from the non-approximated eqn. (7) and the symbol, ○, represents the experimentally obtained k-values. The agreement between the k-values, calculated from eqn. (7), and the experimentally obtained k-values is very good as can be seen in the diagram.

In Fig. 6 log k is plotted as a function of pH for the pH-range 1—13.5. Eqn. (7) was used in calculating the log k values. The symbols are experimentally obtained log k-values. The agreement between the calculated and the obtained k-values is very good except in the pH-range 6—8. In this range the error limits are relatively large owing to experimental difficulties. The kinetic measurements in this pH-range, however, have not been used to calculate any constants in the equilibrium scheeme.

The rate constant k is the rate constant of the total reaction which is manifested as a more or less complete fading of the solution for measurement or a more or less complete restoring of the colour. In the cases when the colour is restored the dye stock solution initially has been more or less decolourized by adding a small amount of a suitable acid or alkaline buffer. When equilibrium has been reached the decolourized solution is mixed with an appropriate buffer and the kinetic measurements can be started.

DISCUSSION

A comparison between the values of the constants for *para*-hydroxy MG and *ortho*-hydroxy MG shows some interesting facts (Table 3). Whether the —OH group is situated *ortho*- or *para* to the central carbon atom of the dye is a matter that does not influence the values of the constants for the reactions in acid solution very much. On the other hand, some of the reactions in alkaline solutions are strongly influenced by the position of the —OH group. The reaction

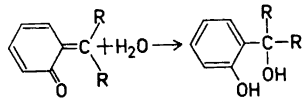

proceeds 3000 times as fast as the reaction

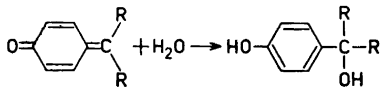

in spite of the fact that the electron-donating —OH group in the *ortho*-position increases the electron density on the central carbon atom more than in the *para*-position and should make a bonding of the negatively polarized oxygen of a water molecule more difficult. The former reaction is facilitated by the favorable conditions for hydrogen bonding and proton transfer between the *ortho*-hydroxy group and the —OH group on the methane carbon atom.

However, the stronger electron repelling property of the *ortho*-hydroxy group is seen in the following reactions (R = $C_6H_4NMe_2$) that proceed about

Table 3. A comparison between the values of the constants for *p*-hydroxy MG and *o*-hydroxy MG.

	K_1	K_2	K_3 × 10^5	K_4 × 10^6	K_6	K_7 × 10^7	K_8 × 10^{10}	K_9
p-hydroxy MG	28.2	2.38	2.5	5.2	600	1.08	1.20	8.4
o-hydroxy MG	29.2	3.93	3.3	4.2	263	0.027	6.1	0.153
	k_1	k_2	k_3	k_4	k_5	k_6	k_7	k_8
p-hydroxy MG	0.111	0.0461	0.00304	1.82	0.00024	0.0020	2.06	1.79 × 10^{-3}
o-hydroxy MG	0.0448	0.0114	0.00129	0.341	0.735	0.113	0.97	3.0 × 10^{-6}

The rate constants k_5, k_6, k_7 and k_8 for *p*-hydroxy MG were not published in Ref.[1] They have been calculated now from earlier measurements.

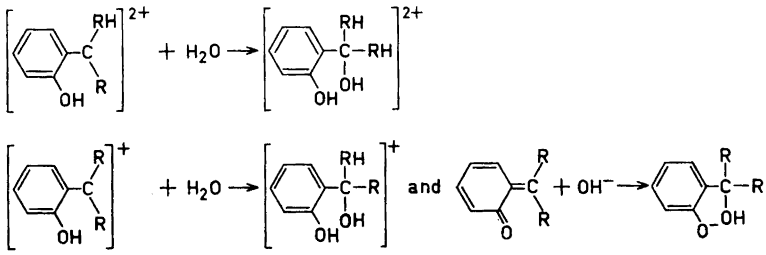

2 times as slowly for *o*-hydroxy MG as the corresponding reactions for *p*-hydroxy MG. But this effect is not seen in the hydration equilibria which are more strongly displaced towards the non-hydrated coloured forms of *p*-hydroxy MG than of *o*-hydroxy MG.

REFERENCES

1. Cigén, R. Protolysengleichgewichte und Reaktionsgeschwindigkeiten einiger basischer Triphenylmethanfarbstoffe *(Diss.)*, University, Lund 1956.
2. Cigén, R. *Acta Chem. Scand.* **14** (1960) 979.
3. Cigén, R. *Acta Chem. Scand.* **15** (1961) 1892.
4. Cigén, R. *Acta Chem. Scand.* **15** (1961) 1905.
5. Cigén, R. *Acta Chem. Scand.* **12** (1958) 1456.
6. Hartridge, H. and Roughton, F. J. W. *Proc. Roy. Soc. London* A **104** (1923) 376.
7. Dalziel, K. *Biochem. J.* **55** (1953) 79.

Received August 2, 1961.

ACTA CHEMICA SCANDINAVICA 16 (1962) 205–208

The Structure of Some Condensation Products of Pulegone

YUAN-LANG CHOW*

Organisk-kemiska Institutionen, Kungl. Tekniska Högskolan, Stockholm, Sweden

Evidence is presented confirming the structures originally assigned by Vorländer *et al.*[1] to pulegone malonic acid ketodilactone and pulegone acetic acid anhydride. Pulegene acetone has been related to pulegone acetic acid anhydride and shown to have structure XV.

Vorländer *et al.*[1] condensed pulegone with sodiomalonic ester and obtained a compound that was hydrolysed to an acid which spontaneously lactonised to give "pulegone malonic acid ketodilactone", formulated as I[1a]. On repeated distillation, carbon dioxide was evolved giving "pulegone acetic acid anhydride" formulated as the enol lactone II [1b]. "Pulegone malonic acid ketodilactone" and "pulegone acetic acid anhydride" have been prepared by Vorländer's procedure and subjected to further investigations.

The dilactone I, containing only six-membered lactone groups, exhibited an unusual infrared absorption with bands at 1775 and 1805 cm^{-1} (in CCl_4) Therefore structures containing five-membered lactone groups such as III or IV could not be excluded. The dilactone was stable to chromic acid oxidation [2] and did not consume periodate in neutral solution. The ketodilactone appears to exist as a dicarboxylate in neutral solution. The calcium salt of the dicarboxylic acid corresponding to I shows absorption bands at 1700 cm^{-1} (keto group) and 1330, 1570 cm^{-1} (carboxylate), and regenerates I upon acidification.

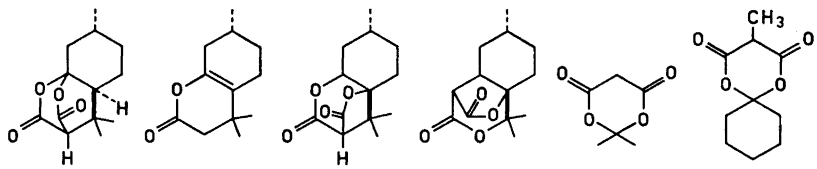

I *II* *III* *IV* *V* *VI*

* Present address: Department of Chemistry, Imperial College, South Kensington, London, S.W. 7.

The abnormally high carbonyl absorptions of the ketodilactone are worthy of comment. Many instances have been discussed where the carbonyl absorption of esters and lactones show a higher frequency than expected [3]. 1,1-Diacetoxypropane absorbs at a higher frequency (1761 cm^{-1})[4] than ethyl acetate (1733 cm^{-1})[6] while cyclic esters of the general type (V) show two carbonyl bands, for example, *iso*propylidenemalonate (V) absorbs at 1750 and 1787 cm^{-1} (in chloroform)[7] while *cyclo*hexylidene methylmalonate (VI) shows bands at 1755 and 1790 cm^{-1}.[5,8] The ketodilactone I embraces the structural features of several of these substances and this fact might explain the observed abnormality.

Controlled pyrolysis of I at 250—290° followed by distillation under reduced pressure, rather than repeated distillation [1b] afforded the crystalline pulegone acetic acid anhydride (II) in high yield. The compound II exhibited an I.R. absorption typical of enol lactones [9] and gave pulegone acetic acid (VII) on alkaline hydrolysis [1b]. The alternative structure (VIII) is ruled out by the fact that the N.M.R. spectrum (at 40 Mc/s, benzene as internal standard) showed no sign of a hydrogen attached to an ethylenic bond. The proton signals observed were: (i) a sharp band at 167.5 c.p.s. (2 protons) due to the methylene group adjacent to the carbonyl group, (ii) a band at 219 c.p.s. (9 protons) due to the three methyl substituents and (iii) two diffused bands centered at 182 c.p.s. (7 protons). The enol lactone II was very resistent to catalytic hydrogenation and was only slowly hydrogenated to give *p*-menthyl-8-acetic acid (IX). The isomeric lactones X and XI have recently been synthesised [10] and differ distinctly from Vorländer's enol lactone.

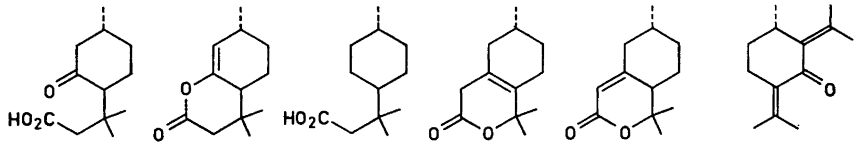

VII VIII IX X XI XII

Pulegone condenses with ethyl acetoacetate under varying conditions [11,12] to give a compound, pulegene acetone, for which several structures have been suggested (XII—XIV). Repetition of the condensation under acidic conditions (zinc chloride-glacial acetic acid)[11] gave two crystalline compounds. One was shown to be the material obtained previously (m.p. 74—76°)[11,1] and the other, a new condensation product, will be described in a future report. The I.R. and U.V. absorption of pulegene acetone are incompatible with any of these formulations but seemed to fit structure XV. The formation of this compound would be easily understandable, assuming 1,4-addition of ethyl acetoacetate to pulegone followed by acetolysis, decarboxylation and ring closure. That structure XV is correct was shown by relating it to II in the following manner. The enol lactone II reacted with methyl magnesium iodide to give a product which was treated with alkali [13] to effect ring closure. The oily reaction product was transformed to pulegene acetone (XV) in excellent yield by zinc chloride treatment. The absolute configuration of pulegone is

known [14] and this ketone on reduction with sodium and alcohol [15] yields D-(—)-menthone in which the side chains are trans. It is therefore probable that the ketodilactone I possesses the absolute configuration XVI.

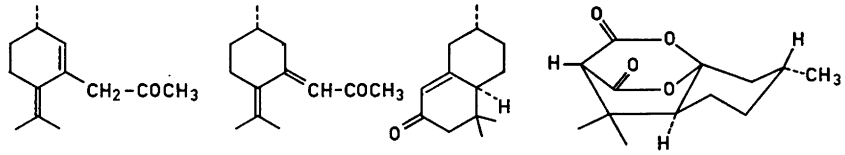

XIII XIV XV XVI

After completion of this work Wolinski and Tyrell [16] also presented evidence confirming the structure XV for pulegene acetone. Their chemical approach is essentially the reverse of that in this report.

EXPERIMENTAL

U.V. spectra and specific rotations are taken in 95 % ethanol. M.p.'s were taken on a Kofler block. Light petroleum refers to a fraction of boiling range 40—60°.

Pulegone malonic acid ketodilactone (I). The compound was prepared according to Vorländer and Köthner [1a] from pulegone (Fluka, $[\alpha]_D + 22°$). M.p. 103—105°, $[\alpha]_D + 12°$. $\nu_{max}^{CCl_4}$ 1775 and 1805 cm^{-1}, ν_{max}^{KBr} 1760 and 1795 cm^{-1}, λ_{max} 208—212 mμ (ε 400).

The calcium salt of pulegone malonic acid was prepared by adding calcium acetate solution to an alkaline solution of the dilactone. The precipitate was collected, washed with ether, 15 % ammonium chloride solution and then with water and dried over P_2O_5. ν_{max} 1570 and 1700 cm^{-1}. On acidification the salt gave the dilactone (I).

Oxidation experiments. (1) A mixture of the dilactone (1.5 g), CrO_3 (3.5 g), acetic acid (30 ml) and conc. sulphuric acid (1 ml) was kept at 50° for 24 h and then diluted with water and the pH adjusted to *ca.* 4. The precipitate (1 g) was unchanged starting material. (2) The dilactone (1 g) was dissolved in 2 N sodium hydroxide solution and pH adjusted to 6—7. Sodium periodate (4.5 g) in water (25 ml) was added. After 20 h at room temperature the solution was acidified. Unchanged dilactone (880 mg) was recovered.

Pulegone acetic acid anhydride (II). The ketodilactone I (4.2 g) was pyrolysed at 240—290° for 30 min and the residue was distilled under a reduced pressure giving the main fraction, b.p. 110—115°/12 mm, (3.5 g) which was recrystallised from light petroleum. The compound, m.p. 46—47°, (lit.[1b] 46°, $[\alpha]_D + 71.6°$ (EtOH)), $[\alpha]_D + 72.2°$, $\nu_{max}^{CCl_4}$ 1420, 1695 and 1770 cm^{-1}, ν_{max} 214 mμ (ε 3400).

Pulegone acetic acid (VII). The sublimed compound had m.p. 70—72° $[\alpha]_D$ —3° (lit.[1b] 67—68°), $[\alpha]_D$ —3.2°. $\nu_{max}^{CCl_4}$ 1705, 2700 and 3400 cm^{-1} in CCl_4. Semicarbazone, crystals from ethanol, m.p. 188—190°, ν_{max} 230 mμ (ε 12 400).

p-*Menthyl-8-acetic acid* (IX). Pulegone acetic acid anhydride (900 mg) in acetic acid (25 ml) was hydrogenated (PtO_2) for 16 h. The uptake of hydrogen was very slow. Addition of water gave an oil which was dissolved in ether. Shaking the ether extract with potassium carbonate solution extracted an acid which was recrystallised from methanol: water (5:1), m.p. 90—92°, $[\alpha]_D$ ±0. (Found: C 72.47; H 11·40. Calc. for $C_{12}H_{22}O_2$: 72.68; H 11.18). ν_{max} 1695, 2700—3200 cm^{-1}.

Pulegene acetone (XV). Pulegone acetic acid anhydride (4 g) in benzene (50 ml) was added, at room temperature, to the Grignard reagent from methyl iodide (4 g) and magnesium (650 mg) in ether (35 ml). The mixture was heated for one hour under reflux. 2 N HCl (30 ml) was added and the aqueous phase was shaken with ether. The combined organic phases were successively shaken with water. Methanol (50 ml) and 50 % NaOH solution (7 ml) were added to the residue from the evaporation of the ether-benzene solution. After 2 h at room temperature, most of the methanol was evaporated *in vacuo*

and water (50 ml) added. The product obtained was distilled *in vacuo* giving two fractions (*a*) and (*b*). (b.p. 107—112°/10 mm, 3.12 g, and b.p. 115—130°/10 mm, *ca.* 0.25 g, respectively). Fraction (*b*) crystallised on cooling and was recrystallised from light petroleum to give white crystals identified as pulegene acetone. Fraction a has the following properties: ν_{max}^{liquid} 1675 and 1625 cm^{-1}, λ_{max} 241 mμ (ε 5100) and 324 (*ca.* 100).

A solution of fraction a (1.7 g) and fused zinc chloride (3 g) in acetic acid (20 ml) was heated on a steam bath for 7 h. Extraction with light petroleum gave a residue which was distilled under reduced pressure, b.p. 130—132°/8 mm (1.4 g). The oil crystallised upon cooling. The product was recrystallised three times from light petroleum, m.p. 74—76°, undepressed on admixture with pulegene acetone prepared according to Barbier[11] $[\alpha]_D$ −126°, ν_{max}^{KBr} 885, 1424, 1622 and 1665 cm^{-1}, $\nu_{max}^{CCl_4}$ 1635 and 1675 cm^{-1}, λ_{max} 240.5 mμ (ε 15 100). (Found: C 81.28; H 10.31. Calc. for $C_{13}H_{20}O$: C 81.20; H 10.48). Semicarbazone, crystals from ethanol, m.p. 177—179°, λ_{max} 269 mμ (ε 22 000). 2,4-Dinitrophenylhydrazone crystals from ethanol m.p. 140—141°, ν_{max} 381 mμ (ε 24 800).

Acknowledgement. The author thanks Professor H. Erdtman for his interest in this work and Dr. S. Forsén for the N.M.R. data.

REFERENCES

1. (*a*) Vorländer, D. and Köthner, E. *Ann.* **345** (1906) 154.
   (*b*) Vorländer, D., May, A. and Konig, W. *Ibid.* 188.
2. Corey, E. J., Ohno, M., Chow, S. W. and Scherrer, R. A. *J. Am. Chem. Soc.* **81** (1959) 6305.
3. Bellamy, L. J. *The Infrared Spectra of Complex Molecules*, 2nd ed., Chapt, 11, Methuen, London 1958.
4. Rasmussen, R. S. and Brattain, D. R. *J. Am. Chem. Soc.* **71** (1949) 2073.
5. Jones, R. N. and Herling, F. *J. Org. Chem.* **19** (1954) 1252.
6. Felton, D. G. I. and Orr, S. F. D. *J. Chem. Soc.* **1955** 2170.
7. Snyder, H. R. and Krause, C. W. *J. Am. Chem. Soc.* **80** (1958) 1942.
8. Personal communication from Professor B. Eistert to whom the author is much indebted.
9. Rosenkranz, H. and Gut, M. *Helv. Chim. Acta* **36** (1953) 1000.
10. Mousseron, M., Mousseron-Canet, M. and Meyrolles, J. *Compt. rend.* **251** (1960) 2447.
11. Barbier, P. *Compt. rend.* **127** (1898) 870.
12. Jupp, L. G., Kon, G. A. R. and Lockton, E. H. *J. Chem. Soc.* **1928** 1639.
13. Heard, R. D. H. and Ziegler, P. *J. Am. Chem. Soc.* **73** (1951) 4036.
14. Fredga, A. *Tetrahedron* **8** (1960) 126.
15. Simonsen, J. L. and Owen, L. N. *The Terpenes*, Vol. I, p. 373, Cambridge University Press 1947.
16. Wolinski, P. and Tyrrell, Ann M. *Chem. & Ind. London* **1960** 1104.

Received August 7, 1961.

ACTA CHEMICA SCANDINAVICA 16 (1962) 209–214

Solubility Studies on Substituted Ammonium Salts of Halide Complexes

I. Theoretical Introduction

G. P. HAIGHT, Jr.

Contribution from Kem. Lab. A, Technical University of Denmark, Copenhagen, Denmark, and Swarthmore College, Swarthmore, Pennsylvania, U.S.A.

The solubility of salts of anionic complexes of metal ions is used as a method for the investigation of step-equilibria in the formation of complex ions in solution. The requisite properties of such compounds are discussed and equations are derived for treating data on solubility as a function of ligand concentration for the class of compound, $(R_4N^+)(ML_m^-)$, where R_4N^+ is a quaternary ammonium ion, M a metal ion of charge $m-1$, and L a halide ion. The use of sulfuric acid as a 1:1 electrolyte to maintain constant ion normality is proposed.

During the past several years a summer student research project at Swarthmore College has shown the possibility of synthesizing a number of salts of low solubility of general formula $(R_4N^+)(ML_m^-)$, where M is an ion of a heavy metal usually in one of the groups following the transition metals, and L is a halide ion. Preliminary studies have shown that in the absence of hydrolysis, the solid phase of these salts in equilibrium with ions in solution remains pure over wide ranges of ligand (halide) concentration. Thus an easily applied method is available for the study of halide complexes of these metal ions in solution. Preliminary observations (unpublished) indicate that the method will certainly give useful results for the halide complexes of Hg(II), Sn(II), Pb(II), and Sb(III). There seems little reason to doubt its application to other central ions in halide complexes. In this paper the equations relating solubility data and concentrations of complex species and of ligand are discussed.

Most salt solubility studies in the literature are concerned with the determination of solubility products. In most cases solubility data have been used for the determination of complexity constants only in cases where equilibrium between solid phase and one complex species is of interest. For example,

Reynolds and Argersinger [1] have discussed the importance of minima in solubility curves, but limited their attention to cases involving simple ions and one complex species. Bjerrum [2] used the solubility of Gerhardtite ($Cu(NO_3)_2 \cdot 3Cu(OH)_2$) as a function of ammonia concentration in his study of step equilibria in ammine formation. Leden [3] has made full use of the potentialities of solubility curves of AgX *vs.* $[X^-]$ in his studies of the complexes of silver ion. Since solubility data on simple salts do not distinguish mono- and polynuclear complexes, Leden generally combined solubility studies with potentiometric measurements. Recently Ahrland [4] has calculated step equilibria for BiI_{3+n}^{-n} complexes from solubility data. By introducing substituted ammonium ions as another controllable variable, it should be possible to calculate step formation constants and to detect polynuclear complex formation from solubility data alone.

MATHEMATICAL RELATIONS PERTAINING TO SOLUBILITY CURVES FOR SALTS OF THE TYPE $A^+ML_m^-$.

Definitions of terms.

S = solubility of the salt in moles per liter
C_M = Total concentration of species containing M
K_s = $[A^+]\,[ML_m^-]$, the solubility product
K_n = $[ML_n]/[L][ML_{n-1}]$
β_n = $\prod_1^n K_n$
n = number of bound ligand atoms per metal ion in a particular complex.
$\bar{n}$ = average number of bound ligands per metal ion in solution
N = maximum coordination number for M.
$[A]$ = concentration of substituted ammonium ion in moles per liter
$[M]$ = Metal ion concentration in moles per liter
$[ML_n]$ = Complex ion concentration in moles per liter
$[L]$ = Free ligand concentration in moles per liter
$[L]_o$ = Ligand concentration before dissolving any salt.

The validity of the mass action law is assumed.

I. For the case in which $A^+ML_m^-$ dissolves in a solvent containing only L^- and inert ions and only mononuclear complexes are formed.

$$S = [M] + [ML] + ML_2] + [ML_3] + \cdots + [ML_N] = C_M = [A] \tag{1}$$

$$C_M = \frac{[ML_m]}{[L]^m\beta_m} + \frac{\beta_1[ML_m]}{[L]^{m-1}\beta_m} + \cdots + \frac{\beta_n[ML_m]}{\beta_m[L]^{m-n}} + \cdots + \frac{\beta_N[ML_m][L]^{N-m}}{\beta_m}$$

Substituting for $[ML_m]$, we obtain

$$S = \frac{K_s}{[A]} \sum_{n=0}^{n=N} \frac{\beta_n[L]^n}{\beta_m[L]^m}$$

$$S^2 = K_s \sum_{n=0}^{n=N} \frac{\beta_n[L]^n}{\beta_m[L]^m} \tag{2}$$

$$\frac{dS^2}{d[L]} = \frac{K_s}{[L]} \sum_0^N \frac{(n-m)\beta_n[L]^n}{\beta_m[L]^m} \quad (3)$$

$$\bar{n} = \frac{[ML] + 2[ML_2] + \cdots + N[ML_N]}{S}$$

$$\bar{n}S = \frac{K_s}{S} \sum_0^N \frac{n\beta_n[L]^n}{\beta^m[L]^m}$$

$$\bar{n}S^2 = K_s \sum_0^N \frac{n\beta_n[L]^n}{\beta_m[L]^m} \quad (4)$$

Combining (2), (3) and (4)

$$\frac{[L]\, dS^2}{d[L]} = \bar{n}S^2 - mS^2$$

$$\frac{d \log S^2}{d \log[L]} = \bar{n} - m \quad (5)$$

Eqn. 5 is the familiar Bjerrum equation [5] for $\bar{n}$ as a function of the species ML_n being measured. The reversal of sign is due to the measured quantity S^2 being inversely proportional to ML_m. The quantity m is given by the formula of the salt. S is measured directly. Where complexes form or dissociate to an extent which effectively alters [L] from $[L]_o$, [L] must be obtained by separate measurement or by a method of successive approximations as follows:

Estimation of [L]. It can be easily shown that

$$[L] = [L]_o - S(n - m) \quad (6)$$

Substituting from eqn. (3) we obtain

$$[L] = [L]_o - [L]\frac{2dS}{d[L]}$$

$$[L] = \frac{[L]_o}{1 + 2dS/d[L])} \quad (7)$$

The denominator of the right hans side of eqn. (7) may be estimated from the slope of the solubility curve for S *vs.* $[L]_o$. An improved curve is then drawn. A second approximation for each point is usually sufficient to give the true S *vs.* [L] curve to which eqns. (1—5) apply.

An interesting consequence of eqn. (7) is that $dS/d[L]$ has a fixed value of 0.5 for $[L]_o = 0$. This in itself is helpful in determining the solubility curve.

Finding points of integer $\bar{n}$. Beck and Huhn have discussed the significance of points where $\bar{n}$ is an integer and described different types of measurements for indicating such points [6]. At such points the concentration of the complex $ML_{n=\bar{n}}$ is a maximum. Any properties of the solution depending mainly upon ML_n should also be maximal at such points. If, in the present case, a minimum appears in the solubility curve, it follows from eqn. (5) that $\bar{n} = m$ at this minimum. It can be shown by similar arguments to those used in developing eqn. (5) that the following equations also apply to the situation under discussion.

$$\mathrm{d}\log(S^2[\mathrm{L}])/(\mathrm{d}\log[\mathrm{L}]) = \bar{n} - m + 1$$

$$\mathrm{d}\log(S^2/[\mathrm{L}])/(\mathrm{d}\log[\mathrm{L}]) = \bar{n} - m - 1$$

or generally that

$$\mathrm{d}\log(S^2[\mathrm{L}]^{(m-n)})/\mathrm{d}\log[\mathrm{L}] = \bar{n} - n \tag{8}$$

where n is an integer.

Thus a plot of log $(S^2[\mathrm{L}]^{(m-n)}$ *vs.* log [L] will show a minimum at the point where $[\mathrm{ML}_n]$ is a maximum *.

It is thus possible using solubility data alone to determine each of the conditions for which $\bar{n}$ has integral values. It should be obvious that similar considerations apply to distribution and other types of measurements used to determine formation functions. This procedure is far simpler than undertaking a different type of measurement for each different $\bar{n}$ value depending on the charge and/or composition of ML_n as suggested by Beck and Huhn [6].

If one assumes that at the points for $[\mathrm{L}]_{n=\bar{n}}$ only the species ML_n, ML_{n+1}, and ML_{n-1} are present, one can approximate the product of K_nK_{n+1} as:

$$K_nK_{n+1} = 1/[\mathrm{L}]^2_{\bar{n}} \tag{9}$$

where n is integral. At half integer values of $\bar{n}$, after Bjerrum [8] we estimate

$$K_n = 1/[\mathrm{L}]_{\bar{n}=n-\frac{1}{2}} \tag{10}$$

Constants so estimated may be used as a starting point for various methods of successive approximation [4,7,8] used in determining values for K_n.

Minima described generally by $\bar{n} - n = 0$ are also useful in determining the presence of higher complexes. In the following paper (II of this series) such a minimum proves the existence of SnCl_4^{2-}, while the absence of a second minimum suggests the absence of SnCl_5^-. Failure to reach a minimum does not exclude the higher complex, but the solubility curve is easily fitted with constants K_1 to K_n up to values of $n = \bar{n}$ at the unattained minimum.

II. In cases where it is convenient to decrease solubilities by including a high (virtually constant) concentration of A^+ in the solvent the derived equations must be modified as follows because S is no longer equal to $[\mathrm{A}^+]$.

$$S = \frac{K_s}{[\mathrm{A}^+]} \sum_{n=0}^{n=N} \frac{\beta_n[\mathrm{L}]^n}{\beta_m[\mathrm{L}]^m} \tag{2a}$$

$$\frac{\mathrm{d}\log S}{\mathrm{d}\log[\mathrm{L}]} = \bar{n} - m \tag{5a}$$

$$[\mathrm{L}] = \frac{[\mathrm{L}]_o}{1 + \mathrm{d}S/\mathrm{d}[\mathrm{L}]} \tag{7a}$$

$$\frac{\mathrm{d}\log(S[\mathrm{L}]^{(m-n)})}{\mathrm{d}\log[\mathrm{L}]} = \bar{n} - n \tag{8a}$$

* It is possible to show from eqn. 7 that plots of $S^2[\mathrm{L}]^{(m-n)}$ *vs.* [L] and plots of $S[\mathrm{L}]^{(m-n)}$ *vs.* [L] give minima at the same points – namely at $[\mathrm{L}]_{n=\bar{n}}$. Thus the points $[\mathrm{L}]_{n=\bar{n}}$ are easily determined from the solubility curve when $[\mathrm{L}] = [\mathrm{L}]_o$.

Other cases can be imagined in which modifications of eqns. (1—7) are required. For instance salts of polyvalent anions such as $(R_4N^+)_2(SnCl_6^{2-})$ would require that $S = [A^+]/2$ in case I and substitution of $[A^+]^2$ for $[A^+]$ in the equations under case II, and that $K_s = [A^+]^2[ML_m]$.

Detecting polynuclear complexes. If solubilities are measured at different values of $[A^+]$ and other conditions remain the same, polynuclear complexes will be detected if S is not inversely proportional to $[A^+]$. Some consequences of polynuclear complex formation in studies involving simple salts are illustrated in Leden's work on silver iodide [3g] and silver thiocyanate [3e].

Is is also possible to alter the solubility of the salt by altering the cation. For instance with $SnCl_3^-$ it is possible to prepare salts with $(CH_3)_3C_6H_5N^+$, (*o*-phenanthroline H^+), and $(CH_3)_4N^+$. Many other univalent cations which might be useful may readily be imagined.

It may be useful to use one cation in the region of the solubility minimum and another at the ends of the curve where solubilities may become very high. If the data overlap the combined curves can be easily used to determine the formation curve.

Solvent media. It is generally customary in studies involving multiple equilibria involving ions to make measurements, if possible, in solutions containing a high and constant concentration of inert ions. The anion generally employed is the perchlorate ion which, unfortunately, precipitates substituted ammonium ions. Sulfates and bisulfates of such ions are very soluble, however. Stokes and Robinson [10] have emphasized that sulfuric acid is a 1:1 electrolyte in solutions more concentrated than 1.0 M. The molarity *vs.* molality and Hammett H_0 functions *vs.* weight percent curves are virtually identical [11] for sulfuric and perchloric acids in the range 1 to 10 M. It thus appears reasonable that sulfuric acid can be used in place of perchloric acid to maintain constant ion normality in concentration regions where the dissociation of the bisulfate ion is suppressed. The following paper describes the use of sulfuric acid in this capacity for a study of the solubility of tetramethylammonium trichlorostannate(II) as a function of chloride ion concentration.

Advantages and limitations. The use of solubilities as suggested will have definite advantages in situations where no good reversible electrode is available for potentiometric measurements, as, for instance, in the studies of complexes of Bi(III) and Sb(III). Measurements should, in general, be less subject to errors from trace impurities in solutions than electrometric measurements.

Solubility studies on the other hand do not in general permit free variation of total concentration of metal ion. Often solubilities are so high that dissociation of ML_n complexes of low n is impossible. In the BiI_n^{3-n} system, Ahrland [4] could not obtain solutions with $\bar{n}$ less than 3 from the solubility of BiI_3, and the author has found (unpublished) that the solubility of tetramethylammonium trichloromercuriate(II) is so high as to prohibit the study of the dissociation of $HgCl_2$ and $HgCl^+$ by this method.

Solubility studies break down if there is a change in the solid phase as the composition of the solution is varied. (If the change is well defined, the solubilities of the various solid phases can be employed in finding step constants, *cf.* Leden [3a,e]).

It is possible that K_s will vary with change in medium. Leden [3b] found that K_s for AgCl changed about 40 % in changing from 5 M $NaClO_4$ to 5 M NaCl. The example treated in the following paper [9] indicates that even smaller variation is to be encountered with complex salts of the type under discussion.

An application of the considerations of this paper to the study of $SnCl_n^{2-n}$ complexes is presented in the following paper [9]. As a rule, the method, using solubilities of salts of complex ions will serve best for information on complexes of higher n, but, as in the illustration to follow, for salts of weakly formed complexes, the entire formation curve may be obtained from the solubility curve. The substituted ammonium salt solubilities appear to have particular applicability to the halide complexes of ions of heavy metals following the transition groups.

The author wishes to thank the Research Corporation for a grant which initiated the studies of tetramethylammonium salts, and the Climax Molybdenum Company for a grant during a leave of absence from Swarthmore College, and particularly Professor J. Bjerrum, Dr. Gwyneth Waind, and the staff at Kem. Lab. A for stimulating and helpful discussions.

REFERENCES

1. Reynolds, C. A. and Argersinger, W. J. *J. Phys. Chem.* **56** (1952) 417.
2. Bjerrum, J. *Kgl. Danske Videnskab. Selskab, Mat.-fys. Medd.* **11** (1931) No. 5.
3. a. Leden, I. *Symposium on Coordination Chemistry*, Copenhagen 1952, p. 77.
   b. Leden, I. *Svensk Kem. Tidskr.* **64** (1952) 249.
   c. Berne, V. E. and Leden, I. *Z. Naturforsch.* **8** (1953) 719.
   d. Leden, I. and Schöön, N. H. *Acta Polytechnica* **4** (1954) No. 2.
   e. Leden, I. and Nilsson, R. *Svensk Kem. Tidskr.* **66** (1954) 126.
   f. Leden, I. and Parck, C. *Acta Chem. Scand.* **10** (1956) 535.
   g. Leden, I. *Acta Chem. Scand.* **10** (1956) 812.
4. Ahrland, S. and Grenthe, I. *Acta Chem. Scand.* **11** (1957) 1111.
5. Bjerrum, J. *Metal Ammine Formation in Aqueous Solution*, P. Haase and Son, Copenhagen 1941. Reprinted 1957, p. 22.
6. Beck, M. T. and Huhn, P. *Acta Chim. Hungarica* **20** (1959) 285.
7. Leden, I. *Z. physik. Chem.* **A 188** (1941)160.
8. Bjerrum, J. Ref.[5], p. 35.
9. Haight, Jr., G. P., Zoltewicz, J. C. and Evans, W. (Paper II). *Acta Chem. Scand.* **16** (1962). *In press.*
10. Stokes, R. H. and Robinson, R. A. *Electrolyte Solutions*, Butterworths, London 1955.
11. Hammett, L. P. and Deyrup, A. J. *J. Am. Chem. Soc.* **54** (1932) 2721.

Received July 25, 1961.

ACTA CHEMICA SCANDINAVICA 16 (1962) 215–220

Determination of the Optical Rotation of β-Fructofuranose by Means of Kinetic Measurements

BJØRN ANDERSEN and HANS DEGN

Universitetets fysisk-kemiske Institut, Copenhagen, Denmark

The furanose form of fructose which is found in sucrose has been investigated. By means of highly active β-fructofuranosidase sucrose has been hydrolyzed to 99 % in 3 minutes. The reaction has been followed by polarimetric measurements directly on the reacting solution. After complete hydrolysis of the sucrose the optical rotation still changes owing to the sum of the further transformations of α-glucopyranose and of β-fructofuranose. From the sum of the two exponentials the one representing the transformation of β-fructofuranose is evaluated by subtracting the one with the small rate constant due to the glucose. It is shown that the rate constant obtained in this way is identical with that obtained by dissolving crystalline fructopyranose in the same enzyme-buffer solution and measuring the change in optical rotation. The optical rotation of the β-fructofuranose has been found by extrapolating the equation to the time when the concentration of β-fructofuranose is identical with the initial sucrose concentration.

The value of $[\alpha]_{546}^{25}$ is found to be 1.7°. The composition of the equilibrium mixture of furanose and pyranose at 25°C based on the optical rotation of the pyranose and the furanose form and the optical rotation of the equilibrium mixture is 31.56 % furanose and 68.44 % pyranose.

As was pointed out in an earlier publication [1], a valuable contribution to the problem of the enzymatic inversion of sucrose would be the determination of the specific optical rotation of β-fructofuranose. The crystalline form of fructose is the pyranose form and the furanose form has not been crystallized. However, when fructose participates in glycosidic linkage as in the disaccharide sucrose it is present in the furanose form. It is therefore possible to follow the reaction β-fructofuranose → equilibrium mixture after very rapid enzymatic hydrolysis of a fructoside if the contributions from the other degradation products to the optical rotation are known at any given time. A technique of this kind was first described by Armstrong [2]. One of the classical investigations is that of Hudson [3]. He has shown that after a rapid hydrolysis of sucrose by invertase, the fructose mutarotates with the same velocity as crystalline

fructose dissolved in the same medium. From these measurements he obtained $+17°$ for the specific optical rotation of β-fructofuranose, using the sodium line. The identity of the velocity constants for the two opposing reactions is not quite convincing, since that from the sucrose splitting was taken from a part of the curve representing both glucose and fructose transformations. The value given for the optical rotation was based on extrapolation of curved lines and is therefore not very reliable. The same value has later been confirmed by Bailey and Hopkins [4] but also in this case the determination was based on extrapolation of curved lines. Furthermore these authors based their calculations on mutarotation constants taken from the literature without ascertaining that the constants were applicable to their solution containing large amounts of β-fructofuranosidase and other proteins. Since these velocity constants are highly dependent on the concentration of hydrogen ions and on the ionic strength, the constants from the literature are hardly applicable. The calculation of Isbell and Pigmann [5] based on the investigation of Purves and Hudson [6] is very convincing concerning the identity of the velocity constants for both directions of the mutarotation of fructose, but in this work no attempt has been made to evaluate the optical rotation of the furanose form. In the following we shall verify that the five-membered fructose after liberation from its glycoside linkage undergoes one and only one reaction and that this reaction is the transformation to the six-membered fructose. Further we shall derive a value for the optical rotation of the five-membered form.

The reaction can be described in the following way:

$$S \rightarrow G_1 + F_1 \qquad \text{(I)}$$
$$G_1 \rightarrow G_2 \qquad \text{(II)}$$
$$F_1 \rightarrow F_2 \qquad \text{(III)}$$

in which S denotes sucrose, G_1 α-glucopyranose and F_1 β-fructofuranose; G_2 denotes the equilibrium mixture which is formed from the α-glucopyranose and F_2 the equilibrium mixture which is formed from the β-fructofuranose. The velocity constants for the three equations are k_S, k_G, k_F. Assuming that reaction I is instantaneous and that reactions II and III are both first order reactions, the optical rotation α as a function of time for the solution is given by the following:

$$(\alpha_t - \alpha_\infty)_{F+G} = (\alpha_o - \alpha_\infty)_F \exp(-k_F t) + (\alpha_o - \alpha_\infty)_G \exp(-k_G t) \qquad \text{(IV)}$$

Since the value of k_F is approximately ten times that of k_G the term containing $\exp(-k_F t)$ will disappear after some time and the equation will be reduced to

$$\ln \frac{(\alpha_t - \alpha_\infty)_{F+G}}{(\alpha_o - \alpha_\infty)_G} = -k_G t$$

This means that a plot of $\ln(\alpha_t - \alpha_\infty)$ *versus* time represents a curve which for large values of t becomes a straight line, with slope $-k_G$ and intercept $\ln(\alpha_o - \alpha_\infty)_G$. In Fig. 1 a graphical representation of this type based on experiments is shown. That this line represents the transformation of α-glucose to the equilibrium mixture of α and β-glucose is clear from the fact that the evaluated k_G is identical with the mutarotation constant obtained by dissolving

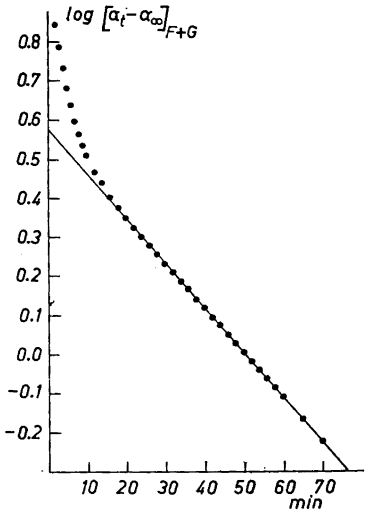

Fig. 1. The experimental values of log $(\alpha_t - \alpha_\infty)_{F+G}$ after rapid hydrolysis of sucrose. α_t represents the resulting optical rotation of the mutarotating glucose and fructose.

α-glucose in the same enzyme-buffer solution. Since we know $(\alpha_o - \alpha_\infty)_G$ and k_G we can calculate the value of $(\alpha_o - \alpha_\infty)_G \exp(-k_G t)$ at any t and subtract this value from the measured total value of $(\alpha_t - \alpha_\infty)_{F+G}$. In that way we obtain a set of values for t and $(\alpha_t - \alpha_\infty)_F$, representing a transformation of the β-fructofuranose to the equilibrium mixture. Our assumption was that this transformation exhibits first order rate behavior and if it holds, the reaction should follow the equation:

$$\ln \frac{(\alpha_t - \alpha_\infty)_F}{(\alpha_o - \alpha_\infty)_F} = -k_F t \qquad (V)$$

This means that by plotting $\ln(\alpha_t - \alpha_\infty)_F$ against time for the values obtained above, the curve should prove to be a straight line. Fig. 2 shows that a graphical

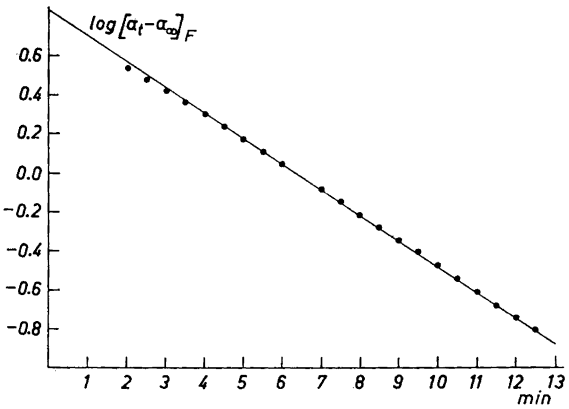

Fig. 2. The calculated values from the same experiment of log $(\alpha_t - \alpha_\infty)_F$ *versus* time. α_t represents the optical rotation of the mutarotating fructose.

representation of this type based on experiments is indeed a straight line, except for the first three minutes (we shall later return to this irregularity). This linear plot shows that the transformation of the liberated β-fructofuranose to its equilibrium mixture follows a first order equation and allows the velocity constant k_F for this reaction to be calculated. Further experiments showed that crystalline fructopyranose brought in solution under exactly the same conditions mutarotates with a velocity constant identical with that evaluated from Fig. 2.

We started with the assumption that the enzymatic splitting of the sucrose in our experiments was instantaneous. This of course is not possible even with the highly active β-fructofuranosidase we used [7]. With 2 mg of the enzyme we obtained a half life of 27 sec. This explains the irregularity of the curve in Fig. 2 mentioned before. The fact that it takes about 3 min. for the sucrose to be hydrolyzed does not affect the calculations up till now, but in the calculations below it cannot be neglected. The calculation of the optical rotation of β-fructofuranose is based on the fact that the straight line in Fig. 2 intersects the y-axis at $\ln(\alpha_o - \alpha_\infty)_F$. Since α_∞ can be measured with great accuracy, the value of α_o can be obtained. However, it is evidently not correct to extrapolate to zero time since at this time the concentration of β-fructofuranose is zero. The concentration of β-fructofuranose in the reaction mixture is determined by the two consecutive reactions I and III.

$$\underset{x}{S} \xrightarrow{k_S} \underset{y}{F_1} \xrightarrow{k_F} \underset{z}{F_2}$$

Assuming in this special case that the enzymatic splitting of sucrose is a first order reaction the following differential equations is found

$$-\frac{dx}{dt} = k_S x \; ; \; -\frac{dy}{dt} = -k_S x + k_F y \; ; \; \frac{dz}{dt} = k_F y$$

Integration of the first equation gives

$$-\ln x = k_S t + I$$

If the concentration of sucrose is a for $t = 0$

$$I = -\ln a$$

and $x = a \exp(-k_S t)$

Substituting this value of x in the second differential equation, we get

$$\frac{dy}{dt} = -k_F y + k_S a \exp(-k_S t)$$

From this first order linear differential equation, y is calculated.

$$y = \exp(-k_F t)\left(\frac{(k_S a \exp(k_F - k_S)t}{k_F - k_S} + P\right)$$

For $t = 0$, $y = 0$ and $P = -a\, k_S/(k_F - k_S)$. We thus obtain $y = -P \exp(-k_S t)$

$+ P \exp(-k_F t)$. Since k_S is far greater than k_F, the first term in this equation can be neglected for large t. We thus get $y = P \exp(-k_F t)$. The correct value of t to which the straight line in Fig. 2 has to be extrapolated is the time when the β-fructofuranose concentration is equal to the initial sucrose concentration. Setting $y = a$, in the equation gives $t = -\ln (a/P)/k_F$ and substituting this value of t in the first order eqn. (V) we obtain $\alpha = (a/P)(\alpha_o - \alpha_\infty) + \alpha_\infty$ in which α denotes the optical rotation of the untransformed β-fructofuranose. Inserting the value of P we get $\alpha = [(k_S - k_F)/k_S] (\alpha_o - \alpha_\infty) + \alpha_\infty$. The specific optical rotation $[\alpha]_{546}^{25}$ can be found from $[\alpha]_{546}^{25} = \alpha/LC$ where C is the concentration in g/cm³ and L the tube length in dm.

EXPERIMENTAL

Polarimetric measurements were performed at 25.0°C in a 10 cm polarimeter tube in a thermostated jacket. The polarimeter was a Zeiss »Lichtelektriches Polarimeter» which allowed readings of the optical rotation with an accuracy of 0.005°. The wavelength used was 546 mμ (the green Hg-line). The change of optical rotation was followed directly in the polarimeter with readings at intervals of 30 sec. The first value after the start of the reaction was usually at 90 sec.

All reaction mixtures consist of:

(1) Acetate buffer, pH 4.75, 0.005 M with respect of sodium acetate and 0.005 M with respect to acetic acid.

(2) One of the following sugars
Sucrose, 10 g/100 ml solution
Fructose, 5.263 g/100 ml solution
Glucose, 5.263 g/100 ml solution
(5.263 g of the monohexoses corresponds to 10 g of sucrose).

(3) Enzyme solution, 1 ml. (Added to the solutions of monohexoses only to assure identical conditions).

The enzyme solution contained 2 mg of β-fructofuranosidase per ml, after being adjusted to pH 4.75. This adjusting of pH was performed either with 1 M acetic acid (in the following refered to as enzyme solution *a*) or with 1 M acetate buffer pH 4.75 (refered to as *b*).

Two experiments with rapid hydrolysis of sucrose were carried out. The only difference between them was the use of enzyme solution *a* in one case, and *b* in the other. The difference in acetate ion concentration due to different adjusting of the pH in the enzyme solution is enough to change the rate constant for the fructose mutarotation. In a later publication we shall treat this problem. For the present it means that two lines of the type in Fig. 2 are obtained with different slopes and the same intercept, which means two different determinations of a_0 for the fructofuranose. (Figs. 1 and 2 refer to case *a*).

The determination of the mutarotation constants for α-glucose and β-fructopyranose was accomplished using the same conditions as in case *a*.

The value of k_S has been determined from experiments in which the 10 % sucrose solution was incubated for 3 min with different amounts of enzyme. With 2 mg, 99 % of the sucrose was hydrolysed after 3 min.

In all cases the slope and the intercept are calculated by means of the method of least squares.

RESULTS

Identity of rate constants

	Velocity constants derived from hydrolyzing sucrose. Enzyme solution *a*.	Velocity constants derived from mutarotating *a*-glucose and *β*-fructopyranose. Enzyme solution *a*.
k_G/ 2.303 min^{-1}	0.01087	0.01085
k_F/ 2.303 min^{-1}	0.0997	0.0943

Determination of optical rotation of the furanose form

	a.	*b*.
k_G/ 2.303 min^{-1}	0.01087	0.01144
k_F/ 2.303 min^{-1}	0.0997	0.1309
$\log(a_o - a_\infty)_G$	0.576	0.576
$\log(a_o - a_\infty)_F$	0.828	0.834
k_S min^{-1}		1.53

equilibrium mixture of 5.263 % glucose ($a_{\infty G}$): 3.29°
equilibrium mixture of 5.263 % fructose ($a_{\infty F}$): −5.52°

a (5.263 %) determined from the correction formula:

	a	*b*	Average
Glucopyranose:	6.99°	6.99°	6.99°
Fructofuranose:	+0.21°	−0.03°	0.09°

From this the specific optical rotation for the *β*-fructofuranose is determined; $[\alpha]_{546}^{25} = 1.7°$.

CONCLUSION

From the identity of rate constants it is proved that the transformation of the *β*-fructofuranose liberated from a glycosidic linkage consists of only one reaction, namely a transformation to an equilibrium mixture of furanose and pyranose. The composition of the equilibrium mixture at 25°C can now be calculated since the optical rotations of both forms and of the equilibrium mixture are known. The result, 31.56 % fructofuranose and 68.44 % pyranose, further permits the calculation of the specific optical rotation of the furanose form at any desired wavelength since the optical rotation of the pyranose and of the equilibrium mixture are always easily determined. In the case of sodium light (589 mμ) $[\alpha]_{589}^{25} = -4.58°$, to be compared with the discussed values from the literature.

Acknowledgement. We gratefully acknowledge discussions with Dr. Thor A. Bak.

REFERENCES

1. Andersen, B. and Bak, T. A. *Acta Chem. Scand.* **14** (1960) 823.
2. Armstrong, E. F. *J. Chem. Soc.* **83** (1903) 1305.
3. Hudson, C. S. *J. Am. Chem. Soc.* **31** (1909) 655.
4. Bailey, K. and Hopkins, R. H. *Biochem. J.* **27** (1933) 1957.
5. Isbell, H. S. and Pigmann, W. W. *J. Research, Natl. Bur. Standards* **20** (1938) 773.
6. Purves, C. B. and Hudson, C. S. *J. Am. Chem. Soc.* **56** (1934) 706.
7. Andersen, B. *Acta Chem. Scand.* **14** (1960) 1849.

Received July 24, 1961.

ACTA CHEMICA SCANDINAVICA 16 (1962) 221–228

The Mechanism of the Reduction of Nitrate

I. Stoichiometry of Molybdate Catalyzed Reductions of Nitrate and Nitrite with Sn(II) in Hydrochloric and Sulfuric Acids

G. P. HAIGHT, Jr.*, PATRICIA MOHILNER** and ALFRED KATZ***

Contribution from Denmarks Technical University, Kem. Lab. A. Copenhagen, Denmark, and the Chemistry Departments of the University of Kansas and of Swarthmore College, U.S.A.

The products of reduction of nitrate and nitrite with Sn(II) in the presence of molybdate catalyst in acid solution depend on the original oxidation state of nitrogen, the acid used, and the order of mixing reagents. In 3.0 M hydrochloric acid, when nitrate or nitrite is added to an excess of Sn(II) in the presence of molybdate, the following reactions have been observed.

$$NO_3^- + 3\,Sn(II) + 8H^+ = NH_3OH^+ + 3\,Sn(IV) + 2\,H_2O$$
$$NH_3OH^+ + Sn(II) + 2\,H^+ = NH_4^+ + Sn(IV) + H_2O$$
$$2HNO_2 + 2\,Sn(II) + 4\,H^+ = N_2O + 2\,Sn(IV) + 3\,H_2O$$

In 3.0 M sulfuric acid, and 1.5 M sulfuric plus 1.5 M hydrochloric acids, nitrous acid gives the same reaction as given above but nitrate is reduced as follows.

$$2\,NO_3^- + 4\,Sn(II) + 10H^+ = N_2O + 4\,Sn(IV) + 5\,H_2O$$

The reduction of nitrate in hydrochloric acid is much faster than in sulfuric acid and proceeds in the two steps indicated. The reduction of hydroxylamine is much slower than the reduction of nitrate making the two steps quite distinct. In the reduction of nitrite some NO is observed if Sn(II) is added to nitrite in excess. Hydroxylamine is a very poor competitor with Sn(II) as a reducing agent for either nitrate or nitrite. It is proposed that in reactions involving excess Sn(II), the question of whether hydroxylamine or nitrous oxide is to be the product depends on the relative rates of dimerization and reduction of the active intermediate HNO.

During the past ten years considerable work has been done on the role of molybdate in the enzymatic reduction of nitrates in plants[1–6]. A number of studies of inorganic systems have shown molybdenum to be an

* Chemistry Department, Swarthmore College (on leave to Kem. Lab. A 1960–1).
** Chemistry Department, Lousiana State University, Baton Rouge.
*** University of Pennsylvania Medical School, Philadelphia.

effective catalyst in the reduction of oxyanions at the dropping mercury electrode [7–9], with zinc metal [10,11] and with stannous chloride [12]. The present study was undertaken in the hope of providing a link in the two lines of research. Molybdate catalyzed reductions of nitrate to ammonia apparently play an important part in the nitrogen cycle of nature. Accordingly we have undertaken an investigation of the stoichiometry and kinetics of the reduction of nitrate in the presence of Sn(II) and molybdate catalyst. Both the stoichiometry and kinetics have proved to be very complex. Therefore we shall divide our findings, reporting the stoichiometry and kinetics, into separate communications. In the present paper we report conditions under which Sn(II) reduces nitrate to nitrous oxide, hydroxylamine, and to ammonia when molybdate is employed as a catalyst. In addition the reduction of nitrous acid to nitrous oxide both in the presence and absence of molybdate is discussed. Results are compared with previous noncatalytic studies of the reduction of nitrate and nitrite with stannous chloride [13–17].

EXPERIMENTAL

A very simple experimental procedure was employed. Standard soiutions of nitrate or nitrite were added by means of a pipette to solutions containing a known excess of Sn(II) and approximately millimolar concentrations of sodium molybdate. Oxygen-free nitrogen was kept bubbling through the test solution at all times. From time to time samples were withdrawn and quenched in an excess of standard iodine-iodide solution which was then titrated with sodium thiosulfate solution. When successive determinations showed no further decrease of Sn(II) concentration with time the reaction was judged to be completed, and the total decrease in number of equivalents of Sn(II) was compared with the number of moles of nitrate or nitrite added. The analytical method was tested and found to be accurate in the presence of nitrate, nitrous oxide, hydroxylamine, and ammonium ions. Sn(II) reacts instantly with nitrous acid and nitrogen dioxide under the conditions of our experiments. NO if formed would be swept out by the nitrogen bubbling through the solution. It turned out that when reagents were mixed in the order indicated no evidence for reduction products other than nitrous oxide, hydroxylamine, and ammonium ions was ever detected.

Hydroxylamine was determined by the method of Bray, Simpson and Mackenzie [18] in which hydroxylamine is oxidized by ferric ions to nitrous oxide at 100°C, and the resulting ferrous ions are titrated with permanganate. If chloride was present, it was diluted one hundred fold before the titration with permanganate. Ammonium ions were determined by the Kjehldahl method after allowance for the hydroxylamine present. Once patterns were established, the number of equivalents of stannous ion consumed could be used to determine the proportions of the various nitrogen containing products at any time during a run.

Nitrous oxide was never determined quantitatively as such. In cases where it was suspected as a product, its odor and ability to support combustion served to indicate that it was a major product. In all such cases the number of equivalents of Sn(II) consumed corresponded to N(I) as the *only* oxidation state of nitrogen produced when neither hydroxylamine or ammonia could be detected.

Reagent grade chemicals were used without further purification. Water purified by double distillation and by ion exchange gave identical results. Solutions of stannous chloride in 3.0 M hydrochloric acid were prepared by dissolving the reagent directly in acid and storing under nitrogen, and by passing solutions of cupric chloride in 3.0 M hydrochloric acid through a tin reductor. In the latter case reaction was complete in one pass. Stannous sulfate was prepared by shaking copper sulfate in 3.0 M sulfuric acid with metallic tin for over a week. The replacement of copper ions by tin proved to be extremely slow in the absence of chloride ions. Stannous ion stock solutions were standardized by titration with permanganate or iodometrically.

Nitric, hydrochloric, and sulfuric acids were standardized by sodium carbonate titrations using methyl orange indicator. Nitric acid was freed from oxides of nitrogen by bubbling oxygen free nitrogen through the solutions for one hour before use. Solutions of sodium nitrite were standardized by reaction with excess standard permanganate which was back titrated with standard ferrous ammonium sulfate solution. We found during these studies that we could also standardize nitrite solutions by reaction with excess Sn(II) and back titration with iodine. This method is not applicable if nitrate is present.

Stannous ions and nitrate ions were found not to react in the absence of molybdate over a two day period. Mixtures deteriorated however, if placed in flasks known to have once contained solutions of molybdate ions, regardless of how thoroughly they were cleaned.

RESULTS

1. *The reduction of nitrate in 3.0 molar hydrochloric acid.* These conditions were selected because of the previous finding that with them hydroxylamine is most easily reduced to ammonia, and hydroxylamine must certainly be an intermediate in the reduction of nitrate to ammonia. Nitrate is in fact reduced to ammonia under these conditions in two distinctive steps.

$$3SnCl_3^- + NO_3^- + H_2O + 2\,H^+ \xrightarrow{\text{Mo(VI) catalyst}} 3\,SnOCl_3^- + NH_3OH^+ \quad (1)$$

$$SnCl_3^- + NH_3OH^+ \xrightarrow{\text{Mo(VI)}} SnOCl_3^- + NH_4^+ \quad (2)$$

The formula $SnCl_3^-$ is used because it has been shown to be the most abundant and most reactive chlorotin(II) complex present in 3.0 M hydrochloric acid.[19-21] The formula $SnOCl_3^-$ is purely speculative, but is a possible initial product if the reactions involve oxygen atom transfer to $SnCl_3^-$.

Fig. 1 shows the pattern of variation of Sn(II) concentration with time for runs containing excess Sn(II), nitrate, and sodium molybdate. A sharp break in the rate is always noted as soon as 3.0 moles of Sn(II) have been consumed for each mole of added nitrate. Table 1 shows how all the nitrogen present can be accounted for as hydroxylamine, ammonium ion, and/or unreacted nitrate at any time before completion of the run. (It is interesting to note that excess nitrate interfered very little with the determination of hydroxylamine.) Conclusive evidence that hydroxylamine is the primary product was found in our ability to calculate the points between $([Sn(II)]_0 - [Sn(II)]/[NO_3^-]^0 = 3$ and 4 from the previously established kinetics of the reduction of hydroxylamine [19].

2. *The reduction of nitrate in sulfuric acid.* In the presence of excess stannous ion and sodium molybdate, nitrate is reduced to nitrous oxide in sulfuric acid of widely varying concentration and in equimolar sulfuric and hydrochloric acids at total ion normality of 3.0 (assuming H_2SO_4 is a 1:1 electrolyte).

$$4\,Sn(II) + 2\,NO_3^- + 10H^+ = 4\,Sn(IV) + N_2O + 5\,H_2O \quad (3)$$

Here nothing can be said about the nature of stannous and stannic species present. In all cases N_2O was detected as a product and the number of equivalents of Sn(II) consumed corresponded almost exactly to reaction (3). This indicates

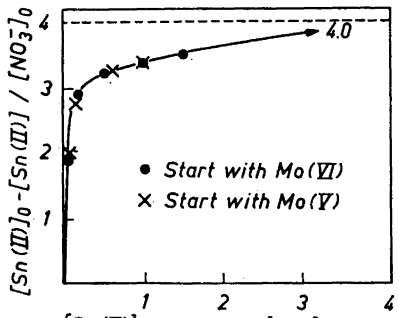

Fig. 1.

that nitrogen in the +1 oxidation state as nitrous oxide or hyponitrous acid ($H_2N_2O_2$) is the only product of the reduction of nitrate under these conditions. This conclusion is strengthened by our inability to detect ammonium ions, hydroxylamine, or nitric oxide among the products. The reaction in 3.0 M sulfuric acid is extremely slow requiring several days time for completion at 25°C, even though one thousand fold more molybdate was used than in the study in hydrochloric acid. Qualitatively it was observed that up to two chloride ions per stannous ion decelerated the reaction somewhat. In equimolar sulfuric and hydrochloric acid the reaction rate was comparable with that in 3.0 M hydrochloric acid, though not quite so fast. The products in the mixed acids were the same as in sulfuric acid. Results obtained in solutions containing sulfuric acid are summarized in Table 2.

3. *The reduction of nitrous acid by Sn(II).* All experiments in which sodium nitrite solutions were added to an excess of Sn(II) in either hydrochloric

Table 1. Nitrate reduction products in 3.0 M hydrochloric acid.

Time, min.	a $Sn(II)_0$ m/l	b $NO_3^-{}_0$ m/l	c Sn(II) m/l	d NH_2OH m/l	e NH_4^+ m/l	f NH_4^+ m/l	g NO_3^- m/l
1	0.234	0.0492	0.1135	0.0383	0.00	0.0014	0.0092
15	0.234	0.0492	0.0770	0.0393	0.0094	0.0099	0.0000
1500	0.234	0.0492	0.0369	0.0000	0.0493	0.0492	0.0000
—	0.0423	0.150	0.0085	0.0113	0.000	0.0007	0.139

10^{-4} M molybdate was present in each solution.

About 30 seconds elapsed between samples used to measure c, and samples used to measure d.

Columns a, b, c and d represent experimental measurements.

e = a − 3b − c if a > 3b

f = b − d, g = 3b−a + c if g > 0.0

The fourth row in Table 1 represents an experiment designed only to show qualitatively the presence of hydroxylamine in a run containing excess nitrate. The nitrate apparently did not interfere with hydroxylamine determination as was expected.

Table 2. Stoichiometry of the reduction of nitrate and nitrite by Sn(II) in sulfuric acid.

Mo m/l	a NO_3^- added millimoles	b NO_2^- added millimoles	c Sn(II) consumed millimoles	c/a	c/b	$[H_2SO_4]$ m/l
none	0.00	5.86	5.71	—	0.97	2
none	0.00	5.86	5.90	—	1.008	2
10^{-3}	0.00	5.86	5.81	—	0.99	2
none	23.5	5.86	6.70	—	1.15	2
none	11.75	5.86	6.46	—	1.10	2
none	22.97	0.00	0.10	0.005	—	2
10^{-3}	2.625	0.00	5.25*	2.00	—	2
10^{-3}	2.625	0.00	5.16*	1.98	—	2
10^{-3}	2.625	0.00	5.29*	2.01	—	3
10^{-2}	4.578	0.00	9.196 **	2.01	—	3.2
10^{-2}	4.578	0.00	9.224 **	2.01_5	—	9.0
0.005	0.150	0.00	0.187 (1 day) 0.307 (2 days)	2.05	—	3.0
0.005	0.150	0.00	0.285 (5 min.) 0.300 (1 h.)	2.00	—	1.5 (+1.5 M HCl)

* 35°C
** 100°C, 10 min.

or sulfuric acids, with or without molybdate present, gave an instantaneous two equivalent reduction of nitrite according to the equation:

$$2\,Sn(II) + 2\,HNO_2 + 4\,H^+ = 2\,Sn(IV) + N_2O + 3\,H_2O \qquad (4)$$

The same results were obtained employing back titration of excess Sn(II) with iodine, or by titrating Sn(II) to a potentiometric end point with the nitrite solution. (Raschig observed nitric oxide (NO) as a product when Sn(II) was added to nitrous acid in excess.) We have the paradoxical result that under conditions where nitrate is reduced to hydroxylamine and ammonia, nitrite is reduced only to nitrous oxide.

Table 3. Stoichiometry of the reduction of nitrite by Sn(II) in hydrochloric acid.

a NO_2^-[a] added millimoles	b Sn(II) consumed millimoles	Other N compounds present	b/a
0.2610	0.2610	none	1.000
4.058	3.996	none	0.985
4.058	4.240	none	1.04
7.250	7.333[a]	none	1.01
1.480	1.475[a]	none	0.995
6.270	6.210[a]	none	0.99
0.478	0.457	0.018 M NH_2OH	0.95
0.821	0.649	0.028 M NH_2OH	0.79
0.1435	0.1207	0.009 M NH_2OH	0.85

In all cases $NaNO_2$ solutions were added to other reagents in 3.0 M hydrochloric acid.

[a] Potentiometric titrations, all other results by iodometric analysis for excess Sn(II).

The fact that nitrate is not reduced when molybdate is absent, but nitrite is reduced quickly and quantitatively suggested that the non-catalyzed reaction could be used to determine nitrite in the presence of nitrate. Attempts to do this proved disappointing since the presence of nitrite evidently causes some reduction of nitrate to take place as is shown in two experiments recorded in Table 2. Similar synergistic effects were recorded by Klemenc and Klima [14] in 1929.

When nitrite solutions are added to solutions containing both hydroxylamine and Sn(II) in 3.0 M hydrochloric acid, somewhat less than one mole of stannous ion per mole of nitrous acid is consumed. The speed of reaction made rate and efficiency of mixing a large factor in the results and only qualitative conclusions can be drawn. It is clear however that hydroxylamine competes only slightly with $SnCl_3^-$, and that the latter is a far more labile reducing agent in this case. Results of all experiments on the reduction of nitrite are summarized in Tables 2 and 3.

DISCUSSION

The patterns of products observed in molybdate catalyzed reductions of nitrate and in the reductions of nitrite with or without molybdate present are very similar to those observed at elevated temperatures without catalysis by Milligan [13], Maumené [15] and Dumreicher [16]. This suggests that molybdate merely activates the robust nitrate ion, but does not further influence the course of reaction. The change in reaction product from hydroxylamine to nitrous oxide when sulfuric acid is substituted for hydrochloric acid is extremely interesting. It is not likely that the various species containing nitrogen in its various oxidation states are much affected by the change from hydrochloric to sulfuric acid at ion normality = 3.0. However, Sn(II) is principally $SnCl_3^-$ in 3.0 M hydrochloric acid. Since this is the most reactive of the chlorotin(II) complexes, the acceleration of reaction due to chloride is explainable, but not necessarily the change in reduction products of nitrate. The change in reduction products is believed to be explicable in terms of the kinetic properties of the active intermediate HNO.

Let us assume that stannous ion functions as a two-electron reducing agent (probably acting as an oxygen atom acceptor). Nitrate ions will then be reduced according to the following steps:

$$Sn^{2+} + H^+ + \overset{(Mo(VI))}{NO_3^-} = SnO^{2+} + HNO_2 \quad (5)$$

$$Sn^{2+} + HNO_2 = SnO^{2+} + HNO \quad (6)$$

$$Sn^{2+} + HNO + H_2O = SnO^{2+} + NH_2OH \quad (7)$$

It is well known that HNO_2 in acid reacts with itself to form the anhydride N_2O_3. It seems reasonable that HNO, which would be a weaker acid, should form its anhydride even more readily. Thus:

$$HNO + HNO = N_2O + H_2O \text{ (or } H_2N_2O_2) \quad (8)$$

is an alternative to reaction (7). The products of reactions (7) and (8) are the two products observed under different conditions. It now remains to explain how the various conditions employed favor one product completely over another.

Reaction (7) will be favored by low concentrations of HNO and by high reactivity of reducing agent. The rate of reaction (8) will increase as the square of the concentration of the active intermediate HNO, and is therefore favored when this concentration is high.

Comparing the reduction of nitrate in hydrochloric and sulfuric acids, we find evidence that reaction (7) is dominant when $SnCl_3^-$ is the dominant form of the reducing agent present. This most reactive species of Sn(II) is able to make (7) the dominant reaction over (8). This is true, however, only when nitrate is the starting material. When nitrous acid is reduced, the initial reaction is very fast producing a large initial concentration of HNO which results in the formation of N_2O by reaction (8). It is hoped that future studies can be undertaken employing conditions where mixtures of products are obtained.

The great reactivity of the postulated species HNO can be used to account for the reduction of nitrate in the presence of nitrite, and for the production of NO when nitrite in excess reacts with solutions of stannous chloride [17]. HNO produced by the reduction of nitrite may give the following reactions as well as (7) and (8).

$$HNO + H^+ + NO_3^- = N_2O_3 + H_2O \quad (9)$$

$$HNO + HNO_2 = 2NO + H_2O \quad (10)$$

Labile HNO_2 traps nearly all the HNO before it can dimerize while only a small, but significant, fraction of the robust nitrate ions are attacked.

The suggestion of Milligan [13], that hydroxylamine is the primary reduction product of nitrate and is reoxidized to nitrous oxide by nitric or nitrous acids, is definitely refuted by our results. Nitrate does not oxidize hydroxylamine during the catalytic reductions, and hydroxylamine does not compete effectively with stannous ion as a reducing agent for nitrous acid. It is likely that the behavior of the very reactive HNO with respect to dimerization or reduction may be a key to the explanation of most observations on the reduction of nitrate which proceed beyond the oxidation states represented by NO_2^- and NO.

The authors wish to express their gratitude for the financial support of the Office of Ordnance Research, U.S. Army and the Climax Molybdenum Company. We also wish to thank Professors Bjerrum and Hofman-Bang for the use of the facilities of Kem. Lab. A.

REFERENCES

1. Nicholas, D. J., Nason, A. and McElroy, W. D. *J. Biol. Chem.* **207** (1954) 341.
2. Nicholas, D. J. and Nason, A. *J. Biol. Chem.* **207** (1954) 353.
3. Nicholas, D. J. and Nason, A. *J. Biol. Chem.* **211** (1954) 183.
4. Nicholas, D. J. and Nason, A. *J. Bacteriol.* **67** (1955) 5, 58.
5. Nicholas, D. J. and Nason, A. *Plant Physiol.* **30** (1955) 135.
6. Nicholas, D. J. and Stevens, H. M. *Nature* **176** (1955) 1066.
7. Haight, Jr., G. P. *Anal. Chem.* **23** (1951) 1505.
8. Johnson, M. G. and Robinson, R. J. *Anal. Chem.* **24** (1952) 366.
9. Haight, Jr., G. P. *Acta Chem. Scand.* **15** (1961) 2012.
10. Haight, Jr., G. P. *Anal. Chem.* **25** (1953) 642.
11. Rechnitz, G. A. *Thesis*, University of Illinois (1961).
12. Haight, Jr., G. P. and Sager, W. F. *J. Am. Chem. Soc.* **74** (1952) 6056.
13. Milligan, L. H. and Gillette, G. R. *J. Phys. Chem.* **28** (1924) 747.
14. Klemenc, A. and Klima, L. *Z. anorg. u. allgem. Chem.* **179** (1929) 379.
15. Maumene, E. J. *Compt. Rend.* **70** (1870) 147.
16. v. Dumreicher *Monatsch.* **1** (1880) 724.
17. Raschig, F. *Z. Anorg. u. allgem. Chem.* **155** (1926) 255.
18. Bray, W. C., Simpson, M. E. and Mackenzie, A. A. *J. Am. Chem. Soc.* **41** (1919) 1362.
19. Haight, Jr., G. P. and von Frankenberg, C. *Acta Chem. Scand.* **15** (1961) 2026.
20. Haight, Jr., G. P., Zoltewicz, J. and Evans, W. *Acta Chem. Scand.* **16** (1962). *In press.*
21. Duke, F. R. and Peterson, N. C. *J. Phys. Chem.* **63** (1959) 2077.

Received August 12, 1961.

ACTA CHEMICA SCANDINAVICA 16 (1962) 229–239

Titration Curves of Polyacids

KATE BAK

Institute for Physical Chemistry, University of Copenhagen, Denmark

The present investigation deals with titration curves of polyacids and the information which can be obtained from them.

The polymer molecule is considered as a one-dimensional lattice, and an expression for the relation between the apparent pK, the degree of neutralization and the energy of interaction is derived.

The analogy of this approach to previous work by Linderstrøm–Lang and J. Bjerrum is demonstrated.

Finally the theory is compared with experimental results for a polyacrylic acid, containing 25–30 monomer units per molecule. The titration curves were corrected for changes in ionic strength during the titration.

It is concluded that the shape of polyacrylic acid in solution is such that each carboxyl group is surrounded by eight other carboxyl groups within a sphere, the approximate radius of which is the distance between two adjacent carboxyl groups.

INTRODUCTION

1. It was early discovered that the titration curves for polyacids, such as gum arabic and pectic acid, differed significantly from those of monobasic acids in that the apparent pK for the polyacid increased during the titration. Originally this was attributed to the existence of different acidic groups, but as the theory of high molecular substances progressed it became clear that in polyacrylic acid, for instance, there is only one type of carboxyl group. The explanation for the increasing pK must therefore rather be sought in the fact that the negative charge of the molecule increases during a titration, thus making it more and more difficult for the protons to be removed.

One way of treating this problem would be a Debye-Hückel approach in which it is assumed that the polymer molecule is a more or less free drained sphere with fixed charges on it. The Poisson-Boltzmann equation for this case has been solved approximately by Hermans and Overbeek [1], and this leads then to an expression for pK as a function of the charge and the ionic strength, as put forward by Overbeek [2]. The agreement between theory and experiment is, however, somewhat unsatisfactory.

An essentially much simpler approach is to elaborate the model for calculation of dissociation constants of acids due to N. Bjerrum [3] in which it is assumed for instance that $pK_1 - pK_2$ for a dibasic acid is determined only by the electrostatic forces and the symmetry of the three molecular species involved in the equilibria. If one assumes that the (linear) polyacid can be treated as a one-dimensional lattice, and that only nearest neighbour interaction need be considered, the problem is an example of a solvable case of the Ising model [4]. Since comparison with experiments shows that in this application of the Ising model the difference between the exact solution and the solution using the Bragg—Williams approximation is negligible, it is possible to drop the assumption of a one-dimensional lattice and also to estimate the influence of next nearest neighbours. In this way, we believe the titration curve can be used as a means of determining the degree of coiling in a polyacid.

Since the Bjerrum approach to dissociation constants also has been used extensively in the theory of the formation of metal complexes, we further compare the results obtained here with formulae given by J. Bjerrum [6] and with analogous expressions derived earlier by Linderstrøm—Lang in a paper on protein solutions [7].

It should be quite clear that the present theory is only a crude one. A large number of factors, such as the effects of binding of counter-ions, and the entropy of distribution of un-ionized groups, ions and bound ion pairs among the possible configurations on the polymer molecule, which are considered for instance in the papers by Harris and Rice [8], have been neglected. In this way it has been possible to obtain simple formulae which can be compared with experiments. In the more involved theories, which only rarely lead to results which can be checked experimentally, it is not always clear which of the many factors considered are the important ones.

EXPERIMENTAL

2. The polyacrylic acid used was presented to us by Dr. V. Shashona, E. I. Du Pont de Nemours and Co. (Inc.), Wilmington, Delaware, U.S.A., as a concentrated aqueous solution. The number-average molecular weight was determined osmometrically by a Christiansen osmometer [9] to be 1.9×10^5, corresponding to about 27 monomer units. This value is the extrapolation of measurements at three different concentrations, performed by Dr. K. Marcker.

The concentration of polyacrylic acid in the solutions titrated was 5.6×10^{-4} g/ml of solution. The base used was 1.2 N NaOH.

The titration curves were determined using a Radiometer pH-meter 3 with glass-electrode and a calomel electrode as a reference. The apparatus was standardized on a 0.05 M solution of potassium hydrogen phthalate, following National Bureau of Standards' standardizing procedure. The titration vessel was stirred with a magnetic stirrer which was switched off during each measurement. In the earlier experiments, CO_2-free air was bubbled through the solution, but since experiments showed that this did not affect the results, this extra precaution was abandoned in later experiments.

The microburette used *, and which was calibrated with mercury, was a syringe, the body of which was made of hard polyethylene, the piston of teflon. The syringe was held in a brass tube and the piston was moved by a micrometer screw. The syringe contains 0.708 ml and can be read with a precision of 0.708/2500 ml.

* Constructed by Dr. Jørgen Koefoed.

The temperature of the solution was kept constant at 25 ± 1°C by surrounding the titration vessel with a small water bath. Titration vessel, water bath and magnetic stirrer were encased in a grounded metal box.

The titrations were carried out two to three times each and were reproducible to within 0.05 pH-unit.

Titration curves for glutaric acid were also determined using solutions which contained the same equivalents of acid as the above solutions of polyacid.

Both for glutaric acid and polyacrylic acid the titrations were performed on solutions containing from 0 to 0.5 mole/l NaCl.

From the titration curves of polyacrylic acid and glutaric acid, the apparent pK was calculated as a function of the degree of neutralization,

$$pK = pH - \log\vartheta/(1-\vartheta)$$

The direct calculation of pK in different salt solutions gave, especially for low salt concentration, curves of a shape as in Fig. 1.

The ionic strength changed considerably during a titration, especially at low salt concentrations. To compensate for this, titration curves were made at eight different concentrations of added NaCl, such that the ionic strength at the start of each run varied from 0 to 0.5. (At higher ionic strength than 0.5 the acid was salted out). For each titration curve the apparent pK was calculated at $\vartheta = 0.1 - 0.9$ (0.05) and the ionic strength was likewise calculated at each point. From the curves of pK *versus* $\sqrt{\mu}$ for each value of ϑ, values of pK at $\sqrt{\mu} = 0.2 - 0.7$ (0.1) were read. In this way one obtains pK as a function of ϑ for various fixed values of μ.

The results are given in Table 1, and it will be seen that $dpK/d\vartheta$ is independent of ϑ, within the error of measurement, such that the curve of pK as a function of ϑ becomes a straight line, which differs markedly from the directly calculated curve given in Fig. 1.

This way of obtaining curves of pK *versus* ϑ is fairly time-consuming, but it is absolutely necessary if one wants significant values, since for instance a titration curve determined at an average ionic strength of 0.025 is almost useless, if for instance μ changes from *ca.* 0.07 to *ca.* 0.045 during the run.

The titration curves of glutaric acid were determined in exactly the same way as those for polyacrylic acid, and were corrected for ionic strength in the same way.

THEORY

3. For a polyacid it is not very profitable to use the dissociation constants for each step in the neutralisation, since they do not differ much from each other. Moreover, the acid would have to be completely homomolecular if we should have any chance of measuring each pK.

To specify the equilibrium between partly neutralized polyacid and hydrogen ions we shall therefore use the apparent pK, defined above.

The apparent pK is a function of ϑ, and is a convenient quantity to work with, in that it measures how much the actual dissociation constant depends on the charge of the acid. However, it can even be advantageous to work with this quantity for a dibasic acid, as we shall see below.

The first to give a theory of the calculation of the ratio of the two dissociation constants for a dibasic acid H_2B was Niels Bjerrum [3] who showed that to a first approximation

$$K_2/K_1 = \tfrac{1}{4} \exp(-e^2/DrkT)$$

In this expression r is the distance between the two carboxyl groups, D is the dielectric constant of the medium, and e is the elementary charge.

This expression is most easily derived in the following way. In the expression

$$K_2/K_1 = [H_2B]\,[B^{2-}]/[HB^-]^2$$

the partition functions are substituted for the concentrations. All the partition functions are identical with respect to translation, vibration, rotation, and electronic state, if we assume the H_2B molecule to be so large that its mass and moment of inertia only undergo negligible changes when one or two protons are taken off. That is, we can set

$$Q_{H_2B} = Q$$

$$Q_{HB^-} = 2Q$$

$$Q_{B^{2-}} = Q \exp(-e^2/DrkT)$$

the molecules B^{2-} and H_2B both being more symmetric than HB^-, such that one obtains their Q's by dividing that of HB^- with a symmetry number $\sigma = 2$. Moreover, the lowest state of energy of B^{2-} contains an electrostatic contribution of e^2/Dr, while the two other species do not contain this contribution, and as we wish to use the partition functions to calculate an equilibrium constant, their energies must be calculated on the same energy scale. By substitution we get Bjerrum's result.

Comparison of Bjerrum's theoretical expression with experiment gives reasonably good agreement for acids with large distances between the carboxyl groups, but for acids like oxalic acid where the carboxyl groups are very near to each other, or for alkyl substituted malonic acids where the material between the carboxyl groups is a hydrocarbon rather than water, there is a considerable discrepancy between theory and experiment.

The work of Bjerrum has been extended in various ways, taking the paraffin part of the molecule into account by assuming it to act as a cavity with a low dielectric constant (Kirkwood—Westheimer theory [10]). It is now well known that this is a highly artificial representation of an organic ion, which only gives reasonable results when one limits oneself to considering solutions of ions in one solvent and at one temperature. Since we are not directly interested in measuring molecular distances, we shall only use that the term appearing in the exponential is the interaction energy between two negative charges located on the carboxyl groups divided by kT. In the following we shall use measured values of K_2/K_1 to calculate the interaction energy $w(\sim e^2/rD)$ and compare w for different acids with each other.

We shall now use N. Bjerrum's method to calculate the titration curve for a polyacid. This method differs considerably from those of Overbeek [2] and of Katchalsky and Spitnik [11], but is in many ways analogous to the treatment given by Marcus [12].

4. As a model for a polyacid we shall use a one dimensional lattice. We shall let the carboxyl groups be the lattice points on which we distribute minus-signs, *i.e.*, from which we take away protons.

If we have M lattice sites ($M \to \infty$) on which we distribute N particles we have for the partition function, if we only take nearest neighbour interaction into account

$$Q(N,M,T) = [q\,e^{-w/kT}]^N \sum_{N_{01}} g(N,M,N_{01})\,(e^{w/2kT})^{N_{01}}$$

where q is the partition function for the individual particle and

$$g = \frac{2N!(M-N)!}{\left(\frac{N_{01}}{2}\right)!\left(N-\frac{N_{01}}{2}\right)!\left(M-N-\frac{N_{01}}{2}\right)!\left(\frac{N_{01}}{2}\right)!}$$

where N_{01} is the number of 01 pairs, *etc.*, see Hill[13], p. 238.

Maximising Q we find that the corresponding number of pairs N_{01}^*, N_{00}^* and N_{11}^* satisfy the equation

$$N_{11}^* N_{00}^*/(N_{01}^*)^2 = \tfrac{1}{4} \exp(-w/kT)$$

that is, for systems where $w/kT \ll 1$ we have $4N_{11}^* N_{00}^* \sim (N_{01}^*)^2$, *i.e.*, we have a random distribution between 01, 00 and 11 pairs. Under these conditions we are therefore justified in using the Bragg—Williams approximation and write the partition function for the molecule with M carboxyl groups, N of which are ionized, as

$$Q(N,M,T) = \frac{M!}{N!(M-N)!}\, q^N\, e^{-N^2 w/MkT}$$

The most serious approximations so far have been the assumption of a linear molecule and the fact that we only take nearest neighbour interaction into account. The assumption of a random distribution is, as we have seen, fairly well justified.

In the Bragg—Williams approximation the difference between a linear lattice and a three-dimensional lattice disappears, and in the following calculations therefore the approximation of primary importance seems to be the assumption of nearest neighbour interaction only.

From this partition function we get the chemical potential of the protons absorbed on the lattice (*i.e.*, which have neutralized the carboxyl groups) by differentiating the logarithm with respect to $(M - N)$, the number of protons on the polymer molecule,

$$\begin{aligned}\mu_{H+}(\text{poly}) &= -kT[\partial \ln Q/\partial(M-N)]_{M,T} \\ &= -kT \ln[\vartheta \exp(2w\vartheta/kT)]/q(1-\vartheta)\end{aligned}$$

using Stirling's formula. $\vartheta = N/M$ is the degree of neutralization used previously.

The chemical potential of the hydrogen ions present in the solution is

$$\mu_{H+}(\text{soln}) = \mu_o + kT \ln c_{H+}$$

and as we define the apparent acid dissociation constant by

$$\ln K = \ln c_{H+} + \ln[\vartheta/(1-\vartheta)]$$

we have by substitution

$$\mu_{H+}(\text{soln}) = \mu_0 + kT \ln K - kT \ln[\vartheta/(1-\vartheta)]$$

The dependence of the apparent dissociation constant on ϑ is now determined by the condition of equilibrium $\mu_{H+}(\text{soln}) = \mu_{H+}$ (poly) and we get

$$-kT\ln[\vartheta\exp(2\vartheta w/kT)]/q(1-\vartheta) = \mu_o + kT \ln K - kT\ln[\vartheta/(1-\vartheta)]$$

or

$$\ln K = (\ln q - \mu_o/kT) - 2w\vartheta/kT$$

The term in parenthesis is $\ln K_0$, *i.e.* the logarithm to the dissociation constant for the first carboxyl group, so that we have

$$pK = pK_o + 2\chi\vartheta \log e$$

where χ is the interaction energy divided by kT.

In the Bragg—Williams approximation therefore $dpK/d\vartheta$ is a constant = 2 log e and one can determine the energy of interaction directly from the slope of the experimental curve. This relation between equilibrium constants and the over-all degree of reaction for molecules with several sites is analogous to equations obtained by J. Bjerrum and by Linderstrøm—Lang.

5. J. Bjerrum considered metal complex formation by the reactions

$$\begin{aligned} &Me + A \rightleftharpoons MeA \\ &MeA + A \rightleftharpoons MeA_2 \\ &\quad\cdot\ \cdot\ \cdot \\ &\quad\cdot\ \cdot\ \cdot \\ &MeA_{M-1} + A \rightleftharpoons MeA_M \end{aligned}$$

M being the maximum number of ligands A that can be attached to the metal atom Me. He further defined $\bar{n}$, the average number of ligand atoms bonded to a metal atom as

$$\bar{n} = \frac{[MeA] + 2[MeA_2] + \ldots + M[MeA_M]}{[Me] + [MeA] + [MeA_2] + \ldots + [MeA_M]}$$

If the kinetics were only determined by statistical factors, we should have very simple ratios of the constants. At equilibrium there will be formed as much of the compound MeA_N as will be broken down. Moreover, the probability of dissociation of an A-unit will be proportional to N, the number of A's already there, whereas the probability for addition of an A-unit will be proportional to $M - N$, the number of free sites. We therefore have for the reactions

$$\begin{aligned} &MeA_{N-1} + A \rightleftharpoons MeA_N \\ &MeA_N + A \rightleftharpoons MeA_{N+1} \\ &(M-N+1)\,[MeA_{N-1}]\,[A]k_{on} = N\,[MeA_N]\,k_{off} \\ &(M-N)\,[MeA_N]\,[A]k_{on} = (N+1)\,[MeA_{N+1}]k_{off} \end{aligned}$$

from which we get

$$\frac{k_{on}}{k_{off}} = \frac{(N)}{(M-N+1)} \frac{[MeA_N]}{[MeA_{N-1}]\,[A]} = \frac{N}{(M-N+1)} k_N$$
$$= \frac{(N+1)}{(M-N)} \frac{[MeA_{N+1}]}{[MeA_N]\,[A]} = \frac{N+1}{M-N} k_{N+1}$$

or

$$\frac{k_N}{k_{N+1}} = \frac{(N+1)(M-N+1)}{(M-N)N}$$

(Bjerrum [4], eqn. (1) p. 24, also Pauli and Valkó [14], p. 114).

To allow for an interaction energy Bjerrum multiplies the right hand side of the equation by x^2, where x is a spreading factor which is a constant characteristic of the whole system, so the equation reads

$$\frac{k_N}{k_{N+1}} = \frac{(M-N+1)(N+1)}{(M-N)N} x^2$$

If we calculate the same ratio on the basis of the partition functions we obtain

$$\frac{k_N}{k_{N+1}} = \frac{(Q_{MeA^{N-}})^2}{Q_{MeA^{(N+1)-}} Q_{MeA^{(N-1)-}}} = \frac{(Q(N,M,T))^2}{Q(N+1,M,T)\,Q(N-1,M,T)}$$
$$= \frac{(N+1)(M-N+1)}{N(M-N)} \exp(2w/MkT)$$

we see that the two results are identical if $x^2 = \exp(2w/MkT)$ or, calling $\chi = w/kT$, $\chi = M\ln x$.

Bjerrum further defines a quantity Δ by $\Delta = (\partial\bar{n}/\partial\ln A)_{\bar{n}=M/2}$ which in our nomenclature corresponds to

$$\Delta = (\partial(M-N)/\partial\ln H^+)_{N=M/2}$$
$$= M \log e\, (\partial\vartheta/\partial pH)_{\vartheta=\frac{1}{2}}$$
$$= \frac{M \log e}{\frac{\partial}{\partial\vartheta}\left[pK + \log(\vartheta/(1-\vartheta))\right]_{\vartheta=\frac{1}{2}}}$$
$$= \frac{M}{2\chi+4}$$

when we insert $\chi = M\ln x$ we get

$$\Delta = M/(2M\ln x+4) = 1/(2\ln x + 4/M)$$

This expression is identical with an expression given by Bjerrum [6] (eqn. 24, p. 34), a formula originally derived by Linderstrøm—Lang [7] in 1924 to describe the average charge on a polyelectrolyte. In his derivation the polyelectrolyte is described as a ball with sites which can adsorb either positive

or negative charges, dependent on the pH of the medium. The average number of charges on each ball is calculated, using the Debye—Hückel theory, the Helmholtz double layer theory, and the law of mass action.

The interaction energy χ stems from the interaction between a pair of nearest neighbours. If next nearest neighbour interaction plays a considerable role, the χ we get from experiments will contain a contribution from this effect also, contributing for a linear lattice at most half of the measured value. However, this contribution should fall off rapidly with increasing ionic strength, as the screening by the medium will make next nearest neighbour interaction negligible, if the molecule remains streched. On the other hand, if the molecule is not stretched, but coiled up in such a way that more than two sites are within the nearest neighbour distance from a single site, this contribution will also be included in the measured χ. This contribution should be expected to increase as the polymer molecule coils up, *i.e.* with increasing ionic strength, although it should not be expected to hide completely the first effect.

Instead of trying to calculate the interaction energy between two sites by considering charges and distances, we have measured it directly by titrating solutions of glutaric acid under conditions identical to those for polyacrylic acid, glutaric acid having the same number of carbon atoms between the two carboxyl groups as has polyacrylic acid.

6. As an illustration of the usefulness of the apparent pK, even for a dibasic acid, we shall derive a connection between K_2/K_1 and $\mathrm{d}pK/\mathrm{d}\vartheta$.

For a dibasic acid H_2B being titrated with NaOH one has

$$x_0 = [H_2B] + [HB^-] + [B^{2-}]$$
$$[Na^+] = 2\vartheta x_0 = 2[B^{2-}] + [HB^-]$$

denoting by x_0 the total concentration of acid. Here again we use ϑ to denote the total degree of neutralization, and we neglect the concentrations of H^+ and OH^- as compared to the other concentrations. Expressing both equations in terms of B^{2-} and dividing the second by the first equation we obtain:

$$[H^+]^2 + [H^+]K_1\left(1 - \frac{1}{2\vartheta}\right) + K_1K_2\left(1 - \frac{1}{\vartheta}\right) = 0$$

From this we see that at $\vartheta = \frac{1}{2}$, $[H^+]^2 = K_1K_2$

Differentiating with respect to ϑ and putting $\vartheta = \frac{1}{2}$ we get

$$K_1 = -\left(\frac{\mathrm{d}[H^+]}{\mathrm{d}\vartheta}\right)_{\vartheta=\frac{1}{2}} - 2[H^+]$$

and so we get for K_2/K_1

$$\begin{aligned} K_2/K_1 &= [H^+]^2/K_1^2 \\ &= [H^+]^2/\{2[H^+] + (\mathrm{d}[H^+]/\mathrm{d}\vartheta)_{\vartheta=\frac{1}{2}}\}^2 \\ &= \{2 + (\mathrm{d}\ln[H^+]/\mathrm{d}\vartheta)_{\vartheta=\frac{1}{2}}\}^{-2} \end{aligned}$$

Another way of calculating this quantity is by using the slope of the apparent pK *versus* ϑ-curve at $\vartheta=\frac{1}{2}$. We differentiate the expression defining pK

$$pK = pH + \log[(1-\vartheta)/\vartheta]$$

with respect to ϑ, and using the previously obtained value of K_1, we get

$$K_1/[H^+] = 2 + \ln 10(\mathrm{dp}K/\mathrm{d}\vartheta)_{\vartheta=\frac{1}{2}}$$

or

$$K_2/K_1 = [2 + \ln 10(\mathrm{dpK}/\mathrm{d}\vartheta)_{\vartheta=\frac{1}{2}}]^{-2}$$

Thus we can calculate χ directly from the experimental curves by $K_2/K_1 = \frac{1}{4}\exp(-\chi)$

COMPARISON WITH EXPERIMENT

7. Table 1 gives values for pK for polyacrylic acid at varying values of ϑ and μ. As will be seen from this, pK *versus* ϑ is a straight line within the experimental error. In Fig. 2 the values of pK are plotted as functions of ϑ. The lowest line in Table 1 shows $\mathrm{dp}K/\mathrm{d}\vartheta$, calculated from the p$K$-values.

Table 2 shows $\chi_P = \frac{1}{2}\ln 10(\mathrm{dp}K/\mathrm{d}\vartheta)$ calculated from the values in Table 1, together with χ_G calculated from K_2/K_1 for glutaric acid from titration curves. As will be seen, both χ_P and χ_G decrease with increasing ionic strength as it was to be expected. The last column in Table 2 shows the interaction energy for polyacrylic acid divided by that for glutaric acid. It will be seen that χ_P is roughly $4\chi_G$, the ratio increasing only very slightly with the ionic strength.

Table 1. pK for polyacrylic acid at different values of ϑ and μ.

	$\mu = 0.040$ $\sqrt{\mu} = 0.20$	$\mu = 0.090$ $\sqrt{\mu} = 0.30$	$\mu = 0.160$ $\sqrt{\mu} = 0.40$	$\mu = 0.250$ $\sqrt{\mu} = 0.50$	$\mu = 0.360$ $\sqrt{\mu} = 0.60$	$\mu = 0.490$ $\sqrt{\mu} = 0.70$
$\vartheta = 0.20$	4.88	4.75	4.64	4.545	4.48	4.43
0.25	5.04	4.86	4.75	4.65	4.57	4.49
0.30	5.18	4.98	4.845	4.725	4.63	4.55
0.35	5.305	5.06	4.92	4.805	4.70	4.61
0.40	5.41	5.16	5.015	4.89	4.78	4.68
0.45	5.54	5.265	5.11	4.97	4.85	4.735
0.50	5.68	5.38	5.20	5.05	4.92	4.80
0.55	5.82	5.49	5.30	5.145	5.00	4.87
0.60	5.965	5.61	5.395	5.23	5.08	4.94
0.65	6.095	5.73	5.51	5.34	5.17	5.02
0.70	6.23	5.85	5.61	5.41	5.24	5.09
0.75	6.38	5.97	5.705	5.49	5.31	5.16
0.80	6.54	6.105	5.81	5.595	5.40	5.235
$\mathrm{dp}K/\mathrm{d}\vartheta$	2.70±0.03	2.23±0.05	1.93±0.03	1.72±0.02	1.52±0.02	1.34±0.02

The fact that χ_P/χ_G is almost independent of the ionic strength shows that the neglect of more than nearest neighbour interaction is reasonable, or alternatively that the coiling of the polymer with increasing ionic strength compensates for the screening effect of the medium. Experimentally one cannot decide between these possibilities, but we believe the latter effect to be of minor importance.

On the other hand, the fact that the measured χ_P is four times what we expected can only be explained by the hypothesis that instead of 2 nearest

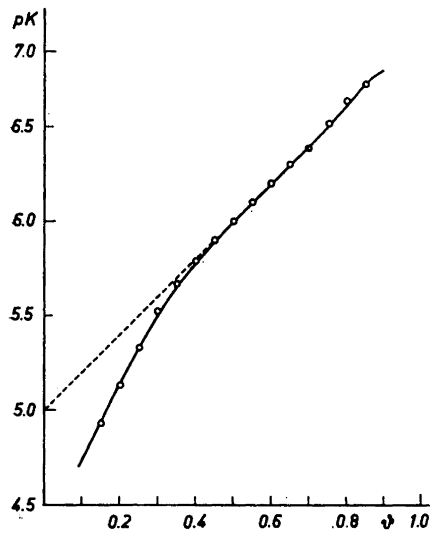

Fig. 1. p*K* *versus* ϑ not corrected for ionic strength.

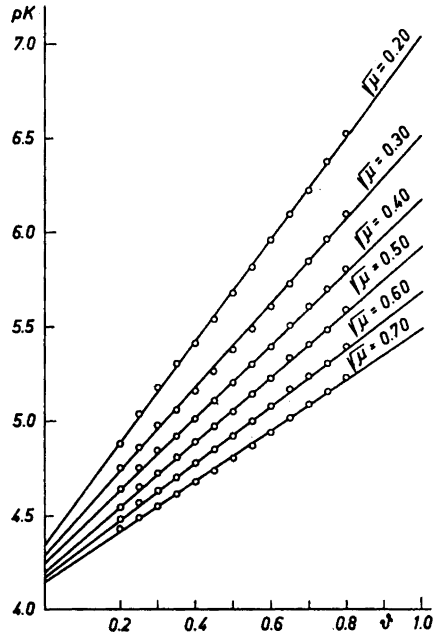

Fig. 2. p*K* *versus* ϑ at different values of the ionic strength.

neighbours each site must have approximately 8 nearest neighbours, *i.e.*, the polymer must be coiled up in such a way that each carboxyl group on the average is surrounded by 8 other carboxyl groups within a sphere, the radius of which is the distance between the carboxyl groups in glutaric acid.

If one tries to build a polyacrylic acid molecule from Catalin models, one finds that it is indeed possible to have a conformation in which every carboxyl group has 8 neighbours within a distance which is only slightly larger than the distance between two carboxyl groups in glutaric acid. This fact renders the hypothesis of eight nearest neighbours in the actual polyacrylic acid molecule somewhat more plausible.

Table 2. Energies of interaction divided by kT for glutaric acid and for polyacrylic acid at various values of the ionic strength.

μ	$\sqrt{\mu}$	χ_G	χ_P	χ_P/χ_G
0.04	0.2	0.812	3.356	3.83
0.09	0.3	0.679	2.568	3.78
0.16	0.4	0.557	2.222	3.99
0.25	0.5	0.475	1.980	4.19
0.36	0.6	0.413	1.750	4.24
0.49	0.7	0.363	1.543	4.25

Acknowledgements. This work was done in partial fulfillment of the requirements for the degree of lic.techn. at the Technical University of Denmark while holding a fellowship from *Det Teknisk-Videnskabelige Forskningsraad.* Some preliminary experiments were made while working on a grant from *Statens Almindelige Videnskabsfond* to Dr. Jørgen Koefoed. To him and to Dr. Thor A. Bak I wish to express my gratitude for many discussions during the work.

REFERENCES

1. Hermans, J. J. and Overbeek, J. Th. G. *Rec. trav. chim.* **67** (1948) 761.
2. Overbeek, J. Th. G. *Bull. Soc. chim. Belge* **57** (1948) 252.
3. Bjerrum, N. *Z. physik. Chem.* **106** (1923) 219.
4. Ising, E. *Z. Physik* **31** (1925) 253.
5. Bragg, W. and Williams, E. J. *Proc. Roy. Soc.* **A 165** (1934) 699.
6. Bjerrum, J. *Metal Ammine Formation in Aqueous Solution,* P. Haase and Son, Copenhagen 1941.
7. Linderstrøm-Lang, K. *Compt. rend. lab. Carlsberg, Sér. chim.,* **15** (1924) No 7.
8. Harris, F. E. and Rice, S. A. *J. Phys. Chem.* **58** (1954) 725, 733.
9. Christiansen, J. A. and Jensen, C. E. *Acta Chem. Scand.* **7** (1953) 1247.
10. Kirkwood, J. G. and Westheimer, F. H. *J. Chem. Phys.* **6** (1938) 506, 513.
11. Katchalsky, A. and Spitnik, P. *J. Polymer Sci.* **2** (1947) 432.
12. Marcus, R. A. *J. Phys. Chem.* **58** (1954) 621.
13. Hill, T. L. *Introduction to Statistical Mechanics,* Addison-Wesley, 1960.
14. Pauli, W. and Valkó, E. *Elektrochemie der Kolloide,* Springer 1929.

Received May 15, 1961.

ACTA CHEMICA SCANDINAVICA 16 (1962) 240–248

Short Communications

On the Specificity of Arylesterases

KLAS-BERTIL AUGUSTINSSON and GUNNAR EKEDAHL

Institute of Organic Chemistry and Biochemistry, University of Stockholm, Sweden

By definition, arylesterases are enzymes which hydrolyse aromatic esters and are resistant to those organophosphorus compounds which strongly inhibit aliesterases and cholinesterases [1]. When this definition was introduced, little was known about the specificity of arylesterases, except for the fact that they hydrolyse phenyl esters at a higher rate than do aliesterases and cholinesterases, the acetate being more readily split than the propionate and butyrate. The present communication extends the specificity study to the description of the influence of the structure of the phenolic/alcoholic moiety of the substrate on the hydrolysis rate, catalysed by human plasma arylesterase.

A partly purified arylesterase preparation (nitrogen content, 13 %) from human plasma was used as enzyme source. It was free from cholinesterase activity. For comparison, a cholinesterase preparation (nitrogen content, 12.6 %) from the same source and free from arylesterase activity was also tested. The Warburg manometric technique was used for esterase determination at pH 7.4, during which the initial substrate concentration was 8 mM. A detergent (Tween 20) was used for solubilization of most esters, and in the concentration used (0.05 %) it had no significant influence on the activity measured. Esterase activity is expressed in μmoles of substrate hydrolysed per h per mg esterase preparation. Corrections were made for spontaneous hydrolysis of substrate, which did not exceed 0.6 μmoles per h in any case under the experimental conditions used.

Among a number of esters tested for enzymatic hydrolysis, the following were not hydrolysed by arylesterase:

benzyl acetate
benzyl benzoate
2-phenylethyl acetate
3-phenylpropyl acetate
ethyl phenylacetate
isoamyl phenylacetate
acetylsalicylate
ethyl benzoate
ethyl *p*-hydroxy-benzoate
ethyl salicylate
diethyl phthalate
diisoamyl phthalate
ethyl gallate
phenyl salicylate
ethyl acetate
isopropyl acetate
amyl acetate
2-ethoxyethyl acetate
vinyl crotonate

The influence of the structure of the phenolic/alcoholic radical of the substrate on the enzymatic hydrolysis is illustrated in Fig. 1, in which the hydrolysis rates of a series of acetic acid esters are compared for arylesterase and cholinesterase. Phenyl acetate (I) was hydrolysed at the highest rate among all esters tested. With the alicyclic analogue of phenyl acetate (cyclohexyl acetate, IV) no hydrolysis was detected. As regards the three cyclohexenyl acetates, it was found that the Δ^1-derivative (II) was hydrolysed but not the Δ^2- (III) and Δ^3-derivatives. This indicates that a double bond nearest to the ester linkage might be prerequisite for enzymatic hydrolysis. Further support for this idea was obtained when it was demonstrated that Δ^1-cyclopentenyl acetate(VI) was hydrolysed, but not cyclopentyl acetate (V). A comparatively high hydrolysis rate was also observed for 3-pyridyl acetate (XIII).

To test this structure-activity relationship further, the hydrolysis of certain

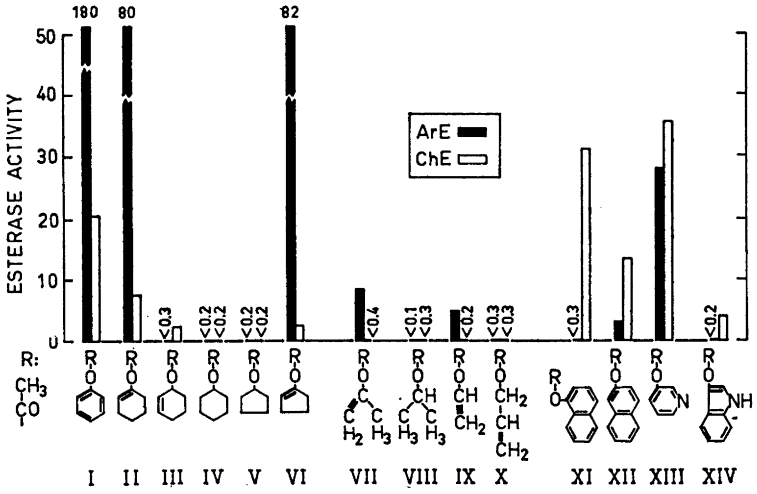

Fig. 1. The enzymatic hydrolysis of various acetates by purified preparations of arylesterase (ArE) and cholinesterase (ChE) from human plasma. Esterase activity is expressed in μmoles of ester hydrolysed per h per mg enzyme preparation.

simple aliphatic acetates were studied. Thus isopropenyl acetate (VII) was found to be split by arylesterase, but not isopropyl acetate (VIII). Moreover, vinyl acetate (IX) was attacked by this enzyme, but not allyl acetate (X).

When naphthyl acetates were tested as substrates, it was found that the 2-naphthyl ester (XII) was hydrolysed at a much higher rate by arylesterase than the 1-naphthyl ester (XI). The hydrolysis rates of these two esters were the reverse for cholinesterase. Steric hindrance is probably the explanation for the difference between the two esters *vis à vis* arylesterase. For the same reason, probably, indoxyl acetate (XIV) and acetyl salicylate were poor substrates for arylesterase.

Human plasma arylesterase was determined to be an acetylarylesterase, since acetates were hydrolysed more rapidly than propionates and butyrates, not only of the phenolic series, but also of the series of vinyl and indoxyl esters. Cholinesterase of human plasma differs in this respect from arylesterase, butyrates (choline, phenyl, indoxyl) being hydrolysed at a higher rate than the corresponding propionates and acetates. As regards arylesterase, substitution by electrophilic and nucleophilic groups in the acyl radical of the ester has a marked influence on the hydrolysis rate. This will be the subject of a following report in this field.

The results reported indicate that the active center of arylesterase contains a structure that reversibly reacts with a C=C group of the alcoholic moiety of an ester; the prerequisite for enzymatic hydrolysis is that this group is bond directly to the alcoholic oxygen atom. It should be mentioned that arylesterase is highly sensitive to mercaptide forming agents (*e.g.*, *p*-hydroxymercuribenzoate) and that the inhibition by these agents is reversed by cysteine [2]. We therefore suggest, as a tentative model for the mechanism of action of arylesterase, that the enzymatic hydrolysis involves the formation of a thioester intermediate from the enzyme SH and the acyl moiety of the substrate. The formation of this intermediate is dependent on the special character of the C-C bond nearest to the ester linkage, as was demonstrated above.

This work was supported by a grant from the *Swedish Natural Science Research Council*. We greatly appreciate the cooperation of Ing. Hans Hasselqvist who synthesised the cyclohexenyl, cyclopentenyl and pyridyl esters.

1. Augustinsson, K.-B. *Nature* **181** (1958) 1786; *Acta Chem. Scand.* **13** (1959) 571.
2. Augustinsson, K.-B. *Ann. N. Y. Acad. Sci.* **94** (1961) 844.

Received December 15, 1961.

Refinement of the Ni_3P Structure

STIG RUNDQVIST, EIVIND HASSLER and LARS LUNDVIK

Institute of Chemistry, University of Uppsala, Uppsala, Sweden

The crystal structure of Ni_3P was originally determined by Aronsson [1]. In the course of crystal-chemical investigations of transition metal phosphides by one of the present authors (S.R.) it became desirable to obtain accurate structural data for Ni_3P. Accordingly, a re-determination of the structure was made by single-crystal methods.

Weissenberg photographs were taken using zirconium-filtered MoK radiation with crystals rotated about the a and c axes. The multiple-film technique, with thin iron foils between successive films, was used. The intensities were estimated visually by comparison with a calibrated scale. The structure was refined from successive electron density maps and from difference maps projected on the ac and ab planes. Corrections for Lorentz and polarisation factors together with Fourier series summations, structure factor calculations, and calculations of interatomic distances were made on the electron digital computer BESK. Atomic scattering factors were interpolated from tables given for nickel by Thomas and Umeda [2] and for phosphorus by Tomiie and Stam [3]. Corrections for absorption were not applied. For the 135 $F(hk0)$-values observed, the final R-value of 0.083 was obtained. An overall, isotropic temperatur factor with $B = 0.29$ Å^2 was applied. The corresponding figures for the 78 $F(h0l)$-values observed were $R = 0.105$, $B = 0.40$ Å^2. (On account of extinction effects, the seven largest $F(hk0)$-values and the largest $F(h0l)$-value were omitted in the refinements, and were not included in the R-values quoted above. Lists of observed and calculated structure factors can be obtained from this Institute on request.)

Final structure data for Ni_3P are given in Table 1. The unit cell dimensions for Ni_3P were determined from powder photographs recorded in Guinier-type focussing cameras with Cu$K\alpha$ and Cr$K\alpha_1$ radiation using silicon ($a = 5.4305$ Å) as the internal calibration standard. The accuracy is estimated to be better than 0.04 %. The standard deviations for the atomic positions quoted in Table 1 were calculated using Cruickshank's [4] equation. Two different sets of x and y parameters for each atom were obtained, one from the $F(hk0)$ and one from the $F(h0l)$ data. The two sets were not significantly different. The parameter values given in Table 1 are weighted averages obtained by giving the parameter values from the centrosymmetric $\varrho(xy)$ projection twice the weight of those from the non-centrosymmetric $\varrho(xz)$ projection.

Table 1. Final structure data for Ni_3P.

Space-group $I\bar{4}$ ($-S_4^2$). $Z = 8$.
$a = 8.954$ Å; $c = 4.386$ Å; $U = 351.6$ Å^3

Atoms in 8(g)	x	$\sigma(x)$	y	$\sigma(y)$	z	$\sigma(z)$
Ni_I	0.0775	0.0003	0.1117	0.0003	0.2391	0.0015
Ni_{II}	0.3649	0.0003	0.0321	0.0003	0.9765	0.0015
Ni_{III}	0.1689	0.0003	0.2200	0.0003	0.7524	0.0015
P	0.2862	0.0005	0.0487	0.0005	0.4807	0.0028

A comparison of the data in Table 1 with those given by Aronsson [1] shows a satisfactory agreement. The x and y parameters are in good agreement, but there are slightly larger differences between the corresponding z parameters. This is explained by the fact that Aronsson derived the z parameters from the positions of the Patterson peaks alone, without subsequent refinements.

Interatomic distances are listed in Table 2.

Acknowledgements. This work has been supported by the *Swedish Technical Research Council State of* and by the *Office of Aerospace Re-*

Table 2. Interatomic distances in Ni_3P (Å). (Distances shorter than 3.6 Å listed)

Ni_I	$-Ni_I$:	2.43_5, $2.71_3(2)$, $2.86_4(2)$
Ni_I	$-Ni_{II}$:	2.64_5, 2.90_8, 3.39_4
Ni_I	$-Ni_{III}$:	2.48_3, 2.58_4, 2.71_3
		2.72_6, 2.81_8
Ni_{II}	$-Ni_{II}$:	2.48_7, $2.65_3(2)$, $2.97_5(2)$
Ni_{II}	$-Ni_{III}$:	2.51_7, 2.54_6
		2.62_2, 3.48_7
Ni_{III}	$-Ni_{III}$:	2.68_5 (2)
Ni_I	$-P$:	2.22_1, 2.28_7, 3.46_7
Ni_{II}	$-P$:	2.29_1, 2.32_2
		2.32_6, 2.34_1
Ni_{III}	$-P$:	2.20_8, 2.27_9
		2.33_5, 3.59_7

search, United States Air Force, through its European Office under Contract No. AF 61 (052)-40. Facilities for use of the electronic digital computer BESK were granted by the *Swedish Board for Computing Machinery.*

1. Aronsson, B. *Acta Chem. Scand.* **9** (1955) 137.
2. Thomas, L. H. and Umeda, K. *J. Chem. Phys.* **26** (1957) 293.
3. Tomiie, Y. and Stam, C. H. *Acta Cryst.* **11** (1958) 126.
4. Cruickshank, D. W. J. *Ibid.* **2** (1949) 65.

Received December 19, 1961.

On the Acceptor Specificity of Rhodanese

BO SÖRBO

Nobel Medical Institute, Biochemical Dept., Stockholm, Sweden

It has previously [1] been shown that rhodanese catalyzes the reaction between thiosulfonates and sulfite to give the corresponding sulfinate and thiosulfate. It could then be expected that rhodanese should also catalyze and exchange reaction between thiosulfate and sulfite

$$S_2O_3^{2-} + {}^{35}SO_3^{2-} = S^{35}SO_3^{2-} + SO_3^{2-}$$

This has now been verified (Table 1), which is of special interest in connection with the experiments on thiosulfate metabolism recently reported by Szczepkowski *et al.*[2,3] These authors injected ^{35}S-labelled cystine into rats and found that most of the radioactivity was excreted into the urine as sulfate, with only a small fraction as thiosulfate. If, however, unlabelled thiosulfate was injected together with the labelled cystine, much more radioactivity was excreted as thiosulfate and less as sulfate. This was interpreted as indicating that thiosulfate is an important metabolic precursor of sulfate, which is in contrast to current opinions[4] on the metabolism of sulfur compounds. The most important precursor of sulfate is usually considered to be sulfite, which is formed from cysteine or cystine with cysteinesulfinate as an intermediate. The results of Szczepkowski *et al.* can in fact be explained by a rhodanese catalyzed dilution of labelled sulfite by unlabelled thiosulfate.

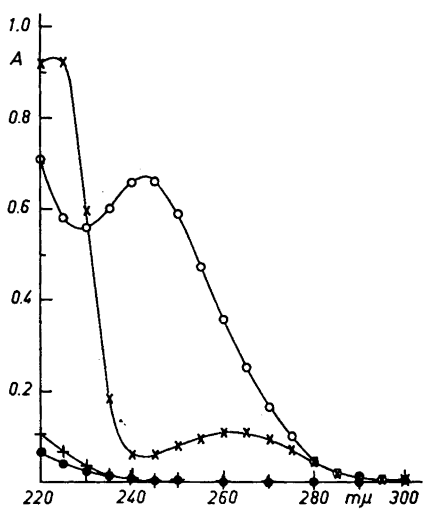

Fig. 1. Absorption spectrum of thiosulfonates and sulfinates. O *p*-toluenethiosulfonate, × *p*-toluenesulfinate, + thiotaurine, ● hypotaurine. Each compound at 1 × 10^{-4} M concentration in 0.05 M phosphate buffer, pH 7.4.

As sulfite is an acceptor for rhodanese, it was of interest to investigate if the structurally related sulfinates (RSO_2^-) could also participate in rhodanese catalyzed transsulfuration reactions. This could be demonstrated to be the case by a spectrophotometric technique, that was based on the fact that arylthiosulfonates (which are very active sulfur donors for rhodanese [5]) show a much stronger light absorption around 240 mμ than do the corresponding sulfinates or alkyl thiosulfonates (Fig. 1). It is thus possible to demonstrate a transsulfuration between an aromatic thiosulfonate and an aliphatic sulfinate or between an aliphatic thiosulfonate and an aromatic sulfinate by following the change in light absorption at 240 mμ. (Other sulfur acceptors, such as sulfite or cyanide, which absorb weakly at 240 mμ, can also be studied in this way). This spectrophotometric technique for following rhodanese catalyzed reactions seems to be of potent value for studies on the reaction mechanism of the enzyme, since it is now possible to rapidly determine what effect different substituents in the donor or acceptor molecule have on the reaction velocity. The rhodanese cata-

search, United States Air Force, through its European Office under Contract No. AF 61 (052)-40. Facilities for use of the electronic digital computer BESK were granted by the *Swedish Board for Computing Machinery.*

1. Aronsson, B. *Acta Chem. Scand.* **9** (1955) 137.
2. Thomas, L. H. and Umeda, K. *J. Chem. Phys.* **26** (1957) 293.
3. Tomiie, Y. and Stam, C. H. *Acta Cryst.* **11** (1958) 126.
4. Cruickshank, D. W. J. *Ibid.* **2** (1949) 65.

Received December 19, 1961.

On the Acceptor Specificity of Rhodanese

BO SÖRBO

Nobel Medical Institute, Biochemical Dept., Stockholm, Sweden

It has previously [1] been shown that rhodanese catalyzes the reaction between thiosulfonates and sulfite to give the corresponding sulfinate and thiosulfate. It could then be expected that rhodanese should also catalyze and exchange reaction between thiosulfate and sulfite

$$S_2O_3^{2-} + {}^{35}SO_3^{2-} = S^{35}SO_3^{2-} + SO_3^{2-}$$

This has now been verified (Table 1), which is of special interest in connection with the experiments on thiosulfate metabolism recently reported by Szczepkowski *et al.*[2,3] These authors injected ^{35}S-labelled cystine into rats and found that most of the radioactivity was excreted into the urine as sulfate, with only a small fraction as thiosulfate. If, however, unlabelled thiosulfate was injected together with the labelled cystine, much more radioactivity was excreted as thiosulfate and less as sulfate. This was interpreted as indicating that thiosulfate is an important metabolic precursor of sulfate, which is in contrast to current opinions[4] on the metabolism of sulfur compounds. The most important precursor of sulfate is usually considered to be sulfite, which is formed from cysteine or cystine with cysteinesulfinate as an intermediate. The results of Szczepkowski *et al.* can in fact be explained by a rhodanese catalyzed dilution of labelled sulfite by unlabelled thiosulfate.

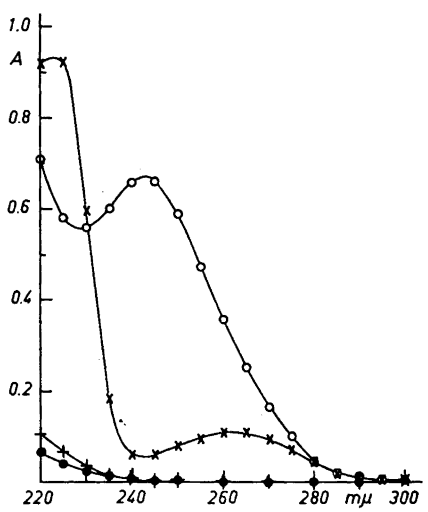

Fig. 1. Absorption spectrum of thiosulfonates and sulfinates. O *p*-toluenethiosulfonate, × *p*-toluenesulfinate, + thiotaurine, ● hypotaurine. Each compound at 1 × 10^{-4} M concentration in 0.05 M phosphate buffer, pH 7.4.

As sulfite is an acceptor for rhodanese, it was of interest to investigate if the structurally related sulfinates (RSO_2^-) could also participate in rhodanese catalyzed transsulfuration reactions. This could be demonstrated to be the case by a spectrophotometric technique, that was based on the fact that arylthiosulfonates (which are very active sulfur donors for rhodanese [5]) show a much stronger light absorption around 240 mμ than do the corresponding sulfinates or alkyl thiosulfonates (Fig. 1). It is thus possible to demonstrate a transsulfuration between an aromatic thiosulfonate and an aliphatic sulfinate or between an aliphatic thiosulfonate and an aromatic sulfinate by following the change in light absorption at 240 mμ. (Other sulfur acceptors, such as sulfite or cyanide, which absorb weakly at 240 mμ, can also be studied in this way). This spectrophotometric technique for following rhodanese catalyzed reactions seems to be of potent value for studies on the reaction mechanism of the enzyme, since it is now possible to rapidly determine what effect different substituents in the donor or acceptor molecule have on the reaction velocity. The rhodanese cata-

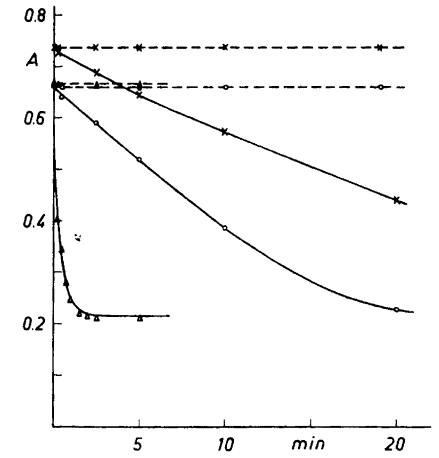

Fig. 2. Reaction between toluenethiosulfonate and sulfinates or sulfite. The test system contained 1×10^{-4} M *p*-toluenethiosulfonate, 5×10^{-4} M sulfinate or sulfite, 0.05 M phosphate buffer pH 7.4 and rhodanese as indicated (3 RU/ml in case iof the sulfinates and 0.6 RU/ml in case of sulfite). Temp. 23°C. O hypotaurine, × cysteinesulfinate, △ sulfite. Dashed curves are without added enzyme.

lyzed reactions between *p*-toluenethiosulfonate and hypotaurine or cysteinesulfinate are shown in Fig. 2. The identity of the reaction products (toluenesulfinate and thiotaurine or thiocysteate, respectively) was established by paper chromatography. Is is also evident from Fig. 2 that sulfite is a better sulfur acceptor than the sulfinates studied. The reaction between a thiosulfonate and sulfinate is reversible as shown in Fig. 3. The equilibrium constant

$$K = \frac{[\text{toluenesulfinate}]\,[\text{thiotaurine}]}{[\text{toluenethiosulfonate}]\,[\text{hypotaurine}]}$$

was calculated to be 1.2 and thus the amino alkylsulfinate has about the same affinity for sulfur as the arylsulfinate. Rhodanese also catalyzed the reaction between thiotaurine and cysteinesulfinate to give hypotaurine and thiocysteate, as demonstrated by paper chromatography. (The test system of pH 7.4 contained 4×10^{-3} M substrate plus 1.4 RU/ml rhodanese, and was incubated 30 min. at 20°C).

Some thiol compounds were also tested as sulfur acceptors for rhodanese at pH 7.4 with *p*-toluenethiosulfonate as the donor. It was found that rhodanese had no catalytic effect with inorganic sulfide, cysteine, cysteamine or glutathione, but that a slow enzyme-catalyzed reaction occurred with mercaptoethanol and thioglycolate. The reaction products are presumably toluenesulfinate and a persulfide of mercaptoethanol and thioglycollate, respectively, but the latter compounds have not yet been identified and are probably rather unstable.

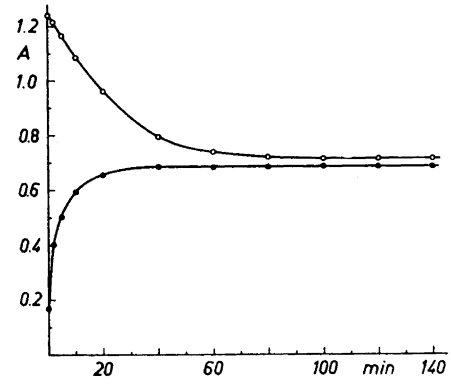

Fig. 3. Reversible reaction between thiosulfonate and sulfinate. The test system contained 2×10^{-4} M substrates and 6 RU/ml rhodanese. Other conditions as in Fig. 2. O *p*-toluenethiosulfonate and hypotaurine, ● *p*-toluenesulfinate and thiotaurine.

Experimental. Crystalline rhodanese, sodium *p*-toluenethiosulfonate, thiotaurine and hypotaurine were prepared as described in earlier publications [5-7], whereas sodium *p*-toluene-

Table 1. Exchange reaction between thiosulfate and sulfite. The test system, at pH 7.4 contained 125 μmoles each of $Na_2S_2O_3$ and $Na_2{}^{35}SO_3$ (7.2×10^3 c.p.m. per μmole), 28 μmoles of NaH_2PO_4 and rhodanese as indicated. Final volume 2.5 ml. The reaction mixtures were incubated for 5 min. at 20°C.

Rhodanese RU*	$S^{35}SO_3^{2-}$ formed μmoles
0	0
1.5	5.7
16.0	48.2

* As defined in Ref.[6]

sulfinate [8] and ^{35}S-labelled sulfite [9] were prepared as described elsewhere. Cysteine sulfinic acid was obtained from the California Corporation for Biochemical Research. Thiosulfate, as the nickel-etylenediamine complex, was isolated from the reaction system of Table 1 by a procedure which was slightly modified from that described by Ames and Willard [10]. Its radioactivity was determined in a windowless gas-flow counter (Frieseke & Hoepfner FH 407), with suitable corrections for self-absorption being applied. Spectrophotometric measurements were made in a Beckman DU spectrophotometer in 1 cm cuvettes. Paper chromatography was carried out with ascending development on Whatman No. 1 paper with acetone-water (4:1) as the solvent. R_F-values in this system are as follows: toluenethiosulfonate 0.87, toluenesulfinate 0.53, thiotaurine 0.42, hypotaurine 0.10, thiocysteate 0.15, cysteinesulfinate 0.07. The samples were dried slowly on the paper with cold air, as this was found to minimize the apparent »spontaneous» reaction described in the case of the reaction between thiotaurine and cysteinesulfinate by De Marco and Coletta [11]. Spots were revealed by iodoplatinate or ninhydrin.

Acknowledgements. This work was supported by a grant from the *Swedish Medical Research Council.* Excellent technical assistance was given by Mr. Ingvar Hedenborg.

1. Sörbo, B. *Acta Chem. Scand.* **11** (1957) 628.
2. Szczepkowski, T. W., Skarżyński, B. and Weber, M. *Nature* **189** (1961) 1007.
3. Weber, M., Szczepkowski, T. W. and Skarżyński, B. *Acta Biochim. Polon.* **8** (1961) 71.
4. Young, L. and Maw, G. A. *The metabolism of sulphur compounds.* Methuen & Co. Ltd., London 1958, p. 30.
5. Sörbo, B. *Acta Chem. Scand.* **7** (1953) 1137.
6. Sörbo, B. *Acta Chem. Scand.* **7** (1953) 1129.
7. Sörbo, B. *Bull. Soc. Chim. Biol.* **40** (1958) 121.
8. Whitmore, F. C. and Hamilton, F. H. *Org. Synthesis* **Coll. Vol. I.** (1944) 492.
9. Chapeville, F. and Fromageot, P. *Biochim. et Biophys. Acta* **14** (1954) 415.
10. Ames, D. P. and Willard, J. E. *J. Am. Chem. Soc.* **73** (1951) 164.
11. De Marco, C. and Coletta, M. *Experientia* **16** (1960) 534.

Received December 28, 1961.

N-Pyrrolidinomethyltetracyclin. Stabilität in Lösungen und Papierchromatographische Prüfung

ARNE BRUNZELL

Statens farmacevtiska laboratorium, Stockholm, Schweden

N-Pyrrolidinomethyltetracyclin (PMT) ist als ein in Wasser leichtlösliches Tetracyclinderivat mit gewissen Vorteilen gegenüber anderen, früher zugänglischen Tetracyclinen [1] introduziert worden. Es wird als Trockensubstanz zur Bereitung von wässrigen Lösungen angeboten. Die Kontrolle der Stabilität des Derivates ist pharmazeutisch und analytisch von besonderem Interesse.

Verschiedene Methoden zur papierchromatographischen Identifizierung von Tetracyclinen sind veröffentlicht worden, von denen hier die von Selzer und Wright [2] als die von verschiedenen Gesichtspunkten aus am besten geeignete hervorgehoben werden soll. Ein wesentlicher Vorteil ist die Schnelligkeit dieser Methode, wodurch die Epimerisierung beim C(4) des Tetracyclins, Chlortetracylins u.s.w. nur in sehr begrenztem Umfange geschehen kann. Von unseren Erfahrungen mit dem System von Selzer und Wright bezügl. Tetracyclin, Chlortetracyclin, Demethylchlortetracyclin und Oxytetracyclin haben wir in anderem Zusammenhang berichtet [3]. Beim Chromatographieren von PMT erschien es uns, als ob sich diese Substanz leicht zersetzte.

Beim Arbeiten nach Selzer und Wright unterschieden sich somit die Chromatogramme, die durch Absetzen von frisch zubereiteter und älterer Lösung in Wasser erhalten wurden. Bei Lagerung der Lösung verschob sich der Schwerpunkt von einem Fleck mit R_F ca. 0.07 (Fleck 1) zu einem Fleck mit R_F ca. 0.28 (Fleck 2) und gleichzeitig erschien ein dritter Fleck mit R_F ca. 0.12 (Fleck 3), der mehr und mehr sichtbar wurde. Die Flecke 2 und 3 stimmten mit denen des Tetracyclins und dessen Epimerisierungsproduktes Quatrimycin überein und deshalb wurde Fleck 1 dem PMT zugeschrieben. Mit frisch zubereiteter wässriger Lösung wurde ein sehr schwacher Tetracyclinfleck und kein Quatrimycinfleck erhalten. Mit frisch zubereiteter methanolischer Lösung wurden dagegen ein

sulfinate [8] and ^{35}S-labelled sulfite [9] were prepared as described elsewhere. Cysteine sulfinic acid was obtained from the California Corporation for Biochemical Research. Thiosulfate, as the nickel-etylenediamine complex, was isolated from the reaction system of Table 1 by a procedure which was slightly modified from that described by Ames and Willard [10]. Its radioactivity was determined in a windowless gas-flow counter (Frieseke & Hoepfner FH 407), with suitable corrections for self-absorption being applied. Spectrophotometric measurements were made in a Beckman DU spectrophotometer in 1 cm cuvettes. Paper chromatography was carried out with ascending development on Whatman No. 1 paper with acetone-water (4:1) as the solvent. R_F-values in this system are as follows: toluenethiosulfonate 0.87, toluenesulfinate 0.53, thiotaurine 0.42, hypotaurine 0.10, thiocysteate 0.15, cysteinesulfinate 0.07. The samples were dried slowly on the paper with cold air, as this was found to minimize the apparent »spontaneous» reaction described in the case of the reaction between thiotaurine and cysteinesulfinate by De Marco and Coletta [11]. Spots were revealed by iodoplatinate or ninhydrin.

Acknowledgements. This work was supported by a grant from the *Swedish Medical Research Council.* Excellent technical assistance was given by Mr. Ingvar Hedenborg.

1. Sörbo, B. *Acta Chem. Scand.* **11** (1957) 628.
2. Szczepkowski, T. W., Skarżyński, B. and Weber, M. *Nature* **189** (1961) 1007.
3. Weber, M., Szczepkowski, T. W. and Skarżyński, B. *Acta Biochim. Polon.* **8** (1961) 71.
4. Young, L. and Maw, G. A. *The metabolism of sulphur compounds.* Methuen & Co. Ltd., London 1958, p. 30.
5. Sörbo, B. *Acta Chem. Scand.* **7** (1953) 1137.
6. Sörbo, B. *Acta Chem. Scand.* **7** (1953) 1129.
7. Sörbo, B. *Bull. Soc. Chim. Biol.* **40** (1958) 121.
8. Whitmore, F. C. and Hamilton, F. H. *Org. Synthesis* **Coll. Vol. I.** (1944) 492.
9. Chapeville, F. and Fromageot, P. *Biochim. et Biophys. Acta* **14** (1954) 415.
10. Ames, D. P. and Willard, J. E. *J. Am. Chem. Soc.* **73** (1951) 164.
11. De Marco, C. and Coletta, M. *Experientia* **16** (1960) 534.

Received December 28, 1961.

N-Pyrrolidinomethyltetracyclin. Stabilität in Lösungen und Papierchromatographische Prüfung

ARNE BRUNZELL

Statens farmacevtiska laboratorium, Stockholm, Schweden

N-Pyrrolidinomethyltetracyclin (PMT) ist als ein in Wasser leichtlösliches Tetracyclinderivat mit gewissen Vorteilen gegenüber anderen, früher zugänglischen Tetracyclinen [1] introduziert worden. Es wird als Trockensubstanz zur Bereitung von wässrigen Lösungen angeboten. Die Kontrolle der Stabilität des Derivates ist pharmazeutisch und analytisch von besonderem Interesse.

Verschiedene Methoden zur papierchromatographischen Identifizierung von Tetracyclinen sind veröffentlicht worden, von denen hier die von Selzer und Wright [2] als die von verschiedenen Gesichtspunkten aus am besten geeignete hervorgehoben werden soll. Ein wesentlicher Vorteil ist die Schnelligkeit dieser Methode, wodurch die Epimerisierung beim C(4) des Tetracyclins, Chlortetracylins u.s.w. nur in sehr begrenztem Umfange geschehen kann. Von unseren Erfahrungen mit dem System von Selzer und Wright bezügl. Tetracyclin, Chlortetracyclin, Demethylchlortetracyclin und Oxytetracyclin haben wir in anderem Zusammenhang berichtet [3]. Beim Chromatographieren von PMT erschien es uns, als ob sich diese Substanz leicht zersetzte.

Beim Arbeiten nach Selzer und Wright unterschieden sich somit die Chromatogramme, die durch Absetzen von frisch zubereiteter und älterer Lösung in Wasser erhalten wurden. Bei Lagerung der Lösung verschob sich der Schwerpunkt von einem Fleck mit R_F ca. 0.07 (Fleck 1) zu einem Fleck mit R_F ca. 0.28 (Fleck 2) und gleichzeitig erschien ein dritter Fleck mit R_F ca. 0.12 (Fleck 3), der mehr und mehr sichtbar wurde. Die Flecke 2 und 3 stimmten mit denen des Tetracyclins und dessen Epimerisierungsproduktes Quatrimycin überein und deshalb wurde Fleck 1 dem PMT zugeschrieben. Mit frisch zubereiteter wässriger Lösung wurde ein sehr schwacher Tetracyclinfleck und kein Quatrimycinfleck erhalten. Mit frisch zubereiteter methanolischer Lösung wurden dagegen ein

relativ schwacher PMT-Fleck, ein deutlicher Quatrimycin- und ein starker Tetracyclinfleck erhalten. Beim Chromatographieren mit einer grossen Anzahl anderer Lösungsmittelssysteme wurde stets Übereinstimmung zwischen den Zersetzungsprodukten des PMT und Tetracyclin samt Quatrimycin erhalten.

Als ein weiterer Beweis für die Zersetzung des PMT zu Tetracyclin kann folgender Versuch dienen.

Eine Lösung von 0.2 g PMT in 4 ml Wasser und 6 ml 0.1 N HCl (pH = 2.0) wurde 4 Tage bei Zimmertemperatur aufbewahrt. Während dieser Zeit zeigten wiederholte papierchromatographische Analysen der herausgenommenen Proben, dass in der Lösung die oben erwähnte Umwandlung geschah. Sodann wurde die Lösung mit NaOH bis pH = 6.2 versetzt und ausgefällte Substanz durch wiederholtes Zentrifugieren isoliert — nach Trocknen im Vakuum insgesamt etwa 93 mg. Die erhaltene Substanz wurde durch Bestimmen des IR-Spektrums (KBr-Platte) als Tetracyclin identifiziert.

Weitere Versuche, das Einwirken verschiedener Lösungsmittel auf PMT zu vergleichen, zeigten, dass keine Zersetzungsprodukte wiedergefunden werden konnten, wenn es auf dem Papier in frisch zubereiteter Lösung in Wasser oder Dioxan abgesetzt wurde, während Lösungen in Alkoholen, wie Methanol, Äthanol und Butanol — selbst bei schnellem Arbeiten — Chromatogramme gaben, die starke Zersetzung aufwiesen.

Ein Chromatographierungsverfahren von Kelly und Buyske [4] mit Butanol als Hauptkomponent der Entwicklungsflüssigkeit gab demzufolge ein Chromatogramm, das auf eine Umwandlung des grössten Teils des PMT in Tetracyclin hindeutete, auch wenn die Absetzungen mit wässriger Lösung gemacht waren.

Wir haben somit die Erfahrung gemacht, dass die Stabilität der PMT-Lösungen sehr stark von der Natur des Lösungsmittels abhängig ist. Da die Zersetzung ausserordentlich schnell einsetzen kann, muss dieser Umstand ebenfalls dann beachtet werden, wenn es sich um eine Behandlung von so kurzer Dauer wie die papierchromatographische Prüfung handelt. Unseren Erfahrungen nach kann Selzer und Wright's Methode für die papierchromatographische Identifizierung und Qualitätsbeurteilung des PMT verwendet werden, wenn die Probe als frisch zubereitete wässrige Lösung abgesetzt wird.

1. Sidel, W., Söder, A. und Lindner, F. *Münch. med. Wochschr.* **100** (1958) 661.
2. Selzer, G. B. und Wright, W. W. *Antibiotics & Chemotherapy* **7** (1957) 292.
3. Brunzell, A. *Pharm. Ztg. ver. Apotheker-Ztg.* **107** (1962) *im Druck.*
4. Kelly, R. G. und Buyske, D. A. *Antibiotics & Chemotherapy* **10** (1960) 604.

Eingegangen am 11. Januar 1962.

New Synthesis of Bicyclo[3.2.1]octane-2-ol

POUL NEDENSKOV, HENNING HEIDE and NIELS CLAUSON-KAAS

Centrallaboratoriet, Sadolin & Holmblad A/S, Copenhagen, Denmark

Hydrogenation of commercial bicyclo[2.2.1]hept-5-ene-2-methanol (I) to bicyclo[2.2.1]heptane-2-methanol (II), tosylation of this compound with toluenesulfonyl chloride in pyridine, and hydrolysis of the resulting tosylester with aqueous acetic acid gives bicyclo[3.2.1]octane-2-ol (III). The synthesis may be carried out without isolating the intermediate compounds pure. The overall yield in the three reactions is 91 %, and the purity of the resulting bicyclooctanol (III) 93 %. If the purities of starting material and reaction product are considered, the overall yield of pure bicyclooctanol based upon pure starting material is 88 %, which is the figure to be used when the yield of the reaction is considered from a theoretical point of view.

The identity of the bicyclooctanol was established by oxidation to the corresponding ketone (IV) (yield 74 %, yield based upon pure materials 80 %), and by preparation of the *p*-nitrobenzoate.

The steric configuration of the hydroxyl group may be inferred from the infrared absorption spectrum to be predominantly *cis* (*cf.* Ref.[1]) to the ethylene bridge.

The synthesis is at present the simplest and cheapest way of preparing the bicyclooctanol (III) in a reasonably pure state. The high yield in the new rearrangement reaction as well as the purity of the reaction product agrees well with the fact, that the original bicycloheptene-

relativ schwacher PMT-Fleck, ein deutlicher Quatrimycin- und ein starker Tetracyclinfleck erhalten. Beim Chromatographieren mit einer grossen Anzahl anderer Lösungsmittelssysteme wurde stets Übereinstimmung zwischen den Zersetzungsprodukten des PMT und Tetracyclin samt Quatrimycin erhalten.

Als ein weiterer Beweis für die Zersetzung des PMT zu Tetracyclin kann folgender Versuch dienen.

Eine Lösung von 0.2 g PMT in 4 ml Wasser und 6 ml 0.1 N HCl (pH = 2.0) wurde 4 Tage bei Zimmertemperatur aufbewahrt. Während dieser Zeit zeigten wiederholte papierchromatographische Analysen der herausgenommenen Proben, dass in der Lösung die oben erwähnte Umwandlung geschah. Sodann wurde die Lösung mit NaOH bis pH = 6.2 versetzt und ausgefällte Substanz durch wiederholtes Zentrifugieren isoliert — nach Trocknen im Vakuum insgesamt etwa 93 mg. Die erhaltene Substanz wurde durch Bestimmen des IR-Spektrums (KBr-Platte) als Tetracyclin identifiziert.

Weitere Versuche, das Einwirken verschiedener Lösungsmittel auf PMT zu vergleichen, zeigten, dass keine Zersetzungsprodukte wiedergefunden werden konnten, wenn es auf dem Papier in frisch zubereiteter Lösung in Wasser oder Dioxan abgesetzt wurde, während Lösungen in Alkoholen, wie Methanol, Äthanol und Butanol — selbst bei schnellem Arbeiten — Chromatogramme gaben, die starke Zersetzung aufwiesen.

Ein Chromatographierungsverfahren von Kelly und Buyske [4] mit Butanol als Hauptkomponent der Entwicklungsflüssigkeit gab demzufolge ein Chromatogramm, das auf eine Umwandlung des grössten Teils des PMT in Tetracyclin hindeutete, auch wenn die Absetzungen mit wässriger Lösung gemacht waren.

Wir haben somit die Erfahrung gemacht, dass die Stabilität der PMT-Lösungen sehr stark von der Natur des Lösungsmittels abhängig ist. Da die Zersetzung ausserordentlich schnell einsetzen kann, muss dieser Umstand ebenfalls dann beachtet werden, wenn es sich um eine Behandlung von so kurzer Dauer wie die papierchromatographische Prüfung handelt. Unseren Erfahrungen nach kann Selzer und Wright's Methode für die papierchromatographische Identifizierung und Qualitätsbeurteilung des PMT verwendet werden, wenn die Probe als frisch zubereitete wässrige Lösung abgesetzt wird.

1. Sidel, W., Söder, A. und Lindner, F. *Münch. med. Wochschr.* **100** (1958) 661.
2. Selzer, G. B. und Wright, W. W. *Antibiotics & Chemotherapy* **7** (1957) 292.
3. Brunzell, A. *Pharm. Ztg. ver. Apotheker-Ztg.* **107** (1962) *im Druck.*
4. Kelly, R. G. und Buyske, D. A. *Antibiotics & Chemotherapy* **10** (1960) 604.

Eingegangen am 11. Januar 1962.

New Synthesis of Bicyclo[3.2.1]octane-2-ol

POUL NEDENSKOV, HENNING HEIDE and NIELS CLAUSON-KAAS

Centrallaboratoriet, Sadolin & Holmblad A/S, Copenhagen, Denmark

Hydrogenation of commercial bicyclo[2.2.1]hept-5-ene-2-methanol (I) to bicyclo[2.2.1]heptane-2-methanol (II), tosylation of this compound with toluenesulfonyl chloride in pyridine, and hydrolysis of the resulting tosylester with aqueous acetic acid gives bicyclo[3.2.1]octane-2-ol (III). The synthesis may be carried out without isolating the intermediate compounds pure. The overall yield in the three reactions is 91 %, and the purity of the resulting bicyclooctanol (III) 93 %. If the purities of starting material and reaction product are considered, the overall yield of pure bicyclooctanol based upon pure starting material is 88 %, which is the figure to be used when the yield of the reaction is considered from a theoretical point of view.

The identity of the bicyclooctanol was established by oxidation to the corresponding ketone (IV) (yield 74 %, yield based upon pure materials 80 %), and by preparation of the *p*-nitrobenzoate.

The steric configuration of the hydroxyl group may be inferred from the infrared absorption spectrum to be predominantly *cis* (*cf.* Ref.[1]) to the ethylene bridge.

The synthesis is at present the simplest and cheapest way of preparing the bicyclooctanol (III) in a reasonably pure state. The high yield in the new rearrangement reaction as well as the purity of the reaction product agrees well with the fact, that the original bicycloheptene-

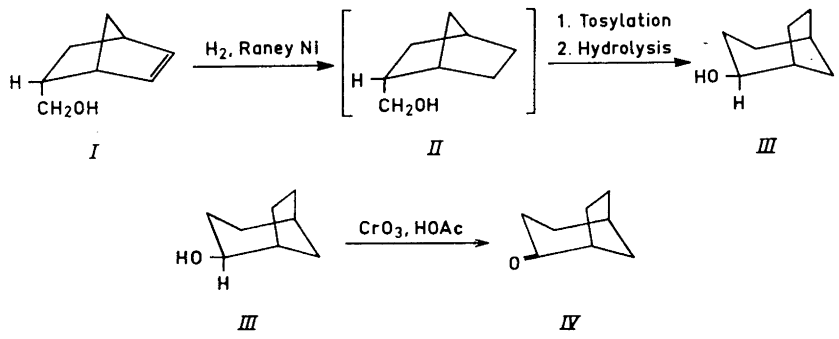

I *II* *III* *III* *IV*

methanol (I) consists mainly of the *endo* isomer [2] (only this isomer is shown in the drawing of the structural formulas).

Experimental. Bicyclo[2.2.1]heptane-2-methanol (II) (cf. Refs.[3,4]). Bicyclo[2.2.1] hept-5-ene-2-methanol (I)* (50.0 g, 0.388 mole of pure product) was shaken (6 h) with Raney nickel (5 g) under hydrogen (25 atm.) at 120°. The nickel was removed by filtration and washed with pyridine (30 ml).

Tosylester of II. The above solution of bicycloheptanemethanol (49.0 g of pure product, 0.388 mole) in pyridine (about 25 ml) was added in one portion to a solution of *p*-toluenesulfonyl chloride (85.0 g, 0.446 mole) in pyridine (100 ml) and the mixture stirred (24 h) at 20° (precipitation of pyridine hydrochloride begins after a few min). The reaction mixture is poured on cracked ice (250 g). Ether (200 ml) is added, and the resulting emulsion brought to pH 3.5 by dropwise addition of concentrated hydrochloric acid (about 85 ml) with cooling and vigorous stirring. The etheral layer is separated, washed with water (2 × 60 ml) (final pH of wash water must be 5 or above), dried over magnesium sulfate, and evaporated from a water bath (75°), at last under 10 mm. The tosylester remains as an oil (104 g), which crystallizes partially on standing.

Bicyclo[3.2.1]octane-2-ol (III). The above tosylester (104 g) is heated with acetic acid (120 ml), *p* toluenesulfonic acid (1.0 g) and water (550 ml) with stirring under reflux (24 h). The heterogeneous reaction mixture is cooled somewhat, 40 % aqueous sodium hydroxide solution (265 g) added, and the mixture heated further under reflux (3 h) to saponify any acetates formed in the rearrangement reaction. The mixture is steam distilled and the crystals formed in the distillate recovered by saturation of the aqueous layer with sodium chloride and extraction three times with ether (400 ml in all). The etheral solution is dried with magnesium sulfate and the ether removed by distillation from a water bath (50°), at last under 15 mm. 46.0 g (91 %) of bicyclooctanol is hereby obtained [m.p. 140–166° (Hershberg app., corr.)]. Considering the purity of the starting material (96 %) and of the reaction product (93 %, see below), the overall yield of pure bicyclooctanol is 88 %.

The product melts at 140–166° (Hershberg app., corr.). Goering *et al.*[1] report 176–177° for *cis*-bicyclooctanol and 194–196° for the *trans* compound. Elementary analyses gave: C 77.1; H 11.1; O 12.0. Calc. for $C_8H_{14}O$ (126.2): C 76.2; H 11.2; O 12.6. The product was chromatographed in the gaseous phase under the conditions recommended by Walborsky *et al.*[5] The product was acetylated in the usual way, and the acetate chromatographed on a 2 m column of 20 % diisooctylphthalate on 60–80 mesh chromosorb at 175° (investigation for bicycloheptanemethanol). Finally the infrared absorption of the product was measured and the spectrum in particular inspected around 965 and around 1040 cm^{-1}, the two regions best suited for an estimation of the *cis-trans* ratio (*cf.* Refs.[1,6]).

The product was oxidized with chromium trioxide in acetic acid as described by Youseff *et al.*[7], using, however, 12 % more chromium trioxide and only one third of the amount of acetic acid recommended by these authors. The reaction mixture was extracted with

* Commercial product from Interchemical Cooperation, U.S.A., n_D^{25} 1.4972, composition minimally 76 % of *endo*, 19 % of *exo* isomer. The product was found by us by acetylation analysis to have an equivalent weight of 129 (calc. 124). If one assumes that the product contains no alcoholic impurities, this figure corresponds to a purity of 96 %.

benzene and the benzene solution found by oxime titration [8] to contain 74 % of the theoretical amount of bicyclo[3.2.1]octane-2-one (IV). The yield is 80 % based upon the content of pure bicyclooctanol in the starting material. From the benzene solution the semicarbazone of bicyclooctanone was prepared in the way recommended for the preparation of camphor semicarbazone [9]. The yield was 73 % of recrystallized, analytically pure material, m.p. 173–174° (previously [1,7] found 171–172°). [Found: C 59.4; H 8.2; N 23.2. Calc. for $C_9H_{15}N_3O$ (181.2): C 59.6; H 8.3; N 23.2].

The product was transformed into the *p*-nitrobenzoate in the usual way. After two crystallizations from pentane the yield of *p*-nitrobenzoate was 60 % and the melting point 78–79°. Further crystallization did not change the melting point (previously [1] found for the *cis* compound 80°).

It was inferred from the above experiments that bicyclooctanol, obtained after the new synthesis as described, contains about 93 % of a 1:20 mixture of *trans*- and *cis*-bicyclo [3.2.1]octane-2-ol, the main impurities (7 % in all) being bicyclic hydrocarbons.

During this investigation one of us (Poul Nedenskov) has received financial aid from *Det teknisk-videnskabelige Forskningsråd*, Denmark.

1. Goering, H. L., Greiner, R. W. and Sloan, M. F. *J. Am. Chem. Soc.* **83** (1961) 1391.
2. Alder, K. and Reubke, R. *Chem. Ber.* **91** (1958) 1525.
3. Alder, K. and Windemuth, E. *Ber.* **71** (1938) 1939.
4. Harry, J. B., U. S. patent 2.638.431 (1953).
5. Walborsky, H. M., Baum, M. E. and Youssef, A. A. *J. Am. Chem. Soc.* **83** (1961) 988.
6. Goering, H. L. and Sloan, M. F. *J. Am. Chem. Soc.* **83** (1961) 1397.
7. Youssef, A. A., Baum, M. E. and Walborsky, H. M. *J. Am. Chem. Soc.* **81** (1959) 4709.
8. Houben-Weyl, *Methoden der organischen Chemie*, Band II (1953) 460.
9. Wallach, O. *Ann.* **353** (1907) 209.

Received December 23, 1961.

ACTA CHEMICA SCANDINAVICA 16 (1962) 249–255

Crystal Structure of the 1 : 3 Addition Compound Iodoform-Quinoline

T. BJORVATTEN and O. HASSEL

Universitetets Kjemiske Institutt, Blindern-Oslo, Norway

Details of the crystal structure determination of the 1:3 addition compound iodoform-quinoline are reported. The structure is trigonal rhombohedral with the (hexagonal) lattice parameters:

$a = 22.40$ Å $\qquad c = 4.59$ Å

both figures with a probable error not exceeding 0.5 %. The primitive (rhombohedral) unit cell contains one molecule of iodoform and three molecules of quinoline. The space group is $R3$. Charge transfer bonds connect every iodine atom with a quinoline nitrogen atom. The I—N distance (3.05 Å) is about 0.60 Å shorter than the van der Waals radius sum of nitrogen and iodine and the C—I—N angle is found equal to 176.8°.

During the last few years the crystal structure of some addition compounds formed by halide molecules and molecules which are known to possess marked electron donor properties have been studied in our laboratory. Among the halides present in the addition compounds studied is iodoform, oxalyl chloride and oxalyl bromide. The donor molecules selected are quinoline, sulphur (S_8), 1,4-dioxan and 1,4-dithiane. In all cases so far examined it has been found that a particular halogen atom of the acceptor molecule is directly linked to an oxygen, sulphur or nitrogen atom belonging to the donor molecule and that the arrangement carbon-halogen-donor atom is approximately *linear* [1,2].

The addition compound between iodoform and quinoline was first prepared by Rhoussopoulos [3]. Dipole moment measurements in carbon tetrachloride solution indicate that the 1:3 complex is present even in dilute solutions[4].

A short communication summing up the main results obtained for the 1:3 compound iodoform-quinoline has been published in 1959 [1]. Here, further details of this investigation will be given and in a forthcoming publication the structure determination of crystals of the 1:3 compound iodoform-sulphur will be described.

The needle-shaped crystals used in the X-ray analysis were obtained from ether solution. The melting point was found equal to 65°C and the measured

density was 1.90 g·cm^{-3}. The hexagonal cross section of the needle was about 0.005 mm^2. Corrections for absorption or secondary extinction were not introduced.

The material on which the structure determination is based consists partly of ordinary Weissenberg diagrams taken with CuK radiation (the hexagonal $hk0$ zone) and the multiple film method was employed with visual estimation of the intensities. For the other zones integrated Weissenberg diagrams with Mo$K\alpha$ radiation were obtained and the intensities measured photometrically.

The space group is $R3$ and the primitive rhombohedral unit cell contains one molecule of iodoform and three molecules of quinoline. X-Ray reflections were however, mainly indexed using the triple primitive "hexagonal" unit cell with the lattice constants:

$$a = 22.40 \text{ Å} \qquad c = 4.59 \text{ Å}$$

The structure determination started with the working out of a two-dimensional Fourier projection along the chief axis. Centers of symmetry and symmetry planes are lacking in the structure, but threefold axes are present on which the iodoform molecules must be situated. The quinoline molecules, however, occupy general positions. These conditions and the presence of the heavy iodine atoms simplifies the determination of the approximate x and y coordinates of the latter atoms and the corresponding coordinates of the iodoform carbon atom are fixed. Even with these simplifications the great number of light atoms in general positions made the task of working out a Fourier projection along the trigonal axis somewhat cumbersome. Taking advantage of the detailed information now available regarding the structure of the pyridine molecule it was possible, however, to choose a model of the quinoline molecule which eventually led to a Fourier projection in which the light atoms were sufficiently well resolved to make possible the refinement of the coordinates by least squares computations. These computations were carried out using a Ferranti Mercury computer.

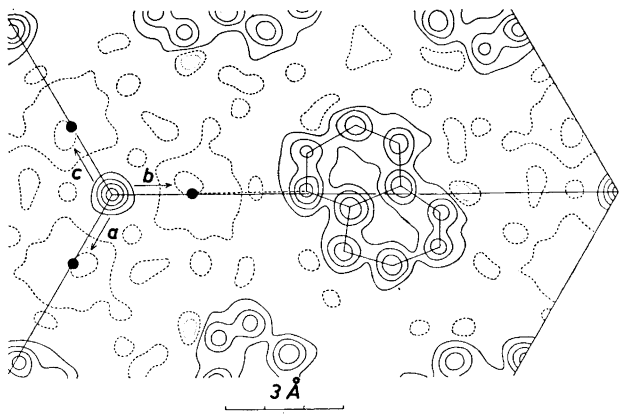

Fig. 1. Electron density projection along the trigonal axis. Contour lines at intervals of 2 e·Å^{-2}. The three axes indicated are the projections of the rhombohedral axes.

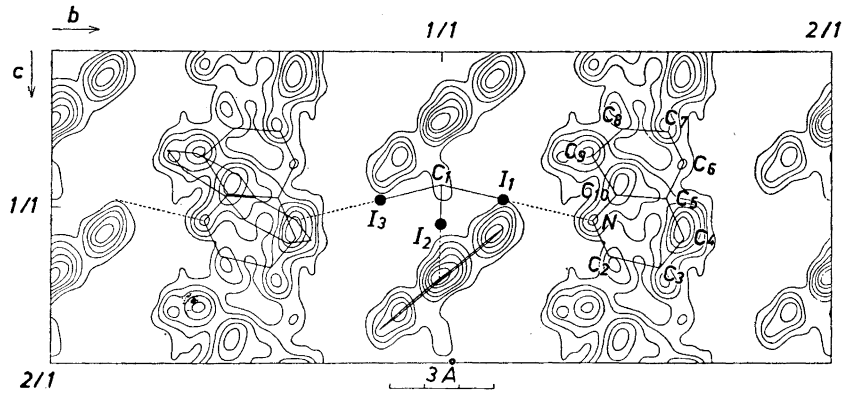

Fig. 2. Electron density projection along [110] (hex. [122]). Contour lines at intervals of 2 e·Å^{-2} from 4 e·Å^{-2} upwards. Contribution from the iodine atoms is subtracted. The axes indicated are the projections of the rhombohedral axes.

The B values of the temperature factor arrived at are as follows: $B_I = 2.14$; $B_N = 1.85$ and B_C (mean value) $= 2.87$. In the final refinement of the coordinates the mean value $B_C = 2.87$ was employed for all carbon atoms. The Fourier map reproduced in Fig. 1 is based on the x and y coordinates thus obtained and by subtracting the contribution from the iodine atoms. The x and y values have been listed in Table 1. The R value corresponding to these coordinates is 0.065 not including unobserved reflections. The number of observed reflections is 107, the number of possible reflections 122.

The results so far (*cf.* Fig. 1) indicated the presence of a bond between each iodoform iodine atom and the nitrogen atom of a particular quinoline molecule and an angle C—I—N of approximately 180°. Final conclusions could not, however, be drawn without determining the z coordinates and a number of two-dimensional Fourier syntheses were therefore worked out with projection along different crystallographic directions. It was found that the most satisfactory resolution could be obtained by choosing the rhombohedral [110] direction (hexagonal [122]).

Table 1.

Atom	x	y	z
I	−0.0531	0.0523	0.0000
N	−0.1302	0.1239	0.2135
C_1	0.0000	0.0000	−0.1249
C_2	−0.1753	0.0810	0.3920
C_3	−0.2398	0.0799	0.4691
C_4	−0.2469	0.1309	0.3268
C_5	−0.1984	0.1813	0.1222
C_6	−0.1931	0.2369	−0.0479
C_7	−0.1530	0.2769	−0.2121
C_8	−0.1003	0.2666	−0.2420
C_9	−0.0852	0.2171	−0.1133
C_{10}	−0.1401	0.1705	0.0874

Table 2. Observed and calculated structure factors and phase angles.

[001] projection

h	k	l	F_o	F_c	a	h	k	l	F_o	F_c	a
0	3	0	117	108	67.4	7	10	0	127	120	109.3
0	6	0	357	396	126.9	7	13	0	158	171	120.4
0	9	0	128	126	144.4	7	16	0	60	57	223.0
0	12	0	229	240	243.1	7	19	0	86	102	239.1
0	15	0	94	87	251.6	8	2	0	47	39	248.2
0	18	0	139	138	12.3	8	5	0	172	162	3.0
0	21	0	95	90	358.2	8	8	0	99	96	3.5
0	24	0	67	81	114.2	8	11	0	155	150	118.5
1	1	0	193	207	355.6	8	14	0	< 54	52	120.2
1	4	0	245	273	123.6	8	17	0	91	75	238.4
1	7	0	262	258	111.9	9	3	0	121	114	24.7
1	10	0	142	129	231.0	9	6	0	124	117	342.0
1	13	0	196	198	243.8	9	9	0	60	51	11.3
1	16	0	113	111	338.2	9	12	0	84	81	104.5
1	19	0	119	126	305.1	9	15	0	< 50	20	316.5
1	22	0	43	51	77.9	9	18	0	58	54	231.3
2	2	0	186	204	356.4	10	1	0	156	150	128.8
2	5	0	270	288	118.2	10	4	0	69	57	31.0
2	8	0	74	60	90.0	10	7	0	107	90	242.0
2	11	0	191	192	246.2	10	10	0	< 55	42	174.7
2	14	0	79	69	214.3	10	13	0	75	72	31.8
2	17	0	134	132	6.3	10	16	0	49	45	298.1
2	20	0	< 49	50	358.2	11	2	0	174	168	115.2
2	23	0	47	54	132.5	11	5	0	81	78	257.5
3	3	0	110	102	170.8	11	8	0	150	141	241.4
3	6	0	142	144	61.3	11	11	0	54	54	0.0
3	9	0	116	108	305.7	11	14	0	98	105	351.4
3	12	0	101	93	208.1	11	17	0	< 31	21	102.7
3	15	0	54	54	90.0	12	3	0	89	81	129.5
3	18	0	82	90	347.5	12	6	0	193	189	241.5
3	21	0	< 42	39	179.6	12	9	0	71	78	247.4
4	1	0	217	228	255.0	12	12	0	113	117	3.0
4	4	0	95	99	178.2	12	15	0	66	63	10.3
4	7	0	140	126	3.7	13	1	0	201	213	116.2
4	10	0	92	87	337.5	13	4	0	159	147	235.7
4	13	0	115	96	119.2	13	7	0	155	156	242.5
4	16	0	< 55	48	99.0	13	10	0	80	84	336.3
4	19	0	74	69	270.0	13	13	0	112	123	4.5
4	22	0	< 32	39	219.8	14	2	0	73	60	170.5
5	2	0	247	264	248.1	14	5	0	140	141	242.4
5	5	0	214	216	355.2	14	8	0	< 54	56	248.9
5	8	0	219	216	3.9	14	11	0	105	99	358.4
5	11	0	95	90	122.2	14	14	0	49	51	6.5
5	14	0	138	141	114.3	15	3	0	< 54	38	275.2
5	17	0	53	42	211.0	15	6	0	95	96	230.2
5	20	0	85	96	240.8	15	9	0	50	42	28.1
6	3	0	129	126	267.3	15	12	0	73	75	348.2
6	6	0	286	312	4.8	16	1	0	99	102	26.6
6	9	0	81	90	23.7	16	4	0	77	69	272.2
6	12	0	182	168	118.2	16	7	0	60	54	153.4
6	15	0	89	84	115.7	16	10	0	49	39	45.0
6	18	0	115	123	242.1	17	2	0	101	96	344.7
7	1	0	262	255	246.6	17	5	0	< 53	44	147.5
7	4	0	229	234	357.0	17	8	0	82	84	111.0
7	7	0	247	255	353.1	17	11	0	< 31	15	296.3

Table 2. Continued.

h	*k*	*l*	F_o	F_c	*a*
18	3	0	62	66	39.1
18	6	0	101	105	118.1
18	9	0	41	48	126.0
19	1	0	146	159	357.7
19	4	0	89	93	109.6
19	7	0	86	102	121.0
20	2	0	64	57	2.7
20	5	0	95	108	115.8
21	3	0	< 42	33	166.8
22	1	0	< 43	23	251.9
22	4	0	< 31	43	129.6
23	2	0	51	57	220.2
			[122] projection		
− 2	1	0	188	201	4.3
− 4	2	0	181	198	3.7
− 6	3	0	98	108	188.9
− 8	4	0	99	99	183.5
−10	5	0	200	210	5.1
−12	6	0	281	288	354.5
−14	7	0	223	225	7.7
−16	8	0	71	72	355.2
−18	9	0	50	57	173.3
−20	10	0	38	36	194.1
−22	11	0	46	39	0.0
−24	12	0	97	90	356.4
−26	13	0	87	84	356.0
−28	14	0	< 50	27	350.5
28	−15	1	< 50	21	17.7
26	−14	1	78	72	349.1
24	−13	1	88	81	352.4
22	−12	1	< 43	27	34.4
20	−11	1	72	57	135.0
18	−10	1	94	99	132.4
16	− 9	1	66	63	43.1
14	− 8	1	142	144	6.1
12	− 7	1	202	207	0.9
10	− 6	1	120	129	26.6
8	− 5	1	165	159	125.4
6	− 4	1	229	222	140.3
4	− 3	1	142	150	40.7
2	− 2	1	194	177	15.1
0	− 1	1	385	375	346.9
− 2	0	1	188	177	14.7
− 4	1	1	241	213	134.5
− 6	2	1	277	270	141.5
− 8	3	1	108	99	131.6
−10	4	1	144	138	28.7
−12	5	1	244	249	353.7
−14	6	1	160	159	3.2
−16	7	1	62	45	58.6
−18	8	1	96	87	143.8
−20	9	1	79	75	136.5
−22	10	1	< 43	24	18.2
−24	11	1	86	81	2.0
−26	12	1	80	72	355.7
−28	13	1	< 50	24	14.8
26	−15	2	< 51	39	350.9
24	−14	2	< 49	42	340.3
22	−13	2	< 46	30	79.2
20	−12	2	117	120	115.9
18	−11	2	105	99	128.1
16	−10	2	79	87	90.0
14	− 9	2	93	96	345.1
12	− 8	2	122	108	344.2
10	− 7	2	87	63	43.6
8	− 6	2	105	99	110.0
6	− 5	2	253	264	124.5
4	− 4	2	95	93	88.2
2	− 3	2	131	117	6.3
0	− 2	2	186	174	355.3
− 2	− 1	2	105	96	11.6
− 4	0	2	93	96	88.2
− 6	1	2	230	240	117.9
− 8	2	2	81	87	90.0
−10	3	2	101	93	17.4
−12	4	2	127	132	351.9
−14	5	2	106	108	345.2
−16	6	2	79	78	103.0
−18	7	2	92	93	128.7
−20	8	2	87	87	116.6
−22	9	2	< 46	33	79.2
−24	10	2	58	60	342.5
−26	11	2	51	45	353.3
22	−14	3	< 51	24	119.1
20	−13	3	75	81	123.7
18	−12	3	93	96	124.7
16	−11	3	46	45	135.0
14	−10	3	44	42	293.2
12	− 9	3	51	60	293.6
10	− 8	3	< 41	30	127.3
8	− 7	3	142	138	121.3
6	− 6	3	190	201	118.2
4	− 5	3	156	159	119.5
2	− 4	3	< 38	3	295.4
0	− 3	3	59	66	306.8
− 2	− 2	3	< 38	12	51.6
− 4	− 1	3	110	105	125.0
− 6	0	3	188	201	118.6
− 8	1	3	147	159	124.3
−10	2	3	42	30	120.3
−12	3	3	< 43	9	185.5
−14	4	3	< 44	36	289.3
−16	5	3	75	75	113.5
−18	6	3	93	93	127.2
−20	7	3	79	84	119.5
−22	8	3	< 51	21	110.6
16	−12	4	< 51	39	131.7
14	−11	4	< 51	48	250.1

Table 2. Continued.

h	k	l	F_o	F_c	α	h	k	l	F_o	F_c	α
12	−10	4	< 51	45	261.2	− 4	− 2	4	72	72	123.2
10	− 9	4	< 49	24	195.0	− 6	− 1	4	102	117	123.2
8	− 8	4	79	99	121.3	− 8	0	4	73	99	119.7
6	− 7	4	118	123	115.3	−10	1	4	< 49	30	194.9
4	− 6	4	63	72	140.9	−12	2	4	< 51	66	265.9
2	− 5	4	< 46	39	218.2	−14	3	4	< 51	42	258.9
0	− 4	4	87	102	260.2	−16	4	4	< 51	15	171.3
− 2	− 3	4	50	57	234.5						

The z coordinate of the three iodine atoms belonging to the iodoform molecule could arbitrarily be put equal to zero and the z coordinate of the carbon atom was computed assuming the I—C—I angle to be 113°.[5] It was further assumed that the C—I—N angle is approximately 180° and that the quinoline molecule is planar. With these assumptions and using the information obtained from the projection along the trigonal axis, an approximate determination of the orientation of the quinoline plane became possible. Subsequently trial and error computations led to a conclusive decision between the four alternatives still remaining for the relative position of the three quinoline molecules and the iodoform molecule. Taking advantage of the results obtained also from Fourier projection along other directions it was possible to compute preliminary values of all the atomic coordinates which served as starting values in the least squares computations. In this way the iodine coordinates and the coordinates of a nitrogen and two carbon atoms (N, C_3, and C_7 of Fig. 2) were refined. The B values arrived at were as follows: For I_1 and I_3 2.67, for I_2 3.46 (*cf.* Fig. 2). The B value chosen for the light atoms (3.0) was kept fixed during the process of least squares refinement.

The final Fourier map with projection along the rhombohedral [110] direction and reproduced in Fig. 2 is based on these coordinates and the x and y coordinates of the other light atoms taken from the final Fourier map with projection along the trigonal axis. The z coordinates used for these light atoms were computed using the planar model of the quinoline molecule mentioned above The final atomic coordinates are listed in Table 1. The y coordinates determined from the Fourier projection along [122] are in good agreement with those obtained from the projection along the trigonal axis. We consider the latter to be the more accurate and these values are therefore listed in Table 1. The phase angles of the reflections and a comparison between observed and calculated structure factors have been listed in Table 2. The R factor for the projection along [110] is 0.063, not including unobserved reflections. The number of observed reflections is 85, the number of possible reflections 110.

The chief aim of the present crystal structure investigation was the determination of the I—N distance and the "valence angle" N—I—C. From the atomic coordinates given in Table 1 the values 3.05 Å and 176.8° are obtained respectively. The standard deviation for the I—N distance is 0.034 Å. These findings are in full agreement with the assumption of comparatively strong

charge transfer bonds between iodine and nitrogen atoms. Other intermolecular separations all agree with those observed in other crystal structures for purely van der Waals type interactions. The I—I distance within the iodoform molecule is found equal to 3.54 Å.

The charge transfer bonds demonstrated in the iodoform-quinoline compound cannot be regarded as exceptional. Analogous bonds are observed in the corresponding compound with sulphur (S_8) and in the 1:1 compound iodoform-dithiane [2,6,7]. Other halides (oxalyl chloride and oxalyl bromide) form addition compounds with dioxan in which charge transfer bonds connect halogen and oxygen, and such bonds are also observed in solid oxalyl bromide [8].

The correctness of the suggestion put forward a few years ago [9] that the forces holding together iodoform and donor molecules in addition compounds depend on bonds between a particular iodine atom and an electron donating atom belonging to the partner molecule has thus been firmly substantiated.

This investigation has in part been sponsored by the *United States Air Force Development Command* under contract AF 61 (052)-71.

REFERENCES

1. Bjorvatten, T. and Hassel, O. *Acta Chem. Scand.* **13** (1959) 1261.
2. Hassel, O. *Tidsskr. Kjemi, Bergvesen, Met.* **21** (1961) 60.
3. Rhoussopoulos, O. *Ber* **16** I (1883) 202.
4. Fruhwirth, O. and Mayer-Pitsch, E. *Z. Elektrochem.* **43** (1937) 304.
5. Bastiansen, O. *Tidsskr. Kjemi, Bergvesen, Met.* **6** (1946) 1.
6. Bjorvatten, T., Hassel, O. and Rømming, Chr. *Nature* **189** (1961) 137.
7. Bjorvatten, T. and Hassel, O. *Acta Chem. Scand.* **15** (1961) 1429.
8. Groth, P. and Hassel, O. *Proc. Chem. Soc.* **1961** 343.
9. Hassel, O. *Proc. Chem. Soc.* **1957** 250.

Received September 7, 1961.

ACTA CHEMICA SCANDINAVICA 16 (1962) 256–262

The Changes of Absorption Spectra of Azo Dyes in Solvent Mixtures

EERO P. J. ELENIUS

Chemistry Department, University of Turku, Finland

The absorption spectra of some azo dyes were measured in mixtures of hexane and ethanol or ethanol and water. The formation of a new species in solutions of some *para* substitued azo dyes through intermolecular hydrogen bonds or the disturbance of an intramolecular hydrogen bond of *o*-methyl red explains one type of changes. The other type, shift of the absorption maximum towards longer wavelengths with increase of OH-group concentration in the solvent, may be due to the action of the dipole field on the dye molecules.

The absorption spectra of dyes in the visible and ultraviolet region are not always the same when measured in different solvents. For example Chako [1] has presented a large number of compounds which have this quality. Often such changes in the absorption spectrum can be explained by certain chemical reactions but solvents of different dielectric constant may cause displacements of absorption bands [1-4].

In this work [5] these problems were studied by using a series of solvent mixtures instead of pure solvents. In this manner the whole effect was divided into a large number of small changes in the hope of arriving at a better understanding of these solvent effects.

The addition of water to alcoholic solutions of substituted azobenzenes also has been studied by Brode and coworkers [6].

EXPERIMENTAL

A. Choice of the solvent. The solution spectra of dyes measured in normal alkanes are most like gaseous spectra of the same dyes. Therefore the action of solvent molecules on the absorbing dye molecules may be at the minimum. Hexane was chosen as a representative of this group of solvents. It was only natural to use water as another solvent. Because these solvents are not miscible a third liquid was needed which was soluble in both hexane and water. Ethanol was suitable for this purpose. A series of solvent mixtures could be made from nonpolar hexane to the highly polar water by using these solvents.

B. Solvents. The anhydrous ethanol was prepared from 95 % ethanol of ALKO using the magnesium alcoholate method [7]. Hexane was a product of British Drug Houses Ltd. and boiled at 67—69°C.

C. Dyes. In connection with another problem [8] several azo dyes were prepared. Some of them were used in this investigation. These are listed below. Only the compound V was a commercial preparation. Before measurements the dyes were purified by two recrystallizations from ethanol. The used azo dyes were: I, 4-monomethylamino-4′-hydroxyazobenzene; II, 4-dimethylamino-4′-hydroxyazobenzene; III, 4-diethylamino-4′-hydroxyazobenzene; IV, 4-dimethylamino-4′-nitroazobenzene, and V, 4-dimethylamino-2′-carboxyazobenzene.

D. Preparation of solutions. A weighed amount of each dye was dissolved in pure ethanol. A series of hexane-ethanol and ethanol-water mixtures having about the same concentrations of dye were made using these stock solutions. The solvent components were measured volumetrically before mixing because the volumes are not completely additive. This quality of the solvents was taken in account when the concentrations of dyes were calculated. Also saturated hexane solutions were used as stock solutions. The concentrations in hexane were estimated spectrophotometrically using the same solvent mixture made from the two stock solutions. The binary solvent mixtures varied by 20 % from each other. The absorption spectra in pure water could not be measured since the solubilities of the dyes were very small.

E. Measurement of the absorption spectra. The absorption spectra were determined by means of Beckman DU quartz spectrophotometer, using fused quartz absorption cells. The lengths of the cells were about 1 cm. In the reference cell there was the same solvent mixture as was used in the dye solutions. The absorbance of pure solvent was taken in

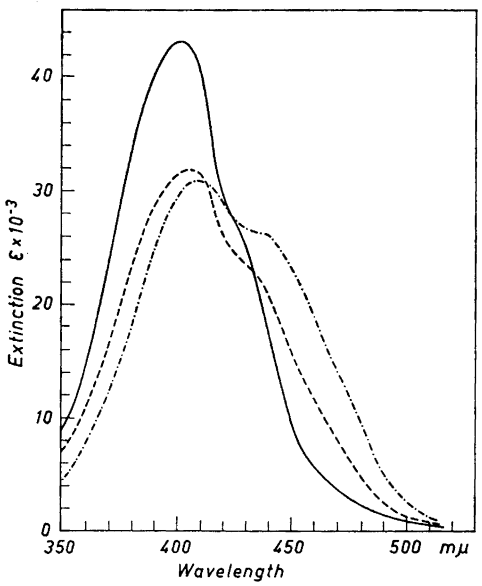

Fig. 1. Absorption spectra of 4-diethylamino-4′-hydroxyazobenzene (dye III) in hexane-ethanol mixtures: 0 % ethanol (———), $C = 1.482 \times 10^{-5}$; 20 % ethanol (— — —), $C = 2.015 \times 10^{-5}$; 100 % ethanol (—·—·—), $C = 2.015 \times 10^{-5}$. The concentrations reported are without the volume corrections.

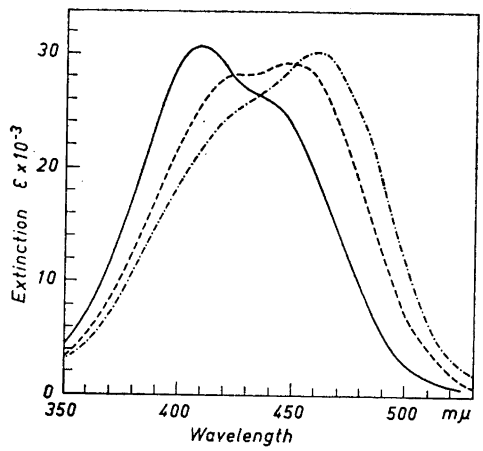

Fig. 2. Absorption spectra of 4-diethylamino-4′-hydroxyazobenzene (dye III) in ethanol-water mixtures: 100 % ethanol (———), $C = 2.015 \times 10^{-5}$; 60 % ethanol (— — —), $C = 4.030 \times 10^{-5}$; 40 % ethanol (—·—·—), $C = 4.030 \times 10^{-5}$.

account when absorption spectra (ε) were calculated according to Lambert-Beer's law. The absorbance values are independent of time.

RESULTS

(a) Aminohydroxy compounds. The spectra of dye III in hexane, ethanol, and in the mixture which includes 20 % ethanol in hexane are shown in Fig. 1 The principal change in the spectrum involves a decrease of the main band observed in hexane at about 400 mμ accompanied by the appearance of a shoulder in the longer wavelengths when ethanol was added. The spectra for the same compound in ethanol-water mixtures containing 100, 60, and 40 % ethanol is shown in Fig. 2. The addition of water also brings about a decrease of the main band accompanied by an increase of a band in the longer wavelengths. A shift towards the longer wavelengths in the spectrum is also possible. Similar effects were observed when the dyes I and II were measured.

(b) Nitroamino compound. The spectrum of dye IV measured in different solvent mixtures is shown in Fig. 3. The main absorption band was observed at 445 mμ in hexane. The addition of ethanol causes a shift in the wavelength of the absorption band. A similar effect can be observed when water is added in ethanol. No sign of the appearance of a new band was observed.

(c) o-Methyl red. The spectra of dye V in hexane-ethanol mixtures including 100, 80, 40, and 0 % hexane are shown in Fig. 4. The absorption maximum was observed at 450 mμ in hexane. The shape of the absorption curves of this dye changes considerably as a result of the addition of ethanol in hexane. The change involves a decrease of absorption in the region of the main absorption band and an increase of a new absorption band at somewhat shorter wavelengths when ethanol has been added. The spectra of the same dye in ethanol-water mixtures including 0, 20, and 60 % of water are shown in Fig. 5. After

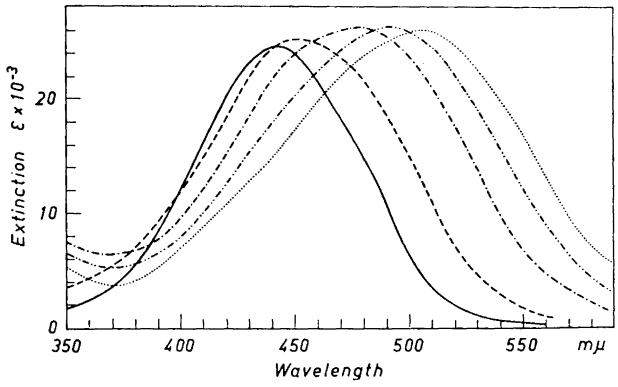

Fig. 3. Absorption spectra of 4-dimethylamino-4'-nitroazobenzene (dye IV) in hexane-ethanol mixtures: 0 % ethanol (———), $C = 3.445 \times 10^{-6}$; 20 % ethanol (— — —), $C = 0.8732 \times 10^{-6}$. The same in ethanol-water mixtures: 100 % ethanol (—·—·—), $C = 4.366 \times 10^{-6}$; 80 % ethanol (—··—··—), $C = 2.620 \times 10^{-6}$; 40 % ethanol (. . . . .), $C = 1.746 \times 10^{-6}$.

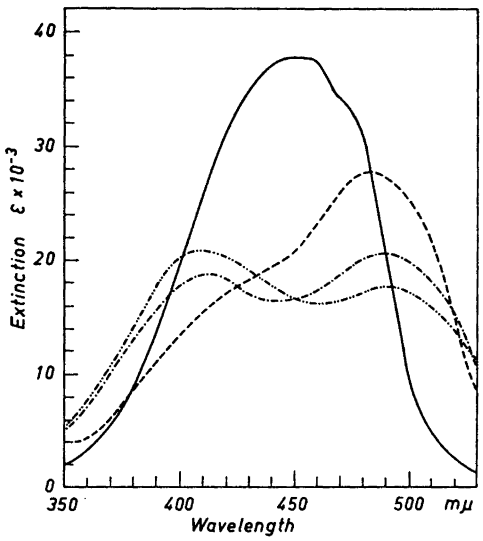

Fig. 4. Absorption spectra of 4-dimethylamino-2'-carboxyazobenzene (dye V) in hexane-ethanol mixtures: 0 % ethanol (———), $C = 0.7530 \times 10^{-5}$; 20 % ethanol (— — —), $C = 0.2742 \times 10^{-5}$; 60 % ethanol (—·—·—), $C = 0.8226 \times 10^{-5}$; 100 % ethanol (—··—··—), $C = 1.371 \times 10^{-5}$.

adding 20 % of water only one absorption maximum is observed. This maximum may also shift toward longer wavelengths upon the addition of water.

DISCUSSION

The appearance of a shoulder on the long wavelength side of the principal absorption band which increases upon addition of ethanol to hexane with

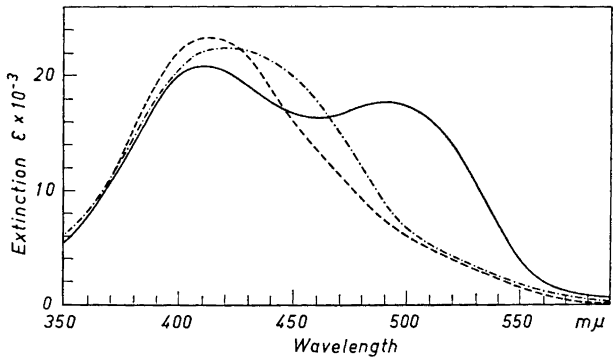

Fig. 5. Absorption spectra of 4-dimethylamino-2'-carboxyazobenzene (dye V) in ethanol-water mixtures: 100 % ethanol (———), $C = 1.371 \times 10^{-5}$; 80 % ethanol (— — —), $C = 0.8226 \times 10^{-5}$; 40 % ethanol (—·—·—), $C = 0.5484 \times 10^{-5}$.

compounds I, II, and III (Fig. 1) suggests the formation of some new species A in the solution. When water was added to solutions of these dyes in ethanol similarly an increase of the absorption band was observed (Fig. 2). Therefore an additional species B may be suggested.

$$R_1R_2N-C_6H_4-N=N-C_6H_4-OH + C_2H_5OH \rightleftharpoons A$$
$$R_1R_2N-C_6H_4-N=N-C_6H_4-OH + H_2O \rightleftharpoons B$$

In the mixtures of ethanol and water both reactions are possible.

A similar effect was reported [6] in aromatic azo compounds having + M groups in the *para* position. These + M groups, possessing an unshared electron pair and thus capable of entering into resonance with the azo group, bring this phenomenon better out but groups of this type are not necessary since also *trans*- and *cis*-azobenzene were found to give a similar change in the absorption spectrum [9].

The observed changes in the spectra of azobenzenes suggest an action of the solvent on the most reactive site in these molecules, the azo group. The *trans* ⇌ *cis* isomerization cannot be the explanation since both forms of azobenzene show the same solvent effect.

The behavior of compound V (*o*-methyl red) seems to be quite different. Upon the addition of ethanol to hexane (Fig. 4) a new strong absorption band shows up but now on the shorter wavelength side of the original absorption maximum. In absolute ethanol solution both bands can be clearly observed. This effect again supports an assumption of a formation of a new species. Upon addition of water to ethanol the original band decreases rapidly (Fig. 5), until in 80 % of ethanol only one maximum can be observed, indicating that water also acts on the dye.

It has been reported [10] that in carbon tetrachloride solution *o*-methyl red shows no infrared band associated with the free OH stretching frequency because of an intramolecular hydrogen bond.

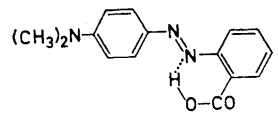

This ring structure is possible also in solutions of the aprotic hexane. The measured absorption band was at 450 mμ (Fig. 4).

A compound like *o*-methyl red having an acetyl group instead of carboxyl group and therefore no hydrogen bond to the azo group showed an absorption maximum at 405 mμ when the spectrum was measured in solution containing 95 % of ethanol in water [10]. Also in indifferent solvent the maximum was at about the same wavelength. Thus the formation of a hydrogen bond with the azo group causes a change toward longer wavelengths in the absorption band from 405 mμ to 450 mμ.

The dyes I, II, and III in pure hexane solution show an absorption band at about 400 mμ. The new bands observed in solutions of ethanol or water appear at about 465 mμ. Therefore the postulated mechanism of solvate formation [6] through hydrogen bonds to the azo group seems to be verified for *para* substituted azobenzenes:

$$Ar_1-N=N-Ar_2 + HOR \rightleftharpoons Ar_1-N=N-Ar_2$$
$$\dot{H}OR$$

(R = C_2H_5 or H)

In solutions of dye V in ethanol or water the situation is different. The most reactive place of the molecule is now the carboxy group and the action of solvent molecules on it seems to disturb the intramolecular hydrogen bond. A new species is formed showing an absorption maximum of only the azo group at 400 mμ.

In the dye IV the contribution of resonance structure C is large because the azo group has a minimum basicity [6]. Here the formation of the solvated

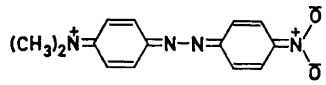

C

species may be inhibited and there is only one species in different solvent mixtures (Fig. 3). The main absorption band of this dye is shifted to lower frequencies (or longer wavelengths) with an increase in the concentration of OH groups (or dipoles) in the solvent. A similar effect can be observed for azobenzenes [9]. In solutions of *cis*-azobenzene the shift is greater than in solutions of the *trans*-form. Since the former has a permanent dipole moment [11] and the latter has not, this phenomenon may be due to the action of the dipolar field of the solvent on the dissolved dye molecules. The resonance structure C of dye IV is also highly polar producing a large shift in the absorption band from 445 mμ in hexane to 505 mμ in a solution of 40 % ethanol in water.

Similar, but smaller shifts can be observed in other series of the spectra (Figs. 1, 2, 4, 5). This effect also explains why the absorption band of the solvated dyes (I, II, III) measured in solutions of 40 % ethanol in water is at wavelengths about 15 mμ longer than the band of *o*-methyl red measured in pure hexane solution.

It seems to be necessary to measure the spectra in both pure solvents and in their mixtures before these chemical and physical solvent effects can be observed and identified. Also a reference spectrum measured in any indifferent solvent is necessary; hexane is recommended for that purpose.

Acknowledgements. The writer gratefully acknowledges the courtesy of Dr. A. Meretoja and Mr. R. Linko for placing dye preparations at his disposal. The writer is also very much obliged to Professors A. Meretoja and H. B. Jonassen (Tulane University, U.S.A.) for interesting discussions.

REFERENCES

1. Chako, N. Q. *J. Chem. Phys.* **2** (1934) 644.
2. Sheppard, S. E. and Newsome, P. T. *J. Am. Chem. Soc.* **64** (1942) 2937.
3. McConnell, H. *J. Chem. Phys.* **20** (1952) 700.
4. Brode, W. R. *J. Phys. Chem.* **30** (1926) 56.
5. Elenius, E. P. J. "*Pro Gradu*", December 2, 1953; M. S. Thesis in Chemistry, University of Turku, Finland.

6. Brode, W. R., Seldin, I. L., Spoerri, P. E. and Wyman, G. M. *J. Am. Chem. Soc.* **77** (1955) 2762.
7. Vogel, A. I. *A Text Book of Practical Organic Chemistry Including Qualitative Organic Analysis*, Spottiswoode, Ballantyne and Co, Ltd, London and Colchester 1948, p. 166.
8. Meretoja, A. and Linko, R. *Suomen Kemistilehti* **B 23** (1950) 26.
9. A work of this author which continues and will be published later.
10. Ross, W. C. J. and Warwick, G. P. *Chem. & Ind. London* **1955** 745.
11. Hartley, G. S. and Le Fèvre, R. J. W. *J. Chem. Soc.* **1939** 531.

Received August 27, 1961.

ACTA CHEMICA SCANDINAVICA 16 (1962) 263–268

Kinetics of the Acid Hydrolysis of Diethoxymethane in Dioxane-Water Mixtures

JOUKO KOSKIKALLIO and IRMA TARVAINEN

Department of Chemistry, University of Oulu, Oulu, Finland

The kinetics of the acid hydrolysis of diethoxymethane has been studied in dioxane-water mixtures with hydrochloric, perchloric, and sulphuric acids as catalysts. In the solvent range from pure water to dioxane containing about 2 moles of water per litre the changes in the rate are small and similar for all the acids used as catalyst. When the concentration of water in dioxane is decreased below about 2 moles per litre, the rate constants decrease or increase depending on the acid catalyst. These results together with those [6] obtained from spectrophotometric measurements show that the acid strength of perchloric acid increases, that of sulphuric acid remains almost unaltered, and that of hydrochloric acid decreases when the concentration of water in dioxane decreases.

The kinetics of the acid hydrolysis of acetic anhydride in acetone-water and dioxane-water mixtures [1] and also the kinetics of the acid hydrolysis of ethyl acetate in acetone-water mixtures have been studied [2] previously. Both reactions are of the bimolecular *A-2* type although the previous results for acetic anhydride indicate a possible change in mechanism from *A-2* to *A-1* as the amount of water in the solvent mixture is decreased. It was therefore of interest to investigate a unimolecular *A-1* type of hydrolysis reaction in the same solvent mixtures. The present investigation was undertaken in order to get values for comparison, the acid hydrolysis of diethoxymethane being chosen as a typical *A-1* reaction.

EXPERIMENTAL

Materials. All the chemicals (E. Merck AG, pro analysi) except dioxane were used as such. Traces of hydroxylic compounds were removed from the dioxane (Fluka AG, purified by the method of Hess and Frahm) by repeated treatment according to the method of Hess and Frahm [3].

Anhydrous perchloric acid was prepared by the method of Smith [4] from 70 % perchloric acid. The solutions of anhydrous perchloric acid and its monohydrate in dioxane were too unstable to be used in the kinetic experiments, but solutions of 70 % perchloric acid in dioxane remained uncolored for several days. Freshly prepared solutions were used in the kinetic experiments.

Table 1. Rate constants, activation energies and entropies of the acid hydrolysis of diethoxymethane in dioxane-water mixtures containing hydrochloric acid 0.100 mole per litre.

$t°$	$[H_2O]$ mole l^{-1}	[HCl] mole l^{-1}	$10^4 \times k$ l $mole^{-1}s^{-1}$	E kcal	ΔS^* e.u.	K $mole^{-1}$ l
10	55.5	0.100	0.142			
25	55.5	0.100	1.39	25.12	6.03	
40	55.5	0.100	10.4			
50	55.5	0.100	38.2			
0	44.0	0.100	0.0188			
25	44.0	0.100	0.832			
40	44.0	0.100	6.67	25.44	6.26	
60	44.0	0.100	74.4			
25	33.9	0.100	0.482			
40	33.9	0.100	3.84	26.31	7.56	
60	33.9	0.100	51.9			
25	22.8	0.100	0.283			
40	22.8	0.100	2.33	26.54	7.52	
60	22.8	0.100	31.7			
25	11.4	0.100	0.267			
40	11.4	0.100	2.19	27.15	9.30	
60	11.4	0.0400	33.5			
40	11.0	0.0400	1.48			
40	5.5	0	1.35			
40	5.5	0.0496	2.96			70
40	5.5	0.0988	4.81			50
40	5.5	0.245	8.60			
40	2.22	0	5.3			
40	2.22	0.0197	8.3			50
40	2.22	0.0396	11.4			40
40	2.22	0.0968	19.4			
40	1.06	0.0194	8.40			60
40	0.52	0.0099	1.39			
40	0.52	0.0240	2.32			160
40	0.26	0.0121	0.88			240

Measurements. The kinetic experiments were performed in the same way as before [5]. When the solvent mixtures contained 11 moles or more of water per litre ampoules were used as reaction vessels; in the case of the other solvent mixtures reaction vessels with no vapour space were used. These vessels were made from 50 ml all-glass syringes to which outlets of capillary tubes were fused. Samples of the reaction mixtures could be obtained within a few seconds by pressing the piston. The samples were weighed before analysis of the formaldehyde formed in the hydrolysis by the bisulphite method [5].

In each case the reaction was allowed to go to completion. Water and hydrochloric acid were added to a few samples which were then heated in ampoules at 60°C for a sufficient time for the reaction to proceed to completion. The equilibrium constant of the reaction was calculated from the analytical data obtained for these samples. The reverse reaction was taken into account when the rate constant of the hydrolysis reaction was calculated. In the rate equations

$$\frac{dx}{dt} = k(a-x) - k'x^3 = k\,(a-x) - k\,\frac{a-x_e}{x_e^3}\,x^3$$

$$\ln(a-x) = k\int\left(1 - \frac{a-x_e}{x_e^3}\,\frac{x^3}{a-x}\right)dt + \text{constant}$$

a is the initial concentration of diethoxymethane, x the concentration of formaldehyde produced in the reaction, x_e the concentration of formaldehyde at equilibrium, k the rate

Table 2. Rate constants, activation energies and entropies of the acid hydrolysis of diethoxymethane catalysed by perchloric acid in dioxane-water mixtures.

$t°$	$[H_2O]$ mole l^{-1}	$[HClO_4]$ mole l^{-1}	$10^4 \times k$ l mole^{-1}s^{-1}	E kcal	ΔS^* *e.u.*	K mole^{-1} l
40	0.275	0	820			
	0.275	0.00051	900			200
	0.275	0.00099	980			260
20	0.55	0.00206	9.05			300
	0.55	0.0102	7.40			250
40	0.55	0	160	29.30	25.30	
	0.55	0.00100	180			180
	0.55	0.00200	210			170
	0.55	0.00490	238			140
60	0.55	0.00106	3290			150
	0.55	0.00199	3990			130
40	1.10	0	31			
	1.10	0.00407	37			80
	1.10	0.00992	45			110
20	2.10	0.0407	0.45			
	2.10	0.0783	0.74			64
40	2.10	0.0193	8.43	29.30	20.20	80
	2.10	0.0398	11.9			110
	2.10	0.0783	22.6			
60	2.10	0.0198	159			70
	2.10	0.075	283			89
40	5.50	0	1.53			
	5.50	0.0407	2.22			
	5.50	0.102	2.84			
	5.50	0.193	5.67			
40	11.0	0	0.81			
	11.0	0.102	1.49			
	11.0	0.203	2.00			
	11.0	0.385	3.84			

constant of the hydrolysis reaction and k' the rate constant of the reverse reaction. The integral on the right was evaluated graphically. The calculated values of k remained constant over the whole range of reaction studied, which was usually from about 10 % to 80 %. When water-rich solvent mixtures were used, the rate constants were calculated from the first-order rate equation. The results are given in Tables 1—4.

The second-order rate constants obtained by dividing the first-order rate constant by the concentration of the catalyst acid increased with the acid concentration; this salt effect was observed in the case of both water and dioxane-water mixtures. In some case the rate constants were extrapolated to zero acid concentration; these values are also given in the tables.

DISCUSSION

The rate constant of the acid hydrolysis of diethoxymethane decreases when dioxane is added to water and has a minimum value when the solvent mixture contains water and dioxane in approximately equimolar ratio. When the proportion of water in the solvent mixture is decreased further, the rate increases rapidly when perchloric acid is used as catalyst. In the concentration range of water in dioxane from 2 to 0.3 mole per litre log k is a linear function of log $[H_2O]$ with slope -2.5, (Fig. 1).

The acidity function H_0 varies in a similar manner in dioxane-water mixtures when the solvent composition is altered [1,6,7]. Measurements [6] on perchloric acid and *o*-chloraniline in dioxane-water mixtures gave equilibrium constants

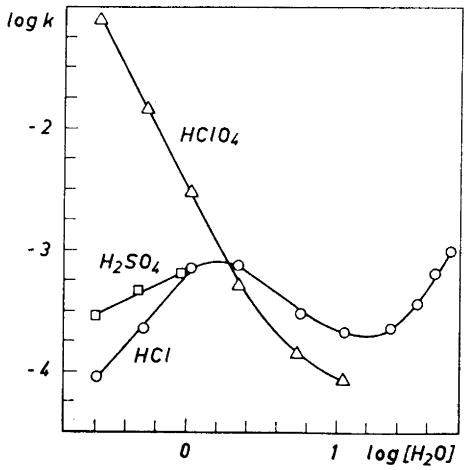

Fig. 1. Plot of log k *versus* log [H_2O].

for the acid-base reaction which varied linearly as log[H_2O] in the range of 0,5 to 11 moles of water per litre in dioxane. The slope of the plot was 1.9.

The similarity of the values of the slopes of the curves shows that the rapid increase of the rate of hydrolysis of diethoxymethane catalysed by perchloric acid is due to changes in the values of the equilibrium constant K of the proton transfer pre-equilibrium and that the rate constant k' of the hydrolysis of the protonated diethoxymethane is approximately independent of changes in the solvent composition as would be expected for a unimolecular reaction of this charge type. The experimental rate constant k of the acid hydrolysis of diethoxymethane is equal to the product of the equilibrium constant K of the proton transfer pre-equilibrium (1) and the rate constant k' of the subsequent slow reaction (2).

$$R + H^+ \rightleftharpoons RH^+ \qquad R = \text{diethoxymethane} \tag{1}$$

$$RH^+ \xrightarrow{\text{slow}} \text{products} \tag{2}$$

In dioxane-rich dioxane-water mixtures perchloric acid is present mainly as ion pairs. When water is added to dioxane the acid strength of perchloric acid decreases rapidly owing to the solvation of perchloric acid by water molecules. The value of the slope of about 2 indicates that in dioxane-rich solvent mixtures perchloric acid is solvated by two water molecules more than protonated diethoxymethane or *o*-chloraniline.

A different situation is found in the acid hydrolysis of diethoxymethane catalysed by hydrochloric acid in dioxane-water mixtures. In water-rich solvent mixtures the rate of hydrolysis changes similarly both when perchloric acid and when hydrochloric acid is the catalyst. The two curves in Fig. 1 differ because the rate constants in the case of perchloric acid were those obtained by extrapolation to zero acid concentration, whereas in the case of hydrochloric acid the rate constants were not extrapolated. In the solvent mixtures containing water less than about 2 moles per litre, the two curves

Table 3. Rate constants of the acid hydrolysis of diethoxymethane catalysed by sulphuric acid in dioxane-water mixtures at 40°C.

$[H_2O]$ mole l^{-1}	$[H_2SO_4]$ mole l^{-1}	$10^4 \times k$ $l\,mole^{-1}s^{-1}$	K $mole^{-1}\,l$
0.250	0.0130	2.84	260
0.474	0.0255	4.43	120
0.93	0.0097	5.72	110
0.93	0.0488	6.85	91
2.14	0.0198	5.76	80
5.36	0.0399	1.43	
10.9	0.0403	0.95	

follow a different course. In the case of hydrochloric acid a maximum value of the rate is observed. When the amount of water is decreased below 1 mole per litre, the rate decreases and the plot of log k *versus* log$[H_2O]$ is linear with slope 1.6.

Spectrophotometric studies [6] reveal that when *o*-chloraniline is used as base the acid strength of hydrochloric acid decreases slightly in these solvent mixtures when the concentration of water decreases. Similarly as when perchloric acid is the catalyst, the changes in the rate of acid hydrolysis of diethoxymethane catalysed by hydrochloric acid are due to changes in the proton transfer pre-equilibrium (1). The rates of acid hydrolysis of acetic anhydride [8] and ethyl acetate [9] vary similarly in dioxane-water mixtures, respective slopes of the log k $-\log[H_2O]$ plots being 1.5 and 1.9 for hydrochloric acid catalyst.

It is interesting to note that whereas the acid strength of hydrochloric acid in dioxane increases when water is added, the acid strength of perchloric acid decreases. The low acid strength of hydrochloric acid in dioxane may be due to a formation of covalent hydrochloric acid molecules which change to solvent separated ion pairs with an increase in acid strength when water is added to dioxane.

Similar curves are obtained with sulphuric acid as catalyst as with hydrochloric and perchloric acids in water-rich solvent mixtures containing two or more moles of water per litre but the curves for solvent mixtures containing only low concentrations of water are different. The rate in dioxane-rich solvent mixtures decreases slightly (Fig. 1) as the amount of water is decreased; the slope of the log k $-\log[H_2O]$ plot is about 0.5. The spectrophotometric studies with *o*-chloraniline gave a similar result with a slope of 0.4.

The activation energies and entropies of the hydrolysis of diethoxymethane (Tables 1 and 2) increase slowly at first when dioxane is added to water and

Table 4. Mean values of the equilibrium constants of the hydrolysis of diethoxymethane at 40°. $K = [\text{acetal}]\,[H_2O]/[CH_2O][ROH]^2$ and $K' = [\text{acetal}]\,[H_2O]^2/[CH_2(OH)_2]\,[ROH]^2$.

$[H_2O]$ mole l^{-1}	K $mole^{-1}\,l$				
	$HClO_4$	HCl	H_2SO_4	mean	$K' = K\,[H_2O]$
0.25	230	240	260	240	60
0.50	160	160	120	150	75
1.0	95	60	100	85	85
2.1	95	45	80	75	160
5.4		60		60	320

more rapidly in the dioxane-rich solvent mixtures. Especially the activation entropy is unusually large in dioxane-water mixtures of low water content.

As shown by the mean values of the equilibrium constants collected in Table 4, the hydrolysis of diethoxymethane does not go to completion in dioxane-rich solvent mixtures. In spite of the fairly large experimental errors in these values, they exhibit no difference in the presence of different acid catalysts, hydrochloric, perchloric and sulphuric acids. This means that the rate of the reverse reaction, the formation of diethoxymethane from formaldehyde and ethanol, changes in a similar way as the rate of the hydrolysis reaction shown in Fig. 1. The variations of the rates of both forward and reverse reactions when the solvent composition is altered, are therefore due to changes in proton transfer pre-equilibria of the type 1.

The values of the equilibrium constants vary as the composition of the solvent mixture is altered. Fromaldehyde is known [10] to be present mainly as methylene glycol in water, but in dry dioxane the formaldehyde molecules are unaltered. It is likely that both forms of formaldehyde are present in concentrations of the same order of magnitude in dioxane-water mixtures containing small amounts of water. As the values of the equilibrium constant of the formaldehyde-methylene glycol reaction in dioxane-water mixtures were not known, the following two equilibria had to be considered:

$$CH_2(OR)_2 + H_2O = CH_2O + 2\ ROH,\ K_1 = \frac{[CH_2O][ROH]^2}{[CH_2(OR)_2][H_2O]} \quad (3)$$

$$CH_2(OR)_2 + 2\,H_2O = CH_2(OH)_2 + 2\,ROH,\ K' = \frac{[CH_2(OH)_2][ROH]^2}{[CH_2(OR)_2][H_2O]^2} \quad (4)$$

Values of these two equilibrium constants were calculated and are given in Table 4. K decreases and K' increases as the amount of water in dioxane is increased. This suggests that both forms of formaldehyde are important in the solvent mixture range and therefore no constancy can be expected. In addition, formaldehyde is partly present as a monoacetal but the concentration of the latter is probably low because water is present in higher concentration than ethanol.

Acknowledgements. The authors wish to record their indebtedness for the financial aid awarded by the *State Commission for Natural Sciences.*

REFERENCES

1. Koskikallio, J. *Acta Chem. Scand.* **14** (1960) 1343.
2. Tommila, E. and Hella, A. *Ann. Acad. Sci. Fennicae A II* (1954) No. 53.
3. Hess, K. and Frahm, H. *Ber.* **71** (1938) 2627.
4. Smith, F. *J. Am. Chem. Soc.* **75** (1953) 184.
5. Koskikallio, J. and Whalley, E. *Trans. Faraday Soc.* **55** (1959) 809.
6. Koskikallio, J. and Ervasti, A. *Acta Chem. Scand.* **16** (1962) *In press.*
7. Braude, E. A. and Stern, E. S. *J. Chem. Soc.* **1948** 1976.
8. Koskikallio, J. and Ervasti, A. *Suomen Kemistilehti* **B 34** (1961) 111.
9. Koskikallio, J. *Unpublished.*
10. Bell, R. P. and MacDougall, A. O. *Trans. Faraday Soc.* **55** (1960) 1281.

Received September 6, 1961.

ACTA CHEMICA SCANDINAVICA 16 (1962) 269–274

The Determination of Chlorinated *o*-Cresols and Chlorinated *o*-Toloxyacetic Acids

BERTIL SJÖBERG

Högre tekniska läroverket, Malmö, Sweden

Methods for the determination of mixtures of chlorinated *o*-cresols by infrared spectroscopy or by partition gas cromatography are described. Chlorinated *o*-toloxyacetic acids are determined as the corresponding chlorinated *o*-cresols after splitting by means of pyridine hydrochloride.

By the chlorination of *o*-cresol a mixture of 4-chloro-, 6-chloro-, 4,6-dichloro-*o*-cresol and unchlorinated *o*-cresol is obtained. The boiling points of these compounds are shown in Table 1.

A distillation will give a low boiling fraction containing *o*-cresol and 6-chloro-*o*-cresol. These two compounds are inseparable by distillation because of their close boiling points. The higher boiling fraction of 4-chloro-*o*-cresol and 4,6-dichloro-*o*-cresol can be resolved by distillation only with great difficulty. Such fractionation is therefore of little use in the analysis of chlorinated *o*-cresols.

In agreement with Freeman, Gardner and Pound [3] it was found that the ultra-violet absorption spectra of the four cresols are too similar to be used for a direct analysis. Much more useful are the infra-red absorption spectra as shown in Figs. 1–4.

By use of suitable absorption maxima the chlorinated *o*-cresols could conveniently be determined by spectrophotometric analyses. Details of the analyses are given in Table 2.

Table 1. The boiling points of *o*-cresol and chlorinated *o*-cresols.

Compound	Boiling point °C/mm Hg
o-Cresol	191/760
6-Chloro-*o*-cresol	191.0–192.3/757 [1]
4-Chloro-*o*-cresol	225/760 [2]
4,6-Dichloro-*o*-cresol	231.6–231.9/739 [1]

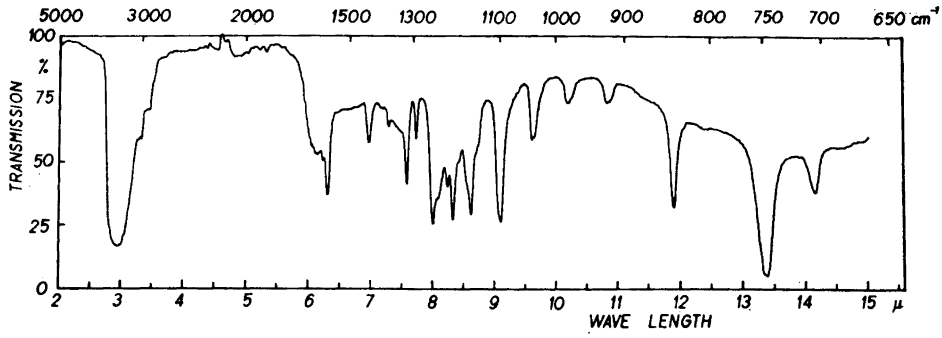

Fig. 1. The infra-red spectrum of *o*-cresol in CS_2-solution.

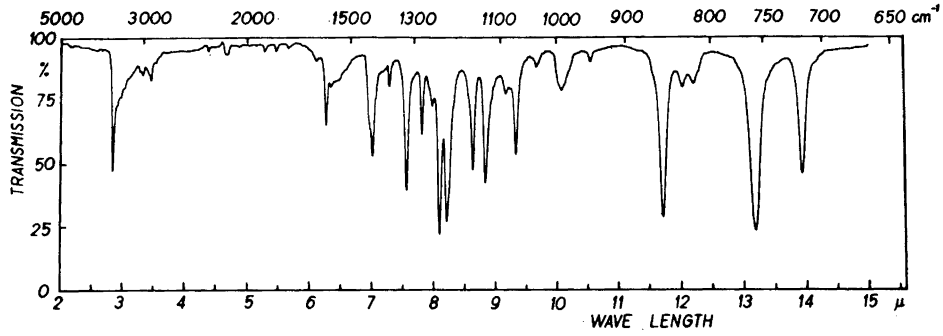

Fig. 2. The infra-red spectrum of 6-chloro-*o*-cresol in CS_2-solution.

The interference of the other compounds at each of these wave-lengths is not very high. It is, however, necessary to prepare a number of solutions of the four cresols in different concentrations and to determine the extinctions at the four wavelengths given in Table 2. In diagrams drawn on millimeter paper the extinctions of the four cresols for each wavelength are plotted as a function of their concentrations [4,5]. By means of these working curves the composition of other samples of these cresols can easily be calculated from the obtained extinction data.

Table 2. Spectrophotometric determination of chlorinated *o*-cresols. Conc. 0.015 g/ml CS_2; Cell 0.4 mm.

Compound	Wave length μ
o-Cresol	13.35
6-Chloro-*o*-cresol	8.80
4-Chloro-*o*-cresol	12.46
4,6-Dichloro-*o*-cresol	13.71

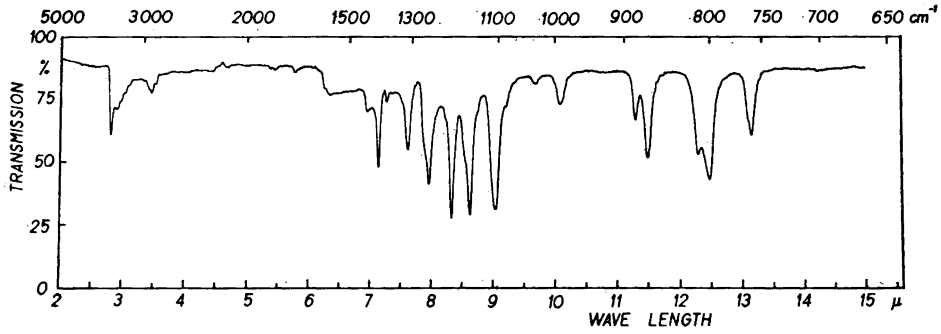

Fig. 3. The infra-red spectrum of 4-chloro-*o*-cresol in CS_2-solution

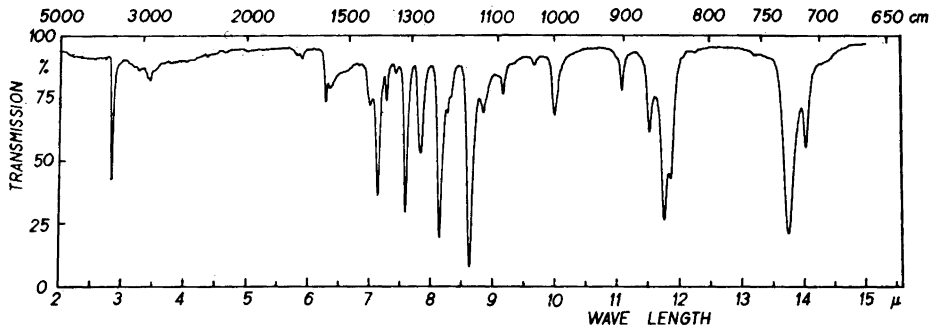

Fig. 4. The infra-red spectrum of 4,6-dichloro-*o*-cresol i CS_2-solution.

This spectrophotometric analytical method has, during a number of years' been used successfully at the Electrochemical Plant, Skoghallsverken, Skoghall, during the manufacture of 4-chloro-*o*-cresol.

For the analysis of chlorinated *o*-cresols partition gas cromatography was also found to be very useful. With a Perkin Elmer Fractometer 116 and Perkin Elmer Standard Packing A in the column the following retention volumes were obtained (Table 3).

Table 3. Relative retention volumes of chlorinated *o*-cresols. Length of column: 2 m. 100 ml He/min. Column packing Perkin Elmer A (20 % Di-decyl-phthalate on Chromosorb)

Compound	Relative retention volume (V_R for *o*-cresol = 1)	
	150°C	175°C
o-Cresol	1.00	1.00
6-Chloro-*o*-cresol	0.70	0.78
4-Chloro-*o*-cresol	5.46	4.65
4,6-Dichloro-*o*-cresol	2.52	2.48

Table 4. Analyses of chlorinated *o*-cresols.

Analysis number	Compound	% Found	% Known weight	Dev.	% Known mole	Dev.
1	*o*-Cresol	25.4	21.4	+4.0	27.6	−2.2
	6-Chloro-*o*-cresol	12.8	13.0	−0.2	12.8	±0
	4-Chloro-*o*-cresol	42.8	41.6	+1.2	40.8	+2.0
	4,6-Dichloro-*o*-cresol	19.0	24.0	−5.0	18.9	+0.1
2	*o*-Cresol	11.9	10.2	+1.7	13.5	−1.6
	6-Chloro-*o*-cresol	14.7	14.6	+0.1	14.6	+0.1
	4-Chloro-*o*-cresol	59.7	57.6	+2.1	57.7	+2.0
	4,6-Dichloro-*o*-cresol	13.8	17.6	−3.8	14.2	−0.4
3	*o*-Cresol	5.8	4.7	+1.1	6.2	−0.4
	6-Cloro-*o*-cresol	12.9	13.1	−0.2	13.2	−0.3
	4-Chloro-*o*-cresol	76.6	76.0	+0.6	75.6	+1.0
	4,6-Dichloro-*o*-cresol	4.8	6.3	−1.5	5.1	−0.3
4	*o*-Cresol	7.0	6.1	+0.9	8.1	−1.1
	6-Chloro-*o*-cresol	7.0	6.8	+0.2	6.8	+0.2
	4-Chloro-*o*-cresol	78.7	77.3	+1.4	77.3	+1.4
	4,6-Dichloro-*o*-cresol	7.3	9.8	−2.5	7.9	−0.6

Elution time at 175°C with column packing A was 60 min. Quite satisfactory separation of the four cresols was obtained. Another useful column packing has been recommended to me by Prawitz,[6] namely 4 g Apiezon and 6 g diglycol on 40 g Silocel C 22.

With column packing Perkin Elmer A and a temperature of 175°C a number of analyses on prepared samples with the four cresols in different concentrations were performed. The results are given in Table 4. The percentages of the four cresols have been calculated from the peak areas without the use of correction factors.

The agreement between known and found values are relatively good at least for 4 chloro-*o*-cresol and 6-chloro-*o*-cresol, which are the main constituents in the technical 4-chloro-*o*-cresol. For higher accuracy, correction factors for the peak areas must be determined. That can easily be done by the preparation and analysis of a suitable number of synthetic mixtures of known compositions.

Having achieved this simple gas cromatographic analysis for the chlorinated *o*-cresols it was found very desirable to try to determine chlorinated *o*-toloxyacetic acids by splitting them into the corresponding chlorinated *o*-cresols. The analysis of the chlorinated toloxyacetic acids has for a long time been an important and difficult problem.

The *o*-toloxyacetic acids cannot be hydrolyzed completely by heating with aqueous solutions of hydrogen halides. Using pyridine hydrochloride [7], however, a quantitative splitting of the chlorinated *o*-toloxyacetic acids to the

corresponding *o*-cresols could be achieved. For this reaction and for the analysis the following procedure was used.

0.5—1.0 g chlorinated *o*-toloxyacetic acid was refluxed with 3 g pyridine hydrochloride for 8 h at 210—220°C. After cooling, the reaction mixture was diluted with 10 ml water. No unreacted toloxyacetic acid could be found. The cresols were extracted with 2 × 2 ml isopropyl ether. The etherial solution was, without further treatment injected into the Gas Fractometer and analyzed. The peaks of the solvent and a small amount of pyridine were not accounted for. The results of the analyses of some prepared mixtures of chlorinated *o*-toloxyacetic acids according to this method are given in Table 5. Correction factors for the peak areas have not been used.

Experiments on a somewhat larger scale have also been made in which it was tried to recover the cresols as completely as possible. Yields of 97—98 % were obtained and the cresols were of high purity.

The author is grateful to Skoghallsverken, Uddeholms AB, Skoghall for permission to publish the details of the infra-red spectrophotometric analyses and for their kindness in supplying the highly purified substances used in this investigation. The author gratefully acknowledges the valuable assistance of ing. Bengt Berglund in the spectrophotometric work.

Table 5. Analyses of chlorinated *o*-toloxyacetic acids.

Analysis number	Compound	% Found	% Known weight	Dev.
1	*o*-Toloxyacetic acid	32.1	32.8	−0.7
	6-Chloro-*o*-toloxyacetic acid	23.8	23.6	+0.2
	4-Chloro-*o*-toloxyacetic acid	21.7	20.6	+1.1
	4,6-Dichloro-*o*-toloxyacetic acid	22.4	23.0	−0.6
2	*o*-Toloxyacetic acid	13.3	13.9	−0.6
	6-Chloro-*o*-toloxyacetic acid	42.5	42.7	−0.2
	4-Chloro-*o*-toloxyacetic acid	26.7	25.2	+1.5
	4,6-Dichloro-*o*-toloxyacetic acid	17.5	18.3	−0.8
3	*o*-Toloxyacetic acid	18.2	17.8	+0.4
	6-Chloro-*o*-toloxyacetic acid	28.3	27.8	+0.5
	4-Chloro-*o*-toloxyacetic acid	42.3	42.3	±0
	4,6-Dichloro-*o*-toloxyacetic acid	11.2	12.2	−1.0
4	*o*-Toloxyacetic acid	10.4	10.7	−0.3
	6-Chloro-*o*-toloxyacetic acid	22.9	23.1	−0.2
	4-Chloro-*o*-toloxyacetic acid	52.3	50.9	+1.4
	4,6-Dichloro-*o*-toloxyacetic acid	14.4	15.3	−0.9
5	*o*-Toloxyacetic acid	4.0	4.1	−0.1
	6-Chloro-*o*-toloxyacetic acid	3.8	3.9	−0.1
	4-Chloro-*o*-toloxyacetic acid	88.3	87.7	+0.6
	4,6-Dichloro-*o*-toloxyacetic acid	3.9	4.4	−0.5

REFERENCES

1. Nord, S. and Sjöberg, B. *Acta Chem. Scand.* **11** (1957) 1753.
2. Sah, P. P. T. and Anderson, H. H. *J. Am. Chem. Soc.* **63** (1941) 3165.
3. Freeman, F., Gardner, K. and Pound, D. W. *J. appl. Chem.* **3** (1953) 160.
4. Daash, L. W. *Anal. Chem.* **19** (1947) 779.
5. Sjöberg, B. *Acta Chem. Scand.* **4** (1950) 802.
6. Prawitz, G. Bönnelyche & Thuröe AB, Malmö, Sweden. *Private communication.*
7. Prey, V. *Ber.* **74 B** (1941) 1219.

Received August 22, 1961.

ACTA CHEMICA SCANDINAVICA 16 (1962) 275–278

Synthese N^1-alkylierter 4-Amino-2-trifluormethyl-benzolsulfonamide

PETER W. FEIT

Forschungslaboratorium der Leo Pharmaceutical Products, Ballerup, Dänemark

4,4′-Dinitro-2,2′-bis-trifluormethyl-diphenyldisulfid wird mit Hydrazinhydrat zur 4,4′-Diaminoverbindung reduziert. Das hieraus nach Acylierung durch oxydierende Chlorierung gewonnene 4-Acetamino-2-trifluormethyl-benzolsulfochlorid liefert bei Umsetzung mit Aminen und anschliessender Entacylierung N^1-alkylierte 4-Amino-2-trifluormethyl-benzolsulfonamide.

5-Trifluormethyl-2,4-bis-aminosulfonyl-anilin zeigt wie das entsprechende 5-Chloranaloge einen diuretischen und saluretischen Effekt, der etwas abgeschwächt auch den entsprechenden N^2, N^4-dimethylierten Verbindungen zu eigen ist [1], eine Tatsache, die mit der im Stoffwechsel stattfindenden Entalkylierung zum freien Sulfonamid gedeutet wird. Da diese Stoffklasse hinsichtlich ihrer Wirkung aus dem Carboanhydrase-Inhibitor Sulfanilamid entwickelt wurde, erschien es in diesem Zusammenhang interessant, mehrere N^1-alkylierte 4-Amino-2-trifluormethyl-benzolsulfonamide zu synthetisieren und auf ihre saluretische Wirkung zu prüfen.

4-Amino-2-trifluormethyl-benzolsulfonamid (XI) ist bekannt. Caldwell und Sayin [2] oxydierten 4,4′-Dinitro-2,2′-bis-trifluormethyl-diphenyldisulfid (I) mit Salpetersäure zu 4-Nitro-2-trifluormethyl-benzolsulfonsäure, setzten deren Natriumsalz mit PCl_5 zum Sulfochlorid um und reduzierten das nach Reaktion mit Ammoniak entstandene 4-Nitro-2-trifluormethyl-benzolsulfonamid zu XI. Oxydierende Chlorierung von I zu dem entsprechenden Sulfochlorid unter verschiedenen Bedingungen verlief nicht zufriedenstellend.

Wir reduzierten I mit Hydrazinhydrat in siedendem Methylcellosolve zum 4,4′-Diamino-2,2′-bis-trifluormethyl-diphenyldisulfid (II)*. Die Reduktion von I mit Eisen und anschliessende Dehydrierung des Reaktionsproduktes mit Wasserstoffperoxyd zu II konnte zwar qualitativ durchgeführt werden, führte jedoch hauptsächlich zum Verlust der Schwefelfunktion durch Reduktion bis zum Schwefelwasserstoff. Die Aminogruppen des Disulfides II wurden durch

* Analoge Reduktion des 2,2′-Dichlor-4,4′-dinitro-diphenyl-disulfides verläuft bereits bei der Temp. des siedenden Alkohols in guter Ausbeute [3].

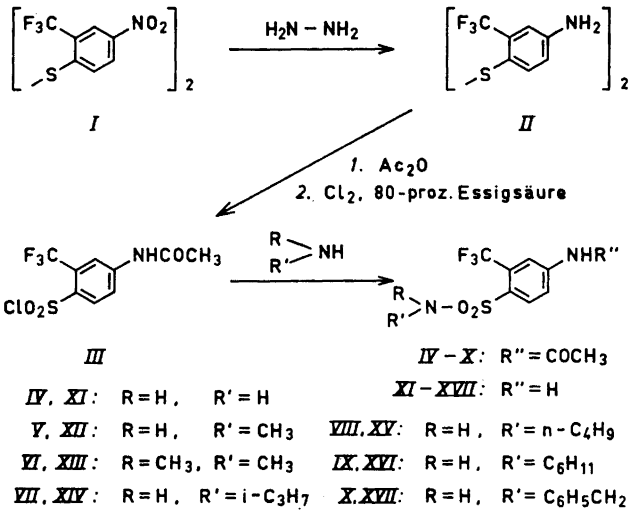

Acetylierung mit Acetanhydrid in Eisessig geschützt, worauf sich die erhaltene 4,4'-Bis-acetamino-Verbindung durch oxydierende Chlorierung in 80-proz. Eisessig glatt in 4-Acetamino-2-trifluormethyl-benzolsulfochlorid (III) überführen liess. Umsetzung mit Ammoniak oder Aminen lieferte die Sulfonamide IV—X, die in siedendem Äthanol/Salzsäure-Gemisch zum 4-Amino-2-trifluormethyl-benzolsulfonamid (XI) bzw. dessen N^1-alkylierten Derivaten XII—XVII entacetyliert wurden. Die Ausbeute an XI, bezogen auf ein aus 4-Chlor-3-trifluormethylnitrobenzol mit Natriumdisulfid in guter Ausbeute erhältliches und nur umständlich und verlustreich zu reinigendes Rohprodukt I[2], betrug über alle Stufen 40 % d. Th.

In Versuchen an Ratten zeigte IV bei peroraler Verabreichung einen saluretischen Effekt, der dem des 5-Trifluormethyl-2,4-bis-aminosulfonyl-anilins gleichkommt. Das entacetylierte XI zeigt eine schwächere Wirkung, während die alkylierten Verbindungen V—X und XII—XVII praktisch als saluretisch unwirksam zu bezeichnen sind.

Herrn Dr. W. Kobinger danke ich für die pharmakologische Untersuchung der Verbindungen.

BESCHREIBUNG DER VERSUCHE *

Alle Schmelzpunkte sind unkorrigiert.

4,4'-Diamino-2,2'-bis-trifluormethyl-diphenyldisulfid (II). Einer eben am Sieden gehaltenen Lösung von 50 g rohem 4,4'-Dinitro-2,2'-bis-trifluormethyl-diphenyldisulfid (I)[2] in 85 ml Methylcellosolve liess man innerhalb von 3 ½ Std. eine Lösung von 40 ml Hydrazinhydrat in 60 ml Methylcellosolve zutropfen, wobei sich die anfangs tiefbraune Lösung nach Rot aufhellte **. Es wurde weitere 30 Min. unter Rückfluss erhitzt, und

* Herrn G. Cornali sei für die Ausführung der Mikroanalysen und meinen Laboranten, Herrn W. Schlichtkrull und Herrn Th. Rolle, für die Mithilfe bei der Ausführung der Versuche gedankt.

** Bei Verwendung von nach Caldwell und Sayin [2] gereinigtem I resultierte eine schwach gelbe Lösung.

Tabelle 1. Übersicht über die dargestellten N^1-alkylierten4-Amino-2-trifluormethylbenzolsulfonamide (XII–XVII) und ihre N^4-Acetylderivate (V–X).

Verb.	Schmp. (Lösungsmittel)	Summenformel (Mol.-Gew.)	Analysendaten				
				C	H	N	S
V	180,5–182 (Methanol und Aceton/Petroläther)	$C_{10}H_{11}F_3N_2O_3S$ (296,2)	Ber.:	40,55	3,74	9,46	10,82
			Gef.:	40,55	3,84	9,30	10,92
XII	128–130 (50-proz. Methanol)	$C_8H_9F_3N_2O_2S$ (254,2)	Ber.:	37,79	3,57	11,02	12,61
			Gef.:	38,00	3,51	11,15	12,70
VI	147,5–149,5 (Methanol)	$C_{11}H_{13}F_3N_2O_3S$ (310,3)	Ber.:	42,58	4,22	9,04	10,33
			Gef.:	42,59	4,37	8,96	10,47
XIII	141,5–143,5 (75-proz. Methanol)	$C_9H_{11}F_3N_2O_2S$ (268,3)	Ber.:	40,29	4,13	10,44	11,95
			Gef.:	40,43	4,18	10,30	11,75
VII	192,5–193,5 (Methanol)	$C_{12}H_{15}F_3N_2O_3S$ (324,3)	Ber.:	44,44	4,66	8,64	9,89
			Gef.:	44,67	4,78	8,74	9,85
XIV	120,5–122,5 (75-proz. Methanol)	$C_{10}H_{13}F_3N_2O_2S$ (282,3)	Ber.:	42,54	4,64	9,93	11,36
			Gef.:	42,54	4,87	10,14	11,42
VIII	181–182,5 (Methanol)	$C_{13}H_{17}F_3N_2O_3S$ (338,4)	Ber.:	46,15	5,07	8,28	9,47
			Gef.:	46,27	5,31	8,27	9,49
XV	122–124 (75-proz. Methanol)	$C_{11}H_{15}F_3N_2O_2S$ (296,3)	Ber.:	44,59	5,10	9,46	10,82
			Gef.:	44,83	5,00	9,38	10,78
IX	151–153 (verd. Methanol)	$C_{15}H_{19}F_3N_2O_3S$ (364,4)	Ber.:	49,44	5,26	7,69	8,80
			Gef.:	49,43	5,42	7,93	8,95
XVI	81–83 (Äthylacetat/Hexan 1:1) 103,5–105,5 (60-proz. Äthanol oder Benzol/Petroläther)	$C_{13}H_{17}F_3N_2O_2S$ (322,4)	Ber.:	48,44	5,32	8,69	9,95
			Gef.:	48,38	5,44	8,64	9,96
X	147–149 (verd. Methanol und Aceton/Petroläther)	$C_{16}H_{15}F_3N_2O_3S$ (372,4)	Ber.:	51,61	4,06	7,53	8,61
			Gef.:	51,49	4,29	7,41	8,67
XVII	117,5–118,5 (75-proz. Methanol)	$C_{14}H_{13}F_3N_2O_2S$ (330,3)	Ber.:	50,90	3,97	8,48	9,71
			Gef.:	50,97	4,06	8,56	9,70

nach dem Erkalten II durch vorsichtigen Zusatz von 300 ml Wasser gefällt. Nach Belassen im Kühlschrank wurde abgesaugt und mit Wasser gewaschen. Ausbeute an gelbgefärbtem Rohprodukt 34,5 g; Schmp. 148–152°C. Die analysenreine Verbindung wurde durch Entacylierung der N^4, $N^{4'}$-Diacetylverbindung (s.u.) gewonnen: Eine Aufschlämmung von 4,4'-Diacetamino-2,2'-bis-trifluormethyl-diphenyldisulfid in der vierfachen Menge 4 N HCl/Äthanol (1:1) wurde 16 Std. erhitzt, die entstandene Lösung warm filtriert und vorsichtig mit konz. Ammoniak neutralisiert. Nach dem Erkalten wurde II abgesaugt und aus Äthanol umkristallisiert. Schmp. 160–161,5°C. (Gef.: C 43,85; H 2,86; N 7,42; S 16,47. Ber. für $C_{14}H_{10}F_6N_2S_2$ (384,4): C 43,74; H 2,62; N 7,29; S 16,68).

4,4'-Diacetamino-2,2'-bis-trifluormethyl-diphenyldisulfid. Eine Aufschlämmung von 34,5 g rohem II in 45 ml Eisessig wurde unter Schütteln portionsweise mit 25 ml Acetanhydrid versetzt. Unter Selbsterwärmung erfolgte zunächst Lösung, wonach das Reaktionsprodukt auszukristallisieren begann. Es wurde noch 2 Std. auf dem Dampfbad erwärmt. Nach Abkühlen wurde die Diacetylverbindung abgesaugt und mit kaltem Eisessig gewaschen. Ausbeute 35,8 g; Schmp. 255,5—259°C. Zur Analyse wurde mehrmals aus Eisessig umkristallisiert; Schmp. 259—260°C. (Gef.: C 46,16; H 3.13; N 5.78; S 13.55. Ber. für $C_{18}H_{14}F_6N_2O_2S_2$ (468,4): C 46,15; H 3,01; N 5,98; S 13,69).

4-Acetamino-2-trifluormethyl-benzolsulfochlorid (III). In eine Aufschlämmung von 234 g 4,4'-Diacetamino-2,2'-bis-trifluormethyl-diphenyldisulfid in 1.2 l 80-proz. Essigsäure wurde bei 10—15°C unter Rühren und Kühlen solange Chlor eingeleitet, bis eine klare Lösung entstanden war, was einige Std. in Anspruch nahm. Es wurde noch 30 Min. gerührt und anschliessend das überschüss. Chlor durch Durchblasen von Luft entfernt. Darauf wurde auf 1.8 l Eiswasser gegossen, das dabei erhaltene Sulfochlorid III abgesaugt und mit Eiswasser gewaschen. Ausbeute 266 g; Schmp. 117,5—119,5°C. Zur Analyse wurde bei Gegenwart von Aktivkohle aus Benzol umkristallisiert (Clathrat mit Benzol: Schmp. 88—90°C; nach Trocknen i. Vak. bei 80°C Schmp. 120—122°C) und einmal aus Eisessig/Wasser umgefällt; Schmp. 119,5—120,5°C. (Gef.: C 35,99; H 2,66; Cl 11,39; N 4,56. Ber. für $C_9H_7ClF_3NO_3S$ (301,7): C 35,83; H 2,34; Cl 11,75; N 4,64).

4-Acetamino-2-trifluormethyl-benzolsulfonamid (IV). 4.5 g III wurden unter Rühren bei 15—20°C in 50 ml konz. Ammoniak eingetragen. Sodann wurde durch 1 stdg. Erwärmen auf dem Dampfbad das überschüssige Ammoniak ausgetrieben. Nach dem Erkalten wurde IV abgesaugt und mit Wasser gewaschen. Ausb. 3,9 g; Schmp. 242,5—244,5°C. Zur Analyse wurde bei Gegenwart von Aktivkohle aus 90-proz. Äthanol umkristallisiert; Schmp. 244,5—246° C. Gef.: C38,14; H 3,26; N 9,88; S 11,50. Ber. für $C_9H_9F_3N_2O_3S$ (282,2): C 38,30; H 3,21; N 9,93; S 11,36).

N^1-Alkylierte 4-Acetamino-2-trifluormethyl-benzolsulfonamide. Allgemeine Arbeitsvorschrift: Das Sulfochlorid III wurde bei 15—20°C unter Rühren portionsweise in die vierfache Menge einer ungefähr 20—30 proz. wässrigen Lösung des entsprechenden Amines eingetragen, und darauf die Reaktionsmischung 1 Std. auf dem Dampfbad erwärmt. Nach dem Erkalten und Neutralisieren mit verdünnter Salzsäure wurde das Sulfonamid abgesaugt und mit Wasser gewaschen.

4-Amino-2-trifluormethyl-benzolsulfonamid (XI). Eine Suspension von 2,25 g IV in einer Mischung aus 15 ml konz. HCl und 5 ml Alkohol wurde 1 Std. am Rückfluss erhitzt. Darauf wurden 4,5 ml einer Mischung aus Alkohol, Äthylacetat und Wasser abdestilliert und die noch warme Reaktionslösung vorsichtig mit Ammoniak neutralisiert. Nach dem Erkalten wurde XI abgesaugt und mit Wasser gewaschen. Ausbeute 1,5 g; Schmp. 196,5—198°C (Lit.[2]: 196—197°C). Umkrist. aus verd. Alkohol ergab gleichbleibenden Schmp.

XII—XVII wurden durch Entacylierung von V—X wie bei XI beschrieben dargestellt.

LITERATUR

1. Sprague, J. M. *Ann. N.Y. Acad. Sci.* **71** (1958) 328; Logemann, W., Giraldi, P. N. und Parenti, M. A. *Nature* **182** (1958) 1510; Lund, F. J. und Kobinger, W. *Acta Pharmacol. Toxicol.* (København) **16** (1960) 297.
2. Caldwell, W. T. und Sayin, A. N. *J. Am. Chem. Soc.* **73** (1951) 5125.
3. Riegel, B., Lappin, G. R., Adelson, B. H., Jackson, R. I., Albisetti, Jr., C. J., Dodson, R. M. und Baker, R. H. *J. Am. Chem. Soc.* **68** (1946) 1264.

Eingegangen am 26. September 1961.

ACTA CHEMICA SCANDINAVICA 16 (1962) 279–282

Dissolution of Cuprous Chloride in Acid Chloride Solution

TOR HURLEN

Central Institute for Industrial Research, Blindern, Oslo, Norway

The dissolution rate (v) of cuprous chloride in various 0.1 N sulphuric acid solutions of potassium chloride and cuprous chloride at 20°C has been studied and in unstirred solutions found to be:

$$v = 6.1\,[(Cu)_s - (Cu)]^{1.25}\,10^{-7}\ \text{mole(CuCl)/cm}^2\text{sec}$$

where (Cu) is the actual cuprous molality in the solution and $(Cu)_s$ its saturation value. The latter value is further found to be given by

$$(Cu)_s = 9.7\ (Cl)\,10^{-2}\ M$$
$$(Cu)_s = 1.4\ (Cl)^2 10^{-1}\ M$$

at chloride concentrations (Cl) below and above about 0.7 M, respectively.

The dissolution rate is greatly increased by stirring, and all results indicate the dissolution to be controlled by the diffusion of cuprous species from the crystal surface to the bulk of the solution.

1.0 INTRODUCTION

During the last decade, electrochemical theories of the type applying to metal/metal ion electrodes have been introduced also to the field of dissolution and growth of ionic crystals in solutions (as reviewed and described by Vetter [1]). Following previous work on the copper/cuprous electrode in complexing chloride solutions [2,3] and on the deposition of cuprous chloride on copper by its reaction with cupric ions in such solutions [4], it was therefore assumed desirable to study also the dissolution of cuprous chloride in solutions of the same type.

2.0 EXPERIMENTAL

The experiments have been performed with high purity copper sheets (14 cm² geometrical surface area) having been immersed for one hour in H_2SO_4 (0.1 N) + $CuSO_4$ (0.1 M) + KCl (0.05 M). This immersion gives a cuprous chloride layer of about 2 mg/cm² on the copper surface [4]. The following three series of solutions have been used:

H_2SO_4 (0.1 N) + KCl(0.1 to 2 M)
H_2SO_4 (0.1 N) + CuCl(x M) + KCl(0.6 + x M)
H_2SO_4 (0.1 N) + CuCl(x M) + KCl(1 + 2x M)

All solutions have been made from A.R. quality acid and salts in water distilled from a rather pure tap water. The cuprous containing solutions were made up in deaerated water and were stored and used under an atmosphere of purified hydrogen (streaming). The cuprous free solutions were exposed to air.

The dissolution rate measurements have been performed both by the semi-continuous quartz helix technique previously described [5] and by intermittent weighing. In all experi-

ments, the cuprous chloride covered copper sheets were vertically immersed in separate portions of 0.5 to 1 l test solution.

The experiments have been carried out in a thermostated room at about 20°C. In most experiments, no stirring has been applied in the solution. In a few cases only, a magnetic stirrer has been used at the bottom of the test beaker. These cases are notified in the text.

3.0 RESULTS

In all solutions applied, the rate curves were nearly linear until most of the cuprous chloride layer was dissolved, whereafter they relatively fast become horizontal as the dissolution rate dropped to zero at complete dissolution of the layer (as already shown by Fig. 3 of Ref.[4]). The slope of the linear part of such a curve is a measure of the dissolution rate.

In Fig. 1, the values obtained for the dissolution rate (v_0) of cuprous chloride in initially cuprous free solutions are plotted *versus* the chloride molality (Cl). The straight lines drawn there correspond to the relationships:

$$v_0 = 3.3(\mathrm{Cl})^{1.25}10^{-8} \text{ mole(CuCl)/cm}^2\text{sec} \quad (1a)$$

$$v_0 = 5.4(\mathrm{Cl})^{2.5}\ 10^{-8} \text{ mole(CuCl)/cm}^2\text{sec} \quad (1b)$$

at low and high chloride concentrations, respectively. Except for the exponential factor of 1.25, these results indicate a transition from a linear to a parabolic chloride dependence at a chloride concentration slightly below 1 M (see Fig. 1). This is analogous to the parabolic/cubic transition previously found for the anodic dissolution of copper in solutions of the same type [2,3].

In Fig. 2, the 1.25-root of the values obtained for the dissolution rate (v) of cuprous chloride in unstirred cuprous containing solutions of essentially

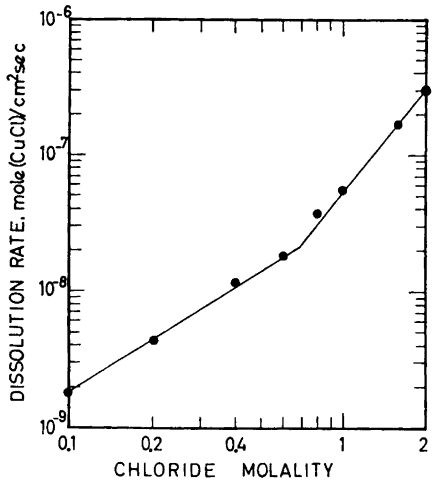

Fig. 1. Rate of dissolution of cuprous chloride in unstirred 0.1 N sulphuric acid solutions of potassium chloride at 20°C.

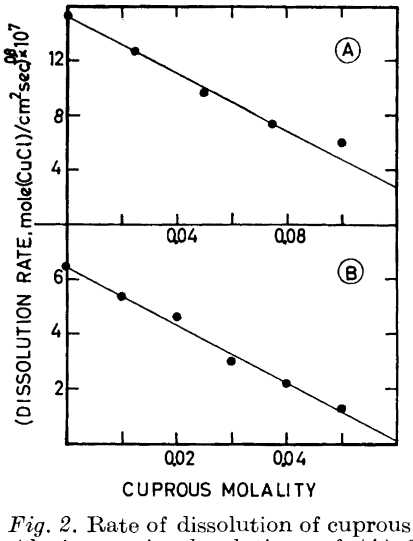

Fig. 2. Rate of dissolution of cuprous chloride in unstirred solutions of (A) 0.1 N sulphuric acid + (1 + 2x) M potassium chloride + x M cuprous chloride and (B) 0.1 N sulphuric acid + (0.6 + x) M potassium chloride + x M cuprous chloride at 20°C.

constant chloride ion molality (0.6 and 1) is plotted *versus* the cuprous molality (Cu). The straight lines drawn there, both correspond to the relationship:

$$v = v_0 \left(1 - \frac{(Cu)}{(Cu)_s}\right)^{1.25} \quad (2)$$

where $(Cu)_s$ is the cuprous molality given by the intersection of the lines with the molality axis, at 0.060 and 0.145 M for the 0.6 and the 1 M chloride solutions, respectively. The two lines in Fig. 2 are further very nearly parallel to each other, both of them giving by their slope:

$$v_0 = 6.1\ (Cu)_s^{1.25}\ 10^{-7}\ \text{mole(CuCl)/cm}^{-2}\text{sec} \quad (3)$$

when $(Cu)_s$ is given in molality units. It is good reason to believe that (2) and (3) apply not only to solutions of the two chloride ion concentrations for which they here have been established.

$(Cu)_s$ most probably represents the saturation concentration of cuprous chloride in the solutions applied. This is somewhat substantiated by the fact that in the 0.6 M chloride series we did not succeed in dissolving all the cuprous chloride weighed in for a 0.07 M cuprous chloride solution, and that some immersion experiments with cuprous chloride covered sheets in this saturated solution did not show any distinct weight changes. From eqns. (1) and (3), it is easily seen that the saturation molality with good approximation is given by

$$(Cu)_s = 9.7\ (Cl)\ \ 10^{-2}\ \text{M} \quad (4a)$$
$$(Cu)_s = 1.4\ (Cl)^2\ 10^{-1}\ \text{M} \quad (4b)$$

at low and high chloride concentrations, respectively.

All the above results concern unstirred solutions. It is possible, however, that (2) to some extent also applies to stirred solutions, but v_0 is strongly increased by stirring. The latter was shown by experiments with a magnetic stirrer in 0.1 N sulphuric acid + 0.3 M potassium chloride. The stirring applied raised the dissolution rate by a factor of about 12. Even though no exact measure is available for the stirring rate, the stirring effect clearly shows the dissolution to be under diffusion control. As is discussed below, this is in agreement also with the results in unstirred solutions.

The reproducibility of the above rate measurements has been well within 5 % in unstirred and 10 % in stirred solutions. The poorer reproducibility in stirred solutions may be due to uncontrolled variations in the stirring rate.

4.0 DISCUSSION

All the above results in unstirred solutions may be represented by the single rate equation:

$$v = 6.1[(Cu)_s - (Cu)]^{1.25}\ 10^{-7}\ \text{mole(CuCl)/cm}^2\text{sec} \quad (5)$$

where $(Cu)_s$ is as given by (4). This is of the right type and magnitude for limiting diffusion currents in the case of natural convection (Ref.[1], pp. 170—174) and indicates the rate determining process to be the diffusion of cuprous species from the crystal surface, where the cuprous concentration is $(Cu)_s$, to the bulk of the solution, where the cuprous concentration is (Cu). The diffusion layer

thickness is thus assumed to be inversely proportional to the 0.25 power of the concentration difference. Stirring should further be expected to reduce this thickness and, thereby, to increase the dissolution rate. This is in accordance with what has been observed in the present case.

The results obtained thus indicate that the exchange of cuprous chloride species between a crystal and a chloride solution of this salt is fast enough to maintain essentially equilibrium conditions at the crystal surface (*i.e.*, to make the solution there saturated) even during relatively rapid dissolution in initially cuprous free solutions. Except for this, the results can tell nothing as to the rate and mechanism of these exchange reactions. The chloride dependence shown by eqns. (4), however, indicates that the dissolution mainly goes to $CuCl_2^-$ at low and to $CuCl_3^{2-}$ at high chloride concentrations (see also Fig. 1). This is in accordance with what has previously been found for the anodic dissolution of copper in solutions of the same type [2,3], and is also what to be expected from stability data for the mentioned complexes [6] and from solubility data for cuprous chloride in chloride solutions [7].

In a more rigorous treatment of the cuprous chloride dissolution, regards have to be made of the possibly different diffusion coefficients of the varies species involved, of the possible reactions between these species in the diffusion layer, and of the possibility of transport influencing electric fields being set up in this layer. Such a treatment necessitates the solution of an intricate system of differential equations and will therefore not be given here. This is even more due to the above simple considerations showing clearly enough what is controlling the dissolution rate. One difficulty in these considerations, however, is that they give a rather satisfactory picture without taking into account that the chloride concentration may possibly be lower at the crystal surface than in the bulk of the solution, especially at high dissolution rates. In the absence of any electric field effects in the diffusion layer and unless the diffusion coefficient should be much lower for the cuprous species than for the chloride ions, one should namely expect such a chloride concentration lowering to have caused an increasing downwards departure in the dissolution rate from the "parabolic" chloride dependence observed. The absence of this departure could probably have some explanation through a more rigorous treatment of the type suggested above.

Acknowledgement. The author is much indebted to Miss E. Husebye, Miss T. Tönderum, and Miss K. Storström for technical assistance, to various members of the staff at the Central Institute for Industrial Research for valuable discussions, and to the *U.S. Department of Army, European Research Office*, for financial support.

REFERENCES

1. Vetter, K. J. *Elektrochemische Kinetik*, Springer, Berlin/Göttingen/Heidelberg 1961.
2. Hurlen, T. *Acta Chem. Scand.* **15** (1961) 1231.
3. Hurlen, T. *Acta Chem. Scand.* **15** (1961) 1239.
4. Hurlen, T. *Acta Chem. Scand.* **15** (1961) 1246.
5. Hurlen, T. *Acta Chem. Scand.* **15** (1961) 615.
6. Bjerrum, J., Schwarzenbach, G. and Sillén, L. G. *Stability Constants. Part II: Inorganic Ligands*, The Chemical Society, London 1958.
7. Bodländer, G. and Storbeck, O. *Z. anorg. Chem.* **31** (1902) 1.

Received September 11, 1961.

ACTA CHEMICA SCANDINAVICA 16 (1962) 283–286

Detection of Drugs other than Barbiturates in the Routine Method for Barbiturate Analysis

A. C. MAEHLY and M. K. LINTURI

*Statens Rättskemiska Laboratorium *, Stockholm 60, Sweden*

When barbiturates are extracted from autopsy tissue, a number of other toxicologically important compounds are extracted at the same time. This paper presents data obtained by paper chromatography and spectrophotometry for more than 20 of these compounds.

In a recent publication [1] we described the isolation, identification, and quantitative determination of barbiturates from human tissue. Several thousand extractions of tissue, blood and urine from autopsy cases have been carried out according to this method. The procedure in brief is as follows:

The tissue (5–50 g) is ground in a blendor (blood or urine is of course taken as such), acidified to pH 3–4 with dilute hydrochloric acid, and extracted with chloroform. The solvent is evaporated and the residue treated with hot dilute hydrochloric acid. The solution is cooled to +4°, fat removed by filtration, and the filltrate reextracted with chloroform. This extract is brought to a known volume (usually 5.0 ml) and aliquots analyzed by paper chromatography and spectrophotometry.

It has been found that quite a number of neutral and acidic compounds of toxicological importance, other than barbiturates, can be detected and assayed at the same time [1]. The advantages of extracting such a variety of drugs in one and the same procedure are obvious. In order to facilitate further analysis it is advisable to separate acidic compounds (barbiturates, salicylic acid, sulfonamides) from the chloroform extract mentioned above and to assay the acidic and the neutral substances separately. To this end we use the following simple procedure:

The chloroform extract (usually 5 ml) is shaken four times with an equal volume of 0.5 N ammonia, separating the solvent layers by centrifugation. The aqueous layers are combined, acidified with hydrochloric acid, and reextracted three times with twice their volume of chloroform. The combined chloroform extracts (containing the acidic compounds) as well as the original chloroform solution (retaining the neutral substances) are each dried over sodium sulfate, filtered, and brought to a known volume, usually 5.0 ml.

* The Government Laboratory for Forensic Chemistry.

Table 1. R_F-values of some non-barbiturate drugs.

Compound		R_F-values			Visibility on the paper
Merck Index name (where possible)	Synonym	diethyl ether	di-*n*-butyl ether **	chloro-form	
p-Acetaminophenol	NAPA	0.30	0	0	UV
Acetophenetidine *	Phenacetine	0.90	0.55	0.95	UV
Acetylcarbromal	Abasin	0.87	0.82	0.93	(*a*)
Aminopyrine	Pyramidon	0.82	0.77	0.94	UV
Antipyrine *	Phenazone	0.55	0.11	0.94	UV, (*c*)
Bemegride	Megimide	0.91	Fr	Fr	(*a*)
Bromisovalum	Bromural	0.90	0.84	0.89	(*b*)
c-Bromovalerylurea	Bromyl	0.90	0.89	0.89	(*b*)
Caffeine *	—	0.24	0.09	0.95	UV
Carbromal	Adalin	0.87	0.88	0.92	(*a*)
Dextromoramide	Palfium	Fr	Fr	Fr	(*c*)
5-Ethyl-3-methyl-5-phenylhydantoin	Difhydan	0.80	0.20	0.56	(*a*) (*a*)
Glutethimide	Doriden	0.90	0.82	0.95	(*d*)
Meprobamate	—	0.80	0.19	0.74	(*e*)
Phenothiazine derivatives	*e.g.*, Lergigan, Chloropromazine	Fr	Fr	Fr	UV, (*c*)
Salicylamide	—	0.25	0.07	0.56	UV, F
Salicylic acid	—	0	0	0	UV, F
Sulfamethazine	Sulfadimidin	0.02	0	0.07	UV
Sulfathiazole	—	0	0	0	UV
Theobromine	—	0	0	0.22	UV
Theophylline	—	0	0	0.15	UV
Truxal	*Trans*-2-chloro-10-(3-dimethylamino-propyliden) thia-xanthene acetate	Fr	Fr	Fr	UV

The following symbols are used:

UV Visible on illumination with ultraviolet light (Hg-line at 254 mμ) when a fluorescent paper is placed under the paper chromatogram as described elsewhere [1]. The compound is listed in Table 2.

F The compound fluoresces on illumination with UV-light.

* The chromatographic and spectral properties of these compounds have been described previously [3].

** Running time 5 h; the solvent front has then left the paper.

Fr At the solvent front.

a) Only large amounts (*ca.* 0.5 mg and more) are visible in UV-light (Hg-line at 254 mμ).

b) Only amounts larger than 0.1 mg are visible in UV-light (Hg-line at 254 mμ).

c) Gives a positive reaction with potassium bismuth iodide (Dragendorff's reagent), described, *e.g.*, by Curry [4].

d) Only visible in UV-light if more than 1 mg is present. A color reaction for gluthetimide, using mercurous nitrate, has been described by Dressler [5].

e) Meprobamate reacts with the chlorine-benzidine reagent described by Vidic [6].

Table 1 shows the R_F-values obtained by using 3 different, water-saturated solvents, *i.e.* diethyl ether, di-*n*-butyl ether and chloroform. Whatman No. 1 paper, previously treated with sodium carbonate solution, and the descend-

ing technique was used. In Table 2 the compounds exhibiting absorption maxima in the ultraviolet are arranged in the order of increasing wavelength of their maxima. The extinction coefficients for 1 % (w/v) solutions, using 1 cm lightpath are also given *. Drugs with distinct absorption peaks can not only be detected but also assayed quantitatively. The compounds lacking

Table 2. Ultraviolet absorption maxima of compounds that are extracted together with barbiturates.

1. *Wavelengths* (λ) in mμ. Accuracy $\pm$ 2 mμ. 2. *Names of compounds:* If possible, the name listed in the »Merck Index», 7th ed., is given. In some cases other names are listed as well. 3. *Solvents:* a-EtOH: ammoniacal 75 % ethanol; pH on diluting with an equal volume of water *ca.* 10. s-EtOH: acidified 75 % ethanol; pH after dilution *ca.* 2. NH_4OH: 0.5 N ammonium hydroxide. H_2SO_4: *ca.* 0.01 N sulfuric acid. KOH: *ca.* 0.1 N potassium hydroxide. 4. *Extinction coefficients:* for 1 % (w/v) solutions, measured in a cuvet with 1.0 cm optical pathlength ($E^{1\%}_{cm}$). Accuracy $\pm$ 3 % except where denoted by »*ca*».

Absorption maxima (mμ)		Compound	Solvent	$E^{1\%}_{1cm}$
maximum	other maxima			
228		Bemegride (Megimide)	NH_4OH	470
228†	(296)	Salicylic acid	a-EtOH	488
230*	(268, 325)	Truxal (Lundbeck)[a]	a-EtOH s-EtOH	287
233†	(300)	Salicylic acid	s-EtOH	558
235†	(302)	Salicylamide	s-EtOH	630
237	(286)	Thiobarbiturates	H_2SO_4	*ca.* 340
240		Barbiturates	NH_4OH	*ca.* 400
242		Br-substituted barbiturates	NH_4OH	*ca.* 400
242	(260)	Sulfamethazine	a-EtOH	730
244		N-alkylated barbiturates	NH_4OH KOH	*ca.* 400
244*	(270)	Antipyrine (Phenazone)	a-EtOH s-EtOH	488
245		Sulfadimethoxine	s-EtOH	350
246		Barbiturates that are Br-substituted and N-alkylated	NH_4OH KOH	*ca.* 400
247		5-Hydroxyethyl-4-methyl-thiazole	a-EtOH	*ca.* 160
248		*p*-Acetaminophenol (NAPA)	a-EtOH s-EtOH	853
250		Acetophenetidine (Phenacetine)	a-EtOH s-EtOH	822
252*		Promethazine (Lergigan)	s-EtOH	955
255*		Promethazine	a-EtOH	915
255		5-Hydroxyethyl-4-methyl-thiazole	s-EtOH	*ca.* 160
255		Barbiturates	KOH	*ca.* 300
255*		Chloropromazine	s-EtOH	1040
256*		Chloropromazine	a-EtOH	990

a) *Trans*-2-chloro-10(3-dimethylaminopropyliden)-thiaxanthene acetate.

* A similar list has been published in other connections by Bradford and Bracket [7].

Table 2. Continued.

256		Sulfathiazole	NH_4OH	256
256	(304)	Thiobarbiturates	NH_4OH	*ca.* 400
257		Br-substituted barbiturates	KOH	*ca.* 300
260	(242)	Sulfamethazine	a-EtOH	740
262		Aminopyrine (Pyramidon)	a-EtOH	406
268*	(230, 325)	Truxal [a]	s-EtOH a-EtOH	122
270		Theophylline	a-EtOH	664
270*	(244)	Antipyrine (Fenazon)	s-EtOH a-EtOH	480
271		Caffeine	s-EtOH	400
272		Caffeine	a-EtOH	420
272		Theobromine	s-EtOH	406
274		Theophylline	a-EtOH	640
275		Theobromine	a-EtOH	550
280		Sulfathiazole	H_2SO_4	180
286	(237)	Thiobarbiturates	H_2SO_4	*ca.* 900
296†	(228)	Salicylic acid	a-EtOH	290
300†	(233)	Salicylic acid	s-EtOH	305
302†	(235)	Salicylamide	s-EtOH	310
304	(256)	Thiobarbiturates	NH_4OH	*ca.* 1160
325*	(230, 268)	Truxal [a]	s-EtOH a-EtOH	28
332†	(235)	Salicylamide	a-EtOH	440

† Fluoresces on the paper.
* Gives a positive reaction with Dragendorff's reagent (potassium bismuth iodide).

such spectral characteristics must be assayed in other ways. For some of them, quantitative methods are available; investigations on the quantitative determination of others are in progress.

Ultraviolet spectra and R_F-values are usually not sufficient for the certain identification of compounds of toxicological importance. A method for identification of micro amounts of compounds that can be sublimated *in vacuo* for both infrared spectrophotometry and melting point determination is described elsewhere [2].

REFERENCES

1. Bonnichsen, R., Maehly, A. C. and Frank, A. *J. Forensic Sci.* **6** (1961) 411.
2. Maehly, A. C. *The Analyst*, **87** (1962) 116.
3. Bonnichsen, R., Maehly, A. C. and Nordlander, S. *J. Chromatography* **3** (1960) 190.
4. Curry, A. S. in Stewart, C. P. and Stolman, A. (Eds.) *Toxicology, Mechanisms and Analytical Methods*, Academic Press, New York 1960, Vol. 1, p. 257 ff.
5. Dressler, A. *Deut. Z. ges. gerichtl. Med.* **50** (1960) 457.
6. Vidic, E. *Arch. Toxikol.* **17** (1959) 373.
7. Bradford, L. W. and Brackett, J. W. *Microchim. Acta* (**1958**) 353.

Received July 19, 1961.

ACTA CHEMICA SCANDINAVICA 16 (1962) 287–292

Phosphides of the *B*31 (MnP) Structure Type

STIG RUNDQVIST

Institute of Chemistry, University of Uppsala, Uppsala, Sweden

The mono-phosphides of Cr, Mn, Fe, Co, W, and Ru crystallize in the *B*31 (MnP) structure type. The unit cell dimensions of these phosphides have been measured, and the structures of MnP, FeP and CoP have been determined accurately by single-crystal methods. Some data for unit cell variations accompanying isomorphous substitution are presented and discussed.

The first X-ray investigation of a phase crystallizing in the *B*31 structure type was made by Hägg [1], who proposed a tentative structure for FeAs. Later, Fylking [2] investigated several arsenides and phosphides isomorphous with FeAs, in particular MnP, and the approximate structure of this phase was determined by single-crystal and powder methods.

Among the phases with the *B*31 structure (a list is given in Ref.[3]) there are six phosphides, *viz.* CrP, MnP, FeP, CoP, WP and RuP. MnP, FeP and CoP were investigated by Fylking [2], CrP by Nowotny and Henglein [4] and by Schönberg [5], WP by Schönberg [5] and RuP by the present author [6].

The present investigation was undertaken in order to provide data for crystal-chemical comparisons in the series of isomorphous *B*31 phosphides.

EXPERIMENTAL

Preparation. The starting materials for the preparation of MnP, FeP and CoP were electrolytic manganese (AB Ferrolegeringar, Stockholm, claimed purity higher than 99.9 %), spectrographically standardized iron and cobalt rods (Johnson, Matthey & Co. Ltd., London) and red phosphorus (purity higher than 99 %). The phosphides were prepared by dropping pellets of red phosphorus into melts of the appropriate metals, contained in crucibles of pure alumina (Degussit Al 23 from Degussa, Frankfurt, Germany). The metals were melted by induction heating in a closed chamber filled with purified argon. No chemical analyses were made. Earlier preparations [7-9] using the technique described above have yielded products with purities higher than 99.5 %.

On account of the high phosphorus pressures over the molten mono-phosphides it was not possible to prepare single-phase MeP alloys [1,10]. The alloys, from which the single-crystals were selected, contained primary MeP crystals embedded in a Me_2P + MeP eutectic. Alloys with higher phosphorus contents were prepared by heating the crushed master alloys and red phosphorus in evacuated and sealed silica tubes at temperatures between 900°C and 1 150°. The phosphides of chromium, tungsten and ruthenium were

prepared by heating metal powder (electrolytic chromium from Gesellschaft für Elektrometallurgie m.b.H., Werk Nürnberg, Germany; tungsten powder, claimed purity 99.9 %, from Söderfors Bruk, Sweden; ruthenium sponge, claimed purity 99.8 %, from Heraeus, Hanau, Germany) and red phosphorus in silica tubes at 1 000°C.

X-Ray work. X-Ray powder photographs were taken with Guinier-type focussing cameras using CrKa_1 radiation, and with silicon (a = 5.4305 Å) as the internal calibration standard. The accuracy of the lattice parameter determinations is estimated to be 0.04 %. For the single-crystal work, needle-shaped crystals of MnP, FeP and CoP(maximum thickness not exceeding 0.05 mm) were used, in which the needle axis corresponded to the b axis of the crystal. Weissenberg photographs were taken about the b axis using zirconium-filtered MoK radiation, and the multiple-film technique with thin iron foils between successive films. The intensities were estimated by visual comparison with calibrated spots. Corrections for Lorentz and polarisation factors, Fourier series summations, structure factor calculations and calculations of interatomic distances were made by the electronic digital computer BESK using programmes available at BESK. Atomic scattering factors were taken from tables given by Watson and Freeman [11] for manganese, Thomas and Umeda [12] for iron and cobalt and Tomiie and Stam [13] for phosphorus. The real part of the dispersion correction, calculated by Dauben and Templeton [14] for each of the metals, was included in the structure factor calculations. Standard deviations of he atomic parameters were estimated by Cruickshank's [15] equation. (Lists of observed and calculated structure factors can be obtained from this Institute on request).

STRUCTURE DETERMINATIONS

According to Hägg [1] and Fylking [2], the $B31$ (MnP) structure, which has the symmetry *Pnma*, can be regarded as an orthorhombic distortion of the hexagonal $B8$ (NiAs) structure. The $B8$ structure (unit cell dimensions a_{B8} and c_{B8}) can also be described by the space group *Pnma* (unit cell dimensions $a = c_{B8}$, $b = a_{B8}$, $c = a_{B8} \times \sqrt{3}$), and the relation between the atomic positions in the NiAs and MnP structures is as follows.

NiAs			MnP		
	x	z		x	z
4 Ni in 4 *(c)*	0	1/4	4 Mn in 4 *(c)*	0.005	0.20
4 As in 4 *(c)*	1/4	7/12	4 P in 4 *(c)*	0.19	0.57

Starting with the approximate atomic parameters quoted above, the structures of MnP, FeP and CoP were refined by successive electron density projections and difference syntheses on the *ac*-plane, until no appreciable shifts in the atomic positions were indicated in the difference maps. An isotropic temperature factor for each crystal was applied in the structure factor calculations.

Table 1. Atomic positions and standard deviations in MnP, FeP and CoP.

Phosphide	Parameters for the metal atoms				Parameters for the phosphorus atoms			
	x	$\sigma(x)$	z	$\sigma(z)$	x	$\sigma(x)$	z	$\sigma(z)$
MnP	0.0049	0.0002	0.1965	0.0002	0.1878	0.0005	0.5686	0.0005
FeP	0.0016	0.0002	0.2006	0.0002	0.1913	0.0005	0.5684	0.0004
CoP	0.0007	0.0002	0.1984	0.0002	0.1917	0.0006	0.5814	0.0006

Table 2. Number of observed (*h0l*) reflexions, reliability index, and temperature factor for MnP, FeP and CoP.

Phosphide	Number of observed (*h0l*) reflexions	Reliability index $\Sigma\|F_o-F_c\|/\Sigma\|F_o\|$	Temperature factor B (Å^2)
MnP	119	0.075	0.29_0
FeP	106	0.054	0.25_7
CoP	101	0.072	0.29_6

Table 3. Unit cell dimensions for *B*31 type phosphides (Å units. Estimated accuracy 0.04 %).

Phosphide	Unit cell dimensions			Volume	$c/(b\times\sqrt{3})$
	a	b	c	U	
CrP	5.362	3.113	6.018	100.5	1.116
MnP	5.258	3.172	5.918	98.7	1.077
FeP	5.191	3.099	5.792	93.2	1.079
CoP	5.077	3.281	5.587	93.1	0.983
WP	5.734	3.249	6.222	115.9	1.106
RuP	5.520	3.168	6.120	107.0	1.115

Table 4. Interatomic distances in MnP, FeP and CoP (Å) (Distances shorter than 3.5 Å listed).

Type of distance	Number of equivalent distances	MnP	FeP	CoP
Me-Me	2	2.70_4	2.65_8	2.60_3
	2	2.81_6	2.79_3	2.75_8
	2	3.17_2	3.09_9	3.28_1
Me-P	1	2.28_9	2.24_1	2.21_5
	2	2.34_0	2.27_9	2.27_1
	1	2.40_3	2.34_7	2.34_9
	2	2.38_7	2.35_1	2.35_7
P-P	2	2.66_0	2.64_1	2.70_3
	2	3.17_2	3.09_9	3.28_1
	2	3.39_4	3.34_1	3.16_1
	4	3.42_0	3.34_1	3.29_3

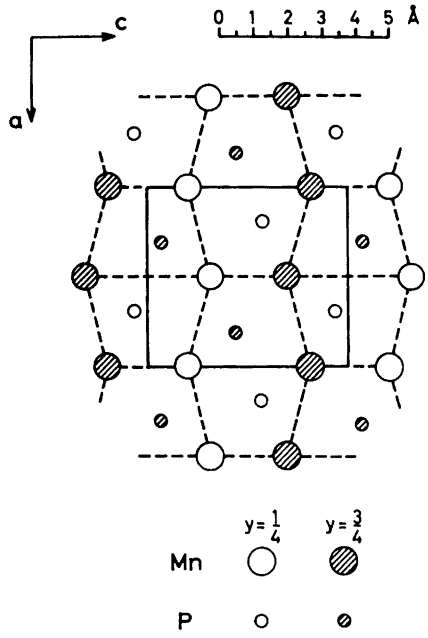

Fig. 1. The structure of MnP projected on (010).

The final atomic parameters are given in Table 1. The number of recorded $F(h0l)$-values, the temperature factor and the reliability index for each crystal are given in Table 2. Unit cell dimensions are listed in Table 3 and interatomic distances in Table 4.

DESCRIPTION OF THE STRUCTURES

A projection of the MnP structure on the *ac*-plane is shown in Fig. 1. The metal atoms have four near metal neighbours, while another two metal neighbours (in the *b* direction) are more distant. Each metal atom has six near phosphorus neighbours situated in a distorted octahedral configuration. The phosphorus atoms are surrounded by six metal atoms at the corners of a highly distorted triangular prism. The triangular prismatic metal coordination about the phosphorus atoms has been found in several phosphides, *e.g.* in Fe_2P ($C22$ type)[16], Co_2P ($C23$ type)[7], Pd_3P (DO_{11} type)[17] and in Rh_4P_3[8]. In the last-mentioned phosphides, the phosphorus atoms have no phosphorus neighbours closer than 3.0 Å. In the $B31$ type phosphides, however, there are zig-zag chains of phosphorus atoms extending in the *b* direction with the P-P distance 2.66 Å in MnP, 2.64 Å in FeP and 2.70 Å in CoP. This may indicate a tendency to P-P bond formation in these phases.

ISOMORPHOUS SUBSTITUTION IN *B*31 STRUCTURES

Unit cell dimensions (as determined in the present investigation) for the six phosphides crystallizing in the *B*31 structure are given in Table 3. The values for MnP, FeP and CoP are in good agreement with those obtained by Fylking [2], whereas the values for CrP and WP are somewhat different from those quoted by Nowotny and Henglein [4] and by Schönberg [5]. Lattice parameter variations indicating extended homogeneity ranges were not observed for any of these phases. As seen from Table 3, the unit cell volumes follow the same sequence as the radii of the metal constituents, but the values for the *b* axis display irregularities. For instance, the largest *b* axis is found for CoP, which has the smallest unit cell volume.

The structural properties of the *B*31 phases have been given particular consideration by Schubert *et al.*[18-21] Schubert divides the *B*31 phases into two classes. In one class, denoted *B*31 *(l)*, the ratio c/b is larger than $\sqrt{3}$ (the value for the ideal *B*8 structure), in the other, denoted *B*31 *(k)* the radio is smaller than $\sqrt{3}$. Schubert points out that *B*31 *(l)* seems to be stable at lower, and *B*31 *(k)* at higher electron concentrations.

Among the phosphides, CoP is the only *B*31 *(k)* phase (see Table 3). The present author has found complete solid solubility of FeP, MnP and CrP in CoP. It is therefore possible to study the "transition" from the *B*31 *(k)* to the *B*31 *(l)* class by the substitution of iron, manganese or chromium for cobalt. Lattice parameter measurements on (Co,Me)P alloys (Me = Fe, Mn, Cr) indicate deviations from Vegard's law. It is interesting to note that the compositions for the alloys with $c/b = \sqrt{3}$ were found to be approximately $Co_{0.6}Fe_{0.4}P$, $Co_{0.8}Mn_{0.2}P$ and $Co_{0.87}Cr_{0.13}P$, which implies that the number of electrons is roughly constant at this c/b ratio.

It is also possible to study the effect of isomorphous substitution for phosphorus by other non-metals in the *B*31 type phosphides. There is, for instance, a considerable solubility of silicon in FeP and CoP, and boron dissolves to some extent in CoP[9]. (There are, however, no indications of any appreciable solubility of sulphur in FeP or CoP). Since the atomic radius of silicon is larger,

Table 5. Unit cell dimensions for ternary *B*31 type phases. (Å units. Estimated accuracy 0.04 %).

Composition	Unit cell dimensions			Volume	$c/(b \times \sqrt{3})$
	a	*b*	*c*	*U*	
CoP	5.077	3.281	5.587	93.0_7	0.983
$CoP_{0.6}Si_{0.4}$	5.060	5.264	5.653	93.4	1.000
$CoP_{0.9}B_{0.1}$	5.050	3.277	5.623	93.0_5	0.991
FeP	5.191	3.099	5.792	93.2	1.079
$FeP_{0.5}Si_{0.5}$	5.242	3.059	5.853	93.9	1.105

and the boron radius is smaller than that of phosphorus, the volume of the CoP unit cell should increase on P/Si substitution and decrease on P/B substitution. If Schubert's hypothesis is correct, the c/b ratio should increase in both cases. The values given in Table 5 show that this is in fact the case. (The compositions given in the table are only approximate).

From the above-mentioned observations it is clear that the unit cell dimensions for $B31$ phases are dependent on "electronic factors" as stressed by Schubert.

The data from the structure determinations do not indicate any marked structural difference between $B31$ *(l)* and $B31$ *(k)* phases.

Acknowledgements. This work has been financially supported by the *Swedish State Council of Technical Research* and by the *Air Force Office of Scientific Research of the Air Research and Development Command, United States Air Force*, through its European Office under contract No. AF 61(052)-40. Facilities for use of the electronic digital computer BESK were given by the *Swedish Board for Computing Machinery.*

The author wishes to thank Professor G. Hägg for his kind interest in this work.

REFERENCES

1. Hägg, G. *Nova Acta Regiae Soc. Sci. Upsaliensis* Ser. IV, **7** (1929) No 1.
2. Fylking, K.-E. *Arkiv Kemi, Mineral. Geol.* **11 B** (1935) No. 48.
3. Pearson, W. B. *A Handbook of Lattice Spacings and Structures of Metals and Alloys.* Pergamon Press, London—New York—Paris—Los Angeles 1958, p. 249.
4. Nowotny, H. and Henglein, E. *Z. anorg. Chem.* **239** (1938) 14.
5. Schönberg, N. *Acta Chem. Scand.* **8** (1954) 226.
6. Rundqvist, S. *Nature* **185** (1960) 31.
7. Rundqvist, S. *Acta Chem. Scand.* **14** (1960) 1961.
8. Rundqvist, S. and Hede, A. *Ibid.* **14** (1960) 893.
9. Rundqvist, S. *Ibid.* **16** (1962) 1.
10. Haughton, J. L. *J. Iron Steel Inst.* **115** (1927) 417.
11. Watson, R. E. and Freeman, A. I. *Acta Cryst.* **14** (1961) 27.
12. Thomas, L. H. and Umeda, K. *J. Chem. Phys.* **26** (1957) 293.
13. Tomiie, Y. and Stàm, C. H. *Acta Cryst.* **11** (1958) 126.
14. Dauben, C. H. and Templeton, D. H. *Ibid.* **8** (1955) 841.
15. Cruickshank, D. W. J. *Ibid.* **2** (1949) 65.
16. Rundqvist, S. and Jellinek, F. *Acta Chem. Scand.* **13** (1959) 451.
17. Rundqvist, S. and Gullman, L.-O. *Ibid.* **14** (1960) 2246.
18. Pfisterer, H. and Schubert, K. *Z. Metallkunde* **41** (1950) 358.
19. Esslinger, P. and Schubert, K. *Ibid.* **48** (1957) 126.
20. Schubert, K. and Esslinger, P. *Ibid.* **48** (1957) 193.
21. Schubert, K. *Z. Naturforsch.* **12** (1957) 310.

Received September 19, 1961.

ACTA CHEMICA SCANDINAVICA 16 (1962) 293–296

Studies on Rutile-Type Phases in Mixed Transition Metal Dioxides II *

BENGT-OLOV MARINDER, EBBA DORM and MADELEINE SELEBORG

Institute of Inorganic and Physical Chemistry, University of Stockholm, Stockholm, Sweden

Rutile-type phases have been found to exist over wide ranges of composition in the systems TiO_2–NbO_2, TiO_2–MoO_2, NbO_2–CrO_2, and NbO_2–MoO_2. The phases show short metal-metal distances which are reflected in the low values of the axial ratio c/a. The relation to the concentration of valence electrons not engaged in metal-oxygen bonding is discussed.

It has previously been shown that remarkably short metal-metal distances exist in several dioxides of transition metals. This is the case for the dioxides of MoO_2 type, for the orthorhombic modification of rhenium dioxide and for rutile type phases observed in several systems of transition metal dioxides [1–3]. It has also been pointed out that there exists a close relationship between the metal-metal distances and the number of excess valence electrons available per close metal-metal contact [1,2]. This relation is particularly evident if some kind of normalized metal-metal distance is used, giving a certain allowance for the different sizes of the metal atoms. For the rutile-type phases the axial ratio c/a has been found to provide an appropriate normalized distance [3]. In order to investigate the validity of this observation, some further pseudo-binary systems of transition metal dioxides have been studied. The investigations have been concentrated on rutile-type phases. A thorough phase analysis was not aimed at.

The samples investigated comprised mixed dioxides of titanium, niobium, chromium and molybdenum. The starting materials were all of high purity. The samples were generally prepared by heating appropriate mixtures of oxides and metals in sealed, evacuated silica tubes and keeping the temperature at about 1 000°C for two days. Since the solubility of MoO_2 in TiO_2 (rutile) was found to be rather limited in specimens prepared in this way, the samples for the $(Ti,Mo)O_2$ systems were melted in an electric arc furnace and then tempered in evacuated silica capsules for two days at about 1 300°C.

* I, see Ref.[4]

Table 1. Methods of preparation and results of phase analyses.

System	Starting materials	Composition of sample	Heating temperature	X-Ray evidence	Unit cell dimensions of rutile type phase			Ref.
					a Å	*c* Å	*c*/*a*	
TiO_2-NbO_2	TiO_2 (anatase)	$Ti_{0.75}Nb_{0.25}O_2$	1 000°C	Rutile	4.659	2.986	0.6409	4
	Nb_2O_5, Nb	$Ti_{0.50}Nb_{0.50}O_2$		»	4.719	2.997	0.6351	4
		$Ti_{0.25}Nb_{0.75}O_2$		»	4.778	2.999	0.6277	4
		$Ti_{0.20}Nb_{0.80}O_2$		»	4.789	2.999	0.6265	
		$Ti_{0.10}Nb_{0.90}O_2$		»	4.822	3.000	0.6221	
TiO_2-MoO_2	TiO_2 (anatase)	$Ti_{0.75}Mo_{0.25}O_2$	1 300°C	»	4.643	2.939	0.6330	
	MoO_3, Mo	$Ti_{0.50}Mo_{0.50}O_2$		»	4.716	2.899	0.6147	
NbO_2-CrO_2	Nb_2O_5, Nb	$Nb_{0.71}Cr_{0.29}O_2$	1 000°C	»	4.735	3.008	0.6353	
	Cr_2O_3	$Nb_{0.69}Cr_{0.31}O_2$		»	4.727	3.004	0.6355	
		$Nb_{0.67}Cr_{0.33}O_2$		»	4.718	3.006	0.6371	
		$Nb_{0.60}Cr_{0.40}O_2$		»	4.691	3.019	0.6436	
		$Nb_{0.50}Cr_{0.50}O_2$		»	4.645	3.014	0.6489	
		CrO_2		»	4.423	2.917	0.6595	5
NbO_2-MoO_2	Nb_2O_5, Nb	$Nb_{0.60}Mo_{0.40}O_2$	1 000°C	»	4.856	2.925	0.6023	
	MoO_3, Mo	$Nb_{0.50}Mo_{0.50}O_2$		»	4.858	2.912	0.5994	
		$Nb_{0.33}Mo_{0.67}O_2$		»	4.855	2.883	0.5938	4
		$Nb_{0.25}Mo_{0.75}O_2$		»	4.855	2.863	0.5897	
VO_2-CrO_2	V_2O_3, V_2O_5, Cr_2O_3	$V_{0.85}Cr_{0.15}O_2$	1 000°C	Distorted rutile				

The preparations were studied by means of X-ray powder photographs obtained in a Guinier focusing camera with strictly monochromatized Cu$K\alpha_1$ radiation.

The methods of preparation and the results of the phase analyses are summarized in Table 1. Fig. 1 represents the volume and the *c*/*a* parameter of the rutile-type phases *versus* the composition of the samples investigated in this and in a previous study [4]. The distortion of the unit cell is obvious for most systems. Thus while the volumes change almost linearly with composition, the axial ratios are far from constant, decreasing markedly with increasing contents of the metal of higher valency except in the systems containing chromium (*v. infra*). This is also demonstrated in Fig. 2 which gives the *c*/*a*-values *versus n*, the number of excess valence electrons per close metal-metal contact. The character of the curves is in general agreement with the previously reported observation that *c*/*a* (and in most cases also the metal-metal distance) decreases with increasing *n*. However, the present data also illustrate the minor influence of the individual character of the various metals on the axial ratio. Thus when comparing systems containing titanium as a common component, the lowering of *c*/*a* is increased by the other metal in the order vanadium, niobium, molybdenum at compositions with the same concentration of valence

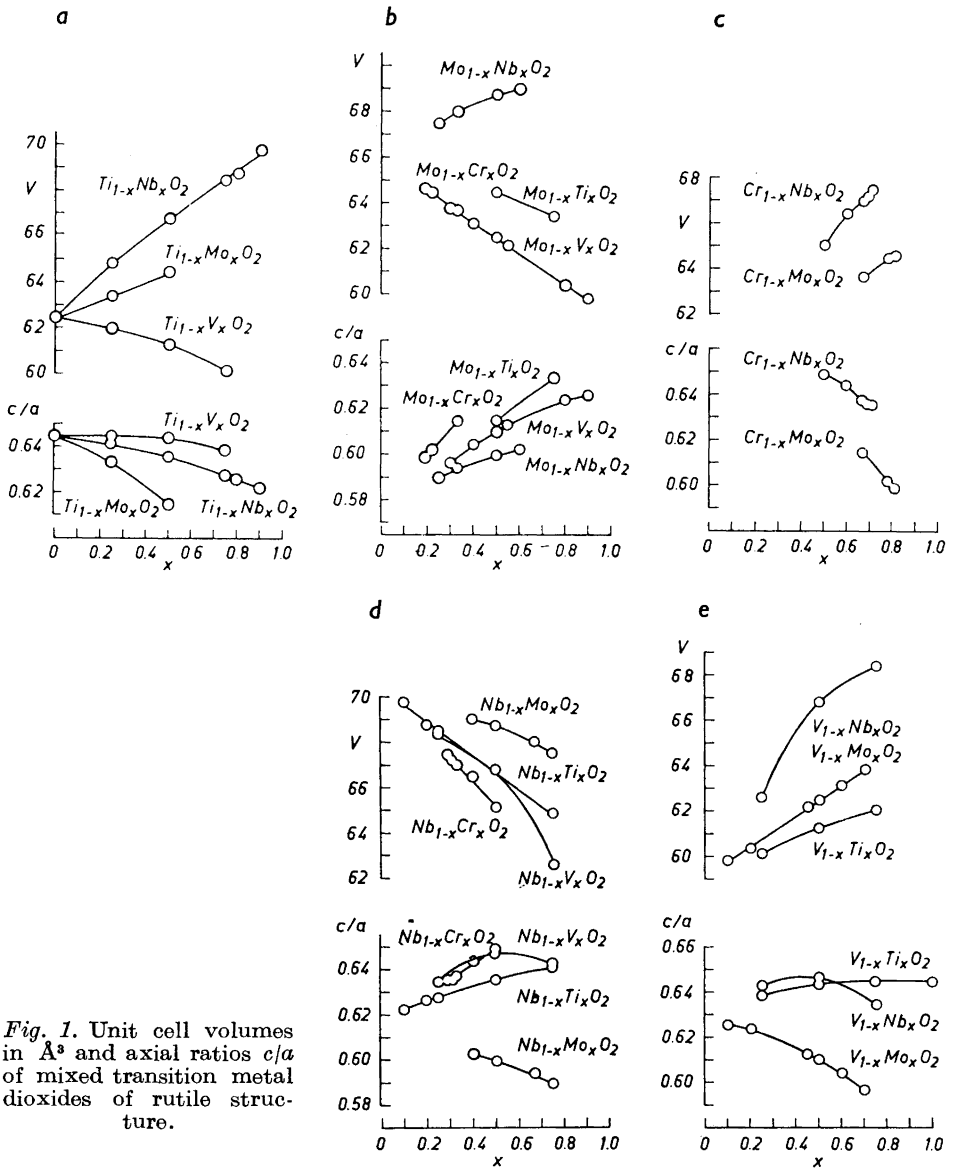

Fig. 1. Unit cell volumes in Å³ and axial ratios c/a of mixed transition metal dioxides of rutile structure.

electrons (*cf.* Fig. 2). In the systems containing molybdenum the axial ratio is lowered more by niobium than by vanadium, the latter two metals contributing the same number of valence electrons. In this connection the variation of c/a with the composition of the $(V,Nb)O_2$ rutile phase is of interest (*cf.* Figs. 1d and 1e).

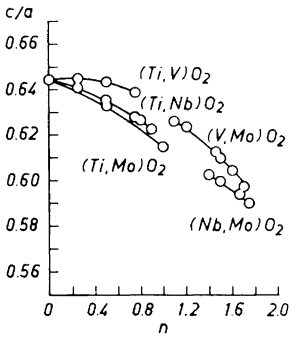

Fig. 2. Axial ratios (c/a) of mixed transition metal dioxides of rutile structure *versus* number of excess valence electrons per close metal-metal contact (n).

The present study confirms the divergent behaviour shown by chromium in rutile-type phases including chromium dioxide [5,6]. Thus the depression of c/a is less for chromium than for titanium and molybdenum in rutile samples containing niobium (Fig. 1d) and less than for titanium, vanadium and niobium in samples with molybdenum as the other component (Fig. 1b). The presence of excess valence electrons contributed by chromium atoms evidently does not cause a reduction of the metal-metal distance or the axial ratio similar to that produced by, for example, the "isoelectronic" molybdenum atoms. The calculation of n values disregarding the chromium electrons is somewhat arbitrary as it involves the assignment of a numerical valency to chromium. On the other hand an estimation of the charge of the chromium atoms from the c/a values of the present rutile phases would be rather uncertain (*cf.* Ref. [6]).

Further studies on these phases including magnetic measurements and X-ray investigations at elevated temperatures are being planned.

The authors wish to express their gratitude to Professor Arne Magnéli for many valuable discussions.

This investigation has been carried out within a research programme financially supported by the *Swedish Natural Science Research Council.*

REFERENCES

1. Magnéli, A. and Andersson, G. *Acta Chem. Scand.* **9** (1955) 1378.
2. Magnéli, A. *Acta Cryst.* **9** (1956) 1038.
3. Marinder, B.-O. and Magnéli, A. *Acta Chem. Scand.* **11** (1957) 1635.
4. Marinder, B.-O. and Magnéli, A. *Acta Chem. Scand.* **12** (1958) 1345.
5. Wilhelmi, K.-A. and Jonsson, O. *Acta Chem. Scand.* **12** (1958) 1532.
6. Sundholm, A., Andersson, S., Magnéli, A. and Marinder, B.-O. *Acta Chem. Scand.* **12** (1958) 1343.

Received September 7, 1961.

ACTA CHEMICA SCANDINAVICA 16 (1962) 297–310

Synthese N^7-alkylierter 7-Aminosulfonyl-6-trifluormethyl-2,3-dihydro-4*H*-1,2,4-benzothiadiazin-1,1-dioxyde

PETER W. FEIT

Forschungslaboratorium der Leo Pharmaceutical Products, Ballerup, Dänemark

Durch Rhodanierung von 2-Amino-4-trifluormethyl-benzolsulfonamid (III) wird die 5-Rhodanverbindung IV dargestellt und über die Rhodanfunktion zum entspr. Diphenyldisulfid V verknüpft. Oxydierende hydrolytische Disproportionierung des Disulfides zur Sulfinsäure VI und anschliessende oxydierende Chlorierung liefert 4-Amino-5-aminosulfonyl-2-trifluormethyl-benzolsulfochlorid (VII). Aus ihm werden auf zwei Wegen (A und B) 3-substituierte N^7-alkylierte 7-Aminosulfonyl-6-trifluormethyl-2,3-dihydro-4*H*-1,2,4-benzothiadiazin-1,1-dioxyde (XII) erhalten. Eine dritte Variation (Weg C) führt von der Disulfidstufe V aus über mehrere Stufen ebenfalls zu XII.

7-Aminosulfonyl-6-trifluormethyl-2,3-dihydro-4*H*-1,2,4-benzothiadiazin-1,1-dioxyd (I) und dessen 3-Alkylderivate [1–5] — insbesondere die 3-Benzylverbindung [1] — zeigen bei peroraler Verabreichung einen ausgeprägten diuretischen und saluretischen Effekt. Es erschien daher interessant, bisher

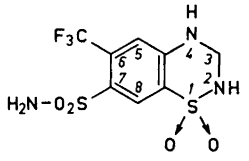

I

unbekannte N^7-alkylierte Vertreter (XII) dieser Verbindungsklasse zu synthetisieren und auf ihre saluretische Wirkung zu prüfen. In vorliegender Arbeit wird eine allgemein anwendbare und konstitutionsbeweisende Synthese solcher Verbindungen beschrieben, die in einer ihrer Varianten gleichzeitig die bisher ebenfalls unbekannten N^4-alkylierten 2,4-Bis-aminosulfonyl-5-trifluormethyl-aniline (VIII) zugänglich macht.

Ein Weg zur Darstellung der den Trifluormethyl-Verbindungen entsprechenden N^4-alkylierten 5-Chlor-2,4-bis-aminosulfonyl-aniline (und somit auch der aus diesen durch Ringschluss mit Aldehyden erhältlichen N^7-alkylierten 6-Chlor-7-aminosulfonyl-2,3-

dihydro-4*H*-1,2,4-benzothiadiazin-1,1-dioxyde) ist inzwischen veröffentlicht worden. Novello und Mitarbb.[3] erhielten durch Umsetzung von 6-Chlor-7-aminosulfonyl-4*H*-1,2,4-benzothiadiazin-1,1-dioxyd mit Chlorsulfonsäure das 7-Sulfochlorid, welches nach Reaktion mit Methylamin bzw. Dimethylamin und anschliessender alkalischer Hydrolyse unter Ringspaltung N^4-Methyl- sowie N^4-Dimethyl-5-chlor-2,4-bis-aminosulfonyl-anilin lieferte. Werner und Mitarbb.[4] beschrieben die partielle Methylierung von 6-Chlor-7-aminosulfonyl-4*H*-1,2,4-benzothiadiazin-1,1-dioxyd mit Dimethylsulfat zur N^7-Methylverbindung. Nach Reduktion mit Natriumborhydrid erhielten die Autoren das entsprechende 2,3-Dihydro-4*H*-1,2,4-benzothiadiazin-1,1-dioxyd. Dieses Resultat steht jedoch nicht in Einklang mit der von Novello und Mitarb.[3] gemachten Erfahrung, nach welcher die Alkylierung vorzugsweise in 4-Stellung hätte erfolgen sollen.

Der hier eingeschlagene Syntheseweg geht aus nachfolgendem Formelschema hervor. Die Einwirkung von nascierendem Rhodan in Eisessig, aus Ammoniumrhodanid und Brom gewonnen *, auf 2-Amino-4-trifluormethyl-benzolsulfonamid (III)[6] ** lieferte 2-Amino-5-rhodan-4-trifluormethyl-benzolsulfonamid (IV). Es war jedoch ein grosser Überschuss an Rhodan notwendig, da sich bei der durch den substitutionshemmenden Einfluss der Trifluormethylgruppe bedingten Reaktionstemperatur ein grosser Teil durch Polyrhodanbildung der Reaktion entzog. Die Behandlung des Rhodanides IV mit wässrigem Alkali bei Raumtemperatur führte wider Erwarten nicht zu dem gewünschten Disulfid V. Nach dem Ansäuern der Reaktionsmischung konnte nur ein unreines Thiophenol isoliert werden, dessen Analyse im Vergleich mit dem ebenfalls zu erwartenden 4-Amino-5-aminosulfonyl-2-trifluormethyl-thiophenol (II) erhöhten Stickstoffgehalt aufwies. Dieses Ergebnis bedarf noch weiterer Untersuchungen und ist wahrscheinlich auf die Bildung eines Harnstoffderivates durch Reaktion mit der bei der alkalischen Spaltung der S-C-Bindung von Rhodaniden entstehenden Cyansäure *** zurückzuführen. Hingegen konnte V aus dem Rhodanid IV durch Erwärmen mit 2,5 proz. wässrigem Ammoniak erhalten werden. Da eine direkte oxydierende Chlorierung von V der ungeschützten aromatischen Aminfunktion wegen aussichtslos erschien, wurde zur Darstellung des Benzolsulfochlorides VII der Weg über die Sulfinsäure VI eingeschlagen. Es zeigte sich nämlich, dass V in 4 N NaOH bei Raumtemperatur leicht hydrolytisch disporportioniert[7], wobei die erhöhte Löslichkeit auf Grund der an der Sulfonamidgruppe erfolgenden Salzbildung von Vorteil war. Das hierbei entstehende, in Wasser schwer lösliche Thiophenol (II) konnte nach Ansäuren leicht von der in Lösung bleibenden Sulfinsäure VI abgetrennt werden. Nach Oxydation von II mit Wasserstoffperoxyd wurde V zurückerhalten. Um die Ausbeute an Sulfinsäure VI zu erhöhen, lag es nahe, die hydrolytische Disproportionierung des Disulfides oxydierend durchzuführen. Da nach Durchleiten von Sauerstoff die isolierbare Menge an Thiophenol kaum abnahm, liessen wir Perhydrol als Oxydations-

* Auch Alkalirhodanid und Brom oder Chlor war anwendbar.

** In den hiesigen Laboratorien wurde III unabhängig von diesen Autoren auf gleichem Wege gewonnen. *m*-Trifluormethyl-anilin ergab im Backverfahren 2-Amino-5-trifluormethyl-benzolsulfonsäure, aus welcher mit Chlorsulfonsäure und Thionylchlorid bei 80°C das Sulfochlorid, und aus diesem mit wässrigem Ammoniak III erhalten wurde. Ausbeute bezogen auf *m*-Trifluormethyl-anilin 50–60 % (Schønfeldt, E. und Thorsteinsson, Th. *Unveröffentlicht*).

*** Zum Mechanismus der S–C-Bindungsspaltung bei Rhodaniden: Tarbell, D. S. und Harnisch, D. P. *Chem. Revs.* **49** (1951) 79.

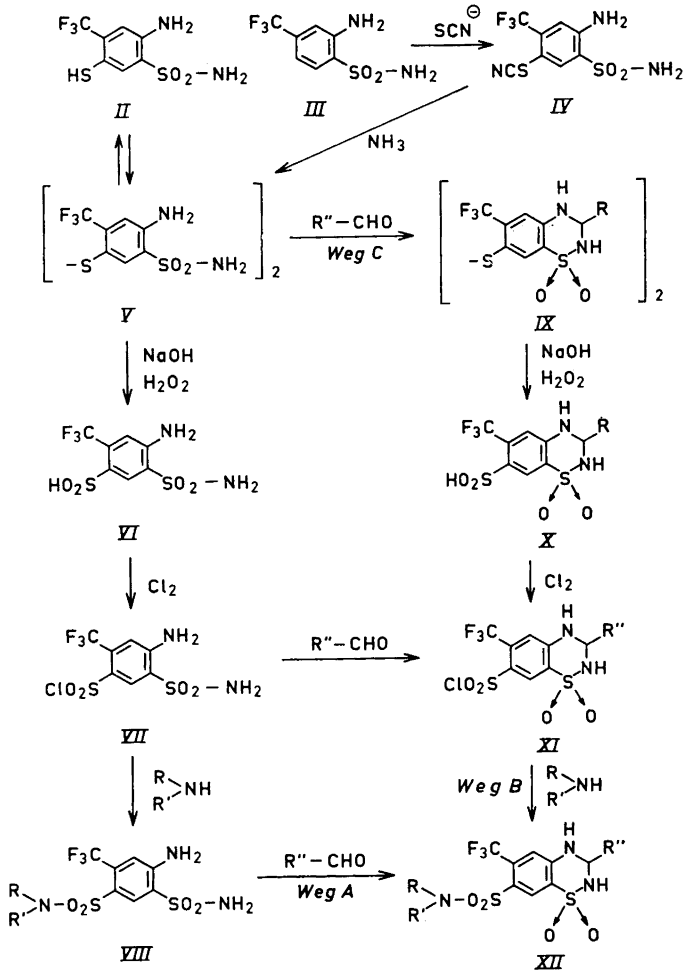

mittel in die Reaktionslösung eintropfen. Um die hierbei nicht restlos zu verhindernde Oxydation der entstehenden Sulfinsäure VI zur Sulfonsäure weitgehend zu unterdrücken und gleichzeitig eine möglichst vollständige Reaktion zu erzielen, wurden die im Versuchsteil angegebenen Reaktionsbedingungen hinsichtlich Temperatur, Wasserstoffperoxydmenge und Zeit durch potentiometrische Verfolgung der Reaktion ermittelt. Die Titrationen wurden in alkalischem Medium an Platinelektroden mit Kaliumpermanganatlösung in Gegenwart von Mangandioxyd durchgeführt und ergaben einen Endgehalt von ungefähr 80 % d. Th. an Sulfinsäure. Die Säure wurde als solche nicht isoliert,

Tab. 1. Saluretischer Effekt der N^4-alkylierten 2,4-Bis-aminosulfonyl-5-trifluormethyl-aniline (VIII).

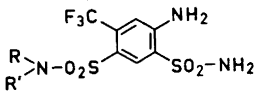

	R	R′	Schmp. °C	Saluretischer Effekt [a]
1	CH_3	H	167,5—169	I
2	CH_3	CH_3	199—200	I
3	i-C_3H_7	H	176,5—178	I
4	n-C_4H_9	H	119—120	0
5	n-C_4H_9	n-C_4H_9	113—114	0
6	C_6H_{11}	H	193,5—195,5	0
7	$CH_2{\cdot}C_6H_5$	H	199,5—201,5	0—I
8	C_6H_5	H	177—178	0

a 0: unwirksam bei 20 mg/kg
I: wirksam in der Grössenordnung von 6-Chlor-7-aminosulfonyl-1,2,4-benzothiadiazin-1,1-dioxyd (Chlorthiazid); vgl. Lund und Kobinger [1].

sondern in salzsaurer Lösung mit der berechneten Menge Chlor oxydierend halogeniert, wobei das Sulfochlorid VII kristallin anfiel. Nachfolgende Umsetzung mit Ammoniak ergab 2,4-Bis-aminosulfonyl-5-trifluormethyl-anilin, welches sich mit auf anderem Wege [1,2,4-6] zugänglichem Material vom gleichen Schmp. als identisch erwies. Mit Aminen wurden die N^4-alkylierten Verbindungen VIII (Tab. 1) erhalten, die durch Kondensation mit Aldehyden unter Ringschluss — in Analogie zum 2,4-Bis-aminosulfonyl-5-trifluormethyl-anilin selbst [1-4] — in die entsprechenden N^7-alkylierten 7-Aminosulfonyl-6-trifluormethyl-2,3-dihydro-4*H*-1,2,4-benzothiadiazin-1,1-dioxyde (XII) (Tab. 2, Weg A) übergeführt werden konnten.

Die verhältnismässig gute Hydrolysenbeständigkeit des Sulfochlorides VII ermöglichte weiterhin dessen Kondensation mit Aldehyden zu den entsprechenden 3-substituierten 6-Trifluormethyl-2,3-dihydro-4*H*-1,2,4-benzothiadiazin-1,1-dioxyd-7-sulfochloriden (XI), wenn durch geeignete Reaktionsbedingungen das entstehende Wasser laufend aus der Reaktionsmischung entfernt wurde. Die wasserfrei durchgeführte Umsetzung von XI mit Aminen ergab wiederum die entsprechenden Dihydro-1,2,4-benzothiadiazin-1,1-dioxyde XII (Tab. 2, Weg B). Wurde mit Phenylacetaldehyd kondensiert und das erhaltene Sulfochlorid XI (R″ = $CH_2 \cdot C_6H_5$) mit Ammoniak in tert. Butylalkohol zur Reaktion gebracht, so entstand 7-Aminosulfonyl-6-trifluormethyl-3-benzyl-2,3-dihydro-4*H*-1,2,4-benzothiadiazin-1,1-dioxyd, welches sich mit authentischem Material [1] als identisch erwies.

Eine weitere Variationsmöglichkeit (Weg C) ergab sich durch Kondensationsreaktion bereits auf der Disulfidstufe. Das Disulfid V wurde mit Phenylacetaldehyd zum 1,1;1′,1′-Bis-dioxyd des Bis-[6-trifluormethyl-3-benzyl-2,3-dihydro-4*H*-1,2,4- benzothiadiazinyl (7)]-disulfids (IX) kondensiert und dieses

Tab. 2. Saluretischer Effekt der N^7-alkylierten 7-Aminosulfonyl-6-trifluormethyl-2,3-dihydro-4*H*-1,2,4-benzothiadiazin-1,1-dioxyde (XII).

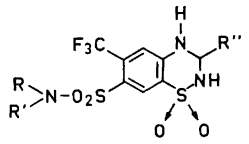

	R	R′	R″	Synthese-weg	Schmp. °C	Saluretischer Effekt [a]
1	*i*-C_3H_7	H	H	A	189,5—191,5	II
2	*n*-C_4H_9	*n*-C_4H_9	H	A	131—132	0
3	C_6H_{11}	H	H	A	283,5—284,5 (280)	<I
4	CH_3	CH_3	CH_3	B	175,5—177,5	II
5	*i*-C_3H_7	H	CH_3	A	258—260	I—II
6	*n*-C_4H_9	*n*-C_4H_9	CH_3	A	136—138	<I
7	C_6H_{11}	H	CH_3	A	212,5—214	<I
8	$CH_2{\cdot}C_6H_5$	H	CH_3	B	210—211,5	I—II
9	*i*-C_3H_7	H	*i*-C_3H_7	A	247—249	I—II
10	*n*-C_4H_9	*n*-C_4H_9	*i*-C_3H_7	A	131—133	<I
11	C_6H_{11}	H	*i*-C_3H_7	A	232—234	I—II
12	CH_3	CH_3	*n*-C_4H_9	B	184,5—186,5	II
13	*i*-C_3H_7	H	*n*-C_4H_9	B	212,5—214,5	II
14	*n*-C_4H_9	*n*-C_4H_9	*n*-C_4H_9	A, B	127—129	I—II
15	C_6H_{11}	H	*n*-C_4H_9	B	192,5—194	I—II
16	*n*-C_4H_9	*n*-C_4H_9	*n*-C_5H_{11}	B	135—137	I—II
17	C_6H_{11}	H	*n*-C_5H_{11}	B	183—185	II
18	$CH_2{\cdot}C_6H_5$	H	*n*-C_5H_{11}	B	145—147	II—III
19	CH_3	H	$CH_2{\cdot}C_6H_5$	B	263,5—265	II—III
20	CH_3	CH_3	$CH_2{\cdot}C_6H_5$	B	240,5—243	II—III
21	*i*-C_3H_7	H	$CH_2{\cdot}C_6H_5$	B	230,5—232	> II
22	*n*-C_4H_9	H	$CH_2{\cdot}C_6H_5$	B	224—225	II—III
23	*n*-C_4H_9	*n*-C_4H_9	$CH_2{\cdot}C_6H_5$	B	197—199	> II
24	C_6H_{11}	H	$CH_2{\cdot}C_6H_5$	B	212—214	> II
25	$CH_2{\cdot}C_6H_5$	H	$CH_2{\cdot}C_6H_5$	B	201,5—202,5	III
26	C_6H_5	H	$CH_2{\cdot}C_6H_5$	B	182,5—183,5	0—I

a 0: unwirksam bei 20 mg/kg
I: wirksam in der Grössenordung von 6-Chlor-7-aminosulfonyl-1,2,4-benzothiadiazin-1,1-dioxyd (Chlorthiazid)
II: wirksam in der Grössenordnung von 7-Aminosulfonyl-6-trifluormethyl-2,3-dihydro-4*H*-1,2,4-benzothiadiazin-1,1-dioxyd (Hydroflumethiazid)
III: wirksam in der Grössenordnung von 7-Aminosulfonyl-6-trifluormethyl-3-benzyl-2,3-dihydro-4*H*-1,2,4-benzothiadiazin-1,1-dioxyd (Benzylhydroflumethiazid).
I:II:III = 1:15:90.
Methodik vgl. Lund und Kobinger [1].

in Analogie zu V über die entsprechende Sulfinsäure X in das Sulfochlorid XI (R″ = $CH_2{\cdot}C_6H_5$) übergeführt. X konnte als Acetonitril- oder auch Acetonaddukt kristallin erhalten werden. Das Natriumsalz erwies sich, ebenso

wie die Sulfinsäure selbst, als in Wasser schwer löslich, was bei der oxydierenden Chlorierung zum Sulfochlorid XI gegenüber der leicht löslichen Sulfinsäure VI veränderte Reaktionsbedingungen erforderte.

Bisher nicht synthetisierte N^2- und verschieden N^2,N^4-alkylierte 2,4-Bis-aminosulfonyl-5-trifluormethyl-aniline sollten auf prinzipiell dem gleichen Weg, der zur Darstellung der N^4-alkylierten Verbindungen beschritten wurde (Formelschema), zugänglich werden, wenn anstatt III die entsprechenden 2-Amino-4-trifluormethyl-benzolsulfonsäure-alkylamide verwendet würden. Um diese Möglichkeit zu prüfen, wurde 2-Amino-4-trifluormethyl-benzolsulfochlorid [6] mit Monomethylamin zum Methylamid umgesetzt, und aus diesem analog III, jedoch unter speziell abgestimmten Reaktionsbedingungen, nach Rhodanierung über das Disulfid und die entsprechende Sulfinsäure 4-Amino-5-methylaminosulfonyl-2-trifluormethyl-benzolsulfochlorid dargestellt. Nach Umsetzung mit Dimethylamin wurde hieraus 2-Methylaminosulfonyl-4-dimethylaminosulfonyl-5-trifluormethyl-anilin erhalten. Die Umsetzung mit Ammoniak ergab die entspr. 4-Aminosulfonylverbindung, identisch mit auf anderem Wege gewonnenem Material *.

Der bei peroraler Verabreichung an Ratten ermittelte saluretische Effekt der alkylierten Sulfonamide VIII und XII ist aus den Tabellen 1 und 2 ersichtlich.

Herrn Dr. W. Kobinger danke ich für die pharmakologische Untersuchung der Verbindungen und für die Überlassung der Ergebnisse. Herrn cand. pharm. P. Mørch sei für die Ausarbeitung der potentiometrischen Titration und Herrn Civil-Ing. E. Juhl Nielsen für wertvolle Diskussion gedankt.

BESCHREIBUNG DER VERSUCHE **

Alle Schmelzpunkte sind unkorrigiert.

2-Amino-5-rhodan-4-trifluormethyl-benzolsulfonamid (IV) Einer Mischung aus 120 g 2-Amino-4-trifluormethyl-benzolsulfonamid [6] (III), 190 g Ammoniumrhodanid und 360 ml Eisessig liess man innerhalb von 1 ½ Std. unter gutem Rühren und Kühlen bei 15—20°C eine Lösung von 60 ml Brom in 90 ml Eisessig zutropfen. Danach wurde noch 2 Std. bei 18—20°C gerührt, wobei durch teilweises Auskristallisieren des Reaktionsproduktes und durch Polyrhodanbildung ein dicker Brei entstand. Es wurde unter Eiskühlung mit 1,5 l Wasser verdünnt, 40 Min. gerührt, abgesaugt und gut mit Wasser gewaschen. Zur Entfernung des Polyrhodan wurde der noch schwach feuchte Filterkuchen mit 1,2 l Methanol gerührt und über Filtererde filtriert. Es wurde dreimal mit insgesamt 300 ml

* Dargestellt analog der entsprechenden 5-Chlorverbindung [5] durch Methylierung von 7-Aminosulfonyl-6-trifluormethyl-3-oxo-2,3-dihydro-4*H*-1,2,4-benzothiadiazin-1,1-dioxyd und nachfolgende Hydrolyse mit 2 N NaOH. Die von Lund und Kobinger [1] irrtümlich als N^2-alkyliert bezeichneten Verbindungen (Subst. 23, 26, 29 und 123) waren durch Alkylierung von 7-Aminosulfonyl-6-trifluormethyl-1,2,4-benzothiadiazin-1,1-dioxyd und anschliessende Hydrolyse bzw. Reduktion gewonnen worden. Ihre Bezeichung muss wie folgt korrigiert werden: N^1-Methyl-2,4-bis-aminosulfonyl-5-trifluormethyl-anilin (Subst. 23); N^1-Carboxymethyl-2,4-bis-aminosulfonyl-5-trifluormethyl-anilin (Subst. 26); 4-Methyl-7-aminosulfonyl-6-trifluormethyl-1,2,4-benzothiadiazin-1,1-dioxyd (Subst. 29); 4-Methyl-7-aminosulfonyl-6-trifluormethyl-2,3-dihydro-4*H*-1,2,4-benzothiadiazin-1,1-dioxyd (Subst. 123). (Lund, F., Leo Pharmaceutical Products, *unveröffentlicht*).

** Herrn G. Cornali sei für die Ausführung der Mikroanalysen und meinen Laboranten, Herrn Th. Rolle und Herrn W. Schlichtkrull, für die Mithilfe bei der Ausführung der Versuche gedankt.

Methanol nachgewaschen und aus den vereinigten Filtraten III mit 1.85 l Eiswasser gefällt. Nach Aufbewahren im Kühlschrank wurde abgesaugt und mit Wasser gewaschen. Ausb. 82,6 g; Schmp. 207—209°C. Zur Analyse wurde aus Methanol Wasser umgefällt, aus wässr. Methanol umkristallisiert und i. Vak. getrocknet. Schmp. 212,5—214,5°C. (Gef.: C 32,23; H 2,13; N 14,31; S 21,60. Ber. für $C_8H_6F_3N_3O_2S_2$ (297,3): C 32,32; H 2,04; N 14,14; S 21,57).

4,4'-Diamino-5,5'-bis-aminosulfonyl-2,2'-bis-trifluormethyl-diphenyl-disulfid (V). (a) Eine Suspension von 120 g der Rhodanverbindung IV in 1.3 l 2.5 % wässr. Ammoniak wurde nach Zugabe eines Antischaummittels unter gutem Rühren 45 Min. auf 80°C erwärmt, wobei sich unter Lösung von IV das Disulfid V als voluminöser, krist. Niederschlag ausschied. Nach dem Abkühlen wurde abgesaugt und gut mit Wasser gewaschen. Ausbeute 81 g; Schmp. (263) 265,5—266,5°C. Aus der Mutterlage konnte durch Zugabe weniger ml Perhydrol noch 4,3 g unreines V gefällt werden. Zur Analyse wurde mehrmals aus der zwanzigfachen Menge 50-proz. Äthanol umkristallisiert und i. Vak. getrocknet. Schmp. 267,5—268°C. (Gef.: C 30,99; H 2,34; N 10,35; S 23,33. Ber. für $C_{14}H_{12}F_6N_4O_4S_4$ (542,5): C 30,99; H 2,23; N 10,33; S 23,64).

(b) Durch Oxydation des Thiophenoles II. 0,5 g II wurden in 3 ml Äthanol gelöst, mit 0,25 ml Perhydrol versetzt und 30 Min. bei Raumtemperatur belassen. Darauf wurde V durch Zusatz von 3 ml Wasser gefällt. Ausbeute 0,4 g; Schmp. 269—270°C ohne Depression mit nach *a* dargestelltem Material, gleichbleibender Schmp. nach Umkristallisieren aus 50-proz. Äthanol. (Gef.: C 30,91; H 2,47; N 10,36; S 23,48).

4-Amino-5-aminosulfonyl-2-trifluormethyl-thiophenol (II). Disproportionierung von V: 2 g V wurden mit 10 ml 4 N NaOH bis zur klaren Lösung geschüttelt und 48 Std. sich selbst überlassen. Darauf wurde mit 4 N HCl auf pH 7 eingestellt, von wenig ausgeschiedenen Verunreinigungen durch Filtration befreit, und aus dem Filtrat II durch Zusatz von 4 N HCl bis pH 2 gefällt (1,4 g; Schmp. 175—178°C). Es wurde aus 6 ml Methanol mit 10 ml Wasser umgefällt. Ausbeute 1,2 g; Schmp. 181,5—184°C. Zur Analyse wurde bei gleichbleibendem Schmp. erneut umgefällt und i. Vak. getrocknet. (Gef.: C 30,80; H 2,63; N 10,31; S 23,54. Ber. für $C_7H_7F_3N_2O_2S_2$ (272,3): C 30,88; H 2,59; N 10,29; S 23,55).

4-Amino-5-aminosulfonyl-2-trifluormethyl-benzolsulfochlorid (VII). 108,5 g des Disulfides V wurden in 400 ml 4 N NaOH aufgeschlämmt und innerhalb 1 Std. unter gutem Rühren und Kühlen bei 18—20°C tropfenweise mit 57,5 ml Perhydrol versetzt. Die entstandene Lösung wurde noch 2 Std. bei gleicher Temperatur belassen und darauf unter Eiskühlung mit 4 N HCl auf pH 7 eingestellt. Ausgeschiedene Verunreinigungen wurden abfiltriert. Die so entstandene Natriumsalzlösung der Sulfinsäure VI (potentiometrisch ermittelter Gehalt an Sulfinsäure 80 % d. Th.) versetzte man bei 10°C mit 275 ml 2 N HCl und leitete sofort darauf bei 10—15°C unter gutem Rühren 23 g Chlor ein, was ungefähr 30 Min. in Anspruch nahm. Nach weiterem 10 Min. langem Rühren wurde das während der Reaktion auskristallisierte Sulfochlorid VII abgesaugt, gut mit Wasser gewaschen und i. Vak. über Phosphorpentoxyd getrocknet. Ausb. 102.5 g; Schmp. 165.5°C (Zers.). Zur Analyse wurden 5 g eines Parallelansatzes aus Eisessig-Wasser umgefällt. Ausb. der Umkrist. 90 %; Schmp. 165—166.5°C (Zers.). (Gef.: C 25,05; H 1.85; Cl 10,45; N 8,28. Ber für $C_7H_6ClF_3N_2O_4S_2$ (338,7): C 24,82; H 1,79; Cl 10,47; N 8,27.

2,4-Bis-aminosulfonyl-5-trifluormethyl-anilin. VII wurde auf übliche Weise mit konz. Ammoniak umgesetzt und aufgearbeitet. Aus verd. Äthanol Schmp. 247—248°C, ohne Depression mit authentischem, aus 5-Trifluormethyl-anilin-disulfochlorid-(2,4) gewonnenem Material [1,2,4-6] vom gleichen Schmp.; auch die IR-Spektren (in KBr) stimmten überein.

N^4-alkylierte 2,4-Bis-aminosulfonyl-5-trifluormethyl-aniline (VIII): Allgemeine Arbeitsvorschrift: Das Sulfochlorid VII wurde portionsweise in eine bei Raumtemperatur gehaltene Lösung des in grossem Überschuss angewandten Amines in tert. Butylalkohol eingetragen. Nach 15—20 stdg. Stehenlassen wurde i. Vak. zur Trockne eingeengt, der Rückstand durch Zusatz von verdünnter Salzsäure kristallisiert und bei Gegenwart von Aktivkohle umkristallisiert. Stark gefärbte Produkte wurden in 4 N NaOH gelöst, die Lösung mit Chloroform extrahiert, und VIII durch verd. Salzsäure aus der wässr. Lösung gefällt. Tab. 3 enthält die dargestellten Verbindungen.

1,1;1',1'-Bis-dioxyd des Bis-[6-trifluormethyl-3-dibenzyl-2,3-dihydro-4H-1,2,4-benzothiadiazinyl-(7)]-disulfids (IX, $R = CH_2 \cdot C_6H_5$). Eine Mischung aus 20 g Disulfid V, 10.1 ml frisch dest. Phenylacetaldehyd und 125 ml Isopropylalkohol wurde mit einer Spatelspitze *p*-Toluolsulfonsäure versetzt und 3 ½ Std. unter Rückfluss erhitzt. Die

Tab. 3. Bis-sulfonamide VIII. (Die Numerierung entspricht der der Tab. 1, aus welcher auch die Schmelzpunkte zu entnehmen sind).

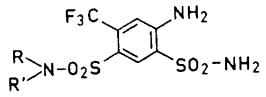

	Zur Reaktion verwendetes Amin R, R′NH		Umkristallisiert aus	Summenformel (Molgew.)	Analyse				
	R	R′				C	H	N	S
1	CH_3	H	30 %Äthanol	$C_8H_{10}F_3N_3O_4S_2$ (333,3)	Ber.	28,83	3,02	12,61	19,24
					Gef.	28,92	3,01	12,41	19,01
2	CH_3	CH_3	30 % Äthanol	$C_9H_{12}F_3N_3O_4S_2$ (347,3)	Ber.	31,12	3,48	12,10	18,46
					Gef.	31,21	3,56	12,17	18,40
3	*i*-C_3H_7	H	Äthylacetat/ Petroläther (warm)	$C_{10}H_{14}F_3N_3O_4S_2$ (361,4)	Ber.	33,24	3,91	11,62	17,74
					Gef.	33,35	4,11	11,85	17,97
4	*n*-C_4H_9	H	50 % Äthanol	$C_{11}H_{16}F_3N_3O_4S_2$ (375,4)	Ber.	35,20	4,19	11,20	17,09
					Gef.	35,39	4,29	11,10	17,11
5	*n*-C_4H_9	*n*-C_4H_9	Benzol	$C_{15}H_{24}F_3N_3O_4S_2$ (431,5)	Ber.	41,75	5,61	9,74	14,86
					Gef.	41,62	5,72	9,96	14,98
6	C_6H_{11}	H	Methanol/Wasser (warm)	$C_{13}H_{18}F_3N_3O_4S_2$ (401,4)	Ber.	38,90	4,52	10,47	15,97
					Gef.	39,04	4,73	10,69	16,13
7	$C_6H_5{\cdot}CH_2$	H	50 % Methanol	$C_{14}H_{14}F_3N_3O_4S_2$ (409,4)	Ber.	41,07	3,45	10,26	15,66
					Gef.	40,91	3,63	10,31	15,51
8	C_6H_5	H	Äthanol/Wasser	$C_{13}H_{12}F_3N_3O_4S_2$ (395,4)	Ber.	39,45	3,06	10,63	16,21
					Gef.	39,61	3,19	10,48	16,28

erhaltene Lösung wurde abgekühlt und die beginnende Kristallisation durch Zugabe von 125 ml Wasser vervollständigt. Nach Aufbewahren im Kühlschrank wurde IX, $R = CH_2{\cdot}C_6H_5$, abgesaugt und mit 50 % Isopropylalkohol gewaschen. Ausbeute 25,2 g; Schmp. 246,5 – 248,5°C (Zers.). Zur Analyse wurde in der 10-fachen Menge heissem Methanol gelöst, über Aktivkohle filtriert und noch warm mit der gleichen Menge Wasser versetzt. Nach dem Erkalten wurde abgesaugt und bei 50°C i. Vak. getrocknet. Schmp. 246,5 – 248,5°C. (Gef.: C 48,28; H 3,23; N 7,45; S 17,08. Ber. für $C_{30}H_{24}F_6N_4O_4S_4$ (746,8): C 48,25; H 3,24; N 7,50; S 17,17).

*6-Trifluormethyl-3-benzyl-2,3-dihydro-4*H*-1,2,4-benzothiadiazin-1,1-dioxyd-sulfinsäure-(7) (X, $R = CH_2{\cdot}C_6H_5$).* 1.5 g des Disulfides IX, $R = CH_2{\cdot}C_6H_5$ schlämmte man in 4,5 ml 4 N NaOH auf und liess innerhalb von 30 Min. bei 20 – 22°C unter Kühlen 0,55 ml Perhydrol eintropfen. Die entstandene Lösung wurde noch 2 Std. bei gleicher Temp. gerührt, im Eisbad abgekühlt und nach Überschichten mit Äther und Verdünnen mit 10 ml Wasser mit 6 ml 4 N HCl angesäuert. Die Ätherschicht wurde abgetrennt, die wässrige Phase noch mehrmals mit Äther extrahiert und die vereinigten ätherischen Lösungen mit wenig Wasser gewaschen und nach Trocknen über Magnesiumsulfat i.

Vak. zur Trockne eingeengt. Der amorphe Rückstand wurde in 1 ml Aceton gelöst, worauf nach Zusatz von Benzol X, R = $CH_2 \cdot C_6H_5$ als Acetonaddukt kristallin erhalten wurde. Ausbeute 1,25 g; Schmp. 112–113°C (Zers.); IR-Absorption: C=O bei 1697 cm^{-1}. (Gef.: C 46,78; H 4,13; N 6,09; S 13,90. Ber. für $C_{15}H_{13}F_3N_2O_4S_2 \cdot C_3H_6O$ (464,5): C 46,54; H 4,12; N 6,03; S 13,80).

Nach Lösen in der 5-fachen Menge Acetonitril und Reiben mit dem Glasstab kristallisierte ein Acetonitriladdukt aus. Schmp. 127°C (Zers.); IR-Absorption: C≡N bei 2279 cm^{-1}. $C_{15}H_{13}F_3N_2O_4S_2 \cdot C_2H_3N$ (447,4) (Gef.: N 8,97. Ber.: N 9,31). Beide Addukte sind ineinander überführbar.

6-Trifluormethyl-3-benzyl-2,3-dihydro-4H-1,2,4-benzothiadiazin-1,1-dioxyd-7-sulfochlorid (XI, R = $CH_2 \cdot C_6H_5$). (a) Aus dem Disulfid IX, R = $CH_2 \cdot C_6H_5$. 6 g IX, R = $CH_2 \cdot C_6H_5$ wurden in 14 ml 4 N NaOH aufgeschlämmt und bei 18–22°C unter gutem Rühren und Kühlen innerhalb von 30 Min. tropfenweise mit 2.6 ml Perhydrol versetzt. Die entstandene Sulfinsäurenatriumsalzlösung verdünnte man mit 20 ml Wasser, kühlte auf 5–10°C und liess sie unter Turbinieren langsam in ein vorher teilweise evakuiertes, 100 ml 0.4 N HCl enthaltenes Reaktionsgefäss bei 10–15°C eintropfen, während gleichzeitig aus einem Gasometer 400 ml Chlor derart eingesaugt wurden, dass stets ein geringer Chlorüberschuss in der Reaktionsmischung vorhanden war. Es wurde noch 20 Min. gerührt, der amorphe Niederschlag abgesaugt, mit Wasser gewaschen und i. Vak. über Phosphorpentoxyd getrocknet (6,34 g). Das Produkt wurde in 50 ml Eisessig gelöst, über Aktivkohle filtriert und XI, R = $CH_2 \cdot C_6H_5$ mit 50 ml Wasser kristallin gefällt. Ausbeute 4.75 g; Schmp. 133–138°C (Zers.). Zur Analyse wurde zweimal wie oben umgefällt und i. Vak. getrocknet. Schmp. 140–141,5°C (Zers.). (Gef.: C 40,95; H 2,91; Cl 7,89; N 6,15. Ber. für $C_{15}H_{12}Cl\,F_3N_2O_4S_2$ (440,9): C 40,86; H 2,75; Cl 8,05; N 6,36).

Beim Verreiben mit Chloroform oder wasserfrei vorgenommenem Umkristallisieren entstand ein Chlatrat mit Chloroform vom Schmp. 102–103°C (Zers.). Mit Benzol wurde ebenfalls ein Chlatrat erhalten, das unscharf bei 150–160°C (Zers.) schmolz (s. auch unter (*b*)). In beiden Fällen wurden keine Analysen erhalten, die auf eine stöchiometrische Zusammensetzung schliessen lassen.

(b) Aus dem Sulfochlorid VII. Eine Aufschlämmung von 102,5 g des Sulfochlorides VII in 1 l trockenem Benzol erhitzte man nach Zusatz von 0,5 g *p*-Toluolsulfonsäure zum Sieden und liess sodann im Verlauf von 45 Min. eine Lösung von 39 ml frisch dest.

Tab. 4. Sulfochloride XI.

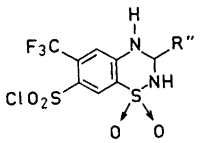

	Eingesetzter Aldehyd	R''	Schmp. (Zers.) °C	Summenformel (Molgew.)	Analyse				
						C	H	Cl	N
1	H_3C-CHO (als Paraldehyd)	CH_3	168–169	$C_9H_8ClF_3N_2O_4S_2$ (364,8)	Ber.	29,63	2,21	9,72	7,68
					Gef.	29,40	2,50	9,50	7,83
2	$H_3C(CH_2)_3 \cdot CHO$	n-C_4H_9	144–145	$C_{12}H_{14}ClF_3N_2O_4S_2$ (406,8)	Ber.	35,43	3,47	8,72	6,89
					Gef.	35,91	3,56	8,54	6,70
3	$H_3C(CH_2)_4 \cdot CHO$	n-C_5H_{11}	143,5–144,5	$C_{13}H_{16}ClF_3N_2O_4S_2$ (420,9)	Ber.	37,10	3,83	8,43	6,66
					Gef.	37,04	3,93	8,45	6,58

Tab. 5. N^7-alkylierte 7-Aminosulfonyl-6-trifluormethyl-2,3-dihydro-4*H*-
der Tab. 2, aus welcher auch die

Weg A:

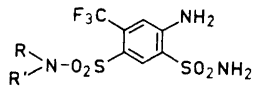

VIII

	Eingesetztes Bis-sulfonamid VIII		R″	Zur Reaktion verwendeter Aldehyd oder Derivat	Lösungsmittel	
	R	R′			1	2
1	*i*-C_3H_7	H	H	$(CH_2O)_x$	Butanol	Heptan
2	*n*-C_4H_9	*n*-C_4H_9	H	$(CH_2O)_x$	Butanol	Heptan
3	C_6H_{11}	H	H	$(CH_2O)_x$	Butanol	Heptan
5	*i*-C_3H_7	H	CH_3	$H_3C{\cdot}CHO$ (als Paraldehyd)	Butanol	Heptan
6	*n*-C_4H_9	*n*-C_4H_9	CH_3	$H_3C{\cdot}CH(OC_2H_5)_2$	Benzol	Heptan
7	C_6H_{11}	H	CH_3	$H_3C{\cdot}CH(OC_2H_5)_2$	Butanol	Heptan
9	*i*-C_3H_7	H	*i*-C_3H_7	$(CH_3)_2CH{\cdot}CHO$	Butanol	Petroläther
10	*n*-C_4H_9	*n*-C_4H_9	*i*-C_3H_7	$(CH_3)_2CH{\cdot}CHO$	Benzol	Petroläther
11	C_6H_{11}	H	*i*-C_3H_7	$(CH_3)_2CH{\cdot}CHO$	Butanol	Hexan
14[a]	*n*-C_4H_9	*n*-C_4H_9	*n*-C_4H_9	$C_4H_9{\cdot}CHO$	Benzol	Heptan

Phenylacetaldehyd in 500 ml Benzol eintropfen. Gleichzeitig mit dem Eintropfen wurde das bei der Reaktion gebildete Wasser mit Benzol azeotrop aus der Reaktionsmischung abdestilliert. Bei grösserem Ansatz erfolgte diese Operation über einen Wasserabscheider mit über Magnesiumsulfat getrocknetem Rücklauf, wobei der Aldehyd dem Rücklauf zugegeben wurde. Nach beendetem Eintropfen wurden aus der entstandenen Lösung noch ungefähr 1 Std. geringe Mengen von Reaktionswasser azeotrop entfernt, wobei das Reaktionsprodukt auszukristallisieren begann. Nach dem Erkalten wurde abgesaugt, mit 300 ml Benzol gewaschen (103 g, bräunlich, kristallin). Es wurde in 1,2 l Eisessig gelöst, über Aktivkohle filtriert und XI, $R=CH_2{\cdot}C_6H_5$ mit 1,7 l Wasser gefällt und i. Vak. getrocknet. Ausbeute 81,5 g; Schmp. 150–160°C. Es handelt sich um ein Chlathrat mit Benzol (s.o.), welches als solches für weitere Reaktionen verwendet wurde. Zur Ana-

1,2,4-benzothiadiazin-1,1-dioxyde (XII). (Die Numerierung entspricht Schmelzpunkte zu entnehmen sind).

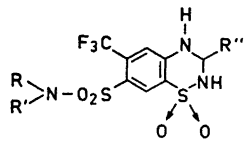

XII

Umgefällt aus	Summenformel (Molgew.)		Analyse			
			C	H	N	S
Methanol/Wasser	$C_{11}H_{14}F_3N_3O_4S_2$ (373,4)	Ber.	35,39	3,78	11,25	17,17
		Gef.	35,59	3,97	10,95	17,08
Äther/Petroläther [b]	$C_{16}H_{24}F_3N_3O_4S_2$ (443,5)	Ber.	43,33	5,45	9,48	14,46
		Gef.	43,51	5,64	9,45	14,47
Aceton/Wasser	$C_{14}H_{18}F_3N_3O_4S_2$ (413,4)	Ber.	40,67	4,39	10,16	15,51
		Gef.	40,75	4,51	10,21	15,38
Methanol/Wasser	$C_{12}H_{16}F_3N_3O_4S_2$ (387,4)	Ber.	37,20	4,16	10,85	16,55
		Gef.	37,18	4,41	10,85	16,49
Benzol/Petroläther	$C_{17}H_{26}F_3N_3O_4S_2$ (457,5)	Ber.	44,63	5,73	9,18	14,01
		Gef.	44,41	5,78	9,05	13,98
Methanol/Wasser	$C_{15}H_{20}F_3N_3O_4S_2$ (427,5)	Ber.	42,15	4,72	9,83	15,00
		Gef.	42,31	4,76	9,76	15,14
Methanol/Wasser	$C_{14}H_{20}F_3N_3O_4S_2$ (415,4)	Ber.	40,47	4,85	10,11	15,43
		Gef.	40,54	4,77	10,07	15,46
Methanol/Wasser Äthylacetat/Petroläther	$C_{19}H_{30}F_3N_3O_4S_2$ (485,6)	Ber.	46,90	6,42	8,64	13,18
		Gef.	46,70	6,39	8,48	13,22
Methanol/Wasser	$C_{17}H_{24}F_3N_3O_4S_2$ (455,5)	Ber.	44,72	5,52	9,21	14,05
		Gef.	44,97	5,44	9,11	14,28
Methanol/Wasser	$C_{20}H_{32}F_3N_3O_4S_2$ (499,6)	Ber.	48,08	6,46	8,41	12,83
		Gef.	47,93	6,53	8,43	12,80

lyse wurde in der 10-fachen Menge Eisessig gelöst, zur Entfernung des Benzols 25 % des Eisessigs i. Vak. abdestilliert, mit Wasser gefällt, und erneut aus Eisessig/Wasser umgefällt. Ausbeute d. Umkrist. 80 %, Schmp. 140–142°C (Zers.), ohne Depression mit nach *(a)* dargestelltem Material. (Gef.: C 40,92; H 2,93; Cl 8,19; N 6,32).

Analog Arbeitsvorschrift *(b)* durch Kondensation mit Aldehyden aus dem Sulfochlorid VII dargestellte Sulfochloride XI sind in Tab. 4 zusammengefasst.

N^7-alkylierte 7-Aminosulfonyl-6-trifluormethyl-2,3-dihydro-4H-1,2,4-benzothiadiazin-1,1-dioxyde (XII). (a) Durch Kondensation N^4-alkylierter 2,4-Bis-aminosulfonyl-5-trifluormethyl-aniline (VIII) mit Aldehyden oder Acetalen (Weg A): Allgemeine Arbeitsvorschrift: Die Verbindungen VIII wurden mit der berechneten Menge des Aldehydes nach Zusatz von *p*-Toluolsulfonsäure als Katalysator im Lösungsmittel 1 (s. Tab. 5) einige

Tab. 5. Fortsetz.

Weg B:

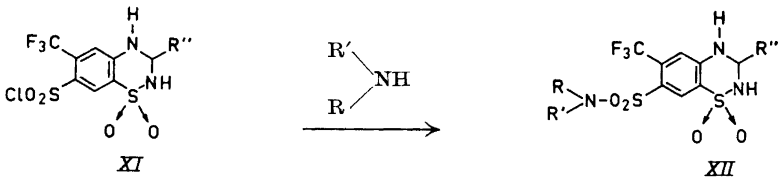

XI *XII*

	Eingesetztes Sulfochlorid XI	Zur Reaktion verwendetes Amin		Umgefällt aus	Summenformel (Molgew.)	Analyse				
	R″	R	R′				C	H	N	S
4	CH_3	CH_3	CH_3	Methanol/Wasser	$C_{11}H_{14}F_3N_3O_4S_2$ (373,4)	Ber.	35,39	3,78	11,25	17,17
						Gef.	35,19	3,81	11,30	17,27
8	CH_3	$CH_2{\cdot}C_6H_5$	H	Methanol/Wasser	$C_{16}H_{16}F_3N_3O_4S_2$ (435,4)	Ber.	44,13	3,70	9,65	14,73
						Gef.	43,99	3,89	9,69	14,94
12	n-C_4H_9	CH_3	CH_3	Methanol/Wasser	$C_{14}H_{20}F_3N_3O_4S_2$ (415,4)	Ber.	40,47	4,85	10,11	15,43
						Gef.	40,62	4,83	9,95	15,43
13	n-C_4H_9	i-C_3H_7	H	Methanol/Wasser	$C_{15}H_{22}F_3N_3O_4S_2$ (429,5)	Ber.	41,95	5,17	9,78	14,93
						Gef.	42,14	5,17	9,96	15,08
4[a]	n-C_4H_9	n-C_4H_9	n-C_4H_9	Methanol/Wasser	$C_{20}H_{34}F_3N_3O_4S_2$ (499,6)	Ber.	48,08	6,46	8,41	12,83
						Gef.	48,19	6,46	8,37	13,05
15	n-C_4H_9	C_6H_{11}	H	Methanol/Wasser	$C_{18}H_{26}F_3N_3O_4S_2$ (469,5)	Ber.	46,04	5,58	8,95	13,65
						Gef.	45,83	5,81	9,05	13,77
16	n-C_5H_{11}	n-C_4H_9	n-C_4H_9	Methanol/Wasser	$C_{21}H_{34}F_3N_3O_4S_2$ (513,6)	Ber.	49,10	6,67	8,18	12,48
						Gef.	48,88	6,71	8,16	12,70
17	n-C_5H_{11}	C_6H_{11}	H	Methanol/Wasser	$C_{19}H_{38}F_3N_3O_4S_2$ (483,6)	Ber.	47,19	5,84	8,69	13,26
						Gef.	47,11	6,06	8,58	13,37
18	n-C_5H_{11}	$CH_2{\cdot}C_6H_5$	H	Methanol/Wasser	$C_{20}H_{24}F_3N_3O_4S_2$ (491,5)	Ber.	48,87	4,92	8,55	13,04
						Gef.	49,03	5,09	8,55	13,18
19	$CH_2{\cdot}C_6H_5$	CH_3	H	Aceton/Wasser	$C_{16}H_{16}F_3N_3O_4S_2$ (435,4)	Ber.	44,13	3,70	9,65	14,73
						Gef.	44,33	3,82	9,43	14,55
20	$CH_2{\cdot}C_6H_5$	CH_3	CH_3	Aceton/Wasser	$C_{17}H_{18}F_3N_3O_4S_2$ (449,5)	Ber.	45,43	4,04	9,35	14,27
						Gef.	45,99	4,17	9,42	14,11
21	$CH_2{\cdot}C_6H_5$	i-C_3H_7	H	Methanol/Wasser (warm)	$C_{18}H_{20}F_3N_3O_4S_2$ (463,5)	Ber.	46,64	4,35	9,07	13,83
						Gef.	46,63	4,44	8,89	13,78
22	$CH_2{\cdot}C_6H_5$	n-C_4H_9	H	Methanol/Wasser (warm)	$C_{19}H_{22}F_3N_3O_4S_2$ (477,5)	Ber.	47,79	4,65	8,80	13,43
						Gef.	48,08	5,05	8,85	13,42
23	$CH_2{\cdot}C_6H_5$	n-C_4H_9	n-C_4H_9	Methanol/Wasser (warm)	$C_{23}H_{30}F_3N_3O_4S_2$ (533,6)	Ber.	51,77	5,67	7,88	12,02
						Gef.	51,76	5,84	7,80	12,01
24	$CH_2{\cdot}C_6H_5$	C_6H_{11}	H	Methanol/Wasser	$C_{21}H_{24}F_3N_3O_4S_2$ (503,5)	Ber.	50,10	4,80	8,35	12,73
						Gef.	50,17	4,96	8,24	12,77
25	$CH_2{\cdot}C_6H_5$	$CH_2{\cdot}C_6H_5$	H	Methanol/Wasser	$C_{22}H_{20}F_3N_3O_4S_2$ (511,5)	Ber.	51,64	3,94	8,22	12,54
						Gef.	51,25	4,12	8,25	12,37
26	$CH_2{\cdot}C_6H_5$	C_6H_5	H	Methanol/Wasser	$C_{21}H_{18}F_3N_3O_4S_2$ (497,5)	Ber.	50,70	3,65	8,45	12,89
						Gef.	50,33	3,93	8,36	12,91

Übereinstimmung der Produkte aus Syntheseweg A und B.
Nach Chromatogr. über Al_2O_3 mit Benzol.

Std. unter Rückfluss erhitzt. Die Reaktionsprodukte XII wurden, z.T. bereits während der Reaktion, durch Zusatz des Lösungsmittels 2 gefällt. Die dargestellten Verbindungen sind in Tab. 5 (Weg A) zusammengefasst.

(b) Durch Reaktion der Sulfochloride XI mit Aminen (Weg B): Allgemeine Arbeitsvorschrift: Die Sulfochloride XI wurden unter Eiskühlung portionsweise in eine Lösung des im Überschuss angewandten Amines in tert. Butylalkohol eingetragen und die Reaktionsmischung darauf einige Stunden bei Raumtemperatur gerührt. Es wurde im Wasserbad von 25°C i. Vak. eingeengt und der Rückstand mit Wasser und verd. Salzsäure kristallisiert. Die dargestellten Verbindungen sind in Tab. 5 (Weg B) zusammengefasst.

7-Aminosulfonyl-6-trifluormethyl-3-benzyl-2,3-dihydro-4H-1,2,4-benzothiadiazin-1,1-dioxyd. Das Sulfochlorid XI, $R'' = CH_2 \cdot C_6H_5$ wurde, wie bei Darstellung der N^7-alkylierten Verbb. XII beschrieben, mit Ammoniak in tert. Butylalkohol umgesetzt und aufgearbeitet. Aus Methanol/Wasser wurde wiederholt umgefällt. Ausbeute 60–70 % d. Th.; Schmp. 226–227°C, ohne Depression mit aus 2,4-Bis-aminosulfonyl-5-trifluormethylanilin durch Kondensation mit Phenylacetaldehyd gewonnenem Material [1] vom gleichen Schmp.; auch die IR-Spektren in KBr stimmten überein.

2-Amino-4-trifluormethyl-benzolsulfonsäure-methylamid. 50 g 2-Amino-4-trifluormethylbenzolsulfochlorid * wurden bei –5°C unter Rühren portionsweise in 200 ml einer 33 % Methylaminlösung eingetragen. Es wurde innerhalb von 2 Std. auf Raumtemperatur erwärmt und anschliessend auf dem Dampfbad das überschüss. Methylamin ausgetrieben. Das ausgeschiedene Öl kristallisierte beim Erkalten zu Kristallklumpen, welche im Mörser zerstossen, mit Wasser gewaschen und aus Äthanol/Wasser umgefällt wurden. Ausbeute 44 g; Schmp. 98–99°C. Zur Analyse wurde bei gleichbleibendem Schmp. zweimal aus Äthanol/Wasser umgefällt und i. Vak. getrocknet. (Gef.: C 37,60; H 3,55; N 11,16; S 12,86. Ber. für $C_8H_9F_3N_2O_2S$ (254,2): C 37,79; H 3,57; N 11,02; S 12.61).

2-Amino-5-rhodan-4-trifluormethyl-benzolsulfonsäure-methylamid. Einer Mischung aus 6,35 g 2-Amino-4-trifluormethyl-benzolsulfonsäure-methylamid, 9,7 g Kaliumrhodanid und 30 ml Eisessig liess man unter Rühren bei 10–15°C innerhalb von 1 ½ Std. eine Lösung von 2.4 ml Brom in 10 ml Eisessig zutropfen. Nach 2 ½ stdg. Rühren bei gleicher Temperatur wurde Aktivkohle und Filtererde zugesetzt, filtriert, und mit 20 ml Eisessig nachgewaschen. Aus den vereinigten Filtraten wurde mit 200 ml Wasser die rohe Rhodanverbindung gefällt. Umfällung erfolgte bei Gegenwart von Aktivkohle aus 30 ml Methanol/90 ml Wasser. Ausb. 4,3 g; Schmp. 114,5–115,5°C. Zur Analyse wurde eine Probe 3-mal aus wenig Eisessig umkristallisiert und i. Vak. getrocknet. Schmp. 117–119°C. Gef.: C 34,96; H 2,80; N 13,32; S 20,50. Ber. für $C_9H_8F_3N_3O_2S_2$ (311,3): C 34,73; H 2,59; N 13,50; S 20,60).

4,4'-Diamino-5,5'-bis-methylaminosulfonyl-2,2'-bis-trifluormethyl-diphenyl-disulfid. 3 g 2-Amino-5-rhodan-4-trifluormethyl-benzolsulfonsäure-methylamid wurden in einer Mischung aus 15 ml Äthanol und 36 ml 2,5 % Ammoniak unter Rühren 30 Min. auf dem Dampfbad erhitzt. Aus der zunächst entstehenden Lösung kristallisierte das Disulfid nach kurzer Zeit aus. Nach dem Erkalten wurde abgesaugt und mit 25 % Äthanol gewaschen. Ausbeute 2,3 g; Schmp. 237–238°C. Zur Analyse wurde aus Äthanol umkristallisiert und i. Hochvak. getrocknet. Schmp. 239–241°C. (Gef.: C 33,77, H 2,82, N 9,74, S 22,27. Ber. für $C_{16}H_{16}F_6N_4O_4S_4$ (570,6): C 33,68; H 2,83; N 9,82; S 22,48).

In einem Fall wurde das Disulfid mit dem Schmp. 178–179,5°C erhalten. Nach mehrmaligem Umkristallisieren aus 50 % Äthanol stieg der Schmp. auf 180,5–181,5°C (Gef.: N 10,01; S 22,50). Nach Lösen in der 10-fachen Menge Äthanol und Impfen mit obiger Kristallform (Schmp. 239–241°C) kristallisierte das Disulfid mit Schmp. 240–241°C aus.

4-Amino-5-methylaminosulfonyl-2-trifluormethyl-benzolsulfochlorid. 2,85 g des vorstehenden Disulfids wurden in 4 N NaOH analog dem Disulfid V oxydierend hydrolytisch disproportioniert und die erhaltene Sulfinsäurelösung oxydierend chloriert. Das erhaltene Sulfochlorid (2,45 g; Schmp. 140°C) wurde aus 15 ml Eisessig/45 ml Wasser umgefällt. Ausb. 1,7 g; Schmp. 150–151°C. Zur Analyse wurde erneut umgefällt (Schmp. 151–152°C) und über Phosphorpentoxyd i. Vak. getrocknet. (Gef.: C 27,36; H 2,41; Cl 10,04; N 7,78; S 18,17. Ber. für $C_8H_8ClF_3N_2O_4S_2$ (352,7): C 27,24; H 2,28; Cl 10,05; N 7,94; S 18,18

4-Aminosulfonyl-2-methylaminosulfonyl-5-trifluormethyl-anilin. 0.5 g des vorstehenden Sulfochlorids wurden in 6 ml konz. Ammoniak eingetragen und darauf das überschüssige NH_3 auf dem Dampfbad ausgetrieben. Nach Zusatz weniger ml Wasser und Erkalten

* vgl. Fussnote Seite 298.

wurde abgesaugt und mit Wasser gewaschen. Umgefällt wurde aus Methanol/Wasser. Ausb. 0.325 g; Schmp. 176—178°C, ohne Depression mit auf anderem Wege gewonnenem Material * vom gleichen Schmp.; auch die IR-Spektren in KBr stimmten überein. Gef.: C 28,71; H 3,20; N 12,54; S 19,20. Ber. für $C_8H_{10}F_3N_3O_4S_2$ (333,3): C 28,83; H 3,02; N 12,61; S 19,24).

2-Methylaminosulfonyl-4-dimethylaminosulfonyl-5-trifluormethyl-anilin. 0.5 g 4-Amino-5-methylaminosulfonyl-2-trifluormethyl-benzolsulfochlorid wurde in 5 ml 30 % Dimethylamin in tert. Butylalkohol eingetragen. Nach einigen Std. wurde i. Vak. zur Trockne eingeengt und mit Wasser kristallisiert. (0,4 g; Schmp. 147—150°C). Es wurde 2-mal aus Äthanol umkristallisiert und i. Vak. bei 60°C getrocknet. Ausbeute 0,3 g; Schmp. 154—155°C. (Gef.: C 33,23; H 3,82; N 11,60; S 17,60. Ber. für $C_{10}H_{14}F_3N_3O_4S_2$ (361,4): C 33,24; H 3,91; N 11,62; S 17,74).

LITERATUR

1. Lund, F. und Kobinger, W. *Acta Pharmacol. Toxicol.* **16** (1960) 297.
2. Holdrege, C. T., Babel, R. B. und Cheney, L. C. *J. Am. Chem. Soc.* **81** (1959) 4807; Yale, H. L., Losee, K. und Bernstein, J. *Ibid.* **82** (1960) 2042; Selleri, R. und Caldini, O. *Ann. chim. Rome* **50** (1960) 170.
3. Novello, F. C., Bell, S. C., Abrams, E. L. A., Ziegler, C. und Sprague, J. M. *J. Org. Chem.* **25** (1960) 970.
4. Werner, L. H., Halamandaris, A., Ricca, Jr., S., Dorfmann, L. und de Stevens, G. *J. Am. Chem. Soc.* **82** (1960) 1161.
5. Close, W. J., Swett, L. R., Brady, L. E., Short, J. H. und Vernstein, M. *J. Am. Chem. Soc.* **82** (1960) 1132.
6. Novello, F. C., Bell, S. C., Abrams, E. L. A., Ziegler, C. und Sprague, J. M. *J. Org. Chem.* **25** (1960) 965.
7. Vgl. *Methoden der organischen Chemie* (Houben-Weyl), Georg Thieme Verlag, Stuttgart 1955, Bd. IX, S. 77, 78.

Eingegangen am 26. September 1961.

* vgl. Fussnote Seite 302.

ACTA CHEMICA SCANDINAVICA 16 (1962) 311–322

Solubility Studies on Substituted Ammonium Salts of Halide Complexes

II. Tetramethylammonium Trichlorostannate(II)

G. P. HAIGHT, Jr.*, JOHN ZOLTEWICZ**, and WARREN EVANS***

Contribution from the Department of Chemistry, Swarthmore College, Pensylvania, U.S.A. and Kem. Lab. A, Technical University of Denmark, Copenhagen, Denmark

Tetramethylammonium trichlorostannate(II) has been found to form a single phase in equilibrium with chloride ion in hydrochloric acid from 2.0 to 9.0 M in concentration. The single phase is also present at ion concentration of 4.0 maintained with mixtures of $H(HSO_4)$ and HCl. Solubility equilibria have been studied assuming the validity of the equations for the formation constants of $SnCl_n^{2-n}$ complexes:

$$K_n = [SnCl_n^{2-n}]/[SnCl_{n-1}^{3-n}]\,[Cl^-]$$

and for the solubility product:

$$K_s = [(CH_3)_4N^+]\,[SnCl_3^-]$$

Analysis of data obtained at $[HCl] + [H_2SO_4] = 4.0$ using the equations of paper I gave consistent results for the various K_n values and a single value for K_s. Analysis of data in varying hydrochloric acid concentration (no other large source of ions present), substituting activity of chloride ion for $[Cl^-]$ also gave consistent results for the various K_n values and the same single value for K_s.

The results of this study confirm the suitability of using H_2SO_4 as an inert 1:1 electrolyte for maintaining constant ion normality.

Stannous ions are found to coordinate with a maximum of four chloride ions in solutions containing up to 6.0 M hydrochloric acid. A comparison of the distribution of various $SnCl_n^{2-n}$ with kinetic data on reactions employing Sn(II) as a reducing agent indicates that $SnCl_3^-$ is the most active reducing agent among the various chlorotin(II) complexes.

* Chemistry Department, Swarthmore College (on leave to Kem. Lab. A 1960–1).
** Organic Chemistry Institute, University of Munich, Germany.
*** National Cancer Institute, Bethesda, Md., U.S.A.

The frequent employment by one of us (GPH) of stannous ion as a reducing agent in kinetic studies [2] of oxidation-reduction reactions has prompted us to investigate further the nature of Sn(II) species in chloride media. Studies reported in the literature describe complexes with ligand number up to four [3-5] and also with ligand number reaching a maximum of three [6], while recently data of Duke and Courtney [5] have been reanalyzed using computer techniques [7] and found to be consistent with a maximum of three chloride ligands per stannous ion. Our discovery that tetramethylammoniumtrichlorostannate(II) is formed in high purity from hydrochloric acid solutions of tetramethylammonium chloride and stannous chloride over wide ranges of chloride ion concentration provided a useful method for settling the question of the presence or absence of a tetrachloro complex and for checking the complexity constants in the literature. A preliminary study of the solubility of the salt *vs.* concentration of hydrochloric acid revealed a sharp minimum at 3.0 M acid. This meant that at higher concentrations of chloride the tetrachlorocomplex and perhaps higher complexes would become the dominant Sn(II) species present. A careful study of the solubility at constant ion strength of 4.0 using sulfuric acid as 1:1 electrolyte has provided a test of the proposition [1] that sulfuric acid could be so used and enabled us to determine the relative concentrations of the various chloro-tin(II) complex species over a wide range of chloride ion concentrations. In the absence of sulfuric acid, activity of hydrochloric acid *vs.* solubility gives the same information up to an activity of 29 (6 molar).

EXPERIMENTAL

Eastman white label tetramethylammonium salts were analyzed argentometrically for halide content and found suitable for use without further purification. Analytical grade hydrochloric and sulfuric acids were diluted with distilled water. Hydrochloric acid was standardized by titration of weighed sodium carbonate using methyl orange indicator and by potentiometric titration with silver nitrate. Sulfuric acid was standardized with sodium carbonate and by measuring its density. All other reagents were of analytical grade and used without further purification.

Preparation of tetramethylammonium trichlorostannate (II). This salt can be precipitated in high yields and high purity simply by mixing solutions of the two ions in 3.0 M hydrochloric acid and cooling to 0°C in an ice bath. The concentration of acid is not critical, salts of the same composition being prepared from solutions 1.0 to 9.0 M in hydrochloric acid. The solubility studies indicate that the concentration of trichlorostannate(II) ion is a maximum in 3.0 M acid, and that hydrolysis may occur if the chloride and hydrogen ion concentrations each are as low as 2.0 M. Commercial stannous chloride gave preparations which were 98.5 to 99.0 % pure, the chief contaminant probably being tin(IV). If stannous chloride solutions are prepared by passing solutions of cupric chloride in hydrochloric acid through a tin reductor in an inert atmosphere, very pure preparations of salt always result. The salt has a large temperature coefficient of solubility and may be recrystallized by dissolving in hot hydrochloric acid and cooling. The salt is washed with alcohol and ether and dried in the absence of oxygen. The dry salt is non-hygroscopic, stable to oxidation by air at room temperature and might well be a good primary standard as a reducing agent. Once in aqueous solution, however, it is as susceptible as stannous chloride to air oxidation. Analysis for tin(II) was made by permanganate titration, chloride was determined by potentiometric titration with silver nitrate after oxidizing tin(II) to tin(IV). Often tin(II) and chloride were determined consecutively on the same sample. Microanalyses for carbon, hydrogen and nitrogen were performed by the Clark Microanalytical Laboratory. The difficult to analyze quaternary nitrogen generally gave poor results. Results on a typical preparation showed: Sn 40.06;

Cl 35.9; C 16.26; H 3.99; N 4.83 %. Calc. for $C_4H_{12}NSnCl_3$: Sn 39.6; Cl 35.6; C 16.1; H 4.04; N 4.68 %.

Solubility studies on the chloro-salt were carried out with solutions from which oxygen had been removed by bubbling through nitrogen or hydrogen scrubbed with chromous sulfate solution. Reproducible results were obtained only when the salt was covered with solution in a wax sealed, completely filled and stoppered weighing bottle. The bottle was placed in a constant temperature bath and shaken at 25.0° for 24 h, equilibrium being reached well within this time. Samples were withdrawn with a filter pipette immediately on breaking the seal and added to a solution containing an excess of standard permanganate solution in dilute sulfuric acid. The permanganate was back titrated with standard sodium oxalate solution. Difficulty was encountered occasionally with colloid formation. Samples that did not become *very* clear shortly after shaking ceased gave slightly high results. Despite the fact that commercial stannous chloride containing 10 to 20 % tin(IV) gave rather good preparations of the complex stannous salt, the presence of the smallest air bubble in a reaction bottle led to low solubilities. Evidently the hydrolyzed stannic chloro complexes do not precipitate the tetramethylammonium ion, but oxidation in a solubility study frees tetramethylammonium ions which suppress the solubility of the stannous salt. This difficulty could be minimized in future work by using a large excess of tetramethylammonium ion in the solvent.

Except for a few measurements on solubility in various hydrochloric acid concentrations, all studies were made with a concentration of 4.0 M hydrogen ion to suppress hydrolysis, and to permit chloride ion concentrations well in excess of that corresponding to the minimum in the curve obtained for hydrochloric acid (Fig. 1). Ion concentrations were maintained using sulfuric acid as a 1:1 electrolyte. (Perchloric acid could not be used owing to the insolubility of tetramethylammonium perchlorate). A nearly exact correspondence exists between concentration and activity properties of $H(HSO_4)$ and $HClO_4$ in the region of 4.0 M concentration [8].

Analysis of data has been carried out by

(*a*) Assuming activity coefficients remain constant at constant ion normality, $[H(HSO_4)] + [HCl] = 4.0$, and using concentrations in expressions for equilibrium constants

$$K_n = [SnCl_n^{2-n}]/[SnCl_{n-1}^{3-n}]\,[Cl^-]$$

and

(*b*) Assuming $K_n = \dfrac{[SnCl_n]}{[SnCl_{n-1}]a_{HCl}}$, where a is activity, in hydrochloric acid solutions

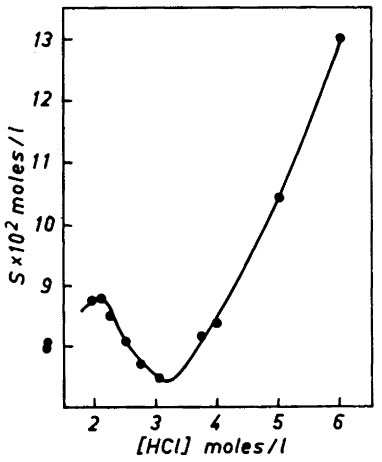

Fig. 1. Solubility curve of tetramethylammonium trichlorostannate(II) *vs.* concentration of hydrochloric acid showing minimum at 3.0 M.

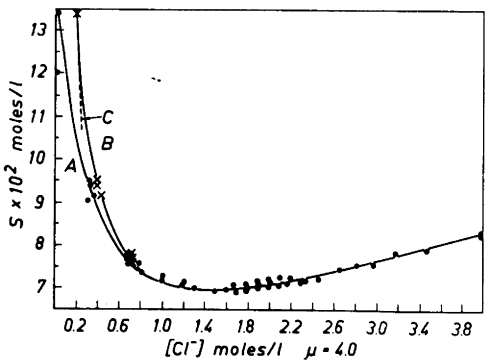

Fig. 2. Solubility of tetramethylammonium trichlorostannate(II) *vs.* added chloride at $H^+ = 4.0$ (curve A). Curve B shows corrections for chloride derived from dissolved salt. The broken line C shows the theoretical limiting slope for the point corresponding to no added chloride. Dots represent raw data. Crosses show corrected chloride concentrations for curve B.

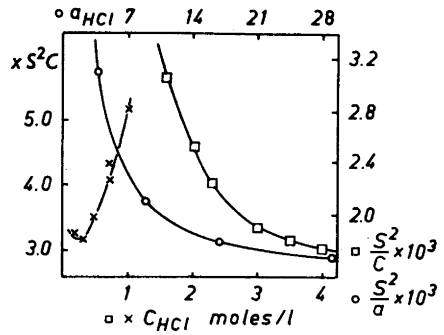

Fig. 3. Plots used in search of evidence for the presence of pentachloro and monochloro complexes in the solutions studied. The minimum at left requires the presence of $SnCl^+$ and/or Sn^{2+}. The absence of a minimum on the right suggests the absence of $SnCl_5^{3-}$ but does not prove it.

in which ion strength is varied and which contain no other substance than hydrochloric acid in large concentration and small concentrations of $(CH_3)_4NSnCl_3$.

RESULTS

The solubility curves *vs.* hydrochloric acid concentration are shown in Figs. 1 and 2. The line drawn through the points in Fig. 2 favors the points deemed most reliable by virtue of increasing experience with the technique. All points which could not definitely be ruled out as having been subject to oxidation, or involving obvious colloid formation are included. At the lower concentrations the correction of the curve for chloride ions derived from the solution of the salt is shown together with the corrected points. This curve with the theoretical limiting slope of 0.5 [1] at zero added chloride is the curve upon which calculation of constants was based, and corresponds nearly identically to a curve calculated from the constants reported. The maximum at 2.0 M acid in the curve obtained in hydrochloric acid alone (Fig. 1) corresponds to a change in the solid phase. The salt became gelatinous in appearance suggesting hydrolysis with the formation of stannous hydroxide or basic chloride. This is consistent with the detection of hydrolysis by Vanderzee and Rhodes [6] at 3.0 M hydrogen ion and low chloride ion concentrations. The data used in calculating constants are summarized in Tables 1 and 2.

Analysis of data. Detection of species present. The minimum of the solubility curve shows clearly the presence of $SnCl_2$, $SnCl_3^-$, and $SnCl_4^{2-}$. Fig. 3 shows plots designed to locate minima corresponding to average ligand numbers ($\bar{n}$) of two and four [1]. There is an apparent minimum for the $S^2[Cl^-]$ *vs.*

Table 1. Solubility data at ion normality = 4.0.

$[HCl]_0$ m/l	$[H_2SO_4]$ m/l	$[Cl^-]$ m/l	S m/l	$S^2 \times 10^3$	$\bar{n}$[a]
0.00	4.0	0.18	0.1340	17.9	1.70
0.30	3.7	0.38	0.0939	8.8	2.20
0.36	3.64	0.43	0.0912	8.3	2.25
0.67	3.33	0.71	0.0757	5.72	2.52
0.80	3.20	0.83	0.0738	5.43	2.70
1.00	3.00	1.00	0.0722	5.20	2.80
1.60	2.40	1.60	0.0698	4.88	3.00
2.00	2.00	2.00	0.0707	5.00	3.27
2.30	1.70	2.30	0.0717	5.12	3.39
3.00	1.00	3.00	0.0755	5.70	3.56
3.50	0.50	3.50	0.0792	6.25	3.66
4.00	0.00	4.00	0.0832	6.91	3.77

[a] from slope of S *vs.* $[Cl^-]$. Corrected for $[Cl^-]$ produced by or added to dissolved salt, using eqn.

$$[Cl^-] = \frac{[Cl^-]_o}{1 + 2dS/d[Cl^-]} \text{ (Ref.}^1\text{)}.$$

$[Cl^-]$ plot very near to the lowest attainable chloride concentration. This corresponds to a maximum concentration of $SnCl_2$, and indicates that $SnCl^+$ must be a minor factor at every experimental point, the fact that Sn^{2+} is the only species present at total chloride concentration equal to zero can be used to extend the data to lower chloride concentrations than the measurements alone allow. At the highest chloride concentration no minimum for $S^2/[Cl^-]$ is observed even at activity 29. Complete conversion to $SnCl_4^{2-}$ without the formation of any $SnCl_5^{3-}$ is apparently the situation, although the failure to reach a minimum corresponding to $\bar{n} = 4.0$ cannot be used to rule out a pentachloro complex. It must be recalled that the data of Duke and Courtney [5] and of Vanderzee and Rhodes [6] did not warrant introduction of $SnCl_4^{2-}$ into their calculations simply because the data did not extend to high enough chloride concentrations. We could fit our data by assuming an $SnCl_5^{3-}$ complex, but could fit it equally well without so assuming.

Table 2. Solubility data in hydrochloric acid solution.

$[HCl]$ m/l	a_{HCl} m/l	S m/l	$S^2 \times 10^3$	$\bar{n}$[a]
6.00	29.0	0.130	17.0	3.90
5.00	17.0	0.1045	10.9	3.82
4.00	8.7	0.0832	6.9	3.77
3.75	6.67	0.0813	6.67	3.75
3.00	4.17	0.0750	5.60	3.00
2.75	3.72	0.0775	6.00	2.92
2.50	3.40	0.0814	6.60	2.85
2.25	2.78	0.0854	7.28	2.70
2.10	2.37	0.0878	7.70	2.57

[a] From slope of S *vs.* a_{HCl} curve.

Attempts to extract $HSnCl_3$ from aqueous solutions in which $SnCl_3^-$ is a prominent species into chloroform ($HCCl_3$) gave negative results. This provides qualitative evidence for the absence of molecular $HSnCl_3$ indicating that it is a very strong acid contrary to the conclusions of Lachman and Tompkins [10].

Determination of complexity constants. Given the species present, and using the notation of the previous paper [1], substituting Sn^{2+} for M, and $(CH_3)_4N^+$ or A^+, the equation for the solubility is:

$$S = [(CH_3)_4N^+] = \sum_0^4 [SnCl_n^{2-n}] \tag{1}$$

where S is the solubility in moles per liter and n the number of chloride ions bound to Sn^{2+}.

If we define a solubility product:

$$K_s = [(CH_3)_4N^+]\,[SnCl_3^-] \tag{2}$$

it follows that

$$S^2 = K_s \sum_0^4 \frac{\beta_n[Cl^-]^n}{\beta_3[Cl^-]^3} \tag{3}$$

and

$$\frac{d \ln S^2}{d \ln [Cl^-]} = \bar{n} - 3 \tag{4}$$

Eqn. 4 is the Bjerrum equation for finding the formation function [11a] modified for the use of solubility data. In Fig. 4 the formation curve obtained through application of this equation is shown. We have chosen to plot $\bar{n}$ *vs.* $[Cl^-]$ rather than $\log[Cl^-]$ in order to make use of the point at the origin. The log plot gives the familiar inflected curve for the last three steps in the formation of $SnCl_4^{2-}$. From the curve *vs.* $[Cl^-]$ it is possible to obtain first estimates of the formation constants by applying the rules:

$$K_n = \frac{1}{[Cl^-]_{\bar{n}=n-0.5}} \quad \text{and} \quad K_n K_{n+1} = \frac{1}{[Cl^-]^2_{\bar{n}=n}}$$

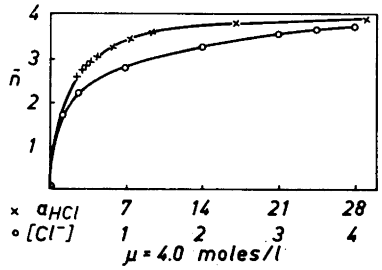

Fig. 4. Formation curves for $SnCl_n^{2-n}$ complexes as a function of chloride concentration at ion normality = 4.0 and of activity of hydrochloric acid in variable ion strength. Note the usefulness of the 0, 0 point when the plot is made in this way.

Table 3. Results of calculations based on Tables 1 and 2.

	Using $[Cl^-]$ in 4 M ($[HCl]+[H_2SO_4]$)		Using a_{HCl} in HCl of varying concentration	
	a	*b*	*a*	*b*
K_1	—	~28		~5.0[c]
K_2	8.00	8.0	5.00	~1.2[c]
K_3	0.90	1.3	0.30	0.40
K_4	0.65	0.7	0.25	0.24
$F_4 = K_sK_4[Cl^-]$	$1.15 \times 10^{-3}/[Cl^-]$		$0.5 \times 10^{-3}/a_{HCl}$	
$F_3 = K_s/K_3[Cl^-]$	$2.0 \times 10^{-3}/[Cl^-]$		$6.5 \times 10^{-3}/a_{HCl}$	
$F_2 = K_s/K_2K_3[Cl^-]^2$	$0.25 \times 10^{-3}/[Cl^-]^2$		$11.0 \times 10^{-3}/a_{HCl}^2$	
$K_s = [(CH_3)_4N^+][SnCl_3^-]$	1.7×10^{-3}		1.7×10^{-3}	

a. Using F values.
b. Using $\bar{n}$ values.
c. From formation curve. Not reliable, unimproved.

As first approximations

$K_1 \sim 33$, $K_2 = 6.0$, $K_3 = 1.4$, and $K_4 = 0.36$
$K_3K_4 = 0.65$, $K_2K_3 = 9.0$, and $K_1K_2 \sim 230$.

The approximate values have been improved by applying the method of Bjerrum [11b] to the experimental points on the formation curve using the formula

$$K_n = \frac{1}{[Cl^-]} \frac{\sum_{t=0}^{t=n-1} \frac{\bar{n} - n + 1 + t}{[Cl^-]^t K_{n-1}K_{n-2}K_{n-3}\ldots K_{n-t}}}{\sum_{t\ 0}^{t=N-n} (n-\bar{n}+t)[Cl^-]^t K_{n+1}K_{n+2}\ldots K_{n+t}} \qquad (5)$$

Eqn. (5) is useful only in the region of the formation curve where the species involved in the expression for a particular K_n are present in appreciable concentrations. The improved values of the constants are summarized in Table 3. It is interesting to note that only the approximate value of K_4 is seriously different from the improved value reported in the table. The values in the table are averages of six or seven points improved by application of eqn. (5) except for values of K_1 where only the three points at lowest chloride gave reasonable results. This implies that significant concentrations of $[Sn^{2+}]$ are present at these points.

Values of constants were also estimated by graphical successive approximations similar to those employed by Leden [12] and Ahrland [13]. This method employs the equation:

$$S^2 = K_s\left[1 + K_4[Cl^-] + \frac{1}{K_3[Cl^-]} + \frac{1}{K_3K_2[Cl^-]^2} + \frac{1}{K_3K_2K_1[Cl^-]^3}\right] \qquad (6)$$

Plotting S^2 *vs.* $[Cl^-]$, one obtains $F_4 = K_sK_4\,[Cl^-]$ from the limiting slope at high $[Cl^-]$. Plotting $S^2 - F_4$ *vs.* $1/[Cl^-]$, one obtains from the slope $F_3 = K_s/K_3\,[Cl^-]$. Plotting $S^2 - F_3$ *vs.* $[Cl^-]$ gives improved values of F_4 and so

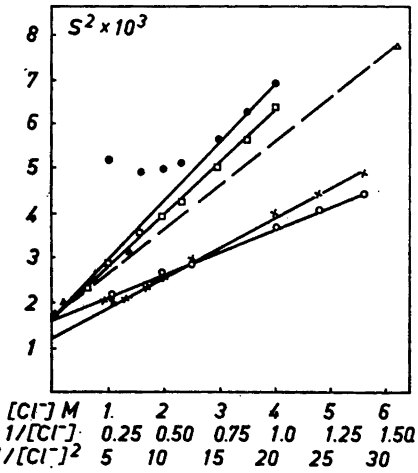

Fig. 5. Analysis of solubility data at ion normality of 4.0 by the method of Leden and Ahrland. Improved plots using F values converge on intercept at $1.7 \times 10^{-3} = K_s$. Curves given by ● and × are used for first approximations for F_4 and F_3 values. Plots given by □, △, and ○ represent best fits of data to eqn. (6).

on. Each plot should give an intercept for $S^2 = K_s$. Successive improvements lead to the convergence of intercepts on the best value of K_s. An illustration of the use of this method to estimate K_n values at ion normality of 4.0 is found in Fig. 5.

The available data cannot give K_1 by this method, but new data at lower $[Cl^-]$ and high $(CH_3)_4N^+$ could conceivably do so. The two methods of calculation give comparable results as shown in Table 3 which summarizes values for constants and final F_n values used in the second method of calculation. The Bjerrum method suffers from the need to determine $\bar{n}$ values from the slopes of curves, while the Leden method places too much reliance on extrapolated values of K_s which must be determined to calculate K_n values. Application of the Leden method should reveal departures from constancy of K_s values at different ligand concentrations, and the Bjerrum method permits estimation of K_n values derived from data at ligand concentrations lower than the limitations of experiment will normally allow.

Use of activity of hydrochloric acid in place of concentration. This substitution gives consistent results only if sulfuric acid is absent. Molal activity coefficients for hydrochloric acid were obtained from published tables [8] and converted to molar activity coefficients. By substituting molar activities for concentration of chloride in the equations previously employed, K_n values may be calculated as before, assuming the formula

$$K_n = \frac{[SnCl_n]}{[SnCl_{n-1}]\, a_{HCl}} \qquad (7)$$

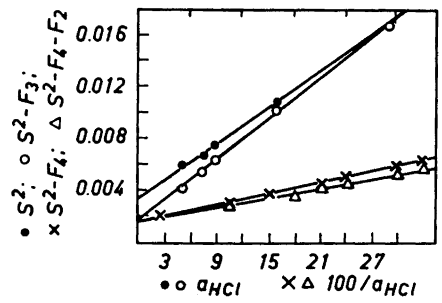

Fig. 6. An illustration of the application of the method of Leden and Ahrland to solubility data at varying activity of hydrochloric acid. Plot for finding F_2 is not shown. Note the convergent intercept corresponding to $K_s = 1.7 \times 10^{-3}$. Activities of hydrochloric acid were used assuming eqn. (7) is applicable.

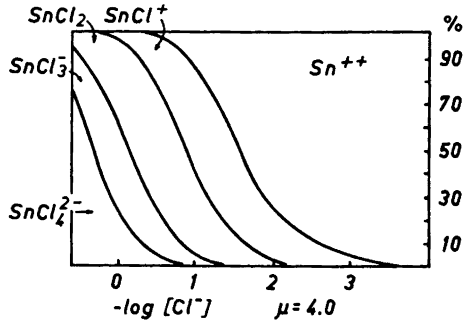

Fig. 7. The distribution of various $SnCl_n^{2-n}$ complexes at ion strength 4.0 and varying chloride ion concentrations.

is valid. The formation curve derived by the Bjerrum method is given in Fig. 4. Fig. 6 illustrates the results of using the Leden technique for calculating K_4 and K_3. Rather surprisingly, the improved F values give not only straight lines, but a common intercept at the same value of K_s which was found in the analysis of data at constant ion normality of 4.0. The results of this analysis of data are summarized in Table 3. In Table 4 a comparison of constants obtained at different ion normalities by various techniques is made. It is seen that the values of the constants divided by the molar activity coefficient of hydrochloric acid when its concentration is equal to the total ion normality give values in fair agreement with those obtained employing eqn. (7).

Table 4. Comparison of K_n from different studies.

	μ = 2.0 M[7]	μ = 3.0 M[6]	μ = 4.0 M*	
			a	*b*
K_1	11.4	14		28
K_2	4.6	3.5	8	8
K_3	0.6	0.95	0.9	1.3
K_4	—	—	0.65	0.70
K_1/y_{HCl}	10.6	9.3		11
K_2/y_{HCl}	4.1	2.3	3.6	3.6
K_3/y_{HCl}	0.4	0.6	0.4	0.6
K_4/y_{HCl}	—	—	0.3	0.3

μ = [HCl] + [H_2SO_4]
y is mean activity coefficient for pure [HCl] = μ.
* Present work.
a. Using F values.
b. Using $\bar{n}$ values.

The relative concentrations of the various $SnCl_n^{2-n}$ species have been determined and are presented graphically for ion normality of 4.0 in Fig. 7. Disagreements with previous studies arise as follows:

(*a*) Vanderzee and Rhodes [6] did not have sufficient data to include K_4 in their calculations.

(*b*) Prytz [3] applied Debye-Hückel activity corrections at ion concentrations too high for them to be valid and apparently ignored hydrolysis effects. In a subsequent publication [14] she reported studies on Sn(II)-OH complexes. Her distribution of $SnCl_n$ species in 3.0 M hydrochloric acid agrees remarkably well with ours.

(*c*) The only serious disagreement appears in the work of Riccobini *et al.*[4] and this too may be attributed to his use of activity corrections based on the Debye-Hückel theory in solutions of high ion normality.

All in all, the agreement between the different methods is excellent and will probably be improved when an adequate theory is available for more concentrated electrolyte solutions, or by simply employing a standard set of assumptions for calculating values of K_n from available data.

DISCUSSION

The results obtained by using eqn. (7) require comment. The analysis indicates not only that eqn. (7) holds within the accuracy of the experimental data, but that K_s is not affected by large changes in ion concentration. There is one precedent for employing eqn. (7) in the work of Bjerrum [15] on the complexes of $CuCl_n^{2-n}$. Bjerrum assumed the existence of a mean activity coefficient:

$$F = \frac{f_{CuCl_n} f_{Cl^-}}{f_{CuCl_{n+1}}}$$

He also noted that for a number of electrolytes at molarities > 3

$$\log f_{\pm} = A + BC$$

where A and B are constants and C is molar concentration. Assuming that F has similar properties to $f_{\pm}$, Bjerrum found for studies in hydrochloric acid that B for the mean activity coefficient, F, was the same as B for HCl and that his data could be fitted to a smooth curve if the A values corresponding to $f_{\pm}$ and F were also the same. Examining his data one finds that eqn. (7) with Cu substituted for Sn would describe the $CuCl_n^{2-n}$ system very well.

Another interesting result of the present study is the apparent constancy of K_s over wide ranges of chloride ion concentration and of total ion normality. The assumption that there is little effect on the activities of minor constituents is put to a rather severe test since concentrations of tetramethylammonium ion rise as high as 0.13 M, yet the K_s obtained by extrapolation remains 1.7×10^{-3} (moles/liter)^2 within a few percent. It may appear that the constancy of K_s has been assumed and built in to the analysis of the data. Insofar as the slopes of plots of F functions are multiples of K_s this is true. The constancy of the intercept and straight lines for F functions are experimental results

Table 5. Comparison of rate constants and $\frac{[SnCl_3^-]}{[Sn(II)]} = a$

Conc. $[Cl^-]$	k^a	a
2.0	0.008	30
3.0	0.020	60
4.0	0.002	10
6.0	3×10^{-6}	<1

[a] Ref.[16]

which we doubt could be obtained if K_s were to vary considerably at different ion strength. The apparent constancy of K_s coupled with the apparent validity of eqn. (7) imply that the assumption that the activity coefficients of ions present in low concentration in solutions of high ion normality are not much affected by changes in the ion normality. The only other reasonable possibility is that this assumption introduces a startling combination of cancelling errors.

The failure to find evidence for formation of $SnCl_5^{3-}$ implies only that its formation constant is extremely low. In preliminary results on the solubility of tetramethylammonium tetrachloroantimonate(III) definite evidence for the existence of $SbCl_5^{3-}$ has been obtained [16]. The higher charge on Sb^{3+} over that on Sn^{2+} means that formation constants will be higher for the antimony complexes. The detection of a higher maximum ligand number for $SbCl_n^{3-n}$ reflects this. It is thus apparent that $SnCl_4^{2-}$ represents an upper limit for ligand numbers for reasons of stability rather than for reasons of structure.

Relative reactivity of the various $SnCl_n^{2-n}$ complexes. It has been observed that the rate constant for the molybdate catalyzed reduction of hydroxylamine by stannous ions varies with hydrochloric acid concentration, having a sharp maximum at 3.0 M hydrochloric acid [17]. Since this maximum corresponds to maximum concentration of $SnCl_3^-$ relative to other chlorotin(II) complexes as shown in this study, the conclusion seems inescapable that $SnCl_3^-$ is the most reactive of the chlorotin(II) species. Table 5 shows the qualitative correlation between the relative amount of $SnCl_3^-$ present and observed rate constants. Duke and Peterson [18] came to the same conclusion as a result of their study of the rate of reduction of methyl orange by stannous ions. This finding is interesting when compared to the finding of Gerischer [19] that $Cd(CN)_3^-$ is the most easily reduced of the cadmium cyanide complexes during electrolysis of their solutions, and the observations of Vlcek [20] showing that complexes of the type MX_5Y are the most reducible of mixed complexes of the octahedral type. There seems to be a strong suggestion that maximum asymmetry leads to maximum reactivity. If $SnCl_3^-$ is in fact $Sn(Cl_3H_2O)^-$, its reactivity is understandable in similar terms.

REFERENCES

1. Haight, Jr., G. P. (Paper I) *Acta Chem. Scand.* **16** (1962) 209.
2. Haight, Jr., G. P. and Bergh, A. Reduction of Mo(VI) and Mo(V) by Sn(II), to be published. *cf.* Bergh, A. *Ph. D. Thesis*, Univ. of Pennsylvania (1959).
3. Prytz, M. *Z. anorg. u. allgem. Chem.* **172** (1928) 147.

4. Riccobini, L., Popoff, P. and Arich, G. *Gazz. chim. ital.* **79** (1949) 547.
5. Duke, F. R. and Courtney, W. G. *Iowa State College J. Sci.* **24** (1950) 397.
6. Vanderzee, C. E. and Rhodes, D. E. *J. Am. Chem. Soc.* **74** (1952) 3552.
7. Rabideau, S. W. and Moore, R. H. *J. Phys. Chem.* **65** (1961) 371.
8. Robinson, R. A. and Stokes, R. H. *Electrolyte Solutions*, Butterworths London 1955.
9. Guggenheim, E. A. *Phil. Mag.* (7) **19** (1935) 588.
10. Lachman, S. J. and Tompkins, F. C. *Trans. Faraday Soc.* **40** (1944) 130, 136.
11. Bjerrum, J. *Metal Ammine Formation in Aqueous Solution*, P. Haase and Son, Copenhagen 1941. Reprinted 1957. (*a*) page 22, (*b*) page 37.
12. Leden, I. *Z.physik. Chem.* **A 188** (1941) 160.
13. Ahrland, S. *Acta Chem. Scand.* **11** (1957) 1111.
14. Prytz, M. *Z. anorg. u. allgem. Chem.* **174** (1928) 355.
15. Bjerrum, J. *Kgl. Danske Videnskab. Selskab, Mat.-fys. Medd.* **22** (1946) No. 18.
16. Haight, Jr., G. P. and Bergh, M. *Unpublished work.*
17. Haight, Jr., G. P. and von Frankenberg, C. *Acta Chem. Scand.* **15** (1961) 2026.
18. Duke, F. R. and Peterson, N. C. *J. Phys. Chem.* **63** (1959) 2077.
19. Gerischer, H. *Z. Elektrochem.* **57** (1953) 604.
20. Vlcek, A. A. *Discussions Faraday Soc.* **26** (1958) 164.

Received July 25, 1961.

ACTA CHEMICA SCANDINAVICA 16 (1962) 323–326

The Effect of the Solvent on the Base Catalyzed Conjugation-Isomerisation of Poly-unsaturated Fatty Acid Compounds

JOHN UGELSTAD, BJÖRN JENSSEN and PREBEN C. MÖRK

Institute of Industrial Chemistry, Norges Tekniske Högskole, Trondheim, Norway

The rate of the conjugation-isomerisation of linseed oil in a solution of K-butoxide in butanol is increased enormously by the presence of an excess of dimethylsulfoxide, dimethylformamide or tetramethylurea. The reaction may thereby be caused to proceed rapidly at room temperature.

In the literature concerning the effect of the solvent on the rate of organic reactions most authors have tried to correlate the effect to the polar properties of the solvent. This theory has led to equations which, for each type of reaction, postulate a certain relationship between the rate and the dielectric constant of the solvent. In two recent publications we discussed these problems [1,2], and gave several examples of reactions where there seems to be no such correlation. In many cases special types of interaction between the reactants and the nearest neighbour solvent molecules seem to outweigh the integral electrostatic effect of the polar forces. As an example of this type of effect we have described briefly some types of base-catalyzed reactions. One of the reactions mentioned was the conjugation-isomerisation of poly-unsaturated fatty acid compounds. In the present paper some of the preliminary results of these investigations are described.

When analyzing a fatty acid compound for the content of different poly-unsaturated fatty acids, conjugation of the double bonds is usually brought about by treatment of the compound at 180°C with a solution of KOH or K-alcoholate in alcohol. From the amount of conjugated diene, triene *etc.*, as determined from UV absorption spectra, the content of the original poly-unsaturated fatty acids may be estimated.

As will be shown below, we have found that the conjugation-isomerisation proceeds rapidly even at 25°C when using a mixture of K-alcoholate in alcohol and an excess of dimethylsulfoxide, dimethylformamide or tetramethylurea as the reaction medium for the conjugation process.

ACTA CHEMICA SCANDINAVICA 16 (1962) 323–326

The Effect of the Solvent on the Base Catalyzed Conjugation-Isomerisation of Poly-unsaturated Fatty Acid Compounds

JOHN UGELSTAD, BJÖRN JENSSEN and PREBEN C. MÖRK

Institute of Industrial Chemistry, Norges Tekniske Högskole, Trondheim, Norway

The rate of the conjugation-isomerisation of linseed oil in a solution of K-butoxide in butanol is increased enormously by the presence of an excess of dimethylsulfoxide, dimethylformamide or tetramethylurea. The reaction may thereby be caused to proceed rapidly at room temperature.

In the literature concerning the effect of the solvent on the rate of organic reactions most authors have tried to correlate the effect to the polar properties of the solvent. This theory has led to equations which, for each type of reaction, postulate a certain relationship between the rate and the dielectric constant of the solvent. In two recent publications we discussed these problems [1,2], and gave several examples of reactions where there seems to be no such correlation. In many cases special types of interaction between the reactants and the nearest neighbour solvent molecules seem to outweigh the integral electrostatic effect of the polar forces. As an example of this type of effect we have described briefly some types of base-catalyzed reactions. One of the reactions mentioned was the conjugation-isomerisation of poly-unsaturated fatty acid compounds. In the present paper some of the preliminary results of these investigations are described.

When analyzing a fatty acid compound for the content of different poly-unsaturated fatty acids, conjugation of the double bonds is usually brought about by treatment of the compound at 180°C with a solution of KOH or K-alcoholate in alcohol. From the amount of conjugated diene, triene *etc.*, as determined from UV absorption spectra, the content of the original poly-unsaturated fatty acids may be estimated.

As will be shown below, we have found that the conjugation-isomerisation proceeds rapidly even at 25°C when using a mixture of K-alcoholate in alcohol and an excess of dimethylsulfoxide, dimethylformamide or tetramethylurea as the reaction medium for the conjugation process.

PROCEDURE

Due to its high content of linolenic acid, linseed oil was chosen as a suitable compound for the preliminary investigation of the effect of the solvent on the rate of the conjugation reaction. 30 mg linseed oil was dissolved in dimethylsulfoxide, dimethylformamide or tetramethylurea. After deaeration of the solution with N_2 the sample was placed in a thermostat bath at 25°C. Then the catalyst solution was added. (The catalyst solution was prepared by dissolving potassium in butanol. In each case the catalyst solution contained 2.3×10^{-3} mole K-butoxide per g solution.) After certain time intervals, the reaction was stopped by dilution with methanol. UV-spectra of the samples were taken with a Beckman Recording Spectrophotometer, Model DK 9500. In the preliminary investigation of the solvent effect on the rate of isomerisation, only the content of conjugated triene, as determined from the absorption peak at ~267 mμ, was considered. This determination gave good reproducible values.

In Table 1 the values for the extinction coefficient k, in a reaction medium consisting of 4 g catalyst-solution and 10 g of dimethylsulfoxide, dimethylformamide or tetramethylurea, are given for various reaction times, ($k = \varepsilon/c \cdot L$ where ε = absorption, c = g/l and L = the length of the cell (= 1 cm)). The results of some experiments with the catalyst-solution only as reaction medium have also been included in the table for comparison.

In Fig. 1 the values for the extinction coefficient are plotted as a function of the reaction time for the mixture of catalyst-solution and dimethylformamide or dimethylsulfoxide. In Fig. 2 the results of some experiments are given where the relative amount of butanol and dimethylsulfoxide in the reaction medium were varied. In these experiments the concentration of catalyst and the reaction time were kept constant.

The linseed oil used in these investigations was also isomerized by the usual method for analysis: treatment at 180°C with 10 g of a solution consisting of 18 % KOH in ethyleneglycol. The extinction coefficient at ~267 mμ after this treatment was 37.5.

Table 1. Extinction coefficient, k, at ~ 267 mμ after different time intervals. Linseed oil, 30 mg. Temp. 25°C.

	Reaction medium	1 min	2 min	5 min	10 min	15 min	20 min	30 min	60 min	120 min	180 min	24 h
A	10 g dimethylsulfoxide, 4 g catalyst-solution	8.2	13.2	24.0	29.0		30.0	31.0	33.0	33.0		
B	10 g N,N-dimethylformamide, 4 g catalyst-solution		3.8	7.4	11.6	19.0		26.0	31.5	34.5	35.0	
C	10 g tetramethylurea 4 g catalyst- solution								32.0	35.0		
D	4 g catalyst- solution									0	0	~0

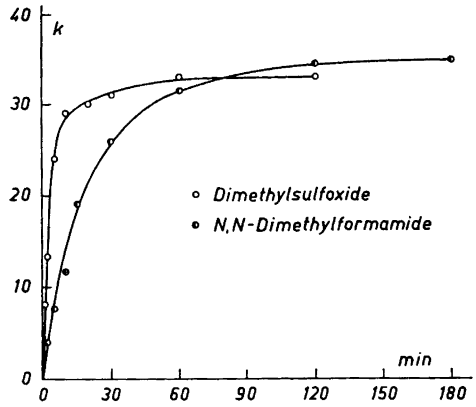

Fig. 1. The extinction coefficient, k, as a function of reaction time. Linseed oil, 30 mg. Catalyst solution, 4 g. DMSO or N,N-dimethylformamide, 10 g. Temp. 25°C.

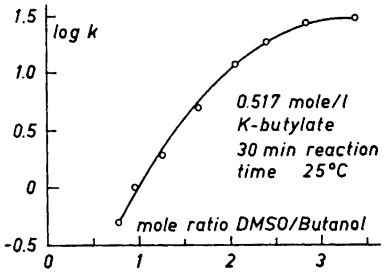

Fig. 2. Log (extinction coefficient) as a function of mole ratio DMSO/butanol.

It may be seen from the table that even after 24 h at 25°C there are only traces of conjugation when the linseed oil is treated with the pure catalyst solution (K-butoxide in butanol). In the mixtures of catalyst solution and dimethylformamide, tetramethylurea or dimethylsulfoxide however, the conjugation-isomerisation takes place with remarkable speed. In each case the extinction coefficient approaches a practically constant value of 33—35, which is reached already after 30 to 60 min.

DISCUSSION

The conjugation reaction is initiated by an attack of the RO^- ion on the CH_2 group in α position to two double bonds. A twostep reaction mechanism may be formulated as follows:

$$-CH=CH-CH_2-CH=CH- + OR^- \rightleftharpoons -\bar{C}H-CH=CH-CH=CH- + ROH \quad (1)$$

$$-\bar{C}H-CH=CH-CH=CH- + ROH \rightarrow -CH_2CH=CH-CH=CH- + OR^- \quad (2)$$

In this case, (1) is most probably the rate determing step. Possibly the proton transfer may also take place without a complete ionization:

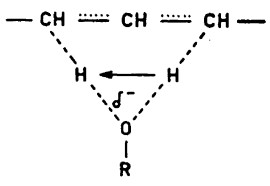

The observed effect of N,N-dimethylformamide, tetramethylurea and dimethylsulfoxide on the rate of the conjugation reaction may possibly be due to: 1. The ability of these substances to act as strong H-acceptors by the formation of H-bonds. 2. Their ability to solvate specifically the K^+-ion.

The effect of H-bond formation may be explained as follows: In alcoholic solution the RO^- ion will be highly solvated by H-bond formation with the alcohol, $RO^- - - - H-OR$, which in turn leads to a deactivation of the catalyst. (It should be noted that alcohol is present in all the experiments.) However, dimethylformamide, tetramethylurea or dimethylsulfoxide present in excess, may effectively bind the alcohol by H-bond formation and thus reduce the deactivation of RO^- by the alcohol. N-Alkylamides are known to act as very strong H-binding "acceptors". The relative strength of dimethylsulfoxide, in this respect is less known. From nuclear resonance studies, Drinkard and Kivelson [3] conclude that dimethylsulfoxide forms stronger H-bonds than acetone with methanol. Lindquist *et al.*[4,5] conclude from measurements of the addition reaction to $SnCl_4$ and $SbCl_5$ that dimethylsulfoxide, like N-alkylamides has a much higher donor-strength than acetone and ethylacetate. A comparison of substances with the same donor atom seems to show a correlation between the electrondonating capacity of the substance and the strength of the H-bond formed.

While the alcohol solvates the catalyst by interaction with the RO^- ion, N-alkylamides and dimethylsulfoxide, with a high electron density at the O atom, might be expected to solvate specificially the K^+ ions. An activation of the catalyst would then occur through a decrease in the $K^+ - - -\overline{O}R$ interaction. Zaugg [6] found that addition of N-alkylamides and dimethylsulfoxide to a solution of sodio malonic esters in benzene markedly increased the rate of the alkylation with alkyl halides, and ascribed this effect to a solvation of the Na^+ ion by these substances. Zaugg concluded that this ability is primarily due to the presence of a region of high electron density in the π-orbital at the O atom of these substances.

REFERENCES

1. Ugelstad, J. and Renolen, P. *Tidskr. Kjemi, Bergvesen Met.* **21** (1961) 88.
2. Ugelstad, J. and Mörk, P. C. *Tidskr. Kjemi, Bergvesen Met.* **21** (1961). *In press.*
3. Drinkard, W. and Kivelson, D. *J. Phys. Chem.* **62** (1958) 1494.
4. Lindqvist, I. and Zackrisson, M. *Acta Chem. Scand.* **14** (1960) 453.
5. Lindqvist, I. and Fjellström, B. *Acta Chem. Scand.* **14** (1960) 2055.
6. Zaugg, H. E. *J. Am. Chem. Soc.* **82** (1960) 2903.

Received September 11, 1961.

ACTA CHEMICA SCANDINAVICA 16 (1962) 327–345

High-Temperature Electrochemical Study of Uranium Oxides in the UO_2 — U_3O_8 Region

KALEVI KIUKKOLA

Metallurgical Laboratory, Institute of Technology, Otaniemi, Finland *

Electromotive force measurements on galvanic cells involving solid electrolytes have been made at temperatures of 800° to 1200°C in order to obtain standard thermodynamic data for the mixing of UO_2 and oxygen gas. Due to the purely anionic conductivity of the electrolyte, a direct evaluation of the relative partial molar free energy of oxygen in uranium oxide as a function of the O/U atomic ratio and temperature has been possible. Therefrom, values for the partial molar heat and entropy of mixing and the corresponding relative integral quantities have been calculated for the whole composition and temperature range investigated. Nonstoichiometry in the homogeneous UO_{2+x} phase is discussed. The solubility of oxygen in this phase was found to be higher than previously known.

In the present investigation, supplementary data to the high-temperature thermodynamic properties of uranium oxides in the UO_2—U_3O_8 region are presented. Following previous suggestions [1,2], an electrochemical technique using galvanic cells with solid electrolytes has been used. The results clarify the phase relations among the stable high-temperature oxide phases and show the dependence of the equilibrium oxygen partial pressure on the composition of the oxide phases or mixtures thereof. Values for the pertinent thermodynamic quantities are evaluated.

In order to obtain the standard molar free energy of formation of uranium oxides with predetermined oxygen-to-uranium ratios, galvanic cells of the previously developed type [3]

$$\mathrm{Fe},\ \mathrm{Fe_xO}\ /\ (0.85\ \mathrm{ZrO_2} + 0.15\ \mathrm{CaO})\ /\ \mathrm{UO_{2+x}}$$

have been investigated. The cell involves at left an iron-wüstite reference electrode with a known equilibrium oxygen partial pressure or the relative partial molar free energy of oxygen. The electrolyte is a solid solution of 85 mole % zirconium dioxide and 15 mole % calcium oxide. Due to its defect

* Present address: Oy Fiskars Ab, Åminnefors, Finland.

structure containing oxygen ion vacancies, this electrolyte is a predominantly anionic conductor over wide variations in the ambient oxygen partial pressure as shown by Kiukkola and Wagner [3] and verified by Kingery *et al.*[4] and Carter [5]. The right-hand electrode is made of uranium oxide with a predetermined oxygen-to-uranium ratio.

EXPERIMENTAL

Uranium oxide electrodes. The various compositions of uranium oxide were prepared in two ways: (1). Reactor grade uranium dioxide powder from Degussa, Germany, was oxidized in air at temperatures below 200°C to the desired overall compositions; (2). Mixtures of UO_3 and U_3O_8 powders, the latter prepared from UO_2 by oxidation in air at 800°C, were heated in evacuated quartz bulbs at 1000°C for about ten days. This method was easier to control.

The prepared uranium oxide powders were pressed into cylindrical pellets of 2 to 3 mm thickness and 8 mm diameter at about 8 ton/cm^2 pressure. The electrolyte and reference electrode pellets were of the same size. In order to reduce contact with the surrounding atmosphere, the uranium oxide pellets were placed into a cup made of thin platinum foil (Fig. 1). For both types of uranium oxide powders, the final homogenization of the electrodes were performed prior to emf measurements by heating the cell initially to the highest possible measuring temperature (1100 to 1200°C). The method of preparation did not influence the equilibrium oxygen pressure values.

Arrangement of the cell. The apparatus and the arrangement of the cell was similar to that previously described [3]. The same procedure was also followed in the preparation of the electrolyte and the reference electrode.

The cell assembly consisting of the electrolyte tablet between the two electrode tablets (Fig. 1) was inserted into a quartz tube of 26 mm inside diameter placed in a vertical, electrically heated tube furnace. The cell was clamped between two horizontal platinum discs which were provided with platinum connecting leads to the potentiometer. An inert atmosphere was maintained around the cell by flowing a slow stream of argon under a slight overpressure. The gas was purified by passing over silica gel, ascarite and magnesium perchlorate and deoxygenated by passing over active copper at 200°C. Emf measurements were taken with a Rubicon precision potentiometer over the temperature range 800 to 1200°C. A complete temperature cycle was always made. The emf of the Pt, Pt + 10 % Rh thermocouple located near the top electrode was measured with the same potentiometer to ± 1°C. One run lasted from 6 to 30 h.

Each iron-wüstite electrode pellet was used successfully for several experiments. For each run, its surfaces were cleaned with sandpaper. Similar precautions were followed with electrolyte pellets. They were used satisfactorily in one or more experiments.

Analysis of uranium oxides. The oxygen-to-uranium ratios of the electrodes were determined after each run by the usual method of oxidizing the weighed elctrode at about 800°C in air in a platinum boat. The oxidized product is assumed to be $U_3O_{8-\delta}$. It is estimated that this will give the composition to better than the nearest 0.01 atom of oxygen. The change of the composition of the electrodes during an emf experiment was found to be within the analytical accuracy.

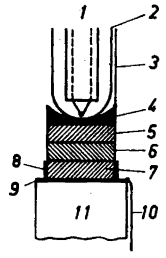

Fig. 1. Cross section of cell with solid electrolyte used in emf measurements. 1. Thermocouple. 2. Quartz tube. 3. Platinum lead. 4. Platinum disc. 5. Reference electrode pellet. 6. Electrolyte pellet. 7. Uranium oxide electrode pellet. 8. Platinum cup. 9. Platinum disc. 10. Platinum lead. 11. Quartz rod.

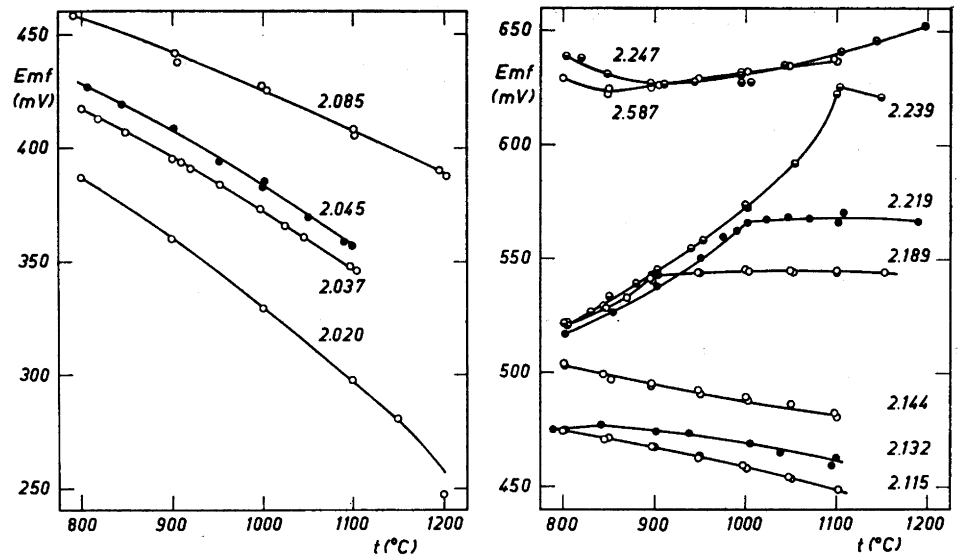

Fig. 2 and 3. Variation of emf of cell Fe, $Fe_xO/(0.85\ ZrO_2 + 0.15\ CaO)/UO_{2+x}$ with temperature for uranium oxides of various O/U atomic ratios.

Solid state coulometric titrations

In addition to the foregoing measurements with uranium oxides of predetermined O/U atomic ratio, a few measurements were performed with the solid state coulometric titration technique developed by Wagner [9,8]. In this method, it is possible to vary the O/U ratio of a given electrode by known amounts and measure the corresponding oxygen partial pressure of the electrode. The galvanic cell was the same as in the other experiments. Prior to measurements, the uranium oxide sample was brought to a composition close to UO_2 by reducing the electrode in hydrogen gas at 1000°C for 4 h and thereafter applying to the assembled cell a positive potential of 0.3 V at 1100°C. The measuring circuit provided instruments for measuring the amount of current passed, the applied potential and the resulting equilibrium potential. All titrations were done at 1100°C to ensure ionic mobility high enough for the homogenization of the electrodes to occur within a reasonable time. For the same reason, the UO_2 electrodes were thin, their weights ranging from 80 to 190 mg.

RESULTS

Electrodes with predetermined composition. Figs. 2 and 3 show plots of emf as a function of composition for some of the uranium oxides with a predetermined O/U atomic ratio. The points shown belong either to descending or ascending temperatures and they deviate from the drawn curves by about $\pm$ 3 mV at most. The emf was found to vary smoothly with temperature at compositions up to $UO_{2.144}$. A definite break in the emf *vs.* temperature curves occurred with the following pellets: $UO_{2.189}$ at about 900°C, $UO_{2.219}$ at about 1000°C, and $UO_{2.239}$ at about 1100°C. These breaks indicate a phase transformation at these temperatures, the homogeneous UO_{2+x} phase prevailing above

these temperatures. The emf values from the composition $UO_{2.250}$ up to $UO_{2.625}$ are practically identical indicating the presence of a two-phase region $UO_{2.250} + UO_{2.667-y}$. Uranium oxide tablets with higher O/U atomic ratio than the above-mentioned, *e.g.* $UO_{2.667}$, gave initially higher emf, too. The final values of emf and composition corresponded to the upper limit of the two-phase region. Due to the high oxygen partial pressures, it was thus impossible to measure the variation of the relative partial molar free energy of oxygen within the $UO_{2.667\pm y}$ one-phase region.

Solid state coulometric titrations. Since the electrolyte is a purely anionic conductor, the passing of current i across the cell during time interval t causes a corresponding transport of oxygen from one electrode to the other. A positive current flowing through the cell from right to left adds oxygen to the UO_2 electrode. The O/U atomic ratio, initially about 2, changes thereby to $2+x$ where x is

$$x = i\,t\,/\,2\,n_U\,F$$

In this equation, n_U is the number of gram atoms of uranium present initially and F is the Faraday constant.

Points of five titrations along with a curve obtained by the conventional method using predetermined electrodes with constant composition are shown in Fig. 4 for the temperature of 1100°C. Due to difficulties in defining the initial composition of the electrodes in titration experiments, it was assumed that they coincided with the conventional curve at a composition defined by their initial emf. The two curves agree at small values of x ($x \leqq 0.2$). At higher O/U ratios, the titrations were not satisfactory presumably due to escape from the uranium oxide electrode of a part of the transported oxygen. It was found that the flow of current, despite its low density, polarized the cell to a potential over 0.9 V which causes oxygen of atmospheric pressure

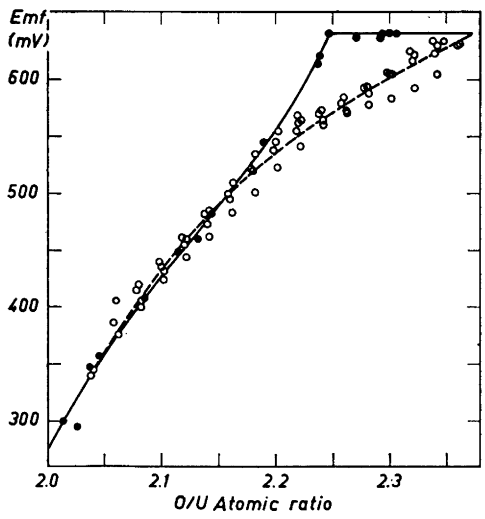

Fig. 4. Variation of emf with uranium oxide composition at 1100°C. —●— measured with cells having predetermined constant composition of uranium oxide, ---O--- experimental points from five coulometric titrations.

Table 1. Relative partial molar free energy of oxygen over iron and wüstite.

	800°C	900°C	1000°C	1100°C	1150°C	1200°C
$\bar{F}_{O_2} - F^\circ_{O_2}$ (kcal)	−93.00	−89.76	−86.69	−83.52	−81.96	−80.40

to develop. Diffusion of the transported oxygen into the uranium oxide pellet was evidently too slow. A comparison of the relevant diffusion coefficients [4,10,11] in the various parts of the cell points to the same conclusion. In addition, the phase change of UO_{2+x} to $UO_{2.25}$ may be slow and cause overshooting since the mobility of uranium is very low as pointed out by Wagner [2]. Finally, it was observed that the titrations were amenable to large hysteresis.

For all these reasons, the conventional measurements with predetermined uranium oxide compositions, the only ones reported in the following, were considered more profitable for the present purposes. In the neighborhood of the ideal O/U ratio the titrations may prove useful.

ANALYSIS AND DISCUSSION OF RESULTS

Evaluation of measurements. Since the electrolyte of the cell shows only predominant ionic conduction due to migration of oxygen ions in the electrolyte, the virtual cell reaction may be expressed in terms of oxygen transfer from the right-hand to the left-hand electrode. Hence the emf E of the cell is

$$E = (\bar{F}''_{O_2} - F^\circ_{O_2}) - (\bar{F}'_{O_2} - F^\circ_{O_2}) / 4F$$

where $\bar{F}'_{O_2}$ and $\bar{F}''_{O_2}$, respectively, are the partial molar free energies of oxygen on the left-hand and the right-hand side of the cell, $\bar{F}^\circ_{O_2}$ is the standard molar free energy of oxygen, and F is the Faraday constant. In all experiments made, a mixture of iron and wüstite was used on the left-hand side of the cell. The values for the relative partial molar free energy over iron and wüstite have been evaluated from gas equilibrium measurements [3] and the corrected values are listed in Table 1.

Equilibrium oxygen pressures. Upon substituting the values in Table 1 and the experimental values of E in the above equation, values of the relative partial molar free energy of oxygen,

$$F^M_{O_2} = \bar{F}_{O_2} - F^\circ_{O_2} = RT \ln p_{O_2},$$

and hence the oxygen partial pressure over uranium oxides can be calculated. The values of the equilibrium oxygen partial pressure as a function of composition are plotted in Fig. 5 at six round temperatures. The corresponding values of the emf were read from large plots of E *vs.* temperature. Fig. 5 includes for comparison some of the data of Biltz and Müller [12] at 1160°C which were determined by a direct manometric measurement. Both type of data agree with

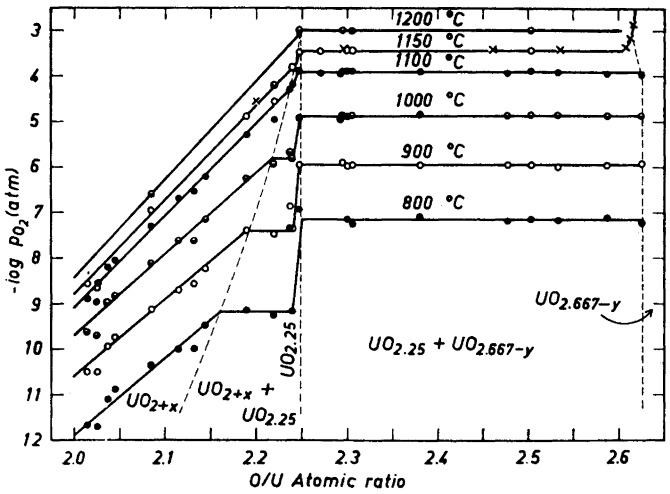

Fig. 5. Variation of equilibrium oxygen pressure with uranium oxide composition at round temperatures between 800°—1200°C. Phase boundaries are indicated with dashed lines. Circles represent data of this study. × represent data of Biltz and Müller [12] at 1160°C.

dan supplement each other very well. The regions were p_{O_2} does not change with composition are two-phase regions. Below $UO_{2.25}$ there is the UO_{2+x} + $UO_{2.25}$ equilibrium and above it the $UO_{2.25}$ + $UO_{2.667-y}$ equilibrium.

The equilibrium oxygen pressures of both two-phase regions are plotted in Fig. 6 as a function of temperature. They are drawn as straight lines which cross at the temperature of 1215° ± 10°C and the log $p_{O_2} = -2.91$. This is the temperature and oxygen pressure above which the UO_{2+x} + $UO_{2.25}$ phase region vanishes (the peritectic point). In the same figure are shown data obtained by Biltz and Müller [12] with manometric pressure measurements, by Blackburn [8] with the Knudsen effusion method, and by Aronson and Belle [13] with the emf method used here. The values of Biltz and Müller for the equilibrium $UO_{2.25}$ + $UO_{2.667-y}$ are in complete agreement with this study. The data of Blackburn are consistently lower. Otherwise, the values are in good agreement.

Phase diagram. Combining the abovementioned facts, it is possible to re-evaluate the usual high-temperature phase diagram for the UO_2 — U_3O_8 range (Fig. 7). In particular, the diagram shows the solubility of oxygen in the UO_{2+x} phase and compares it with the previous evaluations by Grønvold [6], Blackburn [8], Aronson and Belle [13], and Willardson *et al.*[14]. The experimental evidence of Aronson and Belle is fully confirmed. It thus seems established that the solubility of oxygen in the UO_{2+x} phase is greater than is usually shown on phase diagrams which are mainly based on the works by Grønvold and Blackburn.

The $UO_{2.25}$ phase is shown schematically as a straight line since its boundaries are still too inaccurate. The uppper boundary of the $UO_{2.25}$ + $UO_{2.667-y}$

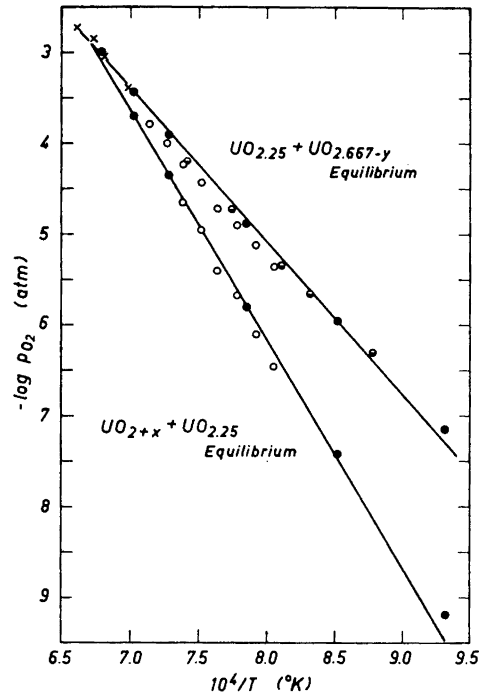

Fig. 6. Plot of log p_{O_2} *vs.* $1/T$ for UO_{2+x} + $UO_{2.25}$ and $UO_{2.25}$ + $UO_{2.667-y}$ equilibria. —●— this study, O Blackburn [8], × Biltz and Müller [12], ◒ Aronson and Belle [13].

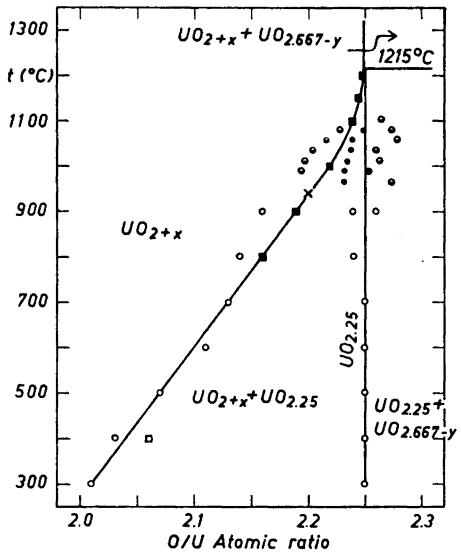

Fig. 7. Phase diagram for the range UO_2 — $UO_{2.3}$. —■— this study, O Grønvold [6], × Aronson and Belle [13], ● & ◒ Blackburn [8], □ Willardson *et al.*[14].

phase field is estimated to be at around $UO_{2.625}$ between 800°—1100°C and, according to Biltz and Müller [12], at around $UO_{2.61}$ above this temperature range. The peritectic temperature, above which the miscibility gap between the phases UO_{2+x} and $UO_{2.25}$ disappears, was estimated by Belle and Auskern [10] to be around 1170°C. A complete miscibility at higher temperatures was inferred by Grønvold [6] from crystallographic considerations.

Integral molar free energies. Choosing the components in uranium oxide of any composition as UO_2 and O_2, then the composition of the oxide is determined by the mole fraction N_{UO_2} or N_{O_2}. If the O/U atomic ratio in the oxide is $2+x$, where $0 \leqq x \leqq 1$, then $N_{UO_2} = 2/(2+x)$ and $N_{O_2} = x/(2+x)$. With the help of the measured values of the relative partial molar free energy of oxygen, $F^M_{O_2}$, it is possible to calculate the relative integral molar free energy F^M for the formation of uranium oxide of any composition from the UO_2 of ideal composition and oxygen gas from the formula [15]

$$F^M = (1-N_{O_2}) \int_0^{N_{O_2}} \frac{F^M_{O_2}}{(1-N_{O_2})^2} \, dN_{O_2}$$

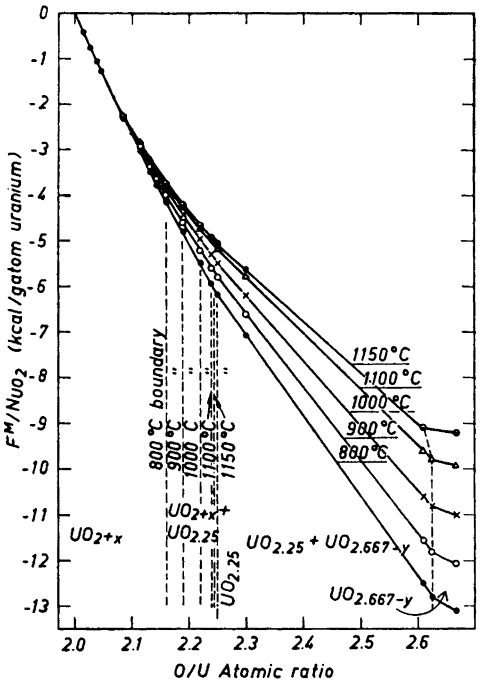

Fig. 8. Integral free energy of formation of uranium oxide from UO_2 and O_2 per gram atom uranium as a function of composition at five round temperatures. Phase boundaries are indicated by dashed lines.

The evaluation of this integral was done graphically in the homogeneous regions and numerically in the two-phase regions where $F^M_{O_2}$ is constant. It was assumed that the phase diagram is of the form shown in Fig. 7 with the phase $UO_{2.25}$ having a very narrow region of homogeneity. The oxygen pressure data for the $UO_{2.667-y}$ phase were estimated from the measurements by Biltz and Müller [12]. Fig. 8 shows the variation with composition of F^M/N_{UO_2}, *i.e.* the relative integral molar free energy per gram atom uranium for five round temperatures, the values for 1200°C being very close to those shown for 1150°C. Table 2 includes a complete list of all thermodynamic data.

Relative partial molar heat of solution of oxygen in uranium oxide. This quantity,

$$H^M_{O_2} = \bar{H}_{O_2} - H^\circ_{O_2}$$

where $H^M_{O_2}$ is the partial molar enthalpy of oxygen gas and $H^\circ_{O_2}$ is the standard molar enthalpy of oxygen gas, is obtained readily from the temperature coefficient of the oxygen pressure at constant composition provided the oxide solution is homogeneous over the whole temperature range. The previously given values of log p_{O_2} were plotted against $1/T$ at constant compositions within the UO_{2+x} phase region. The resulting curves were essentially straight over the temperature range covered. Their slope multiplied by 4.575 gives $H^M_{O_2}$

Table 2. Variation of the thermodynamic properties of uranium oxides with composition and temperature.

O/U atomic ratio	Temp. °C	Relative partial quantities $-H^M_{O_2}$ kcal	$-F^M_{O_2}$ kcal	$-S^M_{O_2}$ e.u.	Relative integral quantities $-H^M/N_{UO_2}$ kcal	$-F^M/N_{UO_2}$ kcal	$-S^M/N_{UO_2}$ e.u.
2.014	800	59.9	57.30	2.39	0.42	0.41	0.01
	900	59.9	56.46	2.90	0.42	0.40	0.01
	1000	59.9	56.06	2.99	0.42	0.40	0.02
	1100	59.9	55.84	2.93	0.42	0.39	0.02
	1150	59.9	55.76	2.88	0.42	0.39	0.02
2.026	800	59.8	57.48	2.15	0.78	0.76	0.02
	900	59.8	56.46	2.84	0.78	0.74	0.04
	1000	59.8	56.48	2.60	0.78	0.73	0.04
	1100	59.8	56.31	2.53	0.78	0.74	0.03
	1150	59.8	56.41	2.38	0.78	0.74	0.03
	1200	59.8	57.6	1.5	0.78	0.75	0.02
2.037	800	63.7	54.53	8.57	1.12	1.07	0.05
	900	63.7	53.27	8.92	1.12	1.04	0.07
	1000	63.7	52.37	8.92	1.12	1.03	0.07
	1100	63.7	51.51	8.90	1.12	1.04	0.06
2.045	800	62.3	53.42	8.23	1.38	1.28	0.09
	900	62.3	52.26	8.52	1.38	1.25	0.10
	1000	62.3	51.36	8.55	1.38	1.24	0.11
	1100	62.3	50.59	8.49	1.38	1.25	0.10
2.085	800	66.6	50.84	14.7	2.70	2.32	0.35
	900	66.6	48.98	15.0	2.70	2.26	0.37
	1000	66.6	47.30	15.2	2.70	2.23	0.37
	1100	66.6	45.93	15.1	2.70	2.22	0.35
	1150	66.6	45.24	15.0	2.70	2.21	0.34
	1200	66.6	44.51	15.0	2.70	2.21	0.33
2.115	800	74.1	49.23	23.2	3.67	3.03	0.60
	900	74.1	46.68	23.4	3.67	2.93	0.63
	1000	74.1	44.35	23.4	3.67	2.88	0.62
	1100	74.1	42.10	23.3	3.67	2.84	0.61
2.132	800	74.8	49.13	23.9	4.35	3.49	0.80
	900	74.8	45.99	24.5	4.35	3.37	0.84
	1000	74.8	44.35	23.9	4.35	3.29	0.83
	1100	74.8	41.08	24.5	4.35	3.23	0.82
2.144	800	73.3	46.55	24.9	4.89	3.78	1.04
	900	73.3	44.14	24.9	4.89	3.64	1.07
	1000	73.3	41.67	24.8	4.89	3.55	1.06
	1100	73.3	39.05	24.9	4.89	3.46	1.04
2.160	800	—[a]	45.11	—[a]	5.38	4.15	1.15
	900	74.8	42.50	27.5	5.38	4.00	1.18
	1000	74.8	39.78	27.5	5.38	3.87	1.18
	1100	74.8	36.94	27.6	5.38	3.76	1.18
	1150	74.8	35.48	27.6	5.38	3.74	1.15

Table 2. Continued.

2.189	800	116.1	44.94	66.4	7.06	4.80	2.11
	900	—[a]	39.67	—[a]	6.48	4.59	1.62
	1000	77.4	36.41	32.2	6.48	4.43	1.62
	1100	77.4	33.24	32.1	6.48	4.27	1.61
	1150	77.4	31.77	32.0	6.48	4.21	1.60
2.219	800	116.1	45.35	66.0	8.81	5.48	3.10
	900	116.1	40.22	64.7	8.22	5.20	2.57
	1000	—[a]	34.57	—[a]	7.60	4.96	2.07
	1100	71.9	31.12	29.7	7.60	4.73	2.09
	1150	71.9	29.65	29.7	7.60	4.65	2.07
	1200	71.9	28.14	29.7	7.60	4.51	2.10
2.239	800	116.1	45.03	66.3	9.97	5.93	3.76
	900	116.1	39.57	65.3	9.39	5.58	3.24
	1000	116.1	33.83	64.7	8.76	5.30	2.72
	1100	—[a]	26.23	—[a]	8.31	5.03	2.39
	1150	69.7	24.67	31.6	8.31	4.92	2.39
2.245	1150	—[a]	24.09	—[a]	8.52	5.00	2.44
2.248	1200	—[a]	21.03	—[a]	8.62	4.87	2.55
2.250	800	—	35.12	—	10.6	6.18	4.13
	900	—	31.97	—	10.0	5.80	3.60
	1000	—	28.41	—	9.40	5.49	3.07
	1100	—	24.57	—	8.95	5.18	2.75
	1150	—	22.36	—	8.81	5.06	2.63
	1200	—	20.17	—	8.74	4.90	2.60
2.300	800	77.1	35.12	39.1	12.5	7.06	5.10
	900	77.1	31.97	38.5	12.0	6.60	4.56
	1000	77.1	28.41	38.2	11.3	6.20	4.03
	1100	77.1	24.57	38.2	10.9	5.79	3.70
	1150	77.1	22.36	38.5	10.7	5.62	3.59
	1200	77.1	20.17	38.7	10.7	5.40	3.58
2.610	1150	—[b]	22.36	—[b]	22.7	9.09	9.55
	1200	—[b]	20.17	—[b]	22.6	8.52	9.56
2.625	800	—[b]	35.12	—[b]	25.1	12.80	11.4
	900	—[b]	31.97	—[b]	24.5	11.80	10.8
	1000	—[b]	28.41	—[b]	23.9	10.81	10.2
	1100	—[b]	24.57	—[b]	23.4	9.78	9.92
2.667	800	50	— 2.5	49	26.2	13.08	12.2
	900	50	— 5.5	47	25.6	12.02	11.6
	1000	50	— 8.4	46	25.0	11.00	11.0
	1100	50	—11.3	45	24.6	9.90	10.7
	1150	50	—12.8	44	24.3	9.19	10.6
	1200	50	—14.3	44	24.3	8.60	10.6

[a] Solubility limit of the UO_{2+x} phase
[b] Upper boundary of the $UO_{2.25}$ + $UO_{2.667-y}$ phase region

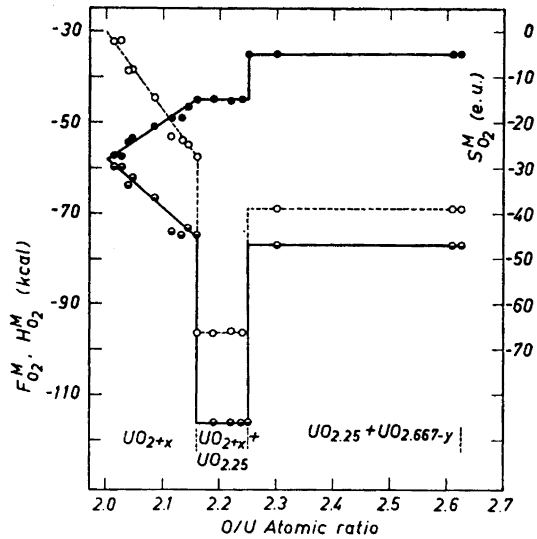

Fig. 9. Variation with uranium oxide composition of relative partial molar free energy $F^M_{O_2}$ (—●—), partial molar heat of mixing $H^M_{O_2}$ (—◒—), and partial molar entropy of mixing $S^M_{O_2}$ (---O---), respectively. Temperature is 800°C.

which is shown as a function of composition in Fig. 9 for the temperature of 800°C. Fig. 9 shows also values for $F^M_{O_2}$, The detailed data are listed in Table 2.

The relative partial molar heat of addition of oxygen increases about linearly with the O/U ratio within the homogeneous UO_{2+x} phase. The appearance of the stable intermediate phase $UO_{2.25}$ causes a large drop in $H^M_{O_2}$ for the two-phase region UO_{2+x} + $UO_{2.25}$. For the second two-phase region $UO_{2.25}$ + $UO_{2.667-y}$ the partial heat of solution is again larger, *i.e.* of the same order of magnitude as at the saturation limit of the UO_{2+x} phase. The evaluation of the partial heats of solution for the two-phase regions is considered later in this paper.

Relative partial molar entropy of oxygen. This quantity,

$$S^M_{O_2} = \bar{S}_{O_2} - S^\circ_{O_2}$$

where $\bar{S}_{O_2}$ is the partial molar entropy of oxygen and $S^\circ_{O_2}$ is the standard molar entropy of oxygen, is obtained from the values of $F^M_{O_2}$ and $H^M_{O_2}$ by the formula

$$S^M_{O_2} = (H^M_{O_2} - F^M_{O_2}) / T$$

The values for 800°C are shown in Fig. 9 and the detailed data are listed in Table 2. The behavior is similar to $H^M_{O_2}$ with a large drop in the UO_{2+x} + $UO_{2.25}$ phase region. Likewise, the partial molar entropies are practically independent of temperature if phase transformations are excluded.

The results are tentatively interpreted to indicate a continuous increase of order in the oxygen sublattice with the dissolution of oxygen in the UO_{2+x} phase. A pronounced increase of order leading to a more stable configuration of atoms is achieved by the transformation of the saturated UO_{2+x} phase to the $UO_{2.25}$ phase. The decrease in the enthalpy, $H^M_{O_2}$, due to the phase transformation is greater than the corresponding change in the subtractive term, $T\,S^M_{O_2}$, of the free energy equation. At higher temperatures the subtractive term, enthalpies and entropies being essentially independent of temperature, becomes the more important and the phase $UO_{2.25}$ tends therefore to grow unstable. The critical point is the peritectic temperature.

In the above qualitative discussion, changes in the electronic consititution of the oxide have not been considered. A simplified treatment of the dependence of the O/U ratio and the concentrations of the individual ionic and electronic lattice defects in the homogeneous UO_{2+x} phase on the oxygen partial pressure of the surrounding gas is presented in the last part of this paper.

All the relative partial quantities of this investigation are at least in fair agreement with the previously published data [8,13].

Relative integral molar heat of mixing. By performing an integration analogous to the one for F^M, it is possible to obtain from the partial heats of mixing the relative integral molar heat of reaction, H^M, of UO_2 and O_2 for the whole composition range studied. In Table 3 results of such evaluations are presented for F^M/N_{UO_2} and H^M/N_{UO_2} at the solubility limit of the phase UO_{2+x}. Included are also the values of $F^M_{O_2}$ for the both two-phase equilibria. Within the UO_{2+x} phase region the integral heat of reaction per mole O_2, *i.e.* H^M/N_{O_2}, is of the same order of magnitude as the relative partial molar heat of addition of oxygen.

In order to obtain the values of H^M beyond the solubility limit of the homogeneous UO_{2+x} phase, it is necessary to evaluate the heat of the equilibrium reaction when 1 gram mole of O_2 reacts with UO_{2+x} to form $UO_{2.25}$ both solid phases being of the appropriate equilibrium compositions. Similarly, it is needed the corresponding heat of the equilibrium reaction for oxygen

Table 3. Relative integral free energy F^M/N_{UO_2} and relative integral heat of mixing H^M/N_{UO_2} per gram atom uranium at the solubility limit of the UO_{2+x} phase. Relative partial molar free energies of oxygen $F^M_{O_2}$ for the two-phase equilibria UO_{2+x} + $UO_{2.25}$ and $UO_{2.25}$ + $UO_{2.667-y}$.

Temp. °C	Solubility limit(O/U)	F^M/N_{UO_2} kcal	H^M/N_{UO_2} kcal	$F^M_{O_2}$ $(UO_{2+x}+UO_{2.25})$ kcal	$F^M_{O_2}$ $(UO_{2.25}+UO_{2.667-y})$ kcal
800	2.160	−4.15	−5.38	−45.11	−35.12
900	2.189	−4.59	−6.48	−39.82	−31.97
1000	2.219	−4.96	−7.60	−33.80	−28.41
1100	2.239	−5.03	−8.31	−27.32	−24.57
1150	2.245	−5.00	−8.52	−24.09	−22.36
1200	2.248	−4.9	−8.6	−21.0	−20.17

and $UO_{2.25}$ forming the $UO_{2.667-y}$ phase. Both values are readily obtained from the slopes of the lines in Fig. 6 which show the two two-phase equilibrium oxygen pressures as a function of temperature.

For the reaction

$$UO_{2+x} + (0.125 - x/2)\, O_2 = UO_{2.25}$$

the heat of reaction per 1 gram mole O_2 is thus -116.1 kcal. For the other equilibrium reaction

$$UO_{2.25} + (0.209 - y/2)\, O_2 = \overline{UO_{2.667-y}}$$

the heat of reaction per gram mole O_2 is -77.1 kcal. Biltz and Müller's[12] results for the same reaction measured in the temperature range 1160—1240°C give about -85 kcal/mole O_2. Blackburn [8] obtained in the range 966—1126°C a value of -78.2 kcal/mole O_2.

With the help of these values and by taking into account the actual amounts of the reacting O_2, it is possible to calculate the H^M-values over the whole range investigated. Finally, it is possible to calculate $H^M_{O_2}$ at any point, especially for the two-phase regions, from the formula [15]

$$H^M_{O_2} = H^M + (1 - N_{O_2}) \left(\frac{\partial H^M}{\partial N_{O_2}} \right)$$

The calculated values are listed in Table 2. Values for the $UO_{2.667-y}$ phase region were estimated from Biltz and Müller's [12] results. It is interesting to note that the relative partial molar heats of addition of oxygen for the both two-phase regions are practically as large as the heats of reaction for the corresponding equilibrium reactions.

A plot of H^M/N_{UO_2} *vs.* O/U atomic ratio is of the same shape as for the free energy in Fig. 8.

Relative integral molar entropy of mixing. The values of this quantity, S^M, were evaluated from the values for H^M and F^M by the usual formula. Results are listed in Table 2. A plot of S^M/N_{UO_2} *vs.* O/U ratio is of the same shape as for the free energy in Fig. 8.

Further comparison of the high-temperature thermodynamic results. Fig. 10 shows the standard free energy change as a function of temperature for the reactions

$$UO_2 + 0.125\, O_2 = \overline{UO_{2.25}}$$

and

$$UO_2 + 0.333\, O_2 = UO_{2.667}$$

The values of Coughlin [16] for the last reaction are about 1.5 kcal less negative. Blackburn's [8] evaluation at 1300°K is in good agreement. A recent evaluation by Ackermann [17] differs markedly only at higher temperatures.

Fig. 11 shows the corresponding standard heats of reaction. The agreement to other evaluations is fairly good.

Extrapolation of the high-temperature results to 25°C. By a straight line extrapolation of the high-temperature free energy values for the reaction

$$UO_2 + 0.125\, O_2 = UO_{2.25}$$

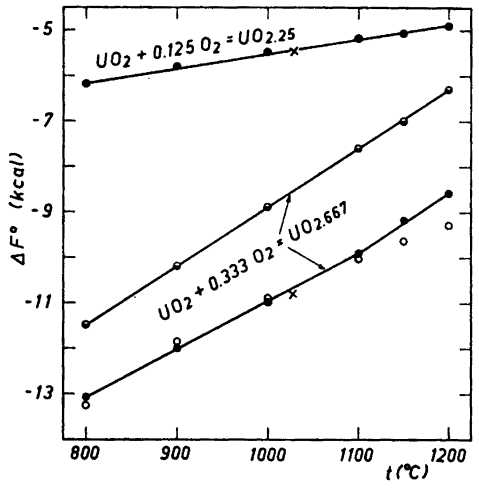

Fig. 10. Variation with temperature of standard free energy change of the reactions $UO_2 + 0.125\ O_2 = UO_{2.25}$ and $UO_2 + 0.333\ O_2 = UO_{2.667}$. —●— this study, × Blackburn [8], ◒ Coughlin [16], O Ackermann [17].

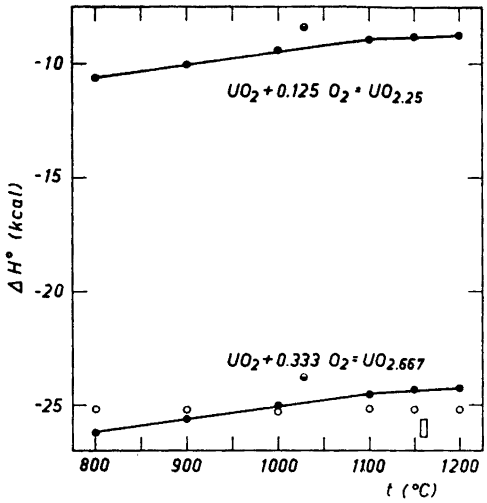

Fig. 11. Variation with temperature of the standard heats of reaction for $UO_2 + 0.125\ O_2 = UO_{2.25}$ and $UO_2 + 0.333\ O_2 = UO_{2.667}$. —●— this study, ◒ Blackburn [8], O Coughlin [16], □ Biltz and Müller [12].

to 25°C one obtains $\Delta F^\circ_{298} = -8.57$ kcal. The standard molar entropies at 25°C are: UO_2 18.623 e.u.[18]; O_2 49.003 e.u.[19]; $UO_{2.25}$ 20.073 e.u.[20]. Thus $\Delta S^\circ_{298} = -4.675$ e.u. and combining this with the extrapolated free energy value one obtains $\Delta H^\circ_{298} = -9.96$ kcal or -79.7 kcal/mole O_2. The corresponding values according to Brewer's [21] estimations are: $\Delta F^\circ_{298} = -9.9$ kcal and $\Delta H^\circ_{298} = -10.8$ kcal or -86.4 kcal/mole O_2.

By a similar extrapolation of the present high-temperature free energy values for the reaction

$$UO_2 + 0.333\ O_2 = UO_{2.667}$$

to 25°C one obtains $\Delta F^\circ_{298} = -21.31$ kcal. The standard molar entropy at 25°C for $UO_{2.667}$ is 22.511 e.u.[22]. The standard entropy change of this reaction is thus $\Delta S^\circ_{298} = -12.446$ e.u. Huber *et al.*[23] have determined the standard heat of the reaction calometrically at 25°C and obtained a value $\Delta H^\circ_{298} = -25.34$ kcal. Combining this value with the standard entropy change one obtains $\Delta F^\circ_{298} = -21.63$ kcal in satisfactory agreement with the extrapolated result of this research.

Using the oxygen pressure data of Biltz and Müller [12] at 580°C and in the composition range $UO_{2.667} - UO_3$ one can evaluate as before for the reaction

$$UO_{2.667} + 0.167\ O_2 = UO_3$$

$\Delta F^\circ_{853} = -160$ cal and $\Delta H^\circ_{853} = -7.5$ kcal. Combining these values with the linearly extrapolated high-temperature results of this study for the reaction

$$UO_2 + 0.333\ O_2 = UO_{2.667}$$

one obtains for the reaction

$$UO_2 + \tfrac{1}{2}\ O_2 = UO_3$$

$\Delta F^\circ_{853} = -15.6$ kcal and $\Delta H^\circ_{853} = -33.7$ kcal. The same quantities according to Coughlin [16] are: $\Delta F^\circ_{853} = -15.3$ kcal and $\Delta H^\circ_{853} = -31.8$ kcal. Upong using the enthalpy and entropy increments of UO_2, O_2, and UO_3 between 298° and 853°K as compiled by Kelley [24], the following values are obtained for the last reaction: $\Delta F^\circ_{298} = -28.5$ kcal and $\Delta H^\circ_{298} = -33.7$ kcal. The corresponding values according to Coughlin [16] are: $\Delta F^\circ_{298} = -25.9$ kcal and $\Delta H^\circ_{298} = -31.8$ kcal.

High-temperature heat-content and entropy data. Upon combining the high-temperature results of this study with the high-temperature heat-content and entropy data for UO_2 and O_2 as compiled by Kelley [24] and the necessary values of ΔH°_{298} and ΔS°_{298} mentioned above, one can evaluate high-temperature heat-content and entropy data for the compounds $UO_{2.25}$ and $UO_{2.667}$ (Table 4). Westrum and Grønvold [22] have determined the heat content of $UO_{2.667}$ over the range from 5° to 350°K. Popov *et al.*[25] have measured the heat capacity of the same compound over the ranges of 100—320°C and 400—600°C. Combining these two investigations and extrapolating the latters' results one obtains for $UO_{2.667}$ the value $H_{1000} - H_{298} = 18.0$ kcal or much higher than the value 13.8 kcal of the present evaluation. The heat capacity values of Popov for UO_3 are also greater than those of Kelley [24].

Non-stoichiometry in uranium dioxide. Wagner [2] has formulated equations for the equilibria of lattice defects in low concentrations within a single phase UO_{2+x} or with a gaseous phase O_2 in terms of the classical law of mass action. The following theoretical relations for the dependence of the oxygen-to-uranium ratio and the concentrations of the individual lattice defects on the oxygen partial pressure of the surrounding gas show the essential results.

Table 4. High-temperature heat content and entropy data for $UO_{2.25}$ and $UO_{2.667}$.

	$UO_{2.25}$		$UO_{2.667}$	
T °K	$H_T - H_{298}$ kcal/mole	$S_T - S_{298}$ e.u.	$H_T - H_{298}$ kcal/mole	$S_T - S_{298}$ e.u.
1000	12.9	23.7	13.8	25.6
1100	15.6	26.3	16.7	28.0
1200	18.4	28.7	19.7	30.7
1300	21.2	30.9	22.6	33.1
1400	23.8	32.9	25.5	35.2
1473	25.6	34.1	27.4	36.4

Assuming that the concentration of interstitial cations and cation vacancies are negligible and disregarding associated lattice defects, it follows from elementary stoichiometry that

$$x - X_O - X_\square = \tfrac{1}{2} X_p - \tfrac{1}{2} X_n \quad (1)$$

where x is the excess of oxygen per uranium ion in oxide of the overall composition UO_{2+x}. X_O, $X_\square$, X_p, and X_n are the ratios of the numbers of interstitial oxygen ions, oxygen ion vacancies, electron holes, and excess electrons to the number of uranium atoms, respectively. These are the principal lattice defects considered.

Electronic defects within the UO_2 phase are created by the reaction

$$\text{electron in valence band} = \text{excess electron} + \text{electron hole} \quad (2)$$

with the equilibrium condition

$$X_n X_p = K_1 \quad (3)$$

The excess oxygen in UO_{2+x} results from the addition of oxygen ions into interstitial positions according to the following reaction between gaseous oxygen and solid UO_2,

$$\tfrac{1}{2} O_2(g) + 2 \text{ electrons in valence band} = \text{interstitial oxygen ion} + 2 \text{ electron holes} \quad (4)$$

with the equilibrium condition

$$X_O X_p^2 / p_{O_2}^{\frac{1}{2}} = K_2 \quad (5)$$

For a uranium oxide with the O/U atomic ratio $\geqq 2$, we may assume that $X_\square \cong 0$. Eqn. (1) becomes then simply

$$x \cong X_O \quad (6)$$

Eqn. (5) yields

$$x = K_2 X_p^{-2} p_{O_2}^{\frac{1}{2}} \quad (7)$$

Two limiting cases are considered. (I) Assume that the oxygen excess, x, is much less than the concentrations of the electronic defects in UO_2 of ideal composition, *i.e.*

$$x \ll K_1^{\frac{1}{2}} \quad (8)$$

Hence

$$X_p \cong X_n \cong K_1^{\frac{1}{2}} \quad (9)$$

From eqn. (7) it follows that

$$x = \overline{K_1^{-1} K_2}\, p_{O_2}^{\frac{1}{2}} \quad (10)$$

Thus under conditions where the concentrations of electronic defects are large in the stoichiometric oxide and the variations of these concentrations with changes in degree of non-stoichiometry is small, the amount of oxygen excess should be linearly proportional to the square root of the ambient oxygen partial pressure.

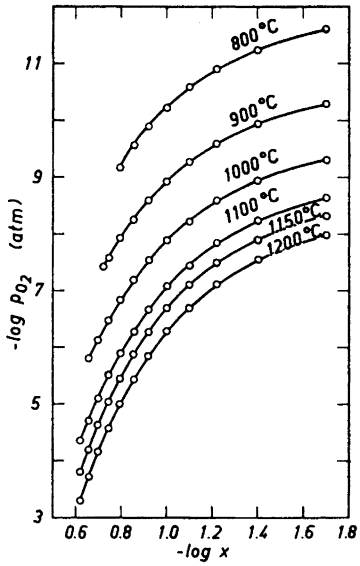

Fig. 12. Change of log p_{O_2} with log x at round temperatures within the UO_{2+x} phase.

(II) Assume an excess of oxygen much greater than the concentrations of electronic defects in UO_2 of ideal composition. Approximately then

$$x \cong X_O \cong \tfrac{1}{2} X_p \tag{11}$$

Substitution in eqn. (5) yields

$$x = X_O = (K_2/4)^{1/6} p_{O_2}^{1/6} \tag{12}$$

The excess of oxygen should under these assumptions be proportional to the 1/6 power of the ambient oxygen pressure.

The foregoing relations may be compared with the experimental results. To this end, eqn. (10) is written as

$$\log p_{O_2} = 2 \log x - 2 \log (K_2/K_1) \tag{13}$$

and eqn. (12) as

$$\log p_{O_2} = 6 \log x - 2 \log (K_2/4) \tag{14}$$

By plotting log p_{O_2} as a function of log x, a slope of 2 or 6 should result if either of the foregoing relations is valid. The data shown in Fig. 5 are plotted in this

Table 5. The initial and final slopes of the log x *vs.* log p_{O_2} curves within the UO_{2+x} phase.

	800°C	900°C	1000°C	1100°C	1150°C	1200°C
Initial slope	1.1	1.1	1.3	1.5	1.4	1.4
Final slope	6.4	6.3	7.0	5.2	9.8	11

Table 6. The equilibrium constant K_2 and the concentrations of the positive holes X_p and excess electrons X_n near the saturation limit of the UO_{2+x} phase.

Temp. (°C)	x	$\log p_{O_2}$	$\log K_2$	K_2	X_p	X_n
800	0.16	−9.19	2.81	630	0.32	0.12
900	0.19	−7.42	2.15	140	0.38	0.098
1000	0.22	−6.13	1.53	34	0.44	0.064
1100	0.24	−4.35	0.92	8.3	0.48	0.032

way in Fig. 12. It is found that the initial slope for small values of x is about 1.1 to 1.5 but increases rapidly with x until near the saturation limit of the UO_{2+x} phase the slope is about 6 (Table 5). The two limiting cases are approached at least semiquantitatively, indicating the applicability of the mass action principle to correlate the significant variables under these conditions.

Eqn. (14), valid for large values of x, gives

$$\log K_2 = 3 \log x - \tfrac{1}{2} \log p_{O_2} + \log 4 \qquad (15)$$

With the help of this equation, one can solve for the equilibrium constant K_2 (Table 6). Under assumption $x = X_O$, one then obtains from eqn. (5) the concentration of positive holes, X_p, and from eqn. (3) the concentration of excess electrons, X_n (the necessary values for K_1 are calculated below). All values are listed in Table 6.

Similarly, eqn. (13) gives for small values of x

$$\log K_1 = \tfrac{1}{2} \log p_{O_2} - \log x + \log K_2 \qquad (16)$$

The values for the equilibrium constant K_1 are given in Table 7. In the same Table are recorded the concentrations of the electronic defects in UO_2 of ideal composition which, according to eqn. (3), are $X_p = X_n = K_1^{\frac{1}{2}}$. The concentrations of electronic defects in UO_2 of ideal composition indicate a large intrinsic electronic disorder which is relatively insensitive to temperature and thus to the equilibrium oxygen partial pressure of the surroundings in agreement with the conductivity measurements of Hauffe [26]. These showed a constant electronic conductivity independent of the oxygen partial pressure in the compound UO_2 at around 1050°C.

Table 7. The equilibrium constant K_1 and the concentrations of the electronic defects in UO_2 of ideal composition.

Temp. (°C)	x	$\log p_{O_2}$	$\log K_1$	K_1	$X_p = X_n$
800	0.04	−11.24	−1.41	0.039	0.20
900	0.04	− 9.95	−1.43	0.037	0.20
1000	0.04	− 8.95	−1.55	0.028	0.17
1100	0.04	− 8.25	−1.81	0.016	0.13

By plotting log K_2 *vs.* $1/T$ a nearly straight line is obtained with a slope of 9270. Thus the heat of reaction (4) is −84.8 kcal/mole O_2. This is of the same order of magnitude as the relative partial molar heat of solution of oxygen in UO_{2+x} obtained previously by plotting log p_{O_2} *vs.* $1/T$ at constant composition.

For reaction (2), the heat of reaction above 900°C is about −14 kcal/mole O_2 and below that temperature about zero, again indicating the insensitivity of the electronic disorder to external conditions.

In an essentially similar treatment of the nonstoichiometry in UO_2, Aronson and Belle [13] obtained also a fairly good correlation between the calculated and observed partial pressures of oxygen by using the principle of mass action.

Acknowledgement. This investigation has been supported by *Suomen atomienergianeuvottelukunta* (Finnish Atomic Energy Commission). Thanks are due to Prof. M. H. Tikkanen for provision of facilities of the Metallurgical Laboratory of the Institute of Technology, Otaniemi, Finland.

REFERENCES

1. Kiukkola, K. and Wagner, C. *J. Electrochem. Soc.* **104** (1957) 308.
2. Wagner, C. *U. S. At. Energy Comm.* **WAPD — 144** (1955).
3. Kiukkola, K. and Wagner, C. *J. Electrochem. Soc.* **104** (1957) 379.
4. Kingery, W. D., Pappis, J., Doty, M. E. and Hill, D. C. *J. Am. Ceram. Soc.* **42** (1959) 393.
5. Carter, R. E. *J. Am. Ceram. Soc.* **43** (1960) 448.
6. Grønvold, F. *J. Inorg. & Nuclear Chem.* **1** (1955) 357.
7. Hoekstra, H. R., Siegel, S., Fuchs, L. H. and Katz, J. J. *J. Phys. Chem.* **59** (1955) 136.
8. Blackburn, P. E. *J. Phys. Chem.* **62** (1958) 897.
9. Wagner, C. *J. Chem. Phys.* **21** (1953) 1819.
10. Belle, J. and Auskern, A. B. in Kingery, W. D. (Ed.) *Kinetics of High-Temperature Processes*, John Wiley & Sons, New York 1959, p. 44.
11. Himmel, L., Mehl, R. F. and Birchenall, C. E. *Trans. AIME* **197** (1953) 827.
12. Biltz, W. and Müller, H. *Z. anorg. u. allgem. Chem.* **163** (1927) 257.
13. Aronson, S. and Belle, J. *J. Chem. Phys.* **29** (1958) 151.
14. Willardson, R. K., Moody, J. W. and Goering, H. L. *J. Inorg. & Nuclear Chem.* **6** (1958) 19.
15. Wagner, C. *Thermodynamics of Alloys*, Addison-Wesley Press, Inc., Cambridge, Mass. 1952.
16. Coughlin, J. P. *U. S. Bur. Mines, Bull.* **542** (1954) 54.
17. Ackermann, R. J., Thorn, R. J., Alexander, C. and Tetenbaum, M. *J. Phys. Chem.* **64** (1960) 350.
18. Jones, W. M., Gordon, J. and Long, E. A. *J. Chem. Phys.* **20** (1952) 695.
19. Rossini, F. D., Wagman, D. D., Evans, E. H., Levine, S. and Jaffe, I. *Natl. Bur. Standards (U.S.), Circ.* **500** (1952).
20. Osborne, D. W., Westrum, Jr., E. F. and Lohr, H. R. *J. Am. Chem. Soc.* **79** (1957) 529.
21. Brewer, L. *Chem. Revs.* **52** (1953) 1.
22. Westrum, Jr., E. F. and Grønvold, F. *J. Am. Chem. Soc.* **81** (1959) 1777.
23. Huber, Jr., E. J., Holley, Jr., C. E. and Meierkord, E. H. *J. Am. Chem. Soc.* **74** (1952) 3406.
24. Kelley, K. K. *U. S. Bur. Mines, Bull.* **584** (1960).
25. Popov, M. M., Gal'chenko, G. L. and Senin, M. D. *Zhur. Neorg. Khim.* **3** (1958) 1734.
26. Hauffe, K. *Z. physik. Chem.* **B 48** (1941) 124.

Received July 26, 1961.

ACTA CHEMICA SCANDINAVICA 16 (1962) 346–350

The Addition of Dibromomalononitrile to Double Bonds. A Route to γ-Lactones

KURT TORSSELL and KJELL DAHLQVIST

Institute of Organic Chemistry and Biochemistry, University of Stockholm, Sweden

Dibromomalononitrile adds to the double bond. It is suggested that the reaction starts with attack of a bromonium ion followed by addition of the negatively charged bromodicyanomethyl group to the other olefinic carbon atom. The adducts can be selectively debrominated. Alkaline hydrolysis of the product affords α-carboxy-γ-lactones.

In view of the strong electronegativity of the cyano group one would expect the bromine atoms of dibromomalononitrile to be easily removable as positive ions, *i.e.*, the compound should act as a brominating agent. In fact, reaction with dimethylaniline in aqueous solution afforded *p*-bromodimethylaniline in 54 % yield, and malononitrile has been converted into monobromomalononitrile by the same reagent [1]. In these reactions a proton is abstracted by the brominating agent with formation of monobromomalononitrile.

We anticipated that reaction of dibromomalononitrile with a double bond would give an adduct, as in (1), although

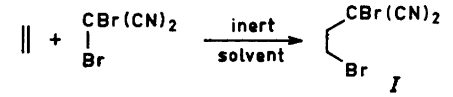

I (1)

allylic bromination was also conceivable. Schmidt *et al.*[2] have published work on the similar reactions between bromonitromethanes or brominated malonic esters and cyclohexene. In methanolic solution 2-bromocyclohexyl methyl ether was formed. The reaction can be depicted in the following manner (2):

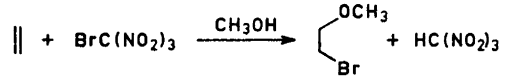

(2)

If an inert solvent had been used the reaction could have taken the course outlined in (1). The Kharash reaction [3] is also of relevance in this connection. Highly halogenated hydrocarbons add to double bonds under the influence of ultraviolet light or peroxides (3). This is a typical radical reaction.

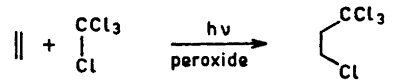

(3)

When styrene and dibromomalononitrile are mixed, heat is evolved and addition of solvent is necessary to moderate the reaction. Cyclohexene on the other hand reacts sluggishly and refluxing in chloroform for several hours is necessary to increase the yield of adduct. Irradiation with ultraviolet light or addition of benzoylperoxide had no marked effect on the yield. Considering the strongly polarized carbon-bromine bond in dibromomalononitrile, we suggest that the mechanism is ionic and is initiated by attack of Br^+. From the reaction mixtures crystalline compounds were isolated analysing correctly for the adducts I. In the case of cyclohexene no 3-bromocyclohexene could be detected. We considered the adducts to be of potential synthetic interest since ring closure of the 1,3 dibromides would give cyclopropane derivatives (4).

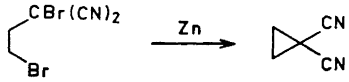

(4)

and selective hydrogenation of one of the bromine atoms, followed by hydrolysis of the cyano groups would lead to γ-lactones or again cyclopropane derivatives (5).

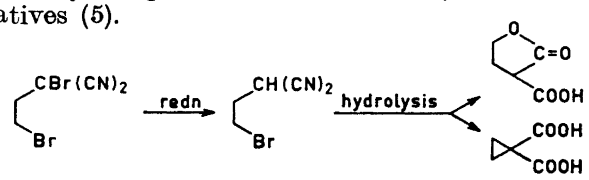

(5)

Zinc reduction of the cyclohexene adduct in acetic acid afforded II in good yield. The same compound was also obtained catalytically using Pt/C. Reduction with zinc in alcoholic solution at 0° gave a product, which showed strong double bond absorption in the IR at 1 650 cm^{-1} and probably consisted mainly of the unsaturated dinitrile III. No cyclopropane formation was detected.

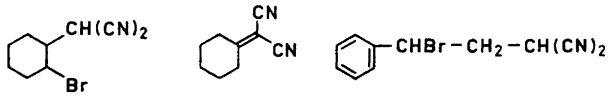

II III IV

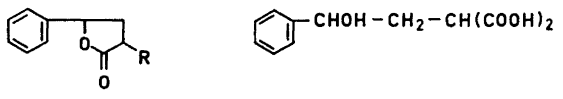

V R=CN
VI R=COOH
VII R=H

VIII

From the catalytic reduction of the crude crystalline styrene adduct the siomer IV was isolated together with a second compound, which besides possessing nitrile absorption in the IR also showed a strong carbonyl band at 1 785 cm^{-1}. This suggested that the compound was V. Alkaline hydrolysis of V gave the carboxylactone VI in a good yield, indentified with an authentic sample prepared by another route. On heating it decarboxylated to VII. Alkaline hydrolysis of the dicyano compound IV gave two products, one of which was identical with VI. The other proved to be VIII and was converted to VI by heating at 90—100° in vacuum for 2 h.

The cyclohexane derivative reacted differently towards alkali. It was easily dissolved in aqueous sodium hydroxide giving a yellow solution from which cyclohexanone separated slowly.

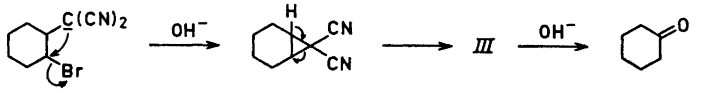

IX X



XI (cis and/or trans) XII XIII XIV

The cyclopropane derivative X is presumably an intermediate, which rearranges *via* III to cyclohexanone. Hydrolysis of II with conc. hydrobromic acid produced a complex mixture of the γ-lactone XI, a carboxy lactone and a compound containing bromine, probably XII. The lactone could be converted to the corresponding amide by the action of ammonia in ethanol and was therefore probably the *trans*-isomer [4]. The acidic materials were difficult to separate and no further work was done with them.

The reaction of some similar compounds such as ethyl bromonitro-malonic ester XIII and carbonyl cyanide XIV was also investigated. XIII is reported to react with double bonds in alcoholic solution according to (2) [2]. From XIII and dimethyl aniline, *p*-bromodimethyl aniline was obtained in 40 % yield using the method previously described [1]. In an inert solvent XIII should add to a double bond according to (6).

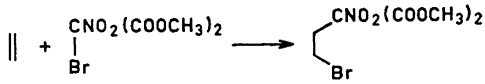

(6)

The intermediate so obtained, on reduction, hydrolysis and decarboxylation would then lead to a γ-hydroxy-amino acid. In fact, the reaction product from styrene or 1-octene no longer showed vinyl double bond absorption in the IR at around 900 cm^{-1}, and on catalytic reduction, hydrolysis and decar-

boxylation a mixture of amino acids was obtained. Paper chromatography showed, besides glycine the presence of one or two unidentified amino acids. However, all attempts to isolate them were unsuccessful.

Recent work by Achmatowich *et al.*[5] on the chemistry of carbonyl cyanide, showed that it adds in a *cis*-fashion to certain types of double bonds (7):

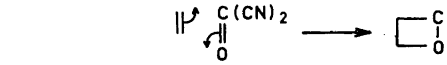

(7)

The action of carbonyl cyanide on β-nitro styrene was therefore investigated, since the adduct formed should be potentially useful for the preparation of serine analogues. However, no reaction between the components could be detected. Radiation with ultraviolet light was without effect.

EXPERIMENTAL

All melting points are corrected.

Dibromomalononitrile. To a cooled mixture of malononitrile (7.0 g) and water (60 ml), bromine (35 g) was added dropwise with stirring. After the addition the solution was stirred for a further hour. The yellow oil which separated was dried over sodium sulphate and distilled in vacuum to give dibromomalononitrile (18 g, 69 %), b.p.$_8$ 48–49°.

(2-Bromocyclohexyl)-bromomalononitrile. A mixture of dibromomalononitrile (5.6 g), cyclohexene (2.0 g), and chloroform (10 ml) was heated under reflux for 48 h. Evaporation of the solvent gave a brown oil, which partially crystallized on addition of methanol at 0° affording the adduct (1.6 g, 22 %). Recrystallisation from methanol gave an analytical sample, m.p. 128–129°. (Found: C 35.29; H 3.38. Calc. for $C_9H_{10}N_2Br_2$ (306.2): C 35.33; H 3.30.)

(2-Bromocyclohexyl)-malononitrile. (a) To a mixture of (2-bromocyclohexyl)-bromomalononitrile (2 g), ethyl acetate (10 ml), acetic acid (40 ml), water (8 ml) and zinc (4 g) was added with stirring at 5°. After 5 min ice-water (200 ml) was added and the aqueous solution extracted three times with ether. The ether was shaken with conc. sodium bicarbonate solution, dried over sodium sulphate and the solvent evaporated. The residue was recrystallized from light petroleum (40–60°) affording (2-bromocyclohexyl)-malononitrile (1.13 g, 77 %) m.p. 65.5–66.5°. (Found: C 47.90; H 5.04; Calc. $C_9H_{11}N_2Br$ (227.0): C 47.62; H 4.85).

(b) (2-Bromocyclohexyl)-bromomalononitrile (0.21 g) in ethyl acetate (20 ml) was reduced catalytically over Pt/C. Hydrogen consumption became slow after the absorption of one mole and on working up 0.14 g of crude product was obtained. After recrystallisation from cyclohexane (2-bromocyclohexyl)-malononitrile, m.p. 65.5–66.5, was obtained, identical with the product from the zinc reduction.

Alkaline hydrolysis of (2-bromocyclohexyl)-malononitrile (II). II (50 mg) in sodium hydroxide (5 N, 0.5 ml) was heated on the water bath for 10 min. An oil separated and the solution turned slightly yellow. Addition of 2,4-dinitrophenylhydrazine solution gave a yellow precipitate (51 mg) which was identified as cyclohexanone 2,4-dinitrophenylhydrazone by m.p. 160–161.5°, and mixed m.p. 159.5–160°.

Acid hydrolysis of II. The malononitrile (0.108 g) was refluxed for one hour with conc. hydrobromic acid (2 ml). Dilution with water and extraction with chloroform gave an oily product (60 mg), which was separated in a neutral fraction (12 mg) and an acidic fraction (46 mg) by extraction with sodium bicarbonate solution. The neutral fraction consisted of the oily lactone XI (IR band at 1 775 cm^{-1}) which was transformed into an amide (amide band in the IR) by treatment with ammonia in ethanol. Distillation of the acid fraction at normal pressure (220°) caused decarboxylation and lactonization (IR band at 1 775 cm^{-1} and a minor peak at 1 725 cm^{-1}, crude product).

The adduct of styrene and dibromomalononitrile. To styrene (6.8 g) in chloroform (50 ml), dibromomalononitrile (14.4 g) was added. The solution became slightly warm and after standing for two days at room temperature the solvent was evaporated affording an oily residue (21 g), which crystallized slowly on standing. This adduct, recrystallized

from light petroleum, had m.p. 75.5–77°. (Found: C 40.22; H 2.79. Calc. for $C_{11}H_8N_2Br_2$ (328.0): C 40.28; H 2.46).

Hydrogenation of the styrene adduct. 1,1-Dicyano-3-bromo-3-phenylpropane. IV. The crude adduct (21 g) in ethyl acetate-ethanol (6:1) was hydrogenated over Pt/C at atmospheric pressure. One mole of hydrogen was absorbed during 2 days. After removal of the solvent in vacuum the product was extracted with cold benzene (20 ml). The yellow insoluble material (1.7 g) was crystallized from ethanol furnishing crystals (0.2 g), m.p. 130–131°, identified as the cyanolactone (V). The light petroleum insoluble part of the benzene extract afforded a further 1.0 g of the cyanolactone V, m.p. 130–131° (lit.[7] 132°), after recrystallization from ethanol. (Found: C 70.32; H 4.89. Calc. for $C_{11}H_9O_2N$ (187.2): C 70.56; H 4.84). The light petroleum soluble part of the benzene extract afforded oily crystals of IV on standing. These were recrystallized from light petroleum and had the m.p. 59–60°, (1.2 g). (Found: C 53.14; H 3.65. Calc. for $C_{11}H_9N_2Br$ (249.1): C 53.19; H 3.64). By evaporation of the mother liquor an additional amount of crude IV (11 g) was obtained. The total yield of IV was 75 %.

α-Carboxy-γ-phenyl-γ-hydroxy butyric acid VIII and α-carboxy-γ-phenyl butyrolactone VI. (a) From crude IV. IV (10 g) was hydrolyzed with 20 % sodium hydroxide (240 ml) on the water bath overnight. A small amount of a yellow insoluble material was filtered off and the filtrate carefully neutralized at 0° with conc. hydrochloric acid. White crystals of VIII (5.0 g, 55 %) separated. After recrystallization from toluene they had m.p. 100–101°. (Found: C 59.06; H 5.20. Calc. for $C_{11}H_{12}O_5$ (224.2): C 58.93; H 5.40). Chloroform extraction of the aqueous phase afforded the lactone VI (0.37 g), identical by mixed melting point and IR spectrum with a sample (m.p. 104–105°) prepared by another route. Decarboxylation of VI at 160° gave γ-phenyl butyrolactone VII in practically 100 % yield.

(b) From the cyanolactone V. The cyanolactone V (80 mg) was hydrolyzed with 20 % sodium hydroxide (2.5 ml). Acidification with conc. hydrochloric acid at room temperature afforded the carboxylactone VI (79 mg crude product). It had m.p. 103–104° after recrystallization from toluene.

α-Carboxy-γ-phenyl butyrolactone. To phenacyl malonic acid[7] (0.23 g) in sodium hydroxide solution (5 ml, 0.8 N) sodium borohydride (70 mg) was added with stirring. After 30 min the solution was acidified with dilute hydrochloric acid. The lactone (125 mg, 59 %) precipitated on standing and had m.p. 104–106° after recrystallization from water (lit.[6] 106°).

Reaction of methyl bromo-nitromalonate with 1-octene and styrene. 1-Octene (1.2 g) and the bromo-nitrodiester XIII[8,9] (2.6 g) were heated on the waterbath for 31 h, after which time the mixture no longer showed vinyl absorbtion in the IR. All attempts to obtain crystalline products from the reaction mixture were unsuccessful. A portion of the product (1.0 g) was refluxed with stannous chloride (4 g) and conc. hydrochloric acid (20 ml) for 0.5 h. Paper chromatography indicated the presence of three amino acids, one of which had the same R_F value as glycine. Attempts to isolate these acids were unsuccessful. Catalytical reduction over Raney-Ni of the crude adduct gave intractable products.

Reaction of styrene and the bromo-nitrodiester XIII also gave an intractable product having no vinyl absorption in the IR.

This work has been supported by grants from the *Swedish Natural Science Research Council* and *Hierta-Retzius Stipendiefond*. The English has been revised by Dr. P. I. L. Daniels.

REFERENCES

1. Ramberg, L. and Wideqvist, S. *Arkiv Kemi, Mineral Geol.* **12 A** (1937) No. 22.
2. Schmidt, E., Ascherl, A. and von Knilling, W. *Ber.* **59** (1956) 1876.
3. Walling, C. *Free Radicals in Solution.* John Wiley, New York 1957, p. 247.
4. Newman, M. S. and VanderWerf, C. A. *J. Am. Chem. Soc.* **67** (1945) 233.
5. Achmatowicz, O. and Leplavy, M. *Roczniki Chem.* **33** (1959) 1349.
6. Bougault, M. J. *Compt. rend.* **146** (1908) 936.
7. Bischoff, C. A. *Ber.* **16** (1883) 1044.
8. Wahl, M. A. *Bull. soc. chim.* [3] **25** (1901) 918, 927.
9. Willstätter, R. and Hottenroth, V. *Ber.* **37 B** (1904) 178.

Received September 9, 1961.

ACTA CHEMICA SCANDINAVICA 16 (1962) 351–358

Gas Chromatographic Separation of Unsaturated Hydrocarbons Using Silver Nitrate in Ethylene Glycol as the Stationary Phase

BENGT SMITH and RAGNAR OHLSON

Institutionen för Organisk Kemi, Chalmers Tekniska Högskola, Göteborg, Sweden

Silver nitrate in ethylene glycol has been investigated as a stationary phase for the separation of unsaturated hydrocarbons by gas chromatography. It is demonstrated, that this substrate has a high selectivity for various types of unsaturated hydrocarbons and is a valuable instrument for solving analytical problems related to hydrocarbons. Retention data are given for about 75 unsaturated hydrocarbons.

The usefulness of silver nitrate solutions as stationary phases for the gas chromatographic analysis of hydrocarbons was first recognized by Bradford *et al.*[1] They separated ethane and ethylene using a column containing silver nitrate in ethylene glycol. A comparative study of ethylene glycol, polyethylene glycol and glycerole as solvents for silver nitrate was made by Bednas and Russel [2] using a material consisting of alkanes and alkenes. They pointed out the difference in retention times between alkanes and alkenes as well as between *cis*- and *trans*-alkenes. The polyethylene glycol column was found to be inferior to the other two columns. Tenney [3], in connection with studies of various liquid substrates used in gas chromatography, also investigated a solution of silver nitrate in triethylene glycol and demonstrated its ability to separate certain types of olefins. Van de Craats [4] and later Luchsinger [5] and Armitage [6] utilized benzyl cyanide as a solvent for the silver nitrate. From the retention values given by Armitage it appears that the selectivity of this stationary phase for various hydrocarbon types is low. This fact can, at least in part, be attributed to the limited solubility of silver nitrate in benzyl cyanide. Thus, although this stationary phase has been stated to be more stable than other silver nitrate solutions, it seems to have a limited analytical value.

Cope *et al.*[7-9] and Sauers [10] used silver nitrate in di- or tetraethylene glycol as stationary phases when analyzing alkenes, methylcycloalkenes, methylenecycloalkanes and menthenes. The same types of unsaturated hydrocarbons have been investigated by means of silver nitrate/ethylene glycol [11,12]. An interesting application of stationary phases containing silver nitrate was made by Cope *et al.*[13] in the analysis of the *cis*- and *trans*-forms of cyclononene,

cyclodecene, cycloundecene and cyclododecene. Camphene and tricyclene were separated at 80°C by Powell and Whiting [14] using silver nitrate/diethylene glycol. It can be questioned whether the silver nitrate plays any roll in this case in view of the reported inactivation of silver nitrate solutions above 65°C [2]. Recently silver nitrate in various solvents has been used in a number of investigations principally dealing with C_2—C_4 hydrocarbons [15-22].

The potential analytical value of silver nitrate solutions as stationary phases in gas chromatography is evident from the preceding review. However, these results have not included enough compounds to permit a thorough evaluation of this kind of packing. On that account it was decided to investigate the performance of about 75 unsaturated hydrocarbons of various types on a stationary phase consisting of silver nitrate in ethylene glycol. The first separation of 3- and 4-methyl-1-pentene by the present authors using this stationary phase was previously reported [23].

EXPERIMENTAL

Material. Most of the hydrocarbons used were prepared in this laboratory. The synthesis of some of them will be described elsewhere.

Apparatus and column. A Perkin-Elmer Vapor Fractometer model 154 was used in the experiments. The preparation of the stationary phase * and of the column has been described previously [23].

Procedure. Relative retention times (R_T), using *trans*-2-pentene as internal standard, were determined throughout. An appropriate number of hydrocarbons were mixed with 2-pentene and the mixture run on a 2 m column at 25°C and 40 ml He/min. The retention times counted from the air top were measured and for each compound the retention time relative to *trans*-2-pentene was calculated.

It will be emphasized that the retention values are dependent on the concentration of silver nitrate in the solvent. As a certain change of composition takes place during use due to elution of the solvent, one might expect a change in the retention data with time. At 25°C, however, no serious variations in retention time have been observed, even after running the column daily for several months. The values obtained are collected in Table 1.

RESULTS AND DISCUSSION

The differing behaviour of the various unsaturated hydrocarbons on the silver nitrate/ethylene glycol stationary phase can largely be attributed to the presence of silver nitrate. Silver ions are known to form complex compounds with unsaturated hydrocarbons. There is also a certain parallelism between the established complex contants [24] and the retention values obtained in this work. This is to be expected since the same forces are active in both cases, although the environments are dissimilar.

The separation obtained between two hydrocarbons on the AgEG stationary phase is largely dependent on three factors, namely the vapour pressure of the compounds, the structural environment of the unsaturated bonds and the nature and number of the latter. Thus, for compounds with the same general structure there is as a rule a steady increase in retention time when going from one compound to the next higher in a series, partly as a consequence of the increased stability of the silver ion complex with decreased vapour pressure (*cf.* Ref.[24]). The structural environment of the unsaturated bond has a pro-

* In the following the silver nitrate/ethylene glycol stationary phase will be denoted the AgEG stationary phase.

found influence on the retention time. Substitution of alkyl groups at the unsaturated bond for hydrogen atoms is often accompanied by a considerable decrease in retention time *. This latter effect dominates over the vapour pressure effect. On that account we get, for example, about the same retention time for 1-butene (b.p. −6°) and 3-methyl-3-hexene (b.p. 95°). *Cis*-isomers are retained more strongly than *trans*-isomers, reflecting another structural influence. The favourable conditions for complex formation present in cyclic alkenes are evident from their appreciably larger retention times in comparison with those for straight chain alkenes with similar structure and boiling point *e.g. cis*-2-pentene (b.p. 37°, $R_T = 3.8$) and cyclopentene (b.p. 44°, $R_T = 18.9$). Naturally, the type and number of the unsaturated bonds are also of importance. The retention time increases with the number of unsaturated bonds in the molecule. Thus diolefins are retarded more than monoolefins **. The retention time is also dependent on the relative position of two or more unsaturated bonds in a molecule. Acetylenic hydrocarbons travel more slowly than olefins in the same boiling range ***.

The gas chromatographic separation of unsaturated hydrocarbons with different boiling points can be achieved using various stationary phases separating according to boiling point. The separation of unsaturated hydrocarbons in the same boiling range presents a more difficult problem. For this purpose a number of stationary phases have been used with more or less success (*cf.* Ref.[26]). The application of the AgEG stationary phase to this problem will now be discussed in some detail. Fig. 1 gives a clear view of the separation possibilities for various types of unsaturated hydrocarbons on this stationary phase.

Saturated and unsaturated hydrocarbons. It has been pointed out previously [2] and will be further stressed here that this stationary phase is ideally suited to the separation of saturated from unsaturated hydrocarbons. Of the unsaturated hydrocarbons investigated *trans*-2-butene (b.p. −1°) has the lowest relative retention time (0.50), the same as that for the saturated hydrocarbon 2,4,4-trimethylpentane (b.p. 99°). This means that any saturated hydrocarbon boiling below about 90° will be released from this column before any unsaturated, even before ethene with the b.p. −104°, and have a relative retention time below 0.50.

Treatment of an unknown sample. Prior to an analysis of an unknown hydrocarbon sample using the AgEG stationary phase, it has to be divided into narrow fractions by distillation or better by gas chromatography using a "boiling point column", *e.g.* a squalane column †. The resulting fractions are then further analyzed on the AgEG stationary phase.

---

* Studies conducted on the stability of complex compounds between unsaturated hydrocarbons and various metal ions indicate that this substitution effect is partly of steric origin, partly connected with the influence exerted by the substituent on the electron density at the unsaturated bond. A bonding theory advanced by Dewar [25] seems to give the best explanation of the experimental facts.

** Certain monoolefins are more strongly retarded than 1,2-dienes in the same boiling range.

*** 1-Alkynes are retained on this column, a fact which may be utilized for the identification of this hydrocarbon type.

† If saturated hydrocarbons are present, it may be advantageous first to sort out these using the AgEG column, the approximate boiling range of the sample being ascertained beforehand.

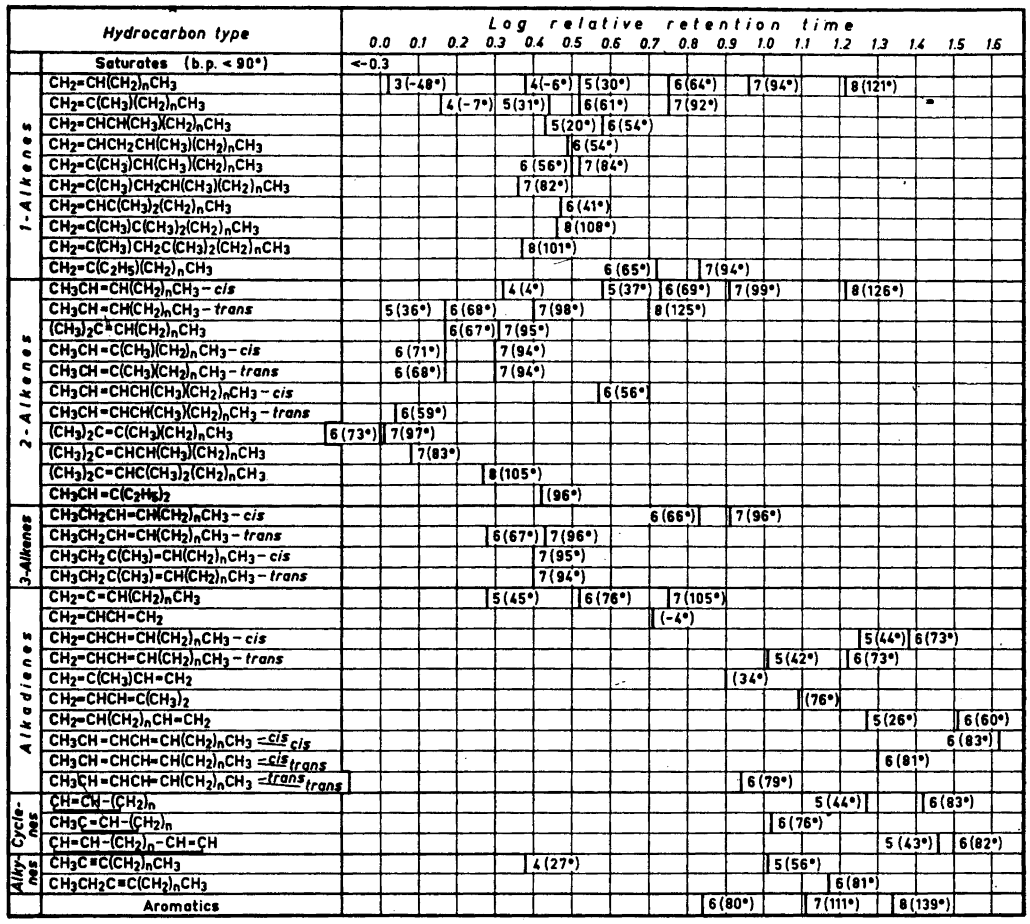

Fig. 1. Log. relative retention time (*trans*-2-pentene internal standard) for various types of unsaturated hydrocarbons on a silver nitrate/ethylene glycol column. (The first number denotes the number of carbon atoms in the molecule and the number within parenthesis denotes the b.p. of the compound.)

Alkene types RCH=CHR(I), R_2C=CHR(II) and R_2C=CR_2(III) *. The possibility of separating close-boiling *cis*- and *trans*-isomers on the AgEG stationary phase was pointed out already by Bednas and Russel [2]. However, not always can a separation be achieved. A necessary condition is that the structural environment of the two forms be distinctly dissimilar. This is the case for the type RCH=CHR(I) but not always for the types RRC=CHR(II) or RRC—CRR(III). In the *cis*-form of type I the hydrogen side is considerably more open than the other and than the two sides in the *trans*-form. In the *cis*-

* R may denote the same or different alkyl groups.

Table 1. Relative retention times for hydrocarbons on a silver nitrate/ethylene glycol column.

Hydrocarbon	Boiling point °C	Relative retention time (R_T) (trans-2-pentene = 1.00)
Saturates		
n-Pentane	36.1	0.07
n-Hexane	68.7	0.14
2,2,4-Trimethylpentane	99.2	0.50
Cyclohexane	60.7	0.37
Aromatics		
Benzene	80.1	6.91
Toluene	110.6	12.9
m-Xylene	139.1	22.0
p-Xylene	138.4	21.8
Alkenes		
C_2 Ethene	−103.7	0.67
C_3 Propene	−47.7	1.04
C_4 1-Butene	−6.3	2.38
cis-2-Butene	3.7	2.09
trans-2-Butene	0.9	0.50
Isobutene	−6.9	1.44
C_5 1-Pentene	30.0	3.29
cis-2-Pentene	36.9	3.77
trans-2-Pentene	36.4	1.00
2-Methyl-1-butene	31.2	2.77
3-Methyl-1-butene	20.1	2.69
2-Methyl-2-butene	38.6	0.71
C_6 1-Hexene	63.5	5.65
cis-2-Hexene	68.8	5.35
trans-2-Hexene	67.9	1.47
cis-3-Hexene	66.4	6.73
trans-3-Hexene	67.1	1.91
2-Methyl-1-pentene	60.7	3.30
3-Methyl-1-pentene	54.1	3.79
4-Methyl-1-pentene	53.9	3.06
2-Methyl-2-pentene	67.3	1.48
3-Methyl-*cis*-2-pentene	70.5	1.49
3-Methyl-*trans*-2-penten	67.6	1.49
4-Methyl-*cis*-2-pentene	56.3	3.73
4-Methyl-*trans*-2-pentene	58.6	1.10
2,3-Dimethyl-1-butene	55.7	3.15
3,3-Dimethyl-1-butene	41.2	2.94
2-Ethyl-1-butene	64.7	5.25
2,3-Dimethyl-2-butene	73.2	1.00
C_7 1-Heptene	93.6	9.14
cis-2-Heptene	98.5	8.17
trans-2-Heptene	98.0	2.50
cis-3-Heptene	95.8	8.17
trans-3-Heptene	95.7	2.70
2-Methyl-1-hexene	92.0	5.65
2-Methyl-2-hexene	95.4	2.06
cis-3-Methyl-2-hexene	94.0	2.00
trans-3-Methyl-2-hexene	94.0	2.00
cis-3-Methyl-3-hexene	95.3	2.50
trans-3-Methyl-3-hexene	93.5	2.50
2,3-Dimethyl-1-pentene	84.3	3.30

Table 1, continued.

	2,4-Dimethyl-1-pentene	81.6	2.30
	2-Ethyl-1-pentene	94.0	6.75
	2,3-Dimethyl-2-pentene	97.4	1.03
	2,4-Dimethyl-2-pentene	83.3	1.19
	3-Ethyl-2-pentene	96.0	2.66
C_8	1-Octene	121.3	16.1
	cis--2-Octene	125.6	16.1
	trans--2-Octene	124.9	5.03
	2,3,3-Trimethyl-1-pentene	108.3	2.89
	2,4,4-Trimethyl-1-pentene	101.4	2.33
	2,4,4-Trimethyl-2-pentene	104.9	1.86
Alkadienes			
C_4	1,3-Butadiene	−4.4	5.17
C_5	1,2-Pentadiene	44.9	1.92
	1,*cis*-3-Pentadiene	44.1	18.0
	1,*trans*-3-Pentadiene	42.0	10.2
	1,4-Pentadiene	26.0	18.7
	2-Methyl-1,3-butadiene	34.1	7.87
C_6	1,2-Hexadiene	76	3.32
	1,*cis*-3-Hexadiene	72.5	24.2
	1,*trans*-3-Hexadiene	72.5	16.5
	1,5-Hexadiene	59.5	32.2
	cis-2-*cis*-4-Hexadiene	83	41.5
	cis-2-*trans*-4-Hexadiene	81	19.8
	trans-2-*trans*-4-Hexadiene	79	8.75
	4-Methyl-1,3-pentadiene	76.3	12.3
C_7	1,2-Heptadiene	105	5.60
Cycloalkenes			
	Cyclopentene	44.2	18.9
	Cyclohexene	83.0	26.6
	1-Methylcyclopentene	75.8	10.4
Cycloalkadienes			
	1,3-Cyclopentadiene	42.5	28.9
	1,3-Cyclohexadiene	81.5	31.9
Alkynes			
	2-Butyne	27.0	2.38
	2-Pentyne	56.1	10.2
	3-Hexyne	81.4	14.9

forms of types II and III the structures on both sides are more alike and similar to those in the *trans*-forms. On that account *cis*- and *trans*-isomers of the two latter types have very nearly the same retention times. The reason for this is obviosuly steric. In the *cis*-form of type I the silver ion can get into closer contact with the double bond than in the *trans*-form and in the isomers of types II and III.

A further consequence is that it will be difficult to separate the *trans*-form of type I from the isomers of type II, if they have similar boiling points. Thus *trans*-2-hexene, 2-methyl-2-pentene and *cis*- and *trans*-3-methyl-2-pentene all boil at about 70°C, while *trans*-2-heptene, 2-methyl-2-hexene and *cis*- and *trans*-3-methyl-2-hexene all boil near 95°C. Neither of these groups is resolved on the AgEG column. Further examples in the latter boiling range are *trans*-3-heptene, *cis*- and *trans*-3-methyl-3-hexene and 3-ethyl-2-pentene. However, the data suggests that alkenes of type III can be separated from the *trans*-

form of type I and alkenes of type II, *cf.* 2,3-dimethyl-2-pentene and the above-mentioned heptenes.

Sometimes one may encounter difficulties in separating *cis*-forms of various alkenes of type I and also these from alkenes of the type CH_2=CHR(IV); *cf.* *cis*-2- and *cis*-3-heptene, 1-octene and *cis*-2-octene.

Alkene types CH_2=CHR(IV) and CH_2=CR_2(V). As might be expected, alkenes belonging to type V generally are released before alkenes belonging to type IV, when they appear in the same boiling range. This fact is exemplified by 1-pentene and 2-methyl-1-butene and by the corresponding hexenes and heptenes. A further example is given by 1-heptene and 2-ethyl-1-pentene. The risk of coincidence between alkenes of type IV and the *cis*-forms of type I was mentioned previously.

Influence of substituents elsewhere than at the C=C bond. It is of particular interest that the retention times of alkenes on the AgEG stationary phase are also influenced by substituents elsewhere than at the ethylenic bond. This is of value since close-boiling isomers only differing in having methyl groups in the β- and γ-positions to the ethylenic bond are difficult to separate on other types of stationary phases. The γ-isomers generally have the shortest retention times *. This difference in retention time was previously utilized for the separation of 3- and 4-methyl-1-pentene [23]. Other examples are given by 2,3-dimethyl-1-pentene and 2,4-dimethyl-1-pentene and by 2,3,3-trimethyl-1-pentene and 2,4,4-trimethyl-1-pentene.

Cycloolefins, alkadienes and alkynes. Hydrocarbons belonging to this group travel more slowly than monounsaturated straight chain alkenes and can generally be separated from the latter ones. There is, however, one exception. 1,2-Alkadienes ** which are released before the other types of hydrocarbons discussed in this section may be mixed up with certain monounsaturated straight chain alkenes.

Thus, while 1,2-alkadienes may be sorted out from the rest of hydrocarbons mentioned in the heading, the separation of close-boiling specimens of other types of alkadienes, cycloolefins and alkynes is not always feasible on the AgEG stationary phase.

Considering the influence of stereoisomerism and replacement of hydrogen atoms at various positions by alkyl groups, the same rules as previously outlined for alkenes apply. The retention data for the three close-boiling isomers of 2,4-hexadiene give a particularly clear demonstration of the influence of stereoisomerism and of the analytical usefulness of this stationary phase.

Aromatic hydrocarbons are, in accordance with their less olefinic nature, less retarded than cyclic unsaturated hydrocarbons, *e.g.* benzene (b.p. 80°, R_T = 6.9) and cyclohexene (b.p. 83°, R_T = 26.6). Because aromatic hydrocarbons appear together with alkenes, it is advantageous to remove them before the separation on the AgEG column, *e.g.* by using a picrate column [27].

Analytical use. The principal analytical use of the AgEG stationary phase may be summarized. (1) For type separation of saturated hydrocarbons from

* The greater shielding of the double bond by a methyl group in γ-position is evident from an inspection of molecular models of the compounds.

** A similar behaviour can be expected from other types of allenes.

all types of unsaturated. (2) For type separation of monounsaturated alkenes from alkadienes (except 1,2-dienes and possibly other allenes), cycloolefins and alkynes. (3) For separating close-boiling isomers of various types of unsaturated hydrocarbons. Of special importance is the possibility of separating *cis*- and *trans*-isomers with certain exceptions. Further separation possibilities arise from substitution at or in the vicinity of the unsaturated bond. (4) For determination, on the basis of the retention time, if a certain hydrocarbon is unsaturated or not. The combination of gas chromatography using the AgEG stationary phase with the hydrogenation methods recently described by the present authors [28] has proved to be especially fruitful for the identification of unsaturated hydrocarbons.

It is hoped that the present attempt to broaden the knowledge of the behaviour of unsaturated hydrocarbons on the AgEG stationary phase will be of use not only for the separation and identification of hydrocarbons in the actual boiling range but will also facilitate the analysis of higher boiling fractions.

Acknowledgement. This work was supported by grants from the *Swedish Technical Research Council* and the *Town Council of Gothenburg.*

REFERENCES

1. Bradford, B. W., Harvey, D. and Chalkley, D. E. *J. Inst. Petrol.* **41** (1955) 80.
2. Bednas, M. E. and Russel, D. S. *Can. J. Chem.* **36** (1958) 1272.
3. Tenney, H. M. *Anal. Chem.* **30** (1958) 2.
4. Van de Craats, F. *Anal. Chim. Acta* **14** (1956) 136.
5. Luchsinger, W. *Gas-Chromatographie 1958*, Abhandlungen der deutschen Akademie der Wissenschaften zu Berlin. Klasse für Chemie, Geologie und Biologie **1959** No. 9, p. 118. Akademie-Verlag, Berlin 1959.
6. Armitage, F. *J. Chromatography* **2** (1959) 655.
7. Cope, A. C., Lebel, N. A., Lee, H. H. and Moore, W. R. *J. Am. Chem. Soc.* **79** (1957) 4720.
8. Cope, A. C., Bumgardner, C. L. and Schweizer, E. E. *J. Am. Chem. Soc.* **79** (1957) 4729.
9. Cope, A. C. and Acton, E. M. *J. Am. Chem. Soc.* **80** (1958) 355.
10. Sauers, R. R. *J. Am. Chem. Soc.* **81** (1959) 4873.
11. Gil-Av, E., Herling, J. and Shabtai, J. *Chem. & Ind. (London)* **1957** 1483; *J. Chromatography* **1** (1958) 508.
12. Shabtai, J., Herling, J. and Gil-Av, E. *J. Chromatography* **2** (1959) 406.
13. Cope, A. C., Moore, P. T. and Moore, W. R. *J. Am. Chem. Soc.* **82** (1960) 1744.
14. Powell, J. W. and Whiting, M. C. *Tetrahedron* **7** (1959) 305.
15. Butler, J. N. and Kistiakowsky, G. B. *J. Am. Chem. Soc.* **82** (1960) 759.
16. Frey, H. M. *Nature* **183** (1959) 743.
17. Luebbe, Jr., R. H. and Willard, J. E. *J. Am. Chem. Soc.* **81** (1959) 761.
18. Barnard, J. A. and Hughes, H. W. D. *Nature* **183** (1959) 250.
19. Hively, R. A. *J. Chem. Eng. Data* **5** (1960) 237.
20. Rabinovitch, B. S. and Michel, K. W. *J. Am. Chem. Soc.* **81** (1959) 5065.
21. Chesick, J. P. *J. Am. Chem. Soc.* **82** (1960) 3277.
22. Zorin, A. D., Ezheleva, A. E. and Devyatykh, G. G. *Trudy Khim. i Khim. Tekhnol.* **1** (1958) 605.
23. Smith, B. and Ohlson, R. *Acta Chem. Scand.* **13** (1959) 1253.
24. Chatt, J. in Plesch, P. H. (ed.) *Cationic polymerisation and related complexes*, W. Heffer and Sons Ltd, Cambridge 1953, p. 40.
25. Dewar, J. S. *Bull. Soc. Chim.* **18** (1951) C 71.
26. Knight, H. S. *Anal. Chem.* **30** (1958) 9.
27. Smith, B. *Acta Chem. Scand.* **13** (1959) 877.
28. Smith, B. and Ohlson, R. *Acta Chem. Scand.* **14** (1960) 1317.

Received September 11, 1961.

ACTA CHEMICA SCANDINAVICA 16 (1962) 359–373

Lipid Formation in *Cryptococcus terricolus*

II. The Effect of Ion Variation on Growth and Lipid Formation

T. A. PEDERSEN*

Royal Institute of Technology, Division of Food Chemistry, Stockholm 70, Sweden

The following medium was found satisfactory for maximum growth and lipid production in *Cryptococcus terricolus:* glucose 40.0 g, urea 0.6 g, KH_2PO_4 0.5 g, $MgSO_4 \cdot 7H_2O$ 1.0 g, Fe(III)-citrate·$3H_2O$ 0.1 g, 0.2 mg of zinc as $ZnSO_4 \cdot 7H_2O$, 0.001 mg of copper as $CuSO_4 \cdot 5H_2O$, and 0.001 mg of manganese as $MnCl_2.4H_2O$ to one litre of redistilled water. Finally, 50 mg of ethylenediamine tetraacetic acid (EDTA) was added per litre. This medium permits the production of approximately 34.5 g of yeast dry matter containing 21 g of lipids per 100 g of assimilated glucose. This yield has been found to remain constant during a large number of transfers in the same medium.

The following ions have to be added to the medium in order to obtain maximum growth: potassium, magnesium, phosphate, sulphate, iron, zinc, and copper. Supraoptimum doses of potassium, zinc, and copper had a markedly inhibiting effect on the growth of the organism. Addition of sodium, calcium, manganese, molybdenum, cobalt, and chlorine seemed to have no effect on the growth.

The lipid content of the cells was influenzed by variations in the different elements in the same manner as the growth. However, contrary to the results obtained in the absence of the other ions, a lack of phosphate or sulphate led to an increased lipid content in the cells. This lipid production may perhaps be compared with the degenerative lipid production found with aging in different organisms. More phosphate and magnesium were required in the medium for producing maximum lipid content, than for producing a maximum amount of yeast dry matter. Manganese, introduced into the medium in a concentration of 0.001 p.p.m., or more, increased the lipid content of the cells. The other elements, which did not affect the growth, had no effect on the lipid content either.

The lipid coefficient generally followed the variations in the lipid content. With increasing magnesium supply, however, it looked as if the effectivity of the conversion of glucose into lipids decreased.

The protein content of the yeast was found to be fairly constant, *viz.* 10–15 % of the dry weight.

* Present address: Department of Microbiology, Agricultural College of Norway, Vollebekk, Norway.

The effects of certain variations in the composition of the medium and the incubation conditions on the growth of *Cryptococcus terricolus* were investigated in earlier experiments [1]. The growth and lipid production of this yeast have, moreover, been found to be closely related [2]. Consequently, it was thought that maximum lipid production should be dependent on optimum growth conditions. However, there is no reason to assume that the *Rhodotorula* medium [3], without beer wort addition, employed as basal medium in earlier investigations [2], should be the best nutrient solution for *C.terricolus*. The amounts of lipids produced by this yeast were found to be independent of the quantities of nitrogen supplied [2]. These results indicated that the lipid production dominates quantitatively in the life activities of this organism, also under conditions found to be unfavourable to lipid production in other "fat" yeast species. It would, therefore, be of general interest to investigate the effect of variations in the composition of the medium on the lipid production.

It is a well-known fact that lipid formation can be brought about in other "fat" yeasts, if the amounts of certain nutrient substances, other than nitrogen, be decreased below critical levels. Reductions in the phosphate [4,5], sulphate, and iron [6] concentrations have been shown to increase the lipid production of various yeasts. With the close relationship between yeast growth and lipid production in *C.terricolus*, it is essential to obtain a balanced nutrient solution that will result in the development of the largest number of cells containing a maximum amount of lipids. With the earlier results in mind, it was hoped that both aims could be attained during one growth phase in a single, unaltered medium.

EXPERIMENTAL

Strain No. 1 of *Cryptococcus terricolus* was used in this investigation. Details concerning treatment of stock cultures, inoculation, and methods of growing the organism have been described earlier [2]. The same paper also contains descriptions of methods used for growth determination, nitrogen and lipid analyses, and determination of sugar consumption.

The *Rhodotorula* medium [3], without addition of beer wort, was employed at the beginning of this investigation. When it was found [2] that urea gave a more rapid growth than did $(NH_4)_2SO_4$, the medium composition was changed as follows: glucose 40.0 g, urea 0.6 g, KH_2PO_4 1.0 g, $MgSO_4 \cdot 7H_2O$ 1.0 g, NaCl 0.5 g, $CaCl_2 \cdot 6H_2O$ 0.5 g, and $FeCl_3 \cdot 6H_2O$ 0.005 g to one litre of distilled water (medium A). These and the other chemicals used were of analytical grade. Urea was autoclaved separately and added to the medium under sterile conditions. This medium was employed only in the first experiments to find the effects of simultaneous variations in the potassium and phosphate contents, supplied as KH_2PO_4, and in the magnesium and sulphate contents, supplied as $MgSO_4 \cdot 7H_2O$. Later on, when each individual ion concentration of interest was varied, it was found more advantageous to work with media prepared by the use of redistilled water. This modification of the composition of the original medium caused a marked decrease in the yeast yield. The decrease could be approximately compensated for by adding 1 ml (per litre nutrient solution) of a trace metal solution containing 39.3 mg of $CuSO_4 \cdot 5H_2O$, 360.3 mg of $MnCl_2 \cdot 4H_2O$, and 879.7 mg of $ZnSO_4 \cdot 7H_2O$ per litre of redistilled water. The final medium contained 0.01 p.p.m. of copper, 0.2 p.p.m. of zinc, and 0.1 p.p.m. of manganese (medium B).

In testing the effect of variations in the iron concentration on the growth of the organism, it was found more practical to use ferric citrate instead of ferric chloride, as a source of this element (medium C). A subsequent modification was obtained by omitting sodium chloride and calcium chloride from this medium (medium C_1).

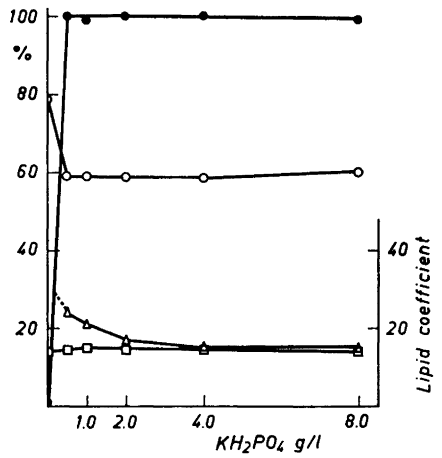

Fig. 1. Effect of different concentrations of KH_2PO_4 on growth, lipid and protein content, and lipid coefficient of *Cryptococcus terricolus*. Medium A.

● — Per cent of maximum growth
□ — Protein content in per cent of dry matter
○ — Lipid content in per cent of dry matter
△ — Lipid coefficient

For further investigations on the effects of additions of different trace metals on the organism, ethylenediamine tetraacetic acid (EDTA) was supplied to the medium to prevent possible precipitation or formation of non-assimilable complexes. This was especially necessary when metal ions were present in rather large quantities. Medium C_1, without additions of copper, zinc, and manganese, but with 50 mg of EDTA per litre, was called medium C_2.

Variations in the concentration of a single ion can be obtained only by changing the supply of a compound containing the desired element. It is of course necessary that the concentrations of the other essential ions present in this compound are kept at a constant level. This is obtained by adding equimolecular amounts of compounds containing the ion to be held constant in combinations with known, non-essential components. The exact methods are described in connection with each particular experiment.

To obtain reproducible results when investigating the effect of micro-elements, it was necessary to cultivate the inoculum twice in media, to which no addition of the actual component had been made, before inoculation of the experimental series. All series were run at least in duplicate, and all experiments repeated.

RESULTS

The contents of glucose and urea in the nutrient solution were kept constant during this investigation. Glucose has been shown to be a satisfactory energy source in the concentration used here [1], and urea has been found to provide an optimum nitrogen source for both growth and lipid production [2]. The other components introduced into the solution at different stages of this investigation, included, in addition to the macro- and micro-elements proved to be generally necessary for growth in most micro-organisms, some components exerting more irregular or undefined effects.

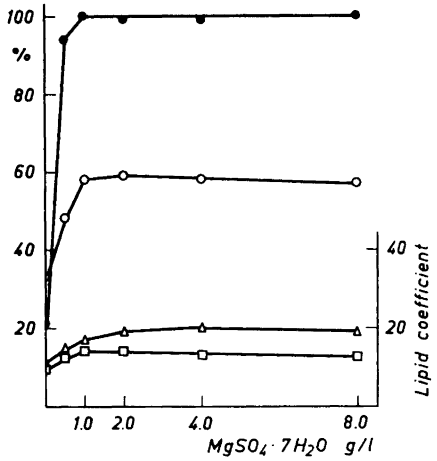

Fig. 2. Effect of different concentrations of $MgSO_4 \cdot 7H_2O$ on growth, lipid and protein content, and lipid coefficient of *Cryptococcus terricolus*. Medium A. Symbols as in Fig. 1.

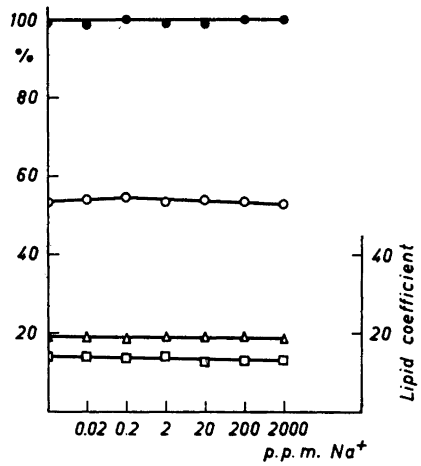

Fig. 3. Effect of different concentrations of Na^+ on growth, lipid and protein content, and lipid coefficient of *Cryptococcus terricolus*. Medium B. Symbols as in Fig. 1.

The optimum concentrations of KH_2PO_4 and $MgSO_4 \cdot 7H_2O$ were determined in a series of preliminary experiments. The concentration of KH_2PO_4 was varied from 8.0 g to 0.0 g per litre of nutrient solution (Fig. 1). As would be expected, the growth decreased rapidly as the amount of KH_2PO_4 approached zero. The protein contents of the cells were independent of the KH_2PO_4 concentration, while the lipid content increased with decreasing supply. This last result is probably connected with the stagnation of the growth. The lipid coefficient (g of newly formed lipids/100 g of assimilated sugar) increased with decreasing KH_2PO_4 supply, evidently as a result of a more economic glucose consumption. In practice, the most effective lipid production was obtained when the content of KH_2PO_4 was kept between 1.0 and 0.5 g per litre. The dotted part of the lipid coefficient curve indicates that a certain lipid formation took place even after the stagnation of the growth and the sugar assimilation. The concentration of KH_2PO_4 in the media employed in the subsequent experiments was kept at 1.0 g per litre.

Variations in the $MgSO_4 \cdot 7H_2O$ content of the medium showed that the maximum yeast production was obtained at 1.0 g of $MgSO_4 \cdot 7H_2O$ per litre (Fig. 2). Further additions seemed to have no effect on the growth, while a reduced concentration, as was to be expected, resulted in a considerable decrease in growth. The lipid content was also kept at its maximum at rates exceeding 1.0 g of $MgSO_4 \cdot 7H_2O$ per litre, while both the lipid content and the effectivity of the lipid production decreased at rates below this level. In addition, it was found that a slight decrease in the protein contents of the yeast cells occurred when the concentration of magnesium sulphate was decreased

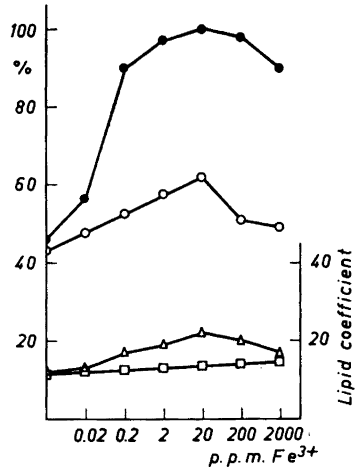

Fig. 4. Effect of different concentrations of Fe^{3+} on growth, lipid and protein content, and lipid coefficient of *Cryptococcus terricolus*. Medium C. Symbols as in Fig. 1.

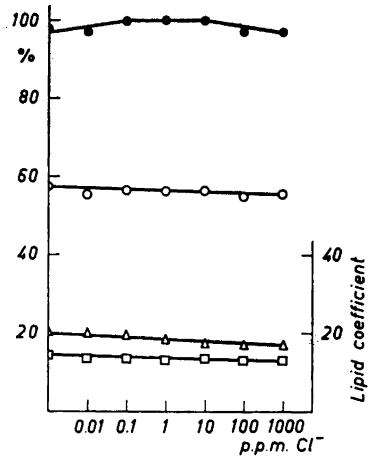

Fig. 5. Effect of different concentrations of Cl^- on growth, lipid and protein content, and lipid coefficient of *Cryptococcus terricolus*. Medium C. Symbols as in Fig. 1.

below 1.0 g per litre. Consequently, the concentration of $MgSO_4 \cdot 7H_2O$ was kept at 1.0 g per litre in the subsequent experiments.

The main interest was now focused on the effect of variations in single nutrient ions. Since it was not possible to vary the ion contents individually, it was necessary first to find elements that had no effect on the organism. These elements could then be combined with the ion to be studied.

The effect of sodium on the organism was tested by means of medium B, in which NaCl had been replaced by various amounts of $NaH_2PO_4 \cdot 2H_2O$. From Fig. 1 it might be assumed that the supply of additional phosphate, as $NaH_2PO_4 \cdot 2H_2O$, to the amount already present in medium B, would have no effect on the organism. Later results (Fig. 8) verified this suggestion. The chlorine content was diminished by the same amount in all series, but this element was still present in the calcium, iron, and manganese salts. The content of sodium varied from 2 000 to 0 p.p.m. No effect on growth, lipid content, protein content, or lipid coefficient resulted from the variations in the sodium content within the limits used here (Fig. 3).

Ferric citrate was used to test the effect of different concentrations of iron on the organism. It was first proved that no difference existed between the standard solution B and the same medium with equivalent iron amounts added as ferric citrate. The iron content was then varied between 2 000 and 0 p.p.m. The growth of the organism was greatly affected by changes in the iron content, a maximum yeast yield being obtained at an addition of 20 p.p.m. (Fig. 4). It also emerges that the changes in both lipid content and lipid coefficient paralleled the alterations in growth. The protein content,

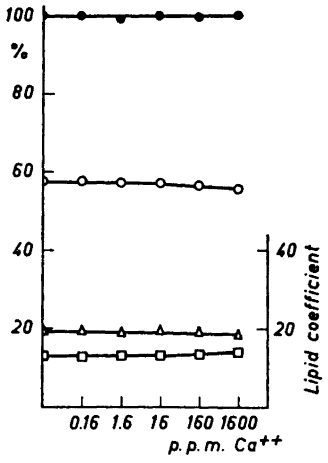

Fig. 6. Effect of different concentrations of Ca^{++} on growth, lipid and protein content, and lipid coefficient of *Cryptococcus terricolus*. Medium C. Symbols as in Fig. 1.

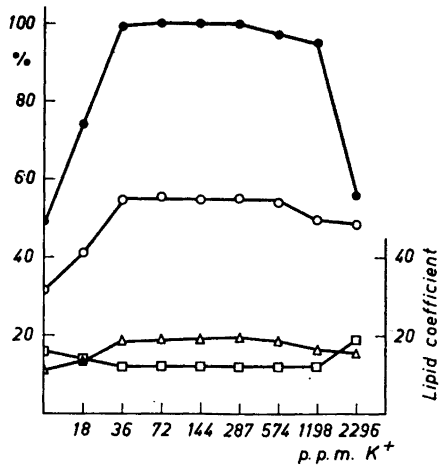

Fig. 7. Effect of different concentrations of K^+ on growth, lipid and protein content, and lipid coefficient of *Cryptococcus terricolus*. Medium C_1. Symbols as in Fig. 1.

however, remained nearly constant, although a slight increase with increasing iron content was perhaps indicated.

The comparatively good growth obtained in media to which no iron had been added (*cf.* Fig. 4) must be due to iron contaminations in the other chemicals, rather than to a growth response in a medium actually iron-free. If a linear dependence is assumed between the iron content and the yeast yield in the lower part of the growth curve, an iron contamination of approximately 90 μg per litre can be calculated for medium C. This amount is far below the purity limits for the chemicals used. It should be pointed out here that similar reservations must be made for any possible contamination when micro- or "non-effective" elements are tested.

Medium C contains chlorine in the following components: NaCl, $CaCl_2 \cdot 6H_2O$, and $MnCl_2 \cdot 4H_2O$. The last component was replaced by equivalent amounts of $MnSO_4 \cdot 4H_2O$. The original $CaCl_2 \cdot 6H_2O$ content could be diminished to 1/10 of the original amount without affecting the growth and lipid production of the organism. This reduced amount was replaced by equivalent amounts of calcium in the form of $Ca(NO_3)_2 \cdot 4H_2O$. A nitrogen-containing compound was chosen since an additional supply of this kind is known to be of no effect on either growth or lipid production [2]. A special testing of this amount of $Ca(NO_3)_2 \cdot 4H_2O$ indicated no differences from the original medium C. Now the chlorine content could be varied simply by altering the NaCl content. Fig. 5 shows that the growth and the lipid and protein contents of the yeast were independent of the chlorine concentrations employed in this investigation.

The effect of calcium was investigated simply by varying the $CaCl_2 \cdot 6H_2O$ content of medium C, since it had been proved that the presence of chlorine had no effect on the organism. Just as for chlorine, the calcium content was

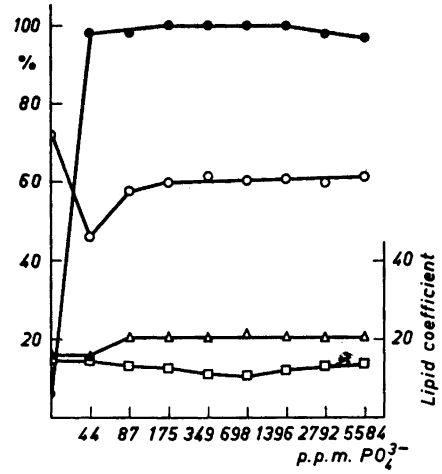

Fig. 8. Effect of different concentrations of PO_4^{3-} on growth, lipid and protein content, and lipid coefficient of *Cryptococcus terricolus*. Medium C_1. Symbols as in Fig. 1.

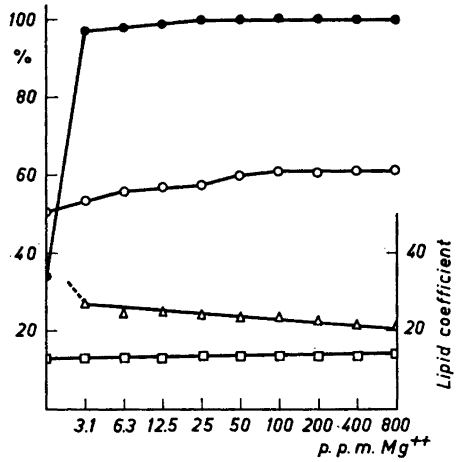

Fig. 9. Effect of different concentrations of Mg^{++} on growth, lipid and protein content, and lipid coefficient of *Cryptococcus terricolus*. Medium C_1. Symbols as in Fig. 1.

found to have no influence on the measured activities of the organism (Fig. 6). The results obtained from the variation of the sodium, calcium, and chlorine contents provide no absolute proof of the yeast being completely independent with respect to these elements, but, at any rate, it has been established that further supply, in addition to the amounts possibly added as contaminants in other chemicals, is unnecessary. Because of these findings, both NaCl and $CaCl_2 \cdot 6H_2O$ were omitted from the medium, which resulted in the modified medium C_1.

It was now possible to investigate the effects of potassium, phosphate, magnesium, and sulphate on the organism. Medium C_1 was used as basal medium. Additional potassium was supplied to the medium as KCl. When the potassium content in the original medium was reduced by decreasing the amount of KH_2PO_4, equivalent amounts of $NaH_2PO_4 \cdot 2H_2O$ were added to keep the phosphate content at a constant level. The growth of the organism was greatly affected by alterations in the potassium content (Fig. 7). Potassium contents less than 36 p.p.m., or exceeding 1198 p.p.m., depressed the growth. The same influence was also found to be present with respect to the lipid content and the lipid coefficient. The relative protein content, however, increased to a certain extent, when the growth conditions became unfavourable to the organism.

A similar method was used to establish the effect of variations in the phosphate supply on the organism. $NaH_2PO_4 \cdot 2H_2O$ was added to the solution to increase the phosphate content beyond that of medium C_1. By reducing the KH_2PO_4 content, on the other hand, a reduction in the phosphate content was obtained. KCl was added in sufficient amounts to keep the potassium con-

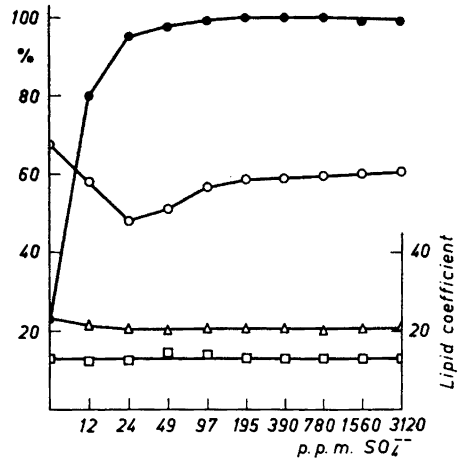

Fig. 10. Effect of different concentrations of SO_4^{--} on growth, lipid and protein content, and lipid coefficient of *Cryptococcus terricolus*. Medium C_1. Symbols as in Fig. 1.

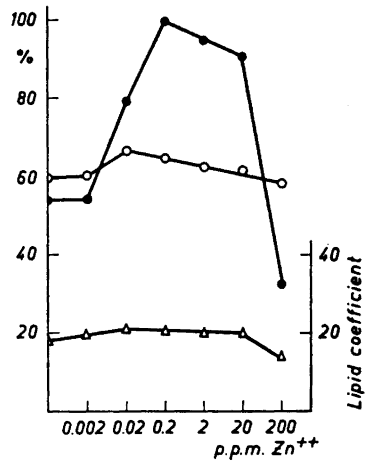

Fig. 11. Effect of different concentrations of Zn^{++} on growth, lipid content, and lipid coefficient of *Cryptococcus terricolus*. Medium C_2. Symbols as in Fig. 1.

centration constant. A rapid decrease in the growth occurred when less than 44 p.p.m. of phosphate was added to the medium (Fig. 8). Larger amounts, however, seemed to have no distinct effect on the growth of the organism. On the other hand, to obtain maximum lipid production, the amount of phosphate must exceed that required for obtaining maximum growth. The lipid content of the cell material decreased by one-fourth when the phosphate supply was reduced from 175 to 44 p.p.m., while the growth remained practically constant. As found in other connections, the stagnation of the growth, in this case due to the absence of phosphate, was accompanied by an abrupt increase in the lipid contents of the cells. The protein content seemed to be unaffected by variations in the amount of phosphate added to the medium.

To study the effect of magnesium on the organism, the amount of this element added to the solution was varied, the sulphate supply being of course kept at a constant level. An increase in the magnesium content was obtained by adding $MgCl_2 \cdot 6H_2O$. When the $MgSO_4 \cdot 7H_2O$ amount was decreased below the original content of medium C_1, the sulphate supply was kept constant by adding $Na_2SO_4 \cdot 10H_2O$. About 3 p.p.m. of magnesium was sufficient for maximum growth (Fig. 9). In contrast to the results obtained for potassium, large quantities of magnesium seemed to have no inhibitory effect on the growth. The lipid contents of the cells increased slightly with increasing magnesium content up to 100 p.p.m., while the economic yield of the transformation of glucose into lipids decreased with increasing amount of magnesium. The highest output of lipids, relative to the amount of sugar consumed, was obtained at 100 p.p.m. of magnesium in the nutrient solution. The protein content seemed to be quantitatively unaffected by variations in the magnesium content.

Table 1. Effect of different concentrations of ethylenediamine tetraacetic acid (EDTA) on the growth of *Cryptococcus terricolus*. Medium C_1.

Added EDTA g/l	Yeast yield g/l
5.0	0
0.5	0
0.05	6.95
0	6.07

Variations in the sulphate content of the medium seemed to result in more pronounced effects on the growth than did alterations in the magnesium content (Fig. 10). The sulphate content was increased by adding $Na_2SO_4 \cdot 10H_2O$ and decreased by reducing the supply of $MgSO_4 \cdot 7H_2O$. In the latter case, $MgCl_2 \cdot 6H_2O$ was added to keep the magnesium content constant. For optimum growth the addition of at least 97 p.p.m. of sulphate was required. Further additions had no effect on the growth. Alterations in the sulphate content of the medium had no quantitative effect on the protein production of the cells. The lipid contents of the cells remained unchanged for additions exceeding 195 p.p.m. of sulphate. Reductions in the sulphate supply led to a decrease in the lipid content, followed by a formation of lipid-richer cells when the sulphate content became so low that the growth was markedly inhibited. Only minor changes in the lipid coefficient were obtained, since the sugar consumption almost paralleled the lipid production of the organism.

The addition of some micro-elements was necessary to obtain maximum growth when the medium was prepared by the use of redistilled water. The effects of additions of copper, zinc, manganese, molybdenum, and cobalt were tested. In recent years, chelating agents, such as EDTA (ethylenediamine

Table 2. The effect produced by excluding different trace metals from a complete medium, on the growth, sugar consumption, and lipid content of *Cryptococcus terricolus*. Medium C_2 to which was added 0.01 p.p.m. of Cu as $CuSO_4 \cdot 5H_2O$, 0.2 p.p.m. of Zn as $ZnSO_4 \cdot 7H_2O$, 0.1 p.p.m. of Mn as $MnCl_2 \cdot 4H_2O$, 0.1 p.p.m. of Mo as $Na_2MoO_4 \cdot 2H_2O$, and 0.1 p.p.m. of Co as $CoCl_2 \cdot 6H_2O$.

Medium	Growth		Sugar consumption		Economic coeff.	Lipid content		Lipid coeff.
	g/l	%	g/l	%		g/l	%	
complete	13.09	95	38.4	96.0	34.1	7.30	55.8	19.0
— Cu	12.40	90	37.4	93.5	33.2	7.11	57.3	19.0
— Zn	6.56	47	16.2	40.5	40.5	3.49	53.2	21.5
— Mn	12.54	91	37.2	93.0	33.7	7.12	56.8	19.1
— Mo	13.56	98	39.2	98.0	34.6	7.70	56.8	19.6
— Co	13.83	100	39.5	98.8	35.0	7.77	56.2	19.7
— all	4.55	33	11.8	29.5	38.6	2.54	55.9	21.5

Table 3. The effect produced by adding different trace metals to medium C_2, on the growth and lipid content of *Cryptococcus terricolus*. When added, the elements were present in the same concentrations as in Table 2.

Addition	Growth		Lipid content	
	g/l	%	g/l	%
None	6.35	46.0	3.77	59.4
+ Cu	8.31	60.2	4.89	58.9
+ Zn	13.29	96.2	7.88	59.3
+ Mn	7.72	55.9	4.48	58.0
+ Cu, Zn	13.39	97.0	8.10	60.5
+ Cu, Mn	7.88	57.1	4.72	59.9
+ Zn, Mn	13.42	97.2	8.00	59.6
+ Cu, Zn, Mn	13.81	100.0	8.11	58.7

tetraacetic acid), have received much attention in similar investigations, because they prevent precipitation and formation of unassimilable complexes.

An addition of 50 mg of EDTA per litre increased growth, while larger amounts inhibited growth completely (Table 1). Medium C_2 was used as a basal medium throughout the subsequent part of the investigation. The addition of micro-elements has been specified in each case.

The effects of various trace metals were tested by using a medium containing all the elements, excluding one element at a time. The composition of the media and the results obtained are given in Table 2.

The growth decreased greatly when zinc was excluded from the medium. The exclusion of copper and manganese seemed to have a slightly growth-decreasing effect, while, on the other hand, molybdenum and cobalt had no effect on the organism. The lipid content in per cent of the dry weights, showed only minor variations, but both the economic coefficient and the lipid coefficient increased when the growth became seriously retarded.

The effects of the three elements, copper, zinc, and manganese were further tested by adding the elements singly, and in different combinations, to the medium. The addition of zinc alone had a marked influence on the growth, whilst copper and manganese added separately, had a more moderate, or a slight effect (Table 3). When zinc was present in the medium, the addition of the other elements resulted in only insignificant effects on the organism. The lipid content in per cent of the dry weights remained almost constant during these experiments.

Since the addition of zinc was so decisive for the development of the organism, the influence of different concentrations of this ion was tested (Fig. 11). 200 p.p.m. of zinc inhibited the growth markedly. To obtain a maximum yeast yield, the concentration had to be decreased to 0.2 p.p.m. With further restrictions in the supply, the yield decreased to approximately 54 % of the maximum yield. The total lipid production was at its maximum at the addition of 0.2 p.p.m. of zinc, but the highest lipid content was obtained at only one-tenth of this concentration. The lipid coefficient showed a maximum between 0.02

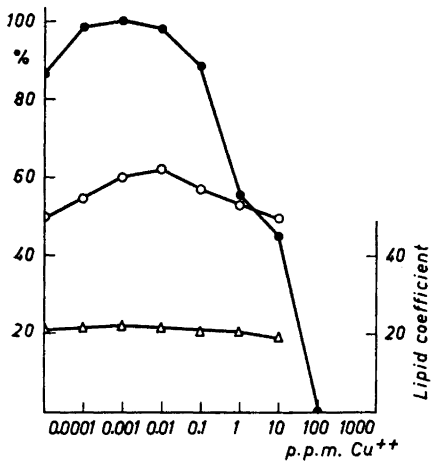

Fig. 12. Effect of different concentrations of Cu^{++} on growth, lipid content, and lipid coefficient of *Cryptococcus terricolus*. Medium C_2 + 0.2 p.p.m. of zinc. Symbols as in Fig. 1.

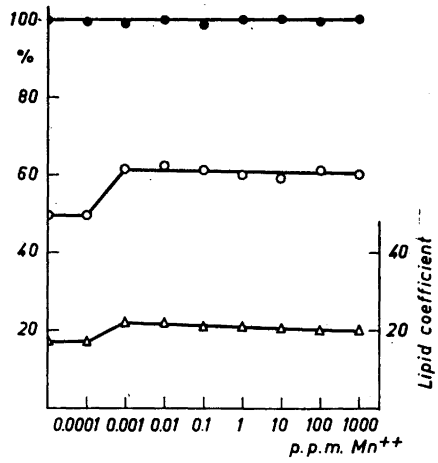

Fig. 13. Effect of different concentrations of Mn^{++} on growth, lipid content, and lipid coefficient of *Cryptococcus terricolus*. Medium C_2 + 0.2 p.p.m. of zinc + 0.001 p.p.m. of copper. Symbols as in Fig. 1.

and 20 p.p.m. of zinc. As a result of these findings, the zinc concentration of the medium was subsequently kept at 0.2 p.p.m.

The influence of variations in the copper content was investigated, by the use of medium C_2, which contained 0.2 p.p.m. of zinc. The growth was completely inhibited when 100 p.p.m. of copper, or more, was added to the medium (Fig. 12). The growth increased with decreasing copper content, maximum yield being obtained at 0.001 p.p.m. A further decrease in the copper supply led to an insignificant decrease in the yeast yield, thus indicating a slightly stimulatory effect of this element. 0.01 p.p.m. of copper gave maximum lipid content, while one-tenth of this concentration gave maximum lipid coefficient. It was therefore considered justifiable to use additions of 0.001 p.p.m. of copper in the subsequent experiments.

Finally, the effect of manganese was investigated. Medium C_2, containing 0.2 p.p.m. of zinc and 0.001 p.p.m. of copper, was used. The results differed markedly from those obtained for varying concentrations of copper and zinc (Fig. 13). No effects on the growth, due to manganese, were found within the concentration limits used here. To obtain the highest lipid production, however, the content of manganese had to be at least 0.001 p.p.m. Further additions had no effect on the lipid content or the effectivity of the lipid production. Consequently, 0.001 p.p.m. of manganese was used in the final medium.

DISCUSSION

The fundamental results obtained in this investigation and in earlier ones [2] on the lipid production of *Cryptococcus terricolus*, are to the effect that growth and lipid production are closely related. This means that, in this yeast, the lipid formation follows the proliferation of the cells, not, as is the case of the other "fat" yeasts, starting after the growth conditions have become unsatisfactory because of restrictions in or a complete assimilation of the supply of a particular nutrient other than the energy- and carbon source. In agreement with this finding, the content of proteins was found throughout to remain at a constant, comparatively low level, only in exceptional cases exceeding 15 % of the dry weight.

However, in spite of the close relationship between the growth and the lipid production in *C. terricolus*, it is of course possible that the optimum conditions for the two processes may be different with respect to the different medium constituents. Since both growth and content of lipids are always determined in the same material, conclusions may be drawn regarding both processes. This is at any rate true of the changes in the amounts of the final products (dry matter, lipids, and proteins).

Both potassium and phosphate are essential to the growth of yeasts. The very low growth of *C. terricolus* found with no addition of KH_2PO_4 is due to the presence of small amounts of these ions in the inoculum, and as contaminants. A comparison of Figs. 7 and 8 with Fig. 1 will show, that the absence of phosphate and potassium decreases the growth, but that the absence of phosphate has the greatest effect. Addition of approximately 44 p.p.m. brought the yeast yield almost to its maximum. In trying to obtain maximum growth in his lipid-forming yeasts, Schulze [7] discovered definite, upper and lower limits with respect to the amount of phosphate, that could be accumulated by the yeast cells. At higher concentrations, the excess of phosphate was left unassimilated, and did not affect the yeast yield. However, in Schulze's investigations, the lipid content was decreased under such conditions, the same phenomenon being observed by Nielsen and Nilsson [4], Maas-Förster [5], and others. Garrido *et al.*[8] working with lipid-producing fungi, found great variations among the phosphate requirements of different organisms. While *Aspergillus nidulans* produced a maximum amount of lipids when supplied with 4 737 p.p.m. of phosphate as KH_2PO_4, *Penicillium javanicum* required only 1/10 of this amount. 175 p.p.m. of phosphate or more was found to result in a maximum lipid production in *Cryptococcus terricolus*. At levels from 175 to 44 p.p.m. of phosphate, an intermediate decrease in the lipid content was found.

Phosphate plays an important role in the carbohydrate metabolism, as well as in the synthesis of the fatty acids. Consequently, the development of energy for the growth of the organism seems to proceed at a normal rate under conditions resulting in a decreased lipid production. When phosphate is not supplied to the medium, the increased production of lipids may probably be compared with the degenerative lipid production following the stagnation of growth in many microorganisms. It is further pointed out that a rich supply of phosphate to the organisms used in the above-mentioned investigations [4,5] led to the production of protein-rich cells. In *C. terricolus*, the protein content remained unaf-

fected by changes in the phosphate addition. This result would be expected if, as has been briefly discussed elsewhere [2], the low protein content is due to a blocking of the amino acid synthesis of the organism.

The function of potassium in yeast growth is not fully understood, but it has been found to be essential. To obtain maximum growth the presence of 36 p.p.m. of potassium is required (Fig. 7). The same is true of maximum lipid production. Maas-Förster [5] found that a lack of potassium decreased the production of yeast cells. The composition of the cells, however, remained constant. Garrido *et al.*[8] obtained similar results regarding the growth of different fungi, finding, however, especially in the case of *Penicillium javanicum* great variations in the lipid content. An addition of 9.7 p.p.m. of potassium to this organism gave a lipid content only about one-third of the maximum value found at an addition of 48.8 p.p.m. A further increase caused the lipid content to decrease by one-third. The large variations found in the growth and lipid production of *P. javanicum* for different potassium concentrations may be compared with those found in *Cryptococcus terricolus* in this investigation.

It is a well known fact that the total intracellular potassium concentration increases in yeast cells with increasing extracellular potassium supply [9]. Due to a decrease in the cell-water content, internal osmotic variations which, in some way, may inhibit the life activities of the cells may occur. Interesting results were obtained by Rothstein and Bruce [10], who found that the sulfhydryl groups of the cell membrane were essential to potassium retention. Since the presence of active coenzyme A plays an important role in the normal development of lipid-forming yeasts, a possible effect on the active sulfhydryl group of coenzyme A should be kept in mind.

1.0 g/l or more of $MgSO_4 \cdot 7H_2O$ is necessary for obtaining maximum growth and maximum lipid production in *C. terricolus*. The effect of increasing $MgSO_4 \cdot 7H_2O$ concentrations on the lipid production seems to be variable, depending on the actual organism under investigation. Garrido *et al.*[8] found that the lipid contents of *Aspergillus nidulans* and *Penicillium spinulosum* increased with increasing $MgSO_4 \cdot 7H_2O$ supply, whereas the reverse was found to be the case with *Penicillium javanicum*. Both magnesium and sulphate are essential to obtain high yields of yeasts. In *Crytococcus terricolus* magnesium and sulphate are also required to obtain a maximum lipid production. Nielsen and Rojowski [6] found that a lipid-rich *Rhodotorula gracilis* yeast was obtained with a reduced sulphate content in the medium. The authors suggested that the primary effect was the decrease in the normal protein content of the cells, followed by a simultaneous increase in the lipid content. Fundamental differences have been found between *R. gracilis* and *Cryptococcus terricolus*, the protein content of the latter species always remaining at a low level. As was the case when the phosphate content was varied, an intermediate decrease in the lipid content occurred at sulphate additions between 195 and 24 p.p.m. When sulphate was absent, the increased production of lipids was probably a result of a degenerative lipid synthesis. Consequently, as far as the effects of both magnesium and sulphate are concerned, optimum growth conditions are accompanied by a maximum lipid production, indicating that, in this case also, a high lipid content is a normal property of the cells.

Addition of iron generally enhances the yield of yeasts. The optimum amount varies from one organism to another. Olson and Johnson [11] found that amounts ranging from 0.025 to 0.15 p.p.m. of iron were necessary for obtaining maximum growth in four different yeasts. Steinberg and Ordal [12] found the addition of iron to be unnecessary for the attainment of maximum lipid synthesis in *Rhodotorula gracilis* grown in a medium containing unrefined carbohydrates. Nielsen and Rojowski [6] succeeded in increasing the lipid content of *R.gracilis* by cultivating the organism with a greatly reduced iron supply. Their results also indicated that the yeast protein in this case decreased from 45 to 20 % of the dry weight.

In *Cryptococcus terricolus*, 0.2 p.p.m. of iron is sufficient to produce approximately 90 % of the maximum yield obtained at 20 p.p.m. Larger doses have a slightly inhibitory effect, the tolerance limits being very wide, however. From 0.2 to 2 000 p.p.m. of iron gives 90 % or more of maximum growth yield. The amounts required for maximum lipid production are the same as those for maximum growth. The positive correlation between healthy growth and maximum lipid production was thus once again stated for *C. terricolus*.

The following ions were shown to have no effect on either the growth or the lipid production of *C.terricolus:* sodium, calcium, cobalt, molybdenum, and chlorine. These results are partly in agreement with those found earlier. Olson and Johnson [11] found that calcium and cobalt were not necessary for maximum yeast growth. No addition of either molybdenum or chlorine was made. Steinberg and Ordal [12] found the amounts of sodium and calcium present in unrefined carbohydrates to be sufficient to meet the requirements for lipid synthesis in *Rhodotorula gracilis*. In the present investigation, the possible presence, as contaminants, of sufficient quantities of the five elements mentioned should not be overlooked. However, no special additions of compounds containing these elements are required.

Ethylenediamine tetraacetic acid (EDTA) is used to keep the concentration of one or more metal ions below certain critical concentrations, above which undesirable precipitates may form, or undesirable reactions occur. The addition of 50 mg of EDTA to the medium resulted in an improvement in growth (*cf.* Table 1). Shukla and Prabhu [13] found that the EDTA effect was due to the prevention of the sugar-salt complex formation, which leads to losses of assimilable sugars in both molasses and synthetic media. More than 500 mg of EDTA per litre of nutrient solution resulted in a total inhibition of the growth. This is probably due to the removal of the free metal ions from the medium, since the equilibrium between free metals, chelating agent, and chelate is strongly shifted towards the metal chelate.

Addition of 50 mg of EDTA per litre was used throughout the investigations of the effects of zinc, copper, and manganese, since no visible precipitation was found to have occurred, even at the highest metal concentrations used. At large metal concentrations, the free metal ions will of course dominate. With a reduced metal supply, an increasing part of the metal ions will be bound in the chelate complexes, but, as the free metal ions are being assimilated, new ions will be set free from the chelates, to an extent depending on the dissociation constants of the different chelate complexes.

The effect of zinc on the growth of the organism is very pronounced. More than 90 % of maximum growth is obtained at 0.2—20 p.p.m. of zinc. The largest lipid production is also found in this interval, although, in this case, also 0.02 p.p.m. must be included in the optimum range. Olson and Johnson [11] found that 0.025—0.2 p.p.m. of zinc caused a maximum growth in four different yeasts. Concentrations within the range 300—500 p.p.m. have generally been found to inhibit the growth of the yeasts partially [14]. Zinc has to be included in the *Rhodotorula gracilis* medium to obtain maximum lipid production [15]. This is also the case with many other lipid-forming microorganisms. To a certain extent, the lipid synthesis seems to be dependent on the addition of zinc.

It is a generally accepted view that, although copper is not essential to yeasts, small concentrations of this metal enhance the growth. Olson and Johnson [11] found that *Torulopsis utilis* 3 required 0.003 p.p.m. of copper for maximum growth — an amount that can be compared with the requirements of *Cryptococcus terricolus*. The requirements for maximum growth and total inhibition seem to vary considerably from one species to another. The growth is generally found to be totally inhibited at an addition of 100 p.p.m. or less.

Usually no effect on the growth is encountered at variations of the manganese content. This element was not required in short experiments on the lipid formation in *Torulopsis lipofera* [16]. In the present experiments, involving cell propagation, however, the lipid production was decreased to a certain extent when the manganese content was decreased below a certain critical value.

Acknowledgements. The author is greatly indebted to the *Royal Norwegian Council for Scientific and Industrial Research* for financial support via the Scandinavian Centres for Advanced Training, Growing Points Programme. Thanks are also due to Professor H. Lundin, Head of the Division of Food Chemistry, for provision of laboratory facilities. The skilful, technical assistance of Mr. L.-G. Bodin is gratefully acknowledged.

REFERENCES

1. Pedersen, T. A. *Physiol. Plantarum* **13** (1960) 64.
2. Pedersen, T. A. *Acta Chem. Scand.* **15** (1961) 651.
3. Lundin, H. *J. Inst. Brewing* **56** (1950) 17.
4. Nielsen, N. and Nilsson, N. G. *Acta Chem. Scand.* **7** (1953) 984.
5. Maas-Förster, M. *Arch. Mikrobiol.* **22** (1955) 115.
6. Nielsen, N. and Rojowski, P. *Acta Chem. Scand.* **4** (1950) 1309.
7. Schulze, K. L. *Appl. Microbiol.* **4** (1956) 207.
8. Garrido, J. M., Woodbine, M. and Walker, T. *An. real. Soc. esp. Fis. Quim.* **49** (1953) 829.
9. Tolberg, A. B. and Pace, N. *Proc. Soc. Exptl. Biol. Med.* **103** (1960) 488.
10. Rothstein, A. and Bruce, M. *J. Cellular Comp. Physiol.* **51** (1958) 439.
11. Olson, B. H. and Johnson, M. J. *J. Bacteriol.* **57** (1949) 235.
12. Steinberg, M. P. and Ordal, Z. J. *J. Agr. Food Chem.* **2** (1954) 873.
13. Shukla, J. P. and Prabhu, K. A. *Nature* **182** (1958) 1316.
14. Morris, E. O. in Cook, A. H. *The chemistry and biology of yeasts*, Academic Press, New York 1958.
15. Blinc, M. and Hočevar, B. *Monatsh.* **84** (1953) 1127.
16. Kleinzeller, A. *Advances in Enzymol.* **8** (1948) 299.

Received September 15, 1961.

ACTA CHEMICA SCANDINAVICA 16 (1962) 374–382

Lipid Formation in *Cryptococcus terricolus*

III. Extraction and Purification of Lipids

T. A. PEDERSEN*

Royal Institute of Technology, Division of Food Chemistry, Stockholm 70, Sweden

Extraction procedures have been developed which release the total lipid content from the yeast *Cryptococcus terricolus* without using hydrolytic or high-temperature treatments. The best results were obtained by extracting freeze-dried yeast material at room temperature. Chloroform-methanol (1:1, v/v) was used as solvent, and the material plus solvent were stirred continuously during three successive three-hour extraction periods. The effectivity of the extraction was found to be dependent on the composition of the solvent mixture and on the length and number of the extraction periods.

An effective purification of the crude lipids was obtained by a thorough mixing of the extract, dissolved in chloroform-methanol (2:1, v/v), with distilled water, followed by separation by centrifugation. The purified lipids were easily redissolved in the usual lipid solvents.

The wash solutions were found to contain only a very small amount of materials of lipid character, varying between 0 and 0.3 % of the lipid content of the organism.

Various methods may be used to separate the lipids from proteins and other components of biological materials. A number of complete procedures for the extraction of lipids from tissues have been described, and a successful extraction of animal preparations is generally obtained with only minor modifications of one of these procedures. However, if a microbial material is to be extracted, it seems difficult to decide which method will give the best result. Various methods have been employed but, in most cases, they include an extreme treatment of the cells, requiring either additions of acids or bases, or extractions at elevated temperatures, or a combination of both treatments. Complete lipid extractions of yeasts have usually been performed by means of such methods. When the interest is concentrated on the determination of the amounts of lipids in phospholipid-poor cell materials, such treatments may be satisfac-

* Present address: Department of Microbiology, Agricultural College of Norway, Vollebekk, Norway.

tory. However, if the extract is to be employed for further analyses to establish the composition of the lipid material, it is essential that the lipids be obtained by the mildest possible procedure.

The main purpose of the present work was to establish an extraction procedure for releasing the total lipid content from *Cryptococcus terricolus* cells without using any undesired pretreatment, and to devise an effective purification procedure for the crude lipid extract. Further analyses of the purified lipid mixture obtained may be performed in the future to give an idea of the composition of the native lipids of this yeast.

EXPERIMENTAL

The yeast was grown in an unbaffled glass fermentation vessel of 10 l capacity. Nutrient solution (7.75 l) of the following composition was poured into the vessel: glucose 40.0 g, KH_2PO_4 1.0 g, $MgSO_4 \cdot 7H_2O$ 1.0 g, Fe-citrate·$3H_2O$ 0.1 g, and 1.0 ml of metal solution (containing 0.2 mg of zinc as $ZnSO_4 \cdot 7H_2O$, 0.1 mg of manganese as $MnCl_2 \cdot 4H_2O$, and 0.01 mg of copper as $CuSO_4 \cdot 5H_2O$) per litre of final solution. The vessel was closed with a stainless steel cover, and autoclaved. 5.4 g of urea in 0.25 l of water was autoclaved separately, and introduced aseptically, together with 1 l of a four-day-old inoculation material, into the fermentation vessel. The vessel was placed in a water bath at 25°C. Compressed air, on being passed through a sterile air filter and a flowmeter at a rate of 1.0 l of air/l of medium/min, was bubbled in continuously at the bottom of the fermentation vessel. In addition, the solution was stirred mechanically throughout the experiment. Foaming was not pronounced, hence no antifoaming agent was added. Intermediate samples of the cell suspension could be taken out for controls and analyses using a sterile pipette. After 3 days, all the sugar had been consumed. The cells were then centrifuged and washed twice with distilled water. One cultivation experiment yielded about 110 g of dry matter. This amount was sufficient for carrying out the investigation. The results from different experiments could thus be directly compared. One part of the cell paste was stored at −20°C. The remainder was immediately freeze-dried to 98−99 % of dry matter and stored in a vacuum desiccator until used.

The following solvents were used for the extractions: diethyl ether anhydrous p.a., petroleum ether (Skellysolve F, residue after evaporation at most 0.0016 %) with a boiling point of 35−60°C, absolute ethanol (99.5 %), chloroform and methanol of analytical grade. The other chemicals used were also of analytical grade.

The following methods, tested for the purification of the crude lipid extracts, were originally described by Folch *et al.*[1,2]

Purification by diffusion. A beaker, slightly larger than the volume of extracts to be washed, is submerged into a larger beaker, nine-tenths full of water, and with a capacity of more than ten times the volume of the extract to be washed. The lipid is dissolved in chloroform-methanol (2:1, v/v) and delivered slowly into the small beaker by means of a volumetric pipette. The system thus obtained is allowed to stand overnight.

Purification by centrifugation. The crude extract, dissolved in chloroform-methanol (2:1, v/v), is mixed thoroughly with one-fifth of its volume of either water or a 0.003 N $MgCl_2 \cdot 6H_2O$ solution, and separated by centrifugation for 15 min at 2 400 r.p.m.

The upper phases obtained with these procedures were removed as completely as possible with a pipette. In the diffusion method, methanol was added to dissolve the cloudy, insoluble matter (fluff) formed at the interface. In the centrifugation procedures, no interfacial fluff was formed. In these cases, the tube wall and the remaining upper phase were washed twice with 1.5-ml portions of a solvent mixture identical with that of the final upper phase.

The lipid samples and the wash solutions were collected and dried on a rotating vacuum drier.

The total carbohydrate content was determined according to the anthrone method described by Trevelyan *et al.*[3] The lipid solutions were poured into the tubes and dried before the adding of the reagent. The sugars in the wash solutions could be easily deter-

mined using a Beckman spectrophotometer at 620 mμ. When lipids were present, yellow and brown colours interfered, making the readings very uncertain. The results were referred to a glucose standard.

The phosphorus content was determined with the Fiske-SubbaRow reagent according to the method modified by Bartlett [4]. Readings were made on a Beckman spectrophotometer at 830 mμ. The lipid solvent was removed on a water bath and any possible residual solvent by repeated blowing with CO_2.

The nitrogen content was determined by the standard Kjeldahl procedure.

Amino nitrogen was determined according to the ninhydrin method modified for use with phospholipids by Wheeldon and Collins [5]. Readings were made on a Beckman spectrophotometer at 570 mμ. Serine was used as standard. In preparations rich in fats and free fatty acids, the total amount of material taken for analysis must not exceed 1 mg. If it does, undissolved particles will disturb the spectrophotometric readings.

The Liebermann-Burchard qualitative test for sterols was performed by dissolving a part of the sample in 2 ml of chloroform and adding 10 drops of acetic anhydride plus 2 drops of concentrated sulphuric acid [6]. Visual readings were made after 2, 10, and 120 min.

RESULTS AND DISCUSSION

When extracting lipids from yeast materials it is usually found that the cells have to be pretreated to give complete extractions.

Table 1 shows the results obtained when a cell paste was extracted directly without any pretreatment. Starkey [7] found only 3.1 % of lipids in *Lipomyces starkeyi* by this extraction procedure. Judging from earlier literature, the poor results obtained by direct extraction using diethyl ether are probably due partly to the impermeability of the yeast cell wall to this solvent, and partly to the formation by the lipids of complexes with the cell proteins not released during this treatment.

It has been known for a long time that a treatment of the cell material with hydrochloric acid increases the amount of extractable lipids. A previous work [8], showed that autoclaving of the *Cryptococcus terricolus* material for 15 min with 1.2 N hydrochloric acid, followed by extraction according to the methods described by Steinberg and Ordal [9], resulted in a complete removal of the lipids (maximum value *ca.* 70 % of the dry matter). The extraction results for *C. terricolus* cells were found to be just as good if the autoclaving was replaced by boiling under reflux for 2 h. This procedure was first introduced by Smedley-MacLean [10]. Milder hydrochloric acid treatments were used successfully by Starkey [7] (boiling with 2 % hydrochloric acid under reflux for 4 h) and by Deinema and Landheer [11] (boiling with 0.5 % hydrochloric acid under reflux for 3 h). The last two procedures were quite as effective for pre-

Table 1. Extraction of lipids with diethyl ether from an untreated paste of *Cryptococcus terricolus* cells.

Material	Extraction method	Extracted lipids. Per cent of dry matter
Wet cell paste	Separatory funnel	7.1
Dried cell paste	Soxhlet	5.1

extraction treatments of *C. terricolus* cells as the stronger methods used previously. Extraction of the hydrolyzed material with petroleum ether in separatory funnels, or extraction of dried hydrolyzed material in Soxhlet extractors with petroleum ether or diethyl ether gave almost identical results.

Direct saponification with ethanolic KOH, followed by acidification of the soap solution and extraction, has also been employed for yeasts [12]. This method, however, was not tried for *C. terricolus* cells.

Large amounts of non-lipids were always extracted whenever the treatment involved a hydrolysis of the cells. The crude extract obtained was exceedingly difficult to purify. After a most particular purification, the lipid extract still had a dark and, as will be shown, unnaturally brown colour. For theoretical reasons, it was also considered desirable to avoid hydrolysis, since destructions of and alterations in the lipid structure most probably increase during such treatments. It is a well known fact that a hydrolytic pretreatment destroys the neutral lipids, especially the phospholipids. Lipids obtained after such treatments are, therefore, poorly suited for further qualitative separations.

Different combinations of solvents were tried for the direct extraction of untreated, dried cell paste in a Soxhlet apparatus. Chloroform [13], ethanol-diethyl ether (3:1, v/v) [13], chloroform-methanol (2:1, v/v) [13], ethanol-benzene (4:1, v/v) [14], and methanol-petroleum ether (1:10, v/v) [15] were used. 20—30% of the lipids were extracted at the most. Anyhow, compared with the diethyl ether extraction, this was at any rate an improvement since greater amounts of the lipids could be extracted directly without pretreatment.

Refluxing the wet cell paste directly with ethanol-diethyl ether as solvent, released still more of the lipids. A combination of the extracts from a 3 hours' reflux treatment with ethanol-diethyl ether (3:1, v/v), followed by two re-extractions with diethyl ether under reflux, each for 2 h, resulted in 45.9 % of extracted matter, corresponding to approximately 3/4 of the lipid content. To get the remainder extracted, a treatment with hydrochloric acid was necessary. It is, in fact, in most cases, advisable to subject the solvent-extracted residue to hydrolysis, followed by new extractions, to check that the extracted material represents the total lipids.

A direct extraction of disintegrated cells was tried in order to obtain a total removal of the cell lipids without hydrolytic pretreatment. The cells in

Table 2. Extraction of an untreated and a disintegrated wet cell paste of *Cryptococcus terricolus*. Refluxed with ethanol-diethyl ether (3:1, v/v), and thereafter subjected to two diethyl ether extractions. The extracted residue hydrolyzed and extracted with petroleum ether.

Material	Lipids. Per cent of dry matter		
	Direct extraction	Rest extracted	Total
Untreated	45.9	13.6	59.5
Disintegrated	50.5	9.2	59.7

a wet cell paste were successfully disintegrated, using a procedure described by Edebo [16]. Microscopic examinations of the material after disintegration indicated a practically total breakage of the individual cell walls. On extraction, the interior of the cells probably came in a more direct contact with the solvents. Table 2 shows that a greater part of the lipids are extracted from a disintegrated material, about 9 % being left for hydrolytic treatment. Even with the solvent mixture used here, the cell wall constitutes a barrier to the solvents, in spite of the fact that diethyl ether, to which the dehydrating agent ethanol has been added, penetrates the wall more effectively than does diethyl ether alone.

Like hydrolysis of the cell material, it is also desirable to avoid the use of elevated temperatures. Hanahan [17] preferred to use extraction at room temperature or at most one at 30—35°C. He found phospholipids from yeasts to be severely affected by extractions with ethanol-diethyl ether (3:1, v/v) at 55—60°C. By the use of this last procedure, they were obtained as very dark, viscous oils, while the extract at 25°C had a light yellow colour.

An attempt was made to extract the disintegrated material directly at room temperature by shaking it in separatory funnels. Large amounts of emulsions were formed, rendering a separation into two phases practically impossible. Lipid extraction, without heating, but by means of continuous stirring with different solvent mixtures, was tried. The first extract, after having been filtered, was found to contain large amounts of contaminations. Upon purification in separating funnels, emulsions were formed which resulted in a difficult separation also in this case.

Hartman *et al.*[15], in extracting freeze-dried *Rhodotorula graminis* material in a Soxhlet apparatus with methanol and light petroleum, obtained 88 % of the total lipids. Judging from these results, freeze-drying seems to have a favourable effect on the extraction procedure. Material obtained from *Cryptococcus terricolus* was freeze-dried and extracted with different solvents and solvent mixtures under continuous stirring at room temperature. The results

Table 3. Extraction of freeze-dried *Cryptococcus terricolus* material under continuous stirring at room temperature with different solvents. Three successive extraction periods of three hours. Extracted residue re-extracted with chloroform-methanol (1:1, v/v) under reflux.

Solvent	Lipids. Per cent of dry matter	Residual lipids. Per cent of dry matter	Total lipids. Per cent of dry matter
Petroleum ether *	58.2	2.5	60.7
Petroleum ether	36.0		
Ethanol-petroleum ether (3:1, v/v)	50.2	7.4	57.6
Diethyl ether	32.5		
Ethanol-diethyl ether (3:1, v/v)	41.6	12.3	53.9
Chloroform	37.5		
Chloroform-methanol (2:1, v/v)	54.5	5.0	59.5

* Material autoclaved before extraction in separatory funnels.

are given in Table 3, and compared with the amount of lipids extracted from an autoclaved material.

Extraction with diethyl ether, petroleum ether, or chloroform alone, released from 54 to 61 % of the total extractable lipids. Consequently, it may be assumed that freeze-drying makes the cell walls more permeable to the various solvents. If dehydrating agents, such as ethanol or methanol, are added, the extraction becomes, of course, more complete. Apart from additional effects upon the cell walls, this might indicate that the lipids are partly present as lipoproteins. Water molecules play an important role in the binding between lipids and proteins [17]. The addition of the dehydrating agent ruptures the lipid-protein linkage, thus making the extraction possible. The best results were obtained with chloroform-methanol, which permitted the extraction of *ca.* 90 % of the lipids, while ethanol-diethyl ether released only 69 % of the lipids. "Maximum extractable lipids" in Tables 4 and 5 give the amounts obtained after re-extraction with chloroform-methanol (1:1, v/v) of the autoclaved, petroleum ether-extracted residue.

It is a well-known fact that the optimum ratio for the solvents may vary considerably from one material to another. Consequently, different chloroform-methanol mixtures were tested.

Table 4. Extraction of freeze-dried *Cryptococcus terricolus* material by continuous stirring at room temperature with different chloroform-methanol mixtures. Three successive extraction periods of three hours.

Chloroform-methanol (v/v)	Lipids. Per cent of dry matter	Percentage of maximum extractable lipids
3:1	44.6	73.5
2:1	54.5	89.8
1:1	60.6	99.8
1:2	52.3	86.2

Table 4 shows that the extraction is practically complete if chloroform-methanol (1:1, v/v) is used as a solvent. The total extraction period comprises nine hours. It would be convenient if this time could be shortened. As shown in Table 5, however, the long extraction period has to be retained in order to obtain satisfactory results.

Table 5. Extraction of freeze-dried *Cryptococcus terricolus* material by continuous stirring at room temperature with chloroform-methanol (1:1, v/v). Length and number of extraction periods varied.

Number of periods	Length of periods in hours	Lipids. Per cent of dry matter	Percentage of maximum extractable lipids
3	1	55.3	91.1
3	2	57.2	94.2
3	3	60.6	99.8
2	3	58.0	95.6
1	3	54.2	89.3

The material obtained after these extraction procedures was of a light yellow colour. This is due to the absence of elevated temperatures during the extractions as well as to the presence of relatively small amounts of contaminants. Sugars in particular, give a brown colour upon heating. However, to avoid misleading results in the subsequent chromatographic separations, the non-lipid contaminants had to be further removed.

Lipid preparations have a remarkable ability to solubilize many non-lipid components. In general, sugars, free amino acids, urea, and also inorganic substances, may be found as contaminations. Partly, the contaminating material is soluble in the lipid solvent used, but mostly the contamination is due to the complexing ability of the varies types of phospholipids. For this reason, selective precipitations are not applicable as purifaction procedures. Liquid-liquid partition methods are effective and widely favoured although they may lead to losses of the most polar lipids. Purification of the crude extract has to be carried out at room temperature.

Re-extraction of the crude extracts in separatory funnels was tried in order to prepare a purified lipid material. The water and solvent phases could hardly be separated after shaking, owing to the formation of large amounts of apparently permanent emulsions. Another method tested consisted in shaking a lipid extract redissolved in chloroform-methanol (2:1, v/v) with a 0.9 % NaCl solution. The formation of emulsion was in this case more moderate and temporary, thus making separation possible, but after drying, large amounts of NaCl crystals were found to be present in the lipids. It was very difficult to free the extract from the NaCl, since, upon repeated shakings with water, the stable emulsions were, to a certain extent, regenerated. Moreover, in this case the addition of the salt increased the problem of contamination.

Reproducible methods for the removal of many of the impurities in a crude lipid extract, are the washing techniques of Folch *et al.*[1,2], mentioned briefly

Table 6. Effect of different washing procedures on the crude lipid extract of *Cryptococcus terricolus* material.

Solutes	Crude extract. Amount	Washed by diffusion in beaker		Washed by centrifugation with H_2O		Washed by centrifugation with 0.003 N $MgCl_2$	
		Amount left	Per cent removed	Amount left	Per cent removed	Amount left	Per cent removed
Total solutes (mg)	221.0	211.5	4.3	214.0	3.2	214.0	3.2
Total nitrogen (mg)	0.42	0.35	16.7	0.32	23.8	0.32	23.8
Amino nitrogen (mg)	0.25	0.17	32.0	0.16	36.0	0.16	36.0
Phosphorus (μg)	126.4	108.5	14.2	83.6	33.9	92.6	28.7
Carbohydrates (as glucose) (μg)	2500	1525	39.0	250	90.0	250	90.0

The qualitative sterol test was negative in the washing solutions removed.

above. These methods were originally applied to brain tissues and some other animal tissues. Folch and his co-workers found that these washing procedures removed the non-lipid contaminants from the extracts, with a concomitant loss of lipids ranging from 0 to at most 0.6 %.

The crude *C.terricolus* lipid extract was purified directly after extraction, without any intermediate drying. The results are given in Table 6.

Washing by means of the two centrifugation procedures seems to have the same effect, 3.2 % of the crude extract materials being removed. The greater loss in total solutes by the beaker diffusion method is probably due to difficulties encountered in removing the upper phase without simultaneously taking away traces of the interfacial fluff. This is the most probable explanation, since the removal of the other compounds investigated was less in this procedure. Carbohydrates were ineffectively removed by the diffusion method, while by the centrifugation methods, the carbohydrate content could be reduced to only 0.1 % of the lipid content. The contents of the other compounds investigated were also very low. The phosphorus content was found to be only about 0.05 %, which indicates a low phospholipid content. The low phospholipid content was verified by preliminary chromatographic separations of the major lipid groups. With the small nitrogen quantities in this material, the determination of the total nitrogen content is, of course, accompanied by relatively large titration errors. From a comparison of the phosphorus and nitrogen contents, it seems likely that the nitrogen contents obtained were too high, especially as the lecithin content according to preliminary chromatographic separations was found to be very low. The amino nitrogen constituted approximately half of the nitrogen found in the purified materials. The losses in total nitrogen during the washing procedures can be accounted for by the removal of amino group-containing compounds.

The washed extract was easily dissolved in the usual lipid solvents without leaving any measurable, undissolved residue. On re-extraction, the wash solutions from the two centrifugation procedures contained at the most 0.3 % of extractable materials of lipid character. In many experiments, no losses at all were detected. The losses of lipids during the washing procedures have consequently been kept at a satisfactory low level.

Acknowledgements. This work has been supported by the *Royal Norwegian Council for Scientific and Industrial Research* via the Scandinavian Centres for Advanced Training, Growing Points Programme. The author wishes to express his gratitude to Dr. Bengt Samuelsson for helpful discussions, to Dr. Lars Edebo for preparing the disintegrated yeast material, and to Mr. Lars-Gunnar Bodin for skilful, technical assistance.

REFERENCES

1. Folch, J., Ascoli, I., Lees, M., Meath, J. A. and LeBaron, F. N. *J. Biol. Chem.* **191** (1951) 833.
2. Folch, J., Lees, M., Meath, J. A. and Sloane Stanley, G. H. *J. Biol. Chem.* **226** (1957) 497.
3. Trevelyan, W. E. and Harrison, J. S. *Biochem. J.* **50** (1952) 298.
4. Bartlett, G. R. *J. Biol. Chem.* **234** (1959) 466.
5. Wheeldon, L. W. and Collins, F. D. *Biochem. J.* **60** (1957) 435.
6. Barron, E. J. and Hanahan, D. J. *J. Biol. Chem.* **231** (1958) 493.

7. Starkey, R. L. *J. Bacteriol.* **51** (1946) 33.
8. Pedersen, T. A. *Acta Chem. Scand.* **15** (1961) 651.
9. Steinberg, M. P. and Ordal, Z. J. *J. Agr. Food Chem.* **2** (1954) 873.
10. Smedley-MacLean, J. *Biochem. J.* **16** (1922) 370.
11. Deinema, M. H. and Landheer, C. A. *Arch. Mikrobiol.* **25** (1956) 193.
12. Kleinzeller, A. *Biochem. J.* **38** (1944) 480.
13. Entenman, C. in Colowick, S. P. and Kaplan, N. O. *Methods in Enzymology*, Vol. III, Academic Press, New York 1957.
14. Gaby, W. L., Hadley, C. and Kaminski, Z. C. *J. Biol. Chem.* **227** (1957) 853.
15. Hartman, L., Hawke, J. C., Shorland, F. B. and diMenna, M. E. *Arch. Biochem. Biophys.* **81** (1959) 346.
16. Edebo, L. *J. Biochem. Microbiol. Techn. Engin.* **2** (1960) 453.
17. Hanahan, D. J. *Lipid Chemistry*, Wiley, New York 1960.

Received September 15, 1961.

ACTA CHEMICA SCANDINAVICA 16 (1962) 383–386

The Synthesis and Characterisation of 4-α,6-β-Bis-D-Glucopyranosido-D-Glucose *

I. J. GOLDSTEIN** and BENGT LINDBERG

Träkemiska avdelningen, Svenska Träforskningsinstitutet, Stockholm, Sweden

The chemical synthesis of 4-α,6-β-bis-D-glucopyranoside-D-glucose has been accomplished. Chemical and enzymic evidence in support of its structure is described. The trisaccharide hendeca-acetate failed to anomerise when treated with titanium tetrachloride.

Although branched polysaccharides have been known for many years, the isolation and proper characterisation of a branched oligosaccharide has not been reported as a product of hydrolysis from such polymers. (The term branched oligosaccharide will be used to refer to saccharides in which at least two sugar residues are glycosidically linked to a third sugar residue). The chemical [1-3] and enzymic [4] syntheses of several branched trisaccharides have been reported. Klemer [1] reported the synthesis of [4-α, 6-β-bis-D-glucopyranosido-D-glucose (I) and in a later communication [5] determined the velocity constants for the hydrolysis of the glycosidic bonds in this substance.

Some years ago one of us [6] (B.L.) tried to synthesise the same trisaccharide; the synthesis was however not accomplished, due to inadequate fractionation of the final product. The present paper describes the synthesis of the trisaccharide by the route previously reported, confirming the specific optical rotation reported by Klemer and adduces chemical and enzymic evidence in support of its structure.

Essentially, the synthesis involves a Koenings-Knorr condensation of tetra-*O*-acetyl-α-D-glucopyranosyl bromide and 1,2,3,2',2',4',6'-β-maltose heptaacetate [6]. The product, after deacetylation was resolved by charcoal column chromatography [7]. The yield of the amorphous trisaccharide was 8.4 %. It had $[\alpha]_D^{20}$ + 83° in water; Klemer [1] reports + 84°.

The following experimental evidence is presented in support of its representation as I:

* This investigation was carried out during a tenure of a Special Fellowship (to I.J.G.) from the Division of General Medical Sciences: United States Public Health Service.

** Present address: School of Medicine, Department of Biochemistry, University of Buffalo, New York, USA.

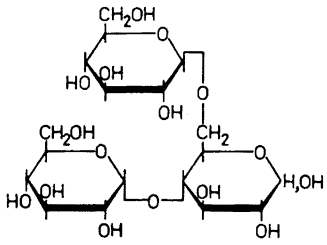

I

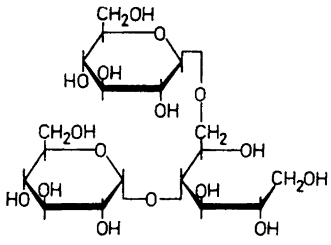

II

(*a*) Partial hydrolysis gives rise to glucose, maltose, gentiobiose and unchanged I.
(*b*) Reduction followed by partial hydrolysis affords glucose as the only saccharide reducing to the *p*-anisidine spray reagent.
(*c*) Emulsin cleaves I to give D-glucose and maltose.
(*d*) Paper electrophoresis in borate buffer of pH 10 (M_G 0.37) indicates the presence of a 1,4- or 1,2-linked residue on the reducing moiety.
(*e*) Reduction of I affords II. Periodate oxidation of II resulted in the consumption of 5.9 moles of periodate with the liberation of 3.1 and 0.95 moles of formic acid and formaldehyde, respectively. (Theory requires 6, 3, and 1 moles).
(*f*) Reduction of periodate oxidised II with borohydride and hydrolysis gives glycerol and erythritol in the relative proportions of 2:1.

The only structure which is in agreement with these facts is I. The conversion of gentiobiose octaacetate to an isomaltose derivative on treatment with titanium tetrachloride [8] suggested that I might undergo a similar transformation to 4-*α*,6-*α*-bis-D-glucosido-D-glucose. This branched trisaccharide would be expected as a product of partial hydrolysis from amylopectin and glycogen. I, however, failed to undergo this anomerisation, possibly because the glucosyl substituent in the 4-*O*-position of the reducing residue of gentiobiose prevents the formation of the reactive intermediate, through which a successful anomerisation must pass.

A further attempt to obtain the *α*-anomer was made using quinoline [9] as the acid acceptor in the condensation of tetra-*O*-acetyl-*α*-D-glucopyranosyl bromide and the maltose heptaacetate.

EXPERIMENTAL

All evaporations were conducted *in vacuo*, bath temp. 35—40°. Paper chromatography was conducted on Whatman No. 1 and preparative separations on Whatman 3 MM.

Chromatographic solvents:

1. Ethyl acetate-pyridine-water (10:4:3)
2. Ethyl acetate-acetic acid-water (3:1:3)
3. Dry benzene (on dimethyl sulphoxide impregnated paper [10])

Chromatographic spray reagents:

1. Acetonic silver nitrate and ethanolic sodium hydroxide.
2. *p*-Anisidine hydrogen chloride.

Melting points are corrected.
Optical rotations determined in water (saccharides) or chloroform (acetates), $c = 1$.

4-α,6-β-Bis-D-glucosido-D-glucose

To a solution of 1,2,3,2′,3′,4′,6′-β-maltose heptaacetate [6] (7.3 g, m.p. 147—149°, $[\alpha]_D^{20}$ +64°) in dry, ethanol-free chloroform (35 ml) was added silver oxide (5.0 g) and Drierite (5.0 g) and the mixture was shaken in the absence of light for 1 h at room temperature. A solution of tetra-*O*-acetyl-α-D-glucopyranosyl bromide (4.9 g) and iodine (0.5 g) in dry, ethanol-free chloroform (30 ml) was added in 4 equal portions over 1 h and the mixture shaken mechanically for 72 h. The reaction mixture was filtered through a layer of Celite, washed with dilute sodium thiosulphate solution and water and dried over sodium sulphate. Concentration of the chloroform solution yielded a yellow syrup which crystallised spontaneously and from which unchanged maltose heptaacetate (0.85 g) was recovered. (Chromatography of the remaining material in solvent 3, spray reagent 1, revealed the presence of maltose heptaacetate and two slower components, having $R_{\text{Maltose heptaacetate}}$ 0.65 and 0.34.)

The acetylated mixture was deacetylated by the method of Zemplén, deionised (Amberlite IR 120 and Dowex 3) and concentrated, to give a clear, colourless syrup (5.1 g). Paper chromatographic analysis in solvent 1 gave glucose, maltose and a trisaccharide (R_{Gl} 0.41) with traces of a slower component (R_{Gl} 0.24).

The syrup was fractionated on a charcoal-Celite column (4 × 43 cm) which was eluted first with water, then with a linear gradient of aqueous ethanol (10 l, 0 — 20 %). 40 ml fractions were collected. D-Glucose (1.8 g), m.p. 148—149°, $[\alpha]_D^{20}$ +52° (final) and maltose (2.6 g), m.p. 163—166°, $[\alpha]_D^{20}$ +126° (final) were obtained and characterised, maltose also as the β-octaacetate, m.p. 159—160°, $[\alpha]_D^{20}$ +61°.

The major portion of the trisaccharide (I) was eluted in fractions 158—176. Concentration followed by extraction with 70 % methanol gave I (0.40 g), $[\alpha]_D^{20}$ +82°, contaminated with a trace of maltose.

Higher fractions, including 50 % ethanol eluant, contained I, contaminated with some saccharides having lower R_F-values. The combined material (0.49 g) was refractionated on a smaller column, yielding further amounts of pure I. The total yield of I was 0.49 g.

Structural studies on I

On electrophoresis in borate buffer (pH 10) maltose, gentiobiose and I had the M_G-values 0.36, 0.71, and 0.37, respectively.

I (2 mg) was hydrolysed in 0.33 N sulphuric acid (0.5 ml) at 100° for 0.5 h. Neutralisation followed by chromatography in solvent 2 gave glucose, maltose (R_{Gl} 0.46), gentiobiose (R_{Gl} 0.36) and unchanged I (R_{Gl} 0.19).

I (20 mg) in water (5 ml) was treated with emulsin at pH 5.5 and 25° for 7 days. A chromatographic investigation of the digest showed the presence of glucose, maltose and unchanged I. The components were separated on paper and glucose and maltose isolated and characterised as the crystalline compounds.

I (33 mg) in water (10 ml) was treated with sodium borohydride (20 mg) After standing overnight at room temperature the solution was deionised and boric acid removed by distillation with methanol. Purification on paper gave the trisaccharide alcohol (II) as a syryp (24 mg), $[\alpha]_D^{20}$ +53°. II and its acetate failed to crystallise. Partial acid hydrolysis of II (same conditions as above) gave glucose as the only reducing sugar, using spray reagent 2. Spray reagent 1 also revealed the presence of II and of disaccharide alcohols.

II (19.0 mg) was dissolved in 0.06 N sodium metaperiodate (10 ml) and stored in the dark for one week. After that period periodate consumption (5.9 moles), liberation of formic acid (3.1 moles), and of formaldehyde [11] (0.95 moles) were determined on 1 ml samples of the solution. The remaining solution was neutralised with barium carbonate, filtered and treated with sodium borohydride (0.030 g). After standing overnight the solution was deionised, concentrated and boric acid removed by distillation with methanol. The residue was dissolved in N sulphuric acid (1 ml) and kept at 70° for one hour. Neutralisation (barium carbonate), filtration, concentration and extraction with methanol gave

a syrup consisting solely of glycerol and erythritol (paper chromatography, solvents 1 and 2). The components were separated on paper and the glycerol:erythritol ratio determined to be 2.1:1 by the method of Lambert and Neish [11].

Attempted synthesis of 4-α,6-α-bis-D-glucopyranosido-D-glucose.

(*a*) I (0.38 g) was acetylated with acetic anhydride and pyridine. The resulting anomeric mixture of hendecaacetates (0.75 g) was dissolved in dry, ethanol-free chloroform (10 ml). A solution of titanium tetrachloride (0.7 ml) in the same solvent (10 ml) was added whereupon a canary-yellow precipitate formed. The mixture was refluxed on a glycerol bath (70°) for 5 h, cooled and worked up according to Lindberg [8], yielding the saccharide acetates as a colourless syrup (0.73 g). The mixture was deacetylated by the method of Zemplén. Chromatography (solvent 1, spray 1) revealed the presence of glucose, maltose and gentiobiose in small amounts, together with the major component, a trisaccharide with the same R_F as I. The latter was purified on paper (solvent 2), yielding the original trisaccharide I (0.25 g), $[\alpha]_D^{20}$ +83°. Treatment as above with emulsin gave glucose, maltose and unchanged I.

(*b*) A mixture of 1,2,3,2′,3′,4′,6′-β-maltose heptaacetate (2.0 g) and tetra-*O*-acetyl-α-D-glucopyranosyl bromide (1.3 g) was dissolved in quinoline, to which had been added Drierite (1.0 g). The mixture was shaken in the absence of light for 24 h and then kept at 50° for 3 h. After cooling chloroform (40 ml) was added and the chloroform solution washed successively with water, dilute sulphuric acid, dilute sodium hydrogen carbonate, water, and dried over sodium sulphate. Concentration of the chloroform solution gave a light red syrup which was deacetylated as above. Chromatographic analysis revealed the presence of glucose, maltose, trisaccharide I and traces of other saccharides. Charcoal column chromatography, followed by fractionation on paper, gave I (65 mg), $[\alpha]_D^{20}$ +79°.

The authors are indebted to *Statens Tekniska Forskningsråd* for financial support and to Mr Christer Marklund for his skilful assistance.

REFERENCES

1. Klemer, A. *Ber* **92** (1959) 218.
2. Klemer, A. and Homberg, K. *Ber.* **93** (1960) 1643.
3. Turvey, J. R. and Evans, J. M. *J. Chem. Soc.* **1960** 2366.
4. Baily, R. W., Barker, S. A., Bourne, E. J., Grant, P. M. and Stacey, M. *J. Chem. Soc.* **1958** 1895.
5. Klemer, A. *Tetrahedron Letters* **22** (1960) 5.
6. Asp, L. and Lindberg, B. *Acta Chem. Scand.* **6** (1952) 941.
7. Whistler, R. L. and Durso, D. F. *J. Am. Chem. Soc.* **72** (1950) 677.
8. Lindberg, B. *Acta Chem. Scand.* **3** (1949) 1355.
9. Helferich, B. and Bredereck, H. *Ann.* **465** (1928) 166.
10. Wickberg, B. *Acta Chem. Scand.* **12** (1958) 615.
11. Lambert, M. and Neish, A. C. *Can. J. Research* **28** (1950) 83.

Received September 1, 1961.

ACTA CHEMICA SCANDINAVICA 16 (1962) 387–391

A Chemically-Synthesised Galactoglucan *

I. J. GOLDSTEIN** and BENGT LINDBERG

Träkemiska Avdelningen, Svenska Träforskningsinstitutet, Stockholm, Sweden

The addition polymerisation of a mixture of 1,6-anhydro-β-D-glucopyranose and 1,6-anhydro-β-D-galactopyranose has given rise to a synthetic galactoglucan. A high molecular weight fraction was selected for study. The results indicate a highly branched structure with a high proportion of α- and 1,6-glycosidic linkages.

The acid-catalysed condensation of simple sugars to afford synthetic polysaccharides has been of increasing interest in recent years [1–5]. An alternative approach to such polysaccharides involves addition polymerisation of anhydro sugars.

Pictet [6] initiated such studies as early as 1918. Recently Carvalho and Schuerch [7] improved the conditions for the polymerisation of 1,6-anhydro-β-D-glucopyranose and investigated the nature of the product formed. The polymerisation of other anhydro sugars was also reported by Schuerch and coworkers.[8,9]

This paper describes the copolymerisation of 1,6-anhydro-β-D-glucopyranose and 1,6-anhydro-β-D-galactopyranose to yield a synthetic heteropolymer. A mixture of these sugar derivatives, in equal proportions, containing monochloroacetic acid as catalyst, was heated in a sealed tube to 106°. The material, a brittle glass, was completely soluble in water and was subjected to fractionation by addition of ethanol to its aqueous solution. After two fractionations a fraction, corresponding to 10 % of the monomers, was obtained, which showed $[\alpha]_D^{20}$ +95° and was completely immobile on paper chromatograms. After dialysis against distilled water 92 % of the material was recovered, and used in subsequent studies. It was found to consist solely of D-glucose (52 %) and D-galactose (48 %) residues and to have a $\overline{DP}_n$ of about 90, as determined osmometrically.

* This investigation was carried out during the tenure of a Special Fellowship (to I.J.G.) from the Division of General Medical Science, United States Public Health Service.

** Present address: School of Medicine, Department of Biochemistry, University of Buffalo, Buffalo, New York, USA.

Table 1. Substances, isolated after periodate oxidation, borohydride reduction and hydrolysis of the synthetic polysaccharide.

Substance	Molar %		
	Quantitative determination	By weight	Calculated [a]
Glycerol	58.6	53.7	55
Erythritol	16.0	16.5	20
D-Glucose	12.9	11.7	25
D-Galactose	10.2	10.3	
Arabinose	2.3	7.0[b]	—

[a]) From consumption of periodate and liberation of formic acid.
[b]) Also containing small amounts of xylose.

Treatment of the synthetic polysaccharide with sodium metaperiodate resulted in the consumption of 1.3 moles of periodate and the liberation of 0.55 moles of formic acid per hexose residue. This is equivalent to a content of 55 % 1 → 6-like bonds, 20 % 1 → 4-like bonds and 25 % 1 → 3-like bonds in the polysaccharide, assuming only pyranosidic residues.

The periodate-oxidised polysaccharide was reduced with sodium borohydride and hydrolysed to afford glycerol, erythritol, D-glucose, D-galactose and small amounts of what appeared to be arabinose and xylose. These products (with the exception of the last two) were identified as the crystalline substances or converted to crystalline derivatives. The amount of each was determined analytically as well as by isolation. These values are collected in Table 1. It can be seen that there is reasonably good agreement between the values noted and the results of the periodate oxidation. The presence of threitol in the "erythritol fraction" was considered a possibility, but paper electrophoresis in sulphonated phenyl boronic [10] acid at pH 6.5 failed to reveal its presence.

Partial hydrolysis gave a mixture of oligosaccharides, one of which was obtained crystalline and proved to be melibiose (6-*O*-*α*-D-galactopyranosyl-D-glucose.

It is apparent from the foregoing that a galactoglucan has been prepared chemically. The fact that the material contains approximately equal amounts of D-glucose and D-galactose residues together with the isolation of melibiose indicates a true heteropolymer as opposed to a mixture of glucan and galactan.

The rotation of the synthetic polymer ($[\alpha]_D^{20}$ + 95° in water) is similar to those of synhtetic glucose polymers [1,7] and indicates the presence of a relatively high content of *α*-glycosidic linkages.

The liberation of 0.55 moles of formic acid on periodate oxidation together with the high proportion of glyceritol isolated from the polyalcohol indicates a highly branched structure or a high content of 1 → 6-linked residues or both possibilities. The latter alternative is considered most probable.

The failure to detect any glycerinaldehyde in the hydrolysate of the polyalcohol suggests the lack of D-glucose or D-galactose residues linked solely in the C-2 position or in the C-2 and C-6 positions. On the other hand, the yields of unoxidised D-glucose (12 %) and D-galactose (10 %) indicates the presence or 1,3-linkages or residues which are multiply linked, *e.g.* containing 1,2- and 1,4-linkages.

Erythritol arises from those D-glucose residues which are linked 1,4 or 1,4 and 1,6; the appearent absence of threitol suggests the lack of D-galactose residues, linked in an analogous manner. The presence of arabinose and xylose cannot be accounted for. They could arise from suitably protected furanosidic residues (cleavage between C-5 and C-6).

EXPERIMENTAL

All melting points corrected.
Paper chromatograms were run on Whatman 1 and preparative separations on Whatman 3 MM.
Chromatographic solvents:
1) Ethyl acetate-pyridine-water (10:4:3).
2) Ethyl acetate-acetic acid-water (3-1-3).
3) 80 % Aqueous acetone.
Chromatographic spray reagents:
1) Acetonic silver nitrate and ethanolic sodium hydroxide.
2) *p*-Anisidine hydrogen chloride.
3) Periodate-benzidine.

Paper electrophoresis was conducted in borate buffer (pH 10), germanate buffer[11] (pH 10.4) and sulphonated phenylboronic acid[10] (pH 6.5).

All optical rotations were determined in water, *c*, 1.0.

Copolymerisation of 1,6-anhydro-D-glucopyranose and 1,6-anhydro-D-galactopyranose. An intimate mixture of 1,6-anhydro-D-glucopyranose (6.70 g), 1,6-anhydro-D-galactopyranose (6.70 g) and monochloroacetic acid (0.670 g) in a Pyrex tube was dried *in vacuo* at 25° for 0.5 h, sealed and heated at 106° for 16 h. The reaction product, a dark, amber-coloured solid, which fissured upon cooling, was dissolved in water (50 ml) containing sodium hydrogen carbonate (0.65 g). The dark brown solution was filtered, the volume was adjusted to 200 ml and ethanol (930 ml) was added slowly with stirring. The syrup which formed was collected by centrifugation and washed with 85 % ethanol. On treatment of the syrup with anhydrous ethanol a brittle powder was obtained which was washed several times with ethanol and ether and dried *in vacuo* at 40°. The product (9.0 g), $[\alpha]_D^{20}$ +94°, on paper chromatography in solvent 1 showed the absence of low molecular weight substances.

Fractionation of the synthetic polysaccharide. The polysaccharide (8.0 g) was dissolved in water (160 ml) and ethanol added dropwise while stirring mechanically. At intervals the precipitate, a syrup, was collected by centrifugation and worked up as before. The following fractions were obtained:

Fraction 1. 65.5 % ethanol. Yield 2.3 g, $[\alpha]_D^{20}$ +95°.

Fraction 2. 71.5 % ethanol. Yield 1.8 g, $[\alpha]_D^{20}$ +92°.

Fraction 3. 76 % ethanol. Yield 1.5 g, $[\alpha]_D^{20}$ +90°.

Fraction 1 was subfractionated by precipitation of its aqueous solution (50 ml) with ethanol.

Fraction 1A 65.5 % ethanol. Yield 1.33 g.
Fraction 1B 71.5 % ethanol. Yield 0.57 g.
Fraction 1C 76 % ethanol. Yield 0.21 g.

Fraction 1A was dialysed against distilled water. A recovery of 1.22 g, $[\alpha]_D^{20}$ +95°, resulted. $\overline{DP}_n$ of fraction 1A, using a Zimm and Myerson [12] osmometer and »Ultrafein allerfeinst" membrans (Membranfiltergesellschaft, Göttingen) was determined in water to be about 90.

Acid hydrolysis of fraction 1A in 1 N sulphuric acid at 100° for 10 h yielded only D-glucose (52 %) and D-galactose (48 %), both sugars being isolated in a crystalline state and characterised.

Periodate oxidation. Icecold 0.061 N sodium periodate solution was added to a sample of fraction 1A (0.350 g, 4.65 % water) to a volume of 200 ml and the mixture kept at 2°. A portion of the periodate solution served as blank. At intervals, aliquots were withdrawn for determination of periodate consumption and formic acid liberation. After 8 days the values became constant: periodate consumption, 1.3 moles per mole hexose residue; formic acid liberation, 0.55 moles per mole hexose residue.

Reduction and hydrolysis of the periodate oxidised polysaccharide. The reaction mixture was neutralised (barium carbonate), centrifuged and the solution poured into a solution of borohydride (1.0 g) in water (25 ml). After standing overnight, the solution was neutralised (acetic acid), deionised (Amberlite IR 120, Dowex 3) and boric acid removed by distillation with methanol.

The product was hydrolysed by treatment with 0.6 N sulphuric acid (25 ml) at 100° for 12 h, neutralized (barium carbonate), filtered, deionised and concentrated to give a yellow syrup (0.2 g). Paper chromatography (solvent 2, spray 1 + 2) showed the presence of glyceritol (R_{Gl} 2.42) erythritol (R_{Gl} 1.93) glucose, galactose (R_{Gl} 0.95), arabinose (R_{Gl} 1.36) and xylose (R_{Gl} 1.51). The last substance was indistinguishable from xylose also on chromatography in solvent 1 and electrophoresis in germanate buffer.

Part of the syrup (0.020 g) was fractionated on thick filter paper, the components eluted with water and determined quantitatively, the polyols according to Lambert and Neish [13], the sugars according to Saeman *et al.*[14]. The results are presented in Table 1.

The remainder of the syrup (0.16 g) was fractionated on filter paper and the various components purified by extraction with methanol and concentrated to give the amounts, shown in Table 1. D-Glucose, m.p. 144—145°, $[\alpha]_D^{20}$ +57° (final), D-galactose, m.p. 165—166°, $[\alpha]_D^{20}$ +80° (final) and erythritol, m.p. 119—120°, crystallised and were indistinguishable from authentic samples. Glycerol was converted to its tri-*O*benzoyl derivative, m.p. and mixed m.p. 71—72°. The mother liquors from the erythritol, when subjected to electrophoresis in borate and sulphonated phenyl boronic acid appeared to contain no threitol.

Partial hydrolysis. A portion of the synthetic polysaccharide (0.75 g) was dissolved in 0.5 N sulphuric acid (100 ml) and kept on a boiling water bath for 3.5 h. The solution was neutralised (barium carbonate), filtered and concentrated to a syrup which upon chromatographic analysis in solvent 1 showed the presence of glucose, galactose and a number of oligosaccharides, all of which having lower R_F-values than that of maltose. The syrup was placed on a charcoal-Celite column (3.5 × 23.5 cm) which was eluted, first with water (2 l), then with a linear gradient of aqueous ethanol (5 l, 0 → 25 %). Fractions (40 ml) were collected and the elution followed by determination of the optical rotation and by chromatography in solvent 3.

Fractions 119—125 were combined and concentrated. Chromatography in solvent 1 showed the presence of two components with R_{Gl} values 0.70 and 0.62, respectively. Separation on paper (solvent 2) gave melibiose (12 mg), R_{Gl} 0.70, which crystallised as the dihydrate upon seeding with authentic material, m.p. and mixed m.p. 81—83°, $[\alpha]_D^{20}$ +125° (final).

The authors are indebted to Mr Christer Marklund for his skilful assistance and to *Statens Tekniska Forskningsråd* for a grant.

REFERENCES

1. Pacsu, E. and Mora, P. T. *J. Am. Chem. Soc.* **72** (1950) 1045.
2. Kent, P. W. *Biochem. J.* **55** (1953) 361.
3. Ricketts, C. R. *J. Chem. Soc.* **1954**. 4031.
4. Bishop, C. T. *Can. J. Chem.* **34** (1956) 1255.
5. O'Colla, P. S. and Lee, E. *Chem. and Ind. London* **1956** 522.
6. Pictet, A. and Sarasin, J. *Helv. Chim. Acta* **1** (1918) 87.
7. Carvalho, J. da Silva, Prins, W. and Schuerch, C. *J. Am. Chem. Soc.* **81** (1959) 4054.
8. Schuerch, C. and Bhattacharyya, A. *Abstract Papers Am. Chem. Soc.* **138** (1960) 6D.
9. Quinn, E., Nevin, R. S., Schuerch, C. and Sarkanen, K. *Abstract Papers Am. Chem. Soc.* **138** (1960) 6D.
10. Garegg, P. and Lindberg, B. *Acta Chem. Scand.* **15** (1961) 1913.
11. Lindberg, B. and Swan, B. *Acta Chem. Scand.* **14** (1960) 1043.
12. Zimm, B. H. and Myerson, I. *J. Am. Chem. Soc.* **68** (1946) 911.
13. Lambert, M. and Neish, A. C. *Can. J. Research. B.* **28** (1950) 83.
14. Saeman, J. F., Moore, W. E., Mitchell, R. L. and Millet, M. A. *Tappi* **37** (1954) 336.

Received September 15, 1961.

ACTA CHEMICA SCANDINAVICA 16 (1962) 392–402

Distribution of Methanol-Water and Ethanol-Water Mixtures in Strongly Basic Polystyrene Anion Exchangers in Free Base Form

EERO SJÖSTRÖM*, LALLI NYKÄNEN** and PEKKA LAITINEN

Lääketehdas Orion Oy, Helsinki, Finland

The distribution of methanol-water and ethanol-water mixtures in two strongly basic anion exchange resins (hydroxyl form) cross-linked with 7.5 % and 0.5 % divinylbenzene has been studied. Centrifugation was used to separate the resin from the surrounding solution and the concentrations in the resin phase were determined after the elution of the solvent components. The hydroxyl-alkoxide ion equilibrium, $ROH + OH^- \rightleftharpoons RO^- + H_2O$, was taken into consideration in the final calculations. For this an equation was derived for the calculation of the hydroxyl and alkoxide ion contents of the resin.

The water concentration was found to be higher inside the resin than in the surrounding solution over the whole solvent composition range. Compared with the same resin in chloride form, the salting-out effect of the hydroxyl resin is greater up to a certain alcohol concentration (about 70 % (w/w) methanol and 83 % (w/w) ethanol) but smaller at higher concentrations. A reasonable explanation for this observation seems to be that the hydroxyl ions are converted into alkoxide ions, as a result of which the ability of the resin to take up alcohol is increased.

The internal solution volumes of the resins were calculated at various alcohol concentrations. The data revealed that, compared with the chloride resin, the hydroxyl resin takes up more solvent and that only small changes take place in the swollen volume with varying alcohol concentration.

Although many investigations have been published on the distribution of solvent mixtures in ion exchange resins in various ionic states (see, *e.g.*, Refs.[1–3]), only very few experiments seem to have been carried out with anion exchange resins in the free base form. The main reason is that an anion

Present address: * (E.S.) Stora Kopparbergs Bergslags AB, Central Laboratory, Falun, Sweden.

** (L.N.) Research Laboratories of the State Alcohol Monopoly, Helsinki, Finland.

exchange resin in its hydroxyl form is more or less unstable to organic solvents. This special case is, however, of considerable interest from the standpoint of a fundamental understanding of the catalysis of reactions by ion exchange resins, for the rate and even the mechanism of a reaction depends on the composition of the solvent in the reacting phase [4]. The present investigation was started in connection with our kinetic studies on resin-catalyzed ester hydrolysis in alcohol-water mixtures.

EXPERIMENTAL

Resins. Two strongly basic polystyrene anion exchange resins cross-linked with 7.5 % and 0.5 % divinylbenzene were used. The former resin, a commercial sample of Dowex 1 (20 to 50 mesh), was ground and sieved in the air-dry state to a particle size of 0.15 to 0.30 mm before use. After the usual purification procedure the resin was air-dried in chloride form and transferred to a glass bottle. The moisture content of the resin, determined by drying to constant weight *in vacuo* over magnesium perchlorate at 60°, was 12.0 %. The total capacity of the dry resin was 2.91 mequiv./g.

The resin containing 0.5 % divinylbenzene was prepared by a method similar to that described by Gregor *et al.*[5] 49.55 g of styrene (Th. Schuchardt) and 0.45 g of a polymer mixture containing 55 % divinylbenzene (Th. Schuchardt) were heated together with 0.5 g of benzoyl peroxide and 400 ml of water to 90° in a 1-l three-necked flask. The mixture was then vigorously stirred for 15 min. After 5 g of soluble starch powder had been added, the stirring was continued for 3 h. The reaction mixture was kept at 90° for a further 24 h after which the product was separated, washed with water, and dried.

The chloromethylation process was exactly the same as described by Pepper, Paisley and Young [6] and Samelson and Hammet [7]. The degree of chloromethylation was determined by burning a sample of the product in the presence of ethylene glycol and sodium peroxide in an IKA-bomb and titrating the residue potentiometrically with silver nitrate. The chloride content was found to be 24.3 % (theoretical value 23.1 %).

The chloromethylated resin was amminated as follows (*cf.* Ref.[6]). 20 g of the chloromethylated resin was added to 500 ml of dioxane and the mixture cooled in an ice bath. After 250 ml of dry trimethylamine (Fluka, purum) had been added, the reaction was allowed to proceed for 48 h with occasional shaking. The amminated resin was purified by alternate treatments with 1 N sodium hydroxide, 5 N hydrochloric acid, and water. The resin was then washed in its chloride form with water to remove excess acid, air-dried to a constant weight, and transferred to a glass bottle. The moisture content of the air-dried resin was found to be 11.7 % by drying at 60° *in vacuo* over magnesium perchlorate to constant weight. The total capacity of the dry resin was 3.80 mequiv./g.

Distribution experiments. Each experiment comprised four steps: (1) equilibration of the resin with a solvent; (2) separation of the outer phase from the resin by centrifugation; (3) elution of the solvent from the resin (water with methanol and alcohol with water); (4) determination of the water and alcohol in the effluents.

In detail, the experiments were carried out as follows. A sample of the air-dried resin (1.000 g of the 7.5 % and 0.1000 g of the 0.5 % cross-linked resin) was introduced into a glass filter-tube (10 × 90 mm) fitted with a sintered glass disc of porosity 1. The resin was allowed to swell in water for 18 to 20 h. It was then converted into the hydroxyl form with 100 ml of 1 N sodium hydroxide solution and washed free of excess alkali with de-ionized water. The resin tube was then placed in an air thermostat maintained at 25 ± 0.2°, and 200 ml of an aqueous alcohol solution at the same temperature was passed through the resin bed at a flow rate of about 0.5 ml/min. The equilibrated resin was allowed to stand for 18 to 20 h, after which it was washed with a further 100 ml of the mixed solvent. The tube was then loosely stoppered, transferred to a centrifuge (Martin Christ, Universal Junior I) and centrifuged for 30 min at a speed of 1 700 r.p.m., which corresponds to 480 *g*. After the centrifugation the water was displaced from the resin phase with absolute methanol into a 100-ml volumetric flask. Similarly, water was used to displace the alcohol. Since duplicate determinations were always performed, four samples in all were required to determine the distribution of the components of each solvent mixture.

The alcohol-water mixtures were prepared by weighing and were allowed to stand several hours in the 25-degree air thermostat before use. Methyl alcohol (guaranteed reagent; water content < 0.03 %) from E. Merck AG, Darmstadt, and ethyl alcohol (quality AaS; water content $\simeq 0.5$ %) from Oy Alkoholiliike Ab, Helsinki, were used in all the experiments. The water used was de-ionized by mixed-bed ion exchange and had a specific conductivity of less than 10^{-6} ohm^{-1} cm^{-1}.

Analytical methods. Water was determined by the Karl Fischer method as modified by Johansson [8]. The difference between duplicate determinations was less than 2 %. *Methanol* was determined by the chromotropic acid method described by Ahlén and Samuelson [9]. A standard and a blank solution were prepared simultaneously with the sample. The measurements were performed at 570 mμ with a Unicam SP 500 spectrophotometer fitted with 1-cm absorption cells. The difference between duplicate determinations did not exceed 2 %. *Ethanol* was determined by titration with potassium dichromate [1,10]. The duplicate determinations differed less than 2 %.

CALCULATIONS

When a strongly basic anion exchange resin in hydroxyl form is equilibrated with an aqueous alcohol solution, the hydroxyl ions are partly replaced by alkoxide ions [4]:

$$ROH + OH^- \rightleftharpoons RO^- + H_2O \qquad (1)$$

Consequently, when the water is displaced from the resin with methanol in the elution step, the hydroxyl ions are converted into an equivalent amount of water. Correspondingly, the alkoxide ions form an equivalent amount of alcohol when the resin is eluted with water. The water and alcohol thus formed must be subtracted from the original water and alcohol contents in order to obtain correct results for the solvent composition in the resin phase. The hydroxyl and alkoxide ion contents of the resin can be calculated as follows.

The equilibrium constant for reaction (1) may be written:

$$\frac{[RO^-]\,[H_2O]}{[ROH]\,[OH^-]} = K \qquad (2)$$

For one equivalent of resin the sum of hydroxyl and alkoxide ion concentrations

$$[OH^-] + [RO^-] = 1$$

hence

$$[RO^-] = 1 - [OH^-] \qquad (3)$$

If $[ROH]_t$ and $[H_2O]_t$ denote the total numbers of moles of alcohol and water found in the effluent per equivalent of resin, then

$$[H_2O] = [H_2O]_t - [OH^-] \qquad (4)$$

and

$$[ROH] = [ROH]_t - (1-[OH^-]) \qquad (5)$$

When $[RO^-]$, $[H_2O]$ and $[ROH]$ are eliminated from eqn. (2) by means of (3), (4) and (5), one obtains

$$\frac{(1-[OH^-])([H_2O]_t-[OH^-])}{([ROH]_t + [OH^-] - 1)[OH^-]} = K \qquad (6)$$

After rearrangement, it is found that

Table 1. Distribution of methanol-water mixtures in Dowex 1 (OH).*

Solution		Resin Phase														
		Experimental values				Calculated values										
MeOH wt. %	X_{MeOH}	MeOH g	H_2O g	MeOH Moles	H_2O Moles	HO^- Equiv.	MeO^- Equiv.	MeOH g	H_2O g	Total solvent g	MeOH wt. %	MeOH Moles	H_2O Moles	Total solvent Moles	X_{MeOH}	V_s ml
0	0	—	425	—	23.6	1.000	0.000	—	407	407	—	—	22.6	22.6	0	408
1	0.0057	5.70	427	0.178	23.7	0.942	0.058	3.84	410	414	0.928	0.120	22.8	22.9	0.0053	415
2	0.0113	11.5	443	0.358	24.6	0.891	0.109	7.97	427	435	1.83	0.249	23.7	24.0	0.0104	437
3	0.0171	17.4	437	0.544	24.3	0.837	0.163	12.2	423	435	2.80	0.381	23.5	23.8	0.0160	438
4	0.0229	20.5	428	0.640	23.8	0.810	0.190	14.4	414	428	3.36	0.450	23.0	23.4	0.0192	431
5	0.0287	25.9	423	0.810	23.5	0.767	0.233	18.5	409	428	4.32	0.577	22.7	23.3	0.0248	431
7.5	0.0436	38.1	418	1.19	23.2	0.686	0.314	28.0	405	433	6.45	0.876	22.5	23.4	0.0374	439
10	0.0588	50.2	407	1.57	22.6	0.612	0.388	37.8	396	434	8.71	1.18	22.0	23.2	0.0509	441
12.5	0.0744	62.4	392	1.95	21.8	0.547	0.453	48.0	383	431	11.1	1.50	21.3	22.8	0.0658	439
15	0.0903	74.2	387	2.32	21.5	0.492	0.508	57.9	378	436	13.3	1.81	21.0	22.8	0.0794	447
17.5	0.107	84.8	373	2.65	20.7	0.450	0.550	67.2	365	432	15.6	2.10	20.3	22.4	0.0938	444
20	0.123	93.8	362	2.93	20.1	0.415	0.585	75.2	355	430	17.5	2.35	19.7	22.0	0.107	443
30	0.194	138	324	4.31	18.0	0.295	0.705	115	319	434	26.5	3.60	17.7	21.3	0.169	454
40	0.273	179	283	5.59	15.7	0.213	0.787	154	279	433	35.6	4.80	15.5	20.2	0.238	460
50	0.360	221	232	6.92	12.9	0.151	0.849	194	229	423	45.9	6.07	12.7	18.8	0.323	458
60	0.458	248	198	7.76	11.0	0.120	0.880	220	196	416	52.9	6.88	10.9	17.8	0.387	458
70	0.568	283	148	8.84	8.24	0.081	0.919	253	147	400	63.3	7.91	8.16	16.1	0.491	451
80	0.692	333	105	10.4	5.81	0.050	0.950	302	104	406	74.7	9.45	5.76	15.3	0.622	472
90	0.835	365	52.7	11.4	2.93	0.023	0.977	333	52.4	385	86.5	10.4	2.91	13.3	0.782	464
100	1.000	362	—	11.3	—	0.000	1.000	330	—	330	100	10.3	—	10.3	1.000	417

* The values are given per one equivalent of resin

Table 2. Distribution of ethanol-water mixtures in Dowex 1 (OH).*

Solution		Resin Phase														
		Experimental values				Calculated values										
EtOH Wt. %	X_{EtOH}	EtOH g	H_2O g	EtOH Moles	H_2O Moles	OH^- Equiv.	EtO^- Equiv.	EtOH g	H_2O g	Total solvent g	EtOH wt. %	EtOH Moles	H_2O Moles	Total solvent Moles	X_{EtOH}	V_s ml
0	0.000	—	425	—	23.6	1.00	0.00	—	407	407	—	—	22.6	22.6	0.000	408
5	0.020	22.7	427	0.492	23.7	0.99	0.01	22.2	409	431	5.15	0.482	22.7	23.2	0.0208	436
8	0.033	35.0	414	0.760	23.0	0.96	0.04	33.2	396	429	7.74	0.720	22.0	22.7	0.0317	435
11	0.046	49.3	401	1.07	22.3	0.96	0.04	47.5	383	431	11.0	1.03	21.3	22.3	0.0462	440
15	0.065	65.4	385	1.42	21.4	0.95	0.05	63.1	367	430	14.7	1.37	20.4	21.8	0.0628	441
20	0.089	80.2	364	1.74	20.2	0.94	0.06	77.4	347	424	18.3	1.68	19.3	21.0	0.0800	436
30	0.143	115	342	2.50	19.0	0.91	0.09	111	326	437	25.4	2.41	18.1	20.5	0.118	454
40	0.207	138	313	3.00	17.4	0.88	0.12	133	297	430	30.9	2.88	16.5	19.4	0.148	452
50	0.281	157	290	3.40	16.1	0.86	0.14	150	274	424	35.4	3.26	15.2	18.5	0.176	449
60	0.369	175	265	3.79	14.7	0.83	0.17	167	250	417	40.0	3.62	13.9	17.5	0.207	446
70	0.477	191	227	4.15	12.6	0.79	0.21	182	212	394	46.2	3.94	11.8	15.7	0.251	427
76	0.553	220	200	4.77	11.1	0.77	0.23	209	185	394	53.0	4.54	10.3	14.8	0.307	434
80	0.610	238	177	5.16	9.81	0.70	0.30	224	164	388	57.7	4.86	9.11	14.0	0.347	435
83	0.656	263	156	5.70	8.64	0.65	0.35	246	144	380	64.7	5.35	7.99	13.3	0.402	432
86	0.723	286	125	6.20	6.94	0.58	0.42	266	114	380	70.0	5.78	6.36	12.1	0.478	438
90	0.779	320	97.7	6.94	5.43	0.49	0.51	296	88.9	385	76.9	6.43	4.94	11.4	0.564	455

* The values are given per one equivalent of resin

Table 3. Distribution of methanol-water mixtures in Dowex 1 (Cl).*

Solution		Resin Phase								
MeOH wt. %	X_{MeOH}	MeOH g	H_2O g	Total solvent g	MeOH wt. %	MeOH Moles	H_2O Moles	Total solvent Moles	X_{MeOH}	V_s ml
0	0.000	—	286	286	—	—	15.9	15.9	0.000	259
20	0.123	51.8	230	282	18.4	1.62	12.8	14.4	0.112	261
30	0.194	78.1	202	280	27.9	2.44	11.2	13.6	0.179	265
50	0.360	122	130	252	48.4	3.82	7.23	11.1	0.346	248
70	0.568	147	87.1	234	62.8	4.60	4.84	9.44	0.487	238
90	0.835	187	34.4	221	84.6	5.84	1.91	7.75	0.753	239
100	1.000	214	—	214	100.0	6.70	—	6.70	1.000	245

* The values are given per one equivalent of resin.

$$[OH^-] = \frac{(K - K[ROH]_t - [H_2O]_t - 1) + \sqrt{(K - K[ROH]_t - [H_2O]_t - 1)^2 + 4[K-1)[H_2O]_t}}{2\,(K-1)} \quad (7)$$

The hydroxyl ion content of the normal resin (Dowex 1), in equilibrium with an aqueous alcohol solution, cannot be exactly calculated using earlier reported values for K. The condition in the resin phase is far from ideal and when the unknown activities are neglected, the K in eqn. (2) will not represent a true thermodynamic equilibrium constant and will probably vary with solvent composition. However, by using earlier reported values for K, it is possible to approximately estimate the influence of the chemical reaction on the analytical figures. Kinetic measurements with a porous resin have given a value of 11.8 for K for methanol-water mixtures [11] (*cf.* Ref.[12]); from other studies the K value for ethanol-water mixtures again, can be evaluated as approximately 0.8 [13] (*cf.* Ref.[14]). As can be seen from Table 1 the calculated values based on these constants differ considerably from experimental values, especially for methanol-water mixtures of low methanol content (Table 1). For ethanol-water mixtures, however, the corrections are smaller owing to the lower K value (Table 2).

Considering a porous resin with an extremely large swollen volume, the additional amounts of water or methanol resulting from chemical reaction can obviously be neglected within the limits of experimental error. For instance, when the hydroxyl ion content of the porous resin in equilibrium with a methanol-water mixture containing not more than 5 % methanol is calculated from eqn. (7) using for K a value of 12, it is seen that the methanol and water formed in the elution step correspond to less than 0.3 % and 3 % of the total (found) methanol and water contents, respectively. For methanol concentrations exceeding 5 % the corresponding figures are 0.2 % and 2 %.

RESULTS AND DISCUSSION

All the experimental data obtained with the normal resin (Dowex 1) and the calculated values are summarized in Tables 1 and 2. For comparison, the

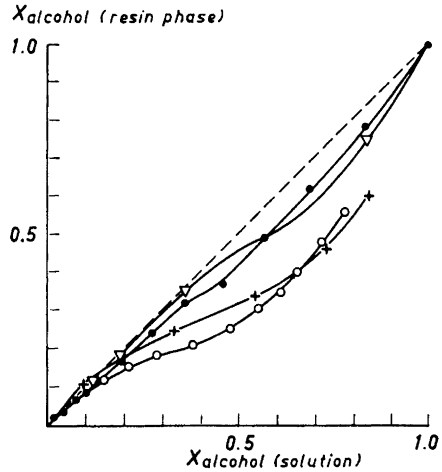

Fig. 1. Distribution of alcohol-water mixtures in Dowex 1.

● Methanol-water mixtures. Resin in OH-form.
▽ Methanol-water mixtures Resin in Cl-form.
○ Ethanol-water mixtures. Resin in OH-form.
\+ Ethanol-water-mixtures. Resin in Cl-form. (Dowex 2). According to data of Rückert and Samuelson [1].

distribution of methanol-water mixtures in the same resin in chloride form was also determined (Table 3). For the ethanol-water mixtures the distribution data reported by Rückert and Samuelson [1] for a resin (Dowex 2) in chloride form were used. The mole fractions of methanol and ethanol in the external solution are plotted agaist the mole fractions in the resin phase in Fig. 1. It is seen, in agreement with general rules presented earlier (see, *e.g.*, Ref.[15]), that the resin favours the more polar solvent component water throughout the whole solvent composition range. The salting-out effect is, of course, more pronounced in ethanol-water mixtures than in methanol-water mixtures. The dipole moments of water, methanol and ethanol are of same order of magnitude ($\mu_{H_2O} = 1.85$ D, $\mu_{MeOH} = 1.68$ D and $\mu_{EtOH} = 1.70$ D)[16] but owing to its largest molar volume, ethanol has the lowest dielectric constant $\varepsilon_{H_2O} = 78.0$ [17], $\varepsilon_{MeOH} = 32.6$ [18], and $\varepsilon_{EtOH} = 24.3$ [18] at 25°).

An interesting difference is noted when data for the hydroxyl resin are compared with data for the chloride resin. As can be seen from Figs. 1 and 2, the salting-out effect of the hydroxyl resin is greater than that of the chloride resin only up to a certain alcohol concentration. The solvent distributions in the hydroxyl and the chloride resins are equal when the methanol concentration in the external solution is about 70 % ($X_{MeOH} = 0.57$) and when the ethanol concentration is 83 % ($X_{EtOH} = 0.66$). At higher alcohol concentrations the distribution is reversed. The experiments of Rückert and Samuelson [1] have shown that the salting-out effect of an anion exchange resin in various ionic states increases for ethanol-water mixtures in the order: $ClO_4^- < Cl^- < SO_4^{2-}$,

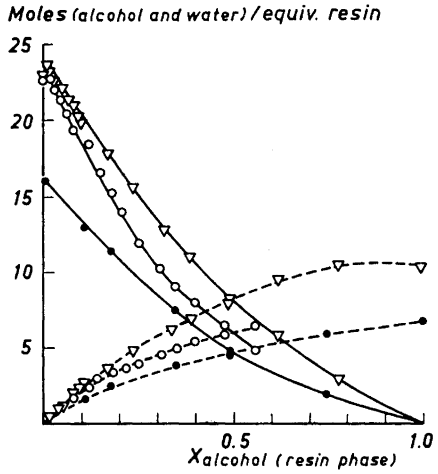

Fig. 2. Uptake of alcohol and water by Dowex 1 as a function of mole fraction of alcohol in the resin phase.

▽---▽ Methanol, ▽—▽ Water. Resin in OH-form.
●---● Methanol, ●—● Water. Resin in Cl-form.
○---○ Ethanol, ○—○ Water. Resin in OH-form.

and that this order prevails throughout the whole solvent composition range. The exceptional behaviour of the hydroxyl resin can be explained by the fact that the hydroxyl ions are replaced by alkoxide ions more and more when the alcohol content of the solvent mixture increases. Consequently the hydroxyl resin is able to take up more alcohol than the chloride resin.

The uptake of water and alcohol (methanol or ethanol) in moles is plotted against the mole fraction of the component in the internal solution in Fig. 2. That the uptake of water by the hydroxyl resin slightly increases with increasing alcohol concentration is indicated by the hardly perceptible maximum at the beginning of the water curve. For comparison, the values from the experiments with the chloride resin are plotted in Fig. 2. It is seen that the hydroxyl resin takes up considerably more solvent than the chloride resin, which is a natural consequence of the greater solvation tendency of the hydroxyl ion compared with that of the chloride ion.

The experiments of Pepper, Reichenberg and Hale [19] with cation exchange resins have shown that there is a linear relationship between the total volume of the system (V_{tot}) and the weight of water absorbed by the resin (W) given by the equation $V_{tot} = W/\varrho + \text{const.}$, where ϱ is the density of water at the temperature in question. The value of the constant in this equation was found to be about 10 % lower than the specific volume of the dry resin as determined pycnometrically. This indicates that when a dry resin is allowed to swell in water the total volume of the system first undergoes a contraction. However, as shown by Boyd and Soldano [20,21], this contraction is in general considerably smaller for anion than for cation exchange resins.

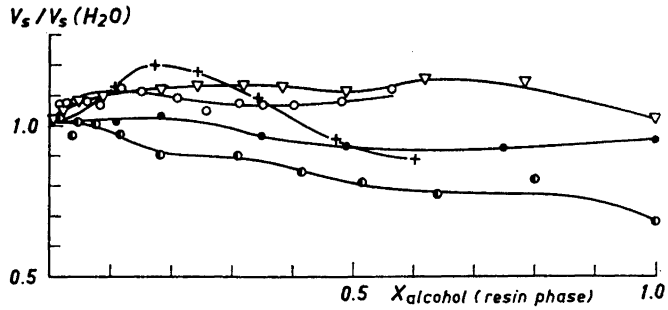

Fig. 3. Relative volume change of the internal solution as a function of alcohol concentration (mole fraction) in the resin phase.

V_s = internal solution volume for alcohol-water mixtures.
V_s (H_2O) = internal solution volume in water.
▽ Methanol-water mixtures. Dowex 1 (OH).
● Methanol-water mixtures. Dowex 1 (Cl).
○ Ethanol-water mixtures. Dowex 1 (OH).
\+ Ethanol-water mixtures. Dowex 2 (Cl). According to data of Rückert and Samuelson [1].
Methanol-water mixtures. Anion exchange resin with 0.5 % DVB (OH).

The volume of the solvent inside the resin (V_s) was calculated by assuming that its density was the same as that of the solvent in the free state. Thus

Table 4. Distribution of methanol-water mixtures in 0.5 % cross-linked resin (OH-form).*

Solution		Resin Phase								
MeOH wt. %	X_{MeOH}	MeOH g	H_2O g	Total solvent g	MeOH wt. %	MeOH Moles	H_2O Moles	Total solvent Moles	X_{MeOH}	V_s ml
0	0.000	—	5994	5994	—	—	333	333	0.000	6000
1	0.0057	61.1	5976	6037	1.01	1.91	332	334	0.0058	6060
2	0.0113	118	6084	6202	1.90	3.68	338	342	0.0107	6240
3	0.0171	152	5868	6020	2.52	4.76	326	331	0.0144	6060
4	0.0229	217	5868	6085	3.57	6.79	326	333	0.0204	6150
5	0.0287	279	5724	6003	4.65	8.71	318	327	0.0267	6060
7.5	0.0436	400	5292	5692	7.03	12.5	294	307	0.0407	5760
10	0.0588	541	5400	5941	9.11	16.9	300	317	0.0534	6030
15	0.0903	810	5040	5850	13.8	25.3	280	305	0.0826	6000
20	0.123	1059	4572	5631	18.8	33.1	254	287	0.115	5790
30	0.194	1434	3762	5196	27.6	44.8	209	254	0.177	5410
40	0.273	1808	3330	5138	35.2	56.5	185	242	0.233	5440
50	0.360	2256	2790	5046	44.7	70.5	155	226	0.313	5440
60	0.458	2592	2052	4644	55.8	81.0	114	195	0.415	5120
70	0.568	2784	1472	4256	65.4	87.0	81.8	169	0.515	4820
80	0.692	2992	938	3930	76.1	93.5	52.1	146	0.642	4590
90	0.835	3232	446	3678	87.9	101	24.8	126	0.802	4940
100	1.000	3264	—	3678	100.0	102	—	102	1.000	4090

* The values are given per one equivalent of resin.

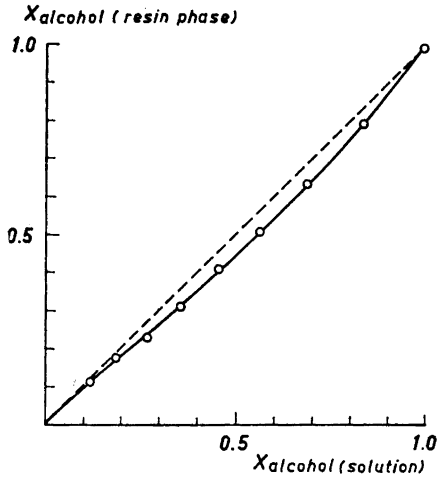

Fig. 4. Distribution of methanol-water mixtures in 0.5 % cross-linked resin (OH-form).

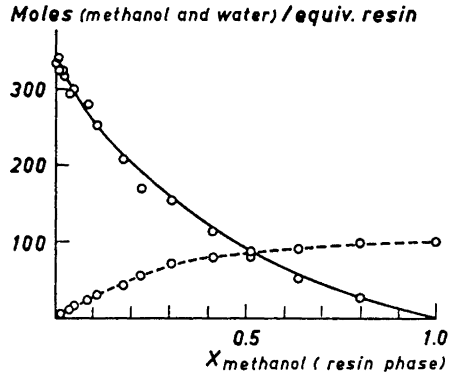

Fig. 5. Uptake of methanol and water by 0.5 % cross-linked resin (OH-form) as a function of mole fraction of methanol in the resin phase. ——— Methanol, ——— Water.

$V_s = W/\varrho$, where W is the weight of solvent in grams absorbed by one equivalent of resin and ϱ the density of the solvent at 25°. Even if this assumption is not fully correct, especially in view of the observations referred to above, the deviations from the true volumes are probably within the limits of the experimental error. The relative volume changes can be seen from Fig. 3, where the ratio V_s/V_s (H_2O) is plotted against the mole fraction of alcohol in the resin phase. It is seen that a slight increase in the internal volume of the hydroxyl resin takes place at very low methanol concentrations. Only a hardly perceptible volume change seems to occur when the methanol concentration is increased, but the volume is somewhat lower in pure methanol. Essentially the same behaviour is noted for the ethanol-water mixtures. Since the hydroxyl resin is not stable in pure ethanol, no experiments were carried out with ethanol concentrations exceeding 90 %. As far as the chloride resin is concerned, it is observed that its volume changes are greater and a maximum appears in the ethanol-water curve.

The solvent distribution data from the experiments with the porous resin are shown in Table 4. Here again, the methanol concentration is lower in the resin phase than in the external solution (Fig. 4). The salting-out effect is, however, much smaller than with the normal resin.

Due to its high degree of swelling, the porous resin absorbs much more solvent than the normal resin. The uptake of water and methanol in moles is plotted against the mole fraction of the internal solution in Fig. 5.

The volume of the solution in the porous resin is about 15 times as great as the volume of solution in the normal resin. Up to an internal methanol concentration of 10 % there is no marked change in the swelling, but then the volume decreases continuously with increasing methanol concentration and is about 33 % smaller in pure methanol than in water (*cf.* Fig. 3).

This work has been supported by *Finnish State Scientific Board.*

REFERENCES

1. Rückert, H. and Samuelson, O. *Acta Chem. Scand.* **11** (1957) 303.
2. Gregor, H. P., Nobel, D. and Gottlieb, M. H. *J. Phys. Chem.* **59** (1955) 10.
3. Gable, R. W. and Strobel, H. A. *J. Phys. Chem.* **60** (1956) 513.
4. Sjöström, E. and Nykänen, L. *J. Org. Chem.* **21** (1956) 1321.
5. Gregor, H. P., Bregman, J. I., Gutoff, F., Broadley, R. D., Baldwin, D. E. and Overberger, C. G. *J. Colloid Sci.* **6** (1951) 20.
6. Pepper, K. W., Paisley, H. M. and Young, M. A. *J. Chem. Soc.* **1953** 4097.
7. Samelson, H. and Hammet, L. P. *J. Am. Chem. Soc.* **78** (1956) 524.
8. Johansson, A. *Svensk Papperstidn.* **50** No. 11 B (1947) 124.
9. Ahlén, L. and Samuelson, O. *Svensk Papperstidn.* **56** (1953) 81.
10. Nogare, S. D. *Anal. Chem.* **25** (1953) 1874.
11. Sjöström, E. and Nykänen, L. *To be published.*
12. Sjöström, E. and Nykänen, L. *Acta Chem. Scand.* **12** (1958) 141.
13. Caldin, E. F. and Long, G. *J. Chem. Soc.* **1954** 3737.
14. Koskikallio, J. *Suomen Kemistilehti* **32 B** (1959) 161.
15. Helfferich, F. *Ionenaustauscher.* Band I. Grundlagen. Verlag Chemie Weinheim/Bergstr. 1959, pp. 96–98, 438.
16. Gurney, R. *Ionic Processes in Solution*, McGraw-Hill Book Co., New York 1953, p. 266.
17. *International Critical Tables*, Vol. VI, p. 78.
18. Weissberger, A. *Technique of Organic Chemistry*, Vol. VII, 2nd Ed., Interscience Publishers, Inc., New York 1955, pp. 90–91.
19. Pepper, K. W., Reichenberg, D. and Hale, D. K. *J. Chem. Soc.* **1952** 3129.
20. Boyd, G. E. and Soldano, B. A. *Z. Elecktrochem.* **57** (1953) 162.
21. Soldano, B. A. and Boyd, G. E. *J. Am. Chem. Soc.* **75** (1953) 6099.

Received September 6, 1961.

ACTA CHEMICA SCANDINAVICA 16 (1962) 403–420

The Crystal Structures of $[Al_2(OH)_2(H_2O)_8](SO_4)_2 \cdot 2H_2O$ and $[Al_2(OH)_2(H_2O)_8](SeO_4)_2 \cdot 2H_2O$

GEORG JOHANSSON

Department of Inorganic Chemistry, Royal Institute of Technology, Stockholm 70, Sweden

The crystal structures of a basic aluminium sulfate, $Al_2O_3 \cdot 2SO_3 \cdot 11H_2O$, and the isomorphous selenate have been investigated by means of X-ray crystallographic methods. The crystals are monoclinic and the space group is $P2_1/n$. The unit cell dimensions are:
$a = 8.15$ Å, $b = 12.48$ Å, $c = 8.40$ Å, $\beta = 101.9°$ for the sulfate and
$a = 8.26$ Å, $b = 12.76$ Å, $c = 8.48$ Å, $\beta = 102.1°$ for the selenate.

The structure contains discrete aluminum-oxygen complexes of the composition Al_2O_{10}, which are built up from two AlO_6 octahedra sharing an edge. The hydrogen atoms have been located by indirect methods. Their positions indicate that the formula for the Al_2O_{10} group should be written $[Al_2(OH)_2(H_2O)_8]^{4+}$. These ions are joined by means of hydrogen bonds to the oxygen atoms of the sulfate or the selenate groups and the water molecules.

According to a previous structure determination [1,2] some of the more basic of the aluminium salts contain discrete $Al_{13}O_{40}$ groups. Since these groups are joined in the crystals only by means of hydrogen bonds [2], it seems reasonable to assume that their structure reflects the structure of the polynuclear complexes that form when an aluminium salt solution is hydrolyzed by the addition of alkali [3,4]. In order to elucidate the intermediate steps in the condensation process leading to these polynuclear ions, the structures of some less basic salts have been investigated. One of these is $Al_2O_3 \cdot 2SO_3 \cdot 11H_2O$, which has a composition corresponding to the loss of one proton for each $Al(H_2O)_6^{3+}$ ion, compared with a ratio of about 2.5 to 1 for the compound containing the $Al_{13}O_{40}$ groups. The structure is of special interest as the number of oxygen atoms is sufficient to give the aluminium ion the expected coordination number of six without involving any of the oxygen atoms of the sulfate groups. This fact makes the existence of discrete aluminium-oxygen complexes possible.

The preparation of $Al_2O_3 \cdot 2SO_3 \cdot 11H_2O$ has been described by several authors. In Gmelin's »Handbuch der Chemie» the formula is given as $Al_2O_3 \cdot 2SO_3 \cdot 12H_2O$, but later work by Bassett and Goodwin [5] has shown that only

11 moles of water are present and not 12. Bassett [5,6] has suggested that the ion $[Al(OH)(H_2O)_5]^{++}$ is present in the structure, but this hypothesis is not supported by the results of the present structure determination.

EXPERIMENTAL

According to the phase diagram given by Bassett and Goodwin [5] for the system $Al_2O_3 - SO_3 - H_2O$ at 25°C, the compound $Al_2O_3 \cdot 2SO_3 \cdot 11H_2O$ has only a small range of stability. Solutions, which according to the diagram should be supersaturated with respect to $Al_2O_3 \cdot 2SO_3 \cdot 11H_2O$, were prepared by dissolving pure aluminium metal (99.99 %) in sulfuric acid (p.a.). To make the reaction more rapid, a small amount of mercury was added as a catalyst. After filtration the solutions were left to crystallize at room temperature. Fairly large crystals were obtained from a solution prepared from 5.3 g Al, 24.5 g H_2SO_4, and 70.2 g H_2O.

The crystals are readily soluble in water forming a clear solution. After some time or on dilution the solution becomes milky and a precipitate is formed.

Analysis. The amount of aluminium was determined by igniting a sample of the air-dried crystals and weighing the residue as Al_2O_3. Water was determined by Brush and Penfield's method as described by Kolthoff and Sandell [8]. Sulfate was determined by precipitating and weighing $BaSO_4$. The results, which are given in Table 1, confirm the results of Bassett and Goodwin that the composition corresponds to $Al_2O_3 \cdot 2SO_3 \cdot 11H_2O$.

Table 1.

	Found	Calculated for $Al_2O_3 \cdot 2SO_3 \cdot 11H_2O$	Calculated for $Al_2O_3 \cdot 2SO_3 \cdot 12H_2O$
% Al_2O_3	22.4	22.15	21.32
% SO_3	34.7	34.79	33.48
% H_2O	43.4	43.06	45.20
Density	1.82	1.829	1.900

X-Ray data. Rotation and Weissenberg photographs showed that the crystals were monoclinic and approximate unit cell dimensions were calculated from them. The following more precise values were calculated from a powder photograph (Table 2) taken with Cu$K\alpha$ radiation in a Guinier focusing camera using KCl (a_0 = 6.293 Å) as internal standard:

$a = 8.15_1$ Å, $b = 12.47_6$ Å, $c = 8.39_9$ Å, $\beta = 101.9_0°$.

The density obtained from the apparent loss of weight in benzene was 1.82 g · cm^{-3}. The calculated density for two formula weights per unit cell is 1.829 (Table 1).

The prism-shaped crystals are extended along the crystallographic a axis. The b and c axes lie in the directions of the diagonals of the base of the prism. Weissenberg photographs were taken about all three axes using CuK radiation. The multiple film technique was used, and the intensities were estimated visually by comparison with an intensity scale (prepared by timed exposures of one of the reflections from the crystal). The maximum dimension of the crystals used was about 0.15 mm. No correction for absorption was applied (μ = 50 cm^{-1}). The intensities were corrected for Lorentz and polarization factors in the usual manner and were placed on a common scale by means of reflections occurring on more than one photograph.

The systematic absences are $h0l$ with h $h+l$ odd and $0k0$ with k odd. This is characteristic for the space group $P2_1/n$.

The isomorphous selenate, $Al_2O_3 \cdot 2SeO_3 \cdot 11H_2O$, was prepared by dissolving aluminium hydroxide in selenic acid in the manner described by Bassett [7]. The crystals seemed to be similar in all respects to those of the sulfate. Rotation and Weissenberg photographs were used to calculate approximate unit cell dimensions and the following more accurate values were determined from Guinier powder photographs:

$a = 8.25_5$ Å, $b = 12.76$ Å, $c = 8.48$ Å, $\beta = 102.1°$

Intensity data were collected in the same way as for the sulfate.

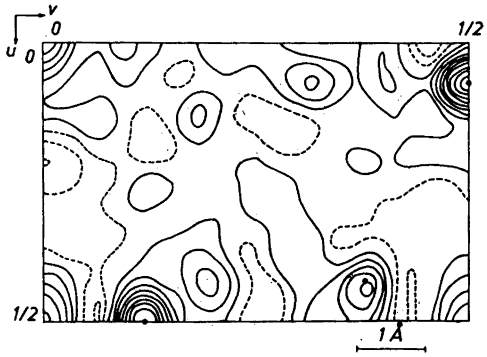

Fig. 1a. Difference Patterson projection along [001]. At the origin only every 5th contour has been drawn. Broken lines indicate negative regions. Small black circles indicate the positions of S—S (Se—Se) vectors.

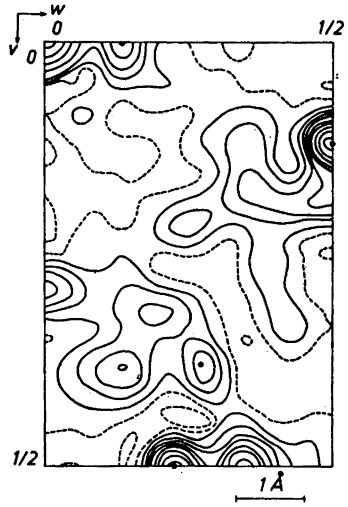

Fig 1b. Difference Patterson projection along [100].

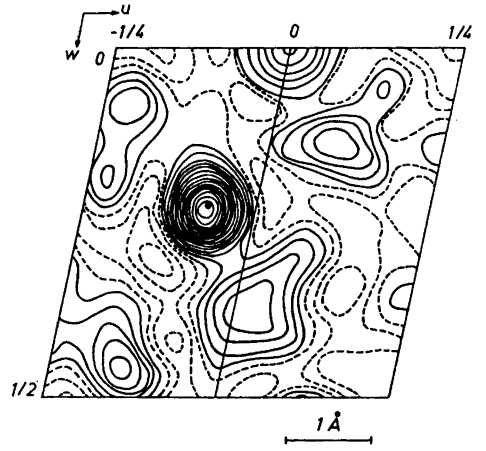

Fig. 1c. Difference Patterson projection along [010].

STRUCTURE DETERMINATION

Preliminary scale and temperature factors for both the sulfate and the selenate were obtained from the *hk*0 and 0*kl* intensities by means of Wilson's method. Difference Patterson projections along the *a*, *b*, and *c* axes were then calculated *. These are shown in Fig. 1. The ratio between the scale factors

* All calculations were carried out on the "Besk" computer using programs designed for the calculation of electron densities [18] and structure factors [19].

for the sulfate and the selenate obtained from the Wilson plot and used for the Patterson maps in Fig. 1 is approximately a factor of 1.3 higher than the ratio calculated from the $|F_c|^2$ values for the final structures, but this difference does not affect the following discussion.

In space group $P2_1/n$ the special positions are all centers of symmetry, and the four S (Se) atoms must therefore occupy one of the general four-fold positions: $\pm (x, y, z) \pm (\frac{1}{2} - x, \frac{1}{2} + y, \frac{1}{2} - z)$.

The vectors connecting these points are:

$\frac{1}{2}\ \frac{1}{2} - 2y\ \frac{1}{2}$	weight 2
$\frac{1}{2} - 2x\ \frac{1}{2}\ \frac{1}{2} - 2z$	» 2
$2x\ 2y\ 2z$	» 1
$2x\ \overline{2y}\ 2z$	» 1

The first two vectors can be identified easily on the $hk0$ and $0kl$ projections (Figs. 1a and 1b). In the $hk0$ projection only the peaks at

$$u = \tfrac{1}{2},\ v = 0.118 \text{ and } u = 0.072,\ v = \tfrac{1}{2}$$

are of sufficient heights to correspond to the difference between a Se — Se and a S — S vector. For the $0kl$ projection possible vectors are:

$$v = 0.120,\ w = \tfrac{1}{2} \text{ and } v = \tfrac{1}{2},\ w = 0.225.$$

These vectors lead to the following parameter values:

$x = \pm 0.214$ or ± 0.714
$y = \pm 0.191$ » ± 0.691
$z = \pm 0.137$ » ± 0.637

The only combinations of these parameters that are crystallographically non-equivalent can be written as

$$\begin{array}{ll} x = 0.214 & x = 0.214 \\ y = 0.191 \text{ and} & y = 0.191 \\ z = 0.137 & z = -0.137 \end{array}$$

Of these only the second set is consistent with the vectors $(\frac{1}{2} - 2x, \frac{1}{2} - 2z)$ occurring in the $h0l$ projection (Fig. 1 c).

There is another possible vector $v = \frac{1}{2}$, $w = \frac{1}{2} - 2z$ in the $0kl$ projection, as the peak at $v = \frac{1}{2}$, $w = 0.350$ is not much lower than the peak selected above. This possibility is ruled out by a comparison with the vectors in the $h0l$ projection.

The Patterson projections thus give the following parameters for the sulfur or the selenium atoms:

$x = 0.214$, $y = 0.191$, $z = 0.863$.

All vectors within the corresponding four-fold position are present as peaks in the Patterson maps (Fig. 1) and have the heights expected from the weights of the corresponding vectors.

The contributions to the structure factors from these atoms were now calculated, and $F_c^{Se} - F_c^{S}$ for each reflection was compared with the differences between the observed structure factors calculated for the four possible

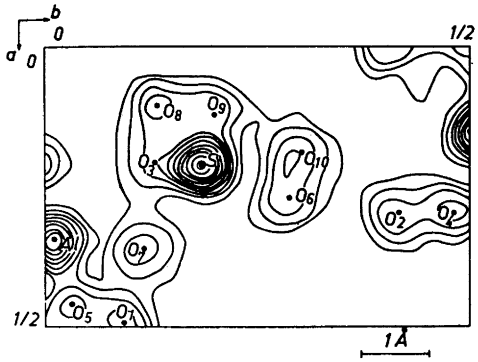

Fig. 2a. c-axis projection of the electron-density. Contours are drawn at intervals of 3 e · Å^{-2}. The zero contour is omitted.

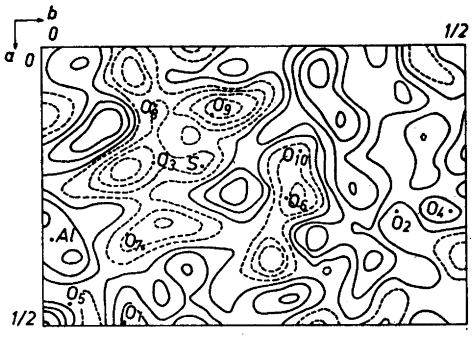

Fig. 2b. $F_o - F_c$ synthesis along [001]. Contours are drawn at intervals of 0.3 e · Å^{-2}. Dashed lines indicate negative regions.

sign combinations: $|F_o^{sel.}| + |F_o^{sulf.}|$, $|F_o^{sel.}| - |F_o^{sulf.}|$, $-|F_o^{sel.}| + |F_o^{sulf.}|$, and $-|F_o^{sel.}| - |F_o^{sulf.}|$. In this way signs were determined for 237 out of 275 observed independent $hk0$, $0kl$, and $h0l$ reflections for the sulfate. Only 12 of these signs were different from the signs calculated for the final structure, and as these were associated with relatively small structure factors, the Fourier maps, calculated at this stage of the structure determination, did not differ much from the final Fourier syntheses shown in Figs. 2a, 3a, and 4a.

The proportion of assigned and erroneous signs for the selenate was approximately the same, and the corresponding Fourier maps were very similar to those for the sulfate.

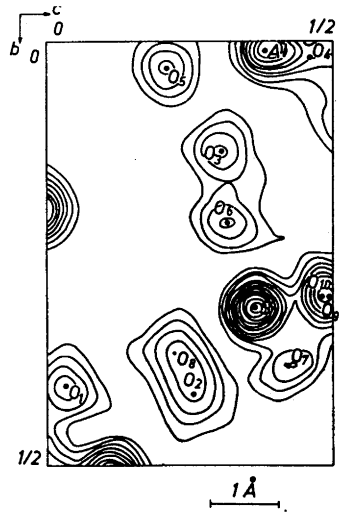

Fig. 3a. a-Axis projection of the electron-density. Contours are drawn at intervals of 3 e . Å^{-2}. The zero contour is omitted.

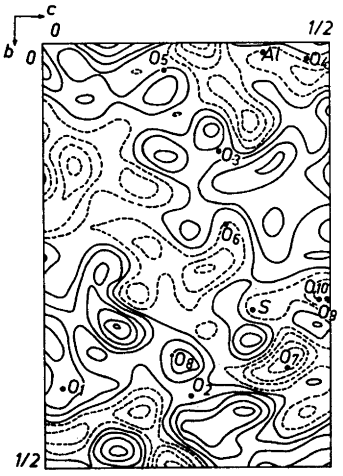

Fig. 3b. $F_o - F_c$ synthesis along [100]. Contours are drawn at intervals of 0.3 e · Å^{-2} Dashed lines indicate negative regions.

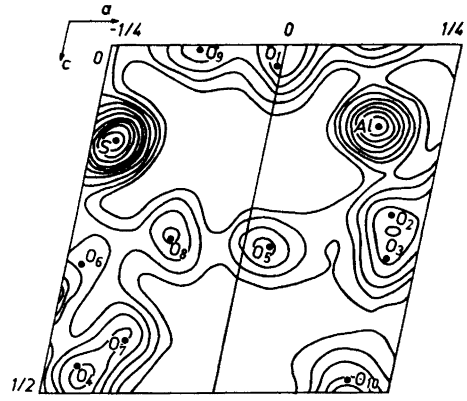

Fig. 4a. *b*-axis projection of the electron-density. Contours are drawn at intervals of 3 e · Å^{-2}. The zero contour is omitted.

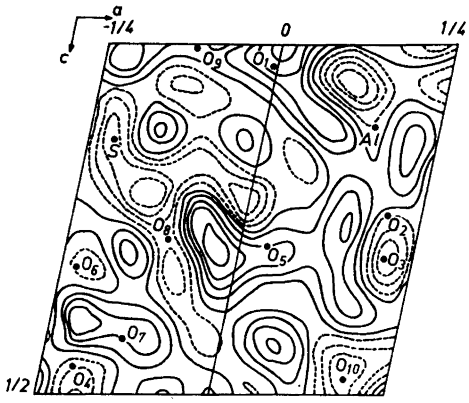

Fig. 4b. $F_o - F_c$ synthesis along [010]. Contours are drawn at intervals of 0.3 e · Å^{-2}. Dashed lines indicate negative regions.

In addition to the maximum at the sulfur position, the *h*0*l* and the *hk*0 projections both contain one peak that is higher than all the others. The x parameters for the two peaks are approximately the same, and in the 0*kl* projection a maximum of about the same height occurs at the point defined by the corresponding y and z parameters. These peaks were assumed to correspond to an aluminium atom in a four-fold position ($x = 0.15$, $y = 0.51$, $z = 0.11$). This assumption is supported by the octahedral arrangement of lower peaks around the assumed aluminium position and also by the smallest distance, 2.9 Å, between the positions — the distance usually observed between two octahedrally coordinated aluminium atoms sharing an edge.

Despite some overlap of peaks the three dimensional arrangement of oxygen atoms in the AlO_6 octahedra could be deduced by a detailed comparison of the three projections, assuming that two AlO_6 octahedra have a shared edge. The Al — O and O — O distances calculated from the resulting parameters are approximately the same as those usually found for AlO_6 octahedra. The oxygen atoms of the sulfate groups were located in the same way by comparing the positions of peaks in the three Fourier projections. The obscuring of the oxygen peaks by diffraction effects from the heavier sulfur atoms and the more serious overlap of peaks in this case result in somewhat more uncertain parameters than above.

None of the oxygen atoms located in this way is shared between a sulfate group and an AlO_6 octahedron. The only oxygen atoms that are associated with more than one cation are those defining the shared edge of the AlO_6 octahedra. The electron density projections thus show the presence of discrete aluminium-oxygen complexes of the composition Al_2O_{10} each built up from two AlO_6 octahedra sharing an edge.

The two Al_2O_{10} groups and the four SO_4 groups in the unit cell account for 36 of the 40 oxygen atoms present. The positions of the remaining four oxygen atoms are uniquely determined by the still unexplained peaks in the Fourier maps.

Table 2. Powder photograph of $Al_2O_3 \cdot 2\,SO_3 \cdot 11H_2O$. Guinier camera. Cu$K\alpha$ radiation..

$h\,k\,l$	$10^4 \sin^2\Theta$ calc	$10^2 \sin^2\Theta$ obs	I obs
0 1 1	0.0126	0.0125	m
1 1 0	0.0131	0.0130	s
1 0 $\bar{1}$	0.0144	0.0143	vw
1 1 $\bar{1}$	0.0182	0.0181	s
1 0 1	0.0218	0.0218	vvw
0 2 1	0.0240	0.0240	m
1 2 0	0.0246	0.0244	m
1 1 1	0.0256	0.0255	vvw
1 2 $\bar{1}$	0.0296	0.0296	s
1 2 1	0.0371	0.0371	s
2 0 0	0.0373	0.0373	s
0 1 2	0.0389	0.0389	s
1 1 $\bar{2}$	0.0408	0.0408	m
2 1 0	0.0411	0.0410	w
2 1 $\bar{1}$	0.0424	0.0423	vw
0 3 1	0.0431	0.0431	s
1 3 0	0.0436	0.0436	m
2 2 0	0.0525	0.0525	w
2 1 1	0.0574	0.0574	w
2 0 $\bar{2}$	0.0575		
2 1 $\bar{2}$	0.0613	0.0613	m
2 2 1	0.0688	0.0688	vvw
1 4 0	0.0703	0.0703	vvw
1 3 $\bar{2}$	0.0713	0.0713	m
2 3 0	0.0716		
2 2 $\bar{2}$	0.0728	0.0728	m
2 3 $\bar{1}$	0.0729		
1 1 $\bar{3}$	0.0810	0.0810	w
3 1 0	0.0877	0.0878	s
2 3 1	0.0879		
2 1 2	0.0912	0.0911	w
2 3 $\bar{2}$	0.0918	0.0917	vw
2 1 $\bar{3}$	0.0978	0.0977	vvw
1 0 3	0.0996	0.0995	vw
2 4 $\bar{1}$	0.0996		
3 1 $\bar{2}$	0.1005	0.1005	vvw
2 2 2	0.1026	0.1026	vw
3 0 $\bar{3}$	0.1294	0.1293	vvw
3 3 $\bar{2}$	0.1310	0.1309	vvw
1 5 $\bar{2}$	0.1323	0.1324	vvw
2 5 0	0.1326		
1 3 3	0.1339	0.1338	vvw
2 5 $\bar{1}$	0.1339		
3 2 $\bar{3}$	0.1446	0.1447	vvw
3 4 0	0.1449		
4 1 $\bar{1}$	0.1469	0.1471	vvw
1 5 2	0.1472		
2 0 $\bar{4}$	0.1480	0.1485	vw
2 4 2	0.1484		
2 5 1	0.1488		
4 0 $\bar{2}$	0.1545	0.1548	vvw
2 4 $\bar{3}$	0.1549		
4 1 $\bar{2}$	0.1583	0.1582	vvw
4 2 $\bar{1}$	0.1583		
1 4 3	0.1606	0.1607	vvw
4 2 0	0.1645	0.1647	m
3 4 1	0.1649		
1 6 $\bar{2}$	0.1742	0.1741	vvw
0 5 3	0.1743		
2 6 0	0.1745		
3 1 $\bar{4}$	0.1835	0.1835	w
4 3 0	0.1835		
3 4 $\bar{3}$	0.1904	0.1906	m
2 6 1	0.1908		
2 6 $\bar{2}$	0.1947	0.1949	vvw
1 5 3	0.1949		
3 2 $\bar{4}$	0.1949		

REFINEMENT OF THE STRUCTURE

With the parameters determined from the electron density projections and the temperature factor obtained from the Wilson plot as a starting point, the sulfate was refined by means of $F_o - F_c$ syntheses on (001), (010), and (100). The three projections were refined simultaneously rather than independently. When the indicated shifts differed from one projection to another, an intermediate value was chosen so as to take into account as far as possible the various amounts of overlap in the three projections. For the following refinement cycle identical shifts were then applied to all three projections.

The starting parameters gave R factors ($R = \Sigma\,||F_o| - |F_c||/\Sigma\,|F_o|$; only observed reflections were included) of 0.28 for the $h0l$, 0.25 for the $hk0$, and 0.25 for the $0kl$ structure factors. Two difference maps reduced the R factors to 0.16 for each of the three projections. At this stage of the refinement it was clear that there was a large difference between the temperature factors

Table 3 a. Final parameters for $[Al_2(OH)_2(H_2O)_8](SO_4)_2 \cdot 2H_2O$

Atom	x	y	z
4 S	0.2130	0.1850	0.8640
4 Al	0.1545	0.5107	0.1160
4 O_1	0.994	0.407	0.031
4 O_2	0.298_5	0.416	0.257
4 O_3	0.292	0.628	0.193
4 O_4	0.296	0.481_5	0.960
4 O_5	0.462	0.031	0.211
4 O_6	0.729	0.713	0.183_5
4 O_7	0.640	0.883	0.079
4 O_8	0.895	0.868_5	0.278
4 O_9	0.879	0.801	0.007
4 O_{10}	0.312	0.802	0.020

of the sulfur and aluminium atoms on the one hand and of the oxygen atoms on the other. Individual isotropic temperature factors were therefore introduced. However, the individual variations for the oxygen atoms did not seem to be so large as to be significant, and throughout the refinement a single temperature factor was used for all oxygen atoms.

After four more difference syntheses significant shifts in positional parameters were no longer indicated, and the refinement was not continued further. The final parameters are given in Table 3a. The temperature factors used for the final calculation of struture factors, listed in Table 4, are 0.9 Å^2 for S and Al and 2.0 Å^2 for O. Atomic scattering factors were calculated from the analytical expressions given by Vand *et al.*[9]. The R factors, including observed reflections only, are 0.086 for the $h0l$, 0.087 for the $hk0$, and 0.091 for the $0kl$ structure factors. The final difference syntheses computed from the F_o and F_c values in Table 4 are shown in Figs. 2b, 3b, and 4b.

In order to check the parameters on some general reflections the hll structure factors were calculated. A comparison between observed and calculated values is given in Table 4. The resulting R factor is 0.091 for the 111 reflections observed.

The selenate was refined in the same way by means of five succesive $F_o - F_c$ syntheses along the three axes. The final R factors are 0.110, 0.092, and 0.097 for the $hk0$, $0kl$, and $h0l$ structure factors, respectively. The tem-

Table 3 b. Final parameters for $[Al_2(OH)_2(H_2O)_8](SeO_4)_2 \cdot 2H_2O$

Atom	x	y	z
4 Se	0.2148	0.1910	0.8610
4 Al	0.1525	0.5154	0.1160
4 O_1	0.001	0.409_5	0.037
4 O_2	0.300	0.428	0.260
4 O_3	0.282	0.635	0.184
4 O_4	0.292	0.488	0.966
4 O_5	0.461	0.033	0.213
4 O_6	0.719	0.700	0.189
4 O_7	0.624	0.887	0.075
4 O_8	0.910	0.867	0.288
4 O_9	0.887	0.795	0.996
4 O_{10}	0.302	0.807	0.020

Table 4. Observed and calculated structure factors for $[Al_2(OH)_2(H_2O)_8](SO_4)_2 \cdot 2H_2O$

h k l	F_o	F_c
0 0 0	—	436
2	118	−122
4	17	16
6	28	26
8	< 6	— 2
1 0	11	12
1 1 0	54	— 48
2	54	— 53
3	48	— 48
4	26	26
5	14	14
6	14	— 14
7	52	— 52
8	22	25
9	23	26
10	6	— 7
0 2 0	17	15
1	58	— 68
2	48	51
3	37	— 38
4	13	— 10
5	6	6
6	33	32
7	9	9
8	< 6	— 2
9	< 5	— 4
10	12	— 16
1 3 0	58	— 64
2	53	54
3	37	36
4	25	— 25
5	9	— 9
6	13	11
7	9	10
8	6	7
9	8	— 11
10	5	4
0 4 0	5	— 3
1	36	37
2	18	— 16
3	25	— 21
4	5	1
5	6	2
6	14	12
7	14	— 11
8	8	— 6
9	16	— 15
1 5 0	6	8
2	51	51
3	15	12
4	24	— 24
5	16	12
6 5 0	30	29
7	20	— 17
8	13	— 12
9	27	30
0 6 0	56	52
1	30	37
2	39	— 40
3	16	— 18
4	14	— 14
5	< 5	— 3
6	< 6	5
7	7	— 6
8	8	— 7
9	7	— 6
1 7 0	9	— 7
2	12	— 13
3	28	28
4	23	25
5	< 6	— 1
6	14	— 11
7	11	— 9
8	19	18
9	5	5
0 8 0	< 5	3
1	29	— 31
2	15	18
3	7	10
4	29	— 33
5	< 6	— 5
6	14	14
7	8	— 8
8	8	7
1 9 0	16	— 14
2	30	30
3	19	17
4	20	— 21
5	10	— 8
6	11	11
7	15	— 13
0 10 0	64	66
1	< 6	— 4
2	29	— 31
3	30	— 30
4	< 6	1
5	19	20
6	16	15
1 11 0	12	— 9
2	10	7
3	7	— 4
4	< 6	— 1

Table 4. Continued.

h k l	F_o	F_c
5 11 0	10	13
6	< 4	− 3
7	20	− 22
0 12 0	< 6	− 7
1	26	− 27
2	< 6	0
3	< 5	4
4	< 5	3
5	< 4	2
6	12	12
1 13 0	6	− 5
2	20	20
3	16	14
4	< 4	− 3
5	6	− 6
0 14 0	< 5	− 4
1	13	14
2	< 4	0
3	10	− 9
4	12	− 12
1 15 0	9	8
2	18	20
3	8	7
0 0 2	< 1	− 1
4	28	29
6	13	14
8	33	29
10	5	3
0 1 1	44	− 41
2	96	94
3	8	− 3
4	13	− 12
5	5	1
6	13	− 14
7	< 4	0
8	17	15
9	5	− 5
10	6	6
0 2 1	53	51
2	16	− 14
3	32	31
4	3	2
5	25	26
6	37	− 39
7	13	− 14
8	< 4	− 1
9	29	25
10	6	6

h k l	F_o	F_c
0 3 1	101	−115
2	15	− 14
3	42	− 40
4	15	16
5	52	51
6	12	− 11
7	49	− 47
8	14	− 13
9	12	− 13
10	11	− 10
0 4 1	19	− 22
2	36	32
3	41	− 39
4	29	− 25
5	25	25
6	9	11
7	< 4	6
8	14	13
9	19	− 21
10	6	6
0 5 1	32	31
2	17	− 17
3	21	19
4	7	9
5	43	42
6	< 4	3
7	22	24
0 6 1	31	− 32
2	12	12
3	7	7
4	46	− 42
5	26	− 25
6	15	11
7	< 4	4
8	23	22
9	13	15
0 7 1	45	− 42
2	36	33
3	6	4
4	13	14
5	< 4	1
6	22	− 23
7	13	− 12
8	23	22
9	16	− 19
0 8 1	20	− 23
2	11	− 13
3	14	− 14
4	< 4	− 3
5	24	− 24

Table 4. Continued.

$h\,k\,l$	F_o	F_c
0 8 6	24	− 25
7	< 4	3
8	16	− 16
9	8	− 8
0 9 1	28	− 27
2	11	− 11
3	32	32
4	27	25
5	< 4	2
6	< 4	3
7	10	− 11
8	< 3	− 3
0 10 1	44	− 44
2	27	25
3	10	− 10
4	11	− 11
5	16	16
6	8	9
7	< 3	1
8	15	19
0 11 1	< 4	5
2	28	30
3	21	− 21
4	11	11
5	9	11
6	< 4	− 6
7	9	9
0 12 1	7	6
2	10	5
3	9	8
4	18	− 16
5	10	− 12
6	7	− 8
0 13 1	32	− 32
2	14	16
3	8	9
4	5	5
5	7	9
6	15	− 19
0 14 1	12	− 14
2	< 3	− 2
3	16	− 20
4	6	8
5	6	7
0 15 1	4	4
2	5	− 6
3	12	18

$h\,k\,l$	F_o	F_c
1 0 $\bar{9}$	< 6	− 4
$\bar{7}$	23	18
$\bar{5}$	10	− 5
$\bar{3}$	10	− 11
$\bar{1}$	14	13
1	38	42
3	79	72
5	35	− 36
7	51	46
9	16	15
2 0 1$\bar{0}$	8	9
$\bar{8}$	44	− 40
$\bar{6}$	20	− 20
$\bar{4}$	58	57
$\bar{2}$	55	53
2	16	− 14
4	16	12
6	< 7	− 6
8	< 6	4
3 0 $\bar{9}$	14	− 13
$\bar{7}$	26	− 26
$\bar{5}$	7	− 5
$\bar{3}$	90	90
$\bar{1}$	40	36
1	13	13
3	21	21
5	61	65
7	24	− 23
9	28	− 29
4 0 1$\bar{0}$	11	− 11
$\bar{8}$	< 7	6
$\bar{6}$	11	11
$\bar{4}$	13	− 15
$\bar{2}$	29	− 28
2	16	− 21
4	17	17
6	30	27
8	20	− 19
5 0 $\bar{9}$	13	− 9
$\bar{7}$	21	23
$\bar{5}$	< 6	− 6
$\bar{3}$	48	− 57
$\bar{1}$	15	− 17
1	15	10
3	< 6	− 3
5	44	− 47
7	< 6	1
6 0 $\bar{8}$	16	17
$\bar{6}$	14	11
$\bar{4}$	7	9
$\bar{2}$	18	− 19

Table 4. Continued.

h k l	F_o	F_c
6 0 2	63	65
4	17	− 17
6	20	− 22
7 0 $\bar{9}$	< 4	5
$\bar{7}$	11	− 13
$\bar{5}$	23	26
$\bar{3}$	8	6
$\bar{4}$	44	46
1	13	− 13
3	20	19
5	7	10
8 0 $\bar{8}$	< 4	− 1
$\bar{6}$	33	− 40
$\bar{4}$	6	6
$\bar{2}$	40	41
2	20	− 22
4	< 5	− 2
9 0 $\bar{7}$	6	6
$\bar{5}$	9	− 13
$\bar{3}$	14	16
$\bar{1}$	13	14
1	< 5	− 1
3	< 4	− 4
10 0 $\bar{4}$	15	18
$\bar{2}$	9	− 13
1 1 $\bar{10}$	11	− 12
$\bar{9}$	< 7	− 2
$\bar{8}$	< 8	5
$\bar{7}$	9	− 12
$\bar{6}$	47	47
$\bar{5}$	28	29
$\bar{4}$	20	16
$\bar{3}$	63	61
$\bar{2}$	83	− 74
$\bar{1}$	71	− 62
1 1 1	24	− 24
2	22	25
3	< 6	7
4	13	10
5	8	11
6	35	− 34
7	37	− 32
8	< 9	− 8
9	< 7	7
10	< 5	− 1
2 1 $\bar{10}$	12	12
$\bar{9}$	11	− 9
$\bar{8}$	< 8	− 3
$\bar{7}$	< 8	− 6
2 1 $\bar{6}$	20	− 20
$\bar{5}$	24	23
$\bar{4}$	48	− 48
$\bar{3}$	50	− 43
$\bar{2}$	72	69
$\bar{1}$	30	− 34
2 1 1	37	35
2	92	− 88
3	< 6	− 5
4	< 7	4
5	< 7	− 2
6	25	− 22
7	26	− 22
8	26	− 25
9	14	12
3 1 $\bar{10}$	12	14
$\bar{9}$	18	18
$\bar{8}$	< 8	6
$\bar{7}$	< 8	− 4
$\bar{6}$	13	− 12
$\bar{5}$	21	− 21
$\bar{4}$	88	− 92
$\bar{3}$	53	− 53
$\bar{2}$	34	32
$\bar{1}$	< 5	6
3 1 1	10	− 9
2	20	18
3	43	− 44
4	20	− 17
5	< 8	2
6	15	− 13
7	20	20
8	11	11
9	14	− 16
4 1 $\bar{10}$	9	− 9
$\bar{9}$	33	33
$\bar{8}$	13	11
$\bar{7}$	< 9	4
$\bar{6}$	26	28
$\bar{5}$	34	− 33
$\bar{4}$	19	23
$\bar{3}$	12	16
$\bar{2}$	7	− 6
$\bar{1}$	30	− 33
4 1 1	< 6	2
2	28	33
3	74	− 80
4	44	− 44
5	< 9	2
6	10	8
7	10	8
8	9	11

Table 4. Continued.

$h\,k\,l$	F_o	F_c
5 1 $\bar{9}$	10	− 13
$\bar{8}$	11	13
$\bar{7}$	18	16
$\bar{6}$	< 9	− 8
$\bar{5}$	23	23
$\bar{4}$	< 8	4
$\bar{3}$	10	10
$\bar{2}$	24	21
$\bar{1}$	< 7	1
5 1 1	< 7	− 1
2	39	− 39
3	28	31
4	17	− 15
5	20	− 21
6	< 8	5
7	21	− 22
8	8	9
6 1 $\bar{9}$	9	− 10
$\bar{8}$	< 7	− 3
$\bar{7}$	25	− 24
$\bar{6}$	< 9	− 8
$\bar{5}$	16	16
$\bar{4}$	29	29
$\bar{3}$	11	− 15
$\bar{2}$	< 8	− 2
$\bar{1}$	15	− 16
6 1 1	22	− 19
2	< 8	− 7
3	14	16
4	30	32
5	11	11
6	< 7	− 3
7	< 5	− 1
7 1 $\bar{9}$	10	16
$\bar{8}$	6	− 7
$\bar{7}$	< 7	− 6
$\bar{6}$	18	19
7 1 $\bar{5}$	< 9	− 1
$\bar{4}$	15	18
$\bar{3}$	28	27
$\bar{2}$	9	− 9
$\bar{1}$	24	26
7 1 1	< 9	1
2	< 9	4
3	< 8	− 6
4	< 8	12
5	10	14
6	< 5	− 6
8 1 $\bar{8}$	11	16
$\bar{7}$	9	10
$\bar{6}$	< 7	5
$\bar{5}$	< 8	1
$\bar{4}$	15	− 16
$\bar{3}$	< 8	6
$\bar{2}$	< 8	4
$\bar{1}$	< 8	− 11
8 1 1	< 8	7
2	< 8	− 6
3	< 7	2
4	9	− 12
9 1 $\bar{7}$	9	17
$\bar{6}$	< 6	2
$\bar{5}$	< 7	− 3
$\bar{4}$	18	− 24
$\bar{3}$	11	− 14
$\bar{2}$	14	− 14
$\bar{1}$	11	− 11
9 1 1	< 5	5
2	< 5	0
3	< 5	− 1
10 1 $\bar{5}$	7	− 13
$\bar{4}$	9	13

perature factors used for the final calculation of structure factors are 0.85 Å^2 for Al, 0.95 Å^2 for Se, and 2.0 Å^2 for O. The final parameters are listed in Table 3b.

For the sulfate the standard deviations in positional parameters calculated by means of Cruickshank's formula [10] are 0.005 Å for sulfur, 0.007 Å for aluminium, and 0.01_6 Å for oxygen atoms. These values lead to standard deviations of 0.01_7 Å in S— O, 0.01_8 Å in Al — O and 0.02_3 Å in O — O distances. For Al—Al and O—O distances between atoms related by centers of symmetry, the standard deviations are 0.01_4 Å and 0.03_2 Å respectively. For the selenate the corresponding values are about twice as large.

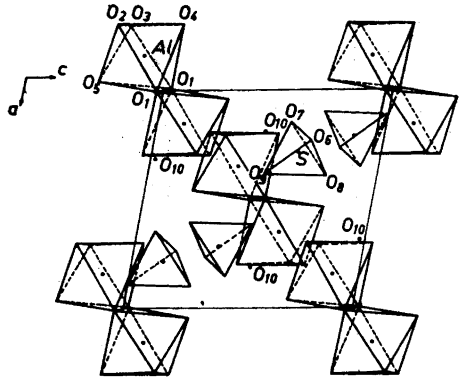

Fig. 5. Projection of the structure along the *b*-axis.

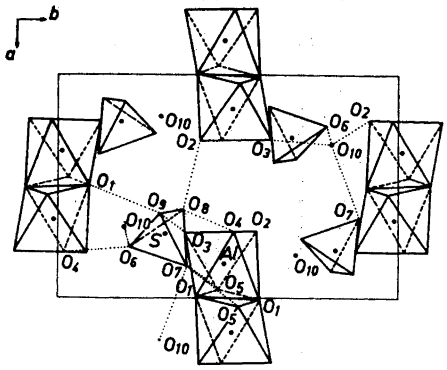

Fig. 6. Projection of the structure along the *c*-axis. Some of the postulated hydrogen bonds have been indicated by means of dotted lines.

The standard deviations calculated in this way may be somewhat too low for the oxygen atoms most affected by overlap. This is especially true for the oxygen atoms of the sulfate and selenate groups, which in all projections are rather close to the heavy atoms. Since for each refinement cycle an average value of the parameter shifts from the three projections was applied, small shifts are still indicated for some of the atoms in the final difference syntheses (Fig. 2b, 3b, and 4b). These remaining shifts are all less than the calculated standard deviations.

DISCUSSION OF THE STRUCTURE

Projections of the structure along the *b* and *c* axes are shown in Figs. 5 and 6.

The unit cell contains two discrete Al_2O_{10} groups, each built up from two AlO_6 octahedra sharing an edge. A projection of the group on a plane through the aluminium atoms and the two bridging oxygens is shown in Fig. 7a, and a projection on a plane perpendicular to this is shown in Fig. 7b. Interatomic distances are given in Table 5. For comparison, the corresponding distances are also given for the selenate.

The average value of the aluminium oxygen bond lengths is 1.89 Å, which is close to the sum of the crystal radii of the ions, 1.90 Å, and is similar to values found for other crystals with octahedral coordination of oxygen ions about aluminium [11]. The bonds to the bridging oxygens are the shortest of the Al—O bond lengths listed in Table 5 although in view of the standard deviations the difference from the average value, 1.89 Å, is not significant.

The contraction of the shared edge, $O_1—O_1$, to 2.39 Å is much more pronounced than is usually found for shared edge lengths in aluminium octahedra in other structures. The O_1 atoms are related by a center of symmetry which

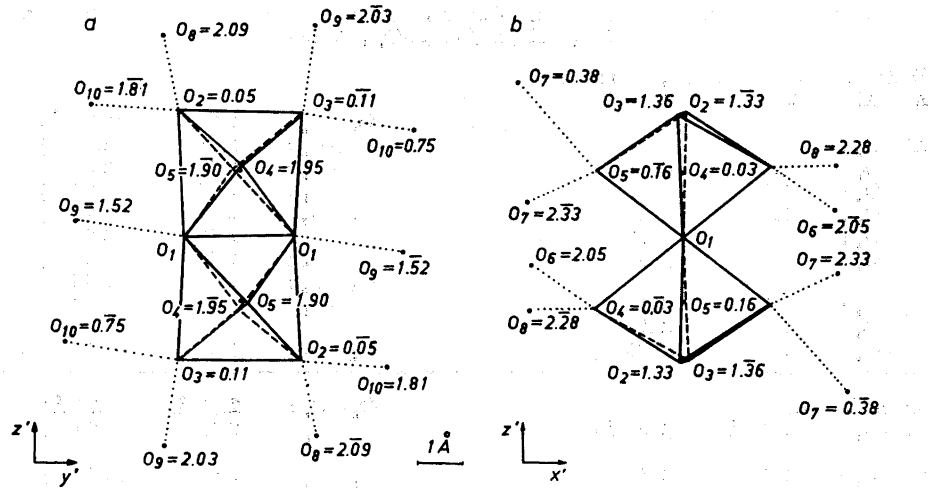

Fig. 7a. Projection of the Al_2O_{10} group on a plane through the aluminium atoms and the two bridging oxygens (O_1). The positions of the hydrogen bonded oxygen atoms are also shown. The height, in Å, above or below the projection plane is given. Dotted lines indicate hydrogen bonds. The aluminium atoms are represented by small filled circles.

Fig. 7b. Projection of the Al_2O_{10} group on a plane through the aluminium atoms and perpendicular to the projection plane in Fig. 7a. Note that the figure is drawn with the y' axis pointing downwards from the viewer.

leads to a rather large standard deviation, 0.03_2 Å, but the occurrence of the same short $O_1—O_1$ distance in both the sulfate and the selenate supports the conclusion that the shortening to 2.39 Å is real. In diaspore [12] the length of an edge shared between two AlO_6 octahedra is 2.46 or 2.54 Å as calculated from the parameters given, and in zunyite [13] the shared edge length is reported to be 2.53 Å. A comparison does not seem entirely justified, however, since in the structures referred to, one of the oxygen atoms of the shared edge also belongs to two other edges shared with a third octahedron. In the structure of $Na[Al_{13}O_4(OH)_{24}(H_2O)_{12}](SeO_4)_4(H_2O)_{13}$ [2] there are two kinds of shared edges; one is analogous to those in diaspore and zunyite and is 2.54 Å, while the other, involving oxygen atoms each belonging to only two octahedra, has a length of 2.37 Å. This is the same within the standard deviations as those found in the present structure determinations. According to a preliminary note on the refinement of dickite, $Al_2Si_2H_4O_5$, a similarly short shared edge length of 2.37 Å occurs in the octahedral layers in this structure [14].

The short O—O distances listed in Table 5 are indicative of hydrogen bonds. The number of such short distances is the same as the number of protons in the structure. Moreover, a comparison between the sulfate and the selenate shows that the short O—O contacts occur between the same atoms in both structures and also that the average difference between these O—O distances in the two structures is much less than between other O—O dis-

Table 5. Interatomic distances. (Values given in parentheses are distances in $[Al_2(OH)_2(H_2O)_8](SeO_4)_2 \cdot 2H_2O$)

Distances within an Al_2O_{10} group					
Al—Al:	2.86 Å	(2.88 Å)			
			$O_1—O_4$:	2.81 Å	(2.78 Å)
Al—O_1 :	1.87	(1.87)	—O_4 :	2.76	(2.75)
—O_1 :	1.85	(1.87)	—O_5 :	2.63	(2.61)
—O_2 :	1.90	(1.90)	—O_5 :	2.76	(2.79)
—O_3 :	1.88	(1.88)	$O_3—O_3$:	2.70	(2.71)
—O_4 :	1.95	(1.92)	—O_4 :	2.62	(2.60)
—O_5 :	1.91	(1.90)	—O_5 :	2.62	(2.59)
			$O_3—O_4$:	2.68	(2.65)
$O_1—O_1$:	2.39	(2.39)	—O_5 :	2.66	(2.69)
—O_2 :	2.80	(2.79)			
—O_3 :	2.71	(2.73)	$O_4—O_5$:	3.08	(3.11)
Short O—O distances			$O_4—O_6$:	2.70 Å	(2.73 Å)
$O_1—O_9$:	2.84 Å	(2.80 Å)	—O_8 :	2.65	(2.69)
$O_2—O_6$:	2.64	(2.63)	$O_5—O_7$:	2.63	(2.60)
—O_{10}:	2.65	(2.69)	—O_7 :	2.72	(2.70)
$O_3—O_9$:	2.73	(2.75)	$O_{10}—O_6$:	2.77	(2.75)
—O_{10}:	2.64	(2.62)	—O_7:	2.80	(2.79)
Other O—O distances < 4 Å					
$O_1—O_6$:	3.50 Å	(3.58 Å)	$O_3—O_6$:	3.73 Å	(3.69 Å)
—O_7 :	3.67	(3.66)	—O_7 :	3.70	(3.82)
—O_8 :	3.87	(4.01)	—O_8 :	3.75	(3.73)
—O_{10}:	3.57	(3.69)			
$O_2—O_2$:	3.71	(3.85)	$O_4—O_4$:	3.29	(3.38)
—O_9 :	3.28	(3.41)	—O_7 :	3.61	(3.68)
—O_9 :	3.61	(3.71)	—O_8 :	3.30	(3.26)
			—O_9 :	3.83	(3.94)
$O_5—O_5$:	3.80 Å	(3.89 Å)			
—O_6 :	3.37	(3.36)	$O_6—O_{10}$:	3.57 Å	(3.70 Å)
—O_9 :	3.66	(3.75)	$O_7—O_7$:	3.77	(3.61)
—O_{10}:	3.38	(3.44)	$O_8—O_{10}$:	3.11	(3.21)
—O_{10}:	3.60	(3.68)	$O_9—O_{10}$:	3.51	(3.39)

Distances within a SO_4 group in $[Al_2(OH)_2(H_2O)_8](SO_4)_2 \cdot 2H_2O$:			
S —O_6 :	1.44 Å	$O_6—O_7$:	2.35 Å
—O_7 :	1.47	—O_8 :	2.40
—O_8 :	1.49	—O_9 :	2.38
—O_9	1.45	$O_7—O_8$:	2.39
		—O_9 :	2.39
		$O_8—O_9$:	2.41

Distances within an SeO_4 group in $[Al_2(OH)_2(H_2O)_8](SeO_4)_2 \cdot 2H_2O$:			
Se—O_6 :	1.58 Å	$O_6—O_7$:	2.63 Å
—O_7 :	1.66	—O_8 :	2.68
—O_8 :	1.63	—O_9 :	2.65
—O_9 :	1.62	$O_7—O_8$:	2.67
		—O_9 :	2.67
		$O_8—O_9$:	2.61

Table 6. Angles about oxygen atoms involved in hydrogen bonds (calculated for $[Al_2(OH)_2(H_2O)_8](SO_4)_2 \cdot 2H_2O$)

O_1:	Al $-O_1-$Al:	100.4°	O_5:	$O_7-O_5-O_7$:	89.6°
	O_9-O_1-Al:	115.6°		O_7-O_5-Al:	127.6°
	O_9-O_1-Al:	129.5°		O_7-O_5-Al:	130.2°
O_2:	$O_{10}-O_2-O_8$:	115.1°	O_{10}:	$O_2-O_{10}-O_8$:	89.1°
	$O_{10}-O_2-$Al:	121.2°		$O_6-O_{10}-O_7$:	103.2°
	O_8-O_2-Al:	123.2°		$O_2-O_{10}-O_6$:	135.1°
				$O_2-O_{10}-O_7$:	97.6°
O_3:	$O_9-O_3-O_{10}$:	103.4°		$O_8-O_{10}-O_6$:	118.4°
	$O_{10}-O_3-$Al:	123.6°		$O_8-O_{10}-O_7$:	111.4°
	O_9-O_3-Al:	127.1°			
O_4:	$O_6-O_4-O_8$:	112.5°			
	O_6-O_4-Al:	117.9°			
	O_8-O_4-Al:	123.3°			

tances (Table 5). Thus, there seem to be strong indications that the oxygen atoms involved in these short O—O contacts are joined together by means of hydrogen bonds. This is supported by considerations of the sum of electrostatic bond strengths for each oxygen atom. Two hydrogen bonds are formed by each of O_2, O_3, O_4, and O_5, which are bonded to only one aluminium atom. The bridging oxygens, O_1, are each involved in one short O—O distance, but the length of this bond, 2.84 Å, indicates that it is rather weak. The oxygen atom, O_{10}, which is not bonded to any aluminium or sulfur atoms and therefore probably is a H_2O molecule, forms four hydrogen bonds. Two of these are directed towards oxygen atoms of the sulfate groups and two towards oxygen atoms of the Al_2O_{10} group. A formula that is consistent with these results should therefore be written: $[Al_2(OH)_2(H_2O)_8](SO_4)_2(H_2O)_2$.

The arrangement of hydrogen bonds around the $[Al_2(OH)_2(H_2O)]_8^{4+}$ group is shown in Fig. 7. For each of O_2, O_3, and O_4 the angle between the short O—O contacts is approximately tetrahedral (Table 6). The sum of the angles about each of the oxygen atoms is rather close to 360°, which shows that the Al—O bond lies, very approximately, in the plane through the pair of hydrogen bonds associated with O_2, O_3, and O_4. The same is true for O_5, but the deviations are larger. In the case of O_1, the single hydrogen bond and the two Al—O bonds are probably more accurately described as pointing towards three corners of a tetrahedron although the angles show rather large deviations from the tetrahedral value.

The average value of the S—O bond lengths in the sulfate group, 1.46 Å, does not differ significantly from those found in other structures, for example 1.44 Å in $Cu(NH_3)_4SO_4 \cdot H_2O$ [15] or 1.49 and 1.48 Å in $CaSO_4 \cdot 2H_2O$ [16].

Of the oxygen atoms of the sulfate groups one (O_7) is involved in three hydrogen bonds and the remaining three (O_6, O_8, O_9) are each involved in two hydrogen bonds.

In the selenate the average value of the Se—O bond lengths is 1.62 Å and of the O—O distances 2.65 Å. For H_2SeO_4 corresponding distances have been reported to be 1.61 Å and 2.64 Å, respectively [17].

Acknowledgements. I am much indebted to Professor Lars Gunnar Sillén for his continuous interest in this work. I also wish to thank Dr. Georg Lundgren and Dr. Howard T. Evans Jr. for discussions in connection with the work. The English text has been corrected by Dr. Denis McWhan. Free time at the "Besk" computer has been made available by the Swedish Board for Computing Machinery. The work has been supported by the *Office of Scientific Research, of the Office of Aerospace Research, United States Air Force,* through its European Office on contract number AF 61 (052)-162.

REFERENCES

1. Johansson, G., Lundgren, G., Sillén, L. G. and Söderquist, R. *Acta Chem. Scand.* **14** (1960) 769.
2. Johansson, G. *Acta Chem. Scand.* **14** (1960) 771.
3. Kohlschütter, H. W. and Hantelmann, P. *Z. anorg. allgem. Chem.* **248** (1941) 319.
4. Brosset, C., Biedermann, G. and Sillén, L. G. *Acta Chem. Scand.* **8** (1954) 1917.
5. Bassett, H. and Goodwin, T. H. *J. Chem. Soc.* **1949** 2239.
6. Bassett, H. *Quart. Revs. London* **1** (1947) 246.
7. Bassett, H. *J. Chem. Soc.* **1950** 1191.
8. Kolthoff, I. M. and Sandell, E. B. *Textbook of Quantitative Inorganic Analysis,* 3rd ed. Macmillan, New York 1952, p. 717.
9. Vand, V., Eiland, P. F. and Pepinsky, R. *Acta Cryst.* **10** (1957) 303.
10. Cruickshank, D. W. J. *Acta Cryst.* **2** (1949) 65.
11. Pauling, L. *The Nature of the Chemical Bond.* New York 1960, p. 539.
12. Busing, W. R. and Levy, H. A. *Acta Cryst.* **11** (1958) 798.
13. Kamb, W. B. *Acta Cryst.* **13** (1960) 15.
14. Newnham, R. E. *Acta Cryst.* **13** (1960) 1004.
15. *Tables of Interatomic Distances and Configuration in Molecules and Ions.* The Chemical Society, Special Publication No. 11, London 1958, p. M74.
16. Atoji, M. and Rundle, R. E. *J. Chem. Phys.* **29** (1958) 1306.
17. Bailey, M. and Wells, A. F. *J. Chem. Soc.* **1951** 968.
18. Edstrand, M. *Unpublished work.*
19. Åsbrink, S., Blomqvist, G. and Westman, S. *Arkiv Kemi* **14** (1959) 545.

Received July 21, 1961.

ACTA CHEMICA SCANDINAVICA 16 (1962) 421–430

The Crystal Structure of Aluminum Niobium Oxide ($AlNbO_4$)

BERIT F. PEDERSEN

Central Institute for Industrial Research, Blindern - Oslo, Norway

The crystal structure of aluminum niobium oxide has been determined by two-dimensional X-ray methods. The oxide crystallizes in the monoclinic system, space group $C2/m$, with a cell content of 4 $AlNbO_4$, and the unit cell dimensions, a = 12.13 Å, b = 3.726 Å, c = 6.46 Å, β = 107.2°

The structure may be described as built up of distorted oxygen-octahedra sharing edges and corners, and linked together to give an infinite three-dimensional network. Both the aluminum and niobium atoms are located in octahedral positions.

In the course of an X-ray study of the system Nb-O performed at this institute an unknown oxide was observed. It was found by heating niobium pentoxide in a corundum crucible to about 1 400°C.

From oscillation and Weissenberg diagrams the dimensions of the unit cell were found to differ markedly from all known modifications of niobium pentoxide. A spectroscopic analysis was therefore made on the sample. The result showed a content of approximately 45 mole % Al_2O_3 in the sample. Consequently the niobium pentoxide must have reacted with the crucible.

The mixed oxide grew as thin colorless platelets on top of the melt, mainly along the edge of the crucible. It is reasonable to believe this to be a 1:1 compound; the deviation from 50 mole % may be accounted for by the bulk of the oxide not having reacted with the crucible, and consequently the difficulty to pick out a pure sample to perform the analysis on.

Previously $AlNbO_4$ has been synthesized in connection with an X-ray investigation on ABO_4 compounds of rutile structure [1]. $AlNbO_4$, however, did not have the rutile type structure, and is only mentioned as probably being monoclinic with b = 3.72 Å. In a recent X-ray investigation [2] of the system niobium pentoxide-aluminum oxide this mixed oxide was found to be the only new phase in the system.

EXPERIMENTAL

A platelet of approximate dimensions (0.02 × 0.2 × 1) mm³ was used in this investigation, which was carried out at room temperature. It turned out that the longest edge of the plate was parallel to the direction of the b-axis, whereas the c-direction was perpendicular to the plate.

Oscillation and zero-, first- and second-layer Weissenberg diagrams were taken rotating about the longest edge of the crystal and using Cu$K\alpha$ radiation. The intensity data consisted of integrated Weissenberg (Wiebenga) diagrams about the same edge using Zr-filtered Mo-radiation (λ_{Mo} = 0.7107 Å). The intensities were recorded photometrically except the very weakest ones which were estimated visually. The number of reflections recorded was 287 (theoretically 449). The intensities were corrected for Lorentz and polarization effects. No absorption corrections were applied although systematic variation in the background blackening of the films indicated an absorption effect. This, however, will be discussed later. The linear absorption coefficient for Mo$K\alpha$ radiation is 47.3 cm^{-1}.

RESULTS

From oscillation- and Weissenberg-diagrams using Cu$K\alpha$ radiation the unit cell dimensions were found to be:

$$a = 12.13 \text{ Å}, \; b = 3.726 \text{ Å}, \; c = 6.46 \text{ Å}, \; \beta = 107.2°$$

These figures are believed to be accurate to within 0.5 %.

With four formula units $AlNbO_4$ in the cell a density of 4.38 g/cm^3 is derived, whereas the calculated density based on the specific volumes of Al_2O_3 and Nb_2O_5 is 4.32 g/cm^3. Due to experimental difficulties a pycnometric density determination was not undertaken.

Systematic absences were, in *hkl;* h + *k* = 2*n* + 1. This gives three possible space groups: *C*2/*m* (No. 12), *Cm* (No. 8), *C*2 (No. 5)

The intensity distribution in the *h*2*l* Weissenberg diagram very closely resembled that of the *h*0*l* film, strongly indicating that all the atoms comprising the structure were situated in, or very close to two planes normal to the *y*-axis and *b*/2 apart, making *C*2/*m* or *Cm* the most probable space group. In both space groups the atoms would be in special positions, the space group *Cm* requiring two $AlNbO_4$ in the asymmetric unit.

Assuming the symmetry to be the higher one (*C*2/*m*), it was possible to find an atomic arrangement compatible with the appearance of the Patterson function and giving calculated *F*-values in acceptable conformity with the observed ones. *C*2/*m* has eight-fold general positions, but as there are only four niobium and four aluminum atoms in the unit cell, these will have to occupy special positions. On the basis of the corrected $(F(h0l))^2$ values a Patterson map was computed. The choice of point positions was restricted by: (1) The absence of a maximum at $u = 0$, $w = 1/2$ in the Patterson map $P(u, w)$. (2) The length of the *b*-axis being only 3.7 Å. From (1) and (2) it can be concluded that four metal or four oxygen atoms can not occupy 2-fold positions. (3) The requirement that at least the heavy atoms are situated in mirror planes. This excludes the 4-fold positions on the rotation axes. Thus the special position *m* of *C*2/*m* is the only possible one. If all the atoms are situated in mirror planes, a complete structure determination can be done based on the (010) projection, as the *y*-coordinates for the atoms will be either 0 or 1/2.

From the Patterson projection $P(u,w)$, Fig. 1, the niobium atom was located. The coordinates for the aluminum atom might also have been determined, but as the Nb-Al peaks were rather irregular it was decided to carry

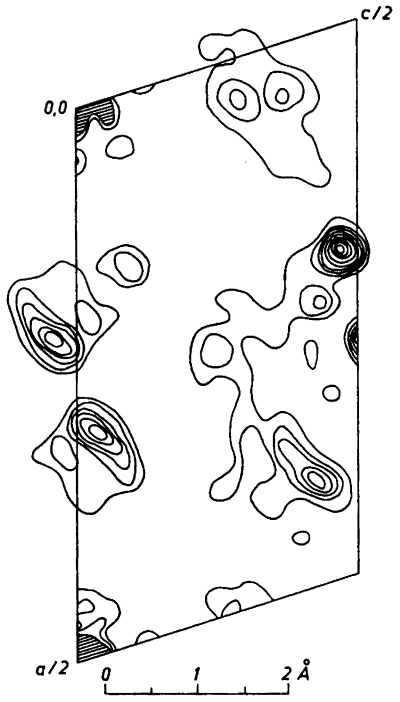

Fig. 1. Patterson projection along the *b*-axis.

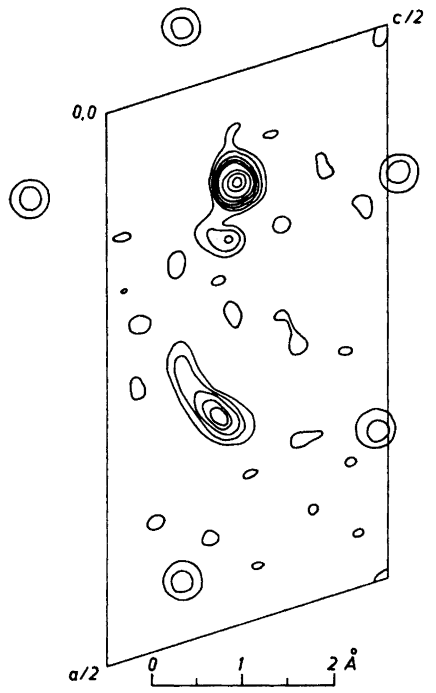

Fig. 2. Electron density projection along the *b*-axis. Contour lines at 5, 10, 15, 20, 25, 50, 75, 100 el/Å².

out a Fourier synthesis based on the strongest reflections. The structure factors were given the signs calculated from the positions of the Nb-atoms. From this Fourier map the aluminum atom could be located. In addition there were several peaks indicating possible positions for the four oxygen atoms. The oxygens were placed in the most probable sites, and a theoretical vector map was drawn including all possible interatomic distances within the unit cell. This drawing showed a close resemblance to the original Patterson projection, and this was taken as a good support for the proposed structure. Structure factors were calculated on the basis of all atoms in the unit cell, and a new Fourier summation was made including all observed reflections. The result is shown in Fig. 2.

Refinements

The structure was refined by the method of least squares and by difference syntheses. As the intensity data were thought to suffer from absorption it was tried to make least squares refinement first on the complete set of data, and secondly by excluding about half of the data suffering most from absorption.

In this calculation the analytical approximation to the scattering factors for the neutral atoms computed by Forsyth and Wells [3] was employed. The omission of the mentioned reflections did not seem to have a marked influence on the results. The parameters for the Nb and Al atoms differed by less than 0.0001 Å in the two cases. Further refinement was carried out varying the parameters for all the atoms. This brought the discrepancy factor down to 0.16. Least squares refinement gave a value of the parameter B in the temperature-correction very close to zero.

At last a total difference synthesis, based on structure factors calculated from the parameters after least squares refinements, and using $B = 0$ was computed. In this calculation the scattering factors for the ions were used. The scattering factor for the Nb ion was taken from Thomas and Umeda [4], for the Al ion from Veenendaal *et al.*[5] and for the 0 ion from James and Brindley [6]. From this Fourier difference map the parameters were corrected in the usual manner. The final coordinates for the atoms together with calculated standard deviation according to Cruickshank [7] are found in Table 1.

Wilson statistics [8] was used to determine the value of the parameter B in the temperature correction. A value of $B = 0.208$ Å^2 was found and this value was applied in calculating a new set of structure factors. At the very end the strongest reflections for low 2Θ values were corrected for secondary extinction [9]. The final Fourier map is shown in Fig. 3. The discrepancy factor including all reflections was calculated to 0.12. (For the unobserved reflections calculated greater than the minimum observable value, the difference between the calculated and half the minimum value were included.) A comparison between observed and calculated structure factors is given in Table 4. It should be pointed out that there might be some deviation from coplanarity of the lighter atoms, as this would not have much influence on the reflections $h2l$ as compared to $h0l$. In that case the correct space group would be $C2$. However, the symmetry of the (010) projection for $C2$ would be equal to the (010) projection for $C2/m$.

DISCUSSION OF THE STRUCTURE

The structure of $AlNbO_4$ is illustrated in Fig. 4. Each metal atom is coordinated to six nearest oxygens forming an octahedral grouping.

The structure may be described as built up of chains of octahedra in the c-direction. The structural unit is actually 4 octahedra sharing edges and linked

Table 1. Final positional parameters as fractions of the cell edges and their standard deviations. All the atoms occupy point positions 4 *(i)* of space group $C2/m$, (0,0,0; ½,½,0) + $x0z$, $\bar{x}0\bar{z}$.

Atom	x	z	$\sigma(x)$	$\sigma(z)$
Nb	0.1030	0.2354	0.0004	0.0008
Al	0.3071	0.1986	0.001	0.002
O_2'	0.364	0.484	0.002	0.004
O_3''	0.443	0.149	0.002	0.004
O_4	0.274	0.149	0.002	0.004
O_1	0.130	0.203	0.002	0.004

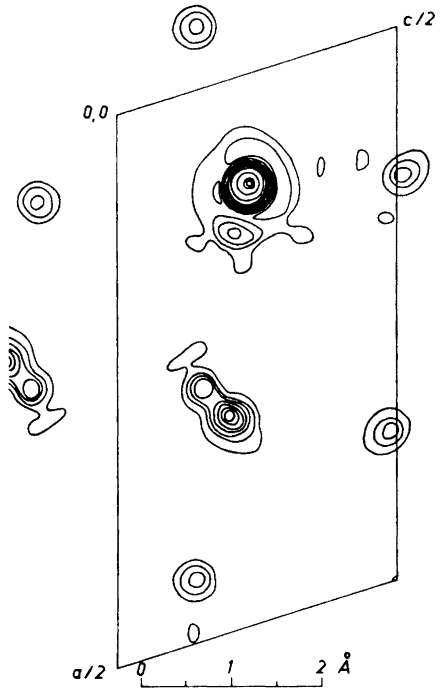

Fig. 3. Final electron density projection along the *b*-axis. Contour lines at 5, 10, ----- 35, 50, 75, 100, 125 el/Å².

to the next unit by sharing two corners. These chains are coupled together by sharing edges with adjacent octahedra displaced $b/2$ in the y-direction. This bonding gives an infinite three-dimensional network of oxygen atoms, having the metal atoms in the octahedral holes. Distances calculated on the assumption that all the atoms are situated in planes normal to the y-axis and $b/2$ apart, are given in Table 2. The atoms are numbered according to Fig. 4.

The niobium-oxygen distances vary between 1.74 Å and 2.38 Å, the distance $Nb\text{-}O_2$ to the shared corner being the shortest one. This is to be expected as the metal atoms on each side of a shared edge tend to be as far apart as

Table 2. Interatomic distances.

$Nb\text{-}O_1$	1.91 Å	$Al\text{-}O_4$	1.89 Å	*O-O distances between shared corners*		
$Nb\text{-}O_2$	1.74 »	$Al\text{-}O_2'$	1.77 »	*(1) In the niobium octahedron*		
$Nb\text{-}O_3$	1.85 »	$Al\text{-}O_3''$	1.77 »	$O_1\text{-}O_3'$	2.87 Å	
$Nb\text{-}O_4$	2.30 »	$Al\text{-}O_4'$	2.17 »	$O_1\text{-}O_3$	2.87 »	
$Nb\text{-}O_3'$	2.38 »	$Al\text{-}O_1$	2.05 »	$O_1\text{-}O_2$	2.73 »	2.91 Å
				$O_2\text{-}O_3$	2.79 »	
O-O distances (shared edge)				$O_2\text{-}O_4$	3.28 »	
$O_4\text{-}O_3'$	2.77 Å					
$O_3\text{-}O_3'$	2.67 »			*(2) In the aluminum octahedron*		
$O_1\text{-}O_4$	2.65 »			$O_3''\text{-}O_4$	2.77 Å	
$O_4\text{-}O_4'$	2.62 »			$O_2'\text{-}O_4$	2.82 »	
				$O_2'\text{-}O_3''$	2.62 »	2.79 Å
				$O_4'\text{-}O_1$	2.85 »	
				$O_1\text{-}O_2'$	2.88 »	

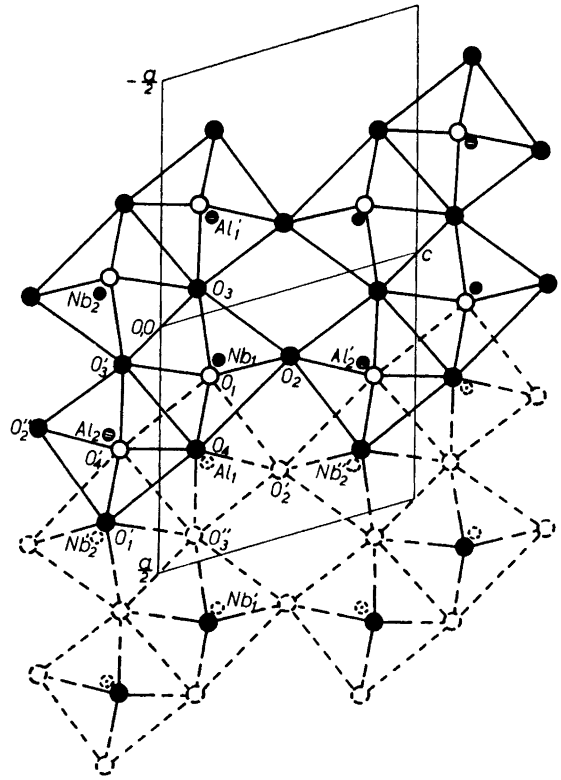

Fig. 4. The structure of $AlNbO_4$. Filled circles indicate atoms situated at $y = 0$. Open circles indicate atoms situated at $y = \pm 1/2$.

possible because of repulsion between equally charged ions. Consequently one could expect Nb-O_2 and Nb-O_3 to be shorter than the other bonds and further Nb-O_2 to be the shortest one. This is exactly what is found. The mean niobium oxygen distance is calculated to 2.07 Å.

The aluminum oxygen distances vary between 1.77 Å and 2.17 Å, the mean value being 1.94 Å. The two shortest distances in this octahedron are, naturally enough, Al-O_2 and Al-O_3.

The oxygen-oxygen distances in the two octahedra vary from 2.73 Å to 3.28 Å in the niobium octahedron and from 2.62 Å to 2.88 Å in the aluminum octahedron. The O-O distances in the two octahedra are not likely to be equal, as the central ion in the two differ in size. The O-O distances in the niobium octahedron have a mean value of 2.91 Å, whereas the O-O distances in the aluminum octahedron have a mean value of 2.79 Å. The overall mean value is 2.85 Å.

From the calculated distances the metal and oxygen radii were determined to:

$$Nb^{5+} = 0.65 \text{ Å}, \quad Al^{3+} = 0.52 \text{ Å}, \quad O^{2-} = 1.42 \text{ Å}$$

Table 3. Metal-metal distances.

	Over shared edge		
2 × Nb_1-Al_1	3.16 Å	2 × Al_1-Al_2	3.14 Å
Nb_1-Al_2	3.30 »	2 × Al_1-Nb_1	3.16 »
Nb_1-Nb_2	3.32 »	Al_1-Nb_2'	3.30 »
	Over shared corner		
Nb_1-Al_1'	3.56 Å	Al_1-Nb_2''	3.50 Å
Nb_1-Al_2'	3.50 »	Al_1-Nb_1'	3.56 »

in fair agreement with the ones reported by Wadsley [10] for (Ti, Nb) and O^{2-}, namely 0.61 Å and 1.38 Å and Paulings values of 0.70 Å, 0.50 Å and 1.40 Å for Nb^{5+}, Al^{3+}, O^{2-}, respectively [11]. Formal valencies may be assigned to the Nb and Al atoms by considering how the adjacent oxygen atoms are held in common by their metal atom neighbours. In this way, valencies of 4 1/6 can be calculated for the Nb atoms and 3 5/6 for the Al atoms.

One common feature throughout the structure is the shortening of the edge shared by two octahedra. This shortening can also be accounted for by repulsion between equally charged ions, in fact this is considered a characteristic feature of ionic structures [12]. This shortening of one edge will give rise to an elongation in the opposite one, which is found to be present in all instances as seen in Table 2. (Shared edges: O_3-O_3', O_4-O_3', O_1-O_4, O_4-O_4', opposite edges: O_2-O_4, O_2-O_3, O_2''-O_1', O_1-O_3, O_3''-O_4 O_2'-O_4.)

There are rather few data with which to compare the interatomic distances obtained in the present investigation. Frevel and Rinn [13] found distances of 1.95 Å and 2.76 Å between metal and anion and anion-anion respectively in NbO_2F. Vousden [14] found 2.00 Å and 2.82 Å in $KNbO_3$ and 1.95 Å and 2.76 Å for $NiNbO_3$. Wadsley [10] reports Me-O distances varying from 1.64 Å to 2.34 Å and O-O distances from 2.52 Å to 3.14 Å in $TiNb_2O_7$.

Each niobium atom is surrounded by six metal atoms forming a very distorted octahedral arrangement. The distances from Nb to its nearest metal neighbours are shown in Table 3. In the same table are given the distances to the seven metal atoms surrounding an aluminum atom.

As one can see there is a marked difference in the metal-metal distances for the two kinds of octahedral coupling. The mean niobium-aluminum distance over a shared edge is 3.21 Å whereas the distance over a shared corner of the oxygen octahedron is pronounced longer, the mean value being 3.53 Å.

In an ideal arrangement of octahedral ions one would expect the metal-metal distance over a shared edge to be 0.71 times the metal-metal distance over a shared corner. However, in a real structure these distances tend to equal out as the figures for $AlNbO_4$ show, where the distance is only shortened by a factor of 0.90.

Acknowledgement. The author wishes to express her gratitude to Dr. N. Norman for having suggested this work, and for many valuable discussions throughout this investigation. The valuable assistence of Miss K. Titlestad and Mrs. L. Bryn is gratefully acknowledged.

This investigation has been sponsored by *Wright Air Development Division* of the *Air Research and Development Command, United States Air Force,* through its European Office, under Contract No. AF 61(052)-460.

Table 4. Observed and calculated structure factors. (Reflections marked * are corrected for secondary extinction).

h	k	l	F_o	F_c	h	k	l	F_o	F_c	h	k	l	F_o	F_c
0	0	1	15	21	4	0	$\bar{13}$	13	− 9	6	0	8	29	−30
0	0	2	88*	−87	4	0	$\bar{12}$	18	−15	6	0	9	<10	− 5
0	0	3	75*	−67	4	0	$\bar{11}$	17	17	6	0	10	30	31
0	0	4	49*	53	4	0	$\bar{10}$	18	19	6	0	11	<10	8
0	0	5	36	35	4	0	$\bar{9}$	20	−17	6	0	12	20	−19
0	0	6	20	−21	4	0	$\bar{8}$	36	−40	6	0	13	14	−17
0	0	7	31	−29	4	0	$\bar{7}$	26	19	6	0	14	13	12
0	0	8	23	20	4	0	$\bar{6}$	50*	53	6	0	15	11	11
0	0	9	25	20	4	0	$\bar{5}$	< 6	8	6	0	$\bar{16}$	< 6	0
0	0	10	20	−12	4	0	$\bar{4}$	84*	−82	8	0	$\bar{17}$	< 8	7
0	0	11	26	−22	4	0	$\bar{3}$	26	−20	8	0	$\bar{16}$	16	17
0	0	12	<10	6	4	0	$\bar{2}$	56*	59	8	0	$\bar{15}$	< 9	− 6
0	0	13	18	17	4	0	$\bar{1}$	64*	60	8	0	$\bar{14}$	17	−18
0	0	14	<10	0	4	0	0	68*	−67	8	0	$\bar{13}$	<10	− 1
0	0	15	13	−11	4	0	1	33*	−35	8	0	$\bar{12}$	28	25
0	0	16	< 9	0	4	0	2	32*	33	8	0	$\bar{11}$	<10	0
0	0	17	< 7	6	4	0	3	51*	51	8	0	$\bar{10}$	30	−27
2	0	$\bar{17}$	< 7	3	4	0	4	23	−28	8	0	$\bar{9}$	20	−12
2	0	$\bar{16}$	12	−13	4	0	5	32	−37	8	0	$\bar{8}$	34	39
2	0	$\bar{15}$	12	−12	4	0	6	< 7	7	8	0	$\bar{7}$	25	18
2	0	$\bar{14}$	14	17	4	0	7	30	33	8	0	$\bar{6}$	27	−34
2	0	$\bar{13}$	10	12	4	0	8	< 7	− 3	8	0	$\bar{5}$	38	−42
2	0	$\bar{12}$	14	−11	4	0	9	26	−22	8	0	$\bar{4}$	28	36
2	0	$\bar{11}$	18	−20	4	0	10	< 8	− 2	8	0	$\bar{3}$	36*	40
2	0	$\bar{10}$	21	15	4	0	11	18	17	8	0	$\bar{2}$	< 5	−10
2	0	$\bar{9}$	22	23	4	0	12	<10	0	8	0	$\bar{1}$	40*	−48
2	0	$\bar{8}$	11	−11	4	0	13	20	−14	8	0	0	20	18
2	0	$\bar{7}$	27*	−36	4	0	14	<10	0	8	0	1	23	28
2	0	$\bar{6}$	13	9	4	0	15	12	13	8	0	2	< 6	− 8
2	0	$\bar{5}$	33*	42	4	0	$\bar{16}$	< 7	4	8	0	3	32	−34
2	0	$\bar{4}$	< 2	2	4	0	$\bar{17}$	< 9	− 9	8	0	4	10	11
2	0	$\bar{3}$	49*	−54	6	0	$\bar{16}$	<10	4	8	0	5	32	31
2	0	$\bar{2}$	6	− 5	6	0	$\bar{15}$	14	15	8	0	6	< 8	− 1
2	0	$\bar{1}$	57*	55	6	0	$\bar{14}$	<10	− 9	8	0	7	30	−30
2	0	0	< 2	− 2	6	0	$\bar{13}$	18	−17	8	0	8	< 9	− 4
2	0	1	63*	−58	6	0	$\bar{12}$	<10	2	8	0	9	21	23
2	0	2	< 4	− 9	6	0	$\bar{11}$	25	26	8	0	10	<10	9
2	0	3	61*	67	6	0	$\bar{10}$	< 9	3	8	0	11	22	−18
2	0	4	18	19	6	0	$\bar{9}$	21	−22	8	0	12	<10	−10
2	0	5	43*	−46	6	0	$\bar{8}$	10	− 9	8	0	13	14	14
2	0	6	38	−38	6	0	$\bar{7}$	13	20	8	0	14	<10	10
2	0	7	30	32	6	0	$\bar{6}$	< 7	0	8	0	$\bar{15}$	< 9	− 9
2	0	8	31	32	6	0	$\bar{5}$	18	−26	10	0	$\bar{17}$	16	14
2	0	9	15	−11	6	0	$\bar{4}$	26	11	10	0	$\bar{16}$	< 8	5
2	0	10	25	−30	6	0	$\bar{3}$	52*	56	10	0	$\bar{15}$	21	−17
2	0	11	<10	6	6	0	$\bar{2}$	12	4	10	0	$\bar{14}$	10	− 6
2	0	12	23	20	6	0	$\bar{1}$	95*	−88	10	0	$\bar{13}$	15	12
2	0	13	<10	2	6	0	0	37*	−39	10	0	$\bar{12}$	<10	8
2	0	14	14	−19	6	0	1	61*	59	10	0	$\bar{11}$	15	−15
2	0	15	< 9	0	6	0	2	67*	66	10	0	$\bar{10}$	< 9	− 4
2	0	16	11	12	6	0	3	30	−33	10	0	$\bar{9}$	20	20
4	0	$\bar{17}$	10	−10	6	0	4	39	−48	10	0	$\bar{8}$	< 8	8
4	0	$\bar{16}$	12	− 9	6	0	5	< 8	8	10	0	$\bar{7}$	35	−32
4	0	$\bar{15}$	12	10	6	0	6	35	42	10	0	$\bar{6}$	22	−20
4	0	$\bar{14}$	13	10	6	0	7	< 9	− 6	10	0	$\bar{5}$	39	38

h k l	F_o	F_c	h k l	F_o	F_c	h k l	F_o	F_c
10 0 $\bar{4}$	34	35	14 0 $\bar{11}$	20	14	18 0 $\bar{14}$	15	−15
10 0 $\bar{3}$	30	−29	14 0 $\bar{10}$	23	18	18 0 $\bar{13}$	17	11
10 0 $\bar{2}$	42	−50	14 0 $\bar{9}$	21	−17	18 0 $\bar{12}$	26	25
10 0 $\bar{1}$	25	24	14 0 $\bar{8}$	34	−26	18 0 $\bar{11}$	<10	− 4
10 0 0	37	46	14 0 $\bar{7}$	17	14	18 0 $\bar{10}$	35	−33
10 0 1	< 7	− 7	14 0 $\bar{6}$	40	39	18 0 $\bar{9}$	< 9	− 7
10 0 2	43	−53	14 0 $\bar{5}$	< 8	− 7	18 0 $\bar{8}$	34	29
10 0 3	< 7	2	14 0 $\bar{4}$	41	−42	18 0 $\bar{7}$	24	19
10 0 4	39	41	14 0 $\bar{3}$	13	−10	18 0 $\bar{6}$	29	−24
10 0 5	17	16	14 0 $\bar{2}$	40	43	18 0 $\bar{5}$	24	−18
10 0 6	31	−36	14 0 $\bar{1}$	21	14	18 0 $\bar{4}$	18	16
10 0 7	10	−17	14 0 0	30	−29	18 0 $\bar{3}$	29	20
10 0 8	17	18	14 0 1	29	−22	18 0 $\bar{2}$	22	−20
10 0 9	20	22	14 0 2	26	27	18 0 $\bar{1}$	28	−18
10 0 10	18	−13	14 0 3	20	16	18 0 0	14	12
10 0 11	13	−13	14 0 4	18	−16	18 0 1	31	26
10 0 12	<10	4	14 0 5	21	−22	18 0 2	< 9	− 9
10 0 13	13	12	14 0 6	17	16	18 0 3	21	−18
10 0 14	< 8	− 6	14 0 7	18	17	18 0 4	<10	− 1
12 0 $\bar{17}$	< 7	4	14 0 8	<10	− 6	18 0 5	21	16
12 0 $\bar{16}$	18	−16	14 0 9	17	−19	18 0 6	<10	− 4
12 0 $\bar{15}$	< 9	− 2	14 0 10	< 9	6	18 0 7	10	− 9
12 0 $\bar{14}$	23	19	14 0 11	13	−12	18 0 8	< 9	3
12 0 $\bar{13}$	13	13	14 0 12	< 8	0	18 0 9	18	16
12 0 $\bar{12}$	25	−25	14 0 13	12	−13	18 0 10	< 8	− 5
12 0 11	26	−21	16 0 $\bar{17}$	14	−14	18 0 11	10	−16
12 0 10	13	15	16 0 $\bar{61}$	18	14	20 0 $\bar{16}$	< 7	− 5
12 0 $\bar{9}$	37	34	16 0 $\bar{15}$	15	17	20 0 $\bar{15}$	13	−15
12 0 $\bar{8}$	< 9	− 8	16 0 $\bar{14}$	<10	− 5	20 0 $\bar{14}$	< 9	− 3
12 0 $\bar{7}$	29	−26	16 0 $\bar{13}$	22	−23	20 0 $\bar{13}$	16	18
12 0 $\bar{6}$	< 8	− 4	16 0 $\bar{12}$	<10	4	20 0 $\bar{12}$	<10	2
12 0 $\bar{5}$	22	25	16 0 $\bar{11}$	15	17	20 0 $\bar{11}$	15	−14
12 0 $\bar{4}$	< 8	− 8	16 0 $\bar{10}$	<10	2	20 0 $\bar{10}$	<10	− 7
12 0 $\bar{3}$	13	−19	16 0 $\bar{9}$	22	−21	20 0 $\bar{9}$	23	20
12 0 $\bar{2}$	< 7	8	16 0 $\bar{8}$	< 9	3	20 0 $\bar{8}$	< 9	5
12 0 $\bar{1}$	32	35	16 0 $\bar{7}$	23	19	20 0 $\bar{7}$	21	−19
12 0 0	11	−10	16 0 $\bar{6}$	< 9	4	20 0 $\bar{6}$	17	−13
12 0 1	33	−34	16 0 $\bar{5}$	31	−28	20 0 $\bar{5}$	27	23
12 0 2	< 8	− 5	16 0 $\bar{4}$	< 8	− 3	20 0 $\bar{4}$	18	17
12 0 3	28	33	16 0 $\bar{3}$	23	23	20 0 $\bar{3}$	17	−18
12 0 4	< 8	7	16 0 $\bar{2}$	15	10	20 0 $\bar{2}$	27	−24
12 0 5	22	−24	16 0 $\bar{1}$	25	−26	20 0 $\bar{1}$	13	14
12 0 6	<10	−10	16 0 0	13	− 8	20 0 0	30	23
12 0 7	21	22	16 0 1	25	23	20 0 1	< 9	− 8
12 0 8	15	12	16 0 2	17	13	20 0 2	23	−23
12 0 9	18	−21	16 0 3	22	−25	20 0 3	<10	3
12 0 10	16	−17	16 0 4	22	−19	20 0 4	21	22
12 0 11	12	13	16 0 5	16	20	20 0 5	<10	0
12 0 12	21	22	16 0 6	21	25	20 0 6	21	−19
12 0 13	< 8	− 4	16 0 7	<10	− 9	20 0 7	<10	− 7
12 0 14	15	−18	16 0 8	18	−25	20 0 8	17	17
14 0 $\bar{17}$	12	−12	16 0 9	<10	1	20 0 9	< 9	7
14 0 $\bar{16}$	< 9	− 9	16 0 10	20	19	20 0 10	< 8	− 9
14 0 $\bar{15}$	14	14	16 0 11	< 8	5	22 0 $\bar{16}$	18	−19
14 0 $\bar{14}$	<10	10	16 0 12	14	−14	22 0 $\bar{15}$	< 8	− 2
14 0 $\bar{13}$	10	−12	18 0 $\bar{16}$	< 7	9	22 0 $\bar{14}$	20	21
14 0 $\bar{12}$	15	−14	18 0 $\bar{15}$	15	−11	22 0 $\bar{13}$	< 9	8

h k l	F_o	F_c	h k l	F_o	F_c	h k l	F_o	F_c
22 0 $\bar{12}$	14	−17	24 0 $\bar{3}$	<10	2	28 0 $\bar{12}$	11	13
22 0 $\bar{11}$	13	−14	24 0 $\bar{2}$	28	23	28 0 $\bar{11}$	< 9	− 5
22 0 $\bar{10}$	17	17	24 0 $\bar{1}$	<10	1	28 0 $\bar{10}$	13	−17
22 0 $\bar{9}$	13	14	24 0 0	27	−24	28 0 $\bar{9}$	< 9	5
22 0 $\bar{8}$	10	−13	24 0 1	<10	− 9	28 0 8	17	19
22 0 $\bar{7}$	22	−22	24 0 2	22	18	28 0 7	< 9	0
22 0 $\bar{6}$	15	13	24 0 3	18	15	28 0 6	22	−23
22 0 $\bar{5}$	25	21	24 0 4	17	−11	28 0 5	< 9	− 7
22 0 $\bar{4}$	<10	− 3	24 0 5	16	−11	28 0 4	20	21
22 0 $\bar{3}$	27	−24	24 0 6	< 9	3	28 0 3	14	15
22 0 $\bar{2}$	< 9	1	24 0 7	< 8	8	28 0 2	14	−13
22 0 $\bar{1}$	18	15	24 0 8	< 7	− 6	28 0 1	14	−17
22 0 0	<10	4	26 0 $\bar{14}$	10	−12	28 0 0	< 9	6
22 0 1	21	−15	26 0 $\bar{13}$	10	−13	28 0 1	< 9	11
22 0 2	<10	3	26 0 $\bar{12}$	< 9	7	28 0 2	< 9	− 2
22 0 3	<10	10	26 0 $\bar{11}$	13	17	28 0 3	< 8	−10
22 0 4	<10	0	26 0 $\bar{10}$	<10	− 7	28 0 4	< 8	5
22 0 5	18	−19	26 0 $\bar{9}$	14	−14	28 0 5	< 7	7
22 0 6	< 9	0	26 0 $\bar{8}$	<10	2	30 0 $\bar{12}$	< 7	− 4
22 0 7	17	15	26 0 $\bar{7}$	15	19	30 0 $\bar{11}$	15	−16
22 0 8	15	9	26 0 $\bar{6}$	<10	− 3	30 0 $\bar{10}$	< 8	2
22 0 9	14	−14	26 0 $\bar{5}$	15	−16	30 0 $\bar{9}$	12	15
24 0 $\bar{15}$	< 8	8	26 0 $\bar{4}$	<10	− 5	30 0 $\bar{8}$	< 9	7
24 0 $\bar{14}$	< 8	2	26 0 $\bar{3}$	20	19	30 0 $\bar{7}$	13	−16
24 0 $\bar{13}$	14	−18	26 0 $\bar{2}$	<10	3	30 0 $\bar{6}$	< 9	− 5
24 0 $\bar{12}$	< 9	− 4	26 0 $\bar{1}$	17	−13	30 0 $\bar{5}$	< 9	10
24 0 $\bar{11}$	16	18	26 0 0	13	− 9	30 0 $\bar{4}$	< 9	9
24 0 $\bar{10}$	15	17	26 0 1	18	15	30 0 $\bar{3}$	12	−14
24 0 $\bar{9}$	18	−17	26 0 2	< 9	5	30 0 $\bar{2}$	< 9	− 6
24 0 $\bar{8}$	18	−20	26 0 3	15	−11	30 0 $\bar{1}$	10	12
24 0 $\bar{7}$	<10	7	26 0 4	14	−10	30 0 0	15	15
24 0 $\bar{6}$	22	23	26 0 5	15	12	30 0 1	10	−11
24 0 $\bar{5}$	<10	− 5	26 0 6	12	10	30 0 2	11	−17
24 0 $\bar{4}$	25	−20	28 0 $\bar{13}$	< 9	10	30 0 3	< 6	0

REFERENCES

1. Brandt, K. *Arkiv Kemi, Mineral. Geol.* **17 A** (1943) No. 15.
2. Goldschmidt, H. J. *Metallurgia* **62**, No. 374 (1960) 241.
3. Forsyth, T. B. and Wells, M. *Acta Cryst.* **12** (1959) 412.
4. Thomas, L. H. and Umeda, K. *J. Chem. Phys.* **26** (1957) 293.
5. Veenendaal, A. L., MacGillavry, D. H., Stam, B., Potters, M. L. and Römgens, M. J. H. *Acta Cryst.* **12** (1959) 242.
6. James, R. W. and Brindley, G. W. *Z. Krist.* **78** (1931) 470.
7. Cruickshank, D. W. T. *Acta Cryst.* **2** (1949) 65.
8. Wilson, A. J. C. *Nature* **150** (1942) 152.
9. Pinnock, P. R., Taylor, C. A. and Lipson, H. *Acta Cryst.* **9** (1956) 175.
10. Wadsley, A. D. *Acta Cryst.* **14** (1961) 660.
11. Pauling, L. *The Nature of the Chemical Bond*, Cornell University Press, Ithaca, N.Y. 1945, p. 346.
12. Wells, A. F. *Structural Inorganic Chemistry*, The University Press, Oxford 1952, p. 93.
13. Frevel, L. K. and Rinn, H. W. *Acta Cryst.* **9** (1956) 626.
14. Vousden, P. *Acta Cryst.* **4** (1951) 373.

Received September 6, 1961.

ACTA CHEMICA SCANDINAVICA 16 (1962) 431–438

The Kinetics of the Water Gas Conversion

II. Investigations at Elevated Pressures

HANS BOHLBRO

The Haldor Topsøe Research Laboratory, Hellerup, Denmark

The validity of the rate equation previously found for the water gas conversion $CO + H_2O \rightarrow CO_2 + H_2$ over a commercial iron oxide-chromium oxide catalyst at atmospheric pressure has been investigated at elevated pressures and 380°C. It was found that the rate equation is satisfactorily obeyed up to at least 20 atm.

Data on the pressure dependence of the rate of the water gas conversion $CO + H_2O \rightarrow CO_2 + H_2$ are rather scarce in the literature. Atwood, Arnold and Appel [1] made their investigation under the assumption that a simple first order expression was valid. Atroshchenko and Bibr [2] also applied a kinetic expression quite different from ours.

In a previous article [3] it was shown that the net rate of the water gas conversion over a commercial iron oxide-chromium oxide catalyst at atmospheric pressure in the temperature range 330–500°C could be adequately described by means of an expression of the exponential type

$$r = r_f - r_b = k\,(CO)^l(H_2O)^m(CO_2)^n(H_2)^q(1-\beta) \qquad (1)$$

where $\beta \equiv (CO_2)(H_2)/K(CO)(H_2O)$.

The exponents vary to some extent with temperature but were found to be situated between the following limits

$$0.80 \leqq l \leqq 1.00,\ 0.20 \leqq m \leqq 0.35,\ -0.65 \leqq n \leqq -0.50 \text{ and } q = 0.$$

The present work was undertaken in order to investigate to which extent eqn. (1) is valid also at elevated pressures (up to 20 atm). The investigation has been performed at 380°C.

EXPERIMENTAL

Gases. All gases employed, CO,N_2 and CO_2 were taken from cylinders.

CO was about 98.5 % pure, the rest being mainly N_2 (about 1 %), H_2 (about 0.5 %), and O_2 (about 0.2 %). CO_2 was less than 0.1 %. Further, traces of iron carbonyl could be found whereas sulphur compounds and hydrocarbons could not be detected. CO was purified by passing over Cu-wire at 300°C (which removes oxygen and iron carbonyl),

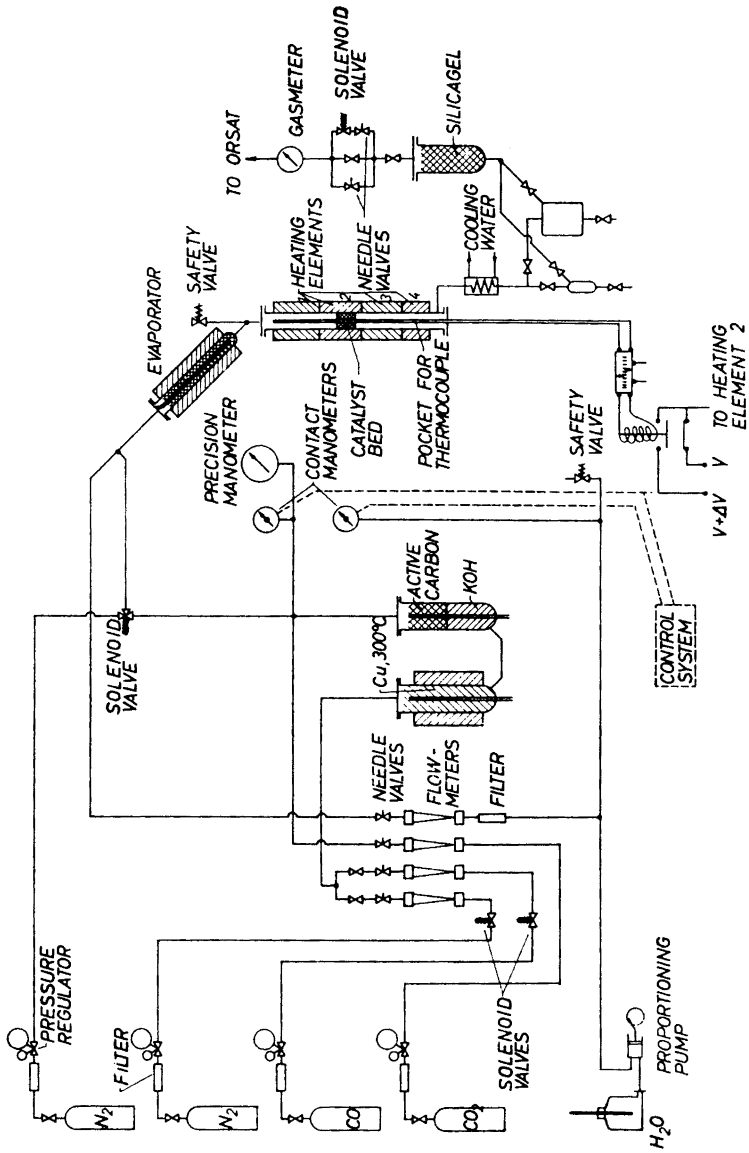

Fig. 1. Schematic drawing of experimental set-up.

alumina, potassium hydroxide pellets and active carbon. N_2 was purified in the same way whereas CO_2 was used without further purification.

Catalyst. The catalyst used was a commercial iron oxide-chromium oxide catalyst similar to the one used previously. Particle size was less than 0.5 mm. The amount of catalyst was 3.00 g (unreduced) diluted by 9.5 cm^3 inert material (quartz) of approx. 1 mm particle size. The total volume of catalyst and diluting material was approx. 12 cm^3. Before starting the measurements the catalyst was reduced and thereafter "aged" by running for about 2 weeks at 380°C and atmospheric pressure. Several dffierent samples of somewhat varying activity have been applied for the investigation.

Experimental set-up. A diagram of the experimental set-up is shown in Fig. 1. The gases were supplied through flowmeters and, in the case of N_2 and CO, through a purification train, to the evaporator where liquid water was introduced by means of a proportioning pump. Mixture of water vapor and gases passed through the reactor containing a preheating zone and then the catalyst layer. The reactor consisted of a stainless steel tube which was heated by four sections of heating elements. A thermocouple tube passed through the catalyst layer so that the temperature could be measured at any level. The temperature of the catalyst layer was regulated by means of the thermocouple and a controller which regulated the voltage of heating element No. 2. After the reactor excess water was condensed and collected in containers (the larger one being used during the night) and the exit gas was dried by silica gel before relieving the pressure. The effluent gas passed through a gasmeter. Constant pressure was maintained automatically by means of a contact manometer for maximum pressure and a solenoid valve in series with an only slightly open needle valve at the exit side. The main stream of the exit gas passed through another needle valve. For the unattended operation during the night the set-up was provided with an automatic control system comprising a number of electronic relays, solenoid valves and a contact manometer for minimum pressure. If, *e.g.*, the water pump would stop the CO stream would be shut off, the apparatus would be flushed with N_2, and the electric current for the heating elements would be interrupted.

Analytical procedure. CO_2 was determined in an Orsat apparatus by absorption in KOH, thereafter CO was determined by oxidation with air over a CuO catalyst and subsequent absorption in KOH. H_2 was determined by gas chromatography. It was ascertained by gaschromatographic analysis that the exit gas did not contain essential amounts of CH_4 or other hydrocarbons at any of the pressures applied. When no CO_2 was included in the feed gas the degree of conversion was calculated on the basis of the CO and CO_2 found in the exit gas. If CO_2 was present in feed gas the H_2 content has been applied instead of the CO_2 content for the calculation of the degree of conversion.

LIST OF SYMBOLS

F = total feed rate (mole/h).
f = feed rate of CO (mole/h).
k = pressure independent part of rate constant for forward reaction (defined by eqn. (1) or (2)).
k_p = reaction rate constant for forward reaction at pressure p (defined by eqn. (3)).
K = equilibrium constant for the water gas conversion.
l, m, n and q = exponents occurring in the reaction rate eqn. (1).
(CO), (H_2O), (CO_2) and (H_2) = partial pressures (atm.) of CO, H_2O, CO_2 and H_2, respectively.
p = total pressure (atm.)
r = net reaction rate (mole CO converted/(h)(g catalyst)).
r_f and r_b = forward and backward reaction rates, respectively.
W = weight of catalyst (g).
x = degree of conversion of CO (mole CO converted/mole CO in feed gas).
y_{CO}, y_{CO_2}, y_{H_2O}, and y_{H_2} = mole fractions of CO, CO_2, H_2O and H_2, respectively. Superscript zero indicates initial mole fraction.
β = $(CO_2)(H_2)/K(CO)(H_2)$.
γ = $y_{CO_2}\, y_{H_2}/K\, y_{CO}\, y_{H_2O}$

THEORETICAL CONSIDERATIONS

Assuming eqn. (1) to be valid also at elevated pressure (with the same exponents) it is possible to substitute

$(CO) = py_{CO}$, $(H_2O) = py_{H_2O}$, $(CO_2) = py_{CO_2}$, and $(H_2) = py_{H_2}$

Eqn. (1) is then replaced by

$$r = k \cdot p^{(l+m+n+q)} y_{CO}^{l} \cdot y_{H_2O}^{m} \cdot y_{CO_2}^{n} \cdot y_{H_2}^{q} (1-\gamma) \qquad (2)$$

where $\gamma \equiv y_{CO_2} y_{H_2} / K y_{CO} y_{H_2O}$

Table 1. Variation of pressure. Approximate feed gas composition: CO : 16 %, CO_2 : 0 %, H_2 : 0 %, N_2 : 63 %, H_2O : 21 %.

No.	Total feed mole/h	Feed gas composition					Conv. exp. %	k_p	Pressure p atm. abs.
		% CO	% CO_2	% H_2	% N_2	% H_2O			
1	3.671	15.80	0	0.06	64.64	19.50	21.8	0.0401	1.00
2	3.604	15.60	0	0.06	65.94	18.40	29.8	0.0708	1.98
3	3.804	15.30	0	0.06	63.14	21.50	39.8	0.124	4.88
4	3.783	16.40	0	0.06	61.54	22.00	51.4	0.225	9.69
5	3.700	17.20	0	0.06	61.24	21.50	59.5	0.330	19.39
6	3.750	16.60	0	0.06	61.94	21.40	50.8	0.221	9.71
7	3.746	16.60	0	0.06	62.34	21.00	42.3	0.148	4.87
8	3.838	15.40	0	0.06	64.84	19.70	29.1	0.0702	1.96

Table 2. Variation of pressure. Approximate feed gas composition: CO : 16 %, CO_2 : 0 %, H_2 :0 %, N_2 : 51 %, H_2O : 33 %.

No.	Total feed mole/h	Feed gas composition					Conv. exp. %	k_p	Pressure p atm. abs.
		% CO	% CO_2	% H_2	% N_2	% H_2O			
1	3.813	15.30	0	0.06	50.74	33.90	21.7	0.0348	1.00
2	3.808	16.40	0	0.06	50.84	32.70	27.5	0.0562	1.99
3	3.729	15.40	0	0.06	51.14	33.40	39.6	0.106	4.87
4	3.721	15.30	0	0.06	51.84	32.80	51.4	0.184	9.67
5	3.779	15.00	0	0.06	51.54	33.40	56.4	0.228	19.39
6	3.804	17.00	0	0.06	48.44	34.50	50.4	0.190	9.66
7	3.725	15.70	0	0.06	51.54	32.70	39.0	0.105	4.87
8	3.754	15.10	0	0.06	52.74	32.10	26.7	0.050	1.98
9	3.708	15.80	0	0.06	51.44	32.70	21.0	0.0329	1.00

Table 3. Variation of pressure. Approximate feed gas composition: CO : 16 %, CO_2 : 0 %, H_2 : 0 %, N_2 : 19 %, H_2O : 65 %.

No.	Total feed mole/h	Feed gas composition					Conv. exp. %	k_p	Pressure p atm. abs.
		% CO	% CO_2	% H_2	% N_2	% H_2O			
1	3.821	15.30	0	0.06	18.64	66.00	31.5	0.0576	1.00
2	3.654	14.70	0	0.06	17.44	67.80	39.0	0.0805	1.96
3	3.721	15.70	0	0.06	18.74	65.50	49.1	0.139	4.89
4	3.675	16.00	0	0.06	19.64	64.30	56.9	0.194	9.72

Table 4. Variation of pressure. Approximate feed gas composition: CO : 40 %, CO_2 : 0 %, H_2 : 0 %, N_2 : 1 %, H_2O : 59 %.

No.	Total feed mole/h	Feed gas composition					Conv. exp. %	k_p	Pressure p atm. abs.
		% CO	% CO_2	% H_2	% N_2	% H_2O			
1	3.750	40.10	0	0.16	0.84	58.90	23.0	0.0595	1.00
2	3.696	39.90	0	0.16	0.84	59.10	31.1	0.102	1.99
3	3.763	38.00	0	0.16	1.64	60.20	41.7	0.179	4.95
4	3.754	39.70	0	0.16	1.24	58.90	48.9	0.257	9.81

Table 5. Variation of pressure. Approximate feed gas composition: CO : 15 %, CO_2 : 33 %, H_2 : 0 %, N_2 : 18 %, H_2O : 34 %.

No.	Total feed mole/h	Feed gas composition					Conv. exp. %	k_p	Pressure p atm. abs.
		% CO	% CO_2	% H_2	% N_2	% H_2O			
1	3.713	14.90	33.20	0.13	17.77	34.00	8.0	0.0722	1.00
2	3.658	14.90	33.30	0.13	17.97	33.70	11.2	0.101	2.04
3	3.775	15.50	33.00	0.13	17.37	34.00	17.6	0.171	4.95
4	3.767	15.40	32.60	0.13	16.77	35.10	24.3	0.246	9.75
5	3.879	14.20	33.40	0.12	19.08	33.20	32.7	0.379	19.66

Table 6. Variation of CO content in feed gas. Constant pressure of about 10 atm.

No.	Total feed mole/h	Feed gas composition					Conv. exp. %	k_p	Pressure p atm. abs.
		% CO	% CO_2	% H_2	% N_2	% H_2O			
1	3.896	5.80	12.10	0.03	37.17	44.90	30.3	0.171	9.76
2	3.733	11.90	13.30	0.07	30.93	43.80	27.6	0.160	9.88
3	3.750	17.00	12.40	0.09	26.51	44.00	27.9	0.163	9.92
4	3.604	23.20	12.80	0.13	21.37	42.50	27.7	0.166	9.92
5	3.663	29.80	13.50	0.17	12.23	44.30	29.0	0.181	9.94

Table 7. Variation of CO_2 content in feed gas. Constant pressure of about 10 atm.

No.	Total feed mole/h	Feed gas composition					Conv. exp. %	k_p	Pressure p atm. abs.
		% CO	% CO_2	% H_2	% N_2	% H_2O			
1	3.667	15.60	0	0.08	51.02	33.30	58.0	0.249	9.90
2	3.879	14.90	16.30	0.08	34.92	33.80	32.1	0.251	9.84
3	3.708	15.50	32.90	0.08	18.42	33.10	21.3	0.212	9.77
4	3.775	16.30	0	0.08	52.62	31.00	54.2	0.226	9.77

i.e., if eqn. (1) is valid also at elevated pressure (with pressure independent exponents) a plot of ln p against the logarithm of an experimental rate constant k_p evaluated from the equation

$$r = f\cdot(\mathrm{d}x/\mathrm{d}w) = k_p \cdot y_{CO}^{l} \cdot y_{H_2O}^{m}\cdot y_{CO_2}^{n}\cdot y_{H_2}^{q}(1-\gamma) \qquad (3)$$

should yield a straight line with the slope $= l + m + n + q$.

The next question which arises is: if a linear relationship between ln k_p thus determined and ln p is obtained, does that mean that l, m, n and q are independent of pressure. It is conceivable if only a single series of runs with varying pressure and constant feed gas is made that l, m, n, and q may vary in such a manner that a straight line with slope equal to that calculated from the atm. pressure equation is obtained. If, however, a linear relationship between ln k_p and ln p is obtained with several feed gases and particularly with a feed gas containing an essential amount of CO_2 as well as with a feed gas without CO_2 it can be concluded that l, m, n and q are at least approximately independent of pressure within the interval investigated.

EVALUATION OF EXPERIMENTAL RESULTS

The procedure for obtaining the experimental data for the evaluation of the relation between ln k_p and ln p has been the following. A series of runs has been made by maintaining a fixed space velocity, feed gas composition and temperature (380°C) and then varying the pressure from 1 to 10 or 20 atm. This procedure has been repeated with other feed gas compositions. In order to determine the exponents l and n independently two series of runs have also been made at the constant pressure of 10 atm. at varying concentrations of CO and CO_2, respectively, in the feed gas (*cf.* Ref.[3]).

From the experimentally found conversions the rate constant k_p has in each case been evaluated by integration of eqn. (3) by means of the electronic digital computer DASK after insertion of the appropriate values of l, m, n and q. In the previous work [3] it was found that the values of the exponents l, m, n and q at 380°C and atmospheric pressure were $l = 1.00$, $m = 0.20$, $n = -0.65$ and $q = 0$; *i.e.* $l + m + n + q = 0.55$. From the preliminary calculations it appeared, however, that a better average value of the slope than 0.55 would be 0.65. This difference is definitely within the experimental uncertainty as each of the exponents is subject to an uncertainty of at least 0.05. In order to obtain the slope 0.65 it seemed the most logical to change the value of m to 0.25 and the value of n to -0.60. The new value of m is actually in better accordance with the values obtained at the neighbouring temperatures 330° and 420° at atmospheric pressure than the previous one (*cf.* Ref.[3]).

By inserting in eqn. (3) these values of the exponents,

$f = y_{CO}^{\circ}\cdot F$, $y_{CO} = y_{CO}^{\circ}(1-x)$, $y_{H_2O} = y_{H_2O}^{\circ} - x\cdot y_{CO}^{\circ}$, and $y_{CO_2} = y_{CO_2}^{\circ} + x\cdot y_{CO}^{\circ}$

we obtain the following eqn. from which the values of k_p have been determined.

$$F\cdot(\mathrm{d}x/\mathrm{d}w) = k_p\cdot(1-x)(y_{H_2O}^{\circ} - x\cdot y_{CO}^{\circ})^{0.25}(y_{CO_2}^{\circ} + x y_{CO}^{\circ})^{-0.60}(1-\gamma) \qquad (4)$$

The technique applied for obtaining k_p has been a little different from that described previously[3]. By application of an arbitrary (approximate) rate

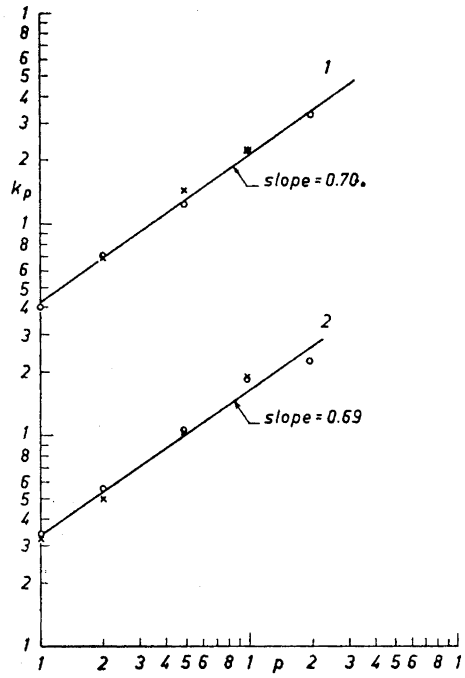

Fig. 2. Plot of ln k_p *vs.* ln p. Data from Tables 1 and 2. o—o: increasing pressure, x—x: decreasing pressure. Numbering of the lines corresponding to that of the tables. Ordinate of line 1 displaced one decade relatively to that of line 2.

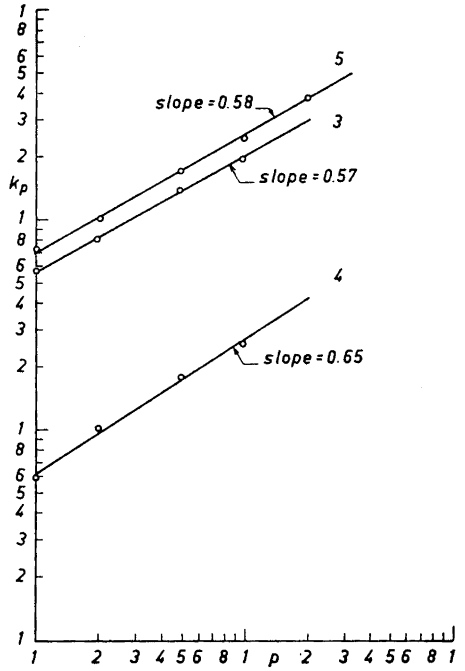

Fig. 3. Plot of ln k_p *vs.* ln p. Data from Tables 3, 4 and 5. Numbering of the lines corresponding to that of the tables. Ordinate of line 4 displaced one decade relatively to that of lines 3 and 5.

constant k_p^* the integration is performed through a catalyst layer of such length that the calculated exit gas composition is equal to the experimentally found exit gas composition. From the amount of catalyst, W^*, thus obtained k_p is calculated from the relation $k_p \cdot W = k_p^* \cdot W^*$ in which W is the actual amount of catalyst.

Table 8. Slopes obtained from the plots of ln k_p *vs.* ln$p$. (Figs. 2 and 3).

Approximate feed gas composition	Pressure range applied	Slope	Line No.
16 % CO, 0 % CO_2, 0 % H_2, 63 % N_2, 21 % H_2O	1—20 atm.	0.70	1
16 % CO, 0 % CO_2, 0 % H_2, 51 % N_2, 33 % H_2O	1—20 atm.	0.69	2
16 % CO, 0 % CO_2, 0 % H_2, 19 % N_2, 65 % H_2O	1—10 atm.	0.57	3
40 % CO, 0 % CO_2, 0 % H_2, 1 % N_2, 59 % H_2O	1—10 atm.	0.65	4
15 % CO, 33 % CO_2, 0 % H_2, 18 % N_2, 34 % H_2O	1—20 atm.	0.58	5

The experimental conditions and the experimentally found conversions together with the values of k_p thus obtained are given in Tables 1—7. The hydrogen appearing in the feed gas originates from that contained in the CO feed gas. The balance gas is listed in the tables as N_2. Figs. 2 and 3 show the plots of ln k_p *vs.* ln p. The slopes obtained from these plots are summarized in Table 8.

DISCUSSION

The question of diffusion restriction has been discussed in the previous article [3] and with the particle size being smaller in the present case it is concluded that the influence of diffusion restriction is again negligible. On the other hand it may be pointed out that for catalyst pellets of industrial sizes (*e.g.* 9 mm) the pressure dependence of the rate of reaction will ordinarily be essentially influenced by diffusion restriction, and the present results therefore in such cases not directly applicable without correction factors.

It appears from the figures that ln k_p to a good approximation is linearly dependent upon ln p in the pressure range 1 to 10 or 20 atm. and that the slope of the straight line is approximately that which should be expected on the basis of the rate equation obtained at atmospheric pressure. The minor variation of the slope (from 0.57 to 0.70) may be at least partly due to experimental uncertainty; there is, however, some indication that an increase of the ratio of H_2O:CO causes a decrease of the slope in a CO_2-free feed gas and that a content of CO_2 in feed gas also lowers the slope. There is no clear indication of a deviation from linearity even at the highest pressures applied (approx. 20 atm.). It should be mentioned that application of erroneous values of l, m, n and q for the calculation of the rate constant k_p has only a slight influence on the slope obtained as long as the errors in the exponents are not exceedingly large. Particularly the influence of minor errors in l and m (and in n when CO_2 is present in feed gas) is completely negligible.

Table 6 shows the results of a series of runs at 10 atm with varying CO content in feed gas. The constancy of k_p, obtained by application of eqn. (4) shows that the value of $l = 1.00$ is also valid at this pressure. Table 7 gives a few runs with varying CO_2 content in feed gas. The k_p's calculated from these do not contradict the value of $n = -0.60$.

In conclusion it may be said that the present results largely confirm the results obtained at atmospheric pressure and further that the same rate equation is valid at total pressures up to about 20 atm.

Acknowledgement. Thanks are due to Mr Haldor Topsøe for permission to publish the results and to Mr. Kjeld Rasmussen for having performed the experimental work.

REFERENCES

1. Atwood, K., Arnold, M. R. and Appel, E. G. *Ind. Eng. Chem.* **43** (1950) 1600.
2. Atroshchenko, V. J. and Bibr, B. *Zhur. Priklad. Khim.* **32** (1959) 997; *Chem. Abstr.* **53** (1959) 15735.
3. Bohlbro, H. *Acta Chem. Scand.* **15** (1961) 502.

Received September 5, 1961.

ACTA CHEMICA SCANDINAVICA 16 (1962) 439–448

Equilibrium Studies of Polyanions
8. On the First Equilibrium Steps in the Hydrolysis of Boric Acid, a Comparison between Equilibria in 0.1 M and 3.0 M $NaClO_4$

NILS INGRI

Department of Inorganic Chemistry, The Royal Institute of Technology, Stockholm 70, Sweden

The first equilibrium steps at 25°C for the hydrolysis of boric acid in 0.1 M and 3.0 M $Na(ClO)_4$ have been studied using a hydrogen electrode. In both media the data for B (the total boric acid concentration) ranging between 0.010 M and 0.200 M could be explained, as in our earlier study [1], by the formation of $B(OH)_4^-$ and $B_3O_3(OH)_4^-$. At higher B (B = 0.4 M and B = 0.6 M) the data could be explained by an additional polynuclear complex, either $B_4O_5(OH)_3^-$ or $B_5O_6(OH)_4^-$; a treatment with Letagrop ("pitmapping", a generalized least square treatment [2], see Table 2) favored $B_5O_6(OH)_4^-$, which is also supported by structural work. The following set of constants is proposed: log $*\beta_1 = -9.00 \pm 0.02$, log $*\beta_{13} = -6.91 \pm 0.03$, log $*\beta_{15} = -6.62 \pm 0.16$ (for 3.0 M $NaClO_4$); log $*\beta_1 = -8.98 \pm 0.01$, log $*\beta_{13} = -7.29 \pm 0.02$, log $*\beta_{15} = -6.77 \pm 0.10$ (for 0.1 M $NaClO_4$).

In a previous emf investigation [1] of alkaline boric acid solutions we found that the first complexes formed when OH^- is added to $B(OH)_3$ are $B(OH)_4^-$ and $B_3O_3(OH)_4^-$. With more OH^- either $B_4O_5(OH)_4^{2-}$ or $B_3O_3(OH)_5^{2-}$ or both, seem also to be formed. Later, evidence [7] in favour of $B_4O_5(OH)_4^{2-}$ was obtained. When so much OH^- has been added that z, the mean charge of the complexes in solution reaches the value -1, all species are transformed to $B(OH)_4^-$.

In the present work a number of new emf measurements in 0.1 M and 3.0 M $Na(ClO_4)$-media at high B and low z will be analysed. Our intention is to see whether our data indicate the formation of any more complexes than B, AB^-, AB_3^- and $A_2B_4^{2-}$ ($A = OH^-$, $B = B(OH)_3$), for instance some of the complexes AB_2^-, AB_4^-, AB_5^-, or AB_6^-. One or more complexes of this type have been proposed by a number of previous workers [3]. The measurements

have been carried out in two different $NaClO_4$-media, 3.0 M and 0.1 M. The aim with measurements in media of such a different total concentration is to see whether the suggestions made by Antikainen [3], that the borate equilibria should be displaced in such a manner, that the predominating polyborate in 3 M $NaClO_4$ should be AB_3 and in 0.1 M $NaClO_4$, AB_4, are also indicated by our emf technique. Antikainen [3] gives the following formation constants, log $*\beta_{13} = -6.725$ (3.0 M $NaClO_4$) and log $*\beta_{14} = -6.840$ (0.1 M $NaClO_4$). If the effect ascribed to larger complexes were really due to unexpected variations in the activity factors, then it was reasonable to except that the effect would be very different in 0.1 and 3.0 M $NaClO_4$; as will be seen, however, the same conclusions could be drawn from data in these two media.

SYMBOLS AND FORMULAS

The symbols used in this work are the same as in Part 2[1] in this series; thus for the species we write in general A_pB_q: B for $B(OH)_3$, A for OH^-, AB for $B(OH)_4^-$, AB_3 for $B_3O_3(OH)_4^-$, *etc.*: for concentrations, h for $[H^+]$, a for $[OH^-]$ and b for $[B(OH)_3]$, B for the total boric acid concentration and H for the total analytical excess concentration of hydrogen ions assuming no hydrolysis; in most experiments H was negative. The notation BZ is used for the number of OH^- bound per boric acid. It can be calculated from the measured E-values (eqn. 2) and from the analytical composition of the solution using the formula

$$BZ = h - H - K_w h^{-1} \quad (1)$$

where K_w is the ionic product of water in 3 M $NaClO_4$. In some cases BZ is divided into the contributions B_1Z_1, B_2Z_2, ... B_qZ_q for the various "nuclearities" present.

The equilibrium concentration of hydrogen ions, h, has been calculated from the relation

$$E = E_{oh} - 59.15 \log h + E_j = E_{oa} + 59.15 \log K_w - 59.15 \log h + E_j \quad (2)$$

where E is the measured potential in mV and E_{oh} and E_{oa} constants. E_j is the liquid junction potential. The E_{oh}-value has been obtained from the range where the hydrolysis of $B(OH)_3$ could be neglected and E_{oa} from the solutions of alkaline unhydrolysed $B(OH)_4^-$-solutions in a manner previously described in Part. 2[1]. E_j has been neglected since $E_j \approx 17h - 8[OH^-]$.

In the cases where normalized curves and projection maps have been used the normalized quantities B, u and v corresponding to B, a and b have been introduced and defined. The other symbols which will be used are defined in the text.

In agreement with the notation in IUPAC, Tables of Stability constants [4], the notations β_{pq} and $*\beta_{pq}$ for the formation constants have been used. For formation of $B_3O_3(OH)_4^-$ from $B(OH)_3$; $*\beta_{13} = h[B_3O_3(OH)_4^-][B(OH)_3]^{-3}$ and $\beta_{13} = [B_3O_3(OH)_4^-][OH^-]^{-1}[B(OH)_3]^{-3}$. In the new edition of Stability constants, it is possible that $B(OH)_4^-$ will be treated as a ligand, and H^+ as the "central group"; the corresponding changes are easily made. (Private communication from L. G. Sillén.)

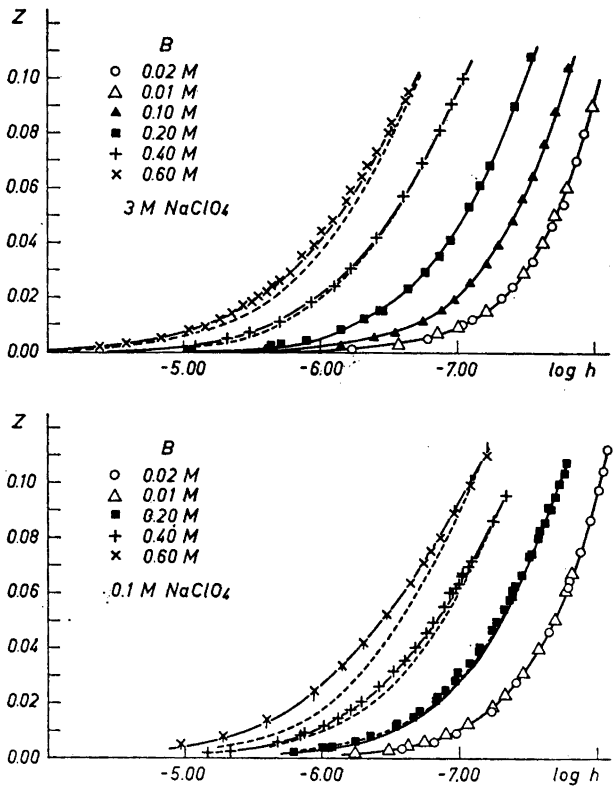

Fig. 1. Average number, Z, of OH^- = A bound per $B(OH)_3$ = B as a function of log h with 3 M and 0.1 M $Na(ClO_4)$ as media. The full curves are calculated assuming the formation of AB^-, AB_3^- and AB_5^-. The curves calculated assuming AB_4^- instead of AB_5^- are practically the same as the full curves; the differences are indicated with vertical lines for B = 0.60 M and 0.1 M $NaClO_4$. The dotted curves are calculated assuming only AB^- and AB_3^-. The equilibrium constants used are given in the text.

EXPERIMENTAL

Reagents and analysis. All chemicals and apparatus used were the same as in Part 2[1] and the composition of the solutions has been determined as described in the same paper.

The titration procedure has also been the same except that in all solutions $[Na^+] + [H^+]$ = constant = 3 M. In Part 2 this sum was constant only in the alkaline solutions.

ASSUMPTIONS ON THE ACTIVITY FACTORS

In the following treatment of data, concentrations will always be used instead of activities. This is based on the assumption that the ratio of activity factors in the law of mass action expression for formation of $B(OH)_3)_q(OH^-)_p$ from $B(OH)_3$ and OH^- stays constant, even though the individual activity factors vary. In the present case we shall see that it is a ratio of activity factors of

Table 1. Data with 0.1 M $Na(ClO_4)$ medium. For the points used in LETAGROP, 10^3 ($Z_{calc}-Z$) is given. For calculating Z_{calc} log $*\beta_1 = -8.98$, log $*\beta_{18} = -7.29$ and log $*\beta_{15} = -6.77$ have been used.

B = 600 mM; Z, 10^3 ($Z_{calc}-Z$), −log [H+]; 0.110, 2, 7.199; 0.099, 2, 7.082; 0.089, 2, 6.962; 0.080, 2, 6.858; 0.071, 6.743; 0.075, 1, 6.792; 0.063, 1, 6.640; 0.052, 1, 6.472; 0.042, 0, 6.300; 0.034, 0, 6.146; 0.024, 0, 5.936; 0.014, −1, 5.592; 0.008, −1, 5.279; 0.005, −1, 4.967;
B = 400 mM; Z, 10^3 ($Z_{calc}-Z$), −log [H+]; 0.067, −1, 7.022; 0.060, 6.953; 0.055, 0, 6.891; 0.049, 6.809; 0.045, 0, 6.760; 0.040, 6.680; 0.035, 0, 6.600; 0.031, 6.522; 0.026, 0, 6.409; 0.020, 6.287; 0.017, 0, 6.207; 0.015, 0, 6.115; 0.012, 0, 6.006; 0.009, 5.868; 0.008, 0, 5.840; 0.006, 5.674; 0.003, 0, 5.328; 0.002, 0, 5.164; 0.095, 1, 7.338; 0.086, 1, 7.249; 0.072, 1, 7.092; 0.070, 7.071; 0.066, 7.018; 0.063, 1, 6.999; 0.062, 1, 6.979; 0.059, −1, 6.930;
B = 200 mM; Z, 10^3 ($Z_{calc}-Z$), −log [H+]; 0.091, −2, 7.648; 0.083, 0, 7.580; 0.073, −2, 7.509; 0.062, −2, 7.408; 0.050, 7.270; 0.039, −2, 7.144; 0.031, −3, 6.993; 0.022, −2, 6.835; 0.015, −1, 6.658; 0.012, −1, 6.531; 0.008, −1, 6.354; 0.059, 6.235; 0.004, 0, 6.048; 0.002, 0, 5.792; 0.107, 1, 7,779; 0.104, 3, 7.772; 0.100, 0, 7.727; 0.095, 7.695; 0.091, −2, 7.648; 0.086, 0, 7.626; 0.080, 0, 7.580; 0.073, −2, 7.509; 0.067, 7.462; 0.060, 7.392; 0.059, 7.385; 0.057, −1, 7.371; 0.054, 7.332; 0.046, −2, 7.244; 0.039, −2, 7.144; 0.034, −1, 7.078; 0.028, 6.972; 0.024, −1, 6.896; 0.021, −1, 6.818; 0.017, −1, 6.707; 0.013, 6.542; 0.004, −1, 6.065; 0.004, 0, 5.997;
B = 10 mM; Z, 10^3 ($Z_{calc}-Z$), −log [H+]; 0.062, 0, 7.797; 0.046, 7.659; 0.027, 0, 7.422; 0.017, 1, 7.238; 0.009, 1, 6.978; 0,006, 1, 6.817; 0.003, 1, 6.583; 0.112, 0, 8.078;, 0.105, 1, 8.048; 0.098, 1, 8.014; 0.087, 7.956; 0.075, 7.886; 0.064, 0, 7.811;
B = 20 mM; Z, 10^3 ($Z_{calc}-Z$), −log [H+]; 0.067, 0, 7.823; 0.061, −1, 7.778; 0.050, 1, 7.703; 0.040, 0, 7.582; 0.031, 0, 7.470; 0.023, 0, 7.336; 0.018, 0, 7.238; 0.012, 0, 7.067; 0.009, 0, 6.902; 0.006, 0, 6.743; 0.004, 6.627; 0.003, 0, 6.482; 0.002, 6.235;

Data with 3 M $Na(ClO_4)$ medium. For the points used in LETAGROP, 10^3 ($Z_{calc}-Z$) is given. For calculating Z_{calc}, log $*\beta_1 = -9.00$, log $*\beta_{18} = -6.91$ and log $*\beta_{15} = -6.62$ have been used.

B = 600 mM: Z,10^3 ($Z_{calc}-Z$), −log [H+]; 0.004, 0, 4.840; 0.009, 0, 5.165; 0.014, 0, 5.360; 0.018, 1, 5.505; 0.022, 1, 5.617; 0.026, 1, 5.708; 0.029, 1, 5.784; 0.039, 0, 5.964; 0.047, 0, 6.099; 0.055, 0, 6.202; 0.063, 0, 6.313; 0.072, −1, 6.422; 0.080, −2, 6.511; 0.092, 6.630; 0.002, 0, 4.387; 0.003, 0, 4.582; 0.008, 0, 5.044; 0.012, −1, 5.272; 0.017, 0, 5.444; 0.020, 0, 5.553; 0.024, 0, 5.650; 0.035, 0, 5,875; 0.044, −1, 6.014; 0.059, −2, 6.229; 0.068, −3, 6.351; 0.084, −3, 6.531; 0.095, −4, 6.652;
B = 400 mM; Z, 10^3 ($Z_{calc}-Z$), −log [H+]; 0.002, 1, 5.091; 0.004, 1, 5.320; 0.007, 0, 5.487; 0.011, 1, 5.665; 0.018, 1, 5.900; 0.024, 2, 6.072; 0.030, 2, 6.198; 0.043, 1, 6.385; 0.059, 1, 6.583; 0.073, 1, 6.725; 0.086, 1, 6.848; 0.095, 1, 6.928; 0.106, 1, 7.023;
B = 200 mM; Z, 10^3 ($Z_{calc}-Z$), −log [H+]; 0.002, 1, 5.648; 0.004, 1, 5.903; 0.015, 1, 6.461; 0.035, 1, 6.878; 0.061, −1, 7.181; 0.000, 5.045; 0.003, 1, 5.720; 0.008, 1, 6.155; 0.011, 1, 6.323; 0.015, 1, 6.457; 0.023, 1, 6.644; 0.029, 1, 6.768; 0.041, 0, 6.958; 0.053, −1, 7.095; 0.068, −2. 7.246; 0.090, −4, 7.427; 0.108, −6, 7.555;
B = 100 mM; Z, 10^3 ($Z_{calc}-Z$), −log [H+]; 0.000, 5.607; 0.002, 1, 6.153; 0.005; 1, 6.398; 0.007, 1, 6.554; 0.011, 1, 6.750; 0.015, 2, 6.885; 0.019, 1, 6.984; 0.025, 0, 7.101; 0.032, 0, 7.219; 0.039, 0, 7.309; 0.048, −1, 7.414; 0.056, −2, 7.489; 0.064, −2, 7.559; 0.076, −3, 7.646; 0.088, −4, 7.727; 0.104, −6, 7.821;
B = 20 mM; Z, 10^3 ($Z_{calc}-Z$), −log [H+]; 0.003, 1, 6.575; 0.007, 0, 6.860; 0.009, 2, 7.009; 0.015, 1, 7.214; 0.029, 2, 7.492; 0.040, 2, 7.629; 0.050, 1, 7.720; 0.060, 2, 7.808; 0,090, 2, 7.999;
B = 10 mM; Z, 10^3 ($Z_{calc}-Z$), −log [H+]; 0.001, 1, 6.242; 0.005, 1, 6.790; 0.010, 1, 7.042; 0.012, 1, 7.117; 0.020, 1, 7.331; 0.024, 1, 7.412; 0.033, 2, 7.561; 0.046, 2, 7.699; 0.054, 3, 7.786; 0.070, 0, 7.878; 0.080, −1, 7.937;

monocharged ions, so that the approximation seems well founded. In addition to that we assumed that E_{oh}, obtained before every titration in the acid "unhydrolysed" boric acid solution is the same also in the hydrolysed solutions used ($Z \leq 0.1$).

ELIMINATION OF THE MONONUCLEAR SPECIES; MEAN COMPOSITION OF THE POLYNUCLEAR COMPLEXES

From our experimental data, $Z(\log h)_B$, given in Table 1 and Fig. 1, we wish to calculate R^{-1}, the average degree of condensation of $B(OH)_3$, and b, the actual concentration of $B(OH)_3$. For this calculation we use the following two general equations given by Sillén [5]

$$R = \text{const} + \int \left(\frac{\mathrm{d} \ln a}{\mathrm{d} \ln B}\right)_Z \mathrm{d}Z \text{ at constant } B \tag{4}$$

$$\ln b = \text{const} + \mathrm{R} - \int Z \mathrm{d}(\ln a) \text{ at constant } B \tag{5}$$

Knowing the position of the mononuclear curve, the contributions, B_1 and B_1Z_1, of the mononuclear species in B and BZ may be calculated

$$B_1 = b + \beta_1 ab \tag{6}$$

$$B_1Z_1 = \beta_1 ab \tag{7}$$

With these data the mean composition of the polynuclear complexes may be calculated from the relations

$$\bar{q}_{poly} = \frac{B - B_1}{BR - B_1} \tag{8}$$

$$p_{poly} = \frac{BZ - B_1Z_1}{BR - B_1} \tag{9}$$

where $\bar{q}_{poly}$ is the average number of boron atoms and $\bar{p}_{poly}$ the average charge of every polynuclear complex.

Calculation of R. Through every set of experimental points, $Z(\log h)$, with a common B-value a smoothed curve was drawn. In the family of curves, $Z(\log h)_B$ so obtained, lines were drawn for a number of round values of Z, $Z = 0.01, 0.02 \ldots 0.1$; for each of these, $\log h$ was read off at the point of intersection with each of the various B-lines. Thus we obtained a set of values $\log h$ $(\log B)_Z$, from which we calculated the derivative in eqn. (4). For this

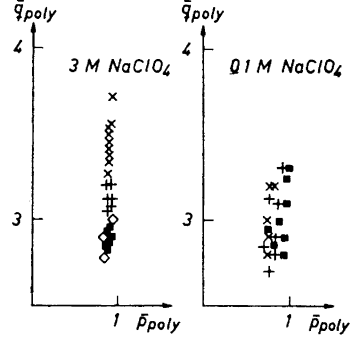

Fig. 2. The average charge, $\bar{p}$, and the average number of boron, $\bar{q}$, of polyborate ions in 3 M and 0.1 M $Na(ClO_4)$.

calculation we determined an approximating polynomial for every Z-value in such a way as to coincide with the function log h (log B) at the points given. The desired derivative at a number of points could then be calculated from the derived polynomial. For every value of B, the derivatives were plotted against Z. These points fell approximately on a straight line and the value of the derivative at $Z = 0$ was obtained by linear extrapolation. The value of the integral in (4) was obtained by calculating the area between the straight line and the coordinate axes from $Z = 0$ up to an arbitrary Z-value. The integration constant was obtained from the lower limit of integration ($Z = 0$), at this limit only the mononuclear boric acid $B(OH)_3$ is present and $R = 1$.

Calculation of ln b. The integral in (5) has been obtained by calculating the area between the log h-axes and the experimental $Z(\log h)_B$-curves from $Z = 0$ up to an arbitrary Z-value and the constant was obtained from the lower limit of integration where ln b = ln B. The determination of the integral for $Z<0.001$ using the experimental points is unsatisfactory and therefore this area has been estimated assuming the formation of one complex AB_3^-. (Ref.[5], eqn. 20 ff.)

The $\bar{q}_{poly}$- and $\bar{p}_{poly}$-values obtained are collected in Fig. 3 and indicate both in 0.1 M and 3.0 M $Na(ClO_4)$

(a) that at least two polynuclear complexes must be formed
(b) that the anions formed all have the charge minus one
(c) that the average number, $\bar{q}_{poly}$, of boron atoms in the polynuclear complexes varies between 2.7 ($\approx$ 3) and 3.7.

ANALYSIS USING NORMALIZED PROJECTION MAPS

On the basis of the results given in the previous section we constructed a number of normalized curves, log **B** (log $u)_{Z,I}$ and compared them with the

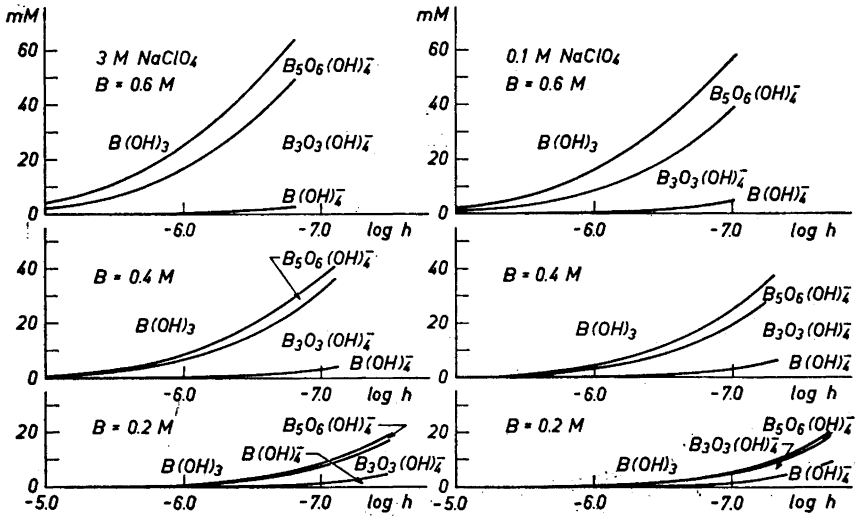

Fig. 3. Distribution of complexes as a function of log h for the total boron concentrations, B = 0.6 M, B = 0.4 M and B = 0.2 M.

corresponding experimental ones. We tried to explain our data with as few complexes as possible. With the data available we do not pretend to be able to determine more than three formation constants at the same time; thus every normalized projection map was constructed assuming not more than two polynuclear complexes $AB_{q'}$ and $AB_{q''}$ besides $B = B(OH)_3$ and $AB = B(OH)_4^-$. On the basis of the deduced $\bar{q}_{poly}$-values we also assumed $\bar{q}_{poly} \leqq 6$.

Our analysis started with testing only one polynuclear complex besides B. Of these combinations, that one containing the polynuclear complex AB_3, $B_3O_3(OH)_4^-$, could explain our experimental data over the broadest B- and Z-range. The explanation was satisfactory only at low B-values ($B \leqq 0.2$ M). In the range of agreement between experimental and calculated points the following equilibrium constants could be deduced:

$\log^*\beta_1 = -8.99$, $\log^*\beta_{13} = -6.85$ (3 M $NaClO_4$) and $\log^*\beta_1 = -8.98$, $\log^*\beta_{13} = -7.28$ (0.1 M $NaClO_4$).

The agreement between calculated and experimental points is illustrated in Fig. 1 (the calculated curve is dotted).

In order to explain the deviation at higher B, we constructed normalized curves for various combinations of two q-values between 2 and 6 which makes $\bar{q}_{poly} \approx 3-4$ and $\bar{p}_{poly} = 1$, and compared them with the experimental data. For these cases the conditions for the concentrations together with the law of mass action gives

$$B = b + {}^*\beta_1 h^{-1} b + q' {}^*\beta_{1q'} h^{-1} b^{q'} + q'' {}^*\beta_{1q''} h^{-1} b^{q''} \tag{10}$$

$$BZ = {}^*\beta_1 h^{-1} b + {}^*\beta_{1q'} h^{-1} b^{q'} + {}^*\beta_{1q''} h^{-1} b^{q''} \tag{11}$$

and by the substitutions

$$u = {}^*\beta_1 h^{-1}\,;\; v = b({}^*\beta_{1q'} {}^*\beta_1^{-1})^{1/(q'-1)}\,;\; B = B({}^*\beta_{1q'} {}^*\beta_1^{-1})^{1/(q'-1)} \tag{12}$$

(10) and (11) may be rewritten in the normalized form

$$B = v + uv + q' uv^{q'} + q'' luv^{q''} \tag{13}$$

$$BZ = uv + uv^{q'} + luv^{q''} \tag{14}$$

$$\text{where } \log l = \log \beta_{1q''} + \frac{(q'' - q')}{(q' - 1)} \log \beta_1 - \frac{(q'' - 1)}{(q' - 1)} \log \beta_{1q'} \tag{15}$$

With a known value of l one may calculate $\log B$ as a function of $\log u$ at constant Z-values. In order to decide whether a combination is possible or not it is necessary to calculate a number of projection maps with different l-values. In the present work about 5—8 l-values have been tested for every combination. The calculation of these projection maps has been carried out using the Ferranti Mercury high speed digital computer, "MATIMA", and an autocode program called PROKA [2c]. Some of the maps have also been calculated on the Swedish computer "BESK" using a program written up for calculation of maps $\log B$ $(\log u)_Z$.

We found from these calculations that the two complex-combinations, $B + AB + AB_3 + AB_4$ and $B + AB + AB_3 + AB_5$ well explained our experi-

mental data. The projection maps which were calculated assuming polynuclear complexes, $AB_2 + AB_4$ and $AB_2 + AB_5$ as well as the mononuclear species, could be ruled out as they explained the experimental data only at high B-values and not at all at low B (0.01 M and 0.02 M); neither did the combination $B + AB + AB_3 + AB_6$ explain our data.

For the two possible combinations the following preliminary equilibrium constants were calculated:

in 3 M $NaClO_4$: $\log {}^*\beta_1 = -8.98$, $\log {}^*\beta_{13} = -6.86$, $\log {}^*\beta_{15} = -6.70$,
$\log {}^*\beta_1 = -8.98$, $\log {}^*\beta_{13} = -6.90$, $\log {}^*\beta_{14} = -6.87$

in 0.1 M $NaClO_4$: $\log {}^*\beta_1 = -8.96$, $\log {}^*\beta_{13} = -7.35$, $\log {}^*\beta_{15} = -6.70$,
$\log {}^*\beta_1 = -8.96$, $\log {}^*\beta_{13} = -7.28$, $\log {}^*\beta_{14} = -7.20$

The use of normalized projection maps and the computer program PROKA[2c] has thus made possible the first assessment of the different complex-combinations. For the final choice and for the refinement of the equilibrium constants it was desirable to compare all experimental data directly with calculated curves. For this purpose the methods of LETAGROP[2c] and KUSKA[2c] seemed to be promising.

REFINEMENT OF THE EQUILIBRIUM CONSTANTS

In the present work we started the refinement of the equilibrium constants for the two possible complex-combinations by calculating a number of maps $Z(\log h)_B$ for different sets of equilibrium constants and compared these ones with the experimental points. For this calculation we used "MATIMA" and the autocode program KUSKA[2c]. This refinement gave the following set of equilibrium constants:

in 3 M $NaClO_4$: $\log {}^*\beta_1 = -9.00 \pm 0.05$, $\log {}^*\beta_{13} = -6.90 \pm 0.1$, $\log {}^*\beta_{15} = -6.65 \pm 0.20$;
$\log {}^*\beta_1 = -9.00 \pm 0.05$, $\log {}^*\beta_{13} = -6.94 \pm 0.1$, $\log {}^*\beta_{14} = -6.95 \pm 0.20$;

in 0.1 M $NaClO_4$: $\log {}^*\beta_1 = -8.98 \pm 0.05$, $\log {}^*\beta_{13} = -7.29 \pm 0.1$, $\log {}^*\beta_{15} = -6.77 \pm 0.20$;
$\log {}^*\beta_1 = -8.98 \pm 0.05$, $\log {}^*\beta_{13} = -7.36 \pm 0.1$, $\log {}^*\beta_{14} = -7.14 \pm 0.20$;

The choice of this set of constants as the "best" one is based on a visual comparison between experimental data and a number of calculated maps, $Z(\log h)_B$. The limits of the errors given are those within which the constants may be varied before "fitting is lost". This treatment is satisfactory considering the reproducibility of analyses and emf measurements. A more quick treatment may be given by using the method of last squares. A suitable form for this calculation has been given by Sillén[2b] and also, a program,LETAGROP, for calculations using a high speed computer has been worked out[2c]. The information obtained by using LETAGROP on data of the present work is collected in Table 2.

Table 2. Equilibrium constants, $*\beta_{pq}$, with the errors, 3 σ, obtained by using the least squares program LETAGROP on data for equilibria in borate solutions. The complexes $AB^-(*\beta_1)$, $AB_3^-(*\beta_{13})$, $AB_5^-(*\beta_{15})$ or $AB_4^-(*\beta_{14})$ are formed from boric acid, B. The experimental points, which have been used in the calculation are denoted in Table 1 and all points have been given the weight, $w = 1$. B stands for $B(OH)_3$.

Reaction	3 M $Na(ClO_4)$		0.1 M $Na(ClO_4)$	
	$\sim AB_4^-$	$\sim AB_5^-$	$\sim AB_4^-$	$\sim AB_5^-$
$B + H_2O \rightleftharpoons B(OH)^- + H^+$				
$-\log *\beta_1 \pm 3\sigma =$	9.00 ± 0.018	9.00 ± 0.015	8.98 ± 0.009	8.98 ± 0.006
$3B + H_2O \rightleftharpoons B_3(OH)^- + H^+$				
$-\log *\beta_{13} \pm 3\sigma =$	6.94 ± 0.051	6.91 ± 0.028	7.36 ± 0.042	7.29 ± 0.015
$4B + H_2O \rightleftharpoons B_4(OH)^- + H^+$				
$-\log *\beta_{14} \pm 3\sigma =$	6.96 ± 0.180	—	7.14 ± 0.108	—
$5B + H_2O \rightleftharpoons B_5(OH)^- + H^+$				
$-\log *\beta_{15} \pm 3\sigma =$	—	6.62 ± 0.156	—	6.77 ± 0.102
Standard deviation in Z, σ (Z) =	± 0.0024	± 0.0021	± 0.0016	± 0.0011

In the calculation using LETAGROP only random errors are considered. Our emf measurements are not better than ± 0.1 mV and the reproducibility of our chemical analysis, 0.3 %.

CONCLUSIONS

Consequently our data for the hydrolysis of boric acid in 3.0 M $NaClO_4$ and 0.1 M $NaClO_4$ could be explained, assuming constant activity factors in each medium, with the species $B(OH)_3$, $B(OH)_4^-$, $B_3O_3(OH)_4^-$ and either $B_5O_6(OH)_4^-$ (best fit) or $B_4O_5(OH)_3^-$. Due to the low solubility of boric acid, B could not be as high as would be desirable for making a choice between $B_4O_5(OH)_3^-$ and $B_5O_6(OH)_4^-$. We are, however, inclined to favour the formula $B_5O_6(OH)_4^-$; it gives a somewhat better agreement with the data, and moreover this ion (but not $B_4O_5(OH)_3^-$) has been found as a separate unit in crystals [6].

One may ask whether it is possible to explain the present data with $B(OH)_3$, $B(OH)_4^-$ and $B_3O_3(OH)_4^-$ only, by analysing each curve, $Z(\log h)_B$, independent of the others, and get a new set of equilibrium constants for every B. Such an analysis has also been made and we found that this treatment also explained the data tolerably. However in this case the fit between the experimental and calculated curves was not as good as by assuming, *e.g.*, $B_5O_4(OH)_4^-$ and therefore we preferred an explanation using the law of mass action. This explanation may also to some extent be supported by the fact that both media give the same answer.

Acknowledgements. The author is indebted to Professor Lars Gunnar Sillén for his suggestion of the present work and also to Professor Pauli Antikainen for valuable discussions at its beginning. I would like to thank Mrs. Mina Frydman and Mr. Frans Ericson for valuable help in the experimental parts. The English of this paper has been corrected by Dr. Derek Lewis. This work forms a part of a program by *Statens naturvetenskapliga forskningsråd.*

REFERENCES

1. Ingri, N., Lagerström, G., Frydman, M. and Sillén, L. G. *Acta Chem. Scand.* **11** (1957) 1034 (Anions, part 2).
2*a*. Dyrssen, D., Ingri, N. and Sillén, L. G. *Acta Chem. Scand.* **15** (1961) 694.
b. Sillén, L. G. *Acta Chem. Scand.* **16** (1962) 159.
c. Ingri, N. and Sillén, L. G. *Acta Chem. Scand.* **16** (1962) 173.
3. Antikainen, P. J. *Suomen Kemistilehti* **B 30** (1957) 74; Lourijsen-Teyssèdre, M. *Bull. soc. chim. France* **1955** 1111. See also references in Part 2, pp. 1036–1037.
4. Bjerrum, J., Schwarzenbach, G. and Sillén, L. G. *Stability constants, Part II, Inorganic ligands*, The Chemical Society Special Publication No. 7, 1958.
5. Sillén, L. G. *Acta Chem. Scand.* **15** (1961) 1981.
6. Zachariasen, W. H. *Z. Krist.* **98** (1937b) 266; Smith, J. B. S. and Richards, R. E. *Trans. Faraday Soc.* **48** (1952) 307.
7. Ingri, N. *To be published.*

Received September 5, 1961.

ACTA CHEMICA SCANDINAVICA 16 (1962) 449–455

The Crystal Structure of $B_{2.89}Si$

BENGT MAGNUSSON and CYRILL BROSSET

Department of Inorganic Chemistry, Chalmers University of Technology, Göteborg, Sweden

The crystal structure of the compound which has earlier been attributed the formulas B_3Si or B_4Si has been determined by two- and three-dimensional X-ray methods. The compound crystallizes in the space group $R\bar{3}m$, with $a = 6.319 \pm 0.005$ Å and $c = 12.713 \pm 0.010$ Å for the hexagonal cell. The structure can be described as a B_4C – structure where groups of two silicon atoms take the places of the chains of three carbon atoms, and where the remaining silicon atoms statistically substitute part of the boron atoms in the boron icosahedrons. The crystallographically determined composition is $B_{2.89}Si$, which is supported by chemical analyses and density measurements.

The original work on the silicon-boron system was carried out by Moissan and Stock [1], who reported two compounds, B_3Si and B_6Si. The compound B_6Si has recently been studied by Cline [2] and Adamsky [3] and is now relatively well-known. Its crystal structure has not yet been determined, but Adamsky reports to work on it and has proposed a configuration. The triboron silicide, which we have reason to refer to as $B_{2.89}Si$, has been extensively studied during the last few years, but the various authors do not agree about its composition and structure. Cline and Sands [4] report the composition B_4Si based on chemical and spectrographic analyses and indicate that it has structual features in common with B_4C. Colton [5] has analysed the compound and obtained a B/Si molar ratio 4.28, and states that it is slightly larger than the expected 4.00 due to the presence of B_6Si. Matkovich [6] has obtained B/Si molar ratios between 3.7 and 4.3 and concludes that the deviation from 4.00 is due to the presence of either silicon or, when silicon is completely removed, some B_6Si and BN. Knarr [7] reports the formula B_3Si based on phase-equilibrium studies. Although the hexagonal unit cell, which he has deduced, differs from the one given by all the other authors mentioned above, his X-ray data reveal that even in this case it is a question of the same compound. Rizzo and Bidwell [8] have analysed the compound very carefully and got a B/Si molar ratio 3.0. They propose that the compound is actually B_4Si, isomorphous with B_4C, with one additional silicon atom per rombohedral unit cell, *i.e.* $B_{12}Si_3 + Si$, an arrangement that is not in agreement with density data. In a recently published work Matkovich [9] has related the compound to other

similar compounds and indicates that it is isomorphous with B_4C. It is evident that a crystal structure determination of this boron silicide would be of great value in order to establish its relationship with the B_4C structure [10,11] and the proposed B_6Si structure [3]. For this reason this work has been performed. The preliminary result has been published earlier [12].

EXPERIMENTAL

Preparation. The crystals of $B_{2.89}Si$ were prepared by melting a mixture of boron (10 %) and silicon (90 %) in a high frequency induction furnace in an argon atmosphere. Crucibles of boron nitride were used. This method usually gives beautiful crystals of this boron silicide embedded in the silicon phase. The excess silicon was dissolved in a nitric acid — fluoric acid mixture [1]. It is not possible to obtain it absolutely pure by this method, as there is always some B_6Si present.

Chemical analysis. Before the analysis the samples were boiled for differing times with HNO_3, which preferentially dissolves B_6Si, and then washed with hot KOH to remove the oxides surrounding the crystals [1]. These were afterwards dissolved in a Na_2CO_3—Na_2O_2-melt in a nickel crucible and analysed for silicon and boron by conventional methods. It is quite evident that the boiling with HNO_3 lowers the B/Si molar ratio. The following are typical figures:

Sample not boiled with HNO_3: B/Si molar ratio = 4.2.

Same sample boiled with HNO_3 for 42 hours: B/Si molar ratio = 3.2.

From our analyses it seems probable that the true B/Si molar ratio is approximately 3.0, and consequently that the analyses performed by Moissan and Stock [1] and Rizzo and Bidwell [8] are substantially correct.

X-Ray methods. In order to determine the cell-dimensions accurately, powder photographs of Guinier type were taken using CuKα radiation and with NaCl as a reference substance. Due regard was taken to film shrinkage by copying a scale on the films before development. The structural investigation was based on single crystal methods. Multiple-film equi-inclination Weissenberg photographs were taken with rotation about the hexagonal c-axis (layer lines 0—6) and the hexagonal a-axis (layer lines 0 and 1) using copper radiation. The reflexion intensities were estimated by visual comparison with standard scales. A subjective correction was made for variation in spot shape. No correction was made for absorption as very small crystals were used. The reflexion intensities were corrected using Lorenz- and polarisation factors.

DETERMINATION OF THE STRUCTURE

The cell dimensions were obtained from powder diffraction data by the method of least squares. $B_{2.89}Si$ is rombohedral. The dimensions of the hexagonal unit cell are the following:

$$a = 6.319 \pm 0.005 \text{ Å}$$
$$c = 12.713 \pm 0.010 \text{ Å}$$

Calculated and observed $\sin^2\Theta$-values are given in Table 1. Here and in the following the indices refer to the hexagonal cell.

In all photographs only reflexions from planes of the following type were observed:

$$-h + k + l = 3n$$

The following rule was obeyed by the intensities:

$$I_{hkl} = I_{kh\bar{l}}$$

Table 1. X-Ray powder diffraction data for $B_{2.89}Si$.

h k l	$10^4 \times \sin^2\Theta_{obs}$	$10^4 \times \sin^2\Theta_{calc}$
0 1 2	345	346
1 1 0	593	595
1 0 4	786	787
0 2 1	832	831
2 1 1	1426	1426
1 1 6	1920	1919
3 0 3, 0 3 3	2118	2117
1 2 5	2307	2308
2 2 0	2384	2381
1 3 1	2615	2616
3 1 2	2725	2727
3 0 6, 0 3 6	3110	3110

The same rule is found in simple rombohedral boron [13]. Of the three possible space groups, $R32$, $R3m$ and $R\bar{3}m$, only the centrosymmetric $R\bar{3}m$ was considered and was found to meet all demands of the data.

The density was found to be 2.44 g/cm³ from a long series of determinations. We have not been able to reproduce the somewhat higher values mentioned in our preliminary report [12]. This, however, does not necessarily mean that these values are erroneous, but they may be interpreted as an indication of a homogeneity range of this boron silicide phase. This idea is supported by the fact that the values of the density of the compound in question in the litterature varies significantly. From the value 2.44 the number of molecules in the hexagonal unit cell is calculated to 10.67, *i.e.*, there are 3.57 molecules per rombohedral unit cell, if the formula is supposed to be B_3Si. This fact implies an unusual structure, provided that the assumption concerning the formula is correct.

From a Patterson projection on (001) it was concluded that the structure is similar to that of the compound B_4C. A three-dimensional Patterson synthesis showed that there are only two atoms in the 0,0,*z*-position, and that all the other atomic positions form icosahedrons in approximately the same way as in B_4C. The atoms in an icosahedron are of two different kinds, the atoms forming the top and bottom of the icosahedrons having higher electron density than the others.

These facts were interpreted in the following way. The structure is a B_4C-structure, where groups of two silicon atoms take the places of the chains of three carbon atoms. The rest of the silicon atoms are statistically substituting boron atoms in one of the two 18*h*-positions, in which the atoms forming the icosahedrons are placed.

This way of interpreting the symmetry of the three-dimensional Patterson synthesis affects the idea of the stoichiometry of the compound. Its formula could thus be given the following general expression:

$$B_{18}(B_{18-x}Si_x)Si_6$$

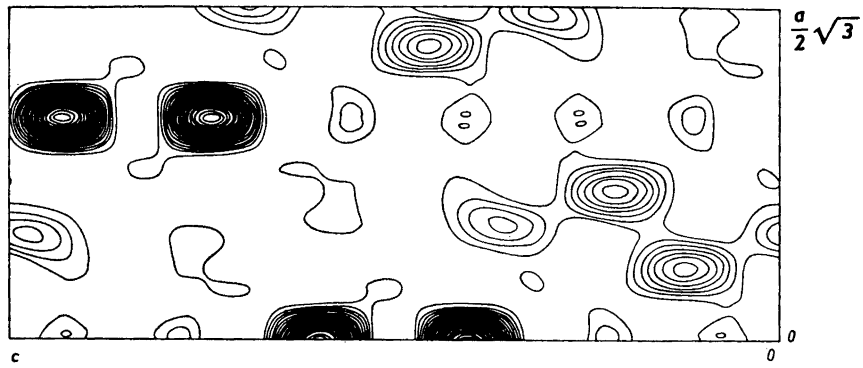

Fig. 1. Electron density, $\varrho(2x,x,z)$, on a mirror plane (120). The contours are at equal but arbitrary intervals.

Analytical data and density measurements indicate that x is in the neighbourhood of 5. If we at first restrict ourselves to whole numbers for x, the following formulas are possible:

$x = 3$	$B_{33}Si_9$
$x = 4$	$B_{32}Si_{10}$
$x = 5$	$B_{31}Si_{11}$
$x = 6$	$B_{30}Si_{12}$
$x = 7$	$B_{29}Si_{13}$

It was plausible to start with the formula $B_{31}Si_{11}$ in trying to account for observed X-ray data, as this formula gives a calculated density of 2.43, which is near the observed value of 2.44. Crystallographic calculations could now be based on parameters obtained from the three-dimensional Patterson synthesis mentioned above and structure factor signs obtained with the assumption of the formula $B_{31}Si_{11}$. This formula states that 5 of the 18 boron atoms in one of the two 18*h* positions (18*h'*) are replaced by silicon atoms. This substitution implies the assigning to the atoms in 18*h'* an atomic form factor:

$$f = 5/18 f_{Si} + 13/18 f_B$$

This operation was easy to perform as the atomic form factors used were of the form [14]:

$$f_i = A_i \cdot \exp(-a_i \sin^2\Theta) + B_i \cdot \exp(-b_i \sin^2\Theta)$$

The electron density calculated in this way for the plane (120) is given in Fig. 1. The oval shape of the peaks is at least partly due to the fact that only reflexions with $l = 0-6$ are used in the Fourier synthesis. From the peaks in this plane, in fact all the parameter values for the structure are obtained. Their final values are given in Table 2. Here, and in the following, the atoms in the 18*h* position in which substitution occurs are denoted as Si,B-atoms.

Table 2. Atomic parameters for $B_{2.89}Si$.

Atom	Position	x	y	z
Si	6c	0	0	0.403_1
Si,B	18h′	0.107_5	-0.107_5	0.877_9
B	18h	0.158_0	-0.158_0	0.025_2

The final structure factors were then calculated. These and the observed values are given in Table 3. The structure factor disagreements,

$$R = \Sigma \, | \, |F_{calc}| - |F_{obs}| \, | \, / \Sigma \, |F_{obs}|$$

of the final coordinates is $R_{hkl} = 9.45$ %, excluding those terms too week to be observed. Observed structure factors have been corrected for thermal

Table 3. Values of observed and calculated structure factors for $B_{2.89}Si$. See the text.

$h\,k\,l$	F_{obs}	F_{calc}	$h\,k\,l$	F_{obs}	F_{calc}
3 0 0	—	+ 1	1 4 3	—	− 5
6 0 0	32	+ 33	2 2 3	31	+ 41
3 3 0	77	+ 77	5 2 3	—	− 11
1 1 0	39	+ 47	2 5 3	—	+ 4
4 1 0	31	+ 27	1 0 4	89	− 92
4 4 0	58	+ 53	4 0 4	—	− 1
2 2 0	71	+ 72	1 3 4	25	− 19
5 2 0	26	+ 24	4 3 4	58	− 61
1 0 1	10	+ 10	1 6 4	—	+ 3
4 0 1	43	− 39	0 2 4	22	− 24
1 3 1	59	− 63	3 2 4	45	− 46
4 3 1	14	− 7	0 5 4	20	− 18
1 6 1	14	− 11	2 1 4	17	− 14
0 2 1	99	− 105	5 1 4	21	− 23
3 2 1	—	+ 4	2 4 4	53	− 48
0 5 1	37	− 37	2 0 5	—	− 2
2 1 1	41	− 39	5 0 5	67	+ 64
5 1 1	52	− 50	2 3 5	31	+ 32
2 4 1	16	− 14	0 1 5	30	+ 36
2 0 2	28	+ 25	3 1 5	42	+ 40
5 0 2	—	− 4	6 1 5	58	+ 59
2 3 2	21	+ 22	0 4 5	48	+ 43
0 1 2	46	+ 38	3 4 5	22	+ 14
3 1 2	62	+ 57	1 2 5	90	+ 87
6 1 2	—	− 3	4 2 5	—	− 11
0 4 2	27	− 39	1 5 5	29	+ 29
3 4 2	—	+ 10	0 0 6	33	− 32
1 2 2	6	− 8	3 0 6	99	− 92
4 2 2	—	− 10	6 0 6	25	+ 26
1 5 2	36	+ 38	0 3 6	10	+ 17
0 0 3	8	+ 7	3 3 6	41	− 39
3 0 3	66	+ 58	0 6 6	51	− 45
6 0 3	13	+ 14	1 1 6	41	− 47
0 3 3	17	− 17	4 1 6	29	− 35
3 3 3	23	− 30	1 4 6	41	− 36
0 6 3	75	+ 71	2 2 6	22	− 17
1 1 3	—	− 3	5 2 6	32	− 35
4 1 3	—	+ 8	2 5 6	32	− 25

Table 4. *R*-factors and calculated densities for various values of x in $B_{18}(B_{18-x}Si_x)Si_6$.

x	Formula	R-factor, %	Calc. density
3	$B_{33}Si_9$	12.63	2.303
4	$B_{32}Si_{10}$	10.44	2.368
4.80	$B_{2.89}Si$	—	2.420
5	$B_{31}Si_{11}$	9.45	2.433
6	$B_{30}Si_{12}$	10.29	2.499
7	$B_{29}Si_{13}$	12.78	2.564

vibration by the factor $\exp[B(\sin\Theta/\lambda)^2]$ with $B = 1.13 \times 10^{-16}$ cm^2 determined by the method of least squares from the final structure factors. An isotropic temperature factor has been applied in spite of the fact that an anisotropic one would have been more satisfactory in this case.

The proposed structure is dependent on the assumption that the formula of the compound is $B_{31}Si_{11}$. It was, however, necessary to verify that the assumed stoichiometry gave the best agreement between observed and calculated intensity data. This has been done by calculating *R*-factors also for structures where the structure factors were based on the formula $B_{18}(B_{18-x}Si_x)Si_6$ with x equal to 3, 4, 6, and 7. The result is given together with the calculated densities in Table 4. From this table it is evident that the formula $B_{31}Si_{11}$ gives the best agreement.

This method of determining the composition, however, is not very good because of the fact that the value of the *R*-factor is not solely depending on the varying substitution in the 18*h*′ position. A better method is to calculate difference syntheses for various compositions and determine the true composition by observing when $\varrho_o - \varrho_c = 0$ at the atomic positions in question. By this method the composition was found to be $B_{2.89}Si$. As there is only a small difference between this composition and $B_{31}Si_{11}$ ($B_{2.82}Si$), no recalculation of structure factors was made.

The standard deviations of atomic coordinates were estimated according to Cruishank's method [15], and the standard deviations in bond lengths were readily calculated from these values. Calculated bond lengths and the standard deviations of these are given in Table 5.

The bond lengths given in Table 5 show that the Si—Si-distance is somewhat longer than the covalent radius sum, while the Si—B-distance and the Si,B—Si,B-distance between two icosahedrons are somewhat shorter than expected. Short bond lengths between icosahedrons are also noted in various forms of boron. [13,16]

Table 5. Bond lengths in $B_{2.89}Si$.

Si—Si	2.463 ± 0.012 Å	
B—B	1.844 ± 0.041 Å	
Si,B—Si,B	2.038 ± 0.018 Å	(within an icosahedron)
Si,B—Si,B	1.721 ± 0.036 Å	(between the icosahedrons)
Si—B	2.002 ± 0.029 Å	
Si,B—B_1	1.964 ± 0.040 Å	
Si,B—B_2	1.952 ± 0.033 Å	

DISCUSSION

The determination of the structure of a boron silicide phase with low boron content has shown that the material used had a composition $B_{2.89}Si$, not far from $B_{31}Si_{11}$. Whether there is a homogeneity range has not been determined, but does not seem improbable.

The structure of this phase has been found to be derivable from the B_4C-structure. This fact has earlier been proposed by several authors. However, it is obviously not quite correct to speak of isomorphism, as silicon atoms in $B_{2.89}Si$ not only correspond to carbon atoms in B_4C but also to part of the boron atoms.

It is interesting to compare the structure of $B_{2.89}Si$ to the structure, which has been hypothetically proposed [3] for B_6Si. This is supposed to be built up from icosahedrons of boron atoms and pairs of silicon atoms. The similarity between this structure and the one of $B_{2.89}Si$, determined in this work, is apparent.

In this connection, it seems justified to mention the principles for the building up of compounds belonging to this category (interstitial boron compounds) given by Matkovich [9]. According to his theory such compounds are built up of intact boron icosahedrons between which are situated groups of two or three atoms or single atoms. The present result seems to introduce a new principle. There seems to be no need for the boron icosahedron to be intact. Evidently, the boron atoms may be replaced by other atoms, which implies that more possibilities of configuration have to be considered than was earlier assumed. A determination of the atomic arrangement in these materials as well as in the compound $B_{11}C_4$, reported by Kranz [17], would be of considerable interest.

Acknowledgements. We wish to thank Dr. N. G. Vannerberg for valuable discussions and Ing. H. Zengler and Ing. L. Randsalu for technical assistance. This work was financially supported by *Statens Tekniska Foskningsråd.*

REFERENCES

1. Moissan, H. and Stock, A. *Compt. rend.* **131** (1900) 139.
2. Cline, C. F. *J. Electrochem. Soc.* **106** (1959) 322.
3. Adamsky, R. F. *Acta Cryst.* **11** (1958) 744.
4. Cline, C. F. and Sands, D. E. *Nature* **185** (1960) 456.
5. Colton, E. *J. Am. Chem. Soc.* **82** (1960) 1002.
6. Matkovich, V. I. *Acta Cryst.* **13** (1960) 679.
7. Knarr, W. A. *Dissertation Abstr.* **20** (1960) 4541.
8. Rizzo, H. F. and Bidwell, L. R. *J. Am. Ceram. Soc.* **43** (1960) 550.
9. Matkovich, V. I. *J. Am. Chem. Soc.* **83** (1961) 1804.
10. Zhdanov, G. S. and Sevast'yanov, N. G. *Compt. rend. Acad. Sci. U.S.S.R.* **32** (1941) 432.
11. Clark, H. K. and Hoard, J. L. *J. Am. Chem. Soc.* **65** (1943) 2115.
12. Brosset, C. and Magnusson, B. *Nature* **187** (1960) 54.
13. Decker, B. F. and Kasper, I. S. *Acta Cryst.* **12** (1959) 503.
14. Vand, V., Eiland, P. F. and Pepinsky, R. *Acta Cryst.* **10** (1957) 303.
15. Cruickshank, D. W. J. *Acta Cryst.* **2** (1949) 65.
16. Hoard, J. L., Hughes, R. E. and Sands, D. E. *J. Am. Chem. Soc.* **80** (1958) 4507.
17. Kranz, R. *Hamburger Beitr. angew. Mineral. u. Kristallphysik.* **2** (1959) 99.

Received September 6, 1961.

ACTA CHEMICA SCANDINAVICA 16 (1962) 456–466

Isoelectric Fractionation, Analysis, and Characterization of Ampholytes in Natural pH Gradients. II. Buffering Capacity and Conductance of Isoionic Ampholytes

HARRY SVENSSON

The Departments of Bacteriology and Physical Chemistry, Karolinska Institutet, Stockholm, Sweden

For a complete separation of proteins in a natural pH gradient, the presence of low-molecular ampholytes with buffering capacity and conductance in the isoelectric state (carrier ampholytes) is necessary. The concentrations of cations and anions in solutions of simple ampholytes are deduced as functions of pH. In the isoionic state, these concentrations are the same, and a simple expression for the degree of ionization is derived. The buffering capacity is deduced as the derivative with respect to pH of the concentration of cations minus the concentration of anions. In the isoionic state, the expression becomes particularly simple and equals that for the degree of ionization but for a numerical factor. Since the conductance is proportional to the concentration of ions, it may be concluded that the conditons for a good buffering capacity and for an appreciable conductance are the same. Both properties rise as the distance pI-pK_1 between the isoionic point and the nearest pK value decreases. Consequently, good carrier ampholytes are those which are isoelectric between two closely spaced pK values.

Conductance measurements are reported for solutions of some ampholytes which can be used as carriers. They are compared with theoretical conductances deduced from the degree of ionization and from estimated, reasonable mobility data of the ions of the ampholytes. These measurements form a semi-quantitative verification of the theory, substantiating the importance of the quantity pI-pK_1.

It is pointed out that the crucial difficulty in stationary electrolysis of proteins is the scarcity of carrier ampholytes isoelectric between pH 4 and 7. Successful separations of proteins isoelectric in this region cannot be expected until useful carrier ampholytes have been synthesized or supplied by other means.

In the preceding article [1] it was proved that two ampholytes can be completely separated by stationary electrolysis only if there is a third ampholyte with an intermediate isoelectric point, or if the two ampholytes are isoelectric on either side of the pH of the pure solvent. For example, histidine may be

completely separated from glutamic acid because a region of pure water may develop between them, but in a run with histidine and lysine there will necessarily be a zone in which the two amino acids remain mixed even in the steady state obtained on prolonged electrolysis.

The above rule also applies to proteins. It is thus impossible to obtain a complete separation between two proteins isoelectric below pH 7 by electrolysis in the absence of other ampholytes. Only a certain degree of purification is possible, which is of course better the greater the difference between the two isoelectric points.

A complete separation of proteins isoelectric on the same side of the neutral point thus requires the presence of amino acids or other low-molecular ampholytes, which may be called *carrier ampholytes*. They will then determine the pH course in the steady state. Because of the very sharp isoelectric points exhibited by proteins, isoelectric separation can be expected to be very selective. Of course each protein is first obtained contaminated by carrier ampholytes, but they can easily be removed by dialysis.

Since even the carrier ampholytes condense in isoelectric zones, the stability of the pH gradient depends on their buffering capacities in and near the isoelectric state. On the other hand, in order to avoid excessive field strengths due to rarefaction of ions, especially in the neutral region, it is also desirable to have access to low-molecular ampholytes with appreciable conductances in the isoelectric state. This article will be devoted to an analysis of the properties of an ampholyte which determine its buffering capacity and conductance in the isoelectric state.

THE ION CONCENTRATIONS OF AN AMPHOLYTE IN THE ISOELECTRIC RANGE

The isoelectric point is defined as the pH at which the ampholyte is immobile in an electric field. At this point, the concentrations of the cationic and anionic subspecies are not necessarily the same. First, the ampholyte may form complexes with other ions than H^+, and second, the mobilities of the cationic and anionic forms need not be the same. A calculation of the state of ionization at the isoelectric point is therefore too complicated and of little practical value. Instead it will be carried out for the isoionic state, in which cations and anions have the same concentration. Experimentally, the isoionic point may be defined as the pH of a solution which does not change its acidity on addition of a small quantity of the ampholyte.

It was pointed out in the previous article [1] that, for the great majority of low-molecular ampholytes, only two pK values exert a measurable influence on the ionization around the isoionic point. One then has the following simple relation between the isoionic point pI and these two pK values:

$$2\ \mathrm{pI} = \mathrm{p}K_1 + \mathrm{p}K_2 \qquad (1)$$

where pK_1 is defined to be smaller than pK_2. If the cation concentration is denoted by C_+, the anion concentration by C_-, and the added concentrations

of zwitterionic and undissociated ampholyte by C_o, then the mass-action law gives the following equations, activity factors being left without consideration:

$$C_+ = C_o \times 10^{pK_1 - pH} \quad (2)$$

$$C_- = C_o \times 10^{pH - pK_2} \quad (3)$$

Further, if C is the total concentration, one has the relation:

$$C = C_+ + C_- + C_o \quad (4)$$

Elimination of C_o gives, after rearrangement:

$$C/C_+ = 1 + 10^{pH - pK_1} + 10^{2(pH - pI)} \quad (5)$$

$$C/C_- = 1 + 10^{pK_2 - pH} + 10^{2(pI - pH)} \quad (6)$$

The degree of ionization must be defined as

$$\alpha = (C_+ + C_-)/C \quad (7)$$

In the isoionic state, one gets the simple expression:

$$\alpha = 2/(2 + 10^{pI - pK_1}) \quad (8)$$

Since pI is never smaller than pK_1, the second term in the denominator is always bigger than unity, and consequently there is an upper limit of $\alpha = 2/3$ for the fraction of ions in an isoionic ampholyte *.

BUFFERING CAPACITY

The mean electric charge of the ampholyte expressed in units of the elementary proton charge is given by the equation:

$$Q = \frac{C_+ - C_-}{C} \quad (9)$$

A plot of Q *versus* pH is identical with the titration curve of the ampholyte; hence the buffering capacity is given by the derivative:

$$-\frac{dQ}{d(pH)} = \frac{d(C_-/C)}{d(pH)} - \frac{d(C_+/C)}{d(pH)} \quad (10)$$

Calculation with the aid of eqns. (5) and (6) gives for the isoionic state, pH = pI:

$$-\frac{dQ}{d(pH)} = \frac{2 \ln 10}{2 + 10^{pI - pK_1}} \quad (11)$$

The buffering capacity as a function of $pI - pK_1$ is shown in Fig. 1. First it falls off linearly, and for $pI - pK_1 = 1$ pH unit as much as 1/4 of the limiting capacity is still retained. The curve then assumes an exponential decline, and

* In another connection [2], the author erroneously stated, without calculation, that α would equal 1/2 for a hypothetical ampholyte with $pK_1 = pK_2$, and that the fractions of zwitterionic and undissociated subspecies were both = 1/4. The relative abundance of the latter two subspecies cannot at all be calculated from titration data alone, but can be derived from other physicochemical measurements together with certain plausible assumptions (Green and Tong [3]; Lumme [4,5]).

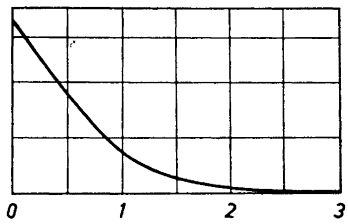

Fig. 1. The buffering capacity of an isoionic ampholyte as a function of pI—pK_1.

for pI—pK_1 = 2 units only 1/34 remains. It can thus be concluded that *carrier ampholytes should have the property of being isoelectric between two closely spaced* pK *values*. Eqn. (11) is also useful as a guide for making up formulas for mixtures of carrier ampholytes. The better the buffering capacity, the smaller amounts of the ampholyte can be taken in order to get a uniform pH gradient.

CONDUCTANCE

The conductance of a solution can be calculated by using one of the well-known equations:

$$\varkappa = F\sum_i c_i z_i u_i = \sum_i c_i z_i \Lambda_i \qquad (12)$$

Here F denotes the Faraday constant = 96 500 coulombs per equivalent, c_i concentrations in moles per cm^3 (always positive), z_i valences with sign according to charge, u_i mobilities in cm^2/V sec. (with positive sign for cathodic, negative for anodic migration), and Λ_i equivalent conductances in cm^2/ohm equiv. (with the same sign as u_i). The subscript i generally refers to the ion constituents (MacInnes [6]) of the solution, and eqns. (12) should be used in that way whenever possible.

For ampholytes in the isoionic state, however, the cation and the anion belong to the same ion constituent, *viz.* the organic radical of the ampholyte. In the isoelectric state, no current is transported by this ion constituent; the whole current is actually transported by the hydrogen ion constituent (Svensson [2]; Van Os and Möller [7]). Since the mobility of the latter cannot be measured in electrolytic systems of this type, the only remaining possibility is to apply eqns. (12) to the free ions actually present and to disregard from the concept of ion constituent. There are three such ions, the cation and the anion of the ampholyte, and in addition the hydrogen ion for acidic and the hydroxyl ion for basic ampholytes. The contribution of the solvent ions is big for strongly acidic and strongly basic ampholytes, but negligible for neutral ones.

The concentration of free ions is given by eqn. (8). Since this expression differs from the buffering capacity, eqn. (11), by a numerical factor only, it is understood that a good conductance and a good buffering capacity are given by the same type of ampholytes, those which are isoelectric between two closely spaced pK values.

The mobilities of ions of ampholytes. Eqn. (12) in conjunction with eqn. (8) is useful for calculation of the conductance of isoionic ampholytes if the mobi-

lities of their ions are known. However, no such data seem to be available in the literature; those for glycine, alanine, and glycyl-glycine reported by Svensson, Benjamisson and Brattsten [8] are without interest in this connection since these ampholytes have practically no conductance in the isoionic state.

For ions of unit charge, the mobility varies inversely with the linear dimensions of the hydrated ions, *i.e.* for spherical ions roughly with the cubic root of the kinetic molecular volume. Consequently a good approximation of the mobility of an ampholytic ion can be obtained by taking the value of an ordinary ion of similar size and structure, and by applying a suitable correction for the difference in molecular volume. The empirical relations between mobilities and molecular volumes presented by Edward [9,10] can be used for this purpose. The procedure will be demonstrated below for a number of easily available ampholytes which can be expected to possess an appreciable conductance in the isoionic state.

The anions of the nicotinic, isonicotinic, and picolinic acids must be expected to be about as mobile as the benzoate ion. In Conway's [11] book, one finds the figure −32.3 for the equivalent conductance of the benzoate ion at infinite dilution and at 25°C. According to Edward, the kinetic molecular volume of the benzoate ion may be estimated to 167.8 Å^3, which corresponds to a sphere radius of 3.42 Å. If this is introduced into Edward's equation for monovalent ions:

$$\Lambda = \pm k/r \qquad (13)$$

the constant k gets the value 110.5. The pyridine-carboxylic acids contain one aromatically bound nitrogen atom instead of one aromatic CH group, which reduces the molecular volume to 165.3 Å^3 and the corresponding radius of a sphere to 3.40 Å. The latter value introduced into (13) gives the figure −32.5 for the equivalent conductance of the pyridine-carboxylic acids. A similar calculation for the cations gives + 37.3 cm^2/ohm equiv.

The amino-benzoic acids are of about the same size and shape as chlorobenzoic acids, for which Saxton and Meier [12] have reported the figures −30.3 (*o*-acid) and −31.0 (*m*-acid). Edward's table gives the molecular volume 184.0 Å^3 for the chlorobenzoate ion and 174.0 Å^3 for an amino-benzoate ion. With a k value of 107.9, one gets an equivalent conductance of −31.2 cm^2/ohm equiv. for the anion of the ampholyte. A similar calculation for the cation gives + 35.7.

In the same way, the probable mobilities of the ions of arsanilic acid, aspartic acid, and glutamic acid have been calulated. For aspartic acid comparison has been made with succinic acid monoamide, for glutamic acid with glutaric acid monoamide, the mobilities of which have been measured by Jeffrey and Vogel [13].

Among the ions for which mobility data are available, the heptanoate ion resembles the lysine anion most closely. Its mobility has been measured by Dippy [14] and can be used to calculate a probable mobility of lysine ions. Similarly, the octanoate ion, also measured by Dippy, is the best one to use for calculating mobilities of arginine ions. Finally, for histidine comparison may be made with phenylpropionic acid, the mobility of which has been measured

Table 1. Probable equivalent conductances in cm^2/ohm equiv. of ions of some ampholytes at 25°C and infinite dilution

Ampholyte	Λ_+	$-\Lambda_-$
Pyridine-carboxylic acids	37.3	32.5
Aminobenzoic acids	35.7	31.2
Arsanilic acids	31.7	29.8
Aspartic acid	36.4	28.1
Glutamic acid	34.2	27.0
Histidine	31.3	31.3
Lysine	29.0	29.0
Arginine	29.3	29.3

by Dippy and Lewis [15]. The probable mobilities thus calculated for ions of ampholytes are collected in Table 1.

The contribution to conductance of the ions of the solvent. The equivalent conductances of the H^+ and OH^- ions are 350 and −192 cm^2/ohm equiv., respectively, at 25°C and infinite dilution. At pH 7, both these ions have a concentration of 10^{-10} moles per cm^3. By the use of eqn. (12), one thus finds the following contribution to conductance of the water ions at 25° and zero ionic strength:

$$\varkappa_w(7) = 0.0542 \times 10^{-6} \text{ ohm}^{-1} \text{ cm}^{-1} \qquad (14)$$

This contribution is too small to require any consideration in the measurements to be described.

Already at pH 6, the conductance contribution of the OH^- ions can be neglected. For that and lower pH values, therefore, one arrives at the following general formula:

$$\varkappa_w(\text{pH}) = 0.35 \times 10^{-\text{pH}} \qquad (\text{pH} < 6) \qquad (15)$$

On the other hand, above pH 8.5, the contribution of the H^+ ions is negligible, and one finds:

$$\varkappa_w(\text{pH}) = 1.92 \times 10^{\text{pH}-15} \qquad (\text{pH} > 8.5) \qquad (16)$$

The equations still refer to zero ionic strength, although this is in itself a contradiction at low and high pH values.

Conductance measurements. In order to test at least semiquantitatively the validity of the theoretical predictions presented above, some conductance measurements have been carried out. A fully quantitative verification would require a more elaborate theory and extensive and careful measurements at varying concentrations on well purified preparations. For the present purpose of finding suitable carrier ampholytes for isoelectric separation of proteins, a semi-quantitative check on the equations is adequate.

Consequently, commercially available ampholytes of analytical grade were in general used without further purification. However, commercial lysine and histidine were found to be partially decomposed. Instead their monohydrochlorides were used, and their solutions were deprived of HCl by passing them through a column of an ion exchanger.

Table 2. The conductance of solutions of pure ampholytes at 25°C.

No.	Ampholyte	Concentration, μmoles/ml	Conductance, μmhos/cm	pH
1	Nicotinic acid	154	527	3.50
2	Isonicotinic acid	16.34	131	3.51
3	Picolinic acid	100	227	3.34
4	*o*-Aminobenzoic acid	54.7	183	3.61
5	*m*-Aminobenzoic acid	54.6	446	3.88
6	*p*-Aminobenzoic acid	36.0	209	3.69
7	*o*-Aminophenylarsonic acid	9.22	432	3.02
8	*p*-Aminophenylarsonic acid	13.04	311	3.17
9	Aspartic acid	56.3	653	2.95
10	Glutamic acid	100	595	3.34
11	Histidine	88.55	172	7.81
12	Lysine	358	2 146	9.96
13	Arginine	100	200	10.84

If possible, the ampholytes were dissolved in distilled water to a concentration of 0.1 M. Slightly soluble ampholytes were dissolved to saturation, and the concentrations were measured by weighing 2 ml samples before and after evaporation of the solvent. The lysine and histidine solutions emerging from the ion exchange column were measured directly, and their concentrations were determined in the same way. The conductances were measured at 25°C on an LKB precision Wheatstone bridge. The pH of each solution was also measured. The results of these measurements are presented in Table 2.

Calculation of conductances. Using the mobility data in Table 1 and the ion concentrations according to eqn. (8), one can now derive theoretical conductances of isoionic ampholytes. The calculation will be explained below with reference to Table 3. For space reasons, the first column of that table contains only a number; the corresponding name of the ampholyte can be found in Table 2. The second column gives the concentration of the solution subjected to conductance measurement. In the third column, the distance from the isoionic point to the nearest pK value is given. The fourth column contains the degree of ionization in the isoionic state, calculated with the aid of eqn. (8). The product of total concentration, degree of ionization, and mean equivalent conductance of cation and anion (Table 1) is the conductance contribution of the ampholytic ions, column 5. From the measured pH data given in Table 2, the contribution of the solvent ions can be calculated by using eqns. (15) or (16), column 6. The figures in column 7 are the sum of those in columns 5 and 6 and represent the conductances of the isoionic solutions that would be expected if the mobility data for infinite dilution could be used at the prevailing concentrations. This is of course not the case, so a correction for the depression of mobilities due to a finite ionic strength must be carried out.

A theoretical correction for the ionic strength effect by Onsager's equation has not been attempted. Instead, the table on pp. 141—42 in Conway's [11] book over the concentration dependence of equivalent conductances of various salts has been studied. Among the mono-mono-valent salts listed there, the two

Table 3. Calculation of theoretical conductances for ampholytes from known concentrations, calculated ionic concentrations, and probable mobilities.

Ampholyte No.	Concentration, μmoles per ml	pI-pK_1	α	$\varkappa_{amph.}$	$\varkappa_w$	$\varkappa$	Ionic strength	Factor	$\varkappa_{corr.}$ μmhos per cm
				μmhos/cm					
1	154	1.37	0.0786	422	111	533	0.00620	0.93	496
2	16.34	1.51	0.0681	39	108	147	0.00071	0.976	143
3	100	2.15	0.0140	49	160	209	0.00093	0.972	203
4	54.7	1.47	0.0635	116	86	202	0.00186	0.96	194
5	54.6	0.81	0.2367	432	46	478	0.00653	0.93	445
6	36.0	1.30	0.0911	110	72	182	0.00174	0.96	175
7	9.22	0.77	0.2532	72	334	406	0.00164	0.962	391
8	13.04	0.92	0.1938	78	236	314	0.00160	0.962	302
9	56.3	0.89	0.2049	372	393	765	0.00632	0.93	711
10	100	1.03	0.1574	482	160	642	0.00810	0.923	592
11	88.55	1.50	0.0595	165	0	165	0.00217	0.956	158
12	358	0.79	0.2448	2 542	17	2 559	0.04385	0.845	2 162
13	100	1.72	0.0367	108	133	241	0.00218	0.956	230

organic salts sodium acetate and sodium butyrate show the strongest concentration dependence. It is therefore possible that the big organic ions in question here have mobilities that are still more concentration-dependent; this would also be in agreement with Onsager's equation. On the other hand, a considerable part of the total conductance is due to H^+ or OH^- ions, which have a small concentration dependence. It is therefore probable that the use of ionic strength factors valid for sodium butyrate will yield conductance corrections of the right order of magnitude; most corrections are also quite small, of the order of 5 %.

The ionic strength of a solutions of a pure ampholyte is identical with the concentration of anions for an acidic and with the concentration of cations for a basic ampholyte. It is obtained by adding the hydrogen or hydroxyl ion concentration to the total concentration of ampholytic ions in the isoionic state, and dividing the sum by 2. These data are given in column 8, and the mobility depression factors pertaining to these ionic strengths are listed in column 9. Column 10, finally, gives the theoretical conductances corrected for the ionic strength effect. They are to be compared with the experimental data in column 4 of Table 2.

RESULTS AND DISCUSSION

As can be seen in Table 3, the degree of ionization varied from 1.40 to 25.32 % among the ampholytes subjected to conductance measurements. The total conductance varied between the limits 143 and 2 162 μmhos/cm. The relative contribution of the solvent ions varied from 0 for histidine to 82.3 % for *o*-aminophenylarsonic acid. In spite of these more than 10-fold variations in the properties of the ampholytes, the calculated conductances lie, with two exceptions, within ± 10 % of the measured ones. In view of the uncertainty

Table 4. Possible carrier ampholytes arranged in the order of increasing isoionic points.

Ampholyte	pI	pI-pK_1
Aspartic acid	2.77	0.89
Glutathion	2.82	0.70
Aspartyl-tyrosine	2.85	0.72
o-Aminophenylarsonic acid	3.00(?)	0.77(?)
Aspartyl-aspartic acid	3.04	0.34
p-Aminophenylarsonic acid	3.15(?)	0.92(?)
Picolinic acid	3.16	2.15
L-Glutamic acid	3.22	1.03
β-Hydroxyglutamic acid	3.29	0.96
Aspartyl-glycine	3.31	1.21
Isonicotinic acid	3.35	1.51
Nicotinic acid	3.44	1.37
Anthranilic acid	3.51	1.47
p-Aminobenzoic acid	3.62	1.30
Glycyl-aspartic acid	3.63	0.82
m-Aminobenzoic acid	3.93	0.81
Diiodotyrosine	4.29	2.17
Cystinyl-diglycine	4.74	1.62
a-Hydroxyasparagine	4.74	2.43
α-Aspartyl-histidine	4.92	1.90
β-Aspartyl-histidine	4.94	2.00
Cysteinyl-cysteine	4.96	2.31
Pentaglycine	5.32	2.27
Tetraglycine	5.40	2.35
Triglycine	5.59	2.33
Tyrosyl-tyrosine	5.60	2.08
Isoglutamine	5.85	2.04
Lysyl-glutamic acid	6.10	1.65
Histidyl-glycine	6.81	1.00
Histidyl-histidine	7.30	0.50
Histidine	7.47	1.50
L-Methylhistidine	7.67	1.19
Carnosine	8.17	1.34
α,β-Diaminopropionic acid	8.20	1.40
Anserine	8.27	1.23
Tyrosyl-arginine	8.38(?)	1.00(?)
	8.68(?)	1.13(?)
L-Ornithine	9.70	1.05
Lysine	9.74	0.79
Lysyl-lysine	10.04	0.59
Arginine	10.76	1.72

of the mobility values, the simplified theory and calculation, and the possibility of impure preparations, the discrepancies are not surprising. Although one cannot speak about a quantitative verification, the measurements nevertheless show that the quantity pI-pK_1 is of a decisive importance for the conductance of isoionic ampholytes. The fact that the same quantity appears in the expression for the buffering capacity, eqn. (11), leads to the conclusion that this quantity, beside the solubility, is the only property that requires consideration in the choice of carrier ampholytes in stationary electrolysis. The smaller the value of pI-pK_1, the more effective is the ampholyte as a carrier.

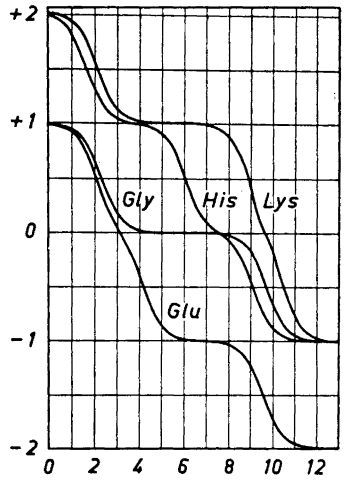

Fig. 2. Titration curves of glutamic acid, glycine, histidine, and lysine. The three amino acids with sharp isoionic points are useful as carrier ampholytes, while glycine, with its extended horizontal part of the curve, is useless.

From pK data available in the monographs of Cohn and Edsall[16], Conway[11], Sahyun[17] Kortüm, *et al.*[18] and in other sources[3–5], a list of possible carrier ampholytes, arranged in the order of increasing isoionic points, has been prepared in Table 4. Ampholytes with pI-pK_1 values bigger than 2.5 units have been excluded as completely useless; to this category belongs the whole group of neutral amino acids. Compounds with pI-pK_1 values between 1.5 and 2.5 units are included, but must be regarded as poor carriers.

The usefulness of an ampholyte as a carrier can also be judged directly from its titration curve. In Fig. 2 the titration curves of glutamic acid, glycine, histidine, and lysine are presented. Good carriers are those with sharp isoionic points. Useless is glycine, which is isoionic over a pH region covering almost four units.

A closer inspection of Table 4 reveals the crucial difficulty in the creation of natural pH gradients suitable for work with proteins. Between pH 3.9 and 7.5 there is only the almost insoluble diiodotyrosine and a number of peptides, either very expensive or not at all on the market. Unfortunately, this is the most important pH range for many proteins. It is thus necessary for continued work along this line to synthesize or to supply by other means new low-molecular ampholytes isoelectric between pH 4 and 7 and with the desired buffering and conductive capacities. The appearence of a number of peptides containing histidine in this region of the table gives a hint of possible ways to solve this problem. Partial hydrolysis of a histidine-rich protein (hemoglobin or globin) can be expected to give a mixture of various peptides containing this amino acid. Experimental work in this direction has been started. The results seem promising and will be dealt with in a forthcoming article.

The data in Table 1 raise some interesting physico-chemical problems. The absence of mobility data for ampholytes in the chemical literature is puzzling, and it appears as very desirable to design moving boundary systems allowing accurate measurements. In particular, it would be most interesting to see if

the big difference in mobility between cation and anion, predicted in Table 1 for many ampholytes, is real. This difference originates in the heavy hydration of carboxylate groups assumed by Edward in order to account for the comparatively low mobilities observed for carboxylate ions. Such a mobility difference, if substantiated by experiments, would results in a marked difference between isoionic and isoelectric points for the ampholytes in question. Such a difference is well known for proteins, but depends on complex formation with other ions than protons.

Acknowledgements. This work was started at the Department of Bacteriology, Karolinska Institutet, Stockholm, and the author wishes to express his sincere thanks to Professor Berndt Malmgren for laboratory facilities there. It was concluded in the recently erected Wallenberg Foundation Jubilee Laboratory at the same address. The author is greatly indebted to the members of the board of this laboratory, the Professors Hugo Theorell and Sune Bergström, for the privilege of establishing a new Department of Physical Chemistry there. Thanks are also due to Miss Birgitta Fagerström and Mr. Alfred Forchheimer for careful measurements. Financially, the work has been supported by the *Medical*, the *Natural Science*, and the *Technical Research Councils of Sweden*, which is gratefully acknowledged.

REFERENCES

1. Svensson, H. *Acta Chem. Scand.* **15** (1961) 325.
2. Svensson, H. *Science Tools* **3** (1956) 30.
3. Green, R. W. and Tong, H. K. *J. Am. Chem. Soc.* **78** (1956) 4896.
4. Lumme, P. O. *Suomen Kemistilehti B* **30** (1957) 168.
5. Lumme, P. O. *Suomen Kemistilehti B* **30** (1957) 176.
6. MacInnes, D. A. *The Principles of Electrochemistry*. Reinold Publ. Corp., New York 1939.
7. Van Os, G. A. J. and Möller, W. *Proc. Koninkl. Ned. Akad. Wetenschap.* **61 B** (1958) 253.
8. Svensson, H., Benjaminsson, A. and Brattsten, I. *Acta Chem. Scand.* **3** (1949) 307.
9. Edward, J. T. *Sci. Proc. Roy. Dublin Soc.* **27** (1956) 273.
10. Edward, J. T. *Chem. & Ind. London* **1956** 774.
11. Conway, B. E. *Electrochemical Data*. Elsevier Publ. Co., London 1952.
12. Saxton, B. and Meier, H. F. *J. Am. Chem. Soc.* **56** (1934) 1918.
13. Jeffrey, G. H. and Vogel, A. I. *J. Chem. Soc.* **1934** 1101.
14. Dippy, J. F. J. *J. Chem. Soc.* **1938** 1222.
15. Dippy, J. F. J. and Lewis, R. H. *J. Chem. Soc.* **1937** 1008.
16. Cohn, E. J. and Edsall, J. T. *Proteins, Amino Acids, and Peptides*. Reinhold Publ. Corp., New York 1943.
17. Sahyun, M. *Outline of the Amino Acids and Proteins*. Reinhold Publ. Corp., New York 1944.
18. Kortüm, G., Vogel, W and Andrussow K. *Dissociation Constants of Organic Acids in Aqueous Solution*. Butterworths, London 1961.

Received September 19, 1961.

ACTA CHEMICA SCANDINAVICA 16 (1962) 467–470

Cell Compartment for Use at Liquid Nitrogen Temperature in a Double-Beam Spectrophotometer

KJ. ROSENGREN*, S. SUNNER and D. TIMM

Thermochemistry Laboratory **, *University of Lund, Lund, Sweden*

A thermally insulated cell compartment accomodating two identical quartz cells, path length less than or equal to 20 mm, has been constructed with which it is possible to work uninterruptedly (without refilling) at liquid nitrogen temperature for at least three hours. The compartment has been used together with a Unicam model SP 700 UV to near IR spectrophotometer.

In the past a considerable number of devices has been designed for spectral analysis of liquid and/or solid samples at moderately low temperatures, *e.g.* that of liquid nitrogen [1–12]. Mostly, a cell compartment has been constructed as a Dewar-vessel, made of quartz or metal, accomodating a single sample cell [1–8]. Thus, with a single-beam instrument, two consecutive spectra have to be taken, one giving the absorption of an appropriate reference system. With a double-beam instrument two spectra still have to be recorded, partial compensation being obtained by introducing a second cell kept at room temperature into the path of the reference beam.

A few authors have described the use of two parallel cells, mounted either in a common double-walled evacuated metal container or in two separate Dewar vessels [9–11].

Nelson [12] describes a single cell construction of considerable interest where he has wholly substituted an insulation of the expanded plastic type (styrofoam) for the Dewar vessel. He glued together sheets of prefabricated styrofoam to a rectangular or cylindrical container for liquid nitrogen. Evacuated quartz cylinders were inserted into the walls of the container and glued in place by use of a synthetic rubber composition (EC 801, Minnesota Mining & Manufacturing Co.). Due to its simplicity this design was very attractive and it appeared that it could easily be used for the manufacture of a two-cell com-

* Research Fellow at *The Swedish Technical Research Council.*

** Sponsored by *The Swedish Natural Science Research Council* and by *The Swedish Technical Research Council.*

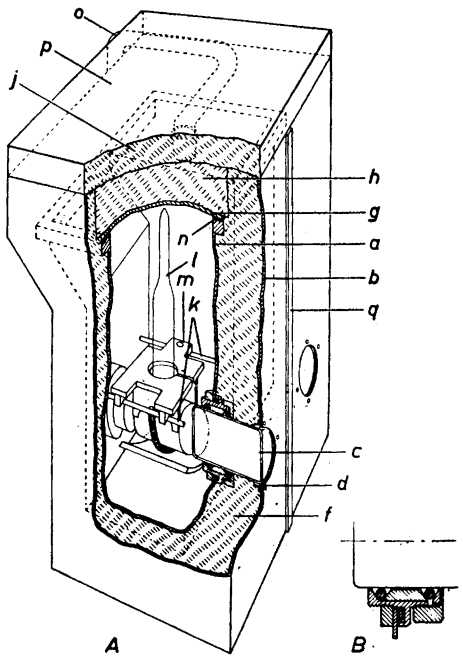

Fig. 1. Cell compartment.

partment. However, in repeating Nelson's work, we encountered a number of difficulties which partly had to do with lack of rigidity of the compartment and partly with difficulties in obtaining a satisfactory seal between the quartz cylinders and the walls made of "Styropor" (Badische Anilin- and Soda-Fabrik AG) *.

These difficulties were overcome by the following changes: In the first place stainless steel was introduced as a constructional material to assure rigidity and a perfectly reproducible mounting of the cells within the compartment. Secondly, the quartz cylinders were fastened using O-rings made of silicon rubber and, thirdly, a foamed-in-place type of polyurethane was used as insulating material.

DESIGN OF THE CELL COMPARTMENT

The cell compartment (Fig. 1 A) consists of an inner can, *a*, made of 1 mm stainless steel and equipped to accomodate two quartz cells, one sample cell and one reference cell, and an outer can, *b*, of the same shape, made of 1,5 mm aluminum plate. The minimum distance between the two cans is 52 mm at the bottom and 38 mm at the walls. The size and shape of the cans were determined from the available space between the monochromator and the detector

* The glue EC 801 with proper accelerator, EC 1 063, was in fact found to be so good as to tear out large pieces of quartz from the cylinder walls thus ruining the high vacuum inside them.

units of the spectrophotometer (Unicam SP 700) as well as from consideration of the storage capacity for liquid nitrogen.

The evacuated cylinders, *c*, with Ultrasil optically polished windows, inner diam. 22 mm, length 50 mm, were mounted in the side walls of the inner can using brass fittings and O-rings (Fig. 1 B). The horizontal distance between the centers of the cylinders was 102 mm and was determined by the beam distance of the spectrophotometer. The cylinders extruded from the inner can so that their outer windows reached the outer can. The distance between the inner windows was 22 mm.

The outer part of each quartz cylinder was equipped with a thin-walled brassflange, *d*, with which the cylinder was secured to the aluminum can, by means of screws. Each flange was equipped with an electrical heater to prevent condensation of moisture on the window *.

The space between the two cans was completely filled with foamed plastic, *f*, in the following manner. The inner can was supported on a prefabricated sheet and an appropriate amount of the foaming composition (Nopco Lockfoam E-302) was introduced and allowed to rise and cure. In order to obtain a uniform structure of the foam we found it advisable to fill the space in two stages.

The inner can was equipped with a lid, *g*, which could be screwed to the can. It was made of a 3 mm brass plate with 3 cm of high density expanded polyurethane insulation on top of it, *h*. In order to assure a close fit between the lid and the Lockfoam plastic during processing, the lid was wrapped in a thin PVC-film and kept in place until the curing of the foam had finished. Afterwards, excess Lockfoam was simply cut away and the surface was smoothened.

The interior of the steel can was divided into two halves by inserting a thin steel plate, *j*, which fitted into light traps in the bottom and in the lid of the can and, in addition, was equipped with two sprung phosphor-bronze blades along each vertical edge giving a complete light seal between the two compartments.

To support the cell holders, the steel can was equipped with two pairs of round brass bars, *k*, screwed to the walls of the can and carefully positioned above and parallel to the light paths. The cells used, *l*, were made of quartz with optically polished Ultrasil windows. The dimensions hitherto used have been o.d. 22 mm, cell length 17 mm. The cells were rigidly placed in brass holders, *m*, machined to allow a kinematic mounting to the brass bars.

As mentioned above, the lid of the inner can was screwed to the rim of the can, a teflon gasket, *n*, giving an almost gas-tight seal.

The inner can held *ca.* 2 litres of liquid nitrogen which was filled in through a short piece of glass tubing carried through the lid by an arrangement with two O-ring gaskets. The tube which had an upper standard joint also served as an escape for the gaseous nitrogen throughout all operations. In order to prevent condensation of moisture on the escape tube, *o*, during experiments, an extra 3 cm of Styropor insulation was placed on top of the lid, *p*.

The assembled cell compartment was inserted into a special housing attached to the Unicam instrument. A track and rail arrangement, *q*, served the

* In a later design, the brass-flanges with heaters were inserted from the outside of the aluminum can, thus facilitating the replacement of a faulty heating wire or of a quartz cylinder with only partial replacement of the plastic foam insulator.

double purpose of keeping the compartment in a fixed position relative to the housing and also acting as a light trap. The escaping nitrogen was carried to the outside of the housing through a tube bent so as to prevent extraneous light from entering the housing. The housing was closed by a tightly fitting metal lid.

Performance. The described cell compartment has now been used in more than 300 runs and proved to be reliable and easy to operate. One filling of liquid nitrogen will last for three to three and a half hours before the surface of the liquid reaches the cell windows.

The fact that the optical path has to pass two one millimeter layers of liquid nitrogen has never caused any trouble even though the recording of spectra down to 200 mμ has become routine [13]. On the contrary, the advantage of having the cell cooled on all surfaces is obvious, particularly in photolysis work using high energy light sources. Gas bubbles can easily be prevented from crossing the optical path by inserting glass troughs beneath the quartz cylinders on both sides of each sample cell.

Acknowledgements. This investigation has been supported by *Directorate of Chemical Science, AFOSR, AFRD of the Air Research and Development Command, United States Air Force,* through its European Office, by the *Swedish Technical Research Council* and by *Knut och Alice Wallenbergs Stiftelse.*

REFERENCES

1. Lewis, G. N. and Lipkin, D. *J. Am. Chem. Soc.* **64** (1942) 2801.
2. Norman, I. and Porter, G. *Proc. Roy. Soc. London* **A 230** (1955) 399.
3. Potts, W. J. *J. Chem. Phys.* **21** (1953) 191.
4. Sowden, R. G. and Davidson, N. *J. Am. Chem. Soc.* **78** (1956) 1291.
5. Hirshberg, Y. and Fischer, E. *Rev. Sci. Instr.* **30** (1959) 197.
6. Jones, T. O. and Willard, J. E. *Rev. Sci. Instr.* **27** (1956) 1037.
7. McConnell, H. M. and Tunnicliff, D. D. *J. Chem. Phys.* **23** (1955) 927.
8. Jones, R. N. and Keir, D. S. *Can. J. Chem.* **34** (1956) 1017.
9. Passerini, R. and Ross, I. G. *J. Sci. Instr.* **30** (1953) 274.
10. Aloisio, C. J. *Rev. Sci. Instr.* **32** (1961) 452.
11. Hirshberg, Y. and Fischer, E. *J. Chem. Soc.* **1953** 629.
12. Nelson, L. S. *Rev. Sci. Instr.* **27** (1956) 655.
13. Rosengren, Kj., Sunner, S. and Timm, D. *Acta Chem. Scand.* **16** (1962) 495.

Received September 30, 1961.

ACTA CHEMICA SCANDINAVICA 16 (1962) 471–478

Heats of Aminolysis and Hydrolysis of Some N-Acetyl Compounds and of Acetic Anhydride

INGEMAR WADSÖ

*Thermochemistry Laboratory *, University of Lund, Sweden*

Enthalphy changes for some aminolysis and hydrolysis reactions involving acetyl compounds have been determined calorimetrically. For the idealized, isothermal (25°C) reaction

$$RNAc(s) + R'NH_2(l) \rightarrow RNH(s) + R'NHAc(l/s)$$

$\Delta H°$ was found to be

-18.07 ± 0.08	kcal/mole for	RNH = imidazole and $R'NH_2$ = butylamine
-20.50 ± 0.06	» »	RNH = 1,2,4-triazole and $R'NH_2$ = butylamine
-17.28 ± 0.08	» »	RNH = 1,2,4-triazole and $R'NH_2$ = aniline
-20.22 ± 0.08	» »	RNH = tetrazole and $R'NH_2$ = aniline

For the reaction

$Ac_2O(l) + R'NH_2(l) \rightarrow HOAc(l) + R'NHAc(l/s)$ $\Delta H°$ was found to be

-27.06 ± 0.11	kcal/mole for	$R'NH_2$ = butylamine
-24.11 ± 0.06	» »	» = aniline

The standard heat of hydrolysis of acetic anhydride has been determined to be -14.00 ± 0.09 kcal/mole. From the obtained data the standard heats of hydrolysis of butyl acetamide and acetanilide have been derived, as well as the heat of combustion of acetanilide.

In a recent paper [1] heats of hydrolysis of N-acetylated imidazole, 1,2,4-triazole and tetrazole were reported. The thermochemical investigation of these compounds has now been extended to include aminolysis reactions with butylamine and aniline. In order to compare the heats of hydrolysis data with those obtained from the aminolysis experiments, the heats of hydrolysis of butyl acetamide and acetanilide must be known. These amides are not easily hydrolyzed at 25°C, but their heats of hydrolysis can be obtained by combining the values of the heat of hydrolysis of acetic anhydride and the heats of amino-

* Sponsored by *The Swedish Natural Science Research Council* and by *The Swedish Technical Research Council.*

lysis of acetic anhydride by butylamine and aniline. The heat of hydrolysis of acetic anhydride is known from the work by Kistiakowsky and co-workers [2]. However, as this value is of prime importance in calorimetry of aminolysis reactions, it has been redetermined in this work.

EXPERIMENTAL

Materials. Imidazole, 1,2,4-triazole, tetrazole, and the corresponding N-acetyl compounds were described in Ref.[1]

Acetic anhydride (Merck, analytical grade) was fractionally distilled through a 25-plate column at atmosphere pressure. A fraction constantly boiling at 139.3°C (754 mm Hg) was collected. Potentiometric titration with sodium hydroxide and gas chromatographic analysis (Pye Argon chromatograph) indicated 99.9 % purity.

Aniline of analytical grade was heated at 100°C with KOH pellets for 2 h, followed by distillation under reduced pressure through a 10-plate column. $n_D^{25} = 1.5838$; $d_4^{25} = 1.0171$.

Acetanilide was prepared from aniline and acetic anhydride and the product obtained was recrystallized from ethanol. Mp. 114.0 – 114.4°C.

Acetic acid (Merck, analytical grade) was purified by freezing out four times. Titration with NaOH indicated 100.0 % purity.

Butylamine of a *purum* grade was dried by refluxing it with KOH pellets for 2 h followed by fractionation at atmosphere pressure in a 25-plate column. Potentiometric titration with standard hydrochloric acid gave an equivalent weight corresponding to 100.0 % purity.

Butyl acetamide was prepared from butylamine and acetic anhydride [3] and fractionally distilled. $n_D^{25} = 1.4389$; $d_4^{25} = 0.8953$.

Benzene of a *purum* quality, free from thiophene, was dried by phosphorus pentoxide and then distilled through a 25-plate column.

Apparatus. The reactions were carried out in an "isothermal-jacket" calorimeter, which has been described in detail elsewhere (Type D in Ref.[4]).

Calibration. The heat equivalent of the calorimeter, including contents, was determined electrically by passing a known current for a given time (300 sec. except for the system with aniline where it was 300 – 900 sec.) through the heating element. The calibrations were performed on the system after the reaction had taken place. No significant correlation between the amount and kind of reactant and the obtained heat capacity values was observed, and therefore mean values of the obtained heat capacities have been used in calculating the results.

Calorimetric procedure. The calorimeter was charged with 100 ml of liquid. Heats of aminolysis and hydrolysis measurements were supplemented by determination of heats of solution in order to obtain the standard enthalpy change, $\Delta H°$, of the reaction.

All reactions investigated were very rapid (< 2 min) except for the aminolysis of the acetylated heterocycles by aniline. Attempts to determine the heat of reaction between aniline and N-acetyl imidazole with the apparatus used in this work failed, as the reaction was too slow. For the reactions between aniline and the acetylated triazole and tetrazole reaction periods had to be taken as long as 20 to 30 min. Thermal leakage in these cases, as well as in the solution experiments with triazole and tetrazole in aniline, was calculated by the Regnault-Pfaundler method [5]. In all other cases the initial and final thermistor resistance values were evaluated graphically.

When butylamine and its mixture with benzene were used as calorimetric liquids small corrections were applied to account for evaporation during the breaking of the ampoule.

The aminolysis reactions were carried out in the pure amines except for the case of acetic anhydride in butylamine, where the reaction was found to be too vigorous and was therefore performed in butylamine-benzene (1:10 parts by volume) solution.

Units of measurements. The results of the calorimetric experiments are expressed in terms of the defined calorie, equal to 4.1840 abs. joules, and refer to the isothermal process at 25°C, and to the true mass.

RESULTS

Aminolysis in pure butylamine

Results from the determination of heats of aminolysis of N-acetyl imidazole and N-acetyl 1,2,4-triazole are given in Table 1. log R_i/R_f is the expression proportional to the temperature change; R_i and R_f are the corrected thermistor resistance values at the start and the end, respectively, of the main period. From four calibration experiments the mean heat equivalent was calculated to be 4 741 + 5 * cal/unit of log R_i/R_f.

Results from determination of heats of solution in butylamine are given in Table 2.

Correction to the standard state. The idealized, isothermal reaction IV is obtained from eqns. I to III.

$RNAc(s) + BuNH_2(l) \rightarrow RNH(soln) + BuNHAc(soln)$	ΔH_1	(I)
$RNH(s) \rightarrow RNH(soln)$	ΔH_2	(II)
$BuNHAc(l) \rightarrow BuNHAc(soln)$	ΔH_3	(III)
$RNAc(s) + BuNH_2(l) \rightarrow RNH(s) + BuNHAc(l)$	$\Delta H°$	(IV)

$\Delta H° = \Delta H_1 - \Delta H_2 - \Delta H_3$

For RNH = Imidazole $\Delta H° = -18.07 \pm 0.06$ and
for RNH = 1,2,4-Triazole $\Delta H° = -20.50 \pm 0.04$ kcal/mole

Taking into consideration possible systematic errors in the analysis and in heat equivalent values, the standard enthalphy change for the reaction with butylamine was found to be -18.07 ± 0.08 and -20.50 ± 0.06 kcal/mole for N-acetyl imidazole and N-acetyl 1,2,4-triazole, respectively.

Aminolysis in butylamine-benzene

From six calibration experiments the mean heat equivalent was calculated to be $4\,012 \pm 2$ cal/unit of log R_i/R_f.

Results from the determination of heat of aminolysis of acetic anhydride are given in Table 3. Results from heats of solution measurements in butylamine-benzene are given in Table 4.

Correction to the standard state. The idealized isothermal reaction IX is obtained from eqns. V to VIII.

$Ac_2O(l) + BuNH_2(soln) \rightarrow HOAc(soln) + BuNHAc(soln)$	ΔH_5	(V)
$BuNHAc(l) \rightarrow BuNHAc(soln)$	ΔH_6	(VI)
$HOAc(l) \rightarrow HOAc(soln)$	ΔH_7	(VII)
$BuNH_2(l) \rightarrow BuNH_2)soln)$	ΔH_8	(VIII)
$Ac_2O(l) + BuNH_2(l) \rightarrow HOAc(l) + BuNHAc(l)$	$\Delta H°$	(IX)

$\Delta H° = \Delta H_5 - \Delta H_6 - \Delta H_7 + \Delta H_8$
$\Delta H° = -27.06 \pm 0.08$ kcal/mole

* When five or more determinations are performed, the uncertainties are given as the standard deviation of the mean. Otherwise they are the average deviation of the mean.

When systematic errors are considered, this value of $\Delta H°$ is -27.06 ± 0.11 kcal/mole.

Aminolysis in aniline

From eight calibration experiments the mean heat equivalent was calculated to be 5066 ± 4 cal/unit of log R_i/R_f.

Results from the determination of heats of aminolysis in aniline are given in Table 5 and results from heats of solution in aniline are given in Table 6.

Corrections to the standard states. The idealized isothermal reactions XIII and XVI are obtained from eqns. X to XII and XIV to XII, respectively.

RNAc(s) + $PhNH_2$(l) → RNH(soln) + PhNHAc(soln)	ΔH_{10}	(X)
RNH(s) → RNH(soln)	ΔH_{11}	(XI)
PhNHAc(s) → PhNHAc(soln)	ΔH_{12}	(XII)
RNAc(s) + $PhNH_2$(l) → RNH(s) + PhNHAc(s)	$\Delta H°$	(XIII)

$\Delta H° = \Delta H_{10} - \Delta H_{11} - \Delta H_{12}$

For RNH = 1,2,4-triazole $\Delta H° = -17.28 \pm 0.07$ and
for RNH = tetrazole $\Delta H° = -20.22 \pm 0.07$ kcal/mole

After systematic errors have been considered, the standard enthalphy change for the reaction with aniline is -17.28 ± 0.08 and -20.22 ± 0.08 kcal/mole for N-acetyl 1,2,4-triazole and N-acetyl tetrazole, respectively.

Ac_2O(l) + $PhNH_2$(l) → HOAc(soln) + PhNHAc(soln)	ΔH_{14}	(XIV)
HOAc(l) → HOAc(soln)	ΔH_{15}	(XV)
PhNHAc(s) → PhNHAc(soln)	ΔH_{12}	(XII)
Ac_2O(l) + $PhNH_2$(l) → HOAc(l) + PhNHAc(s)	$\Delta H°$	(XVI)

$\Delta H° = \Delta H_{14} - \Delta H_{15} - \Delta H_{12}$
$\Delta H° = -24.11 - 0.05$ kcal/mole

When allowances are made for possible systematic errors, this value is $\Delta H° = -24.11 \pm 0.06$ kcal/mole.

Hydrolysis of acetic anhydride

The hydrolysis of acetic anhydride was carried out in 0.8 N aqueous solution of sodium hydroxide (in connection with other hydrolysis measurements [1]). The obtained mean heat equivalent of the system was 9071 ± 5 cal/unit of log R_i/R_f.

Results from the heat of hydrolysis measurements are given in Table 7.

Correction to the standard state. The idealized isothermal reaction XX was obtained from eqns. XVII to XIX. ΔH_{18} and ΔH_{19} were found to be -13.64 and -0.02 kcal/mole, respectively [1].

Ac_2O(l) + H_2O(soln) → 2HOAc(soln)	ΔH_{17}	(XVII)
2HOAc(l) → 2HOAc(soln)	$2 \times \Delta H_{18}$	(XVIII)
H_2O(l) → H_2O(soln)	ΔH_{19}	(XIX)
Ac_2O(l) + H_2O(l) → 2HOAc(l)	$\Delta H°$	(XX)

$\Delta H° = \Delta H_{17} - 2 \times \Delta H_{18} + \Delta H_{19}$
$\Delta H° = -14.00 \pm 0.05$ kcal/mole

After making allowance for systematic errors, $\Delta H°$ was found to be -14.00 ± 0.09 kcal/mole. This value is in fair agreement with that by Kistiakowsky *et al.*[2], -13.92 kcal/mole *. In the following -13.96 ± 0.06 kcal/mole will be used, being the mean between the two determinations.

Table 1. Heats of aminolysis in butylamine

Substance	mmoles	$10^4 \cdot \log R_i/R_f$	$-\Delta H$, kcal/mole
N-acetyl imidazole	1.886	74.85	18.82
	1.888	75.18	18.88
	2.044	81.17	18.83
	2.203	87.00	18.72
			Mean 18.81 ± 0.05
N-acetyl 1,2,4-triazole	2.128	102.28	22.79
	2.872	137.96	22.77
	2.799	134.20	22.73
	2.104	101.16	22.79
			Mean 22.77 ± 0.02

Table 2. Heats of solution in butylamine

Substance	mmoles	$10^4 \cdot \log R_i/R_f$	$-\Delta H$, kcal/mole
Imidazole	2.319	-2.83	-0.58
	2.871	-3.61	-0.60
	2.500	-3.02	-0.57
			Mean -0.58 ± 0.01
1,2,4-Triazole	2.530	5.06	0.95
	2.127	4.23	0.94
	2.261	4.52	0.95
			Mean 0.95 ± 0.01
Butyl acetamide	2.222	6.28	1.34
	2.401	6.52	1.29
	1.898	5.33	1.33
			Mean 1.32 ± 0.02

Table 3. Heat of aminolysis in butylamine-benzene

Substance	mmoles	$10^4 \cdot \log R_i/R_f$	$-\Delta H$, kcal/mole
Acetic anhydride	1.386	135.45	39.21
	1.374	134.50	39.27
	1.489	146.16	39.38
	1.270	124.61	39.37
			Mean 39.31 ± 0.07

* The value is corrected to 25°C; the measurements were performed at 30°C. Uncertainties were not reported.

Table 4. Heats of solution in butylamine-benzene.

Substance	mmoles	$10^4 \cdot \log R_i/R_f$	$-\Delta H$, kcal/mole
Butyl acetamide	1.273	−4.47	−1.41
	1.211	−4.36	−1.44
	1.436	−5.20	−1.45
			Mean −1.43 ± 0.02
Acetic acid	1.269	41.99	13.28
	1.197	39.13	13.12
	1.345	44.47	13.26
	1.206	40.15	13.36
	1.129	37.49	13.32
	1.293	42.76	13.27
			Mean 13.27 ± 0.03
Butylamine	1.165	−1.11	−0.38
	1.040	−1.05	−0.41
	1.045	−1.16	−0.45
			Mean −0.41 ± 0.02

Table 5. Heats of aminolysis in aniline.

Substance	mmoles	$10^4 \cdot \log R_i/R_f$	$-\Delta H$, kcal/mole
N-Acetyl 1,2,4-triazole	3.383	71.91	10.77
	3.003	63.26	10.67
	2.489	53.46	10.88
			Mean 10.77 ± 0.07
N-Acetyl tetrazole	1.621	48.01	15.00
	2.134	63.21	15.01
	1.890	55.68	14.92
			Mean 14.98 ± 0.04
Acetic anhydride	3.056	129.59	21.48
	2.996	128.04	21.65
	2.925	124.99	21.65
	2.831	120.96	21.65
	2.996	128.54	21.73
			Mean 21.63 ± 0.04

Heats of hydrolysis of butyl acetamide and acetanilide

By comparing standard heats of hydrolysis for the heterocyclic acetates and acetic anhydride with the corresponding aminolysis data, it is possible to derive accurate values for the heats of hydrolysis of butyl acetamide and acetanilide, and to check the calorimetric results given in Ref. [1] and those arrived at here.

From the reaction schemes given below three independent values for respective heats of hydrolysis are derived.

Table 6. Heats of solution in aniline

Substance	mmoles	$10^4 \cdot \log R_i/R_f$	$-\Delta H$ kcal/mole
1,2,4-Triazole	2.857	−14.47	−2.57
	2.926	−14.69	−2.54
	2.879	−14.57	−2.56
			Mean −2.56 ± 0.01
Tetrazole	2.223	− 5.35	−1.22
	1.871	− 5.05	−1.37
	2.405	− 5.99	−1.26
	2.483	− 6.36	−1.30
			Mean −1.29 ± 0.05
Acetanilide	3.145	−24.49	−3.94
	2.918	−22.65	−3.93
	2.961	−23.18	−3.97
	3.036	−23.73	−3.96
			Mean −3.95 ± 0.02
Acetic acid	3.016	8.75	1.47
	3.024	8.61	1.44
	3.281	9.64	1.49
	3.346	9.68	1.47
			Mean 1.47 ± 0.01

Table 7. Heat of hydrolysis of acetic anhydride.

Substance	mmoles	$10^4 \cdot \log R_i/R_f$	$-\Delta H$ kcal/mole
Acetic anhydride	1.665	75.91	41.36
	1.874	85.21	41.25
	1.539	69.94	41.22
	1.561	71.04	41.28
	1.512	68.82	41.29
	1.443	65.45	41.14
			Mean 41.26 ± 0.03

		$-\Delta H°$, kcal/mole
A	N-acetyl imidazole(s) + H_2O(l) → imidazole(s) + HOAc(l)	4.83 ± 0.05
	N-acetyl imidazole(s) + $BuNH_2$(l) → imidazole(s) + BuNHAc(l)	18.07 ± 0.08
	BuNHAc(l) + H_2O(l) → HOAc(l) + $BuNH_2$(l)	−13.24 ± 0.09
B	N-acetyl triazole(s) + H_2O(l) → triazole(s) + HOAc(l)	7.29 ± 0.06
	N-acetyl triazole(s) + $BuNH_2$(l) → triazole(s) + BuNHAc(l)	20.50 ± 0.06
	BuNHAc(l) + H_2O(l) → HOAc(l) + $BuNH_2$(l)	−13.21 ± 0.08
C	Ac_2O(l) + H_2O(l) → 2 HOAc(l)	13.96 ± 0.06
	$BuNH_2$(l) + Ac_2O(l) → BuNHAc(l) + HOAc(l)	27.06 ± 0.11
	BuNHAc(l) + H_2O(l) → HOAc(l) + $BuNH_2$(l)	−13.10 ± 0.12

An earlier value, −12.73 ± 0.10 kcal/mole [3], for the heat of the hydrolysis of butyl acetamide derived from measurements according to route C is within twice the sum of

the combined uncertainties and therefore indistinguishable from the value now reported. However, the present experiments were performed with reagents of higher purity and in a more suitable calorimetric system, so that the previous value will not be considered. The heat of hydrolysis of butyl acetamide is given as + 13.20 ± 0.05 kcal/mole, being a weighed mean [6] of the results derived from routes A to C.

		$-\Delta H°$, kcal/mole
D	N-acetyl triazole(s) + H_2O(l) → triazole(s) + HOAc(l)	7.29 ± 0.06
	N-acetyl triazole(s) + $PhNH_2$(l) → triazole(s) + PhNHAc(s)	17.28 ± 0.08
	PhNHAc(s) + H_2O(l) → $PhNH_2$(l) + HOAc(l)	− 9.99 ± 0.10
E	N-acetyl tetrazole(s) + H_2O(l) → tetrazole(s) + HOAc(l)	10.31 ± 0.09
	N-acetyl tetrazole(s) + $PhNH_2$(l) → tetrazole(s) + PhNHAc(s)	20.22 ± 0.08
	PhNHAc(s) + H_2O(l) → $PhNH_2$(l) + HOAc(l)	− 9.91 ± 0.12
F	Ac_2O(l) + H_2O(l) → 2HOAc(l)	13.96 ± 0.06
	Ac_2O(l) + $PhNH_2$(l) → PhNHAc(s) + HOAc(l)	24.11 ± 0.06
	PhNHAc(s) + H_2O(l) → $PhNH_2$(l) + HOAc(l)	−10.15 ± 0.08

The heat of hydrolysis of acetanilide is taken as + 10.05 ± 0.06 kcal/mole, *i.e.*, the weighed mean of the results derived from routes D to F.

Comparison with heats of combustion data

Heats of combustion of acetanilide, aniline, and acetic acid are known and can therefore be checked by the present reaction calorimetric data.

For aniline(l) and acetic acid(l) modern data give the heats of combustion as −810.5[7] and −209.0[8] kcal/mole, respectively.

For acetanilide no recent determinations have been made. The value by Stohmann and Schmidt, as corrected in Kharasch's compilation [9], is −1010.4 kcal/mole. The derived enthalpy change for the standard hydrolysis reaction thus becomes + 9.1 kcal/mole or 0.9 kcal/mole too low in comparison with the data given here. Assuming the data for aniline and acetic acid to be correct, the heat of combustion of acetanilide should be −1009.5 kcal/mole.

REFERENCES

1. Wadsö, I. *Acta Chem. Scand.* **14** (1960) 903.
2. Conn, J. B., Kistiakowsky, G. B., Roberts, R. M. and Smith, E. A. *J. Am. Chem. Soc.* **64** (1942) 1747.
3. Wadsö, I. *Acta Chem. Scand.* **12** (1958) 635.
4. Sunner, S. and Wadsö, I. *Ibid* **13** (1959) 97.
5. See *e.g.*, Sturtevant, J. M. in Weissberger, A. (Ed.) *Physical Methods of Organic Reactions*, 2nd Ed., Part 1. Interscience Publ., New York 1949.
6. Rossini, F. D. in Rossini, F. D. (Ed.) *Experimental Thermochemistry* Interscience Publ., New York 1956.
7. Anderson, C. M. and Gilbert, E. C. *J. Am. Chem. Soc.* **64** (1942) 2369.
8. Evans, F. W. and Skinner, H. A. *Trans. Faraday Soc.* **55** (1959) 260.
9. Kharasch, M. S. *Bur. Standards J. Research* **2** (1929) 359.

Received September 30, 1961

ACTA CHEMICA SCANDINAVICA 16 (1962) 479–486

Heats of Hydrolysis of N-Acetyl Imidazole and Butyl Acetamide in Aqueous Solution

INGEMAR WADSÖ

*Thermochemistry Laboratory *, University of Lund, Sweden*

The heats of hydrolysis of N-acetyl imidazole and butyl acetamide in aqueous solution have been determined by combining standard state data with results from heats of solution measurements. The enthalpy changes were found to be -7.28 ± 0.07 and $+ 10.82 \pm 0.06$ kcal/mole, respectively (hypothetical reaction, no ionization of reaction products). The data have been discussed and compared with data for analogous reactions.

Heats of ionization (ionic strength = 0.2) have been determined for acetic acid, $\Delta H_i = + 0.18 \pm 0.05$ kcal/mole; for imidazolium ion, $\Delta H_i = + 8.79 \pm 0.04$ kcal/mole; and for butylammonium ion, $\Delta H_i = + 13.97 \pm 0.05$ kcal/mole.

Enthalpy data for the hydrolysis of N-acetyl imidazole and butyl acetamide, all reactants being in their standard state **, have recently been determined [1,2]. As these compounds can be looked upon as simple biochemical model compounds, the thermochemical standard data have been converted to apply to the biochemically more interesting state *i.e.* dilute aqueous solution. The enthalpy change in going from the pure compound to *ca.* 0.01 M aqueous solution (ionic strength 0.2) have been measured for the actual reaction components. The heats of ionization of butylammonium ion, imidazolium ion and acetic acid have also been measured.

EXPERIMENTAL

Materials. Butylamine, butyl acetamide and acetic acid were described in Ref.[2]. Imidazole (Fluka, *purum*) was purified by recrystallization from benzene followed by sublimation, m.p. 89.4–89.8°C. Titration with standard hydrochloric acid gave an equivalent weight corresponding to 100.0 % purity. N-Acetyl imidazole was prepared and purified as described in Ref.[1] m.p. 103.4–104.0°C.

Solutions. The solution experiments were performed in aqueous solutions of NaCl, HCl, NaOH, imidazole, and acetic acid. NaCl was added to make the ionic strength equal

* Sponsored by *The Swedish Natural Science Research Council* and *The Swedish Technical Research Council.*

** Referring to the hypothetical process of the pure compounds in their condensed state, at 25°C.

to 0.2. Water used was deionized and electrolytes added were of analytical grade. In the case of imidazole, the water was made free from carbon dioxide by boiling. The imidazole solution was acidified with hydrochloric acid to pH 7.1. When handling the imidazole buffer precautions were taken to avoid uptake of carbon dioxide.

Apparatus. Exept for the last two systems recorded in Table 1 an "isothermal-jacket" metal calorimeter (Type D in Ref.[3]) was used. For the systems with solutions of imidazole and acetic acid as calorimetric liquids, a calorimeter of the same type but made from thin-walled (0.9 mm) glass was used. The time to reach thermal equilibrium (*cf.* Ref.[3]) for the glass calorimeter was about 2 min. The calorimeters were charged with 100 ml of liquid and the substance was contained in a sealed glass ampoule. All reactions were very rapid; the reaction period was *ca.* 2 min and the initial and final thermistor resistance values were evaluated graphically.

Calibration. The heat equivalent of the calorimeter including contents was determined by passing a known current for a given time (360 sec) through the heating element. Each system was calibrated by at least four separate experiments. Calibrations were performed after the solution experiments except for some calibrations of the system with N-acetyl imidazole. Variations in heat equivalent in individual experiments were considered insignificant, the mean values being used.

Units of measurements. The results of the calorimetric experiments are expressed in terms of the defined calorie, equal to 4.1840 abs. joules, and refer to the isothermal process at 25°C and to the true mass.

RESULTS

The experimental results are summarized in Table 1. In the table the symbol log R_i/R_f means the expression proportional to the temperature change: R_i and R_f are the corrected thermistor resistance values at the start and the end, respectively, of the main period. ε is the heat equivalent of the calorimetric system expressed in cal/unit of log R_i/R_f. When five or more determinations were performed, the uncertainties are given as standard deviation of the mean. Otherwise, they are the average deviation of the mean.

In the solution experiments with acetyl imidazole the after-period curve was a straight line, but there was some heat evolution due to the hydrolysis of the ester. If the solution process had been instantaneous this would not cause any systematic error, as the R_f-value was evaluated graphically. In the actual case, however, dissolution was complete after *ca.* 1 min and the R_f-value had to be corrected slightly. The correction amounted to *ca.* 1 % of the log R_i/R_f-value. To avoid ionization of the imidazole when it was dissolved in 0.2 M NaCl solution, the pH was raised to 10.5 with sodium hydroxide.

Heats of ionization of butylammonium ion, imidazolium ion and acetic acid. When butylamine was dissolved in the hydrochloric acid solution, *ca.* one tenth of the hydrogen ions were used up and replaced by butylammonium ions. The heat of dilution of hydrochloric acid over the actual concentration range is very small or 0.02 kcal/mole [4]. It can therefore be assumed with confidence that the difference between the measured heats of solution of butylamine in hydrochloric acid and in sodium hydroxide solution represents the heat of ionization of butylammonium ion, so that this is calculated to be $+ 13.97 \pm 0.05$ kcal/mole.

The dissolution of imidazole under conditions (pH 10.5) allowing only an insignificant amount of the compound to be protonized, was found to be accompanied by a positive enthalpy change equal to + 3.06 kcal/mole. When imidazole was dissolved in 0.1 M hydrochloric acid solution, the obtained en-

Table 1. Heats of solution measurements.

Calorimetric liquid	ε	Substance	mmoles	$10^4 \cdot \log R_i/R_f$	$-\Delta H$ kcal/mole
0.2 M NaCl	9052 ± 12	N-Acetyl imidazole	0.885	−5.15	−5.27
			1.381	−8.09	−5.30
			0.660	−3.69	−5.06
			0.939	−5.26	−5.07
			1.420	−8.18	−5.21
				Mean	−5.18±0.05
		Butyl acetamide	1.561	5.98	3.47
			1.311	5.16	3.56
			1.240	4.80	3.50
			1.278	4.93	3.49
				Mean	3.51±0.03
		Imidazole (pH 10.5)	1.360	−4.51	−3.00
			1.162	−3.94	−3.07
			1.444	−4.94	−3.10
			1.201	−4.05	−3.05
				Mean	−3.06±0.03
0.1 M HCl 0.1 M NaCl	9050 ± 5	Imidazole	1.721	10.91	5.74
			1.349	8.53	5.72
			1.970	12.47	5.73
			1.382	8.76	5.74
				Mean	5.73±0.01
		Butylamine	1.388	30.01	19.57
			1.039	22.38	19.49
			1.360	29.34	19.52
			1.103	23.80	19.53
				Mean	19.53±0.02
		Acetic acid	2.255	0.79	0.32
			3.034	1.07	0.32
			1.736	0.65	0.34
				Mean	0.33±0.01
0.1 M NaOH 0.1 M NaCl	9064 ± 8	Butylamine	1.482	9.05	5.54
			1.742	10.67	5.55
			1.380	8.49	5.58
				Mean	5.56±0.02
0.10 M Imidazole 0.15 M NaCl	8840 ± 8	Acetic acid	1.885	19.06	8.94
			1.271	12.95	9.01
			1.309	13.25	8.95
			1.988	19.91	8.85
				Mean	8.94±0.04
0.20 M HOAc 0.18 M NaCl	8860 ± 7	Imidazole	1.661	10.46	5.58
			1.792	11.22	5.55
			2.088	13.08	5.55
			1.965	12.24	5.52
				Mean	5.55±0.02

thalpy change was −5.73 kcal/mole and the heat of ionization of imidazolium ion, at an ionic strength of 0.2, is thus calculated to be + 8.79 ± 0.04 kcal/mole

The heat of ionization of imidazolium ion has been determined previously from studies of the ionization constant as a function of temperature [5]. The value, referring to zero ionic strength, is only + 7.7 kcal/mole and thus differs considerably from that found here.

The heat of solution of acetic acid in the imidazole buffer was determined to be −8.94 kcal/mole. The final pH of the buffer was 6.85 to 6.90. Using 4.61 as the pK_a'-value for acetic acid, it is found that 0.5 to 0.6 % of the acid was undissociated at the end of the experiments. The heat of solution of acetic acid in the buffer under conditions such that acetate ion is formed quantitatively is thus calculated to be −8.98 ± 0.05 kcal/mole. When acetic acid was dissolved in 0.1 M HCl, the enthalpy change was −0.33 kcal/mole. Using the value + 8.79 for the heat of ionization of imidazolium ion, the heat of ionization of acetic acid is calculated to be + 0.14 ± 0.06 kcal/mole.

Within assigned uncertainties the same value, + 0.20 ± 0.03 kcal/mole, is arrived at when comparing results from the measurements of the heat of solution of imidazole in aqueous acetic acid and in aqueous hydrochloric acid.

It has been reported [6,7] that acetic acid to some extent is dimeric even in aqueous solution. Thus, the above calculations do not strictly apply for the reaction $HOAc + H_2O \rightarrow H_3O^+ + OAc^-$ due to the contribution from the process

$$(HOAc)_2(aq) \rightarrow 2\ HOAc(aq) \qquad (1)$$

However, as shown below, this contribution is insignificant in the present case.

When acetic acid was dissolved in hydrochloric acid, the resulting solution was *ca.* 0.02 M with regard to acetic acid. From the equilibrium constant (0.185 mole/l) [6] given for reaction (1), the amount of acetic acid present in the dimeric form at this concentration is calculated to be *ca.* 0.7 %. The heat of dissociation in the gaseous phase is given [8] as + 7.6 kcal/mole of HOAc and as the heat of dissociation in aqueous solution can be expected to be much smaller, the effect will in this case certainly amount to less then 0.05 kcal/mole.

In a 0.2 M acetic acid solution the amount of HOAc present in dimeric form is calculated to be 6.9 %. In the calorimetric experiments, when 2 mmole of imidazole was added, the same amount of acetic acid was ionized and thus removed from the equilibrium mixture of HOAc and $(HOAc)_2$. In the final solution, where [HOAc] + 2 [$(HOAc)_2$] was *ca.* 0.18 M, the amount of acid present in dimeric form is calculated to be 6.2 %. The measured heat effect, therefore, also involves the enthalpy change when *ca.* 0.2_5 mmole of HOAc is formed from the dimer.

There is no correlation between the amount of imidazole added and the heat of solution value, and the obtained heats of ionization for acetic acid are the same for the two sets of measurements within the assigned uncertainties. It can therefore be concluded that the heat of dimerization of acetic acid in water solution is very small — or that the dimerization is not as extensive as is reported. The values obtained for the heat of ionization of acetic acid can therefore be considered as representing the process when only monomer molecules are involved.

The above experiments with acetic acid were not all performed at a strictly constant ionic strength. When imidazole (*ca.* 2 mmoles) was dissolved in the acetic acid solution, the ionic strength was raised from 0.18 to *ca.* 0.20. For the imidazole buffer the ionic strength was calculated to be 0.20 before the addition of acetic acid and 0.21 to 0.22 afterwards. In this case the observed enthalpy change will include heat effects due to the difference in heat of ionization of the imidazolium ions present in the calorimetric liquid, at the two ionic strengths. Since the results of the two measurements were nearly identical, this effect is not significant.

In the following the value $+ 0.18 \pm 0.05$ kcal/mole will be used for the heat of ionization of acetic acid at an ionic strength of 0.2. This differs significantly from the well documented value [9] at zero ionic strength of -0.07 ± 0.05 kcal/mole.

Heat of hydrolysis of N-acetyl imidazole in aqueous solution. The standard heat of hydrolysis of acetyl imidazole was found to be -4.83 ± 0.05 kcal/mole[1]. From this value and from heat of solution data, the enthalpy change for reaction (2) (INH = imidazole)

$$\text{INAc(aq)} + \text{H}_2\text{O} \rightarrow \text{INH(aq)} + \text{HOAc(aq)} \qquad (2)$$

is calculated to be $\Delta H = -7.28 \pm 0.07$ kcal/mole.

Reaction (2) is hypothetical; the real hydrolysis reaction at pH-values of approximately 7 is given by (3)

$$\text{INAc} + \text{H}_2\text{O} \rightarrow \begin{cases} \alpha\ \text{INH} \\ (1-\alpha)\text{INH}_2^+ \end{cases} + \begin{cases} (1-\beta)\text{HOAc} \\ (\beta\ \text{OAc}^- \end{cases} + (\alpha + \beta - 1)\text{H}^+ \qquad (3)$$

The pK_a'-value for acetyl imidazolium ion has been determined [10] to be *ca.* 3.5 and the ester will thus be insignificantly protonized at a neutral pH-value. Using the derived values for the heat of ionization of acetic acid and of imidazolium ion, the heat of hydrolysis according to eqn. (3) will be *ca.* -12.0 kcal/mole at pH 7.00 and an ionic strength of 0.2 (pK_a for imidazolium ion is 6.95 [11]; pK_a' is estimated to be 7.10).

N-Acetyl imidazole and related compounds have recently attracted a considerable interest as possible models for reactive intermediates in enzyme (*e.g.* chymotrypsin) processes [12,13]. The free energy change of reaction (3), $\Delta G'$, has been derived to -13.3 kcal/mole * [14,15] and the acyl-imidazole grouping has therefore been classified as "energy-rich". The present calorimetric results show, that a substantial part of the free energy, which is released when N-acetyl imidazole is hydrolyzed, can be traced back to the enthalpy change in the hypothetical reaction (2), $\Delta H = -7.3$ kcal/mole. The situation here is strikingly different from the case with O- and S-acetates; the latter also being "energy-rich" compounds according to the definition given by Jencks and co-workers [15]. For these acetates the enthalpy changes for the idealized reactions corresponding to eqn. (2) are *ca.* $+ 0.5$ and -0.9 kcal/mole [16], respectively.

* At pH 7 and *ca.* 25°C, $\Delta G'$ = "standard" free energy change at a specified pH. It is based on total concentrations of reactants, including all ionic spieces. The activity for water is taken to unity.

These low ΔH-values are also reflected in lower $-\Delta G'$-values; -4.9 and -7.4 kcal/mole [15] * respectively.

The $\Delta G'$-value includes the release of free energy accompanying neutralization of the acid formed in the hydrolysis process. For acetic acid this quantity is $-$ 3.1 kcal/mole at pH 7 and 25°C. In calculating $\Delta G'$-values the activity of water is taken to be unity, while other activities are taken equal to molar concentrations. With this convention there will be included in $\Delta G'$ an expression for the "driving force of water" in hydrolysis reactions carried out in aqueous media. Based on a molar scale the activity of water is *ca.* 55 and, therefore, this convention will lower the $\Delta G'$-value by 2.4 kcal/mole at 25°C. Thus in $\Delta G'$-data (pH = 7) given for the hydrolysis of O-, S- or N-acetyl compounds *ca.* -5.6 kcal/mole (*i.e.* the major part of the $\Delta G'$-value for O- and S-acetates) is not related to the ester bond breaking.

When considering the total energy released in a certain reaction, the origin of the different contributions to an energy term are of course insignificant. However, when characterizing compounds as "energy-rich" it is important to stress the type of change behind the energy quantity given.

Heat of hydrolysis of butyl acetamide in the gaseous state and in aqueous solution. The standard heat of hydrolysis of butyl acetamide was determined [2] to be $\Delta H^\circ = + 13.20 \pm 0.05$ kcal/mole. This value refers to the hypothetical reaction where pure butyl acetamide and water react to form pure butylamine and acetic acid; all reaction components being in their condensed states. The ΔH°-value includes energy terms caused by intermolecular interactions, in this case very significant due to the extensive formation of hydrogen bonds. Therefore, to obtain the enthalpy changes for the case where there are no interactions between the molecules the values have to be converted to the ideal gaseous state, for which purpose heats of vaporization, ΔH_v, of the reaction components have to be known.

ΔH_v has been determined calorimetrically, at 25°C, for BuNHAc (17.6 ± 0.2 kcal/mole **) and for $BuNH_2$ (8.26 ± 0.04 kcal/mole [17]). For water ΔH_v is 10.52 ± 0.00 kcal/mole [4].

The enthalpy change for the process HOAc(l) → HOAc(g, equilibrium mixture at saturation pressure) has been determined calorimetrically [17] (25°C) to be 5.58 ± 0.05 kcal/mole. Using Weltner's data [8], the enthalpy change for dissociating dimer molecules present in the equilibrium gas mixture will be 6.91 kcal/mole of HOAc. The heat of vaporization, at 25°C, of acetic acid to form monomer vapor thus will be 12.49 ± 0.07 kcal/mole, (the uncertainty is an estimate). From these vaporization data the heat of hydrolysis of butyl acetamide in the gaseous, monomeric state is derived to be $+ 5.8 \pm 0.2$ kcal/mole.

In the hydrolysis of a peptide bond, C—N and O—H bonds are broken, while N—H and C—O bonds are formed. If no other changes influencing the energy of the system are considered, one would expect, from the values of the thermochemical bond energies, Table 2, the hydrolysis reaction to be endothermic by *ca.* 2 kcal/mole. This value is about 4 kcal/mole lower than that actually

* Corrected to 25°C.

** Results from preliminary measurements in this laboratory (E. Morawetz and S. Sunner).

Table 2. Thermochemical bond energies, E [a].

Bond	E, kcal
C—N	70
O—H	110.6
N—H	93.4
C—O	85.5

[a] E-Values are from Ref.[18] except for $E_{C\text{-}N}$ which has been derived from modern heats of combustion data for butylamine and *sec*-butylamine [19].

obtained, which means that in the ideal, gaseous state a peptide bond grouping is *ca.* 4 kcal/mole more resonance * stabilized than a carboxyl group.
If the standard value, $\Delta H^\circ = +13.20$ kcal/mole, is combined with heats of solution data obtained here, ΔH for reaction (4)

$$\mathrm{BuNHAc(aq) + H_2O \rightarrow BuNH_2(aq) + HOAc(aq)} \quad (4)$$

is calculated to be $+10.82 \pm 0.06$ kcal/mole. At pH 7, however, the dominant product species are those given in eqn. (5)

$$\mathrm{BuNHAc(aq) + H_2O \rightarrow BuNH_3^+(aq) + OAc^-(aq)} \quad (5)$$

If heats of ionization of acetic acid and butylammonium ion are taken to $+0.18$ and $+13.97$ kcal/mole, respectively, the enthalpy change for reaction (5) will be -2.97 ± 0.09 kcal/mole. By comparing the data for the reaction in the standard state, for the gaseous state and for reactions (4) and (5) it is obvious that intermolecular forces and ionization energies play a dominant role in the energetics of peptide hydrolysis. While the isothermal reaction is followed by a heat uptake of 5.8 kcal/mole when the unionized reaction components are isolated from each other, the heat uptake is 10.8 kcal/mole when the molecules taking part in the reaction are solvated by water. In going from the unionized state, eqn. (4), to the ionized, eqn. (5), there is a drastic change from $+10.8$ to -3.0 kcal/mole, which mainly reflects the stabilization of the products when the amino group is protonized.

Sturtevant and co-workers have determined heats of hydrolysis for various peptides, involving splitting of lysine-lysine, tyrosine-glycine, glycine-leucine, glycine-phenylalanine, and benzoic acid-tyrosine bonds [20]. Their results, referring to the fully charged state, vary from -1.2 to -2.6 kcal/mole. The value for butyl acetamide is thus slightly more negative. In the comparison it should, however, be noted that the heat of ionization of butylammonium ion is 3—4 kcal/mole higher than those of the ammonium groups of the amino acids in Ref.[20]. Furthermore, heats of ionization of the carboxyl groups of amino acids and peptides are in the order of 0.5 to 1 kcal/mole **, compared to practically zero for acetic acid and benzoic acid [9]. This means that if comparisons are made for the hypothetical case where no charged products are formed, the heats of

* Here, resonance energy of a compound refers to the difference between the experimental heat of formation and that calculated by adding together thermochemical bond energies.
** See *e.g.* Ref.[21].

hydrolysis of the peptides in Ref.[20] are 2—3 kcal/mole less endothermal than that of butyl acetamide.

The experimental material is not extensive enough to draw any definite conclusions regarding the relationship between heats of hydrolysis and structure. Differences in steric interaction between groups in the vicinity of the peptide bond, however, might account for part of the discrepancy. Another factor, intimately coupled to the steric effects, are differences in solvation energies. When gas phase data and data from water solution were compared it was found that the system (BuNHAc + H_2O)aq was stabilized by an amount of *ca.* 5 kcal/mole more than that of ($BuNH_2$ + HOAc)aq. It is thus obvious that the enthalpy terms involved are very substantial. It seems probable that the open structure of butyl acetamide permits a more extensive solvation of the peptide group than those of the amino acid peptides.

REFERENCES

1. Wadsö, I. *Acta Chem. Scand.* **14** (1960) 903.
2. Wadsö, I. *Ibid.* **16** (1962) 471.
3. Sunner, S. and Wadsö, I. *Ibid.* **13** (1959) 97.
4. Rossini, F D., Wagman, D. D., Evans, W. H., Levine, S. and Jaffe, I. *Selecied Values of Chemical Thermodynamic Properties, Circular of the National Bureau of Standards 500.* US Government Printing Office, Washington 1952.
5. Nozaki, Y., Gurd, F. R. N., Chen, R. F. and Edsall, J. T. *J. Am. Chem. Soc.* **79** (1957) 2123.
6. McDoughall, F. H. and Blumer, D. R. *J. Am. Chem. Soc.* **55** (1933) 2236.
7. Katchalsky, A., Eisenberg, H. and Lifson, S. *J. Am. Chem. Soc.* **73** (1951) 5889.
8. Weltner, Jr., W. *J. Am. Chem. Soc.* **77** (1955) 3941.
9. Laidler, W. J., Papée, H. M. and Leidler, K. J. *Trans. Faraday Soc.* **54** (1958) 502.
10. Jencks, W. P. and Carriuolo, J. *J. Biol. Chem.* **234** (1959) 1272.
11. Kirby, A. H. M. and Neuberger, A. *Biochem. J.* **32** (1938) 1146.
12. Westheimer, F. H. in Boyer, P. D., Lardy, H. and Myrbäck, K. (Editors) *The Enzymes, Vol. 1, 2nd Ed.* Academic Press Inc., New York 1959.
13. Bender, M. L. *Chem. Rev.* **60** (1960) 53.
14. Stadtman, E. R. in McElroy, W. D. and Glass, B. (Editors) *The Mechanism of Enzyme Action*, John Hopkins Press, Baltimore 1954.
15. Jencks, W. P., Cordes, S. and Carriuolo, J. *J. Biol. Chem.* **235** (1960) 3608.
16. Wadsö, I. *Acta Chem. Scand.* **16** (1962) 487.
17. Wadsö, A.-M. and Wadsö, I. *To be published.*
18. Cottrell, T. L. *The Strengths of Chemical Bonds*, 2nd *Ed.* Butterworths Scientific Publications, London 1958.
19. Ewans, F. W., Fairbrother, D. M. and Skinner, H. A. *Trans. Faraday Soc.* **55** (1959) 399.
20. Rawitscher, M., Wadsö, I. and Sturtevant, J. M. *J. Am. Chem. Soc.* **83** (1961) 3180.
21. Edsall, J. T. and Wyman, J. *Biophysical Chemistry, Vol. I* Academic Press, Inc., New York 1958.

Received September 30, 1961.

ACTA CHEMICA SCANDINAVICA 16 (1962) 487–494

Heats of Hydrolysis of Acetates and Thiolacetates in Aqueous Solution

INGEMAR WADSÖ

*Thermochemistry Laboratory *, University of Lund, Sweden*

Enthalpy changes, $\Delta H°$, for the idealized isothermal (25°C) reaction RXAc(s/l) + H_2O(l) → RXH(l) + HOAc(l) have been determined calorimetrically. $\Delta H°$ was found to be + 0.53 ± 0.06 and + 1.75 ± 0.07 kcal/mole for RXAc equal to β-acetylaminoethyl acetate (l) and β-acetylaminoethyl thiolacetate (s), respectively. By heat of solution measurements the enthalpy changes for the hydrolysis reactions in aqueous media (solute concentration *ca.* 0.01 M, no ionization of reaction products), were found to be + 0.47 ± 0.07, −0.91 ± 0.08 and + 0.43 ± 0.06 kcal/mole for RX-Ac equal to $AcNHCH_2CH_2O$-Ac, $AcNHCH_2CH_2S$-Ac and C_2H_5O-Ac, respectively. The heats of hydrolysis of O- and S-acetates and the energetics of the acyl shift O → S in the gaseous state and in aqueous solution are discussed.

In a series of papers [1–3] enthalpy data for heats of hydrolysis of acetates and thiolacetates have been presented. The goal has been to provide some basic experimental data for these classes of compounds, with a special reference to their biochemical significance.

Of the biochemically important thiol esters acetyl coenzyme A is the most studied, and it was therefore felt desirable to determine the heat of hydrolysis of a comparatively simple, but still adequate model compound. In the present investigation β-acetylaminoethyl thiolacetate, $CH_3CONHCH_2CH_2S$-$COCH_3$, has been studied. This compound has been used earlier as a model for acetyl coenzyme A in kinetic studies of the hydrolysis process [4]. To enable a close comparison with the thiol ester, the heat of hydrolysis of the oxygen analogue β-acetylaminoethyl acetate, $CH_3CONHCH_2CH_2O$-$COCH_3$, has been determined. The S- and O-acetyl groups are easily split off in aqueous alkali, while the N-acetyl group is stable under the experimental conditions. Both esters are readily soluble in water and the determined standard enthalpy changes, $\Delta H°$ **

* Sponsored by *The Swedish Natural Science Research Council* and *The Swedish Technical Research Council.*

** Referring to the hypothetical process of the pure compounds in their condensed state, at 25°C.

for the processes have been recalculated to be valid for aqueous solution. For this purpose heats of solution in water (*ca.* 0.01 M solute concentration, ionic strength = 0.2) have been determined for the reaction components, as well as for ethyl acetate and ethanol. Unfortunately, the thiol acetates studied [1,3] earlier are not sufficiently soluble in water to allow measurements of the heat of solution with the calorimetric equipment available.

EXPERIMENTAL

Materials. β-Acetylaminoethanol was prepared[5] from β-aminoethanol (Eastman Kodak, m.p. 9 – 10°C) and acetic anhydride (Merck, analytical grade). The preparation obtained was fractionally distilled at *ca.* 2 mm Hg, b.p. 140°C, and then left for some weeks, after which one of the fractions slowly crystallized. A water solution of the very hygroscopic crystals showed an alkaline reaction. The solution was neutralized to pH 7 and then treated with standard sodium hydroxide (to make a 0.05 M solution) for 20 min. Titration back to pH 7 with hydrochloric acid showed a consumption of alkali corresponding to *ca.* 2 % hydrolyzable acetate. The crystalline preparation was treated with 2 N aqueous potassium hydroxide at room temperature for 5 min followed by neutralization with hydrochloric acid. The water was removed in vacuum at 40°C and the precipitated potassium chloride was filtered off. The residue was distilled quickly through a short Vigreux column at *ca.* 2 mm Hg. The resultant compound reacted weakly alkaline and titrations indicated 0.2 % hydrolyzable acetate.

A sample of this preparation was kept at 200°C, under nitrogen, for one hour. When dissolved in water it showed a strong alkaline reaction. Titration to pH 7 consumed 17 mmoles of HCl per mole of N-acetate. When treated with alkali there was a net consumption equal to 19 mmoles. It thus seems as the N-acetate isomerizes to some extent to the O-ester at high temperatures (*cf.* Ref.[6]) The β-acetylaminoethanol, therefore, cannot be purified by distillation at reasonably high pressures especially as the O-ester would be expected to have a considerably higher vapor pressure.

The alkali-treated and quickly distilled preparation was inoculated with a minute quantity of impure crystals. When two thirds had crystallized the mother liquor was rejected. After the process had been repeated, no O-ester could be detected; $n_D^{25} = 1.4728$; $d_4^{25} = 1.1124$, m.p. 28.0 – 28.8°C.

Acetylation of the hydroxyl group of β-acetylaminoethanol with acetic anhydride according to Roe *et al.*[7] gave a product essentially neutral in water solution.However, the equivalent weight, as determined by alkaline hydrolysis and back titration, was too low, suggesting an extensive formation of N,N,O-triacetate, *ca.* 50 % when the reaction time was as long as 6 h at *ca.* 90°C. The N,O-diacetyl compound could not be purified by careful distillation as the compound was not stable at higher temperatures (an intense odor developed resembling that of pyridine).

To avoid the formation of triacetate, the N,O-diacetate was prepared from the N-acetate by acetylation with an equivalent amount of acetyl chloride in tetrahydrofuran solution at room temperature. Most of the hydrochloride formed was absorbed by the reaction mixture and was removed by ammonia. After filtering off the precipitated ammonium chloride, the excess of ammonia and the solvent was removed in vacuum, at room temperature. The residue was distilled quickly through a 30 cm Vigreux column, yield 83 %. Titration data indicated the product to contain 98 % N,O-diacetate. Attempts to purify the compound by fractional distillation in efficient columns at pressures between 5 and 10 mm Hg were unsuccessful; *ca.* 5 % too low equivalent weights were obtained. However, by repeated fractionation in a 30 cm Vigreux column, at *ca.* 1 mm Hg, an odorless product giving the theoretical equivalent weight was obtained; $n_D^{25} = 1.4510$; $d_4^{25} = 1.1053$.

β-Acetylaminoethane thiol was prepared [8] from freshly distilled ethylenimine [9] and thiolacetic acid [10] (99.5 % according to iodine titration). After repeated fractional distillation at *ca.* 1 mm Hg the substance had the theoretical equivalent weight as determined by iodine titration in acetic acid [11]. $n_D^{25} = 1.5120$.

β-Acetylaminoethyl thiolacetate was prepared [8] from β-acetylaminoethane thiol by acetylation with ketene and purified by repeated fractional distillation at *ca.* 2 mm Hg followed by freezing out. Iodine titrations after alkaline hydrolysis [1] indicated 99.7 % purity. In calculating the enthalpy change it was assumed that 0.3 % inactive impurities were present; m.p. 30—32°C.

Ethyl acetate of analytical grade (Merck) was purified by fractional distillation. The equivalent weight, determined by alkaline hydrolysis and back titration, was equal to the theoretical. Ethyl alcohol of a commercial absolute grade was treated with magnesium [12] and distilled. The acetic acid was that described in Ref. [13].

Apparatus. The measurements were performed with an "isothermal-jacket" glass calorimeter, described in detail elsewhere [14,15]. The calorimeter was charged with 100 ml of liquid and the substance was contained in a sealed glass ampoule. The heat equivalent of the calorimeter including its content was determined by passing a known current for a given time (360 sec) through the heating element. The calibration experiments, at least five for each system, were performed after the reaction had taken place. No significant correlation between amount and kind of reactant and the measured heat capacity values was found and therefore derived mean values have been used in calculating the results.

Procedure. β-Acetylaminoethyl acetate was hydrolyzed in a 0.1 M aqueous solution of sodium hydroxide to which sodium chloride was added to give a total ionic strength of 0.2. The sodium hydroxide concentration was the same as was used in determining the equivalent weight of the ester. As in the analytical experiments, care was taken to avoid absorption of carbon dioxide in the calorimetric liquid. The reaction period was *ca.* 7 min and corrections for heat exchange were calculated by means of the Regnault-Pfaundler method [16]. Normal K-values (K = the constant in Newton's cooling law) were obtained, which indicates that side reactions slower than the main reaction were absent.

The thiol ester was hydrolyzed in 0.8 M sodium hydroxide solution (the same as was used in the analytical experiments). The reaction periods for the calorimetric hydrolysis experiments were 3—7 min; the length of the reaction period was mainly due to the slow dissolution of the crystalline thiol ester. Thiols, formed in an alkaline medium, are rapidly oxidized in the presence of oxygen. Most oxygen could be removed from the calorimetric system, but in order completely to cancel the small unavoidable heat effects due to oxidation the same technique as before [1,3] was used. Thus, 0.5 ml β-acetylaminoethane thiol was substituted for the sodium hydroxide solution. In doing so, normal K-values were obtained. Heat exchange corrections were calculated by means of the Regnault-Pfaundler method.

The hydrolysis experiments were supplemented by heats of solution measurements in the hydrolysis media in order to arrive at enthalpy data for the standard state, $\Delta H°$, and in 0.2 M sodium chloride solution *, to give data for the processes in water solution. These processes were all very rapid, and initial and final thermistor values were evaluated graphically.

Units of measurements. The results of the calorimetric experiments are expressed in terms of the defined calorie, equal to 4.1840 abs. joules, and refer to the isothermal process at 25°C and to the true mass.

RESULTS

The experimental results are summarized in Tables 1—3. In the tables the symbol log R_i/R_f means the expression proportional to the temperature change: R_i and R_f are the corrected thermistor resistance values at the start and the end, respectively, of the main period. ε is the heat equivalent of the calorimetric system expressed in cal/unit of log R_i/R_f. When five or more determinations were performed given uncertainties are standard deviations of the means. Otherwise, they are the average deviation of the mean.

* Here, with only uncharged species present, heats of solution are not expected to be dependent on small differences in the ionic strength. However, to reach conformity with other heats of solution measurements 0.2 M NaCl was used as calorimetric liquid.

The heat of solution of β-acetylaminoethanol was found to be 0.1 kcal/mole more exothermal in aqueous alkali than in water at neutral pH, ionic strengths being the same. The difference is small but seems to be significant.

Corrections to standard states. The ideal isothermal hydrolysis reaction V is obtained from eqns. I—IV, which correspond to the reactions taking place under actual experimental conditions.

X = O, S. R = $AcNHCH_2CH_2$—

RXAc(l/s) + H_2O(soln) → RXH(soln) + HOAc(soln)	ΔH_1	(I)
RXH(l) → RXH(soln)	ΔH_2	(II)
HOAc(l) → HOAc(soln)	ΔH_3	(III)
H_2O(l) → H_2O(soln)	ΔH_4	(IV)
RXAc(l/s) + H_2O(l) → RXH(l) + HOAc(l)	$\Delta H°$	(V)

$\Delta H° = \Delta H_1 - \Delta H_2 - \Delta H_3 + \Delta H_4$

Table 1. Results from heat of hydrolysis and heats of solution measurements performed in aqueous solution containing 0.1 mole NaOH and 0.1 mole NaCl per liter. $\varepsilon = 8882 \pm 7$ cal/unit of log R_i/R_f.

Substance	mmoles	$10^4 \cdot \log R_i/R_f$	$-\Delta H$, kcal/mole
$AcNHCH_2CH_2OAc$	3.266	58.87	16.01
	2.746	49.29	15.94
	2.398	43.21	16.00
	2.897	52.19	16.00
		Mean	15.99 ± 0.03
$AcNHCH_2CH_2OH$	3.387	10.78	2.83
	3.494	11.04	2.81
	2.752	8.80	2.84
		Mean	2.83 ± 0.01
HOAc	3.611	55.73	13.71
	4.306	66.29	13.67
	3.705	57.14	13.70
	3.167	48.73	13.67
	4.353	67.47	13.77
	3.181	48.81	13.63
		Mean	13.69 ± 0.02

Table 2. Results from heat of hydrolysis and heat of solution measurements performed in 0.8 M aqueous NaOH solution. $\varepsilon = 8858 \pm 4$ cal/unit of log R_i/R_f.

Substance	mmoles	$10^4 \cdot \log R_i/R_f$	$-\Delta H$, kcal/mole
$AcNHCH_2CH_2SAc$	2.605	59.79	20.33
	2.416	55.32	20.28
	2.967	68.25	20.38
	2.427	55.73	20.34
		Mean	20.33 ± 0.03
$AcNHCH_2CH_2SH$	2.595	24.60	8.40
	2.550	24.45	8.49
	2.616	24.96	8.45
	3.315	31.84	8.51
		Mean	8.46 ± 0.04

Table 3. Results from heats of solution measurements performed in 0.2 M aqueous solution of NaCl. $\varepsilon = 8878 \pm 7$ cal/unit of log R_i/R_f.

Substance	mmoles	$10^4 \cdot \log R_i/R_f$	$-\Delta H$, kcal/mole
$AcNHCH_2CH_2OAc$	1.572	5.32	3.00
	1.180	3.98	2.99
	2.139	7.11	2.95
		Mean	2.98 ± 0.02
EtOAc	1.262	3.32	2.34
	1.211	3.09	2.27
	0.691	1.74	2.24
	0.950	2.40	2.24
		Mean	2.27 ± 0.03
$AcNHCH_2CH_2SAc$	1.449	−1.42	−0.87
	1.358	−1.43	−0.94
	0.900	−0.91	−0.90
	2.308	−2.46	−0.95
		Mean	−0.92 ± 0.03
$AcNHCH_2CH_2OH$	2.035	6.15	2.68
	2.393	7.36	2.73
	1.399	4.29	2.72
		Mean	2.71 ± 0.02
EtOH	1.405	3.82	2.41
	0.994	2.69	2.40
	1.650	4.47	2.40
	1.573	4.21	2.38
		Mean	2.40 ± 0.01
$AcNHCH_2CH_2SH$	1.654	2.71	1.45
	2.492	3.94	1.40
	3.310	5.31	1.42
	1.404	2.18	1.38
		Mean	1.41 ± 0.02

Table 4.

RXAc	ΔH_1	ΔH_2	ΔH_3	ΔH_4	$\Delta H°$
$AcNHCH_2CH_2OAc$ [a]	−15.99	−2.83	−13.69	0.00 [b]	0.53 ± 0.06
$AcNHCH_2CH_2SAc$	−20.33	−8.46	−13.64 [c]	−0.02 [c]	1.75 ± 0.07

[a]) ΔH_2 refers to the heat of solution of liquid $AcNHCH_2CH_2OH$.
[b]) Ref.[17]
[c]) Ref.[18]

In Table 4 is given a summary of the data in connection with the heats of hydrolysis measurements. The uncertainties assigned for the $\Delta H°$-values include possible systematic errors in the analysis and in the ε-values. All enthalpy values are expressed in kcal/mole.

Heats of hydrolysis in aqueous solution. Enthalpy changes for the hydrolysis reactions in aqueous solution (eqn. X) are derived according to the reaction scheme below.

R = $AcNHCH_2CH_2$—, C_2H_5—
X = O, S

(aq) symbolizes the aqueous medium, ionic strength = 0.2, solute concentration *ca.* 0.01 M.

RXAc(l/s) + H_2O(l) → RXH(l) + HOAc(l)	$\Delta H°$	(V)
RXAc(l/s) → RXAc(aq)	ΔH_6	(VI)
H_2O(l) → H_2O(aq)	ΔH_7	(VII)
RXH(l) → RXH(aq)	ΔH_8	(VIII)
HOAc(l) → HOAc(aq)	ΔH_9	(IX)
RXAc(aq) + H_2O(aq) → RXH(aq) + HOAc(aq)	ΔH_{aq}	(X)

$\Delta H_{aq} = \Delta H° - \Delta H_6 - \Delta H_7 + \Delta H_8 + \Delta H_9$

In Table 5 are summarized data for reactions V—X. ΔH_7 is taken equal to zero [17]. All enthalpy values are expressed in kcal/mole.

Table 5.

RXAc	$\Delta H°$	ΔH_6	ΔH_8	ΔH_9	ΔH_{aq}
$AcNHCH_2CH_2OAc$	0.53	−2.98	−2.71	−0.33 [d]	0.47 ± 0.07
$AcNHCH_2CH_2SAc$	1.75	0.92	−1.41	−0.33 [d]	−0.91 ± 0.08
EtOAc	0.89 [e]	−2.27	−2.40	−0.33 [d]	0.43 ± 0.06

[d] Ref.[14]
[e] Ref.[2]

From the heat of solution of $AcNHCH_2CH_2SH$ in 0.2 M NaCl (−1.41 kcal/mole) and in 0.8 M NaOH (−8.46 kcal/mole) and from the heat of ionization of water (*ca.* + 13.5 kcal/mole) the heat of ionization of the SH-group is calculated to approximately + 6.5 kcal/mole. pK_a' for $AcNHCH_2CH_2SH$ has been reported [19] to be 9.2, which means that ionization of the thiol group will contribute + 0.04 kcal/mole to the heat of hydrolysis of the thiol ester at pH 7. At this pH acetic acid is dissociated almost completely. Using the value + 0.18 ± 0.05 kcal/mole for the heat of ionization of acetic acid, the heats of hydrolysis, at pH 7 and at an ionic strength of 0.2, will be + 0.65 ± 0.09, −0.69 ± 0.09 and + 0.61 ± 0.08 kcal/mole for β-acetylaminoethyl acetate, β-acetylaminoethyl thiolacetate and ethyl acetate, respectively.

DISCUSSION

When an ester is hydrolyzed in aqueous solution, the resulting enthalpy change is a gross effect, which tentatively can be divided into two parts: (*a*) The enthalpy change for the hypothetical hydrolysis reaction where no intermolecular interactions occur, *e.g.* in the ideal gaseous state. (*b*) Enthalpy

changes due to interactions with the solvent. These two enthalpy terms are again gross effects, and further, they cannot be expected to be completely independent of each other. However, in an attempt to analyze the obtained ΔH_{aq}-data the separation is useful.

Heats of vaporization data are not available to allow an accurate calculation of the heats of hydrolysis in the gaseous phase for β-acetylaminoethyl acetate and for the S-analogue. However, for studying enthalpy changes according to (*a*) the gas phase hydrolysis of ethyl acetate and ethyl thiolacetate should serve.

Heats of vaporization, ΔH_v, have been determined calorimetrically at 25°C for ethyl acetate and ethyl thiolacetate and found to be 8.40 ± 0.03 and 9.56 ± 0.05 kcal/mole [20], respectively. For water [17], ethanol [17]* and ethanethiol [21], ΔH_v were taken as 10.52 ± 0.00, 10.17 ± 0.04 and 6.58 ± 0.01 kcal/mole, respectively. Heat of vaporization of acetic acid to the monomer form has been derived to be 12.49 ± 0.07 kcal/mole [14].

From ΔH-data determined [1,2,3] earlier and from the given ΔH_v-data, heats of hydrolysis in the gaseous phase, $\Delta H°_{gas}$, are calculated to be + 4.63 ± 0.11 and −1.82 ± 0.10 kcal/mole for ethyl acetate and ethyl thiolacetate, respectively.

Heats of reaction data for the gaseous state include enthalpy terms due to the formation and breaking of chemical bonds, changes in resonance energies and steric effects. In the hydrolysis of an O-acetate the same type of bonds broken are also formed. Thus, if there is no change in resonance energies, and if steric factors do not contribute to the energy change of the system, the heat of reaction should be zero. The experimentally derived value is + 4.6 kcal/mole, and, therefore, ethyl acetate seems to be more resonance stabilized ** than acetic acid by this amount. In the hydrolysis of a thiol ester, C—S and O—H bonds are broken while S—H and C—O bonds are formed. Using the thermochemical bond energies given in Table 6, $\Delta H°_{gas}$ for the hydrolysis reaction would be expected to be + 7 kcal/mole, neglecting changes in resonance energy.

Table 6. Thermochemical bond energies, *E* [22]

Bond	*E*, kcal
C—S	65
O—H	110.6
S—H	83
C—O	85.5

The $\Delta H°_{gas}$-value actually obtained is *ca.* −2 kcal/mole and a simple thiol acetate, therefore, is 9 kcal less stabilized by resonance than acetic acid or 13—14 kcal/mole less than the corresponding O-ester.

When a simple O-acetate is hydrolyzed in aqueous medium to form unionized acetic acid, the reaction was found to be accompanied by an enthalpy uptake of *ca.* 0.5 kcal/mole, or 4 kcal/mole less than in the gas phase reaction.

* Gas imperfection estimated to 0.05 kcal/mole.

** Here, resonance energy of a compound refers to the difference between the heat of formation value calculated from thermochemical bond energies and that arrived at experimentally.

Apparently, stabilization due to solvation is more pronounced for the reaction products than for the reactants. In case of the thiol ester system the enthalpy change in going from the gaseous state to dilute aqueous solution is + 1 kcal/mole which means that solvation enthalpies are stabilizing the starting system slightly more than the reaction products.

Energetics of acyl shift O → S. Recently, Jencks and co-workers [23] measured the equilibrium, at 39°C, for the isomerization reaction

$$HSCH_2CH_2CH_2OAc(aq) \rightleftharpoons AcSCH_2CH_2CH_2OH(aq)$$

and obtained the standard free energy change, $\Delta G^\circ = -RT \ln \frac{[AcSR]}{[AcOR']}$ to be + 2.50 kcal/mole. As judged from the present calorimetric results the enthalpy change at an acyl shift O → S in aqueous medium will be + 1.3 kcal/mole. Using these values, ΔG° is calculated to be + 2.3 kcal/mole at 25°C. From these data, the entropy term, $T\Delta S$, for a simple transacetylation O→ S in aqueous solution is derived to be −1.0 kcal/mole at 25°C. The ΔH°_{gas}-value for the transacetylation reaction above is estimated to be about + 6.5 kcal/mole and, thus, in the ΔH_{aq}-value of + 1.3 kcal/mole about −5 kcal/mole is due to differences in the heats of solvation of the S-ester (with its OH-group) and the O-ester.

Acknowledgement. The technical assistance of Miss S. Kristoffersson is gratefully acknowledged.

REFERENCES

1. Wadsö, I. *Acta Chem. Scand.* **11** (1957) 1745.
2. Wadsö, I. *Ibid.* **12** (1958) 630.
3. Wadsö, I. *Ibid.* **14** (1960) 561.
4. Hawkins, P. J. and Tarbell, D. S. *J. Am. Chem. Soc.* **75** (1953) 2982.
5. Heyns, K. and v. Bebenburg, W. *Ann.* **595** (1955) 55.
6. Phillips, A. P. and Maggiolo, A. *J. Am. Chem. Soc.* **72** (1950) 4920.
7. Roe, E. T., Miles, T. D. and Swern, D. *J. Am. Chem. Soc.* **74** (1952) 3442.
8. Kuhn, R. and Quadbeck, G. *Chem. Ber.* **84** (1951) 844.
9. Allen, C. F. H., Sprangler, F. W. and Webster, E. R. *Org. Syntheses* **30** (1950) 38.
10. Sjöberg, B. *Svensk Kem. Tidskr.* **63** (1951) 90.
11. Kuhn, R., Birkofer, L. and Quackenbush, F. W. *Chem. Ber.* **72** (1939) 407.
12. Vogel, A. I. *Practical Organic Chemistry* Longmans, Green and Co., London 1948.
13. Wadsö, I. *Acta Chem. Scand.* **16** (1962) 471.
14. Wadsö, I. *Ibid.* **16** (1962) 479.
15. Sunner, S. and Wadsö, I. *Ibid.* **13** (1959) 97.
16. See, *e.g.*, Sturtevant, J. M. in Weissberger, A. (Ed.), *Physical Methods of Organic Reactions*, 2nd Ed., Part 1. Interscience Publ., New York 1949.
17. Rossini, F. D., Wagman, D. D., Evans, W. H., Levine, S. and Jaffe, I. *Selected Values of Chemical Thermodynamic Properties, Circular of the National Bureau of Standards 500.* US Government Printing Office, Washington 1952.
18. Wadsö, I. *Acta Chem. Scand.* **14** (1960) 903.
19. McQuillin, F. J. and Stewart, J. *J. Chem. Soc.* (1955) 2966.
20. Wadsö, A.-M. and Wadsö, I. *To be published.*
21. McCullough, J. P., Hubbard, W. N., Frow, F. R., Hossenlopp, I. A. and Waddington, G. *J. Am. Chem. Soc.* **79** (1957) 561.
22. Cottrell, T. L. *The Strengths of Chemical Bonds*, 2nd Ed. Butterworths Scientific Publications, London 1958.
23. Jencks, W. P., Cordes, S. and Carriuolo, J. *J. Biol. Chem.* **235** (1960) 3608.

Received September 30, 1961.

ACTA CHEMICA SCANDINAVICA 16 (1962) 495–500

An Experimental Approach to the Study of Radical Formation and Recombination Processes

KJ. ROSENGREN*, S. SUNNER and D. TIMM

Thermochemistry Laboratory **, *University of Lund, Lund, Sweden*

An instrumental design is described for the irradiation of light absorbing substances and for the recording of spectra of their decomposition products in a rigid matrix at 77°K, using high pressure mercury lamps and a double-beam recording spectrophotometer. The performance of the assembly has been tested by photolyzing carbon disulfide and ethyl iodide.

The determination of bond energies is one of the principal objects of molecular energetics. For covalent bonds it can be done in one or both of two principally different ways. Either, the direct determination of a specific fragmentation of a molecule may give a value of the *bond dissociation energy* of a particular bond, or, from thermochemical heat of combustion or heat of reaction measurements a value of the *thermochemical bond energy term* may be derived [1].

It should be of considerable theoretical value to devise a method for the direct measurement of *bond formation energies* by studying calorimetrically the radical recombination reaction

$$2\,A\times \rightarrow A_2^{***}$$

Such a method was used by Bichowsky and Copeland [2,3(p. 26)] in determining the heat of formation of H_2 from hydrogen atoms. These were obtained by flowing H_2 through an electric discharge. From measurements of the change in pressure and of the heat release at a platinum surface, the recombination energy was obtained. Obviously, this method is limited to a few cases with very small molecules, where the dissociation process can be unambiguously established.

---

* Research Fellow at *The Swedish Technical Research Council.*

** Sponsored by *The Swedish Natural Science Research Council* and *The Swedish Technical Research Council.*

*** For obvious reasons, this experiment can be performed unambiguously only if the two radicals are identical. In the case of ionic species or formation of bonds of an electron donor-acceptor type the species must of course be different.

To achieve a more general applicability it was deemed necessary to turn to the study of prodution and behaviour of radicals in a condensed state. The problems coped with are here connected with the fulfilment of the following conditions:

1. One — and only one — radical species must be generated in an otherwise non-reactive system.
2. The nature and the amount of the radical must be established. During the procedure the system must be reasonably stable.
3. The recombination reaction must be clean.
4. Further, it must be initiated and completed within the boundaries of a calorimetric system.

Although it was realized that it should be a formidable task to find ways and means by which these conditions could be fulfilled and that the ultimate goal certainly was quite afar, it was felt that results which might be gained could easily justify a careful exploration of the possibilities inherent in this experimental approach.

EXPERIMENTAL APPROACH

The first condition given above was judged to be the most crucial. Although in recent years a very pronounced interest has been shown in the study of free radicals and a considerable amount of information has been gained [4,5], still very little is known about stoichiometric relations in radical formation processes. This being so, the assumption was made that, provided means could be found to split homolytically a symmetrical molecule into two identical radicals, the chemistry of the overall process should be very much simplified. Among a number of possible classes of substances symmetrical aliphatic disulfides were chosen for several reasons. This particular aspect will be elaborated in a later paper [6].

The third condition put severe restrictions on both methods for formation as well as for determination of concentration of reactant and reaction product(s). The calorimetric procedure required the size of the sample container to be at least a few milliliters and its shape to approach spherical symmetry. Thus, some of the most common techniques for radical formation as well as trapping were out of the question. It was therefore decided to start out by exploring the method used by Lewis and Lipkin [7], Norman and Porter [8] and others, namely, to photolyze a compound at liquid nitrogen temperature in a rigid matrix consisting of a mixture of organic solvents and — as a possible analytical tool — to study the spectral changes in the UV and visible regions.

Thus, it was required to design and build a unit for photolysis as well as a compartment for work at liquid nitrogen temperature accomodating an appropriately designed sample cell and an identical reference cell to be used in connection with a recording double-beam spectrophotometer. The construction of the cell compartment has been given in the preceding paper [9]. The present paper gives a description of the photolysis equipment and reports the results of some test experiments.

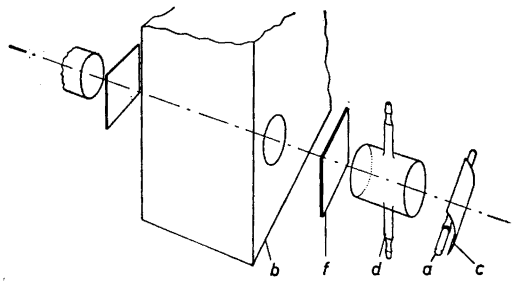

Fig. 1. Lay-out of photolysis equipment.

Apparatus

Photolysis equipment. High pressure mercury lamps, *a*, Philips SP 900 W, were mounted on each side of the cell compartment, *b*, within surface-aluminized parabolic reflectors, *c*, and equipped with appropriate cooling devices and filters (Fig. 1). The filter consisted of 3. 5 cm of a nickel sulphate solution [10] (285 g of $NiSO_4$, 6 H_2O per liter of solution) which was pumped through a cell, *d*, (o.d. 35 mm, cell length 35 mm) and cooled by tap water in a spiral condenser *. The total amount of irradiation has been measured with a uranyl oxalate actinometer and corresponds to 1.8×10^{17} quanta per second and cm^2. Besides, glass filters, *f*, could be inserted into the light beam.

Cells and cell compartment. In the standard procedure cylindrical quartz cells, o.d. 22 mm and i.d. *ca.* 19 mm, cell length 17 mm, were used. The sealed-on, optically polished windows were made of Ultrasil, wall thickness 1.5 mm. The 9 mm inner diameter stem had a quartz to Pyrex graded seal. The cell compartment has been described in a preceding paper [9].

Spectrophotometer. A Unicam model SP 700 double-beam recording spectrophotometer was used, the only change being made was the replacement of the standard cell compartment with the low temperature unit [9]. The recording was made linearly in wave-numbers and, hitherto, with direct reading in percent transmission. The spectrophotometer was calibrated using Philips spectral lamps type 93 106 E (Zn) and type 93 109 E (Hg, low pressure).

Materials

Glass-forming hydrocarbons. Different mixtures of isopentane with 3-methyl pentane were used as glass-forming liquids (6:1 and 2:3 by volume, Ref.[11] and Ref.[8], respectively). In addition, a new mixture of hydrocarbons was tried, *viz.* pentane and *neo*-hexane (3:8 by volume) [12]. The purification and purity determination of the substances will be described elsewhere [13].

Carbon disulfide was purified according to Vogel [14]. From gas-chromatographic studies, the purity was judged to be better than 99.95 %.

Ethyl iodide was purified by fractional distillation. Estimated purity (gaschromatography) better than 99.95 %.

Experimental procedure

Filling of the cells. The stem of the quartz cell was sealed to a shirted standard joint cone by which connection could be established with a high vacuum line. The cells were pumped until the pressure dropped beyond 10^{-4} mm Hg and thereupon they were filled with dry air.

* Metal parts were carefully avoided, the pump being made of lucite. The light transmission of the solution was unaffected after 30 h of operation.

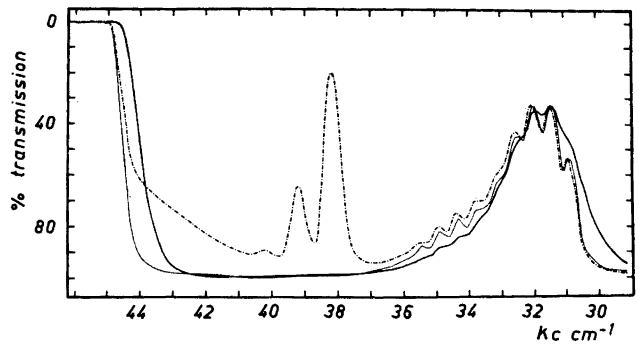

Fig. 2. Spectra of 5 mM solution of carbon disulfide in isopentane/3-methyl pentane (6:1). ——— 298°K; ····· 77°K; —·—·— 77°K after 5 min of photolysis.

All solutions were prepared under careful exclusion of moisture and transferred to the cells through an adapter using a slight overpressure of dry air and under perfectly anhydrous conditions. The amount of solution was so chosen that, after the contraction was completed during cooling, the meniscus was found in the lowest part of the stem. Each cell was then connected to the vacuum-line and the solution was degassed by gentle boiling at room temperature. It was then frozen down to liquid nitrogen temperature, full vacuum was applied, and the cell was sealed off.

Both the sample cell and the reference cell containing pure solvent mixture were inserted into the cell compartment and a spectrum was recorded. Liquid nitrogen of 99.8 % purity (Philips liquifier PW 7 050) was then blown from the storage tank through a vacuum-mantled 250 × 14 mm glass tube packed with quartz-wool (diam. 0.004—0.012 mm) into the cell compartment. The quartz-wool removed even traces of solid impurities from the refrigerant. The duration of the filling operation was *ca.* 30 min whereupon the system was allowed to stand for 10 min to reach thermal equilibrium.

From the start of the filling operation the outer windows of the evacuated quartz cylinders in the cell compartment were electrically heated, a total of *ca.* 20 W being sufficient to prevent condensation.

A spectrum was recorded at 77°K and the cell compartment was brought to the photolysis set-up. The sample was irradiated for a certain time and then reinserted into the spectrophotometer where the spectrum of the irradiated sample was taken. The procedure with intermittent irradiation and spectrum recording could be repeated until the liquid nitrogen level interfered with the light beam, the total possible time of work at 77°K being about 3.5 h before it became necessary to refill with nitrogen.

Spectrophotometer accuracy. Twice a week both cells were filled with pure solvent mixtures and the 100 % line of the spectrophotometer was adjusted using the built-in multipot system. The reproducibility between consecutive control experiments was usually better than 1 % in the hydrogen lamp region and 2 % in the tungsten lamp region. A separate experiment with solvent-filled cells showed that, when liquid nitrogen was introduced into the cell compartment, the curvature produced in the 100 % line was less than ± 2 % in the region 50—13 kc cm^{-1}.

Before a spectrum was recorded the 0 and 100 % lines were adjusted at a wave number where a preliminary experiment had shown no absorption to occur during the experiment. Although the spectrophotometer is equipped with a continuous strip chart recorder, the paper could be rewound and several spectra recorded on the same paper, the reproducibility being better than 10 cm^{-1}.

TESTING OF THE EQUIPMENT

Carbon disulfide. Photolysis of CS_2 in rigid solvents at 77°K has been studied by Norman and Porter [8] and their experiments have been reproduced by Sowden and Davidson [15]. We have photolyzed CS_2 in an isopentane/3-methyl pentane (6:1) glass using 0.2 and 5 mM solutions.

Fig. 2 shows the spectral changes during photolysis, the result from the more concentrated solution being similar to those already published. However, an increased absorption between 32 and 37 kc cm^{-1} indicates the formation of S_2. Upon longer irradiation of the concentrated sample, it becomes turbid (probably caused by aggregates of sulfur atoms) and the light transmission shows a steady decrease starting in the visible and becoming more pronounced throughout the UV region. After a total time of irradiation of 90 min, the sample had a pale yellow colour which persisted on warming up to room temperature.

Accurate measurements of the wave-numbers at the two largest CS peaks give the result 38.16 and 39.20 kc cm^{-1} in agreement with 38.15 and 39.17 kc cm^{-1}, respectively, reported in Ref.[8] Besides these known CS spectral peaks, the more diluted solution upon longer photolysis also showed a decidedly reduced transmission between 45 and 40 kc cm^{-1}.

Ethyl iodide. Photolysis of ethyl iodide has been studied by Norman and Porter [8]. We repeated these experiments in the three hydrocarbon mixtures mentioned above, in concentrations between 0.1 and 1.0 mM, most experiments being performed in a 0.25 mM solution.

In the isopentane/3-methyl pentane (2:3) glass, the only change of the recorded spectrum upon irradiation for 60 min was a marked decrease of the EtI absorption band at 39.2 kc cm^{-1}. However, upon warming the glass above its softening point, the spectrum changed radically and three new absorption bands appeared at 34.6, 25.7 and 21.3 kc cm^{-1}, associated with the formation of molecular iodine, I_2. At the same time the colourless glass became yellow. When EtI was photolyzed, either in the isopentane/3-methyl pentane (6:1) glass or in the pentane/*neo*-hexane (3:8) glass, the same spectral changes occurred even at liquid nitrogen temperature, indicating less rigidity of these matrices [13].

These results — as far as the change in spectrum is concerned — are in agreement with those reported in Ref.[8]

Acknowledgement. This investigation has been supported by *Directorate of Chemical Science, AFOSR, AFRD of the Air Research and Development Command, United States Air Force,* through its European Office, by the *Swedish Technical Research Council* and by *Knut and Alice Wallenbergs Stiftelse.*

REFERENCES

1. Cottrell, T.L. *The Strengths of Chemical Bonds.* 2nd Ed. Butterworths Scientific Publications, London 1958.
2. Bichowsky, F. R. and Copeland, L. C. *J. Am. Chem. Soc.* **50** (1928) 1315.
3. Szwarc, M. *Quart. Rev.* **5** (1951) 22.
4. Bass, A. M. and Broida, H. P. *Formation and Trapping of Free Radicals.* Academic Press, New York and London 1960.

5. Minkoff, G. J. *Frozen Free Radicals.* Interscience Publishers Inc., New York 1960.
6. Rosengren, Kj. *Acta Chem. Scand.* **16** (1962) *In press.*
7. Lewis, G. N. and Lipkin, D. *J. Am. Chem. Soc.* **64** (1942) 2801.
8. Norman, I. and Porter, G. *Proc. Roy. Soc. London* **A230** (1955) 399.
9. Rosengren, Kj., Sunner, S. and Timm, D. *Acta Chem. Scand.* **16** (1962) 467.
10. Kasha, M. *J. Opt. Soc. Amer.* **38** (1948) 929.
11. Potts, W. J. *J. Chem. Phys.* **21** (1953) 191.
12. Rosengren, Kj. and Sunner, S. *Acta Chem. Scand.* **16** (1962) 521.
13. Rosengren, Kj. *Acta Chem. Scand.* **16** (1962) *In press.*
14. Vogel, A. I. *A Text-book of Practical Organic Chemistry.* 3rd Ed. Longmans, Green and Co., London 1956.
15. Sowden, R. G. and Davidson, N. *J. Am. Chem. Soc.* **78** (1956) 1291.

Received September 30, 1961.

ACTA CHEMICA SCANDINAVICA 16 (1962) 501–528

Short Communications

The Structure of Prostaglandin E, F_1 and F_2

SUNE BERGSTROM, R. RYHAGE, B. SAMUELSSON and J. SJÖVALL

Kemiska Institutionen, Karolinska Institutet, Stockholm, Sweden

The smooth muscle stimulating activity discovered in sperm and prostate glands by Goldblatt [1] and von Euler [2] (and earlier refs.) is to a large extent due to a compound recently isolated by Bergström and Sjövall [3] and named prostaglandin E. Its composition was found to be $C_{20}H_{34}O_5$ and more recently we have [4] shown that it contains one carboxyl, one carbonyl (cyclopentanone), 2 hydroxyls and one *trans* double bond. Reduction of the carbonyl with borohydride yielded two isomeric trihydroxy acids PGF_1 and PGF_2. We had earlier also isolated the former from sheep prostate glands [5].

The following degradations have led to the elucidation of the structure of these compounds. Most identifications have been by non-classical means, *i.e.* by masspectrometry [6] (MS) of fractions isolated by gas chromatography (GLC) and the deductions from the masspectrograms have been checked through synthesis and comparison with the MS of the synthetic compounds.

Extensive oxidation with chromic acid in acetic acid at 50° yielded suberic acid in high yield with the consumption of 30 equivalents of oxidant and the formation of 4–5 mole carbon dioxide. Oxidative ozonolysis of the methyl ester acetate yielded α-acetoxy heptanoic acid from all three compounds.

Sodium hydroxide (0.5 N) at room temperature transformed PGE into a compound absorbing at 278 mμ with the loss of one hydroxyl. Oxidative ozonolysis of the methyl ester acetate of this compound yielded suberic acid, succinic acid and α-hydroxyheptanoic acid, *i.e.* 19 of the 20 carbon atoms had been accounted for.

Catalytic reduction of the methyl ester of PGE in ethanol gave a dihydrocompound that on treatment with alkali yielded a compound absorbing at 237 mμ with elimination of one hydroxyl. Oxidative ozonolysis yielded suberic acid and 4-keto-7-hydroxydodecanoic acid, *i.e.* all 20 carbon atoms were accounted for.

Finally catalytic reduction with platinum in acetic acid of PGE yielded among other products compound (I) that was isolated by partition chromatography, identified through GLC and MS and compared with a synthetic specimen. These data support formula II for PGE. *i.e.* 2-(6-carboxyhexyl)-3-(3-hydroxyocten-1-yl)-4-hydroxy-cyclopentanone, or in I.U.P.A.C. notation [9] A5(C_8EIQ3) 1 (7C_7X) 2EQ3Q5.

The facile dehydration of PGE with alkali is indicative of a β-hydroxy ketone. A tertiary β-hydroxyl was ruled out by the ease of acylation of the two hydroxyls in dihydro-PGE and also by NMR-data

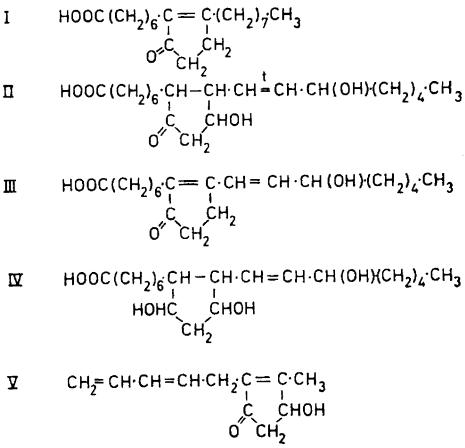

kindly supplied by Dr. G. Slomp, The Upjohn Company, Kalamazoo, Mich., USA. After the elimination of the secondary β-hydroxyl in PGE the double bond migrates into the position indicated in (III).

The two isomeric compounds PGF_1 and PGF_2 must thus have structure IV and only differ in the steric position of the hydroxyl formed by reduction of the carbonyl. Compounds of this type do not seem to have been found in nature earlier. A cyclopentenolone nucleus occurs in the "pyrethrins" present in *Pyrethrium* flowers, *cf.* pyrethrolone (V).

It does not appear unlikely that the prostaglandins are representatives of a group of hormonal compounds of general importance. Their high biological activity makes pharmacological exploration of the activity of similar compounds of interest.

A full report of this work will be published in this journal.

This work has been supported by the Foundations *Therese och Johan Anderssons Minne* and *Gustaf och Thyra Svenssons Minne*. We are also greatly indebted to The Upjohn Company, Kalamazoo, Mich., USA.

1. Goldblatt, M. W. *Chem. & Ind. London* **52** (1933) 1056.
2. v. Euler, U. S. *Scand. Arch. Physiol.* **81** (1939) 65.
3. Bergström, S. and Sjövall, J. *Acta Chem. Scand.* **14** (1960) 1701.
4. Bergström, S., Krabisch, L., Samuelsson, B. and Sjövall, J. *Ibid.* **16** (1962). *In press.*
5. Bergström, S. and Sjövall, J. *Ibid.* **14** (1960) 1693.
6. Ryhage, R. and Stenhagen, E. *J. Lipid Research* **1** (1960) 361.
7. Bergström, S., Eliasson, R., v. Euler, U. S. and Sjövall, J. *Acta Physiol. Scand.* **45** (1959) 133.
8. Bergström, S., Dunér, H., v. Euler, U. S., Pernow, B. and Sjövall, J. *Ibid.* **45** (1959) 145.
9. *Rules for I.U.P.A.C. Notation for Organic Compounds*, Longmans, London 1961.

Received December 12, 1961.

Studies on Ester Sulphates

13. On the Enzymic Synthesis of Steroid Disulphates *

BO WENGLE and HARRY BOSTRÖM

From the Department of Metabolic Research, Wenner-Gren Institute, University of Stockholm and the Pediatric Clinic, Karolinska Sjukhuset, Stockholm, Sweden

Formation of monosulphates of certain steroids in microsome-free liver extracts has been reported by several workers [1-4]. Evidence of the occurrence in rat liver supernatant fluid of two different steroid sulphokinases was presented by Nose and Lipmann in 1958 [5]. One of these enzymes, dehydro*epi*androsterone sulphokinase, was also shown to react with pregnenolone and androsterone, both of which have a hydroxyl group in the 3-position. The other enzyme was capable of sulphurylating the phenolic hydroxyl group of oestrone. On the other hand, no results with bearing on the enzymic *in vitro* formation of disulphates of steroids have so far been reported in the literature. In the present paper, an account is given of certain findings indicating the *in vitro* synthesis of steroid disulphates.

Androst-5-ene-3β-17β-diol **, in a final concentration ranging from 0.016 to 0.083 mM, was incubated for 120 min at 37.5°C in open test tubes, in a medium containing the following constituents: (1) 50 µl of a buffer solution containing equal parts of 0.3 M KH_2PO_4 (pH 6.8), 0.03 M K_2SO_4 and 0.005 M $MgCl_2$; (2) 20 µl of 0.02 M ATP disodium salt***; (3) 50 µl of microsome-free supernatant fluid of female rat liver, homogenized in 2—3 volumes of 0.15 M KCl containing 0.001 M EDTA (pH 7.0), centrifuged at 105 000 *g* for 60 min, and diluted to contain 10 µg of protein per µl; (4) 0.1 mC of carrier-free ^{35}S-labelled sulphate †. Final volume of the incubation mixture: 120 µl. The steroid was added to the empty

* Supported by grants from the *National Institutes of Health*, Bethesda, U.S.A. (A-4410).

** Kindly placed at our disposal by Schering A.-G., Berlin, Germany.

*** Obtained from Sigma Chemical Company, St. Louis, U.S.A.

† Obtained from the Radiochemical Centre, Amersham, England.

kindly supplied by Dr. G. Slomp, The Upjohn Company, Kalamazoo, Mich., USA. After the elimination of the secondary β-hydroxyl in PGE the double bond migrates into the position indicated in (III).

The two isomeric compounds PGF_1 and PGF_2 must thus have structure IV and only differ in the steric position of the hydroxyl formed by reduction of the carbonyl. Compounds of this type do not seem to have been found in nature earlier. A cyclopentenolone nucleus occurs in the "pyrethrins" present in *Pyrethrium* flowers, *cf.* pyrethrolone (V).

It does not appear unlikely that the prostaglandins are representatives of a group of hormonal compounds of general importance. Their high biological activity makes pharmacological exploration of the activity of similar compounds of interest.

A full report of this work will be published in this journal.

This work has been supported by the Foundations *Therese och Johan Anderssons Minne* and *Gustaf och Thyra Svenssons Minne*. We are also greatly indebted to The Upjohn Company, Kalamazoo, Mich., USA.

1. Goldblatt, M. W. *Chem. & Ind. London* **52** (1933) 1056.
2. v. Euler, U. S. *Scand. Arch. Physiol.* **81** (1939) 65.
3. Bergström, S. and Sjövall, J. *Acta Chem. Scand.* **14** (1960) 1701.
4. Bergström, S., Krabisch, L., Samuelsson, B. and Sjövall, J. *Ibid.* **16** (1962). *In press.*
5. Bergström, S. and Sjövall, J. *Ibid.* **14** (1960) 1693.
6. Ryhage, R. and Stenhagen, E. *J. Lipid Research* **1** (1960) 361.
7. Bergström, S., Eliasson, R., v. Euler, U. S. and Sjövall, J. *Acta Physiol. Scand.* **45** (1959) 133.
8. Bergström, S., Dunér, H., v. Euler, U. S., Pernow, B. and Sjövall, J. *Ibid.* **45** (1959) 145.
9. *Rules for I.U.P.A.C. Notation for Organic Compounds*, Longmans, London 1961.

Received December 12, 1961.

Studies on Ester Sulphates

13. On the Enzymic Synthesis of Steroid Disulphates *

BO WENGLE and HARRY BOSTRÖM

From the Department of Metabolic Research, Wenner-Gren Institute, University of Stockholm and the Pediatric Clinic, Karolinska Sjukhuset, Stockholm, Sweden

Formation of monosulphates of certain steroids in microsome-free liver extracts has been reported by several workers [1-4]. Evidence of the occurrence in rat liver supernatant fluid of two different steroid sulphokinases was presented by Nose and Lipmann in 1958 [5]. One of these enzymes, dehydro*epi*androsterone sulphokinase, was also shown to react with pregnenolone and androsterone, both of which have a hydroxyl group in the 3-position. The other enzyme was capable of sulphurylating the phenolic hydroxyl group of oestrone. On the other hand, no results with bearing on the enzymic *in vitro* formation of disulphates of steroids have so far been reported in the literature. In the present paper, an account is given of certain findings indicating the *in vitro* synthesis of steroid disulphates.

Androst-5-ene-3β-17β-diol **, in a final concentration ranging from 0.016 to 0.083 mM, was incubated for 120 min at 37.5°C in open test tubes, in a medium containing the following constituents: (1) 50 µl of a buffer solution containing equal parts of 0.3 M KH_2PO_4 (pH 6.8), 0.03 M K_2SO_4 and 0.005 M $MgCl_2$; (2) 20 µl of 0.02 M ATP disodium salt***; (3) 50 µl of microsome-free supernatant fluid of female rat liver, homogenized in 2—3 volumes of 0.15 M KCl containing 0.001 M EDTA (pH 7.0), centrifuged at 105 000 *g* for 60 min, and diluted to contain 10 µg of protein per µl; (4) 0.1 mC of carrier-free ^{35}S-labelled sulphate †. Final volume of the incubation mixture: 120 µl. The steroid was added to the empty

* Supported by grants from the *National Institutes of Health*, Bethesda, U.S.A. (A-4410).

** Kindly placed at our disposal by Schering A.-G., Berlin, Germany.

*** Obtained from Sigma Chemical Company, St. Louis, U.S.A.

† Obtained from the Radiochemical Centre, Amersham, England.

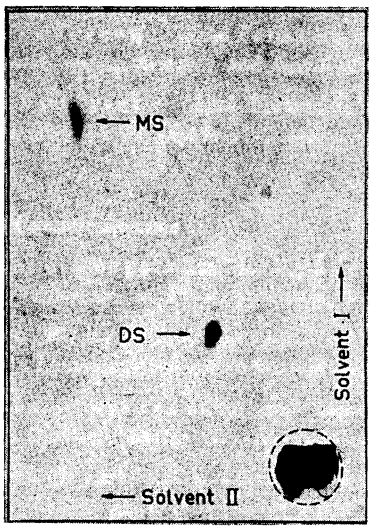

Fig. 1. Autoradiogram of a two-dimensional paper chromatogram, illustrating the separation of compounds MS and DS formed by incubation of androst-5-ene-3β,17β-diol in the sulphurylating system described in the text. The area indicated by the dotted lines contains inorganic and active sulphate. Solvent I: Phenol-water (400 g + 100 g); solvent II: Butanol-acetic acid-water (12/3/5 by vol.).

test tubes in ethanolic solution, the ethanol being evaporated *in vacuo* before addition of the other components.

The ester sulphates formed in the reaction mixture were separated by 2-dimensional ascending paper chromatography (solvent I: phenol-water, 400 g + 100 g; solution II: butanol-acetic acid-water, 12/3/5 by vol.), and by high-voltage electrophoresis, after which they were localized by autoradiography as previously described [6].

The radioactive areas indicated in Fig. 1 were eluted with water, and aliquots of the eluates were counted in a G.-M. counter after plating (infinite thinness) on frosted aluminium plates.

Incubation of androst-5-ene-3β,17β-diol in the sulphurylating system as described above gave rise to two different ^{35}S-labelled compounds (MS and DS), separable on paper chromatograms (Fig. 1) and electrophoretic strips. The sulphates of all sulphate-accepting monohydroxy steroids so far tested in our laboratory migrate to positions identical or close to the position of MS in paper chromatograms and electrophoretic strips [7]. It is therefore assumed that MS constitutes a monosulphate of androst-5-ene-3β,17β-diol. This assumption is further substantiated by the fact that the compound was desulphated by incubation with commercial steroid sulphatase * (37.5°C; pH 7.0; 120 min.).

With respect to the identity of DS, its electrophoretic migration at pH 5.5 suggested a conjugate of greater negative charge than MS. Furthermore, the chromatographic data indicated a higher polarity of DS than MS. On the basis of these facts, it appeared probable that DS was, in fact, a disulphated conjugate. Additional support for this view was obtained by the following findings. (1) When the labelled MS compound was incubated in the sulphurylating system in the absence of labelled inorganic sulphate, the radioactivity was almost quantitatively transformed into DS (Table 1). (2) When the labelled MS compound was incubated as above in the sulphurylating system now containing labelled inorganic sulphate, the radioactivity of DS formed significantly exceeded that of DS in the former experiment. (3) Hydrolysis of DS in an acetate buffer (pH 5.5) for 4 h at 100°C split DS into a

Table 1. Transformation of steroid monosulphate into steroid disulphate. Distribution of radioactivity between the steroid sulphate fractions MS and DS in the incubation medium, before and after incubation for 120′ at 37.5°C in the sulphurylating system described in the text except that ^{35}S-labelled sulphate and androst-5-ene-3β,17β-diol were replaced by partially purified ^{35}S-labelled MS.

Expt. No.	Per cent of total steroid sulphate radioactivity			
	Before incubation		After incubation	
	MS	DS	MS	DS
1	72	28	11	89
2	95	5	7	93

* Obtained from Schering A.-G., Berlin, Germany.

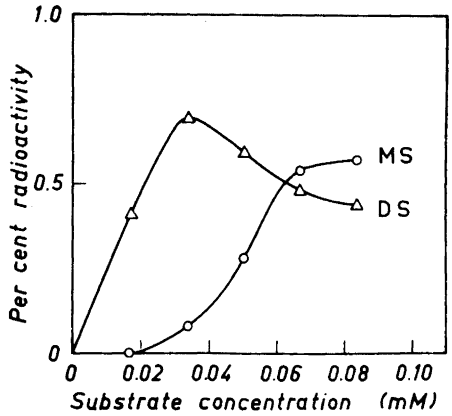

Fig. 2. Formation of MS and DS during incubation in the sulphurylating system described in the text, in relation to different androst-5-ene-3β,17β-diol concentrations of the medium. MS and DS are expressed in per cent of total radioactivity of the incubation mixture.

monosulphate and inorganic sulphate. (4) Desulphation of DS with commercial steroid sulphatase * at 37.5°C, pH 7.0, for 120 min could be demonstrated.

It was concluded from the aforementioned facts that DS is identical with a disulphate of androst-5-ene-3β,17β-diol. According to Bitman and Cohen [8], hydrolytic splitting of steroid sulphates at pH 5.5 under the conditions in question is limited to compounds containing β configuration of the sulphate, and a β,γ-unsaturation to this grouping. The monosulphate left in the hydrolysate, which contained approximately half the activity of DS added, is therefore assumed to be androst-5-ene-3β,17β-diol-17-sulphate. When the MS compound formed during incubation in the sulphurylating system was treated in the same way, almost all radioactivity was revealed as inorganic sulphate, indicating that this monosulphate was probably androst-5-ene-3β,17β-diol-3-sulphate.

Fig. 2 shows the formation in the sulphurylating system of MS and DS, respectively, as a function of androst-5-ene-3β,17β-diol concentration. Formation of DS was found to be optimal at a substrate concentration of approximately 0.035 mM. In low concentrations of the substrate, the only steroid conjugate detected was DS. This might indicate that all MS formed from androst-5-ene-3β,17β-diol at low substrate levels was transformed into DS. At higher concentrations, on the other hand, when DS formation had reached its maximum, greater amounts of MS were found (Fig. 2).

The aforegoing hydrolysis data support the view that MS consisted mainly of the 3-sulphate of androst-5-ene-3β,17β-diol. This fact, as well as the shape of the substrate concentration curves, may imply that two different sulphokinases are operating in the sulphurylating system, one with the ability to transfer sulphate to the 3β-hydroxyl group, and the other to transfer it to the 17β-hydroxyl group. Of these enzymes, the latter seems to be the rate-limiting one for formation of the disulphate in the sulphurylating system used in the present study.

1. De Meio, R. H. and Lewycka, C. *Endocrinology* **56** (1955) 489.
2. Roy, A. B. *Biochem. J.* **63** (1956) 294.
3. Schneider, J. J. and Lewbart, M. L. *J. Biol. Chem.* **222** (1956) 787.
4. De Meio, R. H., Lewycka, C., Wizerkaniuk, M. and Salciunas, O. *Biochem. J.* **68** (1958) 1.
5. Nose, Y. and Lipmann, F. *J. Biol. Chem.* **233** (1958) 1348.
6. Vestermark, A. and Boström, H. *Acta Chem. Scand.* **13** (1959) 827.
7. Boström, H. *Acta Endocrinol.* **37** (1961) 405.
8. Bitman, J. and Cohen, S. L. *J. Biol. Chem.* **191** (1951) 351.

Received January 25, 1962.

* Obtained from Schering A.-G., Berlin, Germany.

Free Radicals in Some Natural Resins

CARL LAGERCRANTZ and MARGARETA YHLAND

Department of Medical Physics, University of Göteborg, Sweden

In this laboratory we have found that some resins derived from pine trees contain varying amounts of free radicals. Thus, the fossile resin amber, fresh oleoresin from *Pinus silvestris*, colophony (gum rosin) and canada balsam exhibited an electron spin resonance (ESR) absorption corresponding to a concentration of 10^{14} — 10^{16} spins per gram substance. The ESR-spectra consisted of a single line of a width between 10 and 15 gauss. The shape of the absorption curve was slightly asymmetrical for some of the specimens investigated. The *g*-value was close to that of diphenylpicrylhydrazyl.

When the samples were kept at an elevated temperature, the ESR-signal was reduced or completely abolished. Thus, the signal from a sample of amber was reduced by a factor of five when kept at 170°C for 10 min. When a specimen of colophony had been melted in the ESR-sample tube by heating to 120°C for some minutes and subsequently was allowed to solidify by cooling to room temperature, it was found that the ESR-signal had almost completely disappeared.

Grinding of such a previously melted and solidified specimen to a finely divided powder restored the ESR-signal. The reappearence and the subsequent increase of the ESR-signal was easily observed when the spectrum was recorded immediately after the specimen had been ground.

When a sample of colophony which exhibited a strong ESR-signal in the powdered form, was dissolved in xylene in the ESR-sample tube, no signal could be detected. An ESR-signal was still present, however, after the specimen had been dissolved in alkaline ethanol.

Irradiation by light from a xenon lamp of a melted and solidified specimen of faintly yellow colophony also restored the signal. Fig. 1 shows the relative radical concentration as a function of time when the sample was irradiated *in situ* through slots in the cavity wall. It is evident that the radical concentration increases during the light periods, and remains constant during the dark periods.

It is obvious that the radicals are connected with the oxidation of some resin components by air oxygen and with the irradiation of the samples by light. Colophony is reported to take up oxygen easily, especially when the surface of the specimen is large as in a powdered form [1]. When photosensitized by dyes as eosine, the resin acids structurally related to levopimaric acid have been shown to add oxygen forming peroxide derivatives [2]. It is believed that the radical content in the resin products is connected in some way with such reactions. This assumption is supported by the fact that more or less crude preparations of abietic acids exhibited an ESR-signal and an analogous behaviour as colophony when melted and solidified. In

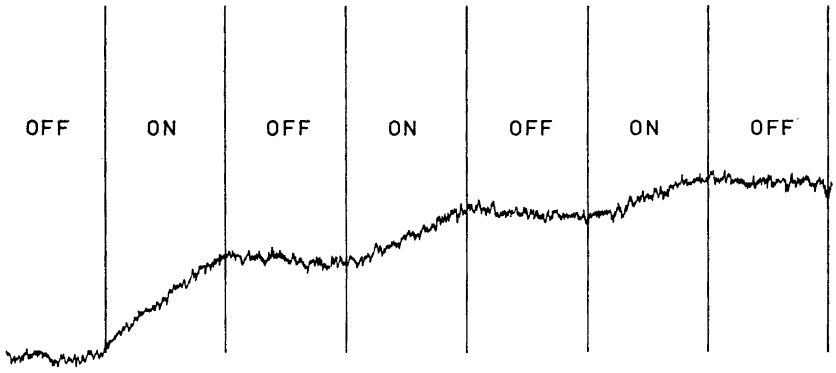

Fig. 1. Light induced free radicals in a solid sample of colophony. Successive periods of light on and off are of 5 min duration. Unfiltered light from a xenon lamp.

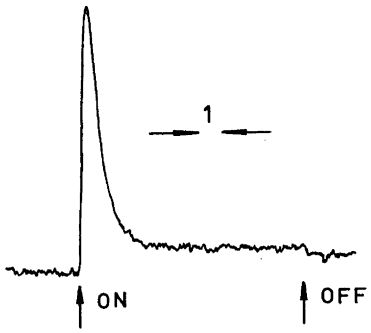

Fig. 2. Light induced free radicals in a solution of levopimaric acid (10^{-2} M) in ethanol containing eosine (10^{-3} M). Time between horizontal arrows = 1 min. Light from a xenon lamp filtered through a 50 mm layer of 10 % $CuSO_4$ solution in H_2O.

contrary no ESR-signal could be detected in a solid sample of dehydroabietic acid, which is reported to be resistent to air oxidation [1].

Further evidence of a free radical mechanism in the reactions discussed was obtained as follows. A sample of highly purified levopimaric acid in ethanol containing eosine as a sensitizer was placed in the ESR-cavity and irradiated *in situ* by visible light as described above. Fig. 2 shows the relative radical concentration as a function of time. The magnetic field was kept constant after being adjusted to maximum response in a previous record. When the light was turned on, there was an immediate rise of the radical concentration, probably very much faster than the time response of the recorder (2 sec.). After having passed through a maximum the radical concentration decays almost completely in a few minutes. Degassing of the solution before the reaction does not seem to alter the shape of the response curve. It was noted that the solution was completely decolourized in the irradiated area of the sample cell. No response could be detected in an analogous experiment performed with pimaric acid.

As long as the resins are in the solid state or in a rigid solution as in colophony, the radicals formed from levopimaric and structurally related resin acids are trapped *in situ*. When the viscosity is lowered by heating or the substances are melted, the radicals become mobile enough to react and disappear. The lack of an ESR-signal of a solution of colophony in xylene is also consistent with this conception. The presence of radicals in a solution of colophony in alkaline ethanol might be interpreted as due to semiquinone radicals derived from transannular peroxides of the resin acids, as semiquinone radicals are known to be stabilized in an alkaline medium.

The process of formation and trapping of free radicals by light irradiation and by oxygen uptake, and their subsequent disappearence when the viscosity decreases, can probably be recycled in natural resins as long as there are substances available which are of the type here considered.

The structure of the radicals related to the resin acids is unknown at present, nor is it clear if the radicals generated by light are identical or not with those formed by air oxidation.

The ESR-spectra were obtained by use of a Varian 100 kc spectrometer equipped with the multipurpose cavity with radiation slots. The irradiation experiments on liquid solutions were performed by use of the flat cell.

The authors are indebted to Dr. H. Bruun for samples of levopimaric and pimaric acid, to Dr. K. J. Karrman for a sample of dehydroabietic acid, and to *Wilhelm och Martina Lundgrens Vetenskapsfond* for financial support.

1. Sandermann, W. *Naturharze, Terpentinöl, Tallöl*, Berlin 1960.
2. Schuller, W. H. and Lawrence, R. V. *J. Am. Chem. Soc.* **83** (1961) 2563.

Received January 23, 1962.

Correction to "A Method for Gas-Liquid Multiplicative Distribution on a Preparative Scale" *

ÖRN WAHLROOS

Laboratory of the Foundation for Chemical Research, Biochemical Institute, Helsinki, Finland

On p. 2055, formula (4) is incorrect and should read

$$n = \sqrt{n_1 n_2} = \frac{b^2}{a^* + (1/a^*) - 2}$$

Received January 31, 1962.

* *Acta Chem. Scand.* **15** (1961) 2053.

Decomposition of Triphenyl Phosphine Oxide in Alcoholic Alkaline Solution

GUNNAR AKSNES and JON SONGSTAD

Chemical Institute, University of Bergen, Norway

Phosphine oxides are compounds of high chemical stability, but it has been observed that when they are fused with alkali hydroxides they will lose their substituent radicals [1]. This decomposition has recently been utilized by Horner *et al.*[2] as a method for preparation of phosphinic acids:

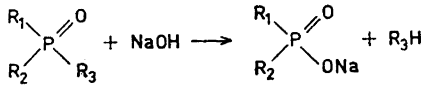

The greater the negativity of the substituents the easier are they lost during the fusion. The above authors observed the following order of stability: alkyl > phenyl > benzyl.

In this communication we wish to report the decomposition of triphenyl phosphine oxide under much milder condition than hitherto described.

When triphenyl phosphine oxide is boiled in an alcoholic solution of alkali hydroxide (*e.g.* 0.1 N NaOH and 0.2 M phosphine oxide in 96 % alcohol) during several hours, a gelatinous compound precipitates in the reaction flask. At the same time it is found that the hydroxide disappears from the alcoholic solution. No salt of phosphinic acid is found in the alcohol.

On treatment of the precipitate with water it decomposes into alkali hydroxide and insoluble inorganic alkali metaphosphate. No salt of phosphinic acid is found in the precipitate.

These observations are in accordance with the following reaction scheme.

This scheme postulates the formation of a pentacovalent intermediate as initiator of the chain process. Although Halmann and Pinchas [3] found no exchange of phosphoryl oxygen in triphenyl phosphine oxide when boiled in ^{18}O-enriched water, it is reasonable to expect that the exchange process is strongly catalysed by hydroxyl ons; Halman and Pinchas [3] do not report i

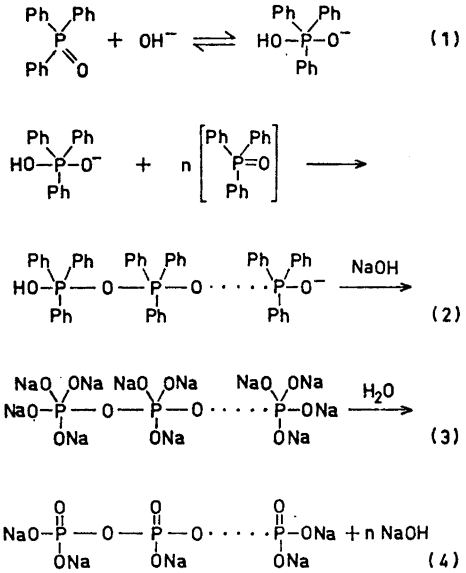

exchange studies in alkaline solution. During formation of the pentacovalent intermediate it seems most reasonable to expect a back side attack on phosphorus opposite to the phosphoryl group to give a trigonal bipyramidal structure with the three phenyl groups in the equatorial positions and the two oxygen atoms in the axial positions. The strong dipole of the phosphoryl group is expected to favour this configuration. In order to explain that diphenyl phosphinic acid is not formed we must assume that release of phenyl groups from the monomeric pentacovalent state requires higher energy than the coupling of the negatively charged oxygen with another phosphine oxide molecule. Since the sodium metaphosphate formed is totally insoluble in water the chains must consist of a great number of phosphate units.

It seems reasonable to assume that the displacement of the phenyl groups by hydroxyl ions from the polymer chains follows immediately upon the polymerisation due to the fact that there is no indication of organic material in the precipitate formed during the reaction.

Horner *et al.*[2] have shown that fusion of triphenyl phosphine oxide with sodium hydroxide quantitatively gives the monomeric product, sodium diphenyl phosphinate. The difference in behaviour can be explained if the first step in the fusion

process consists of a quantitative formation of the pentacovalent intermediate, the decomposition of which can only give monomeric product. Additional evidence for this interpretation is found in the non-proportionality between phosphine oxide decomposition and the hydroxyl concentration in alcoholic solution. Thus, 2 N KOH in 96 % alcohol gives after 48 h boiling 30 % decomposition of a 0.2 M triphenyl phosphine solution as compared with 18 % under the same conditions in 0.2 N NaOH. In 70 % alcohol 0.1 N NaOH gives after only 24 h boiling 45 % decomposition of 0.2 M triphenyl phosphine oxide solution. In the latter case some sodium methaphosphate crystallized directly from the reaction solution. Apparently a greater amount of water in the alcohol will favour the metaphosphate formation from the pentacovalent polymer (step 3). An equivalent amount of hydroxyl ions will then be liberated which can decompose additional amounts of triphenyl phosphine oxide.

Our sincere thanks are due to the *Norwegian Defence Research Establishment* for financial support.

1. Kosolapoff, G. M. *Organophosphorus Compounds*, John Wiley and Sons, Inc., New York 1950, p. 111.
2. Horner, L., Hoffmann, H. and Wippel, H. G. *Chem. Ber.* **91** (1958) 64.
3. Halmann, M. and Pinchas, S. *J. Chem. Soc.* **1958** 3264.

Received January 19, 1962.

Eosine Sensitized Formation of Photo-Radicals in Liquid Solutions

CARL LAGERCRANTZ
and MARGARETA YHLAND

Department of Medical Physics, University of Göteborg, Sweden

It has been established that transient free radicals are formed in the light-induced reaction between levopimaric acid and eosine [1]. In connection with this work other reactions sensitized by eosine were studied by the technique of electron spin resonance (ESR). Some of the results are to be reported here. The experimental arrangements were the same as described earlier [1].

When a solution of eosine and ascorbic acid in pyridine was irradiated by visible light *in situ* at room temperature, Bubnov *et al.*[2] found free radicals by the ESR-technique. The dye sensitizer was considered to be excited to a triplet state when absorbing radiant energy. Subsequently, a hydrogen atom was assumed to be transferred from ascorbic acid to the excited dye molecule. The radical observed was believed to be a semiquinone of eosine, as the ESR-spectrum exhibited a three-line structure with a hyperfine splitting of 4.6 gauss which was considered to be due to the interaction of an unpaired electron with the two hydrogen atoms located on carbon atoms 1 and 8 in the xanthene nucleus of the eosine molecule.

This reaction has been studied in this laboratory using pyridine or ethanol as a solvent. However, an identical three-line spectrum is obtained also when the sodium salt of fluorescein or 4,5-diiodofluorescein is substituted for eosine (the sodium salt of 2,4,5,7-tetrabromofluorescein) in the reaction with ascorbic acid. As there are six hydrogens in fluorescein, and four hydrogens in 4,5-diiodofluorescein available for interaction with the unpaired electron as compared with two hydrogens in eosine, it seems difficult to correlate the three-line structure of the spectra obtained with a semiquinone radical derived from the dye molecule.

Photo-induced radicals have been observed at room temperature in analogous systems containing eosine, in which ascorbic acid has been replaced by other substances using ethanol or pyridine as a solvent. Thus, a three-line spectrum which could not be distinguished from that observed for the reaction of ascorbic acid, was obtained in the case of such widely different substances as benzaldehyde, 1,1-diphenylhydrazine, pyrrole, *p*-toluenethiol and xanthotoxin. When the light is turned on radicals appear immediately and the concentration remains constant until the light is turned off. The reaction rates are certainly much faster than those reproducible with true fidelity by the recorder used.

Considering the three-line ESR-spectrum a simple interpretation does not seem to be possible in terms of a radical derived from the dye sensitizer, the substrate or the solvent. In a recent study of photo-induced reactions similar to those here considered Schenck and Wolgast [3] assume that the radical exhibiting the three-line spectrum is an addition complex built up between

process consists of a quantitative formation of the pentacovalent intermediate, the decomposition of which can only give monomeric product. Additional evidence for this interpretation is found in the non-proportionality between phosphine oxide decomposition and the hydroxyl concentration in alcoholic solution. Thus, 2 N KOH in 96 % alcohol gives after 48 h boiling 30 % decomposition of a 0.2 M triphenyl phosphine solution as compared with 18 % under the same conditions in 0.2 N NaOH. In 70 % alcohol 0.1 N NaOH gives after only 24 h boiling 45 % decomposition of 0.2 M triphenyl phosphine oxide solution. In the latter case some sodium methaphosphate crystallized directly from the reaction solution. Apparently a greater amount of water in the alcohol will favour the metaphosphate formation from the pentacovalent polymer (step 3). An equivalent amount of hydroxyl ions will then be liberated which can decompose additional amounts of triphenyl phosphine oxide.

Our sincere thanks are due to the *Norwegian Defence Research Establishment* for financial support.

1. Kosolapoff, G. M. *Organophosphorus Compounds*, John Wiley and Sons, Inc., New York 1950, p. 111.
2. Horner, L., Hoffmann, H. and Wippel, H. G. *Chem. Ber.* **91** (1958) 64.
3. Halmann, M. and Pinchas, S. *J. Chem. Soc.* **1958** 3264.

Received January 19, 1962.

Eosine Sensitized Formation of Photo-Radicals in Liquid Solutions

CARL LAGERCRANTZ
and MARGARETA YHLAND

Department of Medical Physics, University of Göteborg, Sweden

It has been established that transient free radicals are formed in the light-induced reaction between levopimaric acid and eosine [1]. In connection with this work other reactions sensitized by eosine were studied by the technique of electron spin resonance (ESR). Some of the results are to be reported here. The experimental arrangements were the same as described earlier [1].

When a solution of eosine and ascorbic acid in pyridine was irradiated by visible light *in situ* at room temperature, Bubnov *et al.*[2] found free radicals by the ESR-technique. The dye sensitizer was considered to be excited to a triplet state when absorbing radiant energy. Subsequently, a hydrogen atom was assumed to be transferred from ascorbic acid to the excited dye molecule. The radical observed was believed to be a semiquinone of eosine, as the ESR-spectrum exhibited a three-line structure with a hyperfine splitting of 4.6 gauss which was considered to be due to the interaction of an unpaired electron with the two hydrogen atoms located on carbon atoms 1 and 8 in the xanthene nucleus of the eosine molecule.

This reaction has been studied in this laboratory using pyridine or ethanol as a solvent. However, an identical three-line spectrum is obtained also when the sodium salt of fluorescein or 4,5-diiodofluorescein is substituted for eosine (the sodium salt of 2,4,5,7-tetrabromofluorescein) in the reaction with ascorbic acid. As there are six hydrogens in fluorescein, and four hydrogens in 4,5-diiodofluorescein available for interaction with the unpaired electron as compared with two hydrogens in eosine, it seems difficult to correlate the three-line structure of the spectra obtained with a semiquinone radical derived from the dye molecule.

Photo-induced radicals have been observed at room temperature in analogous systems containing eosine, in which ascorbic acid has been replaced by other substances using ethanol or pyridine as a solvent. Thus, a three-line spectrum which could not be distinguished from that observed for the reaction of ascorbic acid, was obtained in the case of such widely different substances as benzaldehyde, 1,1-diphenylhydrazine, pyrrole, *p*-toluenethiol and xanthotoxin. When the light is turned on radicals appear immediately and the concentration remains constant until the light is turned off. The reaction rates are certainly much faster than those reproducible with true fidelity by the recorder used.

Considering the three-line ESR-spectrum a simple interpretation does not seem to be possible in terms of a radical derived from the dye sensitizer, the substrate or the solvent. In a recent study of photo-induced reactions similar to those here considered Schenck and Wolgast [3] assume that the radical exhibiting the three-line spectrum is an addition complex built up between

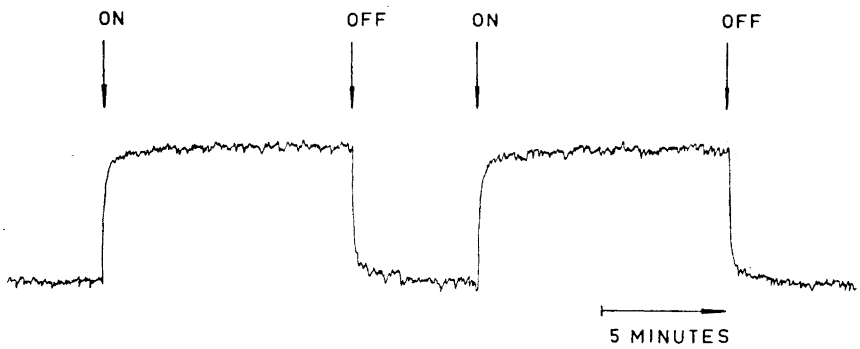

Fig. 1. Photo-induced radicals from a 10^{-2} M solution of 1,4-dihydroxybenzene in H_2O. Eosine concentration 10^{-3} M. The relative radical concentration is recorded as a function of time. The sample was irradiated *in situ* by light from a xenon lamp filtered through a 50 mm layer of 10 % $CuSO_4$ in H_2O. Vertical arrows mark light "on" and "off".

the excited sensitizer and the substrate. Closer details about this complex seem to be lacking.

Although the three-line spectrum is a common phenomenon in photo-reactions sensitized by eosine, other substances have been found which give rise to radicals definitely connected with the substrate molecules. Thus, 1,4-dihydroxybenzene in ethanol or water exhibits the characteristic five-line spectrum of the *p*-semiquinone radical. The radicals appear and disappear synchronously when the light is turned on and off (Fig. 1). An identical spectrum and the same kinetic behaviour were observed also when 1,4-dihydroxybenzene was replaced by *p*-benzoquinone. No radicals could be detected when *p*-dimethoxybenzene was used as a substrate.

N,N-Diphenylamine dissolved in ethanol or pyridine gives rise to photo-induced radicals when sensitized by eosine. The radical concentration increased to a maximum value and then decreased almost to zero in a few minutes. It was found that the decay stopped when the light was turned off as

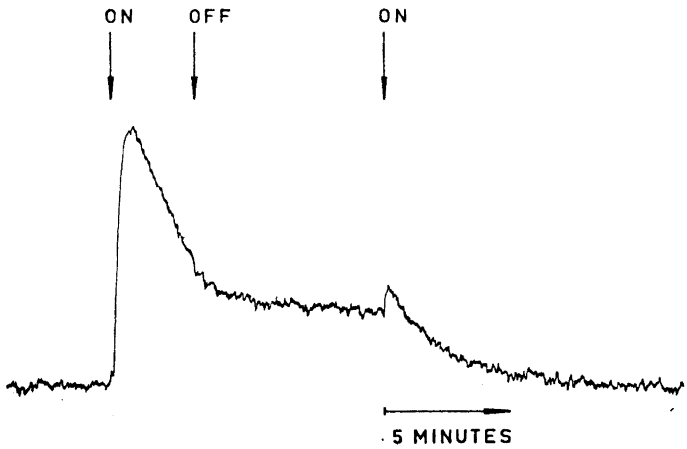

Fig. 2. Photo-induced radicals from a 10^{-2} M solution of N,N-diphenylamine in pyridine. Eosine concentration 10^{-4} M. For other details see legend of Fig. 1.

shown in Fig. 2. Evidently, the radicals are both formed and destroyed by the action of light. The ESR-spectrum, recorded in the dark immediately after the radical concentration had reached the maximum value, exhibited a hyperfine structure, consisting of at least 37 lines in three main groups. The spectrum was nearly identical with that reported by Hoskins [4] for the stable radical obtained when diphenylamine was oxidazed by molecular oxygen in a hot mixture of toluene and alkaline ethanol. This radical was considered to have the structure $(C_6H_5)_2NO\cdot$. It may be suggested that the hydrogen attached to the nitrogen atom of diphenylamine is removed in the photo-induced reaction here described yielding the radical $(C_6H_5)_2N\cdot$.

An ESR-spectrum probably derived from the substrate molecule was obtained in the eosine sensitized reaction of phenothiazine. Due to the instability of the radicals both when the sample was irradiated and when kept in the dark, it was impossible to obtain a complete spectrum under high-resolution conditions. It was observed, however, that there were three main lines separated by about 9.5 gauss, very probably produced by the interaction of the unpaired electron with the nitrogen atom of phenothiazine. The main lines exhibited a splitting into a large number of more or less completely resolved lines. Although the ESR-spectrum does not give precise information, it is believed that the hydrogen atom attached to the nitrogen atom is removed in the radical forming process. To get photo-induced radicals from phenothiazine the presence of this hydrogen seems to be essential, as it was found that no radicals could be detected when N-methylphenothiazine was used as a substrate. However, the radical reactions of unsubstituted phenothiazine are rather complex. Under certain conditions photo-radicals are formed even without eosine as a sensitizer [5].

Thus, the reaction mechanism of N,N-diphenylamine and phenothiazine probably involves an irreversible homolytic extraction of a labile hydrogen. The radicals are derived from the substrate molecules and are present even after the excitation of the sensitizer has ceased. In some other reactions it has been suggested that an addition complex [3] is formed between the excited sensitizer and the substrate. This complex decays rapidly after the excitation has ceased, in some cases obviously reversibly as seen from the kinetic behaviour of 1,4-dihydroxybenzene where the light-induced reaction can be repeated an indefinite number of times.

The authors are indebted to *Wilhelm och Martina Lundgrens Vetenskapsfond* for financial support.

1. Lagercrantz, C. and Yhland, M. *Acta Chem. Scand.* **16** (1962) 505.
2. Bubnov, N. N., Kibalko, L. A., Tsepalov, V. F. and Shliapintokh, V. IA. *Optics and Spectroscopy* **7** (1959) 71.
3. Schenck, G. O. and Wolgast, R. *Naturwiss.* **48** (1961) 737.
4. Hoskins, R. *J. Chem. Physics.* **25** (1956) 788.
5. Lagercrantz, C. and Yhland, M. *To be published.*

Received January 29, 1962.

Synthetic Ascorbigen as a Vitamin C Source for Guinea Pigs and Man

MARTTI KIESVAARA and ARTTURI I. VIRTANEN

Laboratory of the Foundation for Chemical Research, Biochemical Institute, Helsinki, Finland

It was found in this laboratory that 3-hydroxymethylindole (II) is formed during the enzymic splitting of glucose and sulfate from the newly discovered thioglucoside, glucobrassicin (I), present in cabbage plants and isolated in pure form [1,2]. 3-Hydroxymethylindole reacts non-enzymically with the ascorbic acid present in cabbage to form the compound known as ascorbigen (III) [3].

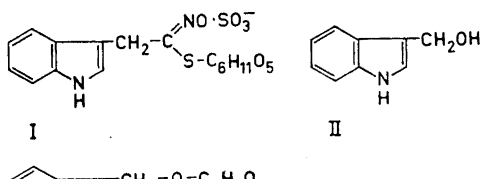

I II

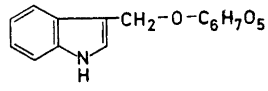

III

shown in Fig. 2. Evidently, the radicals are both formed and destroyed by the action of light. The ESR-spectrum, recorded in the dark immediately after the radical concentration had reached the maximum value, exhibited a hyperfine structure, consisting of at least 37 lines in three main groups. The spectrum was nearly identical with that reported by Hoskins [4] for the stable radical obtained when diphenylamine was oxidazed by molecular oxygen in a hot mixture of toluene and alkaline ethanol. This radical was considered to have the structure $(C_6H_5)_2NO\cdot$. It may be suggested that the hydrogen attached to the nitrogen atom of diphenylamine is removed in the photo-induced reaction here described yielding the radical $(C_6H_5)_2N\cdot$.

An ESR-spectrum probably derived from the substrate molecule was obtained in the eosine sensitized reaction of phenothiazine. Due to the instability of the radicals both when the sample was irradiated and when kept in the dark, it was impossible to obtain a complete spectrum under high-resolution conditions. It was observed, however, that there were three main lines separated by about 9.5 gauss, very probably produced by the interaction of the unpaired electron with the nitrogen atom of phenothiazine. The main lines exhibited a splitting into a large number of more or less completely resolved lines. Although the ESR-spectrum does not give precise information, it is believed that the hydrogen atom attached to the nitrogen atom is removed in the radical forming process. To get photo-induced radicals from phenothiazine the presence of this hydrogen seems to be essential, as it was found that no radicals could be detected when N-methylphenothiazine was used as a substrate. However, the radical reactions of unsubstituted phenothiazine are rather complex. Under certain conditions photo-radicals are formed even without eosine as a sensitizer [5].

Thus, the reaction mechanism of N,N-diphenylamine and phenothiazine probably involves an irreversible homolytic extraction of a labile hydrogen. The radicals are derived from the substrate molecules and are present even after the excitation of the sensitizer has ceased. In some other reactions it has been suggested that an addition complex [3] is formed between the excited sensitizer and the substrate. This complex decays rapidly after the excitation has ceased, in some cases obviously reversibly as seen from the kinetic behaviour of 1,4-dihydroxybenzene where the light-induced reaction can be repeated an indefinite number of times.

The authors are indebted to *Wilhelm och Martina Lundgrens Vetenskapsfond* for financial support.

1. Lagercrantz, C. and Yhland, M. *Acta Chem. Scand.* **16** (1962) 505.
2. Bubnov, N. N., Kibalko, L. A., Tsepalov, V. F. and Shliapintokh, V. IA. *Optics and Spectroscopy* **7** (1959) 71.
3. Schenck, G. O. and Wolgast, R. *Naturwiss.* **48** (1961) 737.
4. Hoskins, R. *J. Chem. Physics.* **25** (1956) 788.
5. Lagercrantz, C. and Yhland, M. *To be published.*

Received January 29, 1962.

Synthetic Ascorbigen as a Vitamin C Source for Guinea Pigs and Man

MARTTI KIESVAARA and ARTTURI I. VIRTANEN

Laboratory of the Foundation for Chemical Research, Biochemical Institute, Helsinki, Finland

It was found in this laboratory that 3-hydroxymethylindole (II) is formed during the enzymic splitting of glucose and sulfate from the newly discovered thioglucoside, glucobrassicin (I), present in cabbage plants and isolated in pure form [1,2]. 3-Hydroxymethylindole reacts non-enzymically with the ascorbic acid present in cabbage to form the compound known as ascorbigen (III) [3].

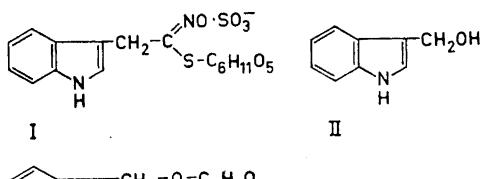

I II

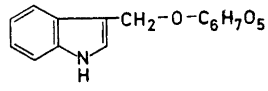

III

Ascorbigen can be prepared synthetically by heating a mixture of 3-hydroxymethylindole and ascorbic acid, or a mixture of indole, formaldehyde, and ascorbic acid in water [3]. On mild acid hydrolysis ascorbic acid is liberated from ascorbigen, as shown by Procházka *et al.*[4], who had isolated ascorbigen from cabbage some years before, considering it to be a genuine plant substance. The structure which these workers proposed for ascorbigen had to be modified, however, in the light of the results obtained by Gmelin and Virtanen. Although the details of its structure are not yet clear, we know that ascorbigen is formed by the splitting of one molecule of water from one molecule of 3-hydroxymethylindole and one molecule of ascorbic acid. Formula III gives an idea of the structure of ascorbigen.

From the above it appears that ascorbigen is an artefact, representing the "bound ascorbic acid" which is supposed to be present in cabbage. Because it is formed when glucobrassicin is split (*e.g.* when cabbage is crushed), it is important to know whether ascorbigen acts as a preventive and curative of scurvy in guinea pigs and in man, — in other words, if it exerts the vitamin C effect.

For the following animal experiments, ascorbigen was prepared synthetically from indole, formaldehyde, and ascorbic acid. 10 g of indole (about 0.085 mole), 30 g of ascorbic acid (about 0.170 mole), 5.1 g of formaldehyde (about 0.170 mole), and 400 ml of citrate buffer (0.05 M) were mixed. The mixture, the pH of which was about 4.0, was heated on a water bath at + 54°C with stirring for about 7 or 8 h. The mixture was filtered after cooling. The filtrate was extracted with 3 × 200 ml of ethyl ether and 5 or 6 × 500 ml of freshly distilled ethyl acetate. The ethyl acetate was evaporated, finally in a small evaporator. The residue was thoroughly dried in a vacuum desiccator. The yield, which according to paper chromatograms and the UV spectrum was pure ascorbigen, was 6 030 mg.

Twenty guinea pigs of a pure albino strain, weighing 250—300 g, were used as test animals. Ten of these were males and ten females. The animals were fed on dry timothy grass. Part of the ascorbic acid had been destroyed in the grass by keeping it in an oven at 40°C for 3 or 4 days. The ascorbic acid content had then decreased to 10 μg/g of grass. The consumption of grass was about 30 g per day and animal. In addition, the guinea pigs were given 10 g per day of a mixture of rolled oats and wheat embryos (4:1). This mixture contained no ascorbic acid at all. The animals were given tap water to drink.

The guinea pigs were weighed every other day. When their weights began to decrease, the animals were divided into the following groups on the 16th day of the experiment: (1) a control group, 4 males and 4 females, (2) an ascorbic acid group, 3 males and 3 females, (3) an ascorbigen group, 3 males and 3 females.

The animals in group 1 were given 1 ml of 50 % saccharose solution *per os* with a pipette daily. The animals in group 2 were given 15 mg of ascorbic acid, and the animals in group 3 26 mg of ascorbigen, likewise in 1 ml of 50 % saccharose solution *per os*. The ascorbigen solution was made up each day immediately before use. The ascorbigen contained 5 μg/mg of free ascorbic acid.

Results. The time course of the weights of the animals is presented graphically in Figs. 1—3. The weights of the control animals decreased continuously after the 10th or 12th day of the experiment. Symptoms of scurvy could be clearly seen as early as the 18th or 20th day of the experiment (lack of appetite, apathy, sore

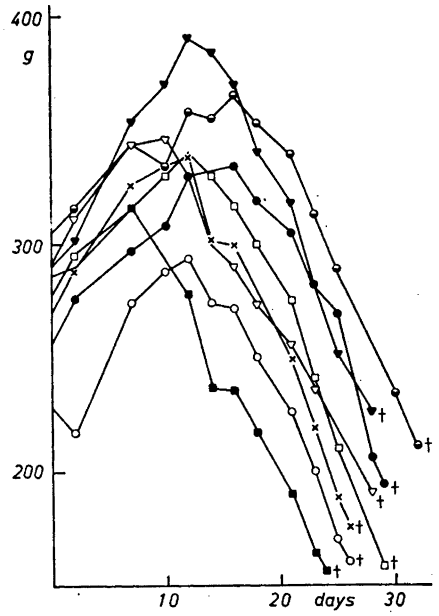

Fig. 1. No ascorbic acid administered to guinea pigs. Group 1.

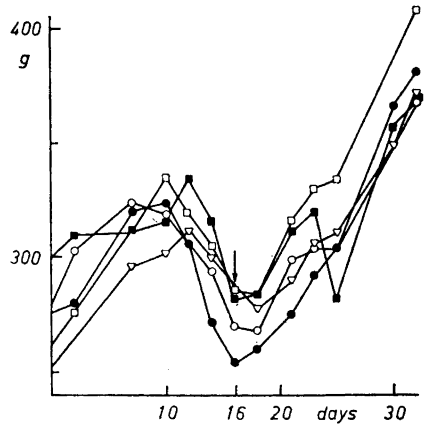

Fig. 2. 15 mg/day of ascorbic acid administered to guinea pigs from the time pointed out by the arrow. Group 2.

joints). These animals died between the 24th and 32nd day of the experiment.

26 mg of ascorbigen per day prevented the development of scurvy, as did 15 mg of ascorbic acid, and the weights of the animals began to increase again at the same rate in both groups. No symptoms of scurvy could be observed in the guinea pigs in the ascorbigen group. In group 2, one animal was taken ill with diarrhea and died on the 27th day of the experiment.

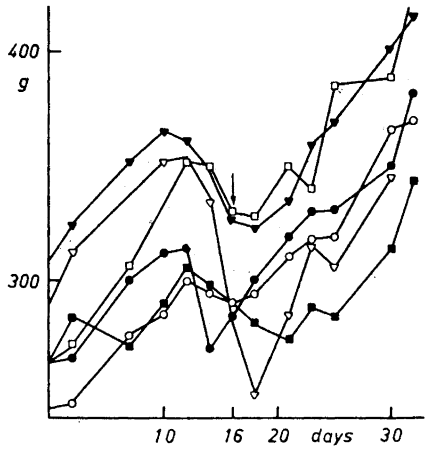

Fig. 3. 26 mg/day of ascorbigen administered to guinea pigs from the time pointed out by the arrow. Group 3.

When investigating the vitamin C effect of ascorbigen on man, the ascorbic acid was determined in the urine of two test persons after the eating first of ascorbic acid and then of the equivalent amount of ascorbigen. The determinations were performed according to the method described by Roe [5].

The test persons were on no special diet during the test, but they avoided to eat fresh fruits. When the vitamin C level in the urine had been followed for some days, they ate 500 mg of ascorbic acid. When the level had sunk again, they ate 875 mg (= 500 mg ascorbic acid) of ascorbigen.

The vitamin C excretion in the urine of both test persons rose sharply after the eating of ascorbic acid, as well as after that of ascorbigen. After the eating of ascorbigen, the vitamin C content in the urine of the first person was about 15 % of the amount excreted after the eating of ascorbic acid. In the second case it was 250 %. Accordingly, the vitamin C effect was established with both persons, even if the excreted amount of ascorbic acid differed greatly. Determinations with several test persons on controlled diets are needed to find out if the ascorbic acid bound in ascorbigen is split quantitatively in the organism, and if there are variations among different individuals in this respect.

This investigation is a part of a research project under U.S. Public Law No. 480, 83rd Congress.

1. Gmelin, R., Saarivirta, M. and Virtanen, A. I. *Suomen Kemistilehti B* **33** (1960) 172.
2. Gmelin, R. and Virtanen, A. I. *Ibid.* **33** (1961) 15.
3. Gmelin, R. and Virtanen, A. I. *Ann. Acad. Sci. Fennicae A II*, **1961** No. 107.
4. Procházka, Z., Šanda, V. and Šorm, F. *Collection Czechoslov. Chem. Communs.* **22** (1957) 654.
5. Roe, J. H. *Chemical Determination of Ascorbic, Dehydroascorbic, and Diketogulonic Acids* in Methods of Biochemical Analysis, Vol. 1, pp. 127–132 and 136. Interscience Publishers Inc., New York 1954.

Received January 22, 1962.

γ-Hydroxyglutaminsäure in *Linaria vulgaris* Miller

SHIN-ICHI HATANAKA

Laboratorium der Stiftung für chemische Forschung, Biochemisches Institut, Helsinki, Finnland

γ-Hydroxyglutaminsäure wurde vor einigen Jahren von Virtanen und Hietala aus *Phlox decussata* als freie Aminosäure isoliert [1]. Sie haben das Vorkommen von γ-Hydroxyglutaminsäure dazu nur in *Linaria vulgaris* auf papierchromatographischer Basis wahrscheinlich gemacht. Es scheint, dass diese Aminosäure im Pflanzenreich wenig verbreitet ist. Vorliegende Mitteilung bestätigt durch einige zusätzliche Versuche die Anwesenheit dieser Aminosäure in *Linaria vulgaris*.

Papierchromatographische Resultate. Zweidimensionale Papierchromatogramme (Butanol-Essigsäure-Wasser 630:100:270 und Phenol-Wasser/NH_3 1 000:365) zeigten, dass die Anfang September gesammelten Pflanzen eine sehr kleine Menge einer Aminosäure X enthielten, die genau wie γ-Hydroxyglutaminsäure wandert. Die R_F-Werte der Aminosäure X wurden bestimmt und mit denen von authentischer γ-Hydroxyglutaminsäure verglichen.

Azidität und Hydrolyse-Beständigkeit. Die saure Aminosäurenfraktion wurde nach der von Virtanen und Hietala beschriebenen Methode aus dem 80 %igem Äthanol-Extrakt der Pflanzen gewonnen. Sie enthielt neben Glutaminsäure und Asparaginsäure auch die zu bestimmende Aminosäure. Nach 24 stündigem Erhitzen dieser Fraktion auf 110°C in 6 N Salzsäure war die Aminosäure unverändert.

Ionenaustausch-Chromatographie an Dowex 1 × 8 200/400. Die saure Aminosäuren-

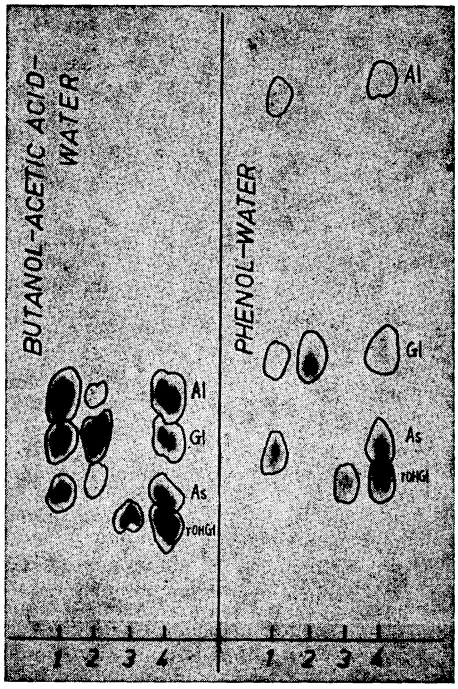

Abb. 1. Das chromatographische Verhalten von γ-Hydroxyglutaminsäure aus *Linaria vulgaris*.
Lösungsmittel: links 1—4 Butanol-Essigsäure-Wasser rechts 1—4 Phenol-Wasser(NH_3)
1 und 4: authentische Proben,
Al: Alanin; Gl: Glutaminsäure,
As: Asparaginsäure, γOHGl: γ-Hydroxyglutaminsäure
2: nach Reduktion der Aminosäure X mit HJ und rotem P.
3: Aminosäure X.

Lösungsmittel	R_F-Werte Glutaminsäure	γ-Hydroxyglutaminsäure	Aminosäure aus *Linaria*
But.-Eisess.-Wasser 630 : 100 : 270	0,11	0,07	0,07
Phenol-Wasser/NH_3 1 000 : 365	0,30	0,17	0,17

Papier Whatman No. 4, Zimmertemperatur, absteigende Methode.

fraktion wurde durch eine Dowex 1-Säule geschickt. Entsprechend dem Ergebnis eines Vorversuches mit einem Gemisch authentischer Glutamin-, Asparagin- und γ-Hydroxyglutaminsäuren wurden Glutaminsäure und Asparaginsäure mit 0,5 N Essigsäure eluiert und danach die zu bestimmende Aminosäure mit 1 N Essigsäure.

Reduktion mit Jodwasserstoffsäure. Da das auf diese Weise erhaltene Präparat noch eine geringe Menge Asparaginsäure enthielt, wurde die Aminosäure X aus einem mit Butanol-Eisessig-Wasser entwickelten Papierchromatogramm extrahiert. Die Reduktion des papierchromatographisch reinen Materials wurde in einem geschlossenen Glasrohr 4,5 Stdn mit 57 %igem HJ (d = 1,70) und rotem Phosphor bei 135—136°C ausgeführt. Nach anschliessender Behandlung mit Amberlite IR-120 wurden die Reaktionsprodukte chromatographiert. Wie aus der Abbildung ersichtlich ist, erwies sich das Hauptprodukt als Glutaminsäure. Dieses Ergebnis beweist, dass die zu bestimmende Substanz eine Hydroxyglutaminsäure sein muss.

Vergleich mit β-Hydroxyglutaminsäure. Auf dem mit Butanol-Eisessig-Wasser entwickelten Chromatogramm wandert β-Hydroxyglutaminsäure etwas schneller als γ-Hydroxyglutaminsäure. Die Aminosäure X zeigte den gleichen R_F-Wert wie γ-Hydroxyglutaminsäure und liess sich somit deutlich von β-Hydroxyglutaminsäure unterscheiden.

Aus diesen experimentellen Resultaten lässt sich folgern, dass *Linaria vulgaris* — obwohl in geringer Menge — γ-Hydroxyglutaminsäure enthält.

Herrn Prof. Dr. A. I. Virtanen bin ich für sein Interesse und Wohlwollen zu besonderem Dank verpflichtet, und Fräulein K. Aalto sei bestens für ihre technische Hilfe gedankt.

1. Virtanen, A. I. und Hietala, P. K. *Acta Chem. Scand.* **9** (1955) 175.

Eingegangen am 2. Januar 1962.

Isolierung und Identifizierung von α-Aminoadipinsäure aus Erbsenkeimlingen (*Pisum sativum* L.)

SHIN-ICHI HATANAKA und
ARTTURI I. VIRTANEN

Laboratorium der Stiftung für chemische Forschung, Biochemisches Institut, Helsinki, Finnland

Wie im hiesigen Institut gezeigt werden konnte, ist das Vorkommen von α-Aminoadipinsäure als freie Aminosäure in höheren Pflanzen (z.B. in Erbsenkeimlingen, in Blättern von *Petasites officinalis*, *Fraxinus excelsior*, den Samen und Keimlingen von *Vicia faba*, *Lupinus angustifolius*, *Phaseolus vulgaris* etc.) recht häufig.[1] Im Falle von *Pisum sativum* war diese Aminosäure ausschliesslich in jungen Keimpflanzen zu finden[2,3]. Beweise für das Vorkommen von freier α-Aminoadipinsäure in Pflanzen gründen sich jedoch nur auf papierchromatographische Bestimmungen. Blass und Macheboeuf haben ihren Befund vom Vorkommen von α-Aminoadipinsäure und Hydroxyaminoadipinsäure in *Vibrio cholerae* zurückgezogen[4]. Da freie α-Aminoadipinsäure früher aus Pflanzen nicht isoliert und folglich auch nicht chemisch charakterisiert ist, war es wichtig die chromatographische Befunde jedenfalls in einem Fall durch Isolierung der Säure zu bestätigen. Vorliegende Mitteilung behandelt die Isolierung und Identifizierung von α-Aminoadipinsäure aus jungen Erbsenkeimlingen.

Beschreibung der Versuche und Ergebnisse. Etwa 3,4 kg Samen von *Pisum sativum* wurden über Nacht in Wasser gequollen und dann auf feuchtes Papier ausgesät. Nach drei- bis viertätiger Keimung bei Zimmertemperatur an einer ziemlich dunklen Stelle wurden die Keimlinge dreimal hintereinander mit 80 %igem Alkohol, insgesamt ca. 27 l, extrahiert. Der Extrakt wurde in Vacuum auf etwa 2 l konzentriert und dann durch Kationenaustauscher Amberlite IR-120 laufen gelassen (300 ml Amberlite pro 1 kg Samen). Danach wurde das Harz sorgfältig mit destilliertem Wasser gewaschen und die Aminosäuren mit 1 N Ammoniak eluiert, bis sich das Eluat als Ninhydrin-negativ erwies. Das Ammoniakeluat wurde in Vacuum auf 260 ml eingeengt. Die Aminosäuren der ammoniak-

fraktion wurde durch eine Dowex 1-Säule geschickt. Entsprechend dem Ergebnis eines Vorversuches mit einem Gemisch authentischer Glutamin-, Asparagin- und γ-Hydroxyglutaminsäuren wurden Glutaminsäure und Asparaginsäure mit 0,5 N Essigsäure eluiert und danach die zu bestimmende Aminosäure mit 1 N Essigsäure.

Reduktion mit Jodwasserstoffsäure. Da das auf diese Weise erhaltene Präparat noch eine geringe Menge Asparaginsäure enthielt, wurde die Aminosäure X aus einem mit Butanol-Eisessig-Wasser entwickelten Papierchromatogramm extrahiert. Die Reduktion des papierchromatographisch reinen Materials wurde in einem geschlossenen Glasrohr 4,5 Stdn mit 57 %igem HJ (d = 1,70) und rotem Phosphor bei 135—136°C ausgeführt. Nach anschliessender Behandlung mit Amberlite IR-120 wurden die Reaktionsprodukte chromatographiert. Wie aus der Abbildung ersichtlich ist, erwies sich das Hauptprodukt als Glutaminsäure. Dieses Ergebnis beweist, dass die zu bestimmende Substanz eine Hydroxyglutaminsäure sein muss.

Vergleich mit β-Hydroxyglutaminsäure. Auf dem mit Butanol-Eisessig-Wasser entwickelten Chromatogramm wandert β-Hydroxyglutaminsäure etwas schneller als γ-Hydroxyglutaminsäure. Die Aminosäure X zeigte den gleichen R_F-Wert wie γ-Hydroxyglutaminsäure und liess sich somit deutlich von β-Hydroxyglutaminsäure unterscheiden.

Aus diesen experimentellen Resultaten lässt sich folgern, dass *Linaria vulgaris* — obwohl in geringer Menge — γ-Hydroxyglutaminsäure enthält.

Herrn Prof. Dr. A. I. Virtanen bin ich für sein Interesse und Wohlwollen zu besonderem Dank verpflichtet, und Fräulein K. Aalto sei bestens für ihre technische Hilfe gedankt.

1. Virtanen, A. I. und Hietala, P. K. *Acta Chem. Scand.* **9** (1955) 175.

Eingegangen am 2. Januar 1962.

Isolierung und Identifizierung von α-Aminoadipinsäure aus Erbsenkeimlingen (*Pisum sativum* L.)

SHIN-ICHI HATANAKA und
ARTTURI I. VIRTANEN

Laboratorium der Stiftung für chemische Forschung, Biochemisches Institut, Helsinki, Finnland

Wie im hiesigen Institut gezeigt werden konnte, ist das Vorkommen von α-Aminoadipinsäure als freie Aminosäure in höheren Pflanzen (z.B. in Erbsenkeimlingen, in Blättern von *Petasites officinalis*, *Fraxinus excelsior*, den Samen und Keimlingen von *Vicia faba*, *Lupinus angustifolius*, *Phaseolus vulgaris* etc.) recht häufig.[1] Im Falle von *Pisum sativum* war diese Aminosäure ausschliesslich in jungen Keimpflanzen zu finden[2,3]. Beweise für das Vorkommen von freier α-Aminoadipinsäure in Pflanzen gründen sich jedoch nur auf papierchromatographische Bestimmungen. Blass und Macheboeuf haben ihren Befund vom Vorkommen von α-Aminoadipinsäure und Hydroxyaminoadipinsäure in *Vibrio cholerae* zurückgezogen[4]. Da freie α-Aminoadipinsäure früher aus Pflanzen nicht isoliert und folglich auch nicht chemisch charakterisiert ist, war es wichtig die chromatographische Befunde jedenfalls in einem Fall durch Isolierung der Säure zu bestätigen. Vorliegende Mitteilung behandelt die Isolierung und Identifizierung von α-Aminoadipinsäure aus jungen Erbsenkeimlingen.

Beschreibung der Versuche und Ergebnisse. Etwa 3,4 kg Samen von *Pisum sativum* wurden über Nacht in Wasser gequollen und dann auf feuchtes Papier ausgesät. Nach drei- bis viertätiger Keimung bei Zimmertemperatur an einer ziemlich dunklen Stelle wurden die Keimlinge dreimal hintereinander mit 80 %igem Alkohol, insgesamt ca. 27 l, extrahiert. Der Extrakt wurde in Vacuum auf etwa 2 l konzentriert und dann durch Kationenaustauscher Amberlite IR-120 laufen gelassen (300 ml Amberlite pro 1 kg Samen). Danach wurde das Harz sorgfältig mit destilliertem Wasser gewaschen und die Aminosäuren mit 1 N Ammoniak eluiert, bis sich das Eluat als Ninhydrin-negativ erwies. Das Ammoniakeluat wurde in Vacuum auf 260 ml eingeengt. Die Aminosäuren der ammoniak-

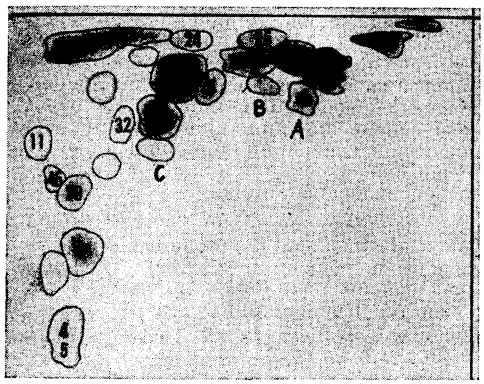

Abb. 1. Chromatogramm der freien Aminosäuren in Keimlingen von *Pisum sativum*. 1 Gly, 2 Ala, 3 Val, 4 Ileu, 5 Leu, 8 Ser, 9 Thr, 11 Pro, 16 Asp, 17 Glu, 24 Glu-NH_2, 25 Asp-NH_2, 29 γ,-Aminobuttersäure, 32 β-Alanin, 45 Äthanolamin, 51 Homoserin, A α-Aminoadipinsäure, B γ-Glutamylalanin, C Tyr.

freien Lösung wurden papierchromatographisch näher untersucht, zweidimensionales Papierchromatogramm, Lösungsmittel: Butanol-Essigsäure-Wasser (630:100:270) und Phenol-Wasser (NH_3) (1 000:365), Papier Whatman No. 4. Das Chromatogramm ist in Abb. 1 zu sehen. Der Fleck A links unterhalb von Glutaminsäure (17) sollte α-Aminoadipinsäure sein. Die Substanz B ist γ-Glutamyl-Alanin [5].

Die neutrale Lösung wurde sodann mit Anionenaustauscher IR-4B (1,5 l) behandelt. Die basischen und neutralen Aminosäuren wurden mit Wasser eluiert und die im Harz verbliebenen sauren Aminosäuren danach mit 1 N Salzsäure eluiert. Die Salzsäure wurde in Vacuum verdampft. Man erhielt so eine Aminosäurenfraktion, welche ausser Glutaminsäure und Asparaginsäure auch die zu identifizierende α-Aminoadipinsäure enthielt. Die zur Trockne eingedampfte Fraktion in wenig Wasser gelöst wurde auf eine (3,2 × 41,5 cm) Säule Dowex 1 gebracht und mit 0,2 N Essigsäure eluiert (16 ml/min). Unter diesen Bedingungen wurde die als α-Aminoadipinsäure betrachtete Aminosäure kurz vor Glutaminsäure eluiert. In einigen Fraktionen kam sie zusammen mit Glutaminsäure aus der Säule und wurde dann durch Wiederholung der Fraktionierung als reine Aminosäure gewonnen.

Bei der Konzentration in Vacuum der Fraktionen, welche praktisch nur noch die zu bestimmende Substanz enthielten, kristallisierte die Aminosäure sofort aus. Die papierchromatographisch reine Aminosäure wurde aus 1 N HCl-Lösung durch Neutralisieren mit 1 N NaOH als kristalline Substanz umgefällt. Nach Abfiltrieren und Waschen mit Äthanol und Äther wurde das Präparat über Phosphorpentoxyd getrocknet. Ausbeute 165 mg. Schmp. 195° (Zers.) (unkorr.) (Kofler Mikroheiztisch). $[\alpha]_D^{22} = +23°$ ($c = 2$; in 6 N HCl). (Gef. C 44.16; H 6.99; N 9.20. Ber. für $C_6H_{11}O_4N$: C 44.71; H 6.88; N 8.69).

Mikro-Stickstoffbestimmung wurde nach Beet [6] ausgeführt. Das Infrarot-Spektrum der Aminosäure war identisch mit dem der synthetischen L-α-Aminoadipinsäure.[7]

Windsor [8], der α-Aminoadipinsäure in sehr kleinen Mengen als Proteinkomponent aus Maissamen nach Säurehydrolyse gewonnen hat, berichtet, dass α-Aminodipinsäure aus einer Dowex 50-Säule mit Salzsäure eluiert, zwischen Glycin und Alanin erscheint. Die von uns isolierte α-Aminoadipinsäure im Gemisch mit authentischen Alanin, Glycin, Glutaminsäure und Asparaginsäure verhielt sich bei der Elution in einer Dowex 50-Säule mit 1 N Salzsäure wie die Aminosäure von Windsor.

Aus den Resultaten geht hervor, dass α-Aminoadipinsäure aus 3—4 Tage alten Erbsenkeimlingen isoliert und chemisch identifiziert werden konnte. Das Vorkommen dieser Aminosäure in grünen Pflanzen wurde dadurch bestätigt.

Fräulein K. Aalto sei für die technische Hilfe und Herrn Lic. Techn. Carl Enebäck, Technische Hochschule Helsinki, für die Bestimmung der Infrarot-Spektren bestens gedankt.

1. Berg, A.-M., Kari, S., Alfthan, M. und Virtanen, A. I. *Acta Chem. Scand.* **8** (1954) 358.
2. Virtanen, A. I., Berg, A.-M. und Kari, S. *Acta Chem. Scand.* **7** (1953) 1423.
3. Miettinen, J. K., *Ann. Acad. Sci. Fennicae A II*, **1955** No 60, p. 520.
4. Blass, J. und Macheboeuf, M. *Bull. soc. chim. biol.* **29** (1947) 903.
5. Virtanen, A. I. und Berg, A.-M. *Acta Chem. Scand.* **8** (1954) 1089.
6. Beet, A. E. *Nature* **175** (1955) 513.
7. Greenstein, J. P. und Winitz, M. *Chemistry of the Amino Acids*, John Wiley, New York 1961 p. 2459.
8. Windsor, E. *J. Biol. Chem.* **192** (1951) 595.

Eingegangen am 2. Januar 1962.

Treatment of Horse Serum Cholinesterase with Sialidase

EDITH HEILBRONN

Research Institute of National Defence, Sundbyberg 4, Sweden

The effect of bacterial sialidase on the electrophoretic properties of human serum cholinesterase suggests that this enzyme is a sialoprotein [1]. A sample of 2 200 fold purified cholinesterase from horse serum, prepared in this laboratory and analyzed for its amount of sialic acid, revealed 3.2 % of this acid [2]. This preparation, however, still does not represent the pure enzyme. It is therefore possible that the sialic acid belonged to other proteins. Further experiments were carried out (on a preparation with a lower degree of purity) in order to answer the question.

Experimental. 25 mg of a preparation obtained by ammonium sulfate fractionation [3] (purification factor about 200) were dissolved in 10 ml of 0.05 M acetate buffer pH 5.5. To the same solution 2 mg of sialidase (Behringwerke, Germany) were added. The solutions were kept at 25°C for 30 days. Twice a week the enzyme activity was determined with an automatic recording titrator at pH 8.0 and 25°C with 5×10^{-3} M butyrylcholine iodide as substrate. The mobility of the enzyme was controlled with paper electrophoresis in Tris buffer pH 8.9 (Schleicher and Schüll paper No. 2043B, 40 × 410 mm, 200 V). The protein was stained with amidoschwarz and the cholinesterase activity was demonstrated with indoxylacetate [2]. Sialidase alone did not stain at the concentration used.

Results. The paper electropherograms of the cholinesterase preparation showed three protein bands. After treatment with sialidase only one band was seen already after one day. The position of the enzyme was changed and closer to the starting line (see Fig. 1). Zone electrophoresis on cellulose of the sialidase treated cholinesterase preparation revealed only one protein peak. Without sialidase treatment this preparation is resolved into three or four peaks [2]. The activity of the sialidase treated cholinesterase solution was constant during 30 days. The results indicate that horse serum cholinesterase as well as some of the impurities of the used preparations are sialoproteins.

1. Svensmark, O. *Acta Physiol. Scand.* **52** (1961) 267.
2. Heilbronn, E. *Biochim. et Biophys. Acta* (1962). *In press.*

Received February 2, 1962.

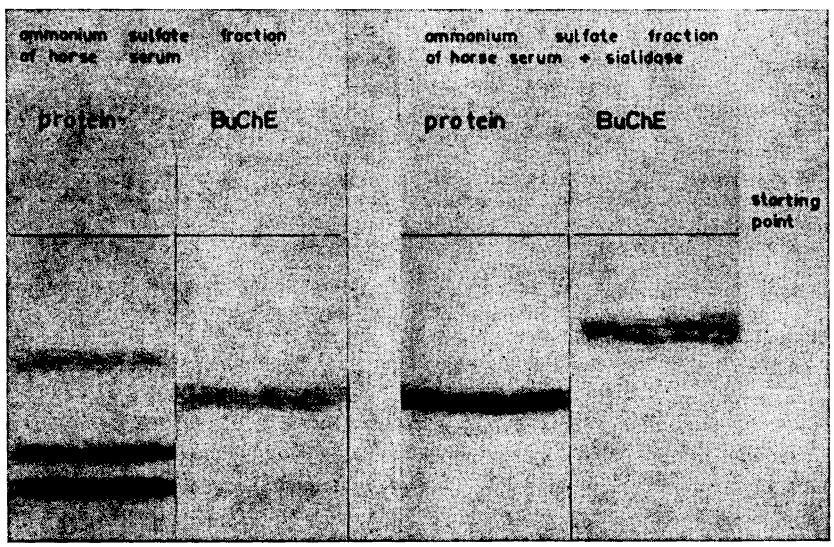

Fig. 1. Paper electropherograms of a cholinesterase preparation from horse serum before and after treatment with sialidase.

Starch Gel Electrophoresis of Basic Water-Soluble Barley Grain Proteins

TOR-MAGNUS ENARI, JUHANI MIKOLA, and MARTTI NUMMI

Laboratory of Brewing, Helsinki, Finland

We have earlier reported the fractionation of water-soluble proteins of barley grain by ion-exchange chromatography on DEAE-cellulose [1,2]. The basic proteins (about 30 % of the total) passed unretarded through the column in 5 mM phosphate buffer of pH 7.5 and the neutral and acid proteins were resolved into 15 components with gradient elution.

The basic protein fraction gives four components on paper electrophoresis at pH 8.6 (Fig. 1). These are apparently identical with the four cathodic components which we have found in the paper electrophoresis of unfractionated barley extracts [3]. Apparently they correspond to the three cathodic fractions which Mourgue and his collaborators have found in the paper electrophoresis of *Ricinus* [4] and *Jatropha* [5] seed extracts.

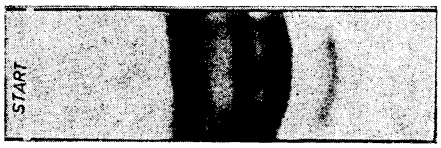

Fig. 1. Paper electrophoresis at pH 8.6 of basic barley proteins.

We have developed a preparative method for the purification of the basic proteins and resolved the material obtained into two anodic and fourteen cathodic components by starch-gel electrophoresis at pH 8.4.

Preparation of basic proteins. 500 g of finely ground and acetone treated barley (Pirkka) was extracted for 2 h with 1 000 ml of water [6] with occasional stirring at 4°C. The slurry was centrifuged at 5 000 r.p.m. for 10 min and the extract was left standing at 4°C for two days. During this period most of the phytic acid and water-soluble polysaccharides are hydrolyzed [7]. The small precipitate which forms on standing was removed by centrifugation. The proteins were then separated from interfering small-molecular substances and simultaneously transferred to 5 mM sodium phosphate buffer of pH 7.5 by gel filtration on Sephadex G-25 equilibrated with this buffer. The solution obtained was run through a 20 g preparative column of DEAE-cellulose (Schleicher & Schüll), equilibrated with the 5 mM buffer, to remove neutral and acid proteins. The solution containing the unretarded basic proteins and polysaccharides was acidified to pH 4.5 and made 0.1 M in respect to acetate with cautious addition of 1 M acetic acid and sodium acetate. The proteins were absorbed on a 20 g column of CM-cellulose (Schleicher & Schüll) at pH 4.5 and, after washing with the starting buffer, eluted with 0.3 M sodium phosphate pH 8.0. The sodium phosphate was removed from the proteins by gel filtration on Sephadex G-25 equilibrated with a 10 mM ammonium formate buffer. The volatile salt was required to suppress the ion-exchange properties of Sephadex G-25. After lyophilization the basic proteins weighed about 700 mg. 60—80 mg of this dry protein material was dissolved in 0.5 ml of water and this solution was used for electrophoretic analyses.

Electrophoretic conditions. The electrophoretic separation was performed by the vertical method described by Smithies [8], with minor alterations. The gels were prepared in plastic trays 30 × 12 × 0.6 cm from starch supplied by *Connaught Medical Research Laboratories, Toronto*. The starch was used at a concentration of 11.3 g/100 ml of buffer solution (for

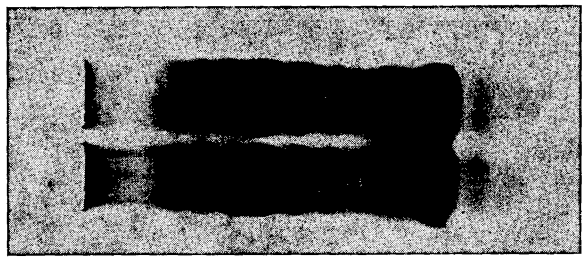

Fig. 2. Starch gel electrophoresis at pH 8.4 of basic barley proteins.

serum 12.3 g/100 ml was recommended). The buffer for gels contained 0.026 mole of H_3BO_3 and 0.014 mole of NaOH per litre, giving a final pH of 8.4 in the settled gel. The bridge solution contained 0.2 mole of H_3BO_3 and 0.04 mole of NaOH per litre. The potential gradient employed was 10 V/cm the positive electrode being in the upper vessel and the basic proteins migrating downwards to the cathode. All runs were made at 4°C. The cut gels were stained for 10 min. with Amido Black B and washed 4–5 times.

Results. The result obtained is shown in Fig. 2, in which 14 cathodic zones can be seen. On the anodic side there is one very diffuse region and one strongly stained band near the start which apparently corresponds to the least basic of the four bands in paper electrophoresis. At pH 7 all the protein material migrated towards the cathode. Thus the two anodic bands at pH 8.4 can also be considered to be basic proteins.

Under the conditions described here, the basic fraction of water-soluble barley grain proteins can be resolved reproducibly into 16 bands of significant intensity, which appear to be native components of barley grain.

Acknowledgements. The investigation has been supported by a grant from the *Finnish State Commission of Natural Sciences (Valtion Luonnontieteellinen Toimikunta)* which is gratefully acknowledged. The authors are indebted to Mrs. Ritva Korhonen and Mr. E. Nikkola for skilful technical assistance.

1. Enari, T.-M. and Mikola, J. *Suomen Kemistilehti* **B 33** (1960) 206.
2. Enari, T.-M. and Mikola, J. *European Brewery Conv. Proc. 8th Congr.* Wien 1961. *In press.*
3. Enari, T.-M., Nummi, M. and Mikola, J. *5th Intern. Congr. Biochem.* Moscow 1961. *In press.*
4. Mourgue, M., Baret, R., Reynaud, J. and Bellini, J. *Bull. soc. chim. biol.* **40** (1958) 1453.
5. Mourgue, R., Baret, R., Kassab, R. and Reynaud, J. *Bull. soc. chim. biol.* **43** (1961) 505.
6. Enari, T.-M., Nummi, M., Mikola, J. and Mäkinen, V. *Finska Kemistsamfundets Medd.* **71** (1962) *In press.*
7. Mikola, J., Nummi, M. and Enari, T.-M. *In press.*
8. Smithies, O. *Biochem. J.* **71** (1959) 585.

Received January 30, 1962.

A Lignan Xyloside from the Sapwood of *Sorbus aucuparia* L.

V. P. ARYA, H. ERDTMAN, M. KROLIKOWSKA and T. NORIN

Institutionen för Organisk Kemi, Kungl. Tekniska Högskolan, Stockholm 70, Sweden

The isolation of two biphenyl derivatives of unusual structure, aucuparin and methoxyaucuparin from the heartwood of mountain ash (*Sorbus aucuparia* L.) has recently been reported from this laboratory.[1] The sapwood contains a lignan xyloside (1–3 % of the dry wood). This xyloside is identical with the lignan xyloside from *Alnus glutinosa* [2] and a *Lyonia* species [3] as shown by a comparison of the physical constants recorded in Table 1.

The investigation of the *Alnus* xyloside [4] showed that the aglycone has the ***structure*** I (X = H).

The *Sorbus* aglycone was obtained by the hydrolysis of the xyloside with acid as well as emulsin. This observation and the small difference in optical rotation between the xyloside and the aglycone indicates that the xyloside is a β-xyloside. Permanganate oxidation of the aglycone dimethyl ether in acetone afforded galloylgallic acid hexamethyl ether, m.p. 190–191°, and gallic acid trimethyl ether. Mild oxidation of the aglycone dimethyl ether with chromic anhydride in pyridine gave a lactone ("α-lactone"), $C_{18}H_{10}O_2(OCH_3)_6$, m.p. 200–201°, $[\alpha]_D$ −103° (a), −122° (c) and a cyclohemiacetal, $C_{18}H_{11}O(OH)(OCH_3)_6$, m.p. 180–181°, $[\alpha]_D$ −6° (c) [monoacetate, $C_{18}H_{11}O(OAc)(OCH_3)_6$, m.p. 158–160°, $[\alpha]_D$ −13° (c)] which on further oxidation furnished the α-lactone. The α-lactone gave the aglycone dimethyl ether on reduction with lithium aluminium hydride. On dehydration with potassium hydrogen sulphate the latter aglycone derivative afforded the anhydro-compound, $C_{18}H_{10}O(OCH_3)_6$, m.p. 145–146°, $[\alpha]_D$ −41.6° (a) as does the *Alnus* aglycone dimethyl ether.

The *Sorbus* xyloside dimethyl ether was oxidised with chromic anhydride in pyridine to an amorphous acid which on hydrolysis furnished the *Sorbus* "α-lactone". The sugar residue must be attached to the methylol group not suffering oxidation and the problem of elucidating the structure of the xyloside is therefore reduced to a determination of the structure of the α-lactone.

serum 12.3 g/100 ml was recommended). The buffer for gels contained 0.026 mole of H_3BO_3 and 0.014 mole of NaOH per litre, giving a final pH of 8.4 in the settled gel. The bridge solution contained 0.2 mole of H_3BO_3 and 0.04 mole of NaOH per litre. The potential gradient employed was 10 V/cm the positive electrode being in the upper vessel and the basic proteins migrating downwards to the cathode. All runs were made at 4°C. The cut gels were stained for 10 min. with Amido Black B and washed 4–5 times.

Results. The result obtained is shown in Fig. 2, in which 14 cathodic zones can be seen. On the anodic side there is one very diffuse region and one strongly stained band near the start which apparently corresponds to the least basic of the four bands in paper electrophoresis. At pH 7 all the protein material migrated towards the cathode. Thus the two anodic bands at pH 8.4 can also be considered to be basic proteins.

Under the conditions described here, the basic fraction of water-soluble barley grain proteins can be resolved reproducibly into 16 bands of significant intensity, which appear to be native components of barley grain.

Acknowledgements. The investigation has been supported by a grant from the *Finnish State Commission of Natural Sciences (Valtion Luonnontieteellinen Toimikunta)* which is gratefully acknowledged. The authors are indebted to Mrs. Ritva Korhonen and Mr. E. Nikkola for skilful technical assistance.

1. Enari, T.-M. and Mikola, J. *Suomen Kemistilehti* **B 33** (1960) 206.
2. Enari, T.-M. and Mikola, J. *European Brewery Conv. Proc. 8th Congr.* Wien 1961. *In press.*
3. Enari, T.-M., Nummi, M. and Mikola, J. *5th Intern. Congr. Biochem.* Moscow 1961. *In press.*
4. Mourgue, M., Baret, R., Reynaud, J. and Bellini, J. *Bull. soc. chim. biol.* **40** (1958) 1453.
5. Mourgue, R., Baret, R., Kassab, R. and Reynaud, J. *Bull. soc. chim. biol.* **43** (1961) 505.
6. Enari, T.-M., Nummi, M., Mikola, J. and Mäkinen, V. *Finska Kemistsamfundets Medd.* **71** (1962) *In press.*
7. Mikola, J., Nummi, M. and Enari, T.-M. *In press.*
8. Smithies, O. *Biochem. J.* **71** (1959) 585.

Received January 30, 1962.

A Lignan Xyloside from the Sapwood of *Sorbus aucuparia* L.

V. P. ARYA, H. ERDTMAN, M. KROLIKOWSKA and T. NORIN

Institutionen för Organisk Kemi, Kungl. Tekniska Högskolan, Stockholm 70, Sweden

The isolation of two biphenyl derivatives of unusual structure, aucuparin and methoxyaucuparin from the heartwood of mountain ash (*Sorbus aucuparia* L.) has recently been reported from this laboratory.[1] The sapwood contains a lignan xyloside (1–3 % of the dry wood). This xyloside is identical with the lignan xyloside from *Alnus glutinosa* [2] and a *Lyonia* species [3] as shown by a comparison of the physical constants recorded in Table 1.

The investigation of the *Alnus* xyloside [4] showed that the aglycone has the ***structure*** I (X = H).

The *Sorbus* aglycone was obtained by the hydrolysis of the xyloside with acid as well as emulsin. This observation and the small difference in optical rotation between the xyloside and the aglycone indicates that the xyloside is a β-xyloside. Permanganate oxidation of the aglycone dimethyl ether in acetone afforded galloylgallic acid hexamethyl ether, m.p. 190–191°, and gallic acid trimethyl ether. Mild oxidation of the aglycone dimethyl ether with chromic anhydride in pyridine gave a lactone ("α-lactone"), $C_{18}H_{10}O_2(OCH_3)_6$, m.p. 200–201°, $[\alpha]_D$ −103° (a), −122° (c) and a cyclohemiacetal, $C_{18}H_{11}O(OH)(OCH_3)_6$, m.p. 180–181°, $[\alpha]_D$ −6° (c) [monoacetate, $C_{18}H_{11}O(OAc)(OCH_3)_6$, m.p. 158–160°, $[\alpha]_D$ −13° (c)] which on further oxidation furnished the α-lactone. The α-lactone gave the aglycone dimethyl ether on reduction with lithium aluminium hydride. On dehydration with potassium hydrogen sulphate the latter aglycone derivative afforded the anhydro-compound, $C_{18}H_{10}O(OCH_3)_6$, m.p. 145–146°, $[\alpha]_D$ −41.6° (a) as does the *Alnus* aglycone dimethyl ether.

The *Sorbus* xyloside dimethyl ether was oxidised with chromic anhydride in pyridine to an amorphous acid which on hydrolysis furnished the *Sorbus* "α-lactone". The sugar residue must be attached to the methylol group not suffering oxidation and the problem of elucidating the structure of the xyloside is therefore reduced to a determination of the structure of the α-lactone.

Table 1. (S,A and L = compounds from *Sorbus*, *Alnus* and *Lyonia*, respectively. $[\alpha]_D$ in acetone = a; in chloroform = c; in methanol = m).

Compound		Composition	M.P.	$[\alpha]_D$
Xyloside	S	$C_{18}H_{10}O(OCH_3)_4(OH)_3^{\alpha}(C_5H_{11}O_4)$	124–125°$^{\beta}$, 165–166°	+ 43° (m)
				+ 38° (a+aq)
	A		122–124°	+ 38° (a+aq)
	L		123°, 165°	+ 27° (a)
dimethyl ether	S	$C_{18}H_{10}O(OCH_3)_6(OH)^{\gamma}(C_5H_{11}O_4)$	143–145°	+ 45° (c)
hexaacetate	S	$C_{18}H_{10}O(OCH_3)_4(OAc)_3(C_5H_8O)(OAc)_2$	98–100°	− 1° (c)
hexabenzoate	S	$C_{18}H_{10}O(OCH_3)_4(OBz)_3(C_5H_8O)(OBz)_3$	138–139°	−2.5° (c)
Aglycone	S	$C_{18}H_{12}(OCH_3)_4(OH)_4^{\alpha}$	115–116°$^{\delta}$	+ 48° (a)
	A		165–167°$^{\delta,\varepsilon}$	+ 52° (a)
dimethyl ether	S	$C_{18}H_{12}(OCH_3)_6(OH)_2^{\gamma}$	163–164°	+ 45° (c)
				+ 32° (a)
	A		152°	- - - - -
	L		158–160°	+ 30° (a)
tetraacetate	S	$C_{18}H_{12}(OCH_3)_4(OAc)_4$	160–161	+ 21° (a), −11° (c)
	A		157–159°	+ 17° (a)
dimethyl ether diacetate	S	$C_{18}H_{12}(OCH_3)_6(OAc)_2$	99–100°	+ 29° (c)
	A		88– 89°	- - - - -

α: Of which two of the OH groups are phenolic. β: Sample containing two moles of water of crystallisation. γ: Alcoholic OH groups. δ: Probably dimorphism. ε: D,L-form [4], m.p. 115–118°.

This lactone could be isomerised with sodium ethoxide to a "β-lactone", $C_{18}H_{10}O_2(OCH_3)_6$, m.p. 152–153°, $[\alpha]_D$ + 13.8° (c), 0° (a), reduced by lithium aluminium hydride to a "β-diol", $C_{18}H_{12}(OCH_3)_6(OH)_2$, m.p. 171–172°, $[\alpha]_D$ +60.7° (c).

The large increase in optical rotation on epimerisation of the α-lactone recalls the similar effect observed on epimerisation of α-conidendrin dimethyl ether to the β-isomer with sodium ethoxide and suggests that the α-lactone might possess a structure and configuration similar to those of α-conidendrin dimethyl ether. However, a retrodendrin structure cannot be excluded since the specific rotation of α-retrodendrin dimethyl ether is similar in magnitude to that of α-conidendrin dimethyl ether and

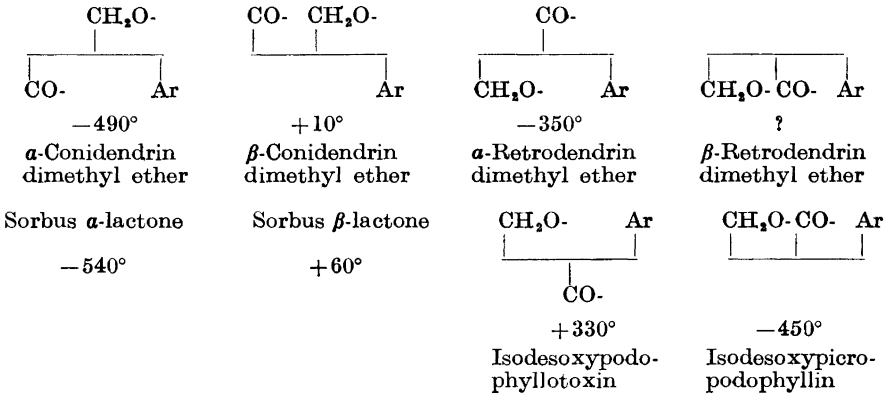

β-retrodendrin dimethyl ether is not known. For the following reason the latter should possess a high positive rotation. Isodesoxypodophyllotoxin and α-retrodendrin dimethyl ether are compounds of antipodal configuration and have rotations of similar magnitude but opposite sign. Similarly, isodesoxypicropodophyllin and β-retrodendrin dimethyl ether have antipodal configurations. Of these two compounds the former has a high negative rotation.

This is illustrated by the partial structures (see p. 519) in which the absolute configurations at C_2 (left), C_3 and C_4 (right) and the molecular rotations (in chloroform) of the relevant lignans are given. Like α-conidendrin dimethyl ether *Sorbus* α-lactone was not epimerised by heating with piperidine or sodium acetate. Under these conditions isodesoxypodophyllotoxin is epimerised to isodesoxypicropodophyllin.[5]

Additional confirmation of this conclusion can be obtained from a comparison of the molecular rotations in chloroform of some diols related to the *Sorbus* aglycone dimethyl ether given above.

The difference (+ 80°) in molecular rotations of the epimeric pair, α- and β-conidendryl alcohol dimethyl ether, is very similar to the difference (+ 72°) in molecular rotations of the *Sorbus* aglycone dimethyl ether and *Sorbus* "β-diol" and is also similar to that of the antipodal pair, isodesoxypodophyllyl alcohol and desoxypicropodophyllyl alcohol (−40°). It is concluded that *Sorbus* xyloside (= *Alnus* and *Lyonia* xyloside) has the structure and *configuration* I (X = xylose).

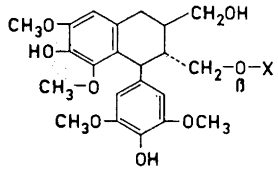

I

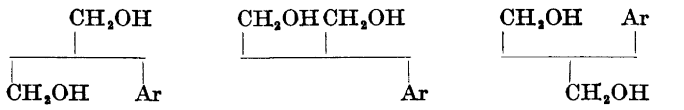

+ 80° α-Conidendryl alcohol dimethyl ether

+ 160° α-Conidendryl alcohol dimethyl ether

−90° Isodesoxypodophyllyl alcohol

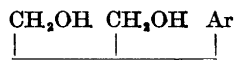

+ 200° *Sorbus* aglycone dimethyl ether

+ 272° *Sorbus* "β-diol"

+ 480° Isodesoxypicropodophyllyl alcohol

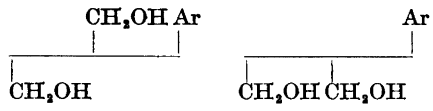

−640° Desoxypodophyllyl alcohol

−130° Desoxypicropodophyllyl alcohol

Acknowledgements. We are grateful to Dr. A. Wettstein, Ciba Ltd., Basel, for several analyses, to the *Swedish Technical Research Council* and the *Office of Research and Development*, U.S. Army Department, for financial support and to the *Ciba Fellowship Trust*, Cambridge, for a fellowship to one of us (V.P.A.).

1. Erdtman, H., Eriksson, G. and Norin, T. *Acta Chem. Scand.* **15** (1961) 1796.
2. Freudenberg, K. and Weinges, K. *Tetrahedron Letters* **17** (1959) 19.
3. Yasue, M. and Kato, Y. *J. Pharm. Soc. (Japan)* **80** (1960) 1013.
4. Weinges, K. *Chem. Ber.* **94** (1961) 2522.
5. Hartwell, J. L., Schrecker, A. W. and Johnson, J. M. *J. Am. Chem. Soc.* **75** (1953) 2138.

Received February 6, 1962.

Some New Glass-Forming Hydrocarbon Mixtures

KJ. ROSENGREN* and S. SUNNER

*Thermochemistry Laboratory**, University of Lund, Lund, Sweden*

In order to study in detail the photolysis reaction mechanisms in a high-viscosity matrix at 77°K it is necessary to devise conditions and means by which reaction between the photolytically active molecules and the surrounding matrix molecules can be prevented or elucidated. The hitherto used glasses [1-4] based on hydrocarbons consist of one or two of the compounds isopentane, 3-methyl pentane and methyl cyclohexane, all containing hydrogen attached to tertiary carbon atoms.

One of the predictable reactions between primary photolysis products and matrix molecules is the hydrogen abstraction from a hydrocarbon by a species of radical nature [5,6]. As the C_{tert}-H bond dissociation energy is about 5 kcal less than that for a $C_{sec.}$—H bond (89 and 94 kcal, respectively) [7], it should be advantageous to have available a matrix without tertiary carbon atoms in the hydrocarbon components. According to the Arrhenius equation, an increase in activation energy of 5 kcal at 77°K changes the rate constant by a factor of 10^{-14}, provided the preexponential factor does not change. Hydrogen bonded to a tertiary carbon atom reacts instantaneously whereas hydrogen bonded to a secondary carbon atom does not react at all.

The following hydrocarbons were purified according to standard procedure [8]: pentane (a), isopentane (b), hexane (c), cyclohexane (d), 3-methyl pentane (e), *neo*-hexane (f), methyl cyclopentane (g) and methyl cyclohexane (h). Binary and ternary mixtures were made and repeatedly cycled between room temperature and 77°K to study their glass-forming properties. The tendency for cracking at 77°K was tested by filling sample tubes with small pieces of broken glass.

The following results were obtained. First, the components of the mixture are given and, secondly, the approximate volume ratio between them, for which a glass with given quality was obtained (in three cases a rather broad ratio interval is given for which glasses have been obtained).

Mixtures forming good glasses at 77°K: a:f, 3:5—3:10; b:e, 0:1—1:0.

Mixtures forming good glasses, which may crack when stored for hours at 77°K: a:c:f, 1:1:9; a:d:f, 5:2:13; b:e:h, 1:1:1; b:h, 3:2; d:f, 1:9; e:h, 1:2—1:6.

Mixtures crystallizing in all proportions during freezing: c:f, e:g, f:g, g:h.

Of the mixtures studied, a:f, a:c:f, a:d:f and d:f do not contain tertiary carbon atoms. However, the only one which has been found to give a very stable glass is pentane and *neo*-hexane. In the proportions 3:8, this glass has been extensively used in our laboratory.

Contraction between 298 and 77°K, relative viscosity and melting behaviour for some of these glasses have been studied [8].

Acknowledgements. This investigation has been supported by *Directorate of Chemical Science, AFOSR, AFRD of the Air Research and Development Command, United States Air Force*, through its European Office and by *Magn. Bergvalls Stiftelse.*

1. Lewis, G. N. and Lipkin, D. *J. Am. Chem. Soc.* **64** (1942) 2801.
2. Norman, I. and Porter, G. *Proc. Roy. Soc. London* **A 230** (1955) 399.
3. Sowden, R. G. and Davidson, N. *J. Am. Chem. Soc.* **78** (1956) 1291.
4. Potts, W. J. *J. Chem. Phys.* **21** (1953) 191.
5. Walling, C. *Free Radicals in Solution.* John Wiley & Sons, New York 1957, p. 323.
6. Gray, P. and Williams, A. *Chem. Rev.* **59** (1959) 267.
7. Cottrell, T. L. *The Strengths of Chemical Bonds.* 2nd Ed. Butterworths Scientific Publications, London 1958.
8. Rosengren, Kj. *Acta Chem. Scand.* **16** (1962) *In press.*

Received February 6, 1962.

* Research Fellow at *The Swedish Technical Research Council.*

** Sponsored by *The Swedish Natural Science Research Council* and by *The Swedish Technical Research Council.*

1,4-Bis-(2-chloräthylamino)-1,4-didesoxy-threit-dihydrochlorid

PETER W. FEIT

Forschungslaboratorium der Leo Pharmaceutical Products, Ballerup, Dänemark

Die Synthese und cytostatische Aktivität des "Degranol's" [1] (1,6-Bis-(2-chloräthylamino)-1,6-didesoxy-D-mannit) veranlasste uns, zu vergleichenden Untersuchungen hinsichtlich einer möglichen antineoplastischen Wirkung und eventuellen Stereospezifität, die stereoisomeren 1,4-Bis-(2-chloräthylamino)-2,3-butandioldihydrochloride darzustellen.

Über das *meso*-Isomere, 1,4-Bis-(2-chloräthylamino)-1,4-didesoxy-erythrit-dihydrochlorid, welches aus *meso*-1,2;3,4-Dioxidobutan durch Reaktion mit Aziridin zu *meso*-1,4-Bis-(1-aziridinyl)-2,3-butandiol und anschliessende Öffnung der Aziridinringe mit wässriger Chlorwasserstoffsäure erhalten wurde, ist inzwischen bereits von anderer Seite berichtet worden [2,3]. Die Konfiguration wurde durch Kristallstrukturmessungen der Aziridinverbindung bestätigt [4]. Die Übertragung der Reaktionsfolge zur Darstellung von 1,4-Bis-(2-chloräthylamino)-1,4-didesoxy-DL-threit-dihydrochlorid blieb nach Reist und Mitarbeitern [3] auf Grund der grossen Polymerisationstendenz des DL-1,4-Bis-(1-aziridinyl)-2,3-butandiols erfolglos. Die von uns gewählten Reaktionsbedingungen ermöglichten es jedoch, aus D-, L- und racemischem 1,2;3,4-Dioxidobutan [5] D-, L- und racemisches 1,4-Bis-(1-aziridinyl)-2,3-butandiol kristallin und analysenrein darzustellen, obgleich die Verbindungen nicht frei von Polymerisationsprodukten waren. Dieses verhinderte eine Messung des optischen Drehvermögens ihrer wässrigen Lösungen. Der Umsatz mit wässriger Chlorwasserstoffsäure lieferte D-, L- und racemisches 1,4-Bis-(2-chloräthylamino)-1,4-didesoxy-threit-dihydrochlorid. Auch bei letzteren Verbindungen muss noch offen gelassen werden, inwieweit sie durch Polymerisationsprodukte verunreinigt sind. Die stereoisomeren Bis-(2-chloräthylamino)-Verbindungen werden vom National Cancer Institut unter National Institut of Health, U.S.A. unter N.S.C. Nr. 39 071 (D-Isomeres), 39 072 (L-Isomeres) und 39 073 (meso-Isomeres) getestet.

Beschreibung der Versuche (Experimentel mitbearbeitet von W. Schlichtkrull).

D-*1,4-Bis-(1-aziridinyl)-2,3-butandiol.* 240 ml Aziridin wurden auf 50° erwärmt und darauf unter gutem Rühren innerhalb von 1 Std. 64,5 g D-1,2;3,4-Dioxidobutan [5] eingetropft, wobei durch Kühlung die Temperatur der Reaktionsmischung zwischen 52 und 53° gehalten wurde. Man rührte noch weitere 3 Stdn. bei gleicher Temperatur und engte darauf i. Vak. bei einer Badtemperatur von nicht über 15° ein. Sobald ein dickflüssiger Kristallbrei vorlag — bei zu weitgehendem Einengen erfolgte spontane Polymerisation unter Selbsterwärmung — wurde mit 150 ml eiskaltem Acetonitril versetzt und nach 14 stdg. Stehen bei 4° die Aziridinverbindung abgesaugt, mit Acetonitril gewaschen und i. Vak. über Natriumhydroxyd getrocknet. Ausb. 71 g, Schmp. 98—99°. Gef.: C 55,51; H 9,37; N 16,30. Ber. für $C_8H_{16}N_2O_2$ (172.2): C 55,79; H 9,36; N 16,27.

L-Isomeres: Schmp. 98—99°; Gef. C 55,51; H 9,25; N 16,25. Racemat.: Schmp. 84—86,5°.

1,4-Bis-(2-chloräthylamino)-1,4-didesoxy-D-threit-dihydrochlorid. Eine Lösung von 64 g D-1,4-Bis-(1-aziridinyl)-2,3-butandiol in 150 ml Wasser liess man bei —5° unter gutem Rühren zu 200 ml konz. Salzsäure tropfen. Darauf wurde die filtrierte Lösung i. Vak. bei einer Badtemperatur von 20° eingeengt, der erhaltene kristalline Rückstand mit 400 ml Äthanol verrieben und nach 15 stdg. Stehen im Kühlschrank abgesaugt und mit Äthanol und Äther gewaschen. Ausb. 104 g, Schmp. 132—136° (Zers.). Zur Analyse wurde mehrmals aus Wasser-Aceton und Dimethylsulfoxyd-Aceton unter Filtrieren über Filtererde umgefällt. Schmp. 235—236° (Zers.); $[\alpha]_D^{20}$ + 30,5° (c = 2, Wasser); (Gef.: C 30,42; H 6,42; N 8,78; Cl 44,60; Cl^- 22,32. Ber. für $C_8H_{18}Cl_{22}N_2O_2 \cdot 2HCl$ (318,1); C 30,22; H 6,34; N 8,81; Cl 44,52; Cl^- 22,30).

L-Isomeres: Schmp. 234—235° (Zers.); $[\alpha]_D^{20}$ —31,1° (c = 2, Wasser); (Gef. C 30,35; H 6,32; N 8,86; Cl 44,50; Cl^- 22,34).

Racemat: Schmp. 234.5° (Zers.).

1. Vargha, L., Toldy, L., Fehér, Ö. und Lendvai, S. *J. Chem. Soc.* **1957** 805; Kellner, B. und Németh, L. *Z. Krebsforschung* **61** (1956) 165; Sellei, C., Eckhardt, S., Hartei, F. und Dumbovich, B. *Lancet* **1956** 785.

2. Vargha, L., Toldy, L. und Kasztreiner, E. *Acta Chim. Acad. Sci. Hung.* **19** (1959) 295.
3. Reist, E. J., Junga, I. E., Wain, M. E., Crews, O. P., Goodman, L. und Baker, B. R. *J. Org. Chem.* **26** (1961) 2139.
4. Could, E. S. und Pasternak, R. A. *J. Am. Chem. Soc.* **83** (1961) 2658.
5. Feit, P. W. *Chem. Ber.* **93** (1960) 116.

Eingegangen am 7. Februar 1962.

4-(Tetracyanoethyl)-2,6-dimethylphenol

BENGT SMITH and ULF PERSMARK

Institutionen för Organisk kemi, Chalmers Tekniska Högskola, Göteborg, Sweden

Sausen, Engelhardt and Middleton [1] have described the formation of 4-(tricyanovinyl)-2,6-dimethylphenol (II) in a reaction between tetracyanoethylene and 2,6-dimethylphenol in tetrahydrofuran-pyridine solution. They assumed that the reaction proceeded over an intermediate 4-(tetracyanoethyl)-2,6-dimethylphenol (I). We wish to report the preparation of the latter compound from tetracyanoethylene and 2,6-dimethylphenol in acetic acid solution. It is a white solid which is reasonably stable in acid solution but, in alkaline solution, is converted to the red 4-(tricyanovinyl)-2,6-dimethylphenol (II). It can, however, be dissolved in sodium bicarbonate solution and reprecipitated with hydrochloric acid.

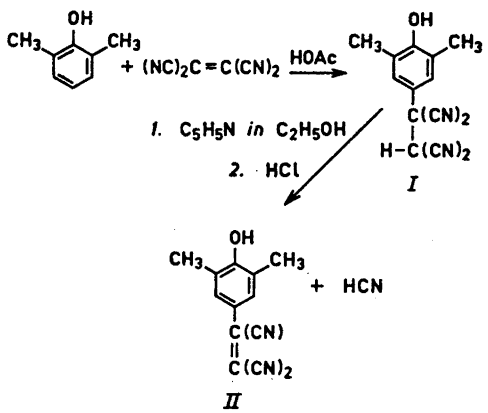

I *II*

We are now studying the scope and limitations of the reaction between tetracyanoethylene and phenols in acidic solution as well as the properties of the tetracyanoethylphenols formed. The results of the study will be presented in a forthcoming paper.

Tetracyanoethylene (0.173 g, 1.35 mmole) and 2,6-dimethylphenol (0.167 g, 1.37 mmole) were dissolved in 15 ml glacial acetic acid and then 1 ml water was added. The reddish-violet solution was discoloured after a few hours and, upon addition of water (10 ml), a white precipitate was formed. It was collected and recrystallized from glacial acetic acid and water (1:1). Yield 0.205 g (61 %). M.p. 154–156° (decomp.). (Found: C 67.4; H 3.97; N 22.2. Calc. for (I), $C_{14}H_{10}ON_4$: C 67.19; H 4.02; N 22.39).

4-(Tetracyanoethyl)-2,6-dimethylphenol (0.145 g, 0.58 mmole) was dissolved in 10 ml ethyl alcohol and 0.5 ml pyridine was added. The solution was heated on a boiling water bath for half an hour. On acidification with 5 N hydrochloric acid, the colour of the dark red solution changed to orange-yellow. Addition of water (10 ml) caused an orange-yellow substance to precipitate. It was collected and recrystallized from glacial acetic acid and water (1:1). Yield 0.122 g (95 %). M.p. 179–181° (decomp.). M.p. for 4-(tricyanovinyl)-2,6-dimethylphenol (II) according to Sausen *et al.*[1] 182–183° (decomp.) *. A specimen of the latter compound obtained from tetracyanoethylene and 2,6-dimethylphenol in alcohol-pyridine solution was found not to depress the melting point of the compound formed from 4-(tetracyanoethyl)-2,6-dimethylphenol.

1. Sausen, G. N., Engelhardt, V. A. and Middleton, W. J. *J. Am. Chem. Soc.* **80** (1958) 2815.

Received February 7, 1962.

* Determined on a preheated block.

2. Vargha, L., Toldy, L. und Kasztreiner, E. *Acta Chim. Acad. Sci. Hung.* **19** (1959) 295.
3. Reist, E. J., Junga, I. E., Wain, M. E., Crews, O. P., Goodman, L. und Baker, B. R. *J. Org. Chem.* **26** (1961) 2139.
4. Could, E. S. und Pasternak, R. A. *J. Am. Chem. Soc.* **83** (1961) 2658.
5. Feit, P. W. *Chem. Ber.* **93** (1960) 116.

Eingegangen am 7. Februar 1962.

4-(Tetracyanoethyl)-2,6-dimethylphenol

BENGT SMITH and ULF PERSMARK

Institutionen för Organisk kemi, Chalmers Tekniska Högskola, Göteborg, Sweden

Sausen, Engelhardt and Middleton [1] have described the formation of 4-(tricyanovinyl)-2,6-dimethylphenol (II) in a reaction between tetracyanoethylene and 2,6-dimethylphenol in tetrahydrofuran-pyridine solution. They assumed that the reaction proceeded over an intermediate 4-(tetracyanoethyl)-2,6-dimethylphenol (I). We wish to report the preparation of the latter compound from tetracyanoethylene and 2,6-dimethylphenol in acetic acid solution. It is a white solid which is reasonably stable in acid solution but, in alkaline solution, is converted to the red 4-(tricyanovinyl)-2,6-dimethylphenol (II). It can, however, be dissolved in sodium bicarbonate solution and reprecipitated with hydrochloric acid.

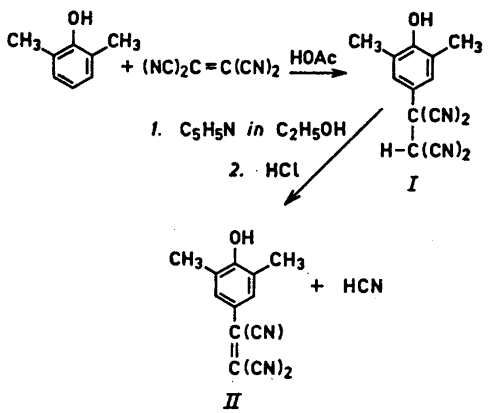

I *II*

We are now studying the scope and limitations of the reaction between tetracyanoethylene and phenols in acidic solution as well as the properties of the tetracyanoethylphenols formed. The results of the study will be presented in a forthcoming paper.

Tetracyanoethylene (0.173 g, 1.35 mmole) and 2,6-dimethylphenol (0.167 g, 1.37 mmole) were dissolved in 15 ml glacial acetic acid and then 1 ml water was added. The reddish-violet solution was discoloured after a few hours and, upon addition of water (10 ml), a white precipitate was formed. It was collected and recrystallized from glacial acetic acid and water (1:1). Yield 0.205 g (61 %). M.p. 154–156° (decomp.). (Found: C 67.4; H 3.97; N 22.2. Calc. for (I), $C_{14}H_{10}ON_4$: C 67.19; H 4.02; N 22.39).

4-(Tetracyanoethyl)-2,6-dimethylphenol (0.145 g, 0.58 mmole) was dissolved in 10 ml ethyl alcohol and 0.5 ml pyridine was added. The solution was heated on a boiling water bath for half an hour. On acidification with 5 N hydrochloric acid, the colour of the dark red solution changed to orange-yellow. Addition of water (10 ml) caused an orange-yellow substance to precipitate. It was collected and recrystallized from glacial acetic acid and water (1:1). Yield 0.122 g (95 %). M.p. 179–181° (decomp.). M.p. for 4-(tricyanovinyl)-2,6-dimethylphenol (II) according to Sausen *et al.*[1] 182–183° (decomp.) *. A specimen of the latter compound obtained from tetracyanoethylene and 2,6-dimethylphenol in alcohol-pyridine solution was found not to depress the melting point of the compound formed from 4-(tetracyanoethyl)-2,6-dimethylphenol.

1. Sausen, G. N., Engelhardt, V. A. and Middleton, W. J. *J. Am. Chem. Soc.* **80** (1958) 2815.

Received February 7, 1962.

* Determined on a preheated block.

Polarography and Reduction of Hydroxylamine-O-sulfonic Acid

HENNING LUND

Department of Chemistry, University of Aarhus, Aarhus, Denmark

During a polarographic investigation of oxime-O-sulfonic acids it became of interest to investigate hydroxylamine-O-sulfonic acid, also called sulfoperamic acid. It was hoped that a polarographic investigation could throw light on the constitution of the compound in solution.

Hydroxylamine-N-sulfonic acid and hydroxylamine-N,N-disulfonic acid are not polarographically reducible [1] and it was found here that hydroxylamine-O,N-disulfonic acid is not reducible between 0 and 2.0 V *vs* S.C.E. in buffered systems, whereas hydroxylamine-O-sulfonic acid is polarographically reducible. This difference is not surprising in view of the fact that hydroxylamine-O-sulfonic acid liberates iodine from iodide whereas the three aforementioned hydroxylaminesulfonic acids do not.

Hydroxylamine-O-sulfonic acid gives rise to a well-defined polarographic wave from pH about 2.5 to 14. Below pH 2.5 the wave is masked by the hydrogen wave. The half-wave potential of the compound is 1.28 V *vs* S.C.E. and it is independent of pH. The height of the wave suggests a two-electron reduction.

Controlled potential reduction at pH 9 shows the electrode reaction to be a two-electron reduction and the reduction products are ammonia and sulfate, the reaction thus being:

$$H_2N-O-SO_3^- + 2\ e^- + H_2O \rightarrow NH_3 + SO_4^{2-} + OH^-$$

Discussion. Several constitutions of hydroxylamine-O-sulfonic acid have been proposed and these have recently been reviewed by Wannagat and Pfeiffenschneider [2]. These authors conclude that hydroxylamine-O-sulfonic acid is an addition compound between SO_3 and the amineoxide form of hydroxylamine, $NH_3^+-O-SO_3^-$.

The result of the controlled potential reduction shows that the compound in buffered solution is not sulfamic acid N-oxide or an inner salt thereof [3] as one would have expected the reduction product from such a compound to be sulfamic acid. This argument can be used against all formulations containing a nitrogen bonded directly to sulfur.

Hydroxylamine-O-sulfonic acid is a strong acid. In the pH-interval in which it is polarographically reducible it exists as the anion. Although some formation of undissociated acid might take place by recombination with hydrogen ions at the electrode surface this is not likely in strongly alkaline solution. The half-wave potential is independent of pH which makes it likely that it is the same species which is reduced in acid and alkaline solution and that it is the anion of hydroxylamine-O-sulfonic acid which is reduced. As the same anion, $H_2N-O-SO_3^-$, is formed from "hydroxylamine-O-sulfonic acid", $H_2N-O-SO_3H$, and from "ammoniaoxide sulfonic acid betain", $H_3N^+-O-SO_3^-$, the polarographic method can not be used to distinguish between the proposed formulations.

Hydroxylamine and derivatives of it like N-alkyl-, N-aryl- or O-alkylhydroxylamine are reduced at the dropping mercury electrode as the hydroxylammonium cation in a pH-dependent wave. In view of that, it seems difficult to explain why the hydroxylamine-O-sulfonic acid is not reducible in the protonated form, *e.g.* the betain, whereas the anion is. The easier reduction of the anion is in accordance with the fact found in a preliminary investigation that the reduction of hydroxylamine-O-sulfonic acid at 0°C by excess of iodide proceeded with a kinetics as a pseudomonomolecular reaction with a rate constant five times as high in an acetate buffer as in N hydrochloric acid.

Experimental. The polarograph was a recording polarograph Radiometer PO4d. The potentiostat was a Wadsworth Controlled Potential Electro-Depositor.

The rate of the chemical oxidation of iodide by hydroxylamine-O-sulfonic acid was found by continuous recording of the polarographic diffusion current of the iodine produced in the reaction. The potential of the electrode was kept at −0.7 V *vs.* S.C.E.

Reduction of hydroxylamine-O-sulfonic acid. 1.0 g of hydroxylamine-O-sulfonic acid was reduced in an aqueous buffer at 1.40 V *vs* S.C.E. The reaction required two electrons per molecule. After completion of the reduction the ammonia formed was distilled off, titrated and characterized as the benzoyl derivative, benzamide. In the remnant sulfate was determined gravimetrically as barium sulfate. The yield of ammonia and sulfate was 91 % and 97 %, respectively.

Acknowledgement. A grant from *Statens almindelige Videnskabsfond* is gratefully acknowledged.

1. Vodrazka, Z. *Chem. listy* **46** (1952) 208.
2. Wannagat, U. and Pfeiffenschneider, R. *Z. anorg. Chem.* **297** (1958) 151.
3. Berlin, A. Ya. *J. Gen. Chem. (U.S.S.R.)* **17** (1947) 95; *Chem. Abstr.* **42** (1948) 51.

Received February 7, 1962.

Electroorganic Preparations X. Polarography and Reduction of α-Naphthoic Acid

HENNING LUND

Department of Chemistry, University of Aarhus, Aarhus, Denmark

Comparatively few compounds containing an ester or an amide group are polarographically reducible. Derivatives of the phthalic acids and of the pyridine mono- and dicarboxylic acids have been investigated polarographically and it has been found that the methyl esters of phthalic and terephthalic acid are reduced to phthalide [1] and *p*-hydroxymethylbenzoic acid methyl ester [2], respectively, and that isonicotinic amide at pH 3 is reduced to γ-pyridyl carbinol [3].

α-Naphthoic amide was found to be polarographically reducible and a controlled potential reduction was made in order to establish the nature of the reduction.

α-Naphthoic acid yields a polarographic wave only in unbuffered or alkaline solution as the wave in acid solution is masked by the hydrogen wave. Only solutions containing lithium or tetraalkylammonium ions as supporting electrolyte can be used. In unbuffered 0.2 M tetraethylammonium bromide solution containing 40 % alcohol the half-wave potential is 1.88_5 V *vs* S.C.E.

By a controlled potential reduction it was shown that the reduction consumed 2 electrons per molecule and a product with m.p. 150° and an analysis corresponding to $C_{11}H_{11}NO$ was obtained. The elementary analysis suggested a reduction in the naphthalene ring rather than in the amide group, the product thus being a dihydronaphthoic amide. As the reduction most probably would take place in the ring to which the amide group was bonded and the melting points of 1,2-dihydronaphthoic amide-1, m.p. 200° [4], and 3,4-dihydronaphthoic amide-1, m.p. 185° [4] or 128° [5], differed considerably from that of the isolated compound, the product might probably be 1,4-dihydronaphthoic amide-1 which apparently has not been described before.

In order to prove that, 1,4-dihydronaphthoic acid-1, m.p. 88°, prepared according to Baeyer [6], was treated with thionyl chloride and the resulting chloride in benzene solution treated with concentrated aqueous ammonia. The compound formed had m.p. 150° and an infrared spectrum identical with that of the product obtained from the electrolytical reduction.

The UV-spectrum of the supposed 1,4-dihydronaphthoic amide, max. at 267 mμ and 273 mμ with ε_{267} 520 and ε_{273} 570, confirmed that no migration of the double bonds had taken place during the preparation from the acid, as 1,2- and 3,4-dihydronaphthoic amide would be expected to show a strong absorption (ε about 10^4) around 250 mμ similar to that of styrene.

The polarographic reduction of α-naphthoic amide in alkaline solution is thus a 1,4-addition to the naphthalene ring. The reduction with sodium amalgam often ressembles the reduction at a mercury electrode, but a reduction of α-naphthoic amide with sodium amalgam in acid solution yields α-naphthyl carbinol [7]. The reduction thus takes place at different positions in acid and alkaline solution. This is also found in the polarographic reduction of isonicotinic amide which in acid solution is reduced in a four electron reduction to γ-pyridyl carbinol [3] and in alkaline solution yields a two-electron wave indicating the formation of a dihydropyridine derivative.

Experimental. The polarograph was a pen-recording polarograph Radiometer Polariter PO4d. The potentiostat was an electromechanical potentiostat of the Lingane-Jones type. The melting point determinations were made with a Leitz "Mikroskop-heiztisch 350". The infrared spectra were recorded at a Perkin-Elmer Infracord and the UV-spectra with a Perkin-Elmer UV-137.

Reduction of α-naphthoic amide. 2.0 g of α-naphthoic amide was suspended in 180 ml 50 % methanol containing 5 g of lithium chloride and 2 g of tetramethylammonium hydroxide and reduced at −1.90 V *vs* S.C.E. The compound dissolved during the reduction which required two electrons per molecule. After completion of the reduction the solution was made slightly acid with acetic acid and the main part of the methanol was removed in vacuo. The product was extracted from

Acknowledgement. A grant from *Statens almindelige Videnskabsfond* is gratefully acknowledged.

1. Vodrazka, Z. *Chem. listy* **46** (1952) 208.
2. Wannagat, U. and Pfeiffenschneider, R. *Z. anorg. Chem.* **297** (1958) 151.
3. Berlin, A. Ya. *J. Gen. Chem. (U.S.S.R.)* **17** (1947) 95; *Chem. Abstr.* **42** (1948) 51.

Received February 7, 1962.

Electroorganic Preparations X. Polarography and Reduction of α-Naphthoic Acid

HENNING LUND

Department of Chemistry, University of Aarhus, Aarhus, Denmark

Comparatively few compounds containing an ester or an amide group are polarographically reducible. Derivatives of the phthalic acids and of the pyridine mono- and dicarboxylic acids have been investigated polarographically and it has been found that the methyl esters of phthalic and terephthalic acid are reduced to phthalide [1] and *p*-hydroxymethylbenzoic acid methyl ester [2], respectively, and that isonicotinic amide at pH 3 is reduced to γ-pyridyl carbinol [3].

α-Naphthoic amide was found to be polarographically reducible and a controlled potential reduction was made in order to establish the nature of the reduction.

α-Naphthoic acid yields a polarographic wave only in unbuffered or alkaline solution as the wave in acid solution is masked by the hydrogen wave. Only solutions containing lithium or tetraalkylammonium ions as supporting electrolyte can be used. In unbuffered 0.2 M tetraethylammonium bromide solution containing 40 % alcohol the half-wave potential is 1.88_5 V *vs* S.C.E.

By a controlled potential reduction it was shown that the reduction consumed 2 electrons per molecule and a product with m.p. 150° and an analysis corresponding to $C_{11}H_{11}NO$ was obtained. The elementary analysis suggested a reduction in the naphthalene ring rather than in the amide group, the product thus being a dihydronaphthoic amide. As the reduction most probably would take place in the ring to which the amide group was bonded and the melting points of 1,2-dihydronaphthoic amide-1, m.p. 200° [4], and 3,4-dihydronaphthoic amide-1, m.p. 185° [4] or 128° [5], differed considerably from that of the isolated compound, the product might probably be 1,4-dihydronaphthoic amide-1 which apparently has not been described before.

In order to prove that, 1,4-dihydronaphthoic acid-1, m.p. 88°, prepared according to Baeyer [6], was treated with thionyl chloride and the resulting chloride in benzene solution treated with concentrated aqueous ammonia. The compound formed had m.p. 150° and an infrared spectrum identical with that of the product obtained from the electrolytical reduction.

The UV-spectrum of the supposed 1,4-dihydronaphthoic amide, max. at 267 mμ and 273 mμ with ε_{267} 520 and ε_{273} 570, confirmed that no migration of the double bonds had taken place during the preparation from the acid, as 1,2- and 3,4-dihydronaphthoic amide would be expected to show a strong absorption (ε about 10^4) around 250 mμ similar to that of styrene.

The polarographic reduction of α-naphthoic amide in alkaline solution is thus a 1,4-addition to the naphthalene ring. The reduction with sodium amalgam often ressembles the reduction at a mercury electrode, but a reduction of α-naphthoic amide with sodium amalgam in acid solution yields α-naphthyl carbinol [7]. The reduction thus takes place at different positions in acid and alkaline solution. This is also found in the polarographic reduction of isonicotinic amide which in acid solution is reduced in a four electron reduction to γ-pyridyl carbinol [3] and in alkaline solution yields a two-electron wave indicating the formation of a dihydropyridine derivative.

Experimental. The polarograph was a pen-recording polarograph Radiometer Polariter PO4d. The potentiostat was an electromechanical potentiostat of the Lingane-Jones type. The melting point determinations were made with a Leitz "Mikroskop-heiztisch 350". The infrared spectra were recorded at a Perkin-Elmer Infracord and the UV-spectra with a Perkin-Elmer UV-137.

Reduction of α-naphthoic amide. 2.0 g of α-naphthoic amide was suspended in 180 ml 50 % methanol containing 5 g of lithium chloride and 2 g of tetramethylammonium hydroxide and reduced at −1.90 V *vs* S.C.E. The compound dissolved during the reduction which required two electrons per molecule. After completion of the reduction the solution was made slightly acid with acetic acid and the main part of the methanol was removed in vacuo. The product was extracted from

the aqueous layer with a 3:1 mixture of chloroform and isopropyl alcohol which was evaporated. The residue was dissolved in a small volume of methanol and on addition of water a precipitate, 1.6 g, was obtained. After two recrystallizations from benzene the compound, 1.3 g, had m.p. 149.5°–150°. (Found: C 76.17; H 6.58; N 8.09. Calc. for $C_{11}H_{11}NO$: C 76.25; H 6.42; N 8.19).

Acknowledgement. A grant from *Statens almindelige Videnskabsfond* is gratefully acknowledged.

1. Whitnack, G. C., Reinhart, J. and Gantz, E. St. C. *Anal. Chem.* **27** (1955) 359.
2. Ono, S. and Nakaya, J. *J. Chem. Soc. Japan.* **74** (1953) 907. *Chem. Abstr.* **48** (1954) 8082.
3. Lund, H. *Collection Czechoslov. Chem. Communs.* **25** (1960) 3313.
4. Ranedo, J. and Leon, A. *Anales soc. espan. fis. quim. Madrid* **25** (1927) 421; *Chem. Abstr.* **22** (1928) 777.
5. Birch, A. J. and Robinson, R. *J. Chem. Soc.* **1944** 503.
6. Baeyer, A. *Ann.* **266** (1891) 169.
7. West, B. L. *J. Am. Chem. Soc.* **42** (1920) 1656.

Received February 7, 1962.

The C-Terminal Amino Acids of Three Variants of Horse Myoglobin

ÅKE ÅKESON

Medicinska Nobelinstitutet, Biokemiska avdelningen, Stockholm, Sweden

In previous communications [1,2] the isolation and analysis of three different horse myoglobins have been reported. The almost identical analytical data for the three components, including the amino acid composition, indicated this to be a case of microheterogeneity, where the difference between the three components consists of an exchange of one amino acid for another or a different distribution of amino acids or charged groups within the molecule. As myoglobin has only one N-terminal amino-acid group [3,4], it is fairly certain to be built up of a single polypeptide chain and identification of the end groups in the three variants would in this case be of singular interest. The N-terminal amino acid has been determined in all three myoglobins and found to be the same [3], while the C-terminal amino acids have been determined only in unseparated horse myoglobin, where one of the components accounts for about 80 % of the material. By following the rate of liberation of amino acids from the apomyoglobin on hydrolysis with carboxypeptidase A the sequence of four C-terminal amino acids was determined [5]. This paper reports the determination of four C-terminal amino acids in the three different myoglobins, using the same method, but with a somewhat different result.

Experimental. The three myoglobin components, designated MbI, II_1 and II_2, were prepared as described previously.[2] Carboxy peptidase A * (CP A) was a commercial product and was treated with diisopropylfluorophosphate (DFP) before use. As the rate of action of CP A on the native as well as denatured myoglobins is extremely slow, the apoproteins were used for the degradation experiments. The latter were prepared by splitting the myoglobins with acid acetone in the cold as described earlier [1]. The native apoproteins, however, proved almost as resistant to attack by the enzyme as unsplit myoglobin. To render them accessible to carboxypeptidase action, the apoproteins were denatured by heating in saltfree solution at pH 8.5 and 90°C for 4 min. Under these conditions a uniform suspension of a finely divided precipitate was obtained, which did not aggregate visibly during the time of hydrolysis. The DFP-treated CP A was dissolved in a 10 % LiCl solution immediately before use.

The hydrolyses were carried out in an unbuffered medium at 37°C and pH 8.5 under continuous stirring. The weight ratio of enzyme to apoprotein was 1:20. The pH was kept constant by addition of 0.1 M NaOH and at suitable intervals 1 ml samples were withdrawn, transferred to centrifuge tubes containing 1 ml of trichloroacetic acid and immediately centrifuged. The supernatant was then analyzed for amino acids in an automatic amino acid analyzer according to Spackman *et al.* [6]. As asparagine and glutamine under these conditions appear exactly coincident with the serine peak on the chromatogram, while aspartic and glutamic acids are well resolved, it was necessary to analyze the supernatant before as well

* Carboxypeptidase, which is equivalent to carboxypeptidase A, was obtained from Worthington Biochemicals, Freehold, New Jersey, as a water suspension of three times recrystallized material.

the aqueous layer with a 3:1 mixture of chloroform and isopropyl alcohol which was evaporated. The residue was dissolved in a small volume of methanol and on addition of water a precipitate, 1.6 g, was obtained. After two recrystallizations from benzene the compound, 1.3 g, had m.p. 149.5°–150°. (Found: C 76.17; H 6.58; N 8.09. Calc. for $C_{11}H_{11}NO$: C 76.25; H 6.42; N 8.19).

Acknowledgement. A grant from *Statens almindelige Videnskabsfond* is gratefully acknowledged.

1. Whitnack, G. C., Reinhart, J. and Gantz, E. St. C. *Anal. Chem.* **27** (1955) 359.
2. Ono, S. and Nakaya, J. *J. Chem. Soc. Japan.* **74** (1953) 907. *Chem. Abstr.* **48** (1954) 8082.
3. Lund, H. *Collection Czechoslov. Chem. Communs.* **25** (1960) 3313.
4. Ranedo, J. and Leon, A. *Anales soc. espan. fis. quim. Madrid* **25** (1927) 421; *Chem. Abstr.* **22** (1928) 777.
5. Birch, A. J. and Robinson, R. *J. Chem. Soc.* **1944** 503.
6. Baeyer, A. *Ann.* **266** (1891) 169.
7. West, B. L. *J. Am. Chem. Soc.* **42** (1920) 1656.

Received February 7, 1962.

The C-Terminal Amino Acids of Three Variants of Horse Myoglobin

ÅKE ÅKESON

Medicinska Nobelinstitutet, Biokemiska avdelningen, Stockholm, Sweden

In previous communications [1,2] the isolation and analysis of three different horse myoglobins have been reported. The almost identical analytical data for the three components, including the amino acid composition, indicated this to be a case of microheterogeneity, where the difference between the three components consists of an exchange of one amino acid for another or a different distribution of amino acids or charged groups within the molecule. As myoglobin has only one N-terminal amino-acid group [3,4], it is fairly certain to be built up of a single polypeptide chain and identification of the end groups in the three variants would in this case be of singular interest. The N-terminal amino acid has been determined in all three myoglobins and found to be the same [3], while the C-terminal amino acids have been determined only in unseparated horse myoglobin, where one of the components accounts for about 80 % of the material. By following the rate of liberation of amino acids from the apomyoglobin on hydrolysis with carboxypeptidase A the sequence of four C-terminal amino acids was determined [5]. This paper reports the determination of four C-terminal amino acids in the three different myoglobins, using the same method, but with a somewhat different result.

Experimental. The three myoglobin components, designated MbI, II_1 and II_2, were prepared as described previously.[2] Carboxy peptidase A * (CP A) was a commercial product and was treated with diisopropylfluorophosphate (DFP) before use. As the rate of action of CP A on the native as well as denatured myoglobins is extremely slow, the apoproteins were used for the degradation experiments. The latter were prepared by splitting the myoglobins with acid acetone in the cold as described earlier [1]. The native apoproteins, however, proved almost as resistant to attack by the enzyme as unsplit myoglobin. To render them accessible to carboxypeptidase action, the apoproteins were denatured by heating in saltfree solution at pH 8.5 and 90°C for 4 min. Under these conditions a uniform suspension of a finely divided precipitate was obtained, which did not aggregate visibly during the time of hydrolysis. The DFP-treated CP A was dissolved in a 10 % LiCl solution immediately before use.

The hydrolyses were carried out in an unbuffered medium at 37°C and pH 8.5 under continuous stirring. The weight ratio of enzyme to apoprotein was 1:20. The pH was kept constant by addition of 0.1 M NaOH and at suitable intervals 1 ml samples were withdrawn, transferred to centrifuge tubes containing 1 ml of trichloroacetic acid and immediately centrifuged. The supernatant was then analyzed for amino acids in an automatic amino acid analyzer according to Spackman *et al.* [6]. As asparagine and glutamine under these conditions appear exactly coincident with the serine peak on the chromatogram, while aspartic and glutamic acids are well resolved, it was necessary to analyze the supernatant before as well

* Carboxypeptidase, which is equivalent to carboxypeptidase A, was obtained from Worthington Biochemicals, Freehold, New Jersey, as a water suspension of three times recrystallized material.

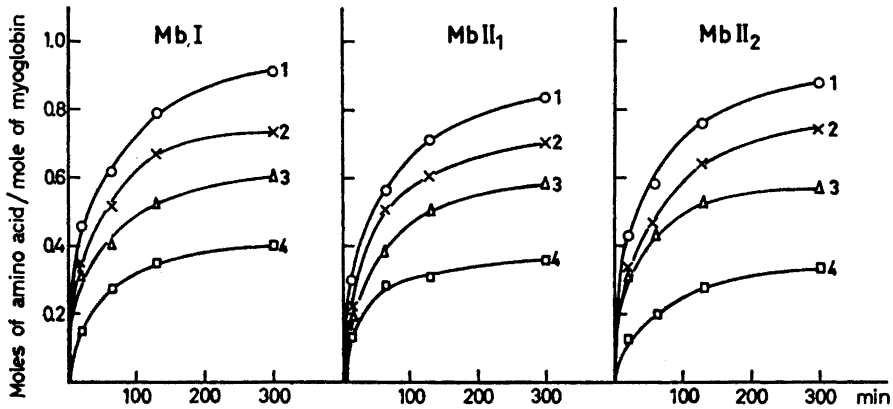

Fig. 1. Liberation of some amino acids from the apoproteins of MbI, $MbII_1$, and $MbII_2$ by carboxypeptidase A. 1 = gly, 2 = glu(NH_2), 3 = phe and 4 = leu.

as after acid hydrolysis. One aliquot was analyzed immediately while another aliquot was hydrolyzed for 3 h with 5 M HCl at 100°C in an evacuated and sealed tube. Most of the HCl was then removed by evaporation *in vacuo* and the hydrolyzed sample analyzed for amino acids as above. Samples of the three denatured apomyoglobins as well as corresponding amounts of CP A were incubated separately under the conditions used for the actual hydrolyses and analyzed for liberated amino acids the same way. In all cases only traces of a few amino acids were released even after prolonged incubation.

Results and discussions. The results of hydrolysis of the apoproteins of the three myoglobins by CP A are shown in Fig. 1.

In addition to the amino acids included in the figure, around 0.2 moles of alanine and tyrosine were released per mole of each apoprotein after 300 min. Their relative rates of release were the same. Smaller amounts of asparagine, isoleucine, threonine, valine and serine in decreasing order were liberated also from all three apomyoglobins. On prolonged hydrolysis for 36 h the molar ratios of amino acid to protein increased to approximately 1 for glycine and glutamine. The corresponding figure for phenylalanine was 0.7 and for leucine 0.6, the values being about the same for all three apoproteins. However, alanine later exceeded tyrosine, the values having increased to 0.4 and 0.3, respectively.

These results show clearly that the sequence of the six C-terminal amino acids is identical in the three myoglobin variants. The similar order of appearance in the different hydrolysates, albeit in rather small quantities, of the other amino acids found, suggests that the likeness stretches even further along the peptide chain. This identity in C-terminal amino acid sequence confirms our earlier conclusion [2] that the three myoglobin variants are distinct, preformed proteins and not artifacts produced during purification, *e.g.* by splitting off or modifying terminal amino acids.

The sequence of the four terminal amino acids can now be established with certainty and it is most probable that the next amino acid is alanine, followed by tyrosine. Investigations of the action by CP A on different peptides [7] have shown that amino acids with short aliphatic side chains are released at a much slower rate than those with an aromatic side chain. It thus seems improbable that the rates of liberation of alanine and tyrosine would be nearly the same if tyrosine was released first. The C-terminal sequence of the three myoglobins would thus be:
(Tyr-Ala-) Leu-Phe-Glu(NH_2)-Gly(COOH).
This sequence differs, however, in several respects from the one reported by Holleman and Biserte [6] for unseparated horse apomyoglobin. They found the sequence leu-asp(NH_2)-phe-gly(COOH) followed by glu-thr or thr-glu, and they evidently did not find tyrosine among the liberated amino acids, and alanine only in negligible quantities. As regards the two penultimate amino acids, the discrepancies between the

two sequences very likely arise from the fact that glutamine and not asparagine is released on the enzymic hydrolysis. Holleman and Biserte converted the liberated amino acids to their DNP-derivatives and analyzed them by paper chromatography. This method does not, however, distinguish between asparagine and glutamine, and even though they, evidently arbitrarily, chose asparagine to represent the amide in the sequence, they really left the question open. The fact that glutamine is the amide in question also explains why they found phenylalanine as the penultimate amino acid instead of glutamine. The present analyses indicated that a large part of the liberated glutamine was converted to pyrrolidone carboxylic acid during the digestion, and thus escaped detection, unless reconverted to glutamic acid by acid hydrolysis.

Acknowledgements. The author wishes to thank Professor Hugo Theorell for his active interest in this work. The valuable technical assistance of Miss Anne-Marie Fridén is gratefully acknowledged.

1. Theorell, H. and Åkeson Å. *Ann. Acad. Sci. Fennicae Ser. A. II*, **1955**, Vol. 60, p. 303.
2. Åkeson, Å. and Theorell, H. *Arch. Biochem. Biophys.* **91** (1960) 319.
3. Porter, R. R. and Sanger, F. *Biochem. J.* **42** (1948) 287.
4. Ingram, V. M. *Biochim. et Biophys. Acta* **16** (1955) 599.
5. Holleman, J. W. and Biserte, G. *Biochim. et Biophys. Acta* **33** (1959) 143.
6. Spackman, D. H., Stein, W. H. and Moore, S. *Anal. Chem.* **30** (1958) 1190.
7. Neurath, H. and Schwert, G. W. *Chem. Revs* **46** (1950) 69.

Received February 22, 1962.

ACTA CHEMICA SCANDINAVICA 16 (1962) 529–540

Perjodatoxydation von Phenolen

VIII *. ^{18}O-Studien zum Mechanismus der oxydativen Spaltung der Monoäther des Brenzcatechins und des Hydrochinons

ERICH ADLER, INGEMAR FALKEHAG und BENGT SMITH

Institutionen för organisk kemi, Chalmers Tekniska Högskola, Göteborg, Schweden

Herrn Professor *Holger Erdtman* zum 60. Geburtstag gewidmet

Die oxydative Entmethylierung von Guajakol und Hydrochinonmonomethyläther mittels Natriumperjodat in Wasser-^{18}O führt zur Bildung von *o*- bzw. *p*-Benzochinon mit einem markierten Sauerstoffatom sowie von unmarkiertem Methanol. Auf Grund dieser Ergebnisse wird angenommen, dass ein zunächst entstehender Perjodsäurearylester (III oder V) direkt oder über ein Aroxylkation (IV) unter Mitwirkung eines Moleküls H_2O in ein *o*-Chinon-halbketal (VI) übergeht, welches seinerseits in die genannten Reaktionsprodukte zerfällt (Schema A). Ein Verlauf nach dem alternativen Schema B, wonach Methanol-^{18}O zu erwarten wäre, wird durch das Ergebnis des Isotopenversuchs ausgeschlossen.

Im Gegensatz hierzu erhält man unmarkierte Chinone, wenn Brenzcatechin oder Hydrochinon mit Perjodat in Wasser-^{18}O oxydiert werden. Hierbei zerfällt also der als Zwischenprodukt anzunehmende Perjodsäureester bzw. das Aroxylkation, ohne dass H_2O in den Kern eingeführt wird (Schema C).

Wie in früheren Mitteilungen [1,2] berichtet wurde, bewirkt Natriumperjodat in wässriger oder wässrig-essigsaurer Lösung eine im allgemeinen rasch verlaufende Oxydation der Monoäther von 1,2- und 1,4-Dihydroxybenzolen. Es entsteht das entsprechende *o*- bzw. *p*-Chinon, während die verätherndе Gruppe als Alkohol freigelegt wird. So wird aus Guajakol (I) und Hydrochinonmonomethyläther (II) neben *o*- bzw. *p*-Benzochinon Methanol in 90 %-iger Ausbeute erhalten.

Die Reaktion mit Guajakolverbindungen wurde einer Bestimmung der Guajacylreste mit freier phenolischer Hydroxylgruppe im Lignin zugrunde gelegt [3]. Sie ist auch allgemein verwendbar als Methode zur Darstellung von *o*-Chinonen und den daraus durch Reduktion zugänglichen Brenzcatechinen aus den entsprechenden Guajakolverbindungen [2], auch in Fällen (z. B. beim Pinoresinol [4]), wo empfindliche Gruppierungen im Molekül die Anwendung

* VII. Mitt. s. Ref. [22].

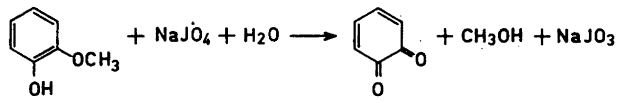

I

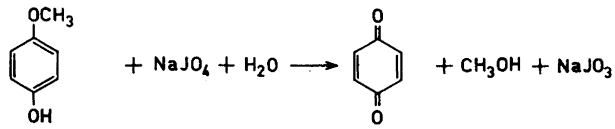

II

konventioneller Entmethylierungsverfahren nicht gestatten. Aus Pyrogallol-1,3-dimethyläther wird durch einseitige oxydative Entmethylierung das 3-Methoxy-*o*-chinon gewonnen [5].

Es schien von Interesse, den Mechanismus dieser Reaktionen näher zu untersuchen. Er sei hier am Beispiel des Guajakols erörtert.

Nach Bunton und Shiner [6] besteht die Initialreaktion zwischen Perjodat und α-Glykolen in einer Koordination der Hydroxylgruppen an das Jodatom unter Bildung eines cyclischen Perjodsäureesters. Eine analoge Einleitungsreaktion würde beim Guajakol zum Arylperjodsäureester III führen.

Da in einer wässrigen Lösung von Natriummetaperjodat (pH 4—5) hauptsächlich das Ion JO_4^- vorliegt, wurde dieses in das Formelschema eingesetzt; die Mitwirkung hydratisierter Formen [7,8] ist jedoch ebenfalls denkbar.

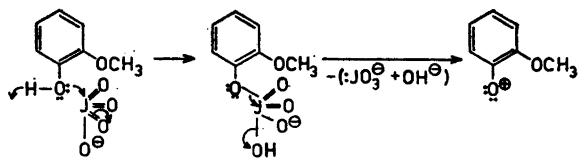

III IV

Am Perjodsäureester III vollzieht sich der eigentliche Oxydationsschritt als ein Zwei-Elektronen-Entzug. Als Reduktionsprodukt entsteht das Jodation, als Oxydationsprodukt das Aroxylkation IV. [Das nach dieser Formulierung auftretende OH^--Ion wird durch ein in der Folgereaktion von IV freigelegtes H^+—Ion (s. unten) neutralisiert.]

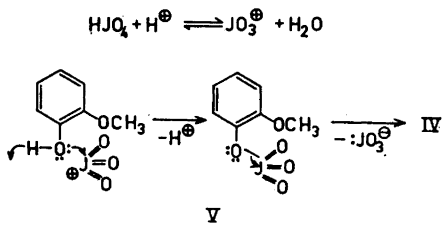

V

Besonders bei Ausführung der Oxydation in stärker saurer Lösung wird man mit Levitt [9] das Auftreten des Perjodonium-Kations JO_2^+ als elektrophilem Agens annehmen können; dessen Attacke würde zur Bildung des Esters V führen, aus dem wiederum durch Loslösung von Jodation das Aroxylkation IV entstünde.

Die vorliegende Untersuchung beschäftigt sich jedoch nicht mit diesen Einleitungsreaktionen; ihr Ziel ist vielmehr, den Mechanismus der Bildung der eigentlichen Reaktionsprodukte, des *o*-Benzochinons und des Methanols, aus dem als Zwischenprodukt anzunehmenden Aroxylkation IV klarzulegen. Für diesen Teil der Reaktion boten sich zwei Erklärungsmöglichkeiten(Schema A bzw. B) an. Nach Schema A konnte das mesomere Kation IV ein Mol. Wasser in die Elektronenlücke einlagern, wobei — nach Eliminierung eines Protons — das Halbketal VI entstünde. Dieses würde spontan in die Endprodukte zerfallen.

Gleichwertig mit dieser Vorstellung (A) ist die Annahme, dass das an der Reaktion beteiligte Mol. H_2O nicht das Aroxylkation (IV) sondern den Perjodsäureester (III oder V) an dem die OCH_3-Gruppe tragenden Ring-C-Atom angreift, wobei in einer "concerted reaction" gleichzeitig das Jodat-anion abgelöst und das Halbketal VI gebildet wird, ohne dass das Kation IV als Zwischenprodukt auftritt.

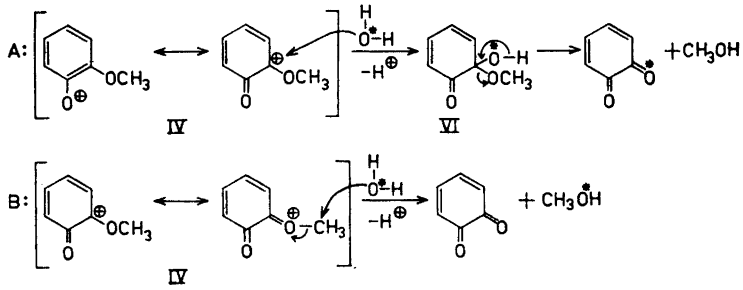

Als eine zweite Möglichkeit (Schema B) war in Betracht zu ziehen, dass das Aroxylkation IV direkt zerfällt, indem ein Mol. H_2O am C-Atom der Methoxylgruppe nucleophil angreift. Ein solcher Mechanismus wäre verständlich auf Grund der Polarisierung der Bindung $O \leftarrow CH_3$, die eine Folge der Ladungsverteilung im mesomeren Kation (vgl. die Grenzstrukturen für IV in Schema B) sein muss.

Eine ähnliche Reaktion könnte auch in diesem Falle direkt am Perjodsäureester stattfinden (Schema B'):

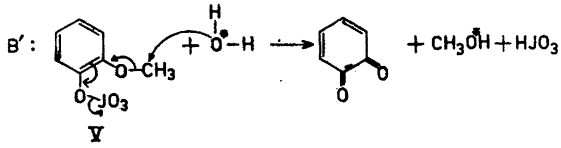

Backman und Havinga [10] diskutierten einen dem Schema B' analogen Mechanismus für die von ihnen beobachtete oxydative Entmethylierung von Guajakol durch Sauerstoff in Gegenwart eines Kupfer-Amin-Komplexes.

Was im voranstehenden am Beispiel des Guajakols für die Oxydation der Monoäther von 1,2-Dihydroxybenzolen entwickelt wurde, gilt sinngemäss auch für die Monoäther von 1,4-Dihydroxybenzolen.

Sowohl an Reaktion A wie an beiden Varianten von B beteiligt sich ein Molekül Wasser, jedoch gelangt der Sauerstoff des Wassers (mit * gekennzeichnet) bei Reaktion A in das Chinon, bei Reaktion B in das Methanol. Es musste deshalb möglich sein, eine Entscheidung zwischen den beiden Mechanismen zu treffen, wenn man die Reaktion in $H_2{}^{18}O$ vor sich gehen liess und den ^{18}O-Gehalt des Chinons sowie des Methanols bestimmte.

Hierzu war zunächst zu untersuchen, ob nicht durch Isotopenaustausch zwischen den Reaktionskomponenten und dem $H_2{}^{18}O$ Störungen auftreten konnten.

Perjodsäure tauscht — über die Hydratformen — ihre Sauerstoffatome rasch — innerhalb von 5 Sek. — gegen den Sauerstoff des Wassers aus [8]. Dieser Austausch kann jedoch bei keinem der gedachten Reaktionsabläufe (A oder B) den ^{18}O-Gehalt der Endprodukte beeinflussen.

Es wäre denkbar, dass die Bildung des Halbketals VI nicht nach Schema A, sondern nach der Variante A′ erfolgt, bei welcher der Perjodsäureester (z.B. V) in einer intramolekularen Oxydoreduktion sich zum Jodsäureester VII umlagert, in welchem nun eines der (markierten) Sauerstoffatome der Jodsäure an den Ring gebunden ist. Der Jodsäureester VII würde aber durch Wasser sehr wahrscheinlich so hydrolysiert werden, dass der Hydroxylsauerstoff des dabei entstehenden Halbketals VI — genau wie bei A — dem Wasser entstammt *. Man wäre also auch bei einem Reaktionsablauf nach A′ vom ^{18}O-Gehalt des Perjodats unabhängig.

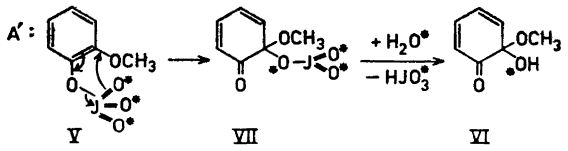

Von besonderer Bedeutung war die Frage, ob Isotopenaustausch bei den gebildeten Chinonen die Ermittlung ihres durch den Reaktionsmechanismus bedingten ^{18}O-Gehaltes störend beeinflussen kann. Es war zu erwarten, dass, wie es von Carbonylverbindungen allgemein bekannt ist, auch die Chinoncarbonyle ihren Sauerstoff durch reversible Hydratisierung gegen den des Wassers austauschen. Über solchen Isotopenaustausch bei *o*-Chinonen liegen in der Literatur keine Angaben vor. Für *p*-Benzochinon ist bekannt geworden [11], dass nach 10-tägiger Kontaktzeit mit Wasser bei Zimmertemperatur der Austausch vollständig ist. Diese Angabe war für die Beurteilung der Verhältnisse bei unseren sehr rasch verlaufenden Oxydationsversuchen unzureichend. Aus Tab. 1, Versuche 1 und 2, geht jedoch hervor, dass die

* Ein zu A′ analoger Mechanismus wurde von Andrew S. Kende und Paul MacGregor für einen ähnlichen Prozess, nämlich die Bildung von 2,6-Dimethyl-*o*-benzochinol bei der Einwirkung von Perchlorylfluorid auf 2,6-Dimethylphenol in Betracht gezogen. Wir danken Herrn Dr. Kende, Lederle Laboratories, Pearl River, N.Y., U.S.A., bestens für die Übersendung des Manuskripts der noch unveröffentlichten Arbeit. *(Anm. bei der Korrektur:* Die genannte Arbeit ist inzwischen erschienen, s. *J. Am. Chem. Soc.* **83** (1961) 4197.)

Tabelle 1. Sauerstoffaustausch zwischen Chinonen und Wasser.

Vers. Nr.	Untersuchtes Chinon	Kontakt mit Wasser-^{18}O		Atom-% ^{18}O-Überschuss [a]		^{18}O-Anreicherung im Chinon % [b]
		Temp.	Zeit (Sek.)	im Wasser- ^{18}O	im Chinon	
1	*o*-Chinon	0°	10	5.52	0.50	9.1
2	*p*-Chinon	20°	300	4.98	0.29	5.8
3	*p*-Chinon	65°	60	4.19	0.33	7.9
4	3,5-Dimethyl-*o*-chinon	20°	30	4.19	0.12	2.9
5	3,5-Dimethyl-*o*-chinon	20°	120	4.98	0.68	13.6

[a] ^{18}O-Überschuss = totaler ^{18}O-Gehalt minus normaler ^{18}O-Gehalt (0.2 Atom-%).
[b] % der theoret. möglichen Anreicherung, d.h. wenn der Isotopenaustausch bei *beiden* Chinonsauerstoffatomen vollständig wäre.

Anreicherung an ^{18}O sowohl in *o*- wie in *p*-Benzochinon < 10 % betrug, wenn diese Chinone unter den in den entsprechenden Oxydationsversuchen (vgl. Tab. 2, Versuche 3 und 4) eingehaltenen Zeit- und Temperatur-Bedingungen mit $H_2{}^{18}O$ behandelt wurden. Dieser geringfügige Austausch störte die Auswertung der Oxydationsergebnisse nicht (s. unten).

Wie in Teil II[5] dieser Untersuchungsserie bereits berichtet wurde, nehmen 3-Methoxy-*o*-chinone (z.B. VIII) eine Ausnahmestellung ein, indem sie beim Lösen in Wasser oder Alkoholen sofort 1 Mol. des Lösungsmittels anlagern unter Ausbildung eines nach der Seite des Adduktes (IX) verschobenen Gleichgewichtes.

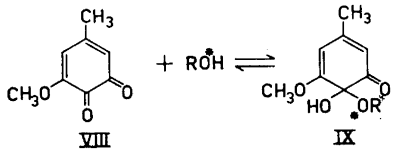

VIII IX

Die Existenz der Addukte IX wurde aus dem charakteristischen Unterschied in der Lichtabsorption der 3-Methoxy-*o*-chinone in hydroxylfreien Lösungsmitteln, z.B. Chloroform (λ_{max} ca. 480 mμ), und hydroxylhaltigen (λ_{max} ca. 370 mμ, schwächere Bande oder Schulter bei ca. 470 mμ) hergeleitet. Dass die Anlagerung des Lösungsmittels an der dem Methoxyl benachbarten Carbonylgruppe erfolgt, wird dadurch gestützt, dass 5-Methoxy-cyclohexan-2,4-dienone (z.B. das Acetonaddukt von VIII, d.h. die Verbindung der Formel IX mit dem Rest $-CH_2COCH_3$ anstelle von $-OR$) ein Absorptionsmaximum bei ca. 360 mμ besitzen [12].

In Übereinstimmung mit der Auffassung vom Vorliegen des oben formulierten Hydratisierungsgleichgewichtes bei 3-Methoxy-*o*-chinonen wurde nun gefunden, dass 5-Methyl-3-methoxy-*o*-chinon (VIII), welches während nur 2 Min. in $H_2{}^{18}O$ gelöst war und dann wieder isoliert wurde, eine Anreicherung von ^{18}O aufwies, die dem vollständigen Austausch eines der beiden Chinonsauerstoffatome entsprach.

Die Strukturspezifität dieser Adduktbildung — sie wurde bisher nur bei 3-Methoxy-*o*-chinonen gefunden — soll in einer späteren Mitteilung näher behandelt werden.

Methanol zeigt in Wasser keinen Sauerstoffaustausch [13].

Um zwischen den Reaktionsmechanismen A und B zu entscheiden, wurden nun Guajakolverbindungen mit Perjodat in Wasser, das einen Überschuss an 3—6 Atom-% ^{18}O enthielt, oxydiert, und der ^{18}O-Überschuss im gebildeten Methanol sowie im *o*-Chinon bestimmt.

Da die Reindarstellung des Methanols einen verhältnismässig grossen Versuchsansatz bedingte, wurde für die entsprechenden Versuche eine leichtlösliche Guajakolverbindung, nämlich das Natriumsalz der 1-(4-Hydroxy-3-methoxyphenyl)-propan-1-sulfonsäure (X) [1] gewählt, wodurch die erforderliche Menge des kostspieligen ^{18}O-markierten Wassers auf ein Minimum gebracht werden konnte. Dass bei der Perjodatoxydation von X 90 % der theoretisch möglichen Menge von Methanol freigelegt werden, wurde bereits früher gezeigt [1].

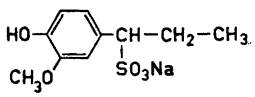

X

Nach Oxydation von X in ^{18}O-markiertem Wasser (15 Min., 20°) wurden überschüssiges Perjodat und gebildetes Jodat als Bleisalze ausgefällt; das Filtrat wurde hierauf über eine Kolonne destilliert, und das als Destillat erhaltene Gemisch von Methanol und Wasser (etwa 70:30) wurde gaschromatographisch getrennt [14]. Im so gewonnenen reinen Methanol wurde der Gehalt an ^{18}O bestimmt.

Zur Bestimmung des ^{18}O-Gehaltes von Methanol kann dieses nach Wiberg [15] direkt in das Massenspektrometer eingeführt werden; aus dem erhaltenen "cracking pattern" wird das Isotopenverhältnis ermittelt. Angaben über die Genauigkeit der Methode fehlen jedoch. Urey und Roberts [16] unterwarfen das Methanol der terMeulen'schen Sauerstoffbestimmung und untersuchten den ^{18}O-Gehalt des dabei erhaltenen H_2O massenspektrometrisch nach Äquilibrierung mit CO_2. Diese Methode erfordert aber verhältnismässig grosse Substanzmengen. Lauder und Zerner [17] führten den Sauerstoff des Methanols in CO über und bestimmten dessen ^{18}O-Gehalt im Massenspektrometer.

Wir verwendeten für die Ermittlung des Verhältnisses der Sauerstoffisotopen im Methanol teils die eben erwähnte direkte massenspektrographische Methode [15], teils unterwarfen wir die aus dem Gaschromatographen austretenden reinen Methanoldämpfe einer Crackung zu CO und H_2 über einem Zn—Cu—Cr-Oxyd-Katalysator [18]*, und oxydierten das CO selektiv mittels J_2O_5 [19] zu CO_2, dessen ^{18}O-Gehalt massenspektrometrisch bestimmt wurde. Die erforderliche Methanolmenge war bei dieser Methode etwa 25 mg.

Beide Bestimmungsmethoden gaben an, dass das bei der Perjodatoxydation von X freigelegte Methanol keinen Überschuss an ^{18}O enthielt (Tab. 2, Vers. 1 und 2). Dies beweist, dass die Reaktion nicht nach Prinzip B verlaufen kann. Die Richtigkeit von Prinzip A bestätigte sich dann bei der Untersuchung der gebildeten Chinone.

Guajakol wurde in ^{18}O-markiertem Wasser bei 0° während ungefähr 10 Sekunden mit Perjodat oxydiert, und das Reaktionsgemisch so schnell wie möglich mit Methylenchlorid ausgeschüttelt. Ähnlich wurde Hydrochinonmonomethyläther behandelt (20°, 30 Sek.). Das gebildete *o*- resp. *p*-Chinon wurde aus den Extrakten rein dargestellt.

* Herrn Dr. J. Marton danken wir bestens für den Hinweis auf diesen Katalysator.

Tabelle 2. ^{18}O-Überschuss in den isolierten Reaktionsprodukten.

Vers. Nr.	Perjodatoxydation von	Isoliertes Produkt	Atom-% ^{18}O-Überschuss[a]		^{18}O-Überschuss im Produkt in % des theor. möglichen
			im Wasser-^{18}O des Reaktionsgemisches[b]	im Produkt	
1	Guajacylpropan-*a*-sulfonsaures Na (X)	CH_3OH [c]	2.68	0	0
2	Wie in Vers. 1	CH_3OH [d]	2.68	0	0
3	Guajakol (0°, 10 Sek.)	*o*-Chinon	5.42	2.61	48 [e]
	» (» » »)	»	5.42	2.44	45
4	Hydrochinon-mono-methyläther (20°, 300 Sek.)	*p*-Chinon	5.36	2.79	52
5	3,5-Dimethylbrenz-catechin (20°, 30 Sek.)	3,5-Dimethyl-*o*-chinon	4.11	0.29	7.0
	» (» » »)	»	4.11	0.27	6.6
6	Hydrochinon (20°, 120 Sek.)	*p*-Chinon	4.09	0.12	2.9

[a] ^{18}O-Überschuss = totaler ^{18}O-Gehalt minus normaler ^{18}O-Gehalt (0.2 Atom-%).

[b] Die hier angegebenen Werte sind korrigiert für die Verminderung des ^{18}O-Überschusses im verwendeten Wasser durch Isotopenaustausch mit dem darin gelösten $NaJO_4$ [8].

[c] Das O-Isotopenverhältnis wurde direkt am CH_3OH bestimmt.

[d] Das O-Isotopenverhältnis wurde nach Überführung in CO_2 bestimmt.

[e] Die Werte für die untersuchten Chinone beziehen sich auf *beide* Sauerstoffatome; d.h. bei vollständiger Markierung *eines* Chinonsauerstoffs ist der theoretische Wert 50 % (ohne Berücksichtigung des eventuellen Isotopenaustauschs mit dem Wasser).

Zur Bestimmung des ^{18}O-Gehaltes in den Chinonen bedienten wir uns der von Dahn, Moll und Menassé [20] beschriebenen Methode, bei welcher die Substanz mit *o*-Phenylendiamin-monohydrochlorid in Gegenwart einer bekannten Menge von unmarkiertem CO_2 bei 300° erhitzt wird. Wie die genannten Autoren gezeigt haben, wird hierbei der Sauerstoff vieler Verbindungstypen als H_2O freigelegt (und in der gleichen Operation mit dem des CO_2 äquilibriert, worauf letzteres massenspektrographisch untersucht wird). Die Methode hat sich nun erwartungsgemäss auch an *o*- und *p*-Chinonen bewährt.

Es zeigte sich (Tab. 2, Vers. 3 und 4), dass beide Chinone einen ^{18}O-Überschuss enthielten, der annähernd einer 50 %-igen Markierung der zwei Sauerstoffatome entsprach, oder m.a.W., es war eines der beiden Chinonsauerstoffatome voll markiert.

Wie oben (S. 533 und Tab. 1) gezeigt, ist bei den angewandten kurzen Reaktionszeiten der Isotopenaustausch zwischen Chinonsauerstoff und Wasser so gering, dass er für die Beurteilung dieses Ergebnisses vernachlässigt werden kann.

Es ist somit bewiesen, dass der eine Chinonsauerstoff aus dem Lösungsmittel (Wasser) stammt. Schema A — das sinngemäss auch auf die Oxydation der Hydrochinon-monoäther zu übertragen ist —, aber nicht Schema B, ist in Einklang mit diesem Befund.

Die in Schema A eingehende intermediäre Bildung des nicht isolierbaren Halbketals VI, bzw. des entsprechenden *p*-chinoliden Produkts bei der Oxydation der Hydrochinon-monoäther, hat ihre Parallele in der Bildung der *o*- und *p*-Benzochinole bei der Perjodatoxydation von Alkylphenolen. In den meisten Fällen sind die *o*-Benzochinole nicht isolierbar, da sie sofort durch Dienaddition dimerisieren [21,22]. Das aus 2,3,5-Trimethylphenol entstehende *o*-Chinol XI erwies sich jedoch als Monomeres stabil [22]; ähnlich wurde bei der Einwirkung von Perjodat auf 1-Methyl-naphthol-2 in 80 %-iger Essigsäure das Naphthochinol XII neben dem entsprechenden Acetat XIII erhalten (s. exptl. Teil).

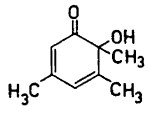

XI

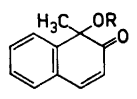

XII :R=H
XIII :R=Ac

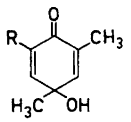

XIV :R=H
XV :R=CH_3

Die *p*-Chinole XIV und XV entstanden als Nebenprodukte bei der Perjodatoxydation von 2,4-Dimethyl- bzw. 2,4,6-Trimethyl-phenol [21,22]. Der Mechanismus der Bildung der *o*- und *p*- Chinole wurde schon in den zitierten Arbeiten [21,22] ganz ähnlich dem nun für die Bildung des Halbketals VI angegebenen formuliert. Criegee [23] erklärte in analoger Weise die Entstehung der Chinolacetate bei der Reaktion von Alkylphenolen mit Bleitetraacetat nach Wessely (Lit. s. Ref. [23]).

Für die Entstehung des *o*-chinoliden Halbketals VI sowie der eben erwähnten *o*-Chinole kann neben A auch die Variante A′ (s. S. 532) in Frage kommen. Für die Bildung der entsprechenden *para*-chinoliden Verbindungen dagegen ist Schema A′ sehr unwahrscheinlich. Die Vorstellung von der intermediären Bildung des Perjodsäurephenylesters (III oder V) und dessen Zerfall nach Schema A unter Mitwirkung des nucleophilen Lösungsmittels, direkt oder über das Aroxylkation IV, vermag die Perjodatoxydation der verschiedenen Typen von Phenolen auf einheitlicher Basis zu erklären.

Es war im Anschluss hieran noch von Interesse, die Perjodatoxydation nicht verätherter 1,2- und 1,4-Dihydroxybenzole zu untersuchen. Erwartungsgemäss werden Brenzcatechin und Hydrochinon durch Perjodat momentan zu *o*- bzw. *p*-Chinon oxydiert. Man könnte sich denken, dass, wie oben für die Monoäther gezeigt, auch bei den freien Dihydroxybenzolen die Reaktion

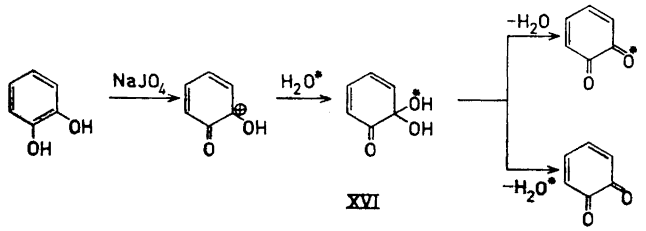

XVI

unter Mitwirkung eines Moleküls Wasser, z.B. im Falle des Brenzcatechins über das Hydrat XVI, verläuft.

Wird die Reaktion in Wasser mit überschüssigem ^{18}O ausgeführt, so müsste der Zerfall von XVI gleiche Teile von markiertem und unmarkiertem *o*-Chinon liefern. (Ein merkbarer Isotopeneffekt dürfte hierbei nicht auftreten.)

Der Versuch wurde in der *ortho*-Serie mit 3,5-Dimethylbrenzcatechin ausgeführt, da das daraus entstehende 3,5-Dimethyl-*o*-chinon [24] verhältnismässig stabil und leicht zu reinigen ist. In der *para*-Serie wurde Hydrochinon verwendet.

In keinem der beiden Fälle enthielt das gebildete Chinon mehr ^{18}O als der in geringem Ausmass stattfindenden Austauschreaktion zugeschrieben werden konnte. (Vgl. Tab. 2, Vers. 5 und 6, und Tab. 1, Vers. 4 und 2.) Die Oxydation der Dihydroxybenzole verläuft demnach — im Gegensatz zur Oxydation ihrer Monoäther — ohne Beteiligung des Wassers; sie kann deshalb analog Schema B nach folgendem Schema (C) formuliert werden:

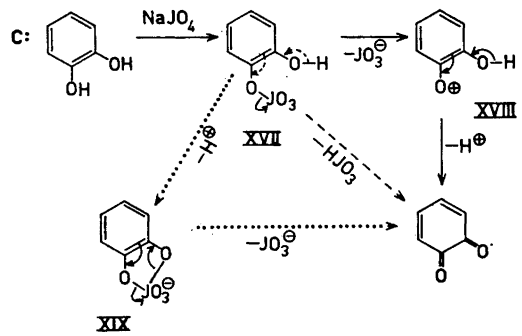

Für die Perjodatspaltung von 1,2-Glykolen in wässrigem Medium ist, u.a. durch kinetische Untersuchungen von Bunton [25], wahrscheinlich gemacht worden, dass der zuerst gebildete Perjodsäure-monoester durch Anlagerung der zweiten OH-gruppe an das Jodatom in einen cyclischen Diester übergeht, der dann in die Reaktionsprodukte zerfällt. Für die Oxydation von Brenzcatechinen kann natürlich ein analoger Reaktionsverlauf (über XVII → XIX) ebenfalls erwogen werden. Da jedoch die Oxydation von Hydrochinon, wo ein cyclischer Diester nicht auftreten kann, ebenso schnell verläuft wie die des Brenzcatechins[2], wird man das Zwischenprodukt XIX als überflüssig betrachten und annehmen dürfen, dass bei den aromatischen (1,2- und 1,4-)Diolen der Zerfall zum Chinon schon am Monoester (vom Typ XVII) direkt oder über das mesomere Kation (vom Typ XVIII) erfolgt.

EXPERIMENTELLES

Natrium-1-(4-hydroxy-3-methoxyphenyl)-propan-1-sulfonat (X). Die nach Adler und Hernestam [1] erhaltene Lösung der freien Sulfonsäure wurde mit verdünnter Natronlauge genau neutralisiert und im Vacuum-Rotationsverdampfer zur Trockene gebracht. Der feste Rückstand wurde durch Lösen in Isopropanol-Wasser (85:15) und Zugabe von Äther umkristallisiert. Farblose Nadeln. (Gef.: C 39.67; H 5.61; S 10.25; OCH_3 10.58. Ber. für $C_{10}H_{13}O_5SNa,2H_2O$: C 39.47; H 5.63; S 10.54; OCH_3 10.20.)

Perjodatoxydation von Natrium-1-(4-hydroxy-3-methoxyphenyl)-propan-1-sulfonat (X). a) Isolierung des gebildeten Methanols. Substanz X (1.6 g = 5.3 mMol) wurde in einer Lösung von Natriummetaperjodat (1.9 g = 8.9 mMol) in 15 ml Wasser, das einen Überschuss von 2.80 Atom-% ^{18}O enthielt, gelöst. Nach 15 Min. bei Zimmertemperatur wurde die Reaktion durch Zugabe von 10 g festem $Pb(NO_3)_2$ unterbrochen, und die Fällung durch Zentrifugieren entfernt. Die Lösung wurde über eine mit Glasspiralen gefüllte Kolonne (0.7 × 25 cm), deren Aufsatz zur Erzielung eines hohen Rückflussverhältnisses mit einem Kühlfinger versehen war, langsam destilliert; es wurden ca. 200 mg eines Gemisches von Methanol und Wasser (etwa 70:30, gaschromatographisch bestimmt [14]) erhalten.

Von diesem Destillat injizierte man 20—40 µl in einen Gaschromatographen (Perkin-Elmer, Modell 154), der mit einer 1 m-Kolonne mit Polyäthylenglykol als stationärer Phase auf Celite als Träger [14] ausgerüstet war. Das Trägergas (He) wurde zwecks Trocknung durch eine in Äthanol-Trockeneis gekühlte Falle und ein P_2O_5-Rohr geleitet. Bei einer Kolonnentemperatur von 65° und einer Gasgeschwindigkeit von 25 ml/Min. war die Zeitspanne zwischen dem Austritt des Methanols und dem des Wassers etwa 20 Min. Aus der Gasfraktion, die das Methanol enthielt, wurde dieses in ein mit Äthanol-Trockeneis gekühltes Röhrchen kondensiert. Eine dahintergeschaltete in gleicher Weise gekühlte Falle schützte die Probe vor Luftfeuchtigkeit. Das die Methanolprobe enthaltende Röhrchen wurde dann unter Kühlung mit flüssiger Luft auf 1 mm Hg evakuiert und abgeschmolzen. Die direkte massenspektrographische Untersuchung des Methanols ergab normale Isotopenzusammensetzung (Tab. 2, Vers. 1).

b) Überführung des Methanols in CO_2. Das aus dem Gaschromatographen austretende methanolhaltige Helium wurde durch ein auf 300° erhitztes Glasrohr (1 × 25 cm) geleitet, das mit einem frisch mittels Methanol reduzierten Zn—Cu—Cr—Oxyd-Katalysator [15] beschickt war; das nunmehr hauptsächlich H_2 und CO anstelle von Methanol enthaltende Gasgemisch wurde dann zur Entfernung von H_2O und CO_2 durch zwei mit $Mg(ClO_4)_2$ bzw. Natronasbest beschickte U-Röhrchen geleitet. Schliesslich wurde das Gasgemisch zwecks Oxydation des CO zu CO_2 durch ein mit Jodpentoxyd [19] gefülltes Röhrchen (0.9 × 13 cm) geschickt. Die Oxydation wurde bei 80° ausgeführt, da bei dieser Temperatur H_2 nicht oxydiert wird [26]. Nach Trocknung in einer mit Alkohol-Kohlensäure gekühlten Falle wurde das CO_2 in ein mit flüssiger Luft gekühltes Röhrchen ausgefroren. Eine dahinter geschaltete ebenso gekühlte Falle diente als Schutz gegen Luftfeuchtigkeit. Das gekühlte Röhrchen wurde evakuiert (1 mm Hg) und abgeschmolzen. Der ^{18}O-Gehalt des CO_2 wurde massenspektrographisch ermittelt (Tab. 2, Vers. 2).

Isolierung der Chinone. o-Benzochinon aus Guajakol (Tab. 2, Vers. 3). Guajakol (100 mg = 0.93 mMol), gelöst in 4.5 ml mit ^{18}O markiertem Wasser (5.52 Atom-% ^{18}O-Überschuss) wurde in einem Scheidetrichter bei 0° während 10 Sek. mit einer Lösung von 350 mg (= 1.63 mMol) $NaJO_4$ in 2.5 ml Wasser des gleichen ^{18}O-Überschusses oxydiert. Das Reaktionsgemisch wurde so rasch wie möglich mit 4 ml Methylenchlorid ausgeschüttelt, der Extrakt mit Na_2SO_4 getrocknet und in einem Rotationsverdampfer i.V. auf einige Zehntel ml konzentriert. Das *o*-Chinon wurde mittels Hexan ausgefällt, abgesaugt, aus Methylenchlorid-Hexan umkristallisiert und i.V. über P_2O_5 getrocknet. Es war nach Schmp. und IR-Spektrum rein.

p-Benzochinon aus Hydrochinon-monomethyläther (Tab. 2, Vers. 4). Der Monomethyläther (100 mg), gelöst in 2 ml Wasser (mit 5.52 Atom-% ^{18}O-Überschuss), wurde bei Zimmertemperatur während 5 Min. mit 400 mg $NaJO_4$ in 2.5 ml Wasser des gleichen Markierungsgrades oxydiert. Das Reaktionsgemisch wurde 3 mal mit je 2 ml Methylenchlorid ausgeschüttelt, der Extrakt mit Na_2SO_4 getrocknet und i.V. zur Trockene gebracht. Das *p*-Chinon wurde durch Sublimation gereinigt und über P_2O_5 verwahrt.

Perjodatoxydation von 1-Methylnaphthol-2. (Versuche ausgeführt von tekn. lic. Britt Berggren). Eine Lösung von 0.5 g des Methylnaphthols in 150 ml Eisessig wurde mit einer Lösung von 0.5 g $NaJO_4$ in 150 ml 60 % Essigsäure versetzt. Nach 30 Min. bei 25° wurde mit Methylenchlorid extrahiert; der Extrakt wurde mit wässriger Arsenitlösung (0.02 N $NaAsO_2$, mit 20 g $NaHCO_3$/l) und mit Wasser gewaschen, mit wasserfreiem $CaSO_4$ getrocknet und eingedampft. Der Rückstand gab beim Umkristallisieren aus Hexan ein unscharf schmelzendes Gemisch, aus dem durch fraktionierte Kristallisation mit Methanol-Wasser und mit Hexan das 2-Methyl-3:4-benzo-*o*-chinol (XII) vom Schmp. 88—89° und dessen Acetat (XIII) vom Schmp. 129—130° erhalten wurden.

Die Produkte waren nach Misch-Schmp. und IR-Spektrum identisch mit authentischen Vergleichsproben [27].

3,5-Dimethyl-brenzcatechin. Aus 1.35 g 2,4-Dimethylphenol nach Teuber und Staiger [26] dargestelltes 3,5-Dimethyl-*o*-chinon wurde als Rohprodukt in 200 ml Wasser mittels SO_2 reduziert, und die Lösung mit Äther extrahiert. Der ölige Abdampfrückstand der ätherischen Lösung wurde wiederholt mit Hexan ausgekocht. Das aus den Hexanlösungen auskristallisierende Produkt wurde aus Cyclohexan umkristallisiert. Schmp. 72.5—73° (Lit.[28] 73—74°). Ausbeute 41 % d. Th., ber. auf 2,4-Dimethylphenol.

3,5-Dimethyl-o-chinon aus 3,5-Dimethyl-brenzcatechin (Tab. 2, Vers. 5). Das Brenzcatechin (50 mg), gelöst in 1.3 ml Wasser-^{18}O wurde bei Zimmertemperatur während 30 Sek. mit 120 mg $NaJO_4$ in 0.8 ml des markierten Wassers oxydiert. Isolierung des 3,5-Dimethyl-*o*-chinons wie für das unsubstituierte *o*-Chinon beschrieben. Es war nach Schmp. und IR-Spektrum mit authentischem Material identisch.

p-Benzochinon aus Hydrochinon (Tab. 2, Vers. 6). Es wurde analog der Darstellung von *p*-Benzochinon aus Hydrochinon-monomethyläther verfahren.

Isotopenaustausch-Versuche (Tab. 1). Das zu untersuchende feingepulverte Chinon (30—40 mg) wurde in 5 ml ^{18}O-markiertem Wasser gelöst und die Lösung unter möglichst gleichen Zeit- und Temperaturbedingungen stehen gelassen (Versuche 1, 2 und 4), wie sie für die Oxydationen der entsprechenden Monomethyläther und der freien Dihydroxybenzole (vgl. Tab. 2) verwendet wurden. In zwei weiteren Fällen (Tab. 1, Vers. 3 und 5) wurden andere Bedingungen gewählt. Isolierung der Chinone wie oben.

Die Bestimmung des ^{18}O-Gehaltes der Chinone wurde nach Dahn, Moll und Menassé [20] ausgeführt. Es wurden Proben von etwa 15 mg des Chinons und 100 mg *o*-Phenylendiamin-monohydrochlorid verwendet. Die Chinone wurden stets sofort nach ihrer Isolierung weiterverarbeitet.

Der *^{18}O-Gehalt des markierten Wassers,* das aus den Versuchsansätzen durch Destillation zurückgewonnen wurde, wurde nach Cohn und Urey [13] nach Äquilibrierung mit CO_2 im letzteren massenspektrographisch bestimmt.

Statens Naturvetenskapliga Forskningsråd danken wir für finanzielle Unterstützung der vorliegenden Arbeit. Die massenspektrometrischen Bestimmungen wurden im Laboratorium für Massenspektrometrie, Karolinska Institutet, Stockholm, ausgeführt. Wir möchten dem Vorstand dieses Laboratoriums, Herrn Docenten R. Ryhage, und seinen Mitarbeitern für ihre Hilfe unseren besten Dank aussprechen.

LITERATUR

1. Adler, E. und Hernestam, S. *Acta Chem. Scand.* **9** (1955) 319.
2. Adler, E. und Magnusson, R. *Acta Chem. Scand.* **13** (1959) 505.
3. Adler, E., Hernestam, S. und Walldén, I. *Svensk Papperstidn.* **61** (1958) 641.
4. Adler, E. und Törnquist, J. *Unveröffentlicht.*
5. Adler, E., Magnusson, R., Berggren, B. und Thomelius, H. *Acta Chem. Scand.* **14** (1960) 515.
6. Bunton, C. A. und Shiner, jun., C. J. *J. Chem. Soc.* **1960** 1593.
7. Crouthamel, C. E., Hayes, A. M. und Martin, D. S. *J. Am. Chem. Soc.* **73** (1951) 82; Shiner, jun., V. J. und Wasmuth, C. R. *J. Am. Chem. Soc.* **81** (1959) 37; Keen, N. und Symons, M. C. R. *Proc. Chem. Soc.* **1960** 383.
8. Brodskii, A. I. und Vysotskaya, N. A. *Doklady Akad. Nauk. SSSR* **101** (1955) 869; Anbar, M. und Guttman, S. *J. Am. Chem. Soc.* **83** (1961) 781.
9. Levitt, L. *J. Org. Chem.* **20** (1955) 1297.
10. Brackman, W. und Havinga, E. *Rec. trav. chim.* **74** (1955) 937, 1107.
11. Fesenko, V. V. und Gragerov, I. P. *Doklady Akad. Nauk. SSSR* **101** (1955) 695; s. auch Samuel, D. und Steckel, F. *Bibliography of the Stable Isotopes of Oxygen,* Pergamon Press, London, 1959.
12. Magnusson, R. *Acta Chem. Scand.* **14** (1960) 1643.
13. Cohn, M. und Urey, H. C. *J. Am. Chem. Soc.* **60** (1938) 679.
14. Smith, B. *Acta Chem. Scand.* **13** (1959) 480.
15. Wiberg, K. *J. Am. Chem. Soc.* **75** (1953) 2665.

16. Urey, H. C. und Roberts, I. *J. Am. Chem. Soc.* **60** (1938) 2391.
17. Lauder, I. und Zerner, B. *Australian J. Chem.* **12** (1959) 621, 630.
18. Fenske, M. R. und Frolich, P. K. *Ind. Eng. Chem.* **21** (1929) 1052; Nussbaum, R. und Frolich, P. K. *Ibid.* **23** (1931) 1386.
19. von E. Doering, W. und Dorfman, E. *J. Am. Chem. Soc.* **75** (1953) 5595.
20. Dahn, H., Moll, H. und Menassé, R. *Helv. Chim. Acta* **42** (1959) 1225.
21. Adler, E., Junghahn, L., Lindberg, U., Berggren, B. und Westin, G. *Acta Chem. Scand.* **14** (1960) 1261.
22. Adler, E., Dahlén, J. und Westin, G. *Acta Chem. Scand.* **14** (1960) 1580.
23. Criegee, R., *Angew. Chem.* **70** (1958) 173.
24. Teuber, H.-J. und Staiger, G. *Chem. Ber.* **88** (1955) 802.
25. Buist, G. J., Bunton, C. A. und Miles, J. H. *J. Chem. Soc.* **1957**, 4567 und 4575.
26. Vandaveer, F. E. und Gregg, R. C. *Ind. Eng. Chem. Anal. Ed.* **1** (1929) 129.
27. Fries, K. und Hübner, E. *Ber.* **39** (1906) 435; Bargellini, G. und Silvestri, S. *Gazz. chim. ital.* **37** (1907) 413.
28. Wessely, F. und Schinzel, E. *Monatsh.* **84** (1953) 969.

Eingegangen am 26. August 1961.

ACTA CHEMICA SCANDINAVICA 16 (1962) 541–542

The Occurrence of Ergosterol in the Lichen *Cornicularia normoerica* (Gunnerus) Lynge

AASE RYE ALERTSEN, TORGER BRUUN and ELLEN HEMMER

Institutt for Organisk Kjemi, Norges Tekniske Høgskole, Trondheim, Norway

Dedicated to Professor *Holger Erdtman* on his 60th birthday

A substance has been isolated from *Cornicularia normoerica* which by direct comparison was identified as ergosterol.

In the literature there are several references to the occurrence of ergosterol in lichens: In *Lobaria pulmonaria*,[1] in *Parmelia saxatilis*,[2] in *Peltigera canina* L.[3], in *Cladonia rangiferina* (L) Hoffm.[4], in *Alectoria ochroleuca* Ehrh.[5], in *Parmelia physodes*[6], in *Gyrophora Dillenii* (Tuck.) Müll. Arg. and *Parmelia furfuracea* L.[7], in *Cetraria islandica*[8], and in *Roccella montagnei*[9]. Ref.[4] lists several other lichens in which the presence of ergosterol was indicated by colour reactions. Of the occurrences the ones reported in Ref.[4,7,9] appear to be the best authenticated, but, curiously, none appear to have made a direct comparison with ergosterol.

During an investigation of the lichen *Cornicularia normoerica* (Gunnerus) Lynge one of us isolated mannitol and minute amounts of a substance which gave colour reactions and a UV spectrum similar to those of ergosterol[10]. We now have repeated the work on larger amounts of material.

The lichen has a very low content of matter which can be extracted with ether, 10.3 g from 4.45 kg of lichen, and subsequent extractions with acetone and with methanol gave comparable amounts of extract. The ether extract appeared to be very complex in composition, and the only substance which was obtained in a reasonably pure, crystalline state, was ergosterol, characterised by m.p. and mixed m.p. with authentic material, optical activity, UV and IR spectra, and by preparation of a benzoate, the m.p. and IR spectrum of which were compared with those of authentic ergosteryl benzoate; for details see Experimental.

EXPERIMENTAL

UV spectra were measured on a Perkin-Elmer Model 13 spectrophotometer in ethanol. IR spectra were measured on a Perkin-Elmer Model 21 Spectrophotometer in KBr. Optical activity was measured in chloroform in a 1 dm tube. In mixed m.p. determinations the m.p.'s of the three samples to be compared were measured at the same time.

The lichen material was collected at the mountain Munken on the northern side of the Trondheim Fjord during April-August 1960. The air dry material, 4.45 kg, contained 13—14 % of moisture as determined by drying at 110°, and an ignition residue of 5—6 %. The ignition residue of carefully cleaned lichen was about 1 %.

The material was extracted with ether in a Soxhlet apparatus for 24 h. Removal of the solvent left 10.3 g of extract. Of this material 4.9 g were neutral towards alkali. It was dissolved in a small volume of acetone, and after standing for some days at low temperature large, needle-like crystals had separated. They melted at 146—150° and absorbed in the UV as did ergosterol. Three more crystallisations from acetone afforded 30 mg of white needles which melted at 149—153°. A mixture with ergosterol melted at 147—150°. $[\alpha]_D$ −122°(*c*, 1.70). λ_{max} 2710, 2800 and 2930 Å, ε 10 500, 11 000 and 6500, respectively. Our comparison sample was a commercial ergosterol which had been crystallised once from acetone and then had the following constants: m.p. 147—151°, $[\alpha]_D$ −121°(*c*, 1.72), λ_{max} 2710, 2810 and 2930 Å, ε 12 500, 13 000 and 7500, respectively. "Elsevier" gives [11] m.p. usually in the 162—167° region with the reservation that it varies with the water content and $[\alpha]_D$ −129° for the monohydrate in chloroform. Barton and Cox [12] give λ_{max} 2710, 2820 and 2920 Å, ε 11 900, 12 500 and 5950, respectively, in ethanol. The IR spectra of the two substances were identical.

The benzoate was prepared with benzoyl chloride in pyridine with boiling for 1 h. It was purified by filtration through alumina in benzene and crystallisation from petroleum ether to give 1.1 mg of benzoate melting at 150—153°. A mixture with ergosteryl benzoate (m.p. 155—156°, prepared in the same way from the commercial ergosterol) melted at 150—153°. The IR spectra of the two substances were essentially identical.

Acknowledgement. We sincerely thank Professor N. A. Sørensen for his interest in the work, and Messrs. Collet and Co., A/S, Oslo, for a generous supply of ergosterol.

REFERENCES

1. Gérard, E. *J. pharm. chim.* [6] **1** (1895) 601; *Compt. rend.* **121** (1895) 723.
2. Keegan, P. Q. *Chemical News* **114** (1916) 74; *Chem. Zentr.* **1916 II** 1166.
3. Zellner, J. *Monatsh.* **59** (1932) 300.
4. Blix, G. and Rydin, H. *Uppsala Läkarfören. Förh.* **37** (1932) 333.
5. Klima, J. *Monatsh.* **62** (1933) 209.
6. Zellner, J. *Monatsh.* **64** (1934) 6.
7. Zellner, J. *Monatsh.* **66** (1935) 81.
8. Montignie, E. *Bull soc. chim. France* [5] **2** (1935) 194.
9. Murty, T. K. and Subramanian, S. S. *J. Sci. Ind. Research (India)* **18B** (1959) 91.
10. Rye, Aa. *Graduation work* 1951.
11. *Elsevier's Encyclopedia of Organic Chemistry*, New York and Amsterdam, Vol. **14** (1940) 68 and Vol. **14s** (1954) 1736 s.
12. Barton, D. H. R. and Cox, J. D. *J. Chem. Soc.* **1948** 1357.

Received September 13, 1961.

ACTA CHEMICA SCANDINAVICA 16 (1962) 543–547

Studies on the Chemistry of Lichens

15 *. Siphulitol, a New Polyol from *Siphula ceratites*

BENGT LINDBERG and HANS MEIER

Institutionen för träkemi, Kungl. Tekn. Högskolan, Stockholm, Sweden

Dedicated to Professor *Holger Erdtman* on his 60th birthday

D-Arabinitol, D-mannitol and a new acyclic polyol, siphulitol, have been isolated from the lichen *Siphula ceratites*. Chemical investigation of the latter, including elementary analysis and periodate oxidation studies, indicated that it was a 1-deoxy-heptitol. The substance was shown to be indistinguishable from 1-deoxy-D-*glycero*-D-*talo*-heptitol, synthesised by unambiguous methods.

In previous papers of this Series, studies on low molecular weight carbohydrates in various lichens, especially of the polyols, have been reported. D-Arabinitol and D-mannitol were found in all lichens studied which belonged to the order Gymnocarpeae [1]. Bruun [2] has recently investigated a lichen of this order, *Siphula ceratites* (Fr.) Th. Fr., and isolated siphulin, a lichen acid, containing a chroman-4-one residue. Dr. Bruun kindly forwarded to us the water-soluble parts of his extracts which should contain the polyols. Paper chromatography of the acetone-extracted material indicated that it contained mannitol, arabinitol and a third component. The latter had a higher R_F-value than arabinitol in solvent system A (see Experimental), a characteristic which we have not observed in the investigation of other lichens.

The mixture was resolved by carbon column chromatography, yielding in the order in which the substances were eluted, D-arabinitol, D-mannitol and the new substance, for which we propose the name siphulitol. The substance crystallised from methanol and showed m.p. 122—123° and $[\alpha]_D$ −8° in water. It could be detected on paper chromatograms with polyol reagents (such as silver nitrate-sodium hydroxide [3] or periodate-benzidine [4]) but not with aldose or ketose reagents. It was unaffected by treatment with acid or alkali. The fact that siphulitol had a higher R_F-value than arabinitol but was more strongly adsorbed on the carbon column, suggests the presence of some lipophilic group, *e.g.* methoxyl, methylene or methyl group. Analysis showed that it did not contain methoxyl. The R_F-value of siphulitol was much lower than that of rhamnitol, suggesting that it was a mono-deoxypolyol with more than six

* Part 14 *Acta Chem. Scand.* **15** (1961) 1695.

carbon atoms. The substance gave a crystalline benzylidene derivative, m.p. 239—242° and $[\alpha]_D$ + 9° in chloroform, the I.R. spectrum of which revealed the absence of free hydroxyl groups. These facts indicated that siphulitol was a monodeoxy heptitol, capable of giving a tribenzylidene derivative; elementary analysis was also in agreement with the formula $C_7H_{16}O_6$.

Assuming a molecular weight corresponding to this formula, siphulitol consumed 5 moles of periodate with the formation of 4 moles of formic acid and 1 mole of formaldehyde. The simultaneous formation of acetaldehyde was demonstrated by a qualitative test. These results are in agreement with the structure of a 1-deoxy-heptitol, *e.g.* II, III or IV.

Two natural heptitols, D-*glycero*-D-*manno*-heptitol or volemitol (I) and D-*glycero*-D-*galacto*-heptitol or perseitol, have been known for a considerable time [5]. A third, D-*glycero*-D-*gluco*-heptitol or β-sedoheptitol, has recently been found by Charlson and Richtmyer [6], who have also isolated an octitol, D-*erythro*-D-*galacto*-octitol. It seemed reasonable to consider possible configurations for siphulitol, related to those of the naturally occurring heptitols. As volemitol (I) is the most widely distributed of these, found also in some lichens, we first considered 1- and 7-deoxy-volemitol (II and III).

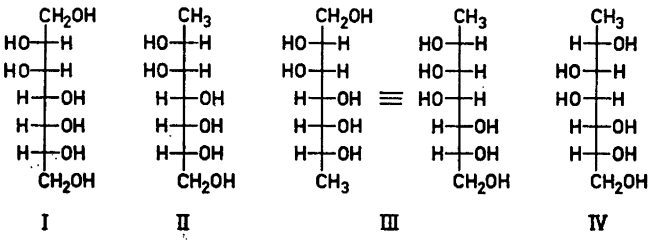

The enantiomorph of 1-deoxy-volemitol (II) is known [7]. Because it is amorphous and gives only a monobenzylidene derivative, it could be excluded as a possibility. The 7-deoxy-volemitol (III) or 1-deoxy-D-*glycero*-D-*talo*-heptitol should give a tribenzylidene derivative (2:4, 3:6, 5:7), analogous to that of mannitol according to the rules for the formation of cyclic acetals, summarised and extended by Barker and Bourne [8]. Further support for structure III was obtained by oxidising siphulitol with a limited amount of periodate and investigating the product by paper chromatography. In addition to a strong spot due to glyceraldehyde and another with high R_F-value possibly due to 4-deoxy erythrose, there was obtained a faint spot with the same R_F-value and colour reactions as arabinose. On similar treatment of 1-deoxy-D-*glycero*-D-*galacto*-heptitol (IV), a strong spot corresponding to arabinose was obtained. Schwartz [9] has demonstrated that *threo*-glycol groups are oxidised more readily than *erythro*-glycol groups; the high yield of arabinose from IV and a low yield from III are in agreement with this observation.

1-Deoxy-D-*glycero*-D-*talo* heptitol (III) was synthesised by the following sequence of reactions. D-Mannose was converted into D-*glycero*-D-*talo*-heptose *via* 1-deoxy-1-nitro-D-*glycero*-D-*talo*-heptitol according to Sowden and Schaffer [10]. The dithioethyl acetal of the heptose was prepared and treated with Raney-nickel, following the procedure devised by Wolfrom and Karabinos [11],

yielding 1-deoxy-D-*glycero*-D-*talo* heptitol. The synthetic product and its benzylidene derivative were identical (m.p., optical rotation, I.R.) with siphulitol and its benzylidene derivative, thereby establishing the structure and configuration of the natural product.

Siphulitol seems to be the first deoxy-alditol to be found in Nature. Generally, there are natural sugars, aldoses or ketoses, which correspond to the naturally occurring alditols, but no natural deoxyheptose or deoxyheptulose is known.

EXPERIMENTAL

Melting points are corrected. Paper chromatography was conducted on Whatman No. 1 filter paper using the following solvent systems:

A. Ethyl acetate-pyridine-water, 2:1:2 (upper phase).
B. Ethyl acetate-pyridine-water, 8:2:1.
C. Ethyl acetate-acetic acid-water, 3:1:3 (upper phase).

Isolation of siphulitol

The water soluble part (about 2 g incompletely dry syrup) of the acetone extract of *Siphula ceratites* (3.6 kg), previously extracted with ether, was supplied by Dr. Bruun. A larger fraction, obtained by subsequent extraction with methanol, contained only traces of siphulitol. Part of the first fraction (300 mg) was added to the top of a carbon-Celite column (3 × 30 cm), which was eluted first with water (2 l) and then with 5 % aqueous ethanol (2 l), and the eluate collected in 15 ml fractions. Tubes 27—39 contained arabinitol (27 mg), tubes 40—52 a mixture of arabinitol and mannitol (19 mg) tubes 52—115 mannitol (42 mg) and tubes 122—137 siphulitol (74 mg). The remainder of the acetone extract was fractionated in a similar manner, yielding a total of 500 mg amorphous siphulitol.

D-*Arabinitol* crystallised from aqueous acetone and melted at 98—100°, undepressed on admixture with an authentic sample.

D-*Mannitol* crystallised from ethanol and melted at 162—164°, undepressed on admixture with an authentic sample.

Siphulitol crystallised from methanol. The substance had a high solubility in that solvent and crystallisation resulted in considerable losses. Only syrup or a mixture of syrup and crystals was obtained on attempted crystallisation from other solvents. An analytical sample melted at 122—123° and showed $[\alpha]_D^{20}$ −8° [*c*, 1.5, H_2O] (Found: C 43.3; H 8.08; O 48.1. Calc. for $C_7H_{16}O_6$: C 42.9. H 8.23; O 48.9). Siphulitol had the same R_F-value as arabinitol in solvent system C but was faster than arabinitol in system A, R_{Glu} = 1.25.

Tri-O-benzylidene derivative of siphulitol. Siphulitol (24 mg) was dissolved in 50 % sulphuric acid (0.6 ml), to which freshly distilled benzaldehyde (400 mg) was added and the mixture shaken for one hour. The crystalline reaction product was filtered and recrystallised from toluene, yielding the pure substance (31 mg), m.p. 239—242° and $[\alpha]_D^{20}$ + 9° (*c*, 1.7, $CHCl_3$) (Found: C 73,0; H 6,18; O 20.9. Calc. for $C_{28}H_{28}O_6$: C 73.0; H 6.13; O 20.8). The I.R. spectrum of this substance (9 mg dissolved in 0.5 ml chloroform) showed the absence of free hydroxyl groups.

Periodate oxidation studies of siphulitol

Siphulitol (20 mg) was dissolved in water (20 ml) and 0.04 M sodium metaperiodate (20 ml) was added. The consumption of periodate, followed spectrophotometrically according to Aspinall and Ferrier [12], reached a constant value, 4.65 moles per mole siphulitol, after one hour.

Under similar conditions 3.7 moles of formic acid and 0.9 moles of formaldehyde were formed, the latter being determined according to Lambert and Neish [13]. All these values are somewhat low; control experiments with galactitol also gave values somewhat lower than the theoretical.

A qualitative test for acetaldehyde in the oxidation products, using the reaction with morpholine and sodium nitroprusside [14], was positive.

Siphulitol (10 mg) in water (10 ml) was treated overnight with an amount of periodate corresponding to 0.25 moles per mole of polyol. The reaction product was analysed by chromatography on paper, impregnated with phosphate buffer of pH 5 [15], using solvent system B. With the anisidine hydrogen chloride reagent [16], there were obtained a strong spot, corresponding to glyceraldehyde, a faint spot corresponding to arabinose and a strong, reddish brown spot with high R_F-value. Under these conditions the four pentoses were well separated, arabinose having the lowest R_F-value. On similar oxidation of 1-deoxy-D-*glycero*-D-*galacto*-heptitol, a similar chromatogram was obtained with the exception that arabinose appeared as a strong spot.

Synthesis of siphulitol

D-Glycero-D-talo-*heptose diethyl dithioacetal.* 1-Deoxy-1-nitro-D-*glycero*-D-*talo*-heptitol (1.5 g) was converted to the heptose by dissolving it in N sodium hydroxide (7.5 ml) adding it drop-wise to a stirred solution of conc. sulphuric acid (1 ml) and water (1.5 ml) at room temperature, and deionising the solution. The syrup obtained on concentrating the solution (1.39 g) was dissolved in conc. hydrochloric acid (2 ml), ethanethiol (2 ml) was added and the mixture shaken, at 0°, for 5 h. The addition of a piece of ice to the mixture resulted in the crystallisation of the thioacetal. It was filtered, washed with ice-water and recrystallised from water, yielding colourless crystals (0.72 g) melting at 165—166°. (Found: S 19.6. Calc. for $C_{11}H_{24}O_6S_2$: S 20.2).

1-Deoxy-D-glycero-D-talo-*heptitol.* The thioacetal above (0.72 g) was dissolved in 70 % ethanol (10 ml), freshly prepared Raney-nickel (5 g) was added and the mixture was refluxed for 4 h. The solids were filtered and washed with water. The combined filtrate and washings were concentrated to a syrup (0.49 g). Paper chromatographic analysis of the product showed a major spot with the same R_F-value as siphulitol but also spots with higher and lower R_F-values. Therefore the syrup was resolved on a cellulose column, using butanol saturated with water as irrigant. A syrup (0.29 g) was obtained which contained the main component chromatographically pure. On attempted crystallisation of this product from methanol, a few mg of crystals, m.p. 150—160°, were obtained. On paper chromatography these gave only one spot with the same R_F-value as siphulitol; however, on paper electrophoresis in sulphonated phenyl boronic acid buffer of pH 6.5 [17], two spots were produced, one of which had the same mobility as siphulitol. The crystals were most probably a mixture of siphulitol and an unidentified impurity. On prolonged standing, siphulitol, m.p. 122—123°, crystallised. The melting point was undepressed on admixture with the natural product and the optical rotations and the IR spectra of the two products were identical.

Part of the syrup (50 mg) was converted to the benzylidene derivative (50 mg) as described above. The derivative melted at 239—242°, undepressed on admixture with the benzylidene derivative of siphulitol, and showed $[\alpha]_D^{20}$ + 9°. The IR spectra of the benzylidene derivatives of the natural and the synthetic product were identical.

Acknowledgement. The authors are indebted to Dr. H. S. Isbell and Dr. N. K. Richtmyer for generous gifts of reference substances and to Mr. L. Nordén for skilful assistance.

REFERENCES

1. Lindberg, B., Missiorny, A. and Wachtmeister, C. A. *Acta Chem. Scand.* **7** (1953)591.
2. Bruun, T. *Tetrahedron Letters* **4** (1960) 1.
3. Trevelyan, W. E., Procter, D. P. and Harrison, J. S. *Nature* **166** (1950) 444.
4. Cifonelli, J. A. and Smith, F. *Anal. Chem.* **26** (1954) 1132.
5. Karrer, W. *Konstitution und Vorkommen der Organischen Pflanzenstoffe.* Birkhäuser, Basel 1958.

6. Charlson, A. J. and Richtmyer, N. K. *J. Am. Chem. Soc.* **82** (1960) 3428.
7. Votoček, E., Valentin, F. and Ràc, T. *Collection Czechoslov. Chem. Communs.* **2** (1930) 402.
8. Barker, S. A. and Bourne, E. J. *Advances in Carbohydrate Chem.* **7** (1952) 138.
9. Schwartz, J. P. C. *J. Chem. Soc.* **1957** 276.
10. Sowden, J. C. and Schaffer, R. *J. Am. Chem. Soc.* **73** (1951) 4662.
11. Wolfrom, M. L. and Karabinos, J. V. *J. Am. Chem. Soc.* **66** (1944) 909.
12. Aspinall, G. O. and Ferrier, R. J. *Chem. and Ind. London* **1957** 1216.
13. Lambert, M. and Neish, A. C. *Can. J. Research.* **28** (1950) 83.
14. Feigl, F. *Spot Tests in Organic Analysis*, Elsevier, Amsterdam 1956.
15. Jayme, G. and Knolle, H. *Angew. Chem.* **68** (1956) 243.
16. Hough, L., Jones, J. K. N. and Wadman, W. H. *J. Chem. Soc.* **1950** 1702.
17. Garegg, P. and Lindberg, B. *Acta Chem. Scand.* **15** (1961) 1913.

Received March 2, 1961.

ACTA CHEMICA SCANDINAVICA 16 (1962) 548–552

Proofs for the Occurrence of Homoprotocatechuic Acid and some Other Pyrocatechol and Guaiacol Derivatives in Pressure Heated Cellulose Spent Liquors

THEODORE ASHORN and TERJE ENKVIST

Department of Chemistry, University of Helsingfors, Finland

Dedicated to Professor *Holger Erdtman* on his 60th birthday

Mixed melting point determinations on crystalline substances or their crystalline derivatives obtained from sodium sulfide enriched pressure heated spent kraft or sulfite liquors have yielded proofs for the occurrence of the following substances: guaiacol, pyrocatechol, *p*-methylcatechol, *p*-ethylcatechol, acetovanillone, vanillin, protocatechualdehyde, *p*-acetopyrocatechol, vanillic acid, and homoprotocatechuic acid. For the separation of the ketonic substances from the aldehydic ones a technique of stepwise acidification of an aqueous solution containing the Girard-P-derivatives of these substances was used.

During many years one of us (T.E.) together with his coworkers has studied the pressure heating of spent kraft or sulfite cellulose liquors to which sodium sulfide has been added. The results have been in part described in several papers [1–7]. Among other things, the occurrence of a series of pyrocatechol and guaiacol derivatives in these liquors has been reported in many cases, until now based on chromatographic evidence only. In the present report these findings have been substantiated by the determinations of mixed melting points of some of these substances or of their crystalline derivatives. The presence of the same substances has been shown also by paper chromatography in several different systems. Qualitative and quantitative chromatographic investigations and methods will be reported in another paper. In the present paper some R_F values only are given. The yields reported in the present paper have been surpassed in other experiments.

SPENT SULFITE LIQUOR

The pressure heated sulfite liquor deferred to in the present paper is identical with the liquor TU 10 described in Ref. [4], Tables 1 and 3. It was obtained by heating continuously a spent commercial calcium base sulfite liquor from the mill of Tainionkoski after addition of sodium sulfide (15.6 % calculated as Na_2S in the organic matter, 1230 g in 7050 ml liquor) for one minute (effective heating time) at about 320° and 155 atmospheres. After

the heating a sample of the liquor was acidified to a pH of about 2 with hydrochloric acid. A current of nitrogen was passed through the liquor which was kept at about 60° in order to remove hydrogen sulfide, the precipitate of "demethylated lignin" obtained was filtered off, and the filtrate extracted continuously with ethyl ether in a liquid-liquid extractor. The ether solution was dried with anhydrous sodium sulfate and the solvent was partly distilled off and finally evaporated *in vacuo* at room temperature.

5 g of the ether extract was dissolved in 75 ml of N sodium hydroxide and the solution extracted continuously with ether in order to remove neutral substances. The aqueous layer was separated from the ether and a stream of carbon dioxide passed through it until the pH had dropped to about 8. A phenolic fraction was isolated by continuous ether extraction of the solution in a yield of about 2.54 g. It was dissolved in 35 ml 99 % methanol. Girard "P" reagent (acethydrazide pyridinium chloride [8]) and several drops of formic acid were added, and the mixture was refluxed for 55 min. The cooled solution was then mixed with 100 ml ether with stirring, and the solution was decanted off from the precipitate consisting of derivatives formed by carbonyl compounds with the reagent. The solvent was evaporated from the solution, the residue was dissolved in 5 ml 75 % ethanol and added to 50 ml of a saturated solution of lead acetate in 50 % ethanol. The precipitate formed (lead salts of pyrocatechol and its derivatives) was separated by centrifugation, washed with alcohol and ether, suspended in acetone and decomposed with hydrogen sulfide. The lead sulfide was filtered off and the filtrate evaporated. The residue was treated with benzoyl chloride and pyridine according to the method of Einhorn [9]). The reaction product was recrystallized three times from aqueous ethanol; m.p. 84°C alone or admixed with an authenthic sample of *pyrocatechol dibenzoate*, prepared according to Ref. [10].

The aqueous-alcoholic supernatant obtained after separation of the lead salts of pyrocatechol and its derivatives was diluted with 2 volumes of water and extracted several times with ether. The ether solution was evaporated without drying and the water and alcohol dissolved in the ether were removed by addition of benzene and distillation through a Vigreux column. The benzene containing residue was treated with 3,5-dinitrobenzoyl chloride and pyridine. The reaction product was recrystallised from alcohol; m.p. 140°C alone or admixed with an autenthic sample of *guaiacol-3,5-dinitrobenzoate*, prepared according to Ref. [11].

The precipitate obtained by treatment with the Girard "P" reagent was extracted with boiling ether and dissolved in 50 ml of water and its separation into a ketonic and aldehydic part was performed by stepwise acidification in the following way:

The pH of the solution was brought to about 6 by the addition of hydrochloric acid and the solution continuously extracted with ether for 5 h. The ether was separated, the aqueous solution acidified to about pH 5.5 and again extracted with ether for 4 h. The fractionation was further continued in the same way, in lowering the pH 0.5 units with hydrochloric acid and extracting with ether for 4 h until pH 1 was reached. Each ether extract was evaporated separately and a sample of the residue analysed by paper chromatography in the ethanol-water-conc. ammonia (80:16:4) system. The fractions obtained at pH 5.5 – 3.5 gave the same two spots and were combined. At pH 3.5 – 1.5 4 spots could be observed but these fractions were not further analysed. The fraction, pH 1.5 – 1, and an additional fraction obtained by a further 4 h ether extraction at pH 1 gave 2 spots not identical with the former and were combined.

The residue, after evaporation of the ether from the fractions between pH 5.5 and 3.5 was dissolved in 1 ml of 75 % aqueous ethanol and precipitated by addition of 3 ml of a saturated solution of lead acetate in 50 % ethanol. The precipitate was centrifuged off, washed with acetone and decomposed in acetone suspension by a current of hydrogen sulfide. The precipitate of lead sulfide was filtered off, the filtrate was evaporated and treated with benzoylchloride in pyridine. The reaction product was recrystallized from aqueous ethanol; m.p. 117°C alone or admixed with an authenthic sample of *3,4-dihydroxyacetophenone-dibenzoate* (dibenzoate of *p*-acetopyrocatechol), prepared according to Ref. [12]

The aqueous alcoholic supernatant left after removal of the precipitate obtained on addition of lead acetate, was diluted with 2 volumes of water and extracted with ether. The ether layer was evaporated and distilled together with benzene as in the above mentioned case of guaiacol. The residue was treated with benzoyl chloride and pyridine as already described, and the reaction product was recrystallized from aqueous ethanol. It showed a m.p. of 106° and did not give any depression of m.p. on admixture with an authenthic sample of *acetovanillone benzoate* prepared according to Ref. [13].

Table 1. R_F values. Chromatography on Whatman No. 1 paper. Descending technique. Spraying with silver nitrate-ammonia, Folin-Denis reagent, diazotized sulfanilic acid or diazotized *p*-nitroaniline.

Eluent	2 % acetic acid	Xylene-butanone [16]	Butanol	Ethanol-ammonia	$CHCl_3$
Impregnation with	—	Formamide	Na_2MO_4 [20]	—	Formamide
Guaiacol	—	0.62	0.94	0.85	0.78
Pyrocatechol	0.72	0.24	0.25	0.81	0.046
p-Methylcatechol	0.72	0.40	0.36	0.81	0.11
p-Ethylcatechol	0.72	0.53	0.69	0.81	0.22
Vanillin	0.64	0.41	0.95	0.69	0.69
Acetovanillone	0.61	0.50	0.96	0.70	0.80
p-Acetopyrocatechol	0.55	—	0.11	0.63	0.79
Protocatechualdehyde	0.59	0.12	0.07	0.63	0.00
Vanillic acid	0.47	0.11	0.28	0.52	0.01
Homovanillic acid	0.77	0.07	0.25	0.61	0.01
Protocatechuic acid	0.46	0.051	0.03	0.45	0.00
Homoprotocatechuic acid	0.75	0.023	0.03	—	0.00
Dihydrocaffeic acid	0.67	0.035	0.03	—	0.00

The fraction obtained at pH 1.5—1 was separated in a similar way. The substance precipitated with lead acetate yielded a benzoate, m.p. 97°, alone or admixed with the *dibenzoate of protocatechualdehyde*, prepared according to Ref. [14]. The supernatant obtained after removal of the lead compound possessed a strong odor of vanillin and gave a benzoate, m.p. 75°, alone or admixed with the *benzoate of vanillin* [15].

The weakly alkaline solution, from which the phenolic fraction had been removed by extraction with ether, was acidified with hydrochloric acid and again extracted with ether, which dissolved a mixture of organic acids. Paper chromatography of this mixture with 2 % aqueous acetic acid as eluent gave three spots, two of which showed R_F identity with protocatechuic acid and homovanillic acid. The third acid was isolated by preparative paper chromatography on Whatman No. 1 paper using a mixture of ethanol-water-conc. ammonia (80:16:4) as eluent. The substance with an R_F value of about 0.5 was eluted from the paper with acetone. The solvent was evaporated and the residue sublimed. The sublimate gave no depression of m.p. on admixture with *vanillic acid*.

KRAFT BLACK LIQUOR

To 450 ml concentrated kraft black liquor from the mill of Enso Gutzeit, **Kotka**, containing 50 % of solids and 239.0 g of organic substance, 116.2 g of crystalline sodium sulfide ($Na_2S \cdot 9H_2O$), 58.41 g of sodium hydroxide and 450 ml of water were added. The mixture was heated in a stainless steel rocking autoclave for 10 min at 285°C.

Phenols. After cooling 1138 g of the heated liquor was neutralized to a pH of about 7 by the addition of 1.41 l of about 2 N sulfuric acid, 200 g sodium hydrogen carbonate was added and a first ether soluble fraction was obtained by continuously extracting the liquor with its suspended precipitate of demethylated lignin with ethyl ether in a liquid-liquid extractor in a slow current of nitrogen and evaporating the solvent. The residue was dissolved in a small amount of acetone and precipitated by addition of a solution of 25 g crystalline lead acetate ($Pb(OCOCH_3)_2 \cdot 3H_2O$) in 130 ml of water and 170 ml of acetone. The precipitate was filtered off, washed with acetone, and decomposed by the addition of dilute sulfuric acid. Pyrocatechol and its derivatives were extracted with ether and the ether solution on evaporation gave a dark syrup weighing 6.0 g. This mixture was separated by preparative paper chromatography on Whatman No. 3 paper impregnated with formamide and using chloroform as eluent (similar to the Freudenberg-Lehmann system

II [16], but using chloroform instead of xylene-methyl-ethyl ketone). Zones with R_F values of 0.046, 0.11. 0.22 and a weak zone with a higher R_F value were obtained. The zones could be located by comparison with parallel chromatograms sprayed with diazotized *p*-nitroaniline or silver nitrate-ammonia reagent and with difficulty, by their dark colour in ultraviolet light. The zones were cut out and eluted with acetone, which also dissolves the residual formamide. Part of this formamide could be removed *in vacuo*.

A sample (127 mg) of the substance from the zone with R_F = 0.22 was dissolved in 2 ml of acetone and refluxed for 30 min together with 440 mg of dinitrofluorobenzene and 0.23 ml of triethylamine (*cf.* Ref. [17]). The reaction mixture was diluted with water and extracted with 15 ml of ethyl ether and the ether layer washed successively with diluted hydrochloric acid, diluted sodium hydroxide solution and water. Evaporation of the ether solution gave a brown oil. Crystallization from ethanol yielded crystals, m.p. 95—97°. Recrystallization from aqueous methanol raised the m.p. to 105—108°. On admixture with an authenthic sample of *2,4-dinitrophenyl ether of p-ethylcatechol*, m.p. 106.5—108°, gave a m.p. of 105—108°. Analysis of the sample obtained from the black liquor (A. Bernhardt, Mülheim, Ruhr): Found: C 51.33; H 3.14; N 12.01. Calc. for $C_{20}H_{14}N_4O_{10}$: C 51.07; H 3.00; N 11.91.

The zone with R_F 0.11 treated in the same way gave a 2,4-dinitrophenyl ether, m.p. 124.5—125.5°, which did not show any depression of m.p. on admixture with an authenthic sample of *2,4-dinitrophenyl ether of methyl catechol*.

Acids. After the ether extraction of the phenolic fraction at pH 7 as described above, the precipitate of "demethylated lignin" was filtered off and the main part of the filtrate (80.2 % by volume) was acidified to a pH of about 2 by the addition of 180 ml sulfuric acid 1:1. A small precipitate was filtered off and the filtrate was extracted continuously with ether in a current of nitrogen. After evaporation of the solvent 51.12 g of liquid residue was obtained, having a strong odor of acetic and formic acids. On drying of a small sample on the water bath, the content of non volatile acids was found to be 46.6 %, corresponding to 23.9 g. Chromatography of a 5 g sample of the non volatile fraction on a column of polycaprolactam (perlon) powder suspended in water (*cf.* Ref.[18]) was carried out. The height of the polycaprolactam layer was 40 cm, the inner diameter of the tube 25 mm. Elution was performed with 1100 ml of water followed by 700 ml of a mixture of isopropanol-water-conc. ammonia 80:16:4. The eluate was collected in 370 test tubes using an automatic fraction collector. Paper chromatography of fractions 138—162 with water as eluent gave one main spot, the same substance was also found in fractions 163—140 although in a lower degree of purity. Ether extraction of fractions 138—162 gave 148 mg of an almost white substance, which crystallized on standing over night at room temperature. Fractions 163—140 gave 119 mg of an ether soluble syrup of brownish color.

A sample of the substance found in fractions 138—162 was recrystallized four times from benzene, once using decolorising carbon (Merck). The purified substance had a m.p. of 127° both alone or when admixed with an authenthic sample of ***homoprotocatechuic acid***, m.p. 127—128°, prepared by Dr. J. Halmekoski by demethylation of synthetic homovanillic acid with hydroiodic acid [19].

Acknowledgement. The authors are indebted to Docent Jaakko Halmekoski for performance and to Mrs. Ulla Enkvist for assistance at some of the chromatographic experiments, and to Docent C. G. Nordström for revision of the English in this manuscript.

REFERENCES

1. Enkvist, T. *Finska Kemistsamfundets Medd.* **64** (1955) 28.
2. Enkvist, T. *Svensk Kemisk Tidskr.* **72** (1960) 93.
3. Enkvist, T. *Teknillisen Kemian Aikakauslehti* **17** (1960) 127.
4. Enkvist, T., Holm, B., Turunen, J. and Turunen, K. *Finska Kemistsamfundets Medd.* **70** (1961) 5.
5. Enkvist, T. *Papper och Trä.* **43** (1961) 657.
6. Enkvist, T., Ashorn, Th. and Hästbacka, K. *IUPAC Journ. In press.*
7. Enkvist, T., Turunen, J. and Ashorn, Th. *Tappi.* **45** (1962) 128.
8. Girard, A. and Sandulesco, G. *Helv. Chim. Acta* **19** (1936) 1095.
9. Einhorn, A. *Ann.* **301** (1898) 95.

10. Döbner, A. *Ann.* **310** (1881) 261.
11. Phillips, M. and Keenan, G. L. *J. Am. Chem. Soc.* **53** (1931) 1924.
12. Neber, P. W., Burgard, A. and Thier, W. *Ann.* **527** (1936) 281.
13. Finnemore, H. *J. Chem. Soc.* **93** (1908) 1515.
14. Haydick, F. *Ber.* **36** (1903) 2930.
15. Popovici, B. *Ber.* **40** (1907) 3505.
16. Freudenberg, K. and Lehmann, B. *Ber.* **93** (1960) 1354.
17. Freudenberg, K. and Sakakibara, A. *Ann.* **623** (1959) 129.
18. Grassmann, W., Endres, H., Pauckner, W. and Mathes, H. *Ber.* **90** (1957) 1125.
19. Halmekoski, J. *Suomen Kemistilehti. In press.*
20. Halmekoski, J. *Ann. Acad. Scient. Fennicæ A II 1959* No. 96; *Suomen Kemistilehti B* **32** (1959) 170, *B* **33** (1960) 74, *B* **34** (1961) 85.

Received September 15, 1961.

ACTA CHEMICA SCANDINAVICA 16 (1962) 553–558

Complex Dibenzofurans

IV *. Syntheses of 2,6′,3′,2″-dioxido-*o*-terphenyl, 2,2′,4′,2″-dioxido-*m*-terphenyl and 2,6′,4′,2″-dioxido-*m*-terphenyl **

NILS E. STJERNSTRÖM

Organisk-kemiska Institutionen, Kungl. Tekniska Högskolan, Stockholm, Sweden

Dedicated to Professor *Holger Erdtman* on his 60th birthday

A phenolic trimeride is obtained when *p*-benzoquinone is treated with acid. Elimination of the phenolic hydroxyl groups by zinc dust distillation affords a neutral compound for which structure II has previously been advanced. This assumption has now been shown to be correct by an unambiguous synthesis of compound II. The syntheses of the *m*-terphenyl derivatives VI and VIIId are described. The five dioxidoterphenyls, II, III, V, VI and VIIId have now been prepared by reliable methods.

A certain interest has recently been shown in compounds of the dioxidoterphenyl type in connection with, *e.g.*, brazanquinone vat dyes [1] and the chemistry of thelephoric acid [2,3], the structure of which has finally been elucidated by Gripenberg [4].

Our interest in compounds of this type stems from previous work with the polymerisation of *p*-benzoquinones. Termolecular coupling products are readily formed when *p*-quinones are treated with strong sulphuric acid [5]. The dihydroxydioxidoterphenyl obtained from *p*-benzoquinone has recently been investigated in this laboratory and structure I was proposed for this compound [6]. Elimination of the phenolic hydroxyl groups by zinc dust distillation gave a neutral product for which structure II was consequently suggested [6].

Other structures were, however, theoretically possible and an unambiguous synthesis of compound II seemed desirable. In the search for a general synthetic route to dioxidoterphenyls Ebel's method [7] was successfully employed for

* Part III. *Acta Chem. Scand.* **15** (1961) 1761.

** Part of this investigation has been presented in a preliminary communication: *Chem. & Ind. London* **1960** 1599.

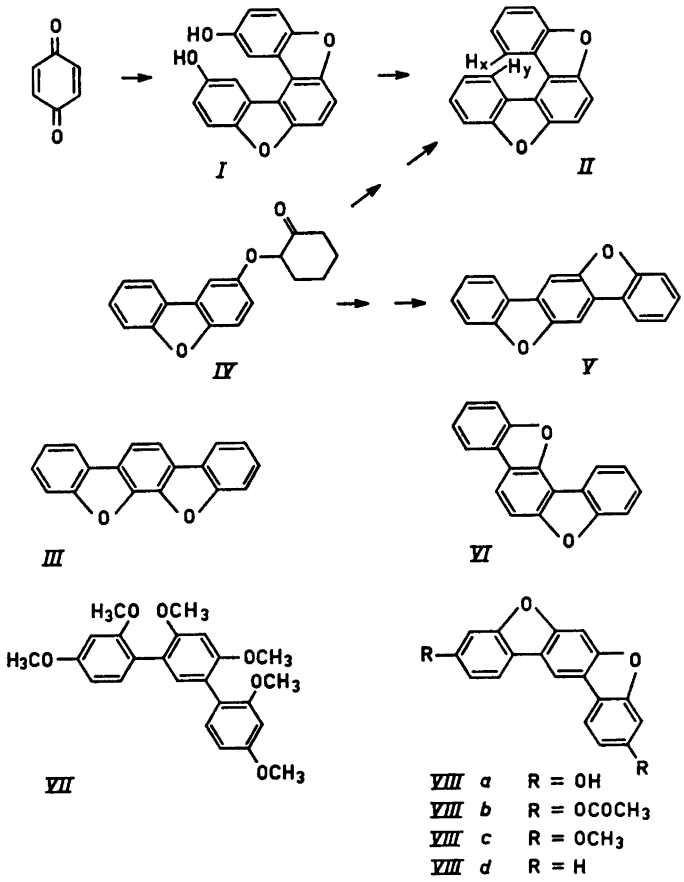

the preparation of 2,2′,3′,2″-dioxido-*p*-terphenyl (III)[8]. Compound II has now been prepared by this procedure.

The sodium salt of 2-hydroxydibenzofuran reacted with 2-bromo*cyclo*hexanone under anhydrous conditions to give 2-(2-keto*cyclo*hexyloxy)-dibenzofuran (IV). Cyclisation of this keto-ether was effected with polyphosphoric acid and a mixture of almost equal amounts of two compounds, A and B, was obtained. These were separated by chromatography on alumina. Compound A was dehydrogenated with palladium to 2,2′,5′,2″-dioxido-*p*-terphenyl (V), identical with an authentic specimen [6,9,10].

Compound A must therefore be 3,4,5,6-tetrahydro-2,2′,5′,2″-dioxido-*p*-terphenyl and B consequently 3,4,5,6-tetrahydro-2,6′,3′,2″-dioxido-*o*-terphenyl (condensation taking place at the 3- and 1-positions of the dibenzofuran moiety, respectively). When compound B was dehydrogenated with palladium it yielded 2,6′3′,2″-dioxido-*o*-terphenyl (II) identical with the above mentioned zinc dust distillation product from *p*-benzoquinone.

During the course of these synthetic experiments the PMR spectrum of the zinc dust distillation product in carbon tetrachloride was recorded at 40 Mc/s and was found to be in complete accordance with the proposed structure II. As only 60 mg of the substance was available at that time the signals were very weak and no fine structure could be observed. The spectrum contained two peaks with a relative intensity of 1:4. Both signals were found at lower fields than an internal *cyclo*hexane reference, the weaker at 268 c/s and the stronger at 240 c/s. As the total number of hydrogens in compound II is ten the PMR signals emanate from two and eight hydrogens, respectively. According to the ring current model [11] for the aromatic system one would expect the hydrogens x and y (II) to absorb at the lowest field. Taking steric interaction [12] into account it seems safe to assign the signal at 268 c/s to the hydrogens x and y (II) and the strong and fairly broad signal at 240 c/s to all the other hydrogens.

The positions of the hydroxyl groups in compound I have not been proved absolutely but considering the origin of the trimeride there can be little doubt about their situation.

Of the five theoretically possible dioxidoterphenyls only the two *m*-terphenyl derivatives VI and VIIId now remained unknown.

2,2′,4′,2″-Dioxido-*m*-terphenyl (VI) was prepared by Ebel's method. The starting material, 1-hydroxydibenzofuran, has previously been synthesised by a rather cumbersome procedure [13]. It was now prepared in the following way. 2-Iodoanisol and 2-iodoresorcinol dimethyl ether were subjected to a mixed Ullmann coupling in a ratio of 8:1 giving a mixture of 2,2′-dimethoxybiphenyl, 2,6,2′,6′-tetramethoxybiphenyl and 2,6,2′-trimethoxybiphenyl. This mixture on prolonged heating with conc. hydrobromic acid yielded 2,2′-dihydroxybiphenyl, 1,9-dihydroxydibenzofuran and 1-hydroxydibenzofuran. No attempt was made to isolate the two former compounds, they were removed from a solution of the reaction mixture in ether by extracting with sodium carbonate solution. The acidity of these two compounds is pronounced, probably due to intramolecular hydrogen bonding (*cf.* Refs.[14],[15]). 1-Hydroxydibenzofuran remained in the ether solution. The yield was about 40 % based on 2-iodoresorcinol dimethyl ether.

The sodium salt of 1-hydroxydibenzofuran reacted with 2-bromo*cyclo*hexanone to give 1-(2-keto*cyclo*hexyloxy)-dibenzofuran which was cyclised with polyphosphoric acid in the usual manner to 3,4,5,6-tetrahydro-2,2′,4′,2″-dioxido-*m*-terphenyl. This compound gave 2,2′,4′,2″-dioxido-*m*-terphenyl (VI) on dehydrogenation with palladium.

A method for preparing dioxido-*p*-terphenyl derivatives, based on dehydration of polyhydroxy-*p*-terphenyls with hydrobromic acid, has recently been developed in this laboratory [10]. This procedure was now successfully employed in the synthesis of 2,6′4′,2″-dioxido-*m*-terphenyl. The starting material, 2,4,4′,6′,2,″4″-hexamethoxy-*m*-terphenyl (VII) was obtained in good yield by a mixed Ullmann coupling of 4,6-diiodoresorcinol dimethyl ether and 4-iodoresorcinol dimethyl ether. It was easily converted to 4,4″-dihydroxy-2,6′,4′,2″-dioxido-*m*-terphenyl (VIIIa) by treatment with hydrobromic acid. The phenol VIIIa then furnished 2,6′,4′,2″-dioxido-*m*-terphenyl (VIIId) when subjected to distillation with zinc dust.

EXPERIMENTAL

All melting points are uncorrected.

2-(2-Ketocyclohexyloxy)-dibenzofuran (IV). Sodium (0.6 g) was dissolved in absolute methanol (20 ml) and 2-hydroxydibenzofuran (4.6 g) in absolute methanol (20 ml) was added, care being taken to exclude moisture and air. The methanol was removed under reduced pressure and 2-bromocyclohexanone [16] (4.5 g) in dry benzene (100 ml) was added with mechanical stirring. The mixture was stirred at room temperature for 0.5 h and at reflux temperature for a further 2 h; it was then extracted first with dilute sodium hydroxide and then with water. The benzene solution was dried over magnesium sulphate and the solvent evaporated under reduced pressure. The remaining slightly yellow oil (6.3 g) was dissolved in a small volume of methanol and crystallised on cooling to −30°. The precipitate (2.5 g) was collected and purified by recrystallisation from methanol and sublimation *in vacuo*, m.p. 107−108.5°. (Found: C 77.0; H 5.7. Calc. for $C_{18}H_{16}O_3$: C 77.1; H 5.8.)

Cyclisation of compound IV. 2-(2-Ketocyclohexyloxy)-dibenzofuran (IV, 1.0 g) was stirred with a mixture of phosphorus pentoxide (15 g) and phosphoric acid (*d* 1.7, 30 ml) for 3 h at 100°. The hot reaction mixture was poured into water. The precipitate (0.9 g, m.p. 95−117°) was collected, washed and dried. A sample (600 mg) was chromatographed on neutral alumina (150 g, column constructed in light petroleum). Two main fractions were obtained: the light petroleum eluate on evaporation gave compound B (265 mg) and the ether eluate gave compound A (271 mg).

Compound A. This substance was purified by recrystallisation from ethanol and sublimation *in vacuo*, m.p. 168−170°. (Found: C 81.9: H 5.6. Calc. for $C_{18}H_{14}O_2$: C 82.4; H 5.4.)

2,2',5',2''-Dioxido-p-terphenyl (V) from compound A. Compound A (50 mg) was thoroughly mixed with a palladium-charcoal catalyst (10 % Pd, 50 mg) and heated at 230° for 5 h in an atmosphere of nitrogen. The product (27 mg) sublimed on the cool walls of the reaction vessel and was purified by recrystallisation from acetic acid, m.p. 273−273.5°. A mixed melting point with a sample of 2.2',5',2''-dioxido-*p*-terphenyl [6,9,10] (m.p. 270.5−271.5°) showed no depression (m.p. 270.5−273°) and the infrared spectra of the two samples were identical. Compound A must therefore be 3,4,5,6-tetrahydro-2,2',5',2''-dioxido-*p*-terphenyl and compound B consequently 3,4,5,6-tetrahydro-2,6',3',2''-dioxido-*o*-terphenyl.

Compound B. 3,4,5,6-tetrahydro-2,6',3',2''-dioxido-o-terphenyl. This substance was purified by recrystallisation from ethanol and sublimation *in vacuo*, m.p. 125.5−126.5°. (Found: C 81.9; H 5.3. Calc. for $C_{18}H_{14}O_2$: C 82.4; H 5.4.)

2,6',3',2''-Dioxido-o-terphenyl (II). Compound B (25 mg) was thoroughly mixed with a palladium-charcoal catalyst (10 % Pd, 25 mg) and heated at 230° for 5 h in an atmosphere of nitrogen. The crude product (*ca.* 25 mg, m.p. 122−141°) sublimed on the cool walls of the reaction vessel and was purified by recrystallisation from acetic acid, m.p. 140−142.5°. A mixed melting point with a sample of the zinc dust distillation product, originating from *p*-benzoquinone [6], (m.p. 140−142.5°) showed no depression (m.p. 140−142.5°) and the infrared spectra of the two samples were identical.

1-Hydroxydibenzofuran. The 2-Iodoresorcinol dimethyl ether, used in this preparation, has been described by Adams *et al.*[17] It is, however, more easily synthesised *via* the lithium compound of resorcinol dimethyl ether (*cf.* the preparation of 3,5-dimethoxy-4-iodotoluene [18]). 2-Iodoresorcinol dimethyl ether (4.8 g), copper bronze (60 g) and 2-iodoanisol (35.5 g) were thoroughly mixed and heated to 220−240°, when a vigorous reaction started which raised the temperature to about 300°. After some minutes the reaction mixture was allowed to cool and the organic products were extracted with chloroform. After evaporation of the solvent a brown crystalline material remained. This was refluxed with hydrobromic acid (48 %, 250 ml) in an atmosphere of nitrogen for 40 h. The reaction mixture was allowed to cool and diluted with water. Ether was added and the ethereal extract washed with water, saturated sodium chloride solution, sodium carbonate solution (2 M) and finally dried over magnesium sulphate. After evaporation of the solvent the reaction product, a brown-red, somewhat oily crystalline material, was recrystallised from water (charcoal). The yield of 1-hydroxydibenzofuran was 1.4 g, m.p. 140−142° (lit.[13] m.p. 140−140.5°).

1-(2-Ketocyclohexyloxy)-dibenzofuran. The sodium salt of 1-hydroxydibenzofuran (prepared as described for 2-hydroxydibenzofuran from 100 mg sodium and 800 mg 1-hydroxydibenzofuran) and 2-bromocyclohexanone[16] (770 mg) in dry benzene (*ca.* 25 ml were stirred at room temperature for 0.5 h and at reflux temperature for an additional 2 h. The reaction mixture was worked up as described above for the preparation of 2-(2-ketocyclohexyloxy)-dibenzofuran (IV). The keto-ether (950 mg) was purified by recrystallisation from methanol, m.p. 138–139°. (Found: C 76.8; H 5.8. Calc. for $C_{18}H_{16}O_3$: C 77.1; H 5.8.)

3,4,5,6-Tetrahydro-2,2',4',2''-dioxido-m-*terphenyl.* 1-(2-Ketocyclohexyloxy)-dibenzofuran (200 mg) was treated with a mixture of phosphorus pentoxide (15 g) and phosphoric acid (*d* 1.7, 30 ml) in the same manner as described above for the cyclisation of compound IV. The conversion was almost quantitative and the product was purified by distillation *in vacuo* and recrystallisation from methanol, m.p. 107–108° (not sharp) (Found: C 82.3; H 5.4. Calc. for $C_{18}H_{14}O_2$: C 82.4: H 5.4.)

2,2',4',2''-Dioxido-m-*terphenyl (VI).* The above compound (90 mg) was thoroughly mixed with a palladium-charcoal catalyst (10 % Pd, 90 mg) and heated at 240° for 5 h in an atmosphere of nitrogen. Compound VI (*ca.* 50 mg) was isolated by extraction with ether. It was purified by recrystallisation from acetic acid and sublimation *in vacuo*, m.p. 169–170°. (Found: C 83.9; H 4.0. Calc. for $C_{18}H_{10}O_2$: C 83.7; H 3.9.)

2,4,4',6',2'',4''-Hexamethoxy-m-*terphenyl (VII).* 4,6-Diiodoresorcinol dimethyl ether (3.9 g, easily obtained from resorcinol dimethyl ether and an equivalent amount of iodine monochloride in acetic acid), copper bronze (35 g) and 4-iodoresorcinol dimethyl ether[10] were thoroughly mixed and heated to 240° when a vigorous reaction started. After some minutes the reaction mixture was allowed to cool to room temperature and extracted with chloroform in a Soxhlet apparatus. The solvent was evaporated and the residue distilled *in vacuo*. The combined products from three runs yielded resorcinol dimethyl ether (2 g), 2,4,2',4'-tetramethoxybiphenyl (22 g) and 2,4,4',6',2'',4''-hexamethoxy-*m*-terphenyl (VII) (7 g, b.p. *ca.* 300°, 1 mm). The terphenyl VII was purified by redistillation but could not be obtained crystalline. No attempt was therefore made to prepare an analytical sample and the product was demethylated directly.

4,4''-Dihydroxy-2,6',4',2''-dioxido-m-*terphenyl (VIIIa) and the corresponding diacetate (VIIIb) and dimethyl ether (VIIIc).* The terphenyl VII (3 g) was refluxed with hydrobromic acid (48 %, 60 ml) for 60 h in an atmosphere of nitrogen. The reaction mixture was allowed to cool to room temperature and the phenol (1.5 g, m.p. *ca.* 320°, decomp.), which was slightly bluish due to superficial oxidation, was collected and washed with water. This crude phenol was converted to the corresponding diacetate, 4,4''-diacetoxy-2,6',4',2''-dioxido-*m*-terphenyl, by acetylation with acetic anhydride and pyridine. The conversion was almost quantitative and the diacetate was purified by recrystallisation from chlorobenzene and sublimation *in vacuo*, m.p. 272–273°. (Found: C 70.2; H 3.9. Calc. for $C_{22}H_{14}O_6$: C 70.6; H 3.8.) The phenol was also methylated with dimethyl sulphate and sodium hydroxide to give a good yield of 4,4''-dimethoxy-2,6',4',2''-dioxido-*m*-terphenyl, which was purified by recrystallisation from chlorobenzene and sublimation *in vacuo*, m.p. 232.5–234°. (Found: C 75.3; H 4.3. Calc. for $C_{20}H_{14}O_4$: C 75.5; H 4.4.)

2,6',4',2''-Dioxido-m-*terphenyl (VIIId).* The preceding crude phenol (320 mg) was thoroughly mixed with zinc dust (10 g) in a test tube with an arrangement for the passage of gas. A brisk nitrogen stream was applied and the phenol-zinc dust mixture was heated to red heat. After only a few minutes the crude product (60 mg) could be collected from the cool walls of the test tube. This product was thoroughly washed first with dilute potassium hydroxide and then with water. The dry product was fractionally sublimed *in vacuo*. A fraction (20 mg), m.p. 219–227°, was collected and recrystallised from acetic acid. The analytical sample was purified by sublimation *in vacuo*, m.p. 229–231°. (Found: C 84.0; H 3.8. Calc. for $C_{18}H_{10}O_2$: C 83.7; H 3.9.)

Acknowledgement. The author is grateful to Dr. Sture Forsén for recording and interpreting the PMR spectrum of 2,6',3',2''-dioxido-*o*-terphenyl, to Professor H. Erdtman for his kind interest and Dr. Ian Wellings for reading the manuscript.

REFERENCES

1. Acharya, R. V., Tilak, B. D. and Venkiteswaran, M. R. *J. Sci. Ind. Research (India)*, **16B** (1957) 400.
2. Read, G. and Vining, L. C. *Can. J. Chem.* **37** (1959) 1442.
3. Aghoramurthy, K., Sarma, K. G. and Seshadri, T. R. *Tetrahedron Letters* **1960** No. 16, p. 4.
4. Gripenberg, J. *Tetrahedron* **10** (1960) 135.
5. Erdtman, H. *Proc. Roy. Soc. London* **A143** (1933) 228.
6. Erdtman, H. and Stjernström, N. E. *Acta Chem. Scand.* **13** (1959) 653.
7. Ebel, F. *Helv. Chim. Acta* **12** (1929) 3.
8. Stjernström, N. E. *Acta Chem. Scand.* **14** (1960) 2191.
9. Schimmelschmidt, K. *Ann.* **566** (1950) 184.
10. Stjernström, N. E. *Acta Chem. Scand.* **14** (1960) 1274.
11. Pople, J. A., Schneider, W. G. and Bernstein, H. J. *High Resolution Nuclear Magnetic Resonance*. Mc Graw Hill, New York 1959. Especially p. 253.
12. Reid, C. *J. Molecular Spectroscopy* **1** (1957) 18.
13. Gilman, H. and Van Ess, P. R. *J. Am. Chem. Soc.* **61** (1939) 1365.
14. Wachtmeister, C. A. *Svensk Kem. Tidskr.* **70** (1958) 117. (Diss.)
15. Musso, H. and Matthies, H-G. *Ber.* **94** (1961) 356.
16. Allinger, J. and Allinger, N. L. *Tetrahedron* **2** (1958) 64.
17. Van Arendonk, A. M., Cupery, M. E. and Adams, R. *J. Am. Chem. Soc.* **55** (1933) 4226.
18. Åkermark, B., Erdtman, H. and Wachtmeister, C. A. *Acta Chem. Scand.* **13** (1959) 1855.

Received March 30, 1961.

ACTA CHEMICA SCANDINAVICA 16 (1962) 559–569

Bisbenzyltetrahydroisoquinoline Alkaloids

III. Counter Current Separation and Crystallization of Methyl Ethers of *l*-Curine

ESKIL HULTIN*

Department of Pharmacology, University of California Medical Center, Los Angeles 24, California, U.S.A.

Dedicated to Professor *Holger Erdtman* on his 60th birthday

Partly methylated *l*-curine ("bebeerine", chondrodendrine) can easily be separated into one unmethylated and one methylated fraction with a counter current procedure using four separatory funnels and three volumes of ether and one volume of buffer pH 12.3. Moreover, the dimethyl ether of *l*-curine can also be easily separated from the fraction of monomethyl ethers at pH about 13.6, using four volumes of buffer and one volume of ether. The *l*-curine dimethyl ether, which has resisted all previous efforts to crystallize it, crystallized from diethyl ether, m.p. 172°C. One of the monomethyl ethers crystallized from benzene, m.p. 142°C, and could also be crystallized from diethyl ether in two forms, m.p. 132°C and 137°C, but did not crystallize from methanol. The other *l*-curine monomethyl ether crystallized from methanol, m.p. 148°C, but did not crystallize from benzene. The *l*-curine monomethyl ether m.p. 206–208°C previously obtained in small yield by Späth and Kuffner was not found, but a monomethyl ether fraction remained after the separation of the monomethyl ethers which had crystallized. The possibility of the natural occurrence of an isomer of *l*-curine is suggested.

The isolation of the alkaloid now called curine was first reported by Wiggers [1]. From roots of a plant referred to as *Cissampelos pareira* he obtained an alkaloid which he called cissampelosine. Later he [2] isolated this substance from *radix pareirae bravae* which at that time was believed to originate from *Cissampelos pareira* L. He shortened the name of the substance to pelosine. A few years later Bödeker [3] also investigated this substance as well as another alkaloid, bebeerine, which had recently been isolated from the bebeeru tree, *Nectandra rodioei* Hook., now called *Ocotea rodiei* (Hook.) Mez. Bödeker concluded that pelosine and bebeerine were different substances.

* Present address: Institutionen för organisk kemi, Tekniska högskolan, Stockholm 70, Sweden.

Some time later Hanbury [4,5,57] came to the conclusion that *radix pareirae bravae* did not originate from *Cissampelos pareira* L. but from *Botryopsis platyphylla* (this name, however, was never formally proposed for the plant [6]), which is now called *Chondrodendron platyphyllum* (A. St. Hil.) Miers. Since Flückiger [7, 8], had been informed early about Hanbury's opinion, he made up and investigated an alkaloid preparation from *Chondrodendron platyphyllum* and also from a safely identified specimen of *Cissampelos pareira*, which he had obtained from Hanbury, and found pelosine in both plants. His results so far have been confirmed: pelosine, now called curine, was identified in *Cissampelos pareira* L. a few years ago [9]. Flückiger did not find any difference between pelosine and the bebeerine from *Nectandra rodioei* Hook., and he agreed with and earlier assumption that bebeerine also was identical with the so called buxine from *Buxus sempervirens* L. Later, it has been denied [10, 11] and disproved [12–15] that pelosine, bebeerine, and buxine are identical. However, the mistake was introduced into Hager's [16] handbook *, where the preferred name is bebeerine; this substance had been sold in England for a long time as a remedy [17]. This seems to have influenced the commercial naming of certain alkaloid preparations of various botanical origins and thus differing chemical compositions; *cf.* Refs. [18–22]. The mistake about the identity also apperas in *Die Pflanzenstoffe* by Husemann *et al.* [23], but there the oldest of the names for these alkaloids, buxine, is preferred, as suggested by Flückiger [7].

Scholtz [24,25] investigated a commercial, crude alkaloid preparation called *bebeerinum purum*, said to originate from *Nectandra rodioei*. He isolated an alkaloid — now called *l*-curine — which he found crystallized so remarkably easily from methanol that he even suggested [20] it be used as a reagent for methanol. However, Dutcher [26] and Anet *et al.* [27] had difficulties in crystallizing this alkaloid from methanol. Scholtz [28] obtained the same alkaloid from *radix pareirae bravae* and, finding support in Bödeker's investigation [3] (which he quoted misleadingly as if Bödeker had discovered the indentity of pelosine and bebeerine instead of finding a difference) and in Flückiger's investigation [7, 8], he considered the identity of bebeerine and pelosine proved. Subsequently Scholtz used the name bebeerine and not pelosine for the alkaloid from *radix pareirae bravae*. It now seems justifiable to doubt that the *bebeerinum purum* he investigated really originated from *Nectandra rodioei* (*cf.* Ref. [17]), particularly since he mentioned not *Nectandra rodioei* but *radix pareirae bravae* as its source in later papers [20,22,29,30], and in quoting from his original investigation [25] of *bebeerinum purum;* in some papers [20, 30] he even stated that *Chondrodendron tomentosum* Ruíz & Pavon was the source of the root. This statement about which of the *Chondrodendron* species is the source of the root is supposed to be the consequence of a misunderstanding [31,58]. A survey of the species of *Chondrodendron* and their geographical distribution has been given by Krukoff and Moldenke [6] and by de Mello Filho [32].

* "Bebeerinum, Bebeerin, Bebirin, Pelosin, Beberia (der Engländer), Buxin ($C^{38}H^{21}NO^6$ oder $C_{19}H_{21}NO_3$ = 311) ein Alkaloid, welches in der Rinde von *Buxus sempervirens* Linn., in der als Färbematerial benutzten Bibirinrinde, Bebeerurinde, Rinde von *Nectandra Rodiaei* Schomburgk, einem in Guyana heimischen Baume aus der Familie der Laurineen, in der Pareirawurzel aufgefunden und als ein Ersatz des Chinins empfohlen wurde". For the peculiar first chemical formula here old atomic weights were used.

Shortly before Scholtz' first papers appeared about the alkaloid he called *d*-bebeerine, Böhm[33–35] published his first results from an investigation of a South American arrow poison, called tubo curare because it was available in tubes of bamboo. Its botanical origin was unknown. Böhm found a substance to which he gave the name *l*-curine. He crystallized it from benzene (m.p. 161°C) and from methanol (m.p. 212°C). Although Böhm [35] and Scholtz [25] submitted each a paper to the same journal within an interval of only slightly more than 8 months, it was 30 years later before it was found — by Späth, Leithe and Ladek [36] — that Böhm's curine and Scholtz' "bebeerine" were *l*- and *d*-forms, respectively, of the same substance.

Scholtz obtained the *l*-form of curine in the beginning of his investigations, but later [29,37] he obtained the *d*-form. It appears from King's [31] work that this has to do with the origin of radix pareirae bravae: *Chondrodendron platyphyllum* (A. St. Hil.) Miers earlier, and *C. microphyllum* (Eichl.) Moldenke later. A third species, *C. tomentosum* Ruíz & Pavon is used by Indians of the upper Amazon for preparing curare [26,58]

In 1933 Späth and Kuffner [38] tried to prepare the two monomethyl ethers of *l*-curine as part of a proof that its composition is $C_{36}H_{38}O_6N_2$ instead of $C_{18}H_{19}O_3N$ as previously assumed [18, 36]. Their efforts were only partly successful. The following procedure was used. Curine was partly methylated with diazomethane. The reaction product was dissolved in a mixture of ether and water containing potassium hydroxide; curine and its monomethyl ethers were extracted from the ether phase with a strong water solution of potassium hydroxide, whereas the dimethyl ether of *l*-curine remained in the ether phase. The separation of *l*-curine and its two monomethyl ethers was not described in detail, but it was mentioned that a tedious series of fractionated crystallizations from methanol and from diethyl ether was used, and that a procedure starting with a series of fractionated extractions was also used. Two different fractions of monophenol bases were finally obtained. One of them, in poor yield, was crystalline; m.p. 206—208°C. This substance was not found in the present investigation. The other was also crystalline, m.p. 154—160°C, but it was considered to still be a mixture of the *l*-curine monomethyl ethers, possibly containing *l*-curine.

The purpose of the present investigation was to elucidate the conditions for preparing the two *l*-curine monomethyl ethers from partly methylated *l*-curine. A similar work, in which the conditions for preparing the two *d*-chondrocurine monomethyl ethers were studied, has recently been reported by the present author [39]. In each of these investigations the problem was divided into two main parts. The first part concerns separating the partly methylated alkaloid into three fractions according to the degree of methylation. The second part of the problem concerns separating the group of monomethyl ethers into its components.

THE USE OF ETHER AND BUFFER FOR THE SEPARATION OF PARTLY METHYLATED *l*-CURINE INTO GROUPS OF ISOMERS

Diethyl ether and buffered water give immiscible solvent systems suitable for the separation of partly O-methylated *l*-curine into three fractions: *l*-curine, the group of monomethyl ethers of *l*-curine, and the dimethyl ether of *l*-curine.

In these experiments, the buffer was made up of potassium phosphate, potassium sulfite (to inhibit as much as possible the formation of coloured substances) and potassium hydroxide. Sodium salts were avoided because a glass electrode was used in the measurements of pH. The partition coefficients for *l*-curine and its monomethyl ethers were measured at various pH values in those ranges which are of main interest in the separation procedure. The technique used was described in a previous paper [40] in this series. The results are given in Fig. 1, where the logarithms of the partition coefficients are plotted *versus* pH. For strongly alkaline buffer solutions the points for *l*-curine are close to a straight line with the inclination −2, and the points for the monomethyl ethers of *l*-curine are close to straight lines with the inclination −1, as can be expected from the presence of 2 and 1 phenolic hydroxyl groups, respectively, in these substances. The straight lines just mentioned are, of course, asymptotes.

It may be added here that the early problem [18, 36, 38] about the molecular weight of curine, *i. e.*, whether $C_{18}H_{21}O_3N$ or $C_{36}H_{41}O_6N_2$ is the correct formula, could easily have been solved if the number of nitrogen atoms or phenolic hydroxyl groups which can participate in acid-base reactions had been computed from measurements of the partition coefficients between ether and a series of acid or alkaline buffers.

It was shown by Baker [41] that a counter current separation of two substances is most efficacious when the ratio of the volumes of the two immiscible solvents equals the inverse value of the geometric mean between the partition coefficients of the two substances. In Fig. 1, where logarithms of partition coefficients for *l*-curine and its monomethyl ethers are given as curves, a line drawn midway between two such curves represents the negative value of the logarithm for the best ratio between the volumes of the two solvent phases. Thus, for a separation of *l*-curine and that monomethyl ether of *l*-curine, whose partition coefficient is nearer to that of *l*-curine, we can read from Fig. 1 that the pH value at which equal volumes of buffer and ether give the best separa-

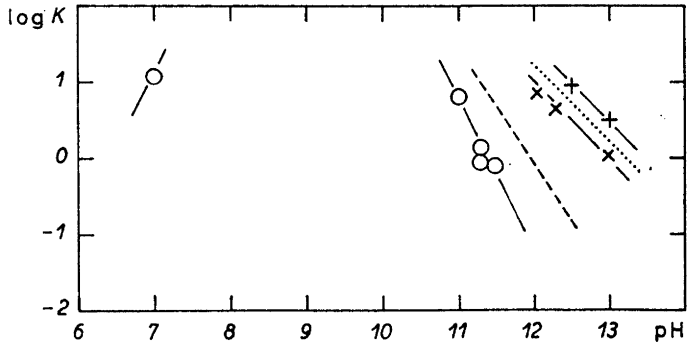

Fig. 1. The influence of pH on the partition coefficient K for *l*-curine (O) and its monomethyl ethers (× and +) between diethyl ether and buffer. The dashed line gives the optimum relationship between volume ratio and pH for separation of *l*-curine from the one of its monomethyl ethers, whose partition coefficient is closest to that of *l*-curine, and the dotted line gives the optimum relationship between volume ratio and pH for separation of the two monomethyl ethers of *l*-curine.

tion (abscissa value zero) is about 11.95, and that, *e. g.*, at pH 12.3 the ordinate value is −0.5 and hence the logarithm for the optimum quotient obtained by dividing the volume of the less polar (ether) phase by the volume of the more polar (buffer) phase is + 0.5, *i. e.*, 3 volumes of ether for 1 volume of buffer. We can also see from Fig. 1 that if we start the separation at pH about 12.3 with 3 volumes of ether and 1 volume of buffer, the difference in abscissa value for the line from which we read the best separation conditions and the line giving the value of the logarithm of the partition coefficient for *l*-curine is about 1.2 in the logarithmic scale. Hence, at pH 12.3 *l*-curine distributes itself in such a way that there will be about 16 times as much *l*-curine in the water phase as in the ether phase. Similarly, one of the monomethyl ethers distributes itself in such a way that there will be about 16 times as much of this substance present in the ether phase as in the water phase. A still larger fraction of the other monomethyl ether and of the dimethyl ether of *l*-curine will be present in the ether phase. The distribution coefficient of *l*-curine dimethyl ether was not measured, but it seems possible to assume safely from Fig. 1 that it is not below 1.5.

Distribution between the two solvent phases in one funnel thus gives a fair separation. The result can easily be greatly improved by adding a few, say two or three more separatory funnels for a counter current separation as previously described [40, 42].

Suitable conditions for an efficacious separation of *l*-curine dimethyl ether from the monomethyl ethers can also be read from Fig. 1. As previously mentioned, the value of the partition coefficient for the dimethyl ether of *l*-curine is probably not less than 1.5; it is more likely larger than 2. Results from several separations have not been contradictory to this. The buffer solution should have as high a pH value as conveniently possible, because the partition coefficient for that *l*-curine monomethyl ether which has the higher partition coefficient decreases with increased pH and is as large as 1 at pH 13.5. It is not too inconvenient to use a solution with pH about 13.6. If the volume of the buffer phase is 4 times as large as that of the ether phase, the monomethyl ether with higher partition ratio distributes itself in such a way that 5 times as much will be present in the water phase as in the ether phase. The other monomethyl ether distributes itself in such a way that about 15 times as much will be present in the water phase as in the ether phase, and the *l*-curine dimethyl ether can reasonably be expected to distribute itself in such a way that at least 10 times more will be present in the ether phase than in the water phase. This implies that in a so called "diamond separation" or "completion of squares" separation [42] with four separatory funnels the recovery of the *l*-curine dimethyl ether in the ether phase can theoretically be expected to be better than 99.8 %. In the water phase the recovery of the monomethyl ether with lower partition ratio can be expected to be still better, whereas the recovery of the monomethyl ether with higher partition ratio can be expected to be about 98 %.

The various fractions are conveniently recovered as described in a previous paper [39]: the pH value of buffer solutions is adjusted to about 8.5, and the precipitate thereby formed ectracted with ether, whereby impurities remain undissolved. Ether solutions are extracted with dilute hydrochloric acid. The substance is precipitated from this water solution by adjusting the pH to

about 8.5, the precipitate is filtered off, washed with distilled water, the pH of which is adjusted to about 8.5, and dried *in vacuo*. It is possible to purify the preparation so obtained still more by extracting it with diethyl ether in a Soxhlet apparatus and evaporating the ether [2, 25].

THE USE OF ETHER AND BUFFER FOR COUNTER CURRENT SEPARATION OF *l*-CURINE MONOMETHYL ETHERS

In Fig. 1 two lines are drawn which show how the partition coefficients of the two *l*-curine monomethyl ethers between diethyl ether and buffer are influenced by pH. Halfway between these lines a dotted line is drawn which indicates how the optimum ratio between the two phases during a separation depends on pH. As previously discussed [39] in the similar problem of separating the two *d*-chondrocurine monomethyl ethers, a fair counter current separation is obviously possible even with a small number of transfers, but a difficulty is that the pH value of the buffer phase must be kept very close to its optimum value. Experiments on the separation of the monomethyl ethers of *l*-curine by a counter current method were discontinued when a convenient way to separate these substances by crystallization was found.

THE USE OF A FLEXIBLE FOUR COMPONENT SYSTEM

The partition coefficients for *l*-curine and its methyl ethers were also determined for various compositions of the four component solvent system previously [39] used in the chondrocurine series.

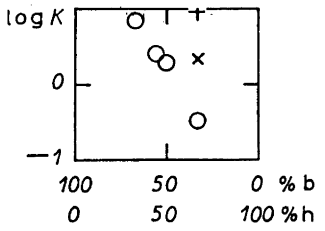

Fig. 2. The influence of the ratio of the volumes of benzene and heptane on the partition coefficient K for *l*-curine (O), and its monomethyl ethers (× and +) between two solvent phases consisting of benzene and heptane in equilibrium with a mixture of equal volumes of methanol and water containing buffering salts (pH about 8).

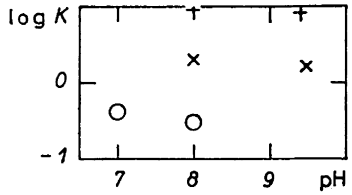

Fig. 3. The influence of pH on the partition coefficient K for *l*-curine (O) and its monomethyl ethers (× and +) between two solvent phases consisting of a mixture of benzene (1/3) and heptane (2/3) in equilibrium with a mixture of equal volumes of methanol and water containing buffer salts (volume ratios 2:4:3).

This solvent system consists of benzene, heptane, methanol, and water, and has proved valuable especially for checking the identity and purity of the alkaloids and the alkaloid derivatives considered here. As part of the procedure for working out separation methods, partition coefficients for *l*-curine and its monomethyl ethers were determined for various compositions of the four component system. The results are given in Figs. 2 and 3. Some preparations used for these measurements were not crystallized. The experiments and the computations were done as described in a previous paper [40].

It can be seen from Fig. 3 that the influence of pH on the value of the partition coefficient for the two *l*-curine monomethyl ethers is rather small in the four component solvent system as compared to the influence of pH in the case of ether and buffer, whereas the quotient between the partition coefficients has about the same order of magnitude for both solvent systems. For distinguishing between the two *l*-curine monomethyl ethers by determining the partition coefficients it is therefore more convenient to use the four component solvent system than ether and buffer.

Thus, a solvent system consisting of 2 volumes of benzene, 4 volumes of heptane, 3 volumes of buffer pH 8.0 containing sodium carbonate and potassium metabisulfite, and 3 volumes of methanol was usually used for this purpose. The monomethyl ether of *l*-curine which crystallized from benzene or ether had a partition ratio about 9, and the monomethyl ether which crystallized from methanol had a partition ratio slightly less than 3. The partition ratio was calculated as the concentration in the less polar phase (mainly benzene and heptane) divided by the concentration in the more polar phase (mainly methanol and water).

However, upon comparison of *l*-curine and the monomethyl ether of *l*-curine with the partition coefficient most close to that of *l*-curine, it is evident from Figs. 1—3 that in the pH range in which a separation can be carried out conveniently the difference between the logarithms of the partition coefficients is roughly about 10 times larger for ether and buffer than for the four component solvent system. Furthermore, the solubility of *l*-curine and its monomethyl ethers is greater in ether and buffer than in the four component solvent system. Hence, the solvent system ether and buffer is better than the four component solvent system for separating *l*-curine from its monomethyl ethers.

CRYSTALLIZATION OF THE METHYL ETHERS OF *l*-CURINE

The crystallization of bisbenzyltetrahydro*iso*quinoline alkaloids is greatly influenced by impurities, and purification in the form of ether extraction [2, 24, 36] is highly advisable. Chloroform, however, has the disadvantage of easily dissolving many of the impurities usually appearing along with these alkaloids.

The *l*-curine dimethyl ether has previously been prepared by several scientists [11, 34, 36, 38, 43, 44] but they all failed to obtain it in crystalline form. Similarly, *l*-curine diethyl ether seems to have been obtained only as an amorphous substance [30, 45]. However, during the counter current separation of a large sample of partly methylated *l*-curine, according to a slightly modified [39, 46] procedure of O'Keeffe *et al.* [47], *l*-curine dimethyl ether started to crystallize after

a few days from the ether phase in the separatory funnel, from which this substance was then recovered.

As described previously in this paper, a preparation consisting of a mixture of the two *l*-curine monomethyl ethers, but almost completely free from *l*-curine and from the dimethyl ether of *l*-curine, can easily be obtained from partly methylated *l*-curine by two counter current separations, using ether and buffer. One of the components of this monomethyl ether preparation crystallized easily from methanol, but never crystallized from benzene, and it was, as already mentioned, identified as the component with the lower partition coeffici ent. The other component crystallized from benzene and from diethyl ether but never crystallized from methanol, and it was identified as the component with the higher partition coefficient. It was actually first crystallized in benzene from a preparation obtained by counter current fractionation (with the four component solvent system) of the *l*-curine monomethyl ethers. Crystals usually appeared over night if the mixture was dissolved in either methanol or benzene. During one counter current separation crystals appeared in the ether phase containing *l*-curine monomethyl ethers. Once crystals were obtained, they were used for seeding in subsequent preparations.

On one occasion 90 g of partly methylated *l*-curine was worked up as described. Thereby all available *l*-curine preparations of varying origin and purity were taken. In this case, there appeared as a result of the separation of the monomethyl ether fraction 13 g of the component which crystallized from benzene, and which has the partition ratio 9 in the normally used four component solvent system, and 10 g of the component which crystallizes from methanol and has the partition ratio 3. In addition to this, after the procedure of crystallizing from benzene and from methanol had been run through twice, 0.5 g was obtained of a substance which crystallized from benzene and had the partition ratio 3, and 8 g were recovered of an amorphous residue with the partition ratio 3.

In this case the appearance of three different main components in the monomethyl ether fraction, surprising as it is at first, is, however, what may be expected if an isomer of *l*-curine occasionally occurs in commercial curare material. A similar situation has been described by Dutcher [48, 49] in the case of tubocurarine and chondrocurarine, *i. e.*, two isomers which, in the normal procedure for preparing tubocurarine, appeared together in the crystallized preparation of tubocurarine. Whereas the distribution of phenolic hydroxyl- and methoxyl groups is the same in tubocurarine and in *l*-curine, no isomer of *l*-curine corresponding to chondrocurarine has yet been reported.

The *l*-curine monomethyl ether with m.p. 206—208°C which Späth and Kuffner [38] obtained only in small amounts, was not found in the present investigation, as already mentioned. It cannot be excluded, however, that this substance occurs in the amorphous rest, m.p. 148°C, which once was obtained after two main components of the *l*-curine monomethyl ether fraction had been separated by crystallization. It may be mentioned here that Späth and Kuffner used a preparation of *l*-curine with the m.p. 221—221.5°C, whereas all others have found the m.p. to be about 213°C. Although Späth and Kuffner started with 6 g of curine, they obtained so little of the monomethyl ether with m.p. 206—208°C that only about 3 mg were taken for methoxyl analysis

instead of the usual about 100 mg. This may illustrate the difficulties they encountered in the separation.

Späth and Kuffner's other crystallized *l*-curine monomethyl ether, which crystallized from ether and from methanol, m.p. 154—160°C, and which they considered to still be a mixture, may have mainly consisted of the same *l*-curine monomethyl ether as that obtained in this investigation as a substance crystallizaing from methanol, m.p. 148°C, but which was not in this investigation obtained in crystalline form from ether. This may possibly be a case of polymorphism. The differences in m.p. for these compounds are about the same as the differences in m.p. found for curine by Späth *et al.* (221—221.5°C), and by others (212—214°C), respectively.

EXPERIMENTAL

Curine. The *l*-curine used in these experiments was prepared from several lots of curare raw material, originating from Peru, by a method similar to those published in earlier investigations. The melting point of preparations recrystallized from methanol, 213—214°C, agreed well with the values obtained by Böhm [34, 35] (212°C), by Scholtz [20, 24, 25, 28, 29] (214°C), by King [31, 50, 51, 52] (215, 213, and 212°C), by Wieland *et al.* [53] (212°C), by Brazil *et al.* [54] (213—214°C), by Anet *et al.* [27] (213—214°C), and by Bhattachari *et al.* [9] (214°C) but did not agree as well with the value obtained by Späth *et al.* [36, 38] (221—221.5°C). Kupchan *et al.* [55] recently for a preparation got m.p. 217—219°C.

pH *measurements.* The pH values refer to the standard buffer pH = 6.885 [56] and are uncorrected. Sodium salts were avoided in strongly alkaline solutions.

Crystallization tubes. The crystallizations were usually carried out in 5 ml partly conical centrifuge tubes, the tip of the bottom of which had been drawn out to a narrow but not capillary tube about 1 cm long, and sealed. The centrifuge tube, thus transformed into a crystallization tube, was placed in a larger centrifuge tube with a somewhat constricted, ground neck, on the top of which was placed a gasket, cut from a rubber tube of the proper size. The rim of the crystallization tube was just large enough to fit well on the top of the gasket. After the crystallization was finished, the narrow tube in the bottom of the crystallization tube was clipped, and the mother liquor was centrifuged off into the larger centrifuge tube.

Procedure for obtaining crystals from the mixture of monomethyl ethers of curine. One gram of the mixture was dissolved in a conical flask in 5 ml of almost boiling benzene, and insoluble impurities were allowed to settle on the bottom of the flask. The solution was filtered hot through cotton into a crystallization tube. On the following day some wart-shaped crystals of one of the monomethyl ethers had formed. They were recovered and used for seeding in the subsequent separation. — One gram of the mixture of *l*-curine monomethyl ethers was dissolved in 3 ml of almost boiling methanol in a conical flask. On the following day crystals could be recovered. They were subsequently used for seeding.

Procedure for separating the components of the mixture of monomethyl ethers of curine. A solution of the mixed *l*-curine monomethyl ethers in almost boiling benzene was prepared, containing 3 ml of benzene for every gram of solute. The solution was filtered hot through cotton into 5 ml crystallization tubes, and they were immediately seeded with several drops of a benzene suspension of crystals obtained by crushing in a mortar the crystals previously obtained, together with benzene. At least 1 mg of crystals per ml solution should be used. After the crystallization was finished, the narrow tube in the bottom of the crystallization tube was clipped, and the mother liquor was centrifuged off into the larger centrifuge tube. The mother liquor was poured into a Petri dish and frozen and then allowed to evaporate, frozen, in a refrigerator at about 4°C. The substance remaining was dissolved in almost boiling methanol, about 3 ml for every gram of solute. The solution was poured into crystallization tubes and immediately seeded with a few drops of a suspension obtained by crushing the proper crystals together with methanol in a mortar. At least 1 mg of crystals should be used for every ml of solution. After the crystallization

was finished, the crystals and the mother liquor were recovered as described. The mother liquor was poured into a dish, and benzene was added. The solution was partly evaporated and then freeze-dried as described. It was found advantageous to purify the substance remaining after this freeze-drying by extracting it with diethyl ether in a Soxhlet apparatus before it was further worked up. More crystalline substance could be recovered by repeating the procedure with the remainder.

The dimethyl ether of l-*curine*. This substance crystallized from diethyl ether, m.p. 172°C. It did not change weight on drying *in vacuo* at 65°C. (Found: C 72.6; H 6.8; N 4.6; CH_3O 20.5. Calc. for $C_{38}H_{42}O_6N_2$: C 72.0; H 6.7; N 4.4; CH_3O 19.5).

The monomethyl ether of l-*curine with higher partition ratio*. 2.0 g of the crude crystallized compound (crystallized in benzene from the mixture of the two *l*-curine monomethyl ethers) were dissolved in 17 ml of boiling benzene. The solution was filtered through cotton into crystallization tubes and seeded. 0.7 g was recovered as recrystallized substance, m.p. 142°C; 1.1 g were recovered from the mother liquor. —1.5 g of the crude crystallized compound were dissolved in dilute hydrochloric acid and thereafter the pH was adjusted to 8.5. The mixture was extracted with about 60 ml of diethyl ether, and the ether phase separated and filtered through cotton. After about 15 min the substance started to crystallize without seeding, both on the glass walls of the container and in the solution. The yield of crystals was 0.4 g, m.p. 132°C; 1.0 g of the substance was recovered from the mother liquor. —6.9 g of the crude crystallized compound were extracted in a Soxhlet apparatus with about 50 ml of diethyl ether. The weight of the undissolved remainder was 0.3 g. Soon after the extraction was begun, small compact separate crystals started to form on the glass wall of the flask. The yield of crystals was 6.0 g, m.p. 137°C, and 0.7 g were recovered from the mother liquor. — Analysis of the substance crystallized from benzene: C 74.7; H 6.8; N 4.3; CH_3O 14.3; the substance recrystallized from wet ether: C 72.4; H 6.9; N 4.5; CH_3O 17.8; an the substance recrystallized from boiling ether: C 73.0; H 6.6; N 4.6; CH_3O 16.1. Calc. for $C_{37}H_{40}O_6N_2 \cdot C_6H_6$: C 75.2; H 6.8; N 4.1; CH_3O 13.6; calc. for $C_{37}H_{40}O_6N_2$: C 73.0; H 6.6; N 4.6; CH_3O 15.3.

The monomethyl ether of l-*curine with lower partition ratio*. 2.0 g of the crude crystallized substance (crystallized in methanol from the residue obtained after one of the *l*-curine monomethyl ethers had been crystallized from a benzene solution) were dissolved in 19 ml of boiling methanol. The solution was poured into crystallization tubes and seeded. Yield of crystals 1.7 g, m.p. 148°C. Recovered from the mother liquor 0.4 g. (Found: C 72.8; H 6.5: N 4.6; CH_3O 15.3. Calc. for $C_{37}H_{40}O_6N_2$: C 73.0; H 6.6; N 4.6; CH_3O 15.3.)

Acknowledgements. The author wishes to express his sincere thanks to *Sverige Amerika Stiftelsen, American Scandinavian Foundation* and *Astra Pharmaceutical Products, Inc.* for fellowships, and to Professor Dermot B. Taylor for granting the privilege of joining his alkaloid research team and for supplying various *Chondrodendron* alkaloids and partly methylated preparations of them.

REFERENCES

1. Wiggers, A. *Annalen der Pharmacie* **27** (1838) 29.
2. Wiggers, A. *Ann. Chem. Pharm.* **33** (1840) 81.
3. Bödeker, C. *Ann. Chem. Pharm.* **69** (1849) 37.
4. Hanbury, D. *Pharm. J.* [3] **4** (1873) 81, 102.
5. Hanbury, D. *Neues Repertorium für Pharmacie* **23** (1874) 279.
6. Krukoff, B. A. and Moldenke, H. N. *Brittonia* **3** (1938) 1.
7. Flückiger, F. A. *Neues Jahrbuch der Pharmacie* **31** (1869) 257.
8. Flückiger, F. A. *Pharm. J.* [2] **11** (1869) 192.
9. Bhattachari, S., Sharma, V. N. and Dhar, M. L. *J. Sci. Ind. Research (India)* **15B** (1956) 363.
10. Faltis, F. *Monatsh.* **42** (1921) 311.
11. Faltis, F., Kadiera, K. and Doblhammer, F. *Ber.* **69** (1936) 1269.
12. Schlittler, I. E., Heusler, K. and Friedrich, W. *Helv. Chim. Acta* **32** (1949) 2209.
13. Grundon, M. F. *Chem. & Ind. (London)* **1955** 1772.
14. McKennis Jr., H., Hearst, P. J., Drisko, R. W., Roe Jr., T. and Alumbaugh, R. L. *J. Am. Chem. Soc.* **78** (1956) 245.

15. Grundon, M. F. and McGarvey, J. E. B. *J. Chem. Soc.* **1960** 2739.
16. Hager, H. *Handbuch der pharmaceutischen Praxis. Erster Theil*, Julius Springer, Berlin 1876, p. 574—576.
17. *The British Pharmacopoea*, Spottiswoode & Co., London 1885.
18. Hildebrandt, H. *Arch. exp. Pathol. Pharmacol. Naunyn-Schmiedeberg's* **57** (1907) 279.
19. Faltis, F. *Monatsh.* **33** (1912) 873.
20. Scholtz, M. *Arch. Pharm.* **250** (1912) 684.
21. Kondo, H., Satomi, M. and Odera, T. *Ann. Rept. ITSUU Lab.* **4** (1953) 59.
22. Scholtz, M. *Arch. Pharm.* **251** (1913) 136.
23. Husemann, A., Hilger, A. and Husemann, T. *Die Pflanzenstoffe in chemischer, physiologischer, pharmacologischer und toxicologischer Hinsicht*, Julius Springer, Berlin 1882 and 1884, p. 542 and 904.
24. Scholtz, M. *Ber.* **29** (1896) 2054.
25. Scholtz, M. *Arch. Pharm.* **236** (1898) 530.
26. Dutcher, J. D. *J. Am. Chem. Soc.* **68** (1946) 419.
27. Anet, F. A. L., Hughes, G. K. and Ritchie, E. *Australian J. Sci. Research Ser A.* **3** (1950) 346.
28. Scholtz, M. *Arch. Pharm.* **237** (1899) 199.
29. Scholtz, M. *Arch. Pharm.* **244** (1906) 555.
30. Scholtz, M. *Arch. Pharm.* **249** (1911) 408.
31. King, H. *J. Chem. Soc.* **1940** 737.
32. de Mello Filho, L. E. in Bovet, D., Bovet-Nitti, F. and Marini-Bettòlo, G. B. *Curare and Curare-like Agents*, Elsevier, Amsterdam 1959, p. 113.
33. Böhm, R. in Ludwig, C. *Beiträge zur Physiologie*, F. C. W. Vogel, Leipzig 1887, p. 173.
34. Böhm, R. *Abhandl. Kgl. sächs. Ges. Wissensch.* **22** (1895) 199.
35. Böhm, R. *Arch. Pharm.* **235** (1897) 660.
36. Späth, E., Leithe, W. and Ladek. F. *Ber.* **61** (1928) 1698.
37. Scholtz, M. *Pharm. Zentralhalle* **47** (1906) 848.
38. Späth, E. and Kuffner, F. *Ber.* **67** (1934) 55.
39. Hultin, E. *Acta Chem. Scand.* **15** (1961) 1130.
40. Hultin, E. *Acta Chem. Scand.* **15** (1961) 879.
41. Bush, M. T., Goth, A. and Dickison, H. L. *J. Pharmacol. Exptl. Therap.* **84** (1945) 262 footnote 6.
42. Bush, M. T. and Densen, P. M. *Anal. Chem.* **20** (1948) 121.
43. Bick, I. R. C. and Clezy, P. S. *J. Chem. Soc.* **1953** 3893.
44. Kidd, D. A. A. and Walker, J. *J. Chem. Soc.* **1954** 669.
45. King, H. *J. Chem. Soc.* **1939** 1157.
46. Jübermann, O. in Müller, E. *Methoden der organischen Chemie* Band I/1, Georg Thieme Verlag, Stuttgart 1958, p. 256.
47. O'Keeffe, A. E., Dolliver, M. A. and Stiller, E. T. *J. Am. Chem. Soc.* **71** (1949) 2452.
48. Dutcher, J. D. *Ann. N.Y. Acad. Sci* **54** (1951) 326.
49. Dutcher, J. D. *J. Am. Chem. Soc.* **74** (1952) 2221.
50. King, H. *J. Chem. Soc.* **1935** 1381.
51. King, H. *J. Chem. Soc.* **1947** 936.
52. King, H. *J. Chem. Soc.* **1948** 1945.
53. Wieland, H., Pistor, H. J. and Bähr, K. *Ann.* **547** (1941) 140.
54. Brazil, O. V., Seba, R. A. and Campos, J. S. *Bol. inst. Vital Brazil* **5** (1945) 79.
55. Kupchan, S. M., Yokoyama, N. and Beal, L. J. *J. Am. Pharm. Assoc.* **49** (1960) 727.
56. Hitchcock, D. I. and Taylor, A. C. *J. Am. Chem. Soc.* **60** (1938) 2710.
57. Hanbury D. and Flückiger. F. A. *Pharmacographica. A history of the principal drugs of vegetable origin, met with in Great Britain and British India*, Macmillan and Co, London 1874, p. 25.
58. Folkers, K. and Unna, K. *Arch. intern. pharmacodynamie* **61** (1939) 370.

Received September 15, 1961.

ACTA CHEMICA SCANDINAVICA 16 (1962) 570–574

Mechanism of Reduction of Sulphur Dioxide by Formic Acid *

MARIT GOLIATH and BENGT O. LINDGREN

Swedish Forest Products Research Laboratory, Stockholm Ö, Sweden

Dedicated to Professor *Holger Erdtman* on his 60th birthday

The oxidation of formic acid with sulphur dioxide was found to follow a second order kinetic. The rate has a maximum at pH 2–3. A mechanism for the reaction has been suggested.

A detrimental by-reaction during the sulphite pulp cooking is the reduction of sulphur dioxide to thiosulphate by monosaccharides and other components of the waste liquor. A simple substance which is present in the liquor and can perform this reduction is formic acid [2] which reacts according to the equation:

$$2\,HCOOH + 2\,SO_2 = 2CO_2 + S_2O_3^{2-} + 2\,H^+ + H_2O.$$

Kinzelberger [3] has reported in a patent dealing with the manufacture of sodium dithionite, that this salt is formed when sodium pyrosulphite is treated with a solution of formic acid and sodium formate in dilute alcohol. When repeating his experiments we obtained no dithionite. When a shorter reaction time was used a small amount of dithionite was found. It is therefore probable that dithionite is the primary reduction product of the formic acid-bisulphite reaction and that it, when formed, rapidly reacts with water yielding bisulphite and thiosulphate. The existence of this reaction path is supported also by the wellknown fact that dithionite is formed from bisulphite or sulphite by many other types of reduction (*e.g.* with sodium amalgam or zinc).

We have examined the kinetics of the bisulphite-formic acid reaction. It was carried out at 135°C in an acetate buffer of pH 5. The reaction was followed by determining the thiosulphate and bisulphite concentrations. The results obtained showed that the reaction was of the second order, the rate being proportional to the concentrations of both bisulphite and formate ions (see experimental part).

* Part 3 in the series Reactions of thiosulphate during sulphite cooking. Part 2, see Ref. [1].

Table 1. The concentrations of thiosulphate formed when sulphur dioxide-sodium sulphite solutions of varying pH were heated with formic acid.

pH at 20°C	Thiosulphate, mM				
	100°C			70°C	
	1 h	2 h	5 h	2 h	5 h
1.3	0.6	0.8	1.3	0.1	0.2
1.7	3.3	3.8	3.9	0.2	0.3
2.1	—	—	—	0.6	1.0
3.0	3.0	3.7	3.9	—	1.3
4.3	—	—	—	0.1	0.1
6.8	0.0	0.0	0.0	—	—
8.2	0.0	0.0	0.0	—	—

Stockman [2] found that the oxidation proceeds more rapidly when the pH is increased and this has recently been confirmed by Slávik [4]. As the pH in their investigations was not increased above about 2 we have determined how the oxidation rate varies over a greater acidity range.

Formic acid was heated in Na_2SO_3—SO_2-solutions, the pH of which ranged from 1.5 to 8 but had the same "total" concentration of sulphur dioxide (that is the concentration sum: $[SO_2] + [HSO_3^-] + [SO_3^{2-}]$). The concentration of formic acid was low (10 mM) compared to that of the other reactant (the "total" concentration of sulphur dioxide was 390 mM). In this way the thiosulphate formed (at most 5 mM) was stabilised by the sulphur dioxide and its degradation could be neglected even in the most acidic of the solutions used.

The reaction was found to proceed fastest in those solutions which at room temperature had pH 2—3 (see Table 1). We have tried to compare the pH dependence with simple functions of the concentrations. Such comparisons can not be carried out exactly because the activity coefficients are not known. It is evident however, from Fig. 1, that the products $[HCOOH][HSO_3^-]$ and $[HCOO^-][SO_2]$ (calculated at 70°C) have maxima at pH 3.0. When the temperature of such a SO_2—HSO_3^- solution is decreased to 20° its pH is changed to about 2.5.

The rate maximum thus falls in the same pH range as the concentration products above have their maxima. The reaction may therefore involve an oxidation of $HCOO^-$ by SO_2 (or H_2SO_3, which is, however, present in only small amounts) [7] or a reaction between HCOOH and HSO_3^-. Of these two alternatives the first is more probable as sulphur dioxide may accept an electron more easily than the negatively charged bisulphite ion, and similarly the formate ion may donate an electron more readily than formic acid.

From these findings the following reaction path for the reaction is suggested.

$$HCOO^- + SO_2 \rightarrow CO_2^- + SO_2^- + H^+$$
$$CO_2^- + SO_2 \rightarrow CO_2 + SO_2^-$$
$$2\ SO_2^- \rightleftharpoons S_2O_4^{2-}$$
$$2\ S_2O_4^{2-} + H_2O \rightarrow S_2O_3^{2-} + 2\ HSO_3^-.$$

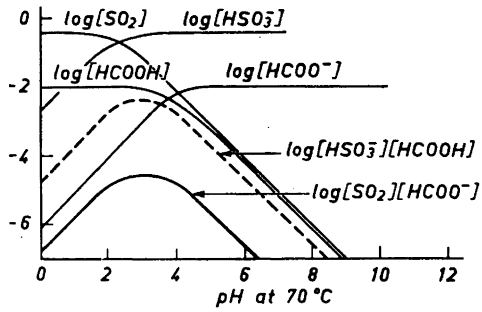

Fig. 1. The concentrations of SO_2, HSO_3^-, HCOOH, $HCOO^-$ and the products $[SO_2]\cdot[HCOO^-]$ and $[HSO_3^-]\cdot[HCOOH]$ *versus* the pH. The total concentration of sulphur dioxide is 0.39 M and that of formic acid 0.01 M.
All values were calculated for 70°C using for pK_a of SO_2 at 70°C the value 2.3 [5] and for HCOOH, 3.8 [6]. The activity coefficients were neglected.
For a $SO_2-HSO_3^-$ solution pH is decreased about 0.5 when the temperature is decreased from 70°C to 20°C as the pK_a for SO_2 is 1.8 at 20°C.

The first step is assumed to be slow compared to the others and should therefore be the rate controlling one.

The intermediate from the formate ion is here written as the radical ion CO_2^-. Another alternative would be the radical HCOO, which is assumed to be formed in the Kolbe electrolytic oxidation of formate [8]. The radical ion SO_2^- suggested to be the primary reduction product of sulphur dioxide is probably in equilibrium with the dithionite ion [9]. Its electronic structure and stability have been discussed in Ref.[10].

EXPERIMENTAL

Bisulphite reduction according to Kinzelberger [8]. Sodium formate (6.8 g) and formic acid (5.2 g) were dissolved in water-ethanol (16:84 w/w, 195 ml). Sodium pyrosulphite (16 g) was added to the solution, which was then heated at 70°C for 3 1/2 h with stirring. The undissolved material was collected and dried in vacuum. In aqueous solution it gave a white precipitate with silver nitrate solution (dithionite gives a black precipitate) and did not decolourise an alkaline resazurin solution (as do dithionite solutions) [11]. Dithionite was therefore not present. An iodometric titration in the presence of formaldehyde showed that the material contained 13 % of sodium thiosulphate. The IR spectrum of the material (peaks at 3.6, 4.3, 6.3, 7.3, 8.5, 9.4, 10.2, 12.9 μ, KBr plate) is composed of the superimposed spectra of sodium bisulphite and sodium formate.

If the reaction mixture was heated for only 1 1/2—2 h the above tests for dithionite were positive. The amount of sodium dithionite formed must however be low, at most a few percent.

Kinetic examination of the formate-bisulphite reaction. Aliquots (50 ml) of a solution containing sodium bisulphite (x mM), sodium formate (y mM) and sodium acetate-acetic acid (0.666 M and 0.277 M, respectively, pH 5) were heated for varying times in steel autoclaves at 135 ± 1°C.

The bisulphite and formate concentrations were in the three kinetic series I: $x = 85.3$ and $y = 100$ mM. II: $x = 258$ and $y = 100$ mM. III: $x = 80.0$ and $y = 200$ mM.

The concentrations of thiosulphate and of bisulphite in the solutions obtained after heating were determined by iodine titrations with and without addition of formalde-

Table 2. Kinetic experiments, series I.

Time min	$[S_2O_3^{2-}]$ mM	$[HSO_3^-]$ mM	$[HCOO^-]$ mM	$k_2 \times 10^4$ $mmole^{-1}\,min^{-1}$
0	—	85.3	100.0	
15	3.5	71.3	93.0	
30	10.3	52.9	79.4	1.8
60	17.9	35.0	64.2	1.5
90	22.9	24.7	54.2	1.9
120	25.7	22.0	48.6	1.6
150	28.1	17.6	43.8	1.8
180	29.3	14.2	41.4	1.1

$\bar{k}_2 = (1.6 \pm 0.25) \times 10^{-4}$ $mmole^{-1}\,min^{-1}$

Table 3. Kinetic experiments, series II.

Time min	$[S_2O_3^{2-}]$ mM	$[HSO_3^-]$ mM	$(HCOO^-]$ mM	$k_2 \times 10^4$ $mmole^{-1}\,min^{-1}$
0	—	258	100.0	
15	6.7	232	86.6	
30	22.1	201	55.8	1.3
45	31.5	185	37.0	1.4
60	38.3	172	23.4	1.7
75	41.9	164	16.2	1.5
90	42.2	160	11.6	1.4

$\bar{k}_2 = (1.5 \pm 0.2) \times 10^{-4}$ $mmole^{-1}\,min^{-1}$

Table 4. Kinetic experiments, series III.

Time min	$[S_2O_3^{2-}]$ mM	$[HSO_3^-]$ mM	$[HCOO^-]$ mM	$k_2 \times 10^4$ $mmole^{-1}\,min^{-1}$
0	—	80	200	
15	5.2	64	190	
30	12.5	49	175	1.5
45	18.8	33	162	1.2
60	23.8	24	152	1.6
75	27.0	18	146	1.3
90	29.3	13	141	1.5
105	30.6	8	138	1.2

$\bar{k}_2 = (1.4 + 0.2) \times 10^{-4}$ $mmole^{-1}\,min^{-1}$

hyde. The solutions obtained gave negative test for dithionite. The results are collected in Tables 2—4. The formate concentrations were calculated by subtraction of twice the thiosulphate concentration from the formate concentration in the starting solutions.

During the first 15 min bisulphite was consumed rather quickly without any corresponding formation of thiosulphate. This was probably due to a rapid oxidation of bisulphite by the oxygen in the autoclave. The rate constant, k_2, was therefore not calculated for the first 15 min of the reaction time. For all the other determinations within a series the sum: $2[HSO_3^-] + [S_2O_3^{2-}]$ was constant ($\pm$ 3 mM) which showed that bisulphite was not consumed in other ways than by thiosulphate formation. The reaction was followed until that reactant, which was present in the smaller amount, had been consumed to about 85 %.

The k_2 values for the three series were, within experimental error, identical ($10^4 \times k_2$ was for I 1.6 $\pm$ 0.25, for II 1.5 $\pm$ 0.2 and for III 1.4 $\pm$ 0.2). The reaction was thus of the second order.

The pH dependence of the reaction. Two aqueous solutions, one of which contained formic acid (5 mM) and sulphur dioxide (0.39 M) and the other the same amount of formic acid but with sodium sulphite (0.39 M) in stead of sulphur dioxide, were mixed in different ratios. Aliquots (50 ml) of the solutions obtained were heated at 100°C and at 70°C for varying times. The amount of thiosulphate formed was determined by iodine titration in the presence of formaldehyde. The results are collected in Table 1.

REFERENCES

1. Goliath, M. and Lindgren, B. O. *Svensk Papperstidn.* **64** (1961) 469.
2. Bergström, H. and Tydén, H. *IVA* **1943** No. 1, p. 12. Stockman, L. *Svensk Papperstidn.* **54** (1951) 621.
3. Kinzelberger *Brit. Pat.* 11 010 (1913).
4. Slávik, I. *Svensk Papperstidn.* **64** (1961) 427.
5. Johnstone, H. F. and Leppla, P. W. *J. Am. Chem. Soc.* **56** (1954) 2233.
6. Embree, H. *J. Am. Chem. Soc.* **56** (1934) 1042.
7. Falk, M. and Giguere, P. A. *Can. J. Chem.* **36** (1958) 1121.
8. Reviewed by Weedon, B.C.L. in *Advances of Organic Chemistry I.* Ed. Raphael, R. A., Tayler, E. C. and Wynberg, H., New York 1960.
9. Hodgson, W. G., Neaves, A. and Parker, C. A. *Nature* **178** (1956) 489; Clark, H. C., Horsfield, A. and Symons, M. C. R. *J. Chem. Soc.* **1961** 7.
10. Dunitz, J. D. *Acta Cryst.* **9** (1956) 579.
11. Eichler, H. *Z. anal. Chem.* **96** (1934) 98; **99** (1934) 270.

Received September 5, 1961.

ACTA CHEMICA SCANDINAVICA 16 (1962) 575–582

Quantitative Gas Chromatography

Quantitative Recovery and Re-injection of a Sample

KERSTIN WIDMARK and GUNNAR WIDMARK

National Institute of Public Health, Stockholm, and Institute of Organic Chemistry and Biochemistry, University of Stockholm, Sweden

Dedicated to Professor *Holger Erdtman* on his 60th birthday

Samples (0.05 μl and 1 μl) of organic compounds (boiling points < 150°C) have been collected at the exhaust tube of a gas chromatograph and then re-injected, using the gas sampling valve of the chromatograph (Perkin-Elmer 116). Two methods have been used to collect the samples, sorption on gel and a freezing-out technique.

The hydrocarbons and chloro compounds, listed in Table 2, have been collected quantitatively on silica gel in U-shaped or F-shaped tubes at room temperature, and then re-injected by rapid heating of the tube to 150°C. The loss of material was found to be very small; samples should be recycled several times in order to permit a determination of the average loss of a collection — re-injection cycle. An average loss of less than 1.5 % was achieved using 1 μl samples, whereas with a sample size of 0.05 μl the loss was found to be somewhat larger.

Interference of water was overcome by the choice of stationary phase or in some cases by applying a CaH_2 pre-column. The importance of ensuring a constant flow-rate of carrier gas for the quantitative estimation of recorded graphs is demonstrated.

Utilizing F-shaped tubes, samples were recycled by a freezing out technique to give a fairly good quantitative yield, in most cases with a loss less than 3 %. This method can be applied more universally since gel was found to interfere with some compounds, *e.g.* 2-pinene decomposed totally, and a loss of 25 % was recorded for butanol.

The presence of an inactive filling (Chromosorb W or glass micro beads) in the F-tube is essential, and with the exception of the low boiling compounds, such as chloroethane and ethyl ether, CO_2-ice gives the same good result as liquid air.

Quantitative gas chromatography may be regarded from at least three different viewpoints. The passage of the sample through the chromatographic instrumentation must proceed without loss, a conception which also includes quantitative injection and recovery of the sample. The instrumentation, including detecting and recording devices, should convert the output

signal to a corresponding quantitative answer, and finally, the physical-chemical background of the response given by the individual chemical compound is to be considered. The publications given in the literature concern the latter two aspects, whereas the first one being the main consideration of this investigation has not, to the knowledge of the authors, been treated earlier.

The technical evolution of commercial chromatographs has advanced considerably during the last years, and there are nowadays no difficulties in running the instruments under such conditions that the important variables are constant enough for a reproducible and quantitative estimation of the graphs. However, an important factor of our investigations, later described, was to keep the flow of carrier gas under control, and the present authors wish to draw the reader's attention to the necessity of checking the flow-rate intermittently during quantitative analysis, *cf.* Fig. 1.

The common errors incurred on estimation of the recorded graphs for quantitative analysis have been thoroughly eluciated in the literature. Janak *et al.*[1,2] have critically compared most methods in use. For this investigation the geometric method has been used when treating sharp and regular peaks, giving the same good result as reported by Janak. However, since changes of flow-rate were sometimes unavoidable, giving an irregular baseline, the planimetric method has been used frequently. For the most part, lower mean errors than those reported by Janak have been obtained for the different peak sizes.

The third viewpoint of quantitative analysis mentioned, *i.e.* the relative signal response of individual compounds using thermal conductivity detectors, has mainly been studied by Rosie and his colleagues [3,4]. We have investigated some of the compounds used in the present investigation, which are also given in the reports of Rosie. As demonstrated by Table 1, fairly good agreement has been obtained both when injecting mixtures of the compounds in benzene (50/50 % by volume), and when injecting equal volumes of the compound sample and benzene separately. However, there are some obvious discrepancies, *e.g.* with 2,2,4-trimethyl pentane, and it is intended to investigate the case further.

Table 1. Relative signal response per mole on thermal conductivity detection (benzene = 100; benzene-compound 50/50 % by volume, average mean error ± 1.5 %

Compounds investigated	Consecutive injection of compound and benzene	Injection of compound-benzene mixtures	
		present authors	Rosie [3,4]
Cyclohexane	103	105	114
Methylcyclohexane	115	113	120
2,2,4-Trimethylpentane	131	134	147
Toluene	113	116	116
Ethanol	67	65	72
Propanol-1	85	83	83
Butanol-1	97	100	95
Ethyl acetate	108	108	111

COLLECTION AND RE-INJECTION OF A SAMPLE

There are several methods in use for collecting a fraction which issues from a gas chromatograph, the purpose of this collection being mostly for further identification by additive analysis. The carrier gas, together with the vapours of the compound of interest, can be carefully drawn by suction into an evacuated container or a syringe. Mostly, the vapours are condensed by cooling, dissolved in a solvent or sorbed on an active surface, and thus more or less effectively freed from the carrier gas. The last three operations are very similar to those for a long time used for sampling vapours in air, but for gas chromatography the problem is not so delicate, since water vapour is not present in large amounts. The quantitative yield of the collection operations mentioned are difficult or impossible to measure by the aid of additive methods, such as UV or IR. It is very obvious that the most convenient way to determine the yield would be gas chromatographic. However, this requires a quantitative re-injection of all the sample collected. *To make this possible, a quantitative circle of gas chromatography is closed, and this makes the gas chromatographic method ready for an enlarged field of analytical work.* The demand for a quantitative re-injection of the collected sample practically eliminates those collecting methods where solvents are used or where the sample is collected together with the carrier gas. To fit the gas chromatographic method the re-injection must proceed rapidly, and thus the only methods which were likely to be applicable were heating techniques of a sorbed or condensed fraction. In this investigation these two methods have been found to give the desired result.

COLLECTION OF A FRACTION ON SILICA GEL

This investigation was begun because of medical interest in benzene vapour, and since the gel technique had been used earlier to collect benzene vapour in air for UV-spectroscopic determination after desorbing with ethanol, attempts were made first to enrich on gel the benzene vapours issuing from the chromatograph. To enable a re-injection into the chromatographs available in these laboratories (Perkin-Elmer 116) the collection tube holding the gel was made U-shaped in order to fit into the gas sampling valve of the apparatus. The U-tube (total length 200 mm pyrex, i.d. 1.5, o.d. 3.0 mm) was filled with 200 mg of activated silica gel, 60—70 mesh, kept in position by plugs of glass yarn.

Since methods of air sampling were simultaneously investigated, and since any disturbance of the base-line height was undesired during collection of the benzene fraction leaving the exhaust tube of the chromatograph, the following method was first adopted. The issuing vapour was drawn by suction into the gel of the U-tube by the aid of a large syringe fastened to one arm of the U-tube by a piece of rubber tubing. The exhaust needle was loosely inserted into the other arm. The rate of suction was kept slightly higher than the flow-rate of carrier gas of the chromatograph to ensure a complete uptake. Due to difficulties in achieving a constant speed when moving the piston of the syringe, an evacuated container was used instead. A constant suction was achieved

during the period of time when benzene was issuing from the chromatograph, by means of attaching a restriction between the U-tube and a vacuum tank of 500 ml capacity.

Later, a third method of collecting the fractions was used. Two U-tubes were carefully calibrated to give exactly the same resistance to gas flow by adjusting the amounts of gel added and the degree of packing. Short teflon tubings were used to connect tightly the two U-tubes to the two way valve of the chromatograph exhaust tube. This arrangement increased the gas pressure at the detector and lifted the baseline. However, on switching the valve from one position to the other, no change of the base-line of the recorder was detected. Thus, one tube could be removed for re-injection without interfering with the recorded graph.

Finally, since the samples were usually recycled several times for determination of the yield of recovery, two uncalibrated gel tubes were interchanged between collection and re-injection positions according to a timed schedule, and the recorded peaks were estimated in two series. This was found to be the most convenient way of collecting the fractions and the procedure rendered it possible to use the more handy F-shaped tubes described later.

RE-INJECTION OF A FRACTION COLLECTED ON SILICA GEL

On re-injection of the collected sample, the U-tube was fastened into the O-fittings of the gas sampling valve of the Perkin-Elmer chromatograph. When opening the valve and flushing the carrier gas through the U-tube, it was found that the gel retained the benzene very effectively at room temperature, and no peak of benzene was detected within 30 min. However, the resistance of the gel layer caused an elevation of the base line. Applying electrical heating to the U-tube (a spiral thread over the tube), the benzene was rapidly desorbed and flushed into the chromatograph, to give a well-defined peak. Heating of the gel layer increased its resistance to the flow of carrier gas, and if heating was continued throughout the analysis, temperature stability was not usually achieved by the time that the sample of benzene entered the detector; thus, the peak of benzene was recorded on a drifting base-line.

It was subsequently demonstrated that the sample of benzene was totally desorbed within 30 sec on heating with the oven used. Thus, the stream of carrier gas through the U-tube or F-tube could be switched off after this time (one minute was used). The peak of benzene appeared usually after 5 min, by which time a good and reproducible baseline had been restored. This made it easier to compare quantitatively the peak areas of repeated re-injections, and thus the yield of each collection — re-injection cycle.

As always on gas analysis, the presence of water vapour interfered. On re-cycling the sample of benzene, the amount of water was increased, giving greater interference on further re-cycling. Furthermore, the water sorbed on the gel was not totally desorbed within 1 min, and sometimes water peaks appeared during subsequent analyses.

The interference of water was successfully overcome by the choice of stationary phase or by the use of a short pre-column containing calcium hydride

Table 2. Average percentage loss of sample at a collecting — re-injection cycle. (Number of cycles minimum 6 and maximum 15).

Substance *a* 0.05 μl *b* 1 μl	Gel method	Freezing-out method Chromosorb-W		Micro glass beads	
		CO_2-ice	liquid air	CO_2-ice	liquid air
Benzene *a*	1.3	4.4	4.4	2.3	
» *b*	0.4	2.7	3.5	2.2	
Toluene *a*	1.1	2.7		2.6	
» *b*	1.0	2.5		2.4	
Ethylbenzene *b*	3.1	3.2		2.6	
Styrene *b*	6.5	3.6			
p-Xylene *b*	2.3			2.7	
Cyclohexane *a*	2.3			15	3.4
» *b*	3.3	2.7	1.5	4.5	
Hexane *b*	3.5	1.3	1.6	29	2.0
Heptane *b*	2.3			2.2	2.0
Pinene *b*	total decomp.	0.5		1.4	
Methanol *a*	6.4 (decomp.)	5.7		9.2	
» *b*	10.3 (decomp.)	6.9	4.5	2.8	
Ethanol *b*	12.7 (decomp.)			2.8	0.6
Propanol-1 *b*	18 (decomp.)			4.1	2.8
Butanol-1 *b*	25 (decomp.)	1.7		2.4	
Ethyl acetat *a*	(decomp.)	10.1	3.3	10.7	5.8
» » *b*				2.1	
Acetone *b*	(decomp.)			9.8	1.4
Methylethyl ketone *b*	(decomp.)	2.3		4.1	
Ethyl ether *b*	(decomp.)	27	4.1	30	2.8
Ethyl chloride *a*	0.3	70	3.9		4.3
» » *b*		34	0.6		0.9
Chloroform *a*	0.6				
Perchloroethylene *a*	2.5				
Dichloroethane *b*	2.9	1.3		2.4	
Trichloroethylene *b*	0.9				

(30 % mixture with Chromosorb-W). The hydride converted the small amounts of water to hydrogen, which did not affect the base-line at these small concentrations, since the thermal conductivity of hydrogen and the carrier gas used were similar.

QUANTITATIVE RESULTS USING SILICA GEL TECHNIQUE

Re-cycling samples of benzene, toluene, chloroform, and trichloro ethylene, and even such a low-boiling compound as ethyl chloride, the loss at each cycle was found to be very small, of the same magnitude as errors made on the estimation of the graphs. Thus, an accurate determination of the mean yield had to be made by re-cycling the sample several times. Up to fourteen cycles have been performed, with a total loss of 10 %. An average loss of 0.4 to 1.0 % for each cycle was achieved for the compounds mentioned when applying a sample size of 1 to 5 μl, the latter being the maximum amount tolerated by our recording device. The loss was found to be somewhat larger

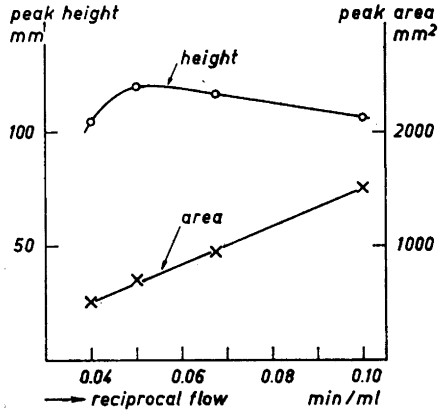

Fig. 1. Effect of flow-rate of carrier gas (helium) on peak height and peak area. Column: 2 m., inner diameter 4 mm., octylphthalate (30 %) on Chromosorb-W; temp. 101°C; sample: 2,2,4-trimethyl pentane, 2 µl; sensitivity 32; chart speed 30 cm/h.

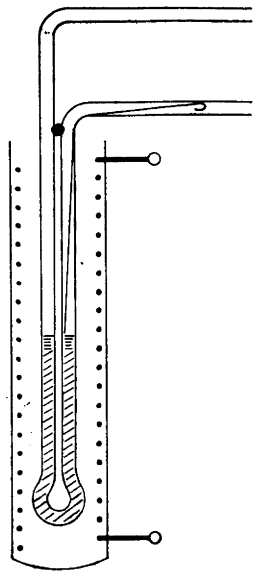

Fig. 2. F- shaped tube and oven. F-shaped tubing of Pyrex glass, o.d. 3 mm, total length about 35 cm, of which the lower 8 cm contained the filling and two small plugs of glass yarn. Since the carrier gas enters *via* the upper arm, the filling is held in position in the lower arm by a stainless steel wire. — The electrical oven consists of a quartz tube holding an inner spiral of resistance wire (4 Ω). With 13 V, the temperature of the F-tube was brought to 170°C within 1 min when the oven was raised over the F-tube.

when 0.05 µl samples were used and the reason for this is now under investigation (*cf.* Table 2).

For the higher boiling aromatic hydrocarbons, a desorbing time of 3 min was found necessary. Slightly distorted peaks were obtained, very likely due to insufficiently high temperatures upon re-injection. For saturated hydrocarbons such as cyclohexane, which were not sorbed as firmly as aromatic hydrocarbons by the gel, the time of uptake on the gel was found to be critical, and should be chosen to be as short as possible and to give no more than the small loss mentioned earlier. Those hydrocarbons isomerized totally by the gel have not been investigated further, *e.g.* 2-pinene.

Certain obstacles were encountered on application of this gel method to lower alcohols, esters, ethers and ketones. These compounds were more or less decomposed on heating the gel upon re-injection. Butanol, for example, gave a loss of 25 %, even more when the CaH_2-pre-column was connected. These findings led to an investigation of the collection method described in the next section.

FREEZING-OUT OF FRACTIONS

Except for work with high vacuum, the freezing-out technique is generally considered not to be quantitative. However, using the F-shaped tubes, shown in Fig. 1, which similarly to the U-tubes could be fitted into the gas sampling valve, fairly quantitative yields were soon obtained. This was achieved when the lower part of the F-tube was filled with packing material to a height of 4 cm; it was demonstrated that the nature of the packing material was of importance. It became apparent that sterchamol and celite-C-22 contained active groups which even at a moderate temperature retained the alcohols, causing tailing. Chromosorb-W (60—80 mesh) or micro glass beads (20—40 mesh) did not give this effect and gave a much lower resistance to the gas than gel. However, on heating at the re-injection of methyl cyclohexanol, an effect was observed which might indicate a decomposition caused by active groups on the filling material.

Cooling of the F-tube was achieved by CO_2-ice; no advantage was found with the use of liquid air when re-cycling benzene or butanol. Naturally, low boiling compounds such as ethyl ether, cyclohexane and ethyl chloride gave better yields by using liquid air. Minimizing the time of collection also increased the yield. Fig. 3 shows chromatograms obtained on re-cycling ethyl ether.

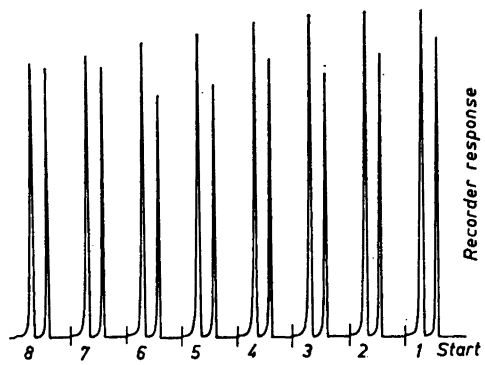

Fig. 3. Chromatograms from recycling of ethyl ether. Chromatogram 1 was given by the injection of 1 μl ethyl ether, and consists of peaks of air and ethyl ether. On repeated re-injection and collection, chromatograms 2—8 were formed. Two F-shaped tubes, filled with micro glass beads, were employed alternatively, and were cooled with liquid air. The first peak of water appeared after the eighth recovery. — Analytical conditions: Reoplex-400 (15 %) on Celite-22; temp. 65°C; pressure 1 kg/cm² (He); sensitivity 128; chart speed 60 cm/h; gas chromatograph Perkin-Elmer 116 e.

Some water vapour was condensed inside the tube, but lessened by protecting the free exit arm of the F-tube with a drying tube containing CaH_2. However, chromatograph columns were chosen where the small peak of water did not interfere, and remaining water was flushed off before a new collection. The use of a pre-column (CaH_2) was omitted since butanol and many other compounds were affected by this pre-column.

On injection, the F-tube was connected rapidly to the gas sampling valve and the hot oven (mostly 150°C) — *cf.* Fig. 2 — was raised over the cooled part of the F-tube. Simultaneously, the valve was opened and the F-tube flushed by the carrier gas. All the samples investigated were vaporized within 45 sec., and after a further 45 sec the valve was turned back to the normal position and base-line stability was rapidly obtained.

The results obtained using the freezing-out technique elaborated up to now are demonstrated by Table 2. For some compounds the yields were quite satisfactory, but mostly the loss was greater than when silica gel was used. At the present stage of the investigation, it is too early to distinguish whether chromosorb or micro glass beads are to be preferred as filling for the collection tubes or to state when cooling by liquid air should be used. With regard to the low resistance to the stream of carrier gas, the micro glass beads seem to be preferable. According to our opinion, the freezing-out technique can be improved further to give a lower loss at each analytical cycle and to allow the treatment of higher boiling compounds.

Acknowledgement. One of the gas chromatographs used in this investigation was aquired thanks to a grant from *Knut och Alice Wallenbergs Stiftelse.*

REFERENCES

1. Krejci, M. and Janak, J. *Chemie* (Prague) **10** (1958) 264–272.
2. Janak, J. *J. Chromatography* **3** (1960) 308–312.
3. Rosie, D. M. and Grob, R. L. *Anal. Chem.* **29** (1957) 1263–1264.
4. Messner, A. E., Rosie, D. M. and Argabright, P. A. *Anal. Chem.* **31** (1959) 230–233.

Received September 15, 1961.

ACTA CHEMICA SCANDINAVICA 16 (1962) 583–590

Spectroscopic Studies on Enols

4 *. Hydrogen Bonding in Usnic Acid

STURE FORSÉN, MARTIN NILSSON and
CARL AXEL WACHTMEISTER

Research Group for Nuclear Magnetic Resonance, Division of Physical Chemistry; Division of Organic Chemistry, Royal Institute of Technology, Stockholm, and Institute of Organic Chemistry and Biochemistry, University of Stockholm, Sweden

Dedicated to Professor *Holger Erdtman* on his 60th birthday

The acetylation of usnic acid has been reinvestigated. A new monoacetate is described and the positions of the *O*-acetyl groups in both acetates are established by spectroscopic methods.

Infrared and proton magnetic resonance spectra show that usnic acid contains three intramolecular hydrogen bonds. The strongest of these is found in the enolised β-triketo-part of the molecule. The hydrogen bond in the aromatic *o*-hydroxyacetyl grouping is stronger than in *o*-hydroxyacetophenone. The third hydrogen bond connects the remaining phenolic hydroxyl group with the tricarbonyl system. As shown by paper chromatography the lipophility of usnic acid is markedly enhanced when this hydroxyl group is acetylated.

Among β-triketones of natural origin, usnic acid (I) is of special interest due to its very wide occurrence — both enantiomers being represented — in lichens of many genera and due to its extreme toxicity. The now accepted structure was proposed independently by Curd and Robertson [1] and by Schöpf and Ross [2,3] but has only recently been confirmed through a total synthesis of usnic acid by Barton, Deflorin and Edwards [4]. The extensive literature on the subject has been reviewed repeatedly, most recently by Shibata [5] and by Hassall [6].

Structure (I) (dibenzofuran numbering) obviously implies several possibilities for formation of intramolecular hydrogen bonds. In fact usnic acid, in spite of its high oxygen content, exhibits pronounced lipophilic properties. It is practically insoluble in the lower alcohols but somewhat soluble in benzene and readily soluble in chloroform.

* Part 3. *Arkiv Kemi* **17** (1961) 523.

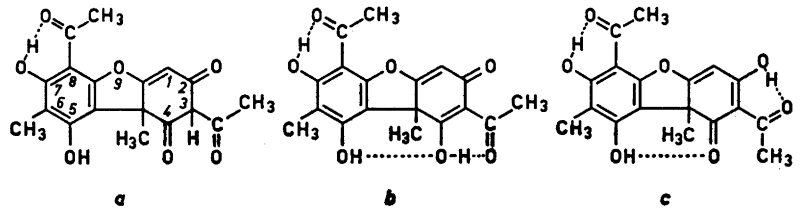

a *b* *c*

I

Usnic acid on mild treatment with acetic anhydride and sulphuric acid affords 5,7-*O*,*O*-diacetylusnic acid [7] which by treatment with sodium carbonate solution readily affords a monoacetate, 5-*O*-acetyl- or 7-*O*-acetylusnic acid, in excellent yield [7]. So far, the position of the acetyl group has not been settled. However, since the phenolic groups in usnic acid would be expected to differ considerably in character, some information might be obtained directly from a consideration of the solubility properties. Such a study proved possible in a simple way by means of paper chromatography, using dimethyl sulphoxide as a stationary phase.

The pronounced trailing of usnic acid, indicative of the strong metal chelating properties of these compounds, was largely eliminated by the use of paper impregnated with ethylenediamine tetraacetic acid (EDTA), as previously tried with advantage in the chromatography of tropolones [8].

As demonstrated by the R_F-values obtained (Table 1), the elimination of one acetyl group from the diacetate causes a remarkable increase in the lipophilic character of the molecule. Hence, the liberated hydroxyl group is presumably largely masked by chelation, as expected in a 5-*O*-acetylusnic acid. Moreover, a reinvestigation of the acetylation reaction revealed the transient occurrence in the reaction mixture of a second monoacetate, presumably 7-*O*-acetylusnic acid, characterised by lower R_F-values even than usnic acid (Table 1). The (−)-form and the racemic form of this derivative were eventually obtained in a pure state.

The dominant role of intramolecular hydrogen bonding in the usnic acid series was still more obvious in view of the highly different properties of the two monoacetates. This suggested a closer investigation using spectroscopic methods. Surprisingly infrared spectroscopy has been little used even in recent work on usnic acid, although its IR spectrum has been published without discussion [9].

Previous investigations in this series of the hydrogen bonding in enolised tricarbonyl systems using infrared and proton magnetic resonance spectroscopy have recently been summarised [10] and provide a necessary background for the interpretation of the complicated spectra of usnic acid. A spectroscopic investigation of the acetates also led to the definite localisation of the acetyl groups in the two monoacetates and gave a more complete understanding of the hydrogen bonding in this unique system.

EXPERIMENTAL

Methods

The PMR spectra were recorded on a Varian V-4 300 spectrometer operating at 40 Mc/s and equipped with a Varian K 3 519 field homogeneity control unit. The measurements were made at 22 ± 1°C. The shifts were determined against an internal tetramethylsilane standard and are given as τ-values according to Tiers [11].

The IR spectra were recorded on a Perkin Elmer No 21 instrument with a sodium chloride prism for 0.1 M solutions in chloroform using mostly 0.1 mm and 1 mm cells. The solvent absorption was compensated.

Paper chromatograms were run on paper (Whatman No. 4) impregnated with an EDTA buffer and dimethyl sulphoxide, using a technique previously described [8]. Hexane and di-isopropyl ether were used as mobile phases. The samples were applied as 1 % solutions in chloroform. The spots were located by means of a UV lamp after drying the paper at 80°. Usnic acid and its derivatives appeared as dark spots. The approximate R_F-values are listed in Table 1.

Table 1. Approximate R_F-values at 25°.

	Mobile phase	
	hexane	di-isopropylether
(±)-Usnic acid	0.10	0.25
(±)-5-*O*-acetylusnic acid	0.55	0.85
(±)-7-*O*-acetylusnic acid	0.03	0.15
(±)-5,7-*O*,*O*-diacetylusnic acid	0.15	0.60

Materials

(±)-*Usnic acid.* (−)-Usnic acid, m.p. 203−204.5°, $[\alpha]_D^{20} = -498°$ (chloroform, *c*, 0.4) from *Haematomma coccineum* (Dicks.) Körb. was racemised by prolonged heating in xylene and was crystallised from chloroform-ethanol to give prisms, m.p. 193−194°C.

(±)-*5,7*-O,O-*diacetylusnic acid* [7]. (±)Usnic acid (5.0 g) was stirred with acetic anhydride (100 ml) containing sulphuric acid (0.4 g) for 7 h at 20°. The crystals were collected, washed with cold methanol and water and dried (yield 3.5 g). Crystallisation from ethyl acetate gave (±)-5,7-*O*,*O*-diacetylusnic acid as yellowish needles, m.p. 205−207° after sintering from 200°.

(±)-*5*-O-*acetylusnic acid* [7]. The diacetate (1.0 g) was stirred with 1 M sodium carbonate solution (150 ml) for 2 h at 25°C. The clear solution was acidified with hydrochloric acid, the precipitate collected, washed with water and dried (yield, 0.9 g). Crystallisation from ethyl acetate gave (±)-5-*O*-acetylusnic acid as yellow needles, m.p. 190−191°.

(±)-*7*-O-*acetyl usnic acid.* Finely pulverised (±)-usnic acid (2.3 g) was stirred at 20°C with acetic anhydride (60 ml) containing sulphuric acid (0.2 g). After 20 min, the solution was freed from undissolved usnic acid by rapid filtration through glass wool and poured with stirring into ice-water (1 200 ml). The precipitate was collected, washed with water and dried (yield 2.1 g). Crystallisations from methyl ethyl ketone and finally from ethyl acetate afforded (±)-7-*O*-acetylusnic acid as pale yellow needles, m.p. 182−183° (yield 0.25 g). (Found: C 62.5; H 4.69. $C_{20}H_{18}O_8$ requires C 62.2; H 4.67.)

(−)-*7*-O-*acetylusnic acid.* Finely pulverised (−)-usnic acid (10 g) was stirred at 24°C with acetic anhydride (200 ml) containing sulphuric acid (0.8 g). After 15 min, undissolved usnic acid (4.0 g) was collected as above and the clear solution poured with stirring into ice-water (2 000 ml). The resinous product was dissolved in ethyl acetate (300 ml). The solution was washed with water (4 × 50 ml) and evaporated to a syrup which was dissolved in hot methanol. The solution on standing in the open air very slowly deposited crystals which were collected (m.p. 120−128°, yield 2.7 g). Crystallisations from methanol, ethyl acetate-methanol (1:4) and finally from ethyl acetate gave (−)-7-*O*-acetyl usnic acid as yellow prisms, m.p. 137−139°, $[\alpha]_D^{20} = -422°$ ($CHCl_3$, $c = 1.1$) (yield 0.45 g). (Found: C 62.3; H 4.66. $C_{20}H_{18}O_8$ requires C 62.2; H 4.67.)

RESULTS

IR and PMR spectra were recorded for usnic acid, its two monoacetates and the diacetate. For comparison, the PMR spectra of 2-hydroxyacetophenone, 2,4-dihydroxyacetophenone and 2,4-dimethoxy-6-hydroxyacetophenone were measured. Previous measurements in this series have mostly been made on carbon tetrachloride solutions, but due to limited solubilities of the compounds mentioned this solvent was only used in a few cases. The structures of the two monoacetates were fully established by these measurements as indicated below. The spectra also indicate the complete enolisation of the β-triketo grouping in the solvents used. IR spectra of the solid compounds, taken on potassium bromide discs, indicate that enolisation is complete also in the solids.

The IR spectra of usnic acid and its derivatives show a number of peaks in the carbonyl region (the figures refer to notations in the spectra, Figs. 1*a*—*d*).

(1) The conjugated chelated carbonyl of the enolised β-tricarbonyl grouping gives a broad band near 1 540 cm^{-1}. Its position should be compared with those of ceroptene (5-methoxy-2-cinnamoyl-6,6-dimethyl-cyclohex-4-ene-1,3-dione) and its transformation products at 1 515—1 525 cm^{-1}.[12]

(2) The enol ether double bond absorbs near 1 610 cm^{-1} as in dimedone methyl ether and the ceroptene derivatives. Absorption of the aromatic ring can also be expected in this region.

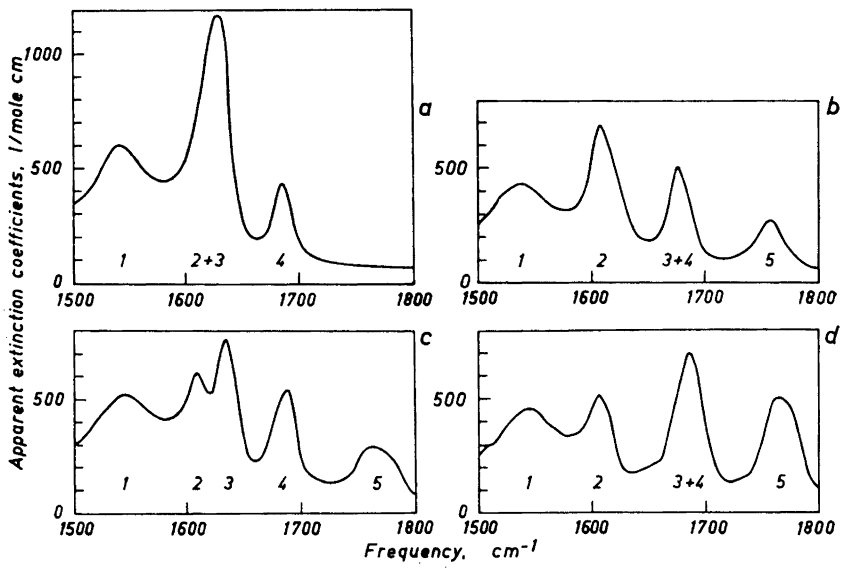

Fig. 1. Carbonyl region in the infrared spectra measured in chloroform solutions. (*a*) Usnic acid; (*b*) 7-*O*-acetylusnic acid; (*c*) 5-*O*-acetylusnic acid; (*d*) 5,7-*O*-*O*-diacetylusnic acid. The numbers 1—5 refer to discussion in the text.

(3) The aromatic *C*-acetyl group in 2,4-dimethoxy-6-hydroxyacetophenone absorbs near 1 620 cm^{-1}. In usnic acid the corresponding band coalesces with the enol ether band and a very intense absorption is observed. On acetylation of the *ortho*-hydroxy group the band is displaced to *ca.* 1 680 cm^{-1}, as expected for a non-chelated aromatic ketone. Acetylation of the *para*-hydroxyl group also affects the carbonyl absorption and in 5-*O*-acetylusnic acid all the bands can be readily seen.

(4) The dienone carbonyl absorbs near 1 670 cm^{-1}.

(5) The *O*-acetyl groups, as expected, absorb near 1 780 cm^{-1}.

The hydroxyl stretching absorptions of enolised β-tricarbonyl compounds are generally far less distinct than those of other chelates. The bands are broad, of low extinction and displaced towards unusually low frequencies. The 2 000—4 000 cm^{-1} region of the IR spectra of the present compounds (Fig. 2) shows three different hydroxyl absorptions, occurring at *ca.* 2 400, 2 800 and 3 000—3 200 cm^{-1}. The first absorption can tentatively be assigned to the very strongly hydrogen bonded enolic hydroxyl group. The absorption in the 2 800 cm^{-1} region agrees with that observed in 2,4-dimethoxy-6-hydroxyacetophenone and therefore can be ascribed to the chelated 7-hydroxy group. The third absorption is shown only by usnic acid and the 7-*O*-acetyl-derivative and must be attributed to the 5-hydroxy group. The position of the band indicates that this hydroxyl group is also engaged in an intramolecular hydrogen bond of by no means negligible strength.

The IR spectra can thus be satisfactorily interpreted and reveal that usnic acid contains three quite distinct hydrogen bonds of different character. Spectra recorded for different concentrations showed no significant changes and it is therefore evident that these hydrogen bonds are intramolecular.

The PMR spectra are very distinct. The figures refer to notations in the spectra of the chloroform solutions (Figs. 3*a*—*d*). The signals from the hydroxyl protons afford straight-forward information about the hydrogen bonding.

(1) The hydroxyl proton of the triketone chelate gives a signal at very low field — for usnic acid at $\tau = -9.20$. For the more dilute carbon tetrachloride solution this signal was observed at $\tau = -8.94$. The signals should be compared with those of ceroptene and its transformation products * and indicate that the enolic hydrogen bond in usnic acid is comparable to the hydrogen bonds in these compounds. The signal is shifted somewhat towards higher field on acetylation of the phenolic hydroxyl groups, especially that in the 5-position.

(2) The phenolic proton of the aromatic conjugated chelate gives a signal at surprisingly low field. Some related compounds were investigated for comparison; thus 2-hydroxyacetophenone, 2,4-dihydroxyacetophenone and 2,4-dimethoxy-6-hydroxyacetophenone in chloroform solutions gave signals for the chelated protons at $\tau = -2.32$, -2.70 and -4.03. The latter values agree in magnitude with those observed in usnic acid and in 5-*O*-acetylusnic

* Ceroptene in carbon tetrachloride solution has been reported [12] to give an enol proton signal at $\tau = -8.91$. Its PMR spectrum has now also been recorded for a more concentrated chloroform solution. Enol proton signals were observed at $\tau = -9.31$ and -9.05. The intensity ratio of 4/1 was also found for the other split peaks in the spectrum.

acid. The position of these signals imply that the hydrogen bonds in these aromatic chelates are rather strong. It should be remembered, however, that diamagnetic anisotropic effects of the aromatic system contribute to the low-field position.

(3) This signal is obviously due to the phenolic hydroxyl group in the 5-position. Its position at a fairly low field indicates that it is engaged in a hydrogen bond comparable in strength to that in salicylaldehyde. This is in agreement with the infrared hydroxyl absorption pattern.

Signal (4), which recurs in all spectra, is obviously due to the proton in the 1-position.

The signals from the methyl groups are generally well separated. Comparison with the model compounds, 2,4-dimethoxy-6-hydroxyacetophenone and 3-methyl-2,4,6-trihydroxyacetophenone, indicates that these signals in usnic acid are, from lower field, coinciding signals from the *C*-acetyl groups, the aromatic methyl and the angular methyl group.

CONCLUSIONS

The IR and PMR spectra thus further confirm the structure (I) for usnic acid and give unambigous evidence concerning the position of the *O*-acetyl groups in the earlier known monoacetate, 5-*O*-acetylusnic acid, and in the new isomer, 7-*O*-acetylusnic acid. Moreover the demonstration of three intramolecular hydrogen bonds of quite different types also accounts for the pronounced lipophility of usnic acid. The exceptionally strong hydrogen bonding in enolised β-tricarbonyl systems has been repeatedly demonstrated in this series. The hydrogen bond in the aromatic chelate is even more pronounced than expected. Unfortunately, only limited information is available on hydrogen bonding in substituted *ortho*-hydroxyacetophenones and related compounds. Our results

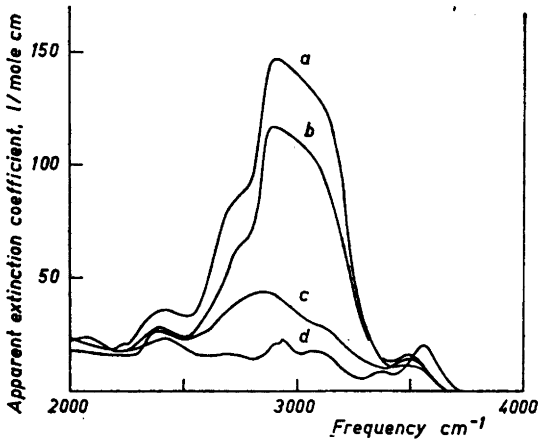

Fig. 2. Hydroxyl region in the infrared spectra of (*a*) usnic acid; (*b*) 7-*O*-acetylusnic acid; (*c*) 5-*O*-acetylusnic acid; (*d*) 5,7-*O*-*O*-diacetylusnic acid. The details of the C—H absorptions between 3 000 and 2 900 cm^{-1} are obscured by solvent absorption.

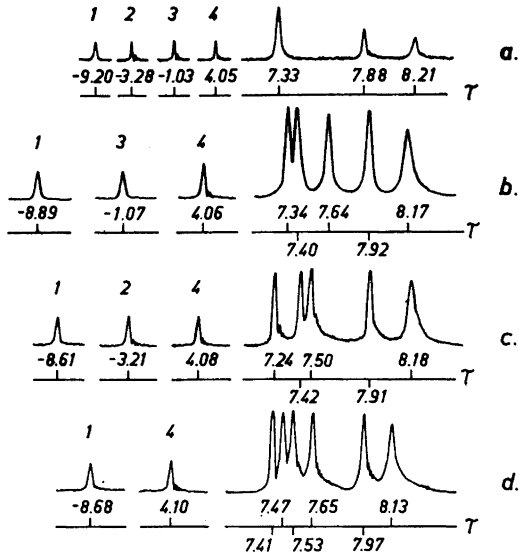

Fig. 3. PMR spectra recorded for chloroform solutions. (*a*) Usnic acid (mole fraction, $x = 0.02$); (*b*) 7-*O*-acetylusnic acid ($x = 0.04$); (*c*) 5-*O*-acetylusnic acid; (*d*) 5,7-*O*-*O*-diacetylusnic acid ($x = 0.04$).

and those obtained by Reeves *et al.*[13] indicate that the strength of the intramolecular hydrogen bond in *o*-hydroxycarbonyl compounds is increased by hydroxy- or methoxysubstitution in *ortho*- or *para*-position to the carbonyl group and by nitro groups in *para*-position to the chelated hydroxyl group.

The third hydrogen bond in usnic acid is weaker but still strong enough to be comparable to that in salicylaldehyde. The reason for its strength is not directly apparent from the formulas drawn. Studies on molecular models, however, show that the distance from the oxygen in the 5-position to the oxygen in the 4-position is rather low. However, the 5-hydroxy-group is probably also capable of distinct intermolecular hydrogen bonding with strongly polar solvents. This is perhaps most obvious from the paper chromatographic data summarised in Table 1, where it is shown that the lipophility is strongly enhanced by acetylation of this group.

In an unsymmetrical β-triketone like usnic acid there are two possibilities for enolisation (I b and I c) (*cf.* Ref.[10,12,14]). In some other β-triketones both forms have been observed to occur simultaneously by the splitting of the peaks in the PMR spectra. In usnic acid or its derivatives no such splitting is observed and it therefore seems probable that one of the forms strongly predominates in the solvents used. It is not possible, however, to judge from the present data whether usnic acid is present as form I b or I c.

Acknowledgements. We thank Professor Holger Erdtman for his kind interest in this work and for a generous supply of usnic acid. We also thank Dr. Erik Forslind for advice and discussions. Miss Gurli Hammarberg has measured the infrared spectra and Dr. P. Daniels has checked the English.

REFERENCES

1. Curd, F. H. and Robertson, A. *J. Chem. Soc.* **1937** 894.
2. Schöpf, C. *Naturwiss.* **26** (1938) 772.
3. Schöpf, C. and Ross, F. *Ann.* **546** (1941) 1.
4. Barton, D. H. R., Deflorin, A. M. and Edwards, O. E. *J. Chem. Soc.* **1956** 530.
5. Shibata, S. in Ruhland, W. *Handbuch der Pflanzenphysiologie*, Vol. X, Springer Verlag, Göttingen 1958.
6. Hassall, C. H. *Progr. in Org. Chem.* **1** (1958) 115.
7. Asahina, Y. and Yanagita, M. *Ber.* **72** (1939) 1140.
8. Wachtmeister, C. A. and Wickberg, B. *Acta Chem. Scand.* **12** (1958) 1335.
9. Cross, A. O. *Introduction to Practical Infra-Red Spectroscopy*, Butterworths, London 1960, p. 45.
10. Nilsson, M. *Svensk Kem. Tidskr.* **73** (1961) 447.
11. Tiers, G. V. D. *J. Phys. Chem.* **62** (1958) 1151.
12. Forsén, S. and Nilsson, M. *Acta Chem. Scand.* **13** (1959) 1383.
13. Reeves, L. W., Allan, E. A. and Strømme, K. O. *Can. J. Chem.* **38** (1960) 1249.
14. Forsén, S. and Nilsson, M. *Acta Chem. Scand.* **14** (1960) 1333.

Received September 15, 1961.

ACTA CHEMICA SCANDINAVICA 16 (1962) 591–598

Isothiocyanates XLII *. Glucocleomin, A New Natural Glucoside, Furnishing (–)-5-Ethyl-5-methyl-2-oxazolidinethione on Enzymic Hydrolysis

ANDERS KJÆR and HELENE THOMSEN

Department of Organic Chemistry, Royal Veterinary and Agricultural College, Copenhagen V, Denmark

Dedicated to Professor *Holger Erdtman* on his 60th birthday

The presence of a new glucoside, *glucocleomin*, in seeds of *Cleome spinosa* Jacq. *(Capparidaceae)* is demonstrated. Acid hydrolysis of glucocleomin produces hydroxylamine whereas enzymic hydrolysis is accompanied by the formation of sulphate, glucose and a 2-oxazolidinethione. On basis of composition, paper chromatography, infra-red and nuclear magnetic resonance spectra the latter is identified as *(–)-5-ethyl-5-methyl-2-oxazolidinethione* with as yet unknown absolute configuration.

The identification is corroborated by synthesis of the heterocyclic hydrolysis product from optically active 1-amino-2-methyl-2-butanol, obtained by resolution of the racemic amino-alcohol with L-mandelic acid. The synthesis of *racemic 5-propyl-* and *5-isopropyl-2-oxazolidinethione* also is described. The combined experimental data provide the basis for a structural formulation of *glucocleomin*. Several botanical sources of glucocleomin are listed.

In a previous communication of this series [1], seed extracts of several species of the family *Capparidaceae* were demonstrated to contain two isothiocyanate-producing glycosides. One of these, glucocapparin, afforded methyl isothiocyanate on enzymic hydrolysis and was subsequently isolated in crystalline form from seeds of *Cleome spinosa* Jacq.[2] It is the purpose of the present paper to describe the structure elucidation of the second glycoside, extracted from the same seed material and constituting an addition to the rapidly growing list of glycosides of this general type [3].

Cleome spinosa Jacq. is a herb of paleotropical distribution, indigeneous to the American continent but naturalized in tropical and subtropical regions

* Part XLI of this series: *Acta Chem. Scand.* **16** (1962) 83.

throughout the world. It affords a popular garden annual ('spider flower') and seed material can be obtained commercially *.

Enzymic hydrolysis of the unknown glycoside did not give rise to the formation of steam-volatile products whereas the expected production of sulphate and glucose was confirmed by paperchromatographic methods. Again, acid hydrolysis of a paper eluate of the unknown glycoside yielded hydroxylamine, a characteristic behaviour of all mustard oil-producing glucosides [4]. It was further established that the enzymic reaction was accompanied by the formation of an ether-extractable hydrolysis product, *cleomin*, yielding a blue colour with Grote's reagent and displaying ultra-violet absorption data (λ_{max}^{EtOH} 242 mμ, displaced to 230 mμ in alkali), analogous to those of several 2-oxazolidinethiones, previously recognized as enzymic hydrolysis products of glucosides containing β-hydroxy-substituted side-chains [3,5]. Paperchromatographic comparison of the enzymically produced compound with all formerly known 2-oxazolidinethiones of natural derivation clearly indicated it to be different from these. The combined evidence at this stage indicated that the glycoside present in *C.spinosa* besides glucocapparin was a new glucoside of the ordinary type, for which the designation *glucocleomin* was introduced in accordance with the common practice for naming compounds within this group of natural products [3] (*cf.* footnote p. 594).

On a preparative scale, a methanolic extract of defatted *C. spinosa* seed powder was subjected to enzymic hydrolysis with a cell-free myrosinase preparation in aqueous citrate buffer at pH 6.4. The mixture was steam-distilled in order to remove methyl isothiocyanate originating from glucocapparin, and the non-volatile hydrolysis product, cleomin, was isolated by continuous ether extraction. After chromatography on alumina and recrystallization from water, cleomin was obtained as a *levo*rotatory, colourless compound, m.p. 52°, possessing the elemental composition $C_6H_{11}NOS$ and exhibiting ultra-violet and infra-red absorption spectra strikingly similar to those of several 2-oxazolidinethiones previously studied in this laboratory and elsewhere [3,5]. Consequently, (I) represents a likely partial structure of cleomin, in which three carbon and ten hydrogen atoms remain to be accomodated.

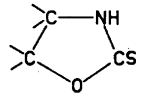

I

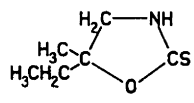

II

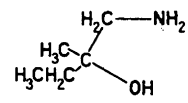

III

Substitution of (I) with propyl- or isopropyl-groupings in 5-position could be ruled out upon comparison of the infra-red spectra of cleomin with those of synthetic samples of these previously unknown substitutes, but also through the higher R_F-values observed on paper chromatography of the 5-substituted propyl-derivatives. Several analogies[5] suggested that the unknown 4-substituted

* The seed material employed in the present studies was purchased from E. Benary, Hann.-Münden, Germany, under the name *Cleome pungens* Willd. (synonym for *C. spinosa* Jacq.). On paperchromatographic evidence two glucosides were likewise reported by Schultz and Wagner [14] in *C. pungens*.

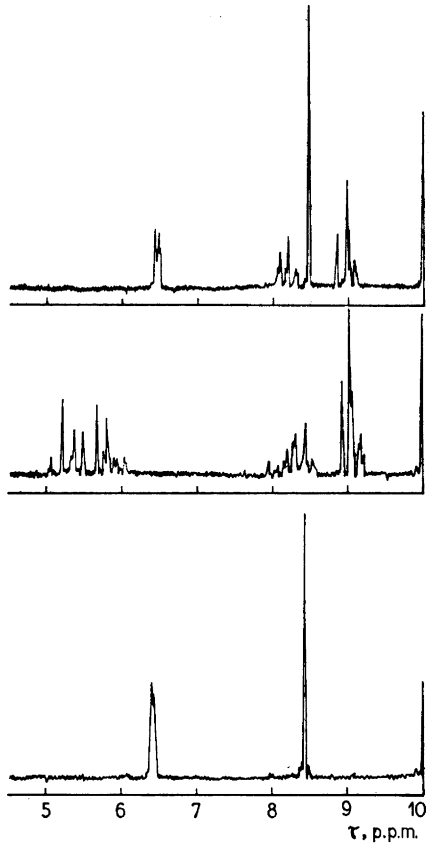

Fig. 1. Proton resonance spectra (60 Mc) of: upper curve: cleomin (II)[(−)-5-ethyl-5-methyl-2-oxazolidinethione]; middle curve: 4-ethyl-2-oxazolidinethione; lower curve: 5,5-dimethyl-2-oxazolidinethione. Solvent: $CDCl_3$.

propyl-isomerides would possess even higher R_F-values and hence could be disregarded as well. The syntheses of the racemic *5-propyl-* and *5-isopropyl-2-oxazolidinethione* were performed by reaction of the appropriate amino-alcohols with thiocarbonyl chloride in the customary way, as described in the experimental section.

A choice between the six possible di-(or tri)-substitutes could be made on basis of n.m.r. spectra (Fig. 1) *. The strong singlet at τ 8.46 precludes structures with hydrogen in both 4- and 5-position, whereas the absence of a doublet at τ 8.5—9.0 is incompatible with structures containing three methyl groups as substituents. Of the remaining possibilities, *viz.* 4-ethyl-4-methyl- and 5-ethyl-5-methyl-2-oxazolidinethione, the former can be excluded since no absorption occurs at τ 5—6, the range for the (5)-CH_2-O-multiplet, as evident from the n.m.r. spectrum of 4-ethyl-2-oxazolidinethione (Fig. 1). The n.m.r. data of

* Nuclear magnetic resonance (n.m.r.) spectra were kindly determined by Varian Associates, Zürich, on an A-60 instrument and are reported here in τ values relative to tetramethylsilane (τ 10.0, Fig. 1).

cleomin are, on the other hand, in perfect agreement with those expected for structure (II), the multiplet at τ 6.45 being assignable to the (4)-CH_2-protons as supported by comparison with the n.m.r. spectrum of 5,5-dimethyl-2-oxazolidinethione (Fig. 1).

Corroboration of this conclusion was provided through infra-red studies. Whereas the solid-phase IR-spectrum of cleomin differed significantly from that of (±)-5-ethyl-5-methyl-2-oxazolidinethione, previously prepared in this laboratory [6], the two compounds gave, as expected, identical infra-red spectra in solution.

A synthesis of cleomin (II) was achieved in the following way. (±)-1-Amino-2-methyl-2-butanol (III), prepared from the cyanohydrin of methyl ethyl ketone as formerly described in this series [6], was resolved through diastereoisomeric salts. Preliminary attempts to effect the resolution by means of (−)-2-(2-naphthoxy)-propionic acid *, successfully employed by Fourneau and Ribas [7] in the resolution of the analogous 1-dimethylamino-2-methyl-2-butanol, were unavailing. Mandelic acid, however, proved to be useful for the desired resolution. The amino-alcohol enantiomer giving a *levo*rotatory neutral oxalate was liberated from the least soluble salt with L(+)-mandelic acid.

On reaction with thiocarbonyl chloride, the active amino-alcohol (III) was converted into (−)-*5-ethyl-5-methyl-2-oxazolidinethione* (II), which proved identical with cleomin, both with regard to sign and magnitude of rotation, m.p. and mixed m.p., as well as ultra-violet, infra-red and n.m.r. spectra. Experimental work is in progress to establish the absolute configuration of cleomin.

No attempts have been made to isolate the parent glucoside, glucocleomin, but the above structure determination of cleomin provides the clue to its structure. Since it has been repeatedly demonstrated [3,5] that enzymically produced 2-oxazolidinethiones arise from cyclization of initially formed 2-hydroxy-substituted isothiocyanates, and in view of the behaviour of glucocleomin towards enzymic and acid hydrolysis, it appears safe to conclude that the glucoside ion ** possesses the structure (IV) with as yet unknown stereochemistry in the side-chain.

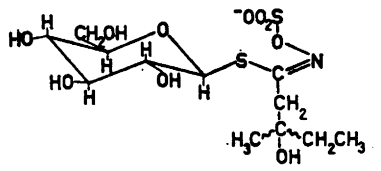

IV

* This acid was conveniently prepared by resolution of the racemate with (+)-2-amino-1-phenylpropane ('dextroamphetamine') according to a proposal of Matell [8] (*cf.* the experimental part).

** Recently, Ettlinger and Dateo [23] suggested the trivial name 'glucosinolate' (*cf.* Greek *σινατ-ελαιον*, mustard oil) for the *S*-β-D-1-glucopyranosyl-formthiohydroximic acid-*O*-sulphonate ion whence all hitherto encountered glucosides of this class derive. In this semisystematic nomenclature, which is considered practical in view of the rapidly growing number of such uniformly constituted glucosides, the glucocleomin ion would be *2-hydroxy-2-methylbutyl-glucosinolate*.

Formally, the new glucoside is closely related to glucoconringiin, a natural glucoside undergoing hydrolysis to 5,5-dimethyl-2-oxazolidinethione [9-11]. As discussed in a recent communication from this laboratory [5], compounds involved in the well-known metabolism of valine, isoleucine and leucine may conceivably function as precursors in the biogenesis of isothiocyanate glucosides containing branched side-chains.

Besides *Cleome spinosa* Jacq. previously published paperchromatographic data [1] indicate seeds of the following *Cleome* species to be sources of glucocleomin: *C. arabica* L., *C. arborea* Bss., *C. gigantea* L., *C. speciosissima* Deppe., *C. viscosa* L., *C. graveolens* Rafin. and *C. trachysperma* (Torr. *et* Gray) Pax *et* K. Hoffm. Other seed specimens containing glucocleomin according to paper chromatography are: *Cleome ornithopoides* L., *C. machycarpa* Rafin., *C. integrifolia* Torr. *et* Gray, *C. serrata* Jacq. and *Crataeva Tapia* L. Whereas no glucocleomin is detectable in seeds of the common caper, *Capparis spinosa* L., fresh green leaves of the same species was found to contain the new glucoside. It is interesting to note that glucocleomin in all of the above listed sources is accompanied by glucocapparin.

Recently, glucocleomin also has been identified in this laboratory as a constituent of seeds of the Indian tree *Putranjiva Roxburghii* Wall., belonging to the family *Euphorbiaceae* and reputed as a source of isothiocyanate glucosides. The results of these studies will be presented in a forthcoming communication [13].

EXPERIMENTAL

Melting points are uncorrected and determined in capillary tubes in liquid baths equipped with fully immersed thermometers. Rotations are measured in 1 dm tubes. Analytical samples are dried *in vacuo* at room temperature over calcium chloride.

Paperchromatographic analysis. A 20 μl aliquot of a 70 % methanol extract (1.0 ml) of finely ground seeds (0.1 g) of *Cleome spinosa* Jacq. was chromatographed on paper with glucotropaeolin as a reference compound in the solvent system butanol: ethanol: water (4:1:4). Besides much glucocapparin (R_B*0.26), a somewhat weaker spot of glucocleomin was observed with an R_B-value of 0.63. Two additional, faint spots with R_B-values of 1.36 and 1.88 indicated the presence of two minor glycosides in the same seed extract.

The total 70 % methanol extract of a 5 g seed sample was evenly distributed along the starting lines of two sheets of Whatman paper No. 3 MM and chromatographed in the above solvent system. The glucocleomin-zones were located by spraying of edge cuts with $AgNO_3/NH_3$ and separately eluted with water. The residue from the eluate of the first sheet was hydrolyzed with 20 % HCl (3 ml) at 50° for 2.5 h. Next day, the hydrolysis residue was chromatographed in methanol : 6 N HCl (7:3), and the formation of hydroxylamine was demonstrated on spraying with picryl chloride [4]. The eluate from the second sheet (100 μl) was subjected to enzymic hydrolysis with a sulphate-free myrosinase preparation. After 1 h, the liberation of sulphate could easily be demonstrated by means of barium acetate. Paper chromatography in *n*-BuOH:EtOH:H_2O (4:1:4) and *n*-BuOH:pyridine:H_2O (6:4:3) served to confirm the concomitant formation of glucose.

Isolation and properties of cleomin. Seeds of *Cleome spinosa* Jacq. (1 kg) were portionwise disintegrated and defatted in a Waring blendor in a total of 3.2 l of carbon tetrachloride. The seed cake was refluxed for 1 h with fresh solvent (3 l) and this operation was repeated once. The dry seed powder (645 g) was extracted by refluxing with three successive 3.5 l-portions of 70 % methanol. The combined filtrates were concentrated *in vacuo*

* *i.e.* the ratio between the distances travelled by the compound and glucotropaeolin, respectively[14].

to remove methanol (end volume 1.4 l) and an orange precipitate was removed by filtration through Celite.

The filtrate was diluted to 4 l and buffered by addition of 150 ml of a 1 M solution of trisodium citrate, containing 3 g of citric acid per l. A cell-free myrosinase solution (100 ml), prepared from white mustard flour, was added together with a small quantity of ascorbic acid [15], and the enzymic hydrolysis was allowed to proceed at room temperature for 24 h. The mixture was then steam-distilled to remove methyl isothiocyanate, a total of 3 l of distillate being collected. After removal of a dark precipitate by filtration, the residue from the steam-distillation was saturated with sodium chloride and subjected to continuous extraction with ether for 24 h.

Cleomin was subsequently transferred from the ether extract to 0.1 N NaOH (400 ml). The aqueous phase was brought to pH 6.5 with hydrochloric acid and the product was retransferred to ether by continuous extraction for 24 h.

The dried ether solution was concentrated to a yellow oil (1.6 g) from which the Grote-positive fraction was quantitatively extracted with hot water. The solid contained in the combined aqueous extracts (1.37 g) was now extracted with several portions of benzene to bring all cleomin into solution. This was then allowed to flow through a column of neutral alumina (65 × 32[o] mm) retaining considerable amounts of extraneous matter. The column was washed with benzene (400 ml) and eluted with the same solvent containing 0.5 % of methanol. The cleomin-containing fractions were pooled and concentrated to dryness. The residue (700 mg) was taken up in hot water, a small quantity of insoluble material was filtered off, and the solution was cooled whereupon slightly yellow crystals separated (270 mg). These were recrystallized twice from water with a little charcoal to give an analytical specimen of *cleomin* (40 mg) as dense, colourless rhombs, m.p. 50—51°, $[\alpha]_D^{24}$—25.4° (*c* 1.0, H_2O). (Found: C 49.34; H 7.78; N 9.62. Calc. for $C_6H_{11}NOS$: C 49.62; H 7.64; N 9.65). The ultra-violet spectrum in ethanol had the following characteristics: λ_{max} 243 mμ (ε 19500), λ_{max} 204 mμ (ε 6650) and λ_{min} 218 mμ (ε 3000), in good agreement with previously reported data for 2-oxazolidinethiones [3]. The infra-red spectrum (in KBr) exhibited conspicuous bands at 3140 vs, 3020 m, 2950 s, 2910 m, 2730 w, 1580 vs, 1470 m, 1455 m, 1380 s, 1348 m, 1330 s, 1300 s, 1250 s, 1200 vs, 1130 s, 1108 s, 1060 m, 1044 m, 1020 w, 1002 m, 962 s, 913 w, 878 m, 787 s and 717 m cm^{-1} (vs very strong, s strong, m medium and w weak). In chloroform solution, the spectrum of cleomin was considerably changed, exhibiting, *e.g.*, two bands at 1530 m and 1500 s cm^{-1}, instead of the 1580 cm^{-1} peak, but indistinguishable from the spectrum of (±)-5-ethyl-5-methyl-2-oxazolidinethione [6] in chloroform solution. In the solid state, however, the enantiomer and the racemic modification possessed markedly different spectra.

On paper chromatography with the upper layer of the solvent system benzene:heptane:water (9:2:9) as the mobile phase, cleomin migrated at an R_{Ph}-value* of 0.83 and was indistinguishable from (±)-5-ethyl-5-methyl-2-oxazolidinethione [6], whereas (±)-5-propyl- and (±)-5-isopropyl-2-oxazolidinethione migrated at rates corresponding to R_{Ph}-values of 0.95 and 0.93, respectively.

Syntheses

Resolution of 1-amino-2-methyl-2-butanol (III). An attempt was made to resolve the racemic amino alcohol by means of (−)-2-(2-naphthoxy)-propionic acid [7]**, which was

* *i.e.* the ratio between the distances travelled by the compound and (+)-5-phenyl-2-oxazolidinethione [16] as a reference.

** This acid was conveniently obtained by resolution of the racemic acid with (+)-1-phenyl-2-aminopropane, liberated from the commercially available sulphate ('Dextroamphetamine sulphate'), according to a suggestion by Matell [8]. The salt produced from equivalent amounts of the acid and amine was recrystallized four times from 85 % ethanol (yield 70 %), m.p. 197—198°, $[\alpha]_D^{23}$ −47.0° (*c* 1.0, CH_3OH). (Found: C 75.05; H 7.23; N 4.02. Calc. for $C_{22}H_{25}NO_3$: C 75.18; H 7.17; N 3.99). (−)-2-(2-Naphthoxy)-propionic acid was liberated from the salt, extracted with ether and recrystallized from benzene, m.p. 118°, $[\alpha]_D^{24}$ −93.5° (*c* 0.5, abs. C_2H_5OH). Lit. values [17]: m.p. 117°, $[\alpha]_D^{20}$ −93.33°.

successfully employed by Fourneau and Ribas [7] in a very similar case, but no fractionation into diastereoisomeric salts could be effected on recrystallization. The following procedure, however, proved useful in achieving the desired resolution:

A solution of the amino-alcohol (4.34 g) in a 3:1 mixture of ethyl acetate and anhydrous ethanol (475 ml) was mixed with another solution of L(+)-mandelic acid (6.40 g) in the same solvent mixture (200 ml), heated to 50° and cooled. The salt (10.6 g), m.p. 115–119°, separated on scratching and was recrystallized seven times from the above solvent system to give one of the diastereoisomeric salts in pure form (2.95 g), m.p. 131°, $[\alpha]_D^{24}$ + 69.0° (*c* 4, H_2O). (Found: C 61.02; H 8.20; N 5.43. Calc. for $C_{13}H_{21}O_4N$: C 61.15; H 8.29; N 5.49). The amino-alcohol was liberated with conc. NaOH and continuously extracted into ether. The dried solution was mixed with an ethereal solution of the calculated amount of oxalic acid dihydrate to form the *neutral oxalate*, which separated from 96 % ethanol in thin colourless plates, m.p. 192°, $[\alpha]_D^{25}$—4.2° (*c* 2.5, H_2O). (Found: C 48.43; H 9.61; N 9.34. Calc. for $C_{13}H_{28}N_2O_6$: C 48.63; H 9.52; N 9.46). On admixture with the racemic oxalate [6], the melting point was depressed to 187–188°. The two preparations gave nearly identical infra-red spectra (in KBr).

Synthesis of (—)-5-ethyl-5-methyl-2-oxazolidinethione (cleomin). The above *levo*rotatory oxalate (675 mg) was suspended in chloroform (15 ml) and cooled in ice. Thiocarbonyl chloride (0.5 ml) was added to the stirred suspension, followed by triethylamine (1.4 g) dissolved in chloroform (5 ml). The reaction mixture was kept at 0° for several hours and then allowed to come to room temperature. The organic phase was extracted with three 5 ml-portions of 0.1 N HCl, washed with water and dried. On evaporation to dryness, a polymeric solid embedded in a yellow oil remained. The latter was thoroughly extracted with hot water until the extracts gave negative Grote-reaction. After concentration to 10 ml, the aqueous solution on cooling and seeding with cleomin slowly deposited colourless, rhombic plates (110 mg), which were recrystallized twice from water to give an analytical specimen, m.p. 50–51°, alone or in admixture with naturally derived cleomin, $[\alpha]_D^{24}$ —25.9° (*c* 1.0, H_2O). (Found: C 49.78; H 7.70; N 9.44). The synthetic specimen was indistinguishable from cleomin on basis of paper chromatography as well as ultra-violet, infra-red and n.m.r. spectra.

5-Propyl-2-oxazolidinethione. (i) *2-Hydroxyvaleronitrile.* Butyraldehyde was converted into the cyanohydrin in 70 % yield on treatment with liquid hydrocyanic acid and a few drops of piperidine, following the general procedure of Linstead and Whalley [18], b.p. 97–98°/11 mm, n_D^{15} 1.4224 (Lit. values: b.p. 110.5–111°/20.5 mm [19], 73–74°/3 mm [20]; $n_D^{15.5}$ 1.42285 [19], n_D^{20} 1.4220 [20]). (ii) *1-Amino-2-pentanol.* The cyanohydrin was reduced in ether solution with a five-fold excess of lithium aluminium hydride, and the reaction mixture was worked up as previously described for analogous cases [9]. The amino-alcohol was obtained in 60 % yield and distilled as a colourless oil, b.p. 83°/10 mm, n_D^{25} 1.4490 (supercooled), which solidified in the receiver, m.p. 29°. (Found: C 58.13; H 12.63; N 13.40. Calc. for $C_5H_{13}NO$: C 58.21; H 12.70; N 13.58). An incorrectly analyzing sample was previously recorded with the b.p. 75–80°/3.5–4 mm [21]. For comparison, the benzamide was prepared as described elsewhere [21], m.p. 112.5° (reported [21] 112–113.5°). The *normal oxalate*, m.p. 212° (decomp.), separated from water (Found: C 48.61; H 9.36; N 9.47). (iii) *(+)-5-Propyl-2-oxazolidinethione.* Upon reaction of 1-amino-2-pentanol with thiocarbonyl chloride in chloroform and addition of triethylamine, a method previously utilized in this laboratory [12], 5-propyl-2-oxazolidinethione was obtained in a 25 % yield. The substance separated from ethyl acetate: pentane mixtures in flat colourless needles, m.p. 51° (Found: C 49.53; H 7.47; N 9.59. Calc. for $C_6H_{11}NOS$: C 49.62; H 7.64; N 9.65). The ultra-violet spectrum (in ethanol) possessed the following characteristics: λ_{max} 243 mμ (ε 18 250), λ_{max} 204 mμ (ε 5100), and λ_{min} 217 mμ (ε 1540). The infra-red spectrum exhibited the expected bands.

5-Isopropyl-2-oxazolidinethione. (i) *2-Hydroxyisovaleronitrile.* Prepared from isobutyraldehyde by the same procedure as employed above for butyraldehyde, b.p. 90°/10 mm, $n_D^{15.5}$ 1.4215 (Lit. values: b.p. 106–106.5°/22 mm [19], n_D^{16} 1.42215 [19]). (ii) *1-Amino-3-methyl-2-butanol.* The reduction of the cyanohydrin proceeded in 80 % yield as described in the above straight-chain series. The amino-alcohol distilled at 76–77°/9 mm as a colour-

less oil, n_D^{26} 1.4501 (supercooled), crystallizing in the receiver, m.p. 27°. (Found: C 58.15; H 12.70; N 13.42). (Lit.values [22]: b,p. 174°/754 mm, m.p. 26–27°). The *benzamide* was prepared for comparison as described above, m.p. 116° (Found: C 70.09; H 8.19; N 6.79. Calc. for $C_{11}H_{17}NO_2$: C 69.52; H 8.26; N 6.76). The *normal oxalate* separated from water, m.p. 229° (decomp.). (Found: C 48.62; H 9.37; N 9.57). (iii) (±)-*5-Isopropyl-2-oxazolidinethione*. The above described procedure was adopted unchanged for the conversion of 1-amino-3-methyl-2-butanol into 5-isopropyl-2-oxazolidinethione, which separated from a mixture of ethyl acetate and pentane in flat, colourless needles, m.p. 99.5°, possessing an ultra-violet spectrum coinciding with that of the 5-propyl derivative. (Found: C 49.62; H 7.72; N 9.44). The infra-red spectrum, however, was markedly different from that of the 5-propyl-substituted compound.

Microanalyses were performed by Mr. G. Cornali.

The authors acknowledge the assistance of Miss E. Vesterager in part of the synthetic work. Thanks are due to Dr. O. Rosenlund, *Ferrosan Ltd.*, for a generous gift of 'Dextro-amphetamine sulphate' and to *The Botanical Garden of the University of Copenhagen* for numerous seed and plant specimens.

The work is part of investigations supported by *The Danish State Research Foundation (Statens Almindelige Videnskabsfond), The Carlsberg Foundation (Carlsbergfondet)* and *Kai Hansen's Fond.*

REFERENCES

1. Kjær, A., Gmelin, R. and Larsen, I. *Acta Chem. Scand.* **9** (1955) 857.
2. Kjær, A. and Gmelin, R. *Acta Chem. Scand.* **10** (1956) 335.
3. Kjær, A. *Fortschr. Chem. Org. Naturstoffe* **18** (1960) 122.
4. Ettlinger, M. G. and Lundeen, A. J. *J. Am. Chem. Soc.* **78** (1958) 4172.
5. Kjær, A. and Christensen, B. W. *Acta Chem. Scand.* **16** (1962) 71.
6. Kjær, A. and Boe Jensen, R. *Acta Chem. Scand.* **12** (1958) 1746.
7. Fourneau, E. and Ribas, I. *Anales soc. españ. fis. y quim.* **25** (1927) 401.
8. Matell, M. *Acta Chem. Scand.* **7** (1953) 698.
9. Kjær, A., Gmelin, R. and Boe Jensen, R. *Acta Chem. Scand.* **10** (1956) 432.
10. Schultz, O.-E. and Wagner, W. *Arch. Pharm.* **289/61** (1956) 597.
11. Gmelin, R. and Virtanen, A. I. *Acta Chem. Scand.* **13** (1959) 1718.
12. Kjær, A. and Christensen, B. W. *Acta Chem. Scand.* **13** (1959) 1575.
13. Kjær, A. and Friis, P. *Acta Chem. Scand.* **16** (1962.) *In press.*
14. Schultz, O.-E. and Wagner, W. *Z. Naturforsch.* **11b** (1956) 73.
15. Schwimmer, S. *Acta Chem. Scand.* **15** (1961) 535.
16. Kjær, A. and Gmelin, R. *Acta Chem. Scand.* **11** (1957) 906.
17. Fourneau, E. and Balaceano *Bull. soc. chim. France* [4] **37** (1925) 1602.
18. Linstead, R. P. and Whalley, M. *J. Chem. Soc.* **1954** 3722.
19. Ultée, A. J. *Rec. trav. chim.* **28** (1909) 248.
20. Nazarov, I. N., Akhrem, A. A. and Kamernitskiĭ, A. V. *Zhur. Obshcheĭ Khim.* **25** (1955) 1345; *Chem. Abstr.* **50** (1956) 4950.
21. Fort, G. and McLean, A. *J. Chem. Soc.* **1948** 1907.
22. Krassuski, K. and Kriwonoss, F. *Ukrain. Khim. Zhur.* **4** (1929) 79; *Chem. Zentr.* **1929 II** 2174.
23. Ettlinger, M.G. and Dateo, Jr.,G.P. *Final Report, Contract DA 19-129-QM-1059.* Departm. of Chemistry, Rice Institute, Houston, Texas (1961) p.12.

Received September 9, 1961.

ACTA CHEMICA SCANDINAVICA 16 (1962) 599–606

Studies on the Chemistry of Lichens

16 *. The Absolute Configuration of Roccellic Acid

BJÖRN ÅKERMARK

Organisk-kemiska Institutionen, Kungl. Tekniska Högskolan, Stockholm, Sweden

Dedicated to Professor *Holger Erdtman* on his 60th birthday

The configurations at the two asymmetric centres of roccellic acid have been established by degradation of its two isomeric monomethylesters (*8*) and (*16*), to (+)-2L-methylpentadecanoic acid (*11*) and (+)-2L-ethyltetradecanoic acid (*19*), respectively. Roccellic acid must thus be (+)-2L-methyl-3L-dodecylsuccinic acid (*3*a).

A number of different lichens contain optically active di- and tricarboxylic acids of the types *1*—*6* [1] (Chart I). It is possible that these acids are derived from alkylated citric acids (type *1*, Chart I). Protolichesterinic acid (*4*a), for example, may be formed from *nor*caperatic acid [2] (*1*, R = $C_{13}H_{27}$, Chart I, II). Nephrosterinic acid (*4b*) and roccellic acid (*3*a) could be formed in similar ways. These transformations should not affect the configuration at the asymmetric carbon atom which is shown in Chart II and common to the acids of the types *1*—*5*. The elucidation of the absolute configuration of some of these acids might therefore be of interest in relation to their biosynthesis. With this possibility in mind, the configuration of the simplest member of the group, roccellic acid (*3*a), has been determined.

DEGRADATIVE WORK

Since a dodecyl group has higher steric requirements than a methyl group, it was possible to prepare the two isomeric monomethyl esters of roccellic acid, (*8*) and (*16*), in a pure state. The monomethylester (*8*), m.p. 45.5—47.5°, was made by treating roccellic acid anhydride (*7*) with dry methanol and the other (*16*), m.p. 56—58°, by hydrolysing dimethyl roccellate (*15*) with an equivalent amount of sodium hydroxide. The monoester (*8*) was decarboxyla-

* Part 15. Lindberg, B. and Meier, H. *Acta Chem. Scand.* 16 (1962) 543.

Chart I

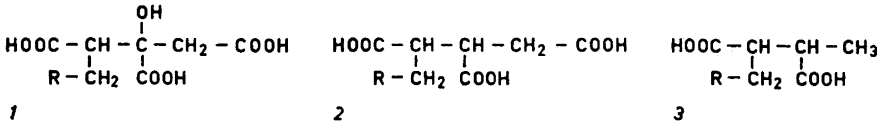

1 *2* *3*

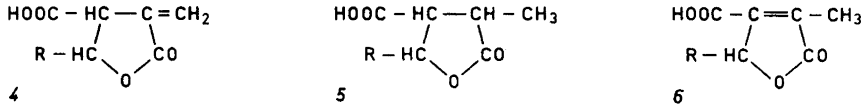

4 *5* *6*

Chart II

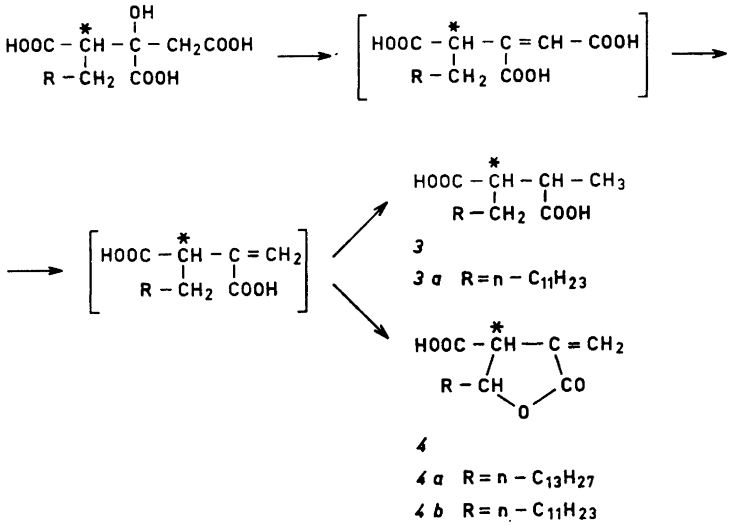

ted by the Hunsdiecker reaction to the bromoester (*9*) which was debrominated with zinc-acetic acid to the ester (*10*) and finally hydrolysed to give (+)-2-methylpentadecanoic acid (*11*; Chart III). Similarly, the monoester (*16*) gave (+)-2-ethyltetradecanoic acid (*19;* Chart IV).

The rotatory dispersion curve * of the morpholinethiocarboxamide (*13*) of (+)-2-methylpentadecanoic acid indicated an L-configuration which was also expected from analogy (*cf.* Ref.[4]). The rotatory dispersion curve of the (+)-2-ethyltetradecanoic acid derivative (*21*), however, failed to show the configuration of this compound. Since roccellic acid anhydride (*7*) is almost optically inactive and a *meso*-form might be expected to have a low rotation due to intramolecular compensation, an L-configuration seemed most probable also for (+)-2-ethyltetradecanoic acid. By stereospecific synthesis the L-configuration was confirmed for both (+)-2-methylpentadecanoic acid (*11*) and for (+)-2-ethyltetradecanoic acid (*19*).

* The measurements and the interpretation of the results were done by Miss A. M. Weidler, Dept. of Chemistry, Stanford University, Calif., U.S.A.

Chart III

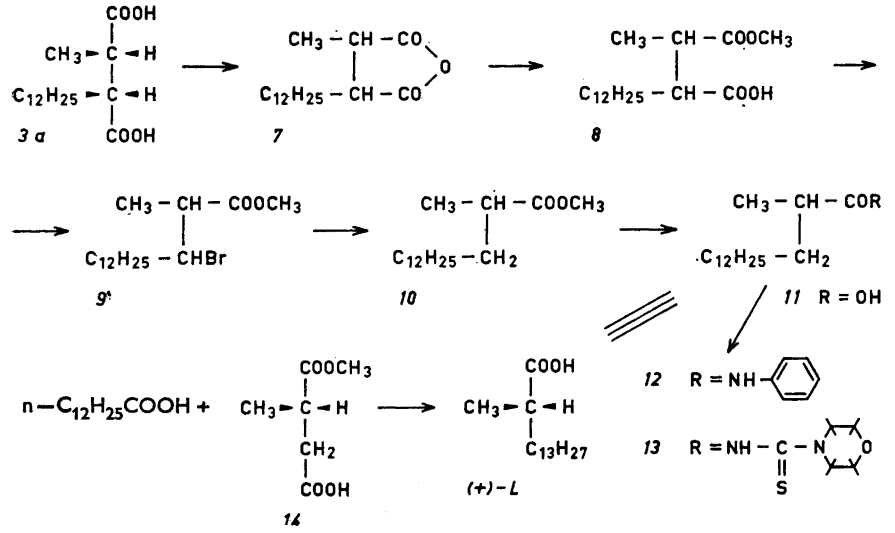

Chart IV

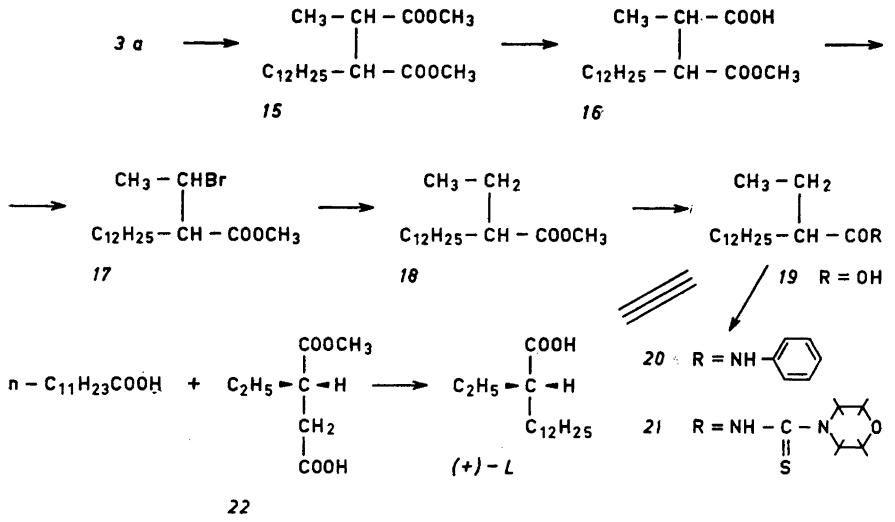

SYNTHETIC WORK

(—)-Methyl 3-carboxy-2L-methylpropanoate (*14*) was made by the procedure described by Ställberg [3]. Mixed electrolysis with tridecanoic acid in methanol containing a small amount of sodium gave (+)-2L-methylpentadecanoic acid (*11*) identical with the degradation product from roccellic acid, although with a slightly higher rotation (*cf.* Ref. [4]).

Similarly, (—)-methyl 3-carboxy-2L-ethylpropanoate (22) was prepared from diethyl allylethylmalonate *via* (—)-2L-ethylpent-4-enoic acid. Since the decarboxylation of allylethylmalonic acid gave a lactone as the main product, the monoethylester of allylethylmalonic acid was decarboxylated and then hydrolysed to 2-ethylpent-4-enoic acid. Several recrystallisations of the quinine salt from acetone gave about 80 % optically pure (—)-2L-ethylpent-4-enoic acid which was methylated and oxidized to (—)-methyl 3-carboxy-2L-ethylpropanoate (*22*) by potassium permanganate in acetone. The configuration and the optical purity of this compound were established by hydrolysis to (—) 2L-ethylsuccinic acid. Mixed electrolysis of (—)-methyl 3-carboxy-2L-ethylpropanoate and lauric acid gave a small amount of (+)-2L,5D-diethyladipic acid and partially racemized (+)-2L-ethyltetradecanoic acid (*19*) having a melting point a few degrees lower than the acid obtained by degradation of roccellic acid. However, the melting point of the synthetic sample was slightly raised on admixture with the degradation product, the infra-red absorption curves of the two acids were identical and the anilides were identical apart from the lower rotation of the synthetic material. A mixture of (—)-2D-ethyltetradecanoic acid (0.010 g) and (+)-2-ethyltetradecanoic acid (0.050 g) from roccellic acid was further identical with the synthetic (+)-2L-tetradecanoic acid in all respects. The acid obtained by degradation of roccellic acid must thus be (+)-2L-tetradecanoic acid (*19*), establishing roccellic acid as (+)-2L-methyl-3L-dodecylsuccinic acid (*3a*; Chart III).

EXPERIMENTAL

Melting points were determined on a Kofler block. Infra-red absorption spectra were taken on a Perkin-Elmer spectrophotometer No. 21, fitted with a sodium chloride prism. The compounds were measured in KBr discs. Microanalysis were carried out by Dr. A. Bernhardt, Mülheim Germany.

Gas chromatography was done on a Pye Argon gas chromatograph, using Apiezon M as the stationary phase and a column temperature of 215°.

Column chromatography was done on silica gel (Gebr. Herrman, Köln, Em 0.15—0.30 mm) using increasing concentrations (0—100 %) of ether in light petroleum (40—60°) as developer.

Roccellic acid (*3a*) was isolated from *Crocynia membranacea* (Dicks.) Zahlbr.[5] M.p. 130.5—132°, $[\alpha]_D^{20}$ + 18.0° (EtOH, *c* 1.94), lit.[6] m.p. 131°, $[\alpha]_D$ + 17.4°.

Roccellic anhydride (*7*). Roccellic acid (12 g) was refluxed with excess of acetyl chloride till the evolution of hydrogen chloride ceased (1.5 h). Distillation of the product at 0.005 mm gave roccellic anhydride (10 g, 89 %) m.p. 26—27.5°, $[\alpha]_D^{20}$ —0.55° ($CHCl_3$, *c* 7.35).

Dimethyl roccellate (*15*) was obtained by methylation of roccellic acid with ethereal diazomethane. Distillation of the product at 0.005 mm gave dimethyl roccellate, m.p. 28.5—30.5°, $[\alpha]_D^{20}$ + 14.5° ($CHCl_3$, *c* 1.67), lit.[6] m.p. 28—29°.

(+)-*Methyl 2-methyl-3-carboxypentadecanoate* (*8*). Roccellic acid anhydride (9.5 g) was refluxed for 0.5 h with dry methanol. The solution was left overnight and excess methanol was then evaporated at room temperature. Chromatography on silica gel (200 g) gave (+)-methyl 2-methyl-3-carboxypentadecanoate (8.0 g, 80 %), m.p. 45.5—47.5°, $[\alpha]_D^{20}$ + 17.6° ($CHCl_3$, *c* 2.96). (Found: C 68.6; H 10.8; equiv. wt. 314. Calc. for $C_{18}H_{34}O_4$: C 68.8; H 10.8; equiv.wt. 314).

(+)-Methyl *3-bromo-2-methylpentadecanoate* (*9*). The monoester (*8*, 9.2 g) was suspended in water (100 ml) and neutralized with sodium hydroxide (1 N). Addition of silver nitrate (6 g in 100 ml water) gave a white silver salt which was washed thoroughly with

water and dried *in vacuo* for 20 h at 100°. The silver salt was then suspended in dry, boiling carbon tetrachloride and bromine was added till presistant colour (4.3 g). The suspension was refluxed for 15 min and then filtered. The precipitate was washed repeatedly with carbon tetrachloride and the combined washings evaporated. Removal of acidic material and distillation gave (+)-methyl 3-bromo-2-methyl-pentadecanoate (7.5 g, 73 %), b.p. 152—154° (1.0 mm), $[\alpha]_D^{20}$ + 10.5° ($CHCl_3$, *c* 4.06), d_4^{20} 1.080. (Found: Br 22.0. Calc. for $C_{17}H_{33}BrO_2$: Br 22.9).

(+)-*Methyl 2-methylpentadecanoate* (10). A mixture of the bromoester (*9*, 7 g), zinc powder (20 g) and potassium iodide (0.1 g) in acetic acid (100 ml) was heated on a water bath for 45 min. After cooling, (+)-methyl 2-methylpentadecanoate (4.8 g, 88 %) was isolated in the usual way. B.p. 141—144° (0.65 mm) $[\alpha]_D^{20}$ + 11.2° (undiluted, *l* 0.5), $[\alpha]_D^{20}$ + 10.9° ($CHCl_3$, *c* 3.31), d_D^{20} 0.868. The purity was proved by gas chromatography. (Found: Saponif. equiv. 265. Calc. for $C_{17}H_{34}O_2$: Saponif. equiv. 270).

(+)-*2-Methylpentadecanoic acid* (*11*). A solution of the ester (*10*, 2.5 g) in dioxan (100 ml) and water (20 ml) containing potassium hydroxide (6 g) was refluxed for 1 h. The crude acid obtained (1.7 g) was chromatographed on silica gel (35 g), giving (+)-2-methylpentadecanoic acid (0.9 g, 40 %). M.p. 39.5—41.5° (from light petroleum at —70° followed by sublimation), identified with a synthetic sample of (+)-2L-methylpentadecanoic acid by means of mixed melting point and infra-red absorption. $[\alpha]_D^{20}$ + 10.5° ($CHCl_3$, *c* 3.06). (Found: C 75.0; H 12.5; equiv. wt. 252. Calc. for $C_{16}H_{32}O_2$: C 75.0; H 12.5; equiv. wt. 256).

The anilide of (+)-*2-methylpentadecanoic acid* (*12*). (+)-2-Methylpentadecanoic acid (*11*; 0.1 g) was treated with thionyl chloride (1 ml) containing a trace of pyridine for 2 h at room temperature. Excess of thionyl chloride was evaporated *in vacuo* and aniline (0.5 g) added. Addition of dilute hydrochloric acid and filtration gave the anilide of (+)-2-methylpentadecanoic acid (0.1 g, 78 %), m.p. 96—97° (from methanol), identified with a synthetic sample by means of mixed melting point determination and infra-red absorption. $[\alpha]_D^{20}$ + 21.0° ($CHCl_3$, *c* 3.21). (Found: C 79.3; H 11.0; N 4.7. Calc. for $C_{22}H_{37}NO$: C 79.8; H 11.2;N 4.2).

The morpholinethiocarboxamide of (+)-*2-methylpentadecanoic acid* (*13*) was prepared according to the method described by Djerassi *et al.*[7] M.p. 110—112° (from cyclohexane). Rotatory dispersion in methanol $[\alpha]^{20}$: + 30° (650) mμ), + 32° (589 mμ), + 153° (373 mμ), —178° (328 mμ), —178° (310 mμ). *c* 0.05625, *l* 0.10 (307—348 mμ); *c* 0.1125, *l* 0.10 (310—400 mμ); *c* 0.1125, *l* 0.50 (372—650 mμ). (Found C 65.1; H 10.4; N 7.0. Calc for $C_{21}H_{40}N_2O_2S$ C 65.5; H 10.4; N 7.3).

(+)-*2L-Methylpentadecanoic acid* (*11*). A mixture of (—)-methyl 3-carboxy-2L-methylpropanoate [3,4] (2.1 g) and tridecanoic acid (6.2 g) in methanol containing sodium methoxide (from 0.1 g sodium) was electrolysed between platinum electrodes. The product was dissolved in light petroleum, the acidic material removed and the solvent evaporated. Hydrolysis by boiling with potassium hydroxide (6 g) in dioxan (250 ml) and water (20 ml) for 1 h gave a mixture of acids (1.5 g) which was chromatographed on silica gel (30 g) furnishing (+)-2L-methylpentadecanoic acid (1.0 g, 28 %), m.p. 39.5—41.5° (from light petroleum at —70°, followed by sublimation), $[\alpha]_D^{20}$ + 11.0° ($CHCl_3$, *c* 2.55). (Found: C 74.6; H 12.3; equiv. wt. 252. Calc. for $C_{16}H_{32}O_2$: C 75.0, H 12.5; equiv.wt. 256).

The anilide of (+)-*2L-methylpentadecanoic acid* (*12*) was prepared as described above. M.p. 96—96.5°, $[\alpha]^{20}$ + 22.4° ($CHCl_3$, *c* 3.08). (Found: C 79.2; H 11.0; N 4.6. Calc. for $C_{22}H_{37}NO$: C 79.8; H 11.2; N 4.2).

(+)-*Methyl 3-carboxy-2-dodecylbutyrate* (*16*). Dimethyl roccellate (*15*; 29 g) in a mixture of dioxan (625 ml) and 1,2-dimethoxyethane (250 ml) was refluxed for 1 h with aqueous sodium hydroxide (3.6 g in 250 ml of water). During the hydrolysis more water (60 ml) was added to keep the mixture homogeneous. The alkali soluble part was isolated in the usual way and washed repeatedly with boiling light petroleum (40—60°). The residue was fairly pure roccellic acid (7.5 g). The light petroleum extracts gave impure monoester (18 g, 65 %), m.p. 51—55°. Chromatography on silica gel (250 g) gave (+)-methyl 3-carboxy-2-dodecylbutyrate (13.5 g, 49 %), m.p. 56—58°, $[\alpha]_D^{20}$ + 11.8° ($CHCl_3$,

c 5.52). (Found: C 69.0; H 10.9; equiv.wt. 315. Calc. for $C_{18}H_{34}O_4$: C 68.8; H 10.8; equiv.wt. 314).

(+)-*Methyl 3-bromo-2-dodecylbutyrate* (*17*). Hunsdiecker degradation of the monoester (*16*; 11.0 g) gave (+)-methyl 3-bromo-2-dodecylbutyrate (10.2 g, 83 %), b.p. 147—148° (0.9 mm), $[\alpha]_D^{20}$ + 9.0° ($CHCl_3$, *c* 4.05), d_4^{20} 1.089. (Found: Br 22.6. Calc. for $C_{17}H_{33}BrO_2$: Br 22.9).

(+)-*Methyl 2-ethyltetradecanoate* (18). Debromination of the bromoester (17; 9.7 g) with zinc-acetic acid gave (+)-methyl 2-ethyltetradecanoate (6.9 g, 92 %), b.p. 116° (0.06 mm), $[\alpha]_D^{20}$ + 8.46° (undiluted, *l* 0.5), $[\alpha]_D^{20}$ + 9.2° ($CHCl_3$, *c* 12.93), d_4^{20} 0.858. The purity was proved by gas chromatography. (Found: Saponif. equiv. 266. Calc. for $C_{17}H_{34}O_2$: Saponif. equiv. 270).

(+)-*2-Ethyltetradecanoic acid* (*19*). The ester (*18*; 4 g) was refluxed for 45 min with a mixture of ethanol (250 ml) and aqueous sodium hydroxide (2 N, 75 ml). The product was chromatographed on silica gel (80 g), giving (+)-2-ethyltetradecanoic acid (3.2 g, 84 %), m.p. 24—27° or 28—30° (dimorphous), $[\alpha]_D^{20}$ + 7.0 ($CHCl_3$, *c* 14.60). On admixture with a synthetic sample, m.p. 24—26°, $[\alpha]_D^{20}$ + 5.2°, the melting point of the high melting modification was depressed to 25—27°. However, the infra-red spectra were identical and a mixture of (+)-2-ethyltetradecanoic acid (0.050 g) from roccellic acid and (−)-2D-ethyltetradecanoic acid (0.010 g) was shown to be identical with the synthetic (+)-2L-ethyltetradecanoic acid by means of rotation, melting point and mixed melting point. (Found: C 75.0; H 12.1, equiv.wt. 259. Calc. for $C_{16}H_{32}O_2$: C 75.0; H 12.5; equiv.wt. 256).

The anilide of (+)-*2-ethyltetradecanoic acid* (*20*) prepared as described above for the isomer (*12*) had m.p. 91—92.5° (from methanol), $[\alpha]_D^{20}$ + 12.2° ($CHCl_3$, *c* 1.81). Apart from a higher rotation this compound was identical with a synthetic sample as shown by means of mixed melting point determination and infra-red absorption. (Found: C 79.7; H 11.45; N 4.2. Calc. for $C_{22}H_{37}NO$: C 79.8; H 11.2; N 4.2).

The morpholinethiocarboxamide of (+)-*2-ethyltetradecanoic acid* (*21*) was prepared according to the procedure described by Djerassi *et al.*[7] M.p. 102—108° and 107—109° (dimorphous), $[\alpha]_D^{20}$ + 9.2° ($CHCl_3$, *c* 2.20), Rotatory dispersion in methanol $[\alpha]^{25}$: + 30° (360 mμ), 0° (500—525 mμ), −12° (600 mμ). *c* 0.0262, *l* 0.50 (350—375 mμ); *c* 0.131, *l a* 0.50 (375—600 mμ). (Found: C 65.3; H 10.8; N 7.0. Calc. for $C_{21}H_{40}N_2O_2S$: C 65.6; H 10.4; N 7.3).

Diethyl allylethylmalonate. Diethyl allylmalonate (300 g) was slowly added to a suspension of sodium hydride (48 % "in oil", 77 g) in a mixture of dioxan (1 l) and 1,2-dimethoxyethane (0.5 l). When the hydrogen evolution had ceased, ethyl iodide (250 g) was added in one protion. The resulting solution was left at room temperature overnight and then refluxed for 1 h. Most of the solvent (1 l) was evaporated and the product isolated in the usual way. The diethyl allylethylmalonate (270 g, 72 %) had b.p. 147—150° (85 mm), lit. 233° [8], 93—95°/0.5 mm [9].

Ethyl 2-carboxy-2-ethylpent-4-enoate. Sodium hydroxide (67 g) in dry ethanol (0.5 l) was added to a solution of diethyl allylethylmalonate (270 g) in dry ethanol (0.5 l). After standing overnight, the mixture was refluxed for 1 h. Acidic and neutral materials were separated by bicarbonate extraction, giving ethyl 2-carboxy-2-ethylpent-4-enoate (154 g, 88 % based on reacted material), which was used without further purification. In addition some unreacted starting material (75 g) was isolated. (Found: Equiv.wt. 195. Calc. for $C_{10}H_{16}O_4$: equiv.wt. 200).

Ethyl 2-ethylpent-4-enoate. Ethyl 2-carboxy-2-ethylpent-4-enoate (154 g) was added from a dropping funnel to high boiling mineral oil heated to 195° at reduced pressure (100 mm), allowing the decarboxylation product to distill off continuously. Redistillation gave ethyl 2-ethylpent-4-enoate (100 g, 83 %) b.p. 165—168°. (Found: Saponif. equiv. 152. Calc. for $C_9H_{16}O_2$: saponif. equiv. 156).

2-Ethylpent-4-enoic acid. Ethyl 2-ethylpent-4-enoate (100 g) was hydrolysed with sodium hydroxide in aqueous ethanol (1 N) giving 2-ethylpent-4-enoic acid (75 g, 98 %), b.p. 104—106° (12 mm, lit.[8] 208°). (Found: C 65.0; H 9.3; equiv.wt. 125. Calc. for $C_7H_{12}O_2$: C 65.6; H 9.4; equiv.wt. 128).

The S-Benzylthiuronium salt of 2-ethylpent-4-enoic acid prepared in the usual way had. m.p. 135.5—137.5°. (Found: C 61.1; H 7.35; N 9.75. Calc. for $C_{15}H_{22}N_2O_2S$: C 61.2; H 7.5; N 9.5).

(—)-*2L-Ethylpent-4-enoic acid.* The salt from 2-ethylpent-4-enoic acid (75 g) and quinine (190 g) was recrystallised eight times from successively smaller amounts of acetone (0.8—0.2 l). The quinine salt was decomposed with dilute hydrochloric acid giving (—)-2L-ethylpent-4-enoic acid (12 g, 16 %), b.p. 90.5—93° (0.5 mm), $[\alpha]_D^{20}$ —2.40° (undiluted, *l* 0.5), $[\alpha]_D^{20}$ —2.8° ($CHCl_3$, *c* 6.20), d_4^{20} 0.963. The configuration was established by degradation to (—)-2L-ethylsuccinic acid as described below.

(—)-*Methyl 3-carboxy-2L-ethylpropanoate* (*22*). (—)-2L-Ethylpent-4-enoic acid (9 g) was methylated with diazomethane. The methyl ester was dissolved in acetone (200 ml), the solution cooled in an ice-salt bath and potassium permanganate (27 g) added over a period of 5 h. The cooling bath was removed and the mixture was left overnight. The precipitate was then filtered off and washed with water containing sodium pyrosulfite. The combined washings were acidified and extracted with ether. Evaporation of the solvent and chromatography on silica gel gave (—)-methyl 3-carboxy-2L-ethylpropanoate (5.1 g, 45 %), b.p. 86—88°/0.05 mm, $[\alpha]_D^{20}$ —9.10° (undiluted, *l* 0.5), $[\alpha]_D^{20}$ —7.36° ($CHCl_3$, *c* 6.79), d_4^{20} 1.119. (Found: C 52.1; H 7.4; equiv.wt. 160; saponif.equiv. 168. Calc. for $C_7H_{12}O_4$: C 52·5; H 7.5; equiv.wt. 160; saponif.equiv. 160).

The S-Benzylthiuronium salt of (—)-*methyl 3-carboxy-2L-ethylpropanoate* was prepared n the usual way from the acid. M.p. 159—162°. (Found: N 8.6. Calc. for $C_{15}H_{22}N_2O_4S$: N 8.6).

(—)-*2L-Ethylsuccinic acid.* (—)-Methyl 3-carboxy-2L-ethylpropanoate (0.3 g) was hydrolysed with 0.5 N sodium hydroxide. The product was sublimed, then dissolved in water and the solution evaporated at room temperature. Crystallisation from benzene gave partially resolved (—)-2L-succinic acid (0.1 g), m.p. 93—95°, $[\alpha]_D^{20}$ —11.5° (H_2O, *c* 5.71). For the pure L-form Berner *et al.*[10] give m.p. 96°, $[\alpha]_D^{20}$ —18.5° (*cf.* Refs.[11,12]).

(+)-*2L-Ethyltetradecanoic acid* (*19*). A mixture of (—)-methyl 3-carboxy-2L-ethylpropanoate (*22*; 1.2 g) and lauric acid (4 g) in methanol containing sodium methoxide (from 0.1 g sodium) was electrolysed between platinum electrodes. The neutral part of the product was refluxed for 3 h with potassium hydroxide (5 g) in dioxan-water (10:1, 500 ml) to give docosane (1.9 g) and a mixture of acids (0.25 g). The acid fraction was repeatedly wased with light petroleum to give a residue of (—)-2L,5D-diethyladipic acid (0.01 g), m.p. 133—136°. The combined light petroleum extracts were chromatographed on silica gel. The main fraction (0.15 g) was washed with light petroleum at —70° and then sublimed, giving partially resolved (+)-2L-ethyltetradecanoic acid (0.10 g, 5.2 %), m.p. 24—26°, $[\alpha]_D^{20}$ + 5.2° ($CHCl_3$, *c* 2.06). (Found: C 74.5; H 12.4; equiv.wt. 253. Calc. for $C_{16}H_{32}O_2$: C 75.0; H 12.5; equiv. wt. 256.

The anilide of (+)-*2L-tetradecanoic acid* (*20*), prepared from a synthetic sample had m.p. 90—92° (from methanol, then from cyclohexane), $[\alpha]_D^{20}$ + 9.5° ($CHCl_3$, *c* 1.05). (Found: C 79.7; H 11.2; N 4.4. Calc. for $C_{22}H_{37}N$ O: C 79.8; H 11.2; 4.2).

(+)-*2L,5D-diethyladipic acid.* (—)-Methyl 3-carboxy-2L-ethylpropanoate (0.10 g) in methanol containing a trance of sodium methoxide, was electrolysed between platinum electrodes. Hydrolysis ofthe neutral part of the product gave (+)-2L,5D-diethyladipic acid (0.025 g, 36 %) m.p. 134—136° (from chloroform) $[\alpha]_D^{20}$ + 8.6° (EtOH, *c* 1.08). Lit m.p. 136°[13] and 136—136.6°[14] for the high melting optically inactive form of 2,5-diethyladipic acid. (Found: C 59.7; H 8.9; equiv. wt. 99. Calc. for $C_{10}H_{18}O_4$: C 59.4; H 8.9; equiv. wt. 101).

(+)-*2D-Ethylpent-4-enoic acid.* The mother liquiors from the preparation of the quinine salt of (—)-2L-ethylpentenoic acid were concentrated and subjected to further crystallisation. Evaporation of the solvent from the most soluble part and subsequent decomposition of the quinine salt with hydrochloric acid yielded (+)-2D-ethylpent-4-enoic acid (15.5 g, 21 %), b.p. 110—112°/13 mm, $[\alpha]_D^{20}$ + 2.0° (unidluted, *l* 0.5), d_4^{20} 0.962.

(+)-*Methyl 3-carboxy-2D-ethylpropanoate.* (+)-2D-Ethylpent-4-enoic acid (15.5 g) was methylated with diazomethane and then oxidized with potassium permanganate

in acetone. The product was chromatographed oh silica gel giving (+)-methyl 3-carboxy-2D-ethylpropanoate (6.9 g, 36 %), b.p. 141—142°/12 mm, $[\alpha]_D^{20}$ + 8.0° (undiluted, *l* 0.5), d^{20} 1.118.

(+)-*Dimethyl 2D-ethylsuccinate.* (+)-Methyl 3-carboxy-2D-ethylpropanoate was methylated with diazomethane furnishing (+)-dimethyl 2D-ethylsuccinate, b.p. 99°/14 mm $[\alpha]_D^{20}$ + 7.92 (undiluted, *l* 0.5) d_4^{20} 1.041. Berner [10] gives $[\alpha]_D^{20}$ −14.89° for the pure (−)-form.

(−)-*2D-Ethyltetradecanoic acid.* A mixture of (+)-methyl 3-carboxy-2D-ethylpropanoate (1.30 g) and lauric acid (3.3 g) in methanol was electrolysed between platinum electrodes. The neutral part of the product was distilled, giving four fractions, I (0.08 g), b.p. 65—70°/1 mm, $[\alpha]_D^{20} \sim 0$ ($CHCl_3$, *c* 7.0); II (0.25 g), b.p. 102—110°/1 mm, $[\alpha]_D^{20}$ −5.2° ($CHCl_3$, *c* 21.4); III (0.65 g), b.p. 110—120°, $[\alpha]_D^{20}$ −4.2° ($CHCl_3$, *c* 20.6), and IV (0.85 g), b.p. 140—160°/1 mm. From infra-red measurements it was clear that fraction (II) consisted partly of dimethyl 2D,5L-diethyladipate and fraction (IV) mainly of docosane. Fraction (III) was hydrolysed and chromatographed to give (−)-2D-ethyltetradecanoic acid (0.40 g, 20 %), m.p. 24—26°, $[\alpha]_D^{20}$ −4.2° ($CHCl_3$, *c* 8.50).

(−)-*2D,5L-Diethyladipic acid.* Dimethyl 2D,5L-diethyladipate from mixed electrolysis of (+)-methyl 3-carboxy-2D-ethylpropanoate and lauric acid (fraction II above) was hydrolysed with sodium hydroxide (0.5 N in ethanol-water 1:1), giving 2D,5L-diethyladipic acid (0.08 g, 10 %), m.p. 134—136° (from chloroform), $[\alpha]_D^{20}$ −7.8° ($CHCl_3$, *c* 2.70).

Acknowledgements. The author would like to thank Professor H. Erdtman and Tekn.-lic. B. Carnmalm for their interest in this work and for valuable discussions. The author is further indebted to Professor C. Djerassi and Miss A. M. Weidler for rotatory dispersion measurements and for a discussion of the results. Thanks are also due to Mr. E. Pettersson for technical assistance, to Miss G. Hammarberg for the infra-red measurements and to Dr. P. Daniels for checking the English.

Financial support form the *Swedish Technical Research Council* is gratefully acknowledged.

REFERENCES

1. Asahina, Y. and Shibata, S. *Chemistry of Lichen Substances*, Maruzen Co, Tokyo 1954, p. 17.
2. Asahina, Y. and Shibata, S. *Ibid.*, p. 205.
3. Ställberg-Stenhagen, S. *Arkiv. Kemi, Mineral. Geol.* **23** A (1946) No 15.
4. Ställberg, G. *Arkiv Kemi* **12** (1958) 153.
5. Åkermark, B., Erdtman, H. and Wachtmeister, C. A. *Acta Chem. Scand.* **13** (1959) 1855.
6. Kennedy, G., Breen, J., Keane, J. and Nolan, T. J. *Sci. Proc. Roy. Dublin Soc.* **21** (N.S.) (1937) 557.
7. Djerassi, C. and Undheim, K. *J. Am. Chem. Soc.* **82** (1960) 5755.
8. Hjelt, E. *Ber.* **29** (1896) 1855.
9. Skinner, G. S. and Huber, R. de V. *J. Am. Chem. Soc.* **73** (1951) 3321.
10. Berner, E. and Leonardsen, R. *Ann.* **538** (1939) 1.
11. Fredga, A. *Tetrahedron* **8** (1960) 126.
12. Freudenberg, K. *Monatsh.* **85** (1954) 537.
13. Lean, B. *J. Chem. Soc.* **65** (1894) 995.
14. Cope, A. and McElwain, S. M. *J. Am. Chem. Soc.* **54** (1932) 4311.

Received September 15, 1961.

ACTA CHEMICA SCANDINAVICA 16 (1962) 607–614

The Constituents of Conifer Needles

II *. Pinifolic Acid, a new Diterpene Acid Isolated from *Pinus silvestris* L.

CURT ENZELL and OLOF THEANDER

Organisk-kemiska Institutionen, Kungl. Tekniska Högskolan and Träkemiska Avdelningen, Svenska Träforskningsinstitutet, Stockholm, Sweden

Dedicated to Professor *Holger Erdtman* on his 60th birthday

A diterpene acid, pinifolic acid, has been isolated from the needles of *Pinus silvestris* L. and shown to have structure (1 a).

In a previous investigation [1] a study was made of the low-molecular carbohydrates present in the needles of *Pinus silvestris* L. The present paper deals with the isolation of a new diterpene acid from the same source and the elucidation of its structure.

Fresh needles, collected in the autumn, were extracted with acetone and the concentrated extract was partitioned between water and chloroform. The acid fraction, obtained from the chloroform phase on extraction with sodium hydrogen carbonate, contained about 65 % of one component and gave, on recrystallisation, a pure diterpene acid, $C_{20}H_{32}O_4$, in 0.27 % yield based on the dry weight of the needles. The name pinifolic acid is proposed for this compound.

The structure (1) is assigned to pinifolic acid on the following evidence. The infrared (Fig. 1) and ultraviolet spectra of the acid indicated the presence of an isolated, unsymmetrically disubstituted double bond and catalytic hydrogenation over Adam's catalyst gave dihydropinifolic acid (2). Pinifolic acid, on dehydrogenation with palladium on charcoal at 290°, gave 1,2,5-trimethyl naphthalene identified by its characteristic ultraviolet absorption [2], together with some volatile acids, which were collected and examined. The first volatile fraction, collected after 10 min, was, according to paper chromatographic results [3], a mixture of acetic and propionic acids; the second fraction, collected after 2 h, appeared to contain very small amounts of (S)-(+)-3-methylpenta-

* Part I. *Acta Chem. Scand.* **12** (1958) 1319.

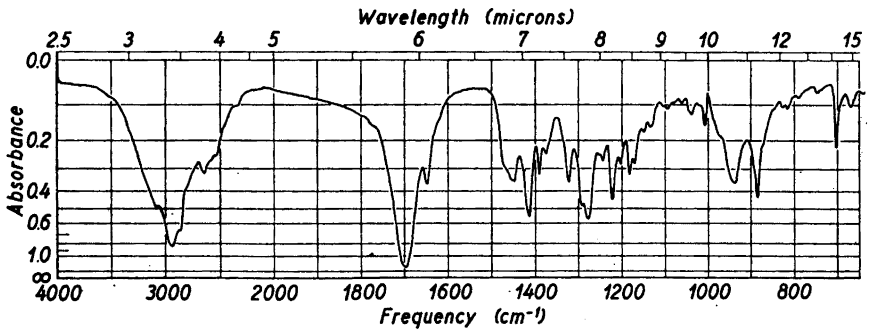

Fig. 1. Infrared spectrum of pinifolic acid.

noic acid [4-6]. In view of the stereochemical importance of this acid further investigation is in progress.

These results suggested that pinifolic acid was closely related to dihydroagathic acid (4), which was prepared from agathic acid [7] (5) by reduction with sodium in butanol [8]. Pinifolic and dihydroagathic acids were found to have similar rotations but somewhat different R_F-values and their dimethyl esters gave infrared spectra which were nearly identical above 1 400 cm^{-1}. The mass spectra of the two dimethylesters (Figs. 2 and 3), discussed below, suggested that the two acids were epimeric at C-(4). Pinifolic acid was therefore related to labdanolic acid [9] (6) in the following manner.

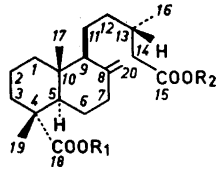

1 a $R_1=R_2=H$
1 b $R_1=R_2=CH_3$
1 c $R_1=CH_3$; $R_2=H$

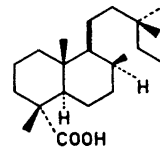

2

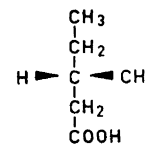

3

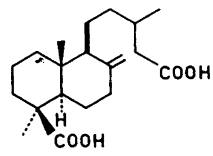

4

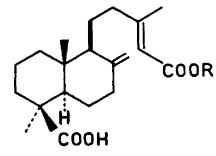

5 a R = H
5 b $R = CH_3$

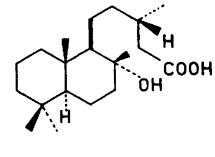

6

Pinifolic acid dimethyl ester on treatment with one equivalent of sodium hydroxide in methanol gave the monoester (1 c), which was reduced with sodium in ethanol or better with lithium in liquid ammonia to the hydroxy acid (7). The methyl ester of this acid was oxidised with chromium trioxide

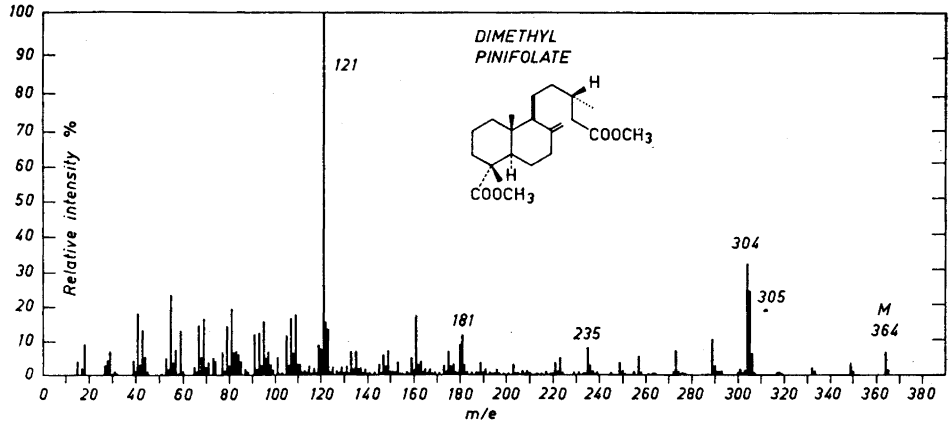

Fig. 2. Mass spectrum of dimethyl pinifolate.

in pyridine to the corresponding oxoester (8), which on Huang-Minlon reduction yielded the acid (9). The cyclohexylamine salt of this acid gave an infrared spectrum identical with that of the corresponding derivative of labd-8(20)-en-15-oate [9] and did not depress the melting point of the latter derivative although the melting points of the two samples were slightly different. The ketoacid (10), obtained on ozonolysis of the acid (9), was identical in all respects (mixed m.p., optical rotation, I.R.) with 20-nor-8-oxo-labdan-15-oic acid [9]. The corresponding oximes were also identical.

The above results settle the structure of pinifolic acid with the exception of the location of the second carboxyl group. The following data are however consistent only with structure (1a) for pinifolic acid. In view of the "finger print" character of mass spectra [10] only the isomer (1b) would be expected to give a mass spectrum (Fig. 2) with all peaks at the same mass numbers as

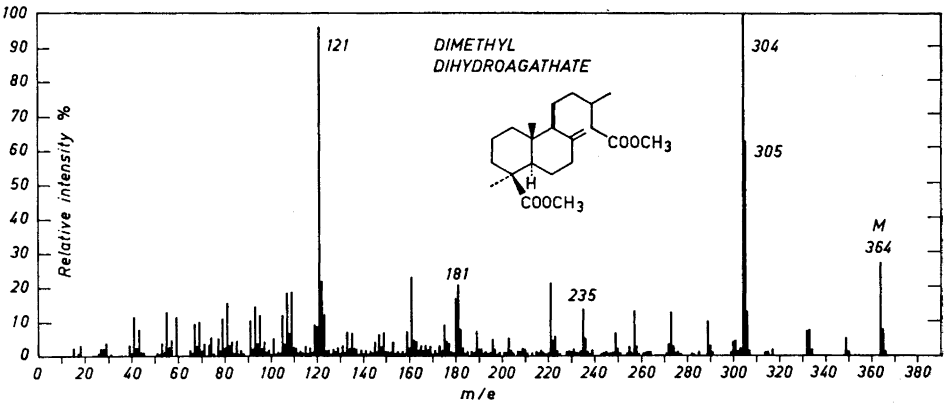

Fig. 3. Mass spectrum of dimethyl dihydroagathate.

those in the spectrum of dimethyl dihydroagathate (Fig. 3). The strong peaks at *m/e* 305 and 304 correspond, respectively, to ions obtained by elimination of the ester group at C(4) and by elimination of this ester group and hydrogen [11,12*]. The peaks at *m/e* 181 and 235 correspond to ions obtained, respectively, from ring A by rupture of the C(6)—C(7) and C(9)—C(10) bonds [13] and from rings A and B by rupture of the C(9)—C(11) bond [11].

Pinifolic acid on titration [14] had the apparent dissociation constants shown in Table 1.

Table 1. Apparent dissociation constants in methylcellosolve/water.

	$pK_1^*{}_{MCS}$	$pK_2^*{}_{MCS}$	$pK^*{}_{MCS}$	Reference
Pinifolic acid (1)	7.24	8.35		Present work
Dihydroagathic acid (4)	7.34	8.85		Present work
Methylsuccinic acid	5.98	8.37		15
Dehydroabietic acid			7.92	16, 17
Agathic acid monomethyl ester (5 b)			8.50	17, 18
Acid (11)			9.49	16

These values clearly eliminate C(10) and C(13) as possible points of attachment of the second carboxyl group. The difference (0.50 pK^*_{MCS}-units) observed between the $pK^*_{2,MCS}$-values for dihydroagathic acid and pinifolic acid is in excellent agreement with the difference (0.50 pK^*_{MCS}-units) calculated by Simon's method [17] on the basis of structures (4) and (1).

Pinifolic acid on treatment with methanol containing catalytic amounts of sulphuric acid gave the dimethyl ester (1b) in nearly quantitative yield while agathic acid (5) on the same treatment only yielded the monoester (5b) [18]. Similarly pinifolic acid gives a dicyclohexylamine salt while dihydroagathic acid yields the monocyclohexylamine salt.

The stereochemistry of pinifolic acid (1) at C(4) follows from the above discussion and at C(5), C(10), C(9), and C(13) from the correlation with labdanolic acid [9] (6). The β-orientation of the side chain at C(9) in labdanolic acid has been deduced from the stability to alkaline treatment of the 20-nor-8-oxoacid (10) obtained on ozonolysis [19] — a proof recently strengthened by the isolation of the less stable isomer of an analogous compound (12) by ozonolysis [20]. Labdanolic acid has been assigned the (S)-configuration [6] at C(13) by analysis of molecular-rotation data [21], the reliability of which is increased by the fact that neither methyl labdanolate nor methyl 13-epilabdanolate exhibit intramolecular hydrogen bonding [22].

The methyl group at C(8) in dihydropinifolic acid is assumed to be β-oriented since the addition of hydrogen should take place preferentially from the sterically less hindered α-side [9].

* Peaks corresponding to ions obtained by removal of the ester group in the side chain of compounds such as methyl cativate, methyl eperuate and methyl labdanolate are absent or of extremely low intensity (below 1 %).

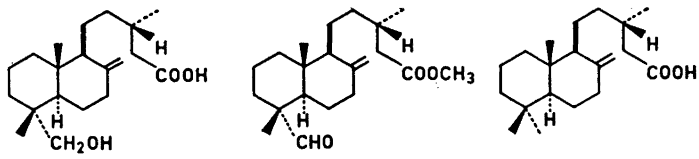

7 8 9

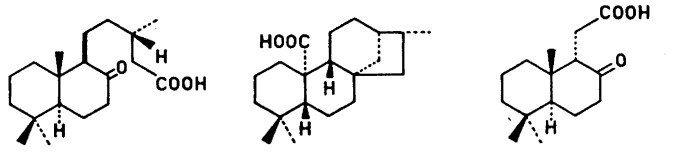

10 11 12

EXPERIMENTAL

Melting points were taken on a Kofler micro hot stage and are corrected. Melting points of the cyclohexylamine salts are dependent upon the rate of heating. Infrared spectra were recorded on a Perkin-Elmer No. 21 instrument (NaCl prism). Ultraviolet spectra were measured on a Beckman recording spectrophotometer, model DK-2. The paper chromatographic studies of the acids were made on dimethyl sulfoxide impregnated papers (Whatman No. 1) using isopropyl ether or ether as solvents [3]. The mass spectra were recorded on an instrument with a heated, all glass inlet system [23] at about 200°. The energy of the electrons was 70 eV. Microanalyses by Dr. A. Bernhardt, Mülheim.

Isolation of pinifolic acid (1a). Needles of *Pinus silvestris* were collected from all parts of the branches in the middle of November. The needles (1 530 g corresponding to 650 g dry material) were covered with acetone and boiled under reflux for 30 min. The needles were removed by filtration, milled in a Wiley-mill and extracted repeatedly (4 × 24 h) with acetone in a Soxhlet apparatus until the concentration of the extract was negligible. The combined acetone solution on cooling gave some greasy material (waxes), which did not contain any pinifolic acid and was subsequently removed by filtration. The acetone solution was concentrated to a small volume and partitioned between water and chloroform. The chloroform phase was extracted with aqueous sodium bicarbonate (10 %). The bicarbonate solution was acidified with dilute sulphuric acid (10 %) and extracted with ether. The ether solution was washed with water, dried (Na_2SO_4) and concentrated to give a lightbrown, partly crystalline residue (2.62 g). One crystallisation from acetone/isopropyl ether gave a paper chromatographically pure product, (1.76 g, 0.27 % of the dry weight of the needles, m.p. 189—191°) which on further recrystallisation gave pure pinifolic acid, m.p. 194—195°, $[\alpha]_D$ + 26° (EtOH, *c* 1.5). (Found: C 71.3; H 9.6; O 19.3; equiv. wt. 167. $C_{20}H_{32}O_4$ requires C 71.4; H 9.6; O 19.0; equiv.wt. 168). The dicyclohexylamine salt had m.p. 164—171°. (Found: N 5.2. $C_{32}H_{58}O_4N_2$ requires N 5.4).

Dihydropinifolic acid (2). Pinifolic acid (60 mg) in ethanol (95 %, 10 ml) was hydrogenated over Adam's catalyst (20 mg) and consumed 1 double bond equivalent of hydrogen in one hour, whereafter the uptake ceased. The catalyst was removed by filtration and the filtrate concentrated to give a crystalline residue which on recrystallisation gave dihydropinifolic acid (47 mg) m.p. 218—219 °, $[\alpha]_D$ + 30° (EtOH, *c* 1.5). (Found: C 70.7; H 10.1. $C_{20}H_{34}O_4$ requires C 71.0; H 10.1).

Dimethyl pinifolate (1b). (*a*) Pinifolic acid (200 mg) on treatment with an ethereal solution of diazomethane (0.5 M, 15 ml) followed by filtration through alumina (neutral activity II, 3 g) gave dimethyl pinifolate (210 mg), n_D^{25} 1.498, $[\alpha]_D$ + 27° ($CHCl_3$, *c* 1.0). (Found: C 72.1; H 10.0. $C_{22}H_{36}O_4$ requires C 72.5; H 10.0). $\nu_{max}^{CCl_4}$ 890, 1 043, 1 060, 1 102, 1 129, 1 147, 1 171, 1 193, 1 232, 1 364, 1 389, 1 437, 1 488, 1 645, 1 727 (broad), 2 880, 2 940, 3 100 cm^{-1}.

(*b*) Pinifolic acid (40 mg), methanol (3 ml) and conc. sulphuric acid (3 drops) were boiled under reflux for 2 h. Dilution with water (20 ml), extraction with ether and filtration of the concentrated ethereal solution through alumina gave dimethyl pinifolate (36 mg), identical with the above product.

Dehydrogenation of pinifolic acid. Pinifolic acid (500 mg) and palladium-charcoal (10 %, 500 mg) were heated at 290° in a small distillation flask. Gas evolution became negligible after 2 h, when 110 ml (3.2 moles/mole acid) had been produced, and the reaction was interrupted. The distillate (*ca.* 5 mg), removed after 10 min, contained according to paper chromatographic results (R_F 0.12 and 0.21, isopropyl ether), acetic and propionic acid. The distillate, (*ca.* 6 mg) removed after 2 h, contained a small amount of 1,2,5-trimethyl naphthalene and an acid, characterised by smell and paper chromatography (R_F 0.47, isopropyl ether) as a caproic acid. The latter was purified by preparative paper chromatography and afforded an acid, $[\alpha]_D$ + 8° (EtOH, *c* 1.0), which gave mass and infrared spectra differing only with respect to the intensity of some peaks from the corresponding spectra of (R)-(−)-3methylpentanoic acid. A third, main fraction (*ca.* 150 mg) was obtained by reducing the pressure to 10 mm and gave on redistillation 1,2,5-trimethyl naphthalene (76 mg) identified by its ultraviolet spectrum, $\lambda_{max}^{light\ petroleum}$ 226 mμ (log ε 4.76), 231 (4.93), 278 (3.78), 289 (3.84), 299 infl. (3.68), 309 (3.18), 324 (3.01). Heilbronner, Frölicher and Plattner [2] give $\lambda_{max}^{light\ petroleum}$ 226 mμ (log ε 4.73), 230 (4.96), 278 (3.78), 288 (3.87), 300 infl. (3.68), 324 (2.96). The additional band at 309 mμ in our spectrum was also observed by Cocker and Halsall [9] at 310 mμ (log ε 3.16).

Dihydroagathic acid. Agathic acid was reduced by adding sodium (3.7 g) to a stirred, refluxing solution of the acid (1.0 g) in butanol (redist., 100 ml) as rapidly as possible. The reaction mixture was boiled under reflux for 45 min, and then water (200 ml) was added and most of the butanol removed by distillation under reduced pressure. The product was diluted with water (300 ml) and extracted with ether, then acidified with dilute sulphuric acid (10 %) and re-extracted with ether to give crude dihydroagathic acid (1.0 g). The crude acid, dissolved in ether (50 ml) was precipitated by addition of cyclohexylamine (2 ml) in ether (10 ml). After one recrystallisation from acetone-methanol the crystalline product (1.10 g) had m.p. 140—180°; on repeated recrystallisation from the same solvent mixture the monocyclohexylamine salt (0.7 g), m.p. 158—188°, $[\alpha]_D$ + 28° (MeOH, *c* 1.2). (Found: C 71.7; H 10.2. $C_{36}H_{66}O_4N$ requires C 71.7; H 10.4) was obtained. Acidification of the salt (300 mg) with dilute hydrochloric acid (10 %) followed by ether extraction gave dihydroagathic acid (4), (230 mg) as a glass, softening point 70—74°, $[\alpha]_D$ + 49° (EtOH, *c* 0.8). (Found: C 71.2; H 9.7. $C_{20}H_{32}O_4$ requires C 71.4; H 9.6). The dimethylester had n_D^{25} 1.4958, $[\alpha]_D$ + 58° ($CHCl_3$, *c* 0.8) $\nu_{max}^{CCl_4}$ 889, 1 031, 1 049, 1 151, 1 195, 1 278, 1 316, 1 331, 1 363, 1 382, 1 437, 1 463, 1 644, 1 720 (broad), 2 840, 2 425, 3 075 cm^{-1}.

18-Hydroxy-labd-8(20)-en-15-oic acid (7). Pinifolic acid dimethyl ester (208 mg), methanol (10 ml) and aqueous potassium hydroxide (1.00 M, 0.60 ml) was left at room temperature (30 min) and then boiled under reflux (15 min). The reaction mixture was cooled, diluted with water (100 ml) and, after addition of aqueous sodium hydroxide (10 %, 3 ml), extracted with ether. The aqueous phase was acidified with dilute sulphuric acid (10 %) and again extracted with ether. The two ether solutions on drying(Na_2SO_4) and evaporation of the solvent gave, respectively, starting material (17 mg) and the paper chromatographically pure monoester (1 c) (183 mg), n_D^{25} 1.4986, $[\alpha]_D$ + 23° ($CHCl_3$, *c* 1.0). This was used in the next step without further purification.

(i) A solution of pinifolic acid monomethyl ester (180 mg) in absolute ethanol (0.5 ml) was added dropwise with stirring to sodium (400 mg) at 130°. Ethanol (4 ml) was then added dropwise over a period of 2 h. After addition of water (2 ml) the reaction mixture was boiled under reflux (1 h), cooled, extracted with ether, acidified with dilute sulphuric acid (10 %) and re-extracted with ether to give a mixture of acids (164 mg). This mixture was chromatographed on silica gel (20 g) to give the hydroxy acid (7) (120 mg) and pinifolic acid (40 mg).

(ii) Pinifolic acid monomethyl ester (630 mg) in dry ether (5 ml) and liquid ammonia (*ca.* 250 ml) was treated with small pieces of lithium until a permanent blue colour was present. The mixture was left for 5 min, then absolute ethanol was added dropwise over a period of 20 min to the solution, which was kept blue by further addition of

lithium. The ammonia was evaporated, the residue diluted with aqueous sulphuric acid (10 %, 100 ml) and extracted with ether. After evaporation of the solvent the residue (556 mg) was adsorbed on silica gel (150 g). Elution with chloroform-ethanol (20:1) gave the paper chromatographically pure hydroxy acid (7), (486 mg), n_D^{25} 1.508, $[\alpha]_D$ + 33° ($CHCl_3$, *c* 0.8), $\nu_{max}^{CCl_4}$ 3 640, 1 703, 1 642, 888 cm^{-1}. (Found: C 74.5; H 10.7. $C_{20}H_{34}O_3$ requires C 74.5; H 10.6). The methylester had n_D^{25} 1.5070, $[\alpha]_D$ + 30° ($CHCl_3$, *c* 1.0).

Methyl 18-oxo-labd-8(20)-en-15-oate (8). The hydroxyester (110 mg) in pyridine (2 ml) was added to chromium trioxide (110 mg) in pyridine (2.5 ml) and the mixture was left overnight at room temperature. Methanol (1 ml) was added and after 1 h the reaction mixture was diluted with aqueous sodium hydroxide (1 %, 50 ml) and extracted with ether. The ether solution was extracted with dilute hydrochloric acid (10 %) and water to give, after drying (Na_2SO_4) and removal of the solvent, a residue (88 mg), which was adsorbed on alumina (3 g, activity II). Elution with light petroleum gave the aldehydo-ester (8), (80 mg), n_D^{25} 1.4988, $[\alpha]_D$ + 31° ($CHCl_3$, *c* 0.9), $\nu_{max}^{CCl_4}$ 2 675, 1 722 (broad).

Labd-8(20)-en-15-oic acid (9). The oxoester (8) (55 mg), hydrazine (95—97 %, 0.3 ml), sodium diethyleneglycolate (from 300 mg sodium) in diethyleneglycol (5 ml) were kept under nitrogen at 160° for 30 min and then at 200—210° for 4 h. The reaction mixture was diluted with water (2 ml), boiled under reflux for 1 h, poured into water (150 ml), acidified with dilute sulphuric acid (10 %) and extracted with ether to give a highly viscous product (40 mg). This was dissolved in ether (5 ml) and gave on addition of cyclohexylamine (0.1 ml) a crystalline precipitate which was removed by filtration, washed with ether and recrystallised from ethyl acetate to give the cyclohexylamine salt (37 mg), m.p. 136—145°, $[\alpha]_D$ + 13° ($CHCl_3$, *c* 0.8), mixed m.p. 135—145° with the cyclohexylamine salt of labd-8(20)-en-15-oate (lit. values m.p. 123—136°, $[\alpha]_D$ + 22°)[9]. The two samples gave identical infrared spectra. Acidification of the salt (37 mg) with dilute hydrochloric acid (10 %) followed by ether extraction gave the acid (8), (27 mg), $[\alpha]_D$ + 24° ($CHCl_3$, *c* 1.0) (lit. value $[\alpha]_D$ + 25°)[9]. The infrared spectra of the two samples of the free acids could not be compared since only a small amount (1.3 mg) of the cyclohexylamine salt of Cocker and Halsall's preparation was available to us.

20-Nor-8-oxo-labdan-15-oic acid. The methyl ester of the acid (9) (25 mg), prepared with diazomethane, was dissolved in methylene chloride and treated with ozone at —70° until the solution was saturated. The excess ozone was removed with dry nitrogen and the solvent evaporated *in vacuo*. The residue was dissolved in a mixture of ethyl acetate (2 ml) and acetic acid (2 ml) and a small amount of activated zinc dust was added. The reaction mixture was stirred for 1 h at room temperature, diluted with water (100 ml) and extracted with ether to give a residue (16 mg) after evaporation. This residue was dissolved in methanol (4 ml) and boiled under reflux for 15 min with aqueous sodium hydroxide (40 %, 1 ml). The solution was diluted with water (50 ml), extracted with ether, acidified and re-extracted with ether to give an acidic material (14 mg), which was absorbed on silica gel (3 g). Elution with chloroform-ethanol (100:1) gave 20-nor-8-oxo-labdan-15-oic acid (10), (11 mg), m.p. and mixed m.p. 107—108° $[\alpha]_D$ —40° ($CHCl_3$, *c* 1.0). (lit. value m.p. 110.5—111° $[\alpha]_D$ —40°)[9]. The infrared spectrum was identical with that of authentic material. Oxime, m.p. and mixed m.p. 184—186° (lit. value 188—189°).

Acknowledgements. We thank Professors H. Erdtman and B. Lindberg for their kind interest, Mrs. S. Strand and Mr. A. Assarsson for skilful assistance, Dr. W. Simon for valuable discussions and the determination of dissociation constants, Dr. T. G. Halsall for samples of labdanolic acid derivatives, and Dr. R. Ryhage for the mass spectrometric determinations. Thanks are also due to the *Swedish Technical Research Council* for financial support.

REFERENCES

1. Assarsson, A. and Theander, O. *Acta Chem. Scand.* **12** (1958) 1319.
2. Heilbronner, E., Frölicher, V. and Plattner, Pl. *Helv. Chim. Acta* **32** (1949) 2479.
3. Hammarberg, G. and Wickberg, B. *Acta Chem. Scand.* **14** (1960) 882.
4. Kögl, F. and Erxleben, H. *Z. physiol. Chem. Hoppe-Seyler's* **235** (1935) 190.
5. Klyne, W. *Progress in Stereochemistry* Bd 1, London 1954, p. 197, 205.

6. Cahn, R., Ingold, C. and Prelog, V. *Experientia* **12** (1956) 81.
7. Simonsen, J. and Barton, D. H. R. *The Terpenes* (2nd Ed.) Vol. III, Cambridge 1951, p. 459.
8. Nakano, T. and Djerassi, C. *J. Org. Chem.* **26** (1961) 167.
9. Cocker, J. and Halsall, T. *J. Chem. Soc.* **1956** 4262.
10. Ryhage, R. and Stenhagen, E. *J. Lipid Research* **1** (1960) 361.
11. Enzell, C. and Ryhage, R. *To be published.*
12. Beynon, J. H. *Mass Spectrometry and its Application to Organic Chemistry*, London 1960, p. 375,
13. Enzell, C. *Acta Chem. Scand.* **15** (1961) 1303.
14. Simon, W. *Helv. Chim. Acta* **41** (1958) 1835.
15. Simon, W., Lyssy, G., Mörikofer, A. and Heilbronner, E. *Zusammenstellung scheinbarer Diassoziationskonstanten im Lösungsmittelsystem Methylcellosolve/Wasser.* Juris-Verlag, Zürich 1959, p. 18.
16. Vorbrüggen, H. and Djerassi, C. *Tetrahedron letters* **1961** 119.
17. Sommer, P. F., Arya, V. P. and Simon, W. *Tetrahedron letters* **1960** No. 20, p. 18.
18. Arya, V., Erdtman, H. and Kubota, T. *Tetrahedron.* **16** (1961) 255.
19. Cocker, J. and Halsall, T. *J. Chem. Soc.* **1957** 4401.
20. Church, R., Ireland, R. and Marshall, J. *Tetrahedron letters* **1961** 34.
21. Bory, S. and Lederer, E. *Croat. Chim. Acta* **29** (1957) 157.
22. Bigley, D., Rogers, N. and Barltrop, J. *J. Chem. Soc.* **1960** 4613.
23. Ryhage, R. *Arkiv Kemi* **16** (1960) 19.

Received September 15, 1961.

ACTA CHEMICA SCANDINAVICA 16 (1962) 615–622

Polysaccharides Elaborated by *Pullularia pullulans*

Part I. The Neutral Glucan Synthesised from Sucrose Solutions

HANS O. BOUVENG, HANS KIESSLING, BENGT LINDBERG and JAMES McKAY

Papperstekniska och träkemiska avdelningarna, Svenska Träforskningsinstitutet, Stockholm Ö, Sweden

Dedicated to Professor *Holger Erdtman* on his 60th birthday

From the crude polysaccharide isolated from cultures of the fungus *Pullularia pullulans* in solutions of sucrose, a neutral glucan and an acidic polysaccharide, containing largely glucose, have been obtained. Structural investigation of the former yielded evidence of an essentially linear molecule of more than 250 α-D-glucopyranose residues linked (1 → 6) and (1 → 4) in the ratio 1:2.

The data compiled up to the present would seem to indicate that the polysaccharides of moulds are based almost without exception on the sugars galactose, glucose and mannose, with the addition of glucosamine in the case of intracellular material [1]. Glucuronic acid and fucose are the most common additives to this basic composition. The distribution of this relatively simple list of ingredients among the occurring molecular species is, however, somewhat varied, both homo- and heteropolymers having been characterised in the limited number of structural investigations reported [2]. More recently, a complex acidic polysaccharide material has been isolated from *Gibberella fujikuroi* [3], containing glucose, galactose, mannose and glucuronic acid, but there is some uncertainty concerning the homogeneity of the preparation. The evidence as it stands does confirm the presence of a polymer in which mannopyranose, galactofuranose and glucuronopyranose residues are combined, the latter forming both terminal and chain units.

Pullularia pullulans has been found to produce two physically distinct polysaccharide components, *viz.* a water-soluble glucan, and a difficultly soluble, jelly-like material, strongly adherent to the cells, and containing glucose, glucuronic acid and small amounts of galactose and mannose [4]. Wallenfels and co-workers [5], in a series of communications, report the isolation of "pullulan", an unbranched glucan of chain length *ca.* 300 glucopyranose units, with α-(1→4)- and α-(1→6)-linkages occurring in the ratio

3:2, from cultures of *P. pullulans* grown on glucose as the carbon source. A brief treatment of this "pullulan" with hot aqueous formic acid yielded a residual polysaccharide which could be converted completely to maltotriose by the action of an enzymic preparation isolated from *Aerobacter aerogenes*.

The present work is directed towards the examination of the polysaccharides elaborated extracellularly by *P. pullulans* from various sugar substrates. Polymer formation has been observed to occur from sucrose, glucose, maltose, mannose, xylose and arabinose as carbon sources but not from either galactose or mannitol. As this list of substrates is traversed from sucrose to arabinose, the associated efficiency of polysaccharide production falls, and the relative amounts of galactose, mannose and glucuronic acid in the polysaccharide mixtures increase. Fractionation of these mixtures with cetyl trimethylammonium hydroxide [6] (CTA—OH), into neutral and acidic components, has shown a clearly defined pattern through the series, *viz.* soluble acidic fractions, rich in galactose and mannose, insoluble acidic fractions, rich in glucose, both types having low specific rotations and containing phosphate and uronic acid; and neutral soluble fractions, rich in glucose, with high specific rotations and free from phosphate and uronic acid. The efficiency of the fractionation is governed by the composition of the crude material to a large extent; both neutral and acidic glucans have been isolated readily from the crude mixtures of polysaccharides obtained from sucrose and maltose cultures, which contained little mannose and galactose initially.

The crude polysaccharide isolated from cultures grown on sucrose yielded 97 % of reducing sugar on hydrolysis, namely glucose, with very small amounts of galactose, mannose and fructose and had specific rotation *ca.* + 190°, 0.44 % nitrogen, and 2.42 % phosphate. On oxidation with periodate, the material consumed 1.41 mole of periodate and released 0.45 mole of formic acid per mole of combined anhydroglucose, indicating the presence of 45 % (1→6)-like and 51 % (1→4)-like linkages.

The purified neutral glucan obtained by fractionation with CTA—OH contained only glucose, was free from phosphate, and showed a single immobile component on paper electrophoresis in borate buffer (pH 10). It had a specific rotation of + 190°, 0.11 % ash, showed no colour reaction with iodine solution and was unattacked by α-amylase. Oxidation with periodate led to the consumption of 1.31 mole of periodate and the liberation of 0.32 mole of formic acid per mole of combined anhydroglucose indicating the presence of 32 % (1→6)-like and 67 % (1→4)-like linkages. Reduction and hydrolysis of the polyaldehyde thus formed yielded 0.63 mole of erythritol, 0.35 mole of glycerol and 0.02 mole of glucose per anhydroglucose residue in the original polysaccharide. Methylation and subsequent hydrolysis yielded 2,3,4-tri-*O*-methyl-D-glucopyranose (33 %), 2,3,6-tri-*O*-methyl-D-glucopyranose (66 %) and 2,3,4,6-tetra-*O*-methyl-glucopyranose (0.4 %). The partial acetolysate of a sample yielded, on deacetylation, glucose (26 %), isomaltose (3 %), maltose (23 %) and higher saccharides including two trisaccharides. These trisaccharides, although not characterised by the formation of crystalline derivatives, appeared, from their chromatographic and electrophoretic mobilities, optical rotations, and behaviour on partial hydrolysis of the reduced and unreduced sugars, to be isomaltotriose (4 %) and maltotriose (> 8 %), respectively.

The acidic glucan was isolated from the polysaccharide mixtures produced in sucrose cultures by means of CTA—OH and copper ethylenediamine. It yielded glucose and uronic acid, mainly as the copper salt, on hydrolysis, was insoluble in water and had $[\alpha]_D$ 0 ± 4° (*c* 0.65 in N NaOH). It contained 66.1 % of reducing sugars (not corrected for combination with uronic acid), 9.9 % of uronic anhydride (decarboxylation), copper (7.8 %) and nitrogen (0.4 %). It consumed 0.74 mole of periodate per mole of anhydrosugar with release of 0.37 mole of formic acid. Reduction and hydrolysis of the periodate-oxidised polysaccharide yielded glycerol and glucose; no erythritol was detected. The structure of this glucan is now being studied.

It is clear that the neutral glucan described above is very closely akin to the material studied by Wallenfels *et al.* and is possibly identical to their "restpullulan" in all but fine structure (Table 1). It should be stated, however,

Table 1.

		Ratio (1→6) to (1→4)-linkages	
	$[\alpha]_D$	By periodate oxidation	By methylation
Crude glucan	+ 194°	0.82	—
Purified glucan	+ 190°	0.48	0.50
"Pullulan" [5]	+ 192°	0.64	0.60
"Restpullulan" [5]	—	0.50	—

that the neutral glucan may well contain a small amount of (1→3)-linkage (1—2 %) for, although no 2,3,6-tri-*O*-methyl glucose was detected in the methylation study, small amounts of unoxidised glucose were detected in experiments based on periodate oxidation.

The polysaccharides produced from the other sugars as sources of carbon have not yet been examined in detail. A neutral glucan has been isolated from cultures grown on maltose, using the CTA—OH fractionation technique, and a preliminary examination shows properties similar to that synthesised from sucrose solutions. The polysaccharide yields only glucose on hydrolysis, has a specific rotation of + 198°, and shows no electrophoretic mobility in borate buffer (pH 10). Periodate oxidation indicates the presence of *ca.* 32 % of (1→6)-linkages, the remainder being ostensibly (1→4). Reduction and hydrolysis of the oxidised polymer yields erythritol, glycerol, and a little glucose. The products of partial acid hydrolysis include components identified chromatographically as maltose, isomaltose and possibly nigerose.

EXPERIMENTAL

Evaporations were carried out under reduced pressure at temperatures not exceeding 40°.

Paper chromatograms were run on Whatman No. 1 and 3MM papers, using the following systems;

A. butanol, ethanol, water, 10:3:5;
B. butanol, pyridine, water, 2:7:2;
C. ethyl acetate, pyridine, water, 10:4:3;
D. ethyl acetate, acetic acid, water, 3:1:3;
E. benzene, dimethylsulphoxide, 20:1, with papers impregnated with dimethyl sulphoxide.

Table 2. Fractionation of crude polysaccharide from *P. pullulans* grown on sucrose-containing cultures.

Fraction	ml CTA—OH added	wt. (g)	$[\alpha]_D$ (NaOH)	Sugars			Phosphate
				Gal	Gl	Man	
1	4	0.163	0 ± 4°	tr.	+	tr.	+
2	4	minute					
3	4	0.510	+ 51°	tr.	+	tr.	4.6 %
4	40	6.645	+ 160°	—	+	—	—
5	40	2.060	+ 170°	—	+	—	—
6	residue	0.293	+ 170°	—	+	—	—

Paper electrophoresis was carried out on Schleicher and Schüll glass fibre papers and on Whatman No. 3 and 3 MM papers in 0.1 M borate buffer of pH 10 at 0.8 kV.

Components were detected by the use of anisidine hydrochloride, α-naphthol-sulphuric acid in butanol, and silver nitrate-sodium hydroxide.

Sugar determinations were made with hypoiodite and Somogyi [8] reagents, those of erythritol and glycerol with periodate-chromotropic [9] acid. Periodate and formic acid were determined iodometrically.

Culture of the organism and the isolation of the polysaccharides. The mould was grown in solutions of the following composition: 0.1 g KH_2PO_4, 0.2 g $CaCl_2.6H_2O$, 0.3 g $MgSO_4.7H_2O$. 0.1 g NaCl, 0.02 g $FeCl_3.6H_2O$, and 2.5 g $NaNO_3$ per litre. As carbon source, 20—50 g of appropriate sugar was used per litre. The inoculated solutions were shaken at 25° for 5—6 days. Usually the time of growth was contrived to be less than that required for the development of the dark colour of the mature organism.

The viscous cultures were heated above 90° for 30 min, cooled and the cells separated by supercentrifugation. The supernatant solutions were de-ionised, concentrated and added dropwise to an excess of ethanol (3—4 volumes). The precipitated polysaccharides were separated by centrifugation or decantation, washed with ethanol and ether and dried *in vacuo* over phosphorus pentoxide.

Polysaccharides synthesised from sucrose. From 3—5 litre batches of culture grown on sucrose solutions (30 g/l) the crude polysaccharides were obtained in quantities of 16—25 g. The white fibrous products proved extremely difficult to redissolve completely in water. Acid hydrolysis yielded glucose along with traces of galactose, mannose and fructose. Paper electrophoresis showed the presence of a major immobile component and a minor mobile component which appeared as an elongated streak on glass fibre papers.

Table 3. Properties of polysaccharide materials from *P. pullulans*.

	Crude polysaccharide	Acidic polysaccharide	Neutral glucan
Specific rotation	+ 190° ± 5	0 ± 4°	+ 190°
Reducing sugars	97 %	66 %	—
Phosphate	2.4 %	—	0
Nitrogen	0.4 %	0.4 %	—
Copper	—	7.8 %	—
Uronic anhydride	—	9.9 %	—
Periodate consumption (moles/mole anhydrosugar)	1.41	0.74	1.31
Formic acid release (same basis)	0.45	0.37	0.32

The polysaccharide (12 g) was dissolved in water (1 000 ml) and fractions were obtained by the addition of 0.23 N CTA—OH as shown in Table 2.

The first three precipitates were washed with water and treated with aqueous acetic acid-hydrochloric acid. The treatment with acid failed to dissolve fractions 1 and 2. The weights mentioned in Table 2 refer to the total material then soluble in N NaOH and precipitable from the neutralised solution with ethanol. Fractions 3, 4 and 5 were easily dissolved in 10 % aqueous acetic acid and the regenerated polysaccharides were precipitated with excess ethanol. Fraction 6 was obtained by passing the solution through cation-exchange resin, concentrating, and adding dropwise to a large excess of ethanol.

Fractions 1 and 3 were combined and dissolved in copper ethylenediamine. The solution on acidification with acetic acid, deposited a blue copper complex which, on dissolving in water and treating with hydrochloric acid, gave a greyish insoluble precipitate. This material was separated and washed with ethanolic hydrochloric acid, ethanol, ether and dried *in vacuo* over phosphorus pentoxide to a grey powder (0.3 g). Hydrolysis of this acidic component yielded glucose and uronic acid. Fractions 4, 5 and 6 were combined to reconstitute the neutral glucan component. Some analytical data are given in Table 3 for the crude polysaccharide, and the components subsequently separated.

Applying the degradative method of Smith *et al.*[7] to the preparations mentioned in Table 3 it was found that both the crude mixture and the neutral glucan produced erythritol and glycerol, along with small amounts of glucose, whereas the acidic polysaccharide yielded only glucose and glycerol.

Degradation of the neutral glucan. The polysaccharide (200 mg) was oxidised at room temperature with 0.16 M periodate solution (50 ml) over a period of 10 days. The solution was neutralised with barium carbonate and the filtrate treated with sodium hydridoborate [7] (200 mg). After 4 h the solution was treated with acetic acid, to destroy excess hydridoborate, de-ionised, and the boric acid removed by repeated distillation with methanol, to leave the polyalcohol (176 mg). The hydrolysate (7 h at 100° with N sulphuric acid) was separated on paper chromatograms (solvent A) and the components estimated, giving glucose (1.88 mg), glycerol (21.9 mg) and erythritol (52.6 mg), the molecular proportions being 1.6, 35.0 and 63.4 %, respectively. Glycerol was characterised as the tri-*O*-benzoate, m.p. and mixed m.p. with an authentic sample 70—71°. The erythritol, m.p. and mixed m.p. 118—119°, was converted to the tetra-acetate, m.p. and mixed m.p. 83—84°.

Methylation of the glucan. The polysaccharide (4 g) was dissolved in dimethyl formamide (75 ml) and the solution was cooled. A mixture of acetic anhydride (25 ml) and pyridine (40 ml) was added slowly with stirring and, after the addition was complete, the solution was was stirred for a further 15 h at room temperature, and finally at 45° for 2 h. The cooled solution was added dropwise with stirring to cold water and the precipitated acetate was collected, dissolved in chloroform, and reprecipitated with light petroleum. The white fibrous solid (6 g) had $[\alpha]_D^{26}$ + 180° (*c* 0.45 in chloroform).

The acetate (6 g) was dissolved in dioxan (100 ml) and dimethyl sulphate (84 ml) and finely powdered sodium hydroxide (70 g) were added with stirring in portions of 12 ml and 10 g over a period of 48 h. The product (4.0 g) was remethylated with methyl iodide (12 ml) and silver oxide (10 g) in dimethyl formamide (100 ml) to give a methyl ether (3.18 g) with a methoxyl content of 44.2 %. Two further methylations gave a product (2.90 g) with 45.9 % methoxyl and $[\alpha]_D^{23}$ + 220° (*c* 1.38 in chloroform). Hydrolysis

Table 4. Fractionation of hydrolysed methylated glucan (2.0 g) from *P. pullulans*.

Fraction	Sugars	Weight	Mole %
32—100	2,3,6-trimethylglucose	1.17 g	65.6
101—275	2,3,4-trimethylglucose	0.58 g	32.5
Residue	trimethyl- and		0.5
	tetramethyl-		0.4
	glucoses	0.033 g	

Table 5. Fractionation of deacetylated partial acetolysate of *P. pullulans* glucan.

Fraction	Sugars	Weight (g)	Weight % of total
25—72	glucose	1.228	25.5
90—108	isomaltose, trace glucose	0.129	2.7
109—140	maltose, trace isomaltose	1.085	22.6
141—153	isomaltotriose, traces maltose, maltotriose	0.200	4.2
154—159	maltotriose, traces maltose, isomaltotriose	0.400	8.3
160—240	maltotriose, higher saccharides, traces acetates	1.769	36.8

of a small sample and examination on a paper chromatogram (solvent A) showed the presence of trimethyl glucose and a very faint trace of tetramethyl glucose.

Hydrolysis of the methylated glucan. Hydrolysis of a portion (2.0 g) of the methyl ether with 90 % formic acid (100 ml; 1 h at 100°) and 0.5 N sulphuric acid (100 ml; 14 h at 100°) yielded a syrupy mixture of sugars (2.04 g) which was adsorbed on a carbon-Celite column (44 × 3.5 cm). Elution was carried out, first, with a gradient of 2.5—5.5 % aqueous methyl ethyl ketone (5 l) and subsequently with 10 % aqueous methyl ethyl ketone to give the sequence of fractions (25 ml) shown in Table 4.

*Characterisation of the methyl ethers. 2,3,6-Tri-*O*-methyl-*D*-glucose.* The ether had m.p. 112—116° on recrystallisation from chloroform-light petroleum and $[\alpha]_D^{24}$ + 92° → + 68° (*c* 0.84 in water). The melting-point was undepressed on admixture with an authentic sample. The derived aldonic acid formed a phenyl hydrazide with m.p. 144—145°, undepressed on admixture with an authentic sample of 2,3,6-tri-*O*-methyl-D-gluconic acid phenyl hydrazide.

*2,3,4-Tri-*O*-methyl-*D*-glucose.* The syrup had $[\alpha]_D^{24}$ + 82° (*c* 1.95 in water). Reaction with *p*-phenylazobenzoyl chloride yielded a product, m.p. 164—165°, undepressed on admixture with authentic 1,6-di-*O*-*p*-phenylazobenzoyl-2,3,4-tri-*O*-methyl-D-glucose.

The residue gave on partition between water and chloroform trimethyl glucose and tetramethyl glucose, 26.4 % and 23.0 %, respectively (by hypoiodite oxidation). The latter component was identified as 2,3,4,6-tetra-*O*-methyl-glucose by its chromatographic mobility (solvents A and E) and colour reaction with *p*-anisidine hydrochloride spray reagent.

Partial acetolysis of the glucan[10]. The polysaccharide (8 g) was dissolved in a mixture (50 ml) of 100 parts acetic anhydride and 9 parts sulphuric acid and kept at 40° for 48 h. The cooled solution was poured into ice-water and the aqueous mixture was extracted with chloroform to give a syrupy mixture of acetates (12.6 g). Deacetylation of this mixture with sodium in methanol-chloroform at −5° for 60 min[11] yielded a mixture of sugars (5.4 g) which was adsorbed on a carbon-Celite column (55 × 6.5 cm). Gradient elution was carried out in the following stages:

(1) 0 −10 % aqueous ethanol (5 l)
(2) 10—35 % aqueous ethanol (5 l)
(3) 35 % aqueous ethanol with a methyl ethyl ketone gradient of 0—10 % (5 l). Fractions (50 ml) were obtained as shown in Table 5.

Characterisation of the sugars. Fractions 25—72. The sugar, on recrystallisation from methanol, had m.p. 140—142° and $[\alpha]_D^{23}$ + 93° → + 52°, and was converted by acetylation with acetic anhydride and sodium acetate to β-penta-acetylglucose, m.p. 130—131°, and $[\alpha]_D^{23}$ + 0° (*c* 0.123 in chloroform).

Fractions 90—108. After purification on filter sheets (solvent C) the sugar was chromatographically and electrophoretically indistinguishable from isomaltose.

Table 6. Fractionation of polysaccharides from *P. pullulans* grown on maltose-containing cultures.

Fraction	ml CTA—OH	ml NaOH	Wt. (mg)	Neutral sugars Gal	Gl	Man
1A	5	2	100	+	+	+
1B			40	—	+	—
2A	10	4	124	+	+	+
2B			50	+	+	+
3	residue		766	—	+	—

Fractions 109—140. The sugar on recrystallisation from methanol-ethanol had m.p. 118—120° and $[\alpha]_D^{24}$ + 109° → + 129°. Acetylation gave maltose β-octa-acetate, m.p. 158.5—159.5° and $[\alpha]_D^{22}$ + 62° (*c* 1.30 in chloroform).

Fractions 141—153. The principal component was purified on filter sheets by chromatography and electrophoresis to give an amorphous solid (98 mg) with $[\alpha]_D^{24}$ + 124° (*c* 0.98 in water), R_G 0.37 (solvent C) and M_G 0.53. Partial acid hydrolysis gave products chromatographically identical to glucose and isomaltose. Partial hydrolysis of the reduced trisaccharide yielded the same sugars as the only reducing products.

Fraction 154—159. The main component was purified on filter sheets by chromatography and electrophoresis to give an amorphous solid (240 mg) with $[\alpha]_D^{24}$ + 144° (*c* 0.52 in water), R_G 0.42 (solvent C), and M_G 0.30.

Partial hydrolysis of the trisaccharide and its reduction product yielded only glucose and maltose. Acetylation afforded a crystalline derivative, m.p. 95—100° and $[\alpha]_D^{25}$ + 81°. Attempts to purify the acetate further by chromatography on Magnesol-Celite columns failed to raise the melting-point.

The mixture of higher saccharides was not examined further.

Polysaccharides synthesised from maltose. The crude polysaccharide mixture resembled those obtained from sucrose cultures but contained rather more combined galactose and mannose. The material (1.5 g) was dissolved in 100 ml aqueous boric acid (0.01 M) and stepwise additions were made alternatively of 0.09 N CTA—OH and 0.01 N NaOH. Fractions were obtained as shown in Table 6.

The precipitates were stirred with 10 % aqueous acetic acid (containing a little HCl), centrifuged, and the soluble matter precipitated by the addition of ethanol (A fractions). The insoluble material was washed with ethanol, ether and dried (B fractions). The supernatant of fraction 2 was de-ionised, the boric acid removed as the volatile methyl ester, and the concentrated aqueous solution added to several volumes of ethanol to precipitate fraction 3.

Fractions 1A and 2A, on paper electrophoresis, moved as elongated streaks while fraction 3 was immobile. Refractionation of the combined fractions 1A, 2A and 2B gave only fractions containing galactose, glucose and mannose. The principal component, fraction 3, gave only glucose on total hydrolysis while the products of partial acid hydrolysis included saccharides corresponding in chromatographic mobility (solvent C) to maltose, isomaltose and possibly nigerose. Periodate oxidation led to the consumption of 1.3 mole of periodate and the liberation of 0.3 mole of formic acid per mole of combined anhydroglucose. Reduction and hydrolysis of the polyaldehyde thus formed showed the presence of erythritol, glycerol and a little glucose, when the products were examined on paper chromatograms (solvent A). The polysaccharide had $[\alpha]_D^{20}$ + 198° (*c* 0.81 in water).

The authors are indebted to *Cellulosaindustrins stiftelse för teknisk och skoglig forskning samt utbildning* and to *Statens Tekniska Forskningsråd* for financial support.

REFERENCES

1. Martin, S. M. and Adams, G. A. *Can. J. Microbiol.* **2** (1956) 715.
2. Stacey, M. and Barker, S. A. *Polysaccharides of Micro-organisms*, Clarendon Press, Oxford 1960, p. 174.
3. Siddiqui, I. R. and Adams, G. A. *Can. J. Chem.* **39** (1961) 1683.
4. Bernier, B. *Can. J. Microbiol.* **4** (1958) 195.
5. Bender, H., Lehmann, J. and Wallenfels, K. *Biochim. et Biophys. Acta* **36** (1959) 309; Wallenfels, K., Bender, H., Keilich, G. and Bechtler, G. *Angew. Chem.* **73** (1961) 245.
6. Scott, J. E. *Methods of Biochemical Analysis* **8** (1960) 145.
7. Abdel-Akher, M., Hamilton, J. K., Montgomery, R. and Smith, F. *J. Am. Chem. Soc.* **74** (1952) 4970.
8. Somogyi, M. *J. Biol. Chem.* **195** (1952) 19.
9. Lambert, M. and Neish, A. C. *Can. J. Research* **B28** (1950) 83.
10. Yamauchi, F. and Azo, K. *Nature* **189** (1961) 752.
11. Zemplén, B. *Ber.* **56** (1923) 1705; **59** (1962) 1258.

Received September 15, 1961.

ACTA CHEMICA SCANDINAVICA 16 (1962) 623–628

The Preparation of 2-Tetrahydropyranyl β-D-Glucopyranosides and Methyl 4-*O*-(2-Tetrahydropyranyl)-β-D-Glucopyranosides

A. N. de BELDER, PER J. GAREGG, BENGT LINDBERG, G. PETROPAVLOVSKII* and OLOF THEANDER

Träkemiska Avdelningen, Svenska Träforskningsinstitutet, Stockholm Ö, Sweden

Dedicated to Professor *Holger Erdtman* on his 60th birthday

The preparations of the two isomeric 2-tetrahydropyranyl β-D-glucopyranosides and the two isomeric 4-*O*-(2-tetrahydropyranyl)-β-D-glucopyranosides and their polyacetates are described.

Although the reaction of dihydropyran with aliphatic and aromatic alcohols has previously been described by Parham and Anderson [1] this reaction has received little attention in the protection of hydroxyl groups in carbohydrates. Each tetrahydropyran group introduced in the molecule gives rise to an additional asymmetric carbon atom and when several hydroxyl groups are reacted this leads to complex mixtures. Dihydropyran has been used to protect hydroxyl groups in ribonucleotide synthesis [2,3] at an intermediate stage without separating the resulting stereoisomers. Amorphous 2-tetrahydropyranyl derivatives were obtained.

The present paper describes the syntheses of the two 2-tetrahydropyranyl β-D-glucopyranosides and the two methyl 4-*O*-(2-tetrahydropyranyl)-β-D-glucopyranosides. The tetrahydropyran groups are stable in alkaline media but are removed under mild acid conditions, and these substances were desired for partial substitution studies.

The two 2-tetrahydropyranyl β-D-glucosides were prepared by reacting 2,3,4,6-tetra-*O*-acetyl-β-D-glucopyranoside (I) with dihydropyran in either acetone or in chloroform solution with hydrochloric acid present as catalyst.

The two isomeric tetraacetates (IIIA and IIIB) could be separated from the crystalline reaction product by fractional crystallisation, by paper chromatography on dimethyl sulphoxide impregnated paper [4] and by chromatography on a silicic acid-dimethyl sulphoxide column [5].

* Royal Swedish Academy of Engineering Sciences research fellow.

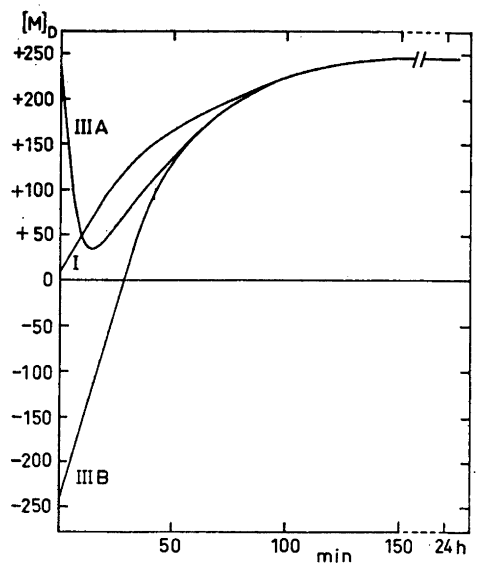

Fig. 1. The rate of hydrolysis in 0.5 N hydrochloric acid in 80 % aqueous acetone at room temperature of (+), IIIA and (−), IIIB, 2-tetrahydropyranyl 2,3,4,6-tetra-*O*-acetyl-β-D-glucopyranosides and the rate of mutarotation of 2,3,4,6-tetra-*O*-acetyl-β-D-glucopyranose under the same conditions.

The infrared spectra of the two acetates, using the potassium bromide pellet technique, showed absorption at 905 cm^{-1} as expected for β-D-glucopyranosides and none in the region expected for the α-D-glucopyranosides [6].

The rate of hydrolysis followed by the change in optical rotation of the two isomeric acetates in 0.5 N hydrochloric acid in 80 % aqueous acetone at room temperature is shown in Fig. 1. From this it appears that the (+), IIIA, isomer is hydrolysed faster than the (−), IIIB isomer. The first-order rate-constants under these conditions were approximately 3×10^{-1} (min^{-1}) for IIIA and 3.4×10^{-2} (min^{-1}) for IIIB. The first-order rate-constant for the mutarotation of I under the same conditions was 1.9×10^{-2} (min^{-1}). The hydrolysis curves indicate that both isomers are β-D-glucosides, the initial rapid hydrolysis being followed by a slower mutarotation of the resulting 2,3,4,6-tetra-*O*-acetyl-β-D-glucopyranose.

The two acetates were deacetylated to yield the two isomeric 2-tetrahydropyranyl β-D-glucosides, of which only the (−) rotating isomer was crystalline. Both deacetylated isomers were cleaved by emulsin as expected for β-D-glucosides.

The two glucosides were easily hydrolysed by N sulphuric, N hydrochloric and 50 % aqueous acetic acid at room temperature in less than 30 min. Some hydrolysis occurred in aqueous solution at pH 5 after a few days.

A paper-chromatographic examination of the reaction of dihydropyran with an equilibrium mixture of 2,3,4,6-tetra-*O*-acetyl-D-glucopyranose in aci-

dic solutions of acetone and chloroform, respectively, indicated that the β-form reacted rapidly but the α-form slowly or not at all, and no α-glucosides were found in the reaction mixture. This may indicate a significant difference in reactivity of axial and equatorial hydroxyl groups towards dihydropyran.

Dihydropyran reacted in the presence of an acid catalyst with methyl 2,3,6-tri-*O*-acetyl-β-D-glucopyranoside to give an isomeric mixture of methyl 2,3,6-tri-*O*-acetyl-4-*O*-(2-tetrahydropyranyl)-β-D-glucopyranosides (VA and VB). The two isomers could be separated from this mixture by fractional crystallisation albeit in low yield. The (+) rotating isomer separated first and the (−) rotating isomer was obtained by crystallisation of the mother-liquors.

The acetates were deacetylated by shaking overnight with a strong anion-exchange resin, in 95 % ethanol. Both isomeric forms of methyl 4-*O*-(2-tetrahydropyranyl)-β-D-glucopyranoside were hygroscopic and had low diffuse melting points.

The position of the tetrahydropyranyl group was confirmed by methylation studies. Only glucoses methylated in the 2-, 3- and 6-positions, but not in the 4- position, were found after methylation and hydrolysis.

The tetrahydropyranyl group was very acid labile and was removed in about 20 min. by 0.0125 N sulphuric acid at 23°. The first-order rate-constants for both the isomers under these conditions were the same, *i.e.* 1.3×10^{-1} (min^{-1}).

The physical constants of the acetylated tetrahydropyranyl derivatives are shown in Table 1. For each pair of derivatives the difference in optical rotation between the isomers is of the same order of magnitude as that for anomeric pairs of glycosides. A determination of the absolute configuration of the tetrahydropyranyl residue would be most difficult. It seems reasonable, however, to assign to the more dextrorotatory isomers the absolute configuration of α-D (β-L) glycosides and the less dextrorotatory the configuration of the β-D (α-L) glycosides.

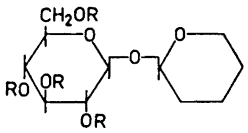

III A: R = −COCH3
IV A: R = −H

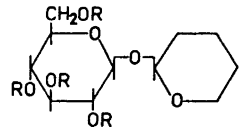

III B: R = −COCH3
IV B: R = −H

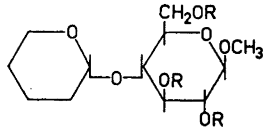

VA: R = −COCH3
VIA: R = −H

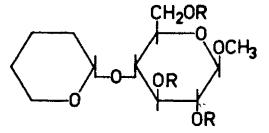

V B: R = −COCH3
VI B: R = −H

Table 1.

Substance	M.p.	$[\alpha]_D^{20}$	$[M]_D$
IIIA	137–138°	+63°	+272°
IIIB	109–111°	−62°	−268°
VA	110–111°	+12°	+ 48.5°
VB	89–90°	−76°	−307°

EXPERIMENTAL

2,3,4,6-Tetra-*O*-acetyl-β-D-glucopyranose (I) was prepared according to McCloskey and Coleman [7] and methyl 2,3,6-tri-*O*-acetyl-β-D-glucopyranoside (II) according to the method by Levene and Raymond [8]. Dihydropyran was distilled over sodium, b.p. 84–86°.

Evaporations were performed at reduced pressure at a bath temperature below 40°. All melting points are corrected.

Chromatography. Paper: Whatman No. 1. Solvents: 1. Isopropyl ether-light petroleum (40–60°), 1:1 (on dimethyl sulphoxide-impregnated paper [4]). 2. Water-saturated methyl ethyl ketone. 3. Butanol-ethanol-water 10:3:5.

Paper electrophoresis. Paper: Whatman No. 1. Buffers: 0.1 M borate at pH 10 [9], 0.05 M germanate at pH 10 [10]. Spray reagents: Anisidine hydrochloride, silver nitrate and sodium hydroxide.

2-Tetrahydropyranyl β-D-glucopyranosides

*Preparation of 2-tetrahydropyranyl-2,3,4,6-tetra-*O*-acetyl-β-D-glucopyranosides. (IIIA and IIIB).* A solution of the tetraacetate I (15 g), dihydropyran (90 ml) and 37 % hydrochloric acid (3 ml) in dry acetone (40 ml) was allowed to stand for 3 h at room temperature, neutralised with sodium hydrogen carbonate, dried over calcium chloride and filtered Concentration to a small volume and addition of ethanol gave crystals (12 g) m.p. 103–105°, $[\alpha]_D^{20}$ 0° (*c*, 1.0 in chloroform). Paper chromatography in solvent 1 gave two spots corresponding to the two isomeric 2-tetrahydropyranyl β-D-glucoside tetraacetates. After several recrystallisations from ethanol, crystals of IIIA were obtained, m.p. 137–138° $[\alpha]_D^{20}$ + 63° (*c*, 1.0 in chloroform). This was the slower-moving compound on paper chromatography in solvent 1.

In another experiment, I (10 g) and dry dihydropyran (10 ml) in anhydrous chloroform (10 ml) containing 0.4 % hydrogen chloride gas was allowed to stand 72 h and worked up as described above. By recrystallisation of the crystalline product a good yield (4.8 g) of almost pure IIIB with m.p. 105–110° and $[\alpha]_D^{20}$ −62° (*c*, 1 in chloroform) was obtained.

The result of the fractional crystallisations is possibly unpredictable and the fact that the above experiments yielded different isomers as pure products may be fortuitous. Better yields of each of the two isomers are obtained by column chromatography.

A silicic acid column (silicic acid, Mallinckrodt AR, 100 mesh, 3 × 28 cm) was prepared according to Lindberg and Wickberg [5] and the mixture (1 g) of the two isomers, from the reaction conducted in acetone solution, was fractionated using solvent 1. IIIB was eluted first (0.35 g) m.p. 109–111°, $[\alpha]_D^{20}$ −62° (*c*, 1.0 in chloroform) after recrystallisation from ethanol, then a mixed fraction which contained both isomers and finally IIIA (0.30 g) with m.p. 137–138° and $[\alpha]_D^{20}$ + 63° (*c*, 1.0 in chloroform) after recrystallisation from ethanol. (IIIA: Found: C 53.0; H 6.60; O 40.5. IIIB: Found: C 52.6; H 6.47; O 41.1. Calc. for $C_{19}H_{28}O_{11}$: C 52.77; H 6.52; O 40.70.)

2-Tetrahydropyranyl β-D-glucopyranosides (IVA and IVB). The acetates were deacetylated in methanolic solutions containing 1.67 % ammonia at room temperature overnight [11]. The solutions were concentrated to dryness. By crystallisation from acetone,

crystals of the glucoside IVB (from IIIB) were obtained with m.p. 176–178°, $[\alpha]_D^{20}$ −110° (*c* 1.0 in water) after recrystallisation from ethanol. (Found: C 50.2; H 7.48; O 42.3. Calc. for $C_{11}H_{20}O_7$: C 49.99; H 7.63; O 42.38.)

The isomer IVA from the acetate IIIA had $[\alpha]_D^{20}$ + 37° (*c*, 1.0 in water) and did not crystallise.

On paper chromatography in solvent 2, IVA had R_F 0.11 and IVB R_F 0.13, on paper electrophoresis in borate[9] IVA had M_G 0.13 and IVB M_G 0.15.

Enzyme hydrolysis. The enzymolyses were conducted in 2 % aqueous solutions buffered at pH 5 and at 25°. The paper chromatograms were run in solvent 3. IVA and IVB and methyl β-D-glucopyranoside were cleaved by emulsin whereas methyl α-D-glucopyranoside was unchanged. Blanks of IVA and IVB in the same buffer containing no enzyme remained mostly unchanged.

A paper chromatographic examination of the reaction of dihydropyran with equilibrated 2,3,4,6-tetra-O-acetyl-D-glucopyranose. The tetraacetate I (2 g) in chloroform containing a few drops 37 % hydrochloric acid was allowed to stand until completely equilibrated, $[\alpha]_D^{20}$ + 80° (*c*, 10.0 in chloroform) (approximately 1 h), neutralised with silver oxide, filtered and separated into two equal volumes which were concentrated to dryness. The reaction with dihydropyran was carried out in acetone and in chloroform solution, respectively, as described above. Samples were withdrawn at intervals and after neutralisation with silver oxide examined by paper chromatography on dimethyl sulphoxide impregnated paper using ethyl ether as solvent. This gave complete separation of 2,3,4,6-tetra-*O*-acetyl-α- and -β-D-glucopyranose with negligible trailing due to mutarotation. The products of the reaction were examined by paper chromatography in solvent 1. It was found that only the α-form of the starting material remained, after 4 h in the experiment conducted in acetone and after 24 h in that conducted in chloroform. Approximately equal amounts of the two tetrahydropyranyl derivatives IIIA and IIIB were formed.

Methyl 4-*O*-(2-tetrahydropyranyl)-β-D-glucopyranosides

Methyl 2,3,6-tri-O-acetyl-4-O-(2-tetrahydropyranyl)-β-D-glucopyranosides. (VA and VB). The triacetate II (1.0 g), dihydropyran (3 ml) and 37 % hydrochloric acid (1 drop) were shaken together for 8 h when no solid material remained. The reaction mixture was diluted with acetone (10 ml), neutralised with silver oxide, concentrated and crystallised from ether-light petroleum (40–60°) overnight to give the mixed isomers VA and VB (0.8 g). Recrystallisation from the same solvent gave the 4-*O*-tetrahydropyranyl derivative VA (0.25 g) m.p. 110–111°, $[\alpha]_D^{20}$ + 12° (*c*, 8.0 in chloroform). (Found: C 53.0; H 6.85. Calc. for $C_{18}H_{28}O_{10}$: C 53.47; H 6.97.) The mother-liquors from above after two recrystallisations from ether-light petroleum (40–60°) yielded the tetrahydropyranyl derivative VB (0.15 g) m.p. 89–90°, $[\alpha]_D^{20}$ −76° (*c*, 0.8 in chloroform). (Found: C 53.2; H 6.77; OCH_3 7.56. Calc. for $C_{18}H_{28}O_{10}$: C 53.47; H 6.97; OCH_3 7.67).

Methyl 4-O-(2-tetrahydropyranyl)-β-D-glucopyranosides. (VIA and VIB). Dowex resin (2-X8 OH^-) was washed with water and then alcohol (95 %). The acetate VA (1.0 g) was shaken with the resin (about 10 g) in ethanol (95 %, 30 ml) overnight. The solution was

Table 2. Rates of hydrolysis of the glucosides VIA and VIB in 0.0125 N sulphuric acid at 23°.

VIA

t (min)	2	4	6	8	10	12	14
$a°_t$	+ 0.16	+ 0.01	−0.06	−0.12	−0.16	−0.19	−0.21
$\log_{10}(a_t - a\infty)$	0.35	0.52	0.64	0.77	0.89	1.00	1.10

VIB

t (min)	3	4	5	6	7	8	9
$a°_t$	−1.74	−1.60	−1.51	−1.43	−1.37	−1.31	−1.26
$\log_{10}(a_t - a\infty)$	0.11	0.20	0.27	0.34	0.40	0.47	0.54

filtered and the resin washed thoroughly with water (made slightly alkaline with ammonia) and then with alcohol. The filtrate and washings were combined and concentrated to give a syrup which crystallised overnight from ethanol-hexane to give needles of the glucoside VIA. This compound was hygroscopic and gave a diffuse m.p. 42—50°, $[\alpha]_D^{20}$ + 39° (*c*, 2.0 in water). (Found: C 52.1; H 8.28. Calc. for $C_{13}H_{22}O_7$: C 51.80; H 7.97.)

The procedure was repeated with the acetate VB to give the glucoside VIB which was also hygroscopic and showed a diffuse m.p. 35—45°, $[\alpha]_D^{20}$ —52° (*c*, 1.2 in water). (Found: C 50.9; H 8.05. Calc. for $C_{13}H_{22}O_7$: C 51.80; H 7.97.)

Rate of hydrolysis of the glucosides. (VIA and VIB). The glucoside (about 0.2 g) was dissolved in water (5 ml). 0.025 N sulphuric acid (5 ml) was added and the rate of hydrolysis followed polarimetrically (Table 2).

Methylations. The glucosides VIA and VIB were methylated in sodium hydroxide with dimethyl sulphate. The products were worked up and hydrolysed as described by Croon [12] and the hydrolysates fractionated by carbon column chromatography. The methyl ethers of glucose were identified by germanate and borate electrophoresis and by paper chromatography in solvents 2 and 3.

REFERENCES

1. Parham, W. E. and Anderson, E. L. *J. Am. Chem. Soc.* **70** (1948) 4187.
2. Smith, M. and Khorana, H. G. *J. Am. Chem. Soc.* **81** (1959) 2911.
3. Khorana, H. G., Turner, A. F. and Vizsolyi, J. P. *J. Am. Chem. Soc.* **83** (1961) 686.
4. Wickberg, B. *Acta Chem. Scand.* **12** (1958) 615.
5. Lindberg, B. and Wickberg, B. *Arkiv Kemi* **13** (1959) 447.
6. Barker, S. A., Bourne, E. J., Stacey, M. and Whiffen, D. H. *J. Chem. Soc.* **1954** 171.
7. McCloskey, C. M. and Coleman, G. H. *Org. Syntheses* **25** (1945) 53.
8. Levene, P. A. and Raymond, A. L. *J. Biol. Chem.* **97** (1932) 763.
9. Foster, A. B. *Advances in Carbohydrate Chem.* **12** (1957) 81.
10. Lindberg, B. and Swan, B. *Acta Chem. Scand.* **14** (1960) 1043.
11. Slotta, K. H. and Heller, H. *Ber.* **63** (1930) 1024.
12. Croon, I. *Acta Chem. Scand.* **13** (1959) 1235.

Received September 15, 1961.

ACTA CHEMICA SCANDINAVICA 16 (1962) 629–639

Über die Wirkung einer Borhydridbehandlung auf die Sulfonierbarkeit von Ligninpräparaten

JOSEF GIERER und SIGURD SÖDERBERG

Schwedisches Holzforschungsinstitut, Holzchemische Abteilung, Stockholm, Schweden

Herrn Professor *Holger Erdtman* zum 60. Geburtstag gewidmet

Treatment of isolated lignins (Brauns' "native lignin" and Björkman-lignin) as well as of finely ground wood powder with borohydride results in a marked decrease of the amount of lignin, soluble under the conditions of acid sulfite cooking (pH 1.4, 135°C, 8 h, Table 1), whereas this treatment essentially has no effect on the sulfonation in neutral solution (pH 6, 135°C, 17 h, Table 2).

An attempt is made to interprete these results in the light of current views on the reactive groups of lignin. The possible role of carbonyl groups in the sulfonation process and in its inhibition by pretreatment with borohydride is discussed.

Die Überführung von Ligninen in wasserlösliche Lignosulfonsäuren wird heute allgemein so gedeutet, dass Sulfogruppen an bestimmte, den aromatischen Kernen benachbarte Kohlenstoffatome der Seitenketten (Benzylkohlenstoffatome) gebunden werden [1]. Durch zahlreiche Versuche mit Modellsubstanzen vom Typus der *p*-Hydroxy- und *p*-Alkoxy-benzylalkohole und -benzyläther [2–7] liess sich diese Auffassung wirkungsvoll stützen und der Einfluss der Acidität auf die Sulfonierung von Ligninen [8–10] mit dem Vorkommen derartiger Strukturelemente erklären [2,3,11].

Die Ergebnisse einer vor kurzem durchgeführten Untersuchung über die Abspaltung von Sulfogruppen aus Lignosulfonsäuren machten jedoch wahrscheinlich, dass nur ein Teil (höchstens 2/3) dieser Gruppen in α- (= Benzyl-) Stellung gebunden ist [12]. Die besondere Reaktionsfreudigkeit der Benzylstellung kann demnach nicht das volle Ausmass der Sulfonierungsreaktion des Lignins erklären und es muss nach weiteren funktionellen Gruppen in den Ligninmolekülen gesucht werden, um diesen komplexen Prozess strukturell befriedigend beschreiben zu können.

Von den bisher in Ligninen nachgewiesenen reaktionsfähigen Gruppen wurden auch Carbonylgruppen als mögliche Ursache der Sulfonierungsreaktion in Betracht gezogen [13]. Vor allem wurden leicht enolisierbare [14], sowie als

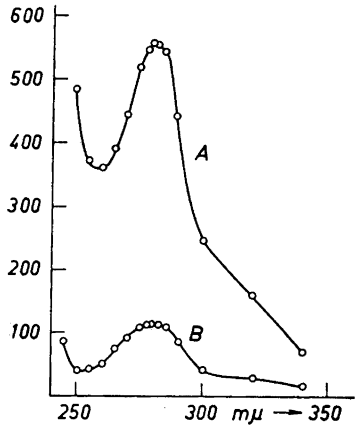

Abb. 1. Ultraviolett-Spektra der Lignosulfonsäuren, hergestellt durch saure Sulfonierung von
A) Brauns' "native lignin"
B) mit Borhydrid behandeltem Brauns' "native lignin".

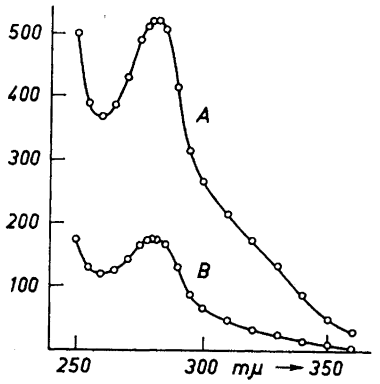

Abb. 2. Ultraviolett-Spektra der Lignosulfonsäuren, hergestellt durch saure Sulfonierung von
A) Björkman-Lignin
B) mit Borhydrid behandeltem Björkman-Lignin

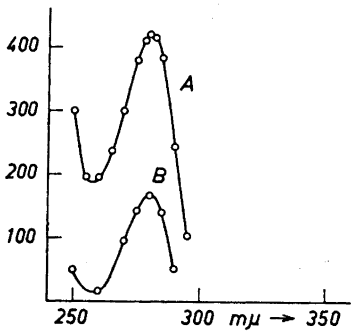

Abb. 3. Ultraviolett-Spektra der Lignosulfonsäuren, hergestellt durch saure Sulfonierung von
A) Holzmehl, mit Äthanol-Benzol (1:1) extrahiert
B) Holzmehl, mit Äthanol-Benzol extrahiert und mit Borhydrid behandelt

Acetale "maskierte" [10a] Carbonyle für diese Reaktion verantwortlich gemacht. Kürzlich wurde erneut die Möglichkeit erwogen, dass Carbonylgruppen sulfonierbare Strukturelemente darstellen [15]. In der vorliegenden Arbeit sollte daher die Rolle der Carbonylgruppen bei der Sulfonierung des Lignins näher studiert werden. Dies wurde auf folgende Weise versucht:

Durch Behandlung mit Borhydrid wurden diese Gruppen in verschiedenen Ligninpräparaten entfernt und die resultierenden Lignine hierauf einer sauren oder einer neutralen und darauffolgenden sauren Sulfitkochung unterworfen. Zum Vergleich wurden auch die entsprechenden unbehandelten Ligninpräparate den gleichen Sulfonierungsbedingungen ausgesetzt. Die Wirkung der Borhydridbehandlungen auf die Sulfonierbarkeit liess sich durch Bestimmung des jeweils in Lösung gegangenen Anteiles und des entsprechenden Sulfonierungsrückstandes, sowie durch Analyse dieser beiden Fraktionen, ermitteln.

Es zeigte sich, dass die Borhydridbehandlung einen stark hemmenden Effekt auf die saure Sulfonierung der untersuchten Ligninpräparate ausübt. Die Abbildungen 1, 2 und 3 veranschaulichen diese Hemmung der sauren Sulfonierung für Brauns' "native lignin", für Björkman-Lignin und für das Protolignin in feingemahlenem, extrahiertem (Benzol-Äthanol 1:1) Fichtenholzmehl. Als grobes Mass für die Menge des jeweils in Lösung gegangenen Lignins dient die Höhe des Extinktionsmaximums bei 280 mμ der gebildeten Lignosulfonsäurelösung. Aus den Abbildungen geht hervor, dass durch Borhydridbehandlung die Grösse des von saurer Sulfitlösung (pH 1,4) bei 135°C innerhalb von 8 Stunden gelösten Ligninanteiles bei Brauns' "native lignin" auf rund 1/5, bei Björkman-Lignin auf rund 1/3 und bei dem Protolignin des Holzes auf ungefähr die Hälfte herabgesetzt wird.

Um diese ausgeprägte Wirkung der Borhydridbehandlung auf die Sulfonierbarkeit durch saure Sulfitlösungen näher zu untersuchen, wurde in einem weiteren Versuch das oben beschriebene Verfahren mit einer grösseren Menge Björkman-Lignin unter Anwendung eines grösseren Borhydridüberschusses wiederholt. Zum Vergleich mit dem Borhydrid-behandelten Präparat wurde die Sulfonierung sowohl mit nicht vorbehandeltem, als auch mit Natronlauge-vorbehandeltem Björkman-Lignin ausgeführt. Die gebildeten Lignosulfonsäuren wurden als Bariumsalze isoliert und, ebenso wie die Sulfonierungsrückstände, auf ihren Methoxyl- und Schwefelgehalt untersucht. Das Ergebnis ist in Tabelle 1 zusammengestellt.

Der bereits in den Abbildungen 1,2 und 3 veranschaulichte, stark hemmende Effekt der Borhydridbehandlung auf die Sulfonierbarkeit von Ligninen in *saurem* Milieu geht aus der Tabelle 1 noch deutlicher hervor. Diese zeigt

Tabelle 1. Saure Sulfonierung von Björkman-Lignin, mit Natronlauge behandeltem Björkman-Lignin und mit Borhydrid behandeltem Björkman-Lignin aus Fichtenholz.

Ausgangsmaterial	OCH_3 %	Sulfonierungsrückstand			Sulfonsäure isoliert als Ba-Salz		
		Menge * in % der Ausg. Menge	OCH_3 %	S %	Menge * in % der Ausg. Menge	OCH_3 %	S %
Björkman-Lignin	15,30	6,1	14,84	2,52	92,8	11,92	5,78
Mit Natronlauge behandeltes Björkman-Lignin	15,31	0,0	—	—	95,3	12,75	4,87
Mit Borhydrid behandeltes Björkman-Lignin	15,28	91,0	14,92	2,24	7,5	11,95	4,98

* umgerechnet auf nicht-sulfoniertes Material

Tabelle 2. Neutrale Sulfonierung von Björkman-Lignin und von mit Borhydrid behandeltem Björkman-Lignin aus Fichtenholz.

Ausgangsmaterial	Sulfonsäure isoliert als Ba-Salz				Bemerkung
	Menge * in % der Ausg. Menge	OCH_3 %	S (%) durch El. Analyse	S (%) durch Titr. v. SO_3H	
Björkman-Lignin	90,5	9,07	6,17	6,15	Kein Sulfonierungsrückstand
Mit Borhydrid behandeltes Björkman-Lignin	87,7	9,93	5,60	5,55	

* umgerechnet auf nicht-sulfoniertes Material

ausserdem, dass auch im Falle des mit Borhydrid vorbehandelten Björkman-Lignins eine gewisse Sulfonierung des Kochungsrückstandes (S = 2.24) eintritt und dass sich mit Natronlauge vorbehandeltes Björkman-Lignin als glatt sulfonierbar erweist.

Vollkommen verschieden verhält sich jedoch mit Borhydrid behandeltes Björkman-Lignin bei einer Kochung mit *neutraler* Sulfitlösung. Es wird in fast gleichem Ausmass wie unbehandeltes Björkman-Lignin sulfoniert und geht wie dieses vollständig in Lösung (Tabelle 2). Wie das Lignosulfonsäurepräparat, das durch Neutralsulfonierung aus unbehandeltem Björkman-Lignin zugänglich ist, bleibt auch das aus Borhydrid-behandeltem Björkman-Lignin bei nachfolgender Sulfitkochung in saurem Milieu in Lösung und nimmt weiteren Schwefel, hauptsächlich in Form von Sulfogruppen, auf (Tabelle 3). Die hemmende Wirkung einer Borhydridbehandlung auf die Sulfonierbarkeit von Björkman-Lignin durch saure Sulfitlösungen kann demnach durch eine der sauren Sulfonierung vorausgehende Sulfitkochung in neutralem Milieu beseitigt werden. Bereits eine Einwirkung einer neutralen Sulfitlösung bei

Tabelle 3. Saure Sulfonierung von neutral sulfoniertem Björkman-Lignin und von mit Borhydrid vorbehandeltem, neutral sulfoniertem Björkman-Lignin aus Fichtenholz.

Ausgangsmaterial	OCH_3 %	S %	Sulfonsäure isoliert als Ba-Salz				Bemerkung
			Menge * in % der Ausg. Menge	OCH_3 %	S % durch El. Analyse	S % durch Titr. v. SO_3H	
Neutral sulfoniertes Björkman-Lignin (freie Säure)	10,65	7,23	75,3	7,67	9,94	9,22	Kein Sulfonierungsrückstand
Neutral sulfoniertes, Borhydrid-vorbeh. Björkman-Lignin (freie Säure)	12,58	6,57	70,9	8,16	9,92	9,05	

* umgerechnet auf nicht-sulfoniertes Material

Zimmertemperatur auf mit Borhydrid vorbehandeltes Björkman-Lignin bewirkt, dass dieses bei nachfolgender saurer Sulfonierung zur Hälfte in Lösung geht (siehe Tabelle 4). Der gelöste Anteil ist — sehr überraschend — noch viel höher sulfoniert als das Produkt der sauren Sulfonierung von Borhydrid-behandeltem und mit neutraler Sulfitlösung bei 135° gekochtem Björkman-Lignin (vgl. Tabelle 4 mit Tabelle 3).

DISKUSSION

Die glatte Sulfonierbarkeit des mit Natronlauge vorbehandelten Björkman-Lignins (siehe Tabelle 1) zeigt, dass der hemmende Effekt der Borhydrid-behandlung auf die Sulfonierbarkeit in saurem Milieu nicht auf die Alkalinität der Borhydridlösung zurückgeführt werden kann (vgl. Ref.[16]), sondern vielmehr den reduzierenden Eigenschaften dieses Agens zuzuschreiben ist. Setzt man voraus, dass die Einwirkung von Borhydrid auf die erwähnten Ligninpräparate keine anderen Veränderungen als eine Reduktion von Carbonyl- zu entsprechenden Carbinolgruppen hervorruft, so können physikalische Faktoren, wie verminderte Löslichkeit und Quellbarkeit, als mögliche Ursachen für die herabgesetzte Sulfonierbarkeit in saurem Milieu ausgeschlossen werden. Eine Überführung von Carbonyl- in Carbinolgruppen sollte im Gegenteil die Löslichkeit bzw. Quellbarkeit in wässrigen Lösungen erhöhen.

Für die rein chemische Deutung der experimentellen Befunde ergeben sich dann folgende Möglichkeiten:

1) Carbonylgruppen sind für die saure, nicht aber für die neutrale, Sulfonierung von entscheidender Bedeutung und/oder
2) Die bei der Reduktion aus den Carbonylgruppen gebildeten Carbinolgruppen hemmen die saure, nicht aber die neutrale Sulfonierung.

Bei Annahme der letztgenannten Alternative lassen sich die Hemmung der Sulfonierungsreaktion des mit Borhydrid vorbehandelten Björkman-Lignins in saurem Milieu (siehe Tabelle 1) und der glatte Verlauf der Sulfonierungsreaktion in neutralem Milieu (siehe Tabelle 2) auf folgende Weise erklären:

Die bei der Borhydridbehandlung eines Ligninpräparates entstehenden reaktionsfähigen Carbinolgruppen gehen bei Einwirkung *saurer* Sulfitlösungen rascher Kondensationsreaktionen ein, als das betreffende Präparat sulfoniert wird. Der Gehalt das Sulfonierungsrückstandes an Sulfogruppen (S = 2,24 %, siehe Tabelle 1) wäre dann auf eine nachträgliche Sulfonierung des Kondensationsproduktes zurückzuführen. Hierfür spricht auch die Tatsache, dass bereits ein viel niedrigerer Gehalt an Sulfogruppen (S = 0,4 %) ausreichen müsste, um das (nicht kondensierte) Präparat einer weiteren Sulfonierung in saurem Milieu zugänglich zu machen (vgl. saure Sulfonierung von bei Zimmertemperatur neutral sulfoniertem, mit Borhydrid vorbehandeltem Björkman-Lignin, Tabelle 4).

In *neutralem* Milieu hingegen ist die Geschwindigkeit der Sulfonierung grösser als die der störenden Kondensationsreaktionen. Sowohl Björkman-Lignin, als auch das mit Borhydrid vorbehandelte Präparat (vgl. Ref.[17]), liefern bei neutraler Sulfonierung in guter Ausbeute Sulfonsäuren mit etwas höheren Schwefelgehalten als bei saurer Sulfonierung (vgl. Tabelle 2 mit Tabelle 1). Bei nachfolgender saurer Sulfonierung dieser Sulfonsäuren nehmen sie eine beträchtliche Menge weiterer Sulfogruppen auf (vgl. Tabelle 3 mit

Tabelle 4. Saure Sulfonierung von mit neutraler Sulfitlösung bei Zimmertemperatur sulfoniertem Björkman-Lignin und von mit Borhydrid vorbehandeltem, mit neutraler Sulfitlösung bei Zimmertemperatur sulfoniertem Björkman-Lignin.

Ausgangsmaterial			Sulfonierungsrückstand			Sulfonsäure, isoliert als Ba-Salz					
						Menge *, in % der Ausg. Menge	OCH_3 %		S %		
	OCH_3 %	S %	Menge *, in % der Ausg. Menge	OCH_3 %	S %		Ba-Salz	freie Säure	Ba-Salz	freie Säure durch Elementaranalyse	freie Säure durch Titration v. SO_3H
Bei Zimmertemperatur neutral sulfoniertes Björkman-Lignin	14,52	1,34	0,0	—	—	81,0	7.21	10.07	11.75	14.27	12.64
Mit Borhydrid vorbehandeltes, bei Zimmertemperatur neutral sulfoniertes Björkman-Lignin	15,10	0,40	42,7	14,31	3,72	46,1	5.66	8.66	15.00	20.45	15.13

* umgerechnet auf nicht-sulfoniertes Material

Tabelle 2), sodass die Produkte dieser "Zweistufensulfonierung" schliesslich einen fast doppelt so hohen Schwefelgehalt wie die nach blosser saurer sulfonierung aufweisen (vgl. Tabelle 3 mit Tabelle 1). Auch diese Befunde können

am besten so erklärt werden, dass bei Neutralsulfonierung die Sulfonierungsreaktion rascher verläuft als die Kondensationsreaktionen, sodass die resultierenden Sulfonsäuren einer weiteren Sulfonierung durch saure Sulfitlösungen zugänglich bleiben.

Es erhebt sich sodann die Frage nach den reaktionsfähigen Carbinolgruppen, welche in Ligninen durch Borhydridbehandlung aus entsprechenden Carbonylgruppen gebildet werden und welche unter den Bedingungen einer sauren Sulfonierung zu Kondensationsreaktionen Anlass geben. Ihre genauere Charakterisierung setzt natürlich die Lokalisierung der verschiedenen im Lignin vorhandenen Carbonylgruppen voraus.

Die Menge der Carbonylgruppen in schonend isolierten Ligninpräparaten (Brauns' "native lignin" und Björkman-Lignin) wurde mit Hilfe der Hydroxylamin-Methode zu 0,12 [18], bzw. zu 0,19 [19,20] per Methoxyl bestimmt. Eine andere Methode, die auf der Reduktion der Carbonylgruppen durch Borhydrid mit nachfolgender volumetrischer Bestimmung des aus dem überschüssigen Borhydrid durch Säure freigesetzten Wasserstoffs beruht [21], ergab ungefähr doppelt so hohe Werte [20]. Diese Diskrepanz wurde dadurch erklärt dass bei der Bestimmung mit Hilfe der Borhydrid-Methode eine durch Schwermetallspuren verursachte, katalytische Oxydation des in der Apparatur befindlichen Wasserstoffs eintreten kann, wodurch zu hohe Carbonylwerte vorgetäuscht werden [22].

Durch Anwendung spektrophotometrischer Methoden konnten vor kurzem 0,1 Carbonylgruppen per Methoxyl (CO/OCH_3) in zu den aromatischen Kernen konjugierter Stellung lokalisiert werden [23]. Hiervon entfallen 0,01 CO/OCH_3 auf α-Carbonyle in Einheiten mit freier phenolischer Hydroxylgruppe und 0,05—0,06 CO/OCH_3 auf α-Carbonyle in Einheiten mit verätherter phenolischer Hydroxylgruppe in p-Stellung zur Carbonylgruppe. Von dem Rest (0,03—0,04 CO/OCH_3) gehören 0,01 CO/OCH_3 Coniferylaldehydgruppen mit freiem phenolischen Hydroxyl und 0,02—0,03 CO/OCH_3 Coniferylaldehydgruppen mit verätherten phenolischen Hydroxyl an.

Es kann angenommen werden, dass ein Teil dieser "konjugierten Carbonyle", v.a. solche in Einheiten mit freier phenolischer Hydroxylgruppe, bei der Reduktion mit Borhydrid Carbinolgruppen (Benzyl- bzw. Zimtalkoholgruppen) liefern, die kondensationsfähig sind. Solche kondensationsfähige Gruppen kommen bekanntlich auch in unbehandelten, unter milden Bedingungen isolierten Ligninpräparaten in geringer Menge vor [24-26]. Möglicherweise sind sie für die Tatsache verantwortlich, dass bei saurer Sulfonierung von Björkman-Lignin ein geringer Rückstand verbleibt (siehe Tabelle 1) und dass ausserdem ein etwas niedrigerer Sulfonierungsgrad als bei neutraler Sulfonierung erreicht wird (vgl. Tabelle 1 mit Tabelle 2). Durch Borhydrid-Reduktion würde demnach die Anzahl der kondensierbaren Gruppen soweit erhöht, dass die Sulfonierbarkeit in saurem Milieu fast vollkommen aufgehoben wird. Ob jedoch die oben erwähnten "konjugierten Carbonyle" zur Erklärung des ausgeprägten Effektes der Borhydridbehandlung auf die saure Sulfonierung ausreichen oder ob noch andere, bisher unbekannte Strukturelemente hierfür verantwortlich sind, lässt sich nicht ohne weiteres entscheiden.

Die andere Möglichkeit zur Erklärung der experimentellen Befunde liegt in der Annahme, dass die in nativen Ligninen vorhandenen Carbonylgruppen

von entscheidender Bedeutung für die Sulfonierung in saurem, nicht aber in neutralem, Milieu sind. Diese Alternative lässt sich strukturmässig nur schwer deuten. Vielleicht ist jedoch die Rolle der Carbonylgruppen so zu verstehen, dass sie durch direkte Teilnahme an der Sulfonierungsreaktion und/oder durch Aktivierung anderer funktioneller Gruppen eine gewisse, sehr rasch verlaufende Anfangssulfonierung ermöglichen[15], wodurch das betreffende Präparat genügend gelöst oder gequollen wird, um weiterer Sulfonierung zugänglich zu sein. Durch Entfernung der Carbonylgruppen wird diese wichtige Initialphase der Sulfonierung so stark gehemmt, dass saure Sulfitlösungen, nicht aber neutrale, das Lignin rasch kondensieren und erst nachträglich sulfonieren.

Diese Hemmung der einleitenden Sulfonierungsphase zeigt sich vielleicht am deutlichsten im unterschiedlichen Verhalten des unbehandelten und des mit Borhydrid vorbehandelten Björkman-Lignins gegenüber einer neutralen Sulfitlösung bei Zimmertemperatur. Das mit Borhydrid vorbehandelte Präparat wird nämlich im Vergleich zum unbehandelten unter diesen Bedingungen nur zu weniger als einem Drittel sulfoniert (S = 0,40 % im Vergleich zu S = 1,34 %, siehe Tabelle 4) und das resultierende Produkt ist im Gegensatz zu dem aus unbehandeltem Björkman-Lignin in Wasser fast unlöslich (siehe exp. Teil).

Eine Entscheidung zwischen den beiden auf S. 633 erwähnten Deutungsmöglichkeiten lässt sich wohl nur durch Untersuchung der Sulfonierung von Ligninpräparaten treffen, in denen die Carbonylgruppen ohne Bildung kondensierbarer Gruppen entfernt wurden.

EXPERIMENTELLER TEIL

Borhydridbehandlung der Ligninpräparate. Je 720 mg aus Fichtenholzmehl gewonnenes Brauns' "native lignin"[14] (OCH_3 = 14,7 %) und Björkman-Lignin [27] (OCH_3 = 15,30 %) wurden mit einer Lösung von 720 mg Natriumborhydrid in 100 ml 80 %igem Äthanol versetzt (pH = 11,9) und 24 Stunden unter Umrührung bei Zimmertemperatur aufbewahrt. Hierauf wurde der Borhydridüberschuss durch Zusatz von Essigsäure zerstört. Die Reaktionsansätze ergaben nach Einengen auf kleines Volumen und Dialyse gegen fliessendes Leitungswasser sehr helle Niederschläge, die abfiltriert, mit Wasser nachgewaschen und durch Umlösen aus 90 %iger Essigsäure — Wasser gereinigt wurden. Nach Trocknen im Vakuum über Ätznatron wurden 520 mg Borhydrid-behandeltes Brauns' "native lignin" (OCH_3 = 14,7 %), bzw. 553 mg Borhydrid-behandeltes Björkman-Lignin (OCH_3 = 15,28 %) erhalten. Beide Präparate gaben erst nach längerem Stehen eine schwache Rotviolett-Färbung mit Phloroglucin — Salzsäure.

Die Borhydridbehandlung von Björkman-Lignin wurde hierauf mit einer grösseren Menge (10 g) unter Anwendung eines starken Borhydridüberschusses (30 g) wiederholt.

Borhydridbehandlung des Fichtenholzmehls. 5 g mit Äthanol — Benzol (1:1) extrahiertes Fichtenholzmehl (OCH_3 = 4,7 %) wurden mit 1,5 g Natriumborhydrid in 100 ml 80 %igem Äthanol versetzt und 24 Stunden bei Zimmertemperatur gerührt. Das fast weisse Produkt wurde abfiltriert, mit Wasser gewaschen und getrocknet. Die Ausbeute betrug 4,7 g, der Methoxylgehalt 4,7 %.

Alkalibehandlung des Björkman-Lignins. 500 mg Björkman-Lignin (OCH_3 = 15,30 %) wurden in 50 ml 0,01 N äthanolischer Natronlauge (80 %iges Äthanol) gelöst (pH = 12,5) und 24 Stunden bei Zimmertemperatur aufbewahrt. Hierauf wurde mit Essigsäure neutralisiert und das Lignin, wie bei den mit Borhydrid behandelten Präparaten beschrieben, wiederisoliert. Es wurden 357 mg Alkali-behandeltes Björkman-Lignin vom Methoxylgehalt 15,31 % zurückerhalten.

Saure Sulfonierung der unbehandelten und der mit Borhydrid behandelten Ligninpräparate. Je 200 mg Ligninpräparat wurden in kleinen Autoklaven aus rostfreiem Stahl mit 10 ml saurer Sulfitlösung (5 % Ges.SO_2, pH = 1,4) versetzt und unter Rotation in einem Ölbad 8 Stunden auf 135°C gehalten. Nach Abkühlen wurde, wenn erforderlich,

von Ungelöstem abfiltriert, einige Male mit Wasser gewaschen und die Rückstände im Vakuum über P_2O_5 getrocknet. Während die unbehandelten Ligninpräparate unter diesen Sulfonierungsbedingungen nahezu restlos in lösliche Lignosulfonsäuren übergeführt wurden (vgl. Ref.[13-15]), ergab mit Borhydrid behandeltes Brauns' "native lignin" einen unlöslichen Rückstand von 161 mg und entsprechend behandeltes Björkman-Lignin einen solchen von 131 mg.

Die Lösungen der gebildeten Lignosulfonsäuren wurden mit den zugehörigen Waschflüssigkeiten vereinigt, durch einen Stickstoffstrom von SO_2 befreit und hierauf auf kleines Volumen eingeengt. Nach erneutem Durchleiten von Stickstoff wurde jeweils auf 50 ml aufgefüllt und von diesen Lösungen mit Wasser Verdünnungen 1:100 hergestellt. Die Ultraviolett-Spektra dieser Verdünnungen gemessen gegen Wasser sind in den Abbildungen 1 und 2 wiedergegeben. Die Höhe des bei 280 mμ liegenden Extinktionsmaximums entspricht ungefähr der Differenz Ausgangslignin (200 mg) minus Sulfonierungsrückstand.

Die vergleichende saure Sulfonierung von unbehandeltem und von mit Borhydrid behandeltem Björkman-Lignin wurde mit grösseren Substanzmengen (je 3 g) unter Einhaltung der unten beschriebenen Arbeitsweise wiederholt. Ausserdem wurde das mit Natronlauge behandelte Björkman-Lignin (siehe oben) den gleichen Sulfonierungsbedingungen unterworfen. Vor der Sulfonierung wurden die 3 Ligninpräparate zwecks Feinverteilung aus 90 %iger Essigsäure-Wasser umgefällt [15], mit Wasser sorgfältig gewaschen und ohne Trocknung in der Sulfonierungslösung (1,4 % NaOH, 4,54 % SO_2, pH 1,4) suspendiert. Die Reaktionstemperatur betrug 135°C, die Reaktionszeit 5 Stunden (Aufheizperiode 1,5 Stunden).

Die Sulfonierungsrückstände wurden abfiltriert, gründlich mit Wasser gewaschen, getrocknet, gewogen und auf OCH_3 und S analysiert (siehe Tabelle 1).

Die Sulfonierungslösungen wurden durch Katjonenaustausch (IR-120) von den Natriumjonen befreit, mit Stickstoff gesättigt und hierauf im Wasserstrahlvakuum auf kleines Volumen eingeengt. Das Verdünnen und Einengen wurde sooft wiederholt, bis das Destillat neutral reagierte. Die konzentrierten Lösungen der freien Lignosulfonsäuren wurden hierauf mit einem Überschuss an Bariumkarbonat neutralisiert, filtriert und im Vakuum zur Trockne eingedunstet. Nach Lösen in wenig Wasser, erneuter Filtration und Einengen zur Trockne wurden die Rückstände gewogen und auf OCH_3 und S analysiert (siehe Tabelle 1).

Saure Sulfonierung des unbehandelten und des mit Borhydrid behandelten Fichtenholzmehls. Je 1 g der beiden Holzmehlpräparate wurde in einem Autoklaven mit 15 ml saurer Sulfitlösung (siehe oben) versetzt und, wie bei den isolierten Ligninpräparaten beschrieben, behandelt. Nicht mit Borhydrid behandeltes Holzmehl gab hierbei einen Sulfonierungsrückstand von 633 mg, mit Borhydrid behandeltes einen solchen von 777 mg. Die Ultraviolett-Spektra der beiden zugehörigen Lignosulfonsäurelösungen (Verdünnungen wie bei den Lignosulfonsäuren aus isolierten Ligninpräparaten angegeben) zeigt Abb. 3.

Neutrale Sulfonierung des unbehandelten und des mit Borhydrid behandelten Björkman-Lignins. Je 3 g der beiden Ligninpräparate wurden aus 90 %iger Essigsäure-Wasser umgefällt [15], mit Wasser und darnach mit neutraler Sulfitlösung (0.31 Mole $Na_2SO_3.7H_2O$ + 0.31 Mole $Na_2S_2O_5$, pH 6,0) gewaschen, die fein verteilten Fällungen in je 260 ml neutraler Sulfitlösung suspendiert und in Autoklaven übergeführt. Die Reaktionstemperatur betrug 135°C, die Reaktionszeit 17 Stunden (Aufheizperiode 1,5 Stunden).

In beiden Fällen ging das gesamte Lignin in Lösung. Die Lösungen wurden durch Einleiten mit Stickstoff gesättigt und durch Jonenaustausch (Dowex 50W—X8) von Natriumjonen befreit. Durch neuerliches Sättigen mit Stickstoff liess sich weiteres SO_2 entfernen, worauf die Lösungen mit überschüssigem Bariumkarbonat neutralisiert und die Bariumsalze, wie bei der sauren Sulfonierung von Björkman-Lignin (siehe oben) beschrieben, isoliert wurden. Die Analysenwerte der beiden Bariumsalze sind in Tabelle 2 zusammengestellt. (Die Schwefelwerte wurden sowohl durch Elementaranalyse, als auch durch potentiometrische Titration der freien Sulfogruppen nach Jonenaustausch ermittelt).

Ungefähr 1/3 der beiden Bariumsalze wurde durch Katjonenaustausch (Dowex 50W—X8) in die freien Säuren übergeführt. Diese konnten durch Gefriertrocknung in Form gelbbrauner Pulver erhalten werden. Ihre weitere Sulfonierung in saurem Milieu wird im Folgenden beschrieben.

Saure Sulfonierung von neutral sulfoniertem Björkman-Lignin und von mit Borhydrid vorbenhandeltem, neutral sulfoniertem Björkman-Lignin. Je 900 mg der beiden freien Sulfonsäuren (siehe oben) wurden in saurer Sulfitlösung gelöst und den gleichen Sulfonierungsbedingungen, wie bei der sauren Sulfonierung von Björkman-Lignin (siehe S. 000) angegeben, ausgesetzt. Hierbei verblieben beide Präparate in Lösung. Die Isolierung der beiden resultierenden Lignosulfonsäuren als Bariumsalze erfolgte wie bei der sauren Sulfonierung des Björkman-Lignins (siehe oben) beschrieben. Ihre Ausbeuten und Analysenwerte sind in Tabelle 3 zusammengestellt.

Neutrale Sulfonierung bei Zimmertemperatur von unbehandeltem und von mit Borhydrid vorbehandeltem Björkman-Lignin. Je 2,0 g der beiden Ligninpräparate wurden in 170 ml neutraler Sulfitlösung (siehe oben) fein verteilt und die Suspensionen unter Umrührung bei Zimmertemperatur 17 Stunden aufbewahrt. Hernach konnten die beiden Präparate weder durch Filtrieren noch durch Zentrifugieren abgetrennt werden. Die kolloiden Suspensionen wurden daher gegen dest. Wasser dialysiert und im Vakuum zur Trockne eingeengt. Ein Versuch, die beiden Präparate durch Umfällen aus 90 %iger Essigsäure-Wasser zu reinigen, misslang. Das Produkt aus nicht-vorbehandeltem Björkman-Lignin blieb hierbei vollkommen in Lösung und das aus Borhydrid-vorbehandeltem Björkman-Lignin ergab lediglich eine milchige Suspension. Auch durch nachfolgende Dialyse (Entfernung der Essigsäure) konnten keine filtrier- oder zentrifugierbare Fällungen erhalten werden. Die beiden Ansätze wurden im Vakuum zur Trockne eingeengt und über P_2O_5 aufbewahrt. Das nicht vorbehandelte Björkman-Lignin ergab 1,48 g, das mit Borhydrid vorbehandelte 1,67 g Sulfonierungsprodukt. Die Analysenwerte dieser Produkte sind in Tabelle 4 enthalten. Das Sulfonierungsprodukt aus Björkman-Lignin ging beim Versetzen mit etwas Wasser zu einem beträchtlichen Teil kolloid in Lösung, das Produkt aus mit Borhydrid vorbehandeltem Björkman-Lignin, hingegen, blieb fast vollkommen ungelöst.

Saure Sulfonierung des bei Zimmertemperatur neutral sulfonierten Björkman-Lignins und des mit Borhydrid vorbehandelten, bei Zimmertemperatur neutral sulfonierten Björkman Lignins. Je 1,0 g der beiden bei Zimmertemperatur neutral sulfonierten Ligninpräparate wurde in 90 ml saurer Sulfitlösung suspendiert und den Bedingungen einer sauren Sulfonierung (siehe oben) unterworfen. Das neutral sulfonierte Björkman-Lignin ging hierbei vollkommen, das mit Borhydrid vorbehandelte, neutral sulfonierte Björkman-Lignin zu etwas mehr als der Hälfte in Lösung. Die beiden Lignosulfonsäuren wurden, wie üblich, als Bariumsalze isoliert und ein Teil durch Jonenaustausch in Freiheit gesetzt. Tabelle 4 zeigt eine Zusammenstellung der Ausbeuten an beiden Bariumsalzen und an ungelöstem Rückstand, sowie der zugehörigen Schwefel- und Methoxylwerte der Bariumsalze und der freien Lignosulfonsäuren.

LITERATUR

1. Übersicht über die Sulfonierung der verschiedenen Strukturelemente, siehe Brauns, F. E. und Brauns, D. A. *The Chemistry of Lignin*, Academic Press, New York and London 1960, S. 373.
2. Lindgren, B. O. *Svensk Papperstidn.* **55** (1952) 78.
3. Adler, E. und Lindgren, B. O. *Svensk Papperstidn.* **55** (1952) 563.
4. Adler, E., Lindgren, B. O. und Saedén, U. *Svensk Papperstidn.* **55** (1952) 245.
5. Adler, E. und Yllner, S. *Svensk Papperstidn.* **55** (1952) 238.
6. Adler, E. und Yllner, S. *Svensk Papperstidn.* **57** (1954) 78.
7. Adler, E. und Yllner, S. *Acta Chem. Scand.* **7** (1953) 570.
8. Hägglund, E. und Johnson, T. *Pappers- och Trävarutidn. Finland* **16** (1934) 282.
9. Erdtman, H. *Svensk Papperstidn.* **43** (1940) 255.
10. Erdtman, H. *Cellulosechemie* **18** (1940) 83.

10a. Erdtman, H. in L. E. Wise und E. C. Jahn, *Wood Chemistry*, Reinhold Publ. Corp. 1952, Bd. 2, S. 999.

11. Adler, E. und Gierer, J. in E. Treiber, *Chemie der Pflanzenzellwand*, Springer Verlag, Heidelberg 1957, S. 464.
12. Gierer, J., Alfredsson, B. und Söderberg, S. *Svensk Papperstidn.* **63** (1960) 201.
13. Brauns, F. E. *Paper Trade J.* **111** (1940) No. 14, 37.
14. Brauns, F. E. *J. Am. Chem. Soc.* **61** (1939) 2120.
15. Björkman, A. und Persson, B. *Svensk Papperstidn.* **60** (1957) 285.

16. Hägglund, E. *Cellulosechem.* **9** (1928) 38., Freudenberg, K., Zocher, H. und Dürr, W. *Ber.* **62** (1929) 1814.
17. Hägglund, E. und Richtzenhain, H. *TAPPI* **35** (1952) 281.
18. Adler, E. und Gierer, J. *Acta Chem. Scand.* **9** (1955) 84.
19. siehe Ref.[11], S. 446.
20. Gierer, J. und Söderberg, S. *Acta Chem. Scand.* **13** (1959) 127.
21. Lindberg, B. und Missiorny, A. *Svensk Papperstidn.* **55** (1952) 13; Lindberg, B. und Theander, O. *Svensk Papperstidn.* **57** (1954) 83.
22. Marton, J., Adler, E. und Persson, K. I. *Acta Chem. Scand.* **15** (1961) 384.
23. Adler, E. und Marton, J. *Acta Chem. Scand.* **13** (1959) 75.
24. Gierer, J. *Acta Chem. Scand.* **8** (1954) 1319; *Chem. Ber.* **80** (1956) 257.
25. Björkman, A. und Persson, B. *Svensk Papperstidn.* **60** (1957) 158.
26. Lindgren, B. O. und Mikawa, H. *Acta Chem. Scand.* **11** (1957) 826.
27. Björkman, A. *Nature* **174** (1954) 1057; *Svensk Papperstidn.* **59** (1956) 477.

Eingegangen am 29. September 1961.

ACTA CHEMICA SCANDINAVICA 16 (1962) 640–648

The Absolute Configuration of the Thujane Group

TORBJÖRN NORIN

Organisk-kemiska Institutionen, Kungl. Tekniska Högskolan, Stockholm, Sweden

Dedicated to Professor *Holger Erdtman* on his 60th birthday

A conjugated addition of hydrogen takes place when (+)-sabinene (3a), (+)-sabinol (3b) and (+)-sabinyl acetate (3c) are hydrogenated catalytically. The structures of the dihydro compounds thus formed are shown to be (7a), (7b), and (7c), respectively.

The main 1,2-addition product from the catalytic hydrogenation of (+)-sabinyl acetate (3c) is shown to be (+)-neoisothujyl alcohol, which now has been characterised for the first time. The stereochemistry of the various thujyl alcohols and thujones are briefly discussed.

The absolute configuration of the dihydro compounds (7b) and (7c) is established by their degradation to the known (+)-α-methyl-α-isopropylsuccinic acid (13). This in turn settles the absolute configuration of (+)-sabinol and (+)-sabinyl acetate, shown in stereoformulae (16b) and (16c). The absolute configuration of all the other monoterpenes of the thujane group follows from known interrelationships.

On catalytic hydrogenation of the alkenylcyclopropane system in thujopsene (1a) and hinokiic acid(1b) a conjugate addition of hydrogen takes place. The structures of the dihydro compounds were proved to be (2a) and (2b), respectively [1,2]. The formation of a new methyl group due to fission of the cyclopropane ring was studied in detail as it conclusively proved the presence and position of this ring. The same type of conjugate addition of hydrogen has been observed in vinylcyclopropane systems [3,4].

However, it has been reported by several authors that the cleavage of the cyclopropane ring occurred in another way during the catalytic hydrogenation of (+)-sabinene (3a), (−)-α-thujene (4) and (+)-sabinol (3b) [5]. The structure of the dihydro compound derived from (+)-sabinene (3a) and (−)-α-thujene (4) was said to be (5a) and that derived from (+)-sabinol (3b) to be (5b). In this paper, evidence is presented showing that the catalytic hydrogenations of (+)-sabinene (3a), (+)-sabinol (3b), and (+)-sabinyl acetate (3c) takes place in the same way as those of thujopsene (1a) and hinokiic acid (1b).

The thujane group is the only important class of monoterpenes in which the absolute configuration has remained unsettled [6]. The absolute configuration of (+)-*cis*umbellularic acid (6) has recently been proposed on the basis of a partial asymmetric synthesis [7]. This acid (6) is related to the monoterpenes of

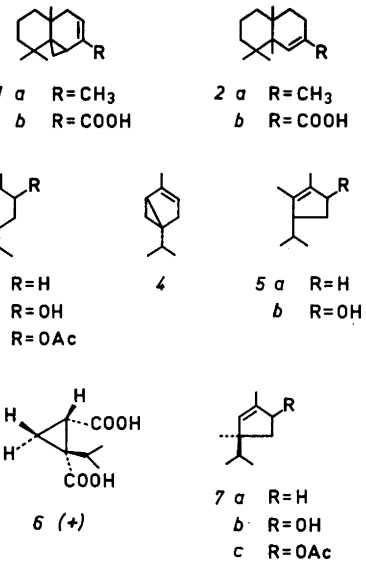

the thujane group and the absolute configuration of the group follows from this assignment. However, an independent solution of this problem was desirable.

The stereospecific opening of the cyclopropane ring during the catalytic hydrogenation of (+)-sabinene (3a), (+)-sabinol (3b) and (+)-sabinyl acetate (3c) and the degradation of the dihydro compounds to compounds of established absolute configuration would completely settle the absolute configuration of the monoterpenes of the thujane group.

The pure (+)-sabinene (3a) and (+)-sabinyl acetate (3c) used for this investigation were obtained from a careful distillation of oil of savin (from *Juniperus sabina* L.). The pure (+)-sabinol (3b) was obtained on hydrolysis of (+)-sabinyl acetate (3c).

(+)-Sabinene (3a) was hydrogenated in methanol using a palladium on charcoal catalyst. A gas liquid chromatogram of the dihydro-product showed only one main peak. Infra red and nuclear magnetic resonance spectra of this crude dihydro compound clearly indicate the presence of a trisubstituted double bond. On ozonisation, the dihydro compound (7a) gave the keto-acid (8). This keto-acid was found to be identical with the (+)-2-methyl-2-isopropyl-5-oxocaproic acid, recently obtained from a degradation of (−)-methylisopulegone [8] (see Table 1). As in the (−)-methylisopulegone work the keto-acid (8) was further degraded to the (+)-α-methyl-α-isopropylglutaric acid (9) and this dicarboxylic acid transformed to the (−)-α-methyl-α-isopropylglutaric anhydride (10).

(+)-Sabinol (3b) was hydrogenated under the same conditions as described for (+)-sabinene (3a). The yield of 1,4-addition product was 30 %, as shown by gas liquid chromatography. The crude dihydro-product was ozonised and the ozonisation product separated into a neutral fraction, containing the 1,2-

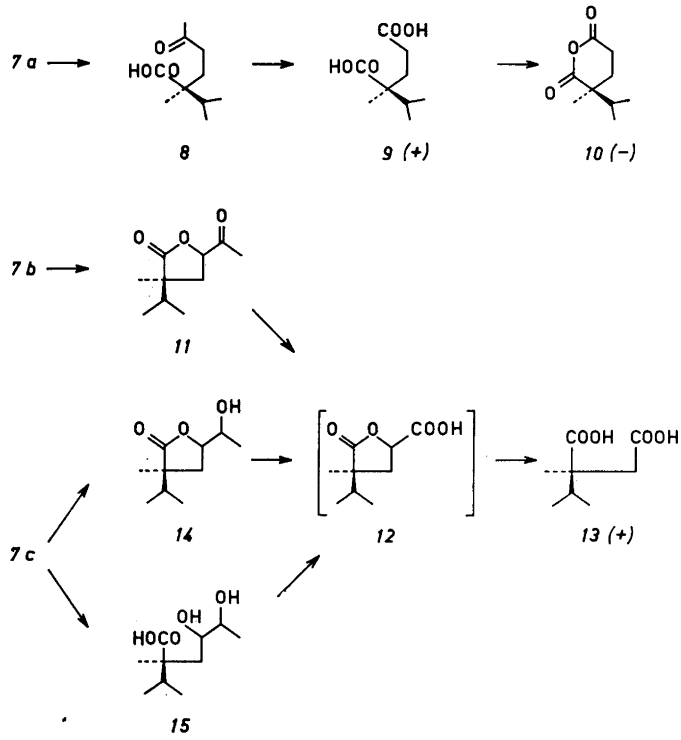

addition products (see below), and an acidic fraction. The acidic fraction was chromatographed on silica gel and the main product isolated was the oily ketolactone (11), further characterized as its crystalline 2,4-dinitrophenylhydrazone. Hypobromite oxidation of this ketolactone (11) gave a product consisting mainly of the lactone-acid (12), as shown by its infra red spectrum. Without further purification this crude product (12) was oxidised with permanganate to a dicarboxylic acid, which after purification by preparative paper chromatography, yielded crystalline (+)-α-methyl-α-isopropylsuccinic acid (13), identified by a direct comparison with an authentic sample [9].

(+)-Sabinyl acetate (3c) was hydrogenated under the same conditions as described for (+)-sabinene (3a) and the yield of 1,4-addition product was 20 % as shown by gas liquid chromatography. The crude dihydro-product was ozonised and the ozonisation product was separated into a neutral fraction, containing the 1,2-addition products, (see below) and an acidic fraction.

Alkaline hydrolysis of the acidic fraction to give the ketolactone (11) afforded a complex mixture as shown by paper chromatography. Treatment of the crude acidic fraction with alkaline potassium borohydride afforded two products, the oily hydroxylactone (14) and the crystalline diol-acid (15), which were isolated by chromatography on silica gel.

The hydroxylactone (14) and the diol-acid (15) were oxidised with hypobromite to give a crude product, the infra red spectrum of which showed that

it consisted mainly of the lactone-acid (12). This product, without further purification, was oxidised with permanganate to a crude dicarboxylic acid from which crystalline (+)-α-methyl-α-isopropylsuccinic acid (13) was isolated after purification by means of preparative paper chromatography.

There were no indications of the presence of a dihydro compound with the structure (5) in any of the hydrogenations discussed above. On the other hand, these hydrogenations are clearly shown to proceed partly by 1,4-addition with formation of the dihydro compounds (7a), (7b), and (7c).

The catalytic hydrogenation of (+)-sabinol (3b) gave 70 % of a 1,2-addition product, the main constituent of which was identified as (−)-neothujyl alcohol in agreement with previous findings [14]. Gas liquid chromatography also indicates the presence of small amounts of (+)-neoisothujylalcohol (see below). (+)-Sabinyl acetate (3c) gave about 80 % of a 1,2-addition product which, after hydrolysis, was shown to be a mixture of about 30 % (−)-neothujyl alcohol and 70 % (+)-neoisothujyl alcohol. These alcohols were separated by fractional crystallisation of the *p*-nitrobenzoates. (+)-Neoisothujyl alcohol has not been characterised previously.* This alcohol gave (+)-isothujone on oxidation with chromic acid. Since (+)-neoisothujyl alcohol and (−)-neothujylalcohol both are formed on catalytic hydrogenation of (+)-sabinyl acetate (3c), these two alcohols must have the same stereochemistry at carbon atom C_2 (for nomenclature and numbering see Refs.[11,12]). The steric relationships previously proposed for the various thujyl alcohols and thujones [11,12] must therefore be changed and may now be expressed as follows:

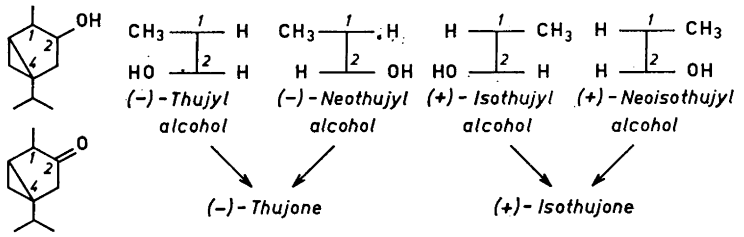

The *cis*- or *trans*-configuration of the C_1-methyl group and the C_4-isopropyl group each of these compounds is still unsettled [7,11,12]. Work on this problem is now in progress.

The absolute configuration of the dihydro compounds (7b) and (7c) is settled by the formation of the known [9] (+)-α-methyl-α-isopropylsuccinic acid (13). This in turn settles the absolute configuration of (+)-sabinol and (+)-sabinyl acetate, which must be represented by the stereoformulae (16b) and (16c), respectively. (+)-Sabinene and (+)-sabinol are both degraded to the same (+)-α-thujadicarboxylic acid [13] and thus (+)-sabinene possesses the absolute configuration shown in the formula (16a). The (+)-α-methyl-α-isopropylglutaric acid obtained from the degradation of the dihydrosabinene

* (+)-Neoisothujyl alcohol may possibly be identical with "δ-thujyl alcohol" isolated from the oil of wormwood, *Artemisia absinthum*, L, (Paolini, V. and Divizza, B. *Atti Accad. Lincei, Roma* **21** (1911) Vol. 1, 570 and Paolini, V. and Lomonaco, R. *ibid.* **23** (1914) Vol. 2, 123; Ref. *Chem. Abstracts* **6** (1912) 2233 and *ibid.* **9** (1915) 1323).

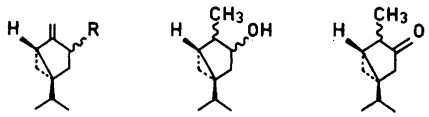

16 a R=H 17 18
b R=OH
c R=OAc

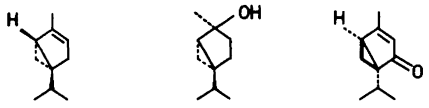

19 20 21

(7a) must accordingly possess the absolute configuration shown in formula (9). The recent degradation of (−)-methylisopulegone [8] led to the identical acid (see Table 1); however, the opposite absolute configuration was assigned to this acid. This discrepancy will be discussed in a separate paper.

The absolute configurations of the various thujyl alcohols (17), thujones (18), of (−)-α-thujene (19), sabinene hydrate (20) [14] and umbellulone (21) follow from known interrelationships [15].

EXPERIMENTAL

Melting points are uncorrected and were taken on a Kofler micro hot stage. The infra red spectra were recorded on a Perkin-Elmer No. 21 instrument (NaCl-prisms; liquids and pure oils in 0.025 mm NaCl-cell; solids, in KBr-discs, unless otherwise stated). Rotations were measured in chloroform (unless otherwise stated). The gas liquid chromatographic (GLC) examinations were made on a Pye Argon Chromatograph; Cat. No 12 000; column length 1.2 m; internal column diameter 5 mm; stationary phase, 100−115 mesh Silocel C 22 brick powder impregnated with 2,4-dinitrophenyl-2-naphthyl ether (15 %) and dibenzyl pyridine (a mixture of 2,4- and 2,6-isomers, 0.75 %) [16]; charge 0.025 μl; temperature 150° (unless otherwise stated).

(+)-Sabinene (3a), (+)-sabinol (3b) and (+)-sabinyl acetate (3c). Oil of savin (40 g) from a steam distillation of the needles and the tops of the branches of *Juniperus sabina* L. (3.9 kg) grown in Stockholm, Sweden, was distilled under reduced pressure (20 mm) in a spinning band column (effective column length about 1.0 m and internal diameter 7 mm). This distillation gave pure (+)-*sabinyl acetate* (*3c*, 3.6 g) which was homogeneous according to GLC, $[\alpha]_D$ + 82° (*c* 1.8), n_D^{25} 1.4678. The first fractions obtained from the distillation were shown to be complex mixtures of hydrocarbons by GLC analysis (stationary phase 100−115 mesh Silocel C 22 brick powder impregnated with 10 % "polyethylene alkatene", a polyester supplied by Perkin-Elmer Co; temperature 60°). These hydrocarbon fractions were combined and redistilled in the same spinning band equipment under atmospheric pressure to give (+)-*sabinene* (*3a*, 1.2 g), $[\alpha]_D$ + 102° (*c* 1.0), n_D^{25} 1.4662 (infra red spectrum identical with that of authentic material [17]). (+)-*Sabinol* (*3b*), $[\alpha]_D$ + 8.3° (*c* 2.0), n_D^{25} 1.4850, was obtained on alkaline hydrolysis of pure (+)-sabinyl acetate (3c) as previously described [10].

Catalytic hydrogenation of (+)-sabinene (3a). (+)-Sabinene (3a, 0.80 g) in methanol (4 ml) was hydrogenated over a 10 % palladium on charcoal catalyst (0.045 g). When the theoretical amount of hydrogen (1 mol. equiv.) had been consumed, the mixture was filtered, diluted with water and extracted with ether. The ether extract was dried (Na_2SO_4) and the solvent evaporated to give the crude *dihydro compound* (*7a*), $[\alpha]_D$ + 34° (*c* 1.7),

n_D^{25} 1.4420. On GLC under the same conditions as described for (+)-sabinene (3a), this crude dihydro compound showed one main peak with an area of about 95 % of the total peak areas and with the retention time 0.63 relative (+)-sabinene (3a). One minor peak was also present in the chromatogram, which had the retention time 0.69 relative (+)-sabinene (3a). The infra red spectrum of this crude dihydro compound (7a) showed characteristic bands at 1 660 and 840 cm^{-1} indicating the presence of a trisubstituted double bond. The nuclear magnetic resonance spectrum showed two signals, at τ 9.22 and 9.03, with areas corresponding to three methyl groups. A signal at τ 8.33 can be assigned to a methyl group on a double bond. The olefinic proton gave rise to a comparatively sharp line at τ 4.86 and the absence of spin-spin splitting suggests the grouping 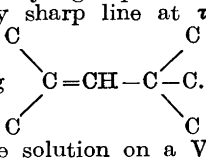 C. The spectrum was obtained with a *ca.* 10 % carbon tetrachloride solution on a Varian V-4300 Spectrometer operating at 40 Mc/s and equipped with a Varian V-K 3506 Stabilizer. Tetramethylsilane was used as internal standard.

(+)-2-Methyl-2-isopropyl-5-oxocaproic acid (8). The crude dihydro compound (7a, 0.7 g) in ethyl acetate/methanol (6:1, 5 ml) was treated with ozone at −70° until a blue colour persisted. Excess ozone was removed by bubbling nitrogen through the solution until the colour disappeared. When the reaction mixture had reached room temperature, zinc dust (1.5 g), previously activated with acetic acid, was added in portions. The decomposition of the ozonides was completed by heating the mixture under gentle reflux for 15 min. Ether (50 ml) was added to the cooled mixture followed by dilute sulphuric acid (1 %, 50 ml). The mixture was filtered and the zinc residue washed with ether and dilute sulphuric acid (1 %). The organic phase was extracted with aqueous sodium hydroxide and separated into acidic (0.40 g) and neutral (0.28 g) fractions.

The acidic fraction was distilled under reduced pressure (p = 0.3 mm) to afford *(+)-2-methyl-2-isopropyl-5-oxocaproic aicd* (*8*, 0.37 g), $[\alpha]_D$ + 15° (*c* 1.0), whose infra red spectrum was identical with that of authentic sample obtained from a degradation of (−)-methylisopulegone [8] (see Table 1).

The neutral fraction contained mainly a keto-aldehyde according to its infra red spectrum, $\nu_{max}^{CCl_4}$ 2 700, 1 735, and 1 715 cm^{-1}. This crude neutral fraction (0.25 g) in dioxane (5 ml) was added to a stirred mixture of silver oxide in water [prepared from a saturated solution of silver nitrate (0.35 g) in water and aqueous sodium hydroxide (4 %, 2 ml)] and heated under reflux for 5 h. A silver mirror was formed. The acidic product (0.11 g), which was obtained from this reaction, was chromatographed on silica gel (4 g). Methanol/chloroform (2 %) eluted the keto-acid (8, 0.08 g) which was purified by distillation.

The *2,4-dinitrophenylhydrazone* of the keto-acid (8) was shown to be identical with an authentic sample, m.p. and mixed m.p. 122°. The infra red spectrum of this derivative was superimposable with that of the authentic sample (see Table 1).

The *methyl ester* of the keto-acid (8) and its *2,4-dinitrophenylhydrazone*, the *(+)-α-methyl-α-isopropylglutaric acid (9)* and the *(−)-α-methyl-α-isopropylglutaric anhydride (10)* were all prepared as described in the (−)-methylisopulegone work [8]. The melting points and rotations of these compounds are given in Table 1 and compared with those of the compounds obtained from (−)-methylisopulegone.

Catalytic hydrogenation of (+)-sabinol (3b). (+)-Sabinol (3b, 1.22 g) in methanol (5 ml) was hydrogenated over a 10 % palladium on charcoal catalyst as described for (+)-sabinene (3a). The dihydro-product showed, on GLC, two peaks with the retention times 0.91 and 0.76 relative (+)-sabinol (3b) and small shoulder with relative retention time 0.77. The areas of the peaks were about 70 % and 30 % of the total peak area, respectively.

The *ozonisation of the dihydro-product obtained from (+)-sabinol (3b)* was carried out as described for the ozonisation of the dihydro compound (7a) and gave similarly an acidic (0.37 g) and a neutral (0.80 g) fraction.

The acidic fraction was chromatographed on silica gel (30 g). Chloroform eluted the *ketolactone* (*11*, 0.15 g), $[\alpha]_D$ −5° (*c* 1.0), $\nu_{max}^{CCl_4}$ 1 775 and 1 720 cm^{-1}. The analytical

Table 1. Compounds obtained from the degradation of dihydrosabinene (7a) compared with those obtained from (−)-methylisopulegone.

Compounds obtained from (−)-methylisopulegone A / Compounds obtained from dihydrosabinene (7a) B		M.p. °C	$[\alpha]_D$ °	*c* in chloroform	Comments
(+)-2-Methyl-2-isopropyl-5-oxocaproic acid (8)	A	oil	+ 3.3	1.52	Identical infra red
	B	oil	+ 16.0	1.0	
2,4-Dinitrophenylhydrazone of this keto-acid (8)	A	122	—	—	Mixed m.p. 122° and identical infra red
	B	122			
Methyl ester of the keto-acid (8)	A	oil	+ 14.1	1.07	
	B	oil	+ 29.0	2.8	
2,4-Dinitrophenylhydrazone of the methyl ester of the keto-acid (8)	A	66−67	+ 32	0.93	
	B	66−67 and 77−78*	+ 34	0.94	
(+)-α-Methyl-α-isopropyl-glutaric acid (9)	A	60−62	+ 8.7	0.8	
	B	60−62 (68−70) **	+ 9.5	0.65	
(−)-α-Methyl-α-isopropyl-glutaric anhydride (10)	A	55−56	− 6.1	0.99	
	B	56−57	− 55	0.94	

* Dimorphous, needles which melt at 77−78° and leaflets with m.p. 66−67°.
** Recrystallised from water. The dried product showed the m.p. 60−62°.

sample was distilled at a pressure of 0.5 mm. (Found: C 65.6; H 8.9. $C_{10}H_{16}O_3$ requires C 65.2; H 8.8). *2,4-Dinitrophenylhydrazone*, m.p. 116−118°. (Found: N 15.2. $C_{16}H_{20}O_6N_4$ requires N 15.4). Methanol/chloroform (4 %) eluted a compound (0.11 g) which was a crude hydroxyketo-acid according to its infra red spectrum, $\nu_{max}^{CCl_4}$ 3 380, 1720 and 1 700 cm^{-1}.

The neutral fraction was distilled at water pump pressure. On GLC, the distilled product showed two peaks with retention times 0.91 and 0.77 relative (+)-sabinol (3b). The areas of the peaks were 98 % and 2 % of the total peak area, respectively. The *p*-nitrobenzoate of this product was recrystallised from methanol to give pure (−)-neothujyl *p*-nitrobenzoate as needles, m.p. 91−92°, $[\alpha]_D$ −12° (*c* 1.6)[10]. Hydrolysis with boiling methanolic potassium hydroxide, followed by steam distillation and distillation under reduced pressure as previously described [10], yielded pure (−)-*neothujyl alcohol*, m.p. 20−22°, $[\alpha]_D$ −9° (*c* 1.1 in ethanol). On GLC, this alcohol showed a peak with the same retention time, 0.91 relative (+)-sabinol (3b), as the "98 %-peak" of the crude neutral fraction. The "2 %-peak" of this neutral fraction had the same retention time as (+)-neoisothujyl alcohol, 0.77 relative (+)-sabinol (3b) (see below).

(+)-α-Methyl-α-isopropylsuccinic acid (13) from the ketolactone (11). The ketolactone (0.11 g) in aqueous sodium hydroxide (10 %, 2 ml) was treated with an ice-cold freshly prepared sodium hypobromite solution [from aqueous sodium hydroxide (10 %, 10 ml) and bromine (0.75 ml)] and the mixture kept at room temperature for 3 h. The bromoform was removed by extraction with ether. The aqueous solution was decolourised with sodium bisulphite, acidified and extracted with ether. Drying (Na_2SO_4) and evaporation of the ether left a viscous liquid (0.093 g). The infra red spectrum showed that this product was the crude *lactone-acid (12)*, $\nu_{max}^{CCl_4}$ 1 773 and 1 702 cm^{-1}, which, without further purification, was oxidised with potassium permanganate (0.085 g) in aqueous sodium carbonate (10 %, 20 ml) at room temperature. After 12 h the mixture was treated with sodium bisulphite, acidified and extracted continously with ether. Drying (Na_2SO_4) and evaporation of the ether left a viscous liquid (0.053 g). This product showed only one main spot when chromatographed on dimethyl sulphoxide-impregnated paper [18] (ether as mobile phase, R_F 0.20). Preparative paper chromatography on dimethyl sulphoxide-impregnated paper (25 × 50 cm, Whatman 3 MM) according to the previous description [2] gave crystalline *(+)-α-methyl-α-isopropylsuccinic acid (13,* 0.032 g), m.p. 132—133°, $[\alpha]_D$ + 12.5 (*c* 1.87 in water). When mixed in the ratio 1:1 with an authentic sample of the (—)-acid [9], the m.p. was 152—153°. This mixture gave an undepressed m.p. when further mixed with the authentic racemic acid. The identity of the (+)-α-methyl-α-isopropylsuccinic acid (13) was also confirmed by comparing its infra red spectrum with that of the authentic (—)-acid.

The crude hydroxyketo-acid from the silica gel chromatography of the acidic ozonisation product (see above) gave a further amount of (+)-α-methyl-α-isopropylsuccinic acid (13), after a similar hypobromite oxidation followed by permanganate oxidation.

Catalytic hydrogenation of (+)-sabinyl acetate (3c). (+)-Sabinyl acetate (3c, 1.5 g) in methanol (5 ml) was hydrogenated over a 10 % palladium on charcoal catalyst as described for (+)-sabinene (3a). On GLC, the dihydro-product showed two peaks with areas corresponding to the relative amounts of about 80 % and 20 %. The retention times relative (+)-sabinol (3b) were 1.23 and 1.05, respectively. The "80 %-peak" was not symmetrical and seemed to consist of two overlapping peaks.

The *ozonisation of the dihydro-product obtained from (+)-sabinyl acetate (3c)* was carried out as described for the ozonisation of the dihydro compound (7a), and gave similarly, an acidic (0.325 g) and a neutral (0.850 g) fraction.

A preliminary experiment in which a small sample (0.020 g) of the acidic fraction was hydrolysed with boiling methanolic potassium hydroxide (5 %, 3 ml) gave an acidic product (0.013 g) which, according to paper chromatography (dimethyl sulphoxide-impregnated paper and ether as mobile phase [18]), was a complex mixture. No ketolactone (11) could be isolated from this product.

The acidic fraction (0.30 g) in methanol (5 ml) was treated with alkaline potassium borohydride [potassium borohydride (0.6 g), potassium hydroxide (0.2 g), water (5 ml) and methanol (5 ml)] for 24 h at room temperature. The alkaline solution was diluted with water, acidified and extracted with ether. Drying (Na_2SO_4) and evaporation of the ether left a viscous liquid which was chromatographed on silia gel (10 g). Chloroform eluted the oily *hydroxylactone (14,* 0.19 g) with characteristic infra red spectrum, $\nu_{max}^{CCl_4}$ 3 600, 3 460, and 1 775 cm^{-1}. The analytical sample was distilled at a pressure of 1.0 mm. (Found: C 65.1; H 9.9. $C_{10}H_{18}O_3$ requires C 64.5; H 9.7). Methanol/chloroform (3 %) eluted the crystalline *diol-acid (15,* 0.067 g) which after one crystallisation from chloroform had m.p. 110—113° (decomp.), $[\alpha]_D$ + 32° (*c* 0.5). (Found: C 59.0; H 9.6. $C_{10}H_{20}O_4$ requires C 58.8; H 9.9).

On GLC, the neutral ozonisation product showed only one peak with the same retention time as the "80 %-peak" of the crude dihydroproduct. This peak also seemed to be an unresolved doublet. The neutral product was hydrolysed with boiling methanolic potassium hydroxide and the hydrolysed product distilled at water pump pressure. GLC of the distilled product showed two peaks with the retention times 0.91 and 0.77 relative (+)-sabinol (3b) and with relative areas of 30 % and 70 %, respectively. This product (0.75 g) was treated with *p*-nitrobenzoyl chloride (1.0 g) in the usual manner to give the oily ester which crystallised on standing. Five crystallisations from methanol furnished pure *(+)-neoisothujyl p-nitrobenzoate* (0.190 g) as needles, m.p. 88—89°, $[\alpha]_D$ + 27° (*c* 1.7). (Found: C 67.1; H 6.9. $C_{17}H_{21}O_4N$ requires C 67.3; H 6.9). The mother liquors from the

first two crystallisations were concentrated and, on seeding with (−)-neothujyl *p*-nitrobenzoate, a crude product crystallised out. After five crystallisations from methanol pure *(−)-neothujyl p-nitrobenzoate* was obtained as needles, m.p. and mixed m.p. 91−92° and infra red spectrum identical with that of an authentic sample.

Hydrolysis of the (+)-neoisothujyl *p*-nitrobenzoate (0.150 g) with boiling methanolic potassium hydroxide (5 %, 5 ml) gave a neutral product (0.050 g) which was distilled under reduced pressure and pure *(+)-neoisothujyl alcohol* was obtained as a colourless oil, $[\alpha]_D$ + 42° (*c* 1.8), n_D^{25} 1.4647. On GLC, this alcohol showed a peak with the same retention time, 0.77 relative (+)-sabinol (3b), as the "70 %-peak" of the crude hydrolysed neutral fraction.

Oxidation of (+)-neoisothujyl alcohol with chromic acid as previously described[10] gave a crude ketone, $[\alpha]_D$ + 51 (*c* 0.63) which had an identical infra red spectrum as (+)-isothujone. The semicarbazone of this crude ketone was purified by crystallisation from methanol/water and gave small amounts of the pure *(+)-isothujone semicarbazone*, m.p. and mixed m.p. 170−172°, $[\alpha]_D$ + 220° (*c* 0.46 in methanol). The infra red spectrum was identical with that of an authentic sample.

(+)-α-Methyl-α-isopropylsuccinic acid (13) from the hydroxylactone (14) and the diol-acid (15). The hypobromite oxidation was carried out as described for the oxidation of the ketolactone (11), to afford a product which was identical with the lactone-acid (12) according to its infra red spectrum and its paper chromatographic behaviour (dimethyl sulphoxide-impregnated paper and ether as mobile phase[18]). This lactone-acid (12) was further oxidised with permanganate and yielded, after purification by means of preparative paper chromatography, as described above, the crystalline *(+)-α-methyl-α-isopropylsuccinic acid (13)*, m.p. and mixed m.p. 132−133°, $[\alpha]_D$ + 12.9 (*c* 1.42 in water).

Similarly the diol-acid (15) was oxidised in two steps, first with hypobromite and then with permanganate, to the (+)-α-methyl-α-isopropylsuccinic acid (13).

Acknowledgements. I wish to thank Professor Holger Erdtman for his interest in this work and for his kind encouragement. Thanks are also due to Professor C. Djerassi for a sample pf (+)-2-methyl-2-isopropyl-5-oxocaproic acid, Professor A. Fredga and Dr. B. Sjöberg for samples of (−)- and racemic α-methyl-α-isopropylsuccinic acid, Dr. S. Forsén for the proton magnetic resonance spectrum, Miss G. Hammarberg for the infra red spectra, Dr. I. Wellings for reading, the manuscript and to *Statens Tekniska Forskningsråd* for a fellowship.

REFERENCES

1. Erdtman, H. and Norin, T. *Chem. & Ind. London* **1960** 622.
2. Norin, T. *Acta Chem. Scand.* **15** (1961) 1676.
3. Ullman, E. F. *J. Am. Chem. Soc.* **81** (1959) 5386.
4. Sarel, S. and Breuer, E. *J. Am. Chem. Soc.* **81** (1959) 6522.
5. For references see Simonsen, J. L. *The Terpenes*, University Press, Cambridge 1949 (2nd Ed.) Vol. II, 13, 20 and 30.
6. Birch, A. J. *Ann. Reports on Progr. Chem. London* **47** (1950) 191.
7. Walborsky, H. M., Sugita, T., Ohno, M. and Inouye, Y. *J. Am. Chem. Soc.* **82** (1960) 5255.
8. Eisenbraun, E. J., Burian, F., Osiecki, J. and Djerassi, C. *J. Am. Chem. Soc.* **82** (1960) 3476.
9. Porath, J. *Arkiv Kemi* **1** (1949) 385.
10. Short, A. G. and Read, J. *J. Chem. Soc.* **1939** 1040.
11. See Ref.[5], p. 25.
12. Simonsen, J. L. and Barton, D. H. R. *The Terpenes*, University Press, Cambridge 1952, Vol. III, p. 533.
13. Semmler, F. W. *Ber.* **35** (1902) 2047.
14. Daly, J. W., Green, F. C. and Eastman, R. H. *J. Am. Chem. Soc.* **80** (1958) 6330.
15. From Simonsen, J. L. *The Terpenes*, University Press, Cambridge 1949 (2nd Ed.) Vol. II, p. 1−60.
16. Groth, A. B. *Svensk Papperstidn.* **61** (1958) 315.
17. Herout, V. *Chem. listy* **46** (1952) 438.
18. Hammarberg, G. and Wickberg, B. *Acta Chem. Scand.* **14** (1960) 882.

Received September 15, 1961.

ACTA CHEMICA SCANDINAVICA 16 (1962) 649–654

Ibamarin, der Bitterstoff aus *Iberis amara* L.

J. B-SON BREDENBERG und ROLF GMELIN

Laboratorium der Stiftung für chemische Forschung, Biochemisches Institut, Helsinki, Finnland

Herrn Professor *Holger Erdtman* zum 60. Geburtstag gewidmet

Ibamarin, $C_{20}H_{28}O_5$, enthält eine enolisierte α-Diketo-Gruppe in einem Sechsring, eine α,β-ungesättigte Keto-Gruppe und zwei nicht-acylierbare Hydroxylgruppen. Ibamarin wird in alkalischer Lösung isomerisiert. Dabei entsteht Isoibamarin, dem die zur Ketogruppe konjugierte Doppelbindung fehlt.

Die *Cruciferae* zeichnen sich durch das Vorkommen einer S-haltigen Naturstoffklasse, der Senfölglucoside [1], aus. Einzelne Gattungen enthalten zusätzliche Inhaltsstoffe wie z. B. Herzglykoside [2], die besonders in Arten der Gattungen *Cheiranthus* und *Erysimum* verbreitet sind. Wir möchten heute über einen Inhaltsstoff verschiedener *Iberis*-Arten, das Ibamarin berichten, das zur Gruppe der pflanzlichen Bitterstoffe gezählt werden kann. Ibamarin wurde erstmals 1954 beschrieben [3] und wurde zunächst irrtümlich als ein glucosidischer Bitterstoff angesehen, was wahrscheinlich der Analyse eines nicht genügend gereinigten Präparats zuzuschreiben war. Ibamarin wurde nun aus den Samen von *Iberis amara* L. im wesentlichen nach der früheren Vorschrift [3] nach mehrmaligem Umkristallisieren aus verdünntem Alkohol in feinen weissen Nadeln erhalten, Schm.p. 143–148° (Zersetzung); $[\alpha]_D^{20}$ −58,5°. Ibamarin schmeckt noch in einer Verdünnung von $1:5 \times 10^6$ deutlich bitter (Grenzwert für Chinin $1:2 \times 10^6$)[4].

Die Verbindung $C_{20}H_{28}O_5$, kristallisiert aus dem verwendeten Lösungsmittel mit einem Mol Kristallwasser, das fest gebunden ist und nur unter teilweiser Zerstörung des Moleküls entfernt werden kann. Ibamarin bildet leicht ein Monoacetat, $C_{22}H_{30}O_6$, Schm.p. 238–241° (Zersetz.); $[\alpha]_D^{20}$ −80,5°, dem der bittere Geschmack fehlt.

In alkalischer Lösung erleidet Ibamarin eine sehr rasche Umlagerung in eine amorphe Substanz, Isoibamarin. Diese Isomerisierung lässt sich UV-spektrometrisch gut verfolgen durch die Veränderung von zwei Maxima bei 234 mμ (log ε 3,98) und 269 mμ (log ε 3,78) zu einem einzelnen Maximum bei 269 mμ (log ε 3,79). Auch in saurer Lösung findet dieselbe Isomerisierung langsam statt, wie sich aus der Veränderung des UV-Spektrums schliessen lässt.

Nach diesen Befunden setzt sich das UV-Spektrum von Ibamarin aus zwei verschiedenen chromophoren Systemen zusammen, von denen das System bei 234 mμ bei der Isomerisierung zerstört wird. Im infraroten Bereich ist als hervortretende Änderung das Verschwinden der Banden bei 1630 und 790 cm^{-1} zu bemerken.

Die Isomerisierung lässt sich folgendermassen erklären: das Maximum bei 234 mμ ist einem α,β-ungesättigten, α,β- oder β, β-disubstituiertem Keton [5a] (wie bei I) (IR[6]:Ketogruppe 1690 cm^{-1}, Doppelbindung 1630, 790 cm^{-1}) zuzuschreiben.

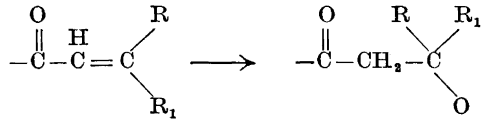

I II

Bei der Isomerisierung verschwindet die Doppelbindung wahrscheinlich durch eine intramolekulare Zyklisierungsreaktion. Eine ähnliche Reaktion ist bei den Bitterstoffen der Cucurbitacin-Gruppe [7] beobachtet worden. In diesem Fall wurde jedoch die Reaktion als eine Anlagerung von Wasser erklärt [8]. Wegen der Geschwindigkeit, mit der die Reaktion stattfindet, ist im hier vorliegenden Fall eine intramolekulare Addition vorzuziehen.

Das zweite UV-Maximum bei 269 mμ ist einer enolisierten α-Diketogruppe in einem Sechsring (Diosphenolgruppe) zuzuschreiben. Folgende Gründe sprechen dafür: Das UV-Maximum erleidet in alkalischer Lösung eine bathochrome Verschiebung nach 312 mμ unter gleichzeitiger Abnahme der Intensität (log ε 3,64). Bei Acetylierung wird das Maximum nach 232 mμ (Ibamarinacetat) bzw. 231 mμ (Isoibamarinacetat) verschoben. Diese Befunde sind in völliger Übereinstimmung mit einer Diosphenol-Gruppe [5b,9,10]. Das IR-Maximum für die Diosphenol-Gruppe [10] liegt im Ibamarin bei 1667 cm^{-1} und im Isoibamarin bei 1660 cm^{-1}. Bei der Azetylierung verschiebt es sich nach 1690 cm^{-1}. Ein enolisiertes Diketon in einem Fünfring absorbiert bei niederer Wellenlänge sowohl im UV- als auch im IR-Bereich [11]. Das Acetat von Ibamarin wird in alkalischer Lösung rasch hydrolysiert. Ausserdem reagiert Ibamarin noch mit *o*-Phenylendiamin und bildet dabei ein (amorphes) Chinoxalin, das durch sein charakteristisches UV-Spektrum identifiziert wurde [12,13]. Beim Erwärmen von Ibamarin in alkalischer Lösung werden Substanzen gebildet, die im IR-Bereich Absorption einer Carboxylgruppe aufweisen. Gleichzeitig verschwindet dabei die Diosphenol-Gruppe, was durch eine Benzilsäure-Umlagerung erklärt werden kann.

Bei Hydrogenierung mit Platin in Äthanol nimmt Ibamarin zwei Mole Wasserstoff auf. Da das UV-Spektrum keinerlei Absorption mehr aufweist, können die Wasserstoff-Atome den zwei Doppelbindungen in den Chromophoren zugeteilt werden.

Die Diosphenol- und die ungesättigte Keto-Gruppe stellen drei von fünf Sauerstoff-Atomen in Ibamarin dar. Aus dem IR-Spektrum (Abb. 1) sieht man, dass die Verbindung keine zusätzlichen Carbonyl-Funktionen enthält. Das Acetat von Ibamarin hat zwei aktive Wasserstoffe, was die Anwesenheit

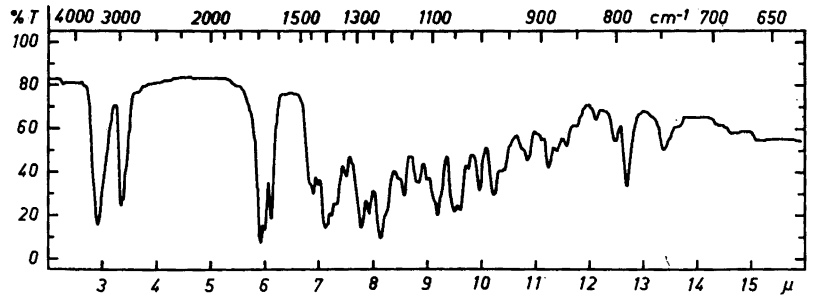

Abb. 1. Infrarot-Spektrum von Ibamarin, 2,4 mg/300 mg KBr.

von zwei Hydroxyl-Guppen anzeigt. Ausserdem absorbiert es bei 3 550 und 3 430 cm^{-1} (in KBr). Diese Banden lassen sich den beiden Hydroxyl-Gruppen zuteilen. Die Möglichkeit einer Aufspaltung der Absorption einer einzelnen Hydroxyl-Gruppe infolge partieller Assoziation kann jedoch nicht ausgeschlossen werden. Die beiden Hydroxyl-Gruppen sind offenbar schwer acetylierbar. Unter energischeren Bedingungen verläuft die Acetylierung von Ibamarin in tiefer eingreifenden Reaktionen. Alle Derivate von Ibamarin zeigen durchweg Hydroxyl-Absorption im IR-Bereich. Die Analyse des Acetats von hydrogeniertem Ibamarin passt jedoch besser zu einer Diacetat-Formel, was auf die Möglichkeit weist, dass unter bestimmten Bedingungen eine der Hydroxyl-Gruppen acetylierbar ist.

Eine Kuhn-Roth-Bestimmung von Ibamarin gibt 1,87 Mole C-Methyl-Gruppen. Dieser Wert gibt einen Hinweis, dass die Verbindung wahrscheinlich drei oder mehr C-Methyl-Gruppen enthält. Dies und die empirische Formel machen es sehr wahrscheinlich, dass Ibamarin ein Diterpen-Derivat, eventuell mit einer tricyklischen Struktur ist. Verschiedene Bitterstoffe vom Diterpen-Typ sind bekannt: Andrographolid [14,15], Clerodin [16,17], Columbin [18], Marrubiin [19], Darutoside [20] und Quassin [21,22]. Die ersteren vier Verbindungen haben alle eine bicyclische Struktur mit einer Furan- oder Butenolid-Gruppe in der Seitenkette gemeinsam. Es sei auf die interessante Tatsache hingewiesen, dass Quassin methylierte Diosphenol-Gruppen besitzt [21,23]. Die folgenden Verbindungen sind wahrscheinlich auch vom Diterpen-Typ: Chasmanthin und Palmarin von *Jatrorrhiza palmata* Miers [24], die Bitterstoffe in *Isodon trichocarpus* Kudo [25-27] und *Simarouba*-Arten [28-30], Chaparrin [31] und Tinosporin [32]. Ein Bitterstoff, Erysimupikron [33], wurde aus der botanisch nahe verwandten Art, *Erysimum crepidifolium* Rchb., isoliert. Eine Formel $C_{20}H_{24}O_5$ wurde für diese Substanz angegeben. Zu wenig ist jedoch für diese Substanz bekannt, um einen näheren Vergleich mit Ibamarin anstellen zu können.

EXPERIMENTELLER TEIL

Alle Schmelzpunkte wurden mit einem Kofler-Mikroheiztisch bestimmt und sind korrigiert. Die Infrarot-Spektren wurden mit einem Beckman IR-5-Gerät, die Ultraviolett-Spektren mit einem Beckman DK-2-Gerät aufgenommen. Die Analysen wurden bei A. Bernhardt, Mülheim a.d.R., Deutschland, ausgeführt.

Isolierung von Ibamarin

Im wesentlichen wurde die früher beschriebene Methode zur Isolierung von Ibamarin verwendet [3]. Das aus Aceton-Petroläther erhaltene Roh-Ibamarin wurde noch dreimal mit verdünntem Äthanol umkristallisiert. Feine, farblose Nadeln, Schm.p. 143–148° (Zers.), $[\alpha]_D^{20}$ −58,5° (c = 2,0; in Methanol). (Gef.: C 65,55; H 8,31; O 21,57; O–CH_3 1,70; C–CH_3 7,67. Ber. für $C_{20}H_{28}O_5 \cdot H_2O$: C 65,55; H 8,25; O 26,20. Nach Trocknung bei 100° im Hochvakuum: Gef.: C 68,24; H 7,87. Ber. für $C_{20}H_{28}O_5$: C 68,94; H 8,10).

Ultraviolett-Spektren: Äthanol λ_{max} 234, 269 mμ (log ε 3,98, 3,78); 0,1 N NaOH in Äthanol-Wasser (1:1), 7 Min nach Auflösung λ_{max} 231, 312 mμ (log ε 3,73, 3,65), keine weitere Veränderung bei längerem Stehen. Ansäuerung der alkalischen Lösung 15 Min nach Alkalisch-Machen λ_{max} 268 mμ (log ε 3,80); 0.05 N HCl, Äthanol-Wasser, unmittelbar nach Auflösen λ_{max} 236, 265 (Schulter) (log ε 3,99, 3,79). Die Intensität bei 236 mμ nahm beim Kochen der Lösung langsam ab (Stunden, log ε: 1, 3,97; 2, 3,95; 3, 3,94), keine Abnahme wurde bei 265 mμ beobachtet; 1 N HCl, Äthanol-Wasser, Siedetemperatur, 236 mμ: Min: 0, 30, 60, 90, log ε 3,98, 3,73, 3,64, 3,62, keine Veränderung bei 265 mμ.

Infrarot-Spektrum: siehe Abb. 1. Beim Trocknen bei höheren Temperaturen färbte sich Ibamarin gelb. Im IR-Spektrum des gelben Ibamarins waren die Maxima im Bereich 1 600–1 700 cm^{-1} verbreitert und zeigten Anzeichen für Nebenbanden. Der "Fingerprint"-Bereich war beinahe flach. Die Intensitäten oder Maxima im Ultraviolett-Gebiet nahmen ebenfalls ab.

Acetylierung

a) Monoacetat. Das Monoacetat wurde durch Acetylierung mit Acetanhydrid und Pyridin zwei Tage bei Zimmertemperatur erhalten. Ein identisches Produkt erhielt man, wenn 2 Std. unter Erwärmen auf dem Wasserbad acetyliert wurde. Die Verbindung kristallisierte aus verdünntem Methanol in kleinen Nadeln, Schm.p. 238–241°, $[\alpha]_D^{20}$ −80,5° (c = 2; in Äthanol). (Gef.: C 67,45, 67,50; H 7,57 ,7,60; Acetyl 10,93; Activ. H 0,53. Ber. für $C_{22}H_{30}O_6$: C 67.67; H 7,74; Acetyl (ein OH) 11,02; Activ. H (zwei) 0,51). Ultraviolett-Spektren: Äthanol, λ_{max} 232 mμ (log ε 4,14); 0.1 N NaOH in Äthanol-Wasser (1:1), 10 Min nach Auflösen, λ_{max} 232, 312 mμ (log ε 3,84, 3,64). Infrarot-Maxima (in KBr): 3 550 (m), 3 430 (m), 1 745 (s), 1 690 (s), 1 630 (m) und 782 (m) cm^{-1}. Die Intensität der Bande bei 1 690 cm^{-1} hatte im Verhältnis zur Bande bei 1 630 cm^{-1} zugenommen, verglichen mit den Banden-Intensitäten von Ibamarin. Das Acetat besass keinen bitteren Geschmack.

b) Acetylierung bei höheren Temperaturen. Ibamarin (32 mg) wurde mit Acetanhydrid (10 ml) und Kaliumacetat (200 mg) durch 24 stdg. Kochen acetyliert. Die Mischung wurde in Wasser gegossen und in üblicher Weise mit Äther extrahiert. Das gelbe amorphe Produkt, das nicht zur Kristallisation gebracht werden konnte, wurde weiter mit Acetanhydrid und Pyridin (2 Tage, Zimmertemperatur) behandelt. Aus Petroläther (K.p. 40–60°) schied sich ein amorphes, gelbes Pulver aus (12 mg), das bei 157–162° schmolz. (Gef.: C 68,09; H 6,94. Ber. für $C_{22}H_{26}O_6$: C 68,36; H 6,77; für $C_{22}H_{28}O_6$: C 68,00; H 7,26). Ultraviolett-Spektrum: Äthanol λ_{max} 236, 267 mμ (log ε 3,92, 3,81); 0.1 N NaOH in Äthanol-Wasser (1:1) λ_{max} 284 mμ (log ε 4,00) (Aromatisierung?). Infrarot-Maxima (in KBr): 3 420 (w), 1 760 (s), 1 695 (m) und 1 615 (w).

Isomerisierung

a) Bei niederer Temperatur. Ibamarin (30 mg) wurde in Äthanol (5 ml) gelöst. 1 N NaOH-Lösung (20 ml) wurde zugegeben. Nach ½ Std. bei Zimmertemperatur wurde die Lösung mit 1 N HCl-Lösung (25 ml) angesäuert und die Mischung mit Äther ausgeschüttelt. Die Ätherlösung wurde gewaschen, getrocknet und im Vakuum zur Trockne gebracht. Der Rückstand bestand aus einen leicht gelblichen amorphen Pulver, das nicht zur Kristallisation gebracht werden konnte. Ultraviolett-Spektren: Äthanol λ_{max} 269 mμ (log ε 3,79); 0.1 N NaOH in Äthanol (1:1) λ_{max} 232, 312 mμ (log ε 3,74, 3,64). Infrarot-Maxima (in KBr): 3 420 (s), 1 690 (s), 1 660 (s) und 1 590 (w) cm^{-1}.

Das Produkt wurde acetyliert (Acetanhydrid-Pyridin, 2 Std. auf dem Wasserbad) und gab 10 mg eines kristallinen Pulvers, Schm.p. 108–112°. Ultraviolett-Spektra:

Äthanol, λ_{max} 231 mμ, 275 mμ (Schulter) (log ε 3.95, 3.19); 0.1 N NaOH in Äthanol-Wasser, λ_{max} 231, 308 mμ (log ε 3,85, 3,65). Infrarot-Maxima (in KBr): 3 440 (m), 1 740 (s), 1 695 (s), 1 630 (w), 1 590 (w) cm^{-1}.

b) Bei höherer Temperatur. Ibamarin (50 mg) wurde in 1 N NaOH-Lösung (25 ml) gelöst und auf dem Wasserbad ½ Std. erhitzt. Nach etwa 10 Min. färbte sich die Lösung gelb. Die Lösung wurde mit Wasser verdünnt, angesäuert und mit Äther extrahiert. Die Ätherphase hinterliess nach Abdampfen ein amorphes Pulver, das nicht zur Kristallisation gebracht werden konnte. Infrarot-Maxima (in KBr): 3 450 (s), breite Absorption 3 400—2 500 und 1 695 (s) cm^{-1}.

Das amorphe Produkt wurde mit Acetanhydrid und Pyridin (½ Std. auf dem Wasserbad, dann Zimmertemperatur über Nacht) acetyliert. Das rohe, amorphe Acetat wurde mit Petroläther und einer kleinen Menge Äther extrahiert. Der Rückstand gab 6 mg Kristalle, Schm.p. 236—239° (Zers). Ultraviolett-Spektrum: Äthanol, keine besondere Absorption ausser einem Maximum geringer Intensität bei 285 mμ. Infrarot-Maxima (in KBr): 3 480 (m), breite Absorption 3 500—2 700, 1 745 (s), 1 715 (m), 1 668 (w) cm^{-1}.

Hydrogenierung

Ibamarin (100 mg) wurde mit Platin in Äthanol bei Zimmertemperatur hydrogeniert. Ein Mol Wasserstoff wurde in 2 Stunden aufgenommen, ein weiteres Mol in etwa 24 Stunden. Die Lösung wurde filtriert und eingedampft. Dabei wurde eine farblose, zähe Masse erhalten (105 mg). Infrarot-Maxima (Film): 3 430 (s) und 1 690 (s) cm^{-1}. Das Produkt wurde acetyliert (Acetanhydrid-Pyridin, Zimmertemperatur, zwei Tage) und gab aus Petroläther ein amorphes Pulver (37 mg) ohne bitteren Geschmack, das bei 120—130° schmolz. (Gef.: C 66,06; H 8,39; O 25,26. Ber. für $C_{32}H_{34}O_6$: C 66,97; H 8,69; O 24,34; für $C_{24}H_{36}O_7$: C 66,04; H 8,31; O 25,66). Ultraviolett-Spektrum: keine besondere Absorption über 230 mμ. Infrarot-Spektrum (in KBr): 3 450 (m), 1 735 (s) und 1 690 (s) cm^{-1}.

Chinoxalin

Ibamarin (20,8 mg) und *o*-Phenylendiamin (6,1 mg) wurden in Eisessig (1 ml) gelöst und auf dem Wasserbad 1 Std. lang erhitzt. Die Lösung war braun gefärbt, aber keine Fällung trat ein. Anschliessend wurde die Lösung über Nacht bei Zimmertemperatur gehalten, in Wasser gegossen und mit Äther extrahiert. Die Ätherphase wurde gründlich mit verdünnter Salzsäure und Wasser gewaschen, getrocknet und eingedampft. Der Rückstand wurde aus Petroläther kristallisiert. 3.2 mg eines feinen Pulvers; Schm.p. 138—145°. Ultraviolett-Spektrum: Äthanol λ_{max} 237, 320 mμ (log ε 4,25, 3,51), Schultern bei 265 und 310 mμ (log ε 3,72, 3,45). Infrarot-Maxima (in KBr): 3 420 (s), 1 690 (s), 1 660 (Schulter, m) und 1 620 (m) cm^{-1}.

Nach der Vollendung des Manuskripts erfuhren wir von einer Arbeit von Pourrat und Decorps (*Bull. soc. chim. France* **1961** 670), in der sie die Isolierung von einem Bitterstoff "Ibamarin" aus *Iberis amara* L. beschreiben. Dieser Bitterstoff ist wahrscheinlich identisch mit unserer Verbindung. Sie erklären jedoch, das die Ergebnisse die Anwesenheit eines Phenol-Hydroxyls, eines nicht-acetylierbaren Hydroxyls, einer Keton- und einer Ester- oder Lacton-Gruppe zeigen. Gemäss unseren Ergebnissen ist die Anwesenheit einer Phenol-, Ester- oder Lacton-Gruppe in Ibamarin ausgechlossen.

LITERATUR

1. Kjær, A. in *Fortschr. Chem. organ. Naturstoffe* **18** (1960) 129.
2. Kowalevski, Z., Jäger, H., Schindler, O. und Reichstein, T. *Helv. Chim. Acta* **43** (1960) 957.
3. Schultz, O. E. und Gmelin, R. *Arch. Pharm.* **59** (1954) 404.
4. Korte, F., Barkemeyer, H. und Korte, I. *Fortschr. Chem. organ. Naturstoffe* **17** (1959) 124.
5. Gillam, A. E. und Stern, E. S. *An Introduction to Electronic Absorption Spectroscopy in Organic Chemistry*, Edward Arnold Ltd, London, 1957, *a* S. 103, *b*. S. 113.

6. Bellamy, L. J. *Ultrarot-Spektrum und chemische Konstitution*, Dietrich Steinkopff, Darmstadt 1955.
7. Lavie, D. und Shvo, Y. *J. Am. Chem. Soc.* **81** (1959) 3058.
8. Lavie, D., Shvo, Y. und Willner, D. *J. Am. Chem. Soc.* **81** (1959) 3062.
9. Stiller, E. T. und Rosenheim, D. *J. Chem. Soc.* **1938** 353.
10. Lavie, D. und Szinai, S. *J. Am. Chem. Soc.* **80** (1958) 707.
11. Bredenberg, J. B. *Acta Chem. Scand.* **13** (1959) 1733.
12. Bohlmann, F. *Chem. Ber.* **84** (1951) 860.
13. Albert, A., Brown, D. J. und Cheeseman, G. *J. Chem. Soc.* **1951** 474.
14. Cava, M. P. und Weinstein, B. *Chem. & Ind. London* **1959** 851.
15. Chan, W. R., Haynes, L. J. und Johnson, L. F. *Chem. & Ind. London* **1960** 22.
16. Sim, G. A., Hamor, T. A., Paul, I. C. und Robertson, J. M. *Proc. Chem. Soc.* **1961** 75.
17. Barton, D. H. R., Cheung, H. T., Cross, A. D., Jackman, L. M. und Martin-Smith, M. *Proc. Chem. Soc.* **1961** 76.
18. Overton, K. H., Weir, N. G. und Wylie, A. *Proc. Chem. Soc.* **1961**, 211.
19. Burn, D. und Rigby, W. *J. Chem. Soc.* **1957**, 2964.
20. Diara, A., Asselineau, C. und Lederer, E. *Bull. soc. chim. France* (5) **1960**, 2171.
21. Valenta, Z., Gray, A. H., Papadopoulos, S. und Podešva, C. *Tetrahedron Letters* **1960**, No. 20, 25.
22. Carman, R. M. und Ward, A. D. *Ibid.* **1961**, 317.
23. Hanson, K. R., Jaquiss, D. B., Lamberton, J. A., Robertson, A. und Savige, W. E. *J. Chem. Soc.* **1954**, 4238.
24. Barton, D. H. R. und Elad, D. *J. Chem. Soc.* **1956** 2085.
25. Naya, K. *Nippon Kagaku Zasshi* **79** (1958) 885; *Chem. Abstracts* **55** (1961) 495.
26. Ikeda, T. und Kanatomo, S. *Yakugaku Zasshi* **78** (1958) 1128; *Chem. Abstracts* **53** (1959) 3389.
27. Takahashi, M., Fujita, T. und Koyama, Y. *Yakugaku Zasshi* **80** (1960) 594; *Chem. Abstracts* **55** (1961) 2590.
28. Glemser, O. und Ott, E. *Ber.* **70 B** (1937) 1513.
29. Ham, E. A., Schafer, H. M., Denkewalter, R. G. und Brink, N. G. *J.Am. Chem. Soc.* **76** (1954) 6066.
30. Polonsky, J. *Bull. soc. chim. France* (5) **1959**, 1546.
31. Geissman, T. A. und Chandorkar, K. R. *J. Org. Chem.* **26** (1961) 1217.
32. Chatterjee, A. und Ghosh, S. *Sci. and Culture (Calcutta)* **26** (1960) 140; *Chem. Abstracts* **55** (1961) 13470.
33. Berger, R. *Heil- und Gewürzpflanzen* **8** (1925) 1.

Received August 28, 1961.

ACTA CHEMICA SCANDINAVICA 16 (1962) 655–658

Iodinated 1-Phenyl*cyclo*alkane-1-carboxylic Acids

RICHARD DAHLBOM* and RENÉ MOLLBERG

Research Laboratories, AB Astra, Södertälje, Sweden

Dedicated to Professor *Holger Erdtman* on his 60th birthday

Some iodinated amino- and hydroxysubstituted 1-phenyl*cyclo*alkane-1-carboxylic acids have been synthesised for investigation as X-ray contrast media.

Iodinated phenylsubstituted alkanoic acids are used clinically as diagnostic agents for visualization of X-rays [1]. The present paper describes the preparation of some related compounds, *viz.* iodinated amino- and hydroxy-substituted 1-phenyl*cyclo*alkane-1-carboxylic acids (I—IV).

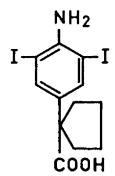

I

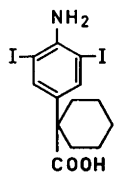

II

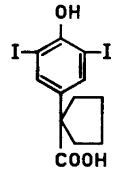

III

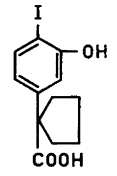

IV

The aminosubstituted acids were prepared according to the following sequence of reactions:

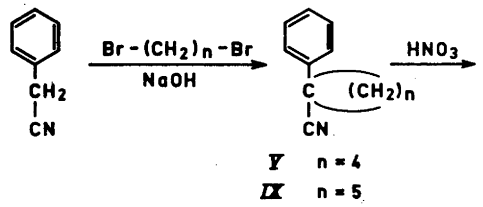

V n = 4
IX n = 5

* Present address: Department of Chemistry, Kungl. Farmaceutiska Institutet, Stockholm, Sweden.

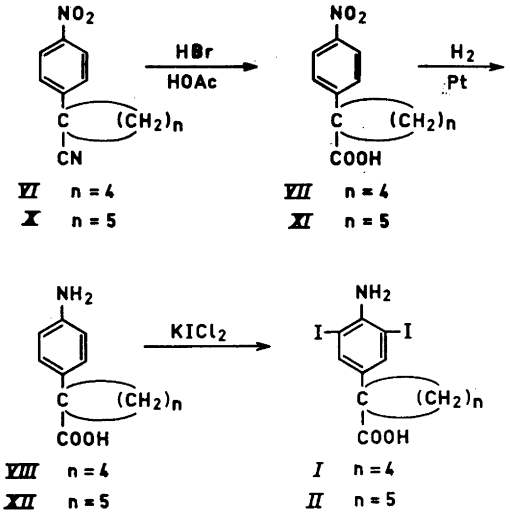

The hydroxysubstituted acids were prepared from *m*- and *p*-methoxybenzylcyanide as follows:

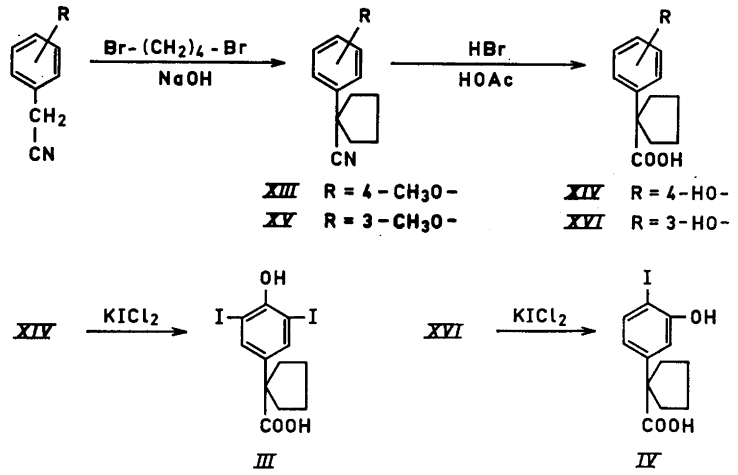

Iodination of 1-(3-hydroxyphenyl)-*cyclo*pentane-1-carboxylic acid yielded only a monoiodo derivative and not a di- or triiodosubstituted product as is the case with several (3-hydroxyphenyl)-alkanoic acids [2]. However, the 2- and 6-positions in the benzene ring of the 1-(3-hydroxyphenyl)-cyclopentane-1-carboxylic acid are hindered sterically by the bulky *cyclo*pentyl group, as is evident from examination of molecular models. We have therefore assumed, that the iodine has entered the 4-position.

The compounds I—IV were tested pharmacologically. No affinity for any special organ was observed, and their toxicities were rather high.

EXPERIMENTAL

*1-Phenyl*cyclo*pentane-1-carbonitrile (V).* This compound has been prepared from benzyl cyanide and 1,4-dibromobutane in the presence of sodium amide [3]. We found that sodium amide could be replaced by sodium hydroxide. A mixture of benzyl cyanide (117 g, 1 mole), 1,4-dibromobutane (216 g, 1 mole) and powdered sodium hydroxide (200 g, 5 mole) was heated at 100—110° in an oil bath with vigorous mechanical stirring. After about half an hour a violent reaction started, which subsided in a few minutes. Stirring was continued at the same temperature for 3 h. The hot reaction mixture was then poured on *ca.* 1 kg of crushed ice. The organic layer was separated and the aqueous solution was extracted with ether (2 × 100 ml). The organic layer and the ether extract were combined and dried over sodium sulphate. The solvent was evaporated and the residue was distilled *in vacuo* giving a colourless oil (132 g, 77 %), b.p. 139—140°/10 mm (lit.[3] 148—153°/20 mm); n_D^{22} 1.5333.

1-(4-Nitrophenyl)-cyclo*pentane-1-carbonitrile (VI).* The nitrile V (34.2 g) was added dropwise with stirring to nitric acid (115 ml, *d* 1.50) at a temperature of −10° to −15° during one hour. The stirring was continued at 0° for 2 h, and the mixture was then poured on 250 g of crushed ice. The precipitated nitro compound was collected, washed with water and crystallised from ethanol, m.p. 76—78° (29 g, 67 %). Recrystallisation from the same solvent raised the m.p. to 77.5—78.5°. (Found: C 66.5; H 5.37; N 13.2. Calc. for $C_{12}H_{12}N_2O_2$: C 66.6; H 5.59; N 13.0).

1-(4-Nitrophenyl)-cyclo*pentane-1-carboxylic acid (VII).* The nitrile VI (29 g) was refluxed for 3 h with a mixture of 48 % hydrobromic acid (150 ml) and glacial acetic acid (100 ml). During the reaction the acid formed gradually crystallised. After cooling the product was collected (28 g, 89 %); m.p. 181—182°. (Found: C 60.9; H 5.59. Calc. for $C_{12}H_{13}NO_4$: C 61.3; H 5.57).

1-(4-Aminophenyl)-cyclo*pentane-1-carboxylic acid (VIII).* The nitro compound VII (26 g) was dissolved in ethanol (250 ml) and hydrogenated at 50° in a Parr hydrogenation apparatus with PtO_2 as catalyst at a pressure of 3—4 kg/cm². The calculated amount of hydrogen was consumed in one hour. During the hydrogenation the amino compound partly separated as white needles. The ethanol was removed *in vacuo* and the residue was dissolved in 2 N hydrochloric acid and the solution was filtered through theorite. The solution was made alkaline with ammonia, and the reaction product was then precipitated with acetic acid and recrystallised from ethanol (22 g, 97 %), m.p. 197—199°. (Found: C 70.0; H 7.49; N 6.79. Calc. for $C_{12}H_{15}NO_2$: C 70.2; H 7.37; N 6.82).

1-(4-Amino-3,5-diiodophenyl)-cyclo*pentane-1-carboxylic acid (I).* The preceding amino compound (20.5 g) was dissolved in 0.1 N hydrochloric acid (4 l) and 2 M potassium iodochloride solution (120 ml, prepared according to the method of Larsen *et al.*[4]) was added with vigorous stirring in one portion. The reaction product started to separate immediately. Stirring was continued for 2 h, and saturated sodium hydrogen sulphite solution was then added in order to remove excess of iodine. The product was collected (40 g, 87 %) and recrystallised from ethanol to give yellow plates, m.p. 180—181° (decomp.). (Found: C 31.5; H 2.84; I 55.1. Calc. for $C_{12}H_{13}I_2NO_2$: C 31.5; H 2.87; I 55.5).

*1-Phenyl*cyclo*hexane-1-carbonitrile (IX).* This compound was prepared from benzyl cyanide, 1,5-dibromopentane and sodium hydroxide by the same method as described for the *cyclo*pentyl analogue V. Formation of solid condensation products lowered the yield to 30 %. The nitrile hade b.p. 148—149°/10 mm; n_D^{22} 1.5334 (lit.[5] b.p. 110—115°/0.7 mm; n_D^{25} 1.5327).

1-(4-Nitrophenyl)-cyclo*hexane-1-carbonitrile (X)* was obtained by nitration of the foregoing nitrile as described for VI. Yield 60 %, m.p. 73—74° (from ethanol). (Found: C 67.6; H 6.11. Calc. for $C_{13}H_{14}N_2O_2$: C 67.8; H 6.13).

1-(4-Nitrophenyl)-cyclo*hexane-1-carboxylic acid (XI).* The nitrile X was refluxed for 3 h with 48 % hydrobromic acid (200 ml) and glacial acetic acid (150 ml). After cooling the separated reaction product was filtered off and recrystallised from ethanol to give colourless crystals (33 g, 78 %) of m.p. 175—177°. This acid has earlier been prepared in 33 % yield by nitration of 1-penyl*cyclo*hexane-1-carboxylic acid [6], m.p. 176—177°.

1-(4-Aminophenyl)-cyclo*hexane-1-carboxylic acid (XII).* The above nitro compound XI (25 g) was hydrogenated in a Parr hydrogenation apparatus as described for compound

VIII. The solution of the amino compound in hydrochloric acid was used directly in the next step. Only one tenth of the solution was worked up and the acid XII was isolated and characterised. It melted at 201—203° after recrystallisation from ethanol. (Found: C 70.7; H 7.40; N 6.38. Calc. for $C_{13}H_{17}NO_2$: C 71.2; H 7.28; N 6.39).

1-(4-Amino-3,5-diiodophenyl)-cyclo*hexane-1-carboxylic acid (II)*. The solution of XII in hydrochloric acid obtained in the foregoing experiment was diluted to 4 l and 2 M potassium iododichloride solution (150 ml) was added. The reaction mixture was stirred at room temperature for 2 h and was then decolourised with saturated sodium hydrogen sulphite solution. The reaction product was collected and recrystallised from ethanol giving light yellow crystals (20 g, 47 % calc. on XI), m.p. 177—178°. (Found C 33.1; H 3.42; I 53.6; N 3.22. Calc. for $C_{13}H_{15}I_2NO_2$: C 33.1; H 3.21; I 53.9; N 2.97).

1-(4-Methoxyphenyl)-cyclo*pentane-1-carbonitrile (XIII)*. 4-Methoxybenzyl cyanide was alkylated with 1,4-dibromobutane in the presence of sodium hydroxide as described for the nitrile V. Yield 76 %, b.p. 121—122°/0.2 mm; n_D^{20} 1.5382. The compound has earlier been prepared [7] using sodium amide as condensation agent.

1-(4-Hydroxyphenyl)-cyclo*pentane-1-carboxylic acid (XIV)*. The nitrile XIII was hydrolysed in the usual way by refluxing it with 48 % hydrobromic acid and glacial acetic acid. Yield 65 %, m.p. 194—196° (from ethanol-water). (Found: C 69.4; H 7.00. Calc. for $C_{12}H_{14}O_3$: C 69.9; H 6.84).

1-(4-Hydroxy-3,5-diiodophenyl)-cyclo*pentane-1-carboxylic acid (III)*. The foregoing acid (31 g) was dissolved in water (7.5 l) at 60°. 2 M potassium iododichloride solution (230 ml) was added, and the mixture was stirred at this temperature for one hour. Excess iodine was removed by addition of sodium hydrogen sulphite solution, and the reaction product was then collected and recrystallised from ethanol-water to give light yellow crystals (35 g, 51 %) of m.p. 205—206°. (Found: C 31.5; H 2.63; I 54.8. Calc. for $C_{12}H_{12}I_2O_3$: C 31.5; H 2.64; I 55.4).

1-(3-Methoxyphenyl)-cyclo*pentane-1-carbonitrile (XV)* was prepared from 3-methoxybenzyl cyanide, 1,4-dibromobutane and sodium hydroxide as described for the nitrile V. Yield 83 %, b.p. 113—114°/ 0.2 mm; n_D^{22} 1.5365. (Found: C 77.7; H 7.48; N 6.90. Calc. for $C_{13}H_{15}NO$: C 77.6; H 7.51; N 6.96).

1-(3-Hydroxyphenyl)-cyclo*pentane-1-carboxylic acid (XVI)*. The nitrile XV was hydrolysed in the usual way by refluxing it with 48 % hydrobromic acid and glacial acetic acid. Yield 68 %, m.p. 168—169° after recrystallisation from water. (Found: C 69.3; H 6.80. Calc. for $C_{12}H_{14}O_3$: C 69.9; H 6.84).

1-(3-Hydroxy-4-iodophenyl)-cyclo*pentane-1-carboxylic acid (IV)*. The foregoing acid (5 g) was dissolved in glacial acetic acid (60 ml) to which had been added some conc. hydrochloric acid (5 ml). 2 M potassium iododichloride solution (50 ml) was then added, and the reaction mixture was heated on the steam bath for 4 h. After cooling, the product which had precipitated was collected. It was then dissolved in alkali and treated with sodium hydrogen sulphite to remove excess of iodine. Precipitation with acid yielded a crystalline product, which was purified further by recrystallisation from ethanol-water to give almost colourless crystals (5 g, 63 %) of m.p. 192—194°. Analysis indicated that only one iodine atom had entered the benzene ring. (Found: C 43.9; H 4.08; I 37.9. Calc. for $C_{12}H_{13}IO_3$: C 43.4; H 3.94; I 38.2).

REFERENCES

1. Burger, A. *Medicinal Chemistry*, 2nd Ed., Interscience, New York 1960, p. 665.
2. Papa, D., Ginsberg, H. F., Lederman, I. and DeCamp, V. *J. Am. Chem. Soc.* **75** (1953) 1107.
3. Tilford, C. H., van Campen, M. G. and Shelton, R. S. *J. Am. Chem. Soc.* **69** (1947) 2902.
4. Larsen, A. A., Moore, C., Sprague, J., Cloke, B., Moss, J. and Hoppe, J. O. *J. Am. Chem. Soc.* **78** (1956) 3210.
5. Lyle, R. E. and Lyle, G. G. *J. Am. Chem. Soc.* **74** (1952) 4059.
6. Rubin, M. and Wishinsky, H. *J. Am. Chem. Soc.* **68** (1946) 828.
7. Ito, T. *Jap. P.* 3427 (1952); *Chem. Abstr.* **48** (1954) 3999.

Received June 2, 1961.

ACTA CHEMICA SCANDINAVICA 16 (1962) 659–672

The Mechanism of Reduction of Nitrate

II. The Kinetics and Mechanism of the Molybdate Catalyzed Reduction of Nitrate by Sn(II) in Acid Solution

G. P. HAIGHT, Jr.* and ALFRED KATZ**

Contribution from Kem. Lab. A., Technical University of Denmark, and the Chemistry Department of Swarthmore College, Swarthmore, Pa., U.S.A.

Molybdate catalyses the reduction of nitrate by Sn(II) in acid solution. In 3.0 M hydrochloric acid the reduction takes place in two steps to hydroxylamine and ammonia. For the reaction

$$3\ Sn(II) + NO_3^- + 8\ H^+(Mo(VI)) = 3\ Sn(IV) + NH_3OH^+ + 2\ H_2O$$

the rate law is:

$$-d[Sn(II)]/dt = \frac{k'[Sn(II)][NO_3^-][Mo]}{1 + k''[Mo]^{1/2} + k'''[NO_3^-]}$$

In 3.0 M sulfuric acid the reaction is much slower and the reduction of nitrate proceeds only to nitrous oxide. For the reaction

$$4\ Sn(II) + 2\ NO_3^- + 10\ H^+ = (Mo(VI))\ 4\ Sn(IV) + N_2O + 5H_2O$$

the rate law is:

$$-d[Sn(II)]/dt = k''''[Mo]^{1/2}[NO_3^-]$$

A general mechanism is derived for these and similar reductions catalyzed by molybdate. Comparisons are made with rate constants derived from catalytic polarographic waves previously reported.

The first paper [1] in this series has described the pattern of products obtained in molybdate catalyzed reductions of nitrate effected by stannous ions. This product pattern apparently depends on events occurring after the initial step in the reduction of nitrate. Since the function of molybdate catalyst is apparently wholly that of rendering the robust nitrate ion reducible, it is important to understand the means by which this initial step is accomplished. In this paper the kinetics of the reduction of nitrate in hydrochloric acid to-

* Chemistry Department, Swarthmore College. On leave to Kem. Lab. A 1960–1.
** University of Pennsylvania Medical School.

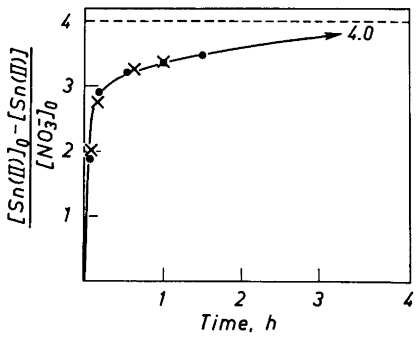

Fig. 1. A plot of the number of moles of Sn(II) consumed per mole of nitrate added *vs.* time demonstrating the sharp change in rate after all the nitrate is converted to hydroxylamine. ● Start with Mo(VI) 2.3 × 10^{-4} M. × Start with Mo(V) 2.3 × 10^{-4} M. $[Sn(II)]_0 = 0.10$ M. $[NO_3^-]_0 = 0.02$ M. $T = 25°C$.

gether with preliminary results in sulfuric acid are described. Previously, Kolthoff, Sandell, and Moskowitz[2] have employed molybdate to catalyze the reduction of nitrate by ferrous ions at 100°C for analytical purposes. Tribalat[3] has reported on the perrhenate catalyzed reductions of nitrate in which she assumes Re(V) to be the catalytic species. Johnson and Robinson [4] have discussed polarographic waves representing molybdate catalyzed reductions of nitrate. Haight [5] has interpreted these catalytic waves as resulting from the catalytic activity of Mo(IV) produced by the reduction of molybdate. Similar catalytic activity of molybdate toward perchlorate [6-8] and hydroxylamine [9] has already been reported. We shall attempt to relate the present findings to those recorded for other systems. The function of molybdate in rendering nitrate reducible is particularly important in view of its required presence for the enzymatic reduction of nitrates occurring in the biochemistry of plants [10].

EXPERIMENTAL

The conditions of experiment, preparation of solutions, and methods of chemical analysis are given in the previous paper [1]. All kinetic runs were performed in a thermostat at 25°C. Ion normality was maintained at 3.0.

RESULTS

Kinetics of the reaction in 3.0 molar hydrochloric acid. The rate of reduction of nitrate to hydroxylamine [1] proved to be so much faster than the subsequent reduction of hydroxylamine to ammonia [9] that it proved possible to consider the reaction:

$$3\ Sn(II) + NO^- + 8\ H^+ \xrightarrow{(Mo(VI))} 3\ Sn(IV) + NH_3OH^+ + 2\ H_2O \qquad (I)$$

as a separate process. In this study, catalysis was so effective that molybdate concentrations employed were in the range of 2 × 10^{-9} to 6 × 10^{-5} M. At such low concentrations it was not possible to ascertain by colorimetric means which oxidation state of molybdenum was the dominant species present during a run as in previous studies [7-9]. It was impossible to distinguish runs begun

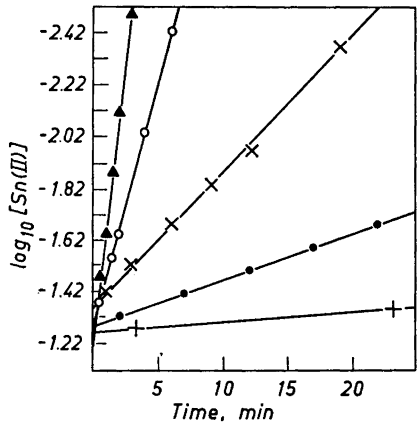

Fig. 2. Plots of log [Sn(II)] *vs.* time for runs containing large excess of nitrate demonstrating 1st order dependence on [Sn(II)]. Slopes are approximately proportional to [Mo(VI)] for constant excess $[NO_3^-]$.

+, ●, O, ▲ 0.16 M NO_3^-
× 0.12 M NO_3^-
\+ 0.37 × 10^{-6} M Mo
● 1.50 × 10^{-6} M Mo
× 4.3 × 10^{-6} M Mo
O 18.7 × 10^{-6} M Mo
▲ 37.5 × 10^{-6} M Mo

with Mo(VI) from those begun with Mo(V). Steady state conditions are achieved at the start of each run contrary to experience with the reduction of perchlorate [7] and hydroxylamine [9] and also contrary to the experience with nitrate in sulfuric acid to be described. Fig. 1 illustrates the separability of the two steps involved in the reduction of nitrate to ammonia and the indistinguishability of runs started with Mo(VI) and with Mo(V).

In the following discussion, overall chemical reactions will be numbered consecutively with Roman numerals. Mathematical equations will be numbered consecutively with Arabic numerals and will be referred to as "eqn. ( )" in the text. Individual chemical steps used in reaction mechanisms will also be numbered consecutively using Arabic numerals and will be referred to as "reaction ( )" in the text. A (±) indicates a reversible reaction. Rate constants k_n and equilibrium constants K_n will be assigned the same number as the

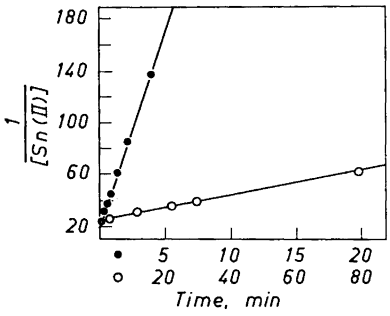

Fig. 3. Plots of 1/[Sn(II)] *vs.* time for runs containing $[Sn(II)]_0 = 3[NO_3^-]_0$.

O 1.5 × 10^{-6} M Mo
● 5.26 × 10^{-5} M Mo

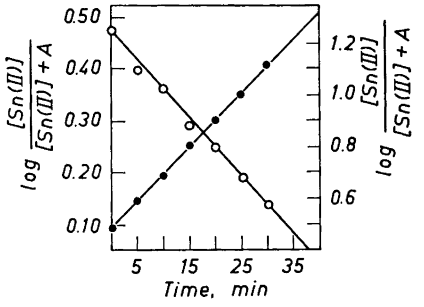

Fig. 4. Plots of log [(Sn(II)]/([Sn(II)] + A) for runs with neither Sn(II) nor NO_3^- present in high excess.

O A = −0.0112 left hand ordinate
● A = +0.1495 right hand ordinate

reaction they represent. Empirical constants used in experimental rate laws will be given distinguishing superscripts.

Determination of the rate law in hydrochloric acid. For runs containing an excess of nitrate, plots of log [Sn(II)] *vs.* time give straight lines with slopes very nearly proportional to the concentration of molybdenum as shown in Fig. 2. In runs in which [Sn(II)] = 3 [NO_3^-] plots of 1/[Sn(II)] *vs.* time gave straight lines as shown in Fig. 3. These combined results suggest a rate law showing first order dependence on all three reagents.

$$-\mathrm{d}[(\mathrm{Sn(II)}]/\mathrm{d}t = k_{\mathrm{obs}}[\mathrm{Sn(II)}][\mathrm{NO_3^-}][\mathrm{Mo}] \qquad (1)$$

Eqn. (1) predicts that for runs in which [Sn(II)] ≠ 3[NO_3^-] plots of log ([Sn(II)]/([Sn(II)] + A) *vs.* t should give straight lines. A = 3[NO_3^-]−[Sn(II)] and is constant for a given run. Fig. 4 demonstrates the validity of the above prediction.

Calculation of k_{obs} from the slopes of the lines obtained in plots such as those given in Fig. 2—4 showed that k_{obs} decreases with increasing molybdenum concentration when nitrate is not present in large excess according to the law:

$$k_{\mathrm{obs}} = k'/(1 + k'''[\mathrm{Mo}]^{1/2}) \qquad (2)$$

This finding is similar to that observed with polarographic catalytic currents which were proportional to the first power of molybdenum concentration if it was below 10^{-5} M and proportional to the square root of the molybdenum concentration if it was above 10^{-4} M.

It was also found that k_{obs} decreased with increasing concentrations of nitrate when it was present in great excess according to the law:

$$k_{\mathrm{obs}} = k'/(1 + k''''[\mathrm{NO_3^-}]) \qquad (3)$$

Plots of $1/k_{\mathrm{obs}}$ *vs.* [Mo]$^{1/2}$ and *vs.* [NO_3^-] are shown in Fig. 5. The considerable scatter shown in the plot of $1/k_{\mathrm{obs}}$ *vs.* [NO_3^-] reflects the interdependence of the two correction terms. Points for a given nitrate concentration converge on the line drawn if the effect due to molybdenum inhibition is allowed for. From the slopes and intercepts of the lines in Fig. 5 estimated values of k', k'', and k''' may be obtained. By successive approximations the values k'' = 312 (l/m)$^{1/2}$ and k''' = 30 l/m were obtained. Using these values, k' was calculated for over thirty runs from plots similar to those in Figs. 2, 3, and 4. The value of k' thus obtained is 1.96 × 10^4 (l/m)$^{3/2}$sec^{-1} with a mean deviation of ± 0.08.

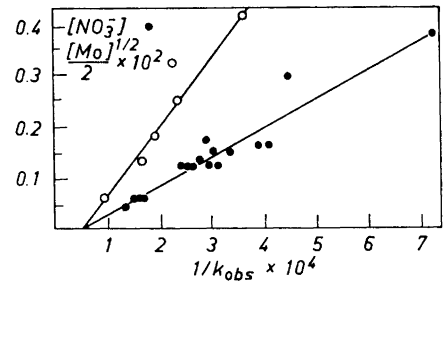

Fig. 5. Estimation of inhibition terms in the rate law. A plot of $1/k_{\mathrm{obs}}$ × 10^4 (abscissa) *vs.* 10^3[Mo]$^{1/2}$ (open dots), and *vs.* [NO_3^-] (closed dots). Intercept gives $1/k'$. Slopes give k''/k' and k'''/k', respectively.

Table 1. Rate constants from individual runs in 3 M HCl. $k'' = 312$. $k''' = 30$.

Run	$[Sn(II)]_0$ m/l	$[NO_3^-]_0$ m/l	[Mo] μm/l	Plot *vs.* t	$k_{obs} \times 10^3$	$k' \times 10^3$	Remarks
8	0.050	0.370	25	log[Sn(II)]	1.38	18.8	
9	0.048	0.159	0.002	»	2.59	15	only 2 points
11	0.048	0.150	1.5	»	3.0	17.7	
12	0.048	0.128	4.26	»	3.6	19.6	
13	0.048	0.160	18.7	»	2.44	17.5	
14	0.048	0.159	37.5	»	2.58	20.0	
17	0.048	0.286	1.43	»	2.22	22.0	
25	0.048	0.150	1.5	»	3.30	19.4	Same as 11
31	0.040	0.122	12.2	»	3.10	17.7	5 duplicates
32	0.040	0.122	6.0	»	3.34	18.3	5 duplicates
33	0.040	0.122	0.5	»	3.88	19.3	5 duplicates
34	0.040	0.122	1.0	»	3.88	19.4	4 duplicates
35	0.040	0.122	2.41	»	4.10	21.2	3 duplicates
36	0.040	0.122	2.41 *	»	4.10	21.2	3 duplicates
37	0.040	0.122	6.00 *	»	3.48	19.2	2 duplicates
38	0.033	0.122	1.00 *	»	4.15	20.8	
45	0.033	0.127	2.00	»	4.00	21.0	2 duplicates
47 a	0.031	0.174	1.57	»	3.62	23.0	25°C
47 b	0.031	0.174	1.57	»	3.05	19.7	22°C
39	0.0322	0.061	2.4	$\log \frac{[Sn(II)]}{[Sn(II)]+A}$	6.24	19.8	
40	0.0279	0.0483	2.4	»	7.03	19.6	
41	0.0645	0.0177	6.0	»	10.29	18.4	
42	0.0645	0.0177	11.7	»	9.81	21.4	
43	0.0627	0.0177	28.6	»	8.19	20.6	
5	0.096	0.024	65.0	»	5.78	19.7	
18	0.0465	0.0158	52.6	1/[Sn(II)]	5.0	17.2	
26	0.0373	0.0124	1.5	1/[Sn(II)]	15.0	22.0	

* Reaction started with Mo(V).

$A = 3[NO_3^-]_0 - [Sn(II)]_0$

Data describing the initial composition of all runs and the values of k_{obs} and k' obtained for each run are collected in Table 1. The rate law has been found valid for nitrate concentrations between 0.005 and 0.37 M, Sn(II) concentrations between 0.002 and 0.10 M, and molybdate concentrations between 10^{-7} and 10^{-4} M. (Two points obtained with a run 10^{-9} M in molybdenum gave gave k_{obs} predicted by the above constants.) The equation best describing the kinetics of this reaction at 25° in 3.0 M hydrochloric acid is then:

$$d[Sn(II)]/dt = \frac{1.96 \times 10^4 [Sn(II)][NO_3^-][Mo]}{1 + 312[Mo]^{1/3} + 30[NO_3^-]} \quad (4)$$

if t is in seconds and concentrations in moles per liter.

Effects of other species present during runs on the reaction rate. Hydroxylamine could not be added initially without giving interference through its reduction. but it seems unlikely that this product could otherwise affect the kinetics. Stannic chloride was added to one run causing a 20 % increase in reaction rate but not altering the form of the rate law. This small effect could have resulted

from an increase in hydrogen ion resulting from hydrolysis or a change in the concentration of free chloride ion. We are confident that Sn[IV] does not inhibit the reaction in any case. Substitution of lithium chloride for hydrogen chloride showed that the rate is roughly proportional to the square of the hydrogen ion concentration in the vicinity of 3.0 M. For $[H^+] < 2.0$ M the reaction order in Sn(II) changes introducing complexities which have not been further investigated as yet. Phosphoric acid in addition to 3.0 M hydrochloric acid had no effect on the reaction rate. The effect of substituting sulfuric acid for hydrochloric acid will be discussed separately.

Eqn. (4) has been tested for typical runs as follows: Let

y = the number of transformations in moles per liter of nitrate ion at time t.
a = the original concentration of nitrate ion in moles per liter.
$3b$ = the original concentration of Sn(II) in moles per liter.
$A = (1 + 312[\mathrm{Mo}]^{1/2})/(1.96 \times 10^4[\mathrm{Mo}])$
$B = 0.0015/[\mathrm{Mo}]$

A and B are constants for any given run but change from run to run. Eqn. (4) may now be transformed to read:

$$\mathrm{d}t/\mathrm{d}t = \frac{A}{(a-y)(b-y)} + \frac{B}{(b-y)}$$

which integrates to give:

$$t = \frac{A}{(a-b)} \ln \frac{b(a-y)}{a)b-y)} + B \ln \frac{b}{|(b-y)} \qquad (5)$$

If $a = b$, eqn. (5) becomes:

$$t = A/(a-y) - A/a + B \ln(a/(a-y))$$

Values of t are calculated for different values of y and compared with observed times. Results of such calculations for typical runs appear in Tables 2—5.

Given the rate law in eqn. (4), it is now possible to test the assumption that reduction of nitrate to hydroxylamine is essentially complete before reduction of hydroxylamine to ammonia becomes significant. The maximum concentration of hydroxylamine will occur when the rate of reduction of hydroxylamine equals the rate of reduction of nitrate. Thus

$$\mathrm{d}[NO_3^-]/\mathrm{d}t = \mathrm{d}[NH_2OH]/\mathrm{d}t$$

For a run employing low molybdate and low nitrate concentrations we can simply employ the numerators of rate laws given by eqn. (4) and in Ref.[10].

$$2 \times 10^4(a-y)(b-y)[\mathrm{Mo}] = 3(0.02(b-y)y[\mathrm{Mo}]^{1/2}) \qquad (6)$$

where y is the concentration of hydroxylamine. The factor 3 appears due to the assumption that $[\mathrm{Sn(II)}] = 3b-3y$. This in fact assumes that virtually no hydroxylamine has been reduced, but the consequences of so assuming are not great as seen below. From eqn. (6) we see that maximum hydroxylamine concentration appears when

$$y/(a-y) = 3.3 \times 10^5 \ [\mathrm{Mo}]^{1/2}$$

Table 2. Chronometric integral for run 33 (excess NO_3^-) *cf.* Eqn. (5). $a = 0.122$. $b = 0.0112$. $A = 122$. $B = 3000$.

t_{obs} sec	$a-y$	$10^3(b-y)$	$\frac{A}{(a-b)} \ln \frac{b(a-y)}{a(b-y)}$	$B \ln[b/(b-y)]$	t_{calc} sec
607	0.118	9.470	147	495	658
1 211	0.1164	8.108	308	972	1 280
1 803	0.1154	6.922	470	1 449	1 919
2 410	0.1144	5.888	640	1 923	2 563
3 000	0.1136	5.052	794	2 390	3 184
3 600	0.1130	4.360	955	2 822	3 777
4 200	0.1120	3.620	1 158	3 370	4 528
4 804	0.1120	3.280	1 367	3 670	5 037

Table 3. Chronometric integral for run 39 (small excess of NO_3^-). $a = 0.0580$. $b = 0.007124$. $A = 31$. $B = 625$. $t = 0$ at first measured point, 5 min after start of run.

t_{obs}	$a-y$	$10^3(b-y)$	$\frac{A}{(a-b)} \ln \frac{b(a-y)}{a(b-y)}$	$B \ln[b/(b-y)]$	t_{calc}
300	0.0562	5.315	155	182	337
600	0.0550	4.109	297	344	641
900	0.0542	3.346	420	472	892
1 200	0.0534	2.520	567	650	1 217
1 500	0.0529	1.975	715	800	1 515

Table 4. Chronometric integral for run 18. (Equivalent Sn(II) and NO_3^-). $a = b = 0.0109$. $A = 3.16$. $B = 28.5$. $t = 0$, one minute after start.

t_{obs}	$a-y$	$A/(a-y)-A/a$	$B \ln[a/(a-y)]$	t_{calc}
60	0.00890	65	13	78
120	0.00757	126	23	149
305	0.00543	292	46	338
600	0.00401	498	63	561
1 200	0.00243	1 010	77	1 087

This run is particularly sensitive to small initial errors which would cause larger and larger deviations from equivalence as the run progressed.

This means that even at the lowest concentrations of molybdate employed, over 99 % of the nitrate has been converted to hydroxylamine before the rates become equal.

Determination of the rate law in 3.0 M sulfuric acid. Only a few runs were made in this medium, but the contrast in the observed kinetics with those observed in hydrochloric acid is so striking that we feel obliged to report our preliminary findings. In the absence of chloride, the reduction of nitrate is extremely slow. In general, we employed one thousand fold more catalyst, yet had to follow reactions for several days to obtain significant change unless a very large excess of nitrate was employed. All the runs employed Mo(VI) as a starting material. Initial periods of faster reaction involving 30 minutes to several hours were observed. Steady state conditions apparently coincided

with the complete conversion of Mo(VI) to Mo(V) which is not a fast process in the absence of chloride. The reaction is slower than the corresponding catalytic reduction of perchlorate under similar conditions. It is inhibited by chloride ions if $[Cl^-]/[Sn(II)] < 2.0$, and then accelerated by higher concentrations of chloride. The reaction stoichiometry is

$$10\,H^+ + 4\,Sn(II) + 2\,NO_3^- = 4\,Sn(IV) + N_2O + 5\,H_2O \qquad (II)\,[1]$$

The reaction rate after the steady state is reached is independent of the concentration of Sn(II), directly proportional to the nitrate concentration and to the square root of the molybdenum concentration. The rate law when essentially all the molybdenum is present as Mo(V) is thus found to be:

$$-d[Sn(II)]/dt = k''''[Mo]^{½}[NO_3^-] \qquad (7)$$

The integrated form of eqn. (7) can be given as

$$t = A\,\ln(a/(a-y))$$

where t is the time in seconds, $A = 2/k''''[Mo]^{½}$, a is the initial concentration of nitrate ion, and y is the number of transformations of nitrate ion in moles per liter. A is contant for a given run, but varies from run to run. Tables 6 to 9 show calculated *vs.* observed times for points obtained after reaching steady state conditions and using $k'''' = 1.2 \times 10^{-4}$ $(l/m)^{½}sec^{-1}$.

The reaction in sulfuric acid needs further investigation both to confirm these preliminary results and to explore the complicated effects of chloride ion upon the kinetics and stoichiometry of the reaction.

MECHANISM OF THE MOLYBDATE CATALYZED REDUCTION OF NITRATE

Reductions in hydrochloric acid

The catalytically active oxidation state of molybdenum must be chosen among the stable VI, V, and III states and the unstable IV state. Mo(VI) forms a complex with nitrate [11] and catalyzes reduction of nitrate by ferrous ion at 100°C.[2] Ferrous ion does not reduce Mo(VI). Dimeric Mo(V) is oxidized directly by perchlorate again at 100°C and this reaction is responsible for the catalytic electroreduction of perchlorate studied by Rechnitz [8]. In previous studies of the reduction of perchlorate, nitrate, and hydroxylamine one of the authors has found, using stannous ions instead of ferrous ions, or, using more negative potentials than those used by Rechnitz, that the unstable species, Mo(IV), is catalytically active. In the latter cases catalyses attributed to Mo(IV) are far more effective than those attributed to Mo(V) or Mo(VI). Mo(III) is noncatalytic in polarographic reductions and can thus be ruled out.

Because Mo (VI) is instantly reduced by Sn(II) in hydrochloric acid and because no difference is observed between reactions started with Mo(VI) and Mo(V) we think it unlikely that Mo(VI) is the active species. In 3.0 M hydrochloric acid Mo(V) is the final product of reduction of Mo(VI) with Sn(II). In order to see if reoxidation of Mo(V) by nitrate ions could be involved in the catalysis, several experiments were performed on the direct oxidation of Mo(V). In each case a period of virtually no reaction was followed by a period of rather

Table 5. Chronometric integral for run 43 in hydrochloic acid. Sn(II) in excess. $t = 0$ at first recorded point, 4 min after start of the run. $a = 0.00770$. $b = 0.01089$. $A = 4.65$. $B = 52.5$.

t_{obs} sec	$10^3(a-y)$ m/l	$10^3(b-y)$ m/l	$\frac{A}{(a-b)} \ln \frac{b(a-y)}{a(b-y)}$	$B \ln[b/(b-y)]$	t_{calc} sec
60	6.80	9.975	61	5	66
240 *	4.80	8.040	243	16	259
360	4.10	7.320	344	19	363
480 *	3.43	6.627	464	27	491
660	2.76	5.963	621	34	655
662 *	2.72	5.920	634	34	668
960	1.91	5.107	934	40	974
960 *	1.98	5.177	894	39	933

* Points from an alternate, identical run.

Table 6. Chronometric integral for run 2 in sulfuric acid. $A = 1.884 \times 10^4$. $a = 0.461$ m/l. $[Sn(II)]_0 = 0.125$ m/l. Mo $= 0.0077$. $k'''' = 1.2 \times 10^{-4}$.

t_{obs} seconds	$(a-y)$ m/l	$A \ln[a/(a-y)] = t_{calc}$ sec.	$-t_{obs}$	$-t_{calc}$
90	0.4469	5 550	90	5 550
270	0.4441	7 050	180	1 390
630	0.4437	7 220	360	170
3 510	0.4366	10 250	2 880	3 030
7 230	0.4266	14 600	3 720	4 350
9 600	0.4171	18 750	2 370	4 150
9 990	0.4164	19 150	390	400
15 790	0.4051	24 400	5 800	5 280

This exploratory run was expected to be over in a few minutes. It shows the initial surge of reaction. Run 5 below shows how greater care eliminates the erratic behavior of later points. Low values of Δt_{obs} are due to the initial surge at the start and to inadequate precautions against air oxidation later in the run.

Table 7. Chronometric integral for run 5 in sulfuric acid. $t = 0$ after 34 min to allow for initial surge. $A = 1.884 \times 10^5$. $a = 0.4420$ m/l. $[Sn(II)]_0 = 0.0736$ m/l.

t_{obs} sec.	$(a-y)$ m/l	$A \ln[a/(a-y)] = t_{calc}$. sec.
3 540	0.4328	3 700
9 190	0.4196	9 770
9 850	0.4179	10 550
12 480	0.4113	13 400

Table 8. Chronometric integral for run 6 in sulfuric acid. $t = 0$ after 168 min to allow for initial surge *. $A = 2.82 \times 10^5$. $a = 0.4415$. $[Sn(II)]_0 = 0.0720$.

t_{obs} sec.	$(a-y)$ m/l	$A \ln[a/(a-y)] = t_{calc}$. sec.
3 180	0.4369	3 240
3 540	0.4365	3 445
19 920	0.4131	19 100

* Note that runs 5 and 6 differ only in [Mo]. Each require the same number of transformations to reach steady state conditions.

Table 9. Chronometric integral for run 7 in sulfuric acid. (Equivalent Sn(II) and NO_3^-). $t = 0$ after 24 h allowed for steady state *. $A = 2.42 \times 10^5$. $a = 0.0240$ m/l $= [Sn(II)]_{0/2}$.

t_{obs} sec.	$(a-y)$ m/l	$A \ln[a/(a-y)] = t_{calc.}$ sec.
67 000	0.01850	63 000
67 700	0.01815	67 400
157 000	0.01215	160 000

* This length of time may not be necessary but was convenient because of the slowness of the reaction.

rapid reaction, indicating that an autocatalytic process was involved. The induction period involving 15 to 30 min convinced us that direct oxidation of Mo(V) by nitrate does not play a significant part in the catalytic process under study. The arguments against the stable states of molybdenum as active catalytic species bring us once again to consider that Mo(IV) is the active catalyst. This conclusion is also consistent with the effectiveness of catalysis in the present case being even greater than in those other cases where Mo(IV) was considered. This conclusion is also interesting in view of the fact that Tribalat [3] found it necessary to assume that Re(V), which is electronically similar to Mo(IV) is the catalytically active state of rhenium in reductions of nitrate by stannous chloride.

Bergh [12] has recently studied the reactions of Sn(II) and the the various oxidation states of molybdenum in hydrochloric acid. In concentrated hydrochloric acid the stoichiometric reaction:

$$2\ Sn(II) + 2\ Mo(VI) = 2\ Sn(IV) + Mo(V) + Mo(III) \qquad (III)$$

occurs, while in dilute hydrochloric acid the following is observed.

$$Sn(II) + 2\ Mo(VI) = Sn(IV) + (Mo(V))_2 \qquad (IV)$$

Sacconi and Cini [13] have studied the reversible dimerization of Mo(V) as concentrated hydrochloric acid is diluted. To explain reactions (III) and (IV) and some features of the catalytic reactions believed to involve Mo(IV) we propose the following closed system. These reactions are believed to be taking place in equilibria involving Sn(II), Sn(IV), and the various oxidation states of molybdenum.

$$Sn(II) + Mo(VI) = Sn(IV) + Mo(IV) \qquad (1)$$
$$2\ Mo(IV) = Mo(V) + Mo(III) \qquad (2)$$
$$Sn(IV) + Mo(III) = Sn(II) + Mo(V) \qquad (3)$$
$$2\ Mo(V) = (Mo(V))_2 \qquad (4)$$
$$(Mo(V))_2 = Mo(VI) + Mo(IV) \qquad (5)$$

Reactions (1) and (2) together account for reaction (III) in concentrated hydrochloric acid. Reaction (1) accounts for initial surges of fast reaction observed when catalyses are started with Mo(VI) [7,9]. If reactions (1) and (2) occur in dilute acid as well, then (3) and (4) are required for obtaining essentially complete production of $(Mo(V))_2$. Reaction (5) is proposed both to close the sequence and as a possible initial source of Mo(IV) for catalyses begun with molybdenum in the (V) state. The known reaction of Mo(III) with Mo(VI) is omitted from

the sequence since its rate is not competitive with the rate of reaction (1)[12]. The kinetics of catalytic reduction of species placed in this system will vary according to the effect of the species on the equilibrium system represented by reactions (1) to (5).

Important features of the kinetics of reaction(I) when compared with other molybdate catalyzed reductions are:

(*a.*) The disappearance of half powers from the rate law as the molybdenum concentration is decreased to 10^{-6} M.
(*b.*) The absence of initial surges and induction periods for reactions begun with Mo(VI) and Mo(V), respectively.
(*c.*) The fact that molybdate concentrations are 1/100 to 1/1 000 those required for Sn(II) reductions of perchlorate [7], hydroxylamine [9], and of nitrate in sulfuric acid.

The development of first order dependence on molybdenum concentration when it is very low agrees with observations made on catalytic polarographic currents [5]. The absence of surges and induction periods at the start of reaction (I) indicate that Mo(IV) is present in its steady state concentration from the start whether the reaction is started with Mo(VI) or Mo(V).

A mechanism consistent with the rate law given by eqn. (4) and with the above observations and assumptions can be derived if it is assumed that Mo(IV) forms an active complex with nitrate which is redued by Sn(II).

$$\text{Mo(IV)} + \text{NO}_3^- = \text{X} \qquad (\pm\ 6)$$
$$\text{X} + \text{SnCl}_3^- = \text{SnOCl}_3^- + \text{NO}_2^- \qquad (7)$$
$$2\text{SnCl}_3^- + \text{NO}_2^- + \text{H}_2\text{O} + 2\text{H}_{aq}^+ = \text{NH}_2\text{OH}^+ + 2\text{SnOCl}_3^- \qquad (8)$$

X is assumed to be an addition complex in equilibrium with Mo(IV) and nitrate ion. $SnCl_3^-$ is the most abundant and most reactive chloro-tin(II) complex in 3.0 M hydrochloric acid [9,14,15]. Reaction (8) is fast [1] and plays no part in the kinetics except to make the number of transformations of Sn(II) three times the number of transformations of nitrate.

From reactions ($\pm$ 6) and (7) we obtain

$$\text{Rate} = K_7K_6[\text{Mo(IV)}][\text{Sn(II)}][\text{NO}_3^-] \qquad (8)$$

Since most of the molybdenum becomes $[\text{Mo(V)}]_2$ in the absence of nitrate we assume $k_1 \gg k_5$ leading to an equation for the steady state in Mo(IV):

$$k_2[\text{Mo(IV)}]^2 = k_5[(\text{Mo(V)})_2] \qquad (9)$$

It may also be argued that the sequence of reactions (1) to (5) describes simply the equilibrium

$$(\text{Mo(V)})_2 \rightleftharpoons \text{Mo(IV)} + \text{Mo(VI)} \qquad (9)$$

If [Mo(IV)] = [Mo(VI)]

$$[(\text{Mo(V)})_2] = k_9[\text{Mo(IV)}]^2 \qquad (9a)$$

which is equivalent to (9) if $k_9 = k_2/k_5$. This simply says the rate of reformation of $[\text{Mo(V)}]_2$ is the same as the rate of disproportionation of Mo(IV) which is a reasonable assumption.

Table 10. Values of rate and equilibrium constants *.

Values	Source
$k' = K_6k_7 = 2.0 \times 10^4$	This paper
$k'' = 2(k_2/k_5)^{1/2} = 312$	This paper
$k''' = K_6 = 30$	This paper
$k_2 \sim 10^4$	Polarography, Ref.[5] ***
$k_5 \sim 0.4$	k'' and k_2
$k_6 \sim 156$ (if $n = 2$) **	Polarography, Ref.[5] ***
625 (if $n = 4$) **	
$k_{-6} \sim 5$ or 20	k_6/K_6
$k_7 = 667$	This paper

* All values in this table derived from the present study refer to kinetics in hydrochloric acid. The results in sulfuric acid are not extensive enough for such analysis as yet.

** The quantity n is the number of elctrons involved in the electrode process associated with the catalytic current. It has not been determined but 2 and 4 are considered the most likely values.

*** Constants obtained polarographically involve work in a different medium and therefore only order of magnitude comparisons can be made.

A material balance in molybdenum requires that

$$[\mathrm{Mo(IV)}] + [\mathrm{X}] + 2[(\mathrm{Mo(V)})_2] = [\mathrm{Mo}] \tag{10}$$

$$[\mathrm{Mo(IV)}] + K_6[\mathrm{Mo(IV)}][\mathrm{NO_3^-}] + 2k_2/k_5)[\mathrm{Mo(IV)}]^2 = [\mathrm{Mo}]$$

$$[\mathrm{Mo(IV)}] = \frac{2[\mathrm{Mo}]}{1 + K_6[\mathrm{NO_3^-}] + [(1 + K_6[\mathrm{NO_3^-}])^2 + 8k_2/k_5[\mathrm{Mo}]]^{1/2}} \tag{11}$$

If eqn. (11) is substituted in eqn. (8) a rate law is obtained which behaves in just the same way as rate law (4) at high $[\mathrm{NO_3^-}]$ and low [Mo]. Rate law (4) requires that

$$[\mathrm{Mo(IV)}] = \frac{[\mathrm{Mo}]}{1 + K_6[\mathrm{NO_3^-}] + [(2\ k_2/k_5)[\mathrm{Mo}]]^{1/2}} \tag{11a}$$

where $K_6 = 30$ and $\sqrt{2k_2/k_5} = 312$. Eqn. (11a) is approximately eqn. (11) under conditions where the right hand sides of eqn. (11) and (11a) approximate one another.

Values of rate and equilibrium constants for steps in the mechanism obtained from this and previous studies are summarized in Table 10.

Mechanism of the reduction of nitrate in sulfuric acid.

Important features of the kinetics of reaction (II) when compared with other molybdate catalyzed reductions are:

(*a*) The reaction is extremely slow. In sulfuric acid the reduction of nitrate is slower than that of perchlorate while the opposite is true in hydrochloric acid.

(*b*) A steady state is observed only when nearly all the molybdenum is in the (V) state. Faster reaction is observed in the presence of Mo(VI) as was the case with hydroxylamine and perchlorate reduction.

(*c*) The slow rate is comparable with rates of reactions catalyzed by Mo(V) at elevated temperatures.
(*d*) The reaction is zero order in Sn(II).
(*e*) The reaction is half order in molybdenum as were all other reactions employing molybdenum concentrations $> 10^{-5}$ M.

If the same reaction scheme is employed as for the kinetics in hydrochloric acid with the substitution of Sn^{++} for $SnCl_3^-$ with only the relative rates of the individual steps changed, we may derive the rate law as follows. If the forward reaction (6) is the rate determining step and reaction (7) is fast compared to (−6) we obtain the rate law with $k'''' = k_6(k_5/k_2)^{½}$. This seems unlikely in view of the fact that Sn^{++} is much less reactive than $SnCl_3^-$. Alternatively, the fact that Sn(II) is so unreactive in sulfuric acid suggests that nitrate is reduced by:

$$Mo(IV) + NO_3^- = Mo(VI) + NO_2^- \qquad (9)$$

Reaction (9) is slow compared with reaction (1) so that the steady state in Mo(IV) is still given by eqn. (9). The function of Sn(II) is merely to restore Mo(IV) lost by reaction (9). That it does this efficiently via reaction (1) is indicated by the faster pace of reaction when Mo(VI) is added initially. If reaction (9) is the rate determining step we have $k'''' = k_9(k_5/k_2)^{½}$.

There is little point in further speculation on the reaction in sulfuric acid until further work is done. The fact that processes are very slow makes it feasible to study individual steps in the reaction in this case. Test tube experiments have shown that reaction (1) is slow enough to study kinetically in sulfuric acid. Study of the direct oxidation of $(Mo(V))_2$ and of Mo(III) by nitrate in sulfuric acid could throw more light on the nature of the catalytic process.

The anomaly that perchlorate is easier to reduce in sulfuric acid and nitrate is easier to reduce in hydrochloric acid using Sn(II) and molybdate catalyst is interesting. Catalytic polarographic waves are ten fold larger for nitrate than for perchlorate even in sulfuric acid [5]. This must mean that more Mo(IV) is available during the perchlorate reduction with Sn(II) than during the nitrate reduction. This is consistent with the observation that a steady state is reached in perchlorate reductions with less than half of the molybdenum in the (V) state [7]. The reduction products of perchlorate such as chlorate, chlorite, and hypochlorite are able to reoxidize Mo(V) to Mo(VI) which is easily converted to Mo(IV). Since nitrite is reduced to nitrous oxide instantly by Sn(II) the only source of Mo(IV) available for nitrate reduction is reaction (5). Apparently the reduction of nitrate in sulfuric acid corresponds to the very slow reaction taking place before a steady state is achieved in perchlorate reductions started by adding Mo(V).

It is probably true that reduction of perchlorate employing only Mo(IV) made available by reaction (5) is slower than reduction of nitrate in both hydrochloric and sulfuric acids, as evidenced by induction periods for reactions started with Mo(V). The ability of perchlorate to furnish oxidants for Mo(V) more than compensates in sulfuric acid, but not in hydrochloric acid.

The authors wish to thank the *Office of Ordnance Research, U. S. Army* for a summer research fellowship for A. K. and the Climax Molybdenum Company for financial support. We are also grateful to Professors Bjerrum and Hofman-Bang for use of the facilities of Kem. Lab. A and to Professor J. A. Christiansen for helpful discussions.

REFERENCES

1. Haight, G. P., Jr., Mohilner, P. and Katz, A. *Acta Chem. Scand* **16** (1962) 221.
2. Kolthoff, I. M., Sandell, E. B. and Moskowitz, B. *J. Am. Chem. Soc.* **55** (1933) 1454.
3. Tribalat, S. *Bull. soc. chim. France* **1951** 131.
4. Johnson, M. G. and Robinson, R. J. *Anal. Chem.* **24** (1952) 366.
5. Haight, Jr., G. P. *Acta Chem. Scand.* **16** (1962) 209.
6. Haight, Jr., G. P. *Anal. Chem.* **23** (1953) 642.
7. Haight, Jr., G.P. and Sager, W. F. *J. Am. Chem. Soc.* **74** (1952) 6056.
8. Rechnitz, G. A. *Thesis. University of Illinois* (1961).
9. Haight, Jr., G. P. and von Frankenberg, C. *Acta Chem. Scand.* **15** (1961) 2026.
10. Nicholas, D. J., Nason, A. and McElroy, W. D. *J. Biol. Chem.* **207** (1954) 341; Nicholas, D. J. and Nason, A. *J. Biol. Chem.* **207** (1954) 353; *J. Biol. Chem.* **211** (1954) 183; *Plant Physiol.* **30** (1955) 135; *J. Bact.* **67** (1955) 5, 58; Nicholas, D. J. and Stevens, H. M. *Nature* **176** (1955) 1066.
11. Coope, P. J. and Thistlethwaite, W. P. *J. Inorg. & Nuclear. Chem.* **2** (1956) 125.
12. Bergh, A. *Thesis, University of Pennsylvania* (1959).
13. Sacconi, L. and Cini, G. *J. Am. Chem. Soc.* **76** (1954) 3800.
14. Haight, Jr., G. P., Zoltewicz, J. and Evans, W. *Acta Chem. Scand.* **16** (1962) 311.
15. Duke, F. R. and Peterson, N. C. *J. Phys. Chem.* **63** (1959) 2077.

Received September 19, 1961.

ACTA CHEMICA SCANDINAVICA 16 (1962) 673–677

Formation of Lithocholic Acid from Ursodeoxycholic Acid in the Rat

Bile Acids and Steroids 116

BELA MATKOVICS* and BENGT SAMUELSSON

Department of Chemistry, Karolinska Institutet, Stockholm, Sweden

Carboxy labelled ursodeoxycholic acid has been synthesized and its metabolism has been studied after intracecal injection into bile duct cannulated rats. The 7β-hydroxyl group of ursodeoxycholic acid is effectively eliminated by microorganisms in the intestine forming lithocholic acid. β-Muricholic acid (3α,6β,7β-trihydroxycholanic acid), chenodeoxycholic acid, and lithocholic acid were identified among the labelled metabolites excreted in the bile.

Cholic and chenodeoxycholic acids are the primary bile acids formed from cholesterol in the rat liver [1]. Chenodeoxycholic acid is metabolized to α-muricholic acid (3α,6β,7α-trihydroxycholanic acid) which is further converted into β-muricholic acid (3α,6β,7β-trihydroxycholanic acid) by an epimerization involving an oxidation-reduction at C7 [2-4]. Two minor metabolites of chenodeoxycholic acid have been isolated, *viz.* 7-ketolithocholic acid (3α-hydroxy-7-ketocholanic acid) and ursodeoxycholic acid (3α,7β-dihydroxycholanic acid). The latter acid is formed by reduction of 7-ketolithocholic acid which yields predominantly the β-epimer [1]. The 7-ketolithocholic acid may be furnished by dehydrogenation of chenodeoxycholic acid either in the liver [4] or in the intestine by microorganisms [5]. In the rat liver ursodeoxycholic acid is hydroxylated in 6β-position to β-muricholic acid and is in addition transformed into chenodeoxycholic acid and an unidentified metabolite [11].

During the enterohepatic circulation of bile acids containing hydroxyl groups in 7α-position, *viz.* cholic, chenodeoxycholic and hyocholic acids, the hydroxyl is eliminated with formation of deoxycholic, lithocholic and hyodeoxycholic acids, respectively [1]. The possibility of eliminating a 7β-hydroxyl group was demonstrated by the transformation of 3α,7β,12α-trihydroxycholanic acid into deoxycholic acid in the intestine [6]. The aim of the present investigation was to find out whether a similar dehydroxylation takes place during the enterohepatic circulation of ursodeoxycholic acid.

EXPERIMENTAL

Ursodeoxycholic acid-24-^{14}C. 7-Ketolithocholic acid-24-^{14}C (m.p. 200—201°) was prepared by oxidation of chenodeoxycholic acid as described earlier [7]. To a solution of 25 mg of this acid in 5 ml of anhydrous propanol was added 0.075 g of sodium. The solution was refluxed for 3 h, diluted with water, acidified and extracted with ether. The residue obtained after evaporation was chromatographed with solvent system F1 which separates ursodeoxycholic acid from chenodeoxycholic acid. Crystallization from ethyl acetate/hexane yeilded 14 mg of ursodeoxycholic acid-24-^{14}C, m.p. 200—201° [8]. Specific actity: 0.55 μC/mg.

Animal experiments. The sodium salt of ursodeoxycholic acid-24-^{14}C (2.0 mg) in 0.9 % sodium chloride solution was injected into the cecal content of three rats (Sprague-Dawley strain, 200—250 g) immediately after cannulation of the bile duct. Bile and feces were collected for two days.

Analysis of feces and bile. Feces were refluxed three times with 80 % aqueous ethanol. After evaporation to dryness the residue was extracted with ether from an acidified water solution.

The bile, collected in ethanol, was filtered, evaporated and hydrolyzed with 2 N NaOH in a closed steel tube for 8 h at 120°.

The free bile acids were separated with reversed phase partition chromatography using the following solvent systems [9,10].

Solvent system	Moving phase (ml)	Stationary phase (ml)
C	Methanol-water 150:150	Chloroform-isooctanol 15:15
F1	Methanol-water 165:135	Chloroform-heptane 45:5
F2	Methanol-water 180:120	Chloroform-heptane 45:5

Four ml of the stationary phase were supported on 4.5 g of hydrophobic Super-Cel. The fractions collected from the columns were titrated with 0.02 N NaOH and the radioactivity was determined by counting of an aliquot in an infinitely thin layer on aluminium planchets. A gas flow counter, Frieseke-Hoepfner FH 51, was used.

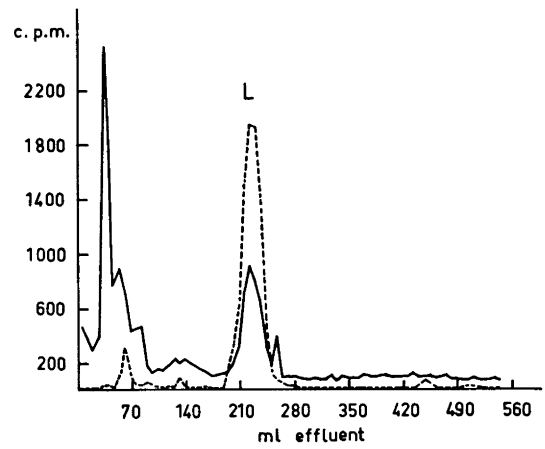

Fig. 1. Chromatographic separation of labelled products in feces after intracecal injection of ursodeoxycholic acid-24-^{14}C into a bile duct cannulated rat. Solvent system F2. Column: 13.5 g. Inactive lithocholic acid (6 mg) added as carrier (L).

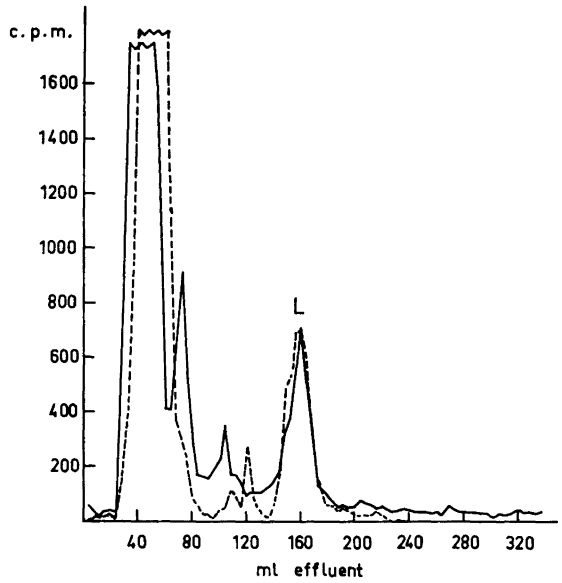

Fig. 2. Chromatographic separation of labelled products excreted in bile after intracecal injection of ursodeoxycholic acid-24-^{14}C into a bile duct cannulated rat. Solvent system: F2. Column: 9 g. Inactive lithocholic acid (5 mg) added as carrier (L).

RESULTS

The sodium salt of ursodeoxycholic acid was injected into the cecal content of bile duct cannulated rats. Of the administered radioactive material

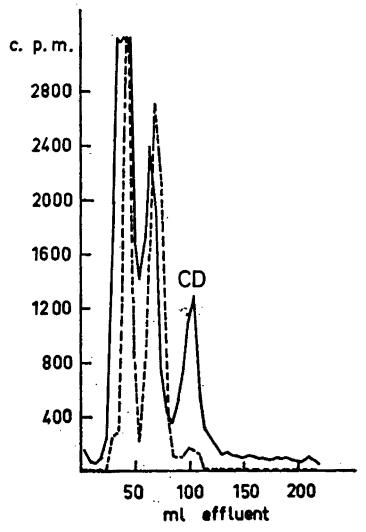

Fig. 3. Rechromatography of 25—85 ml effluent of the chromatography shown in Fig. 2. Solvent system: F1. Column: 9 g. Chenodeoxycholic acid (CD).

about 28—40 % appeared in feces within 36 h whereas the remaining part was absorbed from the intestine and excreted in the bile.

Separation of labelled bile acids in feces. The radioactive compounds excreted in feces were first separated by chromatography with solvent system F2 together with unlabelled lithocholic acid (Fig. 1). The main radioactive peak (200—300 ml) coincided with the peak of the carrier. The identification of labelled lithocholic acid was established by isotope dilution. A minor band of radioactivity appeared at the place of unchanged ursodeoxycholic acid, which was confirmed by rechromatography together with the unlabelled acid with solvent system F1. From 6 to 14 % of the chromatographed radioactive material remained in the column. The nature of these compounds was not further investigated.

Separation of labelled bile acids in bile. The bile acids excreted in the bile were separated after hydrolysis by chromatography with solvent system F2 together with unlabelled lithocholic acid (Fig. 2). A part of the radioactive material coincided with the titration peak of lithocholic acid (140—175 ml). Isotope dilution established the identity. About 3—5 % of the chromatographed radioactivity remained in the stationary phase. The radioactive compounds, which were eluted immediately before (100—130 ml) lithocholic acid were chromatographically similar to 7-ketolithocholic acid but rechromatography with carrier acid showed that they were eluted later. No further attempts were made to determine their structures.

Separation of the more hydrophilic compounds was carried out with solvent system F1 (Fig. 3). In this system chenodeoxycholic acid present in rat bile

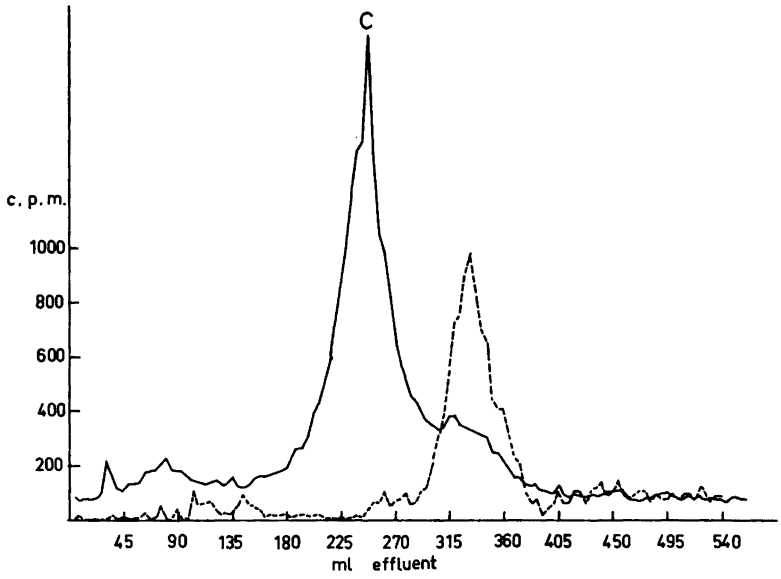

Fig. 4. Rechromatography of 25—50 ml effluent of the chromatography shown in Fig. 3. Solvent system: C. Column: 9 g. Cholic acid (C).

appears at 90—110 ml effluent. A small fraction of the isotope appeared at this place. The radioactive compound eluted immediately before this peak was identified as ursodeoxycholic acid.

The radioactive material in the front peak was chromatographed with solvent system C (Fig. 4). The labelled compound now appeared at the place of β-muricholic acid (3α,6β,7β-trihydroxycholanic acid) immediately after the inactive cholic acid present in the bile. The identity was established by isotope dilution.

DISCUSSION

The results show that the 7β-hydroxyl group of ursodeoxycholic acid is eliminated very efficiently by microorganisms in the intestine forming lithocholic acid. A striking feature is the almost complete absence of other metabolites, which are numerous when chenodeoxycholic acid is administered.

The formation of lithocholic acid from ursodeoxycholic acid is a reaction analogous to the transformation of 3α,7β,12α-trihydroxycholanic acid into deoxycholic acid. As in this case nothing is known about the mechanism of the elimination.

The radioactive compounds found in the bile consist of ursodeoxycholic acid and lithocholic acid absorbed from the intestine together with their liver metabolites, *e.g.* chenodeoxycholic acid and β-muricholic acid.

Acknowledgements. The valuable technical assistance of Miss Cecilia Carlon and Miss Margareta Zetterbom is gratefully acknowledged. This work is part of investigations supported by a grant (H-2 842) from *The National Institutes of Health, U.S. Public Health Service*, Bethesda, Md., USA, and has also been supported by a grant from *Statens Medicinska Forskningsråd.*

REFERENCES

1. Bergström, S., Danielsson, H. and Samuelsson, B. In bloch, K. *Lipide Metabolism.* John Wiley and Sons, Inc., New York 1960, p. 296 ff.
2. Hsia, S. L., Matschiner, J. T., Mahowald, T. A., Elliott, W. H., Doisy, E. A., Jr., Thayer, S. A. and Doisy, E. A. *J. Biol. Chem.* **226** (1957) 667.
3. Hsia, S. L., Matschiner, J. T., Mahowald, T. A., Elliott, W. H., Doisy, E. A., Jr., Thayer, S. A. and Doisy, E. A. *J. Biol. Chem.* **230** (1958) 573.
4. Samuelsson, B. *Acta Chem. Scand.* **13** (1959) 976.
5. Norman, A. and Bergman, S. *Acta Chem. Scand.* **14** (1960) 1781.
6. Samuelsson, B. *Acta Chem. Scand.* **14** (1960) 21.
7. Samuelsson, B. *Acta Chem. Scand.* **13** (1959) 236.
8. Samuelsson, B. *Acta Chem. Scand.* **14** (1960) 17.
9. Bergström, S. and Sjövall, J. *Acta Chem. Scand.* **5** (1951) 1267.
10. Norman, A. *Acta Chem. Scand.* **7** (1953) 1413.
11. Samuelsson, B. *Acta Chem. Scand.* **13** (1959) 970.

Received September 20, 1961.

ACTA CHEMICA SCANDINAVICA 16 (1962) 678–682

Über die Sorption von Eisen(III) an Kationenaustauschern aus Salzsäure

HEINZ TITZE und OLOF SAMUELSON

Institut für technische Chemie, Chalmers Tekniska Högskola, Göteborg, Schweden

Die Sorption von Eisen(III) aus Salzsäurelösungen variierender Konzentration wurde bei verschiedenen Typen von Kationenaustauschern untersucht. In starker Salzsäure erhält man nicht nur bei Austauschern die Sulfonsäuregruppen enthalten eine kräftige Sorption sondern auch bei einem Chelatharz. Das Austauscherskelett besteht in beiden Fällen aus einem Styrol-Divinylbenzolharz. Bei einem Metakrylsäureharz ist eine Sorption kaum nachweisbar. Bei Sulfonsäureharzen steigt die Sorption bei Entsulfonierung. Aus den Versuchen wird der Schluss gezogen, dass in starker Salzsäure das Skelett von Ionenaustauschern aromatischer Struktur sich wie ein effektives Extraktionsmittel für Eisenchloridkomplexe verhält.

Bei Versuchen mit einem Sulfonsäureaustauscher auf Phenolbasis fanden Djurfeldt und Samuelson [1], dass die Eisen(III)-aufnahme als Funktion der Salzsäurekonzentration der Aussenlösung, zum Unterschied von zahlreichen anderen Metallen, bei etwa 5 N HCl ein Minimum durchläuft. Bei noch höheren Salzsäurekonzentrationen nahm die Eisen(III)-aufnahme kräftig zu. Ähnliche Resultate wurden auch mit Kationenaustauschern auf Styrol-Divinylbenzolbasis [2] erhalten. In einer anderen Arbeit zeigten Kraus, Michelson und Nelson [3], dass sich Gallium(III) und Gold(III) ähnlich verhalten wie Eisen(III). Die drei letztgenannten Verfasser weisen darauf hin, dass sich diese drei Elemente sehr leicht mit Äther aus salzsauren Lösungen extrahieren lassen.

Der Zweck der vorliegenden Arbeit ist die Eisen(III)-aufnahme aus salzsauren Lösungen mit verschiedenen Typen von Kationenaustauschern zu untersuchen und hierdurch den Mechanismus dieser Aufnahme zu beleuchten und möglicherweise zusätzliche Unterlagen zu schaffen, die im Zusammenhang mit Ionenaustauschtrennungen von Bedeutung sein können.

EXPERIMENTELLER TEIL

Prinzip der Messungen. Gewogene Austauscherproben wurden mit Lösungen die eine konstante Eisen-(III)-chloridmenge, jedoch unterschiedliche Salzsäurekonzentrationen enthielten geschüttelt. Die Sorption wurde bei sämtlichen Messungen von beiden Seiten

her angestrebt. Zu diesem Zweck wurde je eine der Doppelproben zuerst mit Salzsäure geschüttelt, worauf der Zusatz der Eisen-(III)-chloridlösung erfolgte. Mit den anderen Doppelproben wurde umgekehrt verfahren, das heisst nach Schütteln mit der Eisen-(III)-chloridlösung wurde mit Salzsäure entsprechender Konzentration zum Endvolumen aufgefüllt. Nach Beendigung des Versuches wurde die in der Lösung verbliebene Eisenmenge photometrisch bestimmt.

Ionenaustauscher. Es wurden folgende Kationenaustauscher verwendet:

Dowex A—1 ; 0.15-0.25 mm
» 50-X8; 0,2-0,4 mm
» 50-X8; 0,2-0,4 mm; 55.2 % entsulfoniert
» 50W-X2; 0,15-0,25 mm
» 50W-X8; 0,04-0,08 mm
» 50W-X16; 0,29-0,85 mm
Amberlite IRC-50; 0,17-0,29 mm

Das partiell entsulfonierte Harz wurde von Rückert und Samuelson [4] bereits früher für andere Untersuchungen verwendet.

Sämtliche Austauscher wurden vor den Versuchen in üblichen Austauschersäulen vorbehandelt. Die fabriksneuen Harze wurden einigemale abwechselnd von der Wasserstoffform in die Natriumform überführt. Um die von der Herstellung stammenden Verunreinigungen, bei denen es sich oft um recht beachtliche Eisenmengen handelt, weitgehendst zu entfernen, wurden die Austauscher schliesslich sorgfältig mit 5 N Salzsäure gewaschen. Erst nachdem der salzsaure Auslauf mit Ammoniumrhodanidlösung keine Rosafärbung mehr ergab, wurde mit destilliertem und nachher entionisiertem Wasser säurefrei gewaschen.

Mit Ausnahme des Chelataustauschers Dowex A-1 gelangten alle Harze in der Wasserstofform zur Anwendung. Wegen der begrenzten Haltbarkeit der Wasserstofform dieses schwach sauren Austauschers [5] wurde dieser in der Natriumform eingesetzt.

Durch Zentrifugierung der Austauscher bei 500 *g* während 20 Minuten, wurden sie in eine wägbare Form gebracht und in gut verschlossenen Wägegläsern verwahrt. Eine Probe zur Bestimmung des Wassergehaltes wurde jeweils in einem Exsikkator bei Raumtemperatur über Phosphorpentoxyd zur Gewichtskonstanz getrocknet.

Versuchs- und Messmethodik

Für jede Salzsäurekonzentration wurde je 1,000 g zentrifugiertes Austauscherharz in zwei Erlenmeyer-Glaskolben passender Grösse eingewogen. Die erste Harzprobe wurde mit Salzsäure entsprechender Konzentration, die zweite mit 10 ml Eisen-(III)-chloridstammlösung (im allgemeinen entsprechend 0,1 Millimole Fe) versetzt, mit Plaststopfen verschlossen und 15 Minuten auf einer Schüttelmaschine geschüttelt. Nach Auffüllen der ersten Probe mit 10 ml Eisen-(III)-chloridstammlösung und der zweiten mit Salzsäure zu 100 ml Gesamtvolumen wurde das Schütteln während 16 Stunden, oder noch länger, fortgesetzt.' Die Bestimmung der in der Lösung verbliebenen Eisenmenge wurde mittels 1,10-Phenanthrolin photometrisch ausgeführt [6]. Diese Methode weist neben dem Vorteil einer weitgehenden Unempfindlichkeit gegenüber dem pH-Wert der Lösung auch eine gute Farbkonstanz auf.

Die Eisenstammlösung wurde durch Auflösen einer gewogenen Menge p.a. Klavierdraht in konzentrierter Salzsäure und Oxydation mit Perhydrol erhalten.

Aus den erhaltenen Resultaten wurden die Verteilungskoeffizienten nach folgendem Ausdruck berechnet:

$$D = \frac{(\text{Millimole Fe})_{\text{Aust}} \times \text{Milliliter Lösung}}{(\text{Millimole Fe})_{\text{Lösung}} \times \text{Gramm trock. Aust.}}$$

RESULTATE UND DISKUSSION

Bei den Versuchen mit Sulfonsäureaustauschern normalen Vernetzungsgrades, 8 % oder geringer, wurde nach 16 Stunden von beiden Seiten Gleichgewicht erhalten. Bei stärkerer Vernetzung ist die Harzstruktur so eng, dass

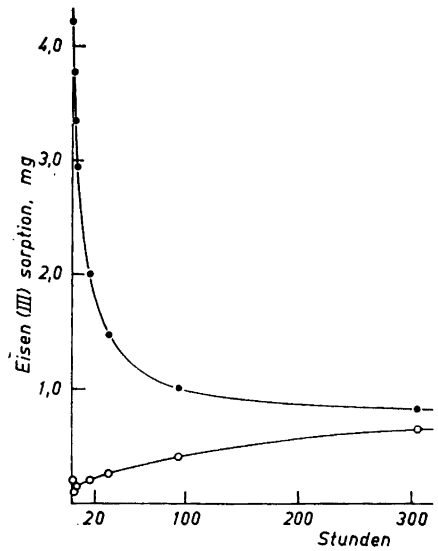

Abb. 1. Die Zeitabhängigkeit der Fe-(III)Aufnahme bzw. Abgabe von Dowex 50W—X16 in 10,6 N HCl.
● Fe(III) zuerst zugesetzt
O HCl zuerst zugesetzt.

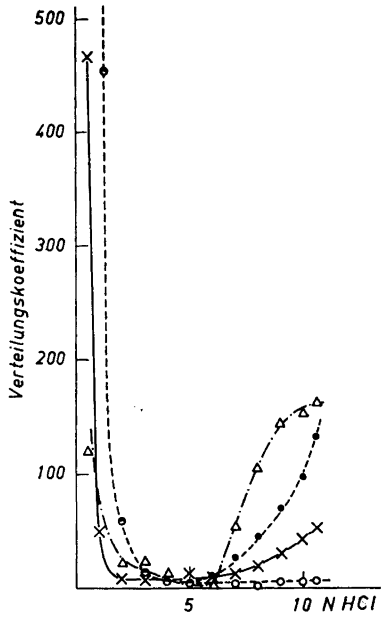

Abb. 2. Die Sorption von Fe(III) an Kationenaustauschern mit verschiedenem Vernetzungsgrad.
△ Dowex 50W—X2
× Dowex 50 X—8
O Dowex 50W—X16. HCl zuerst zugesetzt.
● Dowex 50W—X16. Fe(III) zuerst zugesetzt.

die Gleichgewichtseinstellung nur sehr langsam erfolgt. Dies geht aus den in Abbildung 1 wiedergegebenen Resultaten hervor. Man sieht, dass bei hoher Salzsäurekonzentration auch nach 300 Stunden Reaktionsdauer der Gleichgewichtszustand noch nicht erreicht ist.

Auch beim Versuch mit einem partiell entsulfonierten Austauscher wurde durch sechzehnstündiges Schütteln bei hohen Salzsäurekonzentrationen kein Gleichgewicht erhalten.

Die Abbildung 2 zeigt die Resultate von Versuchen, die mit Sulfonsäureaustauschern auf Styrolbasis mit verschiedenem Vernetzungsgrad ausgeführt wurden. Die Versuchsdauer betrug in allen Fällen 16 Stunden. Die Resultate, die mit Produkten von geringem Vernetzungsgrad (X2 und X8 mit 2 bzw. 8 % Divinylbenzol) erhalten wurden, sind Gleichgewichtswerte, während die aus Versuchen mit X16 errechneten Verteilungskoeffizienten keine Gleichgewichtswerte repräsentieren, sondern einen beträchtlichen Unterschied aufweisen, der auf der Reihenfolge mit welcher die Lösungen zugesetzt wurden, beruht.

Bei hoher Salzsäurekonzentration liegt die Aufnahme von Eisen(III) wesentlich höher bei einem Harz mit 2 % Vernetzung als bei einem mit 8 %. Ein einigermassen sicherer Wert für die Gleichgewichtsmenge in 10,6 N HCl kann aus der Abbildung 1 abgelesen werden. Fügt man auch diesen Wert in die Abbildung 2 ein, so findet man, dass die Eisen(III)-aufnahme mit abnehmenden Vernetzungsgrad zunimmt.

In diesem Zusammenhang sei erwähnt, dass die kräftige Sorption von Eisen(III) in starker Salzsäure nicht auf die Anwesenheit von geringen Mengen fremder Gruppen im Ionenaustauscher (z.B. Carboxylgruppen) zurückgeführt werden kann. Eine kräftige Sorption findet nämlich nicht nur bei Anwendung von Spurenmengen [3] von Eisen(III), sondern auch bei Makromengen [1], statt. Im Zusammenhang mit den vorliegenden Untersuchungen wurde auch ein Austauscher mit verschiedenen Eisen(III)-mengen ins Gleichgewicht gebracht. Bei Dowex 50-X8 zeigte sich, dass die Verteilungskoeffizienten nur wenig von der Konzentration der Aussenlösung abhängig waren, wenn die totale Eisen(III)-menge von 1,1—5,5 mg variierte.

Um den Einfluss der Sulfonsäuregruppen auf die Eisen(III)-sorption in starker Salzsäure zu untersuchen, wurde auch ein partiell entsulfoniertes Präparat verwendet. In Abbildung 3 sind die Resultate denjenigen eines nichtentsulfonierten Harzes gegenübergestellt. Trotzdem in starker Salzsäure voll-

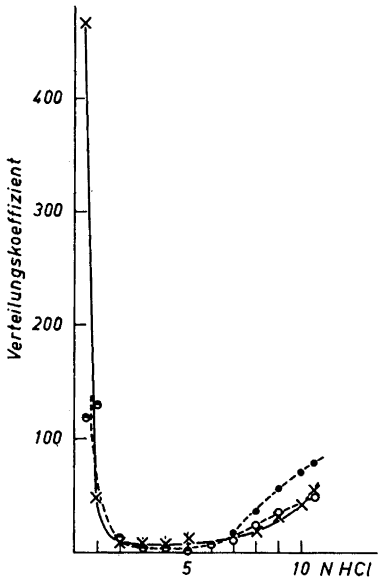

Abb. 3. Die Sorption von Fe(III) an einem entsulfonierten Kationenaustauscher.
× Dowex 50—X8
● Dowex 50—X8 55,2 % entsulf. Fe(III) zuerst zugesetzt.
○ Dowex 50—X8 55,2 % entsulf. HCl zuerst zugesetzt.

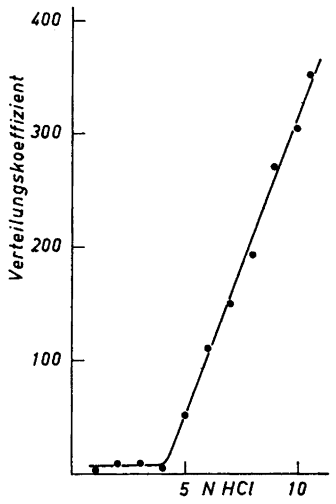

Abb. 4. Die Sorption von Fe(III) an Dowex A—1.

ständiges Gleichgewicht nach 16 Stunden nicht erreicht wurde, ist erkennbar, dass die Eisen(III)-aufnahme bei dem nichtentsulfonierten Austauscher (pro Gramm trockenes Harz) geringer ist. Rechnet man die Resultate zu einer Eisen(III)-aufnahme pro Sulfonsäuregruppe um, so findet man, dass diese bei dem entsulfoniertem Harz mehr als doppelt so hoch wie bei den anderem liegen. Daraus kann man den Schluss ziehen, dass die Sorption nicht durch die Sulfonsäuregruppen verursacht wird, sondern mit dem Austauscherskelett im Zusammenhang steht.

Wenn dies der Fall ist, sollte die Struktur des Skelettes einen bedeutenden Einfluss haben. Wie bereits mit Abbildung 2 gezeigt wurde, hat der Vernetzungsgrad einen solchen Einfluss. Nachdem Sulfonsäureaustauscher mit geringer Vernetzung eine kräftige Eisen(III)-aufnahme zeigen, könnte man erwarten, dass der stark quellbare Austauscher Dowex A-1, der auf Styrolbasis aufgebaut ist und Iminodiessigsäuregruppen enthält, sich ähnlich verhalten würde. In diesem Medium muss man annehmen, dass dieses Harz als Kationenaustauscher vollständig unwirksam ist. Die in Abbildung 4 wiedergegebenen Resultate zeigen, dass die Sorption von Eisen(III) aus starker Salzsäure sogar grösser ist als bei allen anderen untersuchten Harzen. In der bereits genannten Arbeit von Djurfeldt und Samuelson [1] wurde auch mit Wofatit K eine kräftige Eisen(III)-sorption in starker Salzsäure erhalten. Dieser Austauscher ist ein Phenolharz und es erscheint daher naheliegend die Eisen(III)-aufnahme bei allen bisher genannten Produkten auf deren aromatische Struktur zurückzuführen. Als Beispiel eines Austauschers mit hauptsächlich aliphatischer Struktur wurde ein Harz vom Metakrylsäuretyp (Amberlite IRC-50) untersucht. Eine Eisen(III)-aufnahme war über den ganzen Konzentrationsbereich (0,5—10,6 N HCl) kaum nachweisbar.

Man kann aus den vorliegenden Versuchen den Schluss ziehen, dass das Skelett von Ionenaustauschern mit aromatischer Struktur in starker Salzsäure sich als ein effektives Extraktionsmittel erweist, das die Chloridkomplexe des Eisens die sich in diesem Medium bilden, aufnimmt.

Wir danken dem *Schwedischen Technischen Forschungsrat* für die Bereitstellung von Mitteln.

LITERATUR

1. Djurfeldt, R. und Samuelson, O. *Acta Chem. Scand.* **4** (1950) 165.
2. Samuelson, O. Vortrag gehalten beim "120th Meeting of the American Chemical Society", Sept. 1951.
3. Kraus, K. A., Michelson, D. C. und Nelson, F. *J. Am. Chem. Soc.* **81** (1959) 3204.
4. Rückert, H. and Samuelson, O. *Svensk Kem. Tidskr.* **66** (1954) 337.
5. "Dowex Chelating Resin A-1". The Dow Chemical Company, Midland, Mich., 1959.
6. Sandell, E. B. *Colorimetric Determination of Traces of Metals.* Interscience, New York 1959, Seite 541.

Eingegangen am 4. Oktober 1961.

ACTA CHEMICA SCANDINAVICA 16 (1962) 683–688

Synthesis and Metabolism of 3α, 12α-Dihydroxy-Δ^6-cholenic Acid-24-^{14}C

Bile Acids and Steroids 117

BELA MATKOVICS* and BENGT SAMUELSSON

Department of Chemistry, Karolinska Institutet, Stockholm, Sweden

3α,12α-dihydroxy-Δ^6-cholenic acid-24-^{14}C has been synthesized from cholic acid-24-^{14}C. The metabolism of the former acid has been studied after intraperitoneal or intracecal injection to bile duct cannulated rats. The unsaturated acid is reduced in the intestine to deoxycholic acid, which is further oxidized to 12-ketolithocholic acid. Labelled deoxycholic and cholic acids were present in the bile. No transformation of 3α,12α-dihydroxy-Δ^6-cholenic acid occurs in the liver.

Studies concerning the transformation of bile acids during the enterohepatic circulation in different species have demonstrated that deoxycholic acid is formed from cholic acid by the action of intestinal microorganisms on cholic acid. This transformation entails dehydroxylation at C-7, a reaction that has been repeatedly shown to occur for different bile acid species containing either a 7α- or a 7β-hydroxyl group [1,2].

The mechanism of the dehydroxylation has been most thoroughly investigated regarding the transformation of cholic acid into deoxycholic acid whereby the hydroxyl group in 7α-position is eliminated [3,4]. Studies with cholic acid containing tritium in specific positions revealed that the hydrogen atom in 7β-position is retained whereas of the hydrogen atoms bound to carbon atoms adjacent to C-7 (6α,6β, and 8β) one is eliminated in the dehydroxylation, *e.g.* that in 6β position.

The result was interpreted to mean that cholic acid is initially dehydrated by a diaxial trans elimination (6β-H, 7α-OH) in which reaction 3α,12α-dihydroxy-Δ^6-cholenic acid is formed. The reduction of this postulated intermediate to deoxycholic acid was also studied from a stereochemical point of view by observing the change in configuration of the tritium labels retained in deoxy-

* Fellow of the International Atomic Energy Agency 1960–61. Present address: Szeged, Dóm tér 8, Hungary.

cholic acid. By this approach it was evident that if the unsaturated acid were an intermediate reduction must have involved diequatorial transaddition of hydrogen into 6α- and 7β-positions.

In order to get further support for the above mentioned sequence of reactions as well as to make accessible a means of studying this reaction *in vitro* in separate steps we have synthesized ^{14}C labelled 3α,12α-dihydroxy-Δ^6-cholenic acid and studied its metabolism in the rat.

EXPERIMENTAL

Cholic acid-24-^{14}C was synthesized according to the method of Bergström *et al.*[5] Specific activity: 0.6 μC/mg.

Methyl-3α,12α-diacetoxy-7-ketocholanate-24-^{14}C (*I*). The methyl ester from 108 mg of cholic acid-24-^{14}C was dissolved in 5 ml of acetone and 2 ml of water and oxidized with 0.13 g of N-bromosuccinimide during 6 h at room temperature. The solution was diluted with water and extracted with ether. The ether solution was washed with sodium bicarbonate (8 %) and water. The dried ether solution was evaporated and the residue acetylated by refluxing with 2 ml of pyridine and 2 ml of acetic anhydride for 6 h. The reaction mixture was diluted with water and extracted with ether. The ether solution was washed with 2 N hydrochloric acid and water, dried over sodium sulfate and evaporated. Crystallization from aqueous methanol yielded 83 mg of I, m.p. 118–119°[6].

Methyl-3α,12α-diacetoxy-6α-bromo-7-keto cholanate-24-^{14}C (*II*). To a solution of 83 mg of I in 1 ml of acetic acid was added 30.6 mg of bromine and 0.033 ml of 30 % hydrobromic acid in acetic acid. Water was added dropwise to turbidity after 24 h at room temperature. The crystalline product was filtered, washed and dried yielding 84 mg of II, m.p. 164–165°[6].

3α,12α-Dihydroxy-Δ^6-cholenic acid-24-^{14}C (III). An ice-cooled solution of II (80 mg) in 4 ml of methanol was reduced with 80 mg of sodium borohydride for 1 h. Dilution with water, acidification and ether extraction yielded after evaporation 75 mg of residue. This compound was treated without further purification with 0.5 g of Zn in 10 ml of acetic acid and refluxed for 16 h. The solution was diluted with water and extracted with ether. The residue obtained after evaporation was refluxed with 6 ml of aqueous 1 N sodium hydroxide for 4 h. Ether extraction and evaporation gave a residue (43 mg), which was purified by chromatography with solvent system F. Crystallization from ethyl acetate-hexane yielded 32 mg of III, m.p. 157–160°[7]. Specific activity: 0.62 μC/mg. The physical properties of this compound agreed with those given in the reference cited.

Animal experiments. The sodium salt of 3α,12α-dihydroxy-Δ^6-cholenic acid was administered to bile duct cannulated rats[8], Sprague-Dawley strain (200 to 250 g), either by intraperitoneal or intercecal injection. The bile and feces were collected in ethanol for two days.

Isolation procedures and chromatographic methods. Bile acids were extracted from feces by refluxing three times for 3 h with 80 % aqueous ethanol. These extracts were taken to dryness, dissolved in 0.5 N NaOH, acidified and extracted with ether.

The bile was filtered, evaporated and hydrolyzed with 2 N NaOH in a sealed tube at 120°. The free bile acids were extracted with ether after acidification with hydrochloric acid.

The bile acids were separated with reversed phase column chromatography using the following solvent systems[9,10].

Solvent system	Moving phase (ml)	Stationary phase (ml)
C	Methanol-water 150:150	Chloroform-isooctanol 15:15
F1	Methanol-water 165:135	Chloroform-heptane 45:5
F2	Methanol-water 153-147	Chloroform-heptane 45:5

4 ml of the stationary phase were supported on Hydrophobic Super-Cel (Johns Manville, Comp.). When larger columns were needed these amounts were proportionally increased. Radioactivity was determined by counting of an infinitely thin layer in a methane gas-flow counter, (Frieseke-Hoepfner, FH 51).

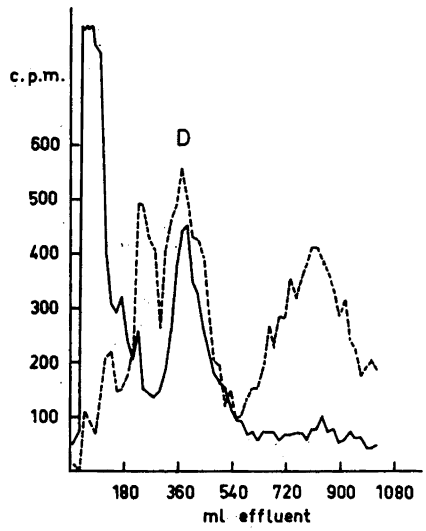

Fig. 1. Chromatographic separation of labelled products in feces after intracecal injection of 3*α*,12*α*-dihydroxy-Δ^6-cholenic acid-24-^{14}C into a bile duct cannulated rat. Solvent system F2. Column: 18 g. Inactive deoxycholic acid (10 mg) added as carrier (D). Solid line: Titration. Broken line: Radioactivity.

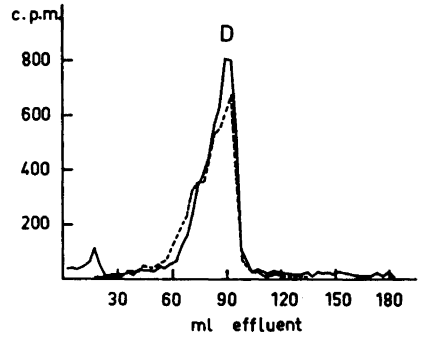

Fig. 2. Rechromatography of 320—450 ml effluent of the chromatography shown in Fig. 1. Solvent system: F2. Column: 4.5 g.

RESULTS

Administration of 3α,12α-dihydroxy-Δ^6-cholenic acid-24^{24}-C into cecum of bile duct cannulated rats. 3α,12α-dihydroxy-Δ^6-cholenic acid-24-^{14}C (2.5 mg) was injected into the cecal content of bile duct cannulated rats. Of the administered radioactivity about 30—40 % were excreted in feces within 48 h, the remainder being excreted with the bile. The radioactive compounds in feces represent the metabolites of 3α,12α-dihydroxy-Δ^6-cholenic acid formed in the intestine by microorganisms. In the bile radioactive compounds can be composed of the injected bile acid or metabolites of it formed in the liver, furthermore intestinal metabolites of the injected acid and finally liver metabolites of the derivatives formed in the intestine.

Radioactive compounds in feces. The radioactive bile acids excreted in feces together with 10 mg of inactive deoxycholic acid were chromatographed with solvent system F2, which was found to be the most suitable system for separation of deoxycholic acid from 3α,12α-dihydroxy-Δ^6-cholenic acid (Fig. 1). The radioactive material eluted from 320—450 ml effluent was rechromatographed with solvent system F2 where the radioactivity coincided with the titration peak of the added carrier (Fig. 2). The identity of this metabolite with deoxycholic acid was finally established by isotope dilution. The radio-

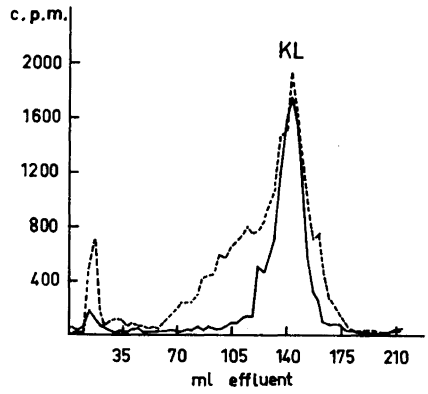

Fig. 3. Rechromatography of 600—1 000 ml effluent of the chromatography shown in Fig. 1. Solvent system: F1. Column: 4.5 g. Inactive 12-ketolithocholic acid (10 mg) added as carrier (KL).

active material (190—300 ml effluent) being eluted immediately before deoxycholic acid was identified as unchanged 3α,12α-dihydroxy-Δ^6-cholenic acid by rechromatography with the inactive acid and by isotope dilution. The broad band (600—1 000 ml effluent) of radioactivity which appears after deoxycholic acid was chromatographed together with 12-ketolithocholic acid (3α-hydroxy-12-ketocholanic acid) with solvent system F1 (Fig. 3). A minor part of the radioactive material is then eluted before 12-ketolithocholic acid whereas most of it coincides with this acid. Isotope dilution established the identity of this latter material. The nature of the more hydrophilic compound has not been investigated.

The radioactive material remaining in the column amounted to 10—15 % of the chromatographed radioactivity.

Radioactive compounds in bile. The free bile acids obtained after hydrolysis of the bile were chromatographed with solvent system F2 after addition of inactive deoxycholic acid (Fig. 4). The main part of the isotope was present as unchanged 3α,12α-dihydroxy-Δ^6-cholenic acid, proved by isotope dilution. The radioactive compound eluted at the same rate as inactive deoxycholic acid (370—500 ml effluent) was identified by isotope dilution.

The front band was rechromatographed with solvent system C (Fig. 5). The titration peak caused by the inactive cholic acid present in rat bile coincided with the main isotope peak. The identity was established by isotope dilution. The nature of the two more hydrophilic radioactive bands was not investigated.

Intraperitoneal administration of 3α,12α-dihydroxy Δ^6-cholenic acid -24-^{14}C to bile duct cannulated rats. This experiment was designed to differentiate between the reactions occurring in the intestine and in the liver. The sodium salt of 3α,12α-dihydroxy-Δ^6-cholenic acid-24-^{14}C was injected intraperitoneally into bile duct cannulated rats and the radioactive material excreted in the bile was separated by chromatography. About 85—90 % of the administered ^{14}C was excreted during the first 24 h. Hydrolysis of this material and chromatographic separation with solvent system F2 revealed that only unchanged 3α,12α-dihydroxy-Δ^6-cholenic acid was present.

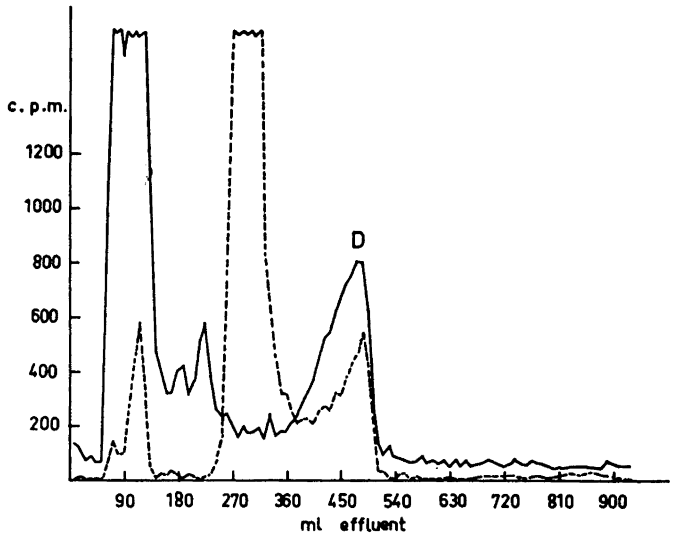

Fig. 4. Chromatographic separation of labelled products excreted in bile after intracecal injection of 3*α*,12*α*-dihydroxy-Δ^6-cholenic acid-24-^{14}C into a bile duct cannulated rat. Solvent system: F2. Column: 18 g. Inactive deoxycholic acid (10 mg) added as carrier (D). Solid line: Titration. Broken line: Radioactivity.

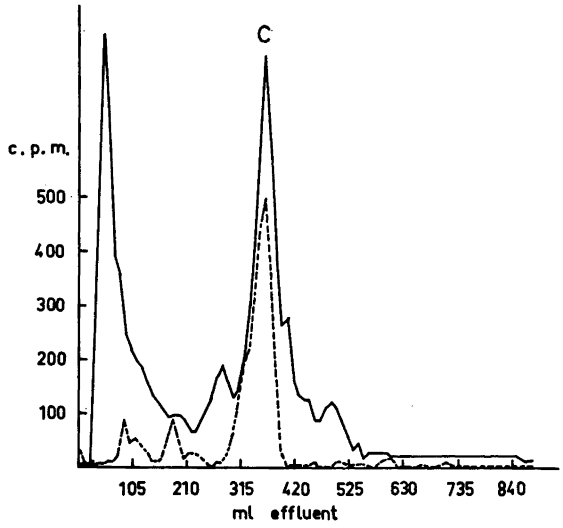

Fig. 5. Rechromatography of 50—140 ml effluent of the chromatography shown in Fig. 4. Solvent system: C. Colunm: 18 g. Cholic acid (C).

DISCUSSION

The identified metabolites of 3α,12α-dihydroxy-Δ^6-cholenic acid formed in the intestine consist of deoxycholic acid and 12-ketolithocholic acid. The former acid is formed by reduction of the unsaturated acid and the latter derivative by oxidation at C-12 of deoxycholic acid. Of the metabolites found in the bile deoxycholic acid is formed primarily in the intestine and a part of it is then 7α-hydroxylated to cholic acid in the liver. The cholenic acid was not attacked during the passage through the liver. The results obtained thus support the earlier postulated biogenesis of deoxycholic acid, although it has not been possible to isolate 3α,12α-dihydroxy-Δ^6-cholenic acid as a metabolite of cholic acid. Similar experiments with 3α,12α-dihydroxy-Δ^7-cholenic acid have shown that this acid is not reduced to deoxycholic acid in the intestine [11].

Acknowledgements. The valuable technical assistance of Miss Cecilia Carlon and Miss Margareta Zetterbom is gratefully acknowledged. This work is part of investigations supported by a grant (H-2 842) from *The National Institutes of Health, U.S. Public Health Service*, Bethesda, Md., USA, and has also been supported by a grant from *Statens Medicinska Forskningsråd.*

REFERENCES

1. Bergström, S., Danielsson, H. and Samuelsson, B. In Bloch, K. *Lipide Metabolism.* John Wiley and Sons, Inc., New York 1960, p. 296 ff.
2. Matkovics, B. and Samuelsson, B. *Acta Chem. Scand.* **16** (1962) 673.
3. Bergström, S., Lindstedt, S. and Samuelsson, B. *J. Biol. Chem.* **234** (1959) 2022.
4. Samuelsson, B. *J. Biol.Chem.* **235** (1960) 361.
5. Bergström, S., Rottenberg, M. and Voltz, J. *Acta Chem. Scand.* **7** (1953) 481.
6. Corey, E. J. *J. Am. Chem. Soc.* **76** (1954) 175.
7. Kagan, H. B. and Jacques, J. *Bull. soc. chim.* France **1960** 871.
8. Bergström, S., Sjövall, J. and Voltz, J. *Acta Physiol. Scand.* **30** (1953) 22.
9. Bergström, S. and Sjövall, J. *Acta Chem. Scand.* **5** (1951) 1267.
10. Norman, A. *Acta Chem. Scand.* **7** (1953) 1413.
11. Samuelsson, B. *Unpublished observations.*

Received September 20, 1961.

ACTA CHEMICA SCANDINAVICA 16 (1962) 689–694

On the Solubility of Carbon Dioxide in Molten Halides

Preliminary communication

K. GRJOTHEIM, P. HEGGELUND, C. KROHN and K. MOTZFELDT

Institute of Inorganic Chemistry, The Technical University of Norway, Trondheim, Norway

Solubilities of CO_2 in molten NaCl and KCl have been determined for the temperature range 810–950°C, at 1 atm pressure of CO_2. The solubilities K_c, expressed as moles CO_2 per ml of solvent (at 1 atm) increase with increasing temperature, being in NaCl 4.6×10^{-6} and 6.0×10^{-6}, in KCl 4.0×10^{-6} and 7.0×10^{-6}, at 850 and 950°C, respectively. The heats of solution, calculated from the slope of log K_c *versus* $1/T$, are 7.1 and 14.8 kcal/mole, in NaCl and KCl, respectively.

A number of different processes have been proposed to explain the low current yield in the electrolytic aluminium process. One of the suggested explanations is that the CO_2 formed on the anode reacts with dissolved Al metal or monovalent Al^+ ions in the molten electrolyte, to form Al^{3+} ions and CO. It is thus assumed that the dissolved metal or monovalent ion, originating at the cathode, is transported upwards by diffusion or convection in the electrolyte, to the vicinity of the anode where it reacts with the CO_2 which is present essentially as gas bubbles.

An alternative explanation suggested here is that the CO_2 formed on the anode dissolves to some extent in the melt, where it may react with the dissolved Al or Al^+ ion, or possibly it may be transported downwards in the electrolyte by convection and diffusion and oxidize the Al metal surface. One should be able to support or reject this latter hypothesis by measuring the solubility of CO_2 in molten cryolite and cryolite-alumina mixtures. In addition, one would gain some fundamental knowledge of the mechanism of CO_2-solution in such melts.

Gas solubilities in molten salts is a rather new field of interest, and most of the work done has been connected with nuclear reactor technology. Grimes *et al.*[1] have determined the solubilities for noble gases in $NaF-ZrF_4$ and $NaF-ZrF_4-UF_4$ melts. Blander *et al.*[2] have measured noble gas solubilities in the $LiF-NaF-KF$ eutectic, while Shaffer *et al.*[3] have investigated the solubilities of HF in $NaF-BeF_2$ and $NaF-ZrF_4$ mixtures. An investigation by Woelk[4] gives some data for Ar solubilities in molten potassium salts. It appears, how-

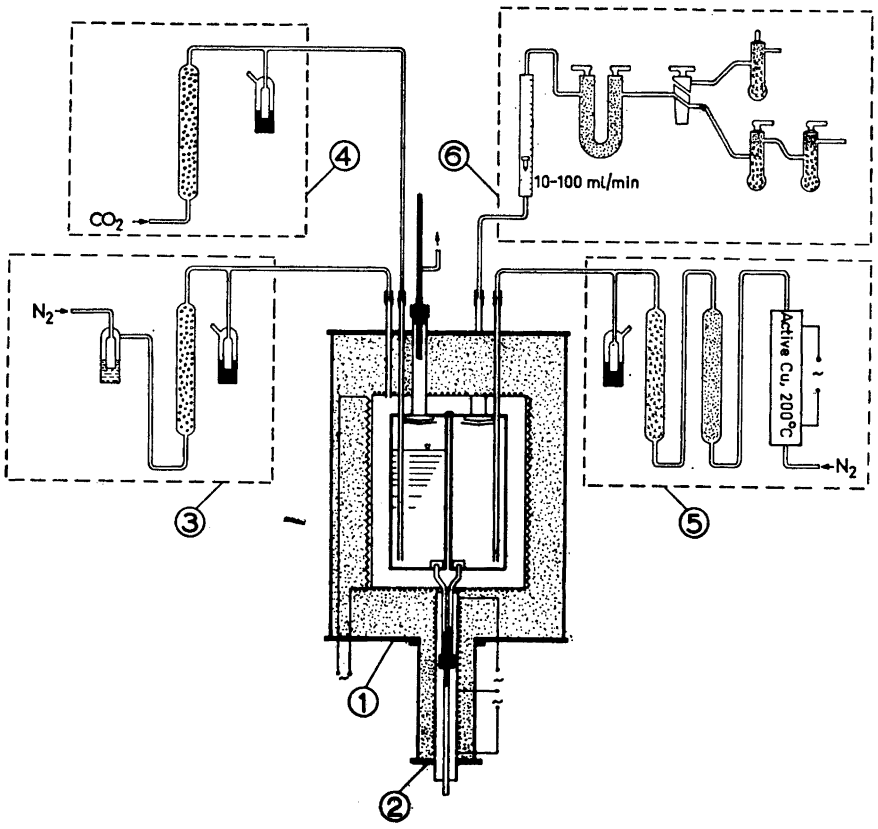

Fig. 1. Diagram of apparatus for measuring solubility of carbon dioxide in molten salt. (1) Furnace with Kanthal A resistors, with nickel vessel consisting of saturating section (left) and stripping section (right) joined by transfer line (bottom). Movable nickel probe shown on top of saturating section. Thermocouple wells not shown. (2) Auxiliary furnace with divided heating element. Top element heated for transfer of melt between nickel sections. Both elements heated for emptying nickel vessel. (3) Drying tube (P_2O_5) and safety outlet for protection gas. (4) Same for CO_2 saturating gas. (5) Purification train (active Cu, magnesium perchlorate, and Ascarite) for stripping gas. (6) Absorbtion train (magnesium perchlorate U tube, and Ascarite vessels for CO_2 absorbtion).

ever, that no data regarding the solubilities of CO_2 in molten salts have been published.

It was decided, then, to investigate the solubility of CO_2 in some simpler alkali halides before attempting the cryolite-alumina system.

EXPERIMENTAL

(*a*) *Apparatus.* The method adopted was essentially the same as the one used by Grimes *et al.*[1] These authors found the solubilities for HF to be approximately 10 times larger than the corresponding noble gas solubilities. Based on the assumption that the

Table 1. Solubility of CO_2 in molten NaCl and KCl.

NaCl		KCl	
Temp. °C	$K_c.10^6$ moles CO_2 / (ml solvent. atm)	Temp. °C	$K_c.10^6$ moles CO_2 / (ml solvent. atm)
812.2	4.20	791.0	2.73
813.0	4.81	792.9	3.02
829.8	4.14	802.0	2.78
830.4	4.18	823.5	3.76
852.0	5.07	835.5	4.14
903.9	5.47	863.1	5.26
948.3	5.71	876.4	4.02
		903.0	4.65
		925.0	6.81
		969.9	8.90

solubilities for CO_2 would be closer to those for HF than to the solubilities for the noble gases, the present apparatus was designed with a volume approximately 1/10 of the one used by Grimes *et al.* Also, the saturating and stripping sections were built into a unit, placed in a single furnace. The apparatus thus modified is shown schematically in Fig. 1, together with gas purification train *etc.*

All sections of the apparatus in contact with the molten salts were made of nickel. The liquid level in the saturating section was determined by means of a movable nickel rod, introduced gas tight and electrically insulated through a packing gland with Teflon gaskets on top of the saturator. The probe was connected in an electric circuit which was completed when the probe made contact with the liquid surface. The relationship between probe position and volume was determined prior to the run by calibration with an aqueous salt solution.

Temperature was measured by Chromel-Alumel thermocouples mounted in thermocouple wells in both saturating and stripping sections. Temperature control was effected by a third thermocouple in the furnace outside the vessel, in connection with a Kent potentiometric controller.

(*b*) *Procedure.* Approximately 0.8 kg of the salt (puriss, from E. Merck) was charged into the saturating section and heated to temperature. During melting, a frozen seal was established in the transfer tube, thus isolating the salt from the stripping section. After saturating by bubbling CO_2 through the melt for 3 h., the frozen seal was destroyed by heating with a small auxiliary furnace, and part of the molten salt was transferred to the stripping section, the exact quantity being determined by means of the nickel probe. The melt thus transferred was stripped of its CO_2-content by bubbling pure nitrogen, and the amount of CO_2 was determined by absorption in Ascarite [5].

(c) *Results.* The results for the solubilities of CO_2 in molten NaCl and KCl, K_c, expressed as moles $CO_2 \times 10^{-6}$ per ml of solvent (at 1 atm), are given in Table 1. In Fig. 2, the values of log K_c are plotted *versus* $1/T$, and a straight line has been fitted to the points for each of the two salts by the method of least squares. It is thus assumed that the heat of solution is constant over the temperature range considered. From the slope of the lines, the heats of solution of CO_2 in NaCl and KCl are 7.1 and 14.8 kcal/mole, respectively.

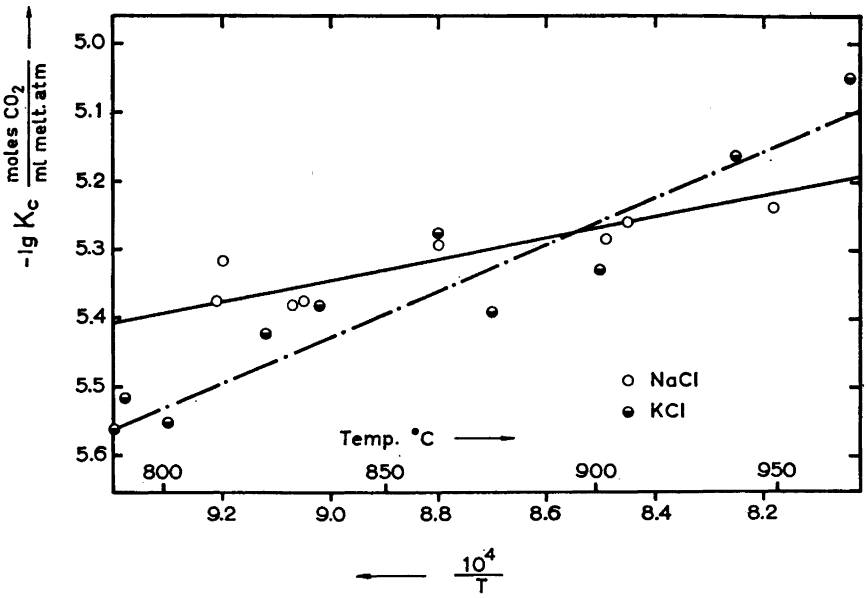

Fig. 2. Solubilities of carbon dioxide in sodium chloride and in potassium chloride melts, plotted as logarithm of solubility *versus* reciprocal temperature. Straight lines show best fit to experimental points by method of least squares.

DISCUSSION

(*a*) *Apparatus.* Generally one might say that the method applied is well suited for the measurement of CO_2-solubilities in molten salts. As can be seen from the fairly large spread in the results, however, there are as yet uncontrolled sources of error.

Preliminary experiments indicated that a saturating time of 3 h was sufficient. The flow rate for the stripping nitrogen was kept at 70 ml/min. With this rate, from 3 to 10 h were needed to effect essentially complete stripping, the observed time being roughly proportional to the amount of CO_2 dissolved. Assuming that Henry's law holds for the solution, and that each bubble of stripping gas reaches equilibrium with the melt, one may calculate the time necessary to effect 99.9 % complete stripping. The times thus calculated agreed rather well with the observed ones. Hence a shortening of the stripping time can be effected only by increasing the stripping gas flow rate.

Severe trouble was caused by corrosion of the nickel vessel by the molten salt. A detailed discussion of these corrosion problems is published elsewhere [6], thus only a few remarks will be given here. Intergranular corrosion in the welds led in most cases to complete penetration after 1—2 weeks of operation. It was then disclosed that, contrary to orders given, the welds had been made with covered electrodes in ordinary atmosphere. This has probably resulted in fairly large amounts of oxygen dissolved in the metal during the welding.

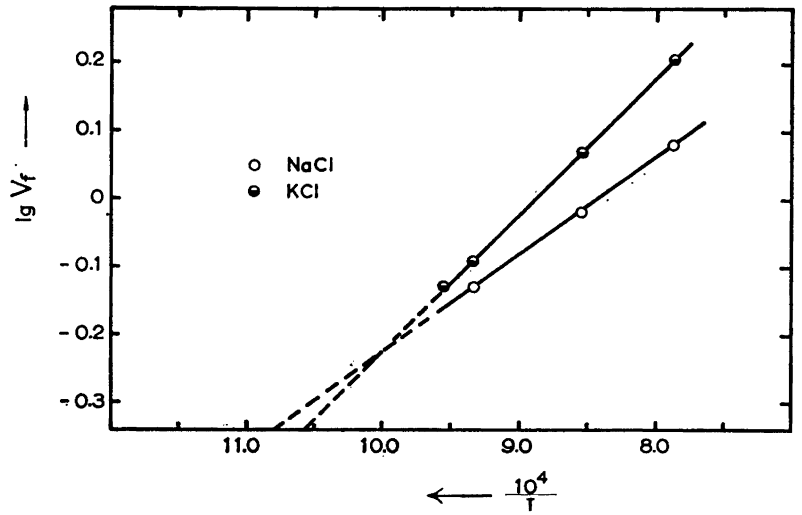

Fig. 3. Logarithm of free volume values for sodium chloride and potassium chloride melts (after Bockris *et al.* [7]) *versus* reciprocal temperature.

Diffusion of this oxygen to the grain boundaries, combined with the stresses from the periodical melting and solidification of the salt, has then resulted in a type of stress corrosion cracking. In the most recent vessel, made with argon welding following the specifications for reactor systems, this source of trouble apparently has been eliminated.

It is expected that larger values for the solubilities of CO_2 will be found when changing to the cryolite-alumina system because of the possible chemical bonding between the carbon dioxide and the oxide in the melt. For this latter system, a volumetric method will be attempted, observing directly the CO_2 uptake of the melt.

(*b*) *Interpretation of results.* Until additional data are available, it seems unwise to draw too definite conclusions from the results, but a few remarks seem justified. At temperatures just above the melting points, the solubility in KCl is lower than that in NaCl, but above approximately 900°C the situation is reversed, the solubility in KCl increasing with temperature about twice as fast as in NaCl. One might at first expect these two chlorides to show a more closely similar behaviour than is actually found. But it should be remembered that the two salts show very marked differences also in other respects, such as, *e.g.*, the temperature dependence of their solubilities in water.

It seems plausible to assume that the dissolution process for CO_2 in these melts is a purely physical one, with no chemical reaction involved. One would then expect some relation between the CO_2 solubility and the free volume in these melts, the solubility being expected to increase with increasing free

volume. Free volume data are available from, *e.g.*, the sonic velocity measurements of Bockris *et al.*[7] The free volumes are found to obey the relation

$$\left(\frac{\partial \ln V_f}{\partial (1/T)}\right)_P = -\frac{E^*_h}{R}$$

For NaCl and KCl, the heat of activation, E^*_h, is essentially constant over the temperature range in question and is found to be 6.6. kcal/mole for NaCl and 8.6 kcal/mole for KCl. A plot of the values of log V_f found by Bockris *et al.* *versus* $1/T$, gives two crossing lines as shown in Fig. 3, with an appearance rather similar to that of the solubility data in Fig. 2.

A correlation between free volume and solubility is thus found for the two salts investigated so far. Further discussions will have to be deferred until data for the other alkali halides have been obtained.

Acknowledgement. The authors wish to thank *The Royal Norwegian Council for Scientific and Industrial Research* for financial support in this work.

REFERENCES

1. Grimes, W. R., Smith, N. V. and Watson, G. M. *J. Phys. Chem.* **62** (1958) 862.
2. Blander, M., Grimes, W. R., Smith, N. V. and Watson, G. M. *J. Phys. Chem.* **63** (1959) 1164.
3. Shaffer, J. H., Grimes, W. R. and Watson, G. M. *J. Phys. Chem.* **63** (1959) 1999.
4. Woelk, H. V. *Nukleonik* **2** (1960) 278.
5. Hillebrand, W. F. *Applied Inorganic Analysis*, Wiley, New York 1953, p. 768.
6. Krohn, C. H. *Tidsskr. Kjemi, Bergvesen Met.* **21** (1961) 183.
7. Bockris, J. O'M. and Richards, N. E. *Proc. Roy. Soc. (London)* **A 241** (1957) 44.

Received October 9, 1961.

ACTA CHEMICA SCANDINAVICA 16 (1962) 695–700

Fractionation of Gelatins using Amberlite CG-50 Resin

E. KULONEN, U. K. VIRTANEN, J. VILJANTO and P. SEPPÄLÄ

Department of Medical Chemistry, University of Turku, Turku 3, Finland

By means of an Amberlite CG-50 resin column, it is possible to separate gelatins into a continuous series of arbitrary fractions by eluting with buffers of increasing pH. The distribution pattern of acid (lime-treated) gelatins was found to occur at a lower pH range than that of neutral gelatins. The fractions which emerged first had a slightly lower molecular weight.

It is suggested that the more acidic and more degraded fractions arise from the surfaces of the fibres.

This work was inspired by the publication by Russell [1] who succeeded in isolating, with a cation exchange resin, a "pH 5.5 fraction" (which passed through the Amberlite cation exchange resin at this pH) from lime-treated gelatin and claimed that it differed from the bulk material by its amino acid composition. We have observed that, with 0.1 N sodium hydroxide, the bulk of the gelatinized collagen from bone can be further fractionated [2]. In the present investigation, we wished to pay special attention to the bulk fractions. The work of Russell was extended by Leach [3] who concluded that the amount of the "pH 5.5 fraction" obtained depended partly on the conditions (pH, salt strength, amount of the sample and surface area of the resin) and partly on the properties of the gelatin (acidity and molecular weight). He did not find any marked differences between the "pH 5.5 fraction" and the bulk material.

Partridge and Boardman [4] have pointed out that the ionic strength is very important in the fractionation of proteins with resins. They stressed the use of higher temperatures which, with most proteins, involves a danger of denaturation but is an advantage with gelatins.

EXPERIMENTAL

A 1 cm diameter, water-jacketed column was filled with a suspension (in the first buffer) of the resin which was allowed to settle to 15 cm height. (Between runs the resin was taken out, regenerated, washed and finally suspended again in the first buffer.) The fraction collector was steered by a timer to accept 2 ml fractions, which took 1 ½ – 3 min. The speed of elution was about 5 – 15 drops per min. This speed could be decreased to one-fourth without any appreciable effect on the fractionation pattern. If the run was interrupted, the next immediate fractions contained erroneously high amounts of protein and several artefact peaks were encountered in this way. The column was kept at a temperature of +36°C (pH 5.5) or +37°C (gradient and NaOH) but check experiments were performed at lower temperatures.

In the initial experiments, two eluents were used: (1) pH 5.5 citric acid-disodium phosphate buffer [5] (McIlwaine) and (2) 0.1 N sodium hydroxide. In the final procedure, the 0.1 N sodium hydroxide was replaced by various gradients of increasing salt strength and/or pH (see the figure legends). Some experiments were made using initially a pH 5.0 buffer.

The sample (usually 50 mg of gelatin, as 1 % solution) was heated to about + 60°C and allowed to cool down to + 37°C before application to the column.

The protein in the fractions was estimated colorimetrically in 0.25—0.5 ml aliquots using a modified biuret reagent [6]. It is known that this reagent does not give equal colours with different fractions but, for the location of the fractions, it is quite satisfactory.

Nine gelatins were studied:

I. commercial, turbid (cleared upon heating), formed poor jelly, pI 5.3;

II. commercial, clear, formed strong jelly, prepared from "cartilage and good bones", pI 5.2;

III. laboratory preparation according to Jackson [7], formed good jelly, turbid even when heated, pI 6.9;

IV. commercial, "for bacteriological purposes", clear, formed strong jelly, pI 7.5;

V. sample specially prepared by Kind & Knox Gelatin Company from porkskin (acid pretreatment), pI 6.8, Bloom value 304;

VI. second run after preparation V, pI 6.8, Bloom value 172;

VII. sample specially prepared by Kind & Knox Gelatin Company from limed calfskins, pI 4.95, Bloom value 244;

VIII. second run after preparation VII, pI 4.9, Bloom value 218;

IX. third run after preparations VI and VII, pI 4.85, Bloom value 124. Fractionation patterns of this sample resembled those of sample VIII and are not given.

The pI was determined as the pH of the gelatin solution which had passed through a mixed-bed resin to remove the ions [8].

The cation exchange resin (Amberlite CG-50, Type 1, 100—200 mesh, Lot 27743) was purchased from British Drug House Ltd., Poole, England.

When the pH of the fractions was raised to 7, a precipitate appeared in most of the fractions, especially when concentrated by evaporation. The physical examinations (diffusion and sedimentation) were therefore performed in an acetate buffer at pH 4.8, + 38°C and ionic strength of 0.15. The sedimentation was studied by means of a Spinco model E ultracentrifuge, and diffusion properties by Antweiler's microelectrophoresis apparatus using the diffusion cell. The diffusion was recorded by means of a built-in interferometric optical system.

RESULTS

Fig. 1. gives the fractionation patterns of samples of different gelatins using the original method of Russell. The "pH 5.5 peak" from the more acid gelatins (I, II) is larger and the fraction eluted with 0.1 N sodium hydroxide is skewed to the left. To find out whether the "pH 5.5 peak" was an independent peak and not an "overflow" fraction, it was rechromatographed twice (Fig. 2) without concentration or any other manipulation. It seems evident that, on rechromatography, only an insignificant amount is retained in the resin. Thus the "pH 5.5 peak" represents a real fraction, but not a homogeneous one as shown below.

To elucidate whether the fractionation depended primarily on the pH of the eluent or on its salt strength, the NaOH elution was replaced by a concentration gradient (by increasing the concentration of McIlwaine's buffer at pH 5.5 threefold) or by a pH gradient (by increasing the pH gradually by means of a decrease in the citric acid in the buffer). No definite fraction emerged as a result of the increase in salt strength but, when the pH was raised, a distinct fraction was obtained.

The result was improved (Fig. 3) when the gradient was made steeper by the use of a more concentrated disodium phosphate solution in the reservoir

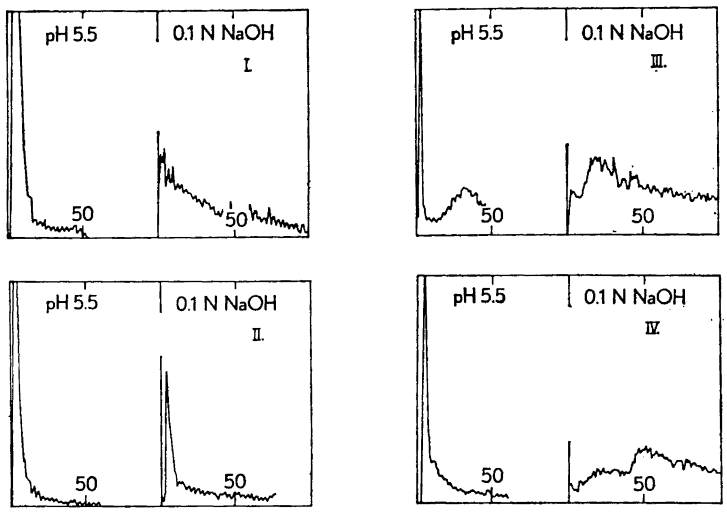

Fig. 1. Fractionation of various gelatins I—IV (specified in the text) with an Amberlite CG-50 resin column which was eluted first with pH 5.5 buffer and then with 0.1 N sodium hydroxide. Number of the fractions is given.

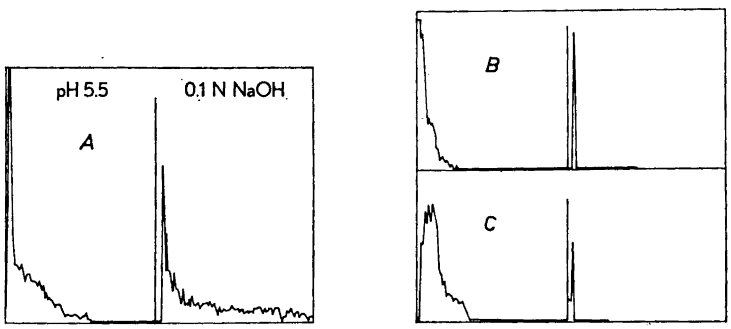

Fig. 2. Rechromatography of the "pH 5.5 fraction" obtained from gelatin II (Fig. 1.); A = original; B = "pH 5.5 fraction" of A, rechromatographed; C = "pH 5.5 fraction" of B, rechromatographed.

vessel. In "neutral" gelatins (III, IV, V, VI), the Na_2HPO_4-gradient fraction is much more marked than in "acid" gelatins (I, II, VII, VIII). From some gelatins (especially IV) a "residual" fraction was recovered using sodium hydroxide. Some additional experiments were made to find out whether the "pH 5.5 peak" could be divided into subfractions. Fig. 4 shows the "pH 5.5 peak" (from gelatin I) rechromatographed in this manner and it is obviously heterogeneous. Using a pH 5.0 citric acid-disodium phosphate buffer instead of the pH 5.5 buffer, a part of the gelatin was still found to pass through the column. When the pH 5.5 buffer was replaced by the pH 5.0 buffer, the bulk of the material emerged as a single fraction which obviously contained some of the material in the "pH 5.5 fraction" together with the "gradient-fraction"

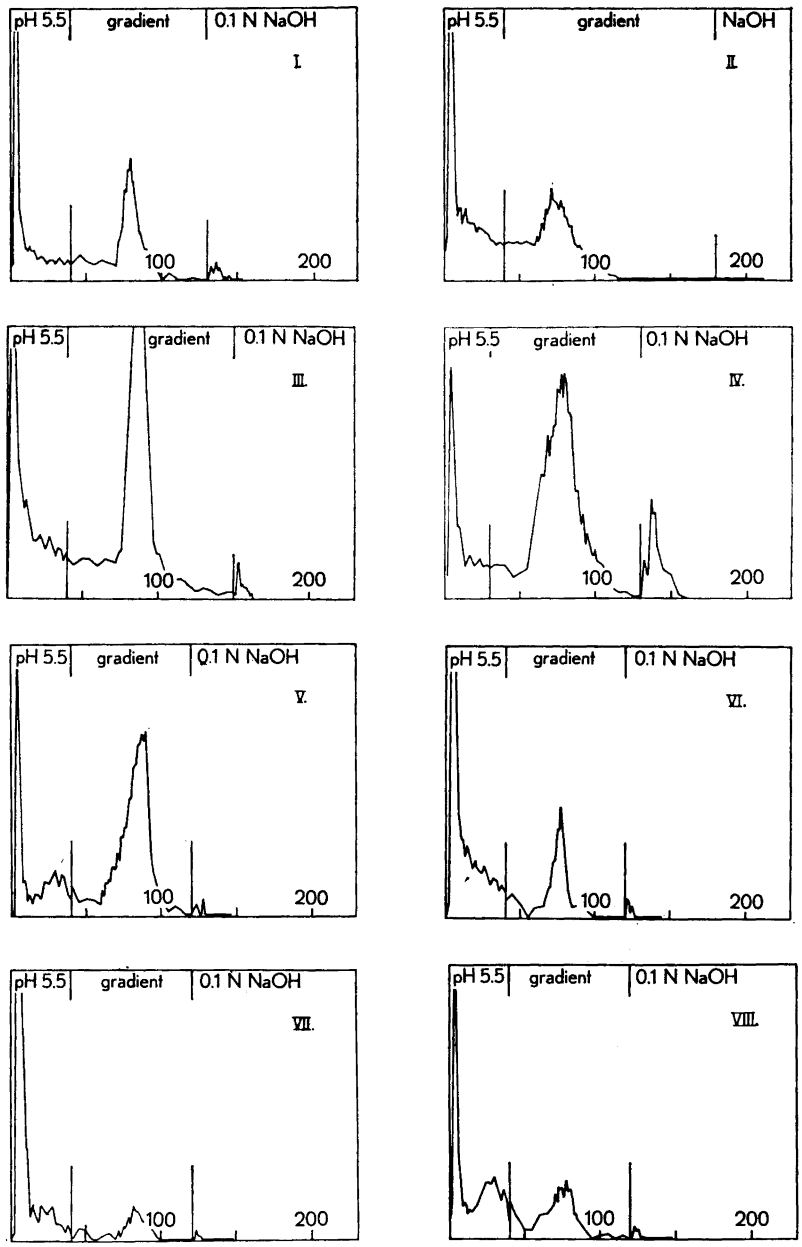

Fig. 3. Chromatography of various gelatins I—VIII (specified in the text) using a pH gradient from pH 5.5 upwards. The volume of the mixing vessel (from which the column was fed) was 100 ml and contained originally McIlwaine's buffer. This was replaced by 0.5 M Na_2HPO_4 from the reservoir vessel. The number of the 2 ml fractions is indicated.

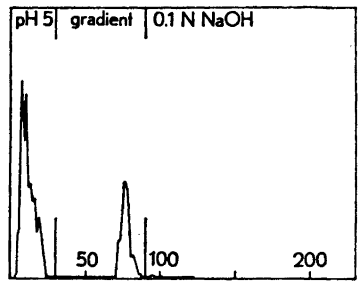

Fig. 4. Rechromatography of the "pH 5.5 fraction" of gelatin I using gradient (as in Fig. 3) beginning at a pH 5.0 (McIlwaine) buffer.

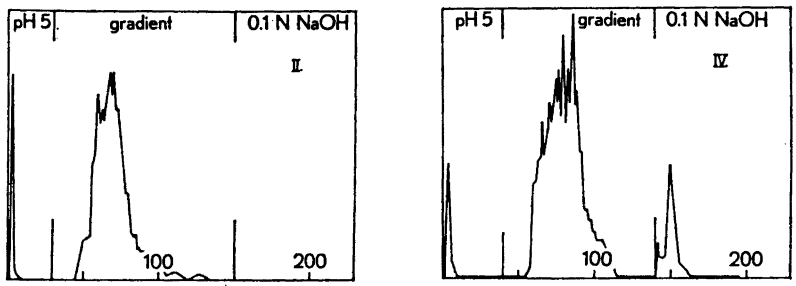

Fig. 5. Chromatography of total gelatins II and IV in the same condition as in Fig. 4.

(Fig. 5). There exists a continuous distribution of fractions which can be separated using buffers of suitable pH. It is not yet quite certain whether there is more than one peak in this distribution and also whether the fractions differ by other properties than their electrical charge. Several unsuccessful attempts were made to modify the gradient in order to split the bulk material which emerged within a range of about one pH unit. The "sodium hydroxide fraction" (*e.g.* from gelatin IV) seems to be different from the bulk fraction.

The sedimentation coefficient ($s°_{20,w}$) of gelatin II was for the "pH 5.5 fraction" 2.64 S and for 0.1 N sodium hydroxide fraction 2.43 S. The diffusion coefficient of the "pH 5.5 fraction" was dependent on the time and $D°_{20,w}$ was estimated to 4.4-5.7 $\times$ 10^{-7} cm^2/sec. For the NaOH-eluted fraction (Fig. 1, II) the diffusion coefficient was 3.0 $\times$ 10^{-7} cm^2/sec. Assuming $\bar{V} = 0.70$, the molecular weight of the "pH 5.5 fraction" was therefore about 40 000—50 000 and of the 0.1 N sodium hydroxide-eluted fraction about 65 000.

DISCUSSION

There is ample evidence for the existence of two fractions in gelatins prepared by mild degradations of soluble collagens [9]. They are known to differ with respect to molecular weight and amino acid composition, *e.g.* the content of histidine. Further studies will show whether the fractions of smaller

particle weight, described above, differ in regard to amino acid composition. In this respect, the "sodium hydroxide fraction" (Fig. 3, IV) is of interest since, judging by its pI, it resembles closest the parent collagen [10,11].

It is not clear to us what is the basic reason for the fractionation. The first fraction emerging is of lower molecular weight. Also, the more acid gelatins contained larger non-adsorbed fractions. In these respects we can confirm the work of Leach [3]. The most plausible, but not necessarily the only reason for the fractionation, seems to us to be the difference in electrical charge. However, attempts to fractionate gelatins by electrophoresis on "Oxoid" cellulose acetate strips at + 37°C and pH 8.6 were not successful.

The technical properties, (jelly strength, turbidity) do not seem to be directly correlated with the fractionation pattern. When the fractionation was performed at + 4°C or in the presence of 4 M urea, that portion of gelatin (II) which was not retained by the column was decreased.

We are of the opinion that these fractions are formed by deamidation (and partly by modification of the arginine residue) during the soaking of the original collagenous material in lime or acid [12]. Some fractions of the collagen may be more exposed to deamidation. If all the amido groups of the collagen were exposed to deamidation at random, we would expect to get whole molecules (or their large parts) of similar acidity. It remains to be proved whether the more acidic fractions arise from the most recent deposits of collagen on or near the surface of the fibres. This suggestion is supported by the fact that soluble collagens yielded in preliminary experiments relatively large "pH 5.5 fractions", presumably because all the molecules were exposed to the degradation simultaneously.

Acknowledgement. This work is a part of a program supported by a grant from the *U.S. Department of Agriculture.* We are especially indebted to Dr. J. Naghski, Eastern Utilization Research and Development Division, Agricultural Research Service of the U.S. Department of Agriculture, who arranged the acquisition of samples V—IX from the Kind & Knox Gelatin Company, Camden, N.J., U.S.A. through the courtesy of Dr. E. M. Marks.

REFERENCES

1. Russell, G. *Nature* **181** (1958) 102.
2. Tuominen, T. and Kulonen, E. *Acta Chem. Scand.* **13** (1959) 2120.
3. Leach, A. A. *Biochem. J.* **74** (1960) 61.
4. Boardman, N. K. and Partridge, S. M. *Biochem. J.* **59** (1955) 543.
5. Hodgman, C. D. (Ed.), *Handbook of Chemistry and Physics*, 31st. Ed., Chemical Rubber Publishing Co., Cleveland, Ohio, 1949, p. 1431.
6. Lowry, O. H., Rosebrough, N. J., Farr, A. L. and Randall, R. J. *J. Biol. Chem.* **193** (1951) 265.
7. Jackson, D. S. *Biochem. J.* **65** (1957) 277.
8. Janus, J. W., Kenchington, A. W. and Ward, A. G. *Research* **4** (1951) 247.
9. Piez, K. A., Weiss, E. and Lewis, M. S. *J. Biol. Chem.* **235** (1960) 1987.
10. Eastoe, J. E. *Biochem. J.* **61** (1955) 589.
11. Eastoe, J. E., Long, J. E. and Willan, A. L. D. *Biochem. J.* **78** (1961) 51.
12. Gustavson, K. H. *The Chemistry and Reactivity of Collagen*, Academic Press, New York 1956, p. 97.

Received October 4, 1961.

ACTA CHEMICA SCANDINAVICA 16 (1962) 701–704

Acid-Base Equilibria in Dioxane-Water Mixtures of Low Water Content

JOUKO KOSKIKALLIO and ANJA ERVASTI

Department of Chemistry, University of Oulu, Oulu, Finland

The apparent equilibrium constants of the proton exchange between *o*-chloroaniline and perchloric, hydrochloric and sulphuric acid in dioxane-water mixtures have been measured spectrophotometrically. The results agree qualitatively with the conclusions drawn from previous kinetic experiments [2,3] that the apparent acid strength of perchloric acid increases greatly, that of sulphuric acid increases slightly, and that of hydrochloric acid decreases as the amount of water in dioxane decreases in dioxane rich solvent mixtures.

Values of the acidity function H_0 in dioxane-water and acetone-water mixtures were measured by Braude and Stern [1], who used fairly concentrated, 1 M and 0.1 M, hydrochloric acid solutions. Recent kinetic studies [2,3] of some acid-catalysed hydrolysis reactions have shown that the apparent acid strengths of strong mineral acids differ greatly in dioxane-water mixtures of low water content. This study was undertaken in order to obtain values of the equilibrium constants for some acid-base reaction which could be compared with the kinetic results. *o*-Chloroaniline was chosen as the base because its basicity is suitable for measurements in solvent mixtures containing mineral acids in concentrations varying from about 10^{-1} to 10^{-3} M.

EXPERIMENTAL

Materials. All the chemicals used (E. Merck AG, *pro analysi*) were used as such except dioxane (Fluka AG, purified by the method of Hess and Frahm) from which traces of hydroxylic compounds were removed by repeated treatment by the method of Hess and Frahm [4]. Hydrogen chloride prepared from sodium chloride and 95 % sulphuric acid was dissolved in dioxane. The solutions containing perchloric acid were prepared from aqueous 70 % perchloric acid. Freshly distilled water was used in all experiments.

Method. A Beckman DU spectrophotometer was used to measure the extinctions of the solutions. The concentration of *o*-chloroaniline was the same, about 10^{-4} M, in all experiments. Absorptions at several wavelengths around that where the absorption was maximal were measured. The extinction E_∞ of the *o*-chloroanilinium ion (or ion pair) was obtained by measuring the absorbtion of solutions containing mineral acid in great excess or by substituting two extinction values obtained at low acid concentrations in eqn. (2).

Table 1. Spectrophotometrically measured values of the equilibrium constant $K = [HA][I]/[IH^+]$ in dioxane-water mixtures at 20°C. I = *o*-chloroaniline, HA = $HClO_4$, HCl or H_2SO_4.

$[H_2O]$ mole/l	Acid	$10^4 \times$ [Acid] mole/l	$K \times 10^4$ mole/l
0.108	$HClO_4$	4.84	0.61
0.108		3.73	0.63
0.22		3.76	2.24
0.45		4.84	7.93
0.45		3.76	8.10
0.45		46.4	6.87
1.11		35.8	63.1
2.22		386	184
2.22		468	173
4.34		364	565
6.56		470	615
8.82		364	851
11.1		364	773
0	HCl	480	451
0		544	582
0.026		840	380
0.069		210	472
0.069		388	300
0.069		908	258
0.278		210	280
1.11		183	129
2.22		207	207
5.48		814	660
11.1		832	1 005
0.11	H_2SO_4	199	86
0.232		262	99
0.55		248	148
0.99		454	193

The ratio of the concentrations of *o*-chloroaniline (I) and *o*-chloroanilinium ion (IH^+) were obtained by substituting the experimental extinction values in eqn. (1) and they were used to calculate the equilibrium constant K, eqn. (2).

$$\frac{[I]}{[IH^+]} = \frac{E_0 - E}{E - E_\infty} \tag{1}$$

E_0 is the extinction of the solution of *o*-chloroaniline and E the extinction of the solution containing *o*-chloroaniline and mineral acid. In dioxane-rich dioxane-water mixtures ions such as the *o*-chloroanilinium ion IH^+ and hydrogen ion H^+ are present mainly as ion pairs which complicates the interpretation of the experimental data [5,6]. The apparent equilibrium constant K was calculated from the experimental data.

$$K = \frac{[HA][I]}{[IH^+]} = [HA]\,\frac{E_0 - E}{E - E_\infty} \tag{2}$$

[HA] is the analytical concentration of the mineral acid.

DISCUSSION

Three different acid concentrations in the ratios 1:2:3 were used in the experiments. The calculated values of K were constant within the chosen concentration ranges when perchloric or sulphuric acid was used but decreased when

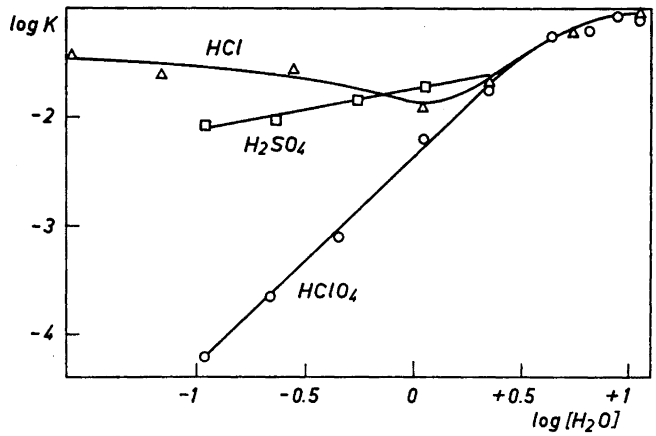

Fig. 1.

the acid concentration increased in the case of hydrochloric acid. The mean values of K obtained at different acid concentrations are given in Table 1 together with the mean values of the acid concentrations. These values show that a tenfold increase in the concentration of perchloric acid has a very small effect on the value of K, but a similar change in the concentration of hydrochloric acid affects the equilibrium constant considerably. This difference may be due to the much higher concentrations of hydrochloric acid used.

In the presence of perchloric acid, a rapid decrease occurs in the value of K when the content of water in dioxane is decreased. The plot (Fig. 1) of log K *versus* log [H_2O] is an approximately straight line with a slope of about 1.9. The apparent acid strength of perchloric acid in dioxane containing 0.1 mole of water per litre is about a thousand times as great as its strength in dioxane containing 10 moles of water per litre. The value 1.9 of the slope indicates that two water molecules are liberated when the proton is transferred to the chloroaniline molecule in reaction 3. The proton is therefore solvated by at least two water molecules in the solvent mixtures studied. It is very likely that the proton is solvated by approximately four water molecules in water and water-rich solutions [7] and by two water molecules in acetic acid-water mixtures containing about 1 to 10 moles of water in acetic acid [5,8] but by only one water molecule in acetic acid containing water less than 0.4 moles per litre [5]. Also in methanol-water and ethanol-water mixtures the proton is solvated by only one water molecule [9].

The hydrolysis rates of diethoxymethane [2] and acetic anhydride [3] in the presence of perchloric acid as catalyst in dioxane-water mixtures increase rapidly when the amount of water decreases from about 10 moles per litre. This also indicates that perchloric acid is a much stronger acid in solvent mixtures containing low concentrations of water. The plots of log k *versus* log [H_2O] are straight lines with slopes of -2.5 and -1.7, respectively. The opposite signs of the slopes derived from kinetic and equilibrium measurements are due

to the way in which K is defined (eqn. 2). In spite of the different nature of the bases in the two cases, the proton being attached to an oxygen atom in case of diethoxymethane and acetic anhydride and to a nitrogen atom in case of *o*-chloroaniline, and the ion pair formation the slopes have similar values. The experiments could not be extended to dry dioxane because of the oxidating power of perchloric acid.

When hydrochloric acid was used the value of K changed in the opposite direction when the solvent composition was altered indicating that hydrochloric acid is a weaker acid than perchloric acid in solvent mixtures containing small amounts of water. The slope of the straight part of the curve in Fig. 1 is about -0.2. In water-dioxane mixtures containing about 2 to 10 moles of water per litre, the values obtained with hydrochloric acid and perchloric acid are practically identical. It seems therefore probable that hydrochloric acid dissolved in dioxane-water looses its solvation water when the concentration of water in the solvent mixtures decreases below about 2 moles per litre.

The kinetic experiments [2,3] revealed somewhat larger effects when hydrochloric acid was used. The rates of the acid-catalysed hydrolyses of diethoxymethane and acetic anhydride decreased when the amount of water in dioxane decreased below about 2 moles per litre. The slopes of the plots of log K *versus* log $[H_2O]$ were 1.5 and 1.6, respectively.

A change in the composition of dioxane-water mixtures altered the equilibrium constant K to only a small extent when sulphuric acid was the acid. The slope of the curve in Fig. 1 is 0.4 and thus close to the values -0.5 and 0.1 obtained in the kinetic experiments [2,3]. The apparent acid strength of sulphuric acid remains almost unaltered in the range of the dioxane-water mixtures used in the present experiments. The apparent acid strength of the mineral acids studied decrease in the order $HClO_4 > H_2SO_4 > HCl$ in dioxane rich solvent mixtures. In acetic acid the pK values and the apparent acid strengts decrease in the same order [5].

Acknowledgement. The authors wish to record their indebtedness to the *State Commission for Natural Sciences* for financial aid.

REFERENCES

1. Braude, E. A. and Stern, E. S. *J. Chem. Soc.* **1948** 1976.
2. Koskikallio, J. and Tarvainen, I. *Acta Chem. Scand.* **16** (1922) 263.
3. Koskikallio, J. and Ervasti, A. *Suomen Kemistilehti* **B34** (1961) 111.
4. Hess, K. and Frahm, H. *Ber.* **71** (1938) 2627.
5. Bruckenstein, S. *J. Am. Chem. Soc.* **82** (1960) 307.
6. Hummelstedt, L. E. and Hume, D. N. *J. Am. Chem. Soc.* **83** (1961) 1564.
7. Bascombe, K. N. and Bell, R. P. *Discussions Faraday Soc.* **24** (1957) 158.
8. Wiberg, K. B. and Evans, R. J. *J. Am. Chem. Soc.* **80** (1958) 3019.
9. Koskikallio, J. *Acta Chem. Scand.* **13** (1959) 671.

Received September 28, 1961.

ACTA CHEMICA SCANDINAVICA 16 (1962) 705–710

The Collagen and Ground Substance of Human Intervertebral Disc at Different Ages

ANUND HALLÉN

Chemistry Department II, Karolinska Institutet, Stockholm, Sweden

The collagen and ground substance of human intervertebral disc has been studied by means of hydroxyproline, hexosamine and nitrogen analyses, as well as extraction experiments. It was found that an increase in a non-soluble fraction containing collagen and components of the ground substance takes place with rising age.

As demonstrated in Schmorl's laboratory by Püschel [1], and verified by several investigators [2–6], the dry substance of the intervertebral disc increases with rising age, and there is a corresponding decrease in its water content. This applies especially to its central part, the *nucleus pulposus (N.P.)*, but also to the peripheral *annulus fibrosus (A.F.)*. A parallel change takes place in the properties of the tissue, which is colourless and has good turgor in the young individual, whereas it is brownishly discolored and almost disintegrating in the highest age groups, as already noted by Luschka [7]. Since postnatal intervertebral disc (from about 1 year of age) is a kind of fibrocartilage containing large quantities of collagen and ester-sulphated mucopolysaccharides [5,8,9], it is highly probable that these changes depend on a change in the composition of the intercellular substances. Sylvén *et al.*[5,8] suggested that an increase in the collagen content might be the responsible factor, and similar explanations have appeared in the case of other connective tissues [10–12]. It nevertheless seems unlikely that this is the whole truth, since there are reasons to believe that changes in the composition and extractability of the mucopolysaccharides [13], as well as the deposition of yellow-brown lipofuscin pigment [6,14], must also be taken into account.

The reasons underlying the changes in the properties of the *N.P.* and *A.F.* with age cannot be known until all the intercellular components have been appropriately characterized, and determined quantitatively. The present investigation was intended as a step in this direction, including a chemical study of the collagen. The components of the "ground substance", *i.e.* the rest of the intercellular substances, are as yet only partly characterized, and at this stage the discussion must be confined to results of hexosamine and nitrogen analyses, and extraction experiments.

EXPERIMENTAL

Preparation of the tissue. Lumbar and lower thoracic parts of the vertebral column were taken from human autopsy cases, and the intervertebral discs were cut out, after freeing them from muscle and loose connective tissue. The *N.P.*, consisting of the most central part, about 2—3 cm^2, was dissected out. The surrounding *A.F.* was also dissected out, after removal of a small peripheral margin of the disc. The intermediate zone between the *N.P.* and *A.F.* was discarded. For the tissue analyses, these specimens were freeze-dried and then minced.

Collagen extraction experiment. A 0.5 g *N.P.* specimen was taken from a 26 year old subject and extracted, without previous drying, for 24 h at room temperature with 10 ml of 0.15 M ammonium carbonate. In this step, the tissue was finely divided with a glass rod. The pH was 9.0 at the beginning of extraction, and 8.6 at the end (glass electrode). The residue was removed by centrifugation at 2 000 *g* for 1 h, washed once with distilled water, and centrifuged down again. Extraction was repeated with 20 ml of 0.2 M citrate buffer, pH 3.8, as described above. At the end of this extraction, the pH was 3.9. The residue was removed and washed as before. The extracts, together with the respective washing water and the residues, were dried in a desiccator, taken up in strong hydrochloric acid and transferred quantitatively to the hydrolysis tubes. After desiccation, hydrolysis and the hydroxyproline analyses were performed essentially as described below.

Preparation of N.P. collagen. About 5 g of pooled *N.P.* from subjects 20—60 years old, that had been stored for several weeks at −15°C, was thawed, minced by hand, and extracted overnight at 0°C with 500 ml of 10 % calcium chloride. The residue obtained on centrifugation was extracted twice more in the same way with 250 ml of 10 % calcium chloride. The residue was then washed with water, freeze-dried, washed with acetone, and ground in a mortar. The yield was 1.3 g of calcium chloride-treated collagen.

83 mg of this collagen preparation was extracted for 2 days at room temperature with 20 ml of 2 % sodium hydroxide. The residue obtained on centrifugation was washed with distilled water, dried by several washings with acetone, and minced in a mortar. 50 mg of sodium hydroxide-treated collagen were obtained.

Hydroxyproline analysis. After hydrolysis of the tissue, the hydroxyproline was oxidized to 4-hydroxypyrrole, and the colour developed with Ehrlich's reagent [15] was read in a photometer according to Neuman and Logan [16], including some important modifications [17,18]. About 8 mg of the dried *N.P.* was hydrolyzed in sealed tubes with 2 ml of 6 M hydrochloric acid for 24 h at 100°C, or for 22 h at 110°C, both conditions giving the same result. The acid was completely removed *in vacuo* in a desiccator over potassium hydroxide. The hydrolysate was dissolved to 25 ml in distilled water, and 2 ml pipetted off into a 2 × 20 cm Pyrex tube. Standards were prepared containing 0, 10, 20 and 30 μg of hydroxyproline in 2 ml of distilled water. To unknowns and standards, about 20 tubes in each experiment, were added 2 ml of equal amounts of 0.01 M copper (II) sulphate and 2.5 M sodium hydroxide mixed immediately before use, and 1 ml of 6 % hydrogen peroxide. The contents were gently mixed, and left standing for 5 min. In order to remove excess peroxide, each tube was vigorously stirred in a mechanical shaker for 5 min, after which the contents were mixed and left standing for 5 min with 0.1 ml of a 0.01 M iron (II) sulphate solution, containing 0.5 % (v/v) sulphuric acid. 6 ml of a solution containing 1 part of 4 M sulphuric acid and 2 parts of 2 % *p*-dimethylaminobenzaldehyde in propanol, mixed immediately before use, was added. After mixing, heating at 70°C for 20 min and cooling with tap water, the red colour was read at 555 mμ in 1 cm absorption cells.

The weight-equivalent colour development of tyrosine was 2 % of that of hydroxyproline, but the absorption spectrum was completely different. The colour of the *N.P.* hydrolysate was found to have the same absorption spectrum as the standard, which implies negligible interference by non-specific chromogens. The hexosamines gave no colour in the reaction, and the colour development of proline was neglected, since it amounted to only some 0.1 % of the hydroxyproline.

Shrinkage-temperature determination. The powdered preparation, immersed in water, was viewed under a cover-glass in the microscope at 75 × magnification during gentle heating, and the temperature for maximal shrinkage recorded as described by Borasky and Nutting [19].

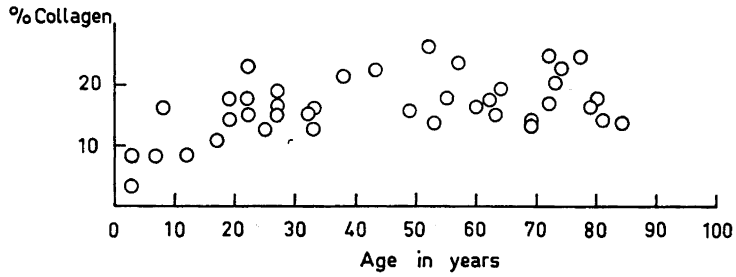

Fig. 1. Collagen content of human freeze-dried *N.P.* at different ages.

Analysis of the ground substance. Hexosamines were determined according to Gardell [20], and nitrogen by a modified Kjeldahl procedure. For further details, reference is made to an earlier paper [13].

RESULTS

Collagen analyses. Fig. 1 is a graphical representation of the results of the hydroxyproline analyses of *N.P.* The hydroxyproline content was multiplied by the factor 7.41, based on the assumption that *N.P.* collagen contains about 13.5 % hydroxyproline, like other mammalian collagens [16,21]. It can be inferred from Fig. 1 that the collagen content of *N.P.* was about 15—20 % of the dry weight, the values increasing slightly with rising age. Since the dry substance increases with age (see Fig. 2), it implies a fairly appreciable increase in collagen per unit volume of native tissue. This is in agreement with the observations of Sylvén *et al.*[5,8]

A.F. contained more collagen, *i.e.* about 50 % of the dry substance. This could be expected from the morphological properties of the tissue [1,9,22].

The extraction experiment showed that the collagen was mainly non-soluble. Thus, only 0.4 mg of collagen was found in the ammonium carbonate extract, and 0.4 mg in the citrate extract, whereas 13.6 mg, *i.e.* 95 %, was present in the residue. These results are in accordance with earlier brief reports [13,23], *i.e.* that only a small percentage of the collagen in *N.P.* can be extracted with physiological saline, slightly acid 10 % calcium chloride or slightly alkaline 30 % potassium chloride.

Attempts to isolate the *N.P.* collagen met with some difficulty, probably because parts of the ground substance were extremely difficult to remove [8,13]. The calcium chloride-treated collagen, obtained in some 95 % yield, contained only 7.4 % hydroxyproline (corresponding to 55 % collagen), and was contaminated by as much as 3 % hexosamine. The sodium hydroxide-treated collagen obtained in some 80 % yield, was practically devoid of hexosamines, and the hydroxyproline content had increased to 10.4 % (corresponding to 77 % collagen).

It proved impossible to see any shrinkage in freeze-dried *N.P.* during heating. In *A.F.*, on the other hand, it was easily visible, and the shrinkage temperature was found to be 60—62°C. In the *N.P.* collagen preparations treated

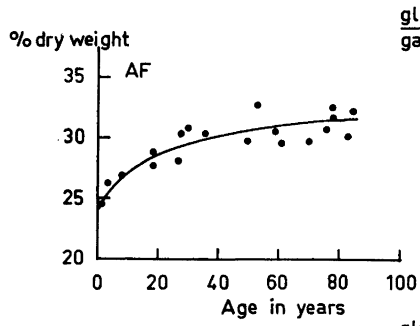

Fig. 2. Dry substance content of human *A.F.* and *N.P.* at different ages. Note the increase in *A.F.* during childhood, and the increase in *N.P.* throughout life. Based on Püschel's data [1].

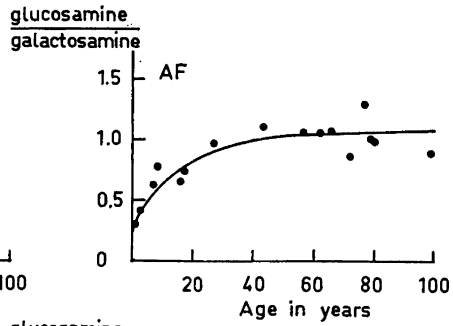

Fig. 3. Ratio of glucosamine/galactosamine of human *A.F.* and *N.P.* at different ages. Note the increase in *A.F.* during childhood, and the increase in *N.P.* throughout life.

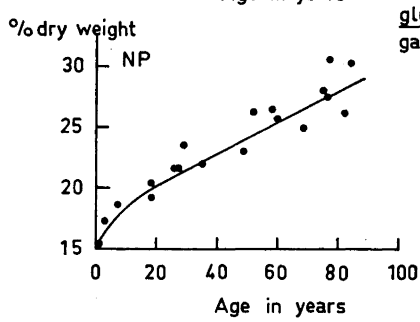

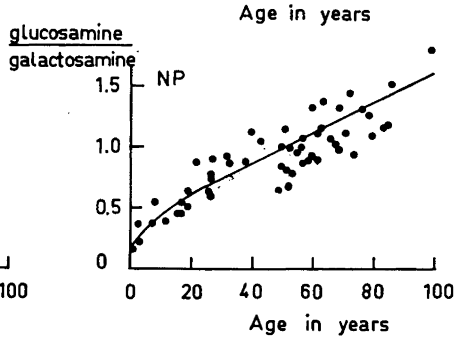

with calcium chloride and sodium hydroxide, the shrinkage could be seen with some difficulty. It occurred at the same temperature as in the case of *A.F.*

These experiments substantiate the view that the collagen of the intervertebral disc is identical with collagen of other mammalian connective tissues[21]. This is also in conformity with the results of Sylvén *et al.*[8], who isolated fibrils from *N.P.* with 600—700 Å periodicity, typical of collagen. The difficulties encountered in determining the shrinkage of *N.P.* may possibly depend on the irregular course of the fibrils here [8], in contrast to their very regular pattern in *A.F.*[22]

Analyses of the ground substance. As reported earlier[13], the hexosamine content of *N.P.* is about 14 % in the 10 to 15 year old, and 6 % in the 90 year old. Such a large decrease in hexosamine content must also mean a decrease per unit of native tissue. The *N.P.* of foetuses and newborns has been found to contain very little hexosamine (a few per cent). This is natural, since at this stage the *N.P.* is an epithelial tissue composed of dorsal cord cells [9].

The hexosamine content of *A.F.* is about 3 %, with a tendency to decreasing values with rising age.

The variation in the ratio of glucosamine/galactosamine in *N.P.* and *A.F.* with age is shown graphically in Fig. 3. It is seen that the ratio increases with

rising age in both. As discussed previously [13], this probably represents a change in the mucopolysaccharide-protein pattern from the chondroitin-6-sulphate of the young tissue to the less easily extractable keratosulphate of the old tissue.

The nitrogen content of *N.P.*, after subtraction of the nitrogen ascribable to collagen (18 % of the collagen content [21]) and hexosamine (8 % of the hexosamine content), was found to increase from a few per cent in the child to almost 10 % in the 90 year old. This probably represents an increase in the non-collagenous protein.

DISCUSSION

It seems that an increase in the collagen content and changes in the composition of the ground substance both contribute to the increase in dry substance of *N.P.* and *A.F.* with age. The contribution of the ground substance is indicated by an increase in the non-collagenous protein, and by the fact that there is a parallel between the increase in dry substance and the increase in the ratio of glucosamine/galactosamine in *A.F.* and *N.P.* (*cf.* Figs. 2 and 3). This parallel can be extended to pathological discs, because very brown *N.P.* with a high content of dry substance [1] (*i.e.* discs that have once ruptured [5,6,14,22]) has also proved to have an exceedingly high glucosamine/galactosamine ratio.

Fairly detailed information has recently been given about the way in which the polypeptide structural unit of the collagen is polymerized to fibrils, and about the increase in the number of cross-linkages and in the stability of the collagen with rising age [24,25]. The corresponding process in the ground substance has not yet been as systematically investigated. Certain observations [13,26–28] nevertheless indicate that, here as well, deposition of a non-soluble, highly cross-linked fraction may take place during aging. The following experiment was made to test this hypothesis.

100.0 mg samples of freeze-dried, minced *N.P.* from subjects aged 7, 22, 60 and 81 years were extracted with 10 ml of 10 % calcium chloride for 24 h at room temperature. The residues obtained after centrifugation were washed with 10 % calcium chloride and distilled water, treated with alcohol and ether, and dried. The weight was found to be 11.8, 19.8, 40.7 and 84.4 mg, respectively.

These results support the hypothesis in question, since such a large increase in the non-soluble fraction (to some 80 % of the dry substance) cannot be explained by the fairly inappreciable increase in collagen content with age (to some 20 % of the dry substance).

It seems reasonable to infer that the changes observed in the chemical composition of the intervertebral disc with rising age (increase in dry substance, collagen content, ratio of keratosulphate/chondroitin sulphate and lipofuscin pigment) are partial manifestations of a generalized, successive deposition of non-soluble, intercellular material.

Acknowledgements. I am greatly indebted to Prof. K. H. Gustavson for valuable discussions.

The investigation was aided by a grant from *Svenska Sällskapet för Medicinsk Forskning.*

REFERENCES

1. Püschel, J. *Beitr. Pathol. Anatom.* **84** (1930) 123.
2. Keyes, D. C. and Compere, E. L. *J. Bone Joint Surg.* **14** (1932) 897.
3. Lindahl, O. *Acta Orthopaed. Scand.* **17** (1948) 134.
4. Schümmelfeder, W. and Schümmelfeder, N. *Der Chirurg* **20** (1949) 395.
5. Hirsch, C., Paulson, S., Sylvén, B. and Snellman, O. *Acta Orthopaed. Scand.* **22** (1952) 175.
6. Hansen, H. J. *Acta Orthopaed. Scand.* **25** (1956) 161.
7. Luschka, H. *Die Halbgelenke des menschlichen Körpers.* Monographie. Berlin 1858, p. 56.
8. Sylvén, B., Paulson, S., Hirsch, C. and Snellman, O. *J. Bone Joint Surg.* **33-A**(1951) 333.
9. Peacock, A. *J. Anatomy* (London) **85** (1951) 260; **86** (1952) 162.
10. Sobel, H., Zutrauen, H. A. and Marmorston, J. *Arch. Biochem. Biophys.* **46** (1953) 221.
11. Sobel, H. and Marmorston, J. *J. Gerontol.* **11** (1956) 2.
12. Boas, N. F. and Foley, J. B. *Proc. Soc. Exptl. Biol. Med.* **86** (1954) 690.
13. Hallén, A. *Acta Chem. Scand.* **12** (1958) 1869; **14** (1960) 1828.
14. Güntz, E. *Deutsche Z. Chirurgie* **254** (1941) 633.
15. Lang, K. *Z. Physiol. Chem. Hoppe-Seyler's* **219** (1933) 148.
16. Neuman, R. E. and Logan, M. A. *J. Biol. Chem.* **184** (1950) 299.
17. Martin, C. J. and Axelrod, A. E. *Proc. Soc. Exptl. Biol. Med.* **83** (1953) 461.
18. Hutterer, F. and Singer, E. J. *Anal. Chem.* **32** (1960) 556.
19. Borasky, R. and Nutting, G. C. *J. Am. Leather Chemists Ass.* **44** (1949) 831. Cited in 21.
20. Gardell, S. *Acta Chem. Scand.* **7** (1953) 207.
21. Gustavson, K. H. *The Chemistry and Reactivity of Collagen.* Academic Press, New York 1956.
22. Hirsch, C. and Schajowicz, F. *Acta Orthopaed. Scand.* **22** (1952) 184.
23. Davidson, E. A. and Woodhall, B. *J. Biol. Chem.* **234** (1959) 2951.
24. Schmitt, F. O., Gross, J. and Jackson, D. in Page's *Connective Tissue, Thrombosis and Atherosclerosis.* Academic Press, New York 1959.
25. Brown, P. C. and Consden, R. *Nature* **181** (1958) 349.
26. Gersh, I. and Catchpole, H. R. *Perspectives in Biology and Medicine* **3** (1960) 282.
27. Gross, J. I., Mathews, M. B. and Dorfman, A. *J. Biol. Chem.* **235** (1960) 2889.
28. Davidson, E. A., Small, W., Perchinelides, P. and Baxley, W. *Biochim. et Biophys. Acta* **46** (1961) 189.

Received September 29, 1961.

ACTA CHEMICA SCANDINAVICA 16 (1962) 711–718

The Synthesis of Certain B_6 Enzymes during the Lag Phase of Growth of *Escherichia coli*

RAIMO RAUNIO and VEIKKO NURMIKKO

Department of Biochemistry, University of Turku, Turku, Finland

1. Using *Escherichia coli* as test organism, the synthesis of glutamic acid and arginine decarboxylases, serine, threonine, and homoserine deaminases, cysteine desulphhydrase, tryptophanase, and tryptophan synthetase was studied during the lag phase of growth.

2. The cells required for inoculation were grown in a medium rich in amino acids and vitamins. Cells in the lag phase of growth that had been transferred to a simple glucose and mineral salt medium were analyzed for enzyme content.

3. No changes were observed in the amounts of glutamic acid and arginine decarboxylases, of serine, threonine, and homoserine deaminases, of cysteine desulphhydrase or of tryptophanase in the cells.

4. The synthesis of tryptophan synthetase started immediately after the cell transfer and the amount of the enzyme increased linearly during the lag phase to four to eight times the original amount.

In spite of the fact that the first period of bacterial growth, the lag phase, is known to be a metabolically active one, and thus no rest phase, the synthesis of enzymes during this phase has not apparently been studied to any greater extent. It is true that in most growth experiments samples have been taken during the period when growth begins, but mostly these samples have been too few in number to give any clear picture of the phase in question and, furthermore, these samples may not always have been taken during the lag phase. Moreover, what literature there is on this growth phase is confusing because, in many cases, the investigators are not agreed upon the exact duration of the lag phase [1].

McGarthy [2] studied the amounts of glucose dehydrogenase and succinic acid dehydrogenase present in cells of *Bact. lactis aerogenes* during the lag phase but he did not observe any changes in the enzyme contents. Rowbury and Woods [3], who investigated the enzymes that synthesize methionine in *Escherichia coli* during the lag phase, found that the ability of cell extract to synthesize methionine increased during the lag phase. Corini and Maas [4] showed that the content of ornithine transcarbamylase in the cell increased between cell divisions.

In previous experiments [5,6] we have found that the amount of vitamin B_6 and certain transaminases increase during the lag phase of growth of *E. coli*. In the present investigation we have studied the synthesis by *E. coli* cells of some other B_6 enzymes during the lag phase. The enzymes we chose to study are the decarboxylases, the serine, threonine, and homoserine deaminases, the cysteine desulphhydrases, tryptophanase and tryptophan synthetase.

EXPERIMENTAL

Growth organism and culture methods. The strain of *Escherichia coli* used in this investigation was isolated as described in a previous paper [23]. Also the media employed have been described in a previous paper [6].

Procedure. Before the experiment *E. coli* cells were transferred from the nutrient agar slant on which they had been maintained to 5 ml of an inoculum medium. The cells were incubated 6—9 h at 37°C in this medium and then transferred aseptically to 1 000 ml of fresh, cold inoculum medium. After incubation for 12—13 h at 37°C the cells were centrifugated at some 2 500 rpm in a Wifug centrifuge for 15 min and washed twice with saline. Immediately after being washed, the cells were transferred in saline to 1 000 ml of growth medium into which they were dispersed with an electric stirrer. The first sample was taken 5 min after this transfer. Later samples were taken at intervals of 5—7 min and placed directly in ice water where the temperature of the medium sank to about 5°C in 1—1 1/2 min. Each sample contained 0.18—0.24 mg (dry weight) of cells per millilitre.

Generally the lag phase lasted 30—50 min. The turbidities of the suspensions were measured with a Klett-Summerson colorimeter employing red filter No. 62. Thirty-five-millilitre volumes of the ice-cold medium were pipetted into tubes of a Servall RC-2 centrifuge and centrifuged 10 min at 10 000 rpm. After this the cells were washed twice with cold saline and centrifuged between washings. During the centrifugation the temperature of the samples was 0°C.

Preparation of enzyme extracts. For the determinations of the *desulphhydrase* and *deaminase* activities the cells were frozen in a small amount of distilled water at —40°C for half an hour and warmed to 37°C. This procedure was repeated. The milky cell suspension obtained was used in the experiments as the enzyme preparation. In a few experiments a toluene powder was employed; this was prepared by a method similar to that described below for the preparation of acetone powder.

For the *decarboxylase*, *tryptophan synthetase*, and *tryptophanase* activity determinations the cells were thoroughly mixed with 30 ml of —20°C acetone for 10—30 min and centrifuged down. The acetone remaining in the sediment was evaporated in a vacuum at room temperature. The acetone powder obtained was autolyzed for decarboxylase determination overnight at 2°C in a M/10 buffer which was the same as the substrate buffer used in the experiment. For the tryptophan synthetase and tryptophanase determinations the powder was autolyzed in M/5 buffer with reduced glutathione for half an hour at room temperature.

Determination of enzyme activities. For the *desulphhydrase* and *deaminase* activity determinations, 0.50-ml volumes of enzyme extract prepared as described were pipetted into 15 × 110 mm tubes. This volume of extract contained approximately 1.00—1.30 mg (dry weight) of cells. The reaction was started by adding a 0.50-ml volume of substrate solution containing 20 μmoles of L-amino acids (40 μmoles of DL-amino acids) in 0.1 M buffer. A borate buffer of pH 9.5 was employed in the determinations of serine and threonine deaminase activities and a phosphate buffer of pH 7.4 in the determination of homoserine deaminase and cysteine desulphhydrase activities. When pyridoxal phosphate was used as activator, the amount added to the reaction system was 20 μg. The reaction was stopped by adding 0.2 ml of 10 N sulphuric acid and heating in a water bath for 2 min. The keto acids formed were determined by the method of Friedemann and Haugen [7]. The absorption of the hydrazone was measured with a Klett-Summerson colorimeter employing filter No. 42. In all experiments the reaction was stopped while the activity increase was still linear.

Table 1. Decarboxylase activities in *Escherichia coli* U 5—41.

Amino acid	Activity (μl CO_2/h).
L-Glutamic acid	232
L-Threonine	4
L-Cysteine	8
DL-Serine	2
L-Tyrosine	0
L-Dopa	0
DL-Ornithine	0
L-Aspartic acid	0
L-Leucine	0
L-Arginine	12
DL-Lysine	4
L-Valine	0
DL-Tryptophan	0
L-Histidine	0

The decarboxylase activity was measured with a Warburg apparatus. For this purpose 1.0 ml of the acetone-dried cell suspension containing 0.056—0.059 mg (dry weight) of cells was pipetted into the main compartment of the Warburg vessel. A 1.0-ml volume of 0.2 M buffer containing 6—10 μmoles of L-amino acid was pipetted into the side arm. The following buffers were used: acetate-buffer (pH 4.5) for histidine and glutamic acid; phosphate buffer (pH 6.0) for lysine, leucine, and valine; phosphate-citrate-buffer (pH 5.2) for arginine, threonine, and cysteine; a phosphate-citrate-buffer of pH 5.5 for ornithine, tyrosine, serine, aspartic acid, and tryptophan; and a phosphate-buffer of pH 6.8 for 3.4-dihydroxyphenylalanine.

The tryptophanase and tryptophan synthetase activities were measured in 15 × 110 mm test tubes by the methods of Gunsalus *et al.*[8] and Yanofsky [9]. No loss of indole was

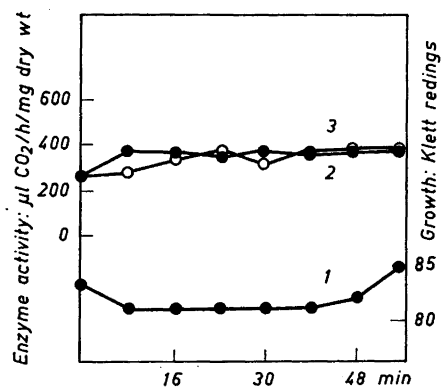

Fig. 1. Glutamic acid decarboxylase activity of *Escherichia coli* cells during the lag phase of growth, 1 = growth curve (right-hand scale), 2 = glutamic acid decarboxylase activity with added pyridoxal-5-phosphate, and 3 = glutamic acid decarboxylase activity without added pyridoxal-5-phosphate.

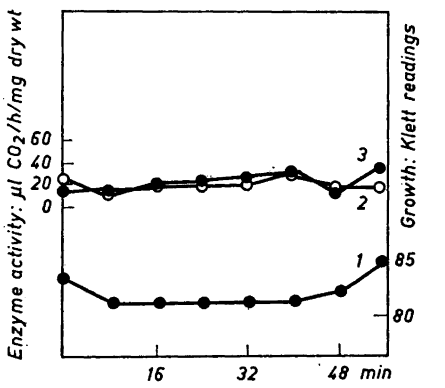

Fig. 2. Arginine decarboxylase activity during the lag phase of growth by *Escherichia coli*. 1 = growth curve (right-hand scale), 2 = arginine decarboxylase activity of cells without added pyridoxal-5-phosphate, and 3 = arginine decarboxylase activity with added pyridoxal-5-phosphate.

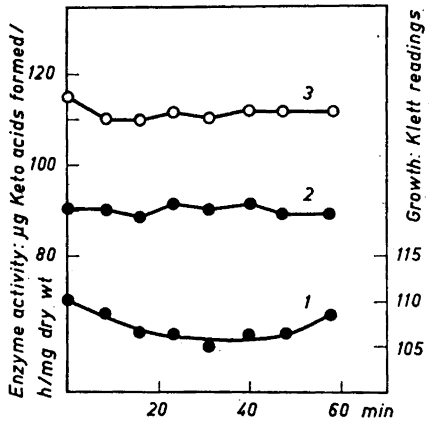

Fig. 3. Serine deaminase activity during the lag phase of growth of *Escherichia coli*. 1 = growth curve (right-hand scale), 2 = serine deaminase activity without pyridoxal-5-phosphate, and 3 = serine deaminase activity with added pyridoxal-5-phosphate.

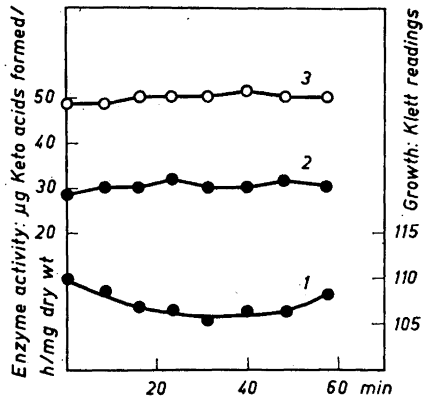

Fig. 4. Threonine deaminase activity by *Escherichia coli* cells during the lag phase of growth. 1 = growth curve (right-hand scale), 2 = threonine deaminase activity without added activator, and 3 = threonine deaminase activity with added pyridoxal-5-phosphate

observed in the determination of tryptophan synthetase during the time of testing when the reaction system lacked serine.

Chemicals. L-Cysteine hydrochloride, DL-serine, DL-threonine, L-histidine, and L-tryptophan were obtained from Hoffmann-La Roche; DL-serine, L-cysteine, DL-valine, L-leucine, L-glutamic acid, DL-lysine, L-arginine, and L-tyrosine from E. Merck AG. DL-Aspartic acid was obtained from Fluka. In paper-chromatographic tests each of the amino acids gave only one spot. Pyridoxal-5-phosphate was obtained from Hoffmann-La Roche. All the other chemicals used were of reagent grade.

RESULTS

The main object of the study was to determine what kinds of amino acid decarboxylases *Escherichia coli* possesses. The results are shown in Table 1.

As can be seen from the table, only glutamic acid was decarboxylated in any marked degree. The glutamic acid and arginine decarboxylase activities were measured in samples taken during the lag phase but the results (shown in Figs. 1 and 2) demonstrate that no variations occurred in the amounts of these enzymes. Addition of pyridoxal-5-phosphate when the activities of the enzymes were measured hardly increased the activities. The activity of glutamic acid decarboxylase varied within the range of 350—400 μl CO_2/mg dry weight/h and that of arginine decarboxylase within the range of 20—30 μl CO_2/mg dry weight/h. The lag phase lasted 40—45 min in these experiments.

No variations were observed in the amounts of serine and threonine deaminases in *E. coli* cells during the lag phase of growth. Fig. 3 shows the amount of serine deaminase in the cells; the activity was within the range of 88—92

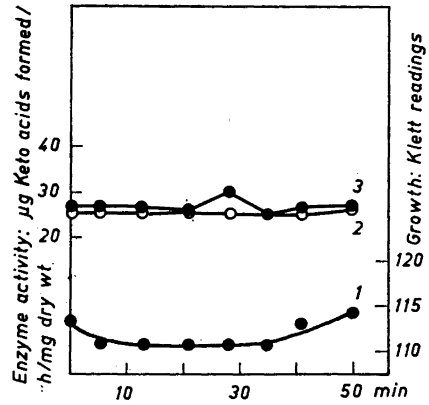

Fig. 5. Cysteine desulphhydrase activity during the lag phase of growth of *Escherichia coli*. 1 = growth curve (right-hand scale), 2 = cysteine desulphhydrase activity without added activator, and 3 = cysteine desulphhydrase activity with added pyridoxal-5-phosphate.

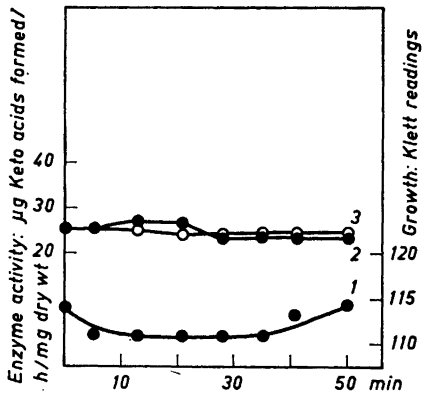

Fig. 6. Homoserine deaminase activity during the lag phase by *Escherichia coli* cells. 1 = growth curve (right-hand scale), 2 = homoserine deaminase activity of cells without added pyridoxal-5-phosphate, and 3 = homoserine deaminase activity with added activator.

µg of keto acid produced per mg (dry weight) of cells during 80 min. In contrast to the decarboxylases, the serine deaminase was strongly activated to the same extent by pyridoxal-5-phosphate throughout the lag phase. The values which were obtained when the activator had been added to the reaction systems for the enzyme determinations, and which correspond to those mentioned above, were 110—115 µg of keto acid produced per mg dry weight in 80 min. The lag phase lasted 40—45 min. The results obtained with threonine deaminase shown in Fig. 4 correspond to those obtained with serine deaminase. Without activator the activity was 28—32 µg of keto acid produced per mg of dry weight in 80 min. The lag phase lasted 40—45 min in these experiments.

No variations were observed in the amounts of cysteine desulphhydrase and homoserine deaminase during the lag phase. As can be seen from Fig. 5, the activity of the cysteine desulphhydrase remained within the range of 25—27 µg of keto acid produced per mg of dry weight during 240 min and was not affected to any marked extent by the addition of pyridoxal-5-phosphate. Such an addition did not either increase the activity of homoserine deaminase, as shown by Fig. 6; during the lag phase this activity remained within the range of 24—26 µg of keto acid produced/mg (dry weight) of cells/240 min. In these experiments the lag phase lasted about 40 min.

The amount of tryptophanase likewise remained constant throughout the lag phase. The activity varied within the limits of 6.2—6.5 µg of indole produced/mg dry weight/140 min, as seen from Fig. 7. Pyridoxal-5-phosphate did not increase the activity during the lag phase, which lasted 40—45 min.

Fig. 8 demonstrates that a marked increase in tryptophan synthetase (tryptophan desmolase) took place in the *E. coli* cells during the lag phase.

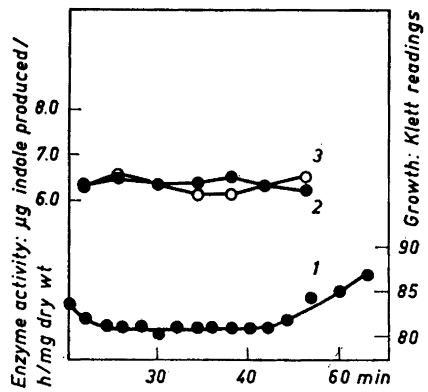

Fig. 7. Tryptophanase activity of *Escherichia coli* cells during the lag phase of growth. 1 = growth curve (right-hand scale), 2 = tryptophanase activity without pyridoxal-5-phosphate, and 3 = tryptophanase activity with added pyridoxal-5-phosphate.

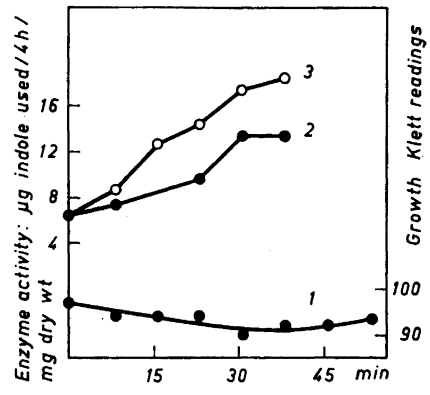

Fig. 8. Tryptophan synthetase activity during the lag phase of growth by *Escherichia coli*. 1 = growth curve (right-hand scale), 2 = tryptophan synthetase activity without added activator, and 3 = tryptophan synthetase with added pyridoxal-5-phosphate.

The enzyme activity in the cells rose from 2.4 to 9.8 µg of indole used/mg (dry weight) of cells/4 h, a fourfold increase. When pyridoxal-5-phosphate was added to the enzyme determination system a still greater increase was observed — the activity increased from 2.4 to 14.6 µg of indole/mg of dry weight/4 h, a sixfold increase. The lag phase lasted 40—45 min in this experiment. In other experiments, the results of which are not given in this paper, the increase was from four- to eightfold (12 experiments) and the lag phase varied between 25 and 35 min in length. The enzyme synthesis always started immediately after the grafting and continued linearly throughout the lag phase.

DISCUSSION

In this investigation the synthesis of certain B_6 enzymes in *Escherichia coli* was studied during the lag phase of growth, which we have taken to be the first period of growth before cell division occurs. In previous works we established that the concentrations of vitamin B_6 and certain transaminases increase greatly in the cells during the lag phase [5,6].

It is a well-known fact that the enzyme content of cells depends on the growth conditions and on the composition of the medium in which the cells are grown before inoculation. Far less known is the fact that the enzymes are not formed at the same rate throughout the growth cycle. An extensive synthesis of enzymes important for catabolic reactions takes place during the late phases of growth. Gale [10] has divided the enzymes into two groups, those of type I active in the early, and those of type II active in the late phases of growth. Under type I he lists, for instance, arginine dehydrolases and the enzymes that

effect glycolysis, under type II decarboxylases, deaminases, and dehydrogenases. The cells employed in our experiments for inoculation were all taken towards the end of the exponential phase or during the retardation phase of growth. Immediately after the cells had been transferred again to the same inoculum medium, they began to grow without lag phase (*cf.* Hinshelwood [11]). Not only the growth phase of the cells but also the repression affects the amounts of enzymes in the cells. In a repression the end product inhibits the enzyme synthesis producing this product. *E. g.*, the amount of tryptophan synthetase produced during cell growth varies with the amount of tryptophan present in the medium as shown by Moyed and Friedman [12] and by Lester and Yanofsky [13] and also by Monod and Cohen-Bazire [14]. We have found in this laboratory that tryptophan inhibits the synthesis of tryptophan synthetase already during the lag phase even if it is added to the medium before the inoculation or during the lag phase of growth [15]. The amounts of amino acid decarboxylases [16–18], tryptophanase [19,20], and serine and threonine deaminases [21,22] increase in cells growing in a medium rich in amino acids. Hence the cells may for various reasons have stored a sufficient amount of enzymes even before the lag phase of growth. Accordingly, the cells do not then synthesize these enzymes during the active growth phases even when they need them for the anabolic reactions. This may be the case with threonine deaminase which is necessary for the biosynthesis of isoleucine.

The *E. coli* cells used as inoculum in our experiments grew in a medium rich in amino acids and vitamins which contained Bacto-tryptone and yeast extract in addition to glucose. The results obtained in this study support previous ones in that large amounts of the enzymes essential to the catabolism of amino acids were present in the cells. The fact that the amount of tryptophan synthetase is low is apparently due to the repression. Cysteine desulphhydrase, serine deaminase, and tryptophanase are enzymes which, as far as we know at present, are required only in the catabolism of amino acids. Therefore variations in the formation of these are not likely to occur at the beginning of the growth.

Threonine deaminase and homoserine deaminase again belong to those enzymes which are essential for both anabolic and catabolic reactions of amino acids; both are required for the biosynthesis of isoleucine. Apparently the cells synthesize the amounts of threonine deaminase and homoserine deaminase necessary for catabolic reactions already in the inoculum cells. Tryptophan synthetase is a purely anabolic enzyme, a fact which explains the large amounts of it that are found in the cells during the lag phase of growth.

REFERENCES

1. Topley, W. W. C. and Wilson, G. S. *The Principles of Bacteriology and Immunology*, 2nd ed., London 1944, p. 67.
2. Mc Garty, B. J. *Proc. Roy. Soc.* B **150** (1959) 410.
3. Rowbury, R. J. and Woods, D. D. *J. Gen. Microbiol.* **24** (1961) 129.
4. Corini, L. and Maas, W. K. *Biochim. et Biophys. Acta* **25** (1957) 208.
5. Nurmikko, V. and Raunio, R. *Acta Chem. Scand.* **15** (1961) 856.
6. Nurmikko, V. and Raunio, R. *Acta Chem. Scand.* **15** (1961) 1263.
7. Friedemann, T. E. and Haugen, G. E. *J. Biol. Chem.* **147** (1943) 415.

8. Gunsalus, I. C., Galeener, C. C. and Stamer, J. R. in Colowick and Kaplan, *Methods in Enzymology*, Acad. Press, N.Y. Vol. **2** (1955) 238.
9. Yanofsky, C. in Colowick and Kaplan, *Methods in Enzymology*, Acad. Press, N.Y. Vol. **2** (1955) 233.
10. Gale, E. F. *The Chemical Activities of Bacteria*, Univ. Tutorial Press, 3rd ed., London 1951, p. 78.
11. Hinshelwood, C. N. *The Chemical Kinetics of Bacterial Cell* Oxford Univ. Press, Oxford 1946.
12. Moyed, H. S. and Friedman, M. *Science* **129** (1959) 968.
13. Lester, G. and Yanofsky, C. *J. Bacteriol.* **81** (1961) 81.
14. Monod, J. and Cohen-Bazire, G. *Compt. rend.* **236** (1953) 530.
15. Nurmikko, V. and Raunio, R. *(Unpublished)*
16. Gale, E. F. *Advances in Enzymol.* **6** (1946) 1.
17. Sehr, I. H. and Mallette, M. F. *Arch. Biochem. Biophys.* **52** (1954) 331.
18. Haughton, B. and King, H. K. *Biochem. J.* **69** (1958) 48 P.
19. Freundlich, M. and Lichstein, H. C. *J. Bacteriol.* **80** (1960) 633.
20. Boyd, W. L. and Lichstein, H. C. *J. Bacteriol.* **69** (1955) 584.
21. Boyd, W. L. and Lichstein, H. C. *J. Bacteriol.* **69** (1955) 545.
22. Pardee, A. B. and Prestidge, L. S. *J. Bacteriol.* **70** (1955) 667.
23. Nurmikko, V. and Laaksonen, S. *Suomen Kemistilehti* B **34** (1961) 7.

Received October 6, 1961.

ACTA CHEMICA SCANDINAVICA 16 (1962) 719–734

Equilibrium Studies on Polyanions

9. The First Steps of Acidification of Chromate Ion in 3 M $Na(ClO_4)$ Medium at 25° C

YUKIYOSHI SASAKI

Department of inorganic chemistry, Royal Institute of Technology, Stockholm 70, Sweden

Emf data (glass electrode, 25°C, 3 M $Na(ClO_4)$) on the reaction of CrO_4^{2-} with H^+ indicated the two products $HCrO_4^-$ and $Cr_2O_7^{2-}$ but gave no evidence for other products, for $[H^+] < 0.03$ M. Spectrophotometric data, with the same medium, gave practically the same equilibrium constants.

	Emf	spectra
$H^+ + CrO_4^{2-} \rightleftharpoons HCrO_4^-$, $\log \beta_{11} = \log K_1 =$	5.89 ± 0.02	5.91 ± 0.01
$2HCrO_4^- \rightleftharpoons Cr_2O_7^{2-} + H_2O$, $\log K_{22} =$	2.20 ± 0.02	2.18 ± 0.08

For higher acidities, both spectrophotometric and emf data gave small deviations which might be due to new complexes.

In two previous investigations [1,2] equilibrium studies of the acidification of WO_4^{2-} and MoO_4^{2-} have been made. In both cases rather complicated equilibria were encountered, the first product being a complex with 6 W, or 7 Mo atoms. According to the literature one might expect much simpler reactions on acidification of CrO_4^{2-} with the dichromate ion, $Cr_2O_7^{2-}$, predominating over a wide range.

The present work on CrO_4^{2-} —H^+ equilibria was started with the aim of determining, by the methods developed in this laboratory, the formulas of the complexes formed and the equilibrium constants for their formation. Unusually enough, the results confirmed those of most previous work on the subject.

It was further thought to be of value to compare, in this relatively simple system, the results that could be obtained with the emf and spectrophotometric methods separately; for the wolframates and molybdates, accurate spectrophotometric studies had been made practically impossible by the occurrence of slow reactions, and by the disturbance from small amounts of silicate, respectively.

NOTATION

In analogy to previous work, we shall consider as reagents, H^+ and $B^{2-} = CrO_4^{2-}$. The concentrations of the free reagents are

$$[H^+] = h;\ [B^{2-}] = [CrO_4^{2-}] = b \tag{1}$$

The equilibrium constant for the formation of a complex H_pB_q (concentration c_{pq}) is called β_{pq}:

$$pH^+ + qB^{2-} \rightleftharpoons H_pB_q^{(2q-p)-};\ [H_pB_q] = c_{pq} = \beta_{pq}h^pb^q \tag{2}$$

(We shall often leave out the charge in the formula for H_pB_q.) For the complexes HB and H_2B_2 we have for instance:

$$H^+ + CrO_4^{2-} \rightleftharpoons HCrO_4^-;\ [HCrO_4^-] = c_{11} = \beta_{11}hb = K_1hb \tag{3}$$

$$2H^+ + CrO_4^{2-} \rightleftharpoons Cr_2O_7^{2-} + H_2O;\ [Cr_2O_7^{2-}] = c_{22} = \beta_{22}h^2b^2 \tag{4}$$

It should be noted that we consider H^+ to be the ligand whereas in the tables of stability constants [3] CrO_4^{2-} is the ligand, and H^+ the "metal", which means that the numbers p and q in (2) are reversed. Fortunately, in the two most important complexes $p = q$ so that the symbols $\beta_{11} = K_1$ and β_{22} will be the same.

We shall sometimes discuss the equilibrium:

$$2HB \rightleftharpoons H_2B_2;\ 2\,HCrO_4^- \rightleftharpoons Cr_2O_7^{2-} + H_2O;\ c_{22}c_{11}^{-2} = K_{22} = \beta_{22}\beta_{11}^{-2} \tag{5}$$

What we call K_{22} is denoted as $\dagger K_{22}$ in the tables of stability constants [3].

If, as usual, B is the total concentration of $B^{2-} = CrO_4^{2-}$, and Z the average number of H^+ bound per B^{2-}, then we have, from the law of mass action and the B and H balance

$$B = b + \Sigma q[H_pB_q] = b + \Sigma q\beta_{pq}h^pb^q \tag{6}$$

$$BZ = \Sigma p[H_pB_q] = \Sigma p\beta_{pq}h^pb^q \tag{7}$$

$$BZ = H - h \tag{8}$$

PREVIOUS WORK

The dichromate ion was one of the earliest, or perhaps the earliest polynuclear ion which, after the advent of the ionic theory, was proved to exist. As early as in 1888, Walden [4] and Ostwald [5] pointed out that the anomalous freezing-points and conductivities of aqueous solutions of CrO_3 could be explained by assuming $Cr_2O_7^{2-}$ as the predominating anion in the solutions. Starting with the work of Sherrill [6] and Spitalsky [7], about twenty papers have been published on the equilibria involving H^+ and CrO_4^{2-}. Usually, emf measurements (glass electrode [10,15–17]) and spectrophotometry [9,12,13,16,17] have been used, but freezing-point [6], conductance [6], vapor pressure [11], calorimetric [14], kinetic [8] and distribution [6] measurements have also been employed. A bibliography of work up to 1957 is given in Ref.[3]

Most of the authors, following Sherrill [6] and Spitalsky [7] find evidence for or presume, the presence of both $HCrO_4^-$ and $Cr_2O_7^{2-}$ (HB and H_2B_2).

For log K_1, eqn. (3), the values reported for 25°C and zero ionic strength agree well [3]: 6.50 (Neuss and Rieman [10] gl) 6.52 (Howard [16] *et al.*, sp, gl) 6.49 (Bailey [17] *et al.*, sp gl), if one neglects a stray value 7.00 from 1928.

For K_{22}, the range at 25°C, and $I = 0$ is somewhat broader: 1.26—1.36 (Stokes *et al.*[11], $p(H_2O)$); 1.64 (Neuss and Rieman [10], gl), 1.55 (Tong and King [13], sp) and 1.52 (Davies and Prue [12], sp).

As always, the activity correction for divalent ions is not as certain as one might wish (compare Güntelberg [18]).

Two species other than HB and H_2B_2 have also been assumed to exist, namely H_2B (H_2CrO_4) and H_3B_2 ($HCr_2O_7^-$). For the formation of H_2B, log $K(H^+ + HCrO_4^- \rightleftharpoons H_2CrO_4) = \log \beta_{21}\beta_{11}^{-1}$ has been given as 4.15 (Job [9], sp, 15°, dil); 0.74 (Neuss and Riemann [10] sp, gl, 25°, 0.16 (KCl)); −0.08 (Tong and King [13], sp, 25°, 1($LiClO_4$)); −0.98 (Bailey *et al.*[17], sp, gl, 25°).

For the formation of H_3B_2 we find the following values for log $K(H^+ + Cr_2O_7^{2-} \rightleftharpoons HCr_2O_7^-) = \beta_{32}\beta_{22}^{-1}$: 3.0 (Beck and Stegmüller [8], from Spitalsky [7], kin, 25°, dil); 0.07 (Tong and King [13], sp 25°, 1($LiClO_4$)); < 1.5 (Schwarzenbach and Meier [15], gl. 20°, 0.1 (KCl)).

As will be seen from the data in the following (*e.g.* Fig. 1), the formation of complexes with more than one H per B such as maybe H_2B or H_3B_2, occurs in a range of high acidity, well separated from the formation range of HB and H_2B_2.

From spectral measurements, Bailey *et al.*[17] have concluded that in concentrated H_2SO_4 there are also other Cr(VI) species, perhaps CrO_2^{2+}, than the H_2CrO_4 assumed by them.

CRYSTAL STRUCTURE

A number of chromates are isomorphous with corresponding sulfates and thus contain chromate groups CrO_4^{2-}. Crystal structure investigations have been made on K_2CrO_4, Na_2CrO_4, $CuCrO_4$, and $CaCrO_4$ (references in Ref.[20]). There seems little doubt that in solution, chromate(VI) is present in the form of tetrahedral CrO_4^{2-}.

Salts described as dichromates, tri- and tetrachromates have been prepared from acidified chromate solutions; if the solution is acidic enough, anhydrous CrO_3 will crystallize.

Byström and Wilhelmi[20] have shown by X-ray methods that $(NH_4)_2Cr_2O_7$(s) contains separate chromate groups, $Cr_2O_7^{2-}$, consisting of two tetrahedra sharing one corner, and Seiter [21] found that $(NH_4)_2Cr_3O_{10}$(s) contains groups $Cr_3O_{10}^{2-}$, also consisting of tetrahedra. Byström and Wilhelmi [19] had earlier found that anhydrous CrO_3(s) contains infinite chains of distorted CrO_4 tetrahedra, linked together by shared corners.

EMF DATA

Reagents and apparatus. Sodium chromate and sodium dichromate, p.a., were recrystallized from twice-distilled water under a stream of nitrogen. The stock solutions were standardized iodometrically; the result was checked by evaporating aliquot portions and weighing the residues.

Sodium perchlorate was prepared from sodium carbonate (Merck, p.a.) and perchloric acid (Kebo, p.a.) as described by Biedermann [22]. Solutions of perchloric acid, sodium hydroxide and silver perchlorate were prepared and standardized as usual in this laboratory (Ingri *et al.* [23]).

All solutions were made up so as to contain 3 M Na^+, with the balance ClO_4^-.

The cell was of the type:

—Ag, AgCl/0.01 M $AgClO_4$, 2.99 M $NaClO_4$/3 M $NaClO_4$/Cr(VI) solution/glass electrode +

Silver chromate electrodes were also used in preliminary experiments, with the aim of measuring $b = [CrO_4^{2-}]$; however, no stable potential was obtained in the acidified solutions.

The vessels for the salt bridge and the reference electrodes were, as usual, of the Wilhelm type [25]. The glass electrodes were Beckman 40498 or Jena H. Silver-silver chloride electrodes were prepared by Brown's method [24]. The cell was kept in an oil thermostat at 25° ± 0.1°C, placed in a 25° thermostat room. The emf of the cell was measured to 0.1 mV with a Radiometer PHM3 valve potentiometer.

Procedure. The experiments were carried out as emf titrations with a series of values for the total chromium concentration, B, between 0.080 and 0.001 M.

As usual, $[H^+] = h$ was calculated from the measured E, by means of the equation [26]

$$E = E_0 + 59.15 \log h - jh \qquad (9)$$

Then, Z was calculated from h and the analytically known B and H using (8).

The data (Figs. 1 and 2) show very clearly that there is a range in log h between −4 and −1.5 were Z is practically constant and = 1.0. The experimental range is thus divided into two separate regions, which can conveniently be treated, for maximum accuracy, in two different sets of experiments.

To study the range with $Z < 1$, H^+ was usually added to a CrO_4^{2-} solution (always keeping B constant and $[Na^+] = 3$ M). In these experiments E_0 and the constant j in $E_j = jh$ (9) could be obtained by adding more acid since for $H < 0.05$ M and $B < 0.08$ M, we could neglect the amount of additional protons bound beyond $Z = 1$. For $B = 0.08$ M, the approximation $h = H - B$ was no longer considered permissible, and E_0 and j were determined by an independent acid titration in 3 M $NaClO_4$ (without chromate), immediately after the chromate titration.

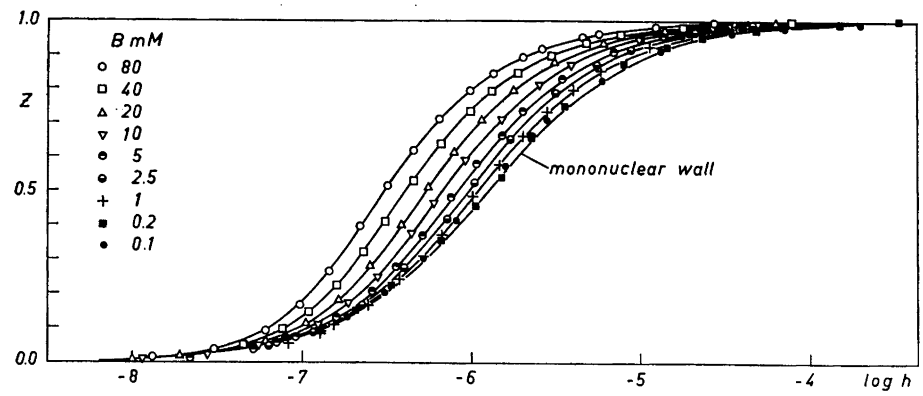

Fig. 1. Glass electrode data (Table 1). Z = average number of H^+ bound per CrO_4^{2-} as a function of log h = log $[H^+]$, for various total Cr(VI) concentrations B. Range with Z between 0 and 1 is given. Data for the more acidic range, with $Z > 1$, are given in Fig. 2.

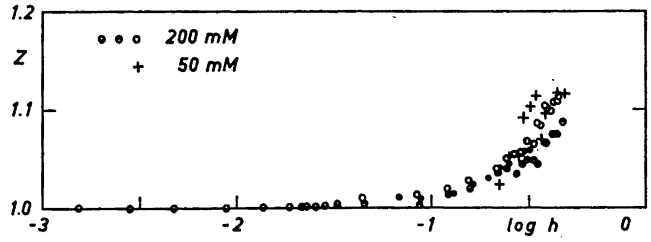

Fig. 2. Continuation of data, Fig. 1, into more acidic range (Table 2.)

For $B = 0.02$ M, a reverse titration was made; NaOH was added to a solution (of $Na_2Cr_2O_7$) initially with $Z = 1$. It fits well with the rest of the family of curves.

In order to study the equilibria with $Z > 1$, separate experiments were performed, starting with a solution with $Z = 1$ (made up using $Na_2Cr_2O_7$, and adding acid. E_0 and j were determined by separate acid titrations in 3 M $NaClO_4$ before and after the chromate titrations. The E_0 before and after sometimes differed by 0.3—0.5 mV and the average was used.

In the whole range of log h covered by the experiments in Fig 1, equilibrium seems to be attained instantaneously (or, to satisfy the kineticists, quicker than we could measure the emf). A few experiments were made with very low B values at $Z < 1$. However with $B \leq 0.0005$ M the emf drifted when log $h < -6$.

Treatment of emf data

The emf data are given in Tables 1 and 2; in Figs. 1 and 2 they are rendered in the form of a family of curves, Z (log $h)_B$.

For log $h < -8$, Z starts at 0, and CrO_4^{2-} is the predominant species. Between log $h = -8$ and -4, Z increases from 0 to 1, and then it remains practically constant up to log $h = -1{,}5$ where it again increases, approaching *ca.* -1.1 at log $h \approx -0.4$, the highest acidity used in the emf work.

We can be brief about the range between $Z = 0$ and 1. At least one polynuclear complex forms, since all the curves for various B do not coincide. In the wide range with $Z \sim 1$, the predominating complexes must have the general formula, $(HB)_n$. One of these must be HB since for low B the curves are seen to approach to a "mononuclear wall", which has the right shape to correspond to the equilibrium of B and BH.

The simplest assumption is that the only complexes present are B, HB and H_2B_2. It can be tested by means of normalized projection maps (Sillén [27]). Eqns. (6) and (7) take the special form

$$B = b + \beta_{11}hb + 2\beta_{22}h^2b^2 \quad (10a); \qquad BZ = \beta_{11}hb + 2\beta_{22}h^2b^2 \quad (10b)$$

Since we have only two equilibrium constants, both can be set equal to unity on normalizing so that the normalized equations are:

$$\mathbf{B} = v + uv + 2u^2v^2 \quad (11a); \qquad \mathbf{B}Z = uv + 2u^2v^2 \quad (11b)$$

We could thus draw the experimental data in the shape of projection maps log B(log $h)_Z$, and construct normalized projection maps log $\mathbf{B}$(log $u)_Z$ using (11), either with the program PROKA in a Ferranti-Mercury computer or

Table 1. Glass electrode data. Corresponding values of Z and $-\log h$.

$B = 0.08206$ M. Z, $-\log h$; 0.012, 7.880; 0.024, 7.655; 0.035, 7.521; 0.047, 7.364; 0.069, 7.310; 0.092, 7.217; 0.113, 7.148; 0.140, 7.077; 0.166, 7.016; 0.192, 6.967; 0.217, 6.921; 0.265, 6.840; 0.311, 6.773; 0.355, 6.710; 0.398, 6.656; 0.439, 6.597; 0.478, 6.544; 0.516, 6.494; 0.552, 6.445; 0.587, 6.394; 0.620, 6.343; 0.652, 6.296; 0.683, 6.242; 0.713, 6.191; 0.743, 6.135; 0.771, 6.075; 0.798, 6.015; 0.824, 5.949, 5.877; 0.874, 5.794; 0.897, 5.701; 0.921, 5.586; 0.954, 5.349; 0.965, 5.250; 0.986, 4.912; 0.996, 4.570;

$B = 0.03964$ M. Z, $-\log h$; 0.012, 7.816; 0.024, 7.589; 0.036, 7.435; 0.048, 7.344; 0.060, 7.275; 0.071, 7.211; 0.095, 7.113; 0.117, 7.036; 0.145, 6.959; 0.172, 7.037; 0.145, 6.959; 0.172, 7.037; 0.224, 6.793; 0.273, 6.708; 0.321, 6.636; 0.367, 6.568; 0.410, 6.509; 0.492, 6.396; 0.532, 6.340; 0.569, 6.289; 0.640, 6.181; 0.673, 6.125, 0.705, 6.068; 0.736, 6.012; 0.766, 5.946; 0.795, 5.880; 0.823, 5.813; 0.849, 5.731; 0.876, 5.646; 0.901, 5.537; 0.926, 5.409; 0.938, 5.331; 0.949, 5.235; 0.961, 5.126; 0.972, 4.983; 0.983, 4.756; 0.994, 4.381; 0.998, 4.112;

* $B = 0.01989$ M. Z, $-\log h$; 0.007, 8.004; 0.015, 7.718; 0.030, 7.479; 0.045, 7.324; 0.060, 7.214; 0.075, 7.139; 0.111, 6.976; 0.146, 6.868; 0.180, 6.783; 0.214, 6.715; 0.247, 6.651; 0.279, 6.597; 0.341, 5.601; 0.400, 6.413; 0.457, 6.332; 0.512, 6.254; 0.564, 6.179; 0.616, 6.102; 0.664, 6.021; 0.711, 5.943; 0.755, 5.855; 0.978, 5.758; 0.839, 5.644; 0.880, 5.514; 0.899, 5.434; 0.918, 5.339; 0.937, 5.225; 0.955, 5.076; 0.973, 4.869; 0.990, 4.515; 0.997, 4.217;

$B = 0.01004$ M. Z, $-\log h$; 0.005, 7.949; 0.009, 7.767; 0.018, 7.562; 0.028, 7.434; 0.037, 7.329; 0.046, 7.253; 0.068, 7.099; 0.090, 6.988; 0.111, 6.903; 0.132, 6.835; 0.152, 6.776; 0.172, 6.724; 0.210, 6.638; 0.247, 6.565; 0.317, 6.446; 0.380, 6.357; 0.466, 6.215; 0.543, 6.103; 0.590, 6.032; 0.634, 5.965; 0.675, 5.897; 0.713, 5.825; 0.749, 5.757; 0.783, 5.670; 0.815, 5.598; 0.845, 5.515; 0.874, 5.417; 0.901, 5.307; 0.950, 5.003; 0.962, 4.896; 0.973, 4.756; 0.978, 4.673; 0.983, 4.575; 0.987, 4.452; 0.992, 4.314;

$B = 0.005095$ M. Z, $-\log h$; 0.009, 7.670; 0.018, 7.522; 0.027, 7.383; 0.036, 7.287; 0.045, 7.213; 0.054, 7.153; 0.063, 7.097; 0.072, 7.040; 0.089, 6.960; 0.165, 6.869; 0.130, 6.802; 0.167, 6.683; 0.207, 6.589; 0.244, 6.514; 0.279, 6.446; 0.312, 6.392; 0.373, 6.291; 0.437, 6.198; 0.486, 6.122; 0.535, 6.046; 0.582, 5.973; 0.624, 5.906; 0.665, 5.826; 0.702, 5.969; 0.738, 5.701; 0.771, 5.630; 0.802, 5.556; 0.833, 5.469; 0.862, 5.375; 0.887, 5.275; 0.913, 5.165; 0.925, 5.101; 0.936, 5.038; 0.959, 4.869; 0.970, 4.771; 0.981, 4.653; 0.987, 4.587; 0.992, 4.371;

$B = 0.002554$ M. Z, $-\log h$; 0.039, 7.263; 0.045, 7.197; 0.053, 7.126; 0.062, 7.060; 0.071, 7.013; 0.088, 6.932; 0.098, 6.846; 0.128, 6.761; 0.148, 6.698; 0.167, 6.641; 0.186, 6.590; 0.205, 6.546; 0.241, 6.467; 0.275, 6.397; 0.309, 6.337; 0.370, 6.232; 0.421, 6.142; 0.479, 6.058; 0.529, 5.985; 0.574, 5.909; 0.617, 5.840; 0.656, 5.775; 0.728, 5.646; 0.792, 5.504; 0.848, 5.346; 0.876, 5.265; 0.898, 5.167; 0.921, 5.059: 0.943, 4.934; 0.952, 4.856; 0.962, 4.766; 0.971, 4.680; 0.978, 4.575; 0.991, 4.342;

$B = 0.001019$ M. Z, $-\log h$; 0.054, 7.080; 0.067, 7.006; 0.089, 6.898; 0.109, 6.810; 0.150, 6.666; 0.169, 6.607; 0.207, 6.506; 0.243, 6.423; 0.309, 6.286; 0.374, 6.174; 0.432, 6.079; 0.485, 5.993; 0.534, 5.914; 0.580, 5.840; 0.623, 5.762; 0.663, 5.694; 0.736, 5.551; 0.798, 5.400; 0.855, 5.243; 0.880, 5.153; 0.904, 5.057; 0.925, 4.947; 0.945, 4.826; 0.961, 4.697; 0.974, 4.553; 0.984, 4.422;

* A reverse titration.

Table 2. Glass electrode data for more acidic range with $Z > 1$. Z as a function of log h. Four independent titrations for $B = 0.2024$ and for $B = 0.05$ M.

B = 0.2024 M. Z, $-\log h$; 0.999, 3.319; 1.000, 3.071; 1.000, 2.917; 1.000, 2.813; 1.000, 2.735; 1.000, 2.672; 1.000, 2.557; 1.000, 2.483; 1.000, 2.325; 1.000, 2.214; 1.001, 2.059; 1.001, 1.950; 1.002, 1.869; 1.002, 1.800; 1.002, 1.722; 1.002, 1.661; 1.002, 1.595; 1.003, 1.546; 1.004, 1.504; 1.005, 1.470;

1.013, 1.168; 1.010, 1.046; 1.015, 0.889; 1.026, 0.786; 1.032, 0.706; 1.042, 0.647; 1.046, 0.596; 1.055, 0.556; 1.059, 0.521; 1.059, 0.488;

1.005, 1.344; 1.008; 1.059; 1.015, 0.906; 1.021, 0.799; 1.036, 0.661; 1.042, 0.610; 1.036, 0.564; 1.045, 0.530; 1.050, 0.500; 1.050, 0.473; 1.045, 0.446; 1.069, 0.409; 1.076, 0.377; 1.076, 0.348; 1.088, 0.326;

1.011, 1.3505; 1.014, 1.066; 1.020, 0.909; 1.029, 0.803; 1.041, 0.663; 1.051, 0.613; 1.056, 0.571; 1.057, 0.534; 1.069, 0.505; 0.066, 0.476; 0.087, 0.456; 0.085, 0.434; 0.105, 0.417; 0.100, 0.382; 0.108, 0.368; 0.110, 0.354; 0.115, 0.343;

B = 0.0500 M. Z, $-\log h$; 1.018, 0.789; 1.024, 0.649; 1.052, 0.600; 1.054, 0.558; 1.092, 0.524; 1.104, 0.493; 1.114, 0.466; 1.070, 0.439; 1.096, 0.469; 1.100, 0.400; 1.126, 0.384; 1.108, 0.367; 1.174, 0.355; 1.166, 0.318;

explicitly by eliminating v from (11a) and (11b). If the maps can be made to fit in some position, one may deduce (12a) and (12b), by comparing (10) and (11) term by term (see also (5)):

$$\log u - \log h = \log\beta_{11} \tag{12a}$$

$$\log \mathbf{B} - \log B = \log \beta_{22} - 2 \log \beta_{11} = \log K_{22} \tag{12b}$$

As a matter of fact, the fit of the experimental and normalized projection was perfect, within the limits of error. Such a good fit over a concentration range of B in the ratio 80:1 would not be likely if the main products had been other than those assumed, HB and H_2B_2. We may even state that there was no evidence for any more complexes. From the position of best fit we obtained the following equilibrium constants,

$$\left.\begin{array}{l} H + B \rightleftharpoons HB; \quad H^+ + CrO_4^{2-} \rightleftharpoons HCrO_4^-; \quad \log \beta_{11} = 5.89 \pm 0.02 \\ 2HB \rightleftharpoons H_2B_2; \quad 2HCrO_4^- \rightleftharpoons Cr_2O_7^{2-} + H_2O; \log K_{22} = 2.20 \pm 0.02 \\ 2H + 2B \rightleftharpoons H_2B_2; 2H^+ + 2CrO_4^{2-} \rightleftharpoons Cr_2O_7^{2-} + H_2O; \log\beta_{22} = 13.98 \pm 0.04 \end{array}\right\} \tag{13}$$

In Fig. 1, the full-drawn curves Z (log $h)_B$ were calculated using the constants in (13); the agreement is as good as might be desired.

Thus we are in the unusual position — for a system with polynuclear complex formation — to have confirmed the practically unanimous conclusion of previous workers as to which complexes are present, and neither to have found evidence for any new complex nor to have disproved earlier evidence for any complex in this range.

The new values (13) for the equilibrium constants are in reasonable agreement with older values considering the difference in ionic medium.

Data for $Z > 1$. The data in Fig. 2 indicate that at high acidities Z goes beyond 1, so that some new product besides HB and H_2B_2 must be formed. However, the accuracy does not permit us to say whether or not Z(log h) is

independent of B in this range. Only data for $B = 0.200$ M and $B = 0.050$ M are available, since for lower B, h was too large as compared with $B(Z-1)$ for an accurate determination of Z.

If the data are significant and independent of B, we may compare the data for $B = 0.2$ M with a normalized curve for the attraction of a single proton and one of the species (mostly H_2B_2) present at $Z = 1$; the association constant is found to be less than $10^{0.6}$.

Thus we would have $\log K(H^+ + Cr_2O_7^{2-} \rightleftharpoons HCr_2O_7^-) \leqq 0.6$, or possibly $\log K(H^+ + HCrO_4^- \rightleftharpoons H_2CrO_4) \leq 1.2$.

However, there are some doubts about the right functioning of the glass electrode in chromic acid solutions.

MacInnes and Longworth [28] found that "at least temporary errors can arise from the use of dehydrating agents, such as chromic acid solution or alcohol, in cleaning the electrodes. Accurate pH values of strongly dehydrating solutions can therefore not be obtained".

Another possible source of error was reported by MacInnes and Belcher [29]. According to them, the glass electrode gives appreciable deviations from the hydrogen electrode showing too high values at pH's lower than 2, and the magnitude of the error depends on the pH, the nature of the anion present and its concentration.

In consequence, a glass electrode calibrated using (9) in perchlorate medium may give low h values in presence of for instance sulfate or phosphate (*cf.* Ref.[29], Fig. 4). In a similar way, our present measurements of h and Z at $Z > 1$ may have been affected by the chromate anions.

Still the values above 0.6 and 1.2 for the two equilibrium constants would remain their maximum values which would correspond to the (unlikely) assumption that the effect of the chromate anion on the glass electrode can be neglected.

Additional data are needed before any certain conclusion can be drawn regarding this region.

SPECTROPHOTOMETRIC DATA

General

Suppose that light of a specified wave length λ passes through a cell of length l containing a solution of total chromate concentration B. In a spectrophotometer one measures by comparison with a blank the ratio between the intensity I, of light that actually passes, and that, I_0, of light that would have passed if no chromate had been present. Ascribing all the difference to the various chromate species, we have the following relationship between the total absorbance A, of the cell and the apparent molar extinction, ε of chromate;

$$A = \log (I_0/I)_\lambda = lB\varepsilon_\lambda \tag{14}$$

We may ascribe to each species: free B (concentration b) and complex H_pB_q (concentration c_{pq}) a molar extinction coefficient, ε_{01} or ε_{pq} which is a function of λ. Leaving out, for brevity the suffix λ, we find

$$B\varepsilon = b\varepsilon_{01} + \Sigma\varepsilon_{pq}c_{pq} = b\varepsilon_{01} + \Sigma\varepsilon_{pq}\beta_{pq}h^p b^q \tag{15}$$

From data $\varepsilon\ (h, B)_\lambda$, one may try to deduce those values for the various molar extinctions ε_{pq} and the equilibrium constants β_{pq} that will give a good agreement with the data. One has more unknown constants to determine than with emf work, but on the other hand one can use a number of wavelengths λ, each of which gives a different set of ε_{pq}, but which ought to give the same values for the equilibrium constants β_{pq}.

The spectrophotometric method can give an independent check on the emf data. Unexpected variations in the activity factors, for instance, might perhaps influence all thermodynamic methods (freezing-point data, extraction equilibria, emf, solubility) and lead to the same erroneous conclusions. The spectra are not likely to be influenced in exactly the same way by variations in the medium.

In general, the emf method has the advantage of covering many more powers of ten in the concentrations of some species; however, in favorable cases, spectrophotometric measurements may help one to measure strongly absorbing species even at very low concentrations.

The data to be presented on the chromate equilibria might be construed as an independent logical proof of the formulas of the complexes present. This may hold true in this relatively simple system (notwithstanding that one has to take log h, and the formula of the first complex, from emf data). However, one should be cautious about generalizing this result. Especially in more complicated systems with polynuclear equilibria, it seems that the usual accuracy of spectrophotometric work does not enable one to distinguish between several possible mechanisms. It is a sobering thought to consider the explanations one might need to invent if on first sight the spectrophotometric data were incompatible with the conclusions drawn from the emf data. For instance, the molar extinctions may themselves sometimes be subject to an unpleasant medium effect which may be mistaken for a chemical reaction.

To sum up, it may be a useful check on the emf results to make a spectrophotometric study of the system whenever this is possible. If the spectral data can be quantitatively explained with the species deduced from the emf data, if they can be used for an independent determination of the equilibrium constants and if this gives the same values, within the limits of error, then one may feel much more certain about the species deduced, and the equilibrium constants. If spectrophotometric and emf data disagree, this gives food for thought.

Experimental

All solutions were made up to contain 3 M $Na(ClO_4)$, as in the emf work. The same emf equipment was used as above to determine log h in the various solutions.

A Hilger Uvispec spectrophotometer was used, with fused quartz cells of thickness 0.1 (only in preliminary experiments), 0.5, 1.0, 2.0, and 4.0 cm. The absorbancy A_λ was read directly to $\pm$ 0.001 unit.

All the measurements were made in a 25°C thermostat room. The temperature in the cell housing was often checked; it proved to keep within 25.0$\pm$0.5°C.

For measurement, one cell was filled with a chromate solution, and another cell, with the same l, with a blank solution, 3 M $NaClO_4$ (in one set of experiments + 0.001 M $HClO_4$). The relative absorbancy A_λ was measured twice, with the cells interchanged, and the average of the two values (they never differed by more than $\pm$ 0.003) taken as the absorbancy of the sample.

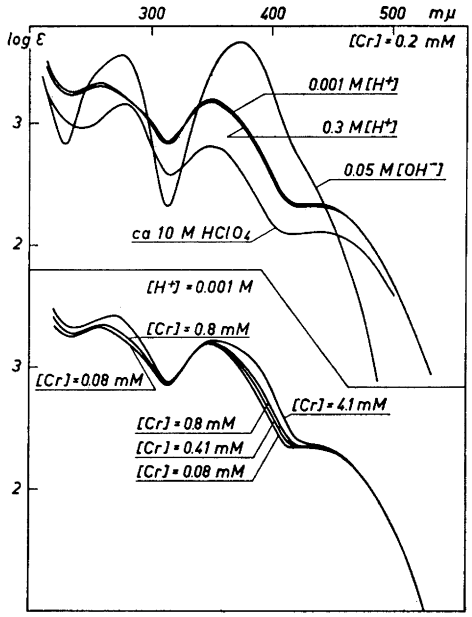

Fig. 3. Spectrophotometric data with constant $B = 0.0002$ M and varying h: log $\varepsilon(\lambda)$ given for 0.05 M OH^- and for h = 0.001, 0.3, and 10 M.

Fig. 4. Spectrophotometric data with constant $h = 0.001$ M and varying B: log $\varepsilon(\lambda)$ given for B = 0.08, 0.41, 0.8 and 4.1 mM.

To determine l, a pair of 1.0 cm cells was arbitrarily chosen as standard ($l = 1.000$ cm). The other sets of cells were calibrated against these for a number of wavelengths, using the same chromate solution and assuming ε to be independent of l in eqn. (14).

Preliminary experiments

In order to find suitable conditions for studying the equilibria, the absorption was studied between $\lambda = 2\,200$ and $5\,500$ Å, with intervals of 20 to 100 Å, first with $B = 0.0002$ M and varying h (Fig. 3), then with $h = 0.001$ M and varying B (Fig. 4). Some typical curves, recalculated to the form log ε (λ) are given in Figs. 3 and 4. In these preliminary experiments, the slit width was adjusted to keep the band width always ≤ 5 Å. The accuracy in Fig. 3 was not so good at $\lambda < 2\,500$ Å, and carbonate was probably present.

In the experiments with small and constant B, a solution that contained 0.05 M OH^- gave practically the same log $\varepsilon(\lambda)$ curve as a neutral Na_2CrO_4 solution. Hence, this curve is likely to be due to CrO_4^{2-}. When the solution was acidified, the curves at first shifted with h; however, for $h = 0.001$ and 0.1 the curve was practically the same; this corresponds to the region with $Z = 1$ from the emf data. For $h = 0.3$ M a small change was noted and in 10 M $HClO_4$ (the only solution used that did not contain 3 M $Na(ClO_4)$), a much lower curve was obtained, indicating new species.

Table 3. Determination of the extinction coefficient in 2.900 M $NaClO_4$, 0.05 M $HClO_4$ medium.

λ = 3740 Å, l = 0.508 cm, slit width 0.19 mm

B, mM	A	ε
0.1001	0.238	4670
0.1501	0.357	4680
0.2002	0.478	4690
0.2502	0.594	4670
0.3003	0.709	4640
0.4004	0.938	4600
0.5005	1.149	4510
0.6006	1.349	4410

λ = 3740 Å, l = 2.00 cm, slit width 0.19 mm

B, mM	A	ε
0.020	0.188	4700
0.040	0.375	4680
0.060	0.561	4660
0.080	0.743	4630
0.100	0.920	4600

λ = 2740 Å, l = 0.508 cm, slit width 0.5 mm

B, mM	A	ε
0.1001	0.191	3750
0.2002	0.378	3720
0.3003	0.568	3720
0.5005	0.944	3710
0.6006	1.132	3710

The experiments with constant h were made at $h = 0.001$ M, which is within the constant range in Fig. 3, or the shelf at $Z = 1$ in Figs. 1 and 2. When B is increased from 0.00008 to 0.004 M, log ε increases, especially around 2 700—2 900 Å and 3 700—4 100 Å, indicating the formation of new species.

Interference of carbonate. The carbonate ion CO_3^{2-} has a certain absorption at low wavelengths, so that CO_2 must be avoided. For instance, in 0.05 M OH^-, the addition of 0.001 M CO_3^{2-} increased A_λ by 0.019 at 2 250 Å, by 0.008 at 2 300 Å, and by 0.006 at 2 400 Å.

Determination of ε_{01}

In the following, more accurate measurements, it was decided to work at 3 740 Å, since at this wavelength the changes in ε were especially great.

At first, A_λ was measured for solutions with 0.050 M OH^- and B from 0.00002 to 0.0006 M. The results are given in Table 3. It was checked for the lowest B that A_λ did not change during three days. Since these solutions are likely to contain only $B^{2-} = CrO_4^{2-}$, we have here $\varepsilon = \varepsilon_{01}$.

For $\lambda = 2\,740$ Å we find $\varepsilon_{01} = 3\,720 \pm 10$, with practically no trend, up to $A_\lambda = 1.1$. For 3 740 Å, on the other hand, a trend in ε is observed. By comparing the data with different cell-widths we can see that ε is a function of A_λ and not of B, and that it keeps practically constant at $4\,680 \pm 10$ for $A_\lambda < 0.6$. Hence it seems that the apparatus does not work linearly for the largest A_λ values.

Similar results were obtained at 4 000 Å: for $A_\lambda < 0.6$, the variations in ε were less than what corresponds to ± 0.001 in A_λ.

Determination of $\beta_{11} = K_1$

These experiments were carried out as alkali titrations, with the same apparatus as in the emf work. We started with a solution with $B = 0.0001$ or 0.0002 M, and $h = 0.001$ M adding equal volumes of an NaOH solution and a solution with double ($2B$) Cr content, to keep B constant. Nitrogen was bubbled through the titration vessel. After each addition, log h was determined using a glass electrode, and then a few ml of the solution were pipetted into a spectrophotometric cell and A_λ determined with 0.19 mm slit width at 3 740 Å, a top of the curve $\varepsilon(\lambda)$.

Stable values were obtained for log h between -3 and -6.6; at lower values for log h, ε began to drift, probably because CO_2 had not been completely excluded from the cell-housing and was absorbed in the solutions, which had a very low buffer capacity.

Table 4 gives corresponding values of log h and ε for $B = 0.1$ and 0.2 mM. In a plot ε(log h), the data for the two B values are seen almost to coincide indicating that we have homonuclear complexes; since one of them is $B^{2-} = CrO_4^{2-}$, they must be mononuclear.

With the assumption that only B and HB need be considered (15), (6) and (7) take the form

$$B\varepsilon = b\varepsilon_{01} + \varepsilon_{11}\beta_{11}hb$$

$$B = b + \beta_{11}hb;\ BZ = \beta_{11}hb$$

By elimination we find

$$Z = (\varepsilon_{01}-\varepsilon)/(\varepsilon_{01}-\varepsilon_{11}) \quad (16)$$

$$\beta_{11} = h^{-1}\ (\varepsilon_{01}-\varepsilon)/(\varepsilon-\varepsilon_{11}) \quad (17)$$

Table 4. Spectrophotometric data, 3 740 Å; corresponding values of $-\log h$, ε.

B = 0.0985 mM. $-\log h$, ε, 3.022, 949; 3.176, 949; 3.483, 964; 3.715 *, 984; 4.151, 1 025; 4.151 *, 1 015; 4.469, 1 096; 4.881 *, 1 279; 5.229 *, 1 593; 5.471, 1 878; 5.520, 2 010; 5.562, 2 050; 5.647, 2 182; 5.807, 2 507; 5.951, 2 822; 6.090, 3 116; 6.286, 3 532; 6.519, 3 908; 6.737, 4 192; 8.801, 4 690; 9.065, 4 690;

B = 0.1970 mM. $-\log h, \varepsilon$; 3.057, 979; 3.238, 979; 3.492, 1 000; 3.696, 994; 3.833, 994; 4.165, 1 030; 4.320, 1 055; 4.636, 1 142; 4.848, 1 253; 5.101, 1 436; 5.216, 1 563; 5.333, 1 710; 5.463, 1 888; 5.655, 2 238; 5.826, 2 664; 5.980, 2 959; 6.187, 3 350; 6.482, 3 847; 6.690, 4 121; 6.901, 4 350; 7.107, 4 421; 8.912, 4 700; 9.131, 4 700; 9.391, 4 700;

* Values obtained by a reverse titration.

Table 5. Spectrophotometric data. Solutions with $h = 0.001$ M, and varying B.

4 000 Å, slit width = 0.05 mm; 1 000 *B*, ε; 0.0997, 334.0; 0.1470, 343.5; 0.1991, 368.0; 0.3972, 385.6; 0.4972, 404.2; 0.5965, 414.9; 0.6979, 427.7; 0.8968, 448.2; 0.9929, 458.2; 1.091, 467.5; 1.191, 482.0; 1.293, 483.1; 1.388, 492.8; 1.491, 497.3; 1.586, 505.6; 1.789, 518.7; 1.991, 532.9;

3 900 Å, slit width = 0.05 mm; 1 000 *B*, ε; 0.1042, 507.2; 0.1871, 532.0; 0.2989, 558.7; 0.3976, 588.5; 0.4989, 611.0; 0.5788, 628.8; 0.6058, 638.8; 0.6767, 647.2; 0.7918, 674.4; 0.9422, 700.4; 0.9939, 705.3; 1.085, 720.7; 1.188, 734.8; 1.291, 749.8; 1.498, 771.0; 1.578, 781.3; 1.684, 793.6;

Values for Z and $\log \beta_{11}$ may be calculated from (16) and (17), setting $\varepsilon_{01} = 4\,700$ and $\varepsilon_{11} = 979$ for 0.2 mM and 949 for 0.2 mM; the latter is the limiting value around $Z = 1$. As an average from the middle range, or from curvefitting we may conclude $\log \beta_{11} \approx 5.9$.

Assuming the main product to be H_2B, and again applying (6), (7) and (15), gave no agreement. If one assumes that both H_2B and HB are present, with $\beta_{11}^2/\beta_{21} = 4$, one might explain the data $\varepsilon(\log h)$, but this would make no sense with the previous emf data.

Determination of β_{22}

A series of solutions with B from 0.0001 M to 0.002 M, all with $h = 0.001$ M, were prepared in 50 ml measuring flasks and kept in the thermostat room for 24 h. Then, measurements were made at 3 900 and 4 000 Å, where $\log \varepsilon$ changes most with B (see Fig. 4). The cell was chosen so as to keep A_λ between 0.15 and 0.6. A_λ was also determined at 3 740 Å, for use in the refinement of the equilibrium constants. It was noted that the absorbance crept for 1 or 2 h before a constant value was obtained.

The data for 3 900 and 4 000 Å are given in Table 5 as $\varepsilon(B)$ and in Fig. 5 as $\log \varepsilon$ $(\log B)_\lambda$.

The variation of ε with B shows that some polynuclear complexes are formed in addition to HB, which is present at $h = 0.001$ and low values for B. Separate experiments showed that ε did not change when $\log h$ was changed from -3.2 to -2.8, keeping B constant; hence their formula is $(HB)_n$.

Assuming that only one complex H_nB_n is formed, eqns. (15) and (6) take the forms:

$$B\varepsilon = \varepsilon_{11}\beta_{11}hb + \varepsilon_{nn}\beta_{nn}h^n b^n \qquad (15b)$$

$$B = \beta_{11}hb + n\beta_{nn}h^n b^n \qquad (6b)$$

We may normalize (15) and (6b) to the following form, removing all constants but one:

$$\mathbf{B}e = rv + v^n \qquad (18a); \qquad \mathbf{B} = v + nv^n \qquad (18b)$$

Eliminating v from (18a) and (18b), or better using it as an auxiliary variable, we may construct a family of curves $\log \varepsilon(\log \mathbf{B})_r$, and try to fit them to the experimental curve $\log e(\log B)$. From the best value of r and the shift between the experimental and normalized variables, at the position of best

fit, we may obtain the various constants by eqns. (19a—c), which may easily be derived, comparing (18) with (15b, 6b):

$$r = \varepsilon_{11}\varepsilon_{nn}^{-1} \quad (19a); \qquad \log\varepsilon - \log e = \log\varepsilon_{nn} \quad (19b)$$

$$\log B - \log \mathbf{B} = \tfrac{1}{n-1}\,(n \log\beta_{11} - \log\beta_{nn}) \quad (19c)$$

A good fit was obtained with $n = 2$ but not, for instance, with $n = 3$. From the position of best fit we calculated
$\log\varepsilon_{nn} = \log\varepsilon_{22} = 2.500 \pm 0.002$ at 4000 Å; 2.676 ± 0.002 at 3 900 Å
$\log\beta_{22} - 2\log\beta_{11} = \log K_{22} = 2.18 \pm 0.08$
$\log\varepsilon_{11} = 1.670 \pm 0.03$ at 4 000 Å; 1.846 ± 0.03 at 3 900 Å
The full-drawn curves for 4 000 Å and 3 900 Å in Fig. 5 are the normalized curves in the position of best fit (thus the calculated curves, $\log\varepsilon(\log B)$).

Refinement of β_{11}

In the treatment of the data at constant B we assumed that only B and HB are present. That this is a reasonable approximation is shown by the close proximity of the curves for $B = 0.1$ and 0.2 mM. Now that K_{22} is known, we may make a small correction for the amount of H_2B_2 present.

First of all, we need the molar extinctions ε_{11} and ε_{22} for 3 740 Å, which we obtain from the values for ε at $h = 0.001$ M at this wave length.

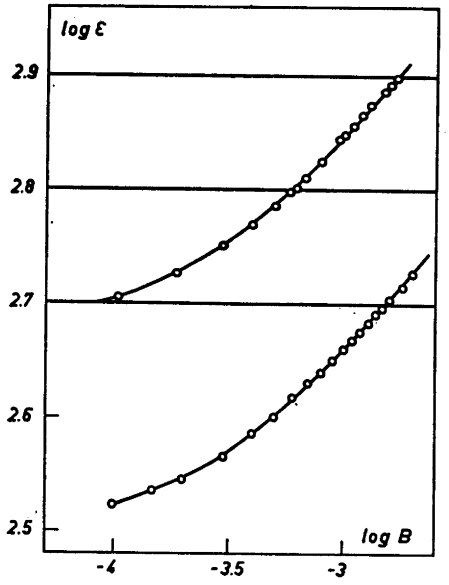

Fig. 5. Spectrophotometric data, $\log\varepsilon(\log B)$ for $h = 0.001$ M, at 3 900 and 4 000 Å.

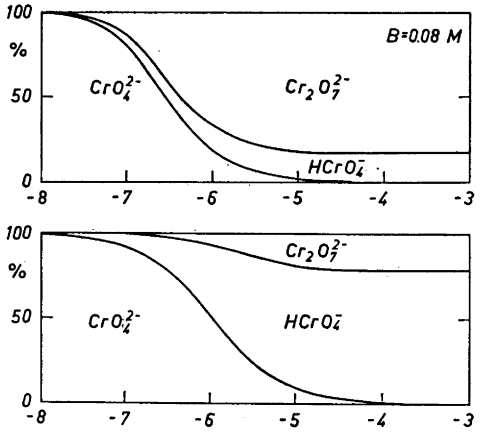

Fig. 6. Distribution of Cr(VI) over the complexes as a function of $\log h$, at two values for B (0.08 and 0.001 M).

Table 6. Calculation of Z and β_{11} from spectrophotometric data shown in Table 5.

$B = 0.09850$ mM			$B = 0.1970$ mM		
$-\log h$	Z	$\log \beta_{11}$	$-\log h$	Z	$\log \beta_{11}$
4.151	0.981	5.84	4.165	0.983	5.90
4.469	0.959	5.81	4.320	0.976	5.92
4.881	0.910	5.86	4.636	0.953	5.91
5.229	0.826	5.88	4.848	0.921	5.90
5.471	0.750	5.93	5.011	0.874	5.92
5.520	0.715	5.91	5.216	0.839	5.91
5.562	0.704	5.92	5.333	0.798	5.91
5.647	0.669	5.93	5.463	0.750	5.91
5.807	0.582	5.93	5.655	0.657	5.92
5.951	0.498	5.93	5.826	0.542	5.88
7.090	0.420	5.93	5.980	0.463	5.91
6.286	0.308	5.91	6.187	0.359	5.92
6.519	0.208	5.91	6.482	0.227	5.91
6.737	0.132	5.85	6.690	0.154	5.92
			6.901	0.093	5.89

At this acidity we need only consider HB and H_2B_2 so that

$$\varepsilon = \varepsilon_{11}c_{11} + \varepsilon_{22}c_{22} = \varepsilon_{11}c_{11} + \varepsilon_{22}K_{22}c_{11}^2 \qquad (20)$$

since $c_{22} = K_{22}c_{11}^2$ (eqn. 5). Knowing K_{22} we may for each point calculate c_{11} from $B = c_{11} + 2K_{22}c_{11}^2$, and then plot, *versus* c_{11}

$$\varepsilon/c_{11} = \varepsilon_{11} + \varepsilon_{22}K_{22}c_{11}$$

The intercept and slope give us $\varepsilon_{11} = 921$ and $\varepsilon_{22} = 1\,790$.

Now we can return to the refinement of β_{11}.

Since only B, HB and H_2B_2 need to be considered, we have $b = B(1-Z)$, and (15) and (7) take the form

$$B\varepsilon = \varepsilon_{01}B(1-Z) + \varepsilon_{11}c_{11} + \varepsilon_{22}K_{22}c_{11}^2 \qquad (20a)$$

$$BZ = c_{11} + 2K_{22}c_{11}^2 \qquad (20b)$$

In (20a) and (20b) we know B, ε, ε_{01}, ε_{11}, ε_{22}, and K_{22} so that only c_{11} and Z are unknown. By successive approximation (two steps suffice) we can find the small correction term $2K_{22}c_{11}^2$ in (20b), and then obtain an improved value for Z and β_{11}. The correction was negligibly small for $B = 0.1$ mM.

The improved values for Z, and the β_{11} calculated from $c_{11} = \beta_{11}Bh(1-Z)$ are given in Table 6. The final value is

$\log \beta_{22} = 5.91 \pm 0.01$.

CONCLUSION

We may summarize our results as follows:

		emf	spectra
$H^+ + CrO_4^{2-} \rightleftharpoons HCrO_4^-$	; $\log \beta_{11} = \log K_1 =$	5.89 ± 0.02	5.91 ± 0.01
$2HCrO_4^- \rightleftharpoons Cr_2O_7^{2-} + H_2O$	; $\log K_{22} =$	2.20 ± 0.02	2.18 ± 0.08
$2H^+ + 2CrO_4^{2-} \rightleftharpoons Cr_2O_7^{2-} + H_2O$	; $\log \beta_{22} =$	13.98 ± 0.04	14.0 ± 0.1

The agreement between the two methods is satisfactory, indicating that no large systematic errors were present in either of them.

As for the reactions in very acidic medium, where a new complex such as H_2CrO_4 or $HCr_2O_7^-$ may be formed, we would not like to draw any certain conclusion from the present emf or spectrophotometric data. The changes in spectra that are obtained with strongly acidic solutions may just as well be due to a medium effect as to the appearance of new species.

There seems to be more hope in an attack using conductiometric measurements, which is at present being made in collaboration with Dr. George Biedermann.

Acknowledgements. The author wishes to express his sincere gratitude to Professor L. G. Sillén for his suggestion of this work and for his valuable criticism.

This investigation has been sponsored in part by the *Air Force Office of Scientific Research of the ARDC, USAF*, through its European Office.

REFERENCES

1. Sasaki, Y. *Acta Chem. Scand.* **15** (1961) 175.
2. Sasaki, Y., Lindqvist, I. and Sillén, L. G. *J. Inorg & Nuclear Chem.* **2** (1959) 93; Sasaki, Y. and Sillén, L. G. *Acta Chem. Scand. To be published.*
3. Bjerrum, J., Schwarzenbach, G. and Sillén, L. G. *Stability constants II, Inorganic ligands, Chem. Soc. Spec. Publ.* **7** (1958).
4. Walden, P. *Z. physik. Chem.* **2** (1888) 49.
5. Ostwald, W. *Z. physik. Chem.* **2** (1888) 78.
6. Sherrill, M. S. *J. Am. Chem. Soc.* **29** (1907) 1641.
7. Spitalsky, E. *Z. anorg. Chem.* **54** (1907) 265.
8. Beck, K. and Stegmüller, P. *Arb. kaiserl. Gesundh.* **34** (1910) 446.
9. Job, P. *Compt. rend.* **186** (1928) 1546.
10. Neuss, J. D. and Rieman, W. III. *J. Am. Chem. Soc.* **56** (1934) 2238.
11. Stokes, R. H., Wilson, J. M. and Robinson, R. A. *Trans. Faraday Soc.* **37** (1941) 566.
12. Davies, W. G. and Prue, J. E. *Trans. Faraday Soc.* **51** (1955) 1045.
13. Tong, J. Y. and King, E. L. *J. Am. Chem. Soc.* **75** (1953) 6180.
14. Hepler, L. G. *J. Am. Chem. Soc.* **80** (1958) 6181.
15. Schwarzenbach, G. and Meier, J. *J. Inorg. & Nuclear Chem.* **8** (1958) 302.
16. Howard, J. R., Nair, V. S. K. and Nancollas, G. H. *Trans. Faraday Soc.* **54** (1958) 1034.
17. Bailey, N., Carrington, A., Lott, K. A. K. and Symons, M. C. R. *J. Chem. Soc.* **1960** 290.
18. Güntelberg, E. *Thesis*, Copenhagen 1937.
19. Byström, A. and Wilhelmi, K.-A. *Acta Chem. Scand.* **4** (1950) 1131.
20. Byström, A. and Wilhelmi, K.-A. *Acta Chem. Scand.* **5** (1951) 1003.
21. Seiter, E. D. *Thesis* 1957, Rutgers Univ., New Brunswick, N. J; Univ. Microfilms 22548.
22. Biedermann, G. *Arkiv Kemi* **9** (1956) 277.
23. Ingri, N., Lagerström, G., Frydman, M. and Sillén, L. G. *Acta Chem. Scand.* **11** (1957) 1034.
24. Brown, A. S. *J. Am. Chem. Soc.* **56** (1934) 646.
25. Forsling, W., Hietanen, S. and Sillén, L.G. *Acta Chem. Scand.* **6** (1952) 901.
26. Biedermann, G. and Sillén, L. G. *Arkiv Kemi* **5** (1953) 425.
27. Sillén, L. G. *Acta Chem. Scand.* **10** (1956) 803.
28. MacInnes, D. A. and Longworth, L. G. *Trans. Electrochem. Soc.* **71** (1937) 73.
29. MacInnes, D. A. and Belcher, D. *J. Am. Chem. Soc.* **53** (1931) 3315.

Received September 25, 1961.

ACTA CHEMICA SCANDINAVICA 16 (1962) 735–748

Studies on Metal Ion Co-ordination in Solution

I. The Complex Formation of Diphenylphosphinobenzene-*m*-sulphonate with Mercury

BJARNE SALVESEN* and JANNIK BJERRUM

Department of Inorganic Chemistry, University of Copenhagen, Copenhagen, Denmark

Ahrland, Chatt *et al* [1]. have extended studies of metal ion complex formation in aqueous solution to such co-ordinating atoms as arsenic and phosphorus. In this paper we have studied the complex formation of mercury(II) with diphenylphosphinobenzene-*m*-sulphonate (proposed by Chatt *et al.* as a water soluble phosphorus ligand). The complex formation of mercury ions was studied both with mercury and platinum electrodes at low metal and ligand concentrations (due to low solubilities of the complexes as well as of the ligand). It could be shown that mercury(I) ions do not form complexes in the region covered, and for mercury(II) it was found that the formation of a tetra-complex was finished at relatively small concentrations of the ligand. A »stop» in the formation curve for $\bar{n} = 1$ as well as for $\bar{n} = 2$ was remarkable. A complex salt of Hg(II) with diphenylphosphinobenzene-*m*-sulphonate (HgL_2) has been prepared. The following values for the complexity constants were determined in $\sim$ 0.01 M HNO_3, 1 M KNO_3 at 25°: $K_1 = 10^{14.3}$ l·mole^{-1}, $\beta_2 = 10^{24.6}$ l^2·mole^{-2}, $\beta_3 = 10^{29.7}$ l^3·mole^{-3}, $\beta_4 = 10^{33.0}$ l^4·mole^{-4}. The great stability of the mono-complex is in agreement with Ahrland and Chatt's findings for the silver(I) ion.

In their studies of the complex formation of silver(I) ions with various types of ligand Ahrland and Chatt *et al.* [1] distinguish between three main types of complex formation: (1) those (*e.g.* NH_3, CN^-, Cl^-, Br^-) which have a stop or inflection at $\bar{n} = 2$; (2) an intermediate type (sulphides, selenides) where the formation of complexes proceeds uniformly to $N = 4$; and (3) those (phosphines, arsines, I^-) with a stop or inflection at $\bar{n} = 1$ and $\bar{n} = 3$.

For mercury(II) ions only complex formation of type (1) with a very pronounced stop at $\bar{n} = 2$ has been examined hitherto. However, it is known that mercury seems to be unable to react with more than one ethylene molecule [2], and that mercury dialkyl and diaryl compounds are easily converted to

* Present address: Pharmaceutical Institute of the University, Blindern, Norway.

compounds in which mercury is attached to only one carbon atom [3]. This suggests that mercury in these compounds has the characteristic number one. Ahrland and Chatt suggest for silver(I) a connection between a high stability of the mono-complex and the possibility of the ligand to accept d-electrons from the metal forming a $d\pi$-bond. On this background it was interesting to see how mercury(II) behaves towards the sulphonated triphenylphosphine used by Chatt *et al.* as a water soluble phosphorus ligand.

NOTATION AND FUNDAMENTAL EQUATIONS.

We are considering the case where the concentration of a metal ion $[M^{\nu}]$ is determined in a constant ionic medium with an electrode of the same metal (Me) or with some other kind of electrode *. Denoting the total concentration of metal salt by (C_M) and the total concentration of complex-forming ligand by (C_L), a half-cell: $Me/C_M,C_L$ is defined. In the special case where $C_L = 0$, the concentration of »free» metal ion $[M^{\nu}]$ can by definition be set equal to C_M. Now combining a half-cell of this type: $Me/[M^{\nu}]_{C_L = 0}$ with a complex one of the same stoichiometrical metal salt concentration in the same ionic medium, we may write, if C_M and C_L are sufficiently small and polynuclear complexes are not formed:

$$E_M = \frac{RT}{\nu F} \ln X = \frac{RT}{\nu F} \ln \sum_0^N \beta_n [L]^n \tag{1}$$

The symbol E_M for the E.M.F. of such a cell as well as the function X were introduced by Fronæus [4], and it will be seen that X is the reciprocal of Bjerrum's [5] degree of formation (α_0) of the metal ion:

$$X = \frac{1}{\alpha_0} = \frac{C_M}{[M^{\nu}]} \tag{2}$$

β_n ($l^n \cdot mole^{-n}$) in (1) denotes the gross complexity constants:

$$\beta_n = K_1 \cdot K_2 \cdot \cdots K_n = \frac{[ML_n]}{[M^{\nu}][L]^n} \tag{3}$$

N denotes the maximum value for n and [L] the concentration of free ligand.

Now considering only the case of mononuclear complexes, it is easily seen that complex solutions of varying composition but with the same value of E_M are corresponding in the sense of Bjerrum [6]. This is tantamount to their having the same distribution of complexes as well as the same concentration of free ligand. In order to obtain the composition of such corresponding solutions Fronæus [4] plotted C_L *versus* the experimentally determined value of E_M for various values of C_M. The concentration of the free ligand is then obtained from a plot of C_L *versus* corresponding C_M values as the value of C_L for $C_M = 0$, and the formation function $\bar{n}$ as the slope of the straight lines in this plot.

* *E.g.* a redox electrode with a metal ion in two valence steps, one of which is not complex forming.

The correctness of this treatment follows from the formulae [6]

$$\bar{n} = \frac{C_L - [L]}{C_M} = \frac{C''_L - C'_L}{C''_M - C'_M} \quad (4)$$

in which the indices to C_L and C_M refer to corresponding solutions. In most cases the upper part of the formation curve can be determined in this way.

In order to determine the remaining part of the formation curve, for which [L] is too small to be determined in this way, we have the Bodländer equation:

$$\frac{\mathrm{d} \log X}{\mathrm{d} \log [L]} = \bar{n} \quad (5)$$

or in its integrated form [7,8]

$$\log \frac{[L]^*}{[L]} = \int_{[L]^*}^{[L]} (1/\bar{n}) \, \mathrm{d} \log X \quad (6)$$

This expression can be directly used to determine the free ligand concentration by numerical integration from a knowledge of $\bar{n}$ and X.

In the present study the mercury electrode was used to follow the complex formation with diphenylphosphinobenzene-*m*-sulphonate. There was the complication that a solution of mercuric ions is reduced to mercurous ions by mercury. However, by measurements with a bright platinum electrode in mixed solutions of mercury(I) and mercury(II) we could show that mercurous ions have only a negligible tendency to form complexes with the phosphine ligand. Therefore (1) a redox electrode of this kind could be used to measure directly the concentration of free mercuric ions as well as X in case the solutions are unsaturated with respect to mercury metal, and (2) if using the mercury electrode a knowledge of the equilibrium constant

$$K_o = \frac{[Hg_2^{2+}]}{[Hg^{2+}]} \quad (7)$$

under the conditions (0.01 M HNO_3, 1 M KNO_3 at 25°C) used in this study is sufficient to correct the measured potentials (E'_M) for cells

$$\mathrm{Hg} \;\Big|\; \begin{matrix}[Hg_2^{++}]\ 1\ \mathrm{M\ KNO_3} \\ C_{Hg(II)} C_L',\ 0.01\ \mathrm{M\ HNO_3}\end{matrix} \;\Big|\; \begin{matrix}1\ \mathrm{M\ KNO_3}\ [Hg_2^{2+}] \\ 0.01\ \mathrm{M\ HNO_3},\ [Hg^{2+}]\end{matrix} \;\Big|\; \mathrm{Hg} \quad (8)$$

with the same total osmotic concentration of mercury

$$C_{Hg} = C_{Hg(II)} + [Hg_2^{2+}] \quad (9)$$

in both half cells to true E_M values as defined in eqn. (1).

The nitric acid concentration used by us ($\sim$ 0.01 M) is high enough to depress the hydrolysis of the mercuric ions. From the hydrolysis constants determined by Hietanen and Sillén [9] it can be estimated that less than 2 % of the mercuric ions is hydrolyzed if $[H^+] \gtrsim 0.01$ M. On the other hand is was considered that protonation of the phosphine ligand could occur at higher acid concentrations. In a single experiment with the glass electrode it was directly shown that addition of the phosphine ligand in a concentration of

Table 1. Infrared spectra of sodium and potassium diphenylphosphinobenzene-*m*-sulphonate in the range from 1000 cm^{-1} to 670 cm^{-1}.

This paper (Na-salt, $2H_2O$)	804s	793s	790s	753s	747s	740s	700s	695s 676m
Ahrland, Chatt *et al.* (»)**	799s	—	788s	753s	746s	738s	700*	691s 673m
This paper (K-salt, $2H_2O$)	800s	—	789s	753s	746s	741s	700*	695s 676m

* Shoulders.

** These authors have in their paper interchanged the spectra of $Ph_2P{\cdot}C_6H_4SO_3Na,2H_2O$ and $As(m\text{-}C_6H_4SO_3Na)_3$.

0.01 M to a 0.01 M hydrochloric acid solution did not diminish the hydrogen ion concentration to a measurable extent. However, extinction measurements in ultraviolet show that phosphonium ions are formed in more concentrated acid solutions.

EXPERIMENTAL

The ligand. Sodium diphenylphosphinobenzene-*m*-sulphonate was prepared according to Ahrland, Chatt *et al.*[1] Recrystallized from water or better from 96 % ethanol, dried at 100°C and kept over silica gel, it gave the dihydrate. (Found: C 54.4; H 4.43; S 7.92. Calc. for $C_{18}H_{14}O_3SPNa$, $2H_2O$ (400.3): C 54.0; H 4.52; S 8.01). We are indebted to Mr. Preben Hansen, who carried out the C, H, and S determinations, and to Mrs. B. Saustrup Kristensen, who examined the salt on a thermo-balance. The dihydrate was found to be stable in the range 100—335°C. The anhydrous salt could not be prepared by further heating. An indefinite transition point found at about 400°C corresponded to a loss of more than 2 moles of water.

The potassium salt was prepared in the same way as the sodium salt using concentrated KOH instead of NaOH. Recrystallized from 96 % alcohol and dried under mild conditions (50 % sulphuric acid), it gave a dihydrate. It began to lose water already at 50°C. A closer examination with the thermobalance showed that the anhydrous salt was formed gradually and was stable in the range 200—300°C. It was less soluble than the sodium salt, and in a 1 M KNO_3 solution the solubility was only about 0.001 M. The sodium salt (the saturated aqueous solution of which is about 0.03 M) dissolved faster in this medium and was used in most of the experiments. Solutions of the salts could be kept unchanged for hours, but after a longer time the ability to complex formation decreased probably due to oxidation of the phosphine group.

We are indebted to Mrs. S. Refn in Professor Stig Veibel's laboratory for an infrared investigation of the two salts (in KBr-tablets). The results are in good agreement with those of Ahrland, Chatt *et al.*[1] (Table 1). None of the salts has bands in the 820 cm^{-1} region where *para*-substituted benzenes have strong bands, and with the above authors we may conclude that all evidence is strongly in favour of *meta*-orientation.

Solutions. The solutions were made up from redistilled water in measuring flasks by pipetting from stock solutions of mercuric nitrate, nitric acid and 2.5 M potassium nitrate. The stock solutions of mercuric nitrate were prepared by dissolving weighed amounts of mercuric oxide in titrated nitric acid. The ligand was either pipetted from stock solutions or directly weighed into the mercuric solution.

Electrodes. The E.M.F. measurements were performed in a similar manner as described before[10,11]. The electrode vessels (with a volume of about 50 ml) have a sealed-in platinum wire in a cavity in the bottom (in order to establish contact with a pool of mercury), and were equipped with a syphon type bridge with stop-cock as well as with inlet and outlet for nitrogen. Thus it was possible to shake the solutions in an inert atmosphere in the electrode vessels in order to reach equilibrium with mercury before the measurement. The cylinder nitrogen used was purified for oxygen by passing through a Meyer-Ronge apparatus. As reference electrode the 1 M KCl-calomel electrode was employed. The electrodes were prepared according to Gjaldbæk[12] in electrode vessels of the model introduced by Lewis, Brighton and Sebastian[13]. The E.M.F. measurements were per-

Table 2. The mercury standard potentials $E^\circ_{0,1}$ and $E^\circ_{1,2}$ relative to the M 1 calomel electrode, and the equilibrium constant K_0 in 1 M KNO_3 at 25°C.

o.	C_{HNO_3}	$[Hg_2^{2+}]$	E	$E^\circ_{0,1}$	$[Hg^{2+}]$	$[Hg_2^{2+}]$	E	$E^\circ_{1,2}$	K_0
1	0.0999	0.0988	0.4552	0.4849	0.0503	0.0494	0.5698	0.6079	120
2	0.0999	0.0985	0.4556	0.4853	0.0503	0.0493	0.5694	0.6075	117
3	0.0499	0.0493	0.4458	0.4844	0.0251	0.0246	0.5592	0.6062	115
4	0.0499	0.0492	0.4454	0.4840	0.0251	0.0246	0.5583	0.6053	113
					0.0169	0.0328	0.5442	0.6052	112
5	0.2135	0.01884	0.4340	0.4850	0.00956	0.00942	0.5450	0.6045	105
6	0.0214	1.884×10^{-3}	0.4045	0.4851	0.958×10^{-3}	0.942×10^{-3}	0.5150	0.6041	103
7	0.0550	0.942×10^{-3}	0.3955	0.4850	0.479×10^{-3}	0.471×10^{-3}	0.5053	0.6033	100
8	0.0150	0.942×10^{-3}	0.3955	0.4850	0.479×10^{-3}	0.471×10^{-3}	0.5049	0.6029	98.5
9	0.0241	0.377×10^{-3}	0.3838	0.4851	0.1916×10^{-3}	0.1884×10^{-3}	0.4930	0.6028	98
0	0.0100	0.377×10^{-3}	0.3837	0.4850	0.1916×10^{-3}	0.1884×10^{-3}	0.4927	0.6025	97
1	0.0500	0.1884×10^{-3}	0.3744	0.4845	0.0958×10^{-3}	0.0942×10^{-3}	0.4831	0.6018	96
2	0.0244	0.1884×10^{-3}	0.3748	0.4849	0.0958×10^{-3}	0.0942×10^{-3}	0.4828	0.6015	93.5
3	0.0150	0.1884×10^{-3}	0.3746	0.4847	0.0958×10^{-3}	0.0942×10^{-3}	0.4826	0.6013	93.5
4	0.0050	0.1884×10^{-3}	0.3744	0.4845	0.0958×10^{-3}	0.0942×10^{-3}	0.4825	0.6012	94
5	0.0020	0.1884×10^{-3}	0.3737	0.4838	0.0958×10^{-3}	0.0942×10^{-3}	0.4790	0.5977	(84)

formed with a precision Vernier potentiometer and a Cambridge galvanometer. The electrodes were placed in a water thermostat and the liquid-liquid junctions between them were established through a 10 M ammonium nitrate solution. Merck's *p.a* chemicals were employed for solutions and electrodes. The mercury was purified in Lothar Meyer's apparatus and distilled in vacuum.

Analytical methods. The mercuric concentration was determined by EDTA titration (addition of excess of complexon III and back titration with zinc sulphate with eriochrom-black as indicator). In a few other cases the total mercury concentration in mercurous containing solutions was determined gravimetrically as calomel after complete reduction with phosphorous acid in the presence of hydrochloric acid [14].

THE MERCURY STANDARD POTENTIALS AND THE EQUILIBRIUM:

$$Hg^{++} + Hg \rightleftharpoons Hg_2^{++} \text{ in 1 M } KNO_3 \text{ at } 25°.$$

In Table 2 are placed together some E.M.F. data at 25° for the cells:

$$(^+)Hg \,|\, [Hg_2^{2+}],\ C_{HNO_3},\ 1\ M\ KNO_3 \,|\, 10\ M\ NH_4NO_3 \,|\, 1\ M\ KCl,\ Hg_2Cl_2 \,|\, Hg^{(-)} \qquad (10)$$

$$(^+)Pt \,|\, [Hg_2^{2+}],\ [Hg^{2+}],\ C_{HNO_3},\ 1\ M\ KNO_3 \,|\, 10\ M\ NH_4NO_3 \,|\, 1\ M\ KCl, Hg_2Cl_2 \,|\, Hg^{(-)} \qquad (11)$$

The mercury-mercurous standard potential $E^\circ_{0,1}$ corresponding to (10) is given by

$$E = E^\circ_{0,1} + 0.02958 \log [Hg_2^{2+}] \qquad (12)$$

and the mercurous-mercuric redox potential $E^\circ_{1,2}$ corresponding to (11) by

$$E = E^\circ_{1,2} + 0.02958 \log \frac{[Hg^{2+}]^2}{[Hg_2^{2+}]} \qquad (13)$$

From the standard potentials $E^\circ_{0,1}$ and $E^\circ_{1,2}$ we get

$$\log K_o = \frac{E^\circ_{1,2} - E^\circ_{0,1}}{0.05916} \tag{14}$$

where K_o is the mercurous-mercuric equilibrium constant (7).

The mercury-mercurous potential was measured in equilibrium solution prepared by shaking mercuric nitrate solutions with liquid mercury in an atmosphere of purified nitrogen. Complete equilibrium was always reached after one night of shaking in thermostat. This was directly checked by determining the total mercury concentration in some of the solutions after the equilibrium establishment. However, we can only confirm the result of Sillén and coworkers [15] that the mercury-mercurous potential is quickly established at the surface of the mercury electrode (if not shaken) long before the solution as a whole has come to an equilibrium. The formal mercurous ion concentration given in the 3rd column of Table 2 is about 1 % less than the mercury concentration in the initial mercuric nitrate solution ($C^\circ_{Hg(NO_3)_2}$), and is directly estimated from the relationship:

$$[Hg_2^{2+}] = \frac{K_o}{1 + K_o} C_{Hg} \tag{15}$$

where C_{Hg} ($=C^\circ_{Hg(NO_3)_2}$) as defined in (9) is unchanged during the mercurous ion formation.

The mercurous-mercuric redox potentials were measured in direct connection with the measurements of the mercury-mercurous potentials. Equal volumes of the mercurous equilibrium solution and the initial mercuric nitrate solution were mixed in an atmosphere of nitrogen and the redox potential measured at a platinum electrode. This redox potential establishes itself more slowly than the mercury-mercurous potential as discussed by several authors [15–17], and in the solutions low in mercury concentrations it could take more than half an hour to reach the equilibrium potential within a tenth of a millivolt. The formal concentrations of $[Hg^{2+}]$ and $[Hg_2^{2+}]$ in the mixed solutions are given in the 6th and 7th columns, respectively. These concentrations fulfill the conditions that the mercurous concentration is half of that in the mercurous equilibrium solution, and that their sum is equal to $C^\circ_{Hg(NO_3)_2}$.

The standard potentials $E^\circ_{0,1}$ and $E^\circ_{1,2}$ relative to the 1 M calomel electrode are given in the 5th and 9th columns and the values for K_o obtained by means of (14) in the last column of Table 2. It will be seen that $E^\circ_{0,1}$ is very constant and independent of variations in the mercurous ion and nitric acid concentrations. On the other hand $E^\circ_{1,2}$ as well as K_o increases slightly with increasing concentrations of the added nitrates in the 1 M potassium nitrate medium. The measurements Nos. 1—4 were performed already in 1944 by one of the authors (J.B.), nevertheless they are seen to compare well with the new measurements.

Schwarzenbach and Anderegg [16] have determined K_o in sodium nitrate solutions, and Sillén *et al.* [15,17] in sodium perchlorate and sodium nitrate solutions. In perchlorate solutions K_o increases much more strongly with the salt concentration than in the nitrate solutions. Hietanen and Sillén [17]

Table 3. Measurements with platinum electrode in mixed solutions of mercury(I) ions and mercury(II)-phosphine complexes in 1 M KNO_3 at 25°C.

$^{(+)}Pt \mid$ sol.Nos. 1–7 $\mid$ 10 M $NH_4NO_3 \mid$ 1 M KCl, $Hg_2Cl_2 \mid Hg^{(-)}$

$[Hg_2^{2+}] = 0.942 \times 10^{-3}$, $C_{Hg(II)} = 0.958 \times 10^{-3}$, $C_{HNO_3} = 0.02$

No.	$C_L \times 10^3$	$C_L/C_{Hg(II)} = \bar{n}$	E	$E_M \times 10^3$	$[Hg^{2+}] \times 10^3$	$\frac{1}{\bar{n}}$	$\log \frac{[L]^*}{[L]}$	[L]
1	0	0	0.5155	0	0.958	—	—	0
2	0.347	0.362	0.5022	13.3	0.571	2.765	2.283	0.268×10^{-14}
3	0.463	0.483	0.4970	18.5	0.466	2.07	2.078	0.429×10^{-14}
4	0.531	0.554	0.4885	23.4	0.385	1.805	1.917	0.623×10^{-14}
5	0.694	0.725	0.4800	35.5	0.241	1.38	1.590	0.132×10^{-13}
6	0.825	0.86	0.4530	62.5	0.0841	1.162	1.020	0.491×10^{-13}
7	1.015	1.06	0.3949	120.6	0.00877	0.944	0	0.515×10^{-12}

$[Hg_2^{2+}) = 0.471 \times 10^{-3}$, $C_{Hg(II)} = 0.958 \times 10^{-3}$, $C_{HNO_3} = 0.02$

1a	0	—	0.5239	0	0.958
4a	0.531	0.554	0.4966	23.7	0.381

explain this in terms of complexity constants estimated under certain assumptions. However, we consider it safer to speak only about different values of the formal equilibrium constant K_0 in the different ionic media. However, it is noteworthy to see that our value in 1 M KNO_3 at 25°C, $K_0 \approxeq 100$, is in very close agreement with the findings of both Schwarzenbach and Anderegg, and Hietanen and Sillén in 1 M $NaNO_3$.

We have carried out some measurements of $E^\circ_{0,1}$ and $E^\circ_{1,2}$ at extremely low mercury concentrations ($\gtrsim 10^{-5}$ M) in order to detect a possible dissociation of the dimeric mercurous ion: $Hg_2^{2+} \rightleftharpoons 2\,Hg^+$. The measurements were performed in potassium nitrate and sodium perchlorate, but the results were somewhat contradictory, and we can only agree with the statement of Linhart [18] that there is no safe experimental evidence for the existence of monomeric mercurous ions in aqueous solutions.

MEASUREMENTS OF THE MERCURY(II)-PHOSPHINE COMPLEX FORMATION WITH A MERCURY(I)-REDOX ELECTRODE

As already mentioned it is possible to show by redox measurement with a bright platinum electrode that mercurous ions have only a negligible tendency to complex formation with the phosphine ligand. The measurements in Table 3 give an example of this. Solutions Nos. 4 aud 4a contain same total concentrations of mercuric nitrate and phosphine ligand, but the concentration of mercurous nitrate in No. 4a is only half of that in No. 4. One should therefore theoretically expect an increase of $0.02958 \log 2 = 0.0089$ V in the measured potential E, if mercurous ions do not form complexes with the ligand. Experimentally one finds 0.0081 V. However, a corresponding comparison of the ligand-free solutions 1 and 1a shows that also here the experimentally found increase $E_{(No.1a)} - E_{(No.1)} = 0.0084$ V is somewhat smaller than the

theoretical increase 0.0089 V. It seems therefore safe to neglect complex formation between mercurous ions and the phosphine ligand. This assumption is supported by the recent studies of Yamane and Davidson [19] who state that mercurous complexes of ligands such as ammonia and cyanide are unstable toward disproportionation to give mercuric complexes but »ionic» chelating ligands such as pyrophosphate and oxalate can form stable mercurous complexes.

From the E.M.F. data in Table 3, one can compute the concentration of free mercuric ions (in column 6) and the variation in the concentration of free ligand (column 9). The differences in the measured potential E between Nos. 1 and 1a (the ligand free solutions) and the rest of the solutions determine E_M for which we have according to the expressions (1) and (2):

$$E_M = 0.05916 \log \frac{0.958 \times 10^{-3}}{[Hg^{2+}]} = 0.05916 \log X \qquad (16)$$

Aqueous solutions of mercurous ions and mercury(II)-complexes are thermodynamically stable with regard to formation of metallic mercury, if $[Hg_2^{2+}] < K_0 [Hg^{2+}] \sim 100 [Hg^{2+}]$. It will be seen that this condition is fulfilled for the solutions Nos. 1—6 and nearly fulfilled for No. 7. Solution No. 7 was completely stable during the measurements, but solutions with higher concentrations of ligand gave shortly after their preparation dark precipitations of mercury.

Log [L]*/[L] in the 8th column of Table 3 determines the concentration of free ligand in the solutions 1—6 relative to that in No. 7. This integral was computed by means of expression (6) from a graph in which $\frac{1}{\bar{n}} \left(= \frac{C_{Hg(II)}}{C_L}\right)$ was plotted *versus* log X as abscissa. The integral was estimated from point to point using Simpson's formula. The concentration of free ligand in solution 7 ($[L]^* = 0.515 \times 10^{-12}$M) and the [L]-concentrations derived from there in the last column of Table 3 were estimated from the measurements with a mercury electrode mentioned in the next section.

MEASUREMENTS OF THE PHOSPHINE COMPLEX FORMATION WITH A MERCURY ELECTRODE

Table 4 gives the experimental data for three series with the initial concentrations of mercuric nitrate 0.00019, 0.00038 and 0.00095 M, respectively, and varying concentrations of ligand. It was not necessary to take special precautions to establish the equilibrium with mercury before measurements of the cells. Mercury(II) solutions with more than 1 mole of ligand per Hg-atom are very close to equilibrium, but also for solutions with a smaller content of ligand the potential E of the cells gave directly the equilibrium potential as discussed in the section on the mercury standard potential. In the series with $C_{Hg} = 0.38 \times 10^{-3}$ M some of the solutions (marked with an asterisk) were prepared as mixed solutions of equal parts of mercuric and mercurous nitrate, but nevertheless gave (as seen from Table 4) the same potential within a few tenths of a millivolt as the initially mercurous-free solutions.

Table 4. Mercury(II)-phosphine complex formation in 1 M KNO_3 at 25°C. Measurements of cells with mercury electrode.

$Hg|C_{Hg},C_L$,0.01 M HNO_3, 1 M KNO_3|10 M NH_4NO_3|1 M KCl,$Hg_2Cl_2|Hg$

$C_{Hg} = 0.19\times10^{-3}$			$C_{Hg} = 0.38\times10^{-3}$			$C_{Hg} = 0.95\times10^{-3}$		
$C_L\times10^3$	E	$E'_M\times10^3$	$C_L\times10^3$	E	$E'_M\times10^3$	$C_L\times10^3$	E	$E'_M\times10^3$
0	0.3748	0	0	0.3837	0	0	0.3955	0
0.1093	0.3668	8.0	0.1126	0.3786	5.1	0.547	0.3845	11.0
0.1125	0.3628	12.0	0.1126*	0.3784	5.3	1.093	0.3507	44.8
0.1408	0.3577	17.1	0.1402	0.3775	6.2	1.366	0.3357	59.8
0.1690	0.3439	30.9	0.1402*	0.3780	5.7	1.640	0.3130	82.5
0.2186	0.3398	35.0	0.1689	0.3762	7.5	1.913	0.2731	122.4
0.2733	0.3014	73.4	0.1689*	0.3760	7.7	2.050	0.0704	325.1
0.328	0.2691	105.7	0.2252	0.3716	12.1	2.186	0.0469	348.6
0.547	−0.0496	424.4	0.2252*	0.3723	11.4	2.186	0.0435	352.0
0.601	−0.0746	449.4	0.2733	0.3678	15.9	2.460	0.0178	377.7
0.656	−0.0982	473.0	0.2815	0.3666	17.1	2.73	−0.0245	420.0
0.683	−0.1080	482.8	0.2815*	0.3669	16.8	3.01	−0.0595	455.0
0.820	−0.1335	508.3	0.3505	0.3535	30.2	3.28	−0.1006	496.1
0.850	−0.1417	516.5	0.547	0.3107	73.0	3.83	−0.1506	546.1
0.929	−0.1472	522.0	0.683	0.2497	144.0	4.37	−0.1685	563.9
1.023	−0.1548	529.6	0.820	0.0459	337.8	4.92	−0.1777	573.2
1.093	−0.1598	534.6	0.957	−0.0030	386.7	5.25	−0.1825	578.0
1.115	−0.1608	535.6	1.093	−0.0472	430.9	5.47	−0.1851	580.6
1.160	−0.1703	545.1	1.366	−0.1190	502.7			
1.64	−0.1893	564.1	1.640	−0.1457	529.4			
1.69	−0.1938	568.6	1.913	−0.1660	549.7			
1.705	−0.1943	569.1	2.186	−0.1788	562.5			
1.79	−0.1956	570.4	2.459	−0.1847	568.4			
			2.733	−0.1931	576.8			

* Solutions prepared as mixed solutions of equal parts of mercuric and mercurous nitrate.

The differences between the potential E of the ligandfree solutions and the rest of the solutions determined the E.M.F. for a cell of type (8):

$$E'_M = 0.02958 \log \frac{K_o \cdot C_{Hg}}{(1+K_o)[Hg_2^{2+}]} = 0.02958 \log \frac{C_{Hg}}{(1+K_o)[Hg^{2+}]} \qquad (17)$$

Complex solutions of different mercury concentrations, but with the same values of E'_M have according to (17) also the same value of $[Hg^{2+}]_{c_L=0}/[Hg^{2+}]$ and are *eo ipso* corresponding solutions. They can therefore be treated according to Fronæus [4] as we know that mercurous ions do not form complexes. In Fig. 1 (in the graph on the left) C_L for each of the three series is plotted *versus* E'_M. Interpolated sets of C_L at rounded-off values of E'_M obtained from this graph are plotted in Fig. 1 (in the graph on the right) *versus* the corresponding values of $C_{Hg(II)}$. In this graph the intercept at the ordinate axis determines directly the free ligand concentration, and the slopes of the straight lines the formation function according to eqns (4). For values of $E'_M \gtrsim 100$ mV $C_{Hg(II)} = C_{Hg}$, but for lower values of E'_M $[Hg^2{}_2{}^+]$ is calculated from the first of the eqns. (17) and $C_{Hg(II)}$ as the difference $C_{Hg} - [Hg^2{}_2{}^+]$ according to (9).

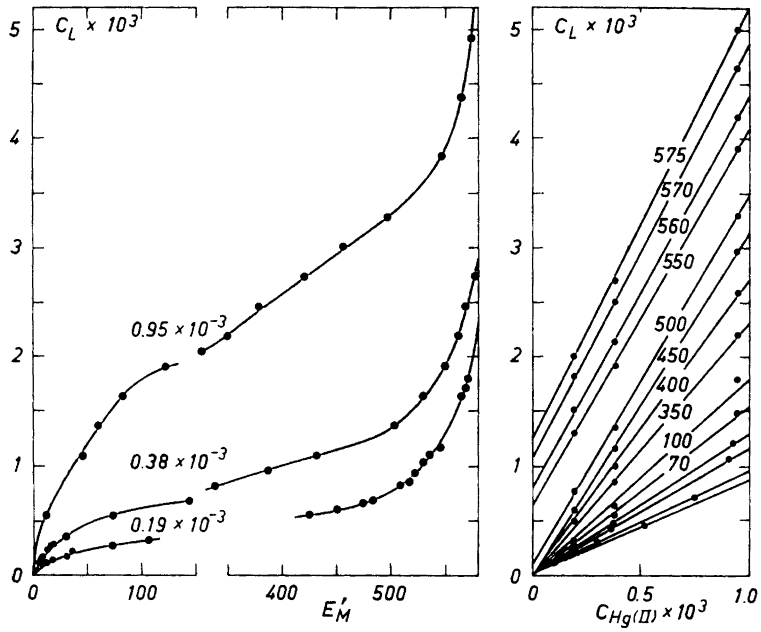

Fig. 1. The E.M.F. measurements are plotted on the left: C_L *versus* E'_M for the three mercury concentrations in Table 4. The straight lines plotted on the right give C_L *versus* $C_{Hg(II)}$ for values of E'_M corresponding to the data in Table 5.

In Table 5 are given (in column 1) the used rounded-off values of E'_M and (in column 2) the interpolated values of C_L for one of the measured series ($C_{Hg} = 0.95 \times 10^{-3}$). Column 3 gives the values of $C_{Hg(II)}$, and columns 4 and 5 the graphically derived values of $\bar{n}$ and [L] from Fig. 1. Column 6 gives the ratio $C_L/C_{Hg(II)}$ which is seen to deviate only a little from $\bar{n}$ as long as the graphically determined [L] (1) is negligible. Column 7 gives the corrected values for E'_M according to the relationships:

$$E_M = E'_M + 0.02958 \log \frac{C_{Hg(II)}}{[Hg^{2+}]_{C_L=0}} = 0.02958 \log X \qquad (18)$$

Finally the last column gives [L] (2), the integrated values of the free ligand concentration computed from a graph in which $1/\bar{n}$ was plotted *versus* log X (eqn. (6)). In this calculation the highest [L] (1) value was taken as reference ($[L]^* = 1.26 \times 10^{-3}$ M).

The data in Table 5 show that using the mercury electrode the complex formation curve for $\bar{n}$-values lower than about one can only be reached with high experimental uncertainty due to mercurous ion formation. It is fortunate that these measurements just overlap the measurements with the platinum electrode in Table 3. By comparison of eqns. (16) and (18) it will be seen that a value of E_M corresponding to a certain value of log X is twice as high as

Table 5. Derived data from Fig. 1. Interpolated values of C_L for one of the measured series ($C_{Hg} = 0.95 \times 10^{-3}$), graphically derived values of $\bar{n}$ and [L] (1) using all three series, and integrated values of [L] (2) using the relation for log ([L]*/[L]).

$[Hg^{2+}]_{C_L=0} = 0.96 \times 10^{-5}$, $[Hg_2^{2+}]_{C_L=0} = 0.94 \times 10^{-3}$

$E'_M \times 10^3$	$C_L \times 10^3$	$C_{Hg(II)} \times 10^3$	$\bar{n}$	[L](1)	$C_L/C_{Hg(II)}$	$E_M \times 10^3$	$\frac{1}{\bar{n}}$	[L](2)
10	0.45	0.518	0.86	0	0.87	61.2	1.162	0.515×10^{-12}
20	0.71	0.752	0.95	0	0.945	76.0	1.052	0.184×10^{-11}
40	1.07	0.908	1.16	0	1.18	98.5	0.862	0.987×10^{-11}
50	1.22	0.931	1.28	0	1.31	108.8	0.782	0.191×10^{-10}
70	1.48	0.946	1.54	0	1.56	129	0.650	0.585×10^{-10}
00	1.79	0.950	1.78	0	1.88	159	0.547†	0.233×10^{-9}
50	2.20	0.950	2.30	0	2.31	409	0.435	0.354×10^{-5}
00	2.59	0.950	2.70	0	2.73	459	0.371	0.170×10^{-4}
50	2.97	0.950	3.10	0	3.13	509	0.323	0.70×10^{-4}
00	3.30	0.950	3.37	0.10×10^{-3}	3.48	559	0.297	0.235×10^{-3}
50	3.92	0.950	3.44	0.64×10^{-3}	4.13	609	0.291	0.74×10^{-3}
60	4.20	0.950	3.57	0.81×10^{-3}	4.42	619	0.280	0.925×10^{-3}
70	4.65	0.950	3.74	1.09×10^{-3}	4.90	629	0.2673	1.14×10^{-3}
75	5.00	0.950	3.92	1.26×10^{-3}	5.26	634	0.255	1.26×10^{-3}*

† Calc. with the average 1.83 of the values found for $C_L/C_{Hg(II)}$ and $\bar{n}$.

in case of the measurements with the mercury electrode. This means that the lowest of the values in Table 5 ($E_M = 61.2$ mV) corresponds very nearly to the value for solution 7 in Table 3 ($E_M = 120.6$ mV). Due to this coincidence [L]* for this solution is taken to be equal to the corresponding ligand concentration [L] (2) $= 0.515 \times 10^{-12}$ M in Table 5.

Fig. 2 shows graphically the complete formation curve as far as $N = 4$. It will be seen that there is a pronounced »stop» in the formation curve for both $\bar{n} = 1$ and $\bar{n} = 2$, but also the separation of the third and fourth steps is much higher than usually found for mercuric complexes. Due to the separation of the steps the consecutive constants are equal to the reciprocal concentrations of free ligand for all half values of $\bar{n}$. From the formation curve is interpolated:

$\bar{n}$	0.5	1.5	2.5	3.0
$-\log$ [L]	14.30	10.30	5.10	4.22

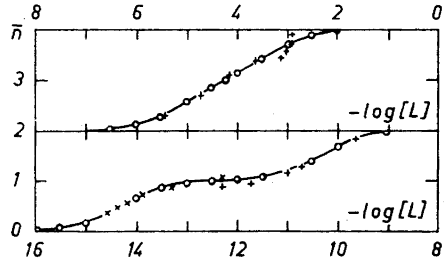

Fig. 2. The complex formation curve of mercury(II) ions and diphenylphosphinobenzene-*m*-sulphonate in 1 M KNO_3 at 25°C. The lower part of the figure gives the curve from $\bar{n} = 0$ to $\bar{n} = 2$, and the upper part from $\bar{n} = 2$ to $N = 4$.
× Exptl. points (Pt-electr.). + Exptl. points (Hg-electr.).
○ Calc. points (from K_1, β_2, β_3, β_4).

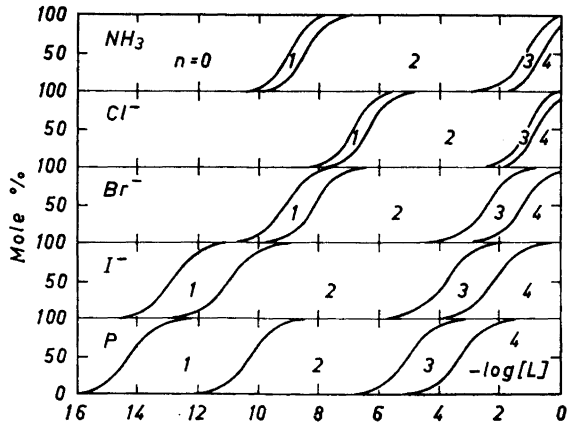

Fig. 3. Comparison of the distribution of mercury(II) between the various complexes as a function of $-\log [L]$ for the ammonia[5], the halide[21], and the phosphine systems.

This gives directly the following values for the complexity constants:

$$\begin{aligned} \log K_1 &= 14.3 \\ \log \beta_2 &= 14.3 + 10.3 = 24.6 \\ \log \beta_3 &= 24.6 + 5.1 = 29.7 \\ \log \beta_4 &= 24.6 + 2 \times 4.22 = 33.0 \end{aligned}$$

There seems to be a higher uncertainty in the experimental points for $\bar{n}$-values between 3 and 4, and this is the reason why the value of $-\log[L]$ for $\bar{n} = 3$ instead of for $\bar{n} = 3.5$ is used in the calculation of β_4.

A MERCURY(II)-PHOSPHINE COMPLEX SALT

Mercuric ions and diphenylphosphinobenzene-*m*-sulphonate can in case of sufficient small concentrations be mixed in all ratios. If the mercuric concentration is essentially higher than 0.001 M, and the concentration of ligand approximately twice that of the metal ion concentration, a complex salt with two moles of ligand per mercuric ion separates out of the solutions on standing overnight. We tried to prepare a complex salt corresponding to the mono complex from a solution of the composition: $C_{Hg} = 0.003$, $C_L = 0.003$, but the infrared spectra of the precipitates (in KBr-tablets) showed that the same complex salt separated in both cases.

The analysis of the white crystalline precipitates dried over silica gel agreed approximately with the formula $Hg[(C_6H_5)_2PC_6H_4SO_3]_2,2H_2O$, corresponding to a formula weight of 919. (Found: C 45.9; H 3.3; S 7.4; Hg 21.9. Calc. for $C_{36}H_{32}O_8P_2Hg$; C 47.0; H 3.5; S 7.0; Hg 21.8). The mercury was

precipitated and weighed as $[Cu\,en_2][HgI_4]$[20] after complete decompostiion of the complex salt with a 1:1 mixture of conc. H_2SO_4 and HNO_3*.

DISCUSSION

In Fig. 3 our results with diphenylphosphinobenzene-*m*-sulphonate and mercury(II) are compared with earlier results for the ammonia system[5] and with Sillén[21] and coworkers' results for the mercury halide systems. The figure shows the distribution of the various complexes HgL_1 to HgL_4 as a function of the ligand exponent $-\log [L]$. The di-complex has in all cases a very large range of existence, but it will be seen that the range of existence of the mono-complex as well as that of the tri-complex increases much from chloride to iodide and again from the iodide to the phosphine system. For this system it is especially the mono-complex which has a great range of existence, and the first coordination number is clearly one. It will be seen that the complex affinity increases in the series: $Cl^- < Br^- < I^-<$ phosphine.

For silver(I) Leden *et al.* have found that the coordination number two decreases in importance for ligands such as chloride and bromide[22], and for both iodide[23] and phosphine[1] the coordination numbers one and three, instead of two, are virtually found. But also here it is remarkable that the complex affinity increases in the series: $Cl^- < Br^- < I^-$ < phosphine.

The first subgroup metal ions Cu^+, Ag^+, Au^+, and Hg^{2+} have all a strong tendency to form linear complexes with ligands which cannot participate in π-bonding as, *e.g.*, ammonia or as cyanide only have p-orbitals available for such bonding. However, after a large range of existence of the linear di-complex a tetrahedral complex is formed in most cases. Our data for the mercury(II)-phosphine system now seem to support the idea of Ahrland and Chatt that ligands furnished with d-orbitals capable of accepting d-electrons from the metal, such as, *e.g.*, phosphines, arsines and the halide ions to an increasing extent from chloride to iodide, interfere with this condition and strongly favour the coordination numbers one and three.

REFERENCES

1. Ahrland, S., Chatt, J., Davies, N. R. and Williams, A. A. *J. Chem. Soc.* **1958** 264, 276.
2. Brandt, P. and Plum, O. *Acta Chem. Scand.* **7** (1953) 97.
3. Jensen, F. R. *J. Am. Chem. Soc.* **82** (1960) 2469.
4. Fronæus, S. *Komplexsystem hos koppar.* Thesis. Lund 1948, pp. 13, 18 ff.
5. Bjerrum, J. *Metal ammine formation in aqueous solution.* Thesis. P. Haase and Son, Copenhagen 1941, pp. 22, 28. Reprinted 1957.
6. Bjerrum, J. *Kgl Danske Videnskab. Selskab, Mat.-fys. Medd.* **21** (1944) No. 4, p. 5.
7. Leden, I. *Potentiometrisk undersökning av några kadmiumsalters komplexitet.* Thesis. Lund 1943, p. 19.
8. Bjerrum, J. *Kemisk Månedsblad* **24** (1943) 22.
9. Hietanen, S. and Sillén, L. G. *Acta Chem. Scand.* **6** (1952) 747.
10. Bjerrum, J. *Kgl. Danske Videnskab. Selskab, Mat.-fys. Medd.* **12** (1934) No. 15.

* We are indebted to Mr. Gunnar Borch, who carried out the Hg determination, and to Mr. Preben Hansen, who carried out the C, H, and S determinations in Professor K. A. Jensen's laboratory.

11. Bjerrum, J. and Nielsen, E. J. *Acta Chem. Scand.* **2** (1948) 297.
12. Gjaldbæk, J. K. *Kgl. Danske Videnskab. Selskab, Mat.-fys. Medd* **5** (1924) No. 9.
13. Lewis, G. N., Brighton, T. B. and Sebastian, R. L. *J. Am. Chem. Soc.* **39** (1917) 2245.
14. Treadwell, F. P. *Lehrbuch der analytischen Chemie*, 5. Aufl. (1911) p. **14**.
15. Jonsson, A., Qvarfort, I. and Sillén, L. G. *Acta Chem. Scand.* **1** (1947) 461.
16. Schwarzenbach, G. and Anderegg, G. *Helv. Chem. Acta* **37** (1954) 1289.
17. Hietanen, S. and Sillén, L. G. *Arkiv Kemi* **10** (1956) 103.
18. Linhart, G. A. *J. Am. Chem. Soc.* **38** (1916) 2356.
19. Yamane, T. and Davidson, N. *J. Am. Chem. Soc.* **82** (1960) 2123.
20. Spacu, G. and Suciu, G. *Z. anal. Chem.* **77** (1929) 334.
21. Sillén, L. G. *Acta Chem. Scand.* **3** (1949) 539.
22. Berne, E. and Leden, I. *Svensk Kem. Tidskr.* **65** (1953) 88; *Z. Naturforsch.* **8a** (1953) 719.
23. Leden I. *Acta Chem. Scand.* **10** (1956) 812.

Received October 7, 1961.

ACTA CHEMICA SCANDINAVICA 16 (1962) 749–754

Crystal Structure of the 1 : 3 Addition Compound Iodoform-Sulphur ($CHI_3 \cdot 3S_8$)

T. BJORVATTEN

Universitetets Kjemiske Institutt, Blindern-Oslo, Norway

The crystal structure of the 1:3 compound iodoform-sulphur, $CHI_3 \cdot 3S_8$, has been determined by X-ray methods. The structure is trigonal rhombohedral with the (hexagonal) lattice parameters: $a = 24.32$ Å; $c = 4.44$ Å. The space group is $R3m$. Charge transfer bonds connect every iodine atom with a sulphur atom belonging to a S_8-ring. The I-S bond distance (3.50 Å) is about 0.50 Å shorter than the van der Waals radius sum of iodine and sulphur and the C-I-S angle is found equal to 177.7°.

Results obtained in this laboratory regarding the structure of iodoform-dithiane [1] clearly prove the existence of charge transfer bonds between iodoform iodine atoms and dithiane sulphur atoms. The apparently isomorphous iodine-sulphur crystals $RI_3 \cdot 3S_8$ (R being CH, P, As or Sb) [2] might be expected to exhibit analogous I—S bonds. In order to check the correctness of this assumption the crystal structures of $CHI_3 \cdot 3S_8$ resp. $SbI_3 \cdot 3S_8$ have been or are being studied in this laboratory.

The present report is dealing with the investigation of the iodoform-sulphur compound. Preliminary results of the structure determination have been given in a survey article by Hassel [3].

EXPERIMENTAL

Needle-shaped crystals of the iodoform-sulphur compound were obtained by evaporation of a solution of sulphur and iodoform in carbon disulphide. The melting point of the compound was found equal to 95°C. The cross section of the crystals used in the X-ray work was about 0.005 mm².

Integrated Weissenberg photographs were taken with rotation about the trigonal axis which is the needle axis. Cu$K\alpha$-radiation was employed and of the 82 $hk0$ reflections attainable, 65 were observed.

Precession diagrams were taken of the rhombohedral $0kl$ zone. Mo$K\alpha$-radiation was employed and of the 95 reflections attainable, 87 were observed. The intensities of the reflections were measured photometrically. No corrections for absorption or secondary extinction were applied. The computation were carried out using a Ferranti Mercury computer. In the calculations the analytical approximations to the atomic scattering factors computed by Forsyth and Wells [4] were employed.

CRYSTAL DATA

The crystals are trigonal rhombohedral with the hexagonal parameters:

$$a = 24.32 \text{ Å}; \qquad c = 4.44 \text{ Å}$$

Both figures are believed to be accurate to within 0.5 % and are in good agreement with those published by West.[5] The density measured using the flotation method was 2.45 g/cm³ leading to the value $Z = 1$ for the number of molecules in the rhombohedral unit cell. The density calculated from the lattice parameters is 2.55 g/cm³. The space group is $R3m$.

STRUCTURE DETERMINATION

The number of formula units in the primitive rhombohedral unit cell is *one* and the sulphur (S_8) molecules are therefore situated in mirror planes, the iodoform molecules on trigonal axes with the iodine atom in a mirror plane. These requirements and the detailed information already available regarding the structure of the iodoform and the sulphur molecules simplified the determination of the approximate hexagonal x and y coordinates by trial and error methods. Using the values of the phase angles obtained from these calculations combined with the observed data, a Fourier map was computed for the projection along the trigonal axis. The coordinates obtained from this Fourier synthesis served as starting values for least squares refinements. The parameters finally arrived at are listed in Table 1. The phase angles of the reflec-

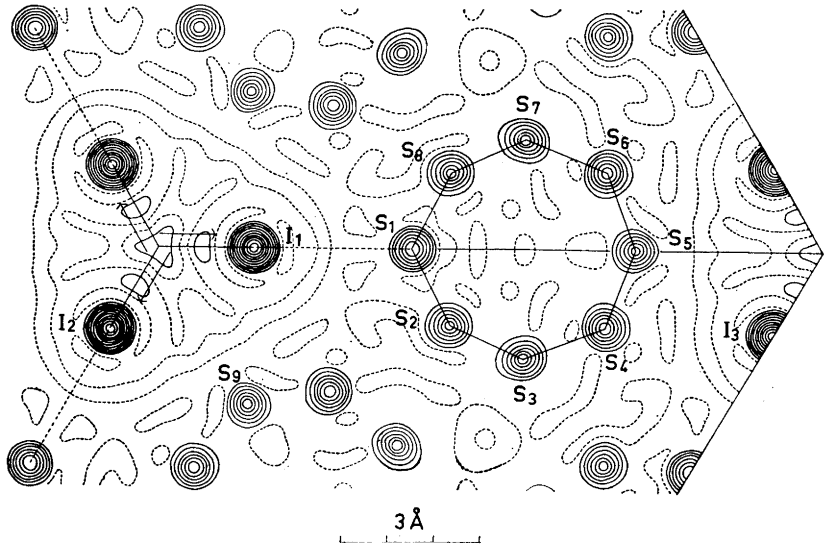

Fig. 1. Electron density projection along the trigonal axis. Contour intervals: 5 e · Å^{-2} for sulphur and carbon atoms, 10 e · Å^{-2} for iodine atoms. The axes indicated are the projections of the rhombohedral axes.

Table 1. Positional and temperature parameters. B_1 and B_2 are temperature factors in the [001] and [211] projection, respectively.

Atom	x	y	z	B_1	B_2
I_1	−0.0487	0.0487	0.0000	2.0	3.3
C	0.0000	0.0000	0.0963	2.0	2.3
S_1	−0.1291	0.1291	−0.1973	1.2	2.3
S_2	−0.0810	0.2158	0.0394	1.5	2.3
S_3	−0.0889	0.2810	−0.2191	1.3	2.3
S_4	−0.1587	0.2928	−0.0410	1.5	2.3
S_5	−0.2407	0.2407	−0.2572	2.4	2.3

Table 2. Interatomic distance and valence angles.

	Distance	Standard deviation		Angle
I_1-I_2	3.56 Å	0.007 Å	I_1-C-I_2	115.9°
I_1-S_1	3.50	0.014	$C-I_1-S_1$	177.7
S_1-S_2	2.11	0.023	$I_1-S_1-S_2$	104.4
S_2-S_3	2.04	0.026	$S_1-S_2-S_3$	106.0
S_3-S_4	2.02	0.022	$S_2-S_3-S_4$	107.6
S_4-S_5	2.00	0.022	$S_3-S_4-S_5$	111.4
$C-I_1$	2.10		$S_4-S_5-S_6$	109.8
I_1-S_9	3.84		$S_8-S_1-S_2$	102.0
I_3-S_4	3.88			

tions and the observed and calculated structure factors have been listed in Table 3. The R factor including only observed reflections is 0.050. A Fourier map based on the final phase angles is reproduced in Fig. 1. In this projection the $C-I-S_1$ arrangement is of course linear as required by the symmetry of the space group.

In order to determine the $C-I-S_1$ angle and the atomic distances, a projection along another direction had to be determined. The hexagonal [211] direction (rhombohedral [100] direction) was chosen for this purpose.

The z coordinates of the iodine atoms could arbitrarily be chosen equal to zero. The $I-C-I$ and $C-I-S_1$ angles were first assumed to be 113° and 180°, respectively. With these assumptions four alternative models could be postulated for the position of the sulphur and iodoform molecules relative to the crystallographic axes. Subsequent trial and error computations led to

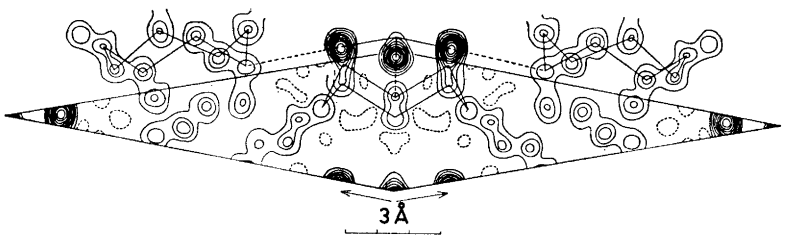

Fig. 2. Electron density projection along a rhombohedral axis. Contour intervals: 10 e · Å^{-2}. The axes indicated are the projections of the rhombohedral axes.

Table 3. Observed and calculated structure factors and phase angles.

[001] projection

h	k	l	F_o	F_c	α	h	k	l	F_o	F_c	α
0	3	0	101	108	5.0	7	10	0	114	114	137.1
0	6	0	408	435	139.4	7	13	0	184	180	110.8
0	9	0	174	168	169.3	7	16	0	<65	57	195.8
0	12	0	319	327	228.8	7	19	0	89	81	244.3
0	15	0	196	195	168.7	7	22	0	115	123	256.7
0	18	0	<65	49	23.6	8	8	0	418	426	0·0
0	21	0	161	162	337.2	8	11	0	79	78	118.4
0	24	0	169	168	12.1	8	14	0	196	201	112.2
1	1	0	141	165	0.0	8	17	0	<68	17	110.7
1	4	0	106	81	90.0	8	20	0	217	228	241.3
1	7	0	307	315	123.1	9	9	0	66	66	180.0
1	10	0	128	102	83.4	9	12	0	83	78	135.0
1	13	0	333	330	257.7	9	15	0	82	81	234.0
1	16	0	<62	71	292.1	9	18	0	<60	20	251.4
1	19	0	159	165	20.8	10	10	0	<63	44	180.0
1	22	0	123	120	1.4	10	13	0	163	156	95.3
1	25	0	116	129	157.4	10	16	0	<65	31	46.6
2	2	0	96	99	0.0	10	19	0	<53	25	96.0
2	5	0	420	438	89.2	11	11	0	<65	34	0.0
2	8	0	193	180	100.6	11	14	0	100	108	13.6
2	11	0	140	144	253.9	11	17	0	79	78	296.6
2	14	0	212	243	245.2	12	12	0	<85	19	180.0
2	17	0	74	66	326.3	12	15	0	125	123	325.6
2	20	0	88	78	23.9	12	18	0	<46	43	61.6
2	23	0	65	48	174.8	13	13	0	136	150	0.0
3	3	0	103	90	180.0	13	16	0	63	66	79.2
3	6	0	181	168	107.3	14	14	0	116	111	0.0
3	9	0	189	180	320.1	15	15	0	156	171	0.0
3	12	0	84	66	123.7						
3	15	0	<62	44	218.3						
3	18	0	128	123	334.0						
3	21	0	<65	11	165.2						
3	24	0	<52	39	131.1						
4	4	0	175	159	180.0						
4	7	0	122	123	-324.8						
4	10	0	80	81	21.8						
4	13	0	103	93	45.0						
4	16	0	141	138	101.0						
4	19	0	123	120	279.7						
4	22	0	83	78	239.7						
5	5	0	188	192	0.0						
5	8	0	67	81	10.3						
5	11	0	105	105	208.7						
5	14	0	172	168	130.1						
5	17	0	132	135	110.8						
5	20	0	<65	37	266.6						
5	23	0	<48	31	286.1						
6	6	0	331	339	0.0						
6	9	0	286	282	358.2						
6	12	0	70	72	102.2						
6	15	0	193	195	119.3						
6	18	0	<62	33	225.6						
6	21	0	108	98	223.9						
7	7	0	323	324	0.0						

[211] projection

h	k	l	F_o	F_c	α
−1	2	0	154	148	0.0
−2	4	0	105	96	0.0
−3	6	0	112	116	180.0
−4	8	0	188	174	180.0
−5	10	0	191	191	0.0
−6	12	0	313	297	0.0
−7	14	0	321	306	0.0
−8	16	0	386	396	0.0
−9	18	0	55	59	180.0
−10	20	0	45	38	180.0
−11	22	0	<20	19	0.0
−12	24	0	<21	22	180.0
−13	26	0	126	122	0.0
−14	28	0	95	83	0.0
−15	30	0	128	119	0.0
−16	32	0	42	45	0.0
−17	34	0	38	30	180.0
−1	1	1	259	302	336.6
−2	3	1	264	273	327.4
−3	5	1	68	62	324.9
−4	7	1	333	330	156.2
−5	9	1	173	159	219.6
−6	11	1	131	123	333.4

h	k	l	F_o	F_c	a	h	k	l	F_o	F_c	a
−7	13	1	266	260	343.5	−10	17	3	45	42	306.9
−8	15	1	227	209	345.3	−11	19	3	27	26	250.6
−9	17	1	104	87	339.4	−12	21	3	98	105	260.3
−10	19	1	62	54	235.2	−13	23	3	27	26	333.4
−11	21	1	107	99	195.6	−14	25	3	22	21	230.7
−12	23	1	105	98	144.9	−15	27	3	66	47	28.9
−13	25	1	70	62	291.6	−16	29	3	62	65	0.0
−14	27	1	145	137	357.0	−2	0	4	65	68	88.7
−15	29	1	39	29	348.7	−3	2	4	133	143	351.5
−16	31	1	73	65	307.3	−4	4	4	119	89	257.5
−17	33	1	49	47	190.6	−5	6	4	94	99	221.7
−1	0	2	304	338	1.1	−6	8	4	60	71	298.5
−2	2	2	147	176	357.6	−7	10	4	69	75	316.8
−3	4	2	94	86	14.9	−8	12	4	55	62	35.0
−4	6	2	191	185	212.4	−9	14	4	85	98	343.5
−5	8	2	81	71	331.0	−10	16	4	21	23	17.1
−6	10	2	101	90	53.5	−11	18	4	95	90	315.0
−7	12	2	131	132	16.8	−12	20	4	73	83	192.0
−8	14	2	162	168	337.5	−13	22	4	42	42	214.8
−9	16	2	119	108	0.0	−14	24	4	44	39	0.0
−10	18	2	98	75	295.8	−15	26	4	35	41	282.3
−11	20	2	42	84	110.7	−3	1	5	21	26	287.1
−12	22	2	35	41	242.3	−4	3	5	27	36	3.2
−13	24	2	55	50	30.1	−5	5	5	56	60	222.8
−14	26	2	79	69	9.8	−6	7	5	62	75	216.0
−15	28	2	32	30	305.2	−7	9	5	35	41	254.1
−16	30	2	42	36	342.8	−8	11	5	<21	27	19.8
−17	32	2	38	38	43.4	−9	13	5	<21	47	315.9
−2	1	3	149	159	342.3	−10	15	5	<20	18	110.0
−3	3	3	71	60	22.2	−11	17	5	42	42	225.0
−4	5	3	116	128	264.7	−12	19	5	<15	6	315.0
−5	7	3	37	41	215.0	−3	0	6	<18	18	312.7
−6	9	3	137	135	252.0	−4	2	6	<18	21	63.4
−7	11	3	53	69	318.0	−5	4	6	22	33	204.8
−8	13	3	144	167	354.6	−6	6	6	45	60	322.0
−9	15	3	67	69	41.3	−7	8	6	19	18	270.0

preliminary values of all the z-coordinates. These coordinates and the coordinates obtained from the [001] projection served as starting values in the least squares computations. In the two final least squares refinements of the parameters a mean value of the temperature factor was employed for the sulphur and carbon atoms.

Observed and calculated structure factors and phase angles finally arrived at in the [211] projection are listed in Table 3. The corresponding R factor is 0.089 including observed reflections only. A Fourier projection along [211] based on the final phase angles is reproduced in Fig. 2. The z coordinates and B values are listed in Table 1. The x and y coordinates determined from the projection along [211] are in good agreement with those obtained from the projection along the trigonal axis. The latter are considered to be more accurate and these values are therefore listed in Table 1.

DISCUSSION OF THE STRUCTURE

Interatomic distances and valence angles are listed in Table 2. The observed $I-S_1$ distance (3.50 Å) is 0.50 Å shorter than the van der Waals radius sum and the $C-I-S_1$ arrangement is nearly linear (angel $C-I-S_1 = 177.7°$). This clearly indicates the presence of a charge transfer bond between iodine and sulphur. The corresponding I—S bond in the iodoform-dithiane compound is somewhat shorter (3.32 Å) [1]. The iodine atom is attached to the ring system in the "equatorial" position.

The distances within the iodoform molecule agree closely with those obtained from crystalline [6] and gaseous [7] iodoform. The mean values for the S—S distances and S—S—S valence angles in the sulphur molecule is 2.043 Å and 107.7°, respectively. This is in very good agreement with the corresponding values reported for orthorhombic sulphur (2.048 Å and 107.9°, respectively) [8]. Differences in valence angles within the sulphur molecule indicate, however, that the ring system is slightly distorted. The mean value for the standard deviation of the S—S—S valence angles is 1.2°. The observed S_1-S_2 distance is 0.06 Å longer and the S_4-S_5 distance is 0.05 Å shorter than the mean S—S distance in orthorhombic sulphur. These differences in S—S distances are probably significant and are believed to be caused by the charge transfer interaction between the sulphur molecule and the relevant iodine atom of the iodoform molecule.

Each iodine atom is closely surrounded by five sulphur atoms belonging to different S_8 molecules. The shortest I—S separation is the one mentioned above. The four additional sulphur atoms which are not situated in the symmetry plane give rise to two further I—S distances which are, respectively, 3.84 Å and 3.88 Å. These four I—S separations are believed to depend on van der Waals type interactions.

Four intermolecular S· · ·S distances are found which are 0.02, 0.12, 0.21 and 0.34 Å shorter than the van der Waals radius sum given by Pauling. Apart from these short distances all intermolecular distances are found to be larger than the sum of the van der Waals radii.

The author is greatly indebted to Professor O. Hassel for his help and very kind interest in this work. The investigation has in part been sponsored by the *United States Air Force Development Command* under contract AF 61 (052)-71.

REFERENCES

1. Bjorvatten, T. and Hassel, O. *Acta Chem. Scand.* **15** (1961) 1429.
2. Auger, V. *Compt. rend.* **146** (1908) 478.
3. Hassel, O. *Tidsskr. Kjemi Bergvesen Met.* **21** (1961) 60.
4. Forsyth, J. B. and Wells, M. *Acta Cryst.* **12** (1959) 412.
5. West, C. D. *Z. Krist.* **96** (1937) 459.
6. Khotsyanova, T. L. Kitaĭgorodskiĭ and Struchkov, Yu.T. *Zhur. Fiz. Khim.* **27** (1953) 647.
7. Bastiansen, O. *Tidsskr. Kjemi, Bergvesen Met.* **6** (1946) 1.
8. Abrahams, S.C. *Acta Cryst.* **14** (1961) 1008.

Received October 3, 1961.

ACTA CHEMICA SCANDINAVICA 16 (1962) 755–759

Some Features of the Ternary System: Myristic Acid, Palmitic Acid and Isopalmitic Acid

SIXTEN ABRAHAMSSON and BERTIL NILSSON

Crystallography Group, Institute of Medical Biochemistry, University of Göteborg, and Institute of Chemistry, University of Uppsala, Sweden

The melting point diagram of the ternary system, myristic acid, palmitic acid and isopalmitic acid has been recorded. A phase analysis of the isothermal section at 25°C by X-ray methods shows the existence of a ternary phase. Its composition is 50 % myristic acid, 15 % palmitic acid and 35 % isopalmitic acid. Structural data are given for the six phases found.

Many solidification point diagrams for ternary systems containing long-chain fatty acids have been recorded. Most of them are discussed by Baily [1]. No X-ray data seem to have been reported for such systems of acids.

This investigation is part of a program of studying multicomponent systems of long-chain compounds. Earlier work has concerned binary systems of normal and branched-chain fatty acids [2–4].

EXPERIMENTAL

The melting points of the different samples representing about one hundred points in the ternary system were obtained in a Kofler heating stage microscope. The acids were fused together and shockfreezed. The samples were then carefully melted, partly resolidified and the temperature recorded when the last crystals again disappeared on heating.

X-Ray Guinier powder photographs of the samples at 25°C were taken with Cu$K\alpha$ and Cr$K\alpha$ radiation. Samples for the X-ray work were obtained by slow crystallization from the melt. The samples were brought to a temperature well above their melting points and the temperature then lowered to room temperature in a thermostat over a period of several days.

The acids were kindly provided by Prof. E. Stenhagen. The melting points of the acids are: myristic acid [5] 54.4°C, palmitic acid [5] 62.9°C and isopalmitic acid [6] 61.6°C.

In the following discussion myristic acid will be called n-C_{14}, isopalmitic acid 14Me-C_{15} *etc.*

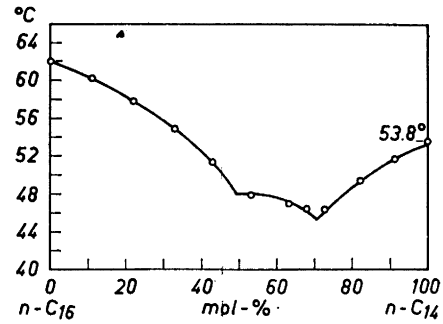

Fig. 1. Melting point diagram of the binary system n-C_{14}—n-C_{16}.

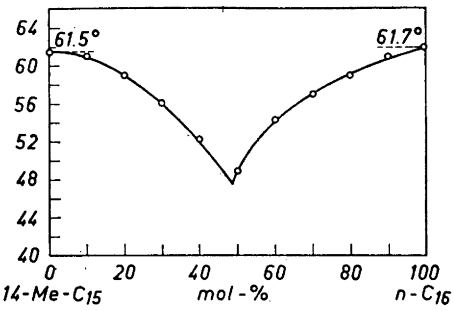

Fig. 2. Melting point diagram of the binary system 14Me-C_{15}—n-C_{16}.

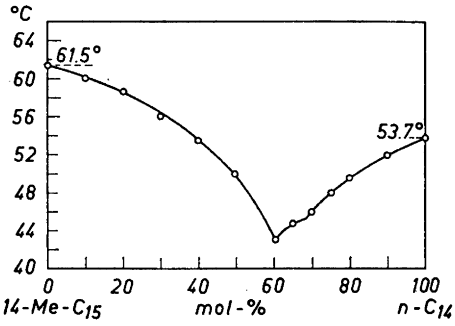

Fig. 3. Melting point diagram of the binary system 14Me-C_{15}—n-C_{14}.

RESULTS AND DISCUSSION

The melting point diagrams of the binary systems of the components are shown in Figs. 1—3. The systems of the normal acids contain a (1:1) molecular compound. The system 14Me-C_{15}—n-C_{16} is of the simple eutectic type whereas the diagram of the system 14Me-C_{15}—n-C_{14} indicates the presence of a (1:3) compound. This is all in accordance with the results of Abrahamsson and von Sydow [4].

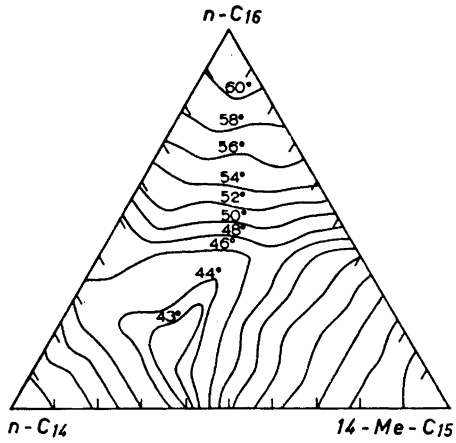

Fig. 4. Melting point isotherms in the ternary system n-C_{14}—n-C_{16}—14Me-C_{15}.

Melting point isotherms in the complete ternary system are given in Fig. 4. A space model was constructed on the recorded melting points but it gave only a crude outline of the melting point surfaces. The lowest melting point is at 42.4°C at a composition of about 60 % n-C_{14}, 10 % n-C_{16} and 30 % 14Me-C_{15}. The ternary system of the normal acids n-C_{14}, n-C_{16} and n-C_{18} is similar in having its lowest melting point at 42.3°C at about 67 % n-C_{14}, 12 % n-C_{16} and 21 % n-C_{18} [1].

The powder photographs of the different samples at 25°C were studied and the phases existing in different regions of the ternary system were determined. The isothermal section is outlined in Fig. 5. It was not possible to find the

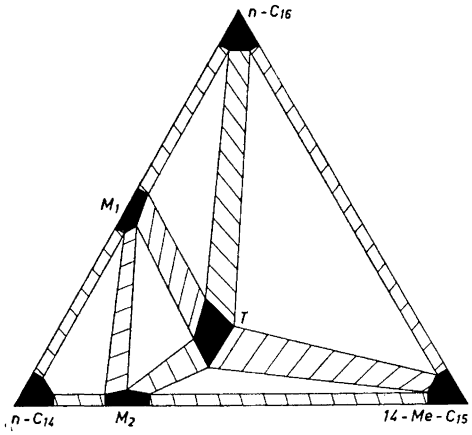

Fig. 5. Isothermal section (25°C) of the ternary system n-C_{14}—n-C_{16}—14M-C_{15}. Black regions represent single phase areas and shaded regions two phase areas.

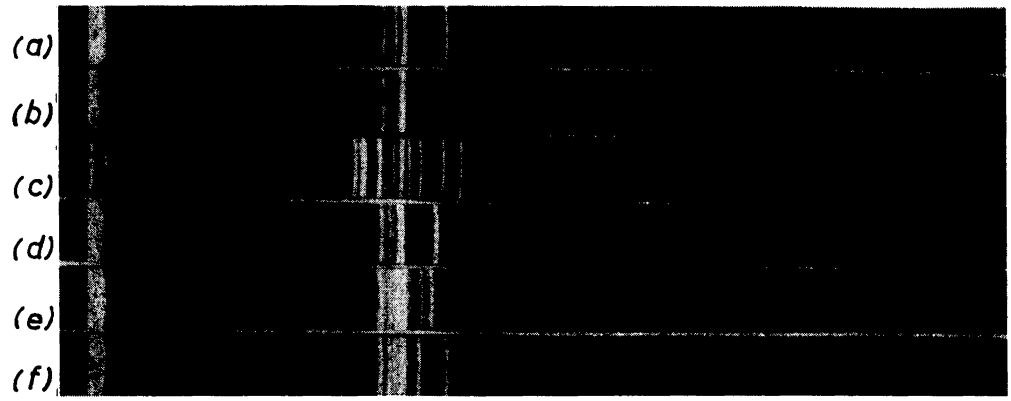

Fig. 6. Powder photographs of the different phases in the ternary system: a) n-C_{14}, b) n-C_{16}, c) 14Me-C_{15}, d) molecular compound M_1, e) molecular compound M_2 and f) ternary compound T. The powder photographs of M_1 and T indicate that they are based on mainly single phase samples whereas that of M_2 shows lines of n-C_{14} as well because M_2 melts incongruently.

actual limits of the different areas and the phase regions drawn are intended to be illustrative only.

As seen from Fig. 5 there exists a ternary compound (T) in the system. It has a composition of 50 % n-C_{14}, 15 % n-C_{16} and 35 % 14 Me-C_{15}. In all, six phases are found in the ternary system and the outlined subdivision seems the only one compatible with the phase analysis.

Phases present. (1) n-C_{14} and (2) n-C_{16}. The normal fatty acids in the system have the C-form structure with the carbon chains in the common orthorhombic chain packing (O$\perp$). Every second chain plane is thus roughly perpendicular to the others. The molecules are held together to dimers by hydrogen bonds and are tilted about 56° towards the end group contact planes (*cf.* von Sydow [7]).

(3) 14Me-C_{15}. The molecules of isoacids are forced to be much more tilted than those of normal acids to allow accomodation for the methyl branches between the tails of the dimer molecules [8]. The angle between the chain axes and the end group planes is thus only about 45°. The chain packing is triclinic with all chain planes parallel (T$\parallel$).

(4) Molecular compound M_1. The compound is analogous to the binary phase in the system stearic acid-palmitic acid. The latter has been shown by Degerman and von Sydow [3] to contain dimers of one molecule stearic acid and one molecule palmitic acid packed essentially the same as the dimers in the C form of normal fatty acids. The long spacing of the molecular compound is accordingly intermediate to those of the components as is also shown in this case where M_1 has $d(001)$ = 33.7 Å whereas n-C_{16} and n-C_{14} have $d(001)$ = 35.7 Å and 31.6 Å, respectively (Table 1). The similarity of the powder photographs of M_1 and the components is obvious from Fig. 6.

Table 1. Long-spacings of the different phases in the ternary system.

Phase	d(001) Å
n-C_{14}(C-form)	31.6
n-C_{16}(C-form)	35.7
14Me-C_{15}	30.2
Molecular compound M_1	33.7
» » M_2	32.2
Ternary compound T	33.7

(5) Molecular compound M_2. In a system corresponding to that of 14Me-C_{15} and n-C_{14} but containing an isoacid with an odd number of carbon atoms (23Me-C_{24}—n-C_{23}) Abrahamsson and von Sydow [4] found that the (1:3) compound has a long spacing similar to that of the normal acid (n-C_{24}) derived from the unbranched part of the isoacid. The carbon chains of the compound follow the orthorhombic chain packing (O⊥). As can be judged from the powder photographs M_2 is similar in having the same chain packing but has a long spacing (32.2 Å) which is shorter than that of the most tilted polymorph of n-C_{15} [5] (34.5 Å). It is not surprising that structural differences should exist in these binary phases depending on whether the isoacid contains an odd or an even number of carbon atoms.

(6) Ternary compound T. The powder photograph of the ternary phase is given in Fig. 5 f. T has the same long spacing as M_1 (Table 1) but shows distinctly different side spacings. The powder diagram indicates that the carbon chains are arranged in the orthorhombic chain packing (O⊥) but it shows no other similarities to the powder patterns of known fatty acid structures.

It has not been possible so far to grow single crystals of M_2 and T and detailed structural information is thus lacking about these two phases.

Acknowledgement. We wish to thank Prof. G. Hägg and Prof. E. Stenhagen for their interest in this work and for laboratory facilities. We also thank Dr. S. Rundqvist for helpful discussions and Mrs. M. Innes and Mr. L. Ahlquist for technical assistance.

The investigation has been supported by grants from the *Swedish National Science Research Council* and (in part) by grant A-4006 from the *U.S. Public Health Service.*

REFERENCES

1. Baily, A. E. *Melting and Solidification of Fats.* Interscience Publishers, New York 1950.
2. von Sydow, E. *Acta Chem. Scand.* **8** (1954) 1513.
3. Degerman, G. and von Sydow, E. *Acta Chem. Scand.* **12** (1958) 1176.
4. Abrahamsson, S. and von Sydow, E. *Arkiv Kemi* **14** (1959) 39.
5. Stenhagen, E. and von Sydow, E. *Arkiv Kemi* **6** (1953) 309.
6. Arosenius, K. E., Ställberg, G., Stenhagen, E. and Tägtström-Eketorp, B. *Arkiv Kemi Mineral Geol.* **26** A (1948) No. 19.
7. von Sydow, E. *Arkiv Kemi* **9** (1956) 231.
8. Abrahamsson, S. *Arkiv Kemi* **14** (1959) 65.

Received October 10, 1961.

ACTA CHEMICA SCANDINAVICA 16 (1962) 760–766

On the Electrical Conductance of KCl in Various Solvent Mixtures at 25 ° C. Test of the Theoretical Equations

SERGIO PETRUCCI

Institute of Inorganic Chemistry, The Technical University of Norway, Trondheim, Norway

Data of electrical conductance of KCl in various solvent mixtures are surveyed. It is pointed out that in some cases the present theoretical equations show some inadequacy.

The Fuoss-Onsager theoretical equation for the equivalent conductance of an unassociated electrolyte can be written [1]:

$$\Lambda = \Lambda_0 - S\sqrt{c} + E\,c\log c + J_1 c - F\Lambda_0 c \qquad (1)$$

where Λ_0 is the limiting conductance at infinite dilution and c is concentration expressed in equivalents per liter. S and E are the Onsager-Fuoss coefficients, both depending on the dielectric constant D, on the viscosity η_0 of the solvent and on the temperature T. J_1 is a coefficient depending upon the same parameters. It is also a function of the so called minimum approach distance a between the two oppositely charged ions. F is the Einstein viscosity coefficient for the solution. It can be neglected for ions that are of approximately the same size as the solvent molecules.

Eqn. (1) has recently been shown [2] to hold for the KCl-water system up to $C = 0.012$ N.

If the electrolyte is partially associated to ion pairs *, the equation expressing the dependence of the equivalent conductance on the concentration becomes [1]:

$$\Lambda = \Lambda_0 - S\sqrt{c\gamma} + Ec\gamma\log(c\gamma) + J_1 c\gamma - K_A c\gamma f^2\Lambda - F\Lambda_0 c \qquad (2)$$

K_A is the association constant, γ the degree of ionization, f the activity coefficient according to Debye-Hückel. (The constant K_A may, of course, be expressed in terms of γ and f, but is retained in the equation because of the convenience in numerical calculation).

* In this paper only ionophores [3] like KCl *etc.* are considered, not ionogenes [3] like acetic acid, etc.

In other words, eqn. (1) is a two-parameter equation and can be written in the general form:

$$\Lambda = f(\Lambda_o, a)$$

since D, η_o and T are properties which are directly measured by independent methods. Similarly, eqn. (2) is a three-parameter equation:

$$\Lambda = f'(\Lambda_o, a, K_A) \qquad (2)$$

This means that the above equations are considered to give satisfactory results only when the experimental $\Lambda - c$ data can be fitted to the equations giving reasonable and consistent values for the parameter Λ_o, a, and K_A if different from zero.

During the last years, eqns. (1) and (2) have been used to analyze conductance-concentration data of large ions, such as tetramethyl- and tetraethylammonium picrate [4], in several solvent mixtures. For such systems the theoretical equations were generally consistent with the experimental data. For KCl in water, eqn. (1) gave an a value of 3.07 Å[1] which is in good agreement with the crystallographic distance of 3.14 Å. Kay [5] has used eqns. (1) and (2) to analyze data found in the literature for KCl (and other salts) in water at various temperatures, in alcohol at 25°C, and in liquid ammonia at −34°C. The analysis for the KCl data gave agreement with the crystallographic distance especially for solutions in water and in methanol.

Eqns. (1) and (2) are derived on the basis of a model considering the ions as discrete particles moving in a continuous medium. The molecular structure of the solvent and the interaction between ions and solvent molecules are thus not taken into account. This model would be expected to show some inadequacy especially for the smaller ions (such as alkali and halide ions) in highly viscous solvents and in mixed solvents with strong interaction between the solvent components. Some research work has been done to clarify this point. For example, conductance measurements have been made for KCl in water-glycerol [6] and in water-ethylene glycol [7] mixtures, with dielectric constants in the range 80 to 40. Analysis of these experimental data by means of eqn. (1) gave values for a in the range 3.3 to 3.8, that is, values in reasonable agreement with the crystallographic distance.

However, when the values of Λ_o for these systems were considered, a positive deviation in the Walden product, compared to the water value, was noticed [6,7]. This was tentatively explained [7] by taking into account the ion-solvent interactions. Indeed it has to be kept in mind that when dealing with limiting values of electrical conductance, every peculiar behaviour must result from ion-solvent interactions. The ion-ion interactions are negligible at zero limiting concentrations.

On Fig. 1 the product of the limiting conductance and the solvent viscosity, $\Lambda_o\eta_o$, is plotted as a function of the dielectric constant.

The system KCl-water-glycerol is shown on curve 1. The Walden product corresponding to $D = 78.5$ is the limiting value for pure water. The last point to the right on curve 1 is the value of $\Lambda_o\eta_o$ in pure glycerine. The KCl-water-glycol system is plotted on curve 2. It is seen that $\Lambda_o\eta_o$ greatly increases from water to glycerol, and also increases from water to glycol.

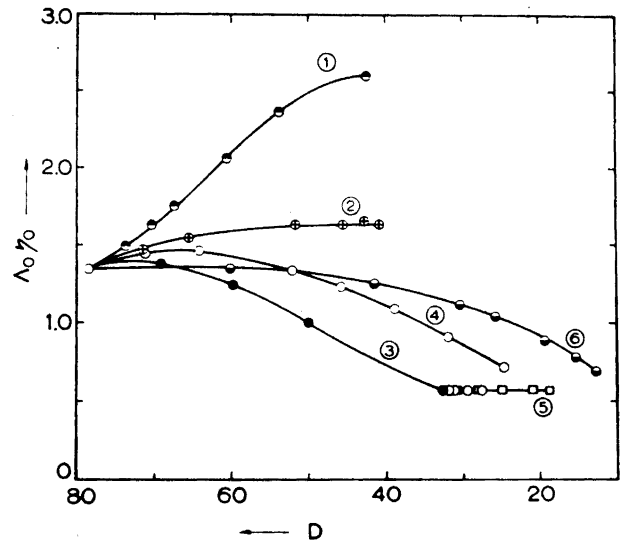

Fig. 1. Walden product *versus* D, for potassium chloride in various solvent mixtures (1) Water-glycerol; (2) Water-glycol; (3) Water-methanol; (4) Water-methylcellosolve. (5) Circles: Methanol-butanol; Squares: Methanol-methylcellosolve. (6) Water-dioxane.

This increase of $\Lambda_0\eta_0$ with decreasing dielectric constant is contrary to the general behaviour noticed by Fuoss for many electrolyte solutions [8]. The data for KCl in water-methanol mixtures [9] (curve 3) show this decrease for smaller values of D, but the curve passes through a slight maximum.

A qualitatively similar change in the Walden product has been noticed for Et_4N-picrate in the same three solvent systems as above [10,20]. This confirms that these deviations depend upon the solvent and not upon a property of KCl.

A slight maximum in the Walden product is also noticed in the system KCl-water-dioxane [11] (curve 6 on Fig. 1).

Fuoss [8] has presented an explanation for the decrease in Walden product with decreasing dielectric constant, according to which the actual viscosity around an ion will be different from the bulk viscosity of the solvent due to an ion-solvent relaxation effect. The actual viscosity η, according to Fuoss can be expressed by the equation:

$$\eta = \eta_0 \left(1 + \frac{B}{R_\infty^2 D}\right) \tag{3}$$

where B is a constant, and R_∞ is the hydrodynamic radius of the ion in a hypotetical medium of infinite dielectric constant.

The increase of the Walden product in water-glycerol, water-glycol and in some of the water-methanol mixtures has been ascribed [7] to the formation of H-bonded solvent complexes. Indeed the anomalous deviation in the Walden product seems to increase with the potential number of H-bonds between

the solvent molecules (*cf.* Fig. 1). This was expressed [7] by a negative term introduced into eqn. (3):

$$\eta = \eta_o \left(1 + \frac{B}{R_\infty^2\ D} - \frac{f(h)}{R_\infty^2\ D}\right) \tag{4}$$

where $f(h)$ is an implicit unknown function of the H-bonds. Indeed in the Walden product, we multiply Λ_o (that is a quantity inversely proportional to the actual viscosity, η, in the vicinity of the moving ion) by the macroscopic viscosity, η_o, of the solvent. If eqn. (4) is correct, it could explain the increase of the Walden product from methanol to glycerol at the same D as shown in Fig. 1. The situation for curve 6 is somewhat different, dioxane being only a H-bond acceptor.

In order to check the hypothesis on which eqn. (4) is based, some further work has recently been carried out by Accascina *et al.*[12], and some of the preliminary results are reported in Table 1 and are incorporated in Fig. 1 for comparison. Curve 4 shows the Walden product for KCl in water-methylcellosolve, while curve 5 is valid for methanol-methylcellosolve and for methanol-butanol. (All the data were analyzed by eqn. (1) assuming the Einstein coefficient equal to zero. No association was noticeable in a trial analysis applying eqn. (2). Details, experimental and final results will be published soon).

It can be seen from Fig. 1 that for water-methylcellosolve the behaviour is similar to the water-methanol mixtures as expected. The non-aqueous mixtures (curve 5) show apparent ideal behaviour with respect to the Walden rule. This is probably due to the weak interaction between the alcohols compared to the water mixtures. The values for the Walden product in the non-aqueous solvent mixtures were analyzed [12] in terms of the semiempirical equation given by Fuoss [8]:

$$R^{\pm}\ D = A + R_\infty^{\pm}\ D \tag{5}$$

where

$$R^{\pm} = (Fe/6\pi)(1/\lambda_o^{\pm}\eta_o) \tag{6}$$

$R^{\pm}$ is the hydrodynamic radius of the K^+ and Cl^- ions, respectively, and $\lambda_o^{\pm}$ their limiting ionic conductance. F is the Faraday, and e the charge of the electron. The transport number of K^+ in the mixtures was assumed constant and equal to the value in methanol at zero concentration [13]. The slopes of the $R^{\pm}\ D$ *versus* D plots gave the radius sum $(R_\infty^+ + R_\infty^-) = 5.7$ Å in methanol-methylcellosolve, and 5.5 Å in methanol-butanol mixtures. These values are much greater than the crystallographic distance. On the other hand, Fuoss [11] has found $(R_\infty^+ + R_\infty^-) = 1.688$ Å for KCl in water-rich dioxane mixtures. This is approximately one half of the crystallographic distance.

This again means that eqn. (5) does not hold in these cases where we have H-bonds between the solvent molecules. Possibly if the $f(h)$ function of eqn. (4) could be found, it would solve the enigma.

Fuoss [11] has proposed an alternative approach: When the ions are of the same size as the solvent molecules, the possibility of a slippage of the ions into

Table 1. Conductance and related data for potassium chloride in various mixed solvents [12]. First four columns: Experimental data. Last three columns: Calculated values.

KCl in water-methylcellosolve mixtures

w % methyl-cellosolve	D	$\eta_0 \times 10^2$ (poises)	Λ_0	$\Lambda_0\eta_0$	$J_1 \pm \Delta J_1$	$a \pm \Delta a$ (cm.10^{-8})
15.25	71.20	1.380	104.7_6	1.446	127 ± 11	2.5 ± 0.2
29.07	64.25	1.923	76.0_2	1.462	137 ± 5	2.9 ± 0.1
50.40	52.10	2.695	49.5_7	1.336	161 ± 3	3.05 ± 0.05
60.23	45.85	2.885	42.6_3	1.230	179 ± 4	2.82 ± 0.06
70.10	38.90	2.865	38.0_0	1.089	257 ± 3	2.88 ± 0.04
80.17	32.00	2.595	35.4_2	0.919	438 ± 3	3.04 ± 0.02
90.47	24.70	2.105	34.7_1	0.731	943 ± 5	3.18 ± 0.02

KCl in methanol-methylcellosolve

w % methyl-cellosolve	D	$\eta_0 \times 10^2$ (poises)	Λ_0	$\Lambda_0\eta_0$	$J_1 \pm \Delta J_1$	$a + \Delta a$ (cm.10^{-8})
20.13	30.75	0.648	88.49	0.573	1 363 ± 14	2.26 ± 0.04
39.71	28.12	0.767	74.15	0.573	1 512 ± 7	2.32 ± 0.02
50.75	25.02	0.938	61.41	0.576	1 768 ± 15	2.43 ± 0.03
80.00	21.05	1.178	48.87	0.576	2 167 ± 11	2.22 ± 0.02
90.06	18.80	1.344	42.29	0.568	2 824 ± 12	2.52 ± 0.02

KCl in methanol — n-butanol

w % butanol	D	$\eta_0 \times 10^2$ (poises)	Λ_0	$\Lambda_0\eta_0$	$J_1 \pm \Delta J_1$	$a \pm \Delta a$ (cm.10^{-8})
5.22	31.87	0.572	99.70	0.570	1 335±6	3.07±0.02
9.01	31.10	0.600	95.12	0.570	1 322±11	2.93±0.03
20.06	29.40	0.668	85.19	0.569	1 400±11	2.99±0.02
29.76	27.62	0.746	75.83	0.566	1 489±10	3.02±0.02

the holes of the liquid may be taken into consideration. According to Sutherland [14], this can be accounted for by replacing the coefficient 6π in the Stokes equation by 4π. For the KCl water-dioxane mixtures the value of $(R_\infty^+ + R_\infty^-)$ is thereby changed from 1.688 Å to 2.53 Å. This latter value is in better accordance with the crystallographic distance than the former.

However, the use of the Sutherland assumption is not consistent with the model on which the equations (1), (2) are based.

Next, some remarks will be added concerning partially associated electrolytes and in particular the correlation between K_A, D and a. Denison and Ram-

sey assumed that an ion pair is only formed when the two ions are in close contact; then the K_A-data obtained from eqn. (2) should fit into the equation [15,16]:

$$K_A = K_o \exp (e^2/aDkT) \quad (7)$$

According to this equation, the association for a certain electrolyte should depend only on the dielectric constant of the solvent (and on the temperature). This is experimentally in accord with some system; *e.g.*, for the large and spherical ions of tetrabutylammonium tetraphenylborate [17], the results for K_A agree rather well with eqn. (7). On the other hand, for a large number of systems eqn. (7) does not hold, as pointed out already by Harned and Owen [18] for pure solvents, and corroborated by some observations for methylammonium picrate in pure solvents and in water-dioxane [19,4a].

Furthermore, the slope of the log K_A *versus* $1/D$ plot (for different compositions of the same mixed-solvent system) in some cases gives an a value far from any expected one [20]. For example, in the case of the system KCl-water-dioxane [11], the log K_A *versus* $1/D$ plot is not even linear. If a straight line is tentatively drawn through the points, the resulting a value is about 6.7 Å. This is more than twice the expected value. The same type of curvature in the log K_A *versus* $1/D$ graph has been noticed for tetrabutylammonium picrate, -iodide and -nitrate in nitrobenzene-carbon tetrachloride mixtures [21]. (Recent spectrophotometric results for the ionization constants of some acids in water-dioxane mixtures [22] show the same concave downward curvature in the pK *versus* $1/D$ plot. Although these results are for ionogenes, they may be taken to indicate that the deviations in question do not depend on the method of measurement). Here again, the deviation between theory and experiment in all probability is due to the neglect of ion-solvent interactions in the theory.

The interaction between solvent and solute may tentatively be taken into account, as proposed by Gilkerson [23], by introducing into eqn. (7) a factor exp $(-E_s/kT)$. According to Gilkerson, E_s is an energy due to the ion-dipole interaction and is proportional to the dipole moment of the solvent. Thus, for a mixed solvent, E_s would be expected to vary with the composition (that is, with the dielectric constant) of the mixture.

Finally, it should be mentioned that the introduction of the $a(0)$ $c^{3/2}$ term [20b] into eqns. (1) and (2) and the use of the Sandved-LaMer activity coefficients [24] would probably avoid trends in the a_J sets of data [11]. These refinements in the calculations look important, especially when the dielectric constant is low or when dealing with 2—2 or 3—3 electrolytes.

This brief survey of the present state of the conductance theory indicates that in a modern approach, short range ion-solvent forces should be taken into account quantitatively. However, this implies a change of the present model.

Acknowledgements. Thanks are expressed to the *Italian Research Council* for research support through a NATO fellowship and to Prof. Kai Grjotheim, Head of the Institute of Inorganic Chemistry, for his kind hospitality.

REFERENCES

1. Fuoss, R. M. and Accascina, F. *Electrolytic Conductance*, Interscience Publ. 1959.
2. Lind, J. E., Zwolenic, J. J. and Fuoss, R. M. *J. Am. Chem. Soc.* **81** (1959) 1557.
3. Fuoss, R. M. *J. Chem. Educ.* **32** (1955) 527.
4. Accascina, F. and Petrucci, S. *Ricerca sci.* **29** (1959) 1383. Accascina, F. and Antonucci, L. *Ricerca sci.* **29** (1959) 1391. Accascina, F. Kay, R. L. and Kraus, C. A. *J. Am. Chem. Soc.* **81** (1959) 2270 and *Proc. Natl. Acad. Sci. U.S.* **45** (1959) 804.
5. Kay, R. L. *J. Am. Chem. Soc.* **82** (1960) 2099.
6. Accascina, F. and Petrucci, S. *Ricerca sci.* **29** (1959) 1640.
7. Accascina, F. and Petrucci, S. *Ricerca sci.* **30** (1960) 808.
8. Fuoss, R. M. *Proc. Natl. Acad. Sci. U.S.* **45** (1959) 807.
9. Foster, N. G. and Amis, S. E. *Z. physik. Chem.* **3** (1955) 365.
10. Accascina, F. and Petrucci, S. *Ricerca sci.* **30** (1960) 1164.
11. Lind, J. E. and Fuoss, R. M. *J. Phys. Chem.* **65** (1961) 999.
12. Accascina, F., Sesta, B. and Petrucci, S. *Unpublished.*
13. Davies, J. A., Kay, R. L. and Gordon, A. R. *J. Chem. Phys.* **19** (1951) 749.
14. Sutherland, W. *Phil. Mag.* **9** (1905) 781.
15. Denison, J. T. and Ramsey, J. B. *J. Am. Chem. Soc.* **77** (1955) 2615.
16. Fuoss, R. M. *J. Am. Chem. Soc.* **80** (1958) 5059.
17. Accascina, F. and Petrucci, S. *Ricerca sci.* **29** (1959) 1633. Berns, R. P. and Fuoss, R. M. *J. Am. Chem. Soc.* **82** (1960) 5585.
18. Harned, H. S. and Owen, B. B., *The Physical Chemistry of Electrolytic Solutions*, 3rd Ed., Reinhold Publ. Co., New York 1958, p. 294.
19. Fuoss, R. M. and Kraus, C. A. *J. Am. Chem. Soc.* **79** (1957) 3301.
20. Accascina, F., D'Aprano, A. and Fuoss, R. M. *J. Am. Chem. Soc.* **81** (1959) 1058.
21. Hirsch, E. and Fuoss, R. M. *J. Am. Chem. Soc.* **82** (1960) 1018.
22. Bell, R. P. and Robinson, R. R. *Trans. Faraday Soc.* **57** (1957) 965.
23. Gilkerson, W. R. *J. Chem. Phys.* **25** (1956) 1199.
24. Gronwall, T. H., LaMer, V. K. and Sandved, K. *Physik. Z.* **29** (1928) 358.

Received October 26, 1961.

ACTA CHEMICA SCANDINAVICA 16 (1962) 767–792

Short Communications

A Novel Synthesis of 1-Bromo-3,5-dinitrobenzene

BO LAMM

Nobel Institute of Chemistry, Stockholm 50, Sweden

1-Bromo-3,5-dinitrobenzene was first prepared by Elion [1]. His method involved bromination of 2,4-dinitroaniline to 2-bromo-4,6-dinitroaniline. The amine group was then replaced with hydrogen by diazotisation and reduction with ethanol. The substance was later prepared by Derbyshire and Waters [2], who simply brominated *m*-dinitrobenzene in conc. sulphuric acid solution containing silver sulphate. The bromide ions resulting from the heterolysis of bromine were continually removed as insoluble silver bromide. Thus, the concentration of bromonium ion could be maintained at a level necessary for the reaction to proceed at a reasonable rate.

The present author wishes to report that 1-bromo-3,5-dinitrobenzene may be prepared in good yield by the Hunsdiecker reaction between silver 3,5-dinitrobenzoate and bromine in carbon tetrachloride solution at reflux temperature under anhydrous conditions. The synthesis is a simple extension of the work by Barnes and Prochaska [3], who found that the silver salts of the three isomeric nitrobenzoic acids all give good yields of the corresponding bromonitrobenzenes. It is interesting to note that the introduction of a second nitro group has practically no influence upon the reaction rate. This supports the generally accepted homolytic mechanism rather than a heterolytic one. Furthermore, the product formed is the expected one. The danger of forming the *m*-dinitrobenzene, owing to the decarboxylation of the 3,5-dinitrobenzoate ion, could not *a priori* be overlooked. However, there seem to be no complications of this kind.

Experimental. Silver 3,5-dinitrobenzoate. The preparation of this salt was carried out as described in the literature. [4] Starting with equimolecular quantities of 3,5-dinitrobenzoic acid (Fluka) and silver nitrate, a 94 % yield of the silver salt was secured. In order to obtain a perfectly dry product, at least two days' storage at 70°C was found necessary.

1-Bromo-3,5-dinitrobenzene. A solution of 65.2 g (0.408 mole) bromine in 100 ml carbon tetrachloride was added during one hour to a vigorously stirred, refluxing mixture of 127.4 g (0.400 mole) silver 3,5-dinitrobenzoate and 500 ml carbon tetrachloride. The stirring and refluxing was then continued for 6 h. During this time, the evolution of carbon dioxide (generated in the reaction) gradually ceased. The course of the reaction could also be followed by the gradual disappearance of the intense bromine colour in the reaction mixture. The carbon tetrachloride solution was then filtered under suction through a sintered glass funnel. The filter cake, consisting of silver bromide, was thoroughly washed with carbon tetrachloride, and the combined filtrate and washings were shaken with sodium bisulphite solution until free from bromine. Acidic substances possibly present were then removed by washing three times with sodium carbonate solution. The carbon tetrachloride solution was finally washed with water until neutral and dried over calcium chloride. The solvent was distilled off at normal pressure, the last traces *in vacuo*, whereupon the remainder suddenly solidified to a yellowish, crystalline mass, melting at 74–75°C (on a Kofler Hot Stage apparatus). The crude product weighed 84.7 g, representing a yield of 86 %. One recrystallization from ligroin raised the melting point to 77°C, reported 77° [1], 77–78° [2]. No depression of the melting point was observed upon admixture with an authentic sample of 1-bromo-3,5-dinitrobenzene, prepared according to Derbyshire and Waters.[2]. Yield of recrystallized product 62.3 g or 63 %.

Financial support from the *Swedish Natural Science Research Council* is gratefully acknowledged.

1. Elion, L. *Rec. trav. chim.* **42** (1923) 145.
2. Derbyshire, D. H. and Waters, W. A. *J. Chem. Soc.* **1950** 573.
3. Barnes, R. A. and Prochaska, R. J. *J. Am. Chem. Soc.* **72** (1950) 3188.
4. Zingaro, R. A., Goodrich, J. E., Kleinberg, J. and VanderWerf, C. A. *J. Am. Chem. Soc.* **71** (1949) 575.

Received February 9, 1962.

Replacement of Bromine and Chlorine in 2-Halo-5-nitrobenzenediazonium Compounds by Chloride Ion

BO LAMM

Nobel Institute of Chemistry, Stockholm 50, Sweden

In a recently published paper [1], the present author reported that nucleophilic halogen exchange reactions take place at room temperature between bromine or chlorine in 4-halo-3-nitrobenzenediazonium ion and chloride ion. Analogous reactions have now been found to take place between bromine and chlorine in 2-halo-5-nitrobenzenediazonium ion and chloride ion.

A kinetic investigation of these reactions is in progress, and some preliminary results will be presented below.

As far as possible, the competitive technique is applied, which means that at least two reactions are studied in the same kinetic run. This makes a safer comparison between their specific reaction rates possible, since the medium effects cancel. For further information about the experimental conditions, reference should be made to previous work. [1] It should be remarked that instead of the infrared spectroscopic technique employed earlier, quantitative gas chromatography has been adopted as the method of assaying the mixtures of dihalonitrobenzenes resulting from the kinetic experiments, since the latter method is considerably faster and has also been found to make possible the quantitative assay of a four-component mixture consisting of two isomeric pairs. Thus, competitive runs with 4-bromo-3-nitrobenzenediazonium ion and 2-bromo-5-nitrobenzenediazonium ion in a large excess of chloride ion have been made.

The competitive runs with the two isomeric bromonitrobenzenediazonium ions and chloride ion mentioned in the previous paragraph were carried out at two different temperatures. At 25°C, the ratio between the rate constants for the 4-bromo-3-nitro isomer and the 2-bromo-5-nitro isomer was found to be 1.32, and at 15°C, the same ratio was 1.61. (An extrapolation in an Arrhenius plot gives the ratio 1.00 at 40°C.)

Figures for the corresponding exchange reactions between ^{36}Cl-labelled chlorine compounds and non-radioactive chloride ion cannot easily be obtained from competitive runs for experimental reasons but may be calculated indirectly. At 25°C, the ratio for the corresponding chlorine compounds is 1.0. No value at 15°C has been obtained as yet.

Finally, the ratio between the specific reaction rates for 2-bromo-5-nitrobenzenediazonium ion and 2-chloro-5-nitrobenzenediazonium ion in the reactions with chloride ion at 25°C has been found to be 2.02. This further confirms the two-step mechanism postulated [1] for these reactions, with the absence of an "element effect". The very close agreement with the ideal value 2 is, however, fortuitous, because experiments which are in progress indicate that the reactions have different temperature coefficients.

One more conclusion may be drawn from the data presented above. Structurally, the 2-halo-5-nitrobenzenediazonium ions may be imagined to arise from the 4-halo-3-nitrobenzenediazonium ions by letting the diazonium group and the nitro group change places. It is interesting to note that this reversal does not have any substantial influence upon the halogen exchange reaction rate constants, since a diazonium group and a nitro group might be expected to interact to a different extent with a large halogen atom like bromine in an *ortho* position, in virtue of their different steric requirements. It is quite probable that solvation of the charged diazonium group makes it "larger" in the thermodynamic sense than would be apparent from the inspection of a molecular model.

Actually, the similarity of the specific reaction rates for the different isomers is nothing but a confirmation of an empirical multiple-substitution-additivity rule for the free-energy-of-activation changes due to substitution. Reference should be made to a review of this subject by Jaffé. [2]

Financial support from the *Swedish Natural Science Research Council* is gratefully acknowledged.

1. Elion, L. *Rec. trav. chim.* **42** (1923) 145.
2. Derbyshire, D. H. and Waters, W. A. *J. Chem. Soc.* **1950** 573.
3. Barnes, R. A. and Prochaska, R. J. *J. Am. Chem. Soc.* **72** (1950) 3188.
4. Zingaro, R. A., Goodrich, J. E., Kleinberg, J. and VanderWerf, C. A. *J. Am. Chem. Soc.* **71** (1949) 575.

Received February 9, 1962.

Replacement of Bromine and Chlorine in 2-Halo-5-nitrobenzenediazonium Compounds by Chloride Ion

BO LAMM

Nobel Institute of Chemistry, Stockholm 50, Sweden

In a recently published paper [1], the present author reported that nucleophilic halogen exchange reactions take place at room temperature between bromine or chlorine in 4-halo-3-nitrobenzenediazonium ion and chloride ion. Analogous reactions have now been found to take place between bromine and chlorine in 2-halo-5-nitrobenzenediazonium ion and chloride ion.

A kinetic investigation of these reactions is in progress, and some preliminary results will be presented below.

As far as possible, the competitive technique is applied, which means that at least two reactions are studied in the same kinetic run. This makes a safer comparison between their specific reaction rates possible, since the medium effects cancel. For further information about the experimental conditions, reference should be made to previous work. [1] It should be remarked that instead of the infrared spectroscopic technique employed earlier, quantitative gas chromatography has been adopted as the method of assaying the mixtures of dihalonitrobenzenes resulting from the kinetic experiments, since the latter method is considerably faster and has also been found to make possible the quantitative assay of a four-component mixture consisting of two isomeric pairs. Thus, competitive runs with 4-bromo-3-nitrobenzenediazonium ion and 2-bromo-5-nitrobenzenediazonium ion in a large excess of chloride ion have been made.

The competitive runs with the two isomeric bromonitrobenzenediazonium ions and chloride ion mentioned in the previous paragraph were carried out at two different temperatures. At 25°C, the ratio between the rate constants for the 4-bromo-3-nitro isomer and the 2-bromo-5-nitro isomer was found to be 1.32, and at 15°C, the same ratio was 1.61. (An extrapolation in an Arrhenius plot gives the ratio 1.00 at 40°C.)

Figures for the corresponding exchange reactions between ^{36}Cl-labelled chlorine compounds and non-radioactive chloride ion cannot easily be obtained from competitive runs for experimental reasons but may be calculated indirectly. At 25°C, the ratio for the corresponding chlorine compounds is 1.0. No value at 15°C has been obtained as yet.

Finally, the ratio between the specific reaction rates for 2-bromo-5-nitrobenzenediazonium ion and 2-chloro-5-nitrobenzenediazonium ion in the reactions with chloride ion at 25°C has been found to be 2.02. This further confirms the two-step mechanism postulated [1] for these reactions, with the absence of an "element effect". The very close agreement with the ideal value 2 is, however, fortuitous, because experiments which are in progress indicate that the reactions have different temperature coefficients.

One more conclusion may be drawn from the data presented above. Structurally, the 2-halo-5-nitrobenzenediazonium ions may be imagined to arise from the 4-halo-3-nitrobenzenediazonium ions by letting the diazonium group and the nitro group change places. It is interesting to note that this reversal does not have any substantial influence upon the halogen exchange reaction rate constants, since a diazonium group and a nitro group might be expected to interact to a different extent with a large halogen atom like bromine in an *ortho* position, in virtue of their different steric requirements. It is quite probable that solvation of the charged diazonium group makes it "larger" in the thermodynamic sense than would be apparent from the inspection of a molecular model.

Actually, the similarity of the specific reaction rates for the different isomers is nothing but a confirmation of an empirical multiple-substitution-additivity rule for the free-energy-of-activation changes due to substitution. Reference should be made to a review of this subject by Jaffé. [2]

A grant from *Knut och Alice Wallenbergs Stiftelse* made possible the purchase of the gas chromatographic apparatus used in this work.

The *Swedish Natural Science Research Council* has provided financial support, which is also gratefully acknowledged.

1. Lamm, B. *Arkiv Kemi* **18** (1961) 79.
2. Jaffé, H. H. *Chem. Revs.* **53** (1953) 191, p. 243.

Received February 9, 1962.

Nucleophilic Substitution of Aromatic Chlorine in Diazonium Ions by Bromide Ion

BO LAMM

Nobel Institute of Chemistry, Stockholm 50, Sweden

It is known [1,2] that aromatic bromine atoms in diazonium compounds may be replaced by chlorine atoms in reactions involving a nucleophilic attack by chloride ion. The opposite reaction, namely substitution of aromatic chlorine by bromide ion has not hitherto been reported to take place in diazonium compounds. However, the substitution of a nitro group by bromide ion in a diazonium compound has been reported by Sihlbom. [3] For comparison it may be mentioned that among the 1-halo-2,4-dinitrobenzenes, substitution of chlorine by bromide ion as well as the opposite reaction take place [4], the specific rates of the two reactions being of the same order of magnitude, so that all four molecular species in question may be present in comparable amounts at equilibrium (measured at 175 and 195°C).

Bearing this evidence in mind, it seems rather difficult to understand why a chlorine atom in a suitably substituted diazonium ion should not be replaced by bromide ion. In actual fact, the present author has found that 2-chloro-5-nitrobenzenediazonium ion and 4-chloro-3-nitrobenzenediazonium ion in a hydrobromic acid-acetic acid-water medium at 25°C are converted to the corresponding bromine compounds through halogen exchange. The conversions are, however, not quantitative for reasons which will be presented below.

Experimental. About 1 g 2-chloro-5-nitroaniline or 4-chloro-3-nitroaniline, prepared by nitration in conc. sulphuric acid solution of *o*-chloroaniline and *p*-chloroaniline, respectively, was dissolved in 75 ml glacial acetic acid and the solution gradually added to a solution of the required amount of sodium nitrite, dissolved in 15 ml conc. sulphuric acid, while cooling in an ice-bath. 75 ml freshly redistilled constant-boiling-point hydrobromic acid was added, and the mixture was placed in a thermostatic bath at 25.0 ± 0.1°C. After one week, no more diazonium compounds were present (negative reaction with 2-naphthol and sodium acetate), and the mixture was distilled with steam until no more organic material was carried over. The distillate was made alkaline and extracted with ether, the combined ether extracts were washed and dried with calcium chloride and finally, the ether was allowed to evaporate at room temperature. The solid remainder was dissolved in 2 ml toluene, and a few microlitres of this solution was analyzed on a Perkin-Elmer Model 116E Fractometer. Conditions: 2 m silicon grease-on-chromosorb column "O", i.d. 4 mm, temp. 185°C, flow

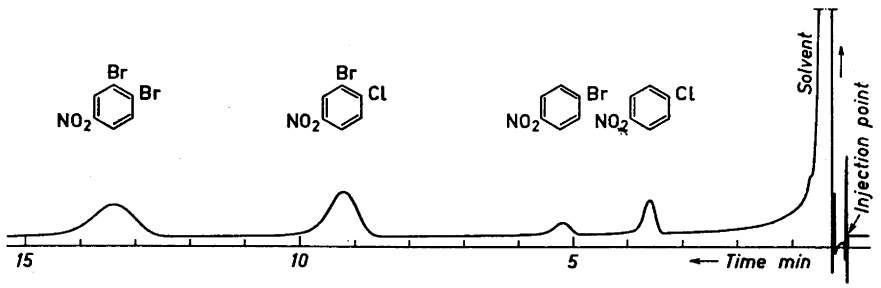

Fig. 1. Fractogram of substances formed in the reactions of 2-chloro-5-nitrobenzenediazonium ion in a hydrobromic acid-acetic acid-water medium.

A grant from *Knut och Alice Wallenbergs Stiftelse* made possible the purchase of the gas chromatographic apparatus used in this work.

The *Swedish Natural Science Research Council* has provided financial support, which is also gratefully acknowledged.

1. Lamm, B. *Arkiv Kemi* **18** (1961) 79.
2. Jaffé, H. H. *Chem. Revs.* **53** (1953) 191, p. 243.

Received February 9, 1962.

Nucleophilic Substitution of Aromatic Chlorine in Diazonium Ions by Bromide Ion

BO LAMM

Nobel Institute of Chemistry, Stockholm 50, Sweden

It is known [1,2] that aromatic bromine atoms in diazonium compounds may be replaced by chlorine atoms in reactions involving a nucleophilic attack by chloride ion. The opposite reaction, namely substitution of aromatic chlorine by bromide ion has not hitherto been reported to take place in diazonium compounds. However, the substitution of a nitro group by bromide ion in a diazonium compound has been reported by Sihlbom. [3] For comparison it may be mentioned that among the 1-halo-2,4-dinitrobenzenes, substitution of chlorine by bromide ion as well as the opposite reaction take place [4], the specific rates of the two reactions being of the same order of magnitude, so that all four molecular species in question may be present in comparable amounts at equilibrium (measured at 175 and 195°C).

Bearing this evidence in mind, it seems rather difficult to understand why a chlorine atom in a suitably substituted diazonium ion should not be replaced by bromide ion. In actual fact, the present author has found that 2-chloro-5-nitrobenzenediazonium ion and 4-chloro-3-nitrobenzenediazonium ion in a hydrobromic acid-acetic acid-water medium at 25°C are converted to the corresponding bromine compounds through halogen exchange. The conversions are, however, not quantitative for reasons which will be presented below.

Experimental. About 1 g 2-chloro-5-nitroaniline or 4-chloro-3-nitroaniline, prepared by nitration in conc. sulphuric acid solution of *o*-chloroaniline and *p*-chloroaniline, respectively, was dissolved in 75 ml glacial acetic acid and the solution gradually added to a solution of the required amount of sodium nitrite, dissolved in 15 ml conc. sulphuric acid, while cooling in an ice-bath. 75 ml freshly redistilled constant-boiling-point hydrobromic acid was added, and the mixture was placed in a thermostatic bath at 25.0 ± 0.1°C. After one week, no more diazonium compounds were present (negative reaction with 2-naphthol and sodium acetate), and the mixture was distilled with steam until no more organic material was carried over. The distillate was made alkaline and extracted with ether, the combined ether extracts were washed and dried with calcium chloride and finally, the ether was allowed to evaporate at room temperature. The solid remainder was dissolved in 2 ml toluene, and a few microlitres of this solution was analyzed on a Perkin-Elmer Model 116E Fractometer. Conditions: 2 m silicon grease-on-chromosorb column "O", i.d. 4 mm, temp. 185°C, flow

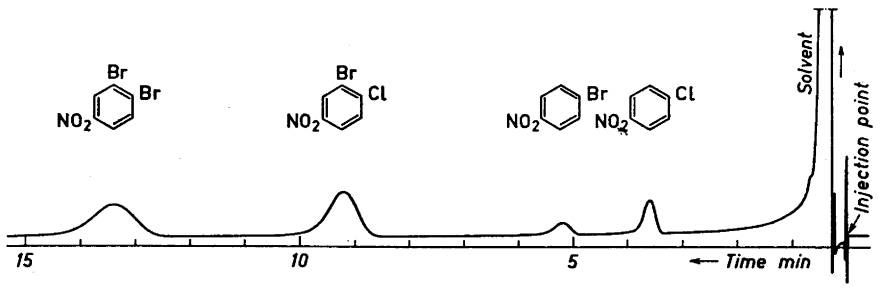

Fig. 1. Fractogram of substances formed in the reactions of 2-chloro-5-nitrobenzenediazonium ion in a hydrobromic acid-acetic acid-water medium.

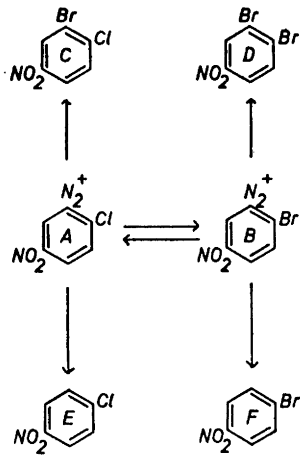

Fig. 2. Reactions of 2-chloro-5-nitrobenzenediazonium ion in a hydrobromic acid-acetic acid-water medium.

rate (He) 85 ml/min. The peaks obtained were easily identified by comparing the retention times with those of authentic samples of the compounds suspected to be present. The fractogram obtained in the experiment with 2-chloro-5-nitrobenzenediazonium ion as the starting material is shown in Fig. 1. The areas under the peaks give a semi-quantitative idea of the molar proportions of the compounds present. In quantitative work, calibrations with known mixtures should always be made.

The experiment with 4-chloro-3-nitrobenzenediazonium ion as the starting material gave a qualitatively analogous result, other isomers being formed.

Discussion. In Fig. 2, a reaction scheme is given for the case of 2-chloro-5-nitrobenzenediazonium ion. In the scheme, all the products observed in the fractogram are accounted for.

One possible explanation for the fact that the compounds are formed in comparable amounts is that the reactions A→C, A→E, B→D and B→F take place at rates comparable to that of A→B (the symbols are taken from Fig. 2). As a consequence, some of the aromatic chlorine will be "frozen in" and thus no quantitative conversion of aromatic chlorine into aromatic bromine can take place.

A further reaction which must be considered is the back-reaction B→A. The rate of this reaction has been studied in previous work[2], and it is considerably more rapid than A→B. It can therefore be estimated, that under the conditions of this work, the small amount of chloride ion generated in the exchange reaction A→B was sufficient to produce a condition of equilibrium at a stage when A and B were present in comparable amounts, despite the large excess of hydrobromic acid. It is, however, impossible to conclude how close to equilibrium the reaction A⇌B had approached before the diazonium compounds were consumed. A possible equilibrium is of course also continually being perturbed by the side-reactions.

The nature of the reactions A→C and B→D is known from the work by Lewis and Hinds[5]. These authors have shown that the rate expression for the reaction between a diazonium ion and bromide ion consists of a monomolecular term arising from the spontaneous decomposition of the diazonium ion, and a bimolecular term ascribed to a nucleophilic attack of bromide ion on the carbon atom carrying the diazonium group. It is thus impossible to suppress the reactions A → C and B → D compared to A → B by increasing the bromide ion concentration.

The reactions A→E and B→F are somewhat unexpected and cannot at present be explained in detail. A plausible mechanism involves the reduction of the diazonium ion by bromide ion as the initiating step. It would be an interesting task to trace the origin of the hydrogen atom which replaces the diazonium group.

The author's thanks are directed to the Head of this Institute, Docent Lars Melander, for valuable discussions.

A grant from *Knut och Alice Wallenbergs Stiftelse* made possible the purchase of the gas chromatographic apparatus used in this work.

Financial support has been provided by the *Swedish Natural Science Research Council.*

1. Hantzsch, A. *Ber.* **30** (1897) 2334; Hantzsch, A. and Smythe, J. S. *Ber.* **33** (1900) 505.
2. Lamm, B. *Arkiv Kemi* **18** (1961) 79.
3. Sihlbom, L. *Acta Chem. Scand.* **7** (1953) 1197.
4. Bennett, G. M. and Vernon, I. H. *J. Chem. Soc.* **1938** 1783.
5. Lewis, E. S. and Hinds, W. H. *J. Am. Chem. Soc.* **74** (1952) 304.

Received February 9, 1962.

Preparation of ^{18}O-Labelled Furan

BØRGE BAK, JØRGEN TORMOD NIELSEN and MARIANNE SCHOTTLÄNDER

Chemical Laboratory of the University of Copenhagen, Copenhagen, Denmark

Furan, enriched with respect to oxygen, has not been prepared earlier. The preparation became of interest to us in connection with structural work on the furan molecule. Here, an unambiguous determination of the oxygen coordinates with respect to the rest of the molecule necessitates that an ^{18}O-enriched sample can be investigated. The same sample is, of course, also of interest for infrared, Raman and ultraviolet spectroscopic work *etc.*

Experimental. The reaction path, found originally by Feist [1] and worked out by him for large quantities of isotopically non-enriched materials, is the following:

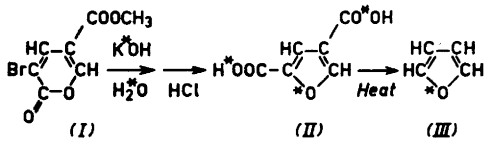

*O designates an oxygen isotope, either ^{16}O or ^{18}O, with a relative abundance of 3:1 in this experiment. O = ^{16}O.

At room temperature 1.10 g (4.8 mmole) of 3-bromocoumalic acid methyl ester [1] (I), m.p. 134.5–135.5°, was dissolved in a solution of 2.20 g (39.4 mmole) of "ordinary" KOH in 4.55 g of water, enriched to 32 % in ^{18}O, the water (~ 242 mmole) acting as reactant and solvent. The reaction flask was flushed with dry nitrogen and heated under reflux to 120°C (oil bath) for 20 min. After cooling to liquid-air temperature, a high vacuum was established whereafter 44 mmoles of dry, gaseous HCl was condensed into the reaction mixture. Under slow elevation of the temperature the HCl applied was absorbed without difficulty, magnetic stirring of the reaction mixture being started as soon as feasible. Stirring at room temperature was continued for 30 min, after which water, methanol, and hydrochloric acid were evaporated *in vacuo* at room temperature and collected at liquid-air temperature (trap 1). The remaining mixture of (II), KBr, KCl, and possibly a small quantity of hydrochloric acid was kept for 24 h over NaOH and P_2O_5 in an evacuated desiccator. The KBr-disc spectrum of 3 mg of the resulting dry mixture showed no sign of an organic compound other than (II).

Conversion of (II) to (III) was carried out in a 350 ml glas ampulla, following the instructions of Ref.[2] except for a slight change in reaction conditions (1 h heating at 250–75°C in an oil bath). After cooling, the CO_2 evolved was removed at −80°C *in vacuo* and collected at liquid-air temperature (trap 2). Thereafter, the available quantity of (III) with a trace of CO_2 was distilled off at 0°C and kept in contact with a small amount of solid NaOH which removed the trace of CO_2 in the course of 24 h. By a final distillation *in vacuo*, 85 mg of (III) (= 1.25 mmole) was collected. The infrared and microwave gas-spectra consistently showed this preparation to consist of a mixture of *ca.* 75 % "ordinary" and *ca.* 25 % [^{18}O]-furan. The yield of (III), based on the amount of (I) applied, was 26 %.

By mass spectroscopy it was shown that the contents of trap 1, as expected, had about the same ^{18}O-abundance as (III) whereas the ^{18}O-abundance of the contents of trap 2 (carbon dioxide) was about *half* of this (11–12 %). This is the reason for believing that the carbonyl oxygen atoms of (II) are *not* exchanged against ^{18}O. The introduction of ^{18}O into the two carboxy groups of (II) takes place during the saponification of the carbomethoxy group and the lactonic part of (I), and not at some later stage. The quantity of ^{18}O which is known to be present in (III) perhaps enters through the generally accepted mechanism:

$$RCH{=}CHOH \rightleftharpoons RCH_2{-}CHO$$
$$RCH_2{-}CHO + H_2{*}O \rightleftharpoons RCH(OH)(*OH)$$
$$\rightleftharpoons RCH_2CH{*}O + H_2O \qquad (IV)$$

(IV) may or may not be accompanied by replacements of the bromine atom of (I) by *OH prior to the final ring closure, but this is without influence on the ^{18}O-abundance of (III).

We are indebted to Dr. Dansgaard of the Biophysical Laboratory of the University of Copenhagen for carrying out the mass spectrometric analyses.

1. Feist, F. *Ber.* **34** (1901) 1992.
2. Bak, B., Nielsen, J. T. and Schottländer, M. *Acta Chem. Scand.* **16** (1962) 123.

Received February 2, 1962.

The Syntheses of a *gem* Dithiol under Mild Conditions

BENGT MAGNUSSON

Department of Organic Chemistry, Chemical Institute, University of Uppsala, Sweden

Preparation of *gem* dithiols has been limited in the past to the reaction of carbonyl compounds with hydrogen sulphide under various conditions. These conditions, however, are rather critical and temperature, pressure and reaction time must be carefully adjusted for each ketone or aldehyde. Certain aldehydes give good yields under moderate pressures (30—50 atm) [1], while other carbonyl compounds require pressures of 7 500—8 500 atm. Chloral, highly fluorinated ketones and aldehydes, and other carbonyl compounds which form stable *gem* diols do not form *gem* dithiols under pressure. Instead *gem* ol-thiols are obtained, sometimes in good yields [2]. 1,3-Diphenyl-2,2-dimercaptopropane was prepared in 80 % yield by Carmack by simply passing hydrogen sulphide and hydrogen chloride at ordinary pressure into a cold ethanol solution of dibenzylketone [3]. Unfortunately, this simple method does not seem to be generally applicable, as attempts by the author to apply it to phenylacetone, dibenzylacetone, α-tetralone, 2-indanone, anthrone, xanthone, and fluorenone have all failed due to the formation of trimers or polymers of the thioketones, or total lack of reaction.

Many attempts have also been made to reduce duplodithioketones to *gem* dithiols, but the duplodithioketones are very stable compounds and it is not possible to reduce them with tin and hydrochloric acid. When they are boiled for an extended period a faint odor of mercaptane is certainly perceptible, but under these conditions the *gem* dithiols are not stable.

Lithium-aluminium hydride splits up the tetrathiane ring, but *gem* dithiols are not stable in alkaline medium. Furthermore, one of the *gem* SH-groups is substituted by hydrogen [1]. Reduction with hydrogen and Raney-nickel was not tried, because the Raney-nickel would cause desulphuration of the tetrathiane ring, as would even copper powder do in boiling dioxane. Moreover, the nickel catalyst would have been poisoned by the sulphur.

Experiments with Carmacks dithiol showed, however, that its disodium salt was stable in ethanol solution at −70° and that it was possible to react this salt with methyl iodide. Therefore attempts were made to reduce duplodithioacetone[4] I with sodium in liquid ammonia. This attempt was successful. The presence of the *gem* dithiol was established by adding benzylchloride to the reaction mixture. β,β-Bis-benzylmercaptopropane III was isolated in 80 % yield. It was identical with a specimen prepared from acetone and benzylmercaptane according to Fromm *et al.*[5]

The free dithiol IV could be isolated by removing the ammonia in vacuum after the reduction with sodium. The solid disodium salt II was dispersed in cold ether and hydrogen chloride was passed into the reaction mixture until the *gem* dithiol was set free. From the ether solution, IV was obtained in 30 % yield after one distillation. It was further purified by sublimation at 0.1 mm. Crystal flakes with a melting point of 6—8° were obtained. (lit. 4—8°)[1]. (Found: C 33.98; H 7.56; S 58.21. Calc. for $C_3H_8S_2$: C 33.29; H 7.45; S 59.26).

The compound gives a yellow precipitate with lead acetate in ethanol, which turns

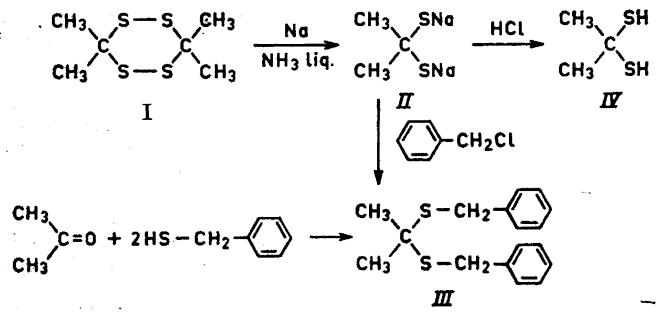

red within one second and is rapidly decomposed to black lead sulphide.

These experiments exclude structures of duplodithioacetone with one thioether bond and one trisulphide bond.

Further they point to a new method to obtain *gem* dithiols.

The author is indebted to Professor A. Fredga for his encouraging interest in this work.

1. Cairns, T. L., Evans, G. L., Larchar, A. W. and McKusick, B. C. *J. Am. Chem. Soc.* **74** (1952) 3982.
2. Harris, Jr, J. F. *J. Org. Chem.* **25** (1960) 2259.
3. Berchold, G. A., Edwards, B. E., Campaigne, E. and Carmack, M. *J. Am. Chem. Soc.* **81** (1959) 3184.
4. Magnusson, B. *Acta Chem. Scand.* **13** (1959) 1031.
5. Fromm, E., Forster, A. and v. Scherschewitski, B. *Ann.* **394** (1912) 343.

Received February 23, 1962.

Studies on Peroxy Compounds XXII * Preparation of 2,3,4,5,4′,5′-Hexahydro-2,2′-dithienyl

CURT BERGLUND and SVEN-OLOV LAWESSON

Department of Organic Chemistry, Chemical Institute, University of Uppsala, Uppsala, Sweden

2-Benzoyloxy tetrahydrothiophene, I, was first prepared in 1957 by Horner and Jürgens [1]. The starting materials were benzoylperoxide and tetrahydrothiophene. Besides I, tetrahydrothiophene sulphoxide, benzoic acid and the anhydride of benzoic acid were obtained.

Sosnovsky [2,3] prepared I by reacting tetrahydrothiophene with *t*-butyl perbenzoate in the presence of cuprous bromide. In that case no oxidation of the sulphide did occur. By pyrolysis of I for 2 h at 110°C a yield of 80 % of 2,3-dihydrothiophene was obtained. In another experiment Sosnovsky heated I in *t*-butanol under reflux for 100 h and isolated a quantitative yield of benzoic acid and a dimer of dihydrothiophene with a b.p. of 90°C/0.5 mm Hg, $n_D^{25} = 1.6006$. Mol. wt. 179. Nothing was said about the structure of the dimer. The present authors had at the same time [4] performed this reaction. When we pyrolyzed I at 160–170°C for 2 h no 2,3-dihydrothiophene could be detected but a 45 % yield of the dimer was obtained. B.p. 88–90°C/0. 2 mm Hg, $n_D^{20} = 1.6023$. Mol. wt. 168. Although 2,3-dihydrothiophene certainly is an intermediate in our case, the dimerization compound is the final product.

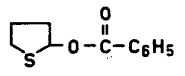

I

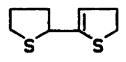

II

Gas chromatographic analysis showed one peak, indicating a single compound, I.R. measurements showed a double bond and elementary analyses agreed well with the formula, $C_8H_{12}S_2$. The dimer was desulphurated with Raney Ni and the hydrocarbon formed was octane which was shown by gas chromatographic analysis. The N.M.R. spectrum of the dimer was also taken and the relative intensities of the bands were 1:1:10, corresponding to one ethylenic, one tertiary and ten methylenic hydrogens. The configuration of the dimer was thus fixed to be II.

A full paper of these and related results is being prepared.

We wish to thank Prof. A. Fredga for his interest in this investigation. Financial support from *Magnus Bergvalls stiftelse* and *Lucidol Division, Wallace & Tiernan, Inc., Buffalo, N.Y. U.S.A.* are also acknowledged.

1. Horner, L. and Jürgens, E. *Ann.* **602** (1957) 135.
2. Sosnovsky, G. *J. Org. Chem.* **26** (1961) 281.
3. Sosnovsky, G. *Tetrahedron* **18** (1962) 15.
4. Lawesson, S.-O. and Berglund, C. *Tetrahedron Letters* **2** (1960) 4.

Received March 12, 1962.

* Part XXI. Lawesson, S.-O., Dahlén, M. and Frisell, C. *Acta Chem. Scand.* **16** (1962). *In press.*

** Present address: Department of Chemistry, University of Aarhus, Aarhus, Denmark.

red within one second and is rapidly decomposed to black lead sulphide.

These experiments exclude structures of duplodithioacetone with one thioether bond and one trisulphide bond.

Further they point to a new method to obtain *gem* dithiols.

The author is indebted to Professor A. Fredga for his encouraging interest in this work.

1. Cairns, T. L., Evans, G. L., Larchar, A. W. and McKusick, B. C. *J. Am. Chem. Soc.* **74** (1952) 3982.
2. Harris, Jr, J. F. *J. Org. Chem.* **25** (1960) 2259.
3. Berchold, G. A., Edwards, B. E., Campaigne, E. and Carmack, M. *J. Am. Chem. Soc.* **81** (1959) 3184.
4. Magnusson, B. *Acta Chem. Scand.* **13** (1959) 1031.
5. Fromm, E., Forster, A. and v. Scherschewitski, B. *Ann.* **394** (1912) 343.

Received February 23, 1962.

Studies on Peroxy Compounds XXII * Preparation of 2,3,4,5,4′,5′-Hexahydro-2,2′-dithienyl

CURT BERGLUND and SVEN-OLOV LAWESSON

Department of Organic Chemistry, Chemical Institute, University of Uppsala, Uppsala, Sweden

2-Benzoyloxy tetrahydrothiophene, I, was first prepared in 1957 by Horner and Jürgens [1]. The starting materials were benzoylperoxide and tetrahydrothiophene. Besides I, tetrahydrothiophene sulphoxide, benzoic acid and the anhydride of benzoic acid were obtained.

Sosnovsky [2,3] prepared I by reacting tetrahydrothiophene with *t*-butyl perbenzoate in the presence of cuprous bromide. In that case no oxidation of the sulphide did occur. By pyrolysis of I for 2 h at 110°C a yield of 80 % of 2,3-dihydrothiophene was obtained. In another experiment Sosnovsky heated I in *t*-butanol under reflux for 100 h and isolated a quantitative yield of benzoic acid and a dimer of dihydrothiophene with a b.p. of 90°C/0.5 mm Hg, $n_D^{25} = 1.6006$. Mol. wt. 179. Nothing was said about the structure of the dimer. The present authors had at the same time [4] performed this reaction. When we pyrolyzed I at 160–170°C for 2 h no 2,3-dihydrothiophene could be detected but a 45 % yield of the dimer was obtained. B.p. 88–90°C/0. 2 mm Hg, $n_D^{20} = 1.6023$. Mol. wt. 168. Although 2,3-dihydrothiophene certainly is an intermediate in our case, the dimerization compound is the final product.

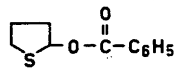

I

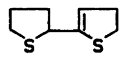

II

Gas chromatographic analysis showed one peak, indicating a single compound, I.R. measurements showed a double bond and elementary analyses agreed well with the formula, $C_8H_{12}S_2$. The dimer was desulphurated with Raney Ni and the hydrocarbon formed was octane which was shown by gas chromatographic analysis. The N.M.R. spectrum of the dimer was also taken and the relative intensities of the bands were 1:1:10, corresponding to one ethylenic, one tertiary and ten methylenic hydrogens. The configuration of the dimer was thus fixed to be II.

A full paper of these and related results is being prepared.

We wish to thank Prof. A. Fredga for his interest in this investigation. Financial support from *Magnus Bergvalls stiftelse* and *Lucidol Division, Wallace & Tiernan, Inc., Buffalo, N.Y. U.S.A.* are also acknowledged.

1. Horner, L. and Jürgens, E. *Ann.* **602** (1957) 135.
2. Sosnovsky, G. *J. Org. Chem.* **26** (1961) 281.
3. Sosnovsky, G. *Tetrahedron* **18** (1962) 15.
4. Lawesson, S.-O. and Berglund, C. *Tetrahedron Letters* **2** (1960) 4.

Received March 12, 1962.

* Part XXI. Lawesson, S.-O., Dahlén, M. and Frisell, C. *Acta Chem. Scand.* **16** (1962). *In press.*

** Present address: Department of Chemistry, University of Aarhus, Aarhus, Denmark.

On the Oxidation of Cholesterol by Blood *in vitro*

Bile Acids and Steroids 119

HENRY DANIELSSON and
MARJORIE G. HORNING*

Department of Chemistry, Karolinska Institutet, Stockholm, Sweden

Although the conversion of cholesterol to bile acids by the liver has been studied extensively [1], very little work has been done on the oxidation of cholesterol by extrahepatic tissue. Meier *et al.*[2] have reported that slices of rat kidney, spleen, adrenals and testes convert the terminal methyl group of 26-^{14}C-cholesterol to $^{14}CO_2$ and suggested that the oxidation by adrenals and testes was directed toward the formation of C-19 and C-21 steroid hormones. Extrahepatic oxidation of cholesterol could be of considerable importance, since by supplying the liver with intermediates in bile acid formation, it would influence the conversion of cholesterol to bile acids.

The observation by Lovelock ** that the cholesterol level in blood, as measured by the Liebermann-Burchard reaction, decreased during the aerobic incubation of blood prompted this investigation of the metabolism of cholesterol by blood using isotopic and chromatographic techniques.

Experimental. "Red blood cells" (likely contaminated whith white blood cells) were isolated from fresh citrated human blood by centrifuging for 10 min at 2 000 × *g*. The packed cells were washed twice by centrifugation with Ringer's solution containing 0.1 % glucose and suspended in an equal volume of the same solution. Lysed cells were prepared by adding an equal volume of distilled water and letting the mixture stand for 5 min at room temperature.

To 10 ml of washed "red blood cells" or lysed cells there was added 1.0 ml of M/10 tris(hydroxymethyl)aminomethane buffer, pH 7.8 and 0.1 ml of 10 % glucose, 2 000 I.U. of benzyl penicillin, 0.1 ml of 1 % versene and 10 μC (160 μg) of 4-^{14}C-cholesterol (Radiochemical Centre, Amersham, England) as a serum albumin suspension [3]. Incubations were carried out aerobically at 37° for 4 h. At the end of the incubation period, the mixture was added dropwise to 5 volumes of ethanol-ether (3:1). The mixture was filtered and the filtrate evaporated to about 20 ml. The filtrate was diluted with water, acidified and extracted twice with butanol saturated with water. The combined butanol extracts were washed with several small volumes of water until neutral and then taken to dryness. The residue was subjected to reversed phase partition chromatography to separate the cholesterol from cholesterol esters and more polar products, using phase-system I[4]. The more polar products were then separated by chromatography into "acidic", "trihydroxy neutral" and "dihydroxy neutral" fractions (*cf.* Ref.[6]) using phase-system III[4]. Rechromatography of the "acidic fraction" was performed with phase systems described by Norman and Sjövall [5].

Results and discussion. Chromatographic analyses of the labeled products isolated from incubations of 4-^{14}C-cholesterol with whole blood, washed "red blood cells", or lysed "red blood cells" showed a small but easily reproducible conversion to more polar products of 2—3 %. The chromatographic pattern of these products was strikingly similar for all types of incubations. The addition of TPNH *, AMP and nicotinamide to washed cells had no stimulatory effects on the oxidation of cholesterol. Significant amounts of cholesterol esters were obtained only from incubations with whole blood.

Partial identification of the more polar products was carried out on material isolated from an incubation of 90 μC of 4-^{14}C-cholesterol with washed "red blood cells". The chromatogram of the more polar products using phase-system III is shown in Fig. 1. The ratio of the "acidic" (8—20 ml of effluent), the "trihydroxy neutral" (25—50 ml of effluent) and the "dihydroxy neutral" fraction (60—150 ml of effluent) was 1:3:6. This was similar to the ratio observed previously for incubations of 4-^{14}C-cholesterol with boiled liver extracts [4]. The results of this experiment were confirmed by analysis of material combined from several small incubations.

The "acidic fraction" was rechromatographed with carrier cholic and chenodeoxy-

* Permanent address: Lipid Research Center, Baylor University College of Medicine, Houston, Texas.

** Personal communication.

* Abbreviations used are: TPNH, triphosphospyridine nucleotide, reduced form; AMP, adenosine monophosphate.

cholic acid. The radioactivity did not coincide with the titration peaks for the carrier acids, but was distributed in three distinct fractions, one slightly less polar than cholic acid and two less polar than chenodeoxycholic acid. Acidic materials with chromatographic properties similar to the last two fractions have been isolated from autoxidized cholesterol [6].

Results obtained from incubations of cholesterol with liver homogenates [6] indicated that the "trihydroxy neutral" fraction might contain 3β,5α,6β-trihydroxycholestane. Upon recrystallization to constant specific activity with carrier triol, 43 % of this fraction was indeed found to be 3β,5α, 6β-trihydroxycholestane. The presence of this triol was confirmed by acetylation of the combined mother liquors and crystals from this experiment. After chromatography on aluminum oxide [6] and recrystallization to constant specific activity, 43 % of the radioactivity was found to be present in the 3,5-diacetate of the triol. The major component (57 %) of the "trihydroxy neutral" fraction was not identified. It did not correspond to any of the known neutral intermediates; after acetylation it was eluted later than the 3,5-diacetate of the triol.

Rechromatography of the "dihydroxy neutral" fraction (75—150 ml of effluent, Fig. 1) showed that the major part of this fraction, about 75 %, had the same elution volume as the epimeric 7-hydroxycholesterols, which can not be separated with this phase system. By isotope dilution it was established that the radioactive material in this peak was a mixture of 7α-, and 7β-hydroxycholesterol; 30 % was identified as 7α-hydroxycholesterol (by crystallization to constant specific activity of the free sterol and of the diacetate) and 74 % as 7β-hydroxycholesterol (by recrystallization of this diacetate and dibenzoate). The remaining 25 % of the "dihydroxy neutral" fraction which was eluted after the epimeric 7-hydroxycholesterols was not identified.

Of the total amount of cholesterol converted to more polar products 65 % was accounted for as 3β,5α,6β-trihydroxycholestane and 7α-, and 7β-hydroxycholesterol. These compounds, together with 7-ketocholesterol, have been shown to be the major autoxidation products of cholesterol (*cf.* Ref.[6]). In spite of the slow oxidation of cholesterol by blood as compared to liver [5], the red and/or the white blood cells could

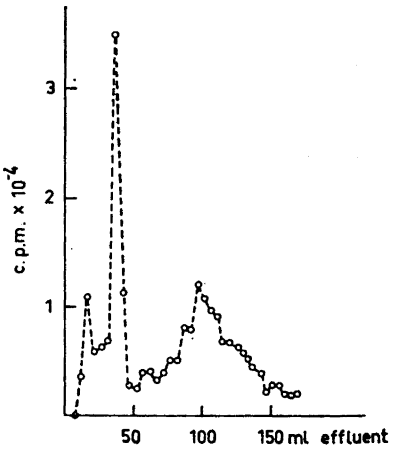

Fig. 1. Rechromatography on phase system III of the more polar fraction obtained from incubation of 90 μC 4-^{14}C-cholesterol with washed "red blood cells". Column: 4.5 g hydrophobic Hyflo Supercel.

play a rôle in the conversion of cholesterol to bile acids if part of the 7α-hydroxycholesterol and of the remaining 35 % of the more polar fraction were formed by enzymic reactions. It appears difficult, however, to establish if this is the case or not.

The present study emphasizes the difficulty of distinguishing enzymic from autoxidation products when microgram quantities of cholesterol are employed in incubations of long duration.

Acknowledgements. This work is part of investigations supported by the National Institutes of Health, Bethesda, Md., USA (Research grant H-2842).

1. Bergström, S., Danielsson, H. and Samuelsson, B. in Bloch, K. *Lipide Metabolism*, John Wiley and Sons, New York 1960, p. 296 ff.
2. Meier, J. R., Siperstein, M. D. and Chaikoff, I. L. *J. Biol. Chem.* **198** (1952) 105.
3. Danielsson, H. *Acta Chem. Scand.* **14** (1960) 348.
4. Danielsson, H. *Biochim. et Biophys. Acta* **27** (1958) 401.
5. Norman, A. and Sjövall, J. *J. Biol. Chem.* **233** (1958) 872.
6. Danielsson, H. *Acta Chem. Scand.* **14** (1960) 846.

Received February 26, 1962.

The Structure of an Alleged Oxepin

G. L. BUCHANAN, Miss J. A. HAMILTON, T. A. HAMOR and G. A. SIM

Chemistry Department, The University, Glasgow, W.2., Scotland

The seven-membered heterocycle, oxepin (I) has recently attracted attention as a potentially flat molecule [1] with eight π-electrons, which would constitute a better test of the Hückel aromaticity rule than cyclo-octatetraene, which is known to be puckered [2]. Benzo-oxepins are known [3], but despite the efforts of many workers [1,4] monocyclic oxepins have so far defied synthesis. Consequently, the recent report [5] of a one-step synthesis of 2-amino-4,7-dimethyloxepin-3-carbonamide (II) from acetonyl acetone and cyanoacetamide is remarkable, and since no structural evidence was offered we have re-examined the reaction product.

A specimen prepared by Westöö's procedure [5] gave m.p., analytical and spectroscopic data in agreement with those reported. The substance is unstable in base, but stable in the presence of acids; it forms a mono-picrate, m.p. 190° (decomp.). (Found: C 44.0; H 3.8; N 17.0. $C_{15}H_{15}O_9N_5$ requires C 44.0; H 3.7; N 17.1) and a mono-hydrobromide, m.p. 230 – 260° (decomp.). (Found: C 41.3; H 5.1; N 10.6; Br 30.4. $C_9H_{12}O_2N_2.HBr$ requires C 41.4; H 5.0; N 10.7; Br 30.65). The infrared spectrum (nujol) shows C=O absorption at 1670 cm^{-1} but no C≡N band, and the nitrile function is thus probably implicated in ring formation. Westöö's formula (II) is one interpretation of this: another possibility is (III), or its double-bond isomers, and an X-ray analysis of the hydrobromide shows that the latter has in fact structure (IV). Westöö's product is thus a highly substituted monomeric cyclopentadiene with the double bonds probably located as in (III).

The hydrobromide crystallizes in the monoclinic system as a monohydrate with cell dimensions $a = 8.44$, $b = 7.45$, $c = 19.05$ Å, $\beta = 102.9°$. There are four units of $C_9H_{13}N_2O_2Br$, H_2O in the unit cell [d(meas.) = 1.59, d (calc.) = 1.588 $g.cm^{-3}$] and the space group is $P2_1/c$. Three-dimensional X-ray intensity data were recorded on equi-inclination Weissenberg photographs and estimated visually; in all 1640 independent structure factors were evaluated.

The position of the bromide ion was deduced initially from Patterson syntheses. The remaining atoms (other than hydrogen) were then located by evaluating two successive three-dimensional Fourier syntheses. Subsequent refinement of the positional and thermal atomic parameters by the method of least squares has reduced the value of R to 15.3 % and the essential details of structure (IV) are now firmly established. The assignment of the double bonds is based on the calculated bond lengths.

For the calculations on the Glasgow University DEUCE computer, programmes [6] devised by Dr. J. S. Rollett and Dr. J. G. Sime were employed. Micro-analyses were by Mr. J. M. L. Cameron, B.Sc., and his staff.

We thank Professor J. Monteath Robertson, F. R. S., for his interest and encouragement, the University of Glasgow for an I.C.I. Research Fellowship to T.A.H.), the Department of Scientific and Industrial Research for financial support (to J.A.H.), and Mr. I. M. Dennler, B.Sc., for preparative assistance.

1. Meinwald, J. and Nozaki, H. *J. Am. Chem. Soc.* **80** (1958) 3132.
2. Lippincott, E. R. and Lord, R. C. *J. Am. Chem. Soc.* **68** (1946) 1868.
3. Huisgen, R., Laschtuvka, E., Ugi, I. and Kammereier, A. *Ann.* **630** (1960) 128; Dimroth, K. and Pohl, G. *Angew. Chem.* **73** (1961) 436.
4. Schweizer, E. E. and Parham, W. E. *J. Am. Chem. Soc.* **82** (1960) 4085; Meinwald, J., Dicker, D. W. and Danieli, N. *J. Am. Chem. Soc.* **82** (1960) 4087; Olsen, S. and Bredoch, R. *Ber.* **91** (1958) 1589.

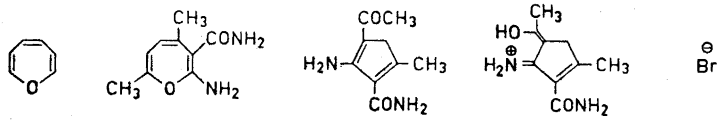

I *II* *III* *IV*

5. Westöö, G. *Acta Chem. Scand.* **13** (1959) 604.
6. Pepinsky, R., Robertson, J. M. and Speakman, J. C. *Computing Methods and the Phase Problem in X-ray Crystal Analysis*, Pergamon Press, Oxford 1961; Rollett, J.S., p. 87; Sime, J. G. p. 301.

Received March 5, 1962.

On the Structure of CrOCl

HANS-ERIK FORSBERG

Department of Inorganic Chemistry, The Royal Institute of Technology, Stockholm 70, Sweden

Some years ago single crystals of CrOCl were prepared from Cr_2O_3 and $CrCl_3$ by Professor H. Schäfer[1], who was kind enough to supply me with specimens suitable for X-ray investigations. From rotation and Weissenberg photographs taken around the *b*-axis with Cu*K* radiation, it was concluded that the crystals are orthorhombic with the following cell dimensions:

$a \approx 3.88$ Å, $b \approx 3.20$ Å, $c \approx 7.72$ Å, $V \approx 95.9$ Å^3.

From the observed density of 3.47 g/ml it was calculated that there should be two formula units of CrOCl in the unit cell.

The extinctions, $hk0$ for $h + k$ = odd, are in agreement with the centrosymmetric space group *Pmmn* and the non-centrosymmetric space group $Pmn2_1$. (Nos. 59 and 31 in the *International Tables for X-ray Crystallography* [2]). Since a plausible structure could be assigned assuming *Pmmn*, the space group of higher symmetry, the lower space group was not considered.

The following preliminary parameters of the atoms were determined from Patterson and Fourier projections on the *xz* plane and geometrical considerations:

2 Cr in 2(*a*): ± (1/4, 1/4, *z*) with $z = 0.109$
2 Cl in 2(*b*): ± (1/4, 3/4, *z*) with $z = 0.327$
2 O in 2(*b*): ± (1/4, 3/4, *z*) with $z = 0.96$

Fig. 1 shows the structure of CrOCl. The chromium and oxygen atoms form Cr—O—Cr layers which are separated by double halogen sheets.

● ○ ⊜ are Cr, O and Cl at $y = 1/4$.
◉ ◎ ⊜ are Cr, O and Cl at $y = 3/4$.

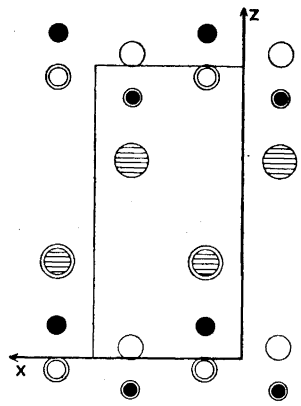

Fig. 1. The structure of CrOCl, viewed along [010].

The atomic arrangement and the space group of CrOCl is the same as in FeOCl (Goldsztaub [3]), InOCl and InOBr (Forsberg [4]), and TiOCl (Schäfer [5]). Thus, as postulated by Schäfer, chromium oxide chloride is isomorphous with these substances.

The following ranges of interatomic distances were found:

Cr—Cr	3.04 Å
Cr—O	1.97—2.01 Å
Cr—Cl	2.32 Å
O—O	2.51 Å
O—Cl	2.83—3.35 Å
Cl—Cl	3.20—3.88 Å

A complete structure determination will be published later.

The research reported in this document has been sponsored by *Air Force Office of Scientific Research, OAR*, through the European Office, Aerospace Research, United States Air Force, under contract No. AF 61(052)-162.

1. Schäfer, H. and Wartenpfuhl, F. *Z. anorg. u. allgem. Chem.* **308** (1961) 282.
2. *International Tables for X-ray Crystallography*, Kynoch Press, Birmingham 1952, Vol I, p. 148 and 117.
3. Goldsztaub, M. S. *Compt. rend.* **198** (1934) 667.
4. Forsberg, H.-E. *Acta Chem. Scand.* **10** (1956) 1286.
5. Schäfer, H., Wartenpfuhl, F. and Weise, E. *Z. anorg. u. allgem. Chem.* **295** (1958) 268.

Received March 8, 1962.

5. Westöö, G. *Acta Chem. Scand.* **13** (1959) 604.
6. Pepinsky, R., Robertson, J. M. and Speakman, J. C. *Computing Methods and the Phase Problem in X-ray Crystal Analysis*, Pergamon Press, Oxford 1961; Rollett, J.S., p. 87; Sime, J. G. p. 301.

Received March 5, 1962.

On the Structure of CrOCl

HANS-ERIK FORSBERG

Department of Inorganic Chemistry, The Royal Institute of Technology, Stockholm 70, Sweden

Some years ago single crystals of CrOCl were prepared from Cr_2O_3 and $CrCl_3$ by Professor H. Schäfer[1], who was kind enough to supply me with specimens suitable for X-ray investigations. From rotation and Weissenberg photographs taken around the *b*-axis with Cu*K* radiation, it was concluded that the crystals are orthorhombic with the following cell dimensions:

$a \approx 3.88$ Å, $b \approx 3.20$ Å, $c \approx 7.72$ Å, $V \approx 95.9$ Å^3.

From the observed density of 3.47 g/ml it was calculated that there should be two formula units of CrOCl in the unit cell.

The extinctions, $hk0$ for $h + k$ = odd, are in agreement with the centrosymmetric space group *Pmmn* and the non-centrosymmetric space group $Pmn2_1$. (Nos. 59 and 31 in the *International Tables for X-ray Crystallography* [2]). Since a plausible structure could be assigned assuming *Pmmn*, the space group of higher symmetry, the lower space group was not considered.

The following preliminary parameters of the atoms were determined from Patterson and Fourier projections on the *xz* plane and geometrical considerations:

2 Cr in 2(*a*): ± (1/4, 1/4, *z*) with $z = 0.109$
2 Cl in 2(*b*): ± (1/4, 3/4, *z*) with $z = 0.327$
2 O in 2(*b*): ± (1/4, 3/4, *z*) with $z = 0.96$

Fig. 1 shows the structure of CrOCl. The chromium and oxygen atoms form Cr—O—Cr layers which are separated by double halogen sheets.

● ○ ⊜ are Cr, O and Cl at $y = 1/4$.
◉ ◎ ⊜ are Cr, O and Cl at $y = 3/4$.

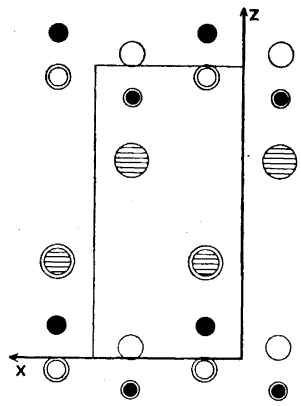

Fig. 1. The structure of CrOCl, viewed along [010].

The atomic arrangement and the space group of CrOCl is the same as in FeOCl (Goldsztaub [3]), InOCl and InOBr (Forsberg [4]), and TiOCl (Schäfer [5]). Thus, as postulated by Schäfer, chromium oxide chloride is isomorphous with these substances.

The following ranges of interatomic distances were found:

Cr—Cr	3.04 Å
Cr—O	1.97—2.01 Å
Cr—Cl	2.32 Å
O—O	2.51 Å
O—Cl	2.83—3.35 Å
Cl—Cl	3.20—3.88 Å

A complete structure determination will be published later.

The research reported in this document has been sponsored by *Air Force Office of Scientific Research, OAR*, through the European Office, Aerospace Research, United States Air Force, under contract No. AF 61(052)-162.

1. Schäfer, H. and Wartenpfuhl, F. *Z. anorg. u. allgem. Chem.* **308** (1961) 282.
2. *International Tables for X-ray Crystallography*, Kynoch Press, Birmingham 1952, Vol I, p. 148 and 117.
3. Goldsztaub, M. S. *Compt. rend.* **198** (1934) 667.
4. Forsberg, H.-E. *Acta Chem. Scand.* **10** (1956) 1286.
5. Schäfer, H., Wartenpfuhl, F. and Weise, E. *Z. anorg. u. allgem. Chem.* **295** (1958) 268.

Received March 8, 1962.

Mean Amplitudes of Vibration and Shrinkage Effect of Boron Trihalides, Calculated from Urey-Bradley Force Constants

E. MEISINGSETH

Institutt for teoretisk kjemi, Norges tekniske høgskole, Trondheim, Norway

In a preliminary report [1] the Urey-Bradley force constants have been calculated for the boron trihalides. It seems reasonable to use these force constants for calculating the mean amplitudes of vibration and the shrinkage effect of the molecules in question. This kind of calculations, based on Urey-Bradley force constants have not been reported previously in the literature.

The mean amplitudes of vibration for the bonded XY atoms (u_{XY}) and non-bonded YY atoms (u_{YY}) have been calculated. Following the teoretical treatment of Cyvin [2], u_{XY} and u_{YY} may be expressed in terms of the elements of the symmetrized mean-square amplitude matrix (Σ):

$$u_{XY} = (1/3(\Sigma_1 + 2\Sigma_3)]^{\frac{1}{2}}$$

$$u_{YY} = [\Sigma_1 + 1/2(\Sigma_3 + 1/3\Sigma_4) - 3^{\frac{1}{2}}\Sigma_{34}]^{\frac{1}{2}}$$

Table 1. Calculated mean amplitudes of vibration (u)*

Molecule	Interatomic distance	u (Å) $T = 0$	298°K
BF_3	B——F	0.0425 (0.0424)	0.0426 (0.0425)
	F——F	0.0521 (0.0517)	0.0558 (0.0552)
BCl_3	B——Cl	0.0478 (0.0478)	0.0491 (0.0491)
	Cl——Cl	0.0532 (0.0536)	0.0683 (0.0683)
BBr_3	B——Br	0.0483 (0.0479)	0.0516 (0.0506)
	Br——Br	0.0485 (0.0461)	0.0768 (0.0726)
BI_3	B——I	0.0613 (0.0508)	0.0587 (0.0570)
	I——I	0.0494 (0.0449)	0.0948 (0.0848)

* Cyvin's [7] values in parentheses.

Table 2. Calculated shrinkage effect (δ) *.

Molecules	δ (Å). $T = 0$	298°K
BF_3	0.00331 (0.00334)	0.00364 (0.00371)
BCl_3	0.00338 (0.00328)	0.00452 (0.00441)
BBr_3	0.00340 (0.00347)	0.00516 (0.00564)
BI_3	0.00325 (0.00311)	0.00541 (0.00510)

* Meisingseth and Cyvin's [6] values in parentheses.

The shrinkage effect which have been observed for linear-chain molecules by electron-diffraction studies of Bastiansen *et al.*[3-5], may be defined as the difference between the observed and calculated interatomic distance. The shrinkage effect for the molecules here considered may be expressed in terms of the Σ-matrix elements [6]:

$$\delta = 1/6R(3^{-\frac{1}{2}}\Sigma_2 - 1/2\,3^{\frac{1}{2}}\Sigma_3 + 1/2\,3^{\frac{1}{2}}\Sigma_4 + \Sigma_{34})$$

where R is the equilibrium interatomic distance.

The results obtained for the mean amplitudes of vibration are given in Table 1 and are in good agreement with those reported by Cyvin [7], as calculated from general quadratic potential function. In Table 2 the calculated shrinkage effects are presented and are compared to those previously calculated by Meisingseth and Cyvin [6]. Here again a good agreement is observed.

1. Meisingseth, E. *Acta Chem. Scand.* **16** (1962) *In press.*
2. Cyvin, S. J. *Acta Chem. Scand.* **13** (1959) 1809.
3. Almenningen, A. Bastiansen, O., and Munthe-Kaas, T. *Acta Chem. Scand.* **10** (1956) 261.
4. Almenningen, A., Bastiansen, O. and Trætteberg, M. *Acta Chem. Scand.* **13** (1959) 1699.
5. Bastiansen, O. and Trætteberg, M. *Acta Cryst.* **13** (1960) 1108.
6. Meisingseth, E. and Cyvin, S. J. *J. Mol. Spectroscopy. In press.*
7. Cyvin, S. J. *Acta Chem. Scand.* **13** (1959) 334.

Received March 6, 1962.

Bond Lengths in Square-Planar Tellurium(II) Complexes

OLAV FOSS

Chemical Institute, University of Bergen, Bergen, Norway

Crystal structure determinations [1] of square-planar tellurium(II) complexes [2-6] have led to the following values for tellurium-ligand bond lengths; the uncertainties quoted are estimated standard deviations.

Tetrathiourea-tellurium(II) dichloride dihydrate [1a,2,3], $Te(tu)_4Cl_2.2H_2O$: Te–S = 2.68 ± 0.01 Å.

Tetrathiourea-tellurium(II) dichloride [1b,3], $Te(tu)_4Cl_2$: Te–S = 2.69 ± 0.01 Å.

trans-Dimethanethiosulphonato-dithiourea-tellurium(II) [1c,4], $Te(tu)_2(S_2O_2CH_3)_2$: Te–S(thiourea) = 2.65 ± 0.015 Å; Te–S-(thiosulphonate) = 2.68 ± 0.015 Å.

trans-Dibromobis(ethylenethiourea)tellurium(II) [1d,5], $Te(etu)_2Br_2$: Te–S = 2.69 ± 0.015 Å; Te–Br = 2.78 ± 0.01 Å.

The results indicate that, with single covalent bond radii for ligands, a bonding radius of 1.64 Å can be assigned to tellurium(II) in square-planar complexes.

In two *cis* complexes, a marked lengthening effect of a thiourea group on a Te–Cl or Te–Br bond *trans* to it is apparent:

cis-Dichloro-dithiourea-tellurium(II) [1e,2,6], $Te(tu)_2Cl_2$: Te–S = 2.48 ± 0.02 Å; Te–Cl = 2.92 ± 0.015 Å.

cis-Dibromo-dithiourea-tellurium(II) [1f,2,6], $Te(tu)_2Br_2$: Te–S = 2.47 ± 0.03 Å; Te–Br = 3.05 ± 0.01 Å.

However, the Te–S bonds are correspondingly shorter; the sum of the Te–Br and Te–S bond lengths in *cis*-$Te(tu)_2Br_2$ is 5.52 Å as compared with 5.47 Å in *trans*-$Te(etu)_2Br_2$. In *cis*-$Te(tu)_2Cl_2$ the sum of the Te–Cl and Te–S bond lengths is 5.40 Å whereas two times 1.64 Å for tellurium plus the single bond radii, 0.99 and 1.04 Å of chlorine and sulphur gives 5.31 Å. Thus, even if the two bonds *trans* to each other are fairly unequal in strength, the sum of their lengths shows only a slight increase. Or in other words, the sum of the bonding radii of tellurium(II) in directions at 180° remains fairly constant.

These observations seem to fit the delocalized molecular orbital scheme based on *p*-functions, developed by Pimentel [7], Hach and Rundle [8,9] and Havinga and Wiebenga [10,11] for bonding in polyhalide ions. In a linear trihalide ion one *p*-orbital of the central atom forms two bonds, at 180°. Support for this type of bonding in polyhalide ions has recently come from nuclear quadrupole resonance measurements [12,13] and studies of bond stretching force constants [14]. Similarly in square-planar tellurium(II) complexes, one tellurium 5*p* orbital would bind two ligands, at 180°; increased engagement of the orbital in bonding to one of the ligands would reduce its bonding capacity for the other ligand.

Krebs [15,16] has pointed out that in half-metals, like tellurium, bonded atoms have nearest non-bonded neighbours in directions approximately linear to the bond. Thus in hexagonal tellurium, an infinite, nearly linear sequence of atoms occurs, with interatomic distances of 2.86, 3.46 and 3.46 Å within the repeat unit; Krebs [15,16] postulates *p*-electron resonance along the chain. It is of interest to note that the average interatomic distance in the chain is two times 1.63 Å.

The extreme asymmetry in strength of two co-linear bonds from an atom, based on one *p*-orbital only of the latter, would be a single covalent bond in one direction and no bond in the other. If the sum of the bonding radii of the atom in the two directions remains constant, the observed "half *p*-bond" radius of 1.64 Å for tellurium(II) would be the average of the single covalent radius, 1.37 Å, and the no-bond radius, *i.e.* the van der Waals radius. This leads to 1.91 Å for the van der Waals radius of tellurium, which is the same as the value, 1.9 Å, given by Briegleb [17]. The slight increase actually observed in the sum of the lengths of the two bonds might then have its cause in an increase in the bonding radius of the more loosely bound ligand; this radius approaches the van der Waals radius, or the ionic radius, as the asymmetry of the complex increases.

For selenium and sulphur, taking as their van der Waals radii about half the shortest non-bonded distances in α-monoclinic [18] and β-monoclinic [19] selenium, 3.53 and 3.48 Å, and in orthorhombic sulphur [20] and cesium hexasulphide [21], 3.37 and 3.39 Å, the above reasoning together with the single covalent radii of 1.17 and 1.04 Å would give about 1.46 and 1.36 Å, respectively, for the "half *p*-bond" radii of divalent selenium and sulphur. Thus, with the radii in the middle column the average of those in the left and right:

	Single covalent	"Half *p*-bond"	No-bond (v. d. Waals)
Sulphur	1.04 Å	1.36 Å	1.68 Å
Selenium	1.17	1.46	1.75
Tellurium	1.37	1.64	1.91

A linear, symmetrical S—S—S arrangement is present in 2,5-dimethyl-thio-thiophthen [23-25]. The expected S—S bond length in such a sulphur(II) complex would be about 1.36 Å + 1.04 Å = 2.40 Å. The observed bond length [25] is 2.35 Å; however, the S—S bonds are here part of a bicyclic unsaturated system and may be subject to shortening through π-bonding.

The work on tellurium(II) complexes was started with a view towards these as model substances for the transition state in nucleophilic displacements on divalent chalcogens. The results, and also kinetic evidence from displacements on sulphur [26], indicate a linear transition state. Furthermore, the picture emerges that in the linear transition state the in- and out-going groups are bonded, at 180°, through a single *p*-orbital of the electrophilic centre. This possibility was considered, and preferred, by Fava *et al.*[27,28] on kinetic grounds. Nucleophilic reactivity may then relate to the ability of the reagent to engage the *p*-orbital in bonding, at the expense of the bond at 180°. Electrophilic reactivity would correspondingly reflect the centre's ability to participate in delocalized *p*-bonding in the transition state.

It appears likely that π-bonding, superimposed on the delocalized σ *p*-bonding, may affect the stabilities of complexes as well as the reactivities, and in the case of different ligands in directions at 180°, influence the relative bond lengths in these directions; for example dative π-bonding from central atom $p\pi$ to ligand $d\pi$ as has been discussed for chloroiodides [9] and phosphinesulphide-iodine complexes [29].

1. Work, to be published, by (*a*) K. Fosheim and A. Scheie, (*b*) S. Solheimsnes, (*c*) K. Marøy, (*d*) H. Kjøge, (*e*) K. Johnsen and K. Marøy, (*f*) K. Maartmann-Moe and the author.
2. Foss, O. and Hauge, S. *Acta Chem. Scand.* **13** (1959) 1252.
3. Foss, O. and Hauge, S. *Acta Chem. Scand.* **15** (1961) 1616.
4. Foss, O. and Johannessen, I.-J. *Acta Chem. Scand.* **15** (1961) 1943.
5. Foss, O. and Fossen, S. *Acta Chem. Scand.* **15** (1961) 1618.
6. Foss, O. and Hauge, S. *Acta Chem. Scand.* **15** (1961) 1615.
7. Pimentel, G. C. *J. Chem. Phys.* **19** (1951) 446.
8. Hach, R. J. and Rundle, R. E. *J. Am. Chem. Soc.* **73** (1951) 4321.
9. Rundle, R. E. *Acta Cryst.* **14** (1961) 585.
10. Havinga, E. E. and Wiebenga, E. H. *Rec. trav. chim.* **78** (1959) 724.
11. Wiebenga, E. H., Havinga, E. E. and Boswijk, K. H. *Advances Inorg. Chem. & Radiochem.* **3** (1961) 133.
12. Cornwell, C. D. and Yamasaki, R. S. *J. Chem. Phys.* **27** (1957) 1060.
13. Yamasaki, R. S. and Cornwell, C. D. *J. Chem. Phys.* **30** (1959) 1265.
14. Person, W. B., Anderson, G. R., Fordemwalt, J. N., Stammreich, H. and Forneris, R. *J. Chem. Phys.* **35** (1961) 908.
15. Krebs, H. *Acta Cryst.* **9** (1956) 95.
16. Krebs, H. *Angew. Chem.* **70** (1958) 615.
17. Briegleb, G. In Müller, E. *Methoden der organischen Chemie, Houben-Weyl's*, 4 th Ed., Thieme, Stuttgart; Vol. III (1), 1955, p. 545.
18. Burbank, R. D. *Acta Cryst.* **4** (1951) 140.
19. Marsh, R. E., Pauling, L. and McCullough, J. D. *Acta Cryst.* **6** (1953) 71.
20. Donohue, J., Caron, A. and Goldish, E. *J. Am. Chem. Soc.* **83** (1961) 3748.
21. Abrahams, S. C. and Grison, E. *Acta Cryst.* **6** (1953) 206.
22. Bezzi, S., Mammi, M. and Garbuglio, C. *Nature* **182** (1958) 247.
23. Bezzi, S., Garbuglio, C., Mammi, M. and Traverso, G. *Gazz. chim. ital.* **88** (1958) 1226.
24. Giacometti, G. and Rigatti, G. *J. Chem. Phys.* **30** (1959) 1633.
25. Mammi, M., Bardi, R., Garbuglio, C. and Bezzi, S. *Acta Cryst.* **13** (1960) 1048.
26. Fava, A. and Iliceto, A. *J. Am. Chem. Soc.* **80** (1958) 3478.
27. Fava, A. and Pajaro, G. *J. Am. Chem. Soc.* **78** (1956) 5203.
28. Fava, A., Iliceto, A. and Camera, E. *J. Am. Chem. Soc.* **79** (1957) 833.
29. Zingaro, R. A. and Hedges, R. M. *J. Phys. Chem.* **65** (1961) 1132.

Received March 16, 1962.

A Simple Apparatus for the Carbonation of Grignard Reagents with Carbon-^{14}C Dioxide

LENNART EBERSON

Division of Organic Chemistry, Draco, Lunds Farmacevtiska AB, Lund, Sweden

The standard apparatus for the carbonation of Grignard reagents with carbon-^{14}C dioxide, as described in several textbooks [1-3], is rather complicated in its construction and operational use, especially for those who only rarely meet with the problem of synthesizing ^{14}C-labelled compounds. It is generally not satisfactory to carry out the reaction in an open vessel by bubbling the carbon-^{14}C dioxide through the Grignard solution, since this process is very likely to cause clogging in the gas-inlet tube and also involves a certain loss of radioactive material.

This paper describes a simple, closed carbonation apparatus, which is easily constructed from commercially available glass equipment at a minimum cost of glass-blowing. It does not require the use of a high-vacuum system, liquid nitrogen temperatures, or a special gas-tight stirrer.

Construction. The apparatus (see Fig. 1) principally consists of a gas evolution vessel A which is in communication with the reaction chamber B through two holes in the top of the drying tube C. A capillary tube through C, connected to the dropping funnel D, allows for the addition of mineral acid to A. E is a high-vacuum stopcock and stirring is effected by means of a Teflon sealed magnet F. The ground glass joints G (B 14*), H (B 34) and I (B 19) permit the apparatus to be easily mounted and dismounted.

Operation. Barium carbonate-^{14}C is weighed into A, and A is fitted to the drying tube C by joint G, which is held together by a spiral spring. C is filled with Drierite which is kept in place by two loose plugs of dry cotton wool. The reaction vessel B is then attached *via* joint H, whereafter the whole system is evacuated and filled with dry nitrogen.

B is removed for a few seconds during which an appropriate amount of the previously prepared Grignard solution is introduced by means of a nitrogen-flushed syringe. Stirring is started and the Grignard reagent is cooled to about −70° in a dry ice-acetone bath. The system is evacuated through E by means of a conventional oil pump whereby the ether solution in B boils up when the pressure has been reduced to about 1 mm Hg. E is closed and the temperature of B is rised to about −15°. Perchloric acid (35 %) is cautiously added from the dropping funnel D, whereby the evolution of carbon-^{14}C dioxide starts. Occasionally, the perchloric acid may collect in the cavity above the capillary tube at the begin of the reaction, but this is easily overcome by cooling at B, which results in a pressure drop in the system and the perchloric acid is sucked into A. When all of the gas has been evolved (a clear solution then remains in A), B is frozen to −80° in order to draw any remaining carbon-^{14}C dioxide into the reaction mixture. The temperature is kept at −80° for about one hour after which time it is allowed to reach room temperature. The reaction mixture is worked up according to conventional procedures.

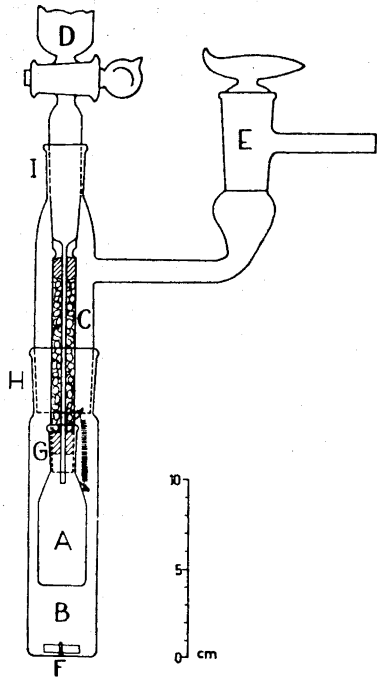

Fig. 1.

* Size designation according to "Quickfit".

When phenyl magnesium bromide or benzyl magnesium chloride was carbonated with inactive carbon dioxide according to this method at the 1.0 mmole level, almost quantitative yields of benzoic and phenylacetic acid were obtained. Phenylacetic-1-^{14}C acid was prepared in 98 % yield (crude product, m.p. 69—74°) from 1.00 mmole of barium carbonate^{14}C.

1. Murray, III, A. and Williams, D. L. *Organic Syntheses with Isotopes, Part I*, Interscience, New York 1958, p. 86.
2. Ronzio, A. R. in Weissberger, A., Ed., *Technique of Organic Chemistry, Volume VI, Micro and Semimicro Methods*, Interscience, New York 1954, p. 391.
3. Weygand, F. and Simon, H. in *Methoden der Organischen Chemie (Houben-Weyl), Band IV, Teil 2, Allgemeine Chemische Methoden*, Thieme, Stuttgart 1955, p. 643.

Received March 6, 1962.

Microdetermination of Protein with Radiocopper and Gel Filtration

RALPH GRÄSBECK and ROLF KARLSSON

Minerva Foundation Institute for Medical Research, Helsinki, Finland

In order to make possible the determination of minute amounts of protein we have developed the following "radiobiuret" techniques:

Sephadex (G-25, coarse) is suspended and allowed to swell in 0.75 N NaOH and packed in the form of a column (diameter up to 1 cm, length about 20 cm). The column is washed overnight with NaOH to remove traces of protein. It is arranged that the protein to be determined is contained in 0.75 N NaOH in a convenient volume (*e.g.* 1—5 ml). To this is added an excess amount (up to 0.5 mg) of radioactive copper with as high specific activity as possible, *e.g.* 1 ml of an aqueous 1:25 dilution of the commercial $^{64}CuCl_2$ solution. All dilutions are made with redistilled water and observing meticulous cleanliness. The mixture is incubated 90 min at room temperature, a measured volume is introduced onto the column followed by NaOH until 25 ml of eluate has been collected. The radioactivity of the eluate is then determined with a scintillation counter. Between samples, the column is washed with NaOH. Known amounts of a standard protein and blanks are run in the same way before and after the unknown. The amount of protein in the unknown sample can be read from the resulting standard curve.

The unbound copper will be retained as the hydroxide in the upper parts of the column, but owing to the low concentration of copper in the original reaction mixture no precipitation will occur there. The determination can also be performed with larger amounts of protein by reading the emerging biuret colour photometrically. However, the free copper will then precipitate, but this can be prevented by complexing the copper ion with citrate as is done in the classic biuret method. When such a mixture is introduced into the column, copper hydroxide will be formed and retained in the upper parts (amino acid complexes are also dissociated). A straight-line relationship *amount of protein/eluted radioactivity* (corrected for radioactive decay) is observable down to at least 1 μg of protein applied onto the column in 5 ml volume, but owing to the obvious advantages of the following method we have made no attempts to reduce further the lower limit of this method.

The reaction may also be performed in another way which enables it to be used for automatic analysis, *e.g.* in continuous registration of protein eluted from chromatographic columns. The chromatographic eluent must first be alkalinized either by the continuous addition of NaOH with a pump or by automatic pH adjustment using a titrator. The mixture is then led to a Sephadex column containing an upper layer of a mixture of radiocopper hydroxide and Sephadex. This can be prepared in a beaker by mixing $^{64}CuCl_2$ with a citrate-carbonate solution (proportions as in Benedict's reagent), pouring the mixture on moist alkaline Sephadex and by shaking until all the copper is adsorbed. The slurry is poured onto the top of a short Sephadex column and the column is then washed with a large volume of NaOH. If desired, the copper hydroxide level can be raised by sucking up acid from below. When the desired level has been reached, NaOH is run in the other direction.

The eluate from the Sephadex column is passed through a glass tube spiral kept in the well of a scintillation crystal fixed in a

When phenyl magnesium bromide or benzyl magnesium chloride was carbonated with inactive carbon dioxide according to this method at the 1.0 mmole level, almost quantitative yields of benzoic and phenylacetic acid were obtained. Phenylacetic-1-^{14}C acid was prepared in 98 % yield (crude product, m.p. 69—74°) from 1.00 mmole of barium carbonate^{14}C.

1. Murray, III, A. and Williams, D. L. *Organic Syntheses with Isotopes, Part I*, Interscience, New York 1958, p. 86.
2. Ronzio, A. R. in Weissberger, A., Ed., *Technique of Organic Chemistry, Volume VI, Micro and Semimicro Methods*, Interscience, New York 1954, p. 391.
3. Weygand, F. and Simon, H. in *Methoden der Organischen Chemie (Houben-Weyl), Band IV, Teil 2, Allgemeine Chemische Methoden*, Thieme, Stuttgart 1955, p. 643.

Received March 6, 1962.

Microdetermination of Protein with Radiocopper and Gel Filtration

RALPH GRÄSBECK and ROLF KARLSSON

Minerva Foundation Institute for Medical Research, Helsinki, Finland

In order to make possible the determination of minute amounts of protein we have developed the following "radiobiuret" techniques:

Sephadex (G-25, coarse) is suspended and allowed to swell in 0.75 N NaOH and packed in the form of a column (diameter up to 1 cm, length about 20 cm). The column is washed overnight with NaOH to remove traces of protein. It is arranged that the protein to be determined is contained in 0.75 N NaOH in a convenient volume (*e.g.* 1—5 ml). To this is added an excess amount (up to 0.5 mg) of radioactive copper with as high specific activity as possible, *e.g.* 1 ml of an aqueous 1:25 dilution of the commercial $^{64}CuCl_2$ solution. All dilutions are made with redistilled water and observing meticulous cleanliness. The mixture is incubated 90 min at room temperature, a measured volume is introduced onto the column followed by NaOH until 25 ml of eluate has been collected. The radioactivity of the eluate is then determined with a scintillation counter. Between samples, the column is washed with NaOH. Known amounts of a standard protein and blanks are run in the same way before and after the unknown. The amount of protein in the unknown sample can be read from the resulting standard curve.

The unbound copper will be retained as the hydroxide in the upper parts of the column, but owing to the low concentration of copper in the original reaction mixture no precipitation will occur there. The determination can also be performed with larger amounts of protein by reading the emerging biuret colour photometrically. However, the free copper will then precipitate, but this can be prevented by complexing the copper ion with citrate as is done in the classic biuret method. When such a mixture is introduced into the column, copper hydroxide will be formed and retained in the upper parts (amino acid complexes are also dissociated). A straight-line relationship *amount of protein/eluted radioactivity* (corrected for radioactive decay) is observable down to at least 1 μg of protein applied onto the column in 5 ml volume, but owing to the obvious advantages of the following method we have made no attempts to reduce further the lower limit of this method.

The reaction may also be performed in another way which enables it to be used for automatic analysis, *e.g.* in continuous registration of protein eluted from chromatographic columns. The chromatographic eluent must first be alkalinized either by the continuous addition of NaOH with a pump or by automatic pH adjustment using a titrator. The mixture is then led to a Sephadex column containing an upper layer of a mixture of radiocopper hydroxide and Sephadex. This can be prepared in a beaker by mixing $^{64}CuCl_2$ with a citrate-carbonate solution (proportions as in Benedict's reagent), pouring the mixture on moist alkaline Sephadex and by shaking until all the copper is adsorbed. The slurry is poured onto the top of a short Sephadex column and the column is then washed with a large volume of NaOH. If desired, the copper hydroxide level can be raised by sucking up acid from below. When the desired level has been reached, NaOH is run in the other direction.

The eluate from the Sephadex column is passed through a glass tube spiral kept in the well of a scintillation crystal fixed in a

counter. The radioactivity is registered with a ratemeter, preferably provided with a pulse-height analyzer, which keeps the background low and makes possible the analysis of the protein content of radioactive eluates, in our case macromolecular ^{57}Co-cyanocobalamin complexes. The readings of the ratemeter are registered graphically with a recorder. Before use, the column is washed with NaOH until the background reading becomes low. Using this system without a pulse-height analyzer we have found 0.45 μg of bovine albumin introduced in 1 ml volume to give noticeable peaks. With the use of better equipment and high-specific activity ^{64}Cu (not available to us due to the distance from the foreign manufacturer) it should be possible to detect still smaller amounts of protein. This system is more sensitive than the preceding one, since by this method the peak radioactivity values are recorded. For practical purposes the method is insensitive to ammonia, since only concentrated solutions elute radioactivity.

The Sephadex functions as a convenient filter and supporting medium, which effectively removes the originally dissolved copper as hydroxide and dissociates small-molecular copper complexes, and which can be prepared rapidly. The main disadvantage of the method is the short half-life of the copper isotope. A longer-lived isotope exists (^{67}Cu), but is not commercially available. On the macro scale our system also works with nickel, but the usual isotope ^{63}Ni emits solely soft beta radiation and is available only in low-specific activity form. Other metals which were tried gave disappointing results.

Acknowledgements. Professor Lennart Simons kindly placed a recorder at our disposal. Grants were obtained from *Sigrid Jusélius Stiftelse, Medicinska Understödsföreningen Liv och Hälsa, Svenska Vetenskapliga Centralrådet,* and the *State Medical Commission.*

Received March 13, 1962.

Isothiocyanates XLIV *. The Isothiocyanate Glucoside (Glucocapparin) in *Crataeva Roxburghii* R.Br. *(Capparidaceae)*

ANDERS KJÆR and
HELENE THOMSEN

Organic Chemistry Department, The Royal Veterinary and Agricultural College, Copenhagen, Denmark

The tree *Crataeva Roxburghii* R.Br. (syn. *C. religiosa* Forst.) of the family *Capparidaceae* grows abundantly in the plains of India and affords a popular local remedy in the treatment of several physical and mental disorders. Of particular interest in connexion with current studies in this laboratory is the paper by Lahiri [1] according to which J. S. Chatterjee from "decomposed" bark of *C. Roxburghii* isolated a crystalline compound, $C_{15}H_{16}N_2S$, reported to be obtainable also from *Moringa pterygosperma* and horse-radish on similar treatment. The compound was demonstrated to be of considerable promise in the clinical treatment of cholera [1]. More recently, Chakravarti [2] established its structure as 1,3-dibenzylthiourea on basis of degradation experiments and comparison with a synthetic specimen **. Unfortunately, Chatterjee's isolation procedure never seems to have been published (*cf.* Ref.[2]). Hence, repetition under exactly the same conditions is not possible. In view of the present knowledge, however, it appeared likely that 1,3-dibenzylthiourea might originate from benzyl isothiocyanate, derivable from glucotropaeolin, a glucosidic progenitor widely distributed in the plant kingdom [4].

* Part XLIII of this series: *Acta Chem. Scand.* 16 (1962). *In press.*

** The same thiourea has been previously reported [3] as a constituent of the unsaponifiable matter from the seed fat ("Khakan fat") of *Salvadora oleoides* Den. (*Salvadoraceae*). On steam distillation, the fat gave about 1.5 % of benzyl isothiocyanate [3], and it appears likely that dibenzylthiourea in this case was an artifact produced from the mustard oil during saponification.

counter. The radioactivity is registered with a ratemeter, preferably provided with a pulse-height analyzer, which keeps the background low and makes possible the analysis of the protein content of radioactive eluates, in our case macromolecular ^{57}Co-cyanocobalamin complexes. The readings of the ratemeter are registered graphically with a recorder. Before use, the column is washed with NaOH until the background reading becomes low. Using this system without a pulse-height analyzer we have found 0.45 μg of bovine albumin introduced in 1 ml volume to give noticeable peaks. With the use of better equipment and high-specific activity ^{64}Cu (not available to us due to the distance from the foreign manufacturer) it should be possible to detect still smaller amounts of protein. This system is more sensitive than the preceding one, since by this method the peak radioactivity values are recorded. For practical purposes the method is insensitive to ammonia, since only concentrated solutions elute radioactivity.

The Sephadex functions as a convenient filter and supporting medium, which effectively removes the originally dissolved copper as hydroxide and dissociates small-molecular copper complexes, and which can be prepared rapidly. The main disadvantage of the method is the short half-life of the copper isotope. A longer-lived isotope exists (^{67}Cu), but is not commercially available. On the macro scale our system also works with nickel, but the usual isotope ^{63}Ni emits solely soft beta radiation and is available only in low-specific activity form. Other metals which were tried gave disappointing results.

Acknowledgements. Professor Lennart Simons kindly placed a recorder at our disposal. Grants were obtained from *Sigrid Jusélius Stiftelse, Medicinska Understödsföreningen Liv och Hälsa, Svenska Vetenskapliga Centralrådet,* and the *State Medical Commission.*

Received March 13, 1962.

Isothiocyanates XLIV *. The Isothiocyanate Glucoside (Glucocapparin) in *Crataeva Roxburghii* R.Br. *(Capparidaceae)*

ANDERS KJÆR and
HELENE THOMSEN

Organic Chemistry Department, The Royal Veterinary and Agricultural College, Copenhagen, Denmark

The tree *Crataeva Roxburghii* R.Br. (syn. *C. religiosa* Forst.) of the family *Capparidaceae* grows abundantly in the plains of India and affords a popular local remedy in the treatment of several physical and mental disorders. Of particular interest in connexion with current studies in this laboratory is the paper by Lahiri [1] according to which J. S. Chatterjee from "decomposed" bark of *C. Roxburghii* isolated a crystalline compound, $C_{15}H_{16}N_2S$, reported to be obtainable also from *Moringa pterygosperma* and horse-radish on similar treatment. The compound was demonstrated to be of considerable promise in the clinical treatment of cholera [1]. More recently, Chakravarti [2] established its structure as 1,3-dibenzylthiourea on basis of degradation experiments and comparison with a synthetic specimen **. Unfortunately, Chatterjee's isolation procedure never seems to have been published (*cf.* Ref.[2]). Hence, repetition under exactly the same conditions is not possible. In view of the present knowledge, however, it appeared likely that 1,3-dibenzylthiourea might originate from benzyl isothiocyanate, derivable from glucotropaeolin, a glucosidic progenitor widely distributed in the plant kingdom [4].

* Part XLIII of this series: *Acta Chem. Scand.* 16 (1962). *In press.*

** The same thiourea has been previously reported [3] as a constituent of the unsaponifiable matter from the seed fat ("Khakan fat") of *Salvadora oleoides* Den. (*Salvadoraceae*). On steam distillation, the fat gave about 1.5 % of benzyl isothiocyanate [3], and it appears likely that dibenzylthiourea in this case was an artifact produced from the mustard oil during saponification.

In this laboratory, bark material of *C. Roxburghii* R.Br.* was reinvestigated and quite different conclusions were attained. On paper chromatography of a methanolic bark extract for isothiocyanate glucosides only one spot was observed, indistinguishable in its R_F-value from that of a reference spot of glucocapparin [5], the predominant glucoside in most species of the family *Capparidaceae* as evident from reported data [6] and a considerable unpublished material in this laboratory. No trace of glucotropæolin was detectable in the bark extract. The alcoholic extracts gave no reaction for thioureas when tested with Grote's reagent.

On enzymic hydrolysis of the methanolic glucoside extract only one isothiocyanate was produced, identified as methyl mustard oil, the expected product from glucocapparin, on conversion into thiourea and paper chromatography of the latter. Finally, an infra-red spectrum served to confirm the identity of the isolate with 1-methylthiourea.

Investigation in this laboratory of an extract of dried leaves of *C. Roxburghii* again revealed exclusively the presence of glucocapparin yielding methyl isothiocyanate on enzymic hydrolysis.

Hence, we have not been able to confirm the presence of 1,3-dibenzylthiourea or any likely precursor of this compound in *C. Roxburghii* and we can offer no explanation for the results reported from Indian laboratories [1,2].

Experimental. Finely pulverized bark of *C. Roxburghii* (200 g) was refluxed for 2 h with 2 l of 70 % methanol, and the extraction was repeated. On paper chromatography in butanol:ethanol:water (4:1:4) and spraying with silver nitrate, this extract gave only one glucoside spot, indistinguishable from that given by an authentic specimen of glucocapparin.

The filtrate was concentrated *in vacuo* (to 450 ml) and filtered through Celite. The solution was buffered at pH 6 with citrate; a trace of ascorbic acid [7] and a myrosinase solution (25 ml) were added, and the enzymic hydrolysis was allowed to proceed for 42 h. Half of the hydrolysis mixture was subjected to steam distillation, the distillate was treated for 3 h with 4 N ammonia, and the solution was evaporated to dryness. The other half was extracted twice with ether and twice with chloroform. The combined extracts were dried and the main part of the solvents were removed over a column. The residue was treated with a solution of ammonia in chloroform for 3 h, and the solvent was removed. Both preparations on paper chromatography in (*a*) water-saturated chloroform, and (*b*) butanol:ethanol:water (spray: Grote's reagent) showed the same pattern, *viz.* one thiourea indistinguishable from a simultaneously run reference sample of methylthiourea.

The combined thiourea preparations were dissolved in a few ml of ethanol and passed through a layer (3 cm) of neutral alumina to remove some yellow contaminations by means of ethanol. The semi-crystalline residue was triturated with a few drops of chloroform and ether and the purified material was employed for infra-red spectroscopy in a KBr-disc. The spectrum was indistinguishable from that of authentic methylthiourea.

A methanolic extract of dried leaves of *C. Roxburghii* was produced in a Waring blendor. Disturbing impurities were removed on precipitation with lead acetate and the purified glucoside solution was chromatographed in the usual way. Only one spot, identical in R_F-value with glucocapparin, was observed. An enzymically hydrolyzed glucoside solution was steam-distilled, converted into thiourea, and chromatographed as described above. Again, only one spot was produced, indistinguishable from that of methylthiourea.

The authors are indebted to Dr. Kai Larsen for the collection of leaves of *C. Roxburghii* in Thailand.

1. Lahiri, S. C. *J. Indian Med. Assoc.* **18** (1949) 155.
2. Chakravarti, R. N. *Indian Med. Gaz.* **86** (1951) 152.
3. Patel, C. K., Iyer, S. N., Sudborough, J. J. and Watson, H. E. *J. Indian Inst. Sci. Sect. A.* **9** (1926) 117.
4. Kjær, A. *Fortschr. Chem. org. Naturstoffe* **18** (1960) 122.
5. Kjær, A. and Gmelin, R. *Acta Chem. Scand.* **10** (1956) 335.
6. Kjær, A., Gmelin, R. and Larsen, I. *Acta Chem. Scand.* **9** (1955) 857.
7. Ettlinger, M. G., Dateo, Jr., G. P., Harrison, B. W., Mabry, T. J. and Thompson, C. P. *Proc. Natl. Acad. Sci. U.S.* **47** (1961) 1924.

Received March 15, 1962.

* The employed bark material was purchased as *Crataeva religiosa* from United Chemical and Allied Products, 10 Clive Row, Calcutta 1, India.

A New Spectrophotometric Method for the Determination of Uranium(VI)

DAVID DYRSSEN and
SOLVEIG EKBERG

Department of Inorganic Chemistry, Royal Institute of Technology, Stockholm, Sweden

Recently Ahrland [1] has presented a critical examination of the three best methods for a spectrophotometric determination of U(VI). He concludes that the thiocyanate method is the most expedient one, but he points out that the absorbance is very sensitive to small variations in the thiocyanate concentration. This drawback has given us reason to look for another procedure that would be more expedient for the determination of the distribution of U(VI) between two liquid phases. A method, which is suitable for such a purpose, should (*a*) have a high sensitivity, (*b*) be independent of the solvent composition of the samples, *i.e.* be insensitive to the acidity of the two phases and to organic solvents and reagents, which in general are colorless but absorb light in the UV-region.

In an extensive investigation [2] of the extraction properties of IPT (β-isopropyltropolone) we observed that the U(VI) complex has an extinction coefficient of 8 000 M^{-1} cm^{-1} at 3 950 Å, and previously Dyrssen [3] showed that the U(VI) complex of tropolone has an extinction coefficient of 6 630 M^{-1} cm^{-1} at 4 000 Å in chloroform. The Fe(III)complex has also a very large extinction coefficient [2], 13 900 M^{-1} cm^{-1} at 4 100 Å. The stability constants of IPT-metal complexes are usually very large [2], so it is in general not difficult to find conditions where a final complex is formed, *i.e.* a complex with a wide stability range. With IPT as with TTA (thenoyltrifluoroacetone) and other chelating acids, U(VI) forms an adduct, a UO_2A_2HA complex. The extra HA can be replaced by solvents that contain ligand-forming atoms (*e.g.* tributyl phosphate, dibutyl sulfoxide, ketones, etc). The use of such a solvent should therefore decrease color changes due the displacement of HA in the uranyl-IPT complex by the sample solvent. A high molarity of the displacing solvent molecule should be favorable, which is more easily obtained if it has a low molecular weight. IPT is a rather weak acid ($pK_a = 7.04$), so to avoid the effect of the acidity of the sample a proton acceptor must be introduced. The acceptor must have a $pK_a < 7.04$ otherwise the yellow anion of IPT (A^-) may be formed. The salt formed between the proton acceptor and the acids in the samples should be soluble in the solution that is measured. The sample, irrespective if it is an aqueous or organic solution (*e.g.* trilaurylamine in dodecane), should be soluble in the IPT reagent solution.

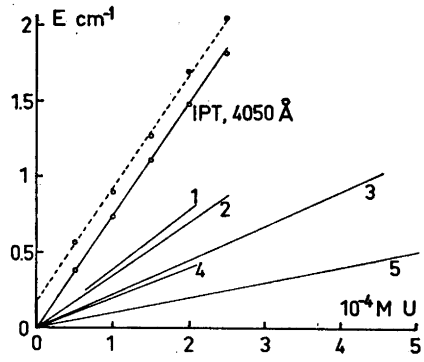

Fig. 1. Comparison of the IPT-method presented in this communication with methods tested by Ahrland: 1 Potassium cyanoferrate (II), 2 Thiocyanate in ethanol, 3 Thiocyanate in water, 4 Sodium cyanoferrate(II), 5 Basic peroxide. The dashed line is the absorbance per cm of the U(VI)-IPT-acetone-pyridine solution using air as reference.

Considering these facts, we have found that a solution of v ml of a liquid sample containing U(VI) + $(10-v)$ ml of 0.05 M IPT + 1 M pyridine in acetone has an extinction coefficient of 0.740 cm^{-1} per mmole of U added to the 10 ml at 405 mμ, which is independent of the solvent composition of the sample as long as $v < 1$ ml (in some cases a larger value of v may be used). The light absorbance per cm using the Hilger Uvispek was a linear function of the U(VI) concentration ($[U_{tot}]$) up to 2 (99 %) (*cf.* Fig. 1). This means that it is possible to determine $[U]_{tot} \geq 10^{-4}$ M in a solution by this method using 1 cm cells. The sensitivity of the method is twice that of the thiocyanate in ethanol or potassium cyanoferrate(II) as demonstrated in Fig. 1.

No attempt has been made to eliminate the influence of Fe(III) as in the case of the thiocyanate method.

We wish to thank the *Swedish Atomic Energy Company* for financial support and for permission to publish this method. We are also indebted to Professor Lars Gunnar Sillén and Docent Sten Ahrland for some helpful comments and to Dr. Derek Lewis for English text revision.

1. Ahrland, S. *Svensk Kem. Tidskr.* **72** (1960) 757 (in English).
2. Dyrssen, D. *Trans. Royal Inst. Technol. Stockholm* (1962) No. 188.
3. Dyrssen, D. *Acta Chem. Scand.* **9** (1955) 1567.

Received March 16, 1962.

Correction to "Formation of Free Radicals from Some Phenothiazine Derivatives as Studied by Electron Spin Resonance" *

CARL LAGERCRANTZ

Department of Medical Physics, University of Göteborg, Sweden

In the reaction scheme on p. 1554 the side chain of the promethazine molecule is erroneously given as 3-dimethylamino-2-methyl-propyl. This is corrected to 2-dimethylaminopropyl and the products obtained in the reaction with conc. sulphuric acid are 10-(hydroxymethyl)-phenothiazine, 1-dimethylaminoethanol and sulphur dioxide.

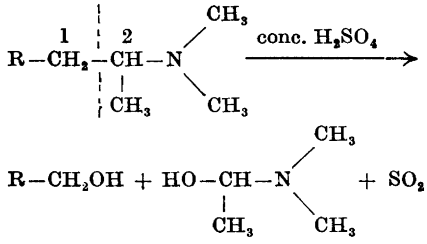

R = phenothiazine nucleus.

* Acta Chem. Scand. **15** (1961) 1545.

Received March 29, 1962.

Optical Rotatory Dispersion of some Nickel Complexes

BERNDT SJÖBERG * and ROLF BACKSTRÖM

Department of Organic Chemistry, Chemical Institute, University of Uppsala, Uppsala, Sweden

In a recent investigation [1] of xanthates it was shown that these compounds often exhibit strong Cotton effects and that the anomalous dispersion curves can be used for stereochemical correlations. However, the amplitudes and at times even the appearance of Cotton effects of xanthates are very dependent upon chemical constitution. Thus rigid compounds, like bornyl xanthates, have Cotton effects of large amplitudes whereas the methyl xanthate of 2-methylbutanol only shows a plain dispersion curve. We thought it possible to increase the interaction between the C=S chromophore and the various substituents of the pertinent molecule by complexing with a metal.

In the preparation of alkyl xanthates the appropriate alcohol is first treated with alkali and carbon disulfide and then with an alkyl halide. If nickel acetate is added instead of the alkyl halide, a coloured metal complex *1* precipitates. Drawert, Reuther and Born [2] recently investigated this type of complex of several racemic alcohols and found a series of absorption bands in the visible and ultraviolet region. The first group of bands are situated at about 480 and 420 mμ, and the extinction of the complexes seems to be fairly dependent on the structure of the alcohol. However, the ε values will generally be of the order of

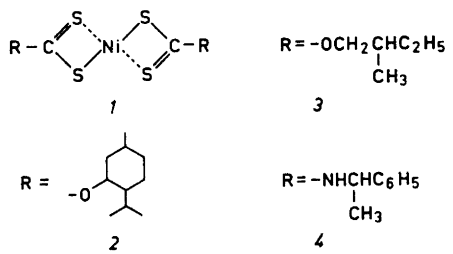

1 *3*

2 *4*

* Present address: AB Astra, Södertälje, Sweden.

No attempt has been made to eliminate the influence of Fe(III) as in the case of the thiocyanate method.

We wish to thank the *Swedish Atomic Energy Company* for financial support and for permission to publish this method. We are also indebted to Professor Lars Gunnar Sillén and Docent Sten Ahrland for some helpful comments and to Dr. Derek Lewis for English text revision.

1. Ahrland, S. *Svensk Kem. Tidskr.* **72** (1960) 757 (in English).
2. Dyrssen, D. *Trans. Royal Inst. Technol. Stockholm* (1962) No. 188.
3. Dyrssen, D. *Acta Chem. Scand.* **9** (1955) 1567.

Received March 16, 1962.

Correction to "Formation of Free Radicals from Some Phenothiazine Derivatives as Studied by Electron Spin Resonance" *

CARL LAGERCRANTZ

Department of Medical Physics, University of Göteborg, Sweden

In the reaction scheme on p. 1554 the side chain of the promethazine molecule is erroneously given as 3-dimethylamino-2-methyl-propyl. This is corrected to 2-dimethylaminopropyl and the products obtained in the reaction with conc. sulphuric acid are 10-(hydroxymethyl)-phenothiazine, 1-dimethylaminoethanol and sulphur dioxide.

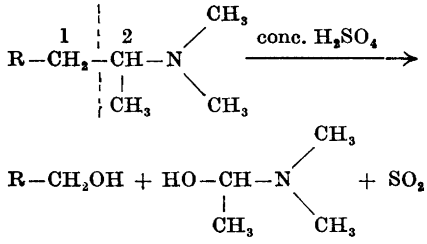

R = phenothiazine nucleus.

* Acta Chem. Scand. **15** (1961) 1545.

Received March 29, 1962.

Optical Rotatory Dispersion of some Nickel Complexes

BERNDT SJÖBERG * and ROLF BACKSTRÖM

Department of Organic Chemistry, Chemical Institute, University of Uppsala, Uppsala, Sweden

In a recent investigation [1] of xanthates it was shown that these compounds often exhibit strong Cotton effects and that the anomalous dispersion curves can be used for stereochemical correlations. However, the amplitudes and at times even the appearance of Cotton effects of xanthates are very dependent upon chemical constitution. Thus rigid compounds, like bornyl xanthates, have Cotton effects of large amplitudes whereas the methyl xanthate of 2-methylbutanol only shows a plain dispersion curve. We thought it possible to increase the interaction between the C=S chromophore and the various substituents of the pertinent molecule by complexing with a metal.

In the preparation of alkyl xanthates the appropriate alcohol is first treated with alkali and carbon disulfide and then with an alkyl halide. If nickel acetate is added instead of the alkyl halide, a coloured metal complex *1* precipitates. Drawert, Reuther and Born [2] recently investigated this type of complex of several racemic alcohols and found a series of absorption bands in the visible and ultraviolet region. The first group of bands are situated at about 480 and 420 mμ, and the extinction of the complexes seems to be fairly dependent on the structure of the alcohol. However, the ε values will generally be of the order of

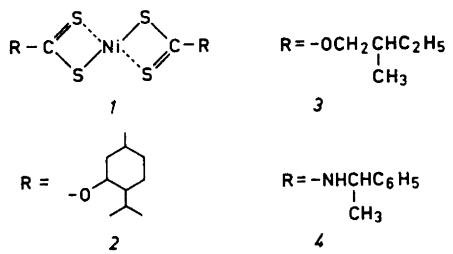

1 *3*

2 *4*

* Present address: AB Astra, Södertälje, Sweden.

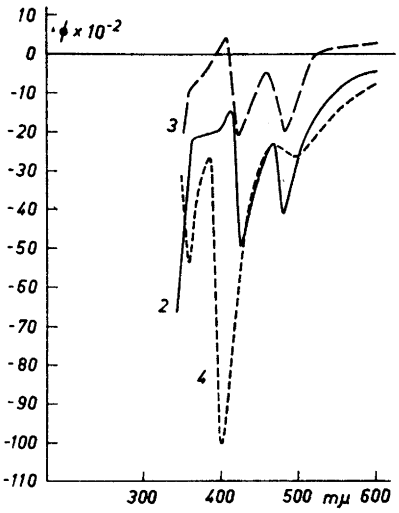

Fig. 1. Optical rotatory dispersion curves of bis[(—)-menthylxanthate]nickel(II) (*2*) bis[(+)-2-methylbutylxanthate)-nickel(II) (*3*) and bis[(—)-α-phenylethyldithiocarbamate)-nickel (II) (*4*).

500—1 000 and 1 000—2 000, respectively. Such high ε values will not allow convenient rotatory dispersion measurements through the absorption region unless the amplitudes of the Cotton effects are large. In order to see if metal complexes related to structure *1* are suitable for rotatory dispersion studies we have prepared this type of nickel complexes from optically active alcohols.

The compounds *2* and *3* prepared from menthol and 2-methylbutanol, respectively, have both absorption bands at 477 and 417 mμ (log ε ~ 3.1 and 3.3); rotatory dispersion curves in Fig. 1. The complex *2*, derived from menthol, has two negative Cotton effects of fairly large amplitudes corresponding to the 477 and 417 mμ bands. But most important the nickel complex *3* prepared from 2-methylbutanol, also exhibits Cotton effects related to the two absorption bands. In this way it seems possible to circumvent the previously mentioned difficulty with rotatory dispersion studies of simple alcohols whose xanthates will not exhibit anomalous dispersion curves.

Optical rotatory dispersion curves of dithiocarbamates have been shown [1,3] to be similar to those of the corresponding xanthates. For that reason we also included amines in our present studies, for example the nickel complex *4* prepared from optically active α-phenylethylamine. This complex has absorption bands at 480 and 385 mμ (log ε ~ 2.3 and 3.6), and strong Cotton effects are found in the rotatory dispersion curve (Fig. 1).

Applications of metal complexes (nickel, copper, etc.) in stereochemical studies of alcohols and amines will be discussed further in our full papers.

Experimental. The bis[xanthate]nickel(II) complexes *2* and *3* were prepared according to the method used on racemic alcohols by Drawert, Reuther and Born [2], and bis[dithiocarbamate]-nickel(II) (4) according to a similar procedure reported by Losanitsch [4].

Bis[(—)-menthylxanthate]nickel(II) (2), m.p. 176°d, λ_{max} dioxane 477 (log ε = 3.08) and 417 mμ (log ε = 3.32). (Found: Ni 11.27. $C_{22}H_{38}O_2S_4Ni$ requires Ni 11.25).

R.D. (Fig. 1), *c*, 0.023 in dioxane: Φ_{589} −450°, Φ_{480} −4 130°, Φ_{467} −2 270°, Φ_{426} −4 990°, Φ_{413} −1 450°, Φ_{345} −6 700°.

Bis[(+)-2-methylbutylxanthate]nickel(II) (3), m.p. 80—84°d., λ_{max} dioxane 477 (log ε = 3.03) and 417 mμ (log ε = 3.32). (Found: Ni 16.81; $C_{12}H_{22}O_2S_4Ni$ requires 15.23).

R.D. (Fig. 1), *c*, 0.021 in dioxane: Φ_{589} + 250°, Φ_{483} −2 020°, Φ_{462} −440°; *c*, 0.011: Φ_{421} −2 130°, Φ_{406} + 440°, Φ_{350} −2 200°.

Bis[(—)-α-phenylethyldithiocarbamate]nickel (II) (4), m.p. 67°d. λ_{max} methanol 480 (log ε = 2.29) and 385 mμ (log ε = 3.62). (Found: Ni 12.89; $C_{18}H_{20}N_2S_4Ni$ requires 12.24).

R.D .(Fig. 1) *c*, 0.020 in methanol: Φ_{589} −880°, Φ_{493} −2 650°, Φ_{464} −2 340°; *c*, 0.010: Φ_{400} −10 100°, Φ_{384} −2 650°, Φ_{359} −5 300°, Φ_{350} −3 180°.

1. Sjöberg, B , Cram, D. J., Wolf, L. and Djerassi, C. *Acta Chem. Scand.* **16** (1962) *In press.*
2. Drawert, F., Reuther, K.-H. and Born, F. *Chem. Ber.* **93** (1960) 3056.
3. Sjöberg, B., Fredga, A. and Djerassi, C. *J. Am. Chem. Soc.* **81** (1959) 5002.
4. Losanitsch, S. M. *Ber.* **24** (1891) 3026.

Received December 19, 1961.

The Structure of N-Methyl-pyridinium-2-aldoxime

LENNART LARSSON and GUN WALLERBERG

Research Institute of National Defence, Dept. 1, Sundbyberg 4, Sweden

The iodide and methane sulphonate salts of N-methyl-pyridinium-2-aldoxime (I), generally denoted as 2-PAM and P2S, respectively, have been reported to be effective antidotes against poisonings caused by toxic organo-phosphorus compounds [1,2]. Studies on the renal excretion of P2S have shown that the excretion is markedly reduced by alkalinization of the urine indicating that the dissociated, basic form (II) is more lipophilic than the acid form (I)[3]. Furthermore the solubility of the basic form in chloroform is about 2.5 % which is unexpectedly high for a "zwitterion".

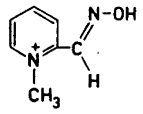

I

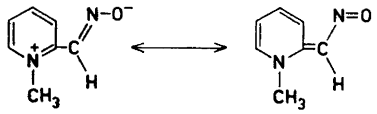

II *III*

These lipophilic properties of the basic form indicate that the basic form may exist as a resonance hybride of the structures II and III. In order to throw light on the resonance conditions in the basic form this compound has been isolated by an anion-exchange technique, and its dipole moment has been determined. Moreover its infrared spectrum has been recorded and compared with the spectrum of 2-PAM.

Presuming a coplanar configuration of the molecule, the dipole moment of the purely ionic structure (II) can approximately be calculated from the bond angles and atomic distances. The lowest moments which in this way can be predicted, are 13.0 D for the *anti* form and 20.6 D for the *syn* form. In which of these forms the compound really exists has not yet been established [4]. The dipole moment of the basic form was found to be 7.7 D in a chloroform solution. This value is probably 20–30 % too low, because the determination was performed in a polar solvent. The found value, however, is considerably lower than the lowest calculated one, which supports that the quinoid structure (II) to a certain extent contributes to the structure of the molecule.

Table 1. The principal absorption frequencies of 2-PAM and its basic form in the region 1 000–1 700 cm^{-1}. (Figures within parentheses denote shoulders.)

Absorption frequencies in cm^{-1} of 2-PAM	Basic form	Assignments [5]
1003	–	N–OH
–	1140	N–O⁻(↔)N=O
1166	1179	C–H
1179	1192	C–H
1235	(1262)	
1292	1285	
1311		O–H (?)
1321	1337	
(1403)		O–H (?)
1427	1431	C–H
(1445)	1456	Pyridine nucleus and C=N (oxime group)
(1456)	1471	
1502	1499	
1575	1560	
1590	–	
1623	1634	

In a comparison between the infrared spectra of the acidic and basic forms in the region 1 000–1 700 cm^{-1} two obvious differences are shown which appears from Table 1 where the principal absorption bands in this region are given. In the spectrum of the acidic form the strong absorption band orginating from the N–OH bond [5] is found at 1 003 cm^{-1} but in the spectrum of the basic form the corresponding band occurs at 1 140 cm^{-1}. A large increase of the frequency is expected to occur when N–OH is changed to N–O⁻ or N=O. The latter structure will cause the largest frequency shift, still larger than the found one, which indicates that the structure II is predominant. More remarkable is the absence of the band in the spectrum of the basic form at 1 590 cm^{-1} which appears in

the spectrum of the acid form. This indicates changes in the double bond structure of the pyridine nucleus or possibly in the C=N bond of the oxime group. Both of these possibilities support a contribution of structure III.

The dipole moment and infrared data indicate that the basic form of a N-methylpyridinium-2-aldoxime salt is a resonance hybride of structures II and III, and that the ionized form predominates, but that the contribution of the quinoid structure is obvious.

Experimental. The preparation of the basic form of N-methyl-pyridinium-2-aldoxime was performed by means of an anion-exchanger (Dowex 2, 20–50 mesh). The column was regenerated by 0.5 M sodium hydroxide solution and washed with methanol. A solution of 5 g of the iodide (2-PAM) in 500 ml of methanol was introduced into the anion-exchanger and the flow rate was kept at about one drop/sec. The dark yellow eluate was concentrated by evaporation under vacuum to a volume of 75–100 ml. By addition of ether to the concentrated solution the basic form was precipitated. The precipitate was filtered off and purified by repeated reprecipitations. Because the product is discoloured by air and light, it had to be dried in a dark vacuum-exsiccator. Yield 50 %. (Found: C 61.5; H 5.86. Calc. for $C_7H_8N_2O$: C 61.8; H 5.92).

Dipole moment measurements. Preliminary experiments showed that the solubility of the basic form was very low in benzene and carbon tetrachloride but about 2.5 % in chloroform. Because of its slight solubility in nonpolar solvents an accurate determination of its dipole will not be successful. Thus for the calculation of the dipole moment the simplified method described by Guggenheim [6] will give a sufficient accuracy. The dielectric constants of five different concentrations of the compound in chloroform were determined by means of a "Dekameter 03" (Dr. N. Slevogt, Germany) at 25°C. In order to check the method of calculation and the instrument, the dipole moment of *p*-nitrosodimethylaniline was determined. It was found to be 5.5 D in chloroform solution and 7.1 D in benzene solution. The latter value agrees well with 6.9 D which has been given by Le Fèvre [7] for this compound in benzene solution.

Infrared spectrophotometric measurements. The infrared spectra of the basic form of N-methyl-pyridinium-2-aldoxime and of its iodide were recorded between 2 and 11 μ on a Perkin-Elmer spectrophotometer, Model 21. The pellet technique was used, and 1 mg of sample was ground mechanically with 300 mg of potassium bromide.

1. Davies, D. R. and Green, A. L. *Brit. J. industr. Med.* **16** (1959) 128.
2. Sundwall, A. *Tidskr. i Militär Hälsovård* (1962). *In press.*
3. Berglund, F., Elwin, C.-E. and Sundwall, A. *Biochem. Pharmacol.* (1962). *In press.*
4. Poziomek, E. J., Kramer, D. N., Fromm, B. W. and Mosher, W. A. *J. Org. Chem.* **26** (1961) 423.
5. Augustinsson, K.-B., Hasselquist, H. and Larsson, L. *Acta Chem. Scand.* **14** (1960) 1253.
6. Guggenheim, E. A. *Trans. Faraday Soc.* **47** (1951) 573.
7. Le Fèvre, R. J. W. *Dipole Moments.* Methuen Co, London 1948, p. 111.

Received March 30, 1962.

Unsaturated γ-Thiolactones II*. The Structures of 3- and 4-Methyl-2-thienols

ANNA-BRITTA HÖRNFELDT and SALO GRONOWITZ

Institute of Chemistry, University of Uppsala, Uppsala, Sweden

It has earlier been shown by NMR-studies that 2-thienol exists in the liquid state as 3-thiolen-2-one (I), and that two tautomeric thiolactone forms of 5-methyl-2-thienol can be prepared, both of which rearrange to an equilibrium mixture consisting of 85 % 5-methyl-3-thiolen-2-one (II) and 15 % 5-methyl-4-thiolen-2-one (III) [1].

We have now extended the investigation of the tautomeric structure of hydroxythiophenes to the two remaining methyl substituted 2-thienols. 3-Methyl-2-thienol was obtained in good yield through hydrogen peroxide cleavage [2] of 3-methyl-2-thiopheneboronic acid, which has been prepared through the reaction of 3-methyl-2-thiophenemagnesium bromide with butyl borate. In a similar way, 4-methyl-2-thienol contaminated with smaller amounts of the

* Part I. Ref.[1]

3-methyl isomer was obtained through metalation of 3-methylthiophene with butyllithium [3] followed by the reaction with butyl borate and peroxide oxidation. This method for the preparation of hydroxythiophenes gives acceptable yields and has also been used by us for the preparations of 2-thienol and the tautomeric forms of 5-methyl-2-thienol, as well as for the preparation of the acetate of the very unstable 3-hydroxythiophene, which was obtained in 30 % yield calculated on 3-bromothiophene. Hydroxythiophenes appear to be available also through acid-catalyzed dealkylation of *t*-butoxythiophenes [4].

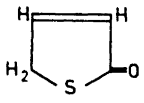

I

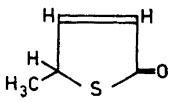

II

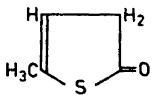

III

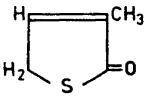

IV

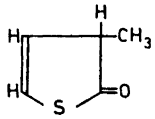

V

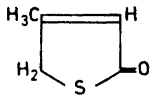

VI

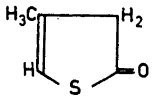

VII

The NMR-spectrum at 60 Mc/s showed that 3-methyl-2-hydroxythiophene exists as 3-methyl-3-thiolen-2-one (IV). Its spectrum showed three bands at τ = 2.70 ppm, τ = 6.03 ppm and τ = 8.07 ppm, with relative intensities of 1:2:3, respectively, and belong thus to the CH-, CH_2- and CH_3-groups of (IV). From the completely resolved spectrum the following coupling constants are obtained: J_{CH-CH_3} = 1.5 c/s, J_{CH-CH_2} = 3.0 c/s and $J_{CH_2-CH_3}$ = 1.9 c/s.

The spectrum of 4-methyl-2-hydroxythiophene consists of three bands at τ = 3.89 ppm, τ = 5.98 ppm and τ = 7.77 ppm with the relative intensities of 1:2:3. The coupling constants are J_{CH-CH_3} = 1.5 c/s, J_{CH-CH_2} = 1.5 c/s and $J_{CH_2-CH_3}$ = 0.75 c/s. From the relative intensities alone it is impossible to determine whether this compound exists as (VI) or (VII). Through a comparison of the chemical shifts of the CH_2-group in this compound and in (I—IV) and of the coupling constants it is evident that this compound is 4-methyl-3-thiolen-2-one (VI). In contrast to the case of the 5-methyl isomer it has not yet been possible to obtain the other thiolactone form (V) of 3-methyl-3-thiolen-2-one by acidifying an alkaline solution.

(IV) reacted in its enol form to give esters and could also be condensed with benzaldehyde in the 5-position to give 5-benzylidene-3-methyl-3-thiolen-2-one.

Experimental. 3-Methyl-3-thiolen-2-one. The Grignard reagent from 35.5 g (0.2 mole) of 3-methyl-2-bromothiophene [5] was added dropwise to 46.4 g (0.2 mole) of butyl borate in 80 ml absolute ether under nitrogen at −70°. The resulting solution was allowed to warm slowly to 0°. The reaction mixture was decomposed with 120 ml of cold sulphuric acid. The aqueous layer was extracted with 200 ml of 1 N cold NaOH and the alkaline solution was acidified with 2 N cold sulphuric acid. The boronic acid was filtered off and immediately dissolved in 250 ml of ether.

135 ml of 10 % hydrogen peroxide was added with stirring to the ethereal boronic acid under nitrogen. When the addition was complete the mixture was refluxed for one hour and the layers separated. The water layer was extracted with ether and the combined ethereal phases were washed five times with 15 ml of 10 % ferrous ammonium sulphate solution, once with water, and dried over $MgSO_4$. Distillation *in vacuo* under nitrogen yielded 9.8 g (43 %) of 3-methyl-3-thiolen-2-one, b.p. 96—98°/8 mm Hg, mp. 35—36°. (Found: C 52.13; H 5.25; S 27.80; Calc. for C_5H_6OS (114.19): C 52.60; H 5.20; S 28.09).

5-Benzylidene-3-methyl-3-thiolen-2-one. 2.3 g (0.02 mole) of 3-methyl-3-thiolen-2-one and 2.2 g (0.02 mole) of benzaldehyde in 20 ml of cold absolute alcohol was treated with gaseous hydrogen chloride yielding 3.0 g (70 %) of 5-benzylidene-3-methyl-3-thiolen-2-one mp.

133–134° (Found: C 70.97; H 4.99; S 15.93. Calc. for $C_{12}H_{10}OS$ (202.27) C 71.25; H 4.98; S 15.85).

3-Acetoxythiophene. 65 g of butyl borate in 170 ml absolute ether was added in a single portion to 3-thienyllithium which had been prepared from 190 ml 1.15 N butyllithium and 32.6 g (0.2 mole) of 3-bromothiophene [6] in 50 ml absolute ether at −70°. The mixture was stirred at −60° for 4 h and the boronic acid [7] isolated and oxidized as above. After the ethereal phases had been washed with ferrous sulphate they were extracted with 80 ml of cold sodium hydroxide solution. The alkaline solution was shaken vigorously for 5 min with crushed ice and 15 ml of acetic anhydride, and then extracted with ether. Distillation *in vacuo* under nitrogen yielded 8.5 g (30 %) of 3-acetoxythiophene b.p. 82–84°/10 mm Hg $n_D^{20} = 1.5200$ (Found: C 50.65; H 4.40; S 22.21. Calc. for $C_6H_6O_2S$ (142.18) C 50.68; H 4.26; S 22.56).

The NMR-spectra were recorded in deuterochloroform-cyclohexane solution on a Varian Associate model A 60 high resolution spectrometer.

Acknowledgements. The authors wish to express their thanks to Prof. Arne Fredga for his interest in this work and for all facilities put at their disposal. The elementary analyses were carried out at the Analytical Department of the Chemical Institute.

1. Gronowitz, S. and Hoffman, R. A. *Arkiv Kemi* **15** (1960) 499.
2. Hawthorne, F. M. *J. Org. Chem.* **22** (1957) 1001.
3. Gronowitz, S., Moses, P., Hörnfeldt, A.-B. and Håkansson, R. *Arkiv Kemi* **17** (1961) 165.
4. Lawesson, S.-O. and Frisell, C. *Arkiv Kemi* **17** (1961) 393.
5. Steinkopf, W. and Jacob, H. *Ann.* **515** (1935) 273.
6. Gronowitz, S. *Acta Chem. Scand.* **13** (1959) 1045.
7. Lawesson, S.-O. *Arkiv Kemi* **11** (1957) 389.

Received April 6, 1962.

A Tetragonal Form of Zirconium Oxide Sulfide, ZrOS

F. JELLINEK

Laboratory of Inorganic Chemistry, University of Groningen, Netherlands, and Institute of Chemistry, University of Uppsala, Sweden

In his study of the system Zr–S Schönberg [1] found a tetragonal phase with cell dimensions $a = 3.55$ Å; $c = 6.31$ Å and space group $P\ 4/nmm-D_{4h}^7$, to which he ascribed a composition of ZrS and a tsructure of the *B* 11 type. Several reinvestigations of the system Zr–S have been undertaken since, *e.g.* by Hahn and coworkers [2], by McTaggart and Wadsley [3] and by the present author. All these investigators agree that ZrS has a cubic superstructure of the NaCl type; no indications were found for the existence of a tetragonal monosulfide, nor indeed for any tetragonal phase in the system Zr–S. (Tetragonal "Zr_4S_3" [2]) has shown to be a ternary phase of composition ZrSiS [4].)

In view of these discrepancies a re-examination of Schönberg's X-ray diagrams of the system Zr–S was undertaken. It was confirmed that in several of his preparations a tetragonal phase with the dimensions and symmetry derived by Schönberg was present. However, all preparations which contain this phase had been partly oxidized: the tetragonal phase was always accompanied by considerable proportions of cubic ZrOS and in some cases even by ZrO_2. It seemed probable, therefore, that the tetragonal phase also contains oxygen.

From the symmetry it is evident that the unit cell must contain an even number of all kinds of atoms; from spatial considerations a unit-cell content of 2 × ZrOS seems the most probable. This hypothesis is strongly supported by the fact the ThOS, UOS and NpOS have the same symmetry and similar cell dimensions as the tetragonal zirconium oxysulfide; the unit cells of ThOS, UOS and NpOS contain two formula units and the structures are of the PbFCl ($E\ 0_1$)-type [5]. It seems most probable, therefore, that the alleged tetragonal ZrS is a new modification of ZrOS, and that its structure is also of the PbFCl type. Zr and S are situated in positions 2(*c*): $0\frac{1}{2}z$; $\frac{1}{2}0\bar{z}$; oxygen in position 2(*a*): 0 0 0; $\frac{1}{2}\frac{1}{2}0$.

133–134° (Found: C 70.97; H 4.99; S 15.93. Calc. for $C_{12}H_{10}OS$ (202.27) C 71.25; H 4.98; S 15.85).

3-Acetoxythiophene. 65 g of butyl borate in 170 ml absolute ether was added in a single portion to 3-thienyllithium which had been prepared from 190 ml 1.15 N butyllithium and 32.6 g (0.2 mole) of 3-bromothiophene [6] in 50 ml absolute ether at −70°. The mixture was stirred at −60° for 4 h and the boronic acid [7] isolated and oxidized as above. After the ethereal phases had been washed with ferrous sulphate they were extracted with 80 ml of cold sodium hydroxide solution. The alkaline solution was shaken vigorously for 5 min with crushed ice and 15 ml of acetic anhydride, and then extracted with ether. Distillation *in vacuo* under nitrogen yielded 8.5 g (30 %) of 3-acetoxythiophene b.p. 82–84°/10 mm Hg $n_D^{20} = 1.5200$ (Found: C 50.65; H 4.40; S 22.21. Calc. for $C_6H_6O_2S$ (142.18) C 50.68; H 4.26; S 22.56).

The NMR-spectra were recorded in deuterochloroform-cyclohexane solution on a Varian Associate model A 60 high resolution spectrometer.

Acknowledgements. The authors wish to express their thanks to Prof. Arne Fredga for his interest in this work and for all facilities put at their disposal. The elementary analyses were carried out at the Analytical Department of the Chemical Institute.

1. Gronowitz, S. and Hoffman, R. A. *Arkiv Kemi* **15** (1960) 499.
2. Hawthorne, F. M. *J. Org. Chem.* **22** (1957) 1001.
3. Gronowitz, S., Moses, P., Hörnfeldt, A.-B. and Håkansson, R. *Arkiv Kemi* **17** (1961) 165.
4. Lawesson, S.-O. and Frisell, C. *Arkiv Kemi* **17** (1961) 393.
5. Steinkopf, W. and Jacob, H. *Ann.* **515** (1935) 273.
6. Gronowitz, S. *Acta Chem. Scand.* **13** (1959) 1045.
7. Lawesson, S.-O. *Arkiv Kemi* **11** (1957) 389.

Received April 6, 1962.

A Tetragonal Form of Zirconium Oxide Sulfide, ZrOS

F. JELLINEK

Laboratory of Inorganic Chemistry, University of Groningen, Netherlands, and Institute of Chemistry, University of Uppsala, Sweden

In his study of the system Zr–S Schönberg [1] found a tetragonal phase with cell dimensions $a = 3.55$ Å; $c = 6.31$ Å and space group $P\ 4/nmm-D_{4h}^7$, to which he ascribed a composition of ZrS and a tsructure of the *B* 11 type. Several reinvestigations of the system Zr–S have been undertaken since, *e.g.* by Hahn and coworkers [2], by McTaggart and Wadsley [3] and by the present author. All these investigators agree that ZrS has a cubic superstructure of the NaCl type; no indications were found for the existence of a tetragonal monosulfide, nor indeed for any tetragonal phase in the system Zr–S. (Tetragonal "Zr_4S_3" [2]) has shown to be a ternary phase of composition ZrSiS [4].)

In view of these discrepancies a re-examination of Schönberg's X-ray diagrams of the system Zr–S was undertaken. It was confirmed that in several of his preparations a tetragonal phase with the dimensions and symmetry derived by Schönberg was present. However, all preparations which contain this phase had been partly oxidized: the tetragonal phase was always accompanied by considerable proportions of cubic ZrOS and in some cases even by ZrO_2. It seemed probable, therefore, that the tetragonal phase also contains oxygen.

From the symmetry it is evident that the unit cell must contain an even number of all kinds of atoms; from spatial considerations a unit-cell content of 2 × ZrOS seems the most probable. This hypothesis is strongly supported by the fact the ThOS, UOS and NpOS have the same symmetry and similar cell dimensions as the tetragonal zirconium oxysulfide; the unit cells of ThOS, UOS and NpOS contain two formula units and the structures are of the PbFCl ($E\ 0_1$)-type [5]. It seems most probable, therefore, that the alleged tetragonal ZrS is a new modification of ZrOS, and that its structure is also of the PbFCl type. Zr and S are situated in positions 2(*c*): $0\frac{1}{2}z$; $\frac{1}{2}0\bar{z}$; oxygen in position 2(*a*): 0 0 0; $\frac{1}{2}\frac{1}{2}0$.

Table 1. Observed and calculated intensities (Cu$K\alpha$ radiation).

$h\,k\,l$	I_{obs}	I_{calc} PbFCl-type	I_{calc} B 11-type
0 0 1	m+	48	33
0 0 2	m+	46	128
1 0 1	v st	216	164
1 1 0	st+ *	178	238
1 0 2	v st	216	190
1 1 1	—	1	12
0 0 3	w⁻	7	15
1 1 2	st	132	136
1 0 3	m+	60	9
2 0 0	st	122	95
2 0 1	w⁻ *	7	6
1 1 3	m+	48	30
0 0 4	—	0	0
2 0 2	m	33	75
2 1 1	st⁻	76	59
1 0 4	st⁻	73	124
2 1 2	st	127	112
2 0 3	w	13	22
1 1 4	v w	5	0
2 1 3	st⁻	58	8
0 0 5		24	5
2 2 0	st⁻	59	49
2 2 1	— *	3	3
1 0 5	—	1	2
2 0 4	—	0	0
2 2 2	m (br)	20	45
3 0 1		21	16
1 1 5	m+ *	50	16
3 1 0	st (br)	64	77
2 1 4		88	154
3 0 2	m *	41	36
3 1 1		0	4

* Intensity estimation inaccurate because of coincidence with line of cubic ZrOS.

The observed intensities are not sufficient for deriving accurate values for the z parameters of Zr and S, but "ideal" values can be calculated by geometrical considerations. Each metal is equidistant from its eight metal neighbours if $z_M = \frac{1}{4}\sqrt{2} \times a/c$. Furthermore, it is equidistant from its five sulfur neighbours, if $z_S = \frac{1}{2} + \frac{a^2}{4c^2(1-2z_M)}$ or, introducing the ideal value of z_M: $z_S = \frac{1}{2} + \frac{a^2}{4c^2 - 2\sqrt{2}ac}$. Substitution of the observed value for c/a leads to "ideal" parameter values of $z_{Zr} = 0.199$ and $z_S = 0.631$.

A comparison with ThOS, UOS, NpOS[5] shows that the "observed" values of z_S closely correspond to the ideal ones, while z_M always is slightly less than the ideal value, the difference being 0.004 on the average. Therefore, the following parameter values were adopted: $z_{Zr} = 0.19_5$; $z_S = 0.63_0$. Using these values, the agreement between observed and calculated intensities (see Table 1) is as good as can be wished; indeed, the agreement is considerably better than that for the structure proposed by Schönberg which is also included in Table 1. (Table 1 of Schönberg's paper [1] should be disregarded, as several errors have crept into both I_{calc} and I_{obs}. The interatomic distances derived from the adopted parameters (Zr—5S = 2.74 Å; Zr—4O = 2.16 Å) are slightly larger than the distances in cubic ZrOS [6], as is to be expected by the increase of the co-ordination number of the metal from seven to nine.

Although all attempts to prepare the phase in a state sufficiently pure for chemical analysis have failed so far, the conclusion that the alleged tetragonal ZrS actually is a new modification of ZrOS with a PbFCl-type structure seems well-supported.

The author wishes to thank Prof. G. Hägg for the loan of N. Schönberg's X-ray diagrams and for valuable discussions.

1. Hägg, G. and Schönberg, N. *Arkiv Kemi* **7** (1954) 371.
2. Hahn, H., Harder, B., Mutschke, U. and Ness, P. *Z. anorg. allgem. Chem.* **292** (1957) 82.
3. McTaggart, F. K. and Wadsley, A. D. *Austral. J. Chem.* **11** (1958) 445.
4. Jellinek, F., and Hahn, H., *Naturwiss.* **49** (1962) 103.
5. Zachariasen, W. H. *Acta Cryst.* **2** (1949) 291.
6. McCullough, J. D., Brewer, L. and Bromley, L. A. *Acta Cryst.* **1** (1948) 287.

Received March 20, 1962.

ACTA CHEMICA SCANDINAVICA 16 (1962) 793–798

Vibrational Structure and Solvent Effects on an Intra-subshell Transition of Osmium(IV) Hexachloro Ions

CHR. KLIXBÜLL JØRGENSEN

Cyanamid European Research Institute, Cologny (Geneva), Switzerland

The narrow absorption band in the yellow of $OsCl_6^{2-}$, caused by an internal transition in the subshell γ_6^4, has an interesting fine structure. The main part is a linear progression (or pseudo-progression) with the characteristic wave-number 170 cm^{-1}, but at a higher wave-number very weak peaks are observed. Their distances from the electronic transition are 1690 cm^{-1} in water, 1450 cm^{-1} in ethanol, and 2980 cm^{-1} in dichloroethane, and may be identified with the O-H bending, C-H bending, and C-H stretching frequencies, respectively.

The narrow lines of lanthanide complexes sometimes have weak satellites caused by co-excitation of vibrations of surrounding molecules. Recently, Young, Gruen, and Satten[1] demonstrated the co-excitation of not only UCl_6^{2-} vibrations, but also C-H vibrations of $[N(CH_3)_4]_2[UCl_6]$. The phenomenon is much more difficult to observe in the 3d, 4d, 5d transition groups, since the absorption bands are so much broader. However, Piper and Koertge[2] succeeded in showing, by deuterium substitution in salts of $Ni(H_2O)^{2+}$, that the weak band at 18 700 cm^{-1} of the latter ion is a superposition of the O-H stretching frequency on the narrow band $^3\Gamma_2 \rightarrow {}^1\Gamma_3$ in the red.

As previously mentioned[3], $OsCl_6^{2-}$ has very narrow bands in the near infra-red and in the yellow, representing internal transitions from $^3\Gamma_4$ (the L, S, coupling component with Bethe's double group quantum number Γ_1) to $^1\Gamma_3$ and $^1\Gamma_5$ (at 10 800 and 11 700 cm^{-1}) and to $^1\Gamma_1$ (at 17 240 cm^{-1}), all energy levels belonging to the same subshell configuration γ_4^5. For an explanation of the notation, see Ref. [17]

There are close analogies between these bands and the bands[4] of $ReCl_6^{2-}$ in the red at 14 030 and 15 400 cm^{-1}. As remarked by the present author at several previous occasions[3], and independently by Eisenstein[5], the original assignment[4] of the excited levels $^2\Gamma_3$ and $^2\Gamma_4$ is not correct. These levels are rather the intermediate coupling components Γ_7 and Γ_8 of the highest term, $^2\Gamma_5$ of the lowest subshell configuration γ_3^5.

The former band, representing the transition to Γ_7, has a vibrational structure[4] consisting of seven equi-distant peaks with the mutual distance

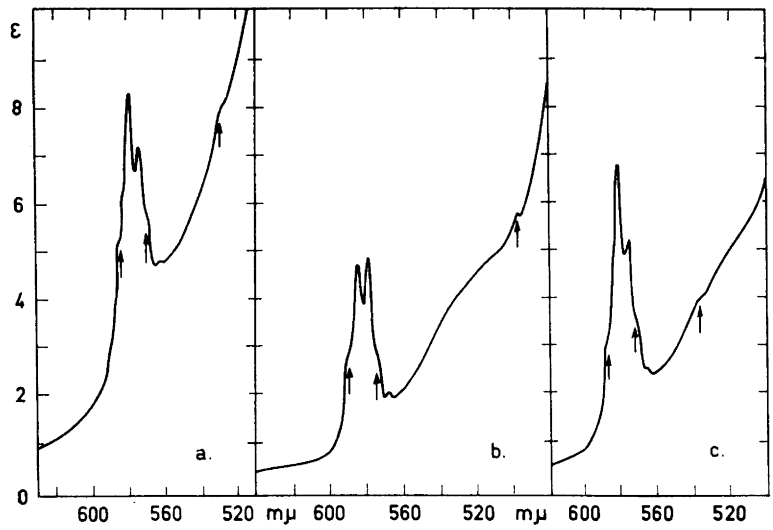

Fig. 1. The absorption spectra of $OsCl_6^{2-}$ in (*a*) 1 M aqueous hydrochloric acid, (*b*) dichloroethane, and (*c*) anhydrous ethanol.

150 to 160 cm^{-1}. The second transition, to Γ_8, produces an irregular band shape[4], and high pressure induces a strong splitting into two parts[6], possibly connected with deviations from the regular octahedral symmetry and removing the degeneracy of the two Kramers doublets in the electronic level Γ_8.

Measurements of $[As(C_6H_5)_4]_2ReCl_6$ in dichloroethane have confirmed the existence[5] of the transition to the nearly degenerate[18] levels Γ_8 and Γ_6 with vibrational structure at 9 110, 9 270, 9 430, 9 570 (maximum, $\varepsilon = 4.5$) and 9 730 cm^{-1}.

The transition in the yellow of $OsCl_6^{2-}$ presents also an equi-distant vibrational structure, as seen in Fig. 1 and in Table 1. The five components observed

Table 1. Wave-number in cm^{-1} of the vibrational components associated with the electronic transition a $\Gamma_1(^3\Gamma_4) \rightarrow {}^1\Gamma_1$ of γ_5^4 in $OsCl_6^{2-}$. Shoulders in parentheses. Three solvents are indicated.

Water	Ethanol	Dichloroethane
(17 090)	(17 000)	(16 960)
17 250	17 170	17 120
17 420	17 330	17 280
(17 540)	(17 500)	(17 430)
17 760	(17 680)	17 600
(18 940)	(18 620)	20 100

have the characteristic wave-number difference σ_c 170 cm^{-1}, slightly higher than in the case of $ReCl_6^{2-}$.

Though these two hexahalides seem to be exceptional by showing vibrational structure of "ligand field" transitions in solution at room temperature, an even more unusual feature is the very weak peak at relatively much higher wave-number. While the oscillator strength P of the main group of peaks roughly is 1.5×10^{-5}, the additional peak at high wave-number has $P \approx 3 \times 10^{-7}$. The position of this peak is highly dependent on the solvent. Professor Ballhausen was kind enough to indicate that the pure electronic transition $0 \rightarrow 0$ without co-excitation of odd vibrations presumably cannot be observed, since the selection rules for electric dipole radiation in O_h are expected to hold as well for $OsCl_6^{2-}$ as for[1] UCl_6^{2-}. Consequently, it must be assumed that absorption of (or emission of) one odd vibrational quantum accompanies each of the absorption lines. The lowest such quantum expected is some 160 cm^{-1} (the bending even Γ_5 mode[13] corresponds to 158 cm^{-1} in $SnCl_6^{2-}$ and to 162 cm^{-1} in $PtCl_6^{2-}$. Similar to the proposals by Liehr and Ballhausen[16], it may hence be assumed that a regular progression of the even, totally symmetric stretching mode Γ_1 might be superposed the odd vibration. The wavenumber of Γ_1 is[13] 311 cm^{-1} in $SnCl_6^{2-}$ and 344 cm^{-1} in $PtCl_6^{2-}$, whereas the three odd normal modes of UCl_6^{2-} are situated[1] at 258 cm^{-1} (stretching), 114 and 94 cm^{-1} (bending). Since the force constants are expected to be slightly larger in the platinum group hexachloride anions than in uranium(IV), the wavenumber intervals 150—170 cm^{-1} would rather be expected to correspond to bending modes. By infrared absorption spectroscopy, Adams[15] found the stretching frequencies of K_2OsCl_6 at 319 and 340 cm^{-1} and of K_2PtCl_6 at 345 cm^{-1}.

However, the equi-distant bands may be a pseudo-progression, caused by the accidental phenomenon that the stretching frequency is twice as large as one of the bending frequencies. Thus, Ballhausen suggested that the two first strong peaks (17 250 and 17 420 cm^{-1} in aqueous solution) are caused by co-excitation of the two odd Γ_4 modes, *i.e.* the mainly bending $\sim$ 160 cm^{-1} and the mainly stretching $\sim$ 330 cm^{-1}.

It seems, from the positions of the "distant peaks" that an odd quantum also might accompany the latter vibrational excitation. If this assumption is correct, the energy above the electronic level of the distant peak is 1690 cm^{-1} in water, 1450 cm^{-1} in ethanol, and 2980 cm^{-1} in dichloroethane.

The possibility that this peak is caused by another electronic level does not look plausible to the present author. The only explanation along this line would involve the Γ_1-component of $^5\Gamma_5$ of $\gamma_5^3\gamma_3$ which might have very low energy (connected with the low interelectronic repulsion energy for the high total spin S), but the necessary effects of intermediate coupling would not be sufficiently efficient to depress the band-width completely from its high value ($\approx$ 1200 cm^{-1}) in a normal $\gamma_5 \rightarrow \gamma_3$. The latter transition is probably responsible for the shoulder at 530 mμ observed in the dichloroethane solution (Fig. 1 b).

Comparing with the vibrational levels of the solvent molecules[7], it is remarkable to note the nearly coincidence of the values given above with the O-H bending wave-number of liquid water 1650 cm^{-1} (vapour 1595 cm^{-1}), the C-H bending of ethanol (broad band at 1380—1450 cm^{-1}), and the C-H stretching of dichloroethane (2959, 3002, 3029 cm^{-1}). An alternative interpretation of the

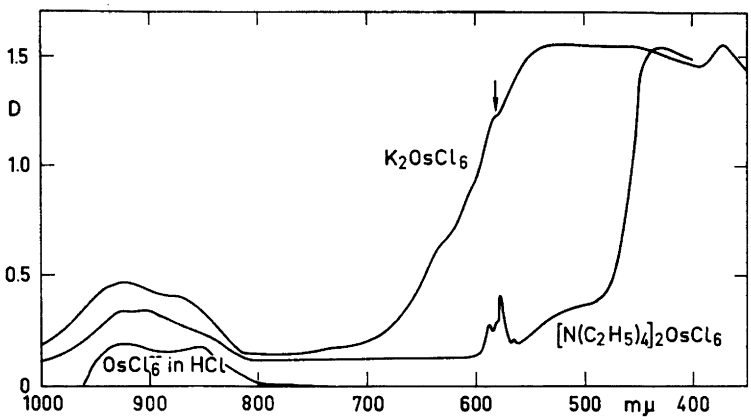

Fig. 2. The reflection spectra of crystalline powders of red $K_2Os_3Cl_6$ and yellow $[N(C_2H_5)_4]_2OsCl_6$. For comparison in the near infra-red, the solution absorption spectrum from Fig. 1 is extended in the region of electronic transitions to $^1\Gamma_3$ and $^1\Gamma_5$ of γ_5^4.

third column of Table 1 would involve the C-H stretching frequencies of the $(n\text{-}C_4H_9)_4N^+$ ion associated with $OsCl_2^{6-}$ in the dichloroethane solution.

In aqueous solution, it is expected that $OsCl_6^{2-}$ polarise surrounding water molecules in such a way that one or both protons are directed towards the anion. Hence, the occurrence of weakly co-excited O-H bending modes is not surprising. It is much more unexpected that C-H bending rather than O-H bending (1000—1100 cm^{-1}) is responsible for the very weak peak in ethanol. It suggests that the methyl end rather than the hydroxo group is close to $OsCl_6^{2-}$. How strange this may be, there is some analogous evidence from the measurement[19] of solvent effects on $IrBr_6^{2-}$ and other 5d-group hexahalide complexes. Thus, $[N(C_4H_9)_4]_2[IrBr_6]$ is not particularly soluble in alcohols (*e.g.* *t*-butanol) while it is very soluble in partly chloro-substituted hydrocarbons such as 1,2-dichloroethane and chloroform.

The electronic level has 80 cm^{-1} lower energy in ethanol and 130 cm^{-1} lower energy in dichloroethane than in the aqueous solution. The simplest interpretation of this fact is that the nephelauxetic effect, *i.e.* the decrese of the apparent term values of interelectronic repulsion parameters, compared to the gaseous ion, is slightly larger in the organic solvents. The parameters[3,8] derived from the spectra of $ReCl_6^{2-}$ and $OsCl_6^{2-}$ in aqueous solution are in cm^{-1}:

$$\begin{array}{lll} ReCl_6^{2-} & K(4,5) \sim (3\,B + C) = 2800 & \zeta_{5d} = 2300 \\ OsCl_6^{2-} & = 2500 & = 2800 \end{array} \qquad (1)$$

and might conceivably be half a per cent smaller in the organic solvents, though higher-order effects of dispersion forces are not excluded. The internuclear distances between the central metal and halogen seem to be larger in aqueous solution than in the organic solvents. The measurements at high pressure by Balchan and Drickamer[9] of electron transfer spectra of 5d group hexahalides show strong shifts to lower wavenumber. The nephelauxetic effect

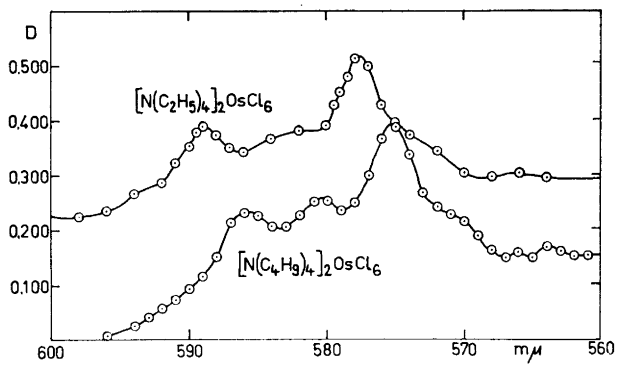

Fig. 3. The reflection spectra of tetra(ethyl)ammonium and tetra(butyl)ammonium osmium(IV) hexachlorides under high dispersion.

seems invariably to become more pronounced by decreased internuclear distance in transition group complexes [10] and in compounds of the trivalent lanthanides [11].

In solid yellow $[N(C_2H_5)_4]_2OsCl_6$, the reflection spectrum shows a complicated structure (Fig. 2) close to 17 310 cm^{-1}, while the dark-red K_2OsCl_6 have stronger electron transfer bands at lower wave-number, and the intra-subshell transition is only seen as a narrow shoulder at 17 120 cm^{-1} on a steep increase (Fig. 2). The yellow crystals of $[N(C_4H_9)_4]_2$ $OsCl_6$ present a similar structure at slightly larger wave-number, the highest band being at 17 380 cm^{-1}. (Fig. 3 and Table 2). Though the intensities vary in a somewhat irregular manner, the wavenumber intervals are invariant (Table 2). By repetition of the latter measurement on the reflection attachment to the Cary-11 spectrophotometer, the same bands were found as given in Table 2, but at 50 cm^{-1} lower wavenumber and further on, the additional small band at 20 100 cm^{-1} was observed, making the crystals closely comparable to the solution in dichloroethane.

The isoelectronic PtF_6 has the corresponding electronic transition [12] at 15 873 cm^{-1}, but only showing weak vibrational structure, compared to many of the complicated band groups of other intra-subshell transitions in the gaseous 5d-hexafluorides.

Table 2. Wave-numbers in cm^{-1} of the vibrational components in the reflection spectra of two solids (see Fig. 3).

$[N(C_2H_5)_4]_2OsCl_6$	$[N(n\text{-}C_4H_9)_4]_2OsCl_6$
16 980	17 070
(17 150)	17 230
17 310	17 380
(17 460)	(17 530)

EXPERIMENTAL

5 g OsO_4 (H. Drijfhout and Zoon, Amsterdam) was reduced by heating with 7 g ascorbic acid in 100 ml 6 M hydrochloric acid. Prolonged boiling has a tendency to produce brown caramellic materials which must be removed by filtration. When the filtrate is added to the solution of 10 g KCl in 50 ml water, brick-red K_2OsCl_6 precipitates. 0.96 g portions of this salt (2 mmoles) can be dissolved in 20 ml of 1 M HCl and yellow precipitates obtained with an excess of tetra(ethyl)ammonium chloride, or even with 2.5 g tetra(butyl)ammonium bromide (Fluka), dissolved in 10 ml ethanol. It is well known that $OsCl_6^{2-}$, once formed, is very robust against ligand exchange in acid solution [14].

The spectra were measured in 5 cm cells on a registering Cary-11 spectrophotometer. The solution of $[N(n\text{-}C_4H_9)_4]_2[OsCl_6]$ in ethanol, measured in Fig. 1, was supersaturated and crystallised after a while.

Analysis of $N(C_4H_9)_2OsCl_6$: Found: C 43.26; H 8.40; N 3.22; Cl 23.84. Calc. C 43.28; H 8.18; N 3.16; Cl 23.96.

REFERENCES

1. Satten, R. A., Young, D. and Gruen, D. M. *J. Chem. Phys.* **33** (1960) 1140.
2. Piper, T. S. and Koertge, N. *J. Chem. Phys.* **32** (1960) 559.
3. Jørgensen, C. K. *Discussions Faraday Soc.* **26** (1958) 175.
4. Jørgensen, C. K. *Acta Chem. Scand.* **9** (1955) 710.
5. Eisenstein, J. C. *J. Chem. Phys.* **32** (1960) 1887 and **34** (1961) 1629.
6. Stephens, D. R. and Drickamer, H. G. *J. Chem. Phys.* **30** (1959) 1364.
7. Landolt-Börnstein, *Tabellenwerte* . . . 6. Aufl., 1. Band, 2. and 3. Teil.
8. Jørgensen, C. K. *Mol. Phys.* **3** (1960) 201.
9. Balchan, A. S. and Drickamer, H. G. *J. Chem. Phys.* **35** (1961) 356.
10. Stephens, D. R. and Drickamer, H. G. *J. Chem. Phys.* **35** (1961) 429.
11. Keating, K. B. and Drickamer, H. G. *J. Chem. Phys.* **34** (1961) 143.
12. Moffitt, W., Goodman, G. L., Fred, M. and Weinstock B. *Mol. Phys.* **2** (1959) 109.
13. Woodward, L. A. and Creighton, J. A. *Spectrochim. Acta* **17** (1961) 594.
14. Larson, L. L. and Garner, C. S. *J. Am. Chem. Soc.* **76** (1954) 1284.
15. Adams, D. M *Proc. Chem. Soc.* **1961** 335.
16. Liehr, A. D. and Ballhausen, C. J. *Phys. Rev.* **106** (1958) 1161.
17. Jørgensen, C. K. *Absorption Spectra and Chemical Bonding in Complexes* Pergamon Press, Oxford, 1962.
18. Runciman, W. A. and Schroeder, K. A. *Proc. Roy. Soc.* (London) **A 265** (1962) 489.
19. Jørgensen, C. K. *J. Inorg. Nucl. Chem. In press.*

Received November 3, 1961

ACTA CHEMICA SCANDINAVICA 16 (1962) 799–806

Studies on the Coagulation of Chicken Blood

III. Differentiation of $\varkappa$-, δ- and φ-Factors by Adsorption

ØYVIND SØRBYE*

Department of Biochemistry and Nutrition, Polytechnic Institute, Copenhagen, Denmark

Studies on the adsorption from oxalated plasma of the coagulation factors, measured as $\varkappa$-, δ- and φ-factor activities with thromboplastin and with Russell's viper venom-cephalin, revealed characteristic differences in the adsorbabilities of these factors by a series of crystalline adsorbents. Differences in the coagulation activity of the factors are thus reflected in differences in their physico-chemical properties. A further differentiation of the φ-factor activity can be made by means of the adsorbents. It is shown that the φ-factor activity represents the combined activities of a calcium carbonate adsorbable φ-factor and one or more φ-factors which are not adsorbed from oxalated plasma by this compound.

In an earlier paper [1] a method was described for estimation of the $\varkappa$-, δ- and φ-factor activities of chicken plasma. The method permitted comparison of the $\varkappa$-, δ- and φ-factor activities of different plasmas and was therefore suitable for a study of the effect of adsorbents on the concentration of the coagulation factors measured as $\varkappa$-, δ- and as φ-factors in the assay systems. It had already been found [1] that the three types of factors could be completely adsorbed from oxalated plasma by typical prothrombin adsorbents, such as barium carbonate and strontium carbonate. The motivation for carrying out further adsorption studies was twofold: In the first place, it was thought possible by systematic testing of other well-defined insoluble compounds to find adsorbents with more selective properties, *i.e.* adsorbents which would adsorb one or two of the coagulation factors and leave the other(s) unaffected — or to find adsorbents with at least different adsorption *capacities* for the three types of factors. In the second place, it was of interest to learn if treatment of plasma with increasing amounts of an adsorbent would result in merely partial adsorption of a certain type of activity ($\varkappa$-, δ- or φ-factor). If this should be the case, it would mean that more than one coagulation factor contributed to the measured activity and would permit a distinction between different coagulation factors with similar effects in the test systems described.

* Fellow of the Royal Norwegian Council for Scientific and Industrial Research.

As reported [1] the dilution curves for φ-factor activity obtained with cephalin, Russell's viper venom (RVV)-cephalin and with thromboplastin as assay accelerators, were of different shapes. It was suggested that the activity measured as φ-factor activity, might represent the combined activities of separate entities (φ_1, φ_2, φ_3. . . .), some of which are active only in the thromboplastin assay system, one or more other factors specific for the cephalin assay system, and one or more factors which are measured as φ-factors in both these systems as well as with RVV-cephalin.

There is at present no evidence indicating the existence of more than one coagulation factor with $\varkappa$-factor activity, or more than one factor with δ-factor activity. In the measurements of $\varkappa$-, and of δ-factor activities of plasmas the three assay systems have so far given identical results. The mechanism by which $\varkappa$- and δ-factor influence the coagulation rate thus appears to be equally important with all three coagulation accelerators.

MATERIALS AND METHODS

The materials and methods for estimation of the $\varkappa$-, δ- and φ-factor activities of chicken plasma were described in a previous paper [1]. The detailed procedure for treatment of plasma with adsorbents was also presented.

Adsorbents. Some of the preparations of the adsorbents used in this work were commercially available, but most of the compounds tested as adsorbents were prepared in the laboratory in an attempt to ensure the greatest possible reproducibility in properties. Yet the adsorption properties of different batches of the same compound, although qualitatively similar, were not always quantitatively identical, *i.e.*, their ability to distinguish between different coagulation factors was the same, but their adsorption *capacities* for each of the various factors could vary somewhat. Amorphous preparations usually did not show the marked selective adsorption properties, typical for crystalline preparations. Therefore, great efforts were taken to prepare the adsorbents in a crystalline or at least a micro-crystalline state. The preparation procedures were adapted from methods described in Gmelin-Kraut's Handbuch der Anorganischen Chemie. All preparations were finally thoroughly washed with distilled water, treated with 96 % ethanol and dried overnight at 80°C.

Oxalates of calcium, strontium and barium were prepared from aqueous solutions of the chlorides with excess of an equimolar mixture of oxalic acid and ammonium oxalate. Precipitation was carried out at 80—90°C. The precipitates were washed several times with hot distilled water by stirring, followed by decantation after settling. The washed products were dissolved in boiling dilute hydrochloric acid (8—10 % for calcium, and 4—5 % for strontium or barium salts) until saturation, quickly cooled to 4—5°C and stored at 5°C for 24—48 h. Microcrystalline oxalates were obtained. Final washing was done with hot distilled water.

Carbonates of calcium, strontium, barium, cadmium, and manganese were prepared from solutions of the chlorides with excess of ammonium bicarbonate. Precipitation was carried out very slowly at 80—90°C. Washing of the precipitates was done with cold distilled water. Use of hot water at this point often gave peptization of the crystals, whereby the preparations lost their selective properties.

Lead chromate. Lead acetate was dissolved in a small volume of 6—7 N nitric acid. Potassium bichromate in excess was added very slowly to the hot solution. Washing of the precipitate was done with hot distilled water.

Barium chromate. A solution of barium chloride was precipitated with excess of potassium bichromate. After washing, the product was dissolved in hot 5 % nitric acid and recrystallized by slow neutralization of the solution with sodium acetate. The crystals were washed with hot distilled water.

Calcium molybdate. Six parts of calcium chloride, two parts of sodium molybdate and four parts of sodium chloride were thoroughly mixed by grinding in a mortar and brought

to melting at 800°C. After cooling, the melt was treated with water to remove the soluble material. The insoluble calcium molybdate was ground to a powder and washed with hot distilled water.

Bismuth fluoride. Bismuth nitrate was dissolved in water with a minimum of nitric acid and precipitated by addition of a concentrated solution of potassium fluoride. Washing of the microcrystalline precipitate was done first with cold, then with hot distilled water.

Calcium fluoride. Five parts of calcium chloride, four parts of sodium fluoride and four parts of sodium chloride were thoroughly mixed by grinding in a mortar and brought to melting at 900°C. The melt was treated as for calcium molybdate.

Lead sulfide. Lead acetate was dissolved in 0.5 N nitric acid. The solution was then treated with hydrogen sulfide gas. During the precipitation the solution was gradually diluted with 1 1/2 volumes of distilled water. The precipitate was washed with dilute nitric acid, followed by hot distilled water.

Magnesium arsenate. A solution of 3.5 g $MgSO_4 \cdot 7H_2O$ in 2 000 ml of water was mixed with 3 g $Na_2HAsO_4 \cdot 7H_2O$ and 0.8 g $NaHCO_3$ dissolved in 1 000 ml of water. The mixture was left at room temperature for at least eight months with occasional stirring. The product ($Mg_3(AsO_4)_2.8H_2O$) was finally washed with cold distilled water.

Treatment of plasma with the adsorbents described here, caused no or at most a very slight pH change. During a preliminary testing of an adsorbent the activity of the adsorbed plasma was compared to that of untreated plasma at different dilutions. Corresponding results were taken to indicate that the reduced activity of the treated plasma was caused by adsorption of coagulation factors and not by release of inhibitory material from the adsorbent. The optimal conditions for elution of the adsorbed factors from the various adsorbents have not been determined, but preliminary experiments have indicated that the factors adsorbed by calcium oxalate may be eluted by citrate buffers of suitable pH and molarity.

EXPERIMENTS AND RESULTS

Comparative studies on the adsorption of $\varkappa$-, δ- and φ-factor activities

A series of adsorbents were tested for approximate capacity to adsorb $\varkappa$-, δ- and φ-factor activity from oxalated plasma. This testing was done in different periods in the course of four years. The plasmas were obtained from normal chickens and had different levels of $\varkappa$-, δ- and φ-factors. A different set of substrate plasmas was used in each experiment, and different batches of thromboplastin, Russell's viper venom and cephalin were employed. The activities of the factors were expressed in arbitrary units. The units for $\varkappa$-and δ-factor activities were related to the differences in $\varkappa$-factor and in δ-factor concentrations between the vitamin K-deficient and the coumachlor plasma used as substrates [1], and appeared not to vary significantly from one set of substrate plasmas to another. Different experiments with the same batch of an adsorbent were therefore comparable. Because of lack of a reliable reference, the φ-factor activity of each untreated plasma was arbitrarily set at 100 %, in spite of possible differences between the plasmas employed. Different experiments with the same batch of an adsorbent could therefore scarcely be expected to give identical results, but were regarded mainly as a guide to more detailed studies on the adsorption of φ-factor activity.

A summary of the results of these experiments is given in Table 1. As anticipated the compounds tested as adsorbents showed some pronounced differences in adsorption capacities for different types of factors ($\varkappa$-, δ- or

φ-factor). Selective adsorption of δ-factor was accomplished with two adsorbents (cadmium carbonate and bismuth fluoride), but none of the adsorbents showed an absolute selectivity for $\varkappa$- or φ-factors. All compounds adsorbing φ-factor activity as measured with thromboplastin, also adsorbed the φ-factor activity which was measured with RVV-cephalin. Selective adsorption of a thromboplastin specific φ-factor was thus not achieved with any of the adsorbents. As for the adsorption of $\varkappa$- and of δ-factor the thromboplastin and the RVV-cephalin assay systems gave concordant results. For a comparison of the effects of the different compounds, it seemed convenient to distinguish between three main groups of adsorbents:

The first group of adsorbents comprised the major part of the compounds. These adsorbents had a smaller or greater adsorption capacity for all three types of coagulation factors ($\varkappa$-, δ- and φ-factors). Considerable differences between the individual adsorbents of this group were noted regarding their relative adsorption capacities for the different factors. Thus calcium oxalate and magnesium arsenate had greater adsorption capacities for δ-factor than for $\varkappa$-factor, whereas adsorbents such as calcium carbonate, manganese carbonate, strontium carbonate, strontium oxalate and lead sulfide had about equal adsorption capacities for these two factors, and barium chromate had definitely greater adsorption capacity for $\varkappa$-factor than for δ-factor. The adsorption studies thus provided additional evidence for the non-identity of the $\varkappa$-factor and δ-factor activities.

In the first group of adsorbents calcium carbonate was found to be fundamentally different from the rest. This adsorbent showed a small, but definite adsorption capacity for $\varkappa$- and δ-factor and, in the range studied, these two coagulation factors were adsorbed proportionally to the amount of adsorbent added. Only a part of the φ-factor activity could, however, be adsorbed by calcium carbonate. This was observed both with thromboplastin and with RVV-cephalin as assay accelerators. The partial absorbability of φ-factor activity by calcium carbonate can probably be explained only by assuming that the activity measured as φ-factor activity with thromboplastin and with RVV-cephalin, represents the combined activities of at least two different coagulation entities: one which can be completely adsorbed from oxalated plasma by treatment with less than 100 mg calcium carbonate per ml of plasma, and one or more factors which cannot be adsorbed by this compound. The designation φ_2-factor was chosen for this coagulation entity, which is a part of the φ-factor activity measured with thromboplastin as well as with RVV-cephalin and can be completely adsorbed from oxalated plasma by treatment with calcium carbonate.

The adsorption of φ_2-factor by calcium carbonate was apparently independent of the adsorption of $\varkappa$- and δ-factors, since maximal adsorption of φ-factor activity was accomplished with adsorbent quantities far below those required for complete adsorption of $\varkappa$- and of δ-factor activities. The adsorption of $\varkappa$- and of δ-factor appeared to be mutually independent, since the $\varkappa$-factor activity adsorbed per unit amount of adsorbent was unrelated to the δ-factor activity of the plasma, and *vice versa*.

Bismuth fluoride and cadmium carbonate represent a second group of adsorbents. In the range studied these two compcunds adsorbed δ-factor only,

Table 1. Effect of adsorbents on δ-, $\varkappa$- and φ-factor levels of plasma.

	Plasma No.	Assay system	Adsorbent in mg per ml plasma	Activities of factors after (before) the adsorption δ	$\varkappa$	φ	Plasma coagulation time in min/100 after (before) adsorption
Group 1	4671 a	Thr.pl.	100 CaC_2O_4	25 (70)	35 (60)	40 (100)	
	8706 b	RVV-ceph.	100 »	40 (90)	25 (50)	50 (100)	30 (20.3)
	4671 b	Thr.pl.	100 $CaMoO_4$	45 (75)	60 (80)	45 (100)	
	8706 a	RVV-ceph.	100 »	5 (30)	50 (75)	78 (100)	25.5 (24)
	4671 b	Thr.pl.	100 $MnCO_3$	55 (75)	60 (80)	75 (100)	
	8706 a	RVV-ceph.	150 »	10 (30)	40 (75)	60 (100)	27.5 (24)
	4702	Thr.pl.	10 $SrCO_3$**	20 (80)	10 (70)	15 (100)	
	8834	RVV-ceph.	10 »	25 (100)	5 (70)	30 (100)	41 (20.8)
	4671 b	Thr.pl.	100 SrC_2O_4	35 (75)	40 (80)	50 (100)	
	8826	RVV-ceph.	100 »	55 (100)	0 (15)	42 (100)	30 (22)
	4702	Thr.pl.	100 PbS	10 (80)	2 (70)	5 (100)	
	8826	RVV-ceph.	100 »	30 (100)	0 (15)	20 (100)	35 (22)
	4702	Thr.pl.	100 BaC_2O_4*	30 (80)	10 (70)	10 (100)	
	8826	RVV-ceph.	100 »	15 (100)	0 (15)	10 (100)	75 (22)
	4671 b	Thr.pl.	10 $BaCO_3$**	0 (75)	0 (80)	1 (100)	
	8834	RVV-ceph.	10 »	15 (100)	10 (70)	15 (100)	51 (20.8)
	4671 b	Thr.pl.	100 $BaCrO_4$	40 (75)	25 (80)	28 (100)	
	8838	RVV-ceph.	100 »	20 (60)	20 (80)	45 (100)	35.6 (21)
	4702	Thr.pl.	100 $Mg_3(AsO_4)_2$	30 (80)	50 (70)	80 (100)	
	8838	RVV-ceph.	150 »	0 (60)	50 (80)	60 (100)	33 (21)
	1212	Thr.pl.	100 $CaCO_3$	55	15	72	
			200 »	45 (65)	5 (25)	72 (100)	
	36	Thr.pl.	100 »	90	90	88	
			200 »	80	80	88	
			300 »	70 (100)	70 (100)	88 (100)	
			400 »	60	60	88	
	8834	RVV-ceph.	200 »	80 (100)	50 (70)	90 (100)	
Group 2	4671 a	Thr.pl.	100 $CdCO_3$	60 (70)	60 (60)	100 (100)	
	2410	»	150 »	33 (48)	— —	100 (100)	
	8848	Thr.pl.	80 »	67	75	100	28.3
			160 »	59 (75)	75 (75)	100 (100)	28.3 (28.3)
			240 »	51	75	100	28.3
	8706 b	RVV-ceph.	200 »	70 (90)	50 (50)	100 (100)	20.3 (20.3)
Group 3	4671 b	Thr.pl.	150 BiF_3	64 (75)	80 (80)	100 (100)	
	2410	»	200 »	34 (48)	— —	100 (100)	
	8849	»	300 »	0 (5)	65 (65)	100 (100)	
	8706	RVV-ceph.	200 »	75 (90)	50 (50)	100 (100)	20.3 (20.3)
	4702	Thr.pl.	150 CaF_2	80 (80)	70 (70)	100 (100)	
	8706 a	RVV-ceph.	200 »	30 (30)	75 (75)	100 (100)	24 (24)
	4671 a	Thr.pl.	100 $PbCrO_4$	70 (70)	60 (60)	100 (100)	
	8834	RVV-ceph.	200 »	100 (100)	70 (70)	100 (100)	20.8 (20.8)

* Different batches of barium oxalate were used in these two experiments.
** Commercial preparations.

Table 2. Effect of column adsorption on δ-, $\varkappa$- and φ-factor levels of normal plasma

Column material	Effluent plasma	Activity of factors in effluent (untreated) plasma			Thromboplastin time in min/100 of effluent (untreated) plasma
2 g CaF_2	0–1 ml	45	90	72	26
	1–2 ml	75 (75)	100 (100)	100 (100)	24.5 (24.5)
	2–3 ml	75	100	100	24.5
2 g $PbCrO_4$	0–1 ml	73	100	98	24.7
	1–2 ml	75 (75)	100 (100)	100 (100)	24.5 (24.5)
	2–3 ml	75	100	100	24.5

proportionally to the amount of adsorbent added. The activities of $\varkappa$- and φ-factors remained unchanged, and no prolongation of the coagulation time of normal plasma could be detected. Complete, selective removal of δ-factor from oxalated plasma might therefore be possible with either of these compounds. It was considered unpracticable and was not attempted since the adsorption capacities for δ-factor were so small *.

A third group of adsorbents is represented by calcium fluoride and lead chromate. Treatment with these compounds had no effect on the activities of $\varkappa$-, δ- or φ-factors as measured with thromboplastin and with RVV-cephalin. Plasma coagulation times was essentially unchanged after adsorption. The coagulation time and $\varkappa$-, δ- and φ-factor levels of normal oxalated plasmas were also found unchanged after passage through a non-wetted column of calcium fluoride or lead chromate, except in the first few drops of effluent plasma (Table 2). These two compounds could thus scarcely be regarded as adsorbents of coagulation factors at all. The experiments do, however, demonstrate that the effects of the other adsorbents (of group 1 and 2) are specific and not simply due to contact of plasma with *any* kind of foreign surface.

Adsorption experiments with "hypoprothrombinemic" plasmas

The coagulation time of plasma is insensitive to variations in $\varkappa$- or δ-factor concentrations above a lower optimal level [1]. A lower optimal level for the concentrations of φ-factors probably also exists. Adsorption of small amounts of $\varkappa$-, δ- or φ-factors from normal plasma would consequently not result in prolonged *plasma coagulation times*. However, the coagulation time of vitamin K-deficient plasma is sensitive to small variations in δ- and φ-factor concentration, and the coagulation time of coumachlor plasma is sensitive to small variations in the concentrations of $\varkappa$- and φ-factors. The effect of some of the

* The procedure for preparation of cadmium carbonate has sometimes given preparation which are less specific than that used in this work. Some preparations showed a small adsorption capacity for φ-factor (but not for $\varkappa$-factor) in addition to the δ-factor adsorption capacity.

Table 3. Adsorption of hypoprothrombinemic plasmas.

Adsorbent in mg per ml plasma	Thromboplastin time of plasma in min/100 after (before) absorption			
	Coumachlor		Vitamin K-deficient*	
50 CaF_2	360	(360)	61	(61)
50 $PbCrO_4$	360		61	
50 $CdCO_3$	360		64.8	
50 BiF_3	360		61.8	
10 $BaCrO_4$	2 000		75	
10 $CaCO_3$	500		73.2	

* The relatively short coagulation time of this plasma indicated a moderately severe vitamin K-deficiency with δ-factor level near, but not below the optimal level.

adsorbents on the coagulation time of these types of plasma was therefore investigated to check the results of the experiments on adsorption of the $\varkappa$-, δ-, and φ-factor activities of normal plasma.

Adsorption with small amounts of calcium fluoride or lead chromate had no effect on the coagulation times of vitamin K-deficient or coumachlor plasma, as seen in Table 3. Similar amounts of cadmium carbonate or bismuth fluoride, however, caused a slight prolongation of the coagulation time of the vitamin K-deficient plasma, but had no such effect on the coagulation time of the coumachlor plasma. The results indicated an adsorption of δ-factor by cadmium carbonate and by bismuth fluoride, and no effect of these adsorbents on $\varkappa$- or φ-factor concentrations. Treatment of the two types of hypoprothrombinemic plasmas with small amounts of barium chromate or calcium carbonate, which reduce the activities of all three types of coagulation factors, definitely prolonged the coagulation times of both plasmas.

The results of these experiments are thus in accordance with the observed effect, or lack of effect, of the respective adsorbents on the activities of $\varkappa$-, φ- and δ-factors.

DISCUSSION

Plasmas from humans with coagulation disorders of genetic origin have been a valuable material for the discovery of previously unknown coagulation factors in man. As far as other species are concerned, hemophilia in dogs has been described by Graham *et al.*[2], and a hemophilia-like disease in swine by Hogan *et al.*[3], but reports on genetic coagulation anomalies in small laboratory animals are lacking. It is, therefore, not possible at present to use genetically deficient chicken plasma for detection of chicken coagulation factors.

This purpose may be accomplished by the use of chicken plasmas with *induced* coagulation deficiencies. The number of coagulation factors which may be studied with such artificial substrates, is limited to the factors which by suitable procedures can be reduced *below optimal levels* in the plasma. These factors do not necessarily correspond to the factors lacking in the different

categories of congenitally deficient human plasmas, recognized at present. The interpretation of the results obtained with artificial test substrates is complicated by the possibility that the reduced coagulation rate of such substrates may be due to lowering of more than one coagulation factor. Thus, the coagulation rate of vitamin K-deficient and of coumachlor plasmas are not determined by the concentrations of one factor only. Vitamin K-deficient plasma has a manifest deficiency in a second factor (δ-factor) and coumachlor plasma in a third ($\varkappa$-factor) in addition to the deficiency in a common factor (φ-factor) [4]. With a substrate of pure vitamin K-deficient plasma the combined activities of δ- and φ-factors would thus be measured, and with pure coumachlor plasma as substrate no distinction between the activities of $\varkappa$- and φ-factors could be made. The information obtained with artifical substrates is therefore of limited value, unless combined with techniques permitting a distinction between the different factors which accelerate the coagulation of the test substrate. Coagulation studies in this laboratory have for some time been devoted to a development of such techniques.

It has been shown that the use of *mixtures* of vitamin K-deficient and coumachlor plasma as substrates permits the differentiation and independent assay of the $\varkappa$-, δ- and φ-factor activities of normal plasma [1]. The present study reveals differences in the adsorbabilities of the factors responsible for these activities. The multiple nature and the non-identity of the activities measured with the pure substrates, could thus have been recognized by studies on the adsorption of the two activities. Adsorbability studies may therefore be of value for differentiation of coagulation activities and for physicochemical characterization of the corresponding coagulation factors.

Thus, adsorption experiments appear to offer a clue to a possible further differentiation of the three activities measured as $\varkappa$-factor, δ-factor and as φ-factor activities. This was indicated by the experiments on adsorption of φ-factor activity by calcium carbonate. The merely partial adsorbability of this activity proves that it is due to at least two different coagulation factors. These preliminary results stressed the necessity of more detailed studies on the effect of adsorbents on the $\varkappa$-, δ- and φ-factor activities of plasma. As will be shown in forthcoming papers, such studies have permitted an even further differentiation of the φ-factor activity and given evidence in favour of the homogeneity of the $\varkappa$-factor and δ-factor activities.

REFERENCES

1. Sørbye, Ø. and Kruse, I. *Acta Chem. Scand.* **14** (1960) 2177.
2. Graham, J. B., Buckwalter, J. A., Hartley, L. J. and Brinkhous, K. M. *J. Exptl. Med.* **90** (1949) 97.
3. Hogan, A. G., Muhrer, M. E. and Bogart, R. *Proc. Soc. Exptl. Biol. Med.* **48** (1941) 217.
4. Dam, H. and Søndergaard, E. *Biochim. et Biophys. Acta* **2** (1948) 409.

Received October 24, 1961.

ACTA CHEMICA SCANDINAVICA 16 (1962) 807–819

Studies of Hydrogen Bonding

Part III *. Intermolecular Hydrogen Bond Association between Nitrogen Compounds and Methanol, Phenol, α-Napththol and Pentachlorophenol

THOR GRAMSTAD

Norwegian Defence Research Establishment, Division for Toxicology, Kjeller, Norway

A linear relationship is shown to exist between the logarithms of the association constants and the pK_a values of the proton acceptors for the system pyridines-phenol. This relationship is not applicable to the aliphatic amines. Pentachlorophenol, unlike phenol, forms 2:1 and 3:1 as well as 1:1 hydrogen bonded complexes with tertiary amines. The effect of steric factors on hydrogen bonding is discussed.

In two previous publications [1,2] it was shown that the logarithms of the association constants, K_{ass}, between organophosphorus compounds and methanol, phenol, α-naphthol and pentachlorophenol respectively, form a linear relationship with the frequency shift, $\Delta\nu_{OH}$, of the O-H band, which accompanies the formation of the hydrogen bond. Furthermore, we concluded that the linear relationships between frequency shift and ΔH, ΔF, ΔS, $\nu_{½}$ and $\nu_{½} \times \varepsilon_{max}$, respectively, were only valid when kept to one system, *e.g.*, OPC-phenol, OPC-methanol etc. It was also shown that the curves ΔH and ΔS *vs.* the frequency shift, $\Delta\nu_{OH}$, flatten with increasing acidity of the proton donors, the sequence of decreasing slope being, methanol > phenol > α-naphthol > pentachlorophenol. The effect of solvent interaction on the hydrogen bond association was considered and the following conclusions drawn: For the system organophosphorus compounds OPC-methanol, the solvent interaction is mainly due to the solvation effect around the hydrogen bonded complex. As the proton-donating power increases, solvent interaction with the proton donor becomes more pronounced, *i.e.*, for the systems OPC-phenol and OPC-α-naphthol both the solvation and the solvent-proton donor effects came into play, and for the system OPC-pentachlorophenol the solvent-proton donor effect predominates. This interpretation may also explain the anomalies ob-

* Part II. *Acta Chem. Scand.* **15** (1961) 1337.

served with pentachlorophenol in comparison with phenol with regard to their relative ability to form intermolecular hydrogen bonds with organophosphorus compounds.

Since hydrogen bond energies between a proton donor and nitrogen compounds have not as yet been studied systematically, we found it of interest to extend our study to compounds containing nitrogen. A particularly interesting paper in this field is that by Sutton *et al.*[3], who present the results of a study of complex formation by partition of a reactant between the vapour phase and solution. By this method they determined K_{ass}, ΔF, ΔH and ΔS values for association between trimethylamine and some hydroxy-compounds and found a linear relationship between the logarithms of the dissociation constants of some hydroxy compounds and their association constants with trimethylamine in cyclohexane as solvent. In a previous paper[4] they had measured the changes of dielectric dipole moment, $\Delta\mu$, which occur when trimethylamine forms complexes with weakly acidic hydroxy-compounds in cyclohexane solution. Here they found that, in general, there is a fairly good correlation between $(\Delta\mu)^2$ and K_{ass}. Another interesting study on ternary solutions has been carried out by Nagakura and Gouterman[5] using ultraviolet spectroscopy. They found the association constants at 25°C in heptane between triethylamine and phenol, α-naphthol and β-naphthol to be 83.8, 121.0 and 103, respectively. For comparison it should be mentioned that the association constants at 25°C obtained by Sutton *et al.*[3] between trimethylamine and phenol, α-naph-

Table 1. Data on hydrogen bonding between nitrogen compounds and phenol

Proton acceptor	PHENOL						
	K_{ass} 20°C	K_{ass} 50°C	ΔH kcal	ΔF kcal	ΔS e.u.	$\Delta\nu_{OH}$ cm^{-1}	$\nu_{½}$ cm^{-1}
Triethylamine	90.9	26.2	−7.8	−2.6	−17.7	380	500
Tripropylamine	22.4	8.7	−5.9	−1.8	−14.1	330	420
Tributylamine	29.2	9.7	−6.9	−2.0	−16.9	350	420
Tribenzylamine	2.7	2.1	−1.6	−0.6	− 3.4	90	406
N-Diethylaniline	2.6	2.1	−1.3	−0.6	− 2.7	67	550
Pyridine	59.8	19.7	−7.0	−2.4	−15.6	492	454
Collidine	137.1	41.6	−7.5	−2.7	−15.7	531	430
2,6-Lutidine	95.2	31.8	−6.9	−2.7	−14.4	535	504
2,4-Lutidine	103.9	35.0	−6.8	−2.7	−14.1	516	466
2-Picoline	74.7	24.8	−6.9	−2.5	−15.0	520	484
3-Picoline	73.1	25.8	−6.5	−2.5	−13.8	491	418
4-Picoline	80.0	27.8	−6.6	−2.6	−13.9	500	404
4-Benzylpyridine	78.3	28.9	−6.2	−2.5	−12.6	—	—
Quinoline	57.4	18.3	−7.2	−2.4	−16.4	498	450
Isoquinoline	61.4	20.4	−6.9	−2.4	−15.4	529	484
Quinaldine	79.9	25.7	−7.1	−2.6	−15.6	532	466
Acridine	67.2	23.4	−6.6	−2.5	−14.1	520	464

thol, and β-naphthol were found to be 86.0, 110, and 230, respectively. The anomalies observed for β-naphthol in comparison with α-naphthol by Sutton *et. al.* with trimethylamine were not observed by Nagakura and Gouterman with triethylamine. Fuson, Pineau and Josien[6] have found by infrared spectroscopy an association constant of 55 for phenol with pyridine in carbon tetrachloride solution. Halleux[7] has also reported some association constants between phenol and a number of pyridines. With regard to hydrogen bond energies only very few results are available. Among the few comparisons that can be made with previously reported values of the enthalpy of association are those obtained by Tsuboi[8], Sutton *et al.*[3] and Becker[9]. Tsuboi's value of −3 kcal/mole and Becker's value of −3,9 kcal/mole for the system methanol-pyridine in CCl_4 solution are consistent with our value of −3.2 kcal/mole (see Table 1), while Tsuboi's value of −5 kcal/mole for phenol-pyridine in CCl_4 solution is somewhat lower than that obtained by us, namely −7.0 kcal/mole.

EXPERIMENTAL

Materials. The following materials were used without further purification: "Merck Guaranteed Reagent" phenol, α-naphthol and carbon disulphide. "Merck Spectroscopic Grade" methanol and carbon tetrachloride. "Fluka puriss" pentachlorophenol. All the nitrogen compounds were of a high standard of purity and in all cases they were purified either by fractional distillation from KOH or by recrystallisation just before use. The *triethylammonium pentachlorophenolate* was prepared by mixing pentachlorophenol (1 g) with an excess of triethylamine (5 g). The mixture was shaken vigorously for a few minutes until all the pentachlorophenol was dissolved, and after few minutes the triethylammonium pentachlorophenolate precipitated out (0.94 g, 68 %. Found: C 39.30; H 4.39; N 3.81; Cl 45.60. $C_{12}H_{16}ONCl_5$ requires C 39.20; H 4.35; N 3.81; Cl 48.27). The salt was purified by washing with ether; it was not appreciably hygroscopic. Attempts to prepare the salt by using solvents, *e.g.*, cyclohexane, ether, ligroin and dioxane were unsuccessful.

Infrared measurements. The instrument, the instrumental conditions and the method of running the spectra were the same as described earlier[2]. For the determination of the frequency shift of the ground state stretching vibration of the O-H band which accompanies the formation of a hydrogen bond, the concentration of the proton donors was kept at 0.06 M, and that of the nitrogen compounds at 0.03 M. The exceptions were, tribenzylamine and N-diethylaniline with phenol, and the systems phenol-pyridines and methanol-amines. The concentrations of the proton acceptors in these systems were 0.12, 0.04 and 0.3 M, and of the proton donors, 0.06, 0.01 and 0.06 M, respectively.

Near-infrared measurements. The instrument, the instrumental conditions, the method of running the spectra, and the method of calculation of association constant were the same as described earlier[2]. The spectra were run immediately after preparing the solutions because of the reaction of the amines, particularly triethylamine, with carbon tetrachloride. This reaction was sufficiently slow, at the low concentrations used, not to interfere seriously. For all thermodynamic data in Table 1, the concentration of the proton donors was kept at 0.006 M to prevent self-association. The concentrations of the proton acceptors were 0.003, 0.006 and 0.012 M, except for the system methanol-nitrogen compounds where they were 0.06, 0.12 and 0.20 M. The concentration range of the proton donors and the acceptors shown in Table 2 is 0−0.006 M.

Refractive index measurements. The refractive index measurements were carried out with a Bausch & Lomb Precision Refractometer, 33−45−02−01, at 20°C. The concentration range of the proton donors and acceptors is 0−0.12 M. The results are shown in Figs. 3 and 4.

Table 2. Data on hydrogen bonding between nitrogen compounds and methanol and α-naphthol.

Proton acceptor	METHANOL							α-NAPHTHOL						
	K_{ass} 20°C	K_{ass} 50°C	$-\Delta H$ kcal	$-\Delta F$ kcal	$-\Delta S$ e.u.	$\Delta\nu_{OH}$ cm^{-1}	$\nu_{½}$ cm^{-1}	K_{ass} 20°C	K_{ass} 50°C	$-\Delta H$ kcal	$-\Delta F$ kcal	$-\Delta S$ e.u.	$\Delta\nu_{OH}$ cm^{-1}	$\nu_{½}$ cm^{-1}
Triethylamine	6.4	3.5	3.8	1.1	9.2	427	352	108.9	38.2	6.6	2.7	13.1	—	—
Tripropylamine	3.4	2.2	2.7	0.7	6.9	413	526	30.9	11.6	6.1	2.0	14.2	380	418
Tributylamine	4.1	2.4	3.5	1.0	8.8	413	532	44.5	17.4	5.9	2.2	12.6	383	342
Tribenzylamine	3.4	2.7	1.5	0.7	2.5	—	—	1.9	1.5	1.3	0.4	3.4	—	—
N-Diethylaniline	1.7	1.3	1.5	0.3	4.1	—	—	—	—	—	—	—	—	—
Pyridine	6.0	3.6	3.2	1.0	7.4	300	304	82.5	33.5	5.7	2.6	10.5	530	514
Collidine	7.6	4.3	3.6	1.2	8.2	356	256	200.8	69.5	6.7	3.1	12.2	535	610

RESULTS AND DISCUSSION

Nitrogen compounds-phenol. The sharp distinction between systems shown to exist in two previous publications [1,2] has further been confirmed in this work. As can be seen in Table 1, the association constants for the system nitrogen compounds-phenol are very small in relation to the great frequency shift, $\Delta\nu_{OH}$, *e.g.*, triethylamine-phenol, K_{ass} = 90.9, $\Delta\nu_{OH}$ = 380, compared with $(C_2H_5)_2NP(O)(OC_2H_5)_2$-phenol[2], K_{ass} = 518.2, $\Delta\nu_{OH}$ = 395. Thus the hydrogen bonding ability of the phosphorus compound with phenol is about 5.5 times that of triethylamine although the frequency shift is almost the same. In general, the ability to form intermolecular hydrogen bonds in relation to frequency shift is very much smaller for nitrogen compounds than for organophosphorus compounds containing the P=O group. Another interesting finding is the marked decrease in hydrogen bonding ability of tripropylamine and tributylamine in comparison with triethylamine (see Table 1). This observation is in agreement with the data reported by Tamres *et al.* [10], who measured the heats of mixing of nitrogen bases with chloroform. They found that the heat of mixing of equimolecular quantities of the nitrogen compound and chloroform is much greater for triethylamine than for tributylamine, *i.e.*, 870 and 438 cal/mole, respectively. These results should be compared with those obtained by us for triethylamine-phenol, K_{ass} = 90.9, ΔH = −7.8 kcal, and for tributylamine-phenol, K_{ass} = 29.2, ΔH = −6.9 kcal (see Table 1). Furthermore, we have found, as shown in Fig. 1, that the correlation between the logarithms of the association constants of nitrogen bases with phenol and the heat of mixing of the same nitrogen bases with chloroform measured by Tamres *et al.* [10] is close to a linear relation, with the exception of triethylamine and tributylamine. This means that the abilities of

pyridines and quinolines to form hydrogen bonds are related to their heat of mixing with chloroform in a linear manner, and that this relationship is not applicable to the aliphatic tertiary bases. There should also exist a linear relationship between the heats of mixing with chloroform and the ΔH values from Table 1, but the calculated enthalpies are too inaccurate for this purpose. It should, however, be noted that the hydrogen bonding abilities of tributylamine and isoquinoline with phenol are very different, K_{ass} = 29.7 and 61.6 l/mole, respectively, although their heats of mixing with chloroform (438 and 440 cal/mole, respectively) and the enthalpies with phenol (—6.9 kcal) are the same. This again supports the view that we have to distinguish between aliphatic tertiary amines and pyridines with regard to their ability to form hydrogen bonds. We have also found, as shown in Fig. 2, a linear relationship between the logarithms of the association constants of pyridines (and quinolines) with phenol and the pK_a values of the bases. The corresponding points for aliphatic tertiary amines are far below the straight lines in Fig. 2. Similar observations have been reported by Halleux[7] who states that there appears to be a linear relationship between log K_{ass} and pK_a for the association of phenol with several pyridines.

The more unfavourable entropy of formation of phenol-nitrogen compounds complexes in comparison with organophosphorus compounds-phenol complexes may depend on (*a*) different solvent interactions on the proton acceptors, *i.e.*, we have to take into account the solvent interaction on the nitrogen compounds in comparison with organophosphorus compounds; (*b*) different steric properties of the complexes, since it is well known that tertiary amines cannot be separated into enantiomers due to the fact that the nitrogen atom is oscillating very quickly through the plane connecting the three different substituents (this oscillating effect may also play a part when aliphatic tertiary amines are compared with pyridines with regard to their ability to form hydrogen bond); (*c*) a difference of polarity in the two types of hydrogen bonds — as pointed out earlier[2], an increase in dipole moment will give a greater orientation of the solvent molecules around the complex which will contribute to a negative entropy of reaction; (*d*) a difference in the mode of formation of the hydrogen bonds, *i.e.*, we have to distinguish between two types of association complexes, one in which there is principally and electronic attraction between the hydrogen atom of the original acid and an electron rich area of the base, and one in which a proton mainly shares the electron pair of another atom to form a covalent bond with the proton acceptor, so that now the bond between the proton

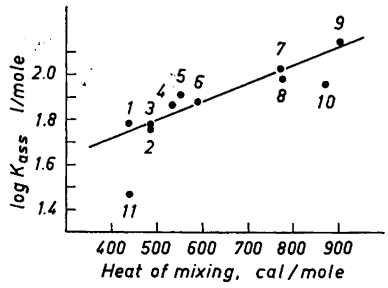

Fig. 1. The relation between the logarithms of the association constants at 20°C for hydrogen bonded complexes between nitrogen compounds and phenol and the heat of mixing of the same bases with chloroform; (1) isoquinoline; (2) quinoline; (3) pyridine; (4) 3-picoline; (5) 4-picoline; (6) 2-picoline; (7) 2,4-lutidine; (8) 2,6-lutidine; (9) 2,4,6-collidine; (10) triethylamine; (11) tributylamine.

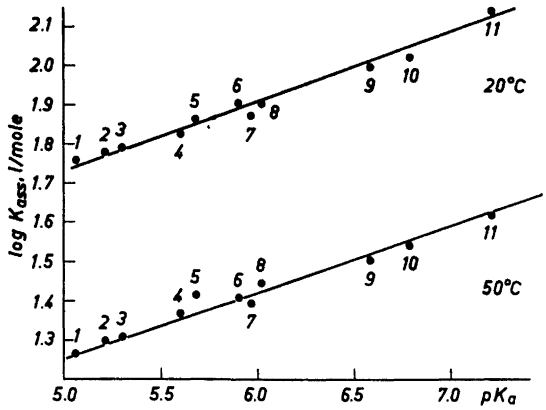

Fig. 2. The relation between pK_a values of proton acceptors and the logarithms of the association constants of the same acceptors with phenol; (1) quinoline; (2) pyridine; (3) isoquinoline; (4) acridine; (5) 3-picoline; (6) quinaldine; (7) 2-picoline; (8) 4-picoline; (9) 2,6-lutidine; (10) 2,4-lutidine; (11) 2,4,6-collidine. Solvent, carbon tetrachloride.

donor and the hydrogen atom becomes mainly electrostatic in character. In the latter case proton-transfer takes place. In the association complex the hydrogen bond is in both cases of the same, unsymmetrical type, but in the latter case the original base holds the hydrogen atom covalently and thus plays the role of the original acid in the former case. A typical example of hydrogen bonding in which electrostatic attraction between proton donor and base predominates is the interaction between phenol and organophosphorus compounds. From this point of view the hydrogen bonding studies in the system organophosphorus compounds-phenol may be considered as a study of the relative electron densities around the oxygen atom in the P=O group. With the nitrogen compounds, however, we should have both types of hydrogen bonds in which either electrostatic attraction or proton-transfer predominates. In the pyridines and quinolines the π electrons in the ring may contribute to the electron density on the nitrogen since nitrogen is more electronegative than carbon. The unshared electron pair on the nitrogen, however, is less available for covalent bond formation because it takes part in resonance in the ring. This may explain the greater hydrogen bonding ability in the electrostatic, non-proton transfer sense of pyridines and quinolines compared with tertiary aliphatic amines in relation to their basicity.

Due to the high electron density around the nitrogen atom in pyridines and quinolines we assume that electrostatic attraction predominates in the hydrogen bonding whereas with amines proton-transfer predominates. However, Table 1 shows that $\Delta\nu_{OH}$ is always $\lesssim$ 380 cm^{-1} for the association of phenol wich tertiary amines, whereas with pyridines it is always $\gtrsim$ 490 cm^{-1}. The smaller frequency shift values for amines-phenol in comparison with pyridines-phenol could be taken to mean that in the latter case the proton-transfer structure should be more pronounced than in the former case, and hence contradict the theory above. The reason for these anomalies may be attributed to steric effects. Strong evidence in support of this view is as shown in Table 2, the greater frequency shift for the system amines-methanol in comparison with pyridines-methanol. This is just the reverse of what is the case with phenol. Furthermore, the association of amines with phenol clearly shows that the effect of steric interaction plays a big part, whereas there is no evidence of steric effects with the system pyridines-phenol, and not even for one between acridine and phenol. The pronounced decrease in the value of the association constant as we proceed from trimethylamine (Sutton *et al.*[3] has found the association constant between trimethylamine and phenol to be 86 l/mole at 25°C) and triethylamine to tripropylamine and tributylamine may also be due to steric effects, *i.e.*, steric interaction between the end of the carbon chain and phenol.

Table 3. Data on hydrogen bonding between nitrogen compounds and pentachlorophenol.

Proton acceptor	PENTACHLOROPHENOL						
	K_{ass} 20°C	K_{ass} 50°C	ΔH kcal	ΔF kcal	ΔS e.u.	$\Delta\nu_{OH}$ cm^{-1}	$\nu_{½}$ cm^{-1}
Triethylamine	—	—	—	—	—	1155	—
Tripropylamine	—	—	—	—	—	1100	—
Tributylamine	—	—	—	—	—	1125	—
Tribenzylamine	1.3	0.8	−3.	−0.2	−10.0	—	—
Pyridine	111.4	44.2	−5.8	−2.7	−10.4	805	922
Collidine	224.7	67.2	−7.6	−3.2	−15.1	1098	1016

Nitrogen compounds-methanol and nitrogen compounds-α-naphthol. It has been found (see Table 2) that the steric effect with amines is less pronounced when phenol is replaced by methanol. This is best illustrated by comparison of tribenzylamine-phenol with tribenzylamine-methanol. Otherwise the association constant and the enthalpies are markedly lower due to the low acidity of methanol. With α-naphthol no enhanced steric effect was observed except with tribenzylamine. As can be seen from Tables 1 and 2, both phenol and α-naphthol have greater frequency shifts with pyridines than for amines, whereas for methanol the reverse is the case. Since the methanol molecule is small there is little steric effect with the amines. This suggests that $\Delta\nu_{OH}$ is larger for amines than for pyridines due to lower basicity of the latter.

Nitrogen compounds-pentachlorophenol. As shown in a previous paper [2] when in the system organophosphorus compounds-phenol and in the system amides-phenol [11] phenol is replaced by pentachlorophenol a drop in association constant occurs, which was suggested to be due to solvent interaction. With the system nitrogen compounds-pentachlorophenol no such drop in association constants was observed. Actually, the association constants, as can be seen in Table 3, are increased considerably on replacing phenol with pentachlorophenol. We suggest that this may be due to the fact that the unshared electron pair on the nitrogen atom in pyridines is more available for covalent bond formation than are those of the oxygen in the P=O group, *i.e.*, there will be a shift in the equilibrium between the electrostatic (I) and the proton-transfer structure (II), towards the latter as the proton-donating power and the ability of the base to form a covalent bond increases.

$$\overset{\delta-}{RO}-H\cdots:\overset{\delta+}{N}- \rightleftharpoons R\overset{-}{O}\cdots H:\overset{+}{N}-$$

(I) (II)

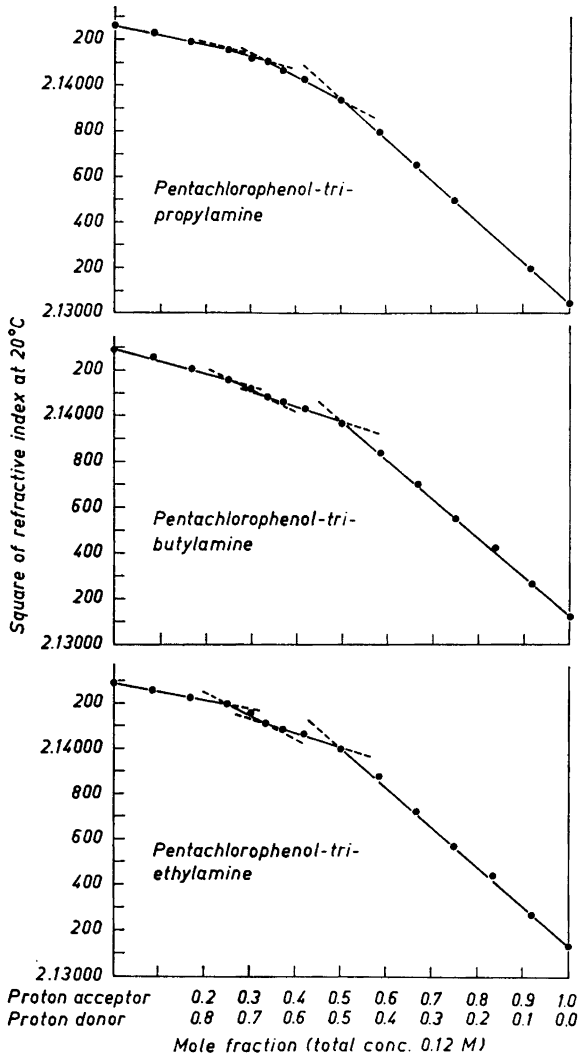

Fig. 3. Square of refractive index *vs.* mole fraction of some hydrogen bonded complexes. The curves show three slope changes corresponding to intermolecular complexes of 1:1, 1:2 and 1:3 ratio. Solvent, carbon tetrachloride.

This view is supported by the fact that the frequency shift $\Delta\nu_{OH}$, and the broadening of the O-H band contour are very much enhanced for the system pyridines-pentachlorophenol in comparison with the system pyridines-phenol, which again may be due to the higher polarity of the proton-transfer structure. In general we suppose that for the system pyridines-phenol the electrostatic structure (I) will predominate. However, as the proton-donating power is

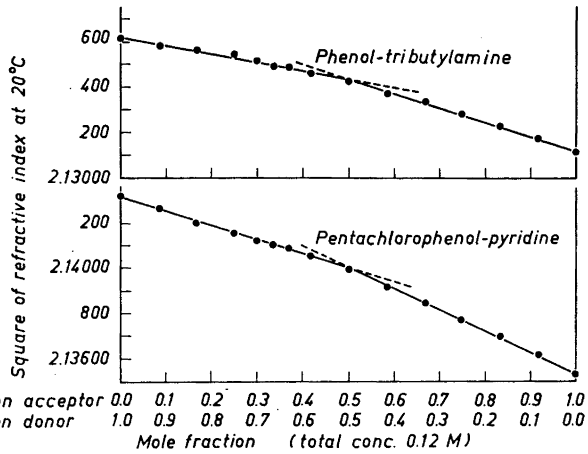

Fig. 4. Square of refractive index *vs.* mole fraction of some hydrogen complexes. The curves show only one slope change corresponding to 1:1 complex. Solvent, carbon tetrachloride.

increased, for example by replacing phenol with pentachlorophenol, the proton-transfer structure (II) becomes more favourable, pyridine utilising its unshared electron pair to form a proton-transfer structure (II) as the acidity of the proton donor increases. This structure is even more pronounced when in the system pyridines-pentachlorophenol the pyridine is replaced by a tertiary aliphatic amine. Due to the stronger basicity of amine the unshared electron pair on the nitrogen will capture the proton and hence the proton-transfer structure will predominate.

Furthermore, it has been found that the polarity of the complexes between amines and pentachlorophenol is increased to such an extent that they react further to give a mixture of 1:1, 1:2 and 1:3 complexes. The results are shown in Fig. 3, using a method described by Giles *et al.*[12] The figure shows the relationship between the square of the refraction index of the solution and the mole fraction of proton donor and acceptor. As can be seen at least 1:1, 2:1 and 3:1 complexes are formed between pentachlorophenol and the amines. For comparison we have shown in Fig. 4, that pyridine-pentachlorophenol and tributylamine-phenol only form 1:1 complexes. Further data on hydrogen bonded complexes are given in Table 4. From this table it can bee seen that if the formal concentrations of, for example, triethylamine and pentachlorophenol are 0.6×10^{-3} and 5.4×10^{-3} moles/l respectively, then the concentration of pentachlorophenol which participates in the complex formation is 0.898×10^{-3} moles/l. This means that the complex must contain more of the proton donor than of the acceptor. This is also the case, as shown in Table 4, for tripropylamine and tributylamine with pentachlorophenol, but not for pyridine and collidine with pentachlorophenol and tributylamine with phenol. These results agree very well with those shown in Figs. 3 and 4. In Fig. 5 some of the

Table 4. Data on hydrogen bonded complexes. Cell length, 10.0 cm. Solvent, carbon tetrachloride. Temperatures, 20° and 50° C (in brackets).

Concentration moles/l × 10^3		Pentachlorophenol + Triethylamine		Pentachlorophenol + Tripropylamine	
Proton donor	Proton acceptor	D^* × 10^2	C^{**} × 10^3	D × 10^2	C × 10^3
6.0	0.0	12.49(12.32)	0	13.31(13.08)	0
5.4	0.6	9.37(10.07)	0.898(0.495)	10.40(11.01)	0.712(0.347)
5.0	1.0	7.47 (8.72)	1.411(0.753)	8.57 (9.85)	1.137(0.480)
4.8	1.2	6.80 (8.09)	1.532(0.859)	7.73 (9.15)	1.315(0.601)
4.5	1.5	5.55 (7.11)	1.833(1.037)	6.60 (8.41)	1.525(0.641)
4.2	1.8	4.58 (6.30)	1.999(1.132)	5.65 (7.62)	1.653(0.703)
4.0	2.0	3.91 (5.80)	2.121(1.175)	5.06 (7.16)	1.718(0.714)
3.6	2.4	2.78 (4.77)	2.264(1.276)	4.10 (6.20)	1.752(0.755)
3.4	2.6	2.37 (4.24)	2.261(1.335)	3.62 (5.75)	1.768(0.762)
3.2	2.8	1.95 (3.86)	2.263(1.320)	3.29 (5.31)	1.717(0.764)
3.0	3.0	1.64 (3.43)	2.212(1.330)	2.92 (4.91)	1.683(0.747)
2.4	3.6	0.88 (2.46)	1.977(1.202)	2.09 (3.67)	1.458(0.715)
2.0	4.0	0.66 (1.95)	1.683(1.050)	1.64 (3.01)	1.261(0.619)
1.0	5.0	0.22 (0.83)	0.894(0.596)	0.61 (1.32)	0.725(0.394)

Concentration moles/l × 10^3		Pentachlorophenol + Tributylamine		Pentachlorophenol + Pyridine	
Proton donor	Proton acceptor	D × 10^2	C × 10^3	D × 10^2	C × 10^3
6.0	0.0	12.90(12.73)	0	13.31(13.08)	0
5.4	0.6	9.69(10.51)	0.893(0.445)	11.49(11.52)	0.219(0.115)
5.0	1.0	8.20 (9.37)	1.185(0.583)	10.35(10.51)	0.334(0.178)
4.8	1.2	7.42 (8.83)	1.349(0.637)	9.75(10.02)	0.405(0.202)
4.5	1.5	6.30 (8.04)	1.568(0.725)	8.94 (9.26)	0.470(0.251)
4.2	1.8	5.26 (7.06)	1.754(0.825)	8.14 (8.57)	0.529(0.268)
4.0	2.0	4.77 (6.70)	1.804(0.841)	7.62 (8.09)	0.564(0.288)
3.6	2.4	3.67 (5.75)	1.893(0.889)	6.65 (7.16)	0.603(0.314)
3.4	2.6	3.29 (5.35)	1.869(0.887)	6.20 (6.75)	0.604(0.303)
3.2	2.8	2.92 (4.91)	1.842(0.885)	5.75 (6.30)	0.608(0.309)
3.0	3.0	2.50 (4.53)	1.838(0.865)	5.26 (5.85)	0.629(0.315)
2.4	3.6	2.68 (3.34)	1.620(0.826)	4.00 (4.58)	0.597(0.298)
2.0	4.0	1.19 (2.69)	1.447(0.731)	3.20 (3.76)	0.558(0.274)
1.0	5.0	0.44 (1.14)	0.795(0.463)	1.46 (1.82)	0.342(0.165)

Table 4, cont.

Concentration moles/l × 10^3		Pentachlorophenol + Collidine		Phenol + Tributylamine	
Proton donor	Proton acceptor	$D \times 10^2$	$C \times 10^3$	$D \times 10^2$	$C \times 10^3$
6.0	0.0	13.08(12.90)	0		0
5.4	0.6	11.07(11.29)	0.321(0.148)	15.49(13.58)	0.081(0.033)
5.0	1.0	9.80(10.24)	0.506(0.237)	12.61(12.55)	0.116(0.039)
4.8	1.2	9.18 (9.72)	0.588(0.278)	12.03(12.00)	0.140(0.057)
4.5	1.5	8.30 (8.94)	0.691(0.341)	11.18(11.24)	0.170(0.056)
4.2	1.8	7.42 (8.25)	0.795(0.362)	10.29(10.46)	0.214(0.065)
4.0	2.0	6.91 (7.73)	0.829(0.404)	9.80 (9.93)	0.204(0.076)
3.6	2.4	5.88 (6.85)	0.901(0.414)	8.72 (8.91)	0.222(0.078)
3.4	2.6	5.40 (6.35)	0.922(0.446)	8.20 (8.41)	0.223(0.076)
3.2	2.8	4.91 (5.90)	0.947(0.455)	7.68 (7.88)	0.225(0.085)
3.0	3.0	4.48 (5.45)	0.944(0.465)	7.16 (7.37)	0.227(0.086)
2.4	3.6	3.27 (4.29)	0.899(0.405)	5.65 (5.88)	0.211(0.075)
2.0	4.0	2.55 (3.48)	0.830(0.381)	4.67 (4.87)	0.191(0.075)
1.0	5.0	1.10 (1.64)	0.495(0.237)	2.27 (2.41)	0.121(0.047)

* D means optical density of free O-H band.
** C means concentration, moles/l, of proton donor participating in complex formation.

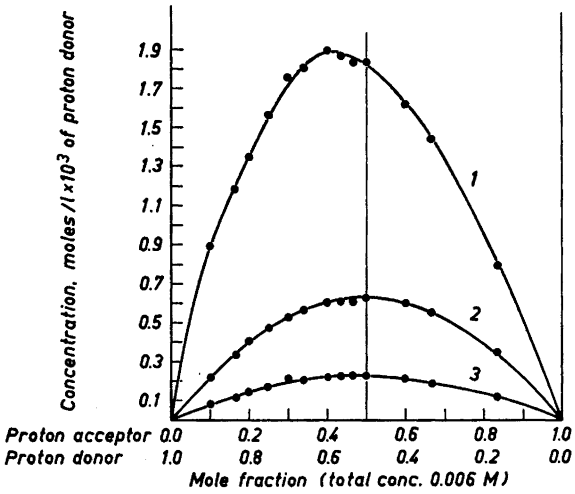

Fig. 5. Concentration of proton donor which participates in hydrogen bonds *vs.* mole fraction. (1) tributylamine-pentachlorophenol; (2) pyridine-pentachlorophenol; (3) tributylamine-phenol. Temperature 20°C.

Table 5. A comparison of thermodynamic data for hydrogen bonds in different solvents.

Compound	K_{ass} 20°C	K_{ass} 50°C	ΔH kcal	ΔF kcal	ΔS e.u.	Solvent
Phenol + Tributylamine	29.2	9.7	−6.9	−2.0	−16.9	CCl_4
	34.3	14.5*	−7.9	−2.1	−19.7	CS_2
Phenol + Pyridine	59.8	19.7	−7.0	−2.4	−15.6	CCl_4
	71.5	31.5*	−7.5	−2.5	−17.0	CS_2
Pentachlorophenol + Pyridine	111.4	44.2	−5.8	−2.7	−10.4	CCl_4
	108.1	48.5*	−7.3	−2.2	−17.5	CS_2

* measured at 40°C.

figures in Table 4 have been plotted to show more clearly the correlation between the concentration of the proton donor participating in complex formation and the mole fraction of the proton donor and acceptor. As can be seen from this figure, the variation of concentration of the proton donor participating in complex formation of pyridine with pentachlorophenol and of tributylamine with phenol is symmetrical with a maximum at mole fraction = 0.5, *i.e.*, we have 1:1 association [13], whereas this is not the case with tributylamine-pentachlorophenol.

We therefore propose the following association scheme for pentachlorophenol with amines:

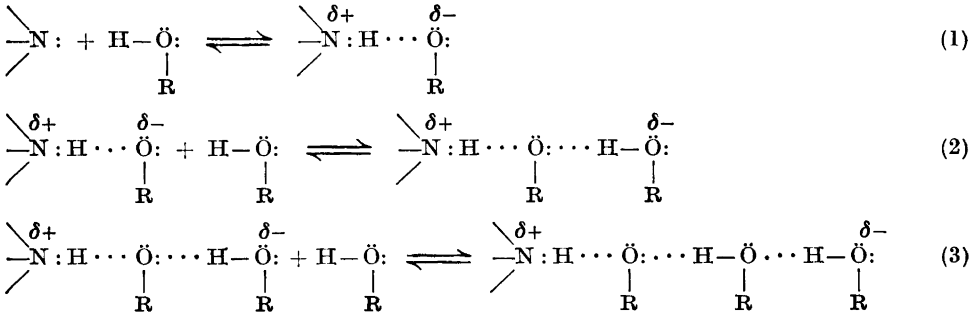

(1)

(2)

(3)

etc.

Eqn. (1) represents the formation of a proton-transfer structure due to the strong acidity of pentachlorophenol. This proton-transfer structure has been confirmed by comparison of its infrared spectrum with that of triethylammonium pentachlorophenolate. Both spectra have a very strong and broad band in the region 1700 to 2800 cm^{-1} and

differ greatly from the spectra of the amines-phenol system. Also, the difference in frequency shift, $\Delta\nu_{OH}$, should be noticed, *e.g.*, 380 cm^{-1} and 1155 cm^{-1}, respectively, for phenol and pentachlorophenol with triethylamine. It is likely that the latter should be attributed to a shift of the N-H frequency upon hydrogen bonding (see eqn. 1). Nevertheless, the electron density on the oxygen atom in pentachlorophenol due to the strong polarity of the complex will increase to such an extent that it will act as base towards a second pentachlorophenol molecule and the result is shown in eqn. (2). This will continue as shown in eqn. (3) until the electron density on the oxygen atoms in the complex due to reduced polarity, is lowered to such an extent that the next pentachlorophenol molecule will associate with a new molecule of amine.

Solvent interaction. As shown in part II [2], the thermodynamic data on hydrogen bonds are very much affected by solvent interaction. It was suggested that the fall in association constants for the system organophosphorus compounds-pentachlorophenol compared with the system organophosphorus compounds-phenol was due at least partly to hydrogen bond formation between the proton donor and the solvent. As discussed above no such fall was found in the association constants in the case of nitrogen compounds. We have found, however, a marked increase in association constants with regard to phenol, but not to pentachlorophenol which remains almost constant, by replacing carbon tetrachloride with carbon disulphide (see Table 5). The reason for this anomaly is not yet clear, and much work needs still to be done, for example by using more differentiated solvents, to reveal the full effect of solvent interaction on hydrogen bonding.

REFERENCES

1. Aksnes, G. and Gramstad, T. *Acta Chem. Scand.* **14** (1960) 1485.
2. Gramstad, T. *Acta Chem. Scand.* **15** (1961) 1337.
3. Denyer, R. L., Gilchrist, A., Pegg, J. A., Smith, J., Tomlinson, T. E. and Sutton, L. E. *J. Chem. Soc.* **1955** 3889.
4. Herlett, J. R., Pegg, J. A. and Sutton, L. E. *J. Chem. Soc.* **1955** 3901.
5. Nagakura, S. and Gouterman, M. *J. Chem. Phys.* **26** (1957) 881.
6. Fuson, N., Pineau, P. and Josien, M-L. *J. Chim. Phys.* **55** (1958) 454.
7. Halleux, A. *Bull. soc. chim. Belges* **68** (1959) 381.
8. Tsuboi, M. *J. Chem. Soc. Japan, Pure Chem. Sect.* **72** (1951) 146.
9. Becker, E. D. *Spectrochim. Acta* **17** (1961) 436.
10. Tamres, M., Searles, S., Leighly, E. M. and Mohrman, D. W. *J. Am. Chem. Soc.* **76** (1954) 3983.
11. Gramstad, T. and Fuglevik, W. J. *Acta Chem. Scand.* **16** (1962). *In press.*
12. Arshid, F. M., Giles, C. H., Melure, E. C., Ogilvie, A. and Rose, T. J. *J. Chem. Soc.* **1955** 67.
13. Aksnes, G. *Acta Chem. Scand.* **14** (1960) 1475.

Received September 13, 1961.

ACTA CHEMICA SCANDINAVICA 16 (1962) 820–826

Vibrational Mean-Square Amplitude Matrices

XVI. In-plane Normal Coordinates and Mean Amplitudes of Vibration in Benzene Molecules

W. V. F. BROOKS* and S. J. CYVIN

Institutt for teoretisk kjemi, Norges tekniske høgskole, Trondheim, Norway

The theory of mean-square amplitude matrices (Σ) is applied to the in-plane vibrations of benzene and benzene-d_6. Numerical values at the absolute zero and 298 °K temperatures are given for (i) the symmetrized Σ-matrix elements, and (ii) the ten mean amplitudes of vibration for the various bonded and non-bonded atom pairs. The calulations are based on L-matrices from Albrecht. The L-matrix elements are given and compared with previously unpublished L-matrix elements of Cyvin.

Calculated in-plane force constants for benzene molecules have been reported by several authors [1–11]. Recently Albrecht [12] has calculated the normal coordinate transformation coefficients for benzenes, using force constants from Whiffen [8]. Mean amplitudes of vibration for benzene [10] and benzene-d_6 [13] have been calculated by Cyvin, and those of benzene compared with values from electron-diffraction data [14–16]. Quite recently calculated mean amplitudes of vibration for benzene have also been reported by Kimura and Kubo [17] in connection with an electron-diffraction reinvestigation of benzene [17,18].

In view of the existing electron-diffraction data of high accuracy for benzene, it was decided to undertake further spectroscopic studies of the mean-square amplitudes of this molecule. In particular it has been planned to perform a calculation of the Bastiansen-Morino shrinkage effects [19,20] for the linearly situated atoms in benzene. These quantities may be calculated by means of the presently given Σ-matrix elements plus the corresponding quantities for the out-of-plane vibrations. Calculations of the latter mean-square amplitude quantities are in progress. In the present work, the in-plane Σ-matrix elements are used to recalculate the mean amplitudes of vibration (which are square roots of the mean-square parallel amplitudes [21]) for the ten interatomic distances in benzene and benzene-d_6. The theoretical foundation of these calculations has been outlined in the previous article of this series [22].

* Permanent address: Department of Chemistry, Ohio University, Athens, Ohio, USA.

Table 1. In-plane symmetry coordinates of benzene.

	S_1	$= 6^{-1/2}\,(d_1+d_2+d_3+d_4+d_5+d_6)$
A_{1g}	S_2	$= 6^{-1/2}\,(r_1+r_2+r_3+r_4+r_5+r_6)$
A_{2g}	S_3	$= 6^{-1/2}R\,(\beta_1+\beta_2+\beta_3+\beta_4+\beta_5+\beta_6)$
B_{1u}	S_{12}	$= 6^{-1/2}D\,(a_1-a_2+a_3-a_4+a_5-a_6)$
	S_{13}	$= 6^{-1/2}(r_1-r_2+r_3-r_4+r_5-r_6)$
B_{2u}	S_{14}	$= 6^{-1/2}(d_1-d_2+d_3-d_4+d_5-d_6)$
	S_{15}	$= 6^{-1/2}R\,(\beta_1-\beta_2+\beta_3-\beta_4+\beta_5-\beta_6)$
	S_{6a}	$= 12^{-1/2}D\,(2a_1-a_2-a_3+2a_4-a_5-a_6)$
	S_{7a}	$= 12^{-1/2}(2r_1-r_2-r_3+2r_4-r_5-r_6)$
$E_{2g(a)}$	S_{8a}	$= 12^{-1/2}(d_1-2d_2+d_3+d_4-2d_5+d_6)$
	S_{9a}	$= (1/2)R(\beta_2-\beta_3+\beta_5-\beta_6)$
	S_{6b}	$= (1/2)D(-a_2+a_3-a_5+a_6)$
	S_{7b}	$= (1/2)\,(-r_2+r_3-r_5+r_6)$
$E_{2g(b)}$	S_{8b}	$= (1/2\,(-d_1+d_3-d_4+d_6)$
	S_{9b}	$= 12^{-1/2}R\,(2\beta_1-\beta_2-\beta_3+2\beta_4-\beta_5-\beta_6)$
	S_{18a}	$= (1/2)R(\beta_2+\beta_3-\beta_5-\beta_6)$
$E_{1u(a)}$	S_{19a}	$= 8^{-1/2}(d_1-d_3-d_4+d_6)$ $-24^{-1/2}D(2a_1+a_2-a_3-2a_4-a_5+a_6)$
	S_{20a}	$= 12^{-1/2}\,(2r_1+r_2-r_3-2r_4-r_5+r_6)$
	S_{18b}	$= 12^{-1/2}R(2\beta_1+\beta_2-\beta_3-2\beta_4-\beta_5+\beta_6)$
$E_{1u(b)}$	S_{19b}	$= 24^{-1/2}(-d_1-2d_2-d_3+d_4+2d_5+d_6)$ $-8^{-1/2}D(-a_2-a_3+a_5+a_6)$
	S_{20b}	$= (1/2)(-r_2-r_3+r_5+r_6)$

Another reason for undertaking the present computations is that the results from benzene may be used as a guide for further calculations on condensed aromatics. Work on naphthalene has been started [23], actuated by the recently published [24] results of an electron-diffraction investigation of condensed aromatics.

SYMMETRY COORDINATES

The in-plane symmetry coordinates are specified in Table 1. The valence force coordinates from which the symmetry coordinates are formed are: r-stretching of a Cl bond, d-stretching of a CC bond, α-bending of a CC angle, β-bending of a CH bond. A diagram and more precise definition of coordinates are given in Ref. [22]

L-MATRICES

Albrecht [12] gives numerical values for the coefficients L_{ij} of the transformation

$$S_i = \sum_j L_{ij}\, Q_j$$

Table 2. Mean amplitudes of vibration in benzene (Å units).

Distance	Symbol	Calculated values: present T = 0°K	present 298°K	Cyvin[10] 298°K	Kimura and Kubo[17] 298°K	Experimental values: Kimura and Kubo[17] 291°K	Bastiansen and Cyvin[16]		Karle[14]
C_1-C_2	$\langle d^2\rangle^{1/2}$	0.0461	0.0464	0.0459	0.0452	0.0456	0.0455	0.0453	0.055
C_1-C_3	$\langle (d^*)^2\rangle^{1/2}$	0.0539	0.0552	0.0547	0.0548	0.0556	0.054	0.054	0.067
C_1-C_4	$\langle (d^{**})^2\rangle^{1/2}$	0.0570	0.0590	0.0597	0.0592	0.0614	0.062	0.059	0.075
C_1-H_1	$\langle r^2\rangle^{1/2}$	0.0771	0.0771	0.0771	0.0771	0.0748	0.073	0.073	0.072
C_2-H_1	$\langle (r^*)^2\rangle^{1/2}$	0.0994	0.0998	0.1004	0.1000	0.0975	0.094	0.092	0.092
C_3-H_1	$\langle (r^{**})^2\rangle^{1/2}$	0.0960	0.0969	0.0960	0.0916	0.0925	0.094	0.087	
C_4-H_1	$\langle (r^{***})^2\rangle^{1/2}$	0.0920	0.0934	0.0942	0.0938	0.0960	0.097	0.099	
H_1-H_2	$\langle t^2\rangle^{1/2}$	0.1573	0.1580	0.1561	0.1597				
H_1-H_3	$\langle (t^*)^2\rangle^{1/2}$	0.1322	0.1332	0.1321	0.1388				
H_1-H_4	$\langle (t^{**})^2\rangle^{1/2}$	0.1171	0.1182	0.1191	0.0966				

relating the symmetry coordinates (S) to the normal coordinates (Q) for both C_6H_6 and C_6D_6. For the calculation of mean-square amplitudes, each of Albrecht's coefficients L_{ij} was multiplied by

$$2\pi 10^{-8}(c\omega_j/hN_o)^{1/2}$$

to give L-matrix elements in (atomic mass units)$^{1/2}$ cm Å^{-1}. N_o is Avogadro's number, h is Planck's constant, c is the velocity of light, and ω_j is the vibrational frequency in cm^{-1} as calculated by Albrecht. Further, the coefficients relating S_{19} to the normal coordinates must be multiplied by $2^{1/2}$ because we have followed Crawford and Califano [11] in dealing with the redundant coordinates of the E_{1u} symmetry type. There are also some changes of sign where our symmetry coordinates have the opposite sense from Albrecht's. The L_{ij} which we have used as well as those which Cyvin used in his earlier calculations, are given in the Appendix.

Table 3. Mean amplitudes of vibration in benzene-d_6 (Å units).

Distance	Symbol	Calculated values: Present T = 0°K	Present 298°K	Cyvin[13] 298°K
C_1-C_2	$\langle d^2\rangle^{1/2}$	0.0459	0.0462	0.0457
C_1-C_3	$\langle (d^*)^2\rangle^{1/2}$	0.0533	0.0547	0.0543
C_1-C_4	$\langle (d^{**})^2\rangle^{1/2}$	0.0563	0.0584	0.0593
C_1-D_1	$\langle r^2\rangle^{1/2}$	0.0658	0.0658	0.0660
C_2-D_1	$\langle (r^*)^2\rangle^{1/2}$	0.0858	0.0868	0.0898
C_3-D_1	$\langle (r^{**})^2\rangle^{1/2}$	0.0839	0.0853	0.0848
C_4-D_1	$\langle (r^{***})^2\rangle^{1/2}$	0.0812	0.0828	0.0839
D_1-D_2	$\langle t^2\rangle^{1/2}$	0.1324	0.1349	0.1296
D_1-D_3	$\langle (t^*)^2\rangle^{1/2}$	0.1122	0.1141	0.1112
D_1-D_4	$\langle (t^{**})^2\rangle^{1/2}$	0.1002	0.1016	0.1028

APPENDIX

A. L-matrix elements for the in-plane vibrations of benzene. ($S = LQ$)
Calculated from Albrecht[12]

Symmetry species	Symmetry coordinate	1	2		
A_{1g}	S_1	0.274256	−0.0897227		
	S_2	0.0353057	1.036393		
		3			
A_{2g}	S_3	1.120128			
		12	13		
B_{1u}	S_{12}	0.949512	0.312328		
	S_{13}	−0.0370822	1.036262		
		14	15		
B_{2u}	S_{14}	0.454584	−0.207611		
	S_{15}	0.676180	0.786109		
		6	7	8	9
	S_6	0.466921	0.244526	−0.522210	−0.271889
	S_7	−0.0105538	1.035481	0.0520144	0.0178191
E_{2g}	S_8	0.107411	−0.0623189	0.426104	0.105617
	S_9	0.177330	0.0668788	−0.646907	0.827350
		18	19	20	
	S_{18}	0.442477	−1.013556	0.0737579	
E_{1u}	S_{19}	0.332233	0.354106	−0.118362	
	S_{20}	0.0222735	0.0373035	1.036050	

B. L-matrix for benzene-d_6. Calculated from Albrecht.

		1	2		
A_{1g}	S_1	0.256399	−0.132374		
	S_2	0.0666245	0.758188		
		3			
A_{2g}	S_3	0.871462			
		12	13		
B_{1u}	S_{12}	0.886128	0.462511		
	S_{13}	−0.0700937	0.757906		
		14	15		
B_{2u}	S_{14}	0.496862	−0.0540145		
	S_{15}	0.362970	0.668948		
		6	7	8	9
	S_6	0.420911	0.389290	−0.476671	−0.261884
	S_7	−0.0176430	0.749349	0.129915	0.0230211
E_{2g}	S_8	0.100693	−0.127683	0.425626	0.0234259
	S_9	0.237911	0.131132	−0.457242	0.600016
		18	19	20	
	S_{18}	0.501042	−0.681429	0.131097	
E_{1u}	S_{19}	0.185197	0.423451	−0.190174	
	S_{20}	0.0206666	0.0894705	0.755538	

C. L-matrix for benzene. Calculated by Cyvin.

		1	2		
A_{1g}	S_1	0.271603	−0.097447		
	S_2	0.064788	1.035015		
		3			
A_{2g}	S_3	1.120176			
		12	13		
B_{1u}	S_{12}	0.942793	0.332066		
	S_{13}	−0.058745	1.035377		
		14	15		
B_{2u}	S_{14}	0.427441	−0.258992		
	S_{15}	0.269399	1.001440		
		6	7	8	9
	S_6	0.492716	0.240582	−0.496631	−0.277777
	S_7	−0.011707	1.035830	0.046600	0.014296
E_{2g}	S_8	−0.094577	−0.059923	0.415108	0.152643
	S_9	0.141868	0.089537	−0.926658	1.002517
		18	19	20	
	S_{18}	1.099641	0.130145	0.051146	
E_{1u}	S_{19}	−0.244451	0.418206	−0.123003	
	S_{20}	−0.010568	0.054548	1.035553	

D. L-matrix for benzene-d_6. Calculated by Cyvin.

		1	2		
A_{1g}	S_1	0.251153	−0.142055		
	S_2	0.095727	0.755373		
		3			
A_{2g}	S_3	0.871262			
		12	13		
B_{1u}	S_{12}	0.872375	0.487942		
	S_{13}	−0.092132	0.755819		
		14	15		
B_{2u}	S_{14}	0.494209	−0.074402		
	S_{15}	−0.180426	0.739730		
		6	7	8	9
	S_6	0.455988	0.376265	−0.468570	−0.235440
	S_7	−0.020647	0.752364	0.114000	0.016726
E_{2g}	S_8	0.092078	−0.118783	0.426885	0.057728
	S_9	0.215819	0.166889	−0.628119	0.774347
		18	19	20	
	S_{18}	0.805535	−0.271485	0.102316	
E_{1u}	S_{19}	−0.097789	0.446346	−0.202469	
	S_{20}	0.0028194	0.113662	0.752878	

E. Σ-matrix elements for benzene and benzene-d_6

	C_6H_6		C_6D_6	
	$T = 0$°K	298°K	0°K	298°K
$\Sigma_{11}(A_{1g})$	0.00132171	0.00134311	0.00130074	0.00132523
$\Sigma_{22}(A_{1g})$	0.00591422	0.00591458	0.00428785	0.00428963
$\Sigma_{12}(A_{1g})$	−0.00034571	−0.00034296	−0.00043014	−0.00042381
$\Sigma(A_{2g})$	0.01568109	0.01571857	0.01209276	0.01223957
$\Sigma_{11}(B_{1u})$	0.01559043	0.01583273	0.01522904	0.01548456
$\Sigma_{22}(B_{1u})$	0.00594632	0.00594667	0.00432447	0.00432620
$\Sigma_{12}(B_{1u})$	0.00119744	0.00118836	0.00150711	0.00148699

$\Sigma_{11}(B_{2u})$	0.00329626	0.00331094	0.00330690	0.00332257
$\Sigma_{22}(B_{2u})$	0.01498288	0.01507659	0.01089051	0.01124770
$\Sigma_{12}(B_{2u})$	0.00155825	0.00155345	0.00163272	0.00161423
$\Sigma_{11}(E_{2g})$	0.01031969	0.01101335	0.01007457	0.01079070
$\Sigma_{22}(E_{2g})$	0.00595446	0.00595487	0.00436412	0.00436596
$\Sigma_{33}(E_{2g})$	0.00241529	0.00245427	0.00238749	0.00242843
$\Sigma_{44}(E_{2g})$	0.01511555	0.01528531	0.01103279	0.01146547
$\Sigma_{12}(E_{2g})$	0.00090501	0.00088883	0.00115857	0.00112613
$\Sigma_{23}(E_{2g})$	−0.00012713	−0.00013029	−0.00015198	−0.00015777
$\Sigma_{34}(E_{2g})$	−0.00114707	−0.00108133	−0.00125970	−0.00116268
$\Sigma_{13}(E_{2g})$	−0.00144739	−0.00129497	−0.00144913	−0.00129435
$\Sigma_{24}(E_{2g})$	0.00018684	0.00018211	0.00023150	0.00022317
$\Sigma_{14}(E_{2g})$	0.00272803	0.00296881	0.00260111	0.00288971
$\Sigma_{11}(E_{1u})$	0.01490241	0.01496376	0.01120122	0.01142895
$\Sigma_{22}(E_{1u})$	0.00329860	0.00332509	0.00324536	0.00328119
$\Sigma_{33}(E_{1u})$	0.00592361	0.00592375	0.00431720	0.00431801
$\Sigma_{12}(E_{1u})$	−0.00174127	−0.00171537	−0.00191171	−0.00184631
$\Sigma_{23}(E_{1u})$	−0.00040337	−0.00040150	−0.00050039	−0.00049571
$\Sigma_{13}(E_{1u})$	0.00015007	0.00015156	0.00017325	0.00017941

F. Numerical values used in the calculations.

R = 1.084 Å (equilibrium C-H distance)
D = 1.397 Å (equilibrium C-C distance)
h = 6.6252×10^{-27} erg sec
N_0 = 6.02472×10^{23} atomic mass units gm^{-1}
c = 2.997929×10^{10} cm sec^{-1}
k = 1.38042×10^{-16} erg deg^{-1}

Σ-MATRIX

The L-matrix elements quoted above were used to calculate the Σ-matrices ($\Sigma = L\Delta\tilde{L}$) for benzene and benzene-d_6. Δ is a diagonal matrix whose elements are

$$(h/8\pi^2 c\omega_i) \coth(hc\omega_i/2kT)$$

where k is the Boltzmann factor and T is the temperature in degrees Kelvin. We used the observed frequencies of gaseous benzene (Brodersen and Langseth [25]) here; thus there is a small inconsistency between the Σ-matrix and the set of force constants from which Albrecht calculated the L-matrix elements. An F-matrix calculated from

$$F = \tilde{L}^{-1} \Lambda L^{-1}$$

would be exactly consistent with our Σ-matrix. The observed and calculated frequencies are sufficiently close that the effect of the inconsistency should be negligible. The Σ-matrix elements are given in the appendix.

MEAN AMPLITUDES OF VIBRATION

The mean-square amplitudes of vibration were calculated from the Σ-matrix using the expressions given in Ref.[22] and the square roots of these are the mean amplitudes of vibration. The calculated mean amplitudes for benzene and benzene-d_6 are given in Tables 2 and 3 along with calculated and observed mean amplitudes from other work.

Note: The digits as given in these and the other tables are not necessarily all significant.

REFERENCES

1. Manneback, C. *Ann.soc. sci. Bruxelles* **55-B** (1935) 237.
2. Redlich, O. and Stricks, W. *Wien. Ber.Math. IIb* **145** (1936).
3. Lord, R. C. and Andrews, D. H. *J.Phys.Chem.* **41** (1937) 149.
4. Bernard, E., Manneback, C. and Verleysen, A. *Ann.soc.sci.Bruxelles* **59** (1939) 367.
5. Bernard, E., Manneback, C. and Verleysen, A. *Ann.soc.sci.Bruxelles* **60** (1940) 45.
6. Bak, B. *Kgl. Danske Videnskab.Selskab, Mat.-fys.Medd.* **22** (1945) No. 9.
7. Crawford, B.L., Jr. and Miller, F. A. *J.Chem.Phys.* **17** (1949) 249.
8. Whiffen, D. H. *Phil.Trans.Roy.Soc. London* **A 248** (1955) 131.
9. Wilson, E. B., Jr., Decius, J. C. and Cross, P. C. *Molecular Vibrations*, McGraw-Hill Book Co., New York, 1955.
10. Cyvin, S. J. *Acta Chem. Scand.* **11** (1957) 1499.
11. Califano, S. and Crawford, B., Jr. *Spectrochim. Acta* **16** (1960) 889.
12. Albrecht, A. C. *J. Mol. Spectroscopy* **5** (1960) 236.
13. Cyvin, S. J. *Acta Chem. Scand.* **12** (1958) 1697.
14. Karle, I. L. *J. Chem. Phys.* **20** (1952) 65.
15. Almenningen, A., Bastiansen, O. and Fernholt, L. *Kgl. Norske Videnskab.Selskabs Skrifter* **1958** No. 3.
16. Bastiansen, O. and Cyvin, S. J. *Nature* **180** (1957) 980.
17. Kimura, K. and Kubo, M. *J. Chem. Phys.* **32** (1960) 1776.
18. Kimura, K. and Kimura, M. *J. Chem. Phys.* **32** (1960) 1398.
19. Bastiansen, O. and Trætteberg, M. *Acta Cryst.* **13** (1960) 1108.
20. Morino, Y. *Acta Cryst.* **13** (1960) 1107.
21. Morino, Y. and Hirota, E. *J. Chem. Phys.* **23** (1955) 737.
22. Brooks, W. V. F. and Cyvin, S. J. *Spectrochim. Acta. In press.*
23. Cyvin, S. J. and Meisingseth, E. *Kgl. Norske Videnskab. Selskabs Skrifter. In press.*
24. Almenningen, A., Bastiansen, O. and Dyvik, F. *Acta Cryst. In press.*

Received October 9, 1961.

ACTA CHEMICA SCANDINAVICA 16 (1962) 827–830

The Isolation of a Xylobiose Monoacetate from the Waste Liquor of a Birch Sulphite Cook

INGEMAR CROON

Billeruds Research Laboratory, Säffle, Sweden

A monoacetate of xylobiose has been isolated by chromatographic methods from the spent liquor of a birch sodium sulphite cook. Periodate oxidation and paper electrophoresis studies indicate that the *O*-acetyl group is located in the 2-position of the non-reducing xylose residue.

The isolation of this compound implies the presence also of other acetylated oligosaccharides in the birch sulphite cooking liquor.

The behaviour of the *O*-acetyl groups of birch xylan during different types of sulphite processes has been studied in this laboratory [1,2]. These studies have indicated that acetylated oligosaccharides should be present in the liquor during certain stages of the acid sulphite cook. An investigation was undertaken in order to follow the dissolution of the carbohydrate material during the cook and to attempt to isolate some partially acetylated oligosaccharides.

The sulphite liquor from a birch cook was purged of free sulfur dioxide and added directly to a carbon-Celite column. The column was irrigated with water to remove inorganic salts. The sugars were eluted using a water-ethanol gradient.

The carbohydrate composition of the waste liquor investigated was very complex. The major part (about 70 % of the material eluted with up to 50 % ethanol) consisted of monosaccharides: xylose, glucose, mannose, galactose, arabinose and rhamnose. These monosaccharides, eluted first from the column, were followed by disaccharides, trisaccharides, aldobiouronic acids, etc. At least 25 different components were indicated by paper chromatographic analysis. Fractions which contained approximately the same components were combined and evaporated *in vacuo*. In this way ten fractions were obtained, some of which contained acetyl groups. The fraction with the highest acetyl content (1.6 %) contained a substance with a R_{xylose}-value of 1.31 in solvent A and 1.20 in solvent B. The other substraces in this fraction were an aldotriouronic acid and xylotetraose, both of which have low R_{xylose}-values in solvent B. The substance with the high R_{xylose}-value was easily isolated therefore by cellulose column chromatography using the latter solvent. The compound

crystallized upon evaporation of the solvent and after two recrystallizations from hot ethanol had m.p. 195—196°C and $[\alpha]_D^{20} = -15$ ($c = 2$ in water). The infrared spectrum of the substance showed absorption at 1 745 cm^{-1} and 1 260 cm^{-1}, thereby indicating the presence of ester groups. Treatment with sodium methoxide in methanol gave a substrance with the same paper chromatographic and electrophoretic mobility as xylobiose. It crystallized from methanol and had m.p. 183—185°C [3]. The phenyl osazone hemihydrate decomposed at 204—206°C in good agreement with reported values for xylobiose phenylosazone-hemihydrate [3].

A quantitative acetyl analysis by gas chromatography gave an *O*-acetyl value of 13.20 % in good agreement with the calculated value 13.27 % for a monoacetyl xylobiose. Elemental analysis (C 44.17, H 6.30, O 49.53 %) was also in agreement with that of a monoacetyl derivative of xylobiose (C 44.4, H 6.18, O 49.38 %). The identity of the compound was further established by complete acetylation affording the crystalline hexa-acetate of xylobiose, melting point (155—156°C), undepressed by admixing with authentic xylobiose hexa-acetate [4].

The substance consumed 2.8 moles of periodate with the liberation of 0.92 moles of formic acid. A unique structure can not be assigned to the compound solely on the basis of this periodate oxidation data. (If position 2 in the reducing xylose unit is free, a formic acid ester will be formed. The determination of the formic acid in this ester depends on the method of analysis employed). However, substitution at the 2-position in the reducing unit and the 3-position in the non-reducing unit may be excluded. As the 4-position in the nonreducing unit is bonded in the xylan chain, the most likely position of the acetyl group should be in the 3-position of the reducing unit or the 2-position of the non-reducing unit.

Garegg and Lindberg [5] in studying the paper electrophoresis of carbohydrates in sulphonated phenyl boric acid at pH 6.5, found pronounced differences between various substituted sugar alcohols, depending upon the site of the substitution. Thus xylitol, 4-*O*-methylxylitol and 3,4-di-*O*-methyl-xylitol had the $M_{mannitol}$-values 0.9, 0.43 and 0.0. Methyl-β-xylopyranoside did not move at all under these conditions. Therefore by studying the electrophoretic mobility of the corresponding mono-*O*-acetyl-xylobiitol, it should be possible to decide whether or not the *O*-acetyl groups are linked to the 3-position in the non-reducing xylose residue. The latter substance was prepared and found to have the $M_{mannitol}$-value 0.50, slightly higher than xylobiitol 0.44. This result strongly indicates that the 3-position in the reducing xylose residue is not substituted and implies that the *O*-acetyl group is located in the 2-position in the nonreducing residue.

DISCUSSION

In natively acetylated birch xylan, the *O*-acetyl groups seem to be linked mainly (about 75 %) in 3-positions of the xylose residues [6,7]. In the isolated xylobiose monoacetate, however, the *O*-acetyl group is most probably located in the 2-position of the non-reducing xylose residue. That it is found in the non-reducing residue seems natural, as bulky substituents in equatorial posi-

tions should render glycosides more stable to acid hydrolysis [8]. Further, the *O*-acetyl group is an electron-withdrawing substituent, and in the sugar residue, they are known to decrease the rate of acid hydrolysis of a glycoside [9]. A substituent in the 2-position, that is closer to the glycosidic linkage should be more efficient than a substituent in the 3-position.

It is probable that some of the *O*-acetyl groups in 3-positions have also survived the sulphite cook and that a number of acetylated oligosaccharides are present in the spent liquor.

EXPERIMENTAL

Paper chromatography. Paper: Whatman No. 1. Solvents:
Solvent A: Butanol, acetone, water, 4:5:1
Solvent B: Ethylacetate, acetic acid, water, 9:2:2.
Spray reagents: Aniline phthalate and silver nitrate/sodium ethoxide.

The waste liquor was obtained from a laboratory cook on birch (*Betula verrucosa*) chips, performed in a 10 litre tumbling stainless steel digester. The cook employed a cooking acid of 6 % total and 1 % combined sulphur dioxide. Heating time 5 h to 150°C and kept 45 min at this maximum temperature; liquor-to-wood ratio 4:1; maximum pressure 7.0 kp/cm². Sodium base was used. Pulp yield was 46 %; roe number 2.7 and pulp viscosity 77 cPT. The acetyl content of the pulp was 1.09 % and the neutral sugar composition: glucose 90.8 %, mannose 0.8 % and xylose 8.4 %.

Fractionation of the mono- and oligosaccharides in the waste liquor. Waste liquor (1 l) was freed from sulphur dioxide by bubbling nitrogen for one hour. The liquor was then added to a carbon-Celite column (3.5 × 55 cm) which was irrigated with water (10 l). The monosaccharides eluted by this treatment were recovered by passage through ion exchange columns and concentration of the solution. A linear gradient from water to 50 % ethanol was then employed and fractions (20 ml) collected, using an automatic fraction collector. Fractions 96–108 contained a component moving faster than xylose. R_{xylose} = 1.31 in solvent A and 1.20 in solvent B. These fractions were combined and taken to dryness by evaporation *in vacuo*.

Isolation of fast moving compound. The latter material (1.24 g), which had an acetyl content of 1.6 %, was dissolved in ethyl acetate-acetic acid-water, 1:1:1 (10 ml), and added to a cellulose column (3 × 30 cm) and eluted with solvent B.

The fractions which contained the component with R_{xylose} = 1.20 were combined and evaporated to dryness whereupon the substance crystallized. After recrystallization from hot ethanol (yield 130 mg) the crystals had m.p. 195–196°C and $[\alpha]_D^{25} = -15°$ (c = 2 in water). The infrared spectrum exhibited absorption maxima at the following frequencies cm^{-1}: 3 350, 2 940, 1 745, 1 650, 1 430, 1 380, 1 260, 1 135, 1 070, 1 030, 990, 970, 940, 890, 860 and 750.

Deacetylation of the substance. The substance (20 mg) was dissolved in sodium methoxide (3 ml) and the solution allowed to stand for 5 h. The sodium ions were removed by cation exchange (IR-120, H^+-form). A gas chromatographic run indicated methyl acetate in the solution. On evaporation of the solvent, the deacetylated compound crystallized, m.p. 183–185°C [3]. The substance gave only xylose upon hydrolysis. To a solution of the crystals (10 mg) in water (1.5 ml) phenyl hydrazine (0.175 g), 20 % acetic acid (1.0 ml) and sodium bisulphite (10 mg) were added. The solution was heated for 2 h at 100°C (bath temp.). The crystals which separated were filtered, washed with water and recrystallized from 60 % ethanol, m.p. 204–206°C in good agreement with reported values for xylobiose phenyl osazone hemihydrate [3].

Determination of the acetyl content of the xylobiose acetyl derivative. The quantitative estimation of the acetyl content of the substance was performed with the gas chromatographic method devised by Spingler and Markert [10]. The substance was found to contain 13.20 % acetyl which corresponds to a monoacetyl derivative of xylobiose (13.27 %).

Acetylation of the monoacetyl derivative of xylobiose. The substance, (10 mg) was heated at 100°C for 1 h with a mixture of acetic acid (0.5 ml), acetic anhydride (4.5 ml) and sodium acetate (0.5 g). The solution was poured into a mixture of ice and water. The acetate

crystallized spontaneously and was filtered after decomposition of all of the acetic anhydride. The crude acetate was washed with dilute sodium bicarbonate and recrystallized from alcohol. M.p. 155–156°C alone or on admixture with authentic β-xylobiose hexaacetate [4].

Periodate oxidation of the substance. The compound was dried *in vacuo* at 40°C for 2 h over P_2O_5. 10.0 mg was weighed into a 10 ml volumetric flask and made up to the mark with an ice-cold solutionof metaperiodate (0.4 g/100 ml). The solution was stored in the refrigerator (+ 3°C).

The periodate consumption was determined by taking aliquots (1 ml) and adding to a solution containing 2 ml of 10 % potassium iodide and 2 ml 3 N sulphuric acid. The solution was diluted with a few ml of water. The iodine liberated was titrated with 0.01 N $Na_2S_2O_3$.

The formic acid production was measured as follows: 1 ml aliquots were withdrawn and added to a solution of ethylene glycol (0.5 ml) in water (5 ml) The mixture was allowed to stand in the dark (refrigerator) for 15 min. 10 % potassium iodide (1 ml) was added and the iodine was titrated with 0.01 N $Na_2S_2O_3$. After 24 h the sample had consumed 2.8 moles of periodate with the liberation of 0.92 moles of formic acid.

Reduction of the xylobiose monoacetate. The substance (2 mg) was refluxed together with Raney-nickel (20 mg) in 70 % ethanol (2 ml) for 3 h. After filtration the reduced material was recovered by evaporation to dryness.

Saponification of the xylobiitol monoacetate. Half of the xylobiitol monoacetate was dissolved in methanol (1 ml) and a solution (0.2 ml) consisted of 10 % ammonia in methanol was added. The mixture was allowed to stand overnight after which the xylobiitol was isolated by evaporation to dryness [11].

Paper electrophoresis. Buffer solution: 0.05 M phenyl boric acid orthosodium sulphonate titrated with sodium hydroxide to pH 6.5 and 0.06 M sodium phosphate buffer solution of pH 6.5. Voltage 0.75 kV; Time 2 ½ h; Temperature 40°C.

Acknowledgement. The author is indebted to Drs. E. Goldstein and P. Garegg for their suggestions and experimental assistance. My thanks are also due to Prof. B. Lindberg for valuable discussions and to Billeruds AB for permission to publish this part of the investigation.

REFERENCES

1. Öhrn, O. E. and Croon, I. *Svensk Papperstidn.* **63** (1960) 601.
2. Annergren, G. E. and Croon, I. *Svensk Papperstidn.* **64** (1961) 618.
3. Whistler, R. L., Bachrach, J. and Tu, C. C. *J. Am. Chem. Soc.* **74** (1952) 3059.
4. Srivastava, H. C. and Smith, F. *J. Am. Chem. Soc.* **79** (1957) 982.
5. Garegg, P. J. and Lindberg, B. *Acta Chem. Scand.* **15** (1961) 1913.
6. Bouveng, H. O., Garegg, P. J. and Lindberg, B. *Acta Chem. Scand.* **14** (1960) 742.
7. Bouveng, H. O. *Acta Chem. Scand.* **15** (1961) 96.
8. Shafizadeh, F. and Thompson, J. *J. Org. Chem.* **21** (1956) 1059.
9. Whistler, R. L. and Richard, G. N. *J. Am. Chem. Soc.* **80** (1958) 4888.
10. Spingler, H. and Markert, F. *Microchim. Acta* **1959** 121.
11. Slotta, K. H. and Heller, N. *Ber.* **63** (1930) 1024.

Received October 30, 1961.

ACTA CHEMICA SCANDINAVICA 16 (1962) 831–836

Crystalline Leghemoglobin

VI. The Comparison of the Two Main Components by Tryptic Peptide Pattern Analysis

NILS ELLFOLK*

Medicinska Nobel Institutet, Biokemiska Avdelningen, Karolinska Institutet, Stockholm, Sweden

The two main components of leghemoglobin have been subjected to tryptic hydrolysis. The resultant peptides have been separated in two dimensions by paper electrophoresis and paper chromatography. Comparison of the peptide patterns of the two components shows many identical peptides, the differences, however, being rather great including several peptides. It is concluded from the results that the two components of Lhb are formed by synthesis by systems that differ genetically.

The concept of the two main components of leghemoglobin (Lhb) being individual proteins is based on recent studies on molecular weight [1], amino acid content [2] and N-terminal amino acids [3]. There are two ways by which these individual components might be formed. One way might be by synthesis *via* individual systems that differ genetically. The other might be a system in which one of the components acts as a precursor for the other. The former possibility has support in the observation that those amino acids, the content of which has been found to differ between the two components, are identical with those amino acids which are known to be interchangeable in specific proteins of different origin, *i.e.* which are synthesized by systems differing genetically. The other possibility, *i.e.* one of the components being a precursor for the other, has particular support in the fact that the two components have different N-terminal amino acids and a slight difference in molecular weight.

In order to elucidate the structural differences between the two components, and to reach a final conclusion as to whether one of the components acts as a precursor for the other or if the two components are synthesized by two

* Permanent address: Research Laboratories of the State Alcohol Monopoly, Helsinki, Finland.

systems under different genetic control, it was decided to study the pattern of their tryptic peptides. The analyses were performed by combined paper electrophoresis and paper chromatography, a technique introduced by Ingram [4] as "the finger printing technique" for detecting small differences in amino acid composition or sequences in proteins, differences which are of importance in the composition of homogeneous proteins from different animal and plant species and those which result from a single gene mutation.

MATERIALS AND METHODS

Leghemoglobin. The two main components of Lhb used in this study were prepared as described previously [5,6]. The electrophoretic homogeneity of the components was checked.

Apoleghemoglobin. The apoproteins of the two components were prepared from the electrophoretically homogeneous components by precipitating in HCl-acetone in the cold as described previously [2].

Trypsin. The trypsin used for the digestions was the crystallized protein salt obtained from Worthington (cryst. Trypsin) and was further purified by electrophoresis in order to remove the chymotrypsin present in the preparation. A typical run was made in the Spinco model E electrophoresis apparatus as follows: A 1.3 % solution of the trypsin was run in the 2 ml cell in a phosphate buffer pH 6.27 and μ 0.1. The preparation showed two components, a main component and a smaller amount of a very slow component. The main component moved to the cathode with a rather high mobility and was found to contain all of the tryptic activity, whereas the smaller component was found to contain the chymotryptic activity. After about 5 h, the separation of the two components had proceeded so far that enough electrophoretically pure trypsin could be isolated. This was done after first adjusting the positions of the two components so that the trypsin-containing component could be removed with a hypodermic needle introduced into the electrophoresis cell. This trypsin preparation showed only slight traces of chymotryptic acitivity.

Assay of chymotrypsin. The chymotrypsin content of the different trypsin preparations was determined by using N-benzoyl-DL-phenylalanine-β-naphthyl ester as a substrate as described by Ravin *el al.* [7].

Assay of trypsin. The trypsin activity of the samples was determined according to Kunitz [8]. 0.5 % casein solutions were hydrolyzed at 35°C for 20 min, the excess casein precipitated with trichloroacetic acid, and the concentration of the split products in the supernatant solutions determined from the optical density at 280 mμ. The amount of active trypsin was determined from the standard curve of Kunitz.

Digestions. The tryptic digestions were performed essentially as described by Ingram [9]: 6.5 ml samples of 0.2 % Lhb solutions were first denaturated by heating in a salt free solution at pH 9 for 5 min at 90°C. The digestions were carried out with continuous stirring at 39°C and pH 9 in an atmosphere of nitrogen. The enzyme to Lhb ratio was 0.01, with the trypsin concentration calculated as active trypsin. The pH was maintained constant by adding 0.2 N NaOH from an Agla micrometer buret. The digestion was continued for 140 min. After digestion, the pH of the solution was brought to pH 4.0 with 4 N acetic acid, after which the solution was lyophilized. These peptide preparations, particularly the hydrolyzate of the faster component, showed a tendency to gelatinize on dissolving in water. The gelatinization tendency was decreased by redissolving the preparations in water, removing the gelatinized material by centrifugation and relyophilizing the supernatant solution.

High-voltage paper electrophoresis. The apparatus consisted of a brass plate coated with a thin layer of polyethylene, and cooled by a system consisting of copper tubing under the plate connected to the tap water [10]. The plate was large enough for a whole sheet of Whatman 3 MM to be used. The electrophoretic separation was carried out in 0.03 M pyridine-acetic acid buffer of pH 4.0 on large sheets of Whatman 3 MM, and at a potential of 27 V/cm. In order to stabilize the temperature of the paper, the current and cooling water were turned on 20 min before the run was started.

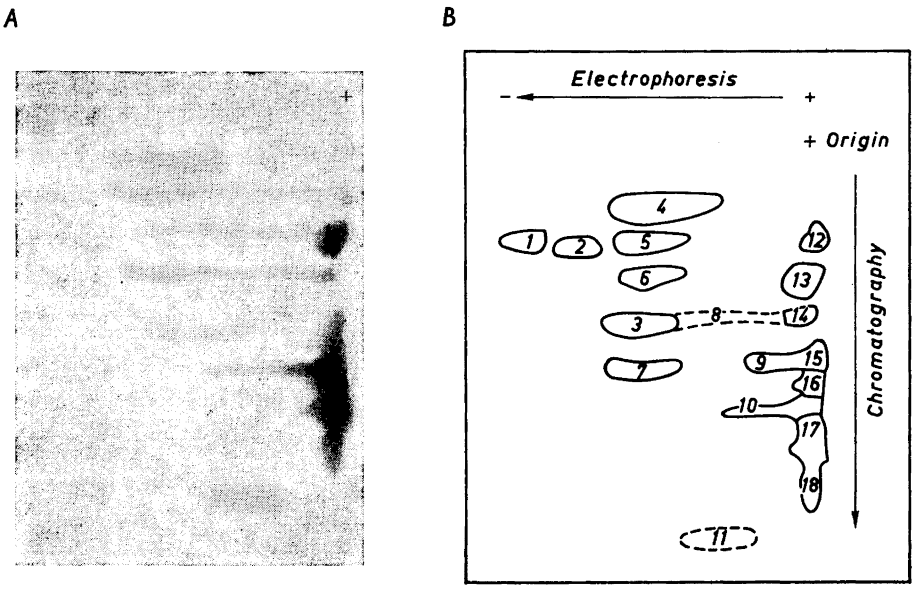

Fig. 1. Two-dimensional separation of tryptic peptides of the faster component of Lhb (A) and its schematic presentation (B). The first dimension is electrophoresis at pH 4.0. The second dimension is chromatography in butanol-acetic acid-water.

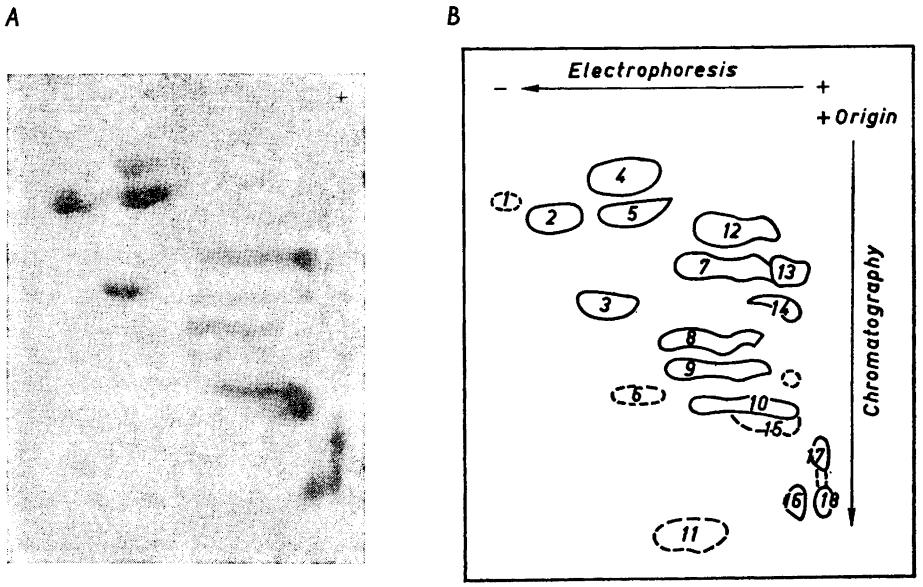

Fig. 2. Two-dimensional separation of tryptic peptides of the slower component of Lbh (A) and its schematic presentation (B). The two dimensions are the same as in Fig. 1.

Peptide pattern analysis. The tryptic hydrolyzates were analyzed by the combination of electrophoresis and chromatography on paper as specified by Ingram [9]. After the temperature of the paper on the plate was stabilized, the sample was put on. The area around the place of application was dried with "Whatman filter paper accelerators" of 1.95 cm diameter [10]. 2—2.5 mg of the tryptic hydrolyzates in 20 μl were put on the dried areas. The electrophoresis was continued for 120 min. The paper was dried, and subjected to descending chromatography in butanol-acetic acid-water (4:1:5 volume ratios) for 6 to 7 h at 37°C in a thermostated room. The spots on the chromatograms were developed by dipping the papers in a 0.4 % ninhydrin solution in acetone containing 2 % pyridine and left at 37°C for color development.

RESULTS

Figs 1 and 2 show tryptic peptide pattern of the faster and slower components and their schematic representation. The polarity of the electrical field is marked on each pattern, and the point of application of the sample is designated by a cross (+).

The fingerprints contain alltogether some 18 peptides. As judged by their ninhydrin colors, the majority are present in good yield. There are slightly more peptides than expected from the amino acid compositions of the two components. Trypsin is well known to split specifically those bonds in the polypeptide chains which are formed by the carboxyl groups of lysine and arginine. There are 13 lysine residues and 1 arginine residue in the fast component, and 13 lysine and 2 arginine residues in the slow component. According to these figures, 14—15 peptides are expected to be formed from the faster component and 15—16 peptides from the slower one after complete trypsin digestion (depending on whether or not there is a lysine or arginine residue as a carboxyl end-group). However, as the amino acid analyses do not account for more than 92.7 % [2] of the apoprotein for the faster component and 95.7 % [2] for slower one, the possible presence of constituents other than amino acids must also be kept in mind.

Peptides numbered 1, 2, 3, 4, 5, and 11 in the digests of both the two components occupy the same relative positions and are therefore considered to have the same chemical structure. Peptides numbered 6 and 7 in the digest of the fast component cannot be found in the digest of the slow component. Peptide number 6 of the fast component might correspond to peptide 7 of the slow component. However, the differences in the peptides of the two components are too great to allow any further conclusions to be drawn on possible changes of the positions of the amino acids in the peptides. A general feature is that the neutral peptides of the fast component (Nos. 12—18) occupy a slightly changed position in the digest of the slow component. This is in part due to a slight increase in the positive electrical charges in the corresponding peptides of the slower component. This finding agrees well with the known electrophoretic behavior of the two components.

The spots numbered 2 in both of the components and that numbered 7 in the fast component were found to turn yellow when kept at room temperature long enough so that the red color of the ninhydrin practically disappeared. This behavior seemed to be reproducible and was therefore assumed to be

specific for the peptides. Perhaps the proline in these peptides is so situated that it is accessible for color formation with ninhydrin (perhaps as an amino endgroup).

DISCUSSION

When the results presented in this paper are examined, the possibility of one of the components being a precursor for the other must be excluded. Instead, it is assumed that the two components are synthesized by systems which differ genetically.

Recent studies on normal and abnormal hemoglobins [11–13] have given valuable insight into the action of a gene and in particular into the firm control exerted by a gene. The chemical structure of a gene is thought to determine the amino acid sequence of the corresponding peptide chain. Any alternation of the gene, *e.g.* a mutation, would result in a chemical change in the peptide chain.

A chromosomal difference has been observed between the cells of the root nodules and those of the root tip. The root-tip cells had the usual diploid number of 14, whereas the root nodules had the tetraploid number of 28 [14]. The doubling of the chromosome number seemed to be associated with the bacterial invasion of the plant cell. It is probably not related to nitrogen fixation. Since nodules formed by inefficient strains also had a double chromosome number as compared with that of the root tip [15], it is difficult to decide the extent to which the synthesis of the two Lhb components is related to it, particularly as a positive correlation exists between the Lhb content in the nodules and the nitrogen fixation [16,17].

The nodule bacteria may, however, cause such changes in the plant cells that the components with chemical difference might be synthesized. It seems less likely that one of the components should be synthesized by the plant cell and the other by the bacterial cell. Recent findings by Bergersen and Briggs [18] revealed a highly organized structure in the soybean root nodules. Electron photomicrographs of mature, nitrogen-fixing nodules showed a system consisting of groups of four to six bacteroids enclosed in well-defined double membranes. It seems unlikely that equal concentration of the two components should always be synthesized on both sides of the double membrane, one component inside the menbrane by the bacteria and the other outside the membrane by the plant cell.

Acknowledgment. The author wishes to express his thanks to Professor Hugo Theorell for his interest in the work. The investigation has been supported by a grant from *Finnish State Commission of Natural Sciences (Statens Naturvetenskapliga Kommission i Finland)* which is gratefully acknowledged.

REFERENCES

1. Ellfolk, N. *Acta Chem. Scand.* **14** (1960) 1819.
2. Ellfolk, N. *Acta Chem. Scand.* **15** (1961) 545.
3. Ellfolk, N. and Levin, K. *Acta Chem. Scand.* **15** (1961) 444.
4. Ingram, V. M. *Nature* **158** (1956) 792.
5. Ellfolk, N. *Acta Chem. Scand.* **13** (1959) 596.
6. Ellfolk, N. *Acta Chem. Scand.* **14** (1960) 609.
7. Ravin, H. A., Bernstein, P. and Seligman, A. M. *J. Biol. Chem.* **208** (1954) 1.
8. Kunitz, M. *J. Gen. Physiol.* **30** (1947) 291.
9. Ingram, V. M. *Biochim. et Biophys. Acta* **28** (1958) 539.
10. Åkeson, Å. and Theorell, H. *Arch. Biochem. Biophys.* **91** (1960) 319.
11. Ingram, V. M. and Stretton, A. O. W. *Nature* **184** (1959) 1903.
12. Hunt, J. A. and Ingram, V. M. *Nature* **181** (1958) 1062.
13. Ingram, V. M. in *Proc. 4th Intern. Congr. Biochem.* Vienna 1958. VIII, p. 95.
14. Wipf, L. and Cooper, D. C. *Natl. Acad. Sci. Proc.* **24** (1938) 87.
15. Wipf, L. *Bot. Gaz.* **101** (1939) 51.
16. Virtanen, A. I., Erkama, J. and Linkola, H. *Acta Chem. Scand.* **1** (1947) 861.
17. Bergersen, F. J. *Biochim. et Biophys. Acta* **50** (1961) 576.
18. Bergersen, F. J. and Briggs, M. J. *J. Gen. Microbiol.* **19** (1958) 482.

Received November 22, 1961.

ACTA CHEMICA SCANDINAVICA 16 (1962) 837–842

Structure of the Maleic Anhydride Bis-Adduct of α, p-Dimethylstyrene

JAAKKO HUKKI

Lääketehdas Orion Oy Pharmaceutical Manufacturers, Helsinki, Finland

The addition reactions of the maleic anhydride bis-adduct of α,p-dimethylstyrene (Id) have been studied. Employing ozonolysis evidence was found for the existence of methyl-methylene tautomerism illustrated by formulas III and III'.

One of the outstanding features of the maleic anhydride bis-adducts of the type I is their "saturated" character regarding addition reactions. So Wagner-Jauregg [1], the discoverer of the first compound (Ia) of this type, found that it did not add bromine and catalytically activated hydrogen and that it was inert to oxidation with perbenzoic acid as well as with potassium permanganate in acetone solution. Thus, being unable to prove the existence of the two double bonds revealed by the structure Ia, he repudiated it in favor of another one by assuming the second step of addition to proceed by substitution mechanism. Similar observations have been made later by Bruckner *et al.*[2,3] in respect to other bis-adducts (Ib and Ic) of the same type. Although the concept of substitution addition has been recently substantiated by Alder and Schmitz-Josten [4] in the case of one of the two maleic anhydride bis-adducts of styrene (II), the original unsaturated type of formula put forward by Wagner-Jauregg still seems to be valid in other cases.

In a previous paper [5] it was shown, that α,p-dimethylstyrene readily adds two molecules of maleic anhydride to form a bis-adduct, for which the formula Id was established. This bis-adduct, too, revealed a "saturated" character when tested with the double bond reagents mentioned above. Only ozone was added in the amount corresponding to one double bond. When, however, the two anhydride rings were opened by converting the dianhydride to the corresponding tetramethyl ester (III), the rigid structure of the bis-adduct became more flexible allowing also the addition of bromine to one double bond. It was shown that the double bond attacked by both ozone and bromine was the one situated in the side ring (not in the bridged ring). First after the cleavage of this double bond by ozonization the existence of the other one could be demonstrated.

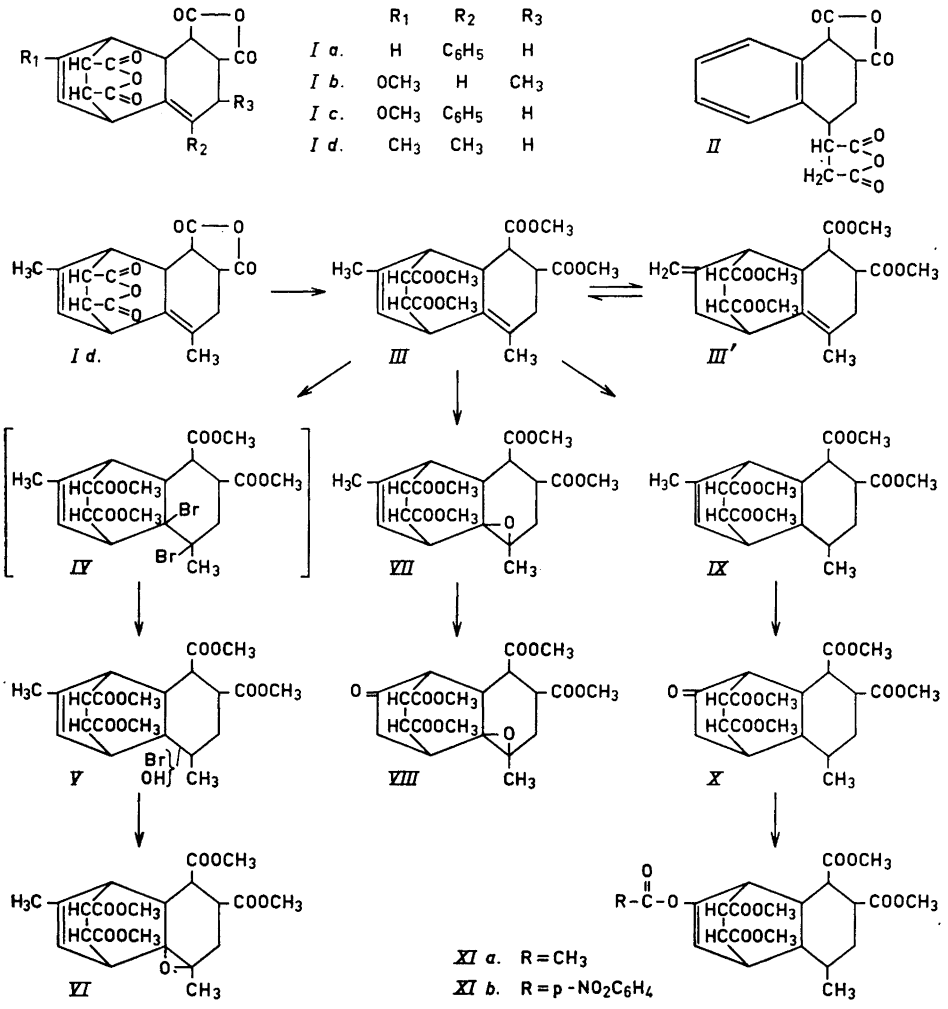

In this paper the addition reactions to the bis-adduct (Id) are further examined. Owing to the easier accessibility by addition reagents and better solubility the tetramethyl ester (III) was used in most experiments. It was prepared by alkaline hydrolysis of the bis-adduct (Id) and methylation of the resulting tetracarboxylic acid by diazomethane. For ascertaining that no change in the position of the double bonds was brought about by the use of strong alkali, the conversion was made in another way also. By methanolysis of the dianhydride and subsequent treatment with diazomethane a monoanhydride dimethyl ester was obtained. This compound, after repetition of the procedure, yielded a tetramethyl ester. It turned out that this ester was identical with the one made by the method including alkaline hydrolysis.

Upon bromination of the tetramethyl ester (III) in carbon tetrachloride solution exactly one molar equivalent of bromine was added. With more bromine the solution turned yellow. It was impossible to isolate the dibromo compound (IV). If, however, the bromination product after evaporation of the solvent was treated with moist methanol, a bromohydrine (V) was obtained. In the formula the mutual orientation of the Br and OH substituents to the double bond is not known. Even the bromohydrine proved rather labile. Upon crystallization from methanol it suffered a loss of one molecule of hydrogen bromide yielding an epoxide (VI). This behaviour is readily understood by considering the tertiary position of the bromine atom in the bromohydrine.

When the tetramethyl ester (III) ($C_{22}H_{28}O_8$) was oxidized with excess of perbenzoic acid in chloroform solution in the cold, exactly one equivalent of active oxygen was consumed and a monoepoxide (VII) ($C_{22}H_{28}O_9$) was the only product that could be isolated (yield 82 %). This epoxide was isomeric but not identical with the one (VI) formed from the bromohydrine by the loss of hydrogen bromide. It proved saturated to bromine and tetranitromethane. So the double bond attacked in both cases must be one and the same and the two epoxides are stereoisomers. When the oxidation was carried out at room temperature, a by-product was isolated along with the epoxide (VII). For this by-product a formula $C_{21}H_{26}O_{10}$ was found by analysis. This same compound could be obtained from the epoxide (VII) by ozonization. The molecular formula of the by-product differs from that of the epoxide by loss of CH_2 and gain of one oxygen atom. For the structure of this compound, see later.

In an attempt to convert the tetramethyl ester (III) into a naphthalene derivative, catalytic hydrogenation formed the first link of the reaction sequence. It was namely intended, after protection of the double bond in the side ring by selective catalytic hydrogenation, to cleave the bicyclo-octene ring system at the other double bond and aromatize the resulting decahydronaphthalene derivative by dehydrogenation. Unfortunately, only the step comprising hydrogenation could be realized. In accordance with earlier statements this adduct also was totally inert to hydrogenation with platinum or palladium catalysts at room temperature and atmospheric or elevated pressure. But when Raney nickel was used as catalyst and the hydrogenation carried out at 105°C and 90 atm. pressure, a dihydro derivative (IV) was readily obtained in a yield of about 70 %. Just as the epoxides this compound, too, proved saturated to bromine and tetranitromethane. All attempts to cleave the bicyclo-octene double bond by oxidation with nitric acid, potassium permanganate or ozone failed. Either unchanged material was recovered or total destruction of the molecule resulted. The only oxidation product that could be isolated was obtained by ozonization. Ozone was consumed very slowly at the temperature of solid carbon dioxide. When an amount of ozone equivalent to two double bonds was passed in, 60 % of the starting material was recovered unchanged. From the reacted material an ozonization product with the molecular formula $C_{21}H_{28}O_9$ was isolated in a yield of 40 %. The formation of this compound from the dihydrotetramethyl ester ($C_{22}H_{30}O_8$) is accordingly exactly analogous with the behaviour of the epoxide (VII) on ozonization. The formation of the ozonization product in both cases may be explained, if a methyl-methylene

tautomerism illustrated by the formulas III and III' is assumed. On this basis the formulas VIII and X are to be derived for the ozonization product of the epoxide (VII) and dihydrotetramethyl ester (IX), respectively. This assumption is supported by the formation of an acetate (XIa) and *p*-nitrobenzoate (XIb) from the ozonization product (X). In addition, the ozonization product (X) dissolved much faster than the parent compound (IX) in dilute sodium hydroxide solution, as may be expected on the basis of keto-enol tautomerism, for which the formula X offers possibility. Besides, ample analogies for the assumed methyl-methylene tautomerism are to be found in the literature, *e.g.* in the case of some terpenes such as eudesmol [6].

It is to be noted that both of the ozonization products (VIII) and (X) were precipitated by methanol directly after evaporation of the solvent. Accordingly, a so-called "spontaneous decomposition of ozonide" [7] should be involved here.

EXPERIMENTAL

Conversion of the dianhydride (Id) into the tetramethyl ester (III). A suspension of 84 g of the dianhydride (Id) in 840 ml of methanol was refluxed until all was dissolved (20 h). From this solution no crystalline compound could be isolated. It was methylated with an ethereal solution of diazomethane. The bulk of the product, 73.6 g, m.p. 170—185°, crystallized almost immediately. Once recrystallized from acetone the compound was obtained as coarse, colorless crystals, m.p. 192—194°. (Found: C 64.30; H 6.07. Calc. for $C_{20}H_{22}O_7$: C 64.16; H 5.92).

On the basis of the above analysis the product must be a monoanhydride dimethyl ester. Which of the two anhydride rings had opened, remained unsettled. The product was difficultly soluble in methanol, even in hot methanol. It dissolved readily in chloroform. This solution did not decolorize bromine. The product dissolved slowly in dilute sodium hydroxide at room temperature.

The monoanhydride dimethyl ester was converted almost quantitatively into the tetramethyl ester (III) by refluxing for 2 days in methanol and subsequent methylating with ethereal diazomethane.

Bromination of the tetramethyl ester (III). Bromohydrine (V). Epoxide (VI). To a solution of 1.0 g of the tetramethyl ester (III) in 10 ml of carbon tetrachloride was added with stirring 380 mg (equivalent to one double bond) of bromine in 9 ml of carbon tetrachloride while the reaction mixture was cooled in an ice-salt bath. During the addition an amorphous brownish precipitate formed. It was filtered off and discarded. After evaporation of the fuming (HBr) solvent a porous resin remained. Upon trituration with moist methanol it deposited the bromohydrine as white crystals. The yield was 432 mg, m.p. about 130° (decomp.). (Found: C 51.62; H 5.49; Br 15.80. Calc. for $C_{22}H_{29}BrO_9$: C 51.18; H 5.66; Br 15.43.)

Upon attempting to crystallize the above bromohydrine from methanol a clear solution was obtained in the hot, but almost immediately a copious amount of colorless crystals separated. These were filtered and dried. The yield was 300 mg, m.p. 196—199° (without decomp.). The test for unsaturation with bromine in chloroform solution was negative. For this compound an epoxide structure was indicated by the lack of bromine. (Found: C 60.37; H 6.35. Calc. for $C_{22}H_{28}O_9$: C 60.54; H 6.47.)

Oxidation of the tetramethyl ester (III) with perbenzoic acid. Epoxide (VII). To a solution of 18.4 g of the tetramethyl ester (III) in 92 ml of chloroform there was added 6.49 g (1.07 equivalents) of perbenzoic acid in 90 ml of chloroform, while the reaction mixture was stirred and cooled in an ice-salt bath. After standing for 24 h at −12°C the perbenzoic acid content of the solution was determined. It appeared that the consumption of the active oxygen corresponded exactly to one double bond. The solution was diluted with ether and washed first with aqueous bicarbonate, then with water. The solvent was evaporated and the solidified residue crystallized from methanol. The yield of the epoxide, m.p. 169—171°, was 15.7 g (82 %). Once recrystallized from methanol the m.p. was unchanged. (Found: C 60.76; H 6.56. Calc. for $C_{22}H_{28}O_9$: C 60.54; H 6.47.)

In another experiment, where 2 g of the tetramethyl ester (III) were oxidized with excess of perbenzoic acid at room temperature, in addition to the epoxide (VII) 265 mg of a by-product, m.p. 215—230°, was obtained. Upon recrystallization from acetone this compound formed large, rectangular plates, m.p. 231—235°. (Found: C 57.42; H 5.92. Calc. for $C_{21}H_{26}O_{10}$: C 57.53; H 5.98.)

Ozonization of the epoxide (VII). Ozonization product (VIII). 5.0 g of the epoxide (VII) were dissolved in 100 ml of chloroform. Ozonized oxygen containing 5.3 % by volume of ozone was passed through this solution with cooling in dry-ice. After absorption of an amount of ozone equivalent to one double bond the solution was evaporated to dryness at room temperature *in vacuo*. The residue, a porous solid, was dissolved in 50 ml of methanol. After a while white crystals begin to separate, yield 1.77 g, m.p. 207—215°. After recrystallization from acetone the compound was obtained as large, rectangular plates, m.p. 230—235°. From the mother liquor of the first fraction a second crop of crystals, m.p. 225—233°, was obtained. The combined yield of the ozonization product was 41 %. (Found: C 57.50; H 5.96. Calc. for $C_{21}H_{26}O_{10}$: C 57.53; H 5.98.)

The ozonization product (VIII) was proved by mixed melting point determination and infrared absorption spectrum to be identical with the above by-product obtained from the tetramethyl ester (III) by excess of perbenzoic acid at room temperature.

Hydrogenation of the tetramethyl ester (III). Dihydrocompound (IX). 10.0 g of the tetramethyl ester (III) in 300 ml of absolute ethanol was hydrogenated for 36 h at 105° and 90 atm. pressure over 3 g of Raney nickel catalyst. After cooling the catalyst was filtered off and the filtrate concentrated. Large, colorless prisms separated. The yield of the hydrogenation product was 7.45 g (74 %), m.p. 156—158°. From the mother liquor 1.47 g of the unchanged starting material, m.p. 120—122°, was recovered. Once recrystallized from methanol the first compound melted at 158—159°. (Found: C 62.60; H 7.20. Calc. for $C_{22}H_{30}O_8$: C 62.54; H 7.16.)

The dihydrocompound was readily soluble in chloroform. The chloroform solution proved saturated toward bromine and tetranitromethane.

Ozonization of the dihydrocompound (IX). Ozonization product (X). Ozonized oxygen was passed through a solution containing 4.72 g of the dihydrocompound (IX) in 100 ml of chloroform with cooling in dry-ice. From the beginning only about a half of the ozone was absorbed. After absorption of one equivalent the ozonization was interrupted. The solvent was evaporated at room temperature *in vacuo*. The residue, a colorless, viscous liquid, was dissolved in methanol. After a while small, colorless crystals, 1.95 g, m.p. 157 158°, separated. This first fraction was shown to be unchanged starting material by mixed melting point determination. From the mother liquor another compound, 0.96 g, m.p. 185—190°, was obtained. It was recrystallized from methanol to give white leaflets, m.p. 191—193°. (Found: C 59.30; H 6.61. Calc. for $C_{21}H_{28}O_9$: C 59.42; H 6.65.)

The ozonization product, contrary to the starting material, dissolved rather readily in dilute sodium hydroxide at room temperature. It was readily soluble in chloroform. The chloroform solution did not decolorize bromine. The test for double bond with tetranitromethane was also negative. The compound did not form an oxime or a semicarbazone.

The acetate (XIa). A mixture of 200 mg of the ozonization product (X), 100 mg of anhydrous sodium acetate and 1 ml of acetic anhydride was refluxed for 1 h. The reaction product was poured in water and extracted with chloroform. The chloroform solution was washed with aqueous sodium bicarbonate and water and evaporated to dryness. Upon trituration with methanol 159 mg of colorless crystals, m.p. 133—134° separated. (Found: C 58.95; H 6.58. Calc. for $C_{23}H_{33}O_{10}$: C 59.22; H 6.48.)

The p-nitrobenzoate (XIb). A mixture of 200 mg of the ozonization product (X) and 120 mg of *p*-nitrobenzoyl chloride in 5 ml of pyridine was refluxed for 1 h. After cooling ether was added. The formed precipitate was brought into solution by means of a few drops of chloroform. After standing for several days 151 mg of yellowish crystals, m.p. 199—205°, separated from the solution. Once recrystallized from a mixture of methanol and acetone small, rectangular plates, m.p. 204—206°, were obtained. (Found: N 2.60. Calc. for $C_{28}H_{31}NO_{12}$: N 2.44.)

REFERENCES

1. Wagner-Jauregg, Th. *Ann.* **491** (1931) 1.
2. Bruckner, V. and Kovács, J. *J. Org. Chem.* **14** (1949) 65.
3. Bruckner, V., Kovács, J. and Huhn, P. *J. Org. Chem.* **16** (1951) 1649.
4. Alder, K. and Schmitz-Josten, R. *Ann.* **595** (1955) 1.
5. Hukki, J. *Ann. Acad. Sci. Fennicae, Ser. A II.* (1952) No. 44.
6. Simonsen, J. *The Terpenes*, Vol. III (1952) 150.
7. Ruzicka, L., Seidel, C., Schinz, H. and Tavel, Ch. *Helv. Chim. Acta* **31** (1948) 257.

Received November 18, 1961.

ACTA CHEMICA SCANDINAVICA 16 (1962) 843–848

A Simple Adsorption Chromatographic Method for the Investigation of Phenolic Structures *

BENGT SMITH

Institutionen för Organisk Kemi, Chalmers Tekniska Högskola, Göteborg, Sweden

A simple adsorption chromatographic method is described which permits a rapid investigation of phenolic structures with the aim of determining the type of phenol and the position of substituents.

Several methods have been utilized for the separation of phenolic mixtures and in the investigation of phenolic structures, *e.g.* paper chromatography [5], gas chromatography [6], electrophoresis [7] and thin layer chromatography [8,9]. Recently an adsorption chromatographic study of steric hindrance in *ortho*-substituted alkyl phenols was made by Carlton and Bradbury [10]. It was shown that the adsorption of this type of phenol on silica gel was considerably influenced by the size and position of the alkyl groups. Since there is a lack of simple methods for the determination of the position of alkyl groups and other groups in phenols, it was decided to investigate the general usefulness of adsorption chromatography on silica gel for this purpose. A novel technique for the detection of the position of the phenol on the column was also developed.

EXPERIMENTAL

Materials. Most of the phenols utilized in this investigation were of commercial origin. Their purity was ascertained by melting point or boiling point determinations and they were, if necessary, recrystallized or redistilled. Silica gel, 100–200 mesh, was used without any pretreatment. The elution was made using "benzene crystallisable". Phenol solutions were made up by dissolving 0.01 g of the phenol in 1 ml of benzene. The permanganate solution used for the detection of the position of the phenols was prepared by dissolving 0.01 mole of potassium permanganate in 1 000 ml of 0.5 % sulphuric acid.

Procedure (*cf.* Fig. 1). A plug of cotton wool was inserted at the end of a glass tube, 6 mm outside diameter and 200 mm long. A dropping tube drawn out to a capillary was placed in the middle of the chromatographic tube and silica gel was then packed to a height of 150 mm.

* Paper No. 5 in a series on analytical investigations of phenols and phenol derivatives. For previous papers, *cf.* Refs. [1-4].

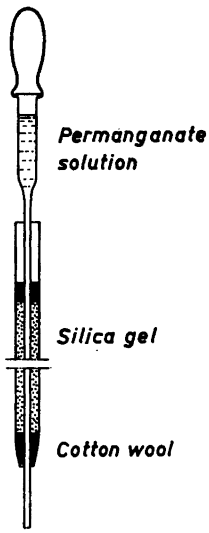

Fig. 1. Equipment used for the determination of R_F-values of phenols.

The dropping tube was filled with permanganate solution. One drop of the benzene solution of the phenol (containing about 100 μg of the phenol) was placed on the top of the column. Elution with benzene was started and allowed to proceed until the solvent reached the bottom of the column. A plug of cotton wool was put on the top of the column in order to hold the silica gel in place during the subsequent withdrawal of the dropping tube. The dropping tube was slowly drawn out and, at the same time, a stream of permanganate solution was evenly ejected into the silica gel layer. At the position of the phenol, the red colour of the permanganate was changed to a nuance between redish-yellow and brown. In some instances the colour disappeared completely. The distance from the middle of the phenolic zone to the beginning of the silica gel layer was measured and the R_F-values were calculated.

The method used for the detection of the position of the phenols was preferred to an extrusion of the column of adsorbent since it was more easy to handle, especially by inexperienced personnel.

RESULTS AND DISCUSSION

The results of the investigation are summarized in Table 1.

Alkylphenols (Nos. 1—18). The influence of *ortho*-situated alkyl groups on the R_F-values of alkylphenols is in accordance with the results obtained by Carlton and Bradbury [10]. The dominating effect seems to be a steric one and the influence of alkyl groups elsewhere than in the *ortho* position is almost negligible (*cf.* however, carvacrol below). As a consequence of different particle size and quality of the silica gel used, the R_F-values obtained here are different from those reported by Carlton and Bradbury [10]. Monohydric alkylphenols without substituents in the *ortho* position have R_F-values between 0.14 and 0.19. One methyl group in the *ortho* position raises the R_F-values to about 0.25 and, with two methyl groups in the *ortho* position, an increase to about 0.40 is obtained. The R_F-values also increase with an increase in the size of the group as shown by the series, *o*-cresol (0.26) — thymol (0.34) — 2,4-di*tert.*-butyl-*m*-cresol (0.70). Two *tert.*butyl groups in the *ortho* position completely

Table 1. R_F-values of various phenols.

No.	Compound	R_F	No.	Compound	R_F
1.	Phenol	0.17	37.	Picric acid	0.20
2.	*m*-Cresol	0.17	38.	*p*-Hydroxydiphenylether	0.17
3.	*p*-Cresol	0.16	39.	*o*-Hydroxydiphenylether	0.35
4.	*p-tert.*-Butylphenol	0.17	40.	Resorcinolmonomethylether	0.12
5.	3,4-Xylenol	0.17	41.	Hydroquinonemonomethylether	0.08
6.	3,5-Xylenol	0.19	42.	Guaiacol	0.30
7.	*o*-Cresol	0.26	43.	Eugenol	0.30
8.	2,3-Xylenol	0.25	44.	Isoeugenol	0.30
9.	2,4-Xylenol	0.26	45.	2,4-Dihydroxyanisol	0.07
10.	2,5-Xylenol	0.27	46.	*m*-Hydroxybenzaldehyde	0.05
11.	2,3,5-Trimethylphenol	0.25	47.	*p*-Hydroxybenzaldehyde	0.04
12.	Carvacrol	0.30	48.	*o*-Hydroxybenzaldehyde	0.30
13.	Thymol	0.34	49.	2,4-Dihydroxybenzaldehyde	0.07
14.	2,4-Di*tert.*-butyl-*m*-cresol	0.70	50.	3,4-Dihydroxybenzaldehyde	0.01
15.	2,6-Xylenol	0.43	51.	*p*-Hydroxyacetophenone	0.03
16.	2,4,6-Trimethylphenol	0.39	52.	*p*-Hydroxypropiophenone	0.02
17.	2,6-Di*tert.*-butylphenol	1.00	53.	*o*-Hydroxyacetophenone	0.22
18.	2,2-Bis(*p*-hydroxyphenyl)-propane	0.07	54.	2,4-Dihydroxyacetophenone	0.02
			55.	*m*-Hydroxybenzoic acid	0.04
19.	*o*-Allylphenol	0.41	56.	*p*-Hydroxybenzoic acid	0.02
20.	*p*-Hydroxydiphenyl	0.19	57.	Salicylic acid	0.06
21.	*o*-Hydroxydiphenyl	0.39	58.	3,4-Dihydroxybenzoic acid	0.02
22.	*o,o'*-Dihydroxydiphenyl	0.11	59.	Gallic acid	0.01
23.	α-Naphthol	0.25	60.	*m*-Hydroxymethylphenol	0.01
24.	β-Naphthol	0.20	61.	*p*-Hydroxymethylphenol	0.02
25.	*m*-Chlorophenol	0.28	62.	*o*-Hydroxymethylphenol	0.04
26.	*p*-Chlorophenol	0.25	63.	2,6-Dimethyl-4-hydroxymethyl-phenol	0.01
27.	*p*-Chloro-*m*-cresol	0.27			
28.	*o*-Chlorophenol	0.42	64.	2,5-Dimethyl-4-hydroxymethyl-phenol	0.05
29.	2-Chloro-5-methylphenol	0.42			
30.	2,4-Dichlorophenol	0.45	65.	Resorcinol	0.03
31.	2,4,5-Trichlorophenol	0.46	66.	Hydroquinone	0.02
32.	*o*-Bromophenol	0.46	67.	Pyrocatechol	0.06
33.	2,4,6-Tribromophenol	> 0.70	68.	Phloroglucinol	0.02
34.	*m*-Nitrophenol	0.04	69.	Pyrogallol	0.04
35.	*p*-Nitrophenol	0.06	70.	*p*-Aminophenol	0.02
36.	*o*-Nitrophenol	0.40	71.	*o*-Aminophenol	0.02

inhibit the adsorption of the phenol on silica gel (*cf.* No. 17). There seems to be a slight steric influence from larger alkyl groups in the *meta* position as evidenced by the high R_F-value obtained for carvacrol (No. 12) in comparison with that obtained for 2,5-xylenol (No. 10). It is of interest to note that, for 2,2-bis-[*p*-hydroxyphenyl]-propane (No. 18), the presence of two hydroxyl groups is indicated by the low R_F-value.

Alkenylphenols, diphenylols and naphthols (Nos. 19—24). The position of the hydroxyl group in the diphenylols is clearly reflected by the R_F-values. The unexpectedly large R_F-value for *o*-allylphenol might be due to internal hydrogen bonding to the allyl group [11]. Similarly, the R_F-value of *o*-hydroxydiphenyl might be influenced by internal hydrogen bonding to the phenyl

group [12,13]. In the naphthols, the proximity of the fused benzene ring makes the R_F-value of α-naphthol slightly higher than that of β-naphthol.

Halophenols (Nos. 25—33). Introduction of a chlorine atom in the *meta* or *para* position relative to the phenolic hydroxyl group increases the R_F-values. This fact throws some light on the way in which the bonding of the halophenols to the surface of the adsorbent takes place. The adsorption of the phenol might occur in several ways. There may be formed a hydrogen bond between the hydrogen atom of the phenolic hydroxyl group and an oxygen atom of the silica gel (Ar—O—H ← O—Si). A hydrogen bond could also be developed the other way, *i.e.* between a hydrogen atom of a hydroxyl group bonded to silicon and the oxygen atom of the phenolic hydroxyl group (Ar—O→ H—O—Si). Other bonding possibilities could arise from the coordination of oxygen or the aromatic ring to silicon. Solvent effects may also influence the adsorption process *.

Because halogen atoms increase the acidity of phenols, the R_F-values should decrease, on account of increased hydrogen bonding, upon substitution of halogen atoms for hydrogen in the phenolic ring if the first bonding alternative dominated. Since an increase is observed, the conclusion seems to be justified that hydrogen bonding from the hydrogen atom of the phenolic hydroxyl group to the adsorbent is not predominant in this case. An interaction between the halogen atom and the adsorbent, obviously, does not need to be considered. The steric effect of *ortho* substitution is considerable, the R_F-values being raised from 0.25—0.28 for chlorophenols with unoccupied *ortho* positions to 0.42—0.46 for chlorophenols with a chlorine atom in one of the *ortho* positions and the other unoccupied.

Nitrophenols (Nos. 34—37). While an increase in the R_F-values followed from a substitution of chlorine atoms for hydrogen *meta* and *para* to the phenolic hydroxyl group, the reverse was observed for nitro groups. Thus, *m*- and *p*-nitrophenol have lower R_F-values than phenol. This fact might, at least in part, be connected with an interaction between the nitro group and the adsorbent. That picric acid has a lower R_F-value than *o*-nitrophenol is also in accordance with this view.

Phenols with various oxygen-containing functional groups and aminophenols (Nos. 38—71) **. A number of phenols with various oxygen-containing functional groups as well as several hydroxyl groups have also been studied. The following groups were considered: Methoxy, phenoxy, formyl, keto, carboxyl and hydroxymethyl. In addition, some aminophenols were investigated.

All these groups confer on the phenol additional possibilities of bonding to the adsorbent. Accordingly, the R_F-values generally are low except in certain instances when the adsorption through the phenolic hydroxyl group is decreased by internal hydrogen bonding to and/or steric hindrance by a

* Attempts to develop formulae for calculating R_F-values for various phenols eluted from silica gel have been made but have not been quite successful [14,15].

** See also Nos. 18 and 22.

functional group in the *ortho* position. This is exemplified by guaiacol, eugenol and isoeugenol (Nos. 42—44), which have a methoxy group in the *ortho* position to the phenolic hydroxyl group and further by *o*-hydroxybenzaldehyde and *o*-hydroxyacetophenone (Nos. 48 and 53). In these cases, the *ortho* position of the functional group is indicated by the high R_F-values. In other instances, however, *ortho* substitution causes only a minor increase in the R_F-values. Thus, a hydroxyl, carboxyl, hydroxymethyl or amino group in the *ortho* position is difficult to trace by means of the R_F-value. In the hydroxydiphenylethers, the presence of the ether oxygen atom hardly influences the R_F-values as indicated by a comparison of the values obtained for *o*- and *p*-hydroxydiphenylether (Nos. 38 and 39) and *o*- and *p*-hydroxydiphenyl (Nos. 20 and 21).

Analytical use. The analytical usefulness of the present adsorption chromatographic method is evident from the preceding discussion. Especially, when combined with other physical and chemical investigation methods, it may give valuable information concerning the structures of phenols.

It is seen that, for alkylphenols, halophenols and certain types of phenols with oxygen-containing functional groups, the R_F-values give a clear indication of the presence of substituent groups in the *ortho* position relative to the phenolic hydroxyl group. Previously, a method for the determination of the number of free *ortho* and *para* positions in phenols has been developed by the present author [3]. This method, however, does not permit any decision as to whether a vacant position is placed *ortho* or *para* to the phenolic hydroxyl group. An additional adsorption chromatographic test, as described here, would in many cases give the required information. For 2,4,6-trialkylphenols, it was found that the justmentioned method, which was based on a bromide-bromate titration, gave erroneous results because of the tendency of these phenols to consume bromine despite the absence of vacant *ortho* and *para* positions. The present adsorption chromatographic method could not help to solve this problem since it is generally not possible to decide from the R_F-values whether an alkyl group is situated in the *meta* or *para* position. One might, for example, expect 2,4,6- and 2,3,6-trimethylphenol to have approximately the same R_F-values. There are, however, chemical methods by which the presence of a vacant *para* position may be proved *.

The presence of several phenolic hydroxyl groups in a molecule gives rise to a low R_F-value. This fact may be utilized for tracing the occurrence of phenolic hydroxyl groups in the *meta* position for which the available chemical tests are less reliable than for phenolic hydroxyl groups in the *ortho* and *para* positions. Similarly, the presence of several hydroxyl groups in phenols like 2,2-bis-[*p*-hydroxyphenyl]-propane (No. 18) is not easily proved by chemical tests but is indicated by the low R_F-value.

Acknowledgement. This work was supported by a grant from the *Town Council of Gothenburg.*

* To be described in a forthcoming paper.

REFERENCES

1. Smith, B. *Acta Chem. Scand.* **10** (1956) 1589.
2. Smith, B. *Acta Chem. Scand.* **11** (1957) 558.
3. Smith, B. *Acta Chem. Scand.* **11** (1957) 839.
4. Smith, B. and Haglund, Å. *Acta Chem. Scand.* **14** (1960) 1349.
5. Reio, L. in Lederer, M. (Ed.) *Chromatographic Reviews*, vol. I, p. 39. Elsevier Publ. Co., Amsterdam 1959.
6. Kreyenbuhl, A. and Weiss, H. *Bull. soc. chim. France* **1959** 1880.
7. Pridham, J. B. *J. Chromatography* **2** (1959) 605.
8. Wagner, G. *Die Pharmazie* **10** (1955) 302.
9. Pastuska, G. *Fresenius Z. f. Analyt. Chem.* **179** (1961) 355.
10. Carlton, J. K. and Bradbury, W. C. *J. Am. Chem. Soc.* **78** (1956) 1069.
11. Baker, A. W. and Shulgin, A. T. *J. Am. Chem. Soc.* **80** (1958) 5358.
12. Wulf, O. R., Liddel, U. and Hendrichs, S. B. *J. Am. Chem. Soc.* **58** (1936) 2287.
13. Lüttke, W. and Mecke, R. *Z. physik. Chem.* **196** (1950) 56.
14. LeRosen, A. L., Monaghan, P. A., Rivet, C. A. and Smith, E. D. *Anal. Chem.* **23** (1951) 730.
15. LeRosen, A. L., Carlton, J. K. and Moseley, P. B. *Anal. Chem.* **25** (1953) 666.

Received November 14, 1961.

ACTA CHEMICA SCANDINAVICA 16 (1962) 849–854

Anion-Exchange Study

I. Adsorption of Some Elements in HBr-Solutions

TORKILD ANDERSEN and A. BYE KNUTSEN

Institute of Chemistry and Institute of Physics, University of Aarhus, Aarhus, Denmark

The anion exchange behaviour of some elements with 18-electron configuration and of Al, Re, Th, Pa, and U was studied in HBr-solutions. Negligible adsorption was shown by Al(III) and Th(IV). Zn(II), Ga(III), Ge(IV), Re(VII), Pa(V), and U(VI) were adsorbed less from HBr-solutions than from HCl-solutions contrary to Cd(II), Hg(II), In(III), Tl(III), Sn(IV), Pb(II), and Sb(III). Improved separation methods are offered for groups of these elements in comparison to earlier HCl-methods.

Recently anion exchange has obtained a widespread application in analytical and nuclear chemistry for separations of the chemical elements. Kraus and Nelson [1] have presented a comprehensive study of the adsorption of the elements by strong base anion resin as a function of the HCl-concentration. Anion exchange data were reported for a number of metals in HF [2] and in mixtures of HCl—HF [3,4]. Less attention has been paid to the application of HBr. Herber and Irvine [5] studied the behaviour of bromide anion complexes of zinc, cobolt, nickel, copper, and gallium; successful separations of these elements were obtained. They indicated that the study of the bromide anion complexes could not be extended beyond ~7 N HBr due to the chemical interaction between the resin and the acid.

Cations with 18-electron configuration have a tendency to form bromo complexes rather than chloro and fluoro complexes [6]. Bromide ions are tied more strongly than chloride ions to the anion exchange resin used, Dowex 1.

In this study a comparison between the adsorption of some elements to a base anion exchange resin from HBr and HCl solutions was carried out in order to improve some of the separation methods using HCl-solutions as elutriant.

EXPERIMENTAL

The resin used was 8 % crosslinked Dowex 1, 200—400 mesh, with a capacity of 3.4 mequiv/g dry resin, in the chloride form. The resin was washed thoroughly with

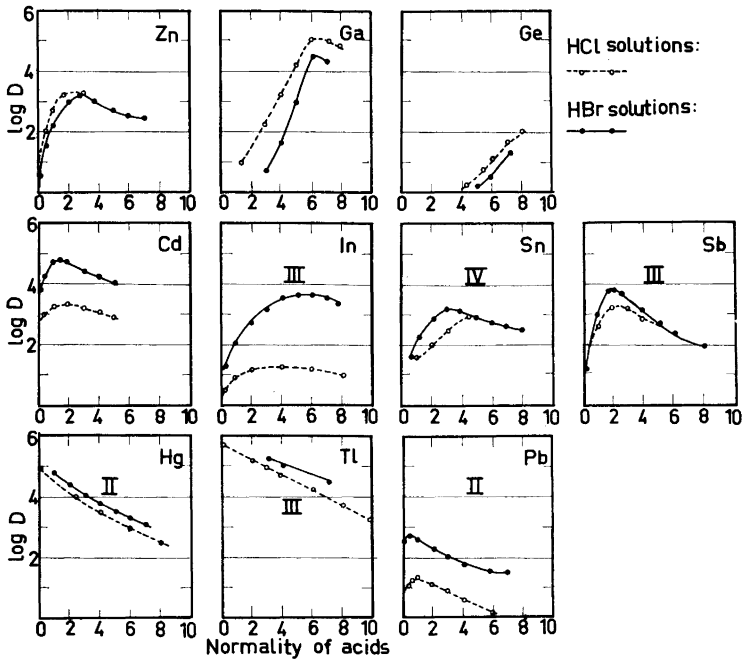

Fig. 1. Adsorption of some elements with 18 electron configuration and of Sb(III), Pb(II) from HBr and HCl solutions.

distilled water and dried at 110°C. In the HBr-investigations the resin was previously converted with HBr.

Adsorbabilities were measured by equilibration methods or column elution as described by Kraus and Nelson [3]. Usually 0.1—0.5 g resin and 5—10 ml liquid were applied. Equilibration was obtained after shaking for 18—20 h. In the case of tin 48 h, of lead 4 h, and of thallium 4 days shaking were applied.

The weight distribution coefficient, D, was calculated from radiometric analysis of the liquid phase before and after equilibration.

$$D = \frac{\text{m.equiv. metal on resin/g dry resin}}{\text{m.equiv. metal. in solution/ml solution}}$$

The volume distribution coefficient, D_v, was determined by the column elution method.

$$D_v = (V/Ad) - i$$

V = total effluent volume necessary to obtain elution peak maximum.
A = cross-sectional area of the column.
d = height of the column.
i = interstitial volume (about 0.4).

The relation between D_v and D is $D_v = D \cdot \varrho$, where ϱ is the bed density (about 0.45 kg/l).

Most of the radioactive tracers were obtained by irradiation of the metals or oxides in the Danish Atomic Energy reactor DR 2. ^{210}Pb was supplied by the Radiochemical Center, Amersham UK. The radiactive tracers were: ^{65}Zn (245 d), ^{115}Cd—^{115}In (54 h-4.5 h), ^{197}Hg (65 h), ^{72}Ga (14.1 h), ^{114}In (49 d), ^{204}Tl (4.1 y), ^{113}Sn—^{113}In(119 d—1.73 h),

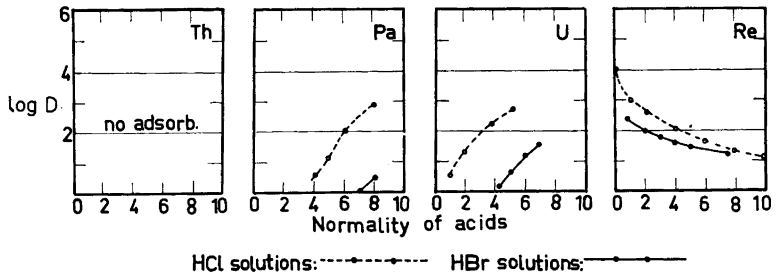

Fig. 2. Adsorption of thorium, protactinium, uranium, and rhenium from HBr and HCl solutions.

^{124}Sb (60 d), and ^{186}Re (91 h). ^{210}Pb was separated from ^{210}Bi by ion exchange [1], and ^{234}Th (24.1 d) from uranium [9]. ^{233}Pa (27 d), formed by neutron irradiation of thorium, was purified by ion exchange [1].

All tracers were converted to bromide form with HBr. Aluminium was dissolved in HBr, germanium dioxide in 2 N NaOH. Uranium nitrate was converted to UO_3 and dissolved in HBr.

^{204}Tl, which is a pure β-emitter, was determined by evaporating aliquots of the liquid phase on polyethylene plates and counted with an endwindow G—M counter. The relative amounts of the other radioactive tracers were determined by a well type scintillation counter. Aluminium was detected with alizarinsulphonic acid [7], germanium with benzidine [8]. Uranium was detected by the yellow colour of the UO_2++-ions.

RESULTS

The logarithms of the distribution coefficients are presented in Figs. 1—2 as a function of hydrobromic acid or hydrochloric acid normality.

Zn(II), Cd(II), Hg(II)

The adsorption of Zn(II) is less in HBr-solutions than in HCl-solutions contrary to Cd(II) and Hg(II). Zn shows significant adsorption at concentrations $> 10^{-1}$N, while Cd is adsorbed at very small concentrations ($< 10^{-3}$ N HBr). Mercury is strongly adsorbed in HBr as well as in HCl-solutions in the concentration range 1—7 N acid.

Separation of Zn—Cd and Zn—Hg is possible on Dowex 1 with HBr as elutriant.

Zn—Cd: Approximately 0.1 ml 2 N HBr containing ^{65}Zn and ^{115}Cd—^{115}In tracers was passed into a 5 cm column with a cross-section of 1 mm^2. Zn was eluted with 0.1 N HBr; Cd was eluted with 4 N HNO_3 as it could not be removed successfully with very dilute HBr-solutions.

Al(III), Ga(III), In(III), Tl(III)

Cations with rare gas electron configuration prefer to form fluoride anion complexes to chloride and bromide complexes [6]. Kraus *et al.*[10] have reported that the alkali metals, the alkaline earths and Al, Y, La, and Yb of group III show no adsorption in HCl.

As a representative of these elements Al showed no adsorption in HBr. The elution constant $E = Axd/V = (i + D_v)^{-1}$ was 2.2—2.3 in the concentration range 1—7 N HBr. Axd is the column volume, V the total effluent volume to reach elution peak maximum. $E = 2.2—2.5$ indicates no adsorption. Herber and Irvine [5] reported that Ga(III) chloride anion complexes are formed at lower halid concentration than bromide anion complexes. Ga(III) is adsorbed in 1 N HCl, but shows no adsorption in HBr-solutions at concentrations lower than 3 N.

In(III) is adsorbed strongly in HBr-solutions contrary to HCl-solutions. The adsorption function of In(III) in HBr rises rapidly with increasing acid concentration.

Thallium was investigated only in the valence state (III). Contrary to Horne [11] Kraus *et al.*[4,10] have shown that Tl(I) is not adsorbed in HCl solution. Reduction of Tl(III) was prevented by addition of bromine or chlorine to the batch samples. It is difficult to obtain exact results on account of the high distribution coefficients, $\sim 10^5$. According to Horne [11] the bromine anion complexes are tied more strongly to the resin than the chloride anion complexes.

Separation of Al(III), Ga(III), In(III), and Tl(III)

Kraus *et al.*[10] separated Al—Ga—In—Tl by means of anion exchange and HCl-elution. Using HBr rather than HCl-solutions as elutriant the separation of Al(III), Ga(III), In(III), and Tl(III) is both faster and better, and smaller columns can be used. The complete separation of Ga—In was confirmed by following the decay of ^{72}Ga. Its half-life was found to be 14.1 h ± 0.1 h. Kraus *et al.* eluted thallium with HNO_3 or $HClO_4$, but these acids do not give a liberation of Tl from the resin in bromide form. However, it is possible to remove thallium from the column with a few column volumes of a 5 % Na_2SO_3-solution (Fig. 3).

Ge(IV), Sn(IV), Pb(II), and Sb(III)

The adsorption of Ge(IV) in HBr occurs at concentrations higher than 5 N, and for HCl at concentrations higher than 3 N. Near 7 N HBr the adsorp-

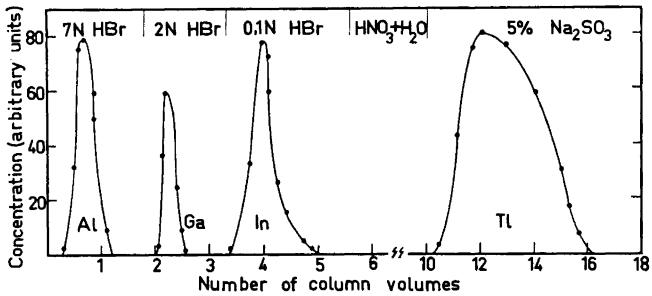

Fig. 3. Separation of Al(III), Ga(III), In(III), and Tl(III) by anion exchange.

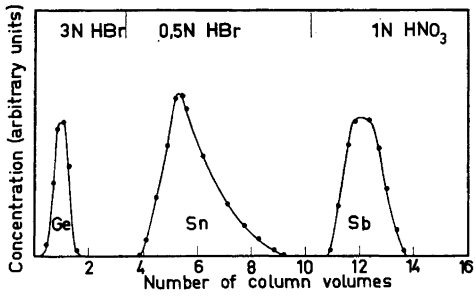

Fig. 4. Separation of Ge(IV), Sn(IV), and Sb(III) by anion exchange.

tion is sufficient to allow separation of germanium from elements which are not adsorbed (*e.g.* aluminium). Tin was only studied in the valence state (IV) because of the oxidation of Sn(II) on the resin. Kraus *et al.*[12] have shown that Sn(IV) is strongly adsorbed in HCl. The authors were not able to reproduce the distribution coefficients given by Kraus; this may be due to different loading of the resin. No investigations were carried out below 0.5 N HBr on account of hydrolysis. Fluoro- and chloro antimony(V) complexes are known, while the existence of antimony(V) bromo complexes is doubtful. Sb(III) shows significant adsorption to the resin in HBr-concentrations > 0.1 N.

Separation of Ge(IV), Sn(IV), and Sb(III) is shown in Fig. 4.

It is possible to separate two or more of the elements: Zn, Cd, Hg, Al, Ga, In, Tl, Ge, Sn, Pb, and Sb using anion exchange resin and HBr-solutions as elutriants, for example Sb(III), In(III), and Cd(II) in Fig. 5.

Th(IV), Pa(V), U(VI), and Re(VII)

Th(IV), Pa(V), and U(VI) show less adsorption to Dowex 1 in HBr- than in HCl-solutions, in agreement with the electron configuration of the ions. Ions with rare gas electron structure prefer to form chloro-complexes rather than bromo-complexes.

The lower adsorbability of Pa(V) agrees well with the lower extractability of this element from HBr than from HCl, as shown by Goble, Golden, and

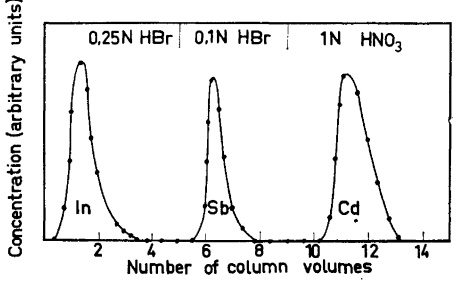

Fig. 5. Separation of Cd(II), In(III), and Sb(III) by anion exchange.

Maddock[13]. Separation of Th—Pa—U is successful with HCl-solutions as elutriant. Only the separation of Th—U and Pa—U is possible with HBr-solutions.

Rhenium shows less adsorption in HBr than in HCl-solutions. Since rhenium (VII) is difficult to remove from the resin with HCl, the application of HBr-solutions as elutriant would be an improvement.

The present results demonstrate that the application of HBr-solutions as elutriant in preference to HCl-solutions can be an advantage in some anion exchange separations. The use of HBr causes less adsorbability of cations with rare gas electron configuration. In the group of cations with 18-electron configuration Cd, Hg, In, Tl, and Sn show greater adsorption from HBr than from HCl solutions contrary to Zn, Ga, and Ge.

REFERENCES

1. Kraus, K. A. and Nelson, F. *Proc. Intern. Conf. Peaceful Uses Atomic Energy* **7** (1956) 113.
2. Faris, J. P. *Anal. Chem.* **32** (1960) 520.
3. Kraus, K. A. and Nelson, F. *A.S.T.M. Spec. Tech. Publ.* **195** (1956).
4. Nelson, F., Rush, R. M. and Kraus, K. A. *J. Am. Chem. Soc.* **82** (1960) 339.
5. Herber, R. H. and Irvine, J. W., Jr. *J. Am. Chem. Soc.* **76** (1954) 987.
6. Schwarzenbach, G. *Rec. trav. chim.* **75** (1956) 699.
7. Feigl, F. *Spot Tests*, Elsevier Publ. Co. New York 1958, p. 183.
8. Feigl, F. *Spot Tests*, Elsevier Publ. Co. New York 1958, p. 112.
9. Buchanan, R. F. and Faris, J. P. *Copenhagen Conf.* IAEA 1960, RICC/173.
10. Kraus, K. A., Nelson, F. and Smith, G. W. *J. Phys. Chem.* **58** (1954) 11.
11. Horne, R. A. *J. Inorg. Nuclear Chem.* **6** (1958) 338.
12. Kraus, K. A., Moore, G. and Nelson, F. *J. Am. Chem. Soc.* **78** (1956) 2692.
13. Goble, A., Golden, J. and Maddock, A. G. *Can. J. Chem.* **34** (1956) 284.

Received October 27, 1961.

ACTA CHEMICA SCANDINAVICA 16 (1962) 855–869

Displacements at Divalent Group VI Elements

A. J. PARKER*

Chemical Institute, University of Bergen, Bergen, Norway

Reactions, spectra and syntheses of aromatic divalent sulphur, selenium and tellurium compounds are described. Displacing tendencies at sulphur and selenium do not correlate with hydrogen or carbon basicity, and decrease in a series of bases

$C_6H_5Se^- > C_6H_5S^- > CN^- > OH^- > SO_3^{2-} > p\text{-}NO_2C_6H_4Se^- > S_2O_3^{2-} \approx p\text{-}NO_2C_6H_4S^- > p\text{-}CH_3C_6H_4SO_2S^- > C_6H_5O^-, p\text{-}NO_2C_6H_4O^-$, in 90 % ethanol-water and $C_6H_5Se^- > C_6H_5S^- > p\text{-}NO_2C_6H_4Se^- > p\text{-}NO_2C_6H_4S^- > C_6H_5O^-, p\text{-}NO_2C_6H_4O^-$ in dimethylformamide. Tellurium-basicities decrease in the same order in 90 % ethanol-water *i.e.* $C_6H_5Te^- > C_6H_5S^- > SO_3^{2-}$, $S_2O_3^{2-} > p\text{-}CH_3C_6H_4SO_2S^-$. Displacements involving multiply charged anions are strongly solvent dependent.

Methods of estimating electrophilic reactivity of divalent Group VI compounds are considered, and spectroscopic evidence for the existence of the conjugate base of *p*-nitrobenzenesulphenic acid is presented.

An investigation of displacements by bases, Y^-, at the divalent Group VI atoms, S, Se and Te (denoted collectively by M throughout this paper) has been made in order to establish whether displacements at all M atoms can be adequately described by eqn. (1) as written, for at least one combination of R, X, and Y^-. R and X are any groups satisfying the bonding requirements of divalent M.

$$RMX + Y^- \rightleftharpoons RMY + X^- \qquad (1)$$

It was of interest to compare reactivities and positions of equilibrium in (1) with similar properties of displacements at another atom such as carbon. Several questions come to mind. For example, is reaction (1) bimolecular, an S_N1-like ionization involving RM^+ as intermediate, or does it have some other mechanism, perhaps non-ionic, associated with oxidation — reduction processes? If bimolecular, what are the steric requirements of (1) and is the direc-

* Royal Norwegian Council for Scientific and Industrial Research Post-doctoral Fellow, 1960–1961; I.C.I. Research Fellow, 1961. Present address: c/o Chemistry Department, University of Western Australia, Nedlands, Western Australia.

tion of most favourable approach by Y^- such that M, X, and Y are linear [1] in the transition state? In the forward reaction (1), what are the relative reactivities (electrophilic tendencies) of RMX if M is the only variable, and what is the effect of intramolecular interactions, between different R and M, on the electrophilic tendency of RMX? What are the relative reactivities (nucleophilic tendencies) of Y^- towards different M atoms, and if Y^- is itself RM^-, what are the nucleophilic tendencies of RM^- in (1), if M (in both RMX and RM^-) is the only variable?

M-Basicities [1] of Y^- and X^-, an equilibrium controlled property, can be estimated from the equilibria (1) and compared with carbon [1] and hydrogen basicities. It was necessary to discover if M-basicities within a series of Y^- remained comparable for all kinds of M in RMX. The effect on the M-basicity of RM^-, of different M atoms, and of intramolecular interactions, between R and M, when RM^- is the displacing base, Y^-, is also of interest [1].

Finally, the influence of the reaction medium on reactivity and the equilibria should be compared with the large changes in carbon-nucleophilic tendencies [2] of Y^-, and smaller changes in carbon-basicities [1(b)], produced by the change from protic to dipolar aprotic solvent. This paper describes some broad preliminary investigations into methods of answering these questions, and reports examples of reactions based on (1). Some observations on the U.V. absorption of organic sulphur, selenium and tellurium compounds have been made and are discussed briefly.

DISCUSSION

Displacements at sulphur, selenium and tellurium, but to a lesser degree at oxygen [1], take place according to (1) provided that R- is more electropositive than —MX, —X is more electronegative than RM—, and Y^- is not a weaker M-base than X^-. Representative displacements, (2), (3), (4), in which the stoichiometry and products fit eqn. (1), have been studied here. Numerous examples exist of displacements at sulphur [1] and to a lesser extent at selenium [7,8,28]. A few displacements at divalent tellurium (5) have been reported [8,9].

$$p\text{-}NO_2C_6H_4SCl + p\text{-}CH_3C_6H_4SO_2S^- \rightarrow p\text{-}NO_2C_6H_4SS_2O_2C_6H_4CH_3\text{-}p + Cl^- \quad (2)$$

$$C_6H_5SeS_2O_2C_6H_4CH_3\text{-}p + C_6H_5S^- \rightarrow C_6H_5SeSC_6H_5 + p\text{-}CH_3C_6H_4SO_2S^- \quad (3)$$

$$C_6H_5TeS_2O_2C_6H_4CH_3\text{-}p + C_6H_5S^- \rightarrow C_6H_5TeSC_6H_5 + p\text{-}CH_3C_6H_4SO_2S^- \quad (4)$$

$$p\text{-}CH_3OC_6H_4TeS_2O_3^- + CH_3OCS_2^- \rightarrow p\text{-}CH_3OC_6H_4TeS_2COCH_3 + S_2O_3^{2-} \quad (5)$$

The reactions generally are too fast for reactivity to be measured by conventional methods, but in the few investigations of rate [3–5], they have been bimolecular, and have had low activation energies (< 14 kcal/mole). Measurable rates are obtained when the reactions have abnormally large negative entropies [6] *i.e.* low log B in the Arrhenius equation, caused by atypical solvent or salt effects.

Although rate measurements of reaction (1) were not practicable, it was hoped to answer the question of relative electrophilic tendencies of M and the effect of interactions between R and M on the reactivity of RMX, by a series of competitive reactions, (6) and (7) respectively, in a well shaken 50/50 hetero-

geneous mixture of chloroform and water, followed by spectrophotometric analysis for $RMS_2O_3^-$ in the aqueous layer and for RMX in the chloroform layer.

$$\underset{(1\ \text{mole})}{RM_1X} + \underset{(1\ \text{mole})}{RM_2X} + \underset{(1\ \text{mole})}{S_2O_3^{2-}} \rightarrow RM_1S_2O_3^- + X^- + RM_2X \quad (6)$$

$$\underset{(1\ \text{mole})}{RMX} + \underset{(1\ \text{mole})}{R^1MX} + \underset{(1\ \text{mole})}{S_2O_3^{2-}} \rightarrow RMS_2O_3^- + X^- + R^1MX \quad (7)$$

(Where X is p-$CH_3C_6H_4SO_2S$-, RM_1- is more electrophilic than RM_2- in (6) and RM- is more electrophilic than R^1M- in (7)).

The method of competitive reactions requires that unchanged RMX should not subsequently equilibrate with $RMS_2O_3^-$ and X^-, *i.e.* that the back reaction of (6) or (7) be very much slower than the forward reaction. This seemed likely since thiosulphate ion is a stronger M-base than p-toluenethiosulphonate ion (X^-) and because the back reactions of (6) or (7) should be slow because of the unfavourable entropy of reaction between two anions (*vide infra*). The products of (6) and (7) should be separated as soon as possible to prevent subsequent equilibration.

Reactions (6) and (7) were influenced by solvation and were not irreversible. In aqueous ethanol, (6) was displaced successively to the left by extraction with chloroform, in which RMX but not the ionic species was soluble. Equimolar amounts of sodium thiosulphate in water and of RMX in the same volume of chloroform, when shaken together for 5 min had an equilibrium constant of approximately 1 when R was phenyl or p-nitrophenyl, M was S, Se, or Te, and X was p-toluenethiosulphonate. Sodium sulphite behaved in the same way as sodium thiosulphate.

Despite these difficulties, competitive reactions (6) and (7) were carried out as outlined, and the aqueous layer was separated as soon as possible and analysed for $RMS_2O_3^-$ by measuring the absorption at 260—350 mμ. All possible pairs of the compounds in the following series, in chloroform, were treated with less than an equimolar amount of sodium thiosulphate in water. The relative concentrations of $RMS_2O_3^-$ found for each pair of compounds suggest an order of electrophilic reactivity towards thiosulphate ion of: p-$NO_2C_6H_4SeX \approx C_6H_5TeX > p$-$CH_3OC_6H_4TeX > C_6H_5SeX$ and of p-$NO_2C_6H_4SeX > p$-$NO_2C_6H_4SX$, where X is the p-toluenethiosulphonate group.

It is not yet possible to decide if these series reflect the electrophilic tendencies of RM- or whether the series is merely controlled by solvation differences between the various RMX and $RMS_2O_3^-$ species, or by variable solvent effects on the rates of the back reaction of (6) and (7) when RM is changed. The results are as expected, if electron withdrawal by R increases the electrophilic reactivity of RMX, and if divalent tellurium is more electrophilic than divalent selenium, than divalent sulphur. Further discussion of the reactivity series will be postponed until other reactions, based on the competitive principle, have been investigated.

The problem of M-basicity of Y^- when Y^- is RM^- in (1), and the effect on this property of intramolecular interactions between R and M in RM^-, was considered in terms of the reactions 1—23, summarized in Table 1. The reactions were carried out in a protic (ethanol) and a dipolar aprotic (dimethyl-

formamide) solvent in order to answer the question of solvent effects on basicity of RM^-. Displacements were very fast in both solvents, so it was not possible to measure rates of reaction, and observe the effect of solvent on reactivity.

The more general question, of relative displacing tendencies at divalent sulphur, selenium and tellurium for a series of Y^-, was investigated by a study of reactions 1—68, Table 1. These reactions unless described as slow, equilibrated before measurements could be made *i.e.* < 1 min after mixing equimolar proportions of the reactants at approximately 10^{-4} M in 90 % ethanol-water. At least one, and usually two, of the reactants or products was analysed spectrophotometrically, and the concentrations at equilibrium of these species are recorded in Table 1 as moles per mole of RMX initially. Reactions were performed under nitrogen, and, except for the "slow" reactions, identical analyses were obtained 5 and 30 min after mixing, confirming that equilibration was complete, or that the reactions were extremely slow. In all reactions of Table 1 and throughout this paper, Ar is *p*-nitrophenyl, and "excess" denotes a concentration > 50 moles per mole of the other reactant. "Slow" reactions had half times > 30 sec at room temperature.

Reactions 1—23 suggest an order of S and Se-basicity, for displacement of both ArS^- and $ArSe^-$ from both ArS- and ArSe- of $C_6H_5S^- \gg ArSe^- > ArS^- \gg C_6H_5O^-$, ArO^-; and for displacement of $C_6H_5S^-$ or $C_6H_5Se^-$ from C_6H_5Se- or C_6H_5S- of $C_6H_5Se^- > C_6H_5S^- \gg C_6H_5O^-$. Thiophenoxide ion did not displace $C_6H_5Te^-$ from diphenyl ditelluride, although an interaction between diphenyl ditelluride and thiophenoxide ion altered the spectrum of a mixture of the two species. An investigation of the origin of this interaction is planned.

The bases, RM^-, used in reactions 1—23, had the same relative displacing tendencies in ethanol, dimethylformamide, dimethylsulphoxide, or acetone. This demonstrates that M-basicity, equilibrium controlled, is not changed to the extent that nucleophilic tendencies of Y^- toward carbon, kinetically controlled, is changed [2] in the transfer from a protic to a dipolar aprotic solvent.

Reactions 1—23 show that electron withdrawal by R in RM^- strongly reduces the displacing tendency of RM^- at divalent selenium, and confirms [10] that the same principal influences S-basicity of RM^-. The M-basicities $RSe^- > RS^- \gg RO^-$ and $RTe^- > RS^- \gg RO^-$, decrease in the same direction as the polarizability of the Group VI elements, and with decreasing ability of RM^- to interact with the *d* orbitals of M in the electrophilic compound RMX. M-Basicities of RM^- decrease with increasing electronegativity of RM-. They do not correlate with hydrogen or carbon basicity. To illustrate, RO^- is generally a stronger carbon [35] and hydrogen base than RS^-, but, as shown here, RS^- is a much stronger M-base than RO^-. The M-basicity, $RS^- > RO^-$ correlates with the relative strengths of the S—S and O—O bonds [36] just as carbon-basicity correlates with bond strength [1(b)]. Unfortunately other bond strength data is not available.

The reactions of Table 1 show that displacing tendencies at both divalent sulphur and selenium, in 90 % ethanol, decrease in the series of bases: $C_6H_5Se^- > C_6H_5S^- > CN^- > OH^- > SO_3^{2-} > ArSe^- > S_2O_3^{2-} \approx ArS^- > CH_3C_6H_4SO_2S^- > C_6H_5O^-$, ArO^-. Displacements at tellurium were observed when synthesizing RTeX and in the competitive experiments already described. These lead to a series of tellurium-basicity of $C_6H_5Te^- > C_6H_5S^- > SO_3^{2-}$,

Table 1. Displacements $RMX + Y^- \rightleftharpoons RMY + X^-$ in 90 % ethanol-water at 20—22°, under nitrogen. Concentrations of X^- and Y^- at equilibrium are expressed as moles per mole of RMX before reaction. Reactions are fast (see text) and are between equimolar proportions of RMX and Y^- at 10^{-4} M, unless stated otherwise. Ar is *p*-nitrophenyl, prefix *n* denotes large excess of Y^-. Reaction number followed by s denotes a slow reaction.

Reaction	RMX	Y^-	$[Y^-]$ or $[RMX]^a$	X^-	$[X^-]$ or $[RMY]^b$	M-basicity
1.	ArSSAr	ArO^-	1.0	ArS^-	0.0	$ArS^- > ArO^-$
2.	ArSSAr	$C_6H_5O^-$	1.0 *	ArS^-	0.0	$ArS^- > C_6H_5O^-$
3.	ArSSAr	$ArSe^-$	0.1	ArS^-	0.9	$ArSe^- > ArS^-$
4.	ArSSAr	$C_6H_5S^-$	(0.0)	ArS^-	1.0	$C_6H_5S^- > ArS^-$
5.	$ArSSC_6H_5$	$C_6H_5S^-$	0.0 *	ArS^-	1.0	$C_6H_5S^- > ArS^-$
6.	ArSeSeAr	ArO^-	1.0	$ArSe^-$	0.0	$ArSe^- > ArO^-$
7.	ArSeSeAr	$C_6H_5O^-$	1.0 *	$ArSe^-$	0.0	$ArSe^- > C_6H_5O^-$
8.	ArSeSeAr	ArS^-	1.0	$ArSe^-$	0.0	$ArSe^- > ArS^-$
9.	ArSeSeAr	2 ArS^-	1.9	$ArSe^-$	0.1	$ArSe^- > ArS^-$
10.	ArSeSeAr	$C_6H_5S^-$	(0.0)	$ArSe^-$	1.0	$C_6H_5S^- > ArSe^-$
11.	$ArSeSC_6H_5$	$C_6H_5S^-$	0.0 *	$ArSe^-$	1.0	$C_6H_5S^- > ArSe^-$
12.	ArSeSAr	ArO^-	1.0	ArS^-	0.0	ArS^-, $ArSe^-$, $> ArO^-$
13.	ArSeSAr	$C_6H_5O^-$	1.0 *	ArS^-	0.0	ArS^-, $ArSe^- > C_6H_5O^-$
14.	ArSeSAr	ArS^-	1.0	$ArSe^-$	0.0	$ArSe^- > ArS^-$
15.	ArSeSAr	2 ArS^-	1.9	$ArSe^-$	0.1	$ArSe^- > ArS^-$
16.	ArSeSAr	$ArSe^-$	0.2	ArS^-	0.8	$ArSe^- > ArS^-$
17.	ArSeSAr	$C_6H_5S^-$	(0.0)	ArS^- + $ArSe^-$	0.8 0.2	$C_6H_5S^- > ArSe^- > ArS^-$
18.	$C_6H_5SSC_6H_5$	$C_6H_5O^-$	1.0 *	$C_6H_5S^-$	0.0	$C_6H_5S^- > C_6H_5O^-$
19.	$C_6H_5SSC_6H_5$	$C_6H_5S^-$	0.5	$C_6H_5S^-$	0.5	Exchange reaction Ref. 4.
20.	$C_6H_5SeSeC_6H_5$	$C_6H_5O^-$	1.0*	$C_6H_5Se^-$	0.0	$C_6H_5Se^- > C_6H_5O^-$
21.	$C_6H_5SeSeC_6H_5$	$C_6H_5S^-$	1.0*1.0	$C_6H_5Se^-$	0.0	$C_6H_5Se^- > C_6H_5S^-$
22.	$C_6H_5SeSC_6H_5$	$C_6H_5S^-$	1.0*1.0	$C_6H_5Se^-$	0.0	$C_6H_5Se^- > C_6H_5S^-$
23.	$C_6H_5TeTeC_6H_5$	$C_6H_5O^-$	1.0 *	$C_6H_5Te^-$	0.0	$C_6H_5Te^- > C_6H_5O^-$
24.	ArSSAr	$CH_3C_6H_4SO_2S^-$	1.0 *	ArS^-	0.0	$ArS^- > CH_3C_6H_4SO_2S^-$
25.	ArSeSeAr	$CH_3C_6H_4SO_2S^-$	1.0 *	$ArSe^-$	0.0	$ArSe^- > CH_3C_6H_4SO_2S^-$
26.	ArSSAr	SO_3^{2-}	(0.0)	ArS^-	1.0	$SO_3^= > ArS^-$
27.	ArSeSeAr	SO_3^{2-}	(0.0)	$ArSe^-$	1.0	$SO_3^= > ArSe^-$
28.	$ArSSO_3^-$	nSO_3^{2-}	1.0 *	ArS^-	0.0	see text
29.	$ArSeSO_3^-$	$n\ SO_3^{2-}$	1.0 *	$ArSe^-$	0.0	see text
30.	$ArSSO_3^-$	$n\ OH^-$	1.0 *	ArS^-	0.0	see text
31.	$ArSeSO_3^-$	$n\ OH^-$	1.0 *	$ArSe^-$	0.0	see text
32s.	$ArSSO_3^-$	$C_6H_5S^-$	(0.0)	ArS^-	1.0	$C_6H_5S^- > SO_3^{2-}$
33s.	$ArSeSO_3^-$	$C_6H_5S^-$	(0.0)	$ArSe^-$	1.0	$C_6H_5S^- > SO_3^{2-}$
34s.	$ArSSO_3^-$	$n\ CN^-$	—	ArS^-	0.2	$SO_3^= > CN^-$
35s.	$ArSeSO_3^-$	$n\ CN^-$	—	$ArSe^-$	0.2	$SO_3^= > CN^-$
36.	ArSSAr	$S_2O_3^{2-}$	(0.0)	ArS^-	1.0	$S_2O_3^= > ArS^-$
37.	ArSeSeAr	$S_2O_3^{-}$	0.7 *	$ArSe^-$	0.3	$ArSe^- > S_2O_3^{2-}$
38.	$ArSS_2O_3^-$	$n\ S_2O^2{}_3^-$	1.0 *	ArS^-	0.0	see text.
39.	$ArSeS_2O_3^-$	$n\ S_2O_3^{2-}$	1.0 *	$ArSe^-$	0.0	see text.
40s.	$ArSS_2O_3^-$	$C_6H_5S^-$	0.0 *	ArS^-	1.0	$C_6H_5S^- > S_2O_3^{2-}$
41s.	$ArSeS_2O_3^-$	$C_6H_5S^-$	0.0 *	$ArSe^-$	1.0	$C_6H_5S^- > S_2O_3^{2-}$
42.	ArSSAr	CN^-	(0.0)	ArS^-	1.0	$CN^- > ArS^-$
43	ArSeSeAr	CN^-	(0.0)	$ArSe^-$	1.0	$CN^- > ArSe^-$
44s.	ArSCN	CN^-	(0.0)	ArS^-	1.0	—
45s.	ArSeCN	CN^-	(0.0)	$ArSe^-$	1.0	—
46.	ArSSAr	$n\ OH^-$	0.0 *	ArS^-	1.0 1.0*	$OH^- > ArS^-$
47.	ArSeSeAr	$n\ OH^-$	0.0 *	$ArSe^-$	1.5	$OH^- > ArSe^-$
48.	$ArSS_2O_2C_6H_4CH_3$	ArS^-	0.0	$CH_3C_6H_4SO_2S^-$	(1.0)	$ArS^- > CH_3C_6H_4SO_2S^-$

Reaction	RMX	Y^-	$[Y^-]$ r $[RMX]^a$	X^-	$[X^-]$ or $[RMY]^b$	M-basicity
49.	$ArSS_2O_2C_6H_4CH_3$	$ArSe^-$	0.0	$CH_3C_6H_4SO_2S^-$	(1.0)	$ArS^- > CH_3C_6H_4SO_2S^-$
50s.	$ArSeS_2O_3^-$	*n* CN^-	0.9 *	$ArSe^-$	0.1	$CN^- > S_2O_3^{2-}$
51.	ArSeSAr	*n* OH^-	(0.0)	ArS^-	1.0	$OH^- > ArSe^- > ArS^-$
				+ $ArSe^-$	0.5	
52.	ArSeSAr	*n* SO_3^{2-}	(0.0)	ArS^-	0.9	$SO_3^{2-} > ArSe^- > ArS^-$
				+ $ArSe^-$	0.1	
53.	ArSeSAr	$S_2O_3^{2-}$	(0.1)	ArS^-	0.8	$S_2O_3^{2-} = ArSe^- > ArS^-$
				+ $ArSe^-$	0.1	
54.	ArSeSAr	CN^-	—	ArS^-	1.0	$CN^- > ArSe^- > ArS^-$
55s.	ArSeSAr	2 CN^-	—	ArS^-	1.0	$CN^- > ArSe^- > ArS^-$
				+ $ArSe^-$	1.0	
56.	$S_4O_6^{2-}$	ArS^-	1.0	$S_2O_3^{2-}$	(0.0)	$S_2O_3^{2-} > ArS^-$
57s.	4 $S_4O_6^{2-}$	ArS^-	0.9	$S_2O_3^{2-}$	0.1 *	$S_2O_3^{2-} > ArS^-$
58s.	$S_4O_6^{2-}$	$ArSe^-$	0.1	$S_2O_3^{2-}$	0.9 *	$ArSe^- > S_2O_3^{2-}$

ArS^- or $ArSe^-$ was not displaced from $ArSS_2O_2C_6H_4CH_3$ or $ArSeS_2C_6H_4CH_3$ by an equimolar proportion of $C_6H_5S^-$, SO_3^{2-}, $S_2O_3^{2-}$ or CN^- or by excess OH^-. Excess SO_3^{2-} or $S_2O_3^{2-}$ did not displace ArS^- or $ArSe^-$ (*cf.* 28, 29, 38, 39), but excess CN^- and $C_6H_5S^-$ displaced ArS^- or $ArSe^-$ (*cf.* 44, 45, 5, and 11).

Displacements in 20 % ethanol-water.

59.	ArSSAr	SO_3^{2-}	(0.0)	ArS^-	1.0	$SO_3^{2-} > ArS^-$
60.	ArSeSeAr	SO_3^{2-}	(0.34)	$ArSe^-$	0.66	$SO_3^{2-} \approx ArSe^-$
61.	ArSeSeAr	2 SO_3^{2-}	(0.26)	$ArSe^-$	0.74	$SO_3^{2-} \approx ArSe^-$
62.	$ArSS_2O_3^-$	n SO_3^{2-}	1.0 *	ArS^-	0.0	see text.
63.	$ArSeS_2O_3^-$	n SO_3^{2-}	1.0 *	$ArSe^-$	0.0	see text.
64.	ArSSAr	$S_2O_3^{2-}$	(0.1)	ArS^-	0.9	$S_2O_3^{2-} > ArS^-$
64s.	$S_4O_6^{2-}$	ArS^-	0.2	$S_2O_3^{2-}$	0.8 *	$ArS^- > S_2O_3^{2-}$
66.	ArSeSeAr	$S_2O_3^{2-}$	0.92	$ArSe^-$	0.08	$ArSe^- > S_2O_3^{2-}$
67.	ArSeSeAr	10 $S_2O_3^{2-}$	0.90	$ArSe^-$	0.10	$ArSe^- > S_2O_3^{2-}$
68s.	$S_4O_6^{2-}$	$ArSe^-$	0.0	$S_2O_3^{2-}$	1.0 *	$ArSe^- > S_2O_3^{2-}$

[a] Concentrations marked with an asterisk are for RMX, others for Y^-.

[b] Concentrations marked with an asterisk are for RMY, others for X^-. Concentrations in parenthesis were not measured, but can be assumed from the stoichiometry of reaction.

$S_2O_3^{2-} > p\text{-}CH_3C_6H_4SO_2S^-$ in aqueous ethanol, and is the same as sulphur or selenium-basicity.

Other features of reactions 1—68 deserve comment. Sulphite and thiosulphate ion reactions, 26—29, 36—39, 59—64, 66, and 67, were strongly solvent dependent. For example, the reaction between thiosulphate ion and ArSeSeAr had an equilibrium constant of 0.2 in 90 % ethanol-water, but of only 0.008 in 20 % ethanol-water; and sulphite ion is a stronger M-base than $ArSe^-$ in 90 % ethanol-water, but is of equivalent strength to $ArSe^-$ in 20 % ethanol-water. This is because the back reaction in each case was between two anions and such reactions tend to be much faster, relative to reaction between an anion and a dipolar molecule, in solvents of high dielectric constant than in solvents of low dielectric constant[36]. Reactions of tetrathionate ion (56—58, 65, 68) were also strongly solvent dependent, because they involve a reaction between two anions. Thus ArS^- slowly displaced $S_2O_3^{2-}$ from $S_4O_6^{2-}$ more

rapidly in 20 % ethanol-water than in 90 % ethanol-water. All displacements involving reaction between two anions (30—35, 38—41, 49, 57 and 58) were "slow" and became faster as the water content (*i.e.* dielectric constant) of the solvent increased. By analogy with the studies made by Bartlett and Davis [6], and Fava and Pajaro [3], we conclude that these reactions have large negative entropies of activation (*i.e.* low log B).

The entropy effect for reactions between anions may reverse the M-basicity of Y^-. Thus thiosulphate ion readily displaced ArS^- from both ArS-[36] and ArSe-[52], but not from $-SSO_3^-$[38] even under highly favourable conditions of solvent and thiosulphate concentration. Displacements from $-SO_3^-$ did not take place (28—35) except by the indirect routes shown in eqns. (8) and (9), because the sulphur of $-SO_3^-$ does not have a vacant d orbital available for occupation in the transition state for displacement, *i.e.* it is not electrophilic.

In the indirect two step displacements like (8) and (9) the base apparently approaches the anion containing electrophilic sulphur or selenium from a direction which is furthest from the negative charge, and least sterically hindered, to form a linear transition state [4].

$$\underset{(S_2O_3^-)}{ArSSO_3^-} + C_6H_5S^- \rightleftharpoons C_6H_5S\text{-}\underset{\displaystyle Ar}{\overset{\displaystyle |}{\overline{S}}}\text{---}\underset{(S_2O_3^-)}{SO_3^-} \rightarrow \underset{}{ArSSC_6H_5} + \underset{(S_2O_3^{2-})}{SO_3^{2-}} \qquad (8)$$

$$\text{then } \underset{}{ArSSC_6H_5} + \underset{(S_2O_3^{2-})}{SO_3^{2-}} \rightleftharpoons \underset{}{C_6H_5SSO_3^-} + \underset{(S_2O_3^-)}{ArS^-} \qquad (9)$$

Apparent displacements of ArS^- from both $-SO_3^-$ and $-S_2O_3^-$ (32—35, 40, 41 and 49) only take place with bases (*e.g.* $C_6H_5S^-$) which are much stronger than SO_3^{2-} or $S_2O_3^{2-}$, respectively, but not with those bases which are merely stronger than ArS^-. This suggests that the reaction path is as in (8) and (9).

Cyanide ion rapidly displaced one mole of ArS^- from ArSSAr and one mole of $ArSe^-$ from ArSeSeAr (*cf.* 42 and 43), but excess cyanide ion only *slowly* displaced a further mole of ArS^- or $ArSe^-$, presumably from ArSCN and ArSeCN respectively. These reactions are a novel example of displacement from unsaturated carbon as shown in eqn. (10), and as such would be slower than displacement from sulphur. ArS^- was displaced faster than $ArSe^-$ from $-CN$.

$$ArMCN + CN^- \rightarrow ArM^- + NC\text{—}CN \qquad (10)$$

The cyanogen formed in (10) would be hydrolysed under the reaction conditions, but no analysis of hydrolysis products was made.

ArSe- behaved as the electrophilic, and ArS- as the displaced portion of ArSeSAr in reactions 15—17, 50—55, in agreement with the M-base strength $ArSe^- > ArS^-$. The opposite mode of displacement was apparent at equilibrium however, because a little $ArSe^-$ was detected. A 50/50 mixture of ArSSAr and ArSeSeAr behaved in the same way as ArSeSAr in reactions 15—17, 50—55, as expected, because any $ArSe^-$ displaced from the mixture subsequently displaced ArS^- from ArSSAr.

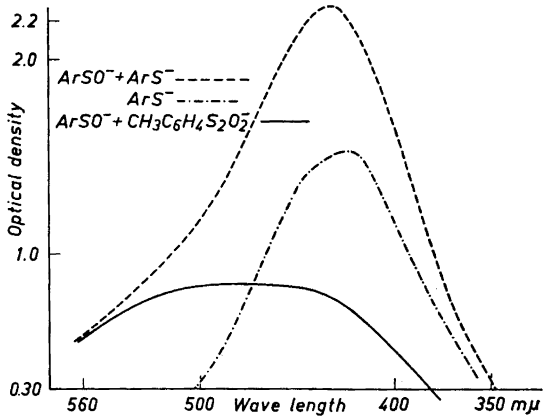

Fig. 1. Evidence for $ArSO^-$. Absorption spectra in 80 % ethanol-water of the reactions:

(1) $ArSS_2O_2C_6H_4CH_3 + 2\ OH^- \rightarrow ArSO^- + CH_3C_6H_4S_2O_2^- + H_2O$
(2) $ArSSAr + 2\ OH^- \rightarrow ArSO^- + ArS^- + H_2O$
(3) $\frac{1}{2}\ ArSSAR + C_6H_5S^- \rightarrow ArS^- + \frac{1}{2}\ (C_6H_5S)_2$
(where 1 mole proportion is 10^{-4} M).

Reactions 28 and 29, suggested that ArSeSAr and the mixture, ArSeSeAr + ArSSAr, might behave differently towards sulphite ion, as in eqns (11) and (12), respectively. The fact that the compound and mixture give the same products, must be due to secondary, rapid reactions of the mixture, (*cf.* eqns. (13) and (14)). Equilibrium (13) lies well to the left as shown by reactions 27 and 51 of Table 1, but apparently sufficient sulphite ion is displaced to enable (14) to proceed to completion.

$$ArSeSAr + SO_3^{2-} \rightleftharpoons ArSeSO_3^- + ArS^- \quad (11)$$

$$1/2\ ArSSAr + 1/2\ ArSeSeAr + SO_3^{2-} \rightleftharpoons 1/2\ ArSeSO_3^- + 1/2\ ArSSO_3^- + 1/2\ ArSe^- + 1/2\ ArS^- \quad (12)$$

$$\text{then } 1/2\ ArSSO_3^- + 1/2\ ArSe^- \rightleftharpoons 1/2\ ArSSeAr + 1/2\ SO_3^- \quad (13)$$

$$\text{and } 1/2\ ArSSeAr + 1/2SO_3^{2-} \rightleftharpoons 1/2\ ArSeSO_3^- + 1/2\ ArS^- \quad (14)$$

Sulphenic acids in displacements at sulphur. Reaction 46, and that between hydroxide ion and $ArSS_2O_2C_6H_4CH_3$ provide evidence for the existence of sulphenic acids [11] as intermediates for displacements by hydroxide ion at divalent sulphur. The spectra for some reactions of hydroxide ion are in Fig. 1. It is apparent that the same species (shown not to be $ArSO_2^-$), absorbing at longer wavelengths than does ArS^-, has been formed in the same concentration from reactions of hydroxide ion with *p*-nitrobenzenesulphenyl *p*-toluenethiosulphonate (ArSX) and with the same concentration of di-*p*-nitrophenyl disulphide (ArSSAr), respectively.

The position of λ_{max} observed for ArS^- (420 mμ), ArSH (316 mμ) ArSSAr (314 mμ), $ArSS_2O_2C_6H_4CH_3$-*p* (290 mμ), and $ArSSO_3^-$ (350 mμ) suggests that

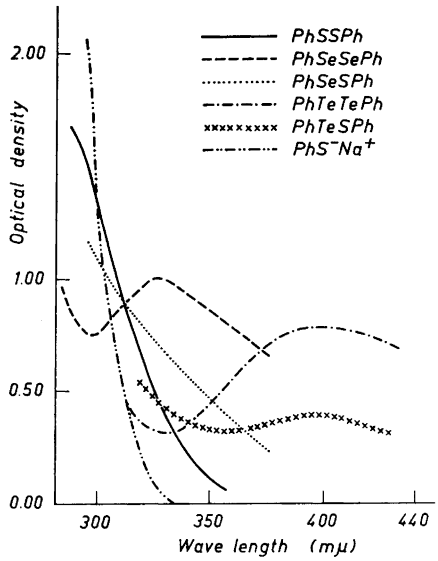

Fig. 2. Absorption spectra of diphenyl disulphide, diphenyl diselenide, benzeneselenenyl thiophenoxide, diphenyl ditelluride, benzenetellurenyl thiophenoxide, and sodium thiophenoxide at 10^{-3} M in 96 % ethanol.

electron withdrawing groups attached to ArS^- cause shifts of ArS absorption to shorter wave lengths, and electron donating groups, or negative charges, cause shifts to longer wave lengths. If this is so, the species with λ_{max} 475 mμ in Fig. 1 must have a group attached to ArS^- which is very strongly electron donating; $ArSO^-$ seems most likely.

In completely aqueous solution, $ArSO^-$ decomposed rapidly. No satisfactory evidence for the existence of $ArSeO^-$ could be obtained. When $ArSeS_2O_2C_6H_4CH_3$ was treated with excess hydroxide ion in ethanol, 1/2 mole proportion of $ArSe^-$ was slowly formed, together with a species absorbing below 400 mμ. ArSeSeAr gave one mole proportion of $ArSe^-$ rapidly and a further 0.5 mole slowly, when treated with excess hydroxide ion in ethanol. These observations could be explained by eqn. (15).

$$ArSeX + OH^- \rightarrow ArSeOH + X^- \rightarrow \tfrac{1}{2}\,ArSeO_2^- + 1/2\ ArSe^- + X^- \qquad (15)$$
(X is p-$CH_3C_6H_4SO_2S$ or ArSe)

Spectra of aromatic sulphur, selenium, and tellurium compounds. Spectra of aromatic disulphides [12,13], diselenides [14,15] and related compounds [12,16] have been reported and discussed in detail. Our results for ditellurides extend the series, and give a set of results measured under identical conditions. No unexpected results were obtained, and, since the intention was to develop a spectrophotometric method of analysing the reactions without disturbing established equilibria, it is sufficient to record the spectra (Fig. 2 and Table 2) and make the following general comments.

Table 2. Absorptions of sulphur, selenium, and tellurium compounds in 90 % ethanol unless stated otherwise. Values in parenthesis denote poorly defined λ_{max} or inflection point.

Compound	λ_{max} (mμ)	log e	λ_{max} (mμ)	log e	λ_{min} (mμ)	log e	λ^a (mμ)	log e^a
$(p\text{-}NO_2C_6H_4S)_2$	314	4.31	(228)	4.15	255	3.83	> 420	< 2
$(p\text{-}NO_2C_6H_4Se)_2$	325	4.22	(232)	4.11	265	3.88	> 442	< 2
$p\text{-}NO_2C_6H_4Se\text{—}SC_6H_4NO_2\text{-}p$	316	4.25	—	—	260	3.87	> 420	< 2
$p\text{-}NO_2C_6H_4O^-$ [e]	406	4.23	433[d]	4.35[d]	—	—	420	3.89
$p\text{-}NO_2C_6H_4S^-$ [e]	420	4.09	504[d]	4.22[d]	—	—	490 442	3.58 4.07
$p\text{-}NO_2C_6H_4Se^-$ [e]	442	4.03	532[d]	4.20[d]	—	—	490 420	3.78 3.99
$p\text{-}NO_2C_6H_4OH$ [f]	314	4.20	—	—	254	—	—	—
$p\text{-}NO_2C_6H_4SH$ [f]	316	4.01	—	—	—	—	—	—
$p\text{-}NO_2C_6H_4SeH$ [f]	326	3.92	—	—	—	—	—	—
$(C_6H_5S)_2$	239	4.23	(300)	2.95	(270)	3.32	—[b]	—
$(C_6H_5Se)_2$	240	4.22	330	2.99	(298)	2.85	—[b]	—
$(C_6H_5Te)_2$	247	4.25	393	2.93	330	2.54	—[b]	—
$C_6H_5TeSC_6H_5$	240	4.24	393	2.63	—	—	—[b]	—
$C_6H_5SeSC_6H_5$	240	4.23	(325)	2.84	—	—	—[b]	—
$C_6H_5S^-$ [e]	269	4.16	—	—	—	—	—[c]	—
$p\text{-}NO_2\text{—}C_6H_4SO^-$ [g]	475	3.90	—	—	—	—	—	—

[a] Reactions were analysed for $p\text{-}NO_2C_6H_4S^-$ and $p\text{-}NO_2C_6H_4Se^-$ at 420, 442, and 490 mμ. Absorption by the substrates in this region therefore does not interfere with the analysis.

[b] Reactions of these compounds with thiophenoxide ion were analysed between 320—400 mμ, their absorption in this region is shown in Fig. 1.

[c] Absorption was very weak above 310 mμ, *cf.* Fig. 1.

[d] Measured in dimethylformamide.

[e] Measured in a solution buffered to pH > 7 by bicarbonate.

[f] In ethanol of pH < 2.

[g] In 80 % ethanol-water.

There was a shift of the first, and a smaller shift of the second, λ_{max} of RMX (where R is an aromatic nucleus, M is O, S, Se, or Te, and X is a group, or negative charge, satisfying the divalent requirements of M) to longer wave lengths as M changed from the smaller to the larger elements of Group VI. If X did not absorb, or if its absorption was known and allowed for, the absorption curves were of almost the same height and shape for the same R group but different M, except that the first and second λ_{max} were most separated in tellurium compounds, but overlapped in sulphur compounds.

The absorption associated with RM- was not shifted or changed by X in a variety of compounds, RMX. However when X was strongly electron withdrawing (*e.g.* RSO_2S—) a shift to shorter wavelengths took place, and when X was strongly electron donating (*e.g.* X the negative charge on M as in ArM^-) a shift to longer wavelengths was observed. Shifts to shorter wavelengths corresponded to a small decrease in intensity, shifts to longer wavelengths were associated with a small increase in intensity.

There was a large solvent shift (27—90 mμ) to longer wave lengths in the absorption of ArM^- (Ar = *p*-nitrophenyl) when changing from the protic

solvent ethanol to the dipolar aprotic solvent dimethylformamide (*cf.* Table 2). Assuming that a shift to longer wavelengths means that the transition energy of the process



was less, the solvent effect agrees with Miller and Parker's postulate [17] that polarizable quinonoid anions are much more solvated in dimethylformamide than in ethanol. As expected [17] the shift was greater when M was more polarizable (*e.g.* Se *vs* O).

Solutions of disulphides, diselenides, and ditellurides obeyed Beer's Law and did not, as has been suggested by some workers [18], dissociate into radicals, RM., at room temperature.

The spectra of Fig. 2 agree with absorption maxima or shoulders between 260—280 mμ found for divalent sulphur compounds, between 300—330 mμ for divalent selenium compounds, and between 380—400 mμ for divalent tellurium compounds such as diaryl and aryl alkyl, but not dialkyl sulphides [12,19,20] and selenides; [12,16,21,22] diaryl and dialkyl disulphides [12,13,23] diselenides [12,15,23] and ditellurides [18,23], elemental sulphur [6], and aromatic thiols [12,20]. We conclude that divalent sulphur absorbs at 260—280 mμ, divalent selenium at 300—330 mμ, and divalent tellurium at 380—400 mμ, provided that at least one weak electron donor (*e.g.* an aromatic nucleus or a conjugated system, or divalent S, Se, or Te), but not a strongly electron perturbing group, is bonded to these elements.

It is felt that the shifts to longer wavelengths of the first absorption of ArM^- when M has increasing atomic weight, depend on electron donation by M^- to Ar (to form $Ar^- = M$) and that the larger elements of Group VI interact with an electron deficient aromatic nucleus (Ar) either in the ground state and/or the excited state, more readily than do the smaller elements of Group VI. The dependence of absorptions on interactions in the excited state makes meaningless any correlation of absorption shifts with M-basicity of ArM^-, because the latter property depends on ground state interactions only.

Analysis of sulphur, selenium and tellurium chromophores. When Z is C_6H_5S, C_6H_5Se or C_6H_5Te, and Y is ArS, ArSe, or ArTe, the absorptions between 300—450 mμ of the compounds, Z—Y, Z—Z, and Y—Y were proportional to the concentrations of the chromophores Z and Y, and were the sum of the absorptions of the appropriate Z and Y for *all combinations* of Z and Y studied. As was shown earlier with the appropriate disulphides [10], Z does not affect the absorption due to Y when they are bound together. It is clear that the spectra of any Z—Y gives the concentration of Z and Y in Z—Y, provided that the spectra of standards, Z—Z and Y—Y have been measured.

An alternative means of analysis of Z—Z, Z—Y, or Y—Y is to displace Z^- or Y^- with a stronger M-base, measure the absorption and compare with that of a standard solution of Z^- or Y^-. This procedure is best suited to compounds in which Z or Y is a nitro substituted benzenesulphenyl or selenenyl group.

The absorption associated with displacing or displaced anions gives their concentrations in a way which does not disturb established equilibria and, as has been demonstrated here, products and positions of equilibria can be determined for a variety of reactions of divalent Group VI compounds.

EXPERIMENTAL

The aromatic sulphur, selenium and tellurium compounds were synthesized from the starting materials and intermediates shown. The method used is referred to by the subscripts A,B,C *etc.*, in the equations. All products were recrystallised to constant melting point. Tellurium compounds were least and sulphur analogues most soluble in the solvent used for recrystallisation. New compounds were analysed for selenium [25] or tellurium [26] by conventional methods. All compounds were analysed for at least one of their constituent chromophores by the spectrophotometric method described above.

Diphenyl disulphide m.p. 60° [27a], colourless crystals from dilute methanol.

$$2C_6H_5SH \xrightarrow[A^{27a}]{I_2} (C_6H_5S)_2 + 2HI$$

Diphenyl diselenide, m.p. 61.5° [27b], yellow crystals from dilute methanol.

$$C_6H_5NH_2 \xrightarrow[B^{27c}]{} C_6H_5N_2^+ \xrightarrow[C^{27c}]{SeCN^-} \underset{I}{C_6H_5SeCN} \xrightarrow[D]{} (C_6H_5Se)_2 + HCN$$

Step D was based on the method of Foss and Svendsen [28]. Phenylselenocyanate (1 mole) was refluxed for 2 h in glacial acetic acid containing 1 mole of water and 0.5 mole of pyridine. Yields was better than those obtained by other methods [27b].

Diphenyl ditelluride, m.p. 66 °[18], orange red needles from methanol.

$$C_6H_5HgCl \xrightarrow[E^{18}]{TeCl_4} \underset{II}{C_6H_5TeCl_3} \xrightarrow[F]{S_2O_5^{2-}} (C_6H_5Te)_2$$

Step F is an improvement on that usually described [18,27d]. The trichloride (II) was treated with excess sodium metabisulphite in cold dilute methanol, water was added, the red oil was extracted with ether and crystallised as red needles as the ether evaporated. The ditelluride was recrystallised from dilute methanol containing a little sodium metabisulphite, and was dried and stored under nitrogen.

Benzenetellurenyl thiophenoxide, m.p. 42—43°, orange needles from dilute methanol.

$$\underset{II}{C_6H_5TeCl_3} \xrightarrow[G]{3p\text{-}CH_3C_6H_4SO_2S^-} \underset{III}{C_6H_5TeS_2O_2C_6H_4CH_3\text{-}p} \xrightarrow[H]{C_6H_5S^-} \underset{IV}{C_6H_5TeSC_6H_5}$$

Step G was used for a variety of reactions of this type (*vide infra*). The trichloride in dry ethyl acetate was treated with 3 moles of potassium *p*-toluenethiosulphonate in boiling methanol. Potassium chloride and colourless insoluble oxidation products were filtered off from the hot solution and the filtrate was concentrated to 5—10 ml and cooled. The orange crystals were recrystallised from methanol, to free them from methanol-soluble oxidation products of the thiosulphonate, then dried and stored under nitrogen. Step H was performed with freshly distilled thiophenol, alkali, and 1 mole of freshly prepared III per mole of thiophenol, in methanol under nitrogen. (Found: Te 40.6. Calc. for $C_{12}H_{10}TeS$: Te 40.6).

Benzeneselenenyl thiophenoxide, m.p. 58° [27e], pale yellow needles from dilute methanol.

$$(C_6H_5Se)_2 \xrightarrow[J^{29}]{Br_2} C_6H_5SeBr_3 \xrightarrow[G]{3p\text{-}CH_3C_6H_4SO_2S^-} C_6H_5SeS_2O_2C_6H_4CH_3\text{-}p \xrightarrow[H]{C_6H_5S^-} C_6H_5SeSC_6H_5$$
V

Benzeneselenenyl p-*toluenethiosulphonate*, m.p. 126—127°, yellow crystals from methanol. Compound V above. (Found: Se 22.9. Calc. for $C_{13}H_{12}SeS_2O_2$: Se 23.0).

Benzenetellurenyl p-*toluenethiosulphonate*, m.p. 138°, orange needles from methanol. Compound III above. (Found: Te 32.4. Calc. for $C_{13}H_{12}TeS_2O_2$: Te 32.5).

p-*Methoxybenzenetellurenyl* p-*toluenethiosulphonate*, m.p. 123—124°, orange-red needles from methanol. (Found: Te 30.2. Calc. for $C_{14}H_{14}TeS_2O_3$: Te 30.2).

$$CH_3OC_6H_5 \xrightarrow[K^{27F}]{TeCl_4} p\text{-}CH_3OC_6H_4TeCl_3 \xrightarrow[G]{3p\text{-}CH_3C_6H_4SO_2S^-} p\text{-}CH_3OC_6H_4TeS_2O_2C_6H_4CH_3\text{-}p$$

Di-p-*nitropenyl disulphide*, m.p. 180° [27g], pale yellow needles from acetic acid.

$$2ArSH \xrightarrow[A^{27a}]{I_2} (ArS)_2 + 2HI$$

Di-p-*nitrophenyl diselenide*, m.p. 179° [27h], deep yellow crystals from acetic acid.

$$2ArSeCN\ ^{27c} \xrightarrow[D]{HOAC/H_2O} (ArSe)_2 + 2HCN$$

Method D gives greatly improved yields (80 %) of diselenide compared with other methods [27h].

p-*Nitrobenzeneselenenyl* p-*nitrothiophenoxide*, m.p. 179—180°, yellow crystals from acetic acid.

$$ArSeCN + ArSH \xrightarrow[M]{HOAC} \underset{VI}{ArSeSAr} + HCN$$

Step M, based on that of Nakasaki [30], was performed in refluxing acetic acid containing a trace of pyridine, under nitrogen for 8 h. (Found: Se 22.8. Calc. for $C_{12}H_8N_2O_4SeS$: Se 22.2).

As has been observed with other disulphides, diselenides and their mixed compounds [31], mixed melting points of many disulphides and diselenides were not depressed, *e.g.* — ArSSAr + ArSeSeAr had m.p. 179°; ArSeSAr + ArSeSeAr had m.p. 179—180°; ArSeSAr + ArSSAr had m.p. 179—180°; ArSSAr had m.p. 180°; and ArSeSeAr had m.p. 179°.

It was therefore necessary to use other criteria to show that ArSeSAr was not a mixture of ArSeSeAr and ArSSAr. A paper chromatogram of a 50/50 mixture of ArSeSeAr and ArSSAr in a dimethylformamide-ligroin-ethanol solvent mixture, on paper saturated with dimethylformamide showed two red bands when sprayed with alcoholic alkali, but ArSeSAr showed only one band. Spectrophotometric measurements confirm the identity of ArSeSAr (*vide infra*).

p-*Nitrobenzenesulphenyl* p-*toluenethiosulphonate*, m.p. 134—135°, colourless crystals from methanol. Analysed spectrophotometrically (*vide infra*).

$$ArSH \xrightarrow[N^{32}]{Cl_2} ArSCl \xrightarrow[G]{p\text{-}CH_4C_6H_4SO_2S^-} \underset{VII}{ArSS_2O_2C_6H_4CH_3\text{-}p}$$

In this case only one mole of *p*-toluenethiosulphonate per mole of ArSCl was used in step G.

p-*Nitrobenzeneselenenyl* p-*toluenethiosulphonate* m.p. 124°, yellow crystals from methanol. (Found: Se 20.3. Calc. for $C_{13}H_{11}NO_4S_2Se$: Se 20.2).

$$ArSeCN \xrightarrow[O^{27k}]{Br_2} ArSeBr_3 \xrightarrow[G]{p\text{-}CH_3C_6H_4SO_2S^-} \underset{VIII}{ArSeS_2O_2C_6H_4CH_3\text{-}p}$$

Tellurium tetrachloride [27m], potassium selenocyanate [33], potassium *p*-toluenethiosulphonate [34], potassium tetrathionate [34], and *p*-nitrothiophenoxide [27n] were prepared as described in the literature. Other reagents were commercial products, purified where necessary by standard methods.

Analysis by ultra violet absorption measurements. Benzenetellurenyl thiophenoxide and benzeneselenenyl thiophenoxide, separately in 90 % ethanol at 10^{-3} M, had absorptions between 300—400 mμ which were identical with those of a 50/50 10^{-3} M mixture of diphenyl ditelluride and diphenyl disulphide and with that of diphenyl diselenide and diphenyl disulphide, respectively. The spectra of the artifical mixtures were changed by recrystallisation from methanol, but those of the compounds were not. *p*-Nitrobenzeneselenenyl *p*-nitrothiophenoxide at 10^{-4} M in 90 % ethanol had an absorption between 260—420 mμ which was identical with a 50/50 mixture at 10^{-4} M of ArSeSeAr and ArSSAr. Between 220—240 mμ the absorption of ArSeSAr is noticeably less than that of the mixture. No point of inflection was observed for ArSeSAr in this region, but ArSSAr, ArSeSeAr, and mixtures of the two have points of inflection at 228 mμ and 232 mμ, respectively, which have been attributed to the S—S [13] and Se—Se [15] bonds. Apparently the Se—S bond does not absorb noticeably in this region.

The following compounds at 10^{-4} M in 90 % ethanol, when treated with an excess of sodium thiophenoxide under nitrogen, had absorptions between 410—480 mμ corresponding exactly to quantitative displacement of ArS^- and $ArSe^-$: Di-*p*-nitrophenyl disulphide, *p*-nitrobenzenesulphenyl *p*-toluenethiosulphonate, *p*-nitrobenzeneselenyl *p*-toluenethiosulphonate, and *p*-nitrobenzeneselenyl *p*-nitrothiophenoxide. This confirms their identity.

Spectrophotometric measurements were made on a Beckmann DU spectrophotometer at 20—22°. Solutions of mercaptides and tellurium compounds, if required for longer than 10 min after preparation, were flushed with nitrogen and kept under nitrogen to prevent oxidation. All solutions obeyed Beer's Law between 10^{-3}—10^{-4} M.

Reactions with bases. The spectra of standard solutions of substrates, of bases, and of expected products in the solvents used were examined between 230—550 mμ. Absorptions were strictly additive when expected products were mixed with either of the reactants, except for those reactions involving unstable equilibria. Beer's Law was obeyed between 10^{-3}—10^{-6} M.

Known concentrations of substrate and base were mixed at 20—22°, and the absorption of the mixture was measured within 5 min of mixing in a region selected so that at least one of the reactants and or products could be readily distinguished. Solutions in ethanol were buffered with excess sodium bicarbonate (provided that the reactants, as shown in a separate experiment, did not react in some other way with bicarbonate) to ensure a pH > 7 when mercaptides, selenides, or other strong bases were involved. Reactions were carried out under nitrogen in oxygen free solvents, although this precaution is rarely necessary if measurements are made without delay.

p-Nitrobenzenesulphenyl *p*-toluenethiosulphonate and the selenenyl analogue in chloroform were treated separately with an equal volume of an equimolar amount of sodium sulphite in water. The two layers were shaken vigorously together for 5 min and separated. The aqueous layer contained 0.5 mole proportion of $ArSSO_3^-$ or $ArSeSO_3^-$ and the chloroform layer, 0.5 mole proportion of $ArSS_2O_2C_6H_4CH_3$ or $ArSeS_2O_2C_6H_6CH_3$. Analysis was by the spectrophotometric method. In the same way it was shown that the reaction between sodium thiosulphate in water and $ArSS_2O_2C_6H_4CH_3$ or $ArSeS_2O_2C_6H_4CH_3$ in chloroform also had an equilibrium constant of 1.

The procedure for competitive reactions of RMX with sodium thiosulphate has been outlined in the discussion. The reactants were shaken together for thirty seconds, and the aqueous and chloroform layers were then separated and analysed spectrophotometrically.

I thank Professor Olav Foss for many helpful discussions. The support of the *Royal Norwegian Council for Scientific and Industrial Research* is gratefully acknowledged.

REFERENCES

1(a) Parker, A. J. and Kharasch, N. *Chem. Revs.* **59** (1959) 610;
(b) Parker, A. J. *Proc. Chem. Soc.* **1961** 371.
2. Parker, A. J. *J. Chem. Soc.* **1961** 1328.
3. Fava, A. and Pajaro, G. *J. Am. Chem. Soc.* **78** (1956) 5203.
4. Fava, A., Iliceto, A. and Camera, E. *J. Am. Chem. Soc.* **79** (1957) 833.
5. McPhee, J. R. *Biochem. J.* **64** (1956) 22.
6. Bartlett, P. D. and Davis, R. E. *J. Am. Chem. Soc.* **80** (1958) 2513.
7. Foss, O. *J. Am. Chem. Soc.* **69** (1947) 2236.
8. Foss, O. *Acta Chem. Scand.* **3** (1949) 1385.
9. Foss, O. *Acta Chem. Scand.* **6** (1952) 306.
10. Parker, A. J. and Kharasch, N. *J. Am. Chem. Soc.* **82** (1960) 3071.
11. Kharasch, N., Potempa, S. J. and Wehrmeister, H. *Chem. Revs.* **39** (1946) 269.
12. Kiss, A. I. and Muth, B. R. *J. Chem. Phys.* **23** (1955) 2189.
13. Leandri, G. and Tundo, A. *Ann. chim. (Rome)* **45** (1955) 180.
14. Bergson, G. *Arkiv Kemi* **13** (1959) 11.
15. Chierici, L. and Passerini, R. *Boll. sci. fac. chim. ind. Bologna* **12** (1954) 131.
16. Chierici, L. and Passerini, R. *Boll. sci. fac. chim. ind. Bologna* **12** (1954) 127.
17. Miller, J. and Parker, A. J. *J. Am. Chem. Soc.* **83** (1961) 117.
18. Farrar, W. V. *Research (London)* **4** (1951) 177.
19. Mangini, A. and Passerini, L. *J. Chem. Soc.* **1952** 1168.
20. Fehnel, E. A. and Carnack, M. *J. Am. Chem. Soc.* **71** (1949) 84.
21. Chierici, L. and Passerini, R. *Atti accad. Nazl. Lincei* **14** (1953) 99.
22. Bergson, G. *Arkiv Kemi* **10** (1957) 127.
23. Bergson, G. *Acta Chem. Scand.* **11** (1957) 571.
24. Bergson, G. *Arkiv Kemi* **9** (1956) 121.
25. Gould, E. S. *Anal. Chem.* **23** (1951) 1502.
26. Vogel, A. I. *A Textbook of Quantitative Inorganic Analysis*, Longmans Green and Co., London, 1947 p. 526.
27. Houben Weyl, *Methoden der Organischen Chemie*, Georg Thieme, Stuttgart, Vol. 9, 1955; (a) p. 61, (b) p. 1096, (c) p. 943, (d) p. 1106, (e) p. 1105, (f) p. 1153, (g) p. 66, (h) p. 1095, (k) p. 1132, (m) p. 1059, (n) p. 26.
28. Foss, O. and Svendsen, S. R. *Acta Chem. Scand.* **8** (1954) 1351.
29. Behagel, O. and Seibert, H. *Ber.* **65** (1932) 816.
30. Nakasaki, M. *J. Inst. Polytech. Osaka City Univ. Ser. C.* **4** (1953) 100; *Chem. Abstr.* **48** (1954) 13653.
31. Rheinboldt, H. and Giesbrecht, E. *Ann.* **568** (1950) 197.
32. Zincke, T. and Lenhardt, S. *Ann.* **400** (1913) 1.
33. Fernelius, W. C. *Inorganic Syntheses* **2** (1946) 186.
34. Foss, O. *Kgl. Norske. Videnskab. Selskab Skrifter* **1945** No. 2.
35. Bunnett, J. F., Hauser, C. F. and Nahabedian, K. V. *Proc. Chem. Soc.* **1961** 305.
36. Cottrell, T. L. *The Strength of Chemical Bonds*, Butterworths, London, 1958.

Received October 17, 1961.

ACTA CHEMICA SCANDINAVICA 16 (1962) 870–874

Chromatographic Separation of Accelerator and Sulphur in Elastomer Vulcanisates Using ^{35}S

H. LETH PEDERSEN

Chemical Research Laboratory, Northern Cable and Wire Works, Ltd., Copenhagen, Denmark

The use of tracers *in casu* ^{35}S for determination of concentrations in chromatographic fractions is well established as an expedient means for the location of the peaks in the chromatogram.

It is shown that a simple technique using dry Al_2O_3 as adsorbent allows a quantitative separation of a mixture of free sulphur and accelerators. The sulphur accumulates in the first few ml of eluent and the accelerators follow appreciably later in the chromatogram.

Using labelled accelerators the decomposition of the accelerator during vulcanisation may be followed quantitatively. The activity is determined by scintillation counting in toluene by means of the Packard Tri-Carb Liquid Scintillation Spectrometer. The accuracy of the determination is about 5 %.

In the analysis of elastomer vulcanisates the determination of free sulphur is an important and complicated procedure, especially when a sulphur bearing accelerator is used. Further, in insulating compounds for wires the sulphur is a deleterious element as the sulphur during ageing might react with the copper conductor. Hence amounts of soluble copper compounds can migrate into the elastomer and drastically catalyse the rate of oxidation and consequently the deterioration.

It is therefore attempted to separate sulphur and accelerator by means of a chromatographic technique [1] and the use of ^{35}S as a tracer facilitates the location of the compounds in the eluent.

The recent advent of the liquid scintillation counting technique based upon the fundamental work of G. Reynold, H. Kallmann and F. N. Hayes permits an easy direct determination of the activity in the fractions from the chromatographic column. Here especially the Packard Tri-Carb LS-spectrometer [2] is very well suited for the purpose.

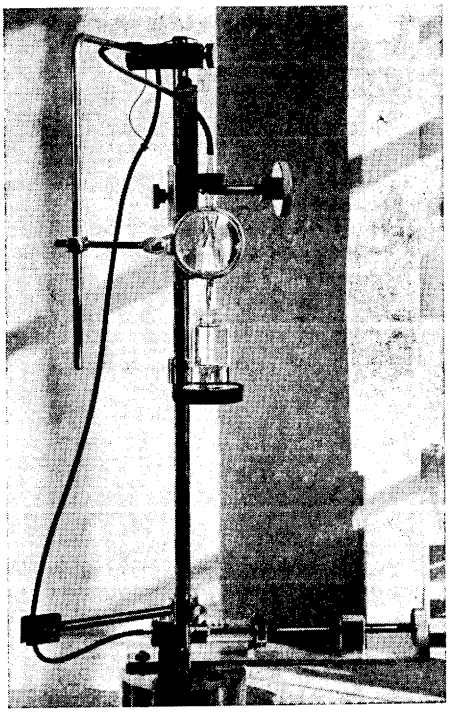

Fig. 1. Pipetting set up.

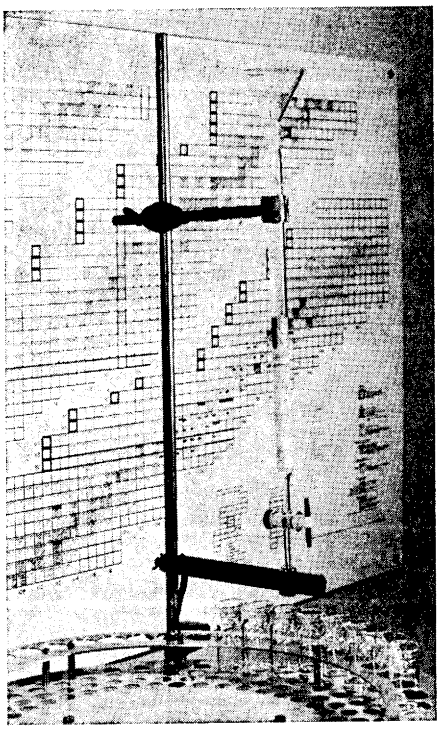

Fig. 2. Fractomate and column in a 300 × 20 mm diameter tube.

THE TECHNIQUE APPLIED

^{35}S and labelled accelerator are dissolved in pure toluene. An aliquot part of the solution having, *e.g.*, 10^4-10^5 cpm* activity in 2 ml is placed in the chromatographic column by means of the pipetting devise shown in Fig. 1. A Carlsberg constriction pipette is operated in conjunction with a hypodermic syringe mounted on a vertical rod by means of an adjustable clamp. A magnifying glass is placed for the inspection of the exact filling of the constriction. All parts of the device are adjustably mounted on the rod.

The column contains a 10 cm filling of dry Al_2O_3 and is placed in the sample collector over the counting vials. In the vials are placed small glass funnels. This ensures that the drops will be safely collected during the shift operation. The active solution is pipetted to the top of the Al_2O_3 and the glass tube washed 3—4 times with small portions of toluene added through a funnel, having a bent tip that touches the glass wall of the column. Finally 30 ml of toluene is added.

First two 1 ml fractions are collected followed by 2 ml fractions until the activity levels off.

* counts per minute.

To the fractions are added 5 ml of toluene containing 5 g 2,5-diphenyloxazole (PPO) and 0.4 g 1,4-bis-2-(5-phenyloxazole)-benzene (POPOP) per liter.

The vials are inserted in the freezer at −3°C and counted after 30 min dark adaption avoiding any exposure to sunlight in the entire procedure.

In the case of elastomer vulcanisates acetone extraction is carried out for 48 h as previously described [3]. A slight greasing of all ground glass joints in the Soxhlet will reduce losses of acetone to a minimum. The extract is evaporated to dryness and transferred to 25 ml toluene and 2 ml are placed in the column. It is advisable to carry out the extraction and evaporation under N_2.

For both the basic solution and the fraction internal standard must be prepared either by use of duplicate samples or a repeated counting cycle after addition of activity. This is normally 1 ml of toluene containing 0.2 mg of ^{35}S or a similar amount of the active accelerator. The raw extracts have a yellow colour and show a definite, although not very pronounced quenching.

If the activities of the fractions are added for the peak and this activity divided by the value obtained with the internal standard the amount of sulphur or accelerator is easily computed.

Normally the accuracy will be better than 5 % and fractions of micrograms can be determined within a standard deviation of about 10 %.

Reagents

Toluene, Merck's pure, distilled once in a 300 mm × 17 mm dia. Klit fractionating column [4]. Stored over $CaCl_2$.

Al_2O_3, Merck's reinst.

S, tetramethylthiuramdisulphide, 4,4'-morpholidedisulphide, Amersham, labelled ^{35}S, initial activity about 500 μCurie/g, if not labelled ordinary technical rubber grade chemicals are used.

PPO, *POPOP*, Packard Scientific Instruments Inc.

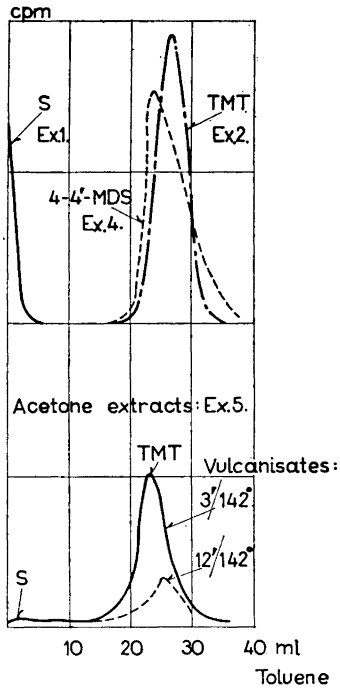

Fig. 3.

DATA

Ex. 1. Elementary rhombic S-35. As shown in Fig. 3 99.6 % of the activity accumulate in the first 6 ml eluent.

	ml	cpm	%	
Added	2	194 000	100.0	(2.031 mg ^{35}S)
Fractions	0—6	193 308	99.6	
	6—30	679	0.35	

The cut from 6—8 ml is very pronounced.

Ex. 2. Tetramethylthiuramdisulphide (TMT), labelled ^{35}S. Fig. 3 shows 0.02 % activity in the first fraction 0—6 ml, whereas 98.1 % are collected from 19—34 ml.

	ml	cpm	%	
Added	1	309 960	100.00	(0.508 mg
Fractions	0—6	60	0.02	TMT-^{35}S)
	6—19	785	0.25	
	19—34	304 368	98.2	
	34—67	2 344	0.75	

Thus the separation of the sulphur is quantitative.

Ex. 3. Equal parts of 2-mercaptobenzothiazolyldisulphide and ^{35}S were boiled in toluene 6 hours under reflux. The solution was transferred to 50 ml and 2 ml corresponding to 0.4 mg ^{35}S chromatographed.

	ml	cpm	%
Added	2	87 674	100.0
Fractions	0—6	85 307	97.3
	6—32	574	0.7

It is seen that there is a negligible exchange to MBTS (expected in the fractions 6—32 ml). The ^{35}S is nicely recovered.

Ex. 4. 4,4'-Morpholidedisulphide, labelled S-35. 2 ml corresponding to about 8 mg (63 870 cpm) gave a peak from 20—40 ml containing 66 940 cpm $\approx$ 105 %.

The separation from ^{35}S is safe. The value of 63 870 cpm is low due to the higher amount of quenching in the concentrated basic solution compared to the fractions and the yield can be considered close to unity.

Ex. 5. Thiuram vulcanisates without sulphur. The compound had the following composition:

Hevea Rubber (RSS 1X)	100 parts
ZnO	10
Stearic acid	1
Whiting	54
Clay	52
TMT	2

Vulcanisation was performed at 142°C.

About 1 g vulcanisate was extracted 48 h with acetone, the extract evaporated to dryness and dissolved in pure toluene. From the chromatograms the content of TMT was calculated based upon the acivity in the fraction from 6—30 ml, *cf.* Fig. 3.

Vulcanised at 142°C	PHR*TMT	
3′	0.110	added
6′	0.085	2.000 PHR
12′	0.042	
24′	0.033	

It is well known that TMT converts to the zinc salt of dithiocarbamic acid during vulcanisation. The data show that this conversion is fast; *e.g.*, after 3 min vulcanisation only about 6 % TMT remains. The further reaction is approximately a first order decomposition of TMT.

CONCLUSIONS

As the examples illustrate, it is possible to locate the pure compounds in the chromatogram and this knowledge can be used for conventional analysis using non-active compounds. Further, some accelerators and the free sulphur can generally be determined with good accuracy even in extremely small quantities.

An important application of the method is the estimation of exchange reaction between accelerator and sulphur by the introduction of either ^{35}S or labelled accelerators and measurements of the distribution of the activity between initial and later fractions. Some experiments regarding this exchange are described by Blokh [5].

Acknowledgement. The author wishes to express his indebtedness to his company, The Northern Cable & Wire Works Ltd., for the permission to publish this paper, and further to Mr. N.C.H. Humphreys of the R.W. Greeff & Co. Ltd. for corrections of the English.

REFERENCES

1. Bellamy, L. J. *et al. Trans. Inst. Rubber Ind.* **22** (1947) 308; **23** (1947) 15.
2. Bell, C. G. and Hayes, F. N. *Liquid Scintillation Counting*, Pergamon Press, N.Y. 1958, p. 50.
3. Leth Pedersen, H. *Rubber Chemistry and Technology* **33** (1960) 181.
4. Klit, A. *Fractional Distillation* (*Diss.*), Copenhagen 1934, p. 45.
5. Blokh, G. A. *Gummi und Asbest* **10** (1957) 610.

Received November 16, 1961.

* parts per hundred parts of rubber.

ACTA CHEMICA SCANDINAVICA 16 (1962) 875–882

Anion-Exchange Study

II. The Indium-Bromide System

TORKILD ANDERSEN and A. BYE KNUTSEN

Institute of Chemistry and Institute of Physics, University of Aarhus, Aarhus, Denmark

The indium-bromide complex system was investigated using the anion-exchange method given by Marcus and Coryell. The mononuclearity of the complexes was tested and confirmed for the range $3 \times 10^{-5} - 3 \times 10^{-4}$ M indium. The distribution of indium between the resin and the solution was determined in the range 0.1 M – 9.3 M LiBr by the batch method using the tracer ^{114}In. A corrected distribution function was constructed showing the complexes from $InBr_2^+$ to $InBr_6^{3-}$, with the successive stepwise formation constants: log $k_2 = 1.3$, log $k_3 = 0.59$, log $k_4 = -0.52$, log $k_5 = -1.6$, and log $k_6 = -2.2$. The values of k_2 and k_3 agree with published data.

The application of anion-exchange to quantitative investigations of complex systems, where the ligand is an anion, was introduced by Fronaeus [1]. He showed that plots of the distribution coefficient *vs.* the ligand concentration gave information about the principal species of complexes in the aqueous phase. Marcus and Coryell [2] extended the application of the adsorption function to allow the determination of the complex formation constants. Marcus studied the systems Ag–Cl [3], Cd–Cl [4], Fe(III)–Cl [5], Ag–S_2O_3 [6], and U(VI)–PO_4 [7] using the anion exchange method [2]. The complex formation constants, obtained by the anion exchange method, were in agreement with data obtained by other physico-chemical methods.

The adsorption of indium into a bromide anion-exchange resin from HBr-solutions is strong ($D_{max} = \sim 4 \times 10^3$) in contrast to the adsorption of indium into a chloride anion-exchange resin from HCl-solutions ($D_{max} = \sim 20$) [8]. The system In–Br was investigated more closely using the anion-exchange method. This method should be useful in evaluating the magnitude of the constants for the higher complexes, in particular the constants for $InBr_3$ and $InBr_4^-$, species with zero or unit charge [2]. Table 1 lists the values of the consecutive formation constants of the In–Br system obtained by earlier investigations together with the values obtained in this investigation. Spectrophotometry was used as a qualitative check of the interpretation of the ion exchange measurements.

Table 1.

Investigator	Method	Ionic strength	log k_1	log k_2	log k_3	log k_4	log k_5	log k_6
Hepler and Hugus [9]	pH	vary	2.20					
Schufle and Eilnad[10]	Ion-exchange	1.00	1.20	0.58	0.70			
DeSesa [11]	Potentiometric	vary	1.82					
Sundén [12]	Potentiometric	2.00	1.98	0.58				
Sundén [13]	Extraction		1.93	0.67				
Cozzi and Vivarelli[14]	Polarography	2.00	3.80	1.00				
Carleson and Irving [15]	Ion-exchange	0.691	2.01	1.09	0.18			
Irving and Rosotti[16]	Extraction	1.00	2.06	1.28	0.36	−0.7		
Burns and Hume [17]	Spectrophotometric	4.00	2.08	1.28	0.60	0.85		
This investigation	Anion-exchange	vary		1.3	0.59	−0.52	−1.6	−2.2

EXPERIMENTAL

The distribution coefficients were measured by the equilibration method [18]. The resin used, Dowex 1 × 10, 200—400 mesh, chloride form, was converted to the bromide form with HBr. The resin was washed with distilled water and dried at 110°C. The capacity was 3.22 mequiv/g dry resin. The water content was 37.0 %.

The indium solutions were prepared from metallic indium, containing ^{114}In as a radioactive tracer. The indium concentration was 3×10^{-5} —3×10^{-4} M. The lithium bromide was prepared from Li_2CO_3 and HBr and recrystallized twice. Bromide was determined by $AgNO_3$-titration.

The batch samples contained 0.1—0.5 g resin and 5—10 ml lithium bromide solution. In order to repress hydrolysis, hydrobromic acid was added to the indium and lithium bromide solutions to give a final concentration of around 0.02 M HBr. The resin was shaken with the solution for 48 h at room temperature. The concentration of indium in the aqueous phase was determined using a well type scintillation counter.

The concentration of Li^+ and Br^- in the resin phase was determined by a method given by Kraus and Moore [19].

The spectrophotometric measurements were carried out with recording Cary 14 spectrophotometer using silica cells of 0.100 and 1.000 cm. lengths, wavelength: 200—300 mμ.

Table 2.

Concentration of ligand m_{LiBr} (mole/litre)	Indium-concentration $\times 10^{-4}$ M	Log of indium distribution coefficient log D.
0.44	0.3	1.20
0.44	1.5	1.15
0.44	3.0	1.20
1.12	0.3	1.76
1.12	1.5	1.75
1.12	3.0	1.78
4.53	0.3	3.78
4.53	1.5	3.80
4.53	3.0	3.74
5.14	0.3	3.97
5.14	1.5	4.01
5.14	3.0	3.98

Table 3. Effects of the variation of the LiBr-concentration.

LiBr-conc. (moles/litre)	Log of Br^- activity function	Log of In-distribution coefficient
0.10	−1.10	0.40
0.21	−0.80	0.76
0.31	−0.63	0.98
0.44	−0.48	1.20
0.68	−0.29	1.52
0.87	−0.17	1.60
0.99	−0.10	1.70
1.18	0.00	1.81
1.38	0.09	2.00
1.58	0.18	2.10
1.97	0.30	2.38
2.46	0.46	2.50
2.95	0.60	3.00
3.44	0.76	3.20
3.80	0.86	3.45
4.72	1.13	3.90
5.24	1.28	4.06
5.66	1.40	4.20
6.16	1.54	4.35
6.56	1.66	4.48
7.08	1.81	4.60
7.50	1.94	4.75
8.03	2.10	4.84
8.44	2.22	4.93
8.88	2.36	4.97
9.35	2.52	4.97

RESULTS

The effect of variation in the indium concentration is shown in Table 2. The results show that the distribution coefficient is unaffected by changes in the indium concentration, indicating that the complexes are mononuclear in the range 3×10^{-5}— 3×10^{-4} M indium. Solvent extraction measurements of Irving and Rosotti [16] were explained by dimerization of indium in aqueous bromide solutions. Johnson and Kraus [20], however, demonstrated by molecular weight measurements using an equilibrium ultracentrifuge that indium(III) in HBr exists only as mononuclear complexes. Table 3 shows the distribution of indium between the resin and the lithium bromide solutions in the range 0.1—9.3 M. The values of the activity function for the bromide ligand $a = m_{\mathrm{LiBr}}\, \gamma_{\pm(\mathrm{LiBr})}$ were obtained from Robinson and Stoke [21]. In Fig. 1 is plotted the logarithms of the distribution coefficient, D, *vs.* the logarithm of the ligand activity.

The spectrophotometric measurements show qualitatively that the complex formation in the system In—Br does not stop at a definite complex (*e.g.* $InBr_3$), but the complex formation is continued for increasing HBr concentrations.

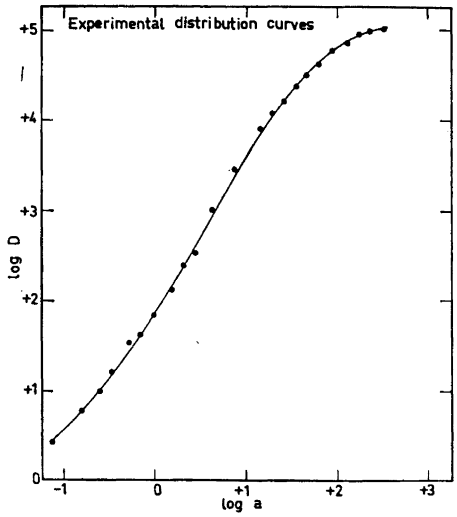

Fig. 1. The anion exchange distribution curve (log D) plotted *vs.* the logarithm of the bromide activity function (log a = log m_{LiBr} + log$\gamma_{\mp LiBr}$) for the absorption of indium from lithium bromide by Dowex 1 bromide-anion exchange resin.

DISCUSSION

Using the terminology of Marcus and Coryell [2] the complexed species of indium may be considered to be formed in the reaction:

$$InBr_3 \rightleftharpoons InBr_{3-i}^{i} + iBr^- \tag{1}$$

where i is the charge of the complex.

The thermodynamic equilibrium constant for the reaction (1) is:

$$\beta_i = (a_{InBr_{3-i}^{i}})(a_{Br})^i / (a_{InBr_3}) = m_i \cdot \gamma_i \cdot a^i \cdot a_0^{-1} \tag{2}$$

where m_i is the concentration of the i-th complex species, γ_i the activity coefficient, a is the ligand activity function and a_0 is the thermodynamic activity of the complex $InBr_3$. The equation

$$\Sigma m_i = a_0 \Sigma \beta_i \gamma_i^{-1} a^{-i} \tag{3}$$

expresses the total concentration of indium in the aqueous phase. An equation analog to (3) expresses the series of complexes ${}_rm$ in the resin phase. If $i = -p$ indicates the charge number of the principal species in the resin, the distribution coefficient D is defined by:

$$D = {}_rm_{-p} / \Sigma m_i = ({}_r\beta_{-p})({}_r\gamma_{-p}^{-1})({}_ra^{-p}) / \Sigma \beta_i \cdot \gamma_i^{-1} \cdot a^{-i} \tag{4}$$

as ${}_ra_0 = a_0$ at equilibrium.

Assuming that γ_i values are essentially independent of a, the activity of the ligand concentration, in the successive regions where the corresponding species $InBr_{3-i}^{i}$ are predominant, and ${}_r\gamma_{-p}$ is independent of a, the log D is expressed by

$$\log D = \log {}_r\beta^*_{-p} + p \log {}_r a - \log \Sigma \beta^*_i a^{-i} \quad (5)$$

when $\beta^*_i = \beta_i \gamma_i^{-1}$

As a Donnan equilibrium ${}_r a_{\mathrm{LiBr}} = a_{\mathrm{LiBr}}$ is proved to exist, the resin ligand activity function ${}_r a$ can be expressed by the equation:

$$\log {}_r a = \log a + 1/2 \, (\log {}_r m_{\mathrm{Br}} - \log {}_r m_{\mathrm{Li}}) \quad (6)$$

If ${}_r a^0$ expresses the resin ligand activity function ${}_r a$ at $a = 1$, a correction function ${}_r F_a$ is defined as:

$$ {}_r \mathrm{F}_a = \log {}_r a - \log {}_r a^0 \quad (7)$$

The ideal or corrected distribution coefficient D° is defined by:

$$\log D^\circ = \log D - p_r F_a = \log K_r - \log \Sigma \beta^*_i a^{-i} \quad (8)$$

in which $K_r = {}_r\beta_{-p} \cdot {}_r\gamma_{-p}^{-1} \cdot {}_r a^0$. According to eqn. (8) the ideal distribution coefficient D° should be a function of the complex formation in the aqueous solution only, for a given ion exchange resin.

The maximal co-ordination number of indium is 6. The ratio between the radius of the indium(III) ion and the radius of the bromide ion shows that the formation of an indium hexabromocomplex is geometrically possible. Woodward and Bill [22] reported from a study of the Raman spectra of indium salts in the presence of a large excess of bromide, that no tetrahedral $InBr_4^-$ ion is present in the aqueous solution. Burns and Hume [17] assumed that the indium tetrabromocomplex is $[In\,(H_2O)_2Br_4]^-$ with a structure as an octahedron, because indium frequently exhibits hexacoordination. The use of eqn. (8) combined with the assumption of the formation of a hexabromocomplex on the resin as R_3InBr_6, results in values of the first complex formation constants in the system In—Br in agreement with published data obtained by other methods (cation-exchange, extraction and spectrophotometry).

The correction function ${}_r F_a$ was calculated by means of the activity values of the bromide ion, the concentration of the lithium ion and the concentration of the bromide ion in the resin phase. The reference point for ${}_r a$, as ${}_r a^0$, at $a = 1$ is calculated like that ${}_r F_a = 0$ at this point; ${}_r a^0$ was determined to 0.46. It is known [19] that the resin invasion is small at a = 1, but still accessible to reasonably accurate measurements. The values of the correction function ${}_r F_a$ are shown in Fig. 2. The function ${}_r F_a$ for the bromide system is nearly identical with the correction function for the chloride system reported by Marcus [2,3].

Using the values of ${}_r F_a$ in Fig. 2, a corrected or ideal distribution coefficient D° is calculated by eqn. (8).

The average charge number $\bar{i}$ and the average ligand number $\bar{n}$ can be calculated from the slopes of the ideal distribution function:

$$\frac{\mathrm{d}(\log D^\circ)}{\mathrm{d}(\log a)} = \bar{i} = 3 - \bar{n}$$

since the parameters K_r and β^*_i are taken as constants.

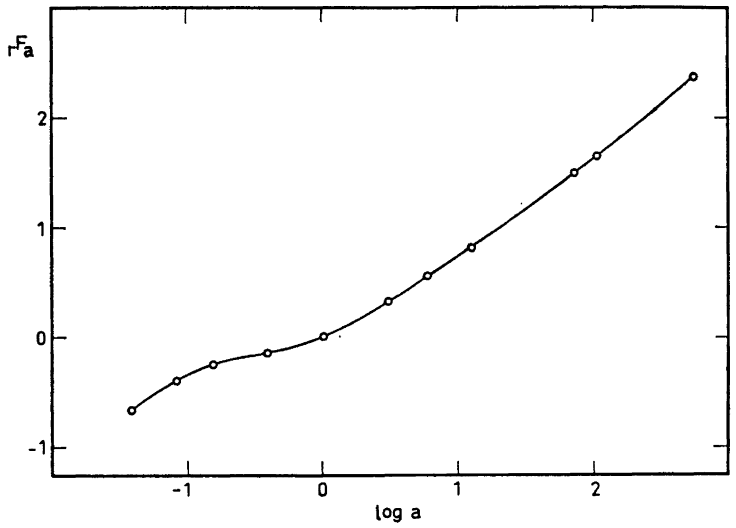

Fig. 2. The activity function $\bar{r}_a$ of bromide in the resin Dowex 1-bromide equilibrated with lithium bromide plotted as a function of the bromide activity function a in lithium bromide solutions (logarithmic scale).

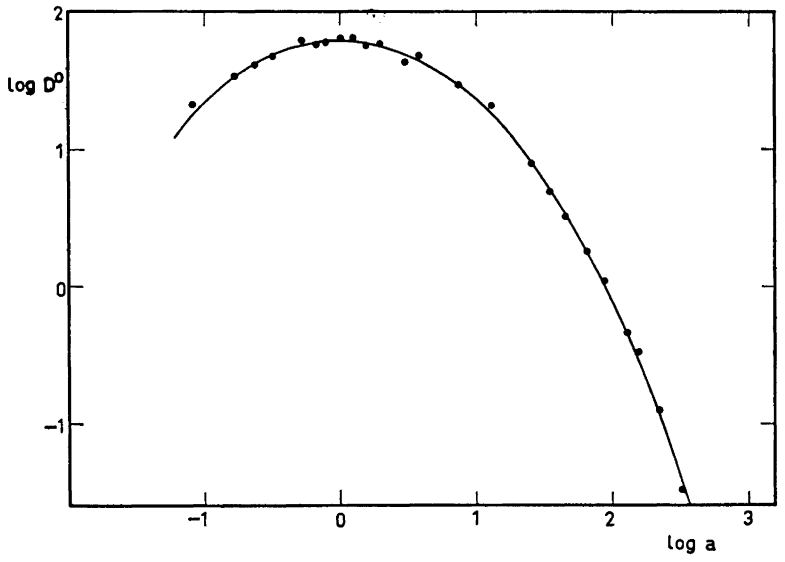

Fig. 3. The corrected distribution curve (log D°) using the parameter $p = 3$ for the predominant resin species R_3InBr_6, plotted *vs.* the bromide activity function (log a).

The curve has slopes ranging from approximately + 1.6 at the lowest concentration to exactly −3.00 at 9 M LiBr. The value + 1.6 refers to $InBr_2^+$ and the value −3.00 to $InBr_6^{3-}$.

The values of the successive formation constants k^*_i were obtained by the Bjerrum's "half-integral $\bar{i}$" method, where, to a first approximation:

$$\log k^* = \log\beta^*_i / \beta^*_{i-1} = -\log a_{(\bar{i}=i-\frac{1}{2})}$$

The preliminary values, obtained by Bjerrum's method, were applied to calculate the formation constants by Sillen's "curve fitting" method [23]. The values so obtained are: $\beta^*_2 = 1.2 \times 10^{-2}$; $\beta^*_1 = 0.26$; $\beta^*_{-1} = 0.30$; $\beta^*_{-2} = 7 \times 10^{-3}$; $\beta^*_{-3} = 5 \times 10^{-5}$. The values of the formation constants $k_n = (InBr_n^{3-n}) / (InBr_{n-1}^{3-(n-1)})(Br^-)$ were calculated: $\log k_2 = 1.3$; $\log k_3 = 0.59 \pm 0.08$; $\log k_4 = -0.52 \pm 0.07$; $\log k_5 = -1.6$ and $\log k_6 = \sim -2.2$. It is not possible to determine k_1 of the experimental results. Log K_r is determined as 2.01 ± 0.04.

The complex formation constants k_2 and k_3 found in the present work are seen to be in reasonable agreement with data obtained by other methods, Table 1. A determination of k_1 was carried out by spectrophotometric methods similar to that of Burns and Hume [17]. The value so obtained agrees with the value reported by Burns and Hume.

The value of k_4 agrees with the result of Irving and Rosotti [16], but deviates from the value reported by Burns and Hume. The spectrophotometric measurements show that the complex formation in the system In—Br does not stop at a decided complex, but the complex formation is continued for increasing HBr-concentration. The value k_4 given by Burns and Hume was determined assuming that the complex $InBr_4^-$ was the only absorbing species of higher complexes. Making a comparison with the complex formation constants of halogen complexes of the group Al, Ga, In, Tl [24] the published data show a marked tendency for the ratio $\log k_3/k_4 > 0$, as in the present work.

The parameter K_r may be used to calculate the equilibrium constant for the reaction

$$InBr_3(aq) + 3\ RBr \rightleftharpoons R_3InBr_6$$

by dividing K_r with the 3rd power of ${}_ra^0$ [2]. This gives $\log K_r - 3{}_ra^0 = 2.01 - 1.38 = 0.63$ for the logarithm of this constant. A comparison between this value and the value for the corresponding reaction in the solution $\log\beta^*_{-3} = -4.3$ shows that the resin stabilizes the indium hexabromocomplex 10^5-fold.

Acknowledgement. The authors are grateful to professor S. E. Rasmussen for his valuable advice and discussions.

REFERENCES

1. Fronaeus, S. *Svensk Kem. Tidsskr.* **65** (1953) 1.
2. Marcus, Y. and Coryell, C. D. *Bull. Research Council Israel* **8A** (1959) 1.
3. Marcus, Y. *Ibid.* **8A** (1959) 17.
4. Marcus, Y. *J. Phys. Chem.* **63** (1959) 1000.
5. Marcus, Y. *J. Inorg. Nuclear Chem.* **12** (1960) 287.
6. Marcus, Y. *Acta Chem. Scand.* **11** (1957) 619.
7. Marcus, Y. *Intern. Conf. Peaceful Use Atomic Energy* **3** (1958) 465.

8. Andersen, T. and Knutsen, A. Bye, Part I. *Acta Chem. Scand.* **16** (1962) 875.
9. Hepler, L. G. and Hugus, Z. Z. *J. Am. Chem. Soc.* **74** (1952) 6115.
10. Schufle, J. A. and Eiland, H. M. *Ibid.* **76** (1954) 960.
11. DeSesa, M. A. *Thesis*, Mass. Inst. of Tech. 1953.
12. Sundén, N. *Svensk Kem. Tidsskr.* **66** (1954) 20, 50, 173.
13. Sundén, N. *Ibid.* **66** (1954) 345.
14. Cozzi, D. and Vivarelli, S. *Z. Elektrochem.* **57** (1953) 408; **58** (1954) 907.
15. Carleson, B. G. F. and Irving, H. *J. Chem. Soc.* **1954** 4390.
16. Irving, H. and Rosotti, F. J. C. *Ibid.* **1955** 1927, 1938, 1946.
17. Burns, E. A. and Hume, D. N. *J. Am. Chem. Soc.* **79** (1957) 2704.
18. Kraus, K. A. and Nelson, F. *A.S.T.M. Spec. Tech. Publ.* **195** (1956).
19. Kraus, K. A. and Moore, G. E. *J. Am. Chem. Soc.* **75** (1953) 1457.
20. Johnson, J. S. and Kraus, K. A. *Ibid.* **79** (1957) 2034.
21. Robinson, R. A. and Stokes, R. H. *Electrolyte Solutions*, Butterworths, London 1955.
22. Woodward, L. A. and Bill, P. T. *J. Chem. Soc.* **1955** 1699.
23. Sillén, L. G. *Acta Chem. Scand.* **10** (1956) 186.
24. Bjerrum, J., Schwarzenbach, G. and Sillen, L. G. *Stability Constants of Metal-ion Complexes. Part II: Inorganic Ligands.* Special publication No. 7 of the Chemical Society, London (1958).

Received October 27, 1961.

ACTA CHEMICA SCANDINAVICA 16 (1962) 883–886

The Hemiacetal of Chloral with Testosterone and Derivatives thereof

POUL BORREVANG

Leo Pharmaceutical Products, Copenhagen, Denmark

Treatment of testosterone with chloral yields the 1-hydroxy-2,2,2-trichloroethyl ether of testosterone. With acid anhydrides or acyl chlorides the corresponding esters are obtained. The hydroxyether reacts with PCl_5 to the 1,2,2,2-tetrachloroethyl ether, which together with KOH in ethanol leads to the 1,2,2-trichlorovinyl ether.

For the purpose of preparing 6-derivatives of testosterone (I) experiments were made with the 3-ethylene ketal of testosterone and chloral in the presence of peroxides to obtain a free-radical reaction. It was possible to isolate a substance of the desired composition $C_{23}H_{33}Cl_3O_4$. The ultraviolet spectrum showed no maxima, but hydrolysis in aqueous acetone with sulphuric acid transformed the substance into testosterone.

The formation of testosterone by hydrolysis indicated that no reaction between the Δ^5-double bond and chloral had taken place. According to the analysis it seemed possible that the free OH-group in the 17-position had reacted with chloral and yielded a hemiacetal. Therefore testosterone was treated with chloral at room temperature without catalysts. This yielded a compound with an elementary analysis in agreement with the hemiacetal of chloral with testosterone (II). This substance, 17-(1-hydroxy-2,2,2-trichloroethoxy)-androst-4-ene-3-one, showed in the infrared spectrum (in KBr) the normal bands for a Δ^4-3-keto group, a band for a hydroxyl-group, and a very strong band at 1 117 cm^{-1}, which indicated an ether-group. Compared to the infrared spectrum of testosterone the new strong bands at 797 and 832 cm^{-1} must be due to the CCl_3-group.

By reaction of II with acetic anhydride in pyridine the corresponding acetate (IIIb) was formed. In the infrared spectrum of testosterone acetate the ester-carbonyl group shows a band at 1 735 cm^{-1}, in the acetate of the hemiacetal of chloral with testosterone this band was shifted to 1 765 cm^{-1}. The ether band, from the hemiacetal, was shifted to 1 142 cm^{-1}, but the bands for the CCl_3-group were identical. A number of esters are listed in Table 1.

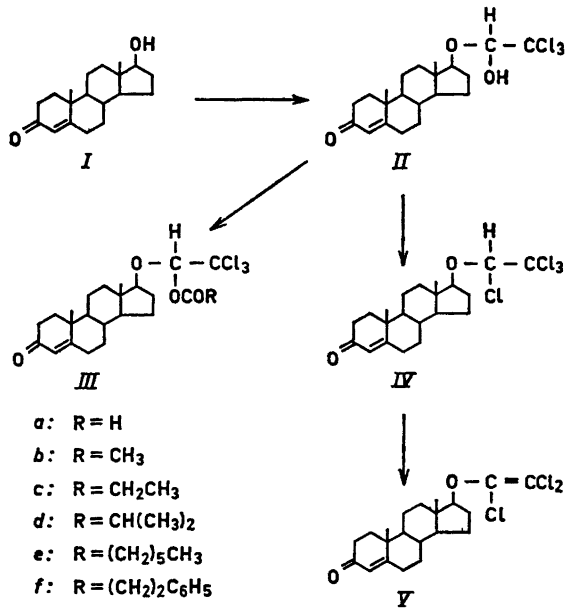

Treatment of II with PCl_5 in chloroform yielded 17-(1,2,2,2-tetrachloroethoxy)-androst-4-ene-3-one (IV) and reflux of IV with KOH in aqueous ethanol yielded 17-(1,2,2-trichloroethenoxy)-androst-4-ene-3-one (V). The two compounds (IV and V) showed in the infrared spectrum normal bands for a Δ^4-3-keto group, and no absorption for a OH-group. The ether band was shifted to 1 150 cm^{-1} for the tetrachloro ether and to 1 165 cm^{-1} for the trichlorovinyl ether. The above-mentioned bands for the CCl_3-group were weak in the tetrachloro ether, but the spectrum showed a new strong band for a C—Cl-group at 700 cm^{-1} whereas in the trichlorovinyl ether the C—Cl frequency is as high as 805 cm^{-1} with a very strong absorption.

Biological properties. Gaunt *et al.*[1] have established that the androgenic activity is greatly reduced by transforming the 17—OH group in testosterone to a methoxy group. The activity of the new ether (II) is in the rat test three to four times that of testosterone propionate whereas the activity of the acetate (IIIb) is only half of that of testosterone propionate, but the acetate shows a markedly protracted action. In aqueous suspension its activity as regards intensity and duration is higher than that of testosterone isobutyrate *. The compounds IV and V showed no androgenic activity.

EXPERIMENTAL

All melting points are uncorrected.

17-(1-Hydroxy-2,2,2-trichloroethoxy)-androst-4-ene-3-one (II). Testosterone (2.9 g) was added to a solution of chloral (1.7 g) in anhydrous benzene (10 ml). By shaking the

* These experiments were carried out in the biological department of Leo Pharmaceutical Products.

Table 1.

Compound	R	Preparation	Recrystallized from	Yield %	M.p. °C	U.V. (ethanol) λ_{max} mμ	U.V. (ethanol) ε	Formula	C % Calc.	C % Found	H % Calc.	H % Found	Cl % Calc.	Cl % Found
The formate IIIa	H		acetone	84	239–41°	241	16 800	$C_{22}H_{29}Cl_3O_4$	56.97	56.98	6.30	6.31	22.93	22.92
The acetate IIIb	CH_3	1	ethyl acetate	88	192–93°	241	16 400	$C_{23}H_{31}Cl_3O_4$	57.81	57.69	6.54	6.61	22.26	22.46
The propionate IIIc	CH_2CH_3	1	methanol	58	151–52°	240	16 800	$C_{24}H_{33}Cl_3O_4$	58.60	58.55	6.76	6.74	21.63	21.59
The isobutyrate IIId	$CH(CH_3)_2$	1	methanol	52	127–28°	242	17 100	$C_{25}H_{35}Cl_3O_4$	59.35	59.41	6.97	7.21	21.03	21.03
The enanthate IIIe	$(CH_2)_5CH_3$	2	96 % ethanol	61	82–83°	241	17 000	$C_{28}H_{41}Cl_3O_4$	61.37	61.21	7.54	7.56	19.41	19.42
The β-phenylpropionate IIIf	$(CH_2)_2C_6H_5$	2	96 % ethanol	72	99–100°	240	16 600	$C_{30}H_{37}Cl_3O_4$	63.44	63.56	6.57	6.62	18.73	18.67

mixture for a few minutes a clear solution was obtained, and after a few more minutes of shaking a solid precipitate was formed. The precipitate was collected on a filter, washed with benzene, and dried at room temp. in order to obtain the hemiacetal (2.5 g), m.p. 194–196°C, raised by crystallization from ethyl acetate to 200–201°C. U.V. λ_{max} 241 mμ in ethanol (ε 16 300). (Found: C 57.62; H 6.70; Cl 24.61. Calc. for $C_{21}H_{29}Cl_3O_3$: C 57.87; H 6.71; Cl 24.41).

The same properties are present if acetic acid is used as solvent. It is also possible to form II with chloral hydrate in chloroform in the presence of benzoyl peroxide.

Esters of the hemiacetal (IIIa, b, c, d, e, and f).

1. *With anhydride.* II (3.0 g) was dissolved in a mixture of the anhydride (10 ml) and pyridine (10 ml). The solution was allowed to stand at room temp. for about 16 h and evaporated *in vacuo*. The residue was crystallized from ethyl acetate, acetone, or methanol to yield the ester.

2. *With acyl chloride.* To a chilled solution of II (2.2 g) in a mixture of dry benzene (10 ml) and pyridine (6 ml), a solution of the acyl chloride (1.3 g) in dry benzene (5 ml) was slowly added while stirred. After standing for about 16 h at + 2°C ether (150 ml) and ethyl acetate (25 ml) were added, and the mixture was washed with 0.5 N H_2SO_4, 0.5 N NaOH and water. The solution was dried with sodium sulphate after which the solvent was removed *in vacuo* and the residue was crystallized from 96 % ethanol in order to yield the ester.

The formate. Formic acid (2.8 ml) was mixed with acetic anhydride (7.5 ml), and the mixture was allowed to stand at room temp. for about 16 h. This solution was added to a solution of II (3.0 g) in pyridine (15 ml), and after standing for 5 h at room temp. the mixture was evaporated to dryness *in vacuo*. The solid residue was triturated with ether, filtered off and dried in order to yield the formate.

17-(1,2,2,2-Tetrachloroethoxy)-androst-4-ene-3-one (IV). To a chilled solution of II (2.0 g) in dry chloroform (50 ml) PCl_5 (1.0 g) was added in small portions under continuous stirring. Having been stirred for about 1 h at + 2°C and for 1 h at room temp. the mixture was poured into a cold NaOH-solution. The chloroform phase was separated from the aqueous phase, washed three times with water, and dried. The solvent was removed *in vacuo*, and the residue was crystallized from methanol to give the tetrachloro ether (1.5 g), m.p. 151–155°C, raised by recrystallization to 156–158°C. U.V. λ_{max} 240 mμ in ethanol (ε = 16 800). (Found: 55.68; H 6.27; Cl 31.00. Calc. for $C_{21}H_{28}Cl_4O_2$: C 55.52; H 6.21; Cl 31.22).

17-(1,2,2-Trichloroethenoxy)-androst-4-ene-3-one (V). IV (2.3 g) in 15 ml of a 5 % solution of KOH in ethanol was refluxed for 20 min. The mixture was then poured into water and the product was extracted with ether (2 × 100 ml). When the extract had been dried the ether was removed *in vacuo* and the residue was crystallized from methanol in order to yield the trichlorovinyl ether (1.6 g), m.p. 120–122°C, raised by recrystallization to 128–130°C. U.V. λ_{max} 240 mμ in ethanol (ε = 19 000). (Found: C 60.48; H 6.56; Cl 25.38. Calc. for $C_{21}H_{27}Cl_3O_2$: C 60.37; H 6.51; Cl 25.46).

Acknowledgements. The author wishes to thank Mr. P. Mørch for ultraviolet and infrared spectra and Mr. G. Cornali for the micronalyses.

REFERENCE

1. Gaunt, R., Tuthill, C.H., Antonchak, N. and Leathem, J.H. *Endocrinology* **52** (1953) 420.

Received November 9, 1961.

ACTA CHEMICA SCANDINAVICA 16 (1962) 887–902

Studies on the Hydrolysis of Metal Ions

38. The Hydrolysis of Mercury(II) in Perchlorate Medium

INGRID AHLBERG

Institute of Chemistry, University of Uppsala, Uppsala, and
Department of Inorganic Chemistry, Royal Institute of Technology, Stockholm, Sweden

The hydrolysis of Hg(II) has been studied at 25.0°C with the media 3.0 M $(Na)ClO_4$, $(Ca)ClO_4$ and $(Mg)ClO_4$. $[H^+]$ was measured with a glass electrode and in the more dilute solutions $[Hg^{2+}]$ was measured with a redox electrode, Hg_2^{2+}, Hg^{2+}/Pt.

The data for $(Mg)ClO_4$ and $(Ca)ClO_4$ media coincide and differences for $(Na)ClO_4$ are attributed to variations in activity factors.

	3 M(Ca,Mg)ClO_4	3 M$(Na)ClO_4$
$Hg^{2+} + H_2O \rightleftharpoons HgOH^+ + H^+$;	$\log \beta_{1,1} = -3.49 \pm 0.06$	-3.55 ± 0.06
$Hg^{2+} + 2H_2O \rightleftharpoons Hg(OH)_2 + 2H^+$;	$\log \beta_{2,1} = -5.96 \pm 0.02$	-6.21 ± 0.02
$2Hg^{2+} + H_2O \rightleftharpoons Hg_2OH^{3+} + H^+$;	$\log \beta_{1,2} = -2.67 \pm 0.03$	$-2.67 \pm 0.03 (B = 1.0\ M)$
$2Hg^{2+} + 2H_2O \rightleftharpoons Hg_2(OH)_2^{2+} + 2H^+$;	$\log \beta_{2,2} = -4.95 \pm 0.08$	$-5.16 \pm 0.09 (B = 1.0\ M)$
$4Hg^{2+} + 3H_2O \rightleftharpoons Hg_4(OH)_3^{5+} + 3H^+$;	$\log \beta_{3,4} = -6.15 \pm 0.08$	$-6.40 \pm 0.08 (B = 1.0\ M)$

The hydrolysis of mercury(II) has been studied by Hietanen and Sillén [1] using 0.5 M $(Na)ClO_4$ as ionic medium and Hg concentrations between 0.015 M and 0.001 M. They found in this range two mononuclear complexes, with $\log \beta_{1,1} = -3.70 \pm 0.07$ and $\log \beta_{2,1} = -6.30 \pm 0.05$. Their rather unusual result, with a second acidity constant larger than the first ($K_1/K_2 = 10^{-1.10} = 0.08$), was later confirmed by Anderegg, Schwarzenbach, Padmayo and Borg [2], who investigated the hydrolysis in nitrate solutions. Extrapolating to ionic strength zero, they got a value of 0.04 for the ratio of the constants for the first and second protonation.

These and other earlier investigations were mostly carried out in dilute solutions and only mononuclear complexes were found. Hayek [3], however, determined the solubility of HgO in concentrated mercury perchlorate and concluded that the solution contained polynuclear ions $Hg(HgO)_2^{2+}$. He was able to isolate the solid compound, $Hg_3O_2(ClO_4)_2$. Crystals of corresponding composition, $Hg_3O_2(NO_3)_2H_2O$ have been found by Bernstein, Pars and Blumenthal [4].

The self-medium method recently used by Hietanen and Sillén [5] in studies of Th^{4+} and UO_2^{2+} seemed to be useful in searching for polynuclear complexes in Hg(II) solutions.

When dealing with complicated equilibria in solution it is desirable to keep the activity coefficients constant, allowing the use of concentrations instead of activities in the calculations This may be brought about through the addition of a large amount of neutral salt as in the inert medium method. If only a minor fraction of the ions in a concentrated metal salt solution is converted into complex species, one might also consider the alteration of the ionic environment to be so small that the same approximation may be made. Since in this work we found it valuable to vary the metal concentration within a very wide range, and were thus forced to substitute a large proportion of the medium ions for mercury ones, we found it advisable also to investigate the influence of the positive medium ion on the activity factors. Sodium, magnesium and calcium perchlorate were used.

The commoner symbols used in the text are the same as in earlier papers in this series (*e.g.* Refs.[5,8]).

B = total Hg(II) concentration
b = concentration of Hg^{2+}
H = analytical hydrogen ion excess concentration
h = actual $[H^+]$
$\beta_{p,q}$ = equilibrium constant for the reaction
$qHg^{2+} + pH_2O \rightleftharpoons Hg_q(OH)_p^{(2q-p)+} + pH^+$
Z average number of hydrogen ions split off by one Hg(II)

$$BZ = h - H = \Sigma p\beta_{p,q} b^q h^{-p} \quad (1)$$

$$\eta = \log \frac{B}{b} = \log(1 + \Sigma q\beta_{p,q} b^{(q-1)} h^{-p}) \quad (2)$$

$y(x)_v = y$ as a function of x at constant v

Other symbols are defined where they appear in the text. All concentrations in tables and figures are expressed in M (mole/l) and equilibrium constants are given on the M scale. In the text the unit mM (millimole/l) will sometimes be used for convenience. The complexes are sometimes written as $Hg_q(OH)_p$, sometimes as A_pB_q where $A = OH^-$ or $(-H^+)$ and $B = Hg^{2+}$.

EXPERIMENTAL

The experiments were carried out as potentiometric titrations. The hydrogen ion concentration, h, was measured with a glass electrode. Quinhydrone, hydrogen or mercury electrodes could not be used because of their reducing effect on mercury(II).

$$(-)\text{ref/S/glass}\ (+) \quad (I)$$

$$E_h = E_{oh} + 59.15 \log h + E_j \quad (3)$$

The composition of the solution, S, was for B = 0.1 M −1.3 M: B M Hg(II), H M H^+, $(3-2B-H)$ M $Na^+(Ca^{2+}_{0.5}, Mg^{2+}_{0.5})$, 3 M ClO_4^- and for B = 0.01 M−0.0025 M B M Hg(II), B' M Hg_2^{2+}, H M H^+, $(3-2B-2B'-H)$ M $Na^+(Ca^{2+}_{0.5}\ Mg^{2+}_{0.5})$, 3 M ClO_4^-
The concentration of free mercury(II) ions, b, was measured with the cell

$$\text{ref/S/Pt} \quad (II)$$

$$E_r = E_{or} + 29.58 \log [Hg^{2+}]^2/[Hg_2^{2+}] + E_j \quad (4)$$

and h as before with a glass electrode. Oxidation during the titration was prevented by bubbling CO_2 through the solution. In solutions with higher B, stirring was performed by bubbling N_2 through the solution during the titration.

The reference half cell was

ref Ag,AgCl/0.01 M NaCl, 2.99 M $Na^+(Ca^{2+}_{0.5}, Mg^{2+}_{0.5})ClO_4$/3 M $Na^+(Ca^{2+}_{0.5}, Mg^{2+}_{0.5})ClO_4$ (III)

Ag,AgCl electrodes were prepared according to Brown [6].

The emf of cell (I) was read on a Radiometer valve potentiometer PHM 4, reading accuracy ± 0.2 mV, calibrated against a Leeds and Northrup compensator type K 3. The latter instrument was used for measuring the emf of cell (II).

The liquid junction potential was measured with a glass electrode and a Ag, AgCl electrode. In 1.5 M $Ca(ClO_4)_2$ with $0.5 > h > 0.006$ M we found $E_j = -(16.5 \pm 0.5)h$ mV and in 1.5 M $Mg(ClO_4)_2$ with $0.2 > h > 0.006$ M $E_j = -(18.5 \pm 1)h$ mV. In 3 M $NaClO_4$ E_j was found to be $-16.7\ h$ mV, in agreement with Biedermann and Sillén [7].

For each value of B, one hydrolysed $Hg(ClO_4)_2$ solution and one with excess acid were prepared. Two sets of titration were then made. In one the acid solution was added to the hydrolysed one, in the other the hydrolysed solution was in the burette. The latter type of titration was used in order to determine E_{oh}.

Materials and analysis

Sodium, magnesium and calcium perchlorate were each prepared by dissolving the carbonate in perchloric acid and recrystallizing the product twice. The concentration of free strong acid was determined as described by Olin [8], and ClO_4^- by ion exchange methods. *Hydrochloric acid* (Kebo p.a.) was standardized against recrystallized Tl_2CO_3 and $KHCO_3$. *Sodium hydroxide* was prepared from 50 % NaOH and standardised against $HClO_4$. *Calcium hydroxide.* By burning $CaCO_3$ in an oven at 900°C we got CaO, which was dissolved in water. The clear solution was standardized against $HClO_4$. *Mercury (II) oxide* (Merck p.a.) was used without purification. *Mercury(I) perchlorate* was prepared by reducing a solution of $Hg(ClO_4)_2$ (see below) with Hg(l).

Determination of remaining Hg^{2+}. After the $Hg(ClO_4)_2$ solution had been in contact with Hg for two days it was analysed for Hg^{2+}. From the reduced solution and stock solutions of $Hg(ClO_4)_2$, $NaClO_4$ and $HClO_4$ two solutions were made up, both 3 M in ClO_4^- and with 50 mM H^+. One, S_1 contained $(c_1 - \delta)$ mM Hg_2^{2+} and δ mM Hg^{2+} and the other, S_2, $(c_1 - \delta)$ mM Hg_2^{2+} and $(c_2 + \delta)$ mM Hg^{2+}. c_1 and c_2 were known, δ was unknown. A potentiometric titration was then made, starting with v_0 ml of S_1 and adding gradually v ml of S_2. The concentration of Hg^{2+} was measured with cell (II). We have [9]

$$[Hg^{2+}] = \delta + vc_2/(v_0 + v)$$

$E_r = E_{or} + 59.15\log[Hg^{2+}]/[Hg_2^{2+}]^{0.5} = E'_0 + 59.15\log[Hg^{2+}]$ since $[Hg_2^{2+}]$ is constant.

$$[Hg^{2+}] = 10^{(E - E_0')/59.15} = \delta + vc_2/(v_0 + v)$$

By analogy with the method developed by Gran [10] for determination of h, $10^{(E-E'')/59.15}$ (E'' = arbitrary constant) was plotted as a function of $vc_2/(v_0 + v)$ and extrapolated to zero; this gave δ as the intercept on the axis. The ratio $[Hg^{2+}]/[Hg_2^{2+}]$ was calculated and found to be close to the value of the equilibrium constant for the reaction $Hg^{2+} + Hg \rightleftharpoons Hg_2^{2+}$ given by Hietanen and Sillén [11] for the actual perchlorate concentration.

Mercury(II) perchlorate. HgO was dissolved in $HClO_4$. A clear solution was obtained only with an excess of acid. Since it was desirable to cover as broad a Z range as possible, we wanted a hydrolysed solution saturated with HgO. First we started by dissolving an excess of HgO in an acid 3 M ClO_4^- solution and filtered off the undissolved oxide. On analysing this solution, however, we came upon several difficulties.

Determination of $[Hg]_{tot}$. Winkler's method, in which Hg is precipitated as Hg_2Cl_2, gave values that agreed very well with each other. To test the accuracy of the analysis we used a solution with a known amount of Hg(II) and found a difference of −0.3 %. With electrolysis, using a rotating platinum net in acid solution, the difference was even greater.

Table 1.

Values of $-\log h$, Z and η with 1.5 M $Ca(ClO_4)_2$ medium

B = 0.0025 M: $-\log h$, Z, η; 3.280, 1.554, 0.7352; 3.194, 1.396, 0.6069; 3.111, 1.250, 0.5023; 3.040, 1.111, 0.4189; 2.970, 0.988, 0.3500; 2.849, 0.743, 0.2475; 2.737, 0.549, 0.1775; 2.631, 0.404, 0.1278; 2.536, 0.301, 0.0954; 2.379, 0.172, 0.0597; 2.255, 0.120, 0.0392; 2.164, 0.090, 0.0318; 2.032, 0.060, 0.0215; 1.941, 0.044, 0.0166; 1.872, 0.024, 0.0142; 1.817, 0.024, 0.0108; 1.743, 0.020, 0.0086; 1.678, — 0.0069; 1.576, — 0.0047; 1.498, — 0.0034;

B = 0.005 M: $-\log h$, Z, η; 2.952, 0.923, 0.3341; 2.862, 0.761, 0.2629; 2.776, 0.615, 0.2046; 2.692, 0.491, 0.1589; 2.612, 0.383, 0.1238; 2.533, 0.299, 0.0964; 2.455, 0.236, 0.0757; 2.326, 0.144, 0.0509; 2.213, 0.111, 0.0367; 2.129, 0.082, 0.0287; 2.002, 0.056, 0.0198; 1.912, 0.040, 0.0154; 1.817, 0.026, 0.0118; 1.750, 0.014, 0.0100; 1.682, 0.022, 0.0068;

Table 2.

Values of $-\log h$, Z and η with 3 M $NaClO_4$ medium.

B = 0.0025 M: $-\log h$, Z, η; 3.104, 1.005, 0.3692; 3.023, 0.845, 0.2954; 2.948, 0.699, 0.2370; 2.872, 0.576, 0.1903; 2.800, 0.472, 0.1541; 2.734, 0.382, 0.1252; 2.668, 0.315, 0.1024; 2.607; 0.259, 0.0839; 2.550, 0.223, 0.0612; 2.455, 0.167, 0.0531; 2.375, 0.135, 0.0415; 2.255, 0.096, 0.0286; 2.171, 0.065, 0.0228; 2.103, 0.062, 0.0189; 2.051, 0.055, 0.0172; 1.828, 0.028, 0.0091; 1.687, — 0.0061; 1.505, — , 0.0046;

B = 0.005 M: $-\log h$, Z, η; 2.827, 0.521, 0.1755; 2.784, 0.462, 0.1550; 2.744, 0.407, 0.1388; 2.702, 0.359, 0.1236; 2.621, 0.277, 0.0964; 2.546, 0.211, 0.0757; 2.473, 0.166, 0.0614; 2.315, 0.102, 0.0384; 2.201, 0.073, 0.0279; 2.117, 0.060, 0.0222; 2.002, 0.040, 0.0168; 1.664, 0.012, 0.0066; 1.488, 0.008, 0.0044;

B = 0.010 M: $-\log h$, Z, η; 2.271, 0.092, 0.0347; 2.326, 0.114, 0.0406; 2.380, 0.137, 0.0472; 2.429, 0.163, 0.0549; 2.482, 0.202, 0.0642; 2.511, 0.224, 0.0707, 2.335, 0.126, 0.0419; 2.191, 0.075, 0.0279; 2.080, 0.049, 0.0205; 1.992, 0.035, 0.0157; 1.836, 0.016, 0.0111; 1.723, 0.012, 0.0076; 1.566, 0.002, 0.0057; 1.456, — , 0.004; 1.373, — , 0.0046; 1.307, — , 0.0041;

Table 3.

Values of $-\log h$, Z with 1.5 M $Ca(ClO_4)_2$ medium.

B = 0.100 M: $-\log h$, Z; 2.032, 0.0929; 1.956, 0.0737; 1.880, 0.0587; 1.807, 0.0476; 1.741, 0.0388; 1.677, 0.0333; 1.625, 0.0283; 1.533,0.0204; 1.454, 0.0178; 1.393, 0.0131; 1.341, 0.0095; 1.295, 0.0071; 1.217, 0.0066; 1.155, 0.0079; 1.107, 0.0032;

B = 0.500 M: $-\log h$, Z; 1.697, 0.0998; 1.670, 0.0913; 1.645, 0.0838; 1.584, 0.0709; 1.523, 0.0595; 1.462, 0.0500; 1.400, 0.0427; 1.332, 0.0355; 1.290, 0.0319; 1.243, 0.0276; 1.155, 0.0227; 1.084, 0.0192; 1.025, 0.0164; 0.950, 0.0148; 0.891, 0.0134; 0.830, 0.0112; 0.783, 0.0086; 0.741, 0.0092; 0.710, 0.0056; 0.673, 0.0052; 0.644, 0.0066; 0.617, 0.0044; 0.587, 0.0040;

B = 1.000 M: $-\log h$, Z; 1.474, 0.0983; 1.446, 0.0895; 1.415, 0.0815; 1.382, 0.0742; 1.346, 0.0680; 1.283, 0.0563; 1.217, 0.0474; 1.156, 0.0403; 1.099, 0.0350; 1.048, 0.0306; 0.984, 0.0254; 0.921, 0.0230; 0.872, 0.0203; 0.832, 0.0175; 0.779, 0.0181; 0.735, 0.0137; 0.700, 0.0122; 0.670, 0.0113; 0.636, 0.0104; 0.583, 0.0089; 0.546, 0.0074; 0.516, 0.0078; 0.494, 0.0067; 0.720, 0.0132; 0.690, 0.0123; 0.656, 0.0114; 0.624, 0.0104; 0.388, 0.0090; 0.551, 0.0070; 0.507, 0.0074; 0.473, 0.0069; 0.438, 0.0059; 0.387, 0.0058; 0.328, 0.0050;

Table 4.

Values of $-\log h$, Z with 1.5 M $Mg(ClO_4)_2$ medium.
B = 0.100 M: $-\log h$, Z; 2.026, 0.0949; 1.966, 0.0794; 1.908, 0.0657; 1.849, 0.0552; 1.793, 0.0466; 1.741, 0.0396; 1.692, 0.0346; 1.606, 0.0269; 1.533, 0.0208; 1.471, 0.0176; 1.371, 0.0116; 1.293, 0.0097; 1.202, 0.0098; 1.134, 0.0072; 1.063, 0.0080; 1.003, 0.0042; 0.954, 0.0050;

B = 0.200 M: $-\log h$, Z; 1.868, 0.0816; 1.817, 0.0700; 1.765, 0.0604; 1.714, 0.0518; 1.660, 0.0458; 1.567, 0.0355; 1.484, 0.0288; 1.415, 0.0231; 1.298; 0.0181; 1.212, 0.0136; 1.145, 0.0095; 1.084, 0.0108; 1.035, 0.0107; 0.996, 0.0080; 0.942, 0.0095; 0.888, 0.0075; 0.845, 0.0045; 0.808, 0.0055;

B = 0.500 M: $-\log h$, Z: 1.701, 0.0998; 1.677, 0.0916; 1.645, 0.0845; 1.584, 0.0714; 1.525, 0.0598; 1.464, 0.0503; 1.403, 0.0426; 1.347, 0.0363; 1.295, 0.0312; 1.244, 0.0277; 1.156, 0.0227; 1.085, 0.0191; 1.030, 0.0149; 0.954, 0.0136; 0.893, 0.0132; 0.834, 0.0096; 0.783, 0.0092; 0.744, 0.0076; 0.708, 0.0062; 0.681, 0.0054; 0.631, 0.0034; 0.558, 0.0062; 0.534, 0.0050;

B = 1.000 M: $-\log h$, Z: 1.488, 0.1014; 1.457, 0.0928; 1.423, 0.0848; 1.393, 0.0773; 1.359, 0.0706; 1.292, 0.0591; 1.227, 0.0497; 1.168, 0.0420; 1.112, 0.0360; 1.060, 0.0315; 0.992, 0.0263; 0.933, 0.0230; 0.884, 0.0197; 0.840, 0.0176; 0.786, 0.0153; 0.744, 0.0128; 0.707, 0.0117; 0.678, 0.0096; 0.644, 0.0081; 0.610, 0.0069; 0.573, 0.0066; 0.544, 0.0058; 0.517, 0.0083: 0.499, 0.0078; 0.451, 0.0077; 0.396, 0.0080; 0.348, 0.0067;

B = 1.300 M: $-\log h$, Z: 1.446, 0.1197; 1.429, 0.1130; 1.407, 0.1070; 1.369, 0.0954; 1.331, 0.0852; 1.292, 0.0763; 1.253, 0.0685; 1.214, 0.0618; 1.178, 0.0557; 1.124, 0.0484; 1.080, 0.0418; 1.033, 0.0370; 0.992, 0.0328; 0.935, 0.0287; 0.888, 0.0255; 0.897, 0.0232; 0.815, 0.0207; 0.774, 0.0192; 0.735, 0.0176; 0.695, 0.0158; 0.663, 0.0145; 0.637, 0.0132; 0.610, 0.0127; 0.830, 0.0222; 0.800, 0.0199; 0.764, 0.0185; 0.729, 0.0165; 0.688, 0.0155; 0.647, 0.0136; 0.604, 0.0123; 0.568, 0.0109; 0.531, 0.0098; 0.504, 0.0096; 0.475, 0.0099; 0.448, 0.0087; 0.418, 0.0085; 0.387, 0.0077;

Table 5.

Values of $-\log h$, Z with 3 M $NaClO_4$ medium.
B = 0.100 M: $-\log h$, Z; 2.088, 0.0817; 2.019, 0.0661; 1.948, 0.0541; 1.880, 0.0445; 1.814, 0.0382; 1.753, 0.0338; 1.701, 0.0296; 1.613, 0.0219; 1.533, 0.0199; 1.473, 0.0156; 1.418, 0.0131; 1.369, 0.0134; 1.292, 0.0107; 1.229, 0.0091; 1.178, 0.0067; 1.112, 0.0078; 1.016, 0.0051;

B = 0.500 M: $-\log h$, Z; 1.758, 0.0945; 1.733, 0.0872; 1.699, 0.0799; 1.635, 0.0663; 1.566, 0.0550; 1.496, 0.0459; 1.429, 0.0386; 1.368, 0.0326; 1.307, 0.0289; 1.256, 0.0251; 1.165, 0.0204; 1.092, 0.0169; 1.033, 0.0137; 0.957, 0.0120; 0.898, 0.0104, 0.834, 0.0096; 0.784, 0.0080; 0.744, 0.0070;

B = 1.000 M: $-\log h$, Z; 1.518, 0.0946; 1.479, 0.0864; 1.446, 0.0784; 1.408, 0.0714; 1.375, 0.0646; 1.304, 0.0535; 1.233, 0.0450; 1.168, 0.0381; 1.107, 0.0331; 1.053, 0.0293; 1.003, 0.0268; 0.923, 0.0223; 0.877, 0.0188; 0.832, 0.0173; 0.778, 0.0154; 0.734, 0.0142; 0.700, 0.0120; 0.668, 0.0120; 0.634, 0.0110; 0.683, 0.0125; 0.656, 0.0110; 0.593, 0.0098; 0.524, 0.0081; 0.456, 0.0068; 0.375, 0.0061; 0.296, 0.0060;

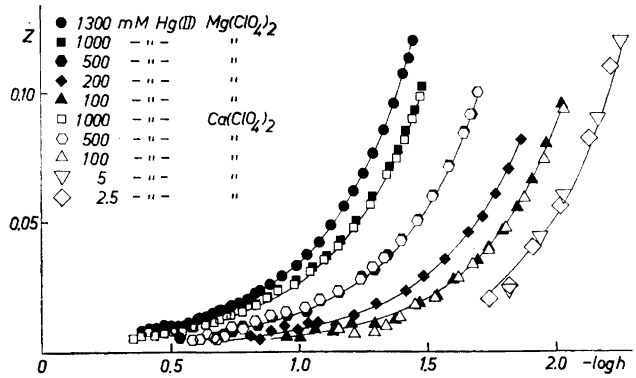

Fig. 1. Hydrolysis of Hg^{2+} in 1.5 M $Ca(Mg)(ClO_4)_2$. Experimental data plotted as $Z(-\log h)_B$. The curves are calculated with the equilibrium constants given in the text.

Determination of H. Several methods are recommended in the literature for the determination of the analytical hydrogen content. Bromide [12] forms strong complexes with mercury and diminishes the hydrolysis, but on adding strong mercury(II) solution to sodium bromide solution we got a precipitate, which it was possible to dissolve only by protracted boiling. Under these conditions there was a strong smell of Br_2, the indicator lost its colour and the equivalence point was transitory. Adding bromide to a diluted mercury (II) solution and bubbling with nitrogen during the titration in order to get rid of carbon dioxide and prevent oxidation by atmospheric oxygen, gave values agreeing to within 0.1 %, but all 1 % lower than the correct one. Potentiometric titration with acid, using a Gran diagram [10] gave a concave curve instead of a straight line, even if both Hg(II) and Br^- were kept constant during the experiment. The results seemed also to depend upon the time of contact between the mercury (II) and bromide solutions. Thus it did not seem likely that this method would give accurate results unless a more complicated technique could be used.

Shaking with liquid Hg and titrating the reduced solution potentiometrically with acid, using the Gran extrapolation, gave too high H-values.

Determination of total perchlorate content. Good results for the total perchlorate content ($= 2B + H$) were obtained by passing a known amount of solution of known $[ClO_4^-]$ through a H^+ saturated ion exchanger and titrating the eluate with NaOH. When mercury was removed by electrolysis and the solution afterwards titrated with NaOH we got slightly lower values for $(2B + H)$. If B is high serious errors in H might arise from the mercury analysis on using the two last methods.

Final preparation. After having tried these different methods of analysis for H with not too good results, we decided to proceed in the simplest way. We could use the approximate information given by the experiments, described above, about the highest Z-value that could be reached. We weighed out 5–25 g oxide and dissolved this in a weighed amount of standard acid by heating on a waterbath for a few days. By this method we got more reproducible results, *i.e.* with separately made solutions we got the same $Z(\log h)_B$ curve.

For each B value we prepared one acid and one hydrolysed solution. The latter frequently became turbid after addition of perchlorate and dilution to the desired volume. The precipitate was filtered off through a procelain filter and weighed after being dried in a desiccator at room temperature. In order to avoid errors arising from changes in air humidity, a second crucible of the same kind was treated in the same way and used as a blank for weight correction. The precipitate weighed about 1 mg/100 ml solution If it is assumed to be HgO, the correction in H may be calculated. It was never as large as 0.1 % of B.

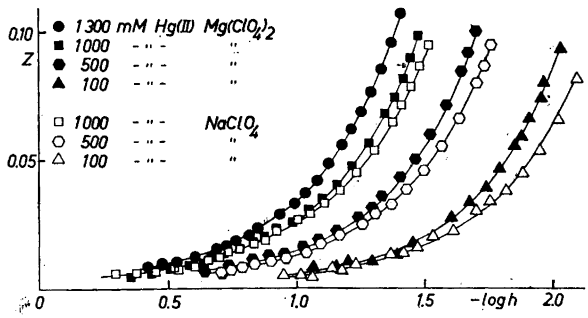

Fig. 2. Hydrolysis of Hg^{2+} in 3 M Na(Mg)ClO_4. Experimental data plotted as $Z(-\log h)_B$. The curves are calculated with the equilibrium constants given in the text.

CALCULATIONS

The experimental data are presented in Tables 1—5 and Figs. 1—4. It should be observed that, on increasing B, the limiting composition will be the same for all three media, namely 1.5 M $Hg(ClO_4)_2$. One may ask how much the activity factors are affected by the change in ionic medium. It is seen that, within the experimental error, the data $Z(\log h)_B$ for 3 M (Mg)ClO_4 coincide with those for 3 M (Ca)ClO_4 in the whole B range studied.

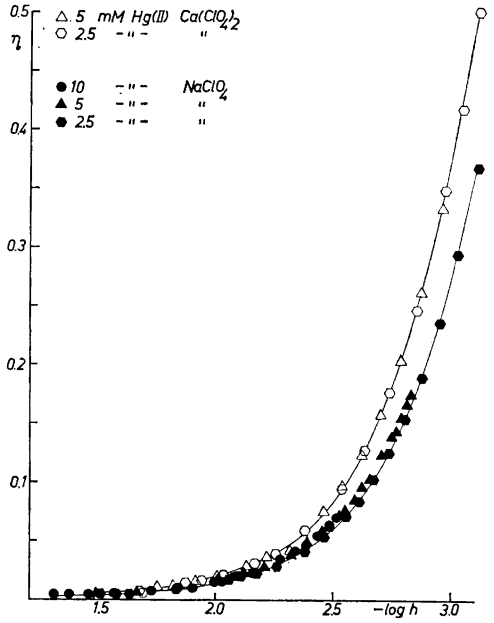

Fig. 3. Experimental data $\eta = \log (B/b)$ as a function of $-\log h$. The curves are calculated with the mononuclear constants given in the text.

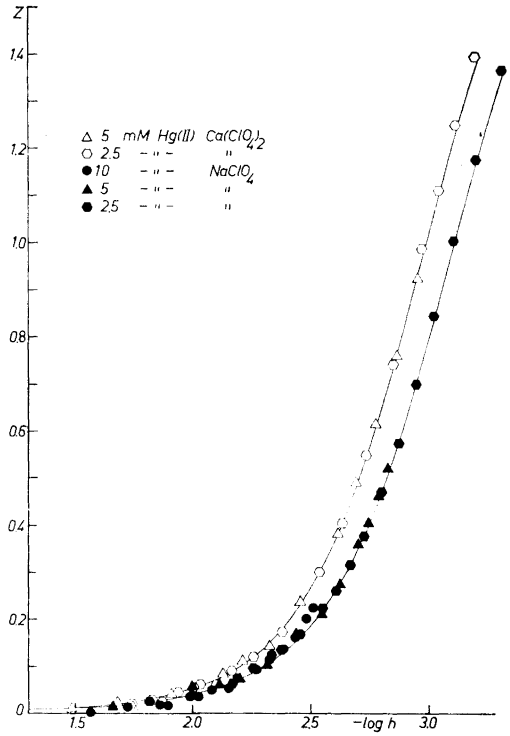

Fig. 4. Experimental data plotted as $Z(-\log h)_B$. The curves are calculated with the equilibrium constants given in the text.

The simplest explanation is that the activity factors are not perceptibly changed when Hg^{2+} is replaced by another bivalent ion, Mg^{2+} or Ca^{2+}. The data in 3 M $(Ca)ClO_4$ and 3 M $(Mg)ClO_4$ will therefore be considered together as one group and the emphasis will be laid on them.

With 3 M $(Na)ClO_4$ on the other hand, the curves for low B deviate considerably from those with 3 M (Ca, Mg)ClO_4. For low B we may still assume constant activity coefficients and equilibrium constants in 3 M $(Na)ClO_4$, but these will be different from those in 3 M (Ca, Mg)ClO_4.

When B increases, separate curves are obtained for different B values (Figs. 1 and 2). This indicates the presence of polynuclear complexes.

Treatment of data in the mononuclear range

For the lowest values of B the points fall on the same $\eta(\log h)_B$ or $Z(\log h)_B$ curve, the "mononuclear wall" (Figs. 3 and 4), *i.e.* only mononuclear complexes are found and this is in agreement with the results of Hietanen and Sillén [1].

Z-data. We have $Z = \dfrac{\beta_{1,1}a + 2\beta_{2,1}a^2}{1 + \beta_{1,1}a + \beta_{2,1}a^2}$ (7)

where $a = h^{-1}$.

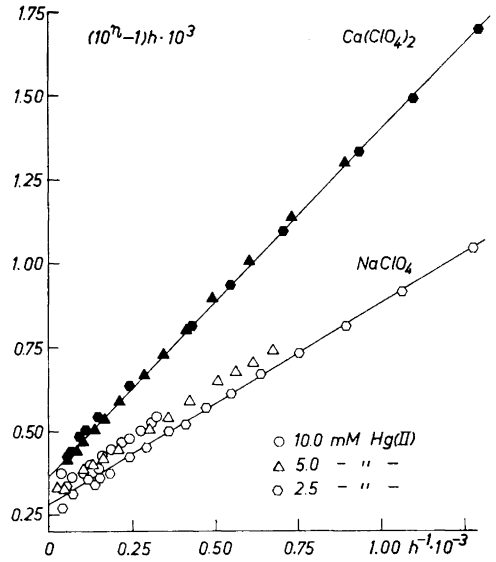

Fig. 5. $(10^{\eta}-1)h$ as a function of h^{-1}. The lines give in 1.5 M $Ca(ClO_4)_2$, $\log \beta_{1,1} = -3.44$, $\log \beta_{2,1} = -5.97$ and in 3 M $NaClO_4$, $\log \beta_{1,1} = -3.53$, $\log \beta_{2,1} = -6.21$.

The experimental curve $Z(\log h)_B$ was compared with normalized curves, $Z(\log u)_B$. Ref.[13]

$$Z = \frac{u + 2ku^2}{1 + u + ku^2} \tag{8}$$

where $u = \beta_{1,1}a$ and $k = \beta_{2,1}\beta_{1,1}^{-2}$.

Redox data. Setting

$$10\eta = B/b = 1 + \beta_{1,1}h^{-1} + \beta_{2,1}h^{-2} \tag{9}$$

and

$$(10\eta-1)h = \beta_{1,1} + \beta_{2,1}h^{-1}$$

$(10\eta-1)h$, plotted as a function of h^{-1} is shown in Fig. 5. To calculate η from E_r, a preliminary value of E_{or} was obtained from the most acid solutions, neglecting the hydrolysis. The plot $(10\eta-1)h$, (h^{-1}) then showed a deviation downwards from the straight line for the lowest h^{-1} values, showing that we had chosen a too low value of E_{or}. A too high value of E_{or} on the other hand caused the points to deviate upwards. The best value of E_{or} was taken as the one which gave the least deviation between the calculated line and the experimental points. In 3 M $(Na)ClO_4$ the correction amounted to 0.15 mV but in 3 M $(Ca)ClO_4$ where the solution was still more acid ($\sim$ 0.1 M), the preliminary E_{or} value could be used without any correction.

The point of intersection with the vertical axis gave $\beta_{1,1}$ and the slope $\beta_{2,1}$. The values are tabled below. Almost the same results were obtained by curve-fitting analogous to (8).

The constants were then refined, using the experimental points and the generalized least squares treatment "Letagrop" (pit-mapping) [18]. The error limits given are three times the "standard" or root mean square deviation (σ).

	3 M (Ca)ClO_4		3 M (Na)ClO_4	
	$\log \beta_{1,1}$	$\log \beta_{2,1}$	$\log \beta_{1,1}$	$\log \beta_{2,1}$
Z data				
B = 0.005 M, 0.0025 M				
Curve-fitting	-3.50 ± 0.06	-6.00 ± 0.04	-3.55 ± 0.06	-6.21 ± 0.02
Letagrop	-3.52 ± 0.03	-5.962 ± 0.003	-3.55 ± 0.04	-6.211 ± 0.003
η data				
B = 0.005 M, 0.0025 M				
Curve-fitting	-3.48 ± 0.04	-5.96 ± 0.02	-3.53 ± 0.04	-6.20 ± 0.02
Linear plot	-3.44 ± 0.04	-5.97 ± 0.02	-3.53 ± 0.04	-6.21 ± 0.02

The larger uncertainty in $\log \beta_{1,1}$ may be understood from the fact that the complex $HgOH^+$ exists in a small amount (at most about 10 % of all Hg(II)) and in a narrow $\log h$ range.

Treatment of data in the polynuclear range

For the higher concentrations only the Z data were used, since the variations of η proved too small to be useful for calculations. The primary data were the measurements $E(H)_B$. To calculate Z and h one needs to know E_0 and E_j in eqn. (3). The first calculations were made using approximate values for E_{oh}, estimated from the most acidic solutions. As the calculations proceeded, E_{oh} and E_j could be refined as will be described below.

From the slope of the curves of the highest B values (self-media) it might be concluded [5] that for low Z values the predominating complexes contain only one OH^- group. A comparison with the value of $\beta_{1,1}$ already determined showed that there must also be polynuclear complexes AB_q besides AB ($HgOH^+$).

Beginning from $$BZ = \Sigma p\beta_{pq}a^p b^q \qquad (1)$$

we subtracted the mononuclear terms, setting as a first approximation $b = B(1-2Z)$ or $b = B(1-Z)$, which gave the same result, since the difference is small. Assuming one polynuclear complex with one OH^- group and another with p OH^- groups we have

$$B_c Z_c = BZ - \beta_{1,1}ab - 2\beta_{2,1}a^2 b = \beta_{1,q'}ab^{q'} + p\beta_{p,q}a^p b^q \qquad (10)$$

Multiplying by $a^{-1} = h$ and extracting the first term we get, after taking logarithms,

$$\log B_c Z_c a^{-1} = \log \beta_{1,q'}b^{q'} + \log (1 + p\beta_{p,q}a^{(p-1)}b^q/\beta_{1,q'}b^{q'}) \qquad (11)$$

Since in each titration $b \approx B$ = constant (11) may be written in the normalized form (v = const.a^{-1}).

$$\log B_c Z_c a^{-1} = \log k + \log(1 + v^{(1-p)}) \qquad (12)$$

where $$\log k = \log \beta_{1,q'} + q' \log B \qquad (12a)$$

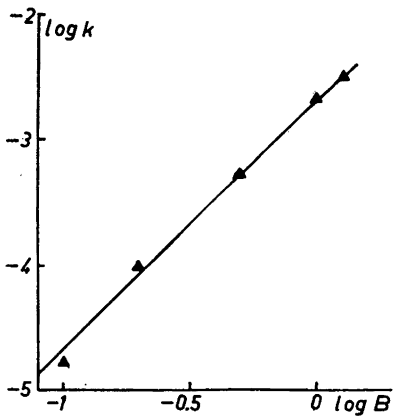

Fig. 6. Log k as a function of log B according to eqn. (12 a). The slope of the line gives $q' = 2$ and the intercept on the vertical axis log $\beta_{1,2} \sim -2.7$.

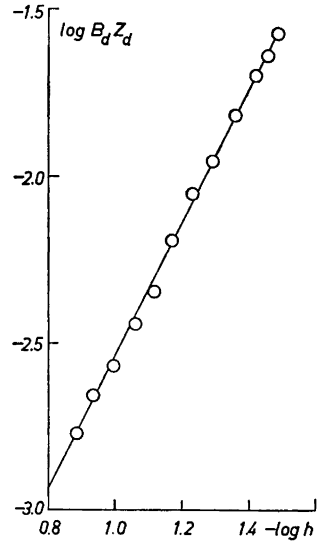

Fig. 7. Log $B_d Z_d$ as a function of $-\log h$ for $B = 1.000$ M according to eqn. (4). B_d Z_d; terms for $HgOH^+$, $Hg(OH)_2$, Hg_2OH^{3+} have been subtracted. The line gives p = 2.

To find log k the experimental plots (log $B_c Z_c h$)(log $h)_B$ were compared with theoretical curves log$(1 + v^{(1-p)})$ (log v) (Ref.[14]), calculated for different values of p. The fit was better with $p = 2$ than with $p = 3$. The following calculation for q and $\beta_{p,q}$ was made with $p = 2$ but with another p value one would obtain a very similar result.

Plotting log k as a function of log B (Fig. 6) gave log $\beta_{1,q'}$ as intercept on the vertical axis. The slope of the line was $q' = 2$. The complex thus seems to be Hg_2OH^{3+} with log $\beta_{1,2}$ approximately $= -2.7$.

With this knowledge we could start again from the experimental data $E(H)_B$ to get a better value of E_{oh}, using a method somewhat modified from that given by Hietanen and Sillén [5]. BZ was obtained for selected values of log h from curves, calculated with the constants found above. From the relation $H = h - BZ$ we got the corresponding H values. From the experimental $E(H)_B$ diagram the corresponding values of E were interpolated. $E + 59.15$ log h was then plotted as a function of h, and the straight line, extrapolated to $h = 0$, gave E_{oh} and the slope E_j. The procedure had to be repeated and the results improved as one gained more knowledge about the complexes appearing; the refinement of E_{oh} and E_j of course led to corresponding small changes in H and Z.

As mentioned above the curve log $(1 + v^{(1-p)})$(log v) for $p = 2$ gave a better fit with the experimental points than that with $p = 3$, which indicates a complex with two OH^- groups. In order to remove any doubt, the term for the new complex with one OH^- was subtracted.

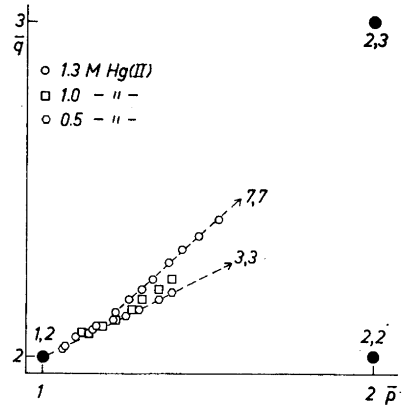

Fig. 8. $\bar{q}$ *versus* $\bar{p}$. The main complex is AB_2 Points for different B values lie on separate lines. The arrows marked 7,7 and 3,3 point to complexes A_7B_7 and A_3B_3.

$$B_dZ_d = BZ - \beta_{1,1}ab - 2\beta_{2,1}a^2b - kh^{-1} = p\beta_{p,q}a^pb^q \tag{13}$$

where $kh^{-1} = \beta_{1,q'}ab^{q'}$

$$\log B_dZ_d = p\log a + \log p\beta_{p,q}b^q \tag{14}$$

In Fig. 7, for $B = 1.0$ M, $\log B_dZ_d(\log a)_B$ gave a straight line with slope $p = 2$. From the intersection with the vertical axis $\beta_{p,q}$ was obtained. Plotting

$$\log B_dZ_d - 2\log a = q\log B + \log \beta_{2,q} + \log 2 \tag{15}$$

versus log B, the slope ($= q$) was intermediate between 2 and 3.

To distinguish between $q = 2$ and 3 several ways were tried. By integration from experimental curves, $Z(\log h)_B$ using general expressions given by Sillén [15], b could be calculated. Starting the integration at $Z = Z_o = 0.01$ and assuming the dominating complex there to be AB_2, we have

$$B = b_o + 2\beta_{1,2}a_ob_o^2 \tag{16}$$

$$BZ_o = \beta_{1,2}a_ob_o^2 \tag{17}$$

$$BR_o = b_o + \beta_{1,2}a_ob_o^2 \tag{18}$$

$$\text{and } \ln\frac{b}{B} = \ln(1-2Z_o) + \int_{Z_o}^{Z}\left(\frac{\log a}{\log B}\right)_Z dZ - \int_{Z_o}^{Z} Z\, d\ln a \tag{19}$$

As the function for the mononuclear species is known, one could subtract it and calculate the average composition of the polynuclear complexes.

$$\bar{q} = \frac{B-B_1}{BR-B_1} \quad (20) \quad \bar{p} = \frac{BZ-B_1Z_1}{BR-B_1} \tag{21}$$

where $B_1Z_1 = b(\beta_{1,1}a + \beta_{2,1}a^2)$ and $B_1 = b(1 + \beta_{1,1}a + \beta_{2,1}a^2)$

The plot $\bar{q}$ against $\bar{p}$ for $B = 1.3$, 1.0 and 0.5 M is shown in Fig. 8. Since the points for different B values lie on diverging lines, we must have at least

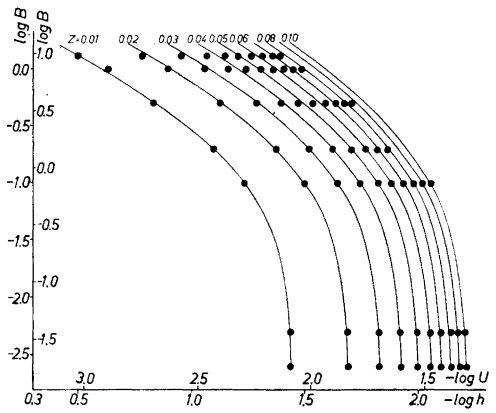

Fig. 9. Projection map: experimental data log $B(-\log h)_Z$ and normalized curves log $B^*(\log u)_Z$, calculated for AB, A_2B. AB_2, A_2B_2, assuming log $\beta_{1,1}^{-2}\beta_{2,1} = 1.1$ and log $\beta_{1,1}^{-1}\beta_{1,2}^{-1}\beta_{2,2} = 1.3$.

two complexes besides the ones found above. As the Z range which it is possible to integrate is very small, definite values of the p and q values cannot be determined from the plot.

The experimental data log $B(\log h)_Z$ were compared with normalized projection maps, log B^* $(\log h)_Z$ (Ref.[16]).

$$B = b + \beta_{1,1}ab + \beta_{2,1}a^2b + 2\beta_{1,2}ab^2 + q\beta_{2,q}a^2b^q \tag{22}$$

$$B^* = v + uv + ku^2v + 2uv^2 + lqu^2v^q \tag{23}$$

where

$$B^* = \beta_{1,1}^{-1}\beta_{1,2}B;\quad v = \beta_{1,1}^{-1}\beta_{1,2}b;\quad u = \beta_{1,1}a \tag{24, 24a, 24b}$$

$$k = \beta_{1,1}^{-2}\beta_{2,1};\quad l = \beta_{1,1}^{(q-3)}\beta_{1,2}^{(1-q)}\beta_{2,q} \tag{24c, 24d}$$

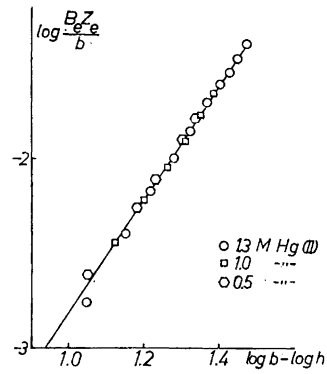

Fig. 10. Log B_eZ_e/b as a function of log b − log h, according to (26). B_eZ_e; terms for $HgOH^+$, $Hg(OH)_2$, Hg_2OH^{3+}, $Hg_2(OH)_2^{2+}$ have been subtracted. The line gives $p = 3$.

The best fit for lower B and Z values was obtained with the assumption $q = 2$, *i.e.* a complex A_2B_2 together with those found earlier (Fig. 9). For higher values of B and Z the experimental points lay on lines more curved towards higher log h values than the normalized ones, thus indicating another complex with higher values of p and q.

With the help of the Ferranti Mercury Computer and the program "KUSKA" [17], several curves $Z(\log h)_B$ were calculated for different values of $\beta_{1,2}$ and $\beta_{2,2}$. From these the one giving the best fit for $B = 0.1$ M, was chosen. The same set of constants could also explain the experimental points for $B = 0.2$ M. When B increased, deviations appeared for high Z-values. Subtracting all four complexes one obtains

$$B_eZ_e = BZ - \beta_{1,1}ab - 2\beta_{2,1}a^2b - \beta_{1,2}ab^2 - 2\beta_{2,2}a^2b^2 = p\beta_{p,q}a^pb^q \qquad (25)$$

In these calculations b was taken from the integration (19).

Setting $q = p + x$

$$\log B_eZ_e/b^x = p \log ab + \log p\beta_{p,q} \qquad (26)$$

Fig. 10 shows $\log B_eZ_e/b^x$ as a function of $\log ab$ for $x = 1$. It is seen that for this value of x the points from different B values fall on the same line. The slope, p, is 3. For all other values of x points for different B values fell on different lines. The complex thus ought to be $Hg_4(OH)_3^{5+}$. The point of intersection with the vertical axis gives an approximate value of $\beta_{p,q}$.

In order to find more accurate values of the five complex constants the generalized least square treatment "LETAGROP" [18] was used.

The deviation given is 3σ as above.

3 M (Ca,Mg)ClO_4	$\log \beta_{1,1}$	$\log \beta_{2,1}$	$\log \beta_{1,2}$	$\log \beta_{2,2}$	$\log \beta_{3,4}$
Letagrop					
(B=1.3−0.0025 M)	−3.52 ± 0.03	−5.962 ± 0.003	−2.66 ± 0.06	−4.91 ± 0.12	−6.18 ± 0.12
(B=1.3−0.1 M)	−3.49 ± 0.02	(−5.96)	−2.67 ± 0.02	−4.95 ± 0.05	−6.15 ± 0.05
Proposed values	−3.49 ± 0.06	−5.96 ± 0.02	−2.67 ± 0.03	−4.95 ± 0.08	−6.15 ± 0.08

In 3 M (Na)ClO_4 the activity coefficients may have a bigger influence, so with help of the same treatment as above the constants were calculated separately for different B values.

3 M (Na)ClO_4	$\log \beta_{1,1}$	$\log \beta_{2,1}$	$\log \beta_{1,2}$	$\log \beta_{2,2}$	$\log \beta_{3,4}$
Letagrop					
(B = 1.0 M)	−3.55 ± 0.06	(−6.21)	−2.65 ± 0.02	−5.16 ± 0.09	−6.40 ± 0.02
(B = 0.5 M)	−3.55 ± 0.09	»	−2.70 ± 0.03	−5.10 ± 0.09	−6.4 ± 0.1
(B = 0.1 M)	−3.56 ± 0.08	»	−2.7 ± 0.1	−5.2 ± 0.1	−

The values given within brackets have not been varied.

CONCLUSION

From the data presented in this paper one may conclude that in Hg(II) perchlorate solutions there are polynuclear species with 1 OH, 2 OH and 3 OH, besides the mononuclear ones found previously by several investigators. The formulas ascribed above have been AB_2, A_2B_2 and A_3B_4, thus Hg_2OH^{3+},

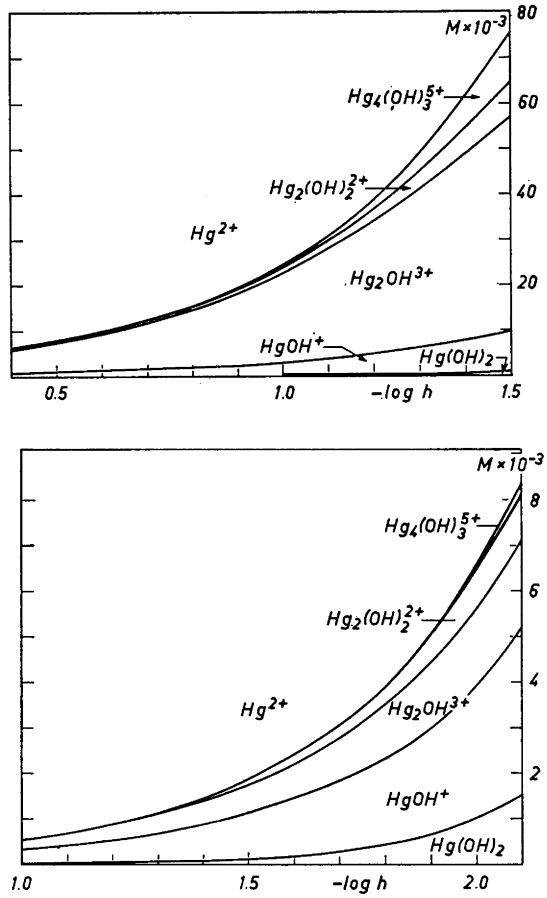

Fig. 11. Distribution of complexes as a function of $-\log h$ for the total mercury concentrations $B = 1.000$ M and $B = 0.100$ M.

$Hg_2(OH)_2^{2+}$ and $Hg_4(OH)_3^{5+}$ as usual with unknown amounts of H_2O and ClO_4^-. A complex AB_2 has also been found in solutions of other divalent metals for instance Pb^{2+} (Ref.[19]) and Cd^{2+} (Ref.[20]), Be^{2+} (Ref.[22]) and Cu^{2+} (Ref.[23]). A_2B_2 was found in Fe^{3+} (Ref.[24]), UO_2^{2+} (Ref.[21]) and Th^{4+} (Ref.[5]) among others.

As may be seen from Fig. 11, which shows the distribution of the various species as a function of $\log h$ for the two limiting concentrations $B = 1.0$ M and 0.1 M, the complexes Hg_2OH^{3+} and $Hg_2(OH)_2^{2+}$ are the most important polynuclear products of hydrolysis, while $[Hg_4(OH)_3^{5+}]$ becomes appreciable only for the higher concentration before precipitation. For this reason the composition of the last complex is somewhat more uncertain than those of Hg_2OH^{3+} and $Hg_2(OH)_2^{2+}$.

It is remarkable that no differences were found if one divalent medium ion Mg^{2+} was substituted with another of the same valency, Ca^{2+}. Even if the positive medium-ion was changed to an univalent one (Na^{+}) the equilibrium constants were not very much affected.

Acknowledgements. The author is greatly indebted to Professor Lars Gunnar Sillén for having suggested the problem, for this continual interest in the work and valuable comments on the manuscript. She also wishes to thank Dr. Georg Biedermann and Dr. Åke Olin for helpful suggestions on various problems connected with this work and Dr. Nils Ingri for help with the use of the computer. Some of the titrations were carried out by Mrs Birgitta Carell. The English of this paper was corrected by Dr. Helen S. Dunsmore.

This work has been supported by the *Office of Scientific Research of the Office of Aerospace Research, U.S.A.F.* through its European Office.

REFERENCES

1. Hietanen, S. and Sillén, L. G. *Acta Chem. Scand.* **6** (1952) 747.
2. Anderegg, G., Schwarzenbach, G., Padmayo, M. and Borg, O. F. *Helv. Chim. Acta* **41** (1958) 988.
3. Hayek, E. *Z. anorg. u. allgem. Chem.* **223** (1935) 382.
4. Bernstein, R., Pars, H. and Blumenthal, D. *J. Am. Chem. Soc.* **79** (1957) 1579.
5. Hietanen, S. and Sillén, L. G. *Acta Chem. Scand.* **13** (1959) 533.
6. Brown, A. S. J. *J. Am. Chem. Soc.* **56** (1934) 646.
7. Biedermann, G. and Sillén, L. G. *Arkiv. Kemi* **5** (1953) 425.
8. Olin, Å. *Acta Chem. Scand.* **14** (1960) 126.
9. Jonsson, A., Qvarfort, I. and Sillén, L. G. *Acta Chem. Scand.* **1** (1947) 461.
10. Gran, G. *Analyst* **77** (1952) 661.
11. Hietanen, S. and Sillén, L. G. *Arkiv Kemi* **10** (1956) 103.
12. Bethge, P. O., Jonevall-Westöö, I. and Sillén, L. G. *Acta Chem. Scand.* **2** (1948) 828.
13. Sillén, L. G. *Acta Chem. Scand.* **10** (1956) 186.
14. Biedermann, G. and Ciavatta, L. *Acta Chem. Scand.* **15** (1961) 1347.
15. Sillén, L. G. *Acta Chem. Scand.* **15** (1961) 1981.
16. Biedermann, G. and Sillén, L. G. *Acta Chem. Scand.* **10** (1956) 1011.
17. Ingri, N. and Sillén, L. G. *Acta Chem. Scand.* **16** (1962) 173.
18. Sillén, L. G. *Acta Chem. Scand.* **16** (1962) 159.
19. Olin Å, *Acta Chem. Scand.* **14** (1960) 814.
20. Biedermann, G. and Ciavatta, L. *Acta Chem. Scand.* **16** (1962). *To be published.*
21. Hietanen, S. and Sillén, L. G. *Acta Chem. Scand.* **13** (1959) 1828.
22. Kakihana, H. and Sillén, L. G. *Acta Chem. Scand.* **10** (1956) 985.
23. Pedersen, K. J. *Kgl. Danske Videnskab. Selskab. Mat.-fys. Medd.* **20** (1943) No. 7.
24. Hedström, B. *Arkiv Kemi* **6** (1953) 1.

Received October 23, 1961.

ACTA CHEMICA SCANDINAVICA 16 (1962) 903–915

Studies on the Coagulation of Chicken Blood

IV. Adsorption of φ-Factor Activity

ØYVIND SØRBYE*

Department of Biochemistry and Nutrition, Polytechnic Institute, Copenhagen, Denmark

Detailed studies on the adsorption of φ-factor activity from oxalated plasma by a series of adsorbents have revealed that this activity is due to the combined activities of at least five different coagulation factors. Three of the factors were inactive when Russell's viper venom-cephalin was substituted for thromboplastin in the assay system. The experiments indicated that the minimum amount of adsorbent necessary for complete adsorption of a (group of) φ-factor(s) from oxalated plasma, may be regarded as an absolute measure of the concentration(s) of the factor(s). It is suggested that the differentiation of the φ-factors obtained by the adsorption technique depends on the presence in the surface of the adsorbents of special adsorption sites, differing in number and specificity with the various adsorbents, each causing adsorption of one or a few φ-factors only.

In a preceding paper [1] it was shown that the differences in effect between κ-, δ- and φ-factors [2] were associated with differences in the adsorbabilities of the factors by a series of adsorbents. Furthermore, it was found that calcium carbonate, which adsorbs all three types of factors, could adsorb only a part of the φ-factor activity as measured with thromboplastin and with Russell's viper venom (RVV)-cephalin. The calcium carbonate adsorbable φ-factor was considered to be a distinct coagulation factor, different from the calcium carbonate non-adsorbable φ-factors, and was designated φ_2-factor.

In the present study the adsorption of φ-factor activity by calcium carbonate and by other φ-factor adsorbing compounds was examined in greater detail to learn if a further differentiation of the φ-factor activity could be accomplished.

Only thromboplastin and RVV-cephalin were used as assay accelerators in this investigation, leaving similar studies with the cephalin assay system [2] to be carried out later.

The materials and methods used in this work have been described in previous communications [1,2].

* Fellow of the Royal Norwegian Council for Scientific and Industrial Research.

EXPERIMENTS AND RESULTS

The adsorption of φ-factor activity from oxalated plasma by the adsorbents of group 1 (*cf.* preceding paper) was studied in detail by determination of the φ-factor activity [2] of plasma aliquots adsorbed with graded amounts of adsorbent. The φ-factor activities determined with thromboplastin (φ_{tpl}-factor activity) and with RVV-cephalin (φ_{Vc}-factor activity) were estimated simultaneously in the adsorbed plasma aliquots.

Adsorption of φ_2-factor by calcium carbonate

A typical experiment with calcium carbonate as adsorbent is shown in Fig. 1. The adsorption of φ-factor activity is proportional to the amount of adsorbent added, until a point is reached where the curve breaks and becomes horizontal. As indicated earlier [1], this shows that only a part of the φ_{tpl}- and the φ_{Vc}-factor activities can be adsorbed by calcium carbonate. The adsorbed activity must consequently be due to a coagulation factor which may be differentiated from all other φ-factors by its adsorbability on calcium carbonate. The designation φ_2-factor was chosen for this coagulation entity.

The designation φ_1-factor has now been chosen for the non-adsorbable (by calcium carbonate) φ-factor, measured both with thromboplastin and with RVV-cephalin, and the terms φ_3-, φ_4-, *etc.* are reserved for the as yet unknown number of φ-factors, which also are non-adsorbable (by calcium carbonate), but specific for the thromboplastin assay system.

Series of comparative measurements of the φ_{tpl}- and φ_{Vc}-factor activities of different plasmas have been carried out. The experiments have shown that plasmas having identical φ_{Vc}-factor activity may have different φ_{tpl}-factor activity. These observations are further evidence for the assumption that the thromboplastin assay system registers variations in the activities of some

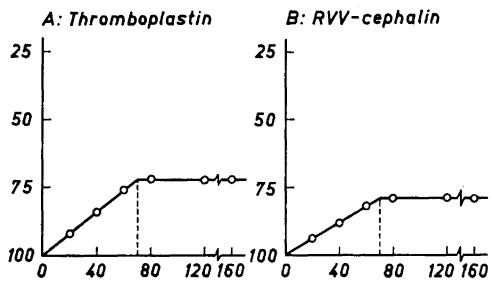

Fig. 1. Adsorption of φ-factor by calcium carbonate. Ordinates: φ-factor activity in % of original plasma. Abscissæ: Calcium carbonate in mg per ml plasma.

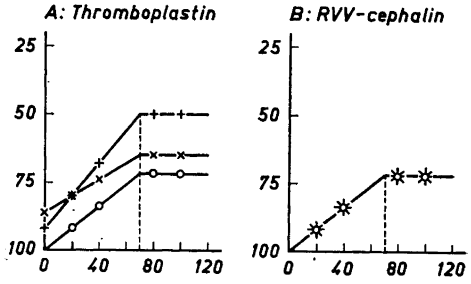

Fig. 2. Adsorption of φ-factor by calcium carbonate.
O: Plasma No. 1217.
+: » » 1219.
×: » » 1218.
Ordinates: φ-factor activity in % of plasma No. 1217.
Abscissæ: Calcium carbonate in mg per ml plasma.

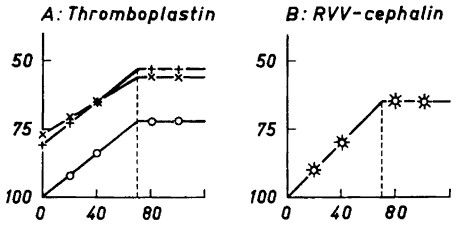

Fig. 3. Adsorption of φ-factor by calcium carbonate.
O: Plasma No. 1722.
+: » » 1721.
×: » » 1724.
Ordinates: φ-factor activity in % of plasma No. 1722.
Abscissæ: Calcium carbonate in mg per ml plasma.

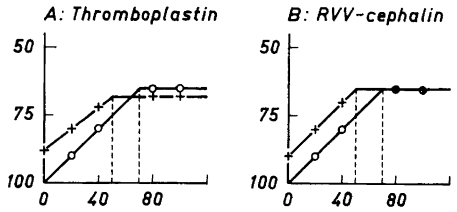

Fig. 4. Adsorption of φ-factor by calcium carbonate.
O: Plasma No. 1221.
+: » » 1220.
Ordinates: φ-factor activity in % of plasma No. 1221.
Abscissæ: Calcium carbonate in mg per ml plasma.

φ-factors which do not influence the results of the RVV-cephalin assay system [2]. Such plasmas were used in the experiments of Figs. 2 and 3. In both these cases the curves for adsorption of the φ_{Vc}-factor activity of three different plasmas were identical. The relation between adsorbed φ_{tpl}-factor activity and amount of adsorbent was, however, not always identical for different plasmas in the same experiment. The three curves of Fig. 2A were not parallel, and the adsorption curve for plasma No. 1 724 (Fig. 3A) differed in slope from the curves for the two other plasmas (Nos. 1 721 and 1 722). However, the minimum amount of adsorbent necessary for maximal adsorption of φ_{tpl}- and φ_{Vc}-factor activities was the same for all plasmas in these experiments, *viz.* 70 mg per ml of plasma. Differences in φ_2-factor activity, as measured with thromboplastin, may thus be found in plasmas having identical φ_2-factor activity as measured with RVV-cephalin. These differences were ascribed to differences in the activity of one or more hypothetical thromboplastin specific factors, acting as synergists for φ_2-factor.

Adsorption experiments were also carried out with plasmas showing different φ_{Vc}-factor activity (Figs. 4 and 5). In each experiment the curves for adsorption of the φ_{Vc}-factor activity of two different plasmas had the same slope. Their φ_{tpl}-factor activity adsorption curves were, however, not parallel. This fact again indicated differences in the activity of one or more thromboplastin specific factors acting as synergists for φ_2-factor. However, for each plasma the two assay systems gave the same value for the minimum amount of adsorbent necessary for maximal adsorption of φ-factor activity, *viz.* 70 mg/ml for plasmas Nos. 1 221 and 1 725, 50 mg/ml for plasma No. 1 220 and 40 mg/ml for plasma No. 1 723.

From Figs. 4 and 5 it was apparent that the observed differences in φ_{Vc}-factor activity of the plasmas were due to differences in the activity of φ_2-factor alone, since the maximally adsorbed plasma had identical φ_{Vc}-factor activity. The φ_2-factor activity of plasmas may consequently be expected to vary independently of the activity of φ_1-factor. The differences in the activi-

ty of φ_2-factor in these plasmas are reflected in proportional differences in the minimum amount of adsorbent necessary for maximal adsorption of φ-factor activity. The observed differences in φ_{tpl}-factor activity of the plasmas were not due to differences in the activity of φ_2-factor only. The activities of the maximally adsorbed plasmas were not identical, indicating additional differences in the activity of thromboplastin specific factors.

A comparison of the experiments in Figs. 1—5 shows that whereas the slope of the curves for adsorption of φ_{Vc}-activity was the same for all plasmas used in the same experiment, the adsorption curves of different experiments varied slightly in slope. This could be expected since a different set of substrate plasmas was used in each experiment. It must be ascribed to small differences in the relative sensitivity of the substrate mixtures to φ_1- and φ_2-factors.

It is thus evident that an estimation of the *concentration* of φ_2-factor in a plasma by determination of its *relative* φ-factor activity ($\varphi_2/\varphi_{total}$) will give different results depending on: (1) whether thromboplastin or RVV-cephalin is used as assay accelerator, (2) the relative sensitivity of the substrate to φ_2-factor and to the calcium carbonate non-adsorbable factor(s), (3) the concentration of φ_1-factor, and (4) the concentrations of thromboplastin specific factors, one or more of which may act as synergists for φ_2-factor. However, the minimum amount of calcium carbonate necessary for maximal adsorption of φ-factor activity appears to be intimately related to the *concentration* of φ_2-factor. It is independent of the nature of the assay accelerator, independent of small differences in the sensitivity of the substrate, and independent of the concentrations of thromboplastin specific factors. It is probably also independent of the concentration of φ_1-factor.

Therefore, the minimum amount of calcium carbonate necessary for maximal adsorption of φ-factor activity from oxalated plasma is regarded as a reliable

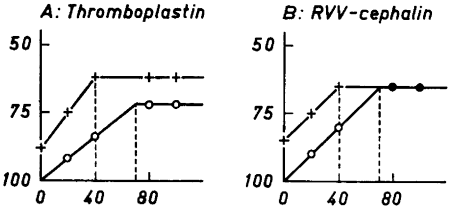

Fig. 5. Adsorption of φ-factor activity by calcium carbonate.
O: Plasma No. 1725.
+: » » 1723.
Ordinates: φ-factor activity in % of plasma No. 1725.
Abscissæ: Calcium carbonate in mg per ml plasma.

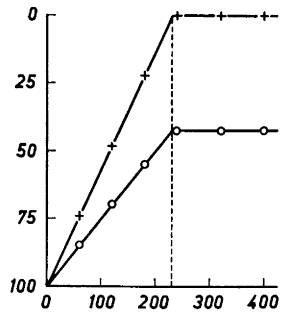

Fig. 6. Adsorption of φ-factor activity by magnesium arsenate.
O: Thromboplastin assay.
+: RVV-cephalin assay.
Ordinate: φ-factor activity in % of original plasma.
Abscissa: Magnesium arsenate in mg per ml plasma.

measure of the concentration of φ_2-factor in the plasma. It appears that a value of 70 (mg calcium carbonate per ml of oxalated plasma) represents the maximum concentration of φ_2-factor in chicken plasma. The experimental background for the lower values occasionally observed will be dealt with in a coming publication.

Adsorption of φ-factor activity by other adsorbents

Less extensive studies on the adsorption of φ-factor activity were carried out with other φ-factor adsorbing compounds (*cf.* preceding article).

Curves for adsorption of φ-factor activity from oxalated plasma by magnesium arsenate are shown in Fig. 6. The φ_{Vc}-factors could be adsorbed completely, whereas only partial adsorption of the φ_{tpl}-factor activity was accomplished with this compound. The experiment indicated that φ_1- and φ_2-factors, and possibly a thromboplastin specific φ-factor were adsorbed simultaneously and proportionally to the amount of adsorbent added to the plasma. Other thromboplastin specific φ-factors appeared to be non-adsorbable by magnesium arsenate.

Fig. 7 shows a typical set of curves for adsorption of φ-factor activity from oxalated plasma by lead sulfide. As with magnesium arsenate, the adsorption of φ_{Vc}-factor activity was proportional to the amount of adsorbent added. The curve indicated that the φ_1- and φ_2-factors could be adsorbed completely and were adsorbed simultaneously. The φ_{tpl}-factor activity was also completely adsorbable by lead sulfide, but the curve for adsorption of this activity was more complex and appeared to be composed of two rectilinear sections. The end point of the curve for adsorption of φ_{Vc}-factor activity coincided with the end point of the second section of the curve for adsorption of φ_{tpl}-factor activity (at B). This point thus represents complete adsorption of a group

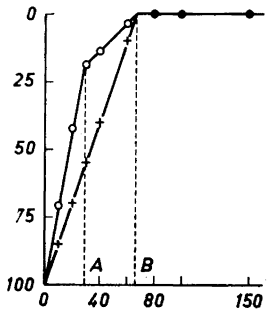

Fig. 7. Adsorption of φ-factor activity by lead sulfide.
O: Thromboplastin assay.
+: RVV-cephalin assay.
Ordinate: φ-factor activity in % of original plasma.
Abscissa: Lead sulfide in mg per ml plasma.

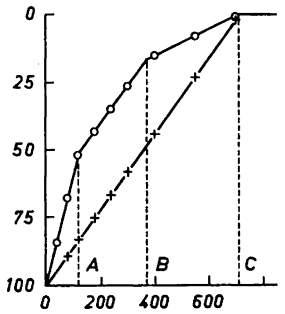

Fig. 8. Adsorption of φ-factor activity by manganese carbonate.
O: Thromboplastin assay.
+: RVV-cephalin assay.
Ordinate: φ-factor activity in % of original plasma.
Abscissa: Manganese carbonate in mg per ml plasma.

of factors which includes the φ_1- and φ_2-factors. It is not known whether or not a thromboplastin specific factor belongs to this group. The end point of the first rectilinear section of the φ_{tpl}-factor adsorption curve (at A) was considered to represent complete adsorption of φ-factors which are thromboplastin specific. It should be stressed that the change in slope occurring at A (29 mg of lead sulfide per ml of plasma), was an abrupt change similar to that occurring at B where the adsorption of the φ_{Vc}-factors was complete. The curve for adsorption of φ_{tpl}-factor activity by lead sulfide should therefore be regarded as two independent adsorption curves superimposed, representing the adsorption of two different groups of φ-factors.

Adsorption of φ-factor activity from oxalated plasma by manganese carbonate is shown in Fig. 8. The curve for adsorption of φ_{Vc}-factor activity showed that the φ_1- and φ_2-factors were completely adsorbable by manganese carbonate and were adsorbed simultaneously. The φ_{tpl}-factors could also be adsorbed completely by this adsorbent, but the curve for adsorption of the latter activity was more complex than the corresponding curve obtained with lead sulfide (Fig. 7). It appeared to be composed of *three* rectilinear sections. The end point of the third section (at C) coincided with the end point of the curve for adsorption of φ_{Vc}-factor activity. This point thus represents complete adsorption of a group of φ-factors which includes φ_1- and φ_2-factors and possibly a thromboplastin specific factor. The end point of the first and of the second rectilinear sections (at A and at B) were considered to represent complete adsorption of two different (groups of) thromboplastin specific φ-factors.

Curves for adsorption of φ_{tpl}- and φ_{Vc}-factor activities from oxalated plasma by calcium oxalate and strontium oxalate are shown in Figs. 9 and 10, respectively. The two sets of curves were very similar. The curves for adsorption of φ_{Vc}-factor activity indicated complete adsorbability and simultaneous

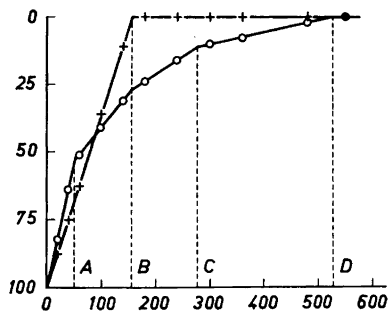

Fig. 9. Adsorption of φ-factor activity by calcium oxalate.
O: Thromboplastin assay.
+: RVV-cephalin assay.
Ordinate: φ-factor activity in % of original plasma.
Abscissa: Calcium oxalate in mg per ml plasma.

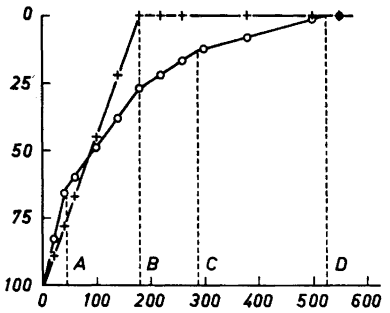

Fig. 10. Adsorption of φ-factor activity by strontium oxalate.
O: Thromboplastin assay.
+: RVV-cephalin assay.
Ordinate: φ-factor activity in % of original plasma.
Abscissa: Strontium oxalate in mg per ml plasma.

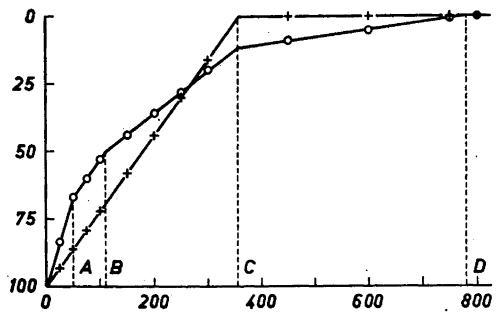

Fig. 11. Adsorption of φ-factor activity by calcium molybdate.
O: Thromboplastin assay.
+: RVV-cephalin assay.
Ordinate: φ-factor activity in % of original plasma.
Abscissa: Calcium molybdate in mg per ml plasma.

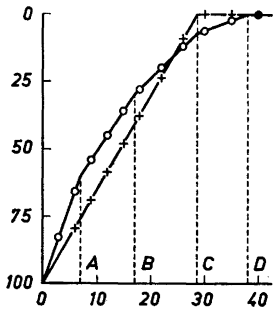

Fig. 12. Adsorption of φ-factor activity by strontium carbonate.
O: Thromboplastin assay.
+: RVV-cephalin assay.
Ordinate: φ-factor activity in % of original plasma.
Abscissa: Strontium carbonate in mg per ml plasma.

adsorption of φ_1- and φ_2-factors by these adsorbents. The curves for adsorption of φ_{tpl}-factor activity by calcium and strontium oxalates were composed of no less than four rectilinear sections. The end points of each of these four sections were throught to represent complete adsorption of four different (groups of) φ-factors. In both curves the end point of the second section (at B) coincided with the point representing complete adsorption of φ_1- and φ_2-factors. The end point of the first, third and of the fourth section (at A, C, and D) may, therefore, represent complete adsorption of three different (groups of) thromboplastin specific φ-factors.

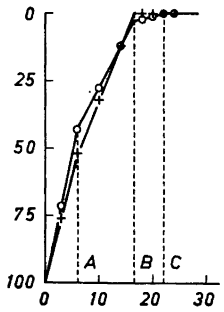

Fig. 13. Adsorption of φ-factor activity by barium carbonate.
O: Thromboplastin assay.
+: RVV-cephalin assay.
Ordinate: φ-factor activity in % of original plasma.
Abscissa: Barium carbonate in mg per ml plasma.

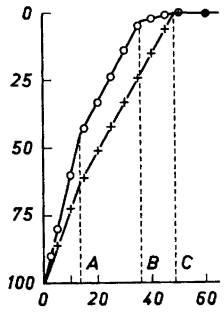

Fig. 14. Adsorption of φ-factor activity by barium oxalate.
O: Thromboplastin assay.
+: RVV-cephalin assay.
Ordinate: φ-factor activity in % of original plasma.
Abscissa: Barium oxalate in mg per ml plasma.

Adsorption of plasma by calcium molybdate and strontium carbonate gave the adsorption curves shown in Figs. 11 and 12. The curves showed a similar complexity as the curves in Figs. 9 and 10, but the adsorption of φ_1- and φ_2-factors by calcium molybdate and strontium carbonate was complete at C *i.e.* at the end point of the *third* part of the four-sectioned curves for adsorption of φ_{tpl}-factor activity.

Figs. 13, 14, and 15 show the curves obtained for adsorption of plasma by barium carbonate, barium oxalate and barium chromate, respectively. The curves for adsorption of the φ_{Vc}-factor activities were composed of two rectilinear sections and indicated that complete adsorption of one φ_{Vc}-factor was accomplished with a smaller amount of adsorbent than that required for complete adsorption of a second φ_{Vc}-factor. The curves for adsorption of the φ_{tpl}-factor activities had three rectilinear sections and indicated independent adsorption of three different (groups of) φ-factors. The end points of two of these sections coincided with the end points of the two sections of the φ_{Vc}-factor adsorption curves. The end point of the third section therefore, represents complete adsorption of a thromboplastin specific φ-factor.

Adsorption of φ-factor activity from preadsorbed plasma

In the interpretation of the curves for adsorption of φ-factor activity from oxalated plasmas, each rectilinear section was thought to represent simultaneous adsorption of one or more (groups of) φ-factors. A sudden change in the slope of the adsorption curve, *i.e.* the end of one rectilinear section and the beginning of a following, was thought to indicate that a (group of) φ-factor(s) had been completely adsorbed at this point, whereas the adsorption of other φ-factor(s) progressed, proportionally to the increase in the amount of adsorbent. This implied that the adsorption of one (group of) φ-factor(s) took place independently of the adsorption of other (groups of) φ-factors. With lead sulfide as adsorbent it was possible to distinguish between two such groups of φ-factors. A similar distinction between three different groups was possible with manganese carbonate, barium carbonate, barium oxalate or barium chromate, and four groups of φ-factors were discernible with calcium oxalate, strontium oxalate, calcium molybdate or strontium carbonate. In general, a two-, three-, or four-sectioned adsorption curve was interpreted as the results of superposition of two, three of four independent adsorption curves, respectively. Each of the independent adsorption curves could be expected to be analogous to the curves obtained with calcium carbonate, and represent the adsorption of one (group of) φ-factor(s).

Adsorption analysis of the φ-factor activity of a plasma with, *e.g.*, strontium carbonate would thus give four characteristic values: A, B, C, and D (*cf.* Fig. 12). Values A, B, and D could be regarded as related to the concentrations of three different (groups of) thromboplastin specific factors. Value C would then be related to the concentrations of a group of factors which includes the φ_1- and φ_2-factors. Two plasma samples, differing only in the concentrations of one of the φ-factors, could consequently be expected to have three of the values in common and differ only in the fourth.

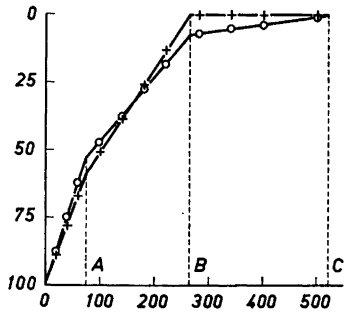

Fig. 15. Adsorption of φ-factor activity by barium chromate.
O: Thromboplastin assay.
+: RVV-cephalin assay.
Ordinate: φ-factor activity in % of original plasma.
Abscissa: Barium chromate in mg per ml plasma.

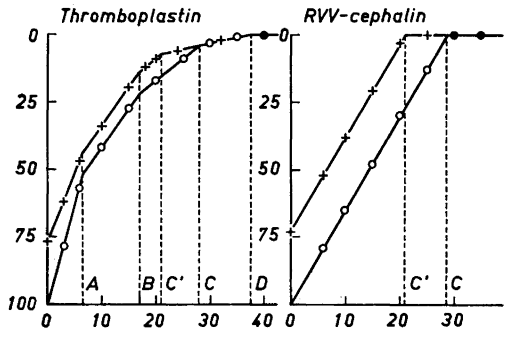

Fig. 16. Adsorption of φ-factor activity by strontium carbonate.
O: Untreated plasma.
+: Plasma preadsorbed with calcium carbonate (80 mg/ml).
Ordinates: φ-factor activity in % of original plasma.
Abscissæ: Strontium carbonate in mg per ml plasma.

The validity of these assumptions has been checked by a few experiments. Plasma pairs, differing only in the concentrations of φ_2-factor, were prepared by adsorbing one portion of a plasma with calcium carbonate to remove φ_2-factor completely. Another portion of the same plasma was left untreated. Curves for adsorption of the φ-factor activity of the untreated plasma were then compared with the curves obtained for the preadsorbed plasma. Typical experiments of this type are shown in Figs. 16—18.

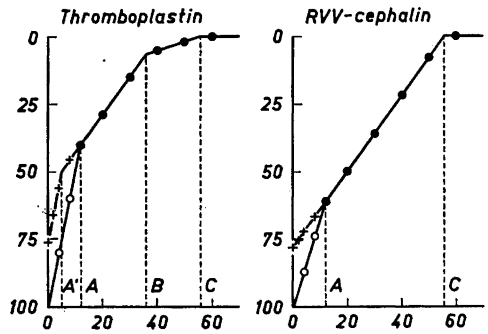

Fig. 17. Adsorption of φ-factor activity by barium oxalate.
O: Untreated plasma.
+: Plasma preadsorbed with calcium carbonate (80 mg/ml).
Ordinates: φ-factor activity in % of original plasma.
Abscissæ: Barium oxalate in mg per ml plasma.

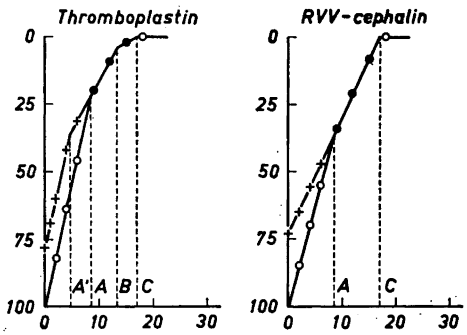

Fig. 18. Adsorption of φ-factor activity by barium carbonate.
O: Untreated plasma.
+: Plasma preadsorbed with calcium carbonate (80 mg/ml).
Ordinates: φ-factor activity in % of original plasma.
Abscissæ: Barium carbonate in mg per ml plasma.

The adsorption by strontium carbonate of the φ-factor activity of untreated and of calcium carbonate preadsorbed plasmas is shown in Fig. 16. It will be seen that the preadsorbed plasma requires less adsorbent (C′) for complete adsorption of the φ_{Vc}-factor activity than does the untreated plasma (C). The quantities of adsorbent causing complete adsorption of the three thromboplastin specific φ-factors (A, B, and D) in the two plasma samples are identical. This experiment thus shows that adsorption of the thromboplastin specific φ-factors occurs independently of the adsorption of φ_2-factor. The latter factor must be considered to compete with φ_1-factor for adsorption on strontium carbonate. The first section of the φ_{tpl}-factor adsorption curves for the untreated and the preadsorbed plasma did not have the same slope, but the following sections of the curves were parallel. This indicates that φ_2-factor may act as a synergist for a factor which is completely adsorbed at A. In fact, this factor may be the hypothetical thromboplastin specific factor, referred to previously (p. 905).

Figs. 17 and 18 show the curves for adsorption of φ-factor activity from untreated and from calcium carbonate preadsorbed plasmas by barium oxalate and barium carbonate, respectively. It will be seen that the curves for adsorption of φ_{Vc}-factor activity from untreated plasma had two rectilinear sections, whereas the curves obtained with preadsorbed plasma were straight lines, merging into the curve for the untreated plasma at A. The φ_{Vc}-factor which was completely adsorbed at A in the untreated plasma was thus no longer present in the preadsorbed plasma. It is concluded that this factor is φ_2-factor, and that φ_1- and φ_2-factor do not compete for adsorption on these adsorbents. The curves for adsorption of φ_{tpl}-factor activity show that the factors completely adsorbed at A in the untreated plasma are completely adsorbed at A′ in the preadsorbed plasma. The amounts of adsorbent required for complete adsorption of the two other groups of φ_{tpl}-factors, are the same for the two plasmas. The experiments show that the φ-factors which are completely adsorbed at B and at C, are adsorbed independently of the adsorption of φ_2-factor. On the other hand, the thromboplastin specific factor which is completely adsorbed at A in the untreated plasma and at A′ in the preadsorbed plasma, competes with φ_2-factor for the adsorption on barium oxalate and barium carbonate. The fact that sections one of the φ_{tpl}-factor adsorption curves for the untreated and for the preadsorbed plasmas are parallel, indicates that the factor adsorbed in competition with φ_2-factor does not act as a synergist for the latter.

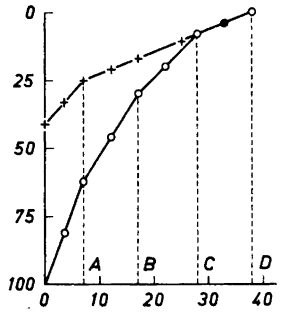

Fig. 19. Adsorption of φ-factor activity by strontium carbonate.
O: Untreated plasma.
+: Plasma preadsorbed with magnesium arsenate (240 mg/ml).
Ordinates: φ-factor activity in % of original plasma.
Abscissæ: Strontium carbonate in mg per ml plasma.

In Fig. 19 are shown the curves for adsorption by strontium carbonate of the φ_{tpl}-factor activities of untreated plasma and of plasma preadsorbed with magnesium arsenate for complete removal of the factors which are adsorbable by this compound (*cf.* Fig. 6). The untreated plasma gave the usual four-sectioned adsorption curve. The adsorption curve for the preadsorbed plasma had only two rectilinear sections. The last part of the second section merged into the fourth section of the curve for the untreated plasma. The changes in slope occurring at B and at C in the curve for the untreated plasma were thus not seen with preadsorbed plasma, whereas the end points of the two sections of the curve for the latter coincided with the end points of sections one and four of the curve for the untreated plasma. It is concluded that the factors removed by preadsorption with magnesium arsenate are the factors which were completely adsorbed at B and at C, and that the adsorption of these factors by strontium carbonate has no influence on the adsorption of the factors adsorbed completely at A and at D. Since the adsorption of φ_1- and φ_2-factors is complete at C and the adsorption of a thromboplastin specific φ-factor is complete at B, it is evident that the factors which are adsorbable by magnesium arsenate include φ_1-factor and φ_2-factor plus a thromboplastin specific φ-factor.

The proposed interpretation of the curves for adsorption of φ-factor activity from oxalated plasma is supported by these experiments. The various shapes of the adsorption curves may be explained as the results of adsorption of different coagulation entities, some of which are adsorbed competitively, whereas the adsorption of others is mutually independent. Factors which are adsorbed competitively by one adsorbent, may be adsorbed independently of each other by another adsorbent. With the adsorbents used in these studies it appears possible to distinguish between three different thromboplastin specific φ-factors (φ_{3-5}), and between two φ-factors (φ_1- and φ_2-factor) with contribute to the measured φ-factor activity both with thromboplastin and with RVV cephalin as assay accelerators. The present differentiation of the φ-factor activity of plasma may not represent the final answer as to the number of different coagulation entities measured as φ-factors in the assay systems used here.

DISCUSSION

The possibility that prothrombin and Stuart factor may be registered as φ_{vc}-factors and proconvertin as a thromboplastin specific φ-factor has been discussed earlier [2]. A final answer to these questions cannot be given at present.

The curves for adsorption of φ-factor activity from oxalated plasma give adequate support for the earlier assumptions [2] that different coagulation entities contribute to the activity measured as φ-factor activity under the conditions described. From the present results it may be concluded that at least five different coagulation factors contribute to the φ-factor activity of plasma as measured with thromboplastin. Three of the factors do not influence the coagulation rate of plasma when RVV-cephalin is used as assay accelerator instead of thromboplastin. They are therefore regarded as thromboplastin specific factors. The two remaining factors (φ_1- and φ_2-factors) are involved in

reactions, the speed of which may limit the coagulation rate of plasma, *both* when thromboplastin and when RVV-cephalin are used as accelerators.

The technique for assay of φ-factor activity [2] usually permits repeated determinations of the clotting times with no more than 0.1 sec. difference. The readings of the φ-factor activity of the adsorbed plasma samples are therefore very accurate. With this in mind it would not be permissible to draw a smooth curve between the observed values so as to fit an adsorption isotherm. Strict proportionality between adsorbed activity and amount of adsorbent is observed for each section of the curves for adsorption of the φ_{Vc}- and the φ_{tpl}-factor activities. The proportionality suggests that the minimum amount of adsorbent necessary for complete adsorption of a (group of) φ-factor(s) may be regarded as an absolute measure of the concentration of the factor(s). This was found to be the case when calcium carbonate was used as adsorbent. With this compound all observed variations in φ_2-factor concentration were associated with proportional variations in the minimum amount of adsorbent necessary for complete adsorption of the factor from oxalated plasma. With the other adsorbents the problem is more complex because of more or less simultaneous adsorption of a number of φ-factors. It is probable that the amount of adsorbent, corresponding to the end point of a rectilinear section of an adsorption curve, is related to the concentration of the factor(s) completely adsorbed at this point, but it is not yet clear if variations in these values for different plasmas can be correlated with variations in the concentrations of the various φ-factors only. Inert plasma material may be adsorbed simultaneously with the φ-factors, but should not be expected to affect the amount of adsorbent necessary for complete adsorption of a φ-factor, *unless it is adsorbed in competition with the factor*. The thromboplastin specific factors behave as inert material in the RVV-cephalin assay. The end points at A in Figs. 13—15, 17, and 18, representing complete adsorption of φ_2-factor and a thromboplastin specific factor in competition, could therefore not be expected to vary with variations in the concentration of φ_2-factor only, but also with variations in the concentration of the inert thromboplastin specific factor. These problems need further consideration. Further experiments with adsorption of preadsorbed plasmas may give additional information concerning the relation between the factors responsible for the adsorption curves obtained with the different adsorbents.

Adsorption of φ-factor by a crystalline adsorbent implies that the adsorbent has a certain spatial pattern of surface molecules which acts as an adsorption site for the factor, probably being the reverse model of a characteristic pattern of molecular groups in the adsorbable factor. Competitive adsorption of some φ-factors by one adsorbent and independent adsorption of the same factors by another adsorbent indicate that different adsorbents can distinguish between different factors. When two or more φ-factors are adsorbed competitively by an adsorbent, the adsorption sites involved are considered to be identical or to have overlapping patterns of surface molecules. In case of independent adsorption entirely different adsorption sites must be engaged in the adsorption of different factors. It would thus seem necessary to regard each adsorbent as having a certain number of adsorption sites with different and very specific adsorption properties. It is not known if the differences

between the various adsorption sites of an adsorbent may be correlated with differences in surface structure between different regions of a single crystal or between crystals of different form. In any case, adsorption analysis appears to represent a valuable technique for differentiation of chicken coagulation factors which cannot be distinguished by other means in the assay systems available at present.

REFERENCES

1. Sørbye, Ø. *Acta Chem. Scand.* **16** (1962) 799.
2. Sørbye, Ø. and Kruse, I. *Acta Chem. Scand.* **14** (1960) 2177.

Received October 24, 1961.

ACTA CHEMICA SCANDINAVICA 16 (1962) 916–921

The Heats of Combustion and Formation of the Three Diazines and their Resonance Energies

JAN TJEBBES

*Thermochemistry Laboratory *, University of Lund, Sweden*

Heat of combustion values have been determined for pyridazine, pyrimidine and pyrazine and found to be, $\Delta Hc°(25°C)$ in kcal.mole^{-1}, -566.59 ± 0.22, -547.88 ± 0.20 and -546.25 ± 0.28, respectively, and heat of formation data are derived. From these values the resonance energies of the diazines have been calculated and the implication on certain thermochemical bond energy terms is discussed.

It is generally accepted that a high degree of stabilization of a simple aromatic system is mainly due to the fact that at least two of the possible valence-bond structures are indistinguishable, as are the Kekulé-structures of benzene. Amongst the six-membered, aromatic heterocyclic ring systems with one or several nitrogen atoms in the ring, pyridine has identical Kekulé-structures. Of the three isomeric diazines, the 1,4- and 1,3-isomers, pyrazine and pyrimidine, respectively, are analogous with pyridine, whereas the 1,2-isomer, pyridazine, has energetically quite different structures (Fig. 1).

It was therefore expected that a determination of the heats of combustion of the three isomers should reveal a considerable difference in the derived resonance stabilization energies — the 1,3- and 1,4-diazines being more stable than the 1,2-isomer.

MATERIALS

Pyridazine. A 40 g sample was kindly provided by Dr. Clauson-Kaas [1], Copenhagen. GLC-analysis (Pye Argon Chromatograph, column: 20 % LAC 3R-728 on C22, $t = 150°$) showed only one minor impurity. Two successive fractional distillations at 94.0° and 16 mm and at 84.0° and 10 mm, gave a product that was free from impurities as judged from the GLC-analysis ($d_4^{25} = 1.1030$).

Pyrimidine. 2-Amino-pyrimidine (Light) was chlorinated to 2-chloropyrimidine as described by Overberger and Kogon [2]. The product was hydrogenated using Pd on $BaSO_4$ as catalyst following the method of Lythgoe and Rayner [3]. The product obtained contain-

* Sponsored by the *Swedish Natural Science Research Council* and the *Swedish Technical Research Council.*

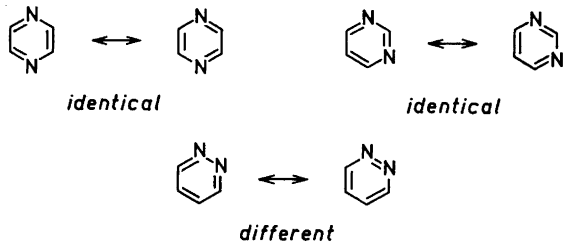

Fig. 1.

ed much water. Separation could be achieved by distillation neither at 760, nor at 100 mm Hg due to formation of azeotropic mixtures (*ca.* 2 % H_2O). After successive treatments with KOH and P_2O_5, as described by Whittaker [4], the substance was distilled twice (60°/89 mm and 122.8°/746 mm). A product was obtained which contained less than 0.01 % H_2O as judged from the GLC-analysis (column as above, t = 100°). d_4^{25} = 1.0792.

Pyrazine. Wyandotte Chem. Corp., Wyandotte, USA, kindly provided a 120 g sample of pyrazine of very high quality. Two distillations over $CaSO_4$ followed by a vacuum sublimation gave a product that was free from impurities to within one part in 10^4 as judged from GLC (column as above, t = 114°, the sample was dissolved in neohexane). M.p. 54.0°, b.p. 116.0° at 760 mm.

COMBUSTION CALORIMETRY

The calorimetric results are expressed in terms of the defined calorie which is equal to 4.1840 abs.joules. All weighings have been reduced to mass. The molecular weights are based upon the 1957 International Atomic Weights. The symbols introduced by Hubbard, Scott and Waddington [5] (and their method of performing the Washburn reduction) have been used.

Apparatus and method. The same combustion calorimeter [6] was used as in previous investigations. Due to a minor change in the head of the bomb two different values of the heat equivalent of the system were used. The calibration experiments reported in this work refer to the combustion of pyrimidine and pyrazine. The heat equivalent value used for the combustions of pyridazine was the same as has been reported elsewhere [6].

Pyridazine and pyrimidine, being liquids, were burnt in soft glass ampoules with paraffin oil as combustion aid. For the solid pyrazine soft glass ampoules were used, each of which had a 3 mm hole in its bottom face through which the molten substance could be introduced. After solidification of the substance, the ampoule was placed in a specially designed platinum crucible, with a depression in the bottom, fitting the base of the ampoule. Experiments showed that no measurable loss of weight occurred during weighing and assembling operations. Enough paraffin oil was added to prevent a direct contact between the oxygen atmosphere and the substance. Therefore, the amount of paraffin oil had to be rather high, accounting for *ca.* 60 % of the heat evolved in the combustion. The analysis for HNO_3 were performed in the usual manner [7].

Table 1. Calibration, Benzoic acid NBS 39h. $\Delta E_c/M$(Benzoic acid) = −6317.88 ± 0.72 cal.g^{-1}. m(Pt) = 23.847 g, ε^i(cont) = 3.95 cal.deg^{-1} (Expts. Nos. 1—5), ε^i(cont) = 3.94 cal.deg^{-1} (Expts. Nos. 6—9).

m' g	m'' g	m^i(cont) g	Δt deg	ΔE(HNO_3) cal	ε°(calor) cal.deg^{-1}
0.825757	0.005474	36.65	0.88851	2.52	5931.63
0.827198	0.005288	36.65	0.88999	1.69	5930.29
0.827939	0.005227	36.66	0.89091	2.37	5929.94
0.826054	0.005159	36.65	0.88889	2.49	5929.78
0.825815	0.005214	36.65	0.88856	2.02	5929.98
0.826013	0.005102	36.42	0.88836	1.96	5931.93
0.827279	0.005474	36.42	0.89027	2.07	5930.04
0.826546	0.005369	36.42	0.88931	1.92	5930.56
0.825211	0.005362	36.42	0.88783	2.21	5931.18
			Mean		5930.59
			Stand. dev. of mean		0.27

ε°(calor) = 5930.59 ± 0.27 cal.deg^{-1}

Table 2. Pyridazine
Series 1: ε°(calor) = 5927.63 ± 0.24 cal.deg^{-1},
m(Pt) = 28.047 g, ε^i(cont) = 4.01 cal.deg^{-1}, $\Delta E\Sigma$ = 2.50 cal.
Series 2: ε°(calor) = 5925.67 ± 0.24 cal.deg^{-1},
m(Pt) = 23.689 g, ε^i(cont) = 3.88 cal.deg^{-1}, $\Delta E\Sigma$ = 2.50 cal.

m' g	m'' g	m''' g	m^i(cont) g	Δt deg	ΔE(HNO_3) cal	$-\Delta E_c^\circ/M$ cal.g
Series 1:						
0.446570	0.182024	0.005480	40.52	0.88219	12.10	7078.24
0.464177	0.175235	0.005587	40.53	0.89079	13.03	7076.65
0.495686	0.150052	0.005398	40.52	0.88122	12.99	7072.86
0.494709	0.150669	0.005311	40.52	0.88165	15.86	7073.15
0.475463	0.166085	0.005853	40.53	0.88747	12.52	7077.84
Series 2:						
0.554773	0.111482	0.005762	36.24	0.88058	15.52	7072.84
0.565616	0.108593	0.004938	36.21	0.88741	14.84	7071.62
0.528986	0.135143	0.005489	36.20	0.89290	13.04	7070.34
				Mean		7074.19
				Stand. dev. of mean		1.02

$\Delta E_c^\circ/M$ = −7074.2 cal.g^{-1}

The combustions are reported in Tables 1—4. All combustion series had in common the following data: t_h = 25.0°C, t_i = 24.1°C, P^i(Gas) = 30.0 atm, V(Bomb) = 0.2751 l, V^i(Water) = 0.820 ml, $\Delta E_c^\circ/M$(Oil) = −10 986.6 ± 0.6 cal.g^{-1} and $\Delta E_c^\circ/M$(Fuse) = −3 971 ± 4 cal.g^{-1}.

Results. The values of $\Delta E_c^\circ/M$ obtained were recalculated to ΔH_c° values. The heats of formation for the compounds were calculated using the standard values for the heats of formation of gaseous CO_2[8] and liquid H_2O[8], −94.05

Table 3. Pyrimidine
ε°(calor) = 5930.59 ± 0.27 cal.deg^{-1}, m(Pt) = 23.841 g,
ε^i(cont) = 3.88 cal.deg^{-1}, $\Delta E\Sigma$ = 2.45 cal.

m' g	m'' g	m''' g	m^i(cont) g	Δt deg	ΔE(HNO_3) cal	$-\Delta E_c^\circ/M$ cal.-g^{-1}
0.454531	0.196203	0.005298	36.35	0.89895	12.87	6842.64
0.475318	0.180673	0.005320	36.35	0.89426	13.38	6842.89
0.432193	0.208901	0.005281	36.33	0.89629	12.05	6839.31
0.444418	0.203413	0.005604	36.33	0.90063	13.41	6838.49
0.447074	0.197778	0.004737	36.34	0.89249	11.89	6840.03
				Mean		6840.67
				Stand. dev. of mean		0.89

$\Delta E_c^\circ/M$ = −6840.7 cal.g^{-1}

Table 4. Pyrazine
ε°(calor) = 5930.59 ± 0.27 cal.deg^{-1}, m(Pt) = 14.048 g,
ε^i(cont) = 3.53 cal.deg^{-1}, $\Delta E\Sigma$ = 2.50 cal

m' g	m'' g	m''' g	m^i(cont g	Δt deg	ΔE(HNO_3) cal	$-\Delta E_c^\circ/M$ cal.g^{-1}
0.298442	0.309073	0.003997	26.46	0.92455	13.88	6815.53
0.349285	0.284236	0.004562	26.46	0.93772	15.01	6817.76
0.339109	0.255077	0.004585	26.46	0.87171	13.81	6820.34
0.329619	0.258763	0.004095	26.46	0.86745	14.12	6822.48
0.293195	0.291620	0.004329	26.46	0.88664	13.25	6825.29
0.293809	0.309140	0.004337	26.46	0.91968	13.12	6820.55
				Mean		6820.32
				Stand. dev. of mean		1.40

$\Delta E_c^\circ/M$ = −6820.3 cal.g^{-1}

Table 5. Thermochemical data at 25°C, in kcal.mole^{-1}. The given uncertainties are twice the final overall standard deviations [10].

Compound	ΔH_c°	ΔH_f°	ΔH_c(gas)	ΔH_f(gas)
Pyridazine	−566.59 ± 0.22	53.75 ± 0.22	−579.37 ± 0.30	66.53 ± 0.30
Pyrimidine	−547.88 ± 0.20	35.04 ± 0.20	−559.83 ± 0.24	46.99 ± 0.24
Pyrazine	−546.25 ± 0.28	33.41 ± 0.28	−559.70 ± 0.36	46.86 ± 0.36

kcal.mole^{-1} and −68.32 kcal.mole^{-1}, respectively. Final overall standard deviations were calculated by the method of Bjellerup [9] based upon the principles of Rossini and Deming [10]. The heat of sublimation of pyrazine and the heat of vaporization of pyrimidine were measured and found to be 13.4_5 ± 0.11 and 11.9_5 ± 0.06 kcal.mole^{-1}, respectively, using the apparatus and technique described by Wadsö [11]. For pyridazine this method could not be used and

Table 6. Atomic heats of formation and resonance energies in kcal.mole^{-1}.

Compound	$-\Delta H_a$ calculated	$-\Delta H_a$ found	$\Delta H_{Res.}$
Benzene	1277.4	1318.2	40.8
Pyridine	1170.1	1194.3	24.2
Pyridazine *	1038.8 *	1051.1	12.3
Pyrimidine	1062.8	1070.8	8.0
Pyrazine	1062.8	1070.9	8.1

* The valence bond structure with a N—N single bond.

therefore a preliminary value for the heat of vaporization, 12.78 ± 0.10 kcal.mole^{-1}, was obtained using a different and more sensitive method *. The results are summarized in Table 5.

RESONANCE ENERGIES

According to standard procedure, the thermochemical resonance energy for a conjugated system equals the difference between the calculated heat of combustion (or formation) value for the most stable valence-bond structure of the molecule and the experimentally determined value. The calculation rests upon the assumption that thermochemical bond energy terms are additive, which is only approximately true. However, by introducing structural refinements the agreement between calculation and experiment for molecules with localized bond orbitals can be as close as a few tenths of a kcal per mole. Table 6 gives the calculated and the experimentally determined atomic heats of formation for benzene [12], pyridine [13] and the three diazines using bond energy terms and heat of atomization values from Cottrell [14]. For pyridazine, the calculated values become 1 038.8 and 1 014.6 kcal.mole^{-1} for the valence bond structures with N—N and N=N bonds, respectively, and the most stable one should be chosen for the comparison.

DISCUSSION

From Table 6 two rather surprising facts emerge. Firstly, that upon substituting a —N= for a —CH= group the resonance energy decreases by as much as 16 kcal per mole, and secondly, that the resonance energy of pyridazine — contrary to all expectations — is higher than those of the 1,4- and 1,3-isomers.

The regular decrease in resonance energy is very questionable and is certainly not supported by chemical evidence. One might even expect *sym*-triazine to show up in the calculation with a negative stabilization energy, which does not make sense at all. Pauling [15] states that the resonance energy

* The assistance of Mr. E. Morawetz, of this laboratory, with this determination is gratefully appreciated.

in pyridine, pyrazine and related six-membered heterocyclic molecules stabilizes them by about 40 kcal.mole^{-1} although a calculation using the values given by Pauling gives a resonance energy of 28 kcal.mole^{-1} for pyridine and 16 kcal.mole^{-1} for pyrazine.

On the other hand it is apparent, either that the importance of identical Kekulé-structures for the stability of the aromatic structure in the present case is far less than is generally accepted, or that at least one of Cottrell's bond energy values is in error. From what has been said the second explanation seems to be most probable, particularly as some of the bond energies involving nitrogen are based on very scanty or old experimental data. The E_{C-N}-value given by Cottrell is 72.8 which is an average value for a number of amines, the spread being as much as $\pm$ 3 kcal.mole^{-1}. Recently, Skinner *et al.*[16] reported heat of combustion values for *n*-butylamine and *sec.*-butylamine. From their results E_{C-N} is calculated to be, on the average, 70 kcal.mole^{-1}. Using this value, the resonance energies become 27, 14, 14, and 12 for pyridine, pyrazine, pyrimidine, and pyridazine, respectively. Still, the situation does not seem satisfactory and it might well be that the bond energies necessary for the calculations must be taken from a comparison material containing the structural element C—N=C (Schiff's bases).

Acknowledgements. The author's thanks are due to Miss Margret Månsson and Mr. B. Nelander for technical assistance, to Dr. N. Clauson-Kaas and Wyandotte Chem. Corp. for gifts of samples and to the University of Lund for financial support.

REFERENCES

1. Clauson-Kaas, N., Si-Oh, L. and Elming, N. *Acta Chem. Scand.* **4** (1950) 1233.
2. Overberger, C. G. and Kogon, I. C. *J. Am. Chem. Soc.* **76** (1954) 1065.
3. Lythgoe, E. W. and Rayner, P. *J. Chem. Soc.* **1951** 2323.
4. Whittaker, N. *J. Chem. Soc.* **1953** 1646.
5. Hubbard, W. N., Scott, D. W. and Waddington, G. *Standard States and Corrections for Combustions in a Bomb at Constant Volume.* Chapter 5 of Rossini, F. D. (Ed.) *Experimental Thermochemistry*, New York 1956.
6. Tjebbes, J. *Acta Chem. Scand.* **14** (1960) 180.
7. Prosen, E. J. *Combustion in a Bomb of Compounds Containing Carbon, Hydrogen, Oxygen and Nitrogen.* Chapter 6 of Ref.[5]
8. Selected Values of Chemical Thermodynamic Properties, *Circular of Natl. Bur. Standards, 500*, Washington D.C. 1952.
9. Bjellerup, L. *Acta Chem. Scand.* **15** (1961) 121.
10. Rossini, F. D. and Deming, W. E. *J. Wash. Acad. Sci.* **29** (1939) 416.
11. Wadsö, I. *Acta Chem. Scand.* **14** (1960) 566.
12. *Selected Values of Properties of Hydrocarbon and Related Compounds*, American Petroleum Institute Research Project 44, Carnegie Institute of Technology, Pittsburgh, Penn.
13. Cox, J. D., Challoner, A. R. and Meetham, A. R. *J. Chem. Soc.* **1954** 265.
14. Cottrell, T. L. *The Strengths of Chemical Bonds, 2nd ed.*, London 1958.
15. Pauling, L. *The Nature of the Chemical Bond, 3rd ed.*, New York 1960.
16. Evans, F. W., Fairbrother, D. M. and Skinner, H. A. *Trans. Faraday Soc.* **55** (1959) 399.

Received November 24, 1961.

ACTA CHEMICA SCANDINAVICA 16 (1962) 922–930

Ein Beitrag zur Bestimmung der absoluten Konfiguration der Anomeren von D-Glucose und D-Mannose durch Änderung der Leitfähigkeit während der Mutarotation in Borsäurelösung

JAKOB BLOM

Tuborg Brauereien, Kopenhagen, Dänemark

Böeseken [1] kam durch Untersuchungen über die Änderung der Leitfähigkeit während der Mutarotation von Zuckern in wässrigen Borsäurelösungen zu dem Resultat, dass α-D-Glucose und β-D-Mannose *cis*-ständige Gruppierung der Hydroxylgruppen bei C_1 und C_2 haben. Im Lichte der neueren Anschauungen über die sterischen Verhältnisse der Stuhl-Konformationen von Pyranosen lassen die experimentellen Daten von Böeseken sich nur mit *trans*-ständiger Gruppierung der Hydroxylgruppen bei C_1 und C_2 in α-D-Glucose und β-D-Mannose korrelieren. Dieses Ergebnis ist in Übereinstimmung mit meinen früheren Untersuchungen [2] über die Säurehydrolyse der Methylglykoside und über die Bromoxydation von Aldosen.

"Unter der Erscheinung Mutarotation verstehen wir im weitesten Sinne jede Reaktion, die sich im Polarimeter verfolgen lässt, im engeren Sinne jedoch nur monomolekulare Reaktionen, bei denen eine optisch aktive Verbindung durch blosses Lösen in einem geeigneten Lösungsmittel teilweise in eine andere Modifikation übergeht. Der weitaus wichtigste Fall ist die Mutarotation der Zucker" (Sørensen [3]). Eine frisch bereitete Lösung von Kristallen eines reduzierenden Zuckers ändert mit der Zeit ihre optische Drehung; nach einiger Zeit wird die Drehung konstant, indem Gleichgewicht eintritt. Folgendes Schema gibt die wichtigsten Vorgänge während der Mutarotation wieder:

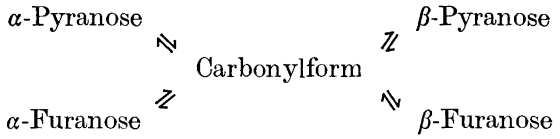

Die Koncentration der als Zwischenstufe auftretenden Carbonylform ist so gering (unter 0,3 %), dass diese für die vorliegenden Betrachtungen ohne Bedeutung ist.

ÜBER DIE RELATIVE KONFIGURATION UND RINGSTRUKTUR DER ANOMEREN D-GLUCOSE, D-MANNOSE UND D-GALACTOSE IN WÄSSRIGER LÖSUNG ZU BEGINN DER MUTAROTATION

Die relative Konfiguration und Ringstruktur der Methylglykoside kann durch Perjodatoxydation nach Jackson und Hudson [4] bestimmt werden. Durch primäre Perjodatoxydation und sekundäre Reduktion der gebildeten Reaktionsprodukte mit Raney-Nickel wird aus Methylglykopyranosiden ein Alkohol gebildet, der das glykosidische Kohlenstoffatom als einziges optisch aktives C-Atom besitzt. Aus den Methylglykosiden von α-D-Glucose (+ 309), α-D-Mannose (+ 154) und α-D-Galactose (+ 381) wird nach Smith und van Cleve [5] derselbe Alkohol, $[\alpha]_D$ ca. −10°, aus den Methylglykosiden von β-D-Glucose (−66), β-D-Mannose (−136) und β-D-Galactose (−1) der enantiomorphe Alkohol, $[\alpha]_D$ ca. + 10°, gebildet. Die genannten α-D-Methylglykoside sind Pyranoside mit derselben Konfiguration bei C_1, die β-D-Methylglykoside sind Pyranoside mit derselben aber entgegengesetzten Konfiguration bei C_1. Die in Klammern eingeführten Zahlen sind die molekularen Drehungen der Verbindungen, [Bates [6]].

Die Differenz der molekularen Drehwerte eines Methylglykosids und des respektiven Zuckers ist konstant, wenn beide dieselbe Konfiguration bei C_1 und dieselbe Ringstruktur haben (Tabelle 1). Die Konstanz der Differenz in den ersten sechs Beispielen deutet darauf hin, dass die genannten anomeren Zucker die gleiche Konfiguration bei C_1 und die gleiche Ringstruktur haben als die respektiven Methylglykoside. Im letztgenannten Fall weiss man, dass sowohl das Glykosid (Augestad und Berner [7]) als der Zucker (Dale [8]) Furanoseringstruktur haben. D-Mannose, $CaCl_2$, $4H_2O$ (−114) gibt bei der Bromoxydation D-Mannonsäure-γ-Lacton. α-D-Glucose (+ 202) und β-D-Glucose (+ 34)

Tabelle 1. Differenz der molekularen Drehung und der Molekularrefraktion.

	$[M]_D$			R_L		
	Methyl-pyranosid	Hexose	Δ	Methyl-pyranosid	Hexose	Δ
α-D-Glucose	+ 309	+ 202	−107	41,80	37,18	4,62
α-D-Mannose	+ 154	+ 53	−101	41,64	37,05	4,59
α-D-Galactose	+ 381	+ 272	−109	41,57	36,97	4,60
β-D-Glucose	− 66	+ 34	+ 100	42,02	37,41	4,61
β-D-Mannose	−136	− 31	+ 105	—	—	—
β-D-Galactose	− 1	+ 99	+ 100	41,78	37,15	4,63
	Methyl-furanosid					
β-D-Mannose $CaCl_2.4H_2O$	−168	−114	+ 54			

Tabelle 2. Differenz der Molekularrefraktionen, ΔR_G, von β- und α-Anomeren.

D-Glucose	0,39
D-Mannose	0,37
D-Galactose	0,42
Methyl-D-Glucosid	0,38
Methyl-D-Galactosid	0,37
Methyl-L-Arabinosid	0,37

sind hingegen Pyranosen, da sie bei der Bromoxydation D-Gluconsäure-δ-Lacton geben.

Nach Riiber [9] ist die Molekularrefraktion ein wertvolles Hilfsmittel für die Korrelierung der Konfiguration anomerer Glykoside und Zucker, da die Erfahrung gezeigt hat, dass die Molekularrefraktion nur in geringem Masse durch Nachbarwirkung der Atome beeinflusst ist. Die Bestimmung der Molekularrefraktion erfordert höchste Präzision in der Messung des Brechungsexponenten und der Dichte, so dass derartige Bestimmungen sehr viel Zeit nehmen. Riiber und Mitarbeiter [10] haben die Molekularrefraktion, R_L, von zahlreichen Methylpyranosiden und den respektiven Zuckern bestimmt. Die Differenz der R_L-Werte war im Mittel 4,61, welches in ausgezeichneter Übereinstimmung mit dem theoretischen Wert für eine CH_2-Gruppe, $R_L = 4{,}618$, ist (Eisenlohr [11]). Ein Methylglykosid unterscheidet sich von dem zugehörigen freien Zucker nur dadurch, dass das glykosidische Wasserstoffatom durch CH_3 ersetzt ist. Weiterhin ist die Differenz der Molekularrefraktionen von den α- und β-Anomeren desselben Zuckers annähernd konstant (Riiber [12]); (Tabelle 2).

Da die am Anfang des Abschnittes aufgezählten Methylglykoside Pyranosen sind, darf man aus den gefundenen Korrelationen schliessen, dass α-D-Glucose (+ 202) β-D-Glucose (+ 34) α-D-Mannose (+ 53) β-D-Mannose (−31) α-D-Galactose (+ 272) und β-D-Galactose (+ 99)[3] in wässriger Lösung am Anfange der Mutarotation Pyranosen-Ring-Struktur haben.

ÜBER DIE UMLAGERUNGEN DER D-GLUCO-, D-MANNO- UND D-GALACTO-PYRANOSEN WÄHREND DER MUTAROTATION

Wie in obigem Schema angedeutet, kann während der Mutarotation Isomerisation sowohl des glykosidischen Kohlenstoffatoms als der Ringstruktur stattfinden. Findet nur eine Umlagerung von Anomeren mit gleicher Ringstruktur statt, spricht man von "einfacher" Mutarotation; tritt gleichzeitig Isomerisation der Ringstruktur ein, spricht man von "komplexer" Mutarotation [6]. Im ersten Falle folgt die Mutarotation dem Verlaufe einer Reaktion erster Ordnung und gibt zufriedenstellend konstante Werte für die Mutarotationskoefficienten. Die Mutarotation von D-Glucose, D-Mannose und Lactose folgt dem Verlaufe einer Reaktion erster Ordnung, wodurch indiciert wird, dass ihre Gleichgewichtslösungen nicht substantielle Mengen von mehr als zwei Modifikationen enthalten. Sørensen [3] hat in einer umfangreichen, sehr gründlichen Arbeit "Beiträge zur Kinetik der Mutarotation" diese Frage untersucht und

diskutiert. Im Allgemeinen studiert man den Verlauf der Mutarotation durch Messung der optischen Drehung, da es am einfachsten ist. Riiber und Mitarbeiter [9] haben ausserdem die viel beschwerlicheren Messungen des Molekular-Volumens und der Molekular-Refraktion durchgeführt. Sørensen hat einige ihrer Versuchsresultate neu berechnet und kommt *in casu* D-Mannose zu folgender, für diese Betrachtungen grundlegenden Konklusion. "Die Mutarotation der Mannose gehorcht dem Konstantsatz und zeigt deshalb keineswegs mehr als zwei Modifikationen an". Weiterhin schreibt Sørensen in der Zusammenfassung: "Die beiden Pyranosen machen bei der Galactose nur etwa 89,4 g/100 g des Gleichgewichtes aus, gegen 97 bis 98 g/100 g bei der Glucose". D-Galactose zeigt "komplexe" Mutarotation; die Gleichung einer Reaktion erster Ordnung ist nicht anwendbar; die berechneten Mutarotationskoefficienten ändern sich während des Fortschreitens der Reaktion.

Isbell und Pigman [13] haben die procentuelle Verteilung der Anomeren verschiedener Zucker in der Gleichgewichtslösung sowohl durch optische Drehung als durch Oxydation mit Brom (0°C, pH = 5.4) bestimmt. Ihre Resultate zeigen für D-Glucose eine gute, für D-Mannose eine ausgezeichnete Übereinstimmung. Gleichgewichtslösungen direkt aus α-D- und β-D-Glucose hergestellt, zeigen keine messbare Änderung in der optischen Drehung, im Brechungsindex und im Volumen.

Dieses Kapitel soll mit den Worten von Bates [6] abgeschlossen werden: "Aldoses which have the glucose and mannose structures establish equilibrium states consisting almost exclusively of α- and β-pyranose modifications."

DIE BESTIMMUNG DER ABSOLUTEN KONFIGURATION DER ANOMEREN D-GLUCOSE UND D-MANNOSE DURCH BÖESEKEN

Basis für die folgende Diskussion ist die letzte von Böeseken publicierte Zusammenfassung [1]: "The use of boric acid for the determination of the configuration of carbohydrates". Böeseken hat sich mit diesem Problem vom Jahre 1913 [14] bis zum Jahre 1949 [1] beschäftigt.

Ausgangspunkt ist das von Vignon [15] entdeckte Phänomen, dass die geringe Acidität einer Borsäurelösung durch Zusatz von gewissen Polyhydroxyverbindungen, wie Mannitol, erheblich grösser wird. Später ging man dazu über die Änderung der elektrischen Leitfähigkeit einer Borsäurelösung beim Auflösen des Polyols zu benutzen, da diese Methode mehr sensibel ist. Mit dieser Methode zeigte Böeseken, dass auch gewisse cyclische Diole mit Borsäure reagieren. Cyclopentan-*cis*-1,2-diol gibt einen starken Leitfähigkeits-Zuwachs, während die *trans*-Verbindung nicht mit Borsäure reagiert. Freie Aldosen und Ketosen reagieren mit Borsäure, während Saccharose die Leitfähigkeit einer Borsäurelösung nicht beeinflusst.

Während die Leitfähigkeit einer Polyol-Borsäurelösung sich nicht beim Stehen ändert, ändert sich die Leitfähigkeit einer frisch bereiteten Lösung einer krystallinischen Aldose, die Borsäure enthält, mit der Zeit. Die Änderung geschieht in Takt mit der Mutarotation des Zuckers. Die Geschwindigkeitskonstanten, nach einer Reaktion erster Ordnung berechnet, sind für α-D-Glucose und β-D-Mannose konstant und haben für jeden Zucker praktisch denselben

Tabelle 3. Die möglichen Konfigurationen am C_1 und C_2 Kohlenstoffatom der anomeren D-Glucose und D-Mannose.

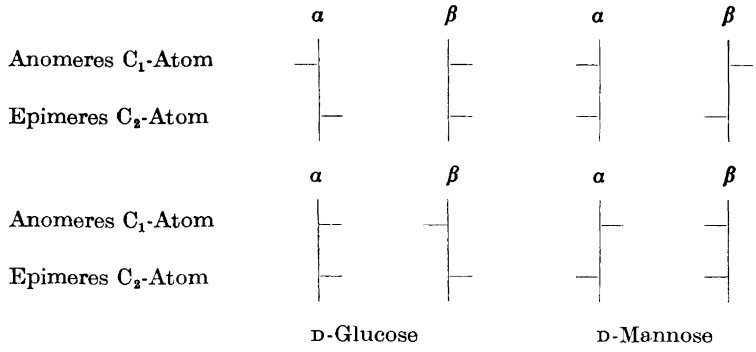

Wert, unangesehen ob sie aus der Änderung der optischen Drehung oder aus der Änderung der Leitfähigkeit berechnet werden. α-D-Glucose und β-D-Mannose zeigen also "einfache" Mutatoration, während α-D-Galactose wiederum "komplexe" Mutarotation zeigt. Bei der Mutarotation der Zucker in Borsäurelösung scheinen also dieselben Reaktionen vor sich zu gehen als bei der Mutarotation in Wasser.

Zu der Zeit (1913) als Böeseken seine ersten Versuche ausführte, war man der Anschauung, dass sowohl die freien Zucker als die Glykoside fünfgliedrige Ringsysteme enthielten. Da α-D-Glucose während der Mutarotation abnehmende Leitfähigkeit zeigt, erteilte Böeseken diesem Anomer *cis*-Konfiguration der Hydroxylgruppen bei C_1 und C_2. β-D-Glucose und β-D-Mannose erteilte er *trans*-Konfiguration, auf Grund des beobachteten Ansteigens der Leitfähigkeit. Als man später erkannte, dass α-D-Glucose und α-D-Mannose die gleiche Konfiguration, β-D-Glucose und β-D-Mannose die gleiche aber entgegengesetzte Konfiguration am glykosidischen Kohlenstoffatom haben, kam Böeseken in eine schwierige Situation, die ich kurz präcisieren möchte. D-Glucose und D-Mannose sind epimere Zucker, d.h. sie unterscheiden sich nur durch die Konfiguration am zweiten Kohlenstoffatom. In der D-Glucose sitzt die Hydroxylgruppe bei C_2 rechts, in der D-Mannose links (C_1 oben, C_5 unten) [Tabelle 3].

α-D-Glucose und β-D-Mannose, respektive β-D-Glucose und α-D-Mannose müssen paarweise entweder *cis*- oder *trans*-Konfiguration bei C_1 und C_2 haben. Die Leitfähigkeitsänderung in einer Borsäurelösung während der Mutarotation müsste für jedes Paar in gleiche Richtung verlaufen. Sie verläuft aber *de facto* für α-D-Glucose und β-D-Mannose in entgegengesetzte Richtung. Um aus diesem Dilemma herauszukommen, introducierte Böeseken die Hypothese, dass während der Mutarotationen eine Änderung der Ringstruktur von Pyranose zu Furanose in grösserem Masstabe eintritt. Die Gleichgewichtslösung der D-Glucose soll nach Böeseken ca. 10 % Furanosen enthalten, und Furanosemodifikationen "must be present in rather large quantities" in der Gleichgewichtslösung der D-Mannose. Da die Gleichgewichtslösung der D-Glucose nur 2—3 %, die Gleichgewichtslösung der D-Mannose kaum Furanosemodifikationen enthält, steht Böesekens Hypothese in direktem Widerspruch mit den experi-

mentellen Daten von Sørensen [3] und gleichzeitig im Widerspruch zu seinen eigenen Daten, da die "einfache" Mutarotation dieser Zucker nur durch Gegenwart zweier und nur zweier Modifikationen verständlich ist.

DIE BESTIMMUNG DER ABSOLUTEN KONFIGURATION DER ANOMEREN VON D-GLUCOSE UND VON D-MANNOSE UNTER ANWENDUNG DER KONFORMATIONSANALYSE UND DER EXPERIMENTELLEN RESULTATE VON BÖESEKEN

Zwei Hydroxylgruppen, welche an vicinalen Kohlenstoffatomen eines Cyclopentanringes gebunden sind, können nur eine *cis*- oder *trans*-Stellung einnehmen, während sie in einer spannungsfreien Stuhl-Konformation:

cis: equatorial-axial *trans:* di-equatorial *trans:* di-axial

an vicinalen Kohlenstoffatomen eines Sechsringes gebunden sein können. Es ist diese Aufteilung in zwei verschiedene *trans*-Konformationen, welche es ermöglicht, das vorliegende Problem zu lösen, indem dadurch die Möglichkeit eintritt, dass die Leitfähigkeit während der Mutarotation sich in entgegengesetzter Richtung ändern kann, selbst wenn ein Anomerenpaar zweier epimerer Zucker *cis*- respektive *trans*-gebundene vicinale Hydroxylgruppen bei C_1 und C_2 hat:

trans e/e ⇌ *cis* e a *cis* a e ⇌ *trans* a/a

Wie bekannt, können sechsgliedrige Ringsysteme wie Cyclohexan und Tetrahydropyran verschiedene Konformationen einnehmen. Die Energiedifferenz zwischen zwei oder mehreren Konformationen einer Verbindung bestimmt welche am stabilsten ist [16]. Die Stuhlkonformationen sind energetisch vorgezogen. Es sind nur diese Konformationen, welche in die vorliegenden Betrachtungen eingehen. In einer grundlegenden Arbeit: "The structure of molecules containing cyclohexane- or pyranose rings" schreiben Hassel und Ottar [17]: "All experimental evidence indicates that the six membered ring form in many sugars will generally have the staggered form (chair). Each pyranose will at least theoretically be able to occur in two different conformations". Reeves [18] bezeichnet die eine Stuhl-Konformation mit C 1 die andere mit 1 C. Es ist nun die Frage, welche Stuhl-Konformation D-Glucose und D-Mannose einnehmen. Die Antwort geben Hassel und Ottar: "In the normal hexoses it seems reasonable to assume that conformations placing both the $-CH_2OH$ group and one $-OH$ group in axial positions on the same side of the ring are energetically unfavourable. If this argument holds it settles the energetically preferred conformations of the following sugars:

α- and β-glucose, α- and β-mannose, α- and β-galactose."

Die vorgezogene Konformation ist in der Nomenklatur von Reeves die C 1 Konformation. Die Substituenten in den Anomeren von D-Glucose und D-Mannose haben in der C 1 resp. 1 C Konformation die in Tabelle 4 skizzierte equatoriale resp. axiale Anknüpfung an die Kohlenstoffatome des Ringes.

Tabelle 4. Die equatoriale und axiale Anknüpfung der Substituenten in D-Glucose und D-Mannose in den möglichen Konfigurationen und den möglichen Stuhl-Konformationen.

	C 1 A		C 1 B		C 1 A		C 1 B		1 C A		1 C B		1 C A		1 C B	
C_1	e		a		e		a		a		e		a		e	
C_2		e	e		a		a			a	a		e			e
C_3	e		e		e		e		a		a		a		a	
C_4		e	e		e		e			a	a		a		a	
C_5	e		e		e		e		a		a		a		a	
	D-Glucose			D-Mannose					D-Glucose				D-Mannose			

Die generelle Ebene des Pyranosenringes wird durch den senkrechten Strich angedeutet. Wie in den Formelbildern von Emil Fischer steht C_1 oben, C_5 unten. Die Anordnung der Hydroxylgruppen bei C_2, C_3, C_4 folgt den bekannten Formeln. Die $-CH_2OH$ Gruppe bei C_5 steht in D-Aldohexopyranosen links. Die Placierung der Hydroxylgruppe bei C_1 ist in allen α-Anomeren auf der einen, in allen β-Anomeren auf der entgegengesetzten Seite.

Reeves kommt durch seine Untersuchungen über die Leitfähigkeit von Cuprammonium in Lösungen der anomeren Methylglykoside von D-Glucose und D-Mannose zu demselben Resultat als Hassel und Ottar für die freien Pyranosen-Zucker. Die vorgezogene Konformation ist die C 1 Konformation, in welcher die grösstmögliche Anzahl von Substituenten, besonders die voluminöse CH_2OH-Gruppe equatoriale Stellungen einnimmt.

Bei der Reaktion zwischen Borsäure und einem Diol, kann kein Zweifel herrschen, wo die Reaktion stattfindet. Bei der Reaktion mit Aldohexosen, welche fünf Hydroxylgruppen haben, bestehen mehrere Möglichkeiten. Macpherson und Percival [19] kamen zu der Konklusion "that the only hydroxyl groups in glucose having any effect on the conductivity of a boric acid solution are those in C_1 and C_2." Weder 2,3,6-Trimethyl-Glucopyranose noch 2,3,4,6-Tetramethyl-glucose reagieren mit Borsäure. Beide Zuckerderivate zeigen Mutarotation.

Der Abstand zwischen den Zentren zweier Sauerstoffatome kann als Mass des Abstandes zweier Hydroxylgruppen gelten. Der Abstand zwischen den Zentren der Sauerstoffatome der Borsäure lässt sich aus den Daten von Zachariasen [20] zu ca. 2,36 Å berechnen. Die Borsäure ist ein planes Molekyl mit symmetrischer Gruppierung der Sauerstoffatome. Borsäure reagiert mit Cyclopentan-*cis*-1,2-Diol, O—O Abstand ca. 2,51 Å [18], nicht aber mit dem *trans*-Isomeren, O—O Abstand ca. 3,45 Å [18]; Borsäure reagiert mit *o*-Dihydroxybenzol, O—O Abstand ca. 2,84 Å, nicht aber mit den *meta*- oder *para*-Isomeren, deren O—O Abstand viel grösser ist als 3,45 Å. Hassel und Ottar [17]

haben gefunden, dass die Abstände der O—O Zentren zweier benachbarter Hydroxylgruppen in einem Pyranosering folgende Werte haben:

trans e/e 2,85 Å *cis* e a 2,96 Å *trans* a/a 3,73 Å

Während der Mutarotation von β-D-Mannose in einer Borsäurelösung steigt die Leitfähigkeit an. Die Lösung enthält nur zwei anomere Pyranosen in der C 1 Konformation. Das Ansteigen der Leitfähigkeit muss durch eine sterische Annäherung der beiden Hydroxylgruppen bei C_1 und C_2 während der Umlagerung vom β-Anomer zum α-Anomer verursacht sein. Da die Hydroxylgruppe bei C_2 in der D-Mannose in der C 1 Konformation axial gebunden ist, muss β-D-Mannose das Anomer sein, welches eine *trans*-axiale Hydroxylgruppe bei C_1 hat und α-D-Mannose das Anomer sein, welches eine *cis*-equatorial gebundene Hydroxylgruppe bei C_1 hat. Nur auf diese Weise besteht die Möglichkeit für eine sterische Annäherung der beiden Hydroxylgruppen, welche sich in einem Ansteigen der Leitfähigkeit bei der Umlagerung von β- zu α-D-Mannopyranose zu erkennen gibt.

Während der Mutarotation von α-D-Glucose in einer Borsäurelösung nimmt die Leitfähigkeit ab. Die Lösung enthält fast ausschliesslich zwei anomere Pyranosen in der C 1 Konformation. Da die Hydroxylgruppe bei C_2 in der D-Glucose in der C 1 Konformation equatorial gebunden ist, muss α-D-Glucose das Anomer sein, welches eine *trans*-equatoriale Hydroxylgruppe bei C_1 hat und β-D-Glucose das Anomer sein, welches eine *cis*-axial gebundene Hydroxylgruppe bei C_1 hat. Nur auf diese Weise besteht die Möglichkeit für ein sterisches "Sich-Entfernen" der beiden Hydroxylgruppen, welche sich in einem Fallen der Leitfähigkeit bei der Umlagerung von α- zu β-D-Glucopyranose zu erkennen gibt.

Betrachtet man nun das Schema in Tabelle 4 mit den soeben angeführten Konklusionen, geben die unter C 1 A angegebenen Formeln ein Bild der Konfiguration und Konformation der α-Anomeren von D-Glucose und D-Mannose, die unter C 1 B angegebenen ein Bild der β-Anomeren. In den Formeln von Emil Fischer, C_1 oben, C_5 unten, wird das endgültige Resultat, dass die Hydroxylgruppe am glykosidischen Kohlenstoffatom von D-Aldohexosen in den α-Anomeren links, in den β-Anomeren rechts gebunden ist. Es ist die umgekehrte Konfiguration derjenigen, welche in der Literatur steht. Das Resultat ist aber in Übereinstimmung mit dem Resultat meiner früheren Untersuchungen über die Reaktionsgeschwindigkeit der Säurehydrolyse von anomeren Methylglykosiden und über die Bromoxydation anomerer Zucker [2] und weiteren Untersuchungen, die in Kürze erscheinen werden.

REFERENZEN

1. Böeseken, J. *Advances in Carbohydrate Chem.* **4** (1949) 189.
2. Blom, J. *Acta Chem. Scand.* **15** (1961) 1667.
3. Sørensen, N. A. *Kgl. Norske Videnskab.* Selskabs Skrifter 1937, No. 2.
4. Jackson, E. L. und Hudson, C. S. *J. Am. Chem. Soc.* **59** (1957) 994.
5. Smith, F. und Cleve, J. W. van *J. Am. Chem. Soc.* **77** (1955) 3091.
6. Bates, F. J. and Associates: *Polarimetry, Saccharimetry and the Sugars.* Circular of the National Bureau of Standards C 440. Washington 1942.
7. Augestad, I. und Berner, E. *Acta Chem. Scand.* **10** (1956) 911.

8. Dale, J. K. *J. Am. Chem. Soc.* **51** (1929) 2788.
9. Riiber, C. N. *Det 4:de Nordiske Kjemikermøte*, Oslo 1932. 106.
10. Riiber, C. N. *Z. physik. Chem.* A **176** (1936) 358.
11. Eisenlohr, F. *Spektrochemie org. Verbindungen*, Stuttgart 1912, p. 48.
12. Riiber, C. N. Tollens-Elsner. *Kurzes Handbuch der Kohlenhydrate*. Leipzig 1935, p. 85.
13. Isbell, H. S. und Pigman, W. W. *J. Research Natl. Bur. Standards* **20** (1938) 773.
14. Böeseken, J. *Ber.* **46** (1913) 2612.
15. Vignon, L. *Comp. rend.* **78** (1874) 148.
16. Dauben, W. G. und Pitzer, K. S. *Conformational Analysis in* Newman, M. S. *Steric Effects in Organic Chemistry*. New York 1956.
17. Hassel, O. und Ottar, B. *Acta Chem. Scand.* **1** (1947) 929.
18. Reeves, R. E. *Advances in Carbohydrate Chem.* **6** (1951) 107.
19. Macpherson, H. T. und Percival, E. G. V. *J. Chem. Soc.* **1937** 1920.
20. Zachariasen, W. H. *Acta cryst.* **7** (1954 a) 305.

Eingegangen am 11. Dezember 1961.

ACTA CHEMICA SCANDINAVICA 16 (1962) 931–935

Studies on Cobaltammines

IV. A Proton Addition Reaction of Some Thiocyanatocobaltammines

RAGNAR LARSSON

Department of Inorganic and Physical Chemistry, Chemical Institute, University of Lund, Lund, Sweden

When $[Co(NH_3)_5NCS](ClO_4)_2$ and *trans*-$[Coen_2(NCS)_2]ClO_4$ are dissolved in concentrated sulphuric acid, a colour change from red to yellow is observed. The absorption curves in the visible and near ultraviolet region are presented. The colour change is shown to be caused by a proton addition reaction, similar to the additions of Ag^+ and Hg^{2+}. It is assumed from the presented data that the Co—NCS—H bond is essentially of the same character as the Co—NCS—Ag and Co—NCS—Hg bonds. This result is put in relation to the current discussion on the covalent bonds of b-class metals [1].

It has long been recognized [2] that silver ions have the ability to coordinate to the thiocyanato group in thiocyanato cobalt(III) ammine complexes. In addition mercury(II) ions have the same coordinating ability [3]. As a result of this reaction the colour of the cobalt complexes shifts from red to yellow [3,4]. According to Werner [2] the colour of the compounds obtained are similar "almost to confusion" to that of the luteo salts. Schaeffer [5] has related this colour shift to the ability of Ag^+ and Hg^{2+} ions to interact with the π electrons of the thiocyanato group.

During investigations on the reactions of thiocyanato cobalt ammines it was observed by the present author, that when these compounds were dissolved in concentrated sulphuric acid a similar change in colour occurred. Although this colour change must have been observed many times during ordinary analytical procedures, it has not been found reported in the available literature. Therefore some experiments were performed to investigate this reaction in detail and to relate it to the already known addition reactions of silver and mercury(II) ion.

MEASUREMENTS

The following experiments were performed:

1. In order to estimate the change of the absorption spectra of cobaltammines when the solvent is changed from water to conc. sulphuric acid the

Table 1. Data of the spectrum of $[Co(NH_3)_6](ClO_4)_3$ dissolved in water and in conc. sulphuric acid.

Solvent	λ_{max1} mμ	$\log \varepsilon_{max1}$	λ_{max2} mμ	$\log \varepsilon_{max2}$
Water	476	1.75	339.5	1.66
Conc. H_2SO_4	479	1.78	339.7	1.69

absorption spectrum of $[Co(NH_3)_6](ClO_4)_3$ was determined in the two solvents. As seen from Table 1 there is only a very small shift in the wavelengths and extinction coefficients of the maxima.

2. In order to relate the change of the absorption spectra of thiocyanatocobaltammines when dissolved in conc. sulphuric acid to that produced by heavy metals, the spectra of $[Co(NH_3)_5NCS](ClO_4)_2$ and *trans*-$[Coen_2(NCS)_2]ClO_4$ were determined in water, in conc. sulphuric acid and in aqueous solutions containing large quantities of mercury nitrate. The results are given in Figs. 1 and 2 and Table 2. The data for the $Coen_2(NCS)_2^+$ ion should be compared to the data given by Shimura and Tsuchida [6] for the *trans*-$Coen_2(NH_3)_2^{3+}$ ion, (λ_{max1} = 467 mμ, log ε_{max1} = 1.77; λ_{max2} = 336 mμ, log ε_{max2} = 1.73). The same spectra were obtained for solutions containing 0.1 M and 0.2 M $Hg(NO_3)_2$, which indicates the completeness of the reaction.

3. The possibility of a substitution reaction in the inner coordination sphere of the cobalt atom is very unlikely as Co(III) thiocyanato complexes

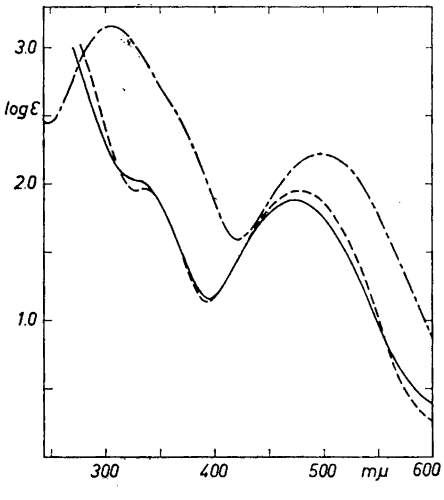

Fig. 1. Spectra of $[Co(NH_3)_5NCS](ClO_4)_2$ dissolved in water (—.—.—), in conc. sulphuric acid (———) and in 0.1 M $Hg(NO_3)_2$ (— — —).

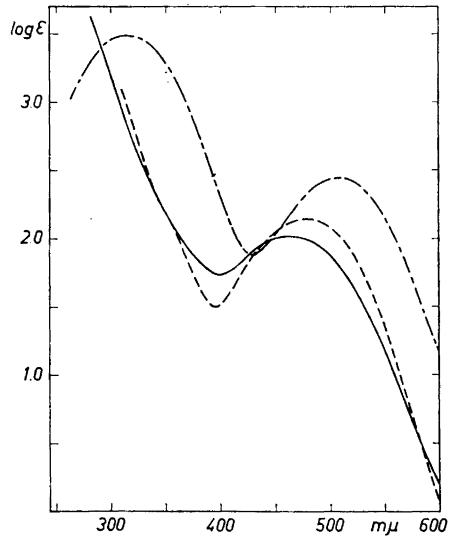

Fig. 2. Spectra of *trans*-$[Coen_2(NCS)_2]ClO_4$ dissolved in water (—.—.—.—), in conc. sulphuric acid (———) and in 0.1 M $Hg(NO_3)_2$ (— — —).

Table 2. Data of observed peaks of spectra of $[Co(NH_3)_5NCS](ClO_4)_2$ and *trans*-$[Coen_2(NCS)_2]ClO_4$ dissolved in water, conc. sulphuric acid and 0.1 M $Hg(NO_3)_2$.

Complex	Solvent	λ_{max1} mμ	log ε_{max1}	λ_{max2} mμ	log ε_{max2}
$[Co(NH_3)_5NCS]^{2+}$	Water	498	2.22	306	3.16
	conc. H_2SO_4	474	1.89	330 *	2.02
	0.1 M $Hg(NO_3)_2$	476	1.95	333	1.96
$[Coen_2(NCS)_2]^+$	Water	509	2.44	315	3.49
	conc. H_2SO_4	465	2.02	—	—
	0.1 M $Hg(NO_3)_2$	479	2.14	—	—

* shoulder

are known to be quite inert [7] and the reaction is apparently momentary. Nevertheless an experiment was performed to investigate this question. A solution of $[Coen_2(NCS)_2]ClO_4$ in conc. H_2SO_4 (17.7 M) was diluted in icecold water and — when the solution had room temperature — diluted so as to give a solution of the complex in 17.7/20 M H_2SO_4. The spectrum of this solution was compared with that of a solution obtained by dissolving the complex directly in 17.7/20 M H_2SO_4. The recovery of the original complex was estimated to be 95—97 % indicating that the colour change is not due to an irreversible decomposition reaction.

4. In spite of the results of experiment 1, there still remains the possibility that the colour change under discussion is caused by a "solvent effect" operating primarly on the thiocyanato group. If this is true one should expect a continous change of the extinction coefficients of the complex for a series of water-sulphuric acid mixtures as solvents. Such measurements for the most simple salt used in this investigation, $[Co(NH_3)_5NCS](ClO_4)_2$ are recorded in Fig. 3. It is seen that there is no "continuous" change but rather a very sharp change of the properties of the solution in the narrow concentration region 14—15 M.

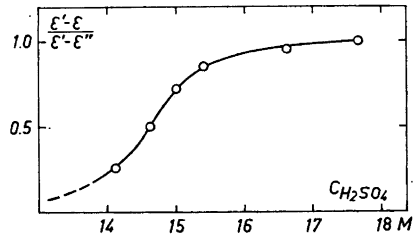

Fig. 3. The function $(\varepsilon'-\varepsilon)/(\varepsilon'-\varepsilon'')$ for the $[Co(NH_3)_5NCS]^{2+}$ complex plotted against the sulphuric acid concentration. The extinction coefficients were read from the curves at 550 mμ.

ε' = extinction coefficient of the complex in pure water
ε'' = » » » » » » conc. H_2SO_4
ε = » » » » » » mixed solvents.

EXPERIMENTAL

The measurements were made with a Beckman DK-1 Recording Spectrophotometer with quartz cells. The concentrations of the metal complexes were chosen so as to give an optical density of the maxima in all cases of the magnitude 0.5—0.8.

Chemicals used. $[Co(NH_3)_6](ClO_4)_3$ and *trans*-$[Coen_2(NCS)_2]ClO_4$ were prepared as before [8,9]. $[Co(NH_3)_5NCS](ClO_4)_2$ was prepared according to the method described by Werner [10] with the additional precipitation of the perchlorate by perchloric acid and final recrystallisation. Cobalt content: calc. 14.69 %; found 14.67 %.

DISCUSSION

It is one of the main theorems of the crystal-field theory [11] that the splitting of the energy levels of the metal ion is strongly dependent upon the distance between the metal ion and the ligand (point-charge or dipole). As it is most probable that in the complexes under discussion, crystal-field effects are the most important ones in determining the visible spectra of the complexes, we can conclude that the electron density around the nitrogen atom in the thiocyanato group is almost the same whether an Hg^{2+}, Ag^+ or H^+ ion coordinates to the sulphur atom. Indeed, the similiarity of the spectra of these association products and of the luteo ions give us the information that the electron density corresponds almost exactly to that of the NH_3-nitrogen atoms in the luteo ions.

The fact that the same electron density is found around the nitrogen atom whether an Hg^{2+} or an H^+ ion is the association partner casts some light upon the discussion on the division of metals into two classes, characterised by their different coordination ability: From the above data we are forced to conclude that the Hg—S and the H—S bonding cause almost the same degree of rehybridization of the thiocyanato group and thus the Hg—S and H—S bonds are of essentially the same character in regard to electronic distribution.

It has been proposed [1] that Hg^{2+} and the other b-group ions owe their strong coordination ability towards sulphur to a d—d π bonding. Because of the above-mentioned similarity between Hg—S and H—S bonds, however, this explanation can be ruled out in the present case as the hydrogen atom cannot participate in any such bonding, nor in any d—p π bonding involving the π-orbitals of the thiocyanate ligand. It seems more likely then, that the explanation given by Williams [12] (see also Ref.[13]) is more appropriate here. This implies that the small and often highly charged ions of the b-group exert a strong polarizing action upon ligands such as sulphur. This polarizing effect is said to be strengthened by the strongly directional orientation of the filled d-orbitals of the b-group metals.

The above-mentioned rehybridization of the thiocyanate group does also manifest itself by a shift of the high intensity peak at about 300 mμ. This peak has been ascribed to an intra-ligand transition (*cf.* Ref.[14], p. 271). Especially in the case of the $[Co(NH_3)_5NCS]^{2+}$ ion (Fig. 1) is this shift easily observed, as here the peak in question and the second "crystal-field peak" ($^1A_{1g} \rightarrow {}^1T_{2g}$-transition) are almost resolved. As the spectra were not recorded in the far ultraviolet, we cannot say anything definite about this shift, but it seems to

be of the same order of magnitude in the case of the Co—NCS—Hg system as in the case of the Co—NCS—H one.

Another point of great interest of the present investigation is the close similarity to the findings of Schilt [15,16] on the proton complexes of the $[Fephen_2(CN)_2]$ molecule. However the bonding mechanism proposed by Schilt [16], implying a direct H—Fe interaction, cannot be applied to the present case as the Ag^+ and Hg^{2+} ions are certainly too large to be situated close to the cobalt nucleus. Rather, it has been concluded recently by Hamer and Orgel [17] tat the explanation offered by Schilt is probably not true, as they [17] could prepare a compound $[Fephen_2(CN-CH_3)_2]$ with a very similar spectrum compared to $[Fephen_2(CN-H)_2]^{2+}$.

This fact, in its turn, gives increased support to our interpretation of the σ-bond character of the S—Hg and S—H bonds in the thiocyanatocobaltammines studied in this paper.

REFERENCES

1. Ahrland, S., Chatt, J. and Davies, N. R. *Quart. Rev.* **12** (1958) 265.
2. Werner, A. *Ann.* **386** (1912) 1.
3. Waggener, W. C., Mattern, J. A. and Cartledge, G. H. *J. Am. Chem. Soc.* **81** (1959) 2958.
4. Chamberlain, M. M. and Bailar, J. C. *J. Am. Chem. Soc.* **81** (1959) 6412.
5. Schäffer, C. E. *Abstracts of Papers Intern. Conf. on Coord. Chem.* London 1959.
6. Shimura, Y. and Tsuchida, R. *Bull. Chem. Soc. Japan* **29** (1956) 311.
7. Adamson, A. W. and Williams, R. G. *J. Am. Chem. Soc.* **76** (1954) 3379.
8. Larsson, R. *Acta Chem. Scand.* **11** (1957) 1405.
9. Larsson, R. *Acta Chem. Scand.* **14** (1960) 697.
10. Werner, A. *Ber.* **40** (1907) 765.
11. Van Vleck, J. H. *J. Chem. Phys.* **7** (1939) 72.
12. Williams, R. J. P. *Proc. Chem. Soc.* **1960** 20.
13. Westland, A. D. *Can. J. Chem.* **38** (1960) 1300.
14. Dunn, T. M. In Lewis, J. and Wilkins, R. G. (Ed.) *Modern Coordination Chemistry*, Interscience Publishers, Inc. New York and London 1960.
15. Schilt, A. A. *J. Am. Chem. Soc.* **82** (1960) 3000.
16. Schilt, A. A. *J. Am. Chem. Soc.* **82** (1960) 5779.
17. Hamer, N. K. and Orgel, L. E. *Nature* **190** (1961) 439.

Received November 21, 1961.

ACTA CHEMICA SCANDINAVICA 16 (1962) 936–946

Isothiocyanates XLIII *. Isothiocyanates from *Putranjiva Roxburghii* Wall. Including *(S)*-2-Methylbutyl Isothiocyanate, A New Mustard Oil of Natural Derivation

ANDERS KJÆR and PALLE FRIIS

Department of Organic Chemistry, Royal Veterinary and Agricultural College, Copenhagen, Denmark

The isothiocyanates produced on enzymic hydrolysis of glycosidic progenitors in seed kernels of the Indian tree *Putranjiva Roxburghii* Wall. *(Euphorbiaceae)* have been reinvestigated. Previous findings of isopropyl and 2-butyl isothiocyanate have been confirmed whereas the volatile hydrolysis product of the minor glucoside, *glucojiaputin*, is demonstrated to be the previously unknown (S)-*2-methylbutyl isothiocyanate* (V), and *not*, as formerly claimed [3,4], phenyl isothiocyanate.

The structure of the new isothiocyanate is established by analysis, optical activity, and n.m.r. spectroscopy of the corresponding thiourea. Its absolute configuration appears from a stereoselective synthesis departing from (*S*)-2-methylbutanol.

In addition to the three volatile mustard oils, identified also by gas chromatography, an enzymically hydrolyzed seed extract is shown to contain (−)-5-ethyl-5-methyl-2-oxazolidinethione (cleomin) (VI), arising from the glucoside *glucocleomin* which recently was established as a wide-spread constituent in species of the family *Capparidaceae* [13].

The isothiocyanate glucosides with branched side-chains encountered thus far are summarized and possible biogenetic pathways discussed.

The tree *Putranjiva Roxburghii* Wall. of the family *Euphorbiaceae* is indigenous to and cultivated as an ornamental throughout tropical India. Since antiquity, curative effects have been attributed to its leaves and seeds, administered in form of decoctions for oral use or as poultices for local application [1,3]. Again, stones of the fruit are reputed to be protective against diseases when placed as rosaries around the necks of children [1] **.

* Part XLII of this series: *Acta Chem. Scand.* **16** (1962) 591.

** In fact, the vernacular names for the tree (*e.g.* Sanskrit *Putra-jiva*, Hindi *Putranjiva* or *Jiputa*) all signify "the life of the child".

Although the high oil content of *Putranjiva* seeds was recognized long ago [1], it was not until 1931 that Krishna and Puntambekar [2] made the first study of the composition of the glycerides. Gambhir and Dutt [3] later extended this investigation and reported the presence in the seed oil of 0.7 % of phenyl isothiocyanate, to which the therapeutic properties of the otherwise normally composed vegetable oil were attributed. The Indian authors based their identification of the steam-volatile mustard oil solely on a sulphur analysis of the corresponding thiourea derivative, m.p. 52°, seemingly inadvertent of the discrepancy between this value and the m.p. 154° of authentic phenylthiourea. This statement prompted Puntambekar [4] to undertake a more detailed study of the steam-volatile isothiocyanates produced on enzymic hydrolysis of glycoside progenitors in seeds of *P. Roxburghii*. Upon fractional distillation, three individual components were partly separated, *viz.* isopropyl isothiocyanate, partly racemized (+)-2-butyl isothiocyanate, and small quantities of a higher-boiling fraction which was claimed to be phenyl isothiocyanate on basis of the sulphur content of the corresponding thiourea. This was reported to melt at 153—154°, alone or in admixture with authentic 1-phenylthiourea. Whereas (+)-2-butyl isothiocyanate, the enzymic hydrolysis product of *glucocochlearin*, occurring in, *e.g.*, several species of the family *Cruciferae* (*cf.* Ref.[5]), presented no novelty within the plant kingdom, the other two isothiocyanates had not formerly been recognized as plant constituents. Puntambekar [4] introduced the designations *glucoputranjivin* and *glucojiaputin* for the glucosidic progenitors affording isopropyl and phenyl isothiocyanate, respectively. The former has since been repeatedly encountered in this laboratory, notably in species of the family *Cruciferae* [5], whereas no other well-authenticated source of phenyl mustard oil has since been reported *.

In connexion with current studies on the distribution and structure of isothiocyanates of natural origin it became of interest to reinvestigate *Putranjiva Roxburghii* Wall., particularly because this plant represents the sole well-documented source of isothiocyanate-producing glycosides within *Euphorbiaceae* **. This family is generally considered to be taxonomically remote from the natural order *Rhoeadales* (*sensu* Wettstein), comprising most of the traditional isothiocyanate glucoside-containing families such as *Capparidaceae*, *Cruciferae*, *Moringaceae* and *Resedaceae*.

On paper chromatography in several solvent systems, a methanolic extract of disintegrated seed kernels of *P. Roxburghii* *** proved to contain at least three mustard oil glucosides (A_1, B and C, Fig. 1), the first two agreeing in their R_B-values [6] with authentic specimens of glucoputranjivin and glucocochlearin, whereas glucoside C appeared at the expected position for a phenyl isothio-

* In a recent study by Bailey *et al.*[14] of the volatile sulphur components in fresh cabbage, phenyl isothiocyanate was tentatively suggested as a trace constituent on basis of an observed peak at mass 135, with isotopic contributions at masses 136 and 137, in mass spectral analyses.

** Freise [15] earlier reported that the latex from *Jatropha multifida* L. (Flor de coral), belonging to the same family, contains a sulphur compound, possibly benzyl isothiocyanate, yet without any experimental documentation.

*** The authors are much indebted to Professor T. R. Govindachari, Presidency College, Madras, India, for the generous gift of the seeds used in the present studies. Seeds can be commercially obtained from United Chemical and Allied Products, 10 Clive Row, Calcutta 1, India.

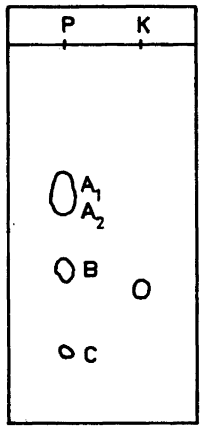

Fig. 1. Paper chromatogram of isothiocyanate glucosides. Solvent system: butanol:ethanol:water (4:1:4). P: Seed extract of *Putranjiva Roxburghii*; K: reference sample of glucotropaeolin. $A_1 + A_2$: Mixture of glucoputranjivin and glucocleomin; B: glucococchlearin; C: glucojiaputin.

cyanate-producing glucoside. No attempts were made in the present work to isolate, separate and characterize the glucosides.

On enzymic hydrolysis of a methanolic seed extract with a crude, cell-free myrosinase preparation, volatile mustard oils were liberated and removed by steam distillation. Paper chromatography in water-saturated chloroform of the corresponding thiourea derivatives [7], formed upon reaction with ammonia, revealed strong spots indistinguishable from those of authentic samples of 1-isopropyl- and (+)-1-(2-butyl)-thiourea. At the expected site of 1-phenylthiourea a minute spot appeared, deviating, however, from that of a reference sample by producing an orthodox blue thiourea colour with Grote's reagent rather than the green-blue tint of phenylthiourea. That this thiourea, corresponding to the minor volatile mustard oil derived from glucojiaputin, was not phenylthiourea or any known thiourea of natural derivation became obvious on comparative paper chromatography in other solvent systems (*cf.* Experimental) in which it migrated at a significantly higher rate than phenylthiourea. The first part of this paper deals with the structure elucidation of the new volatile mustard oil.

On a preparative scale, the crude glucoside mixture, extracted from 850 g of defatted seed kernels of *P. Roxburghii* with 70 % methanol, was hydrolyzed in a citrate buffer at pH 6.5 with a crude, cell-free myrosinase preparation. A mixture of the three volatile isothiocyanates was obtained by steam distillation and subsequent ether extraction, and further converted into a mixture of thioureas (15.4 g) on treatment with methanolic ammonia. Upon systematic, fractional crystallization from ethyl acetate, a homogeneous sample of 1-isopropylthiourea (5.2 g) was obtained. Part of the material present in the mother liquors was subsequently subjected to a 155-plate counter-current distribution between chloroform and water, resulting in virtually complete separation of the three thioureas as estimated from paperchromatographic analysis. From the appropriate tubes, an additional amount of 1-isopropylthiourea was isolated whereas the second "band" afforded the *dextro*rotatory (S)-*1-(2-butyl)-thiourea*, identified on critical comparison with an authentic speci-

men prepared from (+)-2-butyl isothiocyanate. The absolute configuration of the latter was previously established in this laboratory[8]. Contrary to the statement by Puntambekar[4] that partially racemic 2-butyl isothiocyanate is produced in the enzymic reaction, the preparations obtained in the present work possessed full optical activity.

The unknown, more lipophilic thiourea, completely separated from the isopropyl and 2-butyl derivative, was isolated as colourless prisms in amounts corresponding to about 100 mg per kg of seed kernels. The *dextro*rotatory thiourea, m.p. 72°, possessed the elemental composition $C_6H_{14}N_2S$, and exhibited ultraviolet and infra-red absorption data compatible with those expected for an N-pentyl-thiourea. The composition, in connexion with the optical activity, in fact limited the possible structures to (I), (II) or (III).

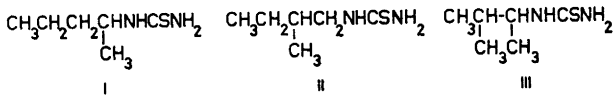

The choice between these was easily made on basis of the n.m.r. spectrum * of the new thiourea (Fig. 2). The presence of six methyl protons and *two* highly deshielded methylene protons (τ 6.8) is compatible only with structure (II).

The absolute configuration of this previously unknown thiourea, and hence of the natural isothiocyanate whence it derives, was established by stereoselective synthesis, departing from *levo*rotatory (*S*)-2-methylbutanol (IV) **. According to described or slightly modified procedures, the alcohol was converted into (+)-2-methylbutyl bromide[9] and this, in turn, into (+)-N-

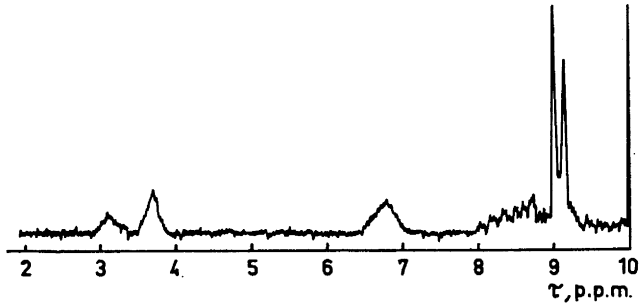

Fig. 2. Proton resonance spectrum (60 Mc) of (+)-1-(2-methylbutyl)-thiourea (II). Solvent: $CDCl_3$; internal standard: $(CH_3)_4Si$ (τ 10.0).

* The authors are indebted to Dr. A. Melera, Varian A-G., Zürich, for the determination of the n.m.r. spectra.

** The authors are grateful to Dr. E. Egelund Pedersen, The Chemical Laboratory of the University of Copenhagen, for a generous gift of optically pure (−)-2-methylbutanol.

(2-methylbutyl)-phthalimide [10] *. Hydrazinolysis of the latter afforded (−)-2-methylbutylamine [10], reacting with thiocarbonyl chloride to give the *dextro*-rotatory (*S*)-2-methylbutyl isothiocyanate (V), which was further converted into (+)-1-(2-methylbutyl)-thiourea on reaction with ammonia. The synthetic specimen proved identical with the thiourea of natural derivation in sign and magnitude of rotation as well as with regard to all other physical properties.

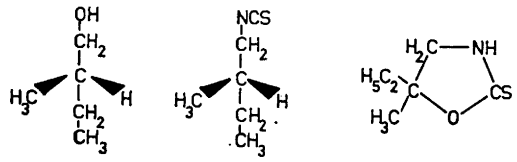

IV V VI

Hence, the volatile isothiocyanate produced on enzymic hydrolysis of glucojiaputin is proved to be *dextro*rotatory (*S*)-2-methylbutyl isothiocyanate (V) ** and *not*, as stated by Puntambekar [4], phenyl mustard oil. No trace of the latter isothiocyanate has been observed in enzymically hydrolyzed seed extracts of *P. Roxburghii* in the course of the present work and we can offer no explanation for the literature records [3,4] of phenyl isothiocyanate as a species of natural derivation.

Gaschromatographic analysis *** of the volatile mustard oil mixture from *Putranjiva* seeds clearly confirmed the presence only of isopropyl, 2-butyl and 2-methylbutyl isothiocyanate. The relative amounts were estimated to be 82 %, 16 % and 2 %, respectively.

A comparative, semi-quantitative evaluation of paper chromatograms of the glucosides (Fig. 1) and the thioureas derivable from the volatile isothiocyanates suggested that an additional glucoside (A_2), inseparable from glucoputranjivin and affording a non-volatile mustard oil on enzymic hydrolysis, was present in *Putranjiva* seeds. The nature of this glucoside was revealed when a paperchromatographic eluate of the combined glucosides, (A_1) and (A_2), was found to give a blue Grote-colour subsequent to enzymic hydrolysis but without addition of ammonia, and when a characteristic UV-absorption pattern was observed for the Grote-positive compound. These data suggested the presence in the seed extract of a glucosidic 2-oxazolidinethione precursor, analogous

* The rotation and other physical constants of our synthetic specimen of this compound were in excellent agreement with the older data of Marckwald [10]. Balenović and Bregant [11] recently reported a considerably higher rotation (+ 24°) for a synthetic, liquid preparation giving correct elemental analysis. The reason for this discrepancy is still obscure. Prof. Balenović kindly compared the infra-red spectra of the two preparations and found them practically identical. The physical constants are at present being reinvestigated in Prof. Balenović's laboratory (personal communication).

** It may be of biogenetic significance that the configuration of the new isothiocyanate is identical with that prevailing at the C_3-atom of natural L-isoleucine.

*** The authors are indebted to Dr. Å. Jart for his assistance in the gaschromatographic analyses.

with those formerly encountered in higher plants (*cf.* Refs. [5,12,13]). Consequently, the filtered residue from the large-scale steam distillation was subjected to continuous extraction with ether, resulting in complete transference of the Grote-positive material to the organic solvent. After extraction with aqueous alkali, adjustment to pH 5.5, and renewed continuous ether extraction, a colourless product (2.0 g) was obtained. After purification, this proved identical with (—)-5-ethyl-5-methyl-2-oxazolidinethione (VI) (cleomin), recently reported from this laboratory [13] as the enzymic hydrolysis product of *glucocleomin*, a glucoside occurring in *Cleome spinosa* Jacq. and several other species of the family *Capparidaceae*. Experiments are in progress to establish the absolute configuration of cleomin.

Puntambekar [4] reported the fruit pulp and the leaves of *P. Roxburghii* to be devoid of isothiocyanates and glycosidic progenitors. Contrary to this statement, a glucoside pattern, qualitatively and quantitatively similar to that observed in seed extracts, was observed during the present work by paper-chromatographic analyses of fresh leaves, stems and roots *. Ultra-violet spectroscopy further served to demonstrate the presence of glucocleomin in all of the plant parts tested.

No experimental reports have as yet appeared on the biosynthesis of isothiocyanate glucosides (VII). As pure speculation it seems attractive, however, to consider at least some of these as derived *in vivo* from activated esters of the corresponding acids (VIII). The branched side-chains encountered thus

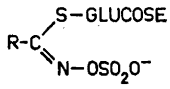

VII

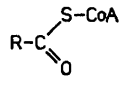

VIII

far in this class of glucosides are presented in Fig. 3. It appears that the corresponding acid derivatives (VIII) are identical with or strikingly similar to those involved in the biosynthesis and catabolism of valine, isoleucine and leucine [21]. Thus, isobutyric acid and 3-hydroxyisobutyric acid are believed to be normal intermediates on the degradative pathway of valine in mammalian tissue [22] whereas 2-methylbutyric acid, in analogy, arises from isoleucine [23]. 2-Ethylhydracrylic acid may be vizualized as resulting from β-oxidation of 2-methylbutyric acid through the shorter chain [12], though such a course admittedly would be at variance with that generally accepted for β-oxidation of α-methyl fatty acids [24].

Again, the acid derivatives (VIII) containing a methylene grouping next to the carboxylic function might conceivably originate from partial or complete reduction of the 2,3-dihydroxy acids, functioning as intermediates in the biosynthesis of valine and isoleucine in microorganisms [21]. If so, this course would represent another deviation in higher plants from the enzymic dehydration of the dihydroxy acids in microorganisms to give the α-keto acids whence

* The authors are indebted to the *Botanical Garden of the University of Copenhagen* for the fresh plant material.

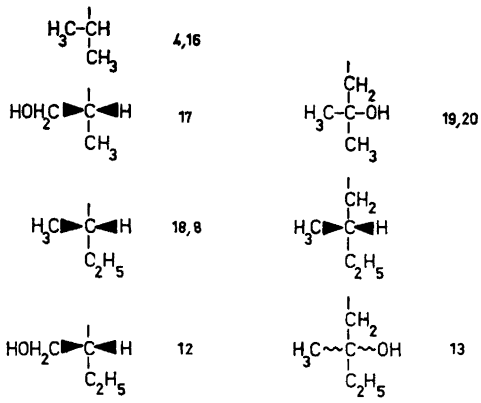

Fig. 3. Known, branched side-chains (R in (VII)) of naturally occurring isothiocyanate glucosides. The figures are literature references.

valine and isoleucine derive [21]. Of course, 3-hydroxyisovaleric acid may equally well be regarded as an established intermediate on the catabolic pathway of leucine [21], and 3-hydroxy-3-methyl-valeric acid as a reduced form of mevalonic acid.

In this connexion, the recent demonstration by Butler and Butler [25] that valine and isoleucine can function as precursors for the cyanogenetic glycosides linamarin and lotaustralin is of interest.

Thus far, isobutyl isothiocyanate has never been encountered as a compound of natural derivation but there may, on basis of biogenetic considerations, be good reasons to expect its future appearance as a product of enzymic glucoside hydrolysis.

EXPERIMENTAL

Melting points are uncorrected and determined in capillary tubes in an Anschütz-Hershberg apparatus. Rotations are measured in a 1 dm tube. Infra-red spectra are determined on a Perkin-Elmer "Infracord"—137 instrument. Analytical samples are dried at room temperature *in vacuo* over calcium chloride.

Paperchromatographic glucoside analysis. A few seed kernels of *P. Roxburghii* were ground in 70 % methanol and the suspension refluxed for 30 min. On paper chromatography in butanol:ethanol:water (4:1:4), followed by spraying with silver-nitrate, the filtrate gave a very strong glucoside spot ($A_1 + A_2$) with an R_B value [6] of 0.58, a medium spot with R_B 0.90 and a weak spot with R_B 1.25 (Fig. 1). The first two glucosides appeared at exactly the positions of glucoputranjivin and glucocochlearin as estimated from controls on the same chromatogram of authentic specimens of these two glucosides, applied in form of an extract of *Cochlearia officinalis* L.[19] Consequently, there can be no doubt that the fast-running component is identical with the glucoside designated *glucojiaputin* by Puntambekar [4].

Paperchromatographic thiourea analysis. A seed portion (10 g) was crushed in water and the suspension was buffered to pH 6.5 with citrate. A trace of ascorbic acid [26,35] and a cell-free myrosinase preparation [27] (1 ml) were added and the mixture was set aside overnight.

Next day, the suspension was steam-distilled, 0.5 l of distillate being collected in conc. ammonia (15 ml). After 2 h at room temperature, the solution was evaporated to

dryness *in vacuo* and the thiourea mixture (50 mg) was dissolved in ethanol (1.8 ml). On paper chromatography of this solution in water-saturated chloroform [7], three thiourea spots were observed with R_{Ph}-values [7] of 0.42, 0.74 and 1.03, the first two being indistinguishable from simultaneously run, authentic samples of isopropyl and 2-butyl thiourea. The very weak spot of the most lipophilic thiourea ran very close to the reference sample of phenylthiourea, yet deviating from this by giving a sky-blue colour with Grote's reagent rather than the green-blue tint of the reference.

Paper chromatography of the same mixture in toluene:ethyl acetate:water (1:1:1) gave the following R_{Ph}-values: 0.58, 0.88 and 1.13, the last value clearly excluding phenylthiourea as a possibility.

Analogously prepared extracts of the thioureas derived from leaves, stems and roots of a fresh plant of *P. Roxburghii* were separately investigated by paper chromatography. Neither the R_{Ph}-values, nor the relative amounts, differed significantly from those observed in the seed extracts.

Isolation and preparation of thioureas. Putranjiva seeds (1.5 kg) were suspended in carbon tetrachloride (4.4 l) and disintegrated in a Waring Blendor. After filtration, the residue was refluxed twice with fresh 4-l portions of the same solvent, and the defatted seed powder was air-dried (850 g). A glucoside extract was prepared by refluxing the seed powder for 1 h with three 5 l-portions of 70 % methanol. The three filtrates were pooled and concentrated to a small volume *in vacuo*. Water was added to a total volume of 4.2 l, and the solution was filtered through Celite. The enzymic hydrolysis was performed in three 1.4 l-portions. To each were added: water (1.3 l), citrate buffer (150 ml, prepared as follows: 1 M sodium citrate (1 l), citric acid (3.0 g), diluted 20 times with water), myrosinase solution [27] (50 ml), and ascorbic acid (25 mg) [35]. The mixtures were set aside for 17 h at room temperature, the pH-value decreasing during this period from 6.4 to 6.0.

The pooled hydrolysis mixtures were steam-distilled and a total of 6 l of distillate collected. This was then extracted with a total of 4 l of ether. Ammonia-saturated methanol (225 ml) was added to the dried ether solution of the volatile isothiocyanates, and the solution was kept for 40 h at room temperature. Ether was distilled off, and the solid residue (15.4 g) was dissolved in hot water (150 ml), filtered hot from sticky impurities, and the filtrate allowed to cool to give a colourless mixture, (A) (13.6 g), of three thioureas (m.p. 149—157°). The material, (B), contained in the mother liquor (2.5 g, m.p. 128—139°), was processed separately as described below.

(i) *Fraction A.* The thiourea mixture (13.6 g) was recrystallized once from water (90 ml), thrice from ethyl acetate, and finally once again from water to give the predominant thiourea (5.2 g), uncontaminated by other thioureas as established from paper-chromatographic analysis. The pure compound, m.p. 168°, proved to be *1-isopropylthiourea* on comparison with an authentic specimen [7]. Identical infrared spectra and undepressed mixed melting points served to establish the identity.

(ii) *Fraction B.* The above mother liquor fraction (2.5 g) was recrystallized thrice from ethyl acetate to give a mixture (1.13 g) of all three thioureas, as estimated from paper chromatography. The solid was partially dissolved in chloroform (60 ml) and the insoluble part (0.48 g), consisting of only the two major thioureas, was discarded. The chloroform solution was equilibrated with water (60 ml) and the combined volumes introduced into the first 6 tubes of a 60-plate Craig-apparatus, preloaded with water-saturated chloroform. After 155 transfers, with single withdrawal of the aqueous phases after 60 distributions, paperchromatographic analyses indicated a high degree of separation of the three thioureas.

Withdrawn tubes No. 5—19: Evaporation to dryness and recrystallization of the residue afforded an additional amount of *1-isopropylthiourea*, m.p. 170°.

Withdrawn tubes No. 34—65: The solid residue was recrystallized twice from water to give colourless needles, m.p. 134°, $[\alpha]_D^{21}$ + 27.7° (*c* 3.4, 96 % ethanol), + 27.2° (*c* 1.6, $CHCl_3$). Comparison of rotation values, coinciding infra-red spectra, and undepressed mixed melting point, served to establish the identity of this thiourea with a synthetic specimen of (S)-*1-(2-butyl)-thiourea* described below.

Tubes No. 35—59 in the apparatus: The semi-crystalline residue from these tubes (259 mg) was recrystallized from water (9 ml), with a little charcoal, to give colourless prisms (119 mg) of the unknown thiourea. An analytical specimen was produced on an

additional recrystallization from water, m.p. 72°, $[\alpha]_D^{20}$ + 7.9° (*c* 1.0, 96 % ethanol) (Found: C 49.13; H 9.68; N 19.08; S 21.90. Calc. for $C_6H_{14}N_2S$: C 49.26; H 9.65; N 19.16; S 21.92). The ultra-violet spectrum in ethanol had the following characteristics: λ_{max} 242 mμ (ε 13 670), 204 mμ (ε 11 300), λ_{min} 224 mμ (ε 3 760). The infra-red spectrum (in KBr) exhibited conspicuous bands at: 3 400 (s), 3 220 (vs), 3 080 (m), 2 950 (s), 2 920 (m,sh), 2 880 (m, sh), 1 605 (s), 1 590 (vs), 1 560 (vs), 1 460 (s), 1 430 (s), 1 375 (m), 1 340 (vs), 1 265 (w), 1 225 (w), 1 165 (m), 1 140 (w),1 015 (w), 970 (w), 940 (w), 890 (w), 770 (w) and 728 (s) cm^{-1} (*vs* very strong, *s* strong, *m* medium, *w* weak and *sh* shoulder). The identity of the thiourea as (S)-*1-(2-methylbutyl)-thiourea* appeared from its n.m.r. spectrum (Fig. 2) and was confirmed upon critical comparison with an authentic specimen of the latter, synthesized as described in the sequel.

(S)-*2-Butyl isothiocyanate*. (*S*)-2-Butylamine hydrochloride (4.78 g, $[\alpha]_D^{19}$ −1.05° (*c* 13.3, H_2O)) [8] was dissolved in 2 N NaOH (21.8 ml), and pure thiocarbonyl chloride (5.0 g) in chloroform (50 ml) was added. Additional 2 N NaOH (44 ml) was added portionwise, and the chloroform layer was separated after ended reaction. It was washed with HCl (4 N) and water, and the solvent was removed. The remaining (S)-*2-butyl isothiocyanate* distilled at 47°/11 mm as a colourless liquid (1.6 g), n_D^{20} 1.4940, d_4^{22} 0.9322, $[\alpha]_D^{22}$ + 66.7° (neat). Literature values: $[\alpha]_D$ + 61.36° [32], $[\alpha]_D^{20}$ + 61.88° [33], $[\alpha]_D$ + 66.0° [28].

(S)-*1-(2-Butyl)-thiourea*. The mustard oil (525 mg) was dissolved in ammonia-saturated methanol (4 ml) and kept at room temperature for a few hours. The solid residue was recrystallized from water to give a pure specimen of (S)-*1(2-butyl)-thiourea*, m.p. 134°, $[\alpha]_D^{25}$ + 29.0° (*c* 1.7, $CHCl_3$). Literature values: m.p. 133—134° [28], 136—137° [18], $[\alpha]_D^{20}$ + 22.77° (*c* 3.568, 94 % ethanol) [18], $[\alpha]_D^{20}$ + 25.65° (*c* 1.65, $CHCl_3$) [29], all referring to preparations of natural derivation. It hence seems likely that the previous isolates [18,29] have been slightly impure or racemized.

(S)-*2-Methylbutyl isothiocyanate* (V). (*S*)-2-Methylbutanol (α_D −9.49° (2 dm tube), n_D^{20} 1.4112) (102 g) was converted into (*S*)-2-methylbutyl bromide (60.0 g) according to the method of Crombie and Harper [9], b.p. 120—121°, n_D^{20} 1.4450, d_4^{21} 1.214, α_D^{23} + 4.90° (1 dm), $[\alpha]_D^{20}$ + 4.04° (neat), in good agreement with numerous literature values, *e.g.* $[\alpha]_D^{20.6}$ + 4.043° [30], n_D^{20} 1.4451 [30], n_D^{20} 1.4451 [31] *. In chloroform solution our bromide gave the rotation value: $[\alpha]_D^{20}$ + 4.30° (*c* 4.6) **.

A mixture of the pure bromide (59 g) and potassium phthalimide (79.7 g) in freshly distilled dimethylformamide (250 ml) was stirred, slowly heated to 100°, and kept at this temperature for 3.5 h. The solid was removed and washed with chloroform, the washings being added to the reaction mixture diluted with chloroform (450 ml). The organic phase was subsequently washed with 2 × 150 ml of water, 6 × 100 ml of 0.2 N NaOH and 3 × 150 ml of water. Chloroform and residual dimethylformamide were distilled off from the dried solution whereafter (S)-*N-(2-methylbutyl)-phthalimide* distilled as a colourless oil, b.p. 129—130°/0.06 mm, crystallizing in the receiver, m.p. 25.5° (60 g). (Found: C 71.74; H 7.04; N 6.49. Calc. for $C_{13}H_{15}NO_2$: C 71.84; H 6.96; N 6.45). The following physical constants were determined: n_D^{25} 1.5384, d_4^{22} 1.0972, $[\alpha]_D^{21}$ + 8.39° (neat), $[\alpha]_D^{22}$ + 8.20° (*c* 0.6, benzene) ***. Literature values [10]: m.p. 23°, d_4^{25} 1.0930, $[\alpha]_D^{25}$ + 7.53° (neat).

The substituted phthalimide (58 g) and hydrazine monohydrate (14 g) were dissolved in methanol (500 ml), and the solution was refluxed for 3 h. Water (200 ml) was added, methanol removed *in vacuo*, and the residue was refluxed for 1 h with water (100 ml) and conc. HCl (50 ml). Water (250 ml) was again added to the cooled mixture which was kept overnight in the icebox. Phthalylhydrazide (44 g) was then filtered off and washed

---

* The value n_D^{20} 1.4552, originally reported by Crombie and Harper [9], has been corrected in this more recent paper.

** We are inclined to believe that the value $[\alpha]_D^{20}$ + 5.81° (*c* 4.8, $CHCl_3$), reported by Crombie and Harper [9], is too high.

*** Balenović and Bregant [11] reported $[\alpha]_D^{25}$ + 24° (*c* 0.56, benzene), *cf.* foot-note on p. 940.

with ice-cold water, and the combined filtrates were concentrated to dryness *in vacuo*. The amine hydrochloride was redissolved in a small volume of water and solid KOH was added, causing the amine to separate as a yellow top layer. Distillation afforded pure *levo*rotatory (S)-*2-methylbutylamine* (10 g), b.p. 95°, n_D^{20} 1.4133, d_4^{23} 0.7490, MR_{23}: Found: 28.93, Calc. 28.71; $[\alpha]_D^{23}$ −6.05° (neat). Literature values [10]: b.p. 95.5−96°, d_4^{25} 0.7505, $[\alpha]_D^{25}$ −5.86° (neat).

A solution of (−)-2-methylbutylamine (3.25 g) in chloroform (100 ml) was dropwise added to a stirred solution of thiocarbonyl chloride (6 g) in chloroform (50 ml) in the course of 1.2 h. The solution was left overnight at room temperature and the major part of the solvent was removed over a small column. The residue was washed with 2 N HCl (10 ml) and the residual chloroform again removed. Pure *dextro*rotatory (S)-*2-methylbutyl isothiocyanate* (V) (1.6 g) distilled as a colourless liquid, b.p. 68.5°/10 mm (Found: C 56.02; H 8.59; N 10.98; S 25.25. Calc. for $C_6H_{11}NS$: C 55.78; H 8.58; N 10.84; S 24.82). The physical constants were: n_D^{20} 1.4984; d_4^{22} 0.9405; $[\alpha]_D^{22}$ + 14.0° (neat, 0.5 dm tube).

Synthesis of (S)-*1-(2-methylbutyl)-thiourea*. The synthetic mustard oil (250 mg) was dissolved in ammonia-saturated methanol (5 ml) and the solution was left for 24 h at room temperature. The crystalline residue was dissolved in hot water, treated with a little charcoal, and filtered. Colourless needles of (S)-*1-(2-methylbutyl)-thiourea* separated on cooling (60 mg), m.p. 73°, alone or in admixture with the specimen of natural derivation described above, $[\alpha]_D^{22}$ + 7.7° (*c* 1.04, 96 % ethanol). The synthetic and the naturally derived sample gave coinciding infra-red spectra.

Gaschromatographic analysis. The crude isothiocyanate fraction, obtained by steam distillation of an enzymically hydrolyzed seed extract of *P. Roxburghii*, was subjected to gaschromatographic analysis according to the procedure recently described by Jart [34]. Squalane served as the stationary phase at a column temperature of 124° and helium as the carrier gas (1.2 l per h).

Isolation of cleomin (VI). The above described enzymically hydrolyzed extract of *Putranjiva* seeds (1.5 kg), from which volatile isothiocyanates had been removed by steam distillation, was filtered through Celite and concentrated *in vacuo* to a volume of 1 l. The aqueous solution was continuously extracted with ether for 36 h, and the ether phase was concentrated to a volume of 500 ml before it was extracted with two 200 ml-portions of 0.2 N NaOH. The ether phase was discarded, and the aqueous solution was adjusted to pH 5.5 with HCl and again extracted continuously with ether for 36 h. The dried ether extract contained an oily residue (6.5 g) that was partly soluble in hot water (115 ml). The solution was treated with charcoal, and the filtrate on cooling deposited colourless needles (317 mg, m.p. 47−48°). A second crop of crystals (2.19 g, m.p. 45−48°) was obtained on concentration of the mother liquor to about 35 ml. A pure specimen was produced on two additional recrystallizations from water, m.p. 52° (Found: C 49.70; H 7.64; N 9.44; S 22.09. Calc. for $C_6H_{11}NOS$: C 49.63; H 7.64; N 9.65; S 22.08). $[\alpha]_D^{22}$ −26.6° (*c* 1.06, H_2O). These data, in addition to paperchromatographic analyses, ultraviolet and infra-red spectra, as well as mixed melting point determination, indicated that the isolate was identical with (−)-*5-ethyl-5-methyl-2-oxazolidinethione* (VI) (cleomin), which was recently established in this laboratory as the enzymic hydrolysis product of glucocleomin, present in *Cleome spinosa* Jacq. and other species of the caper family [13].

The authors are indebted to Mr. G. Cornali and Mr. W. Egger for the microanalyses. The present work is part of investigations supported by *The Danish State Research Foundation (Statens Almindelige Videnskabsfond), The Carlsberg Foundation (Carlsbergfondet), The Research Council of The Technical Sciences (Det Teknisk-Videnskabelige Forskningsråd)* and *Kai Hansen's Fond*.

REFERENCES

1. Nadkarni, K. M. *Indian Materia Medica*, Bombay 1927, p. 727.
2. Krishna, S. and Puntambekar, S. V. *J. Indian Chem. Soc.* **8** (1931) 301.
3. Gambhir, I. R. and Dutt, S. *Indian Soap J.* **11** (1946) 169.

4. Puntambekar, S. V. *Proc. Indian Acad. Sci.* **A32** (1950) 114.
5. Kjær, A. *Fortschr. Chem. Org. Naturstoffe* **18** (1960) 122.
6. Schultz, O.-E. and Wagner, W. *Z. Naturforsch* **11 b** (1956) 73.
7. Kjær, A. and Rubinstein, K. *Acta Chem. Scand.* **7** (1953) 528.
8. Kjær, A. and Hansen, S. E. *Acta Chem. Scand.* **11** (1957) 898.
9. Crombie, L. and Harper, S. H. *J. Chem. Soc.* **1950** 2685.
10. Marckwald, W. *Ber.* **37** (1904) 1046.
11. Balenović, K. and Bregant, N. *Tetrahedron* **5** (1959) 44.
12. Kjær, A. and Christensen, B. W. *Acta Chem. Scand.* **16** (1962) 71.
13. Kjær, A. and Thomsen, H. *Acta Chem. Scand.* **16** (1962) 591.
14. Bailey, S. D., Bazinet, M. L., Driscoll, J. L. and McCarthy, A. I. *J. Food. Sci.* **26** (1961) 163.
15. Freise, F. W. *Perfumery Essent. Oil Record* **26** (1935) 219.
16. Kjær, A. and Conti, J. *Acta Chem. Scand.* **7** (1953) 1011.
17. Kjær, A. and Christensen, B. W. *Acta Chem. Scand.* **13** (1959) 1575.
18. Gadamer, J. *Arch. Pharm.* **237** (1899) 92.
19. Kjær, A., Gmelin, R. and Boe Jensen, R. *Acta Chem. Scand.* **10** (1956) 432.
20. Schultz, O.-E. and Wagner, W. *Arch. Pharm.* **289/61** (1956) 597.
21. Greenberg, D. M. (Ed.) *Metabolic Pathways*, Acad. Press. New York-London 1961, Vol. II.
22. Robinson, W. G., Nagle, R., Bachhawat, B. K., Kupiecki, F. P. and Coon, M. J. *J. Biol. Chem.* **224** (1957) 1.
23. Robinson, W. G., Bachhawat, B. K. and Coon, M. J. *J. Biol. Chem.* **218** (1956) 391.
24. Carter, H. E. *Biol. Symposia* **5** (1941) 47.
25. Butler, G. W. and Butler, B. G. *Nature* **187** (1960) 780.
26. Nagashima, Z. and Uchiyama, M. *Bull. Agr. Chem. Soc. Japan* **23** (1959) 555.
27. Neuberg, C. and Wagner, J. *Biochem. Z.* **174** (1926) 457.
28. Bottomley, W. and White, D. E. *Australian Chem. Inst. J. & Proc.* **17** (1950) 31.
29. Urban, W. *Arch. Pharm.* **242** (1904) 51.
30. Brauns, D. H. *J. Research Natl. Bur. Standards* **18** (1937) 315.
31. Crombie, L., Manzoor-i-Khuda, M. and Smith, R. J. D. *J. Chem. Soc.* **1957** 479.
32. Gadamer, J. *Arch. Pharm.* **239** (1901) 293.
33. Thomé, L. G. *Ber.* **36** (1903) 582.
34. Jart, Aa. *Acta Chem. Scand.* **15** (1961) 1223.
35. Ettlinger, M. G., Dateo, G. P., Harrison, B. W., Mabry, T. J. and Thompson, C. P. *Proc. Natl. Acad. Sci. U.S.* **47** (1961) 1924.

Received December 4, 1961.

ACTA CHEMICA SCANDINAVICA 16 (1962) 947–952

Conjugate Additions of Grignard Reagents to alpha, beta-Unsaturated Esters

XI. The Preparation of Alkylsuccinic Acids from Maleic Esters

VIGGO KØGS ANDERSEN and JON MUNCH-PETERSEN

Organisk-Kemisk Laboratorium, Polyteknisk Læreanstalt, Copenhagen, Denmark

The addition of various alkylmagnesium halides to maleic esters has been worked out as a practical high-yield route to alkylsuccinic acids, including *tert*-butylsuccinic acid. The reaction of phenylmagnesium bromide to give phenylsuccinic acid failed.

Some general aspects of the reaction are considered.

Several methods for the preparation of substituted succinic acids are described in the literature [1]. One of these, which at first sight should be obviously attractive, is the conjugate addition of an organometallic compound to esters (or other derivatives) of ethylenedicarboxylic acids:

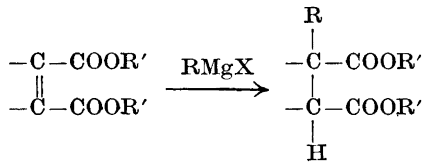

In fact, fair and moderate yields have been reported in many cases from the use of this principle. The results presented in this paper constitute an extention of the work of these earlier investigators. In certain respects substantial improvements have been achieved.

Addition of a Grignard reagent to esters of maleic and fumaric acids has been reported by Marvel *et al.*[2], who obtained a 30 % yield of isopropylsuccinic ester using isopropylmagnesium bromide. By the use of the cadmium reagent instead of the Grignard reagent a 30 % yield is reported also, but this yield is calculated on the basis of unrecovered maleic ester. Actually, only 19 % of the theoretical amount of isopropylsuccinic ester (based on the amount of starting material used) was obtained. Michael [3] has obtained a 20–25 % yield

of diethyl ethylsuccinate by the action of ethyl iodide and zinc on diethyl fumarate.

On the other hand, Hsing and Li [4], by using ethylenetetracarboxylic ester, which is readily available [5], obtained very satisfactory yields of addition products (substituted ethanetetracarboxylic esters) from phenyl-, methyl-, and ethylmagnesium bromides. However, the subsequent transformation of the ethanetetracarboxylic ester into the substituted succinic acid gave only a moderate yield in the case of ethylsuccinic acid, and in the case of methylsuccinic acid the yield was poor. Wideqvist [6] reported the complete failure of the attempted preparation, according to the Hsing and Li procedure [4], of *tert*-butylsuccinic acid; the only product isolated from the reaction between tetraethyl ethylenetetracarboxylate and *tert*-butylmagnesium bromide was tetraethyl ethanetetracarboxylate, the hydrogenation product of the starting material.

In a previous communication [7] the addition of butylmagnesium bromide to the di-*sec*-butyl esters of maleic and fumaric acids was described. The *sec*-butyl esters were used in order to provide a hindrance to the attack of the Grignard reagent on the ester carbonyl group. Nevertheless considerable amounts of lactone were formed as the results of 1,2-addition as well as 1,4-addition:

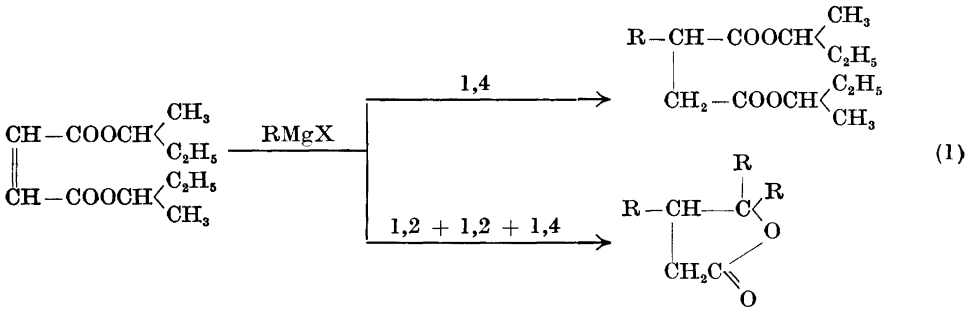

(1)

This was true in the case of both maleic and fumaric ester, although the yields of both reaction products, and more especially of butylsuccinic ester, were much better from maleic than from fumaric ester. Furthermore, whereas by cuprous chloride catalysis, the yields of this latter product from both the two unsaturated esters were greatly increased, the formation of the lactone was largely suppressed in the case of maleic ester, but not in the case of fumaric ester.

Thus, a satisfactory yield of butylsuccinic ester was indeed obtained from maleic ester, and we have now tried to apply this cuprous chloride catalyzed addition reaction with *sec*-butyl maleate to Grignard reagents other than butylmagnesium bromide. The results are summarized in Tables 1 and 2, which also includes the previously reported [7] result with butylmagnesium bromide.

It is seen that, in the case of alkylmagnesium halides, the reaction provides a satisfactory, general, practical route to alkylsuccinic esters. Of particular interest is the preparation of *tert*-butylsuccinic esters, since the corresponding acid has previously been prepared only by a five-step synthesis from ethyl

cyanoacetate, giving an overall yield of 15 % (Wideqvist [6]). We have (from diethyl maleate) obtained a 70 % yield of diethyl *tert*-butylsuccinate, from which the acid was obtained in 91 % yield, giving *tert*-butylsuccinic acid in an overall yield of 64 %. The di-*sec*-butyl ester of *tert*-butylsuccinic acid was obtained in even higher yield, but the isolation of the free acid was in this case troublesome, due to the extremely slow hydrolysis of the ester.

On the other hand, the preparation of phenylsuccinic acid by the addition of phenylmagnesium bromide, which was so successful in the Hsing and Li reaction with ethylenetetracarboxylic ester [4], failed completely for us, both with di-*sec*-butyl and diethyl maleate. This result will be the subject of further studies.

The formation of lactones appears to be suppressed in the case of the branched-chain Grignard reagents (*tert*-butyl and isopropyl). In these cases, analytically pure alkylsuccinic esters are obtained in high yields, without any indication of a lactone product being formed. On the other hand, with ethyl-, propyl-, and butylmagnesium bromides the yields of alkylsuccinic esters are lower, and some lactone is always formed, even in the presence of cuprous chloride. As indicated by the analyses, the resulting alkylsuccinic esters are, in these cases, actually contaminated with some lactone. The lactones formed from ethyl- and propylmagnesium bromide are lower-boiling than the alkylsuccinic ester, that from butylmagnesium bromide higher-boiling.

These results appear to reveal a general feature of the reaction between Grignard reagents and α,β-unsaturated esters. The following two reactions (illustrated for simplicity with crotonic ester as the example) are both competing with the simple conjugate addition reaction:

Table 1. Yields of alkylsuccinic esters from the reaction between maleic esters and alkylmagnesium halides.

Maleic ester	Temp. °C	Alkylmagnesium halide					
		ethyl	propyl	isopropyl	butyl	*tert*-butyl	phenyl
sec-Butyl	0	43 [a,b]		81	67[e]	78[f]	0
	−10	57 [c,b]	63[d]		57[e]	74[g]	0
Ethyl	−10			82.5		70[g]	0

In all cases some non-distillable polymerization product was obtained.
[a] About 25 % *lower*-boiling lactone was obtained. [b] The lactone was not obtained analytically pure. The first fraction (about one fifth) of the ethylsuccinic ester is probably contaminated with a little lactone. [c] About 10 % *lower*-boiling lactone was obtained. [d] No lactone was isolated, but the propylsuccinic ester was not entirely pure; *cf.* Table 2. [e] Very little (6 % or less) *higher*-boiling lactone was obtained. [f] *tert*-Butylmagnesium *bromide* (2.5 qeuiv.) was used. [g] *tert*-Butylmagnesium *chloride* (0.4 equiv.) was used.

A. A 1,2-addition followed either by a 1,4-addition or by another 1,2-addition:

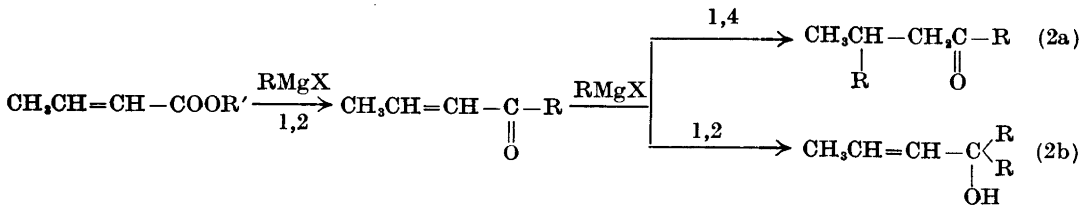

(2a) (2b)

The lactone formation encountered in the case of maleic esters is the result of reaction (2b) above, followed by the addition of the Grignard reagent to the double bond, which is, in this particular case, conjugated to the second ester group (or lactone carbonyl group), *cf.* eqn. (1).

B. A dimerizing Michael condensation (or even poly-condensation), followed by 1,4-addition of the Grignard reagent to the resulting alkylidene-glutaric ester [8]:

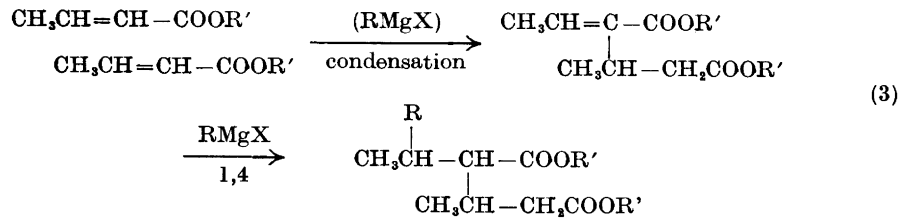

(3)

The simple conjugate addition process is, by the presence of cuprous chloride, favoured over both of these two competing reactions. The 1,2-addition (2) is — in contrast to the dimerization-addition reaction (3) — in most cases largely prevented by the use of *sec*-butyl esters, because the carbonyl group then is sterically protected. A similar steric effect should be expected if bulky Grignard reagents are used in the reaction, although in such a case some steric hindrance to the simple conjugate addition might also be anticipated. In fact, previous results with different Grignard reagents [8,9] indicate this to be true, since, under conditions which had been found favourable for the simple conjugate addition of *prim*-alkylmagnesium bromides, the yields from isopropyl- and especially *tert*-butylmagnesium halides were low *, and the dimerization-addition reaction takes place to a much larger extent. On the other hand, in the present reaction and under the conditions chosen, the 1,2-addition (the lactone formation) is the important competing side-reaction. This fact is presumably due partly to the subsequent, energetically favourable cyclisation to a five-membered ring, and partly to the sluggishness with which maleic esters apparently undergo the dimerization reaction. Accordingly, with the *prim*-alkylmagnesium halides the yield of conjugate addition product is decreased because of the 1,2-addition, which takes place to a considerable degree, whereas, in the case of the bulky isopropyl- and *tert*-butylmagnesium halides no trace of lactone was formed, the yields of conjugate addition pro-

* This difficulty was overcome later by suitable modifications in the procedure, and high yields have been obtained also in these cases [10,11].

Table 2. Di-*sec*-butyl alkylsuccinates: $R-CH(CH_2COOCH(CH_3)C_2H_5)-COOCH(CH_3)C_2H_5$

R	b.p. °C/mm Hg	n_D^{25}	Analyses Found: C H	Calculated: for	C H
Ethyl	86– 88/0.5	1.4277	65.00 10.18	$C_{14}H_{26}O_4$ (258.35)	65.08 10.16
Propyl	102/0.7	1.4302	66.55 10.48	$C_{15}H_{28}O_4$ (272.37)	66.14 10.36
Isopropyl	103–105/1	1.4312	66.15 10.25	$C_{15}H_{28}O_4$ (272.37)	66.14 10.36
Butyl [7]	106–107/0.6	1.4353 (at 20°)	67.85 10.89	$C_{16}H_{30}O_4$ (286.40)	67.09 10.56
tert-Butyl	107/0.9	1.4350	66.90 10.57	$C_{16}H_{30}O_4$ (286.40)	67.09 10.56

ducts therefore being particularly high. Furthermore, similar high yields of simple conjugate addition products were obtained from di*ethyl* maleate with isopropyl- and *tert*-butylmagnesium halides. Apparently, the bulkiness of the alkyl in the Grignard reagent is sufficient to prevent lactone formation (1,2-addition) even in the case of ethyl esters. These considerations are also consistent with the somewhat confusing fact that, whereas *α,β*-unsaturated *esters*, as mentioned above, give lower yields * of conjugate addition products with *tert*-alkylmagnesium halides than with *prim*-alkylmagnesium halides, the opposite is true of the reactions of *α,β*-unsaturated *aldehydes* (crotonaldehyde), in the case of which conjugate addition of a Grignard reagent is reported only with *tert*-alkylmagnesium halides [12]. Again, in the reaction with *α,β*-unsaturated aldehydes, the 1,2-addition (to the aldehyde carbonyl group) and not the dimerization-addition reaction is the chief competing process, and the impedement of this in the case of bulky Grignard alkyls favours the conjugate addition. Similarly, Whitmore and Pedlow [13] found that the reaction of cyclohex-2-enone with *tert*-butylmagnesium chloride resulted in high yield (70 %) of 1,4-addition product, whereas the yield with isopropylmagnesium chloride was somewhat lower (44 %), and the reactions with ethyl- and methylmagnesium bromides took place largely as 1,2-additions.

EXPERIMENTAL

Infra-red spectra have been recorded and interpreted by Mrs. Inger Grete Krogh Andersen, M.Sc., of this laboratory.

Microanalyses are by Mr. Preben Hansen, Microanalytical Division, The Chemical Laboratory, The University of Copenhagen.

Fractional distillations were through a simple 45 cm × 8 mm Podbielniak type column with a tantalum wire spiral, a heated jacket and a partial reflux head. Boiling and melting points are uncorrected.

The preparation of di-*sec*-butyl maleate is previously described [7]. The ethyl ester was a commercial product.

The additions were carried out as previously described [7], except that the cuprous chloride catalyst was added in small portions to the reaction mixture concurrently with the addition of the ester solution [10]. In certain cases cooling in ice-salt has been applied (*cf.* Table 1).

The preparation of free alkylsuccinic acids. The saponification of di-*sec*-butyl butylsuccinate (as well as of the *sec*-butyl esters of the methyl-butylsuccinic acids [7]) has been accomplished previously, using the standard saponification procedure described [8], involving the boiling of the ester under reflux for 6—8 h with three equivalents of potassium hydroxide in ethanol. Butylsuccinic acid, m.p. 81°, was thus obtained in almost quantitative yield. The saponification of di-*sec*-butyl *tert*-butylsuccinate proved to be considerably more difficult to deal with. After 6—8 h of reflux, the mono-*sec*-butyl ester of *tert*-butylsuccinic acid (being insoluble in water) was obtained in almost quantitative yield. It was an oil which gradually crystallized completely, was washed with water and dried, m.p. 57—58°. The infra-red spectrum indicated the presence of a carbonyl group and a *sec*-butyl ester group [7]. (Found: C 62.75; H 9.89. Calc. for $C_{12}H_{22}O_4$ (230.30): C 62.58; H 9.63). On further attempted saponification of the monoester (this time in aqueous solution) slow hydrolysis took place. Even after 12 h still most of the mono-ester was recovered. After another 24 h of saponification only about 20 % of insoluble mono-ester was recovered, and from the filtrate *tert*-butylsuccinic acid, m.p. 128° (*cf.* below) was obtained in an amount corresponding to almost quantitative yield, continuous extraction with ether for 20 h being applied.

Due to these difficulties encountered in the saponification of the di-*sec*-butyl ester, and to the reactivity considerations discussed above, the additions of isopropylmagnesium bromide and *tert*-butylmagnesium chloride to the di*ethyl* ester of maleic acid were tried, and indeed found successful (Table 1).

Diethyl isopropylsuccinate, b.p. 71°/0.6 mm, n_D^{25} 1.4280 (rep.[2]: b.p. 65°/0.5 mm or 82°/1 mm, n_D^{20} 1.4261; 123—125°/20 mm, n_D^{20} 1.4284; 118—126°/20 mm, n_D^{20} 1.4311).

Diethyl *tert*-butylsuccinate, b.p. 75.5—76.0/0.5 mm, n_D^{25} 1.4321 (Found: C 62.65; H 9. 64. Calc. for $C_{12}H_{22}O_4$ (230.30): C 62.58; H 9.63).

The saponification of diethyl *tert*-butylsuccinate was carried out without difficulty in the usual way (see above). *tert*-Butylsuccinic acid, which is readily soluble in water, was obtained in 91 % yield by continuous extraction with ether overnight, distillation of the solvent, and recrystallization from water, m.p. 128° (rep.[6] 132°). (Found: C 55.20; H 8.02. Calc. for $C_8H_{14}O_4$ (174.19): C 55.16; H 8.10).

The authors want to express their gratitude towards *Otto Mønsteds Fond* for financial support.

REFERENCES

1. Diaper, D. G. H. and Kuksis, A. *Chem. Revs.* **59** (1959) 89.
2. Marvel, C. S., Myers, R. L. and Saunders, J. H. *J. Am. Chem. Soc.* **70** (1948) 1694.
3. Michael, A. *Ber.* **29** (1896) 1791.
4. Hsing, C. and Li, L. *J. Am. Chem. Soc.* **71** (1949) 774.
5. Corson, B. B. and Benzon, W. L. *Organic Syntheses* Coll. Vol. **II** (1943) 273.
6. Wideqvist, S. *Arkiv Kemi* **2** (1950) 321.
7. Bjerl Nielsen, E., Munch-Petersen, J., Møller Jørgensen, P. and Refn, S. *Acta Chem. Scand.* **13** (1959) 1943.
8. Munch-Petersen, J. *J. Org. Chem.* **22** (1957) 170.
9. Munch-Petersen, J. *Acta Chem. Scand.* **12** (1958) 967.
10. Munch-Petersen, J. and Andersen, V. K. *Acta Chem. Scand.* **15** (1961) 271.
11. Munch-Petersen, J. and Andersen, V. K. *Acta Chem. Scand.* **15** (1961) 293.
12. Stevens, P. G. *J. Am. Chem. Soc.* **57** (1935) 1112.
13. Whitmore, F. C. and Pedlow, G. W. *J. Am. Chem. Soc.* **63** (1941) 758.

Received November 16, 1961.

ACTA CHEMICA SCANDINAVICA 16 (1962) 953–957

Heats of Combustion of Propanal and 2-Methyl Propanal

JAN TJEBBES

*Thermochemistry Laboratory *, University of Lund, Sweden*

Heat of combustion values have been determined for propanal and 2-methyl-propanal and found to be, ΔH_c°(liq) at 25°C, -434.16 ± 0.18 kcal·mole^{-1} and -589.67 ± 0.18 kcal·mole^{-1}, respectively. From these and previously published data, the C=O bond contribution in calculating heats of combustion by Klages' method has been found to be, on the average, 19.5 kcal.

Until recently accurate heats of combustion and formation data for alkanals have been lacking in the literature. Standard compilations have been using Berthelot's and Thomsen's values from the turn of the century [1,2]. For formaldehyde [3] and acrolein [4] later values have been reported, although long before a modern reliable technique for the experimental determinations was established. In 1960 the present author reported the heats of combustion of two alkanals and two alkenals, and in the same year Nicholson published values for butanal and heptanal [5]. The work reported here gives data for two more alkanals, *viz.* propanal and 2-methyl-propanal.

The importance of approximate methods for the calculation of heats of combustion — and hence heats of formation — for aldehydes is still obvious, and the experimentally determined values have therefore been used to reinvestigate the C=O bond contribution in the calculation of heats of combustion of aldehydes according to Klages' method [6].

MATERIALS

Propanal. The commercial sample (Schuchardt) was distilled twice under nitrogen in a column of 35 theoretical plates (t.p.), the main fraction being the known azeotropic mixture of water and propanal [7]. The purification was followed by use of gas-liquid chromatography (GLC) (column 25 % tricresylphosphate on C22, t = 50°, ionization detector) and already the azeotrope was found to be free from organic impurities. The product was dried three times with anhydrous calcium sulphate and then distilled under nitrogen in a column of 10 t.p. Four middle fractions, which all showed the same boiling point

* Sponsored by the *Swedish Natural Science Research Council* and the *Swedish Technical Research Council.*

Table 1. Propanal
Water content of compound = 0.03 %.
m(Pt) = 23.781 g, m^i(cont) = 36.23 g, ε^i(cont) = 3.85 cal·deg^{-1}, $\Delta E\Sigma$ = 1.70 cal.

m' g	m'' g	m''' g	Δt deg	ΔE(HNO$_3$) cal	$-\Delta E'_c/M$ cal·g^{-1}
0.373625	0.226378	0.004465	0.89818	3.65	7460.66
0.361782	0.229433	0.004865	0.88906	3.69	7458.91
0.369292	0.227385	0.004290	0.89452	3.55	7461.90
0.374259	0.227169	0.003979	0.89991	3.21	7458.39
0.370056	0.223179	0.004910	0.88822	3.64	7464.06
0.373431	0.220557	0.004816	0.88758	3.56	7464.89
				Mean	7461.47
				Stand. dev. of mean	1.09

$\Delta E'_c/M$ = −7461.5 cal·g^{-1}
$\Delta E^\circ_c/M$ = −7463.7 cal·g^{-1}

Table 2. 2-Methyl-propanal
m(Pt) = 23.841 g, ε^i(cont) = 3.85 cal·deg^{-1}, $\Delta E\Sigma$ = 2.10 except in the last combustion where $\Delta E\Sigma$ = 1.71 cal.

m' g	m'' g	m''' g	m^i(cont) g	Δt deg	ΔE(HNO$_3$) cal	$-\Delta E^\circ_c/M$ cal·g^{-1}
0.466268	0.121188	0.004951	36.29	0.87549	3.67	8164.70
0.480440	0.115596	0.004666	36.29	0.88442	3.20	8164.68
0.447774	0.149216	0.005008	36.30	0.90200	3.03	8164.30
0.465133	0.128884	0.004874	36.30	0.88812	3.12	8164.80
0.379532	0.188615	0.004934	36.27	0.88096	2.68	8167.59
				Mean		8165.21
				Stand. dev. of mean		0.60

$\Delta E^\circ_c/M$ = −8165.2 cal·g^{-1}

Table 3. Thermochemical data at 25°C, in kcal·mole^{-1}.

Compound	$-\Delta H^\circ_c$(l)	$-\Delta H^\circ_f$(l)	ΔH_v*	$-\Delta H^\circ_c$(g)	$-\Delta H^\circ_f$(g)
Propanal	434.16 ± 0.18	52.95 ± 0.18	7.1	441.3	45.9
Butanal	592.42 ± 0.34	57.06 ± 0.34	8.1	600.5	49.0
2-Methyl-propanal	589.67 ± 0.18	59.81 ± 0.18	7.7	597.4	52.1
2-Ethyl-hexanal	1215.63 ± 0.36	83.32 ± 0.36	11.3	1226.9	72.0
2-Butenal	546.71 ± 0.18	34.45 ± 0.18	9.2	555.9	25.3
2-Ethyl-2-hexenal	1168.17 ± 0.34	62.46 ± 0.34	11.7	1179.9	50.8

The given uncertainties are twice the final overall standard deviations [13].

* Estimated by Klages' formula: $\Delta H_v(25°C) = (5.4 + 0.036t_B)$ kcal·mole^{-1}.

Table 4. The C=O bond contribution in heats of combustion of alkanals.

Alkane	Alkanal	$-\Delta H_c^\circ$(alkane) kcal.mole^{-1}	$-\Delta H_c^\circ$(alkanal) kcal.mole^{-1}	λ(C=O) kcal.
Propane	Propanal	530.60	441.3	18.7
Butane	Butanal	687.64	600.5	20.9
2-Methyl-propane	2-Methyl-propanal	685.64	597.4	19.8
3-Methyl-heptane	2-Ethyl-hexanal	1316.44	1226.9	18.5
			Mean	19.5

and density, were combined and used in the combustion experiments. B.p. = 47.85°C/760 mm, $d_4^{25} = 0.7919$. From a melting curve (m.p. = −103.0°C) the residual amount of water was estimated to be 0.03 ± 0.02 %.

2-Methyl-propanal. By distilling twice a commercial sample (Light) in the column with 35 t.p. a pure product was obtained. The first fractions from the first distillation contained much water and the last ones fairly large amounts of high boiling substances. A very small fraction, 1/8 of the charge, ($d_4^{25} = 0.7821$) was used in the second distillation, from which half the amount was collected in fractions showing constant density and b.p. Nevertheless, only a small middle fraction was used for the combustion, b.p. = 64.34°C/760 mm, $d_4^{25} = 0.7823$. No impurities could be detected by GLC (column 20 % LAC 3R-728 on C22, t = 50°, ionization detector), and the melting curve (m.p. = −72.15°C) indicated that the total amount of water was less than 0.01 %.

COMBUSTION CALORIMETRY

All calorimetric results are expressed in terms of the defined calorie, which is equal to 4.1840 abs. joules. All weighings have been reduced to mass, and the molecular weights are based upon the 1957 International Atomic Weights. In this work the symbols and calculating procedure introduced by Hubbard, Scott and Waddington [8] have been used.

Apparatus and method. A static, platinum lined bomb [9] was used in the calorimeter described by Bjellerup [10]. The calibration experiments have been published elsewhere [11].

The aldehydes were burnt in soft glass ampoules with paraffin oil as combustion aid. The volatility and explosiveness of propanal made it necessary to use small ampoules, and therefore only 50 % of the total amount of heat evolved originated from the propanal. For 2-methylpropanal the corresponding figure was *ca.* 75 %. The amount of nitric acid formed in each combustion was determined by titration with sodium hydroxide.

The results of the combustion experiments are reported in Tables 1 and 2. Common to the two tables are the following values:

ε°(calor) = 5 930.59 ± 0.27 cal.deg^{-1}, t_h = 25.0°C, t_i = 24.1°C,
P^i(Gas) = 30.0 atm, V(Bomb) = 0.2751 l, V^i(Water) = 0.820 ml,
$\Delta E_c^\circ/M$(Oil) = −10 986.6 ± 0.6 cal.g^{-1} and $\Delta E_c^\circ/M$(Fuse) = −3 971 ± 4 cal·g^{-1}.

Correction for the water content of propanal has been made.

Results. From the found $\Delta E_c^\circ/M$ values, ΔH_c° and ΔH_f° values were calculated. Final overall standard deviations were computed as given elsewhere [9]. Using Klages' formula [12], heats of vaporization data were estimated, and heats of formation and combustion data for the compounds in the gaseous state were derived. Table 3 gives these values for all the aldehydes studied.

DISCUSSION

Although not so many aldehydes have been studied, the data obtained are sufficient to calculate an average value for the C=O bond contribution to estimated heat of combustion data for aldehydes using Klages' method [6].

In order to eliminate possible structural effects, the following method has been used in the calculations. From the heat of combustion of an appropriate alkane two C—H bond contributions, λ(C—H), are subtracted, and one C=O bond contribution, λ(C=O), is added, whereby the heat of combustion of the corresponding aldehyde is obtained.

$$-\Delta H_c^\circ(\text{alkane, g}) - 2\lambda(\text{C—H}) + \lambda(\text{C=O}) = -\Delta H_c^\circ(\text{alkanal, g})$$

The heat of combustion values for the alkanes have been taken from Rossini [14], and Klages' value for λ(C—H) = 54.0 kcal has been used. Table 4 gives the results for the four alkanals studied.

Thus, a strict method of comparison has been used, but nevertheless, the values obtained vary surprisingly. The reason for this is obscure, and it might be argued that the high value for butanal could be due to a systematic error in its heat of combustion value. However, this datum was recently reported by Nicholson [5], who found ΔH_c°(butanal, l) = -592.05 ± 0.34 kcal.mole^{-1} in close agreement with the value used here (*cf.* Table 3).

From the values in Table 3, the heats of hydrogenation of the olefinic bonds in 2-butenal and 2-ethyl-2-hexenal were calculated to be -23.7 ± 0.5 and -21.2 ± 0.5 kcal.mole^{-1}, respectively. Rossini and Rockenfeller [15] have given average values for the heats of hydrogenation of olefinic bonds in different intramolecular environments, and for a *trans* 1,2-dialkylethene their value is -27.0 and for a 1,1,2-trialkylethene -26.4 kcal·mole^{-1}, respectively. The difference between the two sets of values is 3.3 and 5.2 or, on the average, 4.2 kcal·mole^{-1}, which then represents the conjugation stabilization energy in the unsaturated aldehydes. Kistiakowsky and coworkers reported in 1938 the heat of hydrogenation of 2-butenal at 82°C, without giving details of the purity of the compound [16]. Recalculated to 25°C their value becomes 24.8 kcal·mole^{-1}, which is in reasonable agreement with the present result.

In conclusion it might be said that structural effects seem to be more pronounced in alkanals and alkenals than in alkanes or monofunctionally substituted alkanes. Only further work can reveal to what extent this statement is justified.

Acknowledgements. The valuable assistance of Miss Margret Månsson and Mr. B. Nelander with the experiments is gratefully acknowledged. The author's thanks are also due to the University of Lund for financial support of this investigation.

REFERENCES

1. Berthelot, M. and Delépine, A. *Compt. rend.* **129** (1899) 920.
2. Thomsen, J. *Z. physik. Chem.* **52** (1905) 343.
3. v. Wautenberg, H., Muchlinski, A. and Riedler, G. *Angew. Chem.* **37** (1924) 457.
4. Moureu, C., Boutaric, A. and Dufraisse, C. *J. chim. phys.* **18** (1921) 333.
5. Nicholson, G. R. *J. Chem. Soc.* **1960** 2377.
6. Wheland, G. W. *Resonance in Organic Chemistry*, New York 1955, p. 86–89.
7. Smith, T. E. and Bonner, R. F. *Ind. Eng. Chem.* **43** (1951) 1169.
8. Hubbard, W. N., Scott, D. W. and Waddington, G. *Standard States and Corrections for Combustions in a Bomb at Constant Volume.* Chapter 5 of Rossini, F. D. (Ed.) *Experimental Thermochemistry*, New York 1956.
9. Tjebbes, J. *Acta Chem. Scand.* **14** (1960) 180.
10. Bjellerup, L. *Acta Chem. Scand.* **13** (1959) 1511.
11. Tjebbes, J. *Acta Chem. Scand.* **16** (1962) 916.
12. Klages, F. *Chem. Ber.* **82** (1949) 358.
13. Rossini, F. D. and Deming, W. E. *J. Wash. Acad. Sci.* **29** (1939) 416.
14. Rossini, F. D. (Ed.) *Selected Values of Physical and Thermodynamic Properties of Hydrocarbons and Related Compounds*, Pittsburg 1953.
15. Rockenfeller, J. D. and Rossini, F. D. *J. Phys. Chem.* **65** (1961) 267.
16. Dolliver, M. A., Cresham, T. L., Kistiakowsky, G. B., Smith, E. A. and Vaughan, W. E. *J. Am. Chem. Soc.* **60** (1938) 440.

Received November 24, 1961.

ACTA CHEMICA SCANDINAVICA 16 (1962) 958–968

Transfer of Triplet State Energy in Fluid Solutions

II. Further Studies of the Quenching of Biacetyl Phosphorescence in Solution

KJELL SANDROS and HANS L. J. BÄCKSTRÖM

Institutionen för fysikalisk kemi, Chalmers Tekniska Högskola, Göteborg, Sweden

Rate constants for the quenching of biacetyl phosphorescence in benzene solution at 20°C are presented for 21 quenchers of the type for which the quenching mechanism is assumed to be a transfer of the triplet state excitation energy from the biacetyl molecule to a molecule of the quencher, as the result of coupled transitions in the two molecules. The results are discussed on the basis of triplet state energy data from the literature. It is concluded that the energy transfer takes place in molecular encounters, and that the probability of transfer increases with the extent of overlap of the phosphorescence spectrum of biacetyl with the singlet → triplet absorption spectrum of the quencher, as well as with the oscillator strengths of the individual transitions involved in the process. A strong argument in favour of the assumed quenching mechanism is the fact that, at the temperature of the measurements, also substances with triplet state energies somewhat higher than that of biacetyl may act as quenchers, and that for these quenchers the energy transfer may be reversed. As a consequence, their quenching power decreases with increasing biacetyl concentration. As was to be expected, the same effect of the biacetyl concentration on the value of the quenching constant has been found also for quenchers with triplet levels somewhat lower than that of biacetyl.

A previous study [1] of the quenching effect of different types of compounds on biacetyl phosphorescence in benzene solution at 20°C led to the conclusion that the quenching action of certain aromatic compounds is due to a transfer of excitation energy, resulting in a triplet → singlet (T → S) transition in the biacetyl molecule and the reverse (T ← S) transition in the quencher molecule. This interpretation received additional support from experiments on sensitized biacetyl phosphorescence in solution [2]. The present paper gives the results of further work on the relation between quenching power and triplet state energy for quenchers of this type.

EXPERIMENTAL

The method employed was to irradiate the oxygen-free biacetyl solution with a short light flash of moderate intensity and to measure the rate of decay of the phosphorescence with a photomultiplier tube and an oscilloscope. The experimental arrangements were the same as earlier [1]. The solvent was benzene and the temperature 20°C. The concentration of biacetyl was generally about 3×10^{-3} M, one drop of biacetyl being used to 50 ml of solution.

Materials

2-Iodonaphthalene was prepared from 2-naphthylamine by the method of Schmidlin and Huber [3]. It was purified by shaking the solution in methyl isobutyl ketone with dilute sulfuric acid, by treatment with active carbon, by recrystallization from aqueous ethanol, and finally by fractional distillation at 0.05 mm.

All other chemicals were of the highest purity obtainable commercially and were further purified as stated below.

The following substances were recrystallized several times using the solvents indicated. *2,2'-Dinaphthyl*, benzene; *1,2-benzanthracene*, methanol; *1-nitronaphthalene*, aqueous ethanol; *1,8-dinitronaphthalene*, acetone; *2-nitrofluorene*, first aqueous ethanol, then aqueous acetone. *Methyl β-naphthyl ketone* was treated three times with active carbon and then recrystallized from aqueous ethanol. *4,4'-Dinitrobiphenyl* and *1,5-dinitronaphthalene* were freed from basic impurities by shaking their solutions in methyl isobutyl ketone with dilute sulfuric acid. They were then recrystallized from acetone.

The following substances were fractionally distilled at the pressures stated, using an efficient column: *Nitrobenzene*, atmospheric pressure; *1-chloronaphthalene*, 20 mm; *1-bromonaphthalene*, 10 mm; *1-iodonaphthalene*, 0.02 mm. The latter had a refractive index agreeing with the value reported by Krollpfeiffer [4], $n_D^{14} = 1.7054$.

Biacetyl and *benzene* were purified as described earlier [1].

Coronene from Rütgerswerke, Castrop-Rauxel, was used without purification. Its ultraviolet absorption spectrum agreed with that published by Clar [5].

RESULTS OF SYSTEMATIC EXPERIMENTS WITH DIFFERENT QUENCHERS

Table 1 gives the experimental values of the quenching constant k, in l mole^{-1} sec^{-1}, for the different quenchers studied, as well as their triplet state energies E_T, in cm^{-1}, as obtained from the literature.

The k-values for phenanthrene, naphthalene, chrysene, anthracene, pyrene, *trans*-stilbene, and 3,4-benzpyrene, are taken from our previous paper [1]. For nitrobenzene and 1,2-benzanthracene the use of purer preparations resulted in values of k appreciably different from those found earlier.

The results with coronene did not obey the Stern-Volmer quenching formula. The deviations were such that they might be accounted for on the assumption that a dimer was formed which had negligible quenching power. However, this assumption was not supported by light extinction measurements on coronene solutions of varying concentration. The k-value given in the table must be regarded as uncertain.

The E_T-values given represent the energy difference in cm^{-1} between the zero vibrational levels of the lowest triplet state and the singlet ground state of the molecule. Most of the values have been obtained from phosphorescence (T → S emission) spectra of solid solutions at liquid air temperature [6–13]. The values of Evans [14], however, have been obtained from a study of the reverse process (T ← S absorption) in liquid solution at ordinary temperature. For

Table 1. Quenching constants and triplet state energies (E_T) for different quenchers.

	k l mole^{-1} sec^{-1}	E_T cm^{-1}		
Phenanthrene	2.3×10^8	21 600 [7],	21 600 [14],	21 640 [10]
Naphthalene	3.8×10^8	21 300 [6],	21 246 [8],	21 180 [14]
Nitrobenzene	1.4×10^4		21 100 [6]	
2-Iodonaphthalene	1.1×10^6		21 040 [6]	
Methyl β-naphthyl ketone	8.3×10^4		20 700 [7]	
1-Chloronaphthalene	5.9×10^4	20 700 [6],	20 645 [8],	20 700 [12]
1-Bromonaphthalene	1.0×10^5	20 700 [6], 20 650 [12]	20 652 [8],	20 650 [14],
2-Nitrofluorene	1.4×10^6		20 600 [6]	
1-Iodonaphthalene	2.8×10^7		20 500 [12]	
4,4'-Dinitrobiphenyl	3.6×10^6		20 200 [6]	
1,8-Dinitronaphthalene	2.1×10^8		20 000 [6]	
Chrysene	2.4×10^8	20 000 [6],	19 800 [7],	20 040 [10]
1,5-Dinitronaphthalene	2.5×10^8		19 900 [6]	
2,2'-Dinaphthyl	9.7×10^6		19 560 [10]	
1-Nitronaphthalene	1.1×10^8	19 200 [6],	19 250 [13]	
Coronene	2.0×10^8 *	19 100 [7],	19 040 [10]	
trans-Stilbene	4.4×10^9		17 750 [14]	
Pyrene	7.5×10^9	16 800 [7],	16 930 [14],	16 850 [10]
1,2-Benzanthracene	7.0×10^9	16 500 [7],	16 520 [10]	
Anthracene	8.1×10^9	14 700 [6],	14 927 [9],	14 870 [14]
3,4-Benzpyrene	8.2×10^9	14 670 [14],	14 670 [11]	

* Extrapolated to zero quencher concentration.

most substances the T ← S absorption is immeasurably weak under these conditions. As found by Evans, however, the absorption intensity increases in the presence of oxygen. A theoretical treatment of this phenomenon has recently been given by Tsubomura and Mulliken [15]. By saturating the solution with oxygen under pressure, the T ← S absorption bands can often be obtained in sufficient intensity to be measured. The longest-wavelength band of a substance very nearly coincides with the shortest-wavelength band of its phosphorescence spectrum in solid solution at low temperature. Table 1 gives several instances of this agreement. It may be concluded that E_T-values in the table, obtained by the latter method, may be assumed to be valid with good approximation also under our experimental conditions.

In the case of biacetyl it has been possible to measure both T → S and T ← S spectra in solution at ordinary temperature. This is connected with the short natural lifetime of its triplet state (*cf.* p. 964). In solvents like heptane and benzene, Forster [16] found a very weak absorption band at 19 800 ± 100 cm^{-1}, which is probably the 0—0 T ← S absorption band. This sets an upper limit to the triplet state energy of biacetyl under these conditions. On the other hand, examination of the phosphorescence spectrum observed under the same conditions, which is shown in Fig. 1, seems to justify the conclusion that the true value of E_T cannot be much lower than that mentioned above, even though a certain amount of anti-Stokes radiation is to be expected at room temperature [17]. We conclude, therefore, that the true value of E_T under our conditions

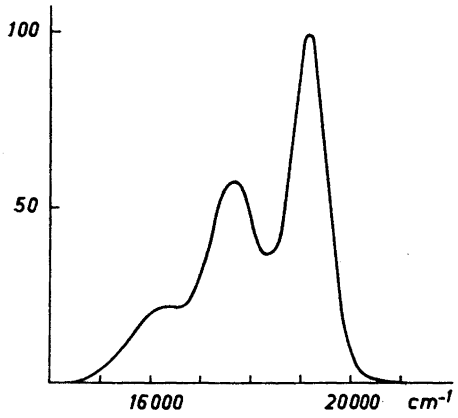

Fig. 1. Phosphorescence spectrum of biacetyl in benzene solution at 20°C, showing relative numbers of light quanta emitted *vs.* wave number in cm^{-1}. (From Ref.[2]).

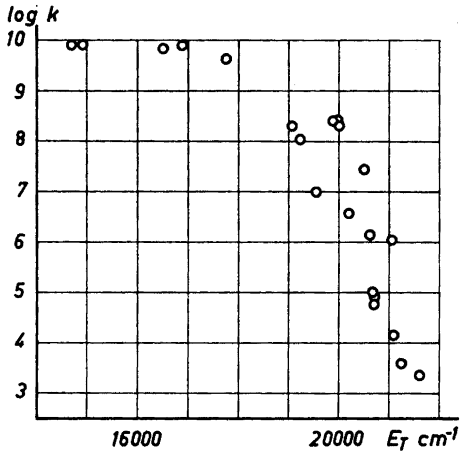

Fig. 2. Log k *vs.* triplet state energy (E_T) for the quenchers listed in Table 1. E_T in cm^{-1}, k in 1 $mole^{-1}$ sec^{-1}.

is about 19 700 cm^{-1}. This value is in general agreement also with the results of low-temperature phosphorescence studies [6,18]. Fortunately, an exact knowledge of the value of E_T for biacetyl is not necessary for the present purpose.

DISCUSSION

The results are represented in graphical form in Fig. 2, where log k is plotted against E_T. From the diagram it is evident that the effectiveness of a quencher of the type studied is mainly determined by the position of its lowest triplet energy level. The results thus confirm our previous conclusion that for substances of this type, quenching is the result of a transfer of triplet state excitation energy from biacetyl to the quencher. In the following we shall discuss the mechanism of this energy transfer, on the basis of the experimental results.

The first thing to be noted is that the strongest quenchers (those with E_T-values below 17 000 cm^{-1}) have practically the same value of k. This value is close to the limit which is set by the rate of diffusion, and which may be estimated by a formula given by Debye [19]. For a bimolecular process in benzene solution at 20°C the calculated limiting value is 1.0×10^{10} l $mole^{-1}$ sec^{-1}. Similarly, a determination of k for anthracene in a somewhat more viscous solvent, methyl benzoate, gave a value of 2.80×10^9 l $mole^{-1}$ sec^{-1} as against 3.15×10^9 l $mole^{-1}$ sec^{-1} according to the formula of Debye.

The viscosity dependence of the quenching constant for strong quenchers shows that the transfer of excitation energy takes place only as a result of molecular encounters and not over larger distances. Experimental and theoretical investigations of sensitized fluorescence in solution have shown that,

under certain conditions, intermolecular transfer of the energy of electronic excitation between singlet states of both donor and acceptor can occur across distances much greater than kinetic-theory collision diameters, by a non-radiative process, generally called "inductive resonance". Transfer over distances of the order of 70 Å has been established in favourable cases. Work in this field has been reviewed in a recent paper by Förster [20], where also other cases of excitation transfer are discussed. As regards the case dealt with in the present paper, he concludes that excitation transfer between triplet states may only be expected to occur at short distances.

Intermolecular transfer of excitation energy between triplet states was first demonstrated by Terenin and Ermolaev [21] as sensitized phosphorescence in solid solutions at low temperature. A closer study of this phenomenon led them to the conclusion [12] that excitation transfer in this case is due to exchange interaction resulting from beginning overlap of the electronic clouds of the two molecules. This would imply that energy transfer would be possible over distances somewhat larger than those of molecular contact. Our results do not exclude this possibility since, in fluid solution, a molecular encounter [22] (involving repeated collisions) would nevertheless be necessary for the transfer to take place.

For quenchers with triplet levels higher than 17 000 cm^{-1} the general trend is a lowering of the quenching constant with increasing triplet state energy, but there are considerable individual variations. This was to be expected. The radiationless transfer of the energy of electronic excitation from an excited donor molecule to an unexcited molecule of the acceptor is the result of coupled transitions in the two molecules. Fig. 3 represents a schematic energy level diagram for donor and acceptor, showing only vibrational levels belonging to the singlet ground states and the lowest triplet states of the two molecules. The temperature is assumed to be so low that both molecules are originally in so-called nonoscillating states. The transitions marked ν_0 are the pure electronic (0—0) transitions. Generally only a small fraction of the transitions actually occurring are of this kind. This is due to the difference between the nuclear equilibrium configurations of ground and of excited states which, in accordance with the Franck-Condon principle, favours transitions to different vibrational levels of the final state (see, *e.g.*, Förster [23]). Two such transitions of equal energy in the two molecules, marked ν^D and ν^A, are shown in the diagram. If the two transitions occur simultaneously, due to quantum-mechanical resonance, the energy of excitation is transferred from donor to acceptor. The energy transferred corresponds to a frequency which is common to the phosphorescence spectrum of the donor and the T ← S absorption spectrum of the acceptor, *i.e.*, it belongs to the region of overlap of the two spectra. With increasing overlap the number of possible coupled transitions will increase, and consequently the possibilities for transfer.

In the present case the donor (biacetyl) is the same throughout. Its T → S emission spectrum at room temperature is shown in Fig. 1. It does not differ essentially from that observed at low temperature [24]. The pure T ← S absorption spectra of the different acceptors (quenchers) are too weak to be measured, but they must extend from the positions of their 0—0 bands, known from phosphorescence spectra, toward higher wave numbers. The extent of spectral

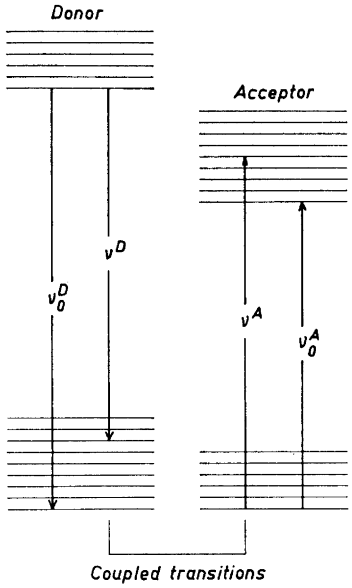

Fig. 3. Schematic energy level diagram illustrating transfer of the triplet state excitation energy from donor to acceptor through coupled transitions. For further explanations see text.

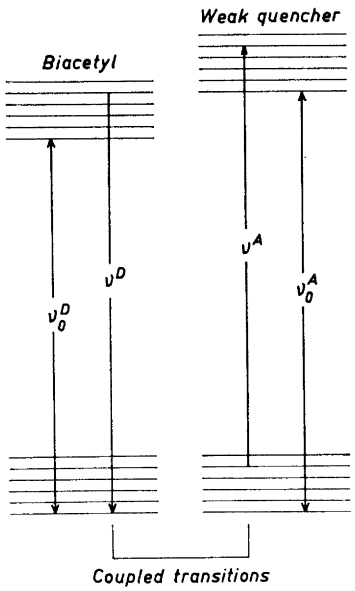

Fig. 4. Schematic energy level diagram illustrating transfer of the excitation energy from a biacetyl molecule in the triplet state to a molecule of a quencher with somewhat higher triplet state energy. For further explanations see text.

overlap must therefore increase with the difference between the triplet state energies of donor and acceptor. A general correlation between quenching constant and triplet state energy for the different quenchers may therefore be expected. However, the probability that coupled transitions will take place in donor and acceptor may be expected to depend also on the oscillator strengths of the individual transitions involved, in a similar way as in long-range excitation transfer according to the theory of Förster [23]. In the present case this means that the intensities of the T←S absorption bands of a quencher as well as their positions should determine the value of its quenching constant. This we believe to be the main cause of the individual variations in the quenching constants observed. We shall return to this point in connection with the discussion of certain experimental results.

At low temperature, where the molecules are originally in vibrationless states, only transitions of the kind illustrated in Fig. 3 are possible. Under these circumstances, a transfer of the excitation energy from the biacetyl to a quencher is possible only if $\nu_o^A \leq \nu_o^D$. At higher temperatures this is no longer true. From Fig. 2 it is also quite evident that substances with triplet state energies higher than that of biacetyl may act as weak quenchers under our experimental conditions.

In the schematic energy level diagram shown in Fig. 4, the triplet state energy of the quencher is assumed to be somewhat higher than that of biacetyl ($\nu_o^A > \nu_o^D$). It is further assumed that the temperature is relatively high, so that transitions from higher vibrational levels may be expected. Two such transitions of equal energy, ν^D and ν^A, are indicated in the diagram. Their occurrence as coupled transitions would transfer the excitation energy from the biacetyl to the quencher. It should be noted in this connection that, as shown by a simple calculation, 1 molecule in 100 has a vibrational energy exceeding 900 cm^{-1} at 20°C.

However, in this case the transfer may evidently be reversed if, during its lifetime, the triplet state quencher molecule should encounter a biacetyl molecule in its ground state. Consequently, for quenchers with triplet levels above that of biacetyl, the quenching constant may be expected to decrease with increasing biacetyl concentration. This has been confirmed, which constitutes another strong argument in favour of the assumed quenching mechanism. As an illustration, results obtained with 1-iodonaphthalene as quencher will be presented in a separate section at the end of this paper. Experiments with other quenchers are in progress and will be reported later by one of us. However, it should be mentioned here that, as was to be expected, the same effect of the biacetyl concentration on the value of the quenching constant has been found also for quenchers with triplet levels somewhat lower than that of biacetyl.

Even though the k-values listed in Table 1 were obtained in experiments where the biacetyl concentration was low, there can be no doubt that many of them do not represent the true quenching constant, uninfluenced by excitation transfer in the reverse direction. In this sense they must be regarded as preliminary. Under these circumstances we prefer to postpone a discussion of the results for individual quenchers. However, an exception will be made for the 1-halogen derivatives of naphthalene. As has already been pointed out by Ermolaev and Terenin [12], these compounds are suitable for testing whether the rate of transfer of triplet state excitation energy depends on the oscillator strengths of the transitions involved in the process. Their phosphorescence spectra are similar as regards both position (*cf.* Table 1) and structure. From the approximate mirror symmetry between absorption and emission spectra [17,23] it may be concluded that the same must be true of their T ← S absorption spectra. On the other hand, the oscillator strengths (f-numbers) of their T ← S transitions must vary markedly. This follows from the relation between the f-number for absorption and the natural mean lifetime, τ_o, for emission [25]. In the case under consideration, where the positions of the absorption bands may be expected to be nearly the same, the f-number should be inversely proportional to τ_o. The mean lifetime of phosphorescence in solid solution at liquid air temperature was found by Ermolaev and Svitashev [13] to be $2.0 \pm 0.2 \times 10^{-3}$ sec for 1-iodonaphthalene and 0.29 sec for 1-chloronaphthalene. Together with the authors' quantum yield determinations, these figures indicate a ratio of the oscillator strengths for these compounds of about 170.

The E_T-value of 1-iodonaphthalene is about 200 cm^{-1} lower than that of the chloro-derivative. As shown by Fig. 2, the general trend of our results is such

that a ratio of their quenching constants of about 4 would appear normal. The experimental value is 450. Our results with these compounds therefore must be said to confirm the expected dependence of the probability of excitation transfer on the oscillator strengths of the individual transitions involved *.

In similar experiments with solid solutions at liquid air temperature, Ermolaev and Terenin [12] obtained quite different results. Naphthalene and its 1-halogen derivatives were found to be equally effective, within limits of error, as quenchers of the phosphorescence of benzophenone. However, the triplet state energy of benzophenone [6] is 24 400 cm^{-1}, *i.e.*, > 3 000 cm^{-1} higher than for naphthalene. There is reason to believe, therefore, that the condition of spectral overlap was in all cases so well fulfilled that some other factor governing the probability of excitation transfer was rate-determining. Obviously, this cannot have been the rate of diffusion, as for quenchers with triplet levels below 17 000 cm^{-1} in the present work. Instead it must have been intermolecular distance. This interpretation fits in very well with the theory proposed by Terenin [26] to explain their results on the influence of the concentration of the acceptor on the quenching of the phosphorescence of benzophenone.

Besides the type of quenchers dealt with in the present paper, there are also quenchers of a different type, characterized by the presence in the molecule of a loosely bound hydrogen atom [1]. For this class of compounds, the quenching mechanism has been assumed to be a photochemical reaction. Since the strongest quenchers in this class are aromatic compounds like hydroquinone and diphenylamine, it may be worth pointing out that their triplet state energies [27,6] are so high (> 23 000 cm^{-1}) that quenching by transfer of the excitation energy is excluded.

RESULTS WITH 1-IODONAPHTHALENE AS QUENCHER AND WITH VARYING BIACETYL CONCENTRATION

The results are given in Table 2. As seen from column 2, raising the biacetyl concentration caused a considerable increase in the phosphorescence mean life. In column 3 the values of τ have been corrected for the slight "self-quenching" of the biacetyl used **. In pure benzene solution τ decreased from 685 to 597 μsec when the biacetyl concentration was raised from 0.0069 to 0.1666 M.

In order to account for the results we have found it necessary to assume that the iodonaphthalene used contained a small fraction of a stronger quencher as an impurity. In the following reaction scheme D denotes biacetyl, A iodonaphthalene, and Q the quenching impurity, all in their ground states.

---

* *Note added in proof:* A redetermination of k for 1-chloronaphthalene, using a preparation of very high purity, gave a value of the quenching constant, corrected for energy transfer in the reverse direction, of 4.1×10^3 l $mole^{-1}$ sec^{-1}. With the corresponding value for 1-iodonaphthalene (p. 967) this gives a ratio of the corrected quenching constants = 8 400.

** *Cf.* Ref.[1], p. 827.

$D + h\nu \rightarrow D_{S'} \rightarrow D_T$

$D_T \rightarrow D + h\nu'$(phosphorescence) (0)

$D_T \rightarrow D$ (radiationless deactivation) (0')

$D_T + A \rightarrow D + A_T$ (energy transfer) (1)

$A_T + D \rightarrow A + D_T$ (reversal of energy transfer) (2)

$A_T \rightarrow A$ (deactivation) (3)

$D_T + Q \rightarrow D + Q_T$ (energy transfer to impurity) (4)

$Q_T \rightarrow Q$ (deactivation) (5)

The first equation represents the formation of a triplet excited biacetyl molecule (D_T), *via* the singlet excited state ($D_{S'}$), as the result of the absorption of a light quantum (*cf.* Ref.[2]). As regards eqn. (0), the natural mean lifetime of biacetyl ($\tau_o = 1/k_o$) must be at least equal to 2.25×10^{-3} sec, the value found for the phosphorescence mean life in solid solution at 77°K [7]. However, the true lifetime under our experimental conditions extrapolated to zero biacetyl concentration, was only 689 μsec, whence the sum of k_o and k_o' equalled 1.45×10^3 sec^{-1}.

As regards the rate constant of reaction (3), the fact that 1-iodonaphthalene exhibits no detectable phosphorescence in solution at ordinary temperature shows that the triplet state lifetime under these conditions must be several orders of magnitude shorter than in solid solution at 77°K, 2×10^{-3} sec. In the present case, therefore, $k_3 \gg k_o + k_o'$.

On the above reaction scheme, the rate of phosphorescence decay after a light flash will be governed by the following differential equations, where symbols within brackets denote concentrations in mole/l.

$$\frac{d[D_T]}{dt} = -(k_o + k_o')[D_T] - k_1[A][D_T] + k_2[D][A_T] - k_4[Q][D_T] \quad (6)$$

$$\frac{d[A_T]}{dt} = k_1[A][D_T] - k_2[D][A_T] - k_3[A_T] \quad (7)$$

According to eqn. (7) the following relation would hold under steady-state conditions (constant illumination):

$$[A_T] = \frac{k_1[A][D_T]}{k_2[D] + k_3} \quad (8)$$

In the particular case under consideration ($k_3 \gg k_o + k_o'$) the same relation may be expected to hold with good approximation. This is confirmed by a study of the general solution of the equation system, which need not be given here. Under these conditions the following expression is obtained for $1/\tau_{corr}$:

$$\frac{1}{\tau_{corr}} = -\frac{d \ln [D_T]}{dt} = k_o + k_o' + k_4[Q] + \frac{k_1 k_3[A]}{k_2[D] + k_3} \quad (9)$$

In order to apply this equation to the experimental data it was transformed into

$$\varphi(\tau) = \frac{\tau_{corr}}{1 - K\,\tau_{corr}} = \frac{1}{k_1[A]} + \frac{k_2[D]}{k_3} \quad (10)$$

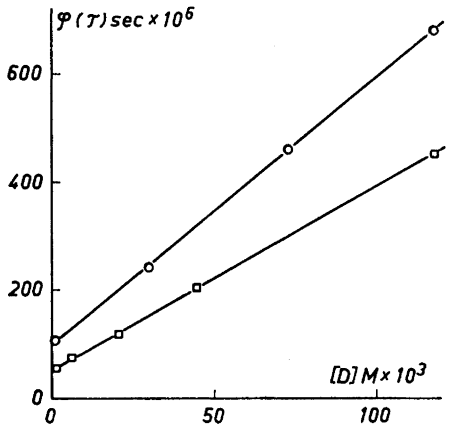

Fig. 5. $\varphi(\tau) = \tau_{corr}/(1-K\ \tau_{corr})$ *vs.* biacetyl concentration [D]. Data from Table 2. □ Series 1, $K = 3280$ sec^{-1}. O Series 2, $K = 2353$ sec^{-1}. For further explanations see text.

where $K = k_o + k_o' + k_4[Q]$. The value of K was varied until a plot of $\varphi(\tau)$ *vs.* [D] gave as nearly as possible a straight line. The result is shown in Fig. 5. The equations of the lines are, with τ in sec

$$\text{Series 1:}\quad \frac{\tau_{corr}}{1-3280\ \tau_{corr}} = 49.9 + 10^{-6} + 3.41 \times 10^{-3}\ [D]$$

$$\text{Series 2:}\quad \frac{\tau_{corr}}{1-2353\ \tau_{corr}} = 97.8 \times 10^{-6} + 4.94 \times 10^{-3}\ [D]$$

Values of τ_{corr} calculated from these equations are given in Table 2, column 4.

The two series of measurements give closely agreeing results as regards the value of k_1, 3.48 and 3.40×10^7 l mole^{-1} sec^{-1}. As regards the value of k_2/k_3 the agreement is less satisfactory, the calculated values being 68 and 51 l mole^{-1}, respectively.

Table 2. Influence of biacetyl concentration [D] on the phosphorescence mean life τ at two concentrations of 1-iodonaphthalene [A]. For further explanations see text.

	[D] M $\times 10^3$	τ_{obs} sec $\times 10^6$	τ_{corr} sec $\times 10^6$	τ_{calc} sec $\times 10^6$
Series 1. [A] = 5.76×10^{-4} M	1.5	46.0	46.0	46.6
	6.1	58.9	58.9	57.4
	20.8	84.9	85.1	86.5
	44.8	121.4	122.3	121.8
	118.0	177.0	182.1	182.1
Series 2. [A] = 3.01×10^{-4} M	1.2	84.5	84.5	83.4
	29.7	152.9	153.8	155.2
	72.9	216.2	220.9	220.4
	117.8	251.0	261.4	261.5

The assumption made, that the iodonaphthalene contained a small fraction of a stronger quencher Q, requires that the term $k_4[Q]$ should be proportional to [A]. This was the case within limits of error. The ratio $k_4[Q]/[A]$, as obtained by subtracting $(k_o + k_o') = 1.45 \times 10^3$ from the above K-values, and dividing by the value of [A], is 3.18×10^6 and 3.00×10^6 l mole^{-1} sec^{-1}, respectively. This would correspond to the presence in the iodonaphthalene of, *e.g.*, 0.04 mole per cent of a quencher as strong as anthracene.

The value of k_1 obtained in these experiments differs relatively little from the corresponding value in Table 1. Results with other quenchers have shown that the difference may in certain cases be considerable.

REFERENCES

1. Bäckström, H. L. J. and Sandros, K. *Acta Chem. Scand.* **12** (1958) 823.
2. Bäckström, H. L. J. and Sandros, K. *Ibid.* **14** (1960) 48.
3. Schmidlin, J. and Huber, M. *Ber.* **43** (1910) 2829.
4. Krollpfeiffer, F. *Ann.* **430** (1923) 204.
5. Clar, E. *Aromatische Kohlenwasserstoffe. Polycyclische Systeme*, 2nd Ed., Springer, Berlin 1952.
6. Lewis, G. N. and Kasha, M. *J. Am. Chem. Soc.* **66** (1944) 2100.
7. McClure, D. S. *J. Chem. Phys.* **17** (1949) 905.
8. Ferguson, J., Iredale, T. and Taylor, J. A. *J. Chem. Soc.* **1954** 3160.
9. Padhye, M. R., McGlynn, S. P. and Kasha, M. *J. Chem. Phys.* **24** (1956) 588.
10. Clar, E. and Zander, M. *Chem. Ber.* **89** (1956) 749.
11. Muel, B. and Hubert-Habart, M. *J. Chim. Phys.* **55** (1958) 377.
12. Ermolaev, V. and Terenin, A. *J. Chim. Phys.* **55** (1958) 698.
13. Ermolaev, V. and Svitashev, K. *Optika i Spektroskopiya* **7** (1959) 664.
14. Evans, D. F. *J. Chem. Soc.* **1957** 1351.
15. Tsubomura, H. and Mulliken, R. S. *J. Am. Chem. Soc.* **82** (1960) 5966.
16. Forster, L. S. *J. Chem. Phys.* **26** (1957) 1761.
17. Pringsheim, P. *Fluorescence and Phosphorescence*, Interscience Publishers, New York 1949.
18. Sidman, J. W. and McClure, D. S. *J. Am. Chem. Soc.* **77** (1955) 6461.
19. Debye, P. *Trans. Electrochem. Soc.* **82** (1942) 265.
20. Förster, Th. *Discussions Faraday Soc.* **27** (1959) 7.
21. Terenin, A. and Ermolaev, V. *Trans. Faraday Soc.* **52** (1956) 1042.
22. Rabinowitch, E. *Trans. Faraday Soc.* **33** (1937) 1225.
23. Förster, Th. *Fluoreszenz organischer Verbindungen*, Vandenhoeck & Ruprecht, Göttingen 1951.
24. Lewis, G. N. and Kasha, M. *J. Am. Chem. Soc.* **67** (1945) 1001.
25. Kasha, M. *Radiation Research, Suppl.* **2** (1960) 251.
26. Terenin, A. N. *Discussions Faraday Soc.* **27** (1959) 97.
27. Zudin, A. A. *Izvest. Akad. Nauk S.S.S.R., Ser. Fiz.* **23** (1959) 142.

Received December 4, 1961.

ACTA CHEMICA SCANDINAVICA 16 (1962) 969–974

Preparation of Prostaglandin F from Prostaglandin E

Prostaglandins and Related Factors 6 *

SUNE BERGSTRÖM, L. KRABISCH, B. SAMUELSSON and J. SJÖVALL

Department of Chemistry, Karolinska Institutet, Stockholm, Sweden

Reduction of prostaglandin E (PGE) ($C_{20}H_{34}O_5$) with sodium borohydride yielded two isomeric reduction products PGF_1 and PGF_2, ($C_{20}H_{36}O_5$) of which PGF_1 was identical with a compound earlier isolated from sheep prostate glands and designated PGF. The data presented indicate that PGE is an unsaturated dihydroxyketocarboxylic acid and that PGF_1 and PGF_2 are stereoisomeric, unsaturated trihydroxycarboxylic acids.

Recently we reported the isolation of two crystalline biologically active compounds from sheep prostate glands, prostaglandin E ($C_{20}H_{34}O_5$) and prostaglandin F ($C_{20}H_{36}O_5$) [1–4]. It has now been found that reduction of PGE with sodium borohydride yielded two compounds one of which proved identical with PGF while the other had different physical and biological properties but the same elementary composition. The former compound is now designated PGF_1 and the new compound PGF_2.

EXPERIMENTAL

Reduction of PGE with sodium borohydride. PGE (100 mg, m.p. 115°) was dissolved in 10 ml of methanol and cooled in an ice bath. A solution of sodium borohydride (300 mg) in 35 ml of methanol was chilled and added. After 20 min at 0° the mixture was left at room temperature for one hour. Water was added and most of the methanol was taken off *in vacuo*. After acidification with hydrochloric acid the aqueous phase was extracted three times with ether, the combined ether extracts were washed with water and brought to dryness at room temperature.

Paper chromatography showed that two new compounds were present whereas the original spot due to PGE had disappeared.

Taking the relative mobility of PGE as 1.00 the values for the two new spots were 0.72 and 0.55, respectively, in a phase system consisting of equal parts of ethylene chloride and heptane as moving phase and 70 % acetic acid as stationary phase [5]. The relative mobility of PGF isolated from sheep prostate glands is 0.72 in the same phase system.

* For earlier papers in this series see Refs.[1-4,7].

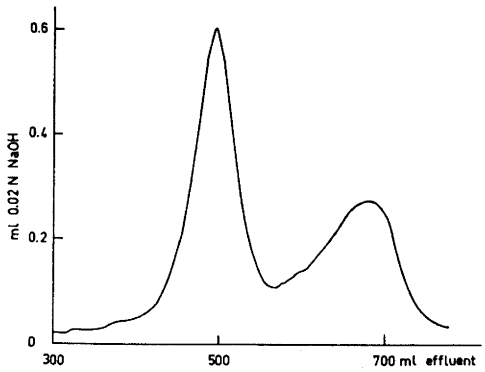

Fig. 1. Reversed phase partition chromatography of reaction product formed by reduction of prostaglandin with sodium borohydride (see text).

Table 1. Interplanar spacings in Ångström units as determined from Guinier powder photographs taken with Cu$K\alpha$ radiation.

P G F		*P G F*$_1$		*P G F*$_2$	
d Å	*I*	*d* Å	*I*	*d* Å	*I*
16.44	s	16.43	s	10.79	vw
9.46	w	9.49	vw	9.15	vw
8.16	w	8.22	vw	8.41	w
6.19	m	6.19	w	7.22	m
5.46	m	5.45	w	5.64	m
5.05	m	5.06	w(d)	4.78	vw
4.71	vw	4.73	w	4.66	vw
4.63	vs	4.62	s(d)	4.53	s
4.54	m	4.53	w	4.37	s
4.46	m	4.45	m(vd)	4.27	w
4.08	m	4.09	m(d)	4.17	m
4.02	s	4.02	m(d)	3.89	m
3.74	w	3.75	w	3.77	m
3.56	w	3.56	vw	3.64	vw
3.45	vw	3.45	vw(d)	3.58	vw
3.07	vw	3.07	w(vd)	3.51	vw
2.93	w	2.95	w(vd)	3.42	vw
2.80	w	2.67	vw(vd)	3.38	vw
2.67	vw	2.58	w(vd)	3.34	vw
2.56	vw	2.49	w(d)	3.12	vw(vd)
2.48	vw	2.39	vw(vd)	3.03	vw
2.39	vw	2.35	vw(vd)	2.96	vw
2.34	vw	2.25	vw(vd)	2.92	vw
2.02	w	2.17	vw(d)	2.83	vw
1.48	w	2.02	vw(vd)	2.70	vw(d)
		1.89	vw(vd)	2.60	w(d)
		1.70	vw(vd)	2.46	vw(d)
				2.40	vw
				2.35	vw
				2.32	vw
				2.25	m
				2.08	vw
				2.00	vw(vd)
				1.69	vw(vd)

s = strong
m = medium
w = weak
vw = very weak

d = diffuse
vd = very diffuse

The residue (100 mg) was then subjected to reversed phase partition chromatography on 18 g of hydrophobic kieselguhr. The solvent system was prepared through mixing of methanol (516 ml), water (684 ml), isooctanol (60 ml) and chloroform (60 ml). 16 ml of the chloroform phase was supported on the kieselguhr. The titration values of the fractions are plotted in Fig. 1.

PGF_1. Fractions 95—133 (600—750 ml effluent) were combined and taken to dryness and crystallized from ethyl acetate-pentane. Yield 37 mg, m.p. 101° not depressed by admixture of PGF isolated from sheep prostate glands. X-Ray diffraction powder pattern, mass spectra and IR-spectra were also identical (see Table 1) with the data published earlier [1].

PGF_2. Fractions 60—85 (440—540 ml effluent) were also combined and yielded 47 mg, m.p. 128°, when crystallized from ethyl acetate-pentane. (Found: C 67.2; H 10.2. Calc. for $C_{20}H_{36}O_5$: C 67.4; H 10.2).

The results of the X-ray diffractions of earlier isolated PGF and PGF_1 and PGF_2 prepared now are listed in Table 1. The mass spectrum of the methyl ester of PGF_2 was practically identical with that of the methyl ester of PGF_1.

Microdetermination of the ratio between the acylable groups and the carboxyl group of PGE, PGF_1 and PGF_2. The method is based on the preparation of the methyl ester with ^{14}C-labeled diazomethane followed by acylation with *p*-nitrobenzoylchloride in pyridine at room temperature. The ratio between the light absorption of the nitrobenzoylgroup at 257 mμ and the radioactivity is then determined.

About one mg of the substance was treated with an excess of diazomethane-^{14}C prepared from nitrosomethyl-^{14}C-urea and then taken to dryness *in vacuo* and dried in a desiccator. The ester was then dissolved in 0.3 ml of dry pyridine and 0.25 ml of a solution of *p*-nitrobenzoylchloride in pyridine (60 mg per ml) was added. After standing overnight at room temperature the solution was cooled in ice and one drop of 50 % aqueous pyridine was added. After 15 min more water was added and the mixture extracted with ether. The combined ether extracts were carefully washed three times with dilute hydrochloric acid followed by 0.2 M sodium carbonate and water. The residue was dissolved in 10 ml of absolute ethanol. The light absorption at 257 mμ was determined after dilution (1:5) and the ^{14}C-content was determined by counting aliquots, plated on aluminium planchets, in a gas flow counter (Frieseke-Hoepfner FH 51) (Table 2).

Table 2.

	(1) c.p.m.	(2) E_{257}	(2)/(1) × 0.475 × 10^3
2-Hydroxystearic acid	3 141	0.69	1.05
9,10-Dihydroxystearic acid	3 293	1.35	1.96
PGE	3 020	0.99	1.53
PGF_1	2 822	1.68	2.8
PGF_2	2 834	1.75	2.95

The data on the mono- and dihydroxystearic acids are reasonably in agreement with one respectively two hydroxyls per methyl ester group. Using these as standards PGF_1 and PGF_2 have approximately three hydroxyl groups in agreement with their preparation from PGE through reduction of a carbonyl group with sodium borohydride. The data for PGE varied in different runs (1.4—1.8) and the reason is apparently that a partial dehydration takes place. The structural implications of these findings will be discussed in a future publication.

Preparation of the methyl ethers of methyl esters of PGE, PGF_1 and PGF_2. For the mass spectrometric analysis the methylation of the methyl esters was carried out essentially as described recently by Müller and Rundel [6].

A solution of 5—10 mg of the methyl ester of PGE, PGF_1 and PGF_2 in 10 ml of dry ether was cooled to —40°. Freshly prepared diazomethane was

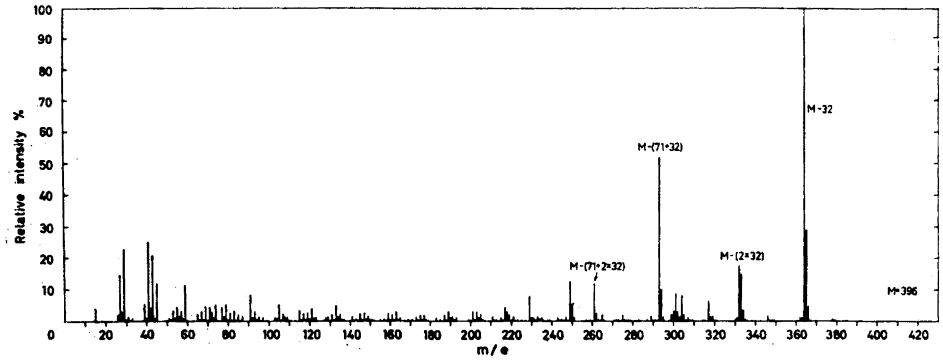

Fig. 2. Masspectrum of the dimethylether methyl ester of prostaglandin E. (PGE).

dried over potassium hydroxide for 2 h, cooled to −40° and added to the solution of the methyl ester immediately after addition of 0.05 ml of boron trifluoride methyl etherate. Diazomethane was added until the yellow colour persisted. After 15 min at −40° and 1 1/2 h at room temperature the solution was filtered from polymethylenes, washed with sodium bicarbonate and water, dried over sodium sulfate and evaporated under reduced pressure.

Gas-liquid chromatography and mass spectrometric analysis of methyl ethers of PGE, PGF_1 and PGF_2 methyl esters. A Pye chromatograph with an argon ionization detector was used. The stationary phase (Apiezon L, Shell Chemicals Ltd.) was supported on 100—120 mesh Celite in the ratio stationary phase: Celite 1:6.4. The retention times for these derivatives of PGE, PGF_1 and PGE_2 at 245° with an argon pressure of 1 kg/cm² are given below.

	Retention time in min.
PGE	48.3
PGF_1	40.5
PGF_2	35.0

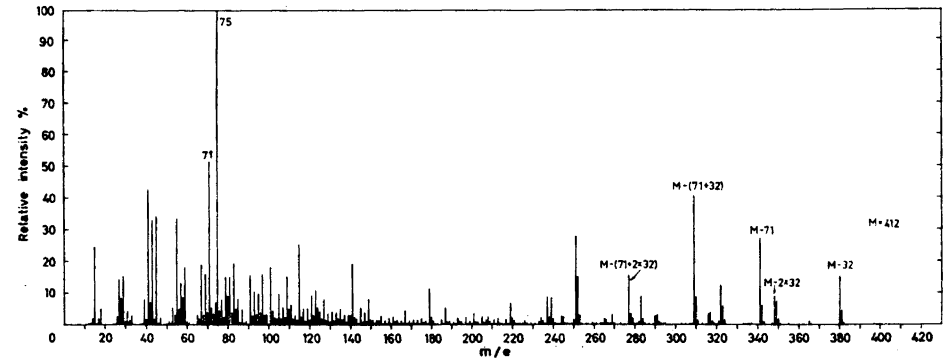

Fig. 3. Masspectrum of the trimethylether methyl ester of prostaglandin F_1 (PGF_1).

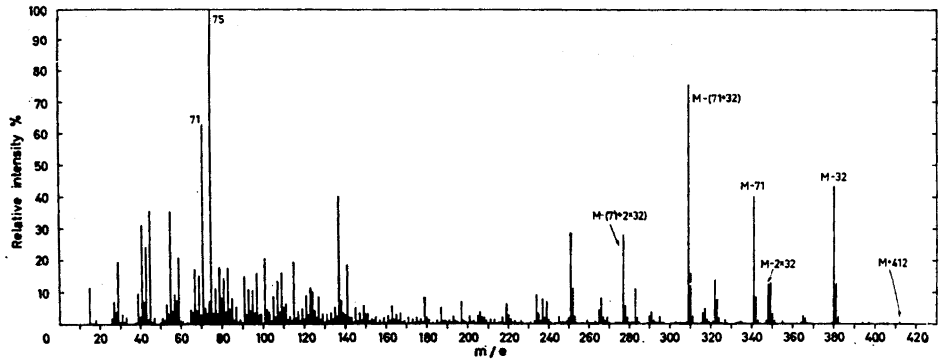

Fig. 4. Masspectrum of the trimethylether methyl ester of prostaglandin F_2 (PGF_2).

Mass spectrometric analysis of the methyl ethers was done after purification with gas chromatography. The analysis was done by Dr. R. Ryhage of this department with the technic described earlier [8]. The mass spectrogram of PGE methyl ester was consistent with the presence of a dimethyl ether with a molecular weight of 396 (= M) with large peaks at M-32, M-2 × 32, M-(32 + 71) and M-(2 × 32 + 71). The mass spectrograms for the two PGF compounds were practically identical, *i.e.* corresponded to trimethyl ethers and showed a molecular weight of 412 and had the same series of marked peaks at M-32, M-2 × 32, M-3 × 32, M-71 + 32 etc., *cf.* Figs. 2, 3 and 4.

The data are in agreement with the successive loss of one, two respectively three molecules of methanol (mol.wt. 32) from the dimethylether of PGE-methyl ester and the trimethylethers of the PGF-methyl esters. All three compounds apparently contain a relatively easily detached grouping with a molecular weight of 71 ($C_5H_{11}^+$?). Further data of the mass spectra will be discussed at a later time.

Biological activity. PGF_2 was found to have 10—20 % of the smooth muscle stimulating activity shown by PGF_1 when tested on the duodenum of the rabbit. The physiological data will be presented in greater detail in a later publication.

DISCUSSION

The formation of the originally isolated prostaglandin F_1 ($C_{20}H_{36}O_5$) when prostaglandin E ($C_{20}H_{34}O_5$) was reduced with sodium borohydride indicates that the two compounds are identical except for the presence of a carbonyl grouping in PGE that can be reduced to the corresponding alcohol in PGF_1. At the same time the other stereoisomeric alcohol PGF_2 is formed.

In this connection it might be mentioned that PGE gave a positive spot test on paper with nitrophenylhydrazine for the presence of a carbonyl whereas the two PGF's gave negative tests.

From the IR-spectra of PGE [2] earlier published it is apparent that only one strong band is present in the carbonyl region at 5.77 μ (1 733 cm^{-1}) indicating that the carbonyl group absorbed at the same wave length as the ester

carbonyl. As aldehydes and alifatic ketones as well as cyclohexanones absorb at longer wave lengths these data indicate that a cyclopentanone might be present that is known to absorb in this region.

As mentioned in earlier publications both PGE and PGF_1 absorbed one mole of hydrogen when reduced with hydrogen and platinum in neutral alcohol. The same was found to take place on reduction of PGF_2. All three compounds showed a band at 10.30 μ (971 cm^{-1}) that disappeared after reduction in a neutral medium indicating that the double bond had the *trans* configuration.

PGE did not show any absorption in the region 210—250 mμ indicating that the original double bond was not in conjugation with the carbonyl or carboxyl group.

From the quantitative acylation experiments it appears that PGF_1 and PGF_2 both contain three hydroxyls. The data for PGE varied somewhat between one and two and apparently some dehydration did occur.

The conclusion that one ring is present is based on the fact that all three compounds contain two hydrogens less than alifatic compounds with these substituents would require. The IR data indicating the presence of a cyclopentanone in PGE supports this conclusion.

The data reported so far thus indicate that the prostaglandins contain the following groups:

PGE	PGF_1 and PGF_2
($C_{20}H_{34}O_5$)	($C_{20}H_{36}O_5$)
1 carboxyl	1 carboxyl
1 carbonyl (cyclopentanone)	
2 hydroxyls	3 hydroxyls
1 double bond (*trans*)	1 double bond (*trans*)
1 ring	1 ring

The work is being continued.

This work has been supported by grants from "Gustaf och Thyra Svenssons Minne" and "Therese och Johan Anderssons Minne", Stockholm, and by the Upjohn Co, Kalamazoo, Mich., USA.

We are greatly indebted to Docent R. Ryhage for the mass spectrometric analysis, to Drs. S. Abrahamsson and Stig Aleby, Uppsala, for the X-ray diffraction data, and to Dr. I. Fischmeister for the IR data and to Miss Anita Ivarsson for able technical assistance.

REFERENCES

1. Bergström, S. and Sjövall, J. *Acta Chem. Scand.* **14** (1960) 1693.
2. Bergström, S. and Sjövall, J. *Acta Chem. Scand.* **14** (1960) 1701.
3. Bergström, S., Eliasson, R., v. Euler, U. S. and Sjövall, J. *Acta Physiol. Scand.* **45** (1959) 133.
4. Bergström, S., Dunér, H., v. Euler, U. S., Pernow, B. and Sjövall, J. *Acta Physiol. Scand.* **45** (1959) 145.
5. Sjövall, J. *Clin. Chim. Acta* **4** (1959) 652.
6. Müller, E. and Rundel, W. *Angew. Chem.* **70** (1958) 105.
7. Bergström, S., Krabisch, L. and Sjövall, J *Acta Chem. Scand.* **14** (1960) 1706.
8. Ryhage, R. *Arkiv Kemi* **16** (1960) 19.

Received November 15, 1961.

ACTA CHEMICA SCANDINAVICA 16 (1962) 975–982

Proteolytic Activity and Trypsin Inhibiting Ability of Serum Fractions Obtained Chromatographically on Anion Exchange Sephadex

GUNNAR LUNDBLAD

National Bacteriological Laboratory, Stockholm, Sweden

The chromatographic separation of normal human serum by means of the anion exchanger DEAE-Sephadex in phosphate buffer at pH 6.6 is described. The presence of two trypsin inhibitors measured on gelatin is confirmed and the occurrence of activated plasmin in the last fraction with a high optical density is suggested. The proteolytic TAMe-esterase activity is found and is assumed to show the presence of the complement factor C'1 in the non-adsorbed fraction.

In an earlier paper [1] the present author reported some studies on the arylesterase activity in normal human serum fractions. The separation was made on the cross-linked dextran gel, Sephadex G-25, introduced by Porath and Flodin [2]. The presence of two arylesterases was indicated. The present communication gives some results obtained upon eluation chromatography of normal human serum on the anion exchanger DEAE-Sephadex A-25 and, in this case, the proteolytic activity and the trypsin-inhibiting ability of the fractions were studied.

It was shown by Bergman and Fruton and their coworkers that proteolytic enzymes possess the ability to hydrolyze not only proteins but also certain synthetic peptides and even some related compounds. Neurath and coworkers [3] found that the amino acid esters, α-benzoyl-L-arginine methyl ester (BAMe) and α-toluenesulphonyl-L-arginine methyl ester (TAMe), are hydrolyzed very rapidly by trypsin. The substrate TAMe has been especially used for investigations of the proteolytic activity of serum and serum components, *cf.* among others, Sherry and Troll [4] and Becker [5]. In this investigation two substrates were used: for the proteinase (endopeptidase) activity gelatin, and for the proteolytic esterase effect the synthetic substrate TAMe.

MATERIAL AND METHODS

Serum from healthy blood donors was investigated. In some experiments, so-called inactivated serum was used, *i.e.* serum that had been kept at 56°C for 30 min.

Fractionation. The chromatographic column was set up as follows. Portions of 15 g DEAE-Sephadex A-25, medium, from Pharmacia, Uppsala, were treated according to the instructions and then suspended in 0.02 M phosphate buffer, pH 6.6. The column, 43 × 1.5 cm inner dimensions and furnished with a jacket, was cooled with water at + 12°C and the fractions were collected in 5 ml portions in a Radirac fraction collector from LKB, Stockholm, at an outflow rate of 90—110 ml/h. The elutions were made with increasing concentrations of NaCl (0.1, 0.2, 0.4, 0.6, and 1.0 M) in the same buffer. The optical density of the fractions was measured at 280 mμ in a Beckman spectrophotometer model DU.

Electrophoresis. Unfractionated serum and "peak fractions" were run electrophoretically on paper, model LKB, Stockholm, in 0.1 M "S:t Eriks" buffer *, at pH 8.6 for 17 h, 300 V and 12 mA, and then stained with naphthalene black 12 B.

Chemicals. The substrate TAMe, HCl was obtained from Hoffman La Roche, Basel, the trypsin (N.B.C. 1:300) from Nutritional Biochemicals Corp., Cleveland, Ohio, the gelatin (U.S.P., granular) from Fisher Sc. and Co., New York, and the merthiolate from Schmitt-Jourdan, Boulogne-sur-Seine, France.

Determination of proteolytic activity. The determination of the gelatin-splitting activity was performed according to the viscosimetrical method which has been suggested by Hultin [6,7] and developed to a high sensitivity by Hultin and Lundblad [8]. The measurements were carried out at 35.5°C in Ostwald viscosimeters. The enzymic activities were calculated according to Hultin's formula [6,7]. The values so obtained were multiplied by 10^6. It is suggested that the unit in which the values are thus expressed and for which the notation mμA has been used previously should be called the Hultin unit (H.U.). The assay of the trypsin-inhibiting ability of the serum fractions was made as follows. Mixtures were made up of 0.50 ml of the various fractions and 0.50 ml of a trypsin solution (0.2 mg/ml in M/15 phosphate buffer, pH 7.25). The mixtures were preincubated for 30 min at + 20°C and then added to 3.00 ml of a 4.00 % solution of gelatin in the same buffer and with 0.01 % of merthiolate added as a sterilizing agent. Measurements were also carried out with buffer substituted for the serum fractions. The gelatinase activity of the fractions was determined in mixtures consisting of 0.50 ml of a fraction, either 0.50 ml of the buffer solution or 0.50 ml of a 0.1 M cysteine solution, and 3.00 ml of the gelatin solution.

Determination of TAMe-esterase activity. The reaction mixtures were made up of 0.50 ml serum fraction, either 0.50 ml of M/15 phosphate buffer, pH 6.6 or 7.9, or 0.50 ml of a 0.1 M cysteine solution, and 1.00 ml of a 0.08 M solution of TAMe in the corresponding buffer. The influence of trypsin on the activity of the serum fractions was measured with reaction mixtures made up as described with, however, a 0.02 mg/ml trypsin solution in the corresponding buffer substituted for the buffer solution. The samples were incubated at 35°C for 20 h and the hydrolysis was measured by titration of the liberated carboxyl groups in an automatic titrator, model TTT 1a from Radiometer, Copenhagen. The activity was expressed in ml of 0.01 N NaOH consumed. Blanks with buffer and without TAMe were always run under the same conditions and corrections were made for the spontaneous hydrolysis of TAMe when necessary.

RESULTS

When the proteolytic activity of the various fractions was measured viscosimetrically with gelatin, very low values were obtained, less than 50 H.U. The main assays of the proteolytic enzymes were therefore carried out by measuring not their ability to split gelatin but, instead, their ability to split TAMe, as will be reported below. Gelatin, however, could be conveniently used for the measurement of the trypsin-inhibiting ability of the serum fractions.

* Na-veronal 18. 2 g, N HCl 12 ml, $Ba(Ac)_2$ 0.96 g, ethylene glycol 90 ml, aq.dest. ad 1 000 ml.

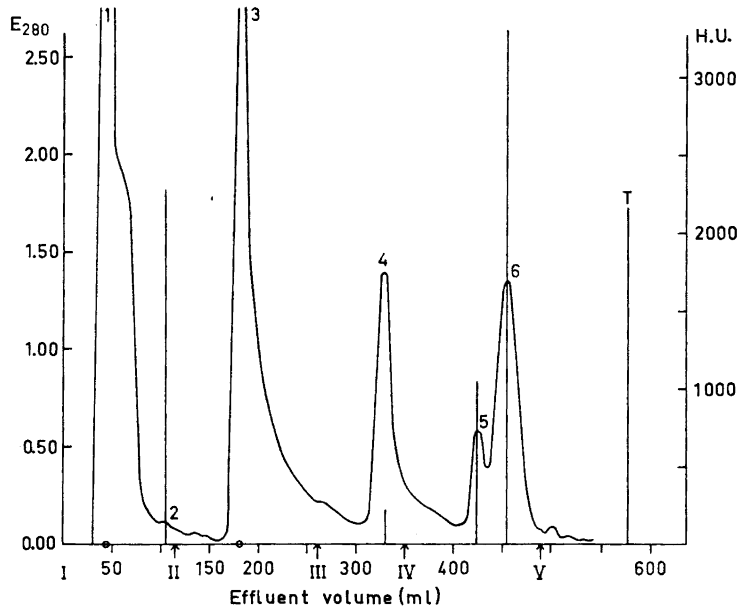

Fig. 1. Trypsin-inhibiting ability in a series of chromatographic fractions of human serum. Column, DEAE-Sephadex, 1.5 cm × 43 cm. Eluent: I, 0.02 M phosphate buffer pH 6.6; II, 0.1 M NaCl; III, 0.2 M NaCl; IV, 0.4 M NaCl; V, 0.6 M NaCl and VI, 1.0 M NaCl, II—VI in buffer I. E_{280} = total optical density at 280 mμ (curve). The straight lines show the gelatin-splitting activity at pH 7.2 of trypsin and the serum fraction. T = gelatin-splitting activity of trypsin alone. The activity is expressed in viscosimetrical Hultin units (H.U.).

The distribution of the trypsin-inhibiting ability in a series of fractions, obtained chromatographically, of normal human serum is shown in Fig. 1. Gelatin was used as substrate and the gelatin-splitting activity in the presence of trypsin in the different fractions can be compared with that of trypsin alone (T). In peaks 1 and 3 there is a complete inhibition, and also in peak 4 a very strong inhibition is found. In peak 5 there is 50 % inhibition whereas in peak 2, where some inhibition might also be expected, there seems however to be a slight increase in activity as compared with the original trypsin activity (T). In peak 6 there is, in fact, an approximately 35 % increase as compared with the gelatin-splitting activity of the trypsin solution.

The distribution of proteolytic TAMe-esterase activity measured at pH 7.9 in a series of chromatographic fractions of serum is shown in Fig. 2. The original TAMe-esterase activity is highest in peaks 1 and 3. With cysteine, a slight activation seems to have occurred in peaks 1, 2, and 3. When trypsin is added to the fractions, there is a rather strong activation in peak 1 whereas the activity in peaks 3—5 has about the same value as the sum of the activity of the trypsin solution and activity of the untreated fraction in question. In peak 2 an inactivation of the trypsin activity by about 35 % was found.

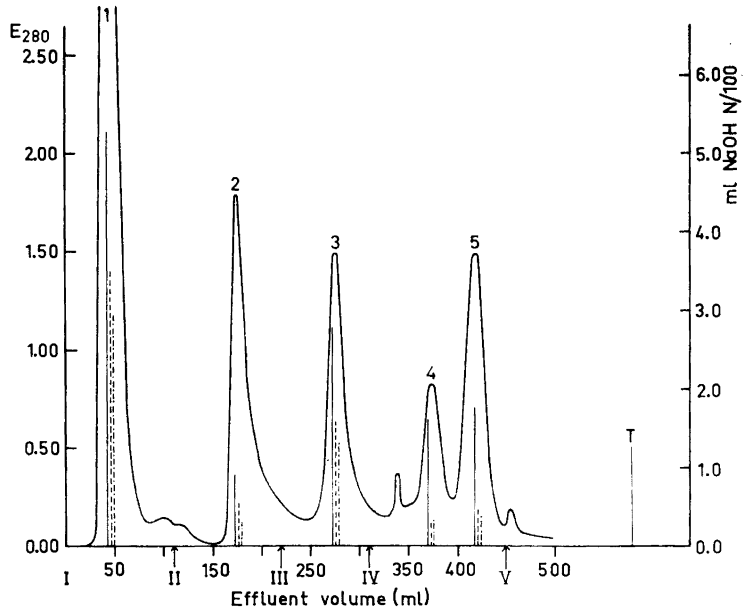

Fig. 2. Protolytic activity and trypsin-inhibiting ability in a series of chromatographic fractions of human serum. Column, DEAE-Sephadex, phosphate buffer pH 6.6. Elution as in Fig. 1. E_{280} = total optical density at 280 mμ (curve). Full lines, TAMe-esterase activity in the presence of trypsin; broken lines, TAMe-esterase activity in the presence of cysteine; dashed and dotted lines, TAMe-esterase activity of fraction only. T = TAMe-esterase activity of trypsin alone. The activity was measured in phosphate buffer at pH 7.9 and expressed as ml NaOH consumed.

The TAMe-esterase activity was measured at pH 6.6 in two series of chromatographic serum fractions, and the result is shown in Fig. 3 A—B. Untreated normal human serum was used in one series (Fig. 3 A) and serum of the same batch, but heated however to 56°C and kept at this temperature for 30 min and then cooled, was used in the other series (Fig. 3 B). In Fig. 3 A, a high TAMe-esterase activity is observed in peak 1. This activity is however considerably reduced in inactivated serum (Fig. 3 B). The activities of peaks 2—6 do not differ very much from each other and no significant difference can be found in the activities of the corresponding peaks in the two chromatograms. The presence of cysteine in the fractions has no effect upon the enzymatic activity. The addition of trypsin at this pH (6.6), as shown in Fig. 3 A—B, brings about no activation in the fraction studied. In the series with untreated serum (Fig. 3 A), the TAMe-esterase activity in peak 1 is about the same as the sum of the activities of fraction and trypsin measured separately. In peaks 2 and 3 the addition of trypsin caused no change in activity and in peaks 4—6 the addition resulted only in a slight increase in activity. In the series with "inactivated" serum (Fig. 3 B), only slight increases in activity were observed.

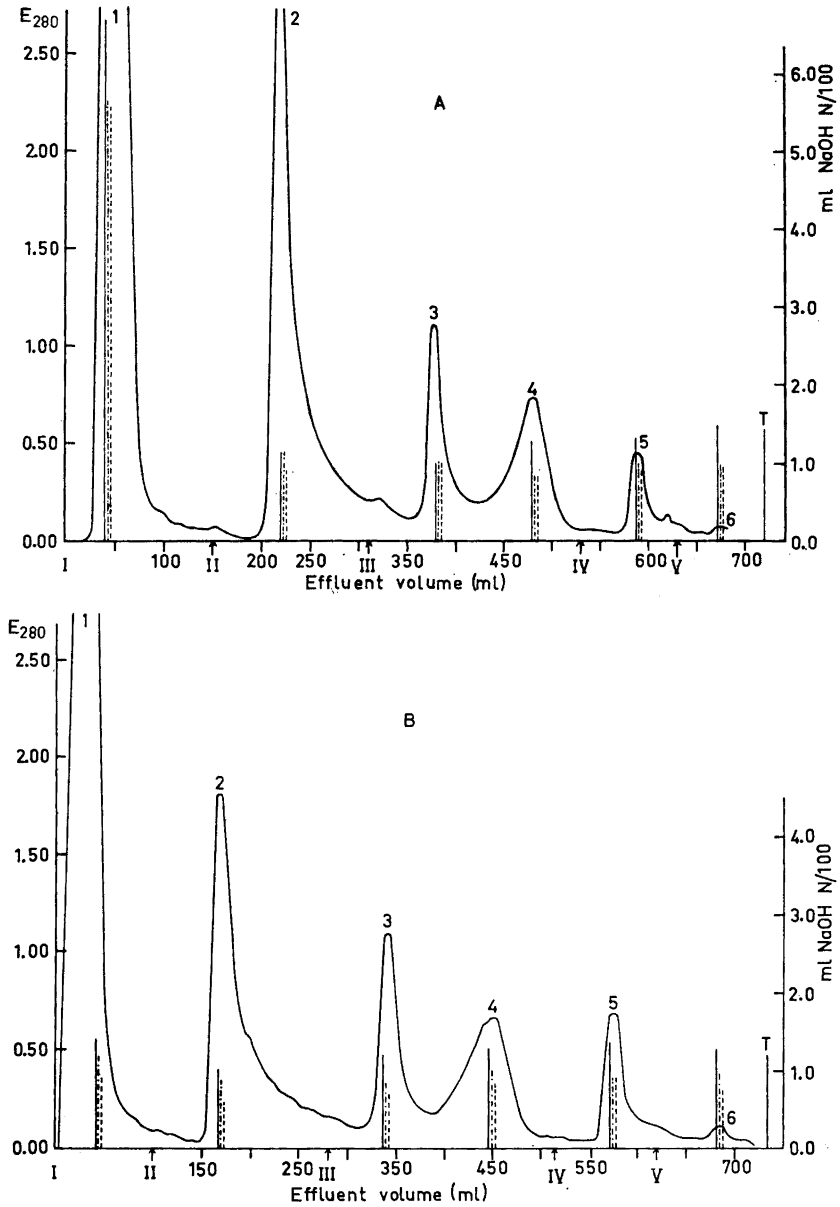

Fig. 3 A—B. TAMe-esterase activity and trypsin-inhibiting ability in a series of chromatographic fractions of human serum. A, Untreated serum; B, Inactivated serum, *i.e.* kept at 56°C for 30 min. Column, DEAE-Sephadex in phosphate buffer, pH 6.6. Elution as in Fig. 1. Full lines, TAMe-esterase activity of fractions in the presence of trypsin; broken lines, TAMe-esterase activity in the presence of cysteine; dashed and dotted lines, TAMe-esterase activity of fraction only. T = TAMe-esterase activity of trypsin alone. The activity was measured in phosphate buffer at pH 6.6 and expressed in ml NaOH consumed.

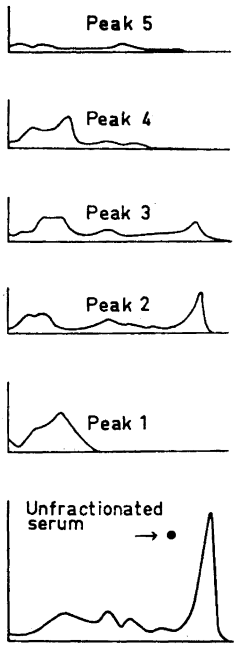

Fig. 4. Electrophoretic diagram of unfractionated serum and of peaks 1—5 in Fig. 2. These fractions are comparable, respectively, with peaks 1 and 3—6 in Fig. 1. Paper electrophoresis in "S:t Eriks" buffer pH 8.6, ionic strength 0.1, 300 V, 12 mA, for 17 h. Protein dye: naphthalene black 12 B.

It may finally be mentioned in this section that unfractionated normal serum and samples corresponding to the five main peaks in the chromatographic separation of the normal serum were taken out for paper electrophoresis. The results are shown in Fig. 4. It can be concluded from this figure that albumin is present in peaks 2 and 3 but not in noticeable quantities in peaks 1, 4, and 5.

DISCUSSION

A comparison between gelatin and TAMe as substrates for the chromatographic fractions might be of interest both concerning the original proteolytic activity of the fractions and the activity of mixtures of trypsin and the fractions. When gelatin is used as substrate and the activity is measured at pH 7.2, trypsin inhibition occurs in several peaks (Fig. 1). When, however, TAMe is used as substrate and the activity is measured at pH 7.9, an apparent inhibition of trypsin occurs only in the second peak (Fig. 2). When the activity is measured at pH 6.6, there is an apparent trypsin inhibition in all the fractions investigated (Fig. 3 A—B).

The influence of serum fractions on trypsin, as shown in Fig. 1, reveals the complete separation of two trypsin inhibitors by the chromatographic procedure since there is a complete inhibition of the trypsin activity in peak 1, no inhibition or only a slight increase in activity in peak 2, and again a complete inactivation in peak 3. The existence of two trypsin inhibitors in serum

has been demonstrated and reviewed by Jacobsson [9]. The increase in gelatin-splitting activity seen in peak 6, Fig. 1, and of TAMe-esterase activity in the presence of trypsin as shown in peak 1, Fig. 2, seems to be due to the well-known ability of trypsin to activate proenzymes as reported by several authors: for trypsinogen and chymotrypsinogen by Northrop and Kunitz [10], far plasminogen by Alkjaerrig *et al.*[11], and for prothrombin by Schultze and Schwick [12]. The intravenous injection of trypsin in rabbits resulted in the circulation of a measurable TAMe-esterase activity for a short time [13].

The influence of cysteine upon the TAMe-esterase activity, as shown in Fig. 2, reveals a slight activation in the first peak. The activation decreases continuously in the subsequent peak fractions. Since none of the proteolytic enzymes of serum with esterase activity (*i.e.* plasmin and thrombin) needs sulfhydryl groups for its activity, complement components might be involved. It has been reported by Pillemer, Lepow and coworkers [14,15] and Becker [5] that the complement factor C'1 is a TAMe-esterase and it was shown by Cushman, Becker and Wirtz [16] that sulfhydryl compounds inhibit immune hemolysis.

The strong esterase activity found in untreated serum (peak 1, Fig. 3 A) was greatly reduced when the serum was "inactivated" (peak 1, Fig. 3 B). It has been long known that the complement factors C'1 and C'2 are completely inactivated when serum is kept at 56°C for 30 min.

Now the question arises about the role of thrombin and plasmin in this connection. It seems unlikely that the activity in peak 1, Fig. 3 A, should be derived from thrombin since calcium was not added but is necessary in higher concentrations than in normal serum for the conversion of prothrombin to thrombin. Furthermore no α_2-β-globulin is present in this fraction (peak 1) as can be seen in Fig. 4. As regards plasmin the activation by trypsin seen in Fig. 1 is localized in peak 6 and is probably derived from activated plasminogen. The heat-labile TAMe-esterase in peak 1, Fig. 3, cannot belong to the plasmin system since the plasmin system is much more heat stable according to Troll and Sherry [17]. It thus seems reasonable to assume that part of the TAMe-esterase activity in peak 1 may be derived from the complement factor C'1.

Acknowledgements. The author wishes to express his thanks to Dr. E. Hultin for valuable discussions and to Mrs. E. von Zeipel, Miss I. Augustsson, Mr. H. Ryttman and Mr. I. Eriksson for skilful technical assistance.

REFERENCES

1. Lundblad, G. *Acta Chem. Scand.* **15** (1961) 212.
2. Porath, J. and Flodin, P. *Nature* **183** (1959) 1657.
3. Schwert, G. W., Neurath, H., Kaufman, S. and Snoke, J. E. *J. Biol. Chem.* **172** (1948) 221.
4. Sherry, S. and Troll, W. *J. Biol. Chem.* **208** (1954) 95.
5. Becker, E. L. *J. Immunol.* **77** (1956) 469.
6. Hultin, E. *Svensk Kem. Tidskr.* **58** (1946) 281.
7. Hultin, E. *Svensk Kem. Tidskr.* **60** (1948) 40.
8. Hultin, E. and Lundblad, G. *Acta Chem. Scand.* **9** (1955) 1610.
9. Jacobsson, K. *Scand. J. Clin. Lab. Invest.* **7** (1955) Suppl. 14, p. 55—102.
10. Northrop, J. H., Kunitz, M. and Herriot, R. M. *Crystalline Enzymes*, 2nd ed. New York 1948.

11. Alkjaerrig, N., Fletcher, A. P. and Sherry, S. *J. Biol. Chem.* **233** (1958) 86.
12. Schultze, H. E. and Schwick, G. *Z. physiol. Chem. Hoppe-Seyler's* **289** (1951) 26.
13. Bastian, J. W., Hill, R. G. and Ercoli, N. *Proc. Soc. Exptl. Biol. Med* **92** (1956) 800.
14. Lepow, I. H., Ratnoff, O. D., Rosen, F. S. and Pillemer, L. *Proc. Soc. Exptl. Biol. Med.* **92** (1956) 32.
15. Lepow, I. H., Ratnoff, O. D. and Pillemer, L. *Proc. Soc. Exptl. Biol. Med* **92** (1956) 111.
16. Cushman, W. F., Becker, E. L. and Wirtz, G. *J. Immunol.* **79** (1957) 80.
17. Troll, W. and Sherry, S. *J. Biol. Chem.* **213** (1955) 881.

Received November 21, 1961.

ACTA CHEMICA SCANDINAVICA 16 (1962) 983–991

Studies on the Hydrolysis of Metal Ions

39. The Hydrolysis of Pb^{2+} in $Mg(ClO_4)_2$ and $Ba(ClO_4)_2$ Medium

LECH PAJDOWSKI* and ÅKE OLIN

Department of Inorganic Chemistry, Royal Institute of Technology, Stockholm 70, Sweden

The hydrolysis of Pb^{2+} in 1.5 M $Mg(ClO_4)_2$ or $Ba(ClO_4)_2$ has been studied by emf methods. In both media the hydrolysis products Pb_2OH^{3+} and $Pb_4(OH)_4^{4+}$ have been identified. These complexes have also been found in a previous investigation [1] with 3 M $NaClO_4$ as salt back-ground. From an analysis of the results at high concentrations of Pb^{2+} it is inferred that the self-medium method of Hietanen and Sillén [2] can yield reliable results in a region where as much as up to 10 % of the free metal ions have been changed to hydrolysis products.

The hydrolysis products of many metal ions have been identified in dilute solution by emf methods [3]. The measurements have been made with solutions containing a high salt back-ground, usually 3 M $NaClO_4$. In such solutions the activity factors vary but little, which is a necessary condition for the successful identification of the complexes formed.

When a metal ion forms polynuclear hydrolysis products, the relative amounts of the species formed will depend both on the total concentration of the metal ion, B, and on the concentration of hydrogen ion, h. It is therefore possible that in concentrated solutions of the metal salt new complexes appear, whose concentrations at low B are so small that they cannot be identified.

The self-medium method proposed by Hietanen and Sillén [2] can be used to identify the hydrolysis products at high values of B. However, from such studies, reliable results can be expected only from measurements with small ranges in Z, since otherwise the variation in the composition of the solutions and hence in the activity factors, may become so large that it will interfere with the interpretation of the data.

Self-medium studies [1,4] on Be^{2+} and Pb^{2+} in 3 M $(Na)ClO_4$ medium have indicated that reliable results can be obtained if the investigation is confined to the Z range $0 < Z < 0.1$. The species identified were Be^{2+}, Be_2OH^{3+} and $Be_3(OH)_3^{3+}$, and Pb^{2+}, Pb_2OH^{3+} and $Pb_4(OH)_4^{4+}$. For higher values of Z, deviations occurred between the experimental data (Z, log h) and those calculated on the assumption that the above-mentioned complexes were

* Present address: Department of Inorganic Chemistry, University of Wroclaw, Poland.

formed. Two possible explanations for this were suggested; the formation of other complexes, or the variation of activity factors.

The present investigation was undertaken in an effort to obtain more information on this point. If substantial changes are found in the shapes of the curves $Z(\log h)_B$ with different media it appears reasonable to ascribe the cause of the deviation to changes in the activity factors and not to new complexes. It should, however, be observed that we can not choose unequivocally between the two hypotheses. The Pb^{2+} ion was used in this study, since $Pb(ClO_4)_2$ solutions are easy to analyse for their analytical hydrogen ion excess, which is essential if accurate values of Z are to be obtained. As salt back-grounds $Mg(ClO_4)_2$ and $Ba(ClO_4)_2$ have been used.

SYMBOLS

B = total metal ion concentration; b = free metal ion concentration; H = analytical hydrogen ion excess (often negative); h = free hydrogen ion concentration; Z = average number of OH^- bound per metal ion (= $(h-H)/B$); $\beta_{p,q}$ = equilibrium constant of the reaction $pA + qB \rightleftharpoons A_pB_q$; $y(x)_v = y$ as a function of x at constant v.

Concentrations are expressed in moles/l (M) and equilibrium constants are given on the M-scale.

MATERIALS AND ANALYSES

Magnesium and barium perchlorate were prepared by reacting $MgCO_3$ and $Ba(OH)_2$ (Merck p.a.) with $HClO_4$ (Kebo p.a.). The products were twice recrystallized from water. The stock solutions of $Mg(ClO_4)_2$ and $Ba(ClO_4)_2$ were analysed by evaporating known quantities with H_2SO_4 and weighing the residues as $MgSO_4$ and $BaSO_4$. The neutrality of these solutions was checked potentiometrically as described in Ref.[5]

The "basic" lead perchlorate stock solution was prepared from PbO (Baker p.a.), which had been repeatedly washed with distilled water, and perchloric acid. An excess of the oxide was used and the mixture of oxide and solution was allowed to stand for a couple of days in order to precipitate foreign metal ions. The solution was then filtered and traces of tetravalent lead removed by bubbling H_2 through the solution using platinum black as a catalyst. Finally the solution was filtered in a N_2 atmosphere and then stored and handled under the same gas. The Pb^{2+} concentration in this solution was found by precipitating lead as $PbSO_4$ and the analytical hydrogen ion excess, which is a negative quantity in this solution, was determined potentiometrically using Gran's [6] method to obtain the equivalence point.

The "neutral" lead perchlorate solution was prepared from stoichiometric amounts of PbO and $HClO_4$. It was analysed in the same way as the "basic" lead perchlorate solution.

EXPERIMENTAL

The experiments were carried out as potentiometric titrations, at 25.0 °C, in an oil thermostat. The hydrogen ion concentration, h, was measured with a calibrated glass electrode and using the cell

glass electrode/equilibrium solution/Ref. (I)

Assuming the activity factors to be constant the emf of cell (I) can be written

$$E = E^\circ - 59.15 \log h - E_j \quad (1)$$

The equilibrium solutions had the following composition

$$B\,\mathrm{M}\,Pb^{2+},\ H\,\mathrm{M}\,H^+,\ (3-2B-H)/2\,\mathrm{M}\ (Mg^{2+},\ Ba^{2+}),\ 3\ \mathrm{M}\ ClO_4^-$$

and the reference half-cell used was

1.5 M (Mg^{2+}, Ba^{2+}) $(ClO_4)_2$/3 M ClO_4^-, 1.495 M (Mg^{2+}, Ba^{2+}), 0.01 M Ag^+/AgCl, Ag (II)

In each experiment B and $[ClO_4^-]$ = 3 M were kept constant and H was varied by the addition of a hydrolysed lead perchlorate solution or by the addition of $HClO_4$. The emf of cell (I) was measured with a Radiometer valve potentiometer (PHM 4) to ± 0.2 mV.

Titration procedure. Two different titration procedures were used depending on the value of B. With B = 0.05 M and 0.1 M three solutions were used, each 3 M in ClO_4^- by addition of the ionic medium;

S_1: The "starting" solution, containing B M $Pb(ClO_4)_2$
S_2: The "basic" solution, containing B M $PbOHClO_4$
S_3: The "acid" solution, containing B M $Pb(ClO_4)_2$ and H M $HClO_4$

Solution S_3, V ml, was gradually added from a buret to a known volume, V_0 ml, of the "starting" solution, S_1, and the emf of cell(I) was measured after each addition ("basic titration"). When the desired volume of S_2 had been added, then solution S_3 was introduced in order to give values of H between 0.005 and 0.025 M ("acid titration").

The values of E measured in the acid titration were used to determine the analytical hydrogen ion concentration (H_b) in the basic lead solution, S_2, by Gran's method [6]. H was then calculated from the analytical data for each point in the acid titration and $E°$ determined from a plot of $E' = E + 59.15 \log H$ *versus* H. The straight line (E + 59.15 log H) (H) was extrapolated to $H = 0$ to give $E°$ (Ref.[7]).

With $E°$ known from the acid titration log h, H and Z in the basic titration can be calculated from

$$\log h = (E° - E)/59.15 \quad (2)$$

$$H = H_b V/(V_0 + V) \quad (3)$$

$$Z = (h - H)/B \quad (4)$$

At the higher Pb^{2+} concentrations, $B \geq 0.25$ M, only two solutions were used. To the starting solution, V_0 ml, containing B M $Pb(ClO_4)_2$ and a known amount of $HClO_4$ (*ca.* 0.025 M), V ml of basic lead solution, S_2, were added from a buret. The first few points in the acid solution were used to determine the analytical hydrogen ion excess in S_2 and $E°$. Two basic solutions were employed. One solution had a OH^-/ClO_4^- ratio equal to 1 and the other had a lower OH^-/ClO_4^- ratio so that accurate results could be obtained at low Z. In these titrations log h was found from eqn. (2) and H from

$$H = H_b(V - V_e)/(V_0 + V) \quad (5)$$

where V_e denotes the equivalence point from the Gran extrapolation. Z was calculated from eqn. (4).

All solutions were carefully protected against CO_2 and were mixed and handled under a N_2 atmosphere. If severe precautions were not taken and CO_2 came into contact with the solution this resulted in the precipitation of lead hydroxide carbonates.

RESULTS AND CALCULATIONS

The experimental data, Z and log h, are presented in Fig. 1 and Table 1. With $Ba(ClO_4)_2$ as medium the following values of B were used; B = 0.05, 0.1, 0.25, 0.5, 1, and 1.45 M. With $Mg(ClO_4)_2$ titrations with B = 0.05, 0.5, 1, and 1.45 M were made. Two titrations with $NaClO_4$ as medium were performed also and they agreed within 0.3 mV with previously published titrations [1], where NaOH was used as the base, and are therefore not included in Table 1.

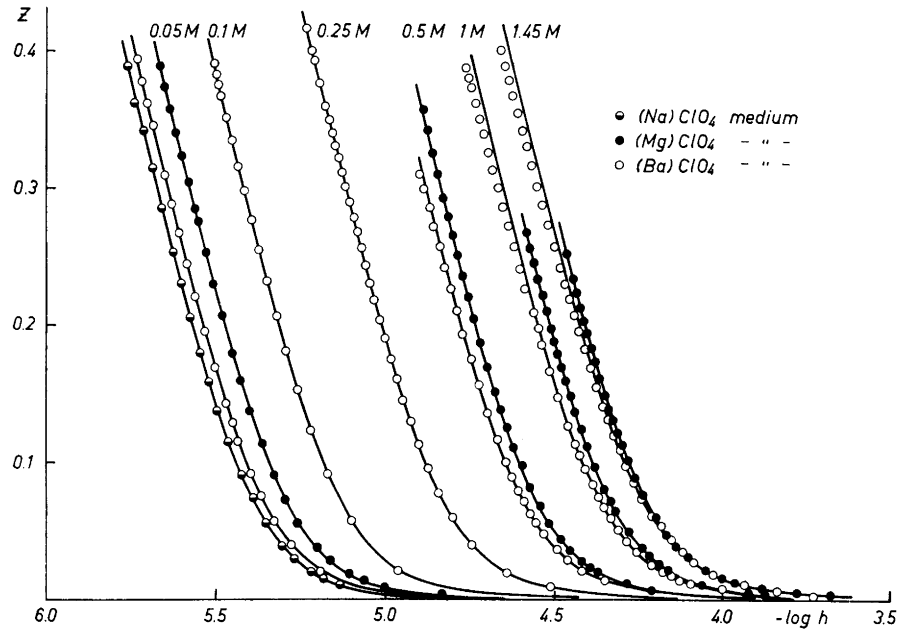

Fig. 1. Z, average number of OH^- bound per Pb(II) atom as a function of log h. Drawn curves have been calculated with the equilibrium constants given in the text.

From the data we observe that for $B \leq 0.25$ M the curves are parallel and considering the data with $Ba(ClO_4)_2$ medium only, $t = (\Delta \log B/\Delta \log h)_Z$ is found to be a constant $= 1.33 \pm 0.02$.

From the data with $B \geq 0.5$ M it is found that the shifts between the curves $Z(\log h)_B$ for the different media tend to diminish as B increases. This is particularly obvious with $B = 1.45$ M for $Z < 0.05$. In this range the curves coincide. This is of course due to the fact the compositions of the solutions tend to become the same, namely $Pb(ClO_4)_2$, as B increases and Z decreases. As Z increases the curves $Z(\log h)_B$ in the three media become separate and the values of $l = |(\Delta Z/\Delta \log h)_B|$ for a given value of Z, always follow the order l (in $NaClO_4$) $< l$ (in $Ba(ClO_4)_2$) $< l$ (in $Mg(ClO_4)_2$).

IDENTIFICATION OF THE COMPLEXES FORMED AT $B \leq 0.25$ M.

As stated above the value of $(\Delta \log B/\Delta \log h)_Z = 1.33 \pm 0.02$ for $B \leq 0.25$ M in 1.5 M $Ba(ClO_4)_2$ medium. The composition of the complexes formed can then, according to Sillén [8], be written $Pb(Pb(OH)_{4/3})_n^{(2+2n/3)+}$. Conceivable values of n are obtained from the relation $n = 3\,m$ with $m = 1, 2, 3$ -- - -. With $n = 3$, which means that the complex $Pb_4(OH)_4^{4+}$ is formed, an excellent fit was found between the experimental curves $Z(\log h)_B$ and the "normalized" curve for the formation of $Pb_4(OH)_4^{4+}$. The formation of $Pb_4(OH)_4^{4+}$. was

Table 1. Corresponding values of $-\log h$ and Z.

$Ba(ClO_4)_2$ medium

$B = 0.05$ M. $-\log h$, Z; 5.166, 0.015; 5.193, 0.019; 5.243, 0.029; 5.279, 0.038; 5.330, 0.056; 5.368, 0.074; 5.397, 0.091; 5.438, 0.115; 5.470, 0.142; 5.505, 0.168; 5.532, 0.195; 5.560, 0.220; 5.585, 0.244; 5.607, 0.267; 5.627, 0.288; 5.649, 0.308; 5.668, 0.327; 5.685, 0.345; 5.701, 0.362; 5.717, 0.378; 5.729, 0.394.
$B = 0.1$ M. $-\log h$, Z; 4.959, 0.019; 5.101, 0.056; 5.171, 0.090; 5.220, 0.122; 5.260, 0.152; 5.293, 0.180; 5.321, 0.206; 5.348, 0.231; 5.370, 0.254; 5.392, 0.275; 5.414, 0.296; 5.433, 0.315; 5.451, 0.334; 5.468, 0.351; 5.484, 0.367; 5.490, 0.375; 5.497, 0.383; 5.506, 0.391.
$B = 0.25$ M. $-\log h$, Z; 4.638, 0.018; 4.743, 0.038; 4.843, 0.077; 4.902, 0.112; 4.948, 0.145; 4.985, 0.175; 5.017, 0.204; 5.032, 0.217; 5.047, 0.230; 5.069, 0.255; 5.093, 0.278; 5.118, 0.300; 5.137, 0.321; 5.155, 0.340; 5.174, 0.359; 5.191, 0.376; 5.206, 0.393; 5.218, 0.405; 5.230, 0.416
$B = 0.5$ M. $-\log h$, Z; 4.178, 0.004; 4.347, 0.013; 4.459, 0.028; 4.516, 0.042; 4.554, 0.055; 4.582, 0.067; 4.604, 0.078; 4.623, 0.088; 4.642, 0.099; 4.670, 0.115; 4.699, 0.135; 4.726, 0.155; 4.748, 0.174; 4.772, 0.192; 4.790, 0.209; 4.809, 0.225; 4.826, 0.241; 4.841, 0.256; 4.858, 0.271; 4.871, 0.285; 4.887, 0.298; 4.900, 0.310.
$B = 1$ M. $-\log h$, Z; 3.967, 0.005; 4.089, 0.012; 4.150, 0.017; 4.197, 0.023; 4.229, 0.029; 4.254, 0.034; 4.275, 0.040; 4.307, 0.049; 4.332, 0.058; 4.351, 0.067; 4.369, 0.075; 4.385, 0.083; 4.407, 0.094; 4.423, 0.104; 4.437, 0.113; 4.461, 0.125; 4.491, 0.146; 4.513, 0.165; 4.540, 0.184; 4.550, 0.196; 4.565, 0.208; 4.589, 0.225; 4.604, 0.241; 4.638, 0.271; 4.668, 0.299; 4.697, 0.325; 4.723, 0.349; 4.746, 0.372; 4.763, 0.386.
$B = 1.45$ M. $-\log h$, Z; 3.898, 0.008; 3.999, 0.015; 4.053, 0.022; 4.107, 0.031; 4.143, 0.040; 4.172, 0.048; 4.202, 0.056; 4.221, 0.064; 4.239, 0.071; 4.260, 0.080; 4.292, 0.096; 4.325, 0.117; 4.359, 0.141; 4.393, 0.168; 4.427, 0.194; 4.456, 0.218; 4.483, 0.241; 4.520, 0.272; 4.552, 0.301; 4.582, 0.329; 4.609, 0.354; 4.636, 0.377; 4.660, 0.399; 4.674, 0.413.

$Mg(ClO_4)_2$ medium

$B = 0.05$ M. $-\log h$, Z; 4.831, 0.004; 4.990, 0.009; 5.061, 0.014; 5.103, 0.018; 5.159, 0.028; 5.201, 0.037; 5.259, 0.055; 5.297, 0.073; 5.328, 0.089; 5.365, 0.113; 5.399, 0.136; 5.428, 0.158; 5.453, 0.179; 5.480, 0.205; 5.507, 0.229; 5.527, 0.252; 5.549, 0.274; 5.560, 0.284; 5.578, 0.304; 5.600, 0.323; 5.617, 0.340; 5.634, 0.357; 5.649, 0.373; 5.663, 0.388.
$B = 0.5$ M. $-\log h$, Z; 3.987, 0.002; 4.207, 0.006; 4.283, 0.010; 4.332, 0.015; 4.369, 0.019; 4.393, 0.023; 4.452, 0.035; 4.481, 0.043; 4.542, 0.067; 4.596, 0.096; 4.640, 0.124; 4.677, 0.150; 4.719, 0.186; 4.756, 0.219; 4.787, 0.250; 4.816, 0.278; 4.846, 0.309; 4.875, 0.341.
$B = 1$ M. $-\log h$, Z; 3.727, 0.002; 3.920, 0.005; 4.004, 0.008; 4.094, 0.013; 4.160, 0.021; 4.216, 0.031; 4.268, 0.045; 4.352, 0.080; 4.403, 0.110; 4.439, 0.135; 4.469, 0.158; 4.493, 0.178; 4.520, 0.204; 4.537, 0.221; 4.562, 0.245; 4.584, 0.266.
$B = 1.45$ M. $-\log h$, Z; 3.276, 0.001; 3.600, 0.002; 3.737, 0.004; 3.839, 0.006; 3.935, 0.010; 4.008, 0.016; 4.067, 0.023; 4.100, 0.030; 4.131, 0.038; 4.167, 0.049; 4.195, 0.059; 4.236, 0.075; 4.281, 0.100; 4.314, 0.120; 4.339, 0.138; 4.366, 0.160; 4.391, 0.182; 4.413, 0.202; 4.435, 0.223; 4.466, 0.251.

confirmed by the "integration method" derived by Sillén [9]. This method gave invariant values of $\bar{p}$ and $\bar{q} = 4$. $\bar{p}$ and $\bar{q}$ are the average values of p and q of the complexes $Pb_q(OH)_p^{(2q-p)+}$ formed. The formation of $Pb_4(OH)_4^{4+}$ in 1.5 M $Ba(ClO_4)_2$ is thus well established. The same complex has also been found in 3 M $NaClO_4$ medium. In 1.5 M $Mg(ClO_4)_2$ it is also likely that the same complex is formed to judge from the good agreement between the experi-

mental $Z(\log h)$ curve for $B = 0.05$ M and the normalized curve. This conclusion is confirmed by the results from the titrations with $B \geq 0.5$ M in this medium.

With $B = 0.05$ M, measurements have been made with all the three media and we observe three $Z(\log h)$ curves which are parallel along the log h axis. The shifts between the curves can be understood, if the activity factors stay constant in each medium but are different from one medium to another.

IDENTIFICATION OF THE COMPLEXES FORMED AT $B \geq 0.5$ M

Whereas for $B \leq 0.25$ M the formation of the complex $Pb_4(OH)_4^{4+}$ can explain the experimental data, additional complexes must be present for $B \geq 0.5$ M at low values of Z. This is indicated by the fact that $(\Delta \log B/\Delta \log h)_Z$ at low Z is no longer 1.33 but tends to diminish with increasing B and that the curves $Z(\log h)_B$ fall off to zero less rapidly than required for "$-(OH)_4$" complexes.

The values of p and q of the complexes formed at low Z, $Pb_q(OH)_p^{(2q-p)+}$, can be estimated from the relations $p = -(\Delta \log Z/\Delta \log h)_B$ and $q = (\Delta \log Z/\Delta \log B)_h + 1$, as described in Ref.[1] When the present data for $0 < Z < 0.01$ were treated as described there, they yielded $p = 1$ and $q = 2$. The new complex formed at low Z would then be Pb_2OH^{3+}. The "integration method" was next applied to all the data and an example of the results is shown in Fig. 2. From this graph we may conclude that the main complexes formed are Pb_2OH^{3+} and $Pb_4(OH)_4^{4+}$. It is thus established that in $NaClO_4$, $Mg(ClO_4)_2$ and $Ba(ClO_4)_2$ medium the main hydrolysis products are the same.

DETERMINATION OF THE EQUILIBRIUM CONSTANTS

From the data with $B \leq 0.25$ M only the equilibrium constant for the formation of $Pb_4(OH)_4^{4+}$

$$4\ Pb^{2+} + 4\ H_2O \rightleftharpoons Pb_4(OH)_4^{4+} + 4\ H^+ \tag{6}$$

$$\beta_{4,4} = [Pb_4(OH)_4^{4+}]\ h^4/b^4 \tag{6a}$$

can be determined, since the concentration of Pb_2OH^{3+} is so small. The determination of $\beta_{4,4}$ has been made by graphical methods using a "normalized" curve, which can be derived from the two basic equations

$$B = b + 4[Pb_4(OH)_4^{4+}] \tag{7}$$

$$BZ = h - H = 4[Pb_4(OH)_4^{4+}] \tag{8}$$

If b is eliminated we obtain

$$X = \log h - 0.25 \log (4\beta_{4,4}B^3) = \log (1-Z) - 0.25 \log Z \tag{9}$$

In position of best fit between the normalized curve $Z(X)$ and the experimental curve $Z(\log h)_B$ the difference between the coordinates on the X- and log h-axes $= -0.25 \log(4\beta_{4,4}B^3)$ which is used to find $\beta_{4,4}$. The values of log $\beta_{4,4}$ so obtained are given below.

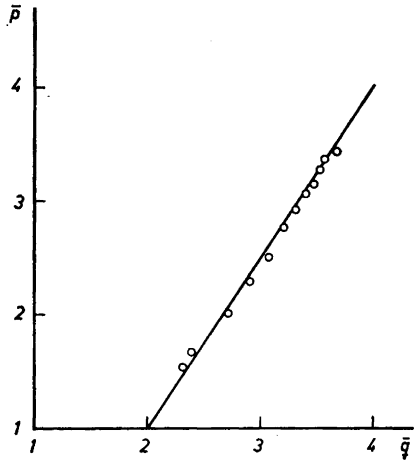

Fig. 2. $\bar{p}$ versus $\bar{q}$ for B = 1 M. The straight line passes through (2,1) and (4,4).

$Ba(ClO_4)_2$: $\log \beta_{4,4} = -19.16 \pm 0.05$ (B = 0.05, 0.1 and 0.25 M)

$Mg(ClO_4)_2$: $\log \beta_{4,4} = -18.90 \pm 0.05$ (B = 0.05 M)

For $B \geq 0.5$ M the complexes Pb_2OH^{3+} and $Pb_4(OH)_4^{4+}$ have definitely been identified. The determination of the equilibrium constants $\beta_{1,2}$ and $\beta_{4,4}$ was therefore started on the assumption that only these two complexes were formed. The agreement between the calculated and experimental $Z(\log h)_B$ curves will then show if this hypothesis is correct or has to be modified.

A first set of values of $\beta_{1,2}$ and $\beta_{4,4}$ (necessary for further calculations with electronic computer programs) was obtained as follows

$$BZ = \beta_{1,2}b^2h^{-1} + 4\beta_{4,4}b^4h^{-4} \quad (10)$$

In this expression b is approximated with

$$b = B(1-2Z) \text{ for } Z < 0.01 \text{ and } b = B(1-Z) \text{ for } Z > 0.01 \quad (11a), (11b)$$

Inserting these values for b in eqn. (10) and rearranging we obtain for $Z < 0.01$

$$Zh/(1-2Z)^2 = B\beta_{1,2} + 4\beta_{4,4}B^3(1-2Z)^2h^{-3} \quad (12a)$$

and for $Z > 0.01$

$$Zh/(1-Z)^2 = B\beta_{1,2} + 4\beta_{4,4}B^3(1-Z)^2h^{-3} \quad (12b)$$

The plots of eqn. (12a), (12b) for the data with $Mg(ClO_4)_2$ medium were straight lines as required by the hypothesis. With $Ba(ClO_4)_2$ medium, however, the lines were curved for $Z > (0.1-0.2)$, the actual value of Z being somewhat dependent on the value of B.

The equilibrium constants found from the plots were used as first approximations in the final adjustment of the constants. This adjustment was done by means of the computer program LETAGROP [10]. The best set of constants found with this program is that, which makes $\Sigma(Z_{exp} - Z_{calc})^2$ a minimum. The following values of the equilibrium constants were obtained for the Z

ranges given in the table. The limits of error given in the log β are three times the standard deviation.

B	$Mg(ClO_4)_2$	Z	$Ba(ClO_4)_2$	Z
0.5 M	$\log \beta_{1,2} = -6.49 \pm 0.09$	<0.3	-6.30 ± 0.2	<0.26
	$\log \beta_{4,4} = -18.949 \pm 0.003$		-19.12 ± 0.02	
1 M	$\log \beta_{1,2} = -6.57 \pm 0.09$	<0.25	-6.39 ± 0.06	<0.12
	$\log \beta_{4,4} = -18.978 \pm 0.003$		-19.11 ± 0.01	
1.45 M	$\log \beta_{1,2} = -6.45 \pm 0.06$	<0.25	-6.24 ± 0.06	<0.12
	$\log \beta_{4,4} = -19.045 \pm 0.003$		-19.12 ± 0.02	

DISCUSSION

With $B = 1.45$ M the two media are almost identical and we should therefore expect the β also to be the same. The fact that two different sets of β are obtained arises from the principle used in selecting the best values of β, namely to find the values of β which reproduce the experimental Z values over as broad a Z range as possible with the restriction that $|Z_{exp} - Z_{calc}|$ should not exceed 0.002 systematically in any part of the range. The standard deviation in Z is less than 0.001 for the data in the table. If the calculations on the $Ba(ClO_4)_2$ data are restricted to the range $Z < 0.05$, values of β are obtained which are closer to the β values with $Mg(ClO_4)_2$ medium. The same is true of the older data with $NaClO_4$ medium for $B = 1.49$ M. We should like here to correct the values given in Ref.[1] for $B = 1.49$ M. Calculations with the program LETAGROP give the new values $\log \beta_{1,2} = -6.30 \pm 0.09$ and $\log \beta_{4,4} = -19.19 \pm 0.02$ ($Z < 0.1$). The values of the equilibrium constants must, however, be regarded as a kind of "average" values in the Z range used in the calculations.

With the $Mg(ClO_4)_2$ data there is very good agreement between the calulated and experimental data whereas the deviation found with $Ba(ClO_4)_2$ would call for additional complexes for the higher values of Z. Let us assume that the activity factors stay constant in a titration and limit the discussion to the titrations with $B = 1.45$ M. The values of the β would then be nearly the same. The differences between the $Z(\log h)$ curves with $NaClO_4$ and $Ba(ClO_4)_2$ and that with $Mg(ClO_4)_2$ suggest that the amount of the unknown species with $Ba(ClO_4)_2$ would be ca. 10 % and with $NaClO_4$ *ca.* 20 % of the total amount of lead hydrolysed. Since there is no evidence of these unknown species in $Mg(ClO_4)_2$ one would estimate that the equilibrium constants of the unknown species would be less by a factor of 10 in $Mg(ClO_4)_2$ as compared with the other two media. This, however, seems very unlikely from the approximate constancy of the values of the $\beta_{4,4}$ and $\beta_{1,2}$.

The deviations are the larger the larger is the value of B. This would require that the unknown complexes have a ratio $OH^-/Pb(II) < 1$ (Ref.[2]). Conceivable complexes of this type, *e.g.* $Pb_4(OH)_3^{5+}$, have values of t smaller than the

experimental value 1.33. The relative positions of the $Z(\log h)_B$ curves along the log h axis do not therefore support the hypothesis that additional complexes are formed.

Since the assumption of constant activity factors leads to a contradiction with the experimental results we may conclude that the deviations are due to variations of the activity factors, which at $Z \approx 0.1$ have become so large as to interfere with the interpretation of the data. If mixed complexes between the cation of the medium and Pb^{2+} and OH^- are formed these complexes will, of course, interfere with the interpretation of the data in the self-medium range. It is, however, unlikely that such complexes are formed since $\beta_{4,4}$ is found to be virtually constant despite changes in the medium and in addition the tendency for Ba^{2+} and Mg^{2+} to associate with OH^- is very weak [11,12].

The inference on the self-medium method which can be drawn from this work would then be that reliable conclusions can be drawn only from the range where $Z \lessapprox 0.05$ with $B > 1$ M. Of course the limit set can claim no general validity but may vary greatly from one system to another as shown by the combination $Pb(ClO_4)_2 + Mg(ClO_4)_2$, where good results are obtained at least up to $Z = 0.25$.

If "finger-prints" of the complexes could be obtained the question whether new complexes are formed or not could be settled. Unfortunately this does not seem possible at present. The Raman spectra of dilute solutions are not sufficiently intense and good infrared spectra are difficult to obtain because of the strong absorption of the water itself.

The same question again arises when attempts are made to determine the structure of complexes in solution by means of X-ray diffraction. Such studies are made with concentrated solutions and the interpretation of the X-ray data is probably best made by correlating such data with a knowledge of the composition of the complexes, as inferred from emf work.

Acknowledgements. We wish to thank Professor Lars Gunnar Sillén for his continual interest in our work and Dr. Derek Lewis for having corrected the English of this paper. This work has been supported by *Statens Tekniska Forskningsråd (Swedish Technical Research Council)* and by a fellowship granted to one of us (L.P.) by *Svenska Institutet för Kulturellt Utbyte med Utlandet (Swedish Institute for Cultural Relations)*.

REFERENCES

1. Olin, Å. *Acta Chem. Scand.* **14** (1960) 814.
2. Hietanen, S. and Sillén, L. G. *Acta Chem. Scand.* **13** (1959) 533.
3. Sillén, L. G. *Quart. Revs. (London)* **13** (1959) 146.
4. Carell, B. and Olin Å. *Acta Chem. Scand.* **15** (1961) 1875.
5. Olin, Å. *Acta Chem. Scand.* **14** (1960) 126.
6. Gran, G. *Analyst* **77** (1952) 661.
7. Biedermann, G. and Sillén, L. G. *Arkiv Kemi* **5** (1953) 425.
8. Sillén, L. G. *Acta Chem. Scand.* **8** (1954) 299.
9. Sillén, L. G. *Acta Chem. Scand.* **16** (1962) 159.
10. Ingri, N. and Sillén, L. G. *Acta Chem. Scand.* **16** (1962) 173.
11. Carell, B. and Olin, Å. *Acta Chem. Scand.* **15** (1961) 727.
12. Stock, D. J. and Davies, C. W. *Trans. Faraday Soc.* **44** (1948) 856.

Received November 28, 1961.

ACTA CHEMICA SCANDINAVICA 16 (1962) 992–998

X-Ray Investigations of Mn_3P, Mn_2P, and Ni_2P

STIG RUNDQVIST

Institute of Chemistry, University of Uppsala, Uppsala, Sweden

The crystal structures of Mn_3P (Fe_3P type), Mn_2P and Ni_2P (revised *C* 22 type) have been refined by single-crystal methods. Both Mn_2P and Ni_2P have appreciable homogeneity ranges. X-Ray powder investigations in the Mn—P system indicate that the existence of the phase described as Mn_3P_2 is doubtful.

The crystal structures of transition metal phosphides with the compositions Me_3P and Me_2P have been the subject of earlier investigations by the author [1–5] in order to provide material for detailed crystal-chemical comparisons within this group of compounds. In the present paper, accurate structure determinations of Mn_3P, Mn_2P, and Ni_2P are reported. In addition, some phase-analytical data for the Mn—P system are presented and discussed.

EXPERIMENTAL

Preparation. The starting materials for the preparations were electrolytic manganese (AB Ferrolegeringar, Stockholm, claimed purity higher than 99.9 %), nickel rods, spectrographically standardized (Johnson, Matthey & Co, Ltd., London), and red phosphorus (purity higher than 99 %). Master alloys were prepared by dropping pellets of red phosphorus into molten metal, contained in crucibles of pure alumina (Degussit Al 23 from Degussa, Frankfurt, Germany). The melting was done by induction heating under a purified argon atmosphere. Alloys of various compositions were made by mixing portions of the crushed master alloys and heating in evacuated and sealed silica tubes. The nickel phosphides did not attack silica appreciably, even after very long heat-treatments. The manganese phosphides, however, attack silica, and the annealing time for manganese phosphides was therefore kept as short as possible.

X-Ray work. The phase analyses were performed by X-ray powder methods only. Powder photographs were recorded in Guinier-type focussing cameras with $CrKa_1$ radiation using silicon (a = 5.4305 Å) as the internal calibration standard. The accuracy of a single lattice parameter measurement is estimated to be 0.04 %, but lattice parameter differences larger than 0.02 % measured for the same phase in different alloys are probably significant.

Single-crystal fragments with roughly uniform cross-sections not exceeding 0.05 mm were selected from the crushed alloys. Weissenberg photographs were taken using zirconium-filtered Mo*K* radiation. The multiple-film technique, with thin iron foils between successive films, was used. The intensities were estimated visually by comparison with calibrated spots. Corrections for Lorentz and polarisation factors, Fourier series summa-

tions, structure factor calculations, and calculations of interatomic distances were made on the electronic digital computer BESK with programmes available at BESK. Atomic scattering factors were taken from tables given for manganese by Watson and Freeman [6], for nickel by Thomas and Umeda [7], and for phosphorus by Tomiie and Stam [8]. The real part of the dispersion correction for the scattering factors of the atoms as given by Dauben and Templeton [9] was inserted for each of the metal atoms in the structure factor calculations. Standard deviations for the atomic positions were estimated using Cruickshank's [10] equation. (List of observed and calculated structure factors can be obtained from this Institute on request).

THE MANGANESE — PHOSPHORUS SYSTEM

Earlier work on the Mn—P system is summarized by Hansen [11]. X-Ray investigations by Årstad and Nowotny [12] showed the existence of Mn_3P, Mn_2P and MnP. Thermal analytical, microscopic, and X-ray investigations by Berak and Heumann [13] confirmed the findings of Årstad and Nowotny, and in addition indicated the existence of Mn_3P_2.

In the present investigation, which is restricted to the range 0—50 atom % phosphorus, the only intermediate phases observed were Mn_3P, Mn_2P and MnP. Within the limits of experimental error, the lattice parameters of Mn_3P and MnP were unchanged in alloys with different compositions and heat-treatments. No appreciable lattice parameter variations for Mn_2P were observed in two-phase Mn_3P + Mn_2P alloys (see Table 1), but variations were observed in alloys containing more than 33 1/3 atom % phosphorus. In order to study this effect more closely, a special investigation of the Mn_2P—MnP part of the system was undertaken. Since the results differ from those obtained by Berak and Heumann, the work will be described in some detail.

A large number of alloys with the composition $Mn_{1.5}P$ were annealed in silica tubes at various temperatures between 800°C and 1090°C for periods varying from one hour to seven days, and subsequently cooled. The rate of cooling was found to have a marked influence on the final state of the samples, and three different methods of cooling the alloys from the annealing temperature to room temperature were therefore used:(1) cooling in air (room temperature attained in 5—10 min), (2) dropping the alloys in water without breaking the silica capsules (room temperature in 10—20 sec), (3) dropping the alloys in water and breaking the capsules (room temperature in less than 3 sec). The last method will be referred to as "rapid quenching" in the following text.

The X-ray powder photographs of all these alloys showed that the two phases Mn_2P and MnP alone were present. The MnP diffraction lines were invariably sharp, whereas the Mn_2P lines were more or less diffuse, depending on the cooling rate. The diffraction lines of Mn_2P were quite sharp for rapidly quenched alloys, which had been annealed

Table 1. Lattice parameters (in Å) of Mn_2P in two-phase Mn_3P + Mn_2P and Mn_2P + MnP alloys, quenched from various temperatures.

Temp. °C	Two-phase Mn_3P + Mn_2P alloys		Two-phase Mn_2P + MnP alloys	
	a	*c*	*a*	*c*
900	6.081	3.460	6.074	3.451
1000	6.081	3.460	6.068	3.446
1070	6.080	3.458	6.059	3.440

at temperatures below approximately 1060°C. The unit cell dimensions decreased progressively with increasing annealing temperature (see Table 1). The aircooled alloys gave rather diffuse Mn_2P lines. The unit cell dimensions were only slightly smaller than those obtained for Mn_2P in two-phase Mn_3P + Mn_2P alloys. The diffraction lines were generally very broad for alloys which had been quenched in water without breaking the silica capcules. In a few cases, two different sets of Mn_2P lines, one sharp and one diffuse, were discernible in the powder photographs of these alloys. For each sharp line, a corresponding diffuse line with a slightly smaller diffraction angle was observed. In some instances, a similar effect was also noticed for rapidly quenched alloys, which had been annelaed at temperatures above 1060°C.

All these observations consistently indicate that Mn_2P has a finite homogeneity range, the phosphorus-rich limit of which moves with increasing temperature towards the phosphorus-rich side of the diagram. MnP is precipitated during the cooling of $Mn_{1.5}P$ alloys, while the Mn_2P phase becomes more metal-rich. In rapidly quenched alloys, the secondary precipitation of MnP is negligible. The powder photographs of these alloys exhibit sharp Mn_2P lines. This indicates a well-crystallized condition of this phase, which has the phosphorus-rich limiting composition corresponding to the annealing temperature used. For lower rates of cooling, the secondary precipitation of MnP is appreciable. The broadening of the Mn_2P diffraction lines is attributable to coring effects. In extreme cases, the supercooling may produce the double set of Mn_2P lines referred to above. The set of sharp lines belongs to phosphorus-rich material retained un-decomposed on quenching, while the set of diffuse lines corresponds to more metal-rich Mn_2P which is formed at lower temperatures. The powder photographs exhibit all types of line intermediate between the extremes of very broad lines on the one hand and two separate sets on the other. There is therefore no reason to believe that the double set of lines indicates a two-phase region, in which equilibrium exists between two Mn_2P-type phases of different composition.

As mentioned above, the only phases observed in the range 33 1/3—50 atom % P are Mn_2P and MnP. This is in contrast to the report by Berak and Heumann [13] *(B & H)*, who claim the existence of an intermediate phase with the composition Mn_3P_2. This phase is stated to form peritectically at 1090°C (only 5°C above the eutectic temperature) and decompose eutectoidally at 1002°C. The failure to detect any Mn_3P_2 phase in the present investigation may be due to unsuccessful annealing and/or quenching techniques. It is felt, however, that the arguments presented by *B & H* for the existence of Mn_3P_2 are not convincing. An attempt to reconcile their observations with the present findings can be made as follows.

The thermal arrest at 1002°C observed by *B & H* (the somewhat scattered experimental points were obtained only on cooling) may be explained by thermal effects, possibly obscured by supercooling, which would accompany the secondary precipitation of MnP from the phosphorus-rich Mn_2P phase. The microscopic examination by *B & H* of an $Mn_{1.5}P$ alloy, quenched from 1080°C, showed a homogeneous phase together with traces of Mn_2P and MnP. The homogeneous phase, claimed to be the new Mn_3P_2 phase, may in fact have been phosphorus-rich Mn_2P, which had been retained undecomposed on quenching. The powder photograph of a further $Mn_{1.5}P$ alloy, quenched from 1080°C, was stated to contain new lines in addition to the Mn_2P pattern. Since the

authors do not claim any high accuracy for their X-ray measurements, and no X-ray data for the new phase were given, it is not unreasonable to believe that their powder photograph contained a double set of Mn_2P lines, possibly in addition to MnP lines. As mentioned before, powder photographs of this type have been obtained by the present author.

THE HOMOGENEITY RANGE OF Ni_2P

In a previous communication [14] on the nickel-phosphorus system the phase $Ni_{12}P_5$ was described. In the present investigation it was found that there exists a two-phase region $Ni_{12}P_5 + Ni_2P$ up to at least 1000°C. The lattice parameters of Ni_2P were measured in two-phase $Ni_{12}P_5 + Ni_2P$ alloys quenched from various temperatures up to 1000°C. The measured unit cell dimensions dit not show detectable variations and were $a = 5.865$ Å, $c = 3.387$ Å. These values are significantly larger than those obtained for the single-phase Ni_2P sample used for the single-crystal work (see below). The unit cell dimensions for Ni_2P in the last-mentioned sample were $a = 5.859$ Å, $c = 3.382$ Å. Ni_2P accordingly exhibits contraction of the unit cell with increasing phosphorus content analoguous to that found for Mn_2P. The equilibria between Ni_2P and more phosphorus-rich intermediate phases are not yet known, and were not studied in the present investigation.

THE STRUCTURE DETERMINATION OF Mn_3P

According to Årstad and Nowotny [12], Mn_3P is isostructural with Fe_3P. This is confirmed by the present investigation. Weissenberg photographs of Mn_3P were taken with crystals rotated about the a and c axes. The structure was refined from successive electron density maps and difference maps projected on the ac and ab planes. For the 129 $F(h\,k\,0)$ values observed, the final R-value of 0.064 was obtained. An overall, isotropic temperature factor with $B = 0.44_9$ Å^2 was applied. The corresponding figures for the 92 $F(h0l)$-values observed were $R = 0.048$, $B = 0.34_5$ Å^2. (The very strong (004) reflection was omitted on account of extinction). For each atom, two sets of x and y parameters were obtained, one from the $\varrho(xy)$ and one from the $\varrho(xz)$ projection. The final differences between these parameter values did not exceed 0.0005 for any atom. The parameter values quoted below are weighted averages, obtained by giving the values from the centrosymmetric xy projection twice the weight of those from the noncentrosymmetric xz projection.

Final structure data for Mn_3P are as follows:

Space group $I\bar{4}-(S_4^2)$, $Z = 8$; $a = 9.181$ Å; $c = 4.568$ Å; $U = 385.0$ Å^3.

Atoms in 8(g)	x	$\sigma(x)$	y	$\sigma(y)$	z	$\sigma(z)$
Mn_I	0.0807	0.0002	0.1071	0.0002	0.2279	0.0006
Mn_{II}	0.3567	0.0002	0.0319	0.0002	0.9863	0.0006
Mn_{III}	0.1721	0.0002	0.2192	0.0002	0.7531	0.0006
P	0.2935	0.0004	0.0450	0.0004	0.4880	0.0011

Table 2. Interatomic distances in Mn_3P (Å). (Distances shorter than 3.7 Å listed).

	Mn_I	Mn_{II}	Mn_{III}	P
Mn_I	2.46_2, 2.71_4 (2) 3.03_5 (2)	2.69_8, 2.84_9, 3.56_5	2.54_3, 2.74_2, 2.77_6, 2.81_9, 2.86_3	2.35_7, 2.43_8, 3.56_9
Mn_{II}	2.69_8, 2.84_9, 3.56_5	2.69_6, 2.88_0 (2) 3.07_2 (2)	2.55_3, 2.60_3, 2.63_9, 3.54_9	2.35_2, 2.36_1, 2.36_7, 2.37_0
Mn_{III}	2.54_3, 2.74_2, 2.77_6, 2.81_9, 2.86_3	2.55_3, 2.60_3, 2.63_9, 3.54_9	2.75_4 (2)	2.29_5, 2.37_7, 2.43_7, 3.62_4
P	2.35_7, 2.43_8, 3.56_9	2.35_2, 2.36_1, 2.36_7, 2.37_0	2.29_5, 2.37_7 2.43_7, 3.62_4	3.50_1 (2) 3.64_1 (2)

Interatomic distances are listed in Table 2.

THE STRUCTURE DETERMINATIONS OF Mn_2P AND Ni_2P

Single-crystals of Mn_2P were selected from a two-phase $Mn_3P + Mn_2P$ alloy. Good single-crystals of Ni_2P proved to be more difficult to obtain, since they were found to be very sensitive to mechanical deformation, which resulted in the X-ray patterns exhibiting elongated and diffuse spots. It was found, however, that crystal fragments picked from crushed alloys gave single-crystals suitable for X-ray work after a 30 min heat-treatment at 930°C.

The hexagonal Mn_2P and Ni_2P structures both belong to the revised $C22$ (Fe_2P) structure type [1]. The space group is $P\bar{6}\ 2m$ with three metal atoms in $3(f)$, three metal atoms in $3(g)$, two phosphorus atoms in $2(c)$ and one phosphorus atom in $1(b)$. Both structures were refined by successive electron density projections on the basal plane. During the refinements it was found that the temperature factor of the $3(g)$ metal atoms was much higher than that of the $3(f)$ atoms. Individual isotropic temperature factors were therefore introduced, which lowered the R-value for Mn_2P from 0.058 to 0.045 for the 67 $F(hk\,0)$-values observed, and for Ni_2P from 0.075 to 0.063 for the 51 $F(hk0)$-values observed. Electron counts did not indicate different scattering parameters for the two sets of metal atoms.

Final structure data for Mn_2P are as follows:

Space group $P\bar{6}\ 2m-(D^3_{3h})$; $Z = 3$; $a = 6.081$ Å; $c = 3.460$ Å; $U = 110.8$ Å^3

	x	$\sigma(x)$	B (Å^2)
3 Mn_I in $3(f)$	0.2546	0.0004	0.23_4
3 Mn_{II} in $3(g)$	0.5943	0.0004	0.43_0
2 P_I in $2(c)$			0.40
1 P_{II} in $1(b)$			0.40

Final data for Ni_2P are as follows:

$a = 5.859$ Å; $c = 3.382$ Å; $U = 100.5$ Å^3

	x	$\sigma(x)$	B (Å^2)
3 Ni_I in 3(f)	0.2575	0.0004	0.32
3 Ni_{II} in 3(g)	0.5957	0.0005	0.69
2 P_I in 2(c)			0.42
1 P_{II} in 1(b)			0.42

The unit cell dimensions for Mn_2P and Ni_2P quoted above were obtained from powder photographs of the alloys from which the single-crystal specimen were selected.

Interatomic distances are given in Table 3. A description of the $C22$ structure is given in Ref.[1]

CONCLUDING REMARKS

The substantial homogeneity ranges of Mn_2P and Ni_2P have escaped the notice of previous investigators. In the present author's opinion, the results of Berak and Heumann in the Mn_2P—MnP part of the Mn—P equilibrium diagram may be explained simply by the extended Mn_2P single-phase field without the introduction of a new intermediate phase. Clearly, an accurate redetermination of the thermal data for the Mn—P system is desirable.

Extended homogeneity ranges seem to be common in Me_2P-type phosphides. According to Haughton [15], secondary precipitation of FeP in two-phase Fe_2P + FeP alloys indicates a wider homogeneity range for Fe_2P at higher temperatures. The existence of an extended homogeneity range for Co_2P has

Table 3. Interatomic distances in Mn_2P and Ni_2P (Å). (Distances shorter than 3.7 Å listed).

Type of distance	Number of equivalent distances	Mn_2P	Ni_2P	Type of distance	Number of equivalent distances	Mn_2P	Ni_2P
Me_I-Me_I	2	2.68_2	2.61_3	P_I-Me_I	3	2.30_4	2.20_9
	2	3.46_0	3.38_2				
Me_I-Me_{II}	2	2.69_4	2.60_5	P_I-Me_{II}	6	2.53_0	2.45_6
	4	2.76_7	2.67_8				
Me_I-P_I	2	2.30_4	2.20_9	P_I-P_I	2	3.46_0	3.38_2
					3	3.51_1	3.38_3
Me_I-P_{II}	2	2.32_2	2.26_6	$Pe_{II}-Me_I$	6	2.32_2	2.26_6
$Me_{II}-Me_{II}$	4	3.19_9	3.08_6	$P_{II}-Me_{II}$	3	2.46_7	2.36_9
	2	3.46_0	3.38_2		3	3.61_4	3.49_0
$Me_{II}-P_I$	4	2.53_0	2.45_6				
$Me_{II}-P_{II}$	1	2.46_7	2.36_9	$P_{II}-P_{II}$	2	3.46_0	3.38_2
	1	3.61_4	3.49_0				

been demonstrated by Nowotny [16] and by the present author [2], and there are also signs of a similar effect for Ru_2P. Variations of the Fe_2P unit cell dimensions have not been measured, but for Mn_2P, Ni_2P, and Co_2P the unit cell volumes decrease with increasing atomic ratios of phosphorus/metal. For Co_2P it has been shown [2] that the homogeneity range extends from the stoichiometric composition towards the phosphorus-rich side of the diagram. This is probably due to a varying number of vacancies on one of the crystallographically non-equivalent cobalt atom sites (Co_{II}). The structure of Co_2P is closely related to that of Mn_2P, Fe_2P, and Ni_2P, and the coordination of the Co_{II} atoms is closely similar to that of the Mn_{II}, Fe_{II} and Ni_{II} atoms. (For more detailed descriptions of these structures, see Refs [1,2]). It is noteworthy that the temperature factors for the Mn_{II} and Ni_{II} atoms are substantially larger than those for Mn_I and Ni_I. The origin of this effect is not easy to explain. However, the effect may indicate that the Mn_{II} and Ni_{II} atomic positions are more likely to be the sites of vacancies or disorder in non-stoichiometric Mn_2P and Ni_2P.

Acknowledgements. This work has been financially supported by the *Swedish State Council of Technical Research* and by the *Air Force Office of Scientific Research of the Air Research and Development Command, United States Air Force* through its European Office under Contract No. AF 61 (052)-40. Facilities for use of the electronic digital computer BESK were given by the *Swedish Board for Computing Machinery.*

The author wishes to thank Professor G. Hägg for his kind interest. Thanks are also due to Mr. O. Olovsson for excellent assistance with numerical computations.

REFERENCES

1. Rundqvist, S. and Jellinek, F. *Acta Chem. Scand.* **13** (1959) 425.
2. Rundqvist, S. *Ibid.* **14** (1960) 1961.
3. Rundqvist, S. *Ibid.* **14** (1960) 2246.
4. Rundqvist, S. *Ibid.* **15** (1961) 342.
5. Rundqvist, S. *Ibid.* **16** (1962). 1.
6. Watson, R. E. and Freeman, A. I. *Acta Cryst.* **14** (1961) 27.
7. Thomas, L. H. and Umeda, K. *J. Chem. Phys.* **26** (1957) 293.
8. Tomiie, Y. and Stam, C. H. *Acta Cryst.* **11** (1958) 126.
9. Dauben, C. H. and Templeton, D. H. *Ibid.* **8** (1955) 841.
10. Cruickshank, D. W. J. *Ibid.* **2** (1949) 65.
11. Hansen, M. *Constitution of Binary Alloys*, Mc Graw-Hill, New York—Toronto—London 1958.
12. Årstad, O. and Nowotny, H. *Z. physik. Chem.* **B38** (1938) 356.
13. Berak, J. and Heumann, Th. *Z. Metallkunde* **41** (1950) 19.
14. Rundqvist, S. and Larsson, E. *Acta Chem. Scand.* **13** (1959) 551.
15. Haughton, J. L. *J. Iron Steel Inst.* **115** (1927) 417.
16. Nowotny, H. *Z. anorg. Chem.* **254** (1947) 31.

Received December 1, 1961.

ACTA CHEMICA SCANDINAVICA 16 (1962) 999–1014

Studies of Hydrogen Bonding

Part IV. A Comparison between the Ability of Organophosporus Compounds to Form Addition Compounds with Iodine and their Ability to Take Part in Hydrogen Bonding

THOR GRAMSTAD and SVEIN IVAR SNAPRUD

Norwegian Defence Research Establishment, Division for Toxicology, Kjeller, Norway

The K_{ass}, ΔH, ΔF and ΔS values for the formation of 1:1 addition compounds between eight organophosphorus compounds and iodine in carbon tetrachloride solution have been determined. The logarithms of the association constants are linearly related to the blue shifts, $\Delta\lambda_{I\text{-}I}$, of the visible iodine band which accompany the formation of the complexes. A linear relationship also exists between the ability of these organophosphorus compounds to form hydrogen bonds with proton donors and addition compounds with iodine. The ultraviolet absorption in the addition compounds which could be attributed to a charge-transfer band is considered to lie at wavelengths shorter than 220 mμ. In the infrared region, addition compound formation with iodine causes a large shift in the P=O stretching frequency of the organophosphorus compounds. The self-association of organophosphorus compounds is also discussed.

It was shown in two previous publications [1,2] that organophosphorus compounds containing the P=O group form very strong intermolecular hydrogen bonds with phenol, methanol, α-naphthol, and pentachlorophenol. It was now of interest to extend our work to see if there was any relation between the ability of organophosphorus compounds to form hydrogen bonds in this way and their ability to form intermolecular addition compounds with halogens, interhalogens and cyanogen halides, respectively. To our knowledge there is only one previous paper on the equilibrium reaction between halogens and organophosphorus compounds, namely by Tsubomura and Kliegman [3] who describe the interaction of iodine and tributyl phosphate. The present paper presents the results of a spectrophotometric investigation of the interaction of iodine with twelve organophosphorus compounds.

Numerous investigators have studied the addition compounds of the halogens and interhalogens with various nitrogen- and oxygen-containing compounds by various methods including X-ray crystallography, thermodynamic

measurements and ultraviolet, visible and infrared spectroscopy. Two theories on the nature of the chemical bond between the two components of these addition compounds have been advanced; the Benesi-Hildebrand donor-acceptor theory [4] in which one of the two reactants acts as an electron donor (Lewis base) and the other as an electron acceptor (Lewis acid), and Mulliken's charge-transfer resonance theory [5] which postulates resonance between so-called "no-bond" and "dative" structures. Hassel *et al.*[6,7] have made a series of X-ray crystallographic studies of the molecular structure of solid addition compounds. In some of the addition compounds studied they found that the electron-donating property was localised on atoms possessing unshared electron pairs, *e.g.*, O, N and S. Furthermore, they found that the electron donor atom was directly linked to one of the halogen atoms to form a co-linear structure. The bond between the donor and acceptor atoms tends to extend or complete a tetrahedral arrangement around the donor atom; sometimes, however, planar structures were found as in the atom complexes of acetone and pyridine. The interatomic distances in addition compounds found by Hassel *et al.* will be compared with spectrophotometric data on hydrogen bonds and addition compounds in the discussion below. Person *et al.*[8] have studied the X—Y stretching vibration of the electron-acceptor molecule by infrared spectroscopy and found a linear relationship between ε_a, the added effective charge, and $\Delta k/k$, the relative change in force constant, due to complex formation. They also found that hydrogen bonded complexes fit this relationship. They interpreted their results in terms of resonance between the structures: $D...X—Y \leftrightarrow (D—X)^+...Y^-$, the latter being a modification of Mulliken's "dative" structure $D^+...(XY)^-$.

de Maine [9] has reported thermodynamic data for complexes of methanol, ethanol and diethyl ether with iodine in carbon tetrachloride and shown that the linear relationships between ΔF and ΔH or ΔS for aromatic complexes of iodine found by Andrews and Keefer [10] do not hold for all iodine complexes. These linear relations appear to hold only for donor molecules of similar geometrical form. Schmulbach and Drago [11] have shown by infrared spectroscopy that for dimethyl acetamide and iodine in carbon tetrachloride solution complex formation occurs through the oxygen atom. They obtained some thermodynamic data by following the changes in the carbonyl absorption on complex formation. A recent paper by Tsubomura and Lang [12] describes a spectrophotometric study of solutions of iodine in acetamide, N,N-dimethylformamide, diethyl sulphide, and diethyl disulphide, and discusses the general features of the spectra of iodine-donor complexes.

EXPERIMENTAL

Materials. The methods of preparation and physical data on the organophosphorus compounds used have, with one exception, $[(C_2H_5)_2N]_2P(O)C_2H_5$, b.p. 100°C/0.7 mm, been published earlier [1]. The phosphorus compounds were purified by fractional distillation or recrystallisation just before use. The iodine was resublimed and dried in a desiccator over phosphorus pentoxide. "Merck Spectroscopic Grade" carbon tetrachloride was used without further purification.

Infared measurements. The infrared spectroscopic measurements were made with a Perkin-Elmer Model 21 Spectrophotometer with sodium chloride optics. This instrument

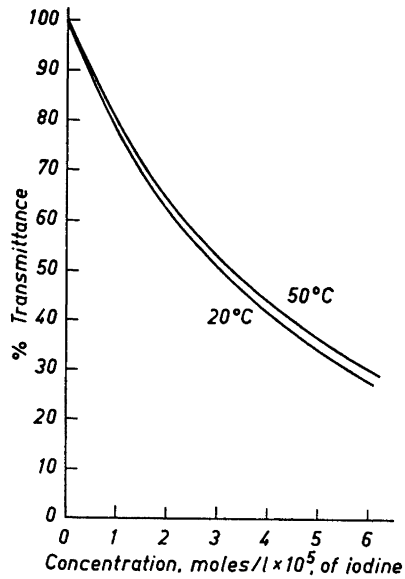

Fig. 1. The relation between percent transmittance and various concentrations of iodine, measured at 518 mμ. Solvent, carbon tetrachloride. Cell length, 10.0 cm.

was also used for the determination of the frequency shift of the ground state stretching vibration of the P=O band which accompanies complex formation with iodine. The association constants of the equilibrium reaction were determined from the decrease in intensity of the free P=O band upon complex formation. These measurements were carried out as a check of the association constants obtained from the decrease in intensity of the iodine visible band upon complexation. The instrumental conditions and the method of running the spectra were the same as described earlier [2]. The concentrations of iodine and phosphorus compounds were, with few exceptions, 0.03 moles/l each for all spectra. For $(CH_3)_3PO$, $(C_2H_5)_3PO$ and $[(C_2H_5)_2N]_2P(O)C_2H_5$ the concentrations were reduced to 0.015 moles/l because of their greater complexing ability. The cell was of 1.00 mm thickness and the temperature was about 30°C.

Visible and ultraviolet measurements. The visible and ultraviolet measurements were carried out with a Beckman Ratio Recording Spectrophotometer Model DK-2. Instrumental conditions were as follows: Scanning time, full scale, 20 min; range, 0—100; sensitivity, 50; time constant, 0.6; percent transmittance. The cell used was the same as described earlier [1]. This instrument was used for the determination of the association constants and the blue shift of the iodine visible band upon complexation with the phosphorus compounds. The concentration of free iodine was determined from the iodine visible band at 518 mμ by using the calibration curves shown in Fig. 1. K_{ass} was calculated as shown below:

$$D + X{-}X \rightleftharpoons D\ldots X{-}X$$

$$K_{ass} = \frac{(D\ldots X{-}X)}{(D)\,(X{-}X)} = \frac{c}{(a-c)\,(b-c)}$$

where c is the concentration in moles/l of the addition compound calculated from the decrease of the free iodine band, and a and b are the initial concentrations in moles/l of electron donor and acceptor, respectively. The spectra were run immediately after preparing the solutions because of the reaction of iodine with carbon tetrachloride and with some of the electron donors. These reactions, however, were sufficiently slow at the low concentrations used to permit exact measurements. The temperatures were kept at 20 and 50°C. The concentration of iodine was kept at 6×10^{-5} moles/l for all spectra and the concentrations of the organophosphorus compounds used are recorded in Table 1.

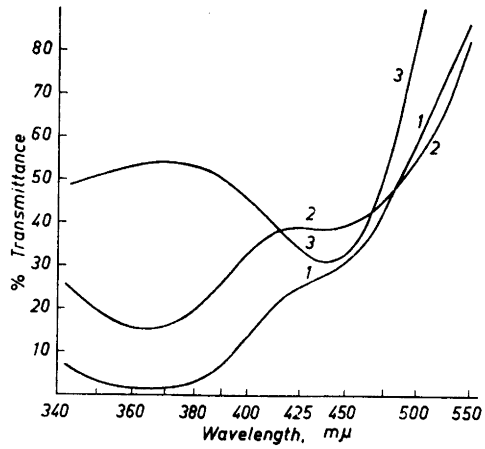

Fig. 2. The visible absorption spectra of $(C_2H_5)_2NP(O)(OC_2H_5)_2-I_2$. Curve 1, 0.27 moles/l of $(C_2H_5)_2NP(O)(OC_2H_5)_2$ and 6×10^{-5} moles/l of I_2, temperature 20°C; curve 2, the same concentration as in curve 1, but the temperature was 50°C; curve 3, 0.20 moles/l of $(C_2H_5)_2NP(O)(OC_2H_5)_2$ and 6×10^{-5} moles/l of I_2, compensated with a reference cell containing 6×10^{-5} moles/l of I_2, temperature 20°C. Solvent, carbon tetrachloride. Cell length, 10.0 cm.

As can be seen, the values of the association constants are the mean values of two or three separate determinations. Table 2 shows the experimental results obtained from the determination of K_{ass} for one of the compounds studied.

RESULTS

Visible absorption spectra. In Fig. 2 are shown the spectra of $(C_2H_5)_2NP(O)(OC_2H_5)_2$ with iodine in carbon tetrachloride solution. These visible absorption spectra are typical for such solutions containing iodine and an organophosphorus compound with a P=O group. Since such phosphorus compounds have no absorption in this region the new absorption band at 438 mμ is assigned to the iodine visible band which has undergone a blue shift upon complex formation. The corresponding free iodine band in carbon tetrachloride solution has its peak at 518 mμ. The assignment for the new absorption band at 364 mμ is not yet clear, but it appears that the intensity of this band is very sensitive to variation in the concentrations of the reactants. As can be seen in Fig. 2, when the concentration of the electron donor is decreased from 0.27 moles/l (curve 1) to 0.20 moles/l (curve 3), the absorption peak at 364 mμ is markedly decreased. Furthermore, comparison of curve 1 with curve 2 (in Fig. 2) shows that both peaks (438 and 364 mμ) are temperature dependent. Tsubomura and Lang [12] also observed a peak at 360 mμ for iodine with amides in methylene chloride solution. The peak, however, disappeared on purification of the amides. The same was also the case with tributyl phosphate and iodine in heptane solution [3]. The observed peak, in this case at 366 mμ, was concluded to be caused either by impurities or by reaction products. We have found, however, in our investigations a strong absorption band at about 364—368 mμ with all the organophosphorus compound-iodine complexes studied. Further-

Table 1. Data of intermolecular addition compounds between organophosphorus compounds and iodine. Solvent, carbon tetrachloride.

Compound	Measurements in infrared region.				
	I $\nu_{P=O}$ cm^{-1}	II $\nu_{P=O}$ cm^{-1}	III $\Delta\nu_{P=O}$ cm^{-1}	IV $\nu_{1/2}$ cm^{-1}	K_{ass} l/mole *ca.* 30°C
$CCl_3PO(OC_2H_5)_2$	1278	1282	32	36	0.69
$CHCl_2PO(OC_2H_5)_2$	1272	1279	38	40	0.82
$CH_3OPO(OCH_3)_2$	1285	1274 1295			
$CH_2ClPO(OC_2H_5)_2$	1267	1270	32	24	1.10
$C_2H_5OPO(OC_2H_5)_2$	1276	1263 1279	36 52	28	5.09
$CH_3PO(OC_2H_5)_2$	1244	1243	35	40	
$C_2H_5PO(OC_2H_5)_2$	1228 1252	1228 1245	28 45	20	4.74
$(C_2H_5)_2NPO(OC_2H_5)_2$	1258	1254	36	28	5.76
$C_6H_5PO(C_6H_5)_2$	1188	1202	40	40	17.48
$C_2H_5PO[N(C_2H_5)_2]_2$	1210 1190	1206 1190	70 54	74	60.21
$CH_3PO(CH_3)_2$	1177	1198	47		
$C_2H_5PO(C_2H_5)_2$	1160	1178	46	52	71.66

more, we observed that this absorption, besides being very concentration dependent, was more enhanced the more the P=O group was polarised. Since this absorption is found at almost the same wavelength for different addition compounds and in different solvents, and is only formed upon complexation, we believe that it may be due to the I_3^- ion. This is in accordance with the results reported by Autrey and Connick [13] and by Buckles *et al.*[14] who found that the I_3^- ion has an absorption peak at 365 mμ.

An attempt to find a charge-transfer absorption band (CT band) between 220 and 300 mμ corresponding to that found for iodine complexes with ether [9], alcohols [9], amines [15], *etc.* was unsuccesful. This result is consistent with the observation by Tsubomura and Kliegman [3] who were unable to find the CT band of the iodine-tributylphosphate complex in heptane solution. However, by using a perfluorocarbon as solvent they did find an absorption tail at about 220 mμ which they considered to be a part of the CT absorption band, and hence concluded that the peak lies at a wavelength shorter than 220 mμ.

Usually the association constants for iodine with electron donors have been evaluated either form the CT band or from the displaced iodine visible band by using the method of Benesi-Hildebrand [17] or a modification thereof [16]. In this work we have evaluated the association constants by measuring the decrease in intensity of the free iodine band upon complex formation. The superposition of the complexed iodine and free iodine bands seems not, at

Table 1, cont.

Compound	Measurements in visible region.									
	$C_p \times 10^2$	$C_i \times 10^5$		$C_c \times 10^5$		K_{ass} l/mole		K_{ass} l/mole		$\Delta\lambda_{I\text{-}I}$ (mμ)shifted.vis. iodine band
		20°	50°	20°	50°	20°	Av.	50°	Av.	
$CCl_3PO(OC_2H_5)_2$										
$CHCl_2PO(OC_2H_5)_2$	10	5.30	5.50	0.70	0.50	1.32		0.91		
	13	5.15	—	0.85	—	1.27	*1.33*	—	*0.96*	65
	15	4.95	5.30	1.05	0.70	1.41		1.00		
$CH_3OPO(OCH_3)_2$	5	5.35	—	0.65	—	2.43		—		
	7	5.00	5.30	1.00	0.70	2.86	*2.64*	1.85	*1.85*	68
	10	4.75	5.07	1.25	0.93	2.63		1.84		
$CH_2ClPO(OC_2H_5)_2$	7	4.95	5.45	1.05	0.55	3.03		1.44		
	10	4.65	5.15	1.35	0.85	2.90	*2.83*	1.65	*1.60*	68
	13	4.50	4.90	1.50	1.10	2.56		1.72		
$C_2H_5OPO(OC_2H_5)_2$	2	5.35	5.60	0.65	0.40	6.08		3.67		
	3	5.10	—	0.90	—	5.90	*6.18*	—	*3.74*	72
	4	4.75	5.20	1.25	0.80	6.57		3.85		
$(C_2H_5)_2NPO(OC_2H_5)_2$	2	5.20	5.45	0.80	0.55	7.70		4.60		
	3	5.00	5.20	1.00	0.80	6.67	*7.19*	5.13	*4.85*	73
	—	—	—	—	—	—		—		
$C_6H_5PO(C_6H_5)_2$	0.8	5.20	5.55	0.80	0.45	19.20		10.15		
	1.0	4.95	5.45	1.05	0.55	21.22	*22.27*	10.10	*10.92*	78
	1.5	4.30	5.05	1.70	0.95	26.40		12.15		
$C_2H_5PO[N(C_2H_5)_2]_2$	0.2	5.25	5.65	0.75	0.35	71.40		31.00		
	0.3	4.90	—	1.10	—	74.80	*75.07*	—	*35.50*	84
	0.5	4.30	5.00	1.70	1.00	79.10		40.00		
$CH_3PO(CH_3)_2$										
$C_2H_5PO(C_2H_5)_2$	0.08	5.60	—	0.40	—	85.30		—		
	0.17	5.30	5.65	0.70	0.35	79.30	*83.17*	37.30	*38.75*	86
	0.25	4.95	5.45	1.05	0.55	84.90		40.20		

I the frequency of pure liquid film or as KBr-disk.
II the frequency of solution in carbon tetrachloride, 0.012 moles/l.
III the frequency shift due to complexation with iodine.
IV the half band width of P=O band when complexed with iodine.
C_p means initial concentration, moles/l, of organophosphours compound
C_i means concentration, moles/l, of free iodine after complex formation
C_c means concentration, moles/l, of complex.

low concentrations, to interfere seriously except in the case of $CCl_3P(O)(OC_2H_5)_2$, where the two bands overlap to such an extent that the K_{ass} value obtained is not very reliable. The agreement of the K_{ass} values determined at various concentrations (Table 1) indicates that 1:1 complexes are formed, and that the superposition of the bands does not in these cases interfere seriously. The K_{ass} values have also been checked by infrared spectroscopy and, as can be seen in Table 1, the association constants evaluated by both methods agree very well. Table 1 also shows the concentrations of reactants, of free iodine after

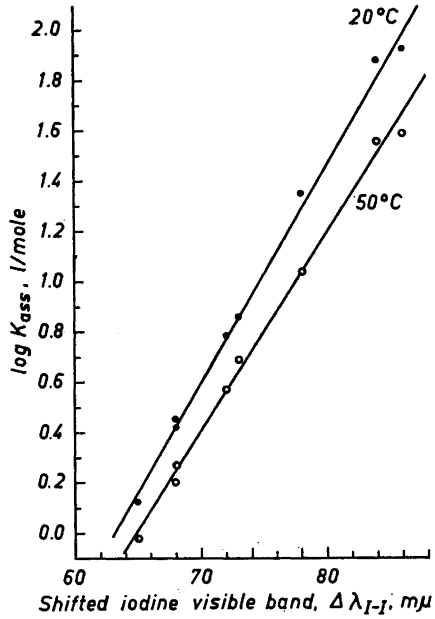

Fig. 3. The relation between the logarithms of the association constants and the shifts in wavelength, $\Delta\lambda_{I\text{-}I}$, of visible iodine band for addition compounds between various organophosphorus compounds and iodine.

complex formation, and of the complexes formed. The association constant of 20.9 l/mole at 20°C for tributyl phosphate and iodine in heptane solution reported by Tsubomura and Kliegman [3] seems very large in comparison with our results, *e.g.*, the association constant of 6.18 l/mole for iodine and triethyl phosphate in carbon tetrachloride solution. The reason for this disagreement may lie either in a difference in the effect of solvent interaction on the complex (or on the reactants) for the two solvents used or in the method of evaluation of the K_{ass} values. (The greater electron release by the butyl group as compared with the ethyl group will also be a factor). On the other hand, their ΔH value of −2.94 kcal/mole is consistent with our result of −3.15 kcal whereas the ΔS values differ greatly, being −3.99 and −7.13 e.u., respectively.

In two previous publications [1,2] it was shown that with experimental error, the logarithms of the association constants, K_{ass}, between organophosphorus compounds (OPC) and phenol, methanol, α-naphthol, and pentachlorophenol, respectively, form a linear relationship with the frequency shift, $\Delta\nu_{O\text{-}H}$, of the O—H band which accompanies the formation of the hydrogen bond. A similar relationship has now been found to be valid for the complexation of organophosphorus compounds with iodine. In Fig. 3 the log K_{ass} values between OPC and iodine are plotted as a function of the blueshift in wavelength, $\Delta\lambda_{I\text{-}I}$, of the iodine visible band upon complex formation. The straight lines drawn through the calculated log K_{ass} values (see Table 1) at 20 and 50°C, are all within experimental error. The smoothed values of log K_{ass} evaluated from the two straight lines in Fig. 3, have been used to determine the corresponding values of ΔH, ΔF, and ΔS. The variation of these with $\Delta\lambda_{I\text{-}I}$ are shown

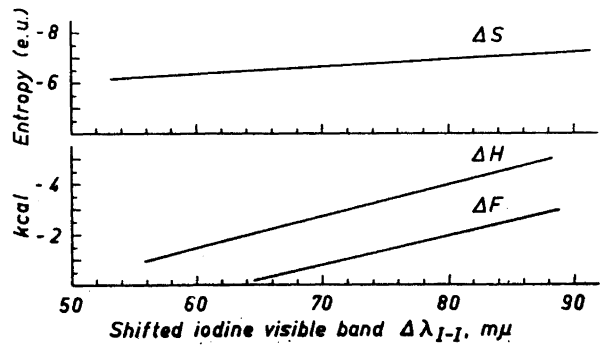

Fig. 4. Enthalpy, $-\Delta H$, free energy, $-\Delta F$, and entropy, $-\Delta S$, *vs.* the blue shifted wavelength, $\Delta\lambda_{I\text{-}I}$, of the iodine visible band upon complexation with various organophosphorus compounds.

in Fig. 4. As can be seen a decrease in enthalpy is compensated by a decrease in the entropy of the system. In the series of OPC studied there is upon complexation with iodine, a decrease of ΔH from approximately -2.1 to -4.8 kcal/mole which is compensated by a decrease of ΔS from -6.6 to -7.1 e.u. Similar results were found for hydrogen bonded complexes of OPC with various proton donors [2], except with pentachlorophenol. The most striking result is perhaps the observation of a linear relationship between the ability of OPC to form hydrogen bonds with phenol and to form addition compounds with iodine, as shown in Fig. 5. The straight lines drawn through the calculated log K_{ass} values at 20 and 50°C for the systems OPC-phenol (see [Part II)[2] and

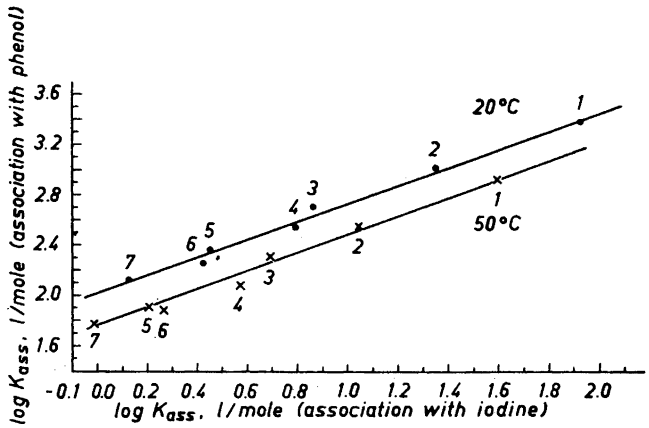

Fig. 5. The relation between the logarithms of the association constants for hydrogen bonded complexes between various organophosphorus compounds and phenol and the logarithms of the association constants of the same phosphorus compounds with iodine, (1) $(C_2H_5)_3PO$, (2) $(C_6H_5)_3PO$, (3) $(C_2H_5)_2NP(O)(OC_2H_5)_2$, (4) $(C_2H_5O)_3PO$, (5) $CH_2ClPO(OC_2H_5)_2$, (6) $(CH_3O)_3PO$, (7) $CHCl_2P(O)(OC_2H_5)_2$. Temperatures, 20 and 50°C.

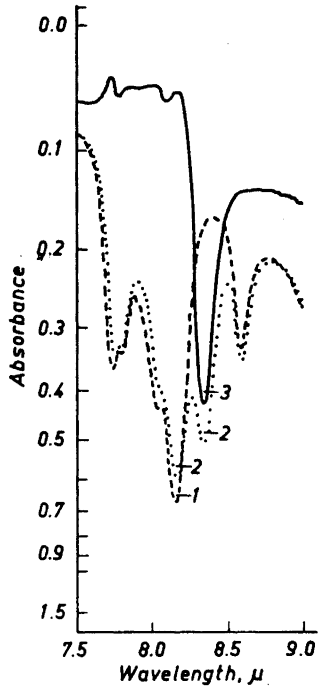

Fig. 6. The infrared absorption spectra of (1) 0.03 moles/l of $C_2H_5P(O)(OC_2H_5)_2$; (2) 0.03 moles/l of $C_2H_5PO(OC_2H_5)_2$ and 0.03 moles/l of I_2; (3) the same concentration as in (2), but compensated with a reference cell containing 0.03 moles/l of $C_2H_5P(O)(OC_2H_5)_2$. Solvent, carbon tetrachloride. Cell length, 1.00 mm. Temperature, *ca.* 30°C.

OPC-iodine are all within experimental error. It should also be noted that the two curves are nearly parallel. This figure demonstrates very clearly that there is a close connection between hydrogen bonding and the bonding in the addition complexes.

Infrared absorption spectra. Fig. 6 shows the effect of iodine on the P=O ground state stretching vibration in a typical case, $C_2H_5P(O)(OC_2H_5)_2$-iodine. The solid curve shows the complexed P=O band when compensated with a reference cell containing the same concentration of organophosphorus compound as in the mixture. As can be seen the complexed P=O band is not very enhanced in broadness in comparison with the free P=O band. This implies that the superposition of the bands does not interfere seriously in the evaluation of the K_{ass} values, which were also found to be consistent with those obtained from the free iodine band. The half band widths of the complexed P=O bands are shown in Table 1. The displacement of the stretching-vibration frequency of the P=O group upon complex formation which should be a measure of the polarisability of the phosphorus compound seems to be larger for the iodine complexes than for the hydrogen bonded complexes, although the K_{ass} and $-\Delta H$ values are larger for the latter. Furthermore, it seems as if the frequency shift of the phosphoryl group is greatest for those compounds containing substituents which contribute to the $+I$ effect and to the $+M$ effect. The strong $-I$ effect of chlorine seems to stabilise the electronic constitution of the P=O group whereas the electromeric effect of particularly the amino group, comes into play upon complexation. These observations are in accordance with

Table 2. Determination of the association constants between iodine and triethylphosphine oxide in carbon tetrachloride. Cell length, 10 cm. Temperature, 20° and 50°C

Concentration (initial)		Percent transmittance	Concentration of free iodine *	Concentration of complex	K_{ass} l/mole	K_{ass} mean value	Temperature
Iodine $M \times 10^5$	Triethylphosphine oxide $M \times 10^3$		$M \times 10^5$	$M \times 10^5$			
6.00	0	26.6	6.00	0	0		
6.00	0.83	29.0	5.60	0.40	85.30		
6.00	1.87	31.0	5.30	0.70	79.30	*83.17*	20°C
6.00	2.50	33.2	4.95	1.05	84.90		
6.00	0	28.8	6.00	0	0		
6.00	1.67	30.6	5.65	0.35	37.30	*38.75*	50°C
6.00	2.50	32.0	5.45	0.55	40.20		

* The concentration of free iodine in this column has been determined by using the calibration curves in Fig. 1.

those predicted in a previous publication [1]. We have also observed that some of the organophosphorus compounds give two new absorption bands upon complexation with iodine, *e.g.*, $CH_2ClP(O)(OC_2H_5)_2$ at 1238 and 1200 cm^{-1}, $(C_2H_5)_2NP(O)(OC_2H_5)_2$ at 1218 and 1207 cm^{-1}, and $(C_6H_5)_3PO$ at 1162 and 1089 cm^{-1}. One of the peaks in the double band is assigned to the complexed P=O stretching vibration band, but the assignment of the other is not quite clear. With regard to the self-association of organophosphorus compounds, we have made some comparisons between the P=O ground state stretching vibration of various phosphorus compounds in pure liquid state (or as a KBr-disk) and in carbon tetrachloride solution. The results are recorded in Table 1.

DISCUSSION OF RESULTS

The present investigation on ternary solutions of iodine with various organophosphorus compounds in carbon tetrachloride has established the following facts: Firstly, the ΔH, ΔF and ΔS values form linear relationships with the blue shift of the wavelength, $\Delta\lambda_{I\text{-}I}$, of the iodine visible band which accompanies the formation of the complex (see Figs. 3 and 4). Secondly, the ability of organophosphorus compounds to form addition compounds with iodine and to form hydrogen bonds with proton donors is related by a linear relationship (see Fig. 5). Thirdly, the frequency shift of the ground state stretching vibration of the P=O band is much larger on complexation with iodine than on hydrogen bonding in relation to the respective association constants; *e.g.*, the K_{ass} and $\Delta\nu_{P=O}$ values for the association of triethylphosphine oxide with pentachlorophenol, α-naphthol, phenol, methanol and iodine are, 2 095.5, 35; 3 763, 20; 2 522, 23; 45.9, 12; and 83.17 l/mole, 46 cm^{-1}, respectively. The extremely large $\Delta\nu_{P=O}$ value for iodine complexation in relation to the low asso-

Table 3. A comparison of data between various hydrogen bonded complexes and the corresponding addition compounds with iodine.

Compound	Iodine				Pentachlorophenol			**Solvent for the addition compounds
	K_{ass} l/mole 20°C	ΔH kcal	$\Delta\lambda_{I\text{-}I}$ mμ	CT λ mμ	K_{ass} l/mole 20°C	ΔH kcal	$\Delta\nu_{O\text{-}H}$ cm^{-1}	
$(C_2H_5)_3N$ [15]	6460	−12.0	108	278			1155	heptane
CH:CHCH:CHCH:N [21]	269	−7.8	100	235	111.4	−5.8	805	»
$HC(O)N(CH_3)_2$ [12]	1.13	−4.0	61	<255	54.1 [26]	−4.6	364	CH_2Cl_2
$C_2H_5OC_2H_5$ [9]	0.97	−4.3	44	249				CCl_4
$C_2H_5OC_2H_5$ [22,23]	1.16	−4.2	60	252				heptane
$CH_3C(O)CH_3$ [24]	0.29*							CS_2
$CH_2(CH_2)_4CO$ [24]	0.56*							»
$CH_3C(O)OCH_3$ [24]	0.34*							»
CH_3OH [9]	0.47	−1.9	72	242.8				CCl_4
C_2H_5OH [9]	0.45	−2.1	69	243.3				»
$CHCl_2P(O)(OC_2H_5)_2$	1.33	−2.1	65	<220	56.3	−5.2	374	»
$(C_2H_5)_3PO$	83.17	−4.9	86	<220	209.5	−6.6	685	»

ciation constant may indicate that we have to differentiate between these addition compounds and hydrogen bonded complexes with regard to the mode of formation of the chemical bond in spite of the linear relationship shown in Fig. 5.

As concluded in a previous publication [2], the relationships between frequency shift, $\Delta\nu_{O\text{-}H}$, and ΔH, ΔF and ΔS are only valid when kept to one system, *e.g.*, OPC-phenol, OPC-methanol, *etc.* Furthermore, it has been shown [18] that there exists for the system phenol-pyridines a linear relationship between the logarithms of the association constants and the pK_a values of the proton acceptors, and that this relationship was not applicable to tertiary aliphatic amines. Similar conclusions can now be drawn with respect to addition compounds with iodine. The data for the iodine complexes of triethylamine, pyridine, ether, *etc.*, as shown in Table 3, do not fit with those obtained for the system OPC-iodine. Table 3 also contains a comparison of data obtained by the present authors and by others for various hydrogen bonded complexes with those for the corresponding addition compounds with iodine. If we compare the abilities of triethylamine and pyridine to form addition compounds with iodine and to form hydrogen bonds we see that both nitrogen compounds form addition compounds more readily than hydrogen bonds, whereas for all the other compounds studied the reverse is the case. This supports the view indicated earlier [18], that a difference exists between hydrogen bonded complexes (and addition compounds) containing nitrogen and those containing oxygen. We there [18] put forward the idea that for the system OPC-hydroxy compounds

Table 3, cont.

Compound	α-Naphthol			Phenol			Methanol			**Solvent for the addition compounds
	K_{ass} l/mole 20°C	ΔH kcal/ mole	$\Delta\nu_{O\text{-}H}$ cm^{-1}	K_{ass} l/mole 20°C	ΔH kcal/ mole	$\Delta\nu_{O\text{-}H}$ cm^{-1}	K_{ass} l/mole 20°C	ΔH kcal/ mole	$\Delta\nu_{O\text{-}H}$ cm^{-1}	
$(C_2H_5)_3N$ [18]	108.9	−6.6		90.9	−7.8	380	6.4	−3.8	427	heptane
CH:CHCH:CHCH:N [18]	82.5	−5.7	530	59.8	7.0	492	6.0	−3.2	300	»
$HC(O)N(CH_3)_2$ [26]				78.6 [26]	−5.4	292				CH_2Cl_2
$C_2H_5OC_2H_5$ [25]				9.6	−4.6	270				CCl_4
$CH_3C(O)CH_3$ [25]				12.3	−4.5	225				CS_2
$CH_2(CH_2)_4CO$ [25]				14.8	4.2	241				»
$CH_3C(O)OCH_3$ [25]				9.5	−5.3	165				»
$CHCl_2P(O)(OC_2H_5)_2$	117.6	−5.7	283	133.1	−5.0	275	7.5	−2.5	148	»
$(C_2H_5)_3PO$	3763	−7.8	530	2522	−6.8	510	45.9	−6.3	270	»

* Association constants at about 30°C.
** Solvent for all hydrogen bonded complexes was carbon tetrachloride (see Refs [2,18])
CT means charge-transfer band.
$\Delta\nu_{I\text{-}I}$ means shift of visible iodine band.

proton transfer does not occur on hydrogen bonding, whereas for nitrogen compounds two types of hydrogen bonds were possible in which the above type (I) or the proton-transfer structure (II) predominates, depending on the nature of the proton donor and acceptor.

$$\overset{\delta-}{\mathrm{RO}}-\mathrm{H}\ldots\overset{\delta+}{\mathrm{N}} \qquad\qquad \overset{-}{\mathrm{RO}}\ldots\mathrm{H}-\overset{+}{\mathrm{N}}$$

(I) (II)

We also gave strong support for the view that for the system tertiary aliphatic amines-pentachlorophenol the structure (II) predominates, whereas for pyridines the structure (I) or (II) is most pronounced depending on the pK_a value of the proton donor. Furthermore, we have found, as pointed out above, that iodine forms addition compounds more readily with nitrogen than with oxygen compounds, whereas the reverse is the case with hydrogen bonding (see Table 3). From these observations the conclusion may be drawn that the ability to form hydrogen bonds is a function of the electron density around the proton acceptor atom, whereas the ability to form addition compounds with iodine is more likely a function of the basicity of the electron donor atom. Thus the ease with which an addition compound with a halogen or interhalogen is formed depends on the ease with which either an electron is transferred to the acceptor atom to give Mulliken's "dative" structure, $D^+\ldots(XY)^-$, or the donor atom can form a covalent bond with the acceptor atom to give the halogen-transfer structure, $(D-X)^+\ldots Y^-$. The former should be function of the ionisation potential of the donor atom, the latter of its basicity.

The reaction mechanism of the complexing of iodine with triethylamine (and pyridine) could thus be described as follows:

$$(C_2H_5)_3N: + \overset{\delta+}{I}\frown\overset{\delta-}{I} \rightleftharpoons [(C_2H_5)_3N{:}I]^+\ldots I^-$$

(III)

On approach of the strongly basic amine, a halogen-transfer structure (III) results. This mechanism is consistent with the large shift in wavelength, $\Delta\lambda_{I\text{-}I}$, of the iodine visible band, the enhanced broadness of the contour of the blue shifted iodine band ($\nu_{\frac{1}{2}}$, 5 700 cm^{-1}), and the very large enthalpy value (ΔH, −12 kcal/mole) found for the system iodine triethylamine-iodine [12,15]. Complex formation between triethylamine and iodine would thus be analogous to that between amines and pentachlorophenol [18] where the proton-transfer structure (II) was found to predominate.

With electron donors containing oxygen (=C=O, $\diagdown\!\!\diagup$P=O, =O), we propose that the electrostatic structure (IV) predominates, and that the association scheme may be written as, for example:

$$\diagdown\!\!\diagup\mathrm{P}{=}\mathrm{O} + \overset{\delta+}{\mathrm{I}}-\overset{\delta-}{\mathrm{I}} \rightleftharpoons \diagdown\!\!\diagup\mathrm{P}{=}\overset{\delta+}{\mathrm{O}}\ldots\mathrm{I}-\overset{\delta-}{\mathrm{I}}$$

(IV)

Table 4. Interatomic distances in some solid addition compounds in Å units, as determined by Hassel and co-workers [6].

Compound	Bond	Length obs.	Sum of covalent radii	Δl*	Bond	Length obs.	Sum of covalent radii	Sum of van der Waals' radii	Δl*	Δw*
Trimethylamine-I_2	I–I	2.84	2.66	0.18	N–I	2.27	2.03	3.65	0.24	1.38
Trimethylamine-ICl	I–Cl	2.53	2.32	0.21	N–I	2.30	2.03	3.65	0.27	1.35
Pyridine-ICl	I–Cl	2.54	2.32	0.22	N–I	2.30	2.03	3.65	0.27	1.35
Acetone-Br_2	Br–Br	2.28	2.28	0.00	O–Br	2.82	1.80	3.35	1.02	.053
1,4-Dioxane-Br_2	Br–Br	2.31	2.28	0.03	O–Br	2.71	1.80	3.35	0.91	0.64
1,4-Dioxane-ICl	I–Cl	2.33	2.32	0.01	O–I	2.57	1.99	3.55	0.58	0.98

* Δl, Δw, means the difference between the interatomic distance observed and the sum of covalent radii, and the sum of van der Waals' radii, respectively.

This mechanism is consistent with the small association constants, the low enthalpies, and the relatively small shift of the iodine visible band found for such complexes.

If we assume that there is some relation between interatomic distances in solid addition compounds and in the corresponding addition compounds in solution our reasoning above is in accordance with X-ray work of Hassel *et al.*[5,7] Some examples are given in Table 4, where the observed distances are compared with the sums of covalent radii and van der Waals' radii of the atoms concerned in the bonding. The observed interhalogen distances are not very much different from those of the free molecules, however Δl (Table 4) is largest for triethylamine and pyridine which indicates a halogen-transfer structure (III), whereas Δl for acetone-Br_2 is nil which indicates an electrostatic structure (IV). The same conclusions may be drawn from the distances between the donor and acceptor atoms. The observed N—I distance in triethylamine and pyridine addition compounds suggests that there is more covalent than electrostatic bonding, whereas for acetone the reverse is the case. Unfortunately no solid addition compounds between organophosphorus compounds and halogens or interhalogens are known since it would be of considerable interest to compare the interatomic distances in these with our results.

Self-association of organophosphorus compounds. Miller, Miller and Rogers[19] have recently shown that organophosphorus compounds have a tendency to form intermolecular association complexes in the pure state. With disubstituted phosphine oxides, $R_2P(O)H$, they found a P=O frequency shift from 1150—1155 cm^{-1} in the solid state to 1190 cm^{-1} in carbon disulphide solution which was attributed to intermolecular association. Furthermore, they found a decrease in the P—H frequency upon solution which is not consistent with bonds of the type $R_2P(O)H\ldots OP(H)R_2$ in the solid state. These results should be compared with those obtained by us for some disubstituted phosphites as shown below.

	$\nu_{P=O}(cm^{-1})$		$\nu_{P-H}(cm^{-1})$	
	Pure State	Solution in CCl_4 0.012 moles/l	Pure state	Solution in CCl_4 0.012 moles/l
$HP(O)(OCH_3)_2$	1267	1265	2420	2432
$HP(O)(OC_2H_5)_2$	1263	1258	2416	2428
$HP(O)[OCH(CH)_2]_2$	1260	1252	2410	2428

As can be seen we have found no increase in the P=O stretching vibration of the phosphites upon solution, rather a small decrease. However, an increase in the P—H frequency was observed upon solution. These results are just the reverse of those reported for disubstituted phosphine oxides [19]. From these observations the conclusion may be drawn that the P=O group in phosphites is not involved in the formation of self-association complexes, whereas in the disubstituted phosphine oxides the P=O group participates. This explanation is consistent with the relative polarity of the P=O bond in the two types of compounds. However, most phosphorus compounds other than the disubstituted phosphites (see Table 1) show an increase in the P=O stretching vibra-

tion frequency upon solution. Furthermore, the shift is greatest for the most polarised phosphine oxides, *e.g.*, the frequency of triethylphosphine oxide is shifted from 1160 cm^{-1} in solid state to 1178 cm^{-1} in carbon tetrachloride solution. This strongly indicates an intermolecular association which may be attributed to a dipole-dipole association, $\equiv\overset{\delta+}{P}=\overset{\delta-}{O}\ldots\overset{\delta+}{\underset{|||}{P}}=\overset{\delta-}{O}$. Hyperconjugation, *e.g.*, $=P(O)CH_2-\overset{\delta+}{H}\ldots\overset{\delta-}{O}=\underset{||}{P}-CH_3$, however, should also be taken into account when considering the association since the shift is largest for trimethylphosphine oxide. The observed reactivity of iodine with all compounds containing the $P-CH_3$ group may also be explained by this methyl hyperconjugation effect. Thus, whereas the triethylphosphine oxide-iodine complex is stable in carbon tetrachloride, trimethylphosphine oxide reacts with iodine. Further evidence for hyperconjugation in the methylphosphines is provided by the fact [20] that they are much stronger bases than other phosphines.

REFERENCES

1. Aksnes, G. and Gramstad, T. *Acta Chem. Scand.* **14** (1960) 1485.
2. Gramstad, T. *Acta Chem. Scand.* **15** (1961) 1337.
3. Tsubomura, H. and Kliegman, J. H. *J. Am. Chem. Soc.* **82** (1960) 1314.
4. Benesi, H. A. and Hildebrand, J. H. *J. Am. Chem. Soc.* **70** (1948) 2832; **71** (1949) 2703.
5. Mulliken, R. S. *J. Am. Chem. Soc.* **72** (1950) 600, **74** (1952) 811; *J. Phys. Chem.* **56** (1952) 801, **23** (1955) 397; *Rec. trav. chim.* **75** (1956) 845.
6. Hassel, O. and Hvoslef, J. *Acta Chem. Scand.* **8** (1954) 873; **10** (1956) 138.
   Hassel, O. and Römming, C. *Acta Chem. Scand.* **10** (1956) 696; **11** (1957) 195.
   Hassel, O. *Proc. Chem. Soc.* **1957** 250.
   Hassel, O. and Strömme, K. O. *Acta Chem. Scand.* **13** (1959) 275.
   Hassel, O. and Hope, H. *Acta Chem. Scand.* **14** (1960) 391.
7. Strömme, K. O. *Acta Chem. Scand.* **13** (1959) 268.
8. Person, W. B., Humphrey, R. E., Deskin, W. A. and Popov, A. J. *J. Am. Chem. Soc.* **80** (1958) 2049; **81** (1959) 273.
   Person, W. B., Erickson, R. E. and Buckles, R. E. *J. Am. Chem. Soc.* **82** (1960) 29.
9. de Maine, P. A. D. *J. Chem. Phys.* **26** (1957) 1189, 1192, 1199.
10. Andrews, L. J. and Keefer, R. M. *J. Am. Chem. Soc.* **77** (1955) 2164.
11. Schmulbach, C. D. and Drago, R. S. *J. Am. Chem. Soc.* **82** (1960) 4484.
12. Tsubomura, H. and Lang, R. P. *J. Am. Chem. Soc.* **83** (1961) 2085.
13. Autrey, A. D. and Connick, R. E. *J. Am. Chem. Soc.* **73** (1951) 1842.
14. Buckles, R. E., Yuk, J. P. and Popov, A. I. *J. Am. Chem. Soc.* **74** (1952) 4379.
15. Nagakura, S. *J. Am. Chem. Soc.* **80** (1958) 520.
16. Tsubomura, H. *J. Am. Chem. Soc.* **82** (1960) 40.
17. Benesi, H. A. and Hildebrand, J. H. *J. Am. Chem. Soc.* **71** (1949) 2703.
18. Gramstad, T. *Acta Chem. Scand.* **16** (1962) 807.
19. Miller, C. D., Miller, R. C. and Rogers, W. *J. Am. Chem. Soc.* **80** (1958) 1562.
20. Kaesz, H. D. and Stone, F. C. A. *J. Am. Chem. Soc.* **82** (1960) 6213.
21. Reid, C. and Mulliken, R. S. *J. Am. Chem. Soc.* **76** (1954) 3869.
22. Brandon, M., Tamres, M. and Searles, S. *J. Am. Chem. Soc.* **82** (1960) 2129.
23. Tamres, M. and Brandon, M. *J. Am. Chem. Soc.* **82** (1960) 2134.
24. Yamada, H. and Kozima, K. *J. Am. Chem. Soc.* **82** (1960) 1543.
25. Gramstad, T. *To be published.*
26. Gramstad, T. and Fuglevik, W. *To be pubslihed.*

Received October 28, 1961.

ACTA CHEMICA SCANDINAVICA 16 (1962) 1015–1026

Lipid Formation in *Cryptococcus terricolus*

IV. Separation of the Lipid Extract by Silicic Acid Column Chromatography

T. A. PEDERSEN*

Royal Institute of Technology, Division of Food Chemistry, Stockholm 70, Sweden

A chromatographic method has been developed which makes possible the separation of the lipids from the yeast *Cryptococcus terricolus*. The phospholipids were separated from the other lipid components by means of their greater adsorption values on a silicic acid column. By a subsequent elution of the adsorbed phospholipids with methanol, a separation of this material into three fractions was obtained. The free fatty acids were removed from the neutral lipids by adsorption on an Amberlite IRA-400 anion exchanger column. The neutral lipids could thereafter be fractionated into sterol esters, triglycerides, free sterols, diglycerides, and monoglycerides by elution with diethyl ether-petroleum ether mixtures from a silicic acid column.

The following composition of the total yeast lipids was established: phospholipids 1.8 %, free fatty acids 2.6 %, sterol esters 0.4 %, triglycerides 91.6 %, free sterols 0.6 %, diglycerides 2.5 %, and monoglycerides 0.3 %. As a contamination in the last part of the free sterol fraction (probably in the form of diglycerides), an amount equal to 0.3 % of the total material was found. The total amount eluted was 100.1 % of the material added. The phospholipid fraction was composed of 38 % of cephalins and 61 % of lecithin. The remaining 1 % consisted of phospholipids containing not only choline, but also nitrogen bases with free amino groups.

With their dominating content of triglycerides, the lipids of *C. terricolus* seem to differ from most other microbial lipids. The possible connection of this result with the extraction procedure used is discussed.

In earlier papers in this series, the effects of varying cultural conditions on the lipid synthesis in *Cryptococcus terricolus* have been investigated [1,2]. Under optimum conditions, the cells were found to contain more than 60 % of lipids on a dry weight basis. After the development of a mild extraction procedure for the yeast lipids [3], it was considered possible, by means of separations of the lipid mixture into its major fractions, to get an idea of the native

* Present address: Department of Microbiology, Agricultural College of Norway, Vollebekk, Norway.

composition of the cell lipids. Only a slight amount of knowledge has been accumulated concerning the composition of the lipids in yeasts. Recently, however, some investigations have been carried out to establish the total fatty acid composition of yeast lipids [4,5]. The separation of the major lipid classes, followed by analyses of the fatty acid composition of the individual fractions, will probably yield some further information on the metabolism of the fatty acids.

The most widely employed adsorbent for lipid separations, when the column chromatographic technique is used, is silicic acid. A separation of the phospholipids from the other lipid components was obtained by Borgström [6], and a fractionation of the individual phospholipid components by Hanahan *et al.*[7] Using model compounds, Borgström [8,9] found that silicic acid was also suitable for the fractionation of the neutral lipids. Barron and Hanahan [10] were able to obtain a separation of the neutral lipids of rat liver, beef liver, and yeast by elution with the non-polar solvent hexane in combinations with benzene and diethyl ether. However, they did not succeed in separating triglycerides and free fatty acids. Hirsch and Ahrens [11] investigated the adsorptive properties of silicic acid for various known lipids, when eluted with petroleum ether-diethyl ether mixtures. Using selected mixtures of this solvent system, they found that effective separations of complex lipid materials, *e.g.* human plasma, could be obtained by elution from a single column. Since this is of great practical advantage, the same method was tried in preliminary experiments, to obtain a separation of the complex *C. terricolus* lipids.

EXPERIMENTAL

The method for growing the organism, the extraction procedures, and the method used for the purification of the lipids have been described elsewhere [3].

Silicic acid powder ("Baker Analyzed" Reagent) was used by Borgström [6] after activation without any further standardizing treatments. To get a convenient flow rate through the column, Celite Analytical Filter-aid (Johns-Manville) has to be added to half the weight of the silicic acid. However, on elution with polar solvents, such as methanol, it was found in the present work that parts of the silicic acid was washed out from the column. This was avoided when the silicic acid was further prepared before use, according to the Hirsch and Ahrens [11] method. 200 g of silicic acid was placed in a 2 l glass cylinder. Absolute methanol was added to the 2 l mark and the silicic acid suspended by rapid agitation. After exactly 30 min settling, the methanol and the suspended silicic acid were decanted and discarded. This procedure was repeated once with methanol and twice with diethyl ether. As a result of the elimination of the part of the silicic acid that could be washed out with polar solvents, the flow rate also increased thus rendering the addition of Celite unnecessary.

To prepare the column, 18 g of treated silicic acid was taken from a batch of adsorbent dried for 24 h at 120°C, and dusted into a glass tube (diameter 20 mm). The tube was furnished with a sintered glass plate, which was covered by a circular disk of diethyl ether-extracted filter paper. After packing the column, the silicic acid was further activated according to the method of Hirsch and Ahrens [11].

The anion exchanger Amberlite IRA-400 column was prepared according to the method described by Borgström [8]. A column 100 mm in height and 20 mm in diameter was used. The elution followed the procedure described by Borgström [8]. To achieve the best possible separation, the first eluate was passed once more through the column.

The yeast lipids were dissolved in a small volume of petroleum ether and pipetted on to the column. The total volume of solvent used for charging the column was always kept under 20 ml. The lipid amount added never exceeded 250 mg.

All solvents used for elution were of reagent grade, redistilled in glass. The diethyl ether was distilled over sodium and stored at 0—5°C. Large elution fractions were collected in Erlenmeyer flasks, while for smaller fractions an automatic collector was used.

The solvent was removed from the large fractions using a rotary vacuum evaporator. The small fractions collected in tubes were dried by a combination of moderate heating on a water bath and simultaneous bubbling with nitrogen. The samples were weighed after drying overnight in a vacuum desiccator. The resulting dry matter was redissolved in a known volume of solvent and aliquots taken out for analyses.

The methods used for the determinations of the phosphorus content, the free amino group content, and the carbohydrate content, as well as the qualitative test for free and esterified sterols, have been briefly described in a previous communication [3].

The content of free fatty acids was determined by titrating with 0.01 M tetramethyl ammonium hydroxide from a micrometer burette (graduated to 0.2 μl), using thymol blue as indicator [12].

The total, esterified fatty acid content was determined using the method modified by Morgan and Kingsbury [13]. This procedure is based on the formation of hydroxamic acids which react with ferric chloride to form coloured complexes having an absorption maximum at 515 mμ. The final, coloured product was compared with a glyceryl monostearate standard.

The quantitative estimation of glycerol followed mainly the method described by Hanahan and Olley [14]. However, the lipid material, usually dissolved in petroleum ether, was pipetted quantitatively into soda glass tubes, and evaporated to dryness. The dry material plus 1 ml of 2 N hydrochloric acid was enclosed in an ampoule and hydrolyzed for 48 h at 100°C. Thereafter, the oxidation of glycerol by periodate and the colorimetric measurement of the chromotropic acid-formaldehyde reaction at 570 mμ, followed strictly the method mentioned.

The sterol content was in some cases determined quantitatively according to the method used by Stadtman [15]. Principally the procedure followed that of Lieberman-Burchard, but, in this case, the colour was measured colorimetrically at 625 mμ. Ergosterol was used as a standard.

The presence of acetal types of phospholipids was investigated with Schiff's reagent, according to the method described by Marinetti *et al.*[16]

As will be shown in these investigations, free amino groups are absent from one fraction of the eluted phospholipids. Consequently, analyses for choline had to be performed. The choline-phosphomolybdate method of Wheeldon and Collins [17] was not sensitive enough for detecting the very small amounts present in the collected phospholipid fractions. Recently, a micro method has been worked out by Ackerman and Chou [18] for the determination of choline down to 1 μg, by precipitating choline reineckate from alkaline solutions, followed by measurements of the absorption at 303 mμ. A Beckman model DU spectrophotometer was used in all of the colorimetric determinations.

RESULTS AND DISCUSSION

To achieve an effective separation of the *C. terricolus* lipids, the method of Hirsch and Ahrens [11] was tried. Judging from Fig. 1, it can be concluded that an absolute separation of the phospholipids from the other components of the lipid mixture was obtained. The phospholipids were further separated into three fractions (Fig. 1A, right) by elution with absolute methanol alone. While the first and third peaks contained free amino groups in their phospholipid nitrogen bases, the material in the tubes 134—137 contained no such bases (Fig. 1B, right).

By multiplying the phosphorus content by the approximate factor 25, the total phospholipid content was found to be 3.0 mg, or 1.5 % of the total lipid material. By multiplying the sum of the serine contents by the mean factor 7.8, it was concluded that half of the phospholipids contained nitrogen bases with free amino groups.

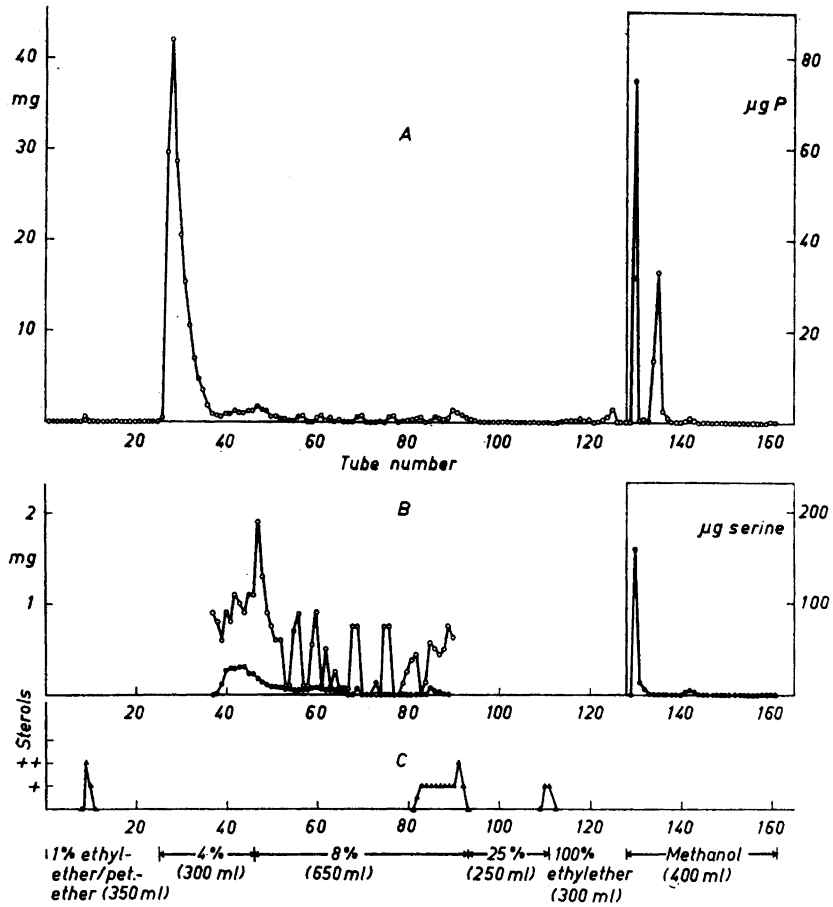

Fig. 1. Separation of *Cryptococcus terricolus* lipids on silicic acid column. The abscissas show the tube number collected fractionally, and the various solvents used to effect elution. Charge: 206.9 mg of lipids. Eluted: 206.2 mg of lipids.

A. ○ Amount eluted in each tube. Phosphorus test negative in the left part of the figure.

B. Left: ● Amount of titratable fatty acids expressed as oleic acid. ○ Total amount eluted in each tube.
Right: ● Amount of free amino groups expressed as serine.

C. ▲ Peaks showing the presence of sterols. Amounts approximately measured by visual readings.

The elution of the neutral lipids and the free fatty acids resulted in a great many peaks (Fig. 1A, left).

All fractions containing esterified fatty acids will be further analyzed at a later stage of this investigation. However, it is convenient to mention the different fractions by their supposed names already in the following.

A single fraction was eluted with 1 % diethyl ether in tubes 9 and 10. This material gave a positive Lieberman-Burchard test (Fig. 1C). As found by

Hirsch and Ahrens [11], the sterol esters were eluted by this solvent mixture, while the free sterols were more strongly adsorbed on the column. The total amount of sterol esters was found to be below 0.5 % of the total material.

The dominant fraction of the lipid material was eluted with 4 % diethyl ether in petroleum ether. Tubes 26—37 contained in all 165.3 mg, or 79.9 % of the lipid material. As shown below, this fraction was composed of triglycerides. The elution of the free fatty acids started in tube 38 and proceeded more or less continuously in the subsequent 50 tubes (Fig. 1B, left). In addition, it will be seen that the amount of free fatty acids present did not constitute the total content of material in these particular tubes. The elution of triglycerides was probably not finished before the elution of the free fatty acids began.

The lipid material contained at least two different free sterols (Fig. 1C). The last peak seemed to be eluted separately but in inweighable amounts. The sterol contents in tubes 81—92 were also very low and could not account for the total contents of eluate in these tubes.

Finally, judging from the elution pattern found by Hirsch and Ahrens [11], it was considered likely that the peak eluted with 100 % diethyl ether was composed of monoglycerides.

The possible difficulties in obtaining effective separations by this elution system were briefly pointed out by Hanahan [19]. The successful separation obtained by Hirsch and Ahrens [11] was due to the comparatively simple composition of the human plasma lipids investigated. It was to be expected that more complex mixtures, especially those with a higher content of unsaturated derivatives, would complicate the fractionation. However, by modifying the

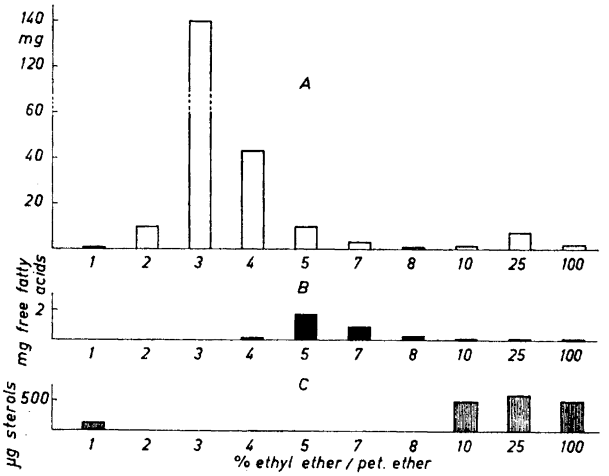

Fig. 2. Separation of *Cryptococcus terricolus* lipids on silicic acid column. Lipids eluted with 200 ml portions of different diethylether/petroleum ether mixtures. Phospholipids removed before start. Charge 215.3 mg of lipids. Eluted: 214.7 mg of lipids.
A. Weight in mg of each fraction.
B. Amount of titratable fatty acids expressed as mg of oleic acid.
C. Content of sterols expressed as µg of ergosterol.

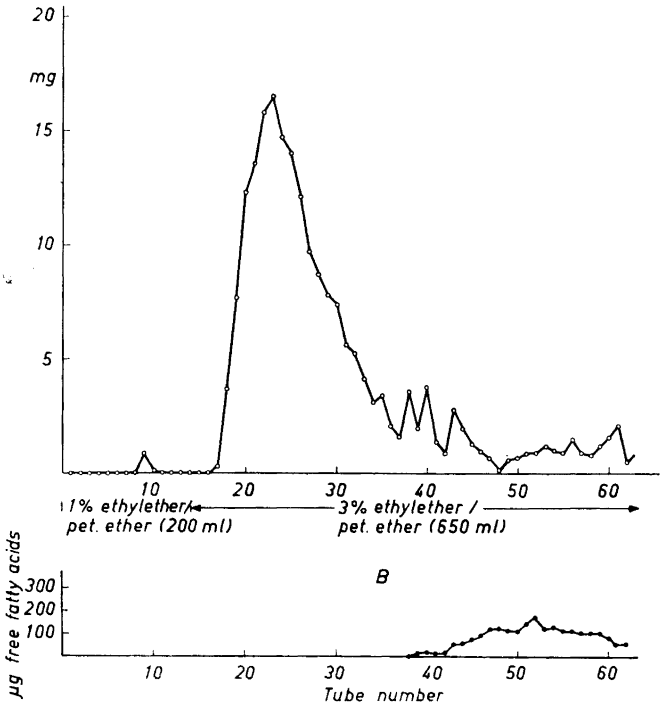

Fig. 3. Separation of *Cryptoccocus terricolus* lipids on silicic acid column. Lipids eluted with 1 and 3 % solvent mixtures.
A. O Weight in mg of each fraction.
B. ● Amount of titratable fatty acids expressed as µg of oleic acid.

solvent system, it was thought possible to obtain a better separation of the triglycerides from the free fatty acids.

The distribution of the lipid fraction, when eluted with 200-ml portions of ten different diethyl ether/petroleum ether mixtures with increasing diethyl ether contents, is shown in Fig. 2. As before, the sterol esters were eluted with 1 % diethyl ether in petroleum ether. By multiplying the amount of free sterols, computed as ergosterol after hydrolysis, by the factor 1.4, it was possible to calculate approximately the content of sterol esters. It will be seen that the sterol ester content was not sufficient to account for the total material eluted in this fraction (Figs. 2A and 2C). The elution of the triglyceride fraction began with the 2 % solvent mixture. The main amount, however, was eluted with 3 % diethyl ether in petroleum ether. The triglyceride fraction had so far been obtained free from titratable fatty acids. When the diethyl ether content in the solvent mixture was further increased, however, the elution of the free fatty acids began. Approximately 80 % of the total free fatty acid content was eluted with the 5 and 7 % mixtures, but traces were found present in all subsequent fractions. With this elution method, approximately 70 %

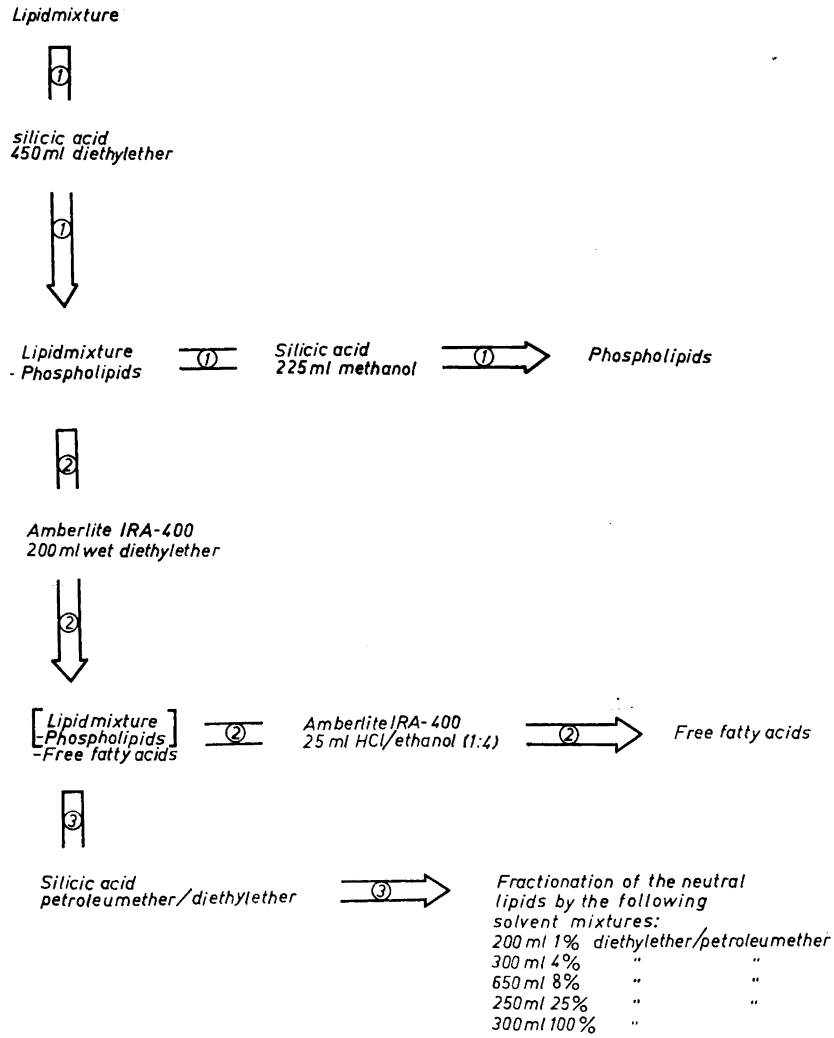

Fig. 4. Elution scheme for fractionation of *Cryptococcus terricolus* lipids. As shown by the numbers, three different columns are used.

of the lipid material was obtained without any content of free fatty acids. Free sterols were present in the last three fractions.

It was assumed that part of the lipid material eluted with 4 % diethyl ether might be obtained free from titratable fatty acids by increasing the amount of the 3 % solvent mixture added to the column. As a result of this procedure (Fig. 3), 81 % of the lipid material was obtained completely free from titratable fatty acids. However, even with the 3 % mixture, the elution of the free

fatty acids began, and continued, as shown in Fig. 2, during the elution of the other neutral lipid components. It was, therefore, assumed that, with this solvent system it would be impossible to obtain a total separation of the free fatty acids from the different glycerides.

It was considered necessary to achieve a total removal of the free fatty acids from the remaining neutral lipids by means of special procedures. Borgström[8] successfully used the Amberlite anion exchanger IRA-400 for this purpose. After passing the material, dissolved in wet petroleum ether, twice through the column, less than 0.1 % of the free fatty acids could be detected in the eluted neutral lipids. No changes in the fatty acid composition were detected, and the elution could be performed quantitatively. However, before adding the lipids to the ion exchanger column, the phospholipids had to be removed, to avoid the simultaneous adsorption of the polar phospholipids. As a consequence of this special removal of both the phospholipids and the free fatty acids, the separations had to be performed on three different columns, two of which, however, were identical (Fig. 4). Three different organic solvents were used throughout the separations, except in the special treatment to release the adsorbed fatty acids from the ion exchanger.

The results of the fractionation obtained with this "three column" technique are shown in Fig. 5. By this procedure the phospholipids were also separated into two large fractions (tubes 2—4 and 4—11) and one very small fraction (tube 15) (Fig. 5A, left). Because of the strong adsorption of the phospholipids to the silicic acid, addition of a larger volume of non-polar solvents had no effect on the elution results. The total phosphorus content was found to be 110.5 μg, corresponding to approximately 2.8 mg of phospholipids. This amount, as well as the fractionation pattern obtained, agrees fairly well with the results given in Fig. 1. The presence of free amino groups (computed as serine) was found in the first and the last fraction of the eluted phospholipids (Fig. 5B, left). The material in each of the three phospholipid fractions was combined and choline determined. No choline was found to be present in the first elution peak of Fig. 5 (tubes 1—3). The next peak (tubes 4—11) contained 290 μg of choline, corresponding to approximately 1 600 μg of lecithin, which agrees very well with the amount of material eluted. The third peak (tubes 14—16) contained 43 μg of choline, indicating that a mixture of lecithin and, perhaps, sphingomyelin, together with some free amino group-containing substance(s) (the serine reaction was also positive) was included in this peak. No further attempts were made to identify these minor substances.

Acetal types of lipids are often found in various phospholipids. No significant results were obtained, however, by using Schiff's test on the three different phospholipid fractions, and these compounds were thus at most present only in trace amounts. The same could be said of the presence of sugars in the eluted phospholipid fractions.

The phospholipid contents of different yeasts have often been found to be very high, varying from 13 up to 80 %, if calculated on the basis of the lipid content [20]. It is essential to point out here that these investigations were performed with yeasts containing only a few per cent of lipids. Nilsson and Nielsen [21] stated that the phospholipid content decreased in proportion to the increase of lipids in *Rhodotorula gracilis*. With 53.6 % of lipids in their

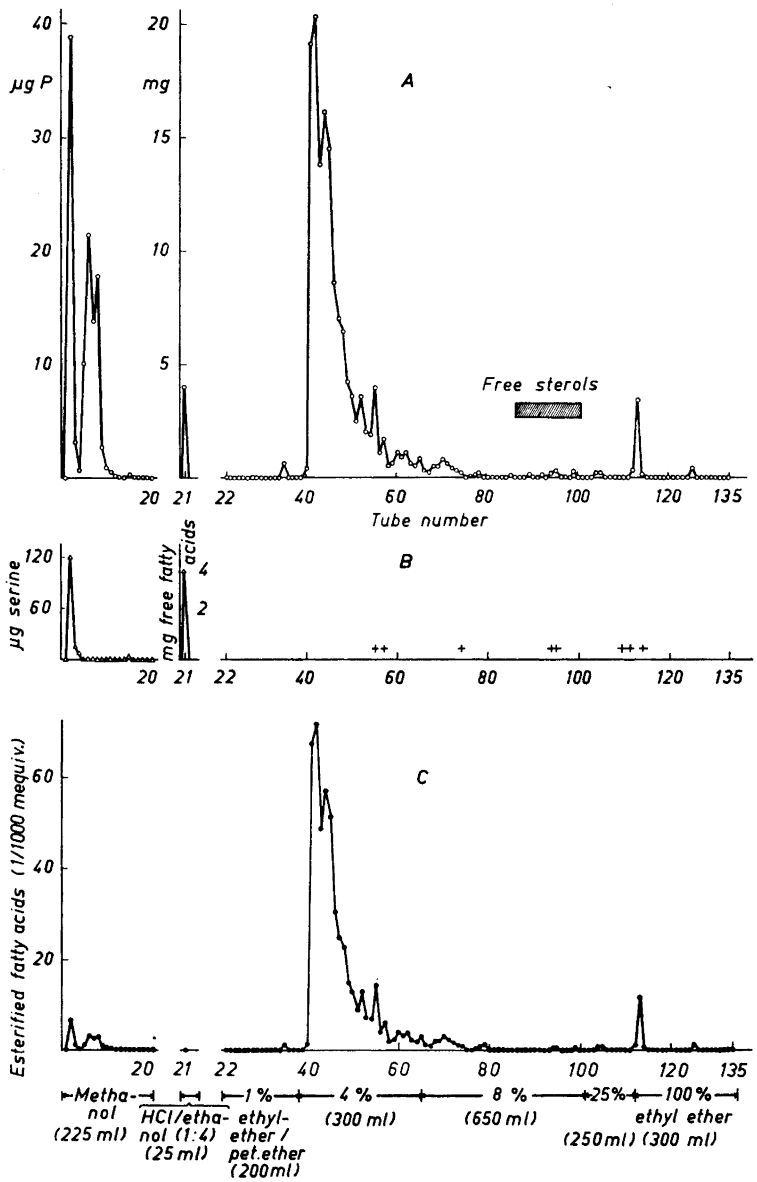

Fig. 5. Separation of *Cryptococcus terricolus* lipids. Charge: 154.0 mg. Eluted: 154.4 mg. Tubes 1—20: Phospholipid fraction. Tube 21: Fatty acids. Tubes 22—135: Neutral lipids.
A. O Amount eluted in each tube.
B. Left: △ Amount of free amino groups expressed as serine.
Right: △ Amount of titratable fatty acids expressed as oleic acid. + indicates traces of free fatty acids.
C. ● 1/1000 mequiv. of esterified fatty acids.

yeast, they found a phospholipid content of the same magnitude as that found for *Cryptococcus terricolus*.

The content of free fatty acids which comprised only 4.0 mg, or 2.6 % of the total eluted lipid material, was collected in tube 21 (Fig. 5A). As pointed out by Kleinzeller [20], there seems to be some clear indications that a considerable amount of free fatty acids may be present in microorganisms. However, as far as yeasts are concerned, the results reviewed by Kleinzeller [20] were obtained by extractions of acid-hydrolyzed cell materials. The possible hydrolytic release of esterified fatty acids as a result of such treatments, should of course be kept in mind. Barron and Hanahan [10] found the free fatty acids to constitute *ca.* 60 % of the total lipids in *Saccharomyces cerevisiae* cells. In their experiments, the lipids were extracted with ethanol-diethyl ether without any pretreatment of the cells. However, repeated 8-hour extraction periods were used, and the presence of fatty acids may perhaps be partly explained as a result of an enzymatic action. It is well known that lecithinases are solvent activated during the extraction procedure. Consequently, in phospholipid-rich materials, or if the same activation phenomenon occurs for the lipolytic enzymes in fat-rich materials, an extensive production of free fatty acids would be possible. By means of the short-time technique used for the extraction of the *Cryptococcus terricolus* lipids, the enzymatic degradation is kept at a minimum. Small amounts of free fatty acids occur in all native lipid mixtures. The amount found in the present material is thus probably not the undesired result of the extraction treatments.

However, the results obtained recently by Hartman *et al.*[4] do not fit in with this view. The high acid value found by them for *Rhodotorula graminis* lipids is of a magnitude often found in earlier investigations with other "fat" yeasts. They supposed that no enzymatic splitting of the neutral fats occurred during their extraction procedure, but, according to the present author, some reservations should be made. The extractions were performed by heating in Soxhlet extractors, or by refluxing, and certain parts of the lipid mixtures (12—21 %) were obtained after acid hydrolysis of the yeast material. These methods do not exclude the possibility of a release of free fatty acids.

After the removal of the free fatty acids, the elution of the neutral lipids resulted in a clearer and more easily identifiable fractionation pattern than that found earlier (Fig. 5A, right). As before, the sterol esters were eluted with 1 % diethyl ether in petroleum ether. The content of esterified fatty acids in this fraction is shown in Fig. 5C. In agreement with the results obtained by Hirsch and Ahrens [11], the free sterols were removed from the column after the elution of the triglyceride fraction. The materials in tubes 86—100 gave a positive Lieberman-Burchard reaction. These tubes contained, in all, approximately 1.0 mg of lipid materials. Using the quantitative sterol test, this amount could be accounted for if the sterols were computed as ergosterol. The free sterol fraction was probably composed of a complex of different sterols, as indicated by the several peaks obtained on elution. Judging from Fig. 5C, however, the sterols in tubes 94—100 seemed to be impure, since, in addition, esterified acids were found. The complete separation of ergosterol and diglycerides was found by Barron and Hanahan [10] to be impossible in their diethyl ether-hexane elution system, although cholesterol and diglycerides were easily

Table 1. Presence of different glyceride types in lipids from *Cryptococcus terricolus*. The italicized alternatives show the actual glyceride in each fraction tested.

Material		EFA 1/1000 mequiv.	EFA mg	EFA per mg of material	mg of glyceride calculated per mg of material		
Tubes	Weight in mg				MG	DG	TG
41— 48	105.8	377	95.76	0.905	1.23	1.07	*1.01*
104—114	3.2	10.65	2.71	0.847	1.15	*1.00*	0.94
125	0.4	1.14	0.29	0.725	*0.99*	0.85	0.81

Abbreviations: EFA- esterified fatty acids, MG-monoglyceride, DG- diglyceride, TG-triglyceride.
Average molecular weight of fatty acids, calculated: 271.

separated. The difficulties in obtaining effective separations when ergosterol is present are due to the larger polarity of ergosterol, as compared with that of cholesterol, resulting in too small chromatographic differences between the ergosterol and the diglycerides. The free sterols amounted to *ca.* 0.6 % and the sterol esters to *ca.* 0.4 % of the total lipid material. These amounts are within the limits usually found for lipid-rich yeasts.

The triglycerides were eluted in tubes 39—79. Many peaks were obtained in this fraction, indicating to a certain extent the complex composition of the triglyceride mixture. The total weight of the contents in these tubes amounted to 141.4 mg, or 91.6 % of the eluted material. By this quantitative dominance of the triglyceride fraction, *Cryptococcus terricolus* differs markedly from other "fat" yeast species studied so far. Barron and Hanahan [10], in one of the few investigations on the separation of yeasts lipids, found their "triglyceride" fraction to constitute 71.0 % of the total cell lipids. However, upon further analysis, 81 % of this fraction was found to be composed of free fatty acids. On the other hand, in tissues of living plants and animals, free fatty acids are generally considered to occur in very small amounts or to be completely lacking. Judging from the above results, the same seems to be the case with *C. terricolus* cells.

The most direct method to determine whether the three main peaks (tubes 40—79, 104—114, and 125, respectively) in the fractionation scheme in Fig. 5A (right) were composed exclusively of tri-, di-, and monoglycerides, respectively, would be to determine the total content of fatty acids and glycerol of each peak individually. However, it was found difficult to obtain reproducible results, within the limits necessary here, with the method used for the glycerol analysis [14]. The varying results were probably due to difficulties encountered in obtaining quantitative hydrolysis of the lipid materials in the different experiments. Instead of performing further investigations concerning this method, the content of esterified fatty acids in each fraction was determined [13]. The material in tubes 41—48 was collected and used as a sample of the proposed triglyceride fraction, while tubes 104—114 and 125 were supposed to contain diglycerides and monoglycerides, respectively. When expressing the results as mg of esterified fatty acids, it was assumed that the various fatty

acids found by preliminary gas-chromatographic analyses were equally distributed over all the fractions. On the basis of this suggestion, the average molecular weight of the fatty acids was calculated at 271.

On the basis of the amounts of esterified fatty acids found per mg of material in each of the three different samples, three alternatives were calculated, *viz.* that the material in question be composed exclusively of either mono-, di-, or triglycerides (Table 1). With the great precision in the experimental techniques used (coefficient of variation far below 1 %), it could be proved that tubes 41—48 contained triglycerides, tubes 104—114 diglycerides, and the last tube (125) monoglycerides. Judging from these results, it may be concluded that the separation of the fat component of the *C. terricolus* lipids into tri-, di-, and monoglycerides can be performed by means of the technique described.

Acknowledgements. This work has been supported by the *Royal Norwegian Council for Scientific and Industrial Research via* the Scandinavian Centres for Advanced Training, Growing Points Programme. The author wishes to express his gratitude to Dr. B. Samuelsson for helpful discussions in the planning of this investigation. The skilful analytical work of Mr. L.-G. Bodin is greatly appreciated.

REFERENCES

1. Pedersen, T. A. *Acta Chem. Scand.* **15** (1961) 651.
2. Pedersen, T. A. *Acta Chem. Scand.* **16** (1962) 359.
3. Pedersen, T. A. *Acta Chem. Scand.* **16** (1962) 374.
4. Hartman, L., Hawke, J. C., Shorland, F. B. and diMenna, M. E. *Arch. Biochem. Biophys.* **81** (1959) 346.
5. Deinema, M. H. *Meded. Landbouwhogeschool, Wageningen* **61** (1961) 1.
6. Borgström, B. *Acta Physiol. Scand.* **25** (1952) 101.
7. Hanahan, D. J., Dittmer, J. C. and Warashina, E. *J. Biol. Chem.* **228** (1957) 685.
8. Borgström, B. *Acta Physiol. Scand.* **25** (1952) 111.
9. Borgström, B. *Acta Physiol. Scand.* **30** (1954) 231.
10. Barron, E. J. and Hanahan, D. J. *J. Biol. Chem.* **231** (1958) 493.
11. Hirsch, J. and Ahrens, Jr., E. H. *J. Biol. Chem.* **233** (1958) 311.
12. Entenman, C. in Colowick, S. P. and Kaplan, N. O. *Methods in Enzymology*, Vol. III, Academic Press, New York 1957.
13. Morgan, D. M. and Kingsbury, K. J. *Analyst* **84** (1959) 409.
14. Hanahan, D. J. and Olley, J. N. *J. Biol. Chem.* **231** (1958) 813.
15. Stadtman, T. G. in Colowick, S. P. and Kaplan, N. O. *Methods in Enzymology*, Vol. III, Academic Press, New York 1957.
16. Marinetti, G. V., Erbland, J. and Kochen, J. *Federation Proc.* **16** (1957) 837.
17. Wheeldon, L. W. and Collins, F. D. *Biochem. J.* **70** (1958) 43.
18. Ackerman, C. J. and Chou, M. *Analyt. Biochem.* **1** (1960) 337.
19. Hanahan, D. J. *Lipide chemistry*, Wiley, New York 1960.
20. Kleinzeller, A. *Advances in Emzymol.* **8** (1948) 299.
21. Nilsson, N. G. and Nielsen, N. *Acta Chem. Scand.* **7** (1953) 1067.

Received December 4, 1961.

ACTA CHEMICA SCANDINAVICA 16 (1962) 1027–1030

The Structure of an Aldopentaouronic Acid from a Birch Wood Xylan

TORE E. TIMELL

Pulp and Paper Research Institute of Canada and McGill University, Montreal, Canada

An aldopentaouronic acid has been isolated after enzymatic hydrolysis of a 4-*O*-methylglucuronoxylan from white birch wood. The compound has been identified as *O*-(4-*O*-methyl-α-D-glucosyluronic acid)-(1 → 2)-*O*-β-D-xylopyranosyl-(1 → 4)-*O*-β-D-xylosyl-(1 → 4)-*O*-β-D-xylosyl-(1 → 4)-D-xylose.

In previous communications [1,2] a brief account was given of preliminary results obtained on treating a 4-*O*-methylglucuronoxylan from white birch wood with a commercial pectinase enzyme The xylan had previously been shown to contain a linear framework of (1→4)-linked β-D-xylose residues, every tenth of which, on the average, carried a (1→2)-linked 4-*O*-methyl-α-D-glucuronic acid residue [3]. The enzymic hydrolysis was carried out inside a semipermeable membrane, suspended in a large volume of water as suggested by Painter [4]. Oligosaccharides formed rapidly diffused through the membrane into the outside water, thus escaping further hydrolysis. Considerable improvement in yield of oligomers was achieved as could also be expected from the theoretical treatment of Kuhn [5]. Two series of oligosaccharides were obtained, one neutral and the other acidic. This paper deals with the constitution of one of the sugar acids, an aldopentaouronic acid.

The enzymatic hydrolysis yielded a mixture of sugars which was resolved into an acid and a neutral portion with an anion exchange resin. The acids were separated by gradient elution from charcoal-Celite. One of the acids with $[\alpha]_D$ + 0.63° had a rate of movement on the paper chromatogram typical of a pentaouronic acid [6]. It was obtained in a yield of 11 % of the original sugar mixture. Its methoxyl content, equivalent weight, and behaviour on partial hydrolysis suggested that it consisted of one *O*-methylglucuronic acid and four xylose residues.

The pentaouronic acid was methylated, first according to Haworth and subsequently by the method of Kuhn *et al.*[7] The fully methylated acid was subjected to methanolysis under conditions known to leave glycuronosidic linkages intact. The methyl ester-methyl glycoside component was saponified

and acidified and the acid and neutral glycosides were separated with an anion exchange resin. The acid fraction contained only one compound, a fully methylated aldobiouronic acid, which was esterified and reduced with lithium aluminum hydride. The partly methylated disaccharide thus obtained could not be induced to crystallize. Hydrolysis gave equimolar amounts of a di-*O*-methylxylose and a tri-*O*-methylglucose, which were separated by paper chromatography. The xylose derivative was identified as 3,4-di-*O*-methyl-D-xylose and the glucose as 2,3,4-tri-*O*-methyl-D-glucose. The methylated aldobiouronic acid was accordingly methyl 2-*O*-[methyl(2,3,4-tri-*O*-methyl-α-D-glucosyl)uronate]-3,4-di-*O*-methyl-D-xyloside. The neutral glycoside fraction was hydrolysed. It contained only one compound, characterized as 2,3-di-*O*-methyl-D-xylose, three moles being obtained per mole of tri-*O*-methylglucose.

Four alternative structures are possible for an aldopentaouronic acid of the present type. Of these, three on methanolysis and subsequent hydrolysis would give rise to one mole of 3-*O*-methylxylose in the acid fraction while the neutral portion would consist of one mole of 2,3,4-tri-*O*-methylxylose and 2 moles of 2,3-di-*O*-methylxylose. The fourth alternative alone, where the acid group is attached to the non-reducing end group of a xylotetraose, is consistent with the present data.

This conclusion was corroborated by the behaviour of the pentaouronic acid on oxidation with periodate, when 6 moles of oxidant were consumed per molecule, with concomitant formation of 2 moles of formic acid. These results could only have been obtained with a compound of the type referred to above. The combined evidence shows that the aldopentaouronic acid was *O*-(4-*O*-methyl-α-D-glucosyluronic acid)-(1→2)-*O*-β-D-xylopyranosyl-(1←4)-*O*-β-D-xylosyl-(1→4)-*O*-β-D-xylosyl-(1→4)-D-xylose.

The nature of the other oligosaccharides formed during the enzymatic hydrolysis and the possible mechanism of the latter will be discussed elsewhere [8].

EXPERIMENTAL

Specific rotations were determined at 20°C and melting points are corrected. Evaporations were carried out *in vacuo* at 40—50°. Sugars were separated on Whatman No. 1 filter paper and, for preparative purposes, on No. 3MM papers provided with a wick of paper No. 50. Solvents (v/v) were (A) ethyl acetate-acetic acid-water (18:7:8), (B) butanone saturated with water and containing 2 % of ammonia, and (C) ethanol-benzene-water (47:200:15). The spray reagent was *o*-aminodiphenyl.

Isolation of the aldopentaouronic acid. The enzymic hydrolysis was carried out with a 4-*O*-methylglucuronoxylan from birch wood [3] and a 0.2 % aqueous solution of a commercial enzyme preparation ("Pectinase", Nutritional Biochemical Corporation, Cleveland, Ohio). Both were kept inside a cellophane dialysing tubing, surrounded by a large quantity of water, as described previously [1,2]. In a typical experiment, neutral and acidic sugars were separated with a Dowex 1-X4 exchange resin (acetate form). The acid mixture (15 g, 40 % of the total) was resolved by gradient elution with aqueous ethanol on a charcoal-Celite column to give a series of uronic acids.

The aldopentaouronic acid was dissolved in water, treated with Amberlite IR-120 exchange resin (acid form), and recovered by repeated evaporations from acetone as a white, amorphous solid (3.6 g), $[\alpha]_D$ + 0.63° (water, *c* 2.6). (Found: OCH_3 4.00; equiv.wt[9]. 737. Calc. for $C_{27}H_{44}O_{23}$: OCH_3 4.21; equiv.wt. 736.3). Partial hydrolysis with 0.22 N sulfuric acid at 100° for 30 min. gave a series of uronic acids, from the mono- to the pen-

taouronic acid, and xylose, xylobiose, xylotriose, and xylotetraose, as indicated by paper chromatography (solvent A).

Methylation of the aldopentaouronic acid. The uronic acid (3.0 g) was dissolved in water (100 ml) containing sodium bicarbonate (5.0 g). Dimethyl sulphate (50 ml) and 40 % (w/w) aqueous sodium hydroxide (50 ml) were added dropwise over a period of 3 h at 10°. Solid sodium hydroxide (30 g) was added, followed by dropwise addition of dimethyl sulphate (50 ml). This process was repeated once. The mixture was acidified to pH 2.0 with sulphuric acid and then extracted with chloroform to give a partly methylated product (3.4 g, OCH_3 37.5 %). The latter was dissolved in dry dimethyl formamide (100 ml) and methylated with silver oxide (75 g) and methyl iodide (100 ml) in the presence of Drierite [7]. Chloroform (300 ml) was added, followed by filtration over Celite. The methylated oligosaccharide (3.2 g) was recovered in the usual way after washing with 5 % aqueous potassium cyanide [7]. Its infrared diagram indicated the absence of hydroxyl groups.

Separation of acidic and neutral sugars. A portion of the methylated compound (2.2 g) was boiled under reflux with N methanolic hydrogen chloride for 8 h. The syrup obtained (2.1 g) was treated with 5 % aqueous barium hydroxide (100 ml) at 60° for 2 h. Solid carbon dioxide was added, barium carbonate was removed by filtration through Celite and the solution was treated with Amberlite IR-120 exchange resin (acid form). The concentrated solution was added to the top of a column containing Dowex 1-X4 exchange resin (acetate form). Elution with water removed neutral glycosides (1.30 g), after which an acid fraction (0.95 g) was recovered by washing with 30 % aqueous acetic acid.

Acid fraction. The acid fraction which contained only one compound was subjected to methanolysis and the methyl ester-methyl glycoside was reduced with lithium aluminum hydride (2.0 g) in tetrahydrofuran (50 ml). The disaccharide obtained was hydrolysed with N-sulphuric acid to give a syrup (330 mg) which contained a di-*O*-methylxylose and a tri-*O*-methylglucose in equimolar quantities. The mixture was resolved by paper chromatography (solvent B).

*3,4-Di-*O*-methyl-*D*-xylose.* This sugar (75 mg) was obtained as a clear syrup with $[\alpha]_D$ + 20° (water, *c* 0.5). Its rate of movement on paper electrophoresis in 0.05 M borate buffer and on paper chromatography (solvents B and C) were the same as those of an authentic specimen. The 3,4-di-*O*-methyl-*N*-phenyl-D-xylopyranosylamine had m.p. 117—118° [10]. Its infrared diagram was identical with that of an authentic sample.

*2,3,4-Tri-*O*-methyl-*D*-glucose.* This syrup (100 mg) had $[\alpha]_D$ + 75° (water, *c* 0.6). The 2,3,4-tri-*O*-methyl-*N*-phenyl-D-glucosylamine had m.p. and mixed m.p. 142—143° [11]. Its infrared spectrum was the same as that of an authentic specimen. (Found: OCH_3 30.5. Calc. for $C_{15}H_{23}O_5N$: OCH_3 31.3.)

Neutral fraction. The neutral portion was hydrolysed with N sulphuric acid. Paper electrophoresis and paper chromatography (solvent C) showed the presence of only 2,3-di-*O*-methyl-D-xylose. The colourless syrup crystallised spontaneously on standing, m.p. 80—82° [12], $[\alpha]_D$ + 23.4° (water, *c* 1.7). (Found: OCH_3 34.4. Calc. for $C_7H_{14}O_5$: OCH_3 34.8). The 2,3-di-*O*-methyl-*N*-phenyl-D-xylopyranosylamine had m.p. and mixed m.p. 123—124° [13]. (Found: OCH_3 24.5. Calc. for $C_{13}H_{19}O_4N$: OCH_3 24.5).

Periodate oxidation of the aldopentaouronic acid. Aliquots (30—40 mg) of the uronic acid were oxidized in the dark with 0.05 M sodium metaperiodate (50 ml) at room temperature for various lengths of time. The results, given as moles oxidant consumed per mole of pentaouronic acid, were as follows:

Time, h	6	24	48	72	96
Periodate consumed	5.2	5.5	5.9	6.0	6.3

Samples (30—40 mg) of the acid were dissolved in water (10 ml) and neutralised with 0.01 N sodium hydroxide. Periodate oxidations were carried out in the same way as before. Oxidation was interrupted by addition of excess ethylene glycol. Formic acid was determined by titration with 0.01 N alkali. The following moles of formic acid were liberated per mole of pentaouronic acid:

Time, h	24	48	72	96
Formic acid	1.84	1.96	2.09	2.24

Acknowledgment. This investigation was supported in part by a United States Public Health Service Research Grant (A-4258) from the *National Institute of Arthritis and Metabolic Diseases, Public Health Service.*

REFERENCES

1. Timell, T. E. *Chem. & Ind. London* **1959** 999.
2. Painter, T. J. and Timell, T. E. *Proc. Sec. Cellulose Conf.* Syracuse, N.Y. **1959** 16.
3. Glaudemans, C. P. J. and Timell, T. E. *J. Am. Chem. Soc.* **80** (1958) 941, 1209.
4. Painter, T. J. *Can. J. Chem.* **37** (1959) 497.
5. Kuhn, W. *Ber.* **63** (1930) 1503.
6. Hamilton, J. K. and Thompson, N. S. *J. Am. Chem. Soc.* **79** (1957) 6464.
7. Kuhn, R., Trischmann, H. and Löw, I. *Angew. Chem.* **67** (1955) 32.
8. Timell, T. E. *To be published.*
9. Hirst, E. L., Hough, L. and Jones, J. K. N. *J. Chem. Soc.* **1949** 928.
10. Jones, J. K. N. and Wise, L. E. *J. Chem. Soc.* **1952** 3389.
11. Peat, S., Schlüchterer, E. and Stacey, M. *J. Chem. Soc.* **1939** 581.
12. Hamilton, J. K., Partlow, E. V. and Thompson, N. S. *Tappi* **41** (1958) 811.
13. Ehrenthal, I., Rafique, M. C. and Smith, F. *J. Am. Chem. Soc.* **74** (1952) 1341.

Received November 30, 1961.

ACTA CHEMICA SCANDINAVICA 16 (1962) 1031–1036

Some Applications of a Benzenoid Proton Chemical Shift Rule

BØRGE BAK, JØRGEN BIRGER JENSEN, ANNE-LISE LARSEN and JOHN RASTRUP-ANDERSEN

Chemical Laboratory of the University of Copenhagen, Copenhagen, Denmark

Proton magnetic resonance spectra of 1,3-$C_6H_4(NO_2)Br$, 1,3-$C_6H_4(NH_2)Cl$, 1,4-$C_6H_4(NH_2)Cl$, 1,2,4,6-$C_2H_2(NH_2)DFD$, and 1,2,4-$C_6H_3(NH_2)DF$ have been recorded on a Varian A60 spectrometer (resonance frequency 60 Mc/s). It is shown how the use of an empirical rule on benzenoid proton chemical shifts helps considerably in an inspectional assignment which may be sufficient in itself, or may be desirable in connection with a rigorous mathematical analysis.

Since precalculation of proton chemical shifts, δ, relative to some chosen standard is practically impossible, the existence of empirical rules, such as Shoolery's rule [1] for CH_2-protons, is of importance. Rules for *benzenoid protons* have also been suggested. Recently, Diehl [2] has reviewed the pertinent literature, and he also contributed by fresh experiments. As stressed by Diehl, observation of benzenoid proton chemical shifts must be carried out on dilute solutions in a magnetically inert solvent such as cyclohexane (in contrast to aromatic solvents), if regularities are to be disclosed.

The law for benzenoid protons [2] may be exemplified as follows.

Suppose that precalculated values for the protons in the compound 1,3-C_6H_4XY are wanted. Suppose that we know the δ's for *ortho*, *meta*, and *para* protons in C_6H_5X and C_6H_5Y. Then the desired precalculation takes place following the scheme indicated in Fig. 1.

In order for the rule to be valid, no pair of substituents may be *ortho* to one another. The rule is, therefore, applicable only to *meta* and *para* disubstituted benzenes, and to 1,3,5 trisubstituted benzenes.

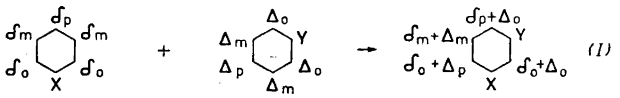

(1)

Fig. 1. Calculation of proton chemical shifts in poly-substituted benzenes from data for mono-substituted benzenes.

Table 1. Proton chemical shifts (δ_o, δ_m, δ_p) of compounds C_6H_5X (5 mole % solution in cyclohexane) in c/s relative to the protons of benzene (5 mole % solution in cyclohexane) as found Spiesecke and Schneider [4], and by Diehl [2].

X	*Spiesecke and Schneider*			*Diehl*		
	δ_o	δ_m	δ_p	δ_o	δ_m	δ_p
F	18.5	1.4	13.0	15.0	0.6	—
Cl	— 1.2	1.5	7.0	— 3.0	3.6	7.8
Br	−13.4	5.1	1.8	−13.2	6.6	3.6
I	−24.0	15.0	2.0	−24.6	13.2	—
OCH_3	26.0	2.4	22.0	25.2	6.0	19.8
NH_2	45.3	12.2	37.5	40.8	13.2	—
$N(CH_3)_2$	36.0	6.0	36.9	—	—	—
CHO	−34.8	−12.8	−16.5	—	—	—
NO_2	−56.9	−12.5	−20.0	−58.8	−12.6	—

Diehl [2] found the δ's by an indirect procedure, studying *meta* and *para* benzene derivatives. The δ's are, of course, also accessible through a direct investigation of C_6H_5X-compounds, but since most benzenoid protons absorb within a 1.5—2.0 p.p.m. range (or 100 c/s at 14 100 Ørsted) the spin-spin coupling constants ($J_{o,o} \sim 10$; $J_{o,m} \sim 3$; $J_{o,p} \sim 1$ c/s) may often be of the order of the δ-differences. When this happens, a complicated pattern arises which is hard to analyze. An *experimental* solution of this difficulty is the use of deuterated species [3,4] since the deuteron-proton spin-spin coupling is only about 1/6 of a corresponding proton-proton coupling. Spiesecke and Schneider [4] have applied this technique. In Table 1 their "direct" results are being compared with Diehl's indirectly derived δ's.

The discrepanices probably reflect the approximate validity of rule (I). We shall demonstrate by means of examples how useful the data of Table 1 are when analysing NMR-spectra of aromatic compounds of the types 1,3-C_6H_4XY, 1,4-C_6H_4XY (X may equal Y), and 1,3,5-C_6H_3XYZ (X, Y and Z may be identical).

EXPERIMENTAL

The instrument applied was a Varian A60 instrument. All solutions investigated were 5 mole % solutions in cyclohexane with an added amount of 5 % tetramethylsilane (TMS). All resonance frequencies of this paper are given in c/s, as measured relative to the internal TMS-standard. The benzene protons absorb at 432 c/s. The δ-value given for a certain type of proton, absorbing at x c/s, is the number $432-x$.

In order to check our experimental procedure against Diehl's we ran samples of 1,4-difluorobenzene, 1,4-dichlorobenzene, and 1,4-dibromobenzene. No interpretational difficulties exist for these spectra. We found, respectively, $\delta = 19.0$ (Spiesecke and Schneider's data; rule (I) 19.9); $\delta = 3.0$ (0.3); $\delta = -2.0$ (−8.3). We are unable to explain the discrepancies, which, however, for the present purpose are less important.

1,3-$C_6H_4(NO_2)Br$

The NMR-spectrum of 1,3-$C_6H_4(NO_2)Br$ is representative of a *simple* type of 1,3-C_6H_4XY spectrum. It has lines at 430.0 (4) *, 438.1 (12) *, 446.2 (9) *, 458.1 (6), 459.4 (8), 459.9 (8), 461.2 (7), 466.0 (3), 467.4 (4), 467.9 (5), 469.3 (4), 479.8 (5), 481.2 (5), 482.0 (7), 483.3 (6), 488.0 (3), 489.2 (4), 490.1 (6), 491.5

Table 2. Calculated and experimental proton chemical shifts of 1,3-$C_6H_4(NO_2)Br$ (5 mole % in cyclohexane) in c/s relative to benzene. Resonance frequency 60 Mc/s. Spin-spin couplings in c/s.

	δ_2	δ_4	δ_5	δ_6
Calculated from rule (I) *	−70.3	−33.4	−7.4	−55.1
Found in this investigation	−66.4	−31.6	−6.0	−53.6
Deviations (numerical)	3.9	1.8	1.4	1.5

$J_{45} = 8.0-8.1$; $J_{56} = 8.1$; $J_{24} = 1.85-2.15$; $J_{26} = 2.15$; $J_{46} = 1.3-1.4$; $J_{25} \sim 0.3$.

* Using Spiesecke and Schneider's δ's.

(5), 496.4 (8) *, 498.4 (12) *, and 500.7 (6) *. The number in parenthesis following the frequency is the peak intensity on an arbitrary scale. Lines marked with * are doublets with a doublet separation of about 0.3 c/s.

Table 2 gives the data resulting almost by inspection of the spectrum.

1,3-$C_6H_4(NH_2)Cl$

The NMR-spectrum of 1,3-$C_6H_4(NH_2)Cl$ is representative of a more complex type of 1,3-C_6H_4XY spectrum. From rule (I), with Spiesecke and Schneider's data, one calculates $\delta_2 = 44.1$; $\delta_4 = 36.3$; $\delta_5 = 13.7$; $\delta_6 = 52.3$. No calculated δ-difference is, therefore, smaller than 8 c/s. Using the estimate $J_{o,o} \sim 10$ c/s we get that $J_{45}/(\delta_5-\delta_4) = 10/22$, $J_{56}/(\delta_6-\delta_5) = 10/38$. Since the occurring J's are all smaller than the occurring δ-differences there is a hope that a reasonable estimate of the J's and the δ's may be made by inspection.

The observed spectrum has lines at 374.2 (3), 375.8 (5), 376.2 (6), 377.9 (5.5), 381.9 (3.5), 383.2 (4.5), 384.1 (7), 385.5 (7.5), 388.0 (5), 388.6 (6), 389.9 (9), 390.5 (10.5), 391.0 (9.5), 392.0 (9.5), 392.9 (11), 399.2 (8), 400.7 (8), 401.2 (8), 402.6 (5.5), 408.5 (8), 409.0 (8), 416.2 (8), 416.9 (8.5), 424.0 (2.5), 424.6 (2.5).

Since the predicted δ_6 equals 52.3, the H(6)-lines are grouped around 432−52 = 380 c/s. This suggests that the octet 374.2−385.5 are "H(6)"-lines. The 8 observed lines are very symmetrically spaced around 379.9 c/s. This would mean $\delta_6 = 52.1$ as compared to 52.3 from rule (I). H(6) couples strongly to H(5), weaker to H(4), and H(2). Thus $J_{65} > J_{64}$ and J_{62}, while $J_{64} \gtrless J_{62}$. This interpretation means that $J_{65} = 7.7$; $J_{64} = 2.15$; $J_{62} = 1.5$, where the values for J_{64} and J_{62} may be interchanged.

As $\delta_5 \sim 14$ (from rule (I)), the H(5) resonances must be located around 418 c/s. The lines could be doublets due to *para* coupling to H(2). Indeed, the three observed doublets at 408.5−409.0; 416.2−416.9; 424.0−424.6 fit this description. The H(4) and H(6) protons cannot exibit such doubling, their *para* positions being occupied by NH_2 and Cl.

From its measured position the doublet at 400.7−401.2 must then be the remaining 2 lines of the expected H(5)-octet. Since $J_{65} = J_{56}$ we get a check on the magnitude of J_{65} from the assigned H(5)-lines mentioned. One finds

$J_{56} = 7.8$ in good agreement with $J_{65} = 7.7$ above. Then, J_{54} must equal 15.5 c/s. Finally, $\delta_5 = 19.4$, as compared to 13.7 from rule (I). This discrepancy is not alarming in view of the somewhat over-simplified procedure applied as evidenced by the intensity difference between, for example, the 424.0 (2.5)—424.6 (2.5) doublet, and the 416.2 (8)—416.9 (8.5) doublet. Obviously, the coupling constant $J_{25} \sim 0.5$ c/s.

According to rule (I), the H(4) resonances should be located around 432—36 = 396, the H(2) resonances around 432—44 = 388 c/s. Hence, their resonances must merge. The H(2) proton couples only weakly to H(4) and H(6), giving rise to an octet (since we already know that $J_{25} \sim 0.5$ c/s) *or* a quartet if either J_{24} or J_{26} is negligible. Since no octet is observed in the spectrum we may conclude that $J_{24} \sim 0$, since $J_{26} = J_{62}$ is known to differ from zero. Considering the intensities, we must assign the lines at 389.9 (9), 390.5 (10.5), 392.0 (9.5), and 392.9 (11) as the quartet looked for. This means $\delta_2 = 40.6$ as compared to 44.1 from rule (I). Also, $J_{26} = 2.20 = J_{62}$ which, by way of exclusion (see above), lets $J_{46} = 1.5$.

Since there is no proton *para* to H(4), the H(4) resonances form a quartet. As $J_{45} = J_{54} = 15.5$ we must look for well-separated lines. This leaves us with no other possibility than the lines at 385.5, 388.6, 399.2, and 402.6. It follows that $\delta_4 = 38$ c/s as compared to 36.3 from rule (I). Also $J_{45} = 13.9$ and $J_{46} = 3.4$. Both values are at variance with $J_{54} = 15.5$ and $J_{64} = 1.5$ found above, but it is to be expected that the estimates involving the very centrally situated H(4)-pattern will be less reliable. The results are summarized in Table 3.

1,4-$C_6H_4(NH_2)F$

The NMR-spectrum of the compound 1,4-$C_6H_4(NH_2)F$ is by no means simple. 15 lines were observed at 376.8 (8), 379.6 (6), 381.7 (11), 383.6 (8), 386.4 (24), 388.5 (8), 391.0 (23), 395.7 (23), 398.5 (7), 401.1 (5), 402.6 (6), 404.3 (23), 406.5 (5), 409.6 (3), 412.5 (10). This spectrum proved identical with the subsequently investigated spectrum of 1,4-$C_6H_4(ND_2)F$ (except for the missing NH_2-absorption at 195 c/s). We may, therefore, ignore the NH_2-protons. By rule (I), $\delta_2 = \delta_6 = 46.7$, and $\delta_3 = \delta_5 = 30.7$. Hence $\delta_2 - \delta_3 > J_{23}$. First, we shall try to interpret the dominant lines of the spectrum by simple inspection. Afterwards, we shall check the estimates by means of data for deuterated derivatives.

Table 3. Calculated and experimental proton chemical shifts of 1,3-$C_6H_4(NH_2)Cl$ (5 mole % in cyclohexane) in c/s relative to benzene. Resonance frequency 60 Mc/s. Spin-spin couplings in c/s.

	δ_2	δ_4	δ_5	δ_6
Calculated from rule (I) *	44.1	36.3	13.7	52.3
Found in this investigation	40.6	38.0	19.4	52.1
Deviations (numerical)	3.5	1.7	5.7	0.2

$J_{45} = 13.9—15.5$; $J_{56} = 7.7—7.8$; $J_{24} \sim 0$; $J_{26} = 2.2$; $J_{46} = 1.5—3.4$; $J_{25} \sim 0.5$.

* Using Spiesecke and Schneider's δ's.

Table 4. Calculated and experimental proton chemical shifts of 1,4-$C_6H_4(NH_2)F$ (5 mole % in cyclohexane) in c/s relative to benzene. Resonance frequency 60Mc/s. Spin-spin couplings in c/s.

	δ_2	δ_3	δ_5	δ_6
Calculated from rule (I) *	46.7	30.7	30.7	46.7
Found in this investigation	49.0	30.0	30.0	49.0
Deviations (numerical)	2.3	0.7	0.7	2.3

$J_{FH(3)} = J_{FH(5)} = 8.5$; $J_{23} = J_{65} = 9.6$; $J_{FH(2)} = J_{FH(6)} = 4.7$; $J_{35} = 3.0$.

* Using Spiesecke and Schneider's δ's.

The H(3), H(5) resonances are expected to occur in the vicinity of 432—31 = 401. They would represent a doublet if only influenced by fluorine, but the interaction with the H(2), H(6) protons will produce a sextet which, dependent upon $J_{FH(3)}$ and J_{32}, may degenerate into a quintet (if $J_{FH(3)} = 2J_{32}$) or into a quartet (if $J_{FH(3)} = J_{32}$).

In all 3 cases it seems clear that the difference 412.5 (10)—404.3 (23) = 8.2 represents $J_{FH(3)}$. This excludes the possibility of assigning a sextet. If a *quintet* is assigned, it is centred around 395.7 (23). If a *quartet* is assigned it is centred around 400, very close to the precalculated position. Since the centre of the H(2), H(6) pattern must be placed somewhere near the strong line at 391.0 (23), we may abandon any further attempt to an analysis by inspection if H(2), H(3) occur as a *quintet*, since in this case $\delta_2 - \delta_3 \sim 5$ while $J_{23} = 8.2 > \delta_2 - \delta_3$. If, however, a H(2), H(3) *quartet* is observed, then $J_{FH(3)} = J_{32} = 8.2$; $\delta_5 = \delta_3 = 32$. This suggest the existence of a H(2), H(6) sextet centred between 391.0 and 386.4 (average value 388.7; calculated from (I): 385.3). In this case $\delta_6 = \delta_2 = 43.3$, $J_{23} = 7.2$, $J_{FH(2)} = 4.6—4.7$. However, $J_{23}/(\delta_2 - \delta_3) \sim 7/11$ so that the simple analysis presented may be incorrect. Signs of its possible invalidity are seen in the intensity irregularities, and in the presence of unassigned, although weak, lines. This was why deuteration was applied.

1,2,4,6-$C_6H_2(NH_2)DFD$ and 1,2,4-$C_6H_3(NH_2)DF$

A 2:1 mixture of 1,2,4,6-$C_6H_2(NH_2)DFD$ and 1,2,4-$C_6H_3(NH_2)DF$ was prepared by two times repeated exchange of 1,4-$C_6H_4(NH_2)F$ in acid D_2O at 110°C, folloved by shaking with H_2O at room temperature ($ND_2 \rightarrow NH_2$). Its spectrum has lines at 375.8 (4), 380.5 (4), 385.5 (9), 390.0 (9) 392.5 (5), 395.5 (11 on the "shoulder" of the following line), 397.7 (17), 400.5 (6), 403.5 (11 on the "shoulder" of the following line), 406.2 (17), and 410.5 (4). By its strong lines at 397.7 and 406.2, this spectrum at once discloses that $J_{FH(3)} = J_{FH(5)} =$ 8.5 c/s and that $\delta_3 = \delta_5 = 432—402 = 30$ as compared to 30.7 from rule (I).

The lines at 375.8—390.0 must stem from H(6) in 1,2,4-$C_6H_3(NH_2)DF$. H(6) is coupled strongly to H(5) and more weakly to fluorine. Hence $J_{65} = J_{23}$ = 9.6 c/s while $J_{FH(2)} = J_{FH(6)} = 4.7$ c/s. Finally, $\delta_2 = \delta_6 = 432—383 = 49$, as compared to 46.7 from rule (I).

H(5) of 1,2,4-$C_6H_3(NH_2)DF$ couples, therefore, almost equally strongly to fluorine and to H(6). The expected quartet degenerates, therefore, into a triplet with its central line at the "unperturbed" H(5) position 402. However, on top of this a *meta* coupling to H(3) should make itself felt. This accounts for the two lines found at 400.5 and 403.5, symmetrically displaced with respect to 402. The assignment means that $J_{35} = 3.0$ c/s. J_{35}, of course, also occurs as the difference 395.5—392.5.

Table 4 summarizes the results.

It is seen that the more laborious analysis by means of spectra of deuterated species confirms the main features found by "inspection" analysis of the spectrum of the parent molecule, relying on rule (I).

REFERENCES

1. Shoolery, J. N. *Techn. Information Bull.* **2** (1959) No. 3. Varian Associates, Palo Alto, California.
2. Diehl, P. *Helv. Chim. Acta* **44** (1961) 829.
3. Bak, B., Shoolery, J. N. and Williams, G. A. III *J. Mol. Spectroscopy* **2** (1958) 525.
4. Spiesecke, H. and Schneider, W. G. *J. Chem. Phys.* **35** (1961) 731.

Received December 9, 1961.

ACTA CHEMICA SCANDINAVICA 16 (1962) 1037–1064

Short Communications

On the Preparation and Properties of Sulfitolysed Fibrinogen and Fibrin

AGNES HENSCHEN

Department of Chemistry II, Karolinska Institutet, Stockholm, Sweden

The possible importance of the sulfur-containing groups in the different steps of blood coagulation has been discussed for a long time. It was, for example, suggested that the fibrinogen-fibrin conversion consisted of an aggregation of fibrinogen molecules due to the oxidation of their sulfhydryl groups and the formation of intermolecular disulfide bonds [1-3]. However, when Bagdy *et al.* and Carter and Warner attempted to determine the sulfhydryl groups present in fibrinogen, no such groups were found [4-6]. Since then we have investigated the presence and number of sulfhydryl groups and disulfide bonds in both fibrinogen and fibrin using several kinds of electrometric titration methods. None of these techniques could reveal any free sulfhydryl groups [7]. The number of disulfide bonds per molecule corresponded closely to the number of half-cystine residues as determined by amino acid analysis after performic acid oxidation [8]. As a further step in the analysis of the function of sulfur-containing groups in the fibrinogen-fibrin conversion, we have studied some properties of fibrinogen and fibrin, which had been treated with disulfide-splitting reagents. A short report on these experiments has already been given by us some time ago [9]. Apart from this no disulfide-modified fibrinogen and fibrin derivatives have been described.

In the present investigation, we have attempted to obtain derivatives of fibrinogen and fibrin in which the sulfur bonds are quantitatively split by sulfite, but in which there are no other modifications. Some of the properties of these derivatives and the thrombin-induced transformation of the fibrinogen-derivative were also studied. Bovine and human fibrinogen and fibrin, purified according to Blombäck and Blombäck, were used [10]. Principally two different methods of sulfitolysis were employed. In most cases we used a slight modification of the method described by Swan [11] and by Pechère *et al.*[12] The protein was dissolved in 8 M urea and treated with sodium sulfite and cupric sulfate usually at a pH of 9.0 at room temperature for one hour. In some cases we used the method described by Bailey and Cole [13]. The protein in an 8 M urea solution was intermittently treated with sodium sulfite and sodium tetrathionate at a pH of 7.4 at + 38°C. After the sulfitolysis, the protein was separated from the reagents by gel filtration on Sephadex G-50 [14] or by dialysis. The number of unchanged disulfide bonds or free sulfhydryl groups was determined by electrometric titration. The yields were calculated from spectrophotometric values [15] and from the weights of the lyophilized material.

The products of sulfitolysis of fibrinogen and fibrin were almost quantitatively recovered. If low molecular weight materials had been formed during sulfitolysis, they should have been lost during isolation by dialysis or gel filtration. This seems not to be the case. For these reasons, the products have been termed S-sulfo-fibrinogen and S-sulfo-fibrin. Some experiments were performed to estimate the size of the derivative molecules. Using Sephadex gels of various molecular sieve properties, no separation of different fractions of the S-sulfo-proteins could be obtained even in 6 M urea solution. Preliminary ultracentrifuge studies showed homogeneity of the substances and a considerable decrease in molecular weight as compared to untreated fibrinogen.

Both the S-sulfo-proteins were, when obtained by dialysis or gel filtration, completely soluble at low concentrations in distilled water. They showed, however, a marked tendency to aggregate when the ionic strength of the solution was increased or its pH was lowered. After lyophilization the products were no longer soluble in water, but dissolved immediately in solutions of, for example, urea or sodium dodecyl sulfate. Solutions of S-sulfo-fibrinogen or S-sulfo-fibrin in distilled water or 0.15 M sodium chloride did not exhibit the precipitability at + 58°C, which is characteristic of untreated fibrinogen.

The S-sulfo-proteins were studied by means of paper and starch gel electrophoresis. The paper electrophoresis pattern varied considerably from one solvent to another. In most urea-containing buffers two to three bands could be distinguished. Whether derived from S-sulfo-fibrinogen or from S-sulfo-fibrin, one or two of the bands showed the same mobility, whereas remaining bands differed according to their source. In all other buffer systems tried, only a single band was demonstrable, even when the buffers contained other reagents, such as sodium dodecyl sulfate or dimethylformamide, capable of splitting hydrogen bonds. Starch gel electrophoresis in 6—7 M urea showed two or three bands, all of which had considerably greater mobility than fibrinogen and fibrin.

The completeness and specificity of the sulfitolytic procedure was controlled. On electrometric titration of the S-sulfo-proteins no remaining sulfhydryl groups or disulfide bonds were found. N-Terminal amino acid analysis, by the phenylisothiocyanate method, showed that the S-sulfo-derivatives had the same N-terminal groups in the same amounts as have the unmodified proteins, which indicates that no peptide bonds were broken during sulfitolysis. The amino acid compositions of the S-sulfo-derivatives seemed to be the same as those of the native proteins.

It was possible to separate different fractions of S-sulfo-fibrinogen and S-sulfo-fibrin on ion exchange Sephadex, diethylaminoethyl- and carboxymethyl-Sephadex. Three components were isolated, which had different electrophoretic mobilities in urea-containing buffers, and which corresponded to the previously observed bands. When recombined the components gave the original pattern.

The possible change in the reaction of the modified fibrinogen in the presence of thrombin was studied. S-Sulfo-fibrinogen was found to be a substrate for thrombin. However, it did not coagulate in the ordinary sense, but formed a fine precipitate. This occurred about as rapidly as the formation of a native fibrin coagulum, provided that the same conditions of pH, ionic strength and temperature were maintained. Approximately 80 % of the S-sulfo-fibrinogen was precipitable with thrombin. S-Sulfo-fibrinogen was apparently more thermostabile than fibrinogen, and the velocity of its reaction with thrombin was unchanged after heating to + 60°C. N-Terminal amino acid analysis indicated that in the presence of thrombin, the peptides were released from S-sulfo-fibrinogen in the same order and at about the same rate as from native fibrinogen. S-Sulfo-fibrin exhibited the same electrophoretic pattern, regardless of whether it had been obtained from S-sulfo-fibrinogen with thrombin or from native fibrin by sulfitolysis.

This work will be described and discussed in detail in the near future.

1. Baumberger, J. P. *Am. J. Physiol.* **133** (1941) 206.
2. Lyons, R. N. *Nature* **155** (1945) 633.
3. Jeener, R. *Experientia* **3** (1947) 243.
4. Bagdy, D., Guba, F., Lorand, L. and Mihalyi, E. *Hung. Acta Physiol.* **1** (1948) 197.
5. Carter, J. R. and Warner, E. D. *Am. J. Physiol.* **179** (1954) 549.
6. Carter, J. R. *Proc. Soc. Exptl. Biol. Med.* **91** (1956) 406.
7. Henschen, A. *To be published.*
8. Henschen, A. and Blombäck, B. *To be published.*
9. Blombäck, B. and Henschen, A. *Umwandlungsformen des Fibrinogens.* Paper presented before the "3. Marburger Symposium", September 6—9, 1961 in Bavaria.
10. Blombäck, B. and Blombäck, M. *Arkiv Kemi* **10** (1956) 415.
11. Swan, J. M. *Nature* **180** (1957) 643.
12. Pechère, J.-F., Dixon, G. H., Maybury, R. H. and Neurath, H. *J. Biol. Chem.* **233** (1958) 1364.
13. Bailey, J. L. and Cole, R. D. *J. Biol. Chem.* **234** (1959) 1733.
14. Porath, J. and Flodin, P. *Nature* **183** (1959) 1657.
15. Blombäck, B. *Arkiv Kemi* **12** (1958) 99.

Received April 13, 1962.

Some Characteristics of a β-Ray Argon Tetrode Detector

ÖRN WAHLROOS
Laboratory of the Foundation for Chemical Research, Biochemical Institute, Helsinki, Finland

Lovelock [1] has suggested that the insertion of a fourth electrode into the argon triode gas chromatographic detector could decrease the noise level and thus increase its sensitivity. Because the author is not aware of any detailed description of the argon tetrode in the literature, some of its properties are reported below.

Experimental. The detector cell is shown in Fig. 1. The collector electrode is connected to the electrometer grid, with a resistance of 95 M Ω to earth. The screen grid voltage is taken from a separate battery. If not otherwise specified, the screen grid has a series resistance of 10 M Ω, and the anode 1 M Ω. 10 mC ^{90}Sr is used as the source of electrons. The high frequency cut-off of the measuring system is at about 50 cps.

The cell was calibrated by the exponential dilution method [1,2]. During most measurements the calibration vessel and the detector were kept at 100°C, and the gas velocity at 100 ml/min. Butane was used as the test substance. The argon gas was purified by means of a trap containing Linde's molecular sieve, 4 Å, kept at −76°C. The detector response was calculated according to formula (1).

$$\ln C = \ln C_0 - \frac{U \cdot t}{V} \qquad (1)$$

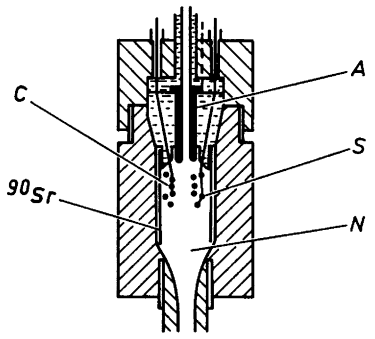

Fig. 1. Lined parts = brass; dotted parts = PTFE; A = anode; S = screen grid; C = collector grid.

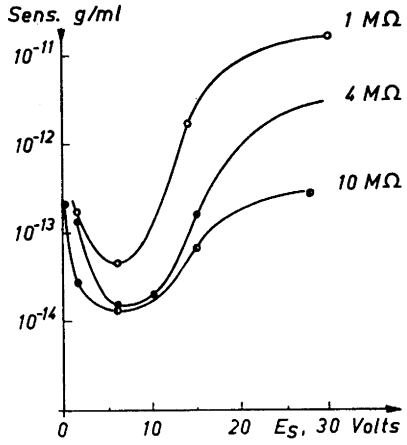

Fig. 2. Dependence of sensitivity on screen grid voltage with the screen grid series resistance as parameter.

(C_0 = initial concentration of butane, C = concentration at time t, U = gas velocity, V = volume of the calibration vessel).

Because the cell was designed for use with packed columns, no scavenge gas is used. The inside of the cell is pear-shaped to give a smoth flow of carrier gas. A diffusion net of wire gauze [1] inserted at N (Fig. 1) had no influence on the signal/noise level.

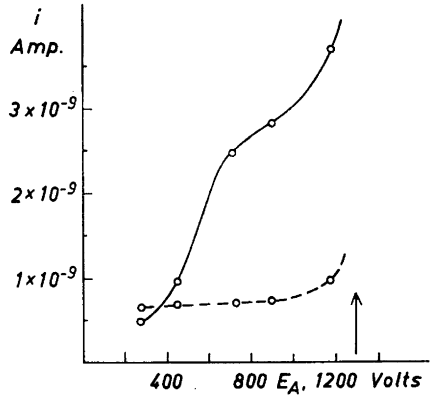

Fig. 3. Anode (— O —) and collector grid (- - - O - - -) currents as a function of anode voltage. Arrow indicates breakdown. Screen + 10 V.

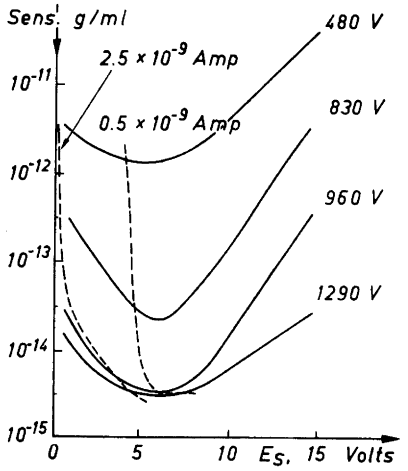

Fig. 4. Ordinate: Concentration of butane giving a signal = 2 × noise. Abscissa: Screen electrode voltage. Solid lines: Sensitivity at different anode voltages. Broken lines connect points with same collector current when pure argon flows through the cell.

The collector grid current with pure argon in the cell, as well as the sensitivity, remained unchanged when the gas velocity was increased from 70 cm³/min to 150 cm³/min.

As shown in Fig. 2, the value of the screen grid series resistance must be at least four times the anode series resistance, or the electron density at the anode will be seriously lowered. Also, the screen current should be kept to a minimum to keep the noise low.

From the plot of the anode voltage, the anode current and the collector current at a constant screen voltage (Fig. 3), it is seen that a measurable collector current exists at low anode voltages. This might be due to a secondary emission of electrons from the collector electrode due to the radiation. The collector current might partly be caused by the reaction[3]

$$A^* + A^* \rightarrow A + A^+ + e^-$$

at the higher anode voltages. The collector current remains fairly constant until the screen grid loses control over the discharge. Then the noise, which during the flat part of the collector current curve is $< 10^{-13}$ A, rises sharply.

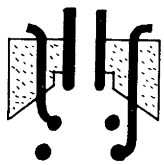

Fig. 5. Second electrode configuration.

At room temperature, the collector current and the noise with pure argon is not markedly dependent on the screen grid voltage within the range + 4 — + 10 V. From the relationships shown in Fig. 4, it is concluded that the positive screen causes an increase in the collecting efficiency of positive ions or a change in the space charge within the cell. Also, the screen prevents the collection of positive argon ions formed near the radiation source.

The ionization efficiency of the cell at maximum sensitivity is about 20 Coul/gr. The linear range is about 10^3.

To keep the detector stable at temperatures above 190°C, the collector electrode should be provided with an earthed guard ring, and precautions against creeping of the PTFE insulation should be taken.

In high sensitivity work it must be observed that the maximum allowed working temperatures for stationary phases will be about 80°C less than the values recorded in the literature.

It may be mentioned that if the electrode configuration in Fig. 5 is used, the maximum sensitivity for organic substances is about ten times lower. However, with this construction the screen electrode may be used for collection of negative ions, formed by electron capture. In this way a sensitivity of about 5×10^{-8} g/ml for oxygen and carbon dioxide has been observed.

The author wishes to thank Professor A. I. Virtanen for his kind interest and Mr. T. Moisio, M. A., for helpful discussions. The investigation is a part of a research project under U. S. Public Law No. 480, 83rd Congress.

1. Lovelock, J. E. in Scott, R. P. W. *Gas Chromatography*, Butterworths, London 1960.
2. Lovelock, J. E. *Anal. Chem.* **33** (1961) 162.
3. Goldstein, L. *Advances in Electronics and Electron Physics* **7** (1955) 401.

Received April 16, 1962.

Syntheses of α-Propylamino-2-methyl-[*carbonyl*-^{14}C] propioanilide

CLAËS TEGNÉR and
KARL-ERIK DOMEIJ

Research Laboratories, AB Astra, Södertälje, Sweden

In studies on the behaviour of drugs in biological systems it is often necessary to be able to trace such compounds in low concentrations. To study the metabolism and distribution of the local anesthetic, α-propylamino-2-methylpropioanilide [1] (Citanest ®), it was necessary to use a radioactive product, hence we prepared a [^{14}C]labelled anilide.

The preparation of diethylamino-2,6-dimethyl-[*carbonyl*-^{14}C]acetanilide in a 20 % yield, based on sodium [^{14}C]acetate, has been outlined by Geddes and Douglas [2] and Geddes [3] but only few experimental details have been published. This synthesis was carried out [4] partly by use of the vacuum line technique. Several synthetic methods have been given [5] for the preparation of similar derivatives, but they involve the use of either elaborate apparatus or of special arrangements such as the vacuum line technique.

This communication describes the preparation of α-propylamino-2-methyl-[*carbonyl*-^{14}C]propioanilide using standard laboratory technique and apparatus. Ethyl magnesium bromide was treated with [^{14}C]carbon dioxide, the propionic acid liberated and heated with red phosphorus and bromine to yield α-bromopropionyl bromide. This was allowed to react with *o*-toluidine and the bromo-2-methylpropioanilide formed was then heated with propylamine, giving the hydrochloride of α-propylamino-2-methyl-[*carbonyl*-^{14}C] propioanilide in an overall yield of 62 %. The purity of the product was ascertained by chromatography by which it was also shown that all radioactivity was located in one spot.

Ethyl magnesium bromide was prepared by adding 125 mmoles (13.6 g) of ethyl bromide (dried over anhydrous sodium sulphate) in 50 ml of dry ether to 125 mmoles (3.20 g) of magnesium filings suspended in 65 ml of dry ether at such a rate as to cause gentle reflux. The mixture was refluxed for a further 15 min to complete the reaction and then cooled, giving 125 ml of an approximately molar solution, from which 100 ml could be pipetted off without contamination from the deposit at the bottom of the flask.

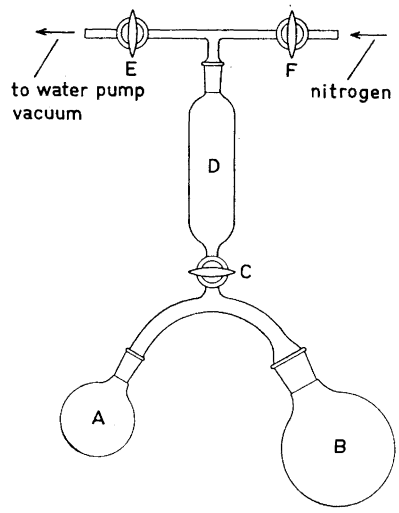

Fig. 1. Apparatus used for the carbonation of Grignard reagent.

Carbonation of the ethylmagnesium bromide was performed in the apparatus shown in Fig. 1. Into flask A (100 ml), containing about fifty 6 mm Ø glass beads, was introduced 50.0 mmoles (9.87 g) of barium [^{14}C]carbonate (radioactivity: 0.2 mC/mmole). The apparatus was evacuated to 10 mm Hg and then filled with nitrogen. The flask B (500 ml) was removed, 100 mmoles of freshly prepared ethyl magnesium bromide (100 ml of the ethereal solution prepared as described above) was quickly introduced and the flask again connected to the apparatus and immersed into an ethanol-dry ice bath of −50°C. (A lower temperature of the cooling-bath or a higher concentration of the Grignard reagent will cause crystallization.) After 5 min, the apparatus was alternately evacuated to 25 mm Hg with a water pump *via* stopcock E and filled with nitrogen *via* stopcock F three times. Finally, the apparatus was evacuated to 25 mm Hg and the stopcock C of the funnel D was closed. The T-tube carrying the cocks E and F was removed and 70 ml of conc. sulfuric acid (p.a.) was introduced into the funnel D (100 ml capacity). With the flask B still in the ethanol-dry ice bath, the apparatus was tilted slightly so as to cause the sulfuric acid to run into flask A (containing the barium [^{14}C]carbonate).

The addition was made dropwise during 20 min while carefully agitating the flask at intervals. Finally, the flask A was heated in an oil bath of 70°C for 5 min. The apparatus was then removed from the baths and allowed to attain room temperature. After frequent shakings during 10 min, flask B was again immersed in the ethanol-dry ice cooling bath (−50°C) and 50 ml of molar sulfuric acid was slowly added during half an hour. The flask was then allowed to warm to room temperature and swirled at intervals, stopcock C being opened to avoid overpressure. The content of flask B was transferred to a separatory funnel, the ethereal layer separated and combined with the ether solutions obtained from extracting the water phase five times with 50 ml portions of ether. After drying overnight over 8 g of magnesium sulfate, the ethereal solution was transferred together with the drying agent to a separatory funnel (500 ml) into which a sintered glass disk had been fused. The separatory funnel was connected to a distillation flask (100 ml), containing ~10 mg of phosphorus pentoxide, and the ether solution was carefully evaporated until about 40 ml was left, whereupon a further ~10 mg of phosphorus pentoxide was introduced. Evaporation was then completed at a bath temperature of 70° until the temperature at the distillation head was 40−42°C.

Bromination was carried out in the same 100 ml distillation flask after it had been equipped with a reflux condenser carrying a $CaCl_2$-drying tube, and a dropping funnel. 20.0 mmoles (0.620 g) of red phosphorus (purified as described by Vogel [6]) and 5 drops of propionic acid anhydride were introduced into the flask, followed by the dropwise addition at room temperature of 120 mmoles (19.2 g = 6.10 ml) of bromine (purified as described by Vogel [7]) at such a rate as to obtain a vigorous reaction. The reaction mixture was then refluxed for one hour. The bromopropionyl bromide thus obtained was distilled under nitrogen at 10 mm Hg into an ice water cooled receiver. (The stem of the receiving adapter extended to the bottom of the receiver.) A maximum bath temperature of 150°C was allowed. When no more distillate was obtained, the distillation flask was removed and the distillation head and condenser were rinsed into the receiver with 75 ml of dry benzene.

The receiver containing the benzenic bromopropionyl bromide was equipped with a separatory funnel, a reflux condenser and a stirrer, and 130 mmoles (13.9 g) of freshly distilled *o*-toluidine in 30 ml of dry benzene were added during 5 min with stirring. The hydrobromide of the *o*-toluidine separated immediately and the mixture was heated to 70° for 15 min to complete the reaction. While still hot, the benzene solution was filtered through a glass filter and the filtrate washed three times with 15 ml portions of hot benzene. To the combined benzene solutions were added 170 mmoles (10.0 g) of propylamine and the solution refluxed for 4 h. The hydrobromide of propylamine separated as colourless crystals and was filtered off on a glass filter and washed with 10 ml of dry benzene. The combined benzene solutions were extracted 4 times with 40 ml of 2 N hydrochloric acid. The extracts were combined and the acidity of the solution was adjusted first with 30 % sodium hydroxide and then with a 2 N solution to pH = 5.7. The solution was then extracted 4 times with 25 ml of ether to remove the excess *o*-toluidine. The ether extracts were discarded and the aqueous solution was made alkaline (pH 10) with 2 N sodium hydroxide. The liberated base was extracted 4 times with 40 ml of ether and the combined extracts evaporated *in vacuo* to dryness using a final bath temperature of 100°C and a pressure of 10 mm Hg. The residue was dissolved in absolute ether and the hydrochloride of the aminoacylanilide was precipitated by the addition of ethereal hydrogen chloride. The precipitate formed was filtered off and after one crystallization from ethanol-ether (1:6) it melted at 165−167°. Yield 8.0 g (62 %). The radioactivity of the product was 0.85 μC/mg.

The procedure described above is also applicable to smaller scale synthesis. Thus, a 5 mmole synthesis gave a 36 % yield of α-propylamino-2-methylpropioanilide hydrochloride. In this smaller scale, the flasks A and B and the funnel D were of 25 ml capacities and the volumes of the solvents used in the reactions and extractions were proportionally reduced.

A 5 mmole synthesis of diethylamino-2,6-dimethylacetanilide hydrochloride from methyl iodide yielded 24 % of final product, applying the above procedure with minor modifications.

1. Löfgren, N. and Tegnér, C. *Acta Chem. Scand.* **14** (1960) 486.
2. Geddes, I. C. and Douglas, D. E. *Federation Proc. London* **15** (1956) 260.
3. Geddes, I. C. *Anest. et Analg. (Paris)* **15** (1958) 908.
4. Geddes, I. C. *Personal communication.*
5. Murray III, A. and Williams, L. *Organic Synthesis with Isotopes*, New York 1958, Part I.
6. Vogel, A. *A Textbook of Practical Organic Chemistry* Longmans, Green and Co., London 1948, p. 188.
7. Ref[6]., p. 185.

Received April 17, 1962.

Photo-Induced Electron Spin Resonance in Solutions of Some Electron-Donor-Acceptor Complexes

CARL LAGERCRANTZ and
MARGARETA YHLAND

Department of Medical Physics, University of Göteborg, Sweden

The charge transfer in molecular complexes composed of an electron donor and an acceptor part (EDA-complexes) will sometimes introduce an unpairing of the electrons involved which gives a detectable electron spin resonance (ESR). Considering complexes in which both the donor and the acceptor parts are organic molecules an ESR-signal has mostly been found in solid state samples. In solutions, however, rather few complexes of this type have been reported to exhibit an ESR-signal [1,2]. (For a recent review on EDA-complexes see Briegleb [3]). We now wish to report that an ESR-signal can be induced in solutions of some organic EDA-complexes when irradiated by light.

Experimental. The electron acceptor was dissolved in an electron donor solvent which had been distilled immediately before use. The solutions to be studied were degassed twice by freezing, evacuating and melting within the sample tube. Before the final melting the volume over the solution was filled with nitrogen of atmospheric pressure. The samples were irradiated *in situ* through the irradiation slots in the cavity wall of a 100 kc Varian spectrometer equipped with the variable temperature accessory. The light source was mounted in an "Universal-Mikroskopierlampe" (Wild, Switzerland) at a distance of 40 cm from the cavity. Two different light-source-filter combinations were used: (A) A high pressure mercury lamp (Osram HBO-200) together with an UV cut off filter (50 % transmission at 408 mμ, 10 % at 387 mμ). Most of the experiments were performed with this source. (B) A high pressure xenon lamp (Osram XBO-150) together with a band pass filter (Wild UG1) with a maximum transmission about 360 mμ. Transmission data

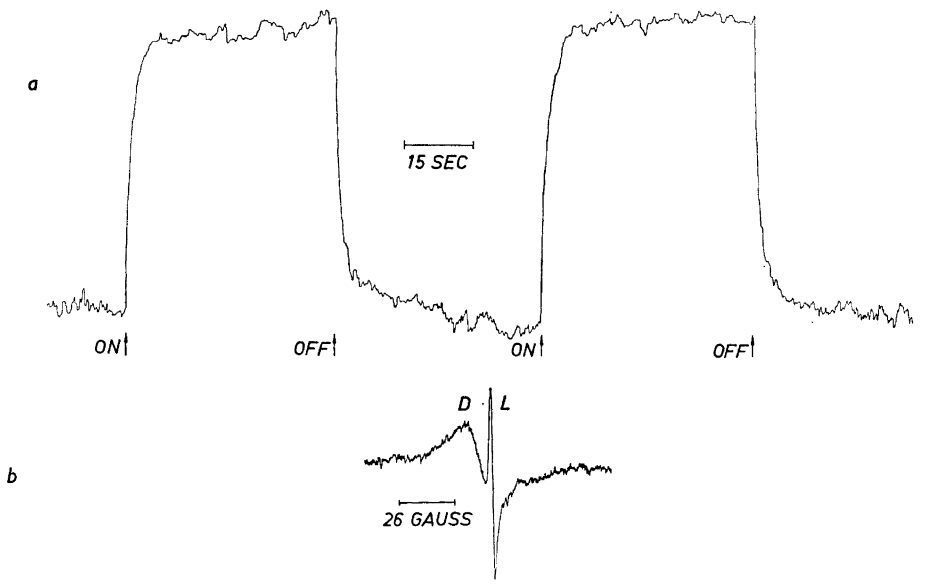

Fig. 1. Photo-induced paramagnetism in a 0.05 M solution of *p*-chloranil in tetrahydrofuran. Light-source-filter: (A).
a. Kinetic curve at −26°C. The relative spin concentration is recorded as a function of time. Constant magnetic field adjusted to maximum response.
b. ESR-spectrum at + 20°C. The first derivative of the absorption is recorded as a function of the magnetic field.

of filters, solvents and solutions were obtained by a Cary model 14 spectrophotometer.

In none of the experiments an ESR-signal could be detected prior to irradiation when the solutions had been prepared and kept in the dark. No ESR-signals could be detected when only the solvents were irradiated.

The kinetic experiments in which the reactions were relatively fast (Fig. 1 a), were performed with a time constant of the detector circuit of 0.3 sec and with a recorder of 0.25 sec response.

Results. Solutions of the electron acceptor *p*-chloranil in electron donor solvents as tetrahydrofuran, *p*-dioxane, xylene, mesitylene and *o*-chlorophenol exhibit a photo-induced ESR-signal. When the light is turned on there is a rapid increase of the signal from zero to a maximum steady state value (Fig. 1 a). When compared with a solution of diphenylpicrylhydrazyl (DPPH) in benzene, it was found that about 0.1 % of the acceptor molecules were transformed to paramagnetic centres. There is also a rapid decay of the signal to zero when the exciting light is turned off. The decay to half-value in a 0.05 M solution of chloranil in tetrahydrofuran was about 1 sec. No dependence on the temperature could be observed in a range of about 50° between −23°C and + 27°C. The reaction could be recycled an infinite number of times with a rather good reproducibility. The ESR-spectra of the chloranil systems recorded during light excitation exhibited a single narrow line (L in Fig. 1 b) with a *g*-value close to that of DPPH. After irradiation of a solution of chloranil in tetrahydrofuran for about one hour (source (A)), a new line (D in Fig. 1 b) appeared which was broader than the original one. This new line did not disappear when the light was turned off. Degassing of the sample had no influence. When chloranil was dissolved in *p*-dioxane no such secondary line could be detected.

Solutions of the electron acceptors *s*-trinitrobenzene, picrylchloride and *m*-dinitrobenzene in donor solvents as tetrahydrofuran, *p*-dioxane, dimethoxyethane, benzaldehyde, xylene and mesitylene exhibit a photo-induced ESR-signal different from that found for chloranil. There is a less rapid response to light (Fig. 2 a). The decay rates are lower than those obtained with chloranil and show a definite temperature dependence. Thus, the time for a decay to half-value was about 1 min at + 20°C in contrast to about 3 min at −10°C for a 0.1 M solution of *s*-trinitrobenzene in tetrahydrofuran. In most of the systems investigated there was a complete decay of the

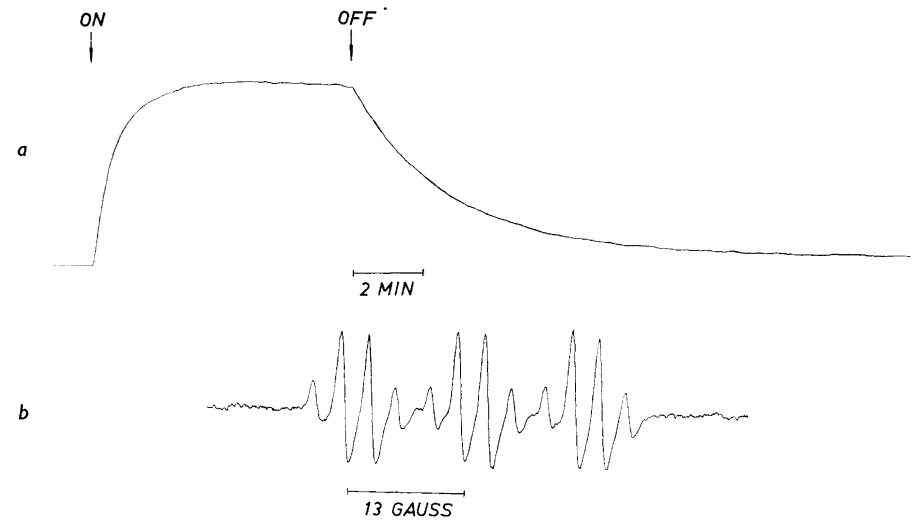

Fig. 2. Photo-induced paramagnetism in a 0.1 M solution of *s*-trinitrobenzene in tetrahydrofuran. Light-source-filter: (A).
a. Kinetic curve at + 11°C.
b. ESR-spectrum at + 20°C.

ESR-signal. Some systems, however, exhibited an ESR-signal detectable even after that the irradiated samples had been kept in the dark overnight. The maximum spin concentration indicated that about 0.1 % of the acceptor molecules had been transformed to paramagnetic centres.

The ESR-spectra recorded during light excitation exhibit a hyperfine structure which can be more or less definitely correlated with a free radical derived from the acceptor part of the EDA-complexes. Fig. 2b shows the light-induced ESR-spectrum of *s*-trinitrobenzene dissolved in tetrahydrofuran. Due to the high symmetry of the molecule the three nitrogen nuclei produce a common splitting into three main lines separated by 13 gauss. Each of these lines is split into a quartet of equally spaced lines (3.0 gauss) by the three hydrogen atoms with the intensity ratio of 1:3:3:1. The appearance of this spectrum did not change even after irradiation for several hours. When dissolved in dimethoxyethane, however, a further splitting of the spectrum initially identical with that obtained in tetrahydrofuran was observed after prolonged irradiation.

The spectral distribution of the energy from light source (A) is well outside the absorption of tetrahydrofuran without any solute, and involves only a rather weak absorption in the solutions here investigated, whereas source (B) emits radiation in a region of relatively high absorption as concerns both the solvent and the solutions. Comparing the results obtained for the systems tetrahydrofuran — chloranil and tetrahydrofuran — *s*-trinitrobenzene by use of (A) and (B) respectively, however, no qualitative differences could be detected.

Discussion. It is believed that a charge transfer which unpairs the electrons involved is produced by the absorption of radiant energy. The subsequent reactions of the paramagnetic complex, a triplet state or, more probable, a biradical may take different paths. The excited chloranil complexes seem to return to the initial state without any dissociation into radical ions as judged from the relatively rapid decay rates and their apparent independence of the temperature. On the other hand the photoactivated complexes involving the nitro substituted derivatives of benzene are dissociated into radical ions as evidenced by their temperature dependent decay rates. The hyperfine structure of the *s*-trinitrobenzene spectrum is consistent with the formation of negative free radical ions by a transfer of one electron without any transfer of hydrogen atoms. In other systems the radical ions formed evidently partake in secondary reactions.

Evidence for positive radical ions derived from the donor part of the EDA-complexes seems to be lacking. A hypothetical explanation may involve a very short life time of these radicals.

1. Lawrence, E. O. *U.S. Atom. Energy Comm.* UCRL-9722 (1961).
2. Miller, R. F. and Wynne-Jones, W. F. K. *Nature* **186** (1960) 149.
3. Briegleb, G. *Elektronen-Donator-Acceptor-Komplexe*, Berlin 1961.

Received April 17, 1962.

Enrichment of Light Isotopes of Sulphur, Carbon and Oxygen Using an Anion Exchanger

KARL ERIK HOLMBERG

Division of Chemistry, Section for Nuclear Chemistry, AB Atomenergi, Studsvik, Tystberga, Sweden

It is known that upon displacement of hydrogensulphite ions from an anion exchanger by a strong acid there is an enrichment of heavy sulphur isotopes at the boundary formed [1]. Similarly it is to be expected that upon absorption of sulphur dioxide from a solution on an anion exchanger column in the acetate ion form there will be an enrichment of the light sulphur isotope at the boundary formed. Several experiments have confirmed this. In the following only one is described.

In the experiment the 7 columns used were of 12 mm inner diameter and about 140 cm length, filled with Dowex 2-x10, 100—200 mesh, acetate ion form. They were connected in series by narrow glass tubes (2 mm inner diameter). On the columns there were absorbed a number of samples of SO_2, pre-enriched in ^{32}S by ion exchange, until there had formed a band of 255 cm length, visible by its yellow color.

ESR-signal. Some systems, however, exhibited an ESR-signal detectable even after that the irradiated samples had been kept in the dark overnight. The maximum spin concentration indicated that about 0.1 % of the acceptor molecules had been transformed to paramagnetic centres.

The ESR-spectra recorded during light excitation exhibit a hyperfine structure which can be more or less definitely correlated with a free radical derived from the acceptor part of the EDA-complexes. Fig. 2b shows the light-induced ESR-spectrum of *s*-trinitrobenzene dissolved in tetrahydrofuran. Due to the high symmetry of the molecule the three nitrogen nuclei produce a common splitting into three main lines separated by 13 gauss. Each of these lines is split into a quartet of equally spaced lines (3.0 gauss) by the three hydrogen atoms with the intensity ratio of 1:3:3:1. The appearance of this spectrum did not change even after irradiation for several hours. When dissolved in dimethoxyethane, however, a further splitting of the spectrum initially identical with that obtained in tetrahydrofuran was observed after prolonged irradiation.

The spectral distribution of the energy from light source (A) is well outside the absorption of tetrahydrofuran without any solute, and involves only a rather weak absorption in the solutions here investigated, whereas source (B) emits radiation in a region of relatively high absorption as concerns both the solvent and the solutions. Comparing the results obtained for the systems tetrahydrofuran — chloranil and tetrahydrofuran — *s*-trinitrobenzene by use of (A) and (B) respectively, however, no qualitative differences could be detected.

Discussion. It is believed that a charge transfer which unpairs the electrons involved is produced by the absorption of radiant energy. The subsequent reactions of the paramagnetic complex, a triplet state or, more probable, a biradical may take different paths. The excited chloranil complexes seem to return to the initial state without any dissociation into radical ions as judged from the relatively rapid decay rates and their apparent independence of the temperature. On the other hand the photoactivated complexes involving the nitro substituted derivatives of benzene are dissociated into radical ions as evidenced by their temperature dependent decay rates. The hyperfine structure of the *s*-trinitrobenzene spectrum is consistent with the formation of negative free radical ions by a transfer of one electron without any transfer of hydrogen atoms. In other systems the radical ions formed evidently partake in secondary reactions.

Evidence for positive radical ions derived from the donor part of the EDA-complexes seems to be lacking. A hypothetical explanation may involve a very short life time of these radicals.

1. Lawrence, E. O. *U.S. Atom. Energy Comm.* UCRL-9722 (1961).
2. Miller, R. F. and Wynne-Jones, W. F. K. *Nature* **186** (1960) 149.
3. Briegleb, G. *Elektronen-Donator-Acceptor-Komplexe*, Berlin 1961.

Received April 17, 1962.

Enrichment of Light Isotopes of Sulphur, Carbon and Oxygen Using an Anion Exchanger

KARL ERIK HOLMBERG

Division of Chemistry, Section for Nuclear Chemistry, AB Atomenergi, Studsvik, Tystberga, Sweden

It is known that upon displacement of hydrogensulphite ions from an anion exchanger by a strong acid there is an enrichment of heavy sulphur isotopes at the boundary formed [1]. Similarly it is to be expected that upon absorption of sulphur dioxide from a solution on an anion exchanger column in the acetate ion form there will be an enrichment of the light sulphur isotope at the boundary formed. Several experiments have confirmed this. In the following only one is described.

In the experiment the 7 columns used were of 12 mm inner diameter and about 140 cm length, filled with Dowex 2-x10, 100—200 mesh, acetate ion form. They were connected in series by narrow glass tubes (2 mm inner diameter). On the columns there were absorbed a number of samples of SO_2, pre-enriched in ^{32}S by ion exchange, until there had formed a band of 255 cm length, visible by its yellow color.

Table 1. Data and analysis of samples of SO_2 from anion exchanger experiment. Travelled length 116.5 m during 43 days at room temperature.

Sample No.	Volume ml	Band length cm	C_{SO_2} mole/l	g SO_2	$Q^{34}/_{32}$
1	2	—	—	—	0.0634
2	75	13	0.343	1.65	0.071
3	100	23	0.355	2.27	0.121
4	200	46.5	0.413	5.28	0.185
5	200	52.5	0.385	4.92	0.267
6	200	39	0.440	5.63	0.347
7	170	37	0.400	4.35	0.704
8	2	—	—	—	1.29
Sum	949	210		24.10	

Table 2. Acetic acid samples from an anion exchanger after 31 m displacement.

Sample No.	Volume ml	Band length cm	C_{CH_3COOH} mole/l	$Q^{13}C$	$Q^{18}O$
1	88	23	0.56	1.00	1.00
3	113	32	0.536	0.997	0.985
3	78	24	0.514	0.912	0.754
4	73	19	0.434	0.778	0.561

The band was displaced with 0.3 M HCl and when leaving the last tube it was returned to the first one, which meanwhile had been regenerated and washed. After 66 meter travel the band had shrunk to 211 cm, probably chiefly due to losses from the back boundary. More SO_2 was added at the middle of the band until its length was 245 cm. The displacement was continued and when the band had travelled a total of 116.5 m it had again shrunk to a length of 212 cm. Then all of the band was taken out as eight samples which were investigated for isotope abundance. For data see Table 1, where Q is the relative abundance of ^{34}S in the sample compared with its natural relative abundance.

If the elementary separation factor is assumed to be $a_{34}/_{32} = 1.0064$, as was found in one experiment, the total separation factor between the ends of the band (20.3) corresponds to 471 theoretical plates. However, completely stationary conditions had probably not been reached.

An isotope enrichment may also be expected on exchange between acetic acid and acetate ion. In order to investigate this, four samples of the acetic acid effluent in front of the sulphurous band were taken after 31 m travel. The acetic acid was transformed to barium acetate. This was pyrolyzed to barium carbonate, which was decomposed with concentrated sulphuric acid to given carbon dioxide for isotopic analysis. In this way the carbon and oxygen isotope content of the acetic acid carboxyl was obtained. The results are given in Table 2.

The high concentration of the acetic acid in the effluent indicates that it is partly bound to the ion exchanger as unionized molecules or single-ionized double molecules. The acetic acid concentration in the effluent is variable and no exact proportionality is found between sample volume and band diplacement length. For these reasons no exact calculation of elementary separation factors can be made. However, a conservative estimate shows that upon exchange between acetate ion plus acetic acid on the exchanger and acetic acid in the solution the carboxyl of the acetic acid in the solution is enriched in ^{13}C by the elementary factor 1.0016 and in ^{18}O by the factor 1.0036.

1. Forberg, S., Barnewik, W., Fogelström-Fineman, I., Westermark, T. and v.Ubisch H. *Proc. Intern. Symposium Isotope Separation*, Amsterdam 1957, North Holland Publishing Co., Amsterdam 1958, p. 243.

Received May 2, 1962.

Preparation of (+)-α-Methoxyphenylacetic Acid

TADEUSZ RAŹNIKIEWICZ
Chemical Institute, University of Uppsala, Sweden

The recent note that a paper on the resolution of α-methoxyphenylacetic acid has been accepted for publication in J. Chem. Soc.[1] has prompted the present author to publish some preliminary results on the optical resolution of this compound. The latter is of interest in connection with studies in progress on the plant-growth regulating properties of such acids [2,3].

Both enantiomorphs of the α-methoxyphenylacetic acid are wellknown. They have been prepared from optically active methyl mandelate by methylation with CH_3I and Ag_2O followed by hydrolysis of the ester [4]. Methylation employing diazomethane with Al-*t*-butylate as catalyst has also been used [5].

Racemic α-methoxyphenylacetic acid was partially resolved on a chromatographic column containing starch [6]. No case could be found in the literature in which alkaloids have been used for resolution.

The present author has found that quinine gave an easily crystallised salt from which the L(+)-acid could be obtained in the pure state after five recrystallisations.

Experimental. *L(+)α-Methoxyphenylacetic acid.* 20.5 g (0.123 mole) α-methoxyphenylacetic acid and 40.1 g (0.124 mole) quinine were dissolved in 250 ml ethanol and 750 ml warm water were added. After two days the crystals were filtered off and recrystallised to maximum activity of the acid. After each recrystallisation a 0.45 g sample was taken, the acid liberated and the rotatory power determined in ethanol solution. The progress of the resolution is seen below.

The acid was liberated from 17.1 g quinine salt with dilute hydrochloric acid and extracted with ether. The ether was evaporated and crude acid (5.0 g) was recrystallised from benzene-petrol-ether (1:2) mixture. It was obtained 4.3 g of acid forming prisms m.p. 65°–67° and $[\alpha]_D^{25} = +148.0°$ ($c = 1.056$, absolute ethanol). Further two recrystallisations of 2.0 g of prisms from ligroin gave 0.78 g of acid forming needles with m.p. 66°–67° and $[\alpha]_D^{25} = +148.3°$ ($c = 1.005$, absolute ethanol). The IR-spectrum was identical with that of the L(+) acid prepared from L(+) mandelic acid.

Crystallisation	1	2	3	4	5
ml ethanol	250	125	60	50	50
ml water	750	375	180	150	150
g salt obtained	32.6	24.1	21.1	19.5	17.6
$[\alpha]_D^{25}$ of acid	+ 83°	+ 132°	+ 142°	+ 147°	+ 147°

Acknowledgement. The author is indebted to prof. A. Fredga for his kind interest and for all facilities put at the author's disposal.

1. Neilson, D. G. and Peters, D. A. V. *J. Chem. Soc.* February 1962.
2. Gronowitz, S. and Raźnikiewicz, T. *Arkiv Kemi* **17** (1961) 561.
3. Mitchell, J. W. and Preston, Jr., W. H. *Science* **118** (1953) 518.
4. Mc Kenzie, A. *J. Chem. Soc.* **75** (1899) 753.
5. Raźnikiewicz, T. *Acta Chem. Scand.* **16** (1962) 1097.
6. Krebs, H., Wagner, J. A. and Diewald, J. *Chem. Ber.* **89** (1956) 1875.

Received April 26, 1962.

Absorption Spectrum of Ruthenium(III) diethyldithiophosphate

CHR. KLIXBÜLL JØRGENSEN

Cyanamid European Research Institute, Cologny(Geneva), Switzerland

The absorption spectra of a series of complexes $Mdtp_3$ with $dtp^- = (C_2H_5O)_2PS_2^-$ and M = Cr, Fe, Rh, In, Ir, and Bi were recently described [1] and a more detailed theoretical discussion attempted [2]. In the case of a few elements, such as cobalt (shortly to be discussed) and ruthenium, the reactions with dtp^- are complicated and yield several products. However, the Ru dtp_3 expected can be isolated from the reaction mixture and the absorption spectrum is studied here.

The actual Ru dtp_3 gives a strong raspberry colour (and not strawberryred as when brown impurities occur) in organic solvents such as ethanol, chloroform and dichloroethane. The absorption bands (wavelength λ in mμ, wavenumber σ in cm^{-1}, molar extinction coefficient ε, half-widths $\delta(-)$ and $\delta(+)$, with shoulders in parentheses) in ethanol are given in Table 1.

Table 1.

λ	σ	ε	$\delta(-)$	$\delta(+)$
511	19 550	2 250	1 650	1 800
421	23 700	2 000	1 800	—
(400)	(25 000)	1 850	—	2 000
280	35 700	10 500	3 200	—
240	41 700	20 000	—	—

The positions of electron transfer bands of this low-spin $4d^5$-system are obviously interesting for comparison with the other diethyldithiophosphates and for a determination [3,4] of the optical electronegativity x_{opt} of the ligand. It is not believed that the first three bands are internal $\gamma_5 \rightarrow \gamma_3$ transitions though they have only twice the intensity of such bands [1] in Rh dtp_3 and Ir dtp_3. However, a comparison with other metals [1] and also a comparison of the weaker bands of $RuCl_6^{3-}$ relative to $RhCl_6^{3-}$ would suggest that the two former compounds are rather exceptional. A very slightly pronounced shoulder at 550–575 mμ observed here of Ru dtp_3 (see Fig. 1) might represent such a transition.

Since $x_{opt} = 2.1$ of Ru(III), the value $x_{opt} = 2.7$ of dtp^- is substantiated by the identification to the band at 19 550 cm^{-1} as the first electron transfer band. The detailed structure of the group of the first three bands may be explained along the lines previously exposed [2].

The high band at 35 700 cm^{-1} is presumably an electron transfer band to the empty γ_3 sub-shell and can be compared to the similar band [1] at 31 200 cm^{-1} of Rh dtp_3 which would be expected to occur at somewhat smaller wavenumber than in

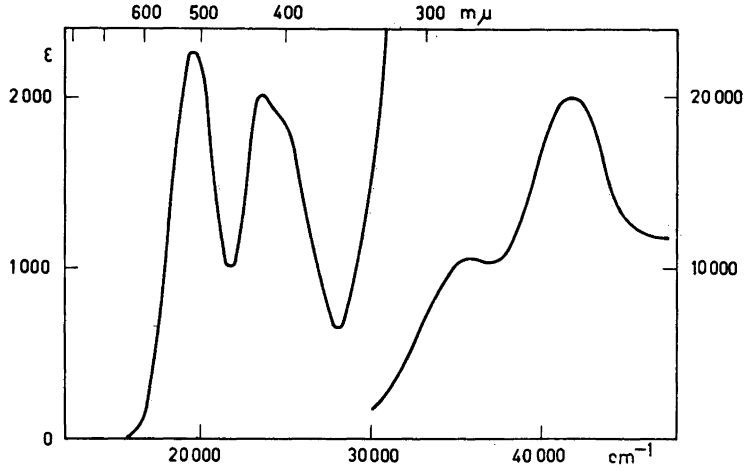

Fig. 1. Absorption spectrum of Ru dtp_3 in ethanol.

Ru dtp_3. However, the band is considerably broader in the latter case ($\delta(-)$ is only 2000 cm^{-1} in Rh dtp_3) as may be explained by the more complicated structure of the excited configuration $\pi^{-1}\gamma_5^5\gamma_3$ of the Ru(III) complexes. Similar remarks apply to the highest band observed at 41 700 cm^{-1} of Ru dtp_3 which may be compared to the band of Rh dtp_3 at 38 800 cm^{-1}.

Experimental 3.8 g "potassium chlororuthenite" (predominantly $K_2[RuCl_5(H_2O)]$ or K_2RuCl_5) from H. Drijfhout and Zoon, Amsterdam, was heated with 100 ml 0.5 M perchloric acid. An olive-brown precipitate (0.9 g) was filtered off, and the filtrate added 40 ml 1 M aqueous solution of ammonium diethyldithiophosphate (from American Cyanamid, Stamford, Conn.). By heating at 80° for 6 h, under stirring, a dark brown precipitate was formed. When boiled with ethanol, this precipitate left 0.6 g of a yellow-brown powder (believed possibly to be dtp_3 RuORu dtp_3, having nearly the same analysis as Ru dtp_3: C 20.93; H 4.39; P 14.79; S 32.67. It is nearly insoluble in ethanol. A solution in dichloroethane shows a broad band at 380 mμ but no maxima in the visible), and the hot filtrate deposited various fractions of dark red, nearly black, crystals. The latter fractions were mixed with small amounts of a brown substance, reversing the intensity ratio between the 420 and 400 mμ bands. On the other hand, the first fraction so prepared (only 0.1 g) was identified as genuine Ru dtp_3. This was not so much because of the analysis. (Found: C 21.50; H 4.52; P 15.18; S 32.95. Calc. for $C_{12}H_{30}O_6P_3S_6Ru$: C 21.92; H 4.66; P 14.14; S 29.27) as because of the fact that colourless In dtp_3, when recrystallized from boiling ethanol together with one of the mixed fractions, syncrystallized with a clear red colour, leaving an orange solution. The visible absorption spectrum of a solution of these In(III), Ru(III) containing crystals was identical with that given above. The reflection spectrum of the red crystals was measured on the attachment to the Cary 14 recording spectrophotometer (on which all solutions were also measured) and showed maxima of the optical density at 509 and 421 mμ and a shoulder at 400 mμ.

1. Jørgensen, C. K. *J. Inorg. Nuclear Chem. In press.*
2. Jørgensen, C. K. *Molecular Physics. In press.*
3. Jørgensen, C. K. *Solid State Physics* **13** (1962) 375.
4. Jørgensen, C. K. *Advances in Chem. Phys. In press.*

Received April 23, 1962.

"The Formation of Polynuclear Complexes"

BROR SKYTTE JENSEN

Danish Atomic Energy Commission, Risø, Denmark

In a recent contribution to *Acta Chem. Scand.*[1] professor L. G. Sillén has criticized my paper "The Formation of Polynuclear Complexes."[2]

The display presented by Sillén clearly shows that I have drawn some wrong conclusions in the case of the hydrolysis of the VO_2^+-ion, but apart from this his criticism is rather surprising both in its form as well as in its examples as will be evident from the following.

It will be clear for readers of my paper that the analysis of experimental data by the method proposed by me is in its present form limited to cases where only two complexes exist simultaneously in major amounts. This is the cause why I did not intend to identify the mononuclear species being formed in the case of the hydrolysis of the vanadyl ion.

Sometimes, however, the trends in the limiting slopes may be of some aid in identifying the new species arising when new reactions start. Such a case do we in fact have in the hydrolysis of the VO^{2+}-ion.

Rosotti by curve-fitting methods claimed the monomeric hydrolysis product to be VO(OH) with a stability constant of $\beta_{11} = 10^{8.2} \pm {}^{0.1}$ and showed how well the calculated curve fitted the experimental data. In his contribution Sillén used this example to demonstrate the superiority of the treatment of experimental data used by him and his group.

By considering the trends shown by the limiting slopes in a log Z *versus* pH plot of the available data it is obvious that the monomeric species $VO(OH)_2$ might as well be the actual species being formed. From the limiting tangent the formation constant is estimated to $\beta_{21} \simeq 10^{19}$.

In Fig. 1 a plot of Z *versus* pH calculated by means of the following formula is compared with experimental data

$$(Z-1) = ((\beta_{21}[OH]^2-1)/(4C_B\beta_{22}[OH]^2))(\sqrt{(\beta_{21}[OH]^2+1)^2+8\beta_{22}[OH]^2C_B} - (\beta_{21}[OH]^2+1))$$

where C_B is the total concentration of vanadium and with $\beta_{21} = 10^{18.8}$ and $\beta_{22} = 10^{21.5}$.

Ru dtp_3. However, the band is considerably broader in the latter case ($\delta(-)$ is only 2000 cm^{-1} in Rh dtp_3) as may be explained by the more complicated structure of the excited configuration $\pi^{-1}\gamma_5^5\gamma_3$ of the Ru(III) complexes. Similar remarks apply to the highest band observed at 41 700 cm^{-1} of Ru dtp_3 which may be compared to the band of Rh dtp_3 at 38 800 cm^{-1}.

Experimental 3.8 g "potassium chlororuthenite" (predominantly $K_2[RuCl_5(H_2O)]$ or K_2RuCl_5) from H. Drijfhout and Zoon, Amsterdam, was heated with 100 ml 0.5 M perchloric acid. An olive-brown precipitate (0.9 g) was filtered off, and the filtrate added 40 ml 1 M aqueous solution of ammonium diethyldithiophosphate (from American Cyanamid, Stamford, Conn.). By heating at 80° for 6 h, under stirring, a dark brown precipitate was formed. When boiled with ethanol, this precipitate left 0.6 g of a yellow-brown powder (believed possibly to be dtp_3 RuORu dtp_3, having nearly the same analysis as Ru dtp_3: C 20.93; H 4.39; P 14.79; S 32.67. It is nearly insoluble in ethanol. A solution in dichloroethane shows a broad band at 380 mμ but no maxima in the visible), and the hot filtrate deposited various fractions of dark red, nearly black, crystals. The latter fractions were mixed with small amounts of a brown substance, reversing the intensity ratio between the 420 and 400 mμ bands. On the other hand, the first fraction so prepared (only 0.1 g) was identified as genuine Ru dtp_3. This was not so much because of the analysis. (Found: C 21.50; H 4.52; P 15.18; S 32.95. Calc. for $C_{12}H_{30}O_6P_3S_6Ru$: C 21.92; H 4.66; P 14.14; S 29.27) as because of the fact that colourless In dtp_3, when recrystallized from boiling ethanol together with one of the mixed fractions, syncrystallized with a clear red colour, leaving an orange solution. The visible absorption spectrum of a solution of these In(III), Ru(III) containing crystals was identical with that given above. The reflection spectrum of the red crystals was measured on the attachment to the Cary 14 recording spectrophotometer (on which all solutions were also measured) and showed maxima of the optical density at 509 and 421 mμ and a shoulder at 400 mμ.

1. Jørgensen, C. K. *J. Inorg. Nuclear Chem. In press.*
2. Jørgensen, C. K. *Molecular Physics. In press.*
3. Jørgensen, C. K. *Solid State Physics* **13** (1962) 375.
4. Jørgensen, C. K. *Advances in Chem. Phys. In press.*

Received April 23, 1962.

"The Formation of Polynuclear Complexes"

BROR SKYTTE JENSEN

Danish Atomic Energy Commission, Risø, Denmark

In a recent contribution to *Acta Chem. Scand.*[1] professor L. G. Sillén has criticized my paper "The Formation of Polynuclear Complexes."[2]

The display presented by Sillén clearly shows that I have drawn some wrong conclusions in the case of the hydrolysis of the VO_2^+-ion, but apart from this his criticism is rather surprising both in its form as well as in its examples as will be evident from the following.

It will be clear for readers of my paper that the analysis of experimental data by the method proposed by me is in its present form limited to cases where only two complexes exist simultaneously in major amounts. This is the cause why I did not intend to identify the mononuclear species being formed in the case of the hydrolysis of the vanadyl ion.

Sometimes, however, the trends in the limiting slopes may be of some aid in identifying the new species arising when new reactions start. Such a case do we in fact have in the hydrolysis of the VO^{2+}-ion.

Rosotti by curve-fitting methods claimed the monomeric hydrolysis product to be VO(OH) with a stability constant of $\beta_{11} = 10^{8.2} \pm {}^{0.1}$ and showed how well the calculated curve fitted the experimental data. In his contribution Sillén used this example to demonstrate the superiority of the treatment of experimental data used by him and his group.

By considering the trends shown by the limiting slopes in a log Z *versus* pH plot of the available data it is obvious that the monomeric species $VO(OH)_2$ might as well be the actual species being formed. From the limiting tangent the formation constant is estimated to $\beta_{21} \simeq 10^{19}$.

In Fig. 1 a plot of Z *versus* pH calculated by means of the following formula is compared with experimental data

$$(Z-1) = ((\beta_{21}[OH]^2-1)/(4C_B\beta_{22}[OH]^2))(\sqrt{(\beta_{21}[OH]^2+1)^2+8\beta_{22}[OH]^2C_B} - (\beta_{21}[OH]^2+1))$$

where C_B is the total concentration of vanadium and with $\beta_{21} = 10^{18.8}$ and $\beta_{22} = 10^{21.5}$.

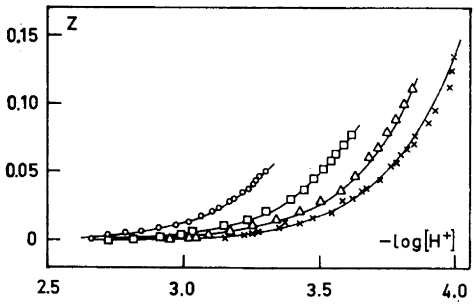

Fig. 1. Hydrolysis of VO^{2+}. Z (average number of OH^- bound per VO^{2+}) as a function of pH for different total concentrations of vanadium. The lines represent theoretical formation curves calculated for $\beta_{22} = 10^{21.5}$ and $\beta_{21} = 10^{18.8}$.

This representation does fit the experimental data as well as does the representation proposed by Rosotti (Fig. 2 of Ref.[3]). By slight changes in the stability constants it is possible to find fits, some of which may suit the investigator better, but with the present set of data it will not be possible to decide, by visual examination, which secondary species is actually being formed.

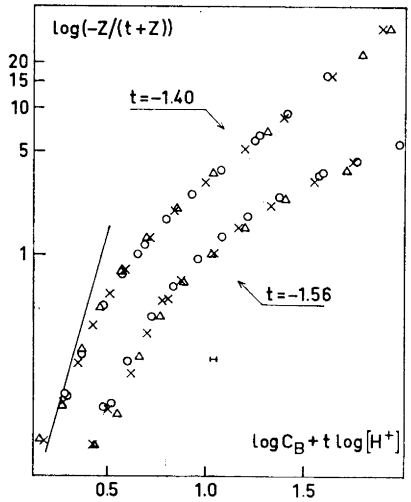

Fig. 2. Hydrolysis of VO_2^+. Values of log $(-Z/(t + Z))$ plotted *versus* $(\log C_B + t\log H^+)$ for $t = -1.40$ and $t = -1.56$. The estimated error is shown in the figure (H). A line of slope 5 is also shown.

To decide which representation does fit the best elaborate least squares calculation might be done leaving the investigator to the choice of regarding a difference found to be significant or not.

To me it seems wise not to state more about the nature of the secondary hydrolysis product than to state it is monomeric as neither of the proposals for the monomeric hydrolysis are much more than guesses. Curve fitting of approximate solutions to experimental data has no chemical meaning and can only be a mathematical art even when it is skillfully done.

To consider my analysis of the hydrolysis of the VO_2^+-ion, the criticism seems at first sight well founded as seen from the comparison of experimental data with theoretical curves based on my formation constants — as displayed by Sillén. The disagreement is impressive but does in fact only prove that my constants are more or less in error.

Whereas a reasonable fit at the onset of the hydrolysis can be obtained by correcting the primary constant within the uncertainty connected to it, this is not the case for the final reaction proposed. If one therefore accepts my proposal for the primary hydrolysis product, additional intermediates must be formed.

As a basis for the analysis by the one or the other method the value of t (for definition see Ref.[2]) is used. In my analysis I used the value $t = -1.40$ whereas Rosotti used the value $t = (-)1.56$.

As a check of which value is to be preferred in the analysis, a plot of log $(-Z/(t + Z))$ *versus* $(\log C_B + t\log[H^+])$ can be made. For the best value of t the best fit with a single curve should be obtained. In Fig. 2 such plots for the experimental data are shown for $t = -1.40$ and $t = -1.56$.

Apart from data referring to the lowest total concentration of vanadium, which are not included in either plot, all experimental data fit very well on a single curve for $t = -1.40$. This is, as is seen from the figure, not the case of $t = -1.56$. The estimated error for the abscissae is shown in the figure. If the actual error is larger, which I do not believe, many reasonable fits can be constructed which are, however, often improbable from a chemical point of view.

Accepting the best fit, an analysis on the basis of the value $t = -1.40$ will be the most reasonable.

The deviation of experimental data corresponding to the lowest total concentration of vanadium may be due to experimental error or may be due to new reactions occurring in this concentration range.

To perform an analysis these data will in any case be neglected in the first attempt and may later be included in a refinement.

The constancy of t over almost the whole range of Z does strongly indicate the existence of series of "core-link" complexes of the general formula $VO_2(VO_2(OH)_{-t})_N$ where $-tN$ must be integers. With the value of $t = -1.40$ only values of $N = 5$, 10, 15-- etc. are possible. The primary hydrolysis product would therefore be expected to be $VO_2(VO_2(OH)_{1.40})_5$ $(=(VO_2)_6(OH)_7)$ as also found by me. It is, however, certain that some of the additional complexes of composition $(VO_2)_{11}(OH)_{14}$,$(VO_2)_{16}(OH)_{21}$, etc. do also exist which I have not pointed out in may paper. If the primary hydrolysis product is $(VO_2)_6(OH)_7$ the limiting slope of a plot of $\log(-Z/(t+Z))$ *versus* $(\log C_B - 1.40 \log [H^+])$ should be 5. That this is the case is seen from Fig. 2.

An enlarged plot of $\log(1.60-Z)$ *versus* pH, (not shown), indicates that new reaction(s) start around $Z \simeq 1.35 \pm 0.03$, a value which corresponds closely to the "core-link" product of composition VO_2 $((VO_2)_5(OH)_7)_5$ with $Z = 1.35$. The pure "core-link" polymerisation does therefore seem to end with this product. The nature of the final reaction(s) cannot be determined with any certainty, but might well be represented by some selected but hypothetical reactions.

Assuming the structure of the hexavanadate $VO_2((VO_2)_5(OH)_7)$ actually to be as formulated in the "core-link" approach, *i.e.* as oxyvanadium(V) pentavanadate, a formulation which has also been proposed by Jander [5] for some solid vanadates, the existence of the solid decavanadates mentioned by Rosotti [4] to support his proposal for the existence of the decavanadate in solution might well be explained. The deviation of the experimental data for low concentrations of vanadium might also be explained as formation of pentavanadates or polypentavanadates in this concentration range.

The formation constants for the species of "core-link" composition can be determined by curve-fitting or other means. When an electronic computer will be at hand I intend to do this determination.

That I still claim—as cited by Sillén with some malice—"A distinct advantage is that the primary polymerisation product often can be determined with certainty", will be obvious from the examples given above.

1. Sillén, L. G. *Acta Chem. Scand.* **15** (1961) 1421.
2. Jensen, B. S. *Ibid.* **15** (1961) 487.
3. Rosotti, F. J. C. and Rosotti, H. S. *Ibid.* **9** (1955) 1177.
4. Rosotti, F. J. C. and Rosotti, H. S. *Ibid.* **10** (1956) 957.
5. Jander, G. and Jahr, K. F. *Z. anorg. U. allgem. Chem.* **212** (1933) 1.

Received April 26, 1962.

Comments to B. S. Jensen's Paper "The Formation of Polynuclear Complexes" *

LARS GUNNAR SILLÉN

Department of inorganic chemistry, The Royal Institute of Technology, Stockholm 70, Sweden

Vanadium(IV) is a minor point. From experience on other systems it seems likely that both $VOOH^+$ and $VO(OH)_2$ are present but that $[VOOH^+] > [VO(OH)_2]$ in the range studied. To determine both constants independently, more data would be needed.

Vanadium(V) is the main problem. Whereas the orange-colored vanadates (the first hydrolysis product of VO_2^+) were earlier supposed to be penta- or hexavanadates, Rossotti's work[1] strongly indicated that they are deca-vanadates. Later work by various methods [2-7], seems to confirm Rossotti's deca-vanadate hypothesis.

B. S. Jensen wants to revive the hexavanadate theory, perhaps with a subsequent series of "core-links" complexes. In his first paper [8] he deduced from Rossotti's data a set of reactions and equilibrium constants. However, a check [9] showed, that with Jensen's theory one would calculate curves $Z(\log h)_B$ far from Rossotti's experimental data, on which the calculations were allegedly founded. In Jensen's new contribution the long discussion does not even end with a set of equilibrium constants. There is little point in continuing this discussion of the revived hexavanadate hypothesis until B. S. Jen-

* *Acta Chem. Scand.* **16** (1962) 1049.

The deviation of experimental data corresponding to the lowest total concentration of vanadium may be due to experimental error or may be due to new reactions occurring in this concentration range.

To perform an analysis these data will in any case be neglected in the first attempt and may later be included in a refinement.

The constancy of t over almost the whole range of Z does strongly indicate the existence of series of "core-link" complexes of the general formula $VO_2(VO_2(OH)_{-t})_N$ where $-tN$ must be integers. With the value of $t = -1.40$ only values of $N = 5$, 10, 15-- etc. are possible. The primary hydrolysis product would therefore be expected to be $VO_2(VO_2(OH)_{1.40})_5$ $(=(VO_2)_6(OH)_7)$ as also found by me. It is, however, certain that some of the additional complexes of composition $(VO_2)_{11}(OH)_{14}$,$(VO_2)_{16}(OH)_{21}$, etc. do also exist which I have not pointed out in may paper. If the primary hydrolysis product is $(VO_2)_6(OH)_7$ the limiting slope of a plot of $\log(-Z/(t+Z))$ *versus* $(\log C_B - 1.40 \log [H^+])$ should be 5. That this is the case is seen from Fig. 2.

An enlarged plot of $\log(1.60-Z)$ *versus* pH, (not shown), indicates that new reaction(s) start around $Z \simeq 1.35 \pm 0.03$, a value which corresponds closely to the "core-link" product of composition VO_2 $((VO_2)_5(OH)_7)_5$ with $Z = 1.35$. The pure "core-link" polymerisation does therefore seem to end with this product. The nature of the final reaction(s) cannot be determined with any certainty, but might well be represented by some selected but hypothetical reactions.

Assuming the structure of the hexavanadate $VO_2((VO_2)_5(OH)_7)$ actually to be as formulated in the "core-link" approach, *i.e.* as oxyvanadium(V) pentavanadate, a formulation which has also been proposed by Jander [5] for some solid vanadates, the existence of the solid decavanadates mentioned by Rosotti [4] to support his proposal for the existence of the decavanadate in solution might well be explained. The deviation of the experimental data for low concentrations of vanadium might also be explained as formation of pentavanadates or polypentavanadates in this concentration range.

The formation constants for the species of "core-link" composition can be determined by curve-fitting or other means. When an electronic computer will be at hand I intend to do this determination.

That I still claim—as cited by Sillén with some malice—"A distinct advantage is that the primary polymerisation product often can be determined with certainty", will be obvious from the examples given above.

1. Sillén, L. G. *Acta Chem. Scand.* **15** (1961) 1421.
2. Jensen, B. S. *Ibid.* **15** (1961) 487.
3. Rosotti, F. J. C. and Rosotti, H. S. *Ibid.* **9** (1955) 1177.
4. Rosotti, F. J. C. and Rosotti, H. S. *Ibid.* **10** (1956) 957.
5. Jander, G. and Jahr, K. F. *Z. anorg. U. allgem. Chem.* **212** (1933) 1.

Received April 26, 1962.

Comments to B. S. Jensen's Paper "The Formation of Polynuclear Complexes" *

LARS GUNNAR SILLÉN

Department of inorganic chemistry, The Royal Institute of Technology, Stockholm 70, Sweden

Vanadium(IV) is a minor point. From experience on other systems it seems likely that both $VOOH^+$ and $VO(OH)_2$ are present but that $[VOOH^+] > [VO(OH)_2]$ in the range studied. To determine both constants independently, more data would be needed.

Vanadium(V) is the main problem. Whereas the orange-colored vanadates (the first hydrolysis product of VO_2^+) were earlier supposed to be penta- or hexavanadates, Rossotti's work[1] strongly indicated that they are deca-vanadates. Later work by various methods [2-7], seems to confirm Rossotti's deca-vanadate hypothesis.

B. S. Jensen wants to revive the hexavanadate theory, perhaps with a subsequent series of "core-links" complexes. In his first paper [8] he deduced from Rossotti's data a set of reactions and equilibrium constants. However, a check [9] showed, that with Jensen's theory one would calculate curves $Z(\log h)_B$ far from Rossotti's experimental data, on which the calculations were allegedly founded. In Jensen's new contribution the long discussion does not even end with a set of equilibrium constants. There is little point in continuing this discussion of the revived hexavanadate hypothesis until B. S. Jen-

* *Acta Chem. Scand.* **16** (1962) 1049.

sen has produced either better data of his own or at least a complete alternative explanation (reactions and equilibrium constants), which can be compared with experimental data.

I might add, that a limited set of core-links complexes, (especially a set of only two species) has often proved a useful approximation but cases with a considerable number of core-links complexes do not seem to be as frequent as I may once have thought on the basis of our earliest data. It is an irony of fate that B. S. Jensen now is trying to revive these concepts too.

1. Rossotti, F. J. C. and Rossotti, H. S. *Acta Chem. Scand.* **10** (1956) 957.
2. Meier, J. and Schwarzenbach, G. *Chimia* **12** (1958) 328.
3. Newman, L. and Quinlan, K. P. *J. Am. Chem. Soc.* **81** (1959) 547.
4. Jahr, K. F. *et al. Z. f. Naturforsch.* **14b** (1959) 468, 469, 470.
5. Chauveau, F. *Bull. soc. chim. France* **1960** 819.
6. Glemser, O. and Preisler, E. *Z. anorg. Chem.* **303** (1960) 303, 316.
7. Schiller, K. and Thilo, E. *Z. anorg. Chem.* **310** (1961) 261.
8. Jensen, B. S. *Acta Chem. Scand.* **15** (1961) 487.
9. Sillén, L. G. *Acta Chem. Scand.* **15** (1961) 1421.

Received May 21, 1962.

Reduction of 2-Mercaptobenzothiazole to Benzothiazole

BENGT WEIBULL

Research Laboratory, Mo och Domsjö AB, Örnsköldsvik, Sweden

2-Mercaptobenzothiazole (I) is widely used as a component in corrosion inhibitors for automotive anti-freezes [1]. Accordingly, its stability in the presence of iron is of great importance. In neutral or alkaline solution it was found to be quite stable, but in acid solution it was reduced by iron powder to benzothiazole (II):

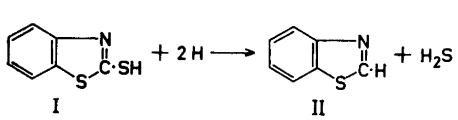

I II

This simple reduction seems not to have been observed for the unsubstituted compound. However, the corresponding reaction was reported for 2-mercapto-6-methylbenzothiazole, while 2-mercapto-4-nitro-6-methyl- and 2-mercapto-4-nitro-6-methoxy-benzothiazole did not yield identifiable products [2], so the reaction is not of general applicability. Reductive degradation of 2-mercaptobenzothiazole under more drastic conditions has been reported. Treatment with Raney nickel [3] or Raney cobalt [4] thus yielded benzothiazole and further degraded compounds. Hydrogenation over a cobalt sulphide catalyst at high pressure and elevated temperature gave equal parts of *o*-aminothiophenol and benzothiazole [5].

Experimental. The directions of Blomquist and Diuguid [2] were partly followed. I (10 g) was mixed with iron powder (Ferrum reductum, 10 g), glacial acetic acid (90 ml), ethanol (25 ml), and water (10 ml). The mixture was heated at 100° for 36 h, after which time no more hydrogen sulphide was evolved. The mixture was made strongly alkaline and distilled with steam until the distillate was clear. It was extracted with ether, the ether solution dried over potassium carbonate, the ether evaporated, and the residue fractionated in vacuum. The main fraction (4.1 g; 51 %) had b.p. 93.0—93.5°/8 mm Hg. Titration with perchloric acid in glacial acetic acid gave equiv. wt. 135.2, calc. for II 135.18. Picrate, m.p. 169° (depends upon rate of heating), lit.[3] 169.5-170°. The identity of the compound was further confirmed by its infrared spectrum, which was found to coincide with that given for benzothiazole by Randall *et al.*[6]

The author is indebted to Mr. L. Rönnbäck for skilful assistance.

1. *British Standard* 3150:1959.
2. Blomquist, A. T. and Diuguid, L. I. *J. Org. Chem.* **12** (1947) 718.
3. Badger, G. M. and Kowanko, N. *J. Chem. Soc.* **1957** 1652.
4. Badger, G. M., Kowanko, N. and Sasse, W. H. F. *J. Chem. Soc.* **1959** 440.
5. Lazier, W. A. and Signaigo, F. K. *U.S. Patent* 2,402,642; *Chem. Abstracts* **40** (1946) 5757.
6. Randall, H. M., Fowler, R. G., Fuson, N. and Dangl, J. R. *Infrared Determination of Organic Structures*, D. Van Nostrand Co., New York 1949, p. 212.

Received May 8, 1962.

sen has produced either better data of his own or at least a complete alternative explanation (reactions and equilibrium constants), which can be compared with experimental data.

I might add, that a limited set of core-links complexes, (especially a set of only two species) has often proved a useful approximation but cases with a considerable number of core-links complexes do not seem to be as frequent as I may once have thought on the basis of our earliest data. It is an irony of fate that B. S. Jensen now is trying to revive these concepts too.

1. Rossotti, F. J. C. and Rossotti, H. S. *Acta Chem. Scand.* **10** (1956) 957.
2. Meier, J. and Schwarzenbach, G. *Chimia* **12** (1958) 328.
3. Newman, L. and Quinlan, K. P. *J. Am. Chem. Soc.* **81** (1959) 547.
4. Jahr, K. F. *et al. Z. f. Naturforsch.* **14b** (1959) 468, 469, 470.
5. Chauveau, F. *Bull. soc. chim. France* **1960** 819.
6. Glemser, O. and Preisler, E. *Z. anorg. Chem.* **303** (1960) 303, 316.
7. Schiller, K. and Thilo, E. *Z. anorg. Chem.* **310** (1961) 261.
8. Jensen, B. S. *Acta Chem. Scand.* **15** (1961) 487.
9. Sillén, L. G. *Acta Chem. Scand.* **15** (1961) 1421.

Received May 21, 1962.

Reduction of 2-Mercaptobenzothiazole to Benzothiazole

BENGT WEIBULL

Research Laboratory, Mo och Domsjö AB, Örnsköldsvik, Sweden

2-Mercaptobenzothiazole (I) is widely used as a component in corrosion inhibitors for automotive anti-freezes [1]. Accordingly, its stability in the presence of iron is of great importance. In neutral or alkaline solution it was found to be quite stable, but in acid solution it was reduced by iron powder to benzothiazole (II):

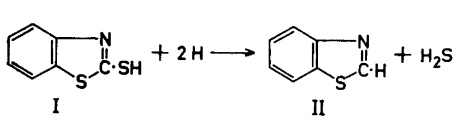

I II

This simple reduction seems not to have been observed for the unsubstituted compound. However, the corresponding reaction was reported for 2-mercapto-6-methylbenzothiazole, while 2-mercapto-4-nitro-6-methyl- and 2-mercapto-4-nitro-6-methoxy-benzothiazole did not yield identifiable products [2], so the reaction is not of general applicability. Reductive degradation of 2-mercaptobenzothiazole under more drastic conditions has been reported. Treatment with Raney nickel [3] or Raney cobalt [4] thus yielded benzothiazole and further degraded compounds. Hydrogenation over a cobalt sulphide catalyst at high pressure and elevated temperature gave equal parts of *o*-aminothiophenol and benzothiazole [5].

Experimental. The directions of Blomquist and Diuguid [2] were partly followed. I (10 g) was mixed with iron powder (Ferrum reductum, 10 g), glacial acetic acid (90 ml), ethanol (25 ml), and water (10 ml). The mixture was heated at 100° for 36 h, after which time no more hydrogen sulphide was evolved. The mixture was made strongly alkaline and distilled with steam until the distillate was clear. It was extracted with ether, the ether solution dried over potassium carbonate, the ether evaporated, and the residue fractionated in vacuum. The main fraction (4.1 g; 51 %) had b.p. 93.0—93.5°/8 mm Hg. Titration with perchloric acid in glacial acetic acid gave equiv. wt. 135.2, calc. for II 135.18. Picrate, m.p. 169° (depends upon rate of heating), lit.[3] 169.5-170°. The identity of the compound was further confirmed by its infrared spectrum, which was found to coincide with that given for benzothiazole by Randall *et al.*[6]

The author is indebted to Mr. L. Rönnbäck for skilful assistance.

1. *British Standard* 3150:1959.
2. Blomquist, A. T. and Diuguid, L. I. *J. Org. Chem.* **12** (1947) 718.
3. Badger, G. M. and Kowanko, N. *J. Chem. Soc.* **1957** 1652.
4. Badger, G. M., Kowanko, N. and Sasse, W. H. F. *J. Chem. Soc.* **1959** 440.
5. Lazier, W. A. and Signaigo, F. K. *U.S. Patent* 2,402,642; *Chem. Abstracts* **40** (1946) 5757.
6. Randall, H. M., Fowler, R. G., Fuson, N. and Dangl, J. R. *Infrared Determination of Organic Structures*, D. Van Nostrand Co., New York 1949, p. 212.

Received May 8, 1962.

The Mechanism of the Biological Formation of Anthraquinones

STEN GATENBECK

Institute of Biochemistry, University of Lund, Lund, Sweden

It has been well established that anthraquinones produced by moulds are derived from acetate [1]. However, the experiments performed with isotopic acetate as an added substrate could not distinguish between the two proposed mechanisms for the formation of the anthraquinones.

As early as 1944 Tatum [2] suggested, on the basis of structural interpretation of monocyclic mould metabolites, that the anthraquinones arise by a condensation of a phthalic acid with a monocylic phenolic carboxylic acid. The other hypothesis [3] involves an overall condensation of acetate throughout the anthraquinone molecule, the most attractive idea being an enzyme-bound linear condensation.

The recent finding of the participation of malonate in fatty acid synthesis has brought about a new trend of thinking about the biosynthesis of acetate-derived compounds. From the experimentally confirmed examples of 6-methylsalicylic acid [4], orsellinic acid [5], oxytetracycline [6], and in the course of this work of rugulosin [7]; the generalization that the so-called acetate-derived compounds are actually made up from an acyl-coenzyme A derivative acting as a primer on the condensation of malonyl units, can be made with great confidence.

On the basis of this generalization the two different mechanisms for the anthraquinone formation can be subjected to experimental investigation. In the first mechanism two monocyclic compounds are individually formed prior to the condensation of the anthraquinone, *i.e.* each of the monocyclic compounds are built up from one acetate unit and three malonate units. The obtained anthraquinone molecule will thus have two acetate units, the other carbon atoms coming from malonate. The positions of the acetate units will be as indicated in Fig. 1.

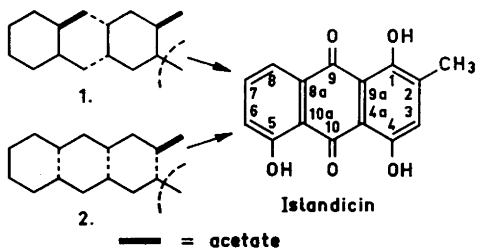

Fig. 1.

On the other hand, if the second mechanism is valid the resulting anthraquinone will carry only one acetate unit as shown in Fig. 1.

In an experiment performed with a culture of *Penicillium islandicum* Sopp (N.R.R.L. 1036) growing on a Czapek-Dox medium, 0.1 mC of malonic acid-2-^{14}C was added. The anthraquinone islandicin was isolated, diluted with nonradioactive carrier and subjected to the following degradations as described in detail elsewhere [1,8]: (*a*) total combustion, (*b*) Kuhn-Roth oxidation and Schmidt degradation of the formed acetic acid, and (*c*) oxidation to 3-hydroxyphthalic acid with subsequent decarboxylation to *m*-hydroxybenzoic acid. Nitration of the latter yielded trinitro-*m*-hydroxybenzoic acid with the carboxyl group representing one of the carbon atoms of special interest in the present problem. The picric acid obtained after decarboxylation was further degraded by a bromopicrin reaction.

The values of the radioactivities listed in Table 1 show that the methyl group of islandicin has a significantly lower specific radioactivity than the position 9 which, on the other hand, has the same specific activity as the positions theoretically directly labelled from malonate in both of the proposed mechanisms.

These results are only compatible with the second of the proposed mechanisms

Table 1.

Substance	*Counts/min/mmole*
Islandicin	108×10^4
Kuhn-Roth acetic acid:	
Carboxyl group (C(2) of islandicin)	0.26×10^4
Methyl group	9×10^4
Trinitro-*m*-hydroxybenzoic acid (C(5, 6, 7, 8, 8a, 9, 10a) of islandicin)	56.56×10^4
Carboxyl group of trinitro-*m*-hydroxy-benzoic acid (C(9) of islandicin)	13.9×10^4
Bromopicrin (C (6, 8, 10a) of islandicin)	13.96×10^4
Carbondioxide from bromopicrin reaction (C (5, 7, 8a) of islandicin)	0.3×10^4

with the modification that one activated acetate unit initiates the condensation of seven malonate units to form the anthraquinone in an over-all reaction.

1. Gatenbeck, S. *Acta Chem. Scand.* **12** (1958) 1211; **14** (1960) 296.
2. Tatum, E. L. *Ann. Rev. Biochem.* **13** (1944) 667.
3. Ehrensvärd, G. and Gatenbeck, S. *Main Lectures, 17th Intern. Congr. Pure and Applied Chem. II (1960) 99.*
4. Bu'Lock, J. D. and Smalley, H. M. *Proc. Chem. Soc.* **1961** 209. Birch, A. J., Cassera, A. and Rickards, R. W. *Chem. and Ind. London* **1961** 792.
5. Mosbach, K. *Naturwiss.* **48** (1961) 525.
6. Gatenbeck, S. *Biochem. Biophys. Research Communs.* **6** (1961/62) 422.
7. Shibata, S. and Ikekawa, T. *Chem. and Ind. London* **1962** 360.
8. Gatenbeck, S. *Acta Chem. Scand.* **12** (1958) 1985.

Received May 2, 1962.

An Attempt to Evaluate a Proton Activity Function from the H_R-Function

ERIK HÖGFELDT

Department of Inorganic Chemistry, Royal Institute of Technology, Stockholm 70, Sweden

Recently a method was developed for the evalution of ion activity functions with the aid of the Hammett acidity function, H_0[1]. It was found by Wyatt [2], that H_0, *i.e.* the proton activity function, is a unique function of the water activity in several strong acids. It was now of interest to learn if other acidity functions give analogous results. The most intensively studied function besides H_0 is H_R defined by the reaction:

$$ROH + H^+ \rightleftharpoons R^+ + H_2O \quad (1)$$

$$H_R = -pK_1 - \log([R^+]/[ROH]) = -\log(y_{ROH}/y_{R+})a_{H+} + \log a_{H_2O} \quad (2)$$

where K_1 is the thermodynamic equilibrium constant of reaction (1) and y_{ROH} and y_{R+} are the activity coefficients of ROH and R^+. ROH is an alcohol of the triphenylcarbinol type and R^+ the corresponding substituted triphenylmethyl cation. For the sake of simplicity of notation we define:

$$y_{ROH}/y_{R+} = \varphi_R \quad (3)$$

From (2) and (3):

$$\log\varphi_R \cdot a_{H+} = -H_R + \log a_{H_2O} \quad (4)$$

If $\varphi_R a_{H+}$ can be used as a measure of the proton activity it should be a unique function of the water activity as found for $\varphi_0 a_{H+}$ where φ_0 is defined by:

$$\varphi_0 = y_B/y_{BH+} \quad (5)$$

i.e. the ratio of the activity coefficients of the base and acid forms of the indicators used in the evaluation of H_0. According to definition:

$$\log\varphi_0 a_{H+} = -H_0 \quad (6)$$

(In preceding papers [1,3] φ_0 has been denoted by φ. By calling it φ_0 the relation to H_0 is indicated in the same manner as with φ_R and H_R). The indicators used in the evaluation of H_0 are mostly substituted anilines.

H_R has recently been measured in the systems $H_2SO_4-H_2O$, $HClO_4-H_2O$ and HNO_3-H_2O by Deno and coworkers [4,5].

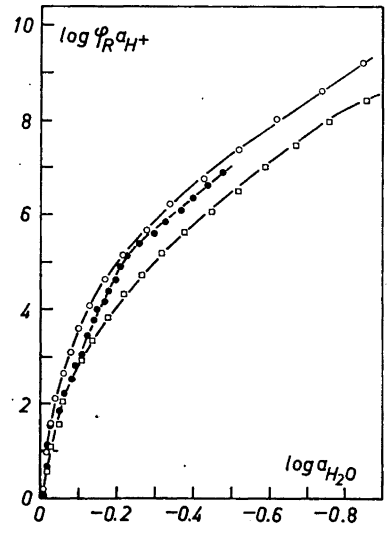

Fig. 1. log $\varphi_R a_{H+}$ plotted against log a_{H_2O} for the three systems:

○ $HClO_4-H_2O$
□ $H_2SO_4-H_2O$
● HNO_3-H_2O

with the modification that one activated acetate unit initiates the condensation of seven malonate units to form the anthraquinone in an over-all reaction.

1. Gatenbeck, S. *Acta Chem. Scand.* **12** (1958) 1211; **14** (1960) 296.
2. Tatum, E. L. *Ann. Rev. Biochem.* **13** (1944) 667.
3. Ehrensvärd, G. and Gatenbeck, S. *Main Lectures, 17th Intern. Congr. Pure and Applied Chem. II (1960) 99.*
4. Bu'Lock, J. D. and Smalley, H. M. *Proc. Chem. Soc.* **1961** 209. Birch, A. J., Cassera, A. and Rickards, R. W. *Chem. and Ind. London* **1961** 792.
5. Mosbach, K. *Naturwiss.* **48** (1961) 525.
6. Gatenbeck, S. *Biochem. Biophys. Research Communs.* **6** (1961/62) 422.
7. Shibata, S. and Ikekawa, T. *Chem. and Ind. London* **1962** 360.
8. Gatenbeck, S. *Acta Chem. Scand.* **12** (1958) 1985.

Received May 2, 1962.

An Attempt to Evaluate a Proton Activity Function from the H_R-Function

ERIK HÖGFELDT

Department of Inorganic Chemistry, Royal Institute of Technology, Stockholm 70, Sweden

Recently a method was developed for the evalution of ion activity functions with the aid of the Hammett acidity function, H_0[1]. It was found by Wyatt [2], that H_0, *i.e.* the proton activity function, is a unique function of the water activity in several strong acids. It was now of interest to learn if other acidity functions give analogous results. The most intensively studied function besides H_0 is H_R defined by the reaction:

$$ROH + H^+ \rightleftharpoons R^+ + H_2O \quad (1)$$

$$H_R = -pK_1 - \log([R^+]/[ROH]) = -\log(y_{ROH}/y_{R+})a_{H+} + \log a_{H_2O} \quad (2)$$

where K_1 is the thermodynamic equilibrium constant of reaction (1) and y_{ROH} and y_{R+} are the activity coefficients of ROH and R^+. ROH is an alcohol of the triphenylcarbinol type and R^+ the corresponding substituted triphenylmethyl cation. For the sake of simplicity of notation we define:

$$y_{ROH}/y_{R+} = \varphi_R \quad (3)$$

From (2) and (3):

$$\log\varphi_R \cdot a_{H+} = -H_R + \log a_{H_2O} \quad (4)$$

If $\varphi_R a_{H+}$ can be used as a measure of the proton activity it should be a unique function of the water activity as found for $\varphi_0 a_{H+}$ where φ_0 is defined by:

$$\varphi_0 = y_B/y_{BH+} \quad (5)$$

i.e. the ratio of the activity coefficients of the base and acid forms of the indicators used in the evaluation of H_0. According to definition:

$$\log\varphi_0 a_{H+} = -H_0 \quad (6)$$

(In preceding papers [1,3] φ_0 has been denoted by φ. By calling it φ_0 the relation to H_0 is indicated in the same manner as with φ_R and H_R). The indicators used in the evaluation of H_0 are mostly substituted anilines.

H_R has recently been measured in the systems $H_2SO_4-H_2O$, $HClO_4-H_2O$ and HNO_3-H_2O by Deno and coworkers [4,5].

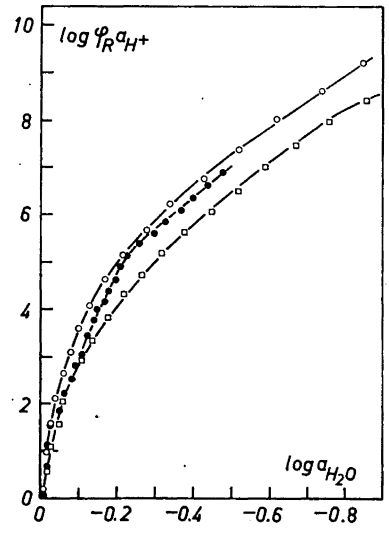

Fig. 1. log $\varphi_R a_{H+}$ plotted against log a_{H_2O} for the three systems:

○ $HClO_4-H_2O$
□ $H_2SO_4-H_2O$
● HNO_3-H_2O

Table 1. $\log \varphi_R \varphi_0^{-1}$ in the system $H_2SO_4 - H_2O$.

$[H_2SO_4]$ M	$\log \varphi_R \varphi_0^{-1}$
10.0	3.99
10.5	4.19
11.0	4.35
11.5	4.53
12.0	4.62
12.5	4.70
13.0	4.78
13.5	4.81
14.0	4.85
14.5	4.89
15.0	4.92
15.5	4.92
16.0	4.98
16.5	4.88
17.0	4.85
17.5	4.74
18.0	4.77
18.1	4.78
18.2	4.86
18.3	4.82

Using these data and the water and acid activities discussed in Ref [1], the function $\varphi_R a_{H^+}$ has been computed according to (4). In Fig. 1 $\log \varphi_R a_{H^+}$ is plotted against $\log a_{H_2O}$ for the three acids. As seen $\varphi_R a_{H^+}$ is not a unique function of the water activity. This indicates individual variations in φ_R and therefore H_R cannot be used for defining a unique proton activity function. However in concentrated sulfuric acid the situation is more hopeful [6]. In Table 1 $\log \varphi_R \varphi_0^{-1}$ obtained by elimination of $\log a_{H^+}$ from (4) and (6) is given from 10.0 – 18.3 M H_2SO_4. In the range 13.0 – 18.3 M H_2SO_4 $\log \varphi_R \varphi_0^{-1}$ is practically constant; the average value is:

$$\log \varphi_R \varphi_0^{-1} = 4.85 \pm 0.07 \qquad (7)$$

This is about the same concentration range where it was found that φ_0 could be regarded as practically constant [1]. In this concentration range the following relation holds between H_R and H_0:

$$H_R = H_0 + \log a_{H_2O} - 4.85 \qquad (8)$$

Any mechanism that correlates with H_R will also correlate with $H_0 + \log a_{H_2O}$ in the range 13.0 – 18.3 M H_2SO_4 and one is as good as the other.

On the other hand for the equilibrium:

$$HNO_2 + H^+ \rightleftharpoons NO^+ + H_2O \qquad (9)$$

H_R is found to correlate better than $H_0 + \log a_{H_2O}$ in concentrated perchloric acid solutions [5]. This is reasonable in view of the possibility that the activity coefficient ratio $y_{HNO_2} \cdot y_{NO^+}^{-1}$ may be subject to the same individual variations as φ_R.

The present state of our knowledge of these systems allows us only to guess the reason for the different behavior of φ_R in the three acids. The measurements by Cigén [7-9] on the proton equilibria of various triphenylmethane dyes show that reaction (1) is only one of several possible reactions. It has been found to hold in concentrated sulfuric acid for the H_R indicators but in dilute aqueous solutions some of the other reactions found by Cigén might interfere.

Recently Deno *et al.* [10] have proposed that H_R' defined by

$$H_R' = H_R - \log a_{H_2O} = -\log \varphi_R a_{H^+} \qquad (10)$$

is a better measure of the proton activity than H_0, because the large triphenyl cations are likely to be practically unhydrated and behave more ideally than the substituted anilines used in the evaluation of H_0. The finding in this paper does not support such a view.

Acknowledgements. This work has received financial support from the *Swedish Atomic Energy Research Council*, which is gratefully acknowledged. Dr Derek Lewis corrected the English text.

1. Högfeldt, E. *Acta Chem. Scand.* **14** (1960) 1627.
2. Wyatt, P. A. H. *Discussions Faraday Soc.* **24** (1957) 162.
3. Högfeldt, E. *J. Inorg. & Nuclear Chem.* **17** (1961) 302.
4. Deno, N. C., Jaruzelski, J. J. and Schriesheim, A. *J. Am. Chem. Soc.* **77** (1955) 3044.
5. Deno, N. C., Berkheimer, H. E., Evans, W. L. and Peterson, H. J. *Ibid.* **81** (1959) 2344.
6. Paul, M. A. and Long, F. A. *Chem. Revs.* **57** (1957), pp. 36 – 39 and references.
7. Cigén, R. *Acta Chem Scand* **12** (1958) 1456.
8. Cigén, R. *Ibid.* **13** (1959) 1113.
9. Cigén, R. *Ibid.* **14** (1960) 979.
10. Deno, N. C. and Spink, C. H. *J. Am. Chem. Soc. In print.*

Received May 11, 1962.

The Hydrogenation of 3-Methylphthalide

PER KOLSAKER

Universitetets kjemiske institutt, Blindern-Oslo, Norway

In order to prepare a substance containing a γ-lactone ring condensed with a cyclohexane ring 3-methylphthalide was hydrogenated catalytically. The product obtained, a liquid boiling at 130—131°C at 10 mm Hg, showed in the infra-red two bands in the carbonyl region, *viz.* 1702 and 1777 cm^{-1}, corresponding to a free carboxyl group and a γ-lactone ring, respectively. The liquid could accordingly be separated in two parts by treatment with a solution of sodium carbonate. Part A (60 %) being insoluble in sodium carbonate was a liquid boiling at 130—131°C at 10 mm Hg. This substance was obviously *cis*- 3-methylhexahydrophthalide as it could be oxidised by means of sodium hypobromite to cyclohexane-*cis*-1,2-dicarboxylic acid.

Part B (40 %) which had dissolved in sodium carbonate could be recovered as a liquid by adding mineral acid. It distilled at 134—135°C at 10 mm Hg and afterwards crystallized spontaneously. The m.p. was 35—37°C and the substance was found to be identical with the acid obtained by hydrogenating 2-ethylbenzoic acid. The 2-ethyl-cyclohexanecarboxylic acid has not been described in the literature and one cannot therefore *a priori* know if the acid with m.p. 35—37° is the *cis* or *trans* isomer. As the lactone (part A) was shown to be the *cis* isomer it would seem probable that the acid m.p. 35—37° is the *trans* isomer formed by a continued hydrogenation of the less stable *trans* lactone.

This could be verified if it were possible to transform the *cis* lactone into the corresponding *cis* 2-ethylcyclohexanecarboxylic acid. We have unsuccessfully tried to prove this by using the following two methods. According to Henecka [1] a γ-lactone reacts with ethanolic hydrogen bromide forming a bromo ester in which the bromine could be removed by reduction. In our case, however, no reaction took place with the ethanolic hydrogen bromide. Giebe [2] found that 3-methylphthalide by treatment with hydrogen iodide and yellow phosphorus gave 2-ethylbenzoic acid, a result which we could verify. When the above *cis* lactone (part A) was treated in the same way no ethylcyclohexanecarboxylic acid was obtained, but a decarboxylation took place and a halogenide $C_8H_{15}I$ was isolated in good yield. The structure of the halogenide is most likely as shown in formula I.

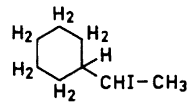

I

On catalytic hydrogenation of acetophenone-*o*-carboxylic acid the same products were obtained as when starting with 3-methylphthalide. Accordingly the hydrogenation of both substances could be expressed by the scheme below.

Experimental. Hydrogenation of acetophenone-o-carboxylic acid. A solution of 5 g acetophenone-*o*-carboxylic acid in 50 ml glacial acetic acid to which 0.5 g platinum oxide had been added was shaken for 15 h with hydrogen at 20°C and 760 mm Hg. In all 3310 ml hydrogen was taken up. On the assumption that 60 % of the starting material had consumed 4 mole and 40 % 5 mole hydrogen the calculated consumption would be 3320 ml. After removing solvent and

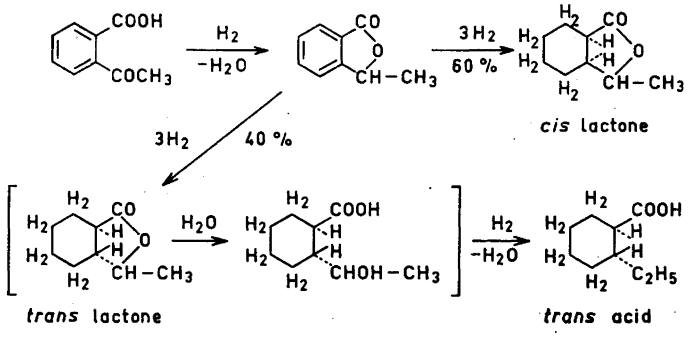

catalyst the residue distilled at 130—131° and 10 mm Hg. Yield 4.7 g.

Hydrogenation of 3-methylphthalide. When hydrogenating 3-methylphthalide as described above, the same product in the same yield was obtained. The infra-red spectra were identical in the two cases.

Separation of the two products of hydrogenation. The hydrogenation product (3 g) dissolved in 50 ml ether was shaken for 5 min with 20 ml 2 N sodium carbonate solution. From the ethereal solution, which had been dried with sodium sulphate 1.7 g oil was isolated which distilled at 130—131°C, 10 mm Hg. The equivalent weight was determined by heating samples dissolved in ethanol for some time with 0.1 N sodium hydroxide and back-titrating with hydrochloric acid. (Found: C 69.76; H 8.84; M 154, 155. Calc. for $C_9H_{14}O_2$: C 70.09; H 9.15; M 154.2). n_D^{20} 1.4748, d_D^{20} 1.0595, $[MR]_{found}$ 40.98. Hexahydro-3-methylphthalide $[MR]_{calc}$ 41.03.

The aqueous solution was acidified with hydrochloric acid and extracted with ether. An oil was obtained, which after distillation at 134—135°, 10 mm Hg, crystallized. M.p. 35—37°C. Yield 1.1 g. The substance could be titrated as an acid.

(Found C 68.94; H 10.13; M 156, 153. Calc. for $C_9H_{16}O_2$: C 69.18; H 10.33; M 156.2). n_D^{20} 1.4648, $d^{20}{}_4$ 1.015, $[MR]_{found}$ 42.85. Ethylcyclohexanecarboxylic acid $[MR]_{calc}$ 43.12.

For further identification of the acid its *p*-bromophenacyl ester was prepared in the usual way. After recrystallization from ethanol m.p. 70—71°C. (Found: C 57.74; H 5.90; Br 22.26. Calc. for $C_{17}H_{21}O_3Br$: C 57.80; H 5.99; Br 22.61).

The m.p. was not depressed on mixing with the *p*-bromophenacyl ester of the acid obtained by hydrogenation of 2-ethylbenzoic acid.

Oxidation of the lactone (part A) with sodium hypobromite. To an ice-cold solution of 9.5 g sodium hydroxide in 150 ml water 12.5 g bromine were added in small portions. The lactone (2.5 g) was dissolved in 15 ml 2 N sodium hydroxide and the two solutions mixed and left at room temperature until the next day. The bromoform formed was extracted with ether and the solution after adding hydrochloric acid again extracted with ether. After removing excess of bromine with sodium sulphite and drying with sodium sulphate the ether was distilled off. The remaining yellow oil (0.5 g) crystallized partly. After washing with benzene and recrystallization from water the substance had m.p. 189—193°C. The *cis*-cyclohexane-1,2-dicarboxylic acid has, according to the literature, m.p. 192°.

Reduction of the lactone with hydrogen iodide. The lactone $C_9H_{14}O_2$ (7.25 g), 25 ml hydrogen iodide (1.7) and 2.9 g of yellow phosphorus were refluxed for 10 h. A yellow layer which formed on top of the solution was isolated, washed with water saturated with sulphur dioxide and dried in a desiccator. After distilling at 49—52°C at 0.15 mm Hg the liquid weighed 6.6 g.

367.0 and 313.7 mg subst. gave 362.1 and 308.7 mg AgI, respectively.
(Found I 53.33, 53.20 %. Calc. for $C_8H_{15}I$ I 53.30 %).
n_D^{20} 1.5300, $d^{20}{}_4$ 1.462, $[MR]_{found}$ 50.09, $[MR]_{calc}$ 49.76.

The author's thanks are due to professor Endre Berner for helpful advice and his kind interest in this work and to *Alf Bjerckes Legat* for a grant.

1. Henecka, H. In Houben-Weyl: *Methoden der organischen Chemie*, 1952, Vol. 8, p. 528.
2. Giebe, G. *Ber.* **29** (1896) 534.

Received April 26, 1962.

Determination of the Configuration of β-Amino and β-Hydroxy Acids by Means of Optical Rotatory Dispersion

BERNDT SJÖBERG*

Department of Organic Chemistry, Chemical Institute, University of Uppsala, Sweden

BIRGITTA HANSSON and
RICHARD DAHLBOM

Department of Chemistry, Royal Institute of Pharmacy, Stockholm, Sweden

It has recently been shown by Sjöberg, Fredga and Djerassi [1], that the absolute configuration of α-amino and α-hydroxy acids can be readily derived from the sign of the Cotton effect in the anomalous rotatory dispersion curves of the dithio-

* Present address: Research Laboratories, AB Astra, Södertälje, Sweden.

catalyst the residue distilled at 130—131° and 10 mm Hg. Yield 4.7 g.

Hydrogenation of 3-methylphthalide. When hydrogenating 3-methylphthalide as described above, the same product in the same yield was obtained. The infra-red spectra were identical in the two cases.

Separation of the two products of hydrogenation. The hydrogenation product (3 g) dissolved in 50 ml ether was shaken for 5 min with 20 ml 2 N sodium carbonate solution. From the ethereal solution, which had been dried with sodium sulphate 1.7 g oil was isolated which distilled at 130—131°C, 10 mm Hg. The equivalent weight was determined by heating samples dissolved in ethanol for some time with 0.1 N sodium hydroxide and back-titrating with hydrochloric acid. (Found: C 69.76; H 8.84; M 154, 155. Calc. for $C_9H_{14}O_2$: C 70.09; H 9.15; M 154.2). n_D^{20} 1.4748, d_D^{20} 1.0595, $[MR]_{found}$ 40.98. Hexahydro-3-methylphthalide $[MR]_{calc}$ 41.03.

The aqueous solution was acidified with hydrochloric acid and extracted with ether. An oil was obtained, which after distillation at 134—135°, 10 mm Hg, crystallized. M.p. 35—37°C. Yield 1.1 g. The substance could be titrated as an acid.

(Found C 68.94; H 10.13; M 156, 153. Calc. for $C_9H_{16}O_2$: C 69.18; H 10.33; M 156.2). n_D^{20} 1.4648, $d^{20}{}_4$ 1.015, $[MR]_{found}$ 42.85. Ethylcyclohexanecarboxylic acid $[MR]_{calc}$ 43.12.

For further identification of the acid its *p*-bromophenacyl ester was prepared in the usual way. After recrystallization from ethanol m.p. 70—71°C. (Found: C 57.74; H 5.90; Br 22.26. Calc. for $C_{17}H_{21}O_3Br$: C 57.80; H 5.99; Br 22.61).

The m.p. was not depressed on mixing with the *p*-bromophenacyl ester of the acid obtained by hydrogenation of 2-ethylbenzoic acid.

Oxidation of the lactone (part A) with sodium hypobromite. To an ice-cold solution of 9.5 g sodium hydroxide in 150 ml water 12.5 g bromine were added in small portions. The lactone (2.5 g) was dissolved in 15 ml 2 N sodium hydroxide and the two solutions mixed and left at room temperature until the next day. The bromoform formed was extracted with ether and the solution after adding hydrochloric acid again extracted with ether. After removing excess of bromine with sodium sulphite and drying with sodium sulphate the ether was distilled off. The remaining yellow oil (0.5 g) crystallized partly. After washing with benzene and recrystallization from water the substance had m.p. 189—193°C. The *cis*-cyclohexane-1,2-dicarboxylic acid has, according to the literature, m.p. 192°.

Reduction of the lactone with hydrogen iodide. The lactone $C_9H_{14}O_2$ (7.25 g), 25 ml hydrogen iodide (1.7) and 2.9 g of yellow phosphorus were refluxed for 10 h. A yellow layer which formed on top of the solution was isolated, washed with water saturated with sulphur dioxide and dried in a desiccator. After distilling at 49—52°C at 0.15 mm Hg the liquid weighed 6.6 g.

367.0 and 313.7 mg subst. gave 362.1 and 308.7 mg AgI, respectively.
(Found I 53.33, 53.20 %. Calc. for $C_8H_{15}I$ I 53.30 %).
n_D^{20} 1.5300, $d^{20}{}_4$ 1.462, $[MR]_{found}$ 50.09, $[MR]_{calc}$ 49.76.

The author's thanks are due to professor Endre Berner for helpful advice and his kind interest in this work and to *Alf Bjerckes Legat* for a grant.

1. Henecka, H. In Houben-Weyl: *Methoden der organischen Chemie*, 1952, Vol. 8, p. 528.
2. Giebe, G. *Ber.* **29** (1896) 534.

Received April 26, 1962.

Determination of the Configuration of β-Amino and β-Hydroxy Acids by Means of Optical Rotatory Dispersion

BERNDT SJÖBERG*

Department of Organic Chemistry, Chemical Institute, University of Uppsala, Sweden

BIRGITTA HANSSON and
RICHARD DAHLBOM

Department of Chemistry, Royal Institute of Pharmacy, Stockholm, Sweden

It has recently been shown by Sjöberg, Fredga and Djerassi [1], that the absolute configuration of α-amino and α-hydroxy acids can be readily derived from the sign of the Cotton effect in the anomalous rotatory dispersion curves of the dithio-

* Present address: Research Laboratories, AB Astra, Södertälje, Sweden.

carbamate and xanthate derivatives, respectively. Other thiono derivatives have also been employed for similar purposes [2,3].

Some β-amino and β-hydroxy acids have recently been isolated from various natural sources. Although the configuration of a number of β-amino and β-hydroxy acids have been determined by chemical means, no well established simple method for the intercorrelation of β-amino and β-hydroxy acids or for the determination of their absolute configuration seems to exist. In fact, even in recent studies [4,5] there have been put forward contradictory interpretations of the steric course of the deamination of β-amino acids. It was therefore interesting to see if dithiocarbamates and xanthates of β-amino and β-hydroxy acids, respectively, would give anomalous rotatory dispersion curves, and if the sign of the Cotton effects could be used in stereochemical work in the same way as has been done in the alpha-series [1].

As model substances in the present study we chose β-aminobutyric acid and β-amino-β-phenylpropionic acid and the corresponding β-hydroxy acids. The absolute configuration of the optically active forms of these acids seems to be well established [6-9]. We used the most readily available antipodes of the four acids; the methyl dithiocarbamates of D-(−)-β-aminobutyric acid (I) and of L-(+)-β-amino-β-phenylpropionic acid (III) as well as the methyl dithiocarbonates (xanthates) of D-(−)-β-hydroxybutyric acid (II) and of L-(+)-β-hydroxy-β-phenylpropionic acid (IV) were prepared in the usual way by the action of carbon disulphide and methyl iodide on the appropriate carboxylic acids. The thiono derivatives of the two substituted butyric acids (I and II) were isolated as the cyclohexylammonium salts.

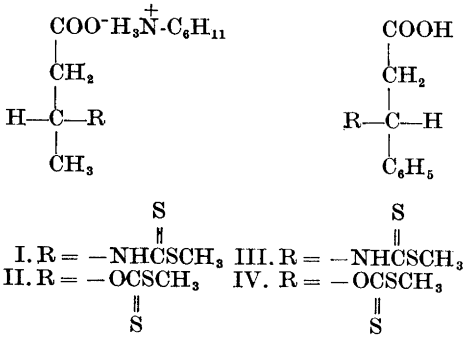

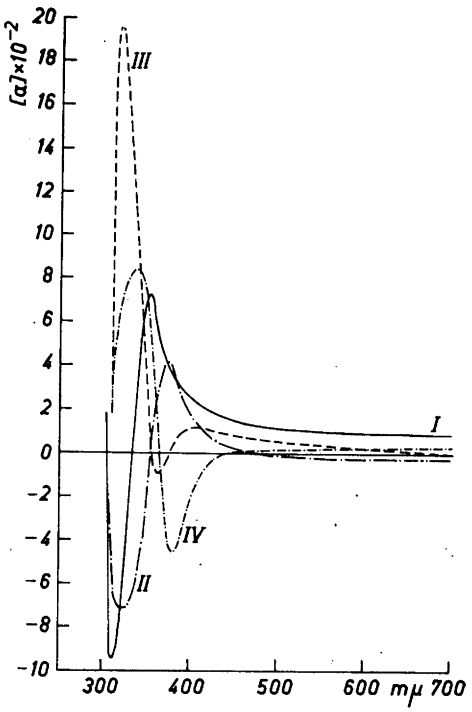

Fig. 1. Optical rotatory dispersion curves of N-dithiocarbomethoxy-D-(−)-β-aminobutyric acid cyclohexylammonium salt (I), O-dithiocarbomethoxy-D-(−)-β-hydroxybutyric acid cyclohexylammonium salt (II), N-dithiocarbomethoxy-L-(+)-β-amino-β-phenylpropionic acid (III) and O-dithiocarbomethoxy-L-(+)-β-hydroxy-β-phenylpropionic acid (IV).

Dithiocarbamates of α-amino and xanthates of α-hydroxy acids have long wave length absorption bands near 330 and 350 mμ, respectively, which are strongly anisotropic, and it has been found that the absolute configuration of the α-asymmetric center can be established from the sign of the Cotton effect: members of the L-series show a positive Cotton effect and members of the D-series exhibit a negative effect [1].

The dithiocarbamates and xanthates (I—IV) of the β-amino and β-hydroxy acids absorb around 330 and 350 mμ. From the optical rotatory dispersion curves of these compounds (Fig. 1) it can be seen that they exhibit strong Cotton effects. The dispersion curves of the cyclohexylammonium salts of N-dithiocarbomethoxy-D-(−)-β-

aminobutyric acid (I) and of O-dithiocarbomethoxy-D-(−)-β-hydroxybutyric acid (II) have positive Cotton effects centered around the 330 and 350 mμ absorption bands, and the dispersion curves of N-dithiocarbomethoxy-L-(+)-β-amino-β-phenylpropionic acid (III) and of O-dithiocarbomethoxy-L-(+)-β-hydroxy-β-phenylpropionic acid (IV) have negative Cotton effects. Although the study of this problem has so far been limited to the investigation of only four structurally varied compounds, it seems as though the sign of the Cotton effect would indicate the absolute configuration of the β-asymmetric center in β-amino and β-hydroxy acids. Since, however, the derivatives of the α- and β-substituted acids of the same configuration have opposite sign of the Cotton effect, the following extension of the previously established relationship [1] is suggested: *If a dithiocarbamate of an amino acid, or a xanthate of a hydroxy acid, has an optical rotatory dispersion curve with a positive Cotton effect, then in the case of an α-amino or an α-hydroxy acid we have the* L*-configuration and in the case of a β-amino or a β-hydroxy acid the* D*-configuration.*

A full report of this work will be published later.

Acknowledgement. A grant from *Statens Naturvetenskapliga Forskningsråd* is gratefully acknowledged.

1. Sjöberg, B., Fredga, A. and Djerassi, C. *J. Am. Chem. Soc.* **81** (1959) 5002.
2. Djerassi, C., Undheim, K., Sheppard, R. C., Terry, W. G. and Sjöberg, B. *Acta Chem. Scand.* **15** (1961) 903.
3. Sjöberg, B., Karlén, B. and Dahlbom, R. *Acta Chem. Scand.* **16** (1962) 1071.
4. English, J. and Bliss, A. D. *J. Am. Chem. Soc.* **78** (1956) 4057.
5. Graf, G. W. and Boeddecker, H. *Ann.* **613** (1958) 111.
6. Balenović, K., Cerar, D. and Fuks, Z. *J. Chem. Soc.* **1952** 3316.
7. Lukeš, R., Kovář, J., Kloubek, J. and Bláha, K. *Chem. Listy* **51** (1957) 1501.
8. Serck-Hanssen, K., Ställberg-Stenhagen, S. and Stenhagen, E. *Arkiv Kemi* **5** (1953) 203.
9. Lukeš, R., Bláha, K. and Kovář, J. *Chem. & Ind. London* **1958** 527.

Received May 18, 1962.

Separation of α- and β-Glucometasaccharinic Acids by Means of Anion Exchange Chromatography

BO ALFREDSSON and OLOF SAMUELSON
Department of Engineering Chemistry, Chalmers Tekniska Högskola, Göteborg, Sweden

In previous papers [1-3] it has been shown that hydroxy acids which are formed during the alkaline degradation of cellulose can be separated chromatographically by means of anion exchange resins. Several hydroxy acids containing 4−6 carbon atoms can be effectively separated by elution with borate solution, whereas with acids such as glycolic and lactic acid the separation is simpler and more efficient in acetate medium [4]. In connection with further work on the separation and identification of hydroxy acids which are formed in various technical processes, it has been found desirable to investigate the possibility of separating the stereoisomeric forms of glucometasaccharinic acids by means of anion exchange chromatography.

As shown by Kenner and Richards [5], β-glucometasaccharinic acid can easily be obtained in a pure form by alkaline degradation of 3-*O*-methylglucose. Large amounts of α-glucometasaccharinic acid are also formed in this reaction. In the present work (Figs. 1 and 3) it is shown that these stereoisomers can be effectively separated by chromatographic elution with 0.07 M sodium tetraborate solution under conditions which have been described in earlier papers for the separation of other saccharinic acids. The fractions were analyzed using the Technicon Auto-Analyzer [6] which means a considerable saving in time compared with the manual dichromate titration used earlier. The elution band corresponding to β-glucometasaccharinic acid appears before that of α-glucometasaccharinic acid and a quantitative separation can be obtained on a fairly short column.

Alkaline degradation of 3-O-methylglucose. The alkaline degradation of 3-*O*-methylglucose and the isolation of β-glucometasaccharinic acid from the reaction mixture has, with small changes, been performed according to the procedure given by Kenner and Richards [5]. A solution of 5.13 g of 3-*O*-methylglucose in

aminobutyric acid (I) and of O-dithiocarbomethoxy-D-(−)-β-hydroxybutyric acid (II) have positive Cotton effects centered around the 330 and 350 mμ absorption bands, and the dispersion curves of N-dithiocarbomethoxy-L-(+)-β-amino-β-phenylpropionic acid (III) and of O-dithiocarbomethoxy-L-(+)-β-hydroxy-β-phenylpropionic acid (IV) have negative Cotton effects. Although the study of this problem has so far been limited to the investigation of only four structurally varied compounds, it seems as though the sign of the Cotton effect would indicate the absolute configuration of the β-asymmetric center in β-amino and β-hydroxy acids. Since, however, the derivatives of the α- and β-substituted acids of the same configuration have opposite sign of the Cotton effect, the following extension of the previously established relationship [1] is suggested: *If a dithiocarbamate of an amino acid, or a xanthate of a hydroxy acid, has an optical rotatory dispersion curve with a positive Cotton effect, then in the case of an α-amino or an α-hydroxy acid we have the* L*-configuration and in the case of a β-amino or a β-hydroxy acid the* D*-configuration.*

A full report of this work will be published later.

Acknowledgement. A grant from *Statens Naturvetenskapliga Forskningsråd* is gratefully acknowledged.

1. Sjöberg, B., Fredga, A. and Djerassi, C. *J. Am. Chem. Soc.* **81** (1959) 5002.
2. Djerassi, C., Undheim, K., Sheppard, R. C., Terry, W. G. and Sjöberg, B. *Acta Chem. Scand.* **15** (1961) 903.
3. Sjöberg, B., Karlén, B. and Dahlbom, R. *Acta Chem. Scand.* **16** (1962) 1071.
4. English, J. and Bliss, A. D. *J. Am. Chem. Soc.* **78** (1956) 4057.
5. Graf, G. W. and Boeddecker, H. *Ann.* **613** (1958) 111.
6. Balenović, K., Cerar, D. and Fuks, Z. *J. Chem. Soc.* **1952** 3316.
7. Lukeš, R., Kovář, J., Kloubek, J. and Bláha, K. *Chem. Listy* **51** (1957) 1501.
8. Serck-Hanssen, K., Ställberg-Stenhagen, S. and Stenhagen, E. *Arkiv Kemi* **5** (1953) 203.
9. Lukeš, R., Bláha, K. and Kovář, J. *Chem. & Ind. London* **1958** 527.

Received May 18, 1962.

Separation of α- and β-Glucometasaccharinic Acids by Means of Anion Exchange Chromatography

BO ALFREDSSON and OLOF SAMUELSON
Department of Engineering Chemistry, Chalmers Tekniska Högskola, Göteborg, Sweden

In previous papers [1-3] it has been shown that hydroxy acids which are formed during the alkaline degradation of cellulose can be separated chromatographically by means of anion exchange resins. Several hydroxy acids containing 4−6 carbon atoms can be effectively separated by elution with borate solution, whereas with acids such as glycolic and lactic acid the separation is simpler and more efficient in acetate medium [4]. In connection with further work on the separation and identification of hydroxy acids which are formed in various technical processes, it has been found desirable to investigate the possibility of separating the stereoisomeric forms of glucometasaccharinic acids by means of anion exchange chromatography.

As shown by Kenner and Richards [5], β-glucometasaccharinic acid can easily be obtained in a pure form by alkaline degradation of 3-*O*-methylglucose. Large amounts of α-glucometasaccharinic acid are also formed in this reaction. In the present work (Figs. 1 and 3) it is shown that these stereoisomers can be effectively separated by chromatographic elution with 0.07 M sodium tetraborate solution under conditions which have been described in earlier papers for the separation of other saccharinic acids. The fractions were analyzed using the Technicon Auto-Analyzer [6] which means a considerable saving in time compared with the manual dichromate titration used earlier. The elution band corresponding to β-glucometasaccharinic acid appears before that of α-glucometasaccharinic acid and a quantitative separation can be obtained on a fairly short column.

Alkaline degradation of 3-O-methylglucose. The alkaline degradation of 3-*O*-methylglucose and the isolation of β-glucometasaccharinic acid from the reaction mixture has, with small changes, been performed according to the procedure given by Kenner and Richards [5]. A solution of 5.13 g of 3-*O*-methylglucose in

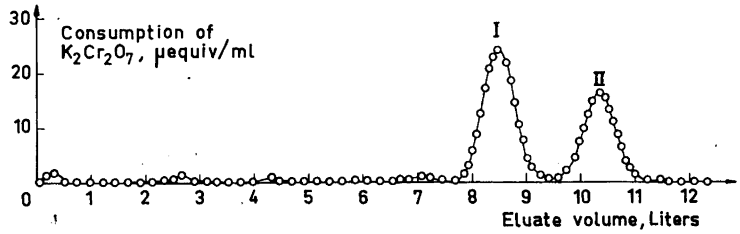

Fig. 1. Chromatographic analysis of the crude salt containing α- and β-glucometasaccharinic acids. (Found: C 35.8; H 5.7. Calc. for $(C_6H_{11}O_6)_2Ca$: C 36.2; H 5.6.
Column: 33 × 332 mm; Dowex 1 X—8 (borate form < 400 mesh). Flow rate: 0.3 ml $cm^{-2}min^{-1}$.

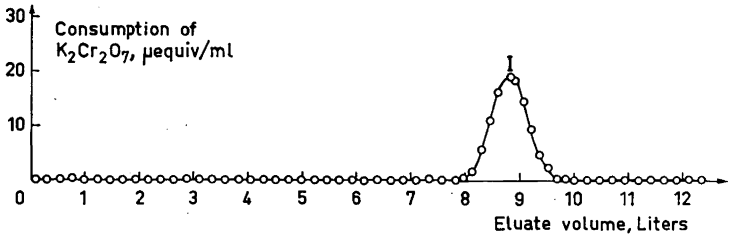

Fig. 2. Chromatographic analysis of β-glucometasaccharinic acid prepared according to Kenner and Richards [5].
Column: 33 × 332 mm; Dowex 1 X—8 (borate form < 400 mesh). Flow rate: 0.3 ml $cm^{-2}min^{-1}$.

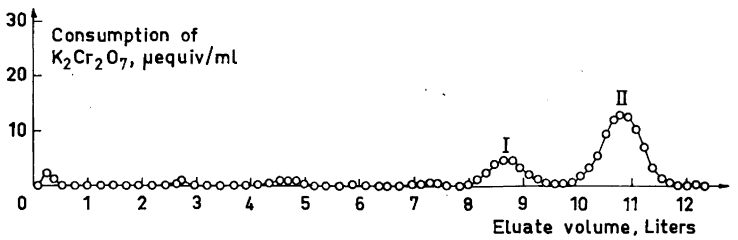

Fig. 3. Chromatographic analysis of the precipitate containing α- and β-glucometasaccharinic acids.
Column: 33 × 332 mm; Dower 1 X—8 (borate form < 400 mesh). Flow rate: 0.3 ml $cm^{-2}min^{-1}$.

1.2 l of oxygen-free lime water (0.062 N) was kept at 29°C for 192 h. The calcium ions were exchanged for hydrogen ions using a cation exchange resin. After washing with water, the effluent was evaporated at 40°C to a syrup which was dissolved in 50 ml of water. After treatment with charcoal, neutralization with calcium carbonate, and filtration, the solution was again evaporated to dryness. After trituration with ethanol, the crude calcium salt was obtained as a yellow crystalline powder (dry weight 5.04 g).

The results from the chromatographic separation (Fig. 1) show that two main fractions have been obtained. The chromatogram reveals traces of some other products. The position of the first elution peak (I) (main fraction) corresponds to that obtained with pure β-glucometasaccharinic acid isolated from the crude fraction according to the method given by Kenner and Richards (Fig. 2). According to these authors, the other main fraction obtained in this synthesis is α-glucometasaccharinic acid and it can therefore be assumed that elution band II contains this acid.

The sodium tetraborate was removed from these fractions by the same method as used in previous work [7]. In a paper chromatographic study (ethyl acetate-acetic acid-water [8,2]) the spots were located using permanganate-metaperiodate. Two distinct spots were obtained for each of the main fractions. The spots obtained from elution band I were identical with those obtained with the authentic β-glucometasaccharinic acid. The slower travelling spot on the paper chromatogram obtained with fraction II was identical with those obtained with fraction I and with authentic β-glucometasaccharinic acid, whereas the faster travelling spot had travelled a longer distance than the corresponding spots obtained with fraction I and with the authentic β-glucometasaccharinic acid. As found by Machell and Richards [9], the α-form of glucometasaccharinic acid travels ahead of the β-form, a fact which further supports the assumption that band II contains α-glucometasaccharinic acid.

The strychnine salt prepared from elution band I and recrystallized from ethanol, sintered and decomposed at 180—185°. The authentic sample of β-glucometasaccharinic acid exhibited the same behavior. No melting point depression was observed.

The brucine salt was prepared from elution band II and was recrystallized from abs. ethanol with slow cooling. The m.p. was 144—147°. Nef [10] reported m.p. 145—150° for brucine α-glucometasaccharinate, whereas Kenner and Richards [5] reported sintering and decomposition at 147—150°.

All these results indicate that elution band I corresponds to β-glucometasaccharinic acid and band II to α-glucometasaccharinic acid. From the areas under the elution curves the amounts of the acids present can be calculated. The ratio between the amounts of α-glucometasaccharinic acid and β-glucometasaccharinic acid was found to be 0.68.

Calcium β-glucometasaccharinate has been isolated from the crude calcium salt obtained by degradation of 3-*O*-methylglucose. The crude calcium salt was dissolved in hot water and the solution kept in a refrigerator at 3—4° for two days. Cubic crystals of calcium β-glucometasaccharinate were formed. The yield was 38 % of the crude salt. Ion exchange chromatography showed that only one elution band was obtained (Fig. 2). Its peak elution volume was the same as that obtained with an earlier work [1].

The mother liquor was treated with ethanol and the precipitated calcium salt, which according to Kenner and Richards [5] should contain a mixture of α- and β-glucometasaccharinic acids, was investigated chromatographically. The results given in Fig. 3 show that two main fractions are obtained corresponding to these two acids. As could be expected, the relative amount of α-glucometasaccharinic acid is much higher in this preparation than in the crude salt.

Acknowledgement. The financial support of the *State Technical Research Council* is gratefully acknowledged.

1. Alfredsson, B., Gedda, L. and Samuelson, O. *Svensk Papperstidn.* **63** (1960) 758.
2. Alfredsson, B., Gedda, L. and Samuelson, O. *Svensk Papperstidn.* **64** (1961) 694.
3. Alfredsson, B., Gedda, L. and Samuelson, O. *Anal. Chim. Acta* **26** (1962) *In press.*
4. Alfredsson, B., Bergdahl, S. and Samuelson, O. *To be published.*
5. Kenner, J. and Richards, G. N. *J. Chem. Soc.* **1954** 278.
6. Samuelson, O. and Simonson, R. *Svensk Papperstidn.* **65** (1962) 363.
7. Samuelson, O., Ljungqvist, K. J. and Parck, C. *Svensk Papperstidn.* **61** (1958) 1043.
8. Richtzenhain, H. and Moilanen, M. *Acta Chem. Scand.* **8** (1954) 704.
9. Machell, G. and Richards, G. N. *J. Chem. Soc.* **1957** 4500.
10. Nef, J. U. *Ann.* **376** (1910) 1.

Received May 11, 1962.

The Synthesis of Some 1,1,1-Trishydroxymethylalkanes

BENGT WEIBULL and MAGNUS MATELL

Research Laboratory, Mo och Domsjö AB, Örnsköldsvik, Sweden

The alkaline condensation of the lower aliphatic aldehydes with formaldehyde is a technically very important reaction. Here mention may be made only of the synthesis of pentaerythritol from acetaldehyde and formaldehyde [1]. The corresponding reaction with higher aldehydes has only met scant interest, presumably on account of the difficulty of obtaining these substances. The expected reaction products, 1,1,1-trishydroxymethylalkanes, might be of potential interest as raw materials for surface active agents (*cf.* Ref.[2]) and were synthesised as model compounds:

$$R{\cdot}CH_2CHO + 3\,HCHO + OH^- \longrightarrow$$
$$\rightarrow R{\cdot}C(CH_2OH)_3 + HCOO^-$$

The branched chain aldehyde, 2-ethylhexanal, was similarly condensed to 3,3-bishydroxymethylheptane. Table 1 summarises the results obtained.

Experimental. Octanal and 2-ethylhexanal were prepared in this laboratory by catalytic air oxidation of the corresponding alcohols. The other aldehydes were commercial products, obtained from Fluka A.G., Switzerland. All syntheses were made in much the same way. A typical experiment is described.

Undecanal (68 g; 0.4 mole) and aqueous formaldehyde (40 %; 224 g; 3 moles) were dissolved in 500 ml of aqueous ethanol (50 %; 500 ml). Potassium hydroxide (22.5 g; 0.4 mole) dissolved in 200 ml of 50 % aqueous ethanol was dropped into the solution with stirring and cooling. Following the addition of the alkali the mixture was stirred for 4 h at room temperature, then for 2 h at 50°. The ethanol was then evaporated and the inhomogeneous mixture extracted with ether. Evaporation of the ether yielded a residue that was distilled in vacuum. The main fraction (43 g; 47 %) had b.p./1 mm Hg 187–190°. It was further purified by recrystallisation from ligroin. M.p. 77–79.

In some experiments sodium hydroxide was used instead. The high proportion of formaldehyde is probably not necessary as some of the aldehydes were reacted with only the theoretical amount without appreciably inferior yield.

The authors are indebted to Mr. C. Engblom and Mr. C. E. Lindahl, who skilfully carried out most of the experimental part of this work.

1. Berlow, E., Barth, R. H. and Snow, J. E. *The Pentaerythritols*, Reinhold Publishing Co., New York 1958.
2. Oda, R. *Fette, Seifen, Anstrichmittel* **59** (1957) 921.
3. Dupont, G., Dulou, R. and Duplessis-Kergomard, A. *Bull. soc. chim. France* **1949** 314.
4. Dermer, O. C. and Solomon, P. W. *J. Am. Chem. Soc.* **76** (1954) 1697.
5. Shortridge, R. W., Craig, R. A., Greenlee, K. W., Derfer, J. M. and Boord, C. E. *J. Am. Chem. Soc.* **70** (1948) 946.

Received May 8, 1962.

Table 1. Properties of compounds $R.C(CH_2OH)_3$.

R	Yield %	B. p. °C/mm Hg	Cryst. from	M.p. °C	Found C	Found H	Found O	Calc. C	Calc. H	Calc. O
C_5H_{11}	61	160–162/1.5	CCl_4	64–65.5[a]	61.3	11.32	27.2	61.3	11.44	27.2
C_6H_{13}[b]	—	—	$CHCl_3$	68–70[c]	—	—	—			
C_8H_{17}	65	190–200/1.5	Ligroin	73.5–75[d]	66.3	11.90	22.1	66.0	12.00	22.0
C_9H_{19}	47	187–190/1	»	77–79	67.3	12.05	20.7	67.2	12.15	20.7
$C_{10}H_{21}$	45	180–186/0.3	»	79.5–81	68.1	12.11	19.6	68.2	12.27	19.5
$C_{12}H_{25}$	51	200–220/2.5	»	83–88	70.0	12.54	17.4	70.1	12.50	17.5
$C_9H_{20}O_2$[e]	83	136–143/8	—	40–42.5[f]	—	—	—			

[a] M.p.[3] 59
[b] Found: OH 26.5; calc.: OH 26.81.
[c] M.p.[4] 68–68.8
[d] M.p.[4] 72–73
[e] The compound is 3.3-bishydroxymethylheptane. Found: OH 21.2; calc.: OH 21.23.
[f] M.p.[5] 41.4–41.9

Synthesis of α,α'-Bis-(3,5-diiodo-4-hydroxyphenyl)-sebacic Acid

RICHARD DAHLBOM and RENÉ MOLLBERG

Department of Chemistry, Royal Institute of Pharmacy, Stockholm, and Research Laboratories, AB Astra, Södertälje, Sweden

Most X-ray contrast media consist of acids containing an iodinated aryl group. When two such acids are joined by an aliphatic chain, compounds posessing good X-ray diagnostic properties and low toxicity may result.

Adipic acid di-(3-carboxy-2,4,6-triiodoanilide) (Biligrafin) is such a compound, having found clinical use as a cholecystographic agent [1].

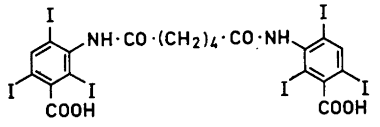

The present note describes the synthesis of a similar type of compound, *viz.* α,α'-bis-(3,5-diiodo-4-hydroxyphenyl)-sebacic acid (III), which was prepared by the sequence of reactions depicted schematically below.

The acids II and III contain two asymmetric carbon atoms, hence the product of the synthesis may consist either of pure racemate or of the meso form, or may be a mixture of both. The product obtained seemed to be uniform. The acid II was partially resolved using (+)-dehydroabietylamine as the optically active base, affording a product exhibiting a small positive rotation at 589 mμ. The optical rotatory dispersion curve, however, showed a considerable rotation at lower wavelengths. Consequently, the acids II and III must have the racemic and not the meso form.

Pharmacological tests in mice showed that acid III had no affinity for any specific part of the test organism, but it exhibited a rather high general toxicity.

α,α'-Bis-(ethoxycarbonyl)-α,α'-bis(4-methoxyphenyl)-sebaconitrile (I). 4-Methoxybenzyl cyanide was treated with diethyl carbonate in the presence of sodium and the resulting sodium salt was treated with 1,6-dibromohexane, according to the procedure outlined by Wideqvist [2].

To a boiling, stirred solution of 29.5 g (0.2 mole) of 4-methoxybenzyl cyanide in 100 ml of diethyl carbonate was added in small portions

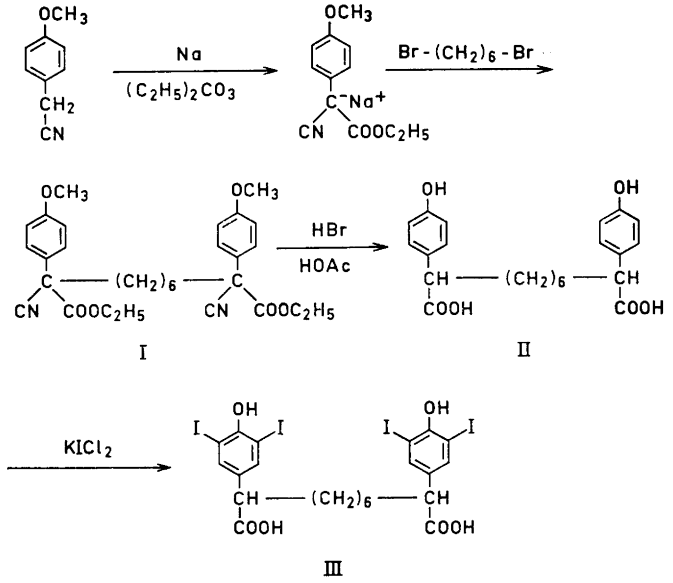

4.6 g (0.2 mole) of sodium shavings. After all the sodium had reacted, the ethanol formed was distilled off and 22.4 g (0.1 mole) of 1,6-dibromohexane was added dropwise to the boiling, stirred solution. The reaction mixture was boiled for a further 5 h, cooled, and treated with 100 ml of ice-water. The alkaline mixture was neutralised with acetic acid, the organic phase was separated, dried with sodium sulphate, and the volatile matter distilled off under vacuum. The residual reddish-brown oil neither crystallised nor could it be distilled without decomposition. It was heated to 240° at 0.5 mm Hg pressure, in order to remove all of the more volatile matter, and the resulting product was used as such in the next step without further purification.

a,a'-Bis-(4-hydroxyphenyl)-sebacic acid (II). 43 g of the crude product I was refluxed for 6 h with 220 ml of 48 % hydrobromic acid and 110 ml of glacial acetic acid. The reaction mixture was then poured onto 1 kg of crushed ice and extracted with 4 × 100 ml of ether. The combined ethereal solution was dried with sodium sulphate and the solvent distilled off, leaving a residue which crystallised upon triturating with a little benzene. The crude product was dissolved in alkali, the solution treated with active carbon and the acid precipitated out with dilute hydrochloric acid. The product thus obtained was further purified through recrystallisation from a large quantity of water (*ca.* 100 ml/g crude product). Obtained 29 g (91 %) of pure white crystals, m.p. 171.5–172.5°. Further recrystallisation did not raise the melting point. (Found: C 68.2; H 6.78. Calc. for $C_{22}H_{26}O_6$: C 68.4; H 6.78).

a,a'-Bis-(3,5-diiodo-4-hydroxyphenyl)-sebacic acid (III). 11.5 g (0.03 mole) of the acid II, prepared as above, was dissolved in a small excess of 5 N sodium hydroxide and heated under vigorous stirring first with 500 ml of conc. hydrochloric acid and then immediately with 65 ml of 2 M $KICl_2$. The resulting yellow-white precipitate was filtered off after one hour and dissolved in sodium bicarbonate solution. After treatment with a saturated bisulphite solution, a light yellow product fell out, which, after recrystallisation from aqueous ethanol, afforded 17 g (63 %) of yellow needles melting at 240–241° (decomp.). (Found: C 30.4; H 2.62; I 55.7. Calc. for $C_{22}H_{22}I_4O_6$: C 29.7; H 2.49; I 57.0).

1. Priewe, H. *Chem. Ber.* **87** (1954) 651.
2. Wideqvist, S. *Arkiv Kemi Mineral. Geol.* **24 B** (1947) No. 14.

Received May 14, 1962.

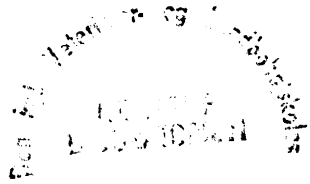

ACTA CHEMICA SCANDINAVICA 16 (1962) 1065–1070

Some Properties of a Ternary System of Optically Active Compounds

MAGNUS MATELL

Research Laboratory, Berol AB, Göteborg 14, Sweden

Submitted in honour of the sixtieth birthday of my teacher, Professor *Arne Fredga*

A ternary system of three optically active acids, two of which are true antipodes, has been investigated. The melting point surface emanating from a quasi-racemate between two of the components extends so far into the ternary space that the melting point maximum is still clearly visible in the pseudo-binary section through the true racemate and the third component. This observation may result in a time-saving improvement of the quasi-racemate method.

The quasi-racemate method has turned out to be most useful for the establishment of configurational relations. As there are several surveys of principles and results [1–4] only a few words are necessary here to present the fundamental idea of the method.

Pair of optical antipodes can form three types of racemates: an eutectic mixture, a solid solution, or a molecular compound, the last case being by far most common. It has been found that structurally related compounds with opposite configurations show a similar tendency to form molecular compounds, which are called quasi-racemates. Compounds with the same configuration, however, form eutectic mixtures or solid solutions. These different possibilities are usually distinguished by a study of the melting point diagrams of the actual systems.

The most serious limitation of the quasi-racemate method is that the conditions for the formation of quasi-racemates are not very well-known. It is not unusual that a pair of rather similar compounds with opposite configurations will not form a quasi-racemate while in other cases structurally rather dissimilar compounds have been found to be quasi-racemate forming [3,5].

The preparation of optically active compounds is a laborious task and the establishment of melting point curves is time-consuming. Much work is thus spent in vain in such cases were an expected quasi-racemate fails to appear. This drawback can be almost completely eliminated in regard to the thermal

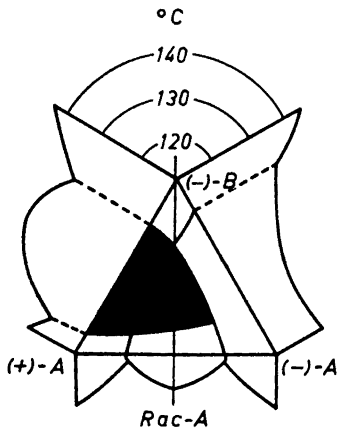

Fig. 1. Schematic projection of the ternary system (+)-A, (−)-A, (−)-B and the three binary systems.

analysis by applying the contact method[6], as suggested by this author [3,7]. Further improvements were discussed in a lecture at "10. Nordiska Kemistmötet" a few years ago [8]. The ideas and experimental evidence underlying this lecture are discussed below.

In a three-component system of a pair of optical antipodes, (+)-A and (−)-A, and a third, optically active compound (−)-B, the melting point surface should be strongly unsymmetrical in respect to the pseudo-binary system rac.-A and (−)-B, if a quasi-racemate exists between (−)-B and one of the A-antipodes. Such a dissymmetry should be provable without access to all three optically pure components, (−)-B and two mixtures of A containing the same excess of each of (+)- and (−)-forms being sufficient. It also seemed reasonable to suppose that a quasi-racemate should have a rather strong influence on the melting point curve in the system rac.-A and (−)-B.

In order to prove these assumptions a three-component system was studied where A was α-(2,4-dichlorophenoxy)propionic acid and B was α-(2,4,5-trichlorophenoxy)propionic acid. Fig. 1 is a schematic projection of the ternary melting point surface. The binary systems, which were described several years

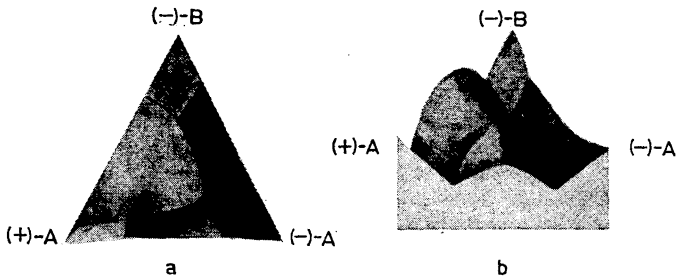

Fig. 2. Space model of the ternary system (+)-A, (−)-A, (−)-B; a. from above, b. from the side.

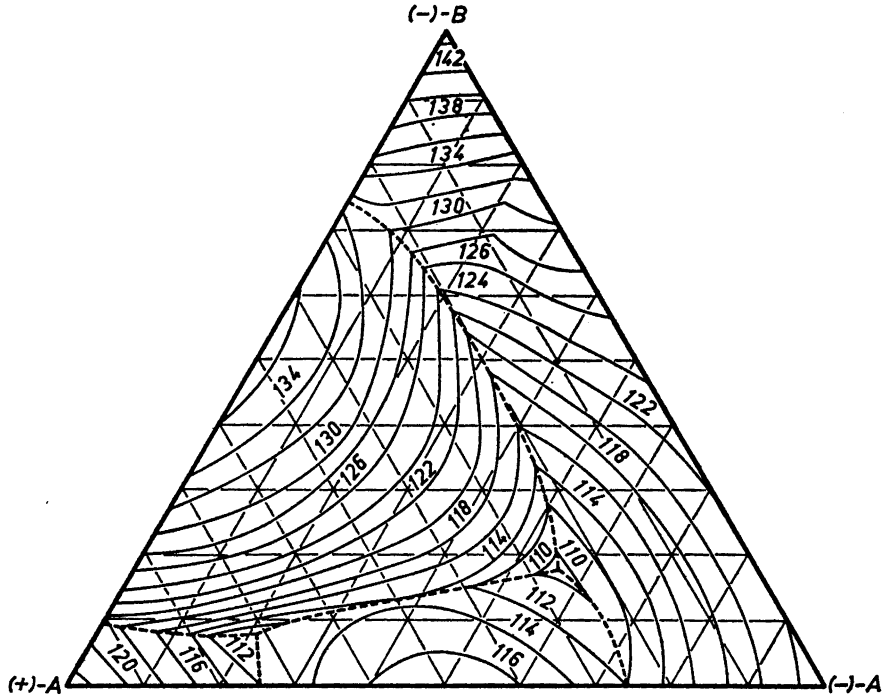

Fig. 3. Melting point isotherms in the ternary system (+)-A, (−)-A, (−)-B.

ago [9], are shown in the same figure. Fig. 2a is a space model seen from above and Fig. 2b is the same model viewed towards the (+)-A:(−)-A side. Melting point isotherms are given in Fig. 3. The space model is based on compositions expressed in per cent by weight, while Fig. 3 is based on mole per cent. The differences are small and are of no account for the discussion.

The strong dissymmetry of the melting point surface is clearly seen in these figures. The binary system (+)-A, (−)-A is symmetrical (Fig. 1), but

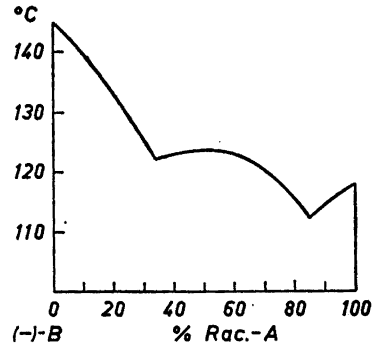

Fig. 4. Melting point diagram of the pseudo-binary system rac.-A, (−)-B.

this symmetry is lost already when a few per cent of (−)-B have been added. There are two ternary eutectic points melting slightly below 110°C. The diagram is dominated by the very characteristic surface emanating from the quasi-racemate and cutting the section rac.-A, (−)-B. The melting point curve of this section is found in Fig. 4. Such a melting point curve may indicate a ternary compound, but a maximum in this section is more probably an indication of a quasi-racemate. The maximum could also be detected in a contact preparation.

In the system now investigated the melting point curve in the quasi-racemic system has a very large maximum. In many cases the middle branch of the melting point curve, representing the quasi-racemate, is much less dominating. As a consequence the ternary melting point surface will not be influenced to the same extent and there is less chance of finding a maximum in the section rac.-A,(−)-B. However, even a rather small maximum, caused by a quasi-racemate, is likely to influence the ternary system to such an extent that some guidance is obtained from a study of (−)-B and partially active A.

As an example of such a system some contact preparations of optically active α-phenoxybutyric acid (A) and α-phenoxyvaleric acid (B) were studied. In this system the maximum of the melting point curve is rather flat [10]. As expected there was only found one eutectic in the system rac.-A,(+)-B. However a maximum and two eutectics could be seen in contact preparations with (+)-B and A containing 60−70 % of the (−)-form.

To sum up, the following steps are suggested when the optically active compound A is to be sterically related to some of the compounds B, C, D . . . available as racemates.

(1) Apply the contact method to the systems AB, AC, AD . . . If a melting point maximum is found in one of these systems, the racemate is resolved. The existence of the quasi-racemate is confirmed by melting point diagrams.

(2) If no system with a melting point maximum can be found, preliminary resolution experiments are carried out. The thermal behaviour of partially active B, C, D . . . containing at least 75 % of one of the antipodes towards (+)-A and (−)-A is studied in contact preparations.

(a) When a melting point maximum is found the resolution is completed and the existence of the quasi-racemate confirmed as in 1.

(b) If no melting point maximum is found the compound giving the biggest thermal difference towards (+)- and (−)-A is resolved etc.

(c) If (+)-A and (−)-A are identical in their thermal behaviour towards partially active B, C, D . . . the probability of a successful application of the quasi-racemate method is extremely small.

(3) The principles in (2) can as well be applied when only one of the antipodes of A is available. In that case the partial resolutions are performed to give two mixtures with opposite but numerically identical optical rotation.

EXPERIMENTAL

References and some properties of the materials used as components in the ternary system are collected in Table 1.

Table 1.

Compound	M.p.(°C)	$[\alpha]_D^{25}$(°) ethanol	Ref.
rac.-α-(2,4-Dichlorophenoxy)propionic acid	117 —118°		11
(+)-α-(2,4-Dichlorophenoxy)propionic acid	122 —123	+ 28.1	11
(—)-α-(2,4-Dichlorophenoxy)propionic acid	122 —123	—28.5	11
(—)-α-(2,4,5-Trichlorophenoxy)propionic acid	143.5—145	—49.5	3

The components were weighed on a torsion balance. The total weight of each mixture was 10 mg. Each sample was dissolved in a small quantity of ether, which was evaporated, the residue dried and powdered.

All melting points were determined in a Kofler hot stage microscope. Contact preparations were studied in the same equipment.

The melting points of different mixtures (mole-%) are found in Fig. 5. Melting points on the same straight lines were used to construct about 15 melting point curves. The compositions corresponding to every second degree were transformed from these to a new triangular diagram and the melting point isotherms drawn to give Fig. 3.

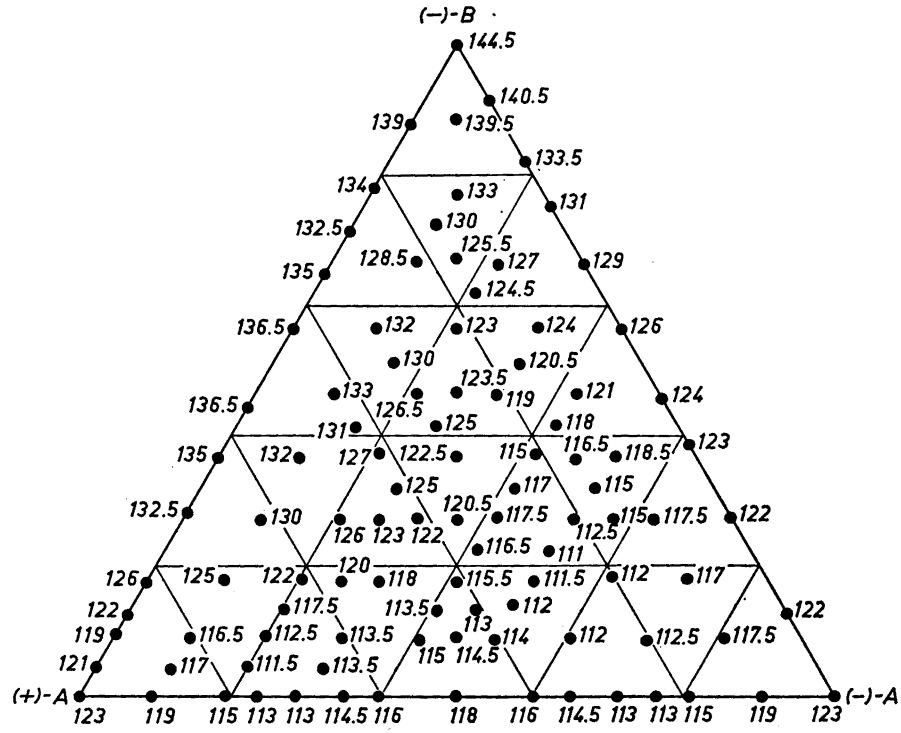

Fig. 5. Melting points of mixtures. Composition in mole-%.

A considerable part of this investigation was carried out at the Institute of Organic Chemistry, Royal Agricultural College, Uppsala. I am much indebted to the head of the institute, Professor Nils Hellström, for all facilities put to my disposal. I also thank Mr. Ants Aamisepp for technical assistance.

This investigation has been supported by a grant from the *Swedish Natural Science Research Council.*

REFERENCES

1. Fredga, A. *The Svedberg 1884–30.8–1944*, Uppsala 1944, p. 261.
2. Timmermans, J. *J. Chim. phys.* **49** (1952) 162.
3. Matell, M. *Ann. Agr. Coll. Swed.* **20** (1953) 205.
4. Fredga, A. *Festschrift Arthur Stoll*, Basel 1957, p. 795.
5. Matell, M. *Arkiv Kemi* **5** (1952) 17.
6. Kofler, L. and Kofler, A. *ThermoMikro-Methoden*, Innsbruck 1954, p. 151, 237.
7. Matell, M. *Mirkrochemie ver. Mikrochim. Acta* **38** (1951) 532.
8. Matell, M. *Sv. Kem. Tidskr.* **71** (1958) 414.
9. Matell, M. *Arkiv Kemi* **5** (1953) 341.
10. Matell, M. *Arkiv Kemi* **8** (1955) 79.
11. Matell, M. *Arkiv Kemi* **4** (1952) 473.

Received December 19, 1961.

ACTA CHEMICA SCANDINAVICA 16 (1962) 1071–1078

Anomalous Rotatory Dispersion Curves of N-Thiobenzoyl and N-Phenylthioacetyl α-Amino Acids

BERNDT SJÖBERG*

Department of Organic Chemistry, Chemical Institute, University of Uppsala, Uppsala, Sweden

BO KARLÉN and RICHARD DAHLBOM

Royal Institute of Pharmacy, Stockholm, Sweden

Submitted in honour of the sixtieth birthday of Professor *Arne Fredga*

N-Thiobenzoyl and N-phenylthioacetyl derivatives of α-amino acids have been shown to possess desirable spectroscopic properties for spectropolarimetric studies; they exhibit absorption bands of low extinction at about 365 and 330 mμ, respectively. Both series of derivatives exhibit Cotton effects related to these absorption bands. N-Phenylthioacetyl derivatives of α-amino acids have strong Cotton effects which are suitable for establishing the absolute configurations.

Recent investigations [1,2] have demonstrated the utility of anomalous rotatory dispersion measurements for stereochemical assignments and conformational problems. Unfortunately, most α-amino acids [3a] and peptides [3b] absorb far down in the ultraviolet region and thus exhibit only plain dispersion curves [4] over the currently accessible spectral range. However, it was found [5] that N-dithiocarbalkoxy (dithiocarbamate) derivatives of α-amino acids absorb at about 330 mμ and yield Cotton effects which can be related to the absolute configuration of the α-asymmetric center — a positive Cotton effect corresponding to the L-configuration, and a negative one to the D-configuration. In an later study [6] it was shown that also N-thionocarbethoxy-α-amino acids and 3-phenyl-2-thiohydantoins have Cotton effect curves which may be used for configurational assignments. In the present work, we have extended the study to other derivatives of amino acids for the same purpose.

* Present address: AB Astra, Södertälje, Sweden.

The C=S chromophore has proved to be useful [7] in this context for several other classes of substances, hence we looked for a suitable thiono derivative of α-amino acids. We were especially interested in investigating the N-thiobenzoyl and N-phenylthioacetyl derivatives of amino acids, since these radicals can easily be introduced into the parent compound. Thus Holmberg [8] prepared in 1944 some N-thiobenzoyl amino acids by the facile introduction of the thiobenzoyl group by means of the very reactive carboxymethyl ester of dithiobenzoic acid, and some years later Kjær [9] prepared a number of N-phenylthioacetyl amino acids by introducing the phenylthioacetyl group with the carboxymethyl ester of phenyldithioacetic acid.

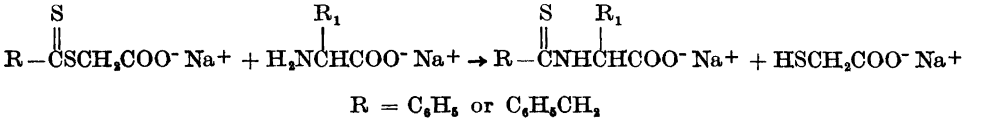

$$R = C_6H_5 \text{ or } C_6H_5CH_2$$

In order to investigate the suitability of N-thiobenzoyl and N-phenylthioacetyl derivatives for rotatory dispersion work, it was first necessary to determine whether the C=S chromophore in these groups possessed suitable ultraviolet absorption bands. Preliminary ultraviolet measurements showed that N-thiobenzoyl α-amino acids have a low extinction band at about 365 mμ (log $\varepsilon \sim 2.4$) and two strong bands at 285 and 240 mμ (log $\varepsilon \sim 3.9$ and 4.1), while N-phenylthioacetyl-α-amino acids exhibit bands at about 330 mμ (log $\varepsilon \sim 1.8$) and 270 mμ (log $\varepsilon \sim 4.1$). The observation of the excellent spectroscopic properties of these derivatives prompted us to synthesize a number of optically active N-thiobenzoyl and N-phenylthioacetyl α-amino acids (I—V

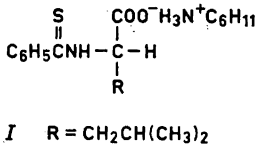

I $R = CH_2CH(CH_3)_2$

II $R = CH_2CONH_2$

III $R = CH_2CH_2COO^-H_3N^+C_6H_{11}$

IV $R = C_6H_5$

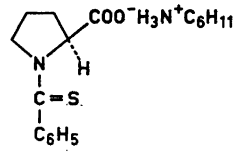

V

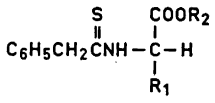

VI $R_1 = CH_3$; $R_2 = H_3NC_6H_{11}$

VII $R_1 = CH(CH_3)_2$; $R_2 = H_3NC_6H_{11}$

VIII $R_1 = CH(CH_3)C_2H_5$; $R_2 = H_3NC_6H_{11}$

IX $R_1 = CH_2CONH_2$; $R_2 = H$

X $R_1 = C_6H_5$; $R_2 = H_3NC_6H_{11}$

XI $R_1 = CH_2C_6H_5$; $R_2 = H_3NC_6H_{11}$

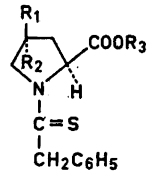

XII $R_1 = R_2 = R_3 = H$

XIII $R_1 = H$; $R_2 = OH$; $R_3 = H_3NC_6H_{11}$

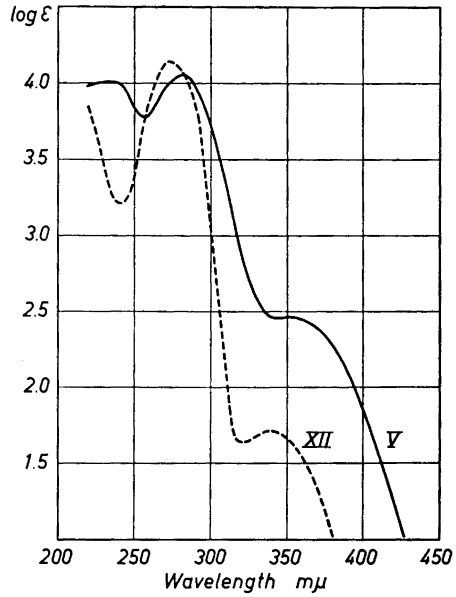

Fig. 1. Ultraviolet absorption in methanol of the cyclohexylammonium salt of N-thiobenzoyl-L-proline (V) and N-phenylthioacetyl-L-proline (XII).

and VI—XIII, respectively), following the experimental procedures described by Holmberg [8] and Kjær [9,10]. The reaction products were usually obtained as non crystallising oils. However, the cyclohexylammonium salts of the thioacylated amino acids crystallised excellently, hence these salts were used for purification and physical measurements. The ultraviolet spectra of one N-thiobenzoyl and one N-phenylthioacetyl amino acid are shown in Fig. 1.

The rotatory dispersion results are summarised in Figs. 2—5. Cotton effects are found in the region of the long wave length absorption bands indicating that these bands are anisotropic ("optically active"). The cyclohexylammonium salts of N-thiobenzoyl-L-leucine (I) as well as of N-thiobenzoyl-L-asparagine (II) exhibit positive Cotton effects (Fig. 2) of very low amplitudes while the corresponding derivative of L-proline (V) apparently has a negative Cotton effect. A positive effect is found for the cyclohexylammonium salt of N-thiobenzoyl-D-α-aminophenylacetic acid (IV). This irregularity is somewhat unexpected in view of the very consistent relationship between configuration and sign of the Cotton effects in the series of dithiocarbamates [5,6], where all the investigated compounds of L-configuration have positive Cotton effects. A similar anomaly was, however, found [6] for the N-thionocarbethoxy derivatives of hydroxyproline and acetoxyproline.

The first absorption band of the N-thiobenzoyl amino acids is situated in a very convenient wave length range for spectropolarimetric studies and the extinction value (log $\varepsilon \sim 2.4$) is generally fairly reasonable. However, bearing in mind the low amplitudes of the Cotton effects this extinction is too high to allow convenient and reliable rotatory dispersion measurements through the absorption region. The corresponding absorption band of the N-phenylthio-

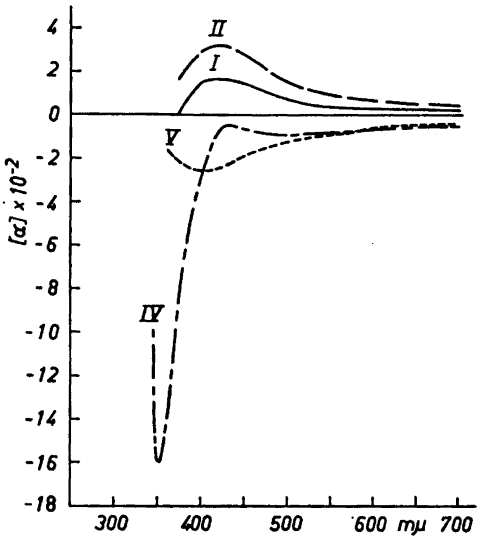

Fig. 2. Optical rotatory dispersion curves of the cyclohexylammonium salts of N-thiobenzoyl-L-leucine (I), N-thiobenzoyl-L-asparagine (II), N-thiobenzoyl-D-α-aminophenylacetic acid (IV) and N-thiobenzoyl-L-proline (V).

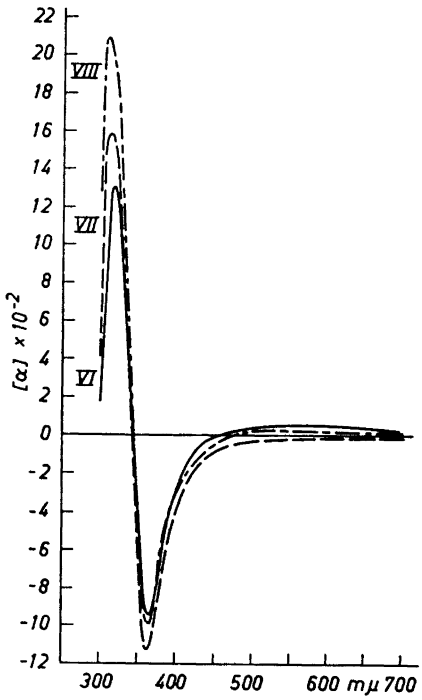

Fig. 3. Optical rotatory dispersion curves of the cyclohexylammonium salts of N-phenylthioacetyl-L-alanine (VI), N-phenylthioacetyl-L-valine (VII) and N-phenylthioacetyl-L-isoleucine (VIII).

acetyl amino acids falls still in a suitable wave length range ($\lambda_{max} \sim 330$ mμ), and in conjunction with the lower extinction value ($\log \varepsilon \sim 1.8$) these derivatives appear to be more suitable for rotatory dispersion studies.

The rotatory dispersion curves of the cyclohexylammonium salts of N-phenylthioacetyl-L-alanine (VI), N-phenylthioacetyl-L-valine (VII) and N-phenylthioacetyl-L-isoleucine (VIII) are shown in Fig. 3. These three compounds have very similar dispersion curves, with negative Cotton effects of large amplitudes. N-Phenylthioacetyl derivatives of asparagine, α-aminophenylacetic acid and β-phenylalanine of L-configuration also exhibit negative Cotton effects (Fig. 4 and Experimental) while those of L-proline (XII) and L-hydroxyproline (XIII) have positive Cotton effects (Fig. 5).

Dithiocarbamates of all the L-α-amino acids which have so far been examined [5,6] show a positive Cotton effect, as well as all the N-thionocarbethoxy derivatives except those of L-hydroxyproline and L-acetoxyproline [6]. In the N-phenylthioacetyl α-amino acids series even proline is exceptional, and it is

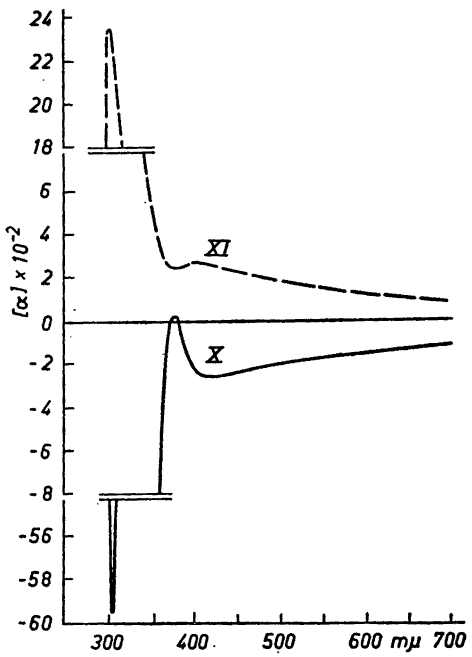

Fig. 4. Optical rotatory dispersion curves of the cyclohexylammonium salts of N-phenylthioacetyl-D-α-aminophenylacetic acid (X) and N-phenylthioacetyl-L-β-phenylalanine (XI).

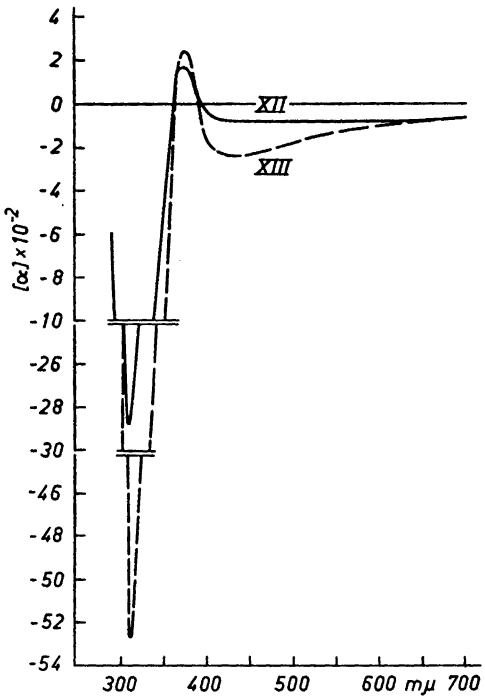

Fig. 5. Optical rotatory dispersion curves of N-phenylthioacetyl-L-proline (XII) and the cyclohexylammonium salt of N-phenylthioacetyl-L-hydroxyproline (XIII).

difficult to rationalise these exceptions. In order to see if the observed anomaly in the proline series will be found for N-phenylthioacetyl derivatives of other α-amino acids and peptides we have undertaken further studies of this subject *, and any possible reason for this anomaly will be discussed when further experimental data will be available.

It is interesting that the sign of the Cotton effects is generally negative for N-phenylthioacetyl L-α-amino acids whereas it is positive for dithiocarbamates and N-thionocarbethoxy derivatives. This reversal of sign is, however, systematic.

N-Phenylthioacetyl α-amino acids are easily prepared [8,9], and in view of the large amplitudes of their rotatory dispersion curves and particularly since their relevant absorption bands have low extinction and occur in a convenient region, these derivatives seem to be very suitable for stereochemical assign-

* When the present paper was prepared we learnt that Professor A. Kjær had started similar studies, and the planned continuation will be a joint work between Professor Kjær and us.

ments of α-amino acids and constitute a valuable complement to the dithiocarbamates and N-thionocarbalkoxy derivatives.

EXPERIMENTAL

The ultraviolet spectra were measured in methanol solution with a Beckman DK-2 spectrophotometer. The rotatory dispersion measurements were determined in methanol solution (25°) by means of an automatically recording Rudolph spectropolarimeter by Mr. Rolf Bäckström, whose assistance is gratefully acknowledged. The data are recorded below as outlined in Ref.[4]

Melting points were determined in an electrically heated metal block, using calibrated Anschütz thermometers.

The microanalyses were carried out in the laboratory of Dr. A. Bernhardt, Mülheim Germany. Before analysis, the compounds were dried at 50° and 0.05 mm.

N-Thioacylamino acids

The L-amino acids were all commercially available.

D-α-Aminophenylacetic acid was prepared according to Marvel and Noyes [11]. Rotation: $[\alpha]_D^{23} = -156.7°$ (c = 7.0 %; in 1.36 equiv. HCl).

Carboxymethyl dithiophenylacetate and *carboxymethyl dithiobenzoate* were prepared as described by Kjær [9,10] by reacting the Grignard reagent obtained from benzyl chloride and bromobenzene, respectively, with carbon disulphide, followed by treatment of the crude reaction mixture with chloroacetic acid.

The amino acids were phenylthioacetylated and thiobenzoylated according to the procedures described by Holmberg [8] and Kjær [9,10]. The amino acid (0.002—0.01 mole) was dissolved in two equivalents (glutamic acid in three equivalents) of N sodium hydroxide followed by the addition of one equivalent of carboxymethyl dithiophenylacetate or carboxymethyl dithiobenzoate. The solution was kept at room temperature overnight and then acidified with 5 N hydrochloric acid. The reaction product separated as an oil, which crystallised only in two cases (compounds IX and XII). The oil was therefore extracted with ether, and the extract washed thoroughly with water to remove the mercaptoacetic acid formed. The thioacylated amino acid was then converted to the well crystallising *cyclohexylammonium salt* by the addition of an ethereal solution of cyclohexylamine. The salt was collected and purified by recrystallisation. By this procedure the following compounds were prepared in yields ranging from 60—80 %.

Cyclohexylammonium salt of N-thiobenzoyl-L-leucine (I). M.p. 159—161° (decomp.), from ethanol-ether. (Found: C 65.2; H 8.48; N 7.87; S 9.33. Calc for $C_{19}H_{30}N_2O_2S$: C 65.1; H 8.63; N 7.99; S 9.15).

Ultraviolet absorptions: $\lambda_{shoulder}$ 365 mμ (log ε 2.43), λ_{max} 285 and 239 mμ (log ε 3.85 and 4.06).

R.D. (Fig. 2), c, 0.109: $[\alpha]_{700}$ + 20°, $[\alpha]_{589}$ + 35°, $[\alpha]_{415}$ + 165°, $[\alpha]_{375}$ 0°.

Cyclohexylammonium salt of N-thiobenzoyl-L-asparagine (II). M.p. 183—184° (decomp.), from ethanol-ether. (Found: C 58.5; H 6.93; N 11.9; S 8.84. Calc. for $C_{17}H_{25}N_3O_3S$: C 58.1; H 7.17; N 12.0; S 9.13).

Ultraviolet absorptions: $\lambda_{shoulder}$ 370 mμ (log ε 2.43), λ_{max} 286 and 241 mμ (log ε 3.87 and 4.08).

R.D. (Fig. 2), c, 0.089: $[\alpha]_{700}$ + 45°, $[\alpha]_{589}$ + 70°, $[\alpha]_{420}$ + 320°, $[\alpha]_{375}$ + 180°.

Cyclohexylammonium salt of N-thiobenzoyl-L-glutamic acid (III). M.p. 207—210° (decomp.), from ethanol-water. (Found: C 61.9; H 8.40; N 8.80; S 6.62. Calc. for $C_{24}H_{39}N_3O_4S$: C 61.9; H 8.44; N 9.02; S 6.89).

Ultraviolet absorptions: $\lambda_{shoulder}$ 365 mμ (log ε 2.42), λ_{max} 286 and 240 mμ (log ε 3.87 and 4.06).

R.D., c, 0.059: $[\alpha]_{700}$ + 30°, $[\alpha]_{589}$ + 45°, $[\alpha]_{420}$ + 145°, $[\alpha]_{380}$ + 55°.

Cyclohexylammonium salt of N-thiobenzoyl-D-α-aminophenylacetic acid (IV). M.p. 188—189.5° (decomp.), from ethanol-ether. (Found: C 68.6; H 7.47; N 8.05; S 8.91. Calc. for $C_{21}H_{26}N_2O_2S$: C 68.1; H 7.07; N 7.56; S 8.66).

Ultraviolet absorptions: λ_{max} 371, 286 and 238 mμ (log ε 2.40, 3.86 and 4.13).

R.D. (Fig. 2), *c*, 0.065: $[\alpha]_{700}$ −65°, $[\alpha]_{589}$ −65°, $[\alpha]_{500}$ −95°, $[\alpha]_{430}$ −45°, $[\alpha]_{353}$ −1600°.

Cyclohexylammonium salt of N-thiobenzoyl-L-proline (V). M.p. 215–216° (decomp.), from ethanol-ether. (Found: C 64.6; H 7.81; N 8.15; S 9.23. Calc. for $C_{18}H_{26}N_2O_2S$: C 64.6; H 7.84; N 8.38; S 9.59).

Ultraviolet absorptions: λ_{max} 352, 281 and 231 mμ (log ε 2.47, 4.06 and 4.02).

R.D. (Fig. 2), *c*, 0.109: $[\alpha]_{700}$ −35°, $[\alpha]_{589}$ −70°, $[\alpha]_{400}$ −250°, $[\alpha]_{360}$ −165°.

Cyclohexylammonium salt of N-phenylthioacetyl-L-alanine (VI). M.p. 129.5–131° (decomp.), from ethanol-ether. (Found: C 62.8; H 8.57; N 8.49. Calc. for $C_{17}H_{26}N_2O_2S$: C 63.3; H 8.12; N 8.69).

Ultraviolet absorptions: λ_{max} 319 and 267 mμ (log ε 1.98 and 4.01).

R.D. (fig. 3), *c*, 0.0624: $[\alpha]_{700}$ + 10°, $[\alpha]_{589}$ + 40°, $[\alpha]_{550}$ + 60°, $[\alpha]_{365}$ −960°, $[\alpha]_{317}$ + 1300°, $[\alpha]_{300}$ + 160°.

Cyclohexylammonium salt of N-phenylthioacetyl-L-valine (VII). M.p. 166.5–167.5° (decomp.), from ethanol-ether. (Found: C 65.7; H 8.93; N 8.14. Calc. for $C_{19}H_{30}N_2O_2S$: C 65.1; H 8.63; N 7.99).

Ultraviolet absorptions: λ_{max} 333 and 271 mμ (log ε 1.83 and 4.08).

R.D. (Fig. 3), *c*, 0.0622, $[\alpha]_{700}$ −5°, $[\alpha]_{589}$ −10°, $[\alpha]_{363}$ −1130°, $[\alpha]_{312}$ + 1590°, $[\alpha]_{300}$ + 430°.

Cyclohexylammonium salt of N-phenylthioacetyl-L-isoleucine (VIII). M.p. 170.5–171.5° (decomp.), from ethanol-ether. (Found: C 66.3; H 8.96; N 7.82. Calc. for $C_{20}H_{32}N_2O_2S$: C 65.9; H 8.85; N 7.69).

Ultraviolet absorptions: λ_{max} 332 and 270 mμ (log ε 1.83 and 4.08).

R.D. (Fig. 3), *c*, 0.0578: $[\alpha]_{700}$ 0°, $[\alpha]_{589}$ + 15°, $[\alpha]_{500}$ + 20°, $[\alpha]_{364}$ −985°, $[\alpha]_{309}$ + 2100°, $[\alpha]_{300}$ + 1350°.

N-Phenylthioacetyl-L-asparagine (IX) was prepared as described by Kjær[9], m.p. 137–138° (decomp.) (lit. 139–140°).

Ultraviolet absorptions: λ_{max} 340 and 267 mμ (log ε 1.75 and 4.05).

R.D., *c*, 0.056: $[\alpha]_{700}$ + 35°, $[\alpha]_{589}$ + 70°, $[\alpha]_{450}$ + 215°, $[\alpha]_{365}$ −35°, $[\alpha]_{305}$ + 1470°, $[\alpha]_{290}$ + 860°.

Cyclohexylammonium salt of N-phenylthioacetyl-D-α-aminophenylacetic acid (X). M.p. 198–200° (decomp.), from ethanol. (Found: C 68.8; H 7.17; N 7.28; S 8.58. Calc. for $C_{22}H_{28}N_2O_2S$: C 68.7; H 7.34; N 7.29; S 8.34).

Ultraviolet absorptions: λ_{max} 334 and 269 mμ (log ε 1.77 and 4.07).

R.D. (Fig. 4), *c*, 0.0447: $[\alpha]_{700}$ −115°, $[\alpha]_{589}$ −150°, $[\alpha]_{425}$ − 270°, $[\alpha]_{380}$ + 20°, $[\alpha]_{305}$ −5950°, $[\alpha]_{300}$ −2420°.

Cyclohexylammonium salt of N-phenylthioacetyl-L-β-phenylalanine (XI). M.p.186.5–187.5° (decomp.), from ethanol-ether. (Found: C 69.7; H 7.81; N 7.09. Calc. for $C_{23}H_{30}N_2O_2S$: C 69.3; H 7.59; N 7.03).

Ultraviolet absorptions: $\lambda_{shoulder}$ 325 mμ (log ε 1.89), λ_{max} 268 mμ (log ε 4.10).

R.D. (Fig. 4), *c*, 0.0887: $[\alpha]_{700}$ + 90°, $[\alpha]_{589}$ +120°, $[\alpha]_{395}$ + 265°, $[\alpha]_{375}$ + 240°, $[\alpha]_{302}$ +2340°, $[\alpha]_{297}$ + 1660°.

N-Phenylthioacetyl-L-proline (XII). M.p. 122–124° (decomp.), from light petroleum-ether. (Found: C 62.5; H 5.81; N 5.91. Calc. for $C_{13}H_{15}NO_2S$: C 62.6; H 6.06; N 5.62).

Ultraviolet absorptions: λ_{max} 339 and 274 mμ (log ε 1.72 and 4.14).

R.D. (Fig. 5), *c*, 0.061: $[\alpha]_{700}$ −65°, $[\alpha]_{589}$ −80°, $[\alpha]_{375}$ + 170°, $[\alpha]_{308}$ −2890°, $[\alpha]_{290}$ −590°.

Cyclohexylammonium salt of N-phenylthioacetyl-L-hydroxyproline (XIII). M.p. 181–181.5° (decomp.), from ethanol-ether. (Found: C 63.0; H 7.59; N 7.51. Calc. for $C_{19}H_{28}N_2O_3S$: C 62.6; H 7.74; N 7.69).

Ultraviolet absorptions: $\lambda_{shoulder}$ 330 mμ (log ε 1.82), λ_{max} 276 mμ (log ε 4.14).

R.D. (Fig. 5), *c*, 0.0672: $[\alpha]_{700}$ −60°, $[\alpha]_{589}$ −90°, $[\alpha]_{435}$ −240°, $[\alpha]_{374}$ + 240°, $[\alpha]_{314}$ −5270°, $[\alpha]_{305}$ −1170°.

REFERENCES

1. Djerassi, C. *Optical Rotatory Dispersion: Applications to Organic Chemistry*, McGraw-Hill Book Co., New York 1960.
2. Djerassi, C. *Pure and Applied Chemistry* **2** (1961) 475.
3. a) Schellman, J. A. Section 15—4 in Ref.[1] b) Blout, E. R. Chapter 17 in Ref.[1]
4. For nomenclature see Chapter 2 in Ref [1]; Djerassi, C. and Klyne, W. *Proc. Chem. Soc.* **1957** 57.
5. Sjöberg, B., Fredga, A. and Djerassi, C. *J. Am. Chem. Soc.* **81** (1959) 5002.
6. Djerassi, C., Undheim, K., Sheppard, R. C., Terry, W. G. and Sjöberg, B. *Acta Chem. Scand.* **15** (1961) 903.
7. Sjöberg, B., Cram, D. J., Wolf, L. and Djerassi, C. *Acta Chem. Scand.* **16** (1962) 1079.
8. Holmberg, B. *The Svedberg 1884—1944*, Almqvist and Wiksell, Uppsala 1944, p. 299.
9. Kjær, A. *Acta Chem. Scand.* **6** (1952) 327.
10. Kjær, A. *Acta Chem. Scand.* **4** (1950) 1347.
11. Marvel, C. S. and Noyes, W. A. *J. Am. Chem. Soc.* **42** (1920) 2259.

Received December 19, 1961.

ACTA CHEMICA SCANDINAVICA 16 (1962) 1079–1096

Optical Rotatory Dispersion Studies

LXX *. Anomalous Rotatory Dispersion of Xanthates: Application in Stereochemical Studies of Alcohols

BERNDT SJÖBERG**

Department of Organic Chemistry, Chemical Institute, University of Uppsala, Uppsala, Sweden

DONALD J. CRAM

Department of Chemistry, University of California, Los Angeles, Calif.

LYNN WOLF and CARL DJERASSI

Department of Chemistry, Stanford University, Stanford, Calif., U.S.A.

Submitted in honour of the sixtieth birthday of Professor *Arne Fredga*

The optical rotatory dispersion of several xanthates has been investigated. The spectroscopic properties of xanthates with absorption bands of low extinction around 355 mμ make them very desirable chromophoric derivatives for anomalous rotatory dispersion measurements among the "transparent" alcohols. The xanthates can be used for stereochemical correlations. The relative configurations of alcohols and their corresponding amines can also be established through the anomalous rotatory dispersion curves of their xanthate and dithiocarbamate derivatives.

Optical rotatory dispersion curves have recently found important applications in many areas of chemistry [1,2]. Plain curves [3] are sometimes quite useful for configurational assignments [4,5] and are to be preferred over monochromatic rotation measurements. However, the most important applications of optical rotatory dispersion measurements in organic chemistry have been

* Paper LXIX, Beard, C., Djerassi, C., Elliott, T. and Tao, R.C.C. *J. Am. Chem. Soc.* **84** (1962) 874.

** Present address: AB Astra, Södertälje, Sweden.

on compounds possessing Cotton effects [1]. Such anomalous dispersion curves are only shown by substances with optically active chromophores absorbing in a presently accessible spectral range, preferably with relatively low extinction (*e.g.*, C=O, C=S, N=O chromophores). There are, however, a number of important classes of organic compounds (*e.g.*, alcohols, amines, carboxylic acids) that do not satisfy these requirements. In order to circumvent this difficulty, we have been searching for easily prepared "chromophoric" derivatives of the "nonchromophoric" parent compound. Thus dithiocarbamates [6] and N-thionocarbethoxy derivatives [7] of α-amino acids as well as xanthates of α-hydroxy acids [6] have been excellent for this approach. The spectroscopic properties of the C=S chromophore have proved to be useful also in a number of other environments [1b], for example in thiourea derivatives of carboxylic acids [8].

Whilst simple alcohols are substantially transparent within the range of quartz spectrographs (the absorption band lies near 185 mμ), xanthates (λ max *ca.* 350 mμ, ε *ca.* 60) satisfy the relevant spectroscopic requirements for anomalous rotatory dispersion studies*. Tschugaeff investigated several dixanthates [9] and subsequently [10] xanthates and dithiourethanes of menthol, borneol, and fenchol. Instrumental limitations precluded rotatory dispersion measurements of xanthates through the region of absorption, and only some 20 years later Lowry and Hudson [11] could demonstrate Cotton effects of a few xanthates. However, no attempts were made to use these anomalous dispersion curves for stereochemical correlations. It was with this latter purpose in mind that we undertook a more extensive rotatory dispersion study of xanthates of a variety of alcohols. Preliminary observations were reported earlier [1a], and details will now be given in the present paper.

The rather high amplitudes observed [11] for xanthates of the cyclic alcohols borneol and fenchol were somewhat fortuitous, since the amplitudes and at times even the appearance of Cotton effects of xanthates are very dependent upon chemical constitution. The methyl xanthate (I) and N-phenyl-N-thiobenzoylthiourethane (II) of 2-methylbutanol exhibit only plain dispersion curves (Fig. 1), and if there are any Cotton effects corresponding to the absorption bands at 350 and 510 mμ, respectively, the amplitudes must be extremely small and within experimental error. The situation is quite altered when the alcohol has a more rigid or bulky structure giving a greater interaction between the C=S chromophore and the various substituents of the molecule. The dispersion curve (Fig. 2) of methyl (−)-1-phenyl-2,2-diphenylethyl xanthate (III) thus has a very pronounced negative Cotton effect with a trough of $[\alpha]_{380}$ −1290° and a peak of $[\alpha]_{335}$ +520°, and similarly N-dithiocarbomethoxy (−)-1-phenyl-2,2-diphenylethylamine (IV) has a negative Cotton effect centered around the dithiocarbamate absorption band at 330 mμ**. The establishment of stereochemical relationships between alcohols and amines or hydroxy and amino acid by chemical interrelations is sometimes complicated [12]. However, it has

* For a discussion of electronic absorption spectra of various thiono compounds, see Janssen, M.J. *Rec. Trav. Chim* **79** (1960) 454.

** Conclusive proof for the configurations III and IV of the two compounds has been obtained by several independent methods; see Ref. [29].

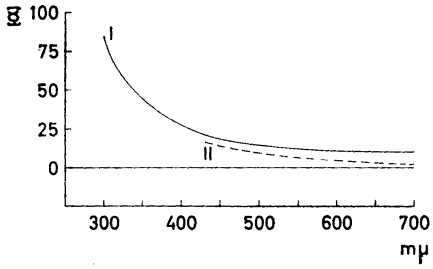

Fig. 1. Optical rotatory dispersion curves of methyl L-2-methylbutyl xanthate (I) and L-2-methylbutyl N-phenyl-N-thiobenzoyl-thiourethane (II).

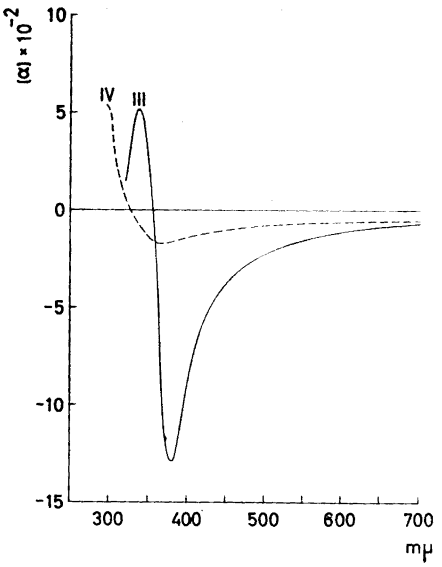

Fig. 2. Optical rotatory dispersion curves of methyl L-1-phenyl-2,2-diphenylethyl xanthate (III) and N-dithiocarbomethoxy L-1-phenyl-2,2-diphenylethylamine (IV).

been shown,[6] that the rotatory dispersion method affords extremely convenient means of assigning configurations to pairs of α-hydroxy and α-amino acids, as the sign of the Cotton effect of the α-hydroxy acid xanthate corresponds to the sign of the Cotton effect of the configurationally related α-amino acid dithiocarbamate. Generally pairs of alcohols and amines can be configurationally related in a similar way by means of the rotatory dispersion curves of their dithiocarbalkoxy derivatives. Dithiocarbalkoxy derivatives of very simple compounds (*e.g.*, 2-methyl-butanol) will apparently not give any Cotton effects, but it would appear that the signs of the plain dispersion curves can be used for stereochemical purposes in an analogous manner to the plain curves of simpler carboxylic acids [4].

Cram and collaborators, in connection with their extensive stereochemical studies,[13] have prepared several diastereoisomeric alcohols of known relative configurations, and in most cases they have also established the absolute configurations. Xanthates of several of these alcohols have now been prepared and their rotatory dispersion investigated in order to see if configurations and conformations could be correlated to any special features of the dispersion curves. Cotton effects with quite large amplitudes are found (Figs. 3—5) for the methyl xanthates V—XIII. The compounds in Fig. 3, all of the L-configuration*, have very similar negative Cotton effect curves with troughs

* The conventions, previously adopted are used, see Cram, D. J. *J. Am. Chem. Soc.* **74** (1952) 2149; Elhafez, F.A.A. and Cram. D. J. *J. Am. Chem. Soc.* **74** (1952) 5846.

around 367 mμ and peaks at 330 mμ. Changes at the α-carbon (*e.g.*, methyl to ethyl to phenyl, V to VI to VII) will apparently not affect the sign of the dispersion curves. Variations at the β-carbon such as methyl to ethyl (V to VIII) or phenyl to cyclohexyl (V to IX) similarly will not change the sign of the dispersion curves as the two L-*threo* compounds (VIII and IX) have negative Cotton effects (Fig. 4). In view of these observations it seems probable that simultaneous variations in substituents both at the α- and β-carbons will be possible without changing the sign of the Cotton effects. The absolute configuration of XIII has been established [14] and the negative Cotton effect indicates that the compound belongs to the L-series. When the configuration is arranged at the α-carbon to give the L-*erythro* compounds (X and XI), positive Cotton effect curves are found (Fig. 5). The absolute configuration of the *erythro* compound (XII) has not previously been established, but considering the similarity in the dispersion curves of XI and XII (Fig. 5) in conjunction with the observations on the xanthates V, VI and VII, we suggest the L-configuration for XII.

Most of the naturally occurring alcohols are cyclic, and we considered it important therefore, to investigate rotatory dispersion curves of xanthates in several different cyclic environments. Rotatory dispersion curves of the methyl xanthates of *cis*- and *trans*-2-methylcyclohexanol (XIV and XV) are shown in Fig. 6, both having negative Cotton effects. The *cis* alcohol was prepared and resolved through the strychnine salt of the acid phthalate according to Gough, Hunter, and Kenyon [15], but for our studies it was not necessary to obtain the pure antipode and an alcohol with the rotation $[\alpha]_D + 4.85°$ (neat) was used. Kenyon *et al.* reports $[\alpha]_D +12.4°$ (neat) for the optically pure alcohol.

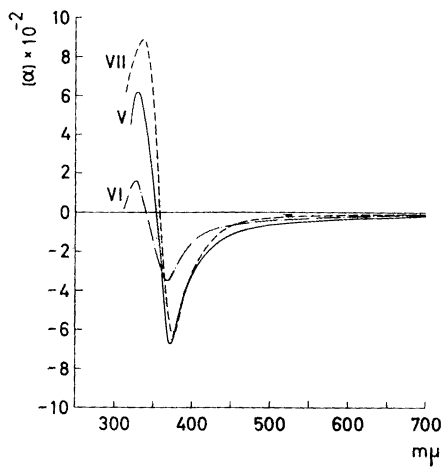

Fig. 3. Optical rotatory dispersion curves of methyl L-*threo*-3-phenyl-2-butyl xanthate (V), methyl L-*threo*-4-phenyl-3-pentyl xanthate (VI) and methyl L-*erythro*-1,2-diphenylpropyl xanthate (VII).

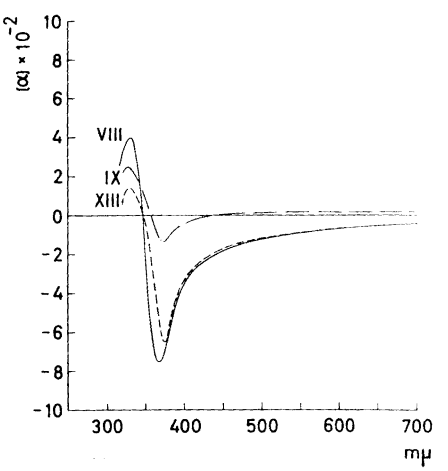

Fig. 4. Optical rotatory dispersion curve of methyl L-*threo*-3-phenyl-2-pentyl xanthate (VIII), methyl L-*threo*-3-cyclohexyl-2-butyl xanthate (IX) and methyl *erythro*-1,2-diphenyl-2-methylbutyl xanthate (XIII).

The racemic *trans*-2-methylcyclohexanol was obtained from commercial 2-methylcyclohexanol by repeated recrystallization of its half phthalate. Since convenient resolutions of alcohols have recently been reported [16,17] through the 3β-acetoxy-Δ^5-etienates we prepared and recrystallized *trans*-2-methylcyclohexanol 3β-acetoxy-Δ^5-etienate. For preparation of the xanthate an alcohol was used with the rotation $[\alpha]_D$ +5.27° (neat), Kenyon reports $[\alpha]_D$ +34.38° (neat) for the optically pure form. At the time that our work was undertaken the absolute configuration of the two epimeric alcohols were not known, but their relative stereochemistry was easily established by oxidation to the corresponding ketone. The *cis*-alcohol gave a ketone having a negative Cotton effect and the *trans*-alcohol a positive*, thus showing that XIV and XV are antipodal around the methyl group, a conclusion in agreement with Kenyon's results [15]. It follows that xanthates of the 2-methylcyclohexanol series exhibit Cotton effects of identical sign, if their hydroxyl-bearing centers possess identical absolute configurations.

* As a result of recent work (Paper LXIX in this series), we now know, that (+)-2-methylcyclohexanone with a positive Cotton effect possesses the following absolute configuration:

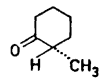

Consequently, XIV and XV represent correct absolute stereoformulas.

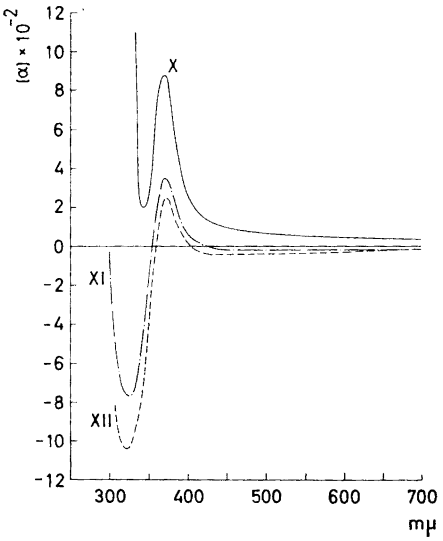

Fig. 5. Optical rotatory dispersion curves of methyl L-*erythro*-3-phenyl-2-butyl xanthate (X), methyl L-*erythro*-3-phenyl-2-pentyl xanthate (XI) and methyl *erythro*-1,2-di(isopropyl)-2-phenylethyl xanthate (XII).

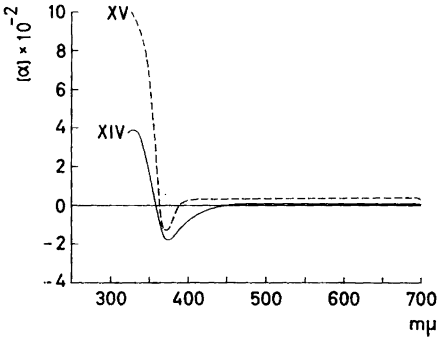

Fig. 6. Optical rotatory dispersion curves of methyl *cis*-2-methylcyclohexyl xanthate (XIV) and methyl *trans*-2-methylcyclohexyl xanthate (XV).

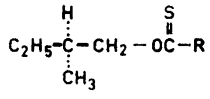

I R=CH_3S

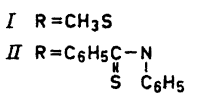

II R=$C_6H_5C(=S)N(C_6H_5)$

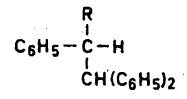

III R=CH_3SCO (=S)

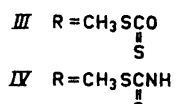

IV R=CH_3SCNH (=S)

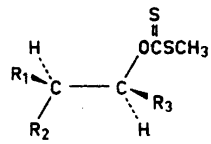

V $R_1=CH_3$; $R_2=C_6H_5$; $R_3=CH_3$.
VI $R_1=CH_3$; $R_2=C_6H_5$; $R_3=C_2H_5$
VII $R_1=CH_3$; $R_2=C_6H_5$; $R_3=C_6H_5$
VIII $R_1=C_2H_5$; $R_2=C_6H_5$; $R_3=CH_3$
IX $R_1=CH_3$; $R_2=C_6H_{11}$; $R_3=CH_3$

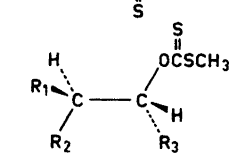

X $R_1=CH_3$; $R_2=C_6H_5$; $R_3=CH_3$
XI $R_1=C_2H_5$; $R_2=C_6H_5$; $R_3=CH_3$
XII $R_1=(CH_3)_2CH$; $R_2=C_6H_5$; $R_3=CH(CH_3)_2$

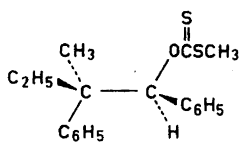

XIII

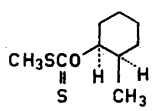

XIV

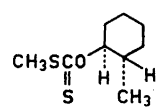

XV

Optically active *cis*- and *trans*-3-methylcyclohexanols of known configurations have been prepared by Hückel and Kurz [18] from (+)-3-methylcyclohexanone, which is easily obtainable [19] from pulegone. From either of these two alcohols we have prepared the methyl (XVI and XIX) and trityl (XVII and XX) xanthates as well as the N-phenyl-N-thiobenzoylthiourethanes (XVIII and XXI). The three derivatives in the *cis*- series are shown in Fig. 7 and those derived from the *trans*-alcohol in Fig. 8. As can be seen the methyl xanthates have both negative Cotton effects with very low amplitudes, while the trityl xanthates have positive Cotton effects of somewhat larger amplitudes. The N-phenyl-N-thiobenzoylthiourethanes both give rotatory dispersion curves with strong positive Cotton effects centered around the low intensity absorption band at 512 mμ. It is interesting to note that the rotatory dispersion curves of the trityl derivatives show opposite signs of the Cotton effects to those of their corresponding methyl xanthates. The reason for this behavior as well as why the *cis*- and *trans*-xanthate derivatives in the 2-series give opposite signs of the Cotton effects while in the 3-series the corresponding *cis* and *trans*-derivatives give the same will be discussed in the last section of this paper.

The menthols are cyclohexanols with an alkyl substituent in the 2-position on one side and another alkyl group in the 3′-position on the opposite side of the hydroxyl function. Thus in the menthol series it will be possible to examine the

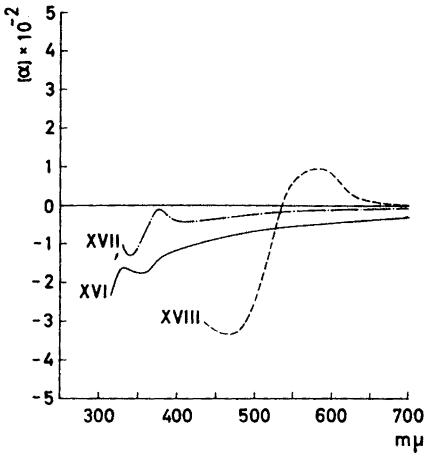

Fig. 7. Optical rotatory dispersion curves of methyl *cis*-3-methylcyclohexyl xanthate (XVI), trityl *cis*-3-methylcyclohexyl xanthate (XVII) and *cis*-3-methylcyclohexyl N-phenyl-N-thiobenzoylthiourethane (XVIII).

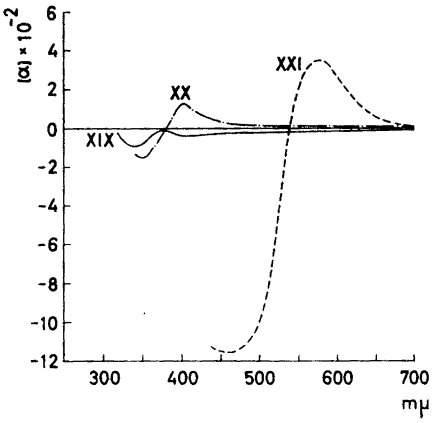

Fig. 8. Optical rotatory dispersion curves of methyl *trans*-3-methylcyclohexyl xanthate (XIX), trityl *trans*-3-methylcyclohexyl xanthate (XX) and *trans*-3-methylcyclohexyl N-phenyl-N-thiobenzoylthiourethane (XXI).

interaction of the two alkyl substituents. For this reason we prepared xanthates of menthol, isomenthol and carvomenthol. The methyl xanthate of (−)-menthol (XXII) exhibits a positive Cotton effect [11], and so does the methyl xanthate of (−)-carvomenthol (XXV) while the same derivative (XXIV) of (+)-isomenthol has a negative one (Fig. 9). The absolute configurations of menthol and isomenthol [20] as well as of carvomenthol [21] have been established beyond doubt. Both in menthol and isomenthol the isopropyl groups are *trans* to the hydroxyls while the hydroxyls and methyls bear a *cis* relationship in menthol and a *trans* relationship in isomenthol. When the methylgroup in the 3′-position (counted from the hydroxyl) is changed from *cis* in (−)-menthol to *trans* in (+)-isomenthol the signs of the Cotton effects are changed from positive for (−)-menthyl methyl xanthate (XXII) to negative for (+)-isomenthyl methyl xanthate (XXIV), an observation which seems consistent with the explanation given at the end of the discussion sections.

Jones and Klyne [5] have studied the plain rotatory dispersion curves of some steroid alcohols as well as of their acetates and benzoates. The intrinsic disadvantage of plain dispersion [1] curves over anomalous ones for complicated molecules prompted us to investigate if the xanthates of steroid alcohols would give suitable Cotton effect curves. As is shown in Fig. 10 the methyl xanthate (XXVI) and trityl xanthate (XXVII) of cholestan-3β-ol exhibit Cotton effect curves of very small amplitude. Considerably larger amplitudes were found [22] for the methyl xanthates of 5α-pregnan-20-ols, these derivatives offering an excellent means of differentiating between 20α- and 20β-ols as the 20α-xanthate exhibits a strong negative Cotton effect and the 20β-xanthate an equally

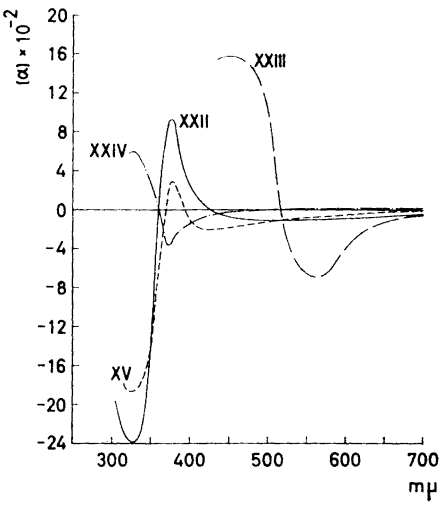

Fig. 9. Optical rotatory dispersion curves of methyl menthyl xanthate (XXII), menthyl N-phenyl-N-thiobenzoylthiourethane (XXIII), methyl isomenthyl xanthate (XXIV) and methyl carvomenthyl xanthate (XXV).

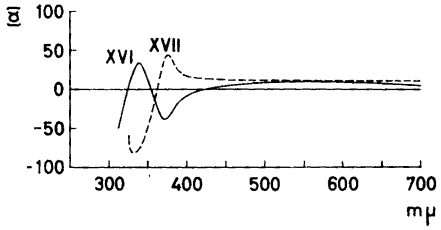

Fig. 10. Optical rotatory dispersion curves of methyl β-cholestanyl xanthate (XXVI) and trityl β-cholestanyl xanthate (XXVII).

strong positive one. As in the cyclohexanol series the methyl and trityl xanthate of cholestan-3β-ol have opposite Cotton effects, and this will be discussed further below.

Already Tschugaeff and Ogorodnikoff studied the rotatory dispersion curves of bornyl methyl xanthate (XXIX) [10a] and bornyl N-phenyl-N-thiobenzoylthiourethane (XXXI) [10b]. They found a positive Cotton effect in the visible wave-length range for the thiourethane, but they were not able to measure below 460 mμ and only obtained the plain part of the dispersion curve for the methyl xanthate. We have now prepared methyl and trityl xanthates and also N-phenyl-N-thiobenzoylthiourethanes of borneol and isoborneol. The optical rotatory dispersion curves of the three derivatives of borneol are found in Fig. 11 (XXIX and XXXI having been measured earlier by Lowry and Hudson [11]) and those of isoborneol in Fig. 12. The methyl xanthate of borneol (XXIX) exhibits a negative Cotton effect with a trough at 380 mμ and a peak at 330 mμ. The Cotton effect is thus almost exactly centered around the low intensity absorption band at 356 mμ. The rotatory dispersion curve of isobornyl methyl xanthate (XXXIII) shows a positive Cotton effect with a peak at 375 mμ and a trough at 330 mμ, this compound having an absorption maximum at 352 mμ. Borneol and isoborneol have opposite signs of rotation at the sodium D-line, but both compounds exhibit positive plain dispersion curves of low rotation. The methyl xanthates (XXIX and XXXIII) have on the other hand distinctly different rotatory dispersion curves with quite large rotations.

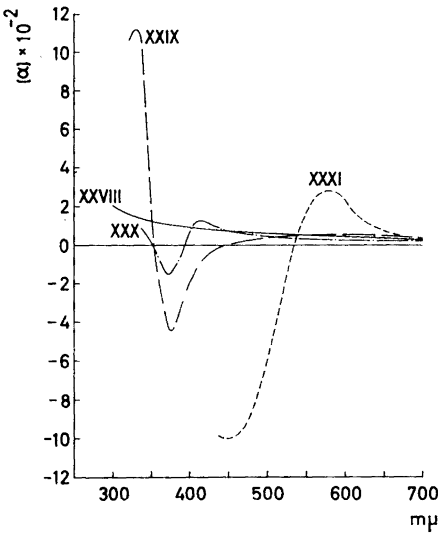

Fig. 11. Optical rotatory dispersion curves of (+)-borneol (XXVIII), methyl bornyl xanthate (XXIX), trityl bornyl xanthate (XXX) and bornyl N-phenyl-N-thiobenzoyl-thiourethane (XXXI).

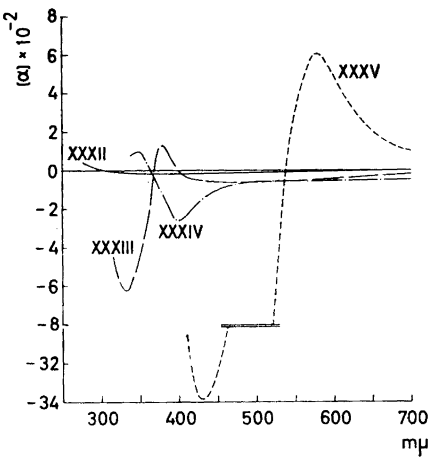

Fig. 12. Optical rotatory dispersion curves of (−)-isoborneol (XXXII), methyl isobornyl xanthate (XXXIII), trityl isobornyl xanthate (XXXIV) and isobornyl N-phenyl-N-thiobenzolthiourethane (XXXV).

The trityl xanthates of cholestan-3β-ol and of *cis*- and *trans*-3-methylcyclohexanol have Cotton effects with larger amplitudes and of opposite sign than those of the corresponding methyl xanthates. The trityl xanthates of borneol (XXX) and isoborneol (XXXIV) exhibit on the contrary Cotton effects of somewhat smaller amplitudes than the methyl xanthates. The rotatory dispersion curve of bornyl trityl xanthate (Fig. 11) has a flat extremum at 425 mμ and a trough at 380 mμ. The Cotton effect must, however, be negative as the absorption maximum is found at 356 mμ, and the peak which should be situated around 325 mμ is not quite resolved. Isobornyl trityl xanthate shows a dispersion curve (Fig. 12) with a negative Cotton effect centered around the 366 mμ absorption band. In the bornyl series the methyl and trityl xanthates have thus the same sign of their Cotton effects whereas they have opposite signs in the isobornyl series. The N-phenyl-N-thiobenzoylthiourethane of borneol (XXXI) as well as that of isoborneol (XXXV) exhibit positive Cotton effects.

Willard and Pacsu [23] recently prepared benzyl xanthates of a few α-D-glucopyranosides, and we have recorded the optical rotatory dispersion curves of methyl α-D-glucopyranoside-6-(S-benzyl) xanthate (XXXVI) and methyl 2,3,4-O-tribenzoyl-α-D-glucopyranoside-6-(S-benzyl) xanthate (XXXVII). These compounds which were kindly supplied by Professor Pacsu (Princeton University), have as expected an absorption band at about 355 mμ of low extinction which evidently is associated with the negative Cotton effects found in their dispersion curves (Fig. 13).

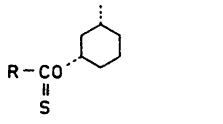

XVI R = CH_3S

XVII R = $(C_6H_5)_3CS$

XVIII R = $C_6H_5C(=S)-N(C_6H_5)$

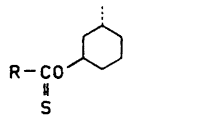

XIX R = CH_3S

XX R = $(C_6H_5)_3CS$

XXI R = $C_6H_5C(=S)-N(C_6H_5)$

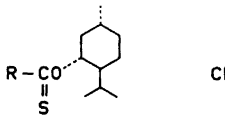

XXII R = CH_3S

XXIII R = $C_6H_5C(=S)-N(C_6H_5)$

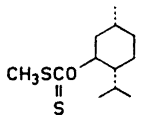

XXIV

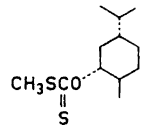

XXV

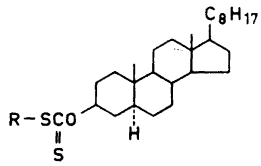

XXVI R = CH_3

XXVII R = $(C_6H_5)_3C$



XXVIII R = H

XXIX R = $CH_3SC(=S)$

XXX R = $(C_6H_5)_3CSC(=S)$

XXXI R = $C_6H_5C(=S)-N(C_6H_5)-C(=S)$



XXXII R = H

XXXIII R = $CH_3SC(=S)$

XXXIV R = $(C_6H_5)_3CSC(=S)$

XXXV R = $C_6H_5C(=S)-N(C_6H_5)-C(=S)$

CONCLUSION

The spectroscopic properties of xanthates with absorption bands around 355 mμ and 275 mμ make them very desirable chromophoric derivatives for anomalous rotatory dispersion measurements among the "transparent" alcohols. The 355 mμ band possesses low extinction ($\log \varepsilon \sim 1.6$) thus allowing rotatory dispersion measurements through this absorption band. The second band has a strong absorption ($\log \varepsilon \sim 4.2$), but the two bands are well separated and the 275 mμ absorption will usually not interfere with spectropolarimetric studies in the 355 mμ absorption region. The strong absorption maximum may also prove useful in analytical applications.

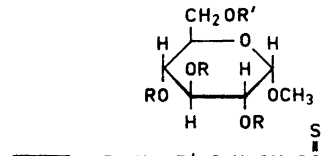

XXXVI R = H; R' = $C_6H_5CH_2SC$(=S)

XXXVII R = C_6H_5C(=O); R' = $C_6H_5CH_2SC$(=S)

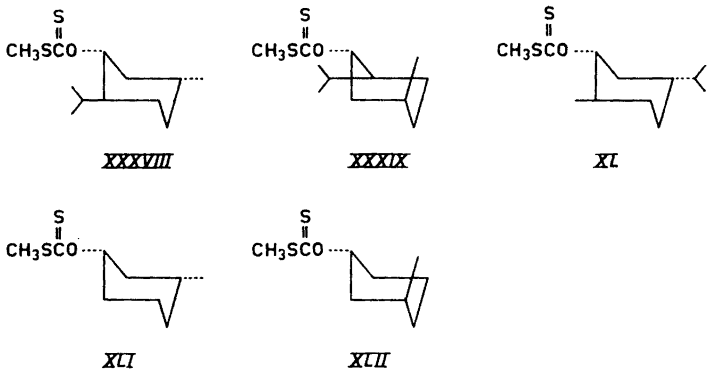

XXXVIII *XXXIX* *XL*

XLI *XLII*

The Cotton effect of xanthates will be due to interaction of the partially unshielded nuclei of various substituents with the electrons of the —C(=S)-S- chromophore. The extent of this interaction depends upon their relative spatial situations, and in view of the free rotation of the xanthate grouping one will observe the effect of an overall rotomer composition. The reason why methyl and trityl xanthates behave differently is that in several instances the large trityl xanthate group may favor a different rotomer composition than the methyl xanthate.

The possibility of free rotation of the xanthate group complicates the situation to such an extent that at the present time a type of "octant rule" [24] approach can not be employed. However, the xanthates can be used for

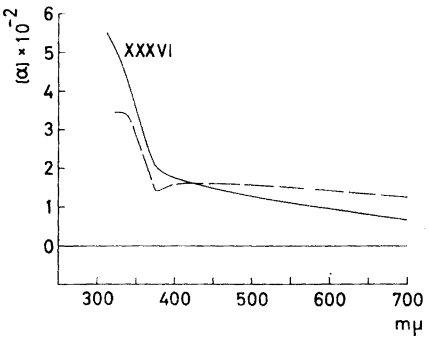

Fig. 13. Optical rotatory dispersion curves of methyl α-D-glucopyranoside-6-(S-benzyl) xanthate (XXXVI) and methyl 2,3,4-O-tribenzoyl-α-D-glucopyranoside-6-(S-benzyl) xanthate (XXXVII) — — —.

stereochemical correlations in closely related series of alcohols (*e.g.*, the alcohols corresponding to the compounds V to XIII), and these derivatives offer excellent means of differentiating between steroid α- and β-ols.

The relative configurations of alcohols and their corresponding amines can also be readily established through the rotatory dispersion curves of the xanthate and dithiocarbamate derivatives. The Cotton effects of xanthates will be centered around 355 mμ and those of dithiocarbamates near 330 mμ, and compounds of the same configurations will exhibit Cotton effects of the same sign.

A comparison of the stereochemistry and rotatory dispersion curves of the compounds III to XIII suggests that the configuration of secondary alcohols may be derived directly from the sign of the Cotton effect of their methyl xanthates in the following way: A model of the methyl xanthate is placed similarly as in the Cahn-Ingold-Prelog R and S convention [26], so that the asymmetric carbon atom is in the center of a "steering wheel", the hydrogen below, the xanthate group and the other two substituents on the wheel. When the groups are arranged clockwise in the order xanthate, large (L) and medium (M) the substance will exhibit a positive Cotton effect, and when the groups are arranged counter clockwise the methyl xanthate will have a negative one.



The situation is more complicated when the xanthate group is situated in a cyclic system, as not only free rotation around the C—O bond is possible but also conformational flipping of one chair form into the other when one of the substituents is axial. The ring conformer composition of various alkyl-substituted cyclohexyl acetates have been derived from rate studies of alkaline hydrolysis and spectroscopic investigations [25]. It is likely that methyl xanthates can be studied in the same way, but qualitatively the conformation of methyl xanthates ought to be obtained simply by equating the methyl xanthate group with an acetate group. From the results of Chapman *et al.* [25] it can then be concluded that menthyl methyl xanthate (XXII) will exist entirely as conformation (XXXVIII) with all three groups equatorial. Isomenthyl methyl xanthate (XXIV) ought to be represented mainly by conformation (XXXIX) with the two larger groups equatorial and the smaller methyl group axial, while carvomenthyl xanthate (XXV) will have all three substituents equatorial (XL). It can be seen that the conformational situation around the xanthate grouping is very similar in all three substances with the exception of the relatively distant (from the C=S chromophore) C—3 substituent. Stereochemically, XXXVIII and XL are identical and exhibit identical signs of their Cotton effects. In XXXIX an antipodal relationship exists around the xanthate grouping, thus explaining the inversion in sign in going from XXXVIII to XXXIX.

A similar explanation can be offered for the observation (Figs. 7 and 8) that the 3-methylcyclohexanol derivatives XVI and XIX, though antipodal

at the asymmetric center carrying the xanthate grouping, exhibit Cotton effect curves of identical sign and weak amplitude. If we assume again that the relatively distant 3-methyl substituent has only a small effect as far as the C=S chromophore is concerned, then it will be noted that in terms of their preferred conformations [25], XLI and XLII, the immediate asymmetric environment around the xanthate grouping in both *cis-* (XVI) and *trans-* (XIX) alcohols *is identical.* The low amplitude of the Cotton effects of these two substances (as well as of the xanthate of cholestan-3β-ol, XXVI) is also understandable, since nuclear substituents are absent in the immediate vicinity of the xanthate function — the principal interaction responsible for the rotation being with the adjacent ring methylene carbons. In the terpene examples, the increased amplitude of the Cotton effect is undoubtedly associated with the presence of an extra-nuclear substituent in relatively close proximity to the electron cloud of the C=S chromophore.

The rotatory dispersion behavior of the 2-methylcyclohexanol xanthates (XIV, XV) cannot be explained in as simple terms, because one of them, the *cis*-isomer, XIV, consists of a mixture of conformers [25] each of which may also have a different rotomer composition as far as free rotation around the $O-C_1$ bond is concerned.

For stereochemical purposes it seems to be better to study methyl xanthates rather then trityl xanthates or N-phenyl-N-thiobenzoylthiourethanes. From a synthetic standpoint the two xanthates are equally easily prepared and are to be preferred to N-phenyl-N-thiobenzoylthiourethanes. However, the recording of the rotatory dispersion curves of N-phenyl-N-thiobenzoylthiourethanes is facilitated as the Cotton effects are found in the visible spectral range and the amplitudes seem to be quite large.

EXPERIMENTAL

All xanthates were prepared by reacting the alcohols in benzene with sodium dispersion and carbon disulfide. When more than one derivative had to be prepared of an alcohol the sodium xanthate was first isolated and then treated with the appropriate halides. N-Phenyl-N-thiobenzoylthiourethanes were obtained from sodium xanthates and diphenylimine chloride [27,28]. The general procedures are given below in the preparation of methyl L-1-phenyl-2,2-diphenylethyl xanthate (III) and the three derivatives XVI–XVIII of *cis*-3-methylcyclohexanol.

The derivatives were filtered in hexane or benzene solution through alumina, and solid compounds were further purified by recrystallization. In case the derivatives were oils they were subjected to vacuum distillation. Partial elimination of the xanthate group evidently happened in some cases as indicated by the low sulfur value in the analysis. However, spectroscopic data showed that the main part was the desired xanthate (in infrared two strong bands at 8.1–8.2 and 9.3–9.5 μ, and in ultraviolet a low extinction band at about 355 mμ).

Methyl L-2-methylbutyl xanthate (I). Prepared from L-(−)-2-methylbutanol; colourless oil.

$\lambda_{max}^{isooctane}$ 355 and 276 mμ, ε 55 and 10 000. R.D. (Fig. 1) in isooctane; *c* 0.45: $[a]_{589}$ +10°, $[a]_{400}$ +24°, $[a]_{310}$ +85°.

L-2-Methylbutyl N-phenyl-N-thiobenzoylthiourethane (II). Prepared from sodium L-2-methylbutyl xanthate and diphenylimine chloride; red oil.

$\lambda_{max}^{isooctane}$ 510 and 315 mμ; ε 240 and 28 700. R.D. (Fig. 1) in isooctane; *c* 0.225: $[a]_{589}$ +5°, $[a]_{430}$ +17°.

Methyl L-*1-phenyl-2,2-diphenylethyl xanthate (III).* To 137 mg (0.5 mmole) of (−)-1-phenyl-2,2-diphenylethanol [29] in 50 ml of dry benzene was added 50 mg of a 50 % sodium dispersion, the mixture was heated under reflux overnight, 100 mg of carbon disulfide was added and heating continued for 5 h, and finally 1 ml of methyl iodide was added and the mixture heated with stirring for a further 5 h period. The benzene was filtered, evaporated and the residue dissolved in hexane and filtered through neutral alumina. The hexane was evaporated *in vacuo* and the residue recrystallized from dilute methanol yielding 130 mg; m.p. 122—124°. (Found: C 72.78; H 5.70; S 17.39. Calc. for $C_{22}H_{20}OS_2$: C 72.48; H 5.53; S 17.59).

$\lambda_{max}^{methanol}$ 355 and 280 mμ, ε 65 and 10 200. R.D. (Fig. 2) in methanol; *c* 0.115: $[a]_{589}$ −120°, $[a]_{380}$ −1290°, $[a]_{335}$ +507°, $[a]_{320}$ +146°.

N-Dithiocarbomethoxy L-*1-phenyl-2,2-diphenylethylamine (IV).* A mixture of 136 mg (0.5 mmole) of (−)-1-phenyl-2,2-diphenylethylamine [29], 5 ml of 0.1 N sodium hydroxide and 100 mg of carbon disulfide in 50 ml of water and 10 ml of dioxane was shaken for 5 h at room temperature. 1 ml of methyl iodide was added and the mixture shaken for another 5 h. The product was extracted with ether, the ether solution washed with dilute hydrochloric acid, water and then dried. The ether was evaporated and the residue chromatographed on Merck acid-washed alumina. The product was eluted with hexane-benzene (1 : 1). It was recrystallized from dilute methanol yielding 85 mg; m.p. 95—96°. (Found: C 72.90; H 5.87; N 3.65; S 17.53. Calc. for $C_{22}H_{21}NS_2$: C 72.68; H 5.83; N 3.86; S 17.64).

$\lambda_{max}^{methanol}$ 330 and 255 mμ, ε 60 and 11 500. R.D. (Fig. 2) in methanol, *c* 0.224: $[a]_{589}$ −54°, $[a]_{370}$ −164°; *c* 0.112; $[a]_{295}$ +540°.

Methyl L-threo-*3-phenyl-2-butyl xanthate (V).* Prepared from L-(+)-*threo*-3-phenyl-2-butanol [30a]; colourless oil. (Found: C 60.04 H 6.86; S 26.50. Calc. for $C_{12}H_{16}OS_2$: C 59.96; H 6.71; S 26.68).

$\lambda_{max}^{methanol}$ 354 mμ, ε 52. R.D. (Fig. 3) in methanol; *c* 0.100: $[a]_{589}$ −35°, $[a]_{370}$ −665°, $[a]_{330}$ +620°, $[a]_{322}$ +420°.

Methyl L-threo-*4-phenyl-3-pentyl xanthate (VI).* Prepared from L-(+)-*threo*-4-phenyl-3-pentanol [30b]; oil. (Found: C 62.67; H 7.47; S 23.88. Calc. for $C_{13}H_{18}OS_2$: C 61.37; H 7.13; S 25.21.

$\lambda_{max}^{methanol}$ 354 mμ, ε 47. R.D. (Fig. 3) in methanol; *c* 0.090: $[a]_{589}$ −25°, $[a]_{365}$ −350°, $[a]_{330}$ +165°.

Methyl L-erythro-*1,2-diphenylpropyl xanthate (VII).* Prepared from L-(+)-*erythro*-1,2-diphenylpropanol [31a]; m.p. 63—64°, sublimed at 35°/0.01 mm. (Found: C 67.74; H 6.01; S 21.19. Calc. for $C_{17}H_{18}OS_2$: C 67.51; H 6.00; S 21.23).

$\lambda_{max}^{methanol}$ 356 mμ, ε 63. R.D. (Fig. 3) in methanol; *c* 0.073: $[a]_{589}$ −11°, $[a]_{376}$ −614°, $[a]_{337}$ +893°, $[a]_{315}$ +613°.

Methyl L-threo-*3-phenyl-2-pentyl xanthate (VIII).* Prepared from L-(−)-*threo*-3-phenyl-2-pentanol [30b]; oil. (Found: C 61.54; H 7.22; S 24.96. Calc. for $C_{13}H_{18}OS_2$; C 61.37; H 7.13; S 25.21).

$\lambda_{max}^{methanol}$ 354 mμ, ε 48. R.D. (Fig. 4) in methanol; *c* 0.115: $[a]_{589}$ −80°, $[a]_{367.5}$ −750°, $[a]_{330}$ +401°, $[a]_{317.5}$ +253°.

Methyl L-threo-*3-cyclohexyl-2-butyl xanthate (IX).* Prepared from L-(+)-*threo*-3-cyclohexyl-2-butanol [31b]; oil. (Found: C 58.90; H 9.35; S 23.94. Calc. for $C_{12}H_{22}OS_2$: C 58.49; H 9.00; S 26.02).

$\lambda_{max}^{methanol}$ 355 mμ, ε 40. R.D. (Fig. 4) in methanol; *c* 0.165: $[a]_{589}$ +15°, $[a]_{345}$ −140°, $[a]_{327.5}$ +245°, $[a]_{315}$ +225°.

Methyl L-erythro-*3-phenyl-2-butyl xanthate (X).* Prepared from L-(+)-*erythro*-3-phenyl-2-butanol [30a]; oil.

$\lambda_{infl.}^{methanol}$ 355 mμ, ε 20. R.D. (Fig. 5) in methanol; *c* 0.050: $[a]_{589}$ +40°, $[a]_{370}$ +835°, $[a]_{342.5}$ +205°, $[a]_{332.5}$ +1100°.

Methyl L-erythro-*3-phenyl-2-pentyl xanthate (XI).* Prepared from L-(−)-*erythro*-3-phenyl-2-pentanol [30b]; oil. (Found: C 61.67; H 7.21; S 24.81. Calc. for $C_{13}H_{18}OS_2$: C 61.37; H 7.13; S 25.21).

$\lambda_{max}^{methanol}$ 354 mμ, ε 58. R.D. (Fig. 5) in methanol: *c* 0.100: $[a]_{589}$ −25°, $[a]_{370}$ +347°, $[a]_{347.5}$ −865°, $[a]_{300}$ −30°.

Methyl erythro-*1,2-di(isopropyl)-2-phenylethyl xanthate (XII).* Prepared from (−)-*erythro*-1,2-di(isopropyl)-2-phenylethanol [32]; m.p. 69−70°, from ligroin. (Found: C 64.77; H 8.20; S 21.16. Calc. for $C_{16}H_{24}OS_2$: C 64.82; H 8.16; S 21.63).

$\lambda_{max}^{methanol}$ 355 mμ, ε 68. R.D. (Fig. 5) in methanol; *c* 0.105: $[a]_{589}$ −18°, $[a]_{372.5}$ +275°, $[a]_{320}$ −1030°, $[a]_{307.5}$ −820°.

Methyl erythro-*1,2-diphenyl-2-methylbutyl xanthate (XIII).* Prepared from (+)-*erythro*-1,2-diphenyl-2-methylbutanol [14]; oil. (Found: C 69.21; H 6.55; S 18.79. Calc. for $C_{19}H_{22}OS_2$: C 69.05; H 6.71; S 19.40).

$\lambda_{infl.}^{methanol}$ 355 mμ, ε 50. R.D. (Fig. 4) in methanol; *c* 0.105: $[a]_{589}$ −70°, $[a]_{375}$ −655°, $[a]_{330}$ +140°, $[a]_{320}$ +50°.

(+)-cis-*2-Methylcyclohexanol.* This alcohol was prepared according to Gough, Hunter and Kenyon [15]. However, recrystallization of the half phthalate strychnine salt was interrupted before full optical purity had been reached, and an alcohol with a specific rotation of +4.85° (neat) was obtained. The optically pure alcohol has a rotation of +12.46° (neat) [15] and hence the alcohol used in our experiments was 39 % resolved.

Oxidation of the alcohol gave a 2-methylcyclohexanone whose rotatory dispersion curve exhibited a negative Cotton effect.

Methyl (+)-cis-*2-methylcyclohexyl xanthate (XIV).* Prepared from an alcohol with the rotation $[a]_D$ +4.85° (neat); oil. (Found: C 53.69; H 7.74. Calc. for $C_9H_{16}OS_2$: C 52.94; H 7.85).

$\lambda_{max}^{isooctane}$ 356 and 276 mμ, ε 46 and 10 300. R.D. (Fig. 6) in isooctane; *c* 0.275: $[a]_{589}$ +11°, $[a]_{375}$ −182°, $[a]_{330}$ +390°, $[a]_{322.5}$ +380°, (these rotations are corrected to 100 % resolution).

trans-*2-Methylcyclohexanol.* The racemic alcohol was prepared according to Gough, Hunter and Kenyon [15], the only difference beeing that commercial 2-methylcyclohexanol (Eastman Kodak, practical) was used.

(+)-trans-*2-Methylcyclohexanol.* This alcohol has previously been prepared by a difficult and tedious method [15]. Partial resolution was readily encountered by recrystallization of the 3β-acetoxy-Δ^5-etienate. 3β-Acetoxy-Δ^5-etienate of racemic *trans*-2-methylcyclohexanol was prepared in a similar way to that described by Djerassi and Staunton [17]. The ester was recrystallized three times from acetone, the ester reduced with lithium aluminium hydride and the partially resolved alcohol was distilled in a hot box at 70°/15 mm. $[a]_D$ +5.27° (neat) as compared to $[a]_D$ +34.38° (neat) for the optically pure alcohol [15]. The sample was thus 15 % resolved.

Oxidation gave a ketone with a positive Cotton effect.

Methyl (+)-trans-*2-methylcyclohexyl xanthate (XV).* Prepared from an alcohol with the rotation $[a]_D$ +5.27 (neat); oil. (Found: C 54.28; H 8.07. Calc. for $C_9H_{16}OS_2$: C 52.94; H 7.85).

$\lambda_{max}^{isooctane}$ 356 and 276 mμ, ε 41 and 10 100. R.D. (Fig. 6) in isooctane; *c* 0.500: $[a]_{589}$ + 35°, $[a]_{370}$ −130°, $[a]_{330}$ +985° (these rotations are corrected to 100 % resolution).

(+)-3-Methylcyclohexanone. The ketone was prepared from pulegone according to McElvain and Eisenbraun [19].

(−)-cis-*3-Methylcyclohexanol.* The optically pure alcohol was prepared according to Hückel and Kurz [18]. However, (+)-3-methylcyclohexanone was reduced with lithium aluminium hydride instead of sodium in alcohol which improved the yield. $[a]_D$ −3.90° (neat). Hückel and Kurz reported $[a]_D^{20}$ −3.91° (neat).

Sodium cis-*3-methylcyclohexyl xanthate.* To 3.2 g (0.028 mole) of (−)-*cis*-3-methylcyclohexanol in 75 ml of dry benzene was added 1.4 g of 50 % sodium dispersion (0.03 gatom), the reaction mixture was stirred for one hour at room temperature and 5 ml of carbon disulfide was added. The mixture was stirred overnight, ether added and the product filtered. The sodium xanthate was recrystallized from benzene-ether, yielding 4.8 g; m.p. 200°(decomp.).

Methyl cis-*3-methylcyclohexyl xanthate (XVI).* To 0.85 g of the sodium xanthate in a mixture of 50 ml of benzene and 25 ml of acetone was added 5 ml of methyl iodide. The reaction mixture was stirred for 24 h at room temperature, filtered and the solvent evaporated *in vacuo*. The residue was dissolved in benzene and filtered through Merck

acid-washed alumina, the benzene evaporated and the xanthate distilled at a bath temperature of 80°/0.2 mm. (Found C 52.85; H 7.61; S 31.22. Calc. for $C_9H_{16}OS_2$: C 52.94; H 7.85; S 31.40).

$\lambda_{max}^{isooctane}$ 355 and 276 mμ, ε 45 and 10 700. R.D. (Fig. 7) in isooctane; *c* 0.193: $[a]_{589}$ −45°, $[a]_{360}$ −175°, $[a]_{335}$ −160°, $[a]_{315}$ −235°.

Trityl cis-*3-methylcyclohexyl xanthate (XVII).* A mixture of 420 mg of sodium *cis*-3-methylcyclohexyl xanthate and 650 mg of trityl bromide in 100 ml of benzene was stirred for 24 h at room temperature, filtered and the solvent evaporated. The residue was dissolved in benzene and filtered through Merck acid-washed alumina. The product was recrystallized from acetone-water and 650 mg was obtained; m.p. 142−143°. (Found: C 74.54; H 6.10; S 14.71. Calc. for $C_{27}H_{28}OS_2$: C 74.96; H 6.52; S 14.82).

$\lambda_{max}^{dioxane}$ 366 and 295 mμ, ε 80 and 11 100. R.D. (Fig. 7). in dioxane; *c* 0.142: $[a]_{589}$ −10°, $[a]_{410}$ −36°, $[a]_{377.5}$ −15°, $[a]_{340}$ −132°, $[a]_{330}$ −100°.

cis-*3-Methylcyclohexyl N-phenyl-N-thiobenzoylthiourethane (XVIII).* A mixture of 420 mg of sodium *cis*-3-methylcyclohexyl xanthate and 440 mg of diphenylimin chloride [33] in 100 ml of dry benzene was stirred at room temperature for 24 h. The mixture was filtered, concentrated and chromatographed on Merck acid-washed alumina. The product was eluted with benzene to yield 575 mg of red crystals. After one recrystallization from hexane there remained 500 mg of red flat plates: m.p. 121−122.5°. (Found C 68.13; H 6.11; N 3.60; S 17.63. Calc. for $C_{21}H_{23}NOS_2$: C 68.22; H 6.28; N 3.79; S 17.35).

$\lambda_{max}^{dioxane}$ 512 and 315 mμ, ε 165 and 8750. R.D. (Fig. 7) in dioxane; *c* 0.140: $[a]_{589}$ +90°, $[a]_{580}$ +95°, $[a]_{467.5}$ −335°, $[a]_{430}$ −300°.

(−)-trans-*3-Methylcyclohexanol.* Prepared according to Hückel and Kurz [18]. $[a]_D$ −7.35° (neat). Hückel and Kurz reported $[a]_D^{20}$ −7.34° (neat).

Methyl trans-*3-methylcyclohexyl xanthate (XIX).* Prepared in the same way as the corresponding *cis*-derivative; oil. (Found: C 52.58; H 7.77; S 31.12. Calc. for $C_9H_{16}OS_2$: C 52.94; H 7.85; S 31.40).

$\lambda_{max}^{isooctane}$ 354 and 276 mμ, ε 43 and 10 700. R.D. (Fig. 8) in isooctane; *c* 0.119: $[a]_{589}$ −18°, $[a]_{410}$ −35°, $[a]_{377.5}$ −11°, $[a]_{340}$ −89°, $[a]_{315}$ −29°.

Trityl trans-*3-methylcyclohexyl xanthate (XX).* Prepared in the same way as the corresponding *cis*-derivative; m.p. 133−135°, from acetone-water. (Found: C 74.50; H 6.20; S 14.53. Calc. for $C_{27}H_{28}OS_2$: C 74.96; H 6.52; S 14.82).

$\lambda_{max}^{dioxane}$ 370 and 295 mμ, ε 80 and 10 700. R.D. (Fig. 8) in dioxane; *c* 0.190: $[a]_{589}$ +5°, $[a]_{402.5}$ +125°, $[a]_{352.5}$ −145°, $[a]_{340}$ −130°.

trans-*3-Methylcyclohexyl N-phenyl-N-thiobenzoylthiourethane (XXI).* Prepared in the same way as the corresponding *cis*-derivative; m.p. 98−99°, from hexane.(Found:C 67.74; H 6.30; N 3.70; S 16.94. Calc. for $C_{21}H_{23}NOS_2$: C 68.22; H 6.28; N 3.79; S 17.35).

$\lambda_{max}^{dioxane}$ 509 and 317 mμ, ε 161 and 8 700. R.D. (Fig. 8) in dioxane; *c* 0.056: $[a]_{589}$ +320°, $[a]_{577.5}$ +325°, $[a]_{460}$ −1150°, $[a]_{437.5}$ −1125°.

Methyl menthyl xanthate (XXII). Prepared from (−)-menthol; oil.

$\lambda_{max}^{isooctane}$ 356 and 276 mμ, ε 44 and 10 850. R.D. (Fig. 9) in isooctane; *c* 0.185: $[a]_{589}$ −69°, $[a]_{375}$ +934°; *c* 0.093: $[a]_{327.5}$ −2370°, $[a]_{305}$ −1935°.

Menthyl N-phenyl-N-thiobenzoylthiourethane (XXIII). Prepared according to Tschugaeff [27]; m.p. 104−106°, from petroleum ether.

$\lambda_{max}^{isooctane}$ 512 and 315 mμ, ε 120 and 8 100. R.D. (Fig. 9) in isooctane; *c* 0.112: $[a]_{589}$ −502°, $[a]_{565}$ −667°, $[a]_{455}$ +1575°, $[a]_{440}$ +1560°.

Methyl isomenthyl xanthate (XXIV). Prepared from (+)-isomenthol [20]; oil. (Found: C 58.89; H 9.02; S 22.42. Calc. for $C_{12}H_{22}OS_2$; C 58.48; H 9.00; S 26.03).

$\lambda_{max}^{isooctane}$ 354 and 276 mμ, ε 44 and 11 900. R.D. (Fig. 9) in isooctane; *c* 0.150: $[a]_{589}$ +9°, $[a]_{372.5}$ −387°, $[a]_{330}$ +584°, $[a]_{320}$ +550°.

Methyl carvomenthyl xanthate (XXV). Prepared from (−)-carvomenthol; oil. (Found: C 58.00; H 8.90; S 23.80. Calc. for $C_{12}H_{22}OS_2$: C 58.48; H 9.00; S 26.03).

$\lambda_{max}^{isooctane}$ 354 and 276 mμ, ε 44 and 11 900. R.D. (Fig. 9) in isooctane; *c* 0.115: $[a]_{589}$ −107°, $[a]_{425}$ −200°, $[a]_{377.5}$ +294°, $[a]_{325}$ −1840°, $[a]_{317.5}$ −1780°.

Methyl β-cholestanyl xanthate (XXVI). The compound was prepared essentially according to O'Conner and Nace [35], but the sodium xanthate was isolated and then reacted with methyl iodide; m.p. 87–88°, from acetone. O'Conner and Nace reported 87.5–88°.

$\lambda_{max}^{isooctane}$ 356 and 276 mμ, ε 51 and 16 100. R.D. (Fig. 10) in isooctane; *c* 0.441: $[a]_{589}$ +9°, $[a]_{370}$ −40°, $[a]_{340}$ +35°, $[a]_{335}$ −50°.

Trityl β-cholestanyl xanthate (XXVII). Prepared from the sodium xanthate and trityl bromide; m.p. 164–166°, from acetone. (Found: C 79.14; H 8.55; S 9.48. Calc. for $C_{46}H_{59}OS_2$: C 79.77; H 8.74; S 9.20).

$\lambda_{max}^{dioxane}$ 356 and 285 mμ, ε 100 and 14 600. R.D. (Fig. 10) in dioxane; *c* 0.210: $[a]_{589}$ +12°, $[a]_{375}$ +45°, $[a]_{335}$ −84°, $[a]_{325}$ −57°.

(+)-Borneol (XXVIII). Camphor was reduced with sodium in dilute ethanol and the borneol purified by repeated recrystallization of its half phthalate from acetic acid and hexane to m.p. 163–164°. The borneol was recrystallized from petroleum ether; m.p. 205–206°, $[a]_D$ +37.1° in chloroform.

Methyl bornyl xanthate (XXIX). From sodium bornyl xanthate and methyl iodide; m.p. 51.5–52°, from dilute methanol. Tschugaeff [10a] reported m.p. 51–52°.

$\lambda_{max}^{isooctane}$ 356 and 274 mμ, ε 42 and 17 700. R.D. (Fig. 11) in isooctane; *c* 0.105: $[a]_{589}$ + 55° $[a]_{380}$ −430°, $[a]_{330}$ +1125°, $[a]_{320}$ + 1060°.

Trityl bornyl xanthate (XXX). From sodium bornyl xanthate and trityl bromide; m.p. 144–146°, from petroleum ether. Tschugaeff [10b] reported 144–146°.

$\lambda_{max}^{dioxane}$ 356 and 297 mμ, ε 38 and 11 000. R.D. (Fig. 11) in dioxane; *c* 0.275: $[a]_{589}$ +35°, $[a]_{415}$ +120° $[a]_{370}$ −147°, $[a]_{335}$ +90°.

Bornyl N-phenyl-N-thiobenzoylthiouretane (XXXI). From sodium bornyl xanthate and diphenylimine chloride; red oil. (Found: C 69.09; H 6.42; S 15.81. Calc. for $C_{24}H_{27}NOS_2$: C 70.37; H 6.64; S 15.66).

$\lambda_{max}^{dioxane}$ 512 and 315 mμ, ε 172 and 17 050. R.D. (Fig. 11) in dioxane; *c* 0.135: $[a]_{589}$ +260°, $[a]_{575}$ +280°; *c* 0.027: $[a]_{450}$ −990°, $[a]_{430}$ −985°.

(−)-Isoborneol (XXXII). Camphor was hydrogenated using Raney nickel as catalyst and the isoborneol was purified by repeated recrystallization of its half phthalate. The alcohol was further purified by recrystallization from petroleum ether and sublimation; m.p. 213–213.5°, $[a]_D$ −29.7° in chloroform. Asahina [34] reported; m.p. 214°, $[a]_D$ −30.6° in ethanol.

Methyl isobornyl xanthate (XXXIII). Prepared in the same way as the corresponding bornyl derivative; oil. (Found: C 60.89; H 8.29; S 24.52. Calc. for $C_{12}H_{20}OS_2$: C 58.97; H 8.25; S 26.24).

$\lambda_{max}^{isooctane}$ 352 and 275½ mμ, ε 215 and 17 200. R.D. (Fig. 12) in isooctane; *c* 0.282: $[a]_{589}$ −48°, $[a]_{470}$ −68°; *c* 0.141: $[a]_{377.5}$ +125°, $[a]_{330}$ −625°, $[a]_{315}$ −460°.

Trityl isobornyl xanthate (XXXIV). Prepared in the same way as the corresponding bornyl derivative; m.p. 134–136°, from petroleum ether. Lowry and Hudson [11] reported 134–136°.

$\lambda_{max}^{dioxane}$ 366 and 296 mμ, ε 35 and 14 700. R.D. (Fig. 12) in dioxane; *c* 0.095: $[a]_{589}$ −45°, $[a]_{400}$ −262°, $[a]_{345}$ +95°, $[a]_{335}$ +75°.

Isobornyl N-phenyl-N-thiobenzoylthiouretane (XXXV). Prepared in the same way as the corresponding bornyl derivative: red oil. (Found: S 15.43. Calc for. $C_{27}H_{25}NOS_2$: S 15.66).

$\lambda_{max}^{dioxane}$ 510 and 315 mμ, ε 256 and 30 600. R.D. (Fig. 12) in dioxane; *c* 0.128: $[a]_{589}$ +525°, $[a]_{575}$ +600°, $[a]_{430}$ −3380°, $[a]_{410}$ −3050°.

Methyl α-D-glucopyranoside-6-(S-benzyl) xanthate (XXXVI). Sample [23] supplied by Prof. Pacsu.

$\lambda_{max}^{dioxane}$ 354 and 281 mμ, ε 62 and 11 900. R.D. (Fig. 13) in dioxane; *c* 0.107: $[a]_{589}$ +80°, $[a]_{375}$ +204°, $[a]_{335}$ +443°, $[a]_{315}$ +555°.

Methyl 2,3,4-O-tribenzoyl-α-D-glucopyranoside-6-(S-benzyl) xanthate (XXXVII). Sample [23] supplied by Prof. Pacsu.

$\lambda_{max}^{dioxane}$ 355 and 281 mμ, ε 83 and 13 700. R.D. (Fig. 13) in dioxane; *c* 0.118: $[a]_{589}$ +123°, $[a]_{377.5}$ +143°, $[a]_{330}$ +345°, $[a]_{315}$ +343°.

Acknowledgements. Grants from the *Swedish Natural Science Research Council* and the *National Cancer Institute* (grant No. CRTY-5061) of the *National Institutes of Health U.S. Public Service*, are gratefully acknowledged. We wish to express out thanks to Mr. Michael Zeppezauer for his valuable assistance in the preparation of some of the xanthates.

REFERENCES

1. a) Djerassi, C. *Optical Rotatory Dispersion: Applications to Organic Chemistry*, McGraw-Hill Book Co., New York 1960. b) Djerassi, C. *Pure and Applied Chemistry* **2** (1961) 475.
2. "Proceedings of a Conference on Rotatory Dispersion" *Tetrahedron* **13** (1961) 1—240.
3. For nomenclature see chapter 2 in Ref. [1a].
4. Sjöberg, B. *Arkiv Kemi* **15** (1960) 451, 497; *Acta Chem. Scand.* **14** (1960) 273.
5. Jones, P. M. and Klyne, W. *J. Chem. Soc.* **1960** 871.
6. Sjöberg, B., Fredga, A. and Djerassi, C. *J. Am. Chem. Soc.* **81** (1959) 5002.
7. Djerassi, C., Undheim, K., Sheppard, R. C., Terry, W. G. and Sjöberg, B. *Acta Chem. Scand.* **15** (1961) 903.
8. Djerassi, C. and Undheim, K. *J. Am. Chem. Soc.* **82** (1960) 5755; Djerassi, C., Undheim, K. and Weidler, A.-M. *Acta Chem. Scand.* **16** (1962) 1147.
9. Tschugaeff, L. *Ber.* **42** (1909) 2244.
10. a) Tschugaeff, L. and Ogorodnikoff, A. *Z. physik. Chem.* **74** (1910) 503. b) *Ibid.* **85** (1913) 481.
11. Lowry, T. M. and Hudson, H. *Phil. Trans. Roy. Soc. London, Ser. A.* **232** (1933) 117.
12. Mills, J. A. and Klyne, W. in Klyne, W. (Ed.) *Progress in Stereochemistry*, Vol. 1, chapter 5, Academic Press, New York 1954.
13. Kingsbury, C. A. and Cram, D. J. *J. Am. Chem. Soc.* **82** (1960) 1810, and preceding papers in the series "Studies in Stereochemistry".
14. a) Cram, D. J. and Allinger, J. *J. Am. Chem. Soc.* **76** (1954) 4516; b) Cram, D. J., Kopecky, K.R., Hauck, F. and Langemann, A. *Ibid.* **81** (1959) 5754.
15. Gough, G. A. C., Hunter, H. and Kenyon, J. *J. Chem. Soc.* **1926** 2052.
16. Woodward, R. B. and Katz, T. J. *Tetrahedron* **5** (1959) 70.
17. Djerassi, C., Warawa, E. J., Wolff, R. E. and Eisenbraun, E. J. *J. Org. Chem.* **25** (1960) 917; Djerassi, C. and Staunton, J. *J. Am. Chem. Soc.* **83** (1961) 736; Djerassi, C., Warawa, E. J., Berdahl, J. M. and Eisenbraun, E. J. *Ibid.* **83** (1961) 3334.
18. Hückel, W. and Kurz, J. *Chem. Ber.* **91** (1958) 1290.
19. McElvain, S. M. and Eisenbraun, E. J. *J. Am. Chem. Soc.* **77** (1955) 3383.
20. McNiven, N. L. and Read, J. *J. Chem. Soc.* **1952** 153.
21. Schmidt, H. *Chem. Ber.* **88** (1955) 459.
22. Djerassi, C., Harrison, I. T., Zagneetko, O. and Nussbaum, A. L. *J. Org. Chem.* **27** (1962) 1173.
23. Willard, I. J. and Pacsu, E. *J. Am. Chem. Soc.* **82** (1960) 4347.
24. Moffitt, W., Woodward, R. B., Moscowitz, A., Klyne, W. and Djerassi, C. *J. Am. Chem. Soc.* **83** (1961) 4013.
25. Chapman, N. B., Parker, R. E. and Smith, P. J. A. *J. Chem. Soc.* **1960** 3634.
26. Cahn, R. S., Ingold, C. K. and Prelog, V. *Experientia* **12** (1956) 81.
27. Tschugaeff, L. A. *Ber.* **35** (1902) 2470.
28. Jamieson, G. S. *J. Am. Chem. Soc.* **26** (1904) 977.
29. Collins, C. J., Christie, J. B. and Raaen, V. F. *J. Am. Chem. Soc.* **83** (1961) 4267.
30. a) Cram, D. J. *J. Am. Chem. Soc.* **71** (1949) 3863; b) Cram, D. J. and Davis, R. *Ibid.* **71** (1949) 3871.
31. a) Elhafez, F. A. A. and Cram, D. J. *J. Am. Chem. Soc.* **74** (1952) 5846; b) Cram, D. J. and Green, F. D. *Ibid.* **75** (1953) 6005.
32. Cram, D. J., Elhafez, F. A. A. and Nyquist, H. L. *J. Am. Chem. Soc.* **76** (1954) 22.
33. Braun, J. von and Pinkernelle, W. *Ber.* **67** (1934) 1218.
34. Asahina, J., Ishidate, M. and Sano, T. *Ber.* **69** (1936) 343.
35. O'Connor, G.L. and Nace, H.R. *J.Am. Chem. Soc.* **74** (1952) 5454.

Received December 19, 1961.

ACTA CHEMICA SCANDINAVICA 16 (1962) 1097–1102

On the Use of Eutectic Melting-point Curves for Sterical Correlations

TADEUSZ RAŻNIKIEWICZ

Organic Department, Chemical Institute, University of Uppsala, Uppsala, Sweden

Submitted in honour of the sixtieth birthday of my teacher, Professor *Arne Fredga*

The melting-point diagrams for mixtures of the (+)- and (−)-forms of α-methoxyphenylacetic acid, α-methoxy-2-thienylacetic acid and α-methoxy-3-thienylacetic acid have been determined. The inactive form of the first-mentioned acid is a true racemate, while the inactive forms of the other two acids constitute conglomerates. The six two-component systems which these three acids give are all of the eutectic type. It is noteworthy that those systems in which the components have opposite configuration give the lower eutectic temperatures. This finding confirms the suggestion made by Fredga [1] that eutectic curves can be used to determine configuration.

The technique of thermal analysis for correlating two optically active compounds whose structures are not too dissimilar has been developed by Fredga into one of the most reliable and convenient methods for determining relative configurations. Using this method, Fredga and his pupils have determined the relative configurations of sulphur and selenium compounds, mercaptosubstituted acids, alkyl- and halogenesubstituted acids and also thiophene derivatives and synthetic plant growth regulators (for review see Ref.[1]). Mislow *et al.*[2] have recently applied this method to determine the configurations of biphenyls.

In most applications of this method antipodes of opposite configuration give a molecular compound in a 1:1 ratio (a quasi-racemate) while antipodes with the same configuration give a solid solution or alternatively a melting-point diagram of the common eutectic type. It is, however, also possible to use the method of thermal analysis in the case where an optically active compound in combination with a second compound gives a solid solution with one enantiomorph and a curve of the eutectic type with its antipode. In this instance the antipode which gives the solid solution has the corresponding configuration. An example of this application is provided by the determina-

tion by Mislow and Meluch [3] of the absolute configuration of α-lipoic acid, from a study of the system 3-methyloctanedioic acid (I) and 3-thioloctanedioic acid (II).

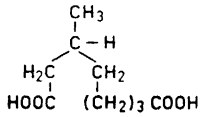

I

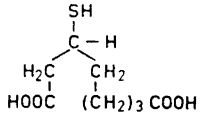

II

The (+)-forms gave a curve of the eutectic type whereas the (+)- and (−)-forms gave solid solutions and were thus shown to have the same configuration.

It is obvious that in the three cases mentioned above the determination of configuration is based on the large differences in the phase behaviour of mixtures of substances with related configurations and mixtures of opposite configurations. The theoretical background for such determinations of configuration rests logically on the analogy with the phase relationships between optically active compounds and their enantiomers which give rise to racemic compounds, solid solutions, or racemic mixtures (conglomerates).

Fredga [1] has pointed out, however, that if an optically active substance gives curves of the common eutectic type with both the enantiomorphs of a second, it appears that the eutectic temperature is always lower when the components have opposite configurations. Hedlund [4] studied the system dithiodilactic acid (III), α-dimethyladipic acid (IV) and found that the

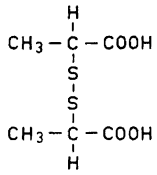

III

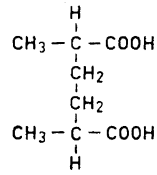

IV

antipodes with opposite directions of rotation gave a lower eutectic temperature and concluded that the antipodes of III and IV with opposite direction of rotation also have opposite configuration. This assignment is in accordance with the results of a more complex determination of chemical configuration.

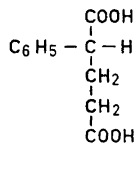

V

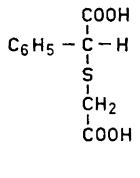

VI

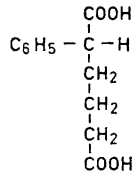

VII

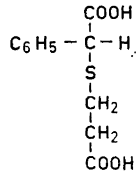

VIII

Similarly Westman [5] used the lower eutectic temperature in the system (−)-α-phenylglutaric acid (V), (+)-phenylthiodiglycolic acid (VI) and in the system (−)-α-phenyladipic acid (VII) and (+)-2-phenyl-3-thiahexanedioic acid (VIII) as an indication of the configurations of VI and VIII

In his recent review Fredga [1] pointed out, however, that the amount of experimental data is too limited to permit any definite conclusions to be drawn regarding the accuracy of this technique.

In the present paper additional evidence will be presented in favour of Fredga's theory. The present author has studied the melting-point diagrams of (+)- and (−)-α-methoxyphenylacetic acid (IX), (+)- and (−)-α-methoxy-2-thienylacetic acid (X) and (+)- and (−)-α-methoxy-3-thienylacetic acid (XI) in addition to those of the mixed systems.

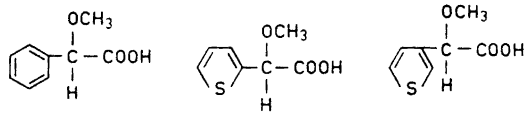

IX X XI

Earlier papers describe the syntheses [6] of the isomeric α-methoxythienylacetic acids and their resolution into enantiomorphs [7]. The configurations of these acids are known [7]. They have been related to the corresponding hydroxy-acids by methylation of the latter with diazomethane using aluminium *t*-butoxide as a catalyst. The thienylglycolic acids have been related to mandelic acid by means of the quasi-racemate method [8,9]. It has been found that both the hydroxy acids and the methoxy acids with the same direction of rotation have the same configuration.

The melting-point diagram of (+)- and (−)-IX (Fig. 1) shows that inactive IX is a true racemate. From Fig. 2 it is evident that inactive X is a conglomerate. Furthermore it was possible to achieve spontaneous resolution of X.

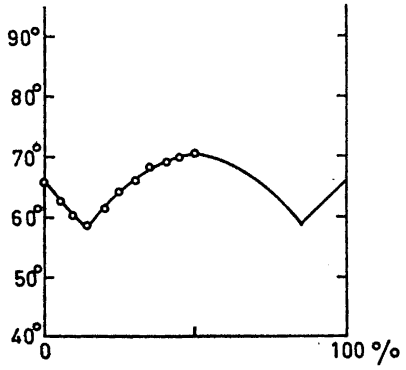

Fig. 1. (+)- and (−)-α-methoxyphenylacetic acid (IX). Abscissa: % (−)-form.

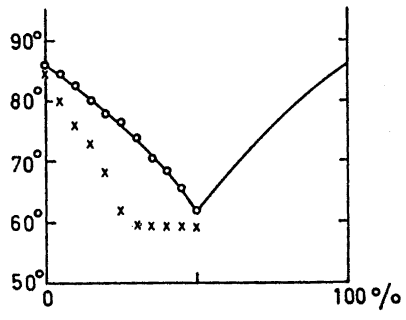

Fig. 2. (+)- and (−)-α-methoxy-2-thienylacetic acid (X). Abscissa: % (−)-form.

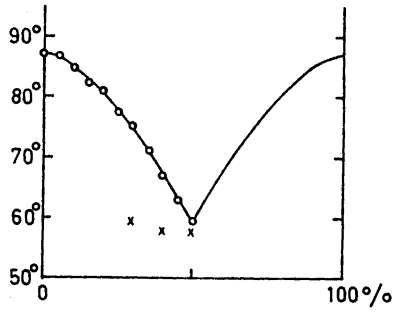

Fig. 3. (+)- and (−)-α-methoxy-3-thienylacetic acid (XI). Abscissa: % (−)-form.

When a solution of inactive X in ether-petrol-ether was allowed to evaporate very slowly, well developed prismatic crystals were formed and isolated individually. One of the larger crystals was shown to be a pure enantiomorph, m.p. 86°, $[\alpha]_D^{25} = +86°$. Crystallisation from benzene-petrol-ether yielded mixtures of less well developed crystals. In some instances, small samples taken for melting point determinations melted sharply at 59—61°, but in most cases the melting process extended over an appreciable temperature range between 60—85°. This effect might be attributed to difficulties in avoiding excesses in the samples of one or other of the antipodes.

The melting-point curve of (+)- and (−)-XI (Fig. 3) is also of the common eutectic type, and inactive XI thus constitutes a conglomerate. In this case, however, spontaneous resolution was not achieved and no difficulties were encountered in the m.p. determinations, which might be due to the fact that XI crystallizes in fine needles.

The apparently complete absence of any racemate-forming tendency in the α-methoxythienylacetic acids makes them ideal for studying the influence of configuration on eutectic-type curves. In addition the geometric differences between the 2-thienyl and the 3-thienyl or phenyl groups are small, and in

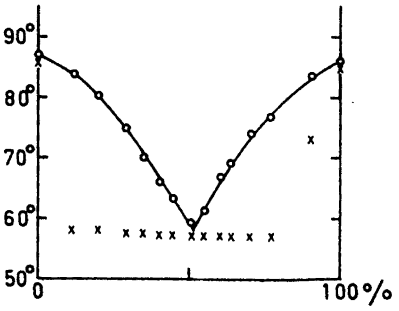

Fig. 4. (+)-α-methoxy-2-thienylacetic acid (X) and (−)-α-methoxy-3-thienylacetic acid (XI). Abscissa: mole % (+)-X.

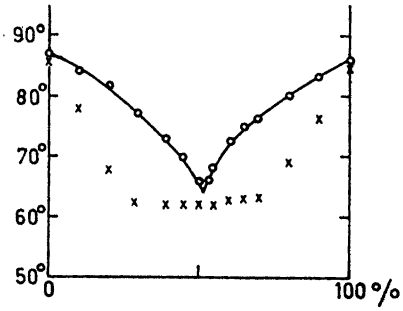

Fig. 5. (−)-α-methoxy-2-thienylacetic acid (X) and (−)-α-methoxy-3-thienylacetic acid (XI). Abscissa: mole % (−)-X.

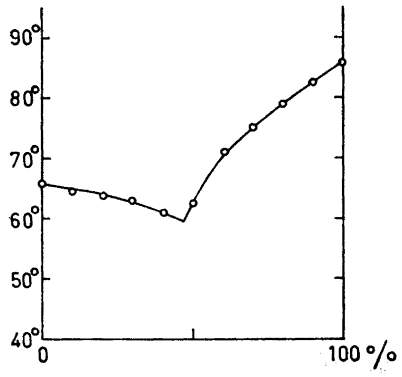

Fig. 6. (+)-α-methoxyphenylacetic acid (IX) and (+)-α-methoxy-2-thienylacetic acid (X). Abscissa: mole % (+)-X.

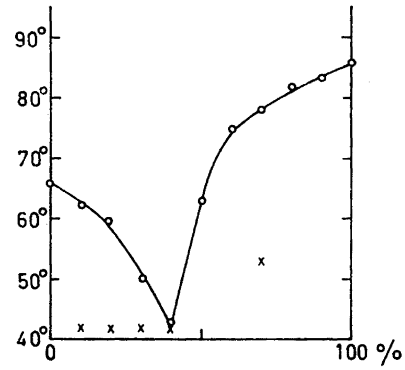

Fig. 7. (+)-α-methoxyphenylacetic acid (IX) and (−)-α-methoxy-2-thienylacetic acid (X). Abscissa: mole % (−)-X.

combination with compounds which have better racemate-forming tendencies, quasi-racemates are often obtained (for review see Ref.[1]).

Figs. 4 and 5 show the melting-point diagrams of (−)-XI with (+)- and (−)-X, respectively. The eutectic temperature is about 6° lower when the components have opposite configurations. More striking are differences shown by the diagrams of (+)-IX with (+)-X (Fig. 6) and (−)-X (Fig. 7) where the eutectic temperature is 16° lower for acids with opposite configurations.

The system IX—XI proved more difficult to study. The diagram for (+)-IX with (−)-XI (Fig. 9) was particularly difficult since some of the mixtures crystallised only after standing for several months at −15°. It is nevertheless clear from Figs. 8 and 9 that in this case mixtures with opposite configurations also show the lower eutectic temperature.

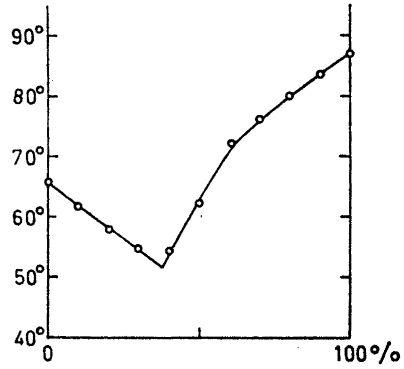

Fig. 8. (+)-α-methoxyphenylacetic acid (IX) and (+)-α-methoxy-3-thienylacetic acid (XI). Abscissa: mole % (+)-XI.

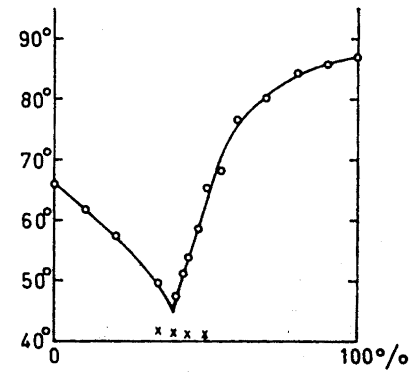

Fig. 9. (+)-α-methoxyphenylacetic acid (IX) and (−)-α-methoxy-3-thienylacetic acid (XI). Abscissa: mole % (−)-XI.

After this investigation was finished and the manuscript prepared, the author learnt that Professor J. E. Ricci (New York University) is also studying the problem of non-identical eutectic diagrams and the stereochemical conclusions which may be drawn from them. A preprint of an article, accepted for publication in the Tetrahedron has kindly been placed at the author's disposal. Starting from pertinent data collected from the literature, Professor Ricci attacks the problem from a more general point of view.

EXPERIMENTAL

(+)-α-Methoxyphenylacetic acid was prepared by the methylation of (+)-mandelic acid with diazomethane using aluminium-*t*-butoxide as a catalyst. The resulting methyl ester was hydrolysed with dilute aqueous sodium hydroxide solution, the sodium salt precipitated with sodium chloride solution and the acid was recrystallised several times from a mixture of petrol-ether and benzene [6], m.p. 65–66°, $[\alpha]_D^{25} = +148.8°$ ($c = 1.028$, ethanol). Literature value [10,11]: m.p. 65–66°, $[\alpha]_D^{25} = -148{,}4°$ ($c = 1.025$, ethanol) resp. m.p. 63–64°, $[\alpha]_D^{25} = -150.6°$ ($c = 0.5412$, ethanol).

Spontaneous resolution of α-methoxy-2-thienylacetic acid. The inactive acid was dissolved in a 1:1 ether petrol-ether mixture and the solvent was allowed to evaporate slowly (during one month) at room temperature. After two weeks crystal formation was observed. It was possible to pick out individual prismatic crystals from the crystalline mass which ultimately formed. Each crystal selected in this way was split into three parts: one was dissolved in ether and the m.p. was determined after evaporating the solvent, a second was mixed with an authentic levorotatory acid and the m.p. of the mixture was determined after evaporating the ether from its ethereal solution, and the third was given similar treatment with a dextrorotatory acid. The m.p. of each of the unmixed samples was 85° while for the mixed samples the melting point was unchanged in one case and depressed in the other, showing that each crystal was a pure enantiomorph. Of ten selected crystals examined in this way, three gave undepressed m.p. with levorotatory acid and seven gave undepressed m.p. with dextrorotatory acid. The largest crystal selected (0.0223 g) was dissolved in 5 ml acetone and the rotation determined: its value was + 0.38° giving $[\alpha]_D^{25} = +86°$.

Melting point diagrams. Weighed amounts of the components were dissolved in acetone. In instances in which crystallisation did not occur after evaporating the solvent, the mixture was kept at −15°. The crystalline mixtures were powdered and dried over conc. sulphuric acid in an desiccator. The melting points were determined using a Kofler hot stage microscope.

Acknowledgements. The author wishes to express his thanks to Professor Arne Fredga for suggesting this work and for all facilities placed at the author's disposal. Thanks are further due to Doc. S. Gronowitz for his interest in this work and for kind help with the manuscript.

REFERENCES

1. Fredga, A. *Tetrahedron* **3** (1960) 126.
2. Mislow, K. and Siegel, M. *J. Am. Chem. Soc.* **80** (1958) 473.
3. Mislow, K. and Meluch, C. *J. Am. Chem. Soc.* **78** (1856) 5920.
4. Hedlund, I. *Arkiv Kemi* **8** (1955) 89.
5. Westman, L. *Arkiv Kemi* **14** (1959) 115.
6. Gronowitz, S. and Raźnikiewicz, T. *Arkiv Kemi* **17** (1961) 661.
7. Raźnikiewicz, T. *Arkiv Kemi* **18** (1961) 467.
8. Gronowitz, S. *Arkiv Kemi* **13** (1958) 87.
9. Gronowitz, S. *Arkiv Kemi* **13** (1958) 231.
10. Bonner, W. A. *J. Am. Chem. Soc.* **73** (1951) 3126.
11. Mc Kenzie, A. *J. Chem. Soc.* **75** (1899) 753.

Received December 18, 1961.

ACTA CHEMICA SCANDINAVICA 16 (1962) 1103–1110

The Alkylation of 5-Benzoylamino-1,3,4-thiadiazoline-2-one

EVA ÅKERBLOM and KURT SKAGIUS

Research Division, AB Pharmacia, Uppsala, Sweden

Submitted in honour of the sixtieth birthday of our teacher, Professor *Arne Fredga*

The methylation of 5-benzoylamino-1,3,4-thiadiazoline-2-one has been studied. It was found that methylation using methyl iodide produced 3-methyl-5-benzoylamino-1,3,4-thiadiazoline-2-one, in contrast to the opinion of Sugii [10]. Using dimethyl sulfate a mixture of 3-methyl-5-benzoylamino-1,3,4-thiadiazoline-2-one and 4-methyl-5-benzoylimino-1,3,4-thiadiazolidine-2-one was obtained. 2-Methoxy-5-benzoylamino-1,3,4-thiadiazole was also synthesized.

Several authors have studied the alkylation of heterocycles which contain a ring nitrogen and an oxygen atom, where the oxygen atom is in a position allowing tautomerism between the oxy and oxo forms. O-Alkylation generally requires the use of diazomethane as the methylation agent [1–3]. When methyl halides or dimethyl sulfate are used, usually the N-methyl derivatives are obtained [3–6], sometimes mixed with the O-alkyl compounds [7,8]. However Ponzio [9] has reported the O-alkylation of 3-phenyl-1,2,4-oxadiazoline-5-one and Sugii [10*] has reported the analogous reaction of 5-acylamino-1,3,4-thiadiazoline-2-one. None of these authors appear to have proved their structures, and since we have found that other thiadiazolones give N-methyl derivatives, a control of Sugii's results seemed justified.

Methylation of 5-benzoylamino-1,3,4-thiadiazoline-2-one (VI) may give five mono-methyl derivatives (I—V) **

We have repeated Sugii's synthesis and have obtained a product with the same melting point. The IR spectrum of this substance (Fig. 1), however, has two carbonyl frequencies (1655 cm^{-1}, 1630 cm^{-1}) but only one strong absorption band in the 1300 cm^{-1} region. This band (1298 cm^{-1}) corresponds to the amide structure of the molecule. There is no other band around 1300 cm^{-1} to indicate a methoxyl group.

* Note that the corresponding abstract in *Chem. Abstr.* **53** (1959) 10033 is incorrect.

** The hydroxythiadiazole structures have been excluded, since it has been shown that similar compounds are present in the oxoform both in solution and in the solid state [14].

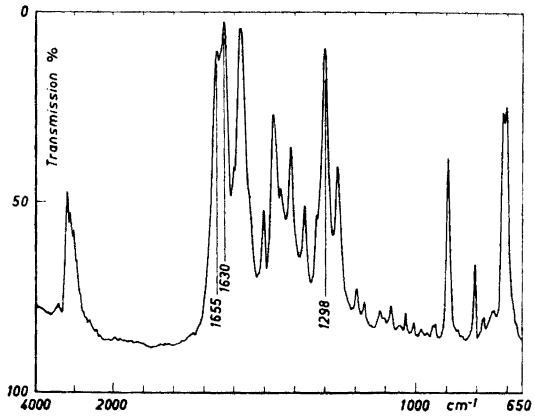

Fig. 1. IR absorption of 3-methyl-5-benzoylamino-1,3,4-thiadiazoline-2-one (I).

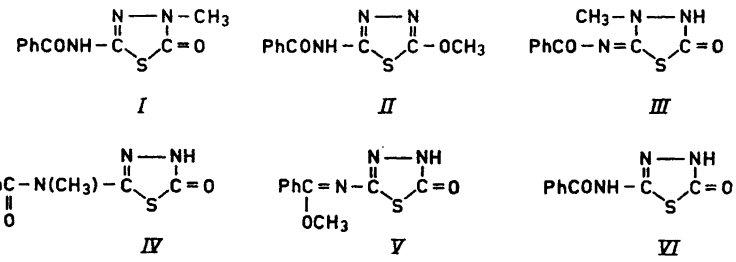

I *II* *III*

IV *V* *VI*

In accordance with this a Zeisel methoxyl determination gives a negative result. Therefore, the 3-methyl derivative (I) was synthesized in a manner which proves its structure (scheme 1). Nitrosation of the methyl derivative (VIII) gave a nitroso compound (IX) which on heating was converted to a thiadiazolone (I), in agreement with the general behaviour of 3-alkyl-2-imino-1,3,4-thiadiazolines [18]. A 4-methyl derivative should give a diazonium salt rather than a nitroso compound.

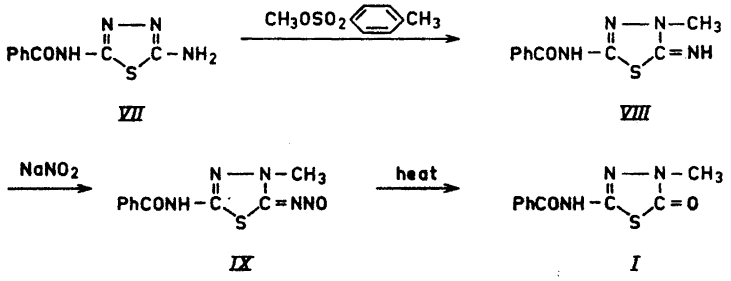

VII *VIII*

IX *I*

Scheme 1.

The substance obtained was identical to Sugii's substance, which thus is shown to be 3-methyl-5-benzoylamino-1,3,4-thiadiazoline-2-one (I).

The preparation of 2-amino-5-benzoylamino-1,3,4-thiadiazole (VII) is described by Sugii [12]. In our hands this method gave mixtures which were hard to separate. Therefore, the ring closure was performed by oxidation with hydrogen peroxide, which gave only the expected benzoyl compound.

In order to obtain a final proof of the preceding result we prepared 2-methoxy-5-benzoylamino-1,3,4-thiadiazole by ring closure of 1-methoxythiocarbonyl-4-benzoyl-3-thiosemicarbazide (scheme 2).

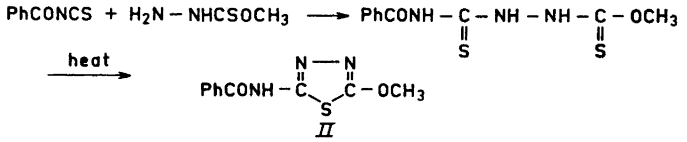

Scheme 2.

The IR spectrum of the compound (II) (Fig. 2) has the expected carbonyl peak at 1670 cm^{-1} and, in addition, two strong absorption bands in the 1300 cm^{-1} region. Here the band at 1310 cm^{-1} may be correlated with the amide structure of the molecule. The other frequency (1279 cm^{-1}) corresponds to a methoxyl group.

In our hands the methylation of 5-benzoylamino-1,3,4-thiadiazoline-2-one (VII) with methyl iodide gave a comparatively low yield. Therefore, an attempt was made to perform the reaction with dimethyl sulfate. We obtained a mixture of at least two substances containing (I) and a substance (A) with the same composition as (I) but differing from this substance and also from (II). By paper chromatography the presence of small amounts of (II) was also indicated.

Determination of the equivalent weight (potentiometrically) and of the molecular weight (ebullioscopically, acetone) shows that substance (A) behaves

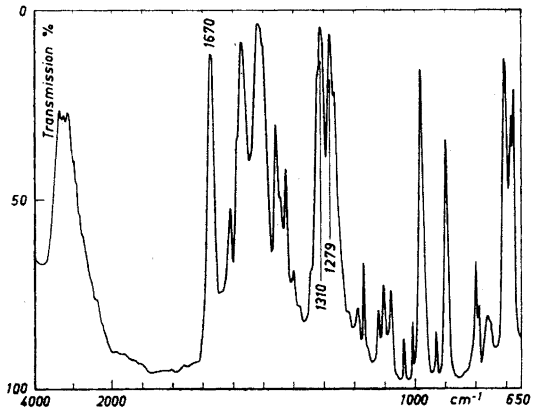

Fig. 2. IR absorption of 2-methoxy-5-benzoylamino-1,3,4-thiadiazole (II).

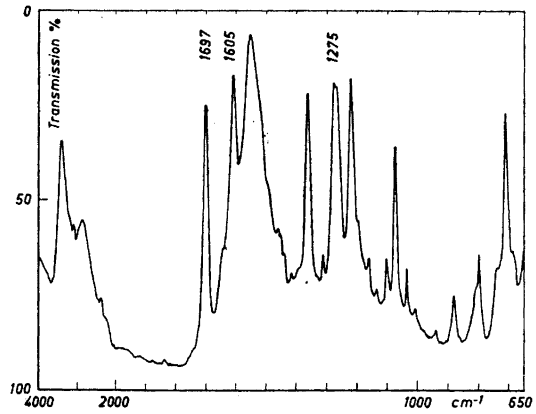

Fig. 3. IR absorption of 4-methyl-5-benzoylimino-1,3,4-thiadiazolidine-2-one (III).

like a monobasic acid with a molecular weight around 230. A Zeisel methoxyl group determination gave about one-half a methoxy group per molecule. This result is confusing, but Karpitschka has reported that sometimes N-methyl groups are split under conditions of a Zeisel test [13]. This may be the case in our determination.

Methoxyl groups exhibit an IR absorption around 1300 cm^{-1}. Actually, substance (A) absorbs at 1275 cm^{-1} (Fig. 3). However, this band disappears when (A) is converted into its sodium salt (Fig. 4). Therefore, it is more likely that this band is caused by an amide structure. A methoxy group absorption should be maintained in the IR spectrum of the salt as is shown by substance (II) (Figs. 2 and 5).

A further inspection of the IR spectrum reveals that compound (A) (Fig. 3) has only one band (1697 cm^{-1}) characteristic of an amide carbonyl grouping,

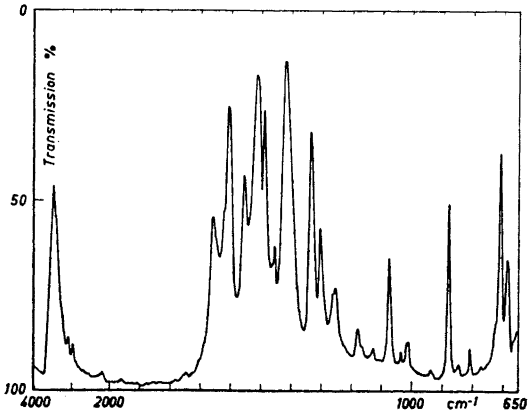

Fig. 4. IR absorption of sodium salt of 4-methyl-5-benzoylimino-1,3,4-thiadiazolidine-2-one.

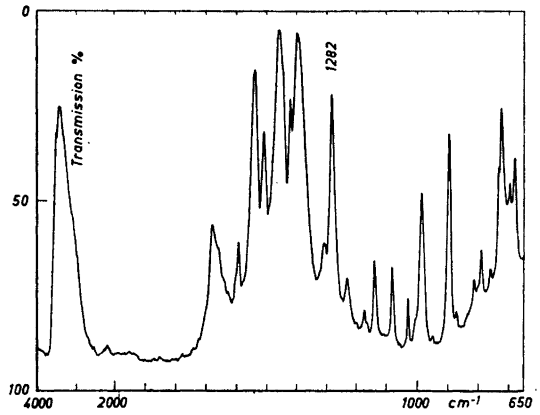

Fig. 5. IR absorption of sodium salt of 2-methoxy-5-benzoylamino-1,3,4-thiadiazole.

whereas (I) (Fig. 1) and (VI) (Fig. 6) exhibit two absorptions (at 1655 and 1630; and at 1668 and 1646 cm^{-1}, respectively). Furthermore substance (A) absorbs at 1605 cm^{-1}, which can be attributed to the presence of an imide structure [14] in the molecule.

Thus, the IR spectra indicate that substance (A) lacks a methoxy group but, instead, possesses an imido group. These fact speak in favour of formula (III) for compound (A).

The UV absorption maxima of the substances (I), (II), (VI), and (A) are collected in Table 1. In an acid medium the substances (I), (II) and (VI), which have amide structures, absorb at 277—282 mμ, whereas substance (A) absorbs at 310 mμ which is characteristic of imido configurations. A similar behaviour has been reported for other heterocycles [14].

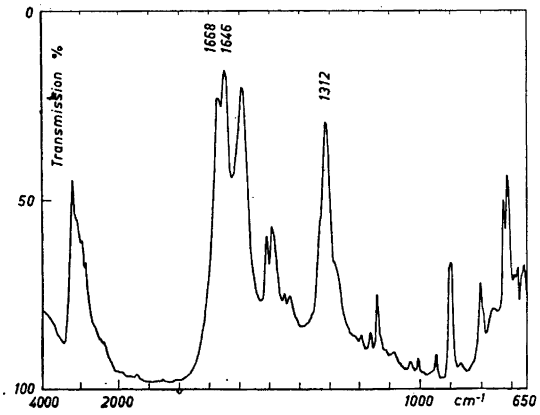

Fig. 6. IR absorption of 5-benzoylamino-1,3,4-thiadiazoline-2-one (VI).

Acid hydrolysis of (A) yields a substance which is identical to the substance (XI) which can be obtained by methylation of 5-amino-1,3,4-thiadiazoline-2-one with methyl *p*-toluenesulfonate (scheme 3). Substance (XI) does not have the same melting-point as 5-methylamino-1,3,4-thiadiazoline-2-one (XII) synthesized by Guha [16].

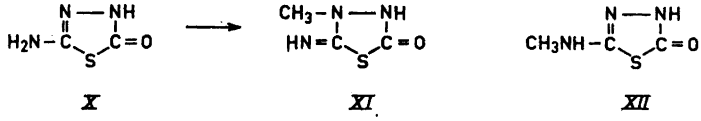

X XI XII

Scheme 3.

The opinion that the alkylation reaction in scheme 3 gives the 4-methyl-5-imino-1,3,4-thiadiazolidine-2-one is supported by the general behaviour of aminothiadiazoles in such reactions [15]; also the nonidentity of (A), (I) and (II) excludes O- or 3-N-substitution.

Thus, the collected chemical and spectral data of substance (A) definitely show it to be 4-methyl-5-benzoylimino-1,3,4-thiadiazolidine-2-one (III). On hydrolysis the molecule (V) should give a non-methylated amino-thiadiazolinone.

EXPERIMENTAL

2-Amino-5-benzoylamino-1,3,4-thiadiazole (VII). 14.8 g (0.058 mole) of 1-benzoyldithiobiurea [12] was stirred with 50 ml of water. 150 ml of 3 % hydrogen peroxide was added and the mixture refluxed for 1 h. After cooling, the mixture was filtered and the precipitate was dissolved in 2 N sodium hydroxide. 1.8 g of undissolved sulfur was filtered off. The filtrate was treated with charcoal, filtered, and acidified with 2 N hydrochloric acid. 11.7 g (91 %) of a colourless substance was obtained. M.p. 277—278.5°C (decomp.). (Found: C 48.9; H 4.0; N 25.3; S 15.0. Calc. for $C_9H_8N_4OS$ (220.2): C 49.1; H 3.7; N 25.4; S 14.6.)

2-Imino-3-methyl-5-benzoylamino-1,3,4-thiadiazoline (VIII). 12.7 g (0.058 mole) of 2-amino-5-benzoylamino-1,3,4-thiadiazole and 21.5 g (0.116 mole) of methyl *p*-toluenesulfonate were mixed and heated in an oil bath at 240°C for 15 min. After cooling, the solidified melt was stirred with acetone and filtered. The precipitate was dissolved in 100 ml of ethanol, the solution treated with charcoal and allowed to cool. 10.8 g (40 %) of 2-imino-3-methyl-5-benzoylamino-1,3,4-thiadiazolinium *p*-toluenesulfonate was obtained as colourless crystals melting at 255.5—260°C.

Table 1. The UV absorption spectra in dimethylformamide-water.

Substance	Maxima (mμ) at pH 2.6	Maxima (mμ) at pH 11.2
3-Methyl-5-benzoylamino-1,3,4-thiadiazoline-2-one (I)	282	315
2-Methoxy-5-benzoylamino-1,3,4-thiadiazole (II)	277	311
4-Methyl-5-benzoylimino-1,3,4-thiadiazolidine-2-one (A)	252, 310	252, 338
5-Benzoylamino-1,3,4-thiadiazoline-2-one (VI)	253, 279	249, 326

The salt was stirred with water, and 2 N sodium hydroxide was added until pH 9 was obtained. The precipitate formed was filtered off and dried. Yield 5.3 g (39 % total yield) of VIII. M.p. 255—257°C (decomp.) (Found: C 51.3; H 4.3; N 24.0; S 13.8. Calc. for $C_{10}H_{10}N_4OS$ (234.3): C 51.3; H 4.3; N 23.9; S 13.7.)

2-Nitrosimino-3-methyl-5-benzoylamino-1,3,4-thiadiazoline (IX). 1.0 g (0.004 mole) of 2-imino-3-methyl-5-benzoylamino-1,3,4-thiadiazoline was dissolved in 30 ml of glacial acetic acid. A solution of 0.36 g (0.005 mole) of sodium nitrite in 5 ml of water was added slowly. The solution turned yellow and after 15 min a yellow substance was precipitated. The mixture was stirred for 1 h at room temperature and filtered. 0.15 g (13 %) of the 2-nitrosimino compound was obtained. The substance decomposes at 200°C.

From the mother liquor 0.7 g of the starting material was recovered after evaporation of the solvent.

3-Methyl-5-benzoylamino-1,3,4-thiadiazoline-2-one (I). 0.15 g (0.6 mmole) of (IX) was refluxed in about 10 ml of chlorobenzene for 30 min. The colour changed from deep yellow to pale yellow. The solution was chilled and 0.1 g (75 %) of an almost colourless substance was collected by filtration. M.p. 257—261°C. After recrystallization from glacial acetic acid 0.06 g of (I), melting at 263.5—267°C, was obtained. Mixed with a substance prepared according to Sugii [10] it showed no melting point depression. (Found: C 50.8; H 3.9; N 18.1; S 13.5. Calc. for $C_{10}H_9N_3O_2S$ (235.2): C 51.1; H 3.9; N 17.9; S 13.6.)

1-Methoxythiocarbonyl-4-benzoyl-3-thiosemicarbazide. 13.3 g (0.125 mole) of methoxythiocarbonylhydrazine was stirred in 100 ml of benzene. A solution of 20.2 g (0.125 mole) of benzoylisothiocyanate in 50 ml of benzene was added carefully. The hydrazine compound was dissolved and the solution became warm. After a while a slightly yellow substance was precipitated. The mixture was stirred for 4 h and finally filtered. Yield 27.5 g (82 %). M.p. 108—109.5°C. (Found: C 44.7; H 4.3; N 15.8; S 23.5. Calc. for $C_{10}H_{11}N_3O_2S_2$ (269.3): C 44.6; H 4.1; N 15.6; S 23.8.)

2-Methoxy-5-benzoylamino-1,3,4-thiadiazole (II). 20 g (0.074 mole) of 1-methoxythiocarbonyl-4-benzoyl-3-thiosemicarbazide was refluxed in chlorobenzene for 3 h. Evolution of hydrogen sulfide was easily recognized. After cooling 14.3 g of colourless crystals were obtained. M.p. 201—215°C. Recrystallization in a mixture of ethanol and acetone. Yield 11.9 g (69 %) of (II). M.p. 217.5—219.5°C. (Found: C 51.2; H 4.2; N 17.9; O 13.8; S 13.5. Calc. for $C_{10}H_9N_3O_2S$ (235.2): C 51.1; H 3.9; N 17.9; O 13.6; S 13.6.)

Acid hydrolysis of 2-methoxy-5-benzoylamino-1,3,4-thiadiazole (II). 1 g of the methoxy compound was refluxed with a mixture of 16 ml of 6 N ethanolic hydrogen chloride and 5 ml of water on a water bath for 1.5 h. The hot mixture was filtered and the precipitate collected. 0.7 g of a subtance, decomposing at 263—271°C, was obtained. The product showed no melting point depression with 5-benzoylamino-1,3,4-thiadiazoline-2-one (VI), prepared according to Sugii [10]. In addition the infrared spectra of the two substances were identical.

Methylation of 5-benzoylamino-1,3,4-thiadiazoline-2-one (VI) with dimethyl sulfate. 4.5 g (0.02 mole) of (VI) was dissolved in 25 ml of 2 N NaOH. 5.0 g (0.04 mole) of dimethyl sulfate was slowly added. After 10 min a precipitate was formed and the mixture turned warm. After stirring for an hour the mixture was filtered. The precipitate (a) and the filtrate (b) were treated as follows:

(a) The precipitate (weight after drying 4.5 g) was stirred with water and the pH was adjusted to 3 with 2 N hydrochloric acid. The mixture was filtered and the precipitate was washed with water and dried. 3.3 g of a substance melting at 136—160°C, was obtained. It was extracted with boiling benzene and 2.5 g of undissolved substance was finally recrystallized from 40 ml of ethanol. 2 g of substance (A) (shown to be (III)), melting at 179.5—181°C was collected. (Found: C 51.2; H 4.0; N 17.7; S 13.7. Calc. for $C_{10}H_9N_3O_2S$ (235.2): C 51.1; H 3.9; N 17.9; S 13.6.)

The solvent was removed from the benzene extract. 0.65 g of a substance melting at 144—165°C was obtained. Chromatography on paper in a 2-butanone-water-methylamine system gave two large spots, one corresponding to (II) and the other unidentified, and further one small spot corresponding to substance (A).

(b) The filtrate was acidified to pH 3 with 2 N hydrogen chloride and filtered. 1.0 g of (I), melting at 257—260°C, was obtained. After recrystallization from glacial acetic acid, the substance melted at 257—260°C, and it showed no melting point depression with the substance prepared according to scheme 1.

Hydrolysis of substance (A). 1 g of substance (A) was refluxed for 1.5 h in ethanolic hydrogen chloride. The solution was chilled and filtered, and 0.45 g of the solid starting material was recovered. The filtrate was evaporated to dryness and 0.3 g of a solid product extracted with boiling acetone. 0.15 g remained undissolved, and it decomposed at 246–249°C. (Found: C 21.9; H 3.7; N 24.9; S 18.9; Cl 21.2. Calc. for $C_3H_6N_3ClOS$ (167.6): C 21.5; H 3.6; N 25.1; Cl 21.2; S 19.1.)

The salt was dissolved in water and NaOH was added to pH 7. The solution was evaporated to dryness and the remainder extracted with hot ethanol. The filtered extract was evaporated to dryness. The resulting base melted with decomposition at 248–249°C and had an IR spectrum identical with (XI), prepared as described below.

4-Methyl-5-imino-1,3,4-thiadiazolidine-2-one (XI). 0.95 g (0.008 mole) of 5-amino-1,3,4-thiadiazoline-2-one [17] was mixed with 3 g of methyl *p*-toluenesulfonate and slowly heated in an oil bath to 125°C. The melt was chilled and extracted with ether, the ether layer decanted, and the undissolved oil was dissolved in acetone. Dry ethanolic hydrogen chloride was added, and the colourless hydrochloride of (XI) was collected and recrystallized from ethanol-ether. 0.25 g was obtained, which decomposed at 250–252°C.

0.2 g of the salt was dissolved in water and the base isolated as described in the previous synthesis. 0.15 g of the base, decomposing at 251.5–253.5°C, was obtained. This substance gave no melting point depression with the substance obtained in the hydrolysis experiment.

Infrared spectra. A Unicam SP 100 spectrophotometer with sodium chloride optics was used. All of the substances were examined with the potassium bromide disc technique.

Acknowledgements. The authors are deeply indebted to Prof. Arne Fredga for his kind interest in this work and to Dr. Bengt Nygård for his contribution to the interpretation of the spectral data. Thanks are also due to Messrs. Martin Sandberg and Jan-Olof Olofsson for help with the spectral work.

REFERENCES

1. Hantzsch, A. *Ber.* **60** (1927) 2537.
2. Hantzsch, A. *Ber.* **61** (1928) 1776.
3. Oliveri-Mandolà, E. and Coppola, A. *Atti reale accad. nazl. Lincei* **20** (1911) 248.
4. Hubacher, K. *Ann.* **259** (1890) 228.
5. Kohler, E. P. and Blatt, A. H. *J. Am. Chem. Soc.* **50** (1928) 504.
6. Lesser, R. and Weiss, R. *Ber.* **57** (1928) 1077.
7. Busch, M. and Limpach, O. *Ber.* **44** (1911) 560.
8. Reissert, A. and Manns, E. *Ber.* **61** (1928) 1308.
9. Ponzio, G. *Gazz. chim. ital.* **53** (1923) 511.
10. Sugii, A. *J. Pharm. Soc. Japan* **79** (1959) 100; *Chem. Zentr.* **131** (1960) 127.
11. Sheinker, Yu. N., Postovskii, I. YA. and Voronina, N. M. *Zhur. Fiz. Khim.* **33** (1959) 302.
12. Sugii, A. *J. Pharm. Soc. Japan* **78** (1958) 306; *Chem. Abstr.* **52** (1958) 11823.
13. Karpitschka, N. *Mikrochim. Acta* **1961** 47.
14. Sheinker, Yu. N., Peresleni, E. M., Zosimova, N. P. and Pomerantsev, Yu. I. *Zhur Fiz. Khim.* **33** (1959) 2096.
15. Bambas, L. L. *The chemistry of heterocyclic compounds*, Interscience Publishers, Inc., New York 1952.
16. Guha, P. C., Chakraborty, T.K. *J. Indian Chem. Soc.* **6** (1929) 102.
17. Guha, P. C. *J. Am. Chem. Soc.* **45** (1923) 1036.
18. Bambas, L. L. *The chemistry of heterocyclic compounds*, Interscience Publishers Inc., New York, 1952, p. 116.

Received December 19, 1961.

ACTA CHEMICA SCANDINAVICA 16 (1962) 1111–1118

Enzymatic Degradation of Water-soluble Cellulose Ethers

SVEN LINDENFORS

Research Laboratory, Mo och Domsjö AB, Örnsköldsvik, Sweden

Submitted in honour of the sixtieth birthday of my teacher, Professor *Arne Fredga*

The degradation of some water-soluble cellulose ethers and one cellulose ester under the influence of cellulase derived from *Aspergillus niger* has been investigated. The influence of enzyme concentration and of the degree of polymerization (D.P.) are discussed. Some factors determining the resistance to degradation are pointed out.

Among the water-soluble high polymers the cellulose ethers are finding an increasing utilisation as suspending, thickening, stabilizing, and film-forming agents. In the solid state the ethers are quite stable in storage; in solution, however, they can undergo deterioration.

The enzyme responsible for the hydrolysis of cellulose and also cellulose derivatives is known as cellulase. Miller *et al.*[1] have recently shown the presence of twenty-four or more electrophoretically distinct, cellulolytically active components in a cellulase preparation from the mould *Myrothecium verrucaria*.

The cellulase used in this investigation (Takamine cellulase 4000 *) is derived from *Aspergillus niger*. It is stated by the manufacturer that it contains appreciable quantities of pectinase and hemicellulase but negligible amounts of protease, amylase, glucose oxidase, and catalase.

The depolymerizing effect of the enzyme on ethyl-hydroxyethyl cellulose in water is seen in Fig. 1. Many other cellulose derivatives are degraded in the same way.

The relation between the quantity of lichenase and the rate of hydrolysis of lichenin (a carbohydrate which resembles cellulose and may be obtained from Iceland moss) has been discussed by Fåhræus [2]. No direct proportion was found to exist. If in this case the remaining viscosity in percent of the original is plotted against the cellulase concentration in percent (calculated on pure and dry cellulose ether) in a semilogarithmic diagram, with time as a parameter, a straight line is obtained, Fig. 2. By changing the enzyme concentration from,

* Manufactured by the Miles Chemical Company, U.S.A.

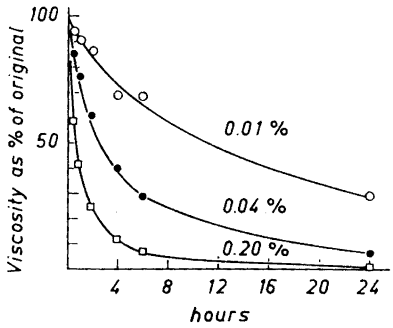

Fig. 1. The decrease in viscosity with time of ethyl-hydroxyethyl cellulose (Modocoll E 600, see experimental part) at different cellulase concentrations (calculated on pure and dry ether). 2.0 % ether in water. Starting viscosity 2 020 cp. pH = 5.8. 20.0°C.

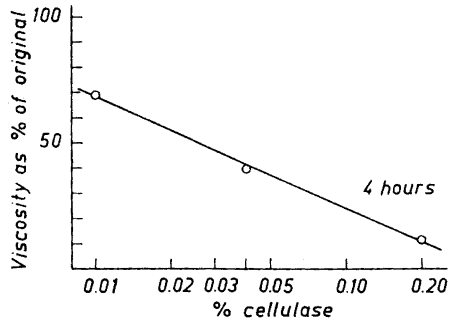

Fig. 2. The relationship between the remaining viscosity and the cellulase concentration (calculated on pure and dry ether) for Modocoll E 600. Reaction time 4 h. 2.0 % ether in water. Starting viscosity 2 020 cp. pH = 5.8. 20.0°C.

for instance, 0.01 % to 0.02 % the remaining viscosity is only decreased by a factor 1.3.

Both temperature and pH have a large influence on the cellulase activity. From Fig. 3 can be seen that the pH optimum for the cellulase used lies between 4 and 5. When comparing the biological resistance of different cellulose derivatives in solution, this fact must be kept in mind. All comparisons between different cellulose derivatives in this investigation are made at constant pH.

Another factor, which must be taken into account when comparing the enzymatic degradation of different cellulose derivatives by following the per-

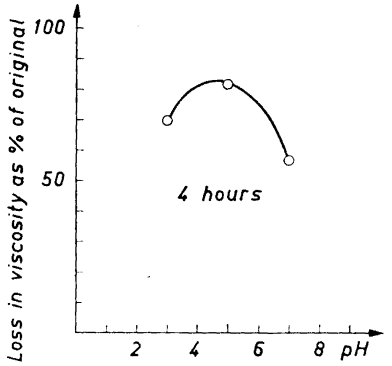

Fig. 3. The loss in viscosity as % of original as a function of pH. 0.20 % cellulase. Temperature 20.0°C. Reaction time 4 h.

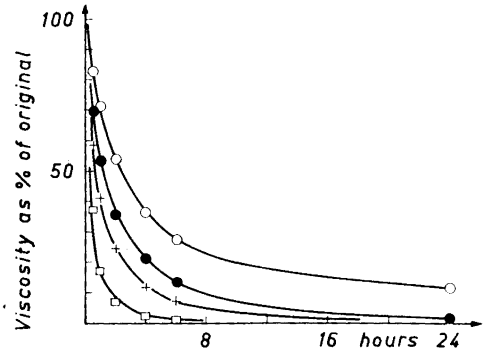

Fig. 4. The decrease in viscosity with time for some ethyl-hydroxyethyl celluloses with different starting viscosities (in all cases the same concentration, 2.0 %). 0.20 % cellulase. 20.0°C. O E 20 (76.0 cp, pH = 6.2); ● E 100 (334 cp, pH = 5.8); + E 600 (1 350 cp, pH = 5.8); □ E 1 200 (8 500 cp, pH = 5.2).

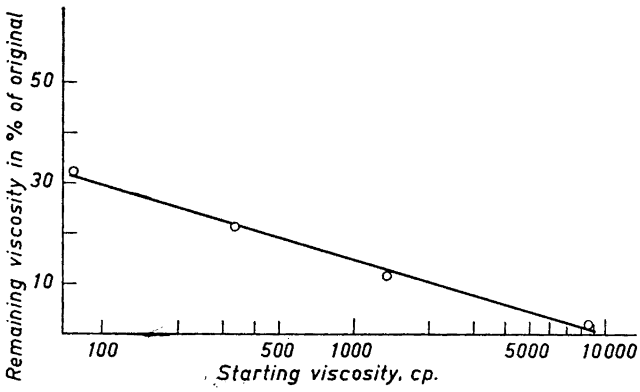

Fig. 5. The remaining viscosity in % of original, as a function of starting viscosity. 0.20 % cellulase. pH = 5.8. Reaction time 4 h. 20.0°C. 2.0 % ether solution in water.

cent loss in viscosity, is the original viscosity of the solution (measured at the same concentration). In Fig. 4 is shown the rate of loss in viscosity for four grades of ethyl-hydroxyethyl cellulose with different starting viscosity (in all cases 2.0 % ether solution in water). The viscosity values at different times are not corrected with respect to the pH influence. The fact that the loss in viscosity, in percent of the original, under identical conditions is less for a low viscosity cellulose ether than for a high one has also been found by Fåhræus and Göransson [3] when degrading the ethers mentioned above with pure cultures of different bacteria and fungi.

This can be expected if it is assumed that the same number of fissions are brought about by the enzyme in a certain period. If in a hypothetic ethyl-hydroxyethyl cellulose, homogeneous with respect to molecular weight (200 000), each chain could be split into three chains of the same length the molecular weight would be 66 700. If in the same amount of a hypothetic ethyl-hydroxyethyl cellulose, with the molecular weight 100 000 each chain is split into two chains of the same length (the same number of fissions in every case) the molecular weight would be 50 000. From eqn. (1) can be calculated that the remaining viscosity in percent of original is higher for the low viscosity than for the high viscosity derivative (14.6 and 1.0 % respectively).

$$M_v^{0.8} = 5113 \cdot \log\eta - 1\,658 \qquad (1)$$

M_v = viscosity average molecular weight
η = Brookfield viscosity in cp

If the remaining viscosity, in percent of the original, is plotted against the starting viscosity (2.0 % solution) at a constant cellulase concentration in a semilogarithmic diagram, with time as a parameter, a straight line is obtained, Fig. 5. The values are corrected with the aid of Fig. 3 to a pH of 5.8 in the solution.

By using the diagrams in Figs. 3 and 5, comparison can be made between the resistance to cellulase degradation of ethyl-hydroxyethyl cellulose and any

cellulose derivative investigated under the conditions, valid for diagram 5 (pH = 5.8, 0.20 % cellulase calculated on pure and dry ether, reaction time 4 h, 20.0°C, 2.0 % ether solution in water). If for instance a cellulose ether with a starting viscosity of 1 000 cp has been found to retain 30 % of the original viscosity under the conditions given above, its biological resistance in comparison to ethyl-hydroxyethyl cellulose can be obtained by dividing 30 by 15 (see Fig. 5 for a starting viscosity of 1 000 cp).

Manley [4] has given the expression below (2) for the relation between the intrinsic viscosity and the viscosity average molecular weight for ethyl-hydroxyethyl cellulose.

$$[\eta] = 3.98 \times 10^{-4} \, M_v^{0.8} \qquad (2)$$

The relation between the intrinsic viscosity and the Brookfield viscosity for a 2.0 % solution of ethyl-hydroxyethyl cellulose in water is also known [5], see eqn. (3).

$$[\eta] = 2.035 \cdot \log\eta \; -0.66 \qquad (3)$$

From eqns. (2) and (3) eqn. (1) is obtained. The decrease in viscosity molecular weights has been calculated for the situations given in Fig. 4. If the remaining viscosity average molecular weight, in percent of the original, is plotted against time the curves for the three products with the lowest starting viscosity (E 20, E 100 and E 600) are very close to each other. The curve for the fourth product (E 1200) lies below the other curves. This product, however, should not, according to the manufacturer, be compared to the others in this situation. This indicates, as Greathouse [6] has pointed out, that the attack of the enzyme is random in which case the degree of polymerisation should have little effect on hydrolysis.

Some data obtained in the way discussed above are given in Table 1 for nine different water-soluble cellulose derivatives. All experiments have been made at the pH which the derivative gives when dissolved in water. Buffer-solutions (sodium hydroxide and potassium biphthalate, pH = 5.0) were first tried in this investigation, but as the influence of electrolytes on different cellulose derivatives varies considerably, the results obtained were not considered representative for the practical situations which are of primary interest in this investigation. The method of using Fig. 3 as a correction curve is in itself not so correct, but it gives, the author believes, a better picture of what happens under practical circumstances.

Although much work has been done to determine the functional group or groups in the cellulose molecule which must be blocked in order to prevent microbiological utilisation the exact mechanism of microbiological attack on cellulose is not known. The maximum possible substitution in cellulose is three groups per anhydroglucose unit. Siu *et al.*[7] investigated the susceptibility of 9 glucose, 3 mannose and 3 cellobiose derivatives to 9 different fungi, and of 11 cellulose derivatives to *Myrothecium verrucaria*. They conclude: "As long as there is at least one firmly bound substituent in every anhydroglucose unit, the resulting derivative is not susceptible to microbiological attack."

From Table 1 is seen that four derivatives have a value in the last column of 0.3—0.4. That means that they are less resistant than ethyl-hydroxyethyl

cellulose (Modocoll, see experimental part) to cellulase attack. This is in agreement with practical experience. All these derivatives contain alkylene oxide groups. With, for instance, hydroxyethyl cellulose substitution occurs on the primary hydroxyls of the introduced hydroxyethyl groups leading to polyethylene oxide side chains. Even if the total substitution as moles of ethylene oxide per anhydroglucose unit (M.S.) is rather high the substitution directly on the three hydroxyl groups of each anhydroglucose unit (D.S.) can be less than one. For the hydroxyethyl cellulose used D.S. can be expected to have a value of about 0.8 [8].

Modocoll has a D.S. of about 1.3. The value of 2.2 in the last column for the methyl cellulose used (D.S. = 1.83) is thus in agreement with the results obtained by Reese *et al.*[9], for carboxymethyl cellulose, which shows that an increase in D.S. from 0.5 to 1.2 increases the resistance to enzymatic attack. The fact that products with D.S.-values over one are degraded is explained by the nonuniform substitution which exists in most technical products and which results in the cleavage of the glycosidic linkages adjacent to the unsubstituted anhydroglucose units. The rule that a D.S. of more than one is required to give protection does not, however, apply to surface modification of fibers [10]. The minimum D.S. for protection of methylated cotton has been found to be 0.7 when diazomethane was used. An equivalent methylation with dimethyl sulfate did not give protection which indicates that the synthetic method used is also of importance.

The relatively high microbiological resistance of the three last derivatives in Table 1 was not expected because of the low D.S.-values. They are all ionic derivatives. Reese [10] has pointed out that the nature of the substituent and its location may be of importance. It is possible that both steric and electronic properties of the substituent play a role together with the D.S. when dealing with microbiological attack on cellulose derivatives.

From what has been said it is clear that there are many factors which are difficult to treat quantitatively but which are of great importance for the resistance to microbiological attack. For testing cellulose derivatives against enzymatic attack the use of a standardised enzyme, like the one used, which is commercially available can simplify the investigation and yet give enough informations.

EXPERIMENTAL

Hydroxyethyl cellulose. Bleached sulphite pulp with an alpha content of 89.5 % was soaked in 19.0 % sodium hydroxide solution for 45 min at 22°C. Excess alkali was removed by pressing to a press factor of 2.42. 121 g of shredded alkali cellulose together with 181 g of ethyl chloride and 35.2 g of ethylene oxide were heated in an autoclave, without stirring, at 55°C for 4 h. The crude product was washed three times in methanol and the last amount of sodium hydroxide was neutralized in the second wash with acetic acid. Total substitution as moles of ethylene oxide per anhydroglucose unit (M.S.) = 1.50 corresponding to a degree of substitution (D.S.) of 0.80 [8].

Ethyl-hydroxyethyl cellulose. This water-soluble cellulose ether is manufactured by Mo och Domsjö AB, Örnsköldsvik, Sweden, and is sold under the name of Modocoll. The different products used, E 20, E 100, E 600 and E 1200 differ mainly in viscosity. The total degree of substitution is, for E 20 1.4, and for the other products 1.7. The ethoxyl and hydroxyethyl substitution is about the same.

Table 1.

Derivative	Schematic formula	D.S.	Starting visc., cp 2.0 % solution	pH	Remaining visc. in % of original after 4 h[b]	Remaining visc. corrected to pH 5.8	Remaining visc. in % of original divided by the corresponding value for Modocoll[c] with the same starting visc.
Hydroxyethyl cellulose	$-O-CH_2-CH_2-OH$	1.50[a]	3 740	6.8	2.1	1.7	0.3
Hydroxypropyl cellulose	$-O-CH_2-\underset{\displaystyle CH_3}{\overset{\displaystyle H}{\underset{\displaystyle |}{\overset{\displaystyle |}{C}}}}-OH$	1.2–1.5	2 150	6.1	4.5	4.4	0.4
Ethyl-hydroxypropyl cellulose	$-O-C_2H_5$ $-O-CH_2-\underset{\displaystyle CH_3}{\overset{\displaystyle H}{\underset{\displaystyle |}{\overset{\displaystyle |}{C}}}}-OH$	1.5–1.7[a]	1 455	5.1	4.7	5.0	0.4
Methyl cellulose	$-O-CH_3$	1.83	6 300	6.2	7.3	6.9	2.2
Methyl-hydroxyethyl cellulose	$-O-CH_3$ $-O-CH_2-CH_2-OH$	1.66	2 450	3.5	3.8	3.8	0.4
Methyl-hydroxypropyl cellulose	$-O-CH_3$ $-O-CH_2-\underset{\displaystyle CH_3}{\overset{\displaystyle H}{\underset{\displaystyle |}{\overset{\displaystyle |}{C}}}}-OH$	–	4 030	6.8	13.2	10.7	1.8
Carboxymethyl cellulose	$-O-CH_2-COONa$	0.70	3 540	7.1	17.8	12.6	1.9
Sulfomethyl cellulose	$-O-CH_2-SO_3Na$	0.28	449	4.4	58.9	55.0	2.8
Cellulose sulfate	$-O-\underset{\displaystyle O}{\overset{\displaystyle O}{\underset{\displaystyle \|\|}{\overset{\displaystyle \|\|}{S}}}}-ONa$	0.40	43.4	3.0	30.4	27.6	0.8

a) M.S. values (total substitution as moles of alkylene oxide per anhydroglucose unit).
b) 0.20 % cellulase calculated on pure and dry derivative. 20.0°C.
c) Ethyl-hydroxyethyl cellulose (see experimental part).

Hydroxypropyl cellulose. Bleached sulphite pulp with an alpha content of 89.5 % was soaked in 19.5 % sodium hydroxide solution for 45 min at 20°C. Excess alkali was removed by pressing to a press factor of 2.39. 95.6 g of shredded alkali cellulose together with 181 g of ethyl chloride and 40.1 g of propylene oxide were heated in an autoclave, without stirring, at 70°C for 4.5 h. The crude product was washed twice in methanol and the last amount of sodium hydroxide was neutralized with acetic acid. The total substitution as moles of propylene oxide per anhydroglucose unit has not been determined. M.S. can be expected to have a value between 1.2 and 1.4.

Ethyl-hydroxypropyl cellulose. Bleached sulphite pulp with an alpha content of 89.5 % was soaked in 19.5 % sodium hydroxide solution for 45 min at 20°C. Excess alkali was removed by pressing to a press factor of 2.40. 96.0 g of shredded alkali cellulose together with 52.3 g of ethyl chloride and 21.5 g of propylene oxide were heated in an autoclave, without stirring, first at 70°C for 60 min, and then at 100°C for 125 min. The crude product was washed three times in methanol and the last amount of sodium hydroxide was neutralized in the second wash with acetic acid. M.S. is not exactly known but can be expected to have a value between 1.5 and 1.7.

Methyl cellulose. The product used, Methocel MC 4 000, is manufactured by the Dow Chemical Company, U.S.A. D.S. = 1.83.

Methyl-hydroxyethyl cellulose. The product used, Tylose MH 1 000, is manufactured by Kalle AG, Germany, D.S.: methoxyl = 1.53; hydroxyethyl = 0.13.

Methyl-hydroxypropyl cellulose. The product used, Methocel 65 HG, NF-grade, is manufactured by the Dow Chemical Company, U.S.A. M.S. or D.S. are not known.

Carboxymethyl cellulose. The product used, Cekol HVB, is manufactured by Uddeholms AB, Skoghall, Sweden. D.S. = 0.70.

Sulfomethyl cellulose. This product was first described by Porath [11,12]. – Bleached sulphite pulp with an alpha content of 89.5 % was soaked in 19.0 % sodium hydroxide solution for 45 min at 20°C. Excess alkali was removed by pressing and the press factor was determined. Alkali cellulose corresponding to 50 g of pulp was shredded, and enough 19.0 % sodium hydroxide solution was added to give a press factor of 4.0. A water solution (120 ml), containing 23.1 g of Na-monochloromethane sulfonate and an equimolar amount of sodium chloride (obtained by reacting dichloromethane with sodium sulphite) was added during a period of 25 min with continuous stirring. The reaction mixture was put into an autoclave and the water was driven off under vacuum and heating. The temperature increased almost continuously during the reaction to about 110°C at the end of the reaction. The crude product was washed three times in 75 % ethanol and the last amount of sodium hydroxide was neutralized with acetic acid. D.S. = 0.28.

Cellulose sulfate. This product differs from the other derivatives used as it is an ester of cellulose. It has been obtained from Eastman Kodak Company, U.S.A. D.S. = 0.40.

2.0 % solutions have been used throughout this investigation. The products have been dissolved at 20°C. The water content in the solid product has been determined by heating at 105°C to constant weight.

The cellulase has been weighed on a precision balance and directly dissolved in the solution under investigation. In most cases the cellulase concentration has been 0.20 % calculated on dry and pure cellulose derivative.

The temperature has in all cases been 20.0°C.

The decrease in viscosity has been followed with a Brookfield viscometer, type LVF. Different spindles and rotation speeds can be used for different viscosity ranges. The combinations of spindles and speeds shown in Table 2 have been used.

Table 2.

Measuring range, cp	Spindle	Rpm
0 — 100	1	30
100 — 500	1	12
500 — 2 500	2	12
2 500 — 10 000	3	12

Acknowledgements. The author is indebted to Dr. I. Jullander, Mo och Domsjö AB, for kind interest in this work and for a critical review of the manuscript.

Most of the experimental work was made by Mrs. I.-M. Leander and Mr. K. Lindström. The author is indebted to them for their valuable assistance. Linguistic assistance by Mr. Derek Gerver is gratefully acknowledged.

REFERENCES

1. Miller, G. L. *et al. J. Chromatog.* **3** (1960) 576.
2. Fåhræus, G. *Handbuch der Pflanzenphysiologie.* Vol. 6, p. 305.
3. Fåhræus, G. and Göransson, B. Royal Agricultural College, Uppsala. *(Personal communication).*
4. Manley, R. St. John. *Arkiv Kemi* **9** (1956) 519.
5. Research Laboratory, Mo och Domsjö AB, Örnsköldsvik, Sweden. *(Unpublished data).*
6. Greathouse, G. A. *Textile Research J.* **20** (1950) 227.
7. Siu, R. G. H. *et al. Ibid.* **19** (1949) 484.
8. Brown, W. *Arkiv Kemi* **18** (1961) 232.
9. Reese, E. T. *et al. J. Bacteriol.* **59:4** (1950) 485.
10. Reese, E. T. *Ind. Eng. Chem.* **49** (1957) 89.
11. Porath, J. *Arkiv Kemi* **11** (1957) 97.
12. Porath, J. U.S.P. 2.891.057.

Received December 19, 1961.

ACTA CHEMICA SCANDINAVICA 16 (1962) 1119–1123

On the Calculation of the Rate Constant Ratio in Consecutive Reactions

SIGVARD WIDEQVIST

Department of Organic Chemistry, University of Uppsala, Sweden

Submitted in honour of the sixtieth birthday of my teacher, Professor *Arne Fredga*

The calculations of the rate constants for consecutive second-order reactions has been discussed, and a method of calculation has been suggested. The method which makes use of numerical or graphical integration has been tested against the data given by Regna and Caldwell for the conversion of a ketopolyhydroxy acid to furfural via ascorbic acid.

Recently Mc Millan [1] published a paper on the calculation of the rate constant ratio in consecutive second-order reactions:

$$A + B \xrightarrow{k_1} C + E$$

$$A + C \xrightarrow{k_2} D + F$$

The statement of Mc Millan that the problem of determining the rate constants k_1 and k_2 has been solved in detail only for the case of equivalent initial reactant concentrations (*i.e.* $B_o = 2A_o$) or for a limited range of the extent of the reaction is not correct (Wideqvist [2]).

The extent of the reaction is usually determined by measuring the concentration of A. From this concentration the rate constants are calculated in some way (Frost and Schwemer [3], Wideqvist [2,4]).

Mc Millan points out that it is a much simpler problem to obtain the ratio $\varkappa = k_2/k_1$ of the two rate constants from a knowledge of the concentrations of *two components* of the reacting system at *the same time*. According to Mc Millan this case assumes greater relevance in view of the increasingly powerful analytical methods, whereby one can often directly determine the concentrations of products and reactants other than A.

The rates of change of the concentrations B and C are

$$dB/dt = -k_1AB \quad (1)$$

$$dC/dt = k_1A(B-\varkappa C) \quad (2)$$

In terms of the reduced concentrations, defined by

$$\beta = B/B_0 \quad (3a)$$

$$\gamma = C/B_0 \quad (3b)$$

the ratio of eqn. (2) to (1) becomes

$$d\gamma/d\beta = (\varkappa\gamma-\beta)/\beta \quad (4)$$

On integrating we obtain

$$\varkappa \ln\beta = \ln[\beta + (1-\varkappa)\gamma] \quad (5)$$

or

$$\gamma = \beta(1-\beta^{\varkappa-1})/(\varkappa-1) \quad (6)$$

For any measured pair (β,γ) of experimental concentrations the value of $\varkappa$ which satisfies eqn. (5) is calculated by determination of the intersection of the left and right hand sides, considered as functions of $\varkappa$ for the given values of the parameters (β,γ). This procedure, recommended by Mc Millan, is, however, very cumbersome. For values of $\varkappa$ less than 0.05 it should be possible to use eqn. (5) in the explicit approximate form

$$\varkappa \approx [\ln(\beta + \gamma)]/[\ln\beta + \gamma/(\beta + \gamma)] \quad (7)$$

Finally Mc Millan states that although the procedure above "is much simpler than in the general case, it also accomplishes less in providing only the ratio $\varkappa$ rather than the values of the individual rate constants k_1 and k_2".

It seems, however, as Mc Millan has overlooked two important facts, namely (1) that $\varkappa$ is already explicitly expressed in eqn. (4) and, (2) that a knowledge of the concentrations B and C also gives the remaining concentration A and thus k_1 and k_2.

The discussion is considerably facilitated by introduction of the reaction variables x and y:

$$\underset{a-x-y}{\mathrm{A}} + \underset{b-x}{\mathrm{B}} \xrightarrow{k_1} \underset{x-y}{\mathrm{C}} + \underset{x}{\mathrm{E}}$$

$$\underset{a-x-y}{\mathrm{A}} + \underset{x-y}{\mathrm{C}} \xrightarrow{k_2} \underset{y}{\mathrm{D}} + \underset{y}{\mathrm{F}}$$

We thus have

$$A_0 = a \text{ and } A = a-x-y$$

$$B_0 = b \text{ and } B = b-x$$

$$C = x-y$$

and then

$$x = B_o - B$$
$$y = B_o - B - C$$
$$A = A_o - 2(B_o - B) + C$$

Every pair of concentrations B and C thus gives a corresponding value of A. By use of the reaction variables we obtain

$$dx/dt = k_1(a-x-y)(b-x) \quad (8)$$

$$dy/dt = k_2(a-x-y)(x-y) \quad (9)$$

By division we get

$$dy/dx = \varkappa(x-y)/(b-x) \quad (10)$$

and on integrating

$$y = \varkappa \int_0^x \frac{x-y}{b-x}\, dx = \varkappa U \quad (11)$$

Thus we get

$$\varkappa = y/U \quad (12)$$

The integral U is easily obtained as the area between the curve $(x-y)/(b-x) = f(x)$ and the x-axis.

Eqn. (8) may be written

$$dx/(b-x) = k_1(a-x-y)dt = k_1 d\Theta \quad (8a)$$

By integration we obtain

$$\frac{1}{\Theta} \ln \frac{b}{b-x} = k_1 \quad (13)$$

where

$$\Theta = \int_0^t (a-x-y)dt \quad (14)$$

A second-order reaction can thus be converted into a first-order reaction by changing the time-variable (Wideqvist [5]). The new time-variable Θ is obtained as the area between the curve $(a-x-y) = f(t)$ and the t-axis. From the knowledge of k_1 and $\varkappa$ we may obtain k_2 from the relation $k_2 = k_1\varkappa$.

It is thus evident that a determination of the reaction variables x and y permits a very simple calculation of the rate constants.

EXAMPLE

Mc Millan gives no example of a reaction which can be treated by his method or by the method described above. However, Regna and Caldwell [6] have described a reaction which can be treated in a similar, although somewhat

simpler way. They have investigated the conversion of a 2-ketopolyhydroxy acid (B) to furfural (F). This is a consecutive first-order process, where ascorbic acid (C) is the intermediate product.

$$\underset{b-x}{\mathrm{B}} \xrightarrow{k_1} \underset{x-y=z}{\mathrm{C}} \xrightarrow{k_2} \underset{y}{\mathrm{F}}$$

The progress of the reaction was followed by determining the concentration $(x-y)$ of the intermediate product ascorbic acid. Analyses were made by titrating samples of the reaction mixture with an iodine solution of approximately 0.025 N. This gives a quantitative indication of the ascorbic acid present, since iodine oxidizes ascorbic acid to its first oxidation product, dehydroascorbic acid.

For the rate of the reactions we get the equations

$$\mathrm{d}x/\mathrm{d}t = k_1(b-x) \tag{15}$$

$$\mathrm{d}y/\mathrm{d}t = k_2(x-y) \tag{16}$$

The rate constant k_2 which evaluates the rate of decomposition of the ascorbic acid was determined directly by measurements on the free ascorbic acid and calculated from the reaction

$$k_2 t = \ln c_o/(c_o-y) \tag{17}$$

where c_o is the initial concentration of ascorbic acid in the separate experiment. Integration of the equation system (15, 16) gives the final equations

Table 1. The conversion of a 2-ketopolyhydroxy acid to furfural *via* ascorbic acid (According to Regna and Caldwell).

t_{min}	$x-y$	Q	$k_2Q = y$	$b-x$	$k_1 \times 10^3$ W	$k_1 \times 10^3$ R & C
0				42.17		
43.6	4.28	93.30	0.046	37.84	2.49	2.53
77.6	7.42	292.2	0.143	34.61	2.54	2.55
114.7	10.32	621.3	0.305	31.54	2.53	2.53
166.0	13.45	1 231	0.604	28.12	2.44	2.44
208.7	16.58	1 872	0.919	24.67	2.57	2.57
278.3	19.89	3 141	1.542	20.74	2.55	2.55
361.9	22.73	4 923	2.417	17.02	2.51	2.50
442.3	25.11	6 846	3.361	13.70	2.54	2.55
480.9	25.98	7 832	3.846	12.34	2.56	2.56
516.8	26.41	8 772	4.307	11.45	2.52	2.53
556.1	27.14	9 825	4.824	10.21	2.55	2.56
602.7	27.56	11 099	5.450	9.16	2.53	2.53
658.0	27.98	12 635	6.204	7.99	2.53	2.53
742.8	28.30	15 021	7.375	6.50	2.52	2.51
770.7	28.04	15 807	7.761	6.37	2.45	2.41
802.1	27.82	16 684	8.192	6.16	2.40	2.34
843.8	27.65	17 841	8.760	5.76	2.36	2.27

$$k_1 t = \ln\, b/(b-x) \tag{18}$$

and

$$x-y = \frac{k_1 b}{k_2-k_1}\,(e^{-k_1 t} - e^{-k_2 t}) \tag{19}$$

From eqn. (19) Regna and Caldwell calculated k_1 by a time-consuming iteration process. The knowledge of the rate constant k_2 and the intermediate concentration $(x-y)$ permits, however, a very simple calculation of k_1. From eqn. (16) we get on integration

$$y = k_2 \int_0^t (x-y)\mathrm{d}t = k_2 Q \tag{20}$$

where Q is the area between the curve $(x-y) = \mathrm{f}(t)$ and the t-axis. As k_2 is known before, we thus also know y. During the reaction the concentration $(x-y) = z$ is measured. Thus we get $x = (y + z) = (z + k_2 Q)$ and $(b-x) = (b-k_2 Q-z)$. The rate constant k_1 is then calculated from eqn. (18).

The results of the calculations are recorded in Table 1. All the concentrations are expressed in "ml of 0.025 N iodine solution". For k_2 Regna and Caldwell obtained the value 4.91×10^{-4}. In Table 1 the values of k_1 calculated in this paper are indicated with (W) and those given by Regna and Caldwell with (R & C).

REFERENCES

1. Mc Millan, W. G. *J. Am. Chem. Soc.* **79** (1957) 4838.
2. Wideqvist, S. *Arkiv Kemi* **8** (1955) 545.
3. Frost, A. A. and Schwemer, W. C. *J. Am. Chem. Soc.* **74** (1952) 1268.
4. Wideqvist, S. *Acta Chem. Scand.* **4** (1950) 1216.
5. Wideqvist, S. *Arkiv Kemi* **8** (1955) 325.
6. Regna, P. and Caldwell, B. P. *J. Am. Chem. Soc.* **66** (1944) 246.

Received December 19, 1961.

ACTA CHEMICA SCANDINAVICA 16 (1962) 1124–1126

The Mechanism of the Acid-catalyzed Hydrolysis of γ-Lactones with a Tertiary Alkyl-Oxygen Bond

RUNE SANDBERG

Department of Organic Chemistry, Chemical Institute, University of Uppsala, Sweden*

Submitted in honour of the sixtieth birthday of my teacher, Professor *Arne Fredga*

It is shown that in aqueous acid solution optically active γ-methyl-γ-caprolactone is formed from the corresponding acid with completely retained configuration. This fact verifies the hypothesis that the acid-catalyzed reversible conversion of a γ-lactone to a hydroxy acid proceeds by mechanism $A_{AC}2$ even with two alkyl groups in γ-position.

In a previous paper [1] it was reported that, in aqueous solution, acid hydrolysis of the γ-lactone ring of terpenylic acid is a bimolecular reaction proceeding through an intermediate complex containing a molecule of water in addition to a proton. This result might be considered somewhat surprising when it is remembered that in terpenylic acid the alkyl-oxygen bond of the lactone ring is tertiary. It is a well-known fact that open-chain esters derived from primary and secondary alcohols are normally hydrolyzed by the bimolecular mechanism $A_{AC}2$ (acyl-oxygen cleavage), while esters from tertiary alcohols are subjected to alkyl-oxygen cleavage without water taking part ($A_{AL}1$).

However, on the part of terpenylic acid two mechanisms had to be considered, either of which should be recognizable by the observed kinetic characteristics. One of these is the $A_{AC}2$ mechanism, which has been shown to be utilized by γ-butyrolactone [2,3], the other a bimolecular mechanism involving acid hydrolysis and esterification with alkyl-oxygen cleavage. The latter, however, has hitherto apparently not been observed. From the fact that changing the hydroxyl group from primary to secondary to tertiary causes an appreciable increase in the rates of lactonization of γ-hydroxy acids and a decrease in the rates for the reverse reaction [4–6], it was concluded that mechanism $A_{AC}2$ applies. It was pointed out that these rate changes, accompanying substitution by alkyl groups, merely could be explained as a result of an increase in the power of ring formation.

* Present address: AB Astra, Södertälje.

It may be worth noting, that Stevens and Tarbell [7] assumed that the above mentioned increase in rates of lactonization was indicative of a carbonium ion mechanism ($A_{AL}1$), when the alkyl-oxygen bond is tertiary.

It was thought that the simplest way to detect the point of bond split in the acid hydrolysis of a γ-dialkylated γ-lactone, or what is equivalent, the point of union in the reverse reaction, should be to make use of an optically active lactone, asymmetric in the γ-position. As the alkaline hydrolysis of various γ-lactones has been shown to obey a second order rate law [1,4,7], in accord with mechanism $B_{AC}2$, it was assumed that no configurational change should occur in this case:

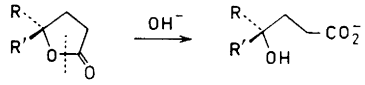

Upon adding an excess of strong acid, the lactonization rapidly goes to an equilibrium mixture of lactone and γ-hydroxy acid containing 1 or 2 % of acid (Sebelius [4] reported 1.8 % of acid in the equilibrium mixture from γ-isocaprolactone). Lactonization by mechanism $A_{AL}2$, being a special case of the bimolecular mechanism of nucleophilic substitution (S_N2), then should give a lactone with inversed configuration, while ring closure by mechanism $A_{AC}2$ should reform the original lactone. (The intermediate complex has in the latter case been assigned the status of a molecule in analogy with what has been found for esters [8]).

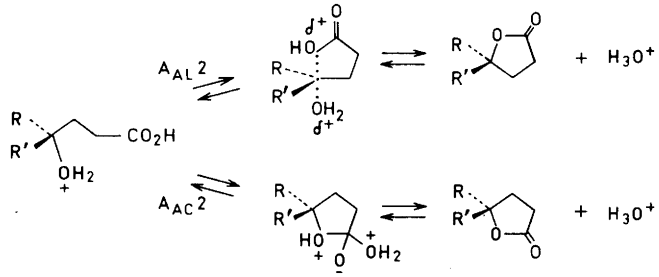

The results from the experiments using optically active γ-methyl-γ-caprolactone are consistent with what is expected for lactonization by acyl-oxygen bonding. When reformed in aqueous alcoholic solution after alkaline hydrolysis, the resulting lactone had the calculated value of rotation in the same direction as the original one.

It should be emphasized that the above discussion has been limited to alkyl substituted γ-lactones. A phenyl group, however, in the γ-position may be expected to create a different situation. In fact some observations by Grace and Symons [9] indicate that the acid hydrolysis of γ-phenyl-γ-valerolactone proceeds by alkyl-oxygen cleavage.

Acknowledgement. The author is grateful to fil.mag. Hans-Gustav Jonsson for the supply of γ-methyl-γ-caprolactone.

EXPERIMENTAL

γ-Methyl-γ-caprolactone, prepared according to Cason *et al.*[10], was purified from accompanying ethyl levulinate by alkaline hydrolysis and subsequent lactonization of the hydroxy acid. The pure lactone had b.p. 106—107°/15 mm, n_D^{25} 1.4400.

The optically active lactone has earlier been prepared from the corresponding hydroxy acid by Kenyon and Symons [11]. The acid was resolved by means of brucine and (−)-1-phenylethylamine. The present author used (+)-1-(2-naphthyl)-ethylamine and (−)-1-phenylethylthiuronium chloride with moderate success.

Preparation of optically active γ-methyl-γ-caprolactone. 25.6 g (0.20 mole) of γ-methyl-γ-caprolactone was dissolved by warming in 30 ml of 6.7 N sodium hydroxide. The solution was neutralized to phenolphthalein with dilute hydrochloric acid and added to a boiling solution of 23.8 g (0.05 mole) of the neutral sulphate of (+)-1-(2-naphthyl)-ethylamine in 200 ml of water. The resulting clear solution was cooled down with swirling in ice-water for a few minutes and then left at room temperature for some hours and finally in the refrigerator over-night. Yield 24.2 g (76 %) of air-dried salt, m.p. 129—132°. Three recrystallizations from acetone gave 10.4 g of salt, m.p. 139—141°. The salt was treated with dilute sodium hydroxide, and the liberated amine extracted with ether. The aqueous phase was acidified with dilute hydrochloric acid, and the hydroxy acid extracted repeatedly with ether. The acid was lactonized by repeated distillation with benzene. Yield 2.65 g of lactone, b.p. 99°/10 mm, n_D^{25} 1.4402, α_D^{25} + 17.99° (2 dm). Kenyon and Symons [11] reported α_D^{25} + 7.15° (0.5 dm).

To the mother liquor from the first crystallization, previously warmed to 50°, was added a hot solution of 21.7 g (0.10 mole) of (−)-1-phenylethylthiuronium chloride in 25 ml of water. The salt began to separate almost immediately. After cooling to room temperature the mixture was left over night in the refrigerator. Yield 22.8 g (70 %) of air-dried salt. Unfortunately the salt tended to decompose when recrystallized from water, and two recrystallizations from acetone plus a little methanol did not seem to improve the quality of the product. The remaining salt (10.4 g, m.p. 128—132°) was shaken between dilute hydrochloric acid and ether and the aqueous phase extracted a few times more with ether, giving 2.4 g of lactone, b.p. 98°/9 mm, n_D^{25} 1.4402, α_D^{25} −11.78° (2 dm).

Lactonization in acid solution. As the lactone is not appreciably soluble in water the experiments were carried out in aqueous alcoholic solutions.

a) *Rotations in the appropriate solvent mixtures.* 0.2275 g of (+)-lactone dissolved up to 15 ml in water containing 22 % alcohol by volume. α_D^{25} + 0.17°, $[\alpha]_D^{25}$ + 5.6°.

0.2301 g of (+)-lactone dissolved up to 15 ml in 0.2 N hydrochloric acid containing 22 % alcohol by volume. α_D^{25} + 0.18°, $[\alpha]_D^{25}$ + 5.9°. The rotation was unchanged after 48 h.

b) *Procedure for lactonization.* 0.5788 g of (+)-lactone was shaken with 5 ml of 2 N sodium hydroxide until solution was complete and then diluted to 15 ml with aqueous alcohol (50 % by volume). The rotation, α_D^{25} + 0.29°, was unchanged after 15 h. To 10 ml of this solution was added 5 ml of 2 N hydrochloric acid. The resulting solution, containing 22 % alcohol by volume had α_D^{25} + 0.29° (calculated α_D^{25} + 0.30°). By potentiometric titration the final solution was found to be 0.219 N in hydrochloric acid.

REFERENCES

1. Sandberg, R. *Arkiv Kemi* **17** (1961) 319.
2. Long, F. A. and Friedman, L. *J. Am. Chem. Soc.* **72** (1950) 3692.
3. Long, F. A., Dunkle, F. B. and McDevit, W. T. *J. Phys. Chem.* **55** (1951) 829.
4. Sebelius, H. *Dissertation*, Lund 1927.
5. Kailan, A. *Z. physik. Chem.* **94** (1920) 111.
6. Kailan, A. *Z. physik. Chem.* **101** (1922) 63.
7. Stevens, C. M. and Tarbell, D. S. *J. Org. Chem.* **19** (1954) 1996.
8. Bender, L. M. *J. Am. Chem. Soc.* **73** (1951) 1626.
9. Grace, J. and Symons, M. C. R. *J. Chem. Soc.* **1961** 47.
10. Cason, J., Brewer, P. B. and Pippen, E. L. *J. Org. Chem.* **13** (1948) 243.
11. Kenyon, J. and Symons, M. C. R. *J. Chem. Soc.* **1953** 3583.

Received December 19, 1961.

ACTA CHEMICA SCANDINAVICA 16 (1962) 1127–1135

Optically Active Bithienyls II. Synthesis and Resolution of 2,2′-Dicarboxy-4,4′-dibromo-5,5′-dimethyl-3,3′-bithienyl *

SALO GRONOWITZ and HARALD FROSTLING

Organic Department, Chemical Institute, University of Uppsala, Uppsala, Sweden

Submitted in honour of the sixtieth birthday of our teacher, Professor *Arne Fredga*

Atropisomerism has been demonstrated for the first time in the 3,3′-bithienyl series. 2,2′-Dicarboxy-4,4′-dibromo-5,5′-dimethyl-3,3′-bithienyl (V) was prepared by first coupling 5-methyl-3-thienyllithium to produce 5,5′-dimethyl-3,3′-bithienyl (III) using $CuCl_2$. Metalation of III with excess butyllithium yielded 2,2′-dicarboxy-5,5′-dimethyl-3,3′-bithienyl (IV) which upon bromination gave (V). This last compound was resolved into its antipodes by fractional crystallization of its cinchonine salt. V exhibits stable optical activity.

Largely owing to the work of Adams *et al.* (for review see Ref.[1]) many biphenyls with hindered rotation about the pivot bond either have been resolved into optical antipodes, or the axial asymmetry has been demonstrated by means of asymmetric transformations. Through these investigations it has been possible to obtain information regarding the relationship between the magnitude and character of the *ortho* substituents and rates of racemization.

During recent years the relative and absolute configurations of optically active biphenyls have attracted considerable interest. Mislow *et al.*[2–5] demonstrated the steric relationships existing between optically active biphenyls by means of chemical [2] and physico-chemical methods [3–5]. In particular the Fredga method of quasi-racemates [6] has proved very useful and convenient also when dealing with axially asymmetric compounds.

Attempts have been made to determine the absolute configuration by kinetic methods [7–11]. Thus Berson [7] has derived the absolute configuration of phenyl dehydrothebaine from a discussion of the stabilities of the possible transition states in the rearrangement which occurs when thebaine reacts with phenylmagnesium bromide. The absolute configurations of biphenyls

* A preliminary report has been given in *Tetrahedron Letters* **1961** 604.

have been determined by application of the Prelog method [12] to phenylglyoxylates of optically active hydroxybiphenyls [8,9,11], and use of the Meerwein-Ponndorf-Verley reduction of biaryl ketones in the presence of optically active alcohols [10]. Comparison of rotation dispersion curves has also been attempted in order to determine the absolute configurations of biphenyls [13].

Due to difficulties in synthesis very few investigations of restricted rotation in non-benzenoid aromatic systems have been undertaken. Adams *et al.* studied a few dipyridyls, phenylpyrroles and dipyrryls (for review see Ref.[1]). Some years ago Nord *et al.*[14,15] investigated two sterically hindered 2- and 3-phenylthiophenes which they synthesized from the appropriate halides by a crossed Ullmann synthesis. They also prepared some 3,3′-bithienyls by the Ullman reaction [16] but it is still difficult to prepare such compounds by this method.

A study of restricted rotation in the bithienyl series should give valuable information about the geometric and electronic properties of such compounds. It should also be possible to determine the configuration of optically active bithienyls relative to suitable biphenyls by the Fredga method. This has proved very useful for the correlation of central asymmetric thiophenes to the corresponding benzenes (for review see Ref.[6]). Desulphurization of such thiophenes with Raney-nickel was introduced by Fredga [17] as a convenient method for determining the configuration of phenylsubstituted optically active compounds relative to aliphatic compounds. It might therefore be possible to obtain information regarding the absolute configuration of bithienyls (and biphenyls) from the Raney-nickel disulphurization of optically active bithienyls.

The reaction of 3-thienyllithium derivatives, obtained by low-temperature halogen-metal interconversion of bromosubstituted thiophenes [18–20] with butyllithium, with cupric chloride, provides a very convenient route to 3,3′-bithienyls [21,22]. Sterically hindered 3,3′-bithienyls should then be easily available by metalation, halogen-metal interconversion, and other substitution reactions with these 3,3′-bithienyls. In this way a study of atropisomerism would be possible, and would entail even less preparative effort than that used in the biphenyl series.

As a first example we have prepared and resolved into its optical antipodes the compound 2,2′-dicarboxy-4,4′-dibromo-5,5′-dimethyl-3,3′-bithienyl (V). 4-Bromo-2-thiophenealdehyde (I) was prepared as described earlier from 4-bromo-2-thienyllithium, obtained through halogen-metal interconversion between 2,4-dibromothiophene and butyllithium at −70°, and N,N-dimethyl formamide [19]. It was found that the yield could be increased to 86 % by increasing the scale twentyfold. Wolff-Kishner reduction of I according to the general description given by King and Nord[23] yields 4-bromo-2-methylthiophene (II) in 84 % yield. Thus in contrast to α-bound bromine, β-bromine is not removed during Wolff-Kishner reduction. Attempts to prepare II in one step by the reaction of 4-bromo-2-thienyllithium with methyl *p*-toluenesulphonate or dimethyl sulphate results in a mixture of isomeric bromo-2-methylthiophenes.

Treatment of II with butyllithium and anhydrous cupric chloride gave 5,5′-dimethyl-3,3′-bithienyl (III), m.p. 135—136° in 27 % yield. This yield

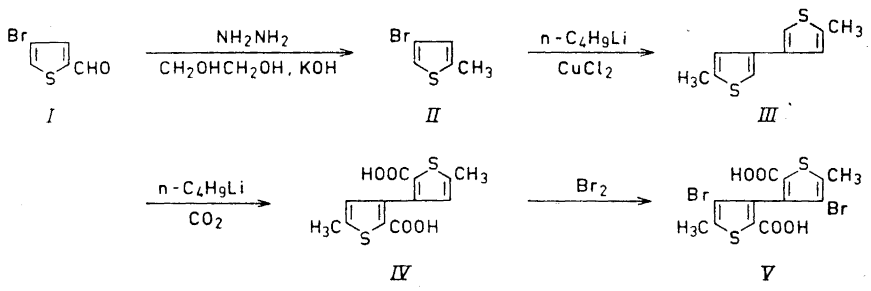

I II III IV V

could not be increased although several variations of this preparation was attempted. Normally 50—60 % yields are obtained in this reaction [21,22]. The structure of III follows from the mode of its formation and reactions (see below). Its physical properties also differ from those of 5,5′-dimethyl-2,2′-bithienyl (m.p. 67° [24]), which would be the product if during the coupling with cupric chloride, 2-methyl-4-thienyllithium rearranged to the thermodynamically more stable lithium derivative [20]. The NMR-spectrum of III confirms this structure assignment. The ring hydrogen part of the NMR-spectrum of III in dimethyl sulphoxide consists of two rather broad bands at 4.85 ppm and 4.62 ppm relative to the solvent. The broadening is caused by unresolved splittings due to mutual couplings between the ring hydrogens and also between the ring hydrogens and the methyl groups. However, the width of the bands ($\approx$ 3 c/s) excludes the presence of any larger ring-coupling constant than J_{24} (1.5 c/s) [25].

Metalation of thiophenes with n-butyllithium is known to occur very selectively at the free α-positions (for review see Ref.[18]). Accordingly the product obtained by metalation of III with excess n-butyllithium followed by carbonation with dry ice was 2,2′-dicarboxy-5,5′-dimethyl-3,3′-bithienyl (IV), m.p. 254—257° (decomp.), obtained in 45 % yield.

The structure of IV is also evident from its NMR-spectrum in dimethyl sulphoxide solution. In this instance the remaining equivalent ring hydrogens at 4.20 ppm relative to the solvent show the coupling of about 1 c/s *, characteristic of a methyl group in the 2-position and a hydrogen in the 3-position of thiophenes [25].

Treatment of IV with excess bromine gave V, m.p. 311—313° (decomp.) in 80 % yield. The occurrence of nuclear bromination as opposed to side-chain bromination was evident from its NMR-spectrum which showed no absorption in the region characteristic of thiophenic hydrogens [25].

Both IV and V melt with decomposition (carbon dioxide evolution) and are best characterized by means of IR-spectra, although relatively reproducible decomposition points can be obtained if their determination is carried out in a specified manner described in the experimental part.

The dimethyl ester of V prepared by esterification with diazomethane, melts at 154—156°.

III was chosen as an intermediate instead of the more easily obtained 3,3′-bithienyl since the metalation of the latter with excess butyllithium gives on

* Only the inner high intensity peaks of the quartet could be resolved.

carbonation a mixture of about equal amounts of 2,2′-dicarboxy-3,3′-bithienyl and 5,5′-dicarboxy-3,3′-bithienyl and these compounds are separated only with difficulty [26].

Resolution of V could be achieved by fractional crystallisation of its cinchonine salts from aqueous ethanol. All other optically active bases tested gave either oils or crystalline salts showing no resolution. Since both the cinchonine salts gave acids with the same maximum activity, it is assumed that complete resolution was obtained. This conclusion, however, is not as valid as if the same maximum activity had been obtained with different bases. The cinchonine salt of the antipode, which was dextrorotatory in acetone or alcohol, was least soluble and was apparently pure after one recrystallization. This antipode is strongly levorotatory in chloroform and in alkaline solution.

In dioxane solution this antipode shows a rotation-dispersion curve with a positive Cotton effect; the peak occurs at 334 mμ. The intense absorption permitted measurements only just beyond the peak.

The optical forms of V are very stable towards racemization. No racemization was observed when optically active V was heated in alkaline solution at 95° for 6 h.

The conjugation band at 249 mμ in the UV-spectrum of biphenyl is very sensitive to the presence of *ortho* substituents. Even a single fluorine substituent in one of the *ortho* positions of biphenyl results in a shift of this band towards shorter wave-lengths accompanied by a reduction of its intensity and in the appearance of a long wave-length band [27], regarded as originating in a benzene type transition. With very bulky *ortho* substituents the conjugation band disappears completely and the composition of the absorption spectrum is almost that provided by adding the spectra of the uncoupled parts [28]. Many attempts have been made to estimate the conformation of biphenyls from their UV-spectra (both from changes in absorption intensities and from wave-lengths displacements), since it is obvious that the amount of conjugation between the rings depends on the mean interplanar angle. However, the effect of *ortho*-substituents is difficult to estimate; more over the functional relation between interplanar angle and resonance energy is not known precisely [29]. From the UV-spectra of 2,2′-ring closed and resolvable biphenyls in which the interplanar angle is practically constant it is evident, however, that the conjugation band is insensitive to small deviations from coplanarity [30,31].

The UV-spectra of bithienyls have been studied very litte. Bantjes [32] investigated the spectra of 2,2′-bithienyl and 2,3′-bithienyl and some of their derivatives and also the spectrum of 3,3′-bithienyl. It seems probable that the high intensity bands at 301 mμ in 2,2′-bithienyl, at 284 mμ in 2,3′-bithienyl and at 260 mμ in 3,3′-bithienyl correspond to the conjugation band at 249 mμ in biphenyl. In III the peak is at 264 mμ. The absorption at the lowest wave-length for 3,3′-bithienyl is in accordance with the smaller degree of conjugation which is known to be present in 3-substituted thiophenes [18].

Carboxyl groups and other carbonyl derivatives, acting as *ortho* substituents, complicate the study of the UV-spectra, however, since not only the conjugation between the rings may be changed but also the more or less coplanar arrangement between the ring and the substituent may be affected considerably [33]. It is therefore evident that considerably more data than is at

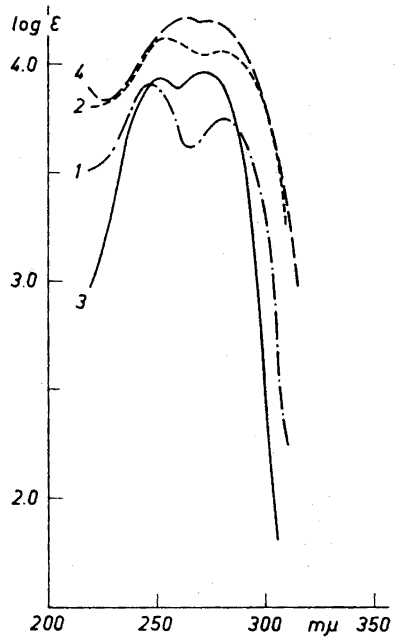

Fig. 1. UV-spectra of 4-bromo-5-methyl-2-thiophenecarboxylic acid (1), 2,2′-dicarboxy-4,4′-dibromo-5,5′-dimethyl-3,3′-bithienyl (2), 5-methyl-2-thiophenecarboxylic acid (3), 2,2′-dicarboxy-5,5′-dimethyl-3,3′-bithienyl (4).

present available is necessary for a more detailed discussion of the UV-spectra of hindered and unhindered bithienyls.

It is apparent, however, from a comparison of the UV-spectrum of V with that of 2-methyl-3-bromo-5-thiophenecarboxylic acid (VI) (Fig. 1), that conjugation between the two rings in V is minimal. There is a close correspondence between the two spectra with V exhibiting doubled extinction. The primary band [34] in V shows a weak bathochromic shift. The spectrum of IV differs still further from that of 5-methyl-2-thiophenecarboxylic acid. In this instance the primary absorption band is shifted from 251 mμ to 262 mμ and partly obscurs the secondary band at 276 mμ, which appears as an inflection.

It is evident however, that two such large groups as the carboxyl must have an appreciable influence on the conjugation band of 3,3′-bithienyl. It is therefore not permissible to regard the UV-spectrum of IV as characteristic of 3,3′-bithienyl derivatives with unhindered rotation.

EXPERIMENTAL

4-Bromo-2-thiophenealdehyde. 202 g (86 %) of 4-bromo-2-thiophenealdehyde, (b.p. 115—116°/10 mm Hg) was obtained from 1130 ml of 1.2 N butyllithium, 300 g (1.24 mole) of 2,4-dibromothiophene [35] in 400 ml of ether and 110 g (1.51 mole) of N,N-dimethyl formamide, as described in Ref.[19]

4-Bromo-2-methylthiophene. 202 g of 4-bromo-2-thiophenealdehyde, 200 ml of hydrazine hydrate (99 %) and 500 ml of ethylene glycol were placed in a 2-l three-necked flask arranged for distillation and equipped with a thermometer extending below the surface of the reaction mixture and a mechanical stirrer. The solution was heated to 130—140° and water and excess hydrazine were distilled off. After 30 min a small amount of water-

insoluble material separated from the distillate and was returned to the reaction flask. The solution was cooled to 40°, 200 g of potassium hydroxide was added and an efficient condenser was fitted to the flask. The flask was carefully heated with stirring, and at about 90° a vigorous reaction with evolution of nitrogen occurred. After the reaction had subsided the mixture was refluxed for an additional 15 min. The 4-bromo-2-methyl thiophene thus formed was steam distilled from the reaction mixture. The distillate was extracted with ether, and the ether extracts were washed with 6 N hydrochloric acid and water, dried and distilled. The yield of 4-bromo-2-methylthiophene was 167 g (88 %) b.p. 61—62°/11 mm Hg, n_D^{20} = 1.5725. (Found: C 34.13; H 2.93. Calc. for C_5H_5BrS (177.1): C 33.91; H 2.84).

5,5'-Dimethyl-3,3'-bithienyl. 160 g (0.91 mole) of 4-bromo-2-methylthiophene in 150 ml of anhydrous ether were added during 5 min under vigorous stirring to 1300 ml of 0.9 N butyllithium, cooled to −70° in the conventional nitrogen-swept four-necked flask. After 5 min 134 g (1 mole) of anhydrous $CuCl_2$ was added and the mixture was stirred for 3 h at −70°. After standing at room temperature for an additional 3h, 750 ml of 5 N hydrochloric acid was added with cooling and stirring. The ether phase was carefully extracted with 5 N hydrochloric acid in order to remove the cuprous chloride formed in the above reaction. After washing the ether phase with water, sodium carbonate solution and water again, followed by drying, ether and butyl bromide were removed *in vacuo*. The crystalline residue was twice recrystallised from ligroin, yielding 19 g (27 %) of 5,5'-dimethyl-3,3'-bithienyl, in the form of colourless flakes, m.p. 135—136°. (Found: C 62.01; H 5.23; S 32.90 Calc. for $C_{10}H_{10}S_2$ (194.3): C 61.81; H 5.19; S 33.00.)

2,2'-Dicarboxy-5,5'-dimethyl-3,3'-bithienyl (IV). 500 ml of 0.9 N butyllithium was added dropwise with stirring to a solution of 18.5 g (0.095 mole) of 5,5'-dimethyl-3,3'-bithienyl in 300 ml of dry ether in the conventional four-necked nitrogen-swept flask. The mixture was refluxed for 2 h and poured onto solid carbon dioxide in ether. After the temperature had risen to −10°, the mixture was hydrolysed with water. The ether phase was extracted with sodium carbonate solution and the combined aqueous phases were acidified with 2 N hydrochloric acid. The crude acid was filtered off, air-dried and then extracted twice with 30 ml of ether to remove some mono acid. The residue was recrystallized from acetic acid yielding 12 g (45 %) of 2,2'-dicarboxy-5,5'-dimethyl-3,3'-bithienyl as colourless crystals, m.p. 254—257° (decomp.). (Found: Equiv. wt 140; C 50.92; H 3.74. Calc. for $C_{12}H_{10}O_4S_2$ (282.3): Equiv. wt 141; C 51.05; H 3.57).

2,2'-Dicarboxy-4,4'-dibromo-5,5'-dimethyl-3,3'-bithienyl (V). An excess of bromine was poured onto 7.0 g (0.025 mole) of 2,2'-dicarboxy-5,5'-dimethyl-3,3'-bithienyl. The bromine was evaporated over night and the residue heated with 200 ml of sodium carbonate solution, filtered and acidified with 2 N hydrochloric acid. The crude acid was filtered off, dried and washed with ether. Recrystallisation from acetic acid yielded 8.5 g (78 %) of 2,2'-dicarboxy-4,4'-dibromo-5,5'-dimethyl-3,3'-bithienyl in the form of white crystals, m.p. 311—313° (decomp.). (Found: C 32.64; H 1.94; Br 36.53. Calc. for $C_{12}H_8Br_2O_4S_2$ (440.2): C 32.74; H 1.83; Br 36.32).

2,2'-Dicarbomethoxy-4,4'-dibromo-5,5'-dimethyl-3,3'-bithienyl was prepared by methylation of the acid with diazomethane. M.p. 154—156° after recrystallisation from ethanol. (Found: C 36.21; H 2.62; Br 33.76. Calc. for $C_{14}H_{12}Br_2O_4S_2$ (468.3) C 35.91; H 2.58; Br 34.15.

5-Methyl-2-thiophenecarboxylic acid [36] was prepared by metalation of 2-methylthiophene with butyllithium followed by carbonation. M.p. 139—140°.

4-Bromo-5-methyl-2-thiophenecarboxylic acid was prepared by bromination of 5-methyl-2-thiophenecarboxylic acid in acetic acid solution. M.p. 197—199° after recrystallisation from aqueous ethanol. (Literature values [37] 197—198°).

Resolution of 2,2'-dicarboxy-4,4'-dibromo-5,5'-dimethyl-3,3'-bithienyl

Preliminary tests on resolution. 0.001 mole of optically inactive acid and 0.002 mole of optically active base were dissolved together in various solvents, *e.g.* water, aqueous ethanol, ethanol, ethyl acetate and acetone. Oils were obtained with cinchonidine, strychnine and quinidine. Phenyl isopropyl amine, α-phenyl ethylamine, brucine and quinine gave crystalline salts of inactive acid. Only cinchonine gave resolution.

Table 1.

Crystallisation	1	2	3
ml 50 % ethanol	1000	300	75
g, salt	6	2	0.6
$[\alpha]_D^{25}$ of acid	+ 42	+ 43	+ 43

7.0 g (0.017 mole) of 2,2′-dicarboxy-4,4′-dibromo-5,5′-dimethyl-3,3′-bithienyl and 10.2 g (0.035 mole) of cinchonine were dissolved in 1 l of hot aqueous ethanol (50 %) and allowed to stand over-night. The precipitate was filtered off and dried. About 0.3 g of the salt was set apart, the acid isolated and the optical activity measured in acetone. The remaining salt was recrystallised from 50 % ethanol. It appears from Table 1 that complete resolution had already been obtained after one crystallisation. The mother-liquors from the second and third crystallisations were therefore evaporated to dryness *in vacuo* and the salt used for the preparation of the (+)-acid *.

Since no base was found which gave a more insoluble salt with the (−)-form, the mother liquor from the first crystallisation of the cinchonine salt was concentrated step-wise *in vacuo*. The salt which separated was filtered off and the activity of the acid measured. The course of resolution is seen in Table 2.

Table 2.

Evaporation	1	2	3	4	5	6
Remaining mother-liquor	500	250	125	75	30	0
g, salt	6	3	1	0.6	0.4	0.11
$[\alpha]_D^{25}$	−10°	−35°	−39°	−41°	−43°	−43°

(+)-2,2′-Dicarboxy-4,4′-dibromo-5,5′-dimethyl-3,3′-bithienyl was obtained almost quantitatively by treating the cinchonine salt with 2 N hydrochloric acid and extracting with ether. The ether was evaporated and the residue recrystallised from acetic acid, yielding white crystals, m.p. 302−305° (decomp.) which had the same IR-spectrum as that of the active acids. R.D. in dioxane (*c* 0.725), temp. 26°: $[M]_{589}$ + 240°, $[M]_{400}$ + 690°, $[M]_{350}$ + 1000°, $[M]_{334}$ + 1300°, $[M]_{327}$ + 810°.

The rotations in some other solvents are given in Table 3.

(−)-2,2′-Dicarboxy-4,4′-dibromo-5,5′-dimethyl-3,3′-bithienyl was obtained by treating the last two fractions of the more soluble cinchonine salt in the same way as described for the (+)-form. M.p. 301−304° (decomp.) ($[\alpha]_D^{25}$ = −43°, *c*, 0.260, acetone).

Melting points of compounds which melted with decomposition were determined by placing the capillary tubes in the m.p. apparatus at a temperature of 10° below the melting point and heating with a rate of about 3°/min.

Racemization experiment. 0.0321 g of the (+)-acid was diluted to 5.00 ml with 0.100 N sodium hydroxide (α_D^{25} = −1.22). After heating in a closed vessel to 95° for 6 h the same rotation was obtained.

Table 3.

Solvent	conc.g acid/dl	α_D^{25}	$[\alpha]_D^{25}$	$[M]_D^{25}$
Acetone	0.836	+ 0.36°	+ 43°	+ 190°
Dimethyl sulphoxide	0.190	+ 0.10°	+ 53°	+ 230°
Ethanol	0.420	+ 0.23°	+ 55°	+ 240°
Chloroform	0.660	−0.38°	− 57.5°	−250°
0.1 N sodium hydroxide	0.642	−1.22°	−190°	−840°

* The antipode which is dextrorotatory in acetone will be designated the (+)-acid.

Table 4. UV-data for some bithienyls and thiophenes.

Compound	Primary band λ_{max} mμ	ε	Secondary band λ_{max} mμ	ε
5-Methyl-2-thiophenecarboxylic acid	252	9 600	273	9 000
4-Bromo-5-methyl-2-thiophenecarboxylic acid	246	8 100	280	5 600
2,2′-Dicarboxy-5,5′-dimethyl-3,3′-bithienyl	262	17 200	(276)	15 500
2,2′-Dicarboxy-4,4′-dibromo-5,5′-dimethyl-3,3′-bithienyl	253	13 400	274	11 200

The UV-spectra were recorded on a Beckman quartz spectrophotometer using ethanol as the solvent. The data are given in Table 4.

The rotation dispersion curve was recorded on a Rudolph selfrecording spectropolarimeter. The *NMR-spectra* were obtained with a Varian Associates model V-4300-B high resolution spectrometer operating at 40 Mc/s in the same way as described earlier [24].

Acknowledgements. The authors wish to express their thanks to the head of this Institute, Prof. Arne Fredga, for his interest in this work and for all facilities put at their disposal. Thanks are due to Dr. R. A. Hoffman for recording the NMR-spectra and to Mr. R. Bäckström for recording the rotation dispersion curve. The elementary analyses were carried out by Dr. A. Bernhardt, Mülheim (Ruhr). A grant from *Hierta-Retzius Foundation* to S.G. is gratefully acknowledged.

REFERENCES

1. Adams, R. and Yuan, H. C. *Chem. Revs.* **12** (1933) 261.
2. Mc Ginn, F. A., Lazarus, A. K., Siegel, M., Ricci, J. E. and Mislow, K. *J. Am. Chem. Soc.* **80** (1958) 476.
3. Fitts, D., Siegel, M. and Mislow, K. *J. Am. Chem. Soc.* **80** (1958) 480.
4. Siegel, M. and Mislow, K. *J. Am. Chem. Soc.* **80** (1958) 473.
5. Mislow, K., Glass, M. A. W., O'Brien, R. E., Rutkin, P., Steinberg, D. H. and Djerassi, C. *J. Am. Chem. Soc.* **82** (1960) 4740.
6. Fredga, A. *Tetrahedron* **8** (1960) 126.
7. Berson, J. A. *J. Am. Chem. Soc.* **78** (1956) 4170.
8. Berson, J. A. and Greenbaum, M. A. *J. Am. Chem. Soc.* **80** (1958) 445.
9. Berson, J. A. and Greenbaum, M. A. *J. Am. Chem. Soc.* **80** (1958) 653.
10. Newman, P., Rutkin, P. and Mislow, K. *J. Am. Chem. Soc.* **80** (1958) 465.
11. Mislow, K., Prelog, V. and Scherrer, H. *Helv. Chim. Acta* **41** (1958) 1410.
12. Prelog, V. *Bull. soc. chim. France* **1956** 987.
13. Mislow, K. and Djerassi, C. *J. Am. Chem. Soc.* **82** (1960) 5247.
14. Owen, L. J. and Nord, F. F. *J. Org. Chem.* **16** (1951) 1864.
15. Jean, G. N. *J. Org. Chem.* **21** (1956) 419.
16. Jean, G. N. and Nord, F. F. *J. Org. Chem.* **20** (1955) 1363.
17. Fredga, A. *Arkiv Kemi* **6** (1953) 277.
18. Gronowitz, S. *Arkiv Kemi* **13** (1958) 295.
19. Gronowitz, S., Moses, P., Hörnfeldt, A.-B. and Håkansson, R. *Arkiv Kemi* **17** (1961) 165.
20. Moses, P. and Gronowitz, S. *Arkiv Kemi* **18** (1961) 119.
21. Gronowitz, S. and Karlsson, H. O. *Arkiv Kemi* **17** (1960) 89.
22. Gronowitz, S. *Acta Chem. Scand.* **15** (1961) 1393.
23. King, V. J. and Nord, F. F. *J. Org. Chem.* **14** (1949) 638.
24. Lescot, jr., E., Buu-Hoi, Ng. Ph. and Xuong, N. D. *J. Chem. Soc.* **1959** 3234.
25. Hoffman, R. A. and Gronowitz, S. *Arkiv Kemi* **16** (1960) 563.
26. Gronowitz, S. and Karlsson, H. O. *Unpublished results.*
27. Beaven, G.H. and Hall, D.M. *J. Chem. Soc.* **1956** 4637.
28. Pickett, L. W., Walter, G. F. and France, H. *J. Am. Chem. Soc.* **58** (1936) 2296.

29. Braude, E. A. and Waight, E. S. in Klyne, W. *Progress in Stereochemistry*, Vol. 1. London 1954, p. 139 ff.
30. Hall, D. M. and Minhaj, F. *J. Chem. Soc.* **1957** 4584.
31. Iffland, D. C. and Siegel, H. *J. Am. Chem. Soc.* **80** (1958) 1947.
32. Bantjes, A. *Thesis*, Leiden 1959.
33. Jean, G. N. and Nord, F. F. *J. Org. Chem.* **20** (1955) 1370.
34. Gronowitz, S. *Arkiv Kemi* **13** (1958) 239.
35. Lawesson, S.-O. *Arkiv Kemi* **11** (1957) 317.
36. Gronowitz, S. and Gestblom, B. *Arkiv Kemi* **18** (1962) 513.
37. Steinkopf, W. *Ann.* **513** (1934) 281.

Received December 19, 1961.

ACTA CHEMICA SCANDINAVICA 16 (1962) 1136–1138

A Small-scale Synthesis of Ferrocene

ANDERS EKEMARK and KURT SKAGIUS

Research Division, AB Pharmacia, Uppsala, Sweden

Submitted in honour of the sixtieth birthday of our teacher, Professor *Arne Fredga*

A small-scale synthesis of ferrocene is described and applied to the preparation of ^{55}Fe- and ^{59}Fe-labelled ferrocene.

In connection with studies on the resorption of iron-containing remedies, it was of interest to analyze blood samples for their content of ^{55}Fe and ^{59}Fe. The purpose of the investigation was to determine the concentration of ^{59}Fe by its γ-radiation, and the ratio of the ^{55}Fe and ^{59}Fe concentrations by liquid scintillation counting based on their radiations. Since the liquid scintillation measurements were performed in toluene solution, it was desirable to convert the iron isotopes into toluene-soluble derivatives. For this purpose, ferrocene seemed to be suitable.

The synthesis of ferrocene from dry ferric chloride, iron powder and cyclopentadiene is described in Organic Syntheses [1]. The method requires anhydrous conditions [2], since the presence of water decreases the yield appreciably *, and, therefore, the first problem we had to solve was to convert the iron of the blood into anhydrous ferric chloride. The destructed blood samples were electrolyzed, using platinum electrodes [3]. The cathode was prepared from coiled platinum wire, which could be heated electrically; allowing the deposited iron to be burned in chlorine. The ferric chloride obtained was dissolved in dry tetrahydrofuran, and used immediately in the synthesis. The ferric chloride solution could not be stored for long periods, since the solute afforded polymerization of the solvent [4].

Usually the reduction of the ferric chloride to ferrous chloride is achieved by means of *ferrum reductum*. In the present case, however, the use of this reducing agent leads to an undesired dilution of the radioactivity. This difficulty was avoided by replacing the iron powder by zinc dust.

* Since the determination was based on the ratio between the ^{55}Fe and ^{59}Fe content of blood, the yield might not necessarily be quantitative; but it was desirable that it should be high.

The method described is quite useful for small-scale synthesis of ferrocene, but, unfortunately, it was impossible to determine the activity by liquid scintillation counting, since the ferrocene involved quenching of the radiation.

EXPERIMENTAL

Preparation of dry ferric chloride *: 30 mg of Fe, obtained as hydroxide from the destructed blood samples, were dissolved in a 5 % solution of oxalic acid, and the pH was adjusted to 4.5 with concentrated ammonia [3]. The volume was then 50 ml. The platinum anode was applied as a stirrer. The cathode was made of a 0.2 mm platinum wire about 90 cm in length which was wound around a U-shaped glass tube. The solution was electrolyzed at 4.5 V and 0.4 A for 2.5 h. During the process it was necessary to correct the pH to 4.5 by adding a few drops of 5 M H_2SO_4. When the electrolysis was completed, the cathode was washed carefully with water and ethanol.

A three-necked flask (Fig. 1) was fitted with a gas inlet tube, a gas outlet

* The destruction of the blood samples was performed by Mr. H. Jenner [3], who also made important contributions to the electrolytical procedure.

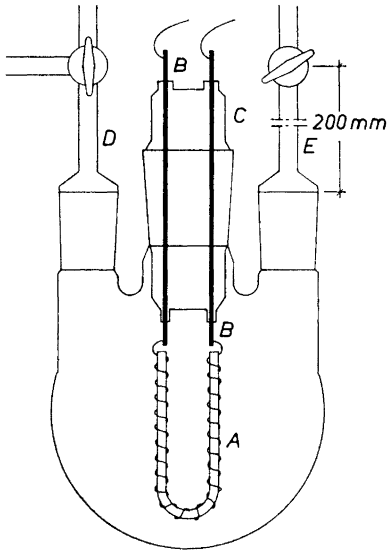

Fig. 1. A. The cathode. B. Pt-wires (Ø 2 mm). C. Glass-stopper. D. Gas inlet tube. E. Gas outlet tube.

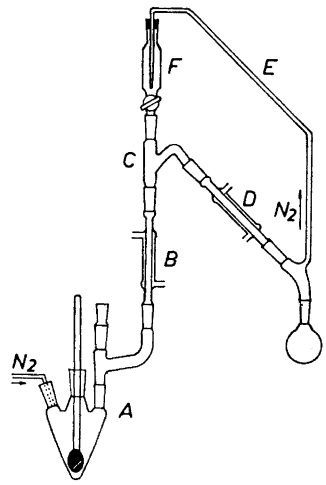

Fig. 2. A. A three-necked flask (25 ml) with a gas inlet tube (Ø 1 mm) of stainless steel for oxygen-free N_2 and a stirrer. B. Reflux condenser. C. Stillhead. D. Distillation condenser. E. A glass tube (Ø 4 mm) through which N_2 is conveyed from the receiver adapter up into the dropping funnel. F. Dropping funnel (10 ml). The upper conical joint is fitted with cotton-wool.

tube, and a glass-stopper through which two platinum wires were drawn. These functioned as holders and contacts for the cathode, thus allowing it to be heated electrically. When the cathode had been put in place, it was dried in a stream of dry nitrogen.

The nitrogen was replaced by chlorine, and the cathode was heated (15 V, 3—4 min), until the iron was burned to iron chloride, which was partly deposited on the walls of the flask. After cooling, the excess of the chlorine was removed by a slow stream of nitrogen, and the ferric salt was dissolved in 7 ml of dry tetrahydrofuran.

Preparation of ferrocene: 28 mg of zinc dust (90 % "active" zinc) was placed in a three-necked flask (Fig. 2) fitted with a gas inlet tube, a mechanical stirrer and a reflux condenser, connected to a distillation condenser via a stillhead. A stream of oxygen-free nitrogen was passed through the apparatus for 20 h.

The freshly prepared chloride solution was placed in a dropping funnel on the stillhead (Fig. 2), and a nitrogen stream was conveyed through the solution for a few minutes. Then the solution was poured out into the reaction vessel through the reflux condenser, and subsequently, the funnel was rinsed with 2 ml of tetrahydrofuran. The mixture was refluxed for 45 min and the bulk of the solvent was removed by distillation; the latter operation required about half an hour.

Meanwhile, 1.4 ml of freshly prepared cyclopentadiene [5] was dissolved in 1.4 ml of diethylamine. The solution was placed in the dropping funnel and a stream of nitrogen was passed through the solution for a few minutes.

When the distillation was finished, the residue was cooled in an ice bath, and the cyclopentadiene solution was added while stirring vigorously. The dark mixture was stirred at room temperature overnight, and the excess of the amine was removed under reduced pressure. The residue was steam-distilled and the distillate extracted with petroleum ether. The solvent was removed and the ferrocene purified by sublimation *in vacuo*. Yield 71 mg (70 %, calculated on the iron content of the original ferric salt solution), melting at 171—174°C.

Acknowledgements. The authors are deeply grateful to Messrs. Adolf Berggren, Hans Jenner and Wolfgang Kirsten for valuable advice and discussions, and to Dr. Karl Johan Öbrink for making the radiation measurements.

REFERENCES

1. *Org. Syntheses* **36** (1956) 31, p. 34.
2. Little, W. F., Koestler, R. C. and Eisenthal, R. *J. Org. Chem.* **25** (1960) 1435.
3. Jenner, H. and Öbrink, K. J. *Scand. J. clin. Lab. Invest. In press.*
4. Meerwein, H., Delfs, D. and Morschel, H. *Angew. Chem.* **72** (1960) 927.
5. *Enjay Co., Technical Bulletin*, No. 12, p. 9.

Received December 19, 1961.

ACTA CHEMICA SCANDINAVICA 16 (1962) 1139–1142

The Synthesis of Tetraiodophthalic-^{131}I Acid Morpholide

KURT SKAGIUS and ANDERS EKEMARK

Research Division, AB Pharmacia, Uppsala, Sweden

Submitted in honour of the sixtieth birthday of our teacher, Professor *Arne Fredga*

In connection with studies of tetraiodophthalic acid amides as potential X-ray diagnostic agents, the title substance was prepared.

During the last decades the evolution of iodine-containing contrast media has proceeded from compounds with one iodine atom at a benzene ring to compounds, containing three atoms. Since the absorption efficiency of a substance is depending upon its iodine content it seemed logical to investigate substances with even more iodine. However, this increase in iodine content must not destroy the possibilities of obtaining high concentrations of the substance in the tissue to be investigated.

The reaction of the easily accessible tetraiodophthalic anhydride with secondary amines gave a series of tetraiodophthalic acid amides. Many of these were difficult to purify by recrystallization and, in addition, they were easily hydrolyzed especially under acid conditions.

In our preliminary pharmacological tests it was rapidly found, that tetraiodophthalic acid morpholide had a comparatively low acute toxicity and, when given intravenously, gave a very high iodine content of the bile flow [1]. Unfortunately, the substance gave indications of renal damage [2] and could not be introduced as a contrast medium. The high iodine concentration in the bile justified, however, a further study of the elimination of the substance through

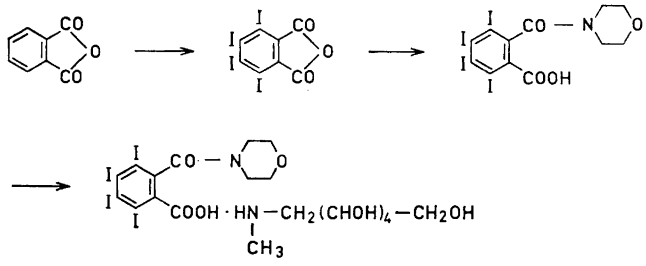

the liver. For this purpose tetraiodophthalic-^{131}I acid morpholide was synthesized.

The synthesis was performed according to the scheme given above.

The iodination of phthalic anhydride is described in Organic Syntheses [3]. After a slight modification this method proved suitable for our purpose. The iodinated anhydride was then converted into the morpholinium salt of the morpholide in a solution of dimethyl sulfoxide in toluene. During the reaction the salt was formed as an oil, which solidified and deposited on the walls of the reaction vessel. The mother liquor could then be removed easily. The acid was isolated and converted to a water solution of its N-methylglucamine salt.

The radioactivity, required for the biological investigation, was fairly high. Therefore it was necessary to perform the synthesis with special care. The iodination of phthalic anhydride was carried out in the equipment, shown in Fig. 1. The whole apparatus was built up on the back of a 12 mm thick plexiglas plate. Parts of the apparatus are fixed in movable holders. Thus, the reaction vessel C can be moved to a position F, allowing the transfer of the reaction mixture to the filter funnel E. Similarly, the dropping funnels K can be brought above the funnel E, facilitating the washing of the filtered crystals.

The remaining steps in the synthesis were performed in the equipment, shown in Fig. 2. This apparatus, too, was built up on the back of a 12 mm plexiglas plate. The equipped plate can be turned around the point of attachment (A) to the stand, thus enabling fluids to be decanted through the joint G.

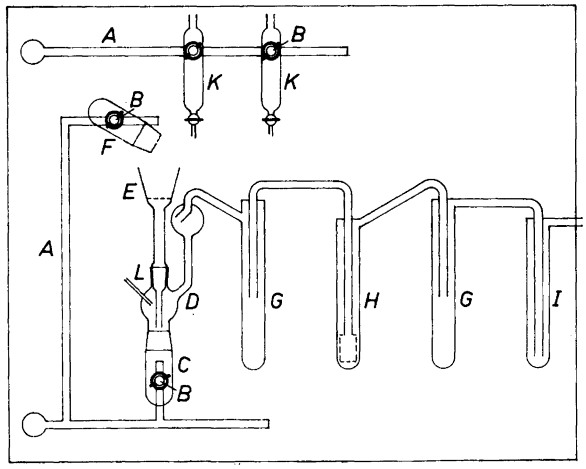

Fig. 1. A. Open cuttings in the plexiglas plate. B. Holders movable in the open cuttings. C. Reaction vessel ($Ø_{inter.}$ 25 mm, length 80 mm). D. Top of the reaction vessel with an air leak tube, an adapter with a splash head and a joint (L). E. Filter funnel. F. Reaction vessel in the upper position. G. Freezing traps. H. Washing bottle with concentrated H_2SO_4. I. Absorption tube with granulated PVC. K. Dropping funnels. L. Joint.

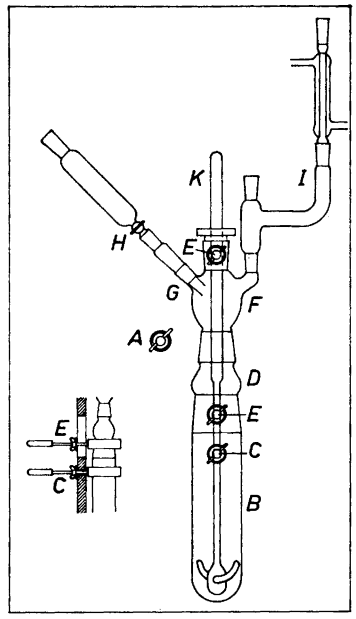

Fig. 2. A. Point of attachment with screw and wing-nut. B. Reaction vessel. C. Holder for reaction vessel. D. Reduction adapter. E. Holder for adapter. F. Three-necked top of reaction vessel. G. Joint. H. Dropping funnel. I. Adapter with reflux condenser.

During operation of the equipment a 5 cm thick lead shelter, fitted with a 14 cm thick lead glass window, was placed in front of the operator.

With the method described, a series of water solutions of the N-methylglucamine salt of tetraiodophthalic-^{131}I acid morpholide was prepared. In a typical experiment 35 ml of a 30 % water solution with a specific activity of 0.1 mC/ml were obtained.

EXPERIMENTAL

Tetraiodophthalic-^{131}I anhydride. 7 mC of iodine-131 (The Radiochemical Centre, Amersham, England) were put in the reaction vessel (C in Fig. 1) in the following way: The sealing of the ampoule was broken, and the ampoule was then inserted into the joint L through a teflon gasket. Most of the iodine fell down into the reaction vessel, which was chilled with dry ice. The upper end of the ampoule was warmed and the iodine on the walls sublimed downwards. The ampoule was then broken about 4 cm from the upper end and 6 ml of oleum (60 % SO_3) were added through the neck of the ampoule. The ice bath was removed and the ampoule replaced by a glass tube of 40 cm length. Through this tube were added 3.0 g (20 mmoles) of phthalic anhydride, 10.2 g (40 mmoles) of iodine and 4 ml of oleum. The tube was replaced by a glass stopper and a very slow stream of air was led through the apparatus by gentle suction. By means of an oil bath the temperature of the reaction vessel was raised to 65°C during an hour and then held there for a further hour. Then the temperature was raised to 170°C within 75 min, and the heating was continued for 30 min. The sublimed iodine was gathered in a gas trap, consisting of two freezing traps, a wash bottle, containing concentrated sulfuric acid, and a tube, filled with granulated polyvinyl chloride.

The heating was stopped and when the temperature was decreased to 125°C the oil bath was removed. When the reaction mixture was cool, the reaction vessel was replaced by an empty one and brought into position F. A filter funnel was fitted into the joint L and the air leak tube was replaced by a stopper. The labelled anhydride was filtered off by suction and washed repeatedly with concentrated sulfuric acid. The vessel, containing the filtrate, was exchanged and stoppered. The anhydride was then washed successively with water, a water solution of sodium pyrosulfite, water and acetone. The yellow needles were air-dried in the funnel over night.

Tetraiodophthalic-^{131}I acid morpholide. The anhydride was placed in the reaction vessel (Fig. 2), 150 ml of dry toluene and 6 ml of freshly distilled dimethyl sulfoxide were added and the mixture was refluxed in an oil bath at 115—120°C. Most of the anhydride dissolved. A solution of 3.0 ml (34 mmoles) of morpholine in 5 ml of toluene was added dropwise. The remaining anhydride rapidly dissolved and at the end of the addition the mixture became turbid. Stirring was continued, and, after about 10 min, the oil bath was removed. The oily salt deposited on the walls of the reaction vessel, and, when room temperature was reached, the mother liquor was removed by decantation. The salt was washed twice with 50 ml of petroleum ether.

140 ml of 95 % ethanol were added and the salt dissolved by heating under reflux on a water bath. The solution was slightly cooled, and 2.2 ml of 8 M methanolic hydrogen chloride were added while stirring vigorously. In a few minutes tetraiodophthalic acid morpholide began to crystallize.

After an hour the acid was filtered off, washed with 300 ml of cold water and air-dried. Yield 10.3 g (69 %). (Found: Equiv. wt. 742. Calc. for $C_{12}H_9I_4NO_4$: 739. An inactive tetraiodophthalic acid morpholide had the following data: Equiv. wt. 744; C 19.8; H 1.3; I 68.7; N 1.9. Calc. for $C_{12}H_9I_4NO_4$: C 19.5; H 1.2; I 68.7; N 1.9.)

N-Methylglucamine salt of tetraiodophthalic-^{131}I acid morpholide. 10.3 g (14 mmoles) of the acid and 2.7 g (14 mmoles) of N-methylglucamine were dissolved in 26 ml of distilled water in a 75 ml reaction vessel of the type, shown in Fig. 2. The solution, which contained 500 mg salt per ml, had a specific activity of 0.15 mC/ml.

REFERENCES

1. Novek, J. *Acta Radiol.* **55** (1961) 359.
2. Edlund, Y. and Zettergren, L. *Acta Radiol.* **55** (1961) 413.
3. *Org. Syntheses*, Coll. Vol. 3 (1955) 796.

Received December 19, 1961.

ACTA CHEMICA SCANDINAVICA 16 (1962) 1143–1146

Structures of the Anhydrides of 3- and 5-Hydroxylaevulic Acid

CHRISTOFFER RAPPE

Chemical Institute, University of Uppsala, Sweden

Submitted in honour of the sixtieth birthday of my teacher, Professor *Arne Fredga*

The anhydrides of 3- and 5-hydroxylaevulic acid are studied, and new structures (VI and VII) are proposed.

Studying 2- and 3-hydroxylaevulic acid Wolff [1] found that these compounds lost water when heated to give crystalline products with high melting points. Wolff suggested that the products were the lactides of the two acids and he proposed the structures I and II for these compounds.

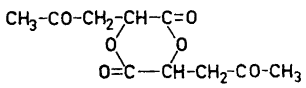

I

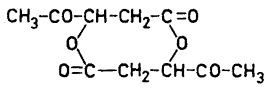

II

However, in a recent paper [2] the present author has pointed out, that Wolff's 2-hydroxylaevulic acid was in fact the 5-isomer. The structure I must therefore be incorrect.

The ethyl ester of the real 2-hydroxylaevulic acid was prepared by Rossi and Lauchenauer [3] and by Wynn and Corwin [4]. These authors found that this ester very easily dehydrated intramolecularily to give β-acetylacrylic acid (III).

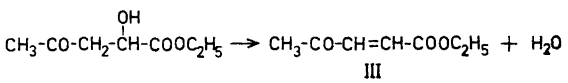

III

Since 5-hydroxylaevulic acid is both a γ-keto and a δ-hydroxy acid and 3-hydroxylaevulic acid is a γ-keto-β-hydroxy acid it would be interesting to study how these acids dehydrate.

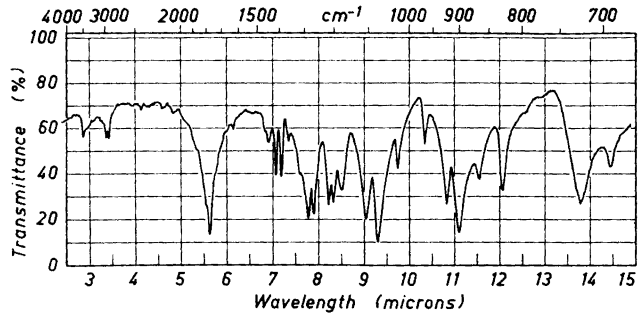

Fig. 1. Infrared spectrum of anhydride of 5-hydroxylaevulic acid (VI). Solid in KBr.

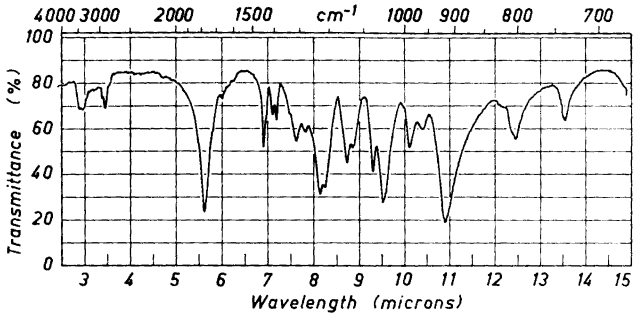

Fig. 2. Infrared spectrum of anhydride of 3-hydroxylaevulic acid (VII). Solid in KBr.

Wolff [1] made no determination of the molecular weights of the anhydrides. but proposed that they were dimers on the grounds of their high melting points. In the present work the molecular weights were determined by the Rast method, and the values 230 (5-anhydride) and 212 (3-anhydride) were obtained showing that the anhydrides are dimers.

The infrared spectra of the anhydrides, Figs. 1 and 2, gave further information about their structures. No peaks were found in the region 5.79—5.88 μ (1725—1700 cm^{-1}) where carbonyl and carboxyl groups are known to have strong vibration absorption bands, *cf.* Bellamy [5,6]. On the other hand, both spectra have strong peaks near the region 5.61—5.68 μ (1780—1760 cm^{-1}) where saturated γ-lactones absorb [7].

Some γ-keto acids, for instance γ-oxopimelic acid and 3-acetylglutaric acid, form bicyclic anhydrides containing two γ-lactone rings IV [8] and V [9].

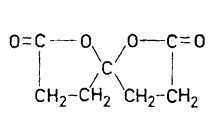

IV

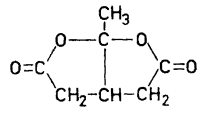

V

The infrared spectra of these also have peaks in the same region as the anhydrides of the two hydroxylaevulic acids, see Table 1. These data indicate that the studied anhydrides also possess γ-lactone rings and the structure VI for the 5-hydroxylaevulic acid anhydride and the structure VII for the 3-isomer anhydride seem probable.

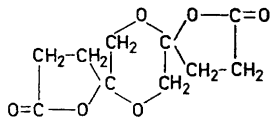

VI

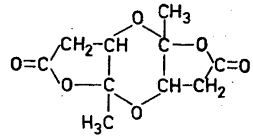

VII

Although these structures seem rather complex, they can be more easily understood if it is supposed that, as in the dehydration of laevulic acid to α-angelica lactone [10], intermediates in their formation are the lactols (VIII and IX) of the corresponding acids, and these dehydrate giving the dimer anhydrides VI and VII.

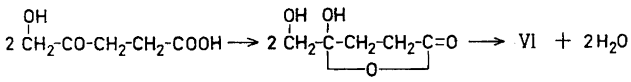

VIII

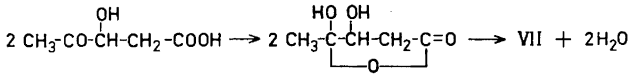

IX

Other 1,2-diols, for instance 1,2-propanediol and 1,2-butanediol can also dehydrate in a similar way to 2,5- (and not 2,6-) derivatives of *p*-dioxane [11,12].

The spectra of the anhydrides VI and VII also contain a series of bands in the region 8.90—9.71 μ (1124—1030 cm^{-1}) where dioxane derivatives absorb [13]. However bands in this region are not specific for dioxane derivatives and therefore this information is of minor importance.

Table 1.

Substance	Band in the region 5.5 — 6.0 μ	
5-Hydroxylaevulic acid	5.81,	5.90
Anhydride of 5-hydroxylaevulic acid (VI)		5.61
Anhydride of 3-hydroxylaevulic acid (VII)		5.59
γ-Oxopimelic acid	5.82,	5.90
Anhydride of γ-oxopimelic acid (IV)		5.58
Anhydride of 3-acetylglutaric acid (V)		5.56

EXPERIMENTAL

The micro analyses were carried out by the Analytical Laboratory of the Chemical Institute, University of Uppsala. The melting point measurements were performed by means of the Kofler microscopic method and the infrared spectra were obtained with a Perkin Elmer Model 137 spectrophotometer provided with a sodium chloride prism.

Anhydride of 5-hydroxylaevulic acid (VI). This compound was prepared according to Wolff [1]. M.p. 265–268°C. The infrared spectrum is given in Fig. 1. (Found: C 52.69; H 5.32; M.W. 230. Calc. for $C_{10}H_{12}O_6$(228.1): C 52.61; H 5.30; M.W. 228).

Anhydride of 3-hydroxylaevulic acid (VII). This compound was prepared according to Wolff [1]. M.p. 238–240°C. The infrared spectrum is given in Fig. 2. (Found: C 52.41; H 5.39; M.W. 212. Calc. for $C_{10}H_{12}O_6$(228.1): C 52.61; H 5.30; M.W. 228).

Acknowledgements. The author is indebted to Professor Arne Fredga for valuable discussions and for all the facilities put at his disposal. The micro analyses were done by Dr. A. Bengtsson.

REFERENCES

1. Wolff, L. *Ann.* **264** (1891) 229.
2. Rappe, C. *Arkiv Kemi* **14** (1959) 467.
3. Rossi, A. and Lauchenauer, A. *Helv. Chim. Acta* **30** (1947) 1501.
4. Wynn, R. and Corwin, A. *J. Org. Chem.* **15** (1950) 203.
5. Bellamy, L. J. *The Infrared Spectra of Complex Molecules*, London 1958, p. 132.
6. *Ref. 5*, p. 162.
7. *Ref. 5*, p. 179.
8. Volhard, J. *Ann.* **253** (1889) 206.
9. Fittig, R. and Roth, E. *Ann.* **314** (1901) 16.
10. Helberger, J. H., Ulubay, S. and Civelekoglu, H. *Ann.* **561** (1949) 215.
11. Noshay, A. and Price, C. *J. Org. Chem.* **23** (1958) 647.
12. Reppe, W. *Ann.* **596** (1955) 67.
13. *Ref. 5*, p. 119.

Received December 8, 1961.

ACTA CHEMICA SCANDINAVICA 16 (1962) 1147–1158

Optical Rotatory Dispersion Studies

LXXIII *. Anomalous Rotatory Dispersion Curves Associated with Acylthioureas. Application to Stereochemical Studies of α-Substituted Carboxylic Acids

CARL DJERASSI, KJELL UNDHEIM** and ANNE-MARIE WEIDLER***

Department of Chemistry, Stanford University, Stanford, California, U.S.A.

Submitted in honour of the sixtieth birthday of Professor *Arne Fredga*

Optically active carboxylic acids show only plain rotatory dispersion curves through the presently accessible spectral range. In an attempt to obtain Cotton effect curves, a number of "chromophoric" derivatives of carboxylic acids have been investigated. Acylthioureas, readily prepared by successive treatment of a carboxylic acid with thionyl chloride, potassium thiocyanate and a secondary amine, proved to be the most desirable derivatives because of their low intensity ultraviolet absorption maximum near 340 mμ, which gave rise to anomalous rotatory dispersion curves. In general, the sign of the Cotton effect can be related to the absolute configuration (*R* or *S*) of the α-substituted carboxylic acid, but caution has to be exercised because of possible complications associated with free-rotational isomerism.

With very few exceptions, the application of anomalous rotatory dispersion measurements to organic chemical problems dates only to our first publications [1] in 1955 dealing with Cotton effect curves of some steroid ketones. In the intervening six years, over three hundred articles have appeared in which such anomalous rotatory dispersion data have been used for the solution of some organic or biochemical problem and there is no doubt that this method has become part of the organic chemist's armamentarium, notably in the field of

* Paper LXXII, Djerassi, C., Records, R., Bunnenberg, E., Mislow, K. and Moscowitz, A. *J. Am. Chem. Soc.* **84** (1962) 870.

** Postdoctorate research fellow 1959—1960; present address, AB Astra, Södertälje, Sweden.

*** Research fellow, 1960—1961 while on leave from the Institute of Chemistry, University of Uppsala, Sweden.

stereochemistry. [2-4] Most of these applications have utilized the carbonyl chromophore, because of its low-intensity absorption maximum near 300 mμ, but in recent years a considerable effort has been expended in our laboratory on converting other functional groups, which are transparent in the 700—250 mμ region, into readily prepared derivatives with spectral properties giving rise to easily measured Cotton effects. This development of "chromophoric" derivatives for rotatory dispersion work has been quite successful [5] and in the present paper we should like to describe our results with carboxylic acids. [6]

Extensive rotatory dispersion measurements by Sjöberg [7] on a variety of optically active carboxylic acids have shown that these substances exhibit only plain dispersion curves. While these curves did prove to be of utility for stereochemical correlations — and certainly are to be preferred over monochromatic rotation measurements at the sodium D line — it was clearly of importance to examine Cotton effect curves of suitable derivatives. Using optically active α-methylbutyric or hydratropic acids as models, a variety of derivatives was examined and we eventually settled on acylthioureas of the type $RCONHC(=S)NR'_2$ for the following reasons: (*a*) as shown in the experimental section, they are easy to prepare; (*b*) they are usually crystalline derivatives (see Table 6), which are readily purified because of their solubility in alkali and their stability to alumina upon chromatography; (*c*) in addition to a high intensity ultraviolet absorption maximum near 280 mμ (log $\varepsilon \sim 4.2$), they exhibit a weaker maximum at 335—345 mμ (log $\varepsilon \sim 2.4$). It was this last feature, which seemed particularly attractive to us, since this relatively weak absorption band — if proven to be optically active — should lead to measurable Cotton effects.

Experimentally, the optically active acid was transformed into its acid chloride with thionyl chloride and treated immediately in acetone solution with potassium thiocyanate. The resulting acylisothiocyanate was not isolated but was converted directly into the corresponding N,N-disubstituted N'-acylthiourea by reaction with a secondary amine. Using (+)-hydratropic acid as the substrate, the corresponding (+)-hydratropyl morpholino (I), piperidino

Table 1. Rotatory dispersion properties of (+)-(S)-hydratropylthiocarbamides. R. D. Cotton effect (methanol)

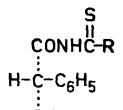

Derivative (R)	First extremum	Second extremum	Last reading	Sign and molecular amplitude
I R = N⟨O⟩	$[\alpha]_{374}$ −961°	$[\alpha]_{325}$ +2 370°	$[\alpha]_{315}$ +1 780°	− 9 160°
II R = N⟨ ⟩	$[\alpha]_{365}$ −944°	$[\alpha]_{320}$ +2 490°	$[\alpha]_{310}$ +1 940°	− 9 480°
III R = N⟨ ⟩	$[\alpha]_{360}$ −982°	$[\alpha]_{312}$ +2 250°	$[\alpha]_{305}$ +1 540°	− 8 475°
IV R = $N(C_2H_5)_2$	$[\alpha]_{370}$ −815°	$[\alpha]_{320}$ +3 140°	$[\alpha]_{310}$ +2 510°	−10 450°

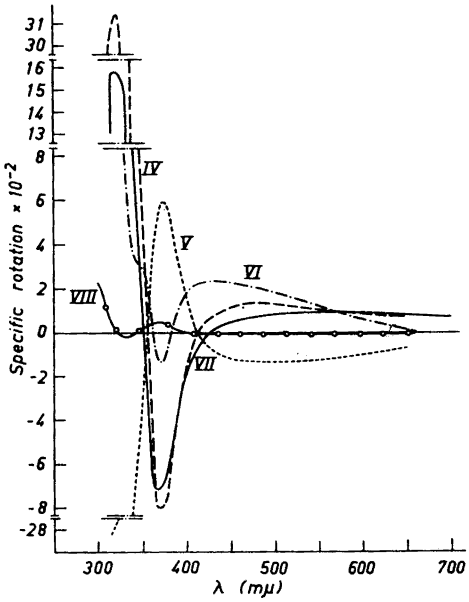

Fig. 1. Optical rotatory dispersion curves (methanol solution) of acylthioureas IV—VIII.

(II), pyrrolidino (III) and diethylamino (IV) thiocarbamides were prepared. As shown in Fig. 1, the (+)-hydratropyl diethylaminothiocarbamide (IV) exhibited a negative Cotton effect of substantial amplitude centered in the 340 mμ region, thus showing that this low-intensity absorption band is indeed optically active. The nature of the amine is not important, since all four hydratropyl derivatives (I—IV) gave negative Cotton effects of approximately identical amplitude (see Table 1). From a synthetic standpoint, the morpholino (I) and diethylamino (IV) derivatives proved to be the most desirable and these were the ones selected for the remaining acids. Before discussing these results, some general comments bearing on the possible relationship of Cotton effect curves and stereochemistry of such acylthioureas seem pertinent.

The sign and magnitude of the Cotton effect (see Fig. 1) of these acylthioureas is associated with the interaction between the partially unshielded nuclei of the various substituents and the electrons involved in the 340 mμ transition of the C=S chromophore. The analogous situation with *cyclic* ketones led to generalizations [2, 4, 8–11] which permit the prediction of the sign and amplitude of Cotton effects of ketones, largely because the spatial relationship between the chromophore and all other substituents is fixed and known. This is obviously not the case with acylthioureas of type A, where theoretically there exists free rotation around all single bonds and where the characteristic feature of the Cotton effect is then made up of the individual contributions of the various free-rotational isomers. Ultimately, this problem can probably be attacked by machine computations [12] but even at the present qualitative stage, some rough generalizations can be made since a considerable number of rotomers will probably be present to only a negligible extent.

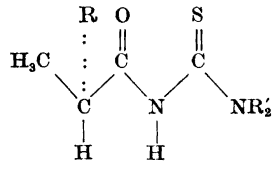

A

As shown in Table 1, variations in the N-dialkyl substituent over the steric range encompassed by I—IV do not affect appreciably the rotomer composition since the Cotton effects of these four hydratropyl derivatives (A, R = C_6H_5) were all negative and of similar amplitude. Free rotation around the two bonds of the central nitrogen will probably also be of little significance, because one and the same rotomer (or rotomer mixture) will be found in virtually all acylthioureas under examination. The most likely arrangement is probably the all-*trans* geometry shown in A, unless the parallel dipoles of theC=O and C=S chromophore favor an alternate arrangement. Since this electrostatic factor is identical in all of the compounds under discussion, it should still lead to roughly the same rotomer composition around the two single bonds of the central nitrogen. This brings us to free rotation around the four bonds connected to the asymmetric carbon atom and it is here that steric factors will play the crucial role. Consequently, differences in the steric requirements of the substituents attached to that carbon atom may lead to variable rotomer mixtures, which may very well result in inversions of the sign of the Cotton effect in spite of the fact that they may possess the same absolute configuration. It is for this reason that any attempted correlation between sign of Cotton effect and absolute configuration be based not on the D and L Fischer convention, but rather on the Cahn-Ingold-Prelog [13] (*R*) and (*S*) system, which usually takes into account the relative bulk of the substituents around the asymmetric center. Even this system may fall down when a hetero-atom is involved, since it will receive priority [13] over a much bulkier carbon-linked substituent. An additional complication may arise when a substituent attached to the carbon atom may undergo hydrogen bonding with either the carbonyl oxygen or the hydrogen atom attached to the central nitrogen in (A), whereupon a new rotomer may become dominant. Taking these factors into consideration, we shall now cover the experimental material at our disposal.

The first group of optically active acids is related to the hydratropic acid derivatives (I—IV, Table 1) in that the asymmetric center has attached to it a small alkyl group (methyl or ethyl), hydrogen and an aromatic system. As shown in Fig. 1 as well as Tables 1 and 2, all of these acylthioureas IV—VIII exhibit a Cotton effect of sign opposite to that of the conventional D line rotation. In each instance, *a negative Cotton effect corresponds to the (S) and a positive Cotton effect to the (R) configuration.* [13]

The second group (IX—XIV) differs from the first in that a hetero-atom (oxygen or sulfur) or a methylene group (IX) is inserted between the aromatic moiety and the asymmetric carbon atom. As can be seen from Fig. 2 and Table 2, the above generalization still holds in that all members with the (*S*)

Table 2. Rotatory dispersion properties of primary acyl morpholino and diethylamino carbamides.

Substance (R = NHC(=S)NEt$_2$) (X = NHC(=S)N⟨O⟩)		Absolute configuration	R. D. Cotton effect (methanol)				
			Sign	First extremum	Second extermum	Last reading	Lit. Reference to acid
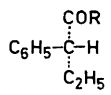	(V)[a]	(*R*)	+	$[\alpha]_{372}$ + 594°	–	$[\alpha]_{320}$ −2800°	(−)[14]
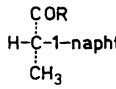	(VI)	(*S*)	−	$[\alpha]_{370}$ −136°	–	$[\alpha]_{330}$ + 757°	(+)[15]
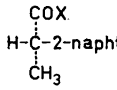	(VII)	(*S*)	−	$[\alpha]_{367.5}$ −715°	$[\alpha]_{320}$ + 1580°	$[\alpha]_{312.5}$ +1060°	(+)[16]
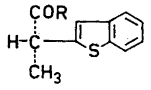	(VIII)	(*R*)	+	$[\alpha]_{370}$ + 44°	$[\alpha]_{330}$ −20°	$[\alpha]_{300}$ + 224°	(+)[17]
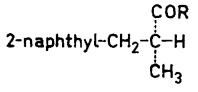	(IX)[b]	(*R*)	+	$[\alpha]_{370}$ + 907°	$[\alpha]_{313}$ −2790°	$[\alpha]_{305}$ −2560°	(−)[18,19]
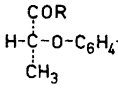	(X)	(*R*)	+	$[\alpha]_{360}$ + 720°	$[\alpha]_{310}$ −195°	$[\alpha]_{300}$ + 870°	(+)[19]
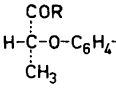	(XI)	(*R*)	+	$[\alpha]_{365}$ + 582°	$[\alpha]_{315}$ −146.5°	$[\alpha]_{310}$ −69°	(+)[20]
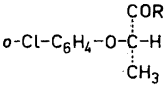	(XII)	(*S*)	−	$[\alpha]_{350}$ −602°	–	$[\alpha]_{320}$ −294°	(−)[21]
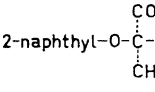	(XIII)	(*S*)	−	$[\alpha]_{365}$ −1420°	$[\alpha]_{330}$ −557°	$[\alpha]_{310}$ −365°	(−)[22]
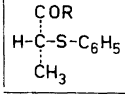	(XIV)	(*R*)	+	$[\alpha]_{350}$ + 113°	$[\alpha]_{335}$ + 57°	$[\alpha]_{310}$ + 191°	(+)[19]

[a] 80 % optical purity.
[b] 88 % optical purity.

configuration exhibit a negative Cotton effect, while the reverse holds true for the (*R*) enantiomers. It is interesting to note from Fig. 2 that in three instances the sign of the Cotton effect coincides with that of the sodium D line rotation,

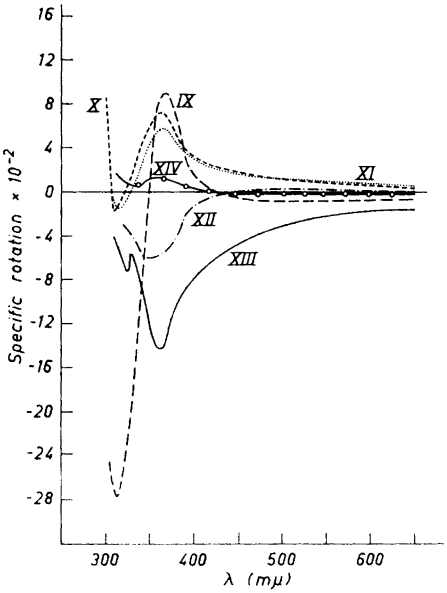

Fig. 2. Optical rotatory dispersion curves (methanol solution) of acylthioureas IX—XIV.

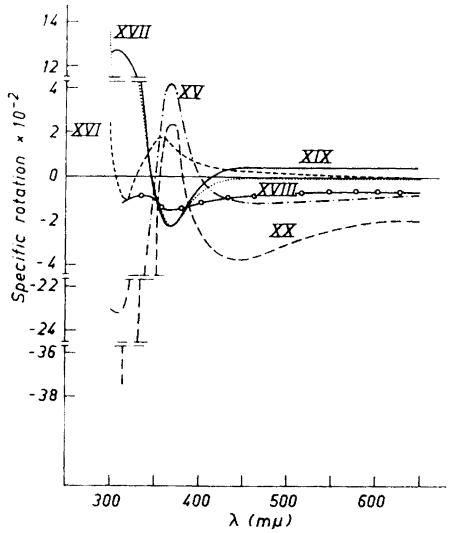

Fig. 3. Optical rotatory dispersion curves (methanol solution) of acylthioureas XV—XX.

while this is not the case in the others (IX, XII, XIV). This illustrates again the great advantage of considering the sign of Cotton effects rather than that of a single wavelength rotation, especially the sodium D line.

The next group of acids (XV—XX in Table 3) differs from the first two in one very important respect, namely that it includes a secondary carboxyl group attached directly to a ring. With one exception (XVIII), the members with the (*S*)-configuration of the carboxyl-bearing asymmetric center exhibit a negative Cotton effect, while a positive Cotton effect is associated with the (*R*)-configuration. The single anomaly XVIII is in our opinion due to a particular rotomer, which is favored in this highly strained, bicyclic system. It is likely that in such a rotomer, some of the more distant ring carbons may be brought in sufficient proximity to the C=S chromophore so as to exert an important rotational contribution. These more distant carbon atoms are, of course, not considered in the (*S*) and (*R*) notation, which is concerned only with the substituents directly connected to the asymmetric carbon atom.

Only three optically active acids were available (XXI—XXIII in Table 4) in which the carboxyl function is tertiary and it is not possible to state, therefore, whether the above emphasized correlation of sign of Cotton effect with (*R*) or (*S*) configuration will hold in such acids. The derivatives of the pair of diterpene acids, O-acetylpodocarpic acid (XXI) and dehydroabietic acid (XXII) do follow the generalization; whether this is fortuitous cannot be determined at this stage, but in any event this result should be useful for absolute configurational assignments among related diterpenes. The cyclopropane

Table 3. Rotatory dispersion properties of secondary (ring attached) acyl diethylamino carbamides.

Substance (R=NHC(=S)NEt$_2$)	Absolute configuration	R. D. Cotton effect (methanol)				
		Sign	First extremum	Second extremum	Last reading	Lit. Reference to acid
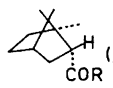 (XV)	(*R*)	+	$[\alpha]_{368}$ + 420°	$[\alpha]_{315}$ −2325°	$[\alpha]_{300}$ −2295°	(−)-endo[23]
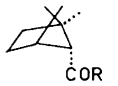 (XVI)	(*R*)	+	$[\alpha]_{358}$ + 181°	$[\alpha]_{320}$ −105°	$[\alpha]_{300}$ + 232°	(+)-endo[24]
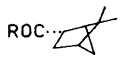 (XVII)	(*S*)	−	$[\alpha]_{370}$ −227°	−	$[\alpha]_{300}$ + 1375°	(+)-2α [25]
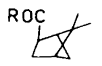 (XVIII)	(*R*)	−	$[\alpha]_{375}$ −155°	$[\alpha]_{340}$ −89°	$[\alpha]_{315}$ −126°	(−)-2β [25]
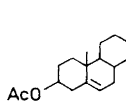 (XIX)	(*S*)	−	$[\alpha]_{374}$ −222°	$[\alpha]_{313}$ + 1263°	$[\alpha]_{310}$ + 1250°	[26]
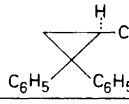 (XX)	(*R*)	+	$[\alpha]_{371}$ + 262°	−	$[\alpha]_{315}$ −3720°	(−)[27]

carboxylic acid derivative XXIII evidently possesses the same absolute configuration as the lower homolog XX as determined [27] by quasi-racemate and rotatory dispersion studies. Consequently, the negative Cotton effect (Fig. 4) of this (*R*)-acid derivative XXIII suggests the presence of a different rotomer composition in XXIII as compared to XX, which is not unreasonable as the presence of the tertiary methyl group may also affect the preferred spatial orientation of the phenyl groups.

The last group of acylthioureas collected in Table 5 (XXIV—XXX) contains several examples, which illustrate the borderline area where such rotatory dispersion results may be used only with caution for stereochemical work. Most of them should be considered as *sui generis* for the time being until additional closely related examples become available. First, there arises the question as to the limiting distance [32] (between the thiourea chromophore and the asymmetric center) which still gives rise to a Cotton effect. A comparison between the α-methylbutyric (XXIV) and β-methylvaleric (XXV) acid derivatives or between the 3β-acetoxy-Δ^5 -bisnor- (XXVIII) and nor (XXIX) -cholenyl thioureas suggests that insertion of a single methylene function is already sufficient to practically obliterate the Cotton effect, only a slight irregularity being noticeable (see Fig. 5) in the β-substituted derivatives. That this does not necessarily follow, however, is illustrated in the 3β-acetoxy-Δ^5-cholenyl

Table 4. Rotatory dispersion properties of tertiary acyl dialkylamino carbamides.

Substance (R = NHC(=S)NEt$_2$) (X = NHC(=S)N⬡O)	Absolute configuration	R. D. Cotton effect (methanol)				
		Sign	First extremum	Second extremum	Last reading	Lit. Reference to acid
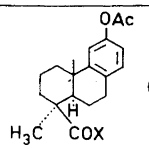 (XXI)	(*S*)	−	$[\alpha]_{378}$ + 87°	−	$[\alpha]_{315}$ + 681°	28
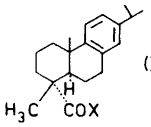 (XXII)	(*R*)	+	$[\alpha]_{367.5}$ + 168°	−	$[\alpha]_{315}$ − 509°	29
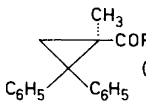 (XXIII)	(*R*)	−	$[\alpha]_{369}$ −439°	−	$[\alpha]_{302}$ + 1610°	(+)[27]

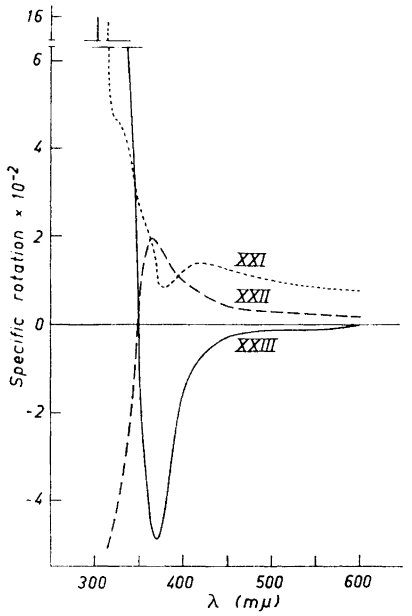

Fig. 4. Opticalrotatory dispersion curves (methanol solution) of acylthioureas XXI −XXIII.

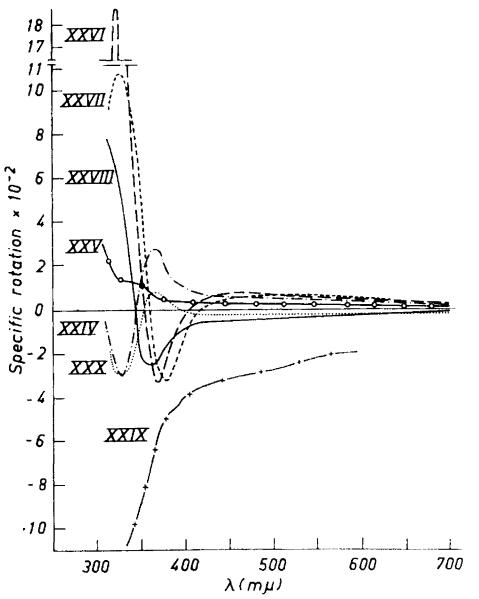

Fig. 5. Optical rotatory dispersion curves of acylthioureas XXIV−XXVII, XXIX and XXX (methanol solution) and XXVIII(dioxane solution).

Table 5. Rotatory dispersion properties of some miscellaneous acylthioureas.

Substance (R = NHC(=S)NEt$_2$) (X = NHC(=S)N⟨⟩O)	Absolute configuration	R. D. Cotton effect (methanol)				
		Sign	First extremum	Second extremum	Last reading	Lit. Reference to acid
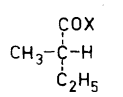 (XXIV)	(*S*)	+	$[\alpha]_{370}$ + 266°	$[\alpha]_{330}$ −311°	$[\alpha]_{310}$ −67°	(+)[30]
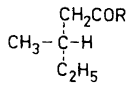 (XXV)	(*S*)	See Fig. 5		—	$[\alpha]_{310}$ + 328°	(+)[31]
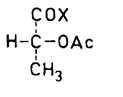 (XXVI)	(*R*)	−	$[\alpha]_{370}$ −340°	$[\alpha]_{322.5}$ +1875°	$[\alpha]_{317}$ + 1700°	(−)[30]
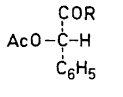 (XXVII)	(*S*)	−	$[\alpha]_{379}$ −337°	$[\alpha]_{329}$ + 1080°	$[\alpha]_{315}$ + 933°	(+)[30]
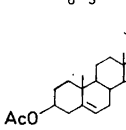 (XXVIII)	(*S*)	−[a]	$[\alpha]_{362}$ −263°	—	$[\alpha]_{312.5}$ + 789°	26
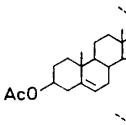 (XXIX)	(*R*)	See Fig. 5		—	$[\alpha]_{335}$ −108°	26
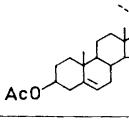 (XXX)	(*R*)	+	$[\alpha]_{365}$ + 74°	$[\alpha]_{320}$ −289°	$[\alpha]_{315}$ −193°	26

[a] In dioxane solution.

thiourea (XXX), where the asymmetric center is located in the γ-position and where a Cotton effect is again observed (Fig. 5). It is very likely, therefore, that in XXX there exist rotomers in which the C=S chromophore is in substantial proximity to some of the asymmetric centers of rings C and/or D, thus resulting in a Cotton effect. Further work with optically active acids is indicated in which the distance of the asymmetric center from the thiourea functionality is varied, before generalizations can be made on the relation of distance with disappearance of Cotton effect.

Of the four acylthioureas in this group (XXIV, XXVI—XXVIII) with an asymmetric center in the α-position, two do not obey the earlier noticed relationship between sign of Cotton effect and the (*R*) or (*S*) configuration. These two exceptions are the derivatives of (+)-α-methylbutyric acid (XXIV) and

of (−)-O-acetyllactic acid (XXVI) and it is interesting to note that when one of the alkyl substituents in these two acids XXIV and XXVI is replaced by phenyl (XXIV *vs.* IV or V; XXVI *vs.* XXVII) then the standard behavior is regained. Two tentative explanations can be offered for this anomaly: (*a*) the rotomer compositions in the two aliphatic examples (XXIV and XXVI) are quite different from those in their aromatic counterparts; (*b*) the rotatory contribution of an aromatic substituent is so much stronger [33] than that of a methyl or ethyl group, that even a relatively small proportion of a given rotomer, in which the C=S chromophore is in close proximity to the aromatic moiety, governs the sign of the Cotton effect. Obviously many more examples of diversely substituted acylthioureas would have to be examined before a firm conclusion could be reached on this point.

Even at this early stage, it is obvious that the examination of "chromophoric" derivatives is quite profitable and may lead to a number of useful applications. In the narrowest sense, derivatives of the type described in the present paper may be used for stereochemical correlations among closely related series (*e.g.* α-arylpropionic or butyric acids), while ultimately subtle conformational points relating to rotomer equilibria may be settled by such an approach. Before this stage is reached, it is necessary to prepare such derivatives of a wide variety of acids (or other substrates [5]), the absolute configuration of which has been determined by some other means. It seems quite appropriate that our initial results be published in a journal issue dedicated to Prof. Arne Fredga, in whose laboratory so many of the presently used acids have been resolved [15–22] and where their absolute configurations have been determined by the quasi-racemate method, which has been pioneered so effectively in the Uppsala laboratories. [34]

EXPERIMENTAL

With one exception (XXVIII), all rotatory dispersion curves were measured in methanol solution (*c*, 0.1−0.04) with a Rudolph automatically recording spectropolarimeter. We are indebted to Mrs. Ruth Records for assistance with these measurements and to Messrs. E. Meier and J. Consul for the microanalyses.

Preparation of acylthioureas. As all thirty derivatives listed in Table 6 were prepared by essentially the same procedure, details are given for only one example (IV):

A mixture of 200 mg of (+)-hydratropic acid (m.p. 31−32°, $[\alpha]_D$ + 80.7° (EtOH) resolved through the strychnine salt [35]) and 1.5 ml of thionyl chloride was heated at 80° for 2 h, the excess reagent was removed under reduced pressure, dry benzene was added and the evaporation process repeated. The resulting acid chloride was dissolved in 4 ml of dry acetone and added slowly to an ice-cold solution of 250 mg of finely powdered potassium thiocyanate (dried at 100°/0.1 mm) in 7 ml of acetone, the entire operation being conducted in a carefully dried apparatus with complete exclusion of moisture. After stirring for 30 min at room temperature, the flask was cooled in ice and a solution of 0.5 ml of diethylamine in 4 ml of acetone added slowly. The mixture was left overnight in the refrigerator, the potassium chloride was filtered and the acetone evaporated. The residual oil was extracted in the cold with 0.4 M sodium hydroxide solution, which left undissolved the diethylamide of hydratropic acid, formed as a by-product. The alkaline extracts were acidified, extracted with ether, washed with water, dried and evaporated. The crystalline residue (240 mg) was chromatographed on 30 g of Merck neutral alumina (activity II) and hydratropyl diethylaminothiocarbamide (IV) was eluted with benzene-ether (4:6); yield 203 mg, m.p. 125−127°. Recrystallization from benzene-hexane provided the analytical specimen with m.p. 130−131°, $\lambda_{max}^{CHCl_3}$ 2.99, 5.88, 6.56, 6.85−7.1 μ, λ_{max}^{MeOH}

Table 6. Physical and analytical properties of acylthioureas.

Substance	m.p. (Kofler)	Empirical formula	Calc.		Found	
			C	H	C	H
I	134–135°	$C_{14}H_{18}N_2O_2S$	60.40	6.52	60.23	6.45
II	102–103°	$C_{15}H_{20}N_2OS$	65.22	7.30	65.10	7.31
III	144–145°	$C_{14}H_{18}N_2OS$	64.06	6.91	64.12	6.96
IV	130–131°	$C_{14}H_{20}N_2OS$	63.58	7.62	63.63	7.65
V	131–132°	$C_{15}H_{22}N_2OS$	64.75	7.97	64.69	8.10
VI	111–112°	$C_{18}H_{22}N_2OS$	68.77	7.05	68.75	6.96
VII	141–142°	$C_{18}H_{20}N_2O_2S$	65.83	6.14	65.64	6.19
VIII	118–119°	$C_{16}H_{20}N_2OS_2$	59.97	6.29	59.84	6.46
IX	88– 90°	$C_{19}H_{24}N_2OS$	69.45	7.36	69.55	7.12
X	116–117°	$C_{15}H_{22}N_2O_2S$	61.22	7.53	61.29	7.58
XI	150–151°	$C_{14}H_{19}ClN_2O_2S$	53.41	6.08	53.69	5.95
XII	95– 96°	$C_{14}H_{19}ClN_2O_2S$	53.41	6.08	53.53	5.82
XIII	119–120°	$C_{18}H_{22}N_2O_2S$	65.45	6.71	65.49	6.56
XIV	66– 68°	$C_{14}H_{20}N_2OS_2$	56.71	6.80	56.96	6.91
XV	123–124°	$C_{16}H_{28}N_2OS$	64.82	9.52	64.93	9.43
XVI	101–102°	$C_{15}H_{26}N_2OS$	63.83	9.29	63.83	9.14
XVII	oil	$C_{14}H_{24}N_2OS$	62.63	9.01	63.01	9.19
XVIII	92– 93°	$C_{14}H_{24}N_2OS$	62.63	9.01	63.18	9.10
XIX	128–130°	$C_{37}H_{42}N_2O_3S$	68.32	8.92	68.28	8.81
XX	131–132°	$C_{21}H_{24}N_2OS$	71.55	6.86	71.30	6.89
XXI	176–177°	$C_{24}H_{32}N_2O_4S$	64.83	7.25	64.79	7.17
XXII	102–104°	$C_{25}H_{36}N_2O_2S$	70.05	8.47	70.38	8.39
XXIII	162–164°	$C_{22}H_{26}N_2OS$	72.08	7.15	72.13	7.11
XXIV	126–127°	$C_{10}H_{18}N_2O_2S$	52.15	7.88	52.44	7.87
XXV	73– 74°	$C_{11}H_{22}N_2OS$	57.34	9.63	57.25	9.49
XXVI	129–130°	$C_{10}H_{16}N_2O_4S$	46.14	6.19	45.98	5.76
XXVII	131–132°	$C_{15}H_{20}N_2O_3S$	58.43	6.41	58.76	6.41
XXVIII	218–219°	$C_{29}H_{44}N_2O_4S$	67.40	8.58	67.69	8.13
XXIX	175–176°	$C_{30}H_{48}N_2O_3S$	69.74	9.36	69.97	9.04
XXX	109–110°	$C_{31}H_{48}N_2O_4S$	68.50	8.89	68.71	9.01

279 and 340 mμ, log ε 4.13 and 2.49. The infrared band at 5.88 μ and the two ultraviolet absorption maxima served as the best spectroscopic criteria for the various thioureas; their homogeneity was also always checked by thin-layer chromatography on silica gel using benzene-ethyl acetate (5:1) or benzene-ether (4:1) as solvent.

Acknowledgement. We are indebted to the various investigators listed in the bibliography and especially to Prof. A. Fredga and Dr. B. Sjöberg for many of the optically active acids used as starting material. We also acknowledge with pleasure a stimulating discussion with Prof J. Meinwald (Cornell University) as well as the financial support provided by grant No. CRTY-5061 from the *National Cancer Institute* of the *National Institutes of Health, U. S. Public Health Service.*

REFERENCES

1. Djerassi, C., Foltz, E. W. and Lippman, A. E. *J. Am. Chem. Soc.* **77** (1955) 4354; Foltz, E. W., Lippman, A. E. and Djerassi, C. *Ibid.* **77** (1955) 4359; Lippman, A. E., Foltz, E. W. and Djerassi, C. *Ibid.* **77** (1955) 4364.
2. Djerassi, C. *Optical Rotatory Dispersion: Applications to Organic Chemistry*, McGraw-Hill Book Co. New York 1960.
3. Djerassi, C. *Pure Appl. Chem* **2** (1961) 475.

4. Klyne, W. in *Advances in Organic Chemistry* (eds. Raphael, R. A., Taylor, E. C. and Wynberg, H.), Interscience Publishers, New York 1960, pp. 239–348.
5. For leading references see Sjöberg, B., Cram, D. J., Wolf, L. and Djerassi, C. *Acta Chem. Scand.* **16** (1962) 1079.
6. For preliminary communication describing some of these results see Djerassi, C. and Undheim, K. *J. Am. Chem. Soc.* **82** (1960) 5755.
7. Sjöberg, B. *Arkiv Kemi* **15** (1960) 451,481; *Acta Chem. Scand.* **14** (1960) 273.
8. Djerassi, C. and Klyne, W. *J. Am. Chem. Soc.* **79** (1957) 1506.
9. Moffit, W., Woodward, R. B., Moscowitz, A., Klyne, W. and Djerassi, C. *J. Am. Chem. Soc.* **83** (1961) 4013.
10. Mislow, K., Glass, M. A. W., Moscowitz, A. and Djerassi, C. *J. Am. Chem. Soc.* **83** (1961) 2771.
11. Djerassi, C. and Klyne, W. *J. Chem. Soc.* **1962** *In press.*
12. See for instance Hendrickson, J. B. *J. Am. Chem. Soc.* **83** (1961) 4537.
13. Cahn, R. S., Ingold, C. K. and Prelog, V. *Experientia* **12** (1956) 81.
14. Levene, P. A. and Marker, R. E. *J. Biol. Chem.* **100** (1933) 685; Petterson, K. *Arkiv Kemi* **10** (1957) 283; Bonner, W. A. and Greenlee, T. W. *J. Am. Chem. Soc.* **81** (1959) 3336.
15. Fredga, A. *Arkiv Kemi* **8** (1955) 463.
16. Sjöberg, B. *Arkiv Kemi* **13** (1958) 1.
17. Sjöberg, B. *Arkiv Kemi* **12** (1958) 565.
18. Matell, M. *Arkiv Kemi* **5** (1953) 187.
19. Sjöberg, B. *Arkiv Kemi* **15** (1960) 451.
20. Matell, M. *Arkiv Kemi* **7** (1954) 437.
21. Fredga, A., Weidler, A-M. and Grönwall, C. *Arkiv Kemi* **17** (1961) 265.
22. Fredga, A. and Matell, M. *Arkiv Kemi* **3** (1952) 429; **4** (1952) 325.
23. Vavon, G. and Riviere, C. *Bull. soc. chim. France* **10** (1943) 460. We are indebted to Prof. H. S. Mosher (Standford University) for this sample of (−)-endocamphane-2-carboxylic acid.
24. Meinwald, J., Lewis, A. and Gassman, P. G. *J. Am. Chem. Soc.* **82** (1960) 2649.
25. Meinwald, J. and Gassman, P. G. *J. Am. Chem. Soc.* **82** (1960) 5445.
26. For stereochemistry see Fieser, L. F. and Fieser, M. *Steroids*, Reinhold Publ. Corp. New York 1959, pp. 337–340. We are indebted to Dr. A. Wettstein (Ciba Ltd., Basel) for these samples.
27. Walborsky, H. M., Barash, L., Young, A. E. and Impastato, F. J. *J. Am. Chem. Soc.* **83** (1961) 2517. The absolute configurations in this paper should be reversed according to a private communication from Prof. Walborsky (Florida State University) to whom we are indebted for the samples of the acids.
28. For leading references to podocarpic acid see Simonsen, J. and Barton, D. H. R. *The Terpenes*, Cambridge University Press 1952, Vol. III, pp. 472 *et sequ.* We are indebted to Prof. E. Wenkert (University of Indiana) for the acid specimen.
29. See Jeger, O., Dürst, O. and Büchi, G. *Helv. Chim. Acta* **30** (1947) 1853 and earlier references. The dehydroabietic acid was donated by Prof. G. Stork (Columbia University).
30. For leading references see Mills, J. A. and Klyne, W. in *Progress in Stereochemistry*, (ed. W. Klyne) Academic Press, New York 1954, Vol. I, chapter 5.
31. Wiberg, K. B. and Rowland, B. I. *J. Am. Chem. Soc.* **77** (1955) 1159; Sax, K. J. and Bergman, W. *Ibid.* **77** (1955) 1910.
32. For a discussion of this factor among aliphatic ketones and aldehydes see Djerassi, C. and Geller, L. E. *J. Am. Chem. Soc.* **81** (1959) 2789.
33. See for instance Table 1 in Brewster, J. H. *J. Am. Chem. Soc.* **81** (1959) 5475.
34. See Fredga, A. *Tetrahedron* **8** (1960) 126.
35. Fredga, A. *Arkiv Kemi* **7** (1954) 241.

Received December 15, 1961.

ACTA CHEMICA SCANDINAVICA 16 (1962) 1159–1174

Ultraviolet Absorption Spectra of Saturated Disulphides and Diselenides

GÖRAN BERGSON, GÖRAN CLAESON and LENNART SCHOTTE

Chemical Institute, University of Uppsala, Sweden

Submitted in honour of the sixtieth birthday of our teacher, Professor *Arne Fredga*

The ultraviolet absorption spectra of a number of saturated aliphatic disulphides and diselenides have been discussed. Special attention is paid to the following problems: (1) The nature of the first absorption band, (2) The red-shift found in small cyclic systems, (3) The effect of unsymmetrical substitution and (4) The interactions found between divalent sulphur atoms and carbonyl- and carboxyl-groups.

The first absorption band originates in a transition from the highest π-orbital (formed by combination of the lonepair atomic-orbitals) to the antibonding σ-orbital in the S—S or Se—Se bond.

The red shift found in small cyclic molecules is explained by the variation of the orbital energy in the highest π-orbital with the dihedral angle of the C—S—S—C group. Unsymmetrical disulphides show only one absorption peak as do symmetrical molecules. This is also true for the highly unsymmetrical molecules containing the Se—S bond.

The interaction between divalent sulphur atoms and carbonyl- or carboxyl-groups is complex. Two different mechanisms can be distinguished. The first results in a perturbation of the $n \rightarrow \pi^*$ transition, and the second is a charge-transfer mechanism.

Many measurements of UV absorption spectra of disulphides and related compounds have been reported, and the interpretations given almost exceed the number of spectra. Owing to the increasing interest in disulphide chemistry it seems justified to collect a number of representative spectra together with their recent interpretations. The present review is, however, incomplete and special reference is paid to the work performed in this field by the Uppsala school. We will deal exclusively with saturated disulphides and diselenides, defined as molecules containing the group:

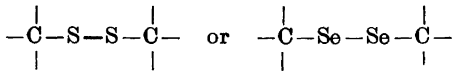

The absorption due to these chromophors is not as simple as at first it might appear. The first absorption peak (*i.e.*, that occurring at longest wavelengths) can vary from about 230 to 370 mμ for disulphides depending on the molecular environment.

It has been found very convenient to compare the disulphide spectra with the spectra of the corresponding diselenides. The diselenides show very similar spectra but they are found at longer wavelengths and this facilitates their study by means of simple commercial instruments. In some instances the disulphides have the first absorption peak near the borderline of the vacuum-ultraviolet region. Ditellurides are even more highly coloured than the diselenides, but their preparation is somewhat more difficult. In Fig. 1 the spectra of some simple compounds illustrate these findings. The three compounds referred to are colourless, yellow and deep-red, respectively. The large variations which may occur in the absorption curves are exemplified in Fig. 2, where the spectra of di-*t*-butyldisulphide (I), 6,8-thioctic acid (II) and 1α,5α-epidithioandrostane-3α,17β-diol (III) are given.

Already in 1936 Fredga [1] pointed out that among the acids with the general formula (IV) those with $n \neq 0$ were colourless whereas the acid with $n = 0$ was yellow, as are other diselenides. The diselenide group accordingly appeared to constitute a special chromophoric system. The spectra of some of the acids cited have now been measured and are given in Fig. 3.

Similar results were reported earlier for sulphur compounds. According to Ley and Arends [2], a maximum at about 250 mμ is characteristic of the disulphide group. In monosulphides with the exception of a few cases [3] the first absorption peak is always found below 250 mμ. It is true that the results quoted so far do not prove the existence of a new type of transition for the disulphides as compared with the monosulphides. They might be attributable instead to displacements of the absorption bands towards longer wavelengths. There are, however, many examples which support the idea of a characteristic absorption peak for the disulphides or diselenides. In Fig. 4, the spectra of 1,3-dithiolane (V) and 1,2-dithiolane (VI) are compared. Although (VI) does not show any

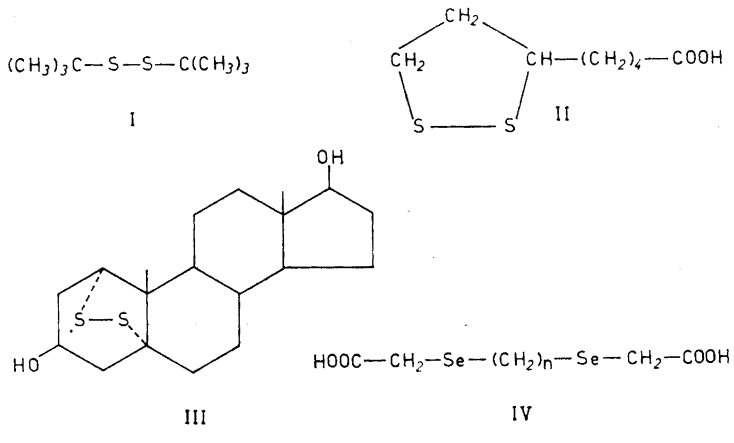

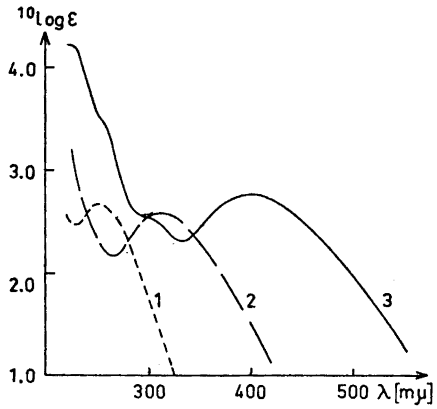

Fig. 1. UV-absorption of: 1. Dipropyl disulphide. 2. Dibutyl diselenide 3. Dibutyl ditelluride.

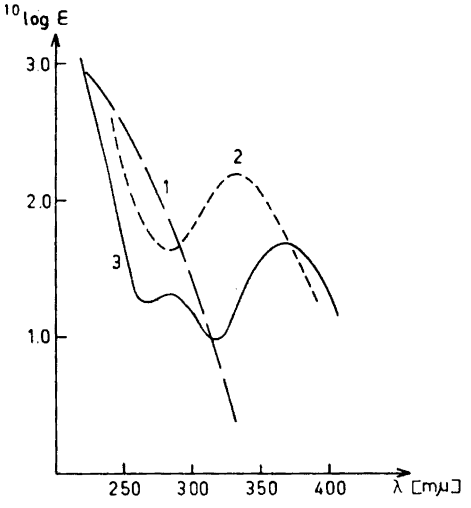

Fig. 2. UV-absorption of: 1. Di-*t*-butyl disulphide (I). 2. 6,8-Thioctic acid (II). 3. 1*α*, 5*α* - Epidithioandrostane - 3*α*, 17*β* - diol (III).

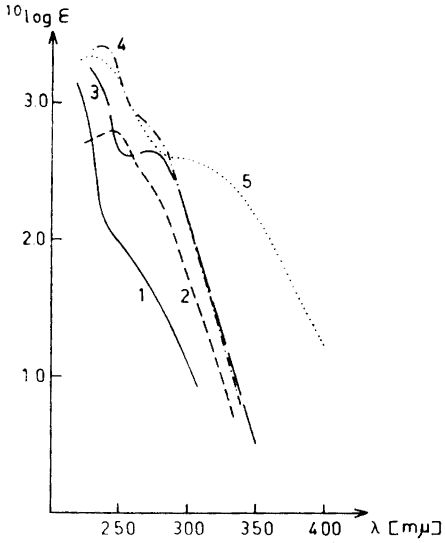

Fig. 3. UV-absorption of: 1. Ethylbutylselenide. 2. Selenium-diacetic acid ($HOOC-CH_2-Se-CH_2-COOH$). 3. Trimethylene-bis-selenium-acetic acid (IV with n = 3). 4. Methylene - bis - selenium-acetic acid (IV with n=1). 5. Diselenium-diacetic acid (IV with n = 0).

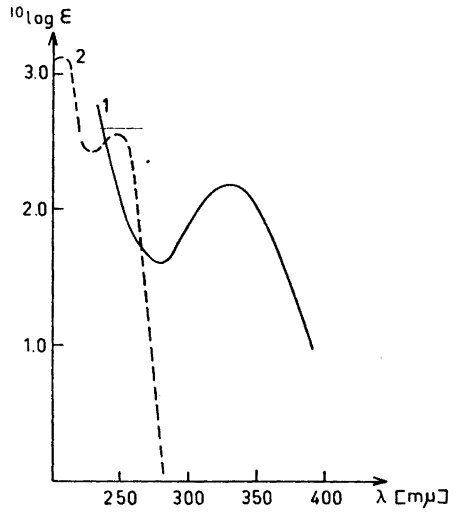

Fig. 4. UV-absorption of: 1. 1,2-Dithiolane (VI). 2. 1,3-Dithiolane (V).

maxima in and below the 250 mμ region, the extinction coefficient is rather high in this region. This indicates that absorption bands may occur at these wavelengths, as is found for (V). The peak at 330 mμ for the disulphide is, however, very pronounced and specific.

In the next paragraph it will be shown that there is also theoretical evidence for the occurrence of a specific absorption peak for disulphides and diselenides. In this connection the important work of Whitney and Calvin [4] on the quantum yield in photolysis with monochromatic light is noteworthy. A quantum yield of almost unity indicates a repulsive upper state, and there is strong evidence for the formation of R—S radicals. This implies that the electronic configuration in the S—S bond changes in the transition.

The nature of the first absorption band. Since in all the molecules considered in this paper the disulphide (or diselenide) group is surrounded by saturated carbon atoms, and the absorption occurs in a region very different from that of hydrocarbon spectra, to a first approximation we can treat the disulphide group as an isolated diatomic unit. Of course this cannot be done if it is part of a conjugated system. According to Pauling [5] the bonds formed by divalent sulphur atoms involve mainly p-orbitals. The two lone-pairs on each sulphur atom therefore occupy an s- and a p-orbital. According to Bergson [6] the simple molecular-orbital theory indicates that the two highest occupied orbitals should be the bonding and antibonding π-orbitals formed by linear combination of the non-bonding $3p_z$-atomic orbitals. The lowest unoccupied orbital

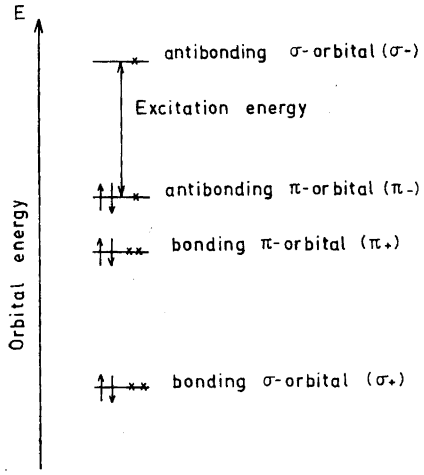

Fig. 5. Schematic representation of molecular-orbital energy levels in a disulphide.

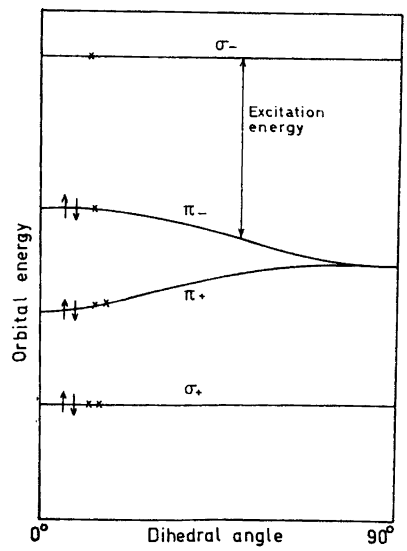

Fig. 6. Orbital energies as a function of the dihedral angle for a symmetrical disulphide. ↑ denotes electrons in the ground state and × electrons in the first excited state. The molecular orbitals have been formed from non-hydridized atomic orbitals.

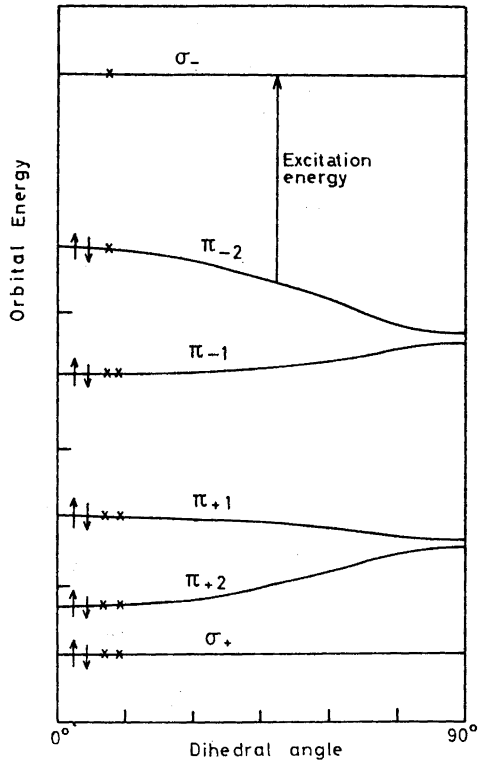

Fig. 7. Orbital energies as a function of the dihedral angle when sp^3-hybridized atomic orbitals have been used.

should be the antibonding σ-orbital between the sulphur atoms (*cf.* Fig. 5). Accordingly the first electronic transition should be a jump from the antibonding π-orbital to the antibonding σ-orbital. The variation of the orbital energies with the dihedral angle of the disulphide group (Fig. 6) has been studied by Bergson [6,7]. These variations account for the stable skew conformation of the disulphide group in the ground state (dihedral angle usually about 90°) and also for the red shift in UV-spectra when the molecule is forced into a conformation with a smaller dihedral angle. This is the case with the five-membered rings for example. According to Foss [8], the dihedral angle in 1,2-dithiolane-4-carboxylic acid is 27°. This model also explains the fission of the disulphide bond upon irradiation [4,9].

The most serious objection to this simple picture is that unhybridized atomic orbitals have been used as a starting point. In reality the lone-pairs often occupy orbitals which are more like sp^3-hybrids. However, Bergson [7] has treated the problem using sp^3-hybridized atomic orbitals and this leads to a very similar picture for the orbitals in question (Fig. 7).

THE SPECTRA OF UNSUBSTITUTED DISULPHIDES AND DISELENIDES

Ley and Arends [2] seem to be the first to have assigned an absorption peak at about 250 mμ to the presence of the S—S group. Since then several investiga-

tors have confirmed this observation. In this connection the extensive work of Koch [10] and Brandt, Emeleus and Hazeldine [11] and also Baer and Carmack [12] may be mentioned. A characteristic absorption curve of this type has already been shown in Fig. 1. The only exceptional case seems to have been di-*t*-butyldisulphide (Fig. 2), where no maximum is present. A phenomenological explanation was advanced by Bergson [13]. The absorption maximum was shown to be displaced to progressive shorter wavelengths in the series $(CH_3)_2S_2$ (λ_{max} = 254.5 mμ), $(C_2H_5)_2S_2$ (λ_{max} = 251.5 mμ) and $(i\text{-}C_3H_7)_2S_2$ (λ_{max} = 245.0 mμ). By extrapolation the peak for $(t\text{-}C_4H_9)_2S_2$ would be expected to occur at about 230 mμ. At such small wavelengths this absorption band must be so strongly overlapped by the higher-intensity bands which always occur in this region, that no maximum is detectable. This interpretation was confirmed by a study of the corresponding diselenide [13]. As mentioned in the introduction (*cf.* Fig. 1) the diselenides show absorption curves very similar to those of the corresponding disulphides, but are more easily studied since their first absorption peak occurs at longer wavelengths. For $(CH_3)_2Se_2$, $(C_2H_5)_2Se_2$, $(i\text{-}C_3H_7)_2Se_2$ and $(t\text{-}C_4H_9)_2Se_2$ the maximum is found at 316, 312, 305, and 286 mμ, respectively. Hyperconjugation is certainly of importance in determining the trend [13].

The maximum for the disulphides mentioned above is thus found between 230 and 255 mμ, and for the diselenides between 286 and 316 mμ. Consequently, the observations made by Calvin and his co-workers [14] in 1954 constitute a great advance. They reported that 1,2-dithiolane (VI) and its derivative, 6,8-thioctic acid (II), had an absorption peak at 330 mμ, and that the peak at 250 mμ was absent (*cf.* Figs. 2 and 4). Although his interpretation that this red-shift originated in ring strain is not wholy true [6,7,9,15] Calvin was the first

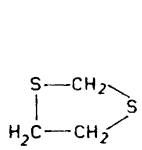

V

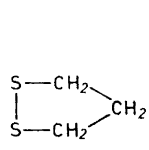

VI

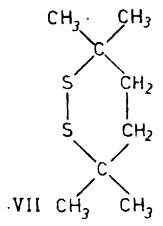

VII

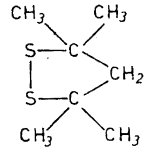

VIII

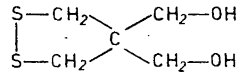

IX

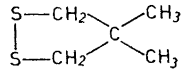

X

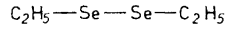

XI

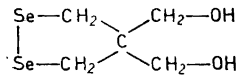

XII

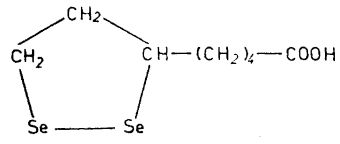

XIII

to point out the relationship between ring size and the position of the first absorption peak. Thus for a seven-membered ring (4,8-thioctic acid) he found the peak at 259 mμ (the same value is also found in 1,2-dithiepan-5-carboxylic acid [16] and is almost that of a noncyclic compound), for a six-membered ring at 286 mμ, and for the five-membered ring at 330 mμ as already stated. He also realized that the dihedral angle of the disulphide group decreased as the number of atoms in the ring decreased. The real cause of the redshift is fully explained from Bergson's theory of the variation of the orbital energies with the dihedral angle (see Figs. 6 and 7).

Schotte [17] investigated some 4-substituted 1,2-dithiolane derivatives prepared by Backer and his co-workers [18], and confirmed the presence of an absorption peak in the 330 mμ region. Some of these spectra are shown in Fig. 8. Claeson [19] prepared and studied the methyl-substituted 5- and 6-membered rings (VII) and (VIII). In the six-membered ring the methyl groups cause an hypsochromic shift as expected. However, by comparison with the unsubstituted ring, methyl substitution in the fivemembered ring results in a red-shift. Evidently, the factors which determine the hypsochromic shift associated with methylsubstitution in non-cyclic systems do not operate in the fivemembered ring. The spectra of (VII) and (VIII) are given in Fig. 9.

A disulphide with an absorption maximum at still longer wavelengths was recently investigated by Bergson and co-workers [20]. This was the steroid with formula (III), for which the spectrum has already been given in Fig. 2. We think that the exceptionally low excitation energy originates in the almost planar conformation of the molecule and in the large S—S distance.

Before concluding this paragraph it remains to mention the bathochromic shift found for diselenides in which the diselenide group is a part of a small ring. The six-membered ring compound 1,2-diselenane has its maximum at 365 mμ and the five-membered 1,2-diselenolane at 444 mμ [9]. In Fig. 10 some examples of diselenide absorption spectra are given. It is true that the examples given of the five-membered rings are not unsubstituted compounds, but the substituents are so far removed from the diselenide group that they cannot influence the first absorption peak.

Some unsymmetrical molecules. The study of unsymmetrical disulphides or diselenides where the two sulphur (or selenium) atoms are not equivalent is of great theoretical importance. Our first studies on unsymmetrical carboxylic substituted disulphides indicated the presence of two absorption peaks which at first we attributed to the unsymmetrical arrangement. However, such an interpretation is not in agreement with our theory of the nature of the absorption band [7,21]. Since the effect of carboxylic groups on the disulphide spectra is complex, however, it was desirable to study simpler unsymmetrical molecules.

Schotte [22] prepared and studied some trichloromethylalkyl disulphides, the spectra of which are given in Fig. 11. No definite absorption peaks are shown by these molecules so that no answer to the asymmetry problem could be obtained from them. The spectra of the unsymmetrical dialkyl disulphides given in Fig. 12 show only one peak, but here the difference between the substitutents is slight.

The thiolselenenates (R—Se—S—R) might be regarded as highly unsymmetrical disulphides or diselenides. Some simple thiolselenenates have now

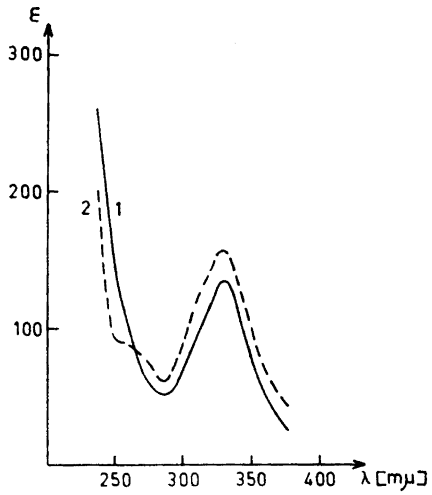

Fig. 8. UV-absorption of: 1. 4,4-Dimethyl-1,2-dithiolane (X). 2. 4,4-Bis-hydroxymethyl-1,2-dithiolane (IX).

been prepared and investigated [21]. The spectrum of ethyl thiolselenenate (XXI) given in Fig. 13 shows only one peak at 285 mμ. This compound is rather unstable and upon heating decomposes into diethyl diselenide and diethyl disulphide which is also given in Fig. 13.

The study of the cyclic 1-thia-2-selena-cyclopentane-4-carboxylic acid (XXII) further confirmed the similarity between the thiolselenenates and the

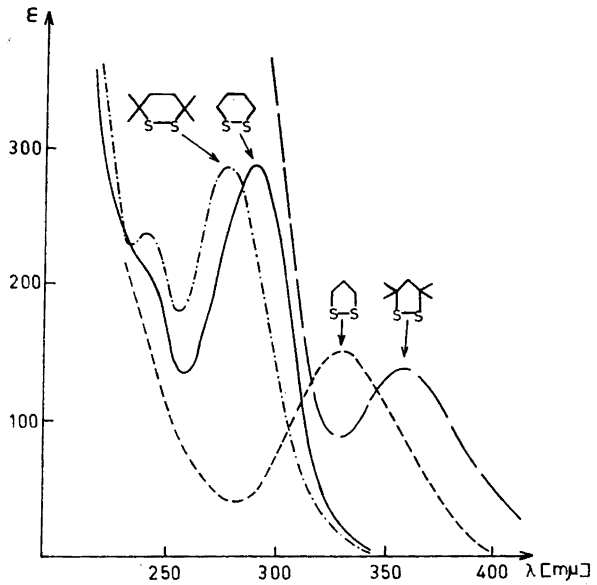

Fig. 9. UV-absorption of the methylsubstituted derivatives VII and VIII as compared with that for the unsubstituted rings.

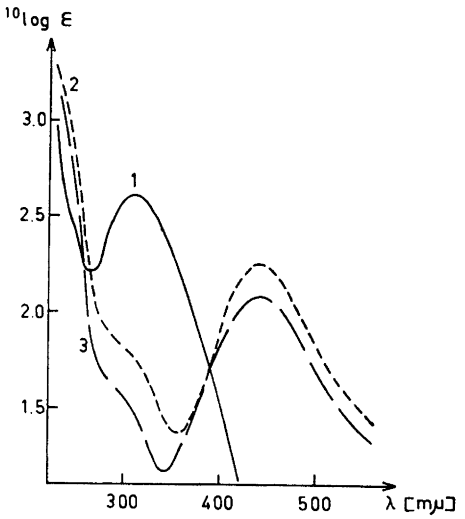

Fig. 10. UV-absorption of: 1. Diethyldiselenide (XI). 2. 4,4-Bis-hydroxymethyl-1,2-diselenolane (XII). 3. 6,8-Selenoctic acid (XIII).

symmetrical disulphides and diselenides [23]. This acid shows a single peak at 386 mμ as shown in Fig. 14 where the spectra of 1,2-dithiolane-4-carboxylic acid and 1,2-diselenolane-4-carboxylic acid (XXIII) and (XXIV) are given for comparison.

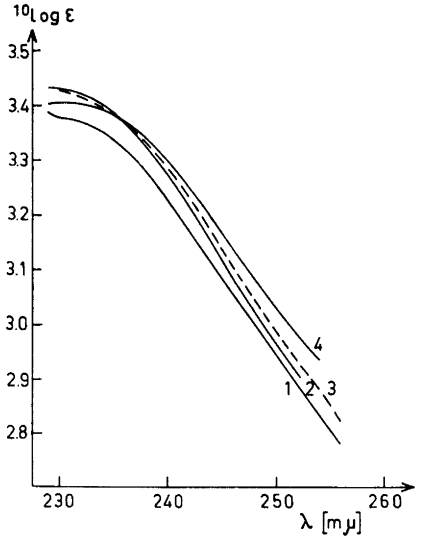

Fig. 11. UV-absorption of: 1. Trichloromethyl-methyldisulphide (XIV). 2. Trichloromethyl-ethyldisulphide (XV). 3. Trichloromethyl-isopropyldisulphide (XVI). 4. Trichloromethyl-*t*-butyldisulphide (XVII).

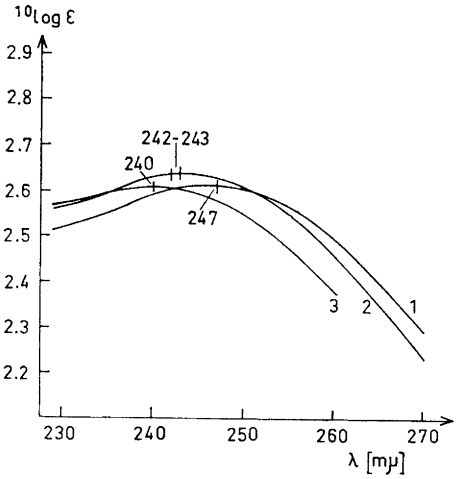

Fig. 12. UV-absorption of: 1. *t*-Butyl-methyldisulphide (XVIII). 2. *t*-Butyl-ethyldisulphide (XIX). 3. *t*-Butyl-isopropyldisulphide (XX).

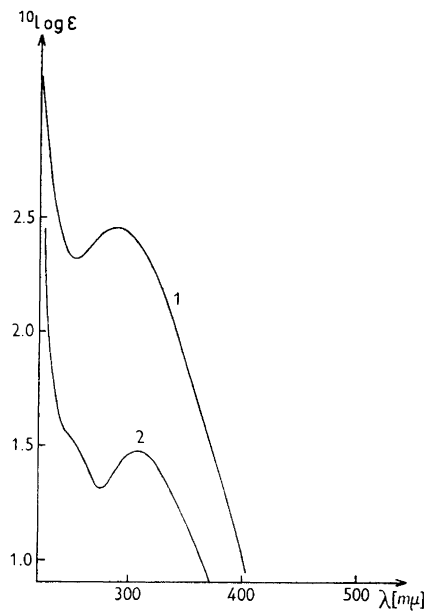

Fig. 13. UV-absorption of: 1. Ethylthiol-selenenate (XXI). 2. The decomposition products of (XXI). *i.e.* diethyldisulphide and diethyldiselenide.

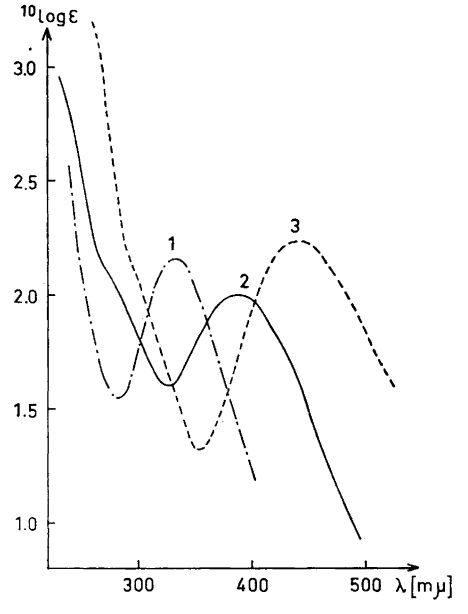

Fig. 14. UV-absorption of: 1. 1,2-Dithiolane-4-carboxylic acid (XXIII). 2. 1-Thia-2-selena-cyclopentane-4-carboxylic acid (XXII). 3. 1,2-Diselenolane-4-carboxylic acid (XXIV).

Accordingly, we conclude that there is no splitting of the first absorption band due to the asymmetry in unsymmetrical disulphides and diselenides or thiolselenates. Reference should also be made to the spectra of some amino-substituted 1,2-dithiolane derivatives which have recently been investigated[34].

$Cl_3C-S-S-CH_3$ XIV

$Cl_3C-S-S-CH_2-CH_3$ XV

$Cl_3C-S-S-CH(CH_3)_2$ XVI

$Cl_3C-S-S-C(CH_3)_3$ XVII

$(CH_3)_3C-S-S-CH_3$ XVIII

$(CH_3)_3C-S-S-CH_2-CH_3$ XIX

$(CH_3)_3C-S-S-CH(CH_3)_2$ XX

$C_2H_5-Se-S-C_2H_5$ XXI

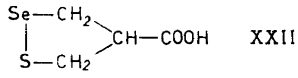

XXII

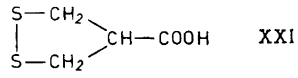

XXIII

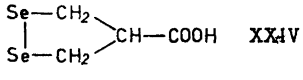

XXIV

THE SPECTRA OF CARBOXYL- AND CARBONYL-SUBSTITUTED DISULPHIDES

During the last six years much work has been done at the Uppsala school on absorption spectra of carboxyl-substituted disulphides and diselenides. Before discussing these studies, attention must be paid to important early work by Fehnel and Carmack [24] on monosulphides. Among other things they have investigated the UV-spectra of ketosulphides of the type (XXV—XXVII). For the compound (XXVII) where the sulphur atom and the carbonyl group are separated by two saturated carbon atoms, the absorption spectrum is almost exactly a superposition of the spectra for a sulphide and a ketone. In compound (XXV), however, an absorption peak at about 300 mμ ($^{10}\log \varepsilon \approx 2.5$) appears. This peak is also present in the methyl-substituted compound (XXVI).

Fehnel and Carmack also investigated the esters (XXVIII—XXX). When the sulphur atom is separated from the ester group by only one carbon atom as in (XXVIII) a new band at 247 mμ ($^{10}\log \varepsilon \approx 2.57$) appeared. The spectra of the other esters were superpositions of the spectra for the isolated chromophores.

The nature of the 300 mμ peak in β-ketosulphides has recently been studied by Bergson and Delin [25]. The investigation of solvent effects has revealed that the excited state is less polar than the ground state. This, together with sensitivity of the intensity to the molecular environment, suggests that the absorption is due to a perturbed carbonyl-transition ($n \rightarrow \pi^*$). The interpretations given by Fehnel and Carmack [24] in terms of resonance formulae involving hyperconjugation and charge transfer are not in accordance with our experi-

$C_2H_5—S—CH_2—CO—CH_3$ XXV

$C_2H_5—S—C(CH_3)_2—CO—CH_3$ XXVI

$C_2H_5—S—CH_2—CH_2—CO—CH_3$ XXVII

$n—C_4H_9—S—CH_2—COOC_2H_5$ XXVIII

$n—C_4H_9—S—CH_2—CH_2—COOC_2H_5$ XXIX

$S(CH_2—CH_2—COOC_2H_5)_2$ XXX

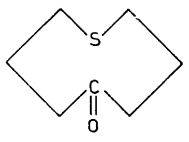

XXXI

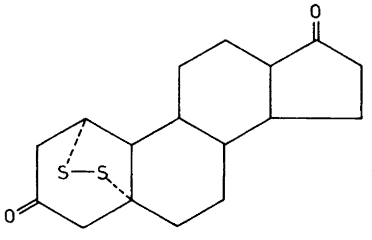

XXXII

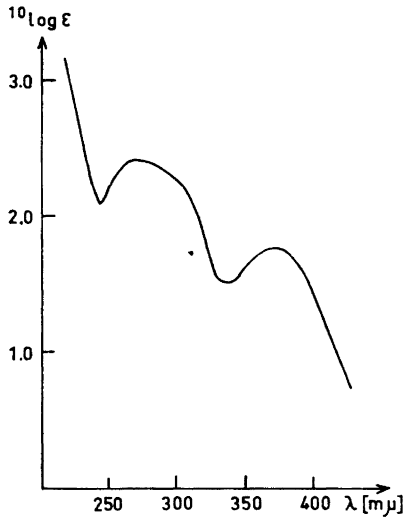

Fig. 15. UV-absorption of: 1α,5α-Epidithioandrostane-3,17-dione (XXXII).

mental findings. We have also investigated some similar selenium derivatives and these too show relatively strong bands in the 300 mμ region [26].

Recently, Leonard *et al.*[27] found a strong interaction between the carbonyl group and the sulphur atom in the cyclic sulphide-ketone (XXXI). This interaction is, however, of a kind different from that discussed above and is best interpreted in terms of charge-transfer.

There are evidently two kinds of interaction between a divalent sulphur atom and a carbonyl group. The first causes a perturbation of the n → π * transition and the second leads to charge-transfer. In order to distinguish between the two alternatives a careful study of solvent effects is necessary. It appears, however, that the charge-transfer effect is characterized by higher intensity and larger departure from the normal carbonyl-wavelengths than the perturbed transitions. Accordingly the effects to be described below are perhaps best interpreted as perturbed carbonyl- or carboxyl-transitions. For a more detailed discussion of the nature of the carboxyl-transitions we refer to the paper by Bergson and Delin [26].

In view of these considerations the detection of similar phenomena in disulphides is scarcely unexpected. The first observation of such an effect was recently made for 1α,5α-epidithioandrostane-3,17-dione (XXXII) where a pronounced absorption peak at 268 mμ appeared [20,28]. The spectrum of this compound is given in Fig. 15 and should be compared with the curve given for 1α,5α-epidithioandrostane-3α,17β-diol in Fig. 2. It is evident that the simultaneous presence of the disulphide and the carbonyl group is necessary for the appearence of the peak at 268 mμ. A detailed analysis of the 268 mμ band reveals that it is in fact composed of two bands, the one occurring at the longer wavelength having the lower intensity. This band is certainly due to the keto-group in the 17-position, which is not so strongly perturbed as that in the 3-position. An attempt can now be made to understand the spectra of the carboxylic substituted disulphides and diselenides in terms of the

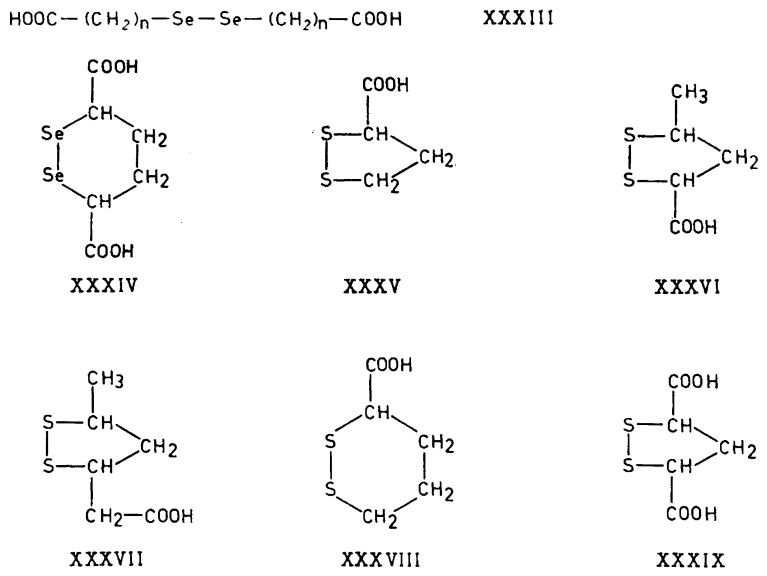

XXXIII XXXIV XXXV XXXVI XXXVII XXXVIII XXXIX

effects discussed above. The acids with the general formula (XXXIII) are considered first. When n = 4 the compound shows a maximum at 311 mμ and the spectrum is in all respects similar to those of simple unsubstituted diselenides. This is also almost true when n = 3 and n = 2, although in these instances a small hypsochromic shift is observed. The maxima are at 308 and 306 mμ when n = 3 and n = 2, respectively. Diselenium-diacetic acid (n = 1) also has an absorption band in the 300 mμ region, but the maximum cannot be determined with certainty owing to overlap by a stronger band with a maximum at 229 mμ. The hypsochromic shift produced by the α-placed carboxylic group is not great, however, as is clearly seen in Fig. 16. It is therefore impossible to draw definite conclusions about its origin. Nevertheless the peak at 229 mμ is not the peak characteristic of the diselenide group, but it may be a perturbed carboxylic absorption band. In diselenium-α-di-propionic acid and diselenium-α-di-isobutyric acid there is also a strong peak at shorter wavelengths together with the usual diselenide peak in the neighbourhood of 300 mμ [9].

The comparison of the spectra of the carboxylic substituted linear disulphides with the corresponding diselenides shows that the diselenides are more suitable for study for the reasons given in the introduction. A typical disulphide peak at 250 mμ is shown by β,β′-dithio-dipropionic acid and γ,γ′-dithio-dibutyric acid, but dithio-diacetic acid shows only end-absorption [29,30]. Judging by the high intensity of the absorption at 250 mμ (Fig. 17) it is evident that the disappearence of the disulphide band is not a real effect. It is also evident that there is another strong band with a maximum below 250 mμ. The same considerations apply also to dithio-α,α′-dipropionic acid and to dithio-α,α′-diisobutyric acid.

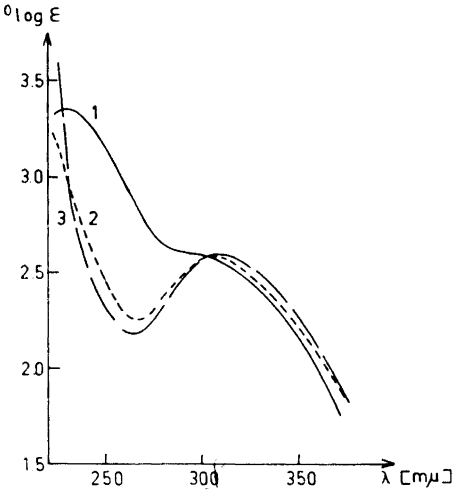

Fig. 16. UV-absorption of the acids (XXXIII). 1. n = 1; 2. n = 2; 3. n = 3.

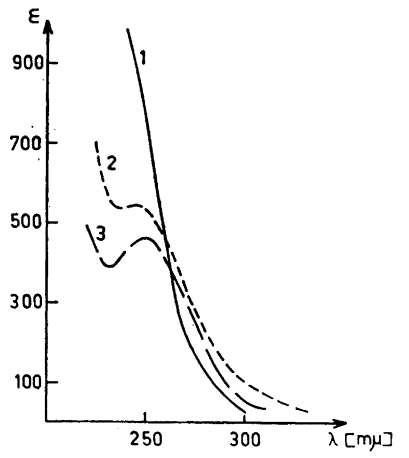

Fig. 17. UV-absorption of:
1. $HOOC-CH_2-S-S-CH_2-COOH$.
2. $HOOC-(CH_2)_2-S-S-(CH_2)_2COOH$.
3. $HOOC-(CH_2)_3-S-S-(CH_2)_3-COOH$.

The six-membered cyclic compound (XXXIV), rac-1,2-diselenane-3,6-dicarboxylic acid, has its first absorption maximum at 343 mμ (Fig. 18). This should be compared with that for the unsubstituted ring at 365 mμ [9]. This difference corresponds to only 0.8 kcal mole^{-1} in excitation energy. In addition it has a band with maximum at about 280 mμ which is strongly

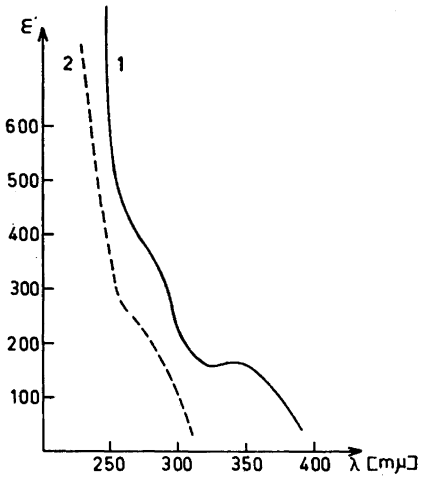

Fig. 18. UV-absorption of: 1. Rac-1,2-diselenane-3,6-dicarboxylic acid (XXXIV). 2. Rac-1,2-dithiane-3,6-dicarboxylic acid.

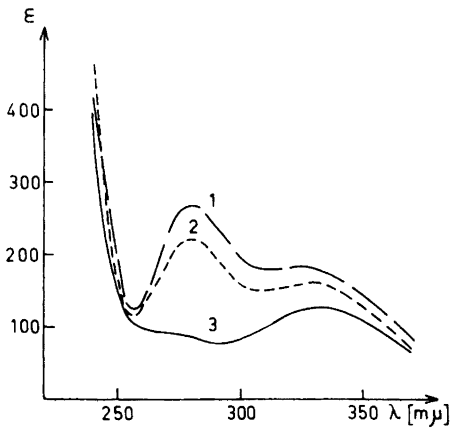

Fig. 19. UV-absorption of 1,2-dithiolane-3-carboxylic acid (XXXV). 1. in 0.6 M HCl. 2. in ethanol. 3. in 0.01 M NaOH.

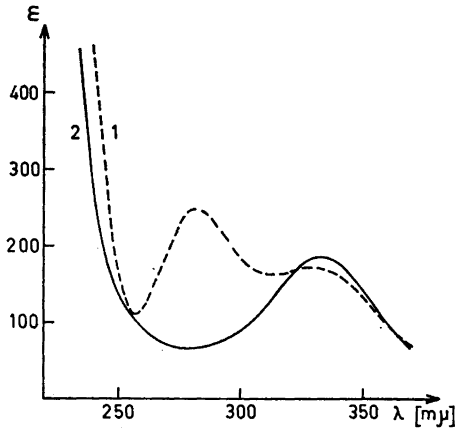

Fig. 20. UV-absorption of: 1. 5-Methyl-1,2-dithiolane-3-carboxylic acid (XXXVI). 2. 5-Methyl-1,2-dithiolane-3-acetic acid (XXXVII).

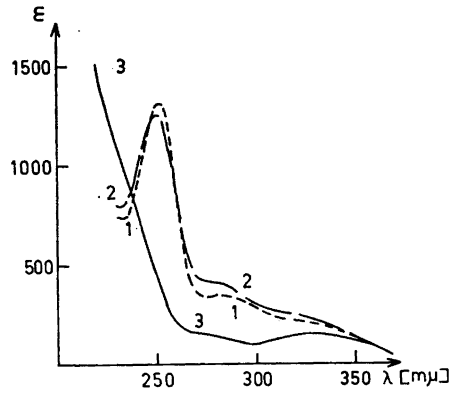

Fig. 21. UV-absorption of: 1. Rac-1,2-dithiolane-3,5-dicarboxylic acid (XXXIX) in 0.1 M H_2SO_4. 2. Rac-dimethyl-1,2-dithiolane-3,5-dicarboxylate (in ethanol). 3. Di-Na-salt of Rac-1,2-dithiolane-3,5-dicarboxylic acid (in water).

overlapped by a band with higher intensity occurring at a shorter wavelength. The 280 mμ band might originate in a transition from the π_{-1} orbital (*cf.* Fig. 7), but this assignment is uncertain. Rac-1,2-dithiane-3,6-dicarboxylic acid has its first absorption band at 275 mμ although it is overlapped by stronger absorptions at shorter wavelengths [30]. The 275 mμ band is displaced little from its position as given by the unsubstituted ring (290 mμ). A possible $\pi_+ \rightarrow \sigma_-$ transition cannot be detected with certainty in this instance owing to the strong absorption at shorter wavelengths, but it can be seen in the unsubstituted 1,2-dithiane and in 3,3,6,6-tetramethyl-1,2-dithiane (Fig. 9).

Among the five-membered acids Claeson [31] has studied 1,2-dithiolane-3-carboxylic acid (XXXV) and 5-methyl-1,2-dithiolane-3-carboxylic acid (XXXVI). Both acids show the typical absorption peak occurring at about 330 mμ and in addition a strong band at 280 mμ is present. This band does not occur when there is a $-CH_2-$ group between the ring and the carboxylic group as was found in (XXXVIII) (Fig. 20), and of course not when the group is as remote as it is in 6,8-thioctic acid. [*Cf.* also 1,2-dithiolane-3-carboxylic acid with 1,2-dithiolane-4-carboxylic acid (Fig. 14) and 1,2-dithiane-3-carboxylic acid with 1,2-dithiane-4-carboxylic acid [32]]. We conclude that the 280 mμ band is best interpreted as a perturbed carboxylic transition, an assignment which is substantiated by its disappearance in alkaline solution (Fig. 19). Similar decreases in the intensity of the bands at short wavelengths as a result of salt formation has also been observed by Schotte for dithio-diacetic acid and 1,2-dithiane-3,6-dicarboxylic acid [30], and by Claeson [33] for 2-methyl-3,4-dithiahexanoic acid.

The existence of a short-wavelengths absorption band which disappears on salt formation is also found in 1,2-dithiane-3-carboxylic acid [31] (XXXVIII), 1,2-dithiane-3,6-dicarboxylic acid and in the five-membered 1,2-dithiolane-

3,5-dicarboxylic acid (XXXIX), which has been carefully investigated by Schotte [29,30]. The methyl ester of this acid has a spectrum very similar to that of the free acid (Fig. 21). The free acid, the ester, and also the salt have the typical 1,2-dithiolane peak in the neighbourhood of 330 mμ. The strong absorption band with maximum at 250 mμ is certainly a perturbed carboxylic transition. In addition to the peaks just mentioned there is also one with maximum at about 280 mμ. This might be another perturbed carboxylic transition.

Acknowledgements. We wish to express our sincere appreciation to Professor Arne Fredga for his constant interest in our work, for many stimulating discussions and for all the facilities placed at our disposal.

REFERENCES

1. Fredga, A. *Svensk Kem. Tidskr.* **48** (1936) 91.
2. Ley, H. and Arends, B. *Z. physik. Chem.* **B15** (1932) 311.
3. Davis, R. E. *J. Org. Chem.* **23** (1958) 1380; Schotte, L. *Arkiv Kemi* **9** (1956) 309.
4. Whitney, R. B. and Calvin, M. *J. Chem. Phys.* **23** (1955) 1750.
5. Pauling, L. *Proc. Natl. Acad. Sci. U.S.* **35** (1949) 495.
6. Bergson, G. *Arkiv Kemi* **12** (1958) 233.
7. Bergson, G. *Arkiv Kemi* **18** (1961) 409. For a review *cf.* Bergson, G. ***Some New Aspects of Organic Disulphides, Diselenides and Related Compounds.*** Abstracts of Uppsala Dissertations in Science **13** (1962).
8. Foss, O. and Tjomsland, O. *Acta Chem. Scand.* **12** (1958) 1810.
9. Bergson, G. *Arkiv Kemi* **13** (1958) 11.
10. Koch, H. P. *J. Chem. Soc.* **1949** 394.
11. Brandt, G. R. A., Emeléus, H. J. and Haszeldine, R. N. *J. Chem. Soc.* **1952** 2549.
12. Baer, J. E. and Carmack, M. *J. Am. Chem. Soc.* **71** (1949) 1215.
13. Bergson, G. *Arkiv Kemi* **9** (1955) 121; *9. Nordiske Kemikermøde i Aarhus* 1956, p. 47.
14. Barltrop, J. A., Hayes, P. M. and Calvin, M. *J. Am. Chem. Soc.* **76** (1954) 4348.
15. Bergson, G. and Schotte, L. *Arkiv Kemi* **13** (1958) 43.
16. Claeson, G. *To be published.*
17. Schotte, L. *Arkiv Kemi* **9** (1956) 309.
18. Backer, H. J. and Tamsma, A. S. *Rec. trav. chim.* **57** (1938) 1183; Backer, H. J. and Evenhuis, N. *Ibid* **56** (1937) 129.
19. Claeson, G. *Svensk Kem. Tidskr.* **69** (1957) 395.
20. Bergson, G., Sjöberg, B., Tweit, R. C. and Dodson, R. M. *Acta Chem. Scand.* **14** (1960) 222.
21. Bergson, G. and Nordström, G. *Arkiv Kemi* **17** (1961) 569.
22. Schotte, L. *Unpublished results.*
23. Bergson, G. and Biezais, A. *Arkiv Kemi*, **18** (1961) 143. *Cf.* also Bergson, G. *Arkiv Kemi* **19** (1962) 75.
24. Fehnel, E. A. and Carmack, M. *J. Am. Chem. Soc.* **71** (1949) 84.
25. Bergson, G. and Delin, A.-L. *Arkiv Kemi* **18** (1962) 489.
26. Bergson, G. and Delin, A.-L. *Arkiv Kemi* **18** (1961) 441.
27. Leonard, N. J., Brown, T. L. and Milligan, T. W. *J. Am. Chem. Soc.* **81** (1959) 504; Leonard, N. J., Milligan, T. W. and Brown, T. L. *J. Am. Chem. Soc.* **82** (1960) 4075.
28. Tweit, R. C. and Dodson, R. M. *J. Am. Chem. Soc.* **81** (1959) 4409.
29. Schotte, L. *Arkiv Kemi* **8** (1955) 579.
30. Schotte, L. *Arkiv Kemi* **9** (1956) 441.
31. Claeson, G. *Acta Chem. Scand.* **13** (1959) 1709.
32. Claeson, G. and Langsjoen, A. *Acta Chem. Scand.* **13** (1959) 840.
33. Claeson, G. *Unpublished results.*
34. Bergson, G. *Arkiv Kemi* **18** (1962) 505; Bergson, G. and Andersson, B. *Ibid.* **19** (1962) 173.

Received December 19, 1961.

ACTA CHEMICA SCANDINAVICA 16 (1962) 1175–1182

Beiträge zur Chemie α-substituierter Sulfide

IX *. Versuche zur Bildung des 4-Thiaisochroman-1-on-systems

ALEXANDER SENNING und SVEN-OLOV LAWESSON**

Laboratorium für Organische Chemie, Chemisches Institut der Universität Uppsala, Uppsala, Schweden

Unserem Lehrer, Professor *Arne Fredga*, zum 60. Geburtstag gewidmet

Zur Abrundung der synthetischen Arbeiten der Verfasser auf dem Gebiet der 4-Thiaisochroman-1-one-derivate (I) [1-4] wurden einige weitere Verbindungen (zumeist phenolische Hydroxylgruppen enthaltend) dargestellt. Diese Verbindungen besitzen, wie auch das schon früher erhaltene 3-(3-Methoxy-4-hydroxyphenyl)-4-thiaisochroman-1-on [4], nach vorläufigen Untersuchungen erhebliche fungizide und bakterizide Aktivität. Nach orientierenden Versuchen zu urteilen, lässt sich das hier angewandte Darstellungsverfahren nicht allgemein zur Gewinnung analoger Derivate aliphatischer Merkaptokarbonsäuren heranziehen. Wie auch gegen Thiosalizylsäure, reagiert Phthalaldehydsäure gegenüber aliphatischen Merkaptokarbonsäuren in der 3-Hydroxyphthalidform. Weder die Umsetzung von Thiosalizylsäure mit Ketonen (mit Chlorwasserstoff oder *p*-Toluolsulfonsäure als Katalysator) oder weniger reaktiven gem-Dihalogeniden, noch die Chlorierung von *o*-Alkylmerkaptobenzoesäuren (Ausnahme: *o*-Methylmerkaptobenzoesäure [1]) erwies sich als gangbarer Weg zur Darstellung von 4-Thiaisochroman-1-on-derivaten.

Senning und Lawesson [1-4] begannen kürzlich eine eingehende Untersuchung der Darstellungsmöglichkeiten für in 3-Stellung substituierte 4-Thiaisochroman-1-one (I), die nach einem amerikanischen Patent [5] als Pflanzenschutzmittel in Frage kommen. Nachdem bei der Chlorierung von *o*-Methylmerkaptobenzoesäure die Bildung von 3,3-Dichlor-4-thiaisochroman-1-on beobachtet worden war [1], wurde die in der aliphatischen Reihe zur Bildung analoger Fünfringe angewandte Methode [6] (Merkaptokarbonsäure und Aldehyd werden in Eisessig gelöst; in die siedende Lösung wird trockener Chlorwasserstoff eingeleitet) zur Darstellung von 3-Alkyl- bzw. 3-Aryl-4-thiaisochroman-1-onen benutzt [2]. Da bei dieser Reaktion gleichzeitig erhebliche Mengen Alkyliden-bis-

* VIII. Mitteilung: Senning, A. und Lawesson, S.-O. *Acta Chem. Scand.* **15** (1961) 1203.

** Neue Anschrift: Chemisches Institut der Universität Aarhus, Aarhus, Dänemark.

(*o*-karboxyphenylsulfid) (II) gebildet werden [2,7], wurde ein neues Verfahren entwickelt, das bessere Ausbeuten an 4-Thiaisochroman-1-on-derivat lieferte [3,4] (Thiosalizylsäure, Aldehyd und *p*-Toluolsulfonsäure werden in siedendem Benzol miteinander umgesetzt, wobei das entstehende Wasser azeotrop abdestilliert wird).

Die schon vorher bekannten insgesamt sechs 4-Thiaisochroman-1-on-derivate sind in den Arbeiten von Böhme und Schmidt [8], Mowry [9,10,5] und Kaufmann [11] beschrieben.

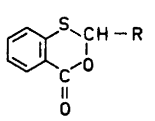

I

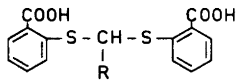

II

Wie uns neuerdings bekannt wurde, sind schon um das Jahr 1906 Patente bzw. Patentanmeldungen erschienen, in denen Produkte aus der Umsetzung von Thiosalizylsäure mit Aldehyden genannt werden. So beschäftigt sich ein deutsches Patent [12] mit einer Verbindung, die aus Thiosalizylsäure und wässrigem Formaldehyd erhalten wird und deren Schmelzpunkt (270°—272°) sich sowohl von dem des 4-Thiaisochroman-1-ons [1] (I, R = H; F: 45°—47°) als auch von dem des Methylen-bis-(*o*-karboxyphenylsulfids) [13] (II, R = H; F: 286°—288°) unterscheidet. Eine deutsche Patentanmeldung [14] enthält Angaben über das Produkt aus Thiosalizylsäure und Chloral, dem auch die richtige Struktur des 3-Trichlormethyl-4-thiaisochroman-1-ons zugeschrieben wird. Beide Verbindung liefern im Laufe weiterer Umsetzungen Schwefelfarbstoffe [15].

Die bisher in der Literatur beschriebenen Umsetzungen, die zu 4-Thiaisochroman-1-on-derivaten führen, sind von Senning und Lawesson [4] diskutiert worden. In der vorliegenden Arbeit haben wir uns hauptsächlich mit der Umsetzung aromatischer Hydroxyaldehyde mit Thiosalizylsäure sowie mit einigen wenig untersuchten Synthesemöglichkeiten beschäftigt und zwar der Umsetzung von Thiosalizylsäure mit Ketonen, der Umsetzung von Thiosalizylsäure mit gem-Dihalogeniden und der Chlorierung von *o*-Alkylmerkaptobenzoesäuren.

Nachdem das 3-(3-Methoxy-4-hydroxyphenyl)-4-thiaisochroman-1-on [4] sich in orientierenden Versuchen als stark fungizid erwiesen hatte, setzten wir weitere hydroxylsubstituierte Benzaldehyde mit Thiosalizylsäure zu den entsprechenden 4-Thiaisochroman-1-on-derivaten um. Diese Verbindungen sind nach vorläufigen Untersuchungen sowohl gegen Pilze als auch Bakterien stark toxisch. Die biologischen Versuchsergebnisse werden demnächst an anderem Ort veröffentlicht.

Die Ausbeuteverhältnisse bei der Reaktion von Thiosalizylsäure mit *m*-Chlorbenzaldehyd in Gegenwart bzw. Abwesenheit von Chlorwasserstoff sind ein weiteres Beispiel für die unterschiedliche Reaktivität von α-Chlorsulfiden (III) bzw. Halbmerkaptalen (α-Hydroxysulfiden) (IV) gegenüber Merkapto- bzw. Karbonsäuregruppen.

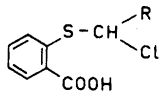

III

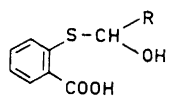

IV

Während sich in Gegenwart von Chlorwasserstoff neben 55 % (3-Chlorbenzal)-bis-(*o*-karboxyphenylsulfid) 34 % 3-(3-Chlorphenyl)-4-thiaisochroman-1-on bilden, entstehen in Abwesenheit von Chlorwasserstoff 63 % 3-(3-Chlorphenyl)-4-thiaisochroman-1-on. In der Tabelle 1 sind die Ergebnisse unserer Versuche zusammengestellt:

Tabelle 1. 1: Katalysator: Chlorwasserstoff (0,15—0,30 Mol Thiosalizylsäure + 0,15—0,30 Mol Aldehyd in 300—500 ml Eisessig)

R =	% I	% II	Referenz
Phenyl	24	69	4
3,4-Methylendioxyphenyl	15	52	7
2-Chlorphenyl	27	57	7
3-Chlorphenyl	34	55	diese Arbeit
4-Chlorphenyl	22	76	7
2-Nitrophenyl	20	0	7
3-Nitrophenyl	43	48	7
4-Nitrophenyl	62	35	7
3-Methoxy-4-hydroxyphenyl	0	84	7
2-Thienyl	2	58	7

2. Katalysator: *p*-Toluolsulfonsäure (0,10 Mol Thiosalizylsäure + 0,12 Mol Aldehyd in 500 ml Benzol).

R =	% I	Referenz
Phenyl	89	4
3-Chlorphenyl	63	diese Arbeit
4-Chlorphenyl	47	4
2-Nitrophenyl	20	4
3-Methoxy-4-hydroxyphenyl	73	4
2-Thienyl	71	4

Während aliphatische Merkaptokarbonsäuren mit Ketonen ohne weiteres Fünf- oder Sechsringe bilden (Bistrzycki und Brenken [6], Fredga [16], Firma du Pont [17]) liess sich Thiosalizylsäure weder mit Hexachlorazeton noch mit Dibenzylketon oder Azeton zur Umsetzung bringen. In allen Fällen, in denen Thiosalizylsäure mit einem Keton zusammen den Bedingungen der Kondensation mit Aldehyden unterworfen wurde, erhielten wir unverändertes Ausgangsmaterial zurück.

Bei der Umsetzung von Thiosalizylsäure mit einem nicht durch benachbarte Gruppierungen aktivierten gem-Dihalogenid wurde das gesuchte Produkt nicht erhalten. Weder die freie Säure in N,N-Dimethylanilin, noch das Natrium-

salz in trockenem Benzol lieferte mit Benzalchlorid 3-Phenyl-4-thiaisochroman-1-on. Dagegen gelang Kaufmann [11] der Ringschluss von Thiosalizylsäure mit Phthalylchlorid [11a] und mit Phosgen [11b].

Die Reaktion mit überschüssigem Chlor, die im Falle der *o*-Methylmerkaptobenzoesäure zum 3,3-Dichlor-4-thiaisochroman-1-on führte [1], nahm im Falle der *o*-Benzylmerkaptobenzoesäure [18] einen anderen Weg. Neben Benzylchlorid bildete sich *o*-Chlorsulfinylbenzoylchlorid [19] (V), dessen Nachweis über das Infrarotspektrum gelang (nach einer privaten Mitteilung von Dr. B. S. Farah sind die beiden charakteristischen Banden bei 1778 cm^{-1} (COCl-Gruppe) und 1158 cm^{-1} (SOCl-Gruppe) der beste Nachweis für *o*-Chlorsulfinylbenzoylchlorid). Durch Vakuumdestillation wurde ein unscharf schmelzendes Substanzgemisch erhalten, das mit Benzolsulfonamid ein charakteristisches Derivat des *o*-Chlorsulfonylbenzoylchlorids [20] lieferte. *o*-Chlorsulfinylbenzoylchlorid erhielten wir auch bei der Chlorierung von *o*-Isopropylmerkaptobenzoesäure [21]. Die

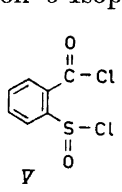

V

Spaltung von Arylbenzylsulfiden durch überschüssiges Chlor wurde erstmals von Zincke [22] beobachtet, der z.B. bei der Chlorierung von *o*-Nitrophenylbenzylsulfid neben Benzalchlorid *o*-Nitrobenzolsulfenylchlorid isolierte. Zincke deutete die Reaktion als Chlorolyse eines polaren Sulfiddichlorids. Im Falle der Chlorierung von *o*-Benzylmerkaptobenzoesäure hat man sich eine intramolekulare Acidolyse des primär entstehenden Arylschwefeltrichlorids zu denken. Das *o*-Chlorsulfinylbenzoylchlorid unterliegt dann leicht sekundär Disproportionierungs- und/oder Oxydationsreaktionen:

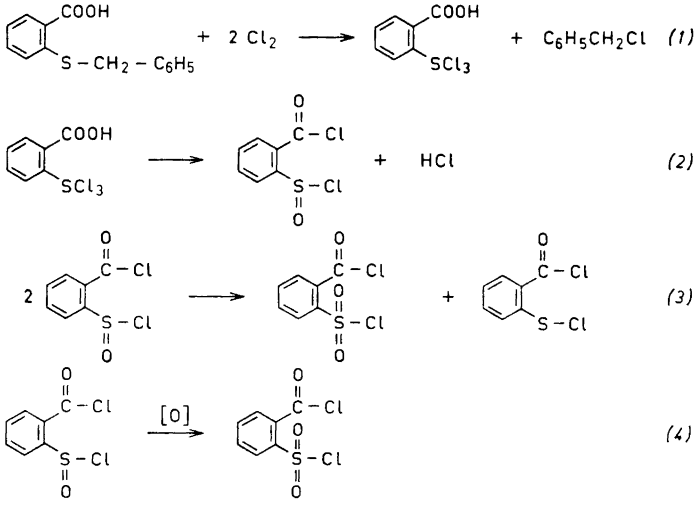

(1)

(2)

(3)

(4)

o-Methylmerkaptobenzoesäure [23] und *o*-Äthylmerkaptobenzoesäure [24] lieferten, mit jeweils einem bzw. zwei Mol Chlor umgesetzt, unscharf schmelzende saure Produkte, die sich in verdünnter Natriumbikarbonatlösung vollständig lösten und demnach kein 4-Thiaisochroman-1-on bzw. 3-Methyl-4-thiaisochroman-1-on enthielten. Das bei der Chlorierung von *o*-Methylmerkaptobenzoesäure (mit einem Überschuss an Chlor) entstehende 3,3-Dichlor-4-thiaisochroman-1-on [1] kann auch durch Chlorierung von 4-Thiaisochroman-1-on erhalten werden, womit die Struktur der Chlorverbindung als bewiesen gelten kann.

Versuche, die schon mehrfach von anderen Autoren (Bistrzycki und Brenken [6], Fredga [16], Firma du Pont [17]) dargestellten 1,3-Thioxolan-4-on- bzw. 1,3-Thioxan-4-on-derivate (VI bzw. VII) auch nach der für die 4-Thiaisochroman-1-on-derivate ausgearbeiteten Methode zu synthetisieren, gelangen in der Mehrzahl der Fälle nicht. Mit Benzaldehyd und Thioglykolsäure wurden keine definierten Produkte erhalten, Thiomilchsäure gab mit Benzaldehyd das von Holmberg [25] beschriebene Benzal-bis-(α-karboxyäthylsulfid) und nur Thioäpfelsäure und Chloral lieferten ein Ringschlussprodukt, für das auf Grund des bifunktionellen Charakters der Thioäpfelsäure sowohl die Fünfring- als auch die Sechsringstruktur denkbar ist (VIII bzw. IX).

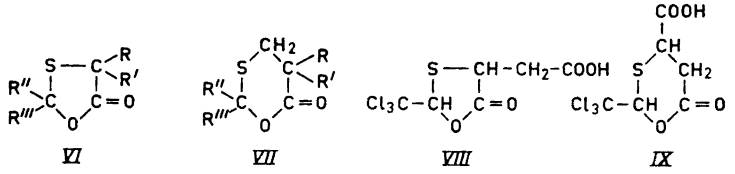

VI VII VIII IX

Bei den Umsetzungen der Phthalaldehydsäure (X) mit aliphatischen Merkaptokarbonsäuren liess sich die *o*-Karboxyaldehydstruktur ebensowenig abfangen wie mit Thiosalizylsäure [4]. Die Reaktionsprodukte (XI) waren in allen Fällen Derivate des 3-Hydroxyphthalids.

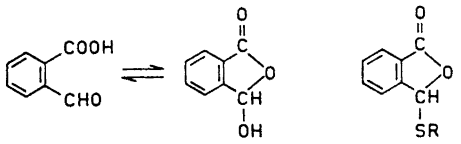

X XI

BESCHREIBUNG DER VERSUCHE

Alle Schmelzpunkte sind unkorrigiert. Die Infrarotspektrogramme wurden mit einem Spektrographen Perkin-Elmer Modell 137 aufgenommen. Die Analysen wurden im Institut für Analytische Chemie der Universität Uppsala sowie von der Firma Alfred Bernhardt, Mülheim (Ruhr), Deutschland ausgeführt.

(1) 4-Thiaisochroman-1-on-derivate

Versuchsanordnung. In einem 1-l-Kolben, der mit einem Rührer und einem Veresterungsaufsatz versehen war, wurde ein Gemisch von 0,15 Mol Thiosalizylsäure, 0,15 Mol Aldehyd, 1 g *p*-Toluolsulfonsäure und 500 ml Benzol bis zur Beendigung der Wasserabscheidung gekocht (etwa 3 Stunden). War das Produkt in Benzol unlöslich, wurde es in der Wärme abfiltriert, andernfalls wurde es nach dem Einengen der Lösung mit Petroläther ausgefällt. Das so erhaltene Rohprodukt wurde mit Natriumbikarbonatlösung digeriert und zur Reinigung umkristallisiert.

3-(2-Hydroxyphenyl)-4-thiaisochroman-1-on. Ausgangsmaterial: 23,1 g (0,15 Mol) Thiosalizylsäure und 18,3 g (0,15 Mol) Salizylaldehyd. Rohausbeute: 29,5 g (76 % der Theorie), F: 214—216°. Nach mehrmaligem Umkristallisieren aus Alkohol und Essigester schmolz das Produkt (farblose mikrokristalline Agglomerate) zwischen 221° und 223°. (Gef. C 64,96; H 4,01; S 12,17. Ber. für $C_{14}H_{10}O_3S$: C 65,10; H 3,90; S 12,41).

3-(3-Hydroxyphenyl)-4-thiaisochroman-1-on. Ausgangsmaterial: 23,1 g (0,15 Mol) Thiosalizylsäure und 18,3 g (0,15 Mol) *m*-Hydroxybenzaldehyd. Rohausbeute: 30,4 g (79 % der Theorie), F: 130°—135°. Nach mehrmaligem Umkristallisieren aus Äther und Petroläther schmolz das Produkt (farblose Spiesse) zwischen 136° und 139°. (Gef. C 65,25; H 3,93; S 12,15. Ber. für $C_{14}H_{10}O_3S$: C 65,10; H 3,90; S 12,41).

3-(4-Hydroxyphenyl)-4-thiaisochroman-1-on. Ausgangsmaterial: 23,1 g (0,15 Mol) Thiosalizylsäure und 18,3 g (0,15 Mol) *p*-Hydroxybenzaldehyd. Rohausbeute: 23,5 g (61 % der Theorie), F: 191°—196°. Nach mehrmaligem Umkristallisieren aus Alkohol schmolz das Produkt (farblose quadratische Prismen) zwischen 191° und 194°. (Gef. C 65,12; H 4,22; S 12,26. Ber. für $C_{14}H_{10}O_3S$: C 65,10; H 3,90; S 12,41).

3-(3,4-Dihydroxyphenyl)-4-thiaisochroman-1-on. Ausgangsmaterial: 15,4 g (0,10 Mol) Thiosalizylsäure und 16,6 g (0,12 Mol) 3,4-Dihydroxybenzaldehyd (Protokatechualdehyd). Rohausbeute: 13,2 g (48 % der Theorie), F: 168°—174°. Nach mehrmaligem Umkristallisieren aus Essigester und Petroläther schmolz das Produkt (farblose Prismen) zwischen 183° und 184°. (Gef. C 61,38; H 3,88; S 12,00. Ber. für $C_{14}H_{10}O_4S$: C 61,02; H 3,70; S 11,78).

3-(3-Chlorphenyl)-4-thiaisochroman-1-on. Ausgangsmaterial: 23,1 g (0,15 Mol) Thiosalizylsäure und 21,0 g (0,15 Mol) *m*-Chlorbenzaldehyd. Rohausbeute: 26,0 g (63 % der Theorie), F: 80°—83°. Nach mehrmaligem Umkristallisieren aus Alkohol schmolz das Produkt (farblose derbe Prismen) zwischen 95° und 97°. (Gef. Cl 12,79; S 11,51. Ber. für $C_{14}H_9ClO_2S$: Cl 12,81; S 11,59).

(3-Chlorbenzal)-bis-(o-karboxyphenylsulfid). 23,1 g (0,15 Mol) Thiosalizylsäure und 21,0 g (0,15 Mol) *m*-Chlorbenzaldehyd wurden in 200 ml Eisessig gelöst. Durch die siedende Lösung wurde 3 Stunden lang trockener Chlorwasserstoff geleitet. Danach wurde die erkaltete Reaktionsmischung in einen Überschuss kaltes Wasser gegossen und die Fällung abfiltriert. Nach Digerieren mit verdünnter Sodalösung hinterblieben 14,0 g (34 % der Theorie) 3-(3-Chlorphenyl)-4-thiaisochroman-1-on, F: 82°—86°. Beim Ansäuern der alkalischen Lösung wurden 17,5 g (55 % der Theorie) (3-Chlorbenzal)-bis-(*o*-karboxyphenylsulfid), F: 185°—189° erhalten. Nach mehrmaligem Umkristallisieren aus Alkohol und Wasser schmolz die Säure (farblose mikrokristalline Agglomerate) zwischen 208° und 210°. (Gef. Cl 8,32; S 14,74. Ber. für $C_{21}H_{15}ClO_4S_2$: Cl 8,23; S 14,88).

(2) Chlorierung von *o*-Benzylmerkaptobenzoesäure

48,8 g (0,20 Mol) *o*-Benzylmerkaptobenzoesäure [18] wurden in 100 ml Tetrachlorkohlenstoff suspendiert und unter Rühren mit 42,6 g (0,60 Mol) Chlor, gelöst in 500 ml Tetrachlorkohlenstoff, versetzt. Nach dem Aufhören der spontanen Chlorwasserstoffentwicklung wurde auf dem Wasserbad erhitzt, bis sich alles gelöst hatte und sich kein Chlorwasserstoff mehr entwickelte (etwa 4 Stunden). Nach Abziehen des Lösungsmittels gingen zwischen 65°/10 mm und 70°/10 mm (Destillation unter Stickstoff) 17,6 g (70 % der Theorie) Benzylchlorid, n_D^{20} 1,5423, über (Lit.: Kp. 179°, n_D^{15} 1,5415). Zwischen 150°/10 mm und 169°/10 mm wurden 37,3 g einer zwischen 54° und 63° schmelzenden Substanz erhalten, die vermutlich überwiegend aus einem Gemisch der symmetrischen (F: 40°) und der unsymmetrischen Form (F: 79°) des *o*-Chlorsulfonylbenzoylchlorids [20] bestand.

Mit Benzolsulfonamid in Pyridin wurde ein Derivat erhalten, das zwischen 203° und 204° schmolz (Schmelzpunkt des 1-Benzolsulfonyl-1,2-dihydrobenzisothiazol-2-on-S,S-dioxyds [19]: 202°).

In einem qualitativen Versuch wurde *o*-Benzylmerkaptobenzoesäure in Methylenchlorid suspendiert. Bei Zimmertemperatur wurde bis zur vollständigen Lösung Chlor eingeleitet (etwa 15 Min.). Der im Vakuum bei Zimmertemperatur von überschüssigem Chlor und dem Lösungsmittel befreite Rückstand wurde in Tetrachlorkohlenstoff gelöst und das Infrarotspektrum dieser Lösung aufgenommen. Es zeigte die charakteristischen Banden des o-Chlorsulfinylbenzoylchlorids bei 1778 cm^{-1} und 1158 cm^{-1}.

(3) Umsetzungen aliphatischer Merkaptokarbonsäuren mit Aldehyden

Versuchsanordnung: Wie unter (1), nur unterblieb die Behandlung mit Natriumbikarbonatlösung.

Thiomilchsäure und Benzaldehyd. Ausgangsmaterial: 53,0 g (0,50 Mol) rac. Thiomilchsäure und 53,0 g (0,50 Mol) Benzaldehyd. Erhalten wurden 41,0 g (55 % der Theorie) rohes Benzal-bis-(α-karboxyäthylsulfid), F: 144°—149° (die Theorie fordert das Auftreten einer razemischen und zweier Mesoformen). Nach mehrmaligem Umkristallisieren aus Benzol schmolz die Säure zwischen 149° und 151°. Die Literatur [25] gibt F: 138°—140° an. Auf Grund dieser Divergenz und da auch der Schmelzpunkt des rac. Bis-(α-karboxyäthyl)-disulfids [26] in der Nähe dieser beiden Schmelzpunkte liegt (F: 148°—149°), wurde die Verbindung analysiert. (Gef. C 51,95; H 5,45; S 20,83. Ber. für $C_{13}H_{16}O_4S_2$: C 51,98; H 5,37; S 21,35).

Thioäpfelsäure und Chloral. Ausgangsmaterial: 15,0 g (0,10 Mol) Thioäpfelsäure und 17,0 g (0,11 Mol) Chloral. Rohausbeute: 24,1 g (83 % der Theorie), F: 135°—139°. Nach mehrmaligem Umkristallisieren aus Alkohol schmolz das Produkt zwischen 145° und 147° (farblose Prismen). Es handelt sich um 2-Trichlormethyl-5-karboxymethyl-1,3-thioxol-4-on oder um 2-Trichlormethyl-6-karboxy-1,3-thioxan-4-on. (Gef. Cl 37,20; S 11,39. Ber. für $C_6H_5Cl_3O_4S$: Cl 38,05; S 11,47).

Thioglykolsäure und Phthalaldehydsäure. Ausgangsmaterial: 9,2 g (0,10 Mol) Thioglykolsäure und 18,0 g (0,12 Mol) Phthalaldehydsäure. Rohausbeute: 17,1 g (76 % der Theorie), F: 138°—141°. Nach mehrmaligem Umkristallisieren aus Alkohol und Wasser schmolz das 3-(Karboxymethylmerkapto)-phthalid zwischen 140° und 142° (farblose Nadeln). (Gef. C 53,63; H 4,09; S 14,04. Ber. für $C_{10}H_8O_4S$: C 53,58; H 3,60; S 14,28).

β-Merkaptopropionsäure und Phthalaldehydsäure. Ausgangsmaterial: 14,0 g (0,13 Mol) β-Merkaptopropionsäure und 23,0 g (0,15 Mol) Phthalaldehydsäure. Rohausbeute: 22,4 g (72 % der Theorie), F: 105°—111°. Nach mehrmaligem Umkristallisieren aus Alkohol schmolz das 3-(β-Karboxyäthylmerkapto)-phthalid zwischen 112° und 114° (farblose Nadeln). (Gef. C 55,58; H 4,24; S 13,39. Ber. für $C_{11}H_{10}O_4S$: C 55,46; H 4,23; S 13,43).

Thioäpfelsäure und Phthalaldehydsäure. Ausgangsmaterial: 7,5 g (0,05 Mol) Thioäpfelsäure und 9,0 g (0,06 Mol) Phthalaldehydsäure. Rohausbeute: 13,1 g (93 % der Theorie), F: 192°—196°. Nach mehrmaligem Umkristallisieren aus Alkohol und Wasser schmolz das 3-(α,β-Dikarboxyäthylmerkapto)-phthalid zwischen 195° und 197,5° (farblose Nadeln). Gef. C 51,72; H 3,72; S 11,23. Ber. für $C_{12}H_{10}O_6S$: S 51,07; H 3,57; S 11,34).

Wir sind dem Institutsvorstand, Herrn Professor A. Fredga, für die Überlassung des Arbeitsplatzes und *Jordbrukets Forskningsråd* für die finanzielle Unterstützung unserer Arbeit zu Dank verpflichtet.

Herrn Professor H. Böhme, Marburg/Lahn, Deutschland und Herrn Dr. B. S. Farah, Allied Chemical Corporation, Morristown, New Jersey, Vereinigte Staaten, danken wir für die anregende Diskussion vorläufiger Versuchsergebnisse und die Erörterung von Reaktionsmechanismen. Die Patentabteilung der Badischen Anilin- & Soda-Fabrik AG, Ludwigshafen am Rhein, Deutschland, war uns freundlicherweise bei der Kontrolle älterer Literaturangaben behilflich und stellte uns Fotokopien schwer zugänglicher Literaturstellen zur Verfügung. Der Firma Aldrich, Milwaukee, Wisconsin, Vereinigte Staaten (Dr. Bader), danken wir für die kostenlose Überlassung von Phthalaldehydsäure.

LITERATUR

1. Senning, A. und Lawesson, S.-O. *Acta Chem. Scand.* **14** (1960) 2230.
2. Senning, A. und Lawesson, S.-O. *Arkiv Kemi* **17** (1961) 261.
3. Senning, A. und Lawesson, S.-O. *Arkiv Kemi* **17** (1961) 387.
4. Senning, A. und Lawesson, S.-O. *Arkiv Kemi* **17** (1961) 489.
5. Monsanto Chemical Company, US Patent 2496741; *Chem. Abstr.* **44** (1950) 5522.
6. Bistrzycki, A. und Brenken, B. *Helv. Chim. Acta* **3** (1920) 447.
7. Senning, A. und Lawesson, S.-O. *Arkiv Kemi* **18** (1961) 95.
8. Böhme, H. und Schmidt, W. *Arch. Pharm.* **286** (1953) 330.
9. Mowry, D. T., Yanko, W. H. und Ringwald, E. L. *J. Am. Chem. Soc.* **69** (1947) 2358.
10. Mowry, D. T. *J. Am. Chem. Soc.* **69** (1947) 2362.
11. a) Kaufmann, H. P. und Rossbach, E. *Ber.* **58** (1925) 1556. b) Kaufmann, H. P., Seher, A. und Hagedorn, P. *Ann.* **587** (1954) 231.
12. Deutsches Patent 219830; *Chem. Zentr.* **1910** *I*, 1075.
13. Brookes, R. F., Cranham, J. E., Cummings, W. A. W., Greenwood, D., Jackson, B. S. und Stevenson, H. A. *J. Sci. Food. Agr.* **1957** No. 1, 31.
14. Deutsche Patentanmeldung B 43607/120; Friedländer, *Fortschritte der Teerfarbenfabrikation* **9** (1913) 572.
15. Deutsches Patent 190477; *Chem. Zentr.* **1907 II**, 2012; vgl. Martinet, *Matières Colorantes*, Paris 1934.
16. Fredga, A. *Ber.* **71** (1938) 289.
17. E. I. du Pont de Nemours and Co., US Patent 2911414; *Chem. Zentr.* **131** (1960) 16567.
18. Apitzsch, H. *Ber.* **46** (1913) 3091.
19. Douglass, I. B. und Farah, B. S. *J. Org. Chem.* **26** (1961) 351.
20. Scheiber, J. und Knothe, M. *Ber.* **45** (1912) 2252.
21. Gilman, H. und Webb, F. J. *J. Am. Chem. Soc.* **71** (1949) 4062.
22. a) Zincke, T. *Ber.* **44** (1911) 769. b) Zincke, T. und Dahm, A. *Ber.* **45** (1912) 3457.
23. Friedländer, P. *Ann.* **351** (1907) 390.
24. Donleavy, J. J. und English, Jr., J. *J. Am. Chem. Soc.* **62** (1940) 220.
25. Holmberg, B. und Mattisson, K. *Ann.* **353** (1907) 123.
26. Fredga, A. *Arkiv Kemi, Mineral. Geol.* **12 A** (1937) No. 13; vgl. Lovén, J. M. *J. prakt. Chem.* [2] **29** (1907) 366.

Eingegangen am 22. Dezember 1961.

ACTA CHEMICA SCANDINAVICA 16 (1962) 1183–1190

Moss Pigments

I. The Anthocyanins of *Bryum cryophilum* O. Mårt.

GERD BENDZ, OLLE MÅRTENSSON and LARS TERENIUS

Chemical Institute, University of Uppsala, and
Pharmacia Research Laboratories, Uppsala, Sweden

Submitted in honour of the sixtieth birthday of our teacher, Professor *Arne Fredga*

Two anthocyanins have been isolated from *Bryum cryophilum* O. Mårt. They have been identified as luteolinidin-5-diglucoside and 5-monoglucoside.

Although the bryophytes form an important group in plant kingdom which is comparatively well explored from taxonomic and systematic points of view, little is known about their chemistry. As to their non-chlorophyllous pigments, which are of particular interest to the taxonomist as giving morphological characters, almost no detailed data regarding their chemical structure seem to have been available in the literature. However, the carotinoid distribution in several species, for example, has been qualitatively investigated recently [1].

Many of the earlier investigations of moss pigments refer to those of the anthocyanin type. Although none of these reddish or purplish pigments had been isolated and identified, their general chemical behaviour, such as their colour reactions, suggested that they are pigments belonging to the anthocyanin group.

Reddish pigments are widely distributed among the mosses and liverworts but those species in which this colour predominates in the general appearance of the plants are comparatively few. Among the "peat mosses" (the order Sphagnales) we have such definitely reddish-coloured species within the groups *Acutifolia* and *Palustria* and in Bryales we find them in genera such as *Bryum*, *Calliergon* and *Drepanocladus*. It should be pointed out, however, that the intensity of colouration may vary greatly within one species depending on nutrition and insolation conditions. These facts are well known to field bryologists and have been verified experimentally [2,3,4].

An extensive work on the occurrence of and the chemical behaviour of brownish and reddish pigments of bryophytes was carried out by Herzfelder [2]. She points out that the resulting colour of a moss or liverworts is a complex phenomenon as the pigmentation occurs in three different ways.

(1) The pigments occur in certain bodies in the cell, the chromatophores. The obligate chlorophyll and at least certain carotenes are fixed to such bodies.

(2) The pigments occur in the cell wall. A general characteristic is that they are often very difficult to extract completely. In addition to chlorophyll, the various cell wall pigments are the most important in the general colouration of moss plants. The cell wall pigments are generally more or less brownish (at least in old tissue) but may sometimes have a red to wine-red colour. This is particularly the case with the stem, the nerve and the border (when present) of the leaf, the cells towards the base of the leaf and the seta and capsula wall of the sporophyte. In some species, for example the genus *Sphagnum*, red cell wall pigments are very important and predominate in the colouration of the plants. According to Herzfelder's paper and our pre-investigations these pigments seem to be anthocyanidin derivatives although not of the same type as the anthocyanidin glycosides occurring in higher plants.

(3) Pigments may occur dissolved in the cell sap. As examples of species with such sap colouration, Herzfelder listed several *Bryum* species such as *B. duvalii* Voit* (a name now replaced by the correct *B. Weigelii* Spreng.), *B. pallens* Schleich., *B. schleicheri* Schwaegr. and *B. turbinatum* (Hedw.) Schwaegr. The reddish cell sap pigments of these species are said to be of anthocyanin type.

To find out whether or not *Bryum* species produce anthocyanins similar to those of the higher plants we have investigated the red pigmentation of *Bryum cryophilum* O. Mårt., a species earlier known under the invalid name *B. obtusifolium* Lindb. As earlier reported [5], two anthocyanins have been isolated from this moss and identified as luteolinidin-5-diglucoside and luteolinidin-5-monoglucoside.

B. cryophilum is a circumpolar species which occurs locally in abundance in arctic areas or mountain areas with an arctic climate. Generally it forms blood-red cushions or borders along small streamlets below snow areas. These investigations have been carried out with air-dried moss collected from the Torneträsk area of Torne Lappmark in northernmost Sweden as well as from Lake Peters in Brooks Range on the arctic slope of Alaska. No significant differences have been observed in the compositions of the anthocyanins in these materials. Provided the moss is carefully air-dried and preserved in a dark place, it may be stored for several years without notable destruction of the pigments. Since mosses are generally very resistant to dry periods — these may be considered as mere interruptions in the vegetation period — we did not consider it necessary to investigate the moss before it was dried. Unless used immediately, etiolation and other growing phenomena make such material less suitable for investigation than the dried material.

All red coloured material was precipitated by ether addition to the extract obtained by treating the air-dried and crushed moss at 0° with methanol

* The author's names have been added by the writers.

Table 1. Visible spectra of the anthocyanins, the corresponding aglycones and luteolinidin.

	λ_{max} in methanol-HCl (mμ)	λ_{max} in methanol-HCl−$AlCl_3$ (mμ)	$\frac{E_{440}}{E_{max}}$ (%)
Anthocyanin I	500	548	22
Aglycone I	498	549	38
Anthocyanin II	499	549	23
Aglycone II	499	549	37
Luteolinidin	499	548	38

containing 1 % of conc. HCl. However, the amount of anthocyanins in this precipitate was only about 10 %, the major part consisting of a complex mixture of yellow and dark-brown compounds.

The anthocyanins were separated from most of these by passing an aqueous acetic acid solution of the precipitate through a Sephadex column, the elution being performed with the same solvent. The two anthocyanins appeared as one orange-red band on the column and it was not possible to separate them from each other on this material. Three fractions were collected. The first one contained two different phenolic glycosides, the second the anthocyanins and the third a mixture of as yet unidentified compounds. The anthocyanin fraction contained at least five substances which were separated on a cellulose powder column with aqueous acetic acid as solvent. Anthocyanin I was obtained almost pure, whereas anthocyanin II had to be further purified by passing through another cellulose powder column before it was chromatographically pure.

It was also possible to isolate and purify the two anthocyanins by repeated chromatography on Whatman No. 3 MM filter paper using different solvents [6]. By this separation method a third red pigment occurring in *B. cryophilum* was also detected and isolated. Only traces of the latter have been obtained but preliminary investigations indicate that it might be an anthocyanidin derivative although not of a glycosidic type as the two isolated anthocyanins.

On acid hydrolysis of the two anthocyanins, two aglycones were obtained which proved to be identical. For example, they gave the same colour reactions,

Table 2. R_F values of the anthocyanins, the corresponding aglycones and luteolinidin.

	butanol-acetic acid-water 6:1:2	water-conc.HCl 97:3	butanol-2 N HCl 1:1 upper phase	acetic acid-conc.HCl-water 15:3:82	acetic acid-conc.HCl-water 30:3:10
Anthocyanin I	0.32	0.44	0.52	0.68	
Aglycone I		0.03			0.64
Anthocyanin II	0.41	0.13	0.31	0.37	
Aglycone II		0.03			0.63
Luteolinidin		0.02			0.63

their spectral and chromatographic properties were identical (Tables 1 and 2) and when co-chromatographed only one spot was obtained.

The R_F-value in water-acetic acid-conc. HCl (10:30:3, by vol.) indicated that the aglycone contains four hydroxyl groups [7] and the bathochromic shift of the maximum in the presence of aluminium chloride suggested that two or more of the hydroxyl groups are adjacent [8]. The aglycone has no hydroxyl group in the 3-position since it was not oxidized by dilute ferric chloride solution and, according to Robinson, only those anthocyanidins with an hydroxyl group in the 3-position are decolourised by this reagent [9].

The infrared spectrum of the aglycone showed all the characteristic features of an anthocyanidin spectrum [10,11]. The absence of a band at about 1460 cm^{-1} confirmed that the aglycone has no methoxyl group. Furthermore, the infrared spectrum was identical with that of luteolinidin (5,7,3′,4′-tetrahydroxyflavylium chloride) synthetized from the triacetate of phloroglucinaldehyde and 3,4-dihydroxyacetophenone diacetate [9,11].

Further evidence for identifying the aglycone as luteolinidin was obtained by comparing their spectral and chromatographic properties (Tables 1 and 2) as well as their colour reactions in acid and alkaline solutions [12]. Another proof of their being identical was that the co-chromatogram gave only one spot.

The position of attachment of the carbohydrates in the two anthocyanins was deduced from spectral data. According to Harborne [13], the percentage intensity at 440 mμ of a 5-substituted anthocyanidin is approximately half that of the corresponding anthocyanidin in which the 5-hydroxyl group is free. The value of the ratios E_{440}/E_{max} for the two anthocyanins as compared to that of the aglycone (Table 1) indicated that the isolated anthocyanins both have a substituted hydroxyl group in the 5-position.

Anthocyanin II was formed by controlled acid hydrolysis of anthocyanin I, the identification being based on chromatography and co-chromatography in different solvents [14]. This indicated that anthocyanin I is a diglycoside and anthocyanin II is the corresponding monoglycoside.

The sugars obtained on acid hydrolysis of the two anthocyanins were identified by paper chromatography in different solvents (Table 3) [15–17] as

Table 3. Identification of the sugars produced by hydrolysis of the anthocyanins.

	butanol [15]-acetic acid-water 4:1:5 upper phase 8 h	phenol [15] 10 h	pyridine [16]-butanol-water 7 h		ethyl acetate [17]-pyridine-water 2:1:2 5 h	
Glucose	0.175	0.42	0.385	0.42	0.54	0.64
Galactose	0.17	0.48	0.34	0.36	0.515	0.62
Fructose	0.25	0.555	0.45	0.47	0.57	0.65
Rhamnose	0.41	0.65	0.62	0.66	0.70	0.78
Sugar from anthocyanin I	0.17	0.42	0.39		0.545	
Sugar from anthocyanin II		0.42		0.41		0.66

glucose. Since the aglycone:glucose ratio in anthocyanin I was found to be 1:1.8, the two isolated anthocyanins must be luteolinidin-5-diglucoside and luteolinidin-5-monoglucoside.

Dr. O. Theander, Stockholm, has made a pre-investigation of the disaccharide obtained by hydrolysis of luteolinidin-5-diglucoside in dilute acetic acid. Although the amount of the disaccharide available was insufficient for a structure determination, the preliminary results indicated that the disaccharide part is 2-*O*-*α*-D-glucopyranosyl-D-glucose (kojibiose). As soon as more material is available this investigation will be continued.

Since the diglucoside is easily hydrolysed to the corresponding monoglucoside, it might be thought that the latter pigment is an artefact formed during the extraction procedure. However, since the relative amounts of the two glucosides are fairly independent of the time of extraction at 0° we suggest that the monoglucoside also occurs in the moss.

Luteolinidin has long been known as a synthetic compound but has not until recently been found to occur naturally as luteolinidin-5-monoglucoside in the petals of *Gesneria cardinalis* and in the sepals and leaves of *Kohleria eriantha* (fam. Gesneriaceae)[18]. Luteolinidin-5-diglucoside has not earlier been found in nature.

It may be pointed out that *B. cryophilum* is considered to be closely related to *B. duvalii* investigated by Herzfelder and found to contain cell sap anthocyanins. Our investigation indicates that *B. cryophilum* contains not only cell sap anthocyanins which are identical with the luteolinidin derivatives isolated but probably also cell wall pigments. This suggestion is substantiated by the fact that it is impossible to extract all the red pigments by merely treating the moss in the cold with methanolic hydrochloric acid. Several hours refluxing with the solvent is necessary to free the remainder from red pigments. The same difficulties connected with the complete extraction of cell wall pigments have been earlier pointed out by Herzfelder and recently by Goodman and Paton when investigating some *Sphagnum* species. This agrees with our extraction experiments on some *Sphagnum* species showing that the cell wall pigments are only partially extracted in the cold by the above mentioned solvent.

Luteolinidin, luteolinidin-5-monoglucoside and the third pigment have been found in the methanolic extract obtained by boiling moss previously extracted in the cold. This fact suggests that some luteolinidin derivative, possibly one or both of the isolated anthocyanins, may also occur fixed in some way to the cell wall. As to the third pigment we have observed a certain resemblance between it and some red cell wall pigments isolated from two *Sphagnum* species suggesting that the former might occur in the cell wall only.

Although only a single moss with cell sap pigments has been investigated, there are reasons to believe that either luteolinidin derivatives or similar anthocyanins may also occur in closely related species of the same genus with cell sap pigments. Regarding the mosses containing only cell wall pigments, our pre-investigations of the red pigments of *Sphagnum magellanicum* Brid. and *S. nemoreum* Scop. (belonging to the groups *Palustria* and *Acutifolia*, respectively) indicate that they are different to the anthocyanins from *B. cryophilum*. At least one of the red pigments in each of these *Sphagnum* species

seems to be an anthocyanidin derivative although not a glycoside since preliminary assays indicate that these two isolated pigments do not contain sugars.

We have also investigated a pleurocarpous moss, *Drepanocladus pseudosarmentosus* (Card. & Thér.) H. Perss., which has reddish cell wall pigmentation. One of the pigments of this moss shows a chemical behaviour somewhat resembling that of the red pigments of anthocyanidin type isolated from the two *Sphagnum* species mentioned above. The other pigment seems to be related to the anthocyanins of *B. cryophilum*.

EXPERIMENTAL

Whatman No. 1 filter paper was used for the paper chromatography unless otherwise stated. The descending chromatographic method was always used. The absorption spectra were measured in methanol containing 0.01 % conc. HCl with a Beckman DU spectrophotometer and the infrared absorption measurements were made with an Unicam 100 spectrophotometer with a sodium chloride prism.

Separation and purification of the anthocyanins. Air-dried moss (22 g) was chopped in a Turmix blendor in methanol-conc. HCl (35:1 v/v) (400 ml), kept at 0° overnight and filtered. Fresh solvent (150 ml) was added to the moss and after a week's storage at 0° it was again filtered. The precipitate formed on addition of ether (15 times the volume) to the combined methanolic extracts was treated with the smallest possible amount of aqueous acetic acid (10 %) and insoluble material removed by centrifugation. The acetic acid solution was passed through a Sephadex (Pharmacia, Uppsala), column, the elution being performed with the same solvent. Three fractions were collected. The second contained the anthocyanins and was evaporated to dryness *in vacuo*. The residue was taken up in aqueous acetic acid (5 %) and chromatographed on a cellulose powder (Grycksbo) column, the same solvent being used for the elution. The eluate was collected in 10 ml fractions and its absorption was recorded at 253 mμ by means of an ultraviolet registrating photometer. Five distinct bands were obtained of which No. 2 and No. 4 contained anthocyanins I and II, respectively. The fractions corresponding to band No. 2 were combined and evaporated to dryness *in vacuo* and the residue (120 mg), consisting of anthocyanin I, was recrystallized from methanol-conc. HCl yielding dark reddish-brown crystals. The fractions containing anthocyanin II were concentrated *in vacuo* to a small volume and again chromatographed on a cellulose powder column as above. After evaporation to dryness *in vacuo* a dark red residue (4 mg) was obtained which was chromatographically pure.

For separation and purification by means of paper chromatography the combined methanolic extracts were concentrated to a small volume *in vacuo* at 30–40°, extracted with petroleum ether and ethyl acetate and finally diluted with methanol-conc. HCl (97:3 v/v). After centrifugation the methanolic solution was applied as a thin band near one edge of a Whatman No. 3 MM filter paper. When developed with the upper phase of butanol-2 N HCl (1/1 v/v) three red bands were obtained, corresponding to anthocyanins I and II and the third red pigment. These were cut out without previous drying and the pigments were eluted with water-methanol-acetic acid (25:70:5, by vol.). Each of the resulting solutions were then concentrated to a small volume *in vacuo*, applied as a streak on No. 3 MM Whatman filter paper and further purified by running in water-acetic acid (85:15 v/v), the elution being made as before. The last traces of impurities were removed by re-running the anthocyanins in the same solvent. Since only a small amount of the third pigment was obtained this could not be satisfactorily purified.

The isolated anthocyanins were tested for homogeneity by paper chromatography in different solvents [19]. The R_F values are given in Table 2 and the spectral data in Table 1.

Identification of the anthocyanins. (*a*) Qualitative hydrolysis. The glucosides were heated with 4 N HCl at 100° for one hour and the solution was then cooled. The aglycones were extracted with pentanol. The combined extracts were washed with water and after removal of the solvent the aglycones were dissolved in methanol-conc. HCl (97:3 v/v). The R_F values, colour reactions and the absorption spectra of the two aglycones were

identical to those of a synthetic sample of luteolinidin (Tables 1 and 2). The infrared spectrum (KBr phase) of the aglycone obtained from anthocyanin I was also identical with that of luteolinidin (KBr phase).

The aqueous phases and the washings from the hydrolysis experiments were combined in order to analyse the sugars and the acid removed by washing with 10 ml portions of a 10 % (w/w) solution of dioctylmethylamine in chloroform until the aqueous solutions were neutral [20]. The aqueous solutions were then concentrated *in vacuo* and chromatographed together with authentic markers in four different solvent systems [15-17]. The sugars were detected by spraying the chromatograms with aniline hydrogen phthalate in butanol and heating at 110° for 5 min.[21] The results are shown in Table 3. The two hydrolysis solutions always yielded a single spot corrresponding to glucose.

(*b*) Quantitative hydrolysis [22]. Anthocyanin I (*ca.* 2.5 mg) in 4 N HCl (1.5 ml) was heated for 30 min in the dark (to prevent decolourization) at 100° under reflux, cooled and diluted with water to 10 ml. The absorbance of this solution at 480 mμ was immediately measured and by means of a standard solution, measured in the same solvent, the concentration of the aglycone was determined.

For determination of the sugar concentration 1 ml of the solution used for the above measurements was added to an anthrone solution (10 ml 0.2 % in 95 % sulphuric acid) and immediately heated for 7 min on a boiling water bath, 10 min after the heating had ceased, the absorption of the solution was measured at 620 mμ and compared with standard glucose solutions [23]. The following results were obtained:

concentration of aglycone:	0.11 mg/ml
» » glucose:	0.12 mg/ml
molar ratio glucose/aglycone:	1.8 : 1

(*c*) Partial hydrolysis of anthocyanin I. Anthocyanin I (2 mg) in 2 N HCl (3 ml) was heated at 100° for 10 min. The mixture was cooled, applied as a streak to No. 3 MM filter paper and developed with the upper phase of butanol-2 N HCl (1:1 v/v). Three red bands were obtained, cut out and eluted with water-methanol-acetic acid (25:70:5 by vol.). The concentrated eluates were re-run in water-acetic acid conc. HCl (82:15:3 by vol.). After elution the pigments were identified as unchanged anthocyanin I, anthocyanin II and luteolinidin by means of chromatography and co-chromatography.

Determination of the disaccharide. Anthocyanin I (20 mg) was refluxed for 5 h with aqueous acetic acid (10 %; 5 ml). After cooling, the solution was extracted with pentanol and the extract washed with water. The acetic acid solution and the washings were evaporated to dryness *in vacuo*. The residue, containing only a very small amount of the disaccharide, has been investigated by Dr. O. Theander, Svenska Träforskningsinstitutet, Träkemiska avdelningen, Stockholm. However, the amount of the disaccharide was not sufficient for a complete determination of the structure.

Investigation of the extract obtained by refluxing the moss. Dried moss extracted twice at 0° with methanol-conc. HCl (35:1 v/v) was refluxed for 4 h with the same solvent and then filtered. After concentration *in vacuo* to a small volume and treatment with petroleum ether and ethyl acetate, the methanolic solution was applied to Whatman No. 3 MM filter paper. When developed with the upper phase of butanol-2 N HCl (1:1 v/v), three red bands were obtained. These were cut out, eluted with water-methanol-acetic acid (25:70:5 by vol.) and concentrated *in vacuo* at 30—40° to a small volume. By chromatographic data the three pigments were identified as luteolinidin, luteolinidin-5-monoglucoside and the third red pigment.

Acknowledgements. The authors are indebted to the head of the organic department, Professor A. Fredga, for his kind interest in this work and for the facilities put at their disposal. They are also indebted to Professor B. Lindberg for advice about and to Dr. O. Theander for studies on the disaccharide. Their thanks are also due to Dr. B. Nygård for the infrared measurements. A grant from the *Swedish Natural Science Research Council* is gratefully acknowledged.

REFERENCES

1. Douin, R. *Compt. rend.* **243** (1956) 1051; **246** (1958) 1248.
2. Herzfelder, H. *Beih. Botan. Centr.* **38** (1921) 355.
3. Goodman, P. J. and Paton, J. A. *Trans. Brit. Bryol. Soc.* **2** (1954) 470.
4. Paton, J. A. and Goodman, P. J. *Ibid*, p. 561.
5. Bendz, G. and Mårtensson, O. *Acta Chem. Scand.* **15** (1961) 1185.
6. Harborne, J. B. *Biochem. J.* **74** (1960) 262.
7. Bate-Smith, E. C. and Westall, R. G. *Biochim. et Biophys. Acta* **4** (1950) 427.
8. Geissman, T. A. and Jurd, L. *Arch. Biochem. Biophys.* **56** (1955) 259.
9. León, A. and Robinson, R. *J. Chem. Soc.* **133** (1931) 2732.
10. Ribéreau-Gayon, P. and Josien, M.-L. *Bull. soc. chim. France* **1960** 934.
11. *To be published.*
12. Pratt, D. D. and Robinson, R. *J. Chem. Soc.* **127** (1925) 1128.
13. Harborne, J. B. *Biochem. J.* **70** (1958) 22.
14. Harborne, J. B. and Sherratt, H. S. A. *Experientia* **13** (1957) 486.
15. Partridge, S. M. and Westall, R. G. *Biochem. J.* **42** (1948) 238.
16. Chargaff, E., Levine, C. and Green, C. *J. Biol. Chem.* **175** (1948) 67.
17. Jermyn, M. A. and Isherwood, F. A. *Biochem. J.* **44** (1949) 402.
18. Harborne, J. B. *Chem. & Ind. London* **1960** 229.
19. Harborne, J. B. *J. Chromat.* **1** (1958) 473.
20. Smith, E. Lester and Page, J. E. *J. Soc. Chem. Ind.* **67** (1948) 48.
21. Partridge, S. M. *Nature* **164** (1949) 443.
22. Nordström, C. G. and Swain, T. *J. Chem. Soc.* **1953** 2764.
23. Hewitt, B. R. *Nature* **182** (1958) 246.

Received December 28, 1961.

ACTA CHEMICA SCANDINAVICA 16 (1962) 1191–1198

Studies on Peroxy Compounds

XXI. The Preparation of 3-Substituted Levulinic Esters *

SVEN-OLOV LAWESSON**, MONICA DAHLÉN and (in part) CHRISTER FRISELL

Department of Organic Chemistry, Chemical Institute, University of Uppsala, Uppsala, Sweden

Submitted in honour of the sixtieth birthday of our teacher, Professor *Arne Fredga*

Heating a tertiary β-ketoester with *p*-toluenesulphonic acid easily causes elimination of the carbo-*t*-butoxy group without side reactions. Starting from derivatives of *t*-butyl acetoacetate, a convenient method for the preparation of 3-alkylsubstituted levulinates is described. 3-Benzoyloxy derivatives of ethyl levulinates were also prepared by reacting benzoyl peroxide with the sodium compounds of different mixed succinates. An attempt to prepare a compound of the acyloin-type by alcoholysis of a benzoyloxy compound only gave an unsaturated ester.

In a series of papers Lawesson *et al.* have recently studied the reaction between benzoyl peroxide and sodium compounds of so-called active methylene compounds. It was found that the benzoyloxy group is easily introduced into diethyl malonates giving O-benzoyltartronates [1], from which diethyl tartronates and tartronic acids could be prepared. Ethyl benzoyloxycyanoacetates [2] were also easily prepared. These compounds are of potential interest in connection with studies on amino acid precursors. β-Ketoesters [3] and β-diketones [4] also react smoothly to give the corresponding benzoyloxy derivatives. *t*-Butyl

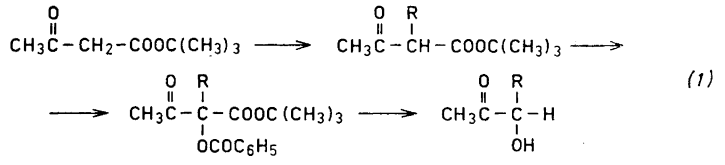

(1)

I

* Part XX. Lawesson, S.-O. and Berglund, C. *Arkiv Kemi* **17** (1961) 485.

** Present address: Department of Chemistry, University of Aarhus, Aarhus, Denmark.

acetoacetate, which is easily prepared from diketene and *t*-butyl alcohol, has been investigated and a novel method of preparing acyloins [5] has been developed according to scheme (1).

The carbo-*t*-butoxy group is easily split off from the *α*-benzoyloxy derivative, I, on heating with *p*-toluenesulphonic acid and, generally, the *β*-carbonyl compound, II, is readily transformed into III under the same conditions (for pertinent references, see Frisell and Lawesson [6]).

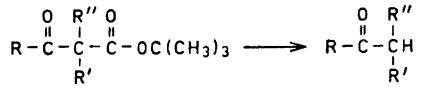

(2)

II III

As an extension of the benzoyl peroxide project [1–5] described in this paper, some work is recorded here on ethyl levulinates with special reference to the preparation of 3-substituted derivatives.

Treibs and Hintermeier [7] prepared ethyl levulinate by reacting the sodium compound of *t*-butyl acetoacetate with ethyl chloroacetate in ethanol as solvent, whereby 1-acetyl-1-carbo-*t*-butoxy-2-carbethoxy-ethane, IV, was first formed. By decomposing IV, ethyl levulinate, V, was obtained in high yields.

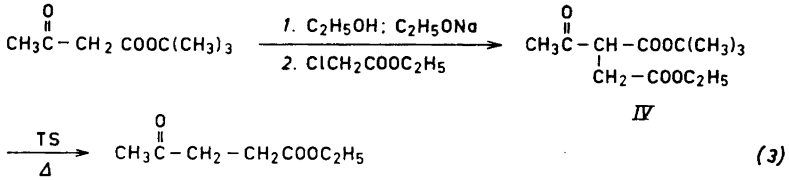

(3)

V

As the oxygen-oxygen bond in benzoyl peroxide is smoothly ruptured when the sodium compound of a so-called active methylene compound is allowed to react with this peroxide, the acetyl succinate, IV, and related compounds should be suitable starting materials for such work, especially as we were interested in extending the new acyloin method [5]. We therefore prepared succinates (VI, a—e)

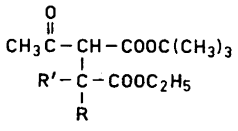

VI

VI *a*: R=R′=H VI *d*: R=R′=CH_3

VI *b*: R=H; R′=CH_3 VI *e*: R=H; R′=n-C_6H_{13}

VI *c*: R=H; R′=C_2H_5

by reacting the sodium compound of *t*-butyl acetoacetate with the appropriate *α*-bromoester. Using ethyl alcohol as solvent, we did not observe any re-esterifi-

action of the *t*-butyl ester. Much lower yields were found when benzene was used as solvent. The succinates VI, a—e, are all rather stable compounds and could be distilled without any observable decomposition. VI (R=H; R′=C_6H_5), however, decomposed on attempted distillation.

The procedure for the subsequent reaction with benzoyl peroxide in benzene was the same as that earlier described [1] and in all cases quantitative yields of benzoic acid were isolated and no gas evolution was observed. No attempts were made to isolate the new products either by crystallization or distillation. Instead, after the usual work-up, catalytic amounts of *p*-toluenesulphonic acid were added and the carbo-*t*-butoxy group eliminated in the usual way. The 3-benzoyloxy levulinates were obtained in high yields. These were stable and did not show any tendency to decompose on distillation.

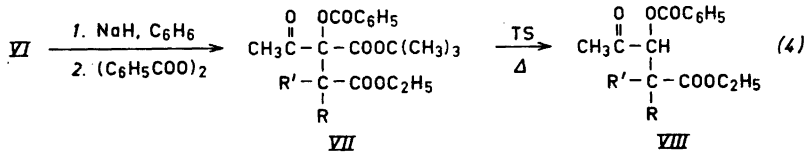

VIII a: R=R′=H VIII d: R=R′=CH_3

VIII b: R=H; R′=CH_3 VIII e: R=H; R′=n-C_6H_{13}

VIII c: R=H; R′=C_2H_5

Having a series of benzoyloxy compounds VIII available, we investigated the possibility of preparing compounds of the acyloin type. It is known that the free acyloin is easily prepared from O-benzoylacyloins by hydrolysis with a base [5]. However, in our case, only small amounts of ethyl acetylacrylate were isolated by alcoholysis of VIII a, indicating that a 1,2-elimination had occurred.

Levulinic ester is the simplest member of γ-ketoesters and is especially attractive as a chemical intermediate because of its various reactive centres. The chemistry of levulinic acid and its esters is not well investigated although their uses as chemical intermediates, solvents, emulsifiers, plasticizers, pharmaceuticals etc. are well known. We have prepared some 3-alkylsubstituted levulinic esters as the starting material for further investigations. Using *t*-butyl acetoacetate instead of ethyl acetoacetate, the elimination of the *t*-butyl ester group under mild conditions is possible without hydrolysis of the ethyl ester group.

Alkylsubstituted *t*-butyl acetoacetates (in the form of the sodium compounds) reacted smoothly with ethyl bromoacetate and some other α-bromoesters and the corresponding levulinic esters were isolated in high yields. In one case, the levulinic ester was hydrolyzed to 3-hexyl levulinic acid which is thought to be a degradation product [8] of Antimycin A_1. A mixed melting point with the 2,4-dinitrophenylhydrazone of the named degradation product * was not depressed and the infrared spectra were superimposable.

* We are grateful to Professors E. E. van Tamelen and F. M. Strong for supplying a sample of this compound.

By reacting the sodium compounds of *t*-butyl iso-propyl acetoacetate and *t*-butyl *sec*-butylacetoacetate with ethyl bromoacetate, either in ethanol or benzene, the expected product was not formed and only diethyl *β*-acetylglutarate could be isolated. At present no explanation can be presented for this unusual observation.

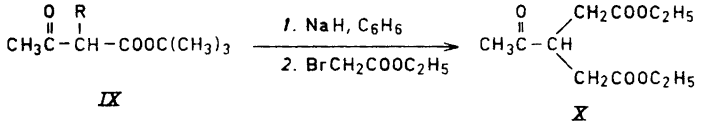

IX a: R = i-C_3H_7

IX b: R = sec-C_4H_9

It was shown that the starting materials actually were IX a and IX b by decomposing them in the presence of *p*-toluenesulphonic acid and isolating the corresponding ketones in high yields. The identity of *β*-acetylglutarate, X, was shown by an unequivocal synthesis.

EXPERIMENTAL

The reactions between benzoyl peroxide and the sodium derivatives were carried out in an atmosphere from which moisture was excluded. Benzoyl peroxide was recrystallized at low temperature from chloroform and methanol. The infrared spectra were recorded on an Infracord. The analyses were made at the Analytical Department of Uppsala University. Boiling and melting points are not corrected.

Starting material

t-Butyl acetoacetate and alkylated derivatives thereof were prepared according to Lawesson *et al.*[5] *t*-Butyl isopropylacetoacetate, a new compound, was prepared as described below. The *α*-bromo carboxylic esters were purchased from Schuchardt, Munich, and used without further purification. Bromoacetone was prepared according to *Organic Syntheses*[9].

t-Butyl isopropylacetoacetate. To a sodium alcoholate solution, prepared from 6.9 g of sodium in 150 ml of ethyl alcohol, 47.4 g (0.3 mole) of *t*-butyl acetoacetate were added. After 15 min 51 g (0.3 mole) of isopropyliodide was added during 30 min and the mixture then refluxed for 7.5 h. The excess ethanol was then immediately stripped off at reduced pressure and the remaining solution poured into water. The water phase was twice extracted with ether. The combined ether extracts were washed with water until neutral and then dried over sodium sulphate. Distillation gave the main fraction at b.p. 90°C/11 mm Hg as a colourless liquid. Yield 47.4 g (79 %), n_D^{20} = 1.4238. (Found: C 65.83; H 10.06. Calc. C 65.97; H 10.07).

Preparation of succinic esters

VI a. Sodium alcoholate was prepared from 6.9 g (0.3 mole) of sodium in 150 ml of ethanol to which 47.4 g (0.3 mole) of *t*-butyl acetoacetate were added. Thereafter 50.3 g (0.3 mole) of ethyl bromoacetate were added dropwise during 15 min and gentle reflux was maintained for 30 min. The ethanol was then stripped off, the remaining solution poured into water + acid. The water phase was extracted with ether several times. The combined ether extracts were washed with water until neutral, dried over sodium sulphate and distilled. The main fraction was a colourless liquid with b.p. 106°C/0.6 mm Hg; n_D^{20} = 1.4338. Yield 58 g (79 %). (Found: C 59.00; H 8.32. Calc.: C 59.00; H 8.25).

When ethyl chloroacetate was used instead of ethyl bromoacetate, the diester was obtained in 62—69 % yield.

VI b. 0.4 mole of sodium ethoxide was prepared in 200 ml of absolute ethanol, and 63 g (0.4 mole) of *t*-butyl acetoacetate were added. After the exothermic reaction had ceased, 72.4 g (0.4 mole) of ethyl *a*-bromopropionate were added and gentle reflux was maintained for 45 min. The ethanol was distilled off and the work-up was performed as above. A colourless liquid was obtained with b.p. 90—92°C/0.3 mm Hg; n_D^{20} = 1.4342. Yield 87.4 g (85 %). (Found: C 60.23; H 8.57. Calc.: C 60.44; H 8.59).

When the sodium compound of *t*-butyl acetoacetate was prepared in benzene from sodium hydride, the following reaction with ethyl *a*-bromoproprionate gave only VI b in 28 % yield.

VI c. The diester was prepared as above from 6.9 g (0.3 mole) of sodium in 150 ml of ethanol, 47.4 g (0.3 mole) of *t*-butyl acetoacetate and 58.5 g (0.3 mole) of ethyl *a*-bromobutyrate (gentle reflux for about 2 h). Distillation gave a colourless liquid with b.p. 120—123°C/0.7 mm Hg; n_D^{02} = 1.4389. Yield 59.6 g (73 %).

VI d. The ester was prepared from 4.6 g (0.2 mole) of sodium in 100 ml of ethanol, 31.6 g (0.2 mole) of *t*-butyl acetoacetate and 39 g (0.2 mole) of ethyl *a*-bromo-isobutyrate (refluxed for 5 h). The usual work-up gave a colourless liquid with b.p. 120—123°C/0.7 mm Hg; n_D^{20} = 1.4433. Yield 13.8 g (25 %).

VI e. The diester was prepared from 79.0 g (0.5 mole) of *t*-butyl acetoacetate and 125.5 g (0.5 mole) of ethyl *a*-bromocaprylate in the usual way (refluxed for 3 h). A colourless liquid with b.p. 130—131°C/0.6 mm Hg; n_D^{20} = 1.4428. Yield 99.1 g (60 %). (Found: C 65.64; H 9.79; Calc.: C 65.82; H 9.82).

The preparation of ethyl *a*-bromocaprylate

88 g (0.74 mole) of redistilled thionyl chloride were placed in a 500 ml three-necked flask, fitted with a stirrer, a dropping funnel and a reflux condenser. After heating the chlorinating agent till gentle reflux, 97.5 g (0.68 mole) of newly distilled caprylic acid were added dropwise during 30 min. Gentle reflux was maintained for a further 30 min, whereafter 0.5 g of red phosphorus were added. After heating till reflux 40 ml (124 g, 0.78 mole) of bromine were added dropwise during 2 ½ h and the mixture was then refluxed for a further 4 ½ h. After cooling, the mixture was poured into the dropping-funnel and in the flask were placed 100 ml of ethanol, to which the mixture was added during on hour. Gentle reflux was maintained for 3 h. Ether was added to the mixture and after washing with sodium bicarbonate and water and drying over sodium sulphate, the ether was stripped off. Distillation gave a colourless liquid with b.p. 118—119°C/11 mm Hg; n_D^{20} = 1.4545. Yield 132.7 g (77 %). (Found: C 47.80; H 7.62. Calc.: C 47.82; H 7.63).

The preparation of ethyl 2-alkyl-3-benzoyloxy-levulinates

VIII a. 4.8 g (0.2 mole) of sodium hydride, covered with 200 ml of dry benzene were placed in a three-necked flask, fitted with a stirrer, reflux condenser and dropping funnel. 48.8 g (0.2 mole) of VI a were added dropwise and when all sodium hydride had been consumed the flask was cooled in an ice-water bath, 36.3 g (0.15 mole) of benzoyl peroxide in 300 ml of benzene were then added during 45 min. After one hour the peroxide test was negative; the mixture was poured out onto water, and the benzene phase separated. The water layer was extracted many times with ether, the combined organic phases washed neutral whit water and dried over sodium sulphate. The solvents were then stripped off and to the remaining solution 0.25 g of *p*-toluenesulphonic acid were added. The distillation vessel was connected to a water pump and warmed on an oil-bath maintained at a temperature of 160°C. When the decomposition was complete (constant pressure) the product was distilled. The main fraction was a pale yellow liquid with b.p. 137—139°C/0.2 mm Hg. n_D^{20} = 1.5022. Yield 33.1 g (86 %). (Found: C 63.30; H 6.19. Calc.: C 63.62; H 6.10). From the water phase 18 g of benzoic acid were isolated.

VIII b. This compound was prepared from 77.4 g (0.3 mole) of VI b and 7.2 g (0.3 mole) of sodium hydride in 225 ml of benzene and 48.4 g (0.2 mole) of benzoyl peroxide

in 400 ml of benzene. The reaction was complete after one hour. The product, which was weakly yellow, had b.p. 142–145°C/0.4 mm Hg. n_D^{20} = 1.4980. Yield 35 g (63 %). (Found: C 64.41; H 6.63. Calc.: C 64.73; H 6.52). Isolated benzoic acid = 24 g.

VIII c. The levulinate was prepared from 54.4 g (0.2 mole) of VI c, 4.8 g (0.2 mole) of sodium hydride and 36 g (0.15 mole) of benzoyl peroxide in a total volume of 450 ml benzene. After the usual work-up, the product was obtained with b.p. 147–150°C/0.4 mm Hg; n_D^{20} = 1.4960. Yield 19.4 g (44 %). (Found: C 65.94; H 6.98. Calc.: C 65.74; H 6.90).

VIII d. The sodium compound of VI d was prepared from 1.4 g (0.06 mole) of sodium hydride and 16.4 g (0.06 mole) of VI d in 75 ml of benzene. 9.7 g (0.04 mole) of benzoyl peroxide in 100 ml of benzene were added and after one hour all peroxides hade been consumed. The work-up gave quantitative yields of benzoic acid and the main product with b.p. 141–144°C/0.3 mm Hg; n_D^{20} = 1.5098. Yield 6.5 g (56 %). (Found: C 65.17; H 6.92. Calc.: C 65.74; H 6.90).

VIII e: The levulinate was prepared as above from 98.4 g (0.3 mole) of VI e and 7.2 g (0.3 mole) of sodium hydride in 225 ml of benzene and 48.4 g (0.2 mole) of benzoyl peroxide dissolved in 400 ml of benzene. No gas was evolved. 20.3 g (84 %) of benzoic acid were isolated and the product had b.p. 169–171°C/0.4 mm Hg; n^{20} = 1.4888. Yield 50.5 g (73 %). (Found: C 68.78; H 8.25. Calc.: 68.94; H 8.10).

Ethanolysis of VIII a. Sodium alcoholate was prepared from 4.6 g (0.2 mole) of sodium in 100 ml of ethanol. 52.8 g (0.2 mole) of ethyl 3-benzoyloxy levulinate were added dropwise during 15 min. A brown-red precipitate was formed immediately and the mixture stirred for 45 h at room temperature. The mixture was then poured onto water and this phase was extracted 5 times with ether. The combined extracts were washed until neutral with water, dried over sodium sulphate and distilled. A product with b.p. 78–80°C/8 mm Hg was obtained, n_D^{20} = 1.4500, yield 6.2 g (22 %) and was indentified as ethyl 3-acetylacrylate. The 2,4-dinitrophenylhydrazone had m.p. 148–149.5°C and the mixed m.p. with the authentic hydrazone was not depressed on admixture. 16.6 g of the starting material (VIII a) were recovered and from the water phase 17.8 g of benzoic acid was isolated.

Preparation of substituted levulinic esters

General procedure. Sodium hydride, covered with dry benzene, was placed under nitrogen in a three-necked flask fitted with a reflux condenser, a stirrer and a dropping funnel. The β-ketoester was added slowly and the sodium hydride was then consumed (in most cases heat was applied). The α-bromoester was then added quickly and the mixture heated under gentle reflux until nearly neutral. The benzene phase was poured into water, the benzene phase separated and the water phase extracted three times with ether. The combined organic phases were washed with water until neutral, dried over sodium sulphate and finally the solvents were stripped off. To the remaining solution 0.25 g of *p*-toluenesulphonic acid were added and the distillation vessel connected to a water pump and warmed on an oilbath, maintained at a temperature of about 150°C. When the decomposition was complete (constant pressure) the product was distilled. Before the final distillation, the product was always taken up in ether and washed with sodium bicarbonate to remove acidic substances.

Ethyl 3-benzyl levulinate. 49.6 g (0.2 mole) of *t*-butyl benzylacetoacetate were added to 4.8 g (0.2 mole) of sodium hydride covered with 150 ml of benzene. 33.5 g (0.2 mole) of ethyl bromoacetate were added and the mixture refluxed for 3 h. After the usual work-up, distillation gave the main fraction as a colourless liquid, b.p. 121–122°C/0.4 mm Hg. Yield 41.1 g (88 %); n_D^{20} = 1.5028. (Found: C 71.44; H 7.73. Calc.: C 71.77; H 7.74).

Ethyl 3-allyl levulinate was prepared from 4.8 g (0.2 mole) of sodium hydride covered with 150 ml of benzene, 40 g (0.2 mole) of redistilled *t*-butyl allyl acetoacetate and 33.5 g (0.2 mole) of ethyl bromoacetate. The product was obtained after the usual work-up and was a colourless liquid with b.p. 67–69°C/0.4 mm Hg. n_D^{20} = 1.4444. Yield 32.5 g (88 %). (Found: C 65.12; H 8.75. Calc.: C 65.19; H 8.75).

Ethyl 3-ethyl levulinate. The sodium compound was prepared from 4.8 g (0.2 mole) of sodium hydride, covered with 150 ml of benzene and 36 g (0.2 mole) of *t*-butyl ethyl acetoacetate. 33.5 g (0.2 mole) of ethyl bromoacetate were added and after reflux for

2.5 h the usual work-up was performed. The main fraction was a colourless liquid and had b.p. 58—60°C/0.4 Hg; n_D^{20} = 1.4312. Yield 29.5 g (86 %). (Found: C 62.34; H 9.34; Calc.: C 62.76; H 9.36).

Ethyl 2-methyl-3-benzyllevulinate. The sodium compound was prepared from 4.8 g (0.2 mole) of sodium hydride and 49.6 g (0.2 mole) of *t*-butyl benzyl acetoacetate. 36.2 g (0.2 mole) of ethyl *a*-bromopropionate were added and after reflux for 5 h the usual work-up gave a colourless liquid with b.p. 125—127°C/0.4 mm Hg; n_D^{20} = 1.5072. Yield 33.4 g (67 %). (Found: C 72.28; H 7.82. Calc.: C 72.55; H 8.12).

Ethyl 2-phenyllevulinate. Sodium alcoholate was prepared from 4.6 g (0.2 mole) of sodium in 100 ml of ethanol and (0.2 mole) of *t*-butyl acetoacetate were added. 48.6 g (0.2 mole) of ethyl *a*-bromophenylacetate were then added during 15 min and the mixture refluxed for 4 h. After the usual work-up, attempted distillation of the diester showed that it decomposed slowly. The carbo-*t*-butoxy group was therefore eliminated by adding TS. The main fraction had b.p. 136—139°C/0.6 mm Hg; n_D^{20} = 1.5038. Yield 30 g (68 %). (Found: C 70.32; H 7.32. Calc.: C 70.89; H 7.32). After some time the liquid crystallized and recrystallization from petrol ether gave needles with m.p. 40—41°C.

The preparation of 2-hexyllevulinic acid

a) *Ethyl 2-hexyllevulinate.* 92 g of VI e were decomposed in the presence of *p*-toluenesulphonic acid and gave 56 g of ethyl 2-hexyllevulinate, n_D^{20} = 1.4418, b.p. 95—97°C/0.4 mm Hg.

b) *2-Hexyllevulinic acid.* 45.6 g of ethyl 2-hexyllevulinate were mixed with 225 ml of 2 M sodium hydroxide solution and the solution was refluxed for 1 ½ h. After cooling, the water phase was acidified and exracted three times with ether. The combined extracts were washed once with water and dried over sodium sulphate. Distillation gave a colourless liquid with b.p. 145°C/0.4 mm Hg; n_D^{20} = 1.4502. Yield 26.4 g (66 %). (Found: C 66.11; H 10.08. Calc.: C 65.97; H 10.07).

The 2,4-dinitrophenylhydrazone of the acid was prepared in the usual waya nd recrystallized from ethanol + acetone to a constant melting point 123—124°C. The mixed m.p. with the degradation product was not depressed. (Found: C 53.76; H 6.43; N 14.68. Calc.: C 53.70; H 6.36; N 14.72).

Attempts to prepare ethyl 3-sec-butyl levulinate. 42.8 g (0.2 mole) of *t*-butyl sec-butyl acetoacetate were added to 4.8 g (0.2 mole) of sodium hydride in 150 ml of benzene. Thereafter, when all hydride was consumed, 33.5 g (0.2 mole) of ethyl bromoacetate were added and the mixture was refluxed for 3 h. The following work-up was performed in the usual way. Distillation gave a colourless product with b.p. 114—116°C/0.3 mm Hg. n_D^{20} = 1.4435. This product was identified as diethyl *β*-acetyl glutarate. Yield 20.2 g (88 %). (Found: C 57.27; H 7.89. Calc. for $C_{11}H_{18}O_5$: C 57.38; H 7.88).

Attempts to prepare t-butyl 3-isopropyl levulinate. 40 g (0.2 mole) of *t*-butyl isopropyl acetoacetate were added to 4.8 g (0.2 mole) of sodium hydride, covered with 150 ml of benzene. After the sodium compound had been formed, 33.5 g (0.2 mole) of ethyl isopropylacetoacetate were added quickly and the mixture was refluxed for 6 h. The work-up gave a product, identified as diethyl *β*-acetylglutarate, with b.p. 115°—118°C/0.3 mm Hg. n_D^{20} = 1.4438. Yield 15.4 g (67 %).

Decomposition of t-butyl sec-butylacetoacetate. 42.8 g (0.2 mole) of IX b were heated to 150°C in the presence of 0.25 g of *p*-toluenesulphonic acid. After the gas evolution ceased, distillation gave a product with b.p. 144—145°C. Yield 18.9 g (83 %). The semicarbazone (from ethanol) had m.p. 120—122°C; lit.[10] 120°C.

Decomposition of t-butyl isopropylacetoacetate. 40 g (0.2 mole) of IX a were decomposed as above. Methyl isobutyl ketone was obtained with b.p. 117°—119°C (lit.[11] 119°C). The 2,4-dinitrophenylhydrazone was prepared and recrystallized from ethanol. M.p. 84—85°C (lit.[11] 95°). (Found: C 51.37; H 5.79; N 19.92. Calc. for $C_{12}H_{16}O_4N_4$: C 51.42; H 5.75; N 19.99).

The preparation of diethyl β-acetylglutarate. Sodium alcoholate was prepared from 6.9 g (0.3 mole) of sodium and 150 ml of ethanol. 73.2 g (0.3 mole) of VI a were added and after another 15 min 50.3 g (0.3 mole) of ethyl bromoacetate were added dropwise and refluxed for 3 h. The alcohol was stripped off and the remainder worked up in the

usual way. After decomposing the product at 150°C distillation gave a colourless liquid with b.p. 120–121°C/0.3 mm Hg. n_D^{20} = 1.4435. Yield 41.4 g (60 %). (Found: C 56.94; H 7.82. Calc.: C 57.38; H 7.88).

Acknowledgements. The authors wish to express their gratitude to the head of this Institute, Professor A. Fredga, for the facilities put at their disposal. Grants from *Statens Naturvetenskapliga Forskningsråd* and *Lucidol Division, Wallace and Tiernan, Inc., Buffalo, N.Y.*, are gratefully acknowledged.

REFERENCES

1. Lawesson, S.-O., Busch, T. and Berglund, C. *Acta Chem. Scand.* **15** (1961) 260.
2. Lawesson, S.-O. and Frisell, C. *Arkiv Kemi* **17** (1961) 409.
3. Lawesson, S.-O., Andersson, M. and Berglund, C. *Arkiv Kemi* **17** (1961) 429.
4. Lawesson, S.-O., Jönsson, P.-G. and Taipale, J. *Arkiv Kemi* **16** (1961) 441.
5. Lawesson, S.-O., Grönwall, S. and Andersson, M. *Arkiv Kemi* **17** (1961) 457.
6. Frisell, C. and Lawesson, S.-O. *Arkiv Kemi* **17** (1961) 401.
7. Treibs, A. and Hintermeier, K. *Ber.* **87** (1954) 1163.
8. Liu, W.-C., van Tamelen, E. E. and Strong, F. M. *J. Am. Chem. Soc.* **82** (1960) 1652.
9. *Org. Syntheses*, Coll. Vol. II, (1943) 88.
10. Cope, A. C., Hofmann, C. M. and Hardy, E. M. *J. Am. Chem. Soc.* **63** (1941) 1852.
11. Shriner, R. L. and Fuson, R. C. *The Systematic Identification of Organic Compounds*, Wiley & Sons, Inc., New York 1948, p. 262.

Received December 22, 1961.

ACTA CHEMICA SCANDINAVICA 16 (1962) 1199–1205

An Optically Active Ferrocene Carboxylic Acid

LARS WESTMAN* and KENNETH L. RINEHART, JR.

Noyes Chemical Laboratory, University of Illinois, Urbana, Illinois, U.S.A.

Submitted in honour of the sixtieth birthday of Professor *Arne Fredga*

1,1′-Dimethylferrocene-2-carboxylic acid and 1,1′-dimethylferrocene-3-carboxylic acid have been separated by chromatography of their mixed *p*-bromobenzyl esters over alumina. The latter acid has been resolved by means of its cinchonidine salt, which gives the (+)-acid, and its quinidine salt, which gives the (−)-acid.

The geometry of ferrocene (I) [1] is unusual in that the two cyclopentadienyl rings are directly above one another, forming a "sandwich" [2] or "Doppelkegel" [3] structure. The unsubstituted nucleus is remarkably symmetrical, but with the introduction of substituents symmetry is lessened and in ferrocenes containing two or more substituents isomers are possible. Positional isomers were initially studied, by Woodward and Rosenblum [4], who acetylated ethylferrocene (II) to a mixture of 1′-, 2-, and 3-acetylethylferrocenes, and by Rinehart, Motz and Moon [5], who obtained mixtures of 2- and 3-acetyldialkylferrocenes from 1,1′-dimethyl- and 1,1′-diisopropyl-ferrocenes (III and IV, respectively). It has been pointed out by each of these groups, and elsewhere [1], that the number of such positional isomers obtained is precisely that predicted for a ferrocene molecule in which the energy barrier to rotation of the two rings with respect to one another is very low, and other evidence also has been accumulated [6] for ready rotation of the cyclopentadienyl rings.

With two or more substituents on each ring, geometrical isomers are possible as has been demonstrated by the isolation of *meso*- and (±)-forms of 3,3′-diacetyl-1,1′-dimethylferrocene (V) and 2,2′-diacetyl-1,1′-dimethylferrocene (VI) [7], and of 1,2; 1′,2′-*bis*-(α-ketotetramethylene)-ferrocene (VII) [8]. Again, the number of isomers obtained corresponds to the number expected for freely rotating rings.

Since the rings are free to rotate, the molecule does not differ greatly from ethane in its possibilities for optical isomerism. Thus, whenever there are at least two different substituents on one ring, optical isomers exist, just as in

* Present address: Glanshammarsgatan 45, Bandhagen 4, Sweden.

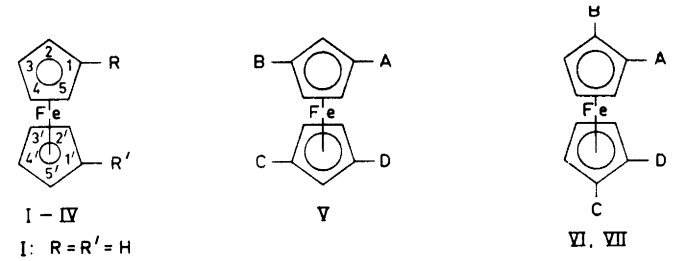

I – IV

I: R = R′ = H

II: R = C_2H_5, R′ = H

III: R = R′ = CH_3

IV: R = R′ = iso-C_3H_7

V

VI, VII

V and VI (*meso*): A = C = CH_3, B = D = $COCH_3$

(±): A = D = CH_3, B = C = $COCH_3$

VII: A + B = C + D = $-(CH_2)_3CO-$

substituted ethanes optical isomers exist whenever one methyl group bears two different substituents (so long as neither of the two substituents is methyl). That this is so is seen by comparison of formulas VIII and IX.

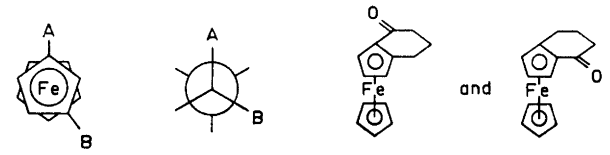

VIII IX X

Optical isomers should, then, be obtainable for homoannularly disubstituted ferrocenes. This was first demonstrated by Thomson [9], who cyclized γ-ferrocenylbutyric acid to 1,2-α-ketotetramethyleneferrocene [8,10] and resolved the latter compounds by means of (−)-menthydrazide. The (+)-ketone obtained had $[\alpha]_D^{15}$ + 550° (*c* 0.3, $CHCl_3$), but the (−)-ketone was not isolated. The present work describes the first resolution of a trisubstituted ferrocene, 1,1′-dimethylferrocene-3-carboxylic acid (XIV), and, apparently, the only reported optically pure enantiomorphic ferrocene. It should be noted, however, that,

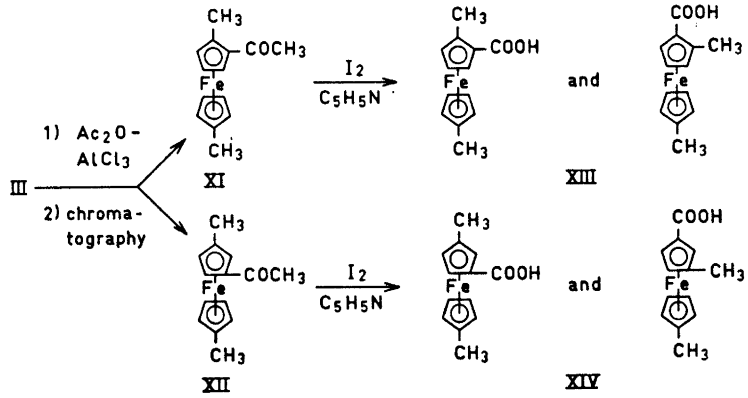

since the mono-substituted ring of XIV is free to rotate with respect to the disubstituted ring, no new element of asymmetry has been introduced beyond that of the 1,2-disubstituted compound X.

Both the 2- and 3-carboxylic acids from 1,1′-dimethylferrocene (XIII and XIV, respectively) were prepared earlier by hypoiodite oxidation of the corresponding 2-acetyl- and 3-acetyl-1,1′-dimethylferrocenes (XI and XII, respectively) [5]. The latter compounds, in turn, had been obtained by acetylation of 1,1′-dimethylferrocene (III) and separation on alumina of the isomeric ketones.

Since the hypoiodite oxidation step of the earlier reaction sequence gave low yields from the difficulty separable isomeric acetyldimethylferrocenes (XI and XII), an alternative route has been developed. In the present method [11] 1,1′-dimethylferrocene was treated with butyllithium * and then with carbon dioxide to give a mixture of acids, which was separated readily into mono- and di-carboxylic acids by the former's solubility and the latter's insolubility in ether [11]. Since earlier attempts to separate the 2- and 3-acids on ion exchange resins and their methyl esters on alumina had failed [11], the acids were converted to their more polar *p*-bromobenzyl esters. These proved readily separable on alumina and the esters XV and XVI were obtained in isomerically pure form. Saponification of these then gave the corresponding acids, which proved identical by melting points and infrared spectra to the acids obtained earlier from hypoiodite oxidation of the acetyl isomers [5]. Evidence for the positions of the acetyl groups in the latter compounds (XI and XII) includes their relative abundance (from acetylation, compared to the proportions of the corresponding acetyldiisopropylferrocenes obtained from acetylation) and their infrared spectra [5], their n.m.r. spectra [13], and their relation to dimethyldiethylferrocenes prepared by unambiguous routes, from ethylmethylcyclopentadienes [7,14].

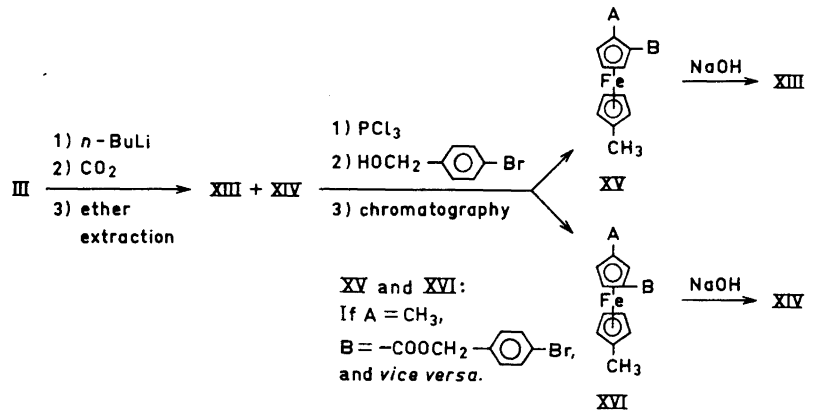

Of the two isomers (XIII and XIV), the more abundant [11] 3-carboxylic acid was chosen for resolution, though resolution of the 2-isomer would pose no new problem beyond supply. A number of alkaloid salts of XIV were inves-

* Although Nesmeyanov, *et al.*, [12] reported that dimethylferrocene did not react with butyllithium, the reaction in fact appears to proceed quite facilely, [11] as noted in the text.

tigated. Cinchonidine and quinine precipitated preferentially the (+) isomer, and cinchonine, brucine, and quinidine the (−)-isomer, while strychnine gave no resolution at all (*cf.* Table 2). Of these, the cinchonidine and quinidine salts were chosen for further study since they gave acids of the highest absolute rotations. Each salt was recrystallized to constant melting point, then decomposed by acid to give the optical isomers. The (+)- and (−)-acids had the same melting point and equal, though opposite, rotation. Their properties are summarized in Table 1.

Table 1. Physical properties of 1,1′-dimethylferrocene monocarboxylic acids.

1,1′-Dimethylferrocene-	M.p.	$[\alpha]_D^{22}$ (*c* 0.8, $CHCl_3$)
(±)-2-carboxylic acid	123−126°	
(±)-3-carboxylic acid	108−109.5°	
(+)-3-carboxylic acid	119−121°	+ 37.5 ± 1.5°
(−)-3-carboxylic acid	119−121°	−36.0 ± 1.0°

EXPERIMENTAL

Melting points were determined on a Kofler micro hot-stage and are uncorrected. Rotations were determined on a Schmidt and Hænsch polarimeter, employing 1-dm cells.

Separation of 1,1′-dimethylferrocene-2-carboxylic and -3-carboxylic acids as their p-*bromobenzyl esters. Run I.* A mixture of 1,1′-dimethylferrocene-2-carboxylic and -3-carboxylic acids (11.6 g, 0.045 mole; obtained as the ether-soluble portion of the monoacid-diacid mixture from treatment of 1,1′-dimethylferrocene with butyllithium followed by carbon dioxide) [11] was mixed with 50 ml of benzene and 50 ml of phosphorus trichloride. The mixture was warmed briefly to dissolve the acids, left overnight at room temperature, finally heated for one hour at reflux, then cooled. The supernatant was decanted, solvent and excess phosphorus trichloride were removed under aspirator pressure. Two fresh 25-ml portions of benzene were added and aspirator evaporation was repeated after each addition.

The dark red residue was dissolved in 100 ml of benzene and 8.4 g (0.045 mole) of *p*-bromobenzyl alcohol in 100 ml of benzene was added. The mixture was warmed briefly on a steam bath, treated with charcoal, filtered and cooled. Ether (300 ml) was added and the solution was extracted four times with 50-ml portions of 5 % sodium bicarbonate, once with 50 ml of water, then dried over magnesium sulfate. Acidification of the bicarbonate solution gave 0.8 g. (7 % of recovered acids, while removal of benzene-ether solvent from the organic phase in a rotary evaporator yielded 17.3 g. (90 % conversion from acids, 96 % yield based on unrecovered acids) of crude ester.

This material, in benzene, was transferred to an alumina column (Merck, acid-washed, 3 cm × 110 cm). Benzene eluted two yellow bands from the column, while a third band remained at the top. Extrusion of the top of the column and extraction with ether and methanol gave 1.4 g of crude recovered acids, apparently formed by saponification on alumina. On evaporation of solvent from the first eluted band, 2.7 g of liquid α ester was obtained, while the second band yielded 5.7 g of solid β ester. An intermediate fraction was rechromatographed (2 × 67-cm column) to give an additional 1.0 g of liquid α ester (total: 3.7 g, 21 % yield, 19 % conversion) and 0.4 g of solid β ester (total: 6.1 g, 34 % yield, 32 % conversion).

A sample of the solid *p*-bromobenzyl 1,1′-dimethylferrocene-3-carboxylate was recrystallized from pentane; m.p. 57−58°. (Found: C 56.71; H 4.80. Calc. for $C_{20}H_{19}BrFeO_2$: C 56.25; H 4.47).

Run II. In a second run employing 1.0 g (0.004 mole) of mixed *a* and *β* mono-acids and 10 ml of phosphorus trichloride in 10 ml of benzene, the mixture stood for 20 h at room temperature, when solvent and excess phosphorus trichloride were removed and 0.75 g (0.005 mole) of *p*-bromobenzyl alcohol in 10 ml of benzene was added. Work-up as in Run I gave 0.10 g (10 %) of recovered acids and 1.6 g (quantitative) of crude esters. Chromatography (1.5 × 58-cm column, Merck acid-washed alumina, benzene eluant) gave 0.80 g (53 % yield, 48 % conversion) of the *a* ester, which did not crystallize during 2 months at deepfreeze temperature, and 0.68 g (46 % yield, 41 % conversion) of the *β* ester, m.p. 55—57° after recrystallization from pentane.

1,1'-Dimethylferrocene-2-carboxylic acid. The liquid *a* ester from Run I (3.7 g) was saponified during 1.5 h in refluxing aqueous alcoholic potassium hydroxide solution (2 g of alkali in 40 ml of ethanol and 10 ml of water). Water (50 ml) was added and most of the alcohol was removed in a rotary evaporator. Then, 50 ml more of water was added and the solution was extracted four times with 25-ml portions of ether. The combined ether extracts were washed twice with 15-ml portions of water which were combined with the main aqueous layer.

From the ether solution was recovered 1.6 g (quantitative) of crude *p*-bromobenzyl alcohol. Addition of 6 N hydrochloric acid to the basic solution precipitated 1,1'-dimethylferrocene-2-carboxylic acid, which was collected, washed with water and dried; 1.9 g (85 % yield from ester) of crude acid, m.p. 105—115°. Recrystallization from ether-pentane gave the analytical sample, m.p. 123—126° (lit.[5] m.p. 118—118.5°). (Found: C 60.54; H 5.48. Calc. for $C_{13}H_{14}FeO_2$: C 60.49; H 5.43).

The infrared spectrum of the acid is identical to that of an authentic sample [15]. The ultraviolet spectrum (absolute ethanol, 9.86×10^{-5} M) has λ_{max} 262 mμ, ε_{max} 5170.

The liquid ester from Run II (0.80 g) was saponified as in the preceding paragraph to yield 0.27 g (56 % yield) of 1,1'-dimethylferrocene-2-carboxylic acid, m.p. 117—122°. Solution in sodium bicarbonate, filtration, and reprecipitation with hydrochloric acid, followed by recrystallization from ether-pentane gave the pure acid, m.p. 122—125°.

1,1'-Dimethylferrocene-3-carboxylic acid. The solid *β* ester (6.1 g) from Run I above was saponified (4 g of potassium hydroxide in 120 ml of ethanol and 20 ml of water) as described for the *a* ester. Work-up as before gave 2.5 g (94 %) of recovered *p*-bromobenzyl alcohol and 3.2 g (87 % from ester) of crude acid, m.p. 105—108°. Recrystallization from ether-pentane gave the pure acid, m.p. 108—109.5° (lit.[5] m.p. 106—106.5°). (Found: C 60.23; H 5.54. Calc. for $C_{13}H_{14}FeO_2$: C 60.49; H 5.43).

The infrared spectrum of this acid was superimposable on that of authentic 1,1'-dimethylferrocene-3-carboxylic acid[15], while the ultraviolet spectrum (10.17×10^{-5} M, absolute ethanol) had λ_{max} 266 mμ, ε_{max} 5210.

In a second run a portion (0.30 g) of the solid *β* ester from Run II was saponified as in other runs to give 0.10 g (56 %) of crude acid, m.p. 95—105°, which was purified by solution in bicarbonate, filtration and reprecipitation with hydrochloric acid, then recrystallized from ether-pentane; m.p. 106—108°.

Table 2. Crystallization of alkaloid salts of 1,1'-dimethylferrocene-3-carboxylic acid.

Alkaloid (mg)	Crystallization 1st *a*	1st *b*	1st *c*	2nd *a*	2nd *b*	2nd *c*	3rd *a*	3rd *b*	3rd *c*	Acid *d*	Acid *e*	Acid *f*
Cinchonidine (294)	10	1	220	10	3	110				+30°	50	190
Quinine (378)	10	6	380	5	4	270	2	2	190	+15°	80	180
Strychnine (334)	7	6	420	5.5	4	230	2.5	2	180	0°	85	125
Cinchonine (294)	7	11	190	3	5	170				−10°	70	170
Brucine (466)	5	14	480	3	7	215				−21°	90	170
Quinidine (369)	8	5	300	5	3	160	3	2	130	−32°	60	160

[a] 95 % ethanol, ml. [b] Water, ml. [c] Salt collected, mg.
[d] Acid recovered from crystallized salts, $[\alpha]_D^{21}$ (c 1.0, in chloroform).
[e] Acid recovered from crystallized salts, mg. [f] Acid recovered from mother liquors, mg.

Optical resolution of 1,1'-dimethylferrocene-3-carboxylic acid. A. Preliminary experiments. Racemic 1,1'-dimethylferrocene-3-carboxylic acid (258 mg, 1.00 mmole) and 1.00 mmole of each of several alkaloids were dissolved in 95 % ethanol-water mixtures and set aside for crystallization. The salts obtained were recrystallized from ethanol-water, then decomposed to give the recovered ferrocene acid, which was tested for optical activity. The remainder of the acid was recovered from the mother liquors. Results are summarized in Table 2.

B. (+)-1,1'-Dimethylferrocene-3-carboxylic acid. Racemic 1,1'-dimethylferrocene-3-carboxylic acid (2.90 g, 0.011 mole, m.p. 108–109.5°) and 3.30 g (0.011 mole) of cinchonidine were dissolved in 90 ml of hot 95 % ethanol. Water (10 ml) was added and the solution was set aside. The cinchonidine salt, which crystallized in yellow needles, was collected, pressed and dried: yield, 3.08 g; m.p. 155–158°. Recrystallizations from ethanol-water are summarized in Table 3. (Found: C 69.47; H 6.46; N 4.86. Calc. for $C_{33}H_{36}FeN_2O_3$: C 69.56; H 6.57; N 5.07). The (+)-acid was obtained by decomposition of the salt with mineral acid.

Table 3. Recrystallizations of (+)-1,1'-dimethylferrocene-3-carboxylic acid cinchonidine salt

No.	95 % EtOH, ml	Water, ml	Salt isolated, g	Salt isolated, m.p.	Acid obtained m.p.	Acid obtained $[\alpha]_D^{22}$ (*c* 0.8, $CHCl_3$)
1	45	5	1.78	161 –164.5°		
2	27	3	1.27	164 –167°		+ 32°
3	18	2	1.02	168 –169.5°		
4	15	1.7	0.87	169 –171°		
5	15	1.7	0.75	168.5–171°	116.5–119°	+ 39°
6	15	1.7	0.47	169 –171°		
7	7.5	0.8	0.40	–		
8	7.5	0.8	0.34	169 –171°	119–121°	+ 36°

C. (−)-1,1'-Dimethylferrocene-3-carboxylic acid. Mother liquors from the initial crystallization and first recrystallization of the cinchonidine salt of the (+)-acid above were combined and acidified to give the crude (−)-acid (2.00 g), which was mixed with 2.86 g of quinidine and dissolved in 62 ml of hot 95 % ethanol. Water (38 ml) was added and the solution was set aside for crystallization. The precipitated salt was collected, pressed and dried: yield, 3.17 g; m.p. 108–115°. Recrystallizations from 95 % ethanol-water are summarized in Table 4. (Found: C 69.82; H 7.45; N 4.85. Calc. for $C_{33}H_{38}FeN_2O_4$: C 68.04; H 6.57; N 4.81.) The (−)-acid was liberated from the salt with mineral acid.

Table 4. Recrystallizations of (−)1,1'-dimethylferrocene-3-carboxylic acid quinidine salt.

No.	95 % EtOH, ml	Water, ml	Salt isolated, g	Salt isolated, m.p.	Acid obtained, m.p.	Acid obtained, $[\alpha]_D^{22}$ (*c* 0.8, $CHCl_3$)
1	50	25	2.22	113–120°		
2	35	17.5	1.82		112–117°	−35°
3	30	15	1.30			
4	30	15	0.95			
5	25	8	0.75	118–122°	119–121°	−37°

Acknowledgment. This work was supported by the Materials Laboratory, Wright Air Development Division, Wright-Patterson Air Force Base, Ohio.

REFERENCES

1. Pauson, P. L. *Quart. Revs. (London)* **9** (1955) 391.
2. Wilkinson, G., Rosenblum, M., Whiting, M. C. and Woodward, R. B. *J. Am. Chem. Soc.* **74** (1952) 2125; Wilkinson, G. *J. Am. Chem. Soc.* **74** (1952) 6148.
3. Fischer, E. O. and Pfab, W. *Z. Naturforsch.* **7b** (1952) 377; Fischer, E. O. and Hafner, W. *Z. Naturforsch.* **9b** (1954) 503.
4. Rosenblum, M. *Ph. D. Thesis*, Harvard University 1953; Rosenblum, M. and Woodward, R. B. *J. Am. Chem. Soc.* **80** (1958) 5443.
5. Rinehart, K. L., Jr., Motz, K. L. and Moon, S. *J. Am. Chem. Soc.* **79** (1957) 2749.
6. *cf.* Pauson, P. L. in *Organometallic Chemistry* (H. Zeiss, ed.) Reinhold Publishing Corp., New York 1960, p. 362.
7. Rinehart, K. L., Jr. and Motz, K. L. *Chem. & Ind. (London)* **1957** 1150.
8. Rinehart, K. L., Jr., Curby, R. J., Jr., Gustafson, D. H., Harbison, K. G. and Bublitz, D. E. *J. Am. Chem. Soc.* **84** (1962). *In press.*
9. Thomson, J. B. *Tetrahedron Letters* **No. 6** (1959) 26.
10. Rinehart, K. L., Jr. and Curby, R. J., Jr. *J. Am. Chem. Soc.* **79** (1957) 3290.
11. Rinehart, K. L., Jr., Marvel, J. T., Miles, F. B. and Westman, L. *Paper in preparation.*
12. Nesmeyanov, A. N., Perevalova, E. G., Beinoravichute, Z. A. and Mølygina, I. L. *Doklady Akad. Nauk. S.S.S.R.*, **120** (1958) 1263.
13. Rinehart, K. L., Jr., Bublitz, D. E. and Gustafson, D. H. *Paper submitted.* Presented at the National American Society Meeting, Washington, D.C., March, 1962.
14. Rinehart, K. L., Jr., Motz, K. L. and Mitchell, C. D. *Paper in preparation.*
15. Motz, K. L. *Ph. D. Thesis*, University of Illinois 1958.

Received December 19, 1961.

ACTA CHEMICA SCANDINAVICA 16 (1962) 1206–1211

A Convenient Method for Determination of Tetramethylthiuram Disulphide

STIG ÅKERSTRÖM

Research Department, AB Bofors, Nobelkrut, Sweden, and Laboratory of Organic Chemistry, Chemical Institute, University of Uppsala, Sweden

P. E. BJÖRN LINDAHL

Institute of Plant Physiology, University of Uppsala, Sweden, and Institute of Plant Physiology, Royal Agricultural College, Uppsala, Sweden

Submitted in honour of the sixtieth birthday of my (S.Å.) teacher, Professor *Arne Fredga*

A new method for the determination of small amounts of tetramethylthiuram disulphide (TMTD) is described. The method is applicable to other tetrasubstituted thiuramdisulphides. The reproducibility of the determination of TMTD is ± 2 %.

Dithiocarbamates and thiuramdisulphides find a variety of applications as plant fungicides, bactericides, analytical reagents, accelerators in the rubber industry and collectors in the flotation of minerals.

During the last ten years many papers concerning these compounds have been published and an increasing need of rapid and exact methods for their determination has arisen.

One of the present authors is studying the inhibition of growth and photosynthesis in submerged plants with tetramethylthiuram disulphide (TMTD) [1]. Further, in some pharmaceutical preparations used in dermatology, *e.g.* Nobecutane, TMTD is the bactericidal and fungicidal component. In such cases a sensitive method for determining TMTD concentrations is required.

As early as 1949 Fredga [2] developed a method for the determination of tetraethylthiuram disulphide (antabuse), which at that time was used for the treatment of chronic alcoholism. Some years later Linderholm and Berg [3] used this method for the determination of small amounts of antabuse in blood and urine. The method is applicable to other tetraalkyl-substituted

thiuramdisulphides and is based on a reduction of the thiuramdisulphide with copper(I) iodide and a spectrophotometric determination of the intensely coloured copper(II) complex formed.

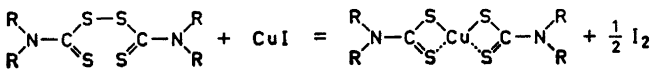

Scheele and Gensch [4] determined TMTD with copper(II) sulphate in the presence of hydroquinone. The same workers [5] also transformed the thiuramdisulphide into the corresponding monosulphide with potassium cyanide and titrated the formed potassium thiocyanate with silver nitrate. Iijima and Eguchi [6] reduced TMTD with sodium thiosulphate to the dithiocarbamate. With copper(II) sulphate this gives the copper(II) N,N-dimethyldithiocarbamate which is then determined spectrophotometrically. Iijima [7] also reduced TMTD with aqueous sodium sulphide and decomposed the dithiocarbamate with acid, the carbon disulphide produced being titrated as the xanthate. Firestone and Vollmer [8] used an infrared spectrophotometric method and Kalasheva [9] developed a polarographic method for TMTD determination. Stepanova [10] has determined TMTD in rubber mixtures and vulcanizates by a photocolorimetric procedure based on the colour reaction of TMTD with cobalt(II) chloride in an ethanol-benzene medium. Salvesen and Domange [11] have determined disulfiram (TMTD) by a colorimetric method. Keppel [12] isolated TMTD by extraction with chloroform. Copper(II) chlorides was then added and the formed complex determined spectrophotometrically at 420 mμ. Barr, Clark and Jacks [13] have worked out a micromethod for the determination of TMTD and dimethyldithiocarbamate based on acid decomposition followed by steam distillation of the formed dimethylamine in excess alkali. The amine is then determined as copper(II) N,N-dimethyldithiocarbamate. In a recent method Lowen [14] titrated TMTD potentiometrically with sodium sulphide in the presence of ferbam (iron(III) N,N-dimethyldithiocarbamate).

None of these methods can be considered as better or simpler than that of Fredga.

The principle of the present method may schematically be written as follows:

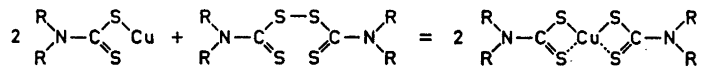

The reaction between the copper(I) compound and the TMTD occurs rapidly and quantitatively. The intensely coloured copper(II) complex formed is determined spectrophotometrically [15,16]. For the determination of TMTD copper(I) N,N-diethyldithiocarbamate was chosen in preference to the corresponding copper(I) N,N-dimethyldithiocarbamate as the solubility of the latter in all common organic solvents is too low. One probably obtains a mixture of the compounds given below owing to the complex constants of the formed copper(II) complexes.

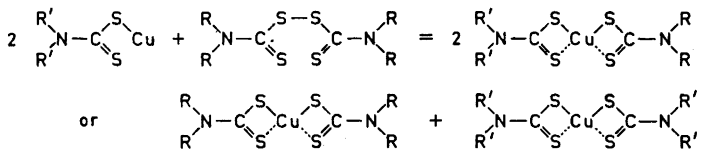

As the extinction coefficients of the copper(II) complexes given below

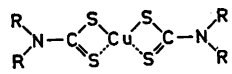

R = methyl, ethyl, propyl, isopropyl.

are the same (within ± 2 % at the absorption maximum of the compounds), this method can also be used for the determination of other tetraalkyl-substituted thiuramdisulphides. For the higher homologues one may also use the corresponding copper(I) N,N-dialkyldithiocarbamate.

In some cases it is necessary to determine dithiocarbamate and thiuramdisulphide in a mixture. For example, TMTD and N,N-dimethyldithiocarbamate ion ($DMDT^-$) can be determined in water. The solution, made weakly alkaline, is extracted with chloroform. The TMTD in the chloroform phase is treated with copper(I) N,N-diethyldithiocarbamate and the intensely coloured complex formed is determined spectrophotometrically. The water phase is treated with copper(II) sulphate at another pH and after extraction of the formed copper(II) complex, the amount of dithiocarbamate is determined spectrophotometrically.

EXPERIMENTAL

Instruments, solvent and reagents

Beckman Spectrophotometer, Model B.
1-cm glass transmission cells.
Chloroform (*pro analysi*), copper(I) N,N-diethyldithiocarbamate [16], tetramethylthiuram disulphide, and copper(II) sulphate pentahydrate.

Procedure I

A sample containing 0.1—0.3 mg of TMTD is weighed in and diluted with chloroform to 50 ml (*a*). About 3 ml of this solution is required for the zero-adjusting of the spectrophotometer. To the rest of the solution 1—10 mg of copper(I) N,N-diethyldithiocarbamate is added (*b*) and shaken well for 10 sec. The optical density of the solution is measured at 433 mμ (*c*).

$$\% \text{ TMTD} = \frac{s \cdot 100}{w}$$

E = optical density
s = mg of TMTD per 50 ml of solution read off from a calibration curve.
w = amount of sample in mg.
Notes. a) For spray packages of Nobecutane (containing 0.016 % of TMTD) 1—1.5 g is sprayed directly into a 50 ml calibrated flask and diluted with chloroform to the mark.

b) Larger quantities than 10 mg should be avoided as the reagent exhibits a slight absorption at the wave-length in question.

c) Measurement of the optical density should be done within 2—5 min. If the solution is allowed to stand too long the copper(I) N,N-diethyldithiocarbamate is autooxidized leading to an increasing extinction giving a TMTD value which is too high. An error of the same kind could also arise if the sample contains some oxidizing agents, extractable with chloroform and able to oxidize copper(I) N,N-diethyldithiocarbamate.

Table 1. Analyses of spray packages of Nobecutane by procedure I.

Nobecutane			
w	*E*	*s*	% TMTD
2212	0.778	0.378	0.0171
1634	0.572	0.276	0.0169
1530	0.545	0.261	0.0171
574	0.205	0.0981	0.0171

Procedure II

Determination of TMTD. A sample of the water solution (20.0 ml) is adjusted to pH 7.6—9.0 (*d*) and the TMTD extracted with three portions of chloroform, each of which is shaken for about 5 sec. The combined extracts are filtered into a 20 ml calibrated flask containing 1 ml of copper(I) N,N-diethyldithiocarbamate solution (*e*). After washing the filter paper and filling the flask with chloroform the optical density of this solution (E_T) is read at 433 mμ using 1 ml of the copper(I) N,N-diethyldithiocarbamate solution diluted with chloroform to 20 ml as reference.

The molecular extinction coefficient of the formed copper(II) complexes is (1.25± 0.02) × 10^4 liter.mole^{-1} . cm^{-1} (Ref.[16]). The concentration of TMTD in the water solution is then given by the expression

Table 2. Analyses of TMTD in water solutions by procedure II.

Solvent	E_T (433 mμ)	$C_{TMTD} \times 10^{-5}$ moles per litre
Tap water	1.808	7.23
	1.798	7.19
	1.780	7.12
Sea water	1.343	5.37
	1.346	5.38
	1.340	5.36
Medium AN1-Sp (g)	1.362	5.45
	1.350	5.40
	1.350	5.40

Note g). This medium is based chiefly on sea water and has been used in manometric photosynthesis experiments [1].

Table 3. Analyses of solutions of TMTD by procedure II. The solutions are diluted with the solvent (AN1-Sp, cf. Table 2) from a standard solution.

Extent of dilution	E_T (433 mμ)	$C_{TMTD} \times 10^{-5}$ moles per litre	Recovery per cent
0 % (standard solution)	1.092	4.37	—
50 %	0.547	2.19	100
75 %	0.284	1.14	104

$$C_{TMTD} = \frac{E_T}{1.25 \times 10^4 \times 2 \times 1} = 4\ E_T \times 10^{-5} \text{ moles per litre.}$$

The reproducibility of this procedure has been tested by repeated analyses (Table 2) and by determination of the recovery from solutions of known dilution (Table 3).

Determination of DMDT⁻. To the solution remaining after the extraction of TMTD is pipetted 1 ml 0.3 % copper(II) sulphate solution (*f*) and the estimated quantity of diluted hydrochloric acid for adjusting the pH to 5—7. The copper(II) complex formed is extracted with three portions of chloroform, each of which is shaken for about 5 sec. The combined extracts are filtered into a 20 ml calibrated flask containing no reagent. After washing the filter paper and filling the flask with chloroform, the optical density of the solution (E_D) is read at 433 mμ with chloroform as reference.

With the molecular extinction coefficient mentioned above, the concentration of $DMDT^-$ is given by the expression

$$C_{DMDT} = \frac{E_D}{1.25 \times 10^4 \times 0.5 \times 1} = 16E_D \times 10^5 \text{ moles per litre.}$$

Values from such analyses are given in Table 4.

Table 4. Analyses of both TMTD and $DMDT^-$ by procedure II. The solutions have been prepared from TMTD or sodium dimethyldithiocarbamate (Na-DMDT) with AN1-Sp (cf. Table 2).

Solution prepared with	E_T	E_D	C_{TMTD}	C_{DMDT^-}
	(433 mμ)		in 10^{-5} moles per litre	
Na-DMDT	0.003 0.005	0.287 0.292	0.01 0.02	4.59 4.67
Na-DMDT	0.009 0.012	0.097 0.096	0.04 0.05	1.55 1.54
TMTD	0.513 0.510	0.003 0.001	2.05 2.04	0.05 0.02
TMTD	0.870 0.885	0.004 0.003	3.48 3.54	0.06 0.05

Notes. d) The amount of diluted hydrochloric acid or sodium hydroxide, required to adjust the pH to within the range 7.6—9.0 in the sample should be previously estimated.

e) Copper(I) N,N-diethyldithiocarbamate (7—10 mg) is dissolved in 10 ml chloroform. The slow autooxidation of Cu(I) to Cu(II) darkens this solution and after about 2 h at room temperature a fresh solution should be prepared. See also note (c).

f) As in note *d*), the amount of acid or base required to adjust the pH to within the range 5—7 should be previously estimated.

Acknowledgements. The authors are indebted to Professors A. Fredga and N. Fries for their kind interest and are also thanksful for the linguistic revision of this manuscript by Dr. Wynford Brown.

REFERENCES

1. Lindhal, P. E. B. *Nature* **191** (1961) 51.
2. Domar, G., Fredga, A. and Linderholm, H. *Acta Chem. Scand.* **3** (1949) 1441.
3. Linderholm, H. and Berg, K. *Scand. J. Clin. Lab. Invest.* **3** (1951) 96.
4. Scheele, W. and Gensch, C. *Kautschuk u. Gummi* **6** WT (1953) 147.
5. Scheele, W. and Gensch, C. *Kautschuk u. Gummi* **7** WT (1954) 122.
6. Iijima, T. and Eguchi, T. *Nippon Gomo Kyokaishi* **29** (1956) 551.
7. Iijima, T. *J. Soc. Rubber Ind. Japan* **29** (1956) 14.
8. Firestone, D. and Vollmer, P. J. *J. Assoc. Offic. Agr. Chemists* **39** (1956) 866.
9. Kalasheva, A. V. *Zavodskaya Lab.* **22** (1956) 420.
10. Stepanova, V. B. *Trudy Nauch-Issledovatd. Inot. Rezin. Prom.* 1955, No. 2, 194; Referat. *Zhur. Khim.* **1956**, Abstr. No. 48628.
11. Salvesen, B. and Domange, L. *Ann. pharm. franc.* **13** (1955) 499.
12. Keppel Geo. E. *J. Assoc. Offic. Agr. Chemists* **39** (1956) 709.
13. Barr, H. E., Clark, P. J. and Jacks, H. *New Zealand J. Sci. Technol.* **38** *B* (1957) 425.
14. Lowen, W. K. *J. Assoc. Office. Agr. Chemists* **44** (1961) 584.
15. Fredga, A. *Rec. trav. chim.* **69** (1950) 416.
16. Åkerström, S. *Arkiv Kemi* **14** (1959) 387, 403.

Received December 27, 1961.

ACTA CHEMICA SCANDINAVICA 16 (1962) 1212–1220

The Crystal Structure of Calcium Carbide II and IV

NILS-GÖSTA VANNERBERG

Institutionen för oorganisk kemi, Chalmers tekniska högskola, Göteborg, Sweden

The crystal structure of CaC_2 II has been determined from two dimensional X-ray data. The structure is built up of calcium and carbide ions arranged in a similar but more complicated way than in CaC_2 I and CaC_2 III. The structure of CaC_2 IV could only be determined from X-ray powder diffraction data. The structure is cubic and disordered.

A review of the literature on the structure of calcium carbide has recently been published in this journal [1]. There seem to exist four modifications, of which CaC_2 I [2] and CaC_2 III [1] have previously been investigated and described. CaC_2 IV [3] is a high temperature modification while CaC_2 II is a low temperature modification stable only in presence of cyanamide ions (CN_2^{2-}) [3].

CALCIUM CARBIDE II

Preparation of the compound. 4 g calcium carbide, 2 g calcium cyanamide and 0.4 g graphite was heated in an induction furnace [1].

A graphite crucible was used. The air was removed from the crucible with the aid of a stream of argon gas. The temperature never exceeded 1700°C. If the temperature was raised to above 2000°C, all nitrogen disappeared and on cooling CaC_2 III was formed.

The compound consisted of smal semi-transparent light brown crystals. They were generally not suited for X-ray work but after many fruitless attempts some useful crystals were found.

Analysis. The carbide content was determined by measuring the amount of gas liberated when a certain amount of water saturated with acetylene gas was added to the sample. Calcium was determined as oxalate. The nitrogen content could be determined by the ordinary Kjeldahl method. The specific gravity was determined by a method described by Schrewelius [4].

The determination of the crystal structure

The structural investigation was based on single crystal methods. The single crystals were mounted inside capillary tubes and rotated about three axes approximately perpendicular to each other. The patterns were generally not of high quality, and twin effects were very common. The reflexion intensities

Table 1. Analysis of CaC_2(tric.)

Sample	% Ca^{2+}	% C_2^{2-}	% CN_2^{2-}	Density
a	60.6	36.4	0.6	2.2
b	60.0	35.6	0.6	2.1
CaC_2(tric.) calculated	62.5	37.4	—	2.17

were estimated by visual comparison with known scales and corrected by Lorenz and polarization factors.

The unit cell was found to be triclinic with

$$a = 8.42 \pm 0.02 \text{ Å} \qquad \alpha = 93.°4 \pm 0.5$$
$$b = 11.84 \pm 0.03 \text{ Å} \qquad \beta = 92.°5 \pm 0.5$$
$$c = 3.94 \pm 0.01 \text{ Å} \qquad \gamma = 89.°9 \pm 0.5$$

The space group was chosen to be base centered $C\bar{1}$, in order to show the resemblance to the cubic superstructure with $a = 5.9$ Å. There are eight formula units in the elementary cell. The calculated density is 2.17 g/cm³, to be compared with 2.17 g/cm³ for CaC_2 III [1] and 2.23 g/cm³ for CaC_2 I [2]. Approximate calcium atom parameters were calculated from Patterson syntheses. With the aid of these parameters the sign of all the reflexions could be calculated and all the atomic parameters could be calculated from electron density maps. The proposed structure model was then refined with the aid of succesive difference syntheses.

The parameter values found were the following:

	x	y	z
4 Ca	0.375	0.141	0.717
4 Ca	0.875	0.109	0.783
4 C	0.066	0.124	0.317
4 C	0.187	0.126	0.192
4 C	0.660	0.090	0.192
4 C	0.590	0.160	0.317

A comparison between observed and calculated structure factors can be found in Table 2. The R factor was found to be 0.18.

Discussion. The distance between the two carbon atoms in a carbide group was found to be 1.14 Å and 1.13 Å, to be compared with 1.20 in CaC_2 I. The difference is not significant. The calcium ions are surrounded by six carbide ions and are in contact with seven carbon atoms. The distances between the calcium ions and carbon atoms are 2.46, 2.55, 2.57, 2.80, 2.82, 2.82 and 2.90 Å. The arrangement can be seen in Fig. 1 and will be discussed below.

Table 2. Observed and calculated structure factors for CaC_2(tric.).

h	k	l	F_{obs}	F_{calc}	h	k	l	F_{obs}	F_{calc}
2	0	0	—	0	0	2	0	—	0
4	0	0	24	− 30	0	4	0	41	− 41
6	0	0	—	0	0	6	0	—	0
8	0	0	12	+ 13	0	8	0	15	+ 18
1	1	0	—	0	0	10	0	—	0
3	1	0	—	0	0	12	0	7	− 6
5	1	0	—	0	0	2	1	19	+ 18
$\bar{1}$	1	0	—	+ 4	0	4	1	—	0
$\bar{3}$	1	0	—	0	0	6	1	14	− 17
$\bar{5}$	1	0	—	0	0	8	1	—	0
0	2	0	—	0	0	10	1	14	+ 12
2	2	0	14	+ 16	0	12	1	—	0
4	2	0	—	0	0	14	1	8	− 6
$\bar{2}$	2	0	14	− 19					
$\bar{4}$	2	0	—	0	0	2	$\bar{1}$	17	− 13
$\bar{6}$	2	0	16	+ 23	0	4	$\bar{1}$	—	0
1	3	0	8	+ 9	0	6	$\bar{1}$	6	+ 8
3	3	0	—	0	0	8	$\bar{1}$	—	0
5	3	0	12	− 12	0	0	$\bar{2}$	30	− 31
$\bar{1}$	3	0	—	0	0	2	2	—	0
$\bar{3}$	3	0	—	− 6	0	4	2	30	+ 26
$\bar{5}$	3	0	—	0	0	6	2	—	0
0	4	0	43	− 41	0	8	2	24	− 17
2	4	0	—	0	0	10	2	—	0
4	4	0	15	+ 26	0	12	2	16	+ 10
6	4	0		0	0	2	$\bar{2}$	—	0
$\bar{2}$	4	0		0	0	4	$\bar{2}$	22	+ 24
$\bar{4}$	4	0	25	+ 21	0	6	$\bar{2}$	—	0
$\bar{6}$	4	0		0	0	8	$\bar{2}$	9	− 11
1	5	0	—	0	0	10	$\bar{2}$	—	0
3	5	0	12	+ 9	0	2	3	15	− 17
5	5	0	—	0	0	4	3	—	0
$\bar{1}$	5	0	17	− 17	0	6	3	17	+ 20
$\bar{3}$	5	0	—	0	0	8	3	—	0
0	6	0	—	0	0	10	3	11	− 16
2	6	0	14	− 12	0	2	$\bar{3}$	13	+ 9
$\bar{4}$	6	0	—	0	0	4	$\bar{3}$	—	0
$\bar{2}$	6	0	17	+ 16	0	6	$\bar{3}$	—	− 1
$\bar{4}$	6	0	—	0	0	0	4	11	+ 12
$\bar{6}$	6	0	18	− 20	0	2	$\bar{4}$	—	0
1	7	0	11	− 12	0	2	$\bar{4}$	—	0
3	7	0	—	0					
5	7	0	16	− 17	2	0	0	—	0
$\bar{1}$	7	0	—	0	4	0	0	31	− 30
$\bar{3}$	7	0	—	+ 9	6	0	0	—	0
$\bar{5}$	7	0	—	0	8	0	0	13	+ 13
0	8	0	19	+ 18	2	0	1	39	− 45
2	8	0	—	0	4	0	1	—	0
4	8	0	15	− 16	6	0	1	20	+ 21
$\bar{2}$	8	0	—	0	8	0	1	—	0
$\bar{4}$	8	0	15	− 10	$\bar{2}$	0	1	28	− 45
1	9	0	—	0	$\bar{4}$	0	1	—	0
3	9	0	16	− 15	$\bar{6}$	0	1	19	+ 19
$\bar{1}$	9	0	17	+ 22	$\bar{8}$	0	1	—	0
$\bar{3}$	9	0	—	0	0	0	2	34	− 31

Table 2. Continued.

h	k	l	F_{obs}	F_{calc}	h	k	l	F_{obs}	F_{calc}
2	0	2	—	0	4	0	2	—	0
4	0	2	28	+ 27	6	0	3	22	− 19
6	0	2	—	0	$\bar{2}$	0	3	15	+ 23
8	0	2	16	− 12	$\bar{4}$	0	3	—	0
$\bar{2}$	0	2	—	0	0	0	4	17	+ 12
$\bar{4}$	0	2	18	+ 27	2	0	4	—	0
$\bar{6}$	0	2			4	0	4	21	− 17
2	0	3	23	+ 23	$\bar{2}$	0	4		

CALCIUM CARBIDE IV

Preparation of the compound. Three specimens containing CaC_2 I, CaC_2 II and CaC_2 III were prepared as described previously. CaC_2 I contained 4 % CaS as impurity, while CaC_2 II contained 1.5 % $CaCN_2$. The compounds were heated to 500°C in a high temperature X-ray diffraction unit. At about 450°C CaC_2 IV is formed from all the modifications. If the temperature is lowered one of the low temperature modifications is formed again. The process is completely reversible. A sample of CaC_2 IV prepared from CaC_2 I always yields CaC_2 I on cooling and so on.

The determination of the crystal structure

The structural investigation was based on X-ray powder photographs taken with a modified Philips' Diffractometer. The specimen temperature was

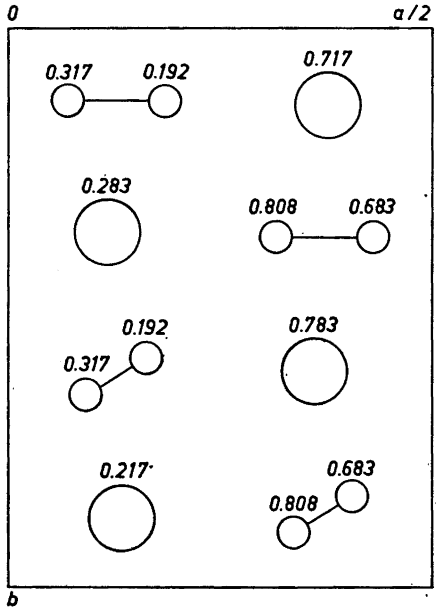

Fig. 1. Projection of the CaC_2(tric.) structure on (001).

Table 3. Observed and calculated $\sin^2\Theta$ values for CaC_2(cub.)

	1		2		3	
h k l	$10^4 \cdot \sin^2\Theta_o$	$10^4 \cdot \sin^2\Theta_c$	$10^4 \cdot \sin^2\Theta_o$	$10^4 \cdot \sin^2\Theta_c$	$10^4 \cdot \sin^2\Theta_o$	$10^4 \cdot \sin^2\Theta_c$
1 1 1	510	513	515	515	513	514
2 0 0	681	684	686	686	683	685
2 2 0	1367	1369	1372	1373	1373	1371
3 1 1	1878	1882	1887	1888	1887	1885
2 2 2			2058	2059		
3 3 1	3257	3251	3259	3260	3259	3257
4 2 0	3422	3422	3430	3432	3422	3427
4 2 2	4100	4106	4116	4118	4100	4112

1. CaC_2(cub.) prepared of CaC_2(tric.)
2. » » » CaC_2(mon.)
3. » » » CaC_2(tetr.)

The reflexions 222 and 422 are disturbed by reflexions from calcium oxide.

500°C. Ni-filtered Cu$K\alpha$ radiation was used and the different peaks were scanned at a speed of 1/8° per minute. The intensities were registered with a Geiger-Müller counter tube. The furnace in which the specimen was placed was very carefully evacuated.

The unit cell was found to be face centered-cubic and the edge length of the elementary cube (Table 3) was

$a = 5.889 \pm 0.005$ for CaC_2 IV from CaC_2 I
$a = 5.894 \pm 0.005$ for CaC_2 IV from CaC_2 II and
$a = 5.886 \pm 0.005$ for CaC_2 IV from CaC_2 III

Table 4. Observed and calculated structure factors for CaC_2(cub.)

		F_c			
h k l	F_o	1	2	3	4
1 1 1	3.2	4.6	4.6	4.6	4.6
2 0 0	11.4	10.1	10.1	10.1	10.2
2 2 0	8.3	7.9	7.9	7.9	7.8
3 1 1	4.6	5.1	5.1	5.1	5.0
3 3 1	4.7	4.7	4.6	4.7	4.7
4 2 0	5.0	5.0	5.0	5.0	5.1

1. Each carbide ion is assumed to rotate.
2. Each carbide ion is assumed to be parallel to one of the four body diagonals.
3. Each carbide ion is assumed to be parallel to one of the six face diagonals.
4. Each carbide ion is assumed to be parallel to one of the three cubic axes.

The differences are not significant. There must be four formula units in the elementary cell. The relative intensity of a certain reflexion is the same regardless if the sample consists of CaC_2 I, II, or III. As mentioned the powder pattern is that of a face centered structure. This excludes the possibility that CaC_2 IV could be isomorphous with pyrite FeS_2. The reflexions (210) and (211), which would be fairly strong, are completely absent.

The only possibility is then that the gravity centers of the carbide ions form a face centered structure while the two carbon atoms of each carbide ion must occur in a disordered way around each main point.

This can be the case, if the carbide ions rotate freely. There are, however, other disordered structures which will also give a face centered cubic cell, *e.g.*, if each pair of carbon atoms is oriented parallel to one of the three cubic axes, or if each pair is parallel to one of the four body diagonals, or if each pair is parallel to one of the six face diagonals [7].

As is clear from Table 4, the calculated structure factors of the four alternatives do not differ appreciably. It must be regarded as impossible to select the correct structure from powder diffraction data only. However, physically there is not a great difference between them. Even if free rotation is not assumed, the disorder at 500°C is certainly dynamic. The only difference would be that the rotation is so strongly hindered that one special orientation is more probable than others.

The calculations are made with the assumption that the distance between the carbon atoms in a carbide group is 1.20 Å.

GENERAL DISCUSSION

Since all the known calcium carbide structures have been determined, it is possible to discuss them, especially their conditions of formation, simultaneously.

All the structures are built up of calcium and carbide ions. The structures have similarities with that of rock salt, *i.e.* each calcium ion is surrounded by six carbide ions and each carbide ion by six calcium ions. The coordinating ions from a more or less distorted octahedron.

The tetragonal calcium carbide CaC_2 I or CaC_2(tetr.) is probably the stable room temperature modification [3], but it is likewise obvious that it is not spontaneously formed without the presence of calcium sulphide [1,3,5]. As the sulphide ion is less space demanding than the carbide ion, it may denote that there are contacts between the carbide ions in the CaC_2(tetr.) structure. An incorporation of a small amount of sulphide ions would reduce these contacts and stabilize the structure. CaC_2(tetr.) is isostructural with barium peroxide, which structure has been carefully described [8]. In this structure type each cation is surrounded by six anions as mentioned above. The carbide axes are all parallel and also coincident with the fourfold axis, thus the calcium ions are in contact with ten carbon atoms each. If contacts between the anions in this structure are to be avoided, the following relation must hold [9].

Table 5. The coordination number of the calcium ions and the conditions of formation of the different calcium carbide modifications.

Phase	The coordination number of the calcium ions	Conditions of formation
CaC_2(cub.)	6	$T > 720°K$
CaC_2(mon.)	8	$T < 720°K$
CaC_2(tric.)	7	$T < 720°K$ presence of $CaCN_2$
CaC_2(tetr.)	10	$T < 720°K$ presence of CaS

$$\frac{r_c}{r_a} > 2\sqrt{\frac{2 + (d/a)^2}{2 + \left(\frac{c}{a} - \frac{2d}{a}\right)^2}} - 1$$

where r_c = the radius of the cation
r_a = the radius of the anion
d = the distance between the carbon atoms in a carbide group
a = the length of the crystallographic a-axis
c = the length of the crystallographic c-axis

In this case d is 1.20 Å, a is 3.89 Å, and c is 6.38 Å. Thus r_c/r_a must be larger than 0.66 but r_c is 0.99 Å and r_a is about 1.55 Å, so r_c/r_a is only 0.63. Accordingly there are contacts between the carbon atoms in this structure and the role of the sulphide ions can be understood.

In triclinic calcium carbide CaC_2 II or CaC_2(tric.), the six carbide ions surround the calcium ion, forming a distorted octahedron. Each calcium ion is in contact with seven carbon atoms. As mentioned the structure is related to the rock salt structure. Now there are two highly symmetric structures containing spherical cations and dumb-bell anions, which are also strongly related to the rock salt structure, *viz.* the pyrite structure and the low temperature sodium cyanide structure [10]. The former is cubic while the latter has a monoclinic structure, but the axes are directly comparable. In the pyrite structure the dumb-bell axes are parallel with the body diagonals in the cubic elementary cell. In the sodium cyanide structure they are parallel with the longest face diagonal in the monoclinic cell. In the former structure the cations become effectively six-coordinated, while in the latter the cations are eight-coordinated.

In triclinic calcium carbide half of the carbide ions are parallel to two of the body diagonals in the cubic subcell, while the other half are parallel to two of the face diagonals in the cubic subcell. The result is that the calcium ions have seven nearest neighbours. The carbon atoms are coordinated by three or four calcium ions. In the first case the carbon atom is surrounded by a tetrahedron consisting of the three calcium ions and the other carbon atom of the

carbide group. In the latter case an irregular tetrahedron is formed by the four calcium ions only.

The structure is stabilized by the incorporation of cyanamide ions. These ions certainly replace carbide ions situated in "pyrite" positions, for there the corresponding cation-anion distance is very little sensitive to changes in the distance between the coordinating atoms belonging to the same anion.

Monoclinic calcium carbide CaC_2 III, CaC_2(mon.) is formed spontaneously when pure calcium carbide is cooled below 450°C. It is very doubtful whether it is really metastable at this temperature, but Bredig reports that it is transformed into CaC_2(tetr.) by grinding at temperatures between 200 and 350°C [3].

As usual the calcium and carbide ions are six-coordinated and the structure is thus related to the rock salt structure. A calcium ion is surrounded by eight carbon atoms forming a structure similar to a dodecahedron. Four of the carbon atoms belong to different carbide groups and lie in about the same plane as the calcium ion. Thus they form a nearly regular square. The other four carbon atoms belong to two carbide ions and are also situated approximately in one plane, perpendicular to the one first mentioned. Thus the structure is very similar to that of the low temperature modification of sodium cyanide.

Each carbon atom is surrounded by four calcium ions, forming a very distorted tetrahedron.

The coordination in the cubic calcium carbide CaC_2 IV or CaC_2(cub.) is less well established. The orientation of the carbide ions is disordered, probably by rotation, but it may also be a completely disordered pyrite structure. The great solubility of calcium cyanamide in calcium carbide above 450°C may then easily be accounted for. In the latter case every calcium ion would be octahedrally surrounded by six carbon atoms. Then the change in the coordination number of the calcium ions is quite in order. At temperatures above 450°C the coordination number is six, just below 450°C it is eight and at still lower temperatures it grows to ten. The triclinic calcium carbide which is only stable in presence of cyanamide ions may be regarded as a hybrid of ordered cubic calcium carbide and monoclinic calcium carbide.

The structures of the strontium and barium carbides are less well established, but the different occurring phases have bee ncharacterized with the aid of their X-ray powder patterns [3]. The tetragonal and cubic phases are known and, besides, strontium carbide in the presence of cyanamide ions forms a phase, which must be very similar to the triclinic calcium carbide. No phase corresponding to the monoclinic structure seems to exist. This is to be expected. As strontium and barium ions are larger than calcium ions the ten-coordination in the tetragonal phase is energetically more favourable than the eight-coordination in the monoclinic phase (see above).

Acknowledgements. The author is indebted to Professor Cyrill Brosset for his interest in this work and for the way he has facilitated its completion. Further the author's thanks are due to the *Swedish Natural Science Research Council* for financial support of this investigation.

REFERENCES

1. Vannerberg, N. G. *Acta Chem. Scand.* **15** (1961) 769.
2. Atoji, M. and Medrud, C. *J. Chem. Phys.* **31** (1959) 332.
3. Bredig, M. A. *J. Phys. Chem.* **46** (1942) 801.
4. Schrewelius, N. *Thesis*. Stockholm 1943.
5. Bochert, W. and Röder, M. *Z. anorg. u. allgem. Chem.* **302** (1959) 253.
6. Bredig, M. A. *Z. anorg. u. allgem. Chem.* **310** (1961) 338.
7. Templeton, D. H. and Dauben, C. H. *J. Am. Chem. Soc.* **72** (1952) 2251.
8. Abrahams, S. C. and Kalnajs, J. *Acta Cryst.* **7** (1954) 838.
9. Vannerberg, N. G. *Thesis* Göteborg 1959. Doktorsavhandlingar vid Chalmers tekniska högskola Nr. 21.
10. Wells, A. F. *Structural Inorganic Chemistry*. 2nd ed. Clarendon Press, Oxford 1960, p. 397, 538.

Received December 8, 1961.

ACTA CHEMICA SCANDINAVICA 16 (1962) 1221–1233

Studies on the Coagulation of Chicken Blood

V. Differentiation and Assay of Labile Factors, Adsorbable by Barium Carbonate

ØYVIND SØRBYE* and INGER KRUSE

Department of Biochemistry and Nutrition, Polytechnic Institute, Copenhagen, Denmark

Studies on the effect of adsorbents on the labile factor activity of fresh oxalated plasmas have revealed that this activity is of a complex nature. Only a part of the labile factor activity can be adsorbed by barium or strontium carbonates, and it is shown that each of these two compounds adsorbs two different labile factors — ψ(psi)-factor and σ(sigma)-factor — which can be adsorbed separately by other selective adsorbents. The minimum amount of adsorbent required for complete adsorption of each labile factor seems to be proportional to the concentration of the factor. ψ-Factor and σ-factor also contribute to the labile factor activity measured when Russell's viper venom, with or without cephalin, is substituted for thromboplastin.

In 1908 Nolf [1] described a plasmatic factor (thrombogène) which accelerated the conversion of prothrombin (thrombozyme) to thrombin. The problem of prothrombin conversion accelerators attracted greater attention when, about 30 years later, Rhoads and Panzer [2], and Quick [3] reported on a prolongation of the coagulation time of plasma during storage. The increase in coagulation time was first ascribed to an alleged lability of prothrombin, but was later [4] shown to be due to destruction of a labile plasma factor, different from prothrombin, but necessary for the conversion of prothrombin to thrombin. Since then, prothrombin conversion accelerators have been studied in several laboratories. The prothrombin accelerator of Fantl and Nance [5], the labile factor of Quick [6], the Ac-globulin of Ware and co-workers [7] and factor V of Owren [8] are all labile plasma factors which accelerate the conversion of prothrombin to thrombin. These coagulation accelerators differ from prothrombin by not being adsorbed by barium carbonate [5], calcium phosphate gel [1,9] or by aluminium hydroxide gel [4]. They are not removed by passage of plasma through asbestos pads [8] and not influenced by dicumarol therapy [4]. At present it is generally agreed that the accelerators described by the different investigators

* Fellow of the *Royal Norwegian Council for Scientific and Industrial Research.*

are identical, and that the terms: prothrombin accelerator, labile factor, Ac-globulin, factor V, and proaccelerin are synonyms for the same coagulation factor.

In this laboratory we have been concerned with the problems of differentiation and assay of coagulation factors in chicken blood in connection with planned studies on the influence of dietary factors on the formation of coagulation factors. The interest in the labile factor activity of fresh chicken plasma was aroused by the experience that the thromboplastin accelerated coagulation time of oxalated chicken plasma increased at least fourfold on storage at 5—6°C for 4—5 days. This gave easy access to substrate plasmas for studies of the coagulation factors which are reduced below optimal levels during short-time storage.

In connection with the studies on the $\varkappa$-, δ-, and φ-factors of normal, vitamin K-deficient and of dicumarol (or coumachlor) plasmas [10,12], the plasmas were also investigated with regard to their *labile factor activity*, defined as the activity of plasma factors which accelerate the coagulation of stored, oxalated normal plasma. It was found that complete adsorption of the $\varkappa$-, δ-, and φ-factors from oxalated plasma by strontium carbonate or barium carbonate also resulted in a limited reduction of the labile factor activity. A further reduction of the labile factor activity could not be obtained by increasing the amounts of adsorbent, nor by renewed treatment with the adsorbent. These experiments indicated that the labile factor activity of fresh oxalated chicken plasma must be due both to strontium carbonate adsorbable and to strontium carbonate non-adsorbable factors, and thus cannot be attributed to a single coagulation factor. In the present and forthcoming papers it will be shown that the labile factor activity of fresh oxalated chicken plasma can be regarded as the combined activity of a number of labile coagulation factors, the differences between which are revealed by adsorption experiments, using crystalline adsorbents. The present study deals with adsorption of the labile factor activity which is adsorbed by barium carbonate or strontium carbonate, simultaneously with the adsorption of the $\varkappa$-, δ-, and φ-factors.

MATERIALS AND METHODS

The materials and methods for coagulation time determinations were described previously [10]. The details of a general adsorption technique were also presented [10]. The adsorbents used in this work were those used in the studies on the adsorption of the $\varkappa$-, δ-, and φ-factors [11].

Stored plasma. Oxalated plasma from normal chickens [10] was stored in cotton plugged or rubber stoppered tubes at 5—6°C. After 4—5 days the thromboplastin coagulation time had increased at least fourfold. Such plasmas were used as substrates for evaluation of the labile factor activities of fresh plasmas.

Coagulation time determination. In addition to the thromboplastin coagulation time (tpl.-time) and the Russell's viper venom (RVV)-cephalin time tests described [10], two modifications of the latter were occasionally used: RVV-buffer times were determined by substituting buffer for cephalin, and RVV-times by leaving out the addition of cephalin or buffer.

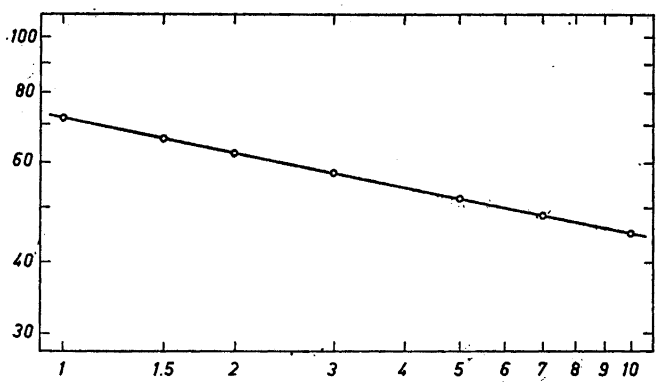

Fig. 1. Dilution curve for labile factor activity. Ordinate: coagulation time in min/100. Abscissa: concentration of fresh plasma in % (v/v)

Determination of the labile factor activity.

Test system: 0.2 ml stored oxalated plasma
0.2 ml dilution of test sample (in buffer)
0.2 ml thromboplastin solution
0.2 ml $CaCl_2$-solution (30 mM).

The coagulation time of this test system varies with the concentration of the coagulation factors which are reduced below optimal levels in the stored plasma. Dilutions of the test sample were made with veronal buffer [10]. A test system with cephalin replacing thromboplastin and RVV-$CaCl_2$[10] replacing $CaCl_2$, and a similar system system without added cephalin, were used to reveal possible differences between the labile factor activity measured by thromboplastin and the similar activities measured by RVV-cephalin or RVV alone, respectively.

EXPERIMENTS AND RESULTS

Determination of labile factor activity. A plot of the coagulation time of stored plasma as a function of the concentration of added fresh plasma gives a straight line on double logarithmic paper for the range 1—10 % (v/v) (Fig. 1). Plasmas with very high or very low activities may show deviations from the straight line at higher or lower concentrations, respectively. When RVV-cephalin or RVV was substituted for thromboplastin, similar dilution curves were obtained, shifted to shorter or longer coagulation times, respectively.

Different fresh plasmas gave identical or parallel lines when tested with the same stored plasma (Fig. 2), showing that the labile factor activities of different plasmas may be different. Curves obtained with one fresh plasma and different stored plasmas were not necessarily identical or of the same slope, as shown in Fig. 3.

The position and slope of the dilution curves may thus vary from one experiment to another, depending on the sensitivity of the substrate and the activity of the fresh plasma. As the potency of the assay accelerator solution (thromboplastin, RVV-cephalin, or RVV) may also be subject to slight variations, a new dilution curve should be prepared in each experiment. A com-

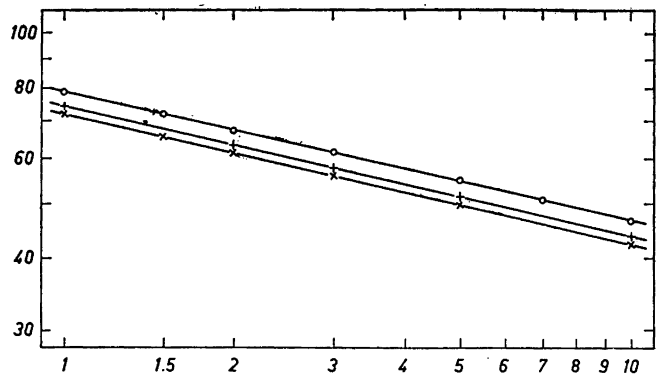

Fig. 2. Dilution curves for three plasmas tested with the same stored plasma. Ordinate: coagulation time in min/100. Abscissa: concentration of fresh plasma in % (v/v). O: plasma A; +: plasma B; ×: plasma C.

parison of the labile factor activities of different plasmas must therefore be done by simultaneous determination of the activities of the plasmas, employing the same sample of stored plasma and the same solution of assay accelerator. Thus, only the relative labile factor activities of different plasmas can be determined by this technique. The results of different experiments could not be expected to be directly comparable without rigorous control of the potency of the accelerator solution and of the sensitivity of the stored plasma. A standard dilution of 5 % was chosen for determination of the labile factor activities of plasmas relative to the activity of a plasma used for preparation of the dilution curve. The recorded coagulation times were reproducible with no more difference than 0.1 sec, corresponding to differences in labile factor activity of less than 1 %.

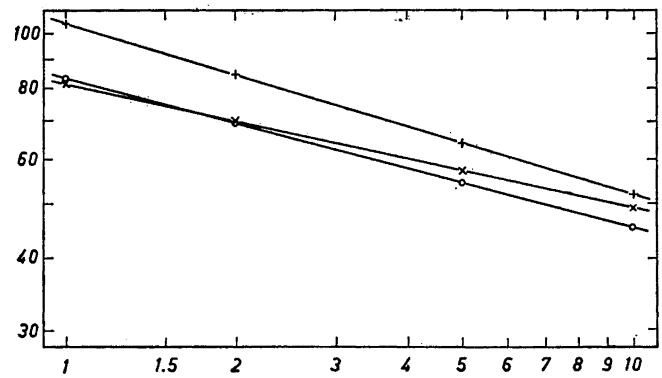

Fig. 3. Dilution curves for a plasma tested with three different stored plasmas. Ordinate: coagulation time in min/100. Abscissa: concentration of fresh plasma in % (v/v). O: stored plasma A; +: stored plasma B; ×: stored plasma C.

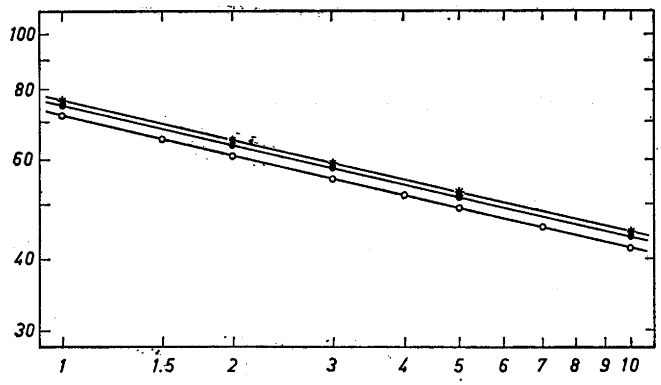

Fig. 4. Dilution curves for untreated and adsorbed plasmas. Ordinate: coagulation time in min/100. Abscissa: concentration of fresh (adsorbed) plasma in % (v/v).

O: untreated plasma.
●: plasma adsorbed with 10 mg/ml barium carbonate.
+: » » » 20 » » »
×: » » » 30 » » »

Adsorption of the labile factor activity. Oxalated plasmas were used for adsorption studies. During a preliminary testing of the adsorbents it was ensured that treatment of the plasma with an adsorbent caused no or only a minimal change in pH. It was also controlled that the adsorbed plasma did not contain significant amounts of inhibitors derived from the adsorbent. This was done by comparing the labile factor activity of the adsorbed plasma to that of the untreated plasma at different dilutions. Absence of inhibitors was indicated by corresponding results. The dilution curves for the untreated and the adsorbed plasma were then parallel as shown for untreated and barium carbonate adsorbed plasmas in Fig. 4, and the activity of the adsorbed plasma could be expressed in terms of the activity of the original plasma.

During the last ten years about one hundred and fifty crystalline inorganic compounds have been tested for adsorption of labile factor activity. More than one hundred of the compounds satisfied the above requirements. Their effects on plasma could thus not be attributed to release of inhibitors or pH changes, but were ascribed to adsorption of labile coagulation factors. The adsorbents were further tested for selectivity, *i.e.* ability to adsorb only a part of the labile factor activity of the plasma with increasing amounts of adsorbent. The present study is confined to the compounds which adsorbed the same or a smaller part of the labile factor activity which could be adsorbed by barium carbonate or strontium carbonate. The results of a preliminary testing are summarized in Table 1. Five of the fifteen adsorbents tested did not reduce the labile factor activity of oxalated plasma. The remaining ten adsorbents were able to adsorb only a part of the total activity and could be classified as selective adsorbents.

During this and subsequent work it was noticed that the ratio of adsorbable to total activity could vary widely in different experiments with the same

Table 1. Adsorption of labile factor activity.

Plasma No.	Adsorbent	mg/ml	Labile factor activity in % of untreated plasma
4128	CaF_2	20	100
		80	100
4128	$PbCrO_4$	20	100
		80	100
4128	BiF_3	20	100
		80	100
4103	$CdCO_3$	20	100
		80	100
4102	$Mg_3(AsO_4)_2$	20	100
		80	100
4103	CaC_2O_4	5	92
		50	92
3511	SrC_2O_4	5	90
		50	90
3522	BaC_2O_4	5	92
		40	92
4102	$CaMoO_4$	20	93
		80	93
4102	$BaCrO_4$	20	89
		80	89
4103	$CaCO_3$	20	92
		80	92
4118	$SrCO_3$	25	87
3508	$SrCO_3$	20	78
		40	78
3516	$BaCO_3$	20	73
		80	73
4118	PbS	20	87
		80	87
4103	$MnCO_3$	50	83
		80	83

adsorbent. Such differences are apparent in the recorded experiments with strontium carbonate as adsorbent, where the ratio in two experiments was 0.87 and 0.78, respectively. Such differences may arise from differences in the *sensitivity of the test substrates* to adsorbable and non-adsorbable factors, but also from differences between *individual fresh plasmas* in the concentrations of adsorbable and non-adsorbable factors.

The adsorption of labile factor activity by the selective adsorbents was studied in greater details by determination of the labile factor activity of a series of plasma aliquots adsorbed with graded amounts of adsorbent. Some of the typical adsorption curves obtained are shown in Figs. 5 A—H. The labile factor activity was adsorbed proportionally to the amount of adsorbent added, until the curve abruptly became horizontal at a certain concentration of adsorbent, indicating that further adsorption of labile factor activity could not be accomplished by increasing the amounts of adsorbent. It was also

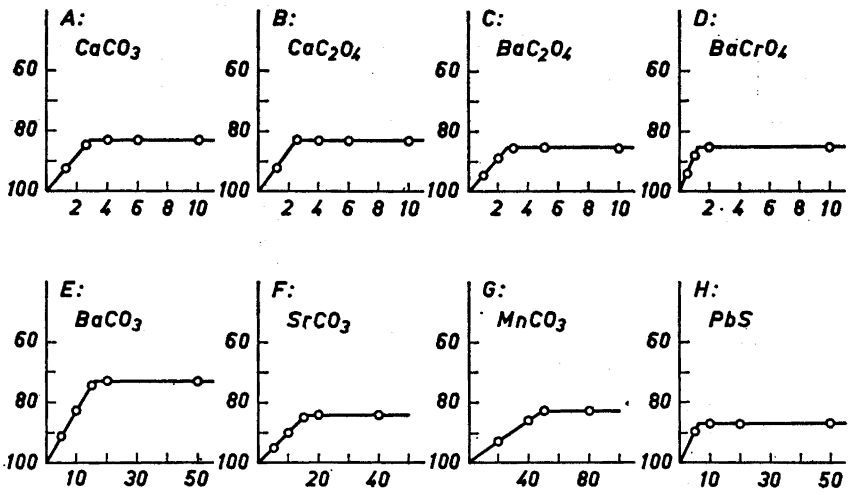

Fig. 5. Adsorption of labile factor activity by selective adsorbents. Ordinates: labile factor activity in % of original plasma. Abscissæ: adsorbent in mg/ml.
A: calcium carbonate, B; calcium oxalate, C: barium oxalate, D: barium chromate, E: barium carbonate, F: strontium carbonate, G: manganese carbonate, H: lead sulfide.

found that renewed treatment with the same adsorbent caused no further reduction of the labile factor activity. Such adsorption curves were obtained with all the selective adsorbents.

The partial adsorbability of the labile factor activity by these adsorbents indicates that the adsorbable and the non-adsorbable activities are not due to the same (groups of) labile coagulation factors. The labile factor activity of fresh oxalated chicken plasma should be regarded, therefore, as the combined activity of separate coagulation factors with characteristic differences in adsorbability.

In Table 2 is shown that the labile factor activity of plasma is reduced by column adsorption to the same extent as by batch adsorption with the same adsorbent except in the first few drops of effluent plasma. The presence or absence of $\varkappa$-factor, δ-factor, φ-factors, and other factors requiring large amounts of adsorbent for complete adsorption, is thus of no consequence for the labile factor activity of the fresh plasma. The plasma concentrations of these factors cannot be reduced to any greater extent during short time storage at 6°C, at least not below optimal levels.

Matching experiments. A comparison of the effects of different adsorbents was carried out in a series of matching experiments: One portion of a plasma was preadsorbed with a certain quantity of an adsorbent. It was generally ensured that the quantity of adsorbent used for preadsorption was sufficient for maximal adsorption of labile factor activity. Another portion of the same plasma was not pretreated. Curves for adsorption of the labile factor activities of the untreated and of the preadsorbed plasmas by another adsorbent were

Table 2. Column adsorption *versus* batch adsorption.

Plasma No.	Adsorption treatment	Tpl.-time in min/100	Labile factor activity in %
3517	Untreated	28	100
	Column of 2 g SrC_2O_4: 0—1 ml effluent	∞	87
	1—2 » »	∞	94
	2—3 » »	78	94
	4—5 » »	43	94
	5—6 » »	36	94
	SrC_2O_4, 5 mg/ml	29	94
	BaC_2O_4, 10 »	29	94
3511	Untreated	26	100
	Column of 2 g BaC_2O_4: 0—1 ml effluent	∞	61
	1—2 » »	∞	94
	2—3 » »	∞	94
	4—5 » »	∞	94
	7—8 » »	∞	94
	BaC_2O_4, 10 mg/ml	27	94
4120	Untreated	22	100
	Column of 1 g $CaCO_3$: 0—1 ml effluent	31	93
	1—2 » »	23	93
	4—5 » »	23	93
	8—9 » »	23	93
	$CaCO_3$, 10 mg/ml	23	93
3510	Untreated	23	100
	Column of 3 g CaC_2O_4: 0—1 ml effluent	∞	82
	1—2 » »	∞	90
	2—3 » »	∞	90
	4—5 » »	∞	90
	CaC_2O_4, 5 mg/ml	24	90
	BaC_2O_4, 5 »	23.8	94
	$SrCO_3$, 25 »	∞	84

then determined simultaneously. The results of such experiments are presented in Figs. 6 and 7 (A—H).

From Fig. 6A it is apparent that the labile factor activity which can be adsorbed by barium oxalate is not affected by preadsorption of the plasma on a calcium oxalate column. The same amount of adsorbent is required for maximal adsorption of the labile factor activity of the untreated and the preadsorbed plasma, and the barium oxalate adsorbable activity is the same in both plasmas, *viz.* 12 % of the original activity. The experiment shows that the labile factors adsorbed by barium and calcium oxalates are different and that the activity of the factor adsorbed by barium oxalate is independent of the activity of the factor adsorbed by calcium oxalate.

Similarly, the labile factor which can be adsorbed by calcium oxalate or calcium carbonate was unaffected by preadsorption of the plasma on a barium oxalate column (Figs. 6B and 6C). The labile factor activity adsorbed by calcium carbonate was also unrelated to the activity removed by preadsorption with barium chromate (20 mg/ml) (Fig. 6D).

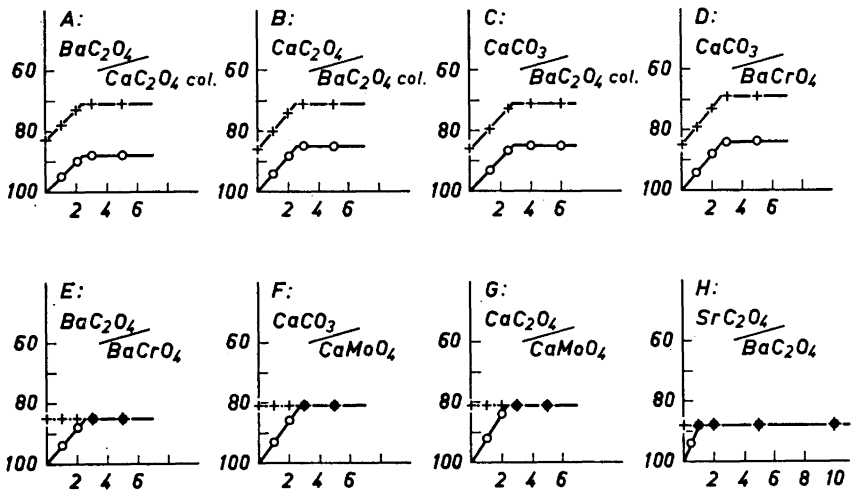

Figs. 6. Adsorption of labile factor activity from untreated and preadsorbed plasmas. Ordinates: labile factor activity in % of original plasma. Abscissæ: adsorbent in mg/ml. O: untreated plasma. +: preadsorbed plasma.
A: barium oxalate adsorption of untreated and calcium oxalate column (4 g) preadsorbed plasma (first ml discarded, the next five ml collected). B: calcium oxalate adsorption of untreated and barium oxalate column (3 g) preadsorbed plasma (first ml discarded, the next five ml collected). C: calcium carbonate adsorption of untreated and barium oxalate column (3 g) preadsorbed plasma (first ml discarded, the next five ml collected). D: calcium carbonate adsorption of untreated and barium chromate (20 mg/ml) preadsorbed plasma. E: barium oxalate adsorption of untreated and barium chromate (20 mg/ml) preadsorbed plasma. F: calcium carbonate adsorption of untreated and calcium molybdate (10 mg/ml) preadsorbed plasma. G: calcium oxalate adsorption of untreated and calcium molybdate (10 mg/ml) preadsorbed plasma. H: strontium oxalate adsorption of untreated and barium oxalate (5 mg/ml) preadsorbed plasma.

Barium oxalate adsorption of untreated plasma reduced the labile factor activity to the same level as obtained with barium chromate, but caused no further reduction of a barium chromate preadsorbed plasma (Fig. 6E). The labile factor adsorbed by these two adsorbents was therefore considered to be identical.

Similar experiments with calcium carbonate, calcium oxalate, and calcium molybdate (Figs. 6F and 6G) established the identity of the labile factor adsorbed by these three adsorbents, and a comparison of the activities adsorbed by strontium and barium oxalates (Figs. 6H and 7A) proved that the latter two adsorbents adsorbed the same labile coagulation factor.

The term σ(sigma)-factor has been chosen for the labile coagulation factor which can be adsorbed from oxalated plasma by barium oxalate, barium chromate or strontium oxalate. The term ψ(psi)-factor was adopted for the labile coagulation factor which can be adsorbed from oxalated plasma by calcium carbonate, calcium oxalate or calcium molybdate.

The labile factor activities adsorbed by strontium carbonate, barium carbonate, lead sulfide, and manganese carbonate were compared in the experi-

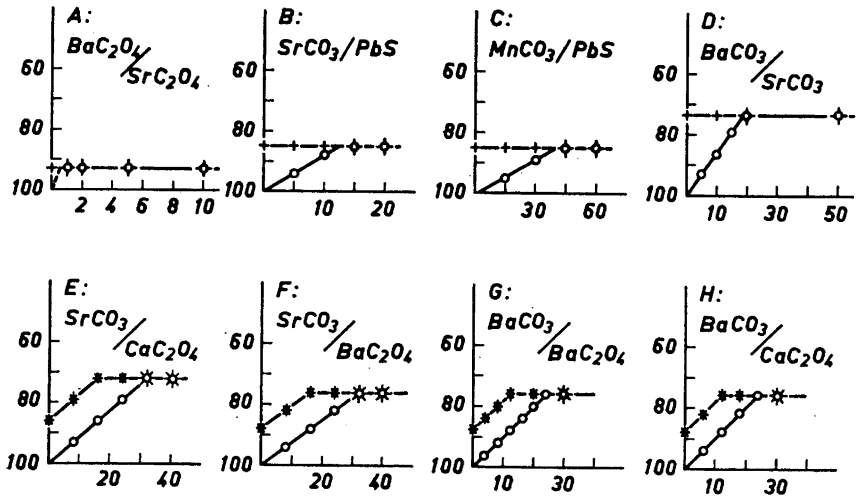

Fig. 7. Adsorption of labile factor activity from untreated and preadsorbed plasmas. Ordinates: labile factor activity in % of original plasma. Abscissæ: adsorbent in mg/ml. O: untreated plasma. + and ×: preadsorbed plasmas.
A: barium oxalate adsorption of untreated and strontium oxalate (5 mg/ml) preadsorbed plasma. B: strontium carbonate adsorption of untreated and lead sulfide (20 mg/ml) preadsorbed plasma. C: manganese carbonate adsorption of untreated and lead sulfide (20 mg/ml) preadsorbed plasma. D: barium carbonate adsorption of untreated and strontium carbonate (25 mg/ml) preadsorbed plasma. E: strontium carbonate adsorption of untreated plasma and plasma preadsorbed with 5 (+) and 200(×) mg/ml calcium oxalate. F: strontium carbonate adsorption of untreated plasma and plasma preadsorbed with 3 (+) and 60 (×) mg/ml barium oxalate. G: barium carbonate adsorption of untreated plasma and plasma preadsorbed with 3 (+) and 60 (×) mg/ml barium oxalate. H: barium carbonate adsorption of untreated plasma and plasma preadsorbed with 5 (+) and 200 (×) mg/ml calcium oxalate.

ments of Figs. 7B—D. It was concluded that the four adsorbents adsorbed the same part of the labile factor activity.

In Figs. 7E—H the labile factor activities adsorbed by strontium or barium carbonates were compared to the activity adsorbed by calcium or barium oxalates. It will be seen that preadsorption by calcium or barium oxalates removes only a part of the labile factor activity which can be adsorbed by barium or strontium carbonates. The amounts of adsorbent required for maximal adsorption of the labile factor activity of the preadsorbed plasma was reduced proportionally. This means that ψ-factor and σ-factor are adsorbed simultaneously by strontium carbonate and by barium carbonate, and the two factors are adsorbed competitively. The curves for plasmas preadsorbed with 5 and 200 mg/ml calcium oxalate were identical as were the curves for plasmas preadsorbed with 3 and 60 mg/ml barium oxalate. It is concluded that the competitive adsorption of ψ-factor and σ-factor by strontium and barium carbonates in independent of the concurrent adsorption of $\varkappa$-, δ-, and φ-factors.

Table 3. Labile factors measured by RVV-cephalin or RVV.

Adsorbent	mg/ml	Labile factor activity in %		
		Tpl.	RVV-ceph.	RVV
Untreated		100	100	100
$CaCO_3$	1	95	94.5	96.5
»	2	90	89	93
»	3	86.5	85	90.5
»	5	86.5	85	90.5
BaC_2O_4	1	94	94	96
»	2	88	88	92
»	3	85	85	90
»	5	85	85	90
$SrCO_3$	25	71.5	70	80.5
Plasma No.		4 679	5 050	5 067

The labile factor activity measured by RVV-cephalin or RVV. In the above experiments thromboplastin was used as assay accelerator. Additional experiments with RVV-cephalin or RVV replacing thromboplastin are summarized in Table 3. It is apparent that both calcium carbonate and barium oxalate reduce the labile factor activity measured by RVV-cephalin or RVV alone. The same amounts of the two adsorbents were required for maximal adsorption of activity in the three test systems, *viz.* 2.7 mg/ml calcium carbonate and 2.5 mg/ml barium oxalate. The maximal effect of strontium carbonate equalled the combined effects of calcium carbonate and barium oxalate. The results indicate that ψ-factor and σ-factor also contribute to the labile factor activity measured with RVV-cephalin or RVV as assay accelerators.

Table 4. Plasma coagulation time and ψ- and σ-factor concentration. Plasma No. 315.

Plasma treatment	Tpl.-time in min/100	Labile factor activity in %
Untreated	25	100
1 mg/ml $CaCO_3$	25	95.5
2 » »	25	91
2.4 » »	25	—
2.5 » »	25.1	88.5
2.6 » »	25.4	—
2.8 » »	26	87.5
3 » »	26	87.5
5 » »	26	87.5
1 mg/ml BaC_2O_4	25	95
2 » »	25	90
2.2 » »	25	—
2.3 » »	25.3	88.5
2.4 » »	25.6	—
2.5 » »	25.9	87.5
3 » »	25.9	87.5
5 » »	25.9	87.5

Influence of ψ- and σ-factor concentrations on the plasma coagulation time. The ψ- and σ-factors do not appear tc be indispensable factors for the coagulation of plasma, but both factors may be important for obtaining the maximal coagulation rate. Complete removal of ψ-factor or σ-factor by adsorption results in a slight prolongation of the coagulation time of plasma. A detailed study of this effect (Table 4) revealed that 85—90 % of either of the two factors could be removed without effect on the coagulation time. The prolongation occurred simultaneously with the removal of the remaining 10—15 % of either activity. An increase in the amounts of adsorbent up to 0.5 % caused no further prolongation of the coagulation time. This means that the ϰ-, δ-, or φ-factors are not reduced below optimal concentrations by the quantities of adsorbent required for complete adsorption of ψ- or σ-factors, and the prolongation of the coagulation time must be due to adsorption of the last 10—15 % of the total ψ- or σ-factor concentration. The accelerating effect of the two labile factors on the coagulation rate of fresh plasma may thus be considered optimal at about 12 % of the normal level.

DISCUSSION

Stored plasma [13–16] or plasma incubated under various conditions [17,18] has regularly been used as a substitute for factor V-deficient plasma in assay of the factor V activity of fresh plasma. The results obtained with artificial substrates are said to be comparable to those obtained with plasma from factor V-deficient patients. Factor V thus appears to be the only plasma factor, limiting thromboplastin coagulation rate, which drops below optimal levels during storage or incubation. In the methods referred to the results are read from standard dilution curves relating coagulation time to activity. A comparison of the results of different experiments seems to depend on a control of the potency of the accelerator solution (thromboplastin) and of the sensitivity of the substrate plasma.

In the proposed method for assay of labile chicken coagulation factors, standard dilution curves could not be used because of the observed differences between the dilution curves obtained with different stored chicken plasmas. The present method, therefore, can only be used for determination of the *relative* labile factor activities of plasmas tested simultaneously. On the other hand, with the use of identical substrates and identical accelerator solutions greater importance could be attributed to small, but reproducible differences in the activities of different plasmas, permitting detailed studies on the effects of adsorbents on the labile factor activity. The results obtained so far strongly suggest that the coagulation deficit in stored chicken plasma cannot be ascribed to a single coagulation factor, but rather to a number of plasma factors. These factors have in common the property of being reduced below optimal levels during short time storage. Their non-identity is inferred from the observed differences in behavior on adsorption of plasma with crystalline adsorbents. The present experiments have shown that the ϰ-, δ-, and φ-factors have no labile factor activity. The factors which determine the coagulation time of stored chicken plasma, therefore, belong to a different group of coagulation factors. The reduction in labile factor activity which occurs on

adsorption of oxalated plasmas by strontium and barium carbonates is solely due to adsorption of two labile coagulation factors for which the terms ψ-factor and σ-factor have been adopted.

The adsorption curves suggest that some adsorbents have special *adsorption sites*[12] for ψ- factor or σ-factor, whereas the two factors compete for the same adsorption sites on other adsorbents. The experiments indicate that these adsorption sites cannot be involved in the adsorption of $\varkappa$-, δ-, or φ-factors.

The observed proportionality between adsorbed activity and amounts of adsorbent indicate that each adsorbent has a definite *adsorption capacity* for the adsorbable labile factor(s) which is independent of the plasma concentration of the factor(s). In analogy with what has been found for adsorption of φ-factor activity by calcium carbonate [11,12], it seems probable that the minimum amount of adsorbent which gives maximal reduction of labile factor activity, *i.e.* complete adsorption of ψ-factor or σ-factor or both, will be proportional to the plasma concentration of the factor(s). Comparison of the concentrations of adsorbable labile factors of plasmas tested in different experiments may thus become possible. However, if inert material is adsorbed *in competition* with the labile factor(s), variations in the concentrations of such material will influence the results in much the same way as variations in the concentrations of the labile factor(s). Great variations in the levels of $\varkappa$-, δ-, and φ-factors, which are adsorbed *independently* of the adsorption of the labile factors, have been shown not to affect the results of this kind of "adsorption titration".

REFERENCES

1. Nolf, P. *Arch. Intern. Physiol.* **6** (1908) 1.
2. Rhoads, J. E. and Panzer, L. M. *J. Am. Med. Ass.* **112** (1939) 309.
3. Quick, A. J. *J. Am. Med. Ass.* **114** (1940) 1342.
4. Quick, A. J. *Am. J. Physiol.* **140** (1943) 212.
5. Fantl, P. and Nance, M. H. *Nature* **158** (1946) 708.
6. Quick, A. J. *Am. J. Physiol.* **151** (1947) 63.
7. Ware, A. G., Guest, M. M. and Seegers, W. H. *Science* **106** (1947) 41.
8. Owren, P. A. *Acta Med. Scand.* Suppl. 194 (1947).
9. Nolf, P. *Arch. Intern. Pharmacodyn. et Thérapie* **70** (1945) 5.
10. Sørbye, Ø. and Kruse, I. *Acta Chem. Scand.* **14** (1960) 2177.
11. Sørbye, Ø. *Acta Chem. Scand.* **16** (1962) 799.
12. Sørbye, Ø. *Acta Chem. Scand.* **16** (1962) 903.
13. Quick, A. J. and Stefanini, M. *J. Lab. Clin. Med.* **33** (1948) 819.
14. Stefanini, M. *Am. J. Clin. Pathol.* **20** (1950) 233.
15. Lewis, M. L. and Ware, A. G. *Proc. Soc. Exptl. Biol. Med.* **84** (1953) 640.
16. Quick, A. J. *J. Clin. Pathol.* **13** (1960) 457.
17. Stormorken, H. *Scand. J. Clin. Lab. Med.* **9** (1957) 273.
18. Borchgrevink, C. F., Pool, J. G. and Stormorken, H. *J. Lab. Clin. Med.* **55** (1960) 625.

Received November 16, 1961.

ACTA CHEMICA SCANDINAVICA 16 (1962) 1234–1244

On the Crystal Structures of $FeOHSO_4$ and $InOHSO_4$

GEORG JOHANSSON

Department of Inorganic Chemistry, Royal Institute of Technology, Stockholm 70, Sweden

The basic iron sulfate, $FeOHSO_4$, forms orthorhombic crystals with lattice parameters $a = 7.33$, $b = 6.42$, and $c = 7.14$ Å. The space group is D_{2h}^{16}—*Pnma* and the unit cell contains four formula weights. Each iron atom is octahedrally coordinated with two hydroxo-groups and four sulfate oxygens. Each hydroxogroup is bonded to two iron atoms. The structure of the basic indium sulfate, $InOHSO_4$, has been shown to be similar.

Crystal structure determinations of a number of basic salts of group 3b metals have shown that the metal atoms in these salts are linked together by means of single or double bridges of hydroxogroups. In crystals of $AlOHSO_4(H_2O)_5$ the aluminum atoms are joined by double OH bridges, which results in the formation of discrete aluminum oxygen complexes [1]. In the corresponding basic sulfates of indium and thallium, $InOHSO_4(H_2O)_2$ [2] and $TlOHSO_4(H_2O)_{2.5}$ [3] the metal atoms are joined by single OH bridges leading to infinite metal-oxygen chains. These basic salts can all be obtained from solutions at room temperature. To see if the same type of bridging occurs in basic salts prepared under different conditions, the structure of an indium sulfate formed by hydrothermal hydrolysis at high temperature has been investigated. It has the composition $In_2O_3 \cdot 2SO_3 \cdot H_2O$. An iron sulfate with the same composition, $Fe_2O_3 \cdot 2SO_3 \cdot H_2O$, can be obtained by the same method of preparation [4]. Structurally the two compounds are closely related.

EXPERIMENTAL

Preparation of crystals. $In_2O_3 \cdot 2SO_3 \cdot H_2O$: Solutions of indium sulfate with concentrations ranging from 0.004 to 1.0 M were prepared by dissolving $In_2(SO_4)_3$ in distilled water or in weak sulfuric acid (< 15 % H_2SO_4). Small samples of the solutions were then heated in sealed pyrex tubes at 100°, 160°, or 190°C for about a week. No precipitates were formed in the tubes heated to 100°C. At the higher temperatures two phases were obtained. One formed only in the most dilute solutions and did not contain sulfate. It was shown by powder photographs to be $In(OH)_3$. The other was the basic sulfate $In_2O_3 \cdot 2SO_3 \cdot H_2O$. It crystallized as thin needles which were bound together into larger aggregates of rather irregular shapes with the needle axes parallel.

$Fe_2O_3 \cdot 2SO_3 \cdot H_2O$: The range of stability has been given by Posjnak and Merwin [4]. Crystals sufficiently large for X-ray work, were obtained by heating a solution containing 4.7 % Fe_2O_3, 12.9 % SO_3, and 82.4 % H_2O at 200°C for about a month.

Analysis. The results of the analysis are compared in Table 1 with calculated values for $In_2O_3 \cdot 2SO_3 \cdot H_2O$ and $Fe_2O_3 \cdot 2SO_3 \cdot H_2O$.

Table 1.

	$In_2O_3 \cdot 2SO_3 \cdot H_2O$ Found	Calc.		$Fe_2O_3 \cdot 2SO_3 \cdot H_2O$ Found	Calc.
% In_2O_3	60.7	60.91	% Fe_2O_3	47.2	47.27
% SO_3	35.1	35.13	% SO_3	47.0	47.40
% H_2O	4.5	3.95	% H_2O	5.9	5.33
Density	3.9$_4$	4.05	Density	3.2$_9$	3.34

The amount of water was determined according to the method of Brush and Penfield [5], and sulfate was determined as $BaSO_4$. In^{3+} and Fe^{3+} were precipitated as hydroxides. After ignition the residue was weighed as In_2O_3 or Fe_2O_3. The density was obtained by comparison of the weight of a sample in benzene and in air.

X-Ray data. Rotation and Weissenberg photographs taken around the three crystallographic axes showed that the crystals are orthorhombic. The following values for the unit cell dimensions were calculated from powder photographs taken with Cu$K\alpha$ radiation (λ = 1.54050 Å) in a Guinier focusing camera with KCl (a_0 = 6.2929 Å) as internal standard:

$a = 7.67_1$ Å $\quad b = 6.64_8$ Å $\quad c = 7.32_3$ Å for $In_2O_3 \cdot 2SO_3 \cdot H_2O$
$a = 7.33_1$ Å $\quad b = 6.41_8$ Å $\quad c = 7.14_3$ Å for $Fe_2O_3 \cdot 2SO_3 \cdot H_2O$

(Estimated accuracy ± 0.005 Å). The first lines on the powder photographs are given in Table 2.

A comparison between observed and calculated densities shows that there are two formula weights, thus 4 Fe(In) atoms, in the unit cell (Table 1).

For $Fe_2O_3 \cdot 2SO_3 \cdot H_2O$ the systematically absent reflections are $0kl$ with $k + l$ odd and $hk0$ with h odd. This is characteristic for the space groups No. 62: *Pnma* and No. 33: $Pn2_1a$. The non-centrosymmetric $Pn2_1a$ was not considered as it was possible to find a satisfactory structure with the higher symmetry.

The crystals are extended along the a axis. The odd layer lines of rotation photographs taken around this axis are very weak. On the even layer lines all reflections with $\frac{1}{2}h + k + l$ odd are absent, which indicates that for every atom at x, y, z there must also be an atom at $1/4 + x$, $\frac{1}{2} + y$, $\frac{1}{2} + z$ or $\frac{3}{4} + x$, $\frac{1}{2} + y$, $\frac{1}{2} + z$.

Difficulties were encountered in finding good single crystals of the corresponding indium compound. The spots on the Weissenberg films were often rather extended and diffuse. This was especially true for crystals prepared at 190°C. Weissenberg photographs showed that the systematic absences are the same as for $Fe_2O_3 \cdot 2SO_3 \cdot H_2O$ except for the presence of very weak reflections $hk0$ for h odd. The odd layer lines around the a axis are extremely weak in comparison with the even layer lines which have the same systematic absences for $\frac{1}{2}h + k + l$ odd as was noted for the Fe salt.

For the collection of intensity data Weissenberg photographs were taken around all three axes using the multiple film technique with MoK radiation for the Fe salt and CuK radiation for the In salt. The maximum dimension of the crystals used were 0.2 mm for the Fe and 0.1 mm for the In salts. The intensities were estimated visually by comparison with a calibrated intensity strip and were corrected for Lorentz and polarization factors.

Because $Fe_2O_3 \cdot 2SO_3 \cdot H_2O$ has a higher symmetry and gave more reliable intensity data, a complete structure determination was carried out only for this compound.

STRUCTURE DETERMINATION

The very weak odd layer lines around the a axis for both the iron and the indium compound indicate that there is no or at least only a very small contri-

bution to these reflections from the metal atoms. Thus, if one Fe atom has the position xyz, there must be a corresponding atom at $\frac{1}{2} + x,y,z$. The extinction on the even layer lines of reflections with $\frac{1}{2}h + k + l$ odd further shows that there must also be Fe atoms at $1/4 + x$, $\frac{1}{2} + y$, $\frac{1}{2} + z$ and $3/4 + x$, $\frac{1}{2} + y$, $\frac{1}{2} + z$. The only position in space group *Pnma* that can accomodate four Fe atoms related in this way, is 4(*c*): $\pm(x, 1/4, z)$, $\pm(\frac{1}{2} + x, 1/4, \frac{1}{2} - z)$. The parameter values must then be $x = \pm 1/8$ or $\pm 3/8$ and $z = \pm 1/4$. All these positions are equivalent and any set of parameters can be chosen, for example: $x = 1/8$, $z = 1/4$, $(y = 1/4)$.

The Fe atoms make a maximum contribution to all $0kl$ reflections and therefore probably determine their signs. On this assumption the electron density projected on the yz plane was calculated. As no signs were later changed because of the contributions from the light atoms, the resulting Fourier map was the same as the final electron density map shown in Fig. 1a. It reveals clearly the positions of the four sulfate groups of the unit cell, and it also indicates the positions of the four oxygen atoms (O_4) not associated with the sulfate groups.

According to Fig. 1a the parameters of O_4 are $y = 1/4$ and $z \approx 0.15$, and O_4 therefore occupies the position 4(*c*). The two nearest Fe atoms are at 1/8, 1/4, 1/4 and 5/8, 1/4, 1/4. The O_4 atom must have a position between these Fe atoms, that is with $x = 3/8$ (or 7/8 which is structurally equivalent), as other values of x would result in Fe—O_4 distances, which are too short. O_4 is therefore in contact with two Fe atoms at distances of approximately 2.0 Å.

The possible x parameters for the sulfur atoms are restricted in the same way as the parameters for the Fe atoms, that is they must be $x = \pm 1/8$ or $\pm 3/8$. With the position of O_4 given ($x = 7/8$, $y = 1/4$, $z \approx 0.35$) and with

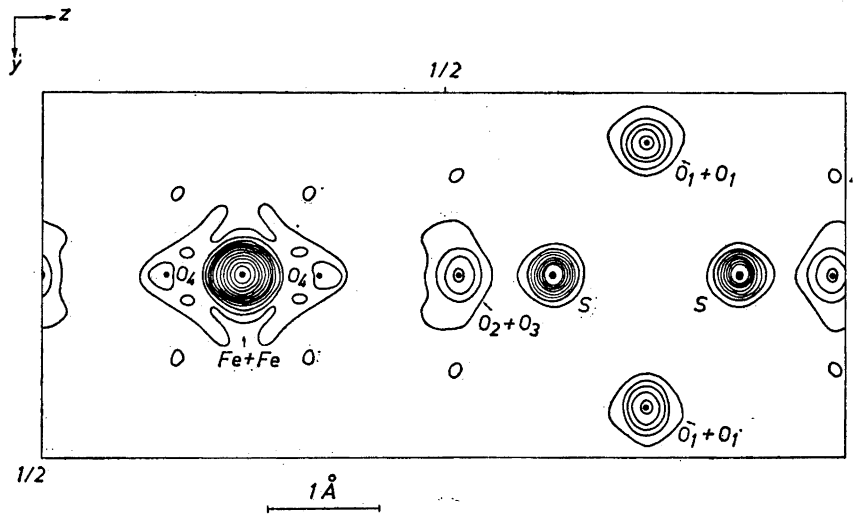

Fig. 1 a. Electron density projection along the *a* axis for $FeOHSO_4$. Contours are drawn at intervals of 10 e·Å^{-2}. The zero contour is omitted. At the Fe peak only every 3rd contour has been drawn above 50 e·Å^{-2}. The final atomic positions are indicated by dots.

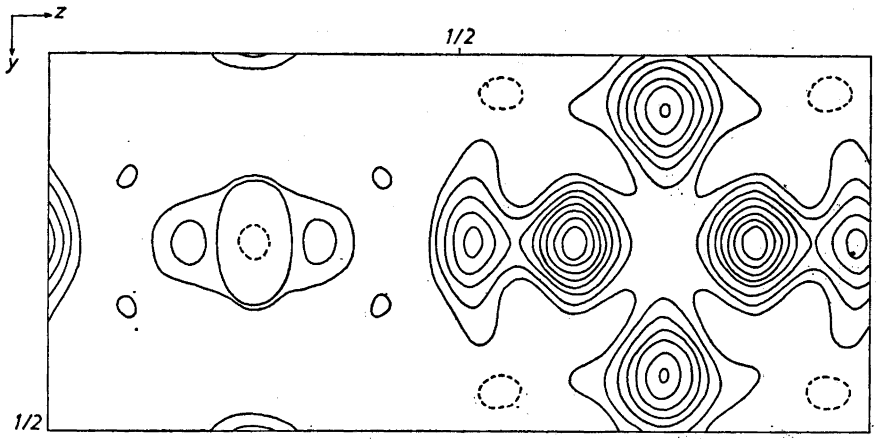

Fig. 1 b. Electron density projection along the *a* axis for $InOHSO_4$ with the contribution from the In atoms subtracted. Contours are drawn at intervals of 4 e·Å^{-2}. The zero contour is omitted. Broken lines indicate negative regions.

the sulfate group oriented as shown by the 0*kl* projection in Fig. 1a, the only possible parameters for the fourfold sulfur position, not leading to O—O distances, which are too short, are $x = 3/8$ and $y = 1/4$, $z \approx 0.63$.

Of the oxygen atoms of the sulfate groups, O_1 occupies an eightfold position since according to Fig. 1a it lies outside the mirror planes at $y = \pm 1/4$. O_2 and O_3 lie on the mirror planes, that is they are in fourfold positions. Their x

Table 2. Powder photographs ($\sin^2\Theta < 0.20$) of $FeOHSO_4$ and $InOHSO_4$, taken with Cu*Ka* radiation in a Guinier camera.

	$FeOHSO_4$				$InOHSO_4$		
h k l	$\sin^2\Theta$ calc.	$\sin^2\Theta$ obs.	*I* obs.	*h k l*	$\sin^2\Theta$ calc.	$\sin^2\Theta$ obs.	*I* obs.
101	0.0227	0.0226	vvw	101	0.0211	0.0211	vvw
011	0.0260	0.0260	m	011	0.0245	0.0245	w+
111	0.0371	0.0370	vvw	002	0.0443	0.0443	w+
002	0.0465	0.0465	w	201	0.0514	0.0514	vs
201	0.0558	0.0558	vs	020	0.0537	0.0537	s
102	0.0575	0.0576	s	210	0.0537		
020	0.0576			102	0.0543	0.0545	vvw
112	0.0719	0.0719	vw	022	0.0979	0.0980	m
212	0.1050	0.1050	vvw	212	0.0980		
221	0.1134	0.1134	w	221	0.1051	0.1052	s
013	0.1190	0.1190	w	013	0.1130	0.1131	w
031	0.1413	0.1413	vw	031	0.1318	0.1318	vw
203	0.1488	0.1488	w	203	0.1399	0.1399	w+
230	0.1738	0.1741	vvw	230	0.1611	0.1612	m
400	0.1766	0.1765	w	400	0.1613		
004	0.1860	0.1859	vvw	004	0.1770	0.1775	vvw
				411	0.1858	0.1857	w
				223	0.1936	0.1935	vw

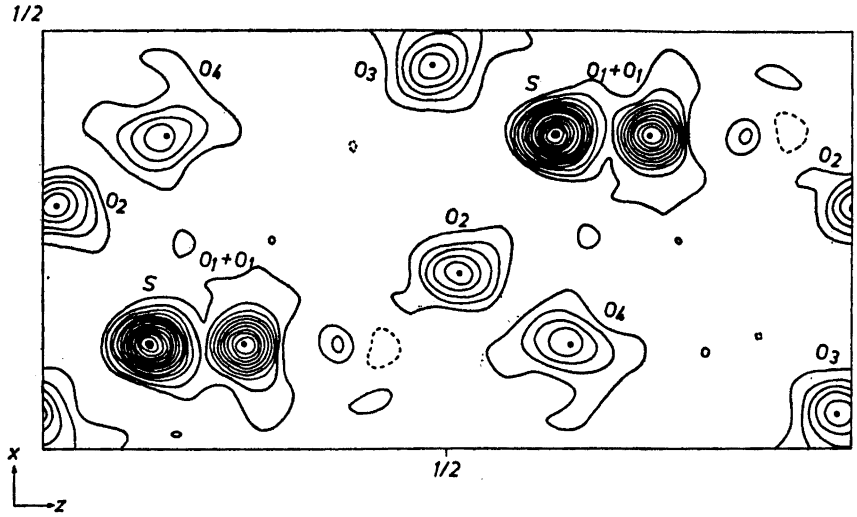

Fig. 2. Electron density projection along the *b* axis for $FeOHSO_4$ with the contribution from the Fe atoms subtracted. Contours are drawn at intervals of 5 e·Å^{-2}. The zero contour is omitted. The final atomic positions are indicated by dots.

parameters can be calculated assuming the O—O distance in a sulfate group to be 2.4 Å.

The resulting parameter values were refined from difference syntheses and electron density projections along the *a*, *b*, and *c* axes. The refinement was continued until the difference maps did not indicate any significant shifts in the positional parameters. The final parameters are given in Table 3. The final electron density projection along the *b* axis with the contribution from the Fe atoms subtracted is shown in Fig. 2.

Of the atoms of the unit cell only O_2 and O_3 give contributions to reflections for which h is even and $\frac{1}{2}h + k + l$ is odd. To maintain the condition that these reflections are systematically absent the parameters of O_2 and O_3 must be related in such a way, that, for example, an O_2 atom at xyz has a corresponding O_3 atom at $1/4 + x$ (or $3/4 + x$), $\frac{1}{2} + y$, $\frac{1}{2} + z$. The final parameters in Table 3 are in accordance with this as there are no indications in the difference maps of any significant deviations from this relation.

Table 3.

Final parameters

	x	y	z
4 Fe in 4(*c*)	0.125	1/4	0.250
4 S in 4(*c*)	0.875	1/4	0.866
8 O_1 in 8(*d*)	0.375	0.067	0.750
4 O_2 in 4(*c*)	0.209	1/4	0.517
4 O_3 in 4(*c*)	0.959	3/4	0.017
4 O_4 in 4(*c*)	0.375	1/4	0.155

For the final calculation of structure factors listed in Table 5, temperature factors of 0.3 Å^2 for Fe and S and 0.5 Å^2 for O atoms were used. The scattering factors were those given by Berghuis *et al.*[6] for O, by Tomiie and Stam [7] for S, and by Thomas and Umeda [8] for Fe. The R factors ($R = \Sigma||F_o|-|F_c||/\Sigma|F_o|$) with only observed reflections included are 0.084 for $0kl$, 0.070 for $h0l$, and 0.086 for $hk0$ reflections. For reflections with h odd there are no contributions from the Fe or O_1 atoms. For this class of reflections the R factors are 0.11 for $h0l$ and 0.13 for $1kl$ reflections. Standard deviations in positional parameters estimated according to the formula given by Cruickshank [9] are about 0.005 Å for S, 0.01_5 Å for O_1, O_2, and O_3, and 0.02 Å for O_4. Since most of the atoms are in special positions, the standard deviations in bond lengths will, however, generally be smaller than might be expected from the values given. The structure of $In_2O_3 \cdot 2SO_3 \cdot H_2O$ is essentially the same as that of $Fe_2O_3 \cdot 2SO_3 \cdot H_2O$. The electron density projection calculated from the $0kl$ structure factors with the contributions from the indium atoms subtracted is shown in Fig. 1b. It is in all essentials identical with that of the iron compound (Fig. 1a), but the presence of weak reflections $hk0$ for h odd shows that the symmetry of the indium salt is lower. The differences probably can be explained by rather small deviations of the parameter values of the light atoms in $In_2O_3 \cdot 2SO_3 \cdot H_2O$ from the *Pnma* symmetry. However, attempts to determine these deviations by means of trial and error were not successful and failed to give an R factor below about 0.30 for the weak $1kl$ and $3kl$ reflections, compared with a R factor of about 0.10 for the $0kl$ and $2kl$ reflections.

DISCUSSION OF THE STRUCTURE

Projections of the structure along the a and b axes are shown in Fig. 3. Each metal atom is octahedrally surrounded by six oxygen atoms. Two of

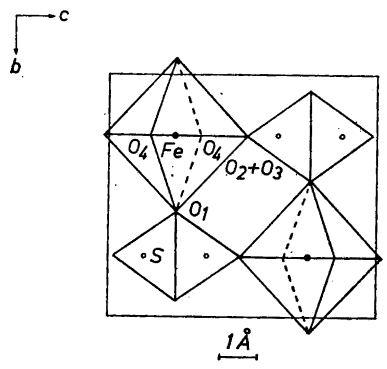

Fig. 3 a. Projection of the structure of $FeOHSO_4$ along the a axis.

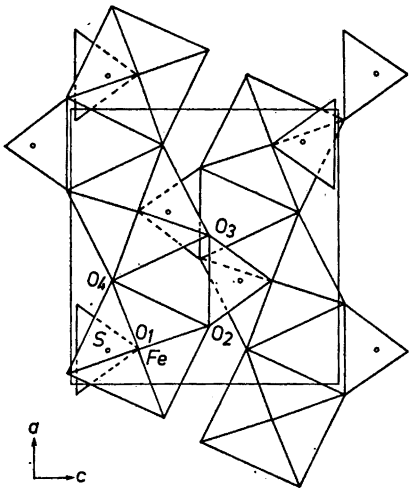

Fig. 3 b. Projection of the structure of $FeOHSO_4$ along the b axis.

Table 4. Interatomic distances.

Distances within a FeO_6 octahedron:

Fe	— 2 O_1	2.03_5 Å	O_1 — O_2	2.86 Å
	— O_2	2.00_3	— O_3	2.86
	— O_3	2.00_3	— O_4	2.82
	— 2 O_4	1.95_4	O_2 — O_4	2.86
			— O_4	2.74
			O_3 — O_4	2.86
			— O_4	2.74

Distances within a SO_4 group:

S	— 2 O_1	1.44 Å	O_1 — O_1	2.35 Å
	— O_2	1.48	— O_2	2.37
	— O_3	1.48	— O_3	2.37
			O_2 — O_3	2.43

Other O—O distances < 4.0 Å

O_1	— O_1	3.67 Å	O_2 — O_3	3.55 Å
	— O_2	3.18	— O_3	3.70
	— O_3	3.18	— O_4	3.41
	— O_4	3.12	O_3 — O_3	3.27
			O_4 — O_4	3.91

these, O_4, are shared between two octahedra. The remaining four belong to sulfate groups. The four hydrogen atoms of the unit cell are probably associated with the bridging oxygens, O_4, as this would increase the sum of electrostatic bond strengths for these atoms from 1 to the expected value of 2. The metal atoms are therefore joined by single hydroxobridges, and the formulae should be written as $FeOHSO_4$ and $InOHSO_4$. The interatomic distances (Table 4) give no evidence for the presence of hydrogen bonds.

The same kind of single hydroxobridges are present in the structure of $InOHSO_4(H_2O)_2$[2]. The two structures are in fact closely related. The two water oxygens of the InO_6 octahedra in $InOHSO_4(H_2O)_2$ are replaced by sulfate oxygens in $InOHSO_4$. The infinite In—OH—In chains, which in the former compound are joined to other similar chains only by means of hydrogen bonds, are in $InOHSO_4$ and $FeOHSO_4$ joined to other chains by means of oxygen atoms belonging to the same sulfate group. The In—In distance, 3.84 Å, within an In—OH—In chain in $InOHSO_4$ is slightly smaller than the corresponding distance in $InOHSO_4(H_2O)_2$, 3.95 Å. Accurate values for the In—O distances can not be calculated, but the approximate structure shows that they do not differ much from the values found for $InOHSO_4(H_2O)_2$[2].

In $FeOHSO_4$, the FeO_6 octahedra are very nearly regular. In view of the standard deviations, however, the difference between the shortest of the Fe—O bond lengths (1.95 Å and involving the bridging oxygens, O_4) and the longest (2.04 Å) is probably significant. The average value of the Fe—O distances, 2.00 Å, is close to the sum of the crystal radii, 2.04 Å [10].

The average S—O distance of 1.46 Å does not differ significantly from S—O distances found for sulfate groups in other structures [1].

Table 5. Observed and calculated structure factors for $FeOHSO_4$.

hkl	F_o	F_c	*hkl*	F_o	F_c
000	—	328	060	112	−116
2	102	−104	2	54	49
4	87	83	4	37	− 37
6	39	− 37	6	28	23
8	83	86	8	60	− 63
10	52	− 53	10	39	41
12	27	27	12	21	− 22
14	< 17	− 17	14	< 17	14
16	23	23	16	20	− 19
18	21	− 23	18	14	20
011	52	− 46			
3	85	91	071	30	30
5	57	− 50	3	65	− 58
7	35	35	5	50	44
9	< 11	− 3	7	31	− 30
11	41	41	9	< 16	8
13	26	− 26	11	34	− 35
15	21	20	13	26	23
			15	19	− 19
020	155	−176			
2	21	20	080	64	65
4	28	− 26	2	20	− 17
6	< 8	3	4	< 14	8
8	63	− 60	6	< 15	− 2
10	32	35	8	36	37
			10	24	− 21
031	88	90			
3	109	−117	091	29	− 27
5	80	76	3	52	50
7	47	− 53	5	46	− 39
9	17	18	7	26	28
11	49	− 51	9	< 17	− 10
13	32	34	11	31	33
15	23	− 27	13	25	− 21
040	131	140			
2	41	− 39	0100	64	− 64
4	32	32	2	34	27
6	16	− 13	4	< 16	− 20
8	60	62	6	18	13
10	36	− 37	8	35	− 40
12	< 17	17	10	30	26
14	< 17	− 9			
16	19	16	0111	< 16	8
18	15	− 17	3	24	− 26
			5	23	19
051	22	− 19			
3	54	53	0120	42	48
5	41	− 36	2	26	− 20
7	20	22	4	< 17	15
9	< 15	2	6	19	10
11	33	32	8	29	31
13	22	− 19	10	21	− 21

hkl	F_o	F_c	*hkl*	F_o	F_c
0131	< 17	− 18	131	25	− 24
3	31	30	2	38	− 39
5	28	− 24	3	< 6	0
7	16	19	4	< 7	7
9	< 15	− 9	5	< 7	5
11	18	22	6	17	17
			7	15	− 15
0140	26	− 29	8	14	− 15
2	< 17	8	9	< 11	− 9
4	< 16	− 6	10	11	− 13
6	< 16	2			
8	16	− 18	141	21	20
			2	33	− 33
0151	< 16	11	3	< 7	− 2
3	< 16	− 20	4	< 8	6
5	18	15	5	< 8	− 5
7	19	− 13	6	13	16
			7	10	15
0160	24	30	8	< 10	− 14
2	< 14	− 14	9	13	9
4	< 13	13	10	16	− 13
6	< 12	− 9			
8	16	21	151	17	17
			2	25	29
101	34	35	3	< 8	− 3
2	53	− 55	4	< 8	− 6
3	9	4	5	11	− 5
4	10	9	6	17	− 15
5	< 7	− 4	7	17	14
6	19	18	8	15	13
7	17	16			
8	16	− 16	161	14	− 15
9	13	10	2	22	25
10	12	− 14	3	< 9	4
			4	< 9	− 5
111	29	33	5	< 9	5
2	49	52	6	14	− 14
3	9	3	7	12	− 13
4	< 6	− 9			
5	10	− 5	171	12	− 14
6	20	− 18	2	18	− 22
7	20	16	3	< 9	4
8	17	16	4	< 10	5
			5	< 10	4
121	30	− 29	6	13	13
2	47	46	7	14	− 12
3	< 6	− 2			
4	13	− 8	181	13	12
5	< 7	5	2	18	− 20
6	14	− 17			
7	11	− 16	191	< 11	11
8	10	16	2	15	18
9	13	− 10			
10	17	14	1101	< 12	− 10
11	12	10	2	14	16

hkl	F_o	F_c	*hkl*	F_o	F_c
201	135	−149	1005	24	− 25
3	97	95	7	44	45
5	55	− 59	9	35	− 36
7	78	79			
9	60	− 59	1101	< 15	− 10
11	30	34	2	19	− 16
301	22	18	1200	56	− 65
2	39	− 34	2	27	30
3	36	31	4	24	− 23
4	21	19	6	< 19	16
5	24	25	8	41	− 41
6	29	29			
			1401	27	34
400	125	−140	3	< 20	− 23
2	116	119	5	< 20	18
4	28	− 29	7	30	− 30
6	55	52			
8	63	− 65	1600	26	31
10	53	56	2	23	− 27
501	19	− 19	210	16	− 16
2	33	32	3	69	64
3	< 9	2	5	< 9	− 4
4	< 9	− 6	7	17	19
5	< 10	5	9	16	− 18
6	17	− 16			
7	18	− 14	420	79	77
8	< 15	14	4	87	− 79
9	< 16	− 9	6	75	78
10	17	12	8	46	− 43
			10	49	46
601	83	88	12	43	− 34
3	47	− 47	14	< 18	19
5	44	50	16	20	− 22
7	47	− 51			
9	61	62	610	18	− 18
			3	12	− 10
701	20	16	5	16	− 17
2	30	25			
			820	58	− 55
800	77	81	4	56	57
2	67	− 66	6	60	− 59
4	18	18	8	36	34
6	37	− 36	10	38	− 37
8	50	50	12	31	28
10	37	− 45	14	19	− 16
901	< 12	− 1	1010	< 17	− 8
2	23	− 18	3	16	22
3	20	− 16			
4	< 16	9	1220	48	49
5	16	− 14	4	45	− 50
6	17	18	6	44	51
			8	29	− 32
1001	50	54	10	25	34
3	33	33	12	25	− 28

hkl	F_o	F_c	*hkl*	F_o	F_c
1620	23	− 21	1680	19	15
4	23	23	10	16	− 18
6	21	− 25			

Acknowledgements. I am indebted to Professor Lars Gunnar Sillén for his interest and helpful criticism. I also wish to thank Mrs Anna-Greta Berg for technical assistance.

The work has been supported by the *Office of Scientific Research, of the Office of Aerospace Research, United States Air Force* through its European Office on contract number AF 61(052)−162. Free time at the "Besk" computer has been made available by the *Swedish Board for Computing Machinery*. The English text has been corrected by Dr. Denis McWhan.

REFERENCES

1. Johansson, G. *Acta Chem. Scand.* **16** (1962) 403.
2. Johansson, G. *Acta Chem. Scand.* **15** (1961) 1437.
3. Johansson, G. *Acta Chem. Scand.* **13** (1959) 925.
4. Posjnak, E. and Merwin, H. E. *J. Am. Chem. Soc.* **44** (1922) 1965.
5. Kolthoff, I. M. and Sandell, E. B. *Textbook of Quantitative Inorganic Analysis* New York 1952, p. 717.
6. Berghuis, J. *et al. Acta Cryst.* **8** (1955) 478.
7. Tomiie, Y. and Stam, C. H. *Acta Cryst.* **11** (1958) 126.
8. Thomas, L. H. and Umeda, K. *J. Chem. Phys.* **26** (1957) 293.
9. Cruickshank, D. W. J. *Acta Cryst.* **2** (1949) 65.
10. Pauling, L. *The Nature of the Chemical Bond.* New York 1960.

Received December 11, 1961.

ACTA CHEMICA SCANDINAVICA 16 (1962) 1245–1250

Disorder and Order in Solid Solutions of Oxygen in α-Titanium

BO HOLMBERG

Institute of Inorganic and Physical Chemistry, University of Stockholm, Stockholm, Sweden

The range of solid solubility of oxygen in α-titanium has been studied by means of X-ray powder and single-crystal techniques. Three phases have been observed, *viz.* a random solution (TiO_{0+x}) and two phases based on an *anti*-$Cd(OH)_2$ structure type. One of the latter (Ti_2O_{1-y}) has a broad range of homogeneity, the oxygen vacancies indicated in the formula being randomly distributed. The other, ($Ti_2O_{1-1/3}$), has one third of the oxygen positions of Ti_2O vacant in an ordered manner. The occurrence of the three phases was found to depend on both the oxygen content and the annealing temperature.

The hexagonal close-packed α-modifications of titanium, zirconium and hafnium are characterized by a remarkable ability to dissolve small nonmetal atoms to a large extent. This is especially so with oxygen which can enter into solid solution up to the compositions $TiO_{0.50}$ [1–4], $ZrO_{0.40}$ [5] and $HfO_{0.26}$ [6] in the three metals, respectively. The solubility mechanism has been thought to imply that the oxygen atoms occupy the major interstices of the metal structure, *i.e.* the octahedral holes, in a perfectly random way [7,8]. Studies recently carried out at this Institute have, however, demonstrated the existence of ordering at higher oxygen contents in the α-zirconium solid solutions [5] while a random arrangement is present in α-hafnium solid solutions [6].

According to previous investigators, the incorporation of oxygen atoms in the α-titanium and α-zirconium structures causes a considerable expansion of the *c* axes while the *a* axes are less affected by the oxygen content. It was, however, found by the present research group that the length of the *a* axes actually passes through a maximum value occurring at the composition $TiO_{0.33}$ [1] and $ZrO_{0.25}$ [5], respectively. At these contents of oxygen, there is also observed a marked acceleration of the rate of increase of the *c* axes.

The present investigation of the α-titanium-oxygen solid solutions has revealed that several preparations may give extra X-ray reflexions which are not compatible with the idea of random solutions of oxygen. The various samples employed in these studies were prepared in the way described in a

Table 1. Structural types identified in samples, $TiO_{0-0.50}$, quenched from the annealing temperature.

Annealing temperature	$TiO_{0.30}$	$TiO_{0.33}$	$TiO_{0.35}$	$TiO_{0.37}$	$TiO_{0.40}$	$TiO_{0.45}$	$TiO_{0.50}$
~ 1800°C	TiO_{0+x}	TiO_{0+x}	TiO_{0+x}	TiO_{0+x}	TiO_{0+x}	TiO_{0+x}	Ti_2O
800°C	»	»	»	»	»	Ti_2O_{1-y}	»
700°C	»	»	»	»	»	»	»
600°C	»	»	»	»	Ti_2O_{1-y}	»	»
500°C	»	»	Ti_2O_{1-y}	Ti_2O_{1-y}	»	»	»
400°C	»	$Ti_2O_{1-\frac{1}{3}}$	»	»			»

previous article [1] which also reports the X-ray techniques used in the phase analysis and the crystal structure determinations.

PHASE ANALYSIS

During the phase analysis of samples $TiO_{0-0.50}$, three types of phases were observed, viz.

(*i*) a phase characterized by the same size (approximately) of the unit cell as that of pure α-titanium metal but showing reflexions such as 003 which are not allowed by the structure of the metal. This phase is called Ti_2O_{1-y} for reasons developed below,

(*ii*) a phase showing the reflexions mentioned under *i* and additional ones corresponding to a unit cell six times the size of the metal unit cell ($Ti_2O_{1-1/4}$),

(*iii*) a phase giving powder patterns in full conformity with those of the metal (TiO_{0+x}).

The occurrence of the three phases depends on both the oxygen content and annealing temperature as shown in Table 1.

Detailed studies on the composition and region of temperature stability of the various phases and also of the characters of the phase transformations are in progress and will be reported at later date.

STRUCTURAL STUDIES

The various phases have been studied by means of single-crystal and powder techniques and the following results have been obtained:

The TiO_{0+x} region

The structure within this region (*cf. iii* above) is identical with the one suggested by Ehrlich [7] for the solid solution of oxygen in titanium *viz.*

Space-group: $P6_3/mmc$ (No. 194)
Unit cell dimensions of the sample $TiO_{0.325}$:
$a = 2.9700$ Å, $c = 4.7751$ Å
Unit cell content: 2 TiO_{0+x}
2 x O in 2(*a*): 0,0,0; 0,0,½ (random distribution)
2 Ti in 2(*c*): $\frac{1}{3},\frac{2}{3},\frac{1}{4}$; $\frac{2}{3},\frac{1}{3},\frac{3}{4}$

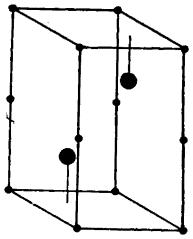

Fig. 1. The structure of α-Ti.

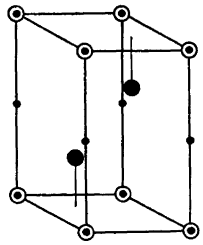

Fig. 2. The structure of Ti_2O.

The structure is illustrated in Fig. 1 which shows the metal atom positions in one unit cell and also the centers of the octahedral interstices in the metal arrangement. The holes are occupied by the oxygen atoms in a random way.

The formula TiO_{0-x} is used to indicate that the pure metal represents the limiting composition of the phase. The maximum content of oxygen (x) is, as mentioned above, dependent on the heat-treatment.

The Ti_2O structure and the Ti_2O_{1-y} region

Single-crystal studies on a sample analysed as $TiO_{0.50}$ were reported in a previous article [9] and gave the following atomic arrangement:

Space-group: $P\bar{3}m1$ (No. 164)
Unit cell dimenions: $a = 2.9593$ Å, $c = 4.8454$ Å.
Unit cell content: Ti_2O.
1 O in 1(*a*): 0,0,0
2 Ti in 2(*d*): $\frac{1}{3},\frac{2}{3},z$; $\frac{2}{3},\frac{1}{3},\bar{z}$; $z = 0.263$

The structure is illustrated in Fig. 2 which shows the atomic positions in one unit cell and also the centers of the octahedral interstices. The structure is of the *anti*-$Cd(OH)_2$ type, which implies that the oxygen atoms occupy the holes in every second layer of octahedral interstices extending parallel to the *ab*-planes. Thus all the holes of these planes are filled while those of the interleaving ones are empty. The metal atoms are not in the ideal positions of the hexagonal close-packed arrangement but somewhat displaced parallel to the *c* axis, away from the oxygen atoms.

For samples of this structure type with lower oxygen contents, a careful comparison of the powder patterns did not reveal any differences except those due to the variation of the unit cell size. This indicates that the structure is essentially unchanged over the entire region of composition. In particular, the intensities of the reflexions 001 and 003 were found to be constant, which shows that the z_{Ti} parameter is not affected by the oxygen content. Samples of the Ti_2O phase with a deficit in oxygen should thus contain vacancies in the oxygen arrangement in a random way. This phase is accordingly formulated Ti_2O_{1-y}.

Table 2. a Comparison of observed and calculated structure factors for Ti_3O. The measured intensities were corrected for absorption, the crystal being approximated to a cylinder of radius 0.020 mm.

hkl	$(hkl)Ti_2O_{1-y}$	$\|F\|_{obs}$	$\|F\|_{calc}$
002	001	—	10
004	002	150	150
006	003	52	53
008	004	141	123
0010	005	41	35
0012	006	71	71
300	110	139	151
302	111	—	2
304	112	121	110
306	113	39	39
308	114	95	103
3010	115	19	31

The Ti_3O structure

The following structure of the $TiO_{0.33}$ sample annealed at 400°C has been derived by applying trial and error techniques on single-crystal data.

Space-group: $P\bar{3}1c$ (No. 163)
Unit cell dimensions $a = 5.1411$ Å, $c = 9.5334$ Å
Unit cell content: 4 Ti_3O
2 O in 2(*a*): 0,0,1/4; 0,0,3/4
2 O in 2(*d*): 2/3,1/3,1/4, 1/3,1/3,1/4
12 Ti in 12(*i*): x,y,z; $\bar{y},x-y,z$; $y-x,\bar{x},z$;
$\bar{x},\bar{y},\bar{z}$; $y,y-x,\bar{z}$; $x-y,x,\bar{z}$;
$y,x,\frac{1}{2}+z$; $\bar{x},y-x,\frac{1}{2}+z$; $x-y,\bar{y},\frac{1}{2}+z$;
$\bar{y},\bar{x},\frac{1}{2}-z$; $x,x-y,\frac{1}{2}-z$; $y-x,y,\frac{1}{2}-z$.
$x = 1/3; y = 0; z = 0.118$

Table 2 a gives a comparison of observed and calculated structure factors for reflexions sensitive to the value of the z_{Ti} parameter. Table 2 b gives a comparison of observed and calculated intensities for reflexions sensitive to the distribution of the oxygen atoms.

Table 2 b. Comparison of observed and calculated Weissenberg intensities for reflexions depending only on the oxygen atom arrangement of the Ti_3O structure.

h k l	I_{obs}	I_{calc}
1 0 0	—	2
1 0 1	vw	5
1 0 2	—	1
1 0 3	—	2
1 0 4	—	0.5
1 0 5	—	0.9
2 0 0	—	0.6
2 0 1	—	2
2 0 2	—	0.4
2 0 3	—	1

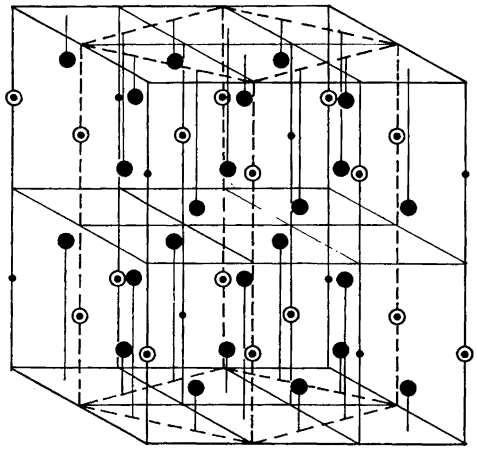

Fig. 3. The structure of Ti_3O.

The structure is a superstructure of the Ti_2O structure having the oxygen vacancies of the Ti_2O structure in an ordered distribution. One oxygen position out of three in every oxygen layer normal to the *c* axis is vacant. The vacant positions have a zigzag arrangement in the direction of the *c* axis. Fig. 3 shows a unit cell of Ti_3O and also the pattern of the basic Ti_2O units.

DISCUSSION

The structural analogy found to exist between the solid solutions of oxygen in α-titanium and α-zirconium does not, upon detailed inspection, exclude structural differences which are of considerable interest. Thus, the analogy is restricted to (*i*) a very high solubility of oxygen in both metals, (*ii*) a peculiar change in the lattice parameters with the oxygen content, and especially the occurrence of a maximum in the *a* parameter, (*iii*) the existence of random solutions of oxygen in the metal at lower oxygen contents and (*iv*) the existence of ordered solutions at higher proportions of oxygen.

The structural differences, on the other hand, manifest themselves in the dissimilar mechanisms of ordering of the oxygen atoms in the two metals. Thus, while in zirconium the oxygen atoms seem to assume an ordered arrangement as soon as a minimum oxygen content is reached, the ordering of the oxygen atoms in titanium is dependent not only on the concentration but also on the temperature. In this connection, it should also be noted that the anomalous change of the unit cell parameters and the process of ordering in the solid solutions are not associated phenomena since they do not occur at the same composition in the zirconium-oxygen system ($ZrO_{0.25}$ and $ZrO_{0.33}$ respectively).

There is a considerable difference in the ways in which the oxygen atoms are arranged in the ordered solid solutions of the two metals. Thus, in the ordered and partly ordered titanium phases, the interstitial atoms occur exclusively

in every second layer of octahedral holes extending normally to the *c* axis, which makes all these phases related to the *anti*-$Cd(OH)_2$ structure type. The metal atoms will thus be in a very asymmetric environment, the asymmetry being accentuated by the fact that the titanium atoms are slightly displaced from their ideal positions, away from the layers of oxygen atoms. In the ordered state of the zirconium-oxygen solid solution however, the oxygen atoms occur evenly distributed over ordered interstitial sites situated in all the layers of octahedral holes extending normally to the *c* axis. This arrangement is not associated with any principal changes in the atomic framework of the pure metal. Moreover, it does not imply large differences in interatomic distances like those found in the titanium-oxygen phases.

Acknowledgements. This investigation has been sponsored by the *Office Chief of Research and Development, U.S. Department of Army*, through its European Research Office and by the *Swedish Natural Science Research Council.*

The author wishes to express his sincere gratitude to Prof. Arne Magnéli and to Dr. Sten Andersson for their never-failing interest and many valuable discussions.

REFERENCES

1. Andersson, S., Collén, B., Kuylenstierna, U. and Magnéli, A. *Acta Chem. Scand.* **11** (1957) 1641.
2. Magnéli, A., Andersson, S., Westman, S., Åsbrink, S. and Holmberg, B. *Final Technical Report* **1** (1958) DA-91-508-EUC-245.
3. Magnéli, A., Andersson, S., Westman, S., Kihlborg, L., Holmberg, B., Åsbrink, S. and Nordmark, C. *Final Technical Report* **1** (1959) DA-91-591-EUC-935.
4. Magnéli, A., Westman, S., Holmberg, B., Kihlborg, L., Åsbrink, S., Nordmark, C., Andersson, S. and Marinder, B.-O. *Final Technical Report* **1** (1960) DA-91-591-EUC-1319.
5. Holmberg, B. and Dagerhamn, T. *Acta Chem. Scand.* **15** (1961) 919.
6. Dagerhamn, T. *Acta Chem. Scand.* **15** (1961) 214.
7. Ehrlich, P. *Z. anorg. Chem.* **247** (1941) 53.
8. Fast, J. D. *Metallwirtschaft* **17** (1938) 641.
9. Andersson, S., Åsbrink, S., Holmberg, B. and Magnéli, A. *Symposium on Crystal Physics, National Institute of Sciences (India), Calcutta, Aug. 1958.*

Received December 19, 1961.

ACTA CHEMICA SCANDINAVICA 16 (1962) 1251–1254

Para-aspidin, a New Phloroglucinol Derivative from Dryopteris Ferns

ANERI PENTTILÄ and JACOBUS SUNDMAN

The Research Laboratories, Medica Ltd., Helsinki, Finland

Para-aspidin (I), isolated from *Dryopteris* species, has been shown to be an isomer of aspidin (II) differing from the same only through the position of the methoxy group. The structure of para-aspidin is confirmed by synthesis.

In our earlier reports concerning the phloroglucinol derivatives from *Dryopteris* ferns the structures of phloropyron [1] and phloraspin [2] are given. In addition to these substances we now have isolated and examined a new compound for which we suggest the name para-aspidin.

Para-aspidin is a yellow substance, melting point 123—125°, soluble in most organic solvents except in methanol and ethanol. It is a monobasic acid the analytical data of which agree with the formula $C_{28}H_{32}O_8$. The molecule was shown to contain one methoxy group. In alcoholic solution the ferric chloride reaction of para-aspidin is brownish red.

The ultraviolet absorption curves of aspidin and para-aspidin in cyclohexane solution are shown in Fig. 1. The maxima of aspidin occur at 230 mμ (ε = 27 100) and at 292 mμ (ε = 20 000), earlier reported 230 mμ (ε = 25 500) and 290 mμ (ε = 21 300) [3]. Para-aspidin has maxima at 228 mμ (ε = 27 100) and at 271 mμ (ε = 21 600).

From the similar solubilities of aspidin and para-aspidin it follows that the paper chromatographic separation of these substances is rather difficult. When the chromatography is performed with benzene-chloroform (1:1) solvent on buffered and formamide impregnated papers [4] para-aspidin appears to have at each pH somewhat lower R_F-values than aspidin, but the differences are too small for identifying the two substances. With tetrazotized di-*o*-anisidine [4] as reagent for detection of the spots they could, however, be identified. With this reagent aspidin yields a yellow spot whereas that of para-aspidin is red-brown.

Among the decomposition products obtained by an alkaline cleavage [5] of para-aspidin either along A - - - A or B - - - B, 3-butyrylfilicinic acid (III), aspidinol (IV) and methylaspidinol (V) could be identified. On the basis of

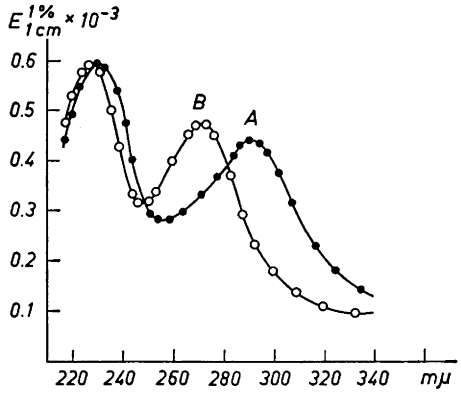

Fig. 1. Ultraviolet absorption spectra of aspidin (A) and para-aspidin (B) in cyclohexane.

these facts the structure of para-aspidin could be represented as (I). The structure is identical with that given by Boehm [6] for aspidin, m.p. 123—124°, which substance later has been shown actually to have the structure (II) [3,7]. Because both of these substances are included in the naturally occurring phloroglucinol derivatives of *Dryopteris* species there is every reason to question whether Boehm really dealt with aspidin or para-aspidin, both being yellow compounds with the formula $C_{25}H_{32}O_8$ and both having equal melting points as well as similar solubilities and ferric chloride reactions. Boehm's descriptions of aspidin include some derivatives of the same namely aniline and phenylhydrazine derivatives. These compounds were first prepared by Poulsson [8]; Boehm made use of them on purpose to prove his aspidin to be identical with the polystichin of Poulsson. Our efforts to carry out the same reactions resulted in an intensive yellow aniline derivative of aspidin, m.p. 132—134°, earlier reported 132° by Boehm [6] and Poulsson [8]. The aniline derivative of para-aspidin was pale yellow in colour and had a m.p. of 168—170° (decomp.). For the phenylhydrazone of aspidin a m.p. of 208—209° was observed, earlier reported 209° by Boehm [6] and 200—203° by Poulsson [8]. By the method of these authors we failed to obtain any crystalline phenylhydrazone of para-aspidin.

These experiments furnish positive proof of the substance examined by Boehm being aspidin (II) and not para-aspidin (I) despite the structural formula given by Boehm.

Semiquantitative paper chromatographic analysis [4] showed that the amounts of para-aspidin in both *Dryopteris austriaca* and *Dr. filix mas* varied considerably, the average content being about 0.2—0.4 % of the air dried rhizomes. The quantities actually isolated from the material were always considerably smaller which is due to the easily occurring decomposition of para-aspidin especially under alkaline conditions. Probably this also is the reason why para-aspidin so long has escaped detection in spite of thorough investigations in this field.

For synthesizing para-aspidin (I) 3-butyrylfilicinic acid (III) and aspidinol (IV) were condensed with formaldehyde in dilute alkaline solution. The yield

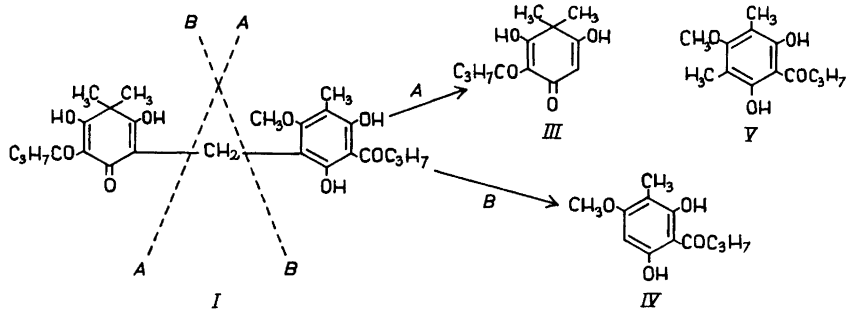

I *III* *V* *IV*

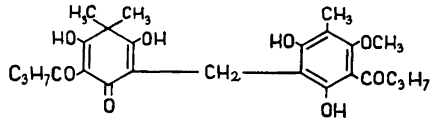

II

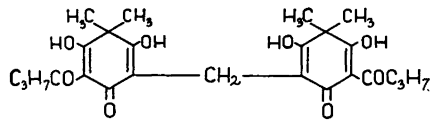

VI

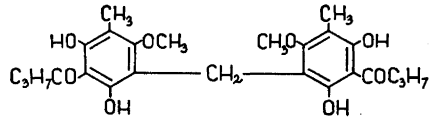

VII

of para-aspidin hereby was remarkably high which was due to the fact that of the two possible symmetrical compounds, albaspidin (VI) and methylene-bis-aspidinol (VII), only small amounts of albaspidin were formed whereas not even traces of methylene-bis-aspidinol could be detected. The synthesis of aspidin is reported to proceed similarly: the reaction yields mainly aspidin at the cost of the two possible symmetrical compounds [7]. Para-aspidin was purified by recrystallizing from methanol and as pure had a melting point of 124—125° showing no depression on mixing with natural para-aspidin.

EXPERIMENTAL

Isolation of para-aspidin. The finely ground rhizomes of *Dryopteris austriaca* (Jacq.) Woynar were extracted with ether for 8 h. (*Subsp. eu-spinulosa* (A. et G.) Hyl. is preferably chosen as source for para-aspidin because of its low content of flavaspidic acid.) The solvent was distilled off and the residue freed of fatty materials by MgO treatment [9]. The "raw aspidin"so obtained was dissolved in methanol and kept for fractional crystal-

lization at 4°. By the help of paper chromatographic analysis [4] the fraction of para-aspidin together with small amounts of albaspidin, aspidin and desaspidin could be separated. Repeated recrystallizations from methanol yielded pure para-aspidin, m.p. 123—125°. (Found: C 64.62; H 7.01; OCH_3 7.16. Calc. for $C_{25}H_{32}O_8$: C 65.22; H 6.95; OCH_3 6.75.)

Alkaline cleavage of para-aspidin. Para-aspidin (100 mg) was dissolved in aqueous sodium hydroxide (5 %, 20 ml), zinc dust (200 mg) was added and the mixture was heated on a steam bath for 5 min. The cooled solution was diluted with water, acidified with sulphuric acid (10 %) and extracted with ether. The ethereal solution was evaporated to dryness and the residue dissolved in acetone and chromatographed on papers buffered to pH 8.8 and 5.0 [4]. On the paper pH 8.8 two main spots were obtained, the R_F-values and colours of which were identical with those obtained by chromatography of authentic specimens of aspidinol, m.p. 142—143°, R_F 0.83, purple spot and methylaspidinol, m.p. 111°, R_F 0.90, yellow spot. On the paper pH 5.0 a carmine red spot with R_F 0.35 was obtained and it was identical with that of 3-butyrylfilicinic acid, m.p. 98°.

Aniline and phenylhydrazine derivatives of aspidin and para-aspidin. According to Boehm [6] the aniline derivatives of aspidin and para-aspidin were prepared as follows: aspidin (460 mg), respectively para-aspidin (460 mg), was mixed with aniline (400 mg, b.p. 184°) and the mixture heated on a steam bath for 5 min and then kept over sulphuric acid over night. After adding abs. ethanol (4 ml) a crystalline precipitate was obtained in a few hours. Recrystallizations from abs. ethanol yielded the aniline derivatives in a pure state showing the melting points mentioned before. An elementary analysis of the aniline derivative of para-aspidin was performed. (Found: C 69.50; H 7.16; N 2.78. Calc. for $C_{31}H_{37}NO_7$: C 69.53; H 6.91; N 2.61.)

The phenylhydrazone of aspidin was prepared according to Boehm [6] whereby a crystalline compound melting at 208—209° was obtained. When para-aspidin was similarly treated with phenylhydrazine only dark coloured amorphous compounds were formed. All attempts to modificate the method in order to obtain crystalline products were unsuccessful.

Synthesis of para-aspidin. 3-Butyrylfilicinic acid (224 mg) and aspidinol (224 mg) were dissolved in aqueous potassium hydroxide (10 ml, 1 %) and formaldehyde (0.75 ml, 4 %) was added. The mixture was kept at room temperature for 15 min and made acidic with hydrochloric acid (10 %). The precipitate was filtered off, washed with water and dried. After recrystallizations from methanol the product had a m.p. of 124—125° and with natural para-aspidin a mixed m.p. of 123—125°. (Found: C 65.72; H 6.90; OCH_3 7.08. Calc. for $C_{25}H_{32}O_8$ C 65.22; H 6.95; OCH_3 6.75.)

REFERENCES

1. Penttilä, A. and Sundman, J. *Acta Chem. Scand.* **15** (1961) 839.
2. Penttilä, A. and Sundman, J. *Acta Chem. Scand.* **15** (1961) 1777.
3. Aebi, A., Kapoor, A. L. and Büchi, J. *Helv. Chim. Acta* **40** (1957) 569.
4. Penttilä, A. and Sundman, J. *J. Pharm. Pharmacol.* **13** (1961) 531.
5. Boehm, R. *Ann.* **318** (1901) 230.
6. Boehm, R. *Ann.* **329** (1903) 321.
7. Riedl, W. and Mitteldorf, R. *Ber.* **89** (1956) 2595.
8. Poulsson, E. *Arch. exptl. Patol. Pharmakol. Naunyn-Schwiedeberg's* **41** (1898) 246.
9. Ackermann, M. and Mühlemann, H. *Pharm. Acta Helv.* **21** (1946) 157.

Received December 20, 1961.

ACTA CHEMICA SCANDINAVICA 16 (1962) 1255–1261

Structural Studies on the Titanium-Nitrogen System

BO HOLMBERG

Institute of Inorganic and Physical Chemistry, University of Stockholm, Stockholm, Sweden

The titanium-nitrogen system has been investigated by X-ray methods using samples quenched after annealing at 900°C. The solubility of nitrogen in α-titanium was found to be 17 at.% ($TiN_{0.20}$), the solid solutions having randomly distributed nitrogen atoms. The crystal structure of the so-called ε phase, which was found to occur within a narrow range of homogeneity at the composition $TiN_{0.50}$, has been determined. It is tetragonal, space-group $P4_2/mnm$, with a unit cell content of 2 Ti_2N and the unit cell dimensions a = 4.9452 Å and c = 3.0342 Å. The structure is of an *anti*-rutile type. The lower limit of the homogeneity range of the TiN phase is at $TiN_{0.6}$.

In connection with structural studies on solid solutions of oxygen in *hcp* titanium, zirconium and hafnium [1–3], it was found to be of interest to examine the titanium-nitrogen system. Previous work by Ehrlich [4] has revealed the existence of a wide range of solid solubility of nitrogen in α-titanium ($TiN_{0-0.22}$) and of the phase $TiN_{0.42-1}$ of a defective $B1$ type of structure. Palty, Margolin and Nielsen [5] reported furthermore a phase (called ε) at a composition of about 26 at. % N with a tetragonal unit cell and suggested the formula to be either Ti_4N or Ti_3N. However, Nowotny, Benesovsky, Brukl and Schob [6] stated that the ε phase exists within a narrow range of homogeneity close to the composition $TiN_{0.5}$ and accordingly suggested the formula Ti_2N.

EXPERIMENTAL

The starting materials were titanium sponge (Johnson, Mathey and Co. Ltd., 99.98 % pure) and TiN prepared from the metal by heating it in a stream of purified nitrogen at 1250°C. The alloys were obtained by melting appropriate mixtures of the starting materials in an electric arc furnace under an argon atmosphere. Part of each melt was then crushed and annealed at 900°C in a sealed, evacuated silica tube for about a month. A tantalum foil protected the specimen from reacting with the silica. The heat-treatment was abruptly stopped by quenching in water. The nitrogen content of the alloys was determined by micro-Kjeldahl techniques.

X-Ray powder photographs were taken of the arc-melted and of the heattreated samples in a Guinier focusing camera with strictly monochromatized CuKa_1 radiation and using KCl (a = 6.2919 Å at 20°C [7]) as an internal standard.

The densities were obtained from the loss of weight in benzene.

Table 1. Unit cell dimensions of the α-titanium solid solutions in alloys TiN_x heat-treated at 900°C for 1 month.

x	a Å	c Å	c/a	V Å^3	
0	2.9506	4.6788	1.5857	35.28 (8)	
0.07	2.959	4.739	1.602	35.93	
0.12	2.9621	4.7547	1.6052	36.13	
0.16	2.9681	4.7732	1.6082	36.42	
0.22	2.9711	4.7843	1.6103	36.57	(two-phase region)
0.32	2.9723	4.7862	1.6103	36.62	» »

Table 2. Unit cell dimensions of the tetragonal ε phase in alloys TiN_x heat-treated at 900°C for 1 month.

x	a Å	c Å	c/a	V Å^3	d_{obs} g/ml	d_{calc} g/ml	
0.32	4.9414	3.0375	0.6147	74.17	4.76	—	(two-phase region)
0.49	4.9428	3.0357	0.6141	74.17	4.86	4.90	
0.52	4.9452	3.0342	0.6136	74.21	4.86	4.91 *	» »

* for the limiting composition $TiN_{0.50}$.

Table 3. Unit cell dimensions of the cubic TiN phase in alloys TiN_x heat-treated at 900°C for 1 month.

x	a Å	V Å^3	d_{obs} g/ml	d_{calc} g/ml	
0.52	4.224	75.36	4.86	—	(two-phase region)
0.61	4.2238	75.35	4.95	(4.97) *	» »
0.71	4.2259	75.47	5.02	5.09 *	

* assuming 100 % occupancy of the metal atom sites.

RESULT OF THE PHASE ANALYSIS

The powder patterns of the samples annealed at 900°C were throughout of good quality showing sharp reflexions. For compositions TiN_x with $x < 0.2$, only lines corresponding to the α-titanium solid solution were present. For higher x values, this was followed by a two-phase region. The additional system of lines, which was found to be in agreement with that of the ε phase reported by Palty *et al.*[5], was free from extra lines at the composition $TiN_{0.5}$. At still higher nitrogen contents, the ε phase was contaminated by the TiN phase which was the only phase present above the composition $TiN_{0.6}$. The general appearance of the system at 900°C is thus in accordance with the findings of Palty *et al.*

The unit cell dimensions of the three phases in the various samples are listed in Tables 1—3. The indexing of the ε phase powder pattern was possible assuming a primitiv tetragonal unit cell (*cf.* Table 4).

For the α region, the maximum solubility of nitrogen at 900°C was found to correspond to the composition $TiN_{0.20}$ (*cf.* Fig. 1). No lines except those of a *hcp* metal atom arrangement were observed, which was taken as evidence

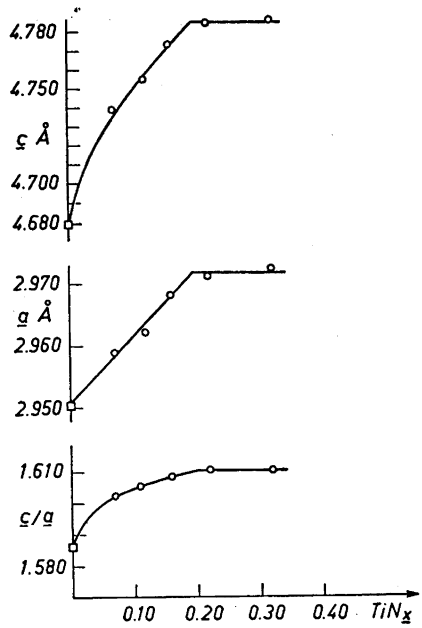

Fig. 1. Lattice parameters of α-titanium solid solutions in alloys TiN_x heat-treated at 900°C.

that the nitrogen atoms occupy interstitial positions in a random way. The mechanism of solubility is evidently the same as the one previously demonstrated in the Hf—O system [3] and for lower contents of oxygen in the Ti—O and Zr—O system [1,2]. The incorporation of the nitrogen atoms causes a continuous increase of both the a and c axes of the titanium lattice.

The ε phase seems to exist over a relatively narrow range of homogeneity close to the composition $TiN_{0.5}$. Some evidence, which is however not considered as conclusive, indicates that the maximum content of nitrogen is at $TiN_{0.50}$. Structural data for this phase are given below.

The lower limit of the nitrogen content of the TiN phase was found to be at $TiN_{0.6}$ for the 900°C samples.

The powder patterns of the samples obtained by quenching from the melt in the arc furnace generally showed rather diffuse reflexions. The displacement of the lines indicated that the ranges of homogeneity exceed the value $x = 0.20$ for the α phase and are below $x = 0.6$ for the TiN phase. These observations are in agreement with those of previous authors. No extra reflexions were found in the α phase pattern. The diffuse character of the photographs should, however, make it difficult to observe such weak reflexions. Thus the present findings are not in conflict with the statement by Nowotny *et al.*[6] that a state of order similar to that of an *anti*-CdI_2 structure should be present in high-temperature samples of the composition $TiN_{0.25}$. Very weak lines correspond-

Table 4. Guinier powder pattern of Ti_2N. Dimensions of the tetragonal unit cell: $a = 4.9452$ Å, $c = 3.0342$ Å.

I	$\sin^2\Theta_{obs}$	hkl	$\sin^2\Theta_{calc}$
w	0.04849	110	0.04852
vw	0.08872	101	0.08870
st	0.09700	200	0.09704
vst	0.11296	111	0.11296
m	0.12137	210	0.12130
m	0.18567	211	0.18574
m	0.19401	220	0.19408
m	0.25774	002	0.25776
st	0.28286	301	0.28278
st	0.30712	311	0.30704
vw	0.31576	320	0.31538
m	0.35475	202	0.35480
m	0.37918	212	0.37906
m	0.37991	321	0.37982

ing to the principal reflexions of the ε phase were observed in some non-equilibrium samples quenched in the arc furnace. This seems to indicate that this phase, although not stable at high temperatures, forms rapidly upon passing its maximum temperature of existence.

THE CRYSTAL STRUCTURE OF Ti_2N

Complete single crystal data for Ti_2N were obtained from Weissenberg photographs taken around [001] and [101] of a slightly ellipsoidal crystal measuring about 0.03 mm. Multiple film technique was applied and the inten-

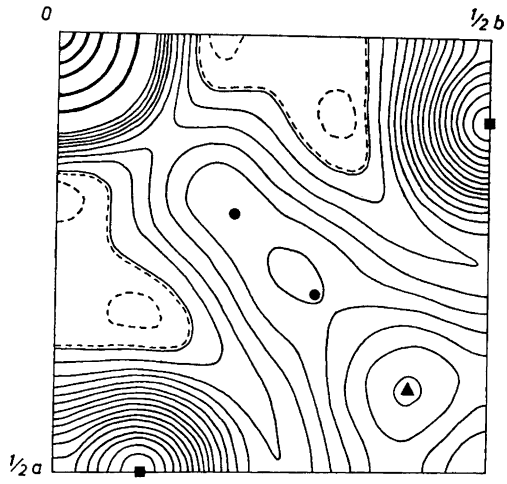

Fig. 2. Patterson projection along [001]. ▲ and ■ represent Ti—Ti vectors of multiplicity one and two respectively, while ● corresponds to Ti—N vectors of multiplicity two.

Table 5. Comparison of observed and calculated structure factors for Ti_2N.

hkl	$\|F\|_{obs}$	$\|F\|_{calc}$	*hkl*	$\|F\|_{obs}$	$\|F\|_{calc}$
200	34.3	38.3	101	10.3	7.6
400	18.4	17.0	301	32.8	34.4
600	5.4	5.5	501	19.4	20.9
110	18.4	16.1	111	36.2 *	49.5
210	28.5	27.8	211	17.1	17.3
310	<7	3.7	311	24.0	22.9
410	25.8	28.1	411	<6	0.1
510	10.0	9.7	511	<5	2.6
220	34.0	37.6	221	13.8	12.1
320	16.6	13.0	321	19.3	17.4
420	8.7	6.3	421	13.8	13.6
520	<6	1.5	521	16.9	20.2
330	22.3	21.7	331	13.0	11.8
430	16.1	15.0	431	10.1	9.8
530	11.0	13.3	531	<3	1.4
440	<7	5.7	441	14.4	16.9

* excluded in the calculation of the reliability index.

sities were estimated visually using a calibrated set of reflexions. A correction for absorption was introduced, the crystal being approximated to a sphere.

The absent reflexions were those characteristic of the space-groups $P4_2nm$, $P\bar{4}n2$ and $P4_2/mnm$. The appearance of the reciprocal lattice planes $hk0$ and $hk2$ was analogous as was also the case with the registered parts of the two planes $hk1$ and $hk3$.

The appearance of the Patterson projection along [001] is shown in Fig. 2. With a cell content of 2 Ti_2N this function could be completely accounted for by the following atomic arrangement:

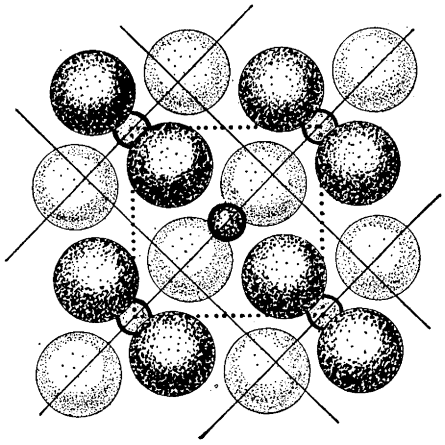

Fig. 3. The crystal structure of Ti_2N projected along the c axis. The large and small circles represent titanium and nitrogen atoms respectively. Light circles have $z = 0$ and dark ones $z = \frac{1}{2}$. The full lines correspond to the β-titanium unit cell.

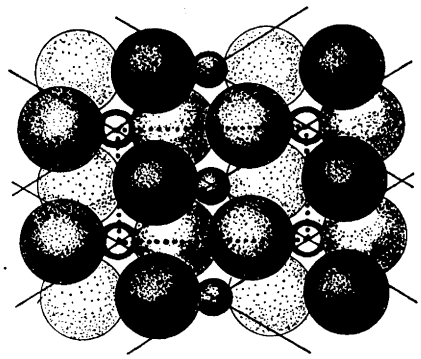

Fig. 4. The crystal structure of Ti_2N projected along the *b* axis. Large circles represent titanium atoms having $y = 0.204$, 0.296, 0.704 and 0.796 respectively, indicated by increasing darkness. Small circles represent nitrogen atoms, light ones having $y = 0$ and dark ones $y = \frac{1}{2}$. The full lines correspond to the *a*-titanium unit cell.

Space-group: $P4_2/mnm$ (No. 136)
Unit cell dimensions: $a = 4.9452$ Å, $c = 3.0342$ Å
Unit cell content: 2 Ti_2N
4 Ti in 4(*f*): $x,x,0$; $\bar{x},\bar{x},0$; $\frac{1}{2}+x,\frac{1}{2}-x,\frac{1}{2}$; $\frac{1}{2}-x,\frac{1}{2}+x,\frac{1}{2}$
2 N in 2(*a*): $0,0,0$; $\frac{1}{2},\frac{1}{2},\frac{1}{2}$

A preliminary value of $x_{Ti} = 0.30$ was obtained from the Patterson projection.

The refinement of the structure was performed by electron density calculations and also by the method of least squares. An isotropic temperature factor of 1.27 Å^2 was employed. In this way the following parameter value was obtained:

$$x_{Ti} = 0.296 \qquad \sigma = \pm 0.001$$

A comparison between the observed and calculated structure factors is given in Table 5. The reliability index, disregarding non-observed reflexions, is 0.094.

The structure thus obtained may be characterized as an *anti*-rutile type. The titanium atoms are arranged to form octahedra that are joined by edges to form strings running parallel to the *c* axis. Neighbouring strings are joined

Table 6. Comparison of the atomic arrangements around the Ti atoms in β-titanium and Ti_2N.

bcc		Ti_2N
Ti — 4 Ti 3.307 Å	Ti — 1 Ti 2.853 Å	(shared edge of Ti_6 octahedron)
	— 2 Ti 3.555	
	— 1 Ti 4.140	(space diagonal of Ti_6 octahedron, a N atom being situated at the centre of this polyhedron)
— 8 Ti 2.864	— 8 Ti 2.936	(oblique edge of Ti_6 octahedron)
— 2 Ti 3.307	— 2 Ti 3.034	(*c* direction)
	— 1 N 2.070	
	— 2 N 2.082	

Table 7. Comparison of the atomic arrangements around the Ti atoms in α-titanium ($TiN_{0.20}$), Ti_2O and Ti_2N.

hcp ($TiN_{0.20}$)		Ti_2O		Ti_2N	
Ti — 6 Ti	2.972 Å	Ti — 6 Ti	2.960 Å	Ti — 2 Ti	3.034 Å
				— 4 Ti	2.936
— 6 Ti	2.944	— 3 Ti	2.860	— 1 Ti	2.853
		— 3 Ti	3.066	— 4 Ti	2.936
				— 1 Ti	3.555
— 6 Ti	4.183	— 3 Ti	4.116	— 1 Ti	3.555
		— 3 Ti	4.262	— 1 Ti	4.140
				— 2 Ti	4.165
				— 2 Ti	4.674
— 6 *x* N	2.092	— 3 O	2.131	— 1 N	2.070
				— 2 N	2.082

mutually by sharing corners. The nitrogen positions are at the centers of the titanium octahedra. The structure is illustrated in Figs. 3 and 4. In the former figure, representing the projection parallel to [001], the relation of Ti_2N to the *bcc* metal structure is demonstrated. The presence of nitrogen atoms in the Ti_2N phase at sites corresponding to the $\frac{1}{2}00$ or $\frac{1}{2}0\frac{1}{2}$ positions of the *bcc* lattice causes the distortion of the latter shown in Table 6.

The projection parallel to [010] given in Fig. 4 shows the relation to α-titanium. Half of the face diagonals (**a** + **c**) of Ti_2N correspond to the a_α (b_α) axes. The metal atom coordinates related to these axes are not $\frac{1}{3},\frac{2}{3}$ and $\frac{2}{3},\frac{1}{3}$ but 0.296, 0.704 and 0.704, 0.296. The *b* axis of Ti_2N corresponds to the c_α axis. In the *hcp* arrangement the atoms form planes $c_\alpha/2$ apart but in Ti_2N the metal atoms are slightly displaced from these planes ($y = 0.250$ and 0.750), y_{Ti} in Ti_2N actually having the values 0.204, 0.296, 0.704 and 0.796.

Table 7 gives a comparison of the atomic arrangements around the Ti atoms in α-titanium, Ti_2O and Ti_2N. Ti_2O has an *anti*-$Cd(OH)_2$ type of structure, the hexagonal unit cell containing two Ti atoms at $\frac{1}{3},\frac{2}{3}, z$ and $\frac{2}{3},\frac{1}{3},\bar{z}$ with $z = 0.263$ and one O atom at 0,0,0 [1]. In this structure the oxygen atoms occupy all the octahedral interstices in every second layer parallel to the *ab* plane while in Ti_2N the nitrogen atoms occupy one half of the octahedral holes in every layer.

Acknowledgement. The author wishes to express his sincere gratitude to Professor A. Ölander for his kind interest and to Professor A. Magnéli for his continuing encouragement and for many valuable discussions.

REFERENCES

1. Holmberg, B. *Acta Chem. Scand.* **16** (1962) 1245.
2. Holmberg, B. and Dagerhamn, T. *Acta Chem. Scand.* **15** (1961) 919.
3. Dagerhamn, T. *Acta Chem. Scand.* **15** (1961) 214.
4. Ehrlich, P. *Z. anorg. Chem.* **259** (1949) 1.
5. Palty, A. E., Margolin, H. and Nielsen, J. P. *Trans. Am. Soc. Metals* **46** (1954) 312.
6. Nowotny, H., Benesovsky, F., Brukl, C. and Schob, O. *Monatsh.* **92** (1961) 403.
7. Hambling, P. G. *Acta Cryst.* **6** (1953) 98.
8. Szànto, I. *Acta Tech. Acad. Sci. Hung.* **13** (1955) 363.

Received December 19, 1961.

ACTA CHEMICA SCANDINAVICA 16 (1962) 1262–1270

Studies on Metal Ion Co-ordination in Solution

II. The Complex Formation of Diphenylphosphinobenzene-*m*-sulphonate with Bismuth

GRAHAM WRIGHT* and JANNIK BJERRUM

Department of Inorganic Chemistry, University of Copenhagen, Copenhagen, Denmark

Diphenylphosphinobenzene-*m*-sulphonate, which was used by Ahrland *et al.*[1,2], and Salvesen and Bjerrum [3] as a phosphorus donor ligand for Ag^+, Cd^{2+} and Hg^{2+}, has been found to be appreciably basic with

$$pK_{L,H^+} = 0.13 + 0.50\ C_{HClO_4}$$

There is evidence that the ligand undergoes self-association when $[L] + [LH^+] >$ ca. 0.01 M, thus limiting the range of concentration useful for determining stability constants. The complex formation between Bi^{3+} and the ligand has been measured using a bismuth amalgam electrode; difficulties with the electrode resulted in low accuracy. A steep formation curve was derived in agreement with the preliminary measurements of Salvesen [4]. The data show that the maximum coordination number is six and only the first and the sixth complex are formed in significant concentration. Stability constants, in 1 M HNO_3 at 25°, are $K_1 = 10^{3.7}$ l·mole^{-1}, $\beta_6 = 10^{21.8}$ l^6·mole^{-6}. These findings are consistent with the stability trend observed by Ahrland and Grenthe [5] for the bismuth halide complexes: $Cl^- < Br^- < I^- < P$. The ranges of existence of intermediary complexes decreases along this series.

It has been shown by Ahrland and Grenthe [5] that bismuth(III) is a class (b) metal ion [6,7], the stability of its halide complexes increasing in the order $Cl^- < Br^- < I^-$. This paper reports further exploration of the class (b) character of bismuth(III) using the water soluble ligand diphenylphosphinobenzene-*m*-sulphonate. The ligand has a phosphorus donor atom; it forms strong silver(I) [1] and mercury(II) [3] complexes and weaker complexes with cadmium(II) [2]. In order to eliminate hydrolysis of the bismuth ion [8] and to maintain a constant salt concentration, 1 M nitric acid has been used as the medium. Salts of the ligand *m*-$(C_6H_5)_2PC_6H_4SO_3^-$ show higher solubility as the acid concentration is increased, hence the ligand is appreciably basic. A

* Present address: Chemistry Department, University of Auckland, Auckland, New Zealand.

UV spectrophotometric method has been used to determine pK_{LH^+} in perchloric acid solutions. Complex stability constants can then be calculated with respect to the unprotonated ligand. A preliminary report of this work has been published with Salvesen as co-author [4].

EXPERIMENTAL

Materials and analysis. *m*-$(C_6H_5)_2PC_6H_4SO_3Na,2H_2O$ has been described previously [1,3]. The ligand decomposes slowly in water and therefore fresh solutions were prepared by weight for each E.M.F. measurement. The spectrophotometric measurements were made using the same stock solution of ligand (0.000616 M); a small correction ($\sim$ 3 % in 2 h) was made for decomposition.

Bismuth solutions were prepared by dissolving pure Merck bismuth nitrate crystals in 1 M HNO_3 and analysing the bismuth gravimetrically as BiOI [5,6].

Pure concentrated nitric acid was diluted to 5 M, boiled to remove nitrous acid, then diluted by trial to 1 M and determined by titration with standard sodium hydroxide. Perchloric acid solutions were prepared by dilution and standardisation of Merck p.a. 70 % $HClO_4$.

Bismuth amalgam (2 %) was prepared by electrolysis of a solution of $Bi(NO_3)_3$ in nitric acid, using a mercury pool as cathode and it was stored in a separatory funnel under distilled water and nitrogen.

Spectrophotometric measurements were made with a Cary 11MS-50 instrument at 25 $\pm$ 2°, using 1 cm silica cells. The reference cell contained the same concentration of perchloric acid as the sample cell, in order to correct for the small background absorption of $HClO_4$.

Potentiometric measurements. The cell was

(−) Hg, Bi	1 M HNO_3	1 M HNO_3	1 M HNO_3	Pt (+)	(1)
	C_{Bi}, C_L		quinhydr.sat.		

A stream of purified nitrogen [10] was passed through the test solution (25 ml) in the electrode vessel. The amalgam was contained in a J-tube of 2 mm bore with a 10 mm cup opening on the short arm immersed in the solution. The longer arm of the J-tube contained a platinum wire which made contact with the amalgam. This design avoided interference caused by a film of solution between the platinum and amalgam: similar precautions have been taken by Holloway and Reilley [11]. Solutions for measurement were transferred to the electrode vessel in the thermostat and nitrogen passed for 20 min. The J-tube electrode was then filled with amalgam and placed in the solution quickly to avoid atmospheric oxidation of the bismuth. The reference electrode, which was a bright platinum foil in 1 M HNO_3 saturated with quinhydrone, was connected by a syphon bridge to the main electrode vessel. Tests of several such reference electrodes against each other showed that their potentials were reproducible and stable for 2−3 h within $\pm$ 0.1 mV. Other details have been described in Part I [3].

Table 1 shows measurements on solutions containing no ligand to test the Nernst law according to the formula valid at 25°C:

$$E = E^\circ + 0.0197 \log [Bi^{3+}] \qquad (2)$$

E° is seen to be a constant for bismuth concentrations between 20.1 mM and 2.01 mM, but below this concentration the potentials are too positive by 1−2 mV. This may be caused by dissolution of small amounts of bismuth from the amalgam during brief exposure to the air. The mean E° of the four highest bismuth concentrations (−423.7 mV) has been used to calculate E at the bismuth concentrations used in all subsequent experiments.

In the presence of the ligand it took about 40 min. to reach the equilibrium potential and the reproducibility was poor, as shown in Fig. 3, where C_L is plotted against E_M. E_M is defined as the potential of the half-cell: Hg,Bi $|C_{Bi},C_L|$ relative to a ligand-free half-cell with the same C_{Bi}, and the directly measured potentials on cell (1) were converted to E_M by means of the above given mean value for E° (−423.7 mV).

Table 1. Nernst law test for the bismuth amalgam electrode in 1 M HNO_3 at 25°. Measurements of the cell:

(−) Hg,Bi | 1 M HNO_3 C_{Bi} | 1 M HNO_3 | 1 M HNO_3 quinhydr. sat. | Pt (+)

C_{Bi} mM	$-E$ mV	$-E°$ mV
20.1	457.0	423.5
10.05	463.2	423.8
4.02	470.9	423.6
2.01	476.9	423.7
1.21	480.4	422.9
0.804	482.2	421.1
0.402	488.6	421.6
0.402	488.2	421.2

A titration procedure was not used; each solution was prepared and measured individually to reduce errors due to ligand decomposition and slow electrode reactions. Preliminary measurements were made using 1 M $HClO_4$ medium; but 1 M HNO_3 was used in the present work because it was hoped that the electrode reaction might be faster in the presence of nitrate [11].

BASICITY OF DIPHENYLPHOSPHINOBENZENE-*m*-SULPHONATE

Fig. 1 shows the UV spectra of the ligand in water, dilute sodium hydroxide and a series of perchloric acid concentrations. The spectra can be simply interpreted as an acid-base equilibrium between two absorbing species, giving an isobiestic point at 241 mμ.

$$LH^+ = L + H^+$$

$$pK_{LH^+} = -\log \frac{(\varepsilon - \varepsilon_{LH^+})C_{HClO_4}}{(\varepsilon_L - \varepsilon)} \qquad (3)$$

ε_L is the molar extinction coefficient for the ligand anion determined in water and dilute sodium hydroxide. ε_{LH^+} is the extinction coefficient of the protonated

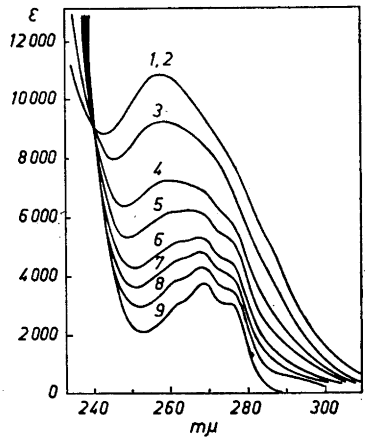

Fig. 1. UV spectra of diphenylphosphinobenzene-*m*-sulphonate in dilute NaOH (1), water (2) and a series of perchloric acid concentrations: 0.184 M (3), 0.415 M (4), 0.599 M (5) 0.829 M (6), 1.00 M (7), 1.38 M (8) and 9.22 M $HClO_4$ (9). The concentration of phosphine ligand was 0.123 mM in al lutions.

Table 2. Spectrophotometric determination of the acid dissoviation constant of *m*-$(C_6H_5)_2PH^+$-$(C_6H_4SO_3^-)$ in perchloric acid at 25°C.

Solution	C_{HClO_4}	$(\varepsilon-\varepsilon_{LH^+})/(\varepsilon_L-\varepsilon)$ at:				pK_{LH^+}	
Curve in Fig. 1	M	252	257	269	276 mμ	exptl.	calc.
3	0.184	3.22	3.33	3.03	3.03	0.24	0.22
4	0.415	1.10	1.19	1.09	1.18	0.33	0.34
5	0.599	0.63	0.67	0.65	0.69	0.40	0.43
6	0.829	0.33	0.34	0.31	0.36	0.56	0.54
7	1.00	0.22	0.25	0.22	0.24	0.63	0.63
8	1.38	0.098	0.118	0.076	0.109	0.86	0.82

ligand, which is assumed to be completely formed in 9.22 M $HClO_4$. ε is the observed extinction coefficient at intermediate acid concentrations. Table 2 gives the ratio $(\varepsilon-\varepsilon_{LH^+})/(\varepsilon_L-\varepsilon)$ measured at four wavelengths. These agree satisfactorily and the mean is used to obtain pK_{LH^+}.

It is known that the pK values of many weak bases in strong acid media are linearly dependent on the concentration of acid [13].

In the present case it is found that

$$pK_{LH^+} = 0.13 + 0.50\ C_{HClO_4} \qquad (4)$$

pK_{LH^+} calculated from this expression is given in Table 2 for comparison. Nitric acid is not a suitable medium for UV spectral measurements therefore it is assumed that the degree of protonation of the ligand in 1 M HNO_3 is 0.8; *i.e.* the same as in 1 M $HClO_4$.

The sulphonate group is known to be a very weak base [14] and hence it is certain that *m*-$(C_6H_5)_2PC_6H_4SO_3^-$ protonates on the phosphorus atom. Henderson and Streuli [16] estimate the pK_{LH^+} of $(C_6H_5)_3P$ in water as 2.73, which is consistent with the present work since a *meta* sulphonate group is known to have an acid strengthening effect [15].

SELF-ASSOCIATION OF DIPHENYLPHOSPHINOBENZENE-*m*-SULPHONATE

The structure of the ion *m*-$(C_6H_5)_2PC_6H_4SO_3^-$ suggests that it is likely to show self-association of the micelle type at higher concentrations, which would interfere with equilibrium studies. The accurate equilibrium measurements of Ahrland *et al.*[1] with the silver ion show that there is no self-association in a neutral medium of ionic strength $I = 0.1$ M, when $C_L < 0.01$ M.

In the present investigation, self-association of the ligand was studied by using the mercury(II) complex and a mercury electrode in the cell:

(−) Hg	0.01 M HNO_3 $I = 0.04$ M C_{Hg}, C_L	0.01 M HNO_3	0.01 M HNO_3 quinhydr. sat.	Pt (+)

(5)

The results of Part I[3] show that when [L] > 0.002 M, the mercury is present almost entirely as the *tetra* complex and in this case:

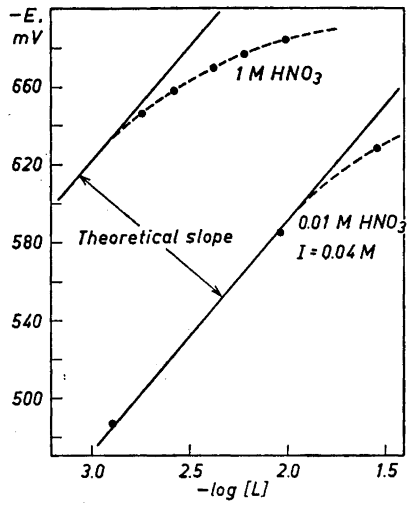

Fig. 2. The potential of cell (5) as a function of log [L] at 25°C. The straight lines have the theoretical slope expected for the *tetra* complex of Hg^{2+} with *m*-$(C_6H_5)_2PC_6H_4SO_3^-$. The mercury concentration was fixed at $C_{Hg} = 0.191$ mM.

$$E = \text{const.} - \frac{RT}{2F} \ln [L]^4 \qquad (6)$$

if C_{Hg} is fixed, and $[L] = C_L - 4\,C_{Hg}$. A graph of E against log [L] should be a straight line with a slope of $4 \times 0.0296 = 0.1184$ V. A decreasing slope as log [L] increases will indicate ligand self-association. Fig. 2 shows that for the conditions of cell (5) self-association occurs above [L] = 0.01 M. Cell (5) has also been used with 1 M HNO_3 as medium and the results are shown in Fig. 2. In this case $[L] = 0.2\ (C_L - 4C_{Hg})$; the factor 0.2 correcting for the protonation of the ligand. In 1 M HNO_3 there is a larger divergence from the theoretical slope; this corresponds to greater self-association and may be caused by self-association of the protonated species or a salt effect on the self-association process. From these preliminary experiments one learns that in 1 M HNO_3 it is not possible to use solutions with [L] > 0.001 M for equilibrium measurements.

COMPLEXING OF DIPHENYLPHOSPHINOBENZENE-*m*-SULPHONATE WITH BISMUTH IONS

The general method and notation has been described in Part I[3]. In 1 M HNO_3 there is partial protonation of the non-complexed ligand:

$$C_L - \bar{n}\ C_{Bi} = [L] + [HL^+] = 5\,[L] \qquad (7)$$

Table 3 gives the results of measurements on cell (1), and they are shown graphically in Fig. 3. From the graphs of C_L *versus* E_M for each bismuth concentration C_{Bi}, it was possible to interpolate at selected E_M values to obtain corresponding values of C_L and C_{Bi}. A graph of C_L *versus* C_{Bi} at constant E_M is a straight line with slope $= \bar{n}$ and intercept = 5 [L], as shown by eqn. (7). Table 4 gives corresponding values of $\bar{n}$ and [L] determined in

Table 3. Measurements of E_M (the potential relative to a ligand-free reference cell with same bismuth concentration) for increasing values of C_L at four different bismuth concentrations. Concentrations are in mM and potentials in mV.

$C_{Bi} = 0.402$		$C_{Bi} = 0.804$		$C_{Bi} = 1.61$	
C_L	E_M	C_L	E_M	C_L	E_M
0.79	4	1.16	3	1.02	0.7
1.14	5	2.19	7	1.68	2.0
2.03	11	2.91	10	2.10	2.9
2.51	19	3.65	17	2.65	4.1
2.60	33	3.87	30	3.31	6.6
2.67	31	4.20	42		
2.86	35	4.31	47	$C_{Bi} = 2.41$	
2.90	44	4.74	48	C_L	E_M
3.04	52	5.52	60	1.89	1.0
3.51	61	6.62	68	2.40	2.1
3.52	58	8.12	85	3.07	3.3
4.73	75			3.48	5.2
4.92	74				
5.63	86				
6.13	88				
7.18	99				

this way; the formation function is plotted in Fig. 4. The smallest values of $\bar{n}$ estimated in this manner are less reliable than the remainder, because they are derived from small, uncertain values of E_M. They are ignored when calculating the constants.

The steep formation curve shows that the maximum co-ordination number is six, and that the concentrations of complexes intermediate between *mono*

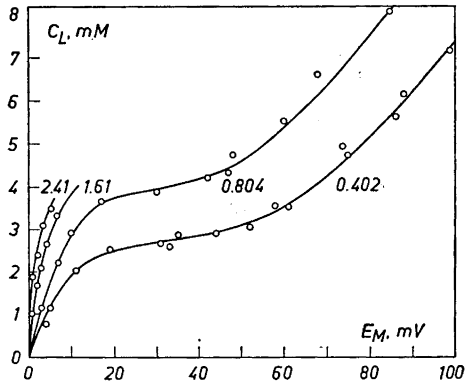

Fig. 3. Graphs of C_L against E_M for the experimental data in Table 3. The bismuth ion concentrations are given in mM for each curve.

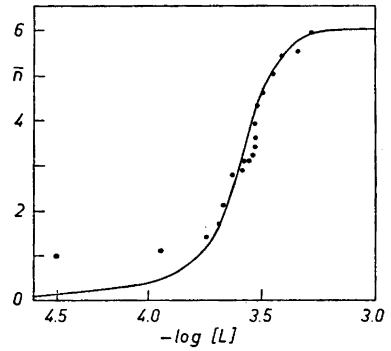

Fig. 4. The complex formation curve of bismuth ions and diphenylphosphinebenzene-*m*-sulphonate. ● Experimental points. The full curve is calculated from the constants $K_1 = 5 \times 10^3$ l·mole^{-1}, $\beta_6 = 6 \times 10^{21}$ l^6·mole^{-6}.

Table 4. Corresponding values of [L] and $\bar{n}$ determined graphically from the data of Table 3. Concentrations in mM and potentials in mV.

E_M	[L]	$\bar{n}$	E_M	[L]	n
2	0.032	1.0	40	0.300	3.4
4	0.116	1.1	45	0.300	3.6
6	0.184	1.4	50	0.304	3.9
8	0.208	1.7	55	0.31	4.3
10	0.220	2.1	60	0.33	4.6
15	0.240	2.8	65	0.36	5.0
20	0.264	2.9	70	0.40	5.4
25	0.272	3.1	75	0.47	5.5
30	0.280	3.1	80	0.54	5.9
35	0.296	3.2			

and *hexa* are small. The experimental formation curve can be best fitted by the constants:

$$K_1 = 5 \times 10^3 \text{ l} \cdot \text{mole}^{-1}, \qquad \beta_6 = 6 \times 10^{21} \text{ l}^6 \cdot \text{mole}^{-6}.$$

The formation function can be calculated with these constants:

$$\bar{n} = \frac{K_1[\text{L}] + 6\beta_6[\text{L}]^6}{1 + K_1[\text{L}] + \beta_6[\text{L}]^6}$$

It is compared with the experimental points in Fig. 4.

The sluggish electrode reaction and the ligand self-association, already mentioned, limit the accuracy of the results. There is also the possibility that mercury may reduce Bi^{3+} in the presence of the ligand, as discussed by Ahrland and Grenthe [5]. But this reaction is likely to be slow and unimportant in the time taken for each measurement. Treatment of the data by the X_i functions of Fronæus or the Bodländer equation as discussed in Part I[3] is unprofitable because of the low precision; but such treatments are consistent with the above constants.

DISCUSSION

Since co-ordination by the sulphonate group [1] or the benzene nucleus [17] is generally very weak, there is undoubtedly co-ordination by a phosphorus donor atom in the present case. The co-ordination number of six found here for the phosphine ligand agrees with that determined by other workers for the halide [5] and thiocyanate ions [18]. It is remarkable that there seems to be no steric hindrance of the formation of the *hexa* complex of m-$(C_6H_5)_2PC_6H_4SO_3^-$. It is reasonable to assume that this is connected with the relatively small C—P—C angle in tertiary aryl phosphines [19] and the relatively large size of the phosphorus atom.

Fig. 5 shows the distribution of bismuth between the various complexes for those systems for which data are available. From this it can be clearly seen that the bismuth ion has a greater affinity for phosphorus than for the halides, confirming the class (b) character of bismuth(III). The ranges of existence of the intermediary complexes decrease from chloride to iodide; and for the phosphine the ranges of existence have decreased so much that

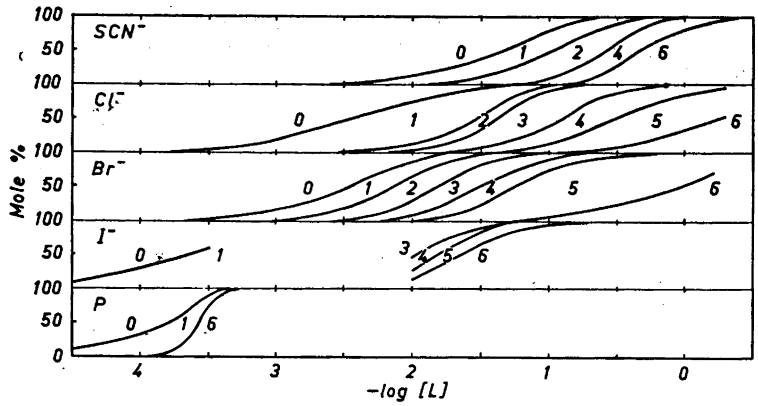

Fig. 5. The distribution of bismuth between the various complexes as a function of log [L]. Conditions: thiocyanate complexes [18] in 0.4 M $HClO_4$ at 20—25°; chloride bromide and higher iodide complexes [5] in 1 M $HClO_4$, 1 M $NaClO_4$ at 25°; *mono*-iodide complex [21] in 1 M $HClO_4$ at 25°. The *m*-$(C_6H_5)_2PC_6H_4SO_3^-$ complexes in 1 M HNO_3 at 25°. Note: Ahrland and Grenthe [5] have incorrectly calculated β_5 and β_6 for the bismuth chloride complexes. In this diagram we have used the corrected constants [22]: log β_5 = 6.72 and log β_6 = 6.56.

we are able to describe the system completely neglecting the complexes intermediary between *mono* and *hexa*. Thus the behaviour of the phosphine as a ligand for bismuth ions can be regarded as an extrapolation of the halide series Cl^-, Br^-, I^-. Similarly previous workers [1,3,4] have shown that for the class (b) metal ions Ag^+ and Hg^{2+}, the phosphine behaves as a halide with properties beyond that of iodide. The thiocyanate ion [18] does not fit into the halide-phosphine series and this may be accounted for by the resonance of the ion SCN^-.

The stability constant data for the halide and phosphine complexes of Ag^+ and Hg^{2+} show an enhanced stability of the *mono* complexes with the heavier donor atoms. Such large and systematic deviations from the statistical ratios of consecutive stability constants indicate that there are important orbital changes accompanying complex formation. Ahrland, Chatt *et al.*[1] have discussed the case of the silver ion in terms of the d_π acceptor properties of the ligand and the hybridisation of the silver ion. Similar considerations apply to the mercuric ion [3,4]. The bismuth ion stability constants deviate from the statistical ratios in the opposite sense to that of Ag^+ and Hg^{2+}. The orbital requirements for π-dative bonding in a *hexa* complex thus appear to be quite different from that in ions of lower co-ordination number.

Williams [20] has suggested that the high polarising power of class (b) metal ions, relative to their size and charge, explains the stability order of complexes of these cations. He has proposed an empirical function of the metal ionisation potential which correlates the data for the phosphine ligand with Ag^+, Cd^{2+}, Hg^{2+} and Bi^{3+} within $\pm$ 2 log K_1 units. However, this correlation applies only to the stability of the *mono* complexes and ignores the relationships

between successive constants. It seems that the symmetry of the orbitals and the overall electronegativity are both important in the stability of class (b) metal complexes.

Acknowledgements. We are grateful for financial assistance to G.W. from *Churchill-trustfondet, Rask-Ørsted Fondet* and the *Rhodes Trust.*

REFERENCES

1. Ahrland, S., Chatt, J., Davies, N. R. and Williams, A. A. *J. Chem. Soc.* **1958** 264, 276.
2. Ahrland, S., Chatt, J., Davies, N. R. and Williams, A. A. *J. Chem. Soc.* **1958** 1403.
3. Salvesen, B. and Bjerrum, J. *Acta Chem. Scand.* **16** (1962) 735.
4. Bjerrum, J., Salvesen, B. and Wright, G. *Proceedings of the 6th International Conference on Coordination Chemistry in Detroit.* The Macmillan Company, New York 1961, p. 126.
5. Ahrland, S. and Grenthe, I. *Acta Chem. Scand.* **11** (1957) 1111.
6. Ahrland, S. *Acta Chem. Scand.* **10** (1956) 723.
7. Ahrland, S., Chatt, J. and Davies, N. R. *Quart. Revs.* **12** (1958) 265.
8. Olin, Å. *Acta Chem. Scand.* **11** (1957) 1445.
9. Vogel, A. I. *Quantitative Inorganic Analysis,* 2nd ed., London 1951, p. 426.
10. Meyer, F. R. and Ronge, G. *Z. angew. Chem.* **52** (1939) 637.
11. Holloway, J. H. and Reilley, C. N. *Anal. Chem.* **32** (1960) 249.
12. Waind, G. M. *Private communication.*
13. Paul, M. A. and Long, F. A. *Chem. Revs.* **57** (1957) 1.
14. Hamer, W. J., Pinching, G. D. and Acree, S. F. *J. Research Natl. Bur. Standards* **31** (1943) 291.
15. McCoy, R. D. and Swinehart, D. F. *J. Am. Chem. Soc.* **76** (1954) 4708.
16. Hendersen, W. A. and Streuli, C. A. *J. Am. Chem. Soc.* **82** (1960) 5791.
17. Andrews, L. J. and Keefer, R. M. *J. Am. Chem. Soc.* **71** (1949) 3644.
18. Kingery, W. D. and Hume, D. N. *J. Am. Chem. Soc.* **71** (1949) 2393.
19. Bartell, L. S. *J. Chem. Phys.* **32** (1960) 832.
20. Williams, R. J. P. *Proc. Chem. Soc.* **1960** 20.
21. Frolen, L. J., Harris, W. S. and Swinehart, D. F. *J. Phys. Chem.* **61** (1957) 1672.
22. Ahrland, S. and Grenthe, I. *Acta Chem. Scand.* **15** (1961) 932.

Received December 20, 1961.

ACTA CHEMICA SCANDINAVICA 16 (1962) 1271–1281

Complex Formation between Borate Ions and *o*-Hydroxy Malachite Green. An Investigation of Equilibria and Reaction Rates

RUNE CIGÉN

Department of Inorganic and Physical Chemistry, Chemical Institute, University of Lund, Lund, Sweden

o-Hydroxy Malachite Green (MG) reacts with borate ions giving complexes analogous to the borate complexes of mannitol and other polyols and diols. Two complexes have been found with the probable structures I and II

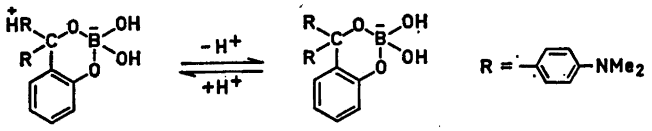

I *II*

The stability constants of the complexes were determined and found to be 4.0×10^3 M^{-1} for Complex I and 2.4×10^4 M^{-1} for Complex II. The protolytic constant for [Complex II] $[H^+]$/[Complex I] was found to be 1.6×10^{-8} M.

The rate constants for the reactions

MG + borate ⇌ Complex I

were determined to 7.5×10^2 min^{-1} M^{-1} for the forward reaction and 0.19 min^{-1} for the backward reaction.

The measurements were carried out spectrophotometrically at 20°C and constant ionic strength 0.5 M

In alkaline solutions borate ions react with *o*-hydroxy Malachite Green (MG) in a manner similar to that in which borate ions react with mannitol, pyrocatechol and other polyols or diols. *o*-Hydroxy Malachite Green behaves like a diol in borate solutions. An aqueous solution of MG is rapidly decoloured when it is mixed with a borate buffer owing to complex formation.

o-Hydroxy MG

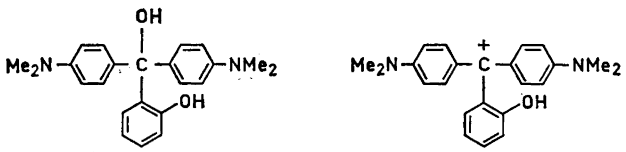

Previous investigations of the complex formation between borate ions and diols show that the following types of complexes are formed [1-7] (**D** = diol, **T** = borate)

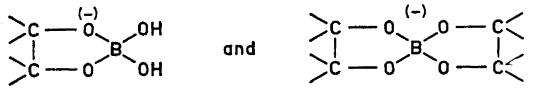

It has also been found that neutral complexes can be formed. Böeseken and Niks (Ref.[2]) suppose that the neutral complex is of the following type

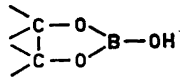

Complexes of the type $\mathbf{TD_2}$ have not been found, however.

The purpose of this investigation is to determine stability constants and reaction rate constants for the complex formation between borate ions and MG.

In weakly alkaline aqueous solutions of MG the dye is present in the form of two coloured and three colourless species. In acid solutions there are two additional forms, one coloured and one colourless. The complicated equilibrium scheme has been analyzed by the author in a previous paper [8]. If borate buffers are used the equilibrium scheme is complicated further by the formation of one or more borate complexes. The investigations carried out now show that two borate complexes are formed which, however, do not exactly correspond to the types of complexes shown above since MG gives six-membered-rings and not the usual five-membered-rings. Complexes with two diols per borate have not been found, a fact that is not surprising since the total concentration of the due stuff was kept as low as 10^{-5} M. Higher concentrations of the dye cannot be used since the preparation of the dye used was the very slightly soluble perchlorate which can be obtained in a very pure state. Further, one of the carbinol forms of the dye is almost insoluble and will precipitate in a certain pH-range if higher concentrations of the dye are used.

The following equilibrium scheme indicates schematically the reactions that can take place if the pH of a solution of MG is changed and borate buffers are used in addition to other buffers:

Scheme I

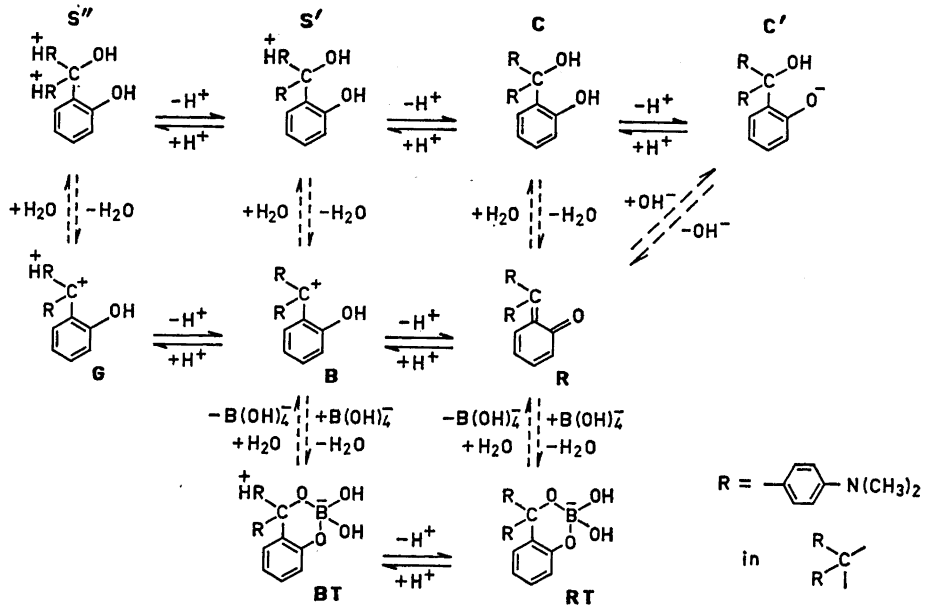

Whole arrows indicate that the reactions proceed with a non-measurable velocity — that is, instantaneously — whereas dashed arrows indicate that the reactions take place with a measurable velocity.

It would seem probable that the borate ions should react with the hydrated forms of the dye, S′ and C, which are diols, and not with the coloured dehydrated forms, B and R. The same complexes can be formed irrespective of the borate ions reacting with the hydrated forms (Scheme II) or with the dehydrated forms (Scheme I). However, kinetic measurements support the reactions according to Scheme I.

Scheme II

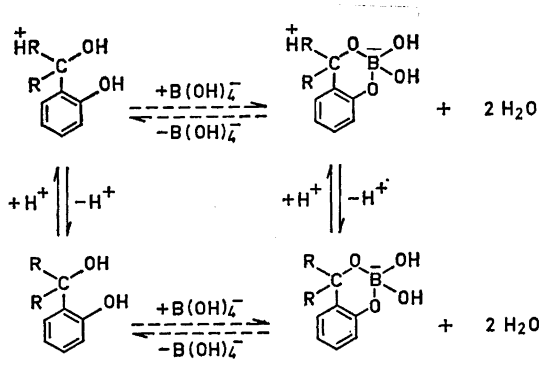

One cannot conclude from the measurements whether the neutral complex has the structure

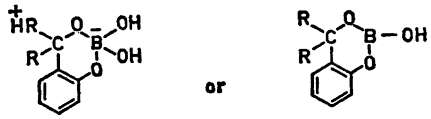

I or II

The latter structure was suggested by Hermans [1] for neutral complexes between borate ions and diols. Compounds of type II with three-coordinated boron have proved to be very weak acids, weaker than boric acid (Hermans [1]). The present investigations show, however, that the complex BT is a considerably stronger acid than boric acid. Therefore, is seems likely that the proton released is bound to a nitrogen in an amino group and not to the oxygen in the group B—OH. This speaks for the structure I. There are, however, no absolutely sure proofs of boron having a four-coordinated configuration (Structure I) or a three-coordinated configuration (Structure II) in complexes between borate ions and polyols.

DEDUCTION OF SOME EQUATIONS USED

The same symbols and definitions have been used as in Ref.[8] Further, the following symbols are defined:

C_T = total concentration of boron

[T] = the concentration of the borate ions which are assumed to be present only as the species $B(OH)_4^-$

$$K_{BT} = \frac{[BT]_\infty}{[B]_\infty[T]_\infty} \quad ; \quad K_{RT} = \frac{[RT]_\infty}{[R]_\infty[T]_\infty} \quad ; \quad K = \frac{[RT][H^+]}{BT]}$$

k_3' = rate constant for the reaction $B + T \rightarrow BT$

k_4' = » » » » » $BT \rightarrow B + T$

k_5' = » » » » » $R + T \rightarrow RT$

k_6' = » » » » » $RT \rightarrow R + T$

A. Equilibrium measurements

The stability constants K_{BT} and K_{RT} were determined by light absorption measurements on solutions of *o*-hydroxy Malachite Green in different borate buffers when equilibrium was reached. The measurements were carried out at the wave length 6090 Å where B and R proved to be the only species in the solutions that absorb light.

In weakly alkaline solutions where the concentrations of the yellow form, G, and its hydrated form, S'', can be omitted in comparison to the concentrations of the other forms of the dye, the following equations are obtained:

$$C_M = [B]_\infty + [R]_\infty + [BT]_\infty + [RT]_\infty + [S']_\infty + [C]_\infty + [C']_\infty \quad (1)$$

According to the definitions of the constants eqn. (1) can be written

$$C_M = [B]_\infty\left[1 + \frac{K_7}{h} + [T]K_{BT} + \frac{K_7}{h}[T]K_{RT} + \frac{1}{K_6}\left(1 + \frac{K_4}{h} + \frac{K_4K_8}{h^2}\right)\right] \quad (2)$$

The absorbancy per cm, e_∞, in a solution is

$$e_\infty = \varepsilon_B[B]_\infty + \varepsilon_R[R]_\infty = \frac{[B]_\infty}{C_M}\left(e_B + e_R\frac{K_7}{h}\right) \quad (3)$$

A combination of eqns. (2) and (3) gives, since $e_B = C_M\varepsilon_B$ and $\varepsilon_R = C_M\varepsilon_R$,

$$\left(K_{BT} + \frac{K_7}{h}K_{RT}\right)[T] = \frac{e_B + e_RK_7/h}{e_\infty} - 1 - \frac{K_7}{h} - \frac{1}{K_6}\left(1 + \frac{K_4}{h} + \frac{K_4K_8}{h^2}\right) \quad (4)$$

In eqn. (4) the terms [T], e_∞, and h can be measured. The terms K_7, e_B, e_R, K_6, K_4, and K_8 are known from earlier investigations (Ref.[8]). Thus the constants K_{BT} and K_{RT} can be determined if the measurements can be carried out in a sufficiently large pH-range.

B. Kinetic measurements

In Ref.[8] there is an equation (eqn. 7) for the total rate constant of the protolytic reactions shown in the equilibrium scheme which is applicable to MG. If we wish to extend this eqn. (7) to include the complex formation with borate ions too, considerable difficulties arise. In kinetic measurements only the colour change, which occurs when the coloured species are transformed to colourless carbinol species and borate complexes, can be followed. An approximate method of determining at least some of the rate constants for the complex formation has been tried based on the following facts: (1) When a solution of MG, containing the dye only in the form of the species B and R, is mixed with a borate buffer the solution fades to about 3—10 % at pH = 8 and 0.3—1 % at pH = 9 of the initial colour intensity. The fading increases when $[B(OH)_4^-]$ increases. (2) The total reaction runs as a first-order reaction, with reasonable accuracy, if the reaction is followed only until 50—75 % of the dye has reacted. Since the total concentration of the dye, C_M, is $\ll [B(OH)_4^-]$ and the measurements are carried out in buffer solutions all reaction steps become pseudomonomolecular. The total reaction deviates from a first-order reaction only in solutions with low pH and high C_T. (3) Since the equilibrium "coloured" $\rightleftharpoons$ "colourless" is strongly displaced towards the right the contribution to the total reaction rate from the reactions $BT \xrightarrow{k_4'} B + T$ and $RT \xrightarrow{k_6'} R + T$ probably can be omitted when only B and R are present at the start of the reactions and nothing of BT or RT.

If k_4' and $k_6' \ll k_3'$ and k_5' the following equations can be deduced:

$$\frac{d}{dt}([R] + [B] + [G]) = k_2[S''] + k_4[S'] + k_6[C] + k_8[C'] - k_1[G] - k_3[B] - k_5[R] - k_3'[B][T] - k_5'[R][T] - k_7[R]oh \quad (5)$$

Eqn. (5) is written

$$U\frac{d[R]}{dt} = Q[S'']-P[R] \text{ where} \quad (6)$$

$$U = 1 + h/K_7 + h^2K_1/K_7 \quad (7)$$

$$Q = k_2 + k_4K_3/h + k_6K_3K_4/h^2 + k_8K_3K_4K_8/h^3 \quad (8)$$

$$P = k_1h^2K_1/K_7 + k_3h/K_7 + k_5 + k_7oh + k_3'[T]h/K_7 + k_5'[T] \quad (9)$$

It further holds that

$$C_M = [R] + [B] + [G] + [S''] + [S'] + [C] + [C'] + [BT] + [RT] \quad (10)$$

which can be written

$$C_M = [R]M + [S'']N \text{ where} \quad (11)$$

$$M = 1 + h/K_7 + h^2K_1/K_7 + [BT]/[R] + [RT]/[R] \quad (12)$$

$$N = 1 + K_3/h + K_3K_4/h^2 + K_3K_4K_8/h^3 \quad (13)$$

Eqn. (6) can now be transformed to

$$\frac{d[R]}{dt} = \frac{QM + PN}{UN}\left(\frac{QC_M^-}{QM + PN} - [R]\right) = k(a-[R]) \quad (14)$$

Integration gives if M is constant (*cf.* Cigén [9], p. 1463)

$$k = \frac{1}{t}\ln\frac{[R]_\infty-[R]_o}{[R]_\infty-[R]_t} = \frac{1}{t}\ln\frac{e_o-e_\infty}{e_o-e_t} \quad (15)$$

The rate constant, k, can be written

$$k = \frac{Q}{N}\left(1 + \frac{[BT] + [RT]}{U[R]} + \frac{V}{U} + \frac{k_3'[T]h/K_7 + k_5'[T])}{U}\right) \quad (16)$$

where

$$V = P - k_3'[T]h/K_7 - k_5'[T] \quad (17)$$

The terms $Q/N + V/U$ are the same as k in eqn. (7) in Ref.[8] and eqn. (26) in Ref.[9] The values of $Q/N + V/U$ at different pH-values are obtained from measurements in borate free solutions. However, k in eqn. (16) becomes approximately constant only if the term $\frac{Q([BT] + [RT])}{NU[R]}$ is small in comparison with the other terms in eqn. (16). If this is true and if $(k_3[T]h/K_7 + k_5'[T])/U \gtrsim Q/N + V/U$ the rate constant k'_3 and (or) k_5' can be determined. Then the rate constant k_4' and (or) k_6' can be calculated from the equations

$$k_4' = k_3'/K_{BT} \quad (18)$$

$$k_6' = k_5'/K_{RT} \quad (19)$$

EXPERIMENTAL

Chemicals used. *o*-Hydroxy Malachite Green was prepared in the form of the perchlorate. The same preparation was used as in Ref.[8] Boric acid, potassium chloride, sodium hydroxide, all of analytical grade, were used in the buffer solutions. Potassium chloride was used to keep the ionic strength constant (0.5 M).

A stock solution of the dye was prepared by shaking a weighed sample of the MG perchlorate for 20 h with a 0.5 M potassium chloride solution which was heated to 70°C before the shaking was started. The volume of the solution was adjusted to the desired one at a temperature of 20°C, and the stock solution was allowed to stand for four days. The concentration of the dye in the stock solution, C_M, was determined spectrophotometrically; $C_M = 1.02 \times 10^{-5}$ M. The weighed sample of MG was calculated to give $C_M = 1.05 \times 10^{-5}$ M. The difference is due partly to the absorption of dyestuff on the walls of the glass flask used and perhaps partly to the fact that some of the very slightly soluble MG perchlorate may have remained undissolved. The method previously used (Ref.[8]) to prepare a stock solution by dissolving the MG perchlorate in acetone which is then diluted with a potassium chloride solution, was not employed in this investigation in order to avoid the possibility of disturbances in the measurements from the acetone.

The borate buffers were prepared from carbon dioxide free solutions of sodium hydroxide, boric acid, and potassium chloride; ionic strength 0.5 M. A solution for measurement was obtained by mixing equal volumes of a borate buffer and a dye stock solution. The pH of the solutions for measurement was determined by emf. measurements at 20.0°C on elements of the following type

H_2, Pt	10 mM HCl 490 mM KCl quinhydrone	conc. KCl	Borate buffer	Pt, H_2

pH means $-\log[H^+]$ and not $-\log a_{H+}$.

Three series of measurements were carried out with different total concentration of boric acid; $C_T = 25$, 12.5, and 6.25 mM. The pH-range used was pH = 8–9.7. The concentration of the borate ions, [T], varied in the three series between 3–22 mM, 1.5–11 mM, and 0.75–5.5 mM. Further it was assumed that no polyborate ions need to be considered at these comparatively low concentrations of boric acid. According to Ingri *et al.*[10] it can be assumed that the greatest part of the boric acid is present as monomer acid and monomer borate ion when $C_T \leq 25$ mM. However, the polyborate formation is strongest at pH-values $\approx pK_s$ of the boric acid, *i.e.* at pH = 9, and it is possible that a certain polyborate formation occurs in the series of measurements with $C_T = 25$ mM.

Apparatus. The equilibrium and kinetic measurements were carried out spectrophotometrically with a Beckman quartz spectrophotometer with photo multiplier. The spectrophotometer was furnished with the arrangements for rapid kinetic studies described in Ref.[8] when the kinetic measurements were carried out.

RESULTS

Equilibrium measurements. In three series of measurements at seven different pH-values in each series the equilibrium absorbancy, E_∞, of the solutions, obtained by mixing equal volumes of borate buffer and dye stock solution, was read. The measurements were carried out at the wavelength $\lambda = 609$ mμ where the coloured species R has an absorption maximum. At this wavelength it also happens that $\varepsilon_R = \varepsilon_B$. Absorption cells of quartz, optical length = 5 cm, were used. The recorded absorbancies were very low but reproducible for the highest borate concentrations. Table 1 contains the corresponding values of E_∞, pH and C_T and the values of K_{RT} and K_{BT} calculated from eqn. (4).

Table 1. Determination of K_{BT} from eqn. (4). K_{BT} is taken = 6 K_{BT}. $C_M = 0.5 \times 10^{-5}$ M. $\lambda = 609$ mμ. $T = 20.0$°C. $d = 5$ cm. $e_B = e_R = 0.420$.

$C_T = 25$ mM				$C_T = 21.5$ mM				$C_T = 6.25$ mM			
pH	[T] mM	$E_\infty = 5\,e_\infty$	$K_{BT} \times 10^{-2}$	pH	[T] mM	$E_\infty = 5\,\infty$	$K_{BT} \times 10^{-2}$	pH	[T] mM	$E_\infty = 5\,e_\infty$	$K_{BT} \times 10^{-2}$
8.04	3.0	0.085	35	8.04	1.50	0.145	37	8.02	0.75	0.256	36
8.25	4.5	0.045	37	8.25	2.25	0.080_5	39	8.24	1.125	0.139	41
8.42	6.0	0.028	39	8.42	3.00	0.049_5	42	8.40	1.50	0.091	42
8.56	7.5	0.021	37	8.56	3.75	0.036	41	8.55	1.875	0.065	42
8.69	9.0	0.015_5	38	8.68	4.50	0.027_5	41	8.67	2.25	0.053	40
8.95	12.5	0.010_5	34	8.93	6.25	0.018	39	8.92	3.125	0.033	40
9.19	16.0	0.008	32	9.17	8.00	0.014	35	9.15	4.00	0.024	39
Mean values			36				39				40

The measurements cannot be carried out within a wider pH-range than pH = 8—9.2 and this is why the constants K_{RT} and K_{BT} cannot be determined separately. By trial and error it was found that the best constancy for K_{RT} and K_{BT} was obtained if K_{RT} was taken = 6 K_{BT}.

From Table 1 it can be seen that the mean value of K_{BT} decreases by 10 % when C_T is increased from 6.25 mM to 25 mM. On the other hand the differences between the K_{BT}-values at C_T = 6.25 mM and 12.5 mM are not significant. A possible formation of polyborate would give too low values of K_{BT}. Therefore the value $K_{BT} = 4.0 \times 10^3$ M^{-1} must be considered as most reliable. This gives $K_{RT} = 2.4 \times 10^4$ M^{-1}.

By definitions $K = K_{BT}K_7/K_{RT}$. From Ref.[8] we get $K_7 = 2.72 \times 10^{-9}$ M and this gives $K = 1.6 \times 10^{-8}$ M^{-1}.

In calculating K_{BT} from eqn. (4) the values of K_7, K_6, K_4, and K_8 were used which had been obtained in a previous investigation on *o*-hydroxy Malachite Green (Ref.[8]). The solutions used in these previous measurements contained 2 % of acetone which, of course, might have influenced the values of the constants determined. However, the influence on the values of K_{BT} and K_{RT} from the above-mentioned small errors that eventually exist in the constants is insignificant. The values of e_B and e_R were determined in solutions free from acetone by the same methods as those used in Ref.[8]

Kinetic measurements. Three series of kinetic measurements, corresponding to the equilibrium measurements but partly at different pH-values, were carried out; Table 2. Furthermore, $Q/N + V/U$ in eqn. (16) (corresponding to k in eqn. (7), Ref.[8]) was determined by kinetic measurements in buffer solutions free from acetone and borate. An attempt to calculate both k_3' and k_5' showed that $k_3' \gg k_5'$ and therefore k_5' cannot be calculated from eqn. (16).

The rate constant k_3' was calculated in the following way. Equal volumes of a borate buffer and a dye stock solution are mixed. In the stock solution all of the dye is present as the coloured ion B, C_M = [B]. The equilibrium B $\rightleftharpoons$ H^+ + R is reached instantaneously and the solution is decolourized owing to the formation of the colourless species S', C, C', BT, and RT. The reactions are followed at low pH until [B] + [R] $\approx \frac{1}{2} C_M$ and at high pH until [B] + [R] $\approx \frac{1}{4} C_M$. The total rate constant k in eqn. (16) is then determined since the term $\frac{Q}{N} \cdot \frac{[BT] + [RT]}{U[R]}$ in eqn. (16) is so small that it can be omitted in comparison with the other terms in eqn. (16). This can be done without large errors since Q/N only amounts to between 1.5 and 14 % of k (see Table 2) and $\frac{[BT] + [RT]}{U[R]} < \frac{1}{4}$ when 50 % of the dye has reacted. Therefore the rate constant k_3' can be calculated from the approximate equation

$$k_3' = \frac{(k - Q/N - V/U)U}{[T]h/K_7} \qquad (20)$$

Table 2 shows that k_3' decreases when pH increases which is in qualitative agreement with the approximations undertaken. The series of measurements with C_T = 25 mM shows, however, that the approximations introduced cannot

Table 2. Determination of k_3' from eqn. (20). $C_M = 1 \times 10^{-5}$ M, $\lambda = 609$ mμ, $T = 20.0$°C.

			$C_T = 25$ mM		$C_T = 12.5$ mM		$C_T = 6.25$ mM	
pH	$Q/N + V/U$ min^{-1}	Q/N min^{-1}	k min^{-1}	k_3' min^{-1} M^{-1}	k min^{-1}	k_3' min^{-1} M^{-1}	k min^{-1}	k_3' min^{-1} M^{-1}
8.04	0.309	0.106	2.16	804	1.23	795	0.765	790
8.42	0.415	0.097	3.13	774	1.75	758	1.105	785
8.68	0.507	0.088	3.40	737	1.98	751	1.23	742
8.93	0.564	0.074	3.36	739	1.98	744	1.29	765
9.17	0.615	0.060	2.83	693	1.72	693	1.225	762
9.42	0.631	0.044	2.28	705	1.48	721	1.09	781
9.72	0.652	0.025	1.63	679	1.16	709	0.93	762
Mean values				733		739		770

alone be responsible for the comparatively large differences of k_3' within this series. The explanation may be that polyborate ions are formed and therefore the k-values obtained become too low. (*Cf.* the low values of K_{BT} in the corresponding series of equilibrium measurements with $C_T = 25$ mM). As a mean of all k_3'-values $k_3' = 7.5 \times 10^2$ min^{-1} M^{-1} was obtained. Eqn. (18) gives then $k_4' = 0.19$ min^{-1}.

In Fig. 1 curve D gives $Q/N + V/U$ as a function of pH. In Fig. 1 is also plotted k as a function of pH calculated from eqn. (20) for different C_T using the mean-value $k_3' = 746$. Curve A, $C_T = 25$ mM; curve B, $C_T = 12.5$ mM; Curve C, $C_T = 6.25$ mM.

If the correction term ([BT] + [RT])/U[R] is introduced into eqn. (20) a better coincidence is obtained between the experimentally found points

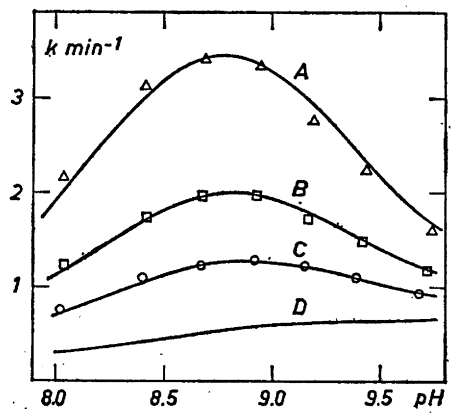

Fig. 1. The rate constant k as a function of pH. Curve A, $C_T = 25$ mM; Curve B, $C_T = 12.5$ mM; Curve C, $C_T = 6.25$ mM. The full drawn curves are calculated from eqn. (20). The symbols are experimentally found k-values. Curve D shows the experimentally found values of $Q/N + V/U$, *i.e.* the rate constant of the total reaction in solutions free from borate, as a function of pH.

(△, □, and ○) and the full drawn calculated curves B and C as well as the left part of curve A. The correction has not been carried out because experimental errors and a possible polyborate formation give an uncertainty of the rate constant k_3' greater than the correction term, except at the lowest pH.

DISCUSSION

In an aqueous solution of *o*-Hydroxy Malachite Green with pH = 5—6 the dye is present as the coloured species B and R. If such a solution is made weakly alkaline with a suitable buffer the solution is decoloured. However, the fading proceeds about ten times faster at pH = 8—9 in borate buffers than in ammonia-ammonium chloride buffers. This high reaction rate in borate buffers shows that the borate complexes are formed by the reactions $B + T \rightarrow BT$ and $R + T \rightarrow RT$ indicated in Scheme I. If the borate complexes were formed according to the reactions indicated in Scheme II the rate of the decolourization should be of the same magnitude as in borate free buffers since the slow reactions $B + H_2O \rightarrow S'$ and $R + H_2O \rightarrow C$ must precede the complex formation $S' + T \rightarrow BT + H_2O$ and $C + T \rightarrow RT + H_2O$.

The kinetic measurements show that the rate of the complex formation is directly proportional to the concentration of the positively charged coloured ion B and to the concentration of the borate ions and that the rate constant $k_3' \gg k_5'$. The complex RT which is considerably stronger than the complex BT is thus formed mainly by the fast reaction $BT \rightarrow RT + H^+$ and not by the slow reaction $R + T \rightarrow RT$.

My thanks are due to Professor Sture Fronæus and Dr. Sten Ahrland for valuable discussions and comments.

REFERENCES

1. Hermans, P. H. *Z. anorg. u. allgem. Chem.* **142** (1924) 83.
2. Böeseken, J. and Niks, A. *Rec. trav. chim.* **59** (1940) 1062.
3. Schäfer, H. *Z. anorg. u. allgem. Chem.* **247** (1941) 96.
4. Böeseken, J. *Advances in Carbohydrate Chem.* **4** (1949) 189.
5. Deutsch, A. and Osoling, S. *J. Am. Chem. Soc.* **71** (1949) 1637.
6. Ross, S. D. and Catotti, A. J. *J. Am. Chem. Soc.* **71** (1949) 3563.
7. Torssell, K. *Arkiv Kemi* **3** (1952) 571.
8. Cigén, R. *Acta Chem. Scand.* **16** (1962) 192.
9. Cigén, R. *Acta Chem. Scand.* **12** (1958) 1456.
10. Ingri, N., Lagerström, G., Frydman, M. and Sillén, L. G. *Acta Chem. Scand.* **11** (1957) 1034.

Received December 13, 1961.

ACTA CHEMICA SCANDINAVICA 16 (1962) 1282–1290

Short Communications

Isolation of Blood Serum Glycolipids

ELISABET SVENNERHOLM and LARS SVENNERHOLM

Department of Medical Biochemistry, University of Gothenburg, Gothenburg, Sweden

In 1958 we described a method for the quantitative determination of plasma cerebrosides and gave figures for their normal plasma concentration [1]. In the same report partial purification of the glycolipids in blood serum by chromatography on magnesium trisilicate and alumina was described. In this process it had soon been evident that the glycolipids with more complex carbohydrate moities were retained on the column. In the method now to be presented the chromatography is performed on silicic acid and ion exchange cellulose.

Materials and methods. Purification of solvents, specifications of silicic acid and DEAE-cellulose and analytical methods for galactose and sulfate were the same as those described by Svennerholm and Thorin [2]. Alumina (standardized according to Brockman) was manufactured by E. Merck AG., Darmstadt. The finest particles were removed by twice suspending the alumina in methanol and decanting the supernatant after 5 min of settling.

Procedure: Preparation of a total serum lipid extract. Normal human blood, without hemolysis, was centrifuged within half an hour after it had been withdrawn. The serum was poured into four volumes of boiling ethanol and stored under ethanol at +4° until it was used. The sampling of serum proceeded for a year. When 17 l of serum had been collected the ethanol extract was evaporated to a volume of about 2 l. The solvent consisted then of about equal volumes of ethanol and water. 60 g of potassium hydroxide pellets were added under gentle stirring, and the extract was stored at +35° for 16 h. After this time the alkaline hydrolysate was extracted three times with 1 l of light petroleum, b.p. 40–45°. The petroleum extracts were pooled and set aside. Then the hydrolysate was acidified with 4 N hydrochloric acid to pH 4–5 and extracted four times with 1 l of chloroform-methanol(4:1, v/v). These extracts were evaporated to dryness (by adding toluene-ethanol 1:1,v/v, several times), redissolved in distilled chloroform and freed from non-lipid contaminants by filtration through a sintered glass filter.

The petroleum extract (P-extract) and the chloroform extract (C-extract) were tested by paper partition chromatography [3]. The P-extract contained mainly cholesterol but also small amounts of glycolipids and sphingomyelins. In the C-extract free fatty acids predominated, but there were also rather large amounts of sphingomyelins and smaller amounts of glycolipids.

Chromatography on silicic acid. The P-extract was evaporated to dryness and redissolved in ethyl ether and filtered. It was added to the top of a 80 g silicic acid column packed in ethyl ether. The column was eluted with 2 l of ethyl ether. The eluate contained large amounts of cholesterol but no glycolipids and sphingomyelins. Afterwards the column was eluted with methanol and samples of about 25 ml were collected on an automatic fraction collector. In the first 250 ml glycolipids were eluted (glycolipid P) and in the following 250 ml sphingomyelins (sphingomyelin P).

The C-extract was divided into four equal volumes and subjected to chromatography on four identical columns with 80 g of silicic acid prepared in chloroform. After the extract had entered the column, it was eluted according to the following scheme:

Chloroform	800 ml
Chloroform-methanol (9:1, v/v)	400 ml
Chloroform-methanol (2:1, v/v)	400 ml
Methanol	800 ml

The chloroform extract was collected in a single batch. It contained only simple lipids (free fatty acids, chloresterol and glycerides). After the eluting solvent had been shifted from chloroform to chloroform-methanol (9:1, v/v) the eluate was collected on the fraction collector and every second fraction was tested by paper chromatography. With chloroform-methanol (9:1, v/v) only glycolipids and autoxidized lipid material were eluted. The more slow moving glycolipids were not eluted until with chloroform-methanol (2:1, v/v) but they were mixed with some sphingomyelins. The methanol eluate contained mainly sphingomyelins. All tubes of the four runnings containing glycolipids but free from sphingomyelins were pooled (glycolipids K 1—4) as the tubes containing sphingomyelins but no detectable amounts of glycolipids (sphingomyelins K 1—4). The tubes containing both glycolipids and sphingomyelins were combined and rechromatographed on a fifth silicic acid column. Glycolipids K 5 and sphingomyelins K 5 were obtained.

Chromatography on alumina. All fractions containing sphingomyelins (sphingomyelin P and K 1—5) were combined, evaporated to dryness, redissolved in 1 l of chloroform-methanol (1:1, v/v), and filtered. The extract was poured onto a column of 50 g of alumina, and the column was eluted with 1 l of chloroform-methanol (1:1, v/v). The total chloroform-methanol extract contained practically all the serum sphingomyelins in pure form. It was later used for gas chromatographic studies of the fatty acid composition of serum sphingomyelins [4]. Afterwards, the alumina was eluted with 1 l of chloroform-ethanol-water (2:5:2,v/v). As this extract contained glycolipids, it was evaporated to 1/4 of its original volume, dialysed against tap water and evaporated to dryness in a rotating evaporator (glycolipid A).

Rechromatography of the glycolipids on silicic acid. As all the glycolipid fractions still contained a large proportion of simple lipids, they were all combined (glycolipid P, K 1—5 and A). They weighed 2.1 g and the hexose content was less than 10 %. They were rechromatographed on 80 g of silicic acid prepared in chloroform. The glycolipids were dissolved in 200 ml of chloroform and poured onto the column. The column was then eluted with: chloroform 800 ml, chloroform-methanol (4:1, v/v) 800 ml, chloroform-methanol (1:1, v/v) 800 ml, and methanol 400 ml. All the eluates were collected in fractions of 25 ml and every second fraction was tested by paper partition chromatography. The pure chloroform eluate did not contain any glycolipids and was discarded. The glycolipids all appeared in the chloroform-methanol eluates, but as there was a distinct difference in mobility between those of tubes 1—40 and those of tubes 41—60 they were divided in two separate fractions (glycolipid I and II), which were evaporated to a small volume and dialysed against running water for 48 h and lyophilized.

Yields:

Glycolipid I	: 477 mg; galactose	16.5 %
Glycolipid II	: 119 mg; galactose	15.0 %

The glycolipid-hexose content of all the serum was 160 mg, and thus the recovery is somewhat more than 60 %. As about 10 % of glycolipids have been used for the chromatographic analyses, the losses due to the isolation are less than 30 %.

Chromatography on DEAE-cellulose. Glycolipids I and II were then subjected to chromatography on DEAE-cellulose in order to divide the glycolipids into a neutral and an acid fraction. Glycolipid I was dissolved in chloroform-methanol (2:1, v/v), poured on a 10 g DEAE cellulose column and eluted as described by Svennerholm and Thorin [2] with 250 ml of (*a*) chloroform-methanol (2:1, v/v), (*b*) same solvent + acetic acid to 5 %, (*c*) same solvent + 1/10 volume of 5 N lithium chloride in water. The neutral eluate was evaporated to dryness without further treatment (glycolipid I A). The other two were evaporated to 1/4 of their original volume, dialysed against running water for 48 h and evaporated to dryness in a rotating evaporator (glycolipid I B and I C, respectively). Glycolipid II was treated in exactly the same way, but only half the amount of cellulose and solvents were used.

Yields:

Glycolipid I	A :	340 mg; galactose	18.0 %
	II A :	16 mg; galactose	21.4 %
	I B :	22 mg; galactose	5.6 %
	II B :	19 mg; galactose	6.3 %
	I C :	74 mg; galactose	8.7 %
	II C :	57 mg; galactose	12.4 %

With paper partition chromatography and thin-layer chromatography on silicic acid acid it could be shown that the fractions A only contained the neutral glycolipids, and that the fractions B contained kephalin B, deranged, (oxidized?) neutral glycolipids and autoxidized lipid material, probably from polyunsaturated fatty acids. The fractions C contained sulfatides and a still unidentified acid lipid. In fraction I C the molar ratio galactose to sulfate was 1.1 : 1.

Preliminary isolation studies indicate that in the neutral fractions there are mono-, di- and trihexosides and neutral aminoglycolipids.

Glucose is the dominating sugar in the monohexosides (cerebrosides), while galactose and glucose occur in about equal amounts in the other neutral glycolipids.

The authors are indebted for financial support given by *Statens Medicinska Forskningsråd* and *Medicinska Fakulteten vid Göteborgs Universitet.*

1. Svennerholm, E. and Svennerholm, L. *Scand. J. Clin. Lab. Invest.* **10** (1958) 97.
2. Svennerholm, L. and Thorin, H. *J. Lipid Research* (Submitted for publication).
3. Beiss, U. and Armbruster, O. *Z. Naturforsch.* **13B** (1958) 79.
4. Stenhagen, E., Svennerholm, E. and Svennerholm, L. *Unpublished experiments.*

Received May 28, 1962.

Hereditary Variation in Content of Isothiocyanates and Thiooxazolidones in Seeds of Rape and Turnip Rape

L.-Å. APPELQVIST

Chemical Division, Swedish Seed Association, Svalöv, Sweden

The use of rapeseed meal in animal nutrition is limited mainly due to its content of glucosides, which in the presence of water are split up and form isothiocyanates and thiooxazolidones. Rather much work has been performed to find the maximum permitted dosage of such meals to various animal species [1]. As rapeseed meal is available in large quantities in several countries considerable effort has been made, *e.g.* in Canada and Sweden, to apply some industrial detoxification process to the meal and thus increase its nutritional value. Even if it is relatively easy to remove the toxic substances industrially [2], it is at present not economically possible as the price for processed rapeseed meal would be to high. If toasting — dry heating — should be efficient in decreasing the toxicity of the meal such high temperatures must be used (130°C for 24 h or 150°C for 5 h [2]) that protein denaturation most probably occurs. Therefore we started this investigation with the object to find out if the hereditary variation in content of these substances are great enough to form a basis for decreasing their content through plant breeding.

The seed samples investigated were taken from the field trials of the Oil Crop Division at the Swedish Seed Association, except for Duro which was received from the General Seed Company, Svalöv. Thus all samples represent carefully handled seed, grown in Sweden under normal conditions.

The determination of isothiocyanates (I) and thiooxazolidones (II) were made essentially according to Wetter [3,4]. All tabulated figures are based upon defatted, dry meal and represent the mean of two analyses. The detailed procedure used in this investigation will be described in a forthcoming, more comprehensive report.

The results thus obtained with rape and turnip rape are shown in Table 1.

Varietal differences in content of these substances in the summerforms of rape and turnip rape have earlier been investigated by Wetter and Craig [5] using seeds grown in different locations in Canada.

Kreula and Kiesvaara [6] investigated the variation in thiooxazolidone content as well in winter as in summer types of rape and turnip rape most probably grown in Finland. Delaveau [7], using a method not quite comparable to the one used in this investigation, has studied varietal differences in content of isothiocyanates in rape and turnip rape, most likely grown in France.

Compared with the figures of Wetter and Craig our results show much greater varietal deviations and lower mean values for both I and II in summer rape. We have found varieties of summer turnip rape with more I and less II than they found. Their findings that the quotient I/II is about 1 in rape and 3.5 in turnip rape can not be of general validity and are most probably due to the rather close relation of the varieties used by them. We have found variations between 0.7 and 1.4 in I/II for summer rape, 2.9 and about 40 in summer turnip rape. The variation reported for the winter types is considerable. It should also be noted that the amount of II is approximately twice as high in winter rape as in summer rape.

The mean value and the variation in content of II in all four groups investigated are not very different from those reported by Kreula and Kiesvaara.

The great variation in content of thiooxazolidone, from 7.9 mg/g for Matador

Glucose is the dominating sugar in the monohexosides (cerebrosides), while galactose and glucose occur in about equal amounts in the other neutral glycolipids.

The authors are indebted for financial support given by *Statens Medicinska Forskningsråd* and *Medicinska Fakulteten vid Göteborgs Universitet.*

1. Svennerholm, E. and Svennerholm, L. *Scand. J. Clin. Lab. Invest.* **10** (1958) 97.
2. Svennerholm, L. and Thorin, H. *J. Lipid Research* (Submitted for publication).
3. Beiss, U. and Armbruster, O. *Z. Naturforsch.* **13B** (1958) 79.
4. Stenhagen, E., Svennerholm, E. and Svennerholm, L. *Unpublished experiments.*

Received May 28, 1962.

Hereditary Variation in Content of Isothiocyanates and Thiooxazolidones in Seeds of Rape and Turnip Rape

L.-Å. APPELQVIST

Chemical Division, Swedish Seed Association, Svalöv, Sweden

The use of rapeseed meal in animal nutrition is limited mainly due to its content of glucosides, which in the presence of water are split up and form isothiocyanates and thiooxazolidones. Rather much work has been performed to find the maximum permitted dosage of such meals to various animal species [1]. As rapeseed meal is available in large quantities in several countries considerable effort has been made, *e.g.* in Canada and Sweden, to apply some industrial detoxification process to the meal and thus increase its nutritional value. Even if it is relatively easy to remove the toxic substances industrially [2], it is at present not economically possible as the price for processed rapeseed meal would be to high. If toasting — dry heating — should be efficient in decreasing the toxicity of the meal such high temperatures must be used (130°C for 24 h or 150°C for 5 h [2]) that protein denaturation most probably occurs. Therefore we started this investigation with the object to find out if the hereditary variation in content of these substances are great enough to form a basis for decreasing their content through plant breeding.

The seed samples investigated were taken from the field trials of the Oil Crop Division at the Swedish Seed Association, except for Duro which was received from the General Seed Company, Svalöv. Thus all samples represent carefully handled seed, grown in Sweden under normal conditions.

The determination of isothiocyanates (I) and thiooxazolidones (II) were made essentially according to Wetter [3,4]. All tabulated figures are based upon defatted, dry meal and represent the mean of two analyses. The detailed procedure used in this investigation will be described in a forthcoming, more comprehensive report.

The results thus obtained with rape and turnip rape are shown in Table 1.

Varietal differences in content of these substances in the summerforms of rape and turnip rape have earlier been investigated by Wetter and Craig [5] using seeds grown in different locations in Canada.

Kreula and Kiesvaara [6] investigated the variation in thiooxazolidone content as well in winter as in summer types of rape and turnip rape most probably grown in Finland. Delaveau [7], using a method not quite comparable to the one used in this investigation, has studied varietal differences in content of isothiocyanates in rape and turnip rape, most likely grown in France.

Compared with the figures of Wetter and Craig our results show much greater varietal deviations and lower mean values for both I and II in summer rape. We have found varieties of summer turnip rape with more I and less II than they found. Their findings that the quotient I/II is about 1 in rape and 3.5 in turnip rape can not be of general validity and are most probably due to the rather close relation of the varieties used by them. We have found variations between 0.7 and 1.4 in I/II for summer rape, 2.9 and about 40 in summer turnip rape. The variation reported for the winter types is considerable. It should also be noted that the amount of II is approximately twice as high in winter rape as in summer rape.

The mean value and the variation in content of II in all four groups investigated are not very different from those reported by Kreula and Kiesvaara.

The great variation in content of thiooxazolidone, from 7.9 mg/g for Matador

Table 1.

Species and varieties	Isothiocyanates mg/g I	Thiooxazolidones mg/g II	I + II	I/II
Brassica napus, wintertype, 59—255 Matador	5.3	7.9	13.2	0.7
— » — , 59—271 Dippes	4.0	7.8	11.8	0.5
— » — , 59—259 from Hungary	3.6	7.2	10.8	0.5
Mean	4.3	7.6	11.9	0.6
Brassica napus, summertype, 61—751 Regina II	3.4	3.2	6.6	1.1
— » — , 61—753 from Canada	3.0	4.4	7.4	0.7
— » — , 61—755 »	3.1	2.5	5.6	1.2
— » — , 61—756 »	2.5	1.8	4.3	1.4
Mean	3.0	3.0	6.0	1.1
Brassica campestris, wintertype, Duro (1959)	7.7	0.5	8.2	5.4
— » — , 59-276 from Poland	8.1	1.3	9.4	6.2
— » — , 61-680 from Austria	9.2	0.3	9.5	30.7
Mean	8.3	0.7	9.0	17.4
Brassica campestris, summertype, 61-880 Bele	5.3	1.8	7.1	2.9
— » — , 61-304 Sv-strain	8.9	0.8	9.7	11.1
— » — , 61-307 »	7.0	0.7	7.7	10.0
— » — , 61-879 »	7.4	0.2	7.6	37.0
Mean	7.2	0.9	8.0	15.2

winter rape to 1.8 for Bele summer turnip rape (or even 0.2 for some non commercial varieties) seems to offer at least a partial explanation why different batches of commercial rapeseed meal (which can contain both rape and turnip rape) in feeding trials have shown great variation in toxicity.

As rape *(Brassica napus)* can be synthesized from kale *(Brassica oleracea)* and turnip rape *(Brassica campestris)* it would be interesting to investigate varietal differences in content of II in kale seed as the genes for high content of II could originate from the kale parent. Work along these lines will be reported in the above mentioned forthcoming report.

The variations found seem to be sufficient for further selection towards lower content of isothiocyanates and thiooxazolidones in rape and turnip rape.

Financial support for this work has been given by the *Nordiska Jordbruksforskares Förenings Kommitté för Foderkvalitet.*

Communications from the Swedish Seed Association, No. 230.

1. Christian, B. C. in Altschul, A. M. *Rapeseed, Mustard-Seed and Poppy-Seed Meals. — Processed Plant Protein Foodstuffs*, Academic Press, New York 1958, p. 577—592.
2. Frölich, A. *Ann. Royal Agric. College* **20** (1953) 105.
3. Wetter, L. R. *Can. J. Biochem. Physiol.* **33** (1955) 980.
4. Wetter, L. R. *Can. J. Biochem. Physiol.* **35** (1957) 293.
5. Wetter, L. R. and Craig, B. M. *Can. J. Plant Sci.* **39** (1959) 395.
6. Kreula, M. and Kiesvaara, M. *Acta Chem. Scand.* **13** (1959) 1375.
7. Delaveau, P. Thèses, Paris 1954.

Received June 1, 1962.

The Synthesis of Ascorbigen from Ascorbic Acid and 3-Hydroxymethylindole

EINO PIIRONEN and
ARTTURI I. VIRTANEN

Laboratory of the Foundation for Chemical Research, Biochemical Institute, Helsinki, Finland

Some years after vitamin C was isolated and characterized as ascorbic acid, it was observed that the content of ascorbic acid in cabbage increased when cabbage was boiled for a short time [1]. McHenry and Graham [2], who detected a rise in the phenol-indophenol titration value in cooked cauliflower and in some other vegetables, believed the increase to be due to the liberation of »bound ascorbic acid», perhaps from an ester. Guha and Pal [3] found that the »bound ascorbic acid», which releases ascorbic acid on hydrolysis, can be extracted from cabbage with organic solvents. Sen-Gupta and Guha [4] gave the name ascorbigen to the substance although they did not isolate it. Procházka *et al.* [5] separated it from other substances. A comparison of their preparation (kindly sent by Dr. Ž. Procházka) with a synthetic ascorbigen prepared in this laboratory (Gmelin and Virtanen [6]) revealed that the former is identical with the synthetic preparation.

Gmelin and Virtanen found that ascorbigen can be synthesized either from 3-hydroxymethylindole and ascorbic acid or from indole, formaldehyde, and ascorbic acid. The synthesis from 3-hydroxymethylindole and ascorbic acid was accomplished in a phosphate buffer (pH 7) by heating for a few minutes on a water bath. Because the yield of ascorbigen varies greatly when this method is used, we have studied the factors that influence the reaction more closely.

In experiments in which ascorbigen was synthesized from 3-hydroxymethylindole and ascorbic acid, the optimum pH for the synthesis was found to be 4 to 5. In the first actual experiment performed after the preliminary experiments, the reaction temperature was 33°C, and the pH range 5 to 7. The same weight of both components was used in the reaction mixture, and hence 21 % of 3-hydroxymethylindole in excess of the theoretical value was added. The decrease in ascorbic acid during the experiment is shown in Table 1.

Table 1. The decrease in ascorbic acid in citrate buffer solutions (0.05 M) containing 9 mg of ascorbic acid and 9 mg of 3-hydroxymethylindole in 5 ml. pH values 5 to 7, temperature 33°C. The mixture was lightly shaken every two minutes during the whole reaction period.

Time	% of the original ascorbic acid consumed at		
min	pH 5	pH 6	pH 7
40	65	25	7
80	72	35	—
120	75	43	—
200	77	55	12

Thin-layer chromatograms of the reaction mixture after a reaction time of 200 min gave after staining with Ehrlich's reagent the following visually determined results.

1. Solvent: butanol saturated with water

	R_F	pH 5	pH 6	pH 7
3,3′-Di-indolyl-methane	0.94	30 %	50 %	35 %
3-Hydroxymethyl-indole	0.89	5 %	10 %	45 %
Ascorbigen	0.83	65 %	40 %	13 %

In addition Ehrlich-positive spots with R_F = 0.72 and 0.16 were obtained which became more intense as the pH rose.

2. Solvent: benzene:ethanol = 2:1

	R_F	pH 5	pH 6	pH 7
3,3′-Di-indolyl-methane	0.80	20 %	50 %	25 %
3-Hydroxymethyl-indole	0.67	0 %	0 %	50 %
Ascorbigen	0.59	80 %	50 %	25 %

In the second experiment the pH range was 2 to 7 and the temperature 37°C. 3-Hydroxymethylindole was used in an excess of 9 % over the theoretical value. The decrease in ascorbic acid at different pH values is shown in Table 2.

The thin-layer chromatogram (benzene: ethanol = 2:1) run after a reaction time of 10 min gave the following visually estimated ratios of the different components at different pH:

Table 2. The decrease in ascorbic acid in citrate-phosphate buffer solutions (McIlvaine) containing 6 mg of ascorbic acid and 5.4 mg of 3-hydroxymethylindole in 3 ml. pH values 2 to 7, temperature 37°C.

pH	mg and % of the orginal ascorbic acid consumed after					
	10 min		40 min		120 min	
	mg/ml	%	mg/ml	%	mg/ml	%
2	—	—	0.31	15	0.42	21
3	—	—	0.93	46	0.97	49
4	1.03	51	1.56	78	1.54	77
5	0.89	45	1.36	69	1.54	77
6	0.09	4	0.47	24	1.07	54
7	0.01	1	0.06	3	0.47	24

3,3′-Di-indolylmethane
pH 2 > pH 3 ≃ pH 4 < pH 5 < pH 6 ≃ pH 7;
3-Hydroxymethylindole
pH 2 < pH 3 > pH 4 > pH 5 > pH 6 < pH 7;
Ascorbigen
pH 2 < pH 3 < pH 4 > pH 5 > pH 6 > pH 7.

The formation of ascorbigen during 10 min at pH 7 was weak; after 40 and 120 min at this pH no ascorbigen was observed. Most of the 3-hydroxymethylindole had condensed to 3,3′-di-indolylmethane. After a reaction time of 120 min at pH 4, the yield of ascorbigen was nearly 80 % of the theoretical value. The photograph of the thin-layer chromatogram (Fig. 1) shows clearly the reaction products and the unchanged 3-hydroxymethylindole after a reaction time of 10 min. No 3-hydroxymethylindole could be detected at any pH value after 40 min.

Summary: Ascorbigen can easily be synthesized from 3-hydroxymethylindole and ascorbic acid at 20 to 37°C. The optimum pH is about 4 and the yield 70 to 80 %. At pH 5 the yield is still almost the same. The reaction time is about 1 h. At pH 7 small amounts of ascorbigen are formed during a short reaction time, but the ascorbigen disappears later on. At pH 6 and 7 large amounts of 3,3′-di-indolylmethane are formed from 3-hydroxymethylindole.

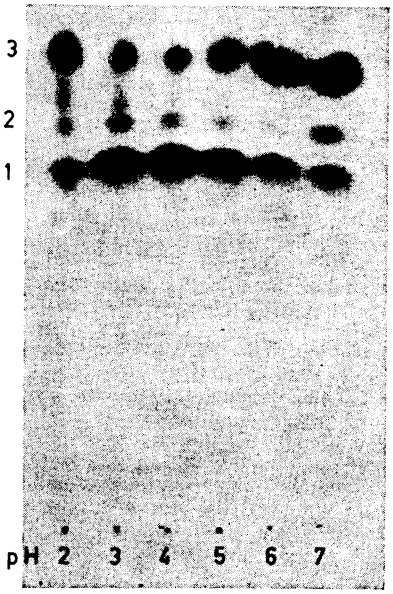

Fig. 1. Synthesis of ascorbigen from 3-hydroxymethylindole and ascorbic acid in water at 37°C and different pH. Reaction time 10 min. A paper chromatogram of the products formed; 1 = ascorbigen, 2 = 3-hydroxymethylindole, 3 = di indolylmethane.

This research has been financed in part by a grant made by the United States Department of Agriculture, Agricultural Research Service.

1. Ahmad, B. *Biochem. J.* **29** (1935) 275.
2. McHenry, E. W. and Graham, M. L. *Nature* **135** (1935) 871.
3. Guha, B. C. and Pal, J. C. *Nature* **137** (1936) 946; **139** (1937) 844.
4. Sen-Gupta, P. N. and Guha, B. C. *Nature* **141** (1938) 974.
5. Procházka, Ž., Šanda, V. and Šorm, F. *Collection Czechoslov. Chem. Communs.* **22** (1957) 333, 654.
6. Gmelin, R. and Virtanen, A. I. *Ann. Acad. Sci. Fennicæ A II*, **1961**, No. 107.

Received May 21, 1962.

Isolation of Acylated α-Alkoxy-glycerylphosphoryl Cholines from Normal Human Serum

OSSI RENKONEN

Department of Serology and Bacteriology, University of Helsinki, Finland

Alkoxy-glycerylphosphoryl cholines were recently isolated from a hydrolysate of highly purified serum lecithin [1]. The present report describes the isolation of the corresponding unhydrolyzed lipids which are shown to be acylated α-alkoxy-glycerylphosphoryl cholines.

The sample of serum lecithin which served as starting material was quite similar to that described previously [1]. It contained 3.2 % ether phosphatides [a] and 1.3 % plasmalogens [b].

Acid and alkali stable lipids (0.49 mg P) were prepared from 0.50 mmole of the lecithin as described previously [1]. Their chromatographic fractionation on silicic acid gave a lecithin-like fraction (0.12 mg P) and a lysolecithin-like one (0.33 mg P).

The lecithin-like fraction was shown to be rather pure acylated alkoxy-glycerylphosphoryl choline. It migrated on thin layer chromatography (TLC) [2] like pure lecithin but it contained acyl esters [3], and phosphorus [4] in molar ratios 1.03:1.00. Strong acid hydrolysis [5] of the preparation released only 0.12 mole free glycerol, but in addition the hydrolysate contained a stable lipid which showed the same mobility as batyl alcohol on TLC. This behaviour is typical of ether phosphatides [1]. The phosphatide contained 0.80 mole choline [6], but it was free of phosphatidyl cholines and choline plasmalogens as 96 % of its phosphorus remained "stable" in a renewed mild acid and alkaline hydrolysis.

The lysolecithin-like fraction isolated from the lecithin hydrolysate was identical with the alkoxy-glycerylphosphoryl cholines described previously [1]. A sample of this preparation (4.5 μmoles) was subjected to acetolysis as described by Carter *et al.*[7] Subsequent chromatography on alkali-free aluminium oxide [8] and silicic acid gave a lipid (3.6 μmoles) [c] which on TLC was identical with batyl alcohol diacetate. The diacetyl compound, after deacylation with alkali, released 1.18 moles formaldehyde by oxidation with periodate. The experimental conditions used gave 1.10 moles formaldehyde from deacylated batyl alcohol diacetate. This shows that the "ether-ester lecithins" of serum are probably α-alkoxy compounds.

A second sample (0.50 mmole) of the serum lecithin was subjected to mild alkaline hydrolysis only, and the stable lipids (0.69 mg P) were fractionated as above.

The lecithin-like fraction (0.18 mg P) thus obtained again moved like pure lecithin on TLC, although it contained carboxylic esters and phosphorus in equimolar amounts. The composition of this preparation became evident after mild acid hydrolysis. After chromatographic fractionation the acid hydrolysate yielded "ether-ester lecithins" identical to those described above, and true lysolecithins which were formed from choline plasmalogens. Thus the preparation was a mixture of unhydrolyzed choline plasmalogens (about 30 %) and "ether-ester lecithins" (about 70 %). It did not contain detectable amounts of "lecithins" of divinylether [d], vinylether-alkoxy [e] or dialkoxy [f] type [9].

The alkaline hydrolysate of the lecithin gave also a lysolecithin-like fraction (0.47 mg P) which was a mixture of choline lysoplasmalogens (about 30 %) and alkoxy-glycerylphosphoryl cholines (about 70 %) [1].

Thus the mild alkaline hydrolysis of serum lecithin caused complete deacylation of phosphatidyl cholines, but at the same time it resulted in only about 75 % deacylation of choline plasmalogens and "ether-ester lecithins". The combination of mild acid and mild alkaline hydrolysis accordingly gave pure "ether-ester lecithins" in about 25 % yield although the starting material contained rather small amounts of these lipids.

These observations confirm and extend the recent finding of Hanahan and Watts [10], who obtained pure acylated α-alkoxy-glycerylphosphoryl ethanolamines by selective alkaline deacylation of a mixture containing about 80 % "ether-ester cephalines" and about 20 % phosphatidyl ethanolamines.

We think that also the slow deacylation of plasmalogens indicated in our experiments will eventually prove useful for isolation of pure native plasmalogens from natural sources.

a. Estimated as stable phosphatides after combined acid and alkaline hydrolysis [1].

b. Estimated as difference between alkali stable phosphatides and ether lipids.

c. Assayed by analysis of carboxylic esters; calculated by assuming that the lipid was a diacyl compound.

d. The phosphorus of the sample remained completely "stable" in mild acid hydrolysis.

e. The lysolecithins formed by the mild acid hydrolysis were free of alkoxy-glycerylphosphoryl cholines as shown by their requimolar content of carboxylic ester and phosphorus.

f. The "ether-ester lecithin" obtained from the mild acid hydrolysate gave nearly quantitative yield of "monochain derivatives" of glycerylphosphoryl choline by prolonged mild alkaline hydrolysis.

Acknowledgements. I wish to thank Mrs. Satu Liusvaara, Mrs. Maire Laakso, and Miss Anneli Miettinen for skilled assistance, and to acknowledge the support of grants from *Jenny and Antti Wihuri Foundation*, *Sigrid Juselius Foundation*, and *The Finnish State Committee for Science*.

1. Renkonen, O. *Biochim. et Biophys. Acta* **59** (1962) 497.
2. Wagner, H., Hörhammer, L. and Wolff, P. *Biochem. Z.* **334** (1961) 175.
3. Renkonen, O. *Biochim. et Biophys. Acta* **54** (1961) 361.
4. Bartlett, G. R. *J. Biol. Chem.* **234** (1959) 466.
5. Renkonen, O. *Biochim. et Biophys. Acta* **56** (1962) 367.
6. Böttcher, C. J. F., Pries, C. and Van Gent, C. M. *Rec. trav. chim.* **80** (1961) 1169.
7. Carter, H. E., Smith, D. and Jones, D. N. *J. Biol. Chem.* **232** (1958) 681.
8. Renkonen, O. *J. Lipid Research* **3** (1962) 181.
9. Marinetti, G. V. *J. Lipid Research* **3** (1962) 1.
10. Hanahan, D. J. and Watts, R. *J. Biol. Chem.* PC 59—60 (1961).

Received June 12, 1962.

Gas Chromatographic Determination of some Volatile Compounds in Urine

ROGER BONNICHSEN
AND MAIRE LINTURI

The Government Laboratory for Forensic Chemistry, Stockholm 60, Sweden

For several years this laboratory has used a chemical as well as an enzymatic method for the determination of alcohol in blood and urine [1]. In some cases large discrepancies were found between the results obtained by the two methods.

The number of cases where these large discrepancies are found as well as the number of cases with smaller but significant differences seem to increase and these findings induced a closer investigation of the cause of the disagreement.

To this purpose a Perkin-Elmer gas fractometer with a flame detector was used. As column filling we used 10 g of Carbowax 1500 (polyethyleneglycol, 10 % by weight on Teflon) in the first part of the column followed by 5 g of Ucon polyglycol LB-550-x (polypropyleneglycol, 20 % by weight on Chromosorb).

This packing ensured complete separation of the volatile compounds which could be expected to be present in the urine samples, without interference of the relatively large amounts of water present. At the same time the water was not, as is the case with polyethyleneglycol alone, unnecessarily retarded which is obviously important as the next sample can not be introduced until all water has left the column.

The temperature was 100°C throughout the procedure and the nitrogen pressure was 1 atm. The urine was injected directly and 2 μl was used. Under these conditions a new sample could be injected every tenth min. At the maximum sensitivity 0.01 % of ethanol in a 2 μl sample gave a deflection of 8 to 10 cm on the recorder.

As could be expected, the chromatographic analysis revealed besides ethanol the presence of methanol, acetone and acetaldehyde which in some but not all cases could account for the differences seen in Table 1. In no cases a higher aliphatic alcohol than ethanol has been found. A typical recording is shown in Fig. 1. Acetone was commonly encountered in diabetic in-

c. Assayed by analysis of carboxylic esters; calculated by assuming that the lipid was a diacyl compound.

d. The phosphorus of the sample remained completely "stable" in mild acid hydrolysis.

e. The lysolecithins formed by the mild acid hydrolysis were free of alkoxy-glycerylphosphoryl cholines as shown by their requimolar content of carboxylic ester and phosphorus.

f. The "ether-ester lecithin" obtained from the mild acid hydrolysate gave nearly quantitative yield of "monochain derivatives" of glycerylphosphoryl choline by prolonged mild alkaline hydrolysis.

Acknowledgements. I wish to thank Mrs. Satu Liusvaara, Mrs. Maire Laakso, and Miss Anneli Miettinen for skilled assistance, and to acknowledge the support of grants from *Jenny and Antti Wihuri Foundation*, *Sigrid Juselius Foundation*, and *The Finnish State Committee for Science*.

1. Renkonen, O. *Biochim. et Biophys. Acta* **59** (1962) 497.
2. Wagner, H., Hörhammer, L. and Wolff, P. *Biochem. Z.* **334** (1961) 175.
3. Renkonen, O. *Biochim. et Biophys. Acta* **54** (1961) 361.
4. Bartlett, G. R. *J. Biol. Chem.* **234** (1959) 466.
5. Renkonen, O. *Biochim. et Biophys. Acta* **56** (1962) 367.
6. Böttcher, C. J. F., Pries, C. and Van Gent, C. M. *Rec. trav. chim.* **80** (1961) 1169.
7. Carter, H. E., Smith, D. and Jones, D. N. *J. Biol. Chem.* **232** (1958) 681.
8. Renkonen, O. *J. Lipid Research* **3** (1962) 181.
9. Marinetti, G. V. *J. Lipid Research* **3** (1962) 1.
10. Hanahan, D. J. and Watts, R. *J. Biol. Chem.* PC 59—60 (1961).

Received June 12, 1962.

Gas Chromatographic Determination of some Volatile Compounds in Urine

ROGER BONNICHSEN
AND MAIRE LINTURI

The Government Laboratory for Forensic Chemistry, Stockholm 60, Sweden

For several years this laboratory has used a chemical as well as an enzymatic method for the determination of alcohol in blood and urine [1]. In some cases large discrepancies were found between the results obtained by the two methods.

The number of cases where these large discrepancies are found as well as the number of cases with smaller but significant differences seem to increase and these findings induced a closer investigation of the cause of the disagreement.

To this purpose a Perkin-Elmer gas fractometer with a flame detector was used. As column filling we used 10 g of Carbowax 1500 (polyethyleneglycol, 10 % by weight on Teflon) in the first part of the column followed by 5 g of Ucon polyglycol LB-550-x (polypropyleneglycol, 20 % by weight on Chromosorb).

This packing ensured complete separation of the volatile compounds which could be expected to be present in the urine samples, without interference of the relatively large amounts of water present. At the same time the water was not, as is the case with polyethyleneglycol alone, unnecessarily retarded which is obviously important as the next sample can not be introduced until all water has left the column.

The temperature was 100°C throughout the procedure and the nitrogen pressure was 1 atm. The urine was injected directly and 2 μl was used. Under these conditions a new sample could be injected every tenth min. At the maximum sensitivity 0.01 % of ethanol in a 2 μl sample gave a deflection of 8 to 10 cm on the recorder.

As could be expected, the chromatographic analysis revealed besides ethanol the presence of methanol, acetone and acetaldehyde which in some but not all cases could account for the differences seen in Table 1. In no cases a higher aliphatic alcohol than ethanol has been found. A typical recording is shown in Fig. 1. Acetone was commonly encountered in diabetic in-

Table 1. Some typical examples of the difference between the two methods. (‰ = g per liter).

Blood		Urine		Gas Chromatography of the Urine			
Widmark ‰	ADH ‰	Widmark ‰	ADH ‰	Ethanol ‰	Methanol ‰	Acetone ‰	Acetal-dehyde ‰
2.73	1.88	3.69	2.47	2.40	0.78	0.02	—
3.45	3.01	4.64	4.25	4.29	0.39	0.02	(0.006 ?)
1.19	0.57	2.39	1.10	0.98	0.66	0.11	—
2.63	2.08	3.23	2.54	2.55	0.39	0.04	0.002
3.34	3.02	3.89	3.93	3.74	—	0.20	—
3.29	2.65	3.61	2.63	2.73	0.69	0.04	—
2.00	1.38	3.29	2.35	2.46	0.45	0.01	unknown
1.00	0.70	1.65	1.12	1.07	0.06	0.17	—

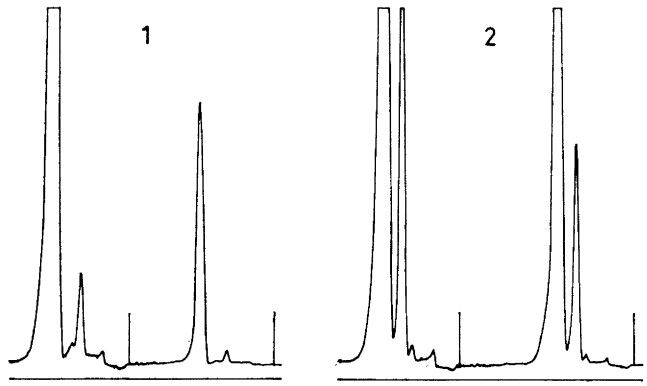

Fig. 1. Recordings of two duplicate analyses with two different sensitivities. The peaks are from left to right, ethanol, methanol, acetone and acetaldehyde. The sensitivities were 32 and 4 in experiment 1, 8 and 4 in experiment 2.

dividuals and the concentration lies mostly around 0.01 ‰. Methanol, acetaldehyde and probably acetone can derive from the drinking of denatured alcohol or home-distilled spirits. In all cases the enzymatic determinations of ethanol agreed closely with the gas chromatographic analysis.

A detailed report with application of the method to blood will be published later.

1. Bonnichsen, R. and Lundgren, G. *Acta Pharmacol. et Toxicol.* **13** (1957) 256.

Received June 25, 1962.

ACTA CHEMICA SCANDINAVICA 16 (1962) 1291–1295

The Chemistry of the Natural Order Cupressales

42 *. Heartwood Constituents of *Tetraclinis articulata* (Vahl) Masters

YUAN-LANG CHOW and H. ERDTMAN

Organisk-kemiska Institutionen, Kungl. Tekniska Högskolan, Stockholm, Sweden

The heartwood of *Tetraclinis articulata* has been investigated. The following constituents have been identified: arabinose, carvacrol, thymohydroquinone, *p*-methoxythymol, thymoquinone, cedrol, hinokiol, hinokione, totarol and three new compounds, an *α,β*-unsaturated ketoalcohol $C_{16}H_{16}O_2$, the phenolic diterpene ketone totarolone $C_{20}H_{28}O_2$ and a diterpene hydroxy acid $C_{20}H_{30}O_3$. The wood also contains an *α,β*-unsaturated ketone, totarolenone, which is hydrogenated to totarolone. Evidence is presented for the presence of *β*- and *γ*-thujaplicin, cedrene and a sesquiterpene alcohol $C_{15}H_{24}O$.

Tetraclinis articulata (Vahl) Masters is a conifer growing in southern Spain and North Africa. It was formerly included in the northern hemispheric genus *Thuja* (*Th. articulata* Vahl) as well as in the southern hemispheric *Callitris* (*C. quadrivalvis* Ventenet).

Tetraclinis articulata is one of the few conifers possessing a lignin containing large amounts of syringyl groups. It is a somewhat isolated genus known from the tertiary period. The genus *Tetraclinis* is monotypic and for that reason it is, at the present stage, less suitable for chemotaxonomic purposes than large genera such as *e.g.*, *Pinus* and *Juniperus*. However, we have included it in our studies because we thought that it might be of some interest to compare its heartwood chemistry with that of other genera of the family Cupressaceae.

Long ago Grimal [1] subjected the steam volatile oil obtained from the fragrant, resistent wood to a brief investigation and isolated carvacrol, thymohydroquinone, thymoquinone and a neutral levorotatory oil.

In this preliminary examination we extracted with acetone the milled heartwood from a tree grown in Morocco. The extract was divided into ether-soluble and ether-insoluble products (I and II, respectively). From II a little arabinose was obtained by extraction with water. Fraction I was further divided into products soluble (III) or insoluble (IV) in light petroleum. From the latter thymohydroquinone was isolated. Fraction III was subjected to steam

* Part 41, *Tetrahedron* **16** (1961) 255 .

distillation and a volatile (V) and a non-volatile (VI) fraction were obtained. The volatile material was shaken successively with sodium bicarbonate and sodium hydroxide solutions yielding a very small, strongly acid fraction (not investigated) and a weakly acid fraction from which carvacrol and *p*-methoxythymol were isolated. The presence of *β*- and *γ*-thujaplicin was demonstrated by paper chromatography.

The neutral fraction (from V) contained thymoquinone and cedrol as well as a liquid which appeared to be a complex mixture of sesquiterpenes similar to many of the "natural cedrene" fractions described by various authors [2]. A gas chromatographic investigation showed the presence of one major and several minor components, none of which, apparently, corresponded to longifolene, thujopsene or cuparene. A small amount of a crystalline substance $C_{10}H_{16}O_2$, m.p. 70°, was also obtained from this fraction. It appears to be an *α,β*-unsaturated ketone containing a hydroxyl group and possibly a monosubstituted vinyl group. There was also a sesquiterpene alcohol which owing to its similarity to cedrol could not be isolated in a pure form, but which furnished a crystalline 3,5-dinitrobenzoate. The composition of this derivative indicated that the sesquiterpene might have the composition $C_{15}H_{24}O$.

The non-steam-volatile fraction VI was similarly divided into strong acids, weak acids and neutral compounds. From the weak acid fraction a very small amount of a diterpene acid $C_{20}H_{30}O_3$, m.p. 260—263°, was obtained. The infrared and ultraviolet spectra indicated that the compound contained a hydroxyl and a carboxyl group and at least one double bond (possibly an unsymmetrically disubstituted vinyl group). Acetylation gave what appeared to be a lactone acetate and an acid acetate. The amount isolated was too small for further investigation.

By a combination of distillation and chromatography, a surprisingly large amount of totarol [3] was isolated from the large neutral fraction (from VI). There were also small amounts of hinokiol and hinokione as well as a mixture of ketonic compounds which has not yet been separated into its components. According to its optical properties and hydrogenation experiments this ketone mixture appeared to consist of two closely related ketophenols, one being a simple ketone and the other an *α,β*-unsaturated ketone. They were called totarolone and totarolenone, respectively. The ketonic diterpenoids were also obtained from the light petroleum soluble fraction III by distillation and extraction of the high boiling fraction with a Girard reagent.

When the totarolone-totarolenone mixture was hydrogenated under mild conditions pure totarolone was obtained in almost quantitative yield.

The structures of hinokiol and hinokione as well as of totarolone and totarolenone have been discussed in earlier preliminary communications [4,5].

No compounds characteristic of *Callitris* have been obtained from *Tetraclinis* which shares with *Thuja* some tropolones. *Thuja*, however, appears to be characterised by sesquiterpenes belonging to the "*trans*-farnesyl group". *Tetraclinis* contains cedrol (*cis*-farnesyl type) like *Platycladus* (= *Biota*), *Chamaecyparis*, *Juniperus* and several other genera of the order Cupressales. Thymohydroquinone occurs in *Tetraclinis* as well as in *Juniperus*. *p*-Methoxythymol has been found in *Calocedrus* (Syn. *Heyderia* and *Libocedrus*), and carvacrol in several tropoloniferous genera. All these characteristics [6] indicate

affinities between *Tetraclinis* and the northern genera of the family Cupressaceae.

From a chemical point of view the co-occurrence of normal and rearranged diterpene phenols such as hinokiol and totarol is of particular interest and certainly indicates biosynthetic interrelations. Such interrelations have already been suggested by Wenkert *et al.*[7]

EXPERIMENTAL

Extraction. Milled wood (8 kg) was extracted continuously with acetone for 24 h. Half of the extract was used for preliminary studies. The acetone was evaporated and the dark brown product poured very slowly into ether (7 l) under vigorous stirring to give an ether soluble (I) and an insoluble (II) product. The precipitate (II) was ground with ether (returned to I) and then with water (insoluble material 64 g). The aqueous extract was treated with charcoal and evaporated to dryness and the residue crystallised from methanol-ethanol (1:1) giving arabinose (0.1 g).

The ether solution (I) was evaporated, yielding a tar (260 g). This was stirred vigorously with light petroleum (5 l). Soluble: (III), insoluble (120 g): (IV). Fraction (III) was evaporated and steam-distilled to give a volatile (V) and a non-volatile fraction (VI). The volatile products were mixed with light petroleum and extracted successively with 5 % sodium bicarbonate and 2 N potassium hydroxide solutions, giving a strongly acid fraction (traces), a weakly acid fraction (VII) (3.5 g) and a neutral fraction (VIII) (68 g). The non-volatile fraction (VI) was dissolved in ether and similarly divided into strongly acid (1.5 g), weakly acid (IX) (13 g) and neutral products (X) (157 g).

Alternatively the solution III was directly divided into neutral products, weak acids and strong acids.

Fraction VII was examined by paper chromatography using dimethyl sulphoxide impregnated paper. Spots were observed corresponding to carvacrol, β-thujaplicin, γ-thujaplicin (trace) and *p*-methoxythymol (or *p*-methoxycarvacrol). The presence of tropolones was also demonstrated by the formation of chloroform-soluble copper complexes.

Fraction VII (545 mg) was dissolved in light petroleum (10 ml), absorbed on silica gel (30 g) and eluted with benzene. The first eluate (60 ml) gave 40 mg, and the second (110 ml) 352 mg, of oil. The latter was converted into a mixture of phenoxyacetic acids which was fractionally crystallised to give carvacroxyacetic acid, m.p. and mixed m.p. 153–155°, and *p*-methoxythymoxyacetic acid, m.p. and mixed m.p. 135–137°. The I.R. spectra were identical with those of authentic specimens.

Part of the neutral fraction VIII (53 g) was distilled through a spinning band column. The following results were obtained (first figure = fraction number, second = boiling range at 10 mm, third = weight in g, fourth = n_D^{25}, fifth = $[\alpha]_D$):

1) 68–72°, 0.05, 1.4753, –; 2) 72–76°, 0.4, 1.4772, + 33°; 3) 76–82°, 0.2, 1.4819, –; 4) 82–86°, 6.2, –, –; 5) 86–91°, 0.55, 1.4982, –; 6) 91–94°, 0.8, –, –; 7) 94–101°, 1.1, 1.4972, –; 8) 101–106°, 0.4, 1.4975, –; 9) 106–110°, 2.4, 1.4979, –; 10) 110°, 19.7, 1.4982, –; 11) 110–120°, 1.7, –, –48.1°; 12) 120–122°, 0.7, –, –; 13) 122°, 4.2, –, –; 14) 122–127°, 0.3, –, –8.9°; 15) 127°, 2.3, –, –19.2°; 16) 127–129°, 1.0, –, –40.6°; 17) 129–142°, 0.6, –, –6.5°; 18) 142–145°, 0.35, –, –; 19) 145°, 4.1, –, –2.9°; 20) 145°, 2.05, –, –;

Fraction 4 solidified on cooling to yellow crystals which were recrystallised from light petroleum, m.p. and mixed m.p. with thymoquinone 46–47°.

Fraction 6 partially crystallised on cooling. The product was recrystallised from light petroleum to give colourless needles, m.p. 70° (unchanged after sublimation), $[\alpha]_D$ + 78°, ν_{max} 900, 990, 1060, 1685 and 3450 cm^{-1}. λ_{max} 234 mμ (ε 8350). (Found: C 72.0; H 9.5. $C_{10}H_{16}O_2$ requires: C 71.4; H 9.6). The amount was insufficient for further investigation.

Fraction 10 was slightly yellowish and was dissolved in light petroleum (10 ml) and absorbed on a column of alumina. Elution with light petroleum gave a colourless oil (17.7 g) followed by thymoquinone (0.8 g). Redistillation of the oil gave a constant boiling main fraction (115°/12 mm), $[\alpha]_D$ –54.4° ($CHCl_3$). The infrared spectrum was similar to that of the neutral "cedrene" described by Naves [2]. The G.L.C.-examination

showed a main peak and several minor peaks, none of which corresponding to longifolene, thujopsene or cuparene.

The I.R. and U.V. spectra of fraction 13 indicated the presence of an aromatic hydrocarbon. It was re-chromatographed on alumina (200 g). The main fraction (3.5 g) was distilled and had b.p. 58–60/0.05 mm, $[\alpha]_D$ −16°, n_D^{25} 1.5068.

Fraction 19 partially crystallised on cooling. A sample (4 g) was dissolved in light petroleum (20 ml) and adsorbed on a column of basic alumina (220 g). The column was eluted successively with light petroleum, light petroleum-benzene and benzene. 32 subfractions were collected. Fraction 19 (1–3) contained a mixture of hydrocarbons, $[\alpha]_D$ −20°. Fraction 19 (10–21) gave cedrol which was recrystallised from acetonitrile $[\alpha]_D$ + 6.5°. M.p. and mixed m.p. with pure cedrol 88–89°.

Fraction 20 showed a strong hydroxyl band. After removal of primary alcohols with phthalic anhydride the residual oil was treated with 3,5-dinitrobenzoyl chloride in pyridine, giving a crystalline product which was recrystallised from ligroin, m.p. 152–153°. It was probably a sesquiterpene alcohol 3,5-dinitrobenzoate. (Found: C 64.0; H 6.8; N 6.6. $C_{22}H_{26}O_6N_2$ requires: C 63.8; H 6.3; N 6.8.)

Fraction IV. This fraction was dissolved in ether, extracted with 1 N potassium hydroxide solution and the aqueous phase was acidified. The acid product was treated with hot benzene and the solution obtained evaporated to a small volume. A mixture of an oil and a crystalline compound was obtained, and the latter was identified as hydrothymoquinone, m.p. and mixed m.p. 145–147°.

The weakly acid *fraction (IX)* was dissolved in light petroleum. A solid (110 mg) slowly separated. This was recrystallised from benzene, m.p. 230–240°. The product was sublimed along a temperature gradient and the main fraction (80 mg) was recrystallised from methanol, giving colourless crystals, m.p. 260–263°, $[\alpha]_D$ −9° (in EtOH), λ_{max} 208 mμ (ε 11 500). ν_{max} 906, 1000, 1635, 1665, 3440 and 1705 cm^{-1}. (Found: C 74.4; H 9.3. $C_{20}H_{30}O_3$ requires: C 75.4; H 9.5.) This compound (50 mg), fused sodium acetate (150 mg), and acetic anhydride (2 ml) were heated on a steam bath for 2 h. Addition of ice water gave a precipitate which was recrystallised from methanol, yielding a mixture of large crystals and a crystal powder. The large crystals were separated and recrystallised from methanol to give a lactone acetate, m.p. 213–215°. (ν_{max} 1000, 1245, 1630 (weak), 1730 and 1800 cm^{-1}). The crystal powder was recrystallised from ligroin three times giving white crystals (acid acetate), m.p. 210–213°. ν_{max} 1230, 1635, 1695, and 1730 cm^{-1}. (Found: C 73.6; H 8.8. $C_{22}H_{33}O_4$ requires: C 73.3; H 8.95.)

The "neutral fraction" (X) consisted of a dark pitch (90 g). It was dissolved in light petroleum (200 ml) and adsorbed on neutral alumina (1.6 kg). The column was successively eluted with light petroleum, benzene, ether, ethyl acetate, acetone, and methanol.

The light petroleum eluate (5 l) gave only 1 g of a resin which was not further investigated. The benzene eluate (7.5 l) gave 32.4 g of a resin which after several weeks deposited crystals, which were distilled in a vacuum (b.p. 130–135/0.2 mm) yielding a solid, m.p. 115–128°. Recrystallisation from light petroleum gave colourless crystals, m.p. 127–128°, not depressed on admixture with authentic totarol, $[\alpha]_D$ + 45° (EtOH). The I.R. spectra of the two samples were superimposable. The substance gave totarol acetate, m.p. and mixed m.p. 124–125°, $[\alpha]_D$ + 51.6° ($CHCl_3$).

Ether (2.5 l) eluted a resin (12.5 g) containing mainly totarol and a small amount of ketonic material. More ether (9.5 l) eluted 25 g of a resin which was triturated with the same amount of light petroleum, yielding a crystalline product (2 g). The analysis of this product showed that it consisted of approximately equal amounts of totarolone ($C_{20}H_{28}O_2$) and totarolenone ($C_{20}H_{26}O_2$), (ν_{max} 806, 815, 1585, 1652, 1680 and 3380 cm^{-1}). Catalytic hydrogenation in ethanol in the presence of a palladium-charcoal catalyst gave a product, totarolone, m.p. 188–189.5°, $[\alpha]_D$ + 101.5° (in EtOH). (ν_{max} 810, 1590, 1685 and 3380 cm^{-1}; λ_{max} 208 mμ (ε 37 700), 222 shoulder (8000), 281 (1900) and 286 (1900)). (Found: C 79.9; H 9.3. $C_{20}H_{28}O_2$ requires: C 80.0; H 9.4.) The acetate (acetic anhydride-pyridine), crystals from methanol, had m.p. 113–115°, $[\alpha]_D$ + 96.6° (EtOH); (ν_{max} 805, 1210, 1704 and 1755 cm^{-1}). (Found: C 77.7; H 8.8. $C_{22}H_{30}O_3$ requires: C 77.2; H 8.9.) The 2,4-dinitrophenylhydrazone, crystals from ethanol, had m.p. 192–194°. (Found: C 65.2; H 6.6; N 11.45. $C_{26}H_{32}N_4O_5$ requires: C 65.0; H 7.0; N 11.6.)

Elution with ethylacetate (3 l) gave a resin (23 g) which was dissolved in light petroleum and kept in an ice box. A crystalline solid (5 g) was deposited which was recrystalli-

sed three times from ethanol and six times from benzene, yielding hinokione (0.9 g), m.p. 191–192°, $[\alpha]_D$ + 111.9° (in EtOH); (ν_{max} 1620, 1695 and 3440 cm^{-1}); λ_{max} 208 mμ (ε 16 900), 219 (7500) and 284 (2400) in ethanol, and 242 (ε 7100), 306 (ε 4590) in 0.1 N sodium ethoxide. (Found: C 80.1; H 9.3. Calc. for $C_{20}H_{28}O_2$: C 80.0; H 9.4.) The acetate, (pyridine-acetic anhydride), m.p. and mixed m.p. with an authentic sample of hinokione acetate 120–122°. ν_{max} 1215, 1702 and 1759 cm^{-1}; λ_{max} 208 mμ (ε 12300), 269 (1200) and 277 (1300). (Found: C 77.1; H 8.8. $C_{22}H_{30}O_3$ requires: C 77.2; H 8.8). Hinokione 2,4-dinitrophenylhydrazone: crystals from ethanol, m.p. 234–236°.

The combined ethanol-benzene mother liquors were evaporated and the residue dissolved in benzene and adsorbed on silica gel (100 g). Elution with benzene furnished small amounts of totarol. Elution with benzene-ether (98:2) gave a totarolone-totarolenone mixture, further elution with benzene-ether (95:5), hinokione (1.1 g) and with benzene-ether (70:30), hinokiol (30 mg) which was recrystallised from benzene. M.p. and mixed m.p. with an authentic sample 240–242°. Superimposable I.R. spectra (peaks at 1030, 3310 and 3560 cm^{-1}).

A fraction (600 g) corresponding to the "neutral fraction" X obtained from a new batch of wood was distilled in a vacuum giving the following fractions.

1) B.p. 80–82°/0.5 mm, (100 g); 2) 88–100°/0.1 mm), (24 g); 3) 98–120°/1 mm, (71 g); 4) 120–128°/0.5 mm, (17 g); 5) 120–139°/0.2 mm, (32 g); 6) 142–170°/0.2 mm, (142 g); 7) 173–175°/0.2 mm, (86 g); 8) a residue (110 g).

Fraction 7 was treated with Girard P reagent (15 g) in ethanol (200 ml) containing acetic acid (30 ml) and a mixture (2.5 g) of carbonyl compounds was isolated. This was hydrogenated in ethanol over palladium on charcoal and the resulting product dissolved in benzene and chromatographed on silica gel using benzene-ether (98:2) as the eluting agent. Totarolone (1.5 g) was obtained. Further elution with benzene-ether (95:5) gave hinokione (1 g).

The non-ketonic products were added to fraction 6 and this mixture was dissolved in 300 ml of light petroleum. On cooling crystallisation took place. The crystals were recrystallised from light petroleum and ethanol, giving totarol (39 g). The mother liquor contained mainly totarol (as shown by the I.R. absorption).

Fractions 4 and 5 were combined and re-distilled. The main fraction, b.p. 90–94°/0.2 mm, was cedrol. The fraction, b.p. 94–105°, contained mainly sesquiterpene alcohols and a compound which according to its I.R. spectrum (ν_{max} 1645, 1685, 2700 and 3620 cm^{-1}) was probably an α,β-unsaturated aldehyde. However, no pure compounds have yet been obtained from this material by chromatography on alumina.

The residue from the distillation of fractions 4 and 5 was dissolved in light petroleum. On standing in a refrigerator, a crude mixture (35 g) of totarolone-totarolenone, hinokione and a trace of hinokiol separated. Part of this mixture (4.4 g) was sublimed in a high vacuum to give a slightly coloured product (4.0 g). It was dissolved in benzene and chromatographed on silica (150 g) using benzene-ether (2, 5, and 25 % ether) as eluents. A totarolone-totarolenone mixture (1.8 g), hinokione (1.5 g) and hinokiol (70 mg) was obtained.

Acknowledgement. This work has been sponsored by the *Office of Research and Development, U.S. Department of Army* through its European Office. We thank Ingeniero J. B. Martinez, Madrid, for the wood samples used in this investigation and Dr. I. Wellings for checking the English of the manuscript.

REFERENCES

1. Grimal, E. *Compt. rend.* **139** (1904) 927.
2. Cf. *e.g.*, Naves, Y. R. *Helv. Chim. Acta* **26** (1943) 302.
3. Simonsen, J. L. and Barton, D. H. R. *The Terpenes*, Vol. III, Cambridge 1952, p. 358.
4. Chow, Y.-L. and Erdtman, H. *Proc. Chem. Soc.* **1960** 174.
5. Chow, Y.-L. and Erdtman, H. *Acta Chem. Scand.* **14** (1960) 1852.
6. Cf. Erdtman, H. *Proc. 4th Intern. Congr. Biochem.* Vienna 1958, *I.U.B. Symposium series* Vol. 4, *Biochemistry of wood.*
7. Wenkert, E. and Jackson, B. G. *J. Am. Chem. Soc.* **80** (1958) 211.

Received December 31, 1961.

ACTA CHEMICA SCANDINAVICA 16 (1962) 1296–1300

The Chemistry of the Natural Order Cupressales

43 *. The Structure and Configuration of Hinokiol and Hinokione **

YUAN-LANG CHOW and H. ERDTMAN

Organisk-kemiska Institutionen, Kungl. Tekniska Högskolan, Stockholm, Sweden

The structures of hinokiol and hinokione have been revised. The oxygen atom of ring A is in the 3-position. The alcoholic hydroxyl group in hinokiol is β-oriented. The A/B-ring junction is the normal 5*a*,10β.

The phenolic diterpene alcohol hinokiol was first isolated from the wood of *Chamaecyparis obtusa* ("hinoki") by Yoshiki and Ishiguro [1a–c]. It has later been encountered in this laboratory in two *Athrotaxis* species [2a], in *Cupressus torulosa* [2b] and in *Tetraclinis articulata* [2c]. Hinokione is the corresponding ketone and a frequent congener of hinokiol [1a,b].

Structures *1a* and *1b* have been suggested for hinokiol and hinokione, respectively [3]. The carbon skeleton has been corroborated by an interrelation with ferruginol [4] but the configuration remained unknown and the location of the secondary hydroxyl group at C_2 rested on inconclusive evidence and appeared improbable to us. In this report we confirm the new structures *2a* and *2b* for hinokione and hinokiol, respectively.

Clemmensen reduction of hinokione afforded ferruginol (*2c*) of known structure and configuration [5]. This shows that rings A and B are *trans*-fused.

Bromination of hinokione acetate (*2d*) furnished a dibromo derivative (*3*). The optical properties of this compound indicated that both bromine atoms were attached to the carbon atom next to the carbonyl group [6]. Dehydrobromination with lithium bromide in dimethylformamide gave an amorphous product, which on boiling with activated zinc and alcohol gave 1,2-didehydro-2-bromohinokione (*4*) and finally the α,β-unsaturated ketone 1,2-didehydrohinokione (*5*) ***. Both (*4*) and (*5*) gave hinokione on mild catalytic reduction.

---

* Part 42, *Acta Chem. Scand.* **16** (1962) 1291.

** Preliminary communication. *Proc. Chem. Soc.* **1960** 174.

*** The debromination of *3* might involve the formation of a zinc-organic intermediate from which ZnBrOEt is released, the latter causing the observed deacetylation. Totarol acetate was not deacetylated under similar conditions.

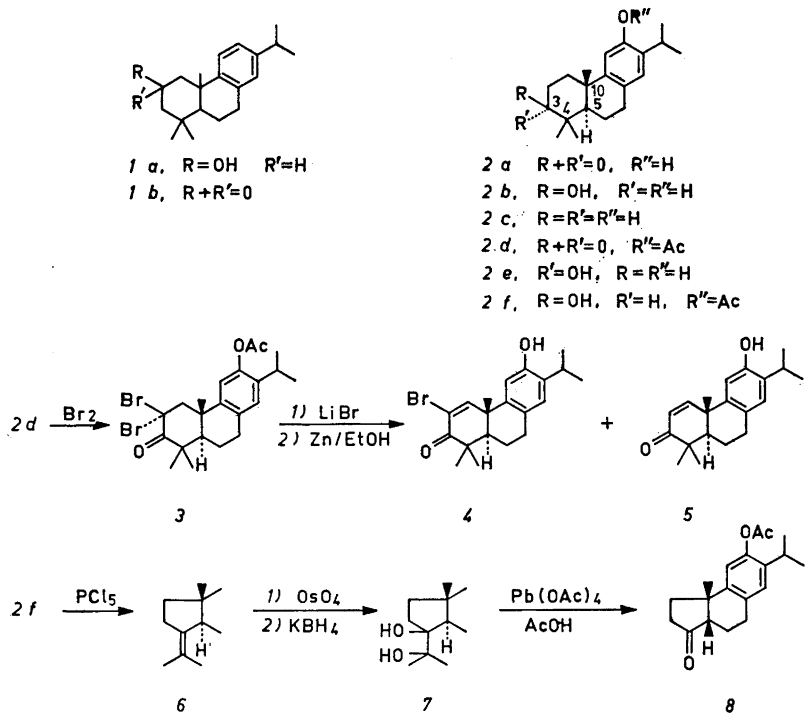

The formation of an α,β-unsaturated ketone would be possible only if the alcoholic hydroxyl group were in position 1 or 3 but not in position 2. The A-ring of dibromohinokione is probably in the boat form, thus relieving the non-bonded interactions between Br at C_2 and the methyl groups at C_4 and C_{10} (*Cf.* Ref.[7]).

Catalytic hydrogenation of hinokione gave isohinokiol (*2e*) and a small amount of hinokiol, whereas reduction with potassium borohydride gave hinokiol in good yield. This indicates that the alcoholic hydroxyl group in hinokiol is equatorial and that in isohinokiol axial [8,9].

Comparison of the molecular rotation of hinokiol and isohinokiol derivatives with those of the corresponding ferruginol derivatives shows that the shifts in rotation are positive for hinokiol and negative for isohinokiol (*cf.* Table 1). By analogy with the similar effects known from 3-hydroxy-triterpenes having

Table 1. Molecular rotation shifts (Molecular rotations, in ethanol within brackets).

Hinokiol diacetate (272) — Ferruginol acetate (188) = + 84°
Isohinokiol diacetate (109) [1b] — Ferruginol acetate (188) = —79°
Hinokiol methylether * acetate (283) — hinokiol methylether * (188) = + 95°
Isohinokiol methylether * acetate (42) — isohinokiol methylether * (144) = —102°

* Phenolic hydroxyl methylated.

$a_{\blacktriangle}^{\blacksquare}5\alpha,10\beta$-absolute configuration [10], this indicates that the alcoholic hydroxyl group in hinokiol is 3β and in isohinokiol 3α.

Treatment of the mono (phenol) acetate of hinokiol (*2f*) with phosphorus pentachloride gave a product possessing an I.R. absorption indicating that dehydration had occurred and that the acetyl group was still present. It therefore appeared that the molecule had undergone the retropinacol rearrangement (*2f—6*) frequently observed in the 3β-hydroxy triterpene series [8,11]. The product was therefore treated with osmium tetroxide and the osmate cleaved with potassium borohydride. The material obtained was subjected to a re-acetylation with acetic anhydride and pyridine to ensure that the phenolic hydroxyl was protected and the product (*7*) oxidised with lead tetraacetate. A high yield (63 %) of acetone was obtained. It is obvious, therefore, that the reaction had proceeded normally and this was confirmed by the fact that the non-volatile fission product exhibited the I.R. absorption expected for a cyclopentanone derivative. The product was re-acetylated and purified by sublimation giving a crystalline semi-pure product (*8*) in small yield which showed a positive Cotton effect similar to that of *cis*-oxotrisnorlupane [11]. (Inversion at C_5 occurred during the oxidation). It is obvious from these results that the alcoholic hydroxyl group in hinokiol is in position 3 and that it is β-oriented. The location of this hydroxyl group has been definitely established by a synthesis of D,L-hinokiol methyl ether recently carried out by one of us [12].

Having the conventional steroid absolute configuration, hinokione should exhibit a positive Cotton effect in analogy with lanost-8-en-3-one [13]. As seen from Table 2 there appears to be a positive peak at 302 mμ but the trough is masked.

Table 2. Specific rotations at different wavelengths.

Hinokione	+ 160°	(450)	+ 1430°	(302)	+ 1375°	(300)
Lanost-8-en-3-one	+ 74°	(589)	+ 610°	(300)	+ 498°	(277.5)
Hinokiol	+ 132°	(450)	+ 332°	(312)		
Ferruginol acetate	+ 118°	(450)	+ 310°	(312)		
Totarolone	+ 167°	(400)	+ 1130°	(312)	+ 130°	(300)

EXPERIMENTAL

Hinokione from the heartwood of *Tetraclinis articulata* had m.p. 191—192°, $[\alpha]_D$ + 111.9° (in EtOH), ν_{max}^{CO} 1695 and ν_{max}^{OH} 3440 cm^{-1}. λ_{max} 208 mμ (ε 16 900); 219 (7480), 284 (2440) (in ethanol); 226 mμ (16 900), 242 (7100), 306 (4600) (in 0.1 N NaOEt-EtOH).

Reduction of hinokione. (a) *With potassium borohydride.* A solution of hinokione (575 mg) in methanol (40 ml) was added to a suspension of potassium borohydride (190 mg) in a mixture of methanol (10 ml), water (1 ml) and 2 N sodium hydroxide solution (8 drops). The mixture was left at room temperature for 10 h. On dilution with water (50 ml) and neutralisation with 2 N sulphuric acid crystals of hinokiol separated (yield 530 mg). After three recrystallisations from benzene the melting point was 240—242°, undepressed on admixture with an authentic specimen of hinokiol.

Further addition of water gave a second crop of crystals (5 mg), m.p. 200—209°. This product was slightly impure isohinokiol. However, chromatography on silica gel failed to give a purer product.

(b) *By catalytic hydrogenation.* Hinokione (100 mg) in glacial acetic acid (20 ml) was hydrogenated in the presence of a platinum oxide catalyst (5 mg) for 4.5 h. After filtration and evaporation of the solvent in a vacuum, a solid, m.p. 205—230°, was obtained. On cooling a hot benzene solution of this product a first crop of crystals was obtained

which, after recrystallisation from benzene, gave pure hinokiol (22 mg). From the mother liquor crude isohinokiol was obtained, which after three crystallisations from benzene melted at 206–209°. (Lit.[1a] 204°.) Yield 50 mg. (ν_{max} 1003, 3240 and 3510 cm^{-1}.)

Clemmensen reduction of hinokione. A mixture of hinokione (320 mg), amalgamated zinc, acetic acid (10 ml) and concentrated hydrochloric acid (3 ml) was refluxed for 5 h, 0.5 ml concentrated hydrochloric acid being added after each hour. The product was dissolved in benzene and purified by filtration through a column of silica gel. The resinous product (270 mg) was acetylated, yielding a resin which on sublimation followed by recrystallisation afforded ferruginol acetate, m.p. 82–84°, $[\alpha]_D$ + 55.1° ($CHCl_3$) identified by direct comparison with an authentic sample.

2,2-Dibromohinokione acetate. A solution of bromine (600 mg) in acetic acid (7 ml) was added drop by drop over 2 h to a cooled solution of hinokione acetate (400 mg) in acetic acid (20 ml containing 2 drops of acetic acid saturated with hydrogen bromide). After 30 min the mixture was poured into water and excess bromine destroyed with sodium thiosulphate. The product (590 mg, m.p. 174–179°) was recrystallised from methanol. Repeated recrystallisations did not change the melting point. (Found: C 54.4; H 6.0; Br 33.8. $C_{22}H_{26}Br_2O_3$ requires: C 52.8; H 5.6; Br 31.95.) ν_{max} 1724 and 1765 cm^{-1}. ν_{max} 208 mμ (ε 3000), 268 (1220), 277 (1230), 313 (97).

Dehydrobromination of 2,2-dibromohinokione acetate. The substance (550 mg), lithium carbonate (1 g) and lithium bromide (1 g) in dimethylformamide (20 ml, redistilled) was heated on the steam bath with stirring under dry nitrogen for 16 h. The solution was poured into 100 ml of cold water, giving a white precipitate. ν_{max} 1210, 1691 and 1762 cm^{-1}. A mixture of this material (460 mg), zinc dust activated with acetic acid (500 mg), and methanol (60 ml) was refluxed for 20 h. The filtrate was evaporated and the residue extracted with cyclohexane. On evaporation a solid (360 mg) was obtained. It was dissolved in benzene and chromatographed on silica gel (30 g), with benzene-ether (19:1) as eluent. On evaporation a solid (180 mg) was obtained which was recrystallised twice from benzene-cyclohexane and sublimed to give 2-bromo-1,2-didehydro-hinokione, m.p. 208–210°, $[\alpha]_D$ + 142° (EtOH). ν_{max} 1668 and 3460 cm^{-1}. λ_{max} 206 mμ (ε 32 300), 258 (11 100) and 283 (5600). (Found: C 64.0; H 6.9. $C_{20}H_{25}O_2Br$ requires: C 63.7; H 6.7.) With Brady's reagent an oil was obtained.

The column was now washed with benzene-ether, giving white crystals (166 mg). These were recrystallised once from benzene and twice from cyclohexane, yielding pure 1,2-didehydro-hinokione, m.p. 175–178°, $[\alpha]_D$ + 163° (EtOH). ν_{max} 1655 and 3280 cm^{-1}. λ_{max} 205 mμ (ε 23 600), 225 (18 900), 284 (3800). (Found: C 80.2; H 8.9; $C_{20}H_{26}O_6$ requires: C 80.5, H 8.8.)

2-Bromo-1,2-didehydro-hinokione was refluxed with zinc and methanol as above for 24 h. A quantitative yield of 1,2-didehydro-hinokione was obtained.

Hydrogenation of 2-bromo-1,2-didehydro-hinokione and of 1,2-didehydro-hinokione. 2-Bromo-1,2-didehydro-hinokione (10 mg) and palladium on charcoal (1 mg) in ethanol was shaken under hydrogen for 24 h. Hinokione (5 mg) was obtained. In the same manner 1,2-didehydro-hinokione also furnished hinokione.

Hinokiol monoacetate. (a) *From hinokiol.* A suspension of hinokiol (1 g) in a mixture of dry benzene (400 ml), acetic anhydride (7 ml) and pyridine (30 drops) was shaken at room temperature for 40 h. The solution obtained was shaken successively with dilute solutions of sodium carbonate, sulphuric acid and finally with water and evaporated. The solid residue was dissolved in benzene and chromatographed on silica gel (50 g). Benzene containing 0–2 % ether eluted a small amount of hinokiol diacetate. With 4 % ether the monoacetate (470 mg) was obtained. It was recrystallised from ether and sublimed, giving pure hinokiol monoacetate (2 *f*), m.p. 186–189°, $[\alpha]_D$ + 59.9° (in EtOH). ν_{max} 1025, 1220, 1730 and 3460 cm^{-1}. (Found: C 76.3; H 9.25. $C_{22}H_{32}O_3$ requires: C 76.7; H 9.4.) Pure ether, finally, eluted hinokiol (190 mg).

(b) *From hinokione acetate.* Hinokione acetate (30 mg) was dissolved in methanol (5 ml), water (2 drops) was added and the solution added to a suspension of potassium borohydride (25 mg) in methanol (2 ml) at room temperature. After 40 min, water (1 ml) and several drops of 2 N sulphuric acid were added with cooling in ice. Further addition of water (7 ml) precipitated a solid (23 mg) which when chromatographed as above furnished 11 mg hinokiol monoacetate (*2f*) and 8 mg of hinokiol.

Action of phosphorus pentachloride etc. on hinokiol monoacetate. A solution of hinokiol monoacetate (155 mg) in light petroleum (150 ml) was evaporated to 120 ml and cooled

in an ice bath to give a fine suspension. Phosphorus pentachloride (420 mg) was added with vigorous shaking. The mixture was kept in an ice box for one hour and then for 3 h at room temperature with occasional shaking. It was then washed successively with 5 % sodium carbonate solution and water. The organic phase was dried and evaporated. The residue was acetylated with acetic anhydride and pyridine. The product was chromatographed on a column of neutral alumina (5 g). Elution with benzene gave a resin (104 mg), $\nu_{max}^{CCl_4}$ 1205 and 1755 cm^{-1}.

A mixture of the above resin (70 mg), osmium tetroxide (100 mg), pyridine (1.5 ml) and dry ether (15 ml) was left in a dark place for 8 days. After removal of the solvents the residue was treated with potassium borohydride (250 mg) in methanol (10 ml) for 10 h. Dilution of the reaction mixture with water, neutralisation with 2 N sulphuric acid and extraction with ether gave a dark coloured extract which was dried and filtered through a silica column to give a purple solid (45 mg) from 250 ml of ether eluent. This solid was acetylated with acetic anhydride and pyridine at room temperature for 10 h, giving 45 mg of a glassy material exhibiting strong absorption at 1210, 1750 and 3400 (broad) cm^{-1}.

The product was treated with lead tetra-acetate (200 mg) in redistilled acetic acid (2 ml) for 12 h. The reaction mixture was warmed to effect solution. The acetone formed was collected by distillation and identified as the 2,4-dinitrophenylhydrazone. (Yield 17 mg).

The residue from the distillation was extracted with ether giving a non-crystalline solid which was acetylated with pyridine and acetic anhydride. The product was chromatographed on neutral alumina using benzene as eluent to give a non-crystalline solid. $\nu_{max}^{CCl_4}$ 1210, 1740 and 1755 cm^{-1} as expected for a compound of structure *8*. The solid gave a red colour and then an oily precipitate with Brady's reagent and on sublimation gave ill-defined crystals, m.p. 104—112°.

Acknowledgement. This work has been sponsored by the *Office of Research and Development, U.S. Department of Army* through its European office. We thank Professor Klyne for the R.D. curves and Dr. I. Wellings for reading the manuscript.

REFERENCES

1. (a) Yoshiki, Y. and Ishiguro, T. *J. Pharm. Soc. Japan* **53** (1913) 1. (b) Simonsen, J. L. and Barton, D. H. R. *The Terpenes*, Vol. **III**, Cambridge University Press, 1952, p. 356. (c) *Ibid.*, p. 355.
2. (a) Erdtman, H. and Vorbrüggen, H. *Acta Chem. Scand.* **14** (1960) 2161. (b) Barreto, H. and Enzell, C. *Ibid.* **15** (1961) 1313. (c) Chow, Y.-L. and Erdtman, H. *Ibid.* **16** (1962) 1291.
3. Fieser, L. and Fieser, M. *Natural Products Related to Phenanthrene*. 3rd Ed., New York 1949, p. 69.
4. Brandt, C. W. and Neubauer, L. G. *J. Chem. Soc.* **1939** 1031; Campbell, W. P. and Todd, D. *J. Am. Chem. Soc.* **62** (1940) 1287.
5. (a) Narashima Rao, P. *Tetrahedron* **4** (1958) 294. (b) King, T. J. and Topliss, L. G. *J. Chem. Soc.* **1957** 573.
6. (a) Jones, R. N. *et al. J. Am. Chem. Soc.* **74** (1952) 2828. (b) Allinger, N. L. and Allinger, J. *Ibid.* **80** (1958) 5476.
7. Barton, D. H. R., Lewis, D. A. and McGhie, J. F. *J. Chem. Soc.* **1957** 2907; Villotti, R., Ringold, H. J. and Djerassi, C. *J. Am. Chem. Soc.* **82** (1960) 5693 and the previous paper quoted therein.
8. Barton, D. H. R. *J. Chem. Soc.* **1953** 1027; *Experientia* **6** (1950) 316.
9. Dauben, W. G., Blanz, Jr., E.J., Jiu, J. and Micheli, R. A. *J. Am. Chem. Soc.* **78** (1956) 3752.
10. Klyne, W. and Stork, W. M. *J. Chem. Soc.* **1954** 1979.
11. Baddeley, G. V., Halsall, T. G. and Jones, E. R. H. *J. Chem. Soc.* **1960** 1715.
12. Chow, Y.-L. *Acta Chem. Scand.* **14** (1960) 1672.
13. Djerassi, C. *et al. J. Am. Chem. Soc.* **80** (1958) 4001; **81** (1959) 4587.

Received December 31, 1961.

ACTA CHEMICA SCANDINAVICA 16 (1962) 1301–1304

The Chemistry of the Natural Order Cupressales

44 *. The Synthesis of DL-Hinokione Methyl Ether **

YUAN-LANG CHOW

Organisk-kemiska Institutionen, Kungl. Tekniska Högskolan, Stockholm, Sweden

A synthesis of DL-hinokione methyl ether from 2-isopropylphenol is described.

The phenolic diterpene ketone hinokione which has now been isolated from several conifer species [1] has recently been shown to possess structure *8* (R = H) [2]. A synthesis of DL-hinokione methyl ether (*8*; R = CH_3) has now been carried out following the general lines of Howell and Taylor's perhydrophenanthrene synthesis [3].

6-Isopropyl-7-methoxy-*a*-tetralone (*3*) was prepared from 2-isopropylanisole and succinic acid anhydride via the intermediates *1* and *2*. The tetralone reacted smoothly with methyl magnesium iodide giving a tertiary alcohol which was dehydrated directly to 1-methyl-6-isopropyl-7-methoxy-3,4-dihydronaphthalene (*4*) with potassium hydrogen sulphate. Epoxidation of *4*

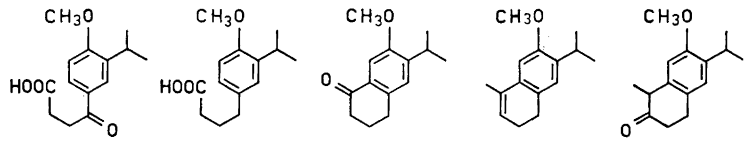

1 *2* *3* *4* *5*

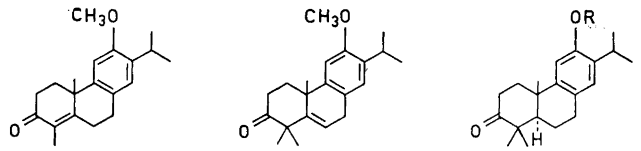

6 *7* *8*

* Part 43. *Acta Chem. Scand.* **16** (1962) 1296.
** Preliminary communication. *Acta Chem. Scand.* **14** (1960) 1672.

and subsequent treatment with dilute sulphuric acid [3] gave liquid 1-methyl-6-isopropyl-7-methoxy-β-tetralone (*5*). Condensation of the β-tetralone with β-chloropentan-3-one in the presence of sodium hydride [3] gave the crystalline α,β-unsaturated ketone *6* which was methylated with methyl iodide and potassium *t*-butoxide [4] to give a non-crystalline resin which on chromatography yielded DL-Δ^5-hinokione methyl ether (*7*) and an isomer (compound A). The methyl ether (*7*) was smoothly hydrogenated in ethanol solution in the presence of a palladium catalyst and a little acetic acid to give DL-hinokione methyl ether. The I.R. spectra of synthetic and natural hinokione methyl ether were superimposable.

EXPERIMENTAL

U.V. spectra were taken in 95 % ethanol solution and I.R. spectra in potassium bromide discs unless otherwise stated. Melting points were taken on a Kofler block.

2-Isopropyl-4-succinoylanisole (1). A solution of succinic anhydride (65 g) and 2-isopropylanisole (80 g) in nitrobenzene (50 ml) was added during one hour to a cold, mechanically stirred solution of aluminium chloride (170 g) in nitrobenzene (400 ml). The mixture was left at room temperature for 10 h and then poured into ice-water (1.5 l) containing hydrochloric acid (100 ml). The nitrobenzene was removed by steam distillation and the resulting organic residue cooled to give a solid. The product was dissolved in hot 10 % sodium carbonate solution (1 l). On cooling the sodium salt precipitated. The salt was collected and washed with cold water and ether. Acidification of the hot aqueous solution gave the keto-acid *1* (115 g). Crystals from ethanol, m.p. 133—135°. (Found: C 66.8; H 7.1. $C_{14}H_{18}O_4$ requires: C 67.2; H 7.25.)

2,4-Dinitrophenylhydrazone, deep red crystals from ethanol, m.p. 85—88°. (Found: C 55.6; H 5.4; N 12.9. $C_{20}H_{22}O_7N_4$ requires: C 55.8; H 5.15; N 13.0.)

4-(3-Carboxypropyl)-2-isopropylanisole (2). A mixture of crude keto-acid *1*, amalgamated mossy zinc (220 g), water (150 ml), concentrated hydrochloric acid (350 ml), and toluene (200 ml) was boiled under reflux for 36 h with constant stirring. Concentrated hydrochloric acid (25 ml) was added every 6 h. The toluene phase was separated and the aqueous phase extracted with ether. The combined organic phases were extracted with 3 N sodium hydroxide solution. The acid products were remethylated with dimethyl sulphate and alkali. The acid was distilled, b.p. 142—145°/0.4 mm. (Yield 95 g or 75 % calculated on 2-isopropyl anisole.) The acid crystallised on cooling. Crystals from ethanol, m.p. 31—34°. (Found: C 71.4; H 8.6. $C_{14}H_{20}O_3$ requires: C 71.2. H 8.5 %.)

5-Isopropyl-6-methoxy-α-tetralone (3). The acid *2* (80 g) and thionyl chloride (160 g) were boiled under reflux for one hour and the excess thionyl chloride was then removed by distillation under reduced pressure. Tetrachloroethane (350 ml) was added to the cold solution, followed by aluminium chloride (75 g) in one lot. When the vigorous evolution of hydrogen chloride had subsided, the mixture was stirred and cooled in an ice bath for one hour. The mixture was left at room temperature for 10 h and then poured into dilute hydrochloric acid. The organic layer was distilled with steam and the residue extracted with ether. After evaporation of the ether, the product was distilled under vacuum giving a main fraction, b.p. 136—138°/1 mm; λ_{max} 210 mμ (ε 13 800), 225 (19 700) and 263 (12 700); ν_{max}^{film} 1675 and 1260 cm^{-1}.

The red 2,4-dinitrophenylhydrazone (from ethyl acetate-ethanol) had m.p. 198—200°. (Found: C 60.2; H 5.5; N 13.8. $C_{20}H_{22}O_5N_4$ requires: C 60.3; H 5.6; N 14.1 %).

1-Methyl-6-isopropyl-7-methoxy-3,4-dihydronaphthalene (4). The α-tetralone (55 g) in ether (200 ml) was added to a Grignard reagent made from magnesium (12.5 g) and methyl iodide (36 ml) in ether (450 ml) and the mixture was boiled under reflux for 5 h. The product was isolated in the usual manner. A mixture of the dry product and fused potassium hydrogen sulphate (70 g) was heated at 120—150° for 2.5 h. The organic material was dissolved in light petroleum and washed with water. After evaporation of the solvent the product was distilled in vacuum. A main fraction, b.p. 101—104°/0.3 mm, was obtained (42 g). ν_{max} 835, 1613 and 1630 cm^{-1}.

1-Methyl-6-isopropyl-7-methoxy-β-tetralone (5). Solutions of compound *4* (40.7 g) in chloroform (250 ml) and perbenzoic acid (27.2 g) in chloroform (350 ml) were mixed at −5° and the mixture kept at 0° for 10 h. The solution was washed with cold 1 N sodium hydroxide and water and the solvent removed by distillation. To the residue a mixture of ethanol (450 ml), water (200 ml), and concentrated sulphuric acid (50 ml) was added and the solution boiled under reflux for 4 h. The reaction product was extracted with ether and distilled giving a main fraction (17 g), b.p. 120−140°/0.4 mm, which was redistilled, b.p. 111−116°/0.1 mm. ν_{max} 1690 and 1718 cm^{-1} (shoulder).

The semicarbazone, crystals from ethanol, melted at 184−187°. (Found: C 66.2; H 8.2; N 14.5. $C_{16}H_{23}O_2N_3$ requires: C 66.4; H 8.0; N 14.5 %).

α,β-Unsaturated ketone 6. β-Chloropent-3-one (1.92 g) was added rapidly with vigorous stirring to a mixture of the β-tetralone (*5*) (3.72 g), a 50 % suspension of sodium hydride (870 mg) and light petroleum (80 ml) kept under a nitrogen atmosphere. The mixture was boiled under reflux for 15 min and then cooled. More sodium hydride suspension was added (870 mg) and the heating continued for another 45 min. 2 N hydrochloric acid (90 ml) was added to the cold mixture and the organic layer separated. The aqueous layer was extracted with ether. The combined organic phases were evaporated and the residue distilled to give a fraction, b.p. 136−148°/0.05 mm (2.8 g), which was chromatographed on alumina (90 g). The fraction eluted with benzene-light petroleum (3:1) gave a crystalline compound which was recrystallised from methanol, m.p. 92−94°; ν_{max} 1615, 1623, 1665 cm^{-1}; λ_{max} 287 mμ (ε 4160), 279 (4720), 247 (17 100), 230 (16 000). (Found: C 80.2; H 8.7. $C_{20}H_{26}O_2$ requires: C 80.5; H 8.8 %.)

2,4-Dinitrophenylhydrazone: red crystals from ethanol, m.p. 225−228°.

Methylation of 6. A solution made from potassium (900 mg) and *t*-butanol (20 ml) was added to a solution of *6* (800 mg) in *t*-butanol (30 ml) and the mixture heated under nitrogen. Methyl iodide (6 ml) was added dropwise and the mixture boiled under reflux for one hour. The solvent was removed under vacuum and the residue dissolved in light petroleum and chromatographed on alumina (30 g). Elution with light petroleum-benzene (5:1, 50 ml) gave a compound (A) (200 mg); m.p. 96−97.5° (from methanol). The I.R. absorption of this compound (ν_{max} 1615, 1673, 1712 cm^{-1}) was very similar to that of *7*. (Found: C 80.8; H 9.2. $C_{21}H_{28}O_2$ requires: C 80.7; H 9.0 %.) Continued elution with the same solvent (150 ml) gave a mixture of A and *7* (175 mg). Elution with light petroleum-benzene (4:1) gave *7* (250 mg) which was recrystallised from methanol and sublimed, m.p. 92−94°, ν_{max} 1614, 1668, 1712 cm^{-1}. (Found: C 80.0; H 8.9. $C_{21}H_{28}O_2$ requires: C 80.7; H 9.0 %.)

The 2,4-dinitrophenylhydrazone, yellow crystals (from methanol), had m.p. 212−214°. A mixture of compound A and *7* melted at 65−85°. Compound A has not been subjected to further investigation but is obviously closely related to *7*. On hydrogenation A gave an amorphous product.

DL-*Hinokione methyl ether (8).* A mixture of *7* (100 mg), prehydrogenated 20 % palladised charcoal (30 mg), ethanol (30 ml), and acetic acid (0.5 ml) was shaken with hydrogen at room temperature for 6 h. Filtration and evaporation gave a resinous product which was recrystallised three times from methanol, m.p. 119−121°. The I.R. spectrum was superimposable with that of natural hinokione methyl ether. (Found: C 80.0; H 9.3. $C_{21}H_{30}O_2$ requires: C 80.2; H 9.6 %.) The 2,4-dinitrophenylhydrazone formed yellow crystals (from ethanol-ethyl acetate) melting at 215−218°.

Acknowledgement. This work was supported by the *U.S. Department of Army*, through its European Research Office under contract number DA-91-591-EUC-1400. The author is indebted to Professor H. Erdtman for his interest in the work, to Dr. D. A. H. Taylor for valuable discussion and to Dr. I. Wellings for reading the manuscript.

REFERENCES

1. (a) Simonsen, J. L. and Barton, D. H. R. *The Terpenes*, Vol. III, Cambridge University Press 1952, p. 358. (b) Erdtman, H. and Vorbrüggen, H. *Acta Chem. Scand.* **14** (1960) 2161. (c) Chow, Y.-L. and Erdtman, H. *Ibid.* **16** (1962) 1291. Barreto, H. and Enzell, C. *Ibid.* **15** (1961) 1313.
2. Chow, Y.-L. and Erdtman, H. *Proc. Chem. Soc.* **1960** 174.
3. Howell, F. H. and Taylor, D. A. H. *J. Chem. Soc.* **1958** 1248.
4. Woodward, R. B., Patchett, A. A., Barton, D. H. R., Ives, D. A. J. and Kelly, R. B. *J. Chem. Soc.* **1957** 1131.

Received December 31, 1961.

ACTA CHEMICA SCANDINAVICA 16 (1962) 1305–1310

The Chemistry of the Natural Order Cupressales

45 *. The Structure and Configuration of Totarol and Totarolone **

YUAN-LANG CHOW and H. ERDTMAN

Organisk-kemiska Institutionen, Kungl. Tekniska Högskolan, Stockholm, Sweden

Totarolone, a constituent of the heartwood of *Tetraclinis articulata* has been reduced to the alcohol totaradiol and to totarol. The alcoholic hydroxyl group of the former compound is situated at C_3. Totarol has been degraded to the dicarboxylic acid (*10*) also obtained from dehydroabietic acid. The structure and absolute configuration of totarolone are therefore represented by formula (*1a*).

A totarol analogue of xanthoperol and some similar compounds have been prepared from totarol.

Totarolone, recently isolated from the heartwood of *Tetraclinis articulata* [1] gives totarol (*2a*) on Clemmensen reduction. Since the structure of totarol is known [2] this proves the nature of the carbon skeleton of totarolone.

Reduction of totarolone with potassium borohydride gives totaradiol *3a*. The molecular rotation shift between totaradiol (*3a*) and its diacetate (*3b*), $[M]_D + 43°$, is very similar to that between hinokiol (*7a*) and its diacetate (*7b*), $[M]_D + 47°$, suggesting that the environments of the asymmetric centres are similar in both series. The carbonyl function of totarolone and the secondary hydroxyl group of totaradiol, therefore, should be at C_3 in analogy with hinokione and hinokiol [3].

Reduction of totarolone benzyl ether (*1c*) with lithium aluminium hydride gave mainly totaradiol benzyl ether (*3c*) also obtained by direct benzylation of totaradiol (*3a*). The infrared absorption of the monobenzyl ether (ν_{max} 1030 cm^{-1}) indicated that the hydroxyl group was equatorial. When heated with phosphorus pentachloride the benzyl ether gave a resin which exhibited a weak band at 1670 cm^{-1} indicating that the usual retropinacol rearrangement had occurred with formation of compound *4*. The resin was therefore successively treated with osmium tetroxide and lead tetraacetate. Acetone was formed together with the A-trisnorcyclopentanone derivative *5* which contained *cis*-fused A/B-rings as the result of inversion at C_5 (*cf.* Ref.[4]). The ketone *5* exhibited the expected absorption at 1260 and 1740 cm^{-1}.

* Part 44. *Acta Chem. Scand.* **16** (1962) 1301.

** Preliminary communication *Acta Chem. Scand.* **14** (1960) 1852.

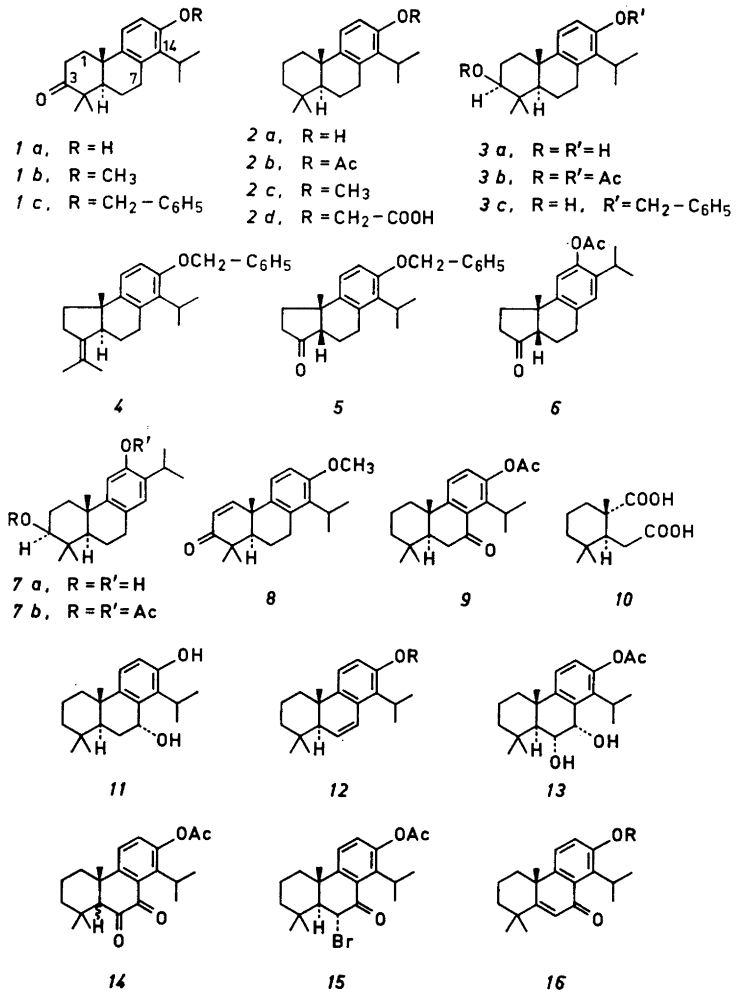

Similar to the crystalline, semipure compound *6* from hinokiol [3], the cyclopentanone *5* showed a positive Cotton effect resembling that of the A/B *cis*-fused 3-keto-A-norcholanic acid [4]. The rotation below 290 mμ was masked by the strong absorption of the aromatic ring.

The rotatory dispersion curves of totarolone and hinokione were very similar showing a positive Cotton effect similar to that of lanost-8-en-3-one [5].

The structure and absolute configuration of totarolone must therefore be represented by *1a*. The α,β-unsaturated totarolenone [1] which accompanies totarolone in *Tetraclinis articulata* and which is hydrogenated to totarolone must consequently have structure *8* (OH instead of OCH_3).

During attempts to relate totarol to dehydroabietic acid totarol acetate (*2b*) was oxidised to 7-ketototarol acetate (*9*) [1]. Attempts to cleave this com-

pound between the carbonyl group and the aromatic ring with hydrazoic acid in trichloroacetic acid failed, the starting material being recovered unchanged. This is obviously due to steric hindrance from the isopropyl group since 7-ketodehydroabietic acid is cleaved under these conditions [7].

On oxidation with trifluoroperacetic acid, however, 7-ketototarol acetate gave an acid product in about 25 % yield. It could not be obtained crystalline but the infrared absorption of the crude product showed, in addition to the hydroxyl peaks in the 3000 cm^{-1} region, a sharp peak at 1730 cm^{-1} attributable to a nonconjugated carboxyl group. The crude acid was therefore ozonised followed by oxidation with alkaline hydrogen peroxide. A complex mixture of acids resulted from which, with considerable difficulty, a small amount of the dicarboxylic acid *10* was isolated. It was identified by mixed melting point with an authentic specimen [7] and by comparison of infrared spectra. This confirms that totarol has the usual steroid configuration (5α,10β).

The phenolic hydroxyl group of ferruginol is said to be resistent to methylation [8]. However, totarolone could be methylated with methyl iodide and potassium carbonate in acetone.

Reduction of the methyl ether (*2c*) as well as the phenoxy acetic acid (*2d*) with lithium-ammonia failed. (An analogous compound without the isopropyl group has been successfully reduced by this method [2].) Attempts to oxidise totarol with potassium nitrosodisulphonate [9] to an orthoquinone suitable for further degradations were also unsuccessful.

Since Δ^6-dehydroferruginol and xanthoperol are found in Nature [10], it was of some interest to prepare similar compounds of the totarol type.

Lithium aluminium hydride reduction of 7-ketototarol acetate gave a mixture of epimeric 7-hydroxytotarols from which the main component (m.p. 215—217.5°) was isolated. This compound must be 7α-hydroxytotarol (*11*) for the following reasons: (1) inspection of molecular models shows that the quasi-equatorial hydroxyl group is more hindered than the quasi-axial due to the presence of the isopropyl group in position C_{14} and (2) because the compound is smoothly dehydrated by oxalic acid in dry toluene to Δ^6-totarol (*12*, R = H). This compound was easily hydrogenated to totarol.

Osmylation of Δ^6-dehydrototarol acetate and subsequent hydrolysis of the osmate with hydrogen sulphide gave a mixture of two diol acetates, from which the main component was isolated in a pure state. Osmium tetroxide will attack the ethylenic linkage from the less hindered α-side and the predominant product should therefore be 6α,7α-dihydroxytotarol acetate (*13*). Mild oxidation of the mixture of the diol acetates with chromium trioxide and sulphuric acid in acetone gave yellow 6,7-diketototarol acetate (*14*). In spite of repeated recrystallisations the product melted over a wide range as does xanthoperol [10] and other related compounds [11].

Bromination of 7-ketototarol acetate (*9*) readily gave a monobromo derivative which, according to the I.R. absorption [12], should be the expected 6α-bromo-7-ketototarol acetate (*15*). Treatment with lithium bromide-lithium carbonate in dry dimethylformamide gave Δ^5-dehydro-7-ketototarol acetate (*16*, R = Ac) in excellent yield. Mild alkaline hydrolysis of this compound gave Δ^5-dehydro-7-ketototarol (*16*, R = H).

EXPERIMENTAL

Clemmensen reduction of totarolone(1a). A mixture of totarolone (230 mg), amalgamated zinc filings (1.5 g) acetic acid (10 ml) and conc. hydrochloric acid (4 ml) was refluxed for 2 h. Amalgamated zinc filings (500 mg) and conc. hydrochloric acid (2 ml) were added and heating continued for 5 h. The hot solution was decanted and on cooling white crystals (150 mg) were obtained, m.p. 120–125°. Recrystallisation from light petroleum gave a crystalline product, m.p. 125–128° (mixed m.p. with authentic totarol 127–128°), $[\alpha]_D$ + 42.5° (in EtOH). The I.R. spectrum was identical with that of totarol.

Totaradiol(3a). A mixture of totarolone (120 mg), 2 N sodium hydroxide solution (5 drops), potassium borohydride (120 mg) and methanol (30 ml) was allowed to stand for 2 h. Water (40 ml) was added and the mixture acidified. Further addition of water (60 ml) gave a crystalline product which was recrystallised from benzene, m.p. 100–102°; resolidifying at 105° (crystal solvent?). It gradually remelted between 169–178°; resolidified at 179° and was completely molten at 183°, $[\alpha]_D$ + 40° (EtOH), ν_{max} 1002, 1180, 1280, 1585, 3380, 3610 cm^{-1}. (Found: C 80.0; H 9.9. Calc. for $C_{20}H_{30}O_2$: C 79.4; H 10.0).

Recrystallisation from carbon tetrachloride gave crystals, m.p. 170–173°, which on sublimation *in vacuo* gave a sample, m.p. 180.5–181.5°.

Totaradiol diacetate (3b) (pyridine-acetic anhydride) gave colourless crystals, m.p. 119–121.5°, from light petroleum. $[\alpha]_D$ + 41° (EtOH), ν_{max} at 1202, 1248, 1725, 1765 cm^{-1}. (Found: C 74.6; H 8.7. Calc. for $C_{24}H_{34}O_4$: C 74.6; H 8.9).

Totaradiol monobenzyl ether (3c). A solution of totarolone benzyl ether (380 mg) in ether (100 ml) was added to a suspension of lithium aluminium hydride (250 mg) in ether (100 ml). The mixture was heated under reflux for 3 h. The excess hydride was destroyed and 0.5 N sulphuric acid added. Extraction with ether gave colourless crystals (400 mg), m.p. 189–193°. The product was crystallised three times from methanol and then sublimed, m.p. 192–193°, $[\alpha]_D$ + 33° (EtOH); ν_{max} 1030, 1264, 1500, 1582, 1590 and 3420 cm^{-1}; λ_{max} 210 mμ (ε 33 880), 277 (1640), 285 (1630). (Found: C 82.3; H 9.1. Calc. for $C_{27}H_{36}O_2$: C 82.6; H 9.2).

Totaradiol (130 mg), anhydrous potassium carbonate (130 mg), and redistilled benzyl bromide (850 mg) in acetone (60 ml) were refluxed for two days. The reaction mixture was diluted with water and the products were extracted with ether. Recrystallisation of the residue from the ether solution with methanol gave totaradiol monobenzyl ether, m.p. 192–193°.

The *acetate* (pyridine-acetic anhydride) formed colourless crystals, m.p. 212–215°, $[\alpha]_D$ + 39° ($CHCl_3$). (Found: C 80.2; H 8.8. Calc. for $C_{29}H_{38}O_3$: 80.1; H 8.8).

Retropinacole rearrangement of totaradiol monobenzyl ether. To a solution of totaradiol monobenzyl ether (200 mg) in light petroleum (200 ml), phosphorus pentachloride (1 g) was added with shaking. The mixture was set aside at room temperature for 18 h with occasional shaking. The solution was then treated with 10 % sodium hydroxide solution and finally with water. The residue from the organic phase was adsorbed on a column of basic alumina (20 g). Light petroleum eluted a colourless resin (140 mg) exhibiting no hydroxyl absorption in the infrared.

This resin, and osmium tetroxide (140 mg), were dissolved in a mixture of ether (20 ml) and pyridine (2 ml). After 3 days the solvents were evaporated *in vacuo* and the residue heated with a solution of sodium sulphite (900 mg) in ethanol (30 ml) and water (15 ml) for a few seconds. The reaction product was extracted with ether. The residue (ν_{max} 3610, 3650 cm^{-1}) was dissolved in acetic acid (10 ml) and lead tetraacetate (400 mg) added. After 12 h water (7 ml) was added. The mixture was heated and the first ml of distillate was collected. Addition of Brady's reagent gave acetone 2,4-dinitro-phenylhydrazone, m.p. and mixed m.p. 128–130°. Yield 50 mg (68 %).

The residual liquid was diluted with water and extracted with ether. The ether solution was then evaporated and the residue chromatographed on silica (15 g). Light petroleum-benzene (1:1, 150 ml) eluted 58 mg of a resin which was distilled in a high vacuum. On trituration with light petroleum a small amount of a crystalline product, m.p. 135–141°, was obtained. ($\nu_{max}^{CCl_4}$: 1260 and 1740 cm^{-1}). The crude material was treated with Brady's reagent giving a yellow product which would not crystallise: λ_{max} 363 mμ (ε 20 200).

Degradation of 7-ketototarol acetate (9). A methylene chloride solution (20 ml) of trifluoroacetic anhydride (4 ml) was added to an ice cooled agitated mixture of 80 % hydrogen peroxide (1 ml) in methylene chloride (10 ml). This peracid solution was slowly (one hour) added to a stirred suspension of 7-ketototarol acetate (3 g) and anhydrous disodium hydrogen phosphate (6.5 g) in methylene chloride. The reaction mixture was stirred for 16 h, heated under reflux for 3 h, then poured into water. The organic layer was washed with 10 % sodium carbonate solution and gave unreacted starting material. From the aqueous layer 810 mg of a solid, acid product was obtained which showed the typical absorption of a carboxylic acid in the 3000 cm^{-1} region and a strong band at 1730 cm^{-1}.

The solid was dissolved in 45 ml of methylene chloride and ozonised for 2.5 h at −20°. The residue from the evaporation of the solvent was oxidised with 30 % hydrogen peroxide (20 ml) in methanol (25 ml) and 2 N sodium hydroxide (15 ml). The acid fraction obtained was chromatographed on silica gel (25 g) using benzene followed by ether as eluents. The fraction eluted with 160 ml of ether gave crystals (30 mg), m.p. 120—158°. Two recrystallisations from methanol-water and one from acetone-cyclohexane gave *trans*-1,3,3-trimethyl-1-carboxycyclohexyl-2-acetic acid (*10*), m.p. and mixed m.p. with an authentic sample 164—168°. $[\alpha]_D$ −4.5° (EtOH). The IR-spectra of the two specimens were superimposable.

The cyclohexylamine salt of the acid was recrystallised from isopropyl alcohol, m.p. 180—183°.

Totarolone methyl ether (1b). A mixture of totarolone (120 mg), anhydrous potassium carbonate (125 mg) and methyl iodide (2 ml) in acetone (15 ml) was heated under reflux for two days. The reaction product was triturated with hot light petroleum (30 ml). The undissolved material was totarolone. The filtrate was evaporated and the residue dissolved in ethanol (3 ml). On cooling the methyl ether crystallised. It was recrystallised from ethanol and sublimed, m.p. 88—100°, $[\alpha]_D$ + 99° (EtOH); ν_{max} 1260, 1705 cm^{-1}. (Found: C 78.8; H 9.3. Calc. for $C_{21}H_{30}O_2$: C 80.2; H 9.6).

Totarol glycolic acid ether (2d). The potassium salt of totarol was prepared by heating and stirring a mixture of totarol (5.16 g) and potassium (850 mg) in benzene (150 ml). To the resulting suspension, a solution of ethyl bromoacetate (3.64 g) in dry benzene was added slowly (mechanical stirring, reflux). At the end of the addition a clear solution was obtained. Heating was continued for another hour. The reaction mixture was shaken with water and the neutral and acidic products isolated. From the acid fraction totarol glycolic acid ether (440 mg) was isolated and gave colourless crystals from methanol-water, m.p. 193—196°, $[\alpha]_D$ + 42.3° (EtOH).

From the neutral fraction the ethyl ester was obtained, (m.p. 73—76°) which on alkaline hydrolysis gave the above acid, m.p. 194—196°. (Found: C 76.4; H 9.6. Calc. for $C_{22}H_{32}O_3$: C 76.7; H 9.4).

7α-Hydroxytotarol (11). A solution of 7-ketototarol acetate (200 mg) in ether (35 ml) was added dropwise to a suspension of lithium aluminium hydride (112 mg) in ether (107 ml). The mixture was heated under reflux for 30 min. The reaction product was isolated in the usual manner and crystallised from benzene, m.p. 215—217.5°, $[\alpha]_D$ + 21.6° ($CHCl_3$), + 30.6° (EtOH); ν_{max} 990, 1275, 1590, 3350 and 3600 cm^{-1}. (Found: C 79.4; H 9.8. Calc. for $C_{20}H_{30}O_2$: C 79.4; H 10.0).

Δ^6-Dehydrototarol acetate (*12*, R = Ac), 7-Hydroxytotarol (3.2 g) and anhydrous oxalic acid (6 g) in dry toluene (100 ml) was distilled with recycling of the toluene for 4 h. The trapped water was removed from time to time. The toluene layer was washed with 2 N sodium hydroxide and water and the toluene removed by distillation. The residue was chromatographed on silica (100 g). Benzene-light petroleum (1:1) eluted an oil (3 g) which did not crystallise. (ν_{max} 690, 1270 cm^{-1}). On hydrogenation with Pd/C in ethanol totarol was obtained.

The oil was acetylated with acetic anhydride and pyridine and the product was crystallised once from light petroleum and twice from ethanol and then sublimed, m.p. 138—140°, $[\alpha]_D$ −114.4° ($CHCl_3$). λ_{max} 267 mμ (ε 9270), 228 shoulder (21 000), 222 (25 900) and 217 shoulder (22 600); ν_{max} 685, 1760 cm^{-1}. (Found: C 80.4; H 9.1. Calc. for $C_{22}H_{30}O_2$: C 80.9; H 9.3.)

6α,7α-Dihydroxytotarol acetate (13). A mixture of the above acetate (590 mg), osmium tetroxide (500 mg), ether (20 ml) and pyridine (1 ml) was kept in a dark place for three days. The solvents were evaporated and the residue dissolved in benzene. This solution

was saturated with hydrogen sulphide and the precipitate obtained was removed by filtration. The benzene solution was washed with water and the solvent evaporated. The residue (510 mg) was recrystallised from benzene-light petroleum giving colourless crystals, (340 mg), m.p. 220–222°, $[\alpha]_D$ + 47.7° (EtOH); ν_{max} 1185, 1760, 3370 (broad) and 3480 cm^{-1}. (Found: C 72.9; H 8.8. Calc. for $C_{32}H_{32}O_4$: C 73.3; H 8.9.)

6,7-Diketototarol acetate (14). To a cold solution of 6,7-dihydroxytotarol acetate (200 mg) in acetone (15 ml) a solution of chromium trioxide (112 mg) in 1 N sulphuric acid (3 ml) was added slowly, with shaking. After 30 min at room temperature the solution was diluted with water and extracted with ether. The yellow solution gave a product (107 mg) which was chromatographed on silica (10 g). The product eluted with ether: benzene (3:97) gave yellow crystals which were recrystallised several times from cyclohexane, m.p. 185–204°; ν_{max} 850, 1585, 1683, 1733, 1762, 3540, 3360 cm^{-1}; λ_{max} 325 mμ (3000), 285 (4950), 208 (14 500).

The compound gave a deep yellow colour reaction with aqueous ferric chloride. (Found: C 72.0; H 7.6. Calc. for $C_{32}H_{38}O_4$, 0.5 H_2O: C 72.3; H 8.00).

6α-Bromo-7-ketototarol acetate (15). To a solution of 7-ketototarol acetate (2.3 g) in acetic acid (75 ml) and one drop of hydrobromic acid, bromine (0.12 g) in acetic acid (12 ml) was added dropwise at room temperature. Decolourisation was instantaneous. An excess of 1 ml was added and after one minute a further addition of water and sodium bisulphite. The precipitate was crystallised from methanol three times to give slightly yellowish needles, m.p. 176–178°, $[\alpha]_D$ −53.1° (EtOH); ν_{max} 1205, 1690 and 1763 cm^{-1}; λ_{max} 208 mμ (ε 13 400), 257 (4860), 293 (1800). (Found: C 62.3; H 6.9; Br 19.6. Calc. for $C_{32}H_{39}O_3Br$: C 62.7; H 6.9; Br 19.0).

Δ^5-Dehydro-7-ketototarol acetate (*16*, R = Ac). A mixture of 6α-bromo-7-ketototarol acetate (550 mg), freshly fused lithium bromide (1.1 g), dry lithium carbonate (250 mg) and dry dimethylformamide (20 ml) was heated to 100° for 40 h with stirring. The reaction mixture was then poured into ice-water. The precipitate was collected and recrystallised from light petroleum, m.p. 163–165°, $[\alpha]_D$ −20.6° (EtOH); ν_{max} 1195, 1595, 1624, 1655 and 1764 cm^{-1}; λ_{max} 259 mμ (ε 12 300), 270 (11 900), 310 shoulder (2600). (Found: C 77.6; H 8.1. Calc. for $C_{32}H_{38}O_3$: C 77.6; H 8.3.)

Δ^5-Dehydro-7-ketototarol (*16*, R = H). Δ^5-Dehydro-7-ketototarol acetate was hydrolysed with sodium hydroxide in methanol. Addition of water gave a precipitate which crystallised from benzene. Pale-yellow crystals, m.p. 243–245°, $[\alpha]_D$ −39.3° (EtOH); ν_{max} 1290, 1607, 1630 and 3300 cm^{-1}; λ_{max} 207 mμ (ε 14 300), 227 (14 300), 249 (10 200), 278 (9600) and 340 (2500).

Acknowledgements. This work has been sponsored by the *Office of Research and Development, U.S. Army Department*, through its European Office. We thank Professor W. Klyne for rotatory dispersion measurements, Professor O. Jeger for a sample of acid (*10*) and Dr. I. Wellings for readings the manuscript.

REFERENCES

1. Chow, Y.-L. and Erdtman, H. *Acta Chem. Scand.* **14** (1960) 1852.
2. Barltrop, J. A. and Rogers, N. A. L. *J. Chem. Soc.* **1958** 2566, and the references quoted therein.
3. Chow, Y.-L. and Erdtman, H. *Proc. Chem. Soc.* **1960** 174; *Acta Chem. Scand.* **16** (1962) 1296.
4. Baddeley, G. B., Halsall, T. G. and Jones, E. R. H. *J. Chem. Soc.* **1960** 1715.
5. Djerassi, C., Halpern, O., Halpern, V. and Riniker, B. *J. Am. Chem. Soc.* **80** (1958) 4001.
6. Brandt, C. W. and Thomas, B. R. *J. Chem. Soc.* **1952** 2442.
7. Schaffner, K., Viterbo, R., Arigoni, B. and Jeger, O. *Helv. Chim. Acta* **39** (1956) 174.
8. Campbell, W. P. and Todd, D. *J. Am. Chem. Soc.* **64** (1942) 928.
9. Teuber, H. J. *Ber.* **86** (1953) 1495.
10. Bredenberg, J. *Acta Chem. Scand.* **11** (1957) 927, 932.
11. Wenkert, E. and Jackson, B. G. *J. Am. Chem. Soc.* **80** (1958) 211.
12. Jones, R. N. *et al. Ibid.* **74** (1952) 2828; Allinger, N. and Allinger, J. *Ibid.* **80** (1958) 5476.

Received December 31, 1961.

ACTA CHEMICA SCANDINAVICA 16 (1962) 1311–1314

The Chemistry of the Natural Order Cupressales

46 *. The Structure of Nootkatone

HOLGER ERDTMAN and YOSHIYUKI HIROSE

Organisk-kemiska Institutionen, Kungl. Tekniska Högskolan, Stockholm, Sweden

A new eudalenoid sesquiterpene ketone, nootkatone, has been isolated from the heartwood of *Chamaecyparis nootkatensis*. It has been shown to possess the structure *1*.

During our investigation of the acetone soluble heartwood constituents of Alaska yellow cedar (*Chamaecyparis nootkatensis* (Lamb.) Spach) several compounds have been isolated, *e.g.* the acidic compounds carvacrol, chamic and chaminic acid and nootkatin. The neutral part contains carvacrol methyl ether and various sesquiterpenes including the triply unsaturated, easily polymerisable, eudalenoid nootkatene. The presence of alcohols and ketones was also indicated [1].

By treating the high boiling neutral fractions with semicarbazide or a Girard reagent a new sesquiterpene ketone, nootkatone, has now been isolated. Nootkatone has the composition $C_{15}H_{22}O$, melts at 36—37° and is dextrorotatory, $[\alpha]_D$ + 195.5°.

The infrared and ultraviolet spectra of nootkatone show that the compound is an α,β-unsaturated ketone. Structure (*1*), which is proposed for this substance, is closely related to α-cyperone (*2*).

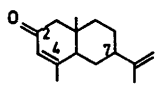

1

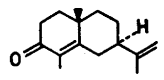

2

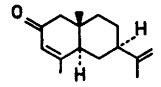

3

Ozonisation of nootkatone gave formaldehyde but no acetone. Hydrogenation with palladium in ethanol furnished a viscous tetrahydro product from which crystalline tetrahydronootkatone semicarbazone was obtained. Similar hydrogenation with platinum oxide gave an alcoholic hexahydro product which on chromatographic purification gave, as the main product (70 %), tetrahydronootkatol, a solid melting at 76.5—77°, $[\alpha]_D$ + 13.9°,

* Part 45. *Acta Chem. Scand.* **16** (1962) 1305.

together with a liquid which is presumably a mixture of isomers. On oxidation tetrahydronootkatol gave a ketone, the semicarbazone of which was identical with that of tetrahydronootkatone.

Reduction of nootkatone with potassium borohydride gave an oily alcohol which on dehydrogenation with selenium afforded eudalene.

In order to locate the carbonyl group, tetrahydronootkatone was treated with methyl magnesium iodide and the resulting alcohol dehydrogenated with selenium. A naphthalene derivative was obtained which was identified as 1,3-dimethyl-7-isopropyl naphthalene. These results clearly indicate that nootkatone possesses structure (*1*). There is no chemical proof of the position of the angular methyl group and an eremophilone-like structure would be an alternative.

Tetrahydronootkatone, prepared from pure, crystalline tetrahydronootkatol, was reduced by Clemmensen's method and the product which, according to its infrared spectrum contained some unsaturated contaminations, was subjected to ozonisation and purified by chromatography on alumina.

The resulting oil had $[\alpha]_D$ + 19.2°, closely similar to that of eudesmane from β-eudesmol and from elemol [2] ($[\alpha]_D$ + 16.2° and 16.3°, resp).

The essential features of the infrared absorption of eudesmane from the latter sources were identical with those of eudesmane from nootkatone. However, it does not appear safe to draw any definite conclusions about the configuration of nootkatone from this result only. The indications are, however, that nootkatone has the same configuration at the active centres as the eudesmols.

The proton magnetic resonance spectrum of nootkatone in carbon tetrachloride with benzene as internal standard showed a signal at 62 cps due to a single proton on a double bond. The low frequency is due to the proton being situated next to a carbonyl group. A signal at 103 cps is due to the two hydrogen atoms on the terminal methylene group of the isopropenyl group. Three sharp lines at 250, 223 and 207 cps correspond to three methyl groups, of which the latter is due to a methyl group in a system of the type $-CO-CH=C(CH_3)-$.

These results are in agreement with the proposed structure *1* as well as with the eremophilone-like alternative. The rotatory dispersion curves of tetrahydronootkatone and of nootkatone have been recorded by Professor Klyne to whom we express our gratitude. The R.D.-curve of nootkatone is very similar to that of 5α-cholest-3-en-2-one[3] kindly provided by Professor C. Djerassi. This indicates that nootkatone has the "ordinary" *trans*-fused ring system (10β,5α).

The configuration at C_7 is not known with absolute certainty. In eudesmol it is β-oriented and the physical properties of the above eudesmane preparation indicate that it is similarly oriented in nootkatone. Assuming this to be correct then the methyl group at C_4 and the hydroxyl group at C_2 of tetrahydronootkatol should be β-oriented, hydrogenation occurring at the least sterically hindered side.

Further work is required to ascertain the absolute configuration of nootkatone and experiments in this direction are in progress. The most likely configuration is *3*.

EXPERIMENTAL

Isolation of nootkatone. (a) The neutral fraction from 28 kg of heartwood of *Chamaecyparis nootkatensis* (370 g) was distilled through an efficient column giving a series of fractions, of which those boiling between 156° and 158° at 5 mm pressure were redistilled through a spinning band column. Series of fractions boiling between 154° and 155° were obtained, the optical rotations of which varied between $[\alpha]_D$ + 91° and + 148°. These were dissolved in six times their volumes of ethanol and treated with sodium acetate and semicarbazide hydrochloride. Crystals separated (about 25 g) which were recrystallised from ethanol yielding pure nootkatone semicarbazone (15 g). The semicarbazone was mixed with phthalic anhydride (15 g) and water (45 ml) and the mixture steam distilled. The volatile organic material was extracted with ether and evaporation of the organic layer gave nootkatone as a pale yellow oil (5 g) which solidified when kept in the ice-box. Recrystallisation from light petroleum gave material, m.p. 36—37°, $[\alpha]_D$ + 195.5° (c = 1.5 in $CHCl_3$). λ_{max} 238 mμ (ε 15 000), ν_{max} 1680 cm^{-1}. (Found: C 82.4; H 10.0, Calc. for $C_{15}H_{22}O$: C 82.5; H 10.2).

(b) The fraction of neutral oil boiling between 155 and 180°/5 mm (105 g) and Girard P reagent (16 g) were dissolved in ethanol (300 ml) containing acetic acid (30 g), and the resultant solution refluxed for 40 min. After cooling to room temperature, the solution was poured into ice-water (2 l), containing sodium carbonate (27 g), and the mixture extracted with ether. The aqueous phase was acidified with sulphuric acid and exhaustively extracted with ether. The latter ether solution was washed with water, dried and evaporated, leaving a brownish oil (10 g) which solidified on cooling. Recrystallisation from light petroleum gave pure nootkatone.

Nootkatone semicarbazone. The semicarbazone was prepared in the usual way and recrystallised from ethanol. It melted at 195—197° (decomp.), $[\alpha]_D$ + 384° (c = 0.51 in $CHCl_3$). (Found: C 69.8; H 9.1; N 15.6. Calc. for $C_{16}H_{25}ON_3$: C 69.9; H 9.15; N 15.3).

The 2,4-dinitrophenylhydrazone melted at 157.5—158.5°. λ_{max} 384 mμ (ε 26 000). (Found: C 62.9; H 6.6; N 14.0. Calc. for $C_{21}H_{26}O_4N_4$: C 63.3; H 6.6; N 14.1).

Ozonolysis of nootkatone. A solution of nootkatone (118 mg) in methylene chloride (20 ml) was treated with ozone for 1.5 h. Water (20 ml) was added and the mixture gently refluxed on a water bath for 2 h. After extraction with light petroleum the aqueous layer was mixed with a saturated solution of dimedone in water (20 ml). The precipitated dimedone derivative (45.3 mg, yield 28.6 %) was identified as the formaldehyde dimedone derivative, m.p. and mixed m.p. 189°.

The filtrate from the formaldehyde dimedone derivative was steam-distilled into 2,4-dinitrophenylhydrazine reagent solution, but no 2,4-dinitrophenylhydrazone was obtained.

Tetrahydronootkatone semicarbazone. Nootkatone (51.9 mg) was hydrogenated in ethanol in the presence of a palladium/charcoal catalyst. The hydrogenation was discontinued when 12.2 ml of hydrogen (2.1 moles) had been consumed. The product obtained was a viscous oil, b.p. 153—155°/7 mm. The semicarbazone was prepared and melted at 210—211° (decomp.) $[\alpha]_D$ + 66.5° (c = 0.9 in $CHCl_3$). (Found: 69.0; H 10.35; N 15.0. Calc. for $C_{16}H_{29}ON_3$: C 68.8; H 10.5; N 15.0).

Tetrahydronootkatol (hexahydronootkatone). Nootkatone (120 mg) was shaken with hydrogen in ethanol in the presence of Adams catalyst. Hydrogen (38.6 ml, 2.9 moles) was absorbed. The product was chromatographed on alumina yielding a liquid (30 %) and crystals (70 %). Recrystallisation of the latter from light petroleum gave material, m.p. 76.5—77°, $[\alpha]_D$ + 13.9° (c = 2.2 in $CHCl_3$). (Found: C 80.2; H 12.1. Calc. for $C_{15}H_{28}O$: C 80.3; H 12.6).

Oxidation of tetrahydronootkatol to tetrahydronootkatone. A solution of the above alcohol (320 mg) in pyridine (5 ml) was added to a solution of CrO_3 (400 mg) in pyridine (5 ml). The mixture was kept overnight at room temperature and was then poured into water and the suspension extracted with ether. The product obtained had b.p. 152°/6 mm, n_D 1.4886, $[\alpha]_D$ + 54.1° (c = 2.4 in $CHCl_3$). It was converted into the semicarbazone, m.p. and mixed m.p. with that of tetrahydronootkatone 210—211° (decomp.). The I.R. spectra were superimposable.

A sample of tetrahydronootkatone prepared in this way was reduced according to the Clemmensen method and the crude product dissolved in methylene chloride and ozonised at room temperature. The reaction product was heated under reflux with water and the organic material dissolved in light petroleum and the solution filtered through a short

alumina column. The filtrate was evaporated and the residue distilled. The product obtained had $[a]_D$ + 19.2° (in $CHCl_3$).

Eudalene from nootkatone. A solution of nootkatone (300 mg) in methanol (5 ml) was added to a solution of potassium borohydride (300 mg) in aqueous methanol and the mixture was kept overnight at room temperature. The reaction mixture was then treated with a cold solution of 5 % sodium hydroxide and shaken with ether. Evaporation of the organic extract gave a viscous oil (300 mg) that did not crystallise.

This oil (300 mg) was heated with selenium (300 mg) for 12 h. The light petroleum ether soluble product was passed through alumina to give a colourless liquid, which yielded a picrate, m.p. 92–93°. The melting point was not depressed by mixing with authentic eudalene picrate and their infrared spectra were superimposable.

1,3-Dimethyl-7-isopropylnaphthalene from tetrahydronootkatone. A solution of tetrahydronootkatone (1.3 g) in dry ether (5 ml) was slowly added to a solution of a Grignard reagent, prepared from magnesium (0.2 g) and methyl iodide (1.5 g) in dry ether (5 ml). The mixture was kept overnight at room temperature. After treatment with a saturated solution of ammonium chloride, followed by extraction with ether, a pale yellow alcohol (0.9 g) was obtained. (ν_{max} 3620 cm^{-1}, no carbonyl band).

The above alcohol (0.9 g) was dehydrogenated with selenium (1.5 g) at 330°C for 30 h. The light petroleum soluble fraction of the product was chromatographed on alumina. Elution with light petroleum gave a colourless liquid (0.4 g), which afforded a picrate, m.p. 104–106° and a trinitrobenzene adduct, m.p. 121–122°. These melting points were not depressed when the derivatives were mixed with the appropriate authentic 1,3-dimethyl-7-isopropylnaphthalene derivatives. The infrared spectra were also identical with those of the 1,3-dimethyl-7-isopropylnaphthalene derivatives. Picrate: Found: C 59.05; H 5.2; N 10.0. Calc. for $C_{21}H_{21}O_7N_3$: C 59.0; H 4.95; N 9.8. Trinitrobenzene adduct: Found: C 61.3; H 5.1; N 10.2. Calc. for $C_{21}H_{21}O_6N_3$: C 61.3; H 5.15; N 10.2.

Acknowledgement. This work has been supported by the *U.S. Department of Army*, through its European Research Office.

REFERENCES

1. Erdtman, H. and Topliss, J. G. *Acta Chem. Scand.* **11** (1957) 1157.
2. Wicki, W., Kalvoda, J. and Jeger, O. *Croat. Chem. Acta* **29** (1957) 265.
3. Djerassi, C. and Nakano, T. *Chem. & Ind. London* **1960** 1385.

Received December 31, 1961.

ACTA CHEMICA SCANDINAVICA 16 (1962) 1315–1320

Polarography of Some Complexes with N-Hydroxyethylethylenediamine-triacetic Acid

KNUT HENNING SCHRØDER

Kjemisk Institutt A, Universitetet i Oslo, Blindern, Norway

The complexes of copper, cadmium and lead with N-hydroxyethylethylenediamine-triacetic acid have been studied by means of the dropping mercury electrode. The half-wave potentials and the diffusion current constants have been determined. It is found that the copper complexes are reduced reversibly while cadmium and lead show irreversible reductions, but all the reductions are diffusion controlled. The complex constants of copper have been calculated.

The complexes of some metals with N-hydroxyethylethylenediamine-triacetic acid (HEDTA) have earlier been studied by potentiometric methods [1–3]. The HEDTA complexes with iron have been studied by pH and redox potential titrations as well as by polarographic and spectrophotometric measurements [4]. The stabilities of the rare earth complexes have been determined by Spedding and co-workers [5].

The present paper is a polarographic study of the copper(II), cadmium and lead complexes formed with HEDTA.

EXPERIMENTAL

Materials. The trisodium hydroxyethylethylenediamine-triacetate, Chel DM-41, and the corresponding HEDTA-acid, Chel DM acid, obtained from Geigy Industrial Chemicals, were used without further purifications and both samples gave identical results. Impurities of sequestering agents with higher stabilities than HEDTA (*e.g.* ethylenediamine-tetraacetic acid, diethylenetriamine-pentaacetic acid, *etc.*) were found not to be present, because the half-wave potentials with the above quality reagents and the potentials of the corresponding complexes with *p.a.* HEDTA were identical (*p.a.* HEDTA was not available until near the end of the experiments). The reagent was standardized by complexometric titration with a standard solution of lead. The remaining chemicals were of reagent grade. Stock solutions of copper, cadmium and lead were prepared by dissolving the corresponding metal salt in redistilled water, and standardized by complexometric titrations with EDTA. A 0.1 M NH_3–NH_4Cl buffer was used if not otherwise stated. To vary pH, NH_3 was added to a 0.1 M HCl solution or HCl was added to a 0.2 M NH_3 solution; to keep the ionic strength constant ($\mu = 0.1$) the first method was preferred when possible. The most alkaline solutions were made up with KOH. The pH was meas-

ured with a conventional pH meter with glass electrode. For studies of the shifts of half-wave potentials with pH, the Beckman so-called "stomach" electrode, directly inserted in the polarographic cell, was found convenient for the pH measurements. Unless specified, the concentration of complexing agent is 12 mM and of metal ions, 0.2 mM.

Apparatus and technique. Polarograms were recorded with a Tast-polarograph, Selector D (Atlas Werken, Bremen, Germany). The conventional type of dropping mercury electrode and of electrolysis cell were used. The capillary characteristics, measured in open circuit at a mercury height of 35 cm were

$$m = 3.015 \text{ mg/sec, and } t = 3.36 \text{ sec.}$$

An external saturated calomel electrode (S.C.E.) served as reference electrode. Dissolved air was removed from the solutions by bubbling oxygen-free nitrogen through the cell for 10 min and passing it over the solution during the electrolysis. All experiments were performed at 25 ± 0.1°C (except in the temperature coefficient studies). The total a.c. resistance of the cell, agar bridge and reference electrode was 800 Ω.

The reversibility of the electrode reactions was tested from the temperature coefficient of the half-wave potentials and the slopes of log $i/(i_d-i)$ *vs.* the potential curves.Corrections were made for the residual current. The data for the log plots were obtained by manual operations of the polarograph. The applied potentials were measured with a Leeds and Northrup Type K potentiometer. Half-wave potentials were taken from the logarithmic plots and were reproducible to ± 1 mV.

Calculations. The HEDTA becomes protonated to varying degrees depending upon the pH of the solution. The following values for the dissociation constants were used to calculate the actual concentrations [2]:

$$pK_1 = 2.64, \qquad pK_2 = 5.33, \qquad pK_3 = 9.73$$

For the reversible processes, the stability constants (pK_c) of the complexes were calculated from the shifts in the half-wave potentials to more negative values on addition of sequestering agent, as described by Kolthoff and Lingane [6].

As the concentration of the free ligand available for complex formation varies with pH of the solution, a plot of $(E_{1/2})_c$ *vs.* pH has a slope a given by

$$a = \frac{0.0591}{n} \cdot Z \qquad \text{(I)}$$

where Z is the number of protons involved in the reduction process:

$$M(H_qX)_p^{[n+p(q-b)]} + Z\,H^+ + n\,e^- + (Hg) = M(Hg) + H_z(H_qX)p^{[Z+p(q-b)]+} \qquad \text{(II)}$$

RESULTS AND DISCUSSION

(*a*) *Copper.* All complexes with copper are reduced directly to the amalgam. The reduction is thermodynamically reversible in the measured pH-range and with all the used concentrations of HEDTA, since the log $i/(i_d-i)$ *vs.* E slopes are all nearly theoretical (n = 2), and since the temperature coefficient of the diffusion current is only + 1.3 %/degree and the shift in half-wave potential only + 0.78 mV/degree.

The slopes of the polarograms are very dependent on the presence of surface active substances. Thus, 0.0004 % Triton X-100 highly affects the diffusion current and half wave-potential and no wave is observed with concentrations of Triton X-100 exceeding 0.005 % before components of the supporting electrolytes are reduced. No maximum suppressor is used in the measurements below.

pH studies. Fig. 1 shows plots of $(E_{1/2})_c$ *vs.* pH for copper(II) with excess of HEDTA. The slope gives the value of Z in eqn. (II). The slopes of log $i/(i_d-i)$ *vs.* E were all in the range 33—36 mV per log unit, giving n = 2. The magnitudes of the half-wave potentials for pH < 2.5 are rather approxi-

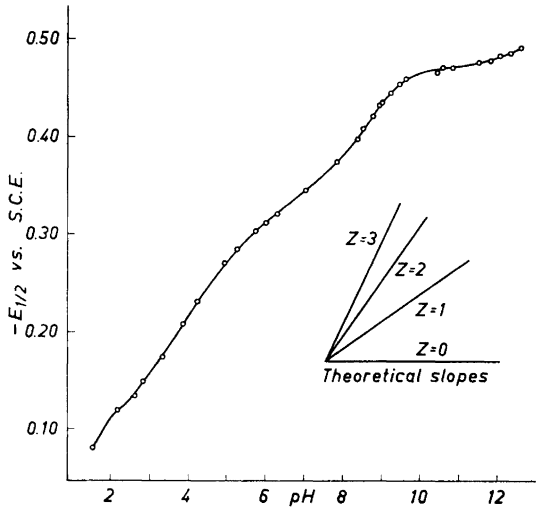

Fig. 1. Variation of half-wave potentials of copper complexes of HEDTA with pH of the solution.

mate because dissolution of mercury took place at almost the same potentials as the reduction of the copper complexes.

A comparison with eqn. (I) indicates that different complexes are formed. The unprotonated complex appears above pH = 8. Up to pH = 9, Z = 2, giving the following reduction process (H_3Y = HEDTA):

$$CuY^- + 2\ e^- + 2\ H^+ + (Hg) = Cu^\circ(Hg) + H_2Y^- \qquad (III)$$

In the pH-range 9—10, Z is changing from 2 to 0. (Z = 1 will give:

$$CuY^- + 2\ e^- + H^+ + (Hg) = Cu^\circ(Hg) + HY^{2-}) \qquad (IV)$$

In the pH-range 10—11.5, Z = 0:

$$CuY^- + 2\ e^- + (Hg) = Cu^\circ(Hg) + Y^{3-} \qquad (V)$$

(Here the mole ratio of metal ion and ligand is assumed to be unity, as stated later.)

It seems that the weak ethanolic group of the ligand possibly dissociates a proton above pH = 11.5, giving a new complex. The slope in Fig. 1 seems to fit for a reaction with Z = 1 ($H_3(OH)Z$ = HEDTA):

$$Cu(ZO)^{2-} + 2\ e^- + H^+ + (Hg) = Cu^\circ(Hg) + Z(OH)^{3-} \qquad (VI)$$

A detailed study of this complex is not possible since this will need to high pH.

In more acid solutions than pH = 8, Fig. 1 shows the appearance of a protonated complex with Z = 1 in the pH-range 5—8:

$$Cu[HY] + 2\ e^- + H^+ + (Hg) = Cu^\circ(Hg) + H_2Y^- \qquad (VII)$$

Below pH = 5, Z = 2 and the reaction is:

$$Cu[HY] + 2\ e^- + 2\ H^+ + (Hg) = Cu^\circ(Hg) + H_3Y \qquad \text{(VIII)}$$

(Here too, the mole ratio of metal ion and ligand is assumed to be unity, as stated later.)

Stability studies. The polarographic data were used to determine the composition of the complexes and the stability constants.

Plots of the values of $(E_{½})_c$ *vs.* the corresponding values of the logarithm of the concentration of the complexing agent show straight lines. In 0.1 M NH_3—NH_4Cl buffer, pH = 9.25, and in 0.1 M sodium acetate-acetic acid buffer, pH = 4.70, the found values of the half-wave potentials in the concentration range 0.3—20 mM HEDTA may be expressed by the following equations:

$$E_{½} = -0.529 - 0.033\ \log\ C_x \text{ and} \qquad \text{(IX)}$$

$$E_{½} = -0.335 - 0.032\ \log\ C_x \qquad \text{(X)}$$

These equations correspond to the complexes CuY^- and Cu[HY], respectively. Therefore, by means of the protolysis constants of HEDTA, C_x is calculated to be the excess of Y^{3-} and HY^{2-} in the two solutions. The slopes of the lines indicate that the mole ratio of metal ion and ligand is unity in both complexes. The half-wave potential of the Cu^{2+}_{aq} complex, $(E_{½})_s$, is taken to be + 0.04 V *vs.* S.C.E. The stability constants are defined as follows:

$$K_{c1} = \frac{[Cu^{2+}]\cdot[Y^{3-}]}{[CuY^-]} \ : \ pK_{c1} = 18.8 \qquad \text{(XI)}$$

$$K'_{c2} = \frac{[Cu^{2+}]\cdot[HY^{2-}]}{[Cu(HY)]} \ ; \ pK'_{c2} = 12.4 \qquad \text{(XII)}$$

To bring eqn. (XII) to a more familiar form, it is combined with (XI) and the dissociation constant pK_3, giving

$$K_{c2} = \frac{[CuY^-]\cdot[H^+]}{[Cu(HY)]} \ ; \quad pK_{c2} = 3.3 \qquad \text{(XIII)}$$

The values become slightly different if calculated with eqn. (IX) and (X) because of deviations from theoretical slopes.

Potentiometrically [2], pK_{c1} has been measured to 17.4. The difference between the potentiometric and polarographic results cannot at present be explained, but similar discrepancy has been observed with related metal complexes.

The reduction of the CuY^- complex is found to be diffusion controlled, obeying Ilkovič's equation, since the diffusion current varies linearly with the concentration of added copper(II) ions in the concentration range studied (from 1.8—9.0 × 10^{-4} M) and with the square root of the height of mercury (from 30—45 cm, corrected for the "back pressure").

The diffusion constant, defined as

$$I = i_d/C \cdot m^{2/3} \cdot t^{1/6}$$

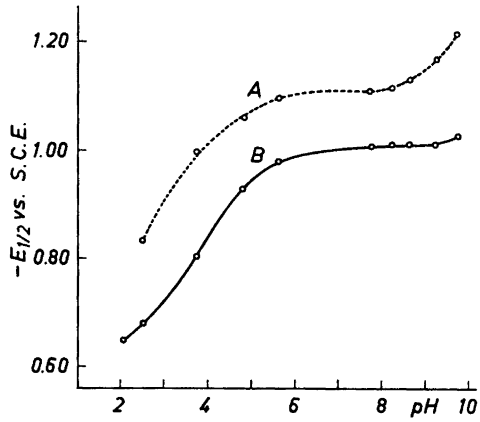

Fig. 2. Variation of half-wave potentials of (A) cadmium- and (B) lead complexes of HEDTA with pH of the solutions.

is measured to 3.03 and 3.13 in solutions containing 1.2×10^{-2} M HEDTA in 0.1 M ammonia or acetic acid buffer (pH = 9.25 and 4.70) and correspond to the complexes CuY^- and Cu[HY].

(*b*) *Cadmium and lead.* The polarographic reduction of these metal complexes with HEDTA was found to be irreversible. The plots of log $i/(i_d - i)$ *vs.* E are curved at all concentrations of the reagent and all values of pH, and the slopes are approximately twice the theoretical values. The irreversibility is probably due to too slow reduction rates. Koryta and Kössler [7] found the same effects with the related sequestering agents nitrilotriacetic acid and ethylenediaminetetraacetic acid.

The polarograms of the cadmium and lead complexes are, like the corresponding copper, complexes, very sensitive to surface active substances.

Plots of the half-wave potentials *vs.* pH for the two metal complexes are shown in Fig. 2. Two waves appeared in acid solutions (pH < 4). The first

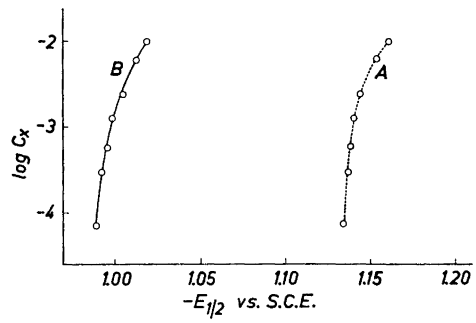

Fig. 3. Variation of half-wave potentials of (A) cadmium- and (B) lead complexes of HEDTA with the logarithm of the concentration of the chelating agent ($C_x = [Y^{3-}]$). pH = 9.25.

one is reversible and is due to reduction of uncomplexed cadmium or lead ions. Because of the irreversibility, no conclusions can be drawn about the nature of the complexes, but comparing with Fig. 3 showing shifts in half-wave potentials with excess of HEDTA, it seems that the reasons for the irreversibility are the same for both complexes since the shapes of the A and B curves are very similar.

The diffusion constants are 2.85 and 3.26 for cadmium and lead complexes, respectively (1.2×10^{-2} M HEDTA, ammonia buffer with pH = 9.25). The diffusion current varies linearly with the square root of the mercury height, measured from 30—45 cm, and with concentrations of metals from $1.8—9 \times 10^{-4}$ M, indicating that the reductions are diffusion controlled. All the polarographic waves are very well defined. The observed half-wave potentials are shown in Figs. 2 and 3.

Chaberek and Martell [2] find that the reduction of iron(III)-HEDTA complexes is reversible and it must be concluded that the mechanism of reduction of the copper and iron complexes is different from that of the cadmium and lead complexes.

REFERENCES

1. Chaberek, S. and Bersworth, F. C. *Science* **118** (1953) 280.
2. Chaberek, S. and Martell, A. E. *J. Am. Chem. Soc.* **77** (1955) 1477.
3. Holloway, J. H. and Reilley, C. N. *Anal. Chem.* **32** (1960) 249.
4. Shochdopole, R. and Chaberek, S. *J. Inorg. & Nuclear. Chem.* **11** (1959) 222.
5. Spedding, F. H., Powell, J. E. and Wheelweight, E. J. *J. Am. Chem. Soc.* **78** (1956) 34.
6. Kolthoff, I. M. and Lingane, J. J. *Polarography*. Interscience, New York 1952, p. 214.
7. Koryta, J. and Kössler, I. *Collection Czechoslov. Chem. Communs.* **15** (1950) 241.

Received December 20, 1961.

ACTA CHEMICA SCANDINAVICA 16 (1962) 1321–1323

Mean Amplitudes of Vibration and Shrinkage Effect of Hydrogen Cyanide from Spectroscopic Data

E. MEISINGSETH and S. J. CYVIN

Institutt for teoretisk kjemi, Norges tekniske høgskole, Trondheim, Norway

Some aspects of the molecular vibrations of the linear YXZ molecular model are studied, and the following calculated quantities for hydrogen cyanide are reported: (*a*) Force constants, (*b*) L matrix elements, (*c*) various mean-square amplitude quantities, (*d*) mean amplitudes of vibration, and (*e*) Bastiansen-Morino shrinkage effect. It has been found at 298°K in Å units: (*d*) $u_{CH} = 0.0731$, $u_{CN} = 0.0342$, $u_{HN} = 0.0941$, and (*e*) $\delta = 0.0164$.

Some spectroscopic calculations for hydrogen cyanide have been performed in addition to the study of cyanogen [1] and acetylene [2]. These computations are believed to be of great value in connection with the recent electron-diffraction study of cyanoacetylene.

THEORY

The present computations are based on the assumption of small harmonic vibrations [3]. It is adhered to the previously chosen internal coordinates as communicated by Cyvin [4].

The cartesian displacement coordinates have been expressed in terms of the symmetry coordinates with the following result.

$$
\begin{aligned}
x_X &= -S_{2a}(R_1R_2)^{1/2}(R_1 + R_2)m_Y m_Z/C \\
y_X &= -S_{2b}(R_1R_2)^{1/2}(R_1 + R_2)m_Y m_Z/C \\
z_X &= (S_1 m_Y - S_3 m_Z)/(m_X + m_Y + m_Z) \\
x_Y &= S_{2a}(R_1R_2)^{1/2}R_2 m_X m_Z/C \\
y_Y &= S_{2b}(R_1R_2)^{1/2}R_2 m_X m_Z/C \\
z_Y &= -[S_1(m_X + m_Z) + S_3 m_Z]/(m_X + m_Y + m_Z) \\
x_Z &= S_{2a}(R_1R_2)^{1/2}R_1 m_X m_Y/C \\
y_Z &= S_{2b}(R_1R_2)^{1/2}R_1 m_X m_Y/C \\
z_Z &= [S_1 m_Y + S_3(m_X + m_Y)]/(m_X + m_Y + m_Z)
\end{aligned}
$$

Here m_X, m_Y and m_Z denote the atomic masses of the X, Y and Z atoms, respectively. The following abbreviation has been used:

$$C = R_1^2\, m_X m_Y + R_2^2\, m_X m_Z + (R_1 + R_2)^2\, m_Y m_Z$$

R_1 and R_2 are used to designate the equilibrium X—Y and X—Z distances, respectively. For further explanation of the symbols, the cited paper [4] should be consulted.

Parallel vibrations. The mean-square parallel amplitudes (or mean-square amplitudes of vibration [5]) for the presently treated molecular model have been studied previously [6]. With the notation $\sigma_{AB} = \langle(z_A - z_B)^2\rangle$, where X, Y and Z may be inserted for A and B, one has

$$\sigma_{XY} = \Sigma_1, \quad \sigma_{XZ} = \Sigma_3, \quad \sigma_{YZ} = \Sigma_1 + \Sigma_3 + 2\,\Sigma_{13}$$

Perpendicular vibrations. The mean-square perpendicular amplitudes [1,4,7] will be identified by the symbol $\tau_{AB} = \langle(x_A - x_B)^2\rangle = \langle(y_A - y_B)^2\rangle$. The following expressions have been found in terms of the mean-square amplitude matrix element $\Sigma_2 = \langle S_{2a}^2\rangle = \langle S_{2b}^2\rangle$.

$$\tau_{XY} = \Sigma_2 R_1 R_2 m_Z^2 [R_2 m_X + (R_1 + R_2) m_Y]^2 / C^2$$
$$\tau_{XZ} = \Sigma_2 R_1 R_2 m_Y^2 [R_1 m_X + (R_1 + R_2) m_Z]^2 / C^2$$
$$\tau_{YZ} = \Sigma_2 R_1 R_2 m_X^2 (R_1 m_Y - R_2 m_Z)^2 / C^2$$

The Σ_2 element is closely connected with the perpendicular vibration frequency (ω_2) according to

$$\Sigma_2 = (hC/8\pi^2 R_1 R_2 m_X m_Y m_Z c\omega_2)\, \coth(hc\omega_2/2kT)$$

where, apart from the symbols used above, only the temperature (T in °K) and fundamental physical constants (h = Planck's constant, c = velocity of light, k = Boltzmann's constant) are present.

Shrinkage effect [1,2,8]. In the presently considered molecular model the Bastiansen-Morino shrinkage effect is given by

$$-\delta = \tau_{YZ}/(R_1 + R_2) - \tau_{XY}/R_1 - \tau_{XZ}/R_2$$

NUMERICAL COMPUTATIONS

The theory has been applied to hydrogen cyanide, identifying the atoms X, Y and Z by C, H and N, respectively.

The adopted equilibrium distance values, *viz.*, $R_1 = 1.0630$ Å and $R_2 = 1.1538$ Å, have been taken from Costain [9]. The normal frequencies (see below) have been obtained from the reported data of Allen, Tidwell and Plyler [10], and are not much different from those of Douglas and Sharma [11].

No.	HCN	DCN
1	2127.6 cm^{-1}	1953.2 cm^{-1}
2	726.8 cm^{-1}	579.9 cm^{-1}
3	3442.8 cm^{-1}	2702.9 cm^{-1}

The force constants were recalculated with the following result (in the notation of Ref.[10]):

$f_1 = 6.249 \times 10^5$ d/cm, $\quad f_2 = 18.689 \times 10^5$ d/cm,
$f_{12} = -0.2140 \times 10^5$ d/cm, $\quad f_a/R_1R_2 = 0.2108 \times 10^5$ d/cm.

The wide applicability of the L-matrix makes it justified to specify its ele-

Table 1. Mean-square amplitude quantities in Å² units for hydrogen cyanide.

Symbol	$T = 0$	298°K
$\Sigma_1 = \sigma_{CH}$	0.005345	0.005345
$\Sigma_3 = \sigma_{CN}$	0.001167	0.001167
Σ_{13}	0.001169	0.001170
Σ_2	0.03425	0.03637
σ_{HN}	0.008852	0.008852
τ_{CH}	0.02264	0.02403
τ_{CN}	0.000870	0.000924
τ_{HN}	0.01463	0.01554

Table 2. Mean amplitudes of vibration (u) and shrinkage effect (δ) in Å units for hydrogen cyanide.

Symbol	$T = 0$	298°K
u_{CH}	0.0731	0.0731
u_{CN}	0.0342	0.0342
u_{HN}	0.0941	0.0941
δ	0.0154	0.0164

ments for the symmetry coordinates of the species Σ^+. It has been found in $(\text{Amu})^{-\frac{1}{2}}$:

$$S_1 = 0.1614\ Q_1 + 1.024\ Q_3$$
$$S_3 = 0.3678\ Q_1 + 0.1393\ Q_3$$

The elements of the Σ-matrix are given numerically in Table 1 at the temperatures of absolute zero and 298°K, along with the mean-square parallel and perpendicular amplitudes. In Table 2 the mean amplitudes of vibration and the shrinkage effect are given.

REFERENCES

1. Cyvin, S. J. and Meisingseth, E. *Acta Chem. Scand.* **15** (1961) 1289.
2. Meisingseth, E. and Cyvin, S. J. *Acta Chem. Scand.* **15** (1961) 2021.
3. Wilson, E. B., Jr., Decius, J. C. and Cross, P. C. *Molecular Vibrations*, McGraw-Hill Book, New York 1955.
4. Cyvin, S. J. *Spectrochim. Acta* **17** (1961) 1219.
5. Cyvin, S. J. *Kgl. Norke Videnskab. Selskabs Skrifter* (1959) No. 2.
6. Cyvin, S. J. *Spectrochim. Acta* **15** (1959) 835.
7. Morino, Y. and Hirota, E. *J. Chem. Phys.* **23** (1955) 737; Cyvin, S. J. *J. Mol. Spectroscopy* **6** (1961) 333.
8. Bastiansen, O. and Trætteberg, M. *Acta Cryst.* **13** (1960) 1108; Morino, Y. *Acta Cryst.* **13** (1960) 1107.
9. Costain, C. C. *J. Chem. Phys.* **29** (1958) 864.
10. Allen, H. C., Jr., Tidwell, E. D. and Plyler, E. K. *J. Chem. Phys.* **25** (1956) 302.
11. Douglas, A. E. and Sharma, D. *J. Chem. Phys.* **21** (1953) 448.

Received December 23, 1961.

ACTA CHEMICA SCANDINAVICA 16 (1962) 1324–1328

Studien über Elimination

IV *. Eine neue Methode zur Darstellung von δ-Ketonitrilen

GUNNEL NÄSLUND, ALEXANDER SENNING** und SVEN-OLOV LAWESSON**

Laboratorium für Organische Chemie, Chemisches Institut der Universität Uppsala, Uppsala, Schweden

t-Butylazetoazetat und alkyl- und aralkylsubstituierte *t*-Butylazetoazetate wurden zyanäthyliert und anschliessend die Karbo-*t*-butoxygruppe durch Erhitzen der Addukte auf 150° in Gegenwart katalytischer Mengen *p*-Toluolsulfonsäure eliminiert. Auf diese Weise wurden hohe Ausbeuten der entsprechenden δ-Ketonitrile erzielt, ohne dass die Zyangruppe angegriffen wurde. In *t*-Butyl-(2-zyanäthyl)-azetoazetat wurde auch die Benzoyloxygruppe durch Umsetzung der Natriumverbindung mit Benzoylperoxyd in Benzol eingeführt. Elimination lieferte dann eine Verbindung vom Azylointyp: 4-Azetyl-4-benzoyloxybutannitril.

Lawesson und Mitarbeiter studierten kürzlich die Chemie des *t*-Butylazetoazetats [1,2], einer Verbindung, die sich leicht aus Diketen und *t*-Butanol darstellen lässt [3]. Hauser und Mitarbeiter [4,5] fanden 1944, dass *t*-Butylhydrogenmalonat beim Erhitzen eine Eliminierungsreaktion erleidet. Auf diesem Gebiet ist auch weiterhin noch gearbeitet worden (ausführliche Literaturhinweise finden sich bei Frisell und Lawesson [6]). Im allgemeinen erleiden β-Karbonylverbindungen vom Typ I beim Erhitzen mit *p*-Toluolsulfonsäure (TS) eine Karbo-*t*-butoxy-Elimination wie folgt:

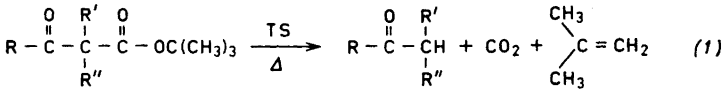

I *II* (1)

* Teil I: Frisell, C. und Lawesson, S.-O. *Arkiv Kemi* **17** (1961) 401; Referenz[1] soll als Teil II und Referenz [2] als Teil III dieser Reihe betrachtet werden.

** Neue Anschrift: Chemisches Institut der Universität Aarhus, Aarhus, Dänemark.

wobei R = OC_2H_5, $OC(CH_3)_3$ oder CH_3, während R′ und R″ verschiedene funktionelle Gruppen oder Alkylgruppen sind. Da *t*-Butylazetoazetat (I, R = CH_3, R′ = R″ = H) die am leichtesten zugängliche Verbindung dieses Typs ist, wurde es in einer Reihe von Untersuchungen [7–9] als Modellsubstanz benutzt; durch Darstellung anderer *t*-Butyl-β-ketoester müsste sich zeigen lassen, dass die hier entwickelten Methoden ganz allgemein für den präparativ-organisch arbeitenden Chemiker von Wert sind.

In Gegenwart eines basischen Katalysators lassen sich Ketone, die mindestens ein α-Wasserstoffatom enthalten, durch Umsetzung mit Akrylnitril zyanäthylieren. Allgemein wird die zweite Zyanäthylgruppe, wenn sich am selben Kohlenstoffatom mehr als ein α-Wasserstoffatom befindet, leichter addiert als die erste und die dritte leichter als die zweite. Überschuss an Keton begünstigt die Bildung des Produkts mit weniger Zyanäthylgruppen [10]. Die Monozyanäthylierung des Zyklohexanons wurde in hohen Ausbeuten dadurch erreicht, dass das Keton vor der Zyanäthylierung in sein Pyrrolidinenamin überführt wurde [11]. Dieses Enamin kann dann leicht zum Ketonitril hydrolysiert werden.

Allerdings wurden unseres Wissens in den wenigen Fällen, in denen Ketone mit Akrylnitril umgesetzt wurden [12,13] nur niedrige Ausbeuten an monozyanäthylierten Ketonen erzielt. Ausserdem muss betont werden, dass man auf Grund von Strukturbetrachtungen bei unsymmetrischen aliphatischen Ketonen monozyanäthylierte Isomere erwarten muss, obwohl eine Methingruppe reaktiver als eine Methylengruppe und eine Methylengruppe reaktiver als eine Methylgruppe (in Nachbarschaft einer Karbonylgruppe) ist; andererseits gibt ein symmetrisches Keton nur ein Monozyanäthylderivat.

Es war daher zu erwarten, dass sich aus *t*-Butylazetoazetat oder seinen Derivaten die entsprechende Zyanäthylverbindung darstellen lassen würde und dass nach Eliminierung der Karbo-*t*-butoxygruppe das entsprechende δ-Ketonitril auf indirektem Wege erhalten werden würde.

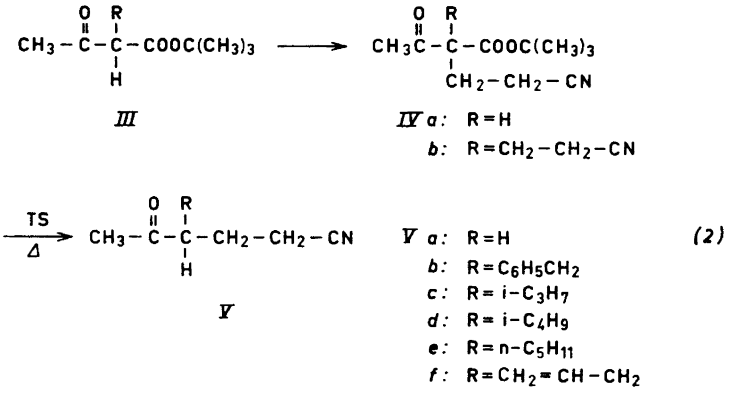

(2)

Die Zyanäthylierung von β-Ketoestern ist bekannt [13], aber nach Verseifung des Addukts werden Glutarsäuren isoliert, da die Zyangruppe sofort angegriffen wird. Albertson [17] stellte jedoch durch Hydrolyse der Estergruppe mit wässriger Natriumkarbonatlösung aus zwei Monozyanäthyl-β-ketoestern δ-Ketoni-

trile dar. Dieselbe Methode wurde später auch unabhängig von Yoho und Levine[18] entwickelt. Wir fanden jetzt, dass die Zyanäthylierung von *t*-Butyl azetoazetaten glatt verläuft und dass die Zyangruppe beim Erhitzen mit *p*-Toluolsulfonsäure nicht hydrolysiert wird. Nur in zwei Fällen wurden analysenreine Addukte isoliert (IVa und b); die anderen Zyanäthylverbindungen zersetzten sich langsam beim Destillieren und wurden daher, ohne erst isoliert zu werden, sofort zu δ-Ketonitrilen pyrolysiert (in Gegenwart von *p*-Toluolsulfonsäure). Beim unsubstituierten *t*-Butylazetoazetat wurden sowohl Mono- als auch Dizyanäthylverbindungen isoliert. Alle substituierten *t*-Butylazetoazetate gaben hohe Ausbeuten mit Ausnahme des sterisch behinderten *t*-Butyl-*i*-propylazetoazetats, das unter abweichenden Bedingungen (Erhitzen, Überschuss an Akrylnitril) nur eine Gesamtausbeute von 20—30 % δ-Ketonitril gab.

Schliesslich wurde die Benzoyloxygruppe in *t*-Butyl-(2-zyanäthyl)-azetoazetat (IVa) eingeführt, indem zuerst die Natriumverbindung von IVa in Benzol hergestellt und diese bei 0° mit Benzoylperoxyd (in Benzol) umgesetzt wurde. Dadurch wird die Sauerstoff-Sauerstoff-Bindung des Peroxyds gespalten und die Benzoyloxygruppe eingeführt:

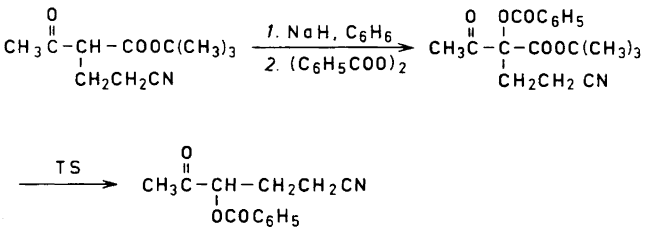

(3)

Diese allgemeingültige Methode zur Einführung von Benzoyloxygruppen in sogenannte aktive Methylenverbindungen wurde kürzlich von Lawesson und Mitarbeitern [1,2,19–22] bearbeitet und vor ganz kurzem wurde der Mechanismus dieser Reaktion aufgeklärt [23].

Die Methode zur Darstellung von δ-Ketonitrilen, die hier beschrieben wird, scheint noch nicht bekannt zu sein. Sie liefert im allgemeinen hohe Ausbeuten, geht von billigen und leicht zugänglichen Substanzen aus und ist ausserordentlich leicht auszuführen. Auf diese Weise lassen sich verschiedene Typen von substituierten δ-Ketonitrilen darstellen, die als Ausgangsmaterial für physiologisch aktive Piperidinderivate und andere Verbindungen von potentiellem Interesse sind.

BESCHREIBUNG DER VERSUCHE

Ausgangsmaterialien. *t*-Butylazetoazetat und dessen Alkylderivate wurden nach bekannten Methoden [1-3] dargestellt. Das Akrylnitril des Handels wurde ohne weitere Reinigung verwendet. Das Benzoylperoxyd wurde bei niedrigen Temperaturen aus Chloroform und Methanol umkristallisiert. Die Analysen wurden von der Firma Alfred Bernhardt, Mülheim (Ruhr), Deutschland, im Institut für Analytische Chemie der Universität Uppsala und im Medizinisch-Chemischen Institut der Universität Uppsala ausgeführt. Alle Schmelz- und Siedepunkte sind unkorrigiert.

Darstellung von t-Butyl-(2-zyanäthyl)-azetoazetat (IVa) und t-Butyl(2,2-biszyanäthyl)-azetoazetat (IVb). In einem 500-ml-Dreihalskolben, der mit einem kräftigen Rührer, einem

Rückflusskühler und einem Tropftrichter versehen war, wurden 158 g (1 Mol) *t*-Butylazetoazetat in 100 ml absolutem Alkohol gelöst. Darauf wurden 0,7 g Natrium zugesetzt. Zu der schwach gelben Lösung wurden 42,5 g (0,8 Mol) Akrylnitril so zugetropft, dass sich die Temperatur zwischen 40° und 45° hielt. Das Reaktionsgemisch wurde 45 Min. gerührt (bis zum Ende der exothermen Reaktion) und dann das Äthanol abdestilliert. Der Rückstand wurde in Äther gelöst und mit 1 ml Essigsäure und Wasser neutral gewaschen. Die Ätherphase wurde über Natriumsulfat getrocknet, der Äther abdestilliert und der Rückstand fraktioniert. Die Hauptfraktion, das Monozyanäthylazetoazetat, hatte Kp. 97°—98°/0,02 mm Hg und n_D^{20} 1,4406. Ausbeute 58,6 g (35 % der Theorie). (Gef. C 62,51; H 7,96. Ber. für $C_{11}H_{17}O_3N$: C 62,54; H 8,11).

Der Destillationsrückstand liess sich nicht unzersetzt destillieren und kristallisierte beim Abkühlen. Nach zweimaligem Umkristallisieren aus Äthanol wurden weisse Nadeln vom Schmelzpunkt 55°—57° erhalten. Ausbeute an Biszyanäthylazetoazetat 43,6 g (21 % der Theorie). (Gef. C 63,81; H 7,73; N 10,68. Ber. für $C_{14}H_{20}O_3N_3$: C 63,61; H 7,63; N 10,60).

Darstellung von δ-Ketonitrilen

*4-Azetyl-*n*-butannitril (Va).* 24,3 g (0,12 Mol) *t*-Butyl-*a*-(2-zyanäthyl)-azetoazetat und 0,1 g *p*-Toluolsulfonsäure wurden in einem Destillationskolben in ein Ölbad von 150° gebracht. Nach etwa 15 Min. hatte die pyrolytische Gasentwicklung aufgehört, so dass im Destillationsapparat konstanter Druck herrschte. Beim Destillieren wurde eine farblose Flüssigkeit vom Kp. 107°—108°/10 mm Hg und n_D^{20} 1,4316 erhalten. Ausbeute: 12,8 g (96 % der Theorie). Das 2,4-Dinitrophenylhydrazon schmolz zwischen 155° und 157° (aus Äthanol).

*4-Azetyl-5-phenyl-*n*-pentannitril (Vb):* In einen 250-ml-Dreihalskolben mit Tropftrichter, Rührer, Thermometer und Rückflusskühler wurden 99,2 g (0,4 Mol) *t*-Butyl-*a*-benzylazetoazetat und 40 ml Äthanol gebracht. In dieser Ester-Alkohol-Lösung wurden 0,3 g Natrium gelöst. Darauf wurden 15,9 g (0,3 Mol) Akrylnitril im Laufe von 40 Min. zugegeben (die Temperatur wurde unter 45° gehalten). Nach weiteren 30 Min. wurde das Äthanol abdestilliert, Äther zugesetzt und die Ätherphase mit 0,5 ml Essigsäure und Wasser neutral gewaschen. Nach Trocknen über Natriumsulfat wurde der Äther und unumgesetztes Akrylnitril und Ester abdestilliert. Dem Rückstand wurden 0,1 g *p*-Toluolsulfonsäure zugesetzt und danach wie oben bei 165°—170° pyrolysiert. Durch Fraktionieren wurde eine farblose Flüssigkeit vom Kp. 122°/0,1 mm Hg, n_D^{20} 1,5182 erhalten. Ausbeute: 59,0 g (98 % der Theorie). (Gef. C 77,70; H 7,30; N 6,99. Ber. für $C_{13}H_{15}ON$: C 77,58; H 7,51; N 6,96).

*4-Azetyl-5-methyl-*n*-hexannitril (Vc).* Zu einer Lösung von 80,0 g (0,4 Mol) *t*-Butyl-*a*-*i*-propylazetoazetat in 45 ml Äthanol wurden 0,3 g Natrium zugesetzt. 15,9 g (0,3 Mol) Akrylnitril wurden zugegeben und das Reaktionsgemisch 5 Stunden auf 35°—40° gehalten. Der Alkohol wurde abdestilliert und der Rückstand wie üblich aufgearbeitet. Nach der Pyrolyse bei 160° wurde beim Fraktionieren eine farblose Flüssigkeit vom Kp. 118°—119°/11 mm Hg und n_D^{20} 1,4427 erhalten. Ausbeute: 10,0 g (22 % der Theorie). (Gef. C 70,88; H 9,42; Ber. für $C_9H_{15}ON$: C 70,55; H 9,87).

*4-Azetyl-6-methyl-*n*-heptannitril (Vd):* 30,0 g (0,14 Mol) *t*-Butyl-*a*-*i*-butylazetoazetat, 14 ml Äthanol, 0,1 g Natrium und 6,9 g (0,13 Mol) Akrylnitril wurden in der üblichen Weise bei 35° miteinander umgesetzt (6 Stunden). Nach der Pyrolyse bei 150°—155° (0,1 g TS) ging beim Fraktionieren zwischen 133°/12 mm Hg und 134°/12 mm Hg eine farblose Flüssigkeit, n_D^{20} 1,4420, über. Ausbeute: 12,7 g (59 % der Theorie). (Gef. C 71,50; H 10,15. Ber. für $C_{10}H_{17}ON$: C 71,80; H 10,25).

*4-Azetyl-*n*-nonannitril (Ve).* 47,9 g (0,21 Mol) *t*-Butyl-*a*-*n*-amylazetoazetat, 21 ml Äthanol, 0,2 g Natrium und 9,0 g (0,17 Mol) Akrylnitril wurden wie oben bei 35° miteinander umgesetzt (5 Stunden). Nach Pyrolyse in Gegenwart von *p*-Toluolsulfonsäure bei 155°—160° wurde eine farblose Flüssigkeit vom Kp. 149°—150°/12 mm Hg, n_D^{20} 1,4450 erhalten. Ausbeute: 29,7 g (97 % der Theorie). (Gef. C 72,56; H 10,90. Ber. für $C_{11}H_{19}ON$: C 72,80; H 10,57).

*4-Azetyl-4-allyl-*n*-butannitril (Vf):* 51,0 g (0,26 Mol) *t*-Butyl-*a*-allylazetoazetat, 25 ml Äthanol, 0,2 g Natrium und 10,6 g (0,20 Mol) Akrylnitril wurden bei 35°—40° miteinander

umgesetzt (3,5 Stunden). Die Karbo-*t*-butoxygruppe wurde bei 150° eliminiert. Das Produkt war eine farblose Flüssigkeit, Kp. 130°—131°/11 mm Hg, n_D^{20} 1,4571. Ausbeute: 25,2 g (84 % der Theorie). (Gef. C 71,24; H 9,06. Ber. für $C_9H_{13}ON$: C 71,49; H 8,67).

*4-Azetyl-4-benzoyloxy-*n*-butannitril:* In einen Dreihalskolben mit Rührer, Rückflusskühler und Tropftrichter wurden 3,4 g (0,14 Mol) Natriumhydrid und 100 ml trockenes Benzol gebracht. 29,0 g (0,14 Mol) *t*-Butyl-*a*-(2-zyanäthyl)-azetoazetat wurden zugesetzt und nach 2,5-Stunden hatte der grösste Teil des Natriumhydrids reagiert und die Gasentwicklung aufgehört. 24,2 g (0,10 Mol) Benzoylperoxyd in 260 ml trockenem Benzol wurden im Laufe von 25 Min. zu der auf 0—4° gekühlten Natriumverbindung zugetropft. Nachdem das Gemisch über Nacht gerührt worden war, wurde es in kaltes Wasser gegossen und mit Salzsäure angesäuert. Die Benzolschicht wurde abgetrennt und die wässrige Phase mehrmals mit Äther ausgeschüttelt. Die vereinigten organischen Phasen wurden mit Natriumhydroxydlösung (zur Entfernung von Benzoesäure) und Wasser geschüttelt und über Natriumsulfat getrocknet (aus der angesäuerten alkalischen Wasserphase wurden 8,0 g Benzoesäure erhalten). Nach Abdestillieren des Lösungsmittels wurde der Rückstand zusammen mit 0,1 g *p*-Toluolsulfonsäure im Ölbad auf 155° erhitzt. Nach Beendigung der Zersetzung lieferte die fraktionierte Destillation eine schwach gelbe Flüssigkeit vom Kp. 160°—162°/0,2 mm Hg, n_D^{20} 1,5207. Ausbeute: 14,3 g (62 % der Theorie). (Gef. C 67,41; H 5,50. Ber. für $C_{13}H_{13}O_3N$: C 67,52; H 5,67).

Die Verfasser sind dem Institutsvorstand, Herrn Professor A. Fredga, für den Arbeitsplatz und dem *Schwedischen Naturwissenschaftlichen Forschungsrat* sowie *Lucidol Division, Wallace and Tiernan, Inc., Buffalo, New York, Vereinigte Staaten*, für finanzielle Unterstützung zu Dank verpflichtet.

LITERATUR

1. Lawesson, S.-O., Grönwall, S. und Andersson, M. *Arkiv Kemi* **17** (1961) 457.
2. Lawesson, S.-O., Dahlén, M. und Frisell, C. *Acta Chem. Scand.* **16** (1962) 1191.
3. Treibs, A. und Hintermeier, K. *Ber.* **87** (1954) 1163.
4. Baumgarten, E. und Hauser, C. R. *J. Am. Chem. Soc.* **66** (1944) 1037.
5. Breslow, D. S., Baumgarten, E. und Hauser, C. R. *J. Am. Chem. Soc.* **66** (1944) 1286.
6. Frisell, C. und Lawesson, S.-O. *Arkiv Kemi* **17** (1961) 401.
7. Frisell, C., Näslund, G. und Lawesson, S.-O. *In Vorbereitung.*
8. Näslund, G., Senning, A. und Lawesson, S.-O. *Acta Chem. Scand.* **16** (1962) 1329.
9. Näslund, G., Senning, A. und Lawesson, S.-O. *In Vorbereitung.*
10. Baumgarten, H. E. und Eifert, R. L. *J. Am. Chem. Soc.* **75** (1953) 3015.
11. Stork, G., Terrell, R. und Szmuszkovicz, J. *J. Am. Chem. Soc.* **76** (1954) 2029.
12. Bruson, H. A. in *Organic Reactions*, Band 5, Kapitel 2, John Wiley and Sons, Inc., New York, N.Y.
13. Bergmann, E. D., Ginsburg, D. und Pappo, R. in *Organic Reactions*, Band 10, John Wiley and Sons, Inc., New York, N.Y., 1959 (Kapitel 3).
14. Barkley, L. B. und Levine, R. *J. Am. Chem. Soc.* **72** (1950) 3699.
15. Campbell, A. D., Carter, C. L. und Slater, S. N. *J. Chem. Soc.* **1948** 1741.
16. Zellars, G. R. und Levine, R. *J. Org. Chem.* **13** (1948) 911.
17. Albertson, N. F. *J. Am. Chem. Soc.* **72** (1950) 2594.
18. Yoho, C. W. und Levine, R. *J. Am. Chem. Soc.* **74** (1952) 5597.
19. Lawesson, S.-O., Busch, T. und Berglund, C. *Acta Chem. Scand.* **15** (1961) 260.
20. Lawesson, S.-O. und Frisell, C. *Arkiv Kemi* **17** (1961) 409.
21. Lawesson, S.-O., Andersson, M. und Berglund, C. *Arkiv Kemi* **17** (1961) 429.
22. Lawesson, S.-O., Jönsson, P.-G. und Taipale, J. *Arkiv Kemi* **17** (1961) 441.
23. Lawesson, S.-O., Frisell, C., Denney, D. Z. und Denney, D. B. *In Vorbereitung.*

Eingegangen am 23. Dezember 1961.

ACTA CHEMICA SCANDINAVICA 16 (1962) 1329–1336

Studien über Elimination

V *. Eine neue Methode zur Darstellung von 1-Methylzyklohexen-1-on-3 und verwandten Verbindungen

GUNNEL NÄSLUND, ALEXANDER SENNING** und SVEN-OLOV LAWESSON**

Laboratorium für Organische Chemie, Chemisches Institut der Universität Uppsala, Uppsala, Schweden

Durch Kondensation von zwei Mol *t*-Butylazetoazetat mit einem Mol verschiedener Aldehyde (Knoevenagel-Reaktion) in Gegenwart von Piperidin wurden "Bis-Verbindungen" (Hydroxyzyklohexanone, VII) dargestellt. Die Struktur dieser Verbindungen (VII) wurde bei der Untersuchung ihrer Infrarotspektren bestätigt. Durch Karbo-*t*-butoxy-Elimination von VII in Gegenwart katalytischer Mengen *p*-Toluolsulfonsäure wurden ausgezeichnete Ausbeuten an 1-Methyl-zyklohexen-1-on-3 und verwandten Verbindungen IX erhalten. Auf Grund gewisser von uns beobachteter Anomalien wird vorgeschlagen, dass eine Hydroxylgruppe in β-Stellung zur Karbo-*t*-butoxygruppe eine notwendige Voraussetzung für die Eliminierung ist.

In der Knoevenagel-Reaktion [1] reagiert ein Mol Aldehyd mit zwei Mol eines β-Ketoesters (oder einer anderen β-Karbonylverbindung) in Gegenwart einer organischen Base zu "Bis-Verbindungen". Der erste Reaktionsschritt ist eine Aldolkondensation, die zu einem α-Methylen-β-ketoester I führt:

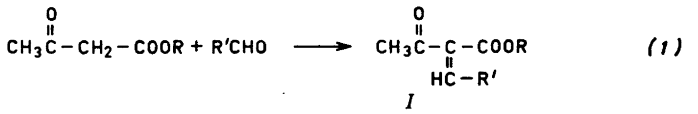

(1)

In der nächsten Stufe liefert I mit einem zweiten Mol β-Ketoester unter Michael-Kondensation (ausführliche Literaturhinweise finden sich bei Bergmann, Ginsburg und Pappo [2]) eine "Bis-Verbindung" II:

* Teil IV: Näslund, G., Senning, A. und Lawesson, S.-O. *Acta Chem. Scand.* **16** (1962) 1324.

** Neue Anschrift: Chemisches Institut der Universität Aarhus, Aarhus, Dänemark.

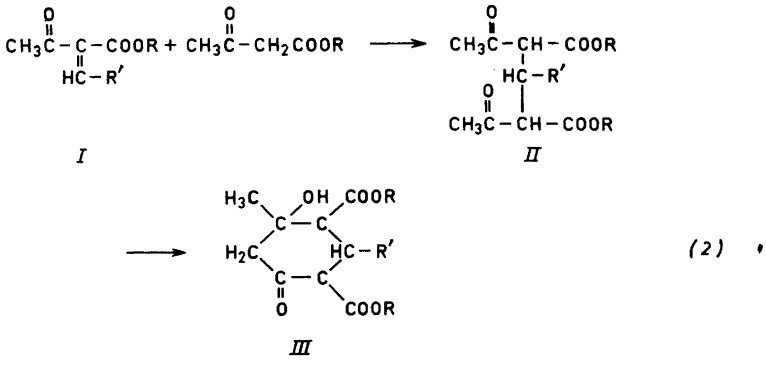

(2)

Die Struktur der "Bis-Verbindung" ist mehrfach diskutiert und in Frage gestellt worden. Knoevenagel [3,4] war zuerst der Ansicht, dass die "Bis-Verbindung" die Struktur II habe, obwohl er glaubte, dass eine Strukturaufklärung mit chemischen Methoden unbefriedigend war; andererseits schrieb Rabe [5–8] den "Bis-Verbindungen" die allgemeine Formel III zu. Der übliche Katalysator für Knoevenagel-Kondensationen ist Piperidin, und die Karbonylverbindung II, die zuerst gebildet wird, liefert in einer intramolekularen Aldolkondensation III, wenn sie unter dem Einfluss des Piperidins verbleibt. Ein Fall ist bekannt, in dem keine Base benötigt wird: Rabe [9,10] zeigte, dass Formaldehyd direkt mit Äthylazetoazetat kondensiert und Isomere vom Typ II und III liefert.

Je nach den Bedingungen, unter denen die Kondensationsreaktionen und die nachfolgende Aufarbeitung durchgeführt wurden, wurden verschiedene Verbindungen isoliert. Das zyklische Primärprodukt III konnte zum Beispiel eine 1,2-Elimination erleiden, wodurch eine Doppelbindung enstand:

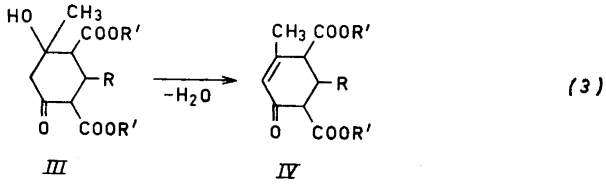

(3)

Nach weiterer Hydrolyse und Dekarboxylierung konnte ein α,β-ungesättigtes Keton (VI) isoliert werden und auch das Monokarbäthoxyderivat (V) wurde in einigen Fällen als Zwischenprodukt erhalten

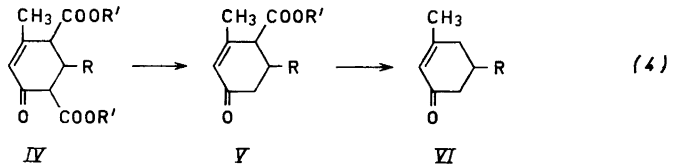

(4)

Horning und Mitarbeiter [11,12] verbesserten ältere Methoden zur Darstellung von Derivaten des 1-Methylzyklohexen-1-on-3 und fanden dabei, dass wenn R (in den Gleichungen 1—4) Aryl ist, V im allgemeinen nicht isoliert werden kann, da beide Estergruppen gleichzeitig hydrolysiert und dekarboxyliert werden.

Lawesson und Mitarbeiter [13–16] haben vor kurzem einige Eliminationsreaktionen untersucht, die für die präparative organische Chemie von Wert sind. Ausgangspunkt war die Tatsache, dass *t*-Alkylester von *β*-Ketosäuren beim Erhitzen in Gegenwart von katalytischen Mengen *p*-Toluolsulfonsäure glatt in Olefin, Kohlendioxyd und eine Karbonylverbindung zerfallen. Aus 1-Methylzyklohexylazetoazetat wurde 1-Methylzyklohexen in hoher Ausbeute dargestellt [13].

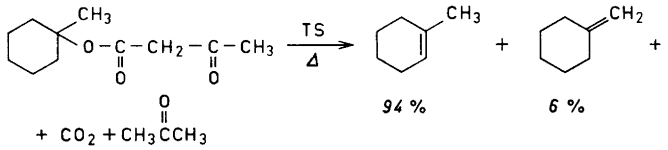

(5)

Wie aus der folgenden Reaktionsgleichung zu ersehen ist, wurde auch ein neues Verfahren zur Darstellung von Azyloinen gefunden [14]:

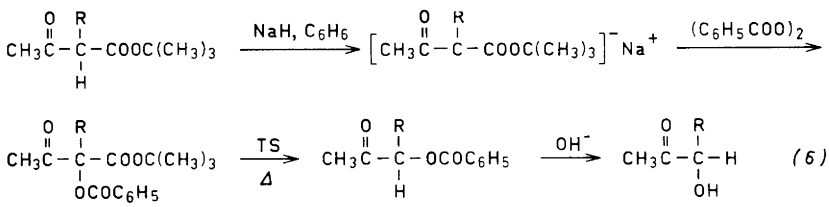

(6)

Eine ähnliche Arbeit [15] beschäftigt sich mit der Darstellung in 3-Stellung substituierter Lävulinsäureester. Des weiteren wurde eine neue Methode zur Darstellung von *δ*-Ketonitrilen [16] ausgearbeitet: Zyanäthylierung von Derivaten des *t*-Butylazetoazetats und anschliessende Karbo-*t*-butoxy-Eliminierung:

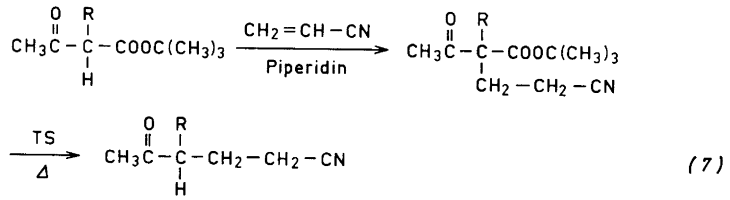

(7)

Da die Elimination der Karbo-*t*-butoxygruppe des *t*-Butylazetoazetats eine ausserordentlich glatt verlaufende Reaktion ist und hohe Ausbeuten an End-

produkten liefert, vermuteten wir, dass sich auch substituierte Derivate des 1-Methylzyklohexen-1-on-3 bequem darstellen lassen würden. In Anlehnung an Hornings Verfahren [11,12] wurden einige einfache Aldehyde im Molverhältnis eins zu zwei mit *t*-Butylazetoazetat umgesetzt, wobei im allgemeinen hohe Ausbeuten erzielt wurden.

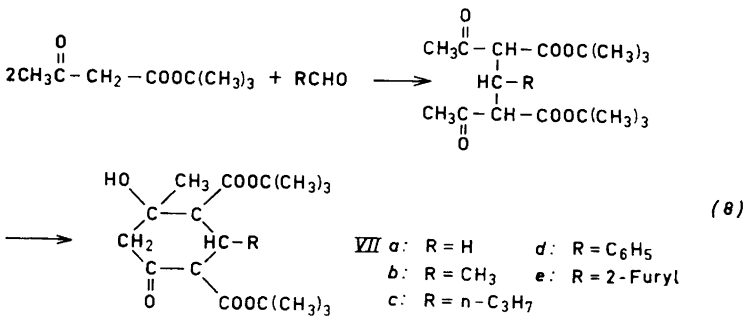

(8)

Die Elementaranalysen zeigten eindeutig, dass den erhaltenen "Bis-Verbindungen" die Formel VII zukommt. Auch die Infrarotspektren der Verbindungen VII a—e gehörten demselben Typ an. Zwischen 3500 und 3400 cm^{-1} trat eine starke Bande auf, die die Gegenwart einer "echten" Hydroxylgruppe im Gegensatz zu einer chelierten enolischen Hydroxylgruppe anzeigte. Die oben genannten Valenzschwingungsfrequenzen könnten auch auf eine intramolekular gebundene Hydroxylgruppe zurückzuführen sein. Auch die Karbonylbanden von VII a—e fallen in den erwarteten Bereich. Alle Spektren enthalten eine Bande in der Nähe von 1150 cm^{-1}, die sich der C—O-Valenzschwingung eines tertiären Alkohols (im allgemeinen bei 1140 cm^{-1}) zuschreiben lässt. Da diese Bande auch durch die CH-"in-plane"-Deformationsschwingung monosubstituierter Benzolderivate [19] hervorgerufen wird, ist der Nachweis einer tertiären Hydroxylgruppe unsicher, wenn die Verbindung einen monosubstituierten Benzolkern enthält. In VII (R = Alkyl) ist diese Bande auch in Abwesenheit eines Benzolkerns vorhanden.

Im Falle der Kondensation von *i*-Butyraldehyd (1 Mol) und *t*-Butylazetoazetat (2 Mol) wurde nicht das 1:2-Addukt, sondern das 1:1-Addukt erhalten (VIII):

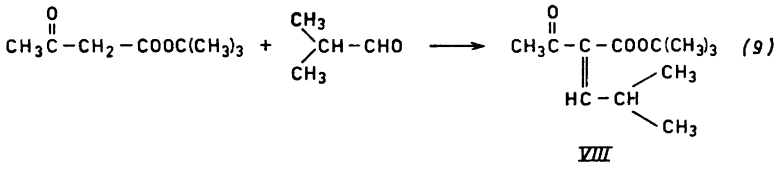

(9)

VIII

Exakte Schlussfolgerungen auf die Faktoren, die für das Ausbleiben der Kondensation verantwortlich sind, lassen sich nicht ziehen. Zweifellos dürften

sterische Einflüsse eine Rolle spielen. Die Weiterführung dieser Eliminationsstudien ergab eine neue allgemeingültige Methode zur Darstellung α,β-ungesättigter Ketone aus Addukten vom Typ VIII. Diese Ergebnisse werden in der nächsten Veröffentlichung dieser Serie [20] enthalten sein:

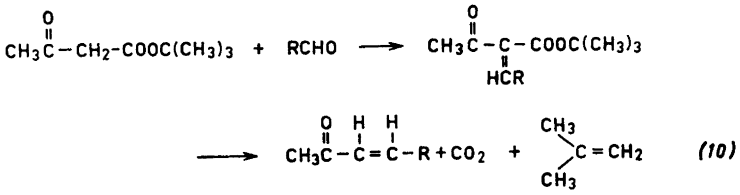

(10)

Aus Gleichung 4 ergibt sich, dass bei der Hydrolyse des Primäraddukts IV die Estergruppe in 4-Stellung in erster Linie eliminiert wird, aber durch weitere Hydrolyse lässt sich auch die Estergruppe in 6-Stellung entfernen. Wir fanden, dass beim Erhitzen des 1:2-Addukts VII in Gegenwart katalytischer Mengen *p*-Toluolsulfonsäure beide Karbo-*t*-butoxygruppen eliminiert werden:

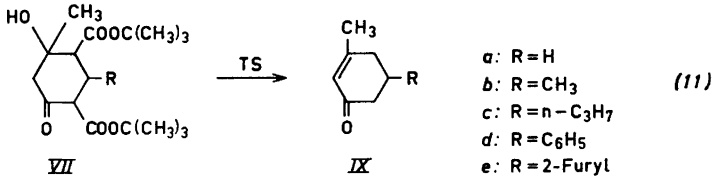

(11)

In allen Fällen wurde IX in ausgezeichneten Ausbeuten ($\approx$ 90 %) erhalten, nur in einem Fall wurden abweichende Verhältnisse beobachtet und zwar als VII (R = 2-Furyl) unter besonders milden Bedingungen zersetzt wurde:

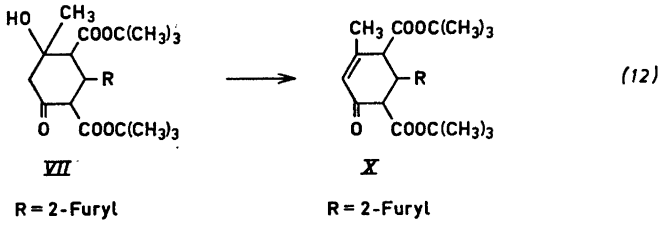

(12)

Eine Karbo-*t*-butoxygruppe blieb also intakt.

Ein gemeinsames Merkmal aller untersuchten Verbindungen (XI)

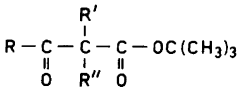

XI

ist, dass alle β-Karbonylverbindungen sind mit R = OC_2H_5, $OC(CH_3)_3$ oder CH_3 und R′ und R″ = verschiedene funktionelle oder Alkylgruppen. Zweifellos handelt es sich bei der Karbo-*t*-butoxy-Elimination in der 4-Stellung von VII um dieselbe Reaktion wie bei anderen *t*-Butyl-β-ketoestern.

Die Karbo-*t*-butoxygruppe in 6-Stellung von VII steht in β-Stellung zu einer Hydroxylgruppe. Während der Elimination in Gegenwart von *p*-Toluolsulfonsäure scheint der erste Reaktionsschritt die Abspaltung von Wasser zu sein. Dann wird die Estergruppe in β-Stellung zur Ketogruppe eliminiert (Gleichung 12), was darauf deutet, dass die β-Hydroxylgruppe eine notwendige Voraussetzung für die Eliminierung ist. Vor kurzem wurden ähnliche Ergebnisse von Vilkas, Abraham und Candehore veröffentlicht [21], nämlich dass beim Erhitzen eines β-Hydroxy-*t*-butylesters (XII) mit Chinolin Isobutylen, Kohlendioxyd und Wasser abgespalten werden.

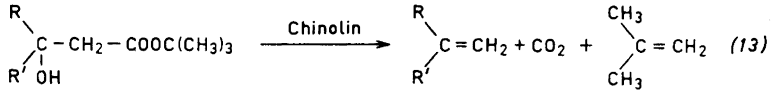

(13)

XII

Ein "concerted mechanism" mit einem zyklischen Zwischenzustand XIII wurde postuliert:

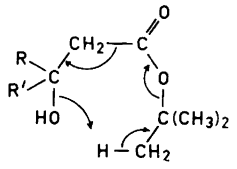

XIII

In unserem Fall dürfte ein ähnlicher Mechanismus bei der Karbo-*t*-butoxy-Elimination der β-Hydroxyester in Gegenwart von *p*-Toluolsulfonsäure wirksam sein.

BESCHREIBUNG DER VERSUCHE

t-Butylazetoazetat wurde nach Treibs und Hintermeier [22] dargestellt. Die Aldehyde waren handelsübliche Qualitäten. Die Analysen wurden im Institut für Analytische Chemie der Universität Uppsala und von der Firma Dr. A. Bernhardt, Mülheim (Ruhr), Deutschland ausgeführt. Alle Siede- und Schmelzpunkte sind unkorrigiert.

Die Darstellung der Addukte VII

Das Verfahren war in allen Fällen das gleiche, so dass eine detaillierte Beschreibung nur für einen Fall angegeben wird.

VII a. In einem 250-ml-Dreihalskolben mit Rührer, Rückflusskühler und Tropftrichter wird die schwach gelbe Mischung von 94,8 g (0,6 Mol) *t*-Butylazetoazetat und 22,5 g (0,3 Mol) Formalin in einem Eisbad auf −5°−0° gekühlt. Darauf werden 1,5 g Piperidin, gelöst in 2−3 g Äthanol, so langsam zugegeben, dass die Temperatur im Kolben unter 0°

bleibt. Nach 6 Stunden bei dieser Temperatur wird das Reaktionsgemisch in einen Weithals-Erlenmeyerkolben gegossen, der zugekorkt und in einen Kühlschrank gestellt wird.

Einmal am Tag werden während der nächsten 3 Tage 1,5 g Piperidin in 2—3 g Äthanol unter Rühren zugesetzt. Dann wurde das Gemisch 24 Stunden bei Zimmertemperatur aufbewahrt, wobei die Flüssigkeit erstarrte. Nach dreimaligem Umkristallisieren aus Azeton wurden weisse Kristalle vom Schmelzpunkt 95,5°—101° erhalten. Ausbeute 62,8 g (64 % der Theorie). (Gef. C 62,17; H 8,59. Ber. für $C_{17}H_{28}O_6$: C 62,26; H 8,62).

VII b. 110,6 g (0,7 Mol) *t*-Butylazetoazetat und 15,4 g (0,35 Mol) Azetaldehyd gaben nach Kondensation in Gegenwart von Piperidin weisse Kristalle (aus Azeton), F: 163°—164°. Ausbeute 77,5 g (65 % der Theorie). (Gef. C 63,25; H 8,56. Ber. für $C_{18}H_{30}O_6$: C 63,13; H 8,83).

VII c. 110,6 g (0,7 Mol) *t*-Butylazetoazetat und 25,2 g (0,35 Mol) *n*-Butyraldehyd lieferten weisse Kristalle (aus Azeton), F: 136,5°—138°. Ausbeute 81,4 g (63 % der Theorie). (Gef. C 64,99; H 9,31. Ber. für $C_{20}H_{34}O_6$: C 64,84; H 9,25).

VII d. 64,8 g (0,41 Mol) *t*-Butylazetoazetat und 22,3 g (0,21 Mol) Benzaldehyd lieferten hellgelbe Kristalle (aus Azeton), F: 176°—177°. Ausbeute: 41,0 g (50 % der Theorie). (Gef. C 68,02; H 8,03. Ber. für $C_{22}H_{32}O_6$: C 67,82; H 8,22).

VII e. 79,0 g (0,5 Mol) *t*-Butylazetoazetat und 24,0 g (0,25 Mol) frisch destilliertes Furfurol lieferten weisse Kristalle (aus Azeton), F: 127,5°—129°. Ausbeute 51,0 g (52 % der Theorie). (Gef. C 63,93; H 7,68. Ber. für $C_{21}H_{30}O_7$: C 63,94; H 7,66).

Darstellung von Derivaten des 1-Methylzyklohexen-1-on-3

Die Karbo-t-butoxy-Elimination wurde in allen Fällen auf die gleiche Weise durchgeführt und zwar wie folgt:

IX a. 23,5 g (0,072 Mol) VII a wurden in einen Destillationskolben gebracht, der an eine Wasserstrahlpumpe angeschlossen war. Nach Zugabe von 0,1 g *p*-Toluolsulfonsäure wurde der Kolben in einem Ölbad auf 155°—160° erhitzt. Nach Beendigung der Zersetzung (konstanter Druck) wurde das Produkt destilliert. Die hellgelbe Hauptfraktion ging zwischen 72°/8 mm Hg und 73°/8 mm Hg über, n_D^{20} 1,4940. Ausbeute 7,2 g (92 % der Theorie) [23]. (Gef. C 75,75; H 9,18. Ber. für $C_7H_{10}O$: C 76,32; H 9,15).

IX b. 19,0 g (0,056 Mol) VII b wurden zwischen 160° und 165° wie oben zersetzt. Das Produkt war eine farblose Flüssigkeit, Kp. 79°—80°/10 mm Hg, n_D^{20} 1,4837. Ausbeute 6,5 g (94 % der Theorie) [23,24]. (Gef. C 77,27; H 9,78. Ber. für $C_8H_{12}O$: C 77,37; H 9,74).

IX c. 10,7 g (0,029 Mol) VII c wurden zwischen 150° und 155° zersetzt. Das Produkt war eine farblose Flüssigkeit, Kp. 109°—110°/10 mm Hg, n_D^{20} 1,4824. Ausbeute 4,0 g (91 % der Theorie) [11]. (Gef. C 78,12; H 10,54. Ber. für $C_{10}H_{16}O$: C 78,89; H 10,59).

IX d. 7,5 g (0,019 Mol) VII d wurden wie oben bei 175°—180° zersetzt. Die Destillation lieferte eine gelbe Flüssigkeit, Kp. 120°—122°/0,4 mm Hg, n_D^{20} 1,5578. Ausbeute 3,5 g (94 % der Theorie) [23]. Oxim: weisse Kristalle, F: 114°—115° (aus Äthanol). Lit.[23]: F: 115°.

IX e. 18,2 g (0,046 Mol) VII e wurden wie oben im Wasserstrahlvakuum bei 165°—170° zersetzt. Das Produkt war eine gelbe Flüssigkeit, Kp. 150°—152°/10 mm Hg, n_D^{20} 1,5332 (Lit.[25]: n_D^{20} 1,5341). Ausbeute 7,2 g (89 % der Theorie). Semikarbazon: gelbe Nadeln, F: 178°—182° (aus Äthanol). Lit.[25]: F: 178°—184°.

Darstellung von X

18,2 g VII e wurden wie oben bei 150°—155° zersetzt, aber statt an eine Wasserstrahlpumpe war die Destillationsapparatur an eine Ölpumpe angeschlossen, die einen Druck von 0,2 mm Hg aufrechterhielt. Nach Beendigung der Zersetzung lieferte fraktionierte Destillation die Hauptfraktion bei Kp. 112°—115°/0,2 mm Hg, n_D^{20} 1,5042. Ausbeute 10,1 g (76 % der Theorie). (Gef. C 69,55; H 7,29. Ber. für $C_{16}H_{20}O_4$: C 69,54; H 7,30).

Die Verfasser sind dem Institutsvorstand, Herrn Professor A. Fredga, für den Arbeitsplatz und *Statens Naturvetenskapliga Forskningsråd* und *Lucidol Division, Wallace and Tiernan, Inc., Buffalo, New York, Vereinigte Staaten*, für finanzielle Unterstützung zu Dank verpflichtet.

LITERATUR

1. Surrey, A. R., *Name Reactions in Organic Chemistry*, New York 1961, S. 147.
2. Bergmann, E. D., Ginsburg, D. und Pappo, R. in Adams, R. *Organic Reactions*, Band 10, S. 179, John Wiley and Sons, N.Y. 1959.
3. Knoevenagel, E. *Ann.* **303** (1898) 223.
4. Knoevenagel, E. *Ber.* **36** (1903) 2118.
5. Rabe, P. und Elze, F. *Ann.* **323** (1902) 83.
6. Rabe, P. *Ann.* **313** (1900) 129.
7. Rabe, P. und Billmann, A. *Ann.* **332** (1904) 22.
8. Rabe, P. *Ber.* **76** (1943) 979.
9. Rabe, P. *Ann.* **332** (1904) 1.
10. Rabe, P. und Rahm, F. *Ann.* **332** (1904) 10.
11. Horning, E. C., Denekas, M. O. und Field, R. E. *J. Org. Chem.* **9** (1944) 547.
12. Horning, E. C. und Field, R. E. *J. Am. Chem. Soc.* **68** (1946) 384.
13. Frisell, C. und Lawesson, S.-O. *Arkiv Kemi* **17** (1961) 401.
14. Lawesson, S.-O., Grönwall, S. und Andersson, M. *Arkiv Kemi* **17** (1961) 457.
15. Lawesson, S.-O., Dahlén, M. und Frisell, C. *Acta Chem. Scand.* **16** (1962) 1191.
16. Näslund, G., Senning, A. und Lawesson, S.-O. *Acta Chem. Scand.* **16** (1962) 1324.
17. Bellamy, L. J. *The Infrared Spectra of Complex Molecules*, Methuen, London 1958, 2. Aufl., S. 102.
18. Referenz [17], S. 109.
19. Referenz [17], S. 82.
20. Näslund, G., Senning, A. und Lawesson, S.-O. *Acta Chem. Scand. Im Vorbereitung.*
21. Vilkas, M., Abraham, N. A. und Candehore, J. *Bull. soc. chim. France* **1960** 1196.
22. Treibs, A. und Hintermeier, K. *Ber.* **87** (1954) 1163.
23. Knoevenagel, E. *Ann.* **281** (1894) 25.
24. Harries, C. *Ber.* **47** (1914) 784.
25. Segel, K.-H. *Ber.* **93** (1960) 2529.

Eingegangen am 28. Dezember 1961.

ACTA CHEMICA SCANDINAVICA 16 (1962) 1337–1345

On the Kinetics of the Zn/Zn_{aq}^{2+} Electrode

TOR HURLEN

Central Institute for Industrial Research, Blindern, Oslo, Norway

Investigations have been made on the anodic dissolution and cathodic deposition of zinc in acid chloride solution at 20°C by means of a slow galvanostatic technique, allowing the "true" rate of these reactions to be determined from the weight change of the electrodes. The reactions have been found to exhibit a combined concentration and activation polarization under the conditions applied, to have mutually symmetric activation controlled Tafel lines with slopes of numerically 2.303 $RT/2F$, and to be independent of the pH of the solution. The activation controlled rate of deposition is moreover found to be proportional to the square of the zinc ion activity. This indicates the kinetic unit equation to be:

$$2\ Zn = 2\ Zn^{2+} + 4e^-$$

In strong chloride solutions, where the polarization behaviour is simplest, the exchange current is found to be:

$$i_0 = 0.7\ a_{Zn^{2+}}\ A/cm^2$$

Comparisons are made to previous results on zinc and to results of analogous experiments on iron and copper.

1.0 INTRODUCTION

It has previously been shown that the reactions of the Fe/Fe_{aq}^{2+} electrode [1] and the Cu/Cu_{aq}^{2+} electrode [2] under stationary conditions seem best represented by the "kinetic unit equations":

$$2\ Fe + OH^- = 2\ Fe^{2+} + OH^- + 4e^- \quad (1)$$

$$2\ Cu = 2\ Cu^{2+} + 4e^- \quad (2)$$

indicating that the anodic and cathodic reactions are second order with respect to the metal and the metal ions, respectively, and that there in the case of iron (but not in the case of copper) is a first order "catalytic" interaction of hydroxyl ions.

As these results were somewhat surprising, it was assumed desirable to carry out the same type of slow amperostatic polarization measurements on some further metals. In the present paper, results thereby obtained on *zinc* in various pure and mixed solutions of hydrochloric acid, potassium chloride, and zinc chloride at 20°C are presented and discussed.

The experimental method applied is especially useful in this case as it allows the rate of the zinc electrode reactions to be determined from the weight change of the electrodes. Account is thereby made of a possible simultaneous corrosion of the electrodes and of a possible current consuming hydrogen evolution accompanying the deposition process.

2.0 PREVIOUS WORK

The anodic dissolution and cathodic deposition of metals have recently been reviewed and discussed by Vetter [3], Hoar [4], Bockris [5], and Fischer [6]. General reference may also be given to the monograph by Mathewson [7]. All these reviews include references to zinc, but do not reveal much data appropriate for a modern analysis of the kinetics of the *active* dissolution and deposition of this metal.

One of the most direct investigations is due to Rojter, Polujan and Jusa [8]. From oscillographically obtained anodic and cathodic potential transients for single crystal zinc in 0.25 M solutions of zinc sulphate in water and in 0.005—0.008 N sulphuric acid at 30°C, they found the Zn/Zn_{aq}^{2+} electrode to behave symmetrically and the polarization at constant current to reach a maximum after about 10^{-2} sec and then to decrease towards a stationary value. Both the maximum values and the stationary values obey the Tafel relationship and give numerical Tafel slopes of approximately 2.303 RT/F and 2.303 $RT/2F$, respectively. This is the same as found for iron [9,10] in experiments of the same type, and the Tafel slope for the stationary potentials also agrees with what is obtained from other types of stationary-state measurements both on iron [1,11] and on copper [2]. Rojter, Polujan and Jusa could moreover find no effect of pH on the Zn/Zn_{aq}^{2+} electrode reactions, which thus seem more analogous to those of the Cu/Cu_{aq}^{2+} electrode [2] than to those of the Fe/Fe_{aq}^{2+} electrode [1,10]. From the maximum polarization values, these authors further estimate the exchange current of the Zn/Zn_{aq}^{2+} electrode to be of the order of 10^{-5} A/cm^2 under the conditions given. This seems to be the only value so far available for the exchange current of this electrode.

Of other polarization studies on the Zn/Zn_{aq}^{2+} electrode reactions may especially be mentioned those of Röntgen and Buchkremer [12], Müller and Barchmann [13], and Piontelli and Poli [14]. The former of these investigations deals with the deposition process and with hydrogen evolution on zinc cathodes. The two latter are mainly concerned with the effect of anions on the deposition and the dissolution process. All three show a rather low Tafel slope for the zinc electrode reactions (not more than 2.303 $RT/2F$) and a very low overvoltage even at current densities of the order of 10^{-3} A/cm^2 at zinc ion concentrations of 0.5 M (see especially Ref.[14]). This may possibly indicate an appreciably higher exchange current for the polycrystalline zinc used by these authors (see also the early work of Allmand and Cocks [15]) than for the single crystals used by Rojter, Polujan and Jusa. The interpretation of the results is impeded, however, by the investigations having been made in acid solutions of low pH without account having been made of the free corrosion of the electrodes.

The rate of corrosion at various crystallographic planes of zinc single crystals in acid solution has been studied by Aminoff[16] and Straumanis[17], both of which have found the close-packed hexagonal basal planes to corrode more slowly than less closely packed planes. The orientation and morphology of electrodeposited zinc have recently been studied by Sato[18].

Much work has been done on the reduction and dissolution of zinc at zinc amalgam electrodes. As this is slightly outside the scope of the present work, no detailed review will be made. However, it may be of interest to give a brief reference to the recent work of Horiuti and Matsuda[19] based on experimental results of Losev. These authors found the mutually reverse reactions of the Zn_{am}/Zn_{aq}^{2+} electrode to have very nearly symmetric Tafel lines with slopes of numerically 2.303 RT/F (see Figs. 1 and 2 in Ref.[19]). This is twice that mentioned above for the stationary reaction on solid zinc electrodes.

3.0 EXPERIMENTAL

The experimental technique has been exactly the same as previously described for analogous experiments on iron[1] and copper[2]. It is a slow amperostatic technique which allows the "true" rate of the dissolution and deposition reaction to be determined from the weight change of the electrodes.

The circular sheet electrodes used were made from *p.a.* zinc rods (E. Merck) by cold-rolling and punching. Prior to use, the electrodes were degreased in chloroform, etched in 1 N hydrochloric acid for 15 min, washed in distilled water and acetone, dried, and weighed. The electrolytes were prepared from A.R. quality acid and salts and were presaturated with purified hydrogen.

The experiments were performed in a thermostated room at about 20°C. The saturated calomel electrodes used have been ascribed a potential of 0.245 V on the normal hydrogen scale (NHS) at this temperature. No attempts have been made to correct for possible liquid junction potentials. When stirring was applied, this was performed with a magnetic stirrer which was placed close to the electrode studied. This stirring was found to raise the limiting deposition current by a factor of about five (see Fig. 4).

4.0 RESULTS

Preliminary experiments showed 0.001 N hydrochloric acid solutions of zinc chloride and potassium chloride to give most suitable pH-conditions for correlating studies to be made on the mutually reverse reactions of the Zn/Zn_{aq}^{2+} electrode. The pH of these solutions seems low enough to exclude difficulties from zinc ion hydrolysis, and high enough to make the corrosion rate negligible as compared to the reaction rates imposed by the applied current (10^{-4}—10^{-2} A/cm^2). The latter was shown by the weight change of the electrodes used. The weight change measurements further showed the deposition efficience in these solutions to be very nearly 100 %, except at current densities exceeding the limiting current for deposition. The main part of the present experiments have therefore been performed with solutions of this type.

Potential-time curves. Fig. 1 gives some examples of anodic potential-time curves at various constant current densities in unstirred 0.001 N hydrochloric acid + 2.999 M potassium chloride. Most of these curves show an initial rise in the potential to a stationary value. This initial rise was usually not observed in the zinc chloride containing solutions used (see below), nor in the initially

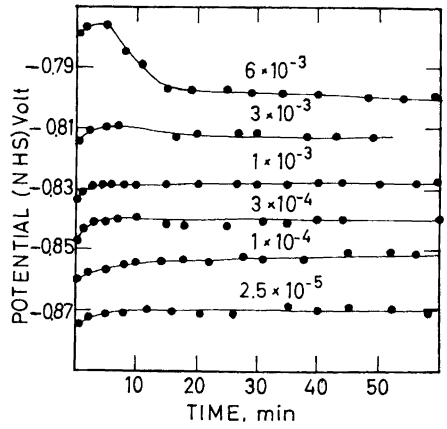

Fig. 1. Anodic potential-time curves for zinc in 0.001 M hydrochloric acid + 2.999 M potassium chloride at various current densities (A/cm²). 20°C.

zinc free solutions when stirring was applied at the anodes. In these cases, the stationary potential either prevailed from the very first reading or was reached after an initial fall in the potential (somewhat as shown by the highest curve in Fig. 1).

Fig. 2 gives some examples of cathodic potential-time curves at various constant current densities in unstirred (A) and stirred (B) 0.001 N hydrochloric acid + 0.05 M zinc chloride + 2.899 M potassium chloride. These curves are representative for those obtained for the deposition of zinc in the

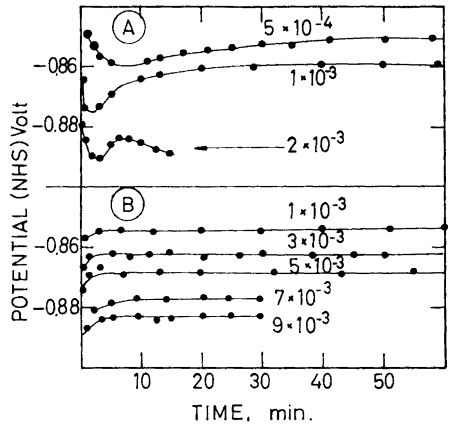

Fig. 2. Cathodic potential-time curves for zinc in unstirred (A) and stirred (B) 0.001 M hydrochloric acid + 2.899 M potassium chloride + 0.05 M zinc chloride at various current densities (A/cm²). 20°C.

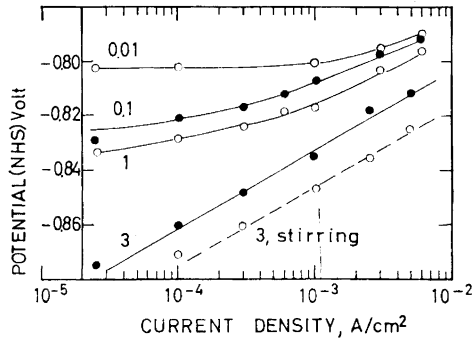

Fig. 3. Anodic polarization curves for zinc in 0.001 M hydrochloric acid solutions of potassium chloride at various total chloride molalities (0.01—3). 20°C.

present work at current densities not exceeding (or approaching too closely) the limiting current.

In constructing polarization ($V/\log i$) curves from the potential-time curves and the weight change data, the potentials representing the lowest numerical polarization have been used (*i.e.* the lowest potentials shown by the anodic and the highest shown by the cathodic potential-time curves).

Polarization curves. Fig. 3 gives some examples of polarization curves obtained for the anodic dissolution of zinc in 0.001 N hydrochloric acid solutions of potassium chloride at various total chloride molalities (0.01—3). Except for one, these curves apply to unstirred solutions, for which case they show a distinct effect of the potassium chloride concentration on the dissolution polarization (especially at low dissolution rates). In stirred solutions, however, this effect is less distinct. This was shown by the application of stirring at anodes in the 1 M solution of this series displacing the corresponding polarization curve almost down to the one given for the stirred 3 M solution in Fig. 3. The author has so far no satisfactory explanation to give for the observed effect of the potassium chloride concentration.

The results in Fig. 3 further show the anodic polarization in the 3 M solution to obey the Tafel relationship with a slope of

$$b_a = 2.303\ RT/2F \tag{3}$$

i.e. 29 mV per logarithmic rate unit at 20°C. This is in agreement with what is indicated above on the basis of previous work on zinc, and it is the same as previously found for the anodic dissolution of iron [1] and copper [2] to divalent ions.

Fig. 4 gives polarization data for the anodic dissolution and cathodic deposition of zinc in 0.001 N hydrochloric acid solutions of zinc chloride (0.01, 0.02 and 0.05 M) and potassium chloride at a total chloride molality of 3. The curves there drawn (solid for unstirred and dashed for stirred solutions) have been constructed from the formula:

$$i/i_0 = \pm \exp\left(\frac{n\alpha F(V-E_R)}{\nu\, RT}\right) \mp \left(1 \pm \frac{i}{i_{lim}}\right)^{1/\nu} \exp\left(\frac{n(\alpha-1)F(V-E_R)}{\nu RT}\right) \tag{4}$$

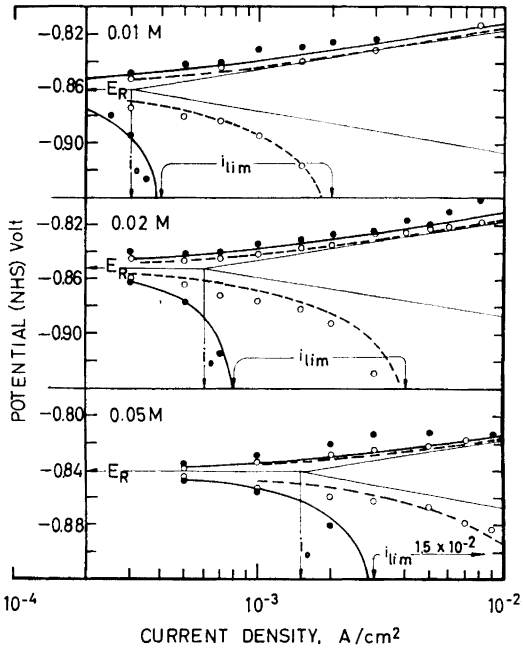

Fig. 4. Polarization curves for anodic dissolution and cathodic deposition of zinc in 0.001 M hydrochloric acid solutions of zinc chloride (0.01, 0.02, and 0.05 M) and potassium chloride at a total chloride molality of 3. The open cricles apply to stirred and the closed to unstirred solutions. 20°C.

by use of the i_0, i_{lim} and E_R values given in Fig. 4, the α and ν values corresponding to the symmetric Tafel lines there suggested, namely

$$\alpha = \nu = 1/2 \tag{5}$$

and a value of 2 for n. Where double signs are used in (4), the upper apply to dissolution and the lower to deposition. All reaction rates are thereby regarded positive, irrespective of the reactions being anodic or cathodic.

Eqn. (4) may be regarded a general polarization equation for simple metal/metalion electrodes for which no other limiting current than the cathodic limiting diffusion current of the metal ions has to be considered [5,20]. It shows the combined effect of activation and concentration polarization and may, by i_0 and ν, possibly also account for what Vetter [3] calls crystallization polarization. The exchange current i_0 must then be assumed to represent the rate of metal ion exchange between the metal lattice and the solution (and not only between possible adatoms and the solution). It is easily seen that (4) involves the simpler equations for pure activation control and pure diffusion control as special cases.

The Tafel lines drawn in Fig. 4 thus represent the absolute rate of the zinc electrode reactions at various potentials and electrolyte compositions (the

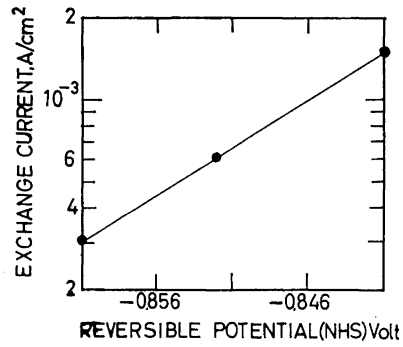

Fig. 5. Exchange current *versus* reversible potential for zinc in 0.001 M hydrochloric acid solutions of zinc chloride and potassium chloride at a total chloride molality of 3. 20°C.

bulk composition of the solutions applied). The relative position of these lines in the diagrams shows:

$$(\mathrm{d}\ \log\ i_a/\mathrm{d}\ \log\ a)_V = 0 \tag{6}$$

$$(\mathrm{d}\ \log\ i_c/\mathrm{d}\ \log\ a)_V = 2 \tag{7}$$

for the effect of the zinc ion activity (estimated from the reversible potentials given) on the absolute rate of the anodic and cathodic reaction, respectively. This is in accordance with what one should expect for a metal/metalion electrode with a stoichiometric factor (ν) of 1/2 (see eqn. (3) and Refs.[3,5,20]).

The relatively good fit of the experimental data in Fig. 4 to the calculated curves lends confidence to the validity of (4)—(7) in the present case and to the values suggested for the exchange current. These values are in Fig. 5 plotted *versus* the reversible potential of zinc in the corresponding solutions. Accepting the value of −0.763 V for the standard potential of zinc [21], the straight line drawn in Fig. 5 corresponds to

$$i_0 = 0.7\ a\ \mathrm{A/cm^2} \tag{8}$$

in the 3 M chloride solutions concerned. This shows the standard exchange current to be 0.7 A/cm². The reversible potential values given in Figs. 4 and 5 are the mean values of the potentials measured in the cell prior to application of current.

From measurements on the corrosion and the anodic dissolution of zinc in more acid solutions (to be published in a subsequent paper on the corrosion of zinc), the pH of the solution could not be found to have any direct effect on the zinc electrode reactions. This is in accordance with the results of Rojter, Polujan, and Jusa [8].

5.0 DISCUSSION

The above results indicate the zinc electrode to exhibit combined diffusion and activation (including crystallization) polarization under the conditions applied, its polarization (at least in strong chloride solutions) being well

described by the "general" polarization equation (4). The equation is here called "general" by being assumed to cover all the mentioned types of polarization and *not* by being assigned general validity. It does, for instance, not account for possible electric field effects in the diffusion layer and the diffuse double layer, nor for possible effects of specific adsorption of ions on the metal surface. The obedience to this equation, as found in the strong (3 M) chloride solutions, may thus be an indication of such effects being negligible. This is what one should expect in the presence of a large excess inert electrolyte [3]. The polarization observed at lower chloride concentrations (see Fig. 3) may include such effects, however.

The way in which the term i/i_{lim} is used in (4), involves the approximation that the diffusion layer thickness is independent of the concentration difference over this layer. This approximation could formally be improved by raising the term to a power of 0.8 (see Ref.[3], p. 172), but this will not have any great effect on the constructed polarization curves. Eqn. (4) also ignores a possible change in the activity coefficient of the zinc ions with their concentration in the diffusion layer. For the strong (3 M) chloride solutions, however, this may seem justified by the observed reversible potentials indicating proportionality between activity and concentration of zinc chloride (at least at zinc ion concentrations from 0.01 to 0.05 M).

The value of 1/2 used in the present case both for the symmetry factor (α) and the stoichiometric number (ν) gives a satisfactory fit to the experimental results. The experimental data are perhaps not accurate enough to prove the absolute correctness of this value for both factors, but they strongly indicate that it cannot be far from correct. It is at least easily seen that other simple values as 1 or 2 for the stoichiometric number do not fit the results at all. The double metal ion mechanism previously found to govern both the Fe/Fe_{aq}^{2+} and the Cu/Cu_{aq}^{2+} electrode reactions [1,2], may thus seem to govern also the Zn/Zn_{aq}^{2+} electrode reactions. The kinetic unit equation may thereby be written:

$$2\ Zn = 2\ Zn_{aq}^{2+} + 4e\text{-} \qquad (9)$$

when also the independence of pH is remembered (compare to (1) and (2) for the iron and copper electrode reactions). This is in accordance with the stationary polarization data of Rojter, Polujan, and Jusa [8].

Eqn. (9) implies that the chloride ions do not directly participate in the electrode reactions. This is substantiated by the relatively small difference shown in Fig. 3 for the anodic polarization of zinc at high current densities in unstirred solutions of widely different chloride concentrations, and also by the results of some preliminary measurements in sulphate solution (not given in this paper) showing the anodic polarization not to be very much different from what it is in chloride solution.

The present results show an appreciably higher exchange current than do the previous results of Rojter, Polujan, and Jusa [8]. It is so far difficult to say whether this is due to the different experimental conditions (polycrystalline zinc in chloride solution *contra* single crystal zinc in sulphate solution) or to the different experimental methods (slow galvanostatic *contra* oscillographic)

applied. The higher values may seem to be more in accordance with the polarization data reported by other authors [12–15], however. These data are already discussed in the above description of previous work.

Acknowledgement. The author is much indebted to Miss T. Tönderum and Miss K. Storström for technical assistance, to various members of the staff at the Central Institute for Industrial Research for helpful discussions, and to the *U.S. Department of Army, European Research Office*, for financial support.

REFERENCES

1. Hurlen, T. *Acta Chem. Scand.* **14** (1960) 1533.
2. Hurlen, T. *Acta Chem. Scand.* **15** (1961) 630.
3. Vetter, K. J. *Elektrochemische Kinetik*, Springer, Berlin/Göttingen/Heidelberg 1961.
4. Hoar, T. P. in Bockris, J. O'M. (Ed.) *Modern Aspects of Electrochemistry No. 2*, Butterworths, London 1959, Chapter 4.
5. Bockris, J. O'M. in Bockris, J. O'M. (Ed.) *Modern Aspects of Electrochemistry No. 1*, Butterworths, London 1954, Chapter 4.
6. Fischer, H. *Elektrokristallization von Metallen*, Springer, Berlin/Göttingen/Heidelberg 1954.
7. Mathewson, C. H. *Zinc, The Metal, Its Alloys and Compounds*, Reinhold, New York 1959.
8. Rojter, W. A., Polujan, E. S. and Jusa, W. A. *Acta Physicochim. URSS* **10** (1939) 845.
9. Rojter, W. A., Jusa, W. A. and Polujan, E. S. *Acta Physicochim. URSS* **10** (1939) 389.
10. Heusler, K. E. *Z. Elektrochem.* **62** (1958) 582.
11. Hoar, T. P. and Hurlen, T. *CITCE VIII (1956)*, Butterworths, London 1957, p. 445.
12. Röntgen, P. and Buchkremer, R. *Metallwirtschaft* **10** (1931) 931.
13. Müller, E. and Barchmann, H. *Z. Elektrochem.* **39** (1933) 341.
14. Piontelli, R. and Poli, G. *Gazz. chim. ital.* **79** (1949) 863.
15. Allmand, A. J. and Cocks, H. C. *Proc. Royal Soc. (London)* **A112** (1926) 259.
16. Aminoff, *Z. Krist.* **65** (1927) 23.
17. Straumanis, M. *Z. physik. Chem.* **147** (1930) 161.
18. Sato, R. *J. Electrochem. Soc.* **106** (1959) 206.
19. Horiuti, J. and Matsuda, A. *J. Res. Inst. Catalysis, Hokkaido Univ.* **7** (1959) 19.
20. Parsons, R. *Trans. Faraday Soc.* **47** (1951) 1332.
21. Latimer, W. M. *Oxidation Potentials (2nd Ed)*, Prentice-Hall, New York 1952, p. 168.

Received December 22, 1961.

ACTA CHEMICA SCANDINAVICA 16 (1962) 1346–1352

Corrosion of Zinc

Effect of pH

TOR HURLEN

Central Institute for Industrial Research, Blindern, Oslo, Norway

The corrosion rate (i_c) and corrosion potential (E_c) of zinc in acid chloride solutions of high chloride content (3 M) are found to vary with the pH according to:

$$\mathrm{d}\log i_c/\mathrm{d}\,\mathrm{pH} = -4/5$$
$$\mathrm{d}E_c/\mathrm{d}\,\mathrm{pH} = -(2/5)2.303\ RT/F$$

At a lower chloride concentration (1 M), deviations occur (especially from the latter relationship) mainly because of the chloride concentration affecting the anodic dissolution reaction.

The anodic dissolution reaction is found to be independent of the pH and of it occurring together with a simultaneous hydrogen evolution reaction. In strong chloride solutions, it has a Tafel slope of approximately $2.303\ RT/2F$.

The hydrogen evolution reaction is found to be strongly stimulated by a simultaneously occuring dissolution reaction. When occuring essentially alone, it is first order in hydrogen ion dependence and has a Tafel slope of approximately $-2.303 \times 2RT/F$ and a standard exchange current (extrapolated) of about 3×10^{-10} A/cm^2.

1.0 INTRODUCTION

It is well known that zinc in acid solution dissolves by a hydrogen evolution type of attack, and that this process is strongly affected by the pH [1–4]. Recent investigations on zinc in sulphuric acid solutions [5,6] have shown its corrosion rate (i_c) and corrosion potential (E_c) to vary with pH approximately as given by:

$$\mathrm{d}\log i_c/\mathrm{d}\,\mathrm{pH} = -4/5 \quad (1)$$
$$\mathrm{d}E_c/\mathrm{d}\,\mathrm{pH} = -(2/5)2.303\ RT/F \quad (2)$$

A main object of the present work is to see if this also is true in hydrochloric acid solutions.

The relationships shown by (1) and (2) are what to be expected on the basis of the theory of mixed potentials [7] when:

(*a*) the hydrogen evolution reaction is first order in hydrogen ion dependence and has a Tafel slope of $-2.303 \times 2RT/F$,

(*b*) the anodic dissolution reaction is pH-independent and has a Tafel slope of 2.303 $RT/2F$, and

(*c*) no interaction — except for the electron balancing — exists between the two different electrode reactions when occuring simultaneously and at equivalent rates on the same metal surface, or an interaction exists which affects the corrosion by the same rate factor and the same potential difference at all pH-values.

This is not only an arbitrary combination of properties suggested to satisfy (1) and (2), but is partly based on direct knowledge of the single electrode reactions.

What is said under (*a*) is in agreement with direct results in sulphuric acid solution [5,6,8], in hydrochloric acid solution [8,9], and in perchloric acid solution [9].

What is said under (*b*) has — to the authors knowledge — direct support only as far as the Tafel slope is concerned [10]. Another object of the present work, therefore, is to elucidate the possible effect of pH on the anodic dissolution reaction.

What is said under (*c*) leaves two possibilities, either the existence or the non-existence of an interaction of the mentioned type. Results by Vonwiller [8] show the former to be true in both sulphuric and hydrochloric acid solutions. For sulphuric acid solutions, this has some support in the cathodic polarization curves given by Rotinyan *et al.*[5,6] The results by Bicelli and Graziano [9] for zinc in hydrochloric and perchloric acid solutions, however, do not show this so clearly. A further elucidation of this matter is a third object of the present work.

2.0 EXPERIMENTAL

The materials used in the present experiments have been the same as previously described [10]. This also applies to the pretreatment of the zinc electrodes (etched for 15 min in 1 N hydrochloric acid).

The experiments have been performed in a thermostated room at about 20°C, partly by cell previously described [11] (both corrosion experiments and galvanostatic polarization experiments) and partly by simple immersion as previously described [12] (except for the quartz helix measurements there described having been replaced by determinations of the weight loss over various periods of immersion). The saturated calomel electrodes used have been ascribed a potential of 0.245 V on the normal hydrogen scale (NHS). No attempts have been made to correct for possible liquid junction potentials.

Experiments have been performed with two series of solutions:

$$\begin{array}{l} \mathrm{HCl}\ (x\ \mathrm{M}) + \mathrm{KCl}\quad (1-x\ \mathrm{M}) \\ \mathrm{HCl}\ (x\ \mathrm{M}) + \mathrm{KCl}\quad (3-x\ \mathrm{M}) \end{array}$$

in which the total chloride content is constant at 1 and 3 M, respectively. The hydrochloric acid molality (x) has been varied from 0.01 to 1 M. A solution of 0.05 M sulphuric acid + 1 M potassium chloride has also been used and may be regarded as belonging to the former of the above series.

3.0 RESULTS

Fig. 1 shows some examples of corrosion rate curves obtained. These curves apply to various hydrochloric acid molalities in the 3 M chloride series, and each experimental point represents the average of at least four experi-

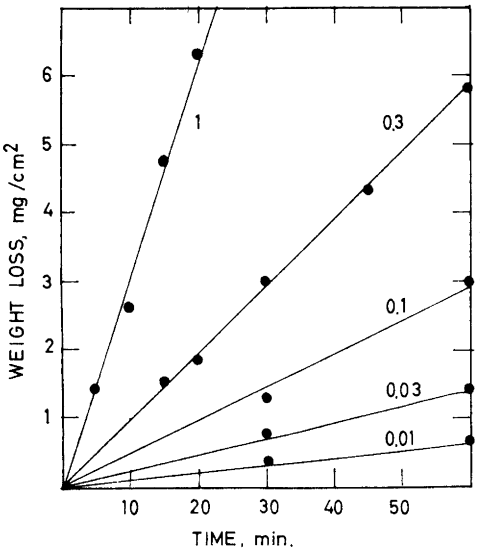

Fig. 1. Weight loss of zinc as function of time in x M hydrochloric acid + $(3-x)$ M potassium chloride at 20°C ($x = 1$, 0.3, 0.1 0.03, and 0.01).

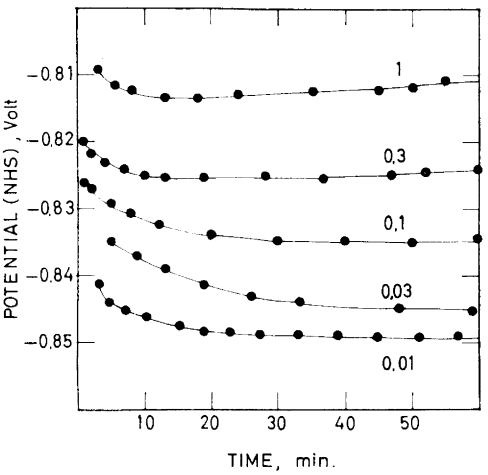

Fig. 2. Corrosion potential of zinc as function of time in x M hydrochloric acid + $(3-x)$ M potassium chloride at 20°C ($x = 1$, 0.3, 0.1, 0.03, and 0.01).

ments. The reproducibility, especially in the most acid solutions, was not always the best, the mean deviation sometimes being as bad as ± 20 %. Analogous results were obtained for the 1 M chloride series, and these combine with those in Fig. 1 in showing the corrosion rate to be essentially constant with time and to increase with the acidity of the solution. The latter is further considered below.

Fig. 2 shows examples of time curves obtained for the corrosion potential at various hydrochloric acid molalities in the 3 M chloride solutions. These curves are representative also for the type of curves obtained in the 1 M chloride solutions. The essentially stationary potential shown by these curves after an initial transient, has generally been well reproducible and is here accepted as the representative corrosion potential.

In Fig. 3, the values thus obtained for the corrosion rate and the corrosion potential of zinc in the mixed HCl/KCl solutions applied are plotted *versus* the hydrochloric acid molality, which, both for the 1 M and the 3 M chloride series, is nearly proportional to the hydrogen ion activity [13]. The corrosion rate is given in current density values which have been calculated from the weight loss data on the basis of the dissolution going to the divalent state [10]. The fully drawn straight lines in Fig. 3 have been given slopes according to (1) and (2), and it may seem that these relationships are not far from being obeyed in the 3 M chloride solutions. In the 1 M chloride solutions, however, the corrosion potential deviates clearly from the relationship (2) by showing a distinctly lower pH-dependence. It is further interesting to note that equal hydrochloric

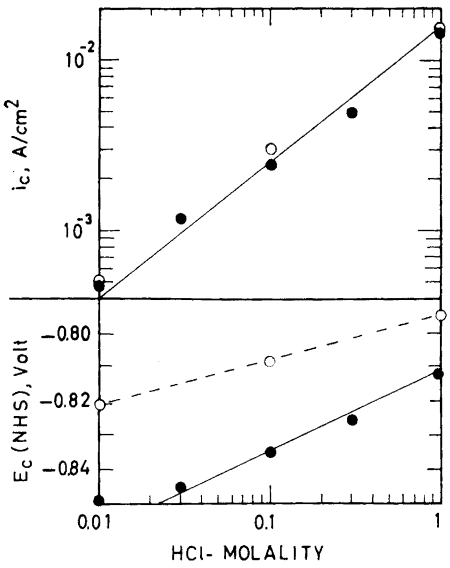

Fig. 3. Corrosion rate (i_c) and corrosion potential (E_c) of zinc as functions of hydrochloric acid molality in HCl/KCl-solutions of total molality 1 (open circles) and 3 (closed circles). 20°C.

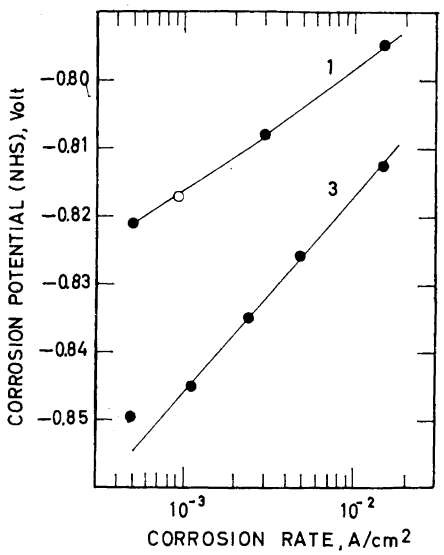

Fig. 4. Corrosion potential *versus* corrosion rate of zinc in HCl/KCl-solutions of total molality 1 and 3. The open circle applies to 0.1 N sulphuric acid + 1 M potassium chloride. 20°C.

acid molalities give almost equal dissolution rates, but distinctly different corrosion potentials at the two different total chloride molalities. The latter is in accordance with what is previously found for the effect of the chloride concentration on the anodic dissolution reaction [10].

In Fig. 4, corresponding values of the corrosion potential and the corrosion rate are plotted *versus* each other in a Tafel diagram. The Tafel line there drawn for the 3 M chloride series has the same slope (29 mV) and nearly the same position as the one previously determined for the activation controlled anodic dissolution of zinc in less acid solutions of the same chloride content [10]. The curve drawn for the 1 M chloride series also compares well with the anodic polarization curve previously found at this chloride concentration [10]. This obviously means that the anodic dissolution reaction neither is pH-dependent, nor is directly affected by being balanced by a simultaneous hydrogen evolution at the same metal surface (except for the reducing influence the gas stirring has on the anodic concentration polarization found to be present in unstirred solutions [10]).

In Fig. 5, results obtained for the dissolution reaction and the hydrogen evolution reaction from experiments with galvanostatically applied currents in a 1 M and 3 M chloride solution of 0.1 M hydrochloric acid, are given in the form of a Tafel diagram plot. The rate of the dissolution reaction has been determined from the weight loss of the zinc electrodes with corrections for

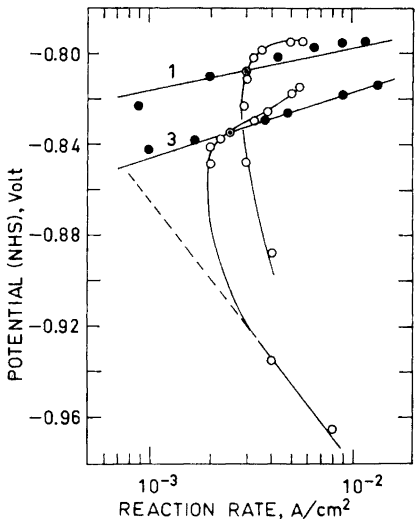

Fig. 5. Tafel diagram for anodic dissolution of zinc (closed circles) and hydrogen evolution on zinc (open circles) in 0.1 M hydrochloric acid solutions of potassium chloride at total molalities of 1 and 3. Corrosion points are given by centred circles. 20°C.

the corrosion occurring in the cell prior to application of current. The rate of the hydrogen evolution reaction has been determined from the same weight loss data by adding (resp. subtracting) the rate corresponding to the cathodic (resp. anodic) current applied in the various cases.

The anodic polarization curves drawn in Fig. 5 have been reproduced from the corrosion curves in Fig. 4. The reasonable fit of the experimental points to these lines is a further verification of the anodic dissolution reaction being essentially independent of the pH and of it occuring simultaneously with a hydrogen evolution reaction on the same metal surfaces.

The polarization data given for the hydrogen evolution reaction in Fig. 5 show this reaction to be strongly stimulated by a simultaneously occurring zinc dissolution reaction, as previously found by Vonwiller [8]. This stimulation is similar to the one previously observed also for hydrogen evolution on iron [11], but appears stronger, especially at and below the corrosion point (the corrosion point being given by centred circles in Fig. 5). Only at potentials low enough to make the dissolution reaction negligibly slow, does the hydrogen evolution reaction seem to follow the Tafel relationship. This is indicated by the partly dashed line in Fig. 5, which have been drawn with a Tafel slope of $-$ 116 mV (*i.e.* $-2.303 \times 2RT/F$). Both the slope and the position of this line is in reasonable agreement with previous results [5,6,8,9] when the comparison is based on the reaction being first order in hydrogen ion dependence. Assuming the suggested Tafel slope and the first order hydrogen ion dependence to be correct, the present results indicate a standard exchange current of about 3×10^{-10} A/cm² for the hydrogen electrode on zinc (in the hypothetical absence of zinc dissolution or of any effect of this dissolution). This is very much lower than the analogous value of about 4×10^{-6} A/cm² previously found for the hydrogen electrode on iron [11].

4.0 DISCUSSION

The present results show that the corrosion of zinc in acid chloride solutions is affected not only by the pH, but also by the salt content of the solutions (see Fig. 3). The salt content mainly affects the corrosion potential, and this seems mainly due to it having a greater effect on the relatively weakly polarizing anodic dissolution reaction than on the more strongly polarizing hydrogen evolution reaction (see Figs. 4 and 5), and to these two effects partly being rate compensating (see Fig. 5). The effect here observed of the salt content on the anodic dissolution reaction is in agreement with previous results [10], but no clear understanding of it has been obtained. For the hydrogen evolution reaction, the observations may indicate the salt effect to be an indirect one, possibly resulting from the influence of the salt content on the anodic dissolution reaction and its interaction with the hydrogen evolution reaction. Because of the salt effect and the mentioned interaction, it is no wonder that the pH-relationships (1) and (2) in the introduction to this paper are not always obeyed by zinc in acid chloride solutions. It is important, however, that reasonable obedience to these relationships is found in strong chloride solutions of constant chloride content (3 M).

The present results give some support for the hydrogen evolution reaction on zinc (when occurring essentially alone on the zinc surface) obeying the Tafel relationship with a slope of $-2.303 \times 2RT/F$, and for it being first order in hydrogen ion dependence (the latter especially by comparing with previous results). They further clearly show that the anodic dissolution reaction is pH-independent, that it to some extent is affected by the salt content of the solution, and that it in strong chloride solutions (3 M) obeys the Tafel relationship with a slope of $2.303\ RT/2F$. The latter two findings are in agreement with previous results [10].

The perhaps most interesting results obtained are those showing the presence of a strong, stimulating interaction of the zinc dissolution reaction with the hydrogen evolution reaction when these occur simultaneously on the same metal surface. As shown in Fig. 5, the stimulation caused by this interaction at a given pH increases with the rate of the anodic dissolution reaction. It even increases so strongly that a reversal occurs in the apparent potential dependence of the hydrogen evolution reaction. At the highest anodic dissolution rates (or most anodic potentials) in Fig. 5, the hydrogen evolution reaction is more than ten times as fast as one should expect from the suggested "interaction free" cathodic Tafel line. From the same diagram is further seen that the corrosion rate is four to five times as high as one should expect in the hypothetical case of no interaction. As further the corrosion rate is found to vary with pH in accordance with (2), one must assume the "stimulation factor" at the corrosion potential to be nearly independent of the pH and, thereby, of the corrosion rate. This may perhaps indicate the stimulation to be more determined by the relationship between the rates of the two simultaneously occuring reactions than by the rate of the dissolution reaction alone.

A quite similar non-mutual interaction between a metal dissolution reaction and a simultaneous hydrogen evolution reaction as here found for zinc, has previously been found also for iron [11]. No clear understanding of this interac-

tion has been obtained, but it may be that the dissolution reaction, when in act of occurring, creates favourable reaction sites for the hydrogen evolution reaction or in other ways facilitates this reaction.

Acknowledgement. The author is much indebted to Miss T. Tönderum and Miss K. Storström for technical assistance, to various members of the staff at the Central Institute for Industrial Research for helpful discussions, and to the *U.S. Department of Army, European Research Office*, for financial support.

REFERENCES

1. Anderson, E. A. and Reinhard, C. E. in Uhlig, H. H. (Ed.) *Corrosion Handbook*, Wiley, New York 1948, p. 331.
2. Evans, U. R. *The Corrosion and Oxidation of Metals*, Arnold, London 1960, pp. 310–11 and 317–19.
3. Katz, W. in Tödt, F. (Ed.) *Korrosion und Korrosionsschutz*, de Gruyter, Berlin, 2nd ed. 1961, p. 198.
4. Marcovic, T., Dugi, Z. and Rubinic, Lj. *Werkstoffe u. Korrosion* **9** (1958) 17.
5. Rotinyan, A. L., Fedot'ev, N. P. and Sok, L. U. *Zhur. Fiz. Khim.***31** (1957) 1295.
6. Sok, L. U., Rotinyan, A. L. and Fedot'ev, N. P. *Zhur. Fiz. Khim.***32** (1958) 2514.
7. Vetter, K. J. *Elektrochemische Kinetik*, Springer, Berlin/Göttingen/Heidelberg 1961, pp. 588–602.
8. Vonwiller, W. *Auflösungsvorgänge und Wasserstoff-Abscheidung an Zink-Elektroden*, Prom. Nr. 2448, Eidg. Techn. Hochschule, Zürich 1955.
9. Bicelli, L. P. and Graziano, M. *Research on Hydrogen Overvoltage on Metallic Single Crystals: Zinc*, Technical Note No. 6, Contract AF 61(052)-44, U.S. Air Force, European Research Office, Brussels, February 1961.
10. Hurlen, T. *Acta Chem. Scand.* **16** (1962) 1337.
11. Hurlen, T. *Acta Chem. Scand.* **14** (1960) 1533.
12. Hurlen, T. *Acta Chem. Scand.* **15** (1961) 615.
13. Harned, H. S. and Gancy, A. B. *J. Phys. Chem.* **62** (1958) 627.

Received December 22, 1961.

ACTA CHEMICA SCANDINAVICA 16 (1962) 1353–1358

Heats of Activation of the Zn/Zn_{aq}^{2+} Electrode

TOR HURLEN

Central Institute for Industrial Research, Blindern, Oslo, Norway

From measurements on the effect of temperature (0–40°C) on the anodic polarization of zinc in 0.001 M hydrochloric acid + 2.999 M potassium chloride and from known data on the isothermal temperature coefficient of the standard potential of this metal, the standard exchange current of the Zn/Zn_{aq}^{2+} electrode has been found to obey the following Arrhenius equation:

$$J_0 = 6.1 \times 10^{10}\ (nFT/\nu)\ \exp\ (-25\,400/RT)\ \text{A/cm}^2$$

showing a mean standard heat of activation of 25.4 kcal.

By comparison with corresponding results for iron and copper and by analogy considerations, indications are found for the mean standard heat of activation of these electrodes being an absolute measure of their standard heat of reaction. This gives −11.0 kcal as the most probable standard heat value for hydrogen evolution on zinc. On this basis, the results further show the standard heat of activation to be zero for zinc dissolution and 50.8 kcal for zinc deposition.

The results otherwise support previous data in showing a Tafel slope of approximately 2.303 $RT/2F$ for the stationary anodic dissolution of zinc, both when under diffusion control and when under activation control. In unstirred solution, activation control predominates at temperatures below about 10°C, while diffusion control takes over at higher temperatures.

The possibility of obtaining absolute electrode potentials by combining kinetic and thermodynamic data is somewhat discussed.

1.0 INTRODUCTION

In a previous work [1], the zinc electrode reactions in strong chloride solutions have been shown to be symmetric ($\alpha = 1/2$) and to be represented by the kinetic unit equation:

$$2\ Zn = 2\ Zn^{2+} + 4e^- \qquad (1)$$

showing the reactions to be second order ($\nu = 1/2$) with respect to the metal and the metal ions, respectively, and to be independent of the pH (see Ref.[2]). The same work clearly shows that the absolute rate of the anodic dissolution reaction at given potentials is independent of the zinc ion activity, and that the standard exchange current of the zinc electrode, therefore, is adequately

given by the intercept of its activation controlled anodic polarization curve in initially zinc free solution with its standard potential.

In the present work, advantage is made of the above findings in determining the standard heats of activation of the zinc electrode from measurements on the effect of temperature (0—40°C) on its anodic polarization in 0.001 M hydrochloric acid + 2.999 M potassium chloride. The theoretical basis for these determinations is as previously described [3]. The particular choice of electrolyte solution is first of all due to it belonging to the series of 3 M chloride solutions with which much work already has been done, and which has proved most suitable for the purpose (see Refs.[1,2]).

2.0 EXPERIMENTAL

The materials and the slow galvanostatic polarization method used in the present work, have been the same as described in the previous paper by the author [1] on the kinetics of the Zn/Zn^{2+}_{aq} electrode at 20°C.

The present experiments have been carried out at approximately 0°C in an ice/water bath and at 10, 30, and 40°C in a water thermostat controlled to 0.1°C. No stirring has been applied in the cell.

The potential measurements have been made isothermally against saturated calomel electrodes, which have been ascribed the following normal hydrogen scale (NHS) values [4]:

0.258 V at 0°C, 0.252 V at 10°C,
0.245 V at 20°C, 0.239 V at 30°C, and
0.232 V at 40°C.

No attempts have been made to correct for the possibly negligible liquid junction potential between the test solution and the saturated potassium chloride solution.

The standard NHS-potential of the zinc electrode is taken to be [4,5]:

−0.765 V at 0°C, −0.764 V at 10°C,
−0.763 V at 20°C, −0.762 V at 30°C, and
−0.761 V at 40°C,

and its standard heat of reaction to be −36.4 kcal (NHS) in anodic direction [5].

3.0 RESULTS

The weight changes found for anodes in the present work, verify previous findings in showing that the anodic reaction of the zinc electrode goes to the divalent state. The anodic potential-time curves obtained, are very much of the same type as those previously shown [1] for analogous experiments at 20°C. The lowest potentials shown by these curves are presented in a Tafel diagram plot in Fig. 1.

The lines in Fig. 1 have all been drawn with Tafel slopes of

$$b = 2.303\ RT/2F \qquad (2)$$

which is in accordance with previous results [1]. The reasonable fit of the experimental points to these lines lends further confidence to the correctness of this Tafel slope value.

In Fig. 2, the current density values (J'_o) obtained by extrapolating the various Tafel lines in Fig. 1 to the corresponding standard potential of zinc, are presented in the form of an Arrhenius plot, $\log(J'_o/T)$ *versus* $1/T$. In the same diagram is also given the value previously determined [1]

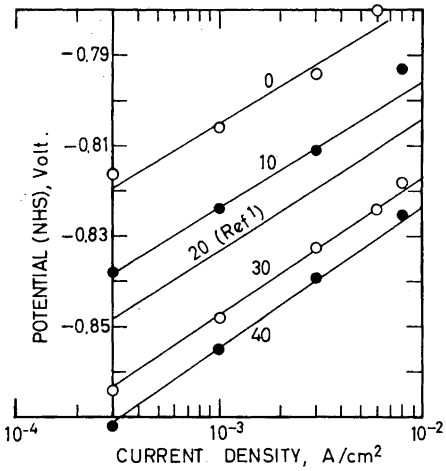

Fig. 1. Tafel diagram for anodic dissolution of zinc in unstirred solution of 0.001 M hydrochloric acid + 2.999 M potassium chloride at various temperatures (°C).

for the standard exchange current (J_o) of the zinc electrode at 20°C. As suggested by the curves there drawn, J_o' in the unstirred solution applied seems essentially identical to J_o at temperatures up to about 10°C, but deviates more and more from it at higher temperatures. This indicates that the zinc electrode, at the lowest temperatures applied, is sluggish enough to make its anodic reaction essentially activation controlled even in unstirred solution, but that diffusion control to some extent comes in already at about 10°C and, from this

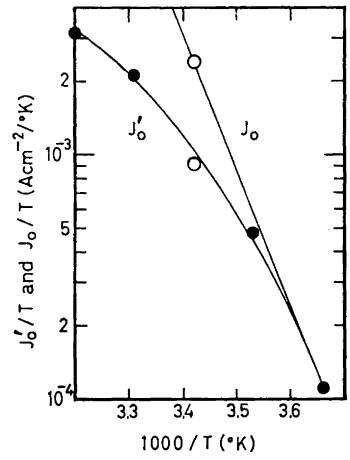

Fig. 2. Arrhenius diagram for the standard exchange current of the Zn/Zn_{aq}^{2+} electrode. The open circles represent results from Ref.[1]

temperature on, increases in importance with increasing temperature until essentially pure diffusion control is attained. This change in control mechanism is obviously due to the ratio between the exchange current and the diffusion current at the zinc electrode increasing with temperature from a value small compared to 1 to a value appreciably higher than 1 within the temperature region covered by the present experiments (see eqn. (4) in Ref.[1]). For zinc anodes in initially zinc free solutions, both the above currents may be regarded as being approximately proportional to the zinc ion concentration at the dissolving electrode surface, whereby the mentioned ratio becomes approximately independent of this concentration and essentially keeps its characteristic meaning also in the present case.

The straight line drawn for the standard exchange current (J_o) in Fig. 2, obeys the following Arrhenius equation:

$$J_o = 6.1 \times 10^{10} \ (nFT/\nu) \ \exp \ (-25\,400/RT) \ \text{A/cm}^2 \tag{3}$$

where n is 2, ν is 1/2 (see the introduction to this paper), and the other factors have their usual meaning. This shows the mean standard heat of activation (as defined in Ref.[3]) to be:

$$\Delta H_o^*(\text{mean}) = 25.4 \text{ kcal} \tag{4}$$

which together with the symmetry factor of 1/2, the stoichiometric number of 1/2, and the accepted standard heat of reaction of the zinc electrode, $\Delta H_{o,a} = -36.4$ kcal (NHS), further gives (see eqn. (5) in Ref.[3]):

$$\Delta H_{o,a}^* = -11.0 \text{ kcal (NHS)} \tag{5a}$$

$$\Delta H_{o,c}^* = +\ 61.8 \text{ kcal (NHS)} \tag{5b}$$

where the subscript (NHS) means that these energy values are referred to the normal hydrogen scale.

4.0 DISCUSSION

The present results support previous findings[1] in showing the anodic reaction of the zinc electrode in unstirred solution to be under mixed diffusion and activation control around room temperature. They further show that the former control mechanism gains predominance at higher and the latter at lower temperatures (below about 10°C), and verify that both of these control mechanisms give rise to a Tafel slope of 2.303 $RT/2F$.

The mean standard heat of activation of 25.4 kcal(absolute) found for the zinc electrode in the present work, is distinctly lower than the numerical hydrogen scale value of 36.4 kcal for its standard heat of reaction. In this respect, the zinc electrode differs from the in many other respects similarly behaving divalent copper and iron electrodes, for both of which the above two standard heat terms are found to be very nearly numerically equal to each other[3]. This equality has been assumed to be an indication that the standard heat of reaction of the hydrogen electrode on iron and copper is near to zero[3]. The present results may thus analogously be taken as an indication of this *not* being true in the case of zinc as electrode material.

The previous results on iron and copper [3] further indicate that the mean standard heat of activation of these metal/metalion electrodes is an absolute measure of their standard heat of reaction (the connection between heat of activation and heat of reaction thereby being quite analogous for metal/metalion electrode reactions as for reactions between a crystal and its vapour). Assuming this to be true also for zinc, one has the following two possibilities for the standard heat of reaction:

Reaction	Possibility I	Possibility II
$Zn = Zn^{2+} + 2e^-(Zn)$	+ 25.4 kcal	−25.4 kcal
$2H^+ + 2e^-(Zn) = H_2$	−61.8 kcal	−11.0 kcal
$Zn + 2H^+ = Zn^{2+} + H_2$	−36.4 kcal	−36.4 kcal

and, thereby, the following corresponding absolute values for the standard heat of activation of the mutually reverse reactions of the zinc electrode:

Reaction	Possibility I	Possibility II
Dissolution	50.8 kcal	0
Deposition	0	50.8 kcal

The values in the latter table are easily obtained by combining those in the former with (4) or (5) above (on the basis of (5) or (6) in Ref.[3]).

By a thermodynamic cycle as the one used in Ref.[3] for the hydrogen evolution reaction, it is found that possibility I and II imply values of about 3.5 and 4.6 eV, respectively, for the heat of electron "evaporation" from zinc. For the electron work function of zinc, experimental values ranging from 3.08 to 4.65 eV are tabulated by Michaelson [6]. The highest of these are the most recently determined ones and probably also the most accurate ones. Unless zinc should have a surface potential of very large magnitude (one volt or so), this indicates that possibility II above is the most likely one.

If the mentioned indications on which the above treatment for zinc and the analogous treatment for copper [3] and iron [7] are based, should prove to be correct, an avenue is obviously open to the evaluation of absolute electrode potentials. These treatments give, namely, the heat of reaction of the single electrode reactions involved, and the entropy change accompanying these reactions is already known [4]. A calculation for iron, copper, and zinc thus yields the following values for the potential difference between metal and solution ($\Delta\emptyset = \emptyset_m - \emptyset_{sl}$) at V(NHS) = 0 and 25°C (in Volt):

Fe	Cu	Zn
+ 0.216	+ 0.255	+ 0.498

These are then the values to be added to hydrogen scale values on these metals (at 25°C) to obtain absolute electrode potentials. However, the validity of the cardinal assumption on which these evaluations are based, namely

that the standard heat content of the activated state of the metal/metalion electrodes concerned is equal to that of their highest end state, remains to be proved. So far, only indications are obtained in this respect (see above and especially Ref.[3]). It may perhaps have some further support however, by the suggested relationship between heat of activation and heat of reaction in case not being a unique one for metal/metalion electrodes. Metal/metal-vapour reactions and also many atom exchange reactions in gases are well known to obey such a relationship. For the latter type of reactions, this relationship has recently even been derived theoretically [8].

The Arrhenius equation (3) for the standard exchange current of the zinc electrode shows the Arrhenius factor (pre-exponential factor) to be:

$$A = 6.1 \times 10^{10}(nFT/\nu) \text{ A/cm}^2 \quad (6)$$

This may be compared to the corresponding values of 35 (nFT/ν) and $8.5 \times 10^{12}(nFT/\nu)$ previously found for the copper [3] and the iron [7] electrode, respectively, what shows this factor to vary strongly for metal/metalion electrodes. There seems to be no doubt that this variation mostly is due to differences in the mean standard entropy of activation of the various electrodes (as already discussed for iron and copper [3]). At present, however, our knowledge of possible other terms involved in the Arrhenius factor for metal/metalion electrodes is too incomplete for reliable values to be calculated for the activation entropy. Further calculations of the type previously performed [3] for iron and copper in this respect, will therefore not be made here.

Acknowledgement. The author is much indebted to Miss Toril Tönderum and Miss Kari Storström for technical assistance, to various members of the staff at the Central Institute for Industrial Research for helpful discussions, and to the *U.S. Department of Army, European Research Office,* for financial support.

REFERENCES

1. Hurlen, T. *Acta Chem. Scand.* **16** (1962) 1337.
2. Hurlen, T. *Acta Chem. Scand.* **16** (1962) 1346.
3. Hurlen, T. *Acta Chem. Scand.* **15** (1961) 621.
4. deBethune, A. J., Licht, T. S. and Swendeman, N. *J. Electrochem. Soc.* **106** (1959) 616.
5. Latimer, W. M. *Oxidation Potentials (2nd Ed.)* Prentice-Hall, New York 1952, p. 168.
6. Michaelson, H. B. in *Handbook of Chemistry and Physics* (38th Ed.), Chemical Rubber Publishing Co., Cleveland 1956–57, p. 2355.
7. Hurlen, T. *Acta Chem. Scand.* **14** (1960) 1564.
8. Kleinpaul, W. *Z. physik. Chem. (Frankfurt)* **29** (1961) 201.

Received December 22, 1961.

ACTA CHEMICA SCANDINAVICA 16 (1962) 1359–1362

Some Problems Related to Detection of Methionine Sulphoxide in Protein Hydrolysates

L. R. NJAA

Governmental Vitamin Laboratory, Norwegian Fischeries Research Institute, Bergen, Norway

Methionine and methionine sulphoxide are completely oxidized to the sulphone stage by H_2O_2 treatment on filter paper if the pH of the solutions applied is less than 1.4. Above this pH a mixture of methionine sulphoxide and methionine sulphone is obtained. At pH about 6.0 practically no sulphone is detected.

Under the conditions used when protein hydrolysates are prepared by heating with 6 N HCl under reflux, methionine sulphoxide is partly reduced to methionine.

It has been suggested that methionine sulphoxide may be formed in fish meal when this contains peroxidized fat [1]. During preliminary work on the possible presence of methionine sulphoxide in hydrolysates of herring-meals, the method of Dent [2,3] for distinguishing between methionine and its sulphoxide was studied. At the same time, the effect of heating methionine sulphoxide under reflux with HCl was examined. It was found that the suggested method [2,3] does not distinguish between methionine and its sulphoxide, and that heating of methionine sulphoxide with 6 N HCl under reflux results in partial reduction of the sulphoxide to methionine.

OXIDATION OF METHIONINE AND METHIONINE SULPHOXIDE WITH H_2O_2 ON FILTER PAPER

The method of Dent [2,3] is based on the observation that methionine and methionine sulphoxide react differently when treated with 30 % H_2O_2 on the filter paper prior to chromatography. It is claimed that methionine is completely oxidized to the sulphone stage by this treatment while the sulphoxide is unaffected.

Portions of aqueous solutions (5 μl, 0.02 M) of DL methionine and of sulphoxides prepared from DL, D and L methionine by methods given in literature [4,5] were applied to sheets of Whatman paper No. 3 and treated with H_2O_2 as described by Dent [2,3]. Ascending chromatograms were run overnight using acetone containing 40 % water and 1 % acetic acid as solvent. Ninhydrine (0.3 % in methanol) was used as spraying reagent. Methionine was oxi-

dized almost completely to the sulphoxide stage by the H_2O_2 treatment while methionine sulphoxide was unaffected.

A clue to the reason for the discrepancy between this result and those reported by Dent [2,3] may lie in his statement that a small amount of HCl was added to dissolve the less soluble of the amino acids [3], which were used as 0.01 M solutions in 75 % (v/v) ethanol. Methionine requires a long time to dissolve in this solvent while the sulphoxide dissolves instantly. It is probable, therefore, that Dent [3] classified methionine among the less soluble amino acids.

Methionine and methionine sulphoxide were therefore prepared in 0.02 M aqueous solutions to which were added 2, 1, 0.5 and 0.25 % concentrated HCl. The corresponding solutions of both substances had the same pH: 1.05, 1.45, 1.85 and 2,30, respectively. Treatment with H_2O_2 prior to chromatography resulted in complete oxidation of both substances to the sulphone stage in the two more acid solutions; in the two less acid solutions both methionine sulphoxide and sulphone were detected on the chromatograms. Thus, complete oxidation to the sulphone stage took place when the pH of the original solution was 1.4 or less. Solutions (0.02 M) of the hydrochlorides were found to have pH's 2.15 and 2.00 for methionine and methionine sulphoxide, respectively; the pH's of the bases were 5.65 and 6.00. Treatment of portions of these solutions with H_2O_2 on the filter paper resulted in more sulphone than sulphoxide for the hydrochlorides while the opposite was true for the bases. By the criteria of Dent [3] the results would have indicated the presence of methionine and methionine sulphoxide in these solutions. Similar treatment of 0.01 M solutions of both substances in 75 % ethanol resulted in complete oxidation of both substances to the sulphone stage when 1 % concentrated HCl was present; without added HCl methionine was oxidized only to the sulphoxide stage while the sulphoxide was unaffected by the treatment. It may be mentioned that HCl was used as a preservative in the urines in which Dent [2] claimed to have detected methionine sulphoxide.

Methionine and methionine sulphoxide did not oxidize when solutions with pH's ranging from 1.0 to 9.0 were applied to the filter paper and left exposed to the air for 23 h prior to chromatography. No sulphone was detected with either substance, and with methionine no sulphoxide was detected. This is rather surprising since methionine when left exposed to the air is often partly oxidized to the sulphoxide [3]. The results taken together seem to indicate that the effect of HCl in the H_2O_2 oxidation of methionine and methionine sulphoxide is through an activating effect on the oxidizing agent and not on the substrate.

EFFECT OF HEATING METHIONINE SULPHOXIDE WITH HYDROCHLORIC ACID

Synge and Wood [6] observed that S-methylcysteine was formed when the corresponding sulphoxide was heated for 24 h with 6 N HCl in a sealed tube at 105°C. Since protein hydrolysates are often made by heating with 6 N HCl under reflux [7], the effect of this treatment on methionine sulphoxide was studied. 0.01 M solutions in 6 N HCl were heated under reflux for 24 h, and then taken to dryness and redissolved in water. The aqueous solutions were then chromatographed by a circular filter paper technique [8] using acetone

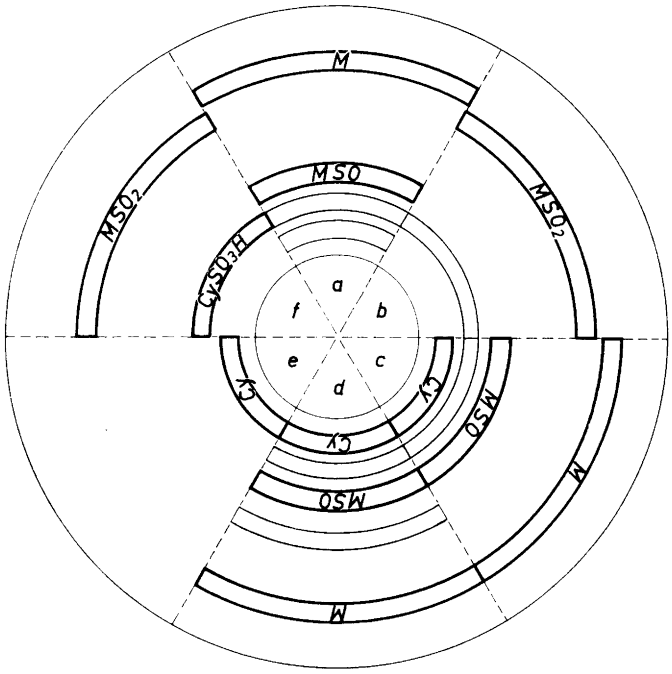

Fig. 1. Circular chromatography on Whatman filter paper No. 3 of 0.01 M solutions in 6 N HCl heated for 24 hours under reflux of methionine sulphoxide (*a*); *a* treated on the starting line with H_2O_2 and ammonium molybdate (*b*); methionine sulphoxide plus cysteine (*c*); methionine sulphoxide plus cystine (*d*); cystine (*e*); *d* treated as *b* (*f*). (Schematic presentation). (M = methionine; MSO = methionine sulphoxide; MSO_2 = methionine sulphone; Cy = cystine; $CySO_3H$ = cysteic acid).

containing 15 % water and 1 % concentrated ammonia. When the chromatograms were run overnight the solvent front moved off the paper but good separation of methionine, methionine sulphoxide and methionine sulphone was obtained. None of the common amino acids moved so fast on the paper that they would have escaped notice.

When methionine sulphoxide alone was heated with 6 N HCl the chromatograms indicated the presence of about equal amounts of methionine and methionine sulphoxide as judged by the intensity of the ninhydrine colour (Fig. 1 a). Two weaker zones were observed between the sulphoxide and the starting line. Treatment on the starting line with H_2O_2 and ammonium molybdate [3] reduced the four zones to two. The stronger one corresponded to methionine sulphone formed from methionine and methionine sulphoxide (Fig. 1 b).

It has been demonstrated that methionine sulphoxide oxidizes cysteine to cystine [4]. It was therefore tested whether the presence of an equivalent amount of cysteine together with methionine sulphoxide resulted in a more complete reduction of the latter to methionine during the heating with HCl. As a control the sulphoxide was also heated with cystine. Neither cysteine, nor cystine

appreciably increased the amount of methionine formed (Fig. 1 c, d). With both substances two zones were observed between the starting line and the methionine sulphoxide zone. The innermost one coincided with cystine (Fig. 1 e) and with the innermost of the zones observed on heating methionine sulphoxide alone (Fig. 1 a). For the mixture methionine sulphoxide and cystine an additional weak zone was observed between methionine sulphoxide and methionine (Fig. 1 d). Treatment of the heated mixture with H_2O_2 and ammonium molybdate on the starting line reduced the number of zones to two. The outermost one corresponded to methionine sulphone, the innermost to cysteic acid (Fig. 1 f). The latter zone also corresponded to the second zone from the starting line formed when methionine sulphoxide was heated alone (Fig. 1 a). The results indicate that when methionine sulphoxide is heated under reflux with 6 N HCl methionine and small amounts of two substances occupying the same zones on the chromatograms as cystine and cysteic acid are formed. It seems likely that the latter substances are homocystine and homocysteic acid. The former was not available, but H_2O_2 treatment of DL homocysteine S lactone gave one zone at the same place on the chromatograms as cysteic acid. It was not attempted to identify more definitely the substances formed. The extra zone formed in the mixture of methionine sulphoxide and cystine is suggested to be cystine disulphoxide.

The extra zones observed beside those corresponding to the substances present in the starting material could not be detected when the substances were dissolved in 6 N HCl and then, without heating under reflux, taken to dryness before redissolving them in water. The reactions responsible for the substances formed seem therefore to require some time of heating. It has not been investigated how long time of heating is required for the reactions to take place.

CONCLUSION

It seems a vain task to search for methionine sulphoxide in protein HCl hydrolysates. If present in the proteins it may be partly reduced during the heating with HCl, and if detected on paper chromatograms it may have been formed by oxidation on the filter paper [3]. By the qualitative means used in the present investigation it cannot be decided whether the presence of cysteine in the proteins may increase the amount of methionine formed from hypothetically present methionine sulphoxide. The method suggested by Dent [3] for the purpose of distinguishing between methionine and methionine sulphoxide in solution is not reliable.

REFERENCES

1. Lea, C. H., Parr, L. J. and Carpenter, K. J. *Brit. J. Nutrition* **12** (1958) 297.
2. Dent, C. E. *Biochem. J.* **41** (1947) 240.
3. Dent, C. E. *Biochem. J.* **43** (1948) 169.
4. Tonnies, G. and Kolb, J. J. *J. Biol. Chem.* **128** (1939) 399.
5. Waelsch, H., Owades, P., Miller, H. K. and Borek, E. *J. Biol. Chem.* **166** (1946) 273.
6. Synge, R. L. M. and Wood, J. C. *Biochem. J.* **64** (1956) 252.
7. Block, R. J., LeStrange, R. and Zweig, G. *Paper Chromatography*, Academic Press, New York 1952, p. 56.
8. Juvvik, P. and Michelsen, K. *To be published.*

Received January 15, 1962.

ACTA CHEMICA SCANDINAVICA 16 (1962) 1363–1368

On the Photo-Transformation of Ergot Alkaloids

IV. Lumilysergic Amides

HANS HELLBERG

Chemical Department, State Pharmaceutical Laboratory, Stockholm, Sweden

An account is given of methods leading to the four possible lumilysergic amides. Three of the substances have been prepared in crystalline form. The physical and chemical properties of the amides are described, as well as their stereochemical relation to the four lumilysergic acids.

In attempts to produce lumilysergic acids on a preparative scale from commercially available mixtures of ergot alkaloids, the yields were very poor. When studying the causes of this drawback, it was observed that if the final alkaline hydrolysis of the lumi alkaloid mixtures was performed too cautiously, considerable quantities of a by-product were obtained, whose chromatographic properties resembled those of the lumiergometrine series. It appeared as a first fraction in partition-chromatographic separation of the expected acids on kieselguhr (celite), impregnated with an ammoniacal aqueous phase. The substance lay close to the front line on ammoniacal paper chromatograms, and separated into three spots, with R_F values ranging from 0.2 to 0.5, on acetic acid paper chromatograms (For methods: see Ref.[2] and Experimental).

As early as 1932, Smith and Timmis [4,5] showed that ergot alkaloids, on moderate treatment with methanolic potassium hydroxide, gave rise to ergine. In their further studies of this substance they found that, on strong alkaline hydrolysis, it yielded lysergic acid [6], but that it was actually the amide of isolysergic acid [7]. Stoll and Hofmann [8] demonstrated that dihydroergotamine I, and corresponding dihydro compounds of other peptide alkaloids, yielded dihydrolysergic amide I on cautious treatment with alkali. They pointed out that a specific cleavage took place, due to the labile nature of the so-called peptide part of the alkaloids.

Consequently, it was reasonable to assume that the by-product obtained on hydrolysis of the lumi ergot alkaloids consisted of lumilysergic amides. In the course of the present work, four such substances appeared — in complete agreement with the theoretical considerations — and were initially denoted arbitrarily as A, B, C, and D.

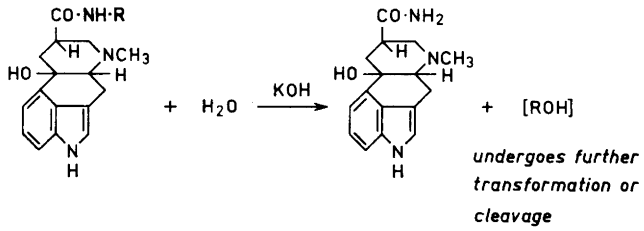

Lumilysergic amides from lumi alkaloids. Paper-chromatographic analysis of the products of alkaline hydrolysis, under the standard conditions used earlier (1 M KOH in 50 % ethanol, boiling water bath), showed that lumiergocristine I and lumiergocristinine II disappeared already within 5 minutes, but that the yield of acids was poor after this short time. Instead, the amide fraction was large. Cleavage of lumiergocristinine I could not be kept in the amide stage, even by this brief treatment, but continued to acids. It was, however, possible to obtain an amide yield from this alkaloid as well by using 95 % ethanol as solvent, and lower temperature (60°C for 45 min). The conditions for amide cleavage of lumiergocristine II, which is relatively difficult to prepare, were not tested separately.

The amide cleavage of available lumiergocristines (described in detail under the heading of Experimental) can be summarized as follows:

Lumiergocristine I	$\xrightarrow{KOH}$	C
Lumiergocristinine I	$\xrightarrow{KOH}$	C
Lumiergocristinine II	$\xrightarrow{KOH}$	A + minute quantity of B

A remarkable feature is that the amide produced from lumiergocristinine I is the same as that from lumiergocristine I. Despite the fact that disrupture of the molecule takes place more than two atoms beyond C_8, epimerization can evidently occur at this carbon atom. This was confirmed by the results obtained with lumiergocristinine II.

Lumilysergic amides from ergine (isolysergic amide). Irradiation of ergine in 0.1 M HCl (in analogy with treatment of the ergometrine alkaloids in Ref.[1]) resulted in only one amide, *i.e.*, substance A, instead of the expected two. When irradiation of ergine was performed in 5 % acetic acid instead, it yielded — in addition to A — a substance that could be presumed to be D. This was the only method which led to recovery of D, and the substance could not, unfortunately, be obtained in crystalline form. In attempts to purify it further, it was rapidly destroyed. This experience, as well as the results of the cleavage of lumi alkaloids, indicates that substance D is labile.

Place of the amides in the stereochemical system. In view of the appearance of substance C on cautious hydrolysis of lumiergocristine I and lumiergocristinine I, it is highly probable that it belongs to series I. Substances A and B

probably belong to series II, since they are obtained in a corresponding way from lumiergocristinine II. A and D, which occur on illumination of the isolysergic amide (ergine), seem likely for this reason to be lumi-isolysergic amides.

Thus, the methods of preparation already seem to afford good reason to use the following denotations:

Substance C: lumilysergic amide I
Substance D: lumi-isolysergic amide I
Substance B: lumilysergic amide II
Substance A: lumi-isolysergic amide II

Additional evidence in favour of this statement is given by the physical and chemical properties of the substances, summarized in Table 1. Thus, decided support is provided by the results of strong alkaline hydrolysis of the amides A, B and C. Although D was an impure product, the results confirm that the substance does, at any rate, belong to series I.

The UV spectra proved, to some extent, to be typical of the various lumilysergic acids and their derivatives. The chief characteristics were the details of the structure around 283 mμ, and the exact position of the maximum close to this wave-length. Substance C showed the distinct maximum at 283 mμ, normal for derivatives in the I series, and an inflexion point at 290 mμ. Substance A had its maximum and inflexion point displaced 2—3 mμ towards shorter wave-lengths, which is normal for derivatives of lumi-isolysergic acid II. Substance B had a flattened peak with a maximum at 284 mμ, which is characteristic of derivatives of lumilysergic acid II.

The order of appearance on chromatograms does not, in view of its highly empirical nature, furnish particularly strong proof for arrangement of isomers in stereochemical systems. The aforementioned denotations are, however, in good agreement with the order of appearance of lumiergometrines on alumina [1], and with that of lumilysergic acids on paper (Ref.[2], acetic acid method). The agreement with the lumiergometrines on paper [1] is not, however, as good.

EXPERIMENTAL

As a rule, the experiments were first made on a micro scale under varying conditions, and the products were studied by paper chromatography, using the methods described earlier [2].

The amides were denoted as A, B, C, and D, according to the order in which they were produced. Amides and acids were identified in the course of the work by paper chromatography, using the solvents benzene, butanol and 20 % acetic acid (1 + 1 + 2), as described in a previous paper [2]. The products obtained by the different procedures were further characterized by means of their crystalline appearance, melting point on the Kofler block, UV spectrum in 0.1 M HCl, and IR spectrum in a KBr plate. Most of these properties are listed in Table 1.

Substances C (lumilysergic amide I) and A (lumi-isolysergic amide II) were produced in sufficient quantities to permit elementary analyses. The following results were obtained:

Lumilysergic amide I, dried in high vacuum at 140°C. Found: C 67.20; H 6.69; N 14.86; O 11.37. Calc. for $C_{16}H_{19}O_2N_3$ (285.34): C 67.34; H 6.71; N 14.73; O 11.21.

Lumi-isolysergic amide II, dried in high vaccum at 100°C. Found: C 66.86; H 6.76; N 14.89; O 11.14. Calc. for $C_{16}H_{19}O_2N_3$ (285.34): C 67.34; H 6.71; N 14.73; O 11.21.

Amides from a lumi alkaloid mixture. 5 g of "Secale Mischalkaloide, Anton v. Waldheim, Wien", containing more than 95 % of ergot alkaloids, was isomerized by boiling

Table 1. Physical and chemical properties of the lumilysergic amides.

	Appearance	Heating on Kofler block	Light absorption in 0.1 M HCl (dry basis)	Optical rotation $[\alpha]_D^{20}$ $c = 1$ in 0.1 M HCl (dry basis)	Lumilysergic acids on strong alkaline hydrolysis (*cf.* Ref.[1])	Paper chromatogram, HAc method (Ref.[1]) ** R_F
Lumilysergic amide I (Substance C)	From methanol: small pillars	Decomposition at 250°C	Max: 283 mμ $E(1\ \%, 1\ cm) = 229$ Infl.pt. 290 mμ	+ 21°	I + small amt. iso I	~ 0.29
Lumi-isolysergic amide I * (Substance D)					I + iso I	~ 0.25
Lumilysergic amide II (Substance B)	From methanol: small prisms	Melting and decomposition at 155°C	Max: 284 mμ $E(1\ \%, 1\ cm) = 199$ *** Flattened peak		II + minute amt. iso II	~ 0.21
Lumi-isolysergic amide II (Substance A)	From methanol: thick, usually broken pillars	Melting point: 153–154°C (decomp.)	Max: 281 mμ $E(1\ \%, 1\ cm) = 231$ Infl. pt. 288 mμ	+ 22°	II + iso II	~ 0.39

* Impure amorphous product.
** R_F values not directly comparable with those in Ref.[1] and Ref.[2]
*** Calculated on undried substance.

with 50 ml of methanol in an N_2 atmosphere for 2 days. The precipitate was filtered off, and allowed to dry in the air. Yield: 3.5 g with high positive optic rotation ($[\alpha]_D$ about + 500° in 1 % $CHCl_3$ solution).

The precipitate was transformed into lumi alkaloids in portions of 0.35 g, which were dissolved in 5 ml of concentrated acetic acid, and diluted to 100 ml with water. Irradiation and extraction were performed as described for ergocristine in Ref.[1] The main part of the coloured material was removed from the product by extraction with ether, using the method given in Ref.[3] Yield 1.4 g.

The lumi alkaloid mixture was boiled with 20 ml of 1 M KOH in 50 % ethanol in a water bath for 15 min and then treated as described below for lumiergocristine I. The first fraction obtained in partition chromatography (column 50 × 3.5 cm) contained three amides, *i.e.*, substances A, B and C. Later fractions contained small quantities of lumilysergic acids. The amide fraction was separated by chromatography on alumina (80 × 2 cm Al_2O_3, according to Brockmann, Merck), using gradient elution with chloroform containing 0 to 10 % ethanol. The content of lumilysergic acid derivatives was measured spectrophotometrically at 283 mμ in the eluates. The three amides separated; A appeared first, followed by B and then by C. There was a large preponderance of A (lumi-isolysergic amide II), the yield being 100 mg, whereas B (lumilysergic amide II) and C (lumilysergic amide I) were obtained in quantities of only about 10 mg. All three were crystallized from methanol.

Amides from lumiergocristine I. 0.5 g of lumiergocristine I was boiled in a water bath for 8 min with 20 ml of 1 M KOH in 50 % ethanol. After cooling, the mixture was saturated with CO_2 to pH 7, when 200 ml of absolute alcohol were added. Saturation with CO_2 was allowed to continue for a short time, after which the precipitate was centrifuged off. The solution was evaporated to dryness. The residue of the alcoholic solution was chromatographed on a kieselguhr (celite) column (50 × 2 cm) with benzene, butanol and 2 M ammonia (1 + 1 + 2). The first fraction contained substance C only, *i.e.*, lumilysergic amide I. (Two additional, smaller fractions were obtained, containing lumi-isolysergic acid I and lumilysergic acid I, respectively). Lumilysergic amide I was crystallized from methanol. Yield 90 mg.

Amides from lumiergocristinine I. 0.1 g of lumiergocristinine I in 5 ml of 1 M KOH in 95 % ethanol was heated in a water bath at 60°C for 45 min under aeration with nitrogen. The ethanolic solution was worked up in the same way as in the case of lumiergocristine I. Two fractions were obtained. The first contained substance C, *i.e.*, lumilysergic amide I, and the second lumi-isolysergic acid I. Paper-chromatographic analyses before and after chromatography on Al_2O_3 showed only an inappreciable quantity of lumilysergic acid I in addition to the aforementioned substances. No spot which could be interpreted as substance D (lumi-isolysergic amide I) was observed. Yield of lumilysergic amide I 9 mg.

Amides from lumiergocristinine II. 0.5 g of lumiergocristinine II was treated in the same way as lumiergocristinine I (see above). The residue after evaporation of the ethanolic solution was chromatographed directly on an Al_2O_3 column (80 × 2 cm) with chloroform containing 0—10 % ethanol (gradient elution). An inappreciable fraction, identified by paper chromatography as substance B (lumilysergic amide II) appeared first, followed by the main fraction, consisting of substance A (lumi-isolysergic amide II). Lumi-isolysergic amide II was obtained by crystallization from a minute quantity of methanol. Yield 60 mg.

Photo-transformation of ergine in 0.1 M HCl. 0.25 g of ergine in 25 ml of 0.1 M HCl was irradiated with an UV lamp, under the conditions described in detail in Ref.[1] for ergocristine. 6.5 g of NaCl and 0.65 g of $Na_2HPO_4.2$ aq were added to the solution, as well as 2 M NaOH to pH 9. The mixture was extracted with 6 × 50 ml of $CHCl_3$. The chloroform phases were dried with anhydrous Na_2SO_4, and evaporated to dryness *in vacuo*. The dry residue was transferred to a small quantity of washed sea sand, and placed on an Al_2O_3 column (80 × 2 cm, according to Brockmann, Merck). The column was eluted with chloroform containing 0—10 % ethanol (gradient elution). Only one fraction of any appreciable size was obtained, and was found to consist of substance A (lumi-isolysergic amide II). Yield 15 mg. None of the small fractions obtained could be shown to contain any lumilysergic amide.

Photo-transformation of ergine in acetic acid solution. 0.25 g of ergine was dissolved in 2.5 ml of concentrated acetic acid, and diluted with 25 ml of water. The solution was

treated as in the preceding experiment. Two fractions were obtained, both containing more than one lysergic acid derivative. The main component of the first fraction was probably substance D. Unfortunately, it could not be obtained in crystalline form, since it was rapidly destroyed on attempts to purify it. The main component of the second fraction from Al_2O_3 chromatography was substance A (lumi-isolysergic amide II).

Acknowledgements. The work was financially supported by *Statens Medicinska Forskningsråd*, which is gratefully acknowledged. My thanks are also due to Miss Kerstin Lindgren for technical assistance, to Dr. Alfred Bernhardt, Max Planck Institut für Kohlenforschung, Mühlheim (Ruhr) for the elementary analyses and to Mrs Erica Odelberg for the translation.

REFERENCES

1. Hellberg, H. *Acta Chem. Scand.* **11** (1957) 219.
2. Hellberg, H. *Acta Chem. Scand.* **12** (1958) 678.
3. Hellberg, H. *Acta Chem. Scand.* **13** (1959) 1106.
4. Smith, G. and Timmis, G. M. *J. Chem. Soc.* **1932** 763.
5. Smith, G. and Timmis, G. M. *J. Chem. Soc.* **1932** 1543.
6. Smith, G. and Timmis, G. M. *J. Chem. Soc.* **1934** 674.
7. Smith, G. and Timmis, G. M. *J. Chem. Soc.* **1936** 1440.
8. Stoll, A. and Hofmann, A. *Helv. Chim. Acta* **33** (1950) 1705.

Received January 24, 1962.

ACTA CHEMICA SCANDINAVICA 16 (1962) 1369–1377

Studies of Hydrogen Bonding

Part V *. The Intermolecular Hydrogen Bond Association of Amides with Phenol and Pentachlorophenol

THOR GRAMSTAD and WILLY JOHANNES FUGLEVIK

Norwegian Defence Research Establishment, Division for Toxicology, Kjeller, Norway

The intermolecular hydrogen bond association constants of twenty-six N,N-disubstituted amides with phenol and pentachlorophenol respectively, have been determined at 20 and 50°C. It has been found that for each system the ΔH, ΔF, ΔS, $\nu_{\frac{1}{2}}$ and $\varepsilon_{max} \times \nu_{\frac{1}{2}}$ values form linear relationships with the hydrogen bond frequency shift.

The influence of various substituents in the amides on the hydrogen bond association constants is discussed. The effect of solvent interaction on the hydrogen bond association is also considered.

It has been shown in two previous publications [1,2] that organophosphorus compounds (OPC) containing the P=O group form very strong intermolecular hydrogen bonds with various hydroxy-compounds. Furthermore, it was shown that the association constants, K_{ass}, form a linear relationship with the frequency shift, ν_{O-H}, of the O—H band, which accompanies the formation of the hydrogen bond. Linear relationships between frequency shift and ΔH, ΔF, ΔS, $\nu_{\frac{1}{2}}$ and $\varepsilon_{max} \times \nu_{\frac{1}{2}}$ respectively, were found to be valid only when kept to one system, *e.g.*, OPC-phenol, OPC-pentachlorophenol *etc.* It was also shown that the curves ΔH and ΔS *vs.* the frequency shift flatten with increasing acidity of the proton donor. With regard to the effect of solvent interaction on hydrogen bond association, it was observed that when carbon tetrachloride was replaced by carbon disulphide as the solvent, the association constant and the enthalpy of association increased, particularly for the system OPC-pentachlorophenol. It was also observed that for each system an increase in the enthalpy was compensated by an increase in the entropy of association, except for OPC-pentachlorophenol where an increase in $-\Delta H$ was accompanied by an decrease in $-\Delta S$. A study of the hydrogen bond association between a number of nitrogen compounds and various hydroxy-compounds revealed

* Part IV: *Acta Chem. Scand.* **16** (1962) 999.

that pentachlorophenol forms 1:1, 2:1 and 3:1 hydrogen bonded complexes with tertiary amines, whereas phenol forms only 1:1 complexes [3]. In addition it was shown that there exists for the system pyridines-phenol a linear relationship between the logarithms of the association constants and the pK_a values of the proton acceptors, and that this relationship was not applicable to tertiary aliphatic amines. In a fourth paper [4] it was shown that the ability of organophosphorus compounds to form addition compounds with iodine and hydrogen bonds with hydroxy-compounds was related by a linear relationship. To our knowledge no systematic study has hitherto been reported concerning the equilibrium reaction of amides with phenol and pentachlorophenol. We therefore found it of interest to extend our research to this field to see if the same fundamental relationships found for organophosphorus compounds containing the P=O group, are valid for N,N-disubstituted amides.

The ability of amides to form intermolecular hydrogen bonds has long been recognised [5-8]. Flett [5] has shown that N,N-dimethylformamide forms hydrogen bonded complexes with phenol, diphenylamine, *p*-benzotoluidide, and benzyl alcohol. He also evaluated the thermodynamic data for these complexes using infrared spectroscopy. Lundgren and Beakley [6] have determined, among others, the equilibrium constant for the association of phenol with N,N-dimethylformamide by using rhodamine-B as indicator. The method involves measurement of the change from colourless rhodamine to the coloured zwitter-ionic form produced by the hydrogen donor. The results obtained were in accordance with those found by Flett [5]. Tsuboi *et al.*[7] have evaluated the thermodynamic data for the system phenol-N,N-dimethylacetamide in various solvents while Becker [8] has studied the interaction between N,N-dimethylform amide and methanol, ethanol, and *t*-butanol.

EXPERIMENTAL

Materials. Phenol, pentachlorophenol, carbon tetrachloride and carbon disulphide were the same as described elsewhere [2]. The amides studied were synthesised from the corresponding acid chlorides and secondary amines. They were purified, either by fractional distillation or by recrystallisation, just before use, and their purity was checked by infrared spectroscopy. Their melting and boiling points are listed in Table 1.

Infrared and near-infrared measurements. The instruments, the instrumental conditions and the methods of running the spectra and the method of calculation of the association constant were the same as described elsewhere [3]. For the determination of the frequency shift of the ground state stretching vibration of the O—H band which accompanies the formation of the hydrogen bond the concentration of the proton donors was kept at 0.06 M, and that of the amides at 0.03 M. For the calculation of association constant in near-infrared region the concentration of the proton donors was kept at 0.006 M to prevent self-association. The concentrations of the proton acceptors for the system amides-phenol, were 0.012, 0.024, 0.036 and 0.06 M, and for the system amides-pentachlorophenol, were 0.003, 0.006, 0.012 and 0.06 M.

RESULTS

Association constant and free energy. It has been shown [1,2] that the logarithms of the association constants, K_{ass}, between organophosphorus compounds and methanol, phenol, α-naphthol and pentachlorophenol respectively, form a near relationship with the frequency shift ν_{O-H}. This relationship was only

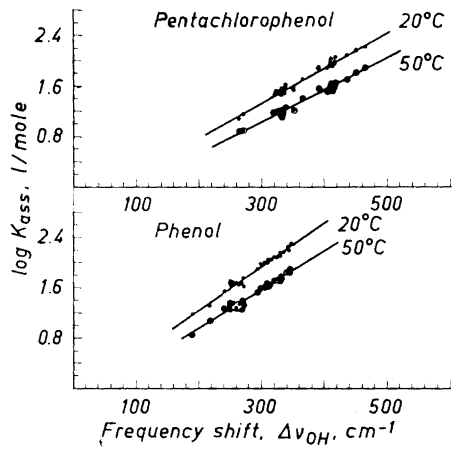

Fig. 1. The relation between the logarithms of the association constants and the frequency shifts for the association of disubstituted amides with phenol and pentachlorophenol. Solvent, carbon tetrachloride.

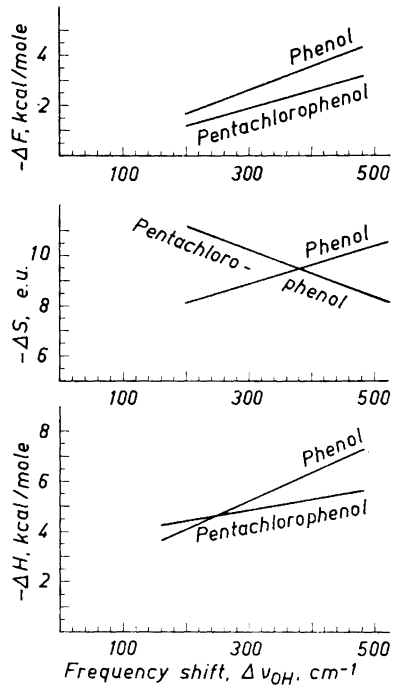

Fig. 2. Free energi $-\Delta F$, entropy $-\Delta S$, and enthalpy $-\Delta H$, *vs.* the frequency shift, $\Delta\nu_{O-H}$ of the O—H bond in hydrogen bonded systems.

valid when kept to one system, *e.g.*, OPC-phenol, OPC-pentachlorophenol, *etc.* As can be seen from Fig. 1 the same relation has now been found to be valid for the association of N,N-disubstituted amides with phenol and pentachlorophenol. A least-squares fit to the calculated log K_{ass} values (see Table 1) at 20 and 50°C, give the straight lines shown in Fig. 1. For each system the lines at 20 and 50°C have different slopes. The sequence is, in order of decreasing divergence, amides-phenol > amides-pentachlorophenol. The difference in slope between the K_{ass} *vs.* $\Delta\nu_{O-H}$ plots for 20 and 50°C for each system, is strongly reflected in the ΔH vs. $\Delta\nu_{O-H}$ and ΔS *vs.* $\Delta\nu_{O-H}$ plots (see Fig. 2). Furthermore, we have found smaller association constants for the system amides-pentachlorophenol than for the system amides-phenol. These observations are all in accordance with those found for the association of organophosphorus compounds with the corresponding proton donors [2]. The anomalies found in the latter study were believed to be due, at least partly, to hydrogen bond formation between the proton donor and the solvent.

Enthalpy and entropy. Fig. 2 shows the relationship ΔH *vs.* $\Delta\nu_{O-H}$ and ΔS *vs.* $\Delta\nu_{O-H}$. The values used are calculated from the smoothed values of

Table 1. Data on the hydrogen bonding of amides to phenol and pentachlorophenol. Solvent, carbon tetrachloride.

Proton acceptor	M.p. °C	ν_{CO} cm^{-1}	Phenol				Pentachlorophenol			
			$\Delta\nu_{O-H}$ cm^{-1}	K_{ass} l/mole 20°C	K_{ass} l/mole 50°C	$\Delta\nu_{CO}$ cm^{-1}	$\Delta\nu_{OH}$ cm^{-1}	K_{ass} l/mole 20°C	K_{ass} l/mole 50°C	$\Delta\nu_{CO}$ cm^{-1}
$CH_3C(O)N(C_6H_{11})_2$	104.5	1652	342	176.7	71.7	22	464	173.7	78.5	39
$CH_3CH_2CH_2C(O)N(C_6H_{11})_2$	39.0	1650	313	112.2	44.6	21	—	—	—	—
$CH_3CH_2C(O)N(C_6H_{11})_2$	63.5	1650	307	104.8	45.6	20	415	101.0	41.8	33
$C_6H_5C(O)N(C_6H_{11})_2$	98.0	1638	311	106.0	41.5	25	410	109.0	44.0	31
$CH_2ClC(O)N(C_6H_{11})_2$	116.0	1656	250	42.5	18.7	15	327	31.3	16.1	23
p-$NO_2C_6H_4C(O)N(C_6H_{11})_2$	175.0	1648	272	41.0	21.0	21	350	34.9	16.7	32
$CH_3C(O)N(C_2H_5)_2$	Bp. 59/6	1657	340	157.2	70.1	17	435	126.5	51.5	32
$CH_3CH_2CH_2C(O)N(C_2H_5)_2$	Bp. 2/0.5	1650	325	123.8	52.3	18	408	80.4	35.2	33
$CH_3CH_2C(O)N(C_2H_5)_2$	Bp. 55/2	1657	329	134.5	55.1	20	415	93.6	38.9	28
$C_6H_5C(O)N(C_2H_5)_2$	Bp. 100/2	1646	298	97.1	40.2	23	390	81.8	37.5	37
$CH_2ClC(O)N(C_2H_5)_2$	Bp. 55/0.2	1667	263	45.7	21.8	18	330	31.8	14.4	25
p-$NO_2C_6H_4C(O)N(C_2H_5)_2$	66.0	1650	267	47.0	18.3	20	330	31.8	13.6	22
$CH_3C(O)N(CH_2)_5$	Bp. 60/0.4	1657	330	135.0	60.1	22	415	112.7	43.7	36
$CH_3CH_2CH_2C(O)N(CH_2)_5$	Bp. 70/1	1651	328	129.1	50.7	22	409	81.9	35.4	30
$CH_3CH_2C(O)N(CH_2)_5$	Bp. 50/4	1652	320	122.1	52.6	19	404	79.4	33.0	34
$C_6H_5C(O)N(CH_2)_5$	45	1648	306	102.6	40.8	26	408	84.6	34.8	36
$CH_2ClC(O)N(CH_2)_5$	Bp. 80/0.5	1664	252	47.7	22.1	16	323	32.3	15.8	21
p-$NO_2C_6H_4C(O)N(CH_2)_5$	122	1650	260	45.3	19.1	19	325	30.3	13.4	22
$CH_3C(O)N(C_6H_5)_2$	102.5	1684	270	59.0	25.9	19	337	41.8	18.5	25
$CH_3CH_2CH_2C(O)N(C_6H_5)_2$	68.0	1685	250	45.5	22.3	24	330	35.1	16.7	30
$CH_3CH_2C(O)N(C_6H_5)_2$	65.0	1687	250	44.0	20.2	22	328	33.3	15.4	29
$C_6H_5C(O)N(C_6H_5)_2$	181.0	1674	240	34.8	18.6	24	318	30.2	15.4	24
$CH_2ClC(O)N(C_6H_5)_2$	121.0	1694	217	21.0	12.0	5	270	14.8	8.0	22
p-$NO_2C_6H_4C(O)N(C_6H_5)_2$	158.5	1673	190	15.3	7.5	14	262	12.2	7.6	21
$HC(O)N(CH_3)_2$	Bp. 94/10	1692	292	78.6	33.0	17	364	54.1	25.9	20
$CH_3NCH{=}CHCH{=}CHC{=}O$	Bp. 63/0.5	1676	345	202.4	77.5	19	448	149.7	65.5	16

log K_{ass} taken from the straight lines in Fig. 1. As can be seen the ΔH and ΔS curves flatten on passing from phenol to pentachlorophenol and this also is in accordance with previously reported observations on organophosphorus compounds [2]. In Table 2 are shown the range of ΔH and ΔS values, and the slope for each system. In the case of the system amides-phenol an increase in

Table 2. Maximum and minimum values of enthalpy and entropy changes on hydrogen bond formation together with the slopes for different systems. Solvent, carbon tetrachloride.

System	ΔH kcal/mole from	to	ΔS e.u. from	to	Slope ** ΔH-curve	ΔS-curve
OPC *-phenol	−4.3	−7.8	− 6.2	−10.5	0.55	0.70
OPC *-pentachlorophenol	−4.1	−6.4	− 7.3	−6.5	0.26	−0.0086
Amides-phenol	−4.0	−5.7	− 8.1	−9.2	0.45	0.30
Amides-pentachlorophenol	−4.7	−5.6	−10.6	−8.7	0.17	−0.38

* OPC means a series of organophosphorus compounds (see Ref.[2]).
** See Fig. 2 and Ref.[2]

the enthalpy of association is compensated by an increase in the entropy of association, whereas the reverse is the case with the system amides-pentachlorophenol.

Half band width and intensity. Fig. 3 shows the observed half band widths, $\nu_{\frac{1}{2}}$, of the hydrogen bonded O—H band plotted as a function of the frequency shift, $\Delta\nu_{O-H}$. The straight lines drawn through the observed values cut the $\nu_{\frac{1}{2}}$-axis at 45 and 50 cm^{-1} which correspond approximately to the half band widths of the hydroxyl groups, in carbon tetrachloride, of phenol and pentachlorophenol, respectively. As can be seen, a fairly good linear relationship is found between $\Delta\nu_{O-H}$ and $\nu_{\frac{1}{2}}$ for each system. Furthermore, we see that for each proton donor there is a systematic increase in $\Delta\nu_{O-H}$ and $\nu_{\frac{1}{2}}$ as the base strength increases. These results are in agreement with those reported elsewhere for organophosphorus compounds and the same proton donors [2]. The correlation between the intensity expressed in terms of $\varepsilon_{max} \times \nu_{\frac{1}{2}}$ and the frequency shift shown in Fig. 4 is close to a linear relation. The straight lines drawn cut the ordinate at 2.43 and 4.0 which correspond to the $\varepsilon_{max} \times \nu_{\frac{1}{2}} \times 10^{-3}$ values of phenol and pentachlorophenol, respectively. ε_{max} is the molecular extinction coefficient at the absorption maximum and is calculated as shown elsewhere [2].

DISCUSSION OF RESULTS

The present study on ternary solutions of N,N-disubstituted amides and phenol or pentachlorophenol in carbon tetrachloride has established the following facts, which also are in accordance with previously reported results on interaction of OPC with various hydroxy-compounds [1,2]: Firstly, in each system, the hydrogen bonded O—H band is enhanced in integrated intensity ($\varepsilon_{max} \times \nu_{\frac{1}{2}}$), broadened in contour, and progressively lowered in frequency as the base strength of the proton acceptor increases. Secondly, phenol forms hydrogen bonds more readily with amides than does pentachlorophenol (see

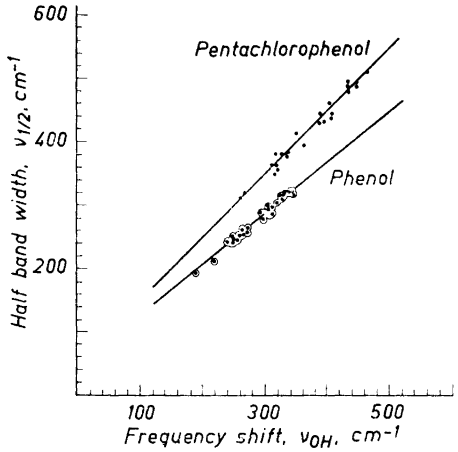

Fig. 3. Half band width $\nu_{1/2}$, *vs.* frequency shift, $\Delta\nu_{O-H}$, of the O—H bond in hydrogen bonded systems.

Table 1). Thirdly, the slopes of the ΔF *vs.* $\Delta\nu_{O-H}$, ΔH *vs.* $\Delta\nu_{O-H}$ and ΔS *vs;* $\Delta\nu_{O-H}$ curves are greater for the system amides-phenol than for the system amides-pentachlorophenol. Fourthly, the association constants for the system OPC-phenol are, in relation to the frequency shift, larger than those for the system amides-phenol, whereas when phenol is replaced by pentachlorophenol the reverse tends to be the case. Some examples are given below:

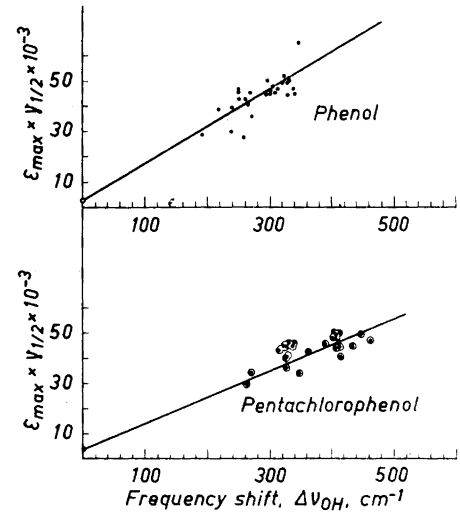

Fig. 4. The frequency shift, $\Delta\nu_{O-H}$, *vs.* intensity, $\varepsilon_{max} \times \nu_{1/2}$, of the O—H bond in hydrogen bonded systems.

	Phenol		Pentachlorophenol	
	$\Delta\nu_{O-H}$	$K_{ass}^{20°C}$	$\Delta\nu_{O-H}$	$K_{ass}^{20°C}$
	cm^{-1}	l/mole	cm^{-1}	l/mole
p-$NO_2C_6H_4C(O)N(C_2H_5)_2$	260	45.3	325	30.3
$CCl_3P(O)(OC_2H_5)_2$ (Ref.[2])	260	73.2	330	29.7
$CH_3NCH{=}CHCH{=}CHCO$	345	202.4	448	149.7
$C_2H_5OP(O)(OC_2H_5)_2$ (Ref.[2])	345	350.5	481	153.1

These results indicate that we have to take into account not only the strong solvent interaction with pentachlorophenol but also the effect of solvent interaction with the amides in comparison with that with the phosphorus compounds, and also with the hydrogen bonded complexes. As shown earlier [2,3], the thermodynamic data of hydrogen bonds are very much affected by solvent interaction. It was suggested that the fall in the values of the association constants for the system OPC-pentachlorophenol when compared with OPC-phenol was due, at least partly, to hydrogen bond formation between the proton and the solvent. In contrast, no such fall was found for the corresponding association constants of pyridine and collidine. As can be seen in Table 1, the results obtained with the amides are consistent with those found with the organophosphorus compounds studied, *i.e.*, the association constant for an amide-pentachlorophenol system is lower than that of the corresponding amide-phenol system. Furthermore, we found (see Table 3) a marked increase in the association constants and enthalpies of association for the systems amides-phenol and amides-pentachlorophenol when carbon tetrachloride was replaced by carbon disulphide as the solvent. These results are also in accordance with those found for organophosphorus compounds[2,3]. The difference in frequency shift should also be noticed, *e.g.*, 448 and 481 cm^{-1}, respectively, for N-methyl-pyridone and triethylphosphate with pentachlorophenol, although with phenol the frequency shift is the same, namely 345 cm^{-1} (see the examples above).

It has been shown earlier [1], that the thermodynamic properties of hydrogen bonds between OPC's and phenols are very much affected by the nature of the substituents in the phosphorus compounds, probably because of the easy deformation of the electronic atmosphere around the phosphorus atom. The same effect, although to a smaller extent, has now been found in amides. The influence of different substituents on the stretching vibration of the carbonyl group is recorded in Table 1. The general tendency is that electron withdrawing substituents, *e.g.*, R′ = CH_2Cl (see structures below) reduce the polarity of the C=O bond and so raise the C=O bond frequency. A phenyl or p-nitrophenyl group in the R′ position, however, reduces its frequency due to direct conjugation of the carbonyl group with the benzene ring, while N-phenyl substitution has the opposite effect. This suggests that in N-phenyl compounds the phenyl group withdraws the unshared electron pair on the nitrogen from conjugation with the carbonyl group. There does, however, seem to be a correlation between the C=O frequency and the ability of the amide to form a hydrogen bond if amides containing the phenyl or p-nitrophenyl group in R′ position are excluded. The sequence, as can be seen from Table 1, is with few exceptions, in order of decreasing ability to form hydrogen bond,

Table 3. A comparison of thermodynamic data for hydrogen bonds in different solvents.

Compound	$\Delta\nu_{OH}$ cm^{-1}	K_{ass} l/mole 20°C	K_{ass} l/mole 50°C	ΔH kcal/mole	ΔF kcal/mole	ΔS e.u.	ν_{CO} cm^{-1}	$\Delta\nu_{CO}$ cm^{-1}	$\nu_{\frac{1}{2}}$ cm^{-1}	Solvent
$C_6H_5OH\cdots OC(H)N(CH_3)_2$	292	78.6	33.0	—5.4	—2.5	—9.9	1692	17	286	CCl_4
	277	116.7	60.5*	—6.0	—2.8	—11.0	1690	20	282	CS_2
$C_6Cl_5OH\cdots OC(H)N(CH_3)_2$	364	54.1	25.9	—4.6	—2.3	—7.8	1688	20	394	CCl_4
	398	74.3	39.1*	—5.8	—2.5	—11.4	1691	22	462	CS_2
$C_6H_5OH\cdots OC(CH_3)N(C_2H_5)_2$	340	157.2	70.1	—5.1	—2.9	—7.2	1657	17	340	CCl_4
	331	259.1	122.4*	—6.8	—3.2	—12.3	1654	34	354	CS_2
$C_6Cl_5OH\cdots OC(CH_3)N(C_2H_5)_2$	435	126.5	51.5	—5.6	—2.1	—9.6	1654	32	478	CCl_4
	440	172.6	92.3*	—5.7	—3.0	—9.2	1653	30	450	CS_2
$C_6H_5OH\cdots OC(CH_3)N(C_6H_{11})_2$	342	167.1	62.7	—6.1	—3.0	—10.8	1652	22	336	CCl_4
	394	257.4	119.1*	—7.0	—3.2	—12.9	1646	33	452	CS_2
$C_6Cl_5OH\cdots OC(CH_3)N(C_6H_{11})_2$	464	151.2	57	—6.1	—2.9	—10.9	1647	39	510	CCl_4
	457	243.0	120.3*	—6.4	—3.2	—10.9	1648	26	460	CS_2

* Measured at 40°C.

$CH_3 > CH_3CH_2CH_2 > CH_3CH_2 > C_6H_5 > CH_2Cl > p\text{-}NO_2C_6H_4$. The enhanced ability of compounds containing the CH_3 group to form a hydrogen bond can be attributed to hyperconjugation through the contribution of the structure 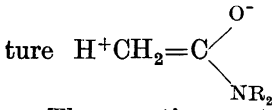

The question as to whether amides protonate on the oxygen or nitrogen atom has remained open for many years. The usual argument for assuming O-protonation is that amides are mesomeric (I ↔ II) and that proton addition

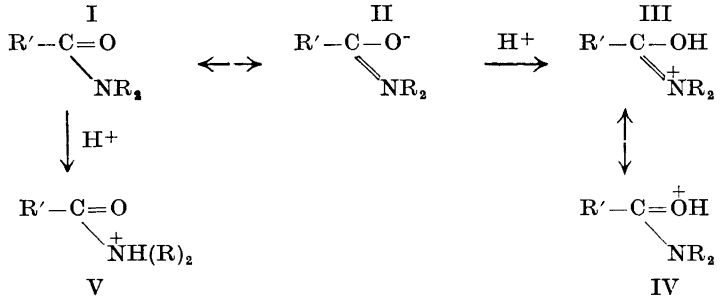

should occur at the atom with highest electron density and hence give the structure III. This O-protonated form is again stabilised by mesomerism (III ↔ IV), unlike the N-protonated form V. Infrared spectroscopy has shown that the carbonyl oxygen in all the amides studied by us participates in hydrogen bonding both with phenol and pentachlorophenol. Recently, Katritzky *et al.*[9] reviewed the protonation of amides and their heterocyclic analogues, and concluded that the evidence as a whole strongly indicates that amides are predominantly protonated at the oxygen atom. The most positive evidence for O-protonation is that from nuclear magnetic resonance spectra which appears to be well-founded. There is, however, also feasible evidence for N-protonation especially from infrared spectroscopy and from application of the Hammett equation [10] to the basicities of *m*- and *p*-substituted benzamides. With regard to hydrogen bonding it may be questionable whether there is any difference in principle between hydrogen bonding and proton-transfer since it is generally accepted that proton-transfer reactions are initiated by the formation of a hydrogen bond.

REFERENCES

1. Aksnes, G. and Gramstad, T. *Acta Chem. Scand.* **14** (1960) 1485.
2. Gramstad, T. *Acta Chem. Scand.* **15** (1961) 1337.
3. Gramstad, T. *Acta Chem. Scand.* **16** (1962) 807.
4. Gramstad, T. and Snaprud, S. I. *Acta Chem. Scand.* **16** (1962) 999.
5. Flett, M. St. C. *J. Soc. Dyers Colourists* **68** (1952) 59.
6. Lundgren, H. P. and Binkley, C. H. *J. Polymer Sci.* **14** (1954) 139.
7. Mizushima, S., Tsuboi, M., Shimanouchi, T. and Tsuda, Y. *Spectrochim. Acta* **7** (1955) 100.
8. Becker, E. D. *Spectrochim. Acta* **17** (1961) 436.
9. Katrizky, A. R., Richard, A. Y. and Jones, B. A. *Chem. & Ind. (London)* **1961** 722.
10. Edward, J. T., Chang, H. S., Yates, K. and Stewart, R. *Can. J. Chem.* **38** (1960) 1518.

Received January 5, 1962.

ACTA CHEMICA SCANDINAVICA 16 (1962) 1378–1384

Neoglucobrassicin, ein zweiter SCN^--Precursor vom Indoltyp in *Brassica*-Arten

ROLF GMELIN und ARTTURI I. VIRTANEN

Biochemisches Forschungsinstitut der Stiftung für chemische Forschung, Helsinki, Finnland

Besides glucobrassicin, isolated from *Brassica* and *Raphanus* species a year ago in this laboratory, another thioglucoside with an indole group in the molecule was found in some *Brassica* species. This glucoside, called neoglucobrassicin by the authors, was isolated as a crystalline brucine salt from the rind of rutabaga (*Brassica napus* var. *napobrassica*). On the basis of the products formed in enzymic cleavage, acid hydrolysis, and hydrogenolysis with Raney nickel, neoglucobrassicin should be N_1-methoxyglucobrassicin. The products were characterized by "Dünnschicht-Chromatographie" and paper chromatography. When the new glucoside was heated, a cleavage product with mass 186 could be found by mass spectrography. Under the same experimental conditions a cleavage product with mass 156 (3-indoleacetonitrile) was formed from glucobrassicin. The mass difference 30 is in accordance with the formula proposed for neoglucobrassicin.

Vor kurzem haben wir über Glucobrassicin [1–3], ein neues Thioglucosid, berichtet, das bisher in Frischpflanzen der Gattungen *Brassica* und *Raphanus* gefunden wurde und als glucosidische Vorstufe von physiologisch bedeutenden Substanzen wie SCN^-, 3-Indolylacetonitril und Ascorbigen von besonderem Interesse ist. Wie wir bereits mitgeteilt haben [3,4], findet sich in einigen Arten, z.B. *Brassica oleracea* var. *acephala* DC, *gongyloides* L., *botrytis* L., *Brassica napus* L. und *Brassica rapa* L. ein zweites, anscheinend nahe verwandtes Thioglucosid. Wegen seiner chemischen Beziehung zu Glucobrassicin bezeichnen wir es als N e o g l u c o b r a s s i c i n.

Neoglucobrassicin wurde aus der Wurzelrinde der Kohlrübe * (*Brassica napus* L. var. *napobrassica*(L.) Peterm. in etwa 0,01 % Ausbeute isoliert. Die Darstellung erfolgte im wesentlichen nach der früheren, für Glucobrassicin angegebenen Vorschrift [3]:

* Die Wurzelrinde der Kohlrübe war als Ausgangsmaterial besonders geeignet, da das Verhältnis des neuen Glucosids zu Glucobrassicin etwa 4:1 war, während in den übrigen Brassica-Arten Glucobrassicin mengenmässig stark überwiegt.

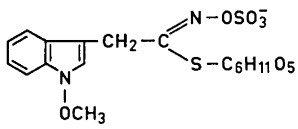

$C_{17}H_{21}N_2O_{10}S_2$

Neoglucobrassicin

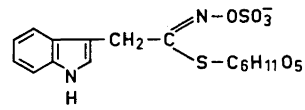

$C_{16}H_{19}N_2O_9S_2$

Glucobrassicin

(*a*) Extraktion der frischen Wurzelrinde mit kochendem Methanol,

(*b*) Anreicherung der Gesamtglucoside durch Ionenaustausch an anionotropem Al_2O_3,

(*c*) Separierung der Glucoside durch präparative Chromatographie auf Zellulose-Pulver,

(*d*) Überführung in eine kristallisationsfähige Salzform.

Bei der präparativen Chromatographie auf Zellulosepulver erschien Neoglucobrassicin in den Fraktionen 20—38 vor Glucobrassicin, das in den Fraktionen 45—55 auftrat (Fraktionen zu 20 ml, Säulengrösse wie bei der Separierung von Glucobrassicin [3]). Nach verschiedenen Versuchen wurde Neoglucobrassicin schliesslich als schwerlösliches Brucin-Salz in langen und sehr dünnen Nadeln erhalten, die sich oberhalb 175°C unter Bräunung zersetzten. Papierchromatographisch trennt sich das Salz in das langsamer wandernde Neoglucobrassicin-Anion und das rascher wandernde Brucin-Kation auf. Das Neoglucobrassicin-Anion weist in verschiedenen Lösungsmittelsystemen gleiche R_F-Werte wie Gluconasturtiin [5] auf, wandert also etwas rascher als Glucobrassicin, das sich papierchromatographisch wie Glucotropaeolin [5] verhält. Es lässt sich auf dem Papierchromatogramm durch verschiedene Sprühreagentien nachweisen: mit Ehrlichs Reagenz oder Zimtaldehyd-Salzsäure entsteht ein orangegelber Fleck, mit ammoniakalischer $AgNO_3$-Lösung beim Erhitzen ein graubrauner Fleck,

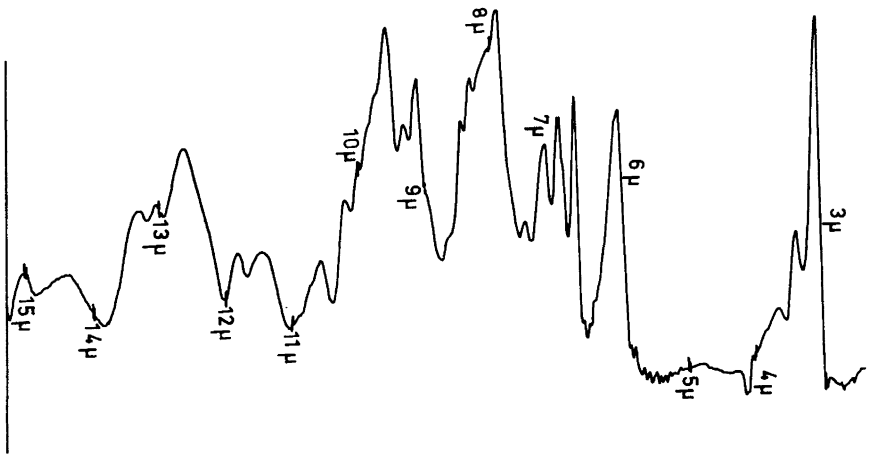

Abb. 1. IR-Spektrum von Neoglucobrassicin-Brucin-Salz (1 mg gepresst in 400 mg KBr).

mit Myrosinase-Ferrinitrat-Reagenz [3] erhält man durch freigesetztes SCN^- einen rotbraunen Fleck. Durch das Ferrinitrat-Reagenz[3] lässt sich Neoglucobrassicin (unspezifisch bräunlicher Fleck) deutlich von Glucobrassicin (intensiv blauvioletter Fleck) unterscheiden. Aus der Elementaranalyse liesss sich die Bruttoformel $C_{40}H_{51}N_4O_{16}S_2$ errechnen, die sich aus dem Brucin-Kation $C_{23}H_{26}N_2O_4$, dem Neoglucobrassicin-Anion $C_{17}H_{21}N_2O_{10}S_2$ und 2 Mol Kristallwasser zusammensetzt. (Gefunden: C 52,87; H 5,98; N 6,21; S 7,31. Berechnet für $C_{40}H_{51}N_4O_{16}S_2$ (908,0): C 52,85; H 5,67; N 6,18; S 7,06. Gefunden 2,77 % H_2O bei 12 stdg. Trocknung im Hochvakuum bei 90°C. Berechnet für 2 H_2O: 3,95 %).

Zur Dokumentation wurde das IR-Spektrum von Neoglucobrassicin (als Brucin Salz) aufgenommen (Abb. 1). UV-Spektrum des papierchromatographisch abgetrennten Neoglucobrassicin-Anions (in Wasser): λ_{max} 288, 276 und 220 mμ (Schulter bei 293—297 mμ) (ε = 5450, 5450 und 4050). λ_{min} 282 und 253 mμ (ε = 5360 und 3550). Das UV-Spektrum von Neoglucobrassicin-Anion weist somit auffallende Ähnlichkeit mit dem eines 1,3-disubstituierten Indols [6] auf.

Da für alle Untersuchungen insgesamt nur etwa 100 mg Substanz zur Verfügung standen, muss sich vorläufig unser Strukturvorschlag für Neoglucobrassicin ausschliesslich auf chromatographische und spektroskopische Analysen und Interpretierung der enzymatisch, hydrolytisch, hydrogenolytisch und thermisch gebildeten Spaltprodukte stützen. Hierbei leisteten die bei Glucobrassicin gesammelten Erfahrungen grosse Dienste, denn ein grosser Teil der dort beobachteten Reaktionstypen [3] galt analog auch für Neoglucobrassicin. — Auf Grund des vorliegenden Tatsachenmaterials schlagen wir für Neoglucobrassicin die Formel (I) vor und begründen sie wie folgt:

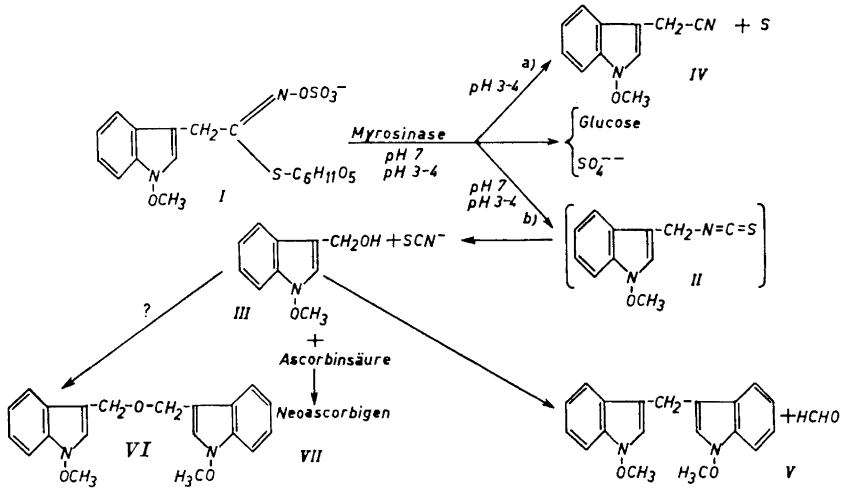

Abb. 2. Enzymatische Spaltung von Neoglucobrassicin und dabei gebildete verschiedene Produkte.

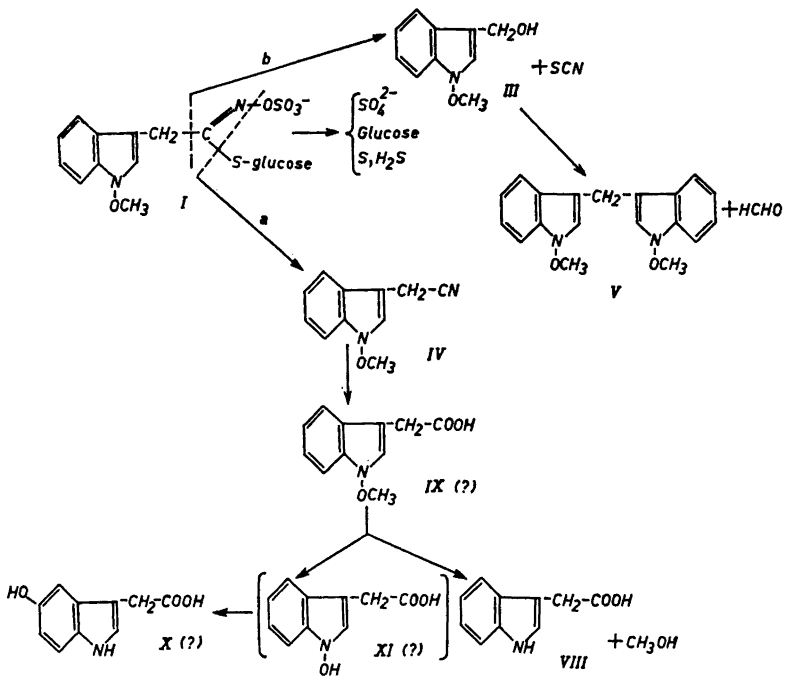

Abb. 3. Hydrolytische Spaltung von Neoglucobrassicin.

Durch Myrosinase wird Neoglucobrassicin analog zu Glucobrassicin gespalten. Nach Abspaltung von Glucose und Sulfat entsteht wahrscheinlich labiles Isothiocyanat, das rasch in SCN^- und ein 1-substituiertes 3-Hydroxymethylindol (III) zerfällt. Diese Verbindung dimerisiert sich nach und nach unter Formaldehyd-Abspaltung zu einem 1,1′-disubstituierten 3,3′-Diindolylmethan

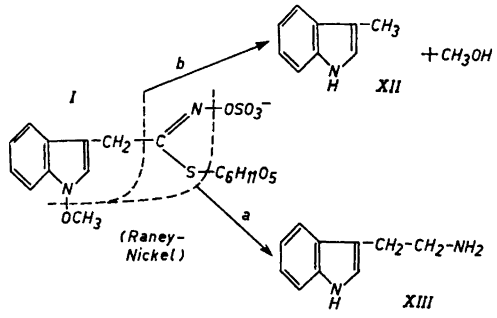

Abb. 4. Hydrogenolytische Spaltung von Neoglucobrassicin.

(V). In geringer Menge wird nebenbei noch ein Produkt, das mit einem Äther der Formel VI identisch sein könnte, gebildet (vgl. Thesing [7]). In Gegenwart von Ascorbinsäure bildet sich bei der enzymatischen Spaltung von Neoglucobrassicin bei pH 7 ein Kondensationsprodukt aus III und Ascorbinsäure, das wir in Analogie zu dem aus Glucobrassicin gebildeten Ascorbigen Neoascorbigen (VII) nennen. Führt man die enzymatische Spaltung bei pH 4 durch, so findet man ein 1-substituiertes 3-Indolylacetonitril (IV). Gleichzeitig kann man jedoch ein Indolderivat beobachten, bei dem es sich eventuell um 1-substituiertes Indol-3-methylisothiocyanat (II) handeln könnte. Es ist doch fraglich ob das Isothiocyanat wirklich so stabil ist, dass man es chromatographisch

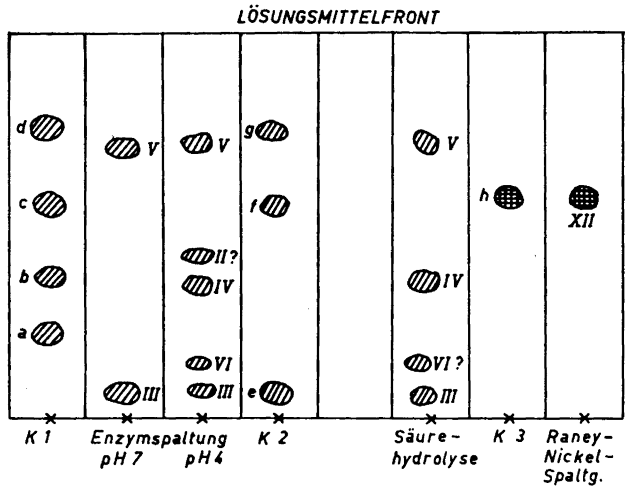

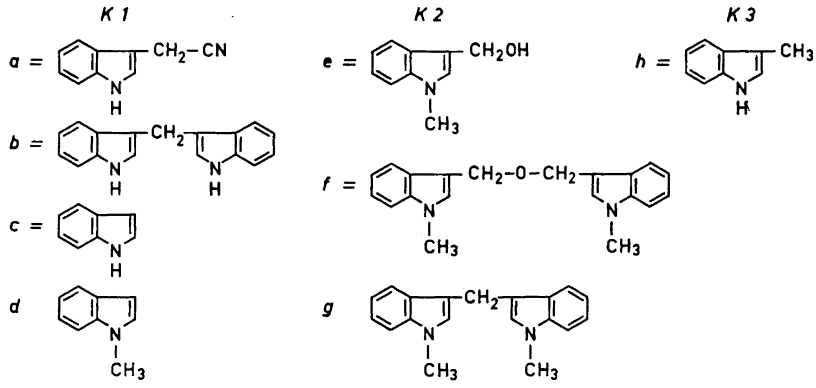

Abb. 5. Dünnschichtschromatogramme von einigen Indolderivaten und Produkten, welche bei der enzymatischen, hydrolytischen und hydrogenolytischen Spaltung von Neoglucobrassicin entstehen. Trägerschicht: Kieselgel G. Fliessmittel: Benzol.

nachweisen kann. Die enzymatischen Spaltungsreaktionen von Neoglucobrassicin sind in Abbildung 2 zusammengefasst.

Bei der sauren Hydrolyse von Neoglucobrassicin werden 3 Säuren gebildet, von denen eine (VIII) papierchromatographisch mit 3-Indolylessigsäure identisch ist. Die beiden anderen werden vorbehaltlich als 1-Methoxyindol-3-essigsäure (IX) und 5-Hydroxyindol-3-essigsäure (X) interpretiert (letztere könnte aus einer intermediär gebildeten 1-Hydroxyindol-3-essigsäure (XI) durch eine Art Phenylhydroxylamin-Umlagerung entstanden sein). Neben dieser normalen Hydrolyse von Neoglucobrassicin als einem Thiohydroxamsäure-Derivat [8] (Reaktionsweg a [3]) kann man unter sauren und alkalischen Bedingungen wie beim Glucobrassicin das Auftreten von Spaltprodukten beobachten, die unter Spaltung der C_a—C_b-Bindung (Reaktionsweg b [3]) entstehen und mit III und V identisch sind. Das Formelschema in Abbildung 3 fasst die hydrolytischen Spaltungsreaktionen zusammen.

Wird Neoglucobrassicin unter schonenden Bedingungen mit Raney-Nickel behandelt, so erhält man als Reaktionsprodukte Skatol (XII) und Tryptamin (XIII), deren Bildung eigentlich nur verständlich sein kann, wenn man einen Substituenten am N_1 über eine Sauerstoff-Brücke gebunden annimmt.

Bei der thermischen Zersetzung von Neoglucobrassicin lässt sich massenspektroskopisch ein Spaltprodukt mit einem maximalen Massenwert von 186 nachweisen. Es dürfte mit Verbindung IV identisch sein, denn unter gleichen Bedingungen erhält man aus Glucobrassicin ein Spaltprodukt der maximalen Masse 156, das mit 3-Indolylacetonitril identisch ist. Aus der Differenz (30) dieser beiden thermischen Zersetzungsprodukte errechnet sich die Grösse des Substituenten am N_1 mit einem Mol. gew. von 31. Dieser Wert entspricht einer Methoxy-Gruppe, und tatsächlich lassen sich die obengenannten Reaktionen und Befunde am besten mit Neoglucobrassicin als einem N_1-Methoxy-Glucobrassicin in Einklang bringen. Auch die bei der Elementaranalyse gefundenen Werte für das Neoglucobrassicin-Anion sind in Übereinstimmung damit.

Für die Erfassung der enzymatisch, hydrolytisch und hydrogenolytisch gebildeten Spaltprodukte hat sich wieder die Dünnschicht-Chromatographie besonders bewährt. Da vorläufig N_1-Methoxyindol-Derivate synthetisch nicht zugänglich waren, wurden Indolderivate, die am N_1 entweder durch H oder durch CH_3 substituiert waren, als Vergleichssubstanzen für die Dünnschicht-Chromatographie verwendet. Wie man aus theoretischen Erwägungen erwarten konnte, liegen die N_1-Methoxy-substituierten Spaltprodukte aus Neoglucobrassicin in ihrem polaren und damit auch in ihrem chromatographischen Verhalten zwischen den entsprechenden, am N_1 durch H bzw. CH_3 substituierten Indolderivaten.

In Abbildung 5 sind die Ergebnisse der dünnschicht-chromatographischen Analyse schematisch wiedergegeben. Die allgemeine Methodik wurde in der letzten Mitteilung [3] ausführlich beschrieben. Die Spaltprodukte VIII, IX, X, VII und XIII wurden papierchromatographisch nachgewiesen.

Neoglucobrassicin repräsentiert somit einen interessanten, neuen Strukturtyp. Seine biogenetische Verwandtschaft zu Glucobrassicin ist leicht erkennbar. — Indolderivate mit einer Sauerstoff-Funktion am N_1 wurden unseres Wissens bisher erst einmal in der Natur vorgefunden und beschrieben (Cypridina-Luciferin [9]). Aufgabe künftiger Studien ist es, die hier vorgebrachten Befunde,

durch Isolierung der Abbauprodukte zu bestätigen und die Biogenese von Neoglucobrassicin sowie seine phytochemische und biologische Bedeutung und Wirkung zu klären.

Dr. E. Honkanen danken wir für die Synthese verschiedener Indolderivate, Mag. T. Moisio für die massenspektroskopische Analyse. Diese Arbeit ist ein Teil des Untersuchungsprojekts unter U.S. Public Law Nr. 480, 83rd Congress.

LITERATUR

1. Gmelin, R., Saarivirta, M. und Virtanen, A. I. *Suomen Kemistilehti B* **33** (1960) 172.
2. Gmelin, R. und Virtanen, A. I. *Ibid. B* **34** (1961) 15.
3. Gmelin, R. und Virtanen, A. I. *Ann. Acad. Sci. Fennicæ A* II, 107 (1961).
4. Virtanen, A. I. *Experientia* **17** (241) 1961.
5. Schultz, O. E. und Gmelin, R. *Z. Naturforsch.* **8b** (1953) 151.
6. Edwards, B. G. *Arch. Biochem. Biophys.* **21** (1949) 103.
7. Thesing, J. *Chem. Ber.* **87** (1954) 692.
8. Ettlinger, M. G. und Lundeen, A. J. *J. Am. Chem. Soc.* **78** (1956) 4172.
9. Hirata, Y., Shimomura, O. und Eguchi, S. *Tetrahedron Letters* **1959** 4.

Eingegangen am 2. Januar 1962.

ACTA CHEMICA SCANDINAVICA 16 (1962) 1385–1392

Binuclear Complexes

I. The Electronic Structure of Copper Acetate

LESLIE S. FORSTER* and C. J. BALLHAUSEN

The Institute for Physical Chemistry, University of Copenhagen, Denmark

The electronic structure of the dimeric copper acetate $Cu_2(Ac)_4 \cdot 2H_2O$ is considered using a molecular orbital scheme. It is proposed that a rather strong σ-bond exists between the two copper-units, in contrast to a former proposal of a δ-bond [4]. The form of the molecular orbital scheme is such that all of the experimental features (antiferromagnetism, absorption spectrum and g-factors) are qualitatively explained. It is suggested that the intensity of the dichroic absorption bands is either of vibronic origin or due to a static dissymmetry.

Copper acetate monohydrate is the prototype of a significant class of complexes, the cupric alkanoates. The basic unit in this complex is a dimer held together principally by acetate bridges [1]. The complex is distinguished from the usual monomeric Cu(II) complexes by the appearance of antiferromagnetism [2-5] and of a new ultraviolet band in the absorption spectrum [6]. The antiferromagnetism has been ascribed to the Cu—Cu interaction and the existence of a δ-bond suggested [4,5]. A theoretical treatment along valence bond lines appeared to be consistent with this conclusion [7]. We will in this note reconsider the problem of the electronic structure of copper acetate as seen from a molecular orbital (L.C.A.O.) viewpoint.

ORBITAL SCHEME

If each copper ion were situated in a regular octahedral environment, the highest occupied molecular orbitals would fall into two groups; the antibonding (or non-bonding) t_{2g}-orbitals characterized by their transformation properties (xy), (yz) and (xz) and the antibonding e_g-orbitals designated (x^2-y^2) and (z^2). For a regular octahedral Cu(II) complex with oxygen ions as ligands

* National Science Foundation Science Faculty Fellow, 1961—62. Permanent address: Department of Chemistry, University of Arizona.

we would expect the separation, $10Dq$, between the e_g and t_{2g} orbitals to be some 10 000 cm^{-1}.

Consider now the actual complex $Cu_2(Ac)_4 \cdot 2H_2O$ where Ac stands for CH_3COO^-. The structure has been given by van Niekerk and Schoening [1]; the four acetate groups make a fourfold bridge holding the complex together (Fig. 1). Furthermore, due to the short Cu—Cu distance (2.64 Å) a direct bond should occur between the two copper atoms. The oxygen atoms in the bridging groups are separated by 2.20 Å.

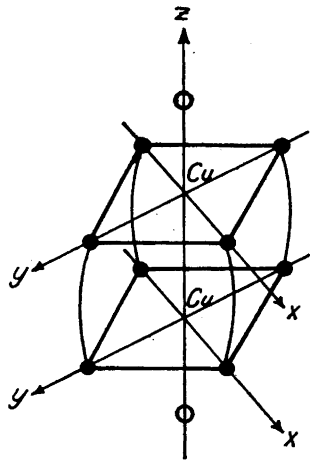

Fig. 1. Molecular structure of $Cu(Ac)_4 \cdot 2H_2O$.

If we now consider the molecule as made up of two units, each containing *one* Cu^{2+} ion we notice that each of these entities has the symmetry C_{4v}. When put together the symmetry of the molecule is D_{4h}. The molecular orbital scheme for the highest occupied levels in the "monomeric complex" $CuO_4 \cdot H_2O$ (pointgroup C_{4v}) would be expected to resemble that of $CuSO_4 \cdot 5H_2O$, that is after Holmes and McClure [8] $E[(xz),(yz)] = 0$, $E(xy) \approx 10\,000$ cm^{-1}, $E(z^2) \approx 13\,000$ cm^{-1} and $E(x^2-y^2) \approx 14\,000$ cm^{-1} (Fig. 2, left and right). Bringing two units of $CuO_4 \cdot H_2O$ together, we would then obtain a molecular orbital scheme as pictured in the middle of Fig. 2.

The reason for the considerable splitting of the two (z^2) molecular orbitals as compared to the other splittings is to be found in the values of the Cu—Cu overlaps. Assuming for a moment that we can consider the molecule as Cu_2^{2+}

Table 1. Overlap integrals for Cu_2^{2+}.

$S(d_{z^2},d_{z^2})$	$S(d_{xy},d_{xy})$ $= S(d_{x^2-y^2},d_{x^2-y^2})$	$S(d_{xz},d_{xz})$ $= S(d_{yz},d_{yz})$
0.019	0.002	0.012

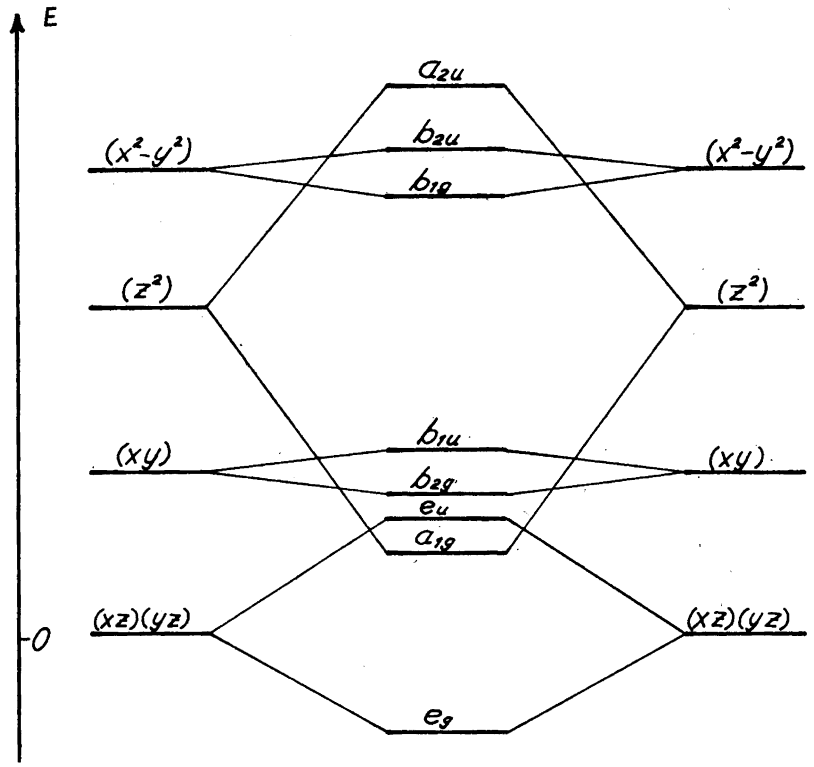

Fig. 2. Highest molecular orbitals for $Cu(Ac)_4 \cdot 2H_2O$. Not drawn to scale. Point group symmetry D_{4h}.

we can calculate the overlap integrals using the analytic SCF $3d^{10}$ (Cu^{+1}) functions given by Watson [9]. These are given in Table 1.

We have assumed some charge neutralization due to the ligand electrons. Whether the effective charge on the copper atom is + 1 or zero is immaterial if the configuration involves $3d^{10}$. Watson [9] has shown that electrons in $3d$ orbitals are not appreciably affected by $4s$ electrons, *i.e.* the $3d$ orbital calculated from $3d^{10}(Cu^{+1})$ is nearly the same as that calculated from $3d^{10}4s(Cu^{\circ})$. Although the SCF orbitals are considerably more contracted than the customary Slater orbitals, in the region of the "tail" the overlap integrals were found to be roughly the same for both sets of orbitals.

The splitting Δ between a given bonding orbital and its antibonding counterpart can be simply expressed as

$$\Delta = \frac{2H_{11}S - 2H_{12}}{1 - S^2} \approx kS$$

where H_{11} and H_{12} has their usual meaning and k is a constant. Hence the greater the overlap S, the greater the magnitude of Δ.

Any direct computation of Δ is however nearly impossible to perform since the orbitals one should use in the calculation of H_{11}, H_{12} and S are molecular orbitals of the form

$$\sigma_1 = ad_{Cu^{2+}} + b\Sigma\sigma_{ligand}$$

where the constants a and b have been determined by a variational calculation for the monomeric molecular unit $CuO_4 \cdot H_2O$. Nevertheless, if we *assume* that no π-bonding takes place, and that $a \approx 1$ (corresponding to *antibonding* e orbitals that are nearly pure metal orbitals) a bonding scheme for the "united" dimer emerges as pictured in Fig. 2.

There are three sets of data that must be rationalized by any model: antiferromagnetism, spectra and g-factors. These will now be considered in that order.

ANTIFERROMAGNETISM

The wavefunction for the ground state of the complex can be written as a determinental wavefunction containing 18 electrons; nine from each Cu^{2+} ion:

$\psi(^1A_{1g}) = |(e_g)^4(a_{1g})^2(e_u)^4(b_{2g})^2(b_{1u})^2(b_{1g})^2(b_{2u})^2|$. The first excited triplet state is then (See Fig. 2) $\psi(^3B_{1g}) = |(e_g)^4(a_{1g})^2(e_u)^4(b_{2g})^2(b_{1u})^2(b_{1g})^2(b_{2u})^1(a_{2u})^1|$ No other deep lying singlet or triplet state is expected to occur.

As first shown by Bleaney and Bowers [2] the magnetic behaviour can be explained in terms of a triplet state lying some 300 cm^{-1} above the ground singlet state. Formally it is of course easy to write down the energies of the above two states in terms of the orbital energies plus the relevant Coulomb (J) and Exchange (K) integrals. Since, however, these latter cannot be calculated with any accuracy, we can only note that the difference in the repulsion energies between the two states must be fairly small.

ABSORPTION SPECTRUM

The crystal absorption spectrum of $Cu(Ac)_4 \cdot 2H_2O$ has been measured by Yamada *et al.*[6] using polarized light. The measurements were presumably performed at room temperature. With a triplet state lying some 300 cm^{-1} above the singlet ground state, we might expect that some of the reported bands were due to transitions from this state to other triplets. Assuming a Boltzmann distribution about 40 % of the molecules should be in the triplet state at room temperature; at $\sim$ 77°K, however, this number has fallen to virtually zero. Consequently one would expect the band intensity of any transition starting from the triplet state to vanish completely by cooling to 77°K. However, measurements indicate that only small intensity changes occur for the "major" bands located at 14 300 cm^{-1} and 27 000 cm^{-1}. We have thus assigned these as singlet-singlet transitions.

In the crystal spectra of cupric acetate monohydrate and several cupric alkanoates, three bands are clearly resolved [6]. The band at 14 300 cm^{-1} has an extinction coefficient in solution of about 200 based upon monomer concentration and therefore the molecular extinction coefficient for the dimer

is about 400. The absorption is more intense in x,y than is z polarization; Yamada *et al.*[6] state that the former is 10 times more intense than the latter. The electric dipole vectors transform like $A_{2u}(\parallel)$ and E_u ($\perp$) with respect to the four-fold axis. The polarization of the band at 14 000 cm^{-1} does therefore correspond to that of an allowed transition $^1A_{1g} \rightarrow {}^1E_u$.

The second band at 27 000 cm^{-1} is somewhat less intense with a molar extinction coefficient of about 100 and ten times stronger in z than in x,y polarization. This band could be assigned to an allowed $^1A_{1g} \rightarrow {}^1A_{2u}$ transition. However, such an assignment as well as the previous one we shall show below to be untenable.

A third band appears at 33 700 cm^{-1} in x,y and at 35 000 cm^{-1} in z polarization. It is difficult to estimate the intensity of this band, since it appears as a shoulder on a more intense band. The origin of this band is unknown.

One electron promotion to the empty a_{2u} orbital from the filled orbitals b_{1g}, b_{2u}, b_{2g}, b_{1u}, e_u, e_g and a_{1g} corresponds to the transitions from the ground state $^1A_{1g}$ to $^1B_{2u}$, $^1B_{1g}$, $^1B_{1u}$, $^1B_{2g}$, ^1E_g, ^1E_u, and $^1A_{2u}$, respectively. It is seen from the level scheme (Fig. 2) that the "parallel" band at 27 000 cm^{-1} in our tentative assignment corresponds to what Mulliken[10] calls a $N \rightarrow V$ transition, that is a transition from a bonding to the corresponding antibonding orbital. With a wavefunction for the excited $^1A_{2u}$ state equal to

$$\psi(^1A_{2u}) = \frac{1}{\sqrt{2}}\Big\{ \mid (e_g)^4(a_{1g}^+)\,(e_u)^4(b_{2g})^2(b_{1u})^2(b_{1g})^2(b_{2u})^2(a_{2u}^-) \mid - \mid (e_g)^4(a_{1g}^-)\,(e_u)^4(b_{2g})^2 (b_{1u})^2(b_{1g})^2(b_{2u})^2(a_{2u}^+) \mid \Big\}$$

we get for the transition moment $P = \int \psi(^1A_{2g})\,\vec{r}\,\psi(^1A_{2u})\mathrm{d}\tau$

$$P = \sqrt{2} \int a_{1g}\,\vec{r}\,a_{2u}\; d\tau$$

Neglecting all overlaps we have

$$a_{1g} = \frac{1}{\sqrt{2}}\Big[(z^2)\,(1) + (z^2)\,(2)\Big]$$

$$a_{2u} = \frac{1}{\sqrt{2}}\Big[(z^2)\,(1) - (z^2)\,(2)\Big]$$

with

$$(z^2) = \alpha d_{z^2} + \sqrt{1-\alpha^2}\sum_1^5 \sigma_{\mathrm{lig}}$$

These wavefunctions lead to the approximate expression

$$P \approx \frac{1}{\sqrt{2}}\Big[\alpha^2 R_1 + (1-\alpha^2)R_2\Big]$$

where R_1 is the distance Cu—Cu and R_2 the distance O—O in a bridge. With $R_1 = 2.6$ Å and $R_2 = 2.2$ Å this expression yields an oscillator strength, f, for the band $f \approx 0.8$. With the molar extinction coefficient $\varepsilon \approx 100$ and $\nu_{1/2} \approx 8 \times 10^3$ cm^{-1} the experimental value of f is about 0.5×10^{-4}.

g-FACTORS

The low-lying triplet state $^3B_{1g}$ is appreciably populated at room temperature and the g-factors have been determined [2], $g_{||} = 2.42 \pm 0.03$, $g_{\perp} = 2.08 \pm 0.03$ ($g_x = 2.34$, $g_x = 2.05$, $g_y = 2.09$) [11]. The configuration of the $^3B_{1g}$ is $(a_{1g})^2(e_u)^4(e_g)^4(b_{2g})^2(b_{1u})^2(b_{2u})\,(a_{2u})$. This state can interact via spin-orbit coupling with $^3E_g(1)$: $(a_{1g})^2(e_u)^3(e_g)^4(b_{2g})^2(b_{1u})^2(b_{2u})^2(a_{2u})$, $^3E_g(2)$: $(a_{1g})^2(e_u)^3(e_g)^4(b_{2g})^2(b_{1u})^2(b_{2u})\,(a_{2u})^2$ and $^3B_{2g}$: $(a_{1g})^2(e_u)^4(e_g)^4(b_{2g})^2(b_{1u})\,(b_{1g})^2(b_{2u})^2(a_{2u})$.

If the L.C.A.O. wave functions for these states are used the expressions for the g-factors are with neglect of overlap effects

$$g_{||} = 2\left(1 - \frac{4\lambda}{E(^3B_{2g}) - E(^3B_{1g})}\right)$$

$$g_{\perp} = 2\left(1 - \frac{\lambda}{E(^3E_g(1)) - E(^3B_{1g})} - \frac{3\lambda}{E(^3E_g(2)) - E(^3B_{1g})}\right)$$

The free Cu^{2+} ion value of $\lambda = -830$ cm^{-1} is too large to use. It is more appropriate to take the spin-orbit coupling parameter for Cu^{+1}, of some -750 cm^{-1}. Using this value we find $E(^3B_{2g}) - E(^3B_{1g}) \approx 14\,000$ cm^{-1}. Due to delocalization effects and state repulsions we would expect the energy of $^3E_g(2)$ to be much higher than the energy of $^3E_g(1)$ and hence we estimate *approximately* $E(^3E_g)\,(1) - E(^3B_{1g}) \approx 17\,000$—$30\,000$ cm^{-1}. In view of the uncertainty of the formula and the values of $g_{||}$ and $g_{\perp}$ these numbers are only reliable to within several thousand cm^{-1}.

We would expect, since the singlet-triplet splitting for these configurations must be small that

$$E(^3B_{2g}) - E(^3B_{1g}) \approx E(^1B_{2g}) - E(^1A_{1g}).$$

Hence we would expect the orbitally forbidden transition $^1A_{1g} \rightarrow {}^1B_{2g}$ to occur at some 14 000 cm^{-1}, and similarly that $^1A_{1g} \rightarrow {}^1E_g(1)$ would occur at some 17 000 to 30 000 cm^{-1}.

DISCUSSION

It should again be stressed, that our proposed molecular orbital scheme is tentative. We can only observe that our model is reasonably consistent with the experimental data. Of course, alternative schemes may also be consistent with the rather limited data. The most conspicious feature in our level scheme is the large splitting of (z^2) in the dimer. This seems certainly reasonable, but this proposal differs from the model considered by Martin *et al.*[4,5] and Ross [7].

The spectral assignments are uncertain. Due to the observed polarizations we have above tentatively assigned these to orbitally allowed transitions. The fact that the orbitally *forbidden* $^1A_{1g} \rightarrow {}^1B_{2g}$ transition arrived at from the g-factor apparently corresponds to the "perpendicular" band in the measured spectrum is, however, suggestive. The experimental values of the band intensities are also much too small for supposedly allowed transitions as demonstrated by the calculated f-value for an allowed $N \rightarrow V$ transition.

If we abandon the idea that the levels are of pure parity, and consider other intensity giving mechanisms, a static dissymmetry or a vibronic mechanism should suffice [12]. Indeed, for use in a vibronic mechanism all possible even and odd vibrational normal modes (with the exception of a_{2g}) are present. Consider for instance the "perpendicular" band at 14 000 cm^{-1}. We now assign this band to the transition $^1A_{1g} \rightarrow {}^1B_{2g}$, but in order to get the observed polarization of the transition the wavefunction for the excited state must be of the type $^1B_{2g} + \lambda^1E_u$. Such a scrambling can be performed via a vibration of ε_u symmetry.

All in all we are inclined to believe that the observed absorption bands are of the latter kind, *i.e.* that the low excited states are predominantly "even", contaminated with "odd" states via a dissymmetry or vibrational scrambling. This proposal also explains that the band at 14 000 cm^{-1} clearly corresponds to the usual copper band [13]. It is thus due to a transition within half of the complex. On the other hand the second band at 27 000 cm^{-1} must involve the whole complex.

Furthermore the triplets and singlets of nearly all configurations are expected to fall approximately on top of each other. Such a feature would explain the absence of temperature effects in the measured spectra.

X-Ray studies have shown that when crystals of Cr(II), Cu(II), Ni(II), and Co(II) acetates are grown from aqueous solution only the chromium and copper acetates dimerize. The heat of hydration of the Ni complex is about the same as that of the Cu complex while the hydration energy of the Co complex is definitely smaller. The explanation for the stability of the dimers could be found in the strength of the metal-metal bond. It is reasonable to assume that the strength of this bond is roughly proportional to the overlap between the metal orbitals. However, calculation of the overlap from Slater or S.C.F. orbitals does not reveal any striking anomaly in the chromium and copper cases. A possible explanation may however be advanced if we examine the electronic configurations of the single species.

An octahedral or pseudo-octahedral configuration of Cr(II) and Cu(II) both possess an E_g ground state. Such a state is subjected to a rather violent Jahn-Teller distortion [14], and it then seems possible that dimerization is the energetically favorable way of lowering the symmetry. It is however well known, that stability criteria and molecular configurations are nearly impossible to infer from *a priori* considerations.

The main result of this note is thus that it is not necessary to postulate a δ-bond between the two copper atoms to account for the electronic features, but that a σ-bond will suffice. Thus, even though the calculations of Ross [7] indicates that a δ-bond would lead to a value for the interaction of the two molecular species of the right order of magnitude we feel that his result does not necessary prove this mechanism, due to his use of approximate wavefunctions. A direct σ interaction seems to us to be more plausible in view of the overlap criteria.

In addition to the direct interaction it is of course also possible to have a "super-exchange" interaction, working through the oxygen bridges. Such a mechanism seems, however, to the present authors to be less likely than the one considered here.

REFERENCES

1. Niekerk, J. N. van and Schoening, F. R. L. *Acta Cryst.* **6** (1953) 227.
2. Bleaney, B. and Bowers, K. D. *Proc. Roy. Soc.* **A 214** (1952) 451.
3. Stevens, K. W. H. *Rev. Mol. Phys.* **25** (1953) 166.
4. Figgis, B. N. and Martin, R. L. *J. Chem. Soc.* **1956** 3837.
5. Martin, R. L. and Waterman, H. *J. Chem. Soc.* **1957** 2545.
6. Yamada, S., Nakamura, H. and Tsuchida, R. *Bull Chem. Soc. Japan* **30** (1957) 953.
7. Ross, I. G. *Trans. Faraday Soc.* **55** (1959) 1057.
8. Holmes, O. G. and McClure, D. S. *J. Chem. Phys.* **26** (1957) 1686.
9. Watson, R. E. *Quart. Progr. Rep. M.I.T.* April 1960.
10. Mulliken, R. S. and Rieke, C. A. *Repts. Progr. in Phys.* **8** (1941) 231.
11. Abe, H. and Shimada, J. *Phys. Rev.* **90** (1953) 316.
12. Ballhausen, C. J. *Progr. Inorg. Chem.* **2** (1960) 251.
13. Bjerrum, J., Ballhausen, C. J. and Jørgensen, C. K. *Acta Chem. Scand.* **8** (1954) 1275.
14. Liehr, A. D. and Ballhausen, C. J. *Ann. of Phys. (N.Y.)* **3** (1958) 304.

Received January 23, 1962.

ACTA CHEMICA SCANDINAVICA 16 (1961) 1393–1396

Polarography of Lead and Cadmium Complexes with Tetraethylenepentamine and Pentaethylenehexamine

EINAR JACOBSEN and KNUT SCHRØDER

Kjemisk Institutt A, Universitetet i Oslo, Blindern, Norway

The complexes of cadmium and lead with tetraethylenepentamine and pentaethylenehexamine have been studied by means of the dropping mercury electrode. The half-wave potentials and the diffusion current constants have been determined and the complex constants calculated. It has been shown that lead exhibits an amine coordination number of four in both complexes. The amine coordination number of cadmium is probably six in the pentaethylenehexamine. The data obtained seem to indicate that cadmium forms two complexes with both polyamines.

The polarography of copper complexes formed with tetraethylenepentamine ("tetren") and pentaethylenehexamine ("penten") has been thoroughly investigated by Jonassen *et al.*[1] The stability of some tetren complexes have been determined by potentiometric titration [2]. The stability of the penten complexes, however, and the polarographic behaviour of the tetren and penten complexes formed with other metals than copper have previously not been investigated. The present paper is a polarographic study of the cadmium and lead complexes formed with tetren and penten.

EXPERIMENTAL

Materials. The technical grade tetraethylenepentamine, obtained from Fluka AG, Switzerland, was purified and standardized as described by Reilley [3]. Pentaethylenehexamine was obtained as a mixture of amines designated "polyamine H, Special" from Carbide and Carbon Chemicals, New York, and was purified and standardized as described by Jonassen [1]. The purity of the reagents was also checked by infra-red analysis. The remaining chemicals were of reagent grade and were used without further purification. Stock solutions of lead and cadmium were prepared by dissolving the metal salt in redistilled water and standardized by complexometric titration with EDTA. 0.5 M phosphate buffer was used as supporting electrolyte. The buffer was prepared by adding potassium hydroxide to phosphoric acid and its pH measured with a pH meter. In order to avoid precipitation of lead phosphate, 1 M ammonia buffer was used as indifferent electrolyte for the lead complexes. The pH of the electrolyte was adjusted to desired value by addition of hydrochloric acid. 0.004 % of Triton x-100, obtained from Rohm and Haas Co, Philadelphia, was found to be effective as maximum suppressor.

Apparatus and technique. Polarograms were recorded with a Tast-Polarograph, Selector D (Atlas Werken, Bremen, Germany). The conventional type of dropping mercury electrode and of electrolysis cell was used. The capillary characteristics, measured in open circuit at a mercury height of 35 cm were $m = 3.015$ mg/sec, and $t = 3.36$ sec. An external saturated calomel electrode (S.C.E.) served as reference electrode. Dissolved air was removed from the solutions by bubbling oxygen-free nitrogen through the cell for 10 min and passing it over the solution during the electrolysis. All experiments were performed at 25 ± 0.1°C.

The reversibility of the electrode reactions was tested by determining the temperature coefficient of the half-wave potentials and the slopes of the curves of log $i/(i_d-i)$ *vs.* the potential. Corrections were made for the residual current. Data for the log plots were taken by manual operation of the polarograph, measuring the applied potential with a Leeds and Northrup Type K potentiometer. Half-wave potentials were taken from the logarithmic plots and were reproducible to ± 1 mV.

RESULTS AND DISCUSSION

The lead complexes with tetren and penten are reduced directly to the amalgam. The plots of log $i/(i_d-i)$ *vs.* the potentials were straight lines and the slopes indicate that the electrode reactions involve reversible two-electron reductions. The plots of the values of $E_{1/2}$ *vs.* the corresponding values of log C_x resulted in straight lines and the slopes of the lines indicate that only one group is coordinated in each complex. In the concentration range 0.3—2.6 mM of the complexing agent the half-wave potentials may be expressed by the following equations:

$$\text{(Pb tetren)}^{2+}: \; E_{1/2} = -0.696 - 0.031 \log C_x$$
$$\text{(Pb penten)}^{2+}: \; E_{1/2} = -0.710 - 0.034 \log C_x$$

The half-wave potentials of both lead complexes are shifted to more negative values with increasing pH. Above pH 10.5 the half-wave potentials are constant, independent of the pH of the supporting electrolyte. The dissociation constant, K_c of the lead complexes was calculated from the half-wave potentials assuming C_x equal to the total concentration in the pH region 10.5—11.5. The following values were calculated:

$$\text{(Pb tetren)}^{2+}: \quad pK_c = 10.9$$
$$\text{(Pb penten)}^{2+}: \quad pK_c = 11.0$$

The pK_c values for the tetren complex is in good agreement with the value ($pK_c = 10-11$) previously determined by potentiometric titration [2]. The pK_c of both complexes is about the same as that of the corresponding triethylenetetramine complex ($pK_c = 10.4$) [4], and seems to indicate that four lead to nitrogen bonds exist in all the three lead polyamine complexes.

The diffusion current constant $I = i_d/C\, m^{2/3}\, t^{1/6}$ at pH 10.3 was found to be 3.3 and 3.1 for the lead tetren and lead penten complex, respectively.

The cadmium complexes with tetren and penten are reduced directly to the amalgam. The half-wave potentials of both complexes are shifted to more negative values with increasing pH. Above pH 10.5 the half-wave potentials were constant and independent of pH of the supporting electrolyte. The plots of log $i/(i_d-i)$ *vs.* the potential were straight lines with the same slope of −0.044 V/log unit for the tetren complex. The log plots of the corresponding penten complex were curved at all concentrations of the reagent in the pH

range 9.5—11.5 of the supporting electrolyte. By careful examination of the undamped so-called Tast polarograms, it was verified that the polarograms of the cadmium penten complex consist of two waves. Exactly the same polarograms were obtained using ammonia buffer as supporting electrolyte.

The polarograms were perfectly reproducible and seem to indicate that the waves are due to two different cadmium complexes being reduced at almost the same potential. Because of the very small difference in half-wave potentials the individual diffusion currents and half-wave potentials could not be measured.

The limiting current of the tetren and penten complexes varied with the height of mercury above the capillary. The value $i/\sqrt{h}$, h being the height of the mercury after correction for the "back pressure", was constant, indicating that the electrode reactions are diffusion controlled. The following values for the diffusion current constants, $I = i_d/C\ m^{2/3}\ t^{1/6}$, were found:

Cadmium tetren (pH 11.2): $I = 2.75$
Cadmium penten (total wave pH 10.5): $I = 2.07$

The half-wave potentials (taking $E_{1/2}$ of the penten complex as the point on the Tast polarogram where $i = i_d/2$) shifted to more negative values with increasing concentration of the reagents. In the concentration range 0.3—8 mM of the complexing agents, the plot of $E_{1/2}$ *vs.* log C_x resulted in straight lines which may be expressed by the equations:

Cadmium tetren: $E_{1/2} = -1.075 - 0.050 \log C_x$
Cadmium penten: $E_{1/2} = -1.22 - 0.050 \log C_x$

The temperature coefficient of the diffusion currents was + 1.3 %/degree and the shift in the half-wave potentials was about + 1 mV/degree for the cadmium tetren and penten complexes. This seems to indicate that both cadmium penten complexes are reversibly reduced at the dropping mercury electrode and that the wave of the tetren complex (slope of log plot = −0.044 V/log unit) also is due to reversible reduction of two complexes being reduced at almost the same potential.

By amperometric titrations of different amounts of cadmium with standardized tetren and penten solutions, it was verified that exactly one mole of the reagent was consumed in the complex formation with one mole of the cadmium ions, indicating that only one ligand is coordinated in each complex. The diffusion current constants of the total waves indicate that the reduction of the complexes involve two electrons.

By assuming reversible reduction of the complexes, the mean values for the dissociation constants of the two tetren and the two penten complexes were calculated. The half-wave potentials obtained from polarograms of solutions with pH > 10.5 were used in the calculation assuming $C_x = C$ in this pH region. The following values were obtained:

Cadmium tetren: $pK_c = 14.7$
Cadmium penten: $pK_c = 19$

The stability of cadmium tetren complex has previously been determined by potentiometric titration [2] and the pK_c value was found to be = 14.0.

Considering the great difference in ionic strength in the potentiometric and the present polarographic determination, the agreement is satisfactory.

The large increase of the stability of the tetren and penten complexes over that of the cadmium triethylenetetramine complex [4] ($pK_c = 10.8$) indicates that the amine coordination number of cadmium is greater than four in the tetren and penten complexes and probably six in the penten complex.

REFERENCES

1. Jonassen, H. B., Bertrand, J. A., Groves, F. R. and Stearns, R. I. *J. Am. Chem. Soc.* **79** (1957) 4279.
2. Reilley, C. N. and Holloway, J. H. *J. Am. Chem. Soc.* **80** (1958) 2917.
3. Reilley, C. N. and Vavoulis, A. *Anal. Chem.* **31** (1959) 243.
4. Reilley, C. N. and Schmid, R. W. *J. Elisha Mitchell Soc.* **73** (1957) 279.

Received January 15, 1962.

ACTA CHEMICA SCANDINAVICA 16 (1962) 1397–1400

Studies on Local Anesthetics XXI *

BJÖRN LÜNING

Institution of Organic Chemistry and Biochemistry, University of Stockholm, Stockholm, Sweden

Three *sec*-butylaminoacetanilides related to Xylocaine® have been synthesized. Their local anesthetic action on rabbit cornea and their subcutaneous toxicity in white mice were determined and compared with those of some of their homologues.

In the preceding investigations of alkylaminoacyl anilides related to Xylocaine®, no compounds containing a *sec*-butylaminoacyl group have been synthesized or tested for their local anesthetic properties. Thus, three *sec*-butylaminoacetanilides (for their structures see Table 1) have been prepared and their durations of anesthesia measured on rabbit cornea. To synthesize the compounds, the appropriate arylamine was condensed with chloroacetyl chloride to give the corresponding α-chloroacetanilide according to the general method of Löfgren [2]. *sec*-Butylamine and the suitable chloroacetanilide were then allowed to react in benzene to form the desired *sec*-butylaminoacetanilide.

The anesthetic potency of the compounds is given as RA ("relative activity") which is obtained by dividing the molarity of a standard Xylocaine solution by that molar concentration of the actual compound which gives the same duration of anesthesia as the Xylocaine standard. Further details regarding the testing of compounds are presented by Löfgren *et al.*[3] LD50 values were obtained by subcutaneous injections in white mice and calculated as (*a*) grams of the base per kilogram of body weight and (*b*) moles per kilogram of body

Table 1. Synthesized compounds.

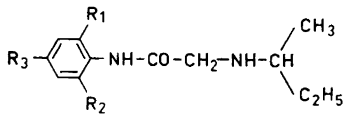

Compound	R_1	R_2	R_3
I	CH_3	H	H
II	CH_3	CH_3	H
III	CH_3	CH_3	CH_3

* For paper XX of this series see Löfgren and Tegnér [1].

Table 2. Local anesthetic activity (rabbit cornea) and subcutaneous toxicity (white mouse) of compounds I—III and four compounds (A—D) synthesized by Löfgren *et al.*[3,4,a].

Compound	Relative anesthetic activity (RA) xylocaine = 1	Toxicity, LD50		Relative toxicity (RT) xylocaine = 1	RA/RT
		g base/kg	moles/kg × 10^3		
Xylocaine	1.0	0.34	1.4	1.0	1.0
I	0.3	~1.7	~9.1	~0.16	~1.9
II	2.0	0.27	1.2	1.3	1.6
III	1.9	0.30	1.2	1.2	1.6
α-(Propylamino)-2,6-dimethylacetanilide (A)[a]	1.0	0.52	2.4	0.61	1.6
α-(Propylamino)-2,4,6-trimethylacetanilide (B)[a]	1.9	0.56	2.4	0.58	3.3
α-(Isopropylamino)-2,6-dimethylacetanilide (C)[a]	0.8	0.48	2.2	0.67	1.2
α-(Isopropylamino)-2,4,6-trimethylacetanilide (D)[a]	0.9	0.47	2.0	0.70	1.3

[a] The pharmacological properties of B and D are found in Löfgren *et al.* [3] For A and C the relative anesthetic activity and the toxicity were obtained by private communication with Dr. S. Wiedling, A.B. Astra, Södertälje, Sweden.

weight ("molar" LD50 value). The term RT ("relative toxicity") is the ratio of the molar LD50 value of Xylocaine and that of the actual compound. The change in RA and RT is indicated by *factors* f_A and f_T; respectively.

The pharmacological data of the compounds are found in Table 2. In Table 2 are also included the pharmacological data of four compounds (A—D) synthesized by Löfgren *et al.*[3,4] *. The material allows a brief study on the relationship between chemical constitution and pharmacological properties:

(1) The introduction of a methyl group into the alkylamino group (R_4NH; *cf.* Table 3: A) at the carbon atom next to the nitrogen atom is in one case (A → II) accompanied by a rise in RA ($f_A = 2.0$), whereas in another case (B → III) RA is not changed ($f_A = 1.0$) **. In both cases the toxicity increases strongly ($f_T = 2.0$) **.

(2) When an isopropylamino group (R_4NH; *cf.* Table 3: B) is replaced by a *sec*-butylamino group, a strong increase in RA ($2.1 < f_A < 2.5$) as well as in RT ($1.7 < f_T < 1.9$) is observed.

(3) The effect on the pharmacological properties of changes in situation and number of methyl groups attached to the benzene nucleus offers some interesting features. The introduction of a methyl group *para* to the amide nitrogen has very little influence on the pharmacological properties, which is

* As regards the pharmacological data of compounds A—D, ses footnote to Table 2.

** The changes in the pharmacological properties which are connected with the same structural change, *i.e.* the introduction of a methyl group at the carbon atom next to the nitrogen atom in the alkylamino group R_4NH (*cf.* Table 3: A), have been studied by Löfgren *et al.* [3] by comparing compounds containing an ethylamino group with those containing an isopropylamino group; see Löfgren *et al.* [3], Table 4:B.

Table 3. Change in relative anesthetic activity (RA) and relative toxicity (RT) when varying the group R_4 (*cf.* formula).

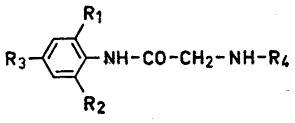

R_1, R_2 or R_3 = H or CH_3
R_4 = *n*-C_3H_7, *i*-C_3H_7 or *sec*-C_4H_9.

Factors f_A and f_T indicate the changes in RA and RT, respectively; *cf.* also text.

Compound					RA	f_A	RT	f_T	RA/RT
No.	R_1	R_2	R_3	R_4					
A. Introduction of a methyl group at the carbon atom next to the nitrogen atom in an alkylamino group R_4NH.									
A	CH_3	CH_3	H	*n*-C_3H_4	1.0	2.0	0.61	2.0	1.6
II	CH_3	CH_3	H	*sec*-C_4H_9	2.0		1.3		1.6
B	CH_3	CH_3	CH_3	*n*-C_3H_7	1.9	1.0	0.58	2.0	3.3
III	CH_3	CH_3	CH_3	*sec*-C_4H_9	1.9		1.2		1.6
B. Introduction of a methyl group at one of the methyl groups of an isopropylamino group R_4NH.									
C	CH_3	CH_3	H	*i*-C_3H_7	0.8	2.5	0.67	1.9	1.2
II	CH_3	CH_3	H	*sec*-C_4H_9	2.0		1.3		1.6
D	CH_3	CH_3	CH_3	*i*-C_3H_7	0.9	2.1	0.70	1.7	1.3
III	CH_3	CH_3	CH_3	*sec*-C_4H_9	1.9		1.2		1.6

demonstrated by the fact that II and III have almost identical RA and RT values. In comparing, I and II, which differ from each other by one *ortho* methyl group, it is found that the local anesthetic activity as well as the toxicity are noticably higher in II than in I ($f_A = 6.7$; $f_T = 8.0$).

EXPERIMENTAL *

α-Chloro-2-methylacetanilide, *α-chloro-2,6-dimethylacetanilide*, and *α-chloro-2,4,6-trimethylacetanilide* were prepared by condensing the suitable arylamine with chloroacetyl chloride in an aqueous sodium acetate buffer, following the general method of Löfgren [2].

α-(sec-Butylamino)-2-methylacetanilide (I). A mixture of 9.2 g (0.050 mole) of α-chloro-2-methylacetanilide, 18 g (0.25 mole) of *sec*-butylamine ** and 40 ml of dry benzene was boiled under reflux for 5 h. The benzene was removed *in vacuo* and the

* The equivalent weights of the bases were determined by titrating them in 30 % ethanol with 0.1 N HCl; mixed indicator methylene blue-methyl red.

** Before use, the *sec*-butylamine was dried over NaOH and distilled.

residue dissolved in 25 ml of concentrated hydrochloric acid. To the solution thus formed, 60 ml of water were added. The slightly soluble α-(*sec*-butylamino)-2-methylacetanilide hydrochloride, which soon deposited, was filtered off and recrystallized twice from isopropanol; yield 8.5 g (0.033 mole, 66 %), m.p. 152° (corr.). (Found: Cl 13.8. Calc. for $C_{13}H_{21}ClN_2O$: Cl 13.9.) The base was liberated from the hydrochloride by addition of dilute aqueous sodium hydroxide, taken up in ether and distilled; b.p. 140°—142°/0.2 mm, n_D^{25} 1.5312. (Found: equiv. wt. 222. Calc. for $C_{13}H_{20}N_2O$: equiv. wt. 220.)

α-(sec-Butylamino)-2,6-dimethylacetanilide (II). α-Chloro-2,6-dimethylacetanilide (9.9 g, 0.050 mole) and *sec*-butylamine (18 g, 0.25 mole) were allowed to react in the same manner as is described under compound I (*cf.* above). The resulting α-(*sec*-butylamino)-2,6-dimethylacetanilide hydrochloride was recrystallized twice from isopropanol; yield 7.4 g (0.027 mole, 55 %), m.p. 180° (corr.). (Found: Cl 12.9. Calc. for $C_{14}H_{23}ClN_2O$: Cl 13.1.) The base was liberated by treatment with dilute aqueous sodium hydroxide and distilled; b.p. 147°—148°/0.2 mm, n_D^{25}1.5206 *. (Found: equiv. wt. 235. Calc. for $C_{14}H_{22}N_2O$: equiv. wt. 234.) The base soon solidified to a crystalline mass; m.p. 46°—47° (corr.).

α-(sec-Butylamino)-2,4,6-trimethylacetanilide (III). α-Chloro-2,4,6-trimethylacetanilide (10.6 g, 0.050 mole) and *sec*-butylamine (18 g, 0.25 mole) were condensed according to the method described under compound I. The α-(*sec*-butylamino)-2,4,6-trimethylacetanilide hydrochloride obtained in the synthesis was recrystallized from isopropanol; yield 8.7 g (0.031 mole, 61 %), m.p. 180° (corr.). (Found: Cl 12.4. Calc. for $C_{15}H_{25}ClN_2O$: Cl 12.4.) The base was liberated from the hydrochloride and distilled; b.p. 152°—154°/0.2 mm. The oily distillate soon solidified to a crystalline mass; m.p. 55°—56° (corr.). (Found: equiv. wt. 247. Calc. for $C_{15}H_{24}N_2O$: equiv. wt. 248.)

Great thanks are due to Dr. S. Wiedling, A.B. Astra, Södertälje, Sweden, for performing the pharmacological tests.

REFERENCES

1. Löfgren, N. and Tegnér, C. *Acta Chem. Scand.* **14** (1960) 486.
2. Löfgren, N. *Studies on Local Anesthetics. Xylocaine, a New Synthetic Drug.* Dissertation, Stockholm 1948.
3. Löfgren, N., Tegnér, C. and Takman, B. *Acta Chem. Scand.* **11** (1957) 1724.
4. Löfgren, N. and Widmark, G. *Svensk Kem. Tidskr.* **58** (1946) 323.

Received December 31, 1961.

* Supercooled.

ACTA CHEMICA SCANDINAVICA 16 (1962) 1401–1417

A Systematic Study of the Photolysis of Some Dialkyl Disulfides in a Rigid Glass at 77°K

KJ. ROSENGREN*

Thermochemistry Laboratory **, *University of Lund, Lund, Sweden*

A number of primary, secondary and tertiary aliphatic disulfides have been photolyzed in a hydrocarbon matrix at 77°K using super high pressure mercury lamps together with appropriate filter. The spectral changes have been recorded and the reaction products, obtained after warm-up, have been identified using GLC.

All primary and secondary disulfides (except Me_2S_2) behave in an analogous stoichiometrically simple way (in contrast to *tert.* butyldisulfide). Strong evidence is presented for the view that the only detectable overall reaction occurring during photolysis is

$$R_1R_2CHSSCHR_1R_2 \rightarrow R_1R_2C{=}S + HSCHR_1R_2.$$

The presence of both reaction products has been established.

The spectral changes during the photolysis of dimethyl disulfide are only initially analogous to those of the other primary disulfides. Upon prolonged irradiation unknown reactions occur, leading to the formation of carbonmonosulfide, CS, among other products.

An experimental study of the possibilities of determining bond-formation energies by direct measurement of the enthalpy change accompanying the radical recombination process

$$2R\cdot \rightarrow R_2$$

must of course start with the elucidation of the conditions under which one specified, known radical can be produced, quantitatively determined and stored for a sufficiently long period of time. Thus, it is obvious that one should first investigate the homolytic splitting of symmetrical compounds, R—R.

In this field the general lack of knowledge, particularly regarding the stoichiometry of radical formation processes, is such that no guidance can be obtained from the literature in selecting the class of compounds to be studied.

* Research Fellow at the *Swedish Technical Research Council.*

** Sponsored by the *Swedish Natural Science Research Council* and by the *Swedish Technical Research Council.*

However, it has been stated repeatedly in the literature that disulfides upon irradiation can be split into intermediate thiyl radicals: $R_2S_2 \rightarrow 2RS\cdot$.

In recent reviews Bateman, Moore and Porter [1] and Parker and Kharasch [2] have summarized the experimental indications for the homolytic splitting of the S—S bond under different conditions and they conclude that convincing evidence exists for the homolysis of this bond in photochemical reactions, whereas purely thermal homolysis of the S—S bond in organic di- and polysulfide molecules at temperatures below 140°C has not yet been conclusively demonstrated. Lewis and Lipkin [3], when illuminating diphenyl disulfide in a rigid matrix at liquid-air temperature, produced a yellow color that disappeared when the sample was brought to room temperature. This color was believed to be due to the free radical $C_6H_5S\cdot$. Barltrop, Hayes and Calvin [4] photolyzed trimethylene disulfide at 77°K in an EPA matrix. Upon photolysis the cell content became pale salmon-colored and the original disulfide peak at 330 mμ disappeared almost completely. When the temperature of the sample was raised a few degrees above liquid nitrogen temperature, the glass lost its rigidity and the cell content rapidly became turbid owing to the formation of polymers. More than 50 % of the original disulfide was recovered. The result from the photolysis was believed to be a diradical $\cdot S(CH_2)_3S\cdot$ which partly polymerized upon warming up. The results of experiments with six simple symmetrical alkyl- and aryl disulfides, aiming at the trapping of free radicals produced under pyrolytic as well as photolytic conditions, have been published by Michaelsen [5]. Among the disulfides sublimed onto a cold finger *in vacuo* and photolyzed *in situ* only the aryl disulfides gave a red deposit, which was thought to be due to free radicals formed through homolysis of the S—S bond. When the disulfides were pyrolyzed in vapor phase by allowing them to pass through a furnace kept above 350°C, a colored deposit collected on the cold finger. This deposit was believed to contain radicals, partly of the type RSS· (yellow deposit) and partly of the type RS· (red deposit); the alkyl disulfides gave a deposit predominantly of the former type.

It seemed therefore reasonable to assume that the photolysis of simple disulfides under conditions favorable for the stabilization of intermediate products formed might lead to the isolation and characterization of thiyl radicals.

The technique chosen (Ref. [9]) was to photolyse the disulfide in a rigid organic matrix at 77°K and to study, primarily, the changes of the UV- and visible spectra. This technique, which has been well established mainly through the work of Norman and Porter [6] and Porter and Strachan [7,8], was early used by Lewis and Lipkin for studying the photolysis of diphenyl disulfide [3]. The present study, however, is only concerned with investigations of aliphatic disulfides. The spectra of these compounds are much less complicated and, moreover, the analysis of possible primary and secondary reaction products is easier to perform.

EXPERIMENTAL TECHNIQUE

Photolysis. The photolysis set-up, consisting of two super high-pressure mercury lamps (900 W each), 35 mm cells filled with nickel sulphate solution (285 g $NiSO_4,6H_2O$ per liter) and exchangeable glass filters, has been described elsewhere [9]. In the present investigation

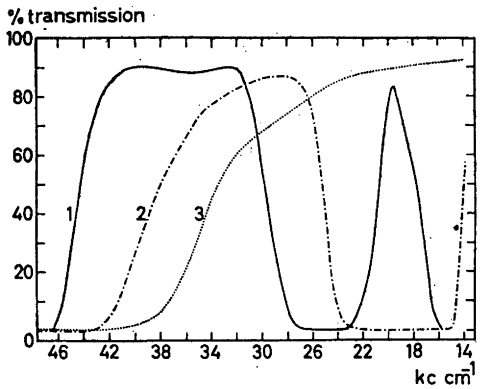

Fig. 1. Light transmission of filters used in the present work. (1) $NiSO_4$, $6H_2O$, 285 g/l, 3.5 cm. (2) Jena filter UG5, high wavenumber cut off 44.3 kc. cm^{-1}. (3) Jena filter WG7, high wavenumber cut off 43.6 kc. cm^{-1}.

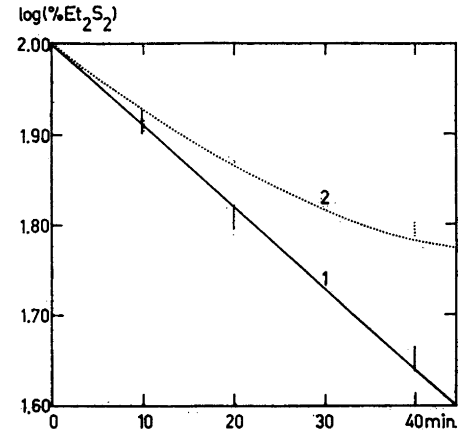

Fig. 2. Log(% remaining ethyl disulfide) from photolysis experiments in matrix B, plotted against time of irradiation (1) at 77°K, (2) at 298°K.

Jena filters (WG7 and UG5) have been used. Fig. 1 shows the light transmission for the solution proper and the filters.

Spectrophotometry. The cell compartment accomodating two 17 × 19 mm quartz cells used both for photolysis and spectrophotometry (Unicam recording spectrophotometer SP 700) has been described elsewhere [10].

Experimental procedure. All solutions were prepared and transferred under rigorously anhydrous conditions as even traces of water interfered, particularly in the short wavelength region [11]. The filling and handling of the quartz cells as well as the general procedure for the photolysis and the spectrophotometer has been described elsewhere [9]. All concentrations given in this paper are referred to room temperature. The actual concentration at 77°K is greater by a factor of 1.32 for solutions in matrix A and 1.30 for solutions in matrix B (see below). The values of molar extinction given have all been corrected for this change in concentration.

Gas-liquid chromatography (GLC) was used to search for reaction products after photolysis. In these experiments disulfide solutions were irradiated in 0.5 mm sealed, clear quartz capillary tubes kept at 77°K in a quartz Dewar vessel equipped with an appropriate heating device to prevent condensation on the outer surface. After photolysis the quarts tubes were opened at 15°C (to avoid evaporation of solvents) and 1 μl samples were withdrawn using a fine glass capillary pipette and transferred to a Pye Argon Chromatograph equipped with an ionization detector. The chromatograph had been rebuilt to accomodate columns of 7 mm inner diam. and 120 cm length, either one or three in series.

Materials

Dimethyl disulfide (British Drug House, b.p. 108.5°/760 mm), *diethyl disulfide* (Eastman chemicals, b.p. 89°/120 mm), *dipropyl disulfide* (Eastman chemicals, b.p. 89°/22 mm), *di-isopropyl disulfide* (Eastman chemicals, b.p. 72°/20 mm), *dibutyl disulfide* (Eastman chemicals, b.p. 101°/10 mm), *di-isobutyl disulfide* (Eastman chemicals, b.p. 85°/10—11 mm), *di-t-butyl disulfide* (Phillips Petr. Co., b.p. 67.5°/9 mm) and *1-butanethiol* (British Drug

House, b.p. 98°/760 mm) were all purified by two successive fractional distillations through a glass column, 50 × 1.2 cm, packed with Fenske helices, 4 mm in diam., main fractions being collected at given b.p.'s and pressures. The samples of the compounds used in the experiments showed no impurities when analyzed with GLC except for dipropyl disulfide, which contained less than 0.1 % of an unknown substance.

Didecyl disulfide was prepared from fractionallydistilled, pure 1-decanethiol by oxidation with iodine. Owing to decomposition, the disulfide obtained could not be further purified by fractional distillation even at low pressures. It was therefore dissolved in absolute ethanol and slowly frozen out on a cold finger using dry ice as a refrigerant. The procedure was repeated twice.

Di-sec-butyl disulfide. A sample of pure 2-butanethiol, prepared from the corresponding bromide and thiourea, Ref. [12], p. 479, was oxidized with iodine. After two successive fractional distillations at 91°/10 mm a faintly yellow product was obtained, which showed less than 0.1 % impurities (GLC).

Di-cyclohexyl disulfide. Pure cyclohexanethiol, prepared from the corresponding bromide and thiourea, was oxidized with iodine. The disulfide was fractionally distilled twice at 98°/2 mm. The colorless main fraction showed less than 0.5 % impurities (GLC).

*Di-neopentyl disulfide. Neo*pentylmercaptan prepared from *neo*pentyl alcohol and *p*-toluene sulfonylchloride [13] was oxidized with iodine. The disulfide was purified by twofold fractional sublimation in vacuum and was recovered as a white solid, m.p. 40–41°C. GLC showed less than 0.1 % impurities.

Cyclohexanethione was prepared from cyclohexanone according to Sen [14]. The substance was fractionally distilled in vacuum into five receiver flasks which were cooled one by one with liquid nitrogen during the distillation and sealed off as soon as a sufficient quantity had been collected. The deep-red colored fraction, boiling at 66°/16 mm, was used for the experiments.

2, 4, 6-Trimethyl trithiane (*a* and *β*) were prepared from thioacetaldehyde, HCl and H_2S [15]. M.p. 101°C and 125–126°C, respectively.

Solvents. All hydrocarbons used, isopentane (techn. grade), pentane (pure grade), *neo*-hexane (pure grade) and 3-methyl pentane (techn. grade), were supplied by Phillips Petroleum Company. They were carefully purified by fractional distillation followed by adsorption on silica gel, the details have been described elsewhere [16].

The matrix forming hydrocarbon mixtures used in this work were:

Isopentane (6 parts) 3-Methyl pentane (1 part)	called matrix A
*Neo*hexane (8 parts) Pentane (3 parts)	called matrix B

Some properties of these mixtures will be given elsewhere [16,17].

RESULTS

Preliminary experiments

In order to see if an extremely low quantum yield at 77°K could make the photolysis of the disulfide molecule impossible, a 20 mM solution of Et_2S_2 in matrix B was photolyzed in quartz capillary tubes both at room temperature and at 77°K. Besides the disulfide, the hydrocarbon mixture contained 0.1 % octane as a reference substance for the gas chromatographic analysis. After photolysis and warm-up, five identical samples were withdrawn from each tube and run through the gas chromatograph. The ratio

$$\frac{\text{area under } Et_2S_2 \text{ peak}}{\text{area under octane peak}}$$

was taken as a measure of the disulfide concentration. The results are given in Table 1 which shows that the quantum yield is of the same order of magnitude at the two different temperatures.

Table 1. Photolysis of 20 mM Et_2S_2 in matrix B, 0.1 % octane added. WG7 filters.

Time of photolysis	Remaining Et_2S_2 % at 298°K	Mean value	at 77°K	Mean value
10 min	80.5		84.4	
	82.5	81.5	80.5	82.5
20 min	76.0		64.3	
	74.6	75.3	64.7	64.5
40 min	62.0		42.4	
	62.7	62.4	47.0	44.7

A plot of log(% remaining Et_2S_2) against the time of photolysis (Fig. 2) indicates the expected first order decay at 77°K, whereas at room temperature the rate constant of the reaction seems to decrease for prolonged photolysis, probably as a result of the formation of light absorbing secondary reaction products which reduce the amount of active light.

When photolyzed under the same conditions methyl disulfide decomposed at about the same ratio as Et_2S_2. However, for 77°K the decay did not fit a first order plot.

When a mixture of methyl- and ethyl-disulfides was exposed to UV-light, the mixed disulfide was formed. The equilibrium for this mixture has recently been studied [18]. To check if this also occurs in a rigid environment, a solution containing 20 mM Et_2S_2, 20 mM Me_2S_2 and 0.1 % octane in matrix B was photolyzed in quartz capillary tubes both at 77°K and at room temperature. The results from the gaschromatographic analyses are shown in Table 2, which

Table 2. Photolysis of 20 mM Me_2S_2 and 20 mM Et_2S_2 in matrix B, 0.1% octane added. WG7 filters.

Time of photolysis	Me_2S_2/octane	MeSSEt/octane	Et_2S_2/octane	K
20 min at room temp.	2.26	4.60	1.97	4.7
	1.81	3.94	1.74	4.9
	1.47	3.88	1.79	5.6
			Mean value	5.1
40 min at room temp.	1.67	3.39	1.42	4.8
	1.95	3.93	1.53	5.1
	1.34	3.49	1.60	5.6
			Mean value	5.2
2 min at 77°K	2.62	0.14	3.45	
5 min at 77°K	2.59	0.17	3.42	
10 min at 77°K	2.13	0.19	3.16	
20 min at 77°K	1.90	0.25	2.94	
30 min at 77°K	1.67	0.22	2.45	
40 min at 77°K	1.31	0.22	1.98	
Blank, unphotolyzed	2.86	0.10	3.63	
	2.80	0.16	3.58	

gives the ratio of "area under disulfide peak"/"area under octane peak". In addition the equilibrium constant $K = \frac{[MeSSEt]^2}{[Me_2S_2][Et_2S_2]}$ is given for the photolysis at room temperature, this constant being corrected for the different response of the detector for various disulfides. This correction is taken from Ref. [18] as the same detector was used in both experiments.

As is seen from Table 2 the mixed disulfide is formed very rapidly at room temperature and the value of K is already after 20 min of photolysis very close to the equilibrium constant previously reported (average 5.6). At 77°K, however, no significant correlation can be found between the amount of mixed disulfide formed and the time of photolysis. The small amount of mixed disulfide found at 77°K is probably formed during the manipulation of the quartz capillary tubes. The reaction may, for instance, be caused by the ultraviolet light produced when the tubes are melted off in a hydrogen flame. It is of interest to notice that most spectrophotometric experiments have been performed in *ca.* 400 times more dilute solutions, in which the average distance between neighbouring disulfide molecules is increased by a factor of 7 (*cf.* below).

From the preliminary experiments it was apparent that, to a considerable extent, disulfide disappears irreversibly during photolysis followed by warm-up. At 77°K the decomposition reaction was found to be, within the limits of error, unimolecular, indicating a direct dependance on the excitational process. Further, the experiments with mixtures of disulfides show that, whatever the reaction mechanism is, an excited disulfide molecule cannot diffuse in the solid matrix to be able to react with a second disulfide molecule.

Although the preliminary results, concerning the possibility of utilizing the chosen method for thermochemical studies of radical recombination energies, were discouraging, it was felt necessary to gain further knowledge of the causes for the apparent failure. Only in this way can one devise experimental conditions, whereby the original idea could be successfully realized.

Spectrophotometric results

Primary alkyl disulfides. A cell containing 0.4 mM butyl disulfide in matrix A together with an appropriate reference cell were cooled down to 77°K inside the cell compartment previously described. An ultraviolet spectrum was recorded after which the solution was photolyzed for a few minutes using WG7 filters. When a new spectrum was recorded shortly after the end of the photolysis period the disulfide peak at 40 kc. cm^{-1} had decreased (Fig. 3). Repeated recordings of the spectrum at various times showed no change in transmission after the end of the photolysis as long as the liquid nitrogen level was kept above the optical path. Repeated photolysis resulted in a further decrease of the disulfide peak and if the spectra after various times of photolysis were recorded on the same paper an isosbestic point at 40.85 kc. cm^{-1} showed up.

The various curves were analyzed and log(% remaining disulfide) at different wavenumbers was plotted against the time of photolysis. A strict first

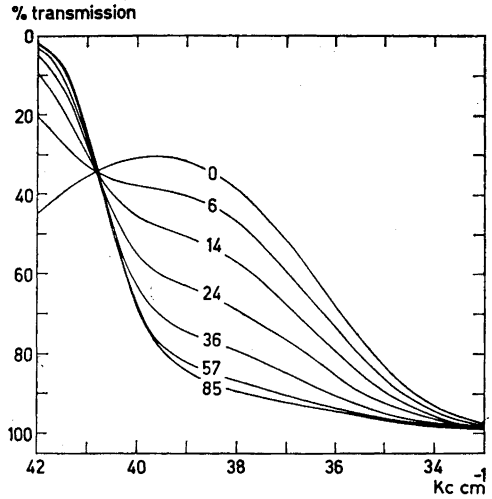

Fig. 3. Photolysis of 0.4 mM butyl disulfide in matrix A at 77°K. The figures give the time of photolysis in minutes.

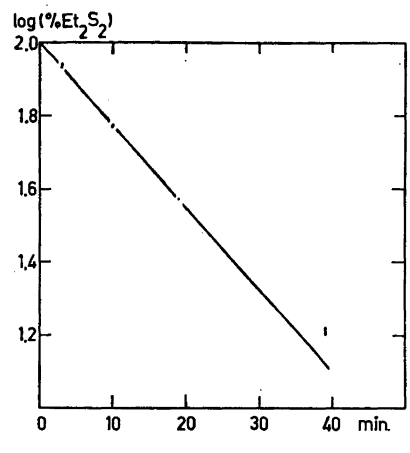

Fig. 4. Log(% remaining butyl disulfide) from photolysis in matrix A at 77°K, plotted against time of irradiation.

order decay was found in a small wavenumber region for photolysis times less than *ca.* 30 min. Fig. 4 shows the results from a typical run; the vertical extent of the four marks represents the maximum deviation when the disulfide concentration is measured at four equally spaced wavenumbers from 37.6 to 38.8 kc. cm^{-1}. Outside this wavenumber region the calculated values did not fit the straight line indicating the formation of light-absorbing reaction products.

The frozen cells were brought to room temperature and the spectrum recorded as soon as possible. This could usually be started within 3—5 min after the disulfide containing cell was lifted up from the liquid nitrogen. Comparison

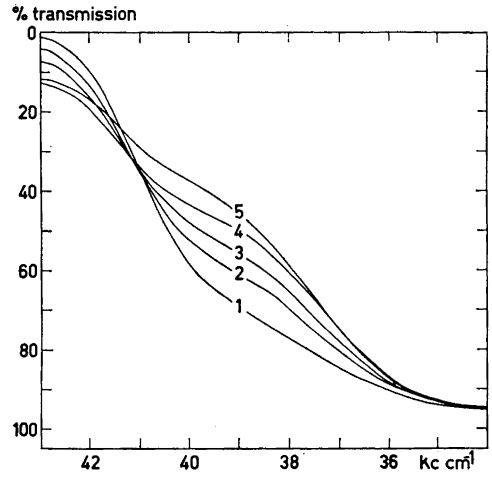

Fig. 5. Spectral changes of a 0.4 mM butyl disulfide, photolyzed at 77°K and brought to room temperature. After (1) 6 min., (2) 15 min., (3) 30 min., (4) 3 h, and (5) 24 h at 298°K.

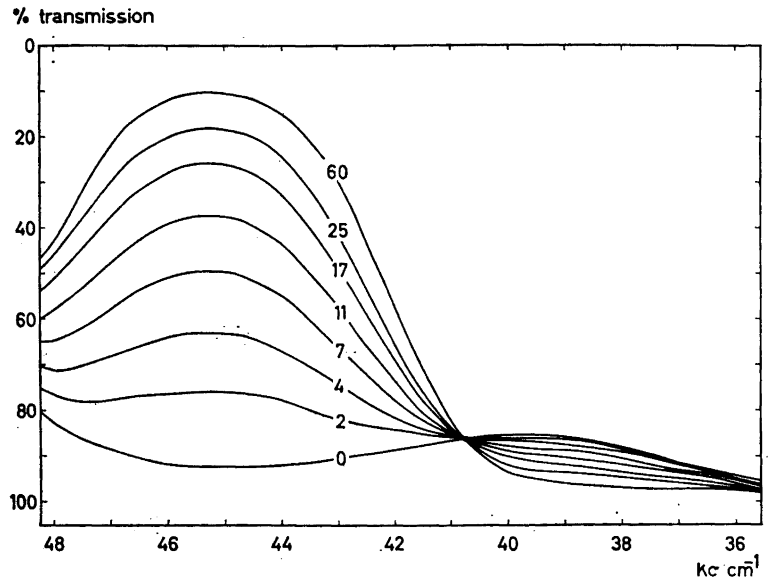

Fig. 6. Photolysis of 0.05 mM butyl disulfide in matrix A at 77°K. The figures give the time of photolysis in minutes.

with the spectrum recorded before the cells were frozen down showed that the amount of remaining disulfide after warm-up was the same as the amount of remaining disulfide measured at 77°K after the last photolysis. The spectrum after warm-up changed slightly with time as shown in Fig. 5.

In order to study more carefully the high absorption peak which was developed during photolysis the experiment was repeated using 0.05 mM disulfide. Fig. 6 shows the spectra recorded after increasing times of photolysis. As is seen from the figure a broad band with a maximum at 45.2 kc. cm^{-1} was created. If the reaction product, responsible for this peak, was formed in the first-order decay reaction, its optical density ought to increase at any wave-number with time of photolysis according to the following equation *:

$$D = \varepsilon\, C_0 l(1-e^{-kt})$$

D = optical density
ε = molar extinction coefficient of the reaction product
C_0 = initial concentration of the disulfide
l = cell length
k = rate constant of the reaction
t = time of photolysis

* It is obvious that this equation is valid also if two identical species are formed per disulfide molecule, the calculated molar extinction coefficient in this case being twice the true one.

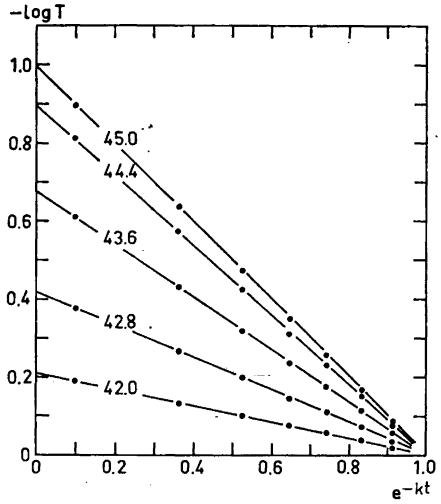

Fig. 7. Optical density plotted against e^{-kt} for various wavenumbers, indicated by figures; k equal to 0.046 min^{-1}.

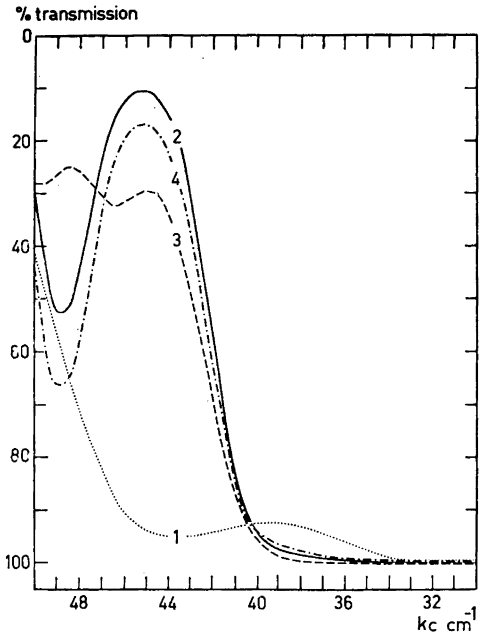

Fig. 8. Spectra of 0.05 mM butyl disulfide in matrix A. (1) Unphotolyzed at 77°K; (2) after 60 min. of photolysis at 77°K and (3) at 298°K; (4) after recooling to 77°K.

Fig. 7 gives the optical density at various wavenumbers plotted against e^{-kt}. The optical density values have all been corrected for remaining unphotolyzed disulfide. A set of different values for k had to be tried until a particular value gave straight lines. In the given experiment k was found to be 0.046 min^{-1}, which corresponded to $t_{½}$ = 15 min. The straight lines could be extrapolated to infinite time of photolysis (e^{-kt} = 0) and thus the molar extinction coefficient for the reaction product at 77°K could be obtained; log ε_{max} = 3.96.

A spectrum recorded a few minutes after the photolyzed solution was brought to room temperature is shown in Fig. 8 (curve 3). The high absorption peak was still present, although somewhat lowered and shifted about 0.2 kc. cm^{-1} towards higher wavenumbers. In addition, a more intensive absorption peak became visible at 48.4 kc. cm^{-1}. The appearence of this peak was fully reversibly dependent on the temperature *. Curve 4 (Fig. 8) shows the spectrum when the optical cells were cooled to 77°K for the second time. The small discrepancy between curves 4 and 2 could be ascribed to dilution of the photolysis product with some unphotolyzed disulfide solution remaining in

* This temperature-dependent absorption is at present without explanation — it has been found in all cases studied with two exceptions — dimethyl and dicyclohexyl disulfide. By independent control experiments it has been established that the spectrophotometer is reliable down to 51 kc. cm^{-1}. *Added in proof:* Reference is made to a later publication [29].

the stem of the optical cell during photolysis. Repeated cycling of the probe between 77°K and room temperature always gave the same result as far as the appearence of the peak at 48.4 kc. cm^{-1} was concerned.

If the photolyzed solution was allowed to stand at room temperature, a slow decrease in absorption, as shown in Fig. 9, could be noticed. It was found that the ratio between the two maxima did not change. Similar experiments repeated with matrix B gave identical results, which was also the case when two sets of filters, other than WG7, were used in the light path, *viz.* WG6 and KG2, high wavenumber cut off at 41.2 and 40.6 kc. cm^{-1}, respectively.

All observations described have been reproduced in a number of runs and, further, experiments with ethyl-, propyl-, isobutyl- and neo-pentyl-disulfides have been performed, all showing the same detailed behaviour with exception of minor differences regarding the spectrophotometric characters of the photolysis product. The results have been summarized in Table 3. Decyl disulfide also gave the same results with the exception that the isosbestic point was observed at 39.7 kc. cm^{-1}. The solutions of this disulfide became turbid when frozen down to 77°K, and no accurate kinetic determinations could therefore be made. However, the rate of photolysis seemed to be considerably lower than that of the other primary disulfides. The spectrum of neo-pentyldisulfide did not differ from other primary or secondary alkyldisulfides. At room temperature in matrix A the maximum appeared at 39.0 kc. cm^{-1}; log ε_{max} = 2.48.

Secondary alkyl disulfides. The investigated secondary alkyl disulfides (isopropyl-, *sec*-butyl- and cyclohexyl) also gave analogous results (Table 3),

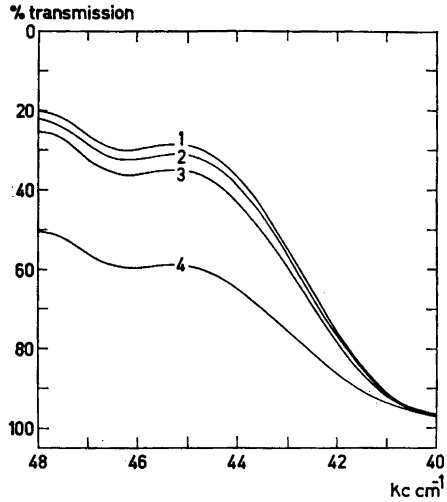

Fig. 9. Spectral changes of a 0.05 mM butyl disulfide, photolyzed at 77°K and brought to room temperature. After (1) 5 min., (2) 60 min., (3) 2.5 h, and (4) 18 h at 298°K.

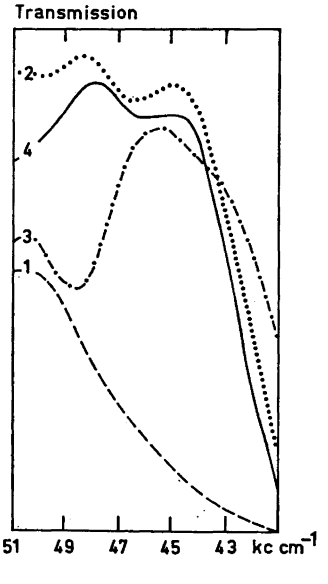

Fig. 10. Spectra of photolyzed disulfides, after warm-up. (1) Me_2S_2; (2) Bu_2S_2; (3) *sec.*-Bu_2S_2 and (4) *neo*pentyl disulfide. The 100% line different for the various disulfides.

although the high absorption peak and the isosbestic point were shifted towards lower wavenumbers, 44.0 and 39.3 kc. cm^{-1}, respectively. The extrapolated log ε_{max} for the photolysis product at 77°K was also in this case about 4. The

Table 3. Spectrophotometric characters at 77°K of the photolysis product for various dialkyl disulfides. Figures in brackets indicate the number of experiments. The uncertainties are expressed as mean deviations.

	Wavenumber of peak	Wavenumber of isosbestic point	log ε_{max}
Me_2S_2	48.07 (1)	43.31 ± 0.04 (4)	(3.8) (1)
Et_2S_2	45.50 ± 0.05 (5)	41.08 ± 0.03 (6)	3.91 ± 0.03 (3)
n-Pr_2S_2	45.27 ± 0.05 (2)	40.96 ± 0.06 (3)	4.0 ± 0.1 (1)
n-Bu_2S_2	45.21 ± 0.03 (7)	40.85 ± 0.04 (10)	3.94 ± 0.03 (6)
i-Bu_2S_2	45.06 ± 0.02 (2)	40.86 ± 0.02 (3)	3.91 ± 0.07 (2)
neo-$Pentyl_2S_2$	44.97 ± 0.02 (2)	40.55 ± 0.04 (2)	4 (2)
i-Pr_2S_2	44.00 ± 0.03 (2)	39.11 ± 0.03 (3)	3.96 ± 0.02 (2)
sec-Bu_2S_2	44.03 ± 0.04 (3)	39.26 ± 0.03 (5)	3.94 ± 0.02 (2)
$Cyclohexyl_2S_2$	44.60 ± 0.03 (2)	40.27 ± 0.03 (3)	3.91 ± 0.04 (2)

secondary disulfides gave somewhat different results after warm-up. For isopropyl- and *sec*-butyl-disulfides the two peaks visible at room temperature were moved closer to each other and the reversible one dominated so strongly in intensity that the original peak at 44 kc. cm^{-1} was visible only as a shoulder (Fig. 10, curve 3). Cyclohexyl disulfide gave no second peak upon warm-up; the maximum appeared at 44.6 kc. cm^{-1} both at 77°K and at room temperature.

Tertiary alkyl disulfides. The spectrum of *tert*-butyl disulfide does not show the disulfide maximum at 40 kc. cm^{-1} [19]; only a weak shoulder is seen at room temperature with inflections at *ca.* 40 and 44 kc. cm^{-1}*. When a solution in matrix A was cooled to 77°K a maximum became visible at 44.6 kc. cm^{-1} (log ε_{max} = 2.97); a minimum appeared at 46.7 kc. cm^{-1} (log ε_{max} = 2.87) and the absorption again increased at higher wavenumbers.

A 0.25 mM solution in matrix A was photolyzed at 77°K using UG5 filters. The disulfide maximum decreased during photolysis in the whole range 48—35 kc. cm^{-1}, neither the isosbestic point nor the high absorption peak was found. When the disulfide concentration had decreased to about 50 % of its initial value, the absorption again rised slowly and a new maximum appeared at 45.5 kc. cm^{-1}. After one and a half hours of photolysis the initial optical density was restored. The complicated kinetic pattern prevented a straightforward analysis. The 45.5 kc. cm^{-1} peak disappeared during warm-up, and the spectrum at room temperature showed only a continuously increasing absorption towards higher wavenumbers. After a second cooling to 77°K the peak became visible again.

Methyl disulfide gave, when photolyzed at 77°K in a 0.05 mM solution in matrix A with WG7 filters, a high absorption peak at 48.1 kc. cm^{-1}, an isosbestic point at 43.3 kc. cm^{-1} and an extrapolated value of log ε_{max} = 3.8; the last value is somewhat uncertain as the high wavenumber region made a precise measurement difficult. The spectrum at room temperature of the

* If log ε is plotted against wave-length, the shoulder almost vanishes; *cf.* Ref.[14]

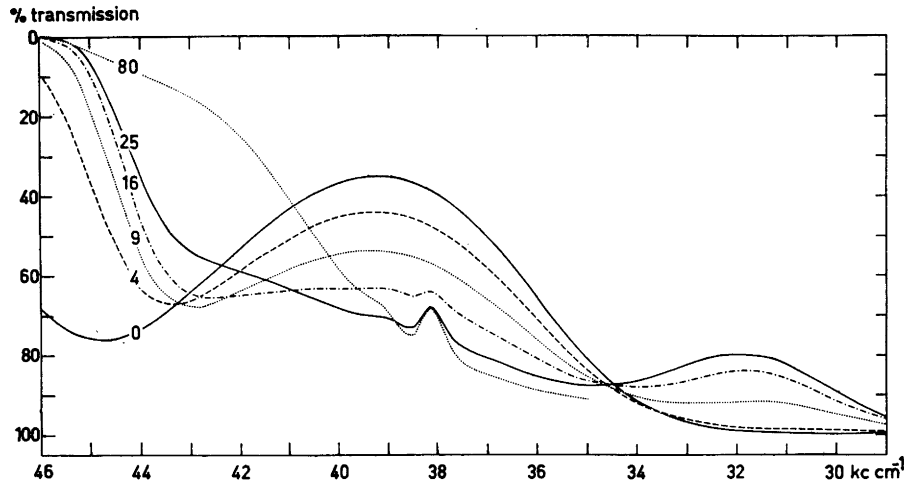

Fig. 11. Photolysis of 0.5 mM methyl disulfide in matrix A at 77°K. The figures give the time of photolysis in minutes.

photolysis product is shown in Fig. 10 (curve 1). The absorption decreased when the sample was allowed to stand at room temperature.

Fig. 11 shows results obtained with a 0.5 mM solution under otherwise identical conditions. The total time of photolysis in minutes is given with each curve. The three first curves all passed through the isosbestic point at 43.3 kc. cm^{-1}, but the curve recorded after 16 min showed a beginning additional absorbance at this wavenumber and a peak at 31.9 kc. cm^{-1} became clearly visible. The last two spectra show these characteristics even more pronounced, a further distinctive feature seen here is a double peak with maxima at 38.18 and 39.20 kc. cm^{-1}. At the end of the photolysis the cell content was turbid, and when the sample was brought to room temperature traces of a colorless precipitate were seen at the bottom of the cell. The spectrum now mainly consisted of one sloping line ranging from 46 to 28 kc. cm^{-1}. An inflection clearly indicated that the broad peak at 31.9 kc. cm^{-1} was still there but that the double peak at 38—39 kc. cm^{-1} had disappeared. It did not become visible again after recooling to 77°K.

Disulfides at high concentrations. Ethyl-, butyl- and cyclohexyl-disulfides have also been photolyzed in 5 mM solutions in matrix A at 77°K using WG7 filters. When irradiated for about an hour these solutions all gave a faint absorption in the visible part of the spectrum ranging from 30 to 17 kc. cm^{-1}. A weak maximum was found around 20 kc. cm^{-1}. The sample cell when lifted up and viewed perpendicularly to the light path showed two thin dark yellow layers close to the two parallel windows. The rest of the cell had a pale rose color which persisted when the sample was brought to room temperature whereas the yellow color disappeared when the cell content lost its rigidity. A spectrum recorded at room temperature showed an absorption between

23 and 17 kc. cm^{-1} with a maximum at 19.5 kc. cm^{-1}. However, the reduction in transmission never exceeded 10 % even at peak maximum.

The yellow color was probably due to the photolysis of mercaptan formed from the disulfide [20]. Several filter combinations were tried, without positive result, in order to achieve a light induced splitting of the disulfide without simultanous photolysis of the mercaptan.

Mercaptans. Alkyl mercaptans when photolyzed at low concentrations (0.05 and 0.4 mM) in matrix A at 77°K using WG7 filters showed very small changes in the spectrum after as much as an hour of irradiation, the most characteristic sign being an *increased transmission* around 48 kc. cm^{-1}. Besides, the transmission was reduced by a few percent at the mercaptan peak for the most concentrated solution.

Cyclohexanethione. The spectrum of cyclohexanethione has been investigated by Sen [21] and by Janssen [22]. Janssen found in cyclohexane a broad band ranging from 25 to 17 kc. cm^{-1} with a maximum at 19.8 kc. cm^{-1}. He also found a rather high ultraviolet absorption owing to impurities but concluded that "cyclohexanethione has no strong absorption band (log $\varepsilon >$ 3.5) at wavelengths above 220 mμ". Owing to the high rate of equilibration between the thione- and its corresponding enethiol-form, 1-cyclohexenethiol, the recorded spectrum cannot, however, be very reliable in the UV-region [14].

A 0.1 mM solution in matrix A was prepared and the recording of a spectrum started within 30 min after the sealed-off flask containing cyclohexanethione was brought to room temperature (see under Materials). The spectrum at 25°C consisted of a rather broad band starting at 35 kc. cm^{-1} with one maximum at 43.8 kc. cm^{-1} and an inflection unveiling a second somewhat lower maximum at about 46.3 kc. cm^{-1}. At 77°K only one peak was seen at 44.3 kc. cm^{-1} (log ε_{max} = 3.74, assuming the substance to be pure thione-form); no trace of the second peak was visible. The 19.8 kc. cm^{-1} absorption maximum could be verified only at high concentrations (calculated total concentration 20 mM, 85 % transmission).

2, 4, 6-Trimethyl-trithiane. The spectrum of *sym*-trithiane was taken in ethanol and in matrix A at room temperature, and the results verified earlier measurements; with an absorption peak at 41.7 kc. cm^{-1} (log ε_{max} = 3.16) [23]. α- and β-2,4,6-trimethyl-trithiane were studied in 0.2 mM solutions in matrix A. Both spectra looked very similar to that of *sym*-trithiane (peak at 41.9 kc. cm^{-1}, log ε_{max} = 2.94).

Control experiments. Pure samples of the hydrocarbon solutions used were photolyzed at 77°K. When WG7 filters were used, half an hour of irradiation did not change the 100 %-line. If the glass filters were removed a further hour of photolysis caused a small change (about 10 %) around 48 kc. cm^{-1}, where the transmission *increased.*

Photolysis of butyl disulfide at room temperature was carried out in a 0.05 mM solution in matrix A. The absorption peak at 45.2 kc. cm^{-1}, found at low temperature, could be easily seen, although the spectrum was very obscure. However, the intensity was reduced by a factor of ten.

Gas chromatographic results

Butyl disulfide was photolyzed in quartz capillary tubes and analyzed for 1-butanethiol by means of the gas chromatograph. All experiments were carried out at 77°K using WG7 filters. After irradiation the tubes were kept in liquid nitrogen until they were opened for analysis. From each tube at least five identical samples were withdrawn and put on the column. The mercaptan could be quantitatively estimated by comparison with octane as reference substance. Measurements were made using initial disulfide concentrations of 10 and 20 mM in matrix A. The time of photolysis varied from 10 to 60 min. Mercaptan was found in all photolyzed samples, the amount varied with the time of photolysis and in some of the tubes irradiated for one hour it corresponded to a 60 % conversion of the initial disulfide assuming a 1:1 ratio. Attempts were made to increase the yield. It seemed, however as if *ca.* 60 % represented an upper limit. Unphotolyzed blanks showed no trace of mercaptan.

DISCUSSION

Even the preliminary experiments have made clear three important points for the elucidation of the chemical reactions occurring after irradiation of disulfides: First, it was found that the disulfide irreversibly disappeared in the reaction; secondly, the decomposition was found to be a first-order reaction. Thirdly, it was shown that diffusion of disulfide molecules or alkyl thiyl radicals must be completely or nearly completely hindered in the matrix at 77°K.

The spectrophotometric investigations in all cases fully confirmed the occurrence of irreversible chemical reactions upon photolysis. The very regular change in spectral pattern obtained for primary and secondary disulfides showing a precise isosbestic point at about 40 kc. cm^{-1} strongly indicated a simple and well-defined chemical reaction to proceed during the irradiation. Further, the kinetics corresponded strictly to that of a first-order reaction as shown by the disappearance of disulfide as well as by the formation of a photolysis product. Although every effort was made to detect spectrophotometrically, after irradiation, the presence of some unstable species that might be of a radical nature, no trace of such a species could be found by the method used.

Taking the given facts into consideration it was concluded that the irradiation initiates a chemical reaction which takes place in the nearest environment of the excited disulfide molecule and leads to the formation of stable molecular species.

Turning to the problem of the nature of this reaction, the following facts must be considered. The difference in behaviour between the primary and the secondary disulfides and the *tert.* butyl disulfide is striking. The spectral change during photolysis of the last compound is complicated and does not allow a simple analysis. The discrepancy can hardly be explained as a result of steric factors, as *neo*-pentyl disulfide behaved normally. In the literature it has often been postulated that hydrogen abstraction from an atom adjacent to a radical

site is very easily achieved. In particular, much evidence has been collected for a disproportionation of alkoxyl radicals according to the reaction [24]:

$$2\ R_1R_2CHX\cdot \rightarrow R_1R_2C{=}X + HXCHR_1R_2$$

where X = O, R = H or Alk.

The same mechanism has been proposed by Coope and Bryce [25] for the thermal degradation of Me_2S_2. These authors found that 1 mole of MeSH was formed per mole of Me_2S_2, together with a product that was assumed to be polymeric thioformaldehyde. It is therefore suggestive that only those disulfides with at least one hydrogen atom in the α-position react in a simple manner as judged from the spectrophotometric evidence. The assumption was therefore made that the analogous reaction, X = S, occurs, following the homolytic splitting of the disulfide to identical thiyl radicals.

In accordance, the experiments showed butanethiol to be formed in increasing amounts during continued photolysis of butyl disulfide. The observation that the yield could not be increased above 60 % is in good agreement with the results obtained by Walling and Rabinowitz [26]. These authors studied the photolysis of 0.2—0.035 M isobutyl disulfide in cumene at 35°C and found that the yield of 2-methyl 1-propanethiol reached a constant level after a certain period of photolysis. They concluded that this level corresponded to a steady state in which the thiol was decomposed by the light at the same rate as it was formed.

Direct evidence for the formation of mercaptans even at 77°K is obtained from the photolysis experiments on disulfides at high concentrations. The yellow color formed upon prolonged photolysis, and irregularly distributed in the sample cell, was also found to be a general feature accompanying photolysis of mercaptans under otherwise similar conditions [20]. The subsequent photolysis of mercaptan formed in the primary chemical reaction also explains the fact that, at 0.4 mM concentrations, the kinetics of the reaction did strictly follow a first-order rate equation only until about 60—70 % of the disulfide was decomposed (Fig. 4).

Provided the above explanation holds, the second reaction product must be a thioaldehyde or a thioketone, depending on whether the disulfide used is primary or secondary. The ease with which the aliphatic thials and thiones trimerize or polymerize makes it extremely difficult to determine the physical properties of the monomers. The only known compound that could be used for the purpose of spectral comparison was cyclohexanethione which further suffers from the disadvantage that it rapidly isomerizes to cyclohexenethiol. Janssen [22] has pointed out that the visible absorption of the thione monomer gradually disappears at room temperature, whereas the ultraviolet absorption remains constant. As expected, both cyclohexenethiol and the trimerized cyclohexanethione exhibit absorption only in the UV-region.

The absorption spectra recorded for the photolysis products from cyclohexyl disulfide and from the sample of freshly distilled cyclohexanethione both show the same peak at 19.8 kc. cm^{-1}. Even if the aforementioned difficulties made a comparison at higher wavenumbers rather doubtful, it is striking that the high absorption maximum was found at 44.3 kc. cm^{-1} ($\log \varepsilon_{max} = 3.74$) for the sample of cyclohexanethione and at 44.6 kc. cm^{-1} ($\log \varepsilon_{max} = 3.91$)

for the photolysis products. In calculating ε_{max} for the sample of cyclohexanethione it was assumed that the substance was pure. According to Sen [14], a freshly distilled sample of cyclohexanethione holds only 62 % of thione-form, the rest being the enethiol isomer. If this is accounted for, the recalculated ε_{max}-value becomes 3.95. The excellent agreement may be fortuitous but strengthens the almost obvious conclusion that the cyclohexanethione found during photolysis cannot protomerize in the matrix. The spectrum extrapolated from the kinetic measurements must therefore be due to pure thione-form together with cyclohexanethiol. The molar extinction of thiol at 44—45 kc. cm^{-1} is in any case less than 3 % of that of the thione and thus the mercaptan does not interfere significantly with the calculation.

After photolysis of a primary or secondary disulfide it has quite generally been found that, after warm-up, the transmission increases at wavenumbers above about 41 kc. cm^{-1} (Fig. 9) and decreases in the range 41—36 kc. cm^{-1} (Fig. 5). This change can best be explained by referring to the trimerization of the thial or thione formed during photolysis *. The trimeric ethanethial has a spectrum with a peak at 41.9 kc. cm^{-1}. The spectrum of the monomer, on the other hand, has a broad maximum extending below 38 kc. cm^{-1} with the doublepeaks at 45.4 and 48.5 kc. cm^{-1} (room temperature, absorption curve corrected for the presence of ethanethiol and remaining disulfide). If the absorption curves are plotted on the same diagram for a molar ratio of monomer to trimer equal to 3:1, the curves intersect at 40.5 kc. cm^{-1} with an estimated error of less than 0.5 kc. cm^{-1}. Thus, if a set of absorption curves were recorded from time to time during the trimerization reaction, an isosbestic point should be found at the intersection wavenumber. From the experiment a value of 40.5 kc. cm^{-1} was found.

As a whole the facts are strongly in favour of the suggested reaction. From a mechanistic point of view the most simple explanation ** would be that the primary step upon excitation is a symmetrical homolytic splitting of the disulfide molecule into two identical thiyl radicals. The subsequent reaction is governed by the close contact between the fragments. Owing to the cage effect [28], the radicals cannot diffuse into the hydrocarbon matrix and have to react either with each other or with matrix molecules. Apparently the α-hydrogen abstraction is the most favoured reaction.

The photolysis of dimethyl disulfide (Fig. 11) initially showed the same characteristics as the other primary disulfides studied, especially at low concentrations. The increase in absorption above 43.3 kc. cm^{-1} with a peak at 48.1 kc. cm^{-1} indicated the formation of monomeric thioformaldehyde. Upon prolonged irradiation, however, presumably secondary photolysis reactions occurred, leading to the formation of several products, one of which could be identified as CS with a double peak at 38.18 and 39.20 kc. cm^{-1}. Carbon monosulfide obtained by photolysis from CS_2 showed the CS double-peaks at 38.16 and 39.20 kc. cm^{-1} under otherwise identical conditions [9]. The reaction

* At an early stage of the present investigation the increase in absorption between 41—36 kc.cm^{-1} was taken as an indication of a recombination reaction leading to an increase in the amount of disulfide present in the solution; *cf.* Ref.[27]

** Owing to the presented experimental facts, an intramolecular rearrangement mechanism with a four-membered ring structure in the transition state can not be excluded.

mechanism is unknown and further experimental studies must be made before an elucidation can be proposed.

Acknowledgements. The technical assistance of Miss S. Kristoffersson and Miss I. Persson is gratefully acknowledged. This investigation has been supported by *Directorate of Chemical Science*, AFOSR, AFRD of the Air Research and Development Command, United States Air Force, through its European Office, and by the *Swedish Technical Research Council.*

REFERENCES

1. Bateman, L., Moore, C. G. and Porter, M. *J. Chem. Soc.* **1958** 2866.
2. Parker, A. J. and Kharasch, N. *Chem. Rev.* **59** (1959) 583.
3. Lewis, G. N. and Lipkin, D. *J. Am. Chem. Soc.* **64** (1942) 2801.
4. Barltrop, J. A., Hayes, P. M. and Calvin, M. *J. Am. Chem. Soc.* **76** (1954) 4348.
5. Michaelsen, J. D. *Dissertation*, Catholic University, Washington, D. C. 1955.
6. Norman, I. and Porter, G. *Proc. Roy. Soc. London* **A 230** (1955) 399.
7. Porter, G. and Strachan, E. *Spectrochim. Acta* **12** (1958) 299.
8. Porter, G. and Strachan, E. *Trans. Faraday Soc.* **54** (1958) 1595.
9. Rosengren, Kj., Sunner, S. and Timm, D. *Acta Chem. Scand.* **16** (1962) 495.
10. Rosengren, Kj., Sunner, S. and Timm, D. *Acta Chem. Scand.* **16** (1962) 467.
11. Passerini, R. and Ross, I. G. *J. Sci. Instr.* **30** (1953) 274.
12. Vogel, A. I. *A Text-book of Practical Organic Chemistry.* 3rd Ed. Longmans, Green and Co., London 1956.
13. Bordwell, F. G., Pitt, B. M. and Knell, M. *J. Am. Chem. Soc.* **73** (1951) 5004.
14. Sen, D. C. *J. Indian Chem. Soc.* **13** (1936) 268.
15. Houben-Weyl *Methoden der organischen Chemie.* 4. Aufl. Georg Thieme, Stuttgart. Band IX, p. 700.
16. Rosengren, Kj. *Acta Chem. Scand.* **16** (1962) 1421.
17. Rosengren, Kj. and Sunner, S. *Acta Chem. Scand.* **16** (1962) 521.
18. Haraldson, L., Olander, C. J., Sunner, S. and Varde, E. *Acta Chem. Scand.* **14** (1960) 1509.
19. Koch, H. P. *J. Chem. Soc.* **1949** 394.
20. Rosengren, Kj. *Acta Chem. Scand.* **16** (1962) 1418.
21. Sen, D. C. *J. Indian Chem. Soc.* **14** (1937) 214.
22. Janssen, M. J. *Rec. trav. chim.* **79** (1960) 464.
23. Fehnel, E. A. and Carmack, M. *J. Am. Chem. Soc.* **71** (1949) 84.
24. Gray, P. and Williams, A. *Chem. Rev.* **59** (1959) 239.
25. Coope, J. A. R. and Bryce, W. A. *Can. J. Chem.* **32** (1954) 768.
26. Walling, C. and Rabinowitz, R. *J. Am. Chem. Soc.* **81** (1959) 1137.
27. Rosengren, Kj., Sunner, S. and Timm, D. *U. S. Dept. Com., Office Tech. Serv., PB Rept.* 145, 677 (1959); *Chem. Abstr.* **55** (1961) 21763 f.
28. Franck, J. and Rabinowitsch, E. *Trans. Faraday Soc.* **30** (1934) 120.
29. Rosengren, Kj. *Acta Chem. Scand.* **16** (1962). *In press.*

Received February 6, 1962.

ACTA CHEMICA SCANDINAVICA 16 (1962) 1418–1420

The Photolysis of Alkanethiols in a Rigid Glass at 77° K with the Possible Formation of Thiyl Radicals

KJ. ROSENGREN*

*Thermochemistry Laboratory***, *University of Lund, Lund, Sweden*

The photolysis of ethanethiol, 2-propanethiol and 1-butanethiol in an organic matrix at 77°K leads to the formation of a rather sharp and fairly stable absorption peak at about 25 kc. cm^{-1}. After warm-up to room temperature, considerable quantities of disulfide were found in the solution. From this and additional experimental evidence, it is concluded that this peak best can be assigned to the thiyl radical.

It has been repeatedly suggested that UV-irradiation of a disulfide leads to the formation of intermediate thiyl radicals (for the literature see, *e.g.*, Ref. [1]). In an attempt to trap thiyl radicals by photolysis in an organic matrix at liquid nitrogen temperature it has been demonstrated that no such trapping occurred as could be detected by UV-spectrophotometry [1]. As an explanation it has been suggested that the negative result is due to the cage-effect (Ref. [2], p. 95) that is, the excited thiyl radicals formed in the initial chemical process were unable to separate and therefore reacted according to

$$R_1R_2CHSSCHR_1R_2 \rightarrow R_1R_2CS + HSCHR_1R_2$$

where R = H or Alk.

Porter *et al.* [3,4] have reported the successful trapping of a number of radical species by the photolysis reaction $RXH \rightarrow RX\cdot + H$ utilizing the fact that hydrogen atoms easily diffuse through the organic matrix even at 77°K. Consequently, photolysis of an alkane thiol might lead to the desired result — formation of a thiyl radical.

RESULTS

The apparatus and technique used have been described elsewhere [5,6]. Ethanethiol, 2-propanethiol and 1-butanethiol, all of satisfactory purity as judged from GLC, were used in the experiments. Isopentane and 3-methyl

* Research Fellow at the *Swedish Technical Research Council.*

** Sponsored by the *Swedish Natural Science Research Council* and by the *Swedish Technical Research Council.*

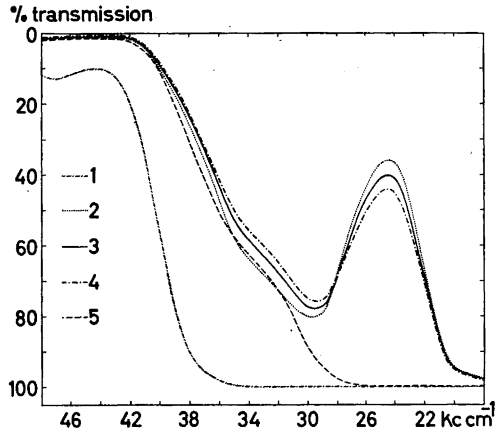

Fig. 1. Photolysis of *n*-BuSH in the matrix. (1) before photolysis at 77°K, (2) immediately after 10 min of photolysis, (3) 30 and (4) 60 min after the end of photolysis. (5) at 298°K.

pentane, 6:1, were used as a matrix-forming mixture. The primary and secondary mercaptans exhibit a weak UV-absorption (ε *ca.* 150) at 43 kc. cm^{-1}; for 0.05 and 5 mM solution the transmission is 100 % below 40 and 34 kc. cm^{-1}, respectively. In the paper cited [1], control photolyses were performed on 0.4 mM 1-butanethiol using WG7 filters. The main change in spectrum during photolysis was a pronounced *increase* in transmission between 50 and 46 kc. cm^{-1}. However, when the photolysis was carried out on 5 mM solutions, all other conditions being equal, the results were as given in Fig. 1. Curve 1 shows the spectrum at 77°K before photolysis. Curve 2 was recorded immediately after 10 min of irradiation. When the sample cell was left at 77°K, curves 3 and 4 were recorded after 30 and 60 min, respectively.

The decrease of the 24.6 kc. cm^{-1} peak is evident as is the formation of an isosbestic point at 28 kc. cm^{-1}. When the irradiation was prolonged no further increase of the peak occurred, probably because the increase in ultraviolet absorption above 30 kc. cm^{-1} prevented further photolysis of the mercaptan molecules.

When the cells were lifted up from the liquid nitrogen an uneven distribution of the yellow color (24.6 kc. cm^{-1} peak) was observed, the layers near the windows being most strongly colored. The color disappeared when the cell content lost its rigidity and no traces of the peak could be seen at room temperature (curve 5); nor did it appear again when the sample was cooled in liquid nitrogen for a second time. Similar experiments performed with ethanethiol and 2-propanethiol gave analogous results, the absorption peak occurring at 25.6 and 24.8 kc. cm^{-1}, respectively.

The following experiment was performed to show the existence of thiyl radicals in the photolyzed glass. A 5 mM ethanethiol solution photolyzed at 77°K was evaporated slightly above room temperature under a stream of nitrogen. An equal amount of the unphotolyzed solution was treated in exactly

the same way. After the solution had been reduced to about a hundredth of the initial volume, samples were withdrawn, put on the gas chromatograph and analyzed for ethyl disulfide. The photolyzed sample gave a large disulfide peak, whereas it was totally absent in the control experiment.

DISCUSSION

The experimental results strongly indicate that the 24.6 kc. cm^{-1} peak should be assigned to the butylthiyl radical. It is commonly supposed that larger molecular species do not migrate in the hydrocarbon glasses at 77°K (Ref. [2], p. 78) and moreover in the preceding paper it was shown that no mixed disulfide was formed at 77°K when a mixture of two alkyl disulfides was photolyzed. Therefore, it can safely be assumed that disulfide cannot be formed in considerable amounts at 77°K by photolysis of a mercaptan. The correspondence between the irreversible disappearance of the 24.6 kc. cm^{-1} peak during warm-up and the simultaneous formation of disulfide lead to the natural conclusion that thiyl radicals were present at 77°K and to the assignment of the 24.6 kc. cm^{-1} peak. The slow decrease of the peak at 77°K must be caused by an unknown reaction. The position of the isosbestic point, at 28 kc. cm^{-1}, conclusively rules out both recombination reactions $2RS\cdot \rightarrow R_2S_2$ and $RS\cdot + H \rightarrow RSH$. Neither the disulfide nor the mercaptan exhibit any absorption at this low wavenumber.

The splitting of the mercaptan leads to the formation of hydrogen atoms. It has been shown that hydrogenation of the glass-forming isopentane — 3-methyl pentane mixtures used in this laboratory lead to a minor significant decrease in light absorption at wavenumbers around 48 kc. cm^{-1} [7]. This may be explained by assuming that minute quantities of unsaturated compounds were present as impurities. In this connection, it is of interest to quote Potts [8], who pointed out that isopentane on standing develops an absorption at 48 to 49 kc. cm^{-1}. It is suggestive to ascribe the decrease in absorption found during the photolysis of the mercaptans in the 50—46 kc. cm^{-1} region to a hydrogenation of olefinic impurities by the hydrogen atoms liberated in the proposed reaction.

Acknowledgements. This investigation has been supported by *Directorate of Chemical Science*, AFOSR, AFRD of the Air Research and Development Command, United States Air Force, through its European Office and by the *Swedish Technical Research Council.*

REFERENCES

1. Rosengren, Kj. *Acta Chem. Scand.* **16** (1962) 1401.
2. Bass, A. M. and Broida, H. P. *Formation and Trapping of Free Radicals.* Academic Press, New York and London 1960.
3. Norman, I. and Porter, G. *Proc. Roy. Soc. London* **A 230** (1955) 399.
4. Porter, G. and Strachan, E. *Trans. Faraday Soc.* **54** (1958) 1595.
5. Rosengren, Kj., Sunner, S. and Timm, D. *Acta Chem. Scand.* **16** (1962) 495.
6. Rosengren, Kj., Sunner, S. and Timm, D. *Acta Chem. Scand.* **16** (1962) 467.
7. Timm, D. *Acta Chem. Scand.* **16** (1962) 1455.
8. Potts, W. J. *J. Chem. Phys.* **20** (1952) 809.

Received February 6, 1962.

ACTA CHEMICA SCANDINAVICA 16 (1962) 1421–1425

A Study on Contraction, Relative Viscosity and Melting Curves of Some Glass-forming Hydrocarbon Mixtures

KJ. ROSENGREN*

Thermochemistry Laboratory **, *University of Lund, Lund, Sweden*

The contraction, relative viscosity and melting curves have been studied for a number of hydrocarbon mixtures that form glassy states upon freezing at 77°K. The commonly used isopentane — 3-methyl pentane glasses as well as three new mixtures have been studied.

During the course of an investigation of the photolysis of organic substances in a rigid matrix at liquid nitrogen temperature it was felt desirable to study, quantitatively, the following properties of the different glass-forming mixtures: the specific volume ratio between 298° and 77°K, the rigidity of the matrix as a function of temperature, and the melting behaviour of the matrix. The contraction of the mixture must be known in order to convert concentration values from room temperature to 77°K. The viscosity of the matrix has a marked influence upon the photolysis path [1, 2] but has, so far, not been quantitatively estimated as a function of temperature. Finally, the heating curve of a particular matrix mixture reveals the possible existence of microcrystalline structures in the glass at 77°K or the formation of crystals during warm-up.

The following glass-forming mixtures have been studied (volume ratios are given):

3-Methyl pentane (pure) [1]
Isopentane — 3-methyl pentane (6:1) [3]
Isopentane — 3-methyl pentane (2:3) [1]
Pentane — neo-hexane (3:8) [4]
3-Methyl pentane — methyl cyclohexane (1:2) [4]
3-Methyl pentane — methyl cyclohexane (1:6) [4]

MATERIALS

All hydrocarbons were Phillips Petroleum Company "pure" grade hydrocarbons, except isopentane and 3-methyl pentane, which were "technical" grade samples from the

* Research Fellow at the *Swedish Technical Research Council.*

** Sponsored by the *Swedish Natural Science Research Council* and by the *Swedish Technical Research Council.*

same company. They were all purified by a routine method, which, in principle, is described in the literature [5].

After the hydrocarbon (about 2 l) had been treated with concentrated sulphuric acid for 5 h, it was neutralized, washed with water and dried over night with "Drierite". The liquid was refluxed over sodium wire, transferred to a still pot, freshly prepared sodium wire was added and the sample was carefully distilled in a 35 plate all glass column packed with Fenske helices; reflux ratio 1:30, 150—200 ml being collected every 24 h. From these fractions samples were withdrawn and analyzed on a gas chromatograph (Pye Argon Chromatograph Type 12000) with dioctyl phthalate as stationary phase. For pentane and neo-hexane all fractions which contained more than 0.05 % impurities were discarded, for cyclohexane the corresponding figure was 0.1 %. *i*-Pentane was allowed to contain max. 0.5 % pentane and for 3-methyl pentane max. 1 % 2-methyl pentane was allowed.

Samples from those fractions which passed the gas chromatographic analysis were tested for ultraviolet transmission below 50 kc. cm^{-1} in a spectrophotometer (Beckman DU equipped with a photomultiplier), and fractions exhibiting a transmission appreciable lower than the pure compound were recycled.

The pure fractions were brought together and allowed to pass a glass column (60 × 2.5 cm) packed with Davidson No. 200 mesh silica gel. The silica gel had been activated in the tube at 350°C. In order to remove the last traces of water, the silica gel tube was evacuated to 1 mm of Hg at 350° and then allowed to cool in vacuum. After the silica gel treatment the ultraviolet transmission was checked again. It was found that a second treatment with fresh silica gel did not improve the spectrum. During all manipulations every precaution was taken to prevent moisture from entering the liquids.

CONTRACTION

Precise quantitative measurements of the contraction which occurs when organic matrix solutions are cooled in liquid nitrogen have been reported for a few hydrocarbons, mainly mixtures of isopentane and methyl cyclohexane [6]. Average values given elsewhere are said to be valid for several different mixtures [1, 3].

A pear-shaped flask (27 ml) was melted on to a 10 ml precision burette equipped with a standard joint. A movable electrical heater, length 5 cm, was wound around the burette and the apparatus was accurately calibrated by weighing. When the hydrocarbon mixture had been poured into the apparatus, the system was out-gassed and closed by means of a stop-cock attached to the burette by means of a standard joint. The volume of the liquid was measured at 293°K in a thermostat and the apparatus was then transferred to a Dewar vessel with liquid nitrogen where it was cooled very slowly. The heater was used to avoid the formation of a deep meniscus in the narrow burette tube. When the volume measurements were made, all portions of the hydrocarbon solutions were in the liquid nitrogen. All mixtures were repeatedly cycled between room temperature and liquid nitrogen, and the measurements were repeated with a second apparatus. The results are given in Table 1.

Table 1. Ratio of specific volume at 77°K and 293°K. The uncertainties are expressed as mean deviations.

Hydrocarbons	$V_{77°K}/V_{293°K}$
Isopentane — 3-methyl pentane (6:1)	0.7605 ± 0.0004
Isopentane — 3-methyl pentane (2:3)	0.7713 ± 0.0004
3-methyl pentane (pure)	0.7845 ± 0.0006
Pentane — neo-hexane (3:8)	0.7694 ± 0.0005

RELATIVE VISCOSITY

The rigidity of a number of hydrocarbon mixtures has been reported in very general terms [1, 3, 7]. Quantitative viscosity comparisons between different mixtures have not been performed as judged from what has been published. A study was therefore undertaken to compare the temperature ranges in which different mixtures start to become fluid. The velocity of fall of a ball-shaped body was taken as a measure of the viscosity.

A cylindrically shaped copper block wound with a heating wire (8 × 5 cm) was placed in the bottom of a Dewar vessel (45 × 5.6 cm); it was thermally insulated from the inner wall of the Dewar by means of thin cork rings. Two holes, both 6 cm deep, were drilled in the block, one centrally, diameter 1.7 cm, the second, diameter 0.6 cm, close to the first one. A small third hole near the edge of the block carried a glass tube from the outside of the Dewar to its bottom. A cylindrical glass vessel (diam. 1.6 cm) provided with a 40 cm long stem (diam. 0.8 cm) could be inserted in the central hole, and a brass ring fastened to the stem served as a lid for the central cavity. Inside the stem a thin rod (35 × 0.3 cm) made from balsa wood could be moved up and down; it was guided by two small rings of steel placed 25 cm apart on the rod. The lower end of the rod was provided with a stainless steel ball (diam. 0.632 cm), the total weight of the movable part being 2.85 g. The temperature inside the copper block could be measured by means of a platinum resistance thermometer (Type Hereaus BS5) placed in the 0.6 cm hole. The dimensions of the coil were 1.2 × 0.5 cm and its resistance at 273°K was 100 Ω. The thermometer was used in connection with a Mueller G 1 bridge (Type Rubicon 1551), and it was calibrated in liquid oxygen, solid carbon dioxide, ice-water and steam.

The hydrocarbon mixture was poured into the glass vessel until it nearly reached the stem. The falling body was inserted and kept in the upper part of the stem by means of a small magnet outside the tube. The liquid was outgassed and the vessel was closed with a stop-cock attached to the stem by means of a standard joint. Liquid nitrogen was poured into the Dewar until the copper block was surrounded with the liquid, while the glass tube with the hydrocarbons was slowly pre-cooled in another Dewar. Great care was taken to prevent the surface of the glassy mixture from forming a deep meniscus.

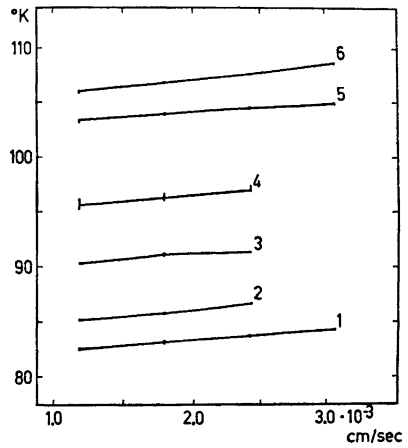

Fig. 1. Relative viscosity for different matrices. (1) *i*-pentane — 3-methyl pentane 6:1, (2) pentane — neo-hexane 3:8, (3) *i*-pentane — 3-methyl pentane 2:3, (4) pure 3-methyl pentane, (5) 3-methyl pentane — methyl cyclohexane 1:2 and (6) 3-methyl pentane — methyl cyclohexane 1:6.

The hydrocarbon mixture was placed in the copper block and allowed to reach liquid nitrogen temperature. The nitrogen was sucked off and the magnet was removed so that the stainless steel ball rested on the hard upper surface of the glass. When the heater was turned on, 1 watt produced a temperature increase of 0.2° per min. The position of the upper end of the balsa rod was measured and, together with the temperature, plotted against time. When the glass softened, the balsa rod started to move at a rate that was directly found from the plotted curve. Obviously, the slope of the curve represents the velocity of fall. Temperatures corresponding to slopes of 10°, 15°, 20° and 25° were evaluated. At least three independent runs were made for each hydrocarbon mixture. The surprisingly good reproducibility is shown in Fig. 1, in which the temperature is plotted against the velocity of fall for a number of hydrocarbons. The vertical extent of the markings represents the maximum deviation between various runs. A few experiments where the temperature rise was 1° per min gave exactly the same result.

According to Stokes Law the viscosity is a linear function of the velocity of fall. Although in this case the contact surface between the falling body and the substance is not constant during a run, the experiment can be used to arrange the hydrocarbon glasses in order of increasing rigidity (Fig. 1). It is of interest to note that the glasses numbered 5 and 6 are of higher viscosity than 3-methyl pentane. Both are mixtures of methyl cyclohexane and 3-methyl pentane, 2:1 and 6:1, respectively, and have not been used previously. However, they tend to crack when stored for several hours at 77°K, which somewhat limits their use.

MELTING CURVES

If the spectral behaviour of a matrix containing trapped unstable species is to be studied as a function of temperature, it is of importance that the specific heat in the melting region does not show any abrupt change. Therefore, the mixtures previously described were studied in a simple specific heat calorimeter.

A cylindrical glass vessel, diam. 3 cm, of 45 ml volume was equipped with an interior heater consisting of a manganin wire wound on a piece of glass tubing, that had been concentrically sealed into the vessel. The vessel was provided with a long stem through which a Heraeus BS5 platinum resistance thermometer could be inserted. The stem was equipped with five circular, highly polished, thin copper discs, equally spaced, serving as heat shields. The vessel fitted into a long, narrow glass Dewar.

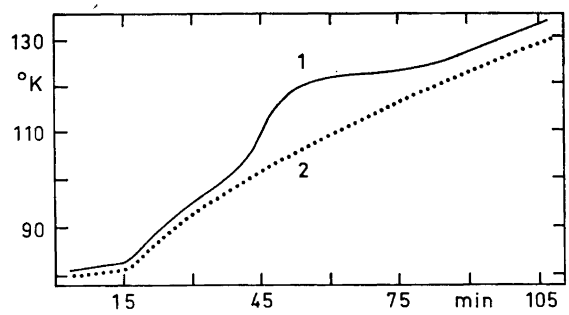

Fig. 2. Melting curves for (1) pentane — neo-hexane 3:8 and (2) isopentane — 3-methyl pentane 6:1.

The glass vessel was filled with the hydrocarbon mixture, the thermometer was inserted and the apparatus was outgassed and closed. The hydrocarbon mixture was cooled to 77°K in the Dewar and when this temperature was reached, the liquid nitrogen was removed. The system was then allowed to attain thermal equilibrium, a steady increase in temperature of about 0.1° per min was reached within 15 min. When 0.5 watt was supplied through the heater, the temperature increased at a rate of about 1° per min (Fig. 2). Although the resistance of the heating wire changed, the power was supplied at a constant rate by means of a circuit described elsewhere [8].

3-Methyl pentane (pure) and isopentane — 3-methyl pentane (6:1 and 2:3) showed an evenly increasing specific heat according to curve 2. Curve 1 represents a typical rum with pentane — neo-hexane (3:8). At about 100°K crystallization started and the crystals melted at 121.9—122.2°K. Beyond 122°, the curve was found to be a direct extension of the curve below 100°K. The same eutecticum was found with varying composition of the glass and it represents neither of the pure components (pentane m.p. 141.7, neo-hexane m.p. 175.0°K). The practical use of the mixture as a matrix is by no means disturbed by the crystallization, which starts at a temperature well above the melting region. Furthermore, crystallization has never been observed during freezing.

The very smooth curves obtained for the isopentane — 3-methyl pentane glasses studied conclusively prove the absence of a microcrystalline structure, which might undergo phase transformation below 150°K.

Acknowledgements. The technical assistance of Miss I. Persson is gratefully acknowledged. This investigation has been supported by *Directorate of Chemical Science*, AFOSR, AFRD of the Air Research and Development Command, United States Air Force, through its European Office, by *Magn. Bergvalls Stiftelse* and by *Knut and Alice Wallenbergs Stiftelse.*

REFERENCES

1. Norman, I. and Porter, G. *Proc. Roy. Soc. London* **A 230** (1955) 399.
2. Timm, D. *Acta Chem. Scand.* **16** (1962) 1455.
3. Potts, W. J. *J. Chem. Phys.* **21** (1953) 191.
4. Rosengren, Kj. and Sunner, S. *Acta Chem. Scand.* **16** (1962) 521.
5. Potts, W. J. *J. Chem. Phys.* **20** (1952) 809.
6. Passerini, R. and Ross, I. G. *J. Sci. Instr.* **30** (1953) 274.
7. Sowden, R. G. and Davidson, N. *J. Am. Chem. Soc.* **78** (1956) 1291.
8. Rosengren, Kj. *Rev. Sci. Instr.* **32** (1961) 1264.

Received February 6, 1962.

ACTA CHEMICA SCANDINAVICA 16 (1962) 1426–1432

Kinetic Study of the Reaction between Phosphonium Compounds and Hydroxyl respectively Alkoxide Ions

GUNNAR AKSNES and JON SONGSTAD

Chemical Institute, University of Bergen, Bergen, Norway

The alkaline decomposition of quaternary phosphonium compounds in different water-alcohol mixtures was found to obey third or second order kinetics dependent on the stability of the leaving negatively charged organic group. Thus, tetraphenyl and triphenylbenzyl phosphonium hydroxides were decomposed according to third order kinetics, first order dependence on the concentration of phosphonium ions and second order on the hydroxyl ions. This is in agreement with the observations of McEwen and co-workers [1]. However, the decomposition of triphenyl-*p*-nitrobenzyl phosphonium hydroxide followed second order kinetics, first order dependence on the concentration of phosphonium ions and first order on the hydroxyl ions. The difference in order is assumed to be due to a greater instability of the pentacovalent intermediate formed when *p*-nitrobenzyl is the leaving group as compared with the intermediates formed from tetraphenyl respectively triphenylbenzyl phosphonium compounds where phenyl respectively benzyl are the leaving groups.

It is shown that the decomposition of tetraphenyl and triphenylbenzyl phosphonium alkoxides obey third order kinetics. However, the dependence of the rate of hydrolysis upon alcohol concentration in the reaction solution, (plot of log *k versus* $1/D$) shows that the rate determining step must be different for the hydroxide and alkoxide reactions. The mechanisms of the decomposition of phosphonium compounds by hydroxide as well as alkoxide ions are discussed.

Ingold and co-workers [2] have postulated that the alkaline decomposition of quaternary phosphonium compounds proceeds through a pentacovalent (trigonal bipyramidal) transition state:

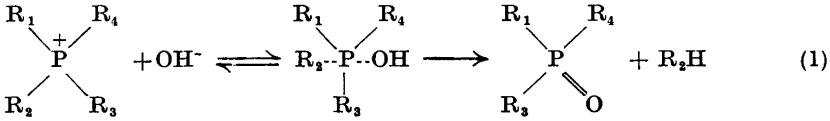

(1)

McEwen and co-workers [1] and Hoffman [7] observed that phosphonium compounds containing benzyl or substituted benzyl groups were decomposed by hydroxyl ions according to third order kinetics, first order dependence on

hydroxyl ion concentration. The benzyl or the substituted benzylgroups were split off as toluene respectively substituted toluenes. The authors explained the decomposition according to the following reaction scheme (tetrabenzyl phosphonium hydroxide as example):

$$\begin{array}{l} \overset{+}{P}(CH_2Ph)_4 + OH^- \overset{\text{fast}}{\rightleftharpoons} HO{\cdot}P(CH_2{\cdot}Ph)_4 + OH^- \overset{\text{fast}}{\rightleftharpoons} \\ H_2O + {}^-O{-}P(CH_2Ph)_4 \overset{\text{slow}}{\longrightarrow} O{=}P(CH_2{\cdot}Ph)_3 + PhCH_2^- \\ \qquad\qquad\qquad\qquad\qquad\qquad\qquad\qquad\qquad\qquad \text{fast} \downarrow H_2O \\ \qquad\qquad\qquad\qquad\qquad\qquad\qquad\qquad\qquad\qquad PhCH_3 + OH^- \end{array} \qquad \text{(II)}$$

Since it is known that phosphonium compounds containing benzyl or substituted benzyl groups very easily form the corresponding phosphoranes in strongly alkaline solution [3], there seemed to exist the possibility that the third order kinetics observed for the alkaline decomposition of benzyl-containing phosphonium compounds might be due to the formation of a phosphorane as an intermediate compound which in turn might be attacked by hydroxyl ions and water to give a pentacovalent transition state:

$$\begin{array}{l} \overset{+}{P}(CH_2Ph)_4 + OH^- \rightleftharpoons (PhCH_2)_3P{=}CH{\cdot}Ph + OH^- \overset{H_2O}{\rightleftharpoons} \\ \qquad\qquad\qquad\qquad\qquad\qquad\qquad\qquad\qquad\

on this question we have studied the alkaline decomposition of tetraphenyl, triphenylbenzyl and triphenyl-*p*-nitrobenzyl phosphonium compounds, in different water-alcohol mixtures. The chief differences between the three phosphonium ions are that benzyl- respectively *p*-nitrobenzyl-containing phosphonium cations easily form phosphoranes in alkaline solution whereas this is not the case with tetraphenyl phosphonium ions. It seems therefore safe to conclude that the only reasonable way in which the tetraphenyl phosphonium cation is attacked by hydroxyl ions is through a direct attack of the hydroxyl ion on the phosphorus atom forming a pentacovalent intermediate or transition state. If the tetraphenyl phosphonium ions are decomposed according to third order kinetics, the formation of a pentacovalent intermediate the decomposition of which is rate determining, appears to be the only reasonable explanation.

EXPERIMENTAL

Tetraphenyl phosphonium bromide was synthesized according to descriptions by Dodonow and Medox [4]. (Found: Br 17.50; 17.65. Calc. for $C_{24}H_{20}PBr,2H_2O$: Br 17.58.)

Triphenylbenzyl phosphonium chloride was made by heating a mixture of equivalent amounts of triphenyl phosphine and benzyl chloride to 120°C for one hour. The crystalline product was recrystallized two times from alcohol-ether mixture. (Found: Cl 9.16; 9.21. Calc for $C_{25}H_{22}PCl$: Cl 9.12.)

*Triphenyl-*p*-nitrobenzyl phosphonium chloride* was synthesized in the same way as the benzyl derivative. The compound was recrystallized two times from alcohol-ether mixture. (Found: Cl 8.16; 8.08. Calc. for $C_{25}H_{20}O_2N$ PCl: Cl 8.17.)

Kinetic measurements. The reactions between tetraphenyl and triphenylbenzyl phosphonium halogenides and sodium hydroxide were performed with equivalent amounts of both reactants. The course of reaction was followed by titration of the unreacted hydroxyl ions after fixed intervals of time. The reactions were normally followed until approximately 70 % hydrolysis. However, in the cases where the hydrolysis were studied below 50 % (by volume) of alcohol in the alcohol-water mixture, the rate constants were calculated from the data below 30 % hydrolysis. This was done in order to avoid precipitation of triphenyl phosphine oxide which was found to accelerate greatly the rate of hydrolysis.

The determination of the rate of reaction between triphenyl-*p*-nitrobenzyl phosphonium chloride and hydroxyl ions was performed with the Radiometer Titrator (T.T.T.I.C.) at pH 10.00, 10.30 and 10.60. The phosphonium compound was always in so great excess that the reaction showed zero order rate dependence with respect to this reactant.

RESULTS AND DISCUSSION

In Fig. 1 are recorded two typical runs for the alkaline decomposition of tetraphenyl and triphenylbenzyl phosphonium compounds where the initial concentrations of the reactants are identical. The third order constant is therefore: $k = \frac{1}{2t}\left(\frac{1}{C^2} - \frac{1}{C_o^2}\right)$ where t = time in min, C_0 = initial concentration of phosphonium cations respectively hydroxyl ions and C = concentration at time t. The data show clearly third order rate dependence in accordance with the observation of McEwen and co-workers [1] from their study of decomposition of tetrabenzyl phosphonium hydroxide. Since thus the alkaline decomposition of tetraphenyl phosphonium compounds shows second order rate dependence on the hydroxyl ions in the same way as the benzyl derivatives a mechanism according to reaction scheme III must be ruled out. In agreement

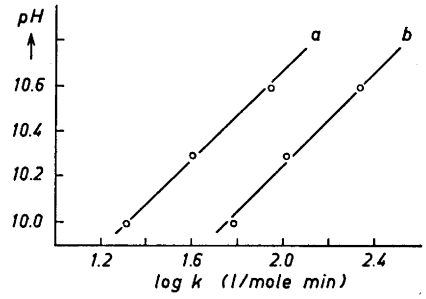

Fig. 2. Plot of log k against pH for the alkaline decomposition of triphenyl-*p*-nitrobenzyl phosphonium chloride, a) 21°C, b) 31°C.

with McEwen *et al.* we therefore conclude that the reaction between tetraphenyl respectively triphenylbenzyl phosphonium cations and hydroxyl ions involves the formation of a pentacovalent intermediate, the decomposition of which is rate determining for the hydrolysis.

However, the rate determining step is dependent on the substituents linked to phosphorus in the quaternary phosphonium compounds. In Fig. 2

Table 1. Rate constants and activation energies for the alkaline decomposition of tetraphenyl, triphenylbenzyl and triphenyl-*p*-nitrobenzyl phosphonium compounds in alcohol-water mixtures. In all experiments are used equivalent concentrations of hydroxyl ions, resp. alkoxide ions, and phosphonium salt (0.05140 N).

Compound	Volume percent alcohol in reaction solution	Rate constant ($l^2mole^{-2}min^{-1}$) 20°C	30°C	40°C	50°C	Activation energy E, kcal
Tetraphenyl phosphonium bromide	100	2.75	21.5	—	—	30.8
	95.6	5.28	30.6	—	—	31.0
	80	—	—	5.92	24.4	26.7
	50	—	—	0.184	0.695	26.7
	20	—	—	—	0.085	—
	0	—	—	—	0.04	—

Compound	Volume percent	Rate constant ($l^2mole^{-2}min^{-1}$) 25°C	35°C	E kcal
Triphenylbenzyl phosphonium chloride	100	17.8	56.0	21.0
	75	24.5	79.5	21.5
	50	4.25	11.2	18.0
	25		−3.6	
	12.5		−2.8	
	0		−0.6	

Compound	Volume percent	pH	Rate constant ($l\ mole^{-1}\ min^{-1}$) 21°C	31°C	E kcal (average)
Triphenyl-*p*-nitrobenzyl phosphonium chloride	50	10.00	20.8	61.8	
	50	10.30	20.3	56.0	18.0
	50	10.60	22.4	56.0	

is plotted log k against pH for the alkaline decomposition of triphenyl-*p*-nitrobenzyl phosphonium chloride at different fixed pH. The linear dependence shows that in this case the hydrolysis of the phosphonium compound is first order dependent on the hydroxyl ion concentration. We assume that the decomposition of the pentacovalent intermediate containing a *p*-nitrobenzyl group is sufficiently rapid to make the first step in reaction scheme II — the formation of the intermediate — rate determining.

By comparing the activation energies for the alkaline decomposition of the three compounds studied (Table 1) we find that there is a decrease of approximately 10 kcal from the tetraphenyl to the triphenylbenzyl phosphonium compound, in agreement with the easier formation of the negatively charged benzyl ion as compared with the phenyl ion. This observation is in accordance with the qualitative results of Ingold and co-workers [2] and Horner *et al.*[5] If the triphenyl-*p*-nitrobenzyl phosphonium compound followed the same kinetics as the tetraphenyl and triphenyl benzyl derivatives one would expect a strong decrease in the activation energy from the benzyl to the *p*-nitrobenzyl derivative due to the strong stabilizing effect of the *p*-nitro group on the benzyl anion. However, the activation energy remains approximately unchanged, which again points to a different kinetic course. The calculated activation energy, 18 kcal, for the decomposition of the *p*-nitrobenzyl compound must therefore be for the formation of the pentacovalent intermediate, whereas the activation energy for the decomposition of the intermediate is expected to lie several kcal lower.

It was observed that on reducing the alcohol content in the reaction solution below a critical value the triphenyl phosphine oxide formed during the reaction began to separate from the solution. The finely divided precipitate

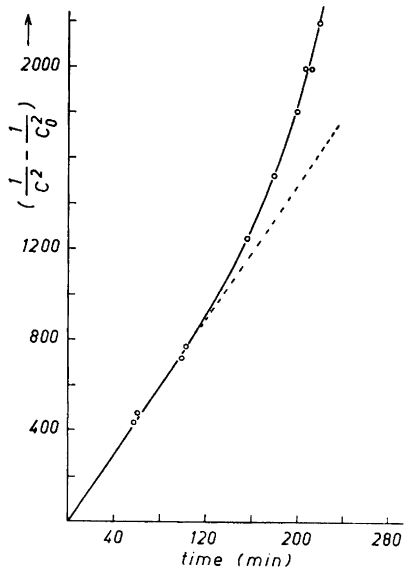

Fig. 3. Hydrolysis of triphenylbenzyl phosphonium hydroxide in 25 % alcohol-water mixture. Concentration 0.0520 M. Temperature 35°C.

of triphenyl phosphine oxide was found to accelerate the rate of hydrolysis. In Fig. 3 is shown a typical experiment for the decomposition of triphenylbenzyl phosphonium hydroxide in 25 % alcohol-water mixture (by volume). As long as the reaction solution keeps the formed phosphine oxide dissolved the rate follows third order kinetics. However, from the moment the separation of the phosphine oxide starts the rate of hydrolysis is greatly increased. We assume that the phosphonium compound is absorbed on the precipitated phosphine oxide thus producing a local high concentration of reactants. If now the reaction with hydroxyl ions take place with the absorbed phosphonium compound the acceleration of the hydrolysis is expected from purely kinetic reasons (*cf.* Hoffmann [7]).

The great increase in the rate of hydrolysis with increasing amount of alcohol in the reaction solution is in accordance with the solvent effect theory. For reactions between two ions the relation between the rate and the dielectric constant of the solution can be expressed in the following way [6]:

$$\ln k = \ln k_0' - \frac{N \cdot Z_A \cdot Z_B \cdot e^2}{DRT \cdot r^*}$$

where k = calculated rate constant, k_0' = rate constant in a medium of infinite dielectric constant, N = Avogadro's number, Z_A and Z_B are the charges of the two ions, e = electron charge, D = dielectric constant, R = gas constant, T = absolute temperature and r^* = distance between the ions in the activated complex. The equation predicts a linear plot of log k against

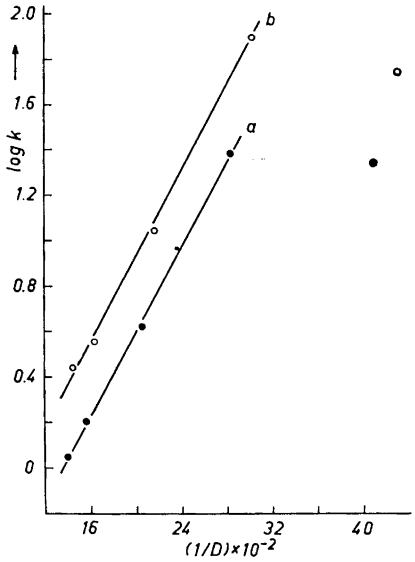

Fig. 4. Plot of log k against $1/D$ for the decomposition of triphenylbenzyl phosphonium hydroxide a) 25°C b) 35°C.

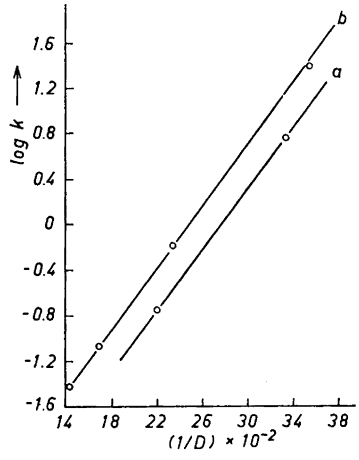

Fig. 5. Plot of log k against $1/D$ for the decomposition of tetraphenylphosphonium hydroxide a) 40°C b) 50°C.

$1/D$ with a positive slope when the charges of the ions are of opposite sign. In the case of the alkaline decomposition of phosphonium compounds the reaction between the two oppositely charged ions have the character of an equilibrium reaction; the observed rate constant includes the product of the different equilibrium constants and the rate constant of the rate determining step. However, the linear dependence between log k and $1/D$ should still be valid. In Fig. 4 and 5 is plotted log k against $1/D$ for the decomposition of triphenylbenzyl and tetraphenyl phosphonium hydroxides. We observe that the values of the rate constants up to 75—80 % alcohol obey the theoretical expression whereas the rates for 100 % alcohol (*i.e.* the rate in pure sodium ethoxide solution) lie far below the predicted values (Fig. 4). Although the rate constants in different alcohol-water mixtures may be influenced through spesific solvent effects, not accounted for in the theoretical equation, the observed drastic decrease in the rate in ethoxide solution can only be explained as due to a different reaction mechanism. In reaction scheme II the dissociation of the proton from the pentacovalent intermediate is formulated as a rapid equilibrium reaction; when the alkoxide ion is the reacting base a corresponding rapid equilibrium reaction is not possible, since there is no hydroxyl proton to dissociate. It seems reasonable to expect that step 2 of the following scheme, the nucleophilic reaction between an alkoxide ion and the alkyl group of the pentacovalent intermediate producing ether and a negatively charged intermediate will now be the rate determining step:

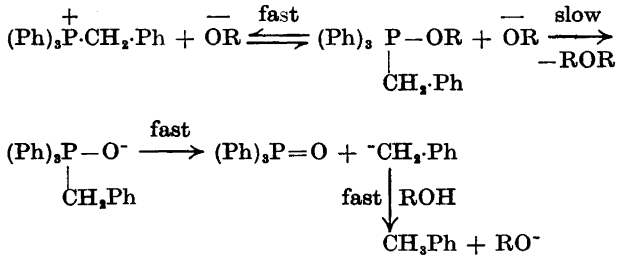

This scheme will still give third order rate dependence in accordance with the experimental data. However, the possibility that the second step consists of a nucleophilic attack of alkoxide ion directly on phosphorus in its pentacovalent state should not be overlooked.

Our sincere thanks are due to the *Norwegian Defence Research Establishment* for financial support.

REFERENCES

1. McEwen, W. E., Vander Werf, C. A. and Zander, M. *J. Am. Chem. Soc.* **81** (1959) 3806.
2. Fenton, G. W. and Ingold, C. K. *J. Chem. Soc.* **1929** 2342.
3. Grayson, M. and Keough, P. T. *J. Am. Chem. Soc.* **82** (1960) 3919.
4. Dodonow, J. and Medox, M. *Ber.* **61** (1928) 907.
5. Horner, L., Hoffman, H., Wippel, H. G. and Hassel, G. *Chem. Ber.* **91** (1958) 52.
6. Scatchard, G. *Chem. Revs.* **10** (1932) 229.
7. Hoffmann, H. *Ann.* **634** (1960) 1.

Received January 19, 1962.

ACTA CHEMICA SCANDINAVICA 16 (1962) 1433–1446

Studies on Metal Complexes in Aqueous Solution by Infrared Spectrophotometry

II. An Investigation on Some First-Row Transition Metal Thiocyanato Complexes

STURE FRONÆUS and RAGNAR LARSSON

Department of Inorganic and Physical Chemistry and Infrared Laboratory, Chemical Institute, University of Lund, Lund, Sweden

The frequency and intensity of the C—N vibration have been measured for the SCN^- ion and the first thiocyanato complex of some divalent first-row transition metals. The stability constants of these complexes have been determined. The data are reported in Table 5. Moreover, it has been found that for the complexes investigated the integrated absorption is constant and equal to that of the free ligand.

It has also been found that a linear relation exists between log β_1 and the frequency shift.

A detailed investigation has been made on the nickel system. The results are in good agreement with earlier determinations on the complex formation. There are some indications that part of the complexity of this system is due to outer-sphere coordination. ($\beta_{1\,in} = 12 \pm 2$ M^{-1}; $\beta_{1\,out} = 3 \pm 2$ M^{-1})

The thiocyanate ion, like the cyanide ion, exhibits a strong infrared absorption due to the stretching vibration of the carbon-nitrogen bond. It has been pointed out by Jones [1] that this fact might make possible examinations of thiocyanato complexes in aqueous solution analogous to the investigations on cyanide systems made by Jones and Penneman [2,3]. As many thiocyanate systems have been investigated in detail by conventional methods [4,5], such an undertaking could be rewarding.

We have accordingly performed infrared absorption measurements on some thiocyanate systems of the first-row transition metals. Our aim has been to verify the assignment of the absorption peaks to certain complexes by using the data for making a calculation of the stability constants of the complexes postulated.

EXPERIMENTAL

The spectrophotometer used was a Perkin-Elmer PE 221 with a grating monochromator. Cells with windows of calcium fluoride and with spacers of equally thick platinum foil were used in both the sample and the reference beam. The solution in the reference cell had a composition equal to that in the sample cell except for a certain amount of sodium perchlorate exchanged for sodium thiocyanate in the latter. In this way an almost complete compensation of the water absorption was obtained in the spectral region under investigation, $1900-2300$ cm^{-1}.

The instrument was operated with the "automatic gain control" characteristic of the model. The setting of the resolution knob was "940" corresponding to a mechanical slit opening of $307-283$ μ. The time for making a scan within the limits given above was about 10 min. As the "speed suppression" of the instrument was set at its maximum value, the greater part of this time was spent in the recording of the absorption peaks. With these arrangements absolute extinction coefficients could be obtained (*vide infra*).

The wave-number readings were checked by measuring the spectra of carbon monoxide in a 10 cm gas cell.

Chemicals used. Sodium thiocyanate of reagent quality was used to make a 3.00 M solution, the concentration of which was checked by Volhard-titration. Most of the metal salts were perchlorates, obtained by treating the corresponding carbonate or chloride with an excess of perchloric acid and recrystallizing the salt from water. From the perchlorates stock solutions were made by weighing; the concentrations were checked by colorimetric methods.

MEASUREMENTS

A. The free thiocyanate ion. In order to verify Beer's law and to test the performance of the apparatus measurements were made of the absorption of the free SCN^- ion in solutions of the composition C_A M NaSCN + $(3.00-C_A)$ M $NaClO_4$. The reference cell then contained 3.00 M $NaClO_4$ (*vide supra*). Two different sets of platinum spacers were used, the thicknesses of which were given by the manufacturer to be 8.8 μ and 20 μ, respectively.

The optical densities obtained are given graphically in Fig. 1. It is seen that straight lines are obtained. Furthermore, if extinction coefficients are calculated from the slopes of the lines using the thicknesses of the spacers given above we obtain the values 535 $M^{-1}cm^{-1}$ (8.8 μ) and 538 $M^{-1}cm^{-1}$ (20 μ). *Throughout this paper the mean value 537 $M^{-1}cm^{-1}$ will be used for the extinction coefficient of the free thiocyanate ion.*

It must be stressed that the good agreement of the two sets of measurements are in striking disagreement with the proposal of Jones and Penneman [2] that the real cell thickness should be considered to be greater than the thickness of the spacer. We noted that with solutions of very strong total absorption (NaSCN with 34 μ spacers) a curvature of the Beer-law plots was obtained, probably because too little energy was reaching the detector. The deviation from straight line appearance was such as to yield too small values of the extinction coefficient. It is also of interest that using the thinnest spacer and with no compensation in the reference beam a few years ago we obtained the value $\varepsilon = 540$ $M^{-1}cm^{-1}$ with a Hilger H 800 Spectrophotometer fitted with a sodium chloride prism and operated at its extreme capacity. Thus we can state that absolute extinction coefficients can be obtained with fair accuracy and that the slit width when properly set is not of critical importance for a good result. That this is so is quite obvious from the rules given by Ramsay [6].

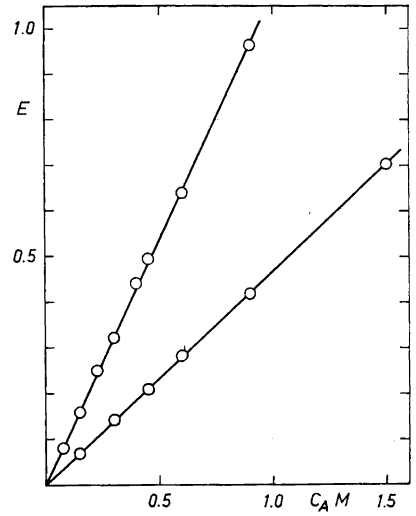

Fig. 1. Optical densities of solutions of NaSCN with a total salt concentration = 3 M. Upper line corresponds to 20.0 μ spacer, lower line to 8.8 μ spacer.

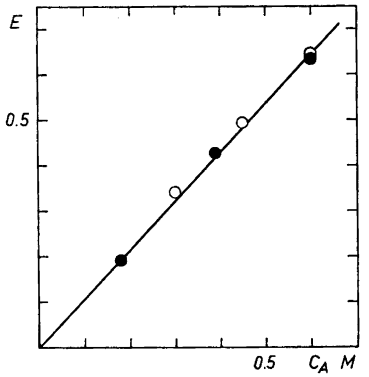

Fig. 2. Optical densities of solutions of NaSCN without extra salt addition (open dots) and with total salt concentration = 6 M (filled dots). Spacer: 20.0 μ. The line is the one drawn in Fig. 1.

The half-width of the absorption peak under discussion was found to be 37 ± 1 cm^{-1}.

The frequency of the SCN^--absorption was found to be 2066 cm^{-1} in good agreement with previously reported infrared [1,7] and Raman [8] data. Within the experimental error no change in the frequency was found as the thiocyanate concentration increased. In order to test the invariance of intensity and frequency of absorption with changing total electrolyte concentration some measurements were made on 6 M salt solutions and on solutions containing only NaSCN. The optical densities are given in Fig. 2 and show no systematic deviation; the frequency of the 6 M salt solutions was shifted to 2069 cm^{-1} whereas the other solutions showed the normal value 2066 cm^{-1}.

B. The metal-thiocyanate systems. In Figs. 3—4 are given representative examples of the spectra obtained.

Common to all the systems there is a new absorption peak at a frequency higher than that of the free thiocyanate ion. The most reasonable explanation is to assume that this peak corresponds to the metal complexes formed in solutions of indicated composition. That this is so will be evident from the following calculations.

In the case of the iron(II)-system some irregularities were observed. At high iron concentrations a decrease of the intensity of the 2099 cm^{-1} peak was observed relative to the peaks at moderate iron concentration. We suggest that in this case more than one iron-containing complex was formed, probably some polynuclear hydrolytic complex. This fact rendered a detailed analysis of the system impossible.

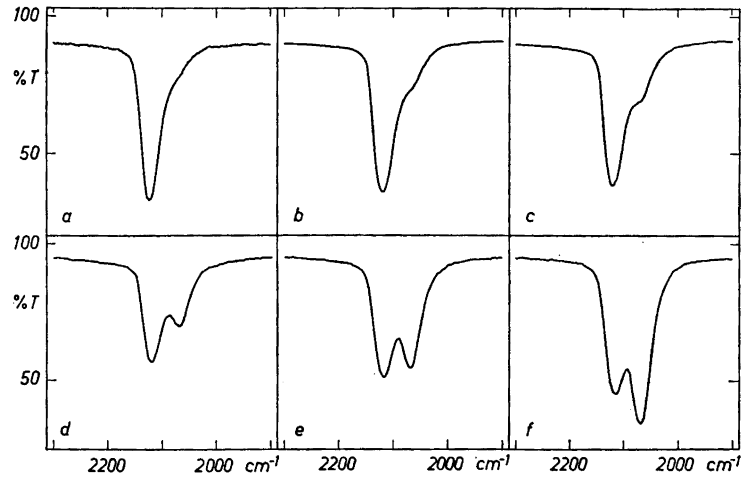

Fig. 3. The Ni^{2+}—SCN- system. Spacer: a.—c. 20.0 μ; d.—f. 8.8 μ.

a. C_M = 1.32 M; C_A = 0.36 M
b. C_M = 0.66 M; C_A = 0.36 M
c. C_M = 0.44 M; C_A = 0.36 M
d. C_M = 0.30 M; C_A = 0.60 M
e. C_M = 0.30 M; C_A = 0.98 M
f. C_M = 0.30 M; C_A = 1.50 M

A QUANTITATIVE TREATMENT OF SOME OF THE SYSTEMS

For the Mn^{2+}, Co^{2+}, Ni^{2+} and Zn^{2+}-systems it was possible to undertake a quantitative analysis of the data, resulting in the determination of the extinction coefficient and the stability constant of the first complex. The calculation method will be presented below.

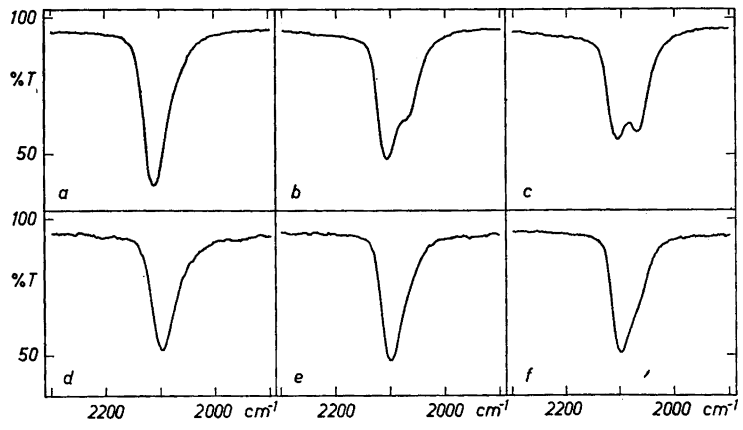

Fig. 4. a.—c. The Zn^{2+}—SCN- system. d.—f. The Fe^{2+}—SCN- system.

a. C_M = 2.89 M; C_A = 0.30 M
b. C_M = 0.49 M; C_A = 0.30 M
c. C_M = 0.25 M; C_A = 0.30 M
d. C_M = 1.8 M; C_A = 0.30 M
e. C_M = 0.90 M; C_A = 0.30 M
f. C_M = 0.45 M; C_A = 0.30 M

C_A = total concentration of ligand
C_M = » » » metal
[A] = free » » ligand
[M] = » » » metal
[MA] = concentration of the first complex
ε_1 = extinction coefficient of the first complex at the maximum of the peak
E = observed optical density at the maximum of the "complex peak"
E_o = the same quantity for $C_M \to \infty$
d = the cell thickness
β_1 = stability constant of the first complex

In the experiments under discussion C_A was kept constant and C_M was varied.

As C_M was always greater than C_A we can assume as an approximation that the first complex MA prevails in regard to the higher complexes MA_2, MA_3 etc.

This approximation gives us the following relations:

$$C_A = [A] + [MA] \tag{1}$$

$$C_M = [M] + [MA] \tag{2}$$

$$E = \varepsilon_1[MA]d \tag{3}$$

Furthermore, by definition:

$$\beta_1 = \frac{[MA]}{[M][A]} \tag{4}$$

Also it must hold:

$$E_o = \varepsilon_1 \cdot C_A \cdot d \tag{5}$$

From eqns. (3) and (5) we obtain:

$$[MA] = \frac{E}{E_o} \cdot C_A \tag{6}$$

and from eqns. (3) and (1):

$$E = \varepsilon_1 d(C_A - [A]) \tag{7}$$

Eqn. (4) is inserted in eqn. (7):

$$E = \varepsilon_1 d\left(C_A - \frac{[MA]}{\beta_1[M]}\right) \tag{8}$$

Now eqns. (2), (5) and (6) are inserted in eqn. (8) and we finally obtain:

$$E = E_o\left(1 - \frac{E/E_o}{\beta_1(C_M - \frac{E}{E_o}C_A)}\right) \tag{9}$$

Table 1. The $Mn^{2+}-SCN^-$ system. Composition of the solutions: C_M M $Mn(ClO_4)_2$ + 0.300 M NaSCN.

C_M M	E_{2093}	$\frac{1}{C_M-C_A}$ M^{-1}	$\frac{E/E_o^1}{C_M-E/E_o^1 \cdot C_A}$ (M^{-1})	$\Delta\nu_{1/2}$ cm^{-1}
1.63	0.332	0.75	0.65	34
1.31	0.327	0.99	0.84	34
1.09	0.308	1.27	0.98	30
0.95	0.292	1.53	1.08	30
0.82	0.280	1.93	1.26	32
0.54	0.233	4.1	1.73	28
0.41	0.205	9.3	2.24	28
$E_o^1 = 0.375$; $E_o = 0.393$ $\varepsilon = 655$ $M^{-1}cm^{-1}$; $\beta_1 = 4.4$ M^{-1}				31 ± 2

Table 2. The $Co^{2+}-SCN^-$ system. Composition of the solutions: C_M M $Co(ClO_4)_2$ + 0.300 M NaSCN.

C_M M	E_{2112}	$\frac{1}{C_M-C_A}$ M^{-1}	$\frac{E/E_o^1}{C_M-E/E_o^1 \cdot C_A}$ (M^{-1})	$\Delta\nu_{1/2}$ cm^{-1}
1.35	0.377	0.95	0.87	31
1.08	0.366	1.28	1.12	28
0.90	0.356	1.67	1.38	30
0.79	0.340	2.05	1.57	26
0.68	0.328	2.67	1.88	31
0.45	0.301	6.7	3.27	30
0.34	0.267	26.3	4.71	30
$E_o^1 = 0.405$; $E_o = 0.417$ $\varepsilon = 696$ $M^{-1}cm^{-1}$; $\beta_1 = 8.9$ M^{-1}				29 ± 1

Thus if the approximation involving the neglection of higher complexes holds true, E plotted against $\frac{E/E_o}{C_M - E/E_o \cdot C_A}$ should yield a straight line with the slope $k = E_o/\beta_1$ and an intercept on the ordinate axis equal to E_o. From these quantities ε_1 and β_1 can be obtained.

The calculation procedure was to make a first plot of E against $1/(C_M-C_A)$ and extrapolate to $1/(C_M-C_A) = 0$. This gave an approximate value of $E_o = E_o^1$. Thereafter $\frac{E/E_o^1}{C_M-E/E_o^1 \cdot C_A}$ could be calculated and E was plotted against this quantity. This gave a new value of $E_o = E_o''$ and from the limiting slope β_1 could be calculated. Renewed plotting using E_o'' gave no perceptible change in the parameters.

Table 3. The $Ni^{2+}-SCN^-$ system. Composition of the solutions: C_M M $Ni(ClO_4)_2$ + 0.360 M NaSCN + (2.64−2 C_M) M $NaClO_4$.

C_M M	E_{2119}	$\frac{1}{C_M - C_A}$ M^{-1}	$\frac{E/E_o^1}{C_M - E/E_o^1 \cdot C_A}$ (M^{-1})	$\Delta\nu_{1/2}$ cm^{-1}
1.32	0.433	1.04	0.95	32
1.10	0.417	1.35	1.16	32
0.99	0.419	1.59	1.36	34
0.88	0.418	1.92	1.63	32
0.77	0.406	2.44	1.93	30
0.66	0.395	3.33	2.42	32
0.61	0.396	3.98	2.82	32
0.54	0.384	5.62	3.47	32
0.49	0.378	7.75	4.18	32
0.44	0.369	12.50	5.21	34
$E_o^1 = 0.463$; $E_o = 0.461$ $\varepsilon = 640$ M^{-1} cm^{-1}; $\beta_1 = 15.0$ M^{-1}				31 ± 2

Table 4. The $Zn^{2+}-SCN^-$ system. Composition of the solutions: C_M M $Zn(NO_3)_2$ + 0.300 M NaSCN.

C_M M	E_{2109}	$\frac{1}{C_M - C_A}$ M^{-1}	$\frac{E/E_o^1}{C_M - E/E_o^1 \cdot C_A}$ (M^{-1})	$\Delta\nu_{1/2}$ cm^{-1}
2.89	0.389	0.39	0.37	38
2.47	0.392	0.46	0.44	34
1.65	0.383	0.74	0.69	34
0.83	0.333	1.90	1.41	32
0.49	0.287	5.15	2.50	32
0.25	0.224		6.75	32
$E_o^1 = 0.407$; $E_o = 0.411$ $\varepsilon_1 = 685$ M^{-1} cm^{-1}; $\beta_1 = 8.2$ M^{-1}				34 ± 2

With this technique the Mn^{2+}, Co^{2+}, Ni^{2+} and Zn^{2+} could be successfully treated. The results are given in Tables 1—4 and Figs. 5 and 6.

The stability constants thus obtained seem to be rather independent of the total salt concentration within the range used in the investigations. Not all systems were investigated under exactly comparable conditions but as no certain rules are known for the variation of the activity coefficients in such highly concentrated solutions, we did not consider it worth while to maintain a rigorously controlled salt medium. The cobalt system was investigated with and without adding sodium perchlorate to constant salt concentration (in equivalents per liter). The results agreed well within experimental error, as seen from Fig. 5.

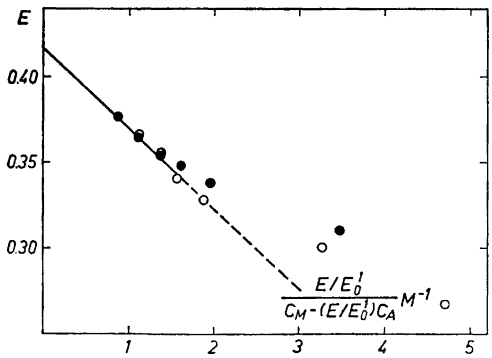

Fig. 5. The $Co^{2+}-SCN^-$ system. Filled dost correspond to measurements in a medium of constant salt concentration = 3 M. The open dots represent the measurements reported in Table 2.

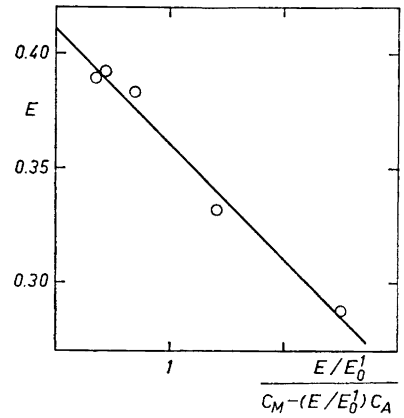

Fig. 6. The $Zn^{2+}-SCN^-$ system. The data are those reported in Table 4.

DISCUSSION

A. General relations between the constants obtained

In Table 5 we report the values obtained for the stability constant and the spectral parameters of the first complex of the metals investigated.

One striking observation emerges from an inspection of the data, namely the constancy of the integrated absorption, for which quantity we have used the approximation $\varepsilon_1 \cdot \Delta\nu_{1/2}$, where $\Delta\nu_{1/2}$ means the half-width of the peak. This fact will be commented upon in a forthcoming paper.

The stability constants reported show the trend expected from the Williams-Irving rule [9]. It is also the trend reported by Yatzimirskii and Korableva [5] at low ionic strength. Especially the perfect agreement between the value of β_1 for the nickel system found here (15 M^{-1}) and that reported earlier (15 M^{-1}) by one of us [10] should be noted. As that work was done at the ionic strength

Table 5. Spectral parameters and stability constants of the investigated complexes.

	ν cm^{-1}	ε $M^{-1}cm^{-1}$	$\Delta\nu_{1/2}$ cm^{-1}	$\varepsilon \cdot \Delta\nu_{1/2} \times 10^{-4}$	β_1 M^{-1} This work	Ref.[5]
SCN^-	2066	537	37	1.99		
$Mn^{2+}-SCN^-$	2093	655	31	2.03	4.4	17.(3)
$Fe^{2+}-SCN^-$	2099					20.(4)
$Co^{2+}-SCN^-$	2112	696	29	2.02	8.9	32.(3)
$Ni^{2+}-SCN^-$	2119	640	32	2.05	15.0	47.(6)
$Zn^{2+}-SCN^-$	2109	685	34	2.32	8.2	15.(4)

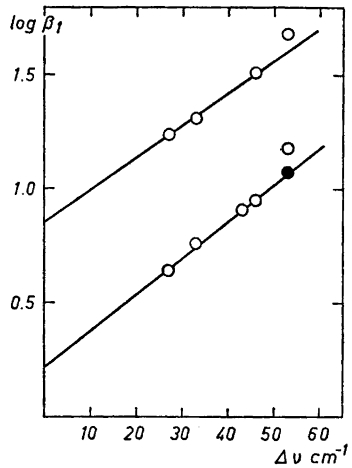

Fig. 7. The logarithm of β_1 as a function of the frequency shift ($\Delta\nu$) of the investigated systems of the first-row transition metals. Upper set: the stability constant reported by Yatzimirskii and Korableva [6]. Lower set: the stability constants obtained in the present investigation ($\beta_{1\,Fe}$ computed by analogy from the data of Ref.[5]). ●: $\beta_{1\,Ni}$ corrected for outer-sphere complexity.

1 M, the good agreement gives support to our somewhat sanguine treatment of the problem of the salt medium of the solutions investigated.

Above all, the agreement between the two determinations of β_1 for the nickel system confirms our working hypothesis that the new peak, observed in the spectra of metal solutions, corresponds really to mononuclear metal-thiocyanato complexes.

A further correlation between the data obtained has been found. If log β_1 for the metals investigated is plotted against the frequency shift a straight line is obtained (Fig. 7). As we could not determine β_1 for the ferrous system because of the disturbing effects caused by the large metal concentration, we have made an estimate founded on the parallellism between our data and those of Yatzimirskii and Korableva [5] for the Mn^{2+}, Ni^{2+} and Co^{2+}-systems.

If it is assumed, as we have done in an earlier paper [11], that the frequency shift of the ligand vibration following upon coordination is proportional to the enthalpy of coordination, and if it is further assumed that the entropy term is almost constant for a sequence of similar metals, then we should expect a linear relation between log β_1 and the frequency shift. Furthermore the line should not go through the origin. Such a relation is actually found here (Fig. 7).

B. The nickel system

As the nickel system exhibited the greatest frequency difference between the complex peak and that of the free ligand, and thus allowed easy absorption determinations, it was selected for a more detailed investigation.

The measurements at a constant value of C_A have already been mentioned. Measurements were also made at a constant value of C_M (*cf.* Fig. 3). The absorption was determined both for the complex peak, E_{2119}, and the free ligand peak, E_{2066}. The absorption was actually measured at the position of the maximum of the peak in question. This position varied a little, to the

Table 6. Determination of $\bar{n}$ of the nickel system. Composition of the solutions: 0.30 M $Ni(ClO_4)_2$ + C_A M NaSCN + (2.40 − C_A) M $NaClO_4$.

C_A M	E_{2066}/d			E_{2119}/d			$\Delta\nu_{1/2}$ cm^{-1}	[A] from E_{2066} mM	$\bar{n}$ eqn. (10)	$\bar{n}$ eqn. (15)	[A] eqn. (10) mM	$\bar{n}$ eqn. (17)	[A] eqn. (10) mM	$\beta_{1\ out}$ M^{-1}
	d=8.8 μ	d=20 μ	MEAN	d=8.8 μ	d=20 μ	MEAN								
0.075	18.2	12.4	15.3	40.2	40.0	40.1		28.5	0.16	0.208	12.6			4.6
0.200	33.6	34.8	34.2	92	100	96	31	63.7	0.46	0.50	50			1.4
0.225	43.9	40.3	42.1	109	116	113	32	78.4	0.49	0.59	49			3.6
0.300	59.7	54.7	57.2	139	144	142	30	106.5	0.53	0.74	79			5.8
0.450	89.5	94.8	92.1	181	197	189	32	171.5	0.93	0.99	154			1.3
0.600	138.6	140.2	139.4	245	240	242	33	259.6	1.13	1.26	222			3±2
0.750	183.5	190.8	187.2	260	271	266	35	349	1.34	1.38	335	1.51	300	
0.975	268.1	273.9	271.0	299	306	302	38	505	1.57	1.58	500	1.87	415	
1.200	361	359	360	325	333	329	40	670	1.77	1.71	690	2.14	560	
1.500	492	462	477	361	364	362	40	888	2.04	1.89	930	2.36	790	

effect that at very high C_A-values the two peaks came a little closer together. As the peaks are not very acuminate, any error thereby introduced is certainly within the random errors. The designations E_{2119} and E_{2066} are thus more of a classificatory type than a descriptive one. Both 8.8 μ and 20 μ spacers were used; the values obtained are reported in Table 6.

It was our aim when performing these measurements to calculate the mean ligand number $\bar{n}$ and compare this quantity with the values obtained from the stability constants reported by Fronæus [10].

By definition

$$\bar{n} = \frac{C_A - [A]}{C_M} \tag{10}$$

One obvious way to calculate $\bar{n}$ is then to use the E_{2066} values and the already determined value of ε_A to determine [A] and thus $\bar{n}$ from eqn. (10). Such a calculation is reported in Table 6.

We will now consider an alternative method for the calculation of $\bar{n}$. It must hold that

$$E_{2119} = d([MA]\varepsilon_1 + [MA_2]\varepsilon_2 + [MA_3]\varepsilon_3 + - - -) \tag{11}$$

It is reasonable as a first approximation to put

$$\varepsilon_2 = 2\,\varepsilon_1, \qquad \varepsilon_3 = 3\;\varepsilon_1 - - - \tag{12}$$

Then we have

$$\frac{E_{2119}}{d \cdot \varepsilon_1} = [MA] + 2[MA_2] + 3[MA_3] + - - - \tag{13}$$

or

$$\frac{E_{2119}}{d\;\varepsilon_1} = C_A - [A] \tag{14}$$

It then follows that

$$\frac{E_{2119}}{d \cdot \varepsilon_1 \cdot C_M} = \bar{n} \tag{15}$$

This approximation can be expected to work well when [A] is rather low so that the first complex MA dominates in the solution. For higher [A] the approximation of eqns. (12) will eventually introduce a systematic error.

However, having established the invariance of the product $\varepsilon_1 \cdot \Delta\nu_{1/2}$ with coordination, we can obtain a successive correction of ε_1 by measuring $\Delta\nu_{1/2}$ for the 2119-peak.

Then we obtain

$$\varepsilon_{1corr} = \frac{(\Delta\nu_{1/2})_1}{\Delta\nu_{1/2}} \cdot \varepsilon_1 \tag{16}$$

and consequently, if ε_1 in eqn. (21) is exchanged for ε_{1corr}

$$\bar{n} = \frac{E_{2119}}{d \cdot C_M \cdot \varepsilon_1} \cdot \frac{\Delta\nu_{1/2}}{(\Delta\nu_{1/2})_1} \tag{17}$$

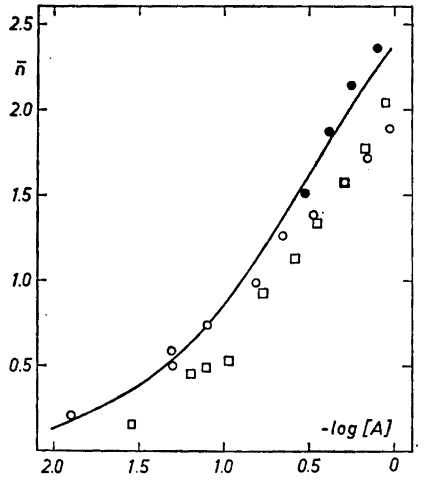

Fig. 8. The complex formation curve of the $Ni^{2+}-SCN^-$ system. Fulldrawn line: $\bar{n}$ according to Fronæus [10]. The dots and squares represent data obtained in the present investigation.
$\bar{n}$ calculated from eqn. (15): ○
$\bar{n}$ » » eqn. (17): ●
$\bar{n}$ » » eqn. (10): □

where $\varepsilon_{1\text{corr}}$ means an average value in which the deviation from eqns. (12) is implied, and $(\Delta\nu_{½})_1$ means the half-width of the 2119-peak determined under such conditions (Table 3) where only the first complex is present in great amount.

The appropriate data for such a calculation and the values of $\bar{n}$ obtained are also included in Table 6.

A comparison between the data reported by Fronæus [10] and our $\bar{n}$-values is found in Fig. 8. It is seen that the values obtained with our second method agree almost completely with Fronæus' $\bar{n}$-curve, whereas those of the first method lie systematically below that curve.

Although the difference is not very great we believe it to be significant and suggest that the cause may be traced to a so called outer-sphere coordination of the thiocyanate ion to the hydrated nickel ion. If we denote such a species as $(M\ aq_6)A_n$ and the inner sphere complex as (MA_n), we obtain for the total concentration of the first complex [MA]:

$$[MA] = [(MA)] + [(M\ aq_6)A] \tag{18}$$

and for the stability constant

$$\beta_1 = \frac{[MA]}{[M][A]} = \frac{[(MA)]}{[M][A]} + \frac{[(M\ aq_6)A]}{[M][A]} \tag{19}$$

or

$$\beta_1 = \beta_{1\text{ in}} + \beta_{1\text{ out}} \tag{20}$$

It is now assumed that the absorption frequency of the thiocyanate ion in the outer-sphere complexes $(M\ aq_6)A_n$ is equal or almost equal to that of the free ligand. The formal quantity calculated from the optical density E_{2066} should then correspond to $[A] + \sum_n [(M\ aq_6)A_n]$, *i.e.* too large a value giving

in its turn too small a value of $\bar{n}$. This is the trend of the discrepancy under discussion.

From this starting-point we have tried a quantitative treatment of the data to obtain $\beta_{1\ out}$.

$$\bar{n}_{\text{eqn. (15)}} = \frac{C_A - [A]}{C_M} \tag{21}$$

$$\bar{n}_{\text{eqn. (10)}} = \frac{C_A - [A] - \Sigma_n[(M\ aq_6)A_n]}{C_M} \tag{22}$$

We define a quantity $\Delta\bar{n}$ as

$$\Delta\bar{n} = \bar{n}_{\text{eqn. (15)}} - \bar{n}_{\text{eqn. (10)}} \tag{23}$$

For small values of [A] where only the first complex is formed in appreciable amounts, we then obtain

$$\Delta\bar{n} = \frac{[(M\ aq_6)A]}{C_M} \tag{24}$$

This expression is easily transformed to

$$\Delta\bar{n} = \frac{\beta_{1\ out}[A]}{1 + \beta_1[A]} \tag{25}$$

Thus we obtain

$$\beta_{1\ out} = \frac{\Delta\bar{n}}{[A]}(1 + \beta_1[A]) \tag{26}$$

In the last column of Table 6 we report $\beta_{1\ out}$ calculated according to eqn. (26) from corresponding values of [A] and $\Delta\bar{n}$, obtained from columns 10, 11 and 12. From eqn. (20) we can then obtain $\beta_{1\ in} = 12\ M^{-1}$. It may be well worth remarking that if we use this value in the log $\beta_1 - \Delta\nu$ plot in Fig. 7, we obtain a much better fit to the linear relationship found for the other systems.

As we have not performed any determination of the degree of outer-sphere complex formation for these other systems we are not in a position to judge whether this better fit is significant or not.

The spectrophotometer has been purchased with a grant from the *Swedish Natural Science Research Council.*

The records of the spectra were made by Miss Kerstin Kulle. As this is the first report from the Infrared Laboratory of this Institute, it is a pleasure and a privilege for us to thank Miss Kulle for her splendid cooperation and assistance in this investigation.

REFERENCES

1. Jones, L. H. *J. Chem. Phys.* **25** (1956) 1069.
2. Jones, L. H. and Penneman, R. A. *J. Chem. Phys.* **22** (1954) 965.
3. Jones, L. H. and Penneman, R. A. *J. Chem. Phys* **24** (1956) 293.

4. Bjerrum, J., Schwarzenbach, G. and Sillén, L. G. *Stability Constants*, Part II, Chemical Society, London 1958.
5. Yatzimirskii, K. B. and Korableva, V. D. *Zhur. Neorg. Khim.* **3** (1958) 339.
6. Ramsay, D. A. *J. Am. Chem. Soc.* **74** (1952) 72.
7. Gordy, W. and Williams, D. *J. Chem. Phys.* **3** (1935) 664.
8. Langseth, A. L., Nielsen, J. R. and Sørensen, J. O. *Z. physik. Chem.* **B 27** (1934) 100.
9. Irving, H. and Williams, R. J. P. *J. Chem. Soc.* **1953** 3192.
10. Fronæus, S. *Acta Chem. Scand.* **7** (1953) 21.
11. Fronæus, S. and Larsson, R. *Acta Chem. Scand.* **14** (1960) 1364.

Received January 26, 1962.

ACTA CHEMICA SCANDINAVICA 16 (1962) 1447–1454

Studies on Metal Complexes in Aqueous Solution by Infrared Spectrophotometry

III. Further Investigations on Thiocyanato Complexes

STURE FRONÆUS and RAGNAR LARSSON

Department of Inorganic and Physical Chemistry and Infrared Laboratory, Chemical Institute, University of Lund, Lund, Sweden

The frequency and intensity of the C—N vibration have been measured for some thiocyanato complexes of widely different metals. The relevant data can be found in Table 4. It is found that the systems can be divided into three classes, depending upon whether the integrated absorption is equal to, greater or less than that quantity for the free thiocyanate ion. It is suggested that these classes correspond to different types of bonding: I. Very small degree of electron exchange between ligand and metal. II. "Lone-pair donation" from the nitrogen atom. III. "Lone-pair donation" from the sulphur atom.

In the case of the cadmium system two absorption peaks are found, which are supposed to correspond to mononuclear and polynuclear complexes, respectively.

In the preceding paper [1] of this series we reported infrared absorption frequencies and intensities for some thiocyanato complexes of the bivalent first-row transition metals. In this paper we report further measurements on some thiocyanato complexes of some typical a- and b-class metals [2].

We have made it our object to correlate changes in absorption frequency and intensity with the structure and bonding characteristics of the complexes. Such measurements have frequently been reported [3–11a] during the last few years. However, with two exceptions [9,11a], all studies have been confined to the solid state. As it has been amply demonstrated by Price, Sherman and Wilkinson [12] that lattice forces can strongly influence the position of the C—N frequency (for the CN^- and OCN^- ions), the value of the information is considerably decreased.

EXPERIMENTAL

The experimental procedure was the same as before.

Chemicals used. Uranyl perchlorate was prepared according to Arhland [13] and $K_3[Cr(NCS)_6]$ and $K_3[Pt(SCN)_6]$ according to the literature. The preparation of

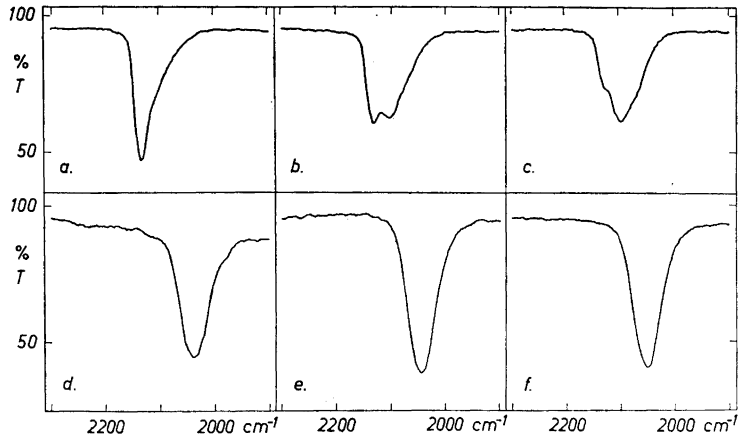

Fig. 1. a.—c. The Cd^{2+}—SCN^- system.

a. $C_M = 2.00$ M; $C_A = 0.30$ M
b. $C_M = 1.08$ M; $C_A = 0.30$ M
c. $C_M = 0.45$ M; $C_A = 0.30$ M

d.—f. The Fe^{3+}—SCN^- system.

d. $C_M = 0.84$ M; $C_A = 0.15$ M
e. $C_M = 0.56$ M; $C_A = 0.15$ M
f. $C_M = 0.28$ M; $C_A = 0.15$ M

$[Co(NH_3)_5NCS](ClO_4)_2$ is described in a recent paper by one of us [14]. $Hg(SCN)_2$ was precipitated from dilute solutions of $Hg(NO_3)_2$ and NaSCN, and washed with water, alcohol and ether. The other salts were perchlorates prepared from reagent quality chlorides.

MEASUREMENTS

The spectra of the following metal-thiocyanato systems were recorded for a constant thiocyanate concentration but a varying metal concentration: Cd^{2+}, UO_2^{2+} and Fe^{3+}. Some representative records for varying composition of the solutions are given in Fig. 1.

In the case of the cadmium system, Fig. 1 a—c, two new peaks are found at 2098 and 2132 cm^{-1}, respectively, the first one dissappearing, the other one increasing in intensity when the metal ion concentration is increased. We suggest that the 2098 cm^{-1} peak corresponds to a mononuclear complex and that the 2132 cm^{-1} peak corresponds to a polynuclear, SCN-bridged complex.

The iron(III)-system exhibits a quite different picture from the systems previously investigated [1]. First of all, the frequency of the new peak (2045 cm^{-1}) is lower than that of the free thiocyanate ion. Furthermore, when the iron concentration is increased the appearance of at least one new absorption peak (present as a shoulder at 2020 cm^{-1} at the highest iron concentration) is evident. The main peak is under the same conditions shifted to 2040 cm^{-1}. We suggest

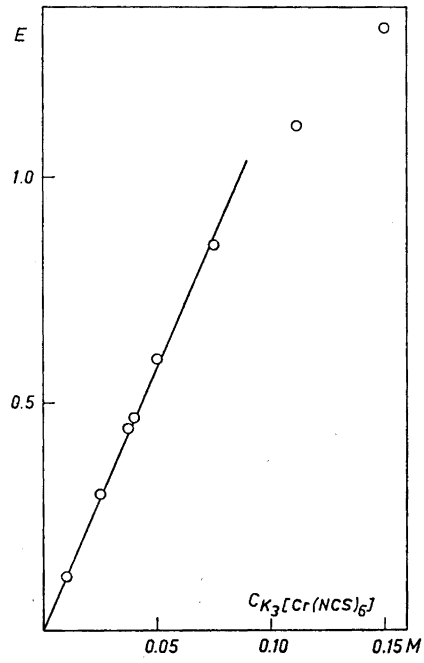

Fig. 2. Total optical density of the absorption peak corresponding to the ion $[Cr(NCS)_6]^{3-}$, The deviation from linearity for very large optical densities is clearly seen (*cf.* Ref.[1] p. 1434).

that the 2045 cm^{-1} peak corresponds to a mononuclear complex, and that a series of polynuclear complexes exists in solution giving rise to the other peaks observed. They are most probably not of the SCN-bridged type.

Also in the case of the uranyl system we must expect the formation of hydrolytic polynuclear complexes. Even though the pH of the solution was kept very low, the high metal concentration must certainly cause a large degree of polymerization.

Because of the complicated nature of these three systems no attempt was made to undertake a calculation of the complexity constants. Only the extinction coefficient of the first thiocyanato complex was determined by extrapolation of the absorbance to $1/(C_M - C_A) = 0$ (*vide* Ref.[1]). The results together with the half-width of the complex peak are reported in Table 3. As the uranyl complex peak was superimposed on the peak of the free ligand, the half-width was determined only from the spectra of the two largest metal : ligand ratios.

Furthermore, the spectra of some inert thiocyanato complex ions have been recorded, *viz.* $[Co(NH_3)_5NCS]^{2+}$, $[Cr(NCS)_6]^{3-}$ and $[Pt(SCN)_6]^{2-}$. In Fig. 2 is given a plot of the optical density of the $[Cr(NCS)_6]^{3-}$ ion *versus* concentration. Due to the low solubility of $K_2[Pt(SCN)_6]$ and $[Co(NH_3)_5NCS](ClO_4)_2$, the instrument was used with ordinate expansion 4 × and 10 × respectively, when recording these complexes. The extinction coefficient of the cobalt complex could not be measured with any great accuracy.

Also some records were made under conditions suitable for the study of the ions $Hg(SCN)_4^{2-}$ and $Co(NCS)_4^{2-}$. In the first case $Hg(SCN)_2$ was dissolved

Table 1. The $Hg^{2+}-SCN^-$ system. $d = 20.0$ μ. $\varepsilon = \dfrac{E}{\bar{n}\, C_M\, d}$

C_M M	C_A M	$\bar{n}$	E	ε $M^{-1}cm^{-1}$	$\Delta\nu_{\frac{1}{2}}$ cm^{-1}
0.200	3.00	3.91	0.638	409	27
0.100	1.50	3.81	0.333	437	27
0.067	1.00	3.78	0.208	411	25
0.133	2.00	3.85	0.435	425	29
			Mean	420	27

in a great excess of NaSCN; from the known stability constants [15] the average number of ligands bound to the metal could be calculated and thus the extinction coefficient (Table 1). In the latter case NaSCN and $Co(ClO_4)_2$ in mole proportions 5:1 were dissolved in water mixed with a succesively increasing amount of methyl-ethyl-ketone (MEK). The spectra are given in Fig. 3. The solutions containing more than 20 % by volume of ketone were bright blue, indicating the presence of the tetrahedral complex $Co(NCS)_4^{2-}$. The optical densities of the peaks are given in Table 2 together with a calculation of ε for each SCN^- group in the complex. It was noted that the exchange of the solvent from water to a water-ketone mixture changed the absorption parameters of the free thiocyanate ion. Thus $\varepsilon = 671$ $M^{-1}cm^{-1}$ and $\nu = 2070$ cm^{-1} and $\Delta\nu_{\frac{1}{2}} = 41$ cm^{-1}. Although this change is significant and indicates a thiocyanate-ketone interaction, it is not of the order of magnitude to disturb the interpretation of the $Co(NCS)_4^{2-}$ spectrum.

The extinction coefficient calculated from the values in Table 2 were obtained from the expression

$$\varepsilon = \frac{E - \frac{1}{5} C_A \cdot \varepsilon_{A,\,2075} \cdot d}{4/5\; C_A d} \qquad (1)$$

where $\varepsilon_{A,\,2075}$ denotes the extinction coefficient of the free thiocyanate ion in 60 % MEK.

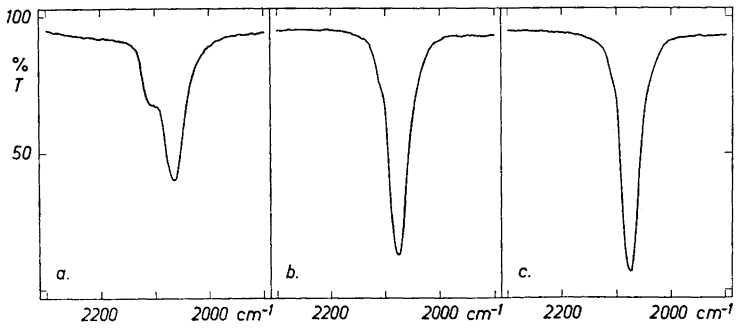

Fig. 3. The $Co^{2+}-SCN^-$ system in water methyl-ethyl-ketone mixtures. a. 0 % MEK, b. 40 % MEK, c. 60 % MEK.

Table 2. Calculation of ε_{SCN^-} of the complex $Co(NCS)_4^{2-}$. MEK = methylethylketone. $C_M = 0.075$ M; $C_A = 0.375$ M.

% MEK	40	60	80
E_{2075}	0.864	1.14	1.26
Mean		1.20	

$\varepsilon_{A,\,2075} = 406\ M^{-1}cm^{-1}$

$$\varepsilon = \frac{1.20 - 0.06}{0.3 \times 20} \times 10^4 = 1900\ M^{-1}cm^{-1}$$

D. Collation of the data for the various systems

The data obtained by the measurements described in this and the preceding paper [1] are collected in Table 3.

As an approximate measure of the integrated absorption the product between the extinction coefficient and the half-width of the band is reported.

It is clearly seen from Table 3 that the systems investigated can be divided into three different classes. For the first one, comprising the bivalent first-row transition metals, it holds that the integrated absorption is constant and — moreover — identical with the same quantity for the free thiocyanate ion.

The second class, tetrahedral Co^{2+}, UO_2^{2+}, Fe^{3+} and Cr^{3+}, is characterized by a definite increase in the integrated absorption, whereas the third one, Pt^{4+} and Hg^{2+}, shows a decrease in the said quantity.

Also it is seen that whereas class I and class III gives frequencies higher than that of the free thiocyanate ion, the class II systems show lower (Fe^{3+}),

Table 3. Spectral parameters of the investigated complexes.

	ν cm^{-1}	ε $M^{-1}cm^{-1}$	$\Delta\nu_{\frac{1}{2}}$ cm^{-1}	$\varepsilon \cdot \Delta\nu_{\frac{1}{2}} \times 10^{-4}$
SCN^-	2066	537	37	1.99
Mn^{2+}-SCN^-	2093	655	31	2.03
Fe^{2+}-SCN^-	2099			
Co^{2+}-SCN^-	2112	696	29	2.02
Ni^{2+}-SCN^-	2119	640	32	2.05
Zn^{2+}-SCN^-	2109	685	34	2.32
$[Co(NH_3)_5NCS]^{2+}$	2123			
$[Co(NCS)_4]^{2-}$	2075	1900	29	4.9
UO_2^{2+}-SCN^-	2066	1100	40	4.4
Fe^{3+}-SCN^-	2045	1310	49	6.4
$[Cr(NCS)_6]^{3-}$	2088	937	39	3.7
Cd^{2+}-SCN^-	2132	635	24	1.5
	2098			
$[Pt(SCN)_6]^{2-}$	2126	246	15	0.4
$[Hg(SCN)_4]^{2-}$	2112	420	27	1.1

identical (UO_2^{2+}), or at least a trend towards lower frequencies (*cf.* Co^{2+}, octahedral, class I, and Co^{2+}, tetrahedral, class II).

It is also obvious that the high frequency peak of the cadmium system exhibits a striking resemblance to the class III systems.

DISCUSSION

The most noteworthy result of this investigation is the classification of the metals in Table 3. To understand the origin of this effect let us first consider classes II and III. These two classes are characterizied by a distinct change of the integrated absorption, the one towards higher, the other towards lower values compared to the free ligand. Keeping in mind that the metal-ligand bond in all cases is much weaker than the bonds in the SCN group, we can consider the effects as a perturbation of the vibration levels in the SCN group, in this case the ν_1 vibration. X-Ray data (for a compilation of existent data, see Ref.[5]) give a clear indication that class II metals coordinate the SCN group *via* the nitrogen atom whereas class III metals coordinate *via* the sulphur atom. — We can then rationalize our findings thus: The class II and III metals are those that form "covalent" bonds with the SCN-group, a lone-pair of the ligand being donated into empty orbitals of the metal; the class II metals interacting with a nitrogen lone-pair, the class III ones interacting with a sulphur lone-pair.

On the basis of this rationalization let us try to understand how such a lone-pair donation will affect IR absorption intensities and frequencies:

From his careful analysis of IR-spectra of the thiocyanate ion Jones[16] suggests the following approximate distribution between the resonance structures:

α	$N\equiv C-S^-$	71 %
β	$^-N=C=S$	12 %
γ	$^{-2}N-C\equiv S^+$	17 %

Now a lone-pair donation from the nitrogen atom giving rise to a M—N σ bond, will benefit from the existense of the β and — above all — the γ canonical structures. In other words, the relative amount of structures β and γ will increase with nitrogen-lone-pair coordination. This means a greater dipole moment over the C—N bond, most probably also implying an increased value of the derivative of dipole moment and thus of the absorption intensity (*vide, e.g.*, Ref.[17], p. 190). This is actually found. Furthermore, the increase of the relative amount of structures β and γ will mean a decrease of bond order of the C—N bond, that is a shift of the absorption frequency towards lower values. This is actually found — at least a trend in that direction is observed (*vide supra* p. 1451).

A lone-pair-donation from the sulphur atom, on the other hand, will give rise to a M—S σ bond. With an analogous argument this might be expected to result in an increase of the relative amount of structure α. This means a decreased polarity of the C—N bond, resulting in a lowered absorption intensity, and an increased bond order, resulting in a shift of the absorption frequency towards higher values. Both these effects are actually found.

We now turn our attention to the invariance of the integrated absorption of the thiocyanate ion when coordinated to metals belonging to class I. We suggest that this means that in these complexes there is very little electron exchange between ligand and metal. However, the observed shifts ($\Delta\nu$) of absorption frequencies and the linear dependence of this quantity on log β_1 (Ref.[1]) are still to be explained.

We consider it probable that the increase of the vibration frequency is of a similar origin as the variation of frequency found for polyatomic ions trapped in ionic matrices [12,18].

The invariance of the integrated absorption tells us that in the cases considered coordination of the thiocyanate ion causes no change in the proportions between the three canonical structures α, β and γ given by Jones [16]. Therefore, the increase of the force constant observed must originate from a repulsion from the electron cloud of the metal acting upon the electron cloud of the nitrogen atom. Qualitatively, it seems plausible that the stronger the metal-ligand bond the closer must the nitrogen atom be to the electron cloud of the metal and thus the greater will be the increase of the force constant. However, we fail to arrive at an explanation of the quantitative connection between $\Delta\nu$ and log β_1.

The effects classified here as characterizing classes I, II and III are most probably additive. Thus the unusual large frequency shift found for SCN-bridged polynuclear complexes (the cadmium system investigated here, and the platinium complexes investigated by Chatt and Duncanson [3]) may arise from a great contribution of class I and class III effects dominating over a less important class II contribution.

Also the position of the absorption peaks of the class II complexes might arise from a superposition of a definite shift towards lower frequencies on a class I effect.

If we compare the classification of the octahedral and tetrahedral Co(II) complexes, we find that the first is a class I complex, *i.e.*, with a very low degree of electron exchange between ligand and metal, whereas the last one is a class II complex, *i.e.*, with a definite "covalent" σ-bonding. This is in striking agreement with the theory for the intensities of electronic spectra, demanding a much stronger electron exchange for tetrahedral than for octahedral complexes. (*cf.*, *e.g.*, Ballhausen [19]).

One more observation may be worthy of comment. It is seen from Table 3 that at least for classes I and III it holds that $\Delta\nu_{\frac{1}{2}}$ is always smaller than the same quantity for the free ligand. This follows, of course, from the more effective shielding of the thiocyanate ion from outer disturbances in the complexes than in the free state.

That the iron(III) system exhibits a very broad peak (*cf.* Table 3) is quite understandable, if as assumed in our discussion above (p. 1449) polynuclear complexes are formed, each contributing with its own absorption peak. The measured half-width is then only a formal quantity. It is most probable that the same holds true also for the uranyl system. However, even if the peaks observed should be composed of several components, the main conclusions drawn from the values of ε_1 and $\Delta\nu_{\frac{1}{2}}$ reported in Table 8 must still hold true.

The measured quantity ε_1 is then smaller than ε would be for a single peak, but as on the other hand $\Delta\nu_{\frac{1}{2}}$ is obviously larger than it would be for a single peak the product may still be of the same order of magnitude as it should be for a single peak.

When this manuscript was close to completion, the paper of Lewis, Nyholm and Smith [11a] appeared. These authors measure the C—N and C—S frequencies of a considerable number of saturated thiocyanato complexes both in the solid state and in solution (acetophenone). They note the difference between the results obtained in these two ways. They also carry on a discussion on the change of bonding in the ligand following upon coordination, which is almost identical to that given here. These authors did not measure the intensity of absorption, and so they must confine their discussion to the change of frequency. As is also reported by Turco and Pecile [11] they find it easier to interpret the change of the C—S frequency than that of the C—N one. This is certainly due to the interference of the electron-repulsion effect discussed above for the class I ions.

The spectra have been recorded by Miss Kerstin Kulle whose work is gratefully acknowledged.

REFERENCES

1. Fronæus, S. and Larsson, R. *Acta Chem. Scand.* **16** (1962) 1433.
2. Ahrland, S., Chatt, J. and Davies, N. R. *Quart. Rev.* **12** (1958) 265.
3. Chatt, J. and Duncanson, J. A. *Nature* **178** (1956) 997.
4. Chamberlain, M. M. and Bailar, J. C. *J. Am. Chem. Soc.* **81** (1959) 6412.
5. Mitchell, P. C. H. and Williams, R. J. P. *J. Chem. Soc.* **1960** 1912.
6. Pecile, C., Giacometti, G. and Turco, A. *Atti accad. Nazl. Lincei, Rend. Classe sci. fis. mat. e nat.* **28** (1960) 189.
7. Vallarino, L. *J. Chem. Soc.* **1957** 2473.
8. Johnson, R. C. and Basolo, F. *J. Inorg. & Nuclear Chem.* **13** (1960) 36.
9. Baldwin, M. E. *J. Chem. Soc.* **1961** 471.
10. Kinell, P. O. and Strandberg, B. *Acta Chem. Scand.* **13** (1959) 1607.
11. Turco, A. and Pecile, C. *Nature* **191** (1961) 66.
11a. Lewis, J., Nyholm, R. S. and Smith, P. W. *J. Chem. Soc.* **1961** 4590.
12. Price, W. C., Sherman, W. F. and Wilkinson, G. R. *Proc. Roy. Soc.* **A 255** (1960) 5.
13. Ahrland, S. *Acta Chem. Scand.* **3** (1949) 374.
14. Larsson, R. *Acta Chem. Scand. To be published.*
15. Gallais, F. and Mounier, J. *Compt. rend.* **233** (1946) 790.
16. Jones, L. H. *J. Chem. Phys.* **25** (1956) 1069.
17. Duncan, A. B. F. *Theory of Infrared and Raman Spectra*, Chapter III in Weissberger, A. (Ed.) *Technique of Organic Chemistry*, Volume IX. Interscience Publ. Inc., New York 1956.
18. Ketelaar, J. A. A. and van der Elsken, J. *J. Chem. Phys.* **30** (1959) 336.
19. Ballhausen, C. J. *Intensities of Spectral Bands in Transition Metal Complexes, Progress in Inorg. Chem.* Vol. 2, p. 251. Ed. F. A. Cotton, Interscience Publishers Inc. New York 1960.

Received January 26, 1962.

ACTA CHEMICA SCANDINAVICA 16 (1962) 1455–1462

The Photolysis of Iodine, Ethyl Iodide and Hydrogen Iodide in a Rigid Glass at 77°K

D. TIMM

*Thermochemistry Laboratory *, University of Lund, Lund, Sweden*

It has been found that the photolysis of iodine in a hydrocarbon matrix at 77°K does not lead to the formation of iodine atoms. That the photolysis of ethyl iodide depends on the viscosity of the matrix has been confirmed and spectral characteristics of intermediates have been recorded. Identical characteristics were found when HI was photolyzed and it has been shown that HI_3 is not involved.

In a search for molecular species that can be split homolytically by photolysis in a glass-forming matrix at the temperature of liquid nitrogen a number of iodine-containing substances have been investigated. The photolysis of iodine, ethyl iodide and hydrogen iodide constitutes the subject of the present paper.

Iodine itself has previously been studied by Norman and Porter [1, 2] and by Sowden and Davidson [3] under similar conditions but with controversial results. Norman and Porter [1] found it possible by photolysis to decolorize a 10^{-3} M iodine solution in a hydrocarbon glass at 86°K and to regain the iodine color during warm-up. On the other hand, Sowden and Davidson [3] found a 10^{-4} M solution to be unchanged even by prolonged irradiation. In a later paper, Norman and Porter [2] described the experimental conditions and results more in detail when using the EPA-matrix (ethanol, ethyl ether and isopentane 2:5:5).

Norman and Porter [2] have also studied the photolysis of EtI in different matrices. These authors suggested that atomic iodine was formed, which is stable at 77°K for several hours in a high-viscosity, "hard" matrix like pure 3-methyl pentane or the mixture 3-methyl pentane, isopentane 3:2, whereas in a low-viscosity, "soft" matrix like pure isopentane diffusional processes lead to the formation of molecular iodine already at liquid nitrogen temperature. Upon warm-up the spectrum of iodine appeared instantly also in hard glasses. In EPA, the authors found that the solid solution irradiated for 1 h remained transparent down to the beginning of absorption by EtI. On warming to room

* Sponsored by the *Swedish Natural Science Research Council* and by the *Swedish Technical Research Council.*

temperature, the absorption spectrum of iodine developed rather slowly, showing also the absorption bands at 290 and 360 mμ attributed to hydrogen tri-iodide [4]. Norman and Porter concluded that the photolysis of EtI leads to the formation of unknown species, which may be HI. They do not give any corresponding results when hydrocarbon matrices were used.

It was felt to be of interest to repeat the photolysis of ethyl iodide with a differential method on a hydrocarbon matrix and to compare the results with those from experiments performed on hydrogen iodide under identical conditions.

MATERIALS

Iodine used was "Baker analyzed" reagent.

Ethyl iodide, Merck analytical grade, was distilled and the main fraction was found to contain less than 0.05 % of gas-chromatographically detectable impurities.

Hydrogen iodide was prepared directly in a 10^{-3} M hydrocarbon solution by reduction with pure hydrogen of an appropriate amount of iodine in the presence of 10—20 % by weight of platinum oxide (Adams catalyst [5]).

Matrix hydrocarbons were purified and tested according to standard procedure [6].

Apparatus and Technique have been described elsewhere [7-8].

RESULTS

Iodine. (Fig. 1) Iodine solutions (1.5×10^{-5} to 4×10^{-5} M) * were prepared in three different glasses: two mixtures of isopentane and 3-methyl pentane, 2:3 by volume [2] (matrix C) and 6:1 by volume [9] (matrix A) and a mixture of pentane and *neo*hexane 3:8 by volume [10] (matrix B). The solutions were cooled to liquid nitrogen temperature (curve 1) and irradiated for 60 min (curve 2). All glasses were yellow and fully transparent in the visible region throughout the experiments. The peaks at 19.9 and 23.0 kc. cm^{-1} were clearly discernible both before and after photolysis. In accordance with the results of Sowden and Davidson no decolorization was obtained, and the spectrum changed only slightly or not at all during the irradiation. After warm-up, the original spectrum was obtained, within the error of reproducibility of the instrument (curve 3). On refreezing, however, the spectrum differed slightly from the unirradiated one at 77°K (curve 4).

Ethyl iodide was irradiated at liquid nitrogen temperature in all three matrices given above at concentrations between 10^{-3} and 10^{-4} M. The spectral changes following upon irradiation depended on the viscosity of the matrix **. In the high-viscosity matrix, C (Fig. 2a), the absorption peak at 38.9 kc. cm^{-1} (curve 1) decreased regularly during the initial 15—20 minutes of photolysis. At the same time the absorption at higher frequencies increased whereas the curve is unchanged at lower frequencies. The curves for different photolysis times cross each other in an isosbestic point at about 42.4 kc. cm^{-1}.

For longer irradiation periods, up to 60 minutes, the absorption increased over the whole UV-region with a recognizable peak at about 23 kc. cm^{-1} (curve 2). This spectrum remained unchanged as long as liquid nitrogen

* Above *ca.* 10^{-4} M, the solution became turbid upon freezing.

** For an experimental study of the viscosity of the different matrices see Ref. [6]

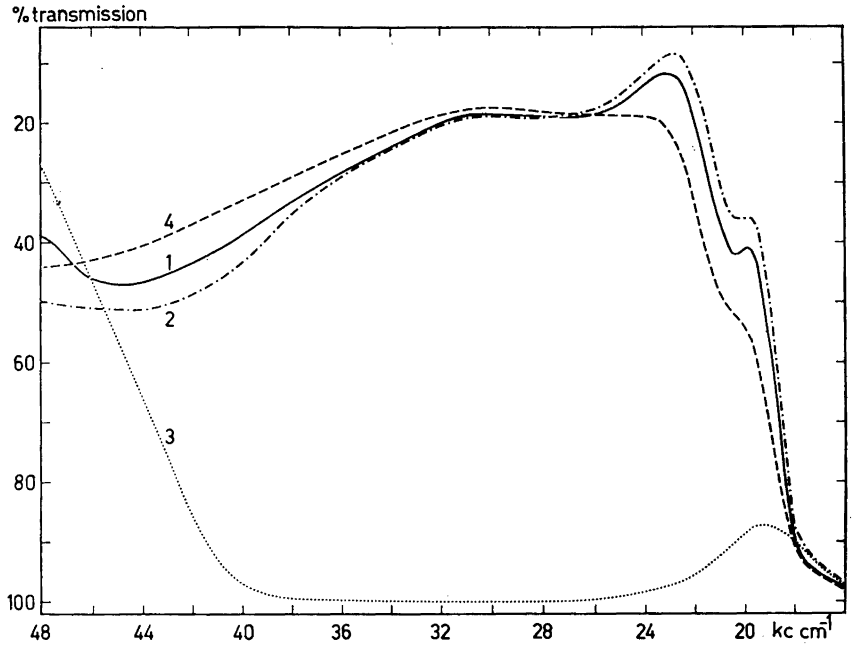

Fig. 1. Spectra of a 3 × 10^{-5} M iodine solution in matrix A. (1) before and (2) after 60 min. of photolysis at 77°K, (3) after warm-up to 298°K and (4) after recooling to 77°K.

surrounded the cell. If the sample was slowly warmed up when still in the cell compartment, the following changes in the spectrum occurred:

A weak maximum appeared at 13.9 kc. cm^{-1}, a strong double peak at 25.8 and 27.4 kc. cm^{-1}, respectively, and a peak at 34.4 kc. cm^{-1} (curve 3). When room temperature was reached the spectrum showed only the presence of iodine: a peak at 19.1 kc. cm^{-1} and an increased absorption in the far UV-region (curve 4). Refreezing to liquid nitrogen temperature, however, did not result in the spectrum of an iodine solution at 77°K (Fig. 1, curve 1); the absorption below about 30 kc. cm^{-1} is lower and above this point higher for the irradiated sample than it is for iodine (curve 5). Besides, a new peak appeared at 22.3 kc. cm^{-1}, which might be an indication of the formation of HI_3 (see below).

In the other matrices spectral changes occurred already during irradiation when the cells were surrounded by liquid nitrogen. Fig. 2b, curve 1 shows the absorption of a 0.25 mM EtI solution in matrix A at 77°K. After 5—10 minutes of irradiation a peak developed at 25.8 kc. cm^{-1} and at about 21 kc. cm^{-1} (curves 2 and 3). On prolonged irradiation peaks at 27.4 and 34.4 kc. cm^{-1} developed faster than the 25.8 kc. cm^{-1} peak, so that the final spectrum at 77°K (curve 4) was similar to that obtained in matrix C. 15 minutes of photolysis of EtI in matrix B gave rise to peaks at 25.6, 27.5 and 34.4 kc. cm^{-1} and a shoulder at about 21 kc. cm^{-1} — that is, the same characteristic frequencies as in the chemically different matrices A and C.

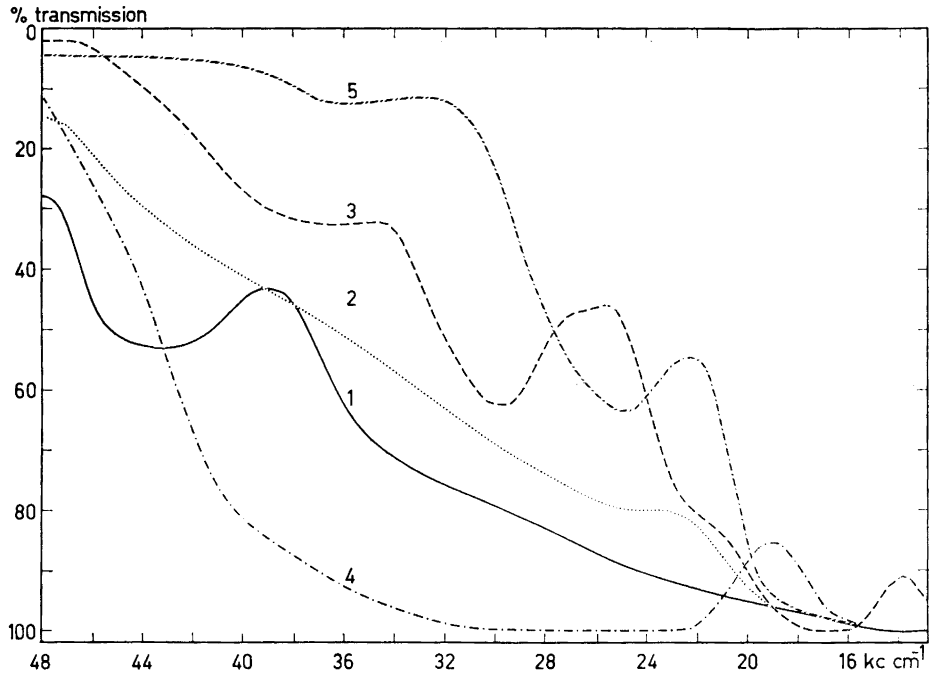

Fig. 2a. Spectra of a 2.5×10^{-4} M ethyl iodide solution in matrix C. (1) before and (2) after 60 min. of photolysis at 77°K, (3) during warm-up, at approximately 90—95°K, (4) after warm-up to 298°K and (5) after recooling to 77°K.

Hydrogen iodide. At room temperature, hydrogen iodide has an absorption maximum at 37.4 kc. cm^{-1} (Fig. 3) in the hydrocarbon mixtures used (curve 1). At liquid nitrogen temperature this maximum is changed to 36.7 kc. cm^{-1} and a new weaker maximum appears at 32.1 kc. cm^{-1} (curve 2).

Hydrogen iodide was irradiated in matrices A and B at concentrations between 2×10^{-4} and 4×10^{-4} M. In the harder matrix C, only one experiment could be performed as the cells almost invariably broke during photolysis. In both glasses the two HI absorption peaks rapidly decreased upon irradiation; after about 10 min. they had practically disappeared. The changes in spectrum as a result of the irradiation were quite analogous to those obtained with ethyl iodide. Thus, the final spectrum at low temperature was dominated by a peak at 34.4 kc. cm^{-1} and a double-peak at 27.4 and 25.8 kc. cm^{-1} (curve 3). After warm-up the spectrum was again that of iodine (curve 4) and after refreezing the spectrum resembled that of irradiated ethyl iodide under the same conditions, with a peak at 22.7 kc. cm^{-1} (curve 5).

Hydrogen iodide and iodine. (Fig. 4) Solutions were prepared in matrix A containing both hydrogen iodide (about 4×10^{-4} M) and iodine (about 3×10^{-5} M). At room temperature the spectrum showed the absorption of both compounds. At 77°K, however, the spectrum did not consist of super-

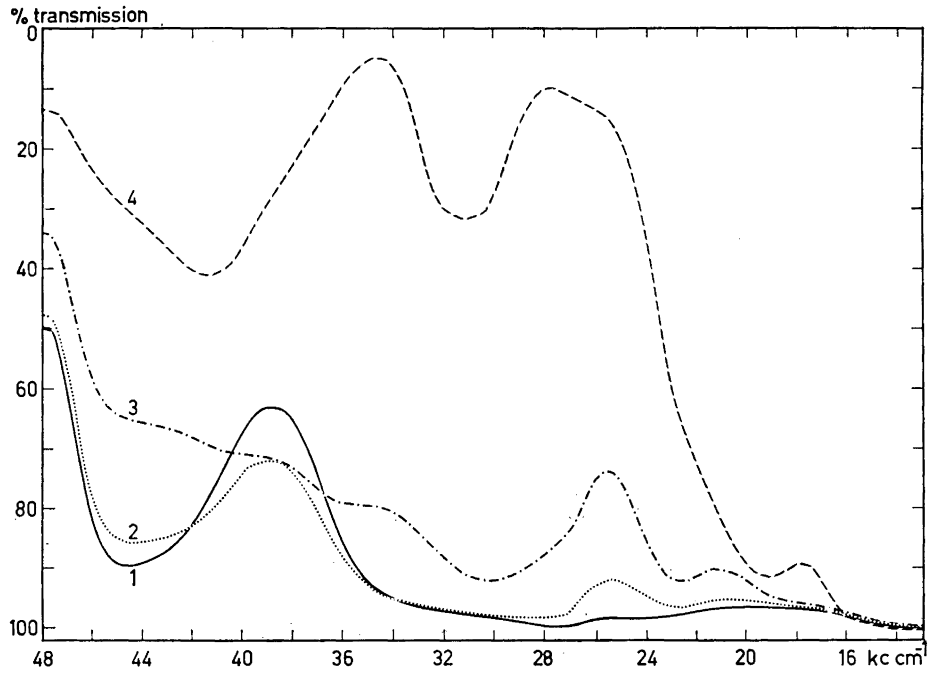

Fig. 2b. Spectra of a 2.5 × 10^{-4} M ethyl iodide solution in matrix A at 77°K. (1) before and after (2) 5 min., (3) 12 min. and (4) 30 min. of photolysis.

imposed spectra of hydrogen iodide and iodine (curve 2). The excess HI could easily be identified on a high absorption background with peaks at 36.7 and 32.1 kc. cm^{-1}. Contrary to this the low temperature absorption of iodine in the wavenumber range 28—18 kc. cm^{-1} was absent and a new sharp peak had developed at 22.1 kc. cm^{-1}. Irradiation of this mixture gave the same spectral changes as a hydrogen iodide solution alone (curve 3).

DISCUSSION

Upon freezing the violet iodine-solution in a hydrocarbon mixture solidified to a yellow, transparent glass, the color change being caused by an increase in light absorption for wavenumbers higher than about 20 kc. cm^{-1}. It has been suggested that the cause may be the low solubility of iodine at 77°K. An extrapolation made by Ham [11] led to an order of magnitude of 10^{-11} M and thus the color of the solution should be caused by microcrystals of iodine. Evans [12] has pointed out that the iodine solution may be colloidal and that Norman and Porter [1], who were able to prepare a transparent 10^{-3} M solution of iodine, probably used solvents containing impurities which formed complexes with I_2.

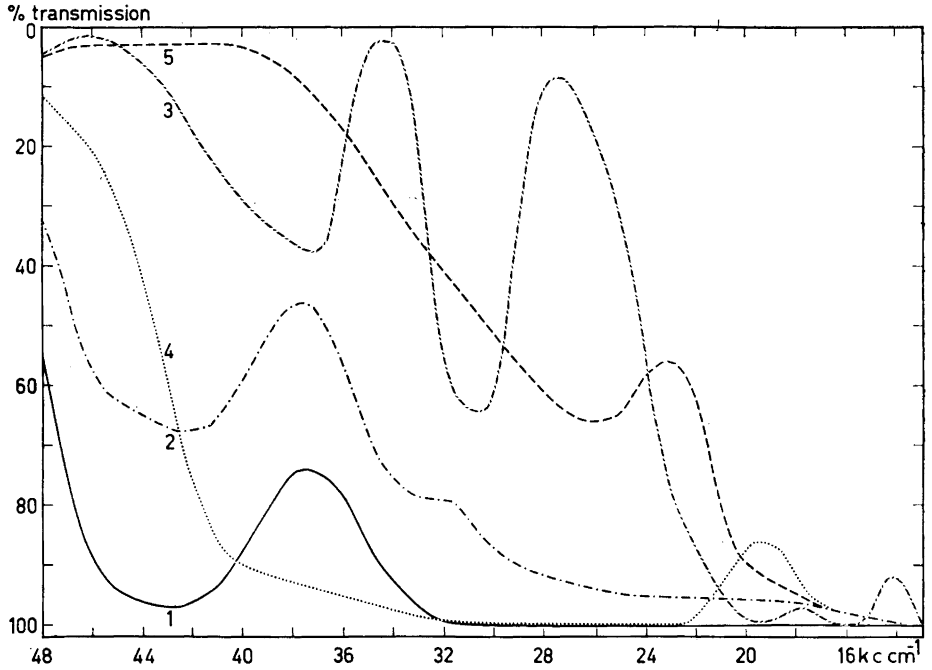

Fig. 3. Spectra of 1.9×10^{-4} M hydrogen iodide solution in matrix A. (1) at 298°K, (2) before and (3) after 60 min. of photolysis at 77°K, (4) after warm-up and (5) after recooling to 77°K.

The existence and the reproducibility of the 23.0 and 19.9 kc. cm^{-1} peaks show that certain complexes between iodine and solvent molecules must be present in all matrix-forming hydrocarbon mixtures and that the peaks probably are superimposed on a continuous background absorption. It may be the presence of complex-forming impurities in the solvents or the formation of contact charge transfer complexes [13, 14] that give rise to the peaks.

From the irradiation experiments it was apparent that iodine did not photolyze under the conditions chosen. The 23.0 kc. cm^{-1} peak, which did not change very much upon photolysis, disappeared, however, after warm-up followed by refreezing. This could simply be explained by assuming that a type of minor impurity present in both glass-forming mixtures reacts during warm-up.

The absorption curves for HI compared with those for the HI-I_2-mixture clearly demonstrated the existence of a complex between HI and I_2 at 77°K with an absorption peak at 21.9 kc. cm^{-1}. Both the photolyzed solution of HI as well as that of EtI showed the formation of I_2 upon warm-up and the same peak became visible upon refreezing at 22.4 and 22.3 kc. cm^{-1}, respectively (corrected for the background absorption).

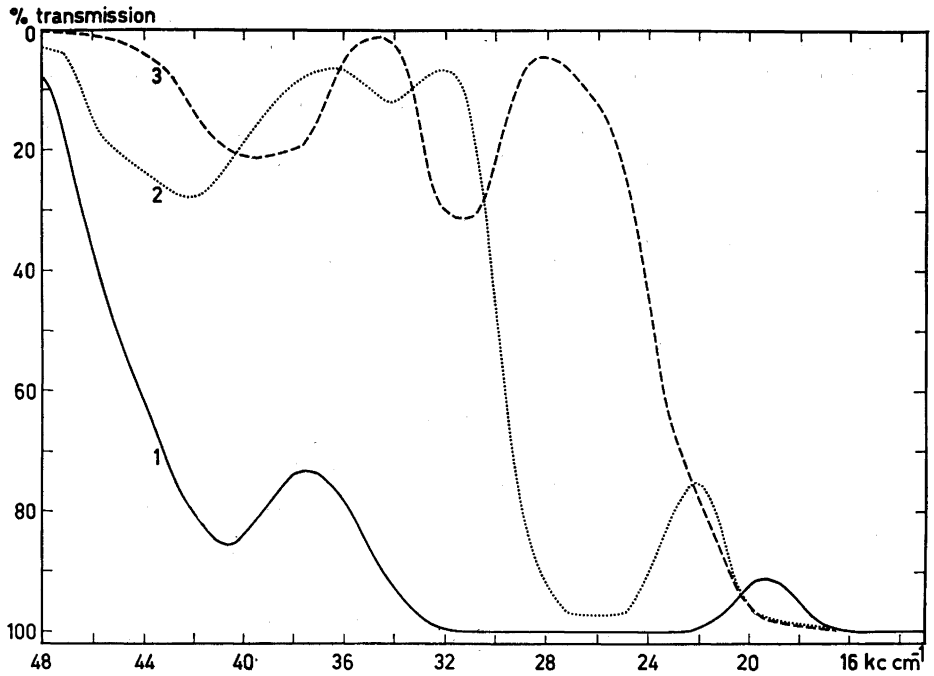

Fig. 4. Spectra of a mixture of 4×10^{-4} M hydrogen iodide plus 3×10^{-5} M iodine in matrix A solution. (1) at 298°K, (2) before and (3) after 10 min. of photolysis at 77°K.

In the experiments with EtI the influence of the viscosity of the matrix was clearly demonstrated, confirming the results of Norman and Porter [2]. In the hard matrix, C, the EtI-peak at 38.9 kc. cm^{-1} diminished continuously during rather short times of photolysis without a simultaneous formation of intermediates, which produce a higher absorption below 42.4 kc. cm^{-1} than EtI itself. The obvious suggestion is that photolysis occurred during the formation of iodine atoms and ethyl radicals [2]. For longer irradiation periods the continuously increasing absorption when going towards higher wavenumbers might be caused by secondary irradiation processes *.

When the photolyzed EtI solution in matrix C was slowly warmed up the same change occurred as in matrices A and B at 77°K, although distinct differences also were apparent. The spectral changes indicated a sequence of reactions and most probably the formation of more than one intermediate species, showing absorption maxima at 34.4, 27.4, 25.8 and 13.9 kc. cm^{-1}. That the photolysis of HI leads to the formation of the same absorption peaks must

* The optical properties of the solid solutions in the different matrices showed quite a variation at 77°K. EtI in matrix C gave a rather high background absorption (Fig. 2a, curve 1). In spite of this, the spectral changes could very well be reproduced although calculations of extinction coefficients became too uncertain to be of value.

have a profound bearing upon the nature of the intermediate products. It therefore seems that they all are related to iodine-containing intermediates and that they have very little, if anything, to do with the existence of a HI_3 complex (*cf.* Fig. 4). It is of interest, however, to note that the well-known peaks produced by an ethanolic iodine solution, at 34.5 and 27.8 kc. cm^{-1}, have been attributed to HI_3 by Batley [4], and that the 34.4 and 27.4 kc. cm^{-1} peaks obtained when EtI and HI are photolyzed develop simultaneously.

Acknowledgements. This investigation has been supported by *Directorate of Chemical Science*, AFOSR, AFRD of the Air Research and Development Command, United States Air Force, through its European Office and by the *Swedish Technical Research Council.*

REFERENCES

1. Norman, I. and Porter, G. *Nature* **174** (1954) 508.
2. Norman, I. and Porter, G. *Proc. Roy. Soc. (London)* **A 230** (1955) 399.
3. Sowden, R. G. and Davidson, N. *J. Am. Chem. Soc.* **78** (1956) 1291.
4. Batley, A. *Trans. Faraday Soc.* **24** (1928) 438.
5. Vogel, A. I. *Practical Organic Chemistry.* 3rd Ed. Longmans, London 1956, p. 470.
6. Rosengren, Kj. *Acta Chem. Scand.* **16** (1962) 1421.
7. Rosengren, Kj., Sunner, S. and Timm, D. *Acta Chem. Scand.* **16** (1962) 467.
8. Rosengren, Kj., Sunner, S. and Timm, D. *Acta Chem. Scand.* **16** (1962) 495.
9. Potts, W. J. *J. Chem. Phys.* **21** (1953) 191.
10. Rosengren, Kj. and Sunner, S. *Acta Chem. Scand.* **16** (1962) 521.
11. Ham, J. *J. Am. Chem. Soc.* **76** (1954) 3875.
12. Evans, D. F. *J. Chem. Soc.* **1957**, 4229.
13. Evans, D. F. *J. Chem. Phys.* **23** (1955) 1424.
14. Briegleb, G. *Elektronen-Donator-Acceptor-Komplexe.* Springer, Berlin 1961.

Received February 6, 1962.

ACTA CHEMICA SCANDINAVICA 16 (1962) 1463–1467

Oxidation as an Aid in the Identification of Unsaturated Hydrocarbons by Gas Chromatography

BENGT SMITH, RAGNAR OHLSON and ANNE-MARIE OLSON

Institutionen för Organisk Kemi, Chalmers Tekniska Högskola, Göteborg, Sweden

Ozone oxidation is shown to be a useful analytical tool for the identification of unsaturated hydrocarbons condensed from analytical gas chromatographs. Several of the products formed on oxidation were determined quantitatively and thus information was obtained about the position and number of various unsaturated bonds in the molecule. The qualitative analysis of the oxidation products was based on the paper chromatographic separation of the dinitrophenylhydrazones prepared from the carbonyl compounds formed on oxidation.

To aid in the identification of unsaturated hydrocarbons separated by gas chromatography, various methods are being studied in this laboratory. Recently [1], a report was published on hydrogenation methods developed for this purpose and in the present paper the utilization of ozone oxidation is described.

Among oxidation methods used in the structural investigation of unsaturated hydrocarbons, ozonolysis has generally been regarded as the best method [2] since a shift in the position of the unsaturated bonds or other rearrangements are not likely to take place (*cf.*, however, below).

Our principal aim was to determine, quantitatively, unsaturated bonds in 1- and 2-position, *i.e.* $>C=CH_2$, $>C=CH-CH_3$, $-C\equiv C-CH_3$ and $>C=C(CH_3)_2$, and further to prove the presence of alkadienes with cumulated and conjugated double bonds. The analysis was based on a quantitative determination of the following ozonolysis products: formaldehyde, acetaldehyde, acetone, glyoxal and carbon dioxide. It was also desired to obtain qualitative analysis of the carbonyl compounds formed on oxidation.

The oxidative cleavage of the unsaturated bonds was found to proceed regularly [3] except in the case of 1,2-alkadienes. According to Bon [4] this reaction can be written

$$H_2C=C=CHR \xrightarrow{O_3} HCHO + RCHO + CO_2$$

Table 1. Oxidation of unsaturated hydrocarbons by ozone.

Hydrocarbon oxidized	Amount	Oxidation products, mmole (yield %)			
Name	mmole	Formaldehyde	Acetaldehyde	Acetone	Carbon dioxide
1-Heptene	0.052	0.050 (96)			
1-Octene	0.095	0.092 (97)			
1-Nonene	0.061	0.064 (105)			
1-Undecene	0.073	0.073 (100)			
2,3,3-Trimethyl-1-butene *	0.108	0.077 (71)			
2,4,4-Trimethyl-1-pentene	0.070	0.060 (86)			
1,5-Hexadiene	0.107	0.206 (96)			
Trans-1,3,5-hexatriene **	0.024	0.042 (88)			
Styrene	0.131	0.127 (97)			
Trans-2-octene	0.027		0.025 (93)		
Trans-2-*trans*-4-hexadiene **	0.030		0.068 (113)		
1,2-Pentadiene	0.152	0.060 (40)	0.048 (32)		0.083 (55)
1,2-Hexadiene	0.104	0.052 (50)	0.042 (40)		0.047 (45)
1,2-Heptadiene	0.152	0.080 (53)	0.060 (39)		0.064 (42)
2-Pentyne	0.159		0.129 (81)		
2,4,4-Trimethyl-2-pentene	0.025			0.022 (88)	

* Criegee [3] has reported that certain olefins of this type ($R_2C{=}CH_2$) are oxidized by ozone to aldehydes $R_2CH{-}CHO$ and carboxylic acids $R_2CH{-}COOH$.

** The yield of glyoxal was not quantitative.

In the ozonolysis of the three 1,2-alkadienes in Table 1, however, acetaldehyde was unexpectedly formed. This fact seems to imply that a rearrangement occurs during the oxidation. The results are consistent with an isomerization to a 2-alkyne *:

$$CH_2{=}C{=}CHR \longrightarrow CH_3{-}C{\equiv}CR$$

According to the formulas given above, the sum of formaldehyde and acetaldehyde or carbon dioxide and acetaldehyde should equal 100 %. This was in fact found to be the case within the limits of error valid for our experiments (*cf.* Table 1). The formation of carbon dioxide is indicative of the presence of an allene. Alkadienes with conjugated double bonds give rise to glyoxal. The yield obtained was, however, rather variable and generally considerably less than expected. Because of this, a quantitative analysis could not be based on the glyoxal determination.

In most cases the yield of oxidation products was over 80 %. This result must be considered satisfactory in view of the losses encountered in the chromatographic separation and during the oxidation procedure. It is seen from Table 1 that the presence of several unsaturated bonds in a molecule, *e.g.* in 1,5- and 2,4-hexadiene and in 1,3,5-hexatriene, is clearly revealed by the amount of formaldehyde and acetaldehyde formed.

* The ready isomerization of allene to methylacetylene is a well-known reaction [5].

To map out the products formed during the ozone oxidation and prior to their quantitative determination a paper chromatographic separation of the dinitrophenylhydrazones formed on reaction of the ozonized solution with 2,4-dinitrophenylhydrazine was made [6]. A measure of the amount of a dinitrophenylhydrazone contained in a spot on the filter paper was obtained by cutting out the spot, extracting the paper with pyridine and titrating the pyridine solution according to Sensabaugh *et al.* [7] using 0.01 N tetrabutylammonium hydroxide. This titration method was found to be useful for determining whether a spot on the filter paper was formed from a major or a minor product in a hydrocarbon mixture. It was also usable for tracing bis-hydrazones formed from difunctional carbonyl compounds since two inflexion points were obtained in the titration curve in this case. It should be emphazised that this titration method does not give an accurate measure of the carbonyl compounds formed in the ozonolysis, since, in the method used, the conversion of the carbonyl compounds into their dinitrophenylhydrazones was not quantitative.

The paper chromatographic method was not too selective, merely giving the carbon number for monofunctional carbonyl compounds up to about C_7. Because of their low R_F-values, the dinitrophenylhydrazones of low molecular difunctional carbonyl compounds, *e.g.* glyoxal and methylglyoxal, could be distinguished from the dinitrophenylhydrazones of monofunctional carbonyl compounds.

The present investigation has proved the utility of ozone oxidation for the identification of unsaturated hydrocarbons separated by gas chromatography. The method, however, is not ideal in all respects. For the qualitative identification of the oxidation products, a more selective and more rapid method than the paper chromatographic one used would be desirable. Furthermore, the quantitative determination is somewhat laborious and only applicable to certain of the oxidation products. The results of the quantitative determinations are collected in Table 1.

It would be a great advantage if the analysis of the oxidation mixture could be made by gas chromatography. We think that the problem could be successfully attacked by utilizing a flame ionisation detector and by performing the ozonolysis in a solvent for which the detector in question is blind.

EXPERIMENTAL

Condensation of fractions from the chromatograph. A known volume of a hydrocarbon fraction was injected into the chromatograph by means of a Hamilton syringe and, after separation, appropriate pure compounds were condensed in a sample tube immersed in a dry ice-acetone bath. The amount of material in the condensed fractions was calculated on the basis of the chromatogram, putting area percentage equal to weight percentage.

Ozonolysis. Among the limited number of usable solvents, ethyl acetate was chosen. When pure, it was not attacked by ozone. It was not necessary to take any special measures in order to decompose the ozonides; the oxidized solution could be treated directly by the various reagents used to determine the carbonyl compounds quantitatively or to transform them into dinitrophenylhydrazones.

Ethyl acetate (0.5 ml) was filled into the sample tube and the level of the solvent marked on the tube. A wash-bottle containing a solution of barium hydroxide (for the absorption of carbon dioxide, *cf.* below) was coupled to the sample tube and the train

was concluded by another wash-bottle with an acidified potassium iodide solution to indicate any break-through of ozone. The sample tube was cooled to 0° in iced water and the reaction train connected to the ozone generator and a stream of 10 ml of oxygen per min. bubbled through until the uptake of ozone was complete as shown by the indicator wash-bottle *.

Ethyl acetate was added to the cool-finger to compensate for losses during the oxidation procedure. Of the contents of the sample tube, 0.1 – 0.2 ml was used for the preparation of dinitrophenylhydrazones. The remainder was used for the quantitative determination of one or several of the following compounds: formaldehyde, acetaldehyde, acetone and glyoxal. As the quality of commercial ethyl acetate, also of analytically pure samples, was rather variable, it was necessary to oxidize a sample and investigate the oxidation products by paper chromatography before using it as solvent in an experiment. Any carbon dioxide formed during the ozonolysis was determined in the barium hydroxide solution as detailed below.

Preparation and paper chromatographic separation of dinitrophenylhydrazones. To the solution of ozonides in ethyl acetate was added 1 ml of a dinitrophenylhydrazine reagent made up by dissolving 1 g of 2,4-dinitrophenylhydrazine in 25 m of 85 % phosphoric acid using a steam bath and, after cooling, diluting the mixture to 50 ml with ethanol [8]. The reaction mixture was heated for some minutes in a water bath (60°) and after cooling allowed to stand for 30 min. The dinitrophenylhydrazones formed were extracted 5 times by 0.5 ml portions of pentane. The pentane was evaporated and the residue dissolved in 0.1 ml pentane. This solution was analyzed by paper chromatography according to Meigh [6] using heptane-methanol, the heptane phase being the mobile one.

Quantitative determinations

Formaldehyde. For the quantitative determination of formaldehyde, the chromotropic acid method was used [9-11]. The density of the red solution formed was measured at 570 mμ against a blank of ethyl acetate treated in the same way as the sample. The amount of formaldehyde in the sample was read from a standard curve prepared by subjecting known amounts of formaldehyde in ethyl acetate, determined by titration [12], to the method.

Acetaldehyde and acetone have been shown to interfere with the determination of formaldehyde by the present method [11]. We have, in accordance with the recommendations of Bricker and Johnson [11], reduced this interference by using larger amounts than usual of chromotropic acid and by dilution with sulphuric acid instead of water.

Acetaldehyde. Eegrive [13] has proposed a colorimetric method for the quantitative determination of acetaldehyde which was found applicable in this case. The procedure developed by Tompsett [14] was used here. It involves a reaction with *p*-hydroxydiphenyl in the presence of copper sulphate and conc. sulphuric acid. A red colour is developed and the density of the solution was measured at 560 mμ against a blank of ethyl acetate treated in the same way as the sample. The amount of acetaldehyde was determined from a calibration curve. We have investigated the influence of a number of lower aldehydes and ketones on the results but have not found any appreciable effect **.

Acetone. For the quantitative determination of acetone, a colorimetric method has been worked out by Ravin [15]. It is based on the reaction of acetone with salicylaldehyde in the presence of strong alkali and heat giving red dihydroxybenzalacetone. The original method was later on modified by Nadeau [16] and Pawan [17]. The density of the solution was measured at 520 mμ against a blank of ethyl acetate treated like the sample. The amount of acetone was obtained from a calibration curve.

Glyoxal. For the quantitative determination of glyoxal, a method devised by Wise *et al.* [18], using dianilinoethane, was employed. The density of the coloured solution formed

* The ozone contents of the oxygen was generally about 5 %.

** Formaldehyde was stated by Tompsett [14] to interfere with the determination of acetaldehyde and he has described an aeration procedure for the separation of these aldehydes prior to the determination of acetaldehyde. Because of the relatively large errors, inherent in our experiments, we have, however, not found it necessary to make any separation.

was measured at 550 mμ. As usual, ethyl acetate treated just like the sample was used in the reference beam and the amount of glyoxal read from a calibration curve. Methylglyoxal was found to interfere with the determination of glyoxal.

Carbon dioxide. Carbon dioxide formed upon the ozonolysis of 1,2-alkadienes was determined by absorbing it in a barium hydroxide solution in a wash-bottle placed after the sample tube in the oxidation train and titrating the excess of base using 0.01 N hydrochloric acid and phenolphthaleine as indicator [19]. A blank was prepared in the same way, using pure ethyl acetate in the sample tube.

Acknowledgement. This work was supported by grants from the *Swedish Technical Research Council* and the *Town Council of Gothenburg.*

REFERENCES

1. Smith, B. and Ohlson, R. *Acta Chem. Scand.* **14** (1960) 1317.
2. Polgar, A. and Jungnickel, J. L. in *Organic Analysis*, vol. III, p. 276, Interscience, New York 1956.
3. Criegee, R. in *Ozone Chemistry and Technology, Advances in Chemistry Series,* No 21, p. 133, Am. Chem. Soc. 1959.
4. Bon, M. D. *Ann. Leningrad State Univ., Chem. Ser.* **3** (1938) 3; *Chem. Zentr.* 1939: II, 366.
5. Fieser, L. F. and Fieser, M. *Introduction to Organic Chemistry*, D. C. Heath and Co., Boston 1957, p. 301.
6. Meigh, D. F. *Nature* **169** (1952) 706; **170** (1952) 579.
7. Sensabaugh, A. J., Cundiff, R. H. and Markunas, P. C. *Anal. Chem.* **30** (1958) 1445.
8. Cheronis, N. D. and Entrikin, J. B. *Semimicro qualitative organic analysis*, 2nd ed. Interscience, New York 1957, p. 392.
9. Eegrive, E. *Z. anal. Chem.* **110** (1937) 22.
10. Boyd, M. J. and Logan, M. A. *J. Biol. Chem.* **146** (1942) 279.
11. Bricher, E. E. and Johnson, K. R. *Ind. Eng. Chem. Anal. Ed.* **17** (1945) 400.
12. Blank, O. and Finkenbeiner, H. *Ber.* **31** (1898) 2979.
13. Eegrive, E. *Z. anal. Chem.* **95** (1933) 323.
14. Tompsett, S. L. *Anal. Chim. Acta* **19** (1958) 360.
15. Ravin, A. *J. Biol. Chem.* **115** (1936) 511.
16. Nadeau, G. *Can. Med. Assoc. J.* **67** (1952) 158.
17. Pawan, G. L. S. *Biochem. J.* **68** (1958) 33 P.
18. Wise, C. S., Mehltretter, C. L. and van Cleve, J. W. *Anal. Chem.* **31** (1959) 1241.
19. Kienitz, H. in Houben-Weyl *Methoden der organischen Chemie*, 4th Ed., part II p. 769. G. Thieme Verlag, Stuttgart 1953.

Received February 7, 1962.

ACTA CHEMICA SCANDINAVICA 16 (1962) 1468–1480

Studies on the Coagulation of Chicken Blood

VI. Use of Cobalt Carbonate, Barium Phosphate, Lead Carbonate and Lead Phosphate for Differentiation and Assay of Strontium Carbonate Non-adsorbable Labile Factors

ØYVIND SØRBYE* and INGER KRUSE

Department of Biochemistry and Nutrition, Polytechnic Institute, Copenhagen, Denmark

The multiple nature of the labile factor activity of strontium carbonate adsorbed oxalated chicken plasma was revealed by adsorption studies. The results obtained with fifty-two selected crystalline adsorbents are explained as adsorption of four different labile coagulation factors by four different groups of adsorbents, represented by the title compounds. Provisional names for these factors are suggested: λ (lambda)-factor is selectively adsorbed by cobalt carbonate, π (pi)-factor by lead carbonate, β (beta)-factor by lead phosphate, and γ (gamma)-factor by barium phosphate. The activity of λ-factor is independent of the concentrations of the other three factors. The activities of β- and π-factors are also mutually independent, whereas γ-factor acts as a synergist both for π-factor and for β-factor. When Russell's viper venom (RVV), with or without cephalin, is substituted for thromboplastin in the assay system, γ- and π-factors are inactive. β-Factor is active only if RVV is supplemented with cephalin. λ-Factor is part of the labile factor activity measured by all three assay accelerators. Determination of the minimum amount of the adsorbents required for maximal adsorption of labile factor activity is suggested as a possibility for quantitative determination of the adsorbable factors.

It was shown in a previous paper[1] that the reduced labile factor activity of strontium (or barium) carbonate adsorbed oxalated chicken plasma was due to adsorption of two labile coagulation factors. The two factors could be adsorbed separately by other adsorbents: ψ-factor by calcium carbonate, calcium oxalate or calcium molybdate and σ-factor by barium oxalate, barium chromate or strontium oxalate.

A number of other insoluble inorganic compounds have been tested for adsorption of the strontium carbonate non-adsorbable labile factor activity.

* Fellow of the Royal Norwegian Council for Scientific and Industrial Research.

In most cases only a part of the total activity could be adsorbed by each of these adsorbents. These results indicated that the labile factor activity of strontium carbonate adsorbed oxalated chicken plasma is of a complex nature and may be regarded as the combined activities of a number of separate labile coagulation factors differing characteristically in adsorbability. Our previous experiences with compounds showing partial adsorption of the strontium carbonate non-adsorbable labile factor activity, were presented in a short communication [2]. The present study deals with fifty-two selected adsorbents by means of which four different strontium carbonate non-adsorbable labile coagulation factors can be adsorbed separately.

MATERIALS AND METHODS

In addition to methods and materials described previously [1,3] the following materials were used in the present study.

Strontium carbonate plasma. Oxalated chicken plasma was adsorbed by strontium carbonate (20—25 mg/ml of a commercial preparation *) to remove the $\varkappa$-, δ-, φ-, ψ- and σ-factors completely.

Adsorbents. The compounds listed below were used as plasma adsorbents in the present study.

Carbonates of Co and Pb, oxides of W, Sb and Bi, Sn mono- and dioxide, sulfates of Pb and Ba, ferri-ferrocyanide, Pb-metaborate, and phosphates of Ba, Sr, Mg, and Co— all were kindly supplied by the Department of Inorganic Chemistry of The Polytechnic Institute. Other adsorbents were prepared in this laboratory, according to procedures described in Gmelin-Kraut's Handbuch der Anorganischen Chemie. These adsorbents were prepared from high purity chemicals by (1) precipitation of aqueous solutions, (2) thermal decomposition of unstable compounds, or (3) reactions between solids in the molten state.

Oxalates of Co and Pb were prepared from hot (90°C) aqueous solutions of soluble salts by precipitation with excess of a hot solution of ammonium oxalate and oxalic acid in equimolar amounts.

Fluorides of Mg and Sr were prepared by melting a mixture containing 5 parts of magnesium chloride or 6 parts of strontium chloride mixed with 4 parts of sodium fluoride and 4 parts of sodium chloride.

Borates of Co and Mn were prepared from the oxide and the carbonate, respectively, by melting with an equimolar mixture of potassium bifluoride and boric acid anhydride.

Oxides of Co, Ni and Cd were prepared by thermal decomposition of the carbonates or oxalates at 500—700°C in air. A commercial preparation of Be-oxide was made crystalline by heating with boric acid anhydride at 1200°C.

Sulfite of Ca was prepared by SO_2-gas saturation of an aqueous suspension of calcium carbonate, followed by filtration and heating of the filtrate on a steam bath.

Sulfides of As and Sb were prepared from dilute hydrochloric acid solutions of the oxides by precipitation with hydrogen sulfide gas or sodium thiosulfate solution. After washing and drying the products were heated in sealed ampullae at 200°C for at least 48 h.

Phosphates of Be, Zr, Th, Fe, Ce and Al ** were prepared from the oxides (Be, Zr), oxalate (Th), carbonate (Fe) and sulfates (Ce, Al), respectively, by melting with 5 parts of sodium metaphosphate at 1000°C.

The phosphate of Mn was prepared by heating of a 10 % phosphoric acid solution saturated with manganese carbonate. The phosphate of Pb was prepared from a lead acetate solution by precipitation with sec. sodium phosphate. A crystalline product was obtained by heating of the washed amorphous precipitate suspended in 8—10 % acetic acid, to 90—100°C.

* From H. Struers chemiske Laboratorium, Copenhagen.

** Whether ortho- or meta-phosphates were formed by this procedure was not investigated.

Basic lead chromate was prepared from a suspension of yellow lead chromate in slightly more than equimolar amounts of sodium hydroxide (as a 5 % (w/v) solution). The suspension was boiled until the colour had changed to bright brick red.

Silicates of Be, Mn and Co were prepared from the sulfates (Be, Mn) and the oxide (Co), respectively, by melting with sodium metasilicate and sodium sulfate or boric acid anhydride.

Aluminates of Co and Be were prepared by melting sodium chloride (sulfate) and sodium aluminate with metal chloride (sulfate) in excess. After washing and drying the insoluble product was remelted with 5 parts of boric acid anhydride.

Tungstates of Ca, Ba, Mn, Fe, Pb, and Co were prepared by melting one part of sodium tungstate with two parts of sodium chloride (sulfate) and a 2—3 fold excess of metal chloride (sulfate). Tungstate of Ce was prepared similarly from cerous sulfate with sodium tungstate in excess.

Molybdates of Ba, Pb, and Co were prepared by melting one part of sodium molybdate with two parts of sodium chloride and a 2—3 fold excess of metal chloride.

All preparations were thoroughly washed with distilled water, treated with 96 % ethanol and dried at 80°C overnight before use. The melts were treated with water to remove soluble material and pulverized before the final washing. The adsorbents were obtained as crystalline or micro-crystalline powders. For comparison, amorphous modifications of a few of the adsorbents were also prepared.

EXPERIMENTS AND RESULTS

Adsorption of strontium carbonate non-adsorbable labile factors. Inorganic insoluble compounds were tested for adsorption of the strontium carbonate non-adsorbable labile factor activity as described previously [1], using strontium carbonate preadsorbed oxalated chicken plasma instead of untreated plasma. The amounts of strontium carbonate used for preadsorption were more than adequate for complete adsorption of the $\varkappa$-, δ-, φ-, ψ-, and σ-factors. No inhibitory effects could be detected in plasmas treated with these adsorbents, and plasma pH was not changed significantly [1].

The results of a preliminary testing of the compounds described in this paper, are summarized in Table 1. The adsorbents listed caused only partial adsorption of the labile factor activity of strontium carbonate plasmas and could thus be classified as selective adsorbents [1].

A detailed study of the effect of the adsorbents revealed that labile factor activity was adsorbed proportionally to the amounts of adsorbent added until, at a certain concentration of adsorbent, no more labile factor activity could be adsorbed by increasing the amounts of adsorbent. Renewed treatment with the same adsorbent caused no further reduction of the labile factor activity. Typical adsorption curves obtained with 8 different adsorbents are shown in Figs. 1 (A—H). All the other adsorbents of Table 1 gave similar adsorption curves.

As pointed out previously [1], partial adsorbability of the labile factor activity by an adsorbent indicates that the adsorbable and the non-adsorbable activities are not due to the same labile coagulation factors. The labile factor activity of strontium carbonate preadsorbed plasmas may be regarded, therefore, as the combined activity of distinct labile coagulation factors with characteristic differences in adsorbability.

Matching experiments. The effects of different adsorbents were compared in a series of matching experiments, carried out as described previously [1]

Table 1. Adsorption of labile factor activity from strontium carbonate plasma.

Plasma No.	Adsorbent	mg/ml	Activity in % of strontium carbonate plasma	Labile factor adsorbed *	Plasma No.	Adsorbent	mg/ml	Activity in % of strontium carbonate plasma	Labile factor adsorbed *
2031	lead carbonate	40	70		5351	cobalt aluminate	40	85	
		80	70				70	85	λ
3162 a	tungsten trioxide	50	89		3571	barium phosphate	70	78	
		100	89				100	78	
3361	cadmium oxide	20	69		3166	strontium phosphate	10	94	
		100	69				60	94	
3375	lead sulfate	20	89		3162 b	magnesium phosphate	50	79	
		100	89	π			100	79	
3600	lead metaborate	50	84		3163	cobalt phosphate	50	86	
		100	84				100	86	
3570	lead oxalate	20	86		1137	manganous phosphate	50	90	
		100	86				100	90	
3523	lead molybdate	20	84		5060 a	cerous phosphate	40	84	
		100	84				60	84	
321	lead phosphate	100	76		5060 b	beryllium phosphate	40	86	
		200	76				60	86	
3505	lead tungstate	50	81		5073	ferric phosphate	40	88	
		100	81	β			60	88	γ
3530	basic lead chromate	20	87		5060 b	aluminium phosphate	40	86	
		80	87				90	86	
1695	cobalt carbonate	120	60		5329 a	thorium phosphate	20	86	
		150	60				40	86	
3585	cobalt oxalate	70	82		5329 b	zirconium phosphate	20	89	
		120	82				40	89	
1113	cobalt borate	20	86		3352	antimony trioxide	20	86	
		50	86				100	86	
3554	cobalt molybdate	60	86	λ	3589	bismuth oxide	40	69	
		120	86				120	69	
3561	cobalt tungstate	60	90		3361	stannous oxide	50	85	
		120	90				100	85	
3696	cobalt solicate	50	78		3361	stannic oxide	50	85	
		100	78				100	85	

* Determined by matching experiments (pp. 1473-1477).

Table 1 (cont.)

Plasma No.	Adsorbent	mg/ml	Activity in % of strontium carbonate plasma	Labile factor adsorbed *	Plasma No.	Adsorbent	mg/ml	Activity in % of strontium carbonate plasma	Labile factor adsorbed *
3162 a	cobaltous oxide	20	78		3530	calcium tungstate	20	89	
		100	78				80	89	
1979	nickel sesquioxide	20	88		3503	barium tungstate	20	92	
		40	88				80	92	
5219	beryllium oxide	40	79		5633	cerous tungstate	40	89	
		70	79				70	89	
5569	arsenic trisulfide	10	90		5889	manganous tungstate	40	86	
		30	90				80	86	
5890	antimony trisulfide	30	83		5890	ferrous tungstate	40	83	
		50	83				60	83	
3568	calcium sulfite	40	88	γ	5209	beryllium silicate	40	86	γ
		80	88				60	86	
3361	barium sulfate	50	85		5889	manganous silicate	40	86	
		100	85				60	86	
3596	ferri-ferro cyanide	20	77		3583	barium molybdate	20	85	
		100	77				100	85	
457	magnesium fluoride	100	75		5896	manganous borate	40	86	
		200	75				60	86	
1110	strontium fluoride	50	92		5209	beryllium aluminate	40	86	
		100	92				60	86	

* Determined by matching experiments (pp. 1473-1477).

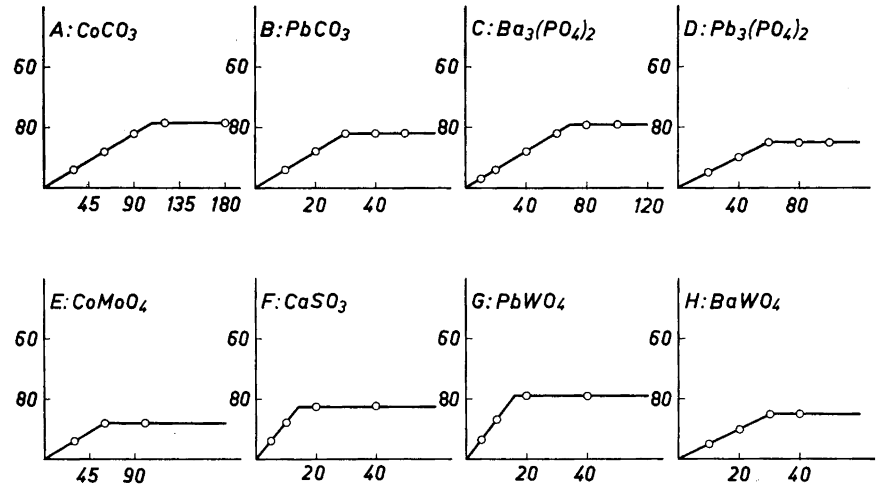

Figs. 1. Adsorption of labile factor activity.

Ordinates: labile factor activity in % of strontium carbonate plasma.
Abscissæ: adsorbent in mg/ml.

A: cobalt carbonate;
B: lead carbonate;
C: barium phosphate;
D: lead phosphate;
E: cobalt molybdate;
F: calcium sulfite;
G: lead tungstate;
H: barium tungstate.

with strontium carbonate plasma instead of untreated plasma. Representative results of such experiments are shown in Figs. 2—4 (A—H). The effects obtained by use of cobalt carbonate, barium phosphate, lead carbonate and lead phosphate were first compared.

The labile factor activities adsorbed by cobalt carbonate and barium phosphate were not reduced after preadsorption of strontium carbonate plasmas by barium phosphate and cobalt carbonate, respectively (Figs. 2A and 2B), and the minimum amounts of each of the two adsorbents required for maximal adsorption of activity remained unchanged after preadsorption by the other adsorbent. The labile factor activities adsorbed by these adsorbents are therefore due to two different labile coagulation factors, and the activities of the factors are mutually independent. Parallel adsorption curves are thus the results of matching experiments with compounds adsorbing different factors with additive effects.

Experiments with lead carbonate and barium phosphate gave the two sets of curves shown in Figs. 2C and 2D. The minimum amounts of each of these adsorbents necessary for maximal adsorption of activity, were not changed after preadsorption by the other adsorbent, but the adsorbable activities were reduced. The experiments indicate that the activities adsorbed by lead carbonate and barium phosphate are due to two different labile factors, the activity of each of which is increased in the presence of the other. Converging

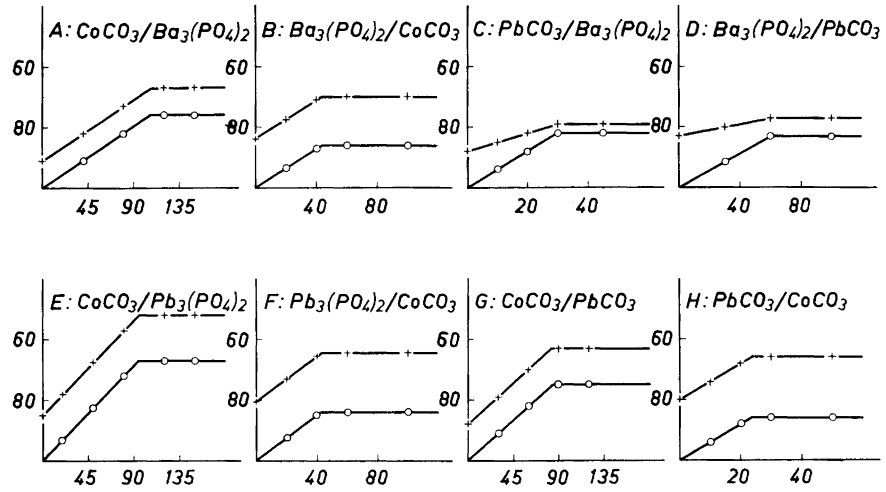

Figs. 2. Comparison of adsorbents I.

Ordinates: labile factor activity in % of strontium carbonate plasma.
Abscissæ: adsorbent in mg/ml.
O: untreated strontium carbonate plasma.
+: preadsorbed strontium carbonate plasma.

A: cobalt carbonate adsorption of untreated and barium phosphate (80 mg/ml) preadsorbed plasma.
B: barium phosphate adsorption of untreated and cobalt carbonate (80 mg/ml) preadsorbed plasma.
C: lead carbonate adsorption of untreated and barium phosphate (80 mg/ml) preadsorbed plasma.
D: barium phosphate adsorption of untreated and lead carbonate (40 mg/ml) preadsorbed plasma.
E: cobalt carbonate adsorption of untreated and lead phosphate (70 mg/ml) preadsorbed plasma.
F: lead phosphate adsorption of untreated and cobalt carbonate (100 mg/ml) preadsorbed plasma.
G: cobalt carbonate adsorption of untreated and lead carbonate (40 mg/ml) preadsorbed plasma.
H: lead carbonate adsorption of untreated and cobalt carbonate (120 mg/ml) preadsorbed plasma.

adsorption curves are thus the results of matching experiments with compounds adsorbing two different labile factors with synergistic effects.

The activities adsorbed by cobalt carbonate and lead phosphate were due to two different labile factors with independent activities (Figs. 2E and 2F). The activities adsorbed by cobalt carbonate and lead carbonate were also different and unrelated (Figs. 2G and 2H).

The activity adsorbed by lead carbonate was different from and unrelated to the activity adsorbed by lead phosphate (Figs. 3A and 3B), whereas the activities adsorbed by barium phosphate and lead phosphate are due to two different factors with synergistic effects (Figs. 3C and 3D).

The results obtained by the use of these four adsorbents can thus be explained as adsorption of four different labile coagulation factors. For these factors we have adopted the following terms:

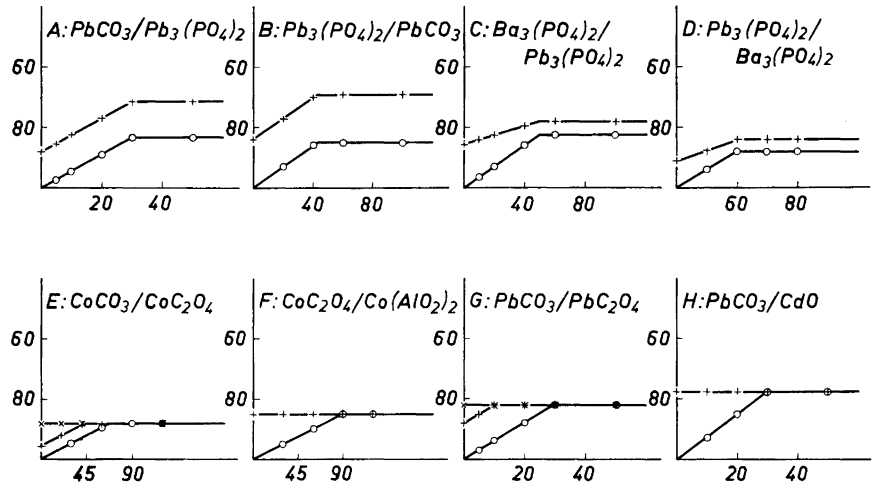

Figs. 3. Comparison of adsorbents II.

Ordinates: labile factor activity in % of strontium carbonate plasma.
Abscissæ: adsorbent in mg/ml.
O: untreated strontium carbonate plasma.
\+ and ×: preadsorbed strontium carbonate plasma.

A: lead carbonate adsorption of untreated and lead phosphate (60 mg/ml) preadsorbed plasma.
B: lead phosphate adsorption of untreated and lead carbonate (40 mg/ml) preadsorbed plasma.
C: barium phosphate adsorption of untreated and lead phosphate (60 mg/ml) preadsorbed plasma.
D: lead phosphate adsorption of untreated and barium phosphate (60 mg/ml) preadsorbed plasma.
E: cobalt carbonate adsorption of untreated plasma and plasma preadsorbed by 20 mg/ml (+) and by 60 mg/ml (×) of cobalt oxalate.
F: cobalt oxalate adsorption of untreated and cobalt aluminate (40 mg/ml) preadsorbed plasma.
G: lead carbonate adsorption of untreated plasma and plasma preadsorbed by 10 mg/ml (+) and by 20 mg/ml (×) of lead oxalate.
H: lead carbonate adsorption of untreated and cadmium oxide (10 mg/ml) preadsorbed plasma.

λ(lambda)-factor for the labile factor adsorbed by cobalt carbonate,
π(pi)-factor for the labile factor adsorbed by lead carbonate,
γ(gamma)-factor for the labile factor adsorbed by barium phosphate, and
β(beta)-factor for the labile factor adsorbed by lead phosphate.

The effects of λ-factor, π-factor and β-factor are apparently purely additive as are the effects of λ-factor and γ-factor. The latter factor, however, appears to act as a synergist both for π-factor and β-factor.

The effects of the other adsorbents could by similar experiments be compared to that of each of these four prototypes of adsorbents.

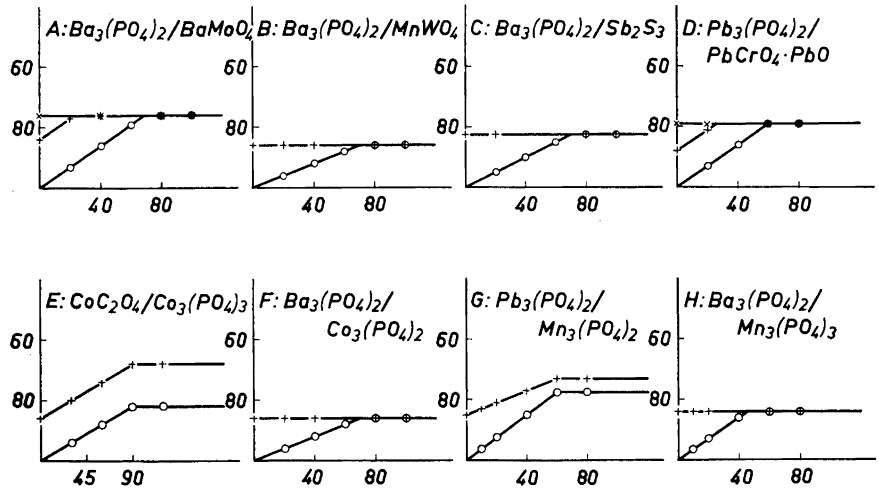

Figs. 4. Comparison of adsorbents III.

Ordinates: labile factor activity in % of strontium carbonate plasma.
Abscissæ: adsorbent im mg/ml.
O: untreated strontium carbonate plasma.
+ and ×: preadsorbed strontium carbonate plasma.

A: barium phosphate adsorption of untreated plasma and plasma preadsorbed by 10 mg/ml (+) and by 20 mg/ml (×) of barium molybdate.
B: barium phosphate adsorption of untreated and manganese tungstate (40 mg/ml) preadsorbed plasma.
C: barium phosphate adsorption of untreated and antimony trisulfide (30 mg/ml) preadsorbed plasma.
D: lead phosphate adsorption of untreated plasma and plasma preadsorbded by 30 mg/ml (+) and by 60 mg/ml (×) of basic lead chromate.
E: cobalt oxalate adsorption of untreated and cobalt phosphate (30 mg/ml) preadsorbed plasma.
F: barium phosphate adsorption of untreated and cobalt phosphate (30 mg/ml) preadsorbed plasma.
G: lead phosphate adsorption of untreated and manganese phosphate (50 mg/ml) preadsorbed plasma.
H: barium phosphate adsorption of untreated and manganese phosphate (50 mg/ml) preadsorbed plasma.

Figs. 3E and 3F show that adsorption by cobalt oxalate and cobalt aluminate can reduce the labile factor activity to the same level as obtained with cobalt carbonate and cobalt oxalate, respectively, and that cobalt carbonate and cobalt oxalate cause no further reduction of the activity of plasmas preadsorbed by adequate amounts of cobalt oxalate or cobalt aluminate, respectively. The effects of the latter two adsorbents are thus due to adsorption of λ-factor.

In the same way it was shown that the effects of lead oxalate or cadmium oxide were due to adsorption of π-factor (Figs. 3G and 3H). Barium molybdate, manganese tungstate and antimony trisulfide were all shown to adsorb γ-factor (Figs. 4 A—C). The factor adsorbed by basic lead chromate was identified as β-factor (Fig. 4D). The factor adsorbed by cobalt phosphate was unrela-

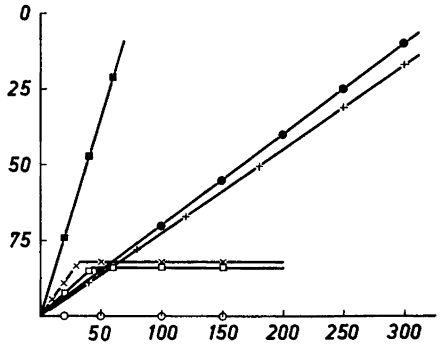

Fig. 5. Differences in effect between crystalline and amorphous adsorbents.

Ordinate: labile factor activity in % of strontium carbonate plasma.
Abscissæ: adsorbent im mg/ml.

○: crystalline barium oxalate, plasma No. 3747.
●: amorphous barium oxalate, plasma No. 3510.
□: crystalline lead phosphate, plasma No. 313.
■: amorphous lead phosphate, plasma No. 222.
×: crystalline lead molybdate, plasma No. 3565.
+: amorphous lead molybdate, plasma No. 3510.

ted to λ-factor (Fig. 4E) and shown to be γ-factor (Fig. 4F). Manganese phosphate adsorbed a factor, acting as a synergist for β-factor (Fig. 4G). It was identified as γ-factor (Fig. 4H). By the same technique the effects of all the other adsorbents could be identified as adsorption of λ-, π-, γ-, or of β-factor. The results of all these experiments are seen from the last column of Table 1.

From the recorded experiments it is apparent that the ratio of adsorbable to total activity of strontium carbonate plasmas can vary in different experiments with the same adsorbent or with compounds shown to adsorb the same factor. Such variations, previously observed for the relative activities of ψ- and σ-factors [1], were ascribed partly to differences in the sensitivity of the substrate plasmas to adsorbable and nonadsorbed factors, and partly to possible differences between individual fresh plasmas in the relative concentrations of these factors. The present discovery of synergistic effects of certain labile factors and purely additive effects of others, shows that the influence of the concentration of non-adsorbed factors on the relative activity of an adsorbable factor is complex. The influence of *increased* concentrations of factors with additive effects is thus equivalent to *decreased* concentrations of factors with synergistic effects.

Crystalline versus amorphous adsorbents. It has been stated [4] that selective adsorption of the $\varkappa$-, δ- and φ-factors was accomplished only by crystalline adsorbents, whereas no clear-cut differentiation of these coagulation activities could be obtained with the corresponding amorphous preparations. For the adsorption of labile factor activity similar phenomena were observed as illustrated by the experiments presented in Fig. 5. The differences in effect of crystalline and amorphous preparations of (1) barium oxalate, of (2) lead phosphate, and of (3) lead molybdate on the labile factor activity of strontium carbonate plasma are quite pronounced.

Table 2. Labile factors measured by RVV-cephalin or RVV.

Treatment of strontium carbonate plasma		Labile factor adsorbed	Labile factor activity in % of strontium carbonate plasma		
Adsorbent	mg/ml		Tpl.	RVV-ceph.	RVV
Untreated			100 [a]	100 [b]	100 [b]
Lead phosphate	20	β	93.5	94.5	100
	40		87	89	100
	60		80.5	83.5	—
	80		80.5	83.5	100
Untreated			100 [c]	100 [b]	100 [b]
Cobalt oxalate	30	λ	95	96	94.5
	60		90	92	89
	90		85	88	83.5
	120		85	88	83.5
Untreated			100 [d,e]	100 [d]	100 [e]
Lead carbonate	10	π	94	100	100
	20		88	—	—
	30		82	—	—
	40		82	100	100
Untreated			100 [d,e]	100 [d]	100 [e]
Barium phosphate	20	γ	95	100	100
	40		90	—	—
	60		85	—	—
	80		82.5	100	100
	100		82.5	100	100

a plasma No. 5617; *b* plasma No. 5045; *c* plasma No. 5351; *d* plasma No. 5051; *e* plasma No. 3445.

*The labile factor activity measured by RVV * cephalin or RVV.* The effects of the adsorbents were also studied with RVV, with or without added cephalin, replacing thromboplastin in the test system [1,3]. Representative experiments are summarized in Table 2.

Adsorption of β-factor (by lead phosphate) reduced the labile factor activity measured by RVV-cephalin, but not that measured by RVV alone. Maximal adsorption of the activities measured by thromboplastin and RVV-cephalin was obtained with the same concentration of lead phosphate, *viz.* 60 mg/ml. Adsorption of λ-factor (by cobalt oxalate) reduced the labile factor activities measured by all three assay accelerators, and maximal adsorption of activity was obtained with the same concentration of adsorbent, *viz.* 90 mg/ml. Removal of π-factor (by lead carbonate) or of γ-factor (by barium phosphate) had no effect on the labile factor activities measured by RVV-cephalin or RVV. By these experiments λ-factor was established as a labile factor common to all three coagulation systems. β-Factor is only active in coagulation systems

* Russell's viper venom, kindly supplied by The Wellcome Research Laboratories, Langley Court, Beckenham, England.

containing added cephalin, as such or in the form of thromboplastin. The π- and γ-factors must be regarded as thromboplastin specific labile factors.

DISCUSSION

The present study is part of a systematic investigation on the effects of adsorbents on the labile factor activity of strontium carbonate preadsorbed oxalated chicken plasma. Partial adsorption of the activity by crystalline adsorbents proved its multiple nature and suggested the use of such adsorbents for characterization of the individual components. By matching experiments fifty-two adsorbents tested in this study were found to belong to four different categories of adsorbents, causing adsorption of four different labile coagulation factors. Differences in physico-chemical properties are thus the basis for regarding these factors as different. Differences in the functions of the factors so defined, were indicated by the observed synergistic effects of certain factors and the merely additive effects of others. λ-Factor is thus functionally different from β- and π-factors because it is not a synergist for γ-factor, and functionally different from γ-factor because of its non-synergistic relations to π- and β-factors. β-Factor and π-factor differ functionally from γ-factor by not being synergists for π-factor or β-factor, respectively.

Further evidence of the functional non-identity of the factors was obtained in experiments with RVV-cephalin or RVV replacing thromboplastin as assay accelerator. Both π-factor and γ-factor were inactive in the RVV-cephalin and RVV assay systems. The activity of β-factor was found to depend on the presence of added cephalin (or thromboplastin). λ-Factor was the only factor active in all three assay systems. These observations and the fact that the effect of each adsorbent can be duplicated by at least two others, appear to rule out the possibility that the results can be due to artifacts.

We have not discovered any simple rules as to which factor is adsorbed by what type of adsorbent. λ-Factor was adsorbed by cobalt compounds only, but cobalt phosphate and cobalt oxide adsorbed γ-factor, sharing this property with a multitude of apparently unrelated compounds. β-Factor was adsorbed by a few lead compounds only. All other lead compounds adsorbed π-factor, duplicating the effects of tungsten and cadmium oxides. The pronounced selective properties of the crystalline adsorbents contrasted sharply with the completely indiscriminate adsorption of labile coagulation factors obtained with amorphous preparations. This is compatible with our previous suggestion [1,5] that selective adsorption of coagulation factors depends on a rigid spatial pattern of molecules in the surface of the adsorbent which "fits" the structure of a characteristic part of the adsorbable factor, permitting adsorption of one or a few factors only.

It has been pointed out previously [1] that in a determination of the relative labile factor activities of different plasmas, the same sample of stored plasma and the same solution of accelerator should be employed. The present results indicate that a comparison of the *activities* adsorbed from two different plasmas by a selected adsorbent, may not permit any conclusions as to the relative *concentrations* of the adsorbable factor since possible differences in adsorbed

activity may be caused by differences in the concentrations of non-adsorbed synergists. Another possibility for quantitative determination of individual labile coagulation factors is suggested by the observed proportionality between adsorbed activity and amounts of adsorbent. The minimum concentration of adsorbent required for maximal adsorption of labile factor activity may thus be proportional to the concentration of the adsorbable factor, and represent an absolute value for the concentration of the factor. Such values will be independent of the concentration of non-adsorbed factors, but may also reflect possible variations in the concentrations of inert plasma factors if such factors are adsorbed in competition with the labile factor.

REFERENCES

1. Sørbye, Ø. and Kruse, I. *Acta Chem. Scand.* **16** (1962) 1221.
2. Sørbye, Ø., Kruse, I. and Dam, H. *Acta Chem. Scand.* **5** (1951) 487.
3. Sørbye, Ø. and Kruse, I. *Acta Chem. Scand.* **14** (1960) 2177.
4. Sørbye, Ø. *Acta Chem. Scand.* **16** (1962) 799.
5. Sørbye, Ø. *Acta Chem. Scand.* **16** (1962) 903.

Received January 12, 1962.

ACTA CHEMICA SCANDINAVICA 16 (1962) 1481–1492

Determination of Barbituric Acid Derivatives as Mercury Compounds III. Composition and Structure of Isolated Compounds

C. O. BJÖRLING, A. BERGGREN and B. NYGÅRD

Research Laboratories, Pharmacia, Uppsala, Sweden

In the compounds between mercury and barbituric acid derivatives, which have been used for the determination of barbiturics, the mercury is attached to the unsubstituted nitrogen atoms with homopolar bonds. One atom of mercury combines with one molecule of a barbituric acid derivative, which has two free NH groups. The resulting compounds are polymers with high molecular weights. One atom of mercury combines with two molecules of a barbituric acid derivative, which has one free NH group. The resulting compounds are monomers.

A new sensitive and quite specific method for the determination of barbituric acid derivatives has recently been developed (Refs.[1-3]). The compounds are extracted together with an equivalent amount of mercury into an organic solvent, and the mercury determined. Mercury(II) salts have been used as precipitating agents for barbiturics in several other methods — both qualitative and quantitative ones — and the compositions of the precipitates have been given (Refs.[4-6]). However, all these methods are concerned with aqueous solutions, and the reaction products may change when taken up in an organic solvent. In this paper the structures of the compounds formed in the analytical procedure have been investigated.

RESULTS AND DISCUSSION

As seen in Table 1 the compounds can be divided into two different groups, one consisting of barbituric acids which are di-substituted at the carbon atom number 5, and the other of acids also substituted at a nitrogen atom. The composition of the mercury compounds of the first group, corresponds closely to a compound, where in one molecule of barbituric acid two hydrogen atoms have been substituted for one atom of mercury. In the second group one atom of mercury substitutes a hydrogen atom in each of two molecules of barbituric acid (Table 3).

Table 1. Barbituric acid investigated.

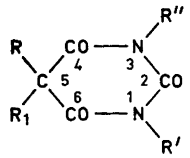

Code used in text	R	R_1	R′	R″
A	C_2H_5	*i*-C_5H_{11}	H	H
B	C_2H_5	C_6H_5	H	H
C	C_3H_5	*neo*-C_5H_{11}	H	H
D	C_2H_5	C_6H_5	CH_3	H
E	C_3H_5	*neo*-C_5H_{11}	CH_3	H
F	C_3H_5	*neo*-C_5H_{11}	CH_3	CH_3
G	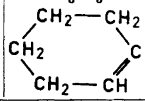	CH_3	CH_3	H

It should be emphasized that none of the mercury compounds investigated contained any appreciable amount of foreign matter, *e.g.* chloride, which might have been introduced from the chloroform. Some of the substances made by former authors contained negative groups, *e.g.* chloride, nitrate, hydroxyl etc.

From Table 2 it may further be concluded that the mercury compounds have molecular weights corresponding to mercuri-(N-methyl-barbituric acid)$_2$ and (mercuri-barbituric acid)$_n$ where the subscript n has a value of about 100. The degree of polymerisation seems to depend on the mode of isolation.

There are some additional differences between the two types of mercury compounds. Those derived from the N-methyl-barbituric acids are more soluble in chloroform than the other cathegory and separate as a fine powder.

Table 2. Molecular weights.

Mercury compound of substance		Boiling point method	Light scattering method	Theory
A	Amobarbital	Too great to be measured	—	(426)*n*
C	Nevental ®			
	Preparation 1	Too great to be measured	50 000 ± 10 %	(437)*n*
	2	» » » » »	30 000 ± 10 %	
	3	» » » » »	32 000 ± 10 %	
	4	» » » » »	51 000 ± 10 %	
E	N-Methyl-Nevental®	781; 938; 836; 710, M = 814	To small to be measured	703
G	Hexobarbital	701; 655; 660; 625, M = 660	To small to be measured	671

Table 3. Analyses of mercury compounds of the substances C, G, E.

	C Nevental ®			G Hexobarbital			E N-Methyl-Nevental ®			
	Per cent			Per cent			Per cent			
	Found		Calc. for $C_{12}H_{16}O_3N_2Hg$	Found		Calc. for $(C_{12}H_{15}O_3N_2)_2Hg$	Found			Calc. for $(C_{13}H_{19}O_3N_2)_2Hg$
C	32.60	32.70	32.99	43.25; 42.93; 43.05		42.95	44.39; 44.78; 44.84			44.41
H	3.98	4.02	3.69	5.44	5.01 5.50	4.51	5.76	5.80	5.76	5.45
N	6.38	6.32	6.41	8.34	8.56 8.39	8.35	7.73	7.72		7.97
Cl	0.04	0.02	0.00				0.8	0.8		0.00
P or S	P: 0.08	0.07	0.00	S: 0.00	0.00	0.00				
Hg	44.85	44.66	45.92	29.79	30.09	29.89	27.83			28.53
Barb. ac.	54.2	54.4	54.08	70.13		70.11	70.0	71.2		71.47

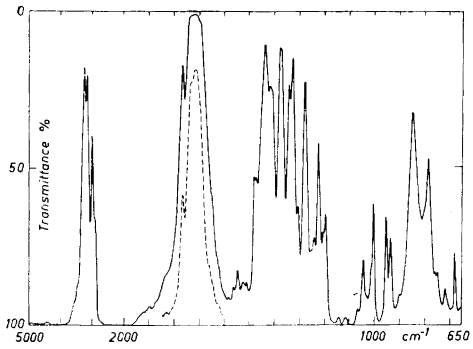

Fig. 1. IR absorption of Neven tal (C) (KBr phase).

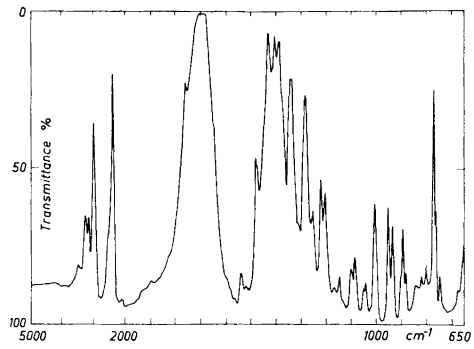

Fig. 2. IR absorption of deuterated Neven-tal (C) (KBr phase).

The high molecular compounds are obtained as a glass. When dry the difference in the rate of dissolution in chloroform is very great. It must be kept in mind that all investigations refer to the substances in chloroform solutions or in the solid state.

Infrared spectra. The characteristic infrared absorption of barbiturates has been studied by several authors. Umberger and Adams [7] identified barbiturates from their IR spectra in chloroform solution. Price *et al.*[8] correlated the pharmacological properties of some barbiturics with their IR absorption in the carbonyl region. Manning and O'Brien [9] proved the value of the method using various group frequencies in the molecules for identification purposes. Recently, Danielsson and Sandberg [10] pointed out the difficulties in classifying N- and N,N′-substituted barbituric acids by their infrared absorption. Levi and Hubley [11] identified barbiturates as copper(II)-pyridine complexes in Nujol and in potassium bromide and related spectral data to structural features.

Table 4. Stretching frequences in the NH and CO regions.

Code	Barbituric acid					Hg(II) compound				
	NH		CO			NH		CO		
A	3220	3100	1763	1732	1702	—	—	1698	1632	
								1701	1637	1541
B	3310	3200 3110	1777	1718	1686	—	—	1700	1632	(1560)
	3300	3170 3110	1774	1716	(1683)			1707	1636	
C	3200	3110	1767	1718	(1696)	—	—	1704	1633	
	3190	3100	1767	1708				1704	1635	(1534)
D	3220	3100	1764	1718	1694	—	—	1727	1667	1631
								1728	1670	1630
E	3220	3140	1749	1723	1673	—	—	1729	1672	1634
								1730	1670	1623
F	—	—	1750	—	1691	—	—	—	—	—

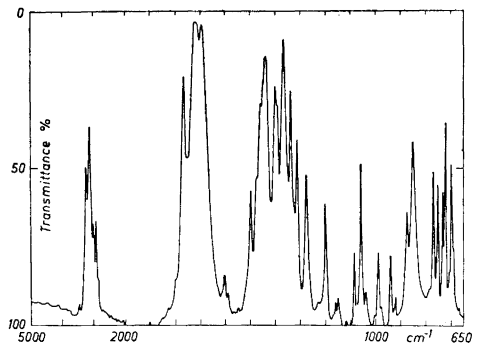

Fig. 3. IR absorption of Methylphenobarbital (D) (KBr phase).

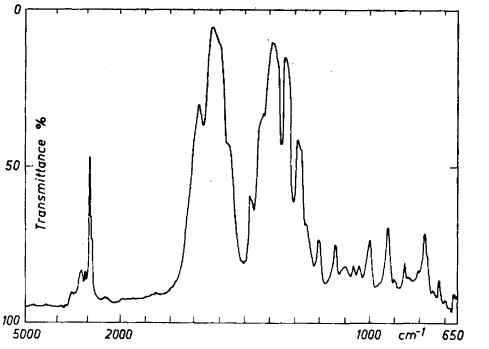

Fig. 4. IR absorption of Hg-Nevental (Hg—C) (KBr phase).

As mainly the NH and CO vibrations of the barbiturate ring are involved in the bond formation with metals, the present discussion is limited to the regions around 3000 and 1700 cm^{-1}, where well-defined absorption bands of these groups appear. The non-N-substituted barbituric acids A—C display the characteristic N—H absorptions around 3200 and 3110 cm^{-1}, which are attributed to the hydrogen-bonded NH groups. Figs. 1 and 2 show the complete spectra of substance C in its normal and in its deuterated state. In the latter case the expected N—D stretching is found at 2360 cm^{-1}. Substance B exhibits an extra band at 3310 cm^{-1} presumably due to free N—H stretching vibrations [11]. The N-methylated barbiturates D and E are characterized by a reduced intensity in the N—H absorptions (Fig. 3), and logically the N,N′-dimethyl substituted compound F has no absorption in the N—H stretching region.

From Table 4 it is evident that no mercury compound of the barbiturates A—E absorbs in the N—H region. On the other hand, among the corresponding sodium and barium barbiturates only the N-methylated compounds have lost their N—H absorption. Compared with the free non-N-methylated acids, the N—H intensities of their sodium and barium salts are reduced to the same degree, indicating *one* unsubstituted N—H group for both kinds of salts.

Of the three different peaks found the lowest frequency is associated with the carbonyl in the 2 position as this may partly assume a single bond character [8]. The two high frequencies are assigned to combined motions where the carbonyl bonds in the 4 and 6 positions are involved. The spectra of the barbiturates A—E comply with these findings. It is interesting that the band at 1720 cm^{-1} has disappeared for the N,N′-methylated compound F whereas the absorption at 1690 cm^{-1} has increased. The inductive effects of the two methyl substituents affect the carbonyl group towards single bond character especially in the 2 position. The two lowest frequencies can no longer be resolved and therefore result in one strong peak.

In the mercury barbiturates we get a drastic shift of the carbonyl stretching frequencies towards low wavenumbers (Table 4) and combined with the disappearance of the N—H stretching frequencies for the compounds A—C this is a strong support for the assumption of nitrogen-mercury bonds. For some metal-urea complexes forming nitrogen-metal bonds Penland *et al.*[12] have shown that a blocking of the resonance between one nitrogen atom and the carbonyl group will cause an increased CO double bond character. Such an explanation is not valid for the mercury barbiturates which have a low frequency band around 1635 cm^{-1} as the dominating absorption in the carbonyl region. The disubstituted acid F has an absorption pattern in the carbonyl region similar to the mercury compounds of A, B, and C but the latter compounds have a greater frequency shift. From this analogy we can conclude that the contribution of single polar bonding in the carbonyls, may partly have an analogous origin.

A methyl group and a mercury atom both exert a negative inductive effect on an adjacent nitrogen which will therefore gain an excess of negative charge. As a net result the carbonyls in the barbiturate ring are weakened and acquire more single polar bond structures. Gierer[13] has observed that the C=O frequency in N-mono-substituted amides is sensitive to the inductive effect of the N-substituent. Thus, he found that the carbonyl frequency in N-chloroacetamide at 1705 cm^{-1} shifted to 1580 cm^{-1} for the corresponding N,N′-mercuri-bis-acetamide.

The absorption spectrum of the mercury compound of substance C is shown in Fig. 4. This compound and its spectrum are typical for the group "A—C" with mercury covalently bonded to both nitrogen atoms.

As a first approximation the inductive forces over both the nitrogen atoms may act in an additive way upon the carbonyl in the 2 position, giving an increased single bond character to this group compared to the other two carbonyls which can be regarded as equivalent. Thus, the dominating low frequency band around 1635 cm^{-1} may be associated with vibrations in the carbonyl bond in the 2 position. To a certain degree this absorption can also be correlated with an in-phase combination of the vibrations of the carbonyls. Further, the combined vibration of the carbonyls in positions 4 and 6 can only occur perpendicularly to the axis of symmetry of the molecule, thus causing the highest frequency band to appear around 1700 cm^{-1}. Although the main influence on the carbonyl groups seems to be caused by the inductive effect of the mercury atoms, an additional effect caused by coordination has to be considered. Mercury has here the coordination number 6 and if a suitable configuration can be established it is possible for the metal to interact with oxygen in adjacent carbonyl groups with coordinative forces. Thus, nothing can be concluded in this respect from the infrared spectra.

The mercury compounds with the barbiturates D and E both contain one methyl group and one mercury atom attached to nitrogen. From Fig. 5a it is obvious that these spectra are distinguished by a splitting of the strongest peak in the carbonyl region, giving absorptions at about 1730, 1670 and 1630 cm^{-1}. This effect is more pronounced for a spectrum run in Nujol mull (Fig. 5b).

The spectra of the two mercury compounds and their corresponding barbituric acids D and E (Figs. 3, 5a and 5b) show the same general carbonyl

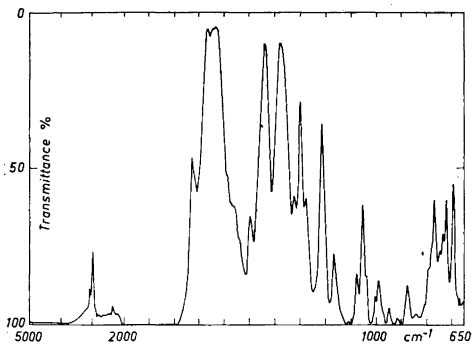

Fig. 5a. IR absorption of Hg-Methyl-phenobarbital (Hg—D) (KBr phase).

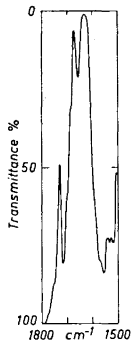

Fig. 5b. IR absorption of Hg-Methyl-phenobarbital (Hg—D) (Nujol suspension).

absorption. We may explain the splitting of the strongest absorption peak as above mainly by the inductive effects in the barbiturate ring. An N-substituted methyl group alone or together with a mercury atom will cause an asymmetry in the ring vibrations.

In the mercury compounds of D and E the low frequency band at 1630 cm^{-1} is little affected by the replacement of a mercury atom for a methyl group. This band is therefore assigned to the vibration of the carbonyl in the 2 position. As the symmetry of the barbituric ring is destroyed the other carbonyls in the 4 and 6 positions are no longer equivalent and give separate bands. The highest frequency at 1730 cm^{-1} may then be assigned to the 6 position carbonyl adjacent to the methyl substituted nitrogen. Finally, the vibration at about 1670 cm^{-1} has to be correlated with the CO group in the 4 position, as here the inductive effects and the coordinative influence are more pronounced because of an adjacent mercury atom.

The carbonyl region for the sodium and barium barbiturates may be interpreted similarly. These compounds contain one equivalent of metal per molecule whether one of the nitrogen atoms is methylated or not. Their car-

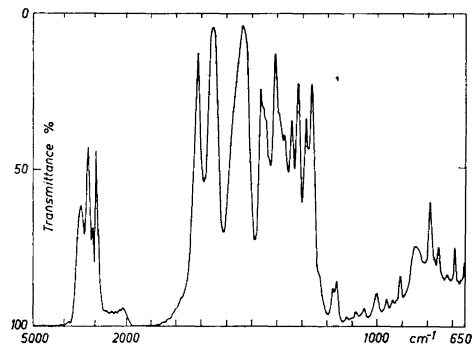

Fig. 6. IR absorption of Ba-Amobarbital (Ba—A) (KBr phase; before heating the disk).

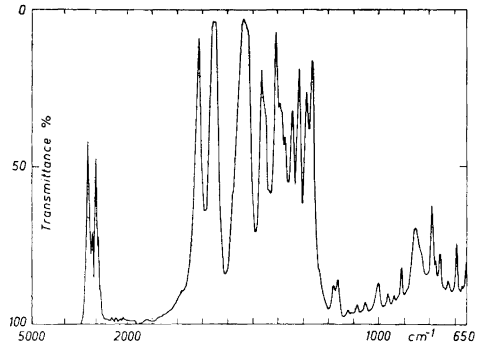

Fig. 7. IR absorption of Ba-Amobarbital (Ba—A) (after heating the disk at 110°C for 10 h)

bonyl absorptions are all very similar exhibiting three distinct peaks in the region from 1520 to 1730 cm^{-1} (Figs. 6—9).

In solution and in the solid state the ionic structures I and II contribute to the electron distribution [14] (Fig. 10). For a methyl substituted compound we have the analogous resonance structure III. Table 5 shows that the position of the band with the highest wave-number is constant, shifting within the range 1710 to 1727 cm^{-1}, which indicates a C=O band.

It is more difficult to explain the second and third absorption bands in the carbonyl region. The second band varies within a relative wide range (1621 to 1670 cm^{-1}) and may be attributed to a conjugated C=N bond frequency. On the other hand, changes in the environment of a C=N linkage may cause considerable frequency shifts. Nor is it possible to find any systematic change in the frequency of the second band in this case. The third low frequency band may be attributed to a carbonyl vibration in an enolate group $=C-O^{(-)}M^{(+)}$. A support for such an explanation is that the sodium barbiturates form a high frequency group (1570 to 1574 cm^{-1}) and the barium barbiturates a low frequency set (1520 to 1540 cm^{-1}) when only the third band is considered. The positions of the three bands just discussed are only slightly influenced by deuterization as seen from Table 5 and Fig. 8. Hence, the N—H bond cannot participate in a band in this region. In conclusion, we refrain

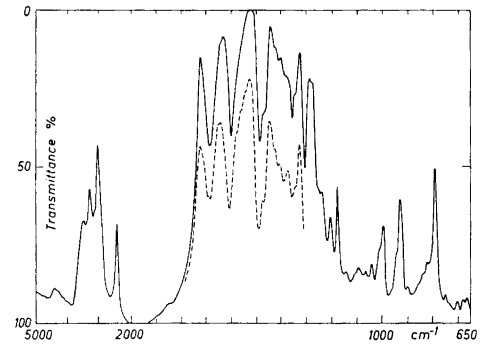

Fig. 8. IR absorption of deuterated Ba-Nevental (Ba—C) (KBr phase).

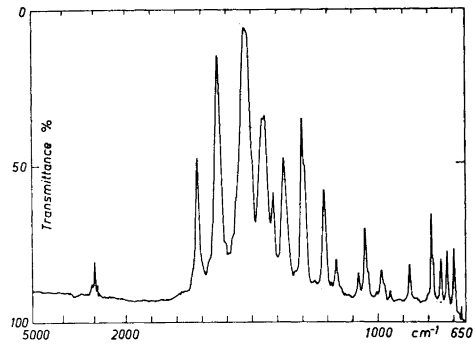

Fig. 9. IR absorption of Ba-Methylphenobarbital (Ba—D) (KBr phase).

from assigning the three absorption peaks to specific groups of the molecules and prefer to identify them with the resonance structures I, II, and III.

Further work with other metals may throw more light on this question.

EXPERIMENTAL

Preparation of mercury compounds. Several modifications of the analytical method were tried until finally the following simple procedure was adopted for preparative work. One gram of the barbituric acid derivative was mechanically shaken with 4 g of mercury(II) oxide (yellow), 20 ml of a 0.05 M sodium carbonate buffer solution with a pH of about 9.5, and 300 ml of chloroform for a couple of hours. The chloroform layer was separated, filtered and evaporated to a volume of about 20 ml. The mercury compound was then precipitated with several hundred milliliters of petroleum ether (b.p. 40—60°). The precipitate was collected, washed with petroleum ether, and dried in vacuum.

For the preparation of the deuterium barbituric acid mercury compound an aliquot of the chloroform solution, corresponding to 100 mg of barbituric acid, was evaporated until only a few ml of chloroform was left. Carbon tetrachloride was added and the

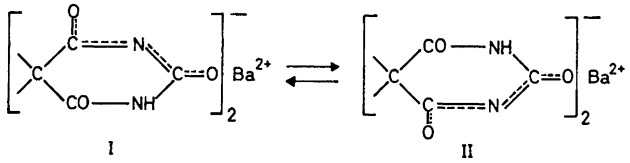

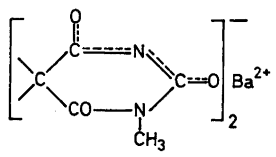

III

Fig. 10.

Table 5. Stretching frequences in the NH and CO regions.

Code	Na compound					Ba compound				
	NH		CO			NH		CO		
A	3220	3090	1710	1667	1570	3210	3090	1712	1653	1533
B	3220	3100	1710	1670	1574	3210	3090	1716	1665	1540
C	3240	3110	1717	1663	1590*	3220	—	1727	1637	1522
						3210	—	1724	1635	1520
								1720	1630	1517**
D						—	—	1717	1634	1527
								1715	1632	1523
E						—	—	1715	1621	1520

* Ca-compound.
** Mainly deuterized product.

solution evaporated to a small volume. This was repeated twice in order to remove all traces of chloroform. The resultant solution, about 20 ml, was shaken for half an hour at room temperature with 10 ml of deuterium oxide, and the mixture evaporated at 0.1 mm Hg. From the introduction of the deuterium oxide, atmospheric moisture was carefully excluded.

Deuterium barbituric acids were prepared by boiling 50 mg of the barbituric acid with 10 ml of deuterium oxide. The solution was then evaporated at 0.1 mm Hg. These procedures give compounds where NH is mainly exchanged for ND.

Analyses. For the determination of *mercury* an amount of substance corresponding to about 20 mg of mercury was dissolved in 5 ml of alcohol and 1 ml of 5 M hydrochloric acid. 15 ml of 0.02 N EDTA was added and then 5 ml of 5 M ammonia. After the addition of 2 ml of buffer, pH = 10 (ammonia 4.5 M, ammonium chloride 1 M), the solution was titrated with 0.02 N zinc sulphate solution using Eriochrome black as indicator.

For the determination of *barbituric acid* in the mercury compound an amount corresponding to about 150 mg of barbituric acid was mixed with 5 ml of water and hydrogen sulphide was bubbled through for 5 min. The mixture was shaken for 10 min, 2 ml of 5 N sulphuric acid added and then extracted four times with chloroform, 15 ml each time. The chloroform was filtered through anhydrous sodium sulphate and evaporated. The residue was dissolved in 10 ml of dimethylformamide and titrated with 0.1 N potassium methylate against thymol blue. A blank was run on the dimethylformamide.

The *molecular weights* of some of the mercury compounds were determined by a boiling point elevation method, using a Gallenkamp apparatus [15]. In this instrument the temperature increase is determined by a thermistor used in conjunction with a Wheatstone bridge.

The boiling vessel was charged with 10 ml of alcohol-free, dry chloroform, containing about 100 mg of glyceryl monostearate, which makes the boiling smooth. When boiling equilibrium had been attained, the galvanometer was brought to zero position and weighed amounts (50 – 100 mg) of the barbituric acid derivative was introduced into the vessel. It was necessary to use the substances as loosely compressed tablets as otherwise some powder adhered to the neck of the boiling vessel. The galvanometer was again brought to zero, another tablet introduced, etc. In this way a calibration curve, a straight line through origo, was obtained, and from experiments with the mercury compounds the results in Table 2 were obtained. The precision was, however, much lower when working with the mercury compounds possibly due to the long equilibration time.

Some determination of the molecular weights were made by light scattering measurement with a Brice-Speiser light scattering photometer [16]. Freshly distilled chloroform was used as solvent and the solutions were clarified by filtering through a Jena G5 sintered glass filter directly into the light scattering cell. The turbidities of a stock solution (about 2 %) and three dilutions were measured at 436 mμ. The refractive index increment for this system was determined with a Rayleigh interferometer and amounted to 0.085 ml/g.

The measurements on the mercury compound of substance C were made on four different solutions.

(1) The compound was prepared by the method given on page 1489, isolated, dried, etc. and then dissolved in the chloroform.

(2) The compound was prepared as above but never isolated. Instead, the chloroform extract containing the compound was concentrated *in vacuo* until the solution contained about 2 per cent of the compound. Part of the solution was analysed and the actual concentration determined and the rest was used for the light scattering experiments.

(3) The compound was prepared as in the preceding paragraph, with the exception that the chloroform extract was concentrated on the waterbath to a 2 % solution.

(4) The compound was prepared as in the preceding paragraph, but the chloroform extract was evaporated to dryness on the water-bath, and the residue was then immediately redissolved in chloroform.

Infrared spectra. A Unicam SP 100 spectrophotometer with sodium chloride optics was used. The solid substances were examined with the potassium bromide disc technique, or in Nujol suspension. In some cases, when a sufficient concentration could be attained, the spectra were also run on chloroform solutions.

Like Jensen [17], we have found some differences between spectra for barbiturates and their salts in Nujol and in potassium bromide tablets. A broad band around 3500 cm^{-1}, indicating an associated O—H stretching frequency, often appears with the disc technique but never with Nujol. Figs. 6 and 7 show that heating the disc at 110°C for some hours eliminates this band. The other parts of the spectrum are little influenced by the heating.

On the other hand, the spectra of the mercury barbiturates often change on heating — the positions of some of the bands may shift by 10 wavenumbers, and the resolution is generally improved.

The Tables 4 and 5 show values obtained on heated discs when the substance did not change at 110°C. When there was a difference between the wavenumbers for treated and untreated discs the absorption was also measured on a Nujol suspension (the values on the second line for each substance in the tables).

Acknowledgement. The authors are indebted to Doc. W. Kirsten for help with the elementary analyses and to Dr. K. Granath for the determination of the molecular weights by light scattering. Thanks are also due to Prof. I. Lindqvist for valuable discussions and to Mrs. B. Willman-Johnson who performed part of the preparative work.

REFERENCES

1. Björling, C. O., Berggren, A., Willman-Johnson, B., Grönwall, A. and Zaar, B. *Acta Chem. Scand.* **12** (1958) 1149.
2. Björling, C. O., Berggren, A. and Willman-Johnson, B. *J. Pharm. Pharmacol* **11** (1959) 297.
3. Zaar, B. and Grönwall, A. *Scand. J. Clin. Lab. Invest.* **13** (1961) 225.
4. Poethke, W. and Fürst, W. *Pharm. Zentralhalle* **98** (1959) 171.
5. Rupp, E. and Müller, K. *Arch. Pharmazie, Ber. deut. pharm. Ges.* **264** (1926) 362.
6. Rupp, E. and Poggendorf, A. *Ibid.* **269** (1931) 607.
7. Umberger, C. J. and Adams, G. *Anal. Chem.* **24** (1952) 1309.
8. Price, W. C., Bradley, J. E. S. and Fraser, R. D. B. *J. Pharm. Pharmacol.* **6** (1954) 522.
9. Manning, J. and O'Brien, K. *Bull. Narcotics* **10** (1958) 25.
10. Danielsson, B. and Sandberg, F. *Svensk Farm. Tidskr.* **63** (1959) 1045.
11. Levi, L. and Hubley, C. *Anal. Chem.* **28** (1956) 1591.

12. Penland, R. B., Mitzushima, S., Curran, C. and Quagliano, J. V. *J. Am. Chem. Soc.* **79** (1957) 1575.
13. Gierer, A. *Z. Naturforsch.* **8b** (1953) 644, 654.
14. Rosén, O. and Sandberg, F. *Acta Chem. Scand.* **4** (1950) 675.
15. A. Gallenkamp & Co Ltd., Sun Street, London, E.C.2.
16. Brice, B. A., Halwere, M. and Speiser, R. *J. Opt. Soc. Amer.* **40** (1950) 768.
17. Buur Jensen, J. *Dansk Tidskr. Farm.* **32** (1958) 221.

Received January 11, 1952.

ACTA CHEMICA SCANDINAVICA 16 (1962) 1493–1510

On the Phase Relationships in the Titanium-Antimony System. The Crystal Structures of Ti_3Sb

ARNE KJEKSHUS, FREDRIK GRØNVOLD and JENS THORBJØRNSEN*

Kjemisk Institutt A, Universitetet i Oslo, Blindern, Norway

By using different melting methods four new titanium antimonides have been identified:

The cubic Ti_3Sb phase, prepared in an arc furnace, is found to have the lattice constant $a = 5.2186$ Å. The pycnometric density is 6.137 g cm^{-3} at 25°C. The crystal structure of the cubic Ti_3Sb phase is of the β-W type.

The tetragonal Ti_3Sb phase, prepared in alumina crucibles in a carbon resistance furnace, is found to have a body-centered unit cell with dimensions: $a = 10.465$ Å, $c = 5.2639$ Å. The pycnometric density is 6.070 g cm^{-3} at 25°C. The space group is $I4/mcm$ (D_{4h}^{18}) and the unit cell contains 24 Ti and 8 Sb in the positions: (0,0,0; 1/2,1/2,1/2) + 4 Ti in (a) ± 0,0,1/4; 4 Ti in (b) 0,1/2,1/4; 1/2,0,1/4; 16 Ti in (k) ± (x,y,0; $\bar{y}$,x,0; x,$\bar{y}$,1/2; y,x,1/2) with $x_1 = 0.0766$, $y_1 = 0.2228$ and 8 Sb in (h) ± (x,1/2 + x,0; 1/2 + x,$\bar{x}$,0) with $x_2 = 0.1635$.

The structure of the tetragonal Ti_3Sb phase is closely related to the β-W type structure of the cubic Ti_3Sb phase.

Cubic crystals are transformed into tetragonal crystals on melting in alumina crucibles, while tetragonal crystals remain tetragonal after melting in the arc furnace. Possible reasons for the apparently irreversible transformation of the two phases are discussed.

The orthorhombic $Ti_{1.7}Sb$ phase, prepared in the carbon resistance furnace, is found to have lattice constants $a = 10.172$ Å, $b = 8.348$ Å and $c = 7.135$ Å. The probable space groups are $Pmma$ (D_{2h}^5), $Pmc2_1$ (C_{2v}^2) and $Pma2$ (C_{2v}^4).

The orthorhombic $Ti_{1.2}Sb$ phase, prepared in the carbon resistance furnace, is found to have lattice constants $a = 14.55$ Å, $b = 16.34$ Å, and $c = 5.31$ Å. The probable space groups are $Pbam$ (D_{2h}^9) and $Pba2$ (C_{2v}^8).

The redetermined lattice constants of the hexagonal TiSb phase, prepared in the carbon resistance furnace, are $a = 4.115$ Å and $c = 6.264$ Å.

* Present address: Reynolds Metals Company, Portland, Oregon, U.S.A.

As result of X-ray studies of titanium antimony alloys Nowotny and coworkers [1–3] reported the existence of four intermediate phases: Ti_4Sb, $Ti_{2.5}Sb$, TiSb and $TiSb_2$. The Ti_4Sb phase [1,2] was prepared by heating weighed amounts of pure antimony and Degussa titanium in porcelain (Pythagoras) tubes in a carbon resistance (Nernst-Tammann) furnace at 1600°C. The alloys were afterwards annealed at 600°C and quenched, or in some cases slowly cooled, to room temperature. The crystallographic properties of this phase were determined from X-ray powder photographs. By comparing visually estimated intensities with those obtained by calculations, Nowotny *et al.*[2] concluded that the Ti_4Sb phase had a structure of the Ni_3Sn-($D0_{19}$)-like type. The deviating composition was accounted for by assuming 0.2 titanium atoms, corresponding to the formula $Ti_3(Ti_{0.2}Sb_{0.8})$, to be distributed at random over the antimony positions.

The $Ti_{2.5}Sb$ phase [3] was synthesized by melting appropriate amounts of the elements in crucibles of carbon using either a Tammann high pressure furnace or a high frequency induction furnace. The crystal structure of $Ti_{2.5}Sb$ was determined by Auer-Welsbach *et al.*[3] by means of single crystal and powder photographs to be of the Cu_2Sb-($C38$)-like type but with doubled c-axis. The parameter values $z_{Ti} = 0.133$ and $z_{Sb} = 0.353$ were determined from the intensities of the $00l$ reflections. Substitution of 0.15 antimony atoms for titanium atoms, corresponding to the formula $Ti_2(Ti_{0.15}Sb_{0.85})$ was thought to explain the excess of titanium and the observed density.

The TiSb phase with NiAs-($B8$)-type structure and the $TiSb_2$ phase with $CuAl_2$-($C16$)-type structure were prepared and examined [1,2] as described for the Ti_4Sb phase. These two phases were also obtained by melting titanium and antimony in the right proportions in open crucibles under halide flux.

Using different methods of preparation, the existence of four different, intermediate phases has been established in this institute [4,5]. The present paper gives an account of the crystal structure determinations for two different phases with composition Ti_3Sb. In addition, some preliminary phase-analytical observations of two more titanium antimonides are reported.

After being informed about the present work, Matthias *et al.*[6] have duplicated the preparation of the cubic Ti_3Sb phase and shown that it is a superconductor with a transition temperature of 5.8°K.

EXPERIMENTAL

The *titanium* metal used in this study was "iodide" titanium in rods supplied through A. D. MacKay, Inc., New York. A spectrographic analysis showed the presence of about 30 ppm of Fe and Mn and less than 10 ppm Cu. No analysis of non-metallic impurities was carried out.

The *antimony* was "High purity antimony" from Bradley Mining Co., San Francisco. According to the supplied analysis it contained the following impurities (in ppm): As (10), Cu (3), Fe (3) and Pb (2).

Several different techniques were tried for preparing the titanium-antimony alloys. In some preliminary experiments alloys were prepared by heating titanium and antimony in evacuated, sealed silica tubes. However, contamination of the alloys due to reaction with silica then always took place. According to Auer-Welsbach *et al.*[3] the compound Ti_5Si_3 is formed by this reaction.

One series of alloys with composition ranging from Ti_6Sb to TiSb was prepared in an electric arc furnace (Degussa Volio) by melting weighed amounts of titanium and antimony, previously mixed and compacted. A protective atmosphere of argon gas was present in the furnace during the melting process. Using a pressure of about 4 atm no preferential loss of antimony from the samples was seen, while melting *in vacuo* gave visible loss of antimony.

In the same composition range a second series of alloys was made by melting weighed quantities of the elements in crucibles of pure alumina, placed inside silica tubes which were evacuated and sealed. The samples were melted in a carbon resistance (Nernst-Tammann) furnace at temperatures ranging from 1400 to 1600°C. Temperatures were measured with an optical pyrometer. When the furnace reached the desired temperature, the sample was immediately removed and quenched in ice water. If the temperature had exceeded 1550°C, the silica tubes often broke during quenching.

The alloys could not be heated in contact with alumina at these temperatures for a longer time, as reactions then were seen to take place. Furthermore it was noticed that pure titanium is able to reduce alumina. This reaction was unsuspected in view of the thermochemical discussion by Kubaschewski and Dench [7] related to the production of Ti—Al alloys from TiO_2 and excess Al at 1000°C. Nevertheless, a reduction of alumina might apparently well take place at higher temperatures.

The melted alloys were bright shiny and metallic looking, while the sintered alloys were in form of a gray to black powder. The alloys were crushed and finely ground and X-ray powder photographs were taken in cameras with 114.6 mm effective diameter and asymmetric film mounting. In most cases filtered copper radiation was used, while chromium radiation was used to obtain greater dispersion in the photographs of the tetragonal Ti_3Sb samples. The lattice constants are expressed in Å units, taking $\lambda_{CuK\alpha_1} = 1.54050$ Å and $\lambda_{CrK\alpha_1} = 2.28962$ Å. Results from Nowotny and coworkers [1-3], expressed in kX, have been transformed to Å by multiplication by the factor 1.00202. The lattice constant of the cubic phase was found by extrapolation according to the method of Nelson and Riley [8].

Oscillation and Weissenberg photographs were taken with Cu*K*-radiation using a Weissenberg camera of 57.3 mm diameter.

The density of the samples was determined pycnometrically at 25°C with kerosene as displacement liquid. To remove gases adsorbed by the sample, the pycnometer was filled with kerosene under vacuum. The samples weighed from 2 to 3 g.

RESULTS

In the titanium-antimony system the existence of four new, intermediate phases was established, *i.e.* the cubic and tetragonal Ti_3Sb phases, the $Ti_{1.7}Sb$ phase and the $Ti_{1.2}Sb$ phase. Furthermore, the existence of the TiSb phase reported by Nowotny and Pesl [1] was confirmed. The $TiSb_2$ phase found by Nowotny and Pesl [1] was not studied here. By the experimental technique used in this study no samples containing the Ti_4Sb and $Ti_{2.5}Sb$ phases reported by Nowotny and coworkers [1-3] were obtained.

A. The cubic Ti_3Sb phase

Powder photographs of samples prepared in the arc furnace showed the presence of a phase which could be indexed on the basis of a cubic unit cell, *cf.* Table 1. Inferred from the powder photographs, the amount of the other phases seems to disappear close to the stoichiometric ratio 3:1. A series of density measurements, *cf.* Table 2, was then carried out for an accurate determination of the composition of this phase. The specific volume *versus* weight % Sb plot shown in Fig. 1 had a break in the linearity at 45.9 weight % Sb (25.0 atomic % Sb), ascertaining the composition to be Ti_3Sb.

Table 1. Powder photograph data of cubic Ti_3Sb taken with CuK-radiation, α_2 and β lines omitted.

$\sin^2\Theta \times 10^4$	hkl	I_{obs}	I_{calc}
—	100	0	0
437	110	12.3	14.3
—	111	0	0
873	200	13.9	15.5
1092	210	14.6	13.8
1312	211	30.2	34.1
1746	220	2.7	2.2
—	300	0	0
—	221		0
2181	310	3.8	3.1
—	311	0	0
—	222	0	0.02
2837	320	3.4	2.6
3056	321	17.7	15.8
3491	400	4.2	3.8
—	410	0	0
—	322		0
3929	411	2.3	1.2
	330		0.6
—	331	0	0
4361	420	4.4	4.5
4582	421	2.8	2.4
4800	332	4.7	4.0
5236	422	0.9	0.8
—	500	0	0
—	430		0

$\sin^2\Theta \times 10^4$	hkl	I_{obs}	I_{calc}
5670	510	2.4	0.8
	431		1.5
—	511	0	0
—	333		0
6330	520	2.5	0.9
	432		1.8
6538	521	6.9	6.6
6978	440	3.6	3.9
—	522	0	0
—	441		0
7412	530	1.8	0.8
	433		0.8
—	531	0	0
7849.6	600	5.5	0.9
	442		3.8
8065	610	1.3	1.1
8284.5	611	12.8	4.0
	532		8.2
8722	620	1.7	1.1
—	621	0	0
—	540		0
—	443		0
9154.0	541	3.4	2.7
—	533	0	0
—	622	0	0.00
9804.5	630	5.6	3.0
	542		6.0

The lattice constant of the sample with the composition Ti_3Sb is found in Table 2 together with the lattice constants of the Ti_3Sb-phase in the samples Ti_4Sb, $Ti_{3.5}Sb$, $Ti_{2.5}Sb$ and Ti_2Sb. As the lattice constant is almost invariant for specimens with different initial proportions of the components, no composition range of the cubic Ti_3Sb-phase is noticeable.

The pycnometric density of Ti_3Sb at 25°C, *cf.* Table 2, is found to be in agreement with the density calculated from the X-ray data, 6.201 g cm^{-3}, assuming two ($Z_c = 1.98$) Ti_3Sb-groups per unit cell.

Table 2. Lattice constants and pycnometric densities of samples containing the cubic Ti_3Sb phase.

Sample	a (Å)	Density (g cm^{-3})
Ti_4Sb	5.2187	5.801
$Ti_{3.5}Sb$	5.2188	5.956
Ti_3Sb	5.2186	6.137
$Ti_{2.5}Sb$	5.2184	6.251
Ti_2Sb	5.2184	6.381

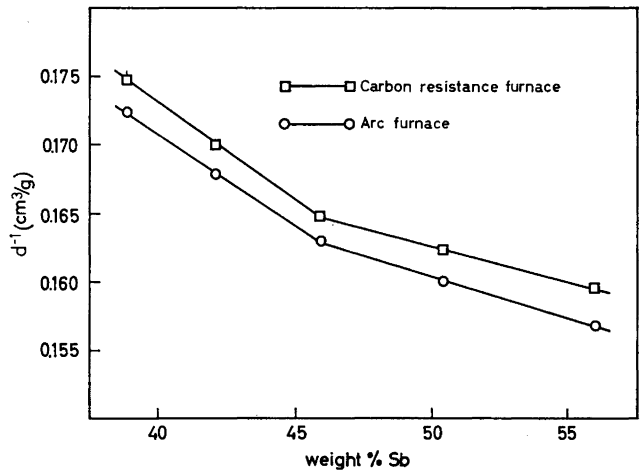

Fig. 1. Reciprocal densities as function of composition for samples synthesized in carbon resistance and arc furnace.

Many related Me_3X compounds of the transition metals have a structure of the β-W (W_3O) type. The β-W structure, *cf.* Fig. 2, is described in space group $Pm3n$ (O_h^3) with

6 Me in (*d*) 1/4,1/2,0; 0,1/4,1/2; 1/2,0,1/4;
3/4,1/2,0; 0,3/4,1/2; 1/2,0,3/4.
2 X in (*a*) 0,0,0; 1/2,1/2,1/2.

As the missing reflections in the powder photographs were in agreement with the extinctions for this space group, a comparison of observed and calculated

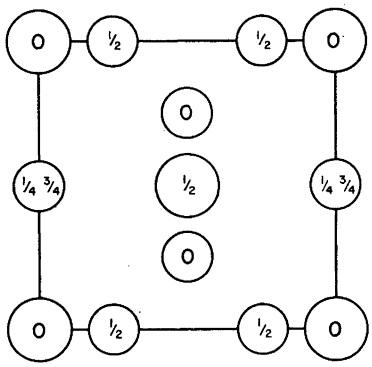

Fig. 2. Projection of one unit cell of the β-W type structure. Large circles represent antimony atoms and small circles titanium atoms. Figures give the *z*-parameters.

Table 3. Powder photograph data of tetragonal Ti_3Sb taken with CrK-radiation, α_2 and β lines omitted.

$\sin^2\Theta \times 10^4$	hkl	I_{obs}	I_{calc}	$\sin^2\Theta \times 10^4$	hkl	I_{obs}	I_{calc}
240	110	8.5	9.4	—	640	0	2.4
481	200	6.5	8.6	6298	413	46	39.2
—	220	0	3.2	—	602	0	0.2
1074	211	40.5	38.1	6690	622	12	10.7
1200	310	14	16.4	6820	721	19.5	18.2
1898	002	35	33.7	6948	730	11.5	8.3
—	400	0	0.0	—	433	0	0.1
2034	321	31.5	26.1	7571	004	18	17.6
—	112	0	1.3	—	800	0	0.3
2159	330	33.5	31.1	7731	523	35	28.3
2378	202	50	48.7	—	114	0	0.4
2398	420	46.5	43.9	—	651	0	2.3
2514	411	113	124.8	7880	712	19	15.9
2853	222	14.5	12.4	—	552		5.7
3094	312	10.5	8.5	—	204	0	1.0
—	510	0	0.0	8119	642	54.5	46.2
—	431	0	0.0	—	820		12.4
3814	402	18.5	14.4	8252	811	40.5	28.2
—	440		2.9		741		8.4
3949	521	43.5	38.5	8328	543	4.5	5.3
4057	332	30.5	23.6	—	224	0	0.7
—	530		7.3	8613	660	32	30.5
4299	422	17	12.9	—	613	0	0.1
—	600		6.7	8765	314	3.5	6.0
—	620	0	0.3	8835	732	31.5	25.4
4865	213	11.5	9.3	—	750	0	1.7
—	611		0.1	9212	831	13.5	14.2
—	512	0	0.0	—	404	0	0.1
5392	541	6.5	4.3	9550	802	33.5	31.7
—	442	0	0.9	9574	840	6	4.2
5821	323	4	5.7	9643	633	11.5	12.1
5868	631	3	4.5	9722	334	35.5	52.5
	532		10.0	9813	910	26.5	38.9
5973	710	26	7.0				
	550		2.5				

intensities for the reflections was carried out. The intensities of the reflections were calculated using the formula

$$I_{calc} = 10^{-5} \times |F|^2 \times Lp \times \nu$$

For the calculation of the structure amplitudes, Thomas-Fermi model values of f, taken from *Internationale Tabellen*, were used throughout this paper. No corrections for absorption and temperature factors were applied. The observed intensities were obtained from photometer recordings and referred to a relative, absolute scale by making the sums of I_{obs} and I_{calc} equal. As can be seen from Table 1 the agreement between the two sets of values is very good, and leaves no doubt about the correctness of the proposed structure.

B. The tetragonal Ti_3Sb phase

Powder photographs of samples prepared in the Nernst-Tammann furnace show the presence of a phase with tetragonal structure, *cf.* Table 3. Powder photographs of various samples of Ti_6Sb, Ti_5Sb and Ti_4Sb contain some of the strongest reflections from α-Ti, while powder photographs of Ti_2Sb contain reflections from a phase richer in antimony with probable composition $Ti_{1.7}Sb$. The additional reflections are weak on photographs of samples with composition $Ti_{3.5}Sb$ and $Ti_{2.5}Sb$ and are absent on photographs of samples with composition Ti_3Sb. A more accurate determination of the composition of the phase was obtained from a plot of the specific volume *versus* weight % Sb, *cf.* Fig. 1, and by means of metallographic methods. Thus the composition of the phase is ascertained to be Ti_3Sb.

The lattice constants of the tetragonal Ti_3Sb phase in the samples Ti_4Sb, $Ti_{3.5}Sb$, Ti_3Sb, $Ti_{2.5}Sb$ and Ti_2Sb are listed in Table 4. The slight expansion of the unit cell, which takes place in the range Ti_3Sb to $Ti_{2.5}Sb$ indicates that the tetragonal Ti_3Sb phase has a narrow range of homogeneity on the antimony-rich side of Ti_3Sb.

The observed density, *cf.* Table 4, indicates that the unit cell contains 8 ($Z_c = 7.94$) Ti_3Sb-groups. The calculated density for Ti_3Sb from the X-ray measurements is 6.116 g cm^{-3}.

Single crystals of Ti_3Sb were found in samples quenched from 1450°C. The single crystals were needle-shaped and oscillation and Weissenberg photographs showed tetragonal symmetry, Laue symmetry $4/mmm$, with the c-axis along the needle axis. Missing reflections on the photographs were:

hkl	when $h + k + l = 2n + 1$
$hk0$	when $(h + k = 2n + 1)$
$0kl$	when $k = 2n + 1$ and $l = 2n + 1$

Characteristic space groups are accordingly $I4/mcm$ (D_{4h}^{18}), $I4cm$ (C_{4v}^{10}) and $I\bar{4}c2$ (D_{2d}^{10}). All possible space groups have symmetry $p4m$ in the 001-projection with $a' = b' = \frac{1}{2}\sqrt{2}\,a$.

Determination of the structure. The intensities of the $hk0$ and $hk1$-reflections were estimated visually from "multiple film" Weissenberg photographs taken with CuK-radiation and were corrected for Lorentz and polarization factors. No corrections for absorption, extinction and temperature factors were applied.

Table 4. Lattice constants and pycnometric densities of samples containing the tetragonal Ti_3Sb phase.

Sample	a (Å)	c (Å)	Density (g cm^{-3})
Ti_4Sb	10.468	5.2640	5.721
$Ti_{3.5}Sb$	10.464	5.2637	5.876
Ti_3Sb	10.465	5.2639	6.070
$Ti_{2.5}Sb$	10.476	5.2688	6.161
Ti_2Sb	10.475	5.2692	6.270

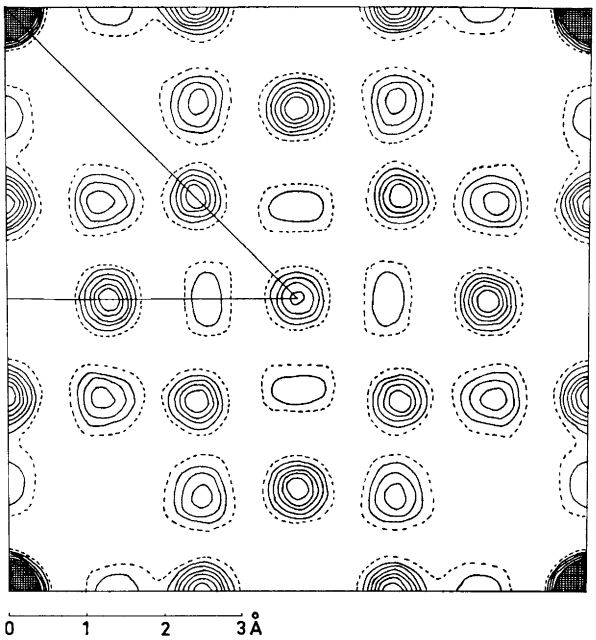

Fig. 3. Patterson projection on 001 of the tetragonal Ti_3Sb. Only the primitive unit cell is drawn. The contours are at equal but arbitrary intervals. Zero contours are broken and negative contours are omitted.

On the basis of the corrected $F(hk0)^2$-values a Patterson map was computed, *cf.* Fig. 3. As the cubic and tetragonal Ti_3Sb phase have related lattice dimensions $a_{tetr} \approx 2a_{cub}$, $c_{tetr} \approx c_{cub}$, relationships with the β-W structure was looked for in the Patterson map. It was indeed possible to rearrange the atoms in the β-W structure in agreement with the Patterson map. Based on these approximate atomic parameters structure factors were calculated, and after adjusting F_o and F_c to the same scale $R = \Sigma\big| |F_o| - |F_c| \big| / \Sigma |F_o| = 0.29$ was found, indicating the main features of the proposed structure to be correct.

The atomic parameters were refined further by means of four Fourier and one difference synthesis. R decreased to 0.19 after the last Fourier synthesis and to 0.132 after the difference synthesis. The observed and calculated $F(hk0)$-values are listed in Table 5 and the final Fourier map is shown in Fig. 4. The corresponding parameters, referred to the body-centered axes, are:

4 Ti I in 0,0 *etc.*
4 Ti II in $0,\frac{1}{2}$ *etc.*
16 Ti III in $x_1 = 0.0766$, $y_1 = 0.2228$ *etc.*
8 Sb in $x_2 = 0.1635$, $y_2 = \frac{1}{2} + x_2 = 0.6635$ *etc.*

In terms of the highest symmetric space group, $I4/mcm$ (D_{4h}^{18}), all atoms are in special positions with fixed z-coordinates. For symmetry reasons only

Table 5. Observed and calculated structure factors for tetragonal Ti_3Sb (CuK-radiation).

hkl	F_o	$\frac{1}{2}F_c$
200	29.3	− 38.2
400	0	− 1.4
600	110.7	+ 114.5
800	16.0	− 23.9
1000	25.6	− 22.9
1200	152.5	+ 142.5
110	22.2	− 27.0
310	70.3	+ 60.7
510	0	− 1.0
710	75.5	− 88.7
910	86.9	+ 91.9
1110	35.8	− 43.2
1310	0	− 5.7
220	42.9	+ 33.2
420	139.1	+ 149.2
620	26.3	+ 18.1
820	101.9	+ 99.8
1020	80.9	+ 70.8
1220	39.9	− 46.8
330	141.5	− 168.4
530	92.3	+ 82.8
730	101.9	+ 92.9
930	93.2	− 96.5
1130	24.2	+ 16.6
1330	51.9	+ 51.3
440	85.5	+ 71.7
640	40.9	− 52.5
840	46.8	+ 37.5
1040	91.4	+ 76.2
1240	0	+ 8.1
550	69.5	+ 75.3
750	27.0	− 31.6
950	0	+ 4.0
1150	34.3	+ 25.4
660	209.9	+ 201.6
860	13.7	+ 8.3
1060	28.8	− 36.4
1260	105.2	+ 117.6
770	39.8	+ 30.5
970	46.4	+ 38.1
1170	0	− 3.9

hkl	F_o	$\frac{1}{2}F_c$
880	45.3	+ 37.8
1080	59.2	+ 51.3
990	105.7	− 114.6

hkl	F_o	$\frac{1}{2}\lvert F_c\rvert$
211	74.6	88.8
411	177.0	186.6
611	0	6.4
811	95.2	103.8
1011	14.0	15.4
1211	14.8	10.4
321	68.0	71.4
521	118.4	132.4
721	86.2	77.4
921	0	3.8
1121	104.4	102.8
1321	59.0	70.0
431	0	4.0
631	48.4	50.2
831	54.6	64.0
1031	0	0.0
1231	45.4	44.0
541	48.6	48.6
741	64.0	57.0
941	41.0	37.2
1141	87.0	84.8
651	37.8	31.4
851	93.8	103.0
1051	134.6	114.6
1251	9.0	11.0
761	11.8	6.4
961	40.2	29.0
1161	20.0	14.6
871	83.8	75.4
1071	81.8	75.8
981	50.4	44.4

the 16 Ti III atoms in (k) and the 8 Sb atoms in (h) contribute to the $hk1$-reflections. The agreement between $|F(hk1)|_o$ and $|F(hk1)|_c$ calculated on this assumption, *cf.* Table 5, is so good, $R = 0.116$, that the space group and atomic parameters x_1, y_1 and x_2 seem correctly chosen.

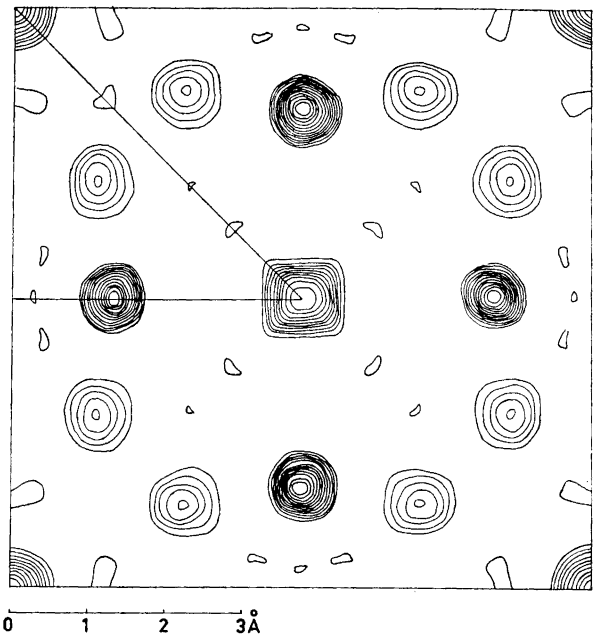

Fig. 4. Fourier projection of the primitive unit cell of tetragonal Ti_3Sb on 001. Contours are drawn at every 10 e $Å^{-2}$. Zero and negative contours omitted.

On the basis of the relationships found between cubic and tetragonal Ti_3Sb is seemed reasonable to assume that the z-coordinates in tetragonal Ti_3Sb were the same as for the corresponding atoms in cubic Ti_3Sb. It turned out, however, that z-values of 0 and ½ for Ti I were unreasonable considering the interatomic distances Ti I—Ti III. Therefore, z-parameter values of 1/4 and 3/4 were chosen for both Ti I and Ti II. In order to verify these z-parameters, intensities was calculated in the same way as for cubic Ti_3Sb and compared with those obtained from photometer recordings of powder photographs. As can be seen from Table 3 the agreement between the two sets of values is good and leaves no doubt about the correctness of the proposed structure.

The deduced atomic arrangement, *cf.* Fig. 5, is thus: (0,0,0; 1/2,1/2,1/2) +

4 Ti I in (*a*) 0,0,1/4; 0,0,3/4.

4 Ti II in (*b*) 0,1/2,1/4; 1/2,0,1/4.

16 Ti III in (*k*) $x,y,0$; $\bar{x},\bar{y},0$; $\bar{y},x,0$; $y,\bar{x},0$; $x,\bar{y},\frac{1}{2}$; $\bar{x},y,\frac{1}{2}$; $y,x,\frac{1}{2}$; $\bar{y},\bar{x},\frac{1}{2}$, with $x_1 = 0.0766$, $y_1 = 0.2228$.

8 Sb in (*h*) $x,\frac{1}{2}+x,0$; $\bar{x},\frac{1}{2}-x,0$; $\frac{1}{2}+x,\bar{x},0$, $\frac{1}{2}-x,x,0$ with $x_2 = 0.1635$.

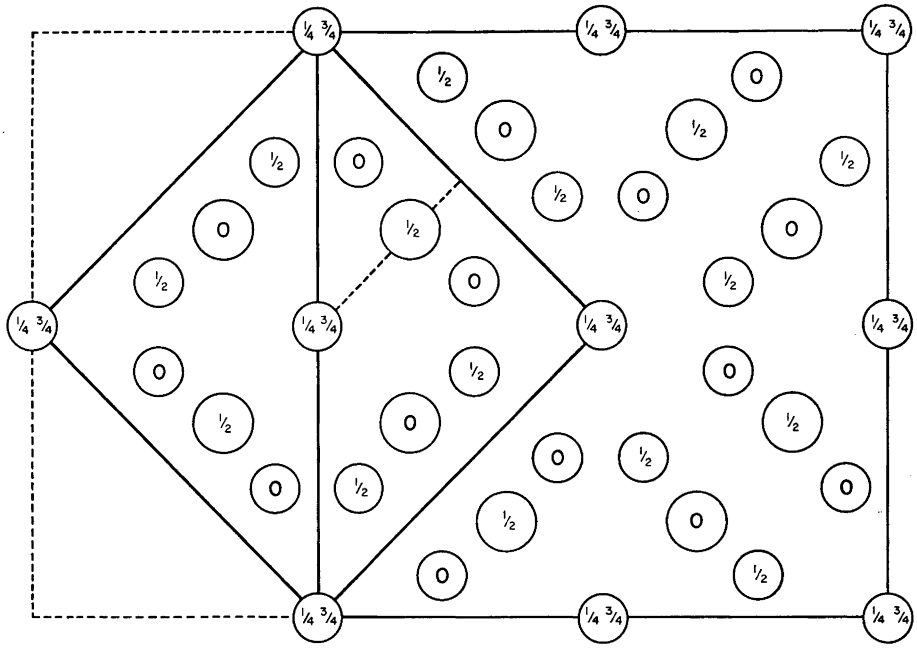

Fig. 5. Projection of the unit cell of tetragonal Ti_3Sb on 001. Large circles represent antimony atoms and small circles titanium atoms. Figures give the z-parameters. Both the primitive and the body-centered unit cell are indicated.

C. Some phase-analytical data

In addition to the two Ti_3Sb phases just reported, two other previously unknown phases, the $Ti_{1.7}Sb$ phase and the $Ti_{1.2}Sb$ phase, were identified in the titanium-rich (> 50 at. % Ti) part of the system. The exact composition ranges of the phases have not been determined, and the formulae only indicate their approximate composition. Phase-analytical work using metallographic and X-ray powder methods and density measurements is still in progress and only a few observations will be mentioned here.

The $Ti_{1.7}Sb$ phase. X-Ray powder photographs of different samples in the range around Ti_2Sb contained reflections from a new phase with composition somewhere in this concentration range. This phase was obtained by either of the melting methods outlined in the experimental part. By means of metallographic methods the approximate composition of this phase is found to be $Ti_{1.7}Sb$, which is in agreement with the composition estimated using the disappearing phase method on the powder photographs.

Single crystals of the $Ti_{1.7}Sb$ phase were obtained with bipyramidal shape in different melts. Oscillation and Weissenberg photographs showed that the crystals had orthorhombic symmetry. With the approximate unit cell dimen-

Table 6. Powder photograph data of $Ti_{1.7}Sb$ taken with CrK-radiation, a_2 and β lines omitted.

I_{obs}	$\sin^2\Theta \times 10^4$ obs	$\sin^2\Theta \times 10^4$ calc	hkl
vw	954	953	211
w	1032	1030	002
m	1140	1137	121
m	1262	1259	220
vw	1348	1345	112
m	1399	1398	301
m	1909	1909	122
vw	1955	1950	031
w	2027	2026	400
vw	2076	2077	131
m	2152	2150	321
st	2287	2284	401
		2289	222
w	2338	2632	113
vw	2476	2472	411
w	2508	2505	013
w	2781	2778	420
vw	2842	2849	132
vw	2920	2922	322
m	3018	3009	040
		3012	213
w	3578	3576	223
vw	3724	3718	430
vw	3808	3808	422
vw	3862	3862	332
vw	4025	4009	033
		4093	042
w	4164	4166	142
vw	4212	4209	323
vw	4309	4307	014
w	4396	4384	512
vw	4513	4516	233
w	5299	5293	441
		5311	620
vw	5460	5448	314
		5453	143
		5466	251
w	5565	5569	621
vw	5814	5811	034
m	6237	6235	523
vw	6572	6563	105
vw	6876	6276	603
m	7180	7175	533
m	7326	7315	125
m	7479	7473	514
m	7988	7987	722
w	8106	8105	800
vw	8272	8268	344
w	8551	8551	811
w	8572	8568	633
m	8796	8796	460
w	8900	8897	552

sions from the single crystal data the lattice constants of the $Ti_{1.7}Sb$ phase were determined from the powder photographs, *cf.* Table 6, to be:

$$a = 10.172 \text{ Å}, \qquad b = 8.346 \text{ Å}, \qquad c = 7.135 \text{ Å}.$$

The only systematic missing reflections were of the type $hk0$ absent when $h = 2n + 1$. The probable space groups are thus $Pmma$ (D_{2h}^5), $Pmc2_1$ (C_{2v}^2) and $Pma2$ (C_{2v}^4).

The $Ti_{1.2}Sb$ phase. Samples with composition in the range about $Ti_{1.2}Sb$ give very complicated powder photographs and the phases are not easily identified by X-ray methods. By metallographic technique, however, two phases with approximate composition $Ti_{1.2}Sb$ and TiSb could be identified. In the same way as the $Ti_{1.7}Sb$ phase, the $Ti_{1.2}Sb$ phase was obtained by either of the melting methods.

Table 7. Powder photograph data of low angle reflections of $Ti_{1.2}Sb$ taken with CuK-radiation, α_2 and β lines omitted.

I_{obs}	$\sin^2\Theta \times 10^4$ obs	$\sin^2\Theta \times 10^4$ calc	hkl
vw	329	327	121
w	386	384	140
w	448	448	400
		452	330
w	489	484	311
vw	536	537	420
w	589	584	150
w	611	608	340
vw	666	668	250
w	678	678	241
w	725	723	510
w	826	818	341
		828	160
w	882	878	251
w	895	892	112
m	1006	1000	521
		1004	450
		1009	600
		1010	061
m	1017	1014	441
		1018	351
st	1039	1031	610
		1038	161
		1043	222
w	1078	1070	132
w	1128	1122	261
vw	1208	1201	270
		1209	630
vw	1310	1308	621
		1310	242
		1312	412
vw	1421	1419	631
		1422	080
		1426	152
vw	1514	1510	252
vw	1607	1605	711
vw	1678	1670	162
		1672	721
m	1780	1775	651
		1783	731
		1790	570
w	1854	1846	452
		1851	602

In most of the samples melted in the Nernst-Tammann furnace long needle-shaped crystals were obtained. Oscillation and Weissenberg photographs showed the crystals to be orthorhombic with unit cell dimensions:

$$a = 14.55 \text{ Å}, \qquad b = 16.34 \text{ Å}, \qquad c = 5.31 \text{ Å}.$$

Missing reflections were: $0kl$ when $k = 2n + 1$ and $h0l$ when $h = 2n + 1$. This is characteristic of the space groups $Pbam$ (D_{2h}^9) and $Pba2$ (C_{2v}^8). In Table 7 are listed the lines found in the low angle region on a powder photograph of the $Ti_{1.2}Sb$ sample.

The TiSb phase. X-Ray powder photographs of the TiSb phase were indexed on the basis of a hexagonal unit cell. The redetermination of the lattice constants gave the result:

$$a = 4.115 \text{ Å}, \qquad c = 6.264 \text{ Å}, \qquad c/a = 1.560$$

Whether the difference between the values given here and the results by Nowotny and Pesl[1] ($a = 4.07_0$ Å; $c = 6.30_6$ Å) reflects the difference in thermal history of the alloys, or indicates an extended homogeneity range, or is due to impurities is not clear at the moment.

DISCUSSION

In the β-W structure of the cubic Ti_3Sb phase, *cf.* Fig. 2, each titanium atom is coordinated to two titanium atoms in linear chains at a distance $a/2$, to eight more titanium atoms at a 22.5 % larger distance, and to four antimony atoms in a tetrahedral arrangement. Each antimony atom is coordinated to twelve titanium atoms at the corners of an icosahedron. The interatomic distances between nearest neighbours in cubic Ti_3Sb are listed in Table 8.

Table 8. Interatomic distances in cubic Ti_3Sb (Å).

Ti	— 2 Ti	: 2.609
	— 8 Ti	: 3.195
	— 4 Sb	: 2.917
Sb	— 12 Ti	: 2.917

The shortest Ti—Ti distance is definitely shorter than in metallic titanium. The shortest interatomic distances are 2.896 Å for α-Ti according to Clark [9] and 2.843 Å for β-Ti according to Levinger [10]. In many of the titanium compounds with β-W structure, listed by Geller [11], even shorter Ti—Ti distances than the one found here are observed.

The observed interatomic distances can also be compared with the values predicted from the metallic radii [12]. If antimony retains one of its usual valences, 1.56 or 3, the twelve Ti—Sb bonds should have bond numbers 0.13 or 0.25. Using the single bond radius value of 1.324 Å for Ti and 1.391 Å for Sb, with an electronegativity correction of 0.008 Å, the expected Ti—Sb bond distances for the two different valence states are 3.239 Å and 3.068 Å, respectively. The observed value 2.917 Å agrees better with that calculated for a valence 3 for Sb than for the usual metallic valence 1.56, but even this value is considerably larger than the observed one. To account for the discrepancy one can either accept a set of special β-W radii (*cf.* Geller [11,13] and Pauling[14]), or assume a higher bond number for the Ti—Sb bonds [14]. Higher bond numbers would obtain, according to Pauling [12], if one electron were transferred from the hyperelectronic Sb atom to the hypoelectronic Ti atom, thus increasing the valences by one. The calculated Ti—Sb bond distance for this valence, 2.993 Å is still appreciably larger than the observed value. Using the effective metallic radius for Ti given by Pauling [14] for the β-W structure, a shorter Ti—Sb bond distance value of 2.940 Å for the same bond number 0.33 is calculated. For the ten Ti—Ti bonds with a bond number of 0.20, and using the β-W radius value for singlebonded Ti of 1.271 Å, the calculated bond distance is 3.058 Å, or rather close to the weighed mean (3.078 Å) of the observed values.

In order to derive the structure of tetragonal Ti_3Sb from the β-W type structure of cubic Ti_3Sb, displacements of some of the atoms must be performed. The main difference between the two structures consists in a movement of the Ti I atoms as indicated by the arrows in Fig. 6 and a translation of these atoms of magnitude $c/4$ along the c-axis. Moreover, a characteristic difference is produced by the change from cubic to tetragonal symmetry, *cf.* Figs. 5 and 6.

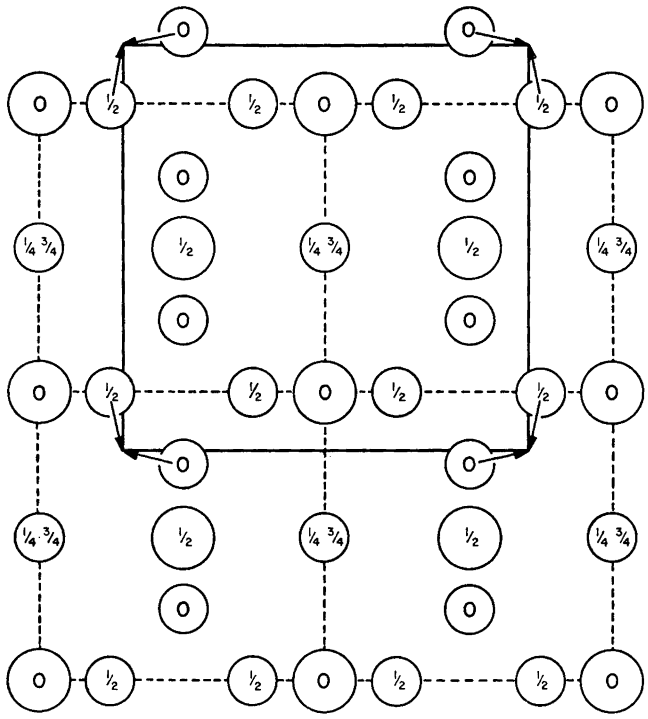

Fig. 6. Projection of four unit cells of cubic Ti_3Sb in relation to the 001 projection of the primitive unit cell of tetragonal Ti_3Sb.

Chains of Ti atoms, characteristic of the cubic Ti_3Sb structure are also present in the tetragonal structure. In the tetragonal structure Ti I and Ti II form chains only along the *c*-axis, while perpendicular to it the chains are broken due to the relative displacement of the Ti I atoms and by the change to tetragonal symmetry. The configuration of the eight Ti III atoms around each Ti I is found to be that of a slightly distorted square antiprism. The Ti II atoms are coordinated to eight Ti III atoms at the corners of an even more distorted rectangular antiprism and to four antimony atoms at the corners of a tetrahedron. Each Ti III atom is surrounded by eleven titanium atoms and four antimony atoms, *cf.* Fig. 5. Each antimony atom is coordinated to ten titanium atoms and two antimony atoms at the corners of an irregular icosahedron.

The interatomic distances between nearest neighbours in tetragonal Ti_3Sb calculated for the final parameters are listed in Table 9. The errors indicated are standard deviations calculated according to Cruickshank [15]. No comparison between observed and calculated bond distances is carried out for tetragonal Ti_3Sb, since even in the case of cubic Ti_3Sb the basis for the calculation is uncertain.

Table 9. Interatomic distances in tetragonal Ti_3Sb (Å).

Ti	I	–	2	Ti	I	: 2.632
		–	12	Ti	III	: 2.794 ± 0.011
Ti	II	–	2	Ti	II	: 2.632
		–	8	Ti	III	: 3.285 ± 0.011
		–	4	Sb		: 2.755 ± 0.003
Ti	III	–	2	Ti	I	: 2.794 ± 0.011
		–	2	Ti	II	: 3.285 ± 0.011
		–	1	Ti	III	: 2.970 ± 0.021
		–	2	Ti	III	: 3.082 ± 0.021
		–	2	Ti	III	: 3.407 ± 0.021
		–	2	Ti	III	: 3.487 ± 0.021
		–	1	Sb		: 2.780 ± 0.012
		–	1	Sb		: 2.790 ± 0.012
		–	2	Sb		: 3.029 ± 0.012
Sb		–	2	Ti	II	: 2.755 ± 0.003
		–	2	Ti	III	: 2.780 ± 0.012
		–	2	Ti	III	: 2.790 ± 0.012
		–	4	Ti	III	: 3.029 ± 0.012
		–	2	Sb		: 3.671 ± 0.004

In order to study relative stabilities of the two crystalline phases, samples first melted in the arc furnace were remelted in the Nernst-Tammann furnace, and *vice versa*. By this treatment, the cubic crystals were changed into tetragonal crystals, while the tetragonal crystals remained unchanged after melting in the arc furnace. Thus, the transformation is apparently irreversible.

It is known in other instances that small amounts of impurities can stabilize more or less foreign structures, *e.g.* a pseudobrookite structure for Ti_3O_5 is found already at an iron concentration of 0.23 weight % Fe ($x = 0.03$ in $(Ti_{1-x}Fe_x)_3O_5$) according to Andersson *et al.*[16] Spectrographic analysis of samples containing the tetragonal Ti_3Sb phase showed the presence of about 3/10 % Al and 3/10 % Si as impurities. Samples of the cubic Ti_3Sb phase were, however, only found to contain the same amounts of impurities as the titanium and antimony used. On melting samples with composition Ti_3Sb in the arc furnace together with different small amounts of Al, Si, Al_2O_3 and SiO_2 they all still gave X-ray photographs characteristic of the cubic Ti_3Sb phase. The presence of impurities like oxygen and nitrogen might perhaps explain the stability of the tetragonal structure. Thus, cubic Ti_3Sb is obtained by remelting tetragonal Ti_3Sb in an arc furnace with small amounts of pure titanium. The explanation of this as due to differences in composition of the two phases, seems unreasonable since, for example, the alloy $Ti_{3.5}Sb$ remains tetragonal after remelting in the arc furnace. Indeed, the pure titanium might act as an absorber of the oxygen and nitrogen present in the alloy.

Including the four phases reported here eight phases have been described in the titanium-antimony system. Their characteristic crystallographic properties are listed in Table 10. In view of the present discussion about the relative stability of cubic and tetragonal Ti_3Sb, and as the present study could not confirm the existence of the Ti_4Sb phase and the $Ti_{2.5}Sb$ phase reported by Nowotny and coworkers [1–3], the possibility that these phases also might be

Table 10. Pycnometric densities and crystallographic data for phases reported in the titanium-antimony system.

Phase	d (g cm^{-3})	a (Å)	b (Å)	c (Å)	c/a	Structure type	Reference
Ti_4Sb	—	5.958	—	4.807	0.807	Hex.-Ni_3Sn	Nowotny *et al.*[2]
Ti_3Sb	6.137	5.2186	—	—	—	Cub.-βW	Present
Ti_3Sb	—	5.217	—	—	—	Cub.-βW	Matthias *et al.*[6]
Ti_3Sb	6.070	10.465	—	5.2639	0.508	Tetr.	Present
$Ti_{2.5}Sb$	5.90	4.01	—	14.5	3.63	Tetr.-Cu_2Sb	Auer-Welsbach *et al.*[3]
$Ti_{1.7}Sb$	—	10.172	8.348	7.135	—	Orthor.	Present
$Ti_{1.2}Sb$	—	14.55	16.34	5.31	—	Orhtor.	Present
TiSb	—	4.07_0	—	6.30_6	1.55	Hex.-NiAs	Nowotny and Pesl[1]
TiSb	—	4.115	—	6.264	1.560	Hex.	Present
$TiSb_2$	—	6.66_6	—	5.81_7	0.87_3	Tetr.-$CuAl_2$	Nowotny and Pesl[1]

stabilized by impurities should not be overlooked. With attention focused on the Ti_4Sb phase it should be noted that a lattice constant variation of only 2 to 4 % between the isostructural phases Ti_4Sb, Ti_4Pb (Nowotny and Pesl [17]) and Ti_3Al * (Anderko *et al.*[18]) is much smaller than the 10 to 23 % difference expected due to the difference in metallic radii of Sb, Pb and Al. This point is perhaps worth a further study in view of the observed reaction between Ti and Al_2O_3.

Acknowledgments. The authors are greatly indebted to Professor Haakon Haraldsen for his kind interest in this study and for placing laboratory facilities at their disposal. They also wish to express their thanks to siviling. Hallstein Kjøllesdal, Sentralinstitutt for Industriell Forskning, for carrying out the meltings in the arc furnace.

REFERENCES

1. Nowotny, H. and Pesl, J. *Monatsh.* **82** (1951) 336.
2. Nowotny, H., Funk, R. and Pesl, J. *Monatsh.* **82** (1951) 513.
3. Auer-Welsbach, H., Nowotny, H. and Kohl, A. *Monatsh.* **89** (1958) 154.
4. Thorbjørnsen, J. *Thesis*, University of Oslo, 1957.
5. Kjekshus, A. *Paper read at the 10th Inter-Scandinavian Chemistry Conference*, Stockholm 1959.
6. Matthias, B. T., Compton, V. B. and Correnzwit, E. *J. Phys. Chem. Solids* **19** (1961) 130.
7. Kubaschewski, O. and Dench, W. A. *Acta Met.* **3** (1955) 339.
8. Nelson, J. B. and Riley, D. P. *Proc. Phys. Soc. (London)* **57** (1945) 160.
9. Clark, H. T. *J. Metals* **1** (1949) 588.
10. Levinger, B. V. *Trans. Am. Soc. Metals* **197** (1953) 195.
11. Geller, S. *Acta Cryst.* **9** (1956) 885.
12. Pauling, L. *The Nature of the Chemical Bond.* Cornell University Press, Ithaca 1960.

* The Ti_2Al phase reported by Ence and Margolin [19] is probably belonging to the homogeneity range of the Ti_3Al phase.

13. Geller, S. *Acta Cryst.* **10** (1957) 380.
14. Pauling, L. *Acta Cryst.* **10** (1957) 374.
15. Cruickshank, D. W. J. *Acta Cryst.* **2** (1949) 65.
16. Andersson, S., Collén, B., Kuylenstierna, U. and Magnéli, A. *Acta Chem. Scand.* **11** (1954) 1641.
17. Nowotny, H. and Pesl, J. *Monatsh.* **82** (1951) 344.
18. Anderko, K., Sagel, K. and Zwicker, U. *Z. Metallkunde* **48** (1957) 57.
19. Ence, E. and Margolin, H. *Trans. Am. Inst. Mining Met. Engrs.* **209** (1957) 484.

Received January 12, 1962.

ACTA CHEMICA SCANDINAVICA 16 (1962) 1511–1518

Amino Acids and γ-Glutamyl Derivatives in Seeds of *Lunaria annua* L.*

P. OLESEN LARSEN

Department of Organic Chemistry, The Royal Veterinary and Agricultural College, Copenhagen, Denmark

Unhydrolyzed seed extracts of *Lunaria annua* L. (family *Cruciferae*) have been investigated for ninhydrin-reacting constituents. *γ-L-Glutamyl-β-alanine*, not previously found in nature, has been isolated and identified on comparison with a synthetic sample. In addition, γ-L-glutamyl-β-aminoisobutyric acid, *m*-carboxy-L-phenylalanine and 3-(3-carboxy-4-hydroxyphenyl)-L-alanine (*m*-carboxy-L-tyrosine), all previously known from higher plants, have been isolated in crystalline form. The presence of still other amino acids, such as several of the ordinary protein constituents, as well as β-alanine, β-aminoisobutyric acid and *m*-carboxyphenylglycine, has been demonstrated by paper chromatography. A minor constituent is tentatively regarded as α- or γ-glutamyl-γ-aminobutyric acid, whereas two additional glutamic acid derivatives are still under consideration.

The *Lunaria* seed extract is the first reported source of the simultaneous occurrence of the three *m*-carboxy-substituted aromatic amino acids encountered so far in higher plants.

The occurrence of the above-mentioned and related compounds in the plant kingdom is briefly discussed.

In the course of investigations on the contents of free amino acids in certain higher plants, containing isothiocyanate-producing glucosides [1], seed extracts of the ornamental crucifer *Lunaria annua* L. (honesty) were examined. Paperchromatographic amino acid analysis revealed a complex picture (Fig. 1), in which, besides common amino acids, a number of unusual spots suggested the presence of other amino acids and peptides. Some of the spots could tentatively be assigned to known compounds, whereas others apparently represented new constituents.

In order to obtain detailed information on the composition of the free amino acids in *Lunaria* seed, investigations were initiated on a larger scale. The total amino acid fraction from 1 kg of seed flour was isolated by means of a strongly acid ion exchange resin and subdivided on other resins as outlined

* Presented in abstract before the *International Symposium on Organic Chemistry of Natural Products*, June 1962, Brussels.

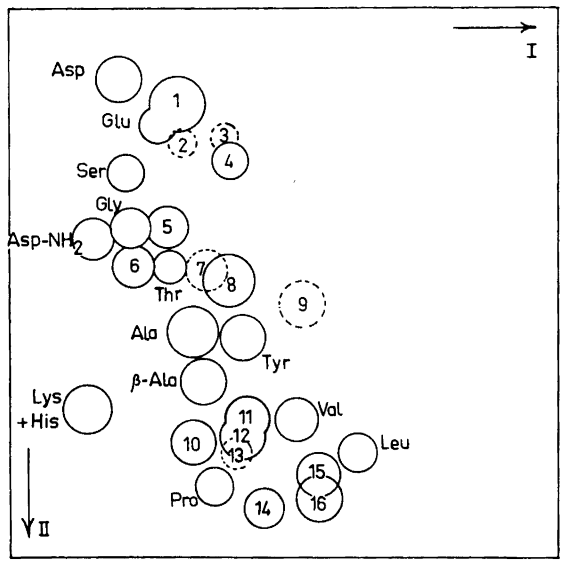

Fig. 1. Two-dimensional paper chromatogram of the amino acid fraction of *Lunaria annua* L. 1. Solvent: butanol:acetic acid: water (12:3:5), 2. Solvent: phenol:water:conc. ammonia (120:30:1). Spots marked by a dotted line are only detectable in highly concentrated fractions. 1: 3-(3-Carboxy-4-hydroxy-phenyl)-L-alanine (*m*-carboxy-L-tyrosine). 2: Unknown acid amino acid. 3: *m*-Carboxyphenylglycine. 4: *m*-Carboxy-L-phenylalanine. 5: γ-L-Glutamyl-β-alanine. 6: Unknown neutral amino acid. 7: Glutamyl-γ-aminobutyric acid. 8: γ-L-Glutamyl-β-aminoisobutyric acid. 9: Unknown acid glutamyl derivative. 10: Unknown neutral glutamic acid derivative. 11: β-Aminoisobutyric acid. 12: γ-Aminobutyric acid. 13: Ethanolamine. 14: Pipecolic acid. 15: γ-Guanidobutyric acid. 16: Unknown neutral glutamic acid derivative.

in Fig. 2. First, a weakly basic ion exchange resin in the acetate form was utilized to separate the amino acids into four fractions. The first of these contained neutral and basic amino acids and derivatives which showed no affinity to the resin. The second and third fraction included acidic compounds displaceable by acetic acid, whereas the fourth fraction contained amino acids sufficiently acid to be displaced only by hydrochloric acid.

In *the first fraction* the neutral and basic compounds were separated by means of a strongly acid resin in the ammonia form. Neutral compounds passed through the resin whereas basic constituents were bound and subsequently eluted with ammonia. The composition of these two fractions is indicated in Fig. 2. When not otherwise indicated the compounds were identified by R_F-values and co-chromatography with authentic samples. In addition, β-aminoisobutyric acid, β-alanine, γ-aminobutyric acid and lysine were controlled by a specific test for amino group position developed in this laboratory [2]. β-Aminoisobutyric acid and γ-aminobutyric acid were distinguished by paper chromatography in 2,4-lutidine:water, a solvent particularly suited for separation of the different aminobutyric and aminoisobutyric acids [3]. Asparagine,

Amino acid fraction

Weakly basic ion exchange resin on the acetate form

- 1. Fraction (unbound neutral and basic amino acids) — Strongly acid ion exchange resin on the ammonia form
  - Unbound fraction of neutral amino acids:
    - Normal protein amino acids (glycine, alanine, valine, leucine and/or isoleucine, serine, threonine, asparagine [A], tyrosine [A], proline [A])
    - Pipecolic acid [A]
    - γ-Aminobutyric acid [A]
    - β-Aminoisobutyric acid [A]
    - β-Alanine [A]
    - γ-Guanidobutyric acid [A;B]
    - Unknown amino acid
    - Two unknown derivatives of glutamic acid [B]
  - Ammonia eluate containing basic amino acids:
    - Lysine [A]
    - Histidine [A]
    - Ethanolamine
    - γ-Guanidobutyric acid [B]
- 2. Fraction (acetic acid eluate) — Strongly basic ion exchange resin in the acetate form
  - Glutamyl-γ-aminobutyric acid [A,B,C]
  - γ-L-Glutamyl-β-aminoisobutyric acid [A,B,D]
  - γ-L-Glutamyl-β-alanine [A,B,D]
  - Unknown glutamyl peptide [A,B,C] and unknown amino acid
  - Glutamic acid
  - Aspartic acid
- 3. Fraction (acetic acid eluate)
  - Aspartic acid
  - *m*-Carboxy-L-phenylalanine [D]
  - *m*-Carboxyphenylglycine [A]
- 4. Fraction (HCl eluate)
  - 3-(3-Carboxy-4-hydroxy-phenyl)-L-alanine (*m*-Carboxy-L-tyrosine) [A,D]

Fig. 2. Fractionation scheme for amino acids in seed extracts of *Lunaria annua* L. A) Identified by specific colour reaction. B) Identified by hydrolysis products. C) Identified by end group analysis. D) Identified by isolation and comparison of infra-red spectra and rotation values with those of authentic samples.

proline, pipecolic acid and β-alanine were recognized by their characteristic colours with ninhydrin. Tyrosine and histidine were identified by reaction with diazotized sulphanilic acid, and γ-guanidobutyric acid by a positive

Sakaguchi reaction coupled with the formation of γ-aminobutyric acid on hydrolysis with barium hydroxide.

The second fraction was shown by paper chromatography to contain aspartic and glutamic acid besides two unknown compounds. Further fractionation was accomplished by chromatography on a strongly basic ion exchange resin in the acetate form, resulting in only partial separation of the two unknown compounds but complete removal of aspartic and glutamic acid. The major component (*ca.* 300 mg) was purified by crystallization and identified as (—)-γ-L-glutamyl-β-aminoisobutyric acid on comparison with an authentic sample [4]. Moreover, the compound on hydrolysis afforded glutamic acid and β-aminoisobutyric acid, both identified by paper chromatography. The minor component, present in a total amount of about 100 mg, was purified by counter current distribution followed by preparative paper chromatography. A crystalline sample, slightly contaminated with γ-glutamyl-β-aminoisobutyric acid, was obtained, which on hydrolysis yielded glutamic acid and β-alanine, both identified by paper chromatography. The identity of the new compound as γ-L-glutamyl-β-alanine, not previously found in nature *, appeared from a critical comparison with a synthetic sample[5]. The infra-red spectra were identical, whereas a slight difference in rotation values could be attributed to a slight contamination with γ-glutamyl-β-aminoisobutyric acid.

β-Alanine and β-aminoisobutyric acid, found in the neutral fraction, could conceivably be artifacts produced by hydrolytic fission of the labile amide bonds in the γ-glutamyl derivatives during isolation of the amino acid fraction. That this was not the case, however, appeared from the fact that the two γ-glutamyl amino acids proved to be stable when subjected to the conditions employed during the preparation of the amino acid fraction.

The third fraction contained aspartic acid in addition to *m*-carboxy-phenylglycine and *m*-carboxy-L-phenylalanine. The latter (18 mg) was isolated in crystalline form and identified on comparison with an authentic sample [6]. The concentrated mother liquor contained *m*-carboxyphenylglycine as apparent from co-chromatography with a synthetic sample and by its specific colour reaction with ninhydrin.

The fourth fraction solely contained 3-(3-carboxy-4-hydroxyphenyl)-L-alanine (*m*-carboxy-L-tyrosine), isolated in substantial amounts (3.7 g) and again identified upon comparison with an authentic sample [1].

γ-L-Glutamyl-β-aminoisobutyric acid [4], as well as (—)-β-aminoisobutyric acid [7], have previously been isolated from bulbs of *Iris tingitana* var. Wedgewood **. (—)-β-Aminoisobutyric acid, of recently established absolute configuration [8], has formerly been observed in human urine [9,10] and in flatworms [11], whereas β-alanine is widely distributed in the plant kingdom and has been isolated from bulbs of *Iris tingitana* var. Wedgewood [12]. It may be significant that the two β-amino acids, occurring together in the same plant in the free state or as γ-glutamyl-derivatives, are regarded as products on the catabolic pathway of pyrimidines [13].

---

* See note added in proof.

** Although no precise author name is quoted, the employed plant material presumably represents a garden variety of *Iris tingitana* Boiss. *et* Reut.

Two other glutamine derivatives may be biogenetically related to γ-glutamyl-β-alanine, *viz.* N^5-ethyl-L-glutamine (theanine), isolated from tea leaves [14] and the fungus *Xenocomus badius* [15], and N^5-(2-cyanoethyl)-L-glutamine, occurring in various *Lathyrus*-species [16] and considered responsible for some of the toxic effects (lathyrism) observed in higher animals after ingestion of these plants.

m-Carboxy-L-phenylalanine and *m*-carboxyphenylglycine have formerly been isolated from *Iris tingitana* var. Wedgewood [6,17], whereas 3-(3-carboxy-4-hydroxy-phenyl)-L-alanine is known as a constituent of seeds of *Reseda odorata* L.[1] For the first time, these three *m*-carboxy-substituted aromatic amino acids have now been identified in the same plant, possibly suggesting a biogenetic relationship between them. Whereas a search for 3-(3-carboxy-4-hydroxyphenyl)-L-alanine in *Iris tingitana* has been without avail [18], *m*-carboxyphenylalanine has been identified in this laboratory by paper chromatography, together with 3-(3-carboxy-4-hydroxy-phenyl)-alanine, in a number of species of *Resedaceae* including *Reseda odorata* L. *m*-Carboxyphenylglycine has not yet been observed in the same species, but may be present in very low concentrations, which, as in the case of *Lunaria annua*, would require highly concentrated fractions to permit detection. The strikingly similar pattern of amino acids and γ-glutamyl-derivatives in *Lunaria annua* L. and *Iris tingitana* var. Wedgewood is surprising in view of the taxonomic remoteness of *Cruciferae* and the monocotyledonous family *Iridaceae*.

In its amino acid picture seed material of *Lunaria annua* L. does not deviate from that of *L. rediviva* L. but is conspicuously different from the patterns observed on seed material of a number of other crucifers studied. Chemically, *Lunaria* species present other unusual features such as the contents of the alkaloid lunarine with as yet unknown structure, producing spermidine on hydrolysis [19]. The occurrence of γ-guanidobutyric acid and pipecolic acid in seeds of *Lunaria* is not too remarkable in view of the wide distribution of these compounds in higher plants [20,21].

Besides the common amino acids and those discussed above, other ninhydrin-reacting compounds were noticed in the amino acid extract of *Lunaria* seeds.

In the neutral fraction three unknown compounds, all with a normal ninhydrin reaction, were present in concentrations high enough to be readily observable on paper chromatograms of the original seed extract (Fig. 1). One of these appears to be an amino acid whereas the two other components may be derivatives of glutamic acid. Work is in progress to establish the identity of these three constituents.

When the second fraction from the weakly basic ion exchange resin was chromatographed on the strongly basic resin, three compounds present in very small amounts were observed. The first of these seems to be an amino acid, the second a glutamyl derivative of an unknown amino acid, whereas the third, after paperchromatographic purification, was hydrolyzed to give glutamic acid and γ-aminobutyric acid, both identified by paper chromatography. Dinitrophenylation of the unhydrolyzed material according to Sanger [22], followed by hydrolysis and paper chromatography of the amino acid fraction, resulted in the appearance of only γ-aminobutyric acid. Hence, it

seems safe to conclude that the compound is either γ-glutamyl-γ-aminobutyric acid or α-glutamyl-γ-aminobutyric acid, none of which have previously been found in nature.

EXPERIMENTAL

Microanalyses were performed by Mr. G. Cornali. Rotations were measured in a 1 dm tube. Infra-red absorption spectra were determined in potassium bromide pellets on a *Perkin-Elmer* "Infracord"-instrument.

The employed material of *Lunaria annua* L. has been stored for several years as seed flour. Comparison with a small specimen of fresh seed material (purchased from I. E. Ohlsen's Enke, Copenhagen), however, revealed no differences in the contents of ninhydrin-postive constituents.

The seed flour (1 kg) was refluxed with carbon tetrachloride (3 l) for 1 h and filtered off after cooling. This procedure was repeated, and the air-dried powder (700 g) was refluxed for 4 h with methanol:water (4 l, 7:3, v/v), cooled and filtered again. The extraction was repeated twice with fresh portions of solvent. The combined filtrates were evaporated *in vacuo* to a dark-brown syrup (220 g), which was partly dissolved in water (750 ml). The filtrate was divided into three equal portions, and the total amino acid fraction in each portion was bound on a strongly acid ion exchange resin (Zeokarb 225, 4 × 50 cm) in the acid form. After washing with water (1 l), the amino acids were eluted with ammonia (2 l, 1 N). The combined eluates from the three portions were evaporated to a dark-brown syrup (30 g). A substantial amount of ammonium acetate of unknown origin condensed in the receiver during the evaporation. The syrup was redissolved in water (450 ml) and again bound to the strongly acid resin and eluted with ammonia. This was done in order to remove some tarry material from the syrup. The final ammonia eluate was again concentrated to a brown syrup (19 g), dissolved in water (250 ml) and applied to a weakly basic resin (Dowex 3, 20—50 mesh, 3.2 × 40 cm) in the acetate form. The effluent was collected in 20-ml fractions. After washing with water (1 l), the column was eluted with acetic acid (2.6 l, 1 N) and subsequently with hydrochloric acid (3 l, 1 N). Fractions 4—30 contained the basic and neutral compounds (first fraction). Fractions 81—109 contained aspartic acid, glutamic acid, and the glutamyl derivatives (second fraction), whereas fractions 110—149 contained aspartic acid and *m*-carboxy-L-phenylalanine (third fraction). Finally, fractions 216—347 contained 3-(3-carboxy-4-hydroxyphenyl)-L-alanine (fourth fraction).

The first fraction was evaporated *in vacuo* to a brown syrup (8.2 g) which was dissolved in water and purified by passing through a column of alumina (Woelm, "annähernd neutral", Akt.-Stufe 1). Most of the coloured material was absorbed on the alumina, whereas the amino acids could be eluted with water, and the solution was concentrated to dryness (4.2 g). The amino acids were applied in aqueous solution (25 ml) to a strongly acid resin (Amberlite IR 120, 2.3 × 18 cm) in the ammonia form. Neutral amino acids were washed through with water (150 ml) and the basic compounds were eluted with ammonia (120 ml, 1 N). Both fractions were evaporated to dryness and the amino acid composition determined by paper chromatography (Fig. 2) (the neutral fraction weighed 3.4 g, the basic fraction 0.3 g).

The second fraction was evaporated *in vacuo* to a brown crystalline residue (1.2 g), which was dissolved in water (50 ml) and applied to a strongly basic ion exchange resin (Dowex 1-X8, 200—400 mesh, 3 × 76 cm) in the acetate form. The column was eluted with acetic acid of a concentration progressively increasing from zero to 0.6 N over a volume of 4 l. The effluate was collected in fractions of 250 drops (*ca.* 20 ml). Fractions 73—79 contained glutamyl-γ-aminobutyric acid, fractions 86—98 γ-L-glutamyl-β-aminoisobutyric acid, fractions 90—99 γ-L-glutamyl-L-alanine, and fractions 98—99 small amounts of two unknown compounds. Glutamic acid and aspartic acid appeared in later fractions.

The fractions 86—94 were evaporated *in vacuo* to a colourless crystalline solid (200 mg). After four crystallizations from water, pure γ-L-glutamyl-β-aminoisobutyric acid resulted (Found: C 46.50; H 7.04; N 12.07. Calc. for $C_9H_{16}N_2O_5$: C 46.54; H 6.95; N 12.06), $[\alpha]_D^{23}$ −1.8° (*c* 1.0, 1 N HCl) (determined 5 min. after preparation of the solution.

No change in rotation was observed during the first 15 min. For rotation of L-glutamine under the same conditions, *cf.* Ref.[23]), $[\alpha]_D^{27}$ −20.0° (*c* 1.0, water (supersaturated)). Lit. value: $[\alpha]_D^{27}$ −33° (*c* 1.0) [4], solvent: water [18]. For a sample of γ-L-glutamyl-β-aminoisobutyric acid from *Iris tingitana* var. Wedgewood [4], the rotation value $[\alpha]_D^{24}$ −18.5° (*c* 1.0, water) was determined in this laboratory. The infra-red absorption spectrum was indistinguish-able from that of the authentic sample [4].

Fractions 95—98 were evaporated *in vacuo* to a colourless crystalline residue (190 mg) and combined with the first two mother liquors from the recrystallization of γ-glutamyl-β-aminoisobutyric acid (content 90 mg). The solid was dissolved in a mixture of water (15 ml), butanol (4 ml) and acetic acid (1 ml) and introduced into a Craig counter-current apparatus with 60 plates (lower and upper phase 10 ml each). The distribution was performed between the two phases of the system butanol:acetic acid:water (4:1:5). After 240 transfers, the tubes 10—34 contained γ-L-glutamyl-β-alanine, contaminated with γ-glutamyl-β-aminoisobutyric acid. The contents of these tubes were evaporated to dryness (70 mg), dissolved in water and chromatographed on Whatman paper No. 3 MM in butanol:acetic acid:water (12:3:5). γ-L-Glutamyl-β-alanine was eluted from the paper and evaporated to dryness (55 mg). Further purification was achieved by application to a strongly basic resin (Dowex 1-X 8, 200—400 mesh, 1 × 6 cm) on the acetate form followed by elution with acetic acid (1 N). The eluate was evaporated to dryness (38 mg) and three recrystallizations from aqueous ethanol afforded a reasonably pure specimen (Found: C 43.35; H 6.59; N 12.56. Calc. for $C_8H_{14}N_2O_5$: C 44.03; H 6.47; N 12.84), $[\alpha]_D^{23}$ + 5.5° (*c* 1.0, water), $[\alpha]_D^{24}$ + 23.0° (*c* 0.366, 0.1 N HCl) (determined 5 min. after preparation of the solution. No change in rotation was observed during the first 15 min.). No value for the rotation is recorded in the literature. A synthetic sample of γ-L-glutamyl-β-alanine [5] gave the value $[\alpha]_D^{25}$ + 25.8° (*c* 0.364, 0.1 N HCl). The infra-red absorption spectrum coincided with that of the synthetic product. Paper chromatography, however, revealed contamination with a small amount of γ-glutamyl-β-aminoisobutyric acid.

The third fraction was evaporated *in vacuo* to a brown oil (300 mg). After solution in water and treatment with charcoal a black resinous material (50 mg) was separated on addition of ethanol. Concentration of the mother liquor yielded *m*-carboxy-L-phenylalanine (18 mg) purified by recrystallization from water, $[\alpha]_D^{24}$ −15.8° (*c* 0.95, water (supersat.)). Lit.value: $[\alpha]_D^{25}$ −17.0° (*c* 1) [6], solvent: water [18] (Ref.[6] erroneously reports the opposite sign of rotation [18]). The infra-red absorption spectrum was identical with that of an authentic sample [6].

The fourth fraction was evaporated *in vacuo* to a brown crystalline residue (4.8 g) Solution in water (40 ml), treatment with charcoal and neutralisation with ammonia to pH 2.5 resulted in the precipitation of 3-(3-carboxy-4-hydroxy-phenyl)-L-alanine (3.2 g). A second crop (460 mg) was obtained from the mother liquor. Recrystallization from water afforded a pure sample, $[\alpha]_D^{26}$ −7.8° (*c* 0.9, 1 N NaOH). Lit.value $[\alpha]_D^{26}$ −7.5° (*c* 0.9, 1 N NaOH) [1]. The infra-red absorption spectrum was indistinguishable from that of an authentic sample [1].

Paper chromatography. The following R_F-values were determined for the new compounds by descending chromatography on Whatman paper No. 1 at 22° in (1) butanol: acetic acid:water (12:3:5), and (2) phenol:water:conc.ammonia (120:30:1) (w/v/v)):

γ-L-Glutamyl-β-alanine:	(1)	0.28,	(2)	0.40.
Glutamyl-γ-aminobutyric acid:	(1)	0.36,	(2)	0.48.

The author wishes to thank professor A. Kjær for encouragement and help during the present work, and expresses his gratitude to Dr. O. Rosenlund Hansen for the employed *Lunaria* seed material, to Dr. J. F. Thompson for samples of *m*-carboxy-L-phenylalanine and γ-L-glutamyl-β-aminoisobutyric acid, to Dr. A. Meister for a specimen of γ-L-glutamyl-β-alanine and to Dr. Y. Robin for a specimen of γ-guanidobutyric acid. Support from *The Carlsberg Memorial Foundation for Brewer I.C. Jacobsen* is gratefully acknowledged.

Added in proof. After the conclusion of the present work, we were privately informed by Dr. J. F. Thompson that γ-L-glutamyl-β-alanine has been isolated from *Iris tingitana* [24]. A sample of the compound from this plant was identical with our product with regard to infra-red spectrum and rotation value.

REFERENCES

1. Olesen Larsen, P. and Kjær, A. *Acta Chem. Scand.* **16** (1962) 142.
2. Olesen Larsen, P. and Kjær, A. *Biochim. et Biophys. Acta* **38** (1960) 148.
3. Awapara, J., Landua, A. J., Fuerst, R. and Seale, B. *J. Biol. Chem.* **187** (1950) 35.
4. Morris, C. J., Thompson, J. F., Asen, S. and Irreverre, F. *J. Biol. Chem.* **236** (1961) 1181.
5. Otani, T. T. and Meister, A. *J. Biol. Chem.* **224** (1957) 137.
6. Thompson, J. F., Morris, C. J., Asen, S. and Irreverre, F. *J. Biol. Chem.* **236** (1961) 1183.
7. Asen, S., Thompson, J. F., Morris, C. J. and Irreverre, F. *J. Biol. Chem.* **234** (1959) 343.
8. Balenović, K. and Bregant, N. *Tetrahedron* **5** (1959) 44.
9. Crumpler, H. R., Dent, C. E., Harris, H. and Westall, R. G. *Nature* **167** (1951) 307.
10. Kahimoto, Y. and Armstrong, M. D. *J. Biol. Chem.* **236** (1961) 3283.
11. Campbell, J. W. *Biol. Bull.* **119** (1960) 75.
12. Morris, C. J., Thompson, J. F., Asen, S. and Irreverre, F. *Nature* **190** (1961) 718.
13. Schulman, M. P. in D. M. Greenberg (Editor), *Metabolic Pathways* vol. **2**, Academic Press, New York 1961, p. 440.
14. Sakato, Y. *J. Agr. Chem. Soc. Japan* **18** (1950) 262, 269; *Chem. Abstr.* **45** (1951) 3528.
15. Casimir, J., Jadot, J. and Renard, M. *Biochim. et Biophys. Acta* **39** (1960) 467.
16. Schilling, E. D. and Strong, F. M. *J. Am. Chem. Soc.* **77** (1955) 2843.
17. Morris, C. J., Thompson, J. F., Asen, S. and Irreverre, F. *J. Am. Chem. Soc.* **81** (1959) 6069.
18. Thompson, J. F. *Personal communication.*
19. Potier, P., LeMen, J., Maurice-Marie, J. and Bladon, P. *Tetrahedron Letters* **No. 18** (1960) 36.
20. Irreverre, F., Evans, R. L., Hayden, A. R. and Silber, R. *Nature* **180** (1957) 704.
21. Hunt, G. E. *Botan. Rev.* **25** (1959) 148.
22. Sanger, F. *Biochem. J.* **39** (1945) 507.
23. Meister, A. *J. Biol. Chem.* **210** (1954) 17.
24. Morris, L. J., Thompson, J. F., Asen, S. and Irreverre, F. *J. Biol. Chem.* **237** (1962) 2180.

Received February 14, 1962.

ACTA CHEMICA SCANDINAVICA 16 (1962) 1519–1538

Short Communications

On the Mutarotation Equilibria of D-Glucose and D-Mannose and the Assignment of Configurations to their α- and β-Anomers

J. BLOM and J. A. CHRISTIANSEN

The Tuborg Breweries, Copenhagen, and Sundvænget 9, Hellerup, Denmark

As well known the interpretation of Roentgen-diffraction-spectra of α-D-glucose [1] seem to have decided the assignment of the two possible configurations at C_1 to the α- and β-anomers as follows: In the Haworth structural picture drawn as usual (C_5,C_4,C_3,C_2,C_1, 12345 clockwise) the configuration at C_1 is for the α-anomer: H above OH, and for the β-anomer: OH above H, where the system of nomenclature of α- and β-anomers is that of Hudson [2].

As shown by one of us in several papers [3] many chemical facts become much easier to understand, when it is assumed that the assignment of configurations to the α- and β-anomers is the reverse of that found roentgenographically. It may be remarked in this connection, that the former assignment has until recently been considered as proved chemically by Böeseken's interpretation of his investigations on the complex-formation between aldoses and boric acid [4]. However, as shown by one of us [5], serious doubt concerning the validity of this interpretation arises when the newer aspects of the conformation of aldohexoses, notably by Hassel and Ottar [6] and by Reeves [7] are taken into account. Whether or not it be permissible to doubt the correctness of the current assignment, it may be of interest to try to use the facts concerning the mutarotation equilibria between the α- and β-anomers to arrive at the assignment in question. For that purpose we have chosen D-glucose and D-mannose because at equilibrium and during their transformations their solutions seem to contain only their α- and β-pyranose modifications [8,9].

In accordance with Hassel-Ottar and Reeves we shall assume, that their most stable structure is the C1 chair conformation, carrying the bulky group at C_5 and the hydroxyl groups at C_4 and C_3 in equatorial positions.

D-Glucose. According to the authors mentioned above, D-glucose has one of the two configurations E or A defined as E: 4e, 3e, 2e, 1e; A: 4e, 3e, 2e, 1a.

We inquire into the equilibrium distribution of the forms E and A. We remark that the quotient $q(E/A)$ of the equilibrium concentrations of molecules in the E-state and in the A-state respectively is

$$q(E/A) = (W_E/W_A)\exp[(H_A - H_E)/RT + (S_E - S_A)/R] \quad (1)$$

where the W's are the "statistical weights" of the states, while the H's and the S's mean enthalpy and entropy, respectively, of the molecules in the states indicated by subscripts.

Inspection of models of the two forms show that the two differences must be small. We therefore expect that approximately

$$q(E/A) = W_E/W_A \quad (2)$$

The problem is thus reduced to estimating the ratio W_E/W_a.

At each of the carbon-atoms 1 to 4 we have evidently a vector represented by H—OH. These four vectors are equal in magnitude and are in planes through the vertical axis of the pyranose ring. Their projection on this axis are also equal in magnitude but are either parallel or antiparallel to each other. The statistical weight w of a certain state means the number of ways in which this state can be realised. Let us take as an example a pair of vectors which are represented by their distances

from the center of a benzene-ring and their directions either in the *ortho-* or in the *para*-position. We first fix one of the vectors and then add the other in the *para*-position. This can only be done in one way and we therefore ascribe the weight unity to the *para*-state. Next we fix one vector and add the other one in the *ortho*-position. This can be done in two ways, and we therefore ascribe the weight 2 to the ortho-state. In other words, if the energies of the molecule in the two states are equal, there must be two parts of the molecules in the *ortho*-state for each part in the *para*-state at equilibrium.

In the *ortho*-state the two vectors form an angle of 60° with each other, but if the angle were decreased to say 10° the situation would be the same as far as the statistical weight is concerned, and this must remain true even if the angle were decreased to zero. Therefore to a pair of vectors of equal length the weight 2 must be ascribed if they are parallel but the weight unity if they are antiparallel. To avoid confusion with the locations in the pyranosering we shall denote the two possible orientations, not as *ortho* and *para*, but as *syn-* and *anti-*, respectively.

In the hexoses there are evidently three pairs of H—OH vectors which include the one at C_1. There are also three pairs not including the one at C_1. The latter ones are obviously equal in the E- and A-forms and may therefore be neglected. For the E-form we denote the former type of pairs by (E2), (E3) and (E4), respectively. Inspection of the model or of the Haworth picture corresponding to D-glucose shows that, the pairs (E2) and (E4) are *anti-*, while (E3) is *syn-*.
Consequently

$$w(\mathrm{E2}) = w(\mathrm{E4}) = 1; w(\mathrm{E3}) = 2. \quad (3)$$

We get the value of W for the whole molecule by combination of the w's for the three pairs or

$$W_\mathrm{E} = w(\mathrm{E2}) \cdot w(\mathrm{E3}) \cdot w(\mathrm{E4}) = 1 \times 2 \times 1 = 2 \quad (4)$$

Similarly the pairs (A2), (A3) and (A4) are, respectively, *syn-*, *anti-*, and *syn-*, and therefore

$$W_\mathrm{A} = w(\mathrm{A2}) \cdot w(\mathrm{A3}) \cdot w(\mathrm{A4}) = 2 \times 1 \times 2 = 4 \quad (5)$$

The equlibrium quotient $q(\mathrm{E/A})$ thus approximates ½. It should be added, that $q(\mathrm{E/A}) = K$, where K is the equilibrium constant for the reaction $\mathrm{A} \rightleftharpoons \mathrm{E}$.

As well known experiments show that at equilibrium the concentration of β-glucose is about twice that of the α-anomer [8,9]. Consequently comparison of theory and experiment shows that, in the α-form of D-glucose the OH at C_1 is located equatorially »northwards» and in the β-form axially »southwards».

Thus we arrive by this argument to an assignment which is the opposite one of that arrived at by interpretation of the Roentgen, diffractionspectra, while it agrees with the one arrived at by means of chemical arguments by one of us [3,5].

D-*Mannose*. Assuming as we did that the arrangement in D-glucose at C_4, C_3 and C_2 is 4e, 3e, 2e, the two anomers of D-mannose must be

$$\mathrm{E}: 4e, 3e, 2a_n, 1e_n; \mathrm{A}: 4e, 3e, 2a_n, 1a_s$$

where the two subscripts n and s mean »pointing northwards» and »pointing southwards», respectively. The model or the Haworth picture then shows, that in this case the pairs (E2), (E3), and (E4) are, respectively, *syn-*, *syn-* and *anti-* while the pairs (A2), (A3), and (A4) are, respectively, *anti-*, *anti-* and *syn-*.

Consequently we get for D-mannose:

$$W_\mathrm{E} = 2 \times 2 \times 1 = 4 \quad (6)$$

$$W_\mathrm{A} = 1 \times 1 \times 2 = 2 \quad (7)$$

Therefore $q(\mathrm{E/A})$ approximates 2 for D-mannose. On the other hand, it is known from experiments [8,9] that there is in the equilibrium solution nearly twice as much of the α-anomer as of the β-anomer. Consequently, by this argument, we find that the OH at C_1 is located equatorially »northwards» in α-D-mannose and axially »southwards» in the β-anomer. In other words, we refind the assignment arrived at in the case of D-glucose.

It might be argued against the considerations above, that equilibrium constants for mutarotation-equilibria are different in different solvents. The answer to this objection is that water is the only solvent, whose molecules have the same composition as the vectors H—OH in question, and that therefore its use as a solvent must lead to the simplest results.

A detailed treatment of some published experimental results concerning mutarotation of glucose and mannose in the light of eqn. (1) will be given by the latter author.

1. McDonald, T. R. R. and Beevers, C. A. *Acta Cryst.* **3** (1950) 394; **5** (1952) 654.
2. Hudson, C. S. *J. Am. Chem. Soc.* **31** (1909)66.
3. Blom, J. *Acta Chem. Scand.* **13** (1959) 388; **15** (1961) 1667.
4. Böeseken, J. *Advances in Carbohydrate Chem.* **4** (1949) 189.
5. Blom, J. *Acta Chem. Scand.* **16** (1962) 922.
6. Hassel, O. and Ottar, B. *Acta Chem. Scand.* **1** (1947) 929.
7. Reeves, R. E. *Advances in Carbohydrate Chem.* **6** (1951) 107.
8. Sørensen, N. A. *Kgl. Norske Videnskab Selskabs Skrifter* **2** (1937) 104, 106.
9. Isbell, H. S. and Pigman, W. W. *J. Research Natl. Bur. Standards* **18** (1937) 141.

Received May 22, 1962.

A Modification for the Determination of Sulphate in Mucopolysaccharides by the Benzidine Method

CRISTOS A. ANTONOPOULOS

Department of Physiological Chemistry, University of Lund, Lund, Sweden

The methods for determination of microgram quantities of sulphate in mucopolysaccharides have been studied. Gravimetric methods have been found to be unsuitable for small amounts of sulphate, while certain colorimetric methods have been found to be generally more suitable. One of the most frequently used techniques is to precipitate the sulphate with benzidine and then to determine the amount of benzidine-sulphate spectrophotometrically.

When using a modification of this procedure described by Kent and Whitehouse [1] difficulties were encountered, particularly in filtering the benzidine-sulphate precipitate through sintred glass to remove the excess benzidine. The process is slow and the results were found to be inconsistent.

A modification of this method in which the benzidine sulphate was separated by centrifugation was also tried [2] but the results obtained were unsatisfactory. With additional modifications of the above methods, more consistent results were obtained with standard solutions as well as with mucopolysaccharides after hydrolysis, and these modifications are described here.

Reagents.

98—100 % Formic acid.
95 % Ethanol.
Benzidine reagent: 0.5 % solution benzidine in 95 % ethanol. Kept in the dark in a refrigerator and renewed every 3 weeks.

Acetone-ethanol mixture, 1:1 (v/v).
1.0 N Hydrochloric acid.
0.5 % (w/v) Thymol in 2 N NaOH.
0.1 N sodium nitrite.

The mucopolysaccharides are hydrolyzed in sealed tubes with 25 % formic acid on a boiling water bath. The hydrolysis curve (Fig. 1) shows that 24 h are sufficient to liberate all the sulphate. Usually 0.75 ml of a mucopolysaccharide solution containing 10—80 μg of sulphate is mixed with 0.25 ml of formic acid.

Standard solutions. 10, 20, 40 and 50 μg SO_4/ml in 25 % formic acid.

Procedure. 0.3 ml of the hydrolysate is placed in a conical centrifuge tube (15 ml) to which 0.5 ml 95 % ethanol, 0.2 ml benzidine reagent and 0.5 ml amyl alcohol are added. The standard solutions are treated in the same way using 0.3 ml aliquots. The tubes are shaken and allowed to stand 60 min at 0°C. They are then centrifuged for 6 min in an ordinary laboratory centrifuge with "swing out" head at 4000 r.p.m. and the supernatant is carefully decanted and discarded. 1 ml acetone-ethanol and 0.5 ml amyl alcohol are added to each tube, the tubes are shaken to disperse the precipitate and then recentrifuged for 6 min. The supernatant is decanted as before, after which 1 ml acetone-ethanol is added, the tubes are shaken and centrifuged again. The supernatant is again decanted.

The precipitate is dissolved in 3 ml of 1.0 N hydrochloric acid and 2 ml of distilled water. The benzidine solutions are diazotized at room temperature by the addition of 1 ml of 0.1 N sodium nitrite. After 3 min, 5 ml of the alkaline thymol solution is added and the contents of the tubes are mixed.

The optical density is measured at 505 mμ in 1 cm cells. The colour is stable for at least 4 h. The amount of sulphate is calculated from a standard curve.

1. McDonald, T. R. R. and Beevers, C. A. *Acta Cryst.* **3** (1950) 394; **5** (1952) 654.
2. Hudson, C. S. *J. Am. Chem. Soc.* **31** (1909)66.
3. Blom, J. *Acta Chem. Scand.* **13** (1959) 388; **15** (1961) 1667.
4. Böeseken, J. *Advances in Carbohydrate Chem.* **4** (1949) 189.
5. Blom, J. *Acta Chem. Scand.* **16** (1962) 922.
6. Hassel, O. and Ottar, B. *Acta Chem. Scand.* **1** (1947) 929.
7. Reeves, R. E. *Advances in Carbohydrate Chem.* **6** (1951) 107.
8. Sørensen, N. A. *Kgl. Norske Videnskab Selskabs Skrifter* **2** (1937) 104, 106.
9. Isbell, H. S. and Pigman, W. W. *J. Research Natl. Bur. Standards* **18** (1937) 141.

Received May 22, 1962.

A Modification for the Determination of Sulphate in Mucopolysaccharides by the Benzidine Method

CRISTOS A. ANTONOPOULOS

Department of Physiological Chemistry, University of Lund, Lund, Sweden

The methods for determination of microgram quantities of sulphate in mucopolysaccharides have been studied. Gravimetric methods have been found to be unsuitable for small amounts of sulphate, while certain colorimetric methods have been found to be generally more suitable. One of the most frequently used techniques is to precipitate the sulphate with benzidine and then to determine the amount of benzidine-sulphate spectrophotometrically.

When using a modification of this procedure described by Kent and Whitehouse [1] difficulties were encountered, particularly in filtering the benzidine-sulphate precipitate through sintred glass to remove the excess benzidine. The process is slow and the results were found to be inconsistent.

A modification of this method in which the benzidine sulphate was separated by centrifugation was also tried [2] but the results obtained were unsatisfactory. With additional modifications of the above methods, more consistent results were obtained with standard solutions as well as with mucopolysaccharides after hydrolysis, and these modifications are described here.

Reagents.

98—100 % Formic acid.
95 % Ethanol.
Benzidine reagent: 0.5 % solution benzidine in 95 % ethanol. Kept in the dark in a refrigerator and renewed every 3 weeks.

Acetone-ethanol mixture, 1:1 (v/v).
1.0 N Hydrochloric acid.
0.5 % (w/v) Thymol in 2 N NaOH.
0.1 N sodium nitrite.

The mucopolysaccharides are hydrolyzed in sealed tubes with 25 % formic acid on a boiling water bath. The hydrolysis curve (Fig. 1) shows that 24 h are sufficient to liberate all the sulphate. Usually 0.75 ml of a mucopolysaccharide solution containing 10—80 μg of sulphate is mixed with 0.25 ml of formic acid.

Standard solutions. 10, 20, 40 and 50 μg SO_4/ml in 25 % formic acid.

Procedure. 0.3 ml of the hydrolysate is placed in a conical centrifuge tube (15 ml) to which 0.5 ml 95 % ethanol, 0.2 ml benzidine reagent and 0.5 ml amyl alcohol are added. The standard solutions are treated in the same way using 0.3 ml aliquots. The tubes are shaken and allowed to stand 60 min at 0°C. They are then centrifuged for 6 min in an ordinary laboratory centrifuge with "swing out" head at 4000 r.p.m. and the supernatant is carefully decanted and discarded. 1 ml acetone-ethanol and 0.5 ml amyl alcohol are added to each tube, the tubes are shaken to disperse the precipitate and then recentrifuged for 6 min. The supernatant is decanted as before, after which 1 ml acetone-ethanol is added, the tubes are shaken and centrifuged again. The supernatant is again decanted.

The precipitate is dissolved in 3 ml of 1.0 N hydrochloric acid and 2 ml of distilled water. The benzidine solutions are diazotized at room temperature by the addition of 1 ml of 0.1 N sodium nitrite. After 3 min, 5 ml of the alkaline thymol solution is added and the contents of the tubes are mixed.

The optical density is measured at 505 mμ in 1 cm cells. The colour is stable for at least 4 h. The amount of sulphate is calculated from a standard curve.

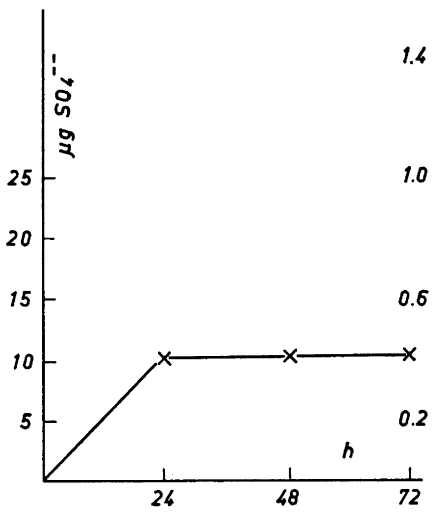

Fig. 1. Liberation of sulphate from chondroitin-sulphate hydrolysed by 25 % formic acid on a boiling waterbath.

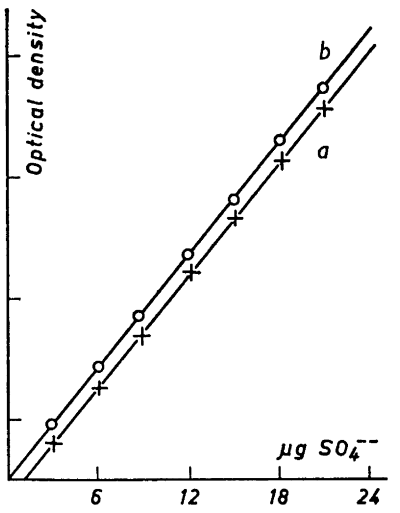

Fig. 2. Curve *a*: Typical standard curve for different amounts of sulphate. Curve *b*: Curve obtained when benzidine corresponding to the amounts of sulphate indicated is diazotized directly.

Results and discussion. Curve *a* in Fig. 2 shows a typical standard curve obtained by the method described. This curve shows a linear relation between the amount of colour formed in the reaction and the amount of sulphate to as little as 3 μg. However, at lower sulphate concentrations deviation from linearity occurs and, moreover, the curve does not pass the origin.

When known amounts of benzidine corresponding to 3—21 μg of sulphate were diazotized a straight line passing through the origin is obtained (Fig. 2, *b*). The two curves are parallel.

The intersection of curve *a* with the ordinate occurs at a point which corresponds to the solubility of benzidine sulphate in the system used. According to Kent and Whitehouse optimum results by this method are found in the pH-range 2.5 to 2.7; the pH under the described conditions was 2.5.

The author is greatly indebted to Dr Sven Gardell for invaluable advice and criticism during the performance of the work.

1. Kent, P. and Whitehouse, M. *Analyst* **80** (1955) 630.
2. Häkkinen, I. *Nature* **186** (1960) 232.

Received May 20, 1962.

On the Role of Leucine in the Carotenoid Synthesis of the Chloroplasts of Higher Plants

L. EHRENBERG and A. F. DÁNIEL

Institute of Organic Chemistry and Biochemistry, University, Stockholm, Sweden

It was previously shown [1-5] that a considerable group of the chloroplast mutants of higher plants possess the ability of chlorophyll synthesis, but that in ordinary light intensities their leaves bleach. Such chloroplast mutants also show an incomplete structural differentiation of the chloroplasts [6]. It has been suggested that carotenoids may play an important role [7-9] in the protection of the chloroplasts from photodestruction. This would be in agreement with isoprenoid abnormalities in chloroplast mutants with increased photosensitivity [10]. Such abnormalities could consist of qualitative deviations in the carotenoid composition — as saturation of some double bonds [11, 12] — or a low concentration of the normal isoprenoid components [13-15]. In the latter case it can be suggested that the carotenoid (or in general the isoprenoid) synthesis is limited by a decreased production of some precursor. The early carotenoid precursors, among which leucine is considered important [16,17], were investigated mainly in fungi. In some chloroplast mutants, deviations from the normal amino acid and protein metabolism have been reported [18-23]. Recently it was reported that the barley mutant xantha-23 can be brought to normal green, *i.e.* with more or less normal chloroplasts, if the seedlings are grown in a leucine containing solution [24]. It is therefore of interest to study whether leucine can serve as a precursor in carotenoid (isoprenoid) synthesis in the leaves.

Experimental. Normal barley seeds (Bonus variety) were sown in Petri dishes and germinated in the dark at room temperature (20°). The leaves of the 6.5 day old seedlings (height 6—7 cm) were cut in 5 mm long pieces, rinsed for 0.5 h in tap water and placed in an aq. dest. solution of 1 % sucrose containing uniformly labelled 2.5 mM L-leucine-^{14}C (1 μC/μM). — The L-leucine-^{14}C was purchased from the Radiochemical Centre, Amersham. The operations were made under weak green light produced by means of an interference filter (Balzer's Broad Band No. 4) with a main transmission between 520 and 580 mμ. One portion of the leaves was kept in the dark continuously, the other was exposed to the light (about 2000 lux) from three 150 W tungsten lamps.

Leaf samples between 0.1 and 0.2 g were taken out from the leucine solution at different times, transferred to a glass filter and washed thoroughly, blotted and weighed. The pigments were extracted with acetone and peroxide-free ether [25]. The bulk carotenoid content was determined by measuring the light absorption at 480 mμ and nominally given as β-carotene [26]. An aliquot of the extract was chromatographed twice in the faster direction on Whatman No. 1 paper with the solvent system of Sapozhnykov [27]. The carotenoid spots were eluted, plated, and their radioactivity measured in a proportional counter (FH 407) with a standard error varying from 1 to 10 %.

The remainder of the extract was repeatedly treated with 70 % ethanol. The combined extracts were used for the determination of the radioactive leucine inside the leaves.

Separate experiments were made with non-labelled leucine to determine the leucine and carotenoid content in the leaves. The leucine content was determined by separating the leucine by repeated one-dimensional paper chromatography and measuring optical density of the leucine-ninhydrin-Cu $^{2+}$ complex [28].

The data reported represent the results of 4 independent incorporation experiments; differencies as great as 25 % have been found between the different experimental series.

Results and discussion. From the radioactivity of the alcoholic extracts it was clear that leucine is taken up rapidly by the leaves (Table 1).

The data in Table 1 demonstrate that the leucine uptake seems to proceed nearly at the same rate in the dark and the light and the tota leucine content was not markedly influenced by the light conditions applied. Saturation of the tissue with leucine solution was reached in the first hour of floating. Later, the specific activity of the leucine was about the same, which indicates that a considerable amount was remaining in the intercellular space, and the incorporation of the leucine into non-soluble compounds was small and/or compensated by the intracellular non-radioactive leu-

* Present address: Institute of Phylogenetics and Genetics, Eötvös Loránd University, Budapest, Hungary.

Table 1. Leucine-^{14}C(*) uptake, leucine content per g fresh weight, and specific activity of leucine in barley leaves floated on leucine solution (1.1×10^6 cpm/μM).

Time	Dark			Light		
	μM*/g	μM/g	$\frac{10^3 \text{ cpm}}{\mu\text{M}}$	μM*/g	μM/g	$\frac{10^3 \text{ cpm}}{\mu\text{M}}$
0 min	—	0.67	—	—	≡ dark	—
10 »	0.15	...	...	0.16	...	...
20 »	0.22	...	...	0.24	...	...
40 »	0.35	...	...	0.40	...	...
1.0 h	0.51	0.92	609	0.53	0.92	634
1.5 »	0.61	1.00	668	0.63	1.00	688
2.0 »	0.74	1.12	727	0.79	1.20	726
3.0 »	0.84	1.35	685	0.88	1.30	743
5.0 »	1.01	2.05	543	1.04	2.09	547
7.0 »	1.13	2.29	542	1.32	2.29	635

cine-pool. In the experiments of Chichester *et al.* [16] it was shown that in *Phycomyces blakesleeanus* grown for 7 days in a medium containing ^{14}C-labelled leucine, only a fragment containing three or at the most four out of the six carbon atoms is utilized directly in the carotenoid synthesis. Consequently, estimating the labelling extent of the carotenoids in the leaves, this part of the molecule had to be considered.

It appears from Table 2 that the ^{14}C of the leucine is incorporated into the carotenoids both in the dark and in the light, with increasingly higher values in the light. Consequently, leucine is used in the light induced carotenoid synthesis. This offers a plausible explanation of the leucine-conditioned normalization of the mutant, xantha-23 [24].

Considering the fact that the carotenoids contain eight isoprenoid units, the highest possible value of the leucine incorporation may be 8. In the investigations using *Phycomyces* [16, 29, 30] labelled DL-leucine was applied, and the duration of the experiments included

Table 2. Incorporation of the ^{14}C into the carotenoids of barley leaves floated on leucine-^{14}C solution (50μC/50μM L-leucine in the solution, illumination started after 1.0 h in the dark).

Time	Dark			Light		
	10^3 cpm in carotenoids per g fr.w.	$\frac{\mu\text{M carot.}}{\text{g fr. w.}}$	$\frac{\mu\text{M leuc.*}(1)}{\mu\text{M carot.}}$	10^3 cpm in carotenoids per g fr. w.	$\frac{\mu\text{M carot.}}{\text{g fr.w.}}$	$\frac{\mu\text{M leuc.*}(1)}{\mu\text{M carot.}}$
1.0 h	1.59	0.111	0.04	—	—	—
1.5 »	2.39	0.111	0.05	2.49	0.108	0.05
2.0 »	3.65	0.109	0.07	4.52	0.105	0.09
3.0 »	4.96	0.109	0.10	9.22	0.112	0.17
5.0 »	6.64	0.110	0.16	14.22	0.134	0.29
7.0 »	8.04	0.110	0.20	21.72	0.164	0.31
7.0 »	Difference (light — dark):			13.68	0.054	0.60 ± 0.24

(1) $\frac{10^3 \text{ cpm/ } \mu\text{M carotenoid} \cdot 6/4}{10^3 \text{ cpm/ } \mu\text{M leucine in the leaf tissue}}$

many cell generations. In such experimental conditions the mean incorporation value for the C_4 fragment of the leucine was found to be 3.37 (3.96 for C(4), C(5), C(5′) and 1.59 for C(3), respectively). Considering that only the L-form of the leucine possesses biological activity, the extent of incorporation found in the *Phycomyces* thus approximates the ideal value. The extent of carotenoid labelling found in the barley leaves was 3 % in the dark, and 8 % in the light induced synthesis, respectively, of the possible maximum in the case of the incorporation of 4 leucine carbons into each of 8 isoprene units per carotenoid molecule. The relatively low incorporation found may be due to the short time of treatment (7 h *versus* the 7 days used in the *Phycomyces* experiments). Furthermore, on entering the cells, the leucine is partly taken up by other active metabolic pools before it can reach the site of the carotenogenesis. It is also possible that some carotenoids are formed from non-radioactive immediate precursors already present in the cells, [17] and that the duration of our experiment was too short to exhaust them. It is clear that in our experiments different carotenoids may utilize leucine to a very different extent; here, the average incorporation has been determined. The present experiment — working with etiolated and illuminated leaves — could be compared with the studies of Braithwaite and Goodwin [31] performed on the precursors of lycopene in tomato slices. Calculating their data by the method applied here it can be concluded that the incorporation of the $^{14}CO_2$ and of the ^{14}C-labelled acetates into the lycopene was about 10^{-2} $\mu M/\mu M$ carotenoid, thus at an order of magnitude less than the incorporation of the C_4 fragment of the leucine into the carotenoids of barley leaves, indicating that the latter is a rather effective early precursor in the carotenoid synthesis in the leaves of higher plants.

Conclusion and summary. The incorporation of the L-leucine-^{14}C into the carotenoids of barley leaves was investigated.

It was found that the ^{14}C originating from uniformly labelled L-leucine is incorporated into the carotenoids of barley leaves.

The extent of labelling was greater in illuminated leaves than in leaves kept in the dark.

It was demonstrated that leucine may serve as an early precursor of carotenoids in the chloroplasts of the leaves of higher plants.

Acknowledgement. Our thanks are due to Professor D. von Wettstein for fruitful discussions. We also appreciate valuable assistence by Mrs Ingrid Lodén. The work was performed as an IAEA fellowship contract with A. F. Dániel and was also supported financially by the *Knut and Alice Wallenberg Foundation* and the *Swedish Agricultural Research Council.*

1. Koski, V. M., Smith, J. H. C. *Arch. Biochem. Biophys.* **34** (1951) 189.
2. Holm, G. *Acta Agr. Scand.* **4** (1954) 457.
3. Röbbelen, G. *Z. Vererbungslehre* **90** (1959) 50.
4. Lyastchenko, I. I. *Biokhimiya* **22** (1957) 942.
5. Faludi, B., Dániel, F. A., Gyurján, I., Száraz, I. *Ann. Univ. Sci. Budapestiensis Sect. biol.* **4** (1961) *(In press).*
6. Wettstein, D. v. *Hereditas* **43** (1957) 303.
7. Lynch, V. H., French, C. S. *Arch. Biochem. Biophys.* **70** (1957) 382.
8. Milner, M., French, C. S., Milner, H. V. *Plant Physiol.* **33** (1958) 367.
9. Bishop, N. I. *Plant. Physiol.* **33** (1958) Suppl.
10. Euler, H. v., Burström, D., Hellström, H. *Hereditas* **18** (1933—34) 225.
11. Anderson, I. C., Robertson, D. S. *Plant Physiol.* **35** (1960) 531.
12. Faludi, B., Dániel, A. F., Kelemen, G. *Physiol. Plantarum* **13** (1960) 227.
13. Tulpule, Sh. H. *Am. J. Botany* **41** (1954) 294.
14. Smith, J. H. C., Durham, L. J., Wurster, C. F. *Plant Physiol.* **34** (1959) 340.
15. Crane, F. L. *Plant Physiol.* **34** (1959) 121.
16. Chichester, C. O., Nakayama, T., MacKinney, G., Goodwin, T. W. *J. Biol. Chem.* **21** (1955) 515.
17. Goodwin, T. *Biochem. J.* **70** (1960) 5.
18. Euler, H. v., Hellström, H., Löfgren, N. *Z. physiol. Chem. Hoppe-Seylers'* **234** (1935) 151.
19. Seltman, H. *Plant Physiol.* **30** (1955) 258.
20. DeKock, P. C., Morrison, R. I. *Biochem. J.* **70** (1958) 266.
21. Fujii, T., Ono, Y. *Proc. Japan. Acad.* **36** (1960) 610.
22. Mossberg, G. Lecture given at the Meeting of the Swedish Mutation Research Group, 26th January, 1962.
23. Holmgren, P. *Ann. Roy. Agr. Coll. Sweden* **22** 354.
24. Eriksson, G., Kahn., A., Walles, B., Wettstein, D. v. *Ber. deut. botan. Ges.* **74** (1961) 221.
25. Koski, V. M. *Arch. Biochem. Biophys.* **29** (1952) 339.

26. Withrow, R. B., Klein, W. H., Price, L., Elstad, W. *Plant Physiol.* **28** (1953) 1.
27. Sapozhnykov, D. I., Bronstein, I. A. and Krasnovskaya, I. A. *Biokhimiya* **20** (1955) 286.
28. Fischer, G. F., Dörfel, H. *Biochem. Z.* **324** (1953) 65.
29. Wuhrman, J. J., Yokoyama, H., Chichester, C. O. *J. Am. Chem. Soc.* **79** (1958) 4569.
30. Yokoyama, H., Chichester, C. O., Nakayama, T., Lukten, A., MacKinney, G. *J. Am. Chem. Soc.* **79** (1957) 2029.
31. Braithwaite, G. D., Goodwin, R. W. *Biochem. J.* **76** (1960) 1.

Received June 8, 1962.

On the Preparation and Properties of Disulfide-Reduced, Alkylated Fibrinogen and Fibrin

AGNES HENSCHEN

Chemistry Department II, Karolinska Institutet, Stockholm, Sweden

Recently we have described the preparation and some properties of sulfitolysed fibrinogen and fibrin [1]. In order to evaluate the completeness and specificity of the sulfite reaction of these proteins, it was desirable to obtain other disulfide-modified derivatives and to compare their properties. In the present investigation, we have chosen to cleave the disulfide bonds by reduction and to block the resulting sulfhydryl groups with an alkylating reagent. Different reducing agents were tried under different conditions.

Bovine fibrinogen and fibrin, purified according to the method of Blombäck and Blombäck [2], were used. Two types of reagents were employed for reduction: sodium borohydride or the mercaptans thioglycollic acid and mercapto-ethanol. Sodium borohydride was used mainly as described by Moore *et al.*[3] The reaction was performed in an 8 M urea solution at a pH between 9 and 11 at + 40°C. Protein and reagent concentrations were about 0.4 %. Sometimes versene or tris were added to the reaction mixture. Thioglycollic acid and mercapto-ethanol were used mainly as described by Sela *et al.*[4] and by Anfinsen and Haber [5] and Crestfield [6], respectively. The reaction mixture was 8 M in urea, 0.4 M in tris and 5×10^{-3} M in versene at a pH of 8.5 and room temperature. Protein concentration was 0.3—1.0 %. Mercaptan was added in approximately 150-fold molar excess regarding the half-cystine content; the solution was kept in a sealed vessel for 4 to 5 h. Alkylation was performed according to the methods of the same authors [3-6]. Only iodoacetic acid was tried. When borohydride was used for reduction, the excess was destroyed by acidification. The reagents and the protein-product were separated by gel-filtration on Sephadex G-50 [7], by dialysis or by precipitation with acetone. The number of unchanged disulfide bonds or freed sulfhydryl groups was determined by electrometric titration. The yields of protein in the procedures were calculated from spectrophotometric values [8] and from the weights of the lyophilized material.

The reduction procedure with sodium borohydride never acted both quantitatively and selectively on the disulfide bonds. Under the conditions described by Moore *et al.*[3] a complete cleavage of the disulfide bonds could be obtained. At the same time, however, some peptide bonds were split as revealed by the formation of new N-terminal amino acids. This side reaction occurred even in the presence of versene. In all these experiments with borohydride the final pH was 10 to 11. In order to obtain a more constant and slightly lower pH some reductions were performed in the presence of tris or with succesive additions of hydrochloric acid in a pH-stat. In these cases no complete cleavage of the disulfide bonds was obtained.

The reduction procedure with the mercaptans thioglycollic acid and mercapto-ethanol acted quantitatively on the disulfide bonds as determined by electrometric titration after alkylation and isolation. In spite of the absence of a nitrogen barrier there was no sign of (not reversed) reoxidation. N-Terminal amino acid analysis of the products gave the same results as with the unmodified proteins. The derivatives obtained by mercaptolysis and alkylation of fibrinogen and fibrin were almost quantitatively recovered. For these reasons, the mercaptolysed, alkylated products were

26. Withrow, R. B., Klein, W. H., Price, L., Elstad, W. *Plant Physiol.* **28** (1953) 1.
27. Sapozhnykov, D. I., Bronstein, I. A. and Krasnovskaya, I. A. *Biokhimiya* **20** (1955) 286.
28. Fischer, G. F., Dörfel, H. *Biochem. Z.* **324** (1953) 65.
29. Wuhrman, J. J., Yokoyama, H., Chichester, C. O. *J. Am. Chem. Soc.* **79** (1958) 4569.
30. Yokoyama, H., Chichester, C. O., Nakayama, T., Lukten, A., MacKinney, G. *J. Am. Chem. Soc.* **79** (1957) 2029.
31. Braithwaite, G. D., Goodwin, R. W. *Biochem. J.* **76** (1960) 1.

Received June 8, 1962.

On the Preparation and Properties of Disulfide-Reduced, Alkylated Fibrinogen and Fibrin

AGNES HENSCHEN

Chemistry Department II, Karolinska Institutet, Stockholm, Sweden

Recently we have described the preparation and some properties of sulfitolysed fibrinogen and fibrin [1]. In order to evaluate the completeness and specificity of the sulfite reaction of these proteins, it was desirable to obtain other disulfide-modified derivatives and to compare their properties. In the present investigation, we have chosen to cleave the disulfide bonds by reduction and to block the resulting sulfhydryl groups with an alkylating reagent. Different reducing agents were tried under different conditions.

Bovine fibrinogen and fibrin, purified according to the method of Blombäck and Blombäck [2], were used. Two types of reagents were employed for reduction: sodium borohydride or the mercaptans thioglycollic acid and mercapto-ethanol. Sodium borohydride was used mainly as described by Moore *et al.*[3] The reaction was performed in an 8 M urea solution at a pH between 9 and 11 at + 40°C. Protein and reagent concentrations were about 0.4 %. Sometimes versene or tris were added to the reaction mixture. Thioglycollic acid and mercapto-ethanol were used mainly as described by Sela *et al.*[4] and by Anfinsen and Haber [5] and Crestfield [6], respectively. The reaction mixture was 8 M in urea, 0.4 M in tris and 5×10^{-3} M in versene at a pH of 8.5 and room temperature. Protein concentration was 0.3—1.0 %. Mercaptan was added in approximately 150-fold molar excess regarding the half-cystine content; the solution was kept in a sealed vessel for 4 to 5 h. Alkylation was performed according to the methods of the same authors [3-6]. Only iodoacetic acid was tried. When borohydride was used for reduction, the excess was destroyed by acidification. The reagents and the protein-product were separated by gel-filtration on Sephadex G-50 [7], by dialysis or by precipitation with acetone. The number of unchanged disulfide bonds or freed sulfhydryl groups was determined by electrometric titration. The yields of protein in the procedures were calculated from spectrophotometric values [8] and from the weights of the lyophilized material.

The reduction procedure with sodium borohydride never acted both quantitatively and selectively on the disulfide bonds. Under the conditions described by Moore *et al.*[3] a complete cleavage of the disulfide bonds could be obtained. At the same time, however, some peptide bonds were split as revealed by the formation of new N-terminal amino acids. This side reaction occurred even in the presence of versene. In all these experiments with borohydride the final pH was 10 to 11. In order to obtain a more constant and slightly lower pH some reductions were performed in the presence of tris or with succesive additions of hydrochloric acid in a pH-stat. In these cases no complete cleavage of the disulfide bonds was obtained.

The reduction procedure with the mercaptans thioglycollic acid and mercapto-ethanol acted quantitatively on the disulfide bonds as determined by electrometric titration after alkylation and isolation. In spite of the absence of a nitrogen barrier there was no sign of (not reversed) reoxidation. N-Terminal amino acid analysis of the products gave the same results as with the unmodified proteins. The derivatives obtained by mercaptolysis and alkylation of fibrinogen and fibrin were almost quantitatively recovered. For these reasons, the mercaptolysed, alkylated products were

termed S-carboxymethyl-fibrinogen and S-carboxymethyl-fibrin. Using Sephadex gels of various molecular sieve properties, no separation of different fractions of the S-carboxymethyl-proteins could be obtained even in 6 M urea solution. Preliminary ultracentrifuge studies (kindly performed by I. Björk) showed homogeneity of the substances and a decrease in molecular weight as compared to untreated fibrinogen.

Both the S-carboxymethyl-proteins were, when obtained by dialysis or gel filtration, completely soluble at low concentrations in distilled water. They showed, however, a marked tendency to aggregate when the ionic strength of the solution was increased or its pH was lowered. After lyophilization the products were no longer soluble in water, but dissolved easily in solutions of, *e.g.*, urea. Solutions of the S-carboxymethyl-proteins in distilled water or 0.15 M sodium chloride did not exhibit the precipitability at + 58°C, which is characteristic of untreated fibrinogen.

The S-carboxymethyl-proteins were studied by means of paper and starch gel electrophoresis. In all buffer systems tried with paper electrophoresis only a single, strong band was demonstrable, even when the buffers contained reagents, such as urea, tergitol NP 35, sodium dodecyl sulfate or dimethylformamide, supposed to be capable of splitting hydrogen bonds. In some preparations of S-carboxymethyl-derivative one or two, extremely faint, additional bands could be distinguished. Starch gel electrophoresis in 6 – 7 M urea pH 9.2 gave the same pattern, with a single, strong band and, in some preparations, two faint additional bands. The main components showed a slightly higher mobility than the corresponding native proteins. The other components had a considerably greater mobility. Thus, the electrophoretic findings were quite different from those obtained with the S-sulfo-derivatives, regarding both the number of components and their mobilities [1].

The reaction of the modified fibrinogen with thrombin was examined. S-Carboxymethyl-fibrinogen was found to be a substrate for thrombin. As with the S-sulfo-derivative no coagulum but a fine precipitate was formed [1]. The precipitation reaction between S-carboxymethyl-fibrinogen and thrombin was unchanged after heating of the derivative to + 60°C. After incubation of S-carboxymethyl-fibrinogen with thrombin two peptides could be isolated in the non-protein supernatant. These peptides showed the same electrophoretic mobilities at pH 4 and gave the same color shades with ninhydrine as the corresponding peptides released from native, bovine fibrinogen. After incubation of S-carboxymethyl-fibrin with thrombin no peptides were found. N-Terminal amino acid analysis indicated that the peptides were released from the fibrinogen derivative in the same order and at about the same rate as from native fibrinogen [9].

The possible re-formation of a saline-soluble, thrombin-coagulable fibrinogen after reduction and reoxidation of the disulfide bonds was studied [5]. Reoxidation in saline and in urea at different dilutions of the reduced fibrinogen was tried. In all instances the protein product was completely insoluble in dilute salt solutions.

The present investigation has shown, that the properties of the S-sulfo-derivative and of the S-carboxymethyl-derivative of fibrinogen and fibrin are very similar except for their behavior in electrophoresis.

This work will be described and discussed in detail in the near future.

1. Henschen, A. *Acta Chem. Scand.* **16** (1962) 1037.
2. Blombäck, B. and Blombäck, M. *Arkiv Kemi* **10** (1956) 415.
3. Moore, S., Cole, R. D., Gundlach, H. G. and Stein, W. H. *Proc. 4th Intern. Congr. Biochem., Vienna* **8** (1958) 52.
4. Sela, M., White, Jr., F. H. and Anfinsen, C. B. *Biochem. Biophys. Acta* **31** (1959) 417.
5. Anfinsen, C. B. and Haber, E. *J. Biol. Chem.* **236** (1961) 1361.
6. Crestfield, A. M. *Personal communication* from Moore, S. (1961).
7. Porath, J. and Flodin, P. *Nature* **183** (1959) 1657.
8. Blombäck, B. *Arkiv Kemi* **12** (1958) 99.
9. Blombäck, B. *Arkiv Kemi* **12** (1958) 321.

Received July 13, 1962.

A Method of Least-Squares for Refining Electron-Diffraction Internuclear Distances using Spectroscopical Shrinkage Effects

S. J. CYVIN

Institutt for teoretisk kjemi, Norges tekniske høgskole, Trondheim, Norway

The Bastiansen-Morino shrinkage effect [1] was first time introduced for linear chains of atoms [2]. As pointed out by Morino, [3] the shrinkage effect may be computed in the linear case from a harmonic-vibration analysis. Recently it has been found that the same situation is present in several cases of non-linear shrinkage effects for highly symmetrical molecules [1]. The Bastiansen-Morino shrinkage effects should be taken into account when electron-diffraction measurements are interpreted. A refinement of the electron-diffraction r^g-values (mean internuclear distances) in germanium tetrachloride has been performed by means of the calculated shrinkage effect from spectroscopic data [4]. This case is very simple as the molecule contains only one structural parameter and one shrinkage effect. The same procedure has been generalized for an arbitrary number of structural parameters and shall be outlined in the following.

Assume a molecule with N types of observable internuclear distances, r_1, r_2, . . ., r_K, r_{K+1}, . . ., r_N, of which K may be considered as independent structural parameters. The remaining $N-K$ distance types are associated with $N-K$ independent shrinkage effects, which may be expressed as

$$-\delta_n = r_n^g - \sum_{k=1}^{K} c_{nk} r_k^g, \; n = K+1, \ldots, N \quad (1)$$

where c_{nk} are constants. This is an extension of the *practical* shrinkage effect for three-particle configurations [1]. Let the observed r^g-values from electron-diffraction be denoted by $(r_i^g)^\circ$, and put

$$r_i^g = (r_i^g)^\circ + \varepsilon_i, \; i = 1, 2, \ldots, N$$

where ε_i represents the correction terms. The corrected values are required to fit accurately the $N-K$ eqns. (1) with "theoretic" δ-values (from spectroscopic calculations). Hence

$$(\sum_k c_{nk}[(r_k^g)^\circ + \varepsilon_k]) - (r_n^g)^\circ - \varepsilon_n = \delta_n \text{ (theor)}$$

or

$$(\sum_k c_{nk}\, \varepsilon_k) - \varepsilon_n = \delta_n \text{ (theor)} - \delta_n \text{ (expt)} \quad (2)$$

This is a set of $N-K$ linear equations with N unknowns (ε_i). Exactly the desired number of K additional linear equations are obtained by minimizing the sum of squares,

$$P = \sum_{i=1}^{N} \varepsilon_i^2 \quad (3)$$

This function may be expressed with the aid of eqns. (2) as a polynomial of second degree in K independent variables, *e.g.*, ε_k ($k = 1, 2, \ldots, K$). In consequence,

$$\frac{\partial}{\partial \varepsilon_k} P(\varepsilon_1, \ldots, \varepsilon_k) = 0 \quad (4)$$

Now the complete set of linear eqns. (2), (4) may be solved for the ε's. This method is adequate if all the observed internuclear distances may be treated indiscriminately, *i.e.*, they are assumed to be of the same accuracy. This condition is very often not fulfilled in practice. In such cases the present method may easily be modified by replacing the expression of (3) by

$$P' = \sum_{i=1}^{N} w_i \varepsilon_i^2 \quad (5)$$

where w_i represents some weight factors.

The method has been applied to benzene, on which a detailed report will be published later.

1. Morino, Y., Cyvin, S. J., Kuchitsu, K. and Iijima, T. *J. Chem. Phys.* **36** (1962) 1109.
2. Bastiansen, O. and Trætteberg, M. *Acta Cryst.* **13** (1960) 1108.
3. Morino, Y. *Acta Cryst.* **13** (1960) 1107.
4. Meisingseth, E. and Cyvin, S. J. *J. Mol. Spectroscopy. In press.*

Received June 12, 1962.

Remark on the Separation of High and Low Vibrational Frequencies *

S. J. CYVIN and B. N. CYVIN

Institutt for teoretisk kjemi, Norges tekniske høgskole, Trondheim, Norway

The approximate method of separation of high and low frequencies [1,2] in Wilson's treatment of molecular vibrations has been utilized by many investigators. In particular, the method is very useful in the case of hydrocarbons, where the high C—H stretching frequencies may be separated from the remaining frequencies with high degree of accuracy.

Separated product rule. As a consequence of the splitting of high and low frequencies, the Teller-Redlich product rule [2,3] splits into separate product rules for the high and low frequencies, respectively. This is true for the frequencies within a specific symmetry species, as well as the frequencies all together. In this connection the authors wish to formulate the following general theorem. When the (approximate) theoretical ratios from the separated product rule within one (or more) symmetry species are multiplied together, the *exact* frequency ratio is obtained.

Example. Ethylene and ethylene-d_4 (symmetry group D_{2h}) are assumed to have the same interatomic distances and interbond angles. Hence the product rule for the frequencies of the totally symmetric species (A_g) reads

$$\omega_1\omega_2\omega_3/\omega_1^*\omega_2^*\omega_3^* = \mu_H/\mu_D \qquad (1)$$

where μ_H and μ_D are the inverse masses of the H and D atoms, respectively. The frequencies of heavy ethylene are identified by an asterisk. From the G matrix of the molecular model in question (see, *e.g.*, Ref.[4]) the following separated product rules have been deduced.

$$\omega_1/\omega_1^* = (\mu_H + 2\mu_C\cos^2A)^{1/2}/(\mu_D + 2\mu_C\cos^2A)^{1/2} \qquad (2)$$

$$\omega_2\omega_3/\omega_2^*\omega_3^* = \mu_H(\mu_H + 2\mu_C\cos^2A)^{-1/2}/\mu_D(\mu_D + 2\mu_C\cos^2A)^{-1/2} \qquad (3)$$

The HCH (or DCD) interbond angle is designated $2A$. The exact relation (1) is seen to be reproduced by multiplying the approximate relations (2) and (3).

Proof of the theorem. Using the symbols of Wilson [2], the separated product rules may be written

$$\Pi\lambda(\text{high})/\Pi\lambda^*(\text{high}) = |\mathfrak{G}_{11}|/|\mathfrak{G}_{11}^*|$$

$$\Pi\lambda(\text{low})/\Pi\lambda^*(\text{low}) = |\mathfrak{G}^\circ|/|\mathfrak{G}^{\circ *}|$$

Here $|\mathfrak{G}^\circ| = |X_{22}|^{-1}$. In order to prove

$$\Pi\lambda(\text{high})\Pi\lambda(\text{low})/\Pi\lambda^*(\text{high})\Pi\lambda^*(\text{low}) = \Pi\lambda/\Pi\lambda^* = |\mathfrak{G}|/|\mathfrak{G}^*|$$

it should be shown that

$$|\mathfrak{G}| = |\mathfrak{G}_{11}| \cdot |\mathfrak{G}^\circ|$$

Wilson [2] has given the relation

$$\mathfrak{G}^\circ = \mathfrak{G}_{22} - \mathfrak{G}_{21}\mathfrak{G}_{11}^{-1}\mathfrak{G}_{12}$$

Hence

$$\mathfrak{G}_{11}\mathfrak{G}^\circ = \mathfrak{G}_{11}\mathfrak{G}_{22} - \mathfrak{G}_{11}\mathfrak{G}_{21}\mathfrak{G}_{11}^{-1}\mathfrak{G}_{12}$$

Notice that $\mathfrak{G}_{21}$ is the transpose of $\mathfrak{G}_{12}$ (because $\mathfrak{G}$ is symmetric). In consequence, one obtains for the determinant:

$$|\mathfrak{G}_{11}\mathfrak{G}^\circ| = |\mathfrak{G}_{11}| \cdot |\mathfrak{G}^\circ| = |\mathfrak{G}_{11}| \cdot |\mathfrak{G}_{22}| - |\mathfrak{G}_{12}|^2 = |\mathfrak{G}|$$

q.e.d. In other words, it has been proved that the original $\mathfrak{G}$-matrix and the splitted $\mathfrak{G}$-matrix, *viz.*

$$\begin{bmatrix} \mathfrak{G}_{11} & \mathfrak{G}_{12} \\ \mathfrak{G}_{21} & \mathfrak{G}_{22} \end{bmatrix} \quad \text{and} \quad \begin{bmatrix} \mathfrak{G}_{11} & 0 \\ 0 & \mathfrak{G}^\circ \end{bmatrix}$$

have identical determinants.

* This project has been supported by *Norges tekniske høgskoles fond*, 1962.

1. Crawford, B. L., Jr. and Edsall, J. T. *J. Chem. Phys.* **7** (1939) 223; Wilson, E. B., Jr. *J. Chem. Phys.* **7** (1939) 1047.
2. Wilson, E. B., Jr. *J. Chem. Phys.* **9** (1941) 76.
3. Redlich, O. *Z. physik. Chem.* **B28** (1935) 371; Angus, W. R., Bailey, C. R., Hale, J. B., Ingold, C. K., Leckie, A. H., Raisin, C. G., Thompson, J. W. and Wilson, C. L. *J. Chem. Soc.* **1936** 971; Edgell, W. F. *J. Chem. Phys.* **13** (1945) 377.
4. Arnett, R. L. and Crawford, B. L., Jr. *J. Chem. Phys.* **18** (1950) 118.

Received June 12, 1962.

Paper Chromatography of Resin Acids

P. DANIELS and C. ENZELL

Organisk-kemiska Institutionen, Kungl. Tekniska Högskolan, Stockholm, Sweden

Several methods of separating and identifying resin acids have been described in the literature. Many of these acids have been obtained in a pure state by fractional crystallisation of their salts with various amines [1,2]. This preparatively important method is however, tedious and less suited for analytical purposes. Partition chromatography has been employed by several workers [3,4], but a satisfactory separation of pimaric, isopimaric, sandaracopimaric ("crytopimaric") [5] and abietic acids has not been obtained [4]. Vapour phase chromatography [6] and mass spectrometry [7] have recently been used in examinations of the methyl esters of resin acids. Vapour phase chromatography suffers, however, from the disadvantages that several stationary phases have to be used and that methyl levopimarate and methyl palustrate are partly isomerised to methyl abietate and methyl dehydroabietate at the high temperatures required. This thermo-lability does not effect the latter method and analysis of mass spectra with the aid of a computer has been found to give good information on the nature of such mixtures [7].

A simpler method is, however, desirable. Wickberg [8] has recently developed a rapid and convenient method for the separation of unsaturated hydrocarbons by partition of their silver complexes between hexadecane and aqueous methanol and this method has now been applied to the methyl esters of resin acids. Methanolic solutions of the esters were applied to fibreglass paper impregnated with hexadecane and the chromatograms were developed with a solution of silver fluoborate [8,9] in aqueous methanol. The compounds were detected by immersing the partially dried paper in a 10 % solution of antimony pentachloride in chloroform. They appeared as round or slightly oval spots. The initial colour of the spots (see Table 1) darkened and intensified when the paper was heated at 100° for a few minutes. The total time required for the separation did not exceed 2 h.

The best results were obtained with a 25–30 % solution of silver fluoborate in ca 80 % aqueous methanol and are given in Table 1. The speed increased but the separation deteroriated when the methanol content was increased. Tailing occurred when the water content was increased and the paper became very brittle when the concentration of silver fluoborate exceeded 30 %. The R_F-values vary somewhat with the distance between the front and the starting line and it is, therefore, advisable to run a complete set of test substances when identifying the components of a mixture.

The increase in R_F-values of the esters containing two conjugated double bonds is found to parallel the increase in wavelength of the ultraviolet absorption maxima of the corresponding acids. Furthermore sandaracopimarate and isopimarate, which possess equatorially oriented vinyl groups, have higher R_F-values than pimarate possessing an axially oriented vinyl group. In a blank experiment it was shown that levopimarate, the most sensitive of the acids used, could be recovered unchanged,

Table 1. R_F-Values of methyl esters of resin acids on hexadecaneimpregnated paper eluted with A (25 g $AgBF_4$, 79 ml MeOH, 16 ml H_2O) and with B (30 g $AgBF_4$, 74 ml MeOH, 19 ml H_2O). Distance front-starting line ca. 130 mm.

Methyl esters	A	B	Colour	λ_{max} of corresponding acids, mμ [4]
Dehydroabietate [10,11]	0.15	0.06	Grey	
Abietate [11,12]	0.22	0.10	Red-brown	240–241
Neoabieatate [11,13]	0.33	0.13	Grey	250–252
Palustrate [11,14]	0.45	0.26	Yellow-brown	265–266
Levopimarate [11,15]	0.53	0.36	Red	272
Pimarate [11,16,17]	0.59	0.45	Grey	
Sandaracopimarate [5,17]	0.68	0.58	Dark grey	
Isopimarate [18,19]	0.68	0.58	Dark grey	

Table 2. R_F-Values of the resin acids on DMS-impregnated paper using light petroleum (b.p. 60 – 71°) as mobile phase.

Acids	R_F-value	
	Dry	Moist
Dehydroabietic	0.35	0.74
Abietic	0.52	0.87
Neoabietic	0.47	0.87
Palustric	0.53	0.90
Levepimaric	0.52	0.89
Pimaric	0.59	0.93
Sandaracopimaric	0.53	0.89
Isopimaric	0.51	0.89

which excludes rearrangement of the double bonds.

An attempt was made to separate the free acids by a method recently developed in this laboratory for the separation of certain carboxylic acids on dimethyl sulphoxide (DMS) impregnated paper [20]. The acids were applied as ether solutions and the chromatogram was developed with light petroleum. They migrated as almost circular spots and, as previously noted for aliphatic acids, the R_F-values were sensitive to the presence of moisture. The separation of the acids, as shown in Table 2, is less satisfactory than that obtained on partition of the silver complexes of their esters. The range within which these R_F-values appear permits simultaneous detection of co-occurring fatty acids of higher molecular weight than myristic acid or of lower molecular weight than nonanic acid [20].

Hexadecane-silver fluoborate-aqueous methanol system. The fibreglass paper (Schleicher and Schüll, 0.17 – 0.23 mm) was cut into strips 23 cm long with the starting line 5 cm from the upper end.

The papers were drawn at an even rate through a 10 %, v/v, solution of hexadecane in light petroleum (b.p. 60 – 71°), uniformly blotted between sheets of filter paper and dried under an infrared lamp.

Ca. 4 % solutions of the methyl esters in methanol were applied to the paper with the aid of a small capillary. The spots were placed 1.5 cm apart and at least 2 cm from the edge of the paper.

The chromatograms were developed by the descending technique using a mixture of (A) 21 ml of a 6 M aqueous solution of silver fluoborate and 79 ml of methanol or of (B) 26 ml of the silver fluoborate solution and 74 ml of methanol as mobile phase. The tank was saturated with a mixture of methanol and water (4:1). All solvents used for development and impregnation were of reagent grade. Freshly prepared solutions of the esters and of the eluent were used on each occasion. The chromatograms were run in the dark to avoid decomposition of the silver solutions.

The papers were partially dried under an infrared lamp and then drawn through a 10 % solution of antimony pentachloride in chloroform. The substances appeared as round or slightly oval spots which became darker and more intense when warmed on a hot plate at 100°.

Stability of methyl levopimarate in the eluting phase. A solution of methyl levopimarate in 30 % silver fluoborate in 80 % methanol-water was allowed to stand in a dark cupboard for 4 h. The solution was then diluted with water and the ester was extracted with ether. The recovered methyl levopimarate had m.p. 61 – 63.5° mixed m.p. 64 – 65° with an authentic sample (m.p. 64 – 65°).

Dimethyl sulphoxide-light petroleum system. The method used was identical to that given by Hammarberg and Wickberg [20]. The acids were applied in 2 – 5 % solution in dimethyl ether. The spots were detected by exposing the paper to ammonia vapour followed by spraying with Duncan and Porteous's indicator solution; the spots appeared light yellow on a green background and were stable for about 3 min.

Acknowledgements. We thank Prof. H. Erdtman for his kind interest and Mrs. S. Strand for skilful assistance. Thanks are also due to the *Swedish Technical Research Council* for financial support.

1. Harris, G. C. and Sparks, J. *J. Am. Chem. Soc.* **70** (1948) 3674 and earlier papers.
2. Desalbus, L. and Dubearnes, R. *Bull. Soc. Chim.* **1958** 229.
3. Loeblich, V. M., Baldwin, D. E., O'Connor, R. T. and Lawrence, R. V. *J. Am. Chem. Soc.* **77** (1955) 6311.
4. Bruun, H. H. and Gåsland, S. *Acta Acad. Aboensis, Mathematica et Physica* XXII, 1. (1960) and ref. quoted therein.
5. Arya, V. P., Enzell, C., Erdtman, H. and Ryhage, R. *Acta Chem. Scand.* **15** (1961) 682.
6. Hudy, J. A. *Anal. Chem.* **31** (1959) 1754.
7. Genge, C. A. *Anal. Chem.* **31** (1959) 1750.
8. Wickberg, B. *Private communication.*

9. Lemal, D. M. and Fry, A. J. *Tetrahedron Letters* **1961** 775.
10. Simonsen, J. and Barton, D. H. R. *The Terpenes* (2nd Ed.) Vol. III. Cambridge 1951, p. 413.
11. Schuller, W. H. and Lawrence, R. V. *Chem. & Ind. London* **1961** 105.
12. Ref.[10], p. 374.
13. Ref.[10], p. 445.
14. Schuller, W. H., Moore, R. N. and Lawrence, R. V. *J. Am. Chem. Soc.* **82** (1960) 1734.
15. Ref.[10], p. 428.
16. Milne, G. W. A. and Smith, H. *Chem. & Ind. London* **1961** 1307.
17. Ireland, R. E. and Schiess, P. W. *Tetrahedron Letters* **1960** No. 25, 37.
18. Antkowiak, W., ApSimon, J. W. and Edwards, O. E. *J. Org. Chem.* **27** (1962) 1930.
19. Ireland, R. E. and Newbould, J. *J. Org. Chem.* **27** (1962) 1931.
20. Hammarberg, G. and Wickberg, B. *Acta Chem. Scand.* **14** (1960) 882.

Received July 2, 1962.

The Hydrolysis of 1,3-Dioxolan and Its Alkyl Derivatives. Part II. The Three Geometric Isomers of 2,4,5-Trimethyl-1,3-dioxolan

PENTTI SALOMAA and
ALPO KANKAANPERÄ

Department of Chemistry, University of Turku, Turku, Finland

In continuation of the previous study of the influence of structure on the kinetics of hydrolysis of derivatives of 1,3-dioxolan [1], the present paper describes the synthesis of, and kinetic data for the three geometric isomers of 2,4,5-trimethyl-1,3-dioxolan.

Experimental. The 2,3-butanediol employed in the synthesis of the examined dioxolans was a technical product (L. Light & Co., Ltd.) consisting mainly of the *meso* form. The *dl*-form present as an impurity was removed by careful distillation in a Todd precision fractionation assembly. Only the middle distillate, which crystallized in the receiver (b.p. 82—84°C/8 mm Hg; $n_D^{25} = 1.4370$), was employed in the subsequent syntheses. The pure *meso*-2,3-butanediol could be employed directly for the preparation of two geometric isomers of 2,4,5-trimethyl-1,3-dioxolan, but the *dl*-2,3-butanediol required in the synthesis of the third isomer was obtained from the *meso* form by the following reaction sequence:

$$\textit{meso}\text{-2,3-butanediol} \xrightarrow{Ac_2O} \textit{meso}\text{-2,3-butanediol diacetate} \xrightarrow{HBr} \textit{dl}\text{-2,3-dibromobutane} \xrightarrow{\text{Ag acetate}} \xrightarrow{\text{alkaline hydrolysis}} \textit{dl}\text{-2,3-butanediol}$$

The diacetate of *meso*-2,3-butanediol and *dl*-2,3-dibromobutane were prepared as described by Wilson and Lucas [2], whereas the preparation of *dl*-2,3-butanediol diacetate and *dl*-2,3-butanediol took place in principle by the method described by Winstein and Buckles [3]. All the intermediates and the final product *dl*-2,3-butanediol (b.p. 80°C/5 mm Hg) were carefully purified by fractional distillation.

The isomers of 2,4,5-trimethyl-1,3-dioxolan were prepared from acetaldehyde *n*-amyl acetal and the 2,3-butanediols by a procedure similar to that used to prepare 2,4-dimethyl-1,3-dioxolans [1]. The 2,*cis*-4,*trans*-5-trimethyl-1,3-dioxolan obtained from *dl*-2,3-butanediol had the following physical constants: b.p. 103.2°C/749.9 mm Hg, $n_D^{25} = 1.3922$, $d_4^{25} = 0.8894$, $[R]_{obs.} = 31.11$ ($[R]_{calc.} = 30.84$).

When *meso*-2,3-butanediol was the starting material, a mixture of 2,*cis*-4,*cis*-5-trimethyl-1,3-dioxolan and 2,*trans*-4,*trans*-5- trimethyl-1,3-dioxolan resulted. The components of the mixture were separated by careful fractional distillation. The physical properties of the lower-boiling component, which was the 2,*cis*-4,*cis*-5-form on the basis of kinetic and other data, were b.p. 109.5°C/751.0 mm Hg, $n_D^{20} = 1.4007$, $d_4^{20} = 0.9123$, $[R]_{obs.} = 30.91$ ($[R]_{calc.} = 30.84$) and those of the higher-boiling component, 2,*trans*-4,*trans*-5-trimethyl-1,3-dioxolan, b.p. 112.4°C/753.4 mm Hg, $n_D^{20} = 1.4038$, $d_4^{20} = 0.9201$, $[R]_{obs.} = 30.87$ ($[R]_{calc.} = 30.84$). The purities of the synthesized 2,4,5-trimethyl-1,3-dioxolans were checked by gas-chromatographic analysis.

The kinetic measurements were carried out as described previously [1].

The rate coefficients of the acid-catalyzed hydrolysis of the three isomers and kinetic quantities calculated from them are shown in Table 1. The assignations of the structures of the isomers were made on the

9. Lemal, D. M. and Fry, A. J. *Tetrahedron Letters* **1961** 775.
10. Simonsen, J. and Barton, D. H. R. *The Terpenes* (2nd Ed.) Vol. III. Cambridge 1951, p. 413.
11. Schuller, W. H. and Lawrence, R. V. *Chem. & Ind. London* **1961** 105.
12. Ref.[10], p. 374.
13. Ref.[10], p. 445.
14. Schuller, W. H., Moore, R. N. and Lawrence, R. V. *J. Am. Chem. Soc.* **82** (1960) 1734.
15. Ref.[10], p. 428.
16. Milne, G. W. A. and Smith, H. *Chem. & Ind. London* **1961** 1307.
17. Ireland, R. E. and Schiess, P. W. *Tetrahedron Letters* **1960** No. 25, 37.
18. Antkowiak, W., ApSimon, J. W. and Edwards, O. E. *J. Org. Chem.* **27** (1962) 1930.
19. Ireland, R. E. and Newbould, J. *J. Org. Chem.* **27** (1962) 1931.
20. Hammarberg, G. and Wickberg, B. *Acta Chem. Scand.* **14** (1960) 882.

Received July 2, 1962.

The Hydrolysis of 1,3-Dioxolan and Its Alkyl Derivatives. Part II. The Three Geometric Isomers of 2,4,5-Trimethyl-1,3-dioxolan

PENTTI SALOMAA and
ALPO KANKAANPERÄ

Department of Chemistry, University of Turku, Turku, Finland

In continuation of the previous study of the influence of structure on the kinetics of hydrolysis of derivatives of 1,3-dioxolan [1], the present paper describes the synthesis of, and kinetic data for the three geometric isomers of 2,4,5-trimethyl-1,3-dioxolan.

Experimental. The 2,3-butanediol employed in the synthesis of the examined dioxolans was a technical product (L. Light & Co., Ltd.) consisting mainly of the *meso* form. The *dl*-form present as an impurity was removed by careful distillation in a Todd precision fractionation assembly. Only the middle distillate, which crystallized in the receiver (b.p. 82—84°C/8 mm Hg; $n_D^{25} = 1.4370$), was employed in the subsequent syntheses. The pure *meso*-2,3-butanediol could be employed directly for the preparation of two geometric isomers of 2,4,5-trimethyl-1,3-dioxolan, but the *dl*-2,3-butanediol required in the synthesis of the third isomer was obtained from the *meso* form by the following reaction sequence:

$$\textit{meso}\text{-2,3-butanediol} \xrightarrow{Ac_2O} \textit{meso}\text{-2,3-butanediol diacetate} \xrightarrow{HBr} \textit{dl}\text{-2,3-dibromobutane} \xrightarrow{\text{Ag acetate}} \xrightarrow{\text{alkaline hydrolysis}} \textit{dl}\text{-2,3-butanediol}$$

The diacetate of *meso*-2,3-butanediol and *dl*-2,3-dibromobutane were prepared as described by Wilson and Lucas [2], whereas the preparation of *dl*-2,3-butanediol diacetate and *dl*-2,3-butanediol took place in principle by the method described by Winstein and Buckles [3]. All the intermediates and the final product *dl*-2,3-butanediol (b.p. 80°C/5 mm Hg) were carefully purified by fractional distillation.

The isomers of 2,4,5-trimethyl-1,3-dioxolan were prepared from acetaldehyde *n*-amyl acetal and the 2,3-butanediols by a procedure similar to that used to prepare 2,4-dimethyl-1,3-dioxolans [1]. The 2,*cis*-4,*trans*-5-trimethyl-1,3-dioxolan obtained from *dl*-2,3-butanediol had the following physical constants: b.p. 103.2°C/749.9 mm Hg, $n_D^{25} = 1.3922$, $d_4^{25} = 0.8894$, $[R]_{obs.} = 31.11$ ($[R]_{calc.} = 30.84$).

When *meso*-2,3-butanediol was the starting material, a mixture of 2,*cis*-4,*cis*-5-trimethyl-1,3-dioxolan and 2,*trans*-4,*trans*-5- trimethyl-1,3-dioxolan resulted. The components of the mixture were separated by careful fractional distillation. The physical properties of the lower-boiling component, which was the 2,*cis*-4,*cis*-5-form on the basis of kinetic and other data, were b.p. 109.5°C/751.0 mm Hg, $n_D^{20} = 1.4007$, $d_4^{20} = 0.9123$, $[R]_{obs.} = 30.91$ ($[R]_{calc.} = 30.84$) and those of the higher-boiling component, 2,*trans*-4,*trans*-5-trimethyl-1,3-dioxolan, b.p. 112.4°C/753.4 mm Hg, $n_D^{20} = 1.4038$, $d_4^{20} = 0.9201$, $[R]_{obs.} = 30.87$ ($[R]_{calc.} = 30.84$). The purities of the synthesized 2,4,5-trimethyl-1,3-dioxolans were checked by gas-chromatographic analysis.

The kinetic measurements were carried out as described previously [1].

The rate coefficients of the acid-catalyzed hydrolysis of the three isomers and kinetic quantities calculated from them are shown in Table 1. The assignations of the structures of the isomers were made on the

Table 1. Values of the rate coefficients k (l mole^{-1}s^{-1}), activation energy E (kcal/mole), logarithm of the frequency factor (log A) and activation entropy $\Delta S^{\ddagger}$ (E.U.) for the acid-catalyzed hydrolysis of the geometric isomers of 2,4,5-trimethyl-1,3-dioxolan.

Parent glycol	Dioxolan	°C	$10^4 \cdot k$	E	log A	$\Delta S^{\ddagger}$
dl-2,3-Butanediol	2,*cis*-4,*trans*-5-Trimethyl-1,3-dioxolan	25	67.8 ± 0.5			
—»—	—»—	35	225 ± 2	21.40	13.52	+ 1.37
—»—	—»—	45	656 ± 7			
meso-2,3-Butanediol	2,*cis*-4,*cis*-5-Trimethyl-1,3-dioxolan [a]	15	30.1 ± 0.2			
—»—	—»—	25	108 ± 1	22.49	14.52	+ 5.93
—»—	—»—	35	363 ± 3			
—»—	2,*trans*-4,*trans*-5-Trimethyl-1,3-dioxolan [b]	15	7.50 ± 0.04			
—»—	—»—	25	24.6 ± 0.2	22.77	14.11	+ 4.05
—»—	—»—	35	93.3 ± 1.1			

[a] the lower-boiling isomer. [b] the higher-boiling isomer.

basis of the following independent information.

The effect of polarity on the rate of hydrolysis is naturally the same for all three isomers and therefore the differences in their rates of hydrolysis must be mainly due to steric factors associated with the opening of the dioxolan ring by the *A 1* mechanism of acetal hydrolysis. In accordance with the explanation of the steric effects suggested previously [1], it may be assumed that the rates of hydrolysis of the three isomers increase in the sequence: 2,*trans*-4,*trans*-5-trimethyl-1,3-dioxolan < 2, *cis*-4,*trans*-5-trimethyl-1,3-dioxolan < 2, *cis*-4,*cis*-5-trimethyl-1,3-dioxolan. This sequence is valid at least as far as the second isomer is concerned because its structure follows from its synthesis from *dl*-2,3-butanediol (Table 1). The structures of the other two isomers derived from *meso*-2,3-butanediol are confirmed, apart from the kinetic data, by their physical constants as compared with those of the isomers of 2,4-dimethyl-1,3-dioxolan [1]. Of the latter isomers, the lower-boiling isomer (the *cis* form) hydrolyzed more rapidly and had a lower density and lower refractive index than the higher-boiling isomer and the same applies to the dioxolans derived from *meso*-2,3-butanediol. In addition, one must expect on the basis of the steric effects discussed earlier [1] that the 2,*trans*-4,*trans*-5-trimethyl-isomer is less likely to hydrolyze more rapidly than the *trans* isomer of 2,4-dimethyl-1,3-dioxolan. This is borne out by the rate coefficients at 25°C, which are 5.07×10^{-3} l mole^{-1}s^{-1} for the latter and 2.46×10^{-3} l mole^{-1}s^{-1} for the former compound.

The financial support of the *State Commission for Natural Sciences* is gratefully acknowledged.

1. Salomaa, P. and Kankaanperä, A. *Acta Chem. Scand.* **15** (1961) 871.
2. Wilson, C. E. and Lucas, H. J. *J. Am. Chem. Soc.* **58** (1936) 2396.
3. Winstein, S. and Buckles, R. E. *J. Am. Chem. Soc.* **64** (1942) 2780, 2787.

Received July 13, 1962.

Conversion of Δ^5-Cholestene-3α-12α-diol to Cholic Acid in the Rabbit

Bile Acids and Steroids 128

HENRY DANIELSSON

Department of Chemistry, Karolinska Institutet, Stockholm, Sweden

The work of Bergström and collaborators (*cf.* Ref.[1]) has demonstrated that during the conversion of cholesterol to cholic acid the steroid nucleus is modified prior to the completion of the side-chain oxidation. Studies of the metabolism of cholesterol and other C_{27}-neutral sterols in liver mitochondrial preparations have shown that the major metabolic event is the introduction of a hydroxyl-group at position 26. The metabolites formed, *e.g.* 26-hydroxycholesterol from cholesterol [2], Δ^5-cholestene-3β,7α,26-triol from 7α-hydroxycholesterol [3], coprostane-3α,7α,26-triol from coprostane-3α,7α-diol [7], are converted mainly to chenodeoxycholic acid when administered to bile-fistula rats. None of the metabolites isolated from these *in vitro* experiments appears to contain a 12α-hydroxyl-group. It seems apparent that the introduction of the 12α-hydroxyl-group which is a necessary step to form the cholic acid nucleus, is a reaction that is not easily reproduced *in vitro*. The nature of the substrate for the 12α-hydroxylase is not entirely known. The work of Lindstedt [5] on the metabolism of 7α-hydroxycholesterol in the bile-fistula rat has suggested the possibility that the formation of 7α-hydroxycholesterol is one of the early steps in the degradation of cholesterol to bile acids. There are, however, no definite reasons to exclude the possibility that the introduction of the 12α-hydroxyl-group could be one of the early steps.

In view of the results of the *in vitro* experiments mentioned above and as a prequisite for *in vitro* studies it seemed of interest to examine the metabolism of 12α-hydroxycholesterol *in vivo*. In a recent communication [6] the synthesis of Δ^5-cholestene-3β,12α-diol, *i.e.* 12α-hydroxycholesterol, was described and the metabolism of this compound in the bile-fistula rat was reported. It was found that 12α-hydroxycholesterol was converted to deoxycholic acid, cholic acid, and one so far unidentified metabolite which was somewhat more polar than deoxycholic acid. As rat liver is known to contain a 7α-hydroxylase which converts deoxycholic acid to cholic acid [7], these results do not unequivocally show that cholic acid is formed directly from 12α-hydroxycholesterol. Hence, it was necessary to repeat these experiments in an animal known not to contain an enzyme that converts deoxycholic acid to cholic acid. Lindstedt and Sjövall [8] have shown that the rabbit is not able to convert deoxycholic acid to cholic acid and the rabbit is therefore the experimental animal of choice for an investigation of the possibly direct formation of cholic acid from 12α-hydroxycholesterol. This communication reports the formation of cholic acid and deoxycholic acid from 12α-hydroxycholesterol in the bile-fistula rabbit.

Experimental. White rabbits, weighing approximately 2.5 kg, were used. Under nembuthal anaesthesia a polyethylene tubing was introduced into the lower part of the common bile duct. Bile was collected in 24 h portions. The bile was saponified in sealed steel tubes with 1 N sodium hydroxide in 50 % ethanol at 110° for 12 h. The free bile acids were obtained by ether extraction of the saponification mixture and were separated by reversed phase chromatography with phase system F 1 [9]. The trihydroxycholanic acid band from these chromatograms were rechromatographed with

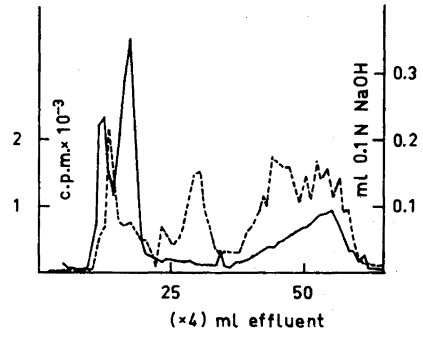

Fig. 1. Chromatography of first 24 h portion of hydrolyzed bile from bile-fistula rabbit injected with tritium labeled 12α-hydroxycholesterol. Column: 18 g hydrophobic Hyflo. Phase system F 1.
Solid line: titration values. Broken line: radioactivity.

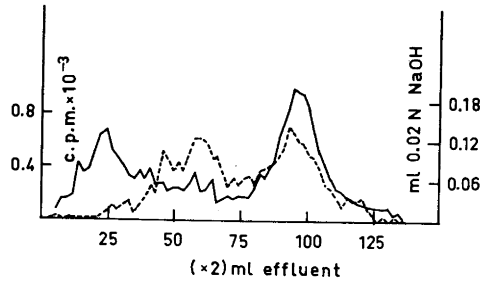

Fig. 2. Rechromatography of the cholic acid band, cf. Fig. 1.
Column: 9 g hydrophobic Hyflo. Phase system C 1.
Solid line: titration values. Broken line radioactivity.

phase system C 1 [9]. The tritium labeled Δ^5-cholestene-3β,12α-diol used was the same material as that described in an earlier paper [6].

Results and discussion. After intraperitoneal administration of a serum albumin stabilized emulsion of Δ^5-cholestene-3β,12α-diol (3 and 6 mg, resp.) 21 and 18 %, resp., of the injected dose was excreted in bile during the subsequent 48 h. Fig. 1 shows a chromatogram of the first 24 h portion of hydrolyzed bile from one rabbit. Three main radioactive bands are seen: one, apparently composed of at least two compounds, is eluted in the vicinity of the titration peak of cholic acid, which has its maximum at 16 ml of effluent; the second radioactive peak appears at 30 ml of effluent and the third is eluted together with deoxycholic acid which has its peak at 55 ml of effluent. Approximately 70 % of the radioactivity eluted together with deoxycholic acid was shown to be identical with deoxycholic acid by crystallization to constant specific radioactivity. The identity of the radioactive material eluted with its maximum at 30 ml of effluent, is not known. A compound with the same chromatographic properties was also formed from 12α-hydroxycholesterol in the rat. The cholic acid band, appearing between 10 and 20 ml of effluent (Fig. 1.) was rechromatographed on a column with phase system C 1 (*cf.* Fig. 2). Approximately half of the radioactivity put on the column was eluted together with cholic acid and the identity of the radioactive material with cholic acid was established by crystallization to constant specific radioactivity. The radioactive material eluted before cholic acid has not been identified. Of the radioactivity excreted in bile after administration of 12α-hydroxycholesterol about 40 % could be accounted for as deoxycholic acid and about 10 % as cholic acid.

The results of this and the previous investigation on the metabolism of 12α-hydroxycholesterol in the bile-fistula rat [6] are summarized in Fig. 3. The conversion of 12α-hydroxycholesterol to cholic acid in the bile-fistula rat is more efficient than what is observed in the rabbit, but in the case of the rat there is an enzyme in the liver that is capable of converting deoxycholic acid to cholic acid. It is therefore not possible to conclude that there is a path-

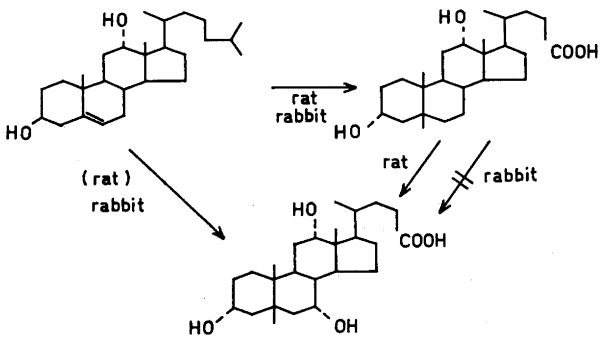

Fig. 3. Summary of the metabolism of 12α-hydroxycholesterol in the bile-fistula rat and bile-fistula rabbit.

way from 12α-hydroxycholesterol to cholic acid that does not entail the intermediary formation of deoxycholic acid. In the rabbit, however, this 7α-hydroxylase is lacking and the results obtained show that there obviously exists such a pathway in this species. The yield of cholic acid from 12α-hydroxycholesterol in the rabbit was rather low, about 10 % of the excreted isotope, while the main product was deoxycholic acid. The present experiments show that the rabbit liver is capable of converting 12α-hydroxycholesterol to cholic acid but do not form any basis for conclusions concerning the possibility that 12α-hydroxycholesterol might be an intermediate in the conversion of cholesterol to cholic acid. The rather low yield of cholic acid does not necessarily mean that this compound is no intermediate, as the metabolism of an intraperitoneally administered compound might not be comparable to that of one formed *in situ*.

Further work is needed to clarify the role of 12α-hydroxycholesterol in bile acid biogenesis.

Acknowledgements. This work is part of investigations supported by *Statens Medicinska Forskningsråd*, Sweden, and the *National Institutes of Health*, Bethesda, Md. (Grant H-2842).

The valuable technical assistance of Mrs. B. Berséus and Miss M.-L. Reinius is gratefully acknowledged.

1. Bergström, S., Danielsson, H. and Samuelsson, B. In Bloch, K. (Ed.) *Lipide Metabolism*, John Wiley and Sons, New York 1960, p. 296 ff.
2. Danielsson, H. *Arkiv Kemi* **17** (1961) 373.
3. Danielsson, H. *Arkiv Kemi* **17** (1961) 363.
4. Berséus, O. and Danielsson, H. *To be published.*
5. Lindstedt, S. *Acta Chem. Scand.* **11** (1957) 417.
6. Danielsson, H. *Arkiv Kemi* **17** (1961) 381.
7. Bergström, S., Rottenberg, M. and Sjövall, J. *Z. physiol. Chem.* **295** (1953) 278.
8. Lindstedt, S. and Sjövall, J. *Acta Chem. Scand.* **11** (1957) 421.
9. Norman, A. and Sjövall, J. *J. Biol. Chem.* **233** (1958) 872.

Received July 19, 1962.

The Preparation of *gem* Dithiols under Mild Conditions

BENGT MAGNUSSON

Department of Organic Chemistry, Chemical Institute, University of Uppsala, Uppsala, Sweden

gem Dithiols have been prepared from carbonyl compounds and hydrogen sulphide under pressure [1], from dibenzylketone and hydrogen sulphide in ethanol at ordinary pressure using hydrogen chloride as a catalyst [2] and by the reduction of duplodithioacetone with sodium in liquid ammonia [3].

During the study of duplodithioketones it was found that ketimines easily add hydrogen sulphide in ether solution at temperatures between $-40°$ and 0°C. After acidifying with dilute hydrochloric acid and extracting the amine hydrochloride with water, *gem* dithiols could be obtained, sometimes in good yields.

In some instances it is not necessary to prepare the ketimine. It is quite sufficient to add the amine to an ether solution of the ketone and pass hydrogen sulphide into the solution at low temperature. The yields are improved if anhydrous potassium carbonate is added to the reaction mixture in order to remove the water formed during the reaction. In both cases the products seem to be quite pure, byproducts with higher boiling points being absent. The products give a positive test for *gem* dithiols with lead acetate in ethanol [1] and a positive test for sulfhydryl with sodium nitroprusside. Infrared absorbtion shows a strong absorbtion maximum at 3.96 – 3.98 μ.

Experimental: (A) *Gem* Dithiols from ketimines. 30 g pentylidene-(3)-butylamine [4] was dissolved in 200 ml dry ether and hydrogen sulphide was passed into the solution at $-30°$C. The reaction mixture became cloudy and a crystalline compound separated. The absorbtion of hydrogen sulphide was very rapid; when absorbtion at $-30°$ ceased the temperature was allowed to rise to 0° and hydrogen sulphide was bubbled through the solution for a further 5 h. The flask and contents were cooled to $-20°$ and 5 M hydrochloric acid was slowly added with stirring until the aqueous phase gave an acid reaction. The ether phase was separated, the aqueous phase extracted with ether and the

way from 12α-hydroxycholesterol to cholic acid that does not entail the intermediary formation of deoxycholic acid. In the rabbit, however, this 7α-hydroxylase is lacking and the results obtained show that there obviously exists such a pathway in this species. The yield of cholic acid from 12α-hydroxycholesterol in the rabbit was rather low, about 10 % of the excreted isotope, while the main product was deoxycholic acid. The present experiments show that the rabbit liver is capable of converting 12α-hydroxycholesterol to cholic acid but do not form any basis for conclusions concerning the possibility that 12α-hydroxycholesterol might be an intermediate in the conversion of cholesterol to cholic acid. The rather low yield of cholic acid does not necessarily mean that this compound is no intermediate, as the metabolism of an intraperitoneally administered compound might not be comparable to that of one formed *in situ*.

Further work is needed to clarify the role of 12α-hydroxycholesterol in bile acid biogenesis.

Acknowledgements. This work is part of investigations supported by *Statens Medicinska Forskningsråd*, Sweden, and the *National Institutes of Health*, Bethesda, Md. (Grant H-2842).

The valuable technical assistance of Mrs. B. Berséus and Miss M.-L. Reinius is gratefully acknowledged.

1. Bergström, S., Danielsson, H. and Samuelsson, B. In Bloch, K. (Ed.) *Lipide Metabolism*, John Wiley and Sons, New York 1960, p. 296 ff.
2. Danielsson, H. *Arkiv Kemi* **17** (1961) 373.
3. Danielsson, H. *Arkiv Kemi* **17** (1961) 363.
4. Berséus, O. and Danielsson, H. *To be published.*
5. Lindstedt, S. *Acta Chem. Scand.* **11** (1957) 417.
6. Danielsson, H. *Arkiv Kemi* **17** (1961) 381.
7. Bergström, S., Rottenberg, M. and Sjövall, J. *Z. physiol. Chem.* **295** (1953) 278.
8. Lindstedt, S. and Sjövall, J. *Acta Chem. Scand.* **11** (1957) 421.
9. Norman, A. and Sjövall, J. *J. Biol. Chem.* **233** (1958) 872.

Received July 19, 1962.

The Preparation of *gem* Dithiols under Mild Conditions

BENGT MAGNUSSON

Department of Organic Chemistry, Chemical Institute, University of Uppsala, Uppsala, Sweden

gem Dithiols have been prepared from carbonyl compounds and hydrogen sulphide under pressure [1], from dibenzylketone and hydrogen sulphide in ethanol at ordinary pressure using hydrogen chloride as a catalyst [2] and by the reduction of duplodithioacetone with sodium in liquid ammonia [3].

During the study of duplodithioketones it was found that ketimines easily add hydrogen sulphide in ether solution at temperatures between $-40°$ and 0°C. After acidifying with dilute hydrochloric acid and extracting the amine hydrochloride with water, *gem* dithiols could be obtained, sometimes in good yields.

In some instances it is not necessary to prepare the ketimine. It is quite sufficient to add the amine to an ether solution of the ketone and pass hydrogen sulphide into the solution at low temperature. The yields are improved if anhydrous potassium carbonate is added to the reaction mixture in order to remove the water formed during the reaction. In both cases the products seem to be quite pure, byproducts with higher boiling points being absent. The products give a positive test for *gem* dithiols with lead acetate in ethanol [1] and a positive test for sulfhydryl with sodium nitroprusside. Infrared absorbtion shows a strong absorbtion maximum at 3.96 – 3.98 μ.

Experimental: (A) *Gem* Dithiols from ketimines. 30 g pentylidene-(3)-butylamine [4] was dissolved in 200 ml dry ether and hydrogen sulphide was passed into the solution at $-30°$C. The reaction mixture became cloudy and a crystalline compound separated. The absorbtion of hydrogen sulphide was very rapid; when absorbtion at $-30°$ ceased the temperature was allowed to rise to 0° and hydrogen sulphide was bubbled through the solution for a further 5 h. The flask and contents were cooled to $-20°$ and 5 M hydrochloric acid was slowly added with stirring until the aqueous phase gave an acid reaction. The ether phase was separated, the aqueous phase extracted with ether and the

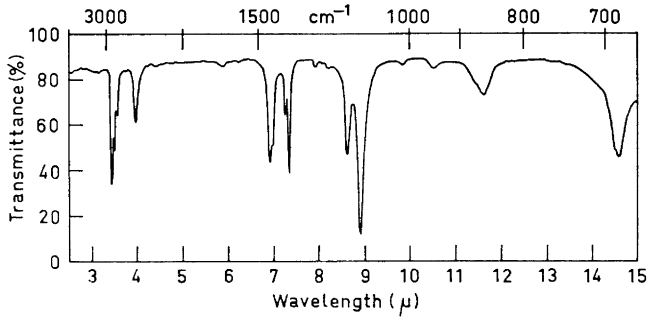

Fig. 1. Infrared spectrum of 2,2-dimercaptopropane.

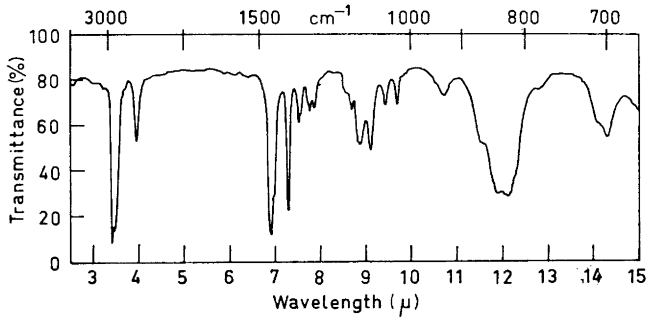

Fig. 2. Infrared spectrum of 3,3-dimercapto-pentane.

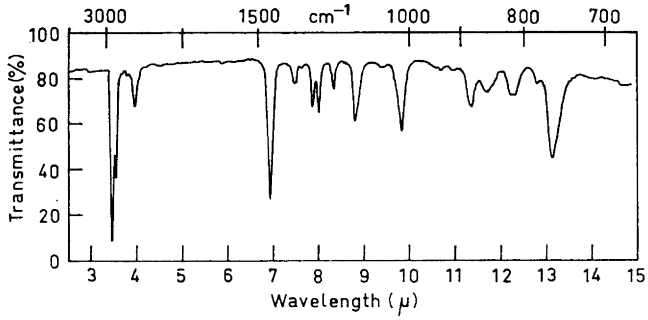

Fig. 3. Infrared spectrum of 1,1-dimercaptocyklohexane.

combined ether solutions were washed with water and dried with anhydrous sodium sulphate. The ether was removed by distillation and the product distilled through a 30 cm Widmer column. After a small forerun of a low-boiling red fluid the 3,3-dimercaptopentane [1] came over as an almost colourless fluid. Yield 24 g (83 %). B.p./12 mm 54°, $n_D^{22} = 1.5053$. (Found: C 44.16; H 8.80; S 47.03. Calc. for $C_5H_{12}S_2$: C 44.07; H 8.88; S 47.06). Ir-Spectrum see Fig. 2.

2,2-Dimercaptopropane [1] was obtained from propylidene-(2)-butylamine in 56 % yield. IR-Spectrum see Fig. 1.

B) *gem* Dithiols from ketones. 58 g Acetone and 10 g butylamine were dissolved in 200 ml dry ether in a 500 ml flask equipped with stirrer, gas-inlet tube, thermometer and calcium chloride guard tube. 100 g anhydrous potassium carbonate was added, the stirrer was started and the mixture cooled to −20°. Hydrogen sulphide was passed into the solution for one hour. The temperature was then allowed to rise to 0° and hydrogen sulphide was passed into the mixture for further 5 h. The potassium carbonate was filtered off and washed with ether, the washings were added to the ethereal reaction product, which was then cooled to −20° and acidified with 5 M hydrochloric acid, the product being then worked up as in A. Yield 49 g 2,2-dimercaptopropane [1] (45 %). B.p/100 mm 57°. $n_D^{22} = 1.5088$. (Found: C 33.38; H 7.36; S 59.13. Calc. for $C_3H_8S_2$: C 33.29; H 7.45; S 59.26).

1,1-Dimercaptocyklohexane [1] was obtained from cyclohexanone in 78 % yield. B.p./2.3 mm 51°, $n_D^{20} = 1.5476$. (Found: C 48.40; H 8.13; S 42.97. Calc. for $C_6H_{12}S_2$: C 48.60; H 8.16; S 43.25).
IR-Spectrum see Fig. 3.

3,3-Dimercaptopentane was obtained from diethylketone in 12 % yield.

d,l-Camphor, dibenzylketone and 2-indanone did not give a dithiol using method B.

After this manuscript has been completed the work of Djerassi and Tursch [5] describing a somewhat similar method of preparing *gem* dithiols became available to the present author.

Acknowledgement. The author is very indebted to professor A. Fredga for his kind interest in this work.

1. Cairns, T. L., Evans, G. L., Larchar, A. W. and McKusick, B. C. *J. Am. Chem. Soc.* **74** (1952) 3982.
2. Berchold, G. A., Edwards, B. E., Campaigne, E. and Carmack, M. *J. Am. Chem. Soc.* **81** (1959) 3148.
3. Magnusson, B. *Acta Chem. Scand.* **16** (1962) 772.
4. Asinger, F., Thiel, M. and Lipfert, G. *Ann.* **627** (1959) 207.
5. Djerassi, C. and Tursch, B. *J. Org. Chem.* **27** (1962) 1041.

Received July 23, 1962.

ACTA CHEMICA SCANDINAVICA 16 (1962) 1539–1548

Crystal and Molecular Structure of the *p*-Bromophenylhydrazone of Arabinose

SVEN FURBERG and CHERRY SCHIANDER PETERSEN

Institute of Chemistry, University of Oslo, Blindern-Oslo, Norway

The structure of the *p*-bromophenylhydrazone of arabinose in the crystalline state has been determined by X-ray crystallographic methods. It is shown that the sugar occurs in the pyranose ring form. The compound is therefore a N,N'-derivative of hydrazine, $R-NH-NH-C_4H_6Br$. The azimuthal angle in hydrazine is about 90°. The bond C(1)–N(1) connecting sugar and hydrazine appears to be significantly shorter than a normal C–N single bond. The arabinose is present in its α-form, with conformation 1e2e3e4a.

The phenylhydrazone and phenylosazone derivatives were originally represented as open-chain compounds, but as they show mutarotation in many cases, other structures have to be considered. In the case of glucose at least two isomeric phenylhydrazones have been isolated. Several types of isomerism are possible, and it has been suggested that they are α-/β-anomers, *syn*- and *anti*-forms, and cyclic-/acyclic isomers [1,2]. Mester [2] applied the formazan reaction to study these compounds. The phenylhydrazone can only yield a formazan when the sugar is present in its acyclic (aldehydo) form. It was found that one of the glucose isomers was acyclic, the others cyclic. Arabinose gave formazan in good yield [3] and its phenylhydrazone therefore probably occurs predominantly in the acyclic form in solution. These results were confirmed by Percival [4] who studied the ultraviolet spectra of the phenylhydrazones. She found that the phenylhydrazone of arabinose and a number of other sugars had absorption characteristics similar to those of the acyclic isomer of glucose. The available evidence thus indicates that acyclic structure is the predominant form of arabinose phenylhydrazone in solution. As for the *p*-bromoderivative, no information on the structure of the sugar in this compound was found in the literature.

We have now determined the structure of the *p*-bromophenylhydrazone of arabinose in the crystalline state, using the methods of X-ray crystallography. Details of the structure analysis are given below. Projections of the electron density in two directions have been calculated (Figs. 1 and 2), from which the positions of the atoms and the molecular structure (Fig. 3) were

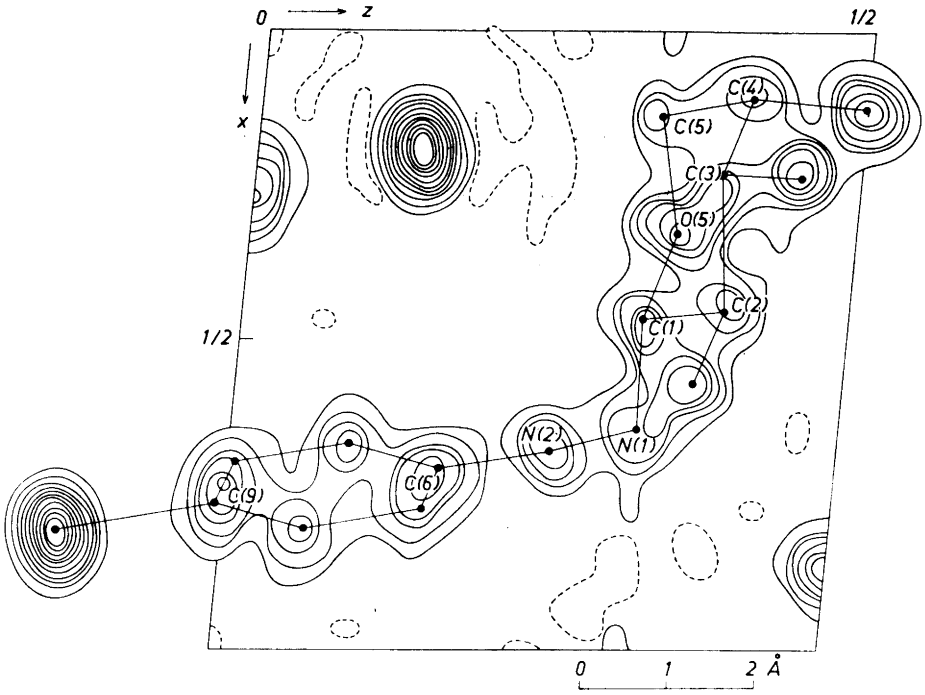

Fig. 1. Electron density projection in direction of *b* axis. Contours at intervals of 5e.Å^{-2} for bromine, 2e.Å^{-2} for the other atoms. The zero contour line is dotted.

determined. As is seen from the figures, the sugar has a cyclic structure, a somewhat unexpected result in view of the investigations referred to above. The compound accordingly should be represented as R—NH—NH—C_6H_4Br.

The sugar occurs in its normal pyranose chair form. The C(1)—N(1) bond is equatorial and the conformation is 1e2e3e4a. The compound is therefore a derivative of *α*-arabinose. The sugar itself crystallizes only in the *β*-form, with conformation 1a2e3e4a. There are four possible pyranose structures of arabinose, 1e2e3e4a ⇌ 1a2a3a4e (*α*-arabinose) and 1a2e3e4a ⇌ 1e2a3a4e (*β*-arabinose). According to the stability rules of Reeves [5] 1e2e3e4a is the most stable of these structures. The mutarotation data, although difficult to interpret, also show that the *α*-form predominates in the equilibrium mixture [6]. In addition, the reactivity of an equatorial hydroxyl group at C(1) is greater, in general, than that of an axial group. It is therefore to be expected that the reaction preferably gives a product in which arabinose has the 1e2e3e4a conformation. Only one isomer of the compound is known, and we have also observed only one crystalline form in our experiments.

The bond lengths and bond angles derived from the final atomic coordinates are given in Table 2 and Fig. 3. No great accuracy can be claimed because of overlap of atoms, lack of centre of symmetry, and the presence of a heavy

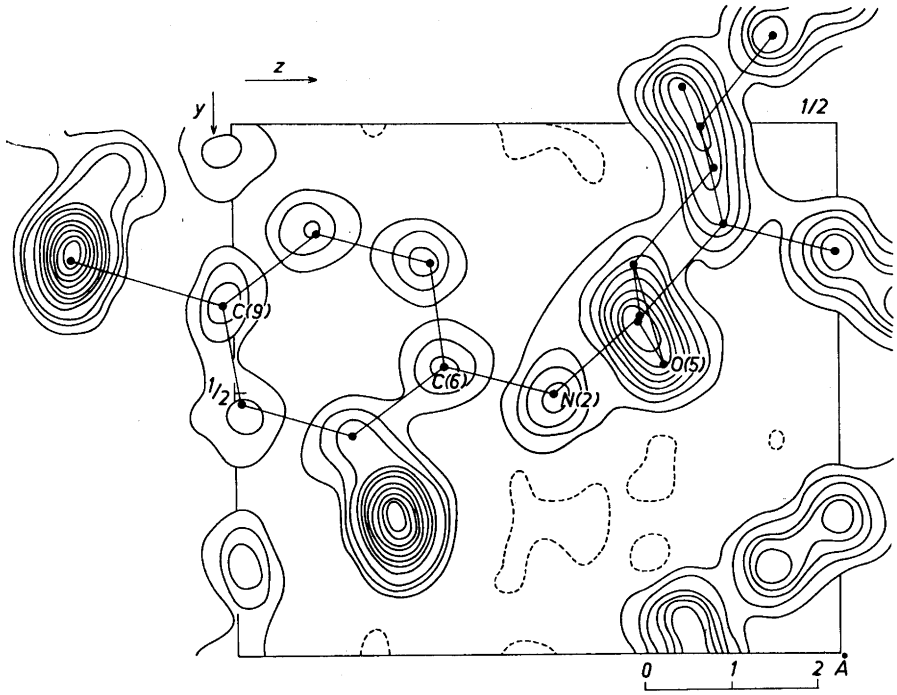

Fig. 2. Electron density projection in direction of *a* axis. Contours as in Fig. 1.

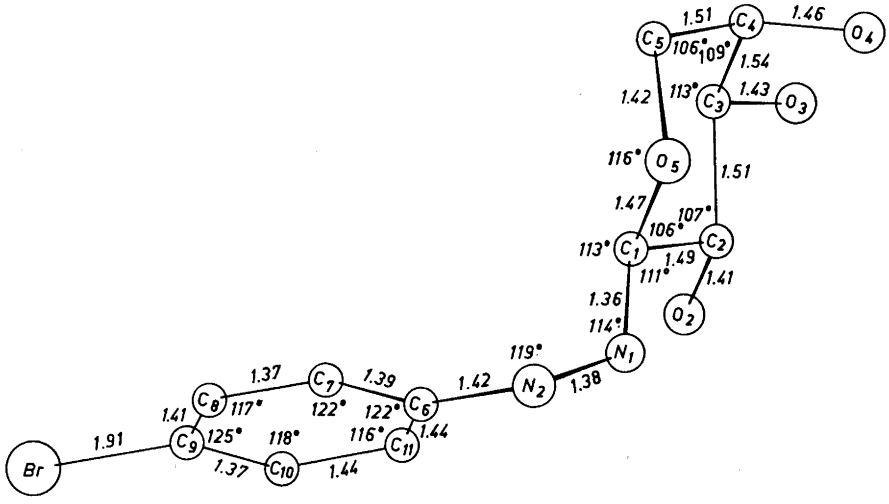

Fig. 3. The molecular structure of arabinose-*p*-bromophenylhydrazone. Bond lengths in Å units.

atom. The standard deviation is estimated to be about 0.02 Å for most distances and 1°—2° for the angles (see below).

The *hydrazine* part of the molecule exhibits some interesting features. The azimuthal angle between the planes N—N—C(6) and N—N—C(1) is close to 90°, in agreement with the calculations of Penny and Sutherland [7] who concluded that the only stable form of hydrazine is that in which the azimuth of one-half of the molecule with respect to the other is approximately 90°. In crystalline diformyl-[8] and diacetyl-hydrazine [9] this angle is 180°, in diacetyl-hydrazine monohydrate [9] 135°, whereas an eclipsed configuration is reported for crystalline hydrazine [10]. The influence of external forces upon the molecular structure is evidently of importance. Gaseous N,N'-dimethylhydrazine has been studied by electron diffraction [11], but the relative position of the methyl groups with respect to each other could not be ascertained. The C—N and N—N bond lengths are all more or less short in the present investigation, the values found being 1.42 Å (N(2)—C(6)), 1.36 Å (N(1)—C(1)) and 1.38 Å (N(1)—N(2)). The N—N bond in hydrazine is 1.46 Å and a normal single bond C—N about 1.49 Å. The calculated standard deviations for the three bonds are in the order of 0.02 Å, but lack of resolution, especially of N(1) and C(1), makes it difficult to estimate whether the deviations are significant or not. We consider the shortening of N(2)—C(6) and N(1)—N(2) possibly significant and that of N(1)—C(1) probably significant. The latter bond connects sugar and hydrazine and is of interest, as in the usual acyclic formulae of sugar phenylhydrazones it is a double bond, whereas the cyclic formula established in the present work gives a single bond. It is noteworthy that the C(1)—O(1) bond in arabinose [12] and other sugars [13] is found to be considerably shorter (1.38 Å) than normal C—O bonds in sugars (1.43 Å). The angles N—N—C(1) and N—N—C(6) are found to be 114° and 119°, respectively.

The dimensions of hydrazine derived in the present work resemble those found in diacetyl-hydrazine, in which there is a significant shortening of both the N—N bond (1.396 Å) and the C—N bond (1.341 Å) due to conjugation effects. In view of the neighbouring benzene ring a similar effect might possibly to a small extent be present also in the phenylhydrazones.

In the *sugar* part of the molecule the only significant deviation from normal molecular dimensions (1.43 Å for C—O, 1.53 Å for C—C and 110° for the angles) occurs in the angle at the ring oxygen atom O(5), which is found to be 116°. In crystalline arabinose [12] this angle is reported to be 113°, in α-rhamnose [13] 120°.

In the *aromatic* part of the molecule the mean C—C distance is 1.40 Å, and all the ring atoms as well as N(2) and the bromine atom lie in the same plane within the limits of error. This plane forms an angle of about 20° with the plane N—N—C(6). The length of the C—Br bond is 1.91 Å, close to the value found in, *e.g.*, tetrabromobenzene [14], where the mean C—Br distance is 1.896 Å. The ring angle at C(9), the carbon atom to which bromine is attached, is possibly significantly greater than 120°. It is interesting to note that this angle is found to be slightly greater than 120° in many cases, such as tetrabromobenzene [14] (122°) and *p*-dichlorobenzene [15] (121°30'). This indicates that the effect possibly is real.

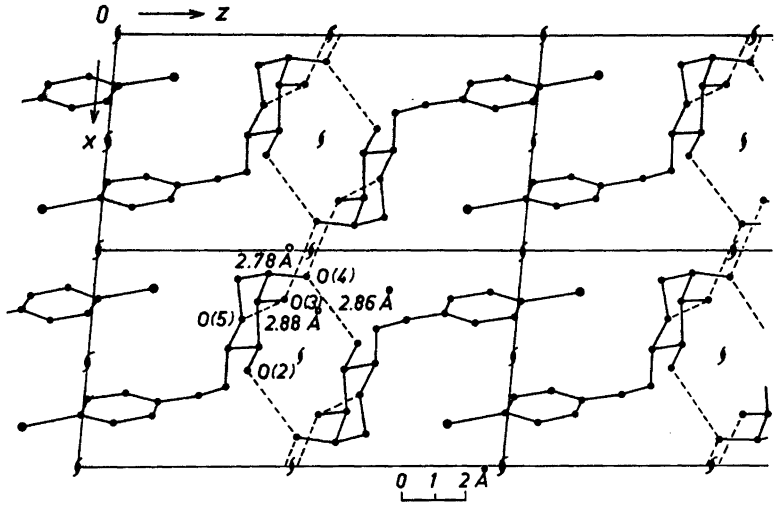

Fig. 4. The *b* projection of the structure. Broken lines indicate hydrogen bonds.

The arrangement of the molecules in the crystal is shown in Fig. 4. Only three intermolecular distances, all involving the oxygen atoms of the sugar, are shorter than 3.2 Å. As there are three hydroxyl hydrogens in the molecule, these interactions are likely to be hydrogen bonds. The atom O(3) is linked to O(5) and O(4) in different molecules by bonds of lengths 2.88 Å and 2.78 Å, respectively. A third bond (2.86 Å) connects O(2) and O(4) in neighbouring molecules, the arabinose residues being linked together in layers parallel to the *xy*-plane. The nitrogen atoms of the hydrazine are not engaged in hydrogen bond formation, apart from a possible weak intramolecular interaction between N(1) and O(2).

EXPERIMENTAL. STRUCTURE ANALYSIS

The compound was prepared by mixing equivalent amounts of *p*-bromophenylhydrazine and β-D-arabinose at room temperature. Acetic acid or 60 % alcohol was used as solvent. In both cases thin long needles melting at 155° – 160°C were obtained. The needle axis corresponds to the crystallographic *b* axis.

X-Ray single crystal diagrams of the Weissenberg type were taken around the *a* and *b* axes, using copper radiation ($\lambda = 1.542$ Å). Small crystals of cross-section about 0.1 × 0.2 mm were used. The diagrams showed that the crystals are monoclinic, with unit cell dimensions $a = 7.12$ Å, $b = 6.15$ Å, $c = 14.09$ Å and $\beta = 96°$ (all ± 0.5 %). The only systematic absences occur in the $0k0$ reflexions for odd values of k. The space group is $P2_1$. The density, measured in a carbon tetrachloride-bromoform mixture, was 1.70 g/cm³, giving two (calc. 1.97) molecules of $C_{11}H_{15}O_4N_2Br$ in the unit cell.

The reflexions were recorded on an integrating Weissenberg camera and their intensities measured by a Hilger & Watts photometer. 208 of the 282 $h0l$ reflexions and 105 of the 122 $0kl$ reflexions obtainable with copper radiation were recorded with measurable intensities. Corrections for absorption and extinction were not applied.

The structure was solved by the standard heavy atom technique.

Table 1. Atomic coordinates as fractions of the corresponding cell edge.

Atom	x	y	z	B_{h0l}	Atom	x	z
Br	0.189	0.756	0.1348	2.8	H(1)	0.484	0.257
O(2)	0.566	0.951	0.3698	3.0	H(2)	0.480	0.460
O(3)	0.226	0.860	0.4461	1.9	H(3)	0.250	0.319
O(4)	0.133	0.290	0.4993	1.7	H(4)	0.970	0.398
O(5)	0.327	0.467	0.3521	2.4	H(5)	0.052	0.351
N(1)	0.645	0.377	0.3334	2.0	H(5)′	0.157	0.273
N(2)	0.676	0.532	0.2655	2.2	H(7)	0.603	0.114
C(1)	0.464	0.302	0.3280	2.1	H(8)	0.320	0.057
C(2)	0.448	0.120	0.3965	1.8	H(10)	0.863	0.046
C(3)	0.247	0.041	0.3839	2.3	H(11)	0.787	0.220
C(4)	0.104	0.221	0.4000	2.2	H(N(1))	0.652	0.387
C(5)	0.134	0.409	0.3342	2.3	H(N(2))	0.596	0.262
C(6)	0.703	0.464	0.1714	1.5	H(O(2))	0.677	0.417
C(7)	0.673	0.608	0.0957	3.2	H(O(3))	0.270	0.410
C(8)	0.704	0.550	0.0050	2.9	H(O(4))	0.981	0.480
C(9)	0.233	0.836	0.0078	1.9			
C(10)	0.801	0.185	0.0634	2.3			
C(11)	0.764	0.244	0.1587	2.3			

The b projection was first determined. The position of the bromine atom was derived from the Patterson synthesis, and the electron density map based on the corresponding signs clearly showed where the benzene ring and the nitrogen atoms had to be placed. The location of the atoms of the arabinose caused considerable difficulties because of overlap of atoms and ambiguity of molecular structure. Several possibilities were tried,

Table 2. Bond lengths (in Å units) and bond angles.

Bond lengths		Bond angles	
C(9)–Br	1.91	Br–C(9)–C(8)	116°
C(9)–C(8)	1.41	C(9)–C(8)–C(7)	117°
C(8)–C(7)	1.37	C(8)–C(7)–C(6)	122°
C(7)–C(6)	1.39	C(7)–C(6)–C(11)	122°
C(6)–C(11)	1.44	C(6)–C(11)–C(10)	116°
C(11)–C(10)	1.44	C(11)–C(10)–C(9)	118°
C(10)–C(9)	1.37	C(10)–C(9)–C(8)	125°
C(6)–N(2)	1.42	Br–C(9)–C(10)	119°
N(2)–N(1)	1.38	C(7)–C(6)–N(2)	120°
N(1)–C(1)	1.36	C(11)–C(6)–N(2)	118°
C(1)–C(2)	1.49	C(6)–N(2)–N(1)	119°
C(2)–C(3)	1.51	N(2)–N(1)–C(1)	114°
C(3)–C(4)	1.54	N(1)–C(1)–C(2)	111°
C(4)–C(5)	1.51	N(1)–C(1)–O(5)	113°
C(5)–O(5)	1.42	C(1)–C(2)–C(3)	107°
C(1)–O(5)	1.47	C(2)–C(3)–C(4)	113°
C(2)–O(2)	1.41	C(3)–C(4)–C(5)	109°
C(3)–O(3)	1.43	C(4)–C(5)–O(5)	106°
C(4)–O(4)	1.46	C(5)–O(5)–C(1)	116°
		O(5)–C(1)–C(2)	106°
		C(1)–C(2)–O(2)	107°
		C(3)–C(2)–O(2)	108°
		C(2)–C(3)–O(3)	110°
		C(4)–C(3)–O(3)	111°
		C(3)–C(4)–O(4)	109°
		C(5)–C(4)–O(4)	111°

Table 3. Observed (F_o) and calculated (F_c) structure factors.

h k l	F_o	F_c	*h k l*	F_o	F_c
0 0 2	18	12	2 0 — 9	15	15
0 0 3	7	1	2 0 — 8	9	— 9
0 0 4	87	— 84	2 0 — 7	52	— 52
0 0 5	13	— 14	2 0 — 6	52	— 52
0 0 6	47	47	2 0 — 5	25	— 26
0 0 7	30	28	2 0 — 4	16	16
0 0 8	53	49	2 0 — 3	52	59
0 0 9	6	5	2 0 — 2	7	5
0 0 10	21	— 21	2 0 — 1	8	11
0 0 11	22	— 21	2 0 0	88	—101
0 0 12	< 6	— 2	2 0 1	99	—108
0 0 13	< 6	2	2 0 2	33	— 30
0 0 14	15	15	2 0 3	12	9
0 0 15	24	25	2 0 4	29	29
0 0 16	12	11	2 0 5	38	34
0 0 17	10	— 8	2 0 6	13	13
1 0 —17	16	13	2 0 7	25	23
1 0 —16	23	24	2 0 8	30	— 29
1 0 —15	5	6	2 0 9	29	— 27
1 0 —14	< 6	— 2	2 0 10	< 6	2
1 0 —13	28	— 28	2 0 11	< 6	2
1 0 —12	23	— 23	2 0 12	11	10
1 0 —11	10	— 9	2 0 13	< 6	3
1 0 —10	34	34	2 0 14	7	— 7
1 0 — 9	33	33	2 0 15	10	— 9
1 0 — 8	21	18	2 0 16	18	— 19
1 0 — 7	6	5	3 0 —17	6	— 5
1 0 — 6	31	— 34	3 0 —16	21	— 19
1 0 — 5	55	— 55	3 0 —15	15	— 16
1 0 — 4	18	— 22	3 0 —14	18	— 16
1 0 — 3	2	— 1	3 0 —13	15	15
1 0 — 2	11	18	3 0 —12	17	16
1 0 — 1	42	43	3 0 —11	31	30
1 0 0	12	— 3	3 0 —10	< 6	1
1 0 1	12	— 16	3 0 — 9	22	— 21
1 0 2	40	32	3 0 — 8	19	— 19
1 0 3	96	— 96	3 0 — 7	19	— 18
1 0 4	33	25	3 0 — 6	< 5	0
1 0 5	26	28	3 0 — 5	26	27
1 0 6	40	37	3 0 — 4	31	34
1 0 7	33	29	3 0 — 3	24	25
1 0 8	4	2	3 0 — 2	16	— 11
1 0 9	38	— 35	3 0 — 1	13	— 19
1 0 10	35	— 33	3 0 0	36	— 36
1 0 11	30	— 28	3 0 1	6	— 3
1 0 12	9	8	3 0 2	21	— 19
1 0 13	23	23	3 0 3	55	55
1 0 14	19	21	3 0 4	23	20
1 0 15	5	4	3 0 5	9	9
1 0 16	12	— 11	3 0 6	21	— 20
1 0 17	11	— 13	3 0 7	29	— 26
2 0 —17	11	10	3 0 8	23	— 22
2 0 —16	< 5	4	3 0 9	19	17
2 0 —15	12	— 12	3 0 10	16	14
2 0 —14	26	— 27	3 0 11	35	35
2 0 —13	14	— 13	3 0 12	16	17
2 0 —12	< 6	0	3 0 13	18	— 20
2 0 —11	10	8	3 0 14	8	— 8
2 0 —10	37	37	3 0 15	13	— 14

$h\,k\,l$	F_o	F_c	$h\,k\,l$	F_o	F_c
3 0 16	< 4	− 5	6 0 −14	9	10
4 0 −16	16	− 15	6 0 −13	26	− 22
4 0 −15	< 5	1	6 0 −12	5	2
4 0 −14	12	10	6 0 −11	5	− 5
4 0 −13	21	20	6 0 −10	6	− 5
4 0 −12	< 6	5	6 0 − 9	23	21
4 0 −11	6	6	6 0 − 8	16	15
4 0 −10	29	− 27	6 0 − 7	< 6	− 2
4 0 − 9	18	− 17	6 0 − 6	8	− 9
4 0 − 8	23	− 21	6 0 − 5	25	− 25
4 0 − 7	26	24	6 0 − 4	21	− 19
4 0 − 6	40	39	6 0 − 3	< 6	− 3
4 0 − 5	37	35	6 0 − 2	13	12
4 0 − 4	12	12	6 0 − 1	13	14
4 0 − 3	17	− 16	6 0 0	13	12
4 0 − 2	28	− 30	6 0 1	8	6
4 0 − 1	19	− 16	6 0 2	26	− 26
4 0 0	< 5	3	6 0 3	10	− 9
4 0 1	46	44	6 0 4	5	6
4 0 2	39	39	6 0 5	14	− 14
4 0 3	7	6	6 0 6	17	17
4 0 4	13	− 11	6 0 7	< 6	3
4 0 5	< 5	1	6 0 8	< 5	− 2
4 0 6	37	− 37	6 0 9	< 5	− 5
4 0 7	11	10	6 0 10	8	− 8
4 0 8	11	10	6 0 11	8	− 8
4 0 9	15	14	7 0 −11	4	1
4 0 10	16	14	7 0 −10	23	20
4 0 11	9	10	7 0 − 9	< 5	3
4 0 12	11	− 11	7 0 − 8	< 5	4
4 0 13	8	9	7 0 − 7	7	− 8
4 0 14	7	− 7	7 0 − 6	6	− 7
4 0 15	< 3	− 2	7 0 − 5	14	− 13
5 0 −14	17	16	7 0 − 4	5	3
5 0 −13	18	16	5 0 − 3	5	5
5 0 −12	17	− 17	7 0 − 2	9	10
5 0 −11	16	− 14	7 0 − 1	< 6	− 2
5 0 −10	19	− 18	7 0 0	< 6	− 4
5 0 − 9	5	− 6	7 0 1	11	− 11
5 0 − 8	10	9	7 0 2	9	− 8
5 0 − 7	21	20	7 0 3	< 6	− 1
5 0 − 6	< 6	4	7 0 4	< 6	5
5 0 − 5	10	9	7 0 5	15	16
5 0 − 4	18	− 18	7 0 6	10	9
5 0 − 3	21	− 21	7 0 7	8	− 7
5 0 − 2	11	− 12	7 0 8	< 4	2
5 0 − 1	17	16	7 0 9	11	− 12
5 0 0	12	11	8 0 − 9	< 4	− 0
5 0 1	19	18	8 0 − 8	10	− 8
5 0 2	16	17	8 0 − 7	8	− 7
5 0 3	18	− 18	8 0 − 6	< 5	1
5 0 4	19	− 20	8 0 − 5	< 5	2
5 0 5	24	− 21	8 0 − 4	17	16
5 0 6	< 6	− 2	8 0 − 3	< 5	− 1
5 0 7	16	15	8 0 − 2	10	9
5 0 8	10	8	8 0 − 1	10	− 11
5 0 9	13	14	8 0 0	9	− 9
5 0 10	11	− 11	8 0 1	6	− 6
5 0 11	12	− 13	8 0 2	< 5	− 1
5 0 12	13	− 15	8 0 3	7	7
5 0 13	< 4	− 3	8 0 4	< 4	4

h k l	F_o	F_c	*h k l*	F_o	F_c
8 0 5	< 5	0	0 2 7	33	34
9 0 — 3	5	5	0 3 7	4	4
9 0 — 2	3	— 3	0 4 7	18	17
9 0 — 1	6	— 6	0 5 7	7	8
9 0 0	11	11	0 6 7	4	8
9 0 1	7	— 7	0 0 8	51	48
0 1 0	0	0	0 1 8	19	18
0 2 0	48	45	0 2 8	17	16
0 3 0	0	0	0 3 8	10	12
0 4 0	23	23	0 4 8	18	23
0 5 0	0	0	0 5 8	3	3
0 6 0	7	6	0 6 8	8	7
0 7 0	0	0	0 0 9	5	6
0 1 1	31	28	0 1 9	36	35
0 2 1	43	43	0 2 9	17	15
0 3 1	21	23	0 3 9	16	19
0 4 1	15	13	0 4 9	12	11
0 5 1	8	6	0 5 9	8	8
0 6 1	5	4	0 6 9	1	3
0 7 1	2	2	0 0 10	20	20
0 0 2	15	13	0 1 10	25	23
0 1 2	77	79	0 2 10	20	16
0 2 2	24	19	0 3 10	18	19
0 3 2	16	21	0 4 10	8	10
0 4 2	9	13	0 5 10	6	6
0 5 2	7	11	0 6 10	1	1
0 6 2	4	3	0 0 11	21	19
0 7 2	4	6	0 1 11	18	15
0 0 3	7	0	0 2 11	37	38
0 1 3	46	40	0 3 11	5	6
0 2 3	73	64	0 4 11	11	11
0 3 3	19	12	0 5 11	2	3
0 4 3	26	21	0 6 11	6	6
0 5 3	5	6	0 0 12	5	3
0 6 3	7	8	0 1 12	13	11
0 7 3	4	4	0 2 12	10	10
0 0 4	79	88	0 3 12	12	11
0 1 4	40	40	0 4 12	7	8
0 2 4	22	25	0 5 12	6	6
0 3 4	19	12	0 0 13	3	2
0 4 4	24	24	0 1 13	29	30
0 5 4	6	7	0 2 13	3	4
0 6 4	9	12	0 3 13	12	12
0 7 4	1	0	0 4 13	4	3
0 0 5	12	12	0 5 13	4	6
0 1 5	20	20	0 0 14	14	15
0 2 5	37	32	0 1 14	9	9
0 3 5	39	38	0 2 14	15	13
0 4 5	8	7	0 3 14	12	13
0 5 5	9	7	0 4 14	9	9
0 6 5	4	4	0 0 15	23	21
0 7 5	3	4	0 1 15	5	5
0 0 6	43	47	0 2 15	14	15
0 1 6	55	55	0 3 15	1	3
0 2 6	40	38	0 4 15	3	5
0 3 6	19	18	0 0 16	10	10
0 4 6	13	12	0 1 16	10	11
0 5 6	8	7	0 2 16	6	7
0 6 6	7	7	0 3 16	7	8
0 7 6	3	3	0 0 17	7	7
0 0 7	26	27	0 1 17	19	17
0 1 7	26	25			

using the agreement factor $R = \Sigma||F_o|-|F_c||/\Sigma|F_o|$ as a criterion. A ring structure gave the lowest R value ($R = 0.23$). This structure was refined, first by difference syntheses ($R = 0.17$), then by least squares calculations ($R = 0.10$) and finally by two more difference syntheses ($R = 0.08$). In the course of the refinement the contributions from the 15 hydrogen atoms were included, their positions being derived partly from the difference syntheses, partly by stereochemical considerations. Isotropic temperature factors $\exp(-B \sin^2\Theta/\lambda^2)$ with B-values between 1.5 and 3.2 were applied to the lighter atoms whereas for bromine $B = 1.5 + 2.9 \cos^2\varphi$, φ being the angle between the normal to the reflecting plane and the direction of maximum vibration. This direction is approximately perpendicular to the Br—C(9) bond. The atomic scattering factors of Hartree (for bromine) and Berghuis *et al.*[16] (for the lighter atoms) were used.

In the *a* projection, which has no centre of symmetry, the first trial structure was derived from the *b* projection and approximately known bond lengths and angles. The structure was first refined by trial, and then by least squares calculations. Four of the atoms, N(1), C(1), O(5) and C(2), lie so close together in this projection that their positions cannot be refined effectively. The final y coordinates of these atoms were derived by trial and are less accurate than those of the other atoms. The final value of R was 0.10. The contributions from the hydrogen atoms were not included in this projection. The value used for B was 2.3 for the oxygens, 2.6 for the nitrogens, 2.7 for aliphatic carbons, 3.0 for aromatic carbons, and 3.8 for bromine, the latter being the mean value of the anisotropic factor. In Table 3 observed (F_o) and calculated (F_c) values for the structure factors are compared. The final coordinates are given in Table 1, and the corresponding bond lengths and angles in Table 2. The z coordinates are those derived from the *b* projection.

The standard deviations of the atomic coordinates were estimated by the Cruickshank formula [17]. The following values were found: $\sigma(x) = \sigma(z) = 0.012$ Å, $\sigma(y) = 0.035$ Å for the carbon and nitrogen atoms; $\sigma(x) = \sigma(z) = 0.009$ Å, $\sigma(y) = 0.025$ Å for the oxygen atoms. For $\sigma(y)$ the lack of centre of symmetry is taken into account by multiplication by 2. The standard deviations in the bond lengths (apart from C—Br) vary between 0.015 Å (for C(4)—O(4)) and about 0.04 Å (for C(6)—C(11) and C(8)—C(9)). If three times the probable error is taken as a limit of error, the corresponding values for this quantity are 0.03 Å and 0.08 Å. For unresolved atoms the error may be even greater, but for all bonds of known length, such as the C—C bonds, the values derived lie well within those limits. The standard deviation of the angles lies in the range 1.0°– 2.3°.

Financial support from *Norges Almenvitenskapelige Forskningsråd* is gratefully acknowledged.

REFERENCES

1. Percival, E. G. *Advances in Carbohydrate Chem.* **3** (1948) 23.
2. Mester, L. and Major, A. *J. Am. Chem. Soc.* **77** (1955) 4297.
3. Mester, L. and Major, A. *J. Am. Chem. Soc.* **78** (1956) 1403.
4. O'Donnell, J. J. and Percival, E. *J. Chem. Soc.* **1959** 2312.
5. Reeves, R. E. *J. Am. Chem. Soc.* **72** (1950) 1499.
6. Austin, W. C. and Walsh, J. P. *J. Am. Chem. Soc.* **56** (1934) 934.
7. Penny, W. G. and Sutherland, G. B. B. M. *J. Chem. Phys.* **2** (1934) 492.
8. Tomiie, Y., Koo, C. H. and Nitta, I. *Acta Cryst.* **11** (1958) 774.
9. Shintani, R. *Acta Cryst.* **13** (1960) 609.
10. Collin, R. L. and Lipscomb, W. N. *Acta Cryst.* **4** (1951) 10.
11. Beamer, W. H. *J. Am. Chem. Soc.* **70** (1948) 2979.
12. Hordvik, A. *Acta Chem. Scand.* **15** (1961) 16.
13. McGeachin, H. McD. and Beevers, C. A. *Acta Cryst.* **10** (1957) 227.
14. Gafner, G. and Herbstein, F. H. *Acta Cryst.* **13** (1960) 706.
15. Frasson, E., Garbuglio, C. and Silvio, B. *Acta Cryst.* **12** (1959) 126.
16. Berghuis, J., Haanappel, I. M., Potters, M., Loopstra, B. O., MacGillavry, C. H. and Veenendaal, A. L. *Acta Cryst.* **8** (1955) 478.
17. Cruickshank, D. W. J. *Acta Cryst.* **2** (1949) 65.

Received February 13, 1962.

ACTA CHEMICA SCANDINAVICA 16 (1962) 1549–1552

Potentiometric Study of a Synthesis of Phosgenite

R. NÄSÄNEN, P. MERILÄINEN and R. HAVANKA

Department of Chemistry, University of Helsinki, Helsinki, Finland

The stability of phosgenite in contact with an aqueous solution of carbon dioxide was investigated. With this purpose the equilibria $PbCl_2(s) + 0.5\ CO_2(g) + 0.5\ H_2O \rightleftharpoons PbCl(CO_3)_{0.5}(s) + H^+ + Cl^-$ and $PbCl(CO_3)_{0.5}(s) + 0.5\ CO_2(g) + 0.5\ H_2O \rightleftharpoons PbCO_3(s) + H^+ + Cl^-$ at 25°C were studied. The respective equilibrium constants were determined by the pH method. The value $10^{-9.89}$ ($I = 0$; 25°C) was calculated for the solubility product of phosgenite, $PbCl(CO_3)_{0.5}$, from the equilibrium constant of the first reaction and known data for lead chloride and carbonic acid. The value $10^{-9.84}$($I = 0$, 25°C) was obtained for this constant from the equilibrium constant of the second reaction and data for lead carbonate and carbonic acid.

The equilibria of phosgenite, $PbCl(CO_3)_{0.5}$, and lead chloride or lead carbonate in contact with an aqueous solution of carbon dioxide have apparently not been studied before although methods for the preparation of phosgenite were presented long ago [1]. The reaction in question are

$$PbCl_2(s) + 0.5\ CO_2(g) + 0.5\ H_2O \rightleftharpoons PbCl(CO_3)_{0.5}(s) + H^+ + Cl^- \quad (1)$$

and

$$PbCl(CO_3)_{0.5}(s) + 0.5\ CO_2(g) + 0.5\ H_2O \rightleftharpoons PbCO_3(s) + H^+ + Cl^- \quad (2)$$

We have investigated these systems proceeding, for the present, from lead chloride only. The method was as follows. A weighed amount of lead chloride was allowed to stand in water to which a given amount of sodium hydroxide had been added and through which carbon dioxide was passed. The pH of the solution was measured and the solid phase was analyzed after equilibrium was reached. The results of one series of such experiments are shown in Fig. 1 where the logarithm of hydrogen ion concentration is plotted as a function of the mole ratio of sodium hydroxide and lead chloride added to the solution. The curve has two buffer ranges of which the lower one is due to reaction (1) and the higher one to reaction (2). When equimolar amounts of lead chloride and sodium hydroxide were used, the solid phase consisted only of well-formed crystals of phosgenite.

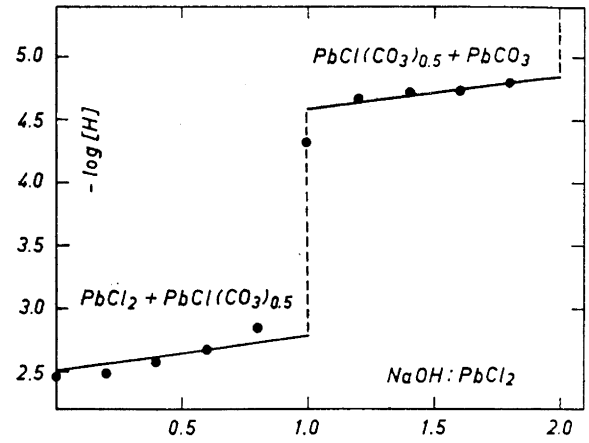

Fig. 1. A plot of $-\log[H]$ against the mole ratio of sodium hydroxide and lead chloride. p_{CO_2} = about 1 atm.

The equilibrium constant of reaction (1)

$$K_p = [H]\ [Cl]/p_{CO_2} \tag{3}$$

can be calculated from experimental values of log [H] and p_{CO_2} referring to the lower buffer range and the calculated value of [Cl]. The last quantity was calculated by iteration from the equation

$$[Cl] = \{2\ K_{sp} + K_{sp}\beta_1\ [Cl] + (c_B + [H])[Cl]^2\}^{1/3} \tag{4}$$

where c_B is the total concentration of added sodium hydroxide, K_{sp} the solubility product of lead chloride and $\beta_1 = [PbCl]/[Pb]\ [Cl]$. The value of K_{sp} for the ionic strength in question was calculated from the equation

$$pK_{sp} = pK^\circ_{sp} - \frac{3.054\ \sqrt{I}}{1 + \alpha\ \sqrt{I}} \tag{5}$$

and the stability constant β_1 from

$$\log\ \beta_1 = \log\ \beta_1^\circ - \frac{2.036\ \sqrt{I}}{1 + \alpha\ \sqrt{I}} \tag{6}$$

Table 1. Computation of the equilibrium constant of reaction (1) at 25°C. p_{CO_2} = 0.976 atm.

$c_B \cdot 10^2$	$-\log[H]$	$\sqrt{I}$	pK_{sp}	$\log \beta_1$	$[Cl] \cdot 10^2$	$[Pb] \cdot 10^2$	$[PbCl] \cdot 10^2$	pK_p	pK°_p
1.920	2.49	0.288	4.17	1.22	6.81	1.46	1.65	3.65	3.84
3.840	2.59	0.298	4.16	1.21	7.81	1.14	1.44	3.68	3.87
5.747	2.68	0.315	4.14	1.20	9.01	0.893	1.27	3.71	3.91
7.667	2.85	0.332	4.12	1.18	10.33	0.711	1.11	3.83	4.03
								Mean	3.91

Table 2. Computation of the equilibrium constant of reaction (2) at 25°C. $p_{CO_2} = 0.967$ atm.; $pS^\circ = 1.464$.

c_B	$\sqrt{I}$	pK_1	pK_2	$-\log[H]$	$[HCO_3]$	[Cl]	pK'_p	pK'^{o}_p
0.115	0.339	6.12	9.88	4.66	0.0011	0.114	5.59	5.79
0.134	0.366	6.11	9.86	4.73	0.0014	0.133	5.59	5.80
0.154	0.392	6.10	9.83	4.73	0.0014	0.153	5.53	5.75
0.173	0.416	6.09	9.82	4.79	0.0017	0.171	5.54	5.78
							Mean	5.78

For pK°_{sp} the value 4.73 (at 25°C) was used. It is the mean of Fromherz's value [2] 4.67 and Nobel and Garrett's value [2] 4.79. For $\log \beta_1^\circ$ the value 1.59 was used. It is the mean of several values ranging from 1.42 to 1.75 taken from the literature [2]. The higher chlorocomplexes were neglected. For the parameter a the value 2 was chosen somewhat arbitrarily. The results relating to the first buffer range are given in Table 1. The ionic strength given in the table was calculated from $I = \frac{1}{2} \Sigma c_i z_i^2$. The values of pK_p were extrapolated to zero ionic strength with the aid of the equation

$$pK^\circ_p = pK_p + \frac{1.018 \sqrt{I}}{1 + a \sqrt{I}} \tag{7}$$

For the parameter a the value 2 was again used.

The equilibrium constant of reaction (2)

$$K'_p = [H]\ [Cl]/p_{CO_2} \tag{8}$$

was computed from experimental values of [H] and p_{CO_2} referring to the higher buffer range of the curve in Fig. 1 and the calculated value of [Cl]. For the calculation of [Cl], the equation

$$[Cl] = c_B - [HCO_3] + 2\ [Pb] + [PbCl] \tag{9}$$

was derived. However, the last two terms on the right-hand side of eqn. (9) can be neglected and also $[HCO_3]$ is only about one per cent of c_B. The values of these terms were calculated from the equations

$$[CO_2] = S p_{CO_2} \tag{10}$$

$$[HCO_3] = K_1[CO_2]/[H] \tag{11}$$

$$[CO_3] = K_2[HCO_3]/[H] \tag{12}$$

$$[Pb] = K'_{sp}/[CO_3] \tag{13}$$

$$[PbCl] = \beta_1[Pb][Cl] \tag{14}$$

where S is the Henry's law constant, K_1 and K_2 the first and second acid dissociation constants of carbonic acid, K'_{sp} the solubility product of lead carbonate and $\beta_1 = [PbCl]/[Pb]\ [Cl]$. The values of the equilibrium constants of carbonic acid were obtained from

$$pK_1 = 6.35 - \frac{1.018\sqrt{I}}{1 + 1.40\sqrt{I}} + 0.055\ I \quad (15)$$

$$pK_2 = 10.33 - \frac{2.036\sqrt{I}}{1 + 1.49\sqrt{I}} + 0.055\ I \quad (16)$$

For the Henry's law constant, the value $S° = 3.44 \times 10^{-2}$ for pure water was used [3]. The value $pK_1^\circ = 6.35$ at zero ionic strength stems from measurements of Harned and Bonner [4] (6.352) and Näsänen [4] (6.349) and the value $pK_2^\circ = 10.33$ from measurements of Harned and Scholes [5]. Näsänen [5] obtained the value 10.32 for the latter constant. The other coefficients in eqns. (15) and (16) were taken from investigations of Näsänen and co-workers [5,6] and the values of the solubility product of lead carbonate from a paper of Näsänen and Meriläinen [6].

The solubility product of phosgenite

$$K_{sp} = [Pb]\ [Cl]\ [CO_3]^{½} \quad (17)$$

can be evaluated from the expression

$$pK_{sp}^\circ = pK_{sp}^\circ(PbCl_2) + 0.5\ pS° + 0.5\ pK_1^\circ + 0.5\ pK_2^\circ - pK_p^\circ \quad (18)$$

as well as from

$$pK_{sp}^\circ = pK_{sp}^\circ(PbCO_3) + pK_p'^\circ - 0.5\ pS° - 0.5\ pK_1^\circ - 0.5\ pK_2^\circ \quad (19)$$

Using the values given above for the constants, we obtained in the first case

$pK_{sp}^\circ = 4.73 + 0.73 + 3.18 + 5.16 - 3.91 = 9.89.$

and in the second case

$pK_{sp}^\circ = 13.13 + 5.78 - 0.73 - 3.18 - 5.16 = 9.84.$

The agreement between these two independent results is thus very good considering the uncertainty of the values of the solubility products of lead chloride and lead carbonate as well as of the values of K_p and K_p'. The extrapolation of K_p and K_p' to zero ionic strength is also somewhat arbitrary. For example, if we use the value 1 instead of 2 for a in eqn. (7), we obtain in the first case $pK_{sp}^\circ = 9.85$ and in the second case $pK_{sp}^\circ = 9.90$. It is obvious that the values originating from the higher buffer range are more accurate. A more thorough study of the equilibrium in this buffer range is in progress.

REFERENCES

1. Mellor, J. W. *A Comprehensive Treatise on Inorganic and Theoretical Chemistry*, London 1930, Vol. 7, p. 852.
2. Bjerrum, J., Schwarzenbach, G. and Sillén, L. G. *Stability Constants of Metal-ion Complexes. Part II: Inorganic Ligands*. London 1958, p. 108.
3. Harned, H. S. and Davis, R. *J. Am. Chem. Soc.* **65** (1943) 2030.
4. Harned, H. S. and Bonner, T. *J. Am. Chem. Soc.* **67** (1945) 1026; Näsänen, R. *Acta Chem. Scand.* **1** (1947) 204.
5. Harned, H. S. and Scholes, S. R. *J. Am. Chem. Soc.* **63** (1941) 1706. Näsänen, R. *Suomen Kemistilehti* **B 19** (1946) 90.
6. Näsänen, R., Meriläinen, P. and Leppänen, K. *Acta Chem. Scand.* **15** (1961) 913.

Received March 8, 1962.

ACTA CHEMICA SCANDINAVICA 16 (1962) 1553–1568

The Chemistry of the Natural Order Cupressales 47 *

The Structures and Absolute Configurations of Widdrol and Widdrol-α-epoxide **

C. ENZELL

Organisk-kemiska institutionen, Kungl. Tekniska Högskolan, Stockholm, Sweden

Widdrol and widdrol-α-epoxide, first isolated from *Widdringtonia* species, are shown to have the structures (3) and (4), respectively.

In 1958 Erdtman and Thomas [1] investigated the heartwood constituents of the species belonging to the South African genus *Widdringtonia*. These trees were found to contain a number of structurally unknown sesquiterpenes, *i.e.* "widdrene" (= thujopsene), [2,3] "widdrene II" (= cuparene) [4], widdrol, "alcohol, $C_{15}H_{26}O_2$, m.p. 154°", "diol, $C_{15}H_{28}O_2$, m.p. 138°" (= selina-4,7-diol) [5], "widdrenic acid" (= hinokiic acid) [2,3], "acid III" (= cuparenic acid) [4], as well as cedrol and eudesmol. Subsequently the structures of all these compounds with the exception of widdrol and the alcohol $C_{15}H_{26}O_2$ have been determined. The elucidation of their structures is the subject of the present paper.

Erdtman and Thomas [1], on the basis of a preliminary investigation, concluded that widdrol was a dicyclic, tertiary sesquiterpene alcohol containing one double bond. They also obtained the unusual 1,7-dimethyl-4-isopropyl naphthalene (1) from the products of the selenium dehydrogenation of widdrol. Recently Nagahama [6] made the important observation that widdrol was formed on attempted acid isomerisation of thujopsene (2) [2,3] with oxalic acid. During the present investigation an epoxidation product of widdrol, widdrol-α-epoxide, was found to be identical with the above alcohol, $C_{15}H_{26}O_2$, isolated from *Widdringtonia juniperoides* [1].

---

* Part 46, *Acta Chem. Scand.* **16** (1962) 1311.

** This structure of widdrol was first reported by H. Erdtman at the Chemical Society Symposium on Terpene Chemistry in London (23.2.1961) *Proc. Chem. Soc.* **1961** 129. Preliminary communication: Enzell, C. *Acta Chem. Scand.* **15** (1961) 1191. Itô, S., Endo, K., Takeshita, H., Nozoe, T. and Stothers, J. B. *Chem. & Ind. London* **1961** 1618, have also arrived at the correct structure for widdrol. Their conclusions were mainly based on spectral data.

Widdrol and widdrol-α-epoxide are assigned the structures (3) and (4), respectively, on the following evidence.

Ozonolysis of widdrol in methylene chloride followed by reduction of the product with lithium aluminium hydride in ether gave a triol (5) together with minor amounts of widdrol-α-epoxide (4). The triol (5) was oxidised under mild conditions to give a hydroxyketoaldehyde (6). This, on treatment with sodium hydroxide in aqueous methanol, gave an octalone (7) and acetaldehyde which were characterised as the 2,4-dinitrophenylhydrazones. The structure of the octalone (7) was established by comparison with synthetic 8,8,10-trimethyl-$\Delta^{1:9}$-2-octalone, recently described in connection with the total synthesis of (±) widdrol [7].

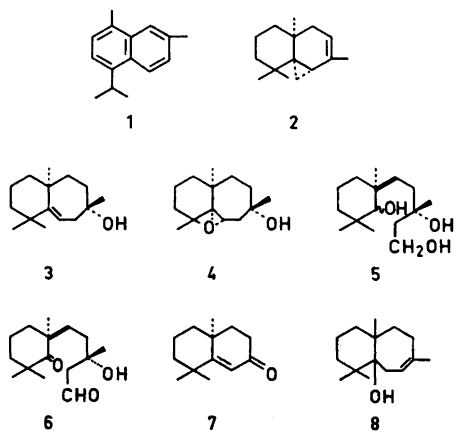

1 2 3 4 5 6 7 8

These results favour structure (3) for widdrol. The alternative structure (8) is excluded by the following reactions. Hydrogenation of widdrol over Adams catalyst in acetic acid gave dihydrowiddrol (9) and a small amount of a hydrocarbon $C_{15}H_{28}$. The latter, probably formed by dehydration and subsequent hydrogenation, is assigned structure (10) of widdrane. Dihydrowiddrol on treatment with acetyl chloride in dimethyl aniline [8], gave the corresponding acetate (11) in good yield. Pyrolysis of the acetate furnished a mixture of unsaturated isomeric hydrocarbons, containing, according to its infrared absorption, minor amounts of the exocyclic isomer. Ozonolysis of the hydrocarbon mixture followed by steam distillation gave a low yield of formaldehyde. The non-volatile material was oxidised with silver oxide to give a ketoacid (12 or 13) as the main product. The ketoacid on oxidation with sodium hypoiodate gave iodoform and the corresponding dicarboxylic acid (14 or 15). These results eliminate structure (8) and widdrol must therefore have structure (3).

The infrared * and mass spectra of widdrol (Figs. 1 and 2) are in good agreement with structure (3). The strongest peak in the mass spectrum of widdrol

* Widdrol in concentrated bromoform or carbon tetrachloride solutions shows a band at 1635 cm^{-1}, attributable to the double bond. The frequency of this band is close to that found for 1,1,10-trimethyl-$\Delta^{8:9}$-octalin (1640 cm^{-1}) and 4,4-dimethylchlolest-5-en-3β-ol (1635 cm^{-1}) but outside the range (1664 – 1672 cm^{-1}) reported for Δ^5-unsaturated steroids [9].

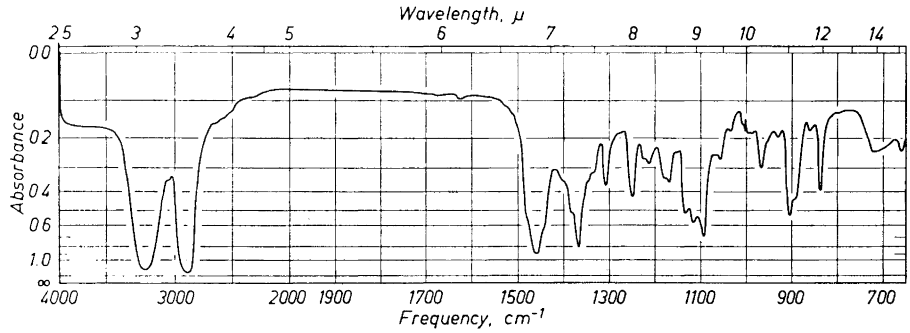

Fig. 1. Infrared spectrum of widdrol (KBr).

occurs at *m/e* 151 and the formation of an ion of this mass number is readily explained since the bonds between C(7) and C(8) and between C(10) and C(11) should be easily cleaved [10]. The resulting ion on uptake of hydrogen would have the required mass number. In agreement with this interpretation the spectrum of dihydrowiddrol exhibits a fairly strong peak at *m/e* 153 corresponding to the cleavage of the same bonds. Similar cleavages have been described in the diterpene series [11]. The proton magnetic resonance spectra of widdrol and many of its derivatives support the structure (3) for widdrol and they will be discussed in a forthcoming publication [12].

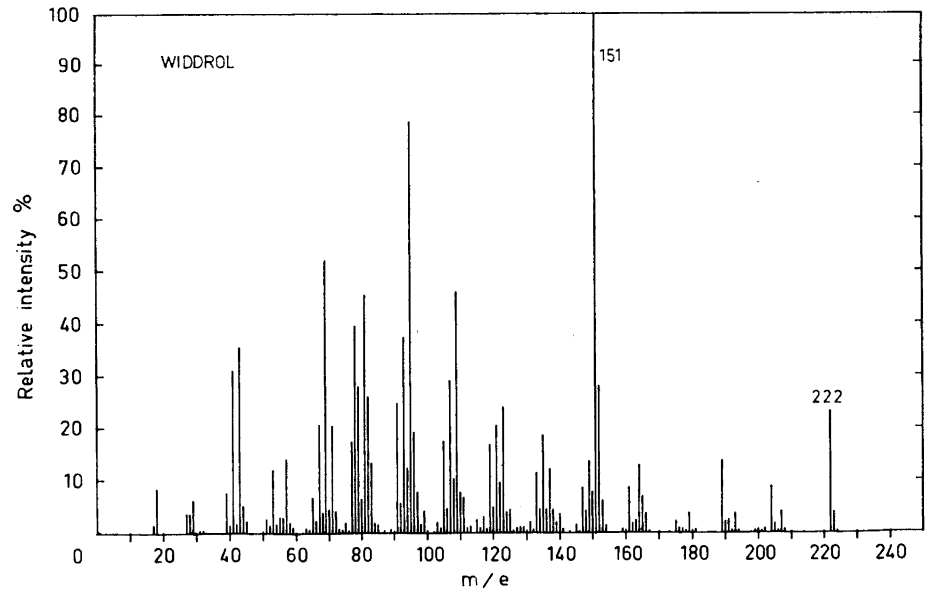

Fig. 2. Mass spectrum of widdrol.

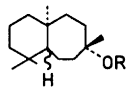

9 (R, H)
11 (R, Ac)

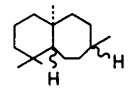

10

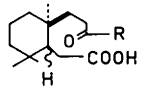

12 (R, CH_3)
14 (R, OH)

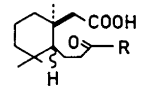

13 (R, CH_3)
15 (R, OH)

The absolute configuration at C(11) in widdrol follows from results obtained by rotatory dispersion measurements, kindly made by Professor W. Klyne. The trimethyl octalone (7) exhibits a positive Cotton effect while 3β-acetoxy-Δ^5-lanosten-7-one (16), 4,4-dimethyl-7-ketocholesteryl acetate (17) and $\Delta^{5,14}$-7-ketoapoeuphadienyl acetate (18), all show negative Cotton effects [13]. Inversions of rotatory dispersion curves of α,β-unsaturated ketones are only known to occur on modification of the adjacent ring to which the α,β-unsaturated carbonyl system is exocyclic [13] whilst modification of the same ring, or of the adjacent ring when the conjugated group is not exocyclic to it, has no major effect [13]. It may therefore be concluded that the octalone (7) has the absolute configuration depicted. Reduction of the octalone (7) with lithium in liquid ammonia gave the decalone (19), which on the basis of the accepted views on the steric course of such reductions is assigned a *trans* ring junction [14]. It exhibits a positive Cotton effect and hence, according to the octant rule [15], the angular methyl group is α-oriented. It therefore follows that the angular methyl group in widdrol is α-oriented.

The conversion [6] of thujopsene (2) into widdrol (3) and the results presented above establish that these compounds have the same configuration at C(11), *i.e.* the angular methyl group in thujopsene is α-oriented. Recent conclusions by Norin [2,16] based on independent evidence confirm this assignment.

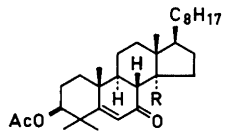

16 (R, CH_3)
17 (R, H)

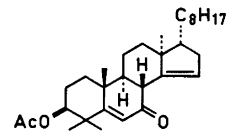

18

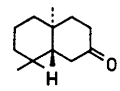

19

The orientations assigned to the hydroxyl group in widdrol (3) and to the 1,2-epoxide group in the naturally occurring widdrol-α-epoxide (4) are based on the following evidence.

Widdrol, on treatment with perphthalic acid in ether, gave widdrol-α-epoxide (4) and widdrol-β-epoxide (20) (ratio 1:2.6), which were readily separated on alumina. Only widdrol-β-epoxide (20) shows an infrared band ($\nu_{max}^{CCl_4}$ 3620 cm^{-1}, *c* 0.005 M) attributable to a non-hydrogen bonded hydroxyl group. This indicates, in agreement with the results given below, that its oxygen atoms are in a *trans*-relationship to each other.

It is known that allylic hydroxyl groups may alter the normal, sterically determined course of epoxidation and this has been attributed to hydrogen bonding of the hydroxyl group with the reagent [17,18]. It appeared possible that a similar effect was responsible for the production of widdrol-α-epoxide and widdrol acetate was therefore oxidised with perphthalic acid. The oxidation product, on treatment with lithium aluminium hydride followed by chromatography, gave, however, both epoxides (4) and (20) but in a lower ratio (1:5.1) than above. It seems that the hydroxyl group has negligible or no *cis*-directing effect and that the introduction of the acetate group only increases the steric hinderance to attack from the α-side.

As mentioned previously ozonisation of widdrol gave widdrol-α-epoxide (4) and the triol (5) (ratio 1:3.5). This result is readily explained by assuming that an attack of ozone from the sterically more hindered side yields the epoxide (4), whereas an attack from the less hindered side gives the normal ozonide. A direct formation of epoxides from sterically hindered olefins is well known [19].

Reduction of widdrol-α-epoxide (4) with lithium in ethylamine gave the 5α,8α-diol (21) and the 6α,8α-diol (22), which were eluted from alumina in this order. Lithium aluminium hydride in tetrahydrofuran gave one product only, the 5α,8α-diol. The 6α,8α-diol (22) is strongly intermolecularly hydrogen bonded as shown by its infrared absorption ($\nu_{max}^{CCl_4}$ 3530 cm^{-1}, *c* 0.0046 M) [20]. This and its chromatographic behaviour show the *cis*-relationship between the two hydroxyl groups in this diol as well as between the two oxygen atoms in the parent compound, widdrol-α-epoxide. Oxidation of the 6α,8α-diol (22) furnished the corresponding hydroxy ketone (23) while the 5α,8α-diol (22) was unaffected.

Widdrol-β-epoxide (20) on reduction with lithium in ethylamine gave the 5β,8α-diol (24) and the 6β,8α-diol (25), which were eluted from alumina in the order mentioned. Attempts to reduce widdrol-β-epoxide with lithium aluminium hydride in tetrahydrofuran gave only starting material. The infrared

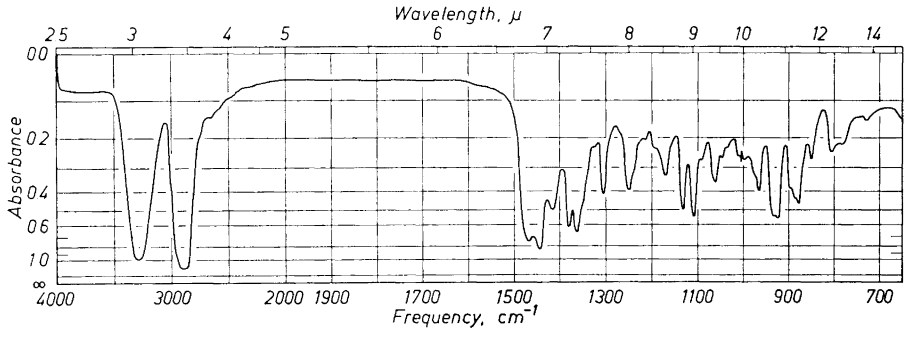

Fig. 3. Infrared spectrum of widdrol-α-epoxide (KBr).

spectrum of the 6β,8α-diol did not exhibit absorption attributable to intramolecular hydrogen bonding. Oxidation of the 6β,8α-diol (25) gave the same hydroxyketone (23) as that obtained from the 6α,8α-diol (22), whereas the 5β,8α-diol (24) was stable to oxidation under similar conditions.

The 6α,8α-diol (22) and the 6β,8α-diol (25) are also obtained on reduction of the hydroxyketone (23) with lithium aluminium hydride and must accordingly have the same configuration at C(5). They are probably the more stable products [14] and are therefore assigned *trans*-fused ring systems by analogy with the more stable isomer of the bicyclo(5,4,0)undecane-2-ones [21]. The difference in reactivity of the two epoxides with lithium aluminium hydride is consistent with the configurations assigned to them, *i.e.* only that epoxide which can be attacked from the sterically less hindered β-side is reduced. Similarly, application of the "benzoate rule" [22] to the difference in molecular rotation ($\Delta[M]_D = +15°$) between the non-hydrogen bonded 6β,8α-diol (25) and its mono-*p*-nitrobenzoate suggests that its secondary hydroxyl group is β-oriented as depicted.

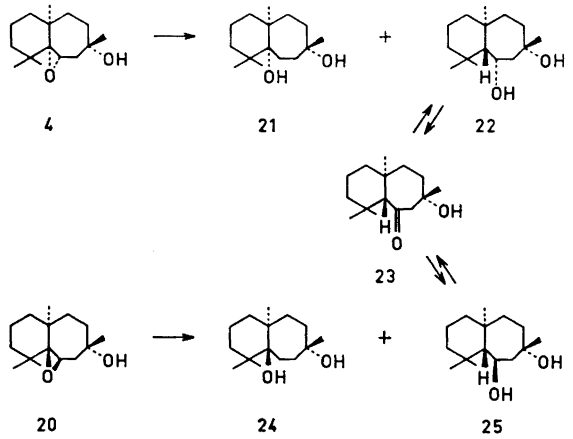

Treatment of widdrol-β-epoxide (20) with aqueous formic acid at room temperature gave the 6β-hydroxyether (26) which may be formed by protonation of the epoxide group and a rear side attack of the hydroxyl group. Oxidation of the hydroxyether gave the corresponding ketoether (27) ($\nu_{max}^{CCl_4}$ 1745 cm^{-1}). Attempts to reduce the ketoether by a modified Wolff-Kishner procedure [23] gave only starting material. Refluxing the ketoether with lithium aluminium hydride in ether for 16 h gave starting material and the 6β-hydroxyether (26) as the main products together with a small amount of the 6α-hydroxyether (28). The preferential formation of the 6β-hydroxyether indicates that reduction takes place mainly by attack from the sterically less hindered side of the ketoether.

The difference in molecular rotation ($\Delta[M]_D = +203°$) between the 6β-hydroxyether and its *p*-nitrobenzoate is consistent with the configuration (26) but not with the alternative (29). The same conclusion is reached on the basis of the negative Cotton effect (*a* −72) * exhibited by the ketoether. A com-

* Amplitudes (*a*) are given as the algebraic difference between [Φ] for peak and through — divided by 100. See Ref.[24]

parison of molecular models (Dreiding) shows that the ether oxygen and C(8) are found in negative octants in structure (27) but in positive octants in the alternative structure (30). Klyne [24] has pointed out that the signs of the Cotton effects shown by cyclopentanones are the same as those of the octants in which are found the atoms of the five-membered ring in the β-position to the carbonyl group, and that this, as well as the large amplitude normally found, is due to "first-order" effects of this ring system. It seems probable that tetrahydrofuranones should exhibit similar effects and that the observed Cotton effect is consistent only with structure (27). Comparison with bicyclo(3,2,1)octan-6-ones gives the same results, *i.e.* the bridge-ring bicyclo(3,2,1)structures of the general type (31), analogous to (27), show negative Cotton effects and those of the enantiomeric type (32), analogous to (30), show positive effects [24].

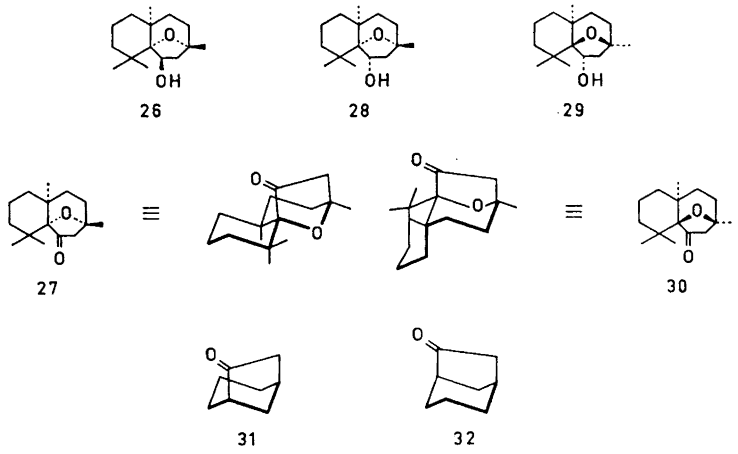

Widdrol-α-epoxide (4) on treatment with boiling water gave two unsaturated diols, which on the basis of their spectral data may be formulated as (33) and (34). In view of the high ionising power of the solvent it seems probable that they are formed *via* a solvated carbonium ion. Oxidation of these diols furnished the corresponding non-conjugated hydroxyketones (35) and (36).

Widdrol was oxidised with osmium tetroxide to give the 5α,6α,8α-triol (37) and the 5β,6β,8α-triol (38). The former structure is assigned to the minor product and the latter structure to the main product (ratio 1:4.5) since the α-side of widdrol should be less readily attacked. In agreement with this the more hindered 5α,6α,8α-triol is not attacked by lead tetracetate [25] and on oxidation with chromium trioxide-sulphuric acid in acetone gives the dihydroxyketone (39), whereas the less hindered 5β,6β,8α-triol yields the hydroxyketoaldehyde (6) with both these reagents. The dihydroxyketone (39) exhibits a negative Cotton effect (a −43) which supports the *cis*-fusion of the rings *.

* The corresponding compound with the rings *trans*-fused has the C(5)-hydroxyl group in a positive octant and would, assuming that its conformation is the same as that of the hydroxyketone (23), be expected to exhibit the same positive Cotton effect as (23) [26].

On treatment with N-bromosuccinimide in aqueous *t*-butyl alcohol widdrol gave a bromoether which is probably formed by attack of bromine from the sterically less hindered side. The bromoether, in agreement with its spectral data, is assigned structure (40). It was possible to reduce this compound to the ether (41) but attempts to convert it to the corresponding hydroxyether failed.

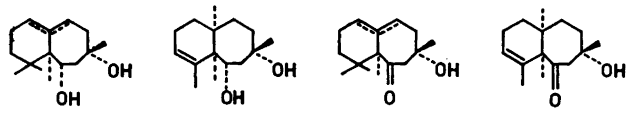

33 34 35 36

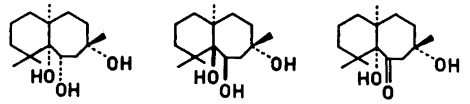

37 38 39



40 (R, Br)
41 (R, H)

42

The conformations of cycloheptane and cycloheptene systems have recently been discussed by several authors [27,28,29]. In those derivatives of widdrol containing a cycloheptane or cycloheptanone ring *trans*-fused to the cyclohexane ring an "all-chair" conformation may be expected to be energetically favoured and this is supported by the positive Cotton effect exhibited by the hydroxyketone (23). Inspection of molecular models indicates that a conformation of widdrol such as that depicted in (42) should be quite rigid. Such a conformation may explain why widdrol on acetylation [8] gives mainly dehydrated material, whereas dihydrowiddrol * gives the corresponding acetate in 92 % yield and why the double bond becomes noticeably less accessible to attack from the α-side in widdrolacetate in comparison to widdrol and, finally, why the mass spectrum of widdrol (Fig. 2) exhibits a parent peak of high intensity (1.85 % of total ion yield) while there is no parent peak in the spectrum of dihydrowiddrol [30].

Erdtman and Thomas [1] obtained a small amount of 1,7-dimethyl-4-isopropyl naphthalene (1), characterised as the picrate, from the selenium dehydrogenation products of widdrol. This result was confirmed and it was found that dehydrogenation with palladium on charcoal gave similar results. Analysis of the dehydrogenation mixture by vapour phase chromatography showed that it consisted of at least nine compounds. It was possible to isolate the naphthalene (1) and to show that one or several of the other compounds were *p*-disubstituted benzene derivatives, since on oxidation with nitric acid the product gave terephthalic acid in low yield. These results show that extensive rearran-

* Dihydrowiddrol should consist largely of the *trans* isomer which, in the more probable of the two "all-chair" conformations has the hydroxyl group "equatorially" oriented.

gements take place during the dehydrogenation of widdrol. The naphthalene (1) has also been isolated from the dehydrogenation products of carotol [31] and thujopsene [3].

Nagahama [6] obtained widdrol on treatment of thujopsene with oxalic acid in aqueous ethanol. In view of the present results it appears probable that this is due to a *trans* diaxial addition of the elements of water to the double bond followed by opening of the three membered ring. Tanka and Yamashita [32] on hydration of thujopsene under mild Bertram-Wahlbaum conditions obtained an alcohol $C_{15}H_{26}O$, m.p. 120—122°, $[\alpha]_D$ + 115°, which may possibly be an intermediate in the isomerisation of thujopsene to widdrol.

In the conifers, widdrol has almost always been found to occur [33] together with cedrene [34,35] cedrol [34], cuparene [4] and thujopsene [2,3]. The corresponding acids, *i.e.* cedrolic acid [36], cuparenic acid [4] and hinokiic acid [2,3] have also been isolated from the same sources.Their co-occurrence and absolute configurations obviously suggest that they arise from a common, properly oriented 2,3-*cis*-farnesyl precursor [37,38]. This will be discussed elsewhere [39].

EXPERIMENTAL

Melting points were determined on a Kofler micro hot stage and are corrected. Infrared spectra were recorded on a Perkin Elmer No 21 instrument (NaCl prism), ultraviolet spectra on a Beckman DK 2 recording spectro-photometer and mass spectra on an instrument [40] with an all glass, heated inlet system (energy of electrons 70 eV). Microanalysis by Dr. A. Bernhardt, Mülheim.

Ozonisation of widdrol (3). Widdrol (1.0 g) in methylene chloride (15 ml) was treated with ozone at −70° until excess ozone was present. Nitrogen was passed through the solution and the solvent removed under reduced pressure at 5—10°. The residue, dissolved in dry ether (20 ml), was added to a stirred suspension of lithium aluminium hydride (0.6 g) in dry ether (100 ml). The reaction mixture was boiled under reflux for one hour, cooled and the excess lithium aluminium hydride destroyed with ethyl acetate. The resulting suspension was acidified and extracted repeatedly with ether. The ether phase gave a residue (1.1 g), which crystallised on treatment with isopropyl ether. Repeated recrystallisation from isopropyl ether gave the triol (5), (0.63 g), m.p. 97—98°, $[\alpha]_D$ −1° ($CHCl_3$, *c* 2.2), (Found C 70.0; H 11.8; O 18.9. $C_{15}H_{30}O_3$ requires C 69.7; H 11.7; O 18.6 %). ν_{max}^{KBr} 3360, 1147, 1062, 1022, 1008 cm^{-1}. Its mass spectrum includes major peaks at *m/e*: 240 (2, *M*-18) *, 225 (10, *M*-18-15), 222 (17, *M*-2 × 18), 207 (14, *M*-2 × 18—15), 204 (7, *M*-3 × 18), 195 (26), 177 (49), 168 (35), 140 (52), 137 (49), 123 (56), 109 (61), 94 (44), 88 (53), 81 (53), 81 (100), 69 (71), 55 (44), 43 (93).

The mother liquors were combined and chromatographed on alumina (neutral, activity III, 30 g). Elution with light petroleum (b.p. 35—60°)-ether (3:1) gave a crystalline material, which on recrystallisation from isopropyl ether gave widdrol-α-epoxide (4), (0.19 g), m.p. and mixed m.p. 156—157°. Infrared spectrum identical with that of widdrol-α-epoxide obtained from perphthalic acid oxidation of widdrol. Elution with ether-ethanol (20:1) gave a further amount (0.04 g) of the triol (5).

Very similar results were obtained when widdrol in methanol was treated with ozone and the solution of the ozonide was added to an aqueous methanolic solution of potassium borohydride.

Trimethyl octalone (7). A solution of chromium trioxide (1.06 g) in water (12 ml) and conc. sulphuric acid (1.8 ml) was added all at once to a stirred solution of the triol (5), (2.0 g) in acetone, which was kept at *ca.* −30°. The reaction mixture was stirred until it reached room temperature (*ca.* 15 min) and then diluted with water (300 ml) and extracted with ether. Work up gave the liquid hydroxyketoaldehyde (6), (1.38 g)

* The figures within brackets give peak intensities as percentages of the strongest peak in the spectrum.

(Found C 70.8; H 9.9. $C_{15}H_{26}O_3$ requires C 70.8; H 10.3). λ_{max}^{EtOH} 301 mμ (*e* 31), $\nu_{max}^{CCl_4}$ 3610; 2720, 1717; 1690 cm^{-1}. Attempts to obtained crystalline derivatives of this compound were unsuccessful.

The hydroxyketoaldehyde (1.2 g) in methanol (p.a., 50 ml) was added to aqueous sodium hydroxide (5 %, 50 ml). This mixture was boiled gently for 3 h under a slow stream of oxygen-free nitrogen and a small amount (*ca.* 10 ml) was removed over a short Vigreux column. The distillate was added to a saturated ethanol solution of 2,4-dinitrophenylhydrazine, which was left for a day and then diluted with water. The resulting crystals were dissolved in benzene and filtered through silica gel. Recrystallisation from ethanol gave acetaldehyde 2,4-dinitrophenylhydrazone (80 mg), m.p. and mixed m.p. 165—167° (decomp.). Infrared spectrum identical with that of authentic material.

The reaction mixture was cooled and steam distilled after addition of water. The distillate (500 ml) was extracted with ether to give an oil (0.66 g), which was chromatographed on alumina (neutral, activity I, 20 g). Elution with light petroleum (b.p. 35—60°)-benzene (5:1) followed by a quick distillation at low pressure gave the trimethyl octalone (7), (0.34 g), n_D^{25} 1.5142, (Found: C 81.1; H 10.4. $C_{13}H_{20}O$ requires C 81.2; H 10.5), λ_{max}^{EtOH} 240 mμ (ε 13 000), $\nu_{max}^{CCl_4}$ 1670, 1597, 1420; 1390, 1380, 1368 cm^{-1}. Rotatory dispersion curve (MeOH): $[\Phi]_{500}$ + 400°, $[\Phi]_{356}$ + 3500°, $[\Phi]_{303}$ −4500°, $[\Phi]_{300}$ −4300°. The mass spectrum includes major peaks at *m/e*: 192, (100, *M*), 177 (17, *M*-15), 164 (49, *M*-28), 149 (69, *M*-28-15), 136 (71), 123 (62), 107 (33), 93 (35), 79 (29), 69 (14), 55 (21), 41 (31), 27 (14), 15 (2). The infrared, ultraviolet and mass spectra were identical with corresponding spectra of 8,8,10-trimethyl-$\Delta^{1:9}$-octalone [7].

The trimethyl octalone (7) 2,4-dinitrophenylhydrazone, m.p. 204—205°, $[\alpha]_D$ + 3° (benzene, *c* 1.0), (Found: C 61.4; H 6.4; N 14.8. $C_{19}H_{24}N_4O_4$ requires C 61.3; H 6.5; N 15.1), λ_{max}^{EtOH} 213 mμ (ε 22 000), 254 mμ (ε 19 000), 298 mμ (ε 12 000), 383 mμ (ε 28 000). Its mass spectrum includes major peaks at m/e: 372 (100, *M*), 357 (29, *M*-15), 302 (17), 287 (14), 267 (12), 183 (7), 175 (9), 159 (22), 147 (10), 131 (14), 119 (18), 105 (33), 91 (46), 79 (29), 69 (20), 55 (25), 41 (30), 18 (16). The infrared, ultraviolet and mass spectra were identical with corresponding spectra of the 2,4-dinitrophenylhydrazone of 8,8,10-trimethyl-$\Delta^{1:9}$-octalone [7].

Trimethyl decalone (19). The trimethyl octalone (7) (350 mg) was dissolved in tetrahydrofuran (7 ml) and added dropwise over 20 min. to a stirred solution of lithium (60 mg) in ammonia (100 ml, distilled over sodium). The solution was stirred for 30 min. Ammonium chloride was added and the ammonia evaporated. The residue was extracted with light petroleum (b.p. 35—60°) and chromatographed on alumina (neutral, activity I, 12 g). Elution with benzene followed by distillation at reduced pressure gave the trimethyl decalone (19) (150 mg), $\nu_{max}^{CCl_4}$ 1707 cm^{-1}. Rotatory dispersion curve (MeOH): $[\Phi]_{500}$ + 550°, $[\Phi]_{313}$ + 1650°, $[\Phi]_{275}$ −1600°, $[\Phi]_{273}$ −1300°. 2,4-Dinitrophenylhydrazone, m.p. 169—184° (slight decomp.), $[\alpha]_D$ + 80° ($CHCl_3$, *c* 0.9), (Found: C 60.7; H 7.1; N 15.1. $C_{19}H_{26}N_4O_4$ requires C 60.9; H 7.0; N 15.0). λ_{max}^{EtOH} 230 mμ (*e* 15 000), 363 mμ (*e* 20 000). Further elution with benzene-ether (20:1) gave starting material (95 mg).

Dihydrowiddrol (9). Widdrol (2.0 g) was hydrogenated at room temperature and atmospheric pressure over Adam's catalyst (180 mg) in acetic acid (20 ml). Hydrogenation ceased after 15 h when 240 ml of hydrogen had been consumed. The catalyst was removed by filtration and the filtrate diluted with water (100 ml), made alkaline and extracted with ether. Removal of the solvent gave a residue (2.0 g), which was chromatographed on alumina (neutral, activity II, 100 g). Elution with light petroleum (b.p. 35—60°) gave the hydrocarbon (10) (0.22 g), n_D^{25} 1.4833, $[\alpha]_D$ + 24° ($CHCl_3$, *c* 5.0), (Found: C 86.6; H 13.3. $C_{15}H_{28}$ requires C 86.5; H 13.5 %). Elution with ether followed by recrystallisation from methanol and sublimation gave dihydrowiddrol (1.6 g), m.p. 54—61°, $[\alpha]_D$ + 51° ($CHCl_3$, *c* 1.1), (Found: C 80.1; H 12.5. $C_{15}H_{28}O$ requires C 80.3; H 12.6 %). The mass spectrum of dihydrowiddrol includes major peaks at *m/e*: 209 (4, *M*-15), 206 (31, *M*-18), 191 (40, *M*-15-18), 178 (20), 163 (22), 153 (33), 137 (33), 123 (90), 109 (92), 95 (100), 83 (55), 69 (69), 55 (57), 41 (62), 29 (18), 18 (13).

Dihydrowiddrol acetate (11). Dihydrowiddrol (1.5 g) was dissolved in dry N-dimethyl aniline (redist.) and acetyl chloride (1.5 ml) was added slowly to the stirred solution. The solution was stirred for 20 h at 40° and the resulting blue solution was diluted with

ether and acidified with ice cold dilute sulphuric acid (5 %). The ether solution was washed with ice-cold dilute sulphuric acid (20 %) and water until neutral, dried and concentrated. The residue (1.77 g) was chromatographed on alumina (neutral, activity I, 100 g) and elution with light petroleum (b.p. 35–60°) gave a small amount (5 mg) of a dehydrated product. Benzene eluted dihydrowiddrol acetate (11), (1.63 g), n_D^{25} 1.4867, $[\alpha]_D$ + 32° ($CHCl_3$, *c* 2.4), (Found: C 76.4; H 11.3. $C_{17}H_{30}O_2$ requires C 76.6; H 11.4), $\nu_{max}^{pure\ oil}$ 1727 cm^{-1}.

Ketoacid (12 or 13). Dihydrowiddrol acetate (0.58 g) was distilled (bath temp. 320°) through a short column (200°) at atmospheric pressure. The distillate, in light petroleum (b.p. 35–60°), was filtered through alumina (neutral, activity I, 50 g) and the filtrate redistilled to give a mixture of hydrocarbons (0.43 g), $\nu_{max}^{pure\ oil}$ 1675, 844; 1643, 885 cm^{-1}. The hydrocarbon mixture in methylene chloride (10 ml) was treated with ozone at −70° until a blue colour persisted and excess ozone was removed by passing through nitrogen. The solution together with the water in the water trap was steam distilled and the distillate collected in an almost saturated aqueous solution of dimedone at 0°. Evaporation of the methylene chloride gave a precipitate, which on recrystallisation from aqueous ethanol gave formaldehyde-dimethon (17 mg), m.p. and mixed m.p. 189–190°. (Negative blank.) The non-volatile part was extracted with ether. The product (0.38 g) was added to a solution of silver nitrate (0.66 g) in water (1 ml). A solution of sodium hydroxide (0.24 g) in water (1 ml) was added and the mixture was stirred for 3 h at 90°, cooled, filtered and washed with ether. The aqueous phase was acidified with dilute sulphuric acid (10 %) and extracted with ether to give a mixture of acids (0.26 g). This was chromatographed on thick, dimethylsulphoxide impregnated paper [41] (2 sheets of Whatman 3 MM, 24 × 36 cm) with ether, saturated with dimethylsulphoxide, as the mobile phase. Ether extraction of the strips gave as the main product the liquid ketoacid (12 or 13) (0.16 g, R_F 0.7), $[\alpha]_D$ −6° ($CHCl_3$, *c* 2.0), (Found: C 71.2; H 10.1. $C_{15}H_{26}O_3$ requires C 70.8; H 10.3), ν_{max}^{CCl} 1700–1715 (broad) cm^{-1}. "Anhydrous 2,4-dinitrophenylhydrazone", m.p. 232–236°, (Found: N 13.5. $C_{21}H_{28}N_4O_5$ requires N 13.5).

Diacid (14 or 15). The ketoacid (140 mg) was dissolved in dilute sodium hydroxide (10 %, 5 ml) and a 10 % solution of iodine in aqueous potassium iodide (20 %) was added dropwise until a slight excess of iodine was present. The reaction mixture was kept at 60° until the iodine colour persisted for 2 min, whereafter it was decolourised by addition of dilute sodium hydroxide (10 %). Addition of water followed by filtration gave iodoform (50 mg), m.p. and mixed m.p. 119–120°. The filtrate, after extraction with ether, was acidified with dilute sulphuric acid (10 %) and extracted with ether. The product (116 mg) was chromatographed on silica gel (20 ml) impregnated with dimethylsulphoxide. Elution with ether, which was almost saturated with dimethylsulphoxide, gave several fractions. Those fractions, which according to paper chromatography contained the diacid, were combined, washed with water and dried. Evaporation of the ether gave the liquid diacid (14 or 15), (95 mg), (Found: C 65.6; H 9.2. $C_{14}H_{24}O_4$ requires C 65.6; H 9.4) $\nu_{max}^{CCl_4}$ 1707 cm^{-1}. Dimethyl ester n_D^{25} 1.4782, $[\alpha]_D$ −2° ($CHCl_3$, *c* 0.9), $\nu_{max}^{CCl_4}$ 1732 cm^{-1}.

Monoperphthalic acid oxidation of widdrol. Widdrol (1.11 g) in dry ether (20 ml) was added to an ethereal solution of monoperphthalic acid (0.2 M, 75 ml) and left for a week at room temperature in a dark place. The solution was washed with aqueous sodium hydroxide (5 %) and water. Evaporation of the solvent gave a crystalline residue (1.21 g), which was chromatographed on alumina (neutral, activity III, 100 g). Elution with benzene gave widdrol-β-epoxide (20), (796 mg, m.p. 95–114°), which after recrystallisation from isopropyl ether had m.p. 120–121°, $[\alpha]_D$ + 36° ($CHCl_3$, *c* 1.0), (Found: C 75.7; H 11.1. $C_{14}H_{24}O_4$ requires C 75.6; H 11.0 %), ν_{max}^{KBr} 1110, 3340, 985, 1258, 1428 cm^{-1}, $\nu_{max}^{CCl_4}$ 3180–3580 (flat), 3620 cm^{-1} (*c* 0.0046 M). Further elution with benzene gave widdrol-α-epoxide (4), (312 mg, m.p. 148–152°), which on recrystallisation from isopropyl ether had m.p. 156–157°, $[\alpha]_D$ −6°, ($CHCl_3$, *c* 1.5), $\nu_{max}^{CCl_4}$ 3180–3600 (flat) cm^{-1} (*c* 0.0050 M).

Widdrol-α-epoxide was identical with the alcohol, $C_{15}H_{26}O$, m.p. 154°, $[\alpha]_D$ −9°, previously obtained from *Widdringtonia dracomontana* [1]. The two compounds had undepressed mixed m.p. 154–155° and identical infrared spectra (Fig. 3).

Both widdrolepoxides (50 mg of each) were recovered unchanged in quantitative yields after treatment overnight at room temperature with chromium trioxide (100 mg) in pyridine (5 ml).

Widdrol acetate. Widdrol (300 mg) was added to a mixture of acetic anhydride (5 ml) and pyridine (5 ml) and the solution left at 20° for three weeks. The reaction mixture was diluted with water (100 ml) and extracted with ether. The product (290 mg) was adsorbed on alumina (neutral, activity II, 12 g). Elution with light petroleum gave a small amount of dehydrated material (14 mg). Elution with light petroleum (b.p. 35—60°)-ether (20:1) gave widdrol acetate (137 mg), n_D^{25} 1.490, $[\alpha]_D$ + 20° ($CHCl_3$, *c* 0.9), $\nu_{max}^{CCl_4}$ 1727 cm^{-1}, (Found: C 77.4; H 10.4; O 12.3. $C_{17}H_{28}O_2$ requires C 77.2; H 10.7; O 12.1). Ether eluted widdrol (114 mg).

Monoperphthalic acid oxidation of widdrol acetate. Widdrol acetate (80 mg) in ether (2 ml) was added to an ethereal solution of monoperphthalic acid (0.6 M, 10 ml) and left for a week at 20° in a dark place. The solution was extracted with aqueous sodium hydroxide (5 %) and water, dried and concentrated to 15 ml. The concentrated solution was stirred with lithium aluminium hydride (200 mg) for 3 h at 20°. The crystalline product (71 mg) was chromatographed on alumina (neutral, activity II, 5 g) to give widdrol-β-epoxide (20), (51 mg) and widdrol-α-epoxide (4), (10 mg) which were identical with authentic material in all respects (mixed m.p. and I.R.).

Reduction of widdrol-α-epoxide (4) with lithium in ethylamine. Lithium (200 mg) and boiling ethylamine (25 ml) were stirred for 10 min. Widdrol-α-epoxide (700 mg) was added and the reaction mixture was stirred for 15 min. Ethanol was added (0.2 ml) and after stirring for an hour excess lithium was destroyed by addition of ammonium chloride. Evaporation of the ethylamine, dilution with water (100 ml) and extraction with ether gave on removal of the solvent a residue (704 mg), which was chromatographed on alumina (neutral, activity II, 50 g). Elution with benzene gave the diol (22), (125 mg), which on recrystallisation from isopropyl ether had m.p. 143—144°, $[\alpha]_D$ + 7° ($CHCl_3$, *c* 0.6), (Found: C 74.8, H 11.4. $C_{15}H_{28}O_2$ requires C 75.0; H 11.7), ν_{max}^{KBr} 896, 1088, 1113, 1160, 3375 cm^{-1}, $\nu_{max}^{CCl_4}$ 3530 cm^{-1} (*c* 0.0045 M). Elution with ether furnished the diol (21), (515 mg), which after recrystallisation from isopropyl ether had m.p. 107—108°, $[\alpha]_D$ + 40° ($CHCl_3$, *c* 0.8), (Found: C 75.1; H 11.9. $C_{15}H_{28}O_2$ requires C 75.0; H 11.7), ν_{max}^{KBr} 917, 1028, 1076, 1110, 1212, 3410, 3475 cm^{-1}.

Reduction of widdrol-β-epoxide (20) with lithium in ethylamine. Lithium (700 mg) and boiling ethylamine (40 ml) were stirred for 20 min. Widdrol-β-epoxide (1.00 g) was added and the mixture stirred for 35 min. After addition of abs. ethanol (0.2 ml) the mixture was stirred for an additional 30 min. before the excess lithium was destroyed with ammonium chloride. The product was worked up according to the above procedure and gave a mixture of diols (960 mg), which was chromatographed on alumina (neutral, activity II, 80 g). Elution with light petroleum (b.p. 35—60°)-ether (10:1) gave the diol (24), (560 mg), which on recrystallisation from isopropyl ether had m.p. 91—92°, $[\alpha]_D$ −33° ($CHCl_3$, *c* 0.9), (Found: C 75.1; H 11.7. $C_{15}H_{28}O_2$ requires C 74.9; H 11.7). ν_{max}^{KBr} 928, 1040, 1136, 3450 cm^{-1}. Elution with ether-ethanol (5:1) gave the diol (25) as a glass (390 mg), $[\alpha]_D$ −2° ($CHCl_3$, *c* 0.9), (Found: C 74.5; H 11.4. $C_{15}H_{28}O_2$ requires C 74.9; H 11.7). $\nu_{max}^{CCl_4}$ 3620 cm^{-1} (*c* 0.005 M). Treatment of this diol with excess *p*-nitrobenzoyl chloride in pyridine for 24 h at room temperature followed by chromatography on alumina and recrystallisation gave a mono *p*-nitrobenzoate, m.p. 135—136°, $[\alpha]_D$ −5° ($CHCl_3$, *c* 0.8), (Found: C 68.2; H 8.2. $C_{22}H_{31}O_5N$ requires C 67.8; H 8.0) and the di *p*-nitrobenzoate, m.p. 195—196°, $[\alpha]_D$ + 112° ($CHCl_3$, *c* 0.9), (Found: N 5.6. $C_{29}H_{34}O_8N_2$ requires N 5.2).

Treatment of the widdrolepoxides with lithium aluminiumhydride. Widdrol-α-epoxide (4), (205 mg) in tetrahydrofuran (15 ml) was refluxed with lithium aluminium hydride (300 mg) for 18 h. The crystalline product (202 mg, m.p. 102—107°), was recrystallised from isopropyl ether to give the diol (21), m.p. and mixed m.p. 107—108°. Identical infrared spectra.

Widdrol-β-epoxide (20) was recovered unchanged after the same treatment.

Both epoxides were recovered unchanged after treatment with lithium aluminium hydride in ether for 12 h at 20°.

Oxidation of diol (22). The diol (50 mg) was oxidised as described for the triol (5). The crystalline product (46 mg, m.p. 80–90°), on recrystallisation from isopropyl ether, gave the hydroketone (23), m.p. 91–92°, $[\alpha]_D$ + 30° ($CHCl_3$, *c* 0.6), (Found: C 75.6; H 10.9. $C_{15}H_{26}O_2$ requires C 75.6; H 11.0). λ_{max}^{EtOH} 309 mμ (36). ν_{max}^{KBr} 1107, 3365: 1700 cm^{-1}, $\nu_{max}^{CCl_4}$ 1106, 3430, 3580; 1700 cm^{-1}. Rotatory dispersion curve (MeOH) $[\Phi]_{596}$ −100°, $[\Phi]_{324}$ + 1230°, $[\Phi]_{310}$ + 50°, $[\Phi]_{279}$ + 1300°, $[\Phi]_{271}$ + 1150°.

The diol (21) was recovered unchanged after the same treatment.

Oxidation of diol (25). The diol (150 mg) was oxidised in the same way as described for the triol (5) except that it was stirred for an additional 30 min at room temperature. The crystalline product (131 mg) was recrystallised to give the hydroxyketone (23), m.p. and mixed m.p. 91–92°. Infrared spectrum identical with that of the hydroxyketone obtained from the diol (22).

The diol (24) was recovered unchanged after the same treatment.

Reduction of hydroxy ketone (23) with lithium aluminium hydride. The hydroxy ketone (185 mg) in ether was added to a suspension of lithium aluminium hydride in ether and refluxed for 3 h. The product (186 mg), was chromatographed on alumina (neutral, activity II, 8 g). Elution with light petroleum (b.p. 35–60°)-ether (5:1) gave the diol (22), (108 mg), m.p. and mixed m.p. 143–144°. Elution with ether gave the diol (25) (73 mg). Infrared spectrum identical with that of authentic material. Di-*p*-nitrobenzoate, m.p. and mixed m.p. 195–196°.

Hydroxyether (26). Widdrol-β-epoxide (20) (100 mg) was added to a solution of formic acid (9 ml) and water (1 ml) and left overnight at room temperature. The solvents were removed by distillation at water pump pressure and the residue was refluxed with a mixture of aqueous potassium hydroxide (40 %, 5 ml) and ethanol (10 ml) for 1 h. Dilution with water (100 ml) followed by extraction with ether gave the hydroxyether (26), (87 mg), which on recrystallisation from light petroleum (b.p. 35–60°) and sublimation had m.p. 99–100°, $[\alpha]_D$ + 7° ($CHCl_3$, *c* 0.9), (Found: 75.5; H 10.8. $C_{15}H_{26}O_2$ requires C 75.6; H 11.0). ν_{max}^{KBr} 1008, 1032, 1084, 1096, 1158, 1267, 3590 cm^{-1}. Its mass spectrum includes major peaks at *m/e*: 238 (9, *M*), 220 (1, *M*-18), 194 (8), 179 (7), 167 (6), 149 (2), 140 (100), 125 (19), 109 (12), 95 (9), 81 (12), 69 (28), 55 (24), 41 (37), 29 (14), 18 (1). *p*-Nitrobenzoate, m.p. 148–149° $[\alpha]_D$ −48° ($CHCl_3$, *c* 1.0), (Found: C 68.4; H 7.6. $C_{22}H_{24}O_5N$ requires C 68.2; H 7.5).

Ketoether (27). The hydroxyether (26), (100 mg) was oxidised as described for the triol (5), and gave the ketoether (27), (94 mg), m.p. 39–40°, $[\alpha]_D$ −71° ($CHCl_3$, *c* 0.9), (Found: C 76.2; H 10.2. $C_{15}H_{26}O_2$ requires C 76.2; H 10.4), ν_{max}^{KBr} 1070, 1125, 1189, 1408, 1745 cm^{-1}, λ_{max}^{EtOH} 219 mμ (ε 402), 305 mμ (ε 34), 315 mμ (ε 42). Rotatory dispersion curve (MeOH) $[\Phi]_{596}$ −100°, $[\Phi]_{323}$ −4000°, $[\Phi]_{292}$ + 3200°, $[\Phi]_{260}$ + 1350°.

Reduction of the ketoether (27) with lithium aluminium hydride. The ketoether (500 mg) and lithium aluminium hydride (750 mg) in dry ether (20 ml) were boiled under reflux for 16 h. The product (455 mg), was chromatographed on alumina (neutral, activity II, 25 g). Elution with light petroleum (b.p. 35–60°) gave starting material (201 mg) and elution with light petroleum-ether (1:1) gave the hydroxyether (26), (124 mg). These compounds were identical in all respects (mixed m.p. and I.R.) with corresponding authentic material. Elution with benzene gave a partly crystalline material (32 mg). Repeated recrystallisation from light petroleum (b.p. 35–60°) followed by sublimation gave a small amount (3 mg) of the hydroxyether (28), m.p. 119–121°. The mass spectrum of this compound was practically identical with that of the hydroxyether (26). The main differences, as expected, were the intensities of certain peaks: *m/e* 238 (1), 194 (2), 179 (4), 169 (1), 125 (43), 95 (55), 18 (31).

Diols (33) and (34). Widdrol-α-epoxide (4), (2.0 g) in distilled water (500 ml) was refluxed for 24 h. Extraction with ether gave a product (2.0 g), which was chromatographed on alumina (neutral, activity III, 60 g). Elution with light petroleum (b.p. 35–60°)-ether (1:1) gave a crystalline product (970 mg) which was recrystallised from isopropyl ether to give the diol (33) m.p. 145–146°, $[\alpha]_D$ + 40° ($CHCl_3$, *c* 0.8) (Found: C 75.4; H 10.9. $C_{15}H_{26}O_2$ requires C 75.6; H 11.0). ν_{max}^{KBr} 870, 1415, 1655; 994, 1095, 1187, 1288, 3250 cm^{-1}, $\nu_{max}^{CCl_4}$ 3490, 3550, 3620 cm^{-1} (*c* 0.0050 M). Elution with ether gave further crystalline material (940 mg), which on recrystallisation from isopropyl ether gave the diol (34), m.p.

124—125°, $[\alpha]_D$ + 31° ($CHCl_3$, *c* 0.9), (Found: C 76.0; H 10.9. $C_{15}H_{26}O_2$ requires C 75.6; H 11.0). ν_{max}^{KBr} 824; 987, 1024, 1120, 1164, 1223, 3340 cm^{-1}, $\nu_{max}^{CCl_4}$ 3530, 3610 cm^{-1} (0.0050 M). The PMR spectra (in $CDCl_3$) of the diol (33) τ 9.13 + 8.87 /2 *s* (6 + 3) CH_3—C(4) and —C(5); 8.80 /*s* (3) CH_3—C(8); 5.89 /2 *d*/ J_{AX} 2.3, J_{BX} 5.8 (1) H_X—C(6); 4.64 /*t* or *m*/ not quite resolved (1) HC=C(11), and of the diol (34) τ 9.17 + 9.00 /2 *s* (3 + 3) CH_3—C(11) and —C(5); 8.81 /*s* (3) CH_3—C(8); 8.34 /*s* (3) CH_3—C(4); 6.21 /2 *d*/ J_{AX} 5.3, J_{BX} 10.3 (1) H_X—C(6); 4.28 /*q*/ *J* 1.5, not quite resolved (1) H—C(3), were determined on a Varian A 60 instrument. Nomenclature, compare Ref.[42]

Hydroxyketones (35) and (36). Oxidation of the diol (33) (35 mg) as described for triol (5), gave the corresponding hydroxyketone (35), (28 mg), m.p. 100—101°, $[\alpha]_D$ + 212° ($CHCl_3$, *c* 0.3), (Found: C 76.2; H 10.2. $C_{15}H_{24}O_2$ requires C 76.2; H 10.2), λ_{max}^{EtOH} 294 mμ (ε 38), $\nu_{max}^{CCl_4}$ 1655, 1686, 3450, 3590 cm^{-1}.

Oxidation of the diol (34) (90 mg), as described for the triol (5), gave the corresponding hydroxyketone (36) (74 mg), m.p. 136—138°, $[\alpha]_D$ + 79° ($CHCl_3$, *c* 1.0), (Found C 76.4; H 10.1. $C_{15}H_{24}O_2$ requires C 76.2; H 10.2). λ_{max}^{EtOH} 294 mμ (ε 45) $\nu_{max}^{CCl_4}$ 1691, 3440, 3580 cm^{-1}.

Triols (37) and (38). Widdrol (2.22 g) and osmium tetroxide (2.54 g) in dry pyridine (25 ml) were left in a dark place for 20 days at 25°. Most of the pyridine was removed *in vacuo* and a mixture of ethanol (30 ml) and benzene (30 ml) was added to the residue followed by mannitol (12 g) and potassium hydroxide (12 g) dissolved in water (30 ml) and ethanol (60 ml). The reaction mixture was boiled under reflux for 7 h, concentrated to 30 ml, and extracted with ether. The highly viscous product (2.48 g), gave, on treatment with a small amount of ether, some crystalline material. This was recrystallised from isopropyl ether to give the triol (37), (0.26 g), m.p. 178—180°, $[\alpha]_D$ + 4° ($CHCl_3$, *c* 1.0), (Found: C 70.3; H 10.9. $C_{15}H_{28}O_3$ requires C 70.3; H 11.0), ν_{max}^{KBr} 973, 1032, 1106, 1177, 1255, 3370 cm^{-1}.

A part (1.65 g) of the combined, concentrated mother liquors was chromatographed on silica gel (300 g). Elution with ether gave the liquid triol (38), (1.43 g), n_D^{25} 1.5179, $[\alpha]_D$ —66° ($CHCl_3$, *c* 1.4), $\nu_{max}^{CCl_4}$ 1048, 1085, 1150, 3440, 3595 cm^{-1}. Further elution with ether gave a small amount (0.13 g) of the crystalline triol (37).

The liquid triol (38), (0.40 g) and *p*-nitrobenzoyl chloride (1.5 g) in dry pyridine (20 ml) were left for 45 h at 20 . The product (0.78 g) was chromatographed on silica gel (50 g). Elution with benzene-ether (4:1) followed by recrystallisation from benzene and ethanol gave the di-*p*-nitrobenzoate (0.38 g), m.p. 176—177°, $[\alpha]_D$ + 48° ($CHCl_3$, *c* 1.1). (Found: C 62.6; H 5.9. $C_{29}H_{34}O_9N_2$ requires C 62.8; H 6.2). Elution with ether followed by recrystallisation from ethanol and isopropyl ether-acetone gave the mono-*p*-nitrobenzoate (0.22 g), m.p. 144—145°, $[\alpha]_D$ + 26° ($CHCl_3$, *c* 0.9). (Found: C 65.2; H 7.8. $C_{22}H_{31}O_6N$ requires C 65.2; H 7.7 %).

Treatment of triols (37) and (38) with lead tetraacetate. Lead tetraacetate (880 mg) was added to the liquid triol (38) (463 mg) in glacial acetic acid (20 ml). After 15 h at 20° glycerine (1 ml) and water (1 ml) were added and the mixture was left for an additional hour. It was diluted with water and extracted with ether to give the hydroxyketoaldehyde (6) (350 mg), exhibiting an infrared spectrum identical with that of the hydroxyketoaldehyde obtained on oxidation of the triol (5).

The crystalline triol (37), on treatment with lead tetraacetate in glacial acid at 20° for 40 h, was recovered unchanged in nearly quantitative yield.

Chromium oxidation of triols (37) and (38). The crystalline triol (37), (100 mg), on oxidation as described for the triol (5), gave a crystalline residue (98 mg), which was recrystallised from isopropyl ether and light petroleum (b.p. 35—60°) to give the dihydroxyketone (39), m.p. 82—83° and 119—120°, $[\alpha]_D$ —47° ($CHCl_3$, *c* 1.0). (Found: C 70.6; H 10.1. $C_{15}H_{26}O_3$ requires C 70.8; H 10.3). λ_{max}^{EtOH} 302 mμ (ε 33), $\nu_{max}^{CCl_4}$ 1048, 1139, 1186, 1280, 1700, 3635 cm^{-1}. Rotatory dispersion curve (MeOH): $[\Phi]_{600}$ —550°, $[\Phi]_{333}$ —2400°, $[\Phi]_{291}$ + 1900°, $[\Phi]_{271}$ + 1300°.

The liquid diol (38) gave, under the same conditions, the hydroxyketoaldehyde (6), exhibiting an infrared spectrum identical with that of the hydroxyketoaldehyde obtained on oxidation of the triol (5).

Bromoether (40). Widdrol (1.54 g) in t-butyl alcohol (20 ml) and water (2 ml) was stirred with N-bromosuccinimide (2.8 g) for 18 h at 20°. The reaction mixture was diluted with water (400 ml) and extracted with light petroleum (b.p. 35—60°). Filtration of the partly crystalline product (2.20 g), gave crystalline material (1.49 g). This was recrystallised from methanol to give the bromoether (40), m.p. 128—129°, $[\alpha]_D$ −26° ($CHCl_3$, *c* 0.8) ν_{max}^{KBr} 1072 cm^{-1}. (Found: C 59.8; H 8.5; Br 26.7. $C_{15}H_{25}OBr$ requires C 59.8; H 8.4, Br 26.5). The same product was also obtained, but in lower yield, on treatment of widdrol in acetic acid with bromine.

Ether (41). Sodium (*ca.* 2 g) was added in pieces to a boiling solution of the bromoether (40), (295 mg) in absolute ethanol (20 ml) over a period of 30 min. The reaction mixture was diluted with water (400 ml) and extracted with light petroleum (b.p. 35—60°). The extract after drying was concentrated and adsorbed on alumina, (neutral, activity I, 13 g). Light petroleum (b.p. 35—60°) eluted the ether (170 mg), which after a quick distillation at low pressure (0.1 mm) had n_D^{25} 1.486, $[\alpha]_D$ + 12° ($CHCl_3$, *c* 0.8), $\nu_{max}^{CCl_4}$ 1045, 1058, 1090 cm^{-1}. (Found: C 80.6; H 11.7. $C_{15}H_{26}O$ requires C 81.0; H 11.8).

Dehydrogenation of widdrol. Widdrol (1 g) was heated at 250—280° for 5 h with palladium on charcoal (10 %, 1 g) in an atmosphere of carbon dioxide. After filtration through alumina the product was distilled to give an oil (0.67 g). This had an ultraviolet spectrum corresponding to the presence of about 30 % of a naphthalene hydrocarbon. Analysis by vapour phase chromatography indicated the presence of 9 compounds. The oil (90 mg) and an ethanolic solution of picric acid gave a crystalline product, which on repeated recrystallisation from ethanol and propanol gave a small amount (12 mg) of the picrate of 1,7-dimethyl-4-isopropylnaphthalene, m.p. and mixed m.p. 90—92°. Oxidation of the oil (230 mg) with aqueous nitric acid (30 %, 24 ml) in a sealed tube overnight at 170° gave a small amount of crystalline material (10 mg). This was esterified with an ethereal solution of diazomethane to give the dimethyl ester of terephthalic acid, m.p. and mixed m.p. 138—140°.

Acknowledgements. I thank Prof. H. Erdtman for his kind interest in this work, Prof. W. Klyne, Westfield College, London, for determining the rotatory dispersion curves and for helpful critisism on their interpretation, Dr. S. Nagahama, Kyushu University, Hakozaki, Fukuoka, for a sample of widdrol, Dr. R. Ryhage, Karolinska Institutet, Stockholm, for the mass spectrometric determinations and Mrs. S. Strand for skilful assistance. Thanks are also due to the *Swedish Technical Research Council* for financial support.

REFERENCES

1. Erdtman, H. and Thomas, B. R. *Acta Chem. Scand.* **12** (1958) 267.
2. Norin, T. *Acta Chem. Scand.* **15** (1961) 1676.
3. Kobayashi, H., Nagahama, S. and Akiyoshi, S. *Bull. Chem. Soc.* Japan **34** (1961) 1123.
4. Enzell, C. and Erdtman, H. *Tetrahedron* **4** (1958) 361.
5. Dolejs, L. and Herout, H. *Collection Czehcoslov. Chem. Communs.* **26** (1961) 2045.
6. Nagahama, S. *Bull. Chem. Soc. Japan* **33** (1960) 1467.
7. Enzell, C. *Tetrahedron Letters* **1962** 185.
8. Ohloff, G. *Helv. Chim. Acta* **41** (1958) 845.
9. Bellamy, L. J. *The Infrared Spectra of Complex Molecules.* London, 1945, p. 33.
10. Beynon, J. H. *Mass Spectrometry and its Application to Organic Chemistry,* Amsterdam 1960, p. 325, 345.
11. Enzell, C. *Acta Chem. Scand.* **15** (1961) 1303.
12. Enzell, C. and Forsén, S. *To be published.*
13. Djerassi, C., Halpern, O., Halpern, V. and Riniker, B. *J. Am. Chem. Soc.* **80** (1958) 4001.
14. Barton, D. H. R. and Morrison, G. A. in Zechmeister, L. *Progress in the Chemistry of Organic Natural Productions,* Springer-Verlag, Wien 1961.
15. Moffitt, W., Woodward, R. B., Moscowitz, A., Klyne, W. and Djerassi, C. *J. Am. Chem. Soc.* **83** (1961) 4013.
16. Norin, T. *To be published.*
17. Henbest, H. B. and Wilson, R. A. L. *J. Chem. Soc.* **1957** 1958.

18. Henbest, H. B., Jackson, W. R., Wilson, R. A. L., Crossley, N. S., Meyers, M. B. and McElhinney, R. S. *Bull. Soc. Chim. France* **1960** 1365.
19. Bailey, P. S. *Chem. Revs.* **58** (1958) 925.
20. Kuhn, L. P. *J. Am. Chem. Soc.* **74** (1952) 2492.
21. Ginsburg, D. and Rosenfelder, W. J. *Tetrahedron* **1** (1957) 1.
22. Brewster, J. H. *Tetrahedron* **13** (1961) 106.
23. Barton, D. H. R., Ives, D. A. J. and Thomas, B. R. *J. Chem. Soc.* **1955** 2056.
24. Klyne, W. *Tetrahedron* **13** (1961) 29.
25. Criegee, R., Büchner, E. and Walther, W. *Ber.* **73** (1940) 571.
26. Djerassi, C. *Optical Rotatory Dispersion*, New York 1960, p. 112.
27. Allinger, N. L. *J. Am. Chem. Soc.* **81** (1959) 5727.
28. Pauncz, R. and Ginsburg, D. *Tetrahedron* **9** (1960) 40.
29. Loewenthal, H. J. E. and Rona, P. *J. Chem. Soc.* **1961** 1429.
30. Bieman, K. and Seibl, J. *J. Am. Chem. Soc.* **81** (1959) 3149.
31. Herout, H., Holub, M., Novotný, L., Šorm, F. and Sýkora, V. *Chem. & Ind. London* **1960** 662.
32. Tanaka, J. and Yamashita, I. *Bull. Osaka Ind. Research Inst.* **9** (1958) 5. From Ref.[6]
33. Erdtman, H. *4th Intern. Congr. Biochem.* Vol. II — Biochemistry of Wood (1958); see also Runeberg, J. *Svensk Kem. Tidskr.* **9** (1961) 465.
34. Stork, G. and Clarke, Jr., F. H. *J. Am. Chem. Soc.* **83** (1961) 3114.
35. Büchi, G. Erickson, R. E., and Wakabayashi, N. *J. Am. Chem. Soc.* **83** (1961) 927.
36. Runeberg, J. *Acta Chem. Scand.* **15** (1961) 945.
37. Hendrickson, J. B. *Tetrahedron* **7** (1959) 82.
38. Ruzicka, L. *Experientia* **9** (1953) 357.
39. Enzell, C. and Norin, T. *To be published.*
40. Ryhage, R. *Arkiv Kemi* **16** (1960) 19.
41. Hammarberg, G. and Wickberg, B. *Acta Chem. Scand.* **14** (1960) 882.
42. Scheidegger, U., Schaffner, K. and Jeger, O. *Helv. Chim. Acta* **45** (1962) 400.

Received April 14, 1962.

ACTA CHEMICA SCANDINAVICA 16 (1962) 1569–1578

Determination of Intrinsic Viscosity of Alginates

ARNE HAUG and OLAV SMIDSRØD

Norwegian Institute of Seaweed Research, N.T.H., Trondheim, Norway

A method for determination of intrinsic viscosity of alginates by extrapolation to zero rate of shear and zero concentration is described, and the importance of the extrapolation to zero rate of shear is discussed. The influence of salts and pH on the viscosity of alginate solutions has been investigated, and the viscosity was found to be independent of pH in the range from 4 to 12. Curves correlating the intrinsic viscosity with the relative viscosity of alginate solution at various concentrations determined at standardized conditions are given. A method for routine determination of intrinsic viscosity without isolation of the alginate by determining the apparent viscosity of the same solution at two different values of rate of shear is described.

From a commercial point of view, the most important property of alginates is their ability to form viscous solutions in water. It is therefore of considerable practical importance to be able to characterize an alginate sample with regard to its ability to form viscous solutions. Most producers describe their products by quoting the viscosity of an aqueous solution containing a certain amount of alginate, usually 0.3 or 1.0 g in 100 ml. In several of the works published about the properties of alginates, the viscosity of an alginate solution containing 0.25 g in 100 ml 0.1 N sodium chloride solution is used for characterizing the samples [1–4].

For scientific purposes it is usual to characterize linear macromolecules by means of the intrinsic viscosity

$$[\eta] = \lim \left(\frac{\eta_r - 1}{c} \right)_{c \to 0}$$

where η_r is the relative viscosity of the polymer solution and c is the concentration, usually given as g per 100 ml. In a number of works the intrinsic viscosity of alginates has been determined. Donnan and Rose [5] investigated a series of alginates varying in intrinsic viscosity from 4.2 to 14.4 (100 ml/g). They reported that dependence of shear stress was only important at viscosities higher than 40 cp. Harkness and Wassermann [6], investigating alginates with intrinsic viscosity in the order of 7 also reported that non-Newtonian

behaviour was only significant at high viscosity and therefore did not affect the intrinsic viscosity. Cook and Smith [7] investigated samples with intrinsic viscosities varying from 3.1 to 17.5. Only the sample with the highest intrinsic viscosity was found to give solutions with non-Newtonian behaviour. Vincent, Goring and Gordon Young [4] prepared alginates from some Canadian brown algae, and found values of intrinsic viscosities varying from 3.6 to 19.2. The influence of rate of shear was not discussed.

Observations in this laboratory [8,9] indicated that non-Newtonian behaviour could be observed at very low concentrations and that intrinsic viscosities, at least above 8—9, determined by extrapolation to zero concentration from measurements carried out at constant shear stress, would be influenced by the shear stress in the measurements.

The purpose of the present paper is to describe a method for the determination of a true intrinsic viscosity of alginate samples by extrapolation to zero rate of shear and zero concentration. The correlation between the intrinsic viscosity and quantities suited for routine determination is given.

As some confusion seems to exist in the literature concerning the effect of pH on the viscosity of alginates, an investigation of this effect and the influence of salts was necessary in order to find suitable conditions for the intrinsic viscosity measurements, and in order to compare the results given in the literature.

EXPERIMENTAL

The sampling of seaweeds and the preparation of alginate have been described earlier [10]. When alginic acid of low molecular weight was desired, the weed, after the usual extraction with dilute acid, was suspended in 1 N H_2SO_4 and maintained at 60°C for a certain time before the usual alkali extraction. The water content of the alginate samples was determined by heating in an oven at 105°C for 6 h, and the intrinsic viscosities are calculated on the basis of dry sodium alginate. All other results are calculated on the basis of sodium alginate containing 90 ± 1 % dry matter.

Solutions were prepared by adding alginate to water and shaking the solution in a slow moving shaker for 15—20 h. After the alginate was completely dissolved, the desired amount of inorganic salt was added and the solution stirred one hour before the measurements.

Five different viscometers were used: Ubbelohde Viscometer No. 1 ($k = 0.00999$) and No. 2 ($k = 0.1001$) (Jena Glas, Mainz), a Wagner-Russell Viscometer [11], Höppler Visco-Waage [8] (glass ball, diameter 99.15 % of tube diameter) and a Höppler Viscometer (glass ball No. 2, diameter 98.00 % of tube diameter). The Ubbelohde viscometers were calibrated at the factory, and the other viscometers were calibrated against the Ubbelohde intruments by means of glycerol-water solutions. All results obtained in the capillary viscometers were corrected for kinetic energy according to the Hagenbach-Couette equation. All viscosity determinations were carried out at 20°C.

A Beckman Zeromatic pH meter, furnished with a glass electrode, was used for pH determinations.

The uronic acid composition of alginates was determined by chromatography of the hydrolysates of alginate samples on an anion exchange column [12] and determination of the amounts of the separated uronic acids by a colour reaction. The detailed procedure will be published later.

RESULTS

The effect of addition of sodium chloride, sodium sulphate and sodium carbonate to a solution of sodium alginate in water is shown in Fig. 1.

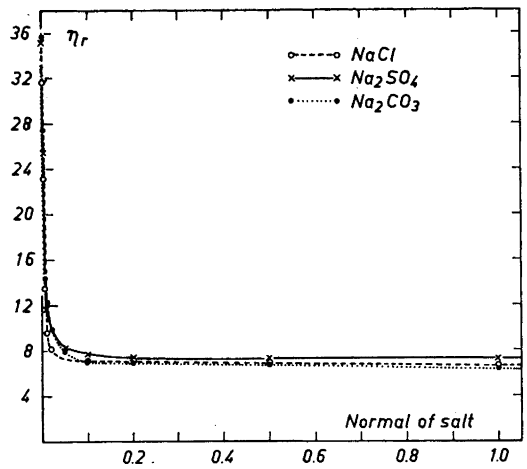

Fig. 1. The relative viscosity of a 0.125 % solution of sodium alginate (*L. digitata*, Munkaunet, 14/2−61, $[\eta] = 27$) containing varying amounts of NaCl, Na_2CO_3 and Na_2SO_4 (Ubbelohde No. 2).

Table 1. The relative viscosity of a 0.125 % solution of sodium alginate (*Laminaria digitata*, Munkaunet, 14/2−61, $[\eta] = 27$) containing potassium and sodium salts in a concentration of 0.25 N (Ubbelohde No. 2).

Salt	pH	η_r
NaCl	7.0	6.96
Na_2CO_3	11.2	6.87
KCl	6.4	6.88
KI	6.3	6.85
KBr	6.3	6.70
KNO_3	6.3	7.17
K_2CO_3	11.1	6.89
K_2SO_4	7.5	7.01
K_3PO_4	11.9	6.46
Na-acetate	8.6	6.70
KH-phthalate	4.0	6.70
Na_3-citrate	7.3	7.25
Dist. water	6.9	31.99

Table 2. The relative viscosity of 0.1 % solution of sodium alginate (*Laminaria digitata*, Munkaunet, 14/2−61, $[\eta] = 27$) at various pH values. (Ubbelohde No. 2).

pH	Ionic strength	η_r	
4.95	0.04	5.68	
6.05	0.06	5.69	Phos-
7.00	0.11	5.56	phates
8.21	0.15	5.48	
8.90	0.15	5.37	Glycine,
9.90	0.15	5.36	NaOH,
11.00	0.15	5.47	KCl
12.00	0.15	5.46	

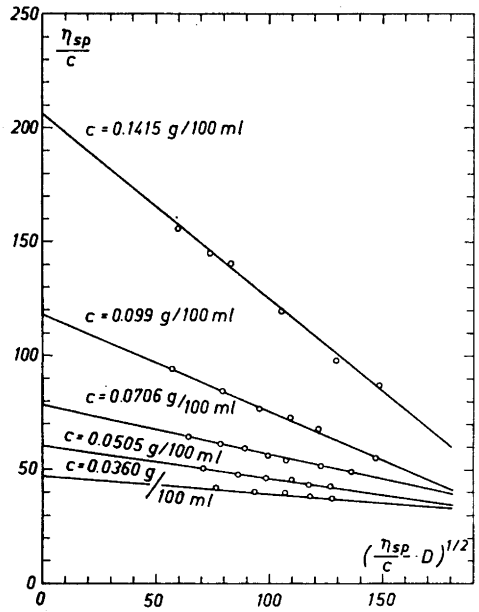

Fig. 2. Extrapolation to zero rate of shear, according to Golub, for sodium alginate from *L. digitata*, Tarva, 3/7—1957 ($[\eta] = 30.0$).

The relative viscosity of solutions of sodium alginate containing various sodium and potassium salts in a concentration of 0.25 N is given in Table 1.

In Table 2 the relative viscosity of sodium alginate solutions at pH values varying from 5 to 12 is shown. The pH of the solutions was adjusted with phosphate or glycine buffers. Potassium chloride was added to the glycine buffer to obtain an ionic strength of approximately 0.15.

For the determination of intrinsic viscosity, 3% (0.565 N) sodium carbonate was chosen as a solvent, and the measurements were carried out in the Wagner-Russell viscometer. As rate of shear (D) the maximum value, at the capillary wall, was used, and calculated according to the formula [13]

$$D = \frac{4\ V}{\pi R^3 t}$$

where V is the volume of the solution passed through the capillary with radius R in the time t. In order to extrapolate to zero rate of shear, the values of the reduced viscosity, η_{sp}/c, were plotted against

$$\left[\left(\frac{\eta_{sp}}{c}\right) \cdot D\right]^{\frac{1}{2}}$$

according to Golub [14]. In Fig. 2 this is shown for five concentrations of a sodium alginate sample with intrinsic viscosity 30 prepared from *Laminaria digitata*. Assuming the curves to be linear over the whole range to $D = 0$, the values of

$$\left(\frac{\eta_{sp}}{c}\right)_{D=0}$$

were determined by extrapolation.

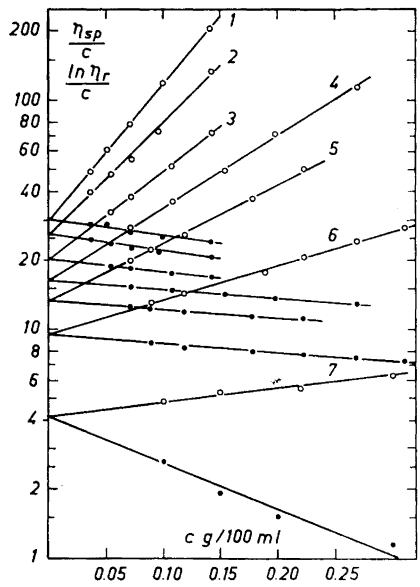

Fig. 3. Extrapolation to zero concentration of η_{sp}/c and $(\ln \eta_r)/c$ for 7 different alginate samples.

1)	*L. digitata*, Tarva, 3/7—57	$[\eta]$: 30.0
2)	» » Kråkvågøy, 3/7—57	$[\eta]$: 26.0
3)	» » Espevær, 8/1—53	$[\eta]$: 20.1
4)	*L. hyperborea* stipes, Hustad, 12/2—59	$[\eta]$: 16.35
5)	*L. digitata*, Munkaunet, 16/3—61 *	$[\eta]$: 13.35
6)	» » » 14/2—61 *	$[\eta]$: 9.6
7)	» » » 14/2—61 *	$[\eta]$: 4.2

* Treated with 1 N H_2SO_4 at 60°C.

The intrinsic viscosity of alginate samples was determined by extrapolation to zero concentration of the curves of

$$\left(\frac{\eta_{sp}}{c}\right)_{D=0}$$

plotted against concentration in a semilogarithmic scale. To facilitate the extrapolation the values of $[(\ln \eta_r)/c]_{D=0}$ were plotted in the same graph. The two expressions extrapolate to the same point at zero concentration. In Fig. 3 the extrapolation to zero concentration is shown for seven different alginate samples.

The importance of extrapolating to zero rate of shear is illustrated in Figs. 4 and 5, which show the extrapolation of η_{sp}/c and $(\ln \eta_r)/c$ for different constant values of rate of shear and shear stress (τ) respectively, for the same alginate sample used for the determinations shown in Fig. 2. The curves for constant rate of shear were determined by interpolation of curves where

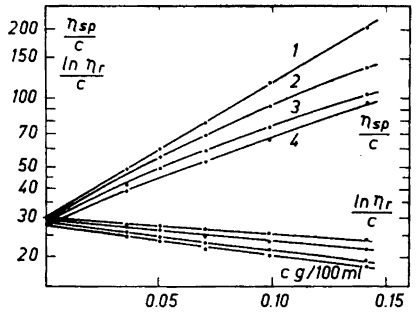

Fig. 4. Extrapolation to zero concentration of η_{sp}/c and $(\ln \eta_r)/c$ for sodium alginate from *L. digitata*, Tarva, 3/7 – 1957 ($[\eta] = 30.0$) for different constant values of rate of shear.

1: $D = 0$ sec^{-1}, $\tau = 0$ dyn/cm^2
2: $D = 40$ » $850 > \tau > 120$ »
3: $D = 140$ » $2200 > \tau > 220$ »
4: $D = 260$ » $3400 > \tau > 400$ »

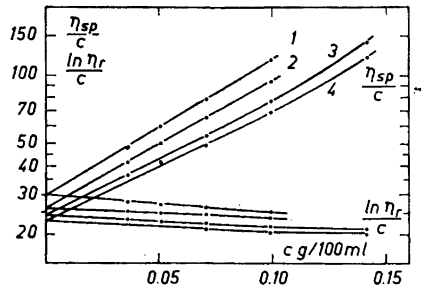

Fig. 5. Extrapolation to zero concentration of η_{sp}/c and $(\ln \eta_r)/c$ for sodium alginate from *L. digitata*, Tarva, 3/7 – 1957 ($[\eta] = 30.0$) for different constant values of shear stress.

1: $\tau = 0$ dyn/cm^2, $D = 0$ sec^{-1}
2: $\tau = 355$ » $140 > D > 35$ »
3: $\tau = 1024$ » $440 > D > 50$ »
4: $\tau = 1682$ » $380 > D > 100$ »

η_{sp}/c was plotted as a function of D (see Ref. 9, p. 21). The same solutions as used for the determination of Fig. 3 were measured in a Höppler viscometer, and the "apparent intrinsic viscosities", $[\eta]_H$, determined by extrapolation.

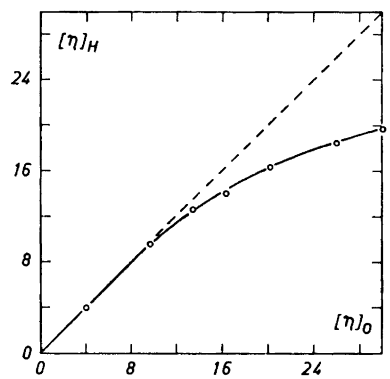

Fig. 6. The relation between the "apparent intrinsic viscosity" $[\eta]_H$ determined from measurements in a Höppler viscometer and $[\eta]_{D=0}$ determined by extrapolation to zero rate of shear.

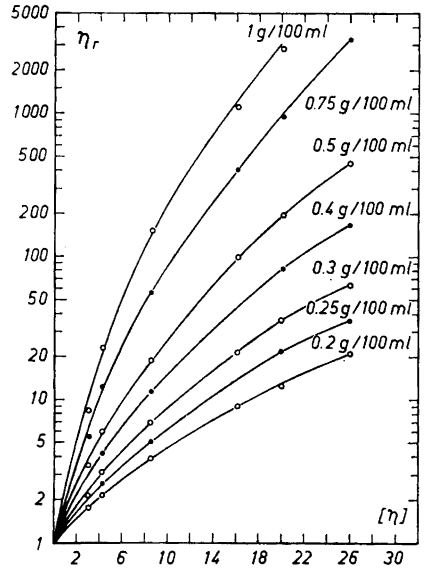

Fig. 7. Viscosity of alginate solutions of varying concentrations in 0.1 N NaCl for samples with different values of intrinsic viscosity (Ubbelohde No. 2).

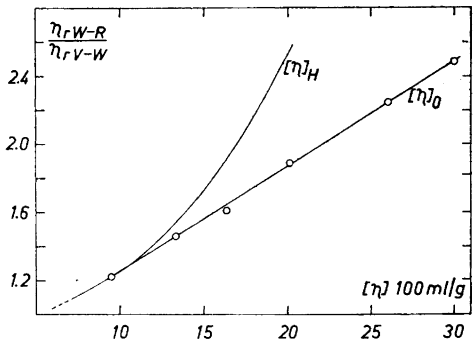

Fig. 8. The quotient between the apparent viscosities determined in the Wagner-Russell viscometer at the lowest rate of shear and in Höppler Visco-Waage with 10 g load as a function of $[\eta]_{D=0}$ and $[\eta]_H$.

Fig. 6 gives the relation between $[\eta]_H$ and intrinsic viscosity determined by extrapolation to zero rate of shear, $[\eta]_{D=0}$.

The correlation between the intrinsic viscosity and the relative viscosity of solutions of various concentrations in 0.1 N sodium chloride measured with Ubbelohde viscometer No. 2 is given in Fig. 7.

The non-Newtonian behaviour of alginate solutions is most pronounced at high values of intrinsic viscosity [8]. The quotient between the apparent viscosities of an alginate solution determined in two viscometers with different rate of shear may, therefore, empirically be correlated to the intrinsic viscosity of the alginate sample. Alginate solutions in 3 % sodium carbonate were adjusted by dilution to an apparent relative viscosity between 4.8 and 5.2, measured in Höppler Visco-Waage with 10 g load. The apparent viscosity of the same solution was then determined in the Wagner-Russell viscometer at the lowest shear stress. The quotient between the two apparent viscosities $\eta_{r\ W-R}/\eta_{r\ V-W}$ as a function of the intrinsic viscosity is shown in Fig. 8. The same quotient as a function of the "apparent intrinsic viscosity", $[\eta]_H$, determined from measurements in the Höppler viscometer is given in the same figure.

Table 3 gives the intrinsic viscosities of some commercial alginates, and some laboratory preparations.

Table 3.

	$[\eta]$
Ascophyllum nodosum, 17/3—57, Leangen	12.5
» » 3/7—57, Tarva	10.5
Laminaria hyperborea, fronds, 26/8, Munkholmen	19.0
» » stipes, 26/8, »	18.4
» » fronds, 24/8, »	13.2
» » stipes, 24/8, »	16.8
Laminaria digitata f. *flexicaulis*, 12/4, Flak	27.7
» » broad fronds, 12/4, »	20.0
Protanal /LF (*Laminaria digitata*)	8.8
» /HF » »	14.0
Manucol SS/LM (*Laminaria hyperborea* stipes)	10.5
» SH/LM (*Ascophyllum nodosum*)	9.6
Noraltex MV (*Laminaria digitata*)	7.9
Kelco SS (*Macrocystis pyrifera*)	10.0

DISCUSSION

Polyelectrolytes dissolved in water give solutions which show a marked drop in viscosity by addition of salts, and at the same time the curves of η_{sp}/c *versus* concentration changes to the shape normal for solutions of uncharged macromolecules.

In pure water at low concentrations the values of η_{sp}/c increase with decreasing concentration [15]. Alginate solutions have previously been shown to behave as typical polyelectrolyte solutions in this respect [8]. The very pronounced effect of addition of small amounts of inorganic salt shown in Fig. 1 should be taken into account when one wants to compare the viscosity of alginate samples. A difference between the viscosity of solutions of two different alginates in water may thus be caused by different amounts of salts as impurities in the two samples, and not by a difference in molecular weight. Determination of viscosity of solutions of alginate in water is, therefore, not suited for characterizing alginate samples. It may be mentioned, however, that the effect of salts is most pronounced at low concentrations of alginate. When the concentration of alginate is increased, the ionic strength increases, and at a sufficiently high alginate concentration (approximately 3 %) an additional increase in ionic strength due to addition of inorganic salt to the solution will have little or no effect on the viscosity.

Harkness and Wassermann [6] and Thiele and Hallich [16] discussed the effect of the addition of different sodium salts on the viscosity of alginate solutions, and claimed that the decrease of viscosity depends on the anion of the sodium salt. As shown in Table 1 some difference between the different salts has been observed. The effect, however, is not very marked. It should be noted that all values of intrinsic viscosity given in this paper refer to 3 % (0.565 N) sodium carbonate solutions. Referring to Fig. 1 and Table 1, it seems that the differences between the intrinsic viscosities in different salt solutions may be disregarded for most practical purposes, provided the amounts of salts are sufficient to reach the horizontal part of the curves in Fig. 1. For one of the samples used for the determination shown in Fig. 3 ($[\eta] = 26.0$), the intrinsic viscosity was also determined in 0.1 N sodium chloride solution, in the way described above. No significant difference between the intrinsic viscosity in 0.1 N sodium chloride solution and 3 % sodium carbonate solution could be observed.

Heen [17] and Bollinger and Münzel [18] claim that the viscosity of alginate solutions has a maximum at pH 7, while Donnan and Rose [5] found that the viscosity was independent of the pH of the solution between pH 6 and 8. Our results, given in Tables 1 and 2, show that the viscosity is independent of pH between pH 4 and 12, and the drop in viscosity observed by Heen and Bollinger and Münzel is probably an effect of increased ionic strength.

The extrapolation method of Golub [14] is derived from a formula of Bueche [19]:

$$\frac{\eta_{sp}}{c} = \left(\frac{\eta_{sp}}{c}\right)_{D=0} \cdot \left[1 - k\left(\frac{\eta_{sp}}{c} \cdot D\right)^{\frac{1}{2}}\right]$$

Golub investigated solutions of rubber in acetone at values of shear rate down to 1 sec^{-1} and found that this formula was in good agreement with the experi-

mental results. As shown in Fig. 2, our results for alginate solutions, plotted according to Golub, gave straight lines in the range of shear rates investigated (20—550 sec^{-1}). Even if the assumption that the formula is valid to zero rate of shear should not be correct, the extrapolation is well-defined and reproducible, and leads to values of intrinsic viscosity that are independent of the viscometer used for the measurements. Of the seven samples described in Fig. 3, only the one with the lowest intrinsic viscosity, $[\eta] = 4.2$, gave solutions which were found to be independent of rate of shear in the range investigated in this work.

The two expressions η_{sp}/c and $(\ln \eta_r)/c$, plotted against concentration on a semilogarithmic scale, give straight lines at low concentrations, as shown in Fig. 3. The extrapolation shown in Fig. 5, at different constant values of shear stress, corresponds to determinations of intrinsic viscosity in the conventional way, using capillary viscometers. The range of shear stress shown in Fig. 5 is very narrow and not outside those employed in ordinary laboratory viscometers of Ostwald or Ubbelohde types. As may be seen from Fig. 6, the values of "apparent intrinsic viscosity", determined from measurements in the Höppler viscometer differ significantly from those determined by extrapolation to zero shear rates for values of intrinsic viscosity higher than 10. It may be noted that the Höppler viscometer has been supposed to give values of apparent viscosity corresponding to zero rate of shear [20].

Extrapolations at constant rate of shear, shown in Fig. 4, gave considerably higher values of "apparent intrinsic viscosity" than extrapolations at constant shear stress. This has earlier been shown to be the case for measurements made in Höppler Visco-Waage [8]. Instruments where the rate of shear is kept constant when measuring a series of solutions with varying polymer concentration, such as rotating cylinder viscometers, will, other conditions being equal, give values more close to the intrinsic viscosity at zero shear rate, than instruments of the capillary or falling ball type where the shear stress is kept constant. This will be the case for all solutions where the viscosity decreases with increasing rate of shear, according to the formula $\eta = \tau/D$.

The determination of intrinsic viscosity by extrapolation to zero rate of shear and zero concentration is a time-consuming process, and not possible to use for routine determinations. It is, however, possible empirically to correlate the intrinsic viscosity, determined as described above, with viscosity measurements carried out at well defined conditions (*e.g.* 0.3 % sodium alginate in 0.1 N sodium chloride solution, measured in Ubbelohde Viscometer No. 2 at 20°C). Correlation curves of this type, for several concentrations of alginate, are given in Fig. 7.

Another method, well suited for routine work, is to measure the apparent viscosity at two different values of rate of shear, and correlate the quotient of the two results with the intrinsic viscosity, as shown in Fig. 8. The solutions must be adjusted by dilution to a certain viscosity in one of the viscometers. This method can only be used for alginates with intrinsic viscosity over a certain value (with the set of instruments used in our laboratory higher than 7), but has the advantage of being independent of the concentration of alginate in the solution. We have in our laboratory found this method very useful, particularly for comparing different raw materials. The intrinsic viscosity can

be determined directly in the sodium carbonate extract, without isolation of the alginate.

Recent investigations have shown that the uronic acid composition of alginates from *Laminaria digitata* and *Laminaria hyperborea* stipes is appreciably different[21]. One of the samples used for the determination of the curve in Fig. 8 was prepared from *Laminaria hyperborea* stipes and the proportion between mannuronic and guluronic acid residues was approximately 0.6. The other samples were all prepared from *Laminaria digitata*, and the proportion between the two different uronic acid residues was approximately 2.5. As the result for the sample with much guluronic acid ($[\eta]$: 16.35) does not deviate from the curve, it may be concluded that the non-Newtonian behaviour of alginate solutions does not depend on the uronic acid composition of the alginate.

REFERENCES

1. Black, W. A. P. and Woodward, F. N. *Advances in Chem. Ser.* **11** (1954) 83.
2. Black, W. A. P., Cornhill, W. J. and Dewar, E. T. *J. Sci. Food Agr.* **3** (1952) 542.
3. Vincent, D. L., Goring, D. A. L. and Gordon Young, E. *J. Appl. Chem. (London)* **5** (1955) 374.
4. Vincent, D. L. *Can. J. Technol.* **34** (1956) 220.
5. Donnan, F. G. and Rose, R. C. *Can. J. Research* **28 B** (1950) 105.
6. Harkness, M. L. R. and Wassermann, A. *J. Chem. Soc.* **1952** 497.
7. Cook, W. H. and Smith, D. B. *Can. J. Biochem. and Physiol.* **32** (1954) 227.
8. Haug, A. *Report No. 8*, Norwegian Institute of Seaweed Research. Oslo 1955.
9. Haug, A. *Viscosity of Alginate Solutions.* In *Report No. 20*, Norwegian Institute of Seaweed Research, Trondheim 1958.
10. Haug, A. *Acta Chem. Scand.* **13** (1959) 601.
11. Wagner, R. H. and Russell, J. *Anal. Chem.* **20** (1948) 151.
12. Larsen, B. and Haug, A. *Acta Chem. Scand.* **15** (1961) 1397.
13. Wilson, K. *Svensk Papperstidn.* **54** (1951) 195.
14. Golub, M. A. *Can. J. Chem.* **35** (1957) 381.
15. Fuoss, R. M. and Strauss, U. P. *J. Polymer. Sci.* **3** (1948) 246.
16. Thiele, H. and Hallich, K. *Z. Naturforsch.* **13 B** (1958) 580.
17. Heen, E. *Kolloid-Z.* **83** (1938) 204.
18. Bollinger, R. and Münzel, K. *Pharm. Acta Helv.* **33** (1958) 225.
19. Bueche, F. *J. Chem. Phys.* **22** (1954) 1570.
20. Schurz, J., Streitig, H. and Wurz, E. *Monatsh.* **87** (1956) 520.
21. Haug, A. *Colloques Internationaux du C.N.R.S.*, No. 103, Dinard 1960, p. 163. Paris 1961.

Received February 23, 1962.

ACTA CHEMICA SCANDINAVICA 16 (1962) 1579–1585

Fractionation of Gelatins with Carboxymethyl Cellulose

E. KULONEN, U. K. VIRTANEN and A. SALMENPERÄ

Department of Medical Chemistry, University of Turku, Turku 3, Finland

Commercial gelatins could be divided into 2 fractions using carboxymethyl cellulose columns which were eluted with various salt strength gradients. The pattern varied according to the history of the gelatin preparation. Analogous experiments with carboxymethyl cellulose papers are also described.

We have earlier described fractionations of commercial gelatins with a cation exchange resin [1] and wished to confirm the findings with a corresponding cation exchange cellulose. Preliminary experiments were carried out on CM-cellulose paper but we could not apply directly the conditions of exchange resin fractionation. It was found instead that with salt solutions the gelatins could be eluted in fractions from the CM-cellulose and this finding was applied to columns. This final phase of the work is related to the experiments of Kessler, Rosen and Levenson [2], who studied acetic acid-solubilized rat tail tendon collagens, and to the work by Piez, Weiss and Lewis [3] on mildly denatured skin collagens.

EXPERIMENTAL

Materials. The carboxymethyl celluloses (referred to here as CM-celluloses) were Whatman products, purchased from H. Reeve Angel & Co. Ltd., London. The powder was labelled "Cation Exchanger Carboxymethylcellulose Powder CM 70" and supplied in sodium form. Two experimental batches of paper (designated CM 50) were used. Even if their ion-binding capacity was reportedly the same, they differed considerably (see Fig. 4). At present the reason for this variation is unknown to us. The manufacturers also informed us that ". . there are subtle differences in the behaviour of different batches . . . ."

The gelatin samples I, II and IV were obtained from commercial sources, III was a laboratory preparation according to Jackson [4], V—IX were specially prepared by Kind & Knox Gelatin Company (Camden, New Jersey, U.S.A.). The preparations III—IX are the same as those used earlier [1] by us. The present designations I and II correspond to II and I, respectively. The pI was determined as the pH of the solution which had passed through a "mixed-bed resin" column [5].

I. clear, strong jelly, prepared from "cartilage and good bones", pI 5.2;
II. turbid (clear when heated), poor jelly, pI 5.3;
III. laboratory preparation, turbid even when heated, good jelly, pI 6.9;
IV. prepared for bacteriological purposes, strong jelly, pI 7.5;
V. specially prepared from pork skin after acidic pretreatment, Bloom value 304, pI 6.8;

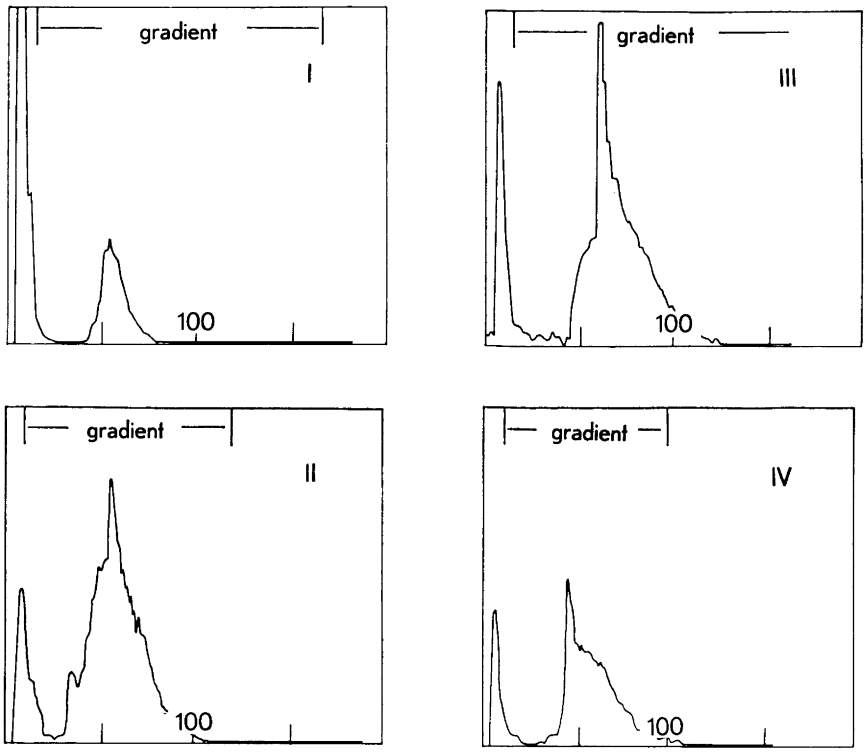

Fig. 1. Fractionation pattern of several samples of gelatins (indicated by numbers I—IX, specified in the text; VIA in Fig. 3 is also comparable) using carboxymethyl cellulose columns. The beginning of the salt gradient and the point when 100 ml eluate had emerged

VI. second run after V; Bloom value 172, pI 6.8;
VII. specially prepared from limed calf skin, Bloom value 244, pI 4.95;
VIII. second run after VII, Bloom value 218, pI 4.9;
IX. third run after VII—VIII, Bloom value 124, pI 4.85.

Fractionation with CM-cellulose columns. The CM-cellulose powder (in sodium form) was suspended in water and allowed to swell overnight. It was washed by decantation and the fine parts were thus removed. The suspension was left to settle in a 1 cm diameter water-jacketed tube in a column of 15 cm height. Finally, air pressure (1 atm) was used to pack the column. A temperature of 37°C was maintained in the column as a rule, but at room temperature the fractionation pattern was almost similar.

If the column was treated with dilute (0.01 M) acetate buffers before the application of the samples, the distribution of the fractions was greatly affected and the significance of pH will be described later.

The gelatin sample (about 40 mg as a 1 % solution which had been passed through a "mixed-bed resin" to remove the ions) was warmed to 40°C and allowed to drain into the column. It was eluted first with water and then with salt solution. Most of the earlier experiments were made using magnesium chloride solution as eluent. The feeding vessel (stirred magnetically) contained initially 100 ml water, and 0.7 % $MgCl_2$ was employed to replace the eluent used from the reservoir flask. Latter, an equivalent concentration of sodium chloride was used. One ml fractions were taken using a "drop-counting" fraction collector.

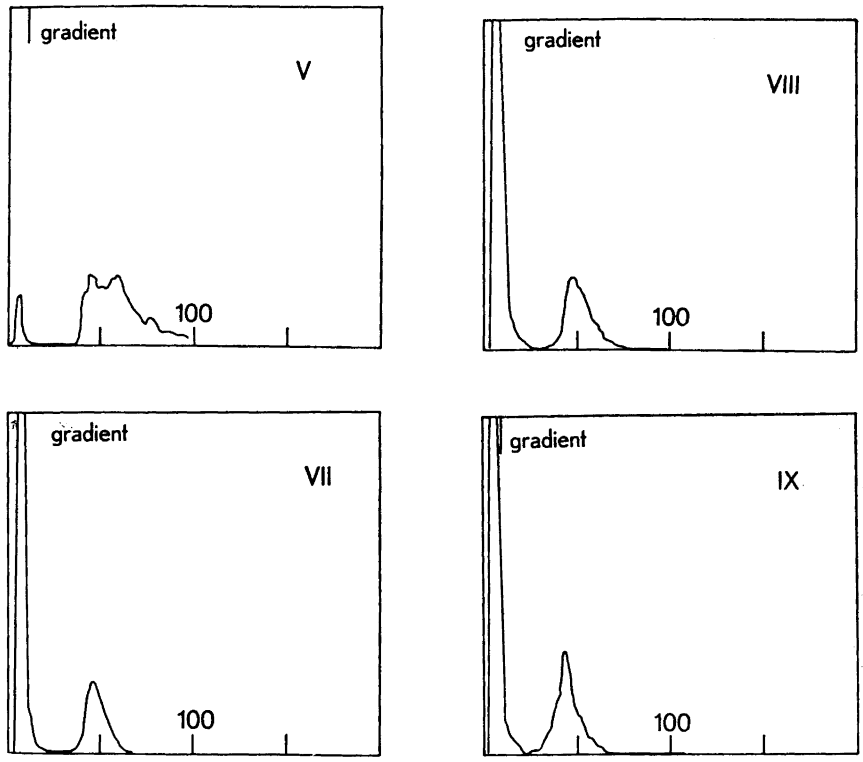

are indicated. At the "100 ml point", the concentration of the salt was about 0.092 N. The total ordinate corresponds to an extinction of 0.9. The analyses are carried out of 0.5 ml eluate, except of 0.3 ml in fractionation of sample V.

Several other salts were tried in equivalent concentrations: potassium chloride, sodium chloride, lithium chloride, calcium chloride, zinc chloride and potassium thiocyanate. However, they did not give markedly different results. Also, the effects of the presence of urea and of pretreatment with hydroxylamine were investigated.

Fractionation on CM-cellulose paper. Two cm broad strips were placed in chromatography troughs for conventional descending elution. A saturation of the paper with water vapour was not necessary. Usually the experiment was carried out at room temperature since at 37°C no improvement was obtained. The gelatin sample (0.010 – 0.050 ml 1 % solution, heated for 10 min at 60 – 70°C) was pipetted on the starting line which had been previously moistened with water. After irrigation with the desired solution, the strip was dried either at room temperature or at 100°C and stained as described below. Additional chromatograms were obtained on washed papers as described in the 'results' section. The difference between the two batches of "CM 50" paper persisted also on the washed paper.

Localization of the fractions. The fractions obtained from the CM-cellulose column were located using a modification of the biuret reaction introduced by Lowry and co-workers [6]. If a precipitate of calcium, magnesium or zinc hydroxide was formed, the fluids were centrifuged clear before the measurement of the colour. In one sample of collagen (V), the magnesium chloride disturbed the development of the colour.

It was necessary to find a satisfactory method for staining the gelatin also on the paper. The following procedure was finally adopted: The dried papers were dipped for

5 min into 1 % tetrabromophenolsulphonphthalein solution [7] (in ethanol and saturated with $HgCl_2$). After washing in 0.5 % acetic acid solution (3 times for 10 min), the papers were dried between blotting papers. Washing with ethanol or methanol did not produce any better contrast. In ammonia vapor, the yellow stain turned blue and distinct but the spots became very soluble. Some other procedures were also tried: spraying with ninhydrin solution (suitable but not very sensitive), collagen staining with aniline blue after treatment with phosphotungstic acid [8] (complicated and not sensitive enough) and staining with lissamine green and subsequent washing with 3 % acetic acid [9] (suitable but not sensitive).

Physicochemical determinations. Sedimentation was measured with a Spinco analytical ultracentrifuge Model E, diffusion with Antweiler's microelectrophoresis apparatus using the diffusion cell and viscosity with an Ostwald type viscosimeter.

RESULTS

Fractionation with CM-cellulose columns. Two fractions were always obtained (Fig. 1). The first fraction seemingly was not attached to the CM-cellulose at all. However, when the CM-cellulose was in the hydrogen form, even the first fraction was bound to the CM-cellulose and was eluted with very dilute magnesium chloride solution. Thus the small amount of sodium in the CM-cellulose was enough to prevent the association of this fraction to the CM-cellulose. The acid gelatins (from limed precursors) yielded a large first fraction which passed straight through the column. We do not give any quantitative estimations concerning the proportions of these fractions since the biuret reaction is approximate only and the amount in the tubes may slightly fluctuate. Fig. 2 shows that the fractions can be reproducibly rechromatographed. The fractionation in the presence of urea did not give markedly different results. A pretreatment with hydroxylamine (pH 9, concentration of hydroxylamine 0.5 M, 90 min at 40°C) of sample V reduced the first fraction.

When some samples got infected and did not form gel any more, the fractionation pattern changed and new fractions appeared (Fig. 3).

Fractionation on CM-cellulose paper. The initial experiments with CM-cellulose paper were made with pH 5.5 citric acid-sodium phosphate buffer (McIlwaine) as eluent. It was observed that a part of the sample (about half) was retained at the origin, the other part migrating with an R_F of about 0.4—0.5. On a paper which had been prewashed with this buffer, the whole sample moved with the front. When a strip was eluted first with pH 5.5 buffer and then with sodium hydroxide, the whole material also migrated at the front. When a strip was developed with the pH 5.5 buffer and sprayed with a suitable pH indicator, it was found that the McIlwaine's buffer was fractionated by "frontal analysis" during the run and a part of the gelatin migrated on the pH boundary line. This conclusion was supported by the finding that, with a pH 8.6 barbiturate buffer, a similar fractionation was obtained.

In addition, 3 % ammonia and 0.1 N hydrochloric acid were tried as eluents but proved unsuccesful. At 4°C, that fraction which was retained at the origin was much augmented.

The best separations were obtained with 0.7 % $MgCl_2$ using the first batch of CM-cellulose paper (Fig. 4). Five bands were registered with R_F values of zero (weak), 0.55 (weak), 0.83, 0.87 (weak) and 1.00 (sample III). From Merck's gelatin (I), only the fraction with $R_F = 0.83$ was obtained.

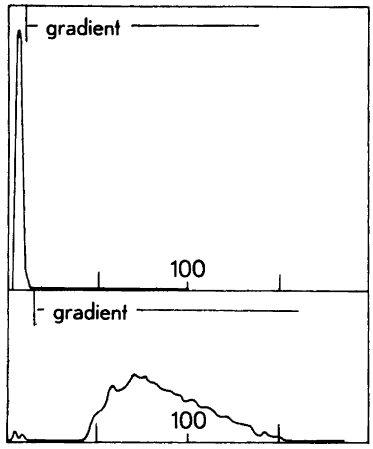

Fig. 2. Rechromatography of the fractions:
Above: First fraction shown in Fig. 1:VII.
Below: Second fraction shown in Fig. 1:III.

To compare different salts, an experiment was made on the second batch of paper at + 37°C with KCl, Na_2SO_4, KSCN, NaCl and $CaCl_2$. The molar concentrations of the eluting fluids were adjusted to correspond to 0.3 % $MgCl_2$. Sodium chloride, potassium chloride and potassium thiocyanate were ineffective and the material remained at the starting line. (In the column fractionation, potassium and sodium chlorides were comparable to $MgCl_2$.) Calcium chloride gave a similar result to $MgCl_2$. Sodium sulphate eluted a part with the front and part was retained at the origin. Similar attempts were made with acetate buffer, pH 4.8. With 0.1 M buffer, the bulk of all the samples migrated with the front. The strength 0.05—0.07 M was found suitable for fractionation.

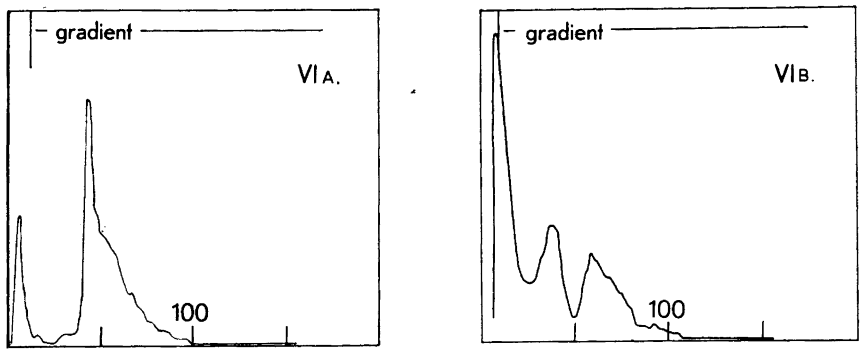

Fig. 3. Effect of microbial degradation on the fractionation pattern. VIA original (without buffer), VIB infected sample (the column pretreated with pH 4.8, 0.01 M acetate buffer). When the original sample VIA was chromatographed in the presence of buffer, only the main peak appeared at about "40 ml point", but no forepeak.

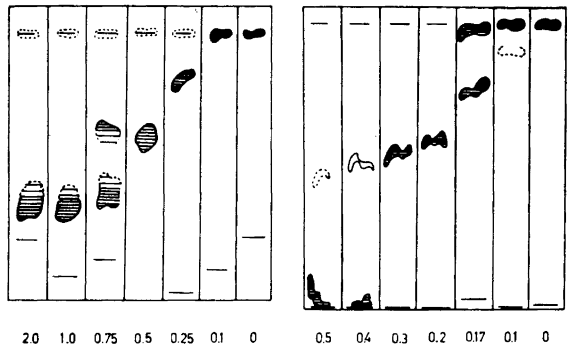

Fig. 4. Elution chromatography of gelatin (III) on carboxymethyl cellulose paper strips. The origin on the top, the solvent front marked below. The figures give the concentration (in %) of magnesium chloride which had been used in the elution. The staining was performed with bromophenolblue [7]. The difference in the two batches of paper is evident.

Most gelatins were then divided into two fractions, one retained at the origin, the other migrating with an R_F of about 0.5. There were differences between the various samples. Sample I (pI 5.2) was retained least under all the conditions studied. An attempt was also made with $MgCl_2$ elution on paper that had been washed with pH 4.8 buffer. As expected, the R_F value of the slower-moving fractions was decreased at pH 4.8 indicating a stronger binding on the CM-cellulose.

Physicochemical data. The two fractions of sample I were studied. The sedimentation coefficients ($s_{20,w}$) were 2.95 *S* and 2.29 *S*. The intrinsic viscosities were 0.39 and 0.25 (c = g/100 ml), respectively. The diffusion coefficient of the first fraction was $D_{20,w} = 3.9 \times 10^{-7}$ cm^2/sec. All measurements were made in pH 4.8, 0.1 M acetate buffer at 37°C. The concentrations were based on the biuret reaction.

DISCUSSION

At present, further experiments on carboxymethyl cellulose paper do not seem advisable because of the heterogeneity of the commercial CM-cellulose papers. Even if the capacity to bind sodium ions is the same, other unknown properties seem to affect significantly the binding of gelatin. However, when this property of the papers becomes understood, methods can be developed for the rapid screening of gelatins.

On the basis of experiments at various hydrogen ion concentrations we believe that the present procedure is related to the fractionation with Amberlite CG-50 resin [1]. The latter is operated with higher salt strengths which affect the apparent isoelectric points of the gelatins and the fractions cannot be directly compared.

We believe that the "forepeak" described by Kessler *et al.* [2] would contain far-degraded gelatins and because we have operated with lower salt strengths, we have actually extended their method to smaller fragments of collagen molecule and divided their "forepeak" to its subfractions. The fractions obtained

by Piez *et al.*[3,10] with sodium acetate buffer gradient from gelatinized soluble collagens can also be separated with the present procedure. Experiments are in progress to elucidate whether the breakdown of these large fragments of collagen can be traced to smaller fractions.

The experience with infected gelatins (Fig. 3) suggests that the present procedure could be applied for the study of the relation of gel-forming capacity and structure of gelatins, for checking their purity and, generally, to follow the degradation of collagens for structural studies. It is useful also for the purification of gelatinized collagen, *e.g.* for the measurement of radioactivity of collagen in metabolic experiments.

Acknowledgement. This work is a part of a program supported by a grant from the *U. S. Department of Agriculture*. We are especially indebted to Dr. J. Naghski, Eastern Utilization Research and Development Division, Agricultural Research Service of U.S. Department of Agriculture, who arranged the supply of the samples V—IX from Kind & Knox Gelatin Company, Camden, N. J., U.S.A., through the courtesy of Dr. E. M. Marks. We also thank Dr. Pentti Seppälä for advice on the determinations of the physicochemical constants.

REFERENCES

1. Kulonen, E., Virtanen, U. K., Viljanto, J. and Seppälä, P. *Acta Chem. Scand.* **16** (1962) 695.
2. Kessler, A., Rosen, H. and Levenson, S. M. *J. Biol. Chem.* **235** (1960) 989.
3. Piez, K. A., Weiss, E. and Lewis, M. S. *J. Biol. Chem.* **235** (1960) 1987.
4. Jackson, D. S. *Biochem. J.* **65** (1957) 277.
5. Janus, J. W., Kenchington, A. W. and Ward, A. G. *Research (London)* **4** (1951) 247.
6. Lowry, O. H., Rosebrough, N. J., Farr, A. L. and Randall, R. J. *J. Biol. Chem.* **193** (1951) 265.
7. Cremer, H. D. and Tiselius, A. *Biochem. Z.* **320** (1950) 273.
8. Heidenhain, M. *Z. wiss. Mikroskopie* **32** (1916) 361.
9. Gorringe, J. A. L. *Clin. Chim. Acta* **2** (1957) 353.
10. Piez, K. A., Lewis, M. S., Martin, G. R. and Gross, J. *Biochim. Biophys. Acta* **53** (1961) 596.

Received January 24, 1962, revised June 4, 1962.

ACTA CHEMICA SCANDINAVICA 16 (1962) 1586–1592

An Apparatus for Partition Chromatography and its Application to the Separation of the Bitter Substances of Hops

LARS-OLOV SPETSIG

Forskningslaboratoriet LKB, Bromma, Sweden

Reversed-phase partition chromatography has proved useful for the separation of hop bitter substances which are then estimated by ultraviolet spectrometry. But hand collection of fractions and determination of ultraviolet absorption are time-consuming and costly. An apparatus has therefore been constructed which measures and records the optical density of the eluant by means of a spectrophotometer connected to a recorder. The apparatus further consists of a chromatographic column with devices of gradient elution and for treating the influent with oxygen-free nitrogen. The elution is carried out with buffer solutions of continuously increasing pH, the value of which is also recorded. The eluted substances may be characterised by their pH of elution, which also enables a rough estimation of the solubility of the substances. Their relative bitterness may be determined after isolation from the eluate. For further characterisation and identification UV and IR spectrometry as well as mass spectrometry have been tried. To facilitate the collection of the samples the tube changes are noted by the recorder.

In 1955, we tried to apply the reversed-phase partition chromatography method of Silk and Hahn [1] to the analysis of humulones, a group of hop bitter substances. The column was packed with kieselguhr treated with dichlorodimethylsilane to make it non-wettable by polar solvents. To begin with, carbon tetrachloride was used as stationary solvent and aqueous methanol as eluant [2]. It soon became evident, however, that chloroform and buffer solutions containing 25 % methanol were superior as solvents [3]. By means of a mixing device gradient elution could then be performed, the pH value of the eluant being raised from pH 3 to pH 11. The separated substances could most easily be estimated by measuring the optical density of the eluate fractions.

But in applying this technique, the collecting of large numbers of fractions and the determination of their ultraviolet absorption were found to be very time-consuming. Furthermore a slow autoxidation of the substances in the fraction collector tubes leads to somewhat erroneous results. An apparatus for automatic absorption measurement was therefore needed. A paper had been published on the use of such a device for measuring and recording the optical

density of eluates continuously and simultaneously at four wavelengths [4]. This apparatus was interesting in principle but seemed too elaborate for our purpose and a simpler construction was worked out, which has now been in use for five years.

This paper will give a detailed description of this apparatus, which automatically measures the pH value of the eluate and its optical density at one wavelength by means of a pH-meter and a spectrophotometer, respectively, connected to a recorder. The application of the apparatus to reversed-phase partition chromatography of hop bitter acids with a pH gradient elution technique is discussed with illustrative examples.

APPARATUS

Most of the apparatus is mounted in a table-type cabinet. On top of the table are placed the column assembly inside a metal shield, the spectrophotometer and the pH-meter. The recorder is placed inside the cabinet as is also the fraction collector, which is thus protected from light. In the cabinet there is also a thermostat, from which water is pumped through the column jacket. A control panel is placed on the rear side of the table.

Column assembly. For analytical purposes a 800 × 8 mm column is used which may be loaded with 20—40 mg of bitter substances. Fig. 1 shows schematically the various Pyrex components of the column assembly. The adapter *A* with a medium fritted-glass disc serves as a support to the packing of the column *B*. On top of the column is placed

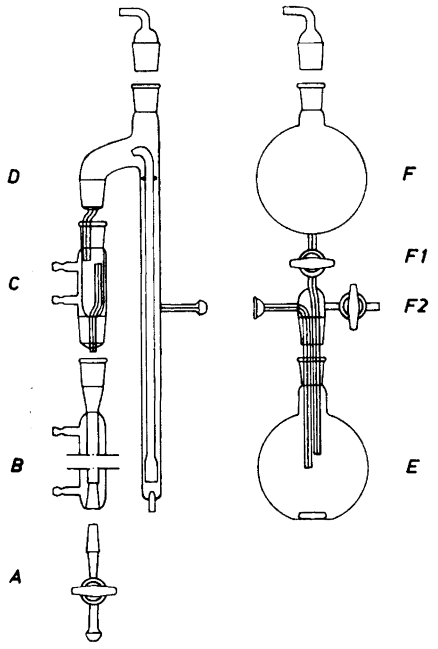

Fig. 1. Column assembly and gradient elution device.

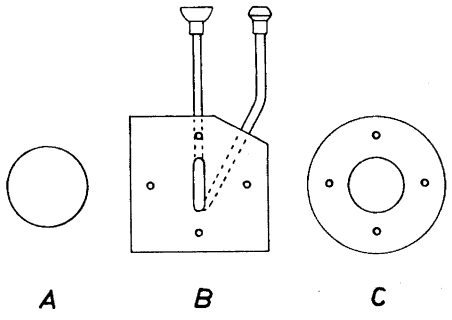

Fig. 2. Absorption cell.

another adapter *C*, in which the eluant is passed through a layer of chloroform for final saturation. Both column *B* and adapter *C* are provided with water jackets. The top piece of the adapter *C* is connected to a gas lift *D*, where the influent is blown with oxygen-free nitrogen to exclude dissolved oxygen, and then transported to the adapter *C*. The gas leaving the apparatus may be led through a series of small mercury-filled gas washing bottles serving as manostats.

For preparative purposes a column of 800 × 25 mm is used which can be loaded with more than 300 mg of bitter substances.

Gradient elution system. This system is composed of a mixing chamber *E* and a feeder *F* (Fig. 1). The mixing chamber is equipped with a magnetic stirrer and contains a buffer solution of low pH and a layer of chloroform. It may be hermetically sealed by means of the stopcock F2. The solution leaving the mixing chamber is replaced by a buffer solution of high pH value stored in the feeder. The pH of the eluant thus rises continuously during the elution, giving a gradient which is a function of the amount and composition of the two solutions. [5] Before filling, both mixing chamber and feeder are flushed with oxygen-free nitrogen.

Absorption cell. The demountable type absorption cell is composed of two optically polished fused silica windows *A* and a 5 mm stainless steel spacer *B* (Fig. 2). The windows are clamped tightly in place by means of stainless steel plates *C* and screws. Two stainless steel tubes with spherical joints form the inlet and outlet tubes of the cell, which is mounted on an extra cover of the spectrophotometer cell compartment.

Spectrophotometer and recorder. A line-operated Hilger Uvispek spectrophotometer connected to a Honeywell Electronik multichannel recorder is used. As the recorder deflections were found to be nonlinear, they have been calibrated by means of an alkaline solution of potassium chromate as described by Haupt. [6]

pH-Meter. The pH value of the eluant leaving the cell is measured by a small combined glass and calomel electrode connected to a Metrohm pH-meter and the recorder.

Fraction collector. The eluate may be fractionated by a fraction collector operated by either a timer or a siphon device. The impulse causing the fraction collector to advance one step also actuates a shutter in the exit opening of the spectrophotometer lamphouse. The shutter is kept closed for one minute by means of a time delay relay. During this period the line of 0 % transmission is recorded. This enables corrections to be made for the slight temperature drift of the spectrophotometer. In addition, the tube changes are noted in the record, which greatly simplifies the picking out of tubes for further investigation.

Nitrogen purification train. The eluant is kept free of dissolved oxygen with purified tank nitrogen. A lift-pump scrubber containing copper ribbon and ammoniacal ammonium chloride solution, as described by Altieri [7], was originally used (*cf.* Vandenheuvel and Richardson [8]). Now amalgamated zinc and vanadium(II) sulphate [9] in dilute sulphuric acid are employed as purification agents. In both cases nitrogen of high purity is obtained.

ANALYTICAL PROCEDURE

Reagents. Mixing chamber solution for hop analysis. 5.4 g of citric acid and 3.4 g of monopotassium orthophosphate in 1 liter of 25 % methanol (v/v), saturated with chloroform.

Feeder solution for hop analysis. 3.1 g of ethylolamine, 5.3 g of diethylolamine. 7.5 g of triethylolamine and 2.0 g of sodium hydroxide in 1 liter of 25 % methanol.

Mixing chamber solution for beer analysis. 5.4 g of citric acid in 1 liter of 25 % methanol, saturated with chloroform.

Feeder solution for beer analysis. 8.9 g of disodium orthophosphate in one liter of 25 % methanol, saturated with chloroform.

Preparation of kieselguhr. Hyflo Super Cel is dried at 110°C, treated with dichlorodimethylsilane, washed with methanol and dried as described earlier[3].

Packing of column. 10—20 ml of chloroform is added slowly to 11 g of hydrophobic Hyflo Super Cel in 300 ml of 35—45 % (v/v) methanol in a top drive macerator. The proper amount of chloroform will depend on the duration of the silane treatment. The slurry is stirred gently for a quarter of an hour to expel entrapped air bubbles and is then transferred to a separating funnel equipped with a stirrer and connected to an 8 mm

column by a ground joint at its neck. The kieselguhr is permitted to settle slowly by gravity into the column, which is filled with air-free 35—45 % methanol saturated with chloroform.

Especially with 25 mm columns good results are also obtained when the packing of the column is carried out in a mixing chamber solution saturated with chloroform.

Preparation of samples. Hop extracts are prepared by macerating 10 g of hops with 150—300 ml of chloroform in a macerator and filtering off the pulp on a glass filter. Beer extracts are obtained by repeated extraction of decarbonised beer in a separatory funnel with chloroform (150 ml/1000 ml beer) after addition of hydrochloric acid to give pH<1 (*cf.* Spetsig *et al.* [3]). The extracts are then evaporated at a temperature not exceeding 30°C to a volume containing 20—40 mg of hop bitter substances or 10—20 mg of beer bitter substances in 0.05 ml.

Loading. The column is loaded by means of a special device consisting of a glass tube with a ground-in glass plunge into which a suitable amount of Hyflo Super Cel is weighed. A small amount of mixing chamber solution is added and the appropriate amount of the sample dissolved in 0.05 ml chloroform. After the mixture has been stirred thoroughly with a thin glass rod, the slurry is added quantitatively by pressing in the plunge to expel the mull into the column, where some of the packing has been sucked off to give a plain surface. The kieselguhr is then gently packed by means of a glass rod with a diskshaped foot. After addition of a small amount of the sucked-off packing over the sample, the column is ready for elution.

Elution. The elution is usually carried out with 1000 ml of eluant. For hop analysis 650 ml of mixing chamber solution is added, giving a gradient from pH 3 to pH 10.5. For beer analysis 1000 ml of mixing chamber solution gives a rise from pH 3 to pH 7, which is sufficient, since beer contains no bitter substances emerging at higher pH values.

Routine analytical procedure. The column mixture is prepared and the column packed as described above. After settling overnight the column is mounted in the apparatus and water of 30°C circulated through the jacket. Then the packing is slowly washed with the appropriate mixing chamber solution in a nitrogen atmosphere. After loading, the column is protected from light with a plastic sleeve and is filled with mixing chamber solution before the adapter is put in place. The adapter, too, is filled completely to exclude air. The gradient elution system, which has previously been flushed with nitrogen, is loaded with the appropriate amount of mixing chamber solution and chloroform and after turning the stopcocks to a closed position also with feeder solution. Nitrogen is then led through the gas lift and the space over the feeder solution. The absorption cell is rinsed with 25 % (v/v) methanol used as a standard through a side tube on the glass tubing connecting column and cell. The spectrophotometer and recorder are standardised at the wavelength chosen, usually 280 or 325 mμ. The stopcock connecting the feeder and the mixing chamber and the stopcock of the column can then be opened, the timer started and the elution begun. If necessary the gas pressure is increased by means of the manostat device to give an elution velocity of 200—400 ml a day. The extinction values are read from the records with a special measuring rule constructed with the aid of the deflection values obtained by calibration and are then plotted against the eluate volume. From the diagram the tubes containing the separated substances are sorted out and the ultraviolet spectra are determined. The compounds can then be extracted with chloroform, dissolved in dilute sodium bicarbonate and their taste tested.

The column may often be used repeatedly. The sample zone is then sucked off and the column is washed with feeder solution in a nitrogen atmosphere.

RESULTS AND DISCUSSION

The bitter substances in hops and beer may be extracted with a number of solvents, *e.g.* chloroform, benzene, methanol, carbon tetrachloride and iso-octane. The most efficient of these solvents is chloroform, which is thus suitable as the stationary solvent in reversed-phase partition chromatography of the bitter substances. Chloroform was therefore used in combination with buffer solutions, which, as eluants, allow an estimation of the solubilities of the acidic

bitter substances. Addition of 25 % methanol was found suitable for producing symmetrical peaks.

Preliminary experiments showed that the front peak and the residue left on the column after the elution contained no bittertasting substances. All the bitter substances must therefore be acids and included in the chromatogram.

With the procedure adopted, sufficient amounts (1—2 mg) of each substance could be isolated from the eluate by extraction with chloroform to make possible an evaluation of the relative bitterness, the most important property of a bitter substance from the practical point of view. Only a few hop substances found in the chromatogram were without a bitter taste. Chloroform extracts of beer gave a number of very small peaks belonging to non-bitter substances, but carbon tetrachloride and isooctane extracts contained mainly bitter compounds.

The pH value of elution proved to be a convenient property for characterising an eluted substance. This pH value is closely related to the solubility of the substance and enables a rough determination of its solubility product by comparison with the values earlier determined for humulinic acid, humulone and lupulone. Hops were found to contain substances over a very wide solubility range with solubility products varying from high values down to 10^{-6}. As beer contains no bitter substances eluted at higher pH values than pH 7, substances with lower solubility products than 10^{-3} are not soluble in wort in unchanged form. The most soluble substances which are first eluted are therefore in general the most interesting.

Another suitable means of characterisation was provided by the ultraviolet absorption curves. A number of peaks gave characteristic spectra with maxima from 325 to 400 mμ. But many substances had rather similar spectra with a maximum in the range 255—275 mμ. A suitable allround wavelength for the recording of the chromatogram was 280 mμ, while 325 mμ was used for special studies, *e.g.* on hulupones, humulones and lupulones. A prefractionation could sometimes be obtained when using a selective solvent such as isooctane for the extraction, which further simplified the study of individual substances.

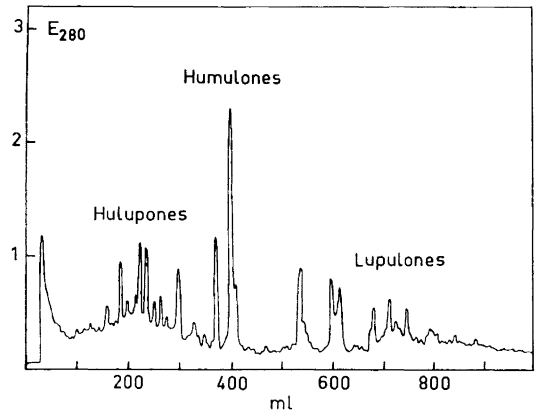

Fig. 3. Chromatogram of bitter substances from Hallertau hops.

The apparatus and procedure has been used to make a survey of all the bitter substances appearing in the brewing process and to study some of the most important of these substances in detail.

When extracts of hops were analysed an extensive resolution of the complex bitter substance mixture was obtained, as is seen from a typical chromatogram in Fig. 3. The chromatogram clearly shows two well-known groups of three substances, the humulones and lupulones. Among the forty or so hitherto unknown substances a further group of three substances named hulupones are included. Many of the other substances are probably oxidation products formed from humulones and lupulones by autoxidation during the storage of the hops. The relative heights of the peaks are altered accordingly as the hops grow older.

A chromatogram of beer bitter substances has a rather different appearance (Fig. 4). The most interesting feature is the group of five high peaks. Hitherto, beer has been supposed to contain as main bitter substances only three iso-humulones formed by rearrangement of the humulones during wort boiling. But the five peaks seem to be caused by six isocompounds, two from each humulone. In addition to these compounds beer is found to contain a number of minor substances, probably oxidation and rearrangement products of hop bitter substances.

Similar analyses have been made of bitter substances from spent hops, from technical extracts of spent hops and from trub. These products contained a mixture of the hop and the beer type bitter substances. A detailed report of all these substances will be given in a separate paper.

By the use of wide columns it became possible to separate individual bitter substances in 100 mg amounts or more for further study. The investigations were concentrated on the hulupones. By means of molecular spectrometry, a method which may very suitably be combined with chromatography, a determination of their structure has been possible [11]. Some of their derivatives have likewise been studied.

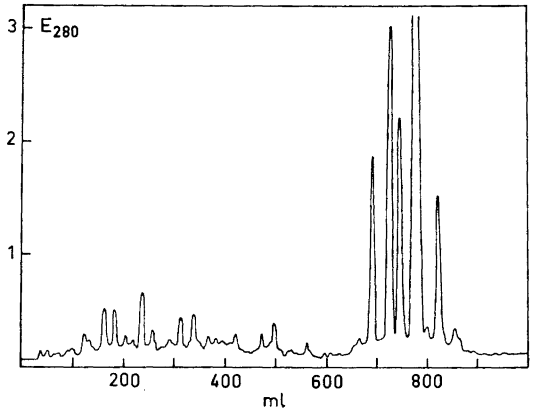

Fig. 4. Chromatogram of bitter substances from Pilsener beer.

The six rearrangement products of the humulones appearing in beer have been isolated for structure determination in combination with a kinetic study of the rearrangement. This investigation will be reported in a separate paper.

Though the method gave good qualitative results, only a semiquantitative determination of bitter substances was possible. The more slowly the elution was carried out, the smaller the areas of the peaks in the last part of the hop chromatograms were found to be. No doubt these substances were slowly oxidised in spite of the nitrogen treatment of the eluate. With a short column and stepwise elution, however, it was possible to obtain in a few hours a number of fractions whose content of substances with characteristic ultraviolet spectra could easily be determined. By a proper choice of the pH values of the eluants in the light of the results of the qualitative analyses, the main components of the bitter substance mixture could be determined with a high degree of accuracy [12].

Acknowledgement. It is gratefully acknowledged that this work has been supported by the Stockholm Brewing Company, Stockholm, as part of its research programme on hops carried out over a period of some years. Thanks are also due to Mr. J. Engblom and the workshop personnel of Forskningslaboratoriet LKB for building the apparatus, and for service and maintenance work.

REFERENCES

1. Silk, M. L. and Hahn, H. H. *Biochem. J.* **56** (1954) 406.
2. Spetsig, L.-O. and Steninger, M. *J. Inst. Brewing* **62** (1956) 333.
3. Spetsig, L.-O., Steninger, M. and Brohult, S. *Proc. European Brewery Conv.* Copenhagen 1957, p. 22.
4. Deutsch, A., Zuckerman, R. and Dunn, M. S. *Anal. Chem.* **24** (1952) 1763.
5. Drake, B. *Arkiv Kemi* **8** (1955) 1.
6. Haupt, G. W. *J. Research Natl. Bur. Standards* **48** (1952) 414.
7. Altieri, V. J. *Gas analysis*, Am. Gas Assoc. New York 1945, p. 261.
8. Vandenheuvel, F. A. and Richardson, G. H. *J. Am. Oil Chem. Soc.* **30** (1953) 104.
9. Meites, L. and Meites, T. *Anal. Chem.* **20** (1948) 984.
10. Rigby, F. L. and Bethune, J. L. *Proc. Am. Soc. Brew. Chem.* **1952** 98.
11. Brohult, S., Ryhage, R., Spetsig, L.-O. and Stenhagen, E. *Proc. European Brewery Conv.* Rome 1959, p. 121.
12. Spetsig, L.-O., *Proc. European Brewery Conv.* Vienna 1961, p. 134.

Received February 9, 1962.

ACTA CHEMICA SCANDINAVICA 16 (1962) 1593–1600

Hammett Series with Biological Activity

O. ROSENLUND HANSEN

A/S Ferrosan, Copenhagen, Denmark

The possibility of relation between biological activity and Hammett's sigma values in appropriate series of benzene derivatives is discussed. A "biological Hammett equation" is set up, based on a number of simplifying conditions, and the limitations of this equation are discussed. Finally, on the basis of data from the literature examples are given of series to which the Hammett equation is or can be applied, and it is mentioned that special deviations occur when certain substituents are used.

Scientists engaged in the production of biologically active substances have always desired to be able to predict the action of a given substance by virtue of its chemical constitution. Many more or less successful theories have been advanced, and still more *ad hoc* explanations have been given, but no fairly general theory is available and may probably not be advanced since biological action cannot be related to one single type of mechanism.

If it is assumed that many substances exert their actions by reacting with cell components, there would be every reason to apply the Hammett equation [1] to appropriate series of benzene derivatives where the action is supposed to be due to a reaction with the side-chain.

The Hammett equation

$$\log k_\sigma - \log k_0 = \varrho\sigma \qquad (1)$$

describes the effect of *meta* and *para* substituents on the rates of side-chain reactions of benzene derivatives and is a linear relationship for the logarithms to the rate constants (and therefore also equilibrium constants) to the σ-values, which are substituent constants independent of the reaction. ϱ is a proportionality constant dependent upon the nature of the reaction and the conditions. k_σ is the rate constant of the member which has a substituent with the value σ, and k_0 is the rate of the unsubstituted member. The degree of biological activity in groups of related compounds is generally believed to depend on the degree of chemical reactivity. It is therefore worth while to plot biological activity against σ-values in appropriate series and try to find simple relationships.

In a review on the Hammett equation [2] Jaffé says that in the literature he has not been able to find a series of substances the biological action of which

has followed the Hammett equation, but on the other hand, he does not consider it inconceivable that such series may be found. Since it is generally assumed that biological action is due to an interaction with enzymes, it is of interest that the velocity constants for hydrolysis of substituted benzoyl cholines with cholinesterase has been found to fit into the Hammett equation [3]. Moreover, Fukuto has shown that the inhibition of cholinesterase with phenyl N-methylcarbamates and with diethyl-phenyl phosphates follows the Hammett equation, and that the insecticide action of the latter with certain exceptions follows the cholinesterase inhibition [4]. As an example of a series of substances with pharmacological effect to which the Hammett equation can be applied, phenylethers of choline with a nicotine-like activity may be mentioned [5].

For the purpose of finding precise expressions of biological activity as a function of σ-values we will regard the growth inhibition. Everywhere in the following, temperature and other environmental conditions other than inhibitors are assumed to be kept constant.

Growth of living organisms is supposed to be an extremely complicated but exactly balanced production of substances. Almost without exception the synthetic activity is proceeding by means of more or less specific enzymes, and an inhibition of one or more of these enzymes will influence the process of growth. Thus, if we affect an organism with a substance which is able to penetrate to an enzyme and to react with it, causing loss of its catalytic ability, we will see that this has an effect on the growth. No effect will generally be seen by adequate low concentrations of the substance because the amount of enzyme may be reduced somewhat before a noticeable decline in the capacity occurs. Increasing concentrations of the inhibitory substance will then show that the rate of growth decreases for at last to become zero. The organism will possibly die when the process of growth has reached a certain low rate. In a living organism proteins and consequently also enzymes are incessantly decomposed and rebuilt, and we assume that an enzyme E_n during the growth is formed at the rate dE_n/dt. If, however, an inhibitory substance is present which reacts with the enzyme by a bimolecular reaction, the enzyme will be destroyed at the rate

$$\left(\frac{dE_n}{dt}\right)_{dest} = k\, E_n\, [I] \qquad (2)$$

where k is the rate constant, and [I] is the concentration of the inhibitor just around the enzyme. The net production of E_n will be reduced partly because some of the output is destroyed and partly because the production may be less than before. The other enzymes of the organism are dependent on E_n which in its turn is dependent on the other enzymes, and by means of this complicated feed back mechanism the organism assumes a lower growth rate.

If the inhibitory substance is a member of a Hammett series (H) we have by analogy with (2)

$$\left(\frac{dE_n}{dt}\right)_{dest} = k_\sigma E_n [H_\sigma] \qquad (3)$$

We now use such a concentration that the growth is inhibited, *e.g.* to q % of uninhibited growth, and we have

$$k_\sigma[H_\sigma]_q = K(q) \tag{4}$$

where $K(q)$ is a constant when q is fixed.

Eqn. (4) must apply to the whole series independent on σ as it is seen from eqn. (3) that the rate of destruction which determines the growth rate is the same when eqn. (4) is satisfied.

From eqn. (4) we get

$$\log\ k_\sigma + \log\ [H_\sigma]_q = \log\ K(q) \tag{5}$$

Specifically applying to the unsubstituted member of the series we have

$$\log\ k_o + \log\ [H_o]_q = \log\ K(q) \tag{6}$$

And from eqns. (5) and (6) we obtain

$$\log\ k_\sigma - \log\ k_o = -\log\ [H_\sigma]_q + \log\ [H_o]_q \tag{7}$$

If the Hammett eqn. (1) is substituted in eqn. (7), we get

$$-\log\ [H_\sigma]_q + \log\ [H_o]_q = \varrho\sigma \tag{8}$$

Eqn. (8) is derived on the assumption of q being a growth inhibition in per cent, but q may generally be interpreted as *equal effect*.

The inhibition of bacterial growth can easily be measured with a reasonable accuracy and can therefore with advantage be used for the verification of the biological Hammett eqn.

When bacteria are transferred to a fresh culture medium, a short time — "the lag" — will often pass before division takes place. If like Hinshelwood [6] we imagine this lag to be a period used for production of substances and reorganization in the cell, we have

$$\int_0^L R\mathrm{d}t = \text{const.} \tag{9}$$

where L is the lag and R the rate of production.

If the culture medium contains an inhibitor reducing R to R' we have

$$\int_0^{L+\Delta L} R'\mathrm{d}t = \text{const.} \tag{10}$$

where ΔL is the increase of lag necessary for the bacterium to reach the same state as the uninhibited bacterium reaches at the time L.

Thus a fixed value of ΔL can be used as a measure of equal effect.

The lag is succeeded by a growth phase in which the bacteria are dividing. This often takes place according to an exponential law

$$N_t/N_o = \exp(kt) \tag{11}$$

where N_t is the number of bacteria at the time t, N_o is the original number of bacteria, and k is a constant. k is a measure of the rate of production in the single cell, and at last k decreases due to the culture medium being consumed at the same time as toxic metabolic products are accumulated.

If as before an inhibitor is added, k is reduced to k' and N_t to N_t'.

Here we can make use of fixed values of N'_t/N_t or of k'/k as a measure of equal effect. In the latter case it is necessary to know the growth curve which moreover has the advantage that ΔL as well as k'/k may be determined independent of each other.

As a measure of inhibition of plants, reduction of the growth in length or of the production of dry metter may, *e.g.*, be used, and in pharmacology the respective responses may be applied.

As appears from eqn. (8) we may plot the negative logarithms of the isotoxic molarities as a function of σ. If the theory holds good, a straight line could be drawn through the points. The slope of this line will be ϱ, and the ϱ-value thus determined appears to be identical with the ϱ-value of the damaging reaction in the cell.

It will, however, hardly be possible to find a series of substances with a considerable number of substituents of different types to which the theory fully applies. The reasons are many, and some of the presumably most important ones are set out below:

1. The reaction was assumed to be "bimolecular". Even though this will often be the case, side-chain reactions of a more complicated nature may well be imagined. The effect may thus be due to a catalytic action in which, *e.g.*, the side-chain is acetylated by active acetyl, whereupon the acetyl group is liberated by hydrolysis. Velocity and equilibrium constants in this cycle will presumably follow the Hammett equation, but the catalytic and consequently the biological effect will not necessarily obey the expressions deduced.

2. In order to enter the cell, the substances must pass the cell-wall, but if the molecule is associated to more than a few molecules of water there will be no free passage, and in order to enable it to pass through, the cell must perform an active transport. Two substances almost similar both in respect of their partition coefficients and their σ-values may therefore be treated quite differently with a consequential difference in biological activity. This fact will be particularly pronounced in more complicated organisms, higher plants and animals where discrimination due to the partition coefficients and permeability is apt to obscure every trace of linearity in the relation between σ-values and activities.

3. One of the conditions of the Hammett equation is that the substituents of the benzene ring only exert their actions *via* the electronic density in the side-chain. In the case of reactions between small molecules this condition will in general be fulfilled. But where it is a question of enzyme reactions in which the reacting molecule as a step in the reaction will be oriented on the enzyme surface, the substituents may take part in the orientation and make irregular contributions to the entropy of reaction. Thus in the above-mentioned diethyl-phenyl phosphate series, the *m*-dimethylamino and *m-tert*-butyl members are *in vitro* much stronger than would appear from the equation. The two groups are far more sterically than chemically alike, and deviations of this type provide valuable information as to the topography of the enzyme surface. As regards the phenyl N-methylcarbamates there are two parallel curves applying to *m*- and *p*-derivatives, respectively.

4. The deduction has been made on the assumption that the inhibitory substance would attack one enzyme only, an assumption which is not always

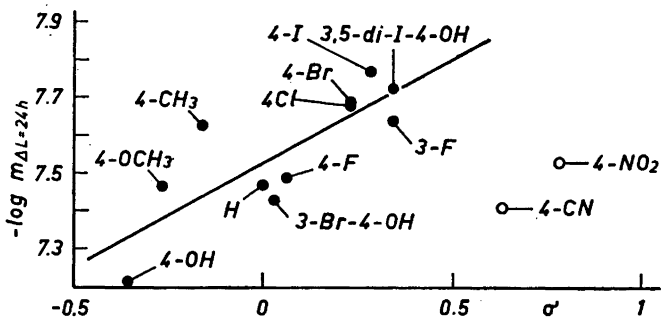

Fig. 1. Activity of substituted G-penicillins plotted against the σ-values of the substituents. The ordinate is the negative logarithm of the molarity which gives a lag of 24 h. A sensitive strain of *Staphylococcus aureus* is used as test organism. Data from Burger [7].

true. Substances reacting with SH-groups must thus be able to attack numerous enzymes simultaneously, and the ϱ-values may vary from one enzyme to another. However, if the reactions with the various enzymes are of the same type, the ϱ-values will not vary much, and what will happen is simply that the "isotoxic curve" will have a curvilinear course.

5. We have used molarity instead of activity, but this error is negligible in comparison with those mentioned above. Very dilute solutions of the inhibitor in the culture medium do, however, present a problem in that the substance will more or less be adsorbed to peptide molecules and to glass surfaces.

No good accordance with eqn. (8) is thus to be expected, at most that rejection of obvious deviations will make it possible to draw a regression line with

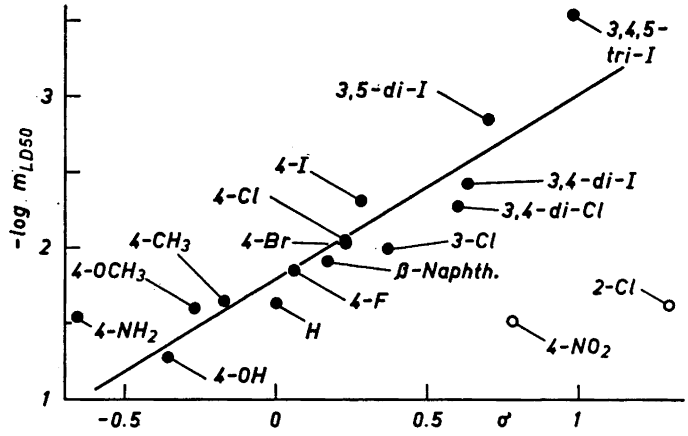

Fig. 2. Activity of substituted benzoic acids plotted against the σ-values of the substituents. The ordinate is the negative logarithm of the molarity which kills 50 % of the larvae of the mosquito *Aedes aegypti* in 24 h. This mortality (LD50) is supposed to be reached when the processes of growth attain a certain low mean value. Data from Casida [8].

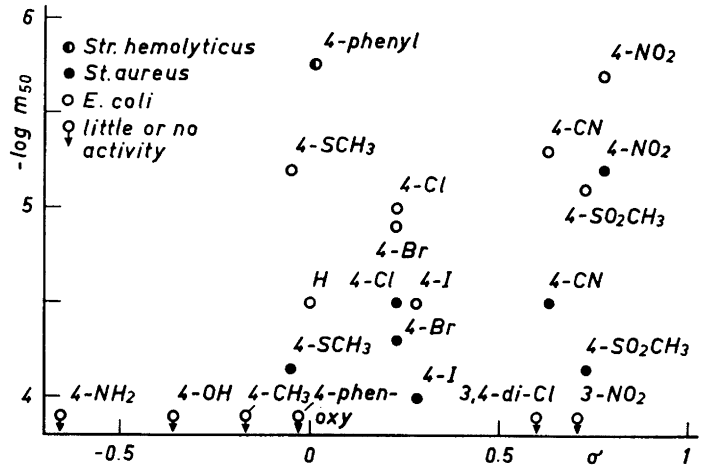

Fig. 3. Activity of chloramphenicol analogues plotted against the σ-values of the substituents. The ordinate is the negative logarithm of the molarity giving 50 % growth of the bacteria *Escherichia coli*, *Staphylococcus aureus* and *Streptococcus hemolyticus*. Data are taken from [13-22], and the values obtained by van der Meer *et al.*[16] have been used as standard values.

reasonable "accidental" deviations. Although such rejection is a difficult and also somewhat questionable matter, it is necessary in order to obtain a ϱ-value which applies to most members of the series and in addition represents the ϱ-value of the enzyme reaction in the cell. In I and II below, the principles for rejection are exemplified.

Biological Hammett series have already been referred to, and some additional series shall be mentioned here:

I. *Substituted G-penicillins* (Fig. 1). The *p*-nitro and *p*-cyano derivatives have not been included in the computation of the regression line. The material is somewhat scanty, and the appearance of a larger material may alter the picture considerably.

II. *Substituted benzoic acids* (Fig. 2). Also in this case it is justifiable to ignore the *p*-nitro derivative. $\varrho = 1.2$ which is approximately the ϱ-value for K_A (1.0). That the effect is not merely a matter of acid strength is seen from

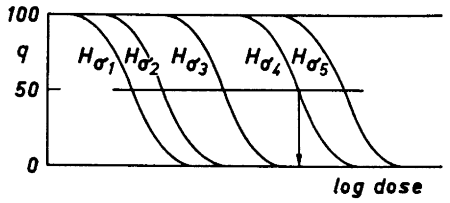

Fig. 4. A curve family showing per cent growth as a function of log dose for five different members of a Hammett series. For the fourth member it is demonstrated how the concentration giving 50 % growth can be estimated.

the fact that the *o*-chlorobenzoic acid, marked in the diagram after acid strength, is far too weak.

These two curves are based primarily on halogen derivatives. In a number of series of substances with antibacterial effect or inhibitory effect on germinating seeds, synthesized in this laboratory for the purpose of investigating the relation between biological activity and σ-values, we have in most instances found such relation by the application of amino, alkyl, hydroxyl, alkoxyl, and halogen groups. Nitro and methylsulfonyl groups, however, as a rule give products with a much lower activity than calculated [9].

It is common procedure to introduce halogen, particularly chlorine, into benzene rings in biologically active substances, this often resulting in more active substances. The trifluoro-methyl group has lately been added to this class of activating substituents. In two antimetabolite series, sulphanilic acid anilides [10] and pantoyltauryl anilides [11], the strongest members are the 3,5-dibromo derivatives, and this has been called a "3,5-dibromoaniline activity". We have synthesized the series in question and furthermore the 3,4,5-trihalogen derivatives which have proved to be stronger than the 3,5-dibromo derivatives [9]. In the present case it would be more reasonable to speak of Hammett effect.

III. *Chloramphenicol analogues* (Fig. 3). This material is difficult to evaluate since it derives from many sources and has been tested on different bacteria. The series has been thoroughly discussed on about the same lines as presented here, and correlation has been found only for the *p*-substituted members, the known *m*-substituted ones being entirely inactive [12]. If the activity of this series is postulated to obey the Hammett equation, it must be added that *m*-substituents prevent the benzene ring from being attached correctly to the enzyme surface. Furthermore, *p*-nitro, *p*-cyano, and *p*-methylsulfonyl are the most activating substituents, contrary to what is found in most other series.

APPENDIX

The deduction of eqn. (8) has been based on a fixed inhibition level of q. A 50 % level is often used, but any other value would have given a straight line parallel to the 50 % line, *i.e.* with the same slope, ϱ.

The isotoxic concentration is obtained by determining the q's for a number of concentrations of each H_σ and plotting them as a function of log $[H_\sigma]$. These curves are parallel because at every value of σ we have eqn. (4)

$$k_\sigma[H_\sigma] = K(q)$$

or

$$\log k_\sigma + \log [H_\sigma] = \log K(q) \tag{12}$$

from which we obtain the slope of each curve in the curve family:

$$\left(\frac{\partial q}{\partial \log [H_\sigma]}\right)_\sigma = 2.30 \frac{K(q)}{K'(q)} \tag{13}$$

i.e. that the slope of all curves is identical for any given q. By intersecting the curve family (Fig. 4) with $q = 50$ we get $\log [H_\sigma]_{50}$ for each substance. The

negative values of these logarithms are plotted against the σ-values, and we get the "isotoxic curve" with the slope ϱ. When choosing another value of q we get the corresponding log $[H_\sigma]_q$ for each substance and a new "isotoxic curve" with the same slope.

The law of the parallel log dose-response curve applies, of course, whether the k's satisfy the Hammett equation or not. It is, indeed, a general assumption within pharmacology that related substances with the same mechanism of action give parallel log dose-response curves. We have here deduced the rule applying to "bimolecular" processes, but conversely, no safe conclusion as to the type of reaction can be drawn from parallel curves.

Acknowledgements. My thanks are due to Dr. J. A. Christensen and Dr. N. F. Gjeddebæk for very valuable suggestions and discussions. I am very grateful to Dr. R. Zahradník, Institute of Physical Chemistry, Praha, for criticism and advice, which has been of great value to me owing to his intimate knowledge of the problems [23].

REFERENCES

1. Hammett, L. P. *Physical Organic Chemistry,* McGraw-Hill, New York and London 1940, p. 186.
2. Jaffé, H. H. *Chem. Rev.* **53** (1953) 191.
3. Ormerod, W. E. *Biochem. J.* **54** (1953) 701.
4. Fukoto, T. R. *Advances in Pest Control Research* **1** (1957) 147.
5. Hey, P. *Brit. J. Pharmacol.* **7** (1952) 117.
6. Hinshelwood, C. N. *The Chemical Kinetics of the Bacterial Cell,* Oxford University Press, London 1946, p. 135.
7. Burger, A. *Medicinal Chemistry,* Interscience Publishers, Inc., New York 1951, p. 882.
8. Casida, J. E. *Biochem. J.* **59** (1955) 216.
9. *To be published.*
10. Goetchius, G. R. and Lawrence, C. A. *J. Bacteriol.* **49** (1945) 575.
11. Winterbottom, R., Clapp, J. W., Miller, W. H., English, J. P. and Roblin, R. O. *J. Am. Chem. Soc.* **69** (1947) 1393.
12. Hahn, F. E., Hayes, J. E., Wisseman, Jr., C. L., Hopps, H. E. and Smedal, J. E. *Antibiotics & Chemotherapy* **9** (1956) 531.
13. Woolley, D. W. *J. Biol. Chem.* **185** (1950) 293.
14. Dann, O., Ulrich, H. and Möller, E. F. *Z. Naturforsch.* **5 b** (1950) 446.
15. Buu-Hoï, N. P., Hoán, N., Jacquignon, P. and Khoï, N. H. *J. Chem. Soc.* **1950** 2766.
16. van der Meer, S., Kofman, H. and Veldstra, H. *Rec. trav. chim.* **72** (1953) 236.
17. Rebstock, M. C., Stratton, C. D. and Bambas, L. L. *J. Am. Chem. Soc.* **77** (1955) 24.
18. Bambas, L. L., Troutman, H. D. and Long, L. M. *J. Am. Chem. Soc.* **72** (1950) 4445.
19. Buu-Hoï, N. P., Hoán, N., Jacquignon, P. and Khoï, N. H. *Compt. rend.* **230** (1950) 662.
20. Buu-Hoï, N. P., Xuong, N. D. and Khoï, N. H. *J. Chem. Soc.* **1951** 255.
21. Rebstock, M. C. and Pfeiffer, E. L. *J. Am. Chem. Soc.* **74** (1952) 3207.
22. Cutler, R. A., Stenger, R. J. and Suter, C. M. *J. Am. Chem. Soc.* **74** (1952) 5475.
23. Zahradník, R. and Chvapil, M. *Experientia* **16** (1960) 511.

Received March 9, 1962.

ACTA CHEMICA SCANDINAVICA 16 (1962) 1601–1606

Calculation of Urey-Bradley Potential Constants

I. Planar XY_3 Molecules

E. MEISINGSETH

Institutt for teoretisk kjemi, Norges tekniske høgskole, Trondheim, Norway

The Urey-Bradley force constants were calculated for $^{11}BY_3$ (Y = F, Cl, Br, I). The forces between non-bonded atoms were assumed to be repulsive, and together with some additional simple assumptions, the relation

$$-0.25 < F'/F < 0$$

was deduced. This condition is in agreement with the usual assumption of $F' = -0.1\ F$. The calculated force constants reproduced the vibrational frequencies of $^{10}BY_3$ with great accuracy. The BY stretching constants (K) and the YY constants (F) were plotted against Pauling's electronegativity showing systematical variations.

The most general form of the potential function in terms of a set of independent internal coordinates, *e.g.*, the valence coordinates, may be expressed as

$$2V = \sum_{i,j} f_{ij}\, \Delta q_i\, \Delta q_j$$

where $f_{ij} = (\partial^2 V/\partial \Delta q_i \partial \Delta q_j)_0$, and Δq are some displacements from equilibrium. When symmetry coordinates are constructed as linear combinations of valence coordinates ($S = U\Delta q$), the potential function reads

$$2V = \sum_{i,j} F_{ij} S_i S_j$$

where the relation between the F's and the f's are given in matrix notation by

$$F = U f \tilde{U}$$

If the vibrational normal frequencies are known, the force constants may be computed by means of Wilson's secular equation [1]

$$|GF - \lambda E| = 0 \qquad (1)$$

In general, however, the number of force constants is greater than the number of normal frequencies. Hence the secular equation cannot be solved without

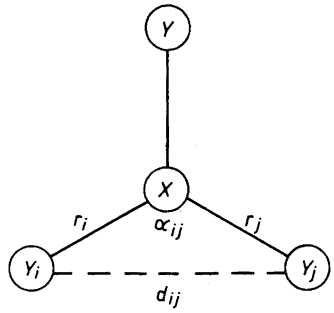

Fig. 1.

ambiguity. Many approximate potential functions have been proposed, one of the most useful ones being suggested by Urey and Bradley [2]. This function is based on the valence force field, but includes central forces between non-bonded atoms.

For small displacements from the equilibrium distance (see Fig. 1) the Urey-Bradley potential function is given by

$$\begin{aligned} V = & \sum_i [K'_i\ r_i \Delta r_i + 1/2\ K_i\ (\Delta r_i)^2] \\ & + \sum_{i<j} [H'_{ij}\ r_{ij}^2\ \Delta\alpha_{ij} + 1/2\ H_{ij}\ (r_{ij}\ \Delta\ \alpha_{ij})^2] \\ & + \sum_{i<j} [F'_{ij}\ d_{ij}\ \Delta d_{ij} + 1/2\ F_{ij}\ (\Delta d_{ij})^2] \end{aligned}$$

Here K', K, H', H, F' and F denote the force constants. r and α represent the bond lengths and interbond angles, respectivily. d is the distance between the non-bonded atoms, and $r_{ij} = (r_i r_j)^{1/2}$. The first order part of the potential function must be included as there is no reason for assuming no strain in the molecules in its equilibrium position. In other words the XY and YY stretches are not independent. Trough the relation

$$d_{ij}^2 = r_i^2 + r_j^2 - 2r_i r_j \cos\ \alpha_{ij}$$

Δd_{ij} may be eliminated, and the following expression for the potential function in terms of the valence coordinates is obtained (Shimanouchi [3]):

$$\begin{aligned} V = & \sum_i [K'_i r_i + \sum_{j(\neq i)} F'_{ij}\ s_{ij}\ d_{ij}]\ (\Delta r_i) \\ & + \sum_{i<j} [H'_{ij} r_{ij} + F'_{ij} d_{ij} (t_{ij} t_{ji})^{1/2}]\ (r_{ij}\ \Delta\ \alpha_{ij}) \\ & + 1/2\ \sum_i [K_i + \sum_{j(\neq i)} (t_{ij}^2 F'_{ij} + s_{ij}^2\ F_{ij})](\Delta r_i)^2 \\ & + 1/2\ \sum_{i<j} [H_{ij} - s_{ij} s_{ji} F'_{ij} + t_{ij} t_{ji} F_{ij}](r_{ij} \Delta\alpha_{ij})^2 \\ & + \sum_{i<j} [-\ t_{ij} t_{ji} F'_{ij} + s_{ij} s_{ji} F_{ij}](\Delta r_i)(\Delta r_j) \\ & + \sum_{i\neq j} [t_{ij} s_{ji} F'_{ij} + t_{ji} s_{ij} F_{ij}](r_j/r_i)^{1/2} (\Delta r_i)(r_{ij}\ \Delta\ \alpha_{ij}) \end{aligned}$$

For the explanation of s and t the cited work [3] should be consulted.

APPLICATION TO THE PLANAR XY_3 MODEL

For the planar symmetrical XY_3 molecule the Δr's are independent variables, but the following redundant condition exists for the $\Delta\alpha$'s

$$\Sigma \Delta\alpha_{ij} = 0$$

Since the redundant condition is exactly of the first order, it is not necessary to introduce the Langrangian undetermined multiplier to obtain a quadratic form of the potential function. From the conditions $(\partial V/\partial \Delta r)_0 = (\partial V/\partial \Delta\alpha)_0 = 0$ one obtains

$$K'_i r_i + \sum_{j\neq i} F'_{ij} s_{ij} d_{ij} = 0$$
$$H'_{ij} r_{ij} + F'_{ij} d_{ij} (t_{ij} t_{ji})^{1/2} = 0$$

Hence the potential function takes the following form:

$$V = 1/2 \sum_i [K_i + \sum_{j(\neq i)} (t_{ij}^2 F'_{ij} + s_{ij}^2 F_{ij})] (\Delta r_i)^2$$
$$+ 1/2 \sum_{i<j} [H_{ij} - s_{ij} s_{ji} F'_{ij} + t_{ij} t_{ji} F_{ij}](r_i r_j)(\Delta\alpha_{ij})^2$$
$$+ \sum_{i<j} [-t_{ij} t_{ji} F'_{ij} + s_{ij} s_{ji} F_{ij}] (\Delta r_i)(\Delta r_j)$$
$$+ \sum_{i\neq j} [t_{ij} s_{ji} F'_{ij} + t_{ji} s_{ij} F_{ij}](r_j/r_i)^{1/2} (\Delta r_i)(r_{ij}\Delta\alpha_{ij})$$

In the present case $s_{ij}^2 = s_{ji}^2 = 3/4$, $t_{ij}^2 = t_{ji}^2 = 1/4$ and $s_{ij} t_{ji} = s_{ii} t_{ji} = \sqrt{3}/4$.

For the F and G matrices the following elements are obtained:

$$F_1 = K + 3F$$
$$F_3 = K + 3/4\, F + 3/4\, F'$$
$$F_4 = H + 1/4\, F - 3/4\, F'$$
$$F_{34} = -\sqrt{3}/4\, (F + F') \qquad (2)$$

$$G_1 = \mu_y$$
$$G_3 = 2/3\, (\mu_x + \mu_y)$$
$$G_4 = 3\, (3/2\, \mu_x + \mu_y) \qquad (3)$$
$$G_{34} = 3/2\, \sqrt{3}\, \mu_x$$

Eqns. (2) and (3) are in agreement with the expressions given by Janz and Mikawa [4].

DISCUSSION OF FORCE CONSTANTS

For a molecule of the here considered type one has four UB force constants, but only three frequencies. Using Eqn. (1) K and H may be eliminated, and F may be expressed as a function of F'. A plot of F vs. F' is shown in Fig. 2 for $^{11}BCl_3$.

As the distance between the non-bonded halogen atoms are shorter than two times the van der Waals' radii (see Table 1), one must expect the internuclear forces to be repulsive. Hence F' is assumed to be negative. Another reasonable assumption is to make H positive. Furthermore, K is assumed to

Table 1. Geometrical data and van der Waals' radii.

	X——Y (Å) [a]	Y.....Y (Å)	v. d. Waals' radii (Å) [b]
BF_3	1.29	2.23	1.37
BCl_3	1.74	3.01	1.81
BBr_3	1.87	3.24	1.95
BI_3	2.10	3.64	2.16

[a] Taken from Ref. [6]
[b] Taken from Ref. [8]

be greater than F, since K is the force constant associated with a bonded and F with a non-bonded atom pair. In consequence, the following relations between the UB force constants are established.

$$F' < 0$$
$$H > 0$$
$$K > F$$

These conditions are represented graphically in Fig. 2 and lead to the conclusion that only the narrow part of the curve between A and B gives reasonable

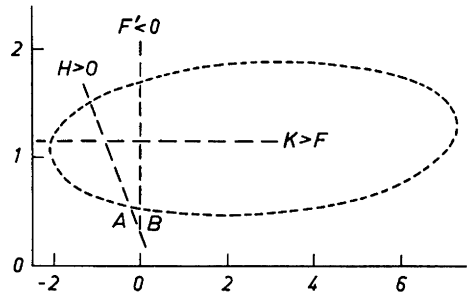

Fig. 2. F plotted against F' for BCl_3.

Table 2. Calculated force constants mdyne/Å units [a].

	BF_3	BCl_3	BBr_3	BI_3
F	0.9263	0.5370	0.4459	0.2860
F'	−0.0926	−0.0537	−0.0446	−0.0286
K	6.0446	3.0212	2.2997	1.8400
H	0.2125	0.0549	0.0880	0.0407
F_1	8.8235	4.6324	3.6373	2.6983
	(8.8236)	(4.6324)	(3.6374)	(2.6984)
F_3	6.6698	3.3837	2.6007	2.0331
	(7.4068)	(3.3424)	(3.3021)	(1.7292)
F_4	0.5135	0.2295	0.2329	0.1337
	(0.5001)	(0.2308)	(0.1807)	(0.1508)
F_{34}	−0.3609	−0.2092	−0.1737	−0.1114
	(−0.6398)	(−0.1958)	(−0.3455)	(−0.0349)

[a] The values in parentheses are calculated by Cyvin [7].

Table 3. Calculated and observed frequencies (cm^{-1}).[a]

		obs.	calc.	% dev.
$^{10}BF_3$	ν_1	888.0	888.0	0
	ν_3	1504.7	1507.0	0.2
	ν_4	480.4	482.3	0.4
$^{10}BCl_3$	ν_1	471.0	471.0	0
	ν_3	993.7	993.4	<0.1
	ν_4	243.0	243.6	0.3
$^{10}BBr_3$	ν_1	278.0	278.0	0
	ν_3	856.0	854.1	0.2
	ν_4	148.0	163.2	10
$^{10}BI_3$	ν_1	190.0	190.0	0
	ν_3	737.0	737.2	<0.1
	ν_4	100.0	100.0	0

[a] The data for BF_3 and BCl_3 are from Ref. [5], and for BBr_3 and BI_3 from Ref. [6].

force-constant values. The variations between A and B are found to be within the order of magnitude of 0.02 mdyne/Å and 0.06 mdyne/Å for F and K respectively. The same conclusion was obtained for the other boron trihalides considered. For all these molecules the following restriction was deduced

$$-0.25 < F'/F < 0$$

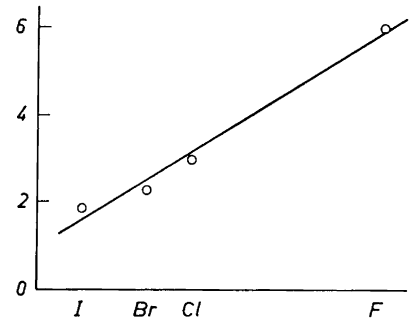

Fig. 3. K plotted against the Pauling electronegativity.

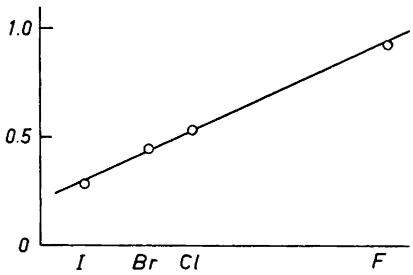

Fig. 4. F plotted against the Pauling electronegativity.

It seems reasonable to choose $F' = -0.1\ F$ for all the boron trihalides. This choise is identical with the frequently applied approximation first proposed by Shimanouchi [3].

NUMERICAL RESULTS

The numerical calculations were carried out using $F' = -0.1\ F$, and based on experimental frequencies from Ref.[5] for BF_3 and BCl_3, and from Ref.[6] for BBr_3 and BI_3. The resulting force constants are given in Table 2. Those for the fluoride, chloride and bromide are in good agreement with recently published UB force constants of Janz and Mikawa [4]. The symmetrized F-matrix elements were calculated according to Eqns. (2) and are included in Table 2. The results are compared to those calculated by Cyvin [7].

The vibrational frequencies for $^{10}BY_3$ (Y = F, Cl, Br, I) were computed from the presently calculated UB force constants. The results are presented in Table 3 and show good agreement with the observed frequencies.

CORRELATION WITH ELECTRONEGATIVITY

The values of K and F change systematically trough the series of the boron trihalides. In Figs. 3 and 4 these constants are plotted against the Pauling electronegativity for the halogenes [8].

REFERENCES

1. Wilson, E. B., Jr., Decius, J. C. and Cross, P. C. *Molecular Vibrations*, McGraw-Hill Book Co., New York 1955.
2. Urey, H. C. and Bradley, C. A., Jr. *Phys. Rev.* **7** (1939) 1969.
3. Shimanouchi, T. *J. Chem. Phys.* **17** (1949) 245.
4. Janz, G. J. and Mikawa, Y. *J. Mol. Spectroscopy* **5** (1960) 92.
5. Lindeman, L. P. and Wilson, M. K. *J. Chem. Phys.* **24** (1956) 242.
6. Wentink, T., Jr. and Tiensuu, V. H. *J. Chem. Phys.* **28** (1958) 826.
7. Cyvin, S. J. *Acta Chem. Scand.* **13** (1959) 334.
8. Pauling, L. *The Nature of the Chemical Bond*, Cornell Univ. Press, New York 1960.

Received January 26, 1962.

ACTA CHEMICA SCANDINAVICA 16 (1962) 1607–1615

The Isolation of Phosphorylhomoserine from Trichloroacetic Acid Extracts of *Lactobacillus casei*

GUNNAR ÅGREN

From the Institute of Medical Chemistry, University of Uppsala, Sweden

Free phosphorylhomoserine has been isolated in considerable amounts from trichloroacetic acid extracts of *Lactobacillus casei*. The mechanism for the formation of the substance is discussed. Some phosphopeptides present in the extract have also been purified and their amino acid composition determined.

In a recent communication from this laboratory evidence was presented for the occurrence in the trichloroacetic acid soluble fraction of *L. casei* of a free phosphorylated amino acid of unknown composition [1]. This paper describes the identification of this compound as phosphorylhomoserine (HserP) *.

EXPERIMENTAL

Preparation. Lactobacillus casei (7461) was cultivated in a medium with the following composition [2]: 10 g of Dextropur **, 10 g of $NaOCOCH_3 \cdot 3H_2O$, 10 g of Bactopeptone *, 1 g of yeast extract **, 25.4 ml of liver extract ***, 0.5 ml of salt mixture **** per 1000 ml of medium at pH 6.8. For large scale cultivation of radioactive labelled bacteria (120 l) the necessary ingredients were first dissolved in 5 l water and heated at 100°C for about 15 min. After cooling a dark precipitate was removed by filtration. The filtrate was evenly distributed in forty 6 liter Erlenmeyer flasks and subsequently water was added to a final volume of 3 l per flask. After adjusting the pH to 6.8, sterilization was accomplished by autoclaving the flasks 15 min. at 118°C.

*Abbreviations: HserP = O-phosphorylhomoserine; Hser = homoserine; ^{32}P = inorganic radioactive phosphate; TCA = trichloroacetic acid; UV = ultra violet; AMP = adenylic acid; MurP = O-phosphorylmuramic acid; ThrP = O-phosphorylthreonine; ATP = adenosine triphosphate; ADP = adenosine diphosphate; P_i = inorganic phosphate; Thr = threonine.

** Glucose manufactured by Corn Products Co., New York.

* Parke, Davis and Co.

** Difco Laboratories.

*** 100 g of Difco Liver was dissolved in 1330 ml and kept at 50° for one hour and subsequently at 80° for 5 min. After filtration and concentration the filtrate was lyophilized. This material was dissolved to contain 15 mg per ml.

**** 4 g of $MgSO_4.H_2O$, 1 g $FeSO_4.7\ H_2O$, 1 g of NaCl, 0.1 g of $MnSO_4.H_2O$ were dissolved to 100 ml.

Inocula for large scale cultivation was prepared by transferring a small amount of growth from a stab culture to two 10 ml flasks, each containing 5 ml of medium. The amount of inocula was increased in the five subsequent steps as previously described [3]. 300 ml suspension from step 5 was then added to each 6 l flask containing 3 l sterilized medium. 1 mC radioactive phosphate per liter medium was added at the same time. Previously it had been shown that the presence of as much as 100 mC per liter medium had no demonstrable effect on growth or acid production over a period of 72 h [4]. Incubation was carried out in an air incubator for 17 h at 37°C. In order to increase the utilization of ^{32}P added to the medium inorganic phosphate was excluded from the salt mixture since preliminary experiments had shown that the phosphorus present in Bactopeptone and liver furnished sufficient total phosphorus (0.005 %) for normal growth.

At the end of the cultivation the radioactive bacteria were separated from the medium in Sharples centrifuges enclosed in a small stainless steel house with a perspex window and with separate effective ventilation. The usual yield of fresh bacteria from a single 120 liter cultivation was about 500–600 g. This material was washed two times with 10 volumes of cold 10 % TCA, each time for about 15 min. The supernatant fluids from the extracted and centrifuged cell suspensions were shaken with ether several times to remove the TCA. The solution was evaporated to a volume of about 300 ml, again shaken several times with ether, and the pH adjusted to 6–7 by addition of a few drops of 1 N NaOH. The concentrate was then run through a 90 × 3 cm Dowex 1 (2 % DVB) formate column mainly according to Hurlbert *et al.*[5] A radioactive peak with inconsiderable UV absorption at 260 or 280 mμ was observed (Fig. 1 in Ref.[6]) located in the position between AMP and inorganic phosphate and eluted between 0.5 M and 2.5 M formic acid concentration. The TCA soluble fraction from each batch of bacteria containing the radioactive, non-UV-absorbing peak was concentrated *in vacuo* to a small volume with repeated additions of water to remove excess formic acid. The concentrated solution was run through a Dowex 50 (8 % DVB) column with 0.01 N HCl (column dimensions 2 cm × 40 cm for a 120 liter culture). Two peaks containing ninhydrin-positive material were eluted following the inorganic phosphate, the first after about 1.0 column volume and the second after about 2.3 column volumes of eluate (effluent volume/resin volume). Fig. 1 in Ref.[1] pictures a typical result.

The material from the second peak which contained the new phosphorylated amino acid was collected and excess of acid removed as described above. Each sample of material was again run through a small Dowex 1 (2 % DVB) formate column (0.9 cm × 50 cm) and eluted mainly according to Hurlbert *et al.*[5] with a gradient 0 → 1 M formic acid and with a volume of 300 ml of the mixer. A large peak appeared when the acidity in the eluate reached a concentration corresponding to 0.60 M formic acid or in the same position as MurP [3]. In Fig. 3 in Ref.[1] the elution curve from a typical experiment is given. The total dry weight of bacteria from five large scale preparations was 650 g. The total weight of the new TCA-soluble compound from the five experiments amounted to 55 mg. Several attempts to crystallize the substance from water, water-methanol or water acetone mixtures failed. The phosphorylated compound was rather soluble in these solvents.

In order to repeat these experiments with larger amounts of material a large scale cultivation of the microorganisms were carried out in a 1000 liter tank on the medium described before *. The yield of fresh bacteria was about 8 kg. The material was washed with cold TCA and the TCA extracts shaken with ether and concentrated *in vacuo* as described before. The concentrated TCA extracts from the unlabelled batch of microorganisms were mixed with a TCA extract from a 120 liter cultivation of labelled bacteria. The mixed extracts were then filtered into five Dowex 1 formate columns (50 × 6.5 cm) and eluted mainly according to Hurlbert *et al.*[5] The eluate was collected in fractions of about 70 to 80 ml every 15 min.

The elution was started with water and about 48 fractions were collected. In the system which followed, a 1700 ml mixing volume was used. The four elution ranges which approximated 1 N formic acid, 4 N formic acid, 0.2 M ammonium formate in 4 N formic acid and 0.4 M ammonium formate in 4 N formic acid were obtained by changing the reservoir to contain these solutions at tubes 48, 200, 600 and 850. Altogether 1000 fractions were collected in each series.

* The cultivation was carried out in the pilot plant of the Department of Bacteriology, Karolinska institutet, Stockholm.

Analytical methods. The nucleotides were assayed as previously described [6]. The radioactivity of the different fractions from the column chromatography of the TCA soluble nucleotides was measured in glass cups with the L.K.B. Robot Scaler. Scanning of the paper chromatogram of HserP, phosphopeptides and nucleotides was made according to Ågren *et al.*[7]

The amino acid composition of phosphopeptides was determined by two-dimensional chromatography [8]. This method was used together with one-dimensional chromatography in 0.1 N ammonium acetate-ethanol (3:7 by vol.), isobutyric acid-ammonia-water (79:1:25 by vol.), butanol-acetic acid-water (4:1:5 by vol., solvent phase) [9]. Phosphopeptides were hydrolyzed with 2 N HCl for 20 h at 120°C in sealed tubes. For chromatography Whatman No. 1 papers were used, and for ionophoresis Whatman No. 3, where the solvents were either a 0.1 M solution of pyridine-acetic acid at pH 5 or 1 N acetic acid.

Synthesis of DL-*phosphorylhomoserine.* The barium salt of DL-phosphorylhomoserine was synthesized according to Levene and Schormüller [10] by phosphorylation of homoserine with phosphoric acid and phosphoric anhydride. Barium was removed by electrodialysis and the substance purified by running through a small Dowex 50 column (55 cm × 0.9 cm) by elution with 0.01 N HCl. The effluent fluid in the tubes was tested for ninhydrin-reacting substance. DL-Phosphorylhomoserine crystallized out of water solutions. The yield was about 5 % of the theoretical. (Found: C 24.9; H 4.88; N 7.16; P 15.0. Calc. for $C_4H_{10}O_6NP$ (199.1): C 24.1; H 5.06; N 7.04; P 15.6).

Dephosphorylation of HserP was performed in sealed glass tubes with 2 N HCl at 120°C for 20 h. Still some phosphorylated product was present and appeared on chromatograms. Hser in the hydrolyzed samples was then purified by preparative paper electrophoresis in 1 N acetic acid. Hser was washed out from the paper strip with distilled water.

RESULTS

Separation of phosphorylhomoserine from phosphopeptides

Also in the 1000 liter cultivation the radioactive peak with inconsiderable UV absorption, containing the desired material was located in the same place of the elution curve as in small scale preparations, *viz.* in the position between AMP and the next large UV-peak (Fig. 1, Ref.[6]). Other parts of the elution diagrams were quite similar to that pictured in this figure.

The ether extracted TCA soluble fraction from the five column eluates containing the peak without UV absorption was concentrated *in vacuo* to a

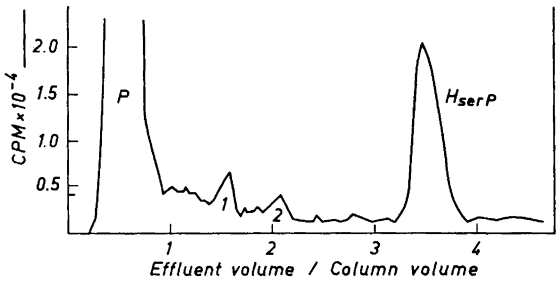

Fig. 1. TCA soluble material collected between 0.7 and 2.5 M formic acid solution on a Dowex 1 column and afterwards separated on a Dowex 50 column. The radioactivity curve is obtained by plotting the number of impulses per min (cpm) in 1 ml aliquots of each tube.

small volume with repeated additions of water to remove excess of formic acid. The concentrated solution was run through a Dowex 50 W (X-8, 200—400 mesh) column with 0.01 N HCl (column dimensions 3 cm × 50 cm). 10 ml fractions were collected at a rate of 0.66 per minute. In Fig. 1 the elution curve is given. A comparison with a similar elution diagram from small scale cultivations (Fig. 1, Ref.[1]) showed some significant differences. In the present diagram two small peaks containing ninhydrin-positive material of phosphopeptide nature were eluted while in earlier experiments only one such peak was observed. Further, these peptide peaks as well as HserP were delayed on the elution curve. Systematic investigations have shown this to be a general phenomenon when Dowex 50 W (white) is used.

Analysis of the phosphopeptide fractions. In the earlier paper it was demonstrated that the single phosphopeptide peak was not homogeneous. A ionophoretic control (pyridine-acetate buffer at pH 5) showed two radioactive peaks. The small amounts of material did not allow rechromatography of this fraction on a second Dowex column. After hydrolysis, two-dimensional paper chromatography of the material showed at least six spots corresponding to the position of aspartic acid, glutamic acid, serine, threonine, alanine and leucine or isoleucine, all members of the phosphopeptide isolated from the enzymatic active center of chymotrypsin or phosphoglucomutase [11].

Consequently a new attempt was made to investigate the homogeneity of the two phosphopeptides which now were separated already on the first Dowex 50 column. The material from peaks 1 and 2 was collected and excess HCl removed as described above. Each sample of material amounted only to a few mg and was run through small Dowex 1 (2 % DVB) formate columns (0.9 cm × 20 cm) and eluted mainly according to Hurlbert *et al.*[5] with a gradient 0→1 M formic acid and with a volume of 150 ml in the mixer. In Figs. 2 and 3 the elution curves are given. Obviously both of the two phosphopeptide fractions from the Dowex 50 column consisted of complex mixtures of peptides. The material from peak No. 1 was resolved into at least three major peaks, A, B and C, weighing from 0.2—1.5 mg which were collected for analysis. The last large peak eluted at 0.9 M formic acid concentration was inorganic phosphate. In ionophoretic controls of the homogeneity of the material from peak A in 1 N acetic acid a radioactive peak could not be found in the scanning

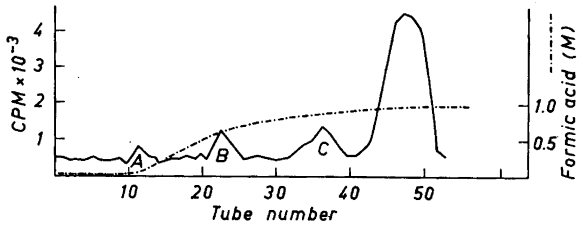

Fig. 2. Radioactivity curve of the material from peptide fraction No. 1, Fig. 1, separated on a Dowex 1 column. The radioactivity curve (the continuous line) is obtained by plotting the number of impulses per min (cpm) in 1 ml aliquots of each tube. The broken line represents formic acid concentration.

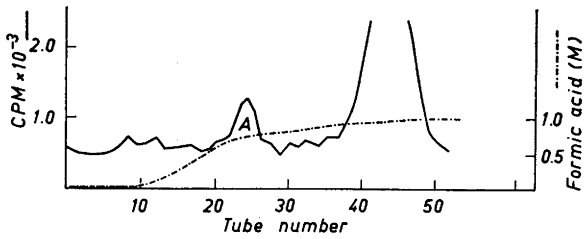

Fig. 3. Radioactivity curve of the material from peptide fraction No. 2, Fig. 1, separated on a Dowex 1 column. The radioactivity curve (the continuous line) is obtained by plotting the number of impulses per min (cpm) in 1 ml aliquots of each tube. The broken line represents formic acid concentration.

of the electropherogram. After acid hydrolysis paper chromatographic analysis showed spots corresponding to the location of aspartic and glutamic acids, serine alanine and three other unidentified amino acids.

The electropherogram of fraction B, 1.5 mg, showed one radioactive and one smaller unlabelled ninhydrin-positive spot. The small amount of material did not allow purification by preparative paper electrophoresis. A two-dimensional chromatogram of the hydrolysate from B showed spots corresponding to the positions of aspartic and glutamic acids, serine, glycine, alanine, a spot with the same color and the same position as β-alanine and one unidentified spot below the glycine spot. The proportions of identified amino acids were other than in the hydrolysate of fraction A. A paper electropherogram of peak C (1.0 mg) showed that it consisted of two radioactive ninhydrin-positive spots too close to each other to allow a preparative electropherographic separation. The hydrolysate contained the same amino acids as in B but in other proportions.

The material from peak No. 2 from the Dowex 50 column gave an elution diagram from the Dowex 1 column as demonstrated in Fig. 3. Only the larger peak A eluted between 0.60 to 0.75 M formic acid was collected. The last large peak on the elution diagram was inorganic phosphate. The weight of A was 2.0 mg. A ionophoretic control of the homogeneity (1 M acetic acid) showed one radioactive and one unlabelled ninhydrin-positive spot well separated from each other. Accordingly, the rest of the material was purified by ionophoresis and elution of the radioactive section of the paper strip with distilled water. As control another section of similar size was also washed with water. Two-dimensional paper chromatography of the purified, hydrolyzed material showed spots corresponding to the position of aspartic and glutamic acids, serine, glycine, threonine, alanine, valine and isoleucine or leucine.

The isolation of phosphorylhomoserine. The material forming the large peak in Fig. 1 labelled HserP was collected and excess HCl removed as described above. The weight was 218 mg. The material was run through a small Dowex 1 (2 % DVB) formate column (0.9 cm × 20 cm) and eluted with a gradient 0 → 1 M formic acid and with a volume of 125 ml in the mixer. Only one large peak appeared between 0.60 and 0.80 M formic acid or in the same position previously found for the same material from small scale cultivations [1] and

also for MurP [3]. The weight of the material from the peak was 210 mg. Since the total dry weight of the bacteria was 1.100 g the yield was better than in the previous small scale preparations [1]. The slightly yellow coloured material was again purified chromatographically on a small Dowex 50 W (X-8, 200—400 mesh) column with 0.01 N HCl (column dimensions 0.9 cm × 55 cm). Only one large symmetrical peak appeared when 3.2 column volume of HCl had passed through or in the same position as in Fig. 1. The dry weight of material was 200 mg.

Identification and characterization

Elementary analysis of the isolated substance was already given in the previous paper. The figures indicated that the substance could be either phosphorylthreonine, previously isolated in this laboratory first from casein [12,13] and later from sheep liver protein [14] or the isomer phosphorylhomoserine. The position of the dephosphorylated amino acid on a two-dimensional paper chromatogram did not coincide with that of threonine. It could be suspected that the new compound was phosphorylhomoserine. With the larger amounts of material from the large scale cultivation the substance could be crystallized by slow evaporation from water solutions as needleshaped crystals.

Elementary analysis of C, H, and N were made by Mr W. Kirsten at this institute. Phosphorus was analyzed according to a modification of Martin and Doty [15].

$C_4H_{10}O_6NP$ (199.1)	Calc.	C 24.1;	H 5.06;	N 7.04;	P 15.6
	Found 1	25.6	4.40	7.12	15.0
	2	24.7	5.24	6.55	14.8
	3	24.7	—	7.07	15.8

Paper ionophoresis and paper chromatography. The ionophoretic migration of HserP in comparison to SerP and ThrP is shown in Table 1. The dephosphorylated compound showed the same mobility as serine and threonine at pH 5. Fig. 4 is a photograph of a chromatogram of the dephosphorylated compound and synthetic Hser running parallely. In the five solvents listed in a preceding paper [9] identical R_F values for the two compounds were obtained. The same result was obtained with 0.1 M ammonium acetate-ethanol (3:7). In several two-dimensional chromatograms the dephosphorylated compound and synthetic Hser only gave a single spot.

X-Ray studies. X-Ray powder photographs of the isolated compound and DL-HserP are given in Fig. 5. The two crystal preparations did not give identical diagram.

Table 1. The ionophoretic mobility of HserP in 1 N acetic acid compared with that of SerP and ThrP (the Pherograph of Wieland-Pfleidern). Time 105 min, 2800 V and 15 mA. + indicate that the substances move toward the anode. The distance measured to slowest part of the spots. Figures are given in cm.

Isol. HserP	Synt. HserP	SerP	ThrP
+ 18	+ 18	+ 21	+ 17

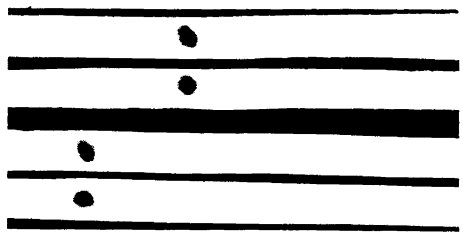

Fig. 4. Two one-dimensional chromatograms run with isobutyric acid-ammonia-water (below) and pyridine-isoamylalcohol-water (above) showing that the dephosphorylated compound gives a spot identical with synthetic homoserine.

Optical rotation. For HserP the following value was obtained $\alpha_D^{22.5}$ + 0.15° (water, *l*, 1; *c* 2.4) which corresponds to $[\alpha]_D^{22.5}$ + 6.25°; $[M]_D^{22.5}$ + 12.4°. M.P. 178° (decomp.).

DISCUSSION

From the results it seems to be proved that the isolated free phosphorylated amino acid in the TCA extracts of *L. casei* is HserP. So far it has not been possible to establish the presence in these extracts of free SerP recently found in the corresponding extracts of animal livers and kidneys [16]. A probable reason for the finding of free SerP in the organ extracts could be the recent observation of Ichihara and Greenberg [17]; using a crude enzyme preparation they presented evidence for the biosynthesis of serine from glyceric acid *via* SerP, which should be dephosphorylated to serine. If that was the single reason for the presence of free SerP in the organ extracts it could have been expected to find free SerP also in the microbial extracts. However, it is quite possible that the bacterial biosynthesis of serine might proceed according to other lines.

About in the same position as SerP on the elution diagram of the bacterical TCA extracts through the Dowex 50 column only two phosphopeptide frac-



Fig. 5. X-Ray powder diagram of HserP from *L. casei* (upper) and synthetic HserP (below). Guinier camera. Nickel-filtered copper *K*-radiation.

tions of complex composition could be observed. From one of these it was possible to purify a phosphopeptide which seemed to be homogeneous on paper electropherogram. It is of considerable interest that the amino acid composition of this peptide is the same as found by Koshland [11] and others [18-20] in the phosphopeptides from the "active site" of phosphoglucomutase and chymotrypsin. The reason for the presence of free peptides of this type in the TCA extracts of *L. casei* is at present not clear.

The optical rotation shows about the same values as SerP as well as ThrP, the latter with different sign [13,21]. Phosphorylserine: $[\alpha]_D^{23}$ + 7.2°; $[M]_{23}^D$ + 13.5. Phosphorylthreonine: $[\alpha]_{24}^D$ −7.4°; $[M]_{24}^D$ −14.6. The optically active and the racemic form of HserP did not give identical X-ray diagrams as was also the case with ThrP [13]. In the latter instance it was probable that the DL-forms were a conglomerate as has been found for the unphosphorylated amino acid [22].

Although this communication seems to be the first report of the isolation of free HserP in extracts of *L. casei* there has been some earlier evidence for a possible presence of the compound in similar extracts. Using ^{14}C labelled glucose it has been shown that homoserine while not a structural component of the bacterial protein is a precursor of threonine in *E. coli* [23]. Wotanabe *et al.*[24-26] using crude enzyme preparations showed that the final step in threonine biosynthesis in yeast required two enzyme fractions, Hser kinase (1) and a second fraction catalyzing an elimination of P_i coupled with the isomeration to form L-Thr from HserP (2).

$$\text{L-Hser} + \text{ATP} \longrightarrow \text{HserP} + \text{ADP} \quad (1)$$

$$\text{HserP} + H_2O \longrightarrow \text{L-Thr} + P_i \quad (2)$$

$$\text{L-Hser} + \text{ATP} + H_2O \longrightarrow \text{L-Thr} + \text{ADP} + P_i \quad (3)$$

The seemingly needless expenditure of phosphate bond energy has been visualized as a device to shift the equilibrium in favor of the accumulation of Thr [27]. According to this scheme HserP should only be an intermediate which once formed ought to disappear. It has not so far been possible to show the occurrence of reaction (1) in extracts of *Neurospora* [27]. Taking all this in consideration the reason for the presence of the comparatively large amounts of HserP in the TCA extracts of *L. casei* is not clear. Meanwhile it can be stated that by following the method described an alternative and easy way is given to obtain considerable amounts of highly labelled HserP. The labelling will be determined by the amount of radioactive inorganic phosphate added to the medium.

Acknowledgements. This investigation was supported by grants from the *Swedish Medical Research Council.* Skilful assistance by Mr. Tage Fransson, Evert Kristensson and Thore Persson is greatfully acknowledged.

REFERENCES

1. Ågren, G. *Acta Soc. Med. Upsaliensis* **64** (1959) 379.
2. Ågren, G. *Acta Physiol. Scand.* **17** (1949) 55.
3. Ågren, G. and de Verdier, C.-H. *Acta Chem. Scand.* **12** (1958) 1927.
4. Ågren, G., de Verdier, C.-H. and Glomset, J. *Acta Chem. Scand.* **9** (1955) 196.
5. Hurlbert, R. B., Schmitz, H., Brumm, A. F. and Potter, V. R. *J. Biol. Chem.* **209** (1954) 23.
6. de Verdier, C.-H. and Ågren, G. *Acta Chem. Scand.* **13** (1959) 1425.
7. Ågren, G., de Verdier, C.-H. and Glomset, J. *Acta Chem. Scand.* **8** (1954) 1570.
8. de Verdier, C.-H. and Ågren, G. *Acta Chem. Scand.* **2** (1948) 783.
9. Ågren, G., de Verdier, C.-H. and Glomset, J. *Acta Soc. Med. Upsaliensis* **60** (1955) 30.
10. Levene, P. A. and Schormüller, A. *J. Biol. Chem.* **105** (1934) 561.
11. Koshland, D. E. and Erwin, M. Y. *J. Am. Chem. Soc.* **79** (1957) 2657.
12. Ågren, G., de Verdier, C.-H. and Glomset, J. *J. Berichte ges. und exper. Pharmakol.* **145** (1951) 226.
13. de Verdier, C.-H. *Acta Chem. Scand.* **7** (1953) 196.
14. Ågren, G., de Verdier, C.-H. and Glomset, J. *Acta Chem. Scand.* **9** (1955) 1041.
15. Martin, J. B. and Doty, D. M. *Anal. Chem.* **21** (1953) 965.
16. Ågren, G. *Acta Soc. Med. Upsaliensis* **65** (1960) 49.
17. Ichihara, A. and Greenberg, D. M. *J. Biol. Chem.* **224** (1957) 331.
18. Cohen, J. A., Oosterbaum, R. A., Warringa, M. G. and Jansz, H. S., *Discussions Faraday Soc.* **20** (1955) 114.
19. Schaffer, N. K., Harshman, S., Engle, R. R. and Drisko, R. W. *Federation Proc.* **14** (1955) 275.
20. Turba, F. and Gundlach, G. *Biochem. Z.* **327** (1955) 186.
21. Ågren, G., de Verdier, C. H. and Glomset, J. *Acta Chem. Scand.* **5** (1951) 324.
22. Shoemaker, D. P., Donohue, J., Shoemaker, V. and Corey, R. B. *J. Am. Chem. Soc.* **72** (1950) 2328.
23. Roberts, R. B., Abelson, P. H., Cowie, D. B., Bolton, E. T. and Britten, R. J. *Studies of biosynthesis in Escherichia Coli.* Carnegie Institute of Washington, Publication No. 607 (1955).
24. Wotanabe, Y., Konishi, S. and Shimura, K. *J. Biochem. Tokyo* **42** (1955) 837.
25. Wotanabe, Y. and Shimura, K. *J. Biochem. Tokyo* **43** (1956) 283.
26. Wotanabe, Y., Konishi, S. and Shimura, K. *J. Biochem. Tokyo* **44** (1957) 299.
27. Flavin, M. and Slaugther, C. *Biochim. et Biophys. Acta* **36** (1959) 554.

Received January 31, 1962.

ACTA CHEMICA SCANDINAVICA 16 (1962) 1616–1626

The Electronic Spectra of Thioamides and Thiohydrazides

Part I. LCAO-MO Treatment and Band Classification for Thiobenzamides

JAN SANDSTRÖM

Department of Organic Chemistry, University of Lund, Lund, Sweden

The ultraviolet spectra of thiobenzamide, N-methylthiobenzamide, and N,N-dimethylthiobenzamide have been recorded in different solvents. A long-wavelength, low-intensity maximum has been assigned to a $n \rightarrow \pi^*$ transition, and a maximum with higher intensity to a $\pi \rightarrow \pi^*$ transition. These assignations and the same ones for thioacetamide are supported by simple LCAO–MO calculations. For dimethylthiobenzamide a steric effect has been included in the calculations, and a prediction of the spectrum of thioacrylamide is given. S-protonation of thioamides in sulphuric acid is supported by NMR spectra.

The light absorption of organic thione compounds has been the subject of investigation for quite a long time due to the remarkable "chromophoric" properties of the thione group. As readily available thiones the thioamides have attracted a special interest. Hantzsch [1] showed by comparing the ultraviolet spectra of suitably substituted derivatives with those of the parent compounds that thioamides mainly occur as thiones and not as the tautomeric imidothiol forms. Burawoy [2,3] made a systematic survey of the ultraviolet spectra of available thiones, and he found a characteristic long-wavelength, low-intensity band, which he called the R-band, and a more intense band, the K-band, at shorter wavelengths. The origin of the R-band has been a matter of dispute for some time [3–5], but it is now fairly well established that the low-intensity band of the thiones is due to the excitation of a nonbonding electron from the sulphur atom to an antibonding π orbital, a $n \rightarrow \pi^*$ transition in the terminology proposed by Kasha [5]. The classification of $n \rightarrow \pi^*$ bands is mainly based on the effects of substituents and solvent polarity, and by such means it has recently been shown [6–10] that the low-intensity bands in simple thioamides are also due to $n \rightarrow \pi^*$ transitions.

In his very thorough investigation of the ultraviolet spectra of organic thiones, Janssen [6–8] has also included a number of thioamides. Regarding

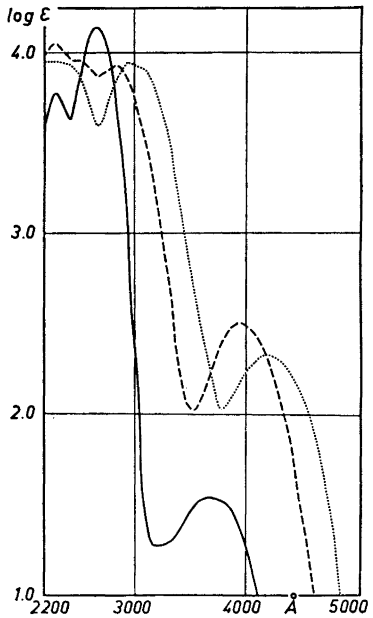

Fig. 1. Ultraviolet spectra of thioacetamide (————), thiobenzamide (.....), and N,N-dimethylthiobenzamide (- - - -) in heptane.

the classification of the strong band of thioacetamide at 2670 Å (log ε 4.14, in heptane) he comes to two conflicting conclusions. His study of the solvent and substituent effects leads to the assignation of the band to a $n \rightarrow \sigma^*$ transition, whereas a LCAO—MO calculation gives better agreement if the band is assumed to be due to a $\pi \rightarrow \pi^*$ transition.

It was hoped that this uncertainty could be removed by an investigation of thioamides where the thioamide group was conjugated with an unsaturated system. A $\pi \rightarrow \pi^*$ transition should occur with lower energy due to the conjugation, whereas a $n \rightarrow \sigma^*$ transition should be less affected. Therefore, if the 2670 Å band is considerably shifted towards a longer wavelength by conjugation, it is probably a $\pi \rightarrow \pi^*$ band, but if it remains in the same region, it should be due to a $n \rightarrow \sigma^*$ transition. As a readily available conjugated thioamide thiobenzamide was chosen, and it was found that the 2670 Å band disappears when the thioamide group is conjugated with a phenyl ring. Instead, a new band appears at 2980 Å (log ε 3.81, in heptane). However, it has been shown by Pullman [11] that enlargment of a conjugated system can sometimes lead to a hypsochromic shift instead of the expected bathochromic one. Therefore it was thought worthwhile to perform a LCAO—MO calculation on thiobenzamide in order to examine the effect of conjugation on the different energy levels. It is well known that the simple Hückel approximation often gives moderately reliable results only for the ground state properties, but the iterative procedure proposed by Wheland and Mann [12] has been of considerable value in the hands of Nagakura [13] for the calculations involving excited levels, and the somewhat simplified procedure of Janssen [8] gives

Table 1.

	Thioacetamide	Conjugate acid (I)	Thioacrylamide	Thiobenzamide	Dimethylthiobenzamide (1)	Dimethylthiobenzamide (2)
Antibonding orbitals	$\alpha - 1.209\beta$	$\alpha - 0.972\beta$	$\alpha - 2.092\beta$ $\alpha - 0.782\beta$	$\alpha - 2.781\beta$ $\alpha - 1.797\beta$ $\alpha - 1.333\beta$ $\alpha - 0.795\beta$	$\alpha - 2.783\beta$ $\alpha - 1.810\beta$ $\alpha - 1.333\beta$ $\alpha - 0.819\beta$	$\alpha - 2.688\beta$ $\alpha - 1.539\beta$ $\alpha - 1.333\beta$ $\alpha - 1.059\beta$
Nonbonding orbital	$\alpha + 0.029\beta$	–	$\alpha + 0.055\beta$	$\alpha + 0.051\beta$	$\alpha + 0.027\beta$	$\alpha + 0.009\beta$
Bonding orbitals	$\alpha + 0.388\beta$ $\alpha + 2.820\beta$	$\alpha + 0.941\beta$ $\alpha + 3.032\beta$	$\alpha + 0.368\beta$ $\alpha + 1.540\beta$ $\alpha + 2.966\beta$	$\alpha + 0.366\beta$ $\alpha + 1.347\beta$ $\alpha + 1.386\beta$ $\alpha + 2.519\beta$ $\alpha + 3.087\beta$	$\alpha + 0.321\beta$ $\alpha + 1.347\beta$ $\alpha + 1.361\beta$ $\alpha + 2.479\beta$ $\alpha + 3.038\beta$	$\alpha + 0.330\beta$ $\alpha + 1.336\beta$ $\alpha + 1.340\beta$ $\alpha + 2.578\beta$ $\alpha + 2.834\beta$
$\Delta E_{n\rightarrow\pi^*}$ $\Delta E_{\pi\rightarrow\pi^*}$	$- 1.238\beta$ $- 1.597\beta$	– $- 1.913\beta$	$- 0.837\beta$ $- 1.150\beta$	$- 0.846\beta$ $- 1.161\beta$	$- 0.846\beta$ $- 1.140\beta$	$- 1.068\beta$ $- 1.389\beta$
Resonance energy *	$- 1.104\beta$	–	$- 2.436\beta$	$- 4.108\beta$	$- 4.176\beta$	$- 3.924\beta$

* -2β substracted for the thiobenzamides. The value for the energy of the C=S bond, -2.312β, is taken from Ref.[8]

good agreement between calculated and found $n \rightarrow \pi^*$ and $\pi \rightarrow \pi^*$ transition energies for a number of different thiones. The method of Janssen can therefore be used with confidence at least to calculate the directions of the shifts imposed upon the energy levels of the thioamide group by conjugation. The calculations were carried out using an electronic digital computor, and the solutions of the secular equations and the calculations of new parameters were combined into one single program. The iterations were continued until $|p_m - p_{m-1}| < 4 \times 10^{-4}$ and $|q_m - q_{m-1}| < 2 \times 10^{-4}$ (p_m and q_m = bond order and charge in the m-th iteration). The Coulomb and resonance integrals are the same as those used by Janssen [8].

The value of $\Delta E_{\pi-\pi^*}$ for thiobenzamide (Table 1) shows that the effect of conjugation actually is to shift the $\pi \rightarrow \pi^*$ band to a lower frequency. The numerical value of the shift is lower than expected from the calculated

Table 2.

$\nu_{\text{thioacetamide}}/\nu_{\text{thiobenzamide}}$		
	$n \rightarrow \pi^*$	$\pi \rightarrow \pi^*$
Calc.	1.46	1.38
Found	1.14	1.12

Table 3.

Compound	Solvent	$n \rightarrow \pi^*$			$\pi \rightarrow \pi^*$					
		λ_{max} Å	log ε	$\Delta\nu^a$ cm.$^{-1}$	λ_{max} Å	log ε	$\Delta\nu^a$ cm.$^{-1}$	λ_{max} Å	log ε	$\Delta\nu^a$ cm.$^{-1}$
CH_3CSNH_2	Heptane	3670[b]	1.55[b]	—	2670	4.14	—	2310	3.77	—
	Ethanol	3270	1.71	—	2660	4.10	—	2100	3.63	—
	Water	3090	1.88	—	2610	4.00	—			
$C_6H_5CSNH_2$	Heptane	4180	2.33	3400	2980	3.81	3900	2390	3.94	1500
	CCl_4	4125	2.40	—	—	—	—	—	—	—
	Ethanol	3700[c]	2.4	—	2960	3.85	—	2410	3.97	—
	Water [d]	3650[c]	2.5	—	2870	3.93	—	2480	3.93	—
$C_6H_5CSNHCH_3$	Heptane	4020	2.48	2400	2880	3.81	2800	2370	4.04	1100
	CCl_4	3960	2.45	—	—	—	—	—	—	—
	Ethanol	3905	2.41	—	2865	3.86	—	2380	4.03	—
	Water [d]	3550[c]	2.4	—	2750	3.92	—	2450	3.97	—
$C_6H_5CSN(CH_3)_2$	Heptane	3950	2.50	2000	2840	3.93	2600	2500	3.95	3300
	CCl_4	3890	2.56	—	—	—	—	—	—	—
	Ethanol	3660	2.47	—	2810	3.97	—	2390	3.99	—
	Water [d]	3520	2.47	—	2710	4.02	—	2300[c]	4.0	—

[a] $\nu_{CH_3CSNH_2} - \nu_{PhCSNR_1R_2}$ [b] Extrapolated value [c] Shoulder [d] With 5 % of ethanol.

transition energies of thioacetamide and thiobenzamide (Table 2), but the same applies to the $n \rightarrow \pi^*$ band and by no means invalidates the argument for the assignation of the 2670 Å band of thioacetamide to a $\pi \rightarrow \pi^*$ transition.

From Table 1 it is apparent that the energies of the highest bonding level and of the nonbonding level are only slightly raised, and therefore the bathochromic shifts of the $n \rightarrow \pi^*$ and $\pi \rightarrow \pi^*$ bands should mainly be due to the considerable decrease in energy of the lowest antibonding π level. If this is correct, the shift in frequency of the $n \rightarrow \pi^*$ and $\pi \rightarrow \pi^*$ bands when going from thioacetamide to thiobenzamide or its N-methyl derivatives ($\Delta\nu$ in Table 3) should be of the same magnitude. This is also the case. The $\Delta\nu$ values have been calculated for heptane solution only, because in ethanol and in water several of the $n \rightarrow \pi^*$ bands are so close to the $\pi \rightarrow \pi^*$ bands that the true positions of the maxima become uncertain, and furthermore the solvent-solute interaction should be as weak as possible, as is the case in heptane solutions.

The effect of methyl substitution on the nitrogen atom does not parallel the one found by Janssen for thioacetamide and several other simple thioamides. Instead, hypsochromic shifts are observed, when two methyl groups are successively introduced (Table 3). It is well known that methyl substitution increases the electron donating capacity of an amino group. This is borne out by the mesomeric dipole moments of the amino, methylamino, and dimethylamino groups, which are 1.67, 1.93, and 2.06 *D*, according to a recent determination by Smith [14]. In the calculations this effect can be accounted for in a simple

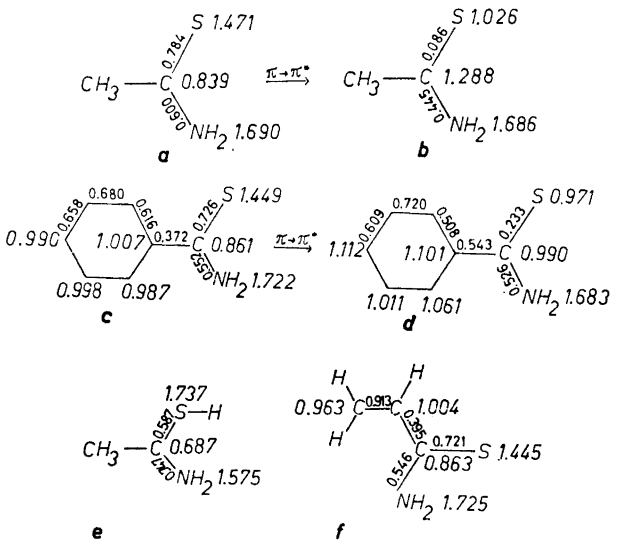

Fig. 2. π Electron distribution and π bond order of thioacetamide in ground state (a) and in excited state (b), thiobenzamide in ground state (c) and excited state (d), thioacetamidium ion in ground state (I, e), and thioacrylamide in ground state (f).

way by giving lower absolute values to the Coulomb integral for the nitrogen atom, when methyl groups are introduced. Janssen [15] has shown that an increase in the electron-donating capacity of a hetero atom attached to a thione group will raise both the nonbonding level and the lowest antibonding π level. For thiobenzamide a calculation has now been performed with the Coulomb integral for nitrogen changed from $\alpha + 1.5\beta$ to $\alpha + 1.3\beta$. The results are found in Table 1, (1). It appears that the nonbonding and lowest antibonding levels are raised by the same amount of energy, but the highest bonding orbital is also raised, and the change in transition energy is negligible both for the $n \rightarrow \pi^*$ and the $\pi \rightarrow \pi^*$ transitions. Thus the change in the Coulomb integral does not seem to account for the hypsochromic shifts on methyl substitution. An examination of the charge diagrams of the ground and excited states in a $\pi \rightarrow \pi^*$ transition (Fig. 2) shows that the inductive effect of the substituents on the nitrogen atom must have little effect on the energy of this transition both in thioacetamide and in thiobenzamide. This conclusion is based on the fact that the charge of the nitrogen atom is hardly affected by the transition. Therefore, as has been shown by Gerson and Heilbronner [16], a change of the Coulomb integral is without effect on the energy of the transition. Instead, hyperconjugation and steric effects must be responsible for the shifts caused by alkyl substitution. An examination of molecular models reveals that the phenyl ring and the thioamide group in N,N-dimethylthiobenzamide cannot be coplanar (Fig. 3). If the steric repulsion is supposed to result in a rotation of the thioamide group out of the plane of

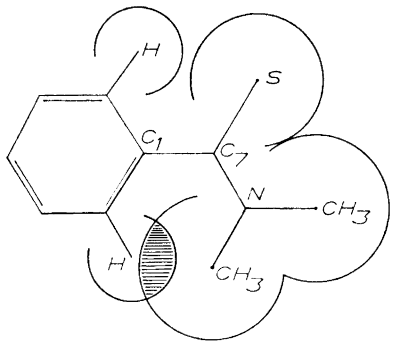

Fig. 3. Steric interference in N,N-dimethylthiobenzamide. As reasonable values for the radii of interaction 0.75 of the van der Waals radii have been chosen (for H 0.9 Å, for S 1.4 Å, and for CH_3 1.5 Å). The C_7—N and C_7—S bond lengths have been taken from Ref.[29]

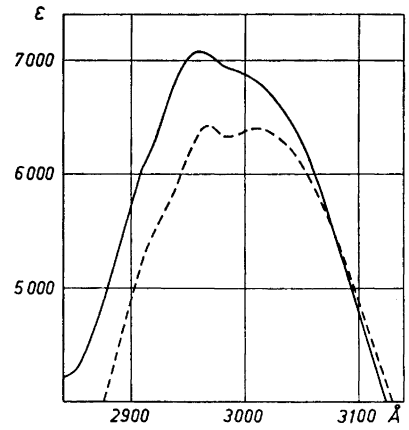

Fig. 4. Ultraviolet spectra of thiobenzamide in heptane (- - - - - -) and in ethanol (————).

the benzene ring, it can be taken into account in a calculation by lowering the absolute value of β for the corresponding bond in the secular equation, as has been shown by Heilbronner and Gerdil [17] and by Coulson [18]. In order to find out the directions of the changes in the energy levels caused by a change in this integral, a calculation was performed on thiobenzamide with $\alpha_N = \alpha_C + 1.3\beta_{CC}$ and $\beta_{1,7} = 0.5\beta_{CC}$ (The C_1—C_7 bond connects the thioamide group with the benzene ring). The results of the calculation are found in Table 1 (2). The effect of the rotation is to increase the $n \rightarrow \pi^*$ and $\pi \rightarrow \pi^*$ transition energies by about the same amounts (-0.22β and -0.25β). In harmony with this, the corresponding spectral shifts (from thiobenzamide to dimethylthiobenzamide) were found to be 1340 and 1650 cm^{-1}, in heptane. One of the common effects of steric inhibition of resonance is a lowering of the intensity of the affected absorption bands. This is found to be the case with the $\pi \rightarrow \pi^*$ band, for which the oscillator strength is lowered from 0.19 to 0.17 in heptane, whereas the oscillator strength for the $n \rightarrow \pi^*$ band increases from 0.0035 in thiobenzamide to 0.0046 in dimethylthiobenzamide. This increase is not surprising in view of the departure from coplanarity in the latter compound. It has been shown in several cases [19-21] that the intensity of $n \rightarrow \pi^*$ transitions in ketones can be considerably increased if the lone pair orbital on the oxygen atom can overlap with a π orbital, which does not necessarily have to be in conjugation with the carbonyl group. However, the steric conditions must be such that the lone pair and π orbitals are not orthogonal, and the result is a partial mixing of the $n \rightarrow \pi^*$ and $\pi \rightarrow \pi^*$ transitions.

The oscillator strengths have been calculated with the aid of the simple formula $f = 4.31 \times 10^{-9} \times \varepsilon_{max} \times 2\ (\nu_{max} - \nu_{0.5})$, where $\nu_{0.5}$ is the wave number on the low frequency side of the band at which the extinction has gone down to half of the maximum value.

Thus it may well be that the increasing hypsochromic shifts caused by methyl substitution are due to increasing departure from coplanarity. Janssen [6] has based a very reasonable explanation of the difference between the spectra of tetramethylthiourea and the other thioureas on a similar steric effect, but here the consequence of the departure from coplanarity is a bathochromic shift, since a heteroatom is turned out of conjugation.

The energy levels, the π electron distribution and the bond orders of thioacrylamide have also been calculated in order to study the effect of a simpler kind of conjugation. As far as is known to the author, no simple α,β-unsaturated thioamide is described in literature. From the calculations (Table 1) it can be concluded that thioacrylamide should have its $n \rightarrow \pi^*$ and $\pi \rightarrow \pi^*$ bands very close to those of thiobenzamide.

The arguments which have been put forward by Janssen [7] and by the present author [9] in favour of a $n \rightarrow \sigma^*$ transition can be reinterpreted in the light of some new evidence to support a $\pi \rightarrow \pi^*$ transition. Like $n \rightarrow \pi^*$ transitions the $n \rightarrow \sigma^*$ transitions must undergo blue shifts when the solvent polarity is increased, since the excited state is less stabilized than the ground state with increasing solvation. This applies in particular to hydroxylic solvents, where hydrogen bonding to the nonbonding electrons is of overwhelming importance for the blue shift [22]. However, a $\pi \rightarrow \pi^*$ transition can also give rise to such a change in the distribution of the π electrons that a blue shift with increasing solvent polarity results. This must be the case when the polarity of a group, which is primarily responsible for the solvation, is considerably diminished or reversed during the transition. As has been pointed out by Janssen [7] this occurs with the thione group in thioamides, and the same applies to thiobenzamide (Fig. 2). This effect must be smaller than the one caused by hydrogen bonding. Now the solvent shifts are of quite different magnitude for the low and high intensity bands in question. For thioacetamide the $n \rightarrow \pi^*$ band is shifted 3400 cm^{-1} and for thiobenzamide about 3100 cm^{-1} when going from heptane to ethanol. The corresponding shift for the high intensity band of thioacetamide is 140 cm^{-1}. For thiobenzamide the matter is somewhat complicated by a slight vibrational structure of the band in heptane (Fig. 4). As a rule the center of gravity of the band is used as the maximum value, but here it is evident that the solvent shift is best represented by the shift of the high frequency vibrational band, which amounts to 120 cm^{-1}. The solvent shifts of $n \rightarrow \pi^*$ and $n \rightarrow \sigma^*$ bands should be of about equal magnitude, since the main effect of increasing the solvent polarity will be a lowering of the n level. This alone renders the assignation of the 2670 Å band of thioacetamide to a $n \rightarrow \sigma^*$ transition somewhat doubtful. Furthermore, Janssen [6] has shown that this band is shifted to 2340 Å in concentrated sulphuric acid. As will be shown later, protonation in concentrated sulphuric acid occurs on the sulphur atom, and the nonbonding electrons in the free thioamide must be regarded essentially as σ electrons in the protonated species. They are therefore not available for transitions giving rise to absorption in

the near ultraviolet. A calculation has been performed to show the effect of S-protonation on the π levels of thioacetamide.

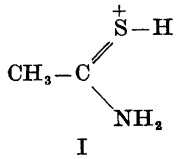

I

The calculations started with the form (I) and with the parameters $\alpha_C = \alpha$, $\alpha_{S+} = \alpha + 1.5\beta$, $\alpha_N = \alpha + 1.5\beta$, $\beta_{CS} = 0.6\beta$, and $\beta_{CN} = 1.2\beta$. The final results are found in Table 1 and Fig. 2. Leroy [23] has shown that the iterative procedure gives a very reasonable result when starting with the form (II). In the final diagram both charge and bond order are symmetrically distributed, and there-

$$H_2N-CH=CH-CH=CH-CH=NH_2^+$$

II

fore the method has also been applied with some confidence to the structure (I). It appears that the energy of the $\pi \rightarrow \pi^*$ transition is increased from -1.597β in thioacetamide to -1.913β in the protonated species, and therefore the band at 2340 Å may well be due to a $\pi \rightarrow \pi^*$ transition. From the excitation energies a $\pi \rightarrow \pi^*$ transition is calculated to appear at 2220 Å in the spectrum of the protonated species, so the agreement is reasonably satisfactory.

It is obvious that the results of the present investigation decidedly attribute the 2670 Å band of thioacetamide and the 2980 Å band of thiobenzamide to $\pi \rightarrow \pi^*$ transitions. This conclusion is further supported by a recent investigation by Hosoya *et al.*[24] As result of a semiempirical molecular orbital calculation with configuration interaction they assign the 2670 Å band to a $\pi \rightarrow \pi^*$ transition, and a second $\pi \rightarrow \pi^*$ transition is calculated to appear at 1670 Å. Despite the poor numerical agreement, this transition is assigned to a band at 2100 Å by means of measurements of the direction of the transition moment in the crystalline state.

Protonation of thioamides

The structure of the conjugate acids of the thioamides has been discussed by several authors with different results. Considerations of resonance stabilization would favour S-protonation, but arguments for N-protonation have also been put forward. Hosoya *et al.*[24] have concluded that N-protonation occurs, since S-protonation ought to raise the energy of the charge transfer state and thereby cause a bathochromic shift of the first $\pi \rightarrow \pi^*$ band. Instead, as mentioned above, a hypsochromic shift is found which is in harmony with the result of a simple calculation. However, Janssen [25] has criticized the theory of

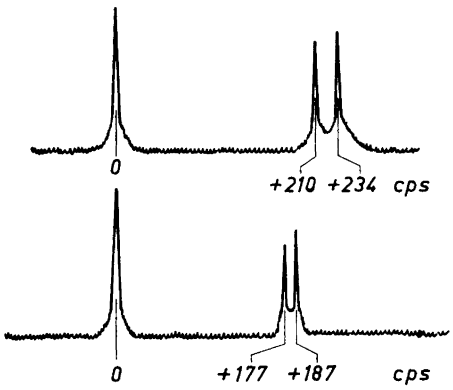

Fig. 5. NMR spectra of N,N-dimethylthiobenzamide in carbon tetrachloride (top) and sulphuric acid (bottom).

Hosoya *et al.* and presented convincing evidence from ultraviolet and infrared spectra of amides and thioamides and their conjugate acids, showing that O- and S-protonation occurs. During recent years a mass of evidence has been accumulated in support of O-protonation of amides, and in several cases (*e.g.* Refs.[26–28]) NMR spectra have been used to show that the rotation around the C—N bond is restricted, which would not have been the case, if N-protonation had occurred. The NMR spectrum has now been recorded for N,N-dimethylthiobenzamide in carbon tetrachloride and in concentrated sulphuric acid (Fig. 5). In both spectra two methyl signals are obtained, showing that the two methyl groups are differently disposed with respect to the thione group. Since N-protonation involves free rotation around the C—N bond, the spectra obtained are only compatible with S-protonation. The chemical shift between the methyl signals is changed from 24 cps in carbon tetrachloride to 10 cps in sulphuric acid. Cryoscopic determination of the van't Hoff i-factor in 100 % sulphuric acid shows that dimethylthiobenzamide is monoprotonated in this solvent (Table 4).

In hydroxylic solvents hydrogen bonding probably also occurs to the sulphur atom. Wheatley [29] and Penfold [30] have shown by X-ray crystallography and Hopkins and Hunter [31] by association measurements that the sulphur atom is the basic center of intermolecular hydrogen bonds in thioamides. Flett [32] has stressed the similarity in infrared spectra of associated thioamides and associated carboxylic acids, where the same type of bonding occurs.

Table 4. van't Hoff i-factors for N,N-dimethylthiobenzamide in 100 % sulphuric acid.

m	Δt°C	i
0.02220	0.282	2.06
0.01298	0.160	2.00
0.02278	0.286	2.01
0.01618	0.208	2.09

EXPERIMENTAL

Thioamides. Thioacetamide was a commercial purissium quality and was recrystallized twice from water without change in melting point (112–113°).

The thiobenzamides were obtained in good yields by reaction between carboxymethyl dithiobenzoate [33] and ammonia or the appropriate amines. Thiobenzamide was recrystallized from benzene and methyl- and N,N-dimethylthiobenzamide from benzene-heptane to constant melting point.

Solvents. Heptane was shaken first with concentrated sulphuric acid and then with water, dried with Drierite and distilled through a 60 cm Vigreux column.

Ethanol, 99.5 %, was refluxed with 1 % of sodium ethoxide for some hours and was then distilled through a 60 cm Vigreux column.

Spectra. The ultraviolet spectra were recorded with a Beckman DU spectrophotometer with photomultiplier attachment. In most cases the readings were followed down to 2150 Å and only in a few cases down to 2050 Å, since the increasing spurious light made the readings uncertain.

The 3670 Å band of thioacetamide in heptane could not be obtained in the pure solvent because of the poor solubility of the compound. Instead, the spectrum was recorded in 5 cm stoppered quartz cells with thioacetamide in pure carbon tetrachloride and in carbon tetrachloride-heptane mixtures (1:4, 2:3, 3:2, and 4:1 v/v). In all these solvents the maximum appeared at 3670 Å, which was therefore taken as the position of the maximum in pure heptane. The molar extinction coefficient at the maximum wavelength decreased gradually with increasing heptane concentration and a value of 35 for pure heptane was obtained by extrapolation.

The NMR spectra were recorded with a Varian Associates model V-4300-B high resolution NMR spectrometer operating at 40 Mc/s, and a flux stabilized 12″ electromagnet from the same company. The magnetic sweep was calibrated with the modulated side band technique.

Cryoscopic measurements. Sulphuric acid containing a slight excess of anhydride was prepared by mixing the calculated amounts of 95–97 % sulphuric acid (Merck, pro analysi) and fuming sulphuric acid with 20 % of anhydride of the same quality. Water was then added in small portions until the horisontal part of the melting point curve was reached. The melting point depressions have been corrected for supercooling, and the calculations have been performed as described by Hammett and Deyrup [34]. N,N-Dimethylthiobenzamide dissolves readily in this sulphuric acid even at a low temperature, and it is recovered unchanged when the solution is poured onto ice.

The author is indebted to *The Swedish Natural Science Research Council* for financial support, to Miss Karin Göransson and Miss Ingeborg Leutiger for recording the ultraviolet spectra, and to Civilingenjör Jan Christer Eriksson for recording the NMR spectra. The author is also indebted to Fil.Kand Leif Robertsson for programming the calculations and to Laborator Carl-Erik Fröberg and Ingenjör Kjell Jönsson at the Institute of Numerical Analysis of the University of Lund for valuable advice concerning the use of the electronic digital computor "SMIL". Laborator Stig Sunner has kindly placed 5 cm quartz cells and a suitable spectrophotometer at the authors disposal.

REFERENCES

1. Hantzsch, A. *Ber.* **64** (1931) 661.
2. Burawoy, A. *Ber.* **63** (1930) 3155.
3. Burawoy, A. *J. Chem. Soc.* **1939** 1177.
4. Lewis, G. N. and Kasha, M. *J. Am. Chem. Soc.* **67** (1945) 994.
5. Kasha, M. *Discussions Faraday Soc.* **9** (1950) 14.
6. Janssen, M. J. *Rec. trav. chim.* **79** (1960) 454.
7. Janssen, M. J. *Rec. trav. chim.* **79** (1960) 464.
8. Janssen, M. J. *Rec. trav. chim.* **79** (1960) 1066.
9. Sandström, J. *Svensk Kem. Tidskr.* **72** (1960) 612.
10. Katagiri, *et al.* Quoted in Ref.[24]

11. Pullman, B. *Chimia* **15** (1961) 4.
12. Wheland, G. W. and Mann, D. E. *J. Chem. Phys.* **17** (1949) 264.
13. Nagakura, S. *Bull. Chem. Soc. Japan* **25** (1952) 164.
14. Smith, J. W. *J. Chem. Soc.* **1961** 81.
15. Jansson, M. J. *The Electronic Structure of Organic Thion Compounds*. Diss. Utrecht 1959, p. 62.
16. Gerson, F. and Heilbronner, E. *Helv. Chim. Acta* **42** (1959) 1877.
17. Heilbronner, E. and Gerdil, R. *Helv. Chim. Acta* **39** (1956) 1996.
18. Coulson, C. A. in *Steric Effects in Conjugated Systems*. Butterworth, London 1958, p. 8.
19. Leonard, N. J. and Owens, F. H. *J. Am. Chem. Soc.* **80** (1958) 6039.
20. Labhart, H. and Wagniere, G. *Helv. Chim. Acta* **42** (1959) 2219.
21. Birnbaum, H., Cookson, R. C. and Lewin, N. *J. Chem. Soc.* **1961** 1224.
22. Pimentel, G. C. *J. Am. Chem. Soc.* **79** (1957) 3323.
23. Leroy, G. *Bull. soc. chim. Belges* **70** (1961) 110.
24. Hosoya, H., Tanaka, J. and Nagakura, S. *Bull. Chem. Soc. Japan* **33** (1960) 850.
25. Janssen, M. J. *Spectrochim. Acta* **17** (1961) 475.
26. Berger, A., Loewenstein, A. and Meiboom, S. *J. Am. Chem. Soc.* **81** (1959) 62.
27. Fraenkel, G. and Franconi, C. *J. Am. Chem. Soc.* **82** (1960) 4478.
28. De Kowalewski, D. G. and Kowalewski, V. J. *Arkiv Kemi* **16** (1961) 373.
29. Wheatley, P. J. *Acta Cryst.* **6** (1953) 369.
30. Penfold, B. R. *Acta Cryst.* **6** (1953) 707.
31. Hopkins, G. and Hunter, L. *J. Chem. Soc.* **1942** 638.
32. Flett, M. St. C. *J. Chem. Soc.* **1953** 347.
33. Holmberg, B. *Arkiv Kemi, Mineral. Geol.* **17 A** (1944) No. 23.
34. Hammett, L. P. and Deyrup, A. J. *J. Am. Chem. Soc.* **55** (1933) 1900.

Received January 17, 1962.

ACTA CHEMICA SCANDINAVICA 16 (1962) 1627–1636

The Crystal Structure of Ba-Ribose-5-phosphate

SVEN FURBERG and ARVID MOSTAD

Institute of Chemistry, University of Oslo, Blindern-Oslo, Norway

The structure of the barium salt of ribose-5-phosphate has been determined by X-ray crystallographic methods with moderate accuracy. The five-membered ring is non-planar with atom C_2 out of the plane of the other atoms. The configuration at the anomeric carbon atom appears to be of the *α*-type. Each barium ion is surrounded by twelve oxygen atoms, three of which are the hydroxyl oxygens of the same molecule.

Continuing our investigations of simple compounds related to the nucleic acids, we have determined the crystal structure of the barium salt of ribose-5-phosphate. This substance was first prepared by Levene and Jacobs [1] by hydrolyzing inosinic acid. They also determined its structure except for the configuration at the anomeric carbon atom which still appears to be unknown. The mutarotation curves are complex [2] and permit no safe conclusions about the structure to be drawn. However, it seems to be generally assumed that the compound is of the *β*-type, as in the nucleotides, from which it is isolated. In view of its relation to nucleic acid structure it would also appear to be of interest to determine the conformation of the ribose in this compound. In earlier studies of cytidine [3] and cytidylic acid [4] we have observed two different conformations of ribose.

EXPERIMENTAL. CRYSTAL DATA

A sample of the compound was supplied by Fluka AG. Crystals were grown by slowly adding alcohol to an aqueous solution, the solution being placed on a watch-glass in a desiccator containing alcohol. From a cluster of crystals a cube with edges approximately 0.1 mm was cut out and used for the investigation. Weissenberg diagrams were taken about the b and c axes using copper radiation ($\lambda = 1.542$ Å). The crystals are monoclinic, with unit cell dimensions $a = 15.38$ Å, $b = 8.56$ Å, $c = 12.86$ Å and $\beta = 118.6°$ (all $\pm$ 0.5 %). All reflections with $h + k$ odd are absent and the lattice is therefore C-centered. As the molecules are optically active, the space group must be $C2$. By flotation in mixtures of bromoform and carbon tetrachloride the density was found to be 2.05 g/cm³, corresponding to four (calculated 4.03) molecules $C_5H_9O_5 \cdot PO_3 \cdot Ba \cdot 5H_2O$ per unit cell.

205 $h0l$ reflections and 52 $hk0$ reflections were recorded with measurable intensity on the films, the numbers obtainable by copper radiation being 220 and 80, respectively. The intensities were estimated visually and corrected for Lorentz-polarization effects. No correction for absorption was made.

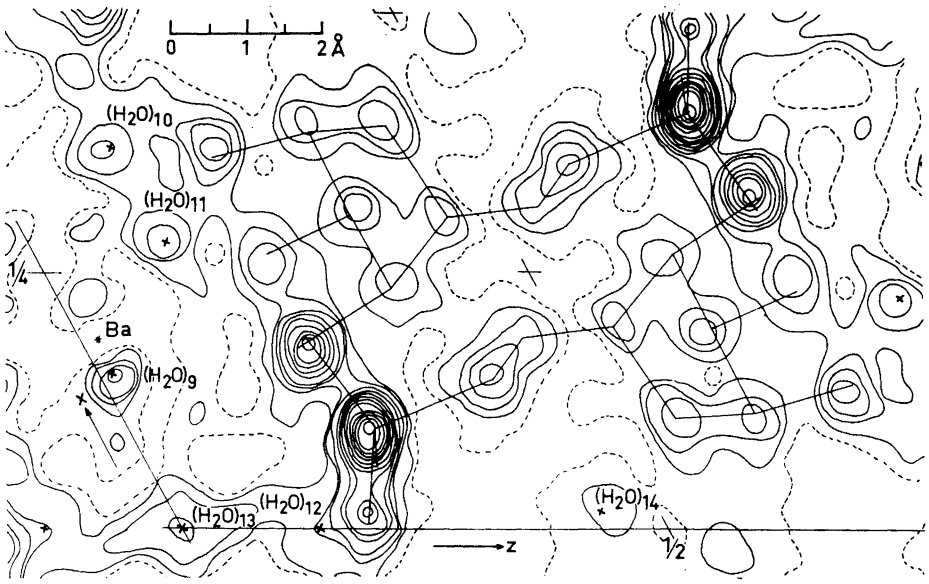

Fig. 1. Electron density projection in direction of *b* axis. Contours at 3, 5, 7 . . .e.Å^{-2}, the first one being dotted. The barium ion is subtracted. Crosses indicate water molecules.

Determination of the structure

The b projection. The barium atom was located by means of the Patterson projection, and a Fourier synthesis based on the corresponding signs indicated the positions of most of the lighter atoms. These were more clearly shown on the difference map reproduced in Fig. 1, which was calculated by subtracting the contribution from the barium atom. The structure was further refined by means of a number of difference syntheses. It was, however, found difficult to locate some of the water molecules unambigously from the maps. Three of the sites are fairly clearly shown, namely those of O_9, O_{10} and O_{11}. In addition there appears to lie a water molecule (O_{13}) on the two-fold axis through origo. The position derived for O_{12} is less certain, as equally good agreement was obtained by substituting it by two half-oxygens with coordinates (0.027, 0.125) and (0.440, 0.140). Finally the water molecule O_{14} lies so near a two-fold axis that the distance to the equivalent atom is only 2.1 Å. This is clearly not possible, and we assume therefore that the water molecules are statistically distributed over these two sites. Consequently, the calculations were based on half an oxygen atom in this position, giving in all five water molecules per barium ion.

The positions finally selected for the atoms are given in Fig. 1 and Table 1. The corresponding values of $R = \Sigma \| F_o | - | F_c \| / \Sigma | F_o |$ is 0.09, including the extinction error occurring in the two strongest reflections (001) and (200). In Table 4 the observed (F_o) and calculated (F_c) values of the structure factors are compared. The analytical approximation to the atomic scattering factors given by Forsyth and Wells [5] was used. The vibrations of the Ba ion are strongly anisotropic. In the temperature factor, $\exp.(B \sin^2\Theta/\lambda^2)$, the value of B varies between 1.1 and 2.5 for the lighter atoms (Table 1), whereas for the Ba ion $B = 0.8 + 1.0 \cos^2\varphi$, φ being the angle between the a axis and the normal to the reflecting plane. The water molecules have B-values in the range 3.5 – 6.0.

The c projection. The coordinates of the barium and phosphorus atoms were derived from the sharpened Patterson synthesis (Fig. 2 b), which showed that their y coordinates

Table 1. Atomic coordinates as fractions of the corresponding cell edge.

	x	y	z	B_{iso}
Ba	0.1862	0.000	0.0262	0.8—1.8
P	0.098	0.495	0.251	1.1
O_1	0.137	0.425	0.765	1.8
O_2	0.231	0.678	0.757	2.0
O_3	0.325	0.395	0.772	2.2
O_4	0.105	0.349	0.570	2.5
O_5	0.145	0.490	0.398	2.0
O_6	0.186	0.450	0.234	2.0
O_7	0.007	0.392	0.197	2.0
O_8	0.060	0.660	0.219	2.0
O_9	0.144	0.307	0.012	3.0
O_{10}	0.365	0.267	0.130	4.5
O_{11}	0.274	0.622	0.139	4.5
O_{12}	0.000	0.093	0.140	6.0
O_{13}	0.000	0.810	0.000	6.0
O_{14}	0.022	0.710	0.438	6.0
C_1	0.112	0.480	0.649	2.2
C_2	0.192	0.578	0.651	2.2
C_3	0.268	0.477	0.653	2.5
C_4	0.199	0.341	0.571	2.2
C_5	0.184	0.341	0.451	2.5

differ by about $b/2$. The y coordinates of the other atoms were derived from the b projection and approximately known bond lengths and bond angles, considering also the Patterson synthesis. They were refined by a number of difference syntheses. The final value obtained for R was 0.12. However, the coordinates derived from this projection are inaccurate because of lack of centre of symmetry and overlap of atoms. The value used for B was

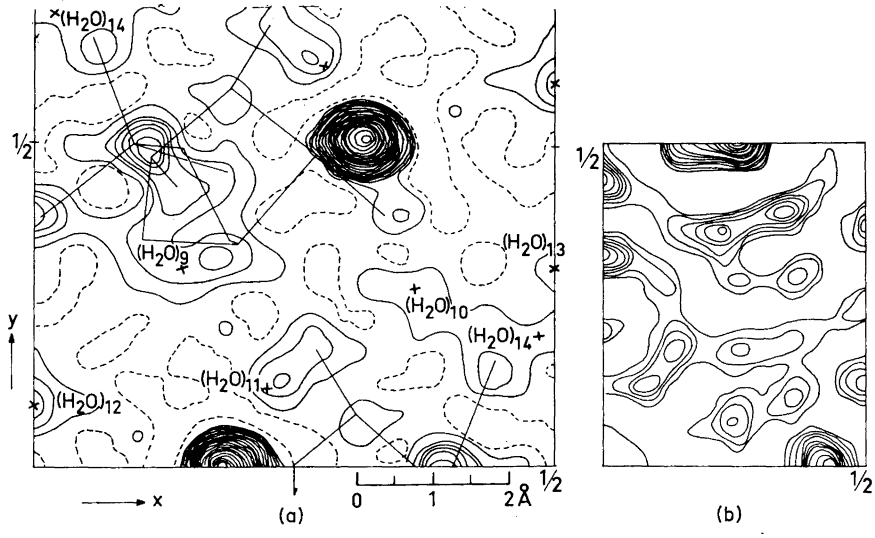

Fig. 2. Electron density (a) and Patterson (b) projections in direction of c axis. Contours as in Fig. 1 in (a), in (b) at arbitrary intervals.

Table 2. Bond lengths (in Å units) and bond angles.

Bond lengths		Bond angles	
$P-O_5$	1.67	O_6-P-O_7	118°
$P-O_6$	1.52	O_6-P-O_8	117°
$P-O_7$	1.51	O_6-P-O_5	103°
$P-O_8$	1.51	O_7-P-O_8	106°
O_5-C_5	1.44	O_7-P-O_5	108°
C_5-C_4	1.45	O_8-P-O_5	104°
C_4-C_3	1.59	$P-O_5-C_5$	115°
C_3-C_2	1.44	$O_5-C_5-C_4$	109°
C_2-C_1	1.48	$C_5-C_4-C_3$	115°
C_1-O_4	1.48	$C_4-C_3-C_2$	99°
O_4-C_4	1.45	$C_3-C_2-C_1$	109°
C_1-O_1	1.43	$C_2-C_1-O_4$	103°
C_2-O_2	1.47	$C_1-O_4-C_4$	107°
C_3-O_3	1.49	$O_4-C_4-C_5$	111°
		$C_4-C_3-O_3$	104°
		$C_2-C_3-O_3$	110°
		$C_3-C_2-O_2$	111°
		$C_1-C_2-O_2$	108°
		$C_2-C_1-O_1$	111°
		$O_4-C_1-O_1$	111°
		$O_4-C_4-C_3$	109°

1.7 for the barium and phosphorus atoms and 2.0—4.0 for the other atoms. The electron density map is shown in Fig. 2 a.

DESCRIPTION AND DISCUSSION OF THE STRUCTURE

The molecular structure. The bond lengths and bond angles calculated from the coordinates in Table 1 are given in Table 2. Lack of resolution and the presence of a very heavy atom make it difficult to determine the structure accurately by two-dimensional methods and we believe that errors as great as about 0.10 Å and 5° may occur. Within these wide limits, the values derived agree with those found in similar compounds. The P—O ester linkage ($P-O_5$) is thus significantly longer than the other P—O distances, as was found also in cytidylic acid [4] and in calcium thymidylate [7].

If our interpretation of the Fourier maps is correct, the hydroxyl groups at C_1, C_2 and C_3 all are in *cis* relation, which means that the compound is

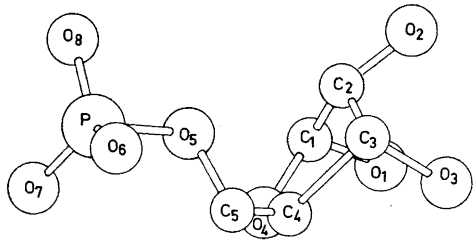

Fig. 3. The molecular structure.

the α-anomer. According to Fluka AG., our sample has the same optical configuration as the natural material. We have tried to accomodate a β-structure on the Fourier- and difference-maps. Although this possibility cannot definitely be excluded due to uncertainty in the positions of some of the water molecules, the α-structure fits the maps much better. We therefore consider it highly probable that this anomer occurs in the crystals. As described below, a complex involving three-point attachment of the Ba ion is present in the crystals. Only α-ribose can form the complex, which thus may favour the crystallization of this anomer.

The phosphate group is pointing away from the ribose ring, the $P-O_8$ bond being nearly parallel to C_5-O_5 and $P-O_5$ to C_4-C_5, as shown in Fig. 3. This makes the molecule as extended as possible. The bond C_5-C_4 is in *gauche* position with respect to the ring bonds to C_4, and there is a staggered arrangement around all the single bonds. The same structural features were found in Ca thymidylate, the only other 5-phosphate hitherto investigated, and are also in exact agreement with space models proposed for nucleic acids [10].

As found in other furanose structures, the five-membered ring is non-planar. Four of the atoms, namely C_1, C_3, C_4 and O_4 lie nearly in one plane, but C_2 is out of this plane by about 0.5 Å in such a direction that O_2 falls nearly on to the plane. The ring angles at carbon atoms C_3 and C_1 are probably significantly smaller than the tetrahedral angle, and the conformation appears to differ from those observed in the ribose derivatives mentioned above [3,4,7].

The water molecules. After recrystallization from water the density corresponds to five molecules of water per molecule, with an accuracy of about half a water molecule. Levene and Jacobs [1] found the number to be five or five and a half. Some of the water of crystallization is, however, easily lost and the sample supplied by Fluka AG. is stated to contain only about three water molecules per barium atom. In the final structure there are, as described above, five water molecules. The electron density maxima corresponding to some of the water sites are considerably lower than found for the other oxygen atoms, and it seems possible that some of the water molecules are lost during the exposure time. We have not tried to take this into account as the data are not accurate enough to disclose such details in the presence of the heavy ion, but have assigned to these atoms anomalously large values of B. This may be interpreted either as thermal motions or as localized disorder, the coordinates given for the water molecules in Table 1 representing the average value of a certain distribution of parameters. This holds particularly for the water molecule at O_{14}. Similar problems as regards the water of crystallization have been encountered in a number of structures, *e.g.* in thymine monohydrate [11].

The ionic environment. In the structure there are corrugated sheets of hydrated barium ions at distances of about 11 Å. The radius of the barium ion is about the same as that of an oxygen atom, and it is recognized that in such cases the most stable anion polyhedron corresponds to coordination numbers in the range nine to twelve. With twelve neighbours the icosahedral configuration appears to be preferred as it is found in a number of barium salts, *e.g.* barium perchlorate trihydrate [8], in which there are twelve Ba to O contacts between 2.96 Å and 3.18 Å. The usual arrangement for coordination number nine arises by adding atoms beyond the centres of the vertical faces

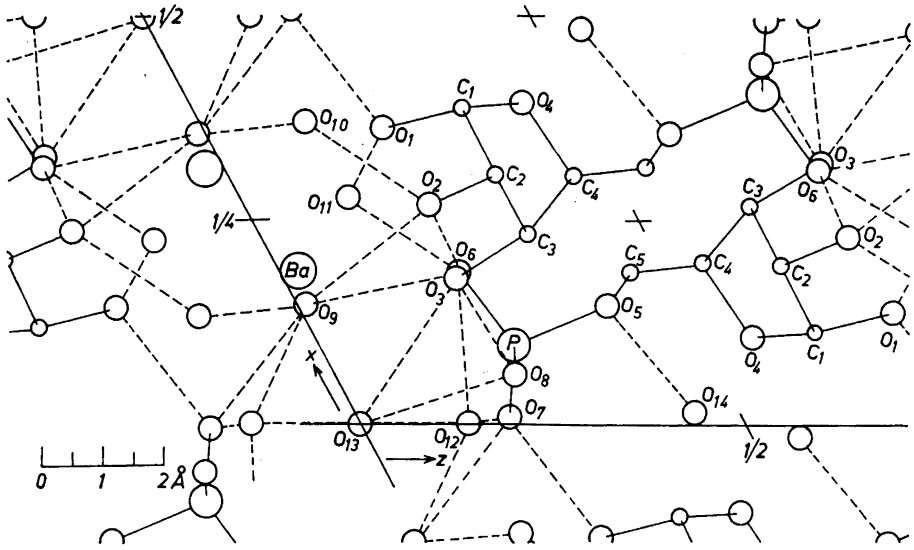

Fig. 4. The *b* projection of the structure. Short O—O contacts are indicated by dotted lines.

of a right triangular prism. An example of a barium salt with an anion polyhedron of this type is provided by barium tetrathionate dihydrate [5], in which the barium ion has nine neighbours at distances 2.73 Å – 2.90 Å. In the present structure there are seven oxygen neighbours with Ba—O separations 2.67 Å—2.88 Å, and in addition five oxygens further apart (3.14 Å—3.80 Å). These twelve neighbours are situated in the corners of a distorted icosahedron. One out of the twenty triangles is common to the anion polyhedra of neighbouring barium ions.

The nature of the linkage between divalent metal ions and ATP, nucleotides and sugar phosphates has been much discussed due to the biological importance of these complexes [9]. Several different modes of attachment have been proposed. The study of the crystal structures of these compounds may contribute to the solution of the problem. In the present structure the barium ion is bonded directly to the hydroxyl groups of α-ribose in a threedentate complex with Ba—O distances 2.84—2.88 Å. It is not linked directly to the phosphate oxygens, but is connected to these three atoms by bridges of the type Ba...O—H...O—P<. In crystals of Ca thymidylate the ion is bonded directly to the phosphate oxygens. In this case, however, the sugar has only one free hydroxyl group.

The hydrogen bonds. The water molecules, the phosphate oxygens and the sugar hydroxyls are all involved in hydrogen bond formation. The three hydroxyl oxygens of α-ribose form a nearly equilateral triangle with edges of

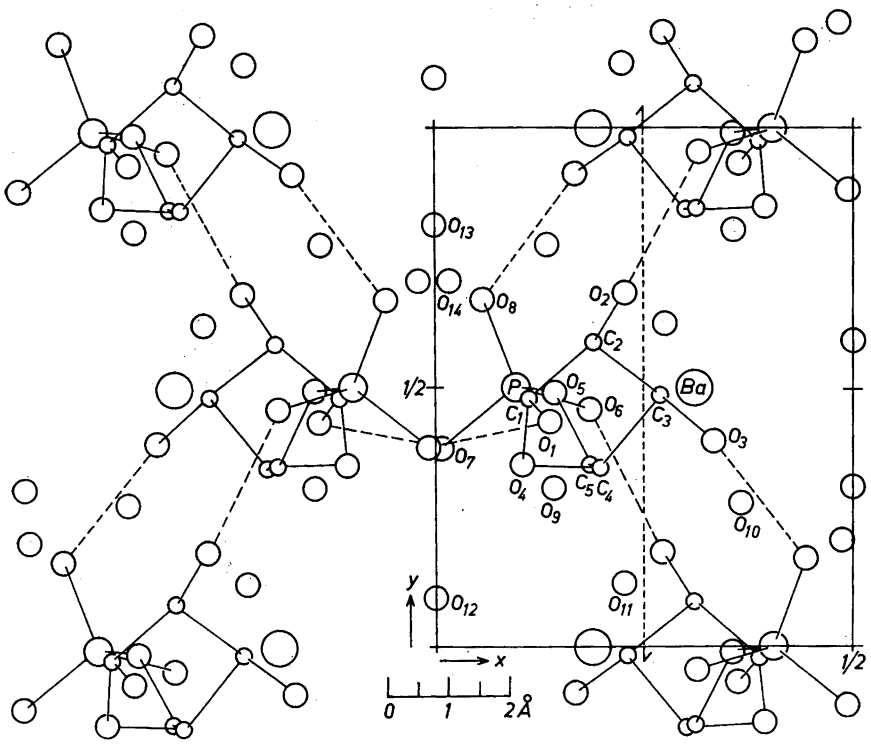

Fig. 5. The *c* projection of the structure. The broken lines show the hydrogen bonds between hydroxyl and phosphate oxygens.

Table 3. Short O—O and Ba—O distances (in Å units).

O_7-O_1	2.50	$Ba-O_1$	2.84
O_6-O_2	2.63	$Ba-O_2$	2.88
O_8-O_3	2.64	$Ba-O_3$	2.86
O_9-O_6	2.88	$Ba-O_9$	2.69
O_9-O_2	2.80	$Ba-O_{10}$	2.67
O_9-O_{12}	2.82	$Ba-O_{11}$	2.69
O_9-O_7	2.68	$Ba-O_{12}$	2.74
O_9-O_{10}	3.01	$Ba-O_{13}$	3.14
$O_{11}-O_1$	2.92	$Ba-O_9$	3.32
$O_{11}-O_6$	2.66	$Ba-O_{10}$	3.33
$O_{10}-O_2$	2.63	$Ba-O_{11}$	3.54
$O_{12}-O_3$	2.90	$Ba-O_{12}$	3.80
$O_{12}-O_7$	2.65		
$O_{12}-O_{13}$	3.02		
$O_{13}-O_3$	2.84		
$O_{13}-O_8$	2.79		
$O_{14}-O_5$	2.80		

Table 4. Observed (F_o) and calculated (F_c) structure factors.

$h\,k\,l$	F_o	F_c	$h\,k\,l$	F_o	F_c	$h\,k\,l$	F_o	F_c
0 0 1	37	48	4 0 $\bar{2}$	10	−11	8 0 $\bar{6}$	12	− 9
0 0 2	15	15	4 0 $\bar{3}$	41	−44	8 0 $\bar{7}$	< 2	3
0 0 3	27	29	4 0 $\bar{4}$	36	−38	8 0 $\bar{8}$	6	4
0 0 4	51	51	4 0 $\bar{5}$	36	−40	8 0 $\bar{9}$	14	−11
0 0 5	59	57	4 0 $\bar{6}$	23	−21	8 0 $\bar{10}$	11	10
0 0 6	8	5	4 0 $\bar{7}$	40	−40	8 0 $\bar{11}$	17	14
0 0 7	14	14	4 0 $\bar{8}$	46	−43	8 0 $\bar{12}$	15	14
0 0 8	25	24	4 0 $\bar{9}$	31	−30	8 0 $\bar{13}$	6	7
0 0 9	18	19	4 0 $\bar{10}$	27	−27	8 0 $\bar{14}$	12	15
0 0 10	13	−14	4 0 $\bar{11}$	30	−29	8 0 $\bar{15}$	26	25
0 0 11	9	−11	4 0 $\bar{12}$	30	−27	8 0 $\bar{16}$	16	20
0 0 12	5	− 4	4 0 $\bar{13}$	21	−20	10 0 0	24	24
0 0 13	12	−11	4 0 $\bar{14}$	15	−15	10 0 1	23	23
0 0 14	14	−14	4 0 $\bar{15}$	11	−13	10 0 2	18	20
2 0 0	35	−48	6 0 0	37	39	10 0 3	14	13
2 0 1	40	−38	6 0 1	25	21	10 0 4	18	18
2 0 2	35	−41	6 0 2	22	19	10 0 5	23	23
2 0 3	30	−31	6 0 3	12	7	10 0 6	14	15
2 0 4	35	−36	6 0 4	10	7	10 0 7	12	14
2 0 5	52	−52	6 0 5	12	7	10 0 8	13	12
2 0 6	39	−41	6 0 6	6	1	10 0 $\bar{1}$	5	− 5
2 0 7	21	−22	6 0 7	14	−12	10 0 $\bar{2}$	5	− 1
2 0 8	27	−29	6 0 8	9	−10	10 0 $\bar{3}$	13	11
2 0 9	27	−28	6 0 9	9	−10	10 0 $\bar{4}$	12	9
2 0 10	11	−12	6 0 10	11	−11	10 0 $\bar{5}$	14	−16
2 0 11	13	−12	6 0 11	18	−17	10 0 $\bar{6}$	15	−13
2 0 12	6	− 7	6 0 $\bar{1}$	41	45	10 0 $\bar{7}$	< 2	2
2 0 13	13	−11	6 0 $\bar{2}$	46	47	10 0 $\bar{8}$	13	−13
2 0 $\bar{1}$	13	− 8	6 0 $\bar{3}$	33	30	10 0 $\bar{9}$	24	−25
2 0 $\bar{2}$	14	−18	6 0 $\bar{4}$	32	32	10 0 $\bar{10}$	33	−38
2 0 $\bar{3}$	41	−45	6 0 $\bar{5}$	50	55	10 0 $\bar{11}$	12	−12
2 0 $\bar{4}$	5	− 7	6 0 $\bar{6}$	43	46	10 0 $\bar{12}$	9	−10
2 0 $\bar{5}$	28	27	6 0 $\bar{7}$	39	38	10 0 $\bar{13}$	27	−26
2 0 $\bar{6}$	25	26	6 0 $\bar{8}$	13	13	10 0 $\bar{14}$	26	−26
2 0 $\bar{7}$	6	9	6 0 $\bar{9}$	29	25	10 0 $\bar{15}$	18	−18
2 0 $\bar{8}$	11	12	6 0 $\bar{10}$	39	32	10 0 $\bar{16}$	9	− 9
2 0 $\bar{9}$	24	21	6 0 $\bar{11}$	17	14	12 0 0	8	5
2 0 $\bar{10}$	27	27	6 0 $\bar{12}$	4	1	12 0 1	4	− 6
2 0 $\bar{11}$	29	27	6 0 $\bar{13}$	6	2	12 0 2	14	−15
2 0 $\bar{12}$	20	19	6 0 $\bar{14}$	7	5	12 0 3	5	2
2 0 $\bar{13}$	29	27	6 0 $\bar{15}$	< 2	0	12 0 4	2	− 4
2 0 $\bar{14}$	23	22	8 0 0	21	−22	12 0 5	17	−16
4 0 0	13	−13	8 0 1	30	−29	12 0 6	11	−11
4 0 1	9	4	8 0 2	26	−27	12 0 $\bar{1}$	18	15
4 0 2	12	5	8 0 3	32	−33	12 0 $\bar{2}$	16	14
4 0 3	18	14	8 0 4	19	−19	12 0 $\bar{3}$	6	− 4
4 0 4	12	13	8 0 5	17	−15	12 0 $\bar{4}$	20	19
4 0 5	20	19	8 0 6	16	−15	12 0 $\bar{5}$	31	32
4 0 6	35	36	8 0 7	10	−12	12 0 $\bar{6}$	16	14
4 0 7	26	27	8 0 8	< 2	− 4	12 0 $\bar{7}$	11	11
4 0 8	17	17	8 0 9	< 2	0	12 0 $\bar{8}$	19	22
4 0 9	20	20	8 0 $\bar{1}$	22	−23	12 0 $\bar{9}$	29	32
4 0 10	26	25	8 0 $\bar{2}$	33	−35	12 0 $\bar{10}$	19	21
4 0 11	25	25	8 0 $\bar{3}$	15	−18	12 0 $\bar{11}$	15	15
4 0 12	12	13	8 0 $\bar{4}$	39	−46	12 0 $\bar{12}$	13	14
4 0 $\bar{1}$	6	8	8 0 $\bar{5}$	24	−20	12 0 $\bar{13}$	20	21

Table 4. Continued.

h k l	F_o	F_c	h k l	F_o	F_c	h k l	F_o	F_c
12 0 $\bar{14}$	13	13	18 0 $\bar{4}$	3	− 1	12 4 0	<13	2
12 0 $\bar{15}$	< 2	2	18 0 $\bar{5}$	5	0	14 4 0	17	15
14 0 0	17	−14	18 0 $\bar{6}$	8	5	1 5 0	<10	2
14 0 1	15	−12	18 0 $\bar{7}$	13	10	3 5 0	25	21
14 0 2	3	− 3	18 0 $\bar{8}$	5	5	5 5 0	39	31
14 0 3	6	− 5	18 0 $\bar{9}$	5	5	7 5 0	<11	7
14 0 4	5	− 6	18 0 $\bar{10}$	9	11	9 5 0	13	13
14 0 $\bar{1}$	5	− 6	18 0 $\bar{11}$	11	14	11 5 0	16	16
14 0 $\bar{2}$	14	−16	18 0 $\bar{12}$	10	12	13 5 0	13	15
14 0 $\bar{3}$	20	−20	1 1 0	12	13	0 6 0	42	40
14 0 $\bar{4}$	19	−22	3 1 0	20	22	2 6 0	25	21
14 0 $\bar{5}$	14	−15	5 1 0	52	52	4 6 0	<11	6
14 0 $\bar{6}$	10	−11	7 1 0	20	13	6 6 0	<12	6
14 0 $\bar{7}$	16	−16	9 1 0	22	18	8 6 0	20	22
14 0 $\bar{8}$	18	−17	11 1 0	20	18	10 6 0	18	15
14 0 $\bar{9}$	11	−12	13 1 0	<13	12	12 6 0	< 9	2
14 0 $\bar{10}$	3	− 2	15 1 0	<11	3	14 6 0	11	13
14 0 $\bar{11}$	14	−14	17 1 0	< 8	9	1 7 0	<12	1
14 0 $\bar{12}$	4	− 5	0 2 0	42	69	3 7 0	27	25
14 0 $\bar{13}$	2	2	2 2 0	29	37	5 7 0	32	28
14 0 $\bar{14}$	< 2	0	4 2 0	29	26	7 7 0	<13	6
16 0 0	12	12	6 2 0	36	29	9 7 0	<11	11
16 0 1	12	14	8 2 0	31	29	11 7 0	< 8	11
16 0 $\bar{1}$	11	10	10 2 0	25	25	13 7 0	< 6	11
16 0 $\bar{2}$	13	13	12 2 0	<13	6	0 8 0	26	25
16 0 $\bar{3}$	14	14	14 2 0	17	17	2 8 0	<13	12
16 0 $\bar{4}$	5	7	1 3 0	26	26	4 8 0	<13	5
16 0 $\bar{5}$	5	8	3 3 0	38	32	6 8 0	<12	10
16 0 $\bar{6}$	13	11	5 3 0	45	43	8 8 0	12	13
16 0 $\bar{7}$	< 2	4	7 3 0	21	18	10 8 0	< 7	13
16 0 $\bar{8}$	< 2	1	9 3 0	25	17	12 8 0	< 3	3
16 0 $\bar{9}$	< 2	0	11 3 0	18	17	1 9 0	<12	7
16 0 $\bar{10}$	< 2	− 3	13 3 0	<12	15	3 9 0	21	21
16 0 $\bar{11}$	< 2	− 3	15 3 0	< 8	7	5 9 0	21	21
16 0 $\bar{12}$	11	−11	0 4 0	34	34	7 9 0	< 7	7
16 0 $\bar{13}$	8	− 9	2 4 0	27	26	9 9 0	9	9
16 0 $\bar{14}$	5	− 7	4 4 0	20	18	0 10 0	20	19
18 0 $\bar{1}$	5	− 6	6 4 0	15	15	2 10 0	< 7	8
18 0 $\bar{2}$	3	− 6	8 4 0	24	22	4 10 0	< 6	1
18 0 $\bar{3}$	3	1	10 4 0	20	14	6 10 0	10	10

about 2.8 Å and the three free phosphate oxygens another such triangle with edges about 2.5 Å. All these triangles lie roughly in planes parallel to the *ab* plane at approximately $z = 0.25$ and 0.75. Each of them is connected by hydrogen bonds to three triangles of the other type in the same plane. The lengths of these bonds are 2.50 Å, 2.63 Å and 2.64 Å, and they are evidently formed by the hydroxyl hydrogen atoms, as is apparent also from their directions. In addition, the water molecules which are associated with the barium ions take part in a number of hydrogen bonds. Thirteen such oxygen-oxygen contacts are shorter than 3.2 Å, lying in the range between 2.63 Å and 3.04 Å. However, only nine of those correspond presumably to hydrogen bonds as

this is the number of available hydrogen atoms (four and a half water molecules). In addition there appears to be a hydrogen bond between $(H_2O)_{14}$ and O_5. In Table 3 oxygen-oxygen contacts shorter than 3.2 Å are given. They are all indicated in Fig. 4 by broken lines. In Fig. 5 only the hydrogen bonds between hydroxyl and phosphate oxygens are shown.

REFERENCES

1. Levene, P. A. and Jacobs, W. A. *Ber.* **44** (1911) 746.
2. Levene, P. A., Harris, S. A. and Stiller, E. T. *J. Biol. Chem.* **105** (1934) 153.
3. Furberg, S. *Acta Cryst.* **3** (1950) 325.
4. Alver, E. and Furberg, S. *Acta Chem. Scand.* **13** (1959) 910.
5. Forsyth, J. B. and Wells, M. *Acta Cryst.* **12** (1959) 412.
6. Foss, O., Furberg, S. and Zachariassen, H. *Acta Chem. Scand.* **8** (1954) 459.
7. Trueblood, K. N. and Horn, P. Luzzati. *Acta Cryst.* **14** (1961) 965.
8. Mani, N. V. and Ramaseshan, S. *Z. Krist.* **114** (1960) 200.
9. Brintzinger, H. *Helv. Chim. Acta* **44** (1961) 199.
10. Furberg, S. *Acta Chem. Scand.* **6** (1952) 634.
11. Gerdil, R. *Acta Cryst.* **14** (1961) 333.

Received March 29, 1962.

ACTA CHEMICA SCANDINAVICA 16 (1962) 1637–1646

Spectroscopic Studies of Charge Transfer Complexes

I. Aldehydes and Iodine

ELSE AUGDAHL and PETER KLÆBOE

Universitetets Kjemiske Institutt, Blindern-Oslo, Norway

Complexes between aldehydes and iodine have been studied in solution by infrared and visible spectroscopic methods. The bond is d rected from the carbonyl oxygen to a halogen atom and is probably of the charge transfer type. Formation constants for these 1:1 complexes in carbon disulphide at 30°C were obtained from intensity changes of the C=O stretching bands. Conjugation and inductive effects had a marked influence on the donor strengths of the aldehydes. The C=O stretching bands of the complexes had lower frequencies (ν), higher integrated intensities (B) and larger half intensity widths ($\nu_{1/2}$) than those of the free aldehydes. Spectral parameters for these bands are given.

During the last decade a number of investigators have studied the complexes between halogens and organic molecules having loose π-electrons or lone pair electrons. Such complexes are believed to be formed by electron transfer from one molecule to another; the organic substance acting as a donor, the halogen as an acceptor of electrons. The theory for this kind of complex formation has been worked out in a series of papers by Mulliken [1]. Since Benesi and Hildebrand's [2] pioneering investigation numerous workers have studied the absorption of halogen addition compounds in the ultraviolet and visible regions [3]. From such data formation constants and thermodynamic functions have frequently been obtained. A number of halogen addition compounds have been studied in the solid state by Hassel and co-workers [4], using X-ray technique.

Infrared spectroscopic technique has also been applied in studies of this type. Vibrational spectral data can more easily be interpreted in terms of changing force constants, charge densities, *etc.* than the ultraviolet data. Previous workers have studied infrared spectral changes of the donor [5–9] as well as of the acceptor [10–16] upon complex formation.

In order to obtain added information about the charge transfer forces acting between halogens and atoms with lone pair electrons, a study of such complexes formed by various types of aldehydes was carried out in this labora-

tory. In the present paper the infrared spectroscopic data obtained for the iodine complexes are presented, followed by a discussion of the results. Subsequent papers will treat the complexes of the same aldehydes with iodine monochloride and iodine monobromide. In the near future complexes formed between various nitriles and halogens will be reported.

EXPERIMENTAL

Chemicals. The best available grades of commercial chemicals were used. Iodine, Merck, resublimated, analytical grade, was used without further purification.

The following aldehydes from Fluka AG had been stabilized with hydroquinone: propionaldehyde, butyraldehyde, *o*- and *m*-tolualdehydes and crotonaldehyde. Hydroquinone had also been added to chloral, a product from Eastman Kodak. These chemicals were all fractionated in a Vigreux column just before use, and their boiling points checked with those given in the literature. Only the middle fractions were used. Cuminaldehyde, 1- and 2-naphthaldehydes, *o*- and *p*-phthaldialdehydes and cinnamic aldehyde, all from Fluka and benzaldehyde, analytical grade from British Drug House had not been stabilized and were studied without further purification. The purity of all the aldehydes was checked by comparing their infrared spectra with those reported in the literature. Carbon disulphide and carbon tetrachloride, analytical grades, both from Merck, were used as solvents. Small impurities are probably not nearly as critical in a quantitative infrared study as in the studies of blue shifted or charge transfer bands. However, as a control the spectrum of a complex between benzaldehyde and halogen was repeated after thorough purification of the halogen and the solvent. No spectral changes were observed.

Stock solutions of the aldehydes and of iodine in carbon disulphide were prepared by weighing into 25 ml volumetric flasks. Carbon disulphide was preferred for the quantitative infrared studies because of the high solubility of iodine in this solvent. The aldehyde-iodine solutions were prepared by pipetting from the stock solutions into 10 ml volumetric flasks. Immediately after preparation the mixed solutions were filled into the absorption cells, and the spectra recorded. The curves were repeated first after a few hours and then after 24 h as a check of eventual irreversible chemical reactions between the aldehydes and iodine.

Instrumental. The infrared spectra were recorded, using a Perkin-Elmer model 21 spectrometer equipped with sodium chloride and calcium fluoride optics. A thermocouple from Charles M. Reeder & Co. was installed, giving twice the previous signal to noise ratio. The quantitative data in the 1700 cm^{-1} region were obtained using the calcium fluoride prism. The slit width was kept constant at 98 μ, corresponding to a computed spectral slit width of approx. 5 cm^{-1}.

Sealed cells of approximately 0.05 and 0.008 cm with sodium chloride windows were used. A variable thickness cell filled with the pure solvent was used as a reference. The wave numbers of the sodium chloride region were calibrated according to standard procedure. The calcium fluoride region was calibrated, using atmospheric water bands [17].

The qualitative spectra recorded in the entire sodium chloride region were obtained at high aldehyde concentrations of approximately 0.1 M and iodine concentrations of 0.5 M in the 0.05 cm cell. In the quantitative runs, however, considerably lower aldehyde concentrations were employed, giving optical densities for the carbonyl stretching band in the interval 0.3—0.5. These spectra were scanned at very low speed in order to obtain the best possible data. No thermostated cell holder was used, but the cell temperature was found to be 30 ± 2°C when measured with a thermocouple. The low solubility of propionaldehyde, butyraldehyde, crotonaldehyde and the *o*- and *p*-phthaldialdehydes in carbon disulphide made it necessary to study these compounds in the thicker cell only. The other aldehydes were studied at two different concentrations, using the thicker and the thinner cells.

Qualitative absorption spectra of the aldehydes and the aldehyde-iodine solutions were obtained in the visible and the ultraviolet region with the aid of a Beckman recording spectrometer DK-1. Carbon tetrachloride was used as the solvent in quartz cells of thicknesses 1 cm.

Table 1. Enhanced and new infrared bands of aldehydes in iodine solutions.

Aldehydes	No.	Enhanced bands	New bands	
Propionaldehyde	1	1729 s[a], 1168 m, 1143 w, 1133 w	*ca.* 1712 s	
Butyraldehyde	2		*ca.* 1718 s	
Chloral	3			
Benzaldehyde	4	1656 vw, 1651 m, 785 w	1689 s, 1218 w	
o-Tolualdehyde	5	1697 w, 1664 w, 1623 w	1678 s, 1217 w	
m-Tolualdehyde	6	1678 w	1690 s	
Cuminaldehyde	7	1692 s, 1667 m, 1658 w	1671 s, 1248 w	
1-Naphthaldehyde	8		1672 s	
2-Naphthaldehyde	9	1655 m	1683 s	
Crotonaldehyde	10		1676 s	R[b]
Cinnamic aldehyde	11	1324 m	1660 s, 1126 m	R
o-Phthaldialdehyde	12		1684 s, 1680 s	
p-Phthaldialdehyde	13		1694 *s*	

a. The intensities are abbreviated as follows: s = strong, m = medium, w = weak.
b. R means that irreversible reactions take place and the data are incomplete.

EXPERIMENTAL RESULTS

A saturated solution of iodine in carbon disulphide at a cell thickness of 0.05 cm showed an infrared spectrum identical with that of the pure solvent. When iodine was added to an aldehyde solution, the majority of the aldehyde bands did not change significantly in position or in intensity. However, for all the aldehydes investigated, with the exception of chloral, some spectral

Table 2. Infrared spectral data for the carbonyl stretching bands of the free aldehydes and their complexes with iodine.

	Free aldehydes			Complexes				
Ald No.[c]	ν_{max} cm^{-1}	$\nu_{1/2}$ cm^{-1}	$B_a \times 10^{-4}$ darks[d]	ν_{max} cm^{-1}	$\nu_{1/2}$ cm^{-1}	$B_c \times 10^{-4}$ darks[d]	$\Delta\nu$[a] cm^{-1}	ΔB[b] $\times 10^{-4}$ darks[d]
1	1738	16	1.1	*ca.* 1718	*ca.* 25	2.6	*ca.* 20	1.5
2	1729	12	1.1	1712	20	2.9	17	1.8
3	1764	6	1.1	—	—	—	—	—
4	1707	7	2.0	1689	13	2.6	18	0.6
5	1701	10	1.6	1678	18	2.6	23	1.0
6	1705	7	1.6	1690	13	2.1	15	0.5
7	1704	7	1.8	1673	15	2.5	31	0.7
8	1696	8	1.9	1672	23	4.2	24	2.3
9	1699	5	2.4	1681	19	5.0	18	2.6
10	1697	7	2.3	1676	15	3.7	23	1.4
11	1686	9	3.0	1660	18	5.0	26	2.0
12	1700	17	2.7	1682	25	4.6	18	1.9
13	1708	11	3.3	1694	23	4.9	14	1.6

a $\Delta\nu = \nu_{max}$ (aldehyde) $-$ ν_{max} (complex).
b. $\Delta B = B_c - B_a$ darks.
c. The numbers refer to the aldehydes as listed in Table 1.
d. 1 dark = 1 cm^{-1} cm^2/mmole.

Table 3. Concentration data and formation constants for the aldehyde complexes [a] with iodine at approximately 30°C.

Ald. No.[f]	C_A[b] mole/l	C_{I_2}[c] mole/l	C_c[d] mole/l	K_c(calc)[e] l/mole	K_c(mean)[e] l/mole
1	0.02561 [g]	0.5284	0.003793	0.23	0.25 ± 0.04
	0.02653 [g]	0.5180	0.002917	0.24	
2	0.02358 [h]	0.5374	0.002694	0.24	0.25 ± 0.04
	0.02386 [h]	0.5556	0.003127	0.27	
3	0.01144 [h]	0.5742	0	0	0. ± 0.05
4	0.008420 [g]	0.6032	0.002104	0.55	0.6 ± 0.05
	0.05635 [i]	0.5741	0.01456	0.62	
5	0.01371 [g]	0.5892	0.003382	0.56	0.6 ± 0.05
	0.07988 [i]	0.5892	0.01775	0.59	
6	0.009484 [g]	0.6115	0.001735	0.40	0.4 ± 0.04
	0.06434 [i]	0.5914	0.01344	0.43	
7	0.009314 [g]	0.6038	0.002474	0.60	0.6 ± 0.05
	0.05709 [i]	0.5209	0.01323	0.60	
8	0.01262 [g]	0.4278	0.001844	0.40	0.4 ± 0.05
	0.07179 [i]	0.5741	0.01212	0.36	
9	0.006626 [g]	0.6155	0.001163	0.35	0.4 ± 0.05
	0.04391 [i]	0.5471	0.007512	0.38	
10	0.007761 [g]	0.5970	0.002195	0.66	0.7 ± 0.06
	0.008053 [h]	0.6079	0.002426	0.71	
11	0.006733 [g]	0.6165	0.002138	0.76	0.75 ± 0.06
	0.05435 [i]	0.5876	0.01599	0.73	
12 *j*	0.01384 [g]	0.6038	0.001265	0.17	0.15 ± 0.04
	0.01468 [h]	0.5944	0.001421	0.17	
13 *j*	0.005731 [h]	0.6143	0.0005872	0.19	0.2 ± 0.05
	0.005614 [h]	0.5832	0.0006193	0.21	

a. Only complexes from the C=O group have been considered.
b. C_A is the initial concentration of aldehyde.
c. C_{I_2} is the initial concentration of iodine.
d. C_c is the equilibrium concentration of the complex.
e. K_c is the formation constant.
f. The numbers refer to the aldehydes as listed in Table 1.
g. Cell thickness 0.0555 cm.
h. Cell thickness 0.0570 cm.
i. Cell thickness 0.0080 cm.
j. The complexes are assumed to be of 1:1 stoichiometry.

changes did occur. These observations are summarized in Table 1, which shows the appearance of some new weak bands and a slight enhancement of some of the original ones. The most prominent changes occur around 1700 cm^{-1}. They appear as a decrease in the intensity of the original carbonyl stretching band and in the formation of a new band on the side toward lower frequencies. The intensity of this new band is enhanced at increasing concentrations of aldehyde or iodine, and is assigned as a band characteristic of a molecular complex. Table 2 lists the spectral parameters observed for the free and the complex carbonyl stretching bands of the aldehydes. The initial concentrations of the aldehydes and the iodine and the calculated values of the complex concentrations in each of the solutions are summarized in Table 3.

The formation constants for the complexes were calculated from the carbonyl stretching bands, assuming a 1:1 complex to the carbonyl group. As an example, the absorption curves for benzaldehyde-iodine are reproduced in Fig. 1. There is an overlap between the free and the complex bands. The experimental curve M has been resolved into two bands represented by the broken curves N and A. Curve N follows the shape of the curve L, characteristic of the free aldehyde; curve N and curve A give the experimental curve M when superimposed. The calculations of the formation constants were based on actual measurements of the areas under the curves L, N and A. Separate backgrounds were drawn for each band, over a frequency range of approximately three times the half band widths. None of the functions proposed for calculating band areas [18] were found satisfactory because of frequent asymmetrical band shapes. Independent measurements showed proportionality of band areas with concentrations and cell thicknesses for each aldehyde.

It is assumed that the integrated absorption intensity of the free carbonyl stretching band does not change upon the addition of iodine. This is verified at least for chloral, which shows no tendency to form a complex with iodine. The concentration C_c of the complex in the solution is given by the expression:

$$C_c = (L-N)\, C_a/L \qquad (1)$$

L and N being the areas under the curves previously named by the same symbols and C_a the initial concentration of the aldehyde. The formation constants have been calculated from the equation:

$$K_c = C_c/(C_a-C_c)(C_{I_2}-C_c) \qquad (2)$$

where C_{I_2} is the initial concentration of iodine of the assumed 1:1 complex. K_c is probably not very different from the true equilibrium constant based on activities. The calculated values for K_c are listed in Table 3. A good agreement has been obtained in most cases between the calculated values at different aldehyde concentrations. The assumption of a 1:1 complex therefore has been justified. The apparent integrated absorption intensities B_a and B_c for the free and the bonded carbonyl absorptions, respectively, have been calculated from eqns. (3) and (4).

$$B_a = L/C_a \cdot l \qquad (3) \qquad\qquad B_c = A/C_c \cdot l \qquad (4)$$

l being the cell thickness, C_a and C_c having the same meaning as before.

No attempt was made to correct for the limited resolving power or to extrapolate to infinite dilution. The values obtained for B_a agree quite well with those reported by Barrow [19].

In order to check the method, a Benesi-Hildebrand [2] calculation of the K_c value was carried out for the cinnamic aldehyde-iodine system, which gave the strongest interaction. In the Scott modification [20], this equation has the form:

$$C_a \cdot C_{I_2} \cdot l/A = 1/K_c \cdot B_c + C_{I_2}/B_c \qquad (5)$$

each symbol having the same meaning as previously described. The spectra of a number of solutions were recorded, the aldehyde concentrations kept constant at 0.02577 M and the iodine concentration varying from 0.1326 M to

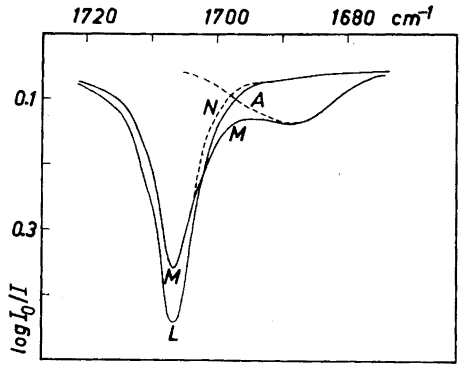

Fig. 1. The carbonyl stretching mode of benzaldehyde (*L*) and benzaldehyde-iodine (*M*) in carbon disulphide. The band *M* is resolved into the band of free benzaldehyde (*N*) and of the complex (*A*).

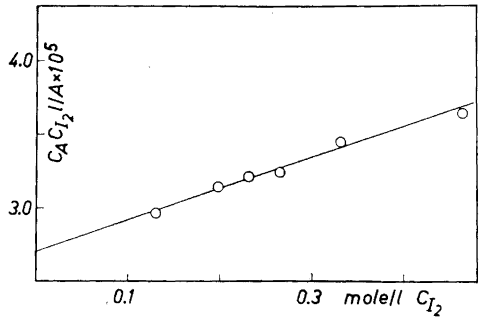

Fig. 2. Benesi-Hildebrand-Scott plot for the cinnamic aldehyde-iodine complex.

0.4642 M. A prerequisite for the validity of eqn. (5) is that $C_{I_2} \gg C_a$, and this is accordingly satisfied.

The data for the Benesi-Hildebrand determination are presented in Table 4. Fig. 2 gives the plot for the cinnamic aldehyde-iodine complex, and the straight line is fitted with a least squares fit. The values obtained for B_c and K_c from Fig. 2 are listed in Table 4. It appears that these values agree quite well with those listed for cinnamic aldehyde-iodine in Tables 2 and 3. This complex is accordingly of the 1:1 type.

Table 2 contains the following data for the free and bonded carbonyl stretching bands of each aldehyde: the frequency ν at maximum absorption, the apparent half intensity width $\nu_{1/2}$, the apparent integrated absorption intensity B, the frequency displacement on complex formation $\Delta\nu$, and finally the difference in the apparent integrated absorption intensities $\Delta B = B_c - B_a$. The listed frequencies of the free carbonyl bands are reliable to within 2 cm^{-1} and the broad complex bands probably within 4 cm^{-1}. Estimated errors in the apparent half intensity widths are probably 1 and 4 cm^{-1} for the free and the bonded carbonyl bands, respectively.

When any of the aldehydes were added to a 1.6×10^{-3} M solution of iodine in carbon tetrachloride, the visible iodine absorption band at 515 mμ was displaced towards higher frequencies. The magnitude of the blue shifts was largest for cinnamic and croton aldehydes, smaller for the aromatic aldehydes (4)—(9), very small for the dialdehydes (12) and (13) and the aliphatic aldehydes (1) and (2). No blue shift was observed for chloral. In each case the free and the blue shifted iodine bands overlapped highly.

Ultraviolet absorption bands around 270 mμ were observed in the propionaldehyde-iodine and in the butyraldehyde-iodine systems, partly overlapped by the $N \rightarrow Q$ transition band of the aldehydes. They can probably be assigned

Table 4. Data for Benesi-Hildebrand-Scott determination of the cinnamic aldehyde-iodine formation constant at approximately 30°C.

C_{I_2} [a] mole/l	A [b] cm^{-1}	C_A[c] . C_{I_2} . l [d] $\times 10^{-4}$	$(C_A . C_{I_2} . l)/A$ $\times 10^{-5}$
0.1326	6.38	1.896	2.973
0.1989	9.05	2.845	3.142
0.2321	10.33	3.319	3.214
0.2652	11.70	3.793	3.241
0.3315	13.76	4.741	3.446
0.4642	18.20	6.639	3.647

$K_c = 0.77$ l/mole $B_c = 4.7 \times 10^4$ darks [e]

a. C_{I_2} is the initial concentration of iodine.
b. A is the integrated area of the 1660 cm^{-1} complex band.
c. C_A is the initial concentration of cinnamic aldehyde: 0.02577 mole/l.
d. l is the cell thickness: 0.0555 cm.
e. 1 dark = 1 cm^{-1} cm^2/mmole.

to charge transfer bands for these complexes. No charge transfer bands of the complexes with the aldehydes (4)—(13) were detected, probably because of the strong overlapping ultraviolet absorption of these aldehydes.

DISCUSSION

The present data can be explained in terms of an interaction between a Lewis base (an aldehyde) and a Lewis acid (the iodine). The small spectral changes observed indicate a very weak interaction. In the much stronger complexes formed between aldehydes and metal halides [21], the normal vibrations of the aldehydes are highly perturbed. The infrared data strongly support the theory that a bond is formed between the carbonyl group and iodine, effected by the oxygen donating lone pair electrons to the halogen. Moreover, in some of the complexes a new infrared band appears around 1200 cm^{-1}, probably connected with a perturbed aldehyde vibration. Similar, but much larger changes have been observed in the aldehyde-interhalogen solutions [22,23] and these effects will be discussed in the following paper.

The blue shifts of the visible iodine absorption band at 515 mμ and the ultraviolet absorptions at 270 mμ observed for two of the iodine-aldehyde complexes suggest that these complexes are of the charge transfer type. According to Mulliken [1] the aldehyde-iodine complexes should be stabilized by resonance between a non-bonded structure

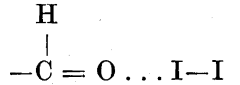

(I)

and a dative structure,

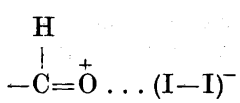

(II)

the latter becoming increasingly important with stronger interaction. The electron which is transferred to give structure (II), supposedly goes into an antibonding orbital, causing a weakening of the I—I bond and a lowering of the I—I stretching frequency. This was verified by Plyler and Mulliken [16] in the pyridine-iodine and benzene-iodine systems and observed in the region around 200 cm^{-1}.

The decrease in the carbonyl stretching frequency of the aldehydes on complex formation with iodine, is in agreement with the results reported by earlier workers on the iodine complexes with ketones [6,8] and dimethylacetamide [9]. The lowering of the frequency may be due partly to a weakening of the carbon-oxygen bond, and partly to an increase in the effective mass on the formation of a partial oxygen iodine charge transfer bond. The former effect is probably more important in accounting for the observed frequency shift $\Delta\nu$.

The carbonyl bond consists of a σ-bond formed by overlapping one of the sp^2 orbitals of the carbon atom with a p orbital of the oxygen atom, the other p orbital of the oxygen forming a π-bond with the unhybridized carbon p orbital. Because oxygen is more electronegative than carbon, the π-electron density will be higher at the oxygen atom. The crystal structure of compounds having hydrogen bonds [24] or charge transfer bonds [25] to the carbonyl group, indicate that the two lone pair orbitals of the latter are in a plane at right angles to the π-bond and making an angle of approximately 120° between the lone pair orbitals and the carbon-oxygen σ-bond. If a lone pair electron of the carbonyl oxygen is transferred to iodine, the π-electron density of the oxygen will increase. According to Yamada and Kozima [8] and based on *M.O.* calculations, the increased π-electron density at the oxygen is accompanied by a decrease in the C=O stretching force constant. Paoloni [26] assumed certain values for the changes in bond lengths and p orbital overlap integrals of the carbon oxygen bond upon complex formation to metal halides. He calculated the frequency shifts $\Delta\nu$ for some aromatic aldehydes and ketones in good agreement with the observations. The increase in the π-electron density at the oxygen atom, accompanying the charge transfer is expected to be different in unconjugated and conjugated systems. For this reason the observed shifts of the various aldehydes are comparable only within their respective systems.

In addition to having lower frequencies, the complex carbonyl stretching bands have generally higher apparent integrated intensities B and larger half intensity widths $\nu_{1/2}$ than the corresponding free bands. The integrated intensity of the carbonyl stretching absorption B is approximately proportional to $(d\mu/dr)^2$, the square of the rate of change in molecular dipole moment with inter-atomic distance. The higher π-electron density on the carbonyl oxygen resulting from larger contribution of the dative resonance structure (II) probably accounts for the increased bond moment. The conjugated aldehydes (4)—(13) seem to give smaller values of ΔB than the saturated, aliphatic aldehydes (1)—(2). These results agree qualitatively with the lower values for ΔB derived from Yamada and Kozima's data [8] in methyl acetate and 3-phenylsydnone compared to saturated ketones. In the two former compounds lone pair electron orbitals of the ether oxygen overlap with the π-orbitals of the carbonyl group, thus causing the same effect as in the conjugated aldehydes.

The close similarity between charge transfer complexes and hydrogen bonding has been emphasized by different authors [12–14]. It is well known [27] that the existence of a hydrogen bond to a carbonyl group perturbs not only the O—H stretching frequency, but also the carbonyl stretching frequency. Barrow [19] observed in infrared that the C=O stretching frequencies of benzaldehyde and propionaldehyde are 8 cm^{-1} lower in chloroform than in carbon tetrachloride. The integrated areas were approximately 23 % and 35 % higher in chloroform for benzaldehyde and propionaldehyde, respectively. Thus, the spectral features of the C=O stretching frequency connected with complex formation to iodine and hydrogen bonding seem qualitatively closely related for the aldehydes. However, the data are too scarce to provide any quantitative correlation.

The enthalpy difference ΔH and entropy difference ΔS can be calculated if the formation constants K_c are observed at different temperatures. The low values expected for ΔH and ΔS in these complexes would make such calculations very inaccurate within the small temperature interval feasible for such measurements. However, the formation constants listed in Table 3 reflect the relative basicities of the aldehydic carbonyl groups towards iodine. The contribution of the dative form (II) and the strength of the complex should increase [1] with lower ionization potential of the aldehyde. Moreover, inductive and conjugation effects are expected to be important for the donor strength of the carbonyl group [28]. The alkyl groups in the saturated aldehydes (1) and (2) give a weak, positive inductive effect and the compounds act as weak donors. Their donor effect is lower than for acetone [8], in agreement with the stronger inductive effect exhibited by an alkyl group compared to a hydrogen atom. The strong, negative inductive effect of the three chlorine atoms adjacent to the carbonyl group in chloral (3), evidently pulls the lone pair electrons close to the oxygen and makes them completely unavailable for donation. This strong inductive effect is also reflected in the high carbonyl stretching frequency of this aldehyde. In the compounds (4)—(10) the carbonyl group is conjugated to an aromatic ring system, and the resulting delocalizing effect on the π-electrons makes these aldehydes stronger donors. The somewhat lower formation constants observed for the complexes with the naphthaldehydes (8) and (9) compared to the benzaldehyde and its derivatives (4)—(7) may be partly due to the lower π-electron density in the naphthalene rings. In crotonaldehyde (10) and cinnamic aldehyde (11) the carbonyl groups are conjugated to an aliphatic double bond, and this arrangement makes these two aldehydes the strongest Lewis bases of those investigated. However, Schmulbach and Drago [9] report a considerably higher formation constant for the corresponding complex between N,N-dimethylacetamide and iodine, indicating a higher basicity of the acetamido group connected with delocalization of the nitrogen lone pair electrons.

It appears that the aromatic dialdehydes (12) and (13) act as very weak donors towards iodine. These compounds should be capable of acting as donors for two iodine molecules. However, the weak donor properties as well as some qualitative spectra obtained for the blue shifted visible iodine peaks indicate the existence of 1:1 complexes under the experimental conditions employed. The mutual negative inductive effects of the aldehyde groups may strongly

inhibit the donation of electrons. A similar example has been reported by Glusker and Thompson [6]. They find that benzil is a weak donor toward iodine compared with other ketones and suggest steric hindrance. Steric hindrance may contribute to the low donor property of *o*-phthaldialdehyde, but not that of *p*-phthaldialdehyde.

The authors are indebted to *Norges almenvitenskapelige forskningsråd* for financial support.

REFERENCES

1. Mulliken, R. S. *J. Am. Chem. Soc.* **74** (1952) 811; *J. Phys. Chem.* **56** (1952) 801; *Rec. trav. chim.* **75** (1955) 845.
2. Benesi, H. A. and Hildebrand, J. H. *J. Am. Chem. Soc.* **71** (1949) 2703.
3. Andrews, L. J. *Chem. Revs.* **54** (1954) 713.
4. Hassel, O. *Proc. Chem. Soc.* **1957** 250; *Molecular Physics* **1** (1958) 241; Hassel, O. and Römming, Chr. *Quart. Revs.* **XVI** (1962) 1.
5. Haller, W., Jura, G. and Pimentel, G. C. *J. Chem. Phys.* **22** (1954) 720.
6. Glusker, D. L. and Thompson, H. W. *J. Chem. Soc.* **1955** 471.
7. Ferguson, E. E. *J. Chem. Phys.* **25** (1956) 577.
8. Yamada, H. and Kozima, K. *J. Am. Chem. Soc.* **82** (1960) 1543.
9. Schmulbach, C. D. and Drago, R. S. *J. Am. Chem. Soc.* **82** (1960) 4484.
10. D'Or, L., Alewaeters, R. and Collin, J. *Rec. trav. chim.* **75** (1956) 862.
11. D'Or, L. and Collin, J. *J. Chem. Phys.* **23** (1955) 397.
12. Person, W. B., Humphrey, R. E., Deskin, W. A. and Popov, A. I. *J. Am. Chem. Soc.* **80** (1958) 2049.
13. Person, W. B., Humphrey, R. E. and Popov, A. I. *J. Am. Chem. Soc.* **81** (1959) 273.
14. Person, W. B., Erickson, R. E. and Buckles, R. E. *J. Am. Chem. Soc.* **82** (1960) 29.
15. Popov, A. I., Humphrey, R. E. and Person, W. B. *J. Am. Chem. Soc.* **82** (1960) 1850.
16. Plyler, E. K. and Mulliken, R. S. *J. Am. Chem. Soc.* **81** (1959) 823.
17. Jones, L. H. *J. Chem. Phys.* **24** (1956) 1250.
18. Jones, R. N. and Sandorfy, C. in *Chemical Applications of Spectroscopy*, Interscience Publishers, New York 1956, p. 280.
19. Barrow, G. M. *J. Chem. Phys.* **21** (1953) 2008.
20. Scott, R. L. *Rec. trav. chim.* **75** (1956) 787.
21. Paoloni, L. and Marini-Bettólo, G. B. *Gazz. chim. ital.* **89** (1959) 1972.
22. Augdahl, E. and Klæboe, P. *Acta Chem. Scand.* **16** (1962) 1647.
23. Augdahl, E. and Klæboe, P. *Acta Chem. Scand.* **16** (1962) 1655.
24. Schneider, W. G. *J. Chem. Phys.* **23** (1955) 26.
25. Hassel, O. and Strömme, K. O. *Acta Chem. Scand.* **13** (1959) 275.
26. Paoloni, L. *Gazz. chim. ital.* **87** (1957) 408.
27. Pimentel, G. C. and McClellan, A. L. *The Hydrogen Bond*, W. H. Freeman & Co., San Fransisco 1960, p. 137.
28. Cook, D. *J. Am. Chem. Soc.* **80** (1958) 49.

Received March 24, 1962.

ACTA CHEMICA SCANDINAVICA 16 (1962) 1647–1654

Spectroscopic Studies of Charge Transfer Complexes

II. Aldehydes and Iodine Monochloride

ELSE AUGDAHL and PETER KLÆBOE

Universitetets Kjemiske Institutt, Blindern-Oslo, Norway

Charge transfer complexes between aldehydes and ICl have been studied in solution by infrared and visible spectroscopic methods. Formation constants for these complexes at 30°C in carbon disulphide were obtained from intensity changes of the C=O stretching bands. ICl is a considerably stronger acceptor than I_2 towards the aldehydes, apparent from the higher formation constants and the larger changes in the infrared and visible spectra. Band displacements and enhancements of weak bands in various parts of the infrared spectra have been listed and these effects have been discussed.

In the first paper of this series [1] the charge transfer complexes [2] between various aldehydes and iodine were studied by means of infrared and visible spectroscopic methods. The present paper presents a study of the complex formation between the same aldehydes and iodine monochloride. It is well known that iodine monochloride can act as a Lewis acid towards substances having loose π-electrons or lone pair electrons. A number of such complexes have been studied by ultraviolet [3], visible [4,5] and infrared [6-8] spectroscopic methods.

EXPERIMENTAL

Chemicals. The origin, the chemical grades of the aldehydes and the method of purification have been described [1]. The iodine monochloride, Merck, was purified by repeated recrystallizations until a constant melting point, 27°C, was obtained [9]. Carbon disulphide and carbon tetrachloride, both Merck, analytical grades, were used as solvents. A careful drying and distillation of the carbon disulphide seemed to have no effect upon the infrared spectra in the carbonyl stretching region. The solvents were therefore used without further purification.

Instrumental. The infrared and the ultraviolet spectrometers and the experimental technique have been described previously [1]. The iodine monochloride solutions were left in the infrared cells only the minimum time required to record the spectra. A certain etching of the sodium chloride windows and the lead spacers was observed, but the cells remained transparent in the region 4000 – 650 cm^{-1}.

Some introductory investigations were carried out in the region 700 – 300 cm^{-1}, with the aid of a caesium bromide prism and sealed cells with KRS-5 windows. However,

the iodine monochloride reacted with the window material, and a strong cell absorption appeared which obscured the spectra. Therefore, no more work was carried out along that line.

EXPERIMENTAL RESULTS

Iodine monochloride has one infrared and Raman active fundamental, observed at 382 cm^{-1} in the gas phase and at 361 cm^{-1} when dissolved in carbon disulphide [6]. In the same solution, three weak infrared bands were observed around 800 cm^{-1} at the concentrations and cell thicknesses employed. Otherwise the spectrum of the solution was identical with that of the pure solvent in the region 4000—650 cm^{-1}.

When iodine monochloride was added to a solution of an aldehyde, a number of changes appeared in the infrared spectra. Particularly in croton aldehyde, but also in some of the other compounds, time dependent spectral variations occurred, obviously caused by addition or substitution reactions. Since most of the new bands did not vary significantly with time, they were ascribed to the molecular complexes. These changes were separated into two groups:

(*a*) Enhancement of some infrared bands, already present in the spectra of the aldehydes.

(*b*) Appearance of new bands and reduction in intensities of adjacent aldehyde peaks.

The enhanced bands and the new peaks appearing in the carbonyl stretching region are listed in Tables 1 and 2, respectively. Reliable data for the new infrared bands in the other spectral regions were obtained only for the aromatic aldehydes (4)—(9) and are given in Table 3. These new bands fall within certain regions, and they are displaced less than 15 cm^{-1} from the free aldehyde

Table 1. Infrared bands enhanced in iodine monochloride solution.

Aldehydes	No.	Enhanced bands					
Propionaldehyde	1	1688 s [a],	1357 m,	1307 w,	1142 w		R [b]
Butyraldehyde	2	1702 w,	1685 m,	1275 w			R
Chloral	3						
Benzaldehyde	4	1687 w,	1656 m,	1651 s,	1598 s, 1491 w,	1583 [c] m, 1284 m	
o-Tolualdehyde	5	1692 w,	1679 w,	1651 s,	1623 w,	1600 s	
m-Tolualdehyde	6	1678 w,	1654 w,	1647 w,	1603 s,	1585 m, 1161 m	
Cuminaldehyde	7	1692 s,	1667 w,	1658 w,	1650 w,	1610 s	
1-Naphthaldehyde	8	1654 w,	1622 w				
2-Naphthaldehyde	9	1655 s,	1631 s				
Crotonaldehyde	10	1034 w					R
Cinnamic aldehyde	11	1650 m,	1228 w				R
o-Phthaldialdehyde	12	1659 s					R
p-Phthaldialdehyde	13						R

[a]. The intensities are abbreviated as follows: s = strong, m = medium and w = weak.

[b]. R means that irreversible reactions take place and the data are incomplete.

[c]. Data in the regions 1600—1580 and 1500—1400 cm^{-1} are obtained from carbon tetrachloride solutions.

Table 2. Infrared spectral data for the carbonyl stretching bands of the aldehyde complexes with iodine monochloride [a].

Aldehydes	No.	ν_{max} cm^{-1}	$\nu_{\frac{1}{2}}$ cm^{-1}	$B_c \times 10^{-4}$ darks [d]	$\Delta\nu$ [b] cm^{-1}	$\Delta B \times 10^{-4}$ [c] darks [d]	
Propionaldehyde	1	1699	20	2.1	39	1.1	R [e]
Butyraldehyde	2	1697	18	2.5	32	1.4	R
Chloral	3						
Benzaldehyde	4	1678	13	3.2	29	1.2	
o-Tolualdehyde	5	1661	12	4.0	40	2.4	
m-Tolualdehyde	6	1659	11	3.9	46	2.3	
Cuminaldehyde	7	1656	14	4.3	48	2.5	
1-Naphthaldehyde	8	1649	10	4.7	47	2.8	
2-Naphthaldehyde	9	1666	17	5.1	33	2.5	
Crotonaldehyde	10	1659			38		R
Cinnamic aldehyde	11	1641	13	6.0	45	3.0	R
o-Phthaldialdehyde	12	1674	14	5.4	26	2.7	R
p-Phthaldialdehyde	13	1678	13	6.5	30	3.2	R

[a]. The spectral data for the carbonyl stretching bands of the free aldehydes are listed in Table 2 (Ref.[1]).
[b]. $\Delta\nu = \nu_{max}$ (aldehyde) $-$ ν_{max} (complex).
[c]. $\Delta B = B_c - B_a$ darks.
[d]. 1 dark = 1 cm^{-1}cm^2/mmole.
[e]. R means that irreversible reactions take place and the data are less reliable.

peaks. Bands in these particular regions have been correlated with vibrations characteristic of aldehydes. Thus, absorption in the range 1400—1370 cm^{-1} has been assigned to the aldehydic δ CH mode [10], and the ranges 1320—1260 cm^{-1} and 1230—1160 cm^{-1} to aromatic aldehyde vibrations [11]. The latter probably involve aromatic skeleton and C—CO stretching modes. The perturbation of these vibrations, as reflected in the band displacements, supports the evidence of complex formation from the carbonyl oxygen atom. Similar effects

Table 3. Infrared bands [a] of aromatic aldehydes perturbed on complex formation with iodine monochloride.

No.[b]	Free [c]	Compl. [c]	Free	Compl.	Free	Compl.	Free	Compl.	Free	Compl.	Free	Compl.
4	1430w [d]	1416w	1387w	1391w	1310m	1314m	1200s	1208s	1164m	1168m	827s	832m
5	1404w	1407m	1383w	1385w	1301w	1306w	1206w	1215m	1157w	1160w	859m	864m
					1284m	1287s	1192s	1198s				
6			1381m	1392m	1295m	1300m			1142s	1150s	905m	908m
					1242s	1247s						
7			1394w	1390w	1305s	1310s	1208s	1218s	1169s	1172s		
8	1447w	1442m	1373w	1375m			1214s	1217s	1170s	1173m	1054s	1058s
9	1441w	1442m	1384w	1383m	1346s	1351w	1254m	1261m	1165m	1172m		

[a]. The carbonyl stretching bands are not included, but are listed in Table 2.
[b]. The numbers refer to the aldehydes as listed in Table 1.
[c]. Data in the region 1500—1400 cm^{-1} are obtained from carbon tetrachloride solutions.
[d]. The intensities are abbreviated as follows: s = strong, m = medium and w = weak.

Table 4. Concentration data and formation constants for the aldehyde complexes [a] with iodine monochloride at approximately 30°C.

Ald [b] No.	C_A [c] mole/l	C_{ICl} [d] mole/l	C_c [e] mole/l	(K_c(calc) [f] l/mole	K_c(mean) l/mole
1	0.02740 [h]	0.2810	0.006874	1.22	1.2 ± 0.2 R [g]
	0.02740 [h]	0.3106	0.007333	1.20	
2	0.02403 [h]	0.3627	0.006974	1.09	1.1 ± 0.2 R
	0.02394 [h]	0.3894	0.007254	1.14	
3	0.01144 [h]	0.6416	0	0.00	0.0 ± 0.1
4	0.008063 [h]	0.3763	0.003715	2.29	2.3 ± 0.1
	0.05635 [i]	0.3237	0.02284	2.21	
5	0.01157 [h]	0.3882	0.005493	2.36	2.3 ± 0.1
	0.08315 [i]	0.5478	0.04379	2.21	
6	0.009484 [h]	0.4333	0.004964	2.59	2.5 ± 0.1
	0.06434 [i]	0.4333	0.03202	2.46	
7	0.009314 [j]	0.4131	0.004360	2.16	2.3 ± 0.1
	0.05734 [i]	0.4390	0.02898	2.49	
8	0.01262 [j]	0.4873	0.007647	2.15	2.1 ± 0.2
	0.07391 [i]	0.5393	0.03664	1.95	
9	0.006626 [j]	0.4188	0.002946	1.92	1.9 ± 0.1
	0.04370 [i]	0.3852	0.01851	2.03	
11	0.007044 [j]	0.04544	0.002362	11.7	11.3 ± 2.0 R
	0.007116 [h]	0.01902	0.001156	10.9	
12 [k]	0.01384 [h]	0.5984	0.003002	0.47	0.5 ± 0.1 R
	0.01417 [h]	0.5619	0.002880	0.46	
13 [k]	0.005636 [h]	0.3679	0.001147	0.70	0.7 ± 0.2 R
	0.005636 [h]	0.5151	0.001544	0.73	

[a]. Only complexes from the C=O group have been considered.
[b]. The numbers refer to the aldehydes as listed in Table 1.
[c]. C_A is the initial concentration of aldehyde.
[d]. C_{ICl} is the initial concentration of iodine monochloride.
[e]. C_c is the equilibrium concentration of the complex.
[f]. K_c is the formation constant.
[g]. R means that irreversible reactions take place, making the calculations less reliable.
[h]. Cell thickness 0.0570 cm.
[i]. Cell thickness 0.0080 cm.
[j]. Cell thickness 0.0555 cm.
[k]. The complexes are assumed to be of 1:1 stoichiometry.

have been observed for complexes between aromatic aldehydes and mercuric chloride [12]. Because of the smaller shifts and the lower intensities, these complex bands were less suitable for quantitative correlations than the carbonyl stretching bands.

The spectral parameters for the complex carbonyl stretching bands are listed in Table 2. These data should be compared with those for the free aldehydes listed in Table 2, Ref.[1] Table 4 contains the initial concentrations of the aldehydes and the halogen, the calculated equilibrium concentrations of the complexes and the formation constants. These calculations are based upon the method described previously [1]. Because of the stronger acceptor properties and higher solubility of iodine monochloride compared to iodine, the experimental conditions could usually be adjusted to make $N \approx 1/2\ L$ (eqn. (1) and

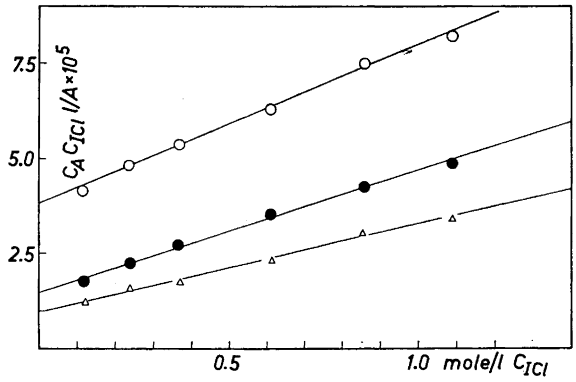

Fig. 1. Benesi-Hildebrand-Scott plots for the complexes between iodine monochloride and the following aldehydes: butyraldehyde (O) $K_c = 1.09$, $B_c = 2.4 \times 10^4$ darks; benzaldehyde (●) $K_c = 2.21$, $B_c = 3.1 \times 10^4$ darks and *o*-tolualdehyde (△) $K_c = 2.29$ and $Bc = 4.4 \times 10^4$ darks.

Fig. 1, Ref.[1]). In that case $C_c \approx 1/2\ C_a$ and the formation constants were calculated at the most favourable conditions. The larger frequency shifts $\Delta\nu$, compared to those observed for the iodine complexes [1] resulted in better resolution of the free and the complex carbonyl stretching bands. However, the enhancement of some weak bands already present in the aldehyde spectrum (Table 1) interfered in some cases. The calculated formation constants have generally smaller relative errors than those reported for the iodine complexes. Crotonaldehyde is not listed in Table 4 since rapid addition reactions with the halogen made quantitative calculations impossible.

Because the complex carbonyl stretching band had a high intensity, the formation constants could be independently determined by the Benesi-Hildebrand equation [13]. If the Scott modification [14] of this method was applied and the integrated intensities of the complex peak were used in eqn. (5) (Ref.[1]), the values obtained for K_c and B_c were in good agreement with those listed in Tables 4 and 2. As representative examples, the Benesi-Hildebrand-Scott plots of the complexes formed by butyraldehyde, benzaldehyde and *o*-tolualdehyde with iodine monochloride are illustrated in Fig. 1 together with the calculated values of K_c and B_c. The scatter of the points in Fig. 1 are not larger than expected when obtained from infrared data, and the plots indicate 1:1 stoichiometries for each of the three systems. However, the Benesi-Hildebrand determinations of B_c and K_c are probably no more precise than the values obtained from the first method and listed in Tables 2 and 4, respectively.

When the aldehydes were added to a 5×10^{-3} M solution of iodine monochloride in carbon tetrachloride, the halogen visible absorption band at 465 mμ was blue shifted. The stronger interactions in these systems compared to the iodine complexes [1], were apparent from the larger blue shifts observed in the former. Chloral appeared again as an exception, giving rise to no blue shift.

The ultraviolet absorption of the mixed solutions above 250 mμ seemed to be a superposition of the aldehyde and halogen absorptions. Possible charge transfer bands may be covered by the strong aldehyde absorption, or they are situated below the transparent region for carbon tetrachloride.

DISCUSSION

As expected, iodine monochloride was found to act as a stronger acceptor than iodine towards the aldehydes. The stronger acidity of iodine monochloride compared to iodine in these systems appeared from the higher formation constants K_c, the larger shifts $\Delta\nu$ of the carbonyl stretching frequency in the infrared and the larger blue shifts observed in the visible region.

Assuming the complexes to be of the charge transfer type, they should be stabilized by the resonance structures [2]

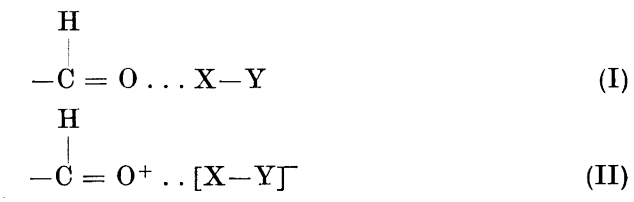

(I)

(II)

The solid lines represent covalent bonds, the dotted lines Coulomb or van der Waals attractions, and X and Y symbolize the halogen atoms. Hassel and co-workers have shown that in charge transfer compounds between iodine monochloride and molecules containing lone pair electrons like 1,4-dioxan [15], pyridine [16] and trimethyl amine [17], the iodine atom is linked to the donor in the crystalline state. Furthermore, they found that the donor atom and the two halogens form a linear (or nearly linear) structure. A similar arrangement probably exists in solution. Referring to the structures (I)—(II) of the complexes, the halogens X and Y will represent iodine and chlorine, respectively. The high electronegativity of chlorine compared to iodine may favour structure (III).



(III)

Person *et al.*[6,7] explained the changes in the infrared spectrum of the acceptor upon complex formation on the basis of this type structure. The stronger acidity of iodine monochloride compared to iodine may be apparent from the larger contribution of structures (II) and (III) to the resonance. It was pointed out by Yamada and Kozima [18] that the increased π-electron density on the oxygen atom in structure (II) results in a decrease of the C=O stretching force constants. It appears from Tables 4 and 2 compared to Tables 3 and 2, Ref.[1], that the formation constants K_c and the spectral shifts $\Delta\nu$ are larger in the iodine monochloride than in the iodine complexes. Furthermore, the aromatic aldehydes (4)—(9) have higher integrated intensities B_c in the iodine monochloride complexes than in the iodine complexes.

The relative donor strengths of the various aldehydes, apparent from the formation constants, K_c, showed a close relationship in the complexes with iodine [1], iodine monochloride and iodine monobromide [19]. The strong field effect or $-I$ effect in chloral completely prevented complex formation. Cinnamic aldehyde formed the strongest complex, the aromatic aldehydes the intermediate, the aliphatic aldehydes the weaker, and the aromatic dialdehydes the weakest complexes. The experimental uncertainties in the formation constants are too high to allow conclusions about the donor strengths of the aromatic aldehydes (4)—(9) relative to the effects of the substituents. It appears, however, that the naphthaldehydes are weaker donors than the benzaldehydes in agreement with the previous results [1].

As listed in Table 1, a number of weak aldehyde bands in the region 2000—650 cm^{-1} were enhanced in iodine monochloride solution. With some exceptions, the same bands which were enhanced in the iodine solutions were also enhanced in the aldehyde interhalogen systems. However, the intensity changes were larger and more frequent in the iodine monochloride solutions. The same effects were observed when carbon tetrachloride was used as a solvent instead of carbon disulphide.

The absorption band at 1651 cm^{-1} in benzaldehyde, having a weak shoulder at 1656 cm^{-1}, increased in intensity in both the iodine monochloride and the iodine monobromide [19] solutions. The integrated area of these overlapping bands was studied as a function of the interhalogen concentration and the data could be fitted with a straight line in the Benesi-Hildebrand-Scott procedure. Furthermore, they gave approximately the same values for the formation constant as those listed in Table 4, and in Table 3, Ref.[19] This indicates that the two enhanced bands increase linearly in intensity with the concentration of the complex. While the bands at 1651 and 1656 cm^{-1} are present as extremely weak bands in benzaldehyde, they should probably be assigned to the benzaldehyde interhalogen complexes. A possible explanation of this effect may be that the symmetry elements of benzaldehyde are reduced upon complex formation, causing inactive fundamentals to become infrared active. If benzaldehyde has the molecular symmetry C_s, the fundamentals belong to species A' and A'' and are all infrared and Raman active. Because of the structural relationship to benzene of symmetry D_{6h}, however, some of the fundamentals may be very weak in the infrared. A further lowering of the molecular symmetry upon complex formation may enhance these infrared absorption bands. Because no detailed vibrational analysis of the present aromatic aldehydes has been made, these explanations are rather speculative. Furthermore, the enhancement of infrared bands in the aliphatic aldehydes (1)—(2) with symmetry C_1 cannot be explained by such arguments. It seems very significant, however, that chloral showed no new or enhanced bands in any of the halogen solutions [1,19]. This strongly suggests that all the enhanced bands listed in Table 1 can be assigned to the complexes. Effects similar to these have been observed by Ferguson [20] in some alkyl benzene-iodine systems. Evidently, much more work is necessary to decide the origin of these enhanced aldehyde bands.

The origin of the three weak infrared bands around 800 cm^{-1} in the spectrum of a concentrated solution of iodine monochloride in carbon disulphide has

not been decided. They cannot be explained as overtones of the fundamental at 380 cm^{-1}. The simultaneous transitions reported by Ketelaar and Hooge [21] in mixtures of halogens and carbon disulphide are expected to give absorptions at other frequencies and of still lower intensities. These bands were not present when cyclohexane was used as a solvent. Furthermore, they coincide with very weak absorption bands of the carbon disulphide. They may be due to enhancement of the solvent bands by solute-solvent interactions.

The authors are indebted to *Norges almenvitenskapelige forskningsråd* for financial support.

REFERENCES

1. Augdahl, E. and Klæboe, P. *Acta Chem. Scand.* **16** (1962) 1637.
2. Mulliken, R. S. *Rec. trav. chim.* **75** (1955) 845, and earlier papers listed there.
3. Andrews, L. J. *Chem. Revs.* **54** (1954) 713.
4. Buckles, R. E. and Mills, J. F. *J. Am. Chem. Soc.* **76** (1954) 4845.
5. Popov, A. I. and Deskin, W. A. *J. Am. Chem. Soc.* **80** (1958) 2976.
6. Person, W. B., Humphrey, R. E., Deskin, W. A. and Popov, A. I. *J. Am. Chem. Soc.* **80** (1958) 2049.
7. Person, W. B., Erickson, R. E. and Buckles, R. E. *J. Am. Chem. Soc.* **82** (1960) 29.
8. Marzocchi, M. and Ferroni, E. *Gazz. chim. ital.* **91** (1961) 1200, 1216.
9. Cornog, J. and Karges, R. A. *Inorganic Syntheses*, Vol. I, McGraw-Hill Book Co. New York 1939, p. 165.
10. Eggers, D. F. and Lingren, W. E. *Anal. Chem.* **28** (1956) 1328.
11. Bellamy, L. J. *The Infra-red Spectra of Complex Molecules*, 2nd ed. Methuen & Co., London 1958, p. 157.
12. Paoloni, L. and Marina-Bettólo, G. B. *Gazz. chim. ital.* **89** (1959) 1972.
13. Benesi, H. A. and Hildebrand, J. H. *J. Am. Chem. Soc.* **71** (1949) 2703.
14. Scott, R. L. *Rec. trav. chim.* **75** (1956) 787.
15. Hassel, O. and Hvoslef, J. *Acta Chem. Scand.* **10** (1956) 138.
16. Hassel, O. and Römming, Chr. *Acta Chem. Scand.* **11** (1957) 696.
17. Hassel, O. and Hope, H. *Acta Chem. Scand.* **14** (1960) 391.
18. Yamada, H. and Kozima, K. *J. Am. Chem. Soc.* **82** (1960) 1543.
19. Augdahl, E. and Klæboe, P. *Acta Chem. Scand.* **16** (1962) 1655.
20. Ferguson, E. E. *Spectrochim. Acta* **10** (1957) 123.
21. Ketelaar, J. A. A. and Hooge, F. N. *J. Chem. Phys.* **23** (1955) 749; **23** (1955) 1549; *Rec. trav. chim.* **76** (1957) 529.

Received March 24, 1962.

ACTA CHEMICA SCANDINAVICA 16 (1962) 1655–1661

Spectroscopic Studies of Charge Transfer Complexes

III. Aldehydes and Iodine Monobromide

ELSE AUGDAHL and PETER KLÆBOE

Universitetets Kjemiske Institutt, Blindern-Oslo, Norway

Charge transfer complexes between aldehydes and IBr have been studied in solution by infrared and visible spectroscopic methods. Formation constants (K_c) for these 1:1 complexes in carbon disulphide at 30°C were obtained from intensity changes of the C=O stretching bands. IBr is a stronger acceptor than I_2 but weaker than ICl towards the aldehydes. In the complexes between each aldehyde and I_2, IBr and ICl, approximately linear relations existed between the C=O frequency shifts ($\Delta\nu$) and ln K_c. Linear relations were also observed in most cases between $\Delta\nu$ and the corresponding integrated intensity changes (ΔB). No monotonic relation was observed between the half intensity widths ($\nu_{1/2}$) and $\Delta\nu$.

In the two previous papers the charge transfer complexes [1] between various aldehydes and iodine [2] and iodine monochloride [3] were studied. The present paper deals with a spectroscopic investigation of the corresponding complexes with iodine monobromide. Only a few complexes between iodine monobromide and donors with lone pair electrons [4–6] have been investigated. Due to the high reactivity of this halogen, the quantitative data in the present paper have been restricted to complexes with aromatic aldehydes.

EXPERIMENTAL

Chemicals. The origin and purity of the aldehydes and the solvents have been described previously [2]. The iodine monobromide, Merck, was purified by recrystallizations to a constant melting point of 42°C.

Instrumental. The infrared and the ultraviolet spectrometers, the absorption cells and the experimental technique have been described [2]. Because of the corrosive properties of iodine monobromide, it was particularly important that these solutions not be left in the cells longer than necessary.

EXPERIMENTAL RESULTS

The fundamental frequency [7] of iodine monobromide appears at 268 cm^{-1}. No overtones have been detected in the region 4000—650 cm^{-1} at the concen-

trations and cell thicknesses employed. A 0.5 M solution of this interhalogen in carbon disulphide seemed to have an infrared spectrum identical to that of the pure solvent in this region.

When iodine monobromide was added to a solution of an aldehyde, infrared spectral changes in the region 4000—650 cm^{-1} occurred in most cases. These changes are listed in Table 1, and they can conveniently be separated into two groups: (*a*) Some weak bands present in the spectra of the aldehydes are enhanced; (*b*) Some bands appear, formerly not present in the aldehydes.

The aldehyde-iodine monobromide solutions were prepared just prior to the recording of the infrared spectra. Irreversible reactions were observed for most of the aldehydes after 24 h. If the spectra were repeated after 30 min, distinct changes occurred with the aldehydes (1), (2), (10), (11), (12) and (13). The remaining aldehyde-iodine monobromide solutions did not change significantly after 30 min. Therefore the complex formation constants are restricted to the aldehydes listed in Table 3.

The spectral features observed for the aldehyde-iodine monobromide solutions are similar to those observed for the corresponding iodine [2] and iodine monochloride [3] systems. This is particularly striking in the two interhalogen systems. Thus, the enhanced, as well as the new bands listed in Table 1, were observed at approximately the same wave numbers in the iodine monochloride solutions. However, the effects were generally much smaller in the iodine monobromide systems. Some of the new complex bands in the region 1400—800 cm^{-1} appeared as barely detectable shoulders in agreement with the weaker interactions expected in the present systems.

The complex formation constants have been calculated according to the method described previously [2] and are listed in Table 3. As a further check the Benesi-Hildebrand [8]-Scott [9] equation was applied to the integrated areas of the complex carbonyl stretching bands in the benzaldehyde and *o*-tolualdehyde solutions. It appears from Fig. 1 that straight lines can be fitted to the data in both systems. Thus, these complexes are of 1:1 stoichiometry, and the calculated values for B_c and K_c agree quite well with those listed in Tables 2 and 3.

The visible absorption band of iodine monobromide situated at 492 mμ in carbon tetrachloride solution was blue shifted when the aldehydes were added, except in the case of chloral. However, the free and the complex iodine monobromide absorption bands overlapped considerably. The blue shifts of the various systems were therefore not easily determined. Neither were the blue shifted bands suitable for a quantitative determination of the formation constants. No charge transfer bands were observed in the transparent region of carbon tetrachloride above 250 mμ.

DISCUSSION

The spectral data observed for the aldehyde-iodine monobromide systems support the prediction that this interhalogen is a stronger Lewis acid than iodine, but weaker than iodine monochloride. In agreement with the iodine monochloride complexes it is highly probable that the iodine atom is linked to

Table 1. Enhanced and new infrared bands of aldehydes in iodine monobromide solutions.

Aldehydes	No.	Enhanced bands			New bands		
Propionaldehyde	1				*ca.* 1704 s[a]		R[b]
Butyraldehyde	2				*ca.* 1702 s		R
Chloral	3						
Benzaldehyde	4	1687 w,	1656 w,	1651 w	1680 s,	1215 w	
o-Tolualdehyde	5	1692 w,	1679 w,	1657 m,	1665 s,	1217 w	
		1651 w,	1639 w,	1623 w			
m-Tolualdehyde	6	1678 w,	1654 w,	1639 w	1664 s,	1148 w	
Cuminaldehyde	7	1692 s,	1667 w,	1656 w	1660 s,	1248 w	
1-Naphthaldehyde	8	1654 m			1656 s,	1057 w	
2-Naphthaldehyde	9	1655 s,	1285 w		1668 s,	1171 w	
Crotonaldehyde	10				1666 s		R
Cinnamic Aldehyde	11				1645 s		R
o-Phthaldialdehyde	12	1659 m			1677 s		R
p-Phthaldialdehyde	13				1681 s		R

[a]. The intensities are abbreviated as follows: s = strong, m = medium, w = weak.
[b]. R means that irreversible reactions take place and the data are incomplete.

the carbonyl group in the present systems. The halogen atoms X and Y in the structures (I)—(III) (Ref.[3]) should therefore represent iodine and bromine, respectively. The smaller electronegativity of bromine compared to chlorine is expected to reduce the contribution of the structure (III) (Ref.[3]) to the resonance in the iodine monobromide complexes. This is in agreement with the lower acidity observed for this interhalogen.

Table 2. Infrared spectral data for the carbonyl stretching bands of the aldehyde complexes with iodine monobromide [a].

Aldehydes	No.	ν_{max} cm^{-1}	$\nu_{1/2}$ cm^{-1}	$B_c \times 10^{-4}$ darks [d]	$\Delta\nu$ [b] cm^{-1}	$\Delta B \times 10^{-4}$ [c] darks [d]	
Propionaldehyde	1	*ca.* 1704	*ca.* 20		*ca.* 34		R [e]
Butyraldehyde	2	*ca.* 1702	*ca.* 15		*ca.* 27		R
Chloral	3						
Benzaldehyde	4	1680	10	3.0	27	1.0	
o-Tolualdehyde	5	1665	12	3.7	36	2.1	
m-Tolualdehyde	6	1664	11	3.6	41	2.0	
Cuminaldehyde	7	1660	13	3.9	44	2.1	
1-Naphthaldehyde	8	1657	15	4.1	39	2.2	
2-Naphthaldehyde	9	1668	17	5.2	31	2.8	
Crotonaldehyde	10	1666			31		R
Cinnamic aldehyde	11	1645			41		R
o-Phthaldialdehyde	12	1677	17	5.0	23	2.3	R
p-Phthaldialdehyde	13	1681	17	5.9	27	2.6	R

[a]. The spectral data for the carbonyl stretching bands of the free aldehydes are listed in Table 2 (Ref.[2]).
[b]. $\Delta\nu = \nu_{max}(\text{aldehyde}) - \nu_{max}(\text{complex})$.
[c]. $\Delta B = B_c - B_a$ darks.
[d]. 1 dark = 1 cm^{-1} cm^2/mmole.
[e]. R means that irreversible reactions take place and the data are less reliable.

Table 3. Concentration data and formation constants for the aldehyde complexes [a] with iodine monobromide at approximately 30°C.

Ald [b] No. [g]	C_A [c] mole/l	C_{IBr} [d] mole/l	C_c [e] mole/l	K_c(calc) [f] l/mole	K_c(mean) l/mole
3	0.01201 [h]	0.4321	0	0	0
4	0.008270 [h]	0.3404	0.002630	1.38	1.4 ± 0.1
	0.06045 [i]	0.4765	0.02343	1.40	
5	0.01301 [h]	0.5964	0.006025	1.46	1.5 ± 0.1
	0.08315 [i]	0.5964	0.03882	1.57	
6	0.009484 [h]	0.6001	0.004475	1.50	1.5 ± 0.1
	0.06434 [i]	0.6001	0.02928	1.46	
7	0.008534 [h]	0.5133	0.003821	1.58	1.6 ± 0.1
	0.05734 [i]	0.4765	0.02421	1.61	
8	0.008524 [h]	0.5134	0.003523	1.38	1.3 ± 0.1
	0.07391 [i]	0.5229	0.02760	1.20	
9	0.006611 [h]	0.5870	0.002846	1.38	1.4 ± 0.1
	0.04370 [i]	0.5229	0.01839	1.50	
12 [j]	0.01417 [h]	0.4022	0.002007	0.41	0.4 ± 0.1
	0.01417 [h]	0.3961	0.001970	0.41	
13 [j]	0.005636 [h]	0.3961	0.001089	0.61	0.6 ± 0.1
	0.005636 [h]	0.4753	0.001265	0.61	

[a]. Only complexes from the C=O group have been considered.
[b]. No reliable data were obtained for the complexes with propionaldehyde, butyraldehyde, crotonaldehyde or cinnamic aldehyde.
[c]. C_A is the initial concentration of aldehyde.
[d]. C_{IBr} is the initial concentration of iodine monobromide.
[e]. C_c is the equilibrium concentration of the complex.
[f]. K_c is the formation constant.
[g]. The numbers refer to the aldehydes as listed in Table 1.
[h]. Cell thickness 0.0570 cm.
[i]. Cell thickness 0.0080 cm.
[j]. The complexes are supposedly of 1:1 stoichiometry.

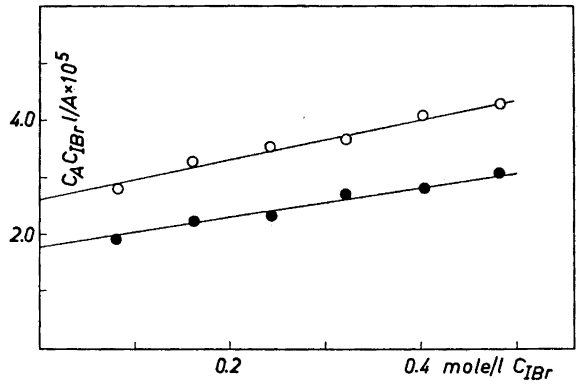

Fig. 1. Benesi-Hildebrand-Scott plots for the complexes between iodine monobromide and benzaldehyde (○) $K_c = 1.32$, $B_c = 2.9 \times 10^4$ darks and *o*-tolualdehyde (●) $K_c = 1.43$, $B_c = 3.9 \times 10^4$ darks.

If the spectral data listed in Tables 2 and 3 are compared with the corresponding data for the iodine [2] and iodine monochloride[3] complexes, the following conclusions can be summarized:

(1) The 1:1 complexes formed between an aldehyde and iodine, iodine monobromide and iodine monochloride, have formation constants K_c increasing in that order.

(2) The spectral shifts $\Delta\nu$ of the aldehydic carbonyl stretching frequencies increase upon complex formation in the order iodine, iodine monobromide and iodine monochloride.

(3) The half intensity widths $\nu_{1/2}$ of the carbonyl stretching frequency increase upon complex formation. However, there seems to be no systematic variation of the band width with higher interaction. Most of the aldehydes have the highest half intensity widths $\nu_{1/2}$ in the iodine complexes, while the values in the interhalogen complexes are somewhat lower.

(4) The integrated intensities B of the carbonyl stretching frequency increase upon complex formation. Moreover, in the aromatic aldehydes (4)—(9) the integrated intensities B seem to increase in the order iodine, iodine monobromide and iodine monochloride.

The data in this and the two previous papers [2,3] indicate that there is no linear relationship between the spectral parameters $\Delta\nu$, B and $\nu_{1/2}$ of the complexes between *different* donors and the *same* acceptor.

Person and co-workers' [10,11] report that both the spectral shifts $\Delta\nu$, the integrated intensities B and the half intensity widths $\nu_{1/2}$ in the acceptor, *e.g.* iodine monochloride, increase with higher interactions. Moreover, Huggins and Pimentel [12] have found a similar relationship between the magnitudes of $\Delta\nu$,

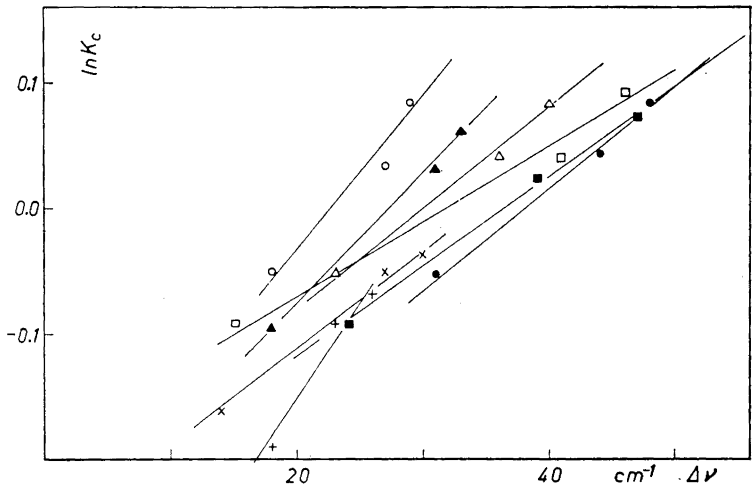

Fig. 2. ln K_c *versus* frequency shift of the carbonyl stretching frequency of aldehydes engaged in complex formation to halogens. Symbols denote the following aldehydes: benzaldehyde (○), *o*-tolualdehyde (△), *m*-tolualdehyde (□), cuminaldehyde (●), 1-naphthaldehyde (■), 2-naphthaldehyde (▲), *o*-phthaldialdehyde (+) and *p*-phthaldialdehyde (×).

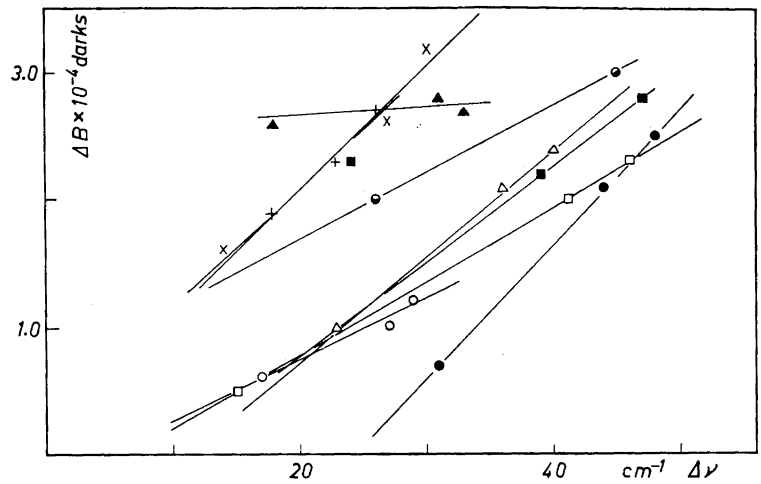

Fig. 3. Integrated intensity change *versus* frequency shift of the carbonyl stretching frequency of aldehydes engaged in complex formation to halogens. Cinnamic aldehyde (◒), other coding defined in *Fig. 2.*

B and $\nu_{1/2}$ of the X—H stretching frequencies with higher interactions in hydrogen bonded systems.

If the spectral parameters $\Delta\nu$, B and $\nu_{1/2}$ and the formation constants K_c are compared for the *same* donor and *different* acceptors, however, some linear relationships have been found. In Fig. 2, ln K_c is plotted against the spectral shifts $\Delta\nu$ obtained from this and the previous papers [2,3]. It appears that points representing the same donor and the three different acceptors in most cases can be fitted with straight lines. The lines representing the different donor systems seem to be fairly parallel. The formation constants are related to the standard free energy changes, according to the equation:

$$\Delta G^\circ_c = -RT \ln K_c$$

and ΔG°_c should accordingly be proportional to $\Delta\nu$ within these systems. It was not possible by the present methods to determine K_c at different temperatures with a very high precision. Accordingly, no data are available concerning the enthalpy differences ΔH and entropy differences ΔS upon complex formation. A correlation between these thermodynamic functions and the parameters $\Delta\nu$, ΔB and $\nu_{1/2}$ might be of interest.

In Fig. 3 the integrated intensity changes ΔB ($\Delta B = B_c - B_a$) are plotted against the spectral shifts $\Delta\nu$. Points representing the same donor can be fitted with straight lines. Furthermore, the lines representing the aromatic aldehydes and the dialdehydes can in many cases be extrapolated to the origin. Only incomplete and less reliable data [3] are available for the aliphatic aldehydes, and these systems have therefore not been included in Figs. 2 and 3.

It is well known that when, *e.g.*, ketones [13] or aldehydes [14] are engaged in hydrogen bonding to the carbonyl oxygen, a lowering of the carbonyl stretching

frequency takes place. To the authors' knowledge the spectral parameters of the carbonyl stretching frequencies have not been extensively studied in hydrogen bonded systems. The proposed close similarity between the charge transfer complexes and the hydrogen bonded systems [10,11] would make a comparison between such data of interest.

The authors express their thanks to Professor O. Hassel for many helpful discussions during the work. Financial support has been granted by *Norges almenvitenskapelige forskningsråd*.

REFERENCES

1. Mulliken, R. S. *Rec. trav. chim.* **75** (1955) 845, and earlier papers listed there.
2. Augdahl, E. and Klæboe, P. *Acta Chem. Scand.* **16** (1962) 1637.
3. Augdahl, E. and Klæboe, P. *Acta Chem. Scand.* **16** (1962) 1647.
4. Popov, A. I. and Skelly, N. E. *J. Am. Chem. Soc.* **77** (1955) 3722.
5. Popov, A. I. and Deskin, W. A. *J. Am. Chem. Soc.* **80** (1958) 2976.
6. Marzocchi, M. and Ferroni, E. *Gazz. chim. ital.* **91** (1961) 1200, 1216.
7. Herzberg, G. *Spectra of Diatomic Molecules*, 2nd ed., D. van Nostrand Co., New York 1950,p. 541.
8. Benesi, H. A. and Hildebrand, J. H. *J. Am. Chem. Soc.* **71** (1949) 2703.
9. Scott, R. L. *Rec. trav. chim.* **75** (1956) 787.
10. Person, W. B., Humphrey, R. E., Deskin, W. A. and Popov, A. I. *J. Am. Chem. Soc.* **80** (1958) 2049.
11. Person, W. B., Erickson, R. E. and Buckles, R. E. *J. Am. Chem. Soc.* **82** (1960) 1850.
12. Huggins, C. M. and Pimentel, G. C. *J. Phys. Chem.* **60** (1956) 1615.
13. Derkosch, J. and Kaltenegger, W. *Monatsh.* **90** (1959) 645.
14. Puranik, G. *J. Chem. Phys.* **26** (1957) 601.

Received March 24, 1962.

ACTA CHEMICA SCANDINAVICA 16 (1962) 1662–1674

Studies on the Coagulation of Chicken Blood

VII. Use of Nickel Oxalate, Bismuth Oxalate, Cadmium Phosphate and Bismuth Phosphate for Differentiation and Assay of Strontium Carbonate Non-adsorbable Labile Factors

ØYVIND SØRBYE* and INGER KRUSE

Department of Biochemistry and Nutrition, Polytechnic Institute, Copenhagen, Denmark

Twenty-five crystalline adsorbents were tested for adsorption of labile factor activity from strontium carbonate preadsorbed oxalated chicken plasma and shown to adsorb only a part of the total activity. The adsorbents belong to four different groups, represented by the title compounds, adsorbing four different labile factors for which provisional names are suggested: ε(epsilon)-factor is selectively adsorbed by nickel oxalate, μ(mu)-factor by bismuth oxalate, ν(nu)-factor by cadmium phosphate, and ϱ(rho)-factor by bismuth phosphate. These factors are different from the λ-, π-, γ- and β-factors selectively adsorbed by adsorbents tested in a previous study. The activity of each of the eight factors depends on the concentration of only one or two of the other seven. None of the factors appear to be functionally identical.

The ε-, μ-, ν-, and ϱ-factors do not contribute to the labile factor activity measured when thromboplastin is replaced by Russell's viper venom, with or without added cephalin. They are regarded as thromboplastin specific labile coagulation factors.

In a previous study on the adsorption of the labile factor activity of strontium carbonate (preadsorbed oxalated chicken) plasma [1], the results obtained with fifty-two selective adsorbents were explained as adsorption of four different labile coagulation factors: λ-factor, selectively adsorbed by cobalt carbonate and six other cobalt compounds, β-factor, selectively adsorbed by lead phosphate and two other insoluble lead salts, π-factor, selectively adsorbed by lead carbonate and six other adsorbents, and γ-factor, selectively adsorbed by a group of thirty-five different adsorbents, represented by barium phosphate.

* Fellow of the Royal Norwegian Council for Scientific and Industrial Research.

The present paper deals with the partial adsorption of labile factor activity from strontium carbonate plasma obtained by use of other groups of adsorbents. It will be shown that the observed effects can be ascribed to selective adsorption of four different labile coagulation factors, which differ from the four labile factors described previously [1].

MATERIALS AND METHODS

Except for the adsorbents the methods and materials used in the present study were as described previously [1-3].

The *adsorbents* were prepared in this laboratory from high purity chemicals by adaption of procedures described in Gmelin-Kraut's Handbuch der anorganischen Chemie (*cf.* preceding paper [1]), with the exception of Cd-sulfide *, red lead oxide (minium) * and oxides of Ti and Zr **.

Oxalate of Ni was prepared from the chloride or sulfate as described for Co-oxalate [1]. Bi-oxalate was prepared from a bismuth-mannitol solution (8 g of Bi-nitrate ground with 3 g of mannitol, diluted with 200–300 ml of water) by precipitation at 50–60°C with oxalic acid in excess.

Borate of Ni was prepared from the oxide as described for Co-borate [1]. Bi-borate was prepared from a bismuth-mannitol solution by precipitation at 50–60°C with a slight excess of Na-tetraborate.

Oxides of Ce, Th, and Cr were prepared by melting of Na-chloride mixed with Ce-oxalate, Th-nitrate and K-bichromate, respectively.

Phosphate of Ni was prepared from a solution of the sulfate, by precipitation with sec. Na-phosphate. The precipitate was crystalline after 2–3 months at room temperature. Bi-phosphate was prepared from the nitrate dissolved in a small volume of nitric acid (7 N) by addition of sec. Na-phosphate, followed by dilution of the hot solution with ten volumes of distilled water. Cd-phosphate was prepared from a hot solution of the sulfate by precipitation with sec. Na-phosphate. A mixed phosphate ($Cd_3(PO_4)_2 \cdot 2CdHPO_4$) is formed.

Pyrophosphates of Ni and Cd were prepared from the sulfates by precipitation with Na-pyrophosphate. The precipitates were dissolved in SO_2-water and crystallized by heating of the solutions on a steam bath.

Phosphate of Cr was prepared from the oxide by melting with Na-metaphosphate. Whether ortho- or meta-phosphate was formed was not investigated.

Arsenates of Cd and Bi were prepared from the sulfate and the nitrate, respectively, with sec. Na-arsenate, in analogy with the procedures for the phosphates.

Ni-arsenate was prepared from the chloride by precipitation with tert. NH_4-arsenate. The product was isolated after four months at room temperature.

Tungstates of Ni and Cd were prepared from the chlorides as described for Ca-tungstate [1].

Bi-tungstate was prepared from the oxide by melting with Na-chloride and Na-tungstate in excess.

Molybdates of Ni and Cd were prepared from the chlorides as described for Ba-molybdate [1].

All adsorbents were thoroughly washed and dried as described [1] and finally obtained as crystalline powders.

EXPERIMENTS AND RESULTS

Adsorption of strontium carbonate non-adsorbable labile factors. The adsorbents were tested for adsorption of the labile factor activity of strontium car-

* kindly supplied by the Department of Inorganic Chemistry, Polytechnic Institute, Copenhagen.

** obtained from H. Struer's chemiske Laboratorium, Copenhagen.

Table 1. Adsorption of labile factor activity from strontium carbonate plasma.

Plasma No.	Adsorbent	mg/ml	Activity in % of strontium carbonate plasma	Labile factor adsorbed *
3585	nickel oxalate	50	82	
		100	82	
2436	nickel borate	20	83	
		40	83	
3532	nickel orthophosphate	50	80	
		80	80	
3557	nickel pyrophosphate	20	93	
		80	93	ε
3554	nickel tungstate	10	85	
		40	85	
3554	nickel molybdate	10	85	
		40	85	
5045	nickel arsenate	10	82	
		20	82	
340	bismuth oxalate	70	91	
		120	91	
621	bismuth borate	50	72	
		150	72	
460	red lead oxide (minium)	30	90	
		50	90	
3080	chromous oxide	50	86	
		80	86	
4419	titanic oxide	40	88	μ
		80	88	
5227	zirconium oxide	30	92	
		50	92	
5227	thorium oxide	30	92	
		50	92	
5575	ceric oxide	10	87	
		20	87	
340	cadmium phosphate	70	85	
		120	85	
3545	cadmium arsenate	60	85	
		100	85	
3545	cadmium pyrophosphate	20	85	
		60	85	
3551	cadmium molybdate	50	85	ν
		80	85	
3505	cadmium tungstate	20	93	
		50	93	
5073	chromous phosphate	10	84	
		50	84	
212	bismuth phosphate	20	92	
		100	92	
3543	bismuth arsenate	20	86	
		40	86	
5604	bismuth tungstate	30	87	ϱ
		50	87	
463	cadmium sulfide	10	89	
		30	89	

* as determined by matching experiments (p. 1665—1669).

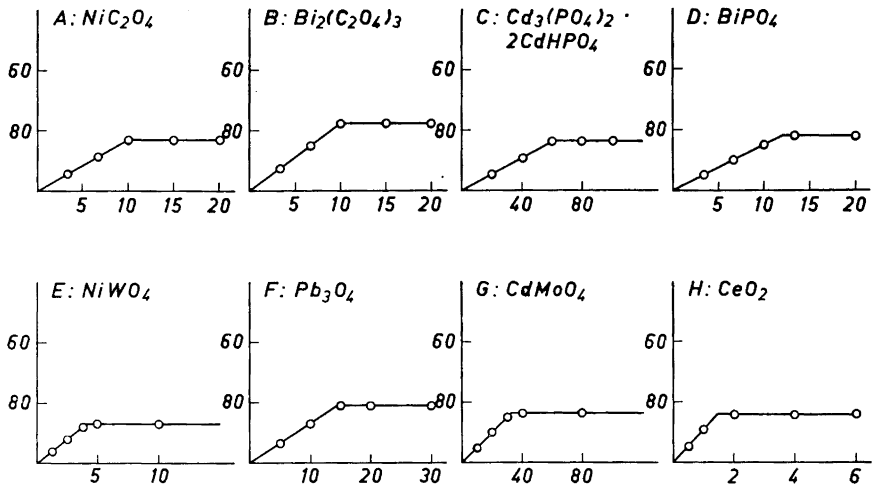

Figs. 1. Adsorption of labile factor activity by selective adsorbents. Ordinates: labile factor activity in % of strontium carbonate plasma. Abscissæ: adsorbent in mg/ml. A: nickel oxalate; B: bismuth oxalate; C: cadmium phosphate; D: bismuth phosphate; E: nickel tungstate; F: red lead oxide; G: cadmium molybdate; H: ceric oxide.

bonate (preadsorbed oxalated chicken) plasma as described in preceding papers [1,3]. No inhibitory effects were detected in the adsorbed plasmas and pH was not significantly altered after adsorption [3].

A summary of the results of a preliminary testing of the adsorbents described in this paper is presented in Table 1. The adsorbents caused only partial adsorption of the labile factor activity of strontium carbonate plasmas and could thus be classified as selective adsorbents.

A detailed study of the effects of the adsorbents showed that labile factor activity was adsorbed proportionally to the amounts of adsorbent added, up to a certain concentration of adsorbent beyond which no further adsorption of activity was obtained. The labile factor activity of plasmas adsorbed once with adequate amounts of a selective adsorbent, could not be reduced further by renewed treatment with the same adsorbent. Adsorption curves obtained with eight different adsorbents are shown in Figs. 1 (A—H). The other adsorbents of Table 1 gave similar adsorption curves. These results were analogous with those obtained by use of the selective adsorbents tested previously [1,3]. The present adsorbents thus offered new possibilities for differentiation of the labile factor activity of strontium carbonate plasma.

Matching experiments. The effects of the various adsorbents of Table 1 were compared in a series of matching experiments, carried out as described previously [1,3]. Representative results of these experiments are presented in Figs. 2 and 3 (A—H).

The labile factor activity adsorbed by nickel oxalate was not reduced after preadsorption of strontium carbonate plasma by bismuth oxalate (Fig. 2 A), and the minimum amount of nickel oxalate required for maximal adsorp-

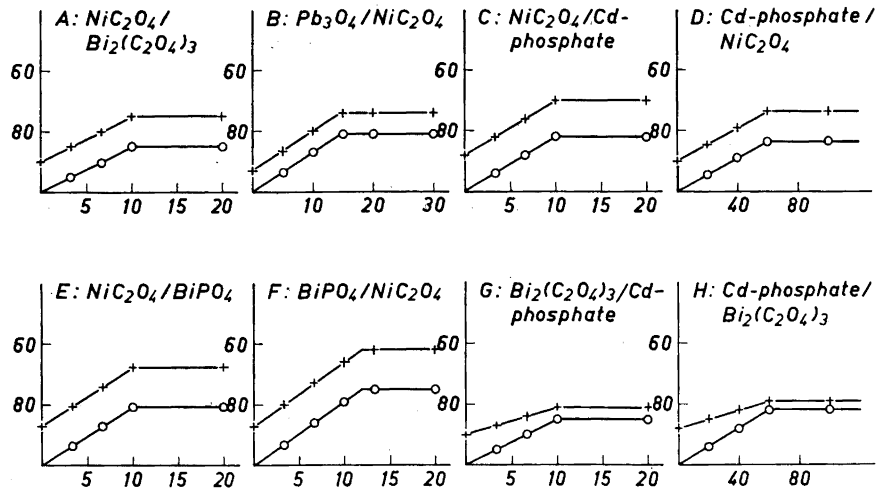

Figs. 2. Comparison of adsorbents I. Ordinates: labile factor activity in % of strontium carbonate plasma. Abscissæ: adsorbent in mg/ml.
O: untreated strontium carbonate plasma. + :preadsorbed strontium carbonate plasma. A: nickel oxalate adsorption of untreated and bismuth oxalate (10 mg/ml) preadsorbed plasma. B: red lead oxide adsorption of untreated and nickel oxalate (10 mg/ml) preadsorbed plasma. C: nickel oxalate adsorption of untreated and cadmium phosphate (60 mg/ml) preadsorbed plasma. D: cadmium phosphate adsorption of untreated and nickel oxalate (10 mg/ml) preadsorbed plasma. E: nickel oxalate adsorption of untreated and bismuth phosphate (12 mg/ml) preadsorbed plasma. F: bismuth phosphate adsorption of untreated and nickel oxalate (10 mg/ml) preadsorbed plasma. G: bismuth oxalate adsorption of untreated and cadmium phosphate (50 mg/ml) preadsorbed plasma. H: cadmium phosphate adsorption of untreated and bismuth oxalate (10 mg/ml) preadsorbed plasma.

tion of activity remained unchanged after preadsorption by bismuth oxalate. The curves for adsorption of labile factor activity by red lead oxide from untreated and from nickel oxalate preadsorbed strontium carbonate plasmas were also parallel (Fig. 2 B). At the time of the latter experiment red lead oxide was used as adsorbent for the factor which is adsorbed by bismuth oxalate (*cf.* Fig. 3 E).

Parallel adsorption curves were also obtained for the adsorbent pairs: nickel oxalate and cadmium phosphate (Figs. 2 C and 2 D), and for nickel oxalate and bismuth phosphate (Figs. 2 E and 2 F).

As in the experiments reported previously [1,3], parallel adsorption curves were interpreted as the results of matching experiments with compounds adsorbing two different labile factors, the activities of which are mutually independent. The factor adsorbed by nickel oxalate is thus different from the factors adsorbed by bismuth oxalate (or red lead oxide), cadmium phosphate and bismuth phosphate.

Matching experiments with bismuth oxalate and cadmium phosphate are shown in Fig. 2 G and 2 H. The minimum amounts of each of these two adsorbents, required for maximal adsorption of activity were not changed after

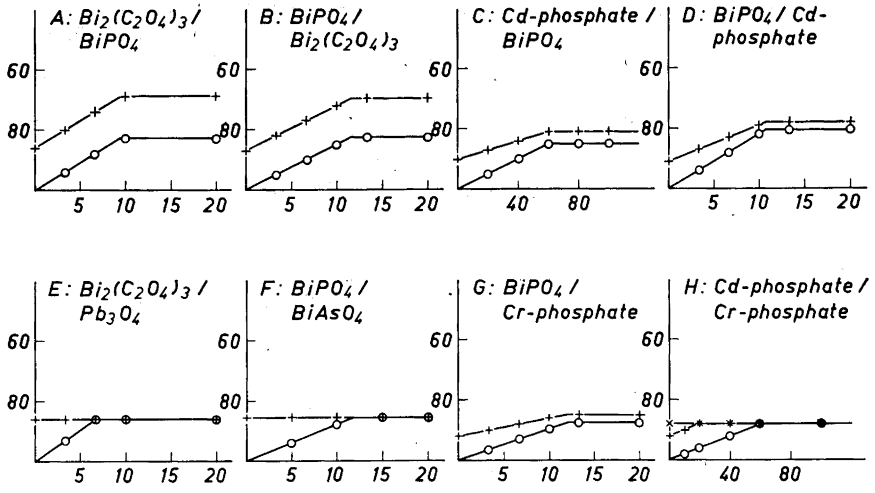

Figs. 3. Comparison of adsorbents II. Ordinates: labile factor activity in % of strontium carbonate plasma. Abscissæ: adsorbent in mg/ml.
O: untreated strontium carbonate plasma. + and ×: preadsorbed strontium carbonate plasma. A: bismuth oxalate adsorption of untreated and bismuth phosphate (10 mg/ml) preadsorbed plasma. B: bismuth phosphate adsorption of untreated and bismuth oxalate (10 mg/ml) preadsorbed plasma. C: cadmium phosphate adsorption of untreated and bismuth phosphate (10 mg/ml) preadsorbed plasma. D: bismuth phosphate adsorption of untreated and cadmium phosphate (50 mg/ml) preadsorbed plasma. E: bismuth oxalate adsorption of untreated and red lead oxide (15 mg/ml) preadsorbed plasma. F: bismuth phosphate adsorption of untreated and bismuth arsenate (20 mg/ml) preadsorbed plasma. G: bismuth phosphate adsorption of untreated and chromous phosphate (40 mg/ml) preadsorbed plasma. H: cadmium phosphate adsorption of untreated plasma and of plasmas preadsorbed by 40 mg/ml (+) and by 60 mg/ml (×) of chromous phosphate.

preadsorption by the other adsorbent, but the adsorbed activities were reduced. Therefore, in agreement with our previous interpretation of converging adsorption curves [1], bismuth phosphate and cadmium phosphate are selective adsorbents for two different labile factors, the activity of each of which is increased in the presence of the other. A synergistic relationship thus exists between these factors.

The activities adsorbed by bismuth oxalate and bismuth phosphate were due to two different labile factors with independent activities (Figs. 3 A and 3 B), whereas the two different factors adsorbed by cadmium phosphate and bismuth phosphate (Figs. 3 C and 3 D), had synergistic effects.

The activity adsorbed by red lead oxide was due to adsorption of the factor which could be adsorbed by bismuth oxalate. Fig. 3 E shows that adsorption by red lead oxide can reduce the labile factor activity to the same level as that obtained by use of bismuth oxalate, and that bismuth oxalate causes no further reduction of the activity of plasma preadsorbed by adequate amounts of red lead oxide. Red lead oxide was therefore, as mentioned above, occasionally used as a substitute for bismuth oxalate.

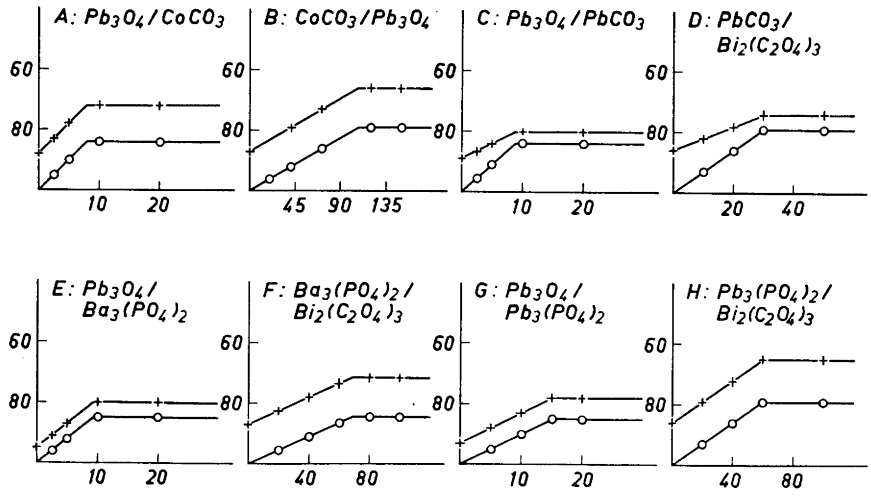

Figs. 4. Comparison of adsorbents III. Ordinates: labile factor activity in % of strontium carbonate plasma. Abscissæ: adsorbent in mg/ml.
O: untreated strontium carbonate plasma. +: preadsorbed strontium carbonate plasma. A: red lead oxide adsorption of untreated and cobalt carbonate (100 mg/ml) preadsorbed plasma. B: cobalt carbonate adsorption of untreated and red lead oxide (20 mg/ml) preadsorbed plasma. C: red lead oxide adsorption of untreated and lead carbonate (40 mg/ml) preadsorbed plasma. D: lead carbonate adsorption of untreated and bismuth oxalate (10 mg/ml) preadsorbed plasma. E: red lead oxide adsorption of untreated and barium phosphate (60 mg/ml) preadsorbed plasma. F: barium phosphate adsorption of untreated and bismuth oxalate (10 mg/ml) preadsorbed plasma. G: red lead oxide adsorption of untreated and lead phosphate (60 mg/ml) preadsorbed plasma. H: lead phosphate adsorpt on of untreated and bismuth oxalate (10 mg/ml) preadsorbed plasma.

The results obtained by use of these five adsorbents can thus be explained as adsorption of four different labile coagulation factors. For these factors we have adopted the following terms: ε(epsilon)-factor for the labile factor selectively adsorbed by nickel oxalate, μ(mu)-factor for the factor selectively adsorbed by bismuth oxalate, ν(nu)-factor for the factor selectively adsorbed by cadmium phosphate, and ϱ(rho)-factor for the labile factor selectively adsorbed by bismuth phosphate. The activities of ε-factor, μ-factor and ϱ-factor are apparently mutually independent as are the activities of ε-factor and ν-factor. The latter factor, however, appears to act as a synergist for μ-factor as well as for ϱ-factor.

The effects of the other adsorbents were by similar experiments compared to that of the adsorbents described. Fig. 3 F shows that bismuth arsenate adsorbed ϱ-factor. Chromium phosphate adsorbed a factor acting as a synergist for ϱ-factor (Fig. 3 G). This factor was shown to be ν-factor (Fig. 3 H). By the same technique the labile factors adsorbed by the remaining adsorbents of Table 1 were identified. The final results of these matching experiments are shown in the last column of Table 1.

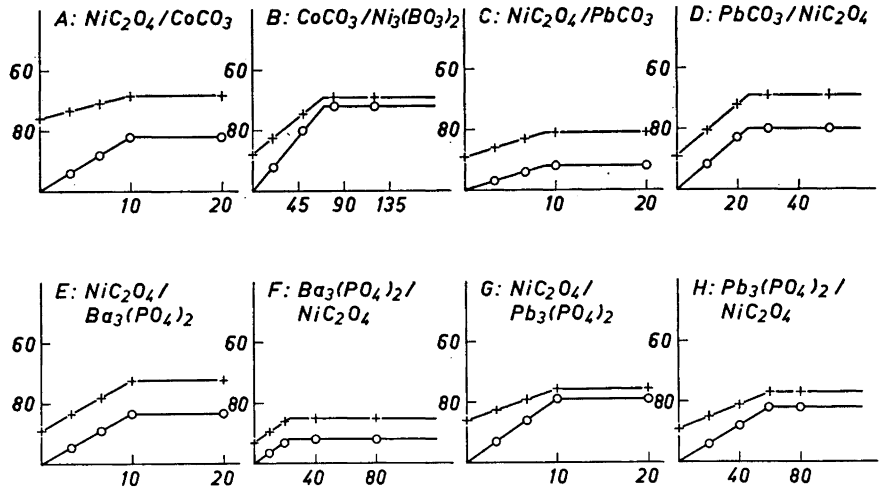

Figs. 5. Comparison of adsorbents IV. Ordinates: labile factor activity in % of strontium carbonate plasma. Abscissæ: adsorbent in mg/ml.
O: untreated strontium carbonate plasma. +: preadsorbed strontium carbonate plasma. A: nickel oxalate adsorption of untreated and cobalt carbonate (80 mg/ml) preadsorbed plasma. B: cobalt carbonate adsorption of untreated and nickel borate (20 mg/ml) preadsorbed plasma. C: nickel oxalate adsorption of untreated and lead carbonate (30 mg/ml) preadsorbed plasma. D: lead carbonate adsorption of untreated and nickel oxalate (20 mg/ml) preadsorbed plasma. E: nickel oxalate adsorption of untreated and barium phosphate (60 mg/ml) preadsorbed plasma. F: barium phosphate adsorption of untreated and nickel oxalate (10 mg/ml) preadsorbed plasma. G: nickel oxalate adsorption of untreated and lead phosphate (60 mg/ml) preadsorbed plasma. H: lead phosphate adsorption of untreated and nickel oxalate (10 mg/ml) preadsorbed plasma.

In analogy with previous observations [1,3], the present experiments show that the relative activity of an adsorbable factor varies in different experiments with the same adsorbents or with compounds shown to adsorb the same factor. As already pointed out [1,3], such variations may be ascribed partly to differences in the sensitivity of the substrate plasmas to adsorbable and non-adsorbed factors, partly to differences in the relative concentrations of these factors in the fresh plasmas employed.

Further matching experiments. The effects of the adsorbents used in this study were also compared with the effects of the adsorbents used previously for selective adsorption of the λ-, π-, γ- and β-factors [1]. The results of these matching experiments are presented in Figs. 4—7 (A—H).

Figs. 4 A and 4 B show that μ-factor and λ-factor (selectively adsorbed by cobalt carbonate) are different labile factors. The activities of the two factors are mutually independent.

The non-identity and synergistic effects of μ-factor and π-factor (selectively adsorbed by lead carbonate) are seen from Figs. 4 C and 4 D. Figs. 4 E and 4 F, and Figs. 4 G and 4 H show that μ-factor is different from γ-factor (selectively adsorbed by barium phosphate) and from β-factor (selectively

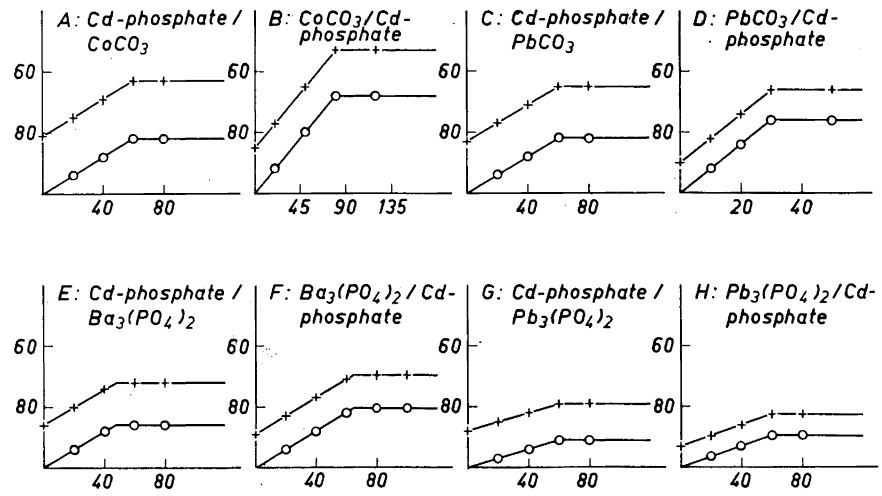

Figs. 6. Comparison of adsorbents V. Ordinates: labile factor activity in % of strontium carbonate plasma. Abscissæ: adsorbent in mg/ml.
O: untreated strontium carbonate plasma. +: preadsorbed strontium carbonate plasma A: cadmium phosphate adsorption of untreated and cobalt carbonate (80 mg/ml) preadsorbed plasma. B: cobalt carbonate adsorption of untreated and cadmium phosphate (60 mg/ml) preadsorbed plasma. C: cadmium phosphate adsorption of untreated and lead carbonate (30 mg/ml) preadsorbed plasma. D: lead carbonate adsorption of untreated and cadmium phosphate (60 mg/ml) preadsorbed plasma. E: cadmium phosphate adsorption of untreated and barium phosphate (70 mg/ml) preadsorbed plasma. F: barium phosphate adsorption of untreated and cadmium phosphate (60 mg/ml) preadsorbed plasma. G: cadmium phosphate adsorption of untreated and lead phosphate (40 mg/ml) preadsorbed plasma. H: lead phosphate adsorption of untreated and cadmium phosphate (60 mg/ml) preadsorbed plasma.

adsorbed by lead phosphate), respectively. The activity of μ-factor is independent of the concentrations of the two latter factors, and *vice versa.*

The matching experiments presented in Figs. 5 were obtained with nickel oxalate (or nickel borate) and selective adsorbents for the λ-, π-, γ- and β-factor activities. It is seen that ε-factor is different from these four factors. It acts as a synergist for λ-factor (Figs. 5 A and 5 B) and for β-factor (Figs. 5 G and 5 H), whereas its activity is independent of the concentrations of π-factor (Figs. 5 C and 5 D) and of γ-factor (Figs. 5 E and 5 F).

Finally, ν-factor and ϱ-factor were both shown to be different from λ-factor, π-factor, γ-factor and from β-factor (Figs. 6 and 7 (A—H)). The ν- and ϱ-factor activities are independent of the λ-, π-, γ-, and β-factor concentrations.

*The labile factor activities measured by RVV-cephalin * and RVV.* The effects of the adsorbents described in this paper were also studied with RVV, with or without added cephalin, replacing thromboplastin in the test system [1-3].

* Russell's viper venom, kindly supplied by The Wellcome Research Laboratories, Langley Court, Beckenham, England.

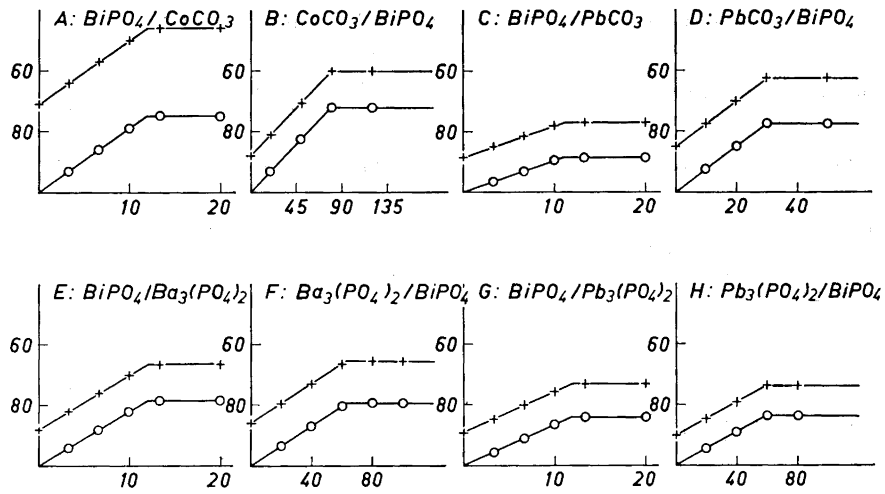

Figs. 7. Comparison of adsorbents VI. Ordinates: labile factor activity in % of strontium carbonate plasma. Abscissæ: adsorbent in mg/ml.
O: untreated plasma. +: preadsorbed strontium carbonate plasma. A: bismuth phosphate adsorption of untreated and cobalt carbonate (80 mg/ml) preadsorbed plasma. B: cobalt carbonate adsorption of untreated and bismuth phosphate (12 mg/ml) preadsorbed plasma. C: bismuth phosphate adsorption of untreated and lead carbonate (30 mg/ml) preadsorbed plasma. D: lead carbonate adsorption of untreated and bismuth phosphate (12 mg/ml) preadsorbed plasma. E: bismuth phosphate adsorption of untreated and barium phosphate (70 mg/ml) preadsorbed plasma. F: barium phosphate adsorption of untreated and bismuth phosphate (10 mg/ml) preadsorbed plasma. G: bismuth phosphate adsorption of untreated and lead phosphate (60 mg/ml) preadsorbed plasma. H: lead phosphate adsorption of untreated and bismuth phosphate (12 mg/ml) preadsorbed plasma.

Representative experiments are summarized in Table 2. Adsorption of ε-factor (by nickel oxalate), of μ-factor (by bismuth oxalate), of ν-factor (by cadmium phosphate) or of ϱ-factor (by bismuth phosphate) had no effect on the labile factor activities measured by RVV-cephalin or by RVV alone. These four factors must consequently be regarded as thromboplastin specific labile coagulation factors.

DISCUSSION

The present study is a continuation of previous studies [1,3] on the effects of crystalline adsorbents on the labile factor activity of fresh oxalated chicken plasma.

Like the adsorbents described in the preceding study [1], the present adsorbents adsorb only a part of the total labile factor activity of strontium carbonate preadsorbed oxalated plasma. This is a further demonstration of the complex nature of this activity and lends additional support to the idea that the labile factor activity of fresh plasma represents the combined activities of discrete labile coagulation factors differing characteristically in adsorbability [1,3]. New possibilities for characterization of the individual components

Table 2. Labile factors measured by RVV-cephalin or RVV.

Treatment of strontium carbonate plasma: Adsorbent	mg/ml	Labile factor adsorbed	Labile factor activity in % of strontium carbonate plasma: Tpl.	RVV-ceph.	RVV
Untreated			100[a] (100)[b]	100[a]	100[b]
Nickel oxalate	3 1/3	ε	95 (95.5)	100	100
	6 2/3	ε	90 (91)	—	—
	10	ε	85 (86.5)	—	100
	20	ε	85 (86.5)	100	100
Untreated			100[a] (100)[b]	100[a]	100[b]
Bismuth oxalate	3 1/3	μ	95 (95.5)	100	100
	6 2/3	μ	90 (91)	—	—
	10	μ	85 (86.5)	—	100
	20	μ	85 (86.5)	100	100
Untreated			100[c] (100)[d]	100[c]	100[d]
Cadmium phosphate	20	ν	95 (96)	100	100
	40	ν	90 (92)	—	—
	60	ν	85 (88)	—	100
	80	ν	85 (88)	100	100
Untreated			100[c] (100)[d]	100[c]	100[d]
Bismuth phosphate	3 1/3	ϱ	96 (96)	100	100
	6 2/3	ϱ	92 (92)	—	—
	10	ϱ	88 (88)	—	—
	13 1/3	ϱ	85.5 (85.5)	100	100
	20	ϱ	85.5 (85.5)	100	100

a: plasma No. 5044; *b:* plasma No. 3589; *c:* plasma No. 5043; *d:* plasma No. 3589.

Table 3. Effect of adsorption of single factors on the specific activities of the others.

Adsorption of	Effect on the specific activity of: ϱ	ν	μ	π	γ	β	ε	λ
ϱ		+	O	O	O	O	O	O
ν	+		+	O	O	O	O	O
μ	O	+		+	O	O	O	O
π	O	O	+		+	O	O	O
γ	O	O	O	+		+	O	O
β	O	O	O	O	+		+	O
ε	O	O	O	O	O	+		+
λ	O	O	O	O	O	O	+	

Symbols: O indicates no change, *i.e.* the factors have independent (additive) effects.
+ indicates reduced specific activity, *i.e.* the factors have synergistic effects.

of this activity were offered by the twenty-five adsorbents described in the present paper. According to results of matching experiments, these adsorbents belong to four different categories of selective adsorbents, adsorbing four different labile coagulation factors. Comparison of the adsorbents described here, with representatives of the four categories of adsorbents described previously [1], showed that the factors adsorbed by the former were different from those adsorbed by the latter. Eight different strontium carbonate non-adsorbable labile coagulation factors can thus be distinguished by us of the adsorbents tested until present. This distinction is based on differences in the physico-chemical properties of the individual factors, and does not *per se* permit definite conclusions concerning their possible *functional* non-identity.

However, the factors, thus defined by their adsorbabilities, do appear to be functionally different entities as judged from the observed synergistic effects of certain factors, and the purely additive effects of others. A summary of these interrelationships (Table 3) shows that none of these factors have identical functional properties. Thus, ϱ-factor differs from all other factors by being a synergist for ν-factor and for none of the other factors, ν-factor is the only factor acting as a synergist for ϱ-factor as well as for μ-factor. μ-Factor is distinguished by its synergistic effects on the ν- and π-factor activities, and π-factor by its synergistic effects on the μ- and γ-factor activities. The functional non-identity of the remaining factors is recognized by similar argumentation.

Further evidence for the functional non-identity of some of the factors was obtained by substituting RVV or RVV-cephalin for thromboplastin as assay accelerator. Six of the factors (ε-, γ-, π-, μ-, ν-, and ϱ-) proved inactive in the RVV and the RVV-cephalin assay systems, and the activity of β-factor was shown to depend on the presence of added cephalin [1]. λ-Factor is thus the only one of these eight factors which is a common component of the labile factor activities measured by these three assay systems, and the ε-, γ-, π-, μ-, ν-, and ϱ-factors must be regarded as thromboplastin specific labile factors. As to the relation between human factor V and chicken labile factor activity, the prolonged thromboplastin and RVV-cephalin accelerated coagulation times of congenitally factor V-deficient human plasma[4] indicate that factor V is a rate limiting coagulation factor in both of these two assay systems. Of the eight labile factors detected in fresh chicken plasma, only λ-factor and β-factor represent activities which may possibly correspond to human factor V activity, if the latter is to be regarded as the activity of a single coagulation factor.

A method for quantitative determination of the ε-, μ-, ν-, and ϱ-factor concentrations in fresh plasma is suggested by the observed proportionality between adsorbed labile factor activity and concentration of adsorbent. The minimum concentration of adsorbent required for maximal adsorption of activity may be proportional to the concentration of the adsorbable factor and represent an absolute value for the concentration of this factor. As pointed out previously [1,3], such values are independent of the concentrations of non-adsorbed factors. However, variations in the concentrations of possible inert plasma factors, adsorbed in competition with the adsorbable labile factor,

must also be considered as a cause of possible variations in the results obtained by this procedure.

In some experiments (unpublished data) the combined activity of the eight labile factors did not account for more than 40 % of the total labile factor activity measured with thromboplastin. Factors differing from those adsorbed by the adsorbents tested until present, are also responsible for the activities measured by RVV and RVV-cephalin, which are not due to λ-factor and the combined activity of the λ- and β-factors, respectively. Selective adsorption of these factors by other categories of adsorbents will be reported in a forthcoming paper.

REFERENCES

1. Sørbye, Ø. and Kruse, I. *Acta Chem. Scand.* **16** (1962) 1468.
2. Sørbye, Ø. and Kruse, I. *Acta Chem. Scand.* **14** (1960) 2177.
3. Sørbye. Ø. and Kruse, I. *Acta Chem. Scand.* **16** (1962) 1221.
4. Rapaport, S. I., Aas, K. and Owren, P. A. *Blood* **9** (1954) 1185.

Received February 28, 1962.

ACTA CHEMICA SCANDINAVICA 16 (1962) 1675–1681

Grindelic and Oxygrindelic Acids

TORGER BRUUN

Institutt for Organisk Kjemi, Norges Tekniske Høgskole, Trondheim, Norway

LLOYD M. JACKMAN

Department of Chemistry, Imperial College of Science and Technology, London, S.W.7, England

EINAR STENHAGEN

Institutionen för Medicinsk Biokemi, Göteborgs Universitet, Göteborg, Sweden

Some observations are recorded on the mass spectra, the nuclear magnetic resonance spectra and the chemistry of grindelic and oxygrindelic acids and certain of their derivatives. The results of these studies confirm the structures (I, R = COOH), and (II, R = COOH) proposed by Panizzi, Mangoni and Belardini [1] for the two acids, respectively.

In the course of an investigation of *Compositae*, which has been pursued for some years in Trondheim, several *Grindelia* species were grown and investigated for their content of acetylenic compounds; *cf.* Ref.[2] During an examination of *Grindelia squarrosa* (Pursh.) it was observed that the flower heads were very sticky, and after steam distillation, extraction of the wet material with ether afforded two acidic substances which could be isolated as their crystalline methyl esters. The one occurring in the higher proportion was crystallised from petroleum to constant melting point, 71—72°, and rotation $[\alpha]_D$ −132°; it is identical with methyl grindelate [1]; *cf.* Table 1. The minor component similarly gave methyl oxygrindelate, m.p. 114—114.5°, $[\alpha]_D$ −106°, and is identical with the ester prepared by Woodward oxidation of methyl grindelate, Table 1.

On the basis of degradative experiments, Panizzi, Mangoni, and Belardini [1] have recently assigned structures (I; R = COOH) and (II; R = COOH) to grindelic and oxygrindelic acids, respectively. We have independently investigated these two acids, and by examination of their infrared, ultraviolet,

nuclear magnetic resonance, and mass spectra, and those of some of their transformation products, we have confirmed the correctnes of the structures (I) and (II).

A number of the compounds investigated have also been prepared by the Italian workers. A comparison of physical constants is made in Table 1. The experimental section includes only those compounds which have not been described by Panizzi and his co-workers.

Grindelic acid, $C_{20}H_{32}O_3$, readily yields methyl and ethyl esters, the infrared spectra of which indicate the absence of hydroxyl groups. Both methyl grindelate and methyl oxygrindelate are readily saponified, indicating the presence of a primary ester grouping. This is confirmed by pK^*_{MCS} values [3,4], very kindly determined by Dr. V. P. Arya, who found the values 7.06 for grindelic acid and 7.04 for oxygrindelic acid. Reduction of the methyl ester with lithium aluminium hydride gives a primary alcohol, grindelenol (I, R = CH_2OH), $C_{20}H_{34}O_2$, which does not possess a carbonyl stretching band in its infrared spectrum. These observations show that the three oxygen atoms in grindelic acid are present as a carboxyl group and an ether. That this ether is not an epoxide, follows from its inertnes to lithium aluminium hydride, and from the fact that grindelic acid was recovered unchanged from an attempted reduction with sodium in propanol.

The n.m.r. spectra of methyl grindelate and methyl oxygrindelate (Table 2) indicate that both compounds contain four methyl groups attached to fully substituted carbon atoms, one of which also carries an oxygen atom (bands near 8.70). Methyl grindelate also gives rise to a broad band at 8.23 assignable to an olefinic methyl group since this methyl group absorbs as a doublet at 9.20 in methyl dihydrogrindelate. The 8.23 band is replaced in the spectrum of methyl oxygrindelate by one equivalent to two protons at 5.93, suggesting

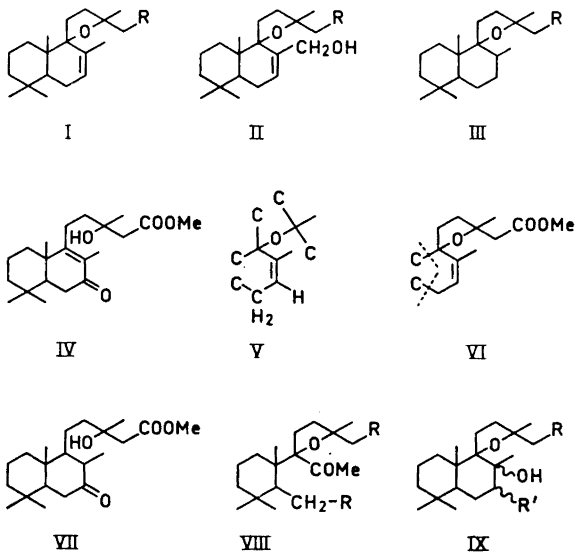

I II III IV V VI VII VIII IX

Table 1.

		M.p.	$[\alpha]_D$	c	λ_{max}	ε
Grindelic acid (I, R = COOH)	*a*	98 – 99	−102	0.71		
Methyl grindelate (I, R = COOMe)	*a,c,d*	70 – 70.5	−134	1.46		
	b	71 – 72	−132	2.67		
Methyl oxygrindelate (II, R = COOMe)	*a,d*	115 −116	−105	0.95		
	b	114 −114.5	−106	2.69		
Methyl dihydroxygrindelate	*a,d*	122 −123	+ 19	0.84		
(IX, R = COOMe, R′ = OH)	*b*	118.5−119	+ 15	2.00		
Isomeric dihydroxygrindelate						
(IX, R = COOMe, R′ = OH)	*b*	152 −154	+ 24	0.84		
Benzoate of methyl dihydroxygrindelate						
(IX, R = COOMe, R′ = OBz)	*b*	193 −194	+ 53	2.00		
Dihydroxygrindelic acid						
(IX, R = COOH, R′ = OH)	*b*	197 −198	+ 25	2.20		
Keto diacid (VIII, R = COOH)	*b*	197 −198	+ 22	2.29		
Keto diester (VIII, R = COOMe)	*a*	102 −103				
	b	98 – 99	– 21	2.20		
13,15-Dihydroxylabdene-8	*a*	104 −105	+ 87	1.0		
13,15-Dihydroxylabdane	*a,d*	121 −122	+ 29	1.3		
	b	119 −120	+ 30	1.05		
Ketol (IV)	*b*	78 – 78.5	+ 65	2.86	2500	17 000
2,4-DNP	*b*	115 −116			3950	28 000
2,4-DNP of dihydro-ketol (VII)	*b*	128 −129			3685	27 000

[a]: See Ref.[1]
[b]: This work.
[c]: Sample for comparison provided by Professor L. Panizzi.
[d]: IR spectrum for comparison provided by Professor L. Panizzi.

that this compound differs from methyl grindelate by having a hydroxymethyl group in place of the olefinic methyl group. We confirmed this conclusion by oxidising methyl grindelate with selenium dioxide to the oxy ester.

The proton spectrum of methyl grindelate also contains a band at 4.50 which is absent in the spectrum of methyl dihydrogrindelate (III, R = COOMe) prepared from the former ester by catalytic hydrogenation. Thus, methyl grindelate contains a trisubstituted double bond. The fine structure of the olefinic proton indicates the presence of a methylene group α to the olefinic proton so that grindelic acid possesses the grouping $-CH_2{\cdot}CH{:}C(CH_3)-$. The absence of further absorption (apart from the ester methoxyl group) below 7.0 shows that the ether oxygen atom is attached at fully substituted carbon atoms. Oxidation of methyl grindelate with sodium dichromate yielded a neutral compound (IV). The U.V. spectrum (λ_{max} 2500 Å, ε 17 000) and infrared spectrum (3480, 1730, 1655, 1610 cm^{-1}) revealed this compound to be an α,β-unsaturated ketol ester. The absence of olefinic absorption and the presence of one methyl absorption at 8.18 in its n.m.r. spectrum requires the double bond to be of the type $\begin{matrix} R' \\ \diagdown \\ R \diagup \end{matrix}C{=}C(CH_3){\cdot}CO-$; R ≠ H or Me. Clearly, this compound is formed by oxidation of the trisubstituted double bond to a ketone, followed by β-elimination of the ether oxygen atom which accordingly must be allylic in grindelic acid. We may now write the part structures (V) in

Table 2. Chemical shifts (τ-values) of protons of grindelic acid derivatives.

Compound	Methyl groups at C(4) and C(10) [a]			8-Me	13-Me	7-H	$-CH_2CO_2Me$
Methyl grindelate (I, R = CO_2Me)	9.20	9.14	9.12	8.23	8.68	4.50	7.40, 7.27 [d]
Methyl oxygrindelate (II, R = CO_2Me)	9.21	9.5	9.12	5.93[b]	8.69	4.53	7.31[e]
Methyl dihydrogrindelate (III, R = CO_2Me)	9.23	9.17	9.15	9.20[c]	8.68	—	7.33[e]
α,β-Unsaturated ketol ester (IV)	9.14	9.11	8.92	8.18	8.705	—	
Grindelenol (I, R = CH_2OH)	9.21	9.16	9.13	8.20	8.74	4.55	7.46[e]
Keto diester (VIII) [1]	9.22	9.09	8.97	7.76	8.75	—	
Diol (IX) [1] m.p. 118–119°	9.19	9.12	8.97	8.62	8.71	—	7.32

[a] The bands are not assigned to specific methyl groups. [b] Hydroxy-methyl group.
[c] Doublet, $J \sim 7$ c/s. [d] AB spectrum, $\delta_{AB} = 7.8$ c/s, $J_{BA} = 14.0$ c/s. [e] Singlet equivalent to two protons.

which the ether oxygen atom is part of a heterocyclic ring since the β-elimination did not result in fragmentation.

The immediate environment of the carboxyl group of grindelic acid is suggested by the n.m.r. spectrum of grindelenol (I, R = CH_2OH) in which the two protons adjacent to the hydroxyl group give rise to a complex multiplet at 6.25. The fine structure of this band is compatible with the grouping $-CH_2CH_2-$. This conclusion is confirmed by the observation that the n.m.r. spectra of a number of compounds (Table 2) in which the carboxyl group is present, exhibits a singlet or an AB multiplet equivalent to two protons near 7.4, which therefore arise from the methylene group $-\overset{|}{\underset{|}{C}}-CH_2COOMe$.

Consideration of the mass spectra of compounds in this series allows an extension of the part structure (V). Methyl grindelate, methyl oxygrindelate, and ethyl grindelate give rise to abundant fragment ions at 210, 226 (210 + O), and 224 (210 + CH_2), respectively, all of which correspond to ion radicals. It is clear that the 210 fragment from methyl grindelate contains the olefinic methyl group and the three oxygen atoms. Similarly, grindelene (I, R = Me), prepared by lithium aluminium hydride reduction of grindelenyl *p*-toluene-

Table 3. Infrared absorption in the region 1030–970 cm^{-1} of grindelic acid derivatives.

Methyl grindelate (I, R = CO_2Me)		1000[b]		985 s
Methyl oxygrindelate (II, R = CO_2Me)		1003		983 s
Grindelene (I, R = Me)	1027 w		997 s[c]	
Methyl dihydrogrindelate (III, R = CO_2Me)	1017	1007[b]		981 vs
Grindelane (III, R = Me)	1015		993 s	979[b]
Diol (IX), m.p. 118–119°[a]	1015			987
Diol (IX), m.p. 152–154°[a]		1006 s	992 s	
Diol			996 vw	
Unsaturated keto/ester (IV)		1003[b]		978 vw
Saturated keto ester (VIII)		1002		970[c]

[a] These diols were obtained from the osmium tetroxide oxidation of methyl grindelate. That with m.p. 118–119° is identical with the diol described by Panizzi *et al.*[1]
[b] Shoulder. [c] Broad.

sulphonate, gives an abundant ion at 166 (210—CO_2). However grindelane (III, R = Me) (obtained by catalytic hydrogenation of grindelene) does not give a strong peak at 168. Evidently, the ion radical (210) is formed from methyl

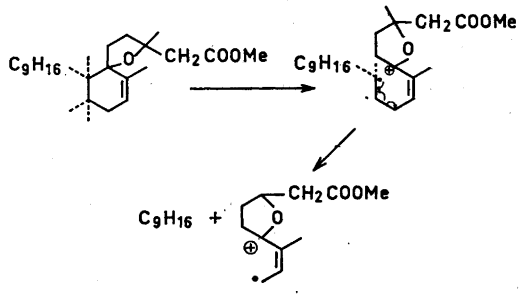

grindelate by cleavage at allylic positions so that the part structure (V) can be extended to (VI). This type of fragmentation is readily explicable if the double bond is part of a six-membered ring (see annexed mechanism). The accompanying molecule, C_9H_{16}, contains three methyl groups which in grindelic acid are attached to fully substituted carbon atoms. Thus grindelic acid must have a structure such as (I, R = COOH) based on decalin with one angular methyl group and one geminal dimethyl group in ring A. Biogenetic considerations favour the 4-position for the geminal methyl groupings. The mass spectra of manoyl oxide and methyl labdanoate, which are known to possess *gem*-dimethyl groups at position 4, show a high peak at *m/e* 109,

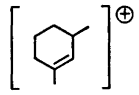

(X)

presumably due to the ion (X). The high peak at *m/e* 109 found in the mass spectra of methyl grindelate, ethyl grindelate and grindelene thus does not contradict the biogenetic considerations.

The structure (I, R = COOH) is firmly established by the elegant degradation of grindelic acid to 14,15,16-trisnorlabdanoic acid reported by the Italian workers.

The infrared spectra of methyl grindelate and methyl oxygrindelate contain a prominent band in the region of 1000 cm^{-1}, see Table 3. It is broad and complex with the highest peak at about 985 cm^{-1}. Its presence appears to have some bearing on the allylic relationship between the double bond and the ether ring in methyl grindelate and methyl oxygrindelate, and also between the double bond and hydroxyl group in methyl oxygrindelate, since on hydrogenation it is split into two distinct bands, and it disappears when the ether ring is opened. The band is strong with an intensity comparable with that of the carbonyl band, and it is stronger in methyl oxygrindelate than in methyl grindelate.

EXPERIMENTAL

All melting points are uncorrected. Mixed melting points were determined simultaneously with the melting points of the pure components. Unless otherwise stated, rotations were measured with chloroform solutions in 1 dm tubes unless specified, ultraviolet spectra were measured with a Perkin-Elmer Model 13 spectrophotometer using ethanol solutions, and infrared spectra were determined with a Perkin-Elmer Model 21 spectrophotometer using chloroform solutions. Nuclear magnetic resonance spectra were obtained with a Varian 4300 spectrometer operating at 56.4 Mc/sec. Deuterochloroform solutions were used, and the spectra were calibrated against tetramethyl silane as an internal reference by the side band method employing a Muirhead-Wigan-D-695-A decade oscillator. Mass spectra were measured with a Dempster type mass spectrometer, *cf.* Ref.[5]

Ethyl grindelate. Pure methyl grindelate (0.2 g) was saponified and the acid converted directly to its silver salt. The dried and powdered salt was refluxed for 8 h in ethyl bromide. Removal of the silver bromide and solvent, and distillation of the residue afforded ethyl grindelate, b.p. 110°/10^{-3} mm, n_D^{22} 1.5037, $[\alpha]_D$ −123° (*c*, 2.22). The ester was subjected to gas-liquid chromatography prior to the determination of its mass spectrum.

Partial synthesis of methyl oxygrindelate. Methyl grindelate (2 g) was refluxed with selenium dioxide (2 g) in 1-butanol (50 ml) for 5 h. After removal of the solvent, ether was added, and the deposited selenium (0.3 g) removed by filtration. Evaporation of the ether, and recrystallisation of the residue from light petroleum containing a little ether yielded methyl oxygrindelate, m.p. 113−114° (undepressed by admixture with the natural ester) $[\alpha]_D$ −105° (*c*, 2.09).

Attempted reduction of grindelic acid with sodium and n-*propanol.* Methyl grindelate (2 g) was saponified and the resulting acid was dissolved in propanol (25 ml). Sodium was added in small pieces to the boiling solution until saturation. The product was poured into water, acidified and extracted with ether. Treatment of the ethereal solution with diazomethane and evaporation of the solvent gave an oil which slowly crystallised to crude methyl grindelate, m.p. 65−72°. A mixture with the starting material melted at 70−72°.

Isomeric methyl dihydroxygrindelates. Osmium tetra-oxide (1.17 g) and methyl grindelate (1.548 g) in ether (35 ml) with pyridine (1 ml) were left in the dark for 5 days. The osmic ester was reduced with hydrogen sulphide [6], and the crude product subjected to a rough chromatographic separation on alumina. With benzene 75 mg of starting material were obtained whilst ether eluted 395 mg and the remainder, 1042 mg, came off with methanol. The material eluted with ether on crystallisation from petroleum furnished methyl dihydroxygrindelate, m.p. 118−119°, *cf.* Ref.[1] Subsequent concentrations of the mother liquors (repeated three times) finally afforded crystals melting at 137−145° (22 mg), $[\alpha]_D$ + 20° (*c*, 2.00). Recrystallisation of this material from petroleum gave an isomeric methyl dihydroxygrindelate, melting at 152−154°, $[\alpha]_D$ + 24° (*c*, 0.84).

Similar treatment of the fraction eluted with methanol furnished only methyl dihydroxygrindelate of the same m.p. (118−119°) and rotation, $[\alpha]_D$ + 15° (*c*, 0.72 for the last crop).

Benzoylation of methyl dihydroxygrindelate with excess benzoyl chloride in pyridine gave the monobenzoate, which was crystallised from petroleum with a trace of chloroform and from carbon tetrachloride until constant m.p., 193−194°, and rotation, $[\alpha]_D$ + 53° (*c*, 2.00).

α,β-Unsaturated ketol ester (IV). A solution of sodium dichromate (3.20 g) in water (2 ml) and acetic acid (25 ml) was added to a solution of methyl grindelate (1.02 g) in acetic acid (5 ml). The mixture was left at room temperature for 72 h and then poured into water. The mixture was extracted with ether. Removal of ether from the dried (Na_2SO_4) extract, and chromatography of the residue afforded a crude product (0.69 g) which on recrystallisation from petroleum gave the *α,β*-unsaturated ketol ester (IV) (0.33 g), m.p. 78−78.5°, $[\alpha]_D$ + 66° (*c*, 2.07), + 65° (*c*, 2.86), λ_{max} 2500 Å, ε 17 000, (Found: C 72.3; H 9.5. $C_{21}H_{34}O_4$ requires C 71.9; H 9.8). This compound yields a 2,4-dinitrophenylhydrazone as fine, red needles from petroleum, m.p. 115−116°, λ_{max} 3950 Å, ε 28 000 in chloroform (Zeiss spectrophotometer, Model PMQ2). (Found: C 61.4; H 7.1; N 10.5. $C_{27}H_{38}N_4O_7$ requires C 61.1; H 7.2; N 10.55).

Hydrogenation of the above ketol ester (IV) over 2 % palladium on barium sulphate in acetic acid afforded a *saturated ketol ester* (VII), b.p. 125°/10^{-3} mm (bath), n_D^{26} 1.4966, $[\alpha]_D$ −17° (*c*, 4.05). (Found: C 71.4; H 9.9. $C_{21}H_{36}O_4$ requires C 71.6; H 10.3). The saturated ketol ester furnished a yellow *2,4-dinitrophenylhydrazone*, m.p. 128−129°, from methanol, λ_{max} 3685 Å, ε 27 000. (Found: C 61.1; H 7.4; N 10.6. $C_{27}H_{40}N_4O_7$ requires C 60.9; H 7.55; N 10.5).

Grindelene (I, R = Me). Methyl grindelate (0.5 g) was treated with a large excess of lithium aluminium hydride in ether. The product was isolated in the usual way and treated with *p*-toluenesulphonyl chloride (1 g) in pyridine (5 ml). After standing for 24 h at room temperature the solution was poured into water and the oily ester was extracted with ether. The etheral extract was dried (Na_2SO_4) and added to a solution of lithium aluminium hydride in large excess in ether. The reaction mixture was treated with dilute sulphuric acid, and the ethereal layer was removed and washed successively with aqueous sodium hydroxide and water. Removal of the solvent from the dried (Na_2SO_4) extract and distillation of the residue gave *grindelene*, b.p. 70−75°/10^{-3} mm, n_D^{21} 1.5069, $[\alpha]_D$ −138° (*c*, 3.03). (Found: C 82.5; H 11.55. $C_{20}H_{34}O$ requires C 82.7; H 11.8). The infrared spectrum showed the absence of OH and C=O and the compound was homogeneous by gas-liquid chromatography.

Grindelane (III, R = Me). Hydrogenation of grindelene over 2 % palladium on barium sulphate in acetic acid afforded *grindelane*, b.p. 70°/10^{-3} mm, n_D^{22} 1.4961, $[\alpha]_D$ −9° (*c*, 1.93). (Found: C 81.7; H 12.2. $C_{20}H_{36}O$ requires C 82.1; H 12.4). Gas-liquid chromatography indicated the presence of a trace of an impurity, possibly an epimer.

Acknowledgements. We are indebted to Dr. R. Ryhage, Karolinska Institutet, Stockholm, for the mass spectra, and to Dr. S. Ställberg-Stenhagen, Medicinsk-kemiska Institutionen, Göteborg, for gas chromatographic separations.

We cordially thank Professor L. Panizzi for an advance copy of the paper to be published in *Gazz. chim. ital.*

REFERENCES

1. Panizzi, L., Mangoni, L. and Belardini, M. *Tetrahedron Letters* **1961**, No. 11, 376; *Gazz. chim. ital. To be published.*
2. Holme, D. and Sørensen, N. A. *Acta Chem. Scand.* **8** (1954) 34.
3. Simon, W. *Helv. Chim. Acta* **41** (1958) 1835.
4. Arya, V. P., Erdtman, H. and Kubota, T. *Tetrahedron* **16** (1961) 255.
5. Ryhage, R. and Stenhagen, E. *J. Lipid Research* **1** (1960) 361.
6. Barton, D. H. R. and Elad, D. *J. Chem. Soc.* **1956** 2085.

Received April 9, 1962.

ACTA CHEMICA SCANDINAVICA 16 (1962) 1682–1694

The Activation of Muscle Hexokinase by Divalent Metal Ions

EVA WALAAS and OTTO WALAAS

Institute of Medical Biochemistry, University of Oslo, Norway

Muscle hexokinase which is rapidly inactivated in solution, can to some extent be stabilized by EDTA and pyrophosphate. A procedure involving fractionation with ethanol is described for the partly purification of muscle hexokinase. The activation of the enzyme by different divalent metal ions has been investigated. The highest maximal activity was obtained by magnesium and at a molar ratio of Mg^{2+}/ATP = 1. Sodium pyrophosphate inhibits hexokinase apparently by the formation of a Mg-pyrophosphate complex, which excludes Mg^{2+} from the activated enzyme substrate complex. In addition, an inhibition of hexokinase by a 1:1 magnesium pyrophosphate complex has been shown. The kinetics of this inhibition is in accordance with a competitive type with respect to the Mg–ATP complex. This gives support for the assumption that the Mg–ATP complex is the actual substrate for muscle hexokinase. At increased concentrations of ATP^{-4} and Mg^{2+} the enzyme activity is inhibited.

Muscle hexokinase is in addition activated by Ca^{2+}, Co^{2+}, Mn^{2+}, and to a small extent by Zn^{2+}. In comparison with the Mg^{2+} effect the activation by these metal ions is characterized as follows. Maximal enzyme activity is less. Activation does occur at lower concentration of these metals and at a molar ratio Me^{2+}/ATP considerable below 1. Half maximal activity for Co^{2+} and Mn^{2+} is observed at a concentration 10 times lower than for Mg^{2+}. At increased concentration of these metal ions, strong inhibition of the enzyme activity is observed.

Since the work by Cori *et al.*[1] the role of hexokinase activity in regulating glucose uptake by muscle has been much discussed. Recently it has been concluded that at least under certain hormonal conditions glucose phosphorylation may be an important limiting step for glucose uptake in the rat diaphragm [2] and in the perfused rat heart[3]. Although this field has attracted considerable interest, small progress has been made concerning the properties of muscle hexokinase following the demonstration of this enzyme in muscle extracts [4,5]. The great lability of muscle hexokinase may be the reason why only slight purification of the enzyme has been obtained [6]. In the present work the possibility of stabilizing the enzyme has been investigated and a partly purified muscle hexokinase has been prepared. The activation of the

enzyme by magnesium has been investigated. Some evidence is obtained that the enzyme is activated by a Mg—ATP complex. It has been shown that muscle hexokinase can also be activated by calcium, manganese, cobalt and zinc *.

MATERIAL AND METHODS

Preparation of muscle extract. Grown rats (weighing 250 g) were decapitated, bled, and skeletal muscle and diaphragm removed, chilled on ice, minced with scissors and transferred to 10 volumes (w/v) of 0.25 M sucrose containing 0.05 M Tris buffer pH 8.2 and EDTA at a final concentration of 0.0018 M. The muscle tissue was homogenized in an all glass Potter-Elvehjem homogenizer for 10 min. All the procedures during the preparation of hexokinase were preformed in the cold room at + 2°C. In some experiments hexokinase activity in a particulate and soluble fraction were investigated separately. The nuclear fraction was removed by centrifugation at 600 × *g* for 10 min, whereupon the supernatant was centrifuged in an International refrigerated centrifuge at 8000 × *g* for 20 min. The soluble fraction (cell sap + microsomes) was removed and the sediment (particulate fraction) containing sarcosomes was resuspended in the medium used for homogenization and centrifuged at 8000 × *g* for 20 min. This procedure was repeated and finally the washed particulate fraction suspended in the same medium. It has previously been shown [7] in experiments on rat diaphragm that 90 % of hexokinase activity is present in the soluble and 10 % in the particulate fraction. The same distribution has been found in rat skeletal muscle. Determination of hexokinase activity in the soluble fraction gave values of 2.8 (rat diaphragm), 2.35 (rat leg muscle) and 2.0 (rat heart muscle). These values are expressed as μmoles glucose phosphorylated in 20 min under standard conditions.

Preparation of acetone powder. Rat skeletal muscle (500 g) was chilled on ice and ground in a meat grinder and extracted with 4 volumes of 0.05 M Tris buffer pH 8.0 containing 0.0018 M EDTA. The extract was added slowly to 9 volumes of acetone at −20°C. A crude hexokinase was prepared by extraction of the acetone powder with Tris buffer pH 8.0 containing 0.0018 M EDTA. Hexokinase extracts of the same activity was obtained by extraction with acetate buffer pH 4.0 or phosphate buffer pH 6.0.

Fractionation with ammonium sulphate. 2 g acetone powder from rat leg muscle extract was ground with 10 volumes 0.03 M Tris buffer — 0.0012 M EDTA pH 7.5 and shaken in the cold for 30 min. The insoluble material was removed by centrifugation at 2000 × *g* for 10 min. The supernatant was fractionated with ammonium sulphate (pH 7.5) and the precipitate between 30 % and 40 % saturation collected and dissolved in 0.03 M Tris buffer — 0.0012 M EDTA pH 8.2. This solution was dialyzed against several shifts of the same buffer for 3 h before hexokinase activity was determined. By this procedure 2- to 4-fold purification of hexokinase per mg nitrogen was obtained. However, marked inactivation of hexokinase did occur and the recovery of the hexokinase initially present was only 30—50 %.

Fractionation with ethanol. 2 g acetone powder was ground with 10 volumes 0.03 M Tris buffer — 0.0012 M EDTA, pH 8.2 and extracted for 20 min in the cold followed by centrifugation at 8000 × *g* for 10 min. Magnesium acetate in the solid state was added to the supernatant to a final concentration of 0.05 M and pH adjusted to 7.5. Fractionation with ethanol was performed at −3°C to −7°C. Ethanol between 5 and 15 % saturation precipitated 50 % of the hexokinase activity. This precipitate was centrifuged at 10 000 × *g* for 15 min at −10°C in an International refrigerated centrifuge. The supernatant was removed and traces of ethanol were evaporated from the residue over night at −20°C. By this procedure 5-fold purification of hexokinase per mg nitrogen was obtained. The enzyme preparation after having been dried *in vacuo* could be stored at −20°C with a constant enzyme activity for two weeks. Attempts to purify this preparation further by fractionation with ammonium sulphate failed, due to extensive inactivation of hexokinase. In a modification of this procedure ethanol fractionation was per-

* *Abbreviations used:* ATP, Adenosine triphosphate; ITP, Inosine triphosphate; GTP, Guanosine triphosphate; UTP, Uridine triphosphate; EDTA, Ethylenediaminetetraacetic acid.

Table 1. Thermal inactivation of muscle hexokinase. The soluble fractions were used in these experiments. Dialysis was performed against 0.03 M Tris buffer pH 8.2 containing 0.0015 M EDTA.

Rat muscle tissue	Procedure	Hexokinase activity * Before	After	Inactivation %
Leg muscle	standing at + 20°C	1.72	0.63	64
» »	for 18 h at + 1°C	1.72	0.80	54
» »	at −20°C	1.72	0.81	54
Diaphragm	at −20°C	2.80	1.70	39
Leg muscle	dialysis for	1.96	0.78	60
Diaphragm	18 h	2.82	0.42	86
Heart	at + 1°C	1.71	0.61	65
Acetone powder from leg muscle	dialysis for 16 h at + 1°C	0.46 **	0.22 **	52

* Activity expressed as μmoles per 50 mg muscle tissue.
** Activity expressed as μmoles per mg protein.

formed without addition of magnesium. In this case hexokinase was precipitated between 15 and 25 % of ethanol and the purification was 3- to 4-fold.

Procedure for assay of hexokinase activity. As a standard procedure hexokinase was incubated with the following mixture (concentrations): 0.001 M glucose, 0.05 M ATP, 0.05 M $MgCl_2$, 0.05 M KCl, 0.03 M Tris buffer pH 8.2. To each incubation vessel was added 0.5 ml enzyme solution and a total volume of 3.0 ml was used. Incubation was performed at + 30°C for 20 min. Hexokinase activity was usually determined by the glucose disappearance method. When incubation was finished precipitation with $ZnSO_4$ + $Ba(OH)_2$

Table 2. Effect of glucose, ATP, $MgCl_2$ and anions on the thermal inactivation of hexokinase. Acetone powder from rat leg muscle extract was used as the enzyme preparation. Dialysis was performed under the conditions stated in Table 1, and the compounds added were present at equal concentractions inside and outside the dialysis bag.

Procedure	Addition	Hexokinase activity Before	After (μmoles per mg protein)	Inactivation %
Standing at + 1°C for 16 hours	0.001 M Glucose	0.68	0.48	30
	0.005 M ATP	0.68	0.48	30
Dialysis at + 1°C for 16 hours	None	0.71	0.30	58
	0.0022 M glucose	0.71	0.39	45
	0.05 M $MgCl_2$	0.71	0	100
Dialysis at + 1°C for 16 hours	None	0.86	0.18	79
	0.1 M KCl	0.71 *	0.15 *	79
	0.1 M K_2HPO_4	0.68 **	0.36 **	44
	None	1.25	0.09	93
	0.03 M Napyrophosphate	0.77 ***	0.68 ***	12

* 0.02 M KCl was present in the incubation medium.
** 0.02 M K_2HPO_4 was present in the incubation medium.
*** 0.005 M sodium pyrophosphate was present in the incubation medium.
Corrections for the inhibitory effect by pyrophosphate present during incubation has been made according to the results given in Table 3.

Table 3. The inhibitory effect by anions on the hexokinase activity. Acetone powder from rat leg muscle extract was used as the enzyme preparation.

Addition	Concentration Moles per l.	Hexokinase activity μmoles per mg protein	Activity per cent of control
Na-pyro-phosphate	0	1.25	100
	0.001	1.48	119
	0.005	0.77	62
	0.01	0.22	18
NaCl	0	0.86	
	0.1	0.71	83
Na_2HPO_4	0	0.86	
	0.1	0.68	79

was performed and residual glucose determined by the method of Nelson [8]. Protein determinations were done by the method of Lowry *et al.*[9]

In the experiments where other divalent metals were substituted for Mg^{2+} in the reaction mixture, some influence on the Nelson method was observed, particularly with Mn^{2+}. Therefore, blanks at zero time were performed at each individual concentration of the metals for appropriate corrections.

Materials. The Ba-salt of ATP from Sigma Chemical Company was converted to the Na-salt before use. The same was done with Ba-salts of ITP, GTP and UTP obtained from Sigma. Analytical grade chemicals from Merck were used in the experiments.

RESULTS

Stabilization of hexokinase by EDTA and anions against thermal inactivation. Muscle hexokinase is subjected to extensive inactivation in solution. As shown previosuly [10] hexokinase in a rat diaphragm muscle extract is protected by EDTA, indicating that trace heavy metals partly are responsible for the inactivation. The addition of EDTA to the solution used for homogenizing the muscle tissue was also found necessary. Hexokinase activity was decreased by 50 % in the soluble as well as in the particulate fraction if EDTA was omitted at this step of the purification procedure. However, other factors are also concerned in the thermal inactivation of muscle hexokinase. As shown in Table 1 crude hexokinase preparations in solution were extensively inactivated by standing, during dialysis or by freezing at −20°C and thawing.

Muscle hexokinase could not satisfactorily be stabilized by addition of reactants of the incubation system (Table 2). Glucose (0.002 M) and ATP (0.005) slightly stabilized the enzyme, while prolonged contact with 0.05 M $MgCl_2$ completely inactivated hexokinase.

The effect by some anions was also investigated. Chloride was without any effect and orthophosphate gave a slight protection. Sodium pyrophosphate, however, at a concentration of 0.03 M was effective in protecting the hexokinase from inactivation during dialysis. On the other hand, pyrophosphate when present at concentrations above 0.005 M during incubation, excerted strong inhibition of hexokinase activity (Table 3). Therefore the use of pyrophosphate as a stabilizing agent is of limited value in the purification procedure. Sodium or potassium chloride and orthophosphate slightly inhibited hexokinase, when present in the incubation system.

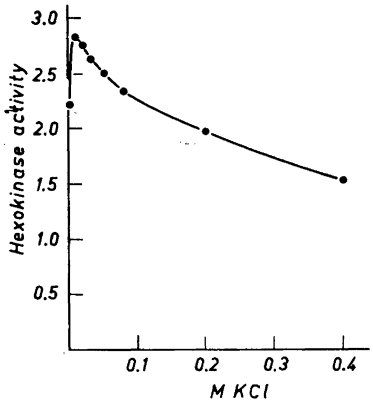

Fig. 1. The influence of KCl on hexokinase activity. Ethanol fractionated hexokinase was used as enzyme preparation.

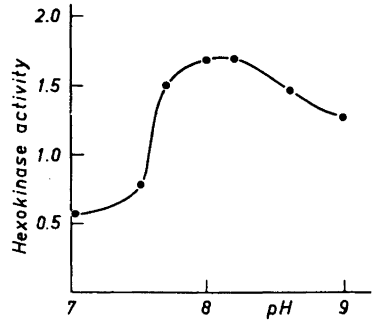

Fig. 2. The influence of pH on muscle hexokinase purified by ethanol fractionation. 0.03 M Tris buffer at the desired pH values was used under standard experimental conditions.

The effect of chloride was thoroughly investigated (Fig. 1). It was observed that KCl in a narrow range 0.02—0.05 M gave a slight activation, followed by inhibition at higher concentrations. Therefore, 0.05 M KCl routinely was added to the incubation mixture to get optimal conditions for hexokinase activity.

Effect of pH on activity. The pH profile of purified hexokinase from skeletal muscle was characterized by an optimum at pH 8.0—8.2 (Fig. 2). The activity rapidly declined at pH below 8 and reached one third maximal activity at pH 7.0. These results are similar to those obtained with crude hexokinase in fresh muscle extracts [7]. It has also been found that hexokinase in fresh homo-

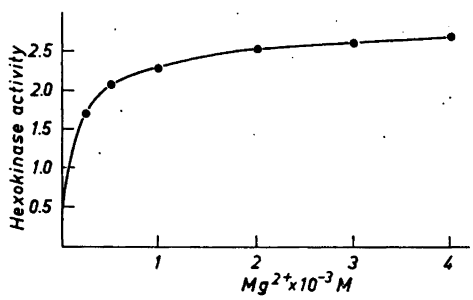

Fig. 3. The influence of $MgCl_2$ on muscle hexokinase at a constant level of ATP. Incubation mixture (concentrations): 0.001 M glucose, 0.001 M ATP, 0.05 M KCl, 0.03 M Tris buffer pH 8.2, ethanol fractionated enzyme preparation. 20 min incubation at 30°C.

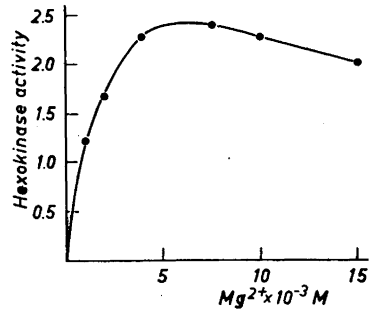

Fig. 4. Inhibition of hexokinase activity by $MgCl_2$ at a concentration above 10^{-2} M. ATP was present at a concentration of 4×10^{-3} M.

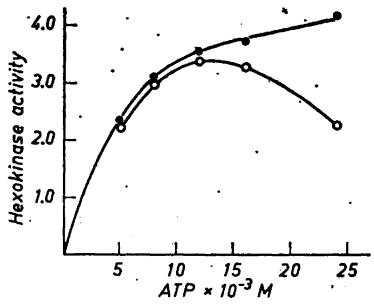

Fig. 5. Inhibition of hexokinase activity by ATP at a molar ratio $Mg^{+2}/ATP \ll 1$. ●: Mg and ATP present at molar ratio of 1. O: Mg present at a constant concentration of 4×10^{-3} M and ATP added at different concentrations. Hexokinase activity was measured by determination of the formation of ADP by an ion exchange resin method [19].

genate is most stable at pH 8, and is partly inactivated at the pH of 7 or below in accordance with previous work [4].

Effect of $MgCl_2$ and magnesium pyrophosphate complex on activity. If hexokinase is saturated with glucose, the activity increases with increasing concentration of Mg^{2+}, and maximum activity is obtained at a molar ratio $Mg^{2+}/ATP = 1$ (Fig. 3). This was found at several different concentrations of ATP. If Mg was added in excess over ATP no inhibitory effect was observed until rather high concentrations of Mg were present (Fig. 4). Similarly, if ATP was present at concentrations considerable higher than Mg ($Mg^{2+}/ATP < 4$), hexokinase activity was decreased (Fig. 5). This was in contrast to the situation when Mg and ATP were present at molar ratio of 1, where inhibition was never observed, even at high concentrations. In these experiments the activity of muscle hexokinase was half maximal at a concentration of ATP and Mg of 1.7×10^{-3} M (Fig. 6). The results are in accordance with those reported by Hers [11] and Liébecq [12] and may suggest that a ATP-magnesium complex is the actual substrate in hexokinase reaction. This was further indicated in experiments where the inhibition of hexokinase activity by inorganic pyrophosphate was studied. The inhibition of hexokinase by sodium pyro-

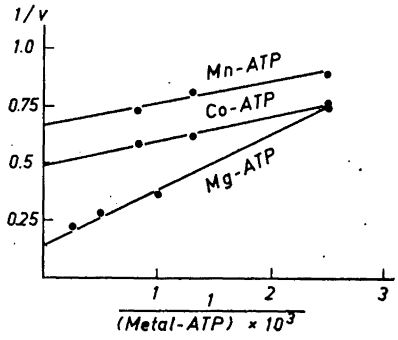

Fig. 6. The effect of different divalent metals on hexokinase activity. Metal and ATP was always added in equimolar concentrations (Mg^{2+} at a range 0.0004—0.004 M, Mn^{2+} and Co^{2+} at a range 0.0004—0.0012 M).

$$\frac{1}{v} = \frac{1}{\mu\text{moles glucose phosphorylated in 20 min at 30°C}}$$

phosphate is demonstrated in Fig. 7, where ATP and Mg were kept constant, and pyrophosphate inhibited the enzyme at higher concentrations. This can be explained by the formation of a Mg-pyrophosphate complex of great stability, which competes for the binding of Mg^{2+} to the enzyme molecule. In this system the molar ratio of Mg^{2+}/ATP was 5, and under these conditions a slight magnesium inhibition is present. Thus, if ATP was kept constant and Mg reduced to a level where the molar ratio Mg^{2+}/ATP = 1, the activity was somewhat increased (Fig. 7). The small activating effect by pyrophosphate at low concentrations therefore can be explained by a release of the Mg^{2+} inhibition of hexokinase. Further experiments indicated that in addition the Mg-pyrophosphate complex itself can act as an inhibitor of hexokinase. A soluble 1:1 complex of the type $MgP_2O_7^{-2}$ has been demonstrated [13]. Fig. 8 shows the inhibition of hexokinase by this complex when ATP was present at different concentrations at a molar ratio of Mg^{2+}/ATP = 1. The curve which is observed corresponds with that expected for a competitive type of inhibition. Accordingly, the results are consistent with the explanation that a 1:1 Mg-pyrophosphate complex can compete with a Mg—ATP complex for active sites on the surface of the enzyme.

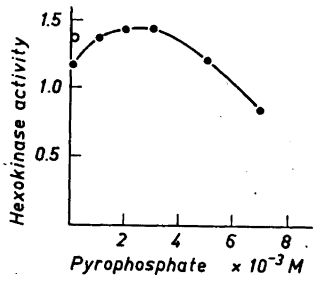

Fig. 7. The influence of sodium pyrophosphate on hexokinase activity. Hexokinase was purified by ethanol fractionation.
●: The system contained 0.002 M ATP and 0.01 M $MgCl_2$ (concentrations).
○: The system contained 0.002 M ATP and 0.002 M $MgCl_2$ (concentrations).

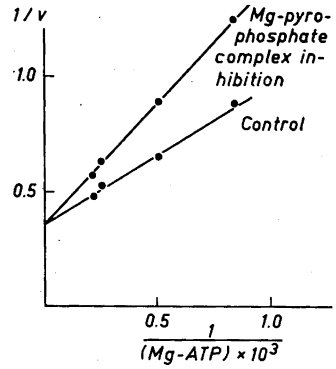

Fig. 8. Inhibition of hexokinase by a soluble magnesium pyrophosphate complex.
The enzyme was preincubated with sodium pyrophosphate and $MgCl_2$ at equimolar concentration (0.01 M) in Tris buffer pH 8.2 for 20 min at 10°C.
During the final incubation ATP and $MgCl_2$ were added at a constant molar ratio of 1:1 (The concentration range varied from 0.001 M to 0.005 M). The Mg pyrophosphate complex was present at a constant concentration in all experiments by dilution of the preincubation mixture 1:2. In unpublished experiments indication have been obtained that a soluble 1:1 complex of pyrophosphate with Mg is formed under these conditions. The final incubation period was 20 min at 30°C.

Table 4. Activation of muscle hexokinase by different divalent metal ions. A concentration of 0.001 M ATP was present with a molar ratio Metal/ATP = 1. Ethanol fractionated hexokinase was used as the enzyme preparation.

Metal ion	Hexokinase activity μmoles per mg protein
Mg^{2+}	2.25
Ca^{2+}	1.70
Co^{2+}	1.40
Mn^{2+}	1.30
Zn^{2+}	0.15
Cu^{2+}	0

Effect of other divalent metals on activity. Muscle hexokinase did not have an absolute requirement for Mg^{2+}. Thus, if magnesium was replaced by one of the divalent metal ions, calcium, cobalt or manganese, activation of the enzyme did occur (Table 4). Only a small activity was observed with Zn^{2+}, and Cu^{2+} was inactive in the system. In some respects the activation of hexokinase by these metal ions differed from that reported for magnesium. When ATP and metal ion were present at a molar ratio of 1, maximal activity with this series of metals was considerably less than with Mg^{2+}. However, half maximal activity

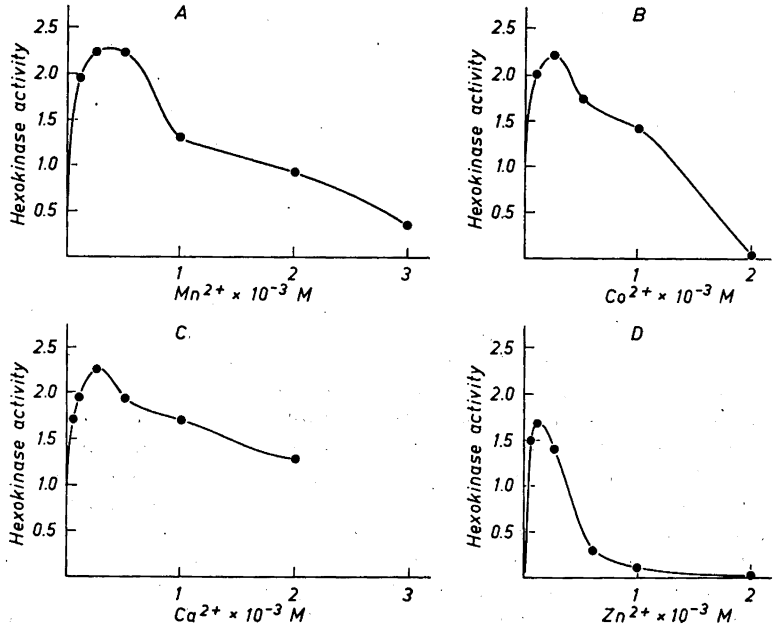

Fig. 9. The influence of $CaCl_2$, $MnCl_2$, $CoCl_2$ and $ZnCl_2$ on muscle hexokinase at a constant level of 0.001 M ATP. These experiments are comparable with those reported in Fig. 3.

with Co^{2+} was observed at 2.3×10^{-4} M and with Mn^{2+} at 1.7×10^{-4} M (Fig. 6) and thus lower than with Mg^{2+} (1.7×10^{-3} M) under the same experimental conditions, *i.e.* when ATP was added at concentrations equal with the metal ion. With these metal ions, hexokinase activity depended upon the concentration of the metal in a manner characteristically different from that described for magnesium. In the experiments, which are shown in Fig. 9, increasing concentrations of the metal ions were added while ATP was kept at a constant level. In contrast to the situation with Mg (Fig. 4), maximal activity was obtained at a ratio metal/ATP considerable below 1. Thus, with Ca^{2+}, Co^{2+}, and Mn^{2+}, the maximal activity appeared at a ratio of 0.5, whereupon strong inhibition did occur when the concentration of the metal was increased. Such an inhibitory effect was still more pronounced with Zn^{2+}, where maximal activity was present at a ratio $Zn^{2+}/ATP = 0.1$. Thus, for all these metal ions the activating effect disappears at higher concentrations. This must be explained by an inhibition of the enzyme at increased concentration of the free metal ions.

The effect of ITP, GTP and UTP on activity. A slow rate of glucose phosphorylation by UTP with muscle hexokinase extract [14] and a small activity of ITP on a partially purified phosphofruktokinase from brain [15] have been reported. This may be due to the contamination of these nucleotides by traces of ADP, since nucleoside diphosphokinase often occurs in these enzyme preparations [16]. However, in a purified preparation of plant hexokinase considerable activition by ITP was observed [17], and ITP and UTP were very active as phosphate donors with highly purified muscle phosphofructokinase [18]. Therefore, experiments on purified hexokinase were performed, where ITP, GTP or UTP purified by an ion exchange resin method [19], were substituted for ATP. However, no measurable glucose phosphorylation could be demonstrated with these nucleotides in the reaction mixture. So far, it must be concluded that muscle hexokinase specifically requires ATP as the phosphate donor.

DISCUSSION

It can be concluded that magnesium is the most effective cation in activating muscle hexokinase. Magnesium gives the highest maximal activity and no inhibitory action takes place until very high concentrations of Mg in excess of ATP are added. The mechanism of this cation activation can be considered as an equilibrium between Mg^{2+} and its complexes with ATP and the enzyme. Thus Najjar [20] has developed the hypothesis that in phosphate transferring enzymes, the function of the metal is to form a complex with the substrate which is the true substrate for the enzyme. Hers [11] working on the phosphofruktokinase and Liébecq [12] investigating muscle hexokinase observed maximal activity at a molar ratio $Mg^{2+}/ATP = 1$ and therefore proposed that the Mg—ATP complex was the actual substrate. On the other hand, Raaflaub and Leupin [21] came to the conclusion that $Mg-ATP^{-2}$ could not act as the substrate for yeast hexokinase. This was denied by Melchior and Melchior [22] who calculated the concentration of the molecular species, Mg^{2+}, $MgATP^{-2}$ and ATP^{-4} which exist in a solution containing ATP and $MgCl_2$. Their experi-

ments on yeast hexokinase could be interpreted by two possible reaction mechanisms.

$$\text{I. } E + MgATP^{-2} \rightleftharpoons E{-}MgATP^{-2}$$
$$\text{II. } E + ATP^{-4} \rightleftharpoons E{-}ATP^{-4}$$
$$E{-}ATP^{-4} + Mg^{2+} \rightleftharpoons E{-}ATP{-}Mg^{2+}$$

The Melchior's were not able to distinguish between the relative importance of the reaction mechanism I and II in the activation of the enzyme. Some information on the mechanism has been given in the experiments on the inhibition of muscle hexokinase by pyrophosphate. The inhibition of hexokinase by sodium pyrophosphate clearly indicates that pyrophosphate complexes Mg^{2+} and thereby competes with the activation of the enzyme. The same conclusion has been reached in studies on polyphosphate inhibition [23] and fluoride inhibition [24] of yeast hexokinase. On the other hand, in the present work the kinetics of the inhibition of muscle hexokinase by a Mg-pyrophosphate complex is in accordance with that of a competitive type with respect to a Mg—ATP complex. This gives some support to the assumption that the $Mg{-}ATP^{-2}$ complex can act as the substrate for the enzyme.

To throw light on this problem, the stability of ATP complexes with different metal cations has been investigated as reported earlier [25]. The formation of 1:1 complexes of the ligand ATP with different metals, Ca^{2+}, Mg^{2+}, Co^{2+}, and Mn^{2+}, were shown. The stability constant of the Mg—ATP complex was calculated to K_f 4.04 in accordance with the value reported by Martell and Schwarzenbach [26]. This does not correspond with the reaction kinetics of muscle hexokinase in activity experiments. As reported, half maximal activity was obtained at a concentration of 1.7×10^{-3} M of magnesium and ATP (Fig. 6). However, the conclusion which can be drawn by comparing activity studies and substrate complex dissociation constants are limited. First, the experimental conditions such as ionic strength, temperature *etc.* have not been completely identical. Further, as pointed out by Melchior [27], ATP at neutral pH in solution exist in several different configurations which can complex with the metal. The catalytic efficiency of a metal ion may therefore be restricted to a complex of a particular molecular shape of ATP which is specially favourable to the required combination with the enzyme.

Williams [28] has further pointed out that the stability of a mixed complex of magnesium with enzyme and substrate will be less than the corresponding Mg-substrate complex. This can be explained by the tendency of magnesium to coordinate with water molecules, especially if coordination through several ligand groups takes place. Therefore, in a mixed enzyme complex, coordination of magnesium with water molecules instead of ligand centres of the enzyme may take place. As a consequence, a mixed hexokinase-ATP complex with magnesium would be less stable than the Mg—ATP complex, which is in accordance with the experimental observations. The nature of the active ligand groups of hexokinase are not known. It is therefore of interest that Ågren and Engström [29] have demonstrated rapid ^{32}P labeling of phosphoserine of purified yeast hexokinase when the enzyme was incubated with ^{32}P labeled ATP. In this connection the hypothesis by Robison and Najjar [30] of the mag-

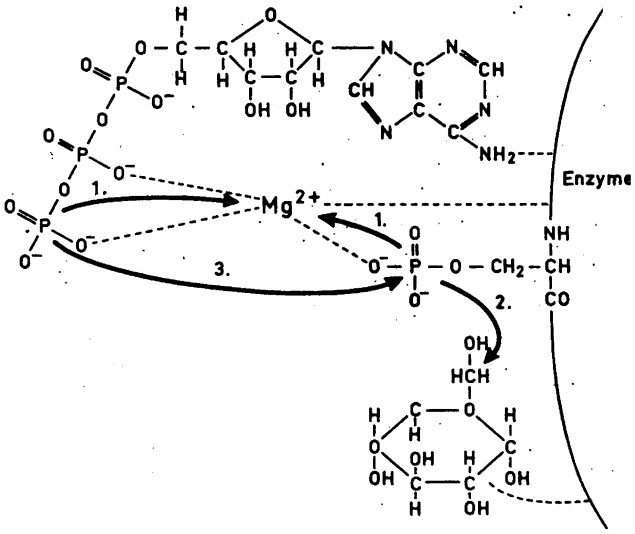

Fig. 10. This illustrates the postulated enzyme-substrate transition complex. By labilization of the phosphate bonds (1), transfer of the phosphate group of phosphorylserine in the enzyme to glucose may occur (2). ATP may serve as the donor for phosphorylation of the serine residue of the enzyme (3) and ADP is formed.

nesium activation of phosphoglucomutase is of interest. In Fig. 10 a tentative scheme for activation of hexokinase is proposed, where Mg^{2+} forms a bridge between ATP^{-2} and the active groups of the enzyme in a ternary transition complex. The positive charge of Mg^{2+} would lower the electron density at the serine phosphate bond of the enzyme and the pyrophosphate bond of ATP. Due to the labilization of these phosphate bonds, the transfer of phosphate from serine phosphate to form glucose-6-phosphate, succeeded by a transfer of phosphate from ATP to the dephosphorylated serine residue of the enzyme would be facilitated. The possible role of an intermediate serine phosphate group in the transphosphorylating process of hexokinase reaction requires further investigation, particularly in view of the results reported by Trayser and Colowick [31].

Compared with Mg^{2+} the activation of muscle hexokinase by the transition series metals Co^{2+} and Mn^{2+}, and by Zn^{2+} as well as by Ca^{2+} is characterized by (*a*) The maximal activity is less, (*b*) Half maximal activity occurs at a lower concentration and (*c*) Strong inhibitory action occurs by increased concentration of the metal ion. These results can be explained as a consequence of the different coordination complexes which is obtained with different metal ions. It has earlier been shown that Mn^{2+}, Co^{2+} (Ref.[25]) and Zn^{2+} (Ref.[32]) form rather stable complexes with ATP compared with the Mg—ATP complex. Different metal ions must also be expected to combine with different ligand centres of the enzyme. While Mg^{2+}, Ca^{2+} and Mn^{2+} mostly combine with oxy-anions under the experimental conditions, Co^{2+} can combine with mixed oxygen anion-nitrogen-ligands, and the Zn^{2+} is likely to be held by

nitrogen groups. The complexing properties of the transition series metals therefore may be the reason why the activation of hexokinase occurs at low concentration of these metal ions. The inhibition of muscle hexokinase at higher concentrations may be due to increased concentration of Me^{2+}-enzyme complex in the presence of excess cations. These complexes are likely to be more stable than the activated mixed complexes and may exert inhibitory action.

Muscle hexokinase is activated by calcium in a manner similar to that observed for Mn^{2+} and Co^{2+}. This occurs in spite of the lower stability of the Ca—ATP complex as reported earlier [25]. The activation of hexokinase by calcium at low concentration may therefore be explained by a high affinity of the enzyme for the Ca—ATP complex.

Finally, it should be pointed out that the metal activation of muscle hexokinase is similar to yeast hexokinase as far as activation by Mg^{2+} and the metals of the transition series is concerned [33]. The only exception is Ca^{2+} which is active in the muscle but inactive on the yeast enzyme.

Acknowledgment. This work has been supported by grants from the *Rockefeller Foundation*, the *Lilly Research Foundation* and from *The Norwegian Research Council for Science and the Humanities*.

Thanks are due to Mrs. Reidun Midthjell for expert technical assistance.

REFERENCES

1. Colowick, S. P., Cori, C. F. and Slein, M. W. *J. Biol. Chem.* **168** (1947) 583.
2. Kipnis, D. M., Helmreich, E. and Cori, C. F. *J. Biol. Chem.* **234** (1959) 177.
3. Park, C. R., Morgan, H. E., Henderson, M. J., Regen, D. M., Cadenas, E. and Post, R. L. *Recent Progr. in Hormone Research* **17** (1961) 493.
4. Colowick, S. P. and Price, W. H. *J. Biol. Chem.* **159** (1945) 563.
5. Cori, C. F. *Harvey Lectures* Ser. 41 (1945—46) 253.
6. Crane, R. K. and Sols, A. in Colowick, S. P. and Kaplan, N. O. (Editors) *Methods in Enzymology*, Academic Press, New York, Vol. 1, 1955, p. 282.
7. Jervell, K. F., Walaas, E. and Walaas, O. *Acta Physiol. Scand.* **35** (1956) 321.
8. Nelson, N. *J. Biol. Chem.* **153** (1944) 375.
9. Lowry, O. H., Rosebrough, N. J., Farr, A. L. and Randall, R. J. *J. Biol. Chem.* **193** (1951) 265.
10. Walaas, E. and Walaas, O. *Biochim. et Biophys. Acta* **20** (1956) 77.
11. Hers, H. G. *Biochim. et Biophys. Acta* **8** (1952) 424.
12. Liébecq, C. *Biochem. J.* **54** (1953) p. xxii.
13. Rogers, L. B. and Reynolds, C. A. *J. Am. Chem. Soc.* **71** (1949) 2081.
14. Kleinzeller, A. *Biochem. J.* **36** (1942) 729.
15. Muntz, J. A. *Arch. Biochem. Biophys.* **42** (1953) 435.
16. Berg, P. and Joklik, W. K. *Nature* **172** (1953) 1008.
17. Saltman, P. *J. Biol. Chem.* **200** (1953) 145.
18. Ling, K.-H. and Lardy, H. A. *J. Am. Chem. Soc.* **76** (1954) 2842.
19. Alertsen, Aa. R., Walaas, O. and Walaas, E. *Acta Physiol. Scand.* **43** (1958) 105.
20. Najjar, V. A. *Phosphorus Metabolism* **1** (1951) 500.
21. Raaflaub, J. and Leupin, I. *Helv. Chim. Acta* **39** (1956) 832.
22. Melchior, N. C. and Melchior, J. B. *J. Biol. Chem.* **231** (1958) 609.
23. Dirheimer, G. and Ebel, J. P. *Bull. soc. chim. biol.* **58** (1956) 1337.
24. Melchior, N. C. and Melchior, J. B. *Science* **124** (1956) 402.
25. Walaas, E. *Acta Chem. Scand.* **12** (1958) 528.
26. Martell, A. E. and Schwarzenbach, G. *Helv. Chim. Acta* **76** (1956) 653.
27. Melchior, N. C. *J. Biol. Chem.* **208** (1954) 615.

28. Williams, R. J. P. in Boyer, P. D., Lardy, H. and Myrbäck, K. (Editors) *The Enzymes*, Academic Press, New York 1959, Vol. I, p. 397.
29. Ågren, G. and Engstrøm, L. *Acta Chem. Scand.* **10** (1956) 489.
30. Robinson, J. P. and Najjar, V. A. *Federation Proc.* **20** (1961) 90.
31. Trayser, K. A. and Colowick, S. P. *Arch. Biochem. Biophys.* **94** (1961) 161.
32. Walaas, E. *Unpublished observation.*
33. Brintzinger, H., Fallab, and Erlenmeyer, H. *Experienta* **15** (1959) 96.

Received April 5, 1962.

ACTA CHEMICA SCANDINAVICA 16 (1962) 1695–1712

On the Stability of the Acetate, Glycolate and Thioglycolate Complexes of Tervalent Europium and Americium

INGMAR GRENTHE

Department of Inorganic and Physical Chemistry, Chemical Institute, University of Lund, Lund, Sweden

The stability constants for the acetate, glycolate and thioglycolate complexes of tervalent europium and americium were determined in a perchlorate medium of the ionic strength $I = 0.5$ M and at a temperature of 20.0°C. The europium complexes were studied by a potentiometric method [1a] and the americium complexes using the cation exchange method of Fronæus [2a-2c]. The quantitative results for the acetate and glycolate systems were checked by an anion exchange study. In all the systems investigated the americium complexes were stronger than the corresponding europium complexes. The difference was most pronounced for the glycolate systems. For both europium and americium the stability constants of the complexes decreased in the following order: glycolate, acetate, thioglycolate.

The acetate and glycolate complexes of several tervalent lanthanides have previously been studied by Sonesson [1a-1e]. Qualitative studies of the cation and anion exchange behaviour of both europium and americium in glycolate solutions have been published by Stewart [3] and Holm *et al* [4]. In the present investigation these measurements were extended in order to determine the stability constants of europium and americium complexes with acetate, glycolate and thioglycolate ions.

As only tracer amounts of ^{241}Am were available, the experimental methods were restricted to ion exchange and solvent extraction studies. In the present investigation the first method, with the cation exchanger in the sodium form, was used. Previous experience [5] did prove that reliable results could be obtained even on the tracer scale. The method has one serious drawback, however: no information about the existence of anionic complexes can be obtained. For this reason an anion exchange study was added to the investigation. Macro amounts of europium oxide were available and therefore the europium systems could be studied by a potentiometric standard method, *viz.* the determination of the concentration free ligand by means of pH-measurements.

All measurements were made at a temperature of 20.0°C and in a perchlorate medium of the ionic strength of $I = 0.5$ M.

CALCULATION OF STABILITY CONSTANTS FROM CATION EXCHANGE DATA

The following notation was used:

C'_M, C'_A = the total concentrations of metal ion and ligand before addition of ion exchanger

C_M, C_A = the total concentrations of metal ion and ligand in equilibrium with the ion exchanger

$[M^{3+}]$, $[MA_j^{3-j}]$ = equilibrium concentrations of the various species in solution

$[M^{3+}]_R$, $[MA_j^{3+j}]_R$ = equilibrium concentrations of the various species in the resin phase.

β_j = the stability constant for the complex MA_j^{3-j} in solution

$l_j = \dfrac{[MA_j^{3-j}]_R}{[MA_j^{3-j}]}$; $(j = 0, 1, 2)$

$l'_j = \beta_j \cdot \dfrac{l_j}{l_0}$; $(j = 1, 2)$

v = the volume of the solution before the addition of the ion exchanger

m = the weight of dried ion exchanger

δ = the swelling factor of the ion exchanger

$X_n = \sum_{j=n}^{N} \beta_j [A^-]^{j-n}$; $(\beta_0 = 1)$

For the determination of the stability constants β_j the functions, φ_1, f and g were used. For further details see Refs.[1a,2b,2c]

$$\varphi = \frac{v}{m}\left(\frac{C'_M}{C_M} - \delta\right) = l_0 \cdot \frac{1 + l'_1[A^-] + l'_2[A^-]^2}{X} \tag{1}$$

$$\varphi_1 = \left(\frac{l_0}{\varphi} - 1\right) \cdot \frac{1}{[A^-]} \tag{2}$$

$$f = \left\{\frac{l_0}{\varphi}\,[(\beta_1 - l'_1)[A^-] - 1] + 1\right\} \cdot \frac{1}{[A^-]^2} = \beta_1\varphi_1 - X_2 - \frac{l'_1 \cdot l_0}{\varphi} \tag{3}$$

$$g = \left\{f - \beta_1\varphi_1 + \frac{l_0}{\varphi}\,(\beta_2 - l'_2)\right\} \cdot \frac{1}{[A^-]} = \beta_2\varphi_1 - \beta_3 - X_4[A^-] \tag{4}$$

$$\lim_{[A^-]\to 0} \varphi_1 = \varphi_1^0 = \beta_1 - l'_1 \tag{5}$$

$$\lim_{[A^-]\to 0} f = f^0 = \beta_1\varphi_1^0 - (\beta_2 - l'_2) \tag{6}$$

$$\Delta\varphi_1 = \varphi_1 - \varphi_1^0 \tag{7}$$

$$\Delta f = f - f^0 \tag{8}$$

$$\beta_1 = \frac{\Delta f}{\Delta\varphi_1} + \beta_3 \cdot \frac{[A^-]}{\Delta\varphi_1} + \beta_4[A^-] \cdot \frac{[A^-]}{\Delta\varphi_1} - l'_2 \cdot \varphi_1 \frac{[A^-]}{\Delta\varphi_1} \tag{9}$$

As a rule β_1 can be determined from eqn. (9) written as

$$\frac{\Delta f}{[A^-]} = \beta_1 \cdot \frac{\Delta\varphi_1}{[A^-]} - \beta_3 - \beta_4[A^-] + l'_2 \cdot \varphi_1 \tag{10}$$

By plotting $\Delta f/[A^-]$ *versus* $\Delta\varphi_1/[A^-]$, β_1 is obtained as the slope. This method could not be used here, because the values of $\Delta f/[A^-]$ and $\Delta\varphi_1/[A^-]$ were approximately constant. The following method of successive approximations was used instead: In the first approximation of β_1 from eqn. (9) all terms except $\Delta f/\Delta\varphi_1$ were neglected. Using this approximate β_1-value the function g was computed. β_2 and β_3 were then determined by plotting g *versus* φ_1. In the second approximation of β_1 all correction terms were included (*vide infra*, p. 1698 and p.1699). In order to compute the last term in eqn. (9) it was necessary to estimate l_2'. This was done using the relation $\beta_1^2 \cdot \beta_2^{-1} = (l_1')^2(l_2')^{-1}$ (*cf.* Ref. [2c], p. 20). A satisfactory value of β_1 was obtained after three approximations.

In order to determine the concentration of free ligand $[A^-]$ from the C_A-values, two corrections had to be applied to the latter figures. The first was due to ligand produced by protolysis of the acid HA. This correction was computed from the acid constant of HA. The second correction was due to ligand produced, when sodium ions in the ion exchanger were replaced by hydrogen ions from the solution. This correction was computed on the assumption (for the validity of this assumption *vide infra*, p. 1699) that $[H^+]_R \cdot [H^+]^{-1} \approx [Na^+]_R \cdot [Na^+]^{-1}$. For further details see Ref. [1d], pp. 1442 and 1445.

EXPERIMENTAL

Chemicals used. A hydrochloric acid solutions of tervalent americium was obtained from A.E.R.E. Harwell. The sample consisted of ^{241}Am to more than 99.93 %, the rest was ^{239}Pu. From this stock solution more dilute americium solutions were prepared by dilution with a 0.5 M sodium perchlorate solution. The acidity of these solutions was determined by a potentiometric determination of their hydrogen ion concentration.

All other chemicals used except thioglycolic acid were of analytical grade. Thioglycolic acid (Fluka purum) was purified by a vacuum distillation before it was used.

The stock solutions of acetic and glycolic acid were standardized by an alkalimetric titration. Thioglycolic acid was standardized by oxidation with a standard iodine solution [6]. The stock solutions of acetate and sodium perchlorate were analysed by passing a known volume of the solutions through an ion exchanger in the hydrogen form followed by an alkalimetric titration of the acid. The cation exchange resin (Dowex 50 W × 8, 50—100 mesh, exchange capacity 3.81 mequiv. · g^{-1}) was used in the sodium form. The swelling factor δ was determined to 0.99 for the value of $v \cdot m^{-1} = 33.9 \times 10^{-3}$ $l \cdot g^{-1}$ used in the following experiments. The buffer solutions used all had the following compositions:

$$C_A \text{ mM NaA}, C_{HA} = k \cdot C_A \text{ mM HA}, \quad I = 0.5 \text{ M}$$

where k is close to unity. Buffer stock solutions were prepared by mixing acetic acid and sodium acetate stock solutions or by partial neutralization of glycolic or thioglycolic acid with sodium hydroxide. Sodium perchlorate was added to give the correct ionic strength. From these stock solutions more dilute solutions were obtained by dilution with a 0.5 M sodium perchlorate solution.

The distribution coefficient φ was determined by shaking 5 ml of the buffer solutions, to which 0.086 ml of the americium stock solutions had been added, with 150 mg ion exchange resin. The time necessary for the attainment of equilibrium was < 20 h. For each ligand, series with varying C_A' were performed at two or three different values of C_M' and each series was repeated at least twice.

The americium concentration of the solutions was determined by measuring the γ-activity of a 4 ml sample in a scintillation counter (Tracerlab P 20, using a NaI (Tl) crystal). In order to determine the absolute concentration of americium the amount in a thin solid sample was determined by measuring the α-activity in a 2 π proportional counter (Tracerlab SC-16 P, was used in this investigation). For details about the preparation of the sample see Ref.[7], p. 1063. By measuring the same amount of americium diluted

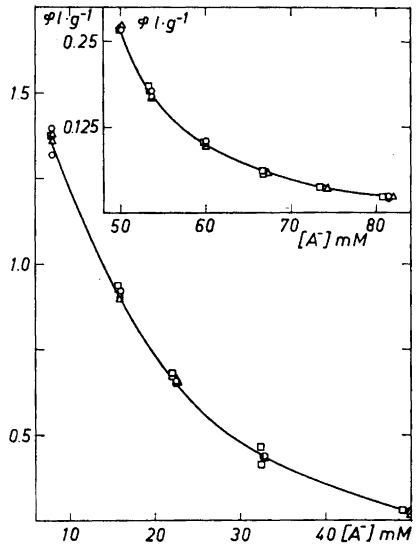

Fig. 1. φ as a function of [A$^-$] for the Am^{3+}-acetate system. $C'_M = 1.14 \times 10^{-7}$ M □, $C'_M = 1.40 \times 10^{-7}$ M ○, $C'_M = 2.12 \times 10^{-7}$ M △.

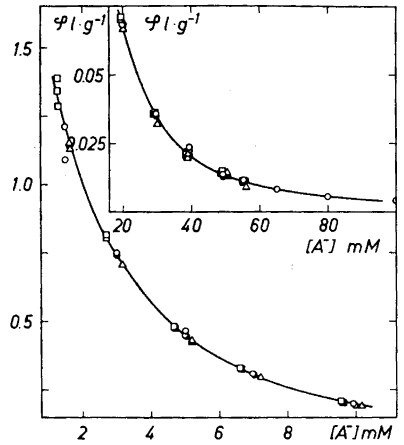

Fig. 2. φ as a function of [A$^-$] for the Am^{3+}-glycolate system. $C'_M = 1.14 \times 10^{-7}$ M □, $C'_M = 1.40 \times 10^{-7}$ M ○, $C'_M = 2.66 \times 10^{-7}$ M △.

to 4 ml in the scintillation counter it was possible to relate the concentration in cpm to the concentration in moles. l^{-1}. 1000 cpm was equal to 1.5×10^{-8} M.

All operations with more concentrated americium solutions were performed in a glove box, while the more dilute solutions were handled in a well ventilated fume hood.

RESULTS

The americium-acetate system

The distribution coefficient φ as a function of the acetate concentration at the different values of C'_M is given in Fig. 1. No corrections needed be applied to the C_A-values because of the low acidity of the buffer solutions (pH $\approx$ 4.5). From Fig. 1 it is evident that there is no variation in φ with the load C_{MR}. The various functions used for the computation of the stability constants are given in Table 1. φ_1 and f were plotted *versus* [A$^-$] and extrapolated to [A$^-$] = 0 to give φ_1^0 and f^0. The following values were obtained:

$$\varphi_1^0 = 94 \pm 2 \text{ M}^{-1}$$
$$f^0 = 7400 \pm 200 \text{ M}^{-2}$$

β_1 was calculated from eqn. (9) in the way described earlier (*vide supra* p. 1697). In the final approximation values of $\beta_2 = 1.9 \times 10^3$ M^{-2}, $\beta_3 = 1 \times 10^4$ M^{-3}, $\beta_4 = 0$ and $l_2' = 6$ M^{-2} were used. The following stability constants were obtained:

$$\beta_1 = 98.5 \pm 3\ M^{-1}$$
$$\beta_2 = (1.9 \pm 0.2) \times 10^3\ M^{-2}$$
$$\beta_3 = (8 \pm 3) \times 10^3\ M^{-3}$$

From eqn. (6) a value of $\beta_2 = 1.86 \times 10^3$ (with the assumption $l_2' = 0$) was obtained.

The americium-glycolate system

The experimental values of φ as a function of $[A^-]$ and C_M' are given in Fig. 2 and the functions used for computing the stability constants in Table 2. The pH of the glycolate buffers was about one unit lower than that of the acetate buffers and the two corrections to the C_A-values (*vide supra* p. 1697) had to be applied. These corrections were checked in a few cases by determining the hydrogen ion concentration of the solutions equilibrated with ion exchanger. The $[A^-]$-values determined by the two methods differed by 0.5 % at most. Values of φ_1^0 and f^0 were determined as described earlier. The following values were obtained:

$$\varphi_1^0 = 630 \pm 5\ M^{-1}$$
$$f^0 = (3.42 \pm 0.03) \times 10^5\ M^{-2}$$

In the final approximation of β_1 from eqn. (9) values of $\beta_2 = 7.2 \times 10^4\ M^{-2}$, $\beta_3 = 2 \times 10^6\ M^{-3}$, $\beta_4 \approx 5 \times 10^6\ M^{-4}$ (estimated from the position of φ_{max} in the anion exchange experiment, *vide infra* p. 1708) and $l_2' = 150\ M^{-2}$ were used.

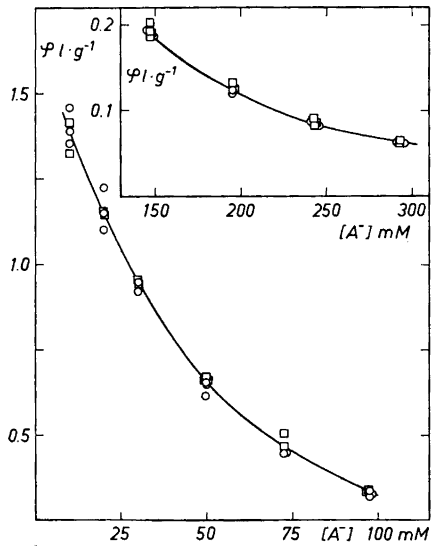

Fig. 3. φ as a function of $[A^-]$ for the Am^{3+}-thioglycolate system. $C_M' = 1.14 \times 10^{-7}$ M □, $C_M' = 2.56 \times 10^{-7}$ M ○.

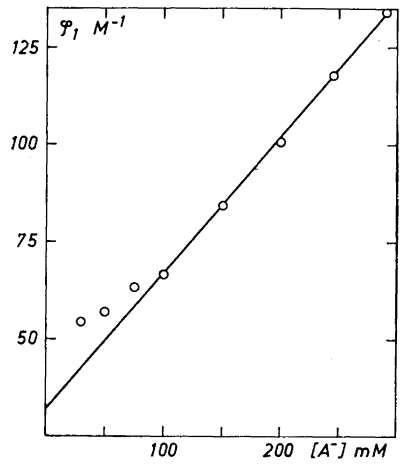

Fig. 4. $\varphi_1 = f([A^-])$ for the Am^{3+}-thioglycolate system.

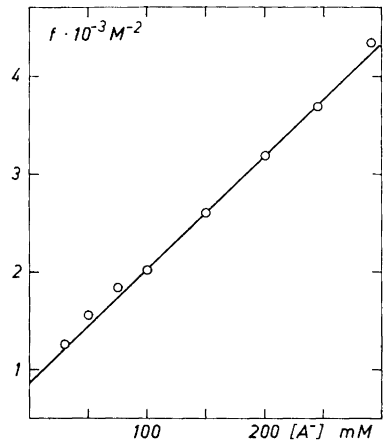

Fig. 5. The function f for the Am^{3+}-thioglycolate system.

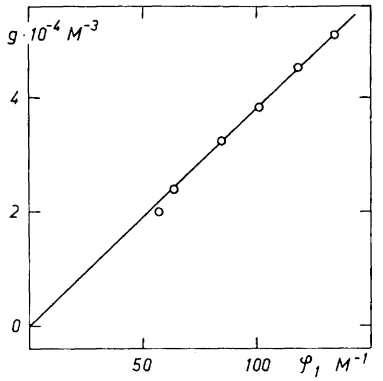

Fig. 6. g as a function of φ_1 for the Am^{3+}-thioglycolate system.

The stability constants obtained were:

$$\beta_1 = 657 \pm 15\ M^{-1}$$
$$\beta_2 = (7.2 \pm 1) \times 10^4\ M^{-2}$$
$$\beta_3 = (2 \pm 1) \times 10^6\ M^{-3}$$

The americium-thioglycolate system

The experimental material is given in Fig. 3 and the functions φ_1, f and g in Table 3. In Figs. 4, 5 and 6 the functions φ_1, f and g are plotted. It is obvious from the figures that the functions deviate from the expected course at lower values of C_A'. This was probably due to an oxidation of the ligand to dithiodi-

Table 1. Corresponding values of $[A^-]$, φ, φ_1, f and g for the americium acetate system. The values of β_1 in column 5 have been computed from eqn. (9) using a value of $\beta_2 = 1.9 \times 10^3\ M^{-2}$, $\beta_3 = 10^4\ M^{-3}$ and $l_2' = 6\ M^{-2}$.

$[A^-]$ mM	φ $l \cdot g^{-1}$	φ_1 M^{-1}	$f \times 10^{-4}$ M^{-2}	β_1 M^{-1}	$g \times 10^{-5}$ M^{-3}
0	2.51	*94*	*0.74*		*−0.8*
8.00	1.37	105	0.85	108.6	1.99
16.00	0.897	112	0.94	120.0	2.24
22.00	0.660	127	1.05	97.7	2.26
33.00	0.430	147	1.22	96.8	2.61
50.00	0.273	164	1.40	101.1	2.99
68.00	0.175	196	1.69	99.4	3.57
100.0	0.101	239	2.10	99.8	4.37
135.0	0.059	308	2.73	98.4	5.64
170.0	0.0375	388	3.47	97.6	7.11
215.0	0.0245	472	4.26	97.3	8.68

Table 2. Corresponding values of $[A^-]$, φ, φ_1, f and g for the americium-glycolate system. The values of β_1 in column 5 have been computed from eqn. (9) using values of $\beta_2 = 7.4 \times 10^4\ M^{-2}$, $\beta_3 = 2 \times 10^6\ M^{-3}$, $l_2' = 150\ M^{-2}$ and $\beta_4 \approx 5 \times 10^6\ M^{-4}$

$[A^-]$ mM	φ l . g^{-1}	φ_1 M^{-1}	$f \times 10^{-5}$ M^{-2}	β_1 M^{-1}	$g \times 10^{-5}$ M^{-3}
0	2.51	*630*	*3.42*		*−1.8*
1.50	1.21	715	3.94	645	4.87
3.00	0.739	799	4.47	655	5.53
5.00	0.450	916	5.20	655	6.38
7.00	0.307	1025	5.89	659	7.20
10.00	0.197	1174	6.85	665	8.30
15.00	0.107	1497	8.85	658	10.59
20.00	0.0670	1823	10.89	657	12.92
30.00	0.0344	2399	14.52	658	17.07
40.00	0.0200	3113	18.99	655	22.20
50.00	0.0135	3698	22.68	655	26.41
55.50	0.0113	3984	24.50	656	28.47
65.00	0.0083	4637	28.62	655	33.17
80.00	0.0054	5798	35.89	652	41.50

glycolic acid. The oxidation was about 10 % in the solutions with the lower values of C_A' and 1—2 % in the solutions with higher C_A'-values. The presence of the oxidation product means that the results for this particular ligand are more uncertain than those for the other two systems. The stability constants however have been computed as before. The following values were obtained:

$$\beta_1 = 35.5 \pm 5\ M^{-1}$$
$$\beta_2 = 400 \pm 100\ M^{-2}$$
$$\beta_3 = 0\ M^{-3}$$

β_1 was computed from eqn. (9) using values of $\beta_3 = \beta_4 = l_2' = 0$.

β_2 was also computed from eqn. (6) with the value of $l_2' = 0$. A value of $\beta_2 = 400\ M^{-2}$ was obtained.

Table 3. Corresponding values of $[A^-]$, φ, φ_1, f and g for the americium-thioglycolate system. β_1 has been computed from eqn. (9) using a value of $\beta_3 = 0$ and $l'_2 = 0$.

$[A^-]$ mM	φ l . g^{-1}	φ_1 M^{-1}	f M^{-2}	β_1 M^{-1}	$g \times 10^{-4}$ M^{-3}
0	2.51	*35*	*860*		*0.00*
10	1.39	80.6			
20	1.15	59.6			
30	0.950	54.7	1258		
50	0.650	57.2	1559	31.5	2.01
75	0.435	63.6	1845	34.4	2.39
100	0.327	66.8	2019	36.4	2.58
150	0.184	84.3	2621	35.7	3.23
200	0.119	100.5	3188	35.5	3.84
245	0.084	117.9	3787	35.3	4.50
290	0.063	133.9	4346	35.2	5.11

Table 4. The distribution coefficients l_j and l'_j for the various americium species.

Ligand	l_0 $l \cdot g^{-1}$	l_1 $l \cdot g^{-1}$	l'_1 M^{-1}	$l_2 \times 10^3$ $l \cdot g^{-1}$	l'_2 M^{-2}
Acetate	2.51	0.11	4.5	7.9	6
Glycolate	2.51	0.10	30	5.3	150
Thioglycolate	2.51	~0.1	~1	0	0

The distribution coefficients l'_j and l_j for the various species in the solutions are given in Table 4. The sorption of the complex species is very much lower than the sorption of the hydrated Am^{3+}-ion. This means that when the first complex is transformed to the second and higher complexes, the absolute decrease in φ will be small and for higher $[A^-]$-values smaller than the random errors. These will thus seriously affect the determination of β_3 and make it impossible to compute any constants for complexes higher than the third.

CALCULATION OF STABILITY CONSTANTS FROM POTENTIOMETRIC DATA

The following notation was used:

$[H^+]$, $[H^+]'$ = the hydrogen ion concentration in buffer solution with and without metal ion.
C_H = the concentration free perchloric acid in the metal perchlorate solution.
C'_{HA}, C'_A = the stoichiometric concentrations of acid and sodium salt in the buffer solutions.
C_A = the actual total concentration of the ligand A, where $C_A = C'_A + [H^+] - C_H$.
$[M^{3+}]$, $[A^-]$ = the concentration of free central ion and free ligand.
β_j = the stability constant of the j:th mononuclear complex.

$$\bar{n} = \frac{C'_A + [H^+] - C_H - [A^-]}{C_M} \tag{10}$$

$$[A^-] = \frac{[H^+]'}{[H^+]} \cdot \frac{(C'_A + [H^+]')(k \cdot C'_A + C_H - [H^+])}{k \cdot C'_A - [H^+]'} \tag{11}$$

If only mononuclear complexes are formed the following expression is valid

$$\ln X([A^-]_j) = \int_0^{[A^-]j} (\bar{n}/[A^-])d[A^-] \tag{12}$$

$X([A^-]_j)$ and k are the same as before (*vide supra*, pp. 1696, 1695). For details of the method of calculation the reader is referred to Refs. [1a–1c].

EXPERIMENTAL

Chemicals used. Europium perchlorate was prepared from Eu_2O_3 (purity > 99.8 %, from Lindsay Chemical Co) by treatment with perchloric acid. The excess of acid was evaporated with a heating lamp. The stock solution was standardized by an ion exchange

analysis. The other chemicals were the same as used in the cation exchange investigation.

Procedure. The emf E of galvanic cells of the following composition were measured:

Au	10.01 mM $HClO_4$ $I = 0.5$ M Quinhydrone	0.5 M Na ClO_4	C_M mM Eu $(ClO_4)_3$ C_H mM H ClO_4 C'_A mM NaA $C'_{HA} = k \cdot C'_A$ mM HA $I = 0.5$ M Quinhydrone	Au

Here A means acetate or glycolate. For the thioglycolate system the quinhydrone electrode could not be used and so the right half-cell had to be replaced according to:

S	C_M mM Eu $(ClO_4)_3$ C_H mM H ClO_4 C'_A mM NaA $C'_{HA} = k \cdot C'_A$ mM Ha I = 0.5 M	glass electrode

The solution in the right half-cell was prepared by adding known amounts of a buffer solution T to 3 ml of a solution S. The small volumes of T were added from an Agla micrometer syringe with an error of 0.5 % at most.

The solutions S and T had the following composition:

S	C_M mM Eu $(ClO_4)_3$ C_H mM H ClO_4 $I = 0.5$ M	T	C_M mM Eu $(ClO_4)_3$ C_H mM H ClO_4 C'_A mM NaA $C'_{HA} = k \cdot C'_A$ mM HA $I = 0.5$ M

The solutions were mixed by passing nitrogen through the right half-cell.

In all the potentiometric titrations described here only one buffer solutions (a 1—1 buffer) was used. For the lanthanide acetate and glycolate systems Sonesson has shown that buffer solutions with different ratios of acid salt give the same $\bar{n}$-values for the same concentration free ligand. Consequently neither the acetate nor the glycolate systems form complexes with HA. This is certainly true also of the europium systems investigated here.

Titrations were also made at $C_M = 0$. The measured emfs were in this case E′. From the titrations with and without central ion present, $[H^+]/[H^+]'$ was computed from the following expression:

$$E'-E = E_A = 58.16 \log [H^+]/[H^+]' \qquad (13)$$

Each titration was repeated at least twice and the reproducibility of the potentials was in general within ± 0.2 mV.

RESULTS

The europium-acetate system

E' and the dissociation constant of acetic acid were determined as a function of the total concentration of ligand C'_A and the results are given in Table 5.

Titrations were performed at two values of C_M (40 mM and 20 mM). It turned out that $\bar{n}/[A^-]$ as a function of $[A^-]$ was dependent on C_M (*cf.* Fig. 7). This might be caused by polynuclear complexes, qualitative changes of the ionic medium, when C_M is varied, or changes of the ionic strength caused by the complex formation. By extrapolation to $C_M = 0$, these possible causes of the variation have all been eliminated and β_j can be calculated from the functions X.

Table 5. E' and the dissociation constant K_c for the various ligands as a function of C'_A.

Acetate buffer			Glycolate buffer			Thioglycolate buffer		
C'_A mM	E' mV	$K_c \times 10^5$ M	C'_A mM	E' mV	$K_c \times 10^4$ M	C'_A mM	E' mV	$K_c \times 10^4$ M
5.00	146.7	3.04	2.48	96.2	2.69	4.95	87.7	3.54
14.70	146.7	3.02	4.90	93.9	2.72	9.80	86.3	3.53
24.04	146.7	3.01	9.62	92.6	2.74	14.56	85.7	3.55
41.67	146.7	3.01	14.15	92.2	2.75	28.30	85.5	3.49
69.57	146.8	3.00	18.52	91.9	2.74	53.57	85.7	3.43
119.2	147.1	2.97	26.79	91.7	2.74	90.16	86.1	3.35
170.0	147.4	2.93	34.48	91.6	2.74	142.9	86.8	3.25
208.8	147.7	2.89	54.69	91.6	2.72	187.5	88.0	3.09
			76.39	91.6	2.72	250.0	89.5	2.91
			93.75	91.7	2.70			
			111.1	91.7	2.70			
			136.4	91.9	2.68			

The functions X, X_1 and X_2 are given in Table 6 for different values of $[A^-]$. All values are referred to solutions with $C_M = 0$. The stability constants were determined by the standard graphical method. The following results were obtained:

Table 6. The functions X, X_1 and X_2 for the europium-acetate system.

$[A^-]$ mM	$\int_0^{[A^-]} \frac{\bar{n}}{[A^-]} d[A^-]$	X	X_1 M^{-1}	$X_2 \times 10^{-3}$ M^{-2}
0.00		*1.000*	*87.5*	*1.54*
1.00	41.75	1.087	87.0	
3.00	122.00	1.276	92.0	
5.00	195.90	1.480	96.0	
7.00	264.00	1.696	99.4	
10.00	357.00	2.042	104.2	1.67
13.00	441.75	2.419	109.2	1.67
16.00	519.90	2.829	114.3	1.68
20.00	615.60	3.426	121.3	1.69
25.00	722.97	4.246	129.8	1.69
30.00	820.47	5.161	138.7	1.71
40.00	994.97	7.315	157.9	1.76
50.00	1146.60	9.906	178.1	1.81
60.00	1281.97	12.99	199.8	1.87
70.00	1405.47	16.63	223.3	1.94
85.00	1571.22	23.16	260.7	2.04
100.0	1717.09	31.01	300.1	2.13
120.0	1890.14	43.83	356.9	2.25
140.0	2040.89	59.25	416.1	2.35

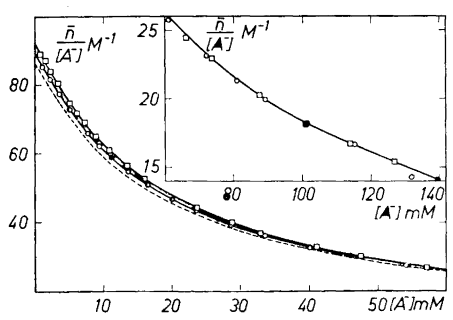

Fig. 7. $\bar{n}/[A^-]$ as a function of $[A^-]$ for the europium-acetate system. □ C_M = 38.98 mM, ○ C_M = 19.49 mM. The dashed curve was obtained on extrapolation to C_M = 0.

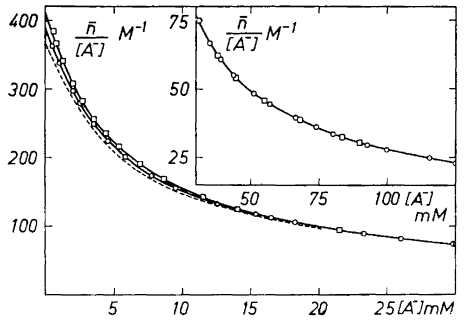

Fig. 8. $\bar{n}/[A^-]$ as a function of $[A^-]$ for the europium glycolate system. □ C_M = 39.60 mM, ○ C_M = 19.80 mM. The dashed curve was obtained on extrapolation to C_M = 0.

$$\beta_1 = 87.5 \pm 1.0\ M^{-1}$$
$$\beta_2 = (1.54 \pm 0.05) \times 10^3\ M^{-2}$$
$$\beta_3 = (6.1 \pm 0.3) \times 10^3\ M^{-3}$$

The europium-glycolate system

This system was investigated in the same way as the acetate system. The experimental values of E' as a function of C'_A are given in Table 5. In Fig. 8 the experimental values of $\bar{n}/[A]$ as a function of $[A^-]$ for C_M = 40 mM, 20 mM and 0 mM (extrapolated) are given. The functions necessary for computing the stability constants are given in Table 7. The following stability constants were obtained:

$$\beta_1 = 369 \pm 3\ M^{-1} \quad ; \quad \beta_3 = (8.1 \pm 0.7) \times 10^5\ M^{-3}$$
$$\beta_2 = (4.1 \pm 0.3) \times 10^4\ M^{-2} \quad ; \quad \beta_4 = (2.3 \pm 0.5) \times 10^6\ M^{-4}$$

The europium-thioglycolate system

The ligand is oxidized by quinhydrone and therefore $[H^+]$ had to be measured by the glass electrode. The emfs were measured with a Radiometer type PHM 4 b pH-meter. E' and E were determined as a function of C'_A as before. Because the complex formation was so weak that at low C_M the E_A-values could not be determined with any accuracy (the E_A-values are small, *cf.* Table 8), only one value of C_M (= 40 mM) was used. The decrease in ionic strength caused by the complex formation was corrected by the addition of solid sodium perchlorate. The titrations could usually be reproduced within ± 0.2 mV. Before and after each titration it was checked that the asymmetry potential of the glass electrode had not changed.

As the ligand was easily oxidized, the experiments were carried out in a nitrogen atmosphere but nevertheless a slight oxidation could not be avoided, amounting to 1—2 % in 5 h at most.

Table 7. The functions X, X_1, X_2 and X_3 for the europium glycolate system.

[A⁻] mM	$\int_0^{[A^-]_j} \frac{\bar{n}}{[A^-]} \cdot d[A^-]$	X	X_1 M^{-1}	$X_2 \times 10^{-4}$ M^{-2}	$X_3 \times 10^{-5}$ M^{-3}
0.00		*1.000*	*369*	*4.10*	*8.1*
1.00	69.45	1.415	415		
2.00	130.38	1.919	460		
3.00	184.45	2.515	505		
5.00	276.85	3.992	598	4.58	
7.00	353.90	5.869	696	4.67	
11.00	479.30	10.99	908	4.90	
17.00	626.60	22.95	1291	5.42	
25.00	777.60	48.82	1913	6.18	5.20
35.00	924.20	101.6	2874	7.16	8.74
50.00	1094.39	237.9	4738	8.74	9.28
70.00	1266.39	562.4	8020	10.93	9.76
90.00	1402.39	1110	12322	13.28	10.20
125.00	1589.48	2829	22620	17.80	10.96

The experimental results for the various titrations are given in Tables 5 and 8. The functions used for the computation of the stability constants are given in Table 9. The following results were obtained:

$$\beta_1 = 35.2 \pm 1.0\ M^{-1}$$
$$\beta_2 = 188 \pm 10\ M^{-2}$$

A slight variation in the $\bar{n}/[A^-]$-values with C_M was found for both the acetate and glycolate systems (see Figs. 7 and 8). This may be caused either by polynuclerar complexes or by changes in the medium. Sonesson did not find any formation of polynuclear complexes for the rare earths before dysprosium, so the second explanation is perhaps the more probable, particularly

Table 8. Experimental values of C'_A, E, E_A, [A⁻] and $\bar{n}/[A^-]$ for the europium thioglycolate system (C_M = 39.60 mM).

C'_A mM	E mV	E_A mV	[A⁻] mM	$\bar{n}/[A^-]$ M^{-1}
0.00	77.3		0.00	*35.2*
4.26	66.1	22.1	1.92	34.2
12.38	65.3	20.3	5.72	30.6
23.64	65.8	19.0	11.3	28.0
37.14	66.7	17.3	19.0	24.5
49.19	68.1	15.8	26.6	21.7
65.00	69.5	14.3	37.2	19.0
90.43	71.9	12.2	56.2	15.5
118.2	73.9	10.8	77.5	13.3
140.0	75.4	9.8	95.4	11.8
173.3	77.5	8.3	125	9.7
204.3	79.3	7.2	154	8.2

Table 9. The functions X and X_1 for the europium-thioglycolate system.

$[A^-]$ mM	$\int_0^{[A^-]_j} \frac{\bar{n}}{[A^-]} d[A^-]$	X	X_1 M^{-1}
0.00		*1.000*	*35.2*
5.00	32.85	1.179	35.8
10.00	62.90	1.370	37.0
15.00	90.40	1.571	38.1
20.00	115.65	1.782	39.1
40.00	199.15	2.707	42.7
60.00	266.35	3.788	46.5
80.00	323.15	5.031	50.4
100.0	371.75	6.417	54.2
120.0	414.35	7.940	57.8
140.0	452.35	9.600	61.4
155.0	478.15	10.92	64.0

as the central ion in this investigation gives a large contribution to the ionic strength of the solutions. This was not the case in Sonessons study because of the higher ionic strength used by him (2 M instead of 0.5 M in the present investigation).

For the thioglycolate system it was not possible to make corrections for these changes in the medium (except for the decrease in ionic strength caused by the complex formation). This fact and the slight oxidation of the ligand imply that the stability constants are more uncertain for this particular system. The maximum deviations are expected to be within the error limits given previously.

INVESTIGATION OF THE EUROPIUM AND AMERICIUM ACETATE AND GLYCOLATE SYSTEMS WITH AN ANION EXCHANGER

A theory for the distribution of a central ion M between a solution phase containing a ligand A and an anion exchange resin saturated with A has been given by Fronæus [8]. This paper should be consulted for further details about the theoretical treatment.

The distribution of the charged species is given by the Donnan equation:

$$[M^{3+}]_R \cdot [A^-]^3_R = K[M^{3+}] \cdot [A^-]^3$$

where the constant K also includes the activity coefficients of the ion species in the two phases. The following relation can be derived:

$$\varphi = \frac{C_{MR}}{C_M} = K \cdot \frac{X([A^-]_R)}{[A^-]^3_R} \cdot \frac{[A^-]^3}{X([A^-])} = l_3 \cdot \frac{\alpha_3}{\alpha_{3R}} \qquad (14)$$

where X ($[A^-]$) and X ($[A^-]_R$) are the functions X for the solution and the resin phases respectively. l_3 is the Nernst distribution coefficient for the third uncharged complex and $l_3 = K \cdot \beta_{3R} \cdot \beta_3^{-1}$.

If anionic complexes are formed, φ should first increase with increasing values of $[A^-]$, then pass through a maximum at the value of $[A^-]$, where $\bar{n} = 3$, in the outer solution and finally decrease again. On the other hand, if no anionic complexes are formed, φ is expected to increase uniformly with increasing values of $[A^-]$. Part of the sorption C_{MR} on the resin at lower values of $[A^-]$ may be due to a surface sorption, as has been pointed out by Froænus [8]. This surface sorption might be estimated by studying a system, where no anionic complexes are formed, in this case the acetate complexes. From Table 10 one can see that the surface sorption will cause the φ-values for the acetate systems to decrease, instead of increasing, as could be expected from the theory.

EXPERIMENTAL

A 2.86×10^{-2} mM $Eu(ClO_4)_3$ solution containing the isotopes $^{152,154}Eu$ was prepared by dissolving 50 mg irradiated Eu_2O_3 (from A.E.R.E. Harwell) in perchloric acid. A solution of the perchlorate was then prepared as described before. A water solution of Am^{3+} was prepared by dilution of the stock solution. The excess of acid was $\approx$ 0.5 mM.

The anion exchanger Dowex 1 × 4, 50–100 mesh was saturated with acetate or glycolate by passing the acids through a column of the ion exchanger in the hydroxyl form. For the value of $v \cdot m^{-1} = 25 \times 10^{-3}\ l \cdot g^{-1}$ used in the following experiments, the swelling factors of the resin in the acetate and glycolate forms were determined to 0.96 and 0.99, respectively. They were constant in the concentration range investigated here.

The experimental procedure was the same as that in the cation exchange experiments. No additional sodium perchlorate was used in the buffer solutions in order to avoid exchange of perchlorate from the solution for ligand from the resin. Because of the very low distribution coefficients it was not possible to obtain sufficiently accurate values of φ by measuring C'_M and C_M. Instead, the resin phase had to be analysed in the way described by Sonesson [1d]. Both the americium and europium concentrations were determined radio metrically as described earlier (*vide supra*, p. 1697).

RESULTS

The experimental results are given in Table 10. In Fig. 9 the distribution coefficient φ_{corr} (the distribution coefficient corrected for the surface sorption) is plotted *versus* $[A^-]$. Both europium and americium were quite strongly sorbed at low acetate concentrations while the φ-values were constant (within

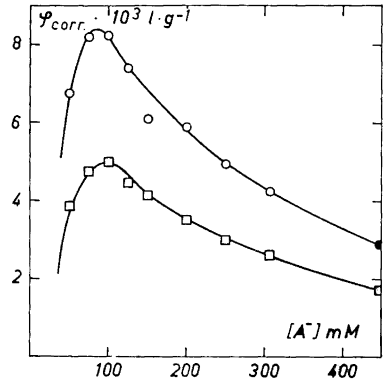

Fig. 9. The anion exchange distributions $\varphi_{corr} = f([A^-])$, for the europium and americium glycolate systems. O the Am^{3+}-glycolate system, □ the Eu^{3+}-glycolate system.

Table 10. The anion exchange distributions for acetate and glycolate systems of europium and americium.

$[A^-]$ mM	$Eu^{3+}-Ac^-$	$Am^{3+}-Ac^-$	$[A^-]$ mM	$Eu^{3+}-glyc^-$	$Am^{3+}-glyc^-$
	$\varphi \times 10^3\ l \cdot g^{-1}$	$\varphi \cdot 10^3\ l \cdot g^{-1}$		$\varphi \cdot 10^3\ l \cdot g^{-1}$	$\varphi \cdot 10^3\ l \cdot g^{-1}$
25	3.95	9.74	25	3.95	9.75
50	0.95	2.22	50	4.83	8.98
75	0.50		75	5.26	9.22
125	0.48	0.69	100	5.49	8.95
250		0.26	125	4.97	8.04
350		0.62	150	4.64	6.73
500	0.47	0.61	200	4.02	6.51
650		0.57	250	3.52	5.56
900		0.53	311	3.12	4.80
			444	2.23	3.43

the experimental error) between $[A^-] = 100$ and 900 mM. Thus no anionic complexes are formed in the resin phase but this does not necessarily imply that no anionic species are present in the solution (see Ref.[1d] p. 1451).

Both the europium and americium glycolate systems have maxima which appear very clearly, when the surface sorption (estimated from the acetate measurements) has been corrected for. The maximum value of φ is much lower for europium than for americium and appears for europium at a higher value of $[A^-]$. It is safe to conclude that anionic glycolate complexes are formed both by europium and americium. In the case of europium this was found already by the potentiometric measurements. The low values of the distribution coefficient for the glycolate system indicate that it is difficult for the anionic complexes to be formed in the resin phase, presumably because of a steric hindrance.

According to Fronæus [8] the values of φ_{max} for systems of equal type should give a qualitative measure of the strength of the anionic complexes. The higher φ_{max} value for the americium glycolate system and the fact that the maximum appears at a slightly lower $[A^-]$-value indicate that americium gives stronger complexes than europium, an already established fact, based on the ion exchange and potentiometric measurements described before. The thioglycolate systems could not be investigated by anion exchangers as the ligand was attacked by the resin.

DISCUSSION

The stability constants for the complexes investigated are collected in Table 11. It is evident that americium forms stronger complexes than europium for all the systems investigated here. This difference is most pronounced for the glycolates, where the stability constants β_j for the americium complexes are $\approx 80\ \%$ greater than those for the corresponding europium complexes. This fact can also be observed in an earlier investigation [3] where cation exchanger columns loaded with europium and americium have been eluted with glycolate

Table 11. The formation constants β_j for the acetate, glycolate and thioglycolate system of europium and americium.

Central ion →	Eu^{3+}				Am^{3+}			
Ligand ↓	β_1 M^{-1}	β_2 M^{-2}	β_3 M^{-3}	β_4 M^{-4}	β_1 M^{-1}	β_2 M^{-2}	β_3 M^{-3}	β_4 M^{-4}
Acetate	87.5 ± 1.0	$(1.54 \pm 0.05) \times 10^3$	$(6.1 \pm 0.3) \times 10^3$	no evidence of anionic complexes	98.5 ± 3.0	$(1.9 \pm 0.2) \times 10^3$	$(8 \pm 3) \times 10^3$	no evidence of anionic complexes
Glycolate	369 ± 3	$(4.1 \pm 0.3) \times 10^4$	$(8.1 \pm 0.7) \times 10^5$	$(2.3 \pm 0.5) \times 10^6$	657 ± 15	$(7.2 \pm 1.0) \times 10^4$	$(2 \pm 1) \times 10^6$	anionic complexes formed
Thioglycolate	35.2 ± 1.0	188 ± 10	0		35.5 ± 5	400 ± 100	0	

buffers and the position of the elution peaks for the two elements has been determined. From the position of the elution peaks the separation factor α_{Am}^{Eu} was determined where:

$$\alpha_{Am}^{Eu} = \frac{\varphi_{Eu}}{\varphi_{Am}} = \frac{^{Eu}l_0 \cdot (1 + {}^{Eu}l'_1 \cdot [A^-] + {}^{Eu}l'_2 \cdot [A^-]^2)}{^{Am}l_0 \cdot (1 + {}^{Am}l'_1 \cdot [A^-] + {}^{Am}l'_2 \cdot [A^-]^2)} \cdot \frac{X^{Am}}{X^{Eu}}$$

Neither the composition of the buffer solutions in Ref. [3] nor the values of l'_1 and l'_2 for the europium and americium complexes are known. This fact makes it impossible to make a quantitative comparison between the two methods. If the ratio between the activity factors for the europium and americium species does not vary with the ionic strength and if the distribution coefficients l'_1 and l'_2 are approximately the same for both the europium and americium glycolates, then the ratio X^{Am}/X^{Eu} can be computed with the use of the values of the separation factor $\alpha_{Am}^{Eu} = 0.69 \pm 0.16$ determined by Stewart [3]. $^{Eu}l_0$ was determined in a separate experiment and was equal to 1.26 $l \cdot g^{-1}$. Thus:

$$\frac{X^{Am}}{X^{Eu}} = (0.69 \pm 0.16) \times \frac{2.51}{1.26} = 1.38 \pm 0.32$$

This ratio is only valid for the constant but unknown value of $[A^-]$ in the buffer solution used by Stewart.

The main factors, affecting the relative stability of the europium and the americium complexes investigated here, are the ionic radius and the properties of the outer electron shells. If the radius factor is the more important one, then europium with its smaller ionic radius is expected to form stronger complexes than americium. This was not the case for the system in the present investigation (see Table 11). As to the properties of the outer electron shells, both elements have the same structure apart from a difference of one unit in the principal quantum number.

The 5f orbitals are more affected by the environment [9] than the 4f orbitals, which means that the former are more available for bond formation. Americium is thus expected to form stronger complexes than europium, if the properties of the outer electron shells are more important than the radius factor. This seems to be the case for the systems in this investigation.

The strongly electropositive lanthanide and actinide elements are according to Ahrland *et al.* [10] class A acceptors and are thus expected to have a greater affinity to oxygen than to sulphur. Glycolate forms stronger complexes than thioglycolate with both europium and americium (see Table 11). From the magnitude of the stability constants it is safe to conclude that the hydroxyl oxygen of the glycolate ion is coordinated to the central ion. A five membered chelate ring is thus formed by the using of this oxygen and the carboxylate group. It is not possible to decide whether the sulphur of the thioglycolate ion is coordinated or not, only that the affinity to sulphur is much smaller than that to oxygen for both europium and americium in accordance with the views given by Ahrland *et al.*

The fact that thioglycolate is even weaker bonded than acetate must be correlated [11] with the greater acidity of thioglycolic acid as compared to acetic acid.

In order to compare Sonessons data[1a-1c] (which were determined at an ionic strength $I = 2$ M) with those of the present investigation, it was necessary to estimate the influence of the ionic strength on the stability constants. The gadolinium systems were assumed to be representative of this variation for all rare earths. For the acetate system no appreciable differences between the stability constants at $I = 0.5$ M and $I = 2$ M were found. For the glycolate systems the β_1-values for $I = 0.5$ M should be decreased by 10 %, the β_2- and β_3-values by 20 % in order to be comparable with the corresponding values at $I = 2$ M. From a comparison with Sonesson's data it is evident that the stability constants of both the acetate and glycolate complexes of Eu^{3+} have values between the corresponding values of Sm^{3+} and Gd^{3+}.

It can be pointed out that the dithiodiglycolate complexes of tervalent americium must be rather weak. The concentration of the ligand is much higher than that of the central ion and the stability constants for the thioglycolate systems are still of the right order of magnitude (estimated from the stability constants of the Eu^{3+}-thioglycolate system). For europium the stability constants can not be influenced more than 1—2 % by the presence of dithiodiglycolate even if the complexes were very stable.

This investigation has been supported by a grant form *Statens Råd för Atomforskning*. The author is indebted to Professor Sture Fronæus and Dr. Sten Ahrland for many fruitful discussions.

REFERENCES

1 a. Sonesson, A. *Acta Chem. Scand.* **12** (1958) 165.
1 b. Sonesson, A. *Ibid.* **12** (1958) 1937.
1 c. Sonesson, A. *Ibid.* **13** (1959) 998.
1 d. Sonesson, A. *Ibid.* **13** (1959) 1437.
1 e. Sonesson, A. *Ibid.* **14** (1960) 1495.
2 a. Fronæus, S. *Acta Chem. Scand.* **5** (1951) 859.
2 b. Fronæus, S. *Svensk Kem. Tidskr.* **64** (1952) 317.
2 c. Fronæus, S. *Ibid.* **65** (1953) 19.
3. Stewart, D. C. *Proc. Intern. Conf. Peaceful Uses Atomic Energy*, Geneva 1955, Vol. 7, p. 321.
4. Holm, L. W., Choppin, G. R. and Moy, D. *J. Inorg. & Nuclear Chem.* **19** (1961) 251.
5. Grenthe, I. and Norén, B. *Acta Chem. Scand.* **14** (1960) 2216.
6. Klason, P. and Carlson, T. *Ber.* **39** (1906) 2216.
7. Ahrland, S., Grenthe, I. and Norén, B. *Acta Chem. Scand.* **14** (1960) 1059.
8. Fronæus, S. *Svensk Kem. Tidskr.* **65** (1953) 1.
9. Katz, J. J. and Seaborg, G. T. *The Chemistry of the Actinide Elements*, Methuen, London 1957, pp. 463—470.
10. Ahrland, S., Chatt, J. and Davies, M. R. *Quart Rev.* 265, vol. XII No. 3, 1958.
11. Lewis, J. and Wilkins, R. G. *Modern Coordination Chemistry*, Interscience New York 1960, pp. 51—57.

Received January 31, 1962.

ACTA CHEMICA SCANDINAVICA 16 (1962) 1713–1729

Über die Reaktionen des Lignins bei der Sulfatkochung

II *. Modellversuche zur Spaltung von Aryl-alkylätherbindungen durch Alkali **

JOSEF GIERER und ISA NORÉN

Schwedisches Holzforschungsinstitut, Holzchemische Abteilung, Stockholm, Schweden

The alkaline degradation of some model substances, representative of the main types of arylether structures assumed to be present in lignin, has been investigated.

β-Arylethers (type A) are hydrolysed on treatment with 2 N sodium hydroxide at 170° for 2 h provided that they contain a free hydroxyl group in the α- or γ-position of the side chain. This reaction proceeds *via* an epoxide and yields the corresponding phenol and 1,2-glycol. If, however, these ethers carry a free phenolic hydroxyl in the *para*-position to the side chain and an α-hydroxyl or ether group they are not hydrolysed but undergo other reactions, the mechanisms of which have been elucidated.

α-Arylethers (type B) are hydrolysed under similar conditions also in the absence of a neighbouring hydroxyl in the β-position provided that they carry a free hydroxyl in the *para*-position. This reaction probably proceeds *via* the methylenequinone.

Von den tiefgreifenden strukturellen Veränderungen, welche Lignin während einer Sulfatkochung erleidet, sind der Einbau von Schwefel und die Freilegung phenolischer Hydroxylgruppen besonders auffallend. Der erstgenannte Vorgang wurde bereits wiederholt mit Hilfe von Modellversuchen [2,3,1] und vor kurzem auch durch Spaltung von Thioligninen [1] näher studiert. Modellversuche über die Freilegung phenolischer Hydroxylgruppen unter den Bedingungen einer Sulfat- oder einer Alkalikochung und über die hierfür erforderlichen strukturellen Voraussetzungen stehen hingegen bisher noch aus. Die Aufsprengung von Arylätherbindungen, die zum Abbau des Lignins in alkalilösliche Bruchstücke führt, darf jedoch als der wichtigste Vorgang des alkalischen Holzaufschlusses überhaupt angesehen werden. In der vorliegenden Arbeit wird

* Teil I, siehe Ref.[1]

** Über die Ergebnisse dieser Arbeit wurde (von J.G.) am Ligninsymposium in Helsinki, 4.–7. Juni 1961, siehe *Paperi ja Puu* 11 (1961) 654 und am Ligninsymposium in Chicago, 14.–16. August 1961 bereits kurz berichtet.

die Spaltbarkeit der im Lignin derzeit angenommenen Typen von Arylalkyläther-bindungen an geeigneten Modellsubstanzen näher untersucht.

Durch analytische Studien an schonend isolierten Ligninpräparaten [4,5] sowie durch Isolierung von Zwischenprodukten der enzymatischen *in vitro*-Synthese von Ligninen [6-8] wurde wahrscheinlich gemacht, dass folgende zwei Bindungsprinzipien zwischen den Phenylpropanmonomeren mengenmässig überwiegen:

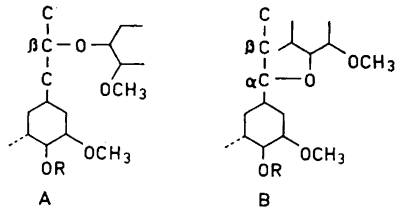

R = H oder Seitenkette der nächsten Einheit

Wie ersichtlich, enthalten beide Verknüpfungsstrukturen (A und B) Arylalkylätherbindungen. Im Zusammenhang mit dem Studium des alkalischen Ligninabbaues kommt dem Verhalten der Strukturelemente des Typus A (β-Aryläthertypus) besondere Bedeutung zu, da ihre Spaltung zu einer vollständigen Trennung zweier benachbarter Phenylpropaneinheiten und damit zum Abbau des Lignins in kleinere Bruchstücke führt. Bei der Spaltung der Strukturelemente des Typus B (Phenylcumarantypus), hingegen, bleibt die βC — Arylbindung zwischen den beiden benachbarten Einheiten erhalten. Dieser Vorgang trägt daher nicht zum Abbau, wohl aber zur Zunahme der Alkalilöslichkeit, bei.

Die β-Aryläther bindung (Typus A)

a) *in nicht-phenolischen Phenylpropaneinheiten* (R = Seitenkette der nächsten Einheit). Leopold [9] stellte im Zusammenhang mit einer Untersuchung über die Oxydation von Lignin durch Nitrobenzol-Alkali fest, dass β-Arylätherbindungen unter den Bedingungen einer Alkalikochung in gewissem Ausmass spaltbar sind. Die α-Ketoverbindungen I und II lieferten 75 % bzw. 87 % der berechneten Menge an phenolischen Substanzen, die entsprechenden Benzylalkohole III und IV, hingegen, nur 18 % bzw. 23 %. Die niedrigen Ausbeuten an phenolischer Substanz (Vinylguajakol) bei der Alkalibehandlung der Substanzen III und IV wurden durch die Annahme sekundärer Kondensations- und Polymerisationsreaktionen erklärt [9].

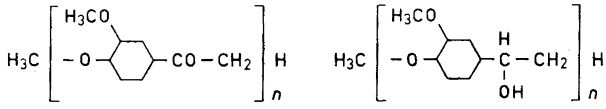

I $n = 2$ III $n = 2$

II $n = 3$ IV $n = 3$

In der vorliegenden Untersuchung wurden vor allem die β-Guajacyläther des α-(3,4-Dimethoxyphenyl)-glycerins (V) und des α-(3-Methoxy-4-hydroxyphenyl)-glycerins (VI) als Modellsubstanzen für die β-Arylätherbindungen in nicht-phenolischen, bzw. in phenolischen Einheiten des Lignins gewählt.

Diese Substanzen enthalten keine zur Arylätherbindung *para*-ständige "ligninähnliche" Seitenkette. In vorläufigen Versuchen konnte jedoch gezeigt werden, dass z. B. *para*-ständige Methylolgruppen (vgl. das Verhalten der Substanzen III und IV [9]) keinen wesentlichen Einfluss auf die im Folgenden beschriebene Arylätherspaltung ausüben.

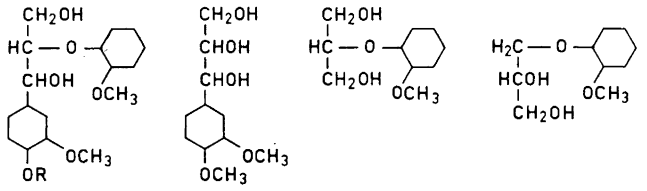

V R = CH_3
VI R = H

VII VIII IX

Die Synthese [10,11] und das Verhalten der Substanzen V und VI unter den Bedingungen anderer wichtiger Ligninreaktionen [10,4] wurden von Adler und Mitarbeitern beschrieben. Über die Einwirkung von Alkali auf diese Substanzen liegen bisher nur kurze Angaben vor. So wurde aus der Substanz V bei Behandlung mit Alkali ein alkalilösliches, amorphes Produkt erhalten, das positive Phenolreaktionen gab [12] und vor kurzem [13] wurden beide Substanzen auf ihre Fähigkeit geprüft, bei der Alkalibehandlung wasserdampfflüchtige Aldehyde und Veratrumaldehyd bzw. Vanillin zu liefern. Näheres über die Spaltbarkeit der β-Arylätherbindung in diesen Substanzen ist bisher nicht bekannt.

Die Alkalilabilität der β-Arylätherbindung in den Substanzen III und IV [9] konnten wir erwartungsgemäss auch bei der Substanz V feststellen. Durch 2-stündiges Erhitzen in 2 N Natronlauge auf 170°C wird der β-ständige Guajacylrest weitgehend abgespaltet (siehe Tab. 1). Nach 15 Min. Reaktionszeit kann bereits die Hälfte der theoretisch zu erwartenden Menge Guajakol isoliert werden. Bei Reaktionstemperaturen um 100°C oder bei Verwendung von 0.2 N Natronlauge tritt hingegen keine nennenswerte Spaltung ein. Eine systematische Untersuchung des Einflusses der verschiedenen Reaktionsbedingungen auf den Umfang der Spaltung wurde bisher nicht durchgeführt.

Die Abspaltung von Guajakol aus der Substanz V ist als alkalische Hydrolyse der β-Arylätherbindung zu betrachten, da im Spaltungsrest die freigelegte Glycerinseitenkette durch Perjodat-Oxydation eindeutig nachgewiesen werden kann. Hierbei werden pro Mol Dimethoxyphenyl-glycerin 2 Mole Oxydationsmittel verbraucht und 1 Mol Ameisensäure gebildet. Beim Studium der sterischen Faktoren der alkalischen Arylätherspaltung, worüber in einer kommenden Mitteilung [14] berichtet werden soll, wurde aus der amorphen Verbindung V das zu erwartende α-(3,4-Dimethoxyphenyl)-glycerin (VII) in kristallisierter Form (Schmp. 109.5—110°) erhalten. Unterwirft man dieses einer Kochung unter den oben genannten Bedingungen, bleibt es vollkommen unverändert und kann praktisch quantitativ zurückgewonnen werden [14].

Vor kurzem wurde gefunden, dass unter den Bedingungen einer Alkalikochung auch der einfache Glycerin-β-guajacyläther VIII, sowie die isomere α-Verbindung IX, glatt gespaltet werden [15]. Die Spaltbarkeit der β-Arylätherbindung in der Substanz V wird daher nicht — oder jedenfalls nicht ausschliesslich — durch den 3,4-Dimethoxyphenylrest bedingt. Vielmehr sind hierfür, wie bei den beiden Glycerinmonoguajacyläthern VIII und IX, die der Arylätherbindung benachbarten Hydroxylgruppen verantwortlich zu machen. Verätherung der beiden Hydroxylgruppen hat nämlich eine weitgehende Blockierung der Spaltungsreaktion zur Folge (siehe Substanz XI in Tab. 1). Selektive Verätherung der benzylalkoholischen Hydroxylgruppe in V, hingegen, setzt die Spaltbarkeit lediglich auf ungefähr die Hälfte herab (siehe Substanz X in Tab. 1).

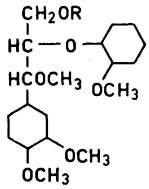

X R=H
XI R=CH$_3$

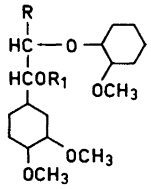

XII R=R$_1$=H
XIII R=CH$_3$, R$_1$=H
XIV R=H, R$_1$=CH$_3$

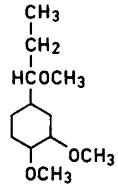

XV

Bei Austausch der endständigen Methylolgruppe in V gegen eine Methylgruppe (Substanz XIII) wird die Spaltbarkeit der β-Arylätherbindung nicht wesentlich beeinflusst, bei Austausch gegen Wasserstoff (Substanz XII), hingegen, wird sie stark herabgesetzt (siehe Tab. 1). Substanz XIV, die wie Substanz XI keine freie, der β-Arylätherbindung benachbarte Hydroxylgruppe enthält, kann nach der Kochung unverändert (kristallisiert) in guter Ausbeute zurückgewonnen werden. Die geringen Spaltungen der Substanzen XI und XIV (siehe Tab. 1) dürften auf eine geringe Alkalilabilität der α-ständigen Methylätherbindung zurückzuführen sein, was auch durch das Verhalten der Substanz XV bei der Alkalikochung angedeutet wird (siehe experimenteller Teil).

Diese Ergebnisse zeigen, dass die alkalische Spaltung der Arylätherbindung in Substanz V, wie in den (nicht substituierten) Glycerin-monoguajacyläthern VIII und IX, unter Mitwirkung der benachbarten Hydroxylgruppe(n) verläuft. Wie bereits mitgeteilt [15], lässt sich die Rolle dieser Gruppen am besten durch die Annahme der Ausbildung intermediärer 1,2-Epoxyde erklären.

Die Richtigkeit dieser Annahme wurde experimentell auf folgende Weise gestützt: Bei Ausführung der Spaltungsreaktionen mit einer Mischung aus Piperidin und Natronlauge können die Epoxydzwischenstufen durch Reaktion mit der Stickstoffbase "aufgefangen" und als Piperidinoverbindungen (α-Piperidino-alkohole) isoliert werden. Der Glycerin-β-guajacyläther (VIII), der bei der Spaltung nur ein 1,2-Epoxyd geben kann, das sich in alkalischem Milieu am primären Kohlenstoffatom öffnet [16], liefert das erwartete 1-Piperidino-propandiol-2,3 (XVI) [15]. Analog hierzu wurde nun aus dem β-Guajacyl-

Tabelle 1. Behandlung der Modellsubstanzen mit 2 N Natronlauge bei 170° (2 Stunden).

Substanz (1)	abgespaltetes, isoliertes und gereinigtes Guajakol % d. Th. (2)	Spaltungsrest, bzw. Reaktionsprodukt, bzw. Ausgangsmaterial (% d. Th.) (3)
α-(3,4-Dimethoxyphenyl)-glycerin-β-guajacyläther (V)	73.3	α-(3,4-Dimethoxyphenyl)-glycerin (VII) (65.1)
α-(3,4-Dimethoxyphenyl)-glycerin-α-methyläther-β-guajacyläther (X)	43.0	Ausgangsmaterial (46.5)
α-(3,4-Dimethoxyphenyl)-glycerin-α,γ-dimethyläther-β-guajacyl-äther (XI)	8.3	Ausgangsmaterial (72.8)
α-(3,4-Dimethoxyphenyl)-äthylen-glykol-β-guajacyläther (XII)	20.2	α-(3,4-Dimethoxyphenyl)-äthylenglykol (17.1)
α-(3,4-Dimethoxyphenyl)-äthylen-glykol-α-methyläther-β-guajacyl-äther (XIV)	10.0	Ausgangsmaterial (89.1)
Methylisoeugenolglykol-β-guajacyl-äther (XIII)	77.5	Methylisoeugenolglykol (65.0)
Methylisoeugenolglykol-α-guajacyl-äther (XXXI)	88.1	Methylisoeugenolglykol (71.2)
Dihydro-dehydro-diisoeugenol (XXVII)	—	Reaktionsprodukt, isoliert als 1-(3-Methoxy-4-acetoxy-phenyl)-2-(2-acetoxy-3-methoxy-5-n-propyl-phenyl)-propen-(1) (XXIX) (67.5)
Dihydro-dehydro-diisoeugenol-methyläther (XXVIII)	—	Ausgangsmaterial (97.8)
Äthyl-veratryl-carbinol-methyl äther (XV)	—	Äthyl-veratryl-carbinol best. durch Acetylierung (12.0)
Pinoresinol (XXXII)	—	Gemisch aus 7 phenol. Substanzen, das kein Ausg. Mat. enthält
Pinoresinol-dimethyläther (XXXIII)	—	Ausgangsmaterial (97.2)

Tabelle 1 Fortsetzung.

Behandlung der Modellsubstanzen mit Piperidin — 2 N Natronlauge (9:1) bei 170° (17 Stunden).

(1)	(2)	(3)
α-(3,4-Dimethoxyphenyl)-glycerin-β-guajacyläther (V)	35.1	Gemisch aus Monopiperidinoverbindungen (XVIII) (38.5)
α-(3,4-Dimethoxyphenyl)-äthylenglykol-β-guajacyläther (XII)	20.5	1-(3,4-Dimethoxyphenyl)-1-hydroxy-2-piperidino-äthan (XVII) (21.7)

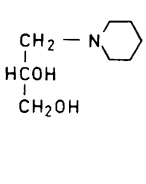

XVI

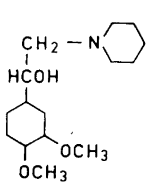

XVII

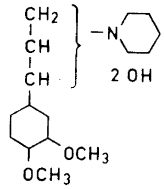

XVIII

äther des α-(3,4-Dimethoxyphenyl)-äthylenglykols (XII) die entsprechende β-Piperidinoverbindung (XVII) in kristallisierter Form erhalten und durch Schmelzpunkt, sowie Misch-Schmelzpunkt mit authentischem 1-(3,4-Dimethoxyphenyl)-1-hydroxy-2-piperidinoäthan (XVII), identifiziert. (Das letztgenannte liess sich durch Umsetzung von ω-Bromacetoveratron mit Piperidin und Reduktion des Umsetzungsproduktes mit Natriumborhydrid gewinnen).

Bei der Spaltung des β-Guajacyläthers des α-(3,4-Dimethoxyphenyl)-glycerins (V), hingegen, kann Epoxydbildung sowohl zwischen dem β- und γ-Kohlenstoffatom, als auch zwischen dem α- und β-Kohlenstoffatom eintreten. Im erstgenannten Fall ist mit der Öffnung des Epoxydringes am primären Kohlenstoffatom (vgl. Spaltung der Substanzen VIII und XII) und der Bildung der entsprechenden γ-Piperidinoverbindung zu rechnen, die in zwei stereoisomeren Formen vorliegen kann. Im zweiten Fall ist die Bildung zweier stereoisomerer Epoxyde (*cis*- und *trans*-) möglich, je nachdem, ob von der *threo*- oder von der *erythro*-Form der Substanz V ausgegangen wird. Die *cis*-Form des α,β-Epoxyds sollte in Analogie zum *cis*-1-Phenyl-2-methyl-äthylenoxyd-1,2 [17] unter Ringöffnung am β-Kohlenstoffatom vorwiegend die *threo*-Form der β-Piperidinoverbindung, die entsprechende *trans*-Form, hingegen, unter Ringöffnung am α-Kohlenstoffatom vorwiegend die *erythro*-Form der α-Piperidinoverbindung liefern. Bei der Spaltung der Substanz V mit Piperidin-Alkali ist daher ein Gemisch struktur- und stereoisomerer Monopiperidinoverbindungen zu erwarten, das durch die Formel XVIII versinnbildlicht werden soll. Tatsächlich wurde hierbei ein Öl erhalten, dessen Analysenwerte gut auf die Formel XVIII stimmen (siehe exp. Teil) und das sich im Dünnschichtschromatogramm als

ein aus vier Hauptkomponenten bestehendes Gemisch erwies. Eine Auftrennung dieses Gemisches wurde nicht durchgeführt.

Bei Anwendung von Piperidin-Natronlauge als spaltendes Agens war der Spaltungsgrad gering (siehe Tab. 1). Er liess sich weder durch Variation des Verhältnisses Piperidin:Natronlauge, noch durch Verlängerung der Reaktionszeit wesentlich erhöhen. Die Ausbeute an Piperidinoverbindung(en) entsprach jedoch ungefähr der Menge des jeweils abgespalteten Guajakols (siehe Tab. 1). Dies zeigt, dass die Spaltungsreaktion vorwiegend — wenn nicht ausschliesslich — über die Epoxyd-Zwischenstufe(n) verläuft. Die Möglichkeit einer nachträglichen Bildung der Piperidinoverbindung(en) aus zunächst entstehenden 1,2-Glykolen, bzw. aus Glycerinen, konnte experimentell ausgeschlossen werden. Nach der Behandlung von Glycerin [15] oder von α-(3,4-Dimethoxyphenyl)-glycerin (VII) mit Piperidin-Natronlauge liessen sich nämlich nicht einmal Spuren von Piperidinoverbindungen chromatographisch nachweisen. Wie bei den entsprechenden Kochungen mit Natronlauge allein, kann in beiden Fällen das Ausgangsmaterial unverändert zurückgewonnen werden.

Die den α-Hydroxy-β-aryläthern V und XII entsprechenden α-Keto-β-aryläther (Phenacyl-aryläther, CO anstatt HCOH) erwiesen sich ebenfalls als weitgehend spaltbar (vgl. Substanzen I und II [9]). Nach Entfernung des Guajakols wurden hochmolekulare, ätherunlösliche, acetonlösliche Produkte erhalten, die nicht näher untersucht wurden. Der Reaktionsverlauf (über polymerisierbare Oxirene oder kondensierbare Ketole?) ist ungeklärt.

b) *in phenolischen Phenylpropaneinheiten* (Typus A, R = H). Vollkommen verschieden von den bisher behandelten β-Arylätherbindungen verhalten sich solche, die in Einheiten mit freier, zur Seitenkette *para*-ständiger phenolischer Hydroxylgruppe liegen. So liefert der der Substanz V entsprechende phenolische β-Aryläther VI bei der Behandlung mit Alkali unter den eingangs erwähnten Bedingungen kein Guajakol. Eine papierchromatographische Untersuchung (siehe experimenteller Teil) zeigt, dass das Reaktionsgemisch nur eine phenolische Substanz enthält, die mit dem Ausgangsmaterial nicht identisch ist. Sie gibt beim Besprühen des Chromatogramms mit einer alkoholischen Lösung von Dibrom-chinonmonochlorimid und mit 0.05 N Natronlauge eine intensive, jedoch instabile Violettfärbung, was zunächst eine (substituierte) Coniferylalkoholstruktur (XIX) andeutete [18,1].

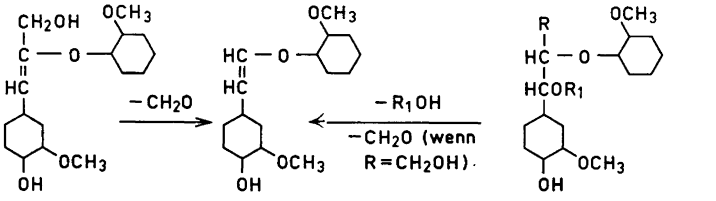

XIX XX

VI R=CH2OH, R1=H
XXI R=R1=H
XXII R=H, R1=CH3
XXIII R=CH2OH, R1=CH3

Authentischer α-Guajakoxy-coniferylalkohol (XIX) gibt zwar mit dem Kupplungsreagenz genau die gleiche, instabile Violettfärbung wie das Produkt der Alkalibehandlung der Substanz VI, besitzt jedoch einen viel kleineren R_F-Wert. Hingegen wird bei der Alkalikochung der Substanz XIX eine phenolische Verbindung erhalten, die sich papierchromatographisch vollkommen gleich wie das untersuchte Produkt aus der Substanz VI verhält. Der α-Guajakoxy-coniferylalkohol (XIX) schien daher eine mögliche Zwischenstufe, nicht aber das Endprodukt der Alkalibehandlung der Substanz VI zu sein und es lag nahe, anzunehmen, dass sich aus ihm bei der Alkalieinwirkung unter Abspaltung von Formaldehyd das 3-Methoxy-4-hydroxy-ω-guajakoxy-styrol (XX) bildet. Die gleiche Substanz sollte dann auch bei der Alkalibehandlung von VI als Endprodukt entstehen. Die Richtigkeit dieser Annahme lässt sich durch Alkalikochung des β-Guajacyläthers des α-(3-Methoxy-4-hydroxyphenyl)-äthylenglykols (XXI) zeigen, in dem die endständige Methylolgruppe der Substanz VI *a priori* fehlt. Es bildet sich nämlich auch in diesem Falle, wie bei der Einwirkung von Alkali auf die Substanzen VI und XIX, das eben erwähnte Styrolderivat (XX). Die Identität der Produkte der Einwirkung von Alkali auf die Substanzen VI, XIX und XXI wurde, wie bereits erwähnt, zunächst durch Papierchromatographie gezeigt, dann aber auch durch Benzylierung und Bestimmung der Schmelzpunkte und Misch-Schmelzpunkte der erhaltenen Benzyläther bewiesen.

Das 3-Methoxy-4-hydroxy-ω-guajakoxy-styrol (XX) ist (als Enoläther) nur in alkalischem Milieu beständig und fällt nach den Kochungen zu einem geringen Teil als Natrium-phenolat aus. In neutraler oder saurer Lösung spaltet es Guajakol ab und bildet, vermutlich durch Polymerisation, eine Reihe anderer phenolischer Substanzen, sowie eine Carbonylverbindung (Papierchromatographie), die nicht näher untersucht wurden.

Unter Berücksichtigung der oben erwähnten experimentellen Befunde schlagen wir für den Verlauf der Reaktion "phenolischer" β-Aryläther vom Typus VI (bzw. XXI—XXIII) mit Alkali folgende Formulierung vor:

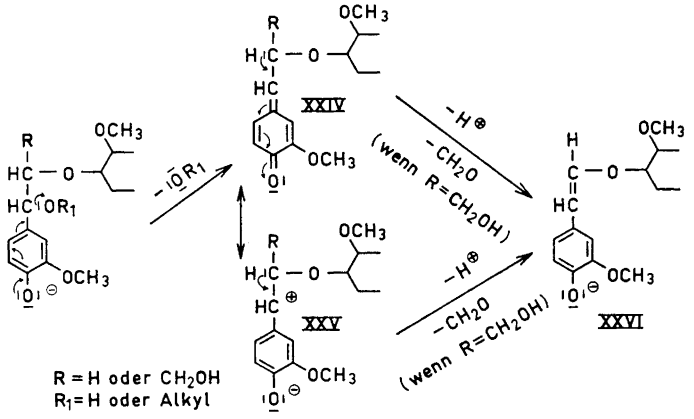

Durch den elektromeren Effekt des Phenolatjons wird unter Übergang in die Chinonmethidstruktur (XXIV) die Abspaltung des in Benzylstellung

befindlichen Substituenten (Hydroxyl oder Alkoxyl) ermöglicht. Das Chinonmethid XXIV, bzw. das hierzu mesomere Zwitterjon XXV, stabilisieren sich durch Protonenabspaltung und (wenn R=CH_2OH) Eliminierung der endständigen Methylolgruppe als Formaldehyd zum kernkonjugierten System XXVI.

Diese Formulierung wird der Tatsache gerecht, dass eine freie phenolische Hydroxylgruppe in *para*-Stellung zur β-Aryläther-Seitenkette Voraussetzung für die Abspaltung der Elemente des Wassers (R_1 = H), bzw. des Alkohols (R_1 = Alkyl, siehe unten), d.h. für die Ausbildung der kernkonjugierten Doppelbindung (in XXVI) ist. Verätherung der phenolischen Hydroxylgruppe (VI → V, XXI → XII) blockiert diesen Reaktionsweg und ermöglicht dadurch die oben beschriebene alkalische Spaltung der β-Arylätherbindung unter Mitwirkung benachbarter alkoholischer Hydroxylgruppen und Ausbildung intermediärer Epoxyde.

Verätherung der α-ständigen (benzylalkoholischen) Hydroxylgruppe, (z. B. in VI oder XXI), hat dagegen, wie oben bereits erwähnt, keinen wesentlichen Einfluss auf den Reaktionsverlauf: Die aus den Substanzen VI und XXI hergestellten α-Methyläther XXIII bzw. XXII geben bei der Behandlung mit Alkali den gleichen Enoläther (XX) wie die Ausgangssubstanzen, was sich ebenfalls durch Benzylierung und Bestimmung der Schmelzpunkte und Misch-Schmelzpunkte der Benzylierungsprodukte zeigen liess.

Die α-Arylätherbindung

Das Verhalten von α-Arylätherbindungen (Benzyl-arylätherbindungen) bei der Alkalikochung wurde vor allem an den beiden Phenylcumaranen (Typus B) Dihydro-dehydro-diisoeugenol (XXVII) und dessen Methyläther (XXVIII) näher untersucht.

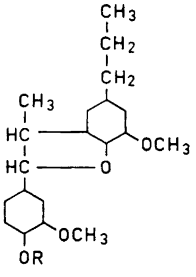

XXVII R = H
XXVIII R = CH_3

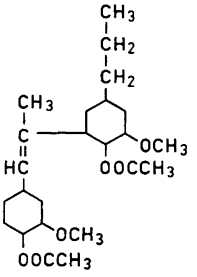

XXIX

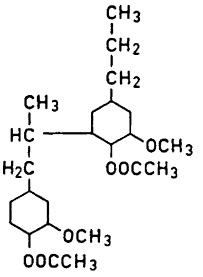

XXX

Die phenolische Verbindung (XXVII) wird unter den gewählten Bedingungen (siehe oben) vollständig gespaltet. Aus dem Reaktionsansatz lässt sich in guter Ausbeute ein Öl isolieren, das bei der Acetylierung mit Essigsäureanhydrid-Pyridin zwei Acetylgruppen aufnimmt. Das Diacetat ist im Hochvakuum gut destillierbar und kristallisiert beim Tiefkühlen seiner konzentrierten Lösung in Methanol aus. Es verhält sich somit wie das Stilbenderi-

vat XXIX, welches Freudenberg und Mitarbeiter vor kurzem [19] aus dem Acetat des Dihydro-dehydrodiisoeugenols durch acetylierende Aufspaltung des Cumaranringes erhielten. Auch die Analysenwerte stimmen hiermit gut überein. Bei der katalytischen Hydrierung (Pd-Tierkohle) nimmt das Diacetat XXIX (Schmp. 111—112°) pro Mol Substanz ein Mol Wasserstoff auf und geht in die gesättigte Verbindung XXX (Schmp. 80.5—81.5°) über.

Die Bildung phenolischer Stilbenstrukturen wurde vor kurzem [20] auch bei der Sulfatkochung von Dihydro-dehydro-diconiferylalkohol (XXVII, jedoch $-CH_2OH$ anstatt $-CH_3$), sowie von Björkman-Lignin beobachtet und durch Bestimmung der Ultraviolett-Spektren belegt. Die Struktur der aus dem Dihydro-dehydro-diconiferylalkohol gebildeten Verbindungen wurde jedoch bisher nicht vollständig geklärt [20]. Es kann erwartet werden, dass die an den Cumaranring gebundene Methylolgruppe im Dihydro-dehydro-diconiferylalkohol für die alkalische Aufspaltung der cyklischen α-Arylätherbindung keine entscheidende Bedeutung hat (vgl. Spaltung von XXVII), und dass sie nach Ausbildung der kernkonjugierten Doppelbindung als Formaldehyd abgespaltet wird (vgl. das Verhalten der Substanzen VI, XIX und XXIII).

Zum Unterschied von Dihydro-dehydro-diisoeugenol (XXVII) erweist sich sein Methyläther (XXVIII) bei der Behandlung mit Alkali unter den eingangs erwähnten Bedingungen als vollkommen stabil und kann schmelzpunktsrein zurückgewonnen werden.

Die bisher behandelten Benzyl-arylätherbindungen (in XXVII und XXVIII) sind Teil eines heterocyklischen Ringsystemes (Typ B, siehe S. 1714). Vor kurzem wurden von Freudenberg und Mitarbeitern [21] auch nicht-cyklische, d.h. nicht einem Phenylcumaran-Ringsystem zugehörige Benzyl-arylätherbindungen als weiteres Bindungsprinzip zwischen den Phenylpropanmonomeren des Lignins in Betracht gezogen. Es kann angenommen werden, dass sich derartige "offene" Benzyl-arylätherstrukturen gegenüber Alkali ähnlich wie die "ringgeschlossenen" (XXVII und XXVIII) verhalten, d. h., dass solche mit einer freien phenolischen Hydroxylgruppe in *para*-Stellung zur Seitenkette unter den gewählten Bedingungen spaltbar und solche mit einer verätherten phenolischen Hydroxylgruppe weitgehend alkalistabil sind.

Die Stabilität von *para*-Alkoxy-benzyl-aryläthern gegenüber Alkali wird jedoch erwartungsgemäss aufgehoben, wenn eine zur Arylätherbindung benachbarte (β-ständige) Hydroxylgruppe vorhanden, m. a. W., wenn, wie bei den β-Aryläthern mit α- und/oder γ-ständigem Hydroxyl (siehe Substanzen V, X, XII und XIII), die Möglichkeit zur Ausbildung intermediärer Epoxyde gegeben ist. So wird z. B. der α-Guajacyläther des Methylisoeugenolglykols

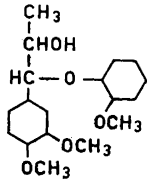

XXXI

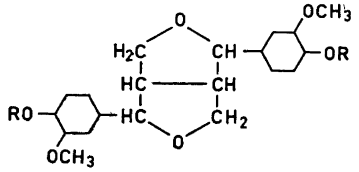

XXXII R = H
XXXIII R = CH_3

(XXXI, Schmp. 105—106°), wie der isomere β-Guajacyläther (XIII), unter den angegebenen Bedingungen weitgehend gespaltet und liefert wie dieser neben Guajakol Methylisoeugenolglykol (Schmp. 124—125°).

Das Verhalten von Benzyl-alkylätherbindungen gegenüber Alkali soll hier nur kurz behandelt werden. Bekanntlich nimmt man im Lignin auch solche Bindungen als wichtige Verknüpfungsart benachbarter Phenylpropanmonomerer (z. B. in Strukturelementen vom Pinoresinoltypus [22]) an. Die bei den *para*-Hydroxy-benzyl-methyläthern XXII und XXIII beobachtete Spaltbarkeit (siehe S. 1719) wurde auch beim zweifachen, cyklischen *para*-Hydroxybenzyl-alkyläther Pinoresinol (XXXII) festgestellt. Er wird unter den angegebenen Bedingungen vollständig gespaltet. Das Reaktionsgemisch enthält mehrere phenolische Substanzen, die bisher nicht näher untersucht wurden.

Der Dimethyläther des Pinoresinols (XXXIII), hingegen, erweist sich als vollkommen stabil und kann nach der Alkalibehandlung in unveränderter Form zurückgewonnen werden.

Benzyl-alkylätherbindungen und Benzyl-arylätherbindungen verhalten sich demnach gegenüber Alkali analog: In Einheiten mit freier, *para*-ständiger phenolischer Hydroxylgruppe (XXII, XXIII, XXXII bzw. XXVII) sind beide Äthertypen spaltbar, in Einheiten mit verätherter, *para*-ständiger phenolischer Hydroxylgruppe (XI, XIV, XV, XXXIII bzw. XXVIII), hingegen, sind sie weitgehend stabil.

Die alkalische Spaltung von Benzyl-arylätherbindungen (z. B. in *para*-Hydroxy-phenylcumaranen, XXVII) und von Benzyl-alkylätherbindungen (z. B. in den *para*-Hydroxy-benzyl-alkyläthern XXII, XXIII und XXXII) scheint daher analog wie die Reaktion "phenolischer" β-Aryläther mit Alkali (siehe S. 1720) über entsprechende Chinonmethid-Strukturen zu verlaufen:

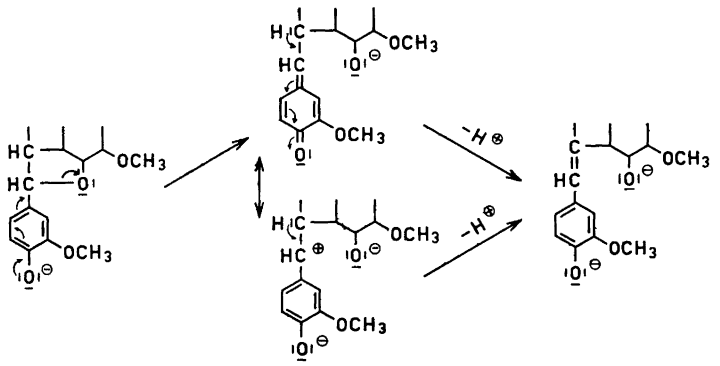

Die Ergebnisse der vorliegenden Arbeit können auf folgende Weise zusammengefasst werden:

Das Verhalten von Aryl-alkylätherbindungen in Strukturelementen, wie sie derzeit in Ligninen angenommen werden, gegenüber Alkali ist abhängig

(a) von der Lage dieser Bindungen in den Seitenketten (vor allem ob sie in α- oder in β-Stellung angreifen),

(b) von der übrigen Struktur der Seitenketten (vor allem ob eine benachbarte Hydroxylgruppe vorhanden ist oder nicht) und
(c) von der An- bzw. Abwesenheit freier phenolischer Hydroxylgruppen in *para*-Stellung zu den Seitenketten.

α-Arylätherbindungen mit freier, *para*-ständiger phenolischer Hydroxylgruppe werden durch 1,2-Eliminierung (siehe S. 1723) gespaltet, solche mit verätherter phenolischer Hydroxylgruppe in *para*-Stellung zur Seitenkette erweisen sich hingegen im allgemeinen als stabil (Ausnahme siehe nächster Absatz).

α- und β-Arylätherbindungen mit verätherter, *para*-ständiger phenolischer Hydroxylgruppe, jedoch freier, benachbarter alkoholischer Hydroxylgruppe, sind über die Zwischenstufe der entsprechenden Epoxyde spaltbar (siehe S. 1722 bzw. 1715).

β-Arylätherbindungen mit freier phenolischer Hydroxylgruppe in *para*-Stellung und mit freier oder verätherter Hydroxylgruppe in α-Stellung, hingegen, sind unter den gewählten Bedingungen alkaliresistent (siehe S. 1719).

EXPERIMENTELLES

Darstellung der Modellsubstanzen

α-(3,4-Dimethoxyphenyl)-äthylenglykol-β-guajacyläther (1-(3,4-Dimethoxyphenyl)-1-hydroxy-2-guajakoxy-äthan, XII). Die Darstellung erfolgte analog zu der der Substanz V [10], durch Reduktion von ω-Guajakoxy-acetoveratron [10] mit Natriumborhydrid. Aus 10.0 g Ausgangsmaterial wurden 8.3 g (= 83 % d. Th.) des obigen Benzylalkohols (XII) erhalten. Er schmolz nach Umkristallisieren aus Aceton bei 133—134° ($C_{17}H_{20}O_5$ (304.2): Ber. OCH_3 30.58. Gef. OCH_3 30.81).

Methylisoeugenolglykol-β-guajacyläther (1-(3,4-Dimethoxyphenyl)-1-hydroxy-2-guajakoxy-propan, XIII) wurde erstmals von E. Adler und S. Delin (siehe Ref.[23]) dargestellt, die Darstellung wurde jedoch bisher nicht näher beschrieben. Die Substanz liess sich analog zu den Substanzen V[10] und XII (siehe oben) durch Reduktion von α-Guajakoxy-propioveratron [23] mit Natriumborhydrid gewinnen. Das farblose Öl kristallisierte zum Teil aus Äthanol-Wasser. Der kristallisierte Anteil schmolz auch nach mehrmaligem Umkristallisieren aus Äthanol-Wasser unscharf zwischen 60 und 65°. ($C_{18}H_{22}O_5$ (318.2): Ber. OCH_3 29.23. Gef. OCH_3 29.30).

α-(3-Methoxy-4-hydroxyphenyl)-äthylenglykol-β-guajacyläther (1-(3-Methoxy-4-hydroxyphenyl)-1-hydroxy-2-guajakoxy-äthan, XXI) wurde durch katalytische Reduktion (Pd-Tierkohle, Lösungsmittel: abs. Äthanol) von ω-Guajakoxy-acetoguajakon-benzyläther [24] erhalten. 3.0 g Ausgangsmaterial ergaben 2.1 g (= 70 % d. Th.) des obigen *para*-Hydroxybenzylalkohols (XXI), der nach Umkristallisieren aus wenig Äthanol bei 129—130° schmolz. ($C_{16}H_{18}O_5$ (290.2): Ber. C 66.22, H 6.20, O 27.57, OCH_3 21.37. Gef. C 66.08, H 5.92, O 27.65, OCH_3 21.45).

Darstellung der Benzyl-methyläther X, XIV, XV, XXII und XXIII. Die oben genannten *para*-Hydroxy- bzw. *para*-Methoxy-benzyl-methyläther wurden durch Einwirkung 0.5 %-iger methanolischer Salzsäure auf die entsprechenden Benzylalkohole dargestellt. Die Methylierung der Substanzen VI [11,24] und XXI (siehe oben) erfolgte bei Zimmertemperatur vgl. Ref.[25], die von V, XII (siehe oben) und von 3,4-Dimethoxyphenyl-äthylcarbinol unter Rückflusskochung. Die Reaktionen wurden durch Dünnschichtschromatographie (siehe unten) laufend verfolgt. In den meisten Fällen liess sich bereits vor Verschwinden der letzten Reste des Ausgangsmaterials der Beginn der Bildung unerwünschter Nebenprodukte nachweisen. Die Methylierungen wurden dann abgebrochen, weshalb die Methoxylwerte der öligen Reaktionsprodukte fast durchwegs etwas zu tief liegen (siehe unten). Der Chlorwasserstoff wurde durch Jonenaustausch (IR-4B) aus den methanolischen Lösungen entfernt und die Lösungen hierauf im Vakuum zur Trockne eingeengt.

α-(3,4-Dimethoxyphenyl)-äthylenglykol-α-methyläther-β-guajacyläther (1-(3,4-Dimethoxyphenyl)-1-methoxy-2-guajakoxy-äthan, XIV). 2.0 g XII (Schmp. 133–134°, siehe oben) lieferten 1.4 g (= 67 % d. Th.) XIV in Form von Kristallen, die nach Umkristallisieren aus Hexan bei 86–87° schmolzen. ($C_{18}H_{22}O_5$ (318.2): Ber. OCH_3 38.99. Gef. OCH_3 38.75).

α-(3,4-Dimethoxyphenyl)-glycerin-α-methyläther-β-guajacyläther (1-(3,4-Dimethoxyphenyl)-1-methoxy-2-guajakoxy-3-hydroxy-propan, X). Aus 1.1 g V[10] wurden 1.1 g (= 97 % d. Th.) X als farbloses Öl erhalten. ($C_{19}H_{24}O_6$ (348.2): Ber. OCH_3 35.62. Gef. OCH_3 35.33).

α-(3-Methoxy-4-hydroxyphenyl)-äthylenglykol-α-methyläther-β-guajacyläther (1-(3-Methoxy-4-hydroxyphenyl)-1-methoxy-2-guajakoxy-äthan, XXII). 2.0 g XXI gaben 1.8 g (= 85.5 % d. Th.) XXII als gelbliches Öl. ($C_{17}H_{20}O_5$ (304.2): Ber. OCH_3 30.58. Gef. OCH_3 29.63).

α-(3-Methoxy-4-hydroxyphenyl)-glycerin-α-methyläther-β-guajacyläther (1-(3-Methoxy-4-hydroxyphenyl)-1-methoxy-2-guajakoxy-3-hydroxypropan, XXIII). Aus 1.5 g VI wurden analog 1.3 g (= 83 % d. Th.) XXIII als schwach gelblich gefärbtes Öl erhalten. ($C_{18}H_{22}O_6$ (334.2): Ber. OCH_3 27.84. Gef. OCH_3 26.96).

3,4-Dimethoxyphenyl-äthyl-carbinol-methyläther (1-(3,4-Dimethoxyphenyl)-1-methoxy-propan, XV). 2.0 g 3,4-Dimethoxyphenyl-äthyl-carbinol ergaben 1.6 g (= 75 % d. Th.) XV als gelbliches Öl. ($C_{12}H_{18}O_3$ (210.1): Ber. OCH_3 44.27. Gef. OCH_3 43.95).

α-(3,4-Dimethoxyphenyl)-glycerin-α,γ-dimethyläther-β-guajacyläther (1-(3,4-Dimethoxyphenyl)-1,3-dimethoxy-2-guajakoxy-propan, XI). Die Darstellung erfolgte durch dreimalige Methylierung der Substanz V [10] mit Methyljodid-Silberoxyd in Dimethylformamid [26]. Aus 3.0 g V wurden 1.8 g (= 55 % d. Th.) XI als schwach gelblich gefärbtes Öl erhalten. Das Produkt enthielt kein Ausgangsmaterial (Dünnschichtschromatographie, siehe unten), jedoch geringe Mengen anderer Verunreinigungen. ($C_{20}H_{26}O_6$ (362.2): Ber. OCH_3 42.80. Gef. OCH_3 41.93).

α-Guajakoxy-coniferylalkohol (XIX) wurde analog zu dem von Freudenberg und Müller [27] beschriebenen α-(2-Methoxy-4-methylphenoxy)-coniferylalkohol durch Reduktion des α-Guajakoxy-acetylferulasäuremethylesters mit Lithium-Aluminiumhydrid als gelbliches Öl erhalten, das nicht zur Kristallisation gebracht werden konnte. Durch Papierchromatographie (siehe unten) konnte gezeigt werden, dass es zum überwiegenden Teil aus einer phenolischen Substanz bestand, die einen R_F-Wert von 0.37 besass und beim Besprühen mit Dibrom-chinonmonochlorimidlösung und mit verd. Natronlauge den gleichen instabilen Indophenolfarbstoff wie die Verbindung XX gab. Auf eine weitere Reinigung musste wegen Materialmangels verzichtet werden.

ω-Piperidino-acetoveratron wurde durch Versetzen einer Lösung von 1.0 g ω-Bromacetoveratron in 25 ml Chloroform mit einer Lösung von 0.7 g Piperidin in 5 ml Chloroform gewonnen. Nach Einengen im Vakuum blieben nadelförmige Kristalle (Piperidiniumbromid) und ein gelbliches Öl zurück, das durch Aufnehmen in Äther abgetrennt und, wie üblich, durch Ausschütteln der alkalischen Lösung mit verd. Salzsäure, Alkalischmachen und Ausschütteln der alkalischen Lösung mit Äther gereinigt wurde. Ausb. 57 % d. Th. Das gelbliche Öl erwies sich auf dem Dünnschichtschromatogramm als einheitlich und wurde direkt weiterverarbeitet (siehe unten).

1-(3,4-Dimethoxyphenyl)-1-hydroxy-2-piperidino-äthan (XVII). 580 mg ω-Piperidinoacetoveratron wurden in 20 ml Äthanol gelöst und mit der Lösung von 600 mg Natriumborhydrid in 5 ml Wasser versetzt. Die blassgelbe Lösung entfärbte sich allmählich und es fiel ein weisser Niederschlag aus. Nach Stehen über Nacht wurde im Vakuum zur Trockne eingeengt und der Rückstand einigemale mit Chloroform unter Rückfluss ausgezogen. Die vereinigten Chloroformextrakte gaben nach Trocknung und Einengen eine weisse Kristallmasse. Ausb. 552 mg (= 95 % d. Th.). Nach Umkristallisieren aus wenig Äthanol wurden Prismen vom Schmp. 108–108.5° erhalten. ($C_{15}H_{23}O_3N$ (265.1): Ber. C 67.94, H 8.67, O 18.10, N 5.28. Gef. C 67.87, H 8.70, O 18.07, N 5.22).

1-(3,4-Dimethoxyphenyl)-1-guajakoxy-propanon-2. 3.0 g α-Brom-veratrylaceton [28] wurden in 70 ml abs. Aceton gelöst und 3.0 g Guajakol, sowie 3.0 g Kaliumkarbonat, zugesetzt. Nach einstündigem Erhitzen unter Rückfluss wurde das Reaktionsgemisch in Wasser gegossen und mit Chloroform ausgeschüttelt. Hierauf wurde das überschüssige Guajakol der Chloroformlösung mit verdünnter Natronlauge entzogen und die Chloroformlösung nach Waschen mit Wasser und Trocknen eingeengt. Das zurückbleibende bräunliche Öl (3.1 g = 89 % d. Th.) erwies sich auf dem Dünnschichtschromatogramm als nur wenig verunreinigt. Destillation im Vakuum (0.1 Torr, Badtemperatur 180–210°) ergab ein gelblich gefärbtes Öl, das nach längerem Stehen kristallisierte. Schmp. nach

Umkristallisieren aus Äthanol 72—72.5°. ($C_{18}H_{20}O_5$ (316.2): Ber. OCH_3 29.42. Gef. OCH_3 29.38).

Methylisoeugenolglykol-α-guajacyläther (1-(3,4-Dimethoxyphenyl)-1-guajakoxy-2-hydroxy-propan, XXXI). 1.9 g des obigen α-Guajakoxy-veratrylacetons wurden in 100 ml 80 %-igem Äthanol mit 2.0 g Natriumborhydrid reduziert. Nach Aufbewahren der Lösung bei Zimmertemperatur über Nacht wurde mit 2 ml Eisessig angesäuert, die Lösung mit Wasser verdünnt und mit Chloroform gründlich ausgeschüttelt. Die Chloroformlösung wurde mit verd. Natronlauge und hierauf mit Wasser gewaschen and nach Trocknung eingeengt. Das Reduktionsprodukt blieb als schwach gelblich gefärbtes Öl zurück, das nach Anreiben in etwas Äther z. T. kristallisierte. Ausb. 1.8 g (= 95 % d. Th.). Umkristallisieren aus wenig Äthanol ergab Kristalle vom Schmp. 105—106°. ($C_{18}H_{22}O_5$ (318.2): Ber. C 67.94, H 6.91, OCH_3 29.24. Gef. C 68.23, H 7.01, OCH_3 29.41).

Acetat von XXXI wurde durch Acetylierung von XXXI mit Essigsäureanhydrid-Pyridin als farbloses Öl erhalten, das nicht kristallisierte. ($C_{20}H_{24}O_6$ (360.2): Ber. OCH_3 25.80, CH_3CO 11.96. Gef. OCH_3 26.21, CH_3CO 11.22).

Behandlung der Modellsubstanzen mit 2 N Natronlauge

Es wurde im wesentlichen die gleiche Arbeitsweise wie bei der Untersuchung der Spaltung der Substanzen VIII und IX, bzw. deren Dimethyläther (siehe Ref.[15]) eingehalten. Das aus den spaltbaren Guajacyläthern freigelegte Guajakol wurde durch Wasserdampfdestillation gereinigt und die Ausbeute (in %) an gereinigtem Guajakol (Reinheitskontrolle durch Dünnschichtschromatographie) in die Tab. 1 eingeführt. Das jeweilige Reaktionsprodukt wurde nach Entfernung des eventuell abgespalteten Guajakols isoliert und, wie im Folgenden beschrieben, charakterisiert.

(a) *Behandlung der nicht-phenolischen β-Aryläther (V, X—XIV) mit 2 N Natronlauge.* Die Spaltungsansätze der Substanzen V, XII und XIII wurden nach Entfernung des Guajakols (Ausb. siehe Tab. 1), wie für die kristallisierte and amorphe Form von V an anderer Stelle [14] beschrieben, aufgearbeitet. Als Spaltungsreste fielen farblose Kristalle [14] — bei Substanz V ein schwach gelblich gefärbtes Öl — in Ausbeuten an, die in Tab. 1 angegeben sind. Der Gehalt an freigelegter Glycerin- bzw. 1,2-Glykolseitenkette wurde durch Oxydation mit Perjodat (siehe Ref.[29]) bestimmt. Der Verbrauch an Oxydationsmittel (ber. auf die Anzahl der im jeweils erwarteten Spaltungsprodukt vorhandenen 1,2-Glykolgruppen) entsprach in allen drei Fällen einem Reinheitsgrad der Spaltungsprodukte von ungefähr 90 %. Im Falle des Spaltungsproduktes aus der Substanz V (α-(3,4-Dimethoxyphenyl)-glycerin, VII) wurde ausserdem die bei der Perjodat-Oxydation aus der mittelständigen Carbinolgruppe gebildete Ameisensäure durch Titration mit Natronlauge bestimmt. Der Verbrauch entsprach 92 % d. Th. Betreffend der sterischen Konfiguration der Spaltungsprodukte aus V und XIII siehe Ref.[14] Substanz X wurde nur zur Hälfte gespaltet (siehe Tabelle 1).

Nach der Alkalibehandlung der Substanzen XI und XIV wurden die Ausgangsmaterialien unverändert zurückgewonnen. XI gab ein gelbliches Öl (Ausb. 73 %), das praktisch frei von 1,2-Glykolgruppen war (Papierelektrophorese, siehe Ref.[14]) und einen Methoxylgehalt von 41.0 % (ber. 42.8 %) besass. Nach der Behandlung konnte nur eine geringe Menge Guajakol (8.3 % d. Th.) isoliert werden. Substanz XIV wurde nach der Alkalibehandlung in kristallisierter Form (Schmp. 132—134°, Misch-Schmp. mit dem Ausg. Mat. 132—134°, Ausb. 89 % d. Th.) zurückerhalten.

(b) *Behandlung der phenolischen β-Aryläther (VI, XXI—XXIII) mit 2 N Natronlauge.* Nach der Alkalibehandlung der Substanzen VI sowie XXI—XXIII wurden die in kleiner Menge (ungefähr 15 % d. Th.) gebildeten Kristalle abfiltriert und die bräunlichen Filtrate zunächst papierchromatographisch (siehe unten) untersucht. Es zeigte sich, dass sie kein Guajakol (R_F = 0.69, blaue Farbe mit dem Kupplungsreagenz), sondern — als einzige phenolische Komponente — eine Substanz mit dem R_F-Wert 0.80 enthielten, die mit dem Kupplungsreagenz einen intensiv violett gefärbten Fleck gab, der sich schon nach kurzer Zeit von der Mitte aus in charakteristischer Weise zu entfärben begann (vgl. Ref.[1,18]). Genau das gleiche papierchromatographische Verhalten wie die Filtrate zeigten die oben erwähnten kristallisierten Anteile, die, wie später gefunden wurde, das Natriumsalz der Substanz XX darstellen. Sie wurden nach der Filtration sorgfältig getrocknet, mit einer

alkoholischen Lösung der äquimolaren Menge Benzylchlorid versetzt und eine Stunde unter Rückfluss erhitzt. Nach Eintragen der Reaktionsgemische in Wasser, Aufnehmen in Äther, Ausschütteln der Ätherlösungen mit verd. Natronlauge und hierauf mit Wasser, Trocknen und Einengen wurde in allen 4 Fällen *3-Methoxy-4-benzyloxy-ω-guajakoxy-styrol* (Benzyläther der Substanz XX) erhalten, das nach Umkristallisieren aus wenig Äthanol bei 80—81° schmolz. ($C_{23}H_{22}O_4$ (326.2): Ber. C 76.26, H 6.07, O 17.67, OCH_3 17.12. Gef. C 76.18, H 5.98, O 17.97, OCH_3 16.86). Aus den Filtraten konnte durch Benzylierung weiterer Benzyläther von XX gewonnen werden. Die Identität der Benzylierungsprodukte aus den Alkalikochungen der Substanzen VI und XXI—XXIII liess sich durch Bestimmung der Misch-Schmp. zeigen, wobei keine Schmp-Erniedrigungen festgestellt werden konnten. Nach Alkalibehandlung des α-Guajakoxy-coniferylalkohols (XIX) liess sich im Reaktionsansatz durch Papierchromatographie (siehe unten) als Hauptkomponente die gleiche Substanz (XX) wie aus VI und aus XXI—XXIII nachweisen (R_F = 0.80, instabile violette Farbe).

(c) *Behandlung der α-Aryläther XXVII, XXVIII und XXXI mit 2 N Natronlauge.* 2.0 g Dihydro-dehydro-diisoeugenol (XXVII) [30] gaben nach der Alkalikochung und üblichen Aufarbeitung ein gelbliches Öl, das bei der Acetylierung mit Essigsäure anhydrid-Pyridin zwei Acetylgruppen aufnahm. Das Diacetat wurde im Vakuum (10^{-3} Torr) destilliert und ging zwischen 170 und 190° (Badtemperatur) als schwach gelblich gefärbtes, sehr zähes Öl über. Ausb. 1.7 g (= 67.5 % d. Th.). In wenig Methanol gelöst und die Lösung unter Umrührung mit Trockeneis-Äthanol auf ungefähr −80° gekühlt, kristallisierte es nach einiger Zeit in Form rechteckiger Platten und schmolz nach zweimaligem Umkristallisieren aus wenig Methanol bei 111—112°. *1-(3-Methoxy-4-acetoxy-phenyl)-2-(2-acetoxy-3-methoxy-5-propyl-phenyl)-propen-(1) (XXIX)* ($C_{24}H_{28}O_6$ (412.2): Ber. C 69.92, H 6.79, O 23.29, OCH_3 15.04, CH_2CO 20.87. Gef. C 70.13, H 6.91, O 23.32, OCH_3 15.01, CH_3CO 20.21).

Das Stilbenderivat XXIX nahm bei der katalytischen Hydrierung (Pd auf Tierkohle, Lösungsmittel: abs. Äthanol) ein Mol Wasserstoff pro Mol Substanz auf. Die gesättigte Verbindung, *1-(3-Methoxy-4-acetoxyphenyl)-2-(2-acetoxy-3-methoxy-5-propyl-phenyl)-propan (XXX)*, kristallisierte nach Anreiben in Ligroin und wurde aus Äthanol umkristallisiert. Schmp. 80.5—81.5°, Misch-Schmp. mit Substanz XXIX 70—74°. ($C_{24}H_{30}O_6$ (414.2): Ber. C 69.58, H 7.24, O 23.17, CH_3CO 20.77. Gef. C 69.95, H 7.09, O 23.30, CH_3CO 19.53).

Der Methyläther des Dihydro-dehydro-diisoeugenols (XXVIII) [31] wurde nach der Behandlung mit 2 N Natronlauge in einer Ausbeute von 98 % der Ausgangsmenge zurückgewonnen. Schmp. nach Umkristallisieren aus Äthanol 95.5—96.5, Misch-Schmp. mit dem Ausgangsmaterial 95.5—96.5°. Auch bei Verwendung von 2 N alkoholischer Natronlauge wurde keinerlei Spaltung erzielt, sondern der Methyläther XXVIII praktisch quantitativ zurückerhalten. Die Alkalistabilität der Substanz XXVIII kann somit nicht durch ihre beschränkte Löslichkeit in 2 N Natronlauge erklärt werden, sondern muss ihre Ursache in der durch Verätherung blockierten, *para*-ständigen phenolischen Hydroxylgruppe (vgl. mit XXVII) haben.

Der α-Guajacyläther des Methylisoeugenolglykols (1-(3,4-Dimethoxyphenyl)-1-guajakoxy-2-hydroxy-propan, XXXI, Schmp. 105—106°) (0.5 g) gab, wie der isomere β-Guajacyläther XIII, bei der Alkalibehandlung die "α-Form" des Methyl-isoeugenolglykols vom Schmp. 124—126° (siehe Ref.[32] und [14]) in einer Ausbeute von 235 mg (= 71 % d. Th.) (siehe Tabelle 1). 170 mg (= 88 % d. Th.) Guajakol wurden isoliert.

(d) *Behandlung der α-Alkyläther (XV, XXXII und XXXIII) mit 2 N Natronlauge* Um die geringe Spaltung der Substanzen XI und XIV (siehe Tabelle 1) erklären zu können, wurde das Verhalten des einfachen Benzylmethyläthers XV unter den Bedingungen einer Alkalikochung untersucht. Es zeigte sich, dass er zu einem geringen Teil gespaltet wurde. Die Bestimmung der freigelegten Hydroxylgruppen im Reaktionsgemisch durch Acetylierung [33], (siehe Ref.[6]) ergab einen Spaltungsgrad von 12 % (siehe Tabelle 1).

Der zweifache *para*-Hydroxybenzyl-alkyläther Pinoresinol (XXXII) lieferte bei der Behandlung mit Alkali ein Gemisch aus 7 phenolischen Substanzen, das kein Ausgangsmaterial enthielt (Papierchromatographie, siehe unten). Eine präparative Auftrennung dieses Gemisches wurde bisher nicht durchgeführt.

Pinoresinol-dimethyläther (XXXIII, Schmp. 102—104°) erwies sich, wie der Methyläther des Dihydro-dehydro-diisoeugenols (XXVIII), bei der Alkalibehandlung sowohl mit wässriger, als auch mit äthanolischer Natronlauge als stabil und wurde praktisch quantitativ zurückgewonnen. Nach Umkristallisieren aus Essigsäure-Wasser schmolz das

wiederisolierte Produkt bei 101—104°. Der Misch-Schmp. mit dem Ausgangsmaterial lag bei 101—104°.

Behandlung der Substanzen V und XII mit Piperidin — 2 N Natronlauge. Es wurde eine ähnliche Arbeitsweise eingehalten, wie bereits bei der Spaltung der Substanzen VIII und IX [15] beschrieben wurde. Nach Entfernung des überschüssigen Piperidins wurde(n) jedoch zunächst der alkalischen Aufschlusslösung die Piperidinoverbindung(en) durch gründliches Ausschütteln mit Chloroform entzogen. Die vereinigten Chloroformlösungen wurden mit verd. Natronlauge und hierauf mit Wasser ausgeschüttelt und ergaben nach Entfernung des Lösungsmittels ein Gemisch, bestehend aus Piperidinoverbindung(en) und Ausgangsmaterial. Zur weiteren Reinigung wurde erneut in Chloroform gelöst und die Chloroformlösungen mit 2 N Salzsäure ausgeschüttelt. Beim Alkalischmachen der salzsauren Lösungen fiel die Piperidinoverbindung aus Substanz XII (XVII) kristallisiert und das Gemisch der Piperidinoverbindungen aus Substanz V (XVIII) als Öl aus. Die alkalischen Lösungen wurden mit Chloroform ausgezogen und das Chloroform nach Trocknen abdestilliert. Die Reinheit der zurückbleibenden Piperidinoverbindung(en) wurde mit Hilfe von Dünnschichtschromatographie (siehe unten) überprüft und die Reinigungsoperation, wenn erforderlich, wiederholt.

Die alkalischen Aufschlusslösungen (nach Entfernung des überschüssigen Piperidins und der gebildeten Piperidinoverbindung(en), siehe oben) wurden angesäuert und gründlich mit Äther ausgeschüttelt. Den vereinigten Ätherlösungen wurde hierauf das Guajakol mit verdünnter Natronlauge entzogen. Das nach Ansäuern der wässrigen Phase, Ausschütteln mit Äther, Trocknen und Einengen der Ätherlösung gewonnene Rohguajakol wurde durch Wasserdampfdestillation gereinigt (Reinheitskontrolle durch Dünnschichtschromatographie, siehe unten).

Aus 2.00 g XII wurden auf diese Weise 0.38 g (= 21.7 %) kristallisiertes 1-(3,4-Dimethoxyphenyl)-1-hydroxy-2-piperidinoäthan (XVII) erhalten, das, aus wenig Äthanol umkristallisiert, bei 107—108.5° schmolz. ($C_{15}H_{23}O_3N$ (265.1): Ber. C 67.94., H 8.67., O 18.10., N 5.28. Gef. C 67.52; H 8.85., O 18.31., N 5.40). Der Misch-Schmp. mit authentischer Substanz XVII (Schmp. 108—108.5°, siehe oben) lag bei 107—108°. Die Ausbeute an gereinigtem Guajakol betrug 168 mg (= 20.5 % d. Th.). 0.525 g Ausgangsmaterial wurden zurückgewonnen.

Aus 2.00 g V wurden 0.68 g (= 38.5 % d. Th.) eines Gemisches von Monopiperidinoverbindungen (XVIII) erhalten, das aus 4 Hauptkomponenten bestand (Dünnschichtschromatographie, siehe unten). ($C_{16}H_{25}O_4N$ (295.2): Ber. C 65.10, H 8.47, O 21.68, N 4.74. Gef. C 64.93, H 8.47, O 21.75, N 4.81). Die Ausbeute an gereinigtem Guajakol betrug 260 mg (= 35 % d. Th.).

Papierchromatographie. Es wurde Whatman No. 1 Filtrierpapier, imprägniert mit einer 20 %-igen Lösung von Formamid in Methanol, und als Lösungsmittelgemisch Xylol:Methyl-äthylketon (1:1), versetzt mit 2 % Formamid, verwendet. Die Entwicklung der an der Luft getrockneten Chromatogramme erfolgte meist durch Besprühen mit einer 0.5 %-igen, alkoholischen Lösung von Dibrom-chinonmonochlorimid und hierauf mit 0.05 N Natronlauge. In einigen Fällen wurde zur weiteren Charakterisierung der Substanzen auch diazotierte Sulfanilsäure als Kupplungsreagenz verwendet.

Dünnschichtschromatographie. Es wurde im wesentlichen die von Stahl [35] angegebene Arbeitsvorschrift eingehalten. Als Adsorbens diente Kieselgel G "Merck", als Lösungsmittel meist Chloroform und in einigen Fällen — vor allem bei Glykolen und Piperidinoverbindungen — Essigsäureäthylester. Die Entwicklung der Chromatogramme erfolgte durch Aufbewahrung der an der Luft getrockneten Platten in einer mit Joddämpfen gesättigten Glaskammer.

Wir danken *Cellulosaindustrins Stiftelse för Teknisk och Skoglig Forskning samt Utbildning* für die Gewährung eines Forschungsbeitrages.

Ein Teil der in der vorliegenden Untersuchung verwendeten Substanz VI wurde uns von Herrn Prof. Dr. K. Kratzl, Wien, zur Verfügung gestellt, wofür auch an dieser Stelle bestens gedankt sei.

LITERATUR

1. Gierer, J. und Alfredsson, B. *Acta Chem. Scand.* **11** (1957) 1516.
2. Enkvist, T. und Moilanen, M. *Svensk Papperstidn.* **52** (1949) 183; **55** (1952) 668.
3. Mikawa, H. *Bull. Chem. Soc. Japan* **27** (1954) 50; Mikawa, H., Sato, K., Takasaki, C. und Ebisawa, K. *Bull. Chem. Soc. Japan* **29** (1956) 265.
4. Adler, E., Pepper, J. M. und Eriksoo, E. *Ind. Eng. Chem.* **49** (1957) 1391.
5. Adler, E., Delin, S. und Lundqvist, K. *Acta Chem. Scand.* **13** (1959) 2149.
6. Freudenberg, K. und Schlüter, H. *Chem. Ber.* **88** (1955) 617.
7. Freudenberg, K. und Hübner, H. H. *Chem. Ber.* **85** (1952) 1181.
8. Freudenberg, K. *Chem. Ber.* **92** (1959) LXXXIX.
9. Leopold, B. *Acta Chem. Scand.* **4** (1950) 1523.
10. Adler, E., Lindgren, B. O. und Saedén, U. *Svensk Papperstidn.* **55** (1952) 245.
11. Adler, E. und Eriksoo, E. *Acta Chem. Scand.* **9** (1955) 341.
12. Adler, E. und Lindgren, B. *Svensk Papperstidn.* **55** (1952) 563.
13. Kratzl, K. *Paperi ja Puu* **11** (1961) 643.
14. Gierer, J. und Norén, I. *Acta Chem. Scand.* **16** (1962). *Im Druck.*
15. Gierer, J. und Kunze, I. *Acta Chem. Scand.* **15** (1961) 803.
16. Eliel, E. L. in Newman, M. S. *Steric Effects in Organic Chemistry*, John Wiley and Sons, New York 1956, Chapman and Hall Limited, London 1956, Seite 107; Gould, E. S. *Mechanism and Structure in Organic Chemistry*, Henry Holt and Co. New York 1960, Seite 294.
17. Fischer, F. und Rönsch, H. *Chem. Ber.* **94** (1961) 901.
18. Gierer, J. *Acta Chem. Scand.* **8** (1954) 1319.
19. Freudenberg, K., Wilk, H., Leuck, H. U., Knof, L. und Fung, Tat Hang *Ann.* **630** (1960) 1.
20. Falkehag, I. *Paperi ja Puu* **11** (1961) 655.
21. Freudenberg, K. und Friedmann, M. *Chem. Ber.* **93** (1960) 2138; Freudenberg, K. und Gurbachan, S. S. *Holzforschung* **15** (1961) 33; Freudenberg, K. *Holz als Roh- und Werkstoff* **18** (1960) 282.
22. Freudenberg, K. und Rasenack, D. *Chem. Ber.* **86** (1953) 755.
23. Adler, E. und Marton, J. *Acta Chem. Scand.* **15** (1961) 357.
24. Kratzl, K., Kisser, W., Gratzl, J. und Silbernagel, H. *Monatsh.* **90** (1959) 771.
25. Adler, E. und Björkqvist, K. J. in Hägglund, E. *Chemistry of Wood*, Academic Press, New York 1951, Seite 288.
26. Kuhn, R., Trischmarn, H. und Löw, I. *Angew. Chem.* **67** (1955) 32.
27. Freudenberg, K. und Müller, H. G. *Ann.* **584** (1953) 40.
28. v. Wacek, A. *Ber.* **77** (1944) 85.
29. Adler, E. und Björkqvist, K. J. *Acta Chem. Scand.* **5** (1951) 241.
30. Aulin-Erdtman, G. *Svensk Kem. Tidskr.* **54** (1942) 168.
31. Erdtman, H. *Ann.* **503** (1933) 283.
32. Kokolow, M. *J. Russ. Phys. Soc.* **29** (1897) 23; *Chem. Zentr.* **1897**, I, 915.
33. Verley, A. und Boelsing, F. *Ber.* **34** (1901) 3354.
34. Stahl, E. *Pharmazeutische Rundschau* **1** No. 2 (1959) 1.

Eingegangen am 19. Februar 1962.

ACTA CHEMICA SCANDINAVICA 16 (1962) 1730–1750

A Thermodynamic Study of the Ternary System, Triethylamine, Water and Heavy Water, with Special Reference to Isotope Separation Problems

C. U. LINDERSTRØM-LANG

The Chemistry Department, The Danish Atomic Energy Commission, Risø, Denmark

1. An experimental isotope separation and solubility study in the two-phase region of the system, water (D_2O + H_2O) — triethylamine (TEA) has been carried out.

Concentrations of D_2O and H_2O in TEA have been determined by their absorption at 4.0 μ and 6.1 μ, respectively.

2. Diethylamine and ethylamine as impurities in the triethylamine used, have been determined by quantitative paper chromatography using a modified Levy-procedure.

3. Fundamental thermodynamic equations pertinent to the calculation of hydrogen isotope separation effects in the system at equilibrium are developed.

4. The total water concentration, x_w, of a phase and the isotopic composition, y_D, of this water (both in mole fractions) are chosen as independent variables. It is presumed that changes in activity coefficients, f, when y_D is varied at constant x_w are small compared to changes when x_w is varied at constant y_D.

On this basis it is postulated that reasonable first-order or second-order approximate relations are obtained when it is assumed that $(\partial \ln f/\partial y_D)_{x_w,T} = 0$ or $(\partial \ln f/\partial y_D)_{x_w,T}$ = a constant (*i.e.* independent of y_D), respectively.

5. These relations are introduced into the fundamental equations and it is shown that in both cases a numerical calculation of the isotope separation effect can be carried through with reasonable accuracy, using available enthalpy data and/or vapour pressure data for pure H_2O-TEA together with two-phase equilibrium data for the binary systems, H_2O-TEA and D_2O-TEA.

The numerical calculation indicates that $\partial \ln f/\partial y_D$ is less than $0.01 \times (\partial \ln f/\partial x_w)$.

6. The relative solubility change of water in TEA, when H_2O is replaced by D_2O at constant temperature, $(\mathrm{d} \ln x'_w/\mathrm{d}y'_D)_{eq,T}$ multiplied by a factor, $Q = 1 + x'_w(\partial \ln f'_w/\partial x_w)$, expressing the degree of ideality in the triethylamine phase, is found to be a simple and convenient measure of the isotope separation effect.

It is shown that the large $\mathrm{d}\ln x'_w/\mathrm{d}y'_D$ found in this system and in other similar systems must be compensated to a great extent by a small Q, so the absence of any high isotope separation effect is easily understood.

The remarkably high difference between the solubility of ordinary water (H_2O) and heavy water (D_2O) in triethylamine (TEA) may seem at first glance to promise a high isotope separation effect when H_2O and D_2O are mixed. However, Carlson [1], using water enriched with a few percent D_2O, found hardly any effect, (for instance, at 35°C the separation factor was 1.004 ± 0.004) and Hahn and Street [2] working with 98 % D_2O found no effect at 15—25°C.

The high expectation probably is based on the often applicable assumption that the solubility of one component in another to a first approximation is independent of the addition of a third component, a condition which, however, is far from being fulfilled when the third component (*e.g.* heavy water), as is the case here, is soluble in both phases.

In order to corroborate these results an experimental study has been undertaken and the system has been given a theoretical treatment. The discussion below is based on elementary thermodynamic principles which, however, do not seem to have been applied to this particular problem before; therefore the solution may have some general interest.

Approximate chemical potential functions are developed and a numerical calculation of the separation effects based on available thermodynamic data is attempted. The resulting figures may furnish only the order of magnitude of the terms involved, however, this appears sufficient to illustrate their relative importance.

EXPERIMENTAL PART

The triethylamine was a Fluka p.a. quality dried for a short time with sodium and decanted.

The heavy water was a 99.8 % quality from which a 20 % D_2O standard solution was prepared.

Procedure. In equilibration tubes shaped as shown on Fig. 1, 3 ml of triethylamine were placed in the horizontal part together with varying amounts (from 0.2 to 1 ml) of H_2O, pure D_2O, or the 20 % mixture. The tubes were shaken in a thermostat (regulating to within 0.01°C). A mercury seal was placed on top of the ground joints.

The shaking was fairly slow and it was extended over night as a convenient routine step though of course much shorter periods would have been sufficient. In order to detect any slow exchange with TEA or impurities in it, even longer periods were used.

After equilibration the mixture, while in the thermostat, was transferred to the vertical section of the tube and the mercury poured off.

A 2 ml sample of the TEA phase was taken and, if necessary for the subsequent determination, diluted with dry TEA.

Then a sample (either 50 μl or 100 μl) of the water phase was drawn with a constriction pipette (Carlsberg). It was noticed that even a few bubbles of expired air through the TEA phase, when passing it with the pipette were enough to produce a turbidity — undoubtedly a carbon dioxide effect. No measures were taken in order to reduce the amount of CO_2 present but as the equilibration procedure was always the same, the relative solubility was probably not affected, nor was the change of solubility with temperature.

The water phase samples were diluted with dry TEA (2—3 ml). In this way the D/H ratio in the two phases became directly comparable.

The concentrations were determined with a "Perkin Elmer 221" infrared spectrophotometer, "H_2O" at 6.1 μ and "D_2O" at 4.0 μ, in 0.125 mm CaF_2-cells. 20 % D_2O for the equilibration was chosen because in this concentration region the ratio of the optical densities at the two wavelengths was near unity (approx. 1.2). An appropriate number of standards was always run simultaneously with the unknowns. It was found impossible to store standards in a satisfactory way, so fresh ones were always made up for each experiment.

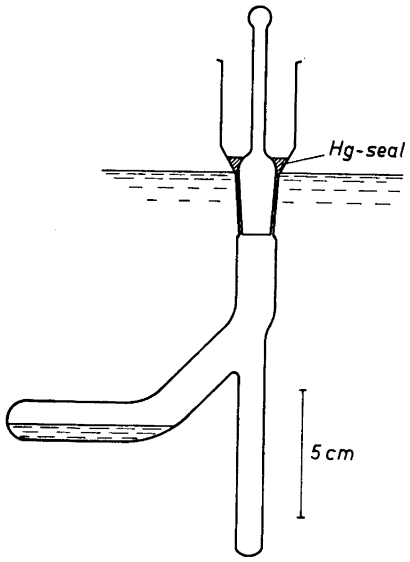

Fig. 1. Equilibration tube.

The varying amount of water phase revealed to what extent disturbing impurities accumulated in the water. The only other source of error that seemed likely to have any importance was a rapid exchange with an impurity in the TEA.

The supplier gave the information that it might contain some diethylamine (DEA) and ethanol. The actual amounts of DEA and, as it turned out, monoethylamine (MEA) present were determined by using a modified Levy procedure [10], *i.e.* reaction with dinitrofluorobenzene and identification and estimation by chromatography on paper. A somewhat higher pH than Levy's was used in order to make the reaction conveniently fast. The DNP derivatives were extracted with ether after neutralizing the reaction mixture to pH 5—6. Dinitrophenol was removed from the ether phase with aquous sodium hydroxide. A 0.1 M phosphate buffer in 50 % ethanol was used as solvent for the chromatographic development; however it is not claimed that the choice is ideal. Otherwise Levy's procedure was followed. The values obtained are believed to be accurate to within 10 % (see Table 1).

Alcohol in TEA was estimated by oxidation for two days with 0.1 N potassium dichromate in 4 N sulphuric acid at 40°C and determination of the excess of dichromate by reaction with iodide and titration of the iodine formed with thiosulphate. The value obtained is believed to be accurate to within 10 % (see Table 1).

TEA, dried for a short time, *i.e.* until bubbles ceased to be evolved, with sodium showed no decrease in alcohol content (tested at different alcohol concentrations) nor was there any detectable residue after evaporation in vacuum.

EXPERIMENTAL RESULTS

There is a slow chemical exchange between 20 % D_2O and TEA which leads to a small decrease in D_2O concentration. It amounts to about 1—2 % (relative) per day. It may be assumed therefore that, if the total amount of water present in an equilibration experiment is 3/2 times the water dissolved in the TEA phase the expected recovery will be approx. 99 %. In most experiments, however, the amount of water is much larger and therefore the correc-

Table 1. Hydrogen exchanging impurities in the triethylamine used, as found by the analytical procedures described in the text.

	mequiv./mole TEA
Diethylamine	1.8
Ethylamine	1.5 (= 0.75 mmole/mole TEA)
Ethanol	1.3
Total	4.6 mequiv. exchangeable hydrogen per mole TEA.

tion much smaller. In agreement with this, the simple recovery average of 21 experiments, corrected for rapid exchange (see below) was 99.6 % (S.D. of the distribution 1 %). Equilibrium is probably attained in much less than one day, so in no case has a correction to the distribution ratio to be made.

Variation of the ratio of water phase to TEA phase had no effect on the optical density ratio of the water phase; therefore, no impurities affecting the spectrophotometric determination appear to accumulate in the water phase.

If a rapidly exchanging impurity is present it may react in the following manner

$$\tfrac{1}{2}\ D_2O + IH \rightleftharpoons \tfrac{1}{2}\ H_2O + ID$$

the equilibrium constant being

$$E = \frac{[ID]\ [H_2O]^{\frac{1}{2}}}{[IH]\ [D_2O]^{\frac{1}{2}}} \simeq 1$$

If $ID \equiv 2\,\varepsilon$ (in moles per mole TEA-phase) and $y_D/(1-y_D) \equiv r$, where y_D is mole fraction of D_2O, *i.e.* $y_D \simeq 0.20$ (see eqn. 8), then

$$\Delta r = \frac{Wy_D - \varepsilon}{W(1-y_D) + \varepsilon} - \frac{Wy_D}{W(1-y_D)} \simeq -\frac{\varepsilon}{(1-y_D)^2 W}$$

Here $(1-y_D) = \frac{4}{5}$ so $\Delta r = -\frac{25}{16}\frac{\varepsilon}{W}$. W is the number of moles of water (20 % D_2O) in equilibrium with, and contained in, one mole of TEA phase (and therefore approx. one mole of TEA). ε is independent of W as long as the amount of impurity is small compared to the amount of D_2O.

The r-values of the water phase samples need no correction for rapidly exchanging impurity, because the standards run simultaneously are treated in exactly the same manner — provided, as already mentioned, the impurities do not accumulate in the water phase and there interfere with the measurements.

The TEA phase r-values will be too high when compared to ordinary standards in which the D_2O concentration (y_D) has been somewhat reduced by the impurities. Relevant standards, which were prepared from TEA "deuterated" with 20 % D_2O and then dried, gave lower TEA phase r-values in agreement with the above; however, a comparison of the different standard curves obtained gave only fair agreement with theory even when this was elaborated to take into account corrections based on: (1) distribution factors

Table 2. Experimental results. 3 ml triethylamine were equilibrated with varying amounts of 20 % D_2O (*i.e.*, $y_D = 0.20$). The isotopic composition of samples drawn from the water phase (and diluted with TEA) and from the TEA phase was determined spectrophotometrically at 6.1 μ ("H_2O") and 4.0 μ ("D_2O"). For details see text.

T °C	Vol. of Water phase μl	Water in TEA phase μl	Isotope separation effect, $\frac{y''_D - y'_D}{y''_D(1-y'_D)}$ uncorrected	corrected for rapid exhange (see Table 1)
27	100	200	+ 0.060	
	100	200	0.000	
	300	200	0.000	
	300	200	− 0.005	
	300	200	+ 0.005	
	800	200	+ 0.005	
	800	200	− 0.005	
	800	200	0.000	
		Average	+ 0.008	0.014
35	140	110	+ 0.025	
	140	110	− 0.005	
	390	110	− 0.003	
	390	110	− 0.010	
	890	110	− 0.007	
	890	110	+ 0.005	
		Average	+ 0.001	0.011
45	175	75	+ 0.010	
	175	75	− 0.010	
	425	75	− 0.005	
	425	75	− 0.010	
	925	75	− 0.020	
	925	75	− 0.020	
		Average	− 0.009	0.006

of the impurities, and (2) their absorptions at the two wavelengths. Deviations from Lambert-Beer's law, caused by shifts, with changing water concentration, in the peak wave-length at 6 μ, were a further complication.

In addition the reduction in TEA r-values was greater than accounted for by chemical analysis and though the explanation may be a trace of water present, it was felt safer to base the TEA phase r-values on a correction calculated from known available exchangeable hydrogen (see Table 1).

Table 2 shows the results of the analytical determinations. The isotope effect, $[y''_D - y'_D]/[y'_D(1-y''_D)]$, (see eqn. 9) has been calculated from the r-values of the TEA phase and the water phase, r' and r'', respectively. One has $[y''_D - y'_D]/[y'_D(1-y''_D)] = (r''-r')/r$ where r with sufficient accuracy is $0.2/0.8 = 1/4$.

The correction for rapid exchange has been calculated as $-\frac{\Delta r}{r} = 4 \cdot \frac{25}{16} \cdot \frac{1}{5} \cdot \frac{4.6}{2} \cdot \frac{10^{-3}}{W}$, where W (in moles per mole TEA) now is the

amount of water in the TEA phase sample (or rather in the corresponding standard).

The standard deviation of $[y''_D - y'_D]/[y'_D(1-y''_D)]$ is estimated to be *ca.* 1—1.5 % (absolute) so the averaged values should be accurate to about 0.5 %. However, the presence of a small amount of water in the TEA employed, a possibility that cannot be excluded, may have introduced a systematic error of about the same magnitude. The solubility determinations are of course less accurate, the estimated standard deviation being 3 % (relative), and, as mentioned earlier, include a systematic error due to the presence of CO_2. The relative position of the two curves is thought to be relevant to the isotope effects found. The calculation is straight forward.

THEORETICAL PART

1. Equilibrium conditions, fundamental equations.

If μ'_D, μ'_H and μ'_A are the chemical potentials of D_2O, H_2O, and TEA in the TEA-rich phase and μ''_D, μ''_H and μ''_A are the corresponding potentials in the water-rich phase, then

$$\begin{aligned} \mu'_D &= \mu''_D \\ \mu'_H &= \mu''_H \\ \mu'_A &= \mu''_A \end{aligned} \tag{1}$$

at equilibrium (denoted below by "eq"), or for any change in composition and temperature (and pressure)

$$d\mu' = d\mu'' \tag{2}$$

for any of the components. The three equations represented by eqn. 2 may be combined in the following way

$$x''_D d\mu''_D + x''_H d\mu''_H + x''_A d\mu''_A = x''_D d\mu'_D + x''_H d\mu'_H + x''_A d\mu'_A, \tag{3}$$

where x_D, x_H and x_A are mole fractions, *i.e.* the number of moles of *pure* component, D_2O, H_2O, and TEA, to be added in order to produce one mole of mixture: $x_D + x_H + x_A = 1$.

Changes in chemical potential may be written (at constant pressure)

$$d\mu = \left(\frac{\partial \mu}{\partial z_1}\right)_{T,z_2} dz_1 + \left(\frac{\partial \mu}{\partial T}\right)_{z_1,z_2} dT; \; (dz_2 = 0) \tag{4}$$

where z_1 and z_2 are any two concentrations, sufficient for describing the composition of the system.

Gibbs-Duhem's equation,

$$x_D \left(\frac{\partial \mu_D}{\partial z_1}\right)_{T,z_2} + x_H \left(\frac{\partial \mu_H}{\partial z_1}\right)_{T,z_2} + x_A \left(\frac{\partial \mu_A}{\partial z_1}\right)_{T,z_2} = 0 \tag{5}$$

and eqn. 4 combined with eqn. 3 gives

$$\left(x_D'' \frac{\partial \mu_D''}{\partial T} + x_H'' \frac{\partial \mu_H''}{\partial T} + x_A'' \frac{\partial \mu_A''}{\partial T}\right) dT =$$

$$\left(x_D'' \frac{\partial \mu_D'}{\partial T} + x_H'' \frac{\partial \mu_H'}{\partial T} + x_A'' \frac{\partial \mu_A'}{\partial T}\right) dT + \left(x_D'' \frac{\partial \mu_D'}{\partial z_1} + x_H'' \frac{\partial \mu_H'}{\partial z_1} + x_A'' \frac{\partial \mu_A'}{\partial z_1}\right) dz_1 \quad (6)$$

Eliminating $\partial \mu_A'/\partial z_1$ (Gibbs-Duhem, eqn. 5) * and introducing $\partial \mu/\partial T = -S$ (the partial molar entropy) give

$$\left[\left(x_D'' - x_D' \frac{x_A''}{x_A'}\right)\frac{\partial \mu_D'}{\partial z_1} + \left(x_H'' - x_H' \frac{x_A''}{x_A'}\right)\frac{\partial \mu_H'}{\partial z_1}\right]\left(\frac{dz_1}{dT}\right)_{eq,x_t} =$$

$$x_D''(S_D' - S_D'') + x_H''(S_H' - S_H'') + x_A''(S_A' - S_A'') \quad (7)$$

Two new variables, y_D and x_W, are now introduced, defined in the following way

$$\begin{aligned} y_D \cdot x_W &\equiv x_D \\ (1-y_D) \cdot x_W &\equiv x_H \\ i.e.,\ x_W + x_A &= 1 \end{aligned} \quad (8)$$

Thus the isotope separation factor, α, may be written

$$\alpha = \frac{y_D''}{1-y_D''} \Big/ \frac{y_D'}{1-y_D'} = 1 + \frac{y_D'' - y_D'}{y_D'(1-y_D'')} \quad (9)$$

The following two relations (*cf.* eqn. 7) may now be obtained

$$x_D'' - x_D' \frac{x_A''}{x_A'} = (y_D'' - y_D')\, x_W'' + y_D' \frac{x_W'' - x_W'}{1 - x_W'} \quad (10)$$

and

$$x_H'' - x_H' \frac{x_A''}{x_A'} = -(y_D'' - y_D')x_W'' + (1 - y_D') \frac{x_W'' - x_W'}{1 - x_W'} \quad (11)$$

The variables, z_1 and z_2 in eqn. 6 or 7 may represent y_D and x_W; correspondingly eqn. 7 yields two equations

$$\left[\frac{x_W'' - x_W'}{1 - x_W'}(y_D'(\partial \mu_D'/\partial x_W)_{T,y_D} + (1 - y_D')(\partial \mu_H'/\partial x_W)_{T,y_D}) + x_W''(y_D'' - y_D')((\partial \mu_D'/\partial x_W)_{T,y_D}\right.$$

$$\left. - (\partial \mu_H'/\partial x_W)_{T,y_D})\right]$$

$$= (dT/dx_W')_{eq,y_D'}[x_W''(y_D''(S_D' - S_D'') + (1 - y_D'')(S_H' - S_H'')) + (1 - x_W'')(S_A' - S_A'')] \quad (12)$$

* When partial derivatives, as here, are supplied with dash, *e.g.* $\partial \mu'/\partial x_W$, it means $(\partial \mu/\partial x_W)_{T,y_D}$ at $x_W = x_W'$, $y_D = y_D'$ and $T = T_{eq}$ where (x_W', y_D', T_{eq}) is a point on the solubility surface.

and

$$\left[\frac{x''_W - x'_W}{1 - x'_W}(y'_D(\partial\mu'_D/\partial y_D)_{T,x_W} + (1-y'_D)(\partial\mu'_H/\partial y_D)_{T,x_W}) + x''_W(y''_D-y'_D)((\partial\mu'_D/\partial y_D)_{T,x_W} - (\partial\mu'_H/\partial y_D)_{T,x_W})\right]$$

$$= (dT/dy'_D)_{eq,x'_W}[x''_W(y''_D(S'_D-S''_D)+(1-y''_D)(S'_H-S''_H))+(1-x''_W)(S'_A-S''_A)] \quad (13)$$

Introducing

$$(dT/dy'_D)_{eq,x'_W} = -(dT/dx'_W)_{eq,y'_D}(dx'_W/dy'_D)_{eq,T} \quad (14)$$

a third equation involving $(dx'_W/dy'_D)_{eq,T}$ is obtained by combining eqns. 12 and 13:

$$-\left[\frac{x''_W - x'_W}{1 - x'_W}(y'_D(\partial\mu'_D/\partial x_W)_{T,y_D} + (1-y'_D)(\partial\mu'_H/\partial x_W)_{T,y_D}) + x''_W(y''_D-y'_D)((\partial\mu'_D/\partial x_W)_{T,y_D} - (\partial\mu'_H/\partial x_W)_{T,y_D})\right](dx'_W/dy'_D)$$

$$= \left[\frac{x''_W - x'_W}{1 - x'_W}(y'_D(\partial\mu'_D/\partial y_D)_{T,x_W} + (1-y'_D)(\partial\mu'_H/\partial y_D)_{T,x_W}) + x''_W(y''_D-y'_D)((\partial\mu'_D/\partial y_D)_{T,x_W} - (\partial\mu'_H/\partial y_D)_{T,x_W})\right] \quad (15)$$

ΔH, the partial molar enthalpy of mixing, may be substituted for S, the partial molar entropy, in the following way:

$$\Delta H - T(S-S_o) = \mu-\mu_o \text{ and } \mu'-\mu_o = \mu''-\mu_o \text{ so}$$

$$S'_D - S''_D = S'_D - S_{Do} - (S''_D - S_{Do}) = (\Delta H'_D - \Delta H''_D)/T, \text{ etc.} \quad (16)$$

where subscript o refers to the pure state.

Eqn. 13 or 15 may form the basis for a calculation of $y''_D - y'_D$ and thereby the isotope separation effect, $[y''_D - y'_D]/[y'_D(1-y''_D)]$ (while the term in eqn. 12 containing $(y''_D - y'_D)$ is of second order only).

2. Approximations

2. 1. *Basic considerations.* Eqns. 12, 13 and 15 are valid regardless of the number of chemical species, due to reactions between the three components, that may be present in the two phases as long, as full equilibrium has been reached. It should be noted, however, that the formulation of approximate chemical potential functions is simplified when information about the presence or non-presence of chemical species, can be introduced. In general three types of reactions leading to the formation of new chemical species should be considered:

1) Equilibrium isotope exchange with the organic component according to the following reaction scheme

$$\tfrac{1}{2}\ D_2O + HB \rightleftharpoons \tfrac{1}{2}\ H_2O + DB \tag{17}$$

where HB is added organic component and DB is the same deuterated. TEA exchanges slowly, if at all, with D_2O. The following theoretical considerations are valid only when this kind of reaction can be neglected.

2) Reaction with the organic component of the following type:

$$H_2O + TEA \rightleftharpoons TEAH^+ + OH^-. \tag{18}$$

Such reaction products may be present in the D_2O-H_2O-TEA system. No accurate information is available and is, in fact, thought to be unnecessary for the following description of the system (where the parameters $[D_2O]$ and $[H_2O]$ include both ions and neutral molecules, and any isotope effects in the reactions are disregarded.) See below (p. 1742) for further comments.

3) $$D_2O + H_2O \rightleftharpoons 2\ HDO \tag{19}$$

This reaction takes place to a degree determined by

$$\frac{f_{HDO}^2[HDO]^2}{f_H f_D[H_2O][D_2O]} = K^* \text{ where } K^* \simeq 4 \tag{20}$$

and f_D, f_H and f_{HDO} are the activity coefficients of D_2O, H_2O, and HDO, respectively.

By taking into account that $K \equiv \frac{1}{4} \cdot \frac{f_H f_D}{f_{HDO}^2} K^*$ is near one (see below) and introducing the two conditions that

$$[D_2O] + [H_2O] + [HDO] = x_W \tag{21a}$$

and

$$[D_2O] + \tfrac{1}{2}[HDO] = y_D x_W \tag{21b}$$

one obtains the following three equations

$$\begin{aligned} [D_2O] &= (1 + a) y_D^2 x_W \\ [H_2O] &= (1 + b)(1-y_D)^2 x_W \\ [HDO] &= 2(1 + c)\, y_D (1-y_D) x_W \end{aligned} \tag{22}$$

Here a, b and c are small compared to one, so the approximation may be made that

$$K = \frac{(1 + c)^2}{(1 + a)(1 + b)} \simeq 1 + 2c - a - b$$

then a, b, and c can be expressed in the following way

$$\begin{aligned} a &= -(K-1)(1-y_D)^2 \\ b &= -(K-1) y_D^2 \\ c &= \ \ (K-1) y_D (1-y_D) \end{aligned} \tag{23}$$

In pure D_2O-H_2O mixtures $K = 0.83$ (Ref.[3]) and the same must be approximately the case in the TEA-water mixture, since f_{DHO} must be near $\sqrt{f_D f_H}$.

2.2. *First approximation.* The change in chemical potential with composition may be written

$$\left(\frac{\partial \mu_D}{\partial z_1}\right)_{T,z_2} = RT\left(\frac{\partial \ln[D_2O]}{\partial z_1}\right)_{T,z_2} + RT\left(\frac{\partial \ln f_D}{\partial z_1}\right)_{T,z_2} \quad (24)$$

and similarly for μ_H and μ_A. The three partial derivatives, $(\partial \ln f/\partial y_D)_{T,x_W}$, result from changes in the medium (triethylamine phase) when D_2O is substituted for H_2O at constant water content (x_W); while the three partial derivatives, $(\partial \ln f/\partial x_W)_{T,y_D}$ result from changes in the medium when the water content is increased at constant y_D, the isotopic composition. $|\partial \ln f/\partial y_D|$ must obviously be considerably smaller than the corresponding $|\partial \ln f/\partial x_W|$, so it would seem to be a justifiable first approximation to assume that

$$\partial \ln f/\partial y_D = 0 \quad (25)$$

This has the following implications:

1) K (eqn. 23) will be independent of y_D.

2) (eqn. 22):
$$\left(\frac{\partial \mu_D}{\partial y_D}\right)_{T,x_W} = RT\left(\frac{\partial \ln[D_2O]}{\partial y_D}\right)_{T,x_W} = \frac{2RT}{y_D} + RT\left(\frac{\partial \ln (1+a)}{\partial y_D}\right)_{T,x_W}$$

$$\left(\frac{\partial \mu_H}{\partial y_D}\right)_{T,x_W} = RT\left(\frac{\partial \ln[H_2O]}{\partial y_D}\right)_{T,x_W} = -\frac{2RT}{1-y_D} + RT\left(\frac{\partial \ln(1+b)}{\partial y_D}\right)_{T,x_W} \quad (26)$$

$$\text{Here } \frac{\partial \ln (1+a)}{\partial y_D} = (K-1)2(1-y_D) \text{ and } \frac{\partial \ln (1+b)}{\partial y_D} = -(K-1)2\, y_D \quad (27)$$

These two derivatives are fairly small correction terms, so

$$y_D \frac{\partial \mu_D}{\partial y_D} + (1-y_D)\frac{\partial \mu_D}{\partial y_D} = 0 \text{ and} \quad (28)$$

$$\frac{\partial \mu_D}{\partial y_D} - \frac{\partial \mu_H}{\partial y_D} = \frac{2RT}{y_D} + \frac{2RT}{1-y_D} + 2RT(K-1) \simeq \frac{2RT}{y_D(1-y_D)} \quad (29)$$

Neglecting $K-1$ probably causes only a 5 % error at maximum, at $y_D = \frac{1}{2}$.

3) From $\partial \ln f_A/\partial y_D = 0$ at any x_W and the Gibbs-Duhem equation applied to pure H_2O-TEA and D_2O-TEA mixtures as follows:

$$x_W \frac{\partial \ln f_{Hh}}{\partial x_W} + (1-x_W)\frac{\partial \ln f_{Ah}}{\partial x_W} = 0$$

and (30)

$$x_W \frac{\partial \ln f_{Dd}}{\partial x_W} + (1-x_W)\frac{\partial \ln f_{Ad}}{\partial x_W} = 0$$

it follows that

$$\frac{\partial \mu_D}{\partial x_W} = \frac{\partial \mu_H}{\partial x_W} \equiv \frac{\partial \mu_W}{\partial x_W} \text{ at any } y_D \quad (31)$$

and

$$y_D \frac{\partial \mu_D}{\partial x_W} + (1-y_D)\frac{\partial \mu_H}{\partial x_W} = \frac{\partial \mu_W}{\partial x_W} \quad (32)$$

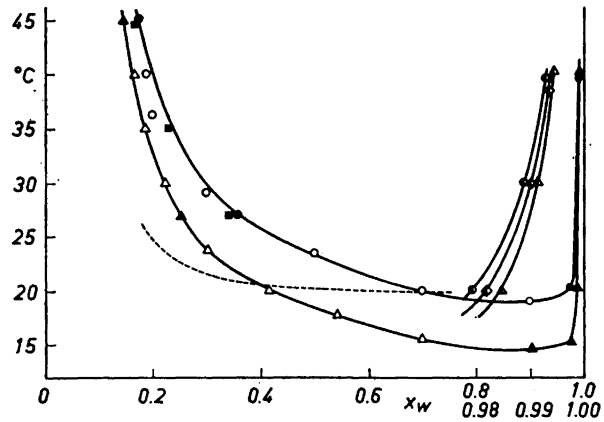

Fig. 2. Solubility curves for mixtures of triethylamine, water and heavy water. x_w is mole fraction of water ($D_2O + H_2O$). The water phase data have been determined by titration.

y_D	Own data: main x_w-scale	Own data: enlarged x_w-scale	Hahn and Street's data[2] (main x_w-scale)
0	●	◐	○
0.20	■		
0.50		◆	
1.00	▲	◭	△

The dashed curve corresponds to the data of Rothmund [9] ($y_D = 0$).

4) With sufficient accuracy it may be assumed that

$$\Delta H_D = \Delta H_H \equiv \Delta H_W \tag{33}$$

These approximations do not imply that there is no difference between f_D and f_H — the activity coefficients of D_2O and H_2O compared at equal x_W — but do imply that the activities or vapour pressures of D_2O and H_2O at any x_W are proportional to $[D_2O]$ and $[H_2O]$, respectively, and that the activity or vapour pressure of TEA at any x_W is independent of y_D. If the latter statement is true for the triethylamine phase it cannot be simultaneously true for the water phase, since the solubility curves (Fig. 2) do not intersect.

2.3. *Second approximations.* The approximate potential functions developed above give simple and useful equations when applied to the fundamental equilibrium conditions (eqns. 12, 13 and 15); it is, however, of interest to estimate the magnitude of the error introduced by neglecting the derivatives $\partial \ln f / \partial y_D$. The data available make in fact this possible if the assumption is made that all three derivatives are constants in the interval $0 \leqq y_D \leqq 1$. This immediately necessitates (the Gibbs-Duhem eqn. 5) that

$$\frac{\partial \ln f_D}{\partial y_D} = \frac{\partial \ln f_H}{\partial y_D} \left(= - \frac{1 - x_W}{x_W} \frac{\partial \ln f_A}{\partial y_D} \right) \equiv M \tag{34}$$

Therefore

$$\ln f_D - \ln f_{Dd} = -M(1-y_D)$$

and

$$\ln f_H - \ln f_{Hh} = My_D \tag{35}$$

$$\text{so} \quad \left(\frac{\partial \ln f_D}{\partial x_W}\right)_{T,y_D} = \left(\frac{\partial \ln f_{Dd}}{\partial x_W}\right)_T - (1-y_D)\left(\frac{\partial M}{\partial x_W}\right)_T \tag{36}$$

$$\text{and} \quad \left(\frac{\partial \ln f_H}{\partial x_W}\right)_{T,y_D} = \left(\frac{\partial \ln f_{Hh}}{\partial x_W}\right)_T + y_D\left(\frac{\partial M}{\partial x_W}\right)_T$$

where d and h refers to pure D_2O- and H_2O-triethylamine systems, respectively. Differentiating eqn. 34 gives

$$\frac{\partial M}{\partial x_W} = -\frac{1-x_W}{x_W}\frac{\partial}{\partial x_W}\left(\frac{\partial \ln f_A}{\partial y_D}\right) + \frac{1}{x_W^2}\frac{\partial \ln f_A}{\partial y_D} \tag{37}$$

The following relations may now be derived:

1) Eqn. 34, with the resonable assumption that also $\partial \ln f_{DHO}/\partial y_D = M$, shows that K of eqn. 23 under these conditions also becomes independent of y_D.

2) From eqns. 34 (*cf.* eqns. 28 and 29) the following results are obtained:

$$y_D\frac{\partial \mu_D}{\partial y_D} + (1-y_D)\frac{\partial \mu_H}{\partial y_D} = RTM = -RT\frac{1-x_W}{x_W}\frac{\partial \ln f_A}{\partial y_D}$$

$$= -RT\frac{1-x_W}{x_W}\left(\ln\frac{f_{Ad}}{f_{Ah}}\right)_{x_W} \tag{38}$$

and

$$\frac{\partial \mu_D}{\partial y_D} - \frac{\partial \mu_H}{\partial y_D} \simeq \frac{2RT}{y_D(1-y_D)} \tag{39}$$

3) From eqns. 36 and 37 it follows that

$$\frac{\partial \ln f_D}{\partial x_W} - \frac{\partial \ln f_H}{\partial x_W} = \frac{\partial \ln(f_{Dd}/f_{Hh})}{\partial x_W} + \frac{1-x_W}{x_W}\frac{\partial}{\partial x_W}\left(\frac{\partial \ln f_A}{\partial y_D}\right) - \frac{1}{x_W^2}\frac{\partial \ln f_A}{\partial y_D}$$

and introducing eqn. 30 gives

$$\frac{\partial \mu_D}{\partial x_W} - \frac{\partial \mu_H}{\partial x_W} = -\frac{RT}{x_W^2}\left(\ln\frac{f_{Ad}}{f_{Ah}}\right)_{x_W} \tag{40}$$

Eqn. 36 yields

$$y_D\frac{\partial \mu_D}{\partial x_W} + (1-y_D)\frac{\partial \mu_H}{\partial x_W} = y_D\frac{\partial \mu_{Dd}}{\partial x_W} + (1-y_D)\frac{\partial \mu_{Hh}}{\partial x_W} \tag{41}$$

4) Differentiation of eqn. 34 with respect to temperature and introduction of

$$\frac{\partial \ln f}{\partial T} = -\frac{\Delta H}{RT^2} \tag{42}$$

(where ΔH is the partial molar enthalpy of mixing) gives

$$-\frac{\partial \Delta H_D}{\partial y_D} = -\frac{\partial \Delta H_H}{\partial y_D} = \frac{1-x_W}{x_W}\frac{\partial \Delta H_A}{\partial y_D} = RT^2\frac{\partial M}{\partial T} \tag{43}$$

So $$-\Delta H_D + \Delta H_{Dd} = -RT^2\frac{\partial M}{\partial T}(1-y_D) \tag{44}$$

and $$-\Delta H_H + H_{Hh} = RT^2\frac{\partial M}{\partial T}\, y_D$$

By subtraction $$(\Delta H_D - \Delta H_H) - (\Delta H_{Dd} - \Delta H_{Hh}) = RT^2\frac{\partial M}{\partial T} \tag{45}$$

while $$y_D\Delta H_D + (1-y_D)\Delta H_H = y_D\Delta H_{Dd} + (1-y_D)\Delta H_{Hh} \tag{46}$$

The preceding systems of equations are based on the assumption that ideal conditions or conditions approaching the ideal are maintained when, in TEA-water mixtures, D_2O is interchanged with H_2O, the total amount of water (x_W) being held constant. It is, however, possible, as mentioned earlier, that reactions of the following type take place: TEA + $H_2O \rightleftharpoons TEAH^+ + OH^-$. The extent to which TEA reacts with H_2O is probably not exactly the same as with D_2O. The ratio of the amounts of the two types of chemical species could have marked influence on the medium, so one could expect that a different parameter in place of x_W might be required. Infrared tests for the presence of NH^+— and ND^+—bonds showed that not more and probably much less than 10 % of the water in the TEA-phase is in the ionized form. An approximate calculation shows that the presence of ions in that concentration probably has so little effect that it is taken into account in a satisfactory manner by the introduction of the second set of approximations (eqn. 34). A comparatively successful determination of $\ln(f_{Ad}/f_{Ah})$ which is discussed below points in the same direction.

3. Application of the approximations to the equilibrium equations.

3.1. *First approximations.* Introducing the simple first approximations represented by eqns. 28, 29, 31, and 32 into eqns. 12, 13, and 15 gives

$$\left(\frac{\partial \mu'_W}{\partial x_W}\right)_{T,y_D}\left(\frac{dx'_W}{dT}\right)_{eq,y'_D} = \frac{\Delta H'_W}{T} \tag{47}$$

$$2RT\,\frac{y''_D - y'_D}{y'_D(1-y'_D)}\left(\frac{dy'_D}{dT}\right)_{eq,x'_W} = \frac{\Delta H'_W}{T} \tag{48}$$

$$\left(\frac{\partial \mu'_W}{\partial x_W}\right)_{T,y_D}\left(\frac{dx'_W}{dy'_D}\right)_{eq,T} = -2RT\,\frac{y''_D - y'_D}{y'_D(1-y'_D)} \tag{49}$$

where x''_W has been set equal to one, $\Delta H''_W$ equal to zero and where $(1-x''_W)(\Delta H'_A - \Delta H''_A) \ll \Delta H'_W$ is neglected (see Fig. 2).

The isotope separation effect, $[y''_D(1-y'_D)/y'_D(1-y''_D)]-1$, for all practical purposes equal to $(y''_D - y'_D)/y'_D(1-y'_D)$, may now be calculated from either eqn. 48 or 49 using available data for the partial vapour pressure of H_2O in

TEA—H_2O mixtures and available determinations of the heat of mixing of TEA and H_2O, together with the solubility curves.

Eqn. 49 is analogous to the Duhem-Margules equation (in one of its forms) for a binary liquid mixture (e.g. D_2O and H_2O) in equilibrium with its vapour: in fact, substituting in eqns. 3 to 5 $x_A d\mu_A$ for $v \cdot dp$ (where v is the molar volume of the gasous mixture and p the total pressure) and choosing as independent variables y_D (the composition of the vapour) (or x_D, since $x_W = 1$) and p, one arrives at three equations analogous to eqns. 47 to 49.

$$RT\left(\frac{\mathrm{d}\ln p}{\mathrm{d}T}\right)_{\mathrm{eq},y} = y''_D(S'_D - S''_D) + (1-y''_D)(S'_H - S''_H) \tag{50}$$

$$2RT\,\frac{y''_D - y'_D}{y'_D(1-y'_D)}\left(\frac{\mathrm{d}y'_D}{\mathrm{d}T}\right)_{\mathrm{eq},p} = y''_D(S'_D - S''_D) + (1-y''_D)(S'_H - S''_H) \tag{51}$$

and the Duhem-Margules equation:

$$RT\left(\frac{\mathrm{d}\ln p}{\mathrm{d}y'_D}\right)_{\mathrm{eq},T} = -\,2RT\,\frac{y''_D - y'_D}{y'_D(1-y'_D)} \tag{52}$$

Eqn. 50 is the equation for the vapour pressure curve.

From eqn. 51 the separation effect may be calculated when the heat of evaporation (and, if necessary, of solution) and the boiling point as a function of vapour composition are known.

Eqn. 52 relates the relative volatility of the pure components to the separation effects. If, in eqn. 49, $\partial\mu'_W/\partial x_W$ is set equal to RT/x'_W, eqns. 49 and 52 become identical in form. It will be shown below that this assumption is not at all permissible; however, eqn. 49, simplified in this manner, is of interest because it may have formed the basis for optimistic estimations of the isotope separation potentialities of this system and other similar systems.

3.2. *Second approximations.* Introducing the second approximation represented by eqns. 38, 39, 40, and 41 into eqns. 12, 13, and 15 gives:

(eqn. 12)

$$\frac{x''_W - x'_W}{1-x'_W}\left(y'_D\frac{\partial\mu_{Dd}}{\partial x_W} + (1-y'_D)\frac{\partial\mu_{Hh}}{\partial x_W}\right) - x''_W\,\frac{(y''_D - y'_D)}{x'^2_W}\,RT\left(\ln\frac{f_{Ad}}{f_{Ah}}\right)_{x'_W} =$$

$$\left(\frac{\mathrm{d}T}{\mathrm{d}x'_W}\right)_{\mathrm{eq},y'_D}\left[x_W\left(y''_D\,\frac{\Delta H'_D - \Delta H''_D}{T} + (1-y''_D)\,\frac{\Delta H'_H - \Delta H''_H}{T}\right) + (1-x''_W)\,\frac{\Delta H'_A - \Delta H''_A}{T}\right] \tag{53}$$

(eqn. 13)

$$-\,\frac{x''_W - x'_W}{x'_W}\left(\ln\frac{f_{Ad}}{f_{Ah}}\right)_{x'_W} RT + 2RT\,\frac{x''_W(y''_D - y'_D)}{y'_D(1-y'_D)} =$$

$$\left(\frac{\mathrm{d}T}{\mathrm{d}y'_D}\right)_{\mathrm{eq},x'_W}\left[x''_W\left(y''_D\,\frac{\Delta H'_D - \Delta H''_D}{T} + (1-y''_D)\,\frac{\Delta H'_H - \Delta H''_H}{T}\right) + (1-x''_W)\,\frac{\Delta H'_A - \Delta H''_A}{T}\right] \tag{54}$$

(eqn. 15)

$$\left[\frac{x''_W-x'_W}{1-x'_W}\left(y'_D\frac{\partial\mu_{Dd}}{\partial x_W}+(1-y'_D)\frac{\partial\mu_{Hh}}{\partial x_W}\right)-\frac{x''_W(y''_D-y'_D)}{x'^2_W}RT\left(\ln\frac{f_{Ad}}{f_{Ah}}\right)_{x'_W}\right]\times$$
$$\times\left(\frac{dx'_W}{dy'_D}\right)_{eq,T}=\frac{x''_W-x'_W}{x'_W}\left(\ln\frac{f_{Ad}}{f_{Ah}}\right)_{x_W}RT-2RT\frac{x''_W(y''_D-y'_D)}{y'_D(1-y'_D)} \quad (55)$$

(It should be noted that $(\partial\mu_{Dd}/\partial x_W)_{x_W=x'_W}$ and $(\ln f_{Ad})_{x'_W}$ apply to the unstable region, because $x'_W > x'_{W,d}$ (the solubility of D_2O).)

The terms that distinguish eqns. 53—55 from eqns. 47—49 contain $\ln(f_{Ad}/f_{Ah})$. When therefore an estimate of this quantity has been made, it will be possible to calculate the separation effect by eqn. 54 or 55. The difference between $\partial\mu_{Dd}/\partial x_W$ and $\partial\mu_{Hh}/\partial x_W$ and between ΔH_D and ΔH_H may be neglected, at least at low y'_D.

3.3. $\ln(f_{Ad}/f_{Ah})$ could be easily calculated, if the vapour pressure curve of pure D_2O—TEA mixtures were known. Failing this the same information may in principle be obtained from the solubility curves (Kohler [4]); however the accuracy of this approach is limited so that the following treatment may furnish only the order of magnitude of $\ln(f_{Ad}/f_{Ah})$.

3.3.1. First an expression for $(\ln(f_{Dd}/f_{Hh}))_{x_W}$ is to be found:

Corresponding to eqn. 1 the following two equations may be written, inserting eqn. 22,

for μ_D at $T = T_D$, $x_W = x'_W$ and $y'_D = 1$:

$$\ln x'_W + \ln f'_{Dd} = \ln x''_{W,D} + \ln f''_{Dd} \quad (56)$$

for μ_H at $T = T_H$, $x_W = x'_W$ and $y'_D = 0$:

$$\ln x'_W + \ln f'_{Hh} = \ln x''_{W,H} + \ln f''_{Hh} \quad (57)$$

where x'_W, T_D and $x''_{W,D}, T_D$ are corresponding points on the D_2O-TEA solubility curve and x'_W, T_H and $x''_{W,H}, T_H$, are corresponding points on the H_2O-TEA curve.

By subtraction and introduction of eqn. 42 (integrated)

$$\left(\ln\frac{f'_{Dd}}{f_{Hh}}\right)_{T=T_D}=\frac{T_D-T_H}{RT_DT_H}\Delta H'_{Hh}+\ln\frac{x''_{W,D}}{x''_{W,H}}+(\ln f''_{Dd})_{T=T_D}-(\ln f''_{Hh})_{T=T_H} \quad (58)$$

The vapour pressure data available show that $\ln f''_{Hh} \simeq 0.01$ and it is unlikely that $\ln f''_{Dd}$ is very much different.

Solubility experiments (see Fig. 2) show that

$$\ln\frac{x''_{W,D}}{x''_{W,H}} \simeq \ln 0.999 = -10^{-3}.$$

Enthalpy data and solubility data (see Table 3 and Fig. 2) show that

$$\frac{T_D-T_H}{RT_DT_H}\Delta H'_{Hh} \simeq 0.03$$

so eqn. 58 may be reduced to

$$\left(\ln\frac{f'_{Dd}}{f_{Hh}}\right)_{T=T_D}=\frac{T_D-T_H}{RT_DT_H}\Delta H'_{Hh} \quad (59)$$

From eqn. 42 it follows that at any temperature, at constant x_W

$$\left(\ln \frac{f_{Dd}}{f_{Hh}}\right)_{x_w,T} = -\frac{T-T_D}{RTT_D}\left[\Delta H_{Dd}-\Delta H_{Hh}\right] + \frac{T_D-T_H}{RT_DT_H}\Delta H_{Hh} \tag{60}$$

which is reduced to eqn. 59 as long as

$$|(T-T_D)(\Delta H_{Dd}-\Delta H_{Hh})| << |(T_D-T_H)\Delta H_{Hh}| \tag{61}$$

This is probably valid in the interval covered by the known parts of the solubility curves. ΔH has been assumed independent of T.

From the reduced form of eqn. 60 it is seen that

$$\frac{\partial \ln(f_{Dd}/f_{Hh})}{\partial x_W} = \frac{d}{dx_W}\left(\frac{T_D-T_H}{RT_DT_H}\Delta H_{Hh}\right) \tag{62}$$

This relationship probably holds even near the critical compositions ($x_{cr,D}$ may be somewhat different from $x_{cr,H}$)as may be seen in the following way:

$\left(\frac{dT_D}{dx'_W}\right)_{eq,y'_D=1}$ and $\left(\frac{dT_H}{dx'_W}\right)_{eq,y'_D=0}$ (subscripts D and H refers to the solubility curves for pure D_2O and H_2O, respectively) are zero at, and very small in an interval around, the critical points. In eqn. 53 the enthalpy terms are proportional to $(x''_W-x'_W)^2$ near the critical composition as expansion of these terms by Taylor's Series will show so, at $x_W \simeq x_{cr}$,

$$\left(\frac{\partial \mu'_{Dd}}{\partial x_W}\right)_{T_D} \simeq \left(\frac{\partial \mu'_{Hh}}{\partial x_W}\right)_{T_H} \simeq 0 \tag{63}$$

this leads to eqn. 62 (*cf.* eqn. 42) noting that

$$\frac{d}{dx_W}\left(\frac{T_D-T_H}{RT_DT_H}\right) \simeq \frac{1}{RT_DT_H}\left(\frac{dT_D}{dx_W} - \frac{dT_H}{dx_W}\right) \simeq 0 \tag{64}$$

Incidentally, a comparison of eqns. 63 and 31 shows the limited applicability of the simple approximations, represented by eqn. 25 near the critical points.

3.3.2. Since $f_{Ad} = f_{Ah} = 1$ for $x_W = 0$ (as has been tacitly assumed above) an integration of eqn. 30 at temp. T between 0 and x'_W yields

$$\left(\ln \frac{f_{Ad}}{f_{Ah}}\right)_{x'_w} = -\int_0^{x'_w} \frac{x_W}{1-x_W}\frac{\partial \ln(f_{Dd}/f_{Hh})}{\partial x_W}\,dx_W \tag{65}$$

$\lim_{x_w \to 0} \frac{x_W}{1-x_W}\frac{\partial \ln(f_{Dd}/f_{Hh})}{\partial x_W} = 0$, so extrapolating eqn. 62 to $x_W = 0$ and inserting it into eqn. 65 probably results in only a relatively small error:

$$\left(\ln \frac{f_{Ad}}{f_{Ah}}\right)_{x'_w} \simeq -\int_0^{x'_w} \frac{x_W}{1-x_W}\frac{d}{dx_W}\left(\frac{T_D-T_H}{RT_DT_H}\Delta H_{Hh}\right)dx_W \tag{66}$$

Integrating by parts

$$\left(\ln \frac{f_{Ad}}{f_{Ah}}\right)_{x'_w} \simeq -\left[\frac{x'_W}{1-x'_W}\frac{T_D-T_H}{RT_DT_H}\Delta H'_{Hh} - \int_0^{1/(1-x'_w)} \frac{T_D-T_H}{RT_DT_H}\Delta H_{Hh}\,d\,\frac{1}{1-x_W}\right]$$

$$\equiv -\frac{x'_W}{1-x'_W}\left[\frac{T_D-T_H}{RT_DT_H}\Delta H'_{Hh} - \overline{\frac{T_D-T_H}{RT_DT_H}\Delta H_{Hh}}\right] \tag{67}$$

where $\frac{T_D-T_H}{RT_D T_H}\Delta H_{Hh}$ is the average of $\frac{T_D-T_H}{RT_D T_H}\Delta H_{Hh}$ as a function of $1/(1-x_W)$ in the interval from 1 to $1/(1-x'_W)$.

NUMERICAL CALCULATION

The simplification that the enthalpy of mixing, ΔH, is independent of temperature is not necessary for the development of the system of equations presented above (though a large temperature coefficient would make the step from eqn. 60 to 59 more uncertain). In the numerical calculation, on the other hand, any appreciable change with temperature should be taken into account. Only enthalpy data below 18°C are available but it is possible to obtain some idea of the temperature dependence of ΔH in the range considered from a comparison between results obtained in different ways (see below). The conclusion reached is that ΔH, with sufficient accuracy, may be considered independent of temperature.

First approximations. The simple eqns. 48 or 49 may be used for the calculation of $(y''_D-y'_D)/y'_D(1-y'_D)$, when $(dT/dy'_D)_{eq,x'_W}$ or $(dx'_W dy'_D)_{eq,T}$, respectively, are assumed to be constant. These conditions are incompatible and it is seen that $(dx'_W/dy'_D)_{eq,T}$ cannot be independent of y'_D (at constant T) near the critical temperature while this is quite possible for $(dT/dy'_D)_{eq,x'_W}$ (at constant x'_W). Eqn. 48 is therefore the more correct. This is, however, of only small importance when the solubility curves are sufficiently close to being straight parallel lines.

Eqn. 49 may be written

$$\frac{y''_D-y'_D}{y'_D(1-y'_D)} = -\frac{x'_{w,d}-x'_{w,h}}{2x'_W} Q \tag{68}$$

where

$$Q = \frac{\partial\mu'_W/\partial x_W}{RT(\partial\ln x'_W/\partial x_W)} = 1 + x'_W \frac{\partial\ln f'_W}{\partial x_W} = x'_W \frac{\partial\ln(P'_W/P_{WO})}{\partial\ln x_W} \tag{69}$$

and $x'_{W,h}$ and $x'_{W,d}$ are the solubilities of pure D_2O and H_2O at temperature T. For the present calculation, Q has been found by extrapolating the vapour pressure data of Kohler [5] at 18°C with the help of the enthalpy data from Copp and Everett [6] at 15°C (see Table 3 and Fig. 3).

Eqn. 48 may be written

$$\frac{y''_D-y'_D}{y'_D(1-y'_D)} = \frac{T_D-T_H}{2RT^2}\Delta H'_W \tag{70}$$

where T_D and T_H are the temperatures at which the solubilities of pure D_2O and H_2O are x'_W. Again the ΔH data from Copp and Everett [6] have been employed, without any temperature corrections (see Table 3 and Fig. 3).

For both sets of calculations the solubility curves shown in Fig. 2 has been used. These are drawn through the experimental points obtained in this labora-

Table 3. Numerical results obtained with the vapour pressure data of Kohler [5], the enthalpy data of Copp and Everett [6] and with the solubility data shown in Fig. 2. $y_D = 0.20$. For further explanation see text.

T	$-\frac{x'_{W,d}-x'_{W,h}}{2x'_W} Q$	$\frac{T_D-T_H}{2RT^2} \Delta H'_W$	$\frac{T_D-T_H}{2RT_DT_H} \Delta H_{Hh}$
°C	(eqn. 68)	(eqn. 70)	(eqn. 72)
22	0.008	0.009	0.018
27	0.017	0.013	0.025
35	0.025	0.021	0.029
45	0.022	0.025	0.030

tory but supported by curves from the paper of Hahn and Street [2]. The absolute position of these curves is not very accurate because small amounts of carbon dioxide may reduce the solubility noticeably (Krichevskii [7]).

The agreement at 35° and 45°C between the separation effects based on eqn. 68 and those based on eqn. 70 may be taken to support the assumption used for their calculation that ΔH varies only little with temperature.

It should be added that such an agreement is not consistent with Kohlers assumption in a later paper [8] according to which ΔH should become zero at 70°C. His conclusion, however, is based on a solubility curve (in a paper by Rothmund [9]) which disagrees with others (*cf.* Fig. 2); in addition, the temperature in question could be anything between 25°C and 145°C, so the disagreement may not be so pronounced as could be expected at first glance.

Second approximations. When $\ln(f_{Ad}/f_{Ah})$ is taken into account in the calculation of the separation effect eqn. 54 should form the basis. It may be simplified

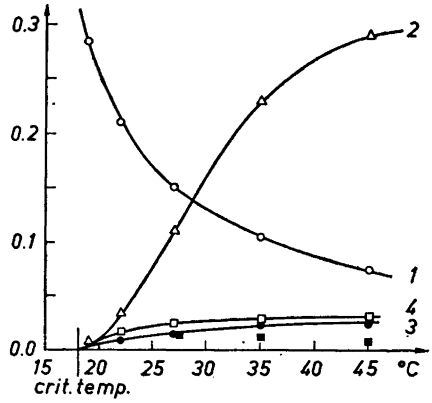

Fig. 3. Calculated (●, eqns. 68 and 70; □, eqn. 72; see Table 3), and experimental (■) isotope separation effects, $(y''_D-y'_D)/y'_D(1-y'_D)$, as compared to a hypothetic separation between ideal mixtures, $\frac{1}{2}(x'_{W,h}-x'_{W,d})/x'_W$ (○, eqn. 52) and the factor $Q = (\partial\mu'_W/\partial x_W)/RT(\partial\ln x'_W/\partial x_W)$ (△, eqn. 69), expressing deviation from ideality.

since

1) $RT^2(\partial M'/\partial T)$ (eqn. 43) is probably small compared to $\Delta H'_{Dd}$ or $\Delta H'_{Hh}$
2) $\Delta H'_{Dd} \simeq \Delta H'_{Hh}$
3) $RT^2(\partial M''/\partial T) \ll \Delta H''_{Hh}$ and $\Delta H''_{Dd} \simeq \Delta H''_{Hh} \ll \Delta H'_{Hh}$
4) $(1-x''_W)(\Delta H'_A - \Delta H''_A) \ll \Delta H'_{Hh}$
5) $x''_W \simeq 1$.

In addition the approximation is again made that $dT/dy'_D = T_D - T_H$. So eqn. 54 becomes

$$\frac{y''_D - y'_D}{y'_D(1-y'_D)} = \frac{T_D - T_H}{2RT^2}\Delta H_{Hh} + \frac{1-x'_W}{2x'_W}\left(\ln\frac{f_{Ad}}{f_{Ah}}\right)_{x'_W} \tag{71}$$

which when eqn. 67 is introduced gives

$$\frac{y''_D - y'_D}{y'_D(1-y'_D)} = \overline{\frac{1}{2}\frac{T_D - T_H}{RT_D T_H}\Delta H_{Hh}} \tag{72}$$

(see Table 3 and Fig. 3).

$\overline{\frac{T_D - T_H}{RT_D T_H}\Delta H_{Hh}}$ has been obtained by graphical integration of

$\frac{T_D - T_H}{RT_D T_H}\Delta H_{Hh}$ as a function of $\frac{1}{1-x_W}$.

Instead of eqn. 54 it may, however, be more instructive to modify eqn. 55 though the resulting equation will be less accurate near the critical point, where $(dx_W/dy_D)_{eq,T} \to \infty$ (while $[y''_D - y'_D]/[y'_D(1-y'_D)] \to 0$):

If the second-order term

$$\frac{x''_W(y''_D - y'_D)}{x'^2_W} RT\left(\ln\frac{f_{Ad}}{f_{Ah}}\right)_{x'_W}\left(\frac{dx'_W}{dy'_D}\right)_{eq,T}$$

is neglected and eqn. 34 is introduced, eqn. 55 may be written

$$\left[\frac{1}{x'_W} + y'_D\frac{\partial \ln f'_D}{\partial x_W} + (1-y'_D)\frac{\partial \ln f'_H}{\partial x_W}\right]\left(\frac{dx'_W}{dy'_D}\right)_{eq,T} = -\frac{\partial \ln f'_H}{\partial y_D} - 2\frac{y''_D - y'_D}{y'_D(1-y'_D)} \tag{73}$$

or, approximately,

$$\frac{y''_D - y'_D}{y'_D(1-y'_D)} \simeq -\frac{x'_{w,d} - x'_{w,h}}{2x'_W} - \frac{x'_{w,d} - x'_{w,h}}{2}\frac{\partial \ln f'_H}{\partial x_W} - \frac{1}{2}\frac{\partial \ln f'_H}{\partial y_D} \tag{74}$$

(*cf.* eqns. 68 and 69). The significance of the different terms in eqn. 74 is illustrated in Fig. 3.

CONCLUSION

The approximate chemical potential functions and other relations developed above rest on the assumption that the numerical value of $\partial \ln f / \partial y_D$ is small compared to $\partial \ln f / \partial x_w$; this has been verified by calculation, the actual result being

$$\frac{1}{500}\frac{\partial \ln f_H}{\partial x_W} < \frac{\partial \ln f_H}{\partial y_D} < \frac{1}{100}\frac{\partial \ln f_H}{\partial x_W} \text{ in the interval } 0.1 < x_W < 0.5$$

In Fig. 3 it is illustrated by the difference between curve 1 and 3 (see Fig. 2 for the numerical value of $x'_{w,d}-x'_{w,h}$) compared to the difference between curve 3 and 4; see eqn. 74 for further explanation. Curve 1, the relative solubility change divided by the statistical factor, 2, would be the isotope separation effect to be expected if the simplified version of eqn. 49, analogous to eqn. 52, were applicable — as it would be in an ideal system. The agreement between experimental (also shown in Fig. 3) and theoretical separation effects is satisfactory if the purpose is to verify that this simplification is not permissible.

When the absolute values of $[y''_D-y'_D]/[y'_D(1-y'_D)]$ are considered, the discrepancy appears somewhat more important (Note that the experimental values include one or two border line cases).

It may be caused by an erroneous $x'_{w,d}-x'_{w,h}$ (eqn. 68); this in fact is the most probable explanation because the effect of introducing $\partial \ln f / \partial y_D \neq 0$, almost certainly must cause an increase in $[y''_D-y'_D]/[y'_D(1-y'_D)]$, due to the less ideal appearance of the D_2O—TEA system in comparison to the corresponding H_2O system.

Expressed in another way: It is probable that T_H-T_D (eqn. 70) is too large as the sign of

$$-\frac{T_D-T_H}{RT_DT_H}\Delta H'_{Hh} + \frac{T_D-T_H}{RT_DT_H}\Delta H_{Hh}$$

or any modification of this term, representing a better approximation to the non-ideality of the systems, almost certainly, is positive (eqn. 72).

The discrepancy may, however, be caused by impurities not accounted for by chemical analysis. A doubling of the amount found would be sufficient to make the discrepancy disappear. It may be shown, as mentioned earlier, that a trace of water would have the same effect.

From the point of view of deuterium oxide separation it may, in general, be said that the difference between the solubilities of D_2O and H_2O in an organic medium ($x'_{w,d}-x'_{w,h}$) furnishes a very poor measure of the degree of separation obtainable because large $x'_{w,d}-x'_{w,h}$ almost invariably must mean that the solubility curve is very flat ($(dx'_w/dT)_{eq,y_D}$ large); this again necessitates values of $(\partial \mu'_w/\partial x_w)_{T,y_D}$ very near zero, *i.e.* very far from the ideal RT/x'_w, unless the absolute values of ΔH or/and T_D-T_H are very large. An equation like 68 or 70 is therefore a simple and better basis for comparison.

A general conclusion would seem to be that it is quite unlikely that large D_2O-H_2O separation effects in liquid-liquid mixtures are possible, at any rate, in the absence of extensive chemical isotope exchange.

The author acknowledges with gratitude pern ission to include water-phase solubility determinations obtained by Mr. P. Solgaard.

The author is greatly indebted to Mr. Th. Rosenberg for numerous stimulating discussions and much critical advice.

REFERENCES

1. Carlson, H. C. Report No. AECD-4085 (1943); *U. S. Atomic Energy Comm. Nuclear Sci. Abstr.* **10** (1956) 6137.
2. Hahn, H. T. and Street, E. B. Report No. HW 48735 (1957); *U. S. Atomic Energy Comm. Nuclear Sci. Abstr.* **11** (1957) 6293.
3. Bebbington, W. P., Thayer, V. R. and Proctor, J. F. DP-400 (1959) Appendix A.
4. Kohler, F. *Monatsh.* **88** (1957) 388.
5. Kohler, F. *Monatsh.* **82** (1951) 913.
6. Copp, J. L. and Everett, D. H. *Discussions Faraday Soc.* 1953, No. 15, 174.
7. Krichevskii, I. R., Khazanova, N. E. and Linshitz, L. R. *Doklady Akad. Nauk, SSSR* **100** (1955) 737.
8. Kohler, F., Arnold, H. and Munn, R. J. *Monatsh.* **92** (1961) 876.
9. Rothmund, V. *Z. physik. Chem.* **26** (1898) 461.
10. Levy, A. L. *Nature* **174** (1954) 126.

Received March 13, 1962.

ACTA CHEMICA SCANDINAVICA 16 (1962) 1751–1756

On the Structure of the Crystal Form C of 11-Bromoundecanoic Acid

KÅRE LARSSON

Crystallography Group, Institute of Medical Biochemistry, University of Göteborg, Sweden

The structure of one crystal form of 11-bromoundecanoic acid has been shown to be isomorphous with the C-form of dodecanoic (lauric) acid and a comparison with that form is made. The bromine contact planes are somewhat closer than the corresponding methyl planes in lauric acid.

The crystal behaviour of 11-bromoundecanoic acid is being investigated. The aim is to study the effect of a bromine atom replacing the terminating methyl group in a simple compound, where the crystal forms of the unsubstituted compound (lauric acid) are known and a direct comparison can be made. The possibility of isomorphous replacement of methyl groups with bromine atoms is of course of great importance for the structure analysis of complicated long-chain compounds.

PREPARATION OF CRYSTALS

Several samples of 11-bromoundecanoic acid were available. Two of them had been prepared by different workers using the method described by Ashton & Smith [1]. This acid is an intermediate in the production of the French polyamide "Rilsan" and an industrial sample of the acid from the Organico company (Paris) was purified and kindly supplied by Mr. K. Serck-Hanssen. The available samples have been purified in different ways and are used for a detailed investigation of the polymorphic behaviour of the bromo acid [2].

Crystallization from the melt gives the C-form, as even-numbered fatty acids do. The C-form has only been obtained from solution when somewhat impure samples have been used. It was found accidentally that beautiful single-crystals of the C-form were formed from a solution of a mixture of the acid and its triglyceride dissolved in light petroleum (b.p. 40–60°). These were used for the X-ray work. The C-form melts at 44.5–45.5°. The melt immediately solidifies in a higher melting modification.

X-RAY DATA

Rotation and Weissenberg photographs were taken with CuK radiation about the a and b axes using a calibrated camera. X-Ray data are listed in

Table 1 together with those of the C-form of lauric acid. The unit cell for lauric acid given by Vand *et al.*[3] has been transformed to suit the choice of a unit cell where β is as near 90° as possible. The transformation matrix is

$$\begin{bmatrix} 1 & 0 & 0 \\ 0 & 1 & 0 \\ 2 & 0 & 1 \end{bmatrix}$$

Absent reflexions are $(h0l)$ when h is odd and $(0k0)$ when k is odd corresponding to space group $P2_1/a$. The unit cell contains four molecules.

The intensities of the $(h0l)$ reflexions were estimated visually using the multiple-film technique with scale. They were corrected for the polarization and Lorentz factors but not for absorption. Absolute values were later obtained by comparison with calculated structure factors.

STRUCTURE DETERMINATION

From the X-ray data it was apparent that the structure was isomorphous with the C-form of lauric acid. The coordinates given by Vand *et al.*[3] were not used as the first trial structure, however, as experiences in the use of the heavy-atom method were desirable for long-chain compounds with a regular distribution of light atoms.

A Patterson (010)-projection was calculated and the bromine position readily derived. A bromine-phased electron density projection showed the whole structure and no other peaks of appreciable height.

All atoms were included in the next cycle of structure-factor and electron density calculation. A difference synthesis was made and new coordinates and temperature factors were derived. The hydrogen atoms were included at this stage with coordinates taken from the data given by Vainshtein and Pinsker [4]. The reliability index R_1 was here 0.25. Anisotropic least-squares refinement for atoms except hydrogens was then applied. Due to the large number of parameters in comparison with the number of independent reflexions the shifts were correlated with difference syntheses. It was found that only the heavy atom showed marked anisotropic vibration whereas the vibrations of the light atoms could be fairly well accounted for by an isotropic temperature factor ($B = 4.5$ Å^2). All positional shifts from the third round of least-squares refinement were considerably less than the estimated standard deviations

Table 1. X-Ray data.

	11-Bromoundecanoic acid	Dodecanoic acid
a	9.66 ± 0.06 Å	9.524 ± 0.02 Å
b	4.96 ± 0.03 Å	4.965 ± 0.01 Å
c	28.07 ± 0.15 Å	27.62 ± 0.05 Å
β	99°54′ ± 1°	96°55′ ± 7′
$c \sin \beta$	27.65 ± 0.15 Å	27.42 ± 0.06 Å
density calc.	1.22 ± 0.02 g.cm^{-3}	1.034 g.cm^{-3}
density obs.	1.24 g.cm^{-3}	1.032 g.cm^{-3}

Table 2. Coordinates of the atoms.

Atom	11-Bromoundecanoic acid		Dodecanoic acid	
	x/a	*z/c*	*x/a*	*z/c*
O_1	0.8725	0.0060	0.8799	0.0067
O_2	0.9495	0.0520	0.9381	0.0538
C_1	0.8703	0.0385	0.8655	0.0429
C_2	0.7680	0.0741	0.7500	0.0750
C_3	0.7570	0.1160	0.7483	0.1208
C_4	0.6384	0.1517	0.6251	0.1483
C_5	0.6296	0.1931	0.6251	0.1958
C_6	0.5314	0.2258	0.4983	0.2242
C_7	0.5150	0.2701	0.4955	0.2739
C_8	0.4055	0.3020	0.3783	0.2992
C_9	0.3948	0.3436	0.3724	0.3483
C_{10}	0.2691	0.3791	0.2499	0.3742
C_{11}	0.2552	0.4215	0.2393	0.4237
C_{12}	—	—	0.1183	0.4492
Br	0.1116	0.4531	—	—

and the R_1-value was 0.14. The final temperature factor used for the bromine atom was $\exp(-0.015\ h^2-0.0013\ l^2-0.0012\ hl)$.

The final electron density projection is shown in Fig. 1. The coordinates of the atoms are given in Table 2 together with those of the C-form of lauric acid transformed to the same unit cell. Observed and calculated structure factors are listed in Table 3. Structure factor calculations, Fourier summations and least-squares refinement were performed on a Mercury computer using programs described by Mills and Rollett [5]. The atomic scattering factors for bromine were taken from Thomas and Umeda [6] and for carbon and oxygen from Berghuis *et al.*[7]

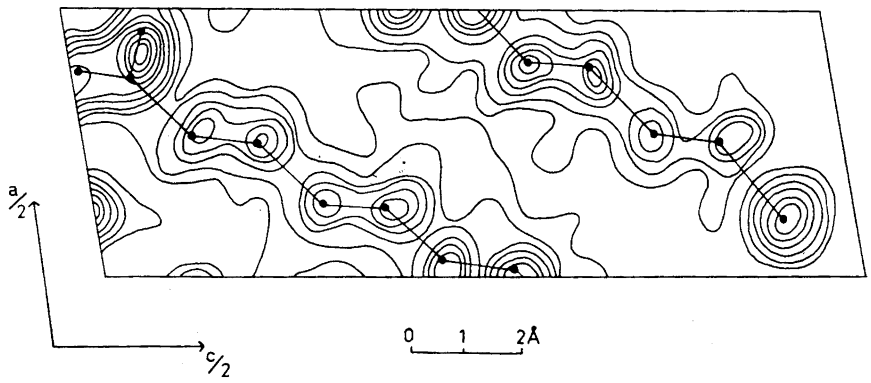

Fig. 1. Electron-density projection along the *b* axis. Contours are given at intervals of 1 eÅ^{-2} for carbon and oxygen and 5 eÅ^{-2} for bromine starting with 1 eÅ^{-2}.

Table 3. Observed and calculated structure factors.

$h\,k\,l$	$\lvert F_o\rvert$	F_c	$h\,k\,l$	$\lvert F_o\rvert$	F_c
0 0 0	—	138	2 0 $\bar{2}\bar{6}$	8.5	10.1
3	5.5	− 5.0	$\bar{2}\bar{7}$	1.7	− 5.4
4	12.8	10.7			
5	5.9	4.7	4 0 0	22.4	−20.7
6	9.8	− 6.8	1	12.5	10.2
7	16.9	14.4	2	12.7	−12.4
8	25.2	−22.5	5	9.8	− 9.9
9	27.0	20.4	6	6.4	− 9.4
10	28.8	−24.4	7	8.7	− 8.6
11	24.1	20.5	8	17.1	18.4
12	29.2	−23.7	9	12.8	−18.0
13	13.5	14.2	10	11.0	12.7
14	6.2	− 4.0	11	11.9	−14.6
15	7.5	7.7	13	4.6	− 8.3
18	8.5	11.5	$\bar{1}$	15.4	14.0
20	9.7	12.4	$\bar{2}$	29.1	−22.7
21	5.0	− 7.9	$\bar{3}$	12.2	12.3
22	8.4	10.5	$\bar{4}$	27.0	−26.6
			$\bar{6}$	27.8	−27.4
2 0 1	8.9	9.7	$\bar{7}$	19.7	−18.0
2	6.9	5.7	$\bar{8}$	11.0	10.2
3	6.1	7.0	$\bar{9}$	17.1	−17.4
4	72.5	−70.7	$\bar{10}$	17.6	16.3
5	22.0	20.5	$\bar{11}$	18.1	−19.3
6	32.7	−31.5	$\bar{12}$	18.7	18.4
7	9.6	14.0	$\bar{13}$	17.6	−16.8
8	10.1	−12.2	$\bar{14}$	19.0	17.1
9	7.9	5.8	$\bar{15}$	12.5	− 8.5
12	9.5	11.5	$\bar{16}$	11.7	9.9
13	7.9	−11.2	$\bar{19}$	12.9	12.4
14	10.8	13.9	$\bar{20}$	22.8	−19.5
15	9.8	−13.1	$\bar{22}$	9.9	−11.8
16	15.5	17.8	$\bar{24}$	8.8	−10.5
17	8.0	−10.5			
$\bar{1}$	5.2	− 4.8	6 0 0	8.2	11.5
$\bar{2}$	14.0	15.0	1	7.9	−11.0
$\bar{3}$	14.0	−12.9	2	8.3	10.1
$\bar{4}$	26.5	27.7	3	9.3	−13.4
$\bar{5}$	18.2	−16.8	4	7.1	8.2
$\bar{6}$	29.1	28.3	$\bar{5}$	8.0	− 9.3
$\bar{7}$	18.4	−15.6	$\bar{2}$	7.0	5.3
$\bar{8}$	25.6	26.9	$\bar{3}$	12.3	12.9
$\bar{9}$	8.5	− 9.4	$\bar{4}$	13.4	−16.0
$\bar{10}$	16.2	21.9	$\bar{5}$	7.4	8.3
$\bar{13}$	9.9	11.8	$\bar{6}$	11.8	−14.7
$\bar{14}$	11.9	−14.4	$\bar{7}$	10.9	13.0
$\bar{15}$	11.8	14.8	$\bar{8}$	13.2	−14.8
$\bar{16}$	17.1	−16.4	$\bar{9}$	8.4	9.8
$\bar{17}$	13.5	15.1	$\bar{10}$	12.4	−12.5
$\bar{18}$	15.5	−15.5	$\bar{15}$	13.5	−13.4
$\bar{19}$	9.7	10.5	$\bar{16}$	15.8	14.0
$\bar{20}$	9.1	−10.4	$\bar{19}$	9.1	−11.3
$\bar{21}$	5.0	4.2	$\bar{20}$	8.4	7.6
$\bar{22}$	5.1	− 5.9	$\bar{21}$	7.6	− 4.6
$\bar{24}$	10.6	12.6			
			8 0 0	9.9	12.2

DISCUSSION

The structure is completely isomorphous with the C-form of lauric acid having the common orthorhombic chain packing ($O_{\perp}$) and the carboxyl groups in the (021)-plane of the subcell. In the C-form of lauric acid the chains are clearly bent in the *a*-axis projection. It is not uncommon that, even in normal long-chain compounds, the molecular packing requires small deviations from the planar zig-zag conformation. As expected, irregularities in the carbon chains become larger when the packing arrangement is more complex such as in branched fatty acids[8,9]. The carbon atoms in the bromine substituted acid do not strictly follow the orthorhombic subcell according to the *b*-axis projection, as the normal to the chain axis through a carbon atom in one chain does not pass through carbon atoms of neighbouring chains. As this also applies to the same projection of lauric acid it seems likely that the chains are bent also in the bromo acid.

Differences in the dimensions and the coordinates are small as can be seen from Tables 1 and 2. The largest differences are found in the distances between alternate carbon atoms which can be calculated if one neglects that the chains are bent. The mean value is 2.65 Å for the bromo acid as compared with 2.51 Å for lauric acid. The standard deviations in the positions estimated from the least-squares treatment are 0.01 Å for the bromine atom, 0.05 Å for the oxygen atoms, and 0.08 Å for the carbon atoms. The angle of tilt of the carbon chains towards the (*a*,*b*)-plane is 54.3°, nearly the same as in lauric acid where it is 54.8°.

The effect of the bromine atom replacing a methyl group can best be studied by a comparison of the packing distances over the bromine and the methyl contact planes, respectively. The fact that lauric acid and 11-bromoundecanoic acid crystallize in isomorphous forms is in itself remarkable and indicates that an ω-bromine atom behaves very similar to a methyl group.

Assuming a bromine-carbon distance of 1.91 Å and that the *y*-coordinate of the carbon atoms are the same as in lauric acid, it is possible to calculate the packing distances over the bromine gap. All distances less than 5.5 Å from one methyl group to carbon atoms on the other side of the methyl gap for the C-form of lauric acid are given by von Sydow [10] as a basis for estimation of the van der Waals interaction. These distances are given in Table 4

Table 4. Distances between the bromine atom and its nearest neighbours on the other side of the bromine gap and corresponding distances for lauric acid.

Number of distances	Atom on the other side of the gap	Distance (Å)	Corresponding distance (Å) for lauric acid
1	Br	3.77	3.85
2	Br	4.15	4.28
1	C_{11}	3.95	4.01
1	C_{11}	4.77	4.72
1	C_{11}	5.40	5.18
1	C_{10}	5.19	5.45
1	C_{10}	5.37	5.45

together with the corresponding distances for 11-bromoundecanoic acid. The bromine-bromine distances are about 0.1 Å shorter than the methyl-methyl distances. The other distances for the bromo acid are smaller or larger than the corresponding ones in lauric acid, due to the effects of a shorter gap but longer chain-terminating bond distance. The end group contact planes are evidently closer in 11-bromoundecanoic acid than in lauric acid corresponding to a van der Waals radius for the bromine atom about 0.05 Å less than that of the methyl group, in accordance with the literature values (*cf.* Ref.[11]).

I wish to thank Dr. S. Abrahamsson for valuable advice during this work and Prof. E. Stenhagen for his interest. I am also indebted to Dr. C. Lagercrantz for providing laboratory space in the Institute of Medical Physics and to Drs. O. S. Mills, K. Prout and J. S. Rollett for use of Mercury programs. Finally I wish to thank Mrs. M. Innes and Mr. L. Ahlquist for technical assistance. Grants in support of the Crystallography group have been obtained from the *National Institute of Arthritis and Metabolic Diseases*, U. S. Public Health Service (A-4006) and from *The Swedish National Science Research Council*, *The Swedish Medical Research Council* and *The Swedish Technical Research Council*.

REFERENCES

1. Ashton, R. and Smith, J. C. *J. Chem. Soc.* **1934** 435.
2. Larsson, K. *To be published.*
3. Vand, V., Morley, W. M. and Lomer, T. R. *Acta Cryst.* **4** (1951) 324.
4. Vainshtein, B. K. and Pinsker, Z. G. *Dokl. Akad. Nauk. SSSR.* **72** (1950) 53.
5. Mills, O. S. and Rollett, J. S. *International Tracts in Computer Science and Technology and Their Application* **4** (1961) 107.
6. Thomas, L. H. and Umeda, K. *J. Chem. Phys.* **26** (1957) 293.
7. Berghuis, J., Haanaapel, Ij. M., Potters, M., Loopstra, B. O., Mac Gillavry, C. H. and Weenendaal, A. L. *Acta Cryst.* **8** (1955) 478.
8. Abrahamsson, S. *Acta Cryst.* **9** (1956) 663.
9. Abrahamsson, S. *Acta Cryst.* **12** (1959) 206.
10. von Sydow, E. *Arkiv Kemi* **9** (1956) 231.
11. Pauling, L. *The Nature of the Chemical Bond*, Cornell Univ. Press, Ithaca 1939, p. 178.

Received March 7, 1962.

ACTA CHEMICA SCANDINAVICA 16 (1962) 1757–1760

Hydrolysis of Vanillyl Methyl Ether

SIGURD LARSSON and BENGT LINDBERG

Istitutionen för träkemi, Kungl. Tekniska Högskolan, Stockholm, Sweden

The hydrolysis of vanillyl methyl ether in the pH-region 3 – 10 at 80° has been studied. The ether was hydrolysed over the whole region, the reaction rate showing a minimum at about pH 5. At pH-values above 6 the kinetics were complicated by side reactions. The results indicate that the reaction proceeds *via* the methylene quinone, formed from the ether by elimination of methanol.

p-Hydroxybenzyl alcohols and ethers are easily transformed into *p*-hydroxybenzyl sulphonic acids on treatment with sulphite not only in acid but also in neutral or alkaline solutions and moreover show greater reactivity than the corresponding *p*-alkoxyderivatives in other reactions. It is believed that groups in lignin, showing similar reactivity, are also of the *p*-hydroxybenzyl alcohol or ether type [1]. In a previous paper from this department [2] dealing with the reaction between vanillyl alcohol (I) and sulphite it was concluded that the formation of the sulphonic acid (III) proceeded *via* the methylene quinone (II), the formation of which should be catalysed by both acids

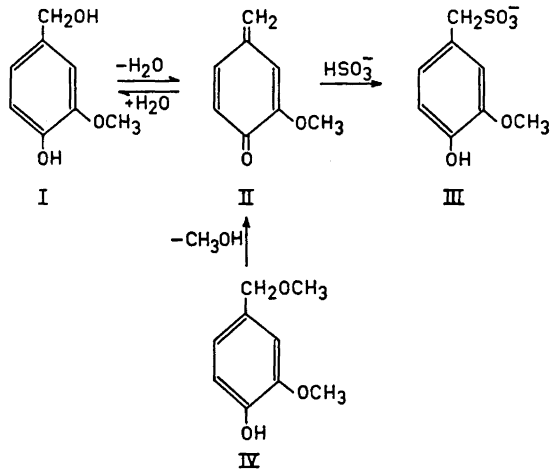

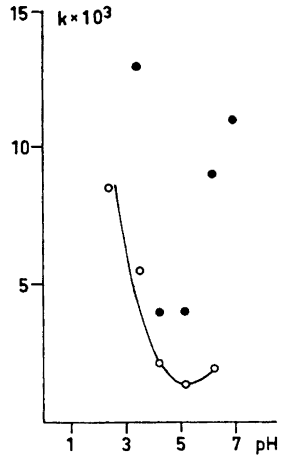

Fig. 1. First rate constant (min^{-1}) for the hydrolysis, at 80°, of vanillyl methyl ether *versus* pH (full line and O). Approximate values for the first order rate constant for formation, at 80°, of the methylene quinone from vanillyl alcohol (●).

and bases. If *p*-hydroxybenzyl ethers, as vanillyl methyl ether (IV), react in an analogous way, then they should also be hydrolysed in acid as well as neutral and alkaline aqueous solutions. In order to test this, a study of the hydrolysis of vanillyl methyl ethers has been conducted.

Vanillyl methyl ether has not been described in the literature but has been prepared by Dr. B. Leopold and by Dr. J. Gierer by treating vanillyl alcohol with methanolic hydrogen chloride (private communications). It is a crystalline substance, m.p. 34—35°. The hydrolysis of the vanillyl methyl ether at 80°

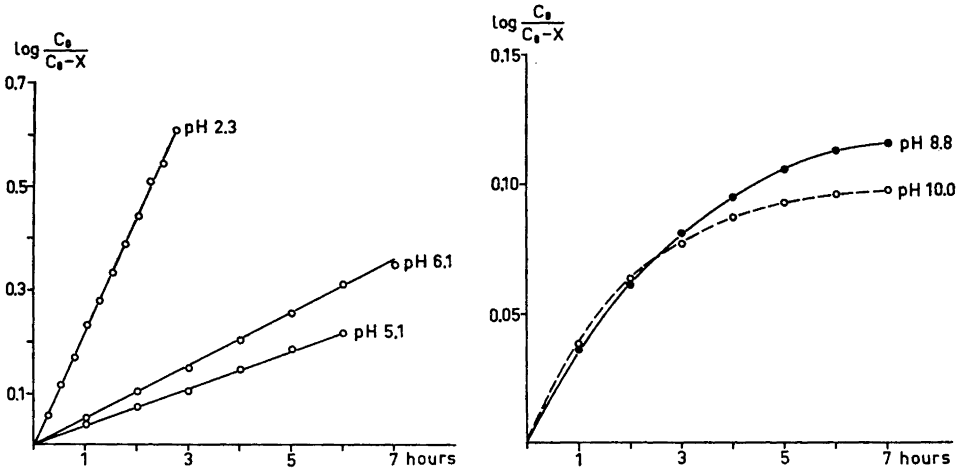

Figs. 2 and 3. Hydrolysis of vanillyl methyl ether at various pH-values.
C_o = original concentration of starting material
X = observed concentration of vanillyl alcohol.

in aqueous buffers between pH 3 and 10 was studied. The ionic strength was the same, 0.3, in all experiments. The reaction was followed by determining the vanillyl alcohol formed by the colour reaction with 2,6-dibromo-benzoquinone-4-chloroimine [3], which gives a blue indophenol with the alcohol but not with the ether. Good first order rate constants were observed up to pH 6 (Fig. 1).

At higher pH-values the significance of the results was obscured by side reactions. The solutions turned dark and a precipitate was formed. This is not unexpected as methylene quinones are known to be extremely labile in alkaline solutions, giving dimers and polymers [4]. The solutions gave the colour reaction with 2,6-dibromo-benzoquinone-4-chloroimine, which indicates the formation of vanillyl alcohol also at these pH-values. The formation of colour went through a maximum, which is expected as the vanillyl alcohol formed should also react further in analogous reactions, proceeding over the methylene quinone. The presence of vanillyl alcohol in the reaction product was demonstrated by thin layer chromatography, which also revealed the presence of products other than vanillyl alcohol and the starting material.

In our previous communication [2] were included approximate values for the rate of formation of the methylene quinone from vanillyl alcohol determined at 80° and various pH-values. The values obtained are plotted in Fig. 1 together with values for the hydrolysis of vanillyl methyl ether under the same conditions. The two sets of values are of the same order of magnitude and show the same pH-dependence, with a minimum around pH 5.

Vanillyl methyl ether is thus hydrolysed at all the pH-values studied. Further the rate of hydrolysis and the analogous rate of formation of the methylene quinone from vanillyl alcohol are of similar orders of magnitude and show the same pH-dependency. The similar high reactivity of *p*-hydroxybenzyl alcohols and *p*-hydroxybenzyl ethers towards sulphite, sulphides, methanolic hydrogen chloride and other reagents, as well as the reactivity of the corresponding groups in the lignin molecule towards the same reagents, are readily understood if it is assumed that they proceed over a methylene quinone intermediate, formed by elimination of water or alcohol from the *p*-hydroxybenzyl derivative.

In a recent paper Filar and Winstein [5] have stated that all nucleophilic substitutions of substances of the type V, including the alkaline hydrolysis of

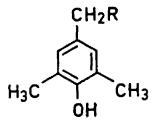

V

the acetate (R = OAc), proceed over the corresponding methylene quinone. This lends further support to the conclusions reached in the present study.

The hydrolysis of vanillyl methyl ether at pH 5.1 and 70° and 90° was also studied. From the values of the rate constants obtained, the apparent activation energy could be determined to be 26 kcal/mole.

EXPERIMENTAL

Vanillyl methyl ether. Vanillyl alcohol (2 g) was dissolved in 0.5 % methanolic hydrogen chloride (100 ml) and kept at room temperature overnight. The solution was neutralised with silver carbonate, filtered, concentrated to dryness and the residue distilled under reduced pressure. The crystalline product was recrystallised several times from ethyl ether-light petroleum, yielding the pure substance (0.8 g), m.p. 34—35°. (Found: OCH_3 37.4. Calc. for $C_9H_{12}O_3$: OCH_3 36.9).

Kinetic determinations. The buffers used, all about 0.2 M, were acetate-hydrochloric acid (pH 2.3), citrate (pH 3.4), acetate (pH 4.1 and 5.1), phosphate (pH 6.1, 6.9, 7.2 and 7.5) and borate (pH 7.9, 8.8 and 10.0). Sodium chloride was added to the buffers to an ionic strength of 1.0. For each pH-value known amounts of vanillyl alcohol were dissolved in buffer-water (3:7). To one ml of the solution 14 ml of 0.043 N aqueous sodium hydroxide and 0.2 ml of 0.5 % 2,6-dibromo-benzoquinone-4-chloroimine in ethanol were added. After exactly 10 min at room temperature the extinction was determined at 640 mμ. Linear calibration curves, differing only slightly for the different pH-values, were obtained.

Buffer and a 0.0015 M solution of vanillyl methyl ether in the proportions 3:7 were mixed and kept at 80° ± 0.1 in a thermostatically controlled polyethylene glycol bath. 1 ml samples were withdrawn at regular intervals, and poured into 0.043 N aqueous sodium hydroxide (14 ml), after which the vanillyl alcohol in the sample was determined as above. Some typical diagrams, showing the first order kinetics observed at lower pH-values and the undefinable kinetics found at higher pH-values are given in Figs. 2 and 3.

Thin layer chromatography. The reaction products were investigated by thin layer chromatography on silica gel G, using as solvent chloroform. The fast moving starting material and the slower vanillyl alcohol were observed at all pH-values, while at the higher values unidentified spots with lower mobilities than vanillyl alcohol were also observed.

REFERENCES

1. Adler, E. and Gierer, J. in Treiber, E. *Die Chemie der Pflanzencellwand*, Springer Verlag 1957.
2. Ivnäs, L. and Lindberg, B. *Acta Chem. Scand.* **15** (1961) 1081.
3. Gierer, J. *Acta Chem. Scand.* **8** (1954) 1319.
4. Hultzsch, K. *Chemie der Phenolharze*, Springer Verlag 1950, p. 63; Martin, R. K. *The Chemistry of Phenolic Resins*, Wiley 1956, p. 139.
5. Filar, L. J. and Winstein, S. *Tetrahedron Letters* **25** (1960) 9.

Received February 24, 1962.

ACTA CHEMICA SCANDINAVICA 16 (1962) 1761–1764

Qualitative Analysis of Bile Acids by Gas Chromatography

Bile Acids and Steroids 124

JAN SJÖVALL

Department of Chemistry, Karolinska Institutet, Stockholm, Sweden

A method for the gas chromatographic analysis of bile acid methyl esters before and after the treatment with trifluoroacetic anhydride using the fluoroalkyl silicone QF-1 as stationary phase is described.

In connection with work on fecal bile acids a method was required for the separation of complex bile acid mixtures. A few papers have been published on the gas chromatography of bile acids [1-4] but the stationary phases previously described do not give separation factors large enough to allow the analysis of fecal bile acid mixtures. Recently VandenHeuvel, Haahti and Horning described the use of a fluoroalkyl silicone as stationary phase for the separation of steroids [5]. Dr. Horning has kindly sent us a sample of this phase (QF-1 Dow Corning Corp.) which has now been tested and found to be extremely valuable for separation of bile acid methyl esters and their trifluoroacetates [6].

EXPERIMENTAL

A Pye Argon chromatograph was modified so that a 6 foot × 5 mm U-tube column could be used. Column temperature was kept constant or was linearly programmed with a Model 40 temperature programmer (F & M Scientific Corp.). The standard ionization detector was kept in a separately heated oven at about 240°C. An independently heated metal block was placed as a flash heater around the region where samples were injected. Connections between column and detector were made by stainless steel tubing (1.8 mm o.d.), teflon tubing and through-hole silicone stoppers.

Column packings were prepared essentially as described previously [2] and approximately 0.5 % QF-1 [5] or a mixture of 0.5 % QF-1 and 0.05 % ethylene glycol isophthalate was applied on acid washed, acetone washed and siliconized Gas Chrom P (Applied Science Laboratories). Methyl esters of bile acids were made and injected into the column as described previously. Trifluoroacetates were prepared by heating 0.3 – 1 mg of the methyl ester in 0.2 ml of trifluoroacetic anhydride in a small glass stoppered test tube at 30°C for 15 min. The reagent was then evaporated under a stream of nitrogen and the residue dissolved in 0.1 ml of acetone.

RESULTS AND DISCUSSION

Compounds without trifluoroacetoxy groups were run with the flash heater at 280—300°C; when trifluoroacetoxy compounds were present the flash heater was kept at 250°C. The compounds with hydroxyl and/or keto groups showed no signs of degradation. Slight tailing was observed with di- and trihydroxy compounds but did not disturb qualitative analysis. A separation of disubstituted bile acid methyl esters and methyl cholate is shown in Fig. 1. Trifluoroacetates always gave very sharp and symmetrical peaks. In some cases these compounds showed minor signs of degradation on the column as evidenced by a slight rise in the base line just before the appearance of the peak (one exception noted below). Although quantitative studies have not yet been carried out it was evident that trihydroxy compounds gave significantly lower responses with the detector (see Ref.[7]). The trifluoroacetate of methyl 3β,7α,12α-trihydroxycholanate gave no response or a negative peak unless 1500 V was applied to the detector. Other trifluoroacetates tested always gave positive peaks with the potentials applied (1000—1500 V).

The relative retention times of the compounds tested are summarized in Table 1. As pointed out by VandenHeuvel, Haahti and Horning [5] the ketones are generally retained much longer than the corresponding hydroxy compounds on QF-1. From the results obtained with mono- and disubstituted compounds it is seen that substitution at C12, C7 and C3 increase the retention time in this order. Exceptions are the 3,7-diketo- and 3,12-diketocholanic acid methyl esters that have about the same retention time. Furthermore it is seen that

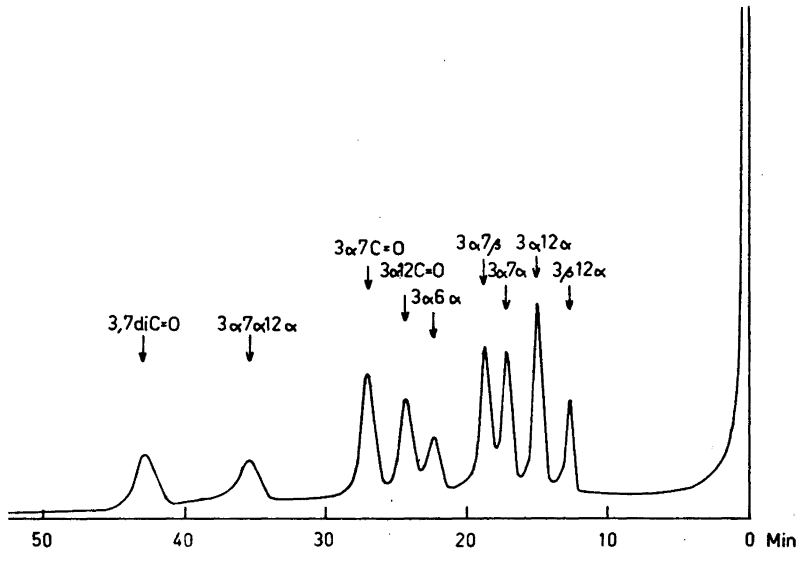

Fig. 1. Separation of some methyl esters of naturally occurring bile acids. Column: 0.5 % QF-1 on Gas-Chrom P. Temperature: 219°C. Argon pressure: 1.0 kg/cm².

Table 1. Retention times relative to methyl deoxycholate of various bile acid methyl esters before and after treatment with trifluoroacetic anhydride. Conditions were as described in Fig. 1.

Substituents	Free hydroxyl(s) (ROH)	Trifluoroacetate (TFA)	Ratio ROH/TFA
12α	0.31	0.22	1.41
12β	0.34	0.25	1.36
7α	0.35	0.26	1.35
7β	0.39	0.32	1.22
3β	0.44	0.41	1.07
3α	0.49	0.42	1.17
12-keto	0.49	—	—
7-keto	0.57	—	—
3-keto	0.95	—	—
3β,12α	0.85	0.58	1.47
3α,12α	1.00	0.67	1.50
3α,12β	1.08	0.78	1.39
3α,7α	1.15	0.85	1.35
3α,7β	1.25	1.00	1.25
3α,6α	1.47	0.98	1.50
3α,12-keto	1.62	1.54	1.05
3-keto,12α	1.83	1.42	1.29
3α,7-keto	1.79	1.68	1.07
3-keto,7α	2.17	1.76	1.23
3,12-diketo	2.86	—	—
3,7-diketo	2.83	—	—
3α,7α,12α	2.33	1.39	1.68
3α,7β,12α	2.44	1.33	1.83
3β,7α,12α	1.86	1.17	1.59
3α,6α,7α	2.61	1.24	2.10
3α,6β,7α	2.39	0.85	2.81
3α,6β,7β	2.27	1.50	1.51
3α,12α,7-keto	3.70	2.54	1.46
3α,7α,12-keto	4.00	2.80	1.43
3-keto,7α,12α	4.79	2.79	1.72
3α,7,12-diketo	4.48	4.30	1.04
3,7,12-triketo	6.33	—	—

an equatorial hydroxyl group gives a longer retention time than an axial one at the same carbon atom. Similar but not so regular effects can also be seen with the trisubstituted compounds studied.

Trifluoroacetylation generally decreases the retention times of compounds containing hydroxyl groups. Trifluoroacetylation of a compound having only one hydroxyl group at C3, changes the retention time but slightly. The retention times of C7 and C12 monohydroxy and di- and trihydroxy compounds decrease markedly after treatment with trifluoroacetic anhydride. There is a tendency for this decrease to be more pronounced with hydroxyl groups at C12 than at C7. The change of retention time on trifluoroacetylation of trihydroxy compounds is of particular value since these compounds show only small differences in retention time. An exceptionally short retention time of methyl 3α,6β,7α-trihydroxycholanate is observed after treatment with trifluoroacetic

anhydride. The same retention time is obtained with the trifluoroacetate of 3α,7α-dihydroxycholanic acid methyl ester. This might possibly be explained by an elimination of the 6β-trifluoroacetoxy group in the flash heater.

When analyzing unknown samples of bile acid methyl esters we have found it very useful to analyze the sample before and after treatment with trifluoroacetic anhydride. When using QF-1 as stationary phase this gives much information on the nature of the bile acid. If the trifluoroacetylation is carried out at room temperature it is also possible to follow the course of the reaction and hydroxyl groups that are difficult to acylate can thus be detected. Certain hydroxyls (*e.g.*, 12α) react so slowly that a partial acylation can be effected.

For special purposes we have found a mixture of 0.5 % QF-1 and 0.05 % polyethylene glycol isophthalate useful. This stationary phase gives as good peaks as QF-1 alone. The differences in retention times between hydroxyl groups and keto groups are diminished and the decrease in retention time after treatment with trifluoroacetic anhydride becomes more pronounced. In some cases the separation factor between two compounds is increased and it is possible for example to separate partially the methyl esters of 12β-hydroxy- and 7α-hydroxycholanic acids which is not possible with QF-1 alone.

An increased resolution can also be obtained by temperature programming [8]. The flash heater and the detector are kept at the constant temperatures already described. The column temperature at which the analysis is started will depend to some extent on the type of bile acids to be separated. It was found suitable to increase the temperature by 1—2°C per minute.

The method described in this paper has been of great value for the analysis of fecal bile acids as will be described in following papers. It has made possible the isolation of a hitherto unknown naturally occurring bile acid to which the structure could be tentatively assigned on the basis of the chromatographic data [9].

Acknowledgements. I am indebted to Prof. S. Bergström and to Drs. H. Danielsson, A. Norman and B. Samuelsson for supplying many of the bile acids used.

This work has been supported by *Statens Medicinska Forskningsråd.*

REFERENCES

1. VandenHeuvel, W. J. A., Sweeley, C. C. and Horning, E. C. *Biochem. Biophys. Research Communs* **3** (1960) 33.
2. Sjövall, J., Meloni, C. R. and Turner, D. A. *J. Lipid Research* **2** (1961) 317.
3. Blomstrand, R. *Proc. Soc. Exptl. Biol. Med.* **107** (1961) 126.
4. Holmes, W. L. and Stack, E. *Biochim. et Biophys. Acta* **56** (1962) 163.
5. VandenHeuvel, W. J. A., Haahti, E. O. A. and Horning, E. C. *J. Am. Chem. Soc.* **83** (1961) 1513.
6. VandenHeuvel, W. J. A., Sjövall, J. and Horning, E. C. *Biochim. et Biophys. Acta* **48** (1961) 596.
7. Sweeley, C. C. and Chang, T. L. *Anal. Chem.* **33** (1961) 1860.
8. Haahti, E. O. A. *Scand. J. Clin. Invest.* **13** (1961) Suppl. 59.
9. Danielsson, H., Eneroth, P., Hellström, K. and Sjövall, J. *J. Biol. Chem. In press.*

Received April 6, 1962.

ACTA CHEMICA SCANDINAVICA 16 (1962) 1765–1769

On the Extent of the Conversion of Scymnol to Cholic Acid in the Rat

Bile Acids and Steroids 120

H. DANIELSSON and A. KALLNER

Department of Chemistry, Karolinska Institutet, Stockholm, Sweden

R. J. BRIDGWATER, T. BRIGGS and G. A. D. HASLEWOOD

Guy's Hospital Medical School, London, S. E. 1.

After intraperiotoneal administration of tritium labeled scymnol (VII) to bile fistula rats about 90 % of the radioactivity was excreted in bile during the first 24 h. Scymnol and two compounds which upon alkaline hydrolysis yielded material with chromatographic properties similar to those of anhydroscymnol, were the main metabolites. Cholic acid (I) accounted for only 0.5 % of the radioactivity excreted in bile. The bearing of these results on the theory that the mechanism of conversion of cholesterol to cholic acid in mammals represents a recapitulation of the evolution of bile salts is discussed.

The elucidation of the structure of bile alcohols and bile acids in different species has revealed that the composition of bile salts in the bile of an animal can often be correlated with its position in the evolutionary series [1,2]. Thus, bile alcohols and acids with 27 carbon atoms are found in more primitive animals, *e.g.* sharks, amphibians and certain reptiles, while acids with 24 carbon atoms are typical for the "modern" vertebrates, such as most bony fishes, snakes, birds and mammals. Cholesterol is the precursor of C_{27} as well as C_{24} bile salts, and it has been proposed that the mechanism of the conversion of cholesterol to C_{24} bile acids in mammals would entail the intermediary formation of C_{27} steroids similar to or the same as those found in the bile of lower species.

Studies on the mechanism of formation of cholic acid (I) in the rat have shown that the steroid nucleus of cholesterol is modified prior to the final oxidation of the side-chain and that 3α,7α,12α-trihydroxycoprostane (II) and the corresponding coprostanic acid (III), an acid found in the bile of amphi-

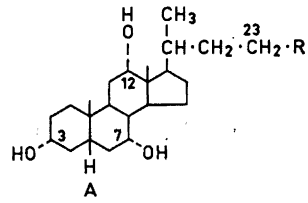

(I) A, R = $-{}^{24}COOH$

(II) A, R = $-{}^{24}CH_2\cdot{}^{25}CH(^{26}CH_3)(^{27}CH_3)$

(III) A, R = $-CH_2\cdot CH(COOH)(CH_3)$

(IV) A, R = $-CH_2\cdot CH(CH_2OH)(CH_3)$

(V) A, R = $-CH(O-CH_2)\cdot CH\cdot CH_2OH$

(VI) A, R = $-CHOH\cdot CH(CH_2O\cdot SO_3^-)(CH_2OH)$

(VII) A, R = $-{}^{24}CHOH\cdot CH(CH_2OH)(CH_2OH)$

bians and crocodiles, are rapidly degraded to cholic acid [3]. The conversion of cholesterol to these two compounds has, however, not yet been demonstrated in the rat [3]. The formation of trihydroxycoprostanic acid from trihydroxycoprostane has been shown to occur in rat and mouse liver *in vitro* [4] and the reaction involves the introduction of a hydroxyl group at C_{26} to yield the tetrol (IV) which is subsequently oxidized to the acid (III). It has been suggested that these changes represent the initial steps in the oxidation of the C_{27} side-chain. The later steps in the transformation of trihydroxycoprostanic to cholic acid have not been fully elucidated, but it appears likely that a β-oxidation occurs, splitting the side-chain between C_{24} and C_{25} yielding cholyl-CoA and propionyl-CoA [3–6].

In 1930, Windaus *et al.*[7] suggested that "scymnol", a C_{27} steroid alcohol obtained from the bile of sharks and carps and originally isolated by Hammarsten [8] in 1898, could be an intermediate in the conversion of cholesterol to cholic acid in mammals. However, as shown by Thannhauser [9], administration of a sample of Windaus' "scymnol" did not cause an increased formation of cholic acid in the bile fistula dog.

Structure (V) for "scymnol" was finally established [10], and it was further shown that this substance is an artefact, being formed during alkaline hydrolysis from the sulphate (VI) present in biles [11]. Because of this, it has been agreed [10,11] to rename the substance (V) "anhydroscymnol" and to transfer the name "scymnol" to the native bile alcohol (VII), which is the object of study now reported. Scymnol (VII) has been prepared from shark bile salts and also made by partial synthesis from cholic acid [11].

The structure of scymnol does not fit into the above formulated mechanism for the oxidation of the side-chain in the formation of C_{24} bile acids. Thus, if scymnol were a precursor of cholic acid in mammals, this would indicate the presence of an alternative and quite different pathway in the side-chain oxidation. The existence of such a pathway would be inconsistent with the hypothesis that the conversion of cholesterol to cholic acid in mam-

mals is a recapitulation of the evolution of bile salts, for selachians phylogenetically represent a development of an early side-branch of the path of evolution leading to mammals.

The partial synthesis of scymnol has made it possible to study accurately its metabolism. This communication is a report on the metabolism of randomly tritium labeled scymnol in the bile fistula rat.

EXPERIMENTAL

A sample of partially synthetic scymnol [11] was exposed to 2 C of tritium gas for 3 weeks according to the method of Wilzbach [12] in the apparatus described by Bergström and Lindstedt [13]. The sample was then treated with 5 % (w/v) KOH in methanol for 2 h at room temperature. The solution was acidified with HCl, extracted with water-saturated butanol and the butanol extract washed with water until neutral. After evaporation of the butanol the residue was chromatographed twice on a column of hydrophobic kieselguhr with solvent system C:3 [14]. The main radioactive peak was pooled, unlabeled scymnol added, and the mixture was again chromatographed with system C:3. The radioactive peak was eluted at the same place as the carrier added. The labeled scymnol obtained had a specific activity of ~8 μC/mg.

4–8 μC of tritium labeled scymnol was injected intraperitoneally as serum albumin stabilized emulsions [4] into bile fistula rats. Bile was collected in 24 h portions. The bile was acidified with HCl and extracted with water-saturated butanol. The butanol extracts were washed with water until neutral and evaporated. The residue was chromatographed with solvent system D[15]. Bile and chromatographically isolated fractions were hydrolyzed with 2 N NaOH at 120° in a sealed steel tube for 14 h. The saponification mixtures were acidified and extracted with butanol. The residues of the butanol extracts were chromatographed first with solvent system C:1 [14] and then with system C:3.

RESULTS AND DISCUSSION

After intraperitoneal administration of tritium labeled scymnol about 90 % of the radioactivity was excreted in bile in 24 h. No significant amounts of radioactivity were excreted in bile during the following days or in the urine collected during the first two days.

Chromatography with system C:1 of hydrolysed bile obtained during the first 24 h showed that only 5 % of the radioactivity was eluted within the titration peak of cholic acid, while most of the remaining radioactivity appeared considerably earlier, with elution volume similar to that of scymnol and anhydroscymnol, which are eluted close to each other with this solvent system. As scymnol sulphate upon vigorous alkaline hydrolysis is converted into anhydroscymnol, as mentioned earlier, it is obvious that chromatography of hydrolysed bile does not distinguish between free and conjugated scymnol excreted in bile.

In order to obtain information on this point, unhydrolysed bile, collected during the first 24 h after injection of labeled scymnol, was chromatographed with solvent system D (Fig. 1). About 50 % of the radioactivity put on the column was retained in the stationary phase. Rechromatography of this labeled material, together with unlabeled scymnol, in system C:3 showed that the peaks of radioactivity and added carrier coincided.

As shown in Fig. 1, the radioactivity in the effluent of the column was distributed in several peaks appearing in connection with the two main titra-

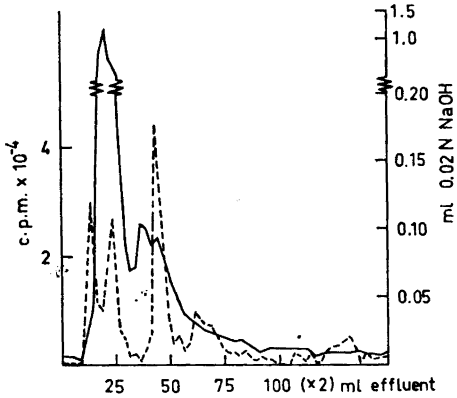

Fig. 1. Chromatography of the first 24 h portion of unhydrolysed bile after intraperitoneal administration of 8 μC of tritium labeled scymnol. Column: 9 g hydrophobic kieselguhr. Phase system D. Solid line: titration values. Broken line: radioactivity.

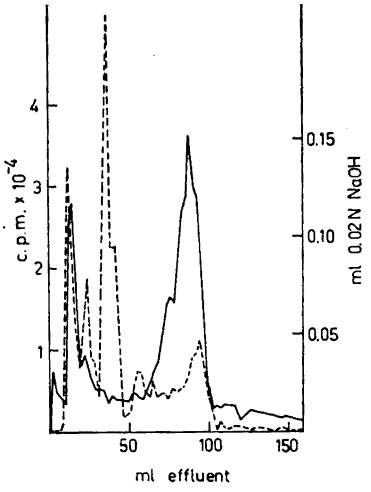

Fig. 2. Chromatography of hydrolysed taurocholic acid band, 13—30 ml effluent, Fig. 1. Column: 4.5 g hydrophobic kieselguhr. Phase system C:1. Solid line: titration values. Broken line: radioactivity.

tion peaks caused by taurocholic (13—30 ml effluent) and taurochenodeoxycholic acid (34—60 ml effluent). The taurocholic acid band was pooled, hydrolysed and chromatographed on phase system C:1 (Fig. 2). The main part of the radioactivity was eluted as three distinct peaks, more polar than cholic acid while about 25 %, which corresponds to 5 % of the total radioactivity excreted in the bile, appeared within the titration peak of cholic acid. The fractions containing the cholic acid were combined and after addition of unlabeled cholic acid crystallized repeatedly from ethyl acetate. The specific activity reached a constant value after 5 crystallizations. The radioactivity thus identified as cholic acid represents 0.5 % of the total radioactivity excreted in bile. This must be considered a minimum value, as it can be expected that tritium labeled scymnol on conversion to cholic acid loses a part of the tritium located in the side-chain. However, as the amount of radioactivity excreted in bile nearly equals that administered, this loss of tritium cannot have had a very pronounced influence on the order of magnitude found for the conversion of scymnol to cholic acid.

The isotope eluted between 30 and 50 ml effluent (Fig. 2) showed chromatographic properties similar to those of anhydroscymnol when rechromatographed with system C:3, but the identity of the radioactive compound with anhydroscymnol was not further established. The preceding two radioactive peaks were not identified.

Chromatography of the hydrolysed taurochenodeoxycholic acid fraction (*cf.* Fig. 1) demonstrated that about one third of the radioactivity in this

fraction had chromatographic behaviour similar to that of anhydroscymnol while the remainder consisted of two unknown compounds more polar than anhydroscymnol.

The results obtained thus show that the main part, about 70 %, of intraperitoneally administered scymnol was excreted in bile as scymnol and two compounds that yielded material chromatographically similar to anhydroscymnol upon alkaline hydrolysis. The original structure of the latter two compounds is not known but it appears likely that they represent conjugates of scymnol with, *e.g.*, sulfuric acid, as they are much more polar than scymnol. Cholic acid accounted for only 0.5 % of the radioactivity excreted in bile, while the remaining 30 % was distributed chiefly in two uknown compounds more polar than scymnol before as well as after hydrolysis.

The very poor conversion of scymnol to cholic acid by rat liver can be considered as evidence in favour of the hypothesis that the conversion of cholesterol to cholic acid in mammals follows a pathway, which does not include scymnol, and may be different from that leading to cholic acid in most teleostean fishes. This view accords with what seems obvious from the natural distribution of cholic acid: that this substance has been produced at least twice during evolution [11].

Acknowledgements. The skilful technical assistance of Miss C. Carlon is gratefully acknowledged.

This work is part of investigations supported by the *National Institutes of Health*, Bethesda, Md., USA (Research Grants H-2842 and A-4303 and Research Fellowship HF 7600).

REFERENCES

1. Haslewood, G. A. D. *Physiol. Revs.* **35** (1955) 178.
2. Haslewood, G. A. D. In Wolstenholme, G. E. W. and O'Connor, M. *The Biosynthesis of Terpenes and Sterols*, Churchill, London 1959, p. 206 ff.
3. Bergström, S., Danielsson, H. and Samuelsson, B. In Block, K. *Lipide Metabolism*, John Wiley and Sons, New York 1960, p. 296 ff.
4. Danielsson, H. *Acta Chem. Scand.* **14** (1960) 348.
5. Danielsson, H. *Arkiv Kemi* **17** (1961) 373.
6. Suld, H. M., Staple, E. and Gurin, S. *Federation Proc.* **20** (1961) 284 a.
7. Windaus, A., Bergmann, W. and Konig, G. *Z. physiol. Chem. Hoppe-Seyler's* **189** (1930) 148.
8. Hammarsten, O. *Z. physiol. Chem. Hoppe-Seyler's* **24** (1898) 322.
9. Thannhauser, S. J. *Unpublished work* referred to in Ref.[7]
10. Cross, A. D. *J. Chem. Soc.* **1961** 2817.
11. Bridgwater, R. J., Briggs, T. and Haslewood, G. A. D. *Biochem. J.* **82** (1962) 285.
12. Wilzbach, K. E. *J. Am. Chem. Soc.* **79** (1957) 1013.
13. Bergström, S. and Lindstedt, S. *Acta Chem. Scand.* **11** (1957) 1275.
14. Norman, A. and Sjövall, J. *J. Biol. Chem.* **233** (1958) 872.
15. Norman, A. *Acta Chem. Scand.* **7** (1953) 1413.

Received March 6, 1962

ACTA CHEMICA SCANDINAVICA 16 (1962) 1770–1778

The Incorporation of Phosphorus into Human Erythrocyte Ghosts

GUNNAR ÅGREN, BIRGITTA HALLBERG and GUNNAR RONQUIST

Institute of Medical Chemistry, University of Uppsala, Sweden

About 30 labelled phosphopeptides and phosphorylserine have been isolated from red-cells ghosts incubated with radioactive inorganic phosphate. The rate of incorporation and the pH-dependence of the labelling have been determined.

It was demonstrated in a previous paper that the main part of the phosphoproteins in *Escherichia coli* are located in the cell-wall preparations [1]. It was therefore of interest to carry out a similar investigation with some animal cell-wall material. The erythrocyte ghosts seemed to be appropriate for this purpose. It was also shown [2] that labelled phosphorylserine could be isolated from erythrocyte ghosts which had been suspended in 0.1 M tris * at pH 7.4 in the presence of ^{32}P. These experiments indicated that the ghosts contain phosphoproteins which may be active in the phosphorus metabolism of the erythrocytes.

It has now been possible to isolate several phosphopeptides from the acid-hydrolyzed protein residue of the ghosts, and the qualitative amino acid composition of the phosphopeptides has been studied in greater detail. A study has also been made of the initial rate of ^{32}P-labelling of the phosphopeptides, as well as of the pH-dependence of the labelling.

METHODS

Incubation of red cell ghosts with ^{32}P. After some preliminary work with earlier methods, the ghosts were finally prepared in the following way.

2000–3000 ml samples of human blood obtained from the University Hospital, Uppsala, were centrifuged and washed at least twice with cold physiologic sodium chloride solution, in a refrigerated Stock centrifuge taking 7.5 l. All further procedures were carried out at 2°C. After each centrifugation, the leucocytes were removed by skimming and suction. Nine volumes of cold distilled water were added, and the pH adjusted to 6.0 by means of CO_2. The ghosts settled to the bottom during storage overnight in the cold room. The clear supernatant was removed by decantation and suction.

* Tris = tris(hydroxymethyl)aminomethane; ^{32}P = radioactive inorganic phosphate; TCA = trichloroacetic acid; SerP = phosphorylserine; cpm. = counts per minute; UV = ultraviolet.

The ghosts from 1000–1500 ml samples of red cells were washed mainly according to Post *et al.* [3] They were first suspended in 7.5 l of 10^{-3}M tris-acetate buffer, adjusted to pH 6.5 by CO_2. Centrifugation at 3000 r.p.m. for 20 min in the Stock centrifuge, and resuspension in the dilute buffer, were repeated 6 or more times until the supernatant was colourless. The volume of the faintly pink ghosts usually diminished to 50–80 % of the corresponding red cells. The average dry weight of ghosts from 1000 ml of red cells was 6 g.

To the ghosts (about 1000 ml) were added 2 volumes of 2×10^{-2} M tris-glycylglycine buffer, pH 8.2. After mixing, the suspension was centrifuged at 20 000 r.p.m. for 60 min in the Spinco ultracentrifuge (Model L, rotor No. 21). The precitate was washed about 6 times by resuspension and centrifugation. Tris-glycylglycine, 10^{-2} M, pH 8,2 was used twice, and 2×10^{-4} M buffer was used in the final washings (4 times) until the supernatant was colourless. The volume of the practically colourless ghosts, when prepared from about 1000 ml of red cells, usually amounted to around 300 ml, with a decrease in the dry weight from about 6 to 2 g. Ghosts from totally 25 l of human red cells were prepared in this way.

For labelling with ^{32}P, the ghosts (300 ml) were diluted to about 2 l with 2×10^{-4}M tris-glycylglycine buffer at pH 7.4, and incubated with approximately 10 mC of ^{32}P for 30 min at 20°C. The ghosts were then precipitated by addition of cold TCA to a final concentration of 10 % (w/v). The precipitate was centrifuged, washed with 10 % TCA and dried with ethanol. The lipids were removed by extraction twice with ethanol/ether at 45°C, followed by ether. The residue contained the Schneider protein fraction and nucleic acid.

Isolation of SerP and phosphopeptides. To obtain these substances, the protein fraction was partially hydrolyzed according to Lipmann [4], with 10 times the protein weight of 2 N HCl under reflux on a water bath for 20 h. After most of the HCl had been removed by repeated evaporation *in vacuo*, the hydrolysate of ghosts from a 1000 ml sample of red cells was applied to a Dowex 50 column (40 × 2 cm), and eluted with 6 column volumes of 0.01 N HCl. The four ^{32}P-labelled fractions following inorganic phosphate were further separated into several fractions on 25 × 0.9 cm columns of Dowex (2 % DVB) formate with gradient elution 0 → 1 M formic acid, using the procedure of Busch *et al.* [5] The volume in the mixer was 150 ml, and the eluate was collected in fractions of 5 ml every 20 min.

Analytical methods. The purity of the labelled subfractions from the Dowex 1 formate columns was analyzed by high-voltage electrophoresis, using Whatman No. 3 paper. The electropherograms were run in the Wieland-Pfleiderer apparatus at 2650 V and 35 mA for 60 min at 4–6°C, using 1 N acetic acid as solvent. Several of the subfractions were found to contain up to five non-labelled ninhydrin-positive fractions, and one or several labelled fractions. All fractions from the Dowex 1 formate columns were therefore further purified by preparative paper electrophoresis. Scanning of the electropherograms was performed according to Ågren *et al.* [6] The labelled spots were eluted with water, and the solutions concentrated to dryness *in vacuo*.

The radioactivity of the different fractions from column chromatography of the hydrolyzed protein residues was measured in glass cups, using an L. K. B. Robot Scaler. Determinations of the specific activity were made on stainless steel planchettes with the Tracerlab Superscaler. At least 1000 counts were measured. The specific activity of the different phosphorylated compounds was calculated as cpm./μg phosphorus. All activity values were recalculated to the time of incubation.

The qualitative amino acid composition of the purified phosphopeptides was determined by one-dimensional high-voltage electrophoresis at 2600 V and 40 mA for 60 min using 1 N acetic acid as solvent, and Whatman No. 1 paper. The phosphopeptides were hydrolyzed with 2 N HCl in sealed tubes for 20 h at 120°C.

RESULTS

Isolation of phosphopeptides. Fig. 1 illustrates a typical elution diagram of the hydrolyzed protein residue of ghosts from 1150 ml of red cells passing through a Dowex 50 column with 0.01 N HCl. A large peak containing nin-

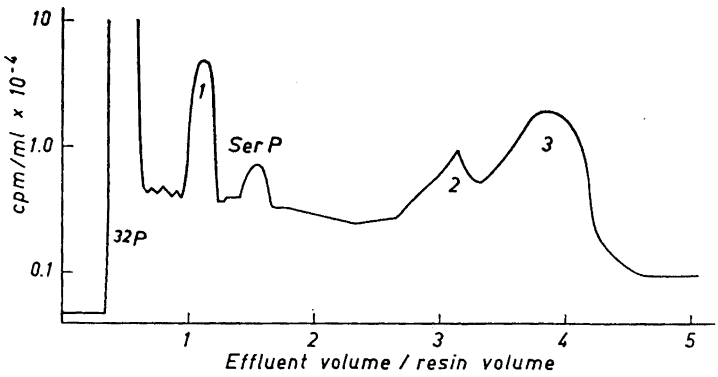

Fig. 1. Radioactivity curve from a hydrolysate of red cell ghosts separated on a Dowex 50 (8 % DVB) column. The curve was obtained by plotting the number of impulses per min (cpm) in 1 ml aliquots of each tube. The ghosts had been incubated for 30 min with ^{32}P.

hydrin-positive material was eluted in a position between ^{32}P- and SerP. Two additional large peaks containing ninhydrinpositive material appeared after SerP, the first after 3.0 column volumes and the second after 4.0 column volumes of eluate (effluent volume/resin volume). The following total amounts of material were obtained from 21 similar experiments: No. 1 fraction after ^{32}P = 98 mg; SerP = 43 mg; fraction No. 1 after SerP = 38 mg; fraction No.2 after SerP = 27 mg.

The material from each of the four peaks after ^{32}P was collected, and run through small Dowex 1 colums with gradient elution 0 → 1 M formic acid. The results were as follows.

Fig. 2 shows the elution chromatogram of 34 mg of radioactive material from peak No. 1 in Fig. 1, after running through the Dowex 1 column. Three

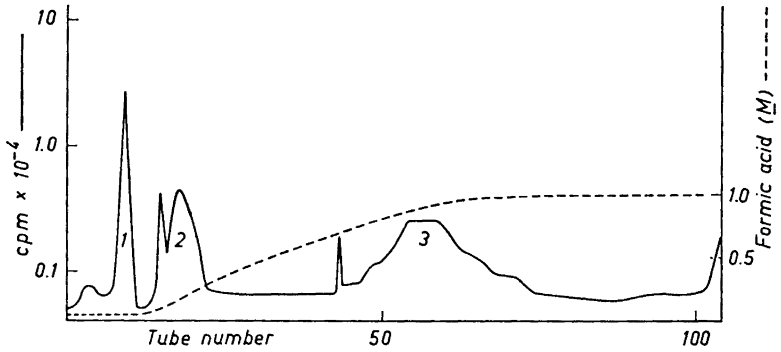

Fig. 2. Radioactivity curve of the material from peak No. 1, Fig. 1, separated on a Dowex 1 (2 % DVB) column. The radioactivity curve (the continuous line) was obtained by plotting the number of impulses per min (cpm) in 1 ml aliquots of each tube. The broken line represents formic acid concentration.

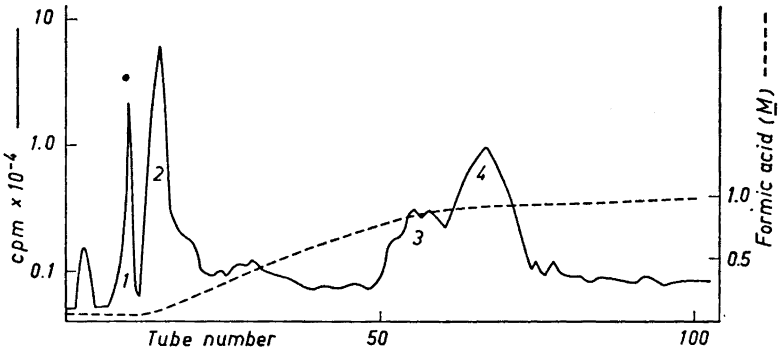

Fig. 3. Radioactivity curve of the material from the SerP-peak, Fig. 1. See legend for Fig. 2.

large labelled peaks were obtained. Their weight was 3.0, 3.9 and 0.8 mg, respectively. The material from each fraction was further purified by preparative paper ionophoresis. In many cases, nonlabelled ninhydrinpositive material could be separated from a labelled compound. This was eluted from the electropherogram, hydrolyzed and analyzed by paper electrophoresis. The amino acid composition of the phosphopeptides is given in Table 1. The low recovery of labelled material must imply that a considerable proportion of it was not eluted with the gradient system used. By succeeding gradient elution 1 → 4 M formic acid 2 large labelled peaks were obtained, which contained phosphopeptides.

The elution chromatogram of 14 mg of radioactive material from the SerP peak in Fig. 1, when run through the Dowex 1 column with gradient 0 → 1 M formic acid, is presented in Fig. 3. This material, as well as the other amounts used in the experiments illustrated in Figs. 2—5, was obtained from 6 samples of red cells, representing approximately 8 l of cells. Four large labelled peaks were obtained from the SerP fraction. They weighed 3.0, 0.5, 1.0 and 2.5 mg, re-

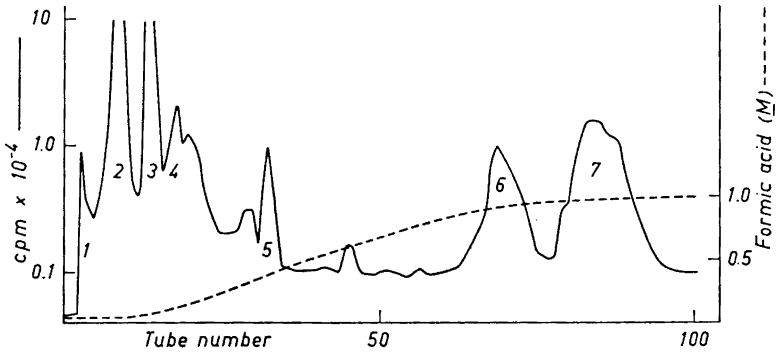

Fig. 4. Radioactivity curve of the material from peak No. 2, Fig. 1. See legend for Fig. 2.

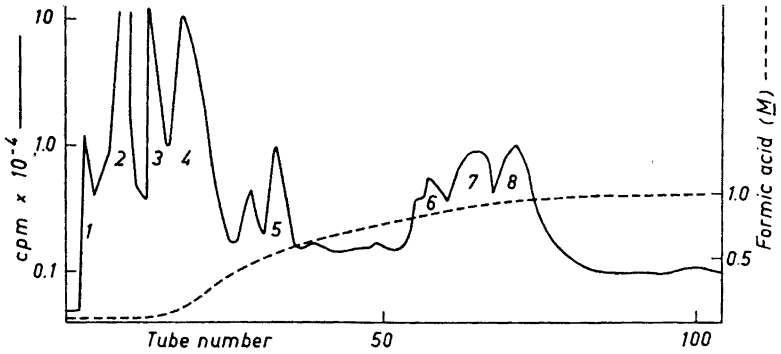

Fig. 5. Radioactivity curve of the material from peak No. 3, Fig. 1. See legend for Fig. 2.

spectively. The last fraction contained mainly SerP. The amino acid composition of the other three phosphopeptides, which had been further purified by paper electrophoresis, is given in Table 1. A purer SerP sample was obtained when the SerP fraction from the Dowex 50 fraction was instead run through a Dowex 1 (10 % DVB) chloride column with 0.01 N HCl.

Fig. 4 shows the elution chromatogram of 21 mg of radioactive material from peak 2 in Fig. 1, when run through a Dowex 1 formate column. Seven large labelled peaks were obtained. Their weight was 3.2, 3.2, 2.0, 3.0, 2.2, 1.5 and 1.4 mg, respectively. The recovery was satisfactory. The material from the 7 fractions was further purified by preparative paper electrophoresis, hydrolyzed and analyzed for amino acids. The results are given in Table 1.

In a similar way, Fig. 5 shows the elution chromatogram of 12 mg of radioactive material from peak 3 in Fig. 1, after running through the Dowex 1 formate column. Eight large labelled peaks were obtained, and their pattern seemed to be about the same as in Fig. 4. The weight of the different fractions was 3.4, 4.8, 2.2, 1.5, 1.0, 1.2, 0.8 and 1.4 mg, respectively. As before all fractions were further purified by preparative paper ionophoresis, and analyzed for amino acids. The results are given in Table 1.

It is evident from the table that more than 30 phosphopeptides could be prepared in this way. The simplest phosphopeptide consisted of serine and glutamic acid. Three different phosphopeptides containing glutamic acid and serine, and either glycine, aspartic acid or alanine were also identified. In addition, several tetra- and pentaphosphopeptides were obtained which had the same amino acid pattern, but which differed with respect to their content of the individual amino acids. In the pentapeptides, the most usual combination was aspartic acid, glutamic acid, serine, glycine and alanine. Proline was present in one hexapeptide, and threonine in another. The two phosphopeptides containing 8 amino acids and hexosamine had the same amino acid pattern. In some fractions, the amount of material was insufficient for analysis.

In some experiments, the two first fractions from the Dowex 50 columns were run through a Dowex 1 (10 % DVB) chloride column. A hexapeptide containing glutamic acid, alanine, proline, β-alanine, threonine and glycine

Table 1. Amino acid pattern of phosphopeptides separated on Dowex 50 columns with 0.01 N HCl in four fractions (Fig. 1). Each fraction subsequently separated into several fractions first on Dowex 1 formate columns (Figs. 2—5) and in a few cases by the succeeding paper electrophoresis (a, b, c).

Amino acid	Fraction No. 1 (Fig. 1) divided into fractions				SerP fraction divided into fractions			Fraction No. 2 (Fig. 1) divided into fractions on Dowex 1 columns												Fraction No. 3 (Fig. 1) divided into fractions on Dowex 1 columns																	
	1	2	4	5	1	2	4	1	2	3	4	5			6			7				1	2	3	4	5			6			7			8		
												a	b	a	b	c										a	b	a	b	c	a	b	a	b	c		
Asp	+	+	+	+	+			+	+	+	+	+	+			+	+					+	+	+	+		+	+		+	+	+		+	+	
Glu	+	+	+	+	+	+	+	+	+	+	+	+	+	+	+	+	+					+	+	+		+	+	+	+	+	+	+	+	+	+	
Ser	+	+	+	+	+	+	+	+	+	+	+	+	+	+	+	+	+					+	+	+	+	+	+	+	+	+	+	+	+	+	+	
Ala	+	+	+	+	+	+	+	+	+	+	+	+	+	+	+	+	+					+	+		+	+	+	+	+		+	+	+		+	
Gly	+	+	+	+	+	+		+	+	+	+	+	+	+	+	+	+					+	+		+	+	+	+	+		+	+	+	+	+	
Pro	+	+							+	+													+		+											
Lys									+														+													
Thr	+																																		+	+	
Hexos-amine	+				+	+		+	+														+													
β-Ala									+														+													

Table 2. Specific activities of red cell ghosts incubated for different times with ^{32}P. Phosphopeptides and SerP separated first on Dowex 50 and subsequently on Dowex 1 (10 % DVB) 10 columns.

Time of incubation	Fraction No. 4 Fig. 2	Fractions No. 1 & 2 Fig. 3	Fraction No. 4 Fig. 3 (SerP)	Fraction No. 2 Fig. 4	Fraction No. 2 Fig. 5
10 sec	496*	—	34	—	203
5 min	1 860	1 990	930	9 940	14 300
30 min	19 700	6 800	3 410	67 100	93 100

* Counts per min and μg of phosphorus.

was isolated from fraction No. 1 after ^{32}P. Since serine was present in all the other phosphopeptides isolated, the acid-stable phosphorus must have been linked to this amino acid.

Rate of incorporation of ^{32}P. Washed red-cell ghosts from 1500 ml of cells were suspended in 1000 ml of this-glycylglycine buffer at pH 7.4, and 3 equal parts of the suspension were incubated with 10 mC of ^{32}P for 10 sec, 5 min, and 10 min, respectively. The ghost suspensions were precipitated with TCA, and prepared and treated as previously described. The fractions from the Dowex 50 columns were further separated, using Dowex 1 (10 % DVB) chloride columns and 0.01 N HCl, without a gradient system. The values for the specific activity are given in Table 2.

Only the first part of fraction No. 4 (from fraction No. 1, Fig. 1) is visible at the end of the elution curve in Fig. 2. It was eluted with gradient 1 → 4 N formic acid on a Dowex 1 (2 % DVB) formate column. When the original fraction (No. 1, Fig. 1) was purified on a Dowex 1 (10 % DVB) chloride column, it appeared comparatively rapidly in the eluate. When further purified by paper electrophoresis, it could be separated into three fractions, *i.e.*, one unlabelled UV-absorbing fraction, one labelled UV-quenching fraction, and one labelled fraction without UV absorption. In view of the small amount of material in the latter two fractions, no detailed analysis could be made of the rate of ^{32}P incorporation.

It is evident from the figures in Table 2 that the maximal incorporation of activity may not be attained even after 30 min incubation. Another interesting feature is the low values for the specific activity of the SerP isolated (fraction No. 4, Fig. 3).

Table 3. Total radioactivity of phosphopeptides and SerP calculated as cpm per gm dry weight of ghosts incubated with ^{32}P at three different pH for 30 min.

pH	Fraction No. 1 Fig. 1	SerP Fig. 1	Fraction No. 2 Fig. 1	Fraction No. 3 Fig. 1
7.2	76.6×10^5	14.5×10^5	24.0×10^5	14.2×10^5
6.2	22.9×10^5	19.5×10^5	23.0×10^5	44.7×10^5
5.5	2.15×10^5	3.35×10^5	4.1×10^5	7.3×10^5

Table 4. Specific activity of phosphopeptides and SerP isolated by Dowex 50 chromatography (Fig. 1). The material from each peak was resolved into several fractions by Dowex 1 (2% DVB) chromatography (Figs. 2–5). The ghosts had been incubated with ^{32}P at three different pH.

Fraction No. (Figs. 2–5)	Peak No. 1 (Fig. 1)			SerP–Peak (Fig. 1)			Peak No. 3 (Fig. 1)		
	pH 7.2	pH 6.2	pH 5.5	pH 7.2	pH 6.2	pH 5.5	pH 7.2	pH 6.2	pH 5.5
1	223 000*	148 000	9 100	282 000	—	29 500	792 000	18 500	7 770
2	51 000	18 000	7 800	34 700	—	4 100	16 600	435 000	210 900
3	24 500	11 800	9 030	94 500	—	1 600	16 700	—	2 700
4	101 000	—	4 800	413 000	10 700	1 140	16 900	—	2 600
5	631 000	10 700	24 200				3 500	—	4 800
6							4 870	11 100	26 600
7							60 000	20 700	22 200
8							520	10 100	2 900

* Counts per min and μg of phosphorus.

pH dependance of ^{32}P incorporation. Washed red-cell ghosts from 1200 ml of cells were suspended in 1000 ml 2×10^{-2} M tris-glycylglycine buffer at pH 7.2, and divided into three equal parts. The pH of two of the samples was adjusted to 6.2 and 5.5, respectively. Each sample was incubated with 8 mC of ^{32}P for 30 min. The suspensions were precipitated with TCA. Phosphopeptides and SerP were isolated by Dowex 50 chromatography. The total activity of the 4 fractions isolated in these three experiments is given in Table 3 (*cf.* Fig. 1). These values indicate that the total activity was maximal at pH 7.2 and minimal at pH 5.5. The ghosts had, however, a tendency to precipitate rapidly from the suspension when the pH fell from 6.2 to 5.0. The four fractions were resolved into several subfractions by Dowex 1 chromatography. Their specific activity is shown in Table 4. It is evident from this table that the highest values for specific activity were recorded chiefly in the samples isolated from the fraction incubated with ^{32}P at pH 7.2, with intermediate values in incubation at pH 6.2, and minimum values at pH 5.5.

DISCUSSION

Several experiments were carried out to compare the labelling of ghosts which had been washed 6 or 12 times with the two types of buffer. The more thoroughly washed ghosts showed greater incorporation of ^{32}P in the different peaks. Similar determinations were made when part of the fresh blood had been stored for 3 weeks at +2°C. These experiments also showed more marked labelling of the ghosts washed 12 times. A comparison indicated that the degree of labelling of the ghosts was about the same when they were prepared from fresh or from stored blood.

The phosphorus content of the protein residues from the ghosts was low, *i.e.* 0.06 %. The dry weight of ghosts decreased considerably when they were washed with the more alkaline buffer. Several experiments showed that the clear centrifugates from the washings contained material which incorporated

^{32}P in about the same way as the ghosts. An account of these results will be given in a later paper.

Although the amino acid sequence in the isolated phosphopeptides was not determined, it can be pointed out that the composition of each peptide in Table 1, as well as the comparative order of lower and higher peptides (Asp Ser Glu Ala Gly Pro), is almost the same as the sequence for chymotrypsin [7] or phosphoglucomutase [8]. The probability that so many phosphopeptides isolated from the ghosts would nearly agree with this sequence by chance is fairly small. Consequently, the data indicate that the amino acid sequence of the active site is almost the same for at least 5 amino acids as for some enzymes which specifically hydrolyze proteins, or transfer a phosphate group between glucose donator and acceptor molecules.

The rate of ^{32}P-labelling is a comparatively slow process, and of the same order as that previously found for several rat organs [10]. It is conceivable that enzymes, as phosphatases, are engaged in the labelling of the phosphoproteins of the red-cell wall. It has previously been shown that dephosphorylated phosphopeptone can, in the presence of alkaline phosphatase and ^{32}P-labelled glycerophosphate, act as a phosphate acceptor [10]. Some preliminary results obtained in this work seem, however, to indicate that a labelled nucleotide can also be isolated from the hydrolyzed cell ghosts. Schauer and Hillman [11] recently obtained some evidence of the presence in the red-cell ghosts of an acid-labile, UV-absorbing substance which may play a role in the labelling of the membrane.

The function of cellular phosphoproteins of a non-enzymic type is not known, although it has been suggested that they may be involved in ion transport [12]. The localization of the labelled phosphoprotein to the red-cell membrane, as well as the possibility of extracting it from this site, suggest that it may operate in the cell as a metabolically activated natural ion-exchange material, the results of this activation being the transport of phosphorus across the cell membrane.

Acknowledgement. The authors are indebted to Mr. Roman Bijan and Mr. Tore Persson for skilful assistance. This investigation forms a part of a programme supported by grants from the *Swedish Medical Research Council.*

REFERENCES

1. Ågren, G. *Acta Chem. Scand.* **10** (1956) 152.
2. Ågren, G. and Engström, L. *Acta Chem. Scand.* **10** (1956) 876.
3. Post, R. L., Merrit, C. R., Kinsolving, C. R. and Albright, C. D. *J. Biol. Chem.* **235** (1960) 1796.
4. Lipmann, F. *Biochem. Z.* **262** (1933) 3.
5. Busch, H., Hurlbert, R. B. and Potter, V. R. *J. Biol. Chem.* **196** (1952) 717.
6. Ågren, G., de Verdier, C.-H. and Glomset, J. *Acta Chem. Scand.* **8** (1954) 1570.
7. Turba, F. and Grundlach G. *Biochem. Z.* **327** (1955) 186.
8. Koshland, D. E. and Erwin, M. Y. *J. Am. Chem. Soc.* **79** (1957) 2657.
9. Ågren, G., de Verdier, C.-H. and Glomset, J. *Acta Chem. Scand.* **8** (1954) 503.
10. Ågren, G. *Acta Chem. Scand.* **13** (1959) 1048.
11. Schauer, R. and Hillman, G. *Z. physiol. Chem. Hoppe-Seyler's* **325** (1961) 9.
12. Heald, P. J. *Biochem. J.* **80** (1961) 510.

Received March 2, 1962.

ACTA CHEMICA SCANDINAVICA 16 (1962) 1779–1784

Über die Konfiguration anomerer Methylglykoside; chromatographisches Verhalten und sterische Hinderung

JAKOB BLOM

Tuborg Brauereien, Kopenhagen, Dänemark

Verschiedene Autoren haben über die Trennung anomerer Methylglykoside durch Säulenchromatographie berichtet. Nach Umkehrung der konventionellen Konfiguration der Methoxylgruppe von α- resp. β-Anomeren lassen sich die relativen Wanderungsgeschwindigkeiten von Anomeren mit gleichem Ringsystem mit einer sterischen Hinderung der Hydroxylgruppe, welche der Methoxylgruppe am nächsten steht, korrelieren. Die Korrelation der grösseren sterischen Hinderung mit der grösseren Wanderungsgeschwindigkeit und der langsameren Säurehydrolysengeschwindigkeit ist in Übereinstimmung mit einer von Gastambide aufgestellten Regel über Wanderungsgeschwindigkeit und sterische Hinderung der aktiven Gruppe. Das Resultat der vorliegenden Arbeit über die Konfiguration anomerer Methylglykoside stimmt mit dem Ergebnis meiner früheren Untersuchungen überein, kommt jedoch mit der konventionellen Anschauung in Streit.

Anomere Methylglykofuranoside und anomere Methylglykopyranoside lassen sich durch Säulenchromatographie trennen [1–7]. Bei der Glykosidbildung aus freiem Zucker und Methylalkohol unter dem katalytischen Einfluss von Salzsäure werden sowohl anomere Furanoside als anomere Pyranoside gebildet. Bei der Säulenchromatographie einer solchen, maximal vier Isomere enthaltenden Lösung sind für anomere Methylglykoside mit gleichem Ringsystem alle Faktoren mit Ausnahme eines einzigen gleich. Es ist dieselbe stationäre Phase, dieselbe optisch inaktive, mobile Phase, dieselbe Anzahl von HO-Gruppen, räumlich in derselben Weise an denselben C-Atomen des gleichen Ringsystemes gebunden. Der einzige Faktor, welcher verschieden ist, ist die räumliche Anknüpfung der CH_3O-Gruppe an dem glykosidischen C-Atom, C_1. Es besteht eine gewisse Wahrscheinlichkeit, dass der Unterschied in der Wanderungsgeschwindigkeit bei der Säulenchromatographie zweier Anomere mit gleichem Ringsystem in Unterschieden im sterischen Aufbau und eine dadurch bedingte Ungleichheit der sterischen Hinderung zu suchen ist. Es ist dabei zu erinnern, dass die CH_3O-Gruppe eine Gruppe mit grosser Raumerfüllung ist.

CHROMATOGRAPHISCHE TRENNUNG VON STEREOISOMEREN

"The mobility of carbohydrates and their derivatives on cellulose paper is dependent upon adsorption on the cellulose support and on partition between the stationary aqueous phase and the mobile organic phase." [8] "Resolutions of several amino acids have been effected by paper chromatography. Since in these separations optically inactive solvents are as satisfactory as active ones, the molecular dissymmetry of the cellulose from which the paper is made must be the determining factor." [9] "It is a consequence of Martins theory that isomers having the same groups would be expected to have the same partition coefficient, and that they therefore should not be resolvable on the paper-partition chromatogram. A deviation from this rule will be largely the result of steric factors. The resolution of the optical isomers of certain amino acids by paper chromatography, without use of optically-active solvent mixtures, requires a role for the asymmetric cellulose fibres not consonant with the concept of partition." [10] "Da es sich bei der Verteilungschromatographie überwiegend um energetisch verschiedene intermolekulare Wasserstoffbrückenbindungen zwischen der mobilen und der stationäre Phase handelt, offenbart sich z. B. eine Schwächung dieser Bindung infolge sterischer Hinderung durch Unterschied in den R_M-Werten." [11]

Vavon und Gastambide [12] vermochten cyclische *cis*- und *trans*-Isomere durch Säulenchromatographie zu trennen (Menthol und Neomenthol, Borneol und Isoborneol). Die *trans*-Isomeren wurden stärker adsorbiert als die *cis*-Isomeren. Gastambide [13] stellt in seiner Abhandlung "Chromatographie et empêchement stérique" folgende Regel für die Adsorption isomerer, nahe verwandter Verbindungen auf: "Soit deux composés R1—F—R2 et R3—F—R4 où F est une fonction quelconque. R1 et R3, de même R2 et R4 sont des radicaux hydrocarbonés saturés isomères ou très voisins. Le composé dont la fonction F présente le plus d'empêchement stérique est le moins adsorbé. Conclusions: Avec les divers couples de composés organiques étudiés, les séparations chromatographiques vérifient la règle. Il existe, semble-t-il, tout au moins pour les alcools et les cétones, un certain parallélisme entre la chromatographie et l'empêchement stérique: l'isomère ou l'homologue qui s'élue en tête est celui dont la fonction active dans l'adsorption possède d'avantage d'empêchement stérique." Die sterische Hinderung wurde durch die Geschwindigkeit der Ester- und Oximbildung bestimmt.

CHROMATOGRAPHISCHE TRENNUNG ANOMERER METHYLGLYKOSIDE

Bei der Verteilungschromatographie scheint es sich u.a. um energetisch verschiedene Wasserstoffbrückenbindungen zwischen den Molekülen in der mobilen Phase und den HO-Gruppen der stationären Cellulose zu handeln. Der Energiewert oder die Stärke einer Wasserstoffbrückenbindung zwischen zwei HO-Gruppen ist nach Kuhn [14] umgekehrt proportional der Länge der Wasserstoffbrücke. Eine Gruppe mit grosser Raumerfüllung wie die CH_3O-Gruppe kann eine nahestehende HO-Gruppe überschatten, so dass alle Möglichkeiten für die Bildung zwischenmolekularer Wasserstoffbrücken nicht zum Ausdruck kommen können. Für den sterischen Effekt der CH_3O-Gruppe auf

Tabelle 1.

	Ringsystem Konfiguration	"Projected valency angle"		Abstände Å	
	Konformation	C_2-C_1	C_3-C_1	O_2---O_1	O_3---O_1
I	Furanosen *cis* 2—1 *trans* 2—1	 0° 120°		 2.51 3.45	
II	Pyranosen, C 1 e_3 a_2 e_1 e_3 a_2 a_1	 60° 180°		 2.96 3.73	
III	e_3 e_2 e_1 e_3 e_2 a_1	60° 60°		2.85 2.96	
IV	a_3 e_2 a_1 a_3 e_2 e_1	60° 60°	0°	2.96 2.85	2.78
V	a_3 a_2 a_1 a_3 a_2 e_1	180° 60°	0°	3.73 2.96	2.78

O---O Abstände grösser als 3.37 Å sind nicht angeführt.
a bzw. e deutet eine axiale bzw. equatoriale Anknüpfung der Substituenten an.

die nächst stehende HO-Gruppe muss einerseits der O- - -O Abstand der Gruppen andrerseits der "projected valency angle" nach Reeves[15] von Einfluss sein. In Tabelle 1 sind die Abstände zwischen dem Sauerstoffatom der CH_3O-Gruppe und dem Sauerstoffatom der nächst stehenden HO-Gruppe und "the projected valency angle" zwischen diesen Gruppen zusammengestellt. Die Werte sind teils der Abhandlung von Reeves teils einer Abhandlung von Hassel und Ottar[16] entnommen. Wie man aus Tabelle 1 ablesen kann, ist bei anomeren Methylglykofuranosiden, I, der Unterschied in den O- - - O Abständen und in den Winkeln so gross, dass es verständlich ist, dass anomere Methylglykofuranoside sich chromatographisch trennen lassen können. Dasselbe gilt für anomere Methylglykopyranoside mit D-Mannose- und L-Rhamnoseringsystem, II. Reeves (Ref.[15] Seite 131) fand experimentell (im Gegensatz zu seiner Voraussage), dass die D-Mannose-methylglykoside die C 1 Konformation haben. Für L-Rhamnose muss man, da es eine L-Hexose ist, die 1 C Konformation erwarten. D-Mannose und L-Rhamnose haben in den respektiven Konformationen bei C_2 eine a-HO-Gruppe. Der Unterschied in den Abständen und den Winkeln ist für diese Anomere ebenso gross als für die anomeren Furanoside. Dies macht es verständlich, dass anomere Methylglykopyranoside mit D-Mannose respektive L-Rhamnose Ringsystem sich chromatographisch trennen lassen können. D-Glukose, III, hat in der C 1 Konformation eine C_2 e HO-Gruppe. Dies bedingt, dass der Unterschied in den

O - - - O Abständen klein und der Unterschied in den Winkeln gleich Null wird. Es ist verständlich, dass die chromatographische Trennung der anomeren Methyl-D-Glukopyranoside Schwierigkeiten begegnet hat. "The relative R_F values of the anomeric methyl-D-glucopyranosides suggest that it is hardly possible, with the systems used, to separate one from the other. This has been borne out by experience in these laboratories." [17] Es ist einerseits möglich gewesen die Anomeren mit dem homomorphen Ringsystem der D-Galactopyranose, III, welche gleichfalls eine C_2 e HO-Gruppe besitzen, zu trennen [4]; andrerseits berichtet Mowery [7], dass es nicht möglich war, die anomeren Methylpyranoside der L-Arabinose zu trennen. Selbst wenn es mit gewissen Schwierigkeiten verbunden war, ist es möglich gewesen, die Methylpyranoside der D-Ribose, IV, zu trennen. Die D-Ribose hat in der C 1 Konformation ebenfalls eine C_2 e HO-Gruppe aber im Gegensatz zu den bisher genannten Zucker eine C_3 a HO-Gruppe. Bei dieser Konfiguration in dieser Konformation wird der O_3 - - - O_1 Abstand kleiner als jeder andere O - - - O Abstand in einer Stuhl-Konformation und der Winkel gleich Null. Eine a CH_3O-Gruppe muss einen stark abschirmenden Effekt auf die *cis* C_3 a HO-Gruppe haben. Es ist verständlich, dass der Unterschied zum andern Anomer mit *trans*-diequatorial gebundenen Gruppen so gross wird, dass die anomeren Methyl-D-Ribopyranoside sich chromatographisch trennen lassen können. In Tabelle 1 ist das theoretisch am meisten sterisch behinderte Anomer in jeder Gruppe zuerst angeführt.

Tabelle 2. Am schnellsten wanderndes, am langsamsten hydrolysierbares von anomeren Methylglykosiden.

Methylglykosid		$[\alpha]_D$	Verfasser	
			Chromatographie	Säurehydrolyse
Furanoside				
D-Arabinose	α	+ 128	A.B.	A.B.
L-Fucose	β	+ 113	A.B.	A.B.
D-Mannose	α	+ 109	A.B. M.	A.B.
D-Xylose	β	− 89.5	A.B.	A.B.
D-Ribose	β	− 62.4	B.S.	—
L-Arabinose	α	− 128	A.B. M.	A.B.
L-Rhamnose	α	− 98.6	A.B.	—
D-Galactose	β	− 112	A.B.	A.B.
Pyranoside				
D-Mannose	α	+ 80	A.B. M.	I.F.
L-Rhamnose	α	− 63	H.J.W.	R.S.
L-Arabinose	β	+ 245.5	A.B. M.	R.S.
D-Galactose	α	+ 196.6	A.B.	R.S.
D-Ribose	β	− 106.5	B.S.	—

A.B. Augestad, Berner
B.S. Barker, Smith
H.J.W. Hough, Jones, Wadman
M. Mowery
R.S. Riiber, Sørensen
I.F. Isbell, Frusch.

In Tabelle 2 ist das bei der Säulenchromatographie zuerst eluierte, also am schnellsten wandernde anomere Methylglykofuranosid resp. -pyranosid angeführt. Es ist in allen bisher untersuchten Fällen dasselbe Anomer, welches am langsamsten durch Säure hydrolysiert wird [3,4,18,19]. Um Platz zu sparen, sei auf meine zweite Publikation, welche die Geschwindigkeit der Säurehydrolyse anomerer Methylglykoside zum Thema hat, hingewiesen [21]. Die Korrelation der grösseren sterischen Hinderung mit der grösseren Wanderungsgeschwindigkeit und der langsameren Säurehydrolyse ist in Übereinstimmung mit den Resultaten ähnlicher Untersuchungen von Gastambide [13].

In Tabelle 3. ist das am schnellsten wandernde, am langsamsten hydrolysierbare von anomeren Methylglykosiden mit gleichem Ringsystem nach der Konfiguration der Hydroxylgruppe, welche der Methoxylgruppe am nächsten steht, in Kolonnen geordnet. In den Formeln nach Haworth mit Nummerierung der Ringkohlenstoffatome in Sinne des Uhrzeigers haben die Glykoside der D-Arabinose, L-Fucose, D-Mannose eine nach oben gerichtete, die Glykoside der D-Xylose, D-Ribose, L-Arabinose, L-Rhamnose, D-Galactose eine nach unten gerichtete Hydroxylgruppe bei C_2. Nach Gastambide besteht die Regel: "L'isomère qui s'élue en tête est celui dont la fonction active dans l'adsorption possède d'avantage d'empêchement stérique." Folgt man dieser Regel, muss

Tabelle 3.

		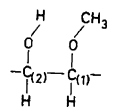	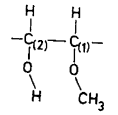
	Furanoside	Drehung	Drehung
I	D-Arabinose α	+	
	L-Fucose β	+	
	D-Mannose α	+	
	D-Xylose β		−
	D-Ribose β		−
	L-Arabinose α		−
	L-Rhamnose α		−
	D-Galactose β		−
	Pyranoside		
II	D-Mannose α	+	
	L-Rhamnose α		−
		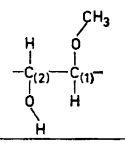	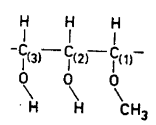
	Pyranoside		
III	L-Arabinose β	+	
	D-Galactose α	+	
IV	D-Ribose β		−

dasjenige anomere Methylglykosid der Gruppen I und II, in welchem die Hydroxylgruppe bei C_2 und die Methoxylgruppe *cis* Konfiguration haben, "d'avantage empêchement stérique" besitzen und daher "l'isomère qui s'élue en tête" sein. Folgt man den Gedankengang weiter, müssen die Methylglykoside der Gruppen I und II von α-D-Arabinose, β-L-Fucose, α-D-Mannose eine nach oben und die Methylglykoside von β-D-Xylose, β-D-Ribose, α-L-Arabinose, α-L-Rhamnose, β-D-Galactose eine nach unten gerichtete Methoxylgruppe haben. In Methylglykosiden der Gruppen III und IV ist der Unterschied in den O - - - O Abständen weit geringer als in den Glykosiden der Gruppen I und II. Nichtsdestoweniger folgen die in Tabelle 3 angeführten Methylglykoside der Gruppen III und IV der Regel von Gastambide.

In den konventionellen Formeln nach Haworth haben die α-D- und β-L-Methylglykoside eine nach unten gerichtete, die β-D- und α-L-Methylglykoside eine nach oben gerichtete Methoxylgruppe. Dieses gilt sowohl für Pyranoside als Furanoside. Vergleicht man die konventionellen Formeln mit den in Tabelle 3 angeführten, sieht man, dass sie sich in der Konfiguration der Methoxylgruppe widersprechen [20]. Das Resultat dieser Arbeit ist in Übereinstimmung mit den Ergebnissen meiner früheren Untersuchungen [21].

LITERATUR

1. Hough, L., Jones, J. K. N. und Wadman, W. H. *J. Chem. Soc.* **1950** 1702.
2. Augestad, I., Berner, E. und Weigner, E. *Chem. & Ind. London* **1953** 376.
3. Augestad, I. und Berner, E. *Acta Chem. Scand.* **8** (1954) 251.
4. Augestad, I. und Berner, E. *Acta Chem. Scand.* **10** (1956) 911.
5. Watkins, W. M. *J. Chem. Soc.* **1955** 2054.
6. Barker, G. R. und Smith, D. C. C. *J. Chem. Soc.* **1954** 2151
7. Mowery, D. F. *Anal. Chem.* **29** (1957) 1451; Mowery, D. F. *Anal. Chem.* **31** (1959) 1911.
8. Ferrier, R. J. und Overend, W. G. *Quart. Rev.* **13** (1959) 285.
9. Wheland, G. W. *Advanced Organic Chemistry*, John Wiley and Sons 1960, p. 309.
10. Kowkabany, G. N. *Advances in Carbohydrate Chem.* **9** (1954) 309.
11. Franc, J. *Z. Elektrochem.* **61** (1957) 1069.
12. Vavon, G. und Gastambide, B. *Compt. rend.* **226** (1948) 1201.
13. Gastambide, B. *Bull. soc. chim.* **21** (1954) 842.
14. Kuhn Lester, P. *J. Am. Chem. Soc.* **74** (1952) 2492.
15. Reeves, R. E. *Advances in Carbohydrate Chem.* **6** (1951) 108.
16. Hassel, O. und Ottar, B. *Acta Chem. Scand.* **1** (1947) 929.
17. Bollenback, G. N. *Methyl Glucoside*, Academic Press, New York 1958.
18. Riiber, C. N. und Sørensen, N. A. *Kgl. Norske Videnskab. Selskabs Skrifter*, No. 1. 1938.
19. Isbell, H. S. und Frush, H. L. *J. Research Natl. Bur. Standards* **24** (1940) 125.
20. Kjær, A. und Lindberg, B. *Acta Chem. Scand* **13** (1959) 1713.
21. Blom, J. *Acta Chem. Scand.* **13** (1959) 388; **15** (1961) 1667; **16** (1962) 922.

Eingegangen am 29. März 1962.

ACTA CHEMICA SCANDINAVICA 16 (1962) 1785–1793

Studies on the Hydrolysis of Metal Ions 40

A Liquid Distribution Study of the Hydrolysis of Cd^{2+}

DAVID DYRSSEN and PAAVO LUMME*

Department of Inorganic Chemistry, Royal Institute of Technology, Stockholm 70, Sweden

The distribution of cadmium at 25°C between the liquid amine LA-1 in benzene and 3 M $Na(ClO_4,OH)$ has been measured, as a function of $[OH^-]$, with radioactive cadmium. The distribution data could be explained by Dyrssen and Sillén's [1] two-parameter approximation for the stepwise formation of $Cd(OH)_4^{2-}$ from Cd^{2+}. High-speed refinement of the parameters obtained by curve-fitting gave the following values with the σ-deviations:

$$a = \tfrac{1}{4} \log \beta_4 = 3.012 \pm 0.043$$
$$b = \tfrac{1}{2} \log K_n K_{n+1}^{-1} = 0.429 \pm 0.047$$
$$\log \gamma_2\beta_2(20\ \%\ \text{LA-1}) = 10.345 \pm 0.082$$

The value for the formation constant of $Cd(OH)^+$, $\log K_1 = 4.30 \pm 0.18$, agrees very well with the value in 3 M $LiClO_4$ determined by Biedermann and Ciavatta [2].

Some experiments were also carried out with radioactive $Cd(OH)_2$ in a solubility column [3], but the solubility is lower than that predicted from the values of a and b and Schindler's [4] value of the solubility product of $Cd(OH)_2$ in 3 M $NaClO_4$.

Biedermann and Ciavatta [2] have investigated the hydrolysis of Cd^{2+} in the concentration range above 0.1 M by emf titrations. In this connection it seemed worthwhile to study the hydrolysis of cadmium also at low concentrations, where only mononuclear species might be formed. Previously we had carried out both solubility and distribution experiments [3,5,6] to study the hydrolysis of Hg^{2+}, Ag^+ and VO_2^+, and at a present no other methods seem to be more favorable at low metal concentrations.

A previous investigation by Gayer and Woontner [7] of the solubility of $Cd(OH)_2$ as a function of pH ($-\log [OH^-]$, see below and Fig. 4) did not agree with reasonable values of the solubility product [8], and indicated that difficulties could be met in measuring the solubility even if a column with radio

* On leave from the University, Helsinki, Finland.

active $Cd(OH)_2$ was used. Some experiments with a solubility column (see below and Fig. 2) confirmed this.

After some preliminary distribution experiments carried out by Mr. John Crabtree, it was found that cadmium(II) could be extracted with benzene (as $Cd(OH)_2$, as was proved later), if the liquid amine Amberlite LA-1 was added to the benzene phase. Similarly Ag^+ is extracted with quinoline in benzene [5], except that in this case $AgClO_4$ is extracted instead of AgOH.

EXPERIMENTAL

Extraction with amine. The amine used was an Amberlite LA-1 product (Rohm & Haas), which is a mixture of highly branched unsaturated, secondary aliphatic amines. A structure formula for the mixture has been indicated as follows:

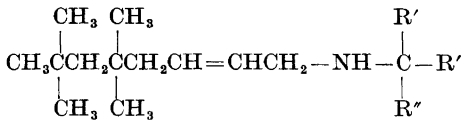

where R + R′ + R″ = 11—14 carbon atoms. It is liquid at room temperature. The mean molecular weight of the commercial product is 372 and its molarity at 25°C is about 2.25.

Organic amines may contain more or less carbonate and therefore the 20 % (vol.) amine solutions in benzene (p.a. Merck), were shaken overnight with half their volume of 0.1 M barium chloride or nitrate (barium hydroxide might be more effective) and the two phases then centrifuged. The lighter benzene phase was pipetted off and this amine solution was used in the experiments; lower amine concentrations were obtained by dilution with benzene.

Sodium perchlorate was prepared by dissolving the theoretically needed amount of sodium carbonate (p.a. Merck) in concentrated perchloric acid (p.a. Kebo) and crystallizing the product two times from water. A stock solution (about 6 M) was prepared from this material. The concentration of the sodium perchlorate stock solution was determined by evaporating a 5 ml sample to dryness and weighing.

A dilute perchloric acid solution was titrated against crystallized thallium carbonate using a bromocresol green-methyl red mixture in alcohol as indicator (Ref.[9], p. 83). Sodium hydroxide stock solution was prepared according to Sörensen (Ref.[9], p. 70) in a plastic flask, in which it was kept under an atmosphere of nitrogen. The 1.0, 0.1 and 0.001 M sodium hydroxide solutions were prepared by diluting this stock solution with sodium perchlorate so that the ionic strength of the solutions came to be 3.0 M. The concentrations were determined by means of standard perchloric acid solutions using the same indicator as above.

A stock solution of 0.04 M borax (Merck, p.a.) in 2.92 M sodium perchlorate was also prepared.

Cadmium oxide was prepared by dissolving cadmium metal (p.a.) in conc. nitric acid (Merck, p.a.), evaporating the solution to dryness in a platinum crucible, and heating the residue to about 600°C for about half an hour. A part of this product was irradiated in the Swedish reactor R1. The cadmium isotope used was ^{115m}Cd with the half-life of 43 days; ^{115}Cd (2.3 days) with its daughter ^{115m}In were allowed to die out, in most experiments. The active cadmium oxide was dissolved into 3 M perchloric acid and diluted with 3 M sodium perchlorate.

Equal total volumes (10 or 15 ml) of the aqueous and organic phases were equilibrated in 50 ml Pyrex stoppered centrifuge tubes. The phases were mixed by repeated slow inversion of the tubes at 25°C in a thermostated room. The acidity (or basicity) of the aqueous phase was varied, but the ionic strength was always kept at 3 M with sodium perchlorate. Equilibrium was obtained in 2 h, but in many cases the samples were shaken overnight. No time-dependent differences between the samples were observed.

After shaking, the samples were centrifuged and 5 ml of the aqueous phase taken to measure its pH (or $-\log [OH^-]$) and 2 ml to measure the γ-activity or 10 ml to measure the β-activity. Activity measurements were also made with the organic phase. The measurements of the γ-activity of the solutions, which were contained in plastic tubes, were made with a Tracerlab Versa/Matic II spectrometer connected with a Tracerlab SC-57 low background well scintillation counter. The β-activity measurements were made with a Tracerlab SC-18 Superscaler or SC-19 Utility Scaler connected with SC-31 Interval Timer and a Century Electronics M6 GM-tube for liquid samples. The results reported are mainly based on γ-activity measurements.

The measurements of $-\log [OH^-]$ were made with a Radiometer pH meter Type 4 using a Beckman glass electrode type E and a "Wilhelm" reference bridge of the type:

$$|3\ M\ NaClO_4|\ 2.9\ M\ NaClO_4 + 0.1\ M\ AgClO_4|\ AgCl,Ag$$

The reference buffer solution was 2.99 M with respect to sodium perchlorate and 0.01 M with respect to sodium hydroxide ($-\log [OH^-] = 2.00$). The value $pK_w = 14.22$ for the ionic product [10] of water in 3 M sodium perchlorate at 25°C was used to calculate $-\log [H^+]$ (pH).

Solubility column. The crystalline cadmium hydroxide used in the solubility measurements was prepared from cadmium nitrate by the ammonia method (*cf.* Schindler [4]). $Cd(NO_3)_2(H_2O)_4$ (Merck) was dissolved in water to give 0.5 liter of about 0.6 M solution, which was heated under reflux in an all-ground glass system. So much concentrated ammonia (p.a. Merck) was added to the solution that the cadmium hydroxide first precipitated redissolved again. The solution was refluxed as slowly as possible so as to reduce the rate of loss of ammonia. After refluxing overnight crystals of cadmium hydroxide (diameter about 1 mm) were found in the bottom of the flask. The refluxing was continued until no more crystals seemed to be formed. The crystals were then filtered under an atmosphere of nitrogen, washed with a little water and dried in a desiccator which contained ascarite.

About 1.5 g of the prepared cadmium hydroxide, enclosed in a quartz ampoule, was irradiated at Harwell, England for two months in a strong neutron flux. The short-lived isotope was allowed to die out, before the product was placed in the solubility column (about 1.3 g). A standard reference solution from the radiated product was also prepared. This had the composition: 9.438×10^{-3} M $Cd(ClO_4)_2$, 1.112×10^{-2} M $HClO_4$ and 2.97 M $NaClO_4$, and in the beginning of the experiments gave 119 400 cpm/ml in the β-tube (see above).

The solubility column and method used have been described previously by Dyrssen and Tyrrell [3]. The solution circulated in the column was 0.005 M in borax and the pH was varied by changing the sodium hydroxide concentration. The ionic strength of the solution was kept constant at 3 M with sodium perchlorate. One sample was taken per day and after this the solution in the column was changed. The pH and β-activity of the samples were measured as in extraction experiments above.

All experiments were performed at 25°C.

The data. In Fig. 1 the extraction data are given in the form of the logarithm of the distribution ratio $q = [Cd]_{tot,org}/[Cd]_{tot,aq}$ *versus* $-\log (OH^-)$. In Fig. 2 the solubility data are given in the form of the logarithm of the total cadmium concentration in solution, $[Cd]_{tot}$ *versus* $-\log [OH^-]$. The points in Fig. 1 represent the mean of six distribution experiments at different initial concentrations of cadmium(II) in the aqueous phase (3.9×10^{-5} to 3.9×10^{-4} M). The two sets of points in Fig. 2 represent two runs with the solubility column starting from each side of the solubility minimum.

Equilibrium constants

General equilibria:

$$\log K_w = \log [H^+][OH^-] = -14.22 \pm 0.02 \text{ (Ref.[10])}$$
$$\beta_n = [Cd(OH)_n][Cd]^{-1}[OH]^{-n}$$
$$K_n = [Cd(OH)_n][Cd(OH)_{n-1}]^{-1}[OH]^{-1}$$

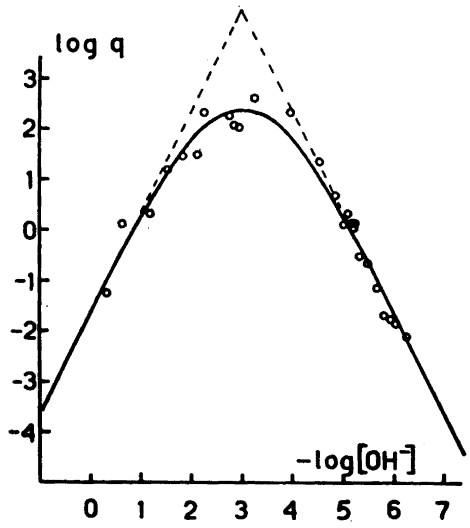

Fig. 1. Distribution of radioactive Cd(II) between benzene with 20 % Amberlite LA-1 and 3 M Na(OH,ClO_4) at 25°C. Each point is the mean value of six measurements. The curve is calculated with three parameters: $a = 3.01$, $b = 0.43$ and $\log \beta_2\lambda_2 = 10.35$ (see text). The equations for the asymptotes (dashed lines) to the distribution curve are given in the text.

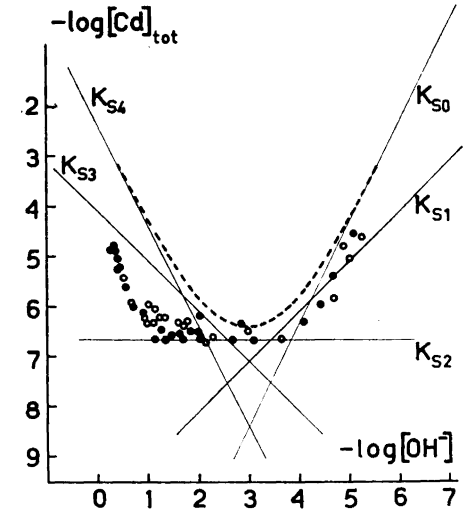

Fig. 2. Solubility of radioactive $Cd(OH)_2$ in 3 M Na(OH,ClO_4) at 25°C. The two different sets of points represent two different runs. The thin straight lines represent the equations $\log [Cd]_{tot} = \log K_{sn} + (n-2) \log [OH^-]$. The dashed curve has the same form as in Fig. 1 and is calculated with $a = 3.01$, $b = 0.43$ and $\log K_{s0} = -14.41$ (Schindler [4]); K_{sn} are also calculated from these constants.

Two-parameter approximation [1]:

$a = \frac{1}{4} \log \beta_4$
$b = \frac{1}{2} \log K_n K_{n+1}^{-1}$
$\log \beta_n = na - nb \quad (4-n)$
$\log K_n = a + b \quad (5-2n)$

Distribution constant:

$\lambda_2 = [Cd(OH)_2]_{org}[Cd(OH)_2]^{-1}$:

Solubility equilibria:

$K_{s0} = [Cd^{2+}][OH^-]^2$
$K_{s1} = [CdOH^+][OH^-] = \beta_1 K_{s0}$
$K_{s2} = [Cd(OH)_2] = \beta_2 K_{s0}$
$K_{s3} = [Cd(OH)_3^-][OH^-]^{-1} = \beta_3 K_{s0}$
$K_{s4} = [Cd(OH)_4^{2-}][OH^-]^{-2} = \beta_4 K_{s0}$
$[Cd]_{tot} = K_{s0}([OH^-]^{-2} + \beta_1[OH^-]^{-1} + \beta_2 + \beta_3[OH^-] + \beta_4[OH^-]^2)$

TREATMENT OF THE DISTRIBUTION DATA

The data are not accurate enough to allow a treatment which can be accepted without discussion. We shall therefore give several arguments below which support the results obtained by the following treatment:

It is known [2] that at low concentrations of Cd(II), Cd^{2+} is the main species in 3 M perchlorate solutions below pH 9 (above $-\log [OH^-] = 5$). For values of $-\log [OH^-]$ between 4.5 and 6.3 the distribution ratio, q, is approximately proportional to $[OH^-]^2$, which gives the slope -2 in Fig. 1. This shows that cadmium is extracted as $Cd(OH)_2$ in this $[OH^-]$ region. We now make the assumption that this is the only cadmium species extracted into the benzene phase and that the distribution ratio λ_2 is independent of the OH^- and ClO_4^- content in 3 M $Na(OH,ClO_4)$.

By variation of the amine concentration, $[L]_{org}$, in the benzene phase between 2 and 20 % we found that $q\,[L]_{org}^{-2}\,[OH^-]^{-2}$ was approximately constant, which indicated that two amine molecules are bound to $Cd(OH)_2$ and thus that four ligands are attached to Cd(II) in the organic phase.

When $[OH^-]$ is increased above 0.001 M the distribution ratio decreases which indicates that negative hydroxo complexes are formed in the aqueous phase.

We also found that there was no systematic change of distribution ratio when the initial total concentration of cadmium was varied between 3.9×10^{-5} and 3.9×10^{-4} M. Thus we seem to be dealing only with mononuclear species.

In formulating a quantitative expression for the distribution ratio over the whole $[OH^-]$ region there is no chemical reason to leave out any of the complexes $CdOH^+$, $Cd(OH)_2$, $Cd(OH)_3^-$ and $Cd(OH)_4^{2-}$ especially as the curve has a tendency to approach the slope + 2 in Fig. 1. On the other hand the accuracy is too low to allow the determination of five parameters: β_1, β_2, β_3, β_4 and λ_2 or $\beta_2\lambda_2$. We therefore decided to use the two-parameter approximation given by Dyrssen and Sillén [1], especially as this approximation can very well

describe the complex formation of Cd^{2+} with NH_3. In fact it was shown by Dyrssen and Sillén [1] that a curve of the present type should be obtained when an intermediate complex is extracted (case II). Thus

$$q = \frac{[Cd(OH)_2]_{org}}{[Cd^{2+}] + [CdOH^+] + [Cd(OH)_2] + [Cd(OH)_3^-] + [Cd(OH)_4^{2-}]}$$

or

$$q = \frac{\beta_2\lambda_2[OH^-]^2}{1 + \beta_1[OH^-] + \beta_2[OH^-]^2 + \beta_3[OH^-]^3 + \beta_4[OH^-]^4}$$

The asymptotes of the log q ($-\log [OH^-]$) curve in Fig. 1 are

$$\log q = \log \beta_2\lambda_2[OH^-]^2 = \log \lambda_2 + 2a - 4b + 2 \log [OH^-]$$
$$\log q = \log \beta_2\lambda_2\beta_4^{-1} [OH^-]^{-2} = \log \lambda_2 - 2a - 4b - 2 \log [OH^-]$$

and they intersect at the point

$$-\log [OH^-] = a$$
$$\log q = \log \lambda_2 - 4b$$

The point on the curve below this point has

$$\log q = \log \lambda_2 - 4b - \log (2 \times 10^{-3b} + 10^{-4b})$$

Approximate values of a, b and $\log \lambda_2$ could then be obtained by curvefitting [1,11].

These constants were then refined by high-speed computing using a Ferranti-Mercury computer and the LETAGROP program [12,13] with the following SP:

1) Title; cadmiumdistr 3 par weight log q; newline; jump 2
3) $X = 0$; $K = P$; $i = 1(1)N$; print (e_i) 1,3; repeat;
   $i = 1$ (1) 4; $W = ie_1 + 4ie_2 - iie_2$; print (W) 1,3;
   $b_i = \psi\exp(HW)$; repeat; $b_5 = \psi\exp(He_3)$
5) $U = \psi \exp(-HU_K)$
7) $W = b_4UUUU + b_3UUU + b_2UU + b_1U + 1$; $V = b_5UU/W$
10) $G_o = 1$; $W = \psi \log (V)$; $Z_o = W/H$; $Z_K = F_K$; jump 11; ψ exp; ψ log; close; →

Then followed the 26 data as $F_K = \log q$; $U_K = -\log [OH^-]$; $Z_K = 0$ and the DS part as 3; $e_1 = a = 3.00$; $e_2 = b = 0.45$; $e_3 = \log \beta_2\lambda_2 = 10.30$; $E = 0.0001$. The values of h_1 and h_2 were taken as 0.05 and h_3 as 0.10.

The computer found the error-pit easily and printed the following values and standard deviations:

$$a = 3.012 \pm 0.043$$
$$b = 0.429 \pm 0.047$$
$$\log \beta_2\lambda_2 = 10.345 \pm 0.082$$

The error sum, $U = \sum_1^{26} (\log q_{calc} - \log q_{exp})^2$, was 1.911 and $\sigma = \sqrt{U/23} = 0.288$.

In Fig. 3 a and b the iso-error lines for combinations of the parameters are shown with a rectangle which encloses the error-level $U + \sigma^2$ (the D-boundary). Other levels with $U + 2\sigma^2$, $3\sigma^2$ and $4\sigma^2$ are also shown. These

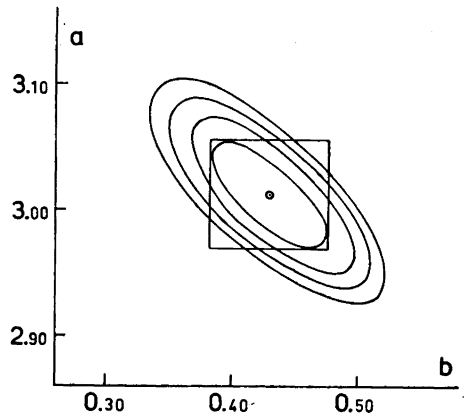

Fig. 3. Error-square sum ellipses for $U + \sigma^2$, 2 σ^2, 3 σ^2 and 4 σ^2 which show the way the parameters a and b influence each other. The rectangle encloses the D-boundary obtained by the LETAGROP computer program [13] and the point is the values of a and b which together with log $\beta_2\lambda_2 = 10.345$ give the minimum error-square sum.

ellipses (or ellipsoids if the error in log $\beta_2\lambda_2$ is included) have been calculated by the aid of a simple program. We may see from Fig. 3 that the constants a and b are not independent.

From the values of the three parameters the following approximate values of the stepwise formation constants may be calculated:

$$\log K_1 = 4.30 \pm 0.18$$
$$\log K_2 = 3.44 \pm 0.09$$
$$\log K_3 = 2.58 \pm 0.09$$
$$\log K_4 = 1.72 \pm 0.18$$
$$\log \lambda_2(20\ \%\ \text{LA-1}) = 2.60 \pm 0.36$$

Biedermann and Ciavatta [2] found $14.22 - 10.2 \pm 0.2 = 4.0 \pm 0.2$ for log K_1 in good agreement with our value. The value given by Marcus [14] seems too high.

Comparison with other d^{10} ions

In order to see how reasonable the constants obtained above are, we may compare the formation constants of Ag^+, Cd^{2+} and Hg^{2+} with the ligands OH^- and NH_3:

	log K_1	log K_2	log K_3	log K_4	Ref. No.
OH^- — 3 M $NaClO_4$					
Ag^+	1.5	2.0	< 0.3	—	$5(K_1K_2)$, $15(K_2)$
Cd^{2+}	4.3	3.4	2.6	1.7	this work
Hg^{2+}	10.7	11.6	< 0	—	16
NH_3 — 2 M NH_4NO_3					
Ag^+	3.20	3.83	—	—	8
Cd^{2+}	2.65	2.10	1.44	0.93	8
Hg^{2+}	8.8	8.7	1.0	0.8	8

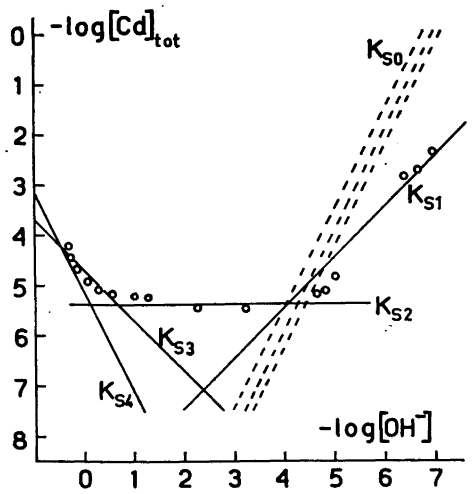

Fig. 4. Solubility data of Gayer and Woontner [7] plotted as log $[Cd]_{tot}$ against $-\log [OH^-]$. The fulldrawn lines are based on their values of K_{s1}, K_{s2}, K_{s3} and K_{s4} (for equations see definition of equilibrium constants). The dashed lines represent different values of the solubility product (see text).

It may be seen that Ag^+ and Hg^{2+} form complexes with two OH^- and NH_3 readily, but additional ligands are only added with difficulty. The two ligands are coordinated linearly. The first constant is small as compared with the second one. Cd^{2+} on the other hand forms four complexes with NH_3 and the stepwise formation constants decrease regularly in nearly equal steps. Orgel [17] has explained this difference by the small d—s separation of Ag^+ and Hg^{2+} (5 eV against 10 for Cd^{2+}).

The formation constants of the OH^- complexes are larger than for NH_3 in the case of the divalent ions Cd^{2+} and Hg^{2+}, but smaller in the case of Ag^+. This may be a charge effect.

The comparison with other data which is made here gives some confidence in the data we have obtained for the complex formation between Cd^{2+} and OH^-.

THE SOLUBILITY MEASUREMENTS

As mentioned in the introduction Gayer and Woontner [7] have measured the solubility of $Cd(OH)_2$ at different pH. We have plotted their data as log $[Cd]_{tot}$ against $-\log [OH^-]$ in Fig. 4 together with four straight lines (fulldrawn) which are determined by the values of log K_{s1}, log K_{s2}, log K_{s3} and log K_{s4} (tentative lower limit) given by Gayer and Woontner [7]. The most serious objection against the data is that they do not fit with reported values of the solubility product, K_{s0}; the lines (dashed), which are determined by log K_{s0} values of Moeller and Rhymer [8] (−13.49), Ishikawa and Shibata [8] (−13.93) and Feitknecht and Reinmann [8] (−14.20), are also shown in Fig. 4.

It should be mentioned that the straight lines in Fig. 4 are only asymptotes to the solubility curve. Their real positions relative to the curve are shown in Fig. 2.

Our solubility work was carried out in 3 M Na(OH, ClO_4) with a solubility column. The data differ from Gayer's and Woontner's [7] in two ways: The solubility minimum is about 20 times lower in our case; this may be a salt effect. The increase in solubility in the strongly alkaline region is more marked in our case.

However, our data also do not fit the values of K_{s0}. The value by Schindler [4] in 3 M $NaClO_4$ (−14.41, *cf.* also Ref.[2]) was used to fix the straight line with slope + 2 in Fig. 2. This line may be used to fit the curve obtained in the distribution experiments (Fig. 1) to the axes. As we do this we assume that we have only mononuclear complexes in the aqueous solution. Obviously, the solubility data are too low to fit the curve. One reason might be that in spite of our precautions the surface of the $Cd(OH)_2$ in the column might have been covered with $CdCO_3$ which is less soluble. By using another procedure to prepare $Cd(OH)_2$ it might be possible to solve this problem in the future.

Acknowledgements. We wish to thank Professor Lars Gunnar Sillén, Drs. Georg Biedermann and Liberato Ciavatta for valuable discussions and Mr. John Crabtree from Harwell, England, for his preliminary experiments. The English has been revised by Dr. Derek Lewis. The investigation has been supported by *Office of Scientific Research* of the Office of Aerospace Research USAF through its European office and by a grant from the *Finnish State Commission for Natural Sciences*. The apparatus used is purchased by a grant from the *Swedish Atomic Energy Research Council*.

REFERENCES

1. Dyrssen, D. and Sillén, L. G. *Acta Chem. Scand.* **7** (1953) 663.
2. Biedermann, G. and Ciavatta, L. *Acta Chem. Scand.* **16** (1962). *In press.*
3. Dyrssen, D. and Tyrrell, V. *Acta Chem. Scand.* **15** (1961) 393.
4. Schindler, P. *Helv. Chim. Acta* **42** (1959) 2736.
5. Antikainen, P. J. and Dyrssen, D. *Acta Chem. Scand.* **14** (1960) 86.
6. Dyrssen, D. and Sekine, T. *Acta Chem. Scand.* **15** (1961) 1399; Full paper to be published in *J. Inorg & Nuclear Chem.*
7. Gayer, K. H. and Woontner, L. *J. Phys. Chem.* **61** (1957) 364.
8. Bjerrum, J., Schwarzenbach, G. and Sillén, L. G. *Stability Constants, part II*, The Chemical Society, London 1958.
9. Kolthoff, I. M. and Stenger, V. A. *Volumetric Analysis II*, Interscience Publishers, New York 1947.
10. Ingri, N., Lagerström, G., Frydman, M. and Sillén, L. G. *Acta Chem. Scand.* **11** (1957) 1034.
11. Sillén, L. G. *Acta Chem. Scand.* **10** (1956) 186.
12. Dyrssen, D., Ingri, N. and Sillén, L. G. *Acta Chem. Scand.* **15** (1961) 694.
13. Ingri, N. and Sillén, L. G. *Acta Chem. Scand.* **16** (1962) 173.
14. Marcus, Y. *Acta Chem. Scand.* **11** (1957) 690.
15. Biedermann, G. and Sillén, L. G. *Acta Chem. Scand.* **14** (1960) 717.
16. Ahlberg, I. *Acta Chem. Scand.* **16** (1962) 887.
17. Orgel, L. E. *An introduction to transition-metal chemistry: Ligand-field theory*, Methuen, London 1960, p. 66–68.

Received March 26, 1962.

ACTA CHEMICA SCANDINAVICA 16 (1962) 1794–1798

The Separation of Buffer Salts at Gel Filtration

BÖRJE LINDQVIST

Central Laboratory, Mjölkcentralen, Stockholm, Sweden

During gel filtration of proteins, artefacts were observed which led to the observation that the salts of the buffers used were separated simultaneously with the proteins. Tests with pure salt solutions indicated that during sieving as well as during displacement chromatography all kinds of salt fractionation could occur. Even pure water "sieved" through the column produced several conductivity peaks when the column was in equilibrium with a buffer containing polyvalent ions.

Actual separation of both simple anions and cations in mixtures have been analytically demonstrated under conditions varying from 0.1 N acetic acid to 0.1 N ammonium hydroxide in the column. It is suggested that ions retarded by the gel matrix give the gel the property of an amphoteric ion exchanger with respect to the non-retarded ions outside the matrix.

In an experiment to fractionate and desalt [1] solutions containing enzymatically digested casein [2] (cheese preparation) through columns of Sephadex G 25*, we found that the inorganic salt ions present were fractionated simultaneously. This caused artefacts in the form of false peptide peaks. The reason for this is probably that the phosphopolypeptides formed micells at certain points in the column where a combination of pH-decrease and Ca-increase occurred and thus moved at a greater speed than otherwise.

A series of experiments was carried out in order to obtain some understanding of this undesirable distribution of salts during fractionation. The immediate purpose was to eliminate the disturbances, although the results may quite possibly be applicable to the intentional fractionation of similar substances.

A chromatograph column, 2 × 110 cm, was packed with Sephadex G 25 treated according to the manufacturer's instructions [3]. To permit the continuous registration of changes in conductivity of the eluate, the eluate was led through the conductivity cell of a Conductolyzer ** at 25°C ± 0.01°C and the changes were measured and registered. In some instances, the eluate was led further to a fraction collector.

* Manufactured by AB Pharmacia, Uppsala, Sweden.
** Manufactured by LKB-Produkter AB, Stockholm 12, Sweden.

When boric acid was not included in the buffer, the Sephadex column was kept at somewhat varying room temperatures. When boric acid was present, it was necessary to maintain a constant temperature since the equilibrium of the Sephadex-boric acid complex is markedly dependent on temperature, and the only possibility of obtaining straight base lines is therefore to keep the temperature constant. The rate of flow through the column was kept constant in all experiments at 30 ml/h. The input of the Conductolyzer was connected in parallel with a resistor of 8.2 kΩ, so that the extreme changes in conductivity which occurred in certain cases could be kept within the limits of the diagram paper. The position of the base line and the sensitivity of the recording instrument were adjusted according to experience to give suitable curves. The paper speed of the recorder was kept at 1 cm/h in all experiments except for those illustrated in Fig. 4.

The experiments were divided into four parts: displacement of one buffer in the column by another; filtration of distilled water through columns in equilibrium with buffers of various ionic types; filtration of 0.1 N NaCl under the same conditions as above; and filtration of mixtures of anions or cations through a column equilibrated with 0.1 N acetic acid or 0.1 N ammonia.

The buffer solutions used were: 0.1 N NaOH + citric acid to pH 6.7; phosphate buffer, μ 0.1, at pH 7.5; 0.1 N HN_4OH; 0.1 N acetic acid; 0.1 N trishydroxymethyl-aminomethane ("Tris"); 0.1 N NaOH + boric acid to pH 10.5; Aronsson-Grönwall's high resolution buffer [4], 0.1 N with respect to "Tris" (12.10 g/l "Tris", 1.20 g/l EDTA, 0.92 g/l boric acid), and a couple of equiconductive buffers of the same pH-value, obtained through neutralizing 0.1 N NaOH with conc. H_3PO_4 or citric acid to pH 7.00.

The procedure in the experiments was to adjust the column to complete equilibrium with the buffer used by letting the buffer run through until the conductivity of the eluate remained constant for at least 2 h. By means of the customary chromatographic technique, 10 ml of the test solution was then applied to the column. Elution with the buffer followed immediately and the recorder was started simultaneously. The procedure in the displacement tests was analogous. The ions in the fractions were identified with the aid of the usual analytical techniques.

Some of the conductivity curves obtained have been re-traced and are given in Figs. 1—4. This was done in order to correct for some maladjustments during some of the first experiments before sufficient experience had been acquired.

Fig. 1 gives the results when water was filtered through the column. When the water passed the conductivity cell, the recorder indicated lower conductivity. Depending on the degree of diffusion of water and salts, the peak registered will have the basic character of an ordinary Gaussian curve rather than being rectangular. However, the water curves shown in the figure have different shapes and deviate from a Gaussian curve in some instances, indicating that the water does not pass through the column without interference with the gel and the buffer salts. This is demonstrated more clearly by the fact that, for each of the different buffers used, there are marked variations in the flow rate of the water through the column in relation to the rate for the eluating buffer. Migration is fastest in the citrate buffer and slowest in the borate buffer. In a composite buffer such as the Aronsson-Grönwall buffer, the water

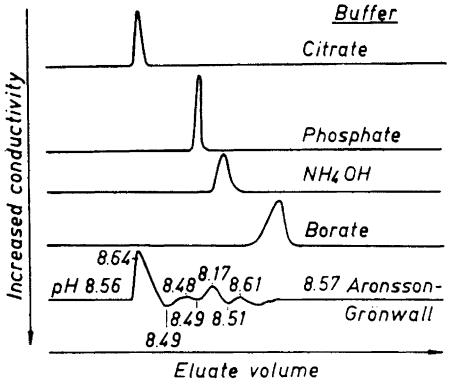

Fig. 1. Gel filtration of 10 ml water through a column packed with Sephadex G 25 in equilibrium with the buffers stated. The interaction between the water and the gel is illustrated by the different shapes and positions of the water peaks in the conductivity curve. Separation of the components in the Aronsson-Grönwall buffer is indicated by the shape of the curve and the pH-value of the eluate corresponding to the peaks obtained.

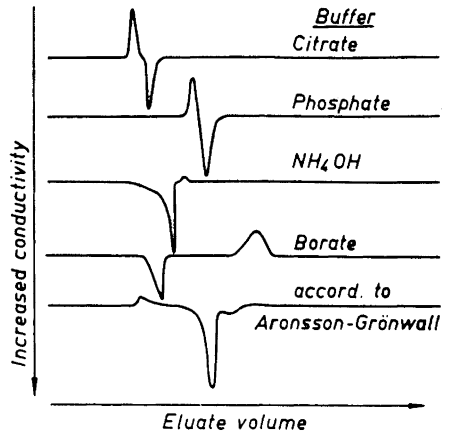

Fig. 2. Gel filtration of 10 ml 0.1 N NaCl under the same conditions as in Fig. 1. When buffers with polyvalent anions are used, the shape of the curve indicates the separation of water and NaCl. Peak heights correspond to a conductivity change of 2—10 %.

will even give rise to a whole series of peaks which represent conductivities both higher and lower than that of the eluating buffer. The eluate fractions corresponding to these peaks were found to vary in their pH-values and buffer capacity, which confirmed fractionation of the buffer when the water passed through the column. The pH-values obtained have been included in the figure.

Fig. 2 illustrates the the result of the corresponding gel filtration of 0.1 N NaCl. Monovalent buffers gave distorted Gaussian curves of the type exemplified by the ammonium hydroxide curve. Polyvalent anion types, on the other hand, gave complex curves. Citrate, phosphate, and borate buffers all gave two peaks for the gel filtration of NaCl, the one showing a quite low conductivity and the other showing a high conductivity in relation to the conductivity of the buffer before and after the peaks. In the case of the citrate and phosphate buffers, the high conductivity peaks follow immediately after the low conductivity peaks. In the case of the borate buffer, the high conductivity peak appears first and is followed by a long interval before the low conductivity peak is apparent. When the Aronsson-Grönwall buffer is used, the curve is again rather complex. However, it is not possible to discard *a priori* the assumption that the single peaks observed, such as with NH_4OH, consist of superimposed curves of different types. It would therefore be too presumptuous to draw extensive conclusions from these observations although it is

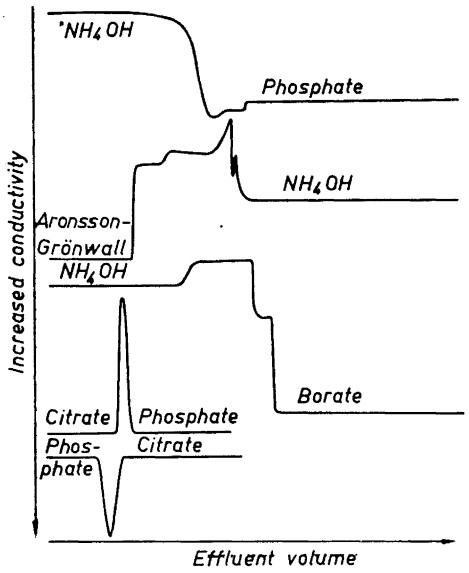

Fig. 3. Displacement of one buffer in the Sephadex G 25 column by another. The steps in the conductivity curves indicate a strong interaction between the buffer ions and the gel or the original ions retarded by the gel.

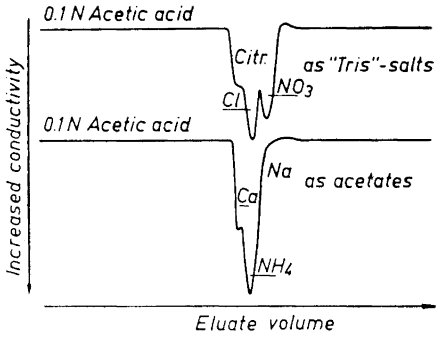

Fig. 4. Under similar conditions, Sephadex G 25 is able to bring about at least a partial separation of both anions and cations in the mixtures. The gel appears to act as an amphoteric ion exchanger.

clear that water and NaCl do become separated during the passage through the column.

In the displacement of one buffer in the column by another, the curves obtained show more or less distinct steps. This is illustrated by some examples in Fig. 3. Even here, each of the superimposed effects appears as a step which is modified in the direction of either low or high conductivity.

In one experiment, buffers having almost equivalent conductivity, ionic strength and pH were permitted to replace each other. The buffers used were sodium phosphate and sodium citrate, both being made by neutralizing 0.1 N NaOH with the respective acids in concentrated or solid form to pH 7.00 $\pm$ 0.005. When the Sephadex column is saturated with the citrate buffer and the displacement made with phosphate buffer, a solitary sharp peak with low conductivity appears (water?). When the displacement procedure is reversed, there is a similar single peak but this is in the direction of increased conductivity, indicating that the salts have partially migrated over each other.

Finally, in order to demonstrate the separation of ions and groups of ions in the eluates, several experiments were performed, some of which are presented in Fig. 4. Two experiments were carried out with the column saturated with 0.1 N acetic acid. In one of these, a mixture of citric acid, hydrochloric acid and nitric acid was filtered through the gel, all of these substances at 0.1 N

and dissolved in 0.1 N acetic acid. The fractions obtained were analyzed and showed a relatively good separation of the acids. The separation was improved if the solution was made 0.3 N with regard to "Tris", before filtration. The citric acid is the first to appear, the other acids following as shown in Fig. 4. When not neutralized with "Tris" the citric acid appeared last.

In the second of these experiments, Ca^{2+}, NH_4^+ and Na^+ were separated from each other as acetates. There was poor separation, however, between NH_4^+ and Na^+. In this case, too, factors were observed which reversed the order of the ions (presence of other anions, pyridine, etc.).

DISCUSSION

The phenomena observed are associated with some form of retardation of the ions moving through the column. It is not possible to state definitely whether this retardation is caused by filtration according to molecular size, partition chromatography, ion exchange chromatography or by other effects. When buffers containing boric acid are used, a marked ion exchange effect is to be expected since the boric acid is bound to the Sephadex gel and gives a relatively strongly ionized complex. A possible explanation of the effects occurring with the other types of buffers might be that the anions and cations which are more or less bound by the gel matrix give the gel the character of amphoteric ion exchanger in its relationship to the mobile ions outside the gel. In this case, the amphoteric ion exchanger would exhibit an unique property in that its ionized groups would migrate steadily through the column with a characteristic migration rate of their own, determined by the ion form and size.

Ion exchange properties of the gel *per se*, as discussed by Miranda *et al.*[5], seem less likely. Even if the ion exchanger is amphoteric, one can scarcely expect the simultaneous separation of both anions and cations within the wide pH interval provided by 0.1 N HAc—0.1 N NH_4OH.

REFERENCES

1. Flodin, P. *J. Chromatography* **5** (1960) 103.
2. Lindqvist, B. *Intern. Dairy Congr. Proc. 16th Congr.*, Copenhagen **1962 B** 673.
3. Pharmacia, *Sephadex in Gel Filtration* Uppsala, Sweden, 1961.
4. Aronsson, T. and Grönwall, A. *Scand. J. Clin. & Lab. Invest.* **9** (1957) 338, also in *Science Tools, The LKB Instrument J.* **5** (1958) 17.
5. Miranda, F., Rochat, H. and Lissitzky, S. *J. Chromatography* **7** (1962) 142.

Received March 26, 1962.

ACTA CHEMICA SCANDINAVICA 16 (1962) 1799–1818

Short Communications

On the Interpretation of the Electron Spin Resonance Spectrum of the Light-Induced Radicals from *s*-Trinitrobenzene Dissolved in Tetrahydrofuran

CARL LAGERCRANTZ and MARGARETA YHLAND

Department of Medical Physics, University of Göteborg, Göteborg, Sweden

We have recently described the generation of free radicals when a solution of *s*-trinitrobenzene in tetrahydrofuran was irradiated by light [1]. It was believed that the radiant energy absorbed promoted a charge transfer in an electron-donor-acceptor complex built up from tetrahydrofuran (donor) and *s*-trinitrobenzene (acceptor) leading to an unpairing of the electrons involved. The electron spin resonance (ESR) spectrum exhibited a 12-lines structure with four lines of the intensity ratio 1:3:3:1 distributed into three equal groups. This spectrum is consistent with the interaction of the unpaired electron with one nitrogen atom and three equivalent protons.

In the note [1] the spectrum was tentatively connected with the formation of a negative radical ion derived from *s*-trinitrobenzene in spite of the presence of only one nitrogen hyperfine interaction. The suggestion was made that this single interaction was dependent on a splitting common to the three nitrogen nuclei due to the high symmetry of the molecule. The three protons, however, were assumed to interact in a conventional way. This explanation can of course be questioned, and other interpretations can be suggested.

A radical which is formed by the transfer of an electron to *s*-trinitrobenzene would be expected to give rise to a splitting into seven energy levels by the interaction of the three equivalent nitrogen nuclei. The three equivalent protons would split each of these levels into four, giving rise to $4 \times 7 = 28$ lines, if no overlapping is present. The intensity ratio of these lines should be: 1:3:3:1:3:9:9:3:6:18:18:6:7:21:21:7:6:18:18:6:3:9:9:3:1:3:3:1. It is obvious that the spectrum described by us is not consistent with this hypothetical spectrum. Consequently, the structure of the radicals giving rise to the recorded spectrum has to be explained in other terms than those of a negative radical ion derived directly from *s*-trinitrobenzene.

A situation very similar to the one discussed has been encountered by Ward [2] in a study of the ESR-spectra of radicals produced by the action of alkali metals on nitro-substituted derivatives of benzene dissolved in dimethoxyethane and tetrahydrofuran. In agreement with our results one single nitrogen hyperfine interaction was found for *m*-dinitrobenzene, *p*-dinitrobenzene, *s*-trinitrobenzene and trinitromesitylene. In *s*-trinitrobenzene the single nitrogen hyperfine interaction was combined with the interaction of three equivalent protons. The spectra of the chemically prepared negative radical ions described by Ward were found to be different from those prepared by electrogeneration [3]. The spectra of the dinitrobenzenes obtained by the last method exhibit the interaction of two nitrogen nuclei. The difference in the spectra of the electrogenerated and the chemically produced dinitrobenzene negative ions was tentatively explained by Ward to be due to the existence of a tight complex between the alkali metal and the nitro-substituted hydrocarbon. Through the formation of this complex the equivalence of the three nitrogen atoms would be completely removed.

No spectrum of *s*-trinitrobenzene radicals obtained by electrogeneration seems to have been reported. The chemically obtained radicals of *s*-trinitrobenzene reported by Ward were produced in dimethoxy-

ethane, and the spectrum was recorded with a relatively low resolution. A direct comparison between this spectrum and that reported by us is therefore rather difficult.

In view of the findings described by Ward, it is not impossible, however, to still assign our spectrum to negative ions derived from *s*-trinitrobenzene. The peculiar single nitrogen interaction of our system in which no alkali metals were present, is perhaps connected with some kind of interaction with the tetrahydrofuran molecules. It may be suggested that the complex between tetrahydrofuran and *s*-trinitro benzene involves three molecules of tetrahydrofuran and one molecule of *s*-trinitrobenzene according to the formula given below. The presence of three simultaneous spin systems each enclosing the aromatic nucleus with the three protons and one nitro-group with the attached tetrahydrofuran molecule, could possibly explain the obtained spectrum.

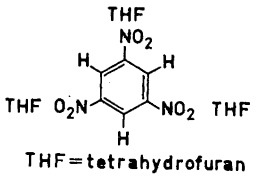

THF = tetrahydrofuran

1. Lagercrantz, C. and Yhland, M. *Acta Chem. Scand.* **16** (1962) 1043.
2. Ward, R. L. *J. Am. Chem. Soc.* **83** (1961) 1296.
3. Maki, A. H. and Geske, D. H. *J. Chem. Phys.* **33** (1960) 825.

Received July 31, 1962.

Interconversion of 1-Phenyl-5-mercapto-1,2,3-triazole and 5-Phenylamino-1,2,3-thiadiazole

T. KINDT-LARSEN and CHRISTIAN PEDERSEN

Department of Organic Chemistry, University of Technology, Copenhagen, Denmark

From the reaction between 1-phenyl-5-chloro-1,2,3-triazole (I) and sodium hydrogen sulphide one would expect to get 1-phenyl-5-mercapto-1,2,3-triazole (II). Hess has, however, shown [1] that this reaction produces a mixture of two compounds one of which is a sulphide with the structure (VIII). The other product, with melting point 173°, has the composition corresponding to (II) but since it shows no acidic properties it cannot be a mercaptotriazole and Hess proposed that it has the structure (III). Hess, furthermore, found that this compound would dissolve in hot, aqueous sodium hydroxide; acidification of the alkaline solution gave a new, isomeric compound with m.p. 65° for which the structure (II) was proposed. The lower melting isomer, when heated in ligroin, rearranged to the higher melting isomer.

Since the structures (II) and (III) are tautomeric it is unlikely that they should represent two different compounds and it has now been shown that the higher melting isomer is identical with the known 5-phenylamino-1,2,3-thiadiazole (IV) which is easily prepared from phenyl isothiocyanate and diazomethane [2].

The lower melting isomer was prepared from authentic 5-phenylamino-1,2,3-thiadiazole (IV) by heating with sodium hydroxide according to Hess [1]. That it is 1-phenyl-5-mercapto-1,2,3-triazole (II), as proposed by Hess, was shown by convert-

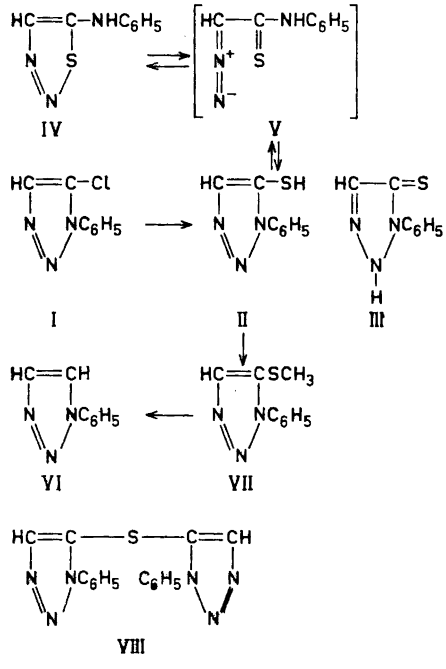

ethane, and the spectrum was recorded with a relatively low resolution. A direct comparison between this spectrum and that reported by us is therefore rather difficult.

In view of the findings described by Ward, it is not impossible, however, to still assign our spectrum to negative ions derived from *s*-trinitrobenzene. The peculiar single nitrogen interaction of our system in which no alkali metals were present, is perhaps connected with some kind of interaction with the tetrahydrofuran molecules. It may be suggested that the complex between tetrahydrofuran and *s*-trinitro benzene involves three molecules of tetrahydrofuran and one molecule of *s*-trinitrobenzene according to the formula given below. The presence of three simultaneous spin systems each enclosing the aromatic nucleus with the three protons and one nitro-group with the attached tetrahydrofuran molecule, could possibly explain the obtained spectrum.

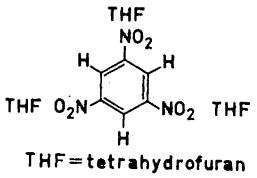

THF = tetrahydrofuran

1. Lagercrantz, C. and Yhland, M. *Acta Chem. Scand.* **16** (1962) 1043.
2. Ward, R. L. *J. Am. Chem. Soc.* **83** (1961) 1296.
3. Maki, A. H. and Geske, D. H. *J. Chem. Phys.* **33** (1960) 825.

Received July 31, 1962.

Interconversion of 1-Phenyl-5-mercapto-1,2,3-triazole and 5-Phenylamino-1,2,3-thiadiazole

T. KINDT-LARSEN and CHRISTIAN PEDERSEN

Department of Organic Chemistry, University of Technology, Copenhagen, Denmark

From the reaction between 1-phenyl-5-chloro-1,2,3-triazole (I) and sodium hydrogen sulphide one would expect to get 1-phenyl-5-mercapto-1,2,3-triazole (II). Hess has, however, shown [1] that this reaction produces a mixture of two compounds one of which is a sulphide with the structure (VIII). The other product, with melting point 173°, has the composition corresponding to (II) but since it shows no acidic properties it cannot be a mercaptotriazole and Hess proposed that it has the structure (III). Hess, furthermore, found that this compound would dissolve in hot, aqueous sodium hydroxide; acidification of the alkaline solution gave a new, isomeric compound with m.p. 65° for which the structure (II) was proposed. The lower melting isomer, when heated in ligroin, rearranged to the higher melting isomer.

Since the structures (II) and (III) are tautomeric it is unlikely that they should represent two different compounds and it has now been shown that the higher melting isomer is identical with the known 5-phenylamino-1,2,3-thiadiazole (IV) which is easily prepared from phenyl isothiocyanate and diazomethane [2].

The lower melting isomer was prepared from authentic 5-phenylamino-1,2,3-thiadiazole (IV) by heating with sodium hydroxide according to Hess [1]. That it is 1-phenyl-5-mercapto-1,2,3-triazole (II), as proposed by Hess, was shown by convert-

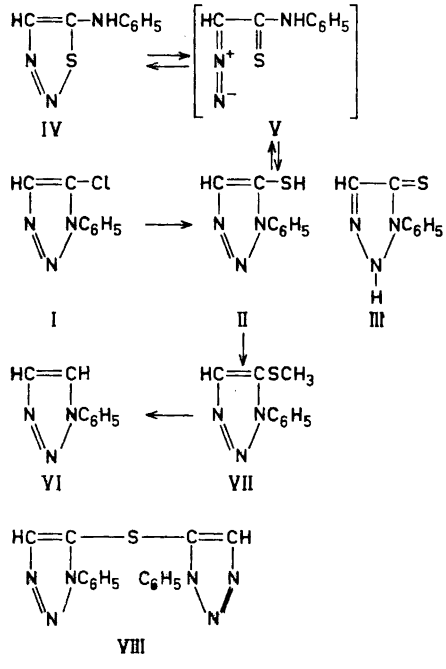

ing it to 1-phenyl-5-methylmercapto-1,2,3-triazole (VII) which, when desulphurized with Raney nickel, gave the known 1-phenyl-1,2,3-triazole (VI). The direct desulphurization of (II) was not attempted because of the instability of this compound.

The primary product in the reaction of 1-phenyl-5-chloro-1,2,3-triazole (I) and sodium hydrogen sulphide is probably the mercaptotriazole (II) which then, under the conditions of the reaction, rearranges into (IV). The interconversion of (II) and (IV) is probably taking place *via* the diazothioacetic anilide (V) in analogy with the rearrangement between 1-phenyl-5-amino-1,2,3-triazole and 5-phenylamino-1,2,3-triazole where a diazocompound similar to (V) is assumed to be an intermediate [3]. Sheehan and Izzo [2] assumed a tautomeric form of (V) to be an intermediate in the formation of 5-phenylamino-1,2,3-thiadiazole from phenyl isothiocyanate and diazomethane.

Experimental. Reaction of 1-phenyl-5-chloro-1,2,3-triazole with sodium hydrogen sulphide. To a solution of 1-phenyl-5-chloro-1,2,3-triazole [4,5] (2.5 g) in ethanol (35 ml) was added 7.5 ml of 22 % aqueous sodium hydrogen sulphide (prepared by saturating a solution of sodium hydroxide (8.0 g) in water (37 ml) with hydrogen sulphide at room temperature). The solution was kept at room temperature for 7 days during which time a crystalline precipitate formed; it was filtered off, washed with water and ethanol and dried. Yield 0.70 g (28 %), m.p. 168–170°. After two recrystallizations from ethanol the compound melted at 172–173°. (Found: C 53.95; H 4.00; N 23.80. Calc. for $C_8H_7N_3S$: C 54.19; H 3.99; N 23.72). The product was identical in infra red spectrum and mixed melting point with 5-phenylamino-1,2,3-thiadizole (IV) prepared according to Sheehan [2]. When the reaction was performed at 100° in a sealed tube the only product that could be isolated was the sulphide (VIII).

1-Phenyl-5-mercapto-1,2,3-triazole. 4.0 g of 5-phenylamino-1,2,3-thiadiazole was added to a solution of sodium hydroxide (1.0 g) in water (25 ml). The mixture was heated to *ca.* 90° for a few minutes until the thiadiazole was dissolved, and the slightly coloured solution was filtered through activated carbon. The filtrate was cooled in ice; when acidified with dilute hydrochloric acid an oil was precipitated which crystallized on scratching. The product was filtered off and washed with water. Yield 3.30 g (82 %), m.p. 63–65°. Two recrystallizations from ether-pentane gave pure 1-phenyl-5-mercapto-1,2,3-triazole with m.p. 64–65 (Hess [1] reported m.p. 65°). (Found: C 54.35; H 4.02; N 23.86; S 18.03. Calc. for $C_8H_7N_3S$: C 54.19; H 3.99; N 23.72; S 18.08). The compound was decomposed when kept at room temperature for a few weeks.

1-Phenyl-5-methylmercapto-1,2,3-triazole. 5-Phenylamino-1,2,3-thiadiazole (10.0 g) was suspended in 150 ml of 1 N sodium hydroxide and heated to *ca.* 90° for a few minutes until it was dissolved. The solution was filtered through activated carbon, cooled and stirred with methyl iodide (20 ml) for 2 h at room temperature. Excess methyl iodide was removed by blowing air through the mixture and the product was then extracted with ether. The ether solution was washed with water and dried with magnesium sulphate. The ether was removed *in vacuo* and the residue was distilled yielding 6.6 g (61 %) of 1-phenyl-5-methylmercapto-1,2,3-triazole as a yellow oil with b.p. 140° (0.5 mm). (Found: C 56.50; H 4.88; N 22.80; S 16.88. Calc. for $C_9H_9N_3S$: C 56.50; H 4.75; N 22.00; S 16.76).

1-Phenyl-1,2,3-triazole. To a solution of 1-phenyl-5-methylmercapto-1,2,3-triazole (1.0 g) in ethanol (20 ml) was added *ca.* 5 g of Raney nickel and the mixture was heated on the steam bath for 8 h. The Raney nickel was filtered off and washed twice with hot ethanol and the ethanol was removed *in vacuo* at room temperature. The residue was dissolved in ether and treated with activated carbon. Addition of pentane precipitated 430 mg (56 %) of 1-phenyl-1,2,3-triazole with m.p. 54–55° (Dimroth [6] recorded 55–56°). Mixed melting point and infrared spectrum proved that the product was identical with an authentic sample.

Microanalysis were made by Mr. Preben Hansen.

This work is part of an investigation supported by *Kai Hansen's Fond.*

1. Hess, F. *Diss.*, München 1909.
2. Sheehan, J. C. and Izzo, P. T. *J. Am. Chem. Soc.* **71** (1949) 4059.
3. Lieber, E., Ramachandra Rao, C. N. and Chao, T. S. *J. Am. Chem. Soc.* **79** (1957) 5962.
4. Dimroth, O. *Ann.* **364** (1909) 203.
5. Lieber, E., Chao, T. S. and Ramachandra Rao, C. N. *J. Org. Chem.* **22** (1957) 654.
6. Dimroth, O. *Ber.* **35** (1902) 1029.

Received July 29, 1962.

Über das Vorkommen von Cucurbitacin E und I in *Iberis amara* L. *(Cruciferae)* und die Identität von "Ibamarin" mit Cucurbitacin I

J. B-SON BREDENBERG

Department of Chemistry, Indiana University, Bloomington, Indiana, U.S.A.,

R. GMELIN

Biochemische Abteilung, Chemie Grünenthal G.m.b.H., Stolberg/Rheinland

Die Cucurbitacine sind in der Familie *Cucurbitaceae* weit verbreitet. Nach den bis heute geltenden chemotaxonomischen Erfahrungen schienen sie — wie auch der Name ausdrückt — auf diese Familie beschränkt zu sein [1,2].

Wir haben nun gefunden, dass die Cucurbitacine E und I auch in *Iberis amara* L. (*Cruciferae*) vorkommen und deren stark bitteren Geschmack verursachen.

Ein Bitterstoff "Ibamarin", aus den Samen von *Iberis amara* isoliert, wurde erstmals von Schultz und Gmelin 1954 erwähnt [3]. Pourrat und Decorps [4] beschrieben kürzlich eine Verbindung aus dem gleichen Pflanzenmaterial, die sie ebenfalls "Ibamarin" benannten und die offensichtlich identisch mit dem früher beschriebenen Bitterstoff gleichen Namens ist [5]. Die chemischen Eigenschaften von "Ibamarin" wurden inzwischen näher studiert [5], und eine Bruttoformel $C_{20}H_{28}O_5$ wurde dafür vorgeschlagen [4,5].

Nachdem unsere Versuche, das Molekulargewicht nach der Methode von Rast zu bestimmen, falsche Resultate ergeben hatten, und auch eine massenspektroskopische Molekulargewichtsbestimmung wegen der zu geringen Flüchtigkeit der Substanz erfolglos war, ergab ein Kernresonanzspektrum, dass "Ibamarin" mehr Wasserstoff enthielt als in dem ursprünglichen Formelvorschlag angegeben war.

Auf eine auffallende Ähnlichkeit zwischen den chemischen Eigenschaften von "Ibamarin" und den Cucurbitacinen war schon früher hingewiesen [5]. Wir haben nun gefunden, dass die physikalischen Eigenschaften von "Ibamarin" in sehr guter Übereinstimmung mit denen von Cucurbitacin I (Elatericin B) sind [6-9]. Beim Vergleich mit authentischem Material, das uns freundlicherweise durch Prof. Lavie, Rehovoth, Israel, zur Verfügung gestellt worden war, erwies sich "Ibamarin" tatsächlich als identisch mit Cucurbitacin I. Der Name "Ibamarin" ist also zu streichen und durch Cucurbitacin I zu ersetzen. Bei einer erneuten Aufarbeitung der Samen von *Iberis amara* nach einem modifizierten Verfahren erhielten wir eine zweite Substanz, $C_{32}H_{44}O_8$, Fp. 234–237°. Diese Substanz wurde als Cucurbitacin E (*a*-Elaterin) [9-12] identifiziert, welches auch in verschiedenen *Cucurbitaceae*-Arten als Begleiter von Cucurbitacin I vorkommt [1].

Das nunmehr sicher bewiesene Vorkommen von zwei Cucurbitacinen in einer *Cruciferen*-Art zeigt, dass diese Naturstoff-Klasse sauerstoffreicher Triterpene in Pflanzenreich weiter verbreitet ist als ursprünglich angenommen worden war.

Vorläufige Untersuchungen, bei denen wir zur Identifizierung von Cucurbitacin E und I die Dünnschichtchromatographie heranzogen, ergaben, dass die Gattung *Iberis* hinsichtlich des Vorkommens dieser Bitterstoffe nicht einheitlich ist. Während in den Samen von *Iberis amara* L. und *Ib. umbellata* L. die beiden Bitterstoffe sich nachweisen liessen, enthielt *Iberis sempervirens* L., die sich auch sonst phytochemisch deutlich von den anderen Arten unterscheidet, keine Bitterstoffe. Systema tische Untersuchungen mit weiteren *Iberis*-Arten sind im Gange.

Versuchsteil. 230 g Samen von *Iberis amara* L. (var. "White Rocket") (Harry E. Saier, Dimondale, Michigan) wurden gemahlen und im Soxhlet mit Hexan entfettet. Der nur schwach bittere, gelbliche Ölrückstand (25 g) wurde verworfen. Die Samen wurden anschliessend in gleicher Weise mit Aceton extrahiert, wonach ein nur noch schwach bitter schmeckendes Samenpulver zurückblieb. Der Aceton-Auszug wurde eingeengt, und der Trockenrückstand wurde mit 100 ml $CHCl_3$ ausgekocht. Die filtrierte Chloroformlösung wurde auf 100 g neutrales Al_2O_3 (Woelm, Aktivitätsstufe 3) gebracht. Die Entwicklung erfolgte durchlaufend mit Chloroform, Chloroform-Äthanol (1:1) und Äthanol. Der Bitterstoff erschien in den Chloroform-Äthanol-Fraktionen. Das Roh-Produkt (1,6 g) wurde in 5 ml Benzol gelöst. Beim Stehen über Nacht im Kühlschrank schieden sich 154 mg einer Substanz aus (Fp. 229–232°). Weitere 38 mg der gleichen Substanz wurden nach Eindampfen der Mutterlauge, Auflösen des Rückstands in 5 ml Aceton und mehrstündigem Stehen bei −10° erhalten. Der Rückstand der Mutterlauge ergab aus Benzol, dem etwas Wasser zugesetzt war,

940 mg (0,4 %) kristallines "Ibamarin", das mit unserem früheren Vergleichsmaterial identisch war. Die vereinten Mutterlaugen gaben nach erneuter Chromatographie weitere 50 mg der Verbindung mit Fp. 229–232°, deren Gesamtausbeute somit 0,1 % betrug.

"Ibamarin". "Ibamarin" wurde aus Benzol mit einem Zusatz von etwas Wasser umkristallisiert und analysenrein erhalten, Fp. 148–150°. Mischschmelzpunkt mit Cucurbitacin I (Fp. 148–150°) ergab keine Depression. Die IR-Spektren in Nujol und Chloroform waren identisch.

Substanz Fp. 234–237°. Der kristalline Stoff, Fp. 229–232°, wurde aus Benzol umkristallisiert, wobei farblose Blättchen, Fp. 234–237°, erhalten wurden, $[\alpha]_D^{22} - 60°$ ($CHCl_3$, *c* 1 %). (Gefunden: C 68,99; H 7,77; O 22,87. Berechnet für $C_{32}H_{44}O_8$: C 69,04; H 7,95; O 22,99). Der Mischschmelzpunkt mit Cucurbitacin E (Fp. 235–237°) gab keine Depression. Die IR-Spektren in Nujol und Chloroform waren identisch.

Dünnschicht-Chromatographie. (*a*) Cucurbitacin E, (*b*) Cucurbitacin I, (*c*) "Ibamarin", (*d*) "Acetyl-Ibamarin", und (*e*) Substanz Fp. 234–237°, wurden in 5–20 μg-Mengen auf Glasplatten mit Kieselgel G-Merck in üblicher Weise dünnschichtchromatographisch entwickelt. Als Fliessmittel diente Chloroform mit 5 % Äthanol-Zusatz. Die Flecken wurden durch Besprühen mit äthanolischer $FeCl_3$-Lösung (rotbraune Flecken) oder mit einem Gemisch aus 2 Teilen konz. H_3PO_4 und 8 Teilen Äthanol (graubraune Flecken nach Erhitzen auf 140°, mattgelbe Fluoreszenz unter UV-Licht) sichtbar gemacht. R_F-Werte: (*a*) und (*e*) 0,41, (*b*) und (*c*) 0,23, (*d*) 0,37.

Wir danken Dr. R. W. King für die Aufnahme der NMR-Spektren.

1. Rehm, S., Enslin, P. R., Meeuse, A. D. J. und Wessels, J. H. *J. Sci. Food. Agr.* **8** (1957) 679; *Chem. Abstr.* **52** (1958) 4931.
2. Eisenhut, W. O. und Noller, C. R. *J. Org. Chem.* **23** (1958) 1984.
3. Schultz, O. E. und Gmelin, R. *Arch. Pharm.* **59** (1954) 404.
4. Pourrat, H. und Decorps, P. *Bull. soc. chim. France* **1961** 670.
5. Bredenberg, J. B. und Gmelin, R. *Acta Chem. Scand.* **16** (1962) 649.
6. Enslin, P. R., Rehm, S. und Rivett, D. E. A. *J. Sci. Food Agr.* **8** (1957) 673; *Chem. Abstr.* **52** (1958) 4931.
7. Lavie, D. und Willner, D. *J. Am. Chem. Soc.* **80** (1958) 710.
8. Lavie, D. und Shvo, Y. *J. Am. Chem Soc.* **82** (1960) 966.
9. Lavie, D., Shvo, Y., Gottlieb, O. R. und Glotter, E. *Tetrahedron Letters* **1961** 615.
10. Lavie, D. und Szinai, S. *J. Am. Chem. Soc.* **80** (1958) 707.
11. Gilbert, J.N.T. und Mathieson, D. W. *Tetrahedron* **4** (1958) 302.
12. deKoch, W. T., Enslin, P. R., Norton, K. B., Barton, D. H. R., Sklarz, B. und Bothner-By, A. A. *Tetrahedron Letters* **1962** 309.

Received July 17, 1962.

Production of some Amino Acids and B-Vitamins by the Corn Smut Fungus *U. maydis* (DC) Cda.

W. G KURZ and L.-E. ERICSON

Division of Food Chemistry, Royal Institute of Technology, Stockholm, Sweden

During recent years we have studied some of the factors influencing the biosynthesis of lysine and threonine by *U. maydis* (DC) Cda. as well as the ability of this organism to utilize various sources of carbon and nitrogen for growth and amino acid production. [1,2] As a sideline to this work, we have also made a limited number of observations on the ability of *U. maydis* (DC) Cda. to produce valine and glutamic acid as well as a few B-vitamins when cultivated on different media in 10-litre fermentation vessels. It should be emphasized that this investigation was of an exploratory nature only and that no attempt was made to obtain maximal yields for the different substances studied.

A culture of *Ustilago maydis* (DC) Cda. was purchased from the Centralbureau voor Schimmelcultures, Baarn, Holland. This culture is identical with *U. maydis* ATCC 11427, P.R.L. 119 and N.R.R.L. 2321. It was maintained on agar slants, prepared by adding 1.5 % agar to the medium suggested by Dulaney.[9]

Four different media were used. Medium I was a synthetic medium and had the composition given in Table V, Ref.[2] Maltose (100 g/l) and a mixture of ammonium sulphate (6.0 g/l) and urea (1.8 g/l) were used as sources of carbon and nitrogen. It also contained all the mineral constituents that were found to be necessary for the growth of *U. maydis* (DC) Cda. Medium II was made up entirely from unhopped lager wort, which was diluted 1:1 with distilled

940 mg (0,4 %) kristallines "Ibamarin", das mit unserem früheren Vergleichsmaterial identisch war. Die vereinten Mutterlaugen gaben nach erneuter Chromatographie weitere 50 mg der Verbindung mit Fp. 229–232°, deren Gesamtausbeute somit 0,1 % betrug.

"Ibamarin". "Ibamarin" wurde aus Benzol mit einem Zusatz von etwas Wasser umkristallisiert und analysenrein erhalten, Fp. 148–150°. Mischschmelzpunkt mit Cucurbitacin I (Fp. 148–150°) ergab keine Depression. Die IR-Spektren in Nujol und Chloroform waren identisch.

Substanz Fp. 234–237°. Der kristalline Stoff, Fp. 229–232°, wurde aus Benzol umkristallisiert, wobei farblose Blättchen, Fp. 234–237°, erhalten wurden, $[\alpha]_D^{22} - 60°$ ($CHCl_3$, *c* 1 %). (Gefunden: C 68,99; H 7,77; O 22,87. Berechnet für $C_{32}H_{44}O_8$: C 69,04; H 7,95; O 22,99). Der Mischschmelzpunkt mit Cucurbitacin E (Fp. 235–237°) gab keine Depression. Die IR-Spektren in Nujol und Chloroform waren identisch.

Dünnschicht-Chromatographie. (*a*) Cucurbitacin E, (*b*) Cucurbitacin I, (*c*) "Ibamarin", (*d*) "Acetyl-Ibamarin", und (*e*) Substanz Fp. 234–237°, wurden in 5–20 μg-Mengen auf Glasplatten mit Kieselgel G-Merck in üblicher Weise dünnschichtchromatographisch entwickelt. Als Fliessmittel diente Chloroform mit 5 % Äthanol-Zusatz. Die Flecken wurden durch Besprühen mit äthanolischer $FeCl_3$-Lösung (rotbraune Flecken) oder mit einem Gemisch aus 2 Teilen konz. H_3PO_4 und 8 Teilen Äthanol (graubraune Flecken nach Erhitzen auf 140°, mattgelbe Fluoreszenz unter UV-Licht) sichtbar gemacht. R_F-Werte: (*a*) und (*e*) 0,41, (*b*) und (*c*) 0,23, (*d*) 0,37.

Wir danken Dr. R. W. King für die Aufnahme der NMR-Spektren.

1. Rehm, S., Enslin, P. R., Meeuse, A. D. J. und Wessels, J. H. *J. Sci. Food. Agr.* **8** (1957) 679; *Chem. Abstr.* **52** (1958) 4931.
2. Eisenhut, W. O. und Noller, C. R. *J. Org. Chem.* **23** (1958) 1984.
3. Schultz, O. E. und Gmelin, R. *Arch. Pharm.* **59** (1954) 404.
4. Pourrat, H. und Decorps, P. *Bull. soc. chim. France* **1961** 670.
5. Bredenberg, J. B. und Gmelin, R. *Acta Chem. Scand.* **16** (1962) 649.
6. Enslin, P. R., Rehm, S. und Rivett, D. E. A. *J. Sci. Food Agr.* **8** (1957) 673; *Chem. Abstr.* **52** (1958) 4931.
7. Lavie, D. und Willner, D. *J. Am. Chem. Soc.* **80** (1958) 710.
8. Lavie, D. und Shvo, Y. *J. Am. Chem Soc.* **82** (1960) 966.
9. Lavie, D., Shvo, Y., Gottlieb, O. R. und Glotter, E. *Tetrahedron Letters* **1961** 615.
10. Lavie, D. und Szinai, S. *J. Am. Chem. Soc.* **80** (1958) 707.
11. Gilbert, J.N.T. und Mathieson, D. W. *Tetrahedron* **4** (1958) 302.
12. deKoch, W. T., Enslin, P. R., Norton, K. B., Barton, D. H. R., Sklarz, B. und Bothner-By, A. A. *Tetrahedron Letters* **1962** 309.

Received July 17, 1962.

Production of some Amino Acids and B-Vitamins by the Corn Smut Fungus *U. maydis* (DC) Cda.

W. G KURZ and L.-E. ERICSON

Division of Food Chemistry, Royal Institute of Technology, Stockholm, Sweden

During recent years we have studied some of the factors influencing the biosynthesis of lysine and threonine by *U. maydis* (DC) Cda. as well as the ability of this organism to utilize various sources of carbon and nitrogen for growth and amino acid production. [1,2] As a sideline to this work, we have also made a limited number of observations on the ability of *U. maydis* (DC) Cda. to produce valine and glutamic acid as well as a few B-vitamins when cultivated on different media in 10-litre fermentation vessels. It should be emphasized that this investigation was of an exploratory nature only and that no attempt was made to obtain maximal yields for the different substances studied.

A culture of *Ustilago maydis* (DC) Cda. was purchased from the Centralbureau voor Schimmelcultures, Baarn, Holland. This culture is identical with *U. maydis* ATCC 11427, P.R.L. 119 and N.R.R.L. 2321. It was maintained on agar slants, prepared by adding 1.5 % agar to the medium suggested by Dulaney.[9]

Four different media were used. Medium I was a synthetic medium and had the composition given in Table V, Ref.[2] Maltose (100 g/l) and a mixture of ammonium sulphate (6.0 g/l) and urea (1.8 g/l) were used as sources of carbon and nitrogen. It also contained all the mineral constituents that were found to be necessary for the growth of *U. maydis* (DC) Cda. Medium II was made up entirely from unhopped lager wort, which was diluted 1:1 with distilled

water. The carbohydrate content of the final medium was approximately 100 g/l, 80 % of which was fermentable with *Saccharomyces cereviseae*. The concentration of assimilable nitrogen was approximately 0.6 mg/ml. No minerals were added to this medium. Medium III contained beet sugar molasses as the carbon source and diammonium phosphate (10 g/l) as the nitrogen source. By dissolving 208 g of molasses in one litre of distilled water, a sugar content of about 100 g/l medium was obtained. No mineral constituents were added. Medium IV was identical with medium III but the supernatant fluid from the anaerobic digestion tanks for sewage sludge was used instead of water for the dilution of the molasses. The supernatant fluid from the sewage works was freed from particles before being used.

The organism, in all cases reported here, was grown in 10-liter fermentation vessels. The rate of aeration was 0.3 l per litre medium per min and the broth was stirred at about 700 r.p.m. The temperature was kept at 27°C. Inocula were prepared by growing the organism in shaking flasks at 25°C for 48 – 72 h.

Samples for analysis were withdrawn immediately after inoculation of the tanks and after 10 and 25 days. Each sample was incubated at 45°C for 24 h at pH 4.0 as this had been found to give maximal values for lysine and threonine. Before being submitted to the analytical procedures the incubation mixture was centrifuged to remove cell debris.

Microbiological methods were used for the estimation of the amino acids and vitamins under study. Lysine and glutamic acid were determined according to the tube assays of Steele *et al.* using *Leuconostoc mesenteroides* P-60 (ATCC 8042) as test organism [3]. Threonine and valine were also estimated by the procedures outlined by Steele *et al.* but in these cases *Streptococcus faecalis* ATCC 8043 was employed as test organism. For all amino acid determinations we used Difco's Bacto Assay Media. Growth was measured turbidimetrically after 24 h at 37° C in a Coleman Model 11 Universal spectrophotometer at 640 mμ.

Riboflavin was released by HCl treatment as described in the method of analysis of the *Association of Official Agricultural Chemists*, Eigth Edition [4]. *L. casei* ATCC 7469 served as test organism in the Difco's Bacto Riboflavin Assay Medium. For this as for the other vitamins cup plate assays were applied. The agar plates were incubated overnight at 37°C.

Niacin was also set free according to the method recommended by A.O.A.C., by autoclaving in 1 N H_2SO_4. The test medium was that of Bolinder and Larsen [5] using *S. faecalis* ATCC 8043. Niacin was used as standard.

An estimate of the total folic- and folinic acid activity was obtained in the following manner. The pH of the samples was adjusted with 1 M K_2HPO_4 to 6.5. To 10 ml samples was added 80 mg of the Bacto chicken pancreas conjugase preparation sold by Difco Laboratories, Detroit, USA. The mixture was then incubated under toluene overnight at 37°C. It was thereafter boiled for 5 min and centrifuged. The total folic- and folinic acid activity was estimated with *S. faecalis* ATCC 8043 as test organism. The same medium was used as for the niacin assay with the omission of folic acid and the addition of 1 mg of niacin per l medium (single strength). It should be pointed out that since the samples probably contained several members of the folic- and folinic acid group of factors, whereas pteroylglutamic acid served as standard, this assay merely gives an indication of the presence of large or small amounts of folic- and/or folinic acid activity. It does not give an estimate of the content of pteroylglutamic acid content of the samples.

The biotin assay was preceeded by autoclaving the samples in 1 N H_2SO_4 at about 120°C for 30 min. After neutralization the samples were assayed for biotin using *L. fermenti* ATCC 9338 as test organism. The basal medium was the same as the acetate medium described by Bolinder and Larsen [5] with the modifications mentioned by Sjöstedt and Ericson [6].

Vitamin B_{12} (cyanocobalamin) and related growth factors were released by boiling in dilute KCN at approximately pH 5 for 15 min. *E. coli* 113 – 3 was used as test organism in the medium suggested by Diding [7] but modified by the addition of 100 mg thiomalic acid and 10 mg KCN per litre medium (single strength). Cyanocobalamin served as standard.

The results are summarized in Table 1. For the sake of brevity only the initial values and the highest or lowest values observed during the fermentation are presented. It should be mentioned that the growth in medium I was poorer than previously encountered and that the values for lysine and threonine are far below those reported earlier. The data from this experiment are nevertheless included as they clearly demonstrate the ability of *U. maydis* to produce all the vitamins tested with the exception of vitamin B_{12}. We have been unable to detect any ability of *U. maydis* to synthesize this vitamin (or related factors) which is contrary to the report by Haskins *et al.* [8] In fact the B_{12}-activity present in medium IV which contained sewage sludge was utilized by the organism in a few days. In general the

Table 1. Concentration of some amino acids and vitamins in incubated (45°C, pH 4.0) *U. maydis* broth. The figures within brackets give the number of days of fermentation.

Medium	Cell number × 10^6	pH	Amino acids				Vitamins					
			Lysine	Threonine	Valine	Glutamic acid	Ribo-flavine	Niacin	Biotin	B_{12}-activity	Folic- and folinic acid activity direct treated	
			μg/ml	μg/ml	μg/ml	μg/ml	mμg/ml	mμg/ml	mμg/ml	mμg/ml	mμg/ml	mμg/ml
I	11.2(0)	6.5(0)	10(0)	10(0)	25(0)	10(0)	10(0)	35(0)	5(0)	0(0)	6(0)	3(0)
	325(5)	8.2(5)	50(5)	50(5)	50(2)	80(5)	75(5)	120(5)	12(5)	0(5)	150(10)	190(10)
II	15.0(0)	6.4(0)	100(0)	100(0)	140(0)	60(0)	25(0)	320(0)	10(0)	25*(0)	30(0)	75(0)
	1150(10)	5.4(10)	310(5)	250(5)	210(2)	110(2)	450(10)	470(5)	80(10)	70*(5)	100(5)	130(5)
III	24(0)	7.1(0)	35(0)	100(0)	180(0)	250(0)	30(0)	560(0)	6(0)	10*(0)	20(0)	20(0)
	900(5)	6.3(5)	35(5)	40(5)	90(5)	190(5)	75(5)	560(5)	5(0)	5*(5)	130(5)	130(5)
IV	24(0)	7.1(0)	35(0)	100(0)	200(0)	280(0)	30(0)	380(0)	30(0)	35(0)	20(0)	20(0)
	750(10)	5.6(10)	70(10)	80(10)	110(10)	320(5)	180(10)	560(2)	40(5)	7*(10)	75(5)	380(10)

* Diffuse growth zones not due to B_{12}-like factors but more likely to methionine.

concentrations of the vitamins present at any stage of the fermentation were low for all media. Also the ability to synthesize lysine, threonine, valine and glutamic acid was poor under the conditions of this experiment.

1. Ericson, L.-E. and Kurz, W. G. *Biotechnology and Bioengineering* **4** (1962) 23.
2. Kurz, W. G. and Ericson, L.-E. *Biotechnology and Bioengineering* **4** (1962) 37.
3. Steele, B. F., Sauberlich, H. E., Reynolds, M. S. and Baumann, C. A. *J. Biol. Chem.* **177** (1949) 533.
4. *Official methods of analysis of the Association of official agricultural chemists*, Eigth Edition, Washington D. C. 1955.
5. Bolinder, A. E. and Larsen, B. *Acta Chem. Scand.* **15** (1961) 823.
6. Sjöstedt, M. and Ericson, L.-E. *Acta Chem. Scand.* **16** (1962). *In press.*
7. Diding, N. Å. *Scand. J. Clin. & Lab Invest.* **3** (1951) 215.
8. Haskins, R. H., Lemicux, R. U., Thorn, J. A. and Ledingham, G. A. *Intern. Congr. Microbiol., Abstrs of Papers*, Rio de Janeiro 1950, p. 189.
9. Dulaney, E. L. *Can. J. Microbiol.* **3** (1957) 467.

Received August 7, 1962.

Crystal Structure Data for the Compounds $TaCl_5 \cdot POCl_3$ and $TiCl_4 \cdot 2POCl_3$

CARL-IVAR BRÄNDÉN*

University of Uppsala, Institute of Chemistry, Uppsala, Sweden

Preliminary studies of the compounds $TaCl_5 \cdot POCl_3$ and $TiCl_4 \cdot 2POCl_3$ have been made as part of an investigation of the crystal structures of addition compounds formed between metal halides and $POCl_3$ or $PO(CH_3)_3$. Single crystals were prepared in sealed capillary tubes using a zone melting technique. Rotation and Weissenberg photographs (layer-lines 0—2) were taken with CuK radiation. From the space group and the approximate unit cell dimensions thus obtained and from a comparison of the intensities it was found that the compound $TaCl_5 \cdot POCl_3$ is isostructural with $SbCl_5 \cdot POCl_3$ [1] and the compound $TiCl_4 \cdot 2POCl_3$ is isostructural with $SnCl_4 \cdot 2POCl_3$. [2]

No further work on these compounds is intended at present.

I wish to thank Professor G. Hägg for all the facilities placed at my disposal and Professor I. Lindqvist for continued interest and stimulating discussions. This work has been sponsored by a grant from Air Force Office of Scientific Research, OAR, through the European Office, Aerospace Research, United States Air Force under Contract No. AF 61(052)—43. This grant is gratefully acknowledged.

I am indebted to Mr. S. Sandborg for help with the X-ray examination of $TaCl_5 \cdot POCl_3$.

The approximate cell dimensions are:

1. $TaCl_5 \cdot POCl_3$:	Orthorhombic,	Space group,	$P\,n\,m\,a$.
	$a = 16.4$ Å	$b = 8.1$ Å	$c = 9.0$ Å
2. $TiCl_5 \cdot 2POCl_3$:	Orthorhombic,	Space group,	$P\,n\,n\,m$.
	$a = 13.4$ Å	$b = 13.5$ Å	$c = 7.7$ Å

* Present address: Laboratory of Molecular Biology, University Postgraduate Medical School, Hills Road, Cambridge, England.

1. Lindqvist, I. and Brändén, C.-I. *Acta Cryst.* **12** (1959) 642.
2. Brändén, C.-I. *Acta Chem. Scand.* **17** (1963). *In press.*

Received August 6, 1962.

concentrations of the vitamins present at any stage of the fermentation were low for all media. Also the ability to synthesize lysine, threonine, valine and glutamic acid was poor under the conditions of this experiment.

1. Ericson, L.-E. and Kurz, W. G. *Biotechnology and Bioengineering* **4** (1962) 23.
2. Kurz, W. G. and Ericson, L.-E. *Biotechnology and Bioengineering* **4** (1962) 37.
3. Steele, B. F., Sauberlich, H. E., Reynolds, M. S. and Baumann, C. A. *J. Biol. Chem.* **177** (1949) 533.
4. *Official methods of analysis of the Association of official agricultural chemists*, Eigth Edition, Washington D. C. 1955.
5. Bolinder, A. E. and Larsen, B. *Acta Chem. Scand.* **15** (1961) 823.
6. Sjöstedt, M. and Ericson, L.-E. *Acta Chem. Scand.* **16** (1962). *In press.*
7. Diding, N. Å. *Scand. J. Clin. & Lab Invest.* **3** (1951) 215.
8. Haskins, R. H., Lemicux, R. U., Thorn, J. A. and Ledingham, G. A. *Intern. Congr. Microbiol., Abstrs of Papers*, Rio de Janeiro 1950, p. 189.
9. Dulaney, E. L. *Can. J. Microbiol.* **3** (1957) 467.

Received August 7, 1962.

Crystal Structure Data for the Compounds $TaCl_5 \cdot POCl_3$ and $TiCl_4 \cdot 2POCl_3$

CARL-IVAR BRÄNDÉN*

University of Uppsala, Institute of Chemistry, Uppsala, Sweden

Preliminary studies of the compounds $TaCl_5 \cdot POCl_3$ and $TiCl_4 \cdot 2POCl_3$ have been made as part of an investigation of the crystal structures of addition compounds formed between metal halides and $POCl_3$ or $PO(CH_3)_3$. Single crystals were prepared in sealed capillary tubes using a zone melting technique. Rotation and Weissenberg photographs (layer-lines 0—2) were taken with CuK radiation. From the space group and the approximate unit cell dimensions thus obtained and from a comparison of the intensities it was found that the compound $TaCl_5 \cdot POCl_3$ is isostructural with $SbCl_5 \cdot POCl_3$ [1] and the compound $TiCl_4 \cdot 2POCl_3$ is isostructural with $SnCl_4 \cdot 2POCl_3$. [2]

No further work on these compounds is intended at present.

I wish to thank Professor G. Hägg for all the facilities placed at my disposal and Professor I. Lindqvist for continued interest and stimulating discussions. This work has been sponsored by a grant from Air Force Office of Scientific Research, OAR, through the European Office, Aerospace Research, United States Air Force under Contract No. AF 61(052)—43. This grant is gratefully acknowledged.

I am indebted to Mr. S. Sandborg for help with the X-ray examination of $TaCl_5 \cdot POCl_3$.

The approximate cell dimensions are:

1. $TaCl_5 \cdot POCl_3$:	Orthorhombic,	Space group,	$P\,n\,m\,a$.
	$a = 16.4$ Å	$b = 8.1$ Å	$c = 9.0$ Å
2. $TiCl_5 \cdot 2POCl_3$:	Orthorhombic,	Space group,	$P\,n\,n\,m$.
	$a = 13.4$ Å	$b = 13.5$ Å	$c = 7.7$ Å

* Present address: Laboratory of Molecular Biology, University Postgraduate Medical School, Hills Road, Cambridge, England.

1. Lindqvist, I. and Brändén, C.-I. *Acta Cryst.* **12** (1959) 642.
2. Brändén, C.-I. *Acta Chem. Scand.* **17** (1963). *In press.*

Received August 6, 1962.

Light-Induced Free Radicals in Solutions of Some Unsaturated Compounds and Tetranitromethane

CARL LAGERCRANTZ and
MARGARETA YHLAND

Department of Medical Physics, University of Göteborg, Göteborg, Sweden

It is generally assumed that the coloured products formed in solutions of many unsaturated compounds and tetranitromethane (TNM) are electron-donor-acceptor (EDA) complexes built up from unsaturated compounds which release electrons to TNM [1]. We now wish to report that such systems exhibit an electron spin resonance (ESR) absorption when irradiated by light at room temperature. The spectra recorded were found to be more or less characteristic for the molecular structure of the donor substances. Light-induced radicals in solutions of some other EDA-complexes have recently been described [2].

The ESR-spectra were obtained by a Varian 100 kc spectrometer. The specimens were irradiated *in situ* through the slots of the ESR-cavity. The light source was a mercury lamp equipped with two sets of filters isolating either the lines 365.0/366.5 mμ (source UV) or the lines 405/407 mμ (source Blue). Substances liquid at room temperature were used either undiluted or diluted by an equal volume of chloroform. Solid substances were dissolved in chloroform. The mole ratio of the substances to TNM was made 10:1. The radical spectra were recorded either during irradiation or in the dark immediately after a period of irradiation. If no radicals were observed after an irradiation period of 10 min, the reaction was considered as negative. No radicals could be observed in a reaction mixture composed of a substance and TNM which had been irradiated separately before mixing.

The results obtained can be divided into four groups as follows.

I. The ESR-spectra of this group exhibited a triplet structure, the lines of which are equally spaced, and are of equal intensity. The width of the individual lines is rather narrow. A characteristic feature is a large splitting amounting to between 26 and 30 gauss for different substances. Some of the spectra exhibited a very narrow secondary splitting of the three main lines. The following substances were found to belong to this group:

(*a*) β-oxo compounds: acetylacetone, benzoylacetone (Fig. 1); (*b*) β-keto esters: ethyl acetoacetate, ethyl benzoylacetate and diethyl acetonedicarboxylate; (*c*) aliphatic ketones such as methyl nonylketone (reaction mixture: colourless); (*d*) cyclic ketones: cyclopentanone and cyclohexanone (reaction mixtures: colourless). The spectra of the cyclic ketones exhibited a superposition of two individual spectra. Besides the large-spaced triplet structure of group I, there was another triplet with a closer spacing.

II. The ESR-spectra of this group exhibited also a triplet structure similar to that of group I but the splittings were smaller, and were found to be between 6—13 gauss. Further splittings of the main lines were a common feature of this group.

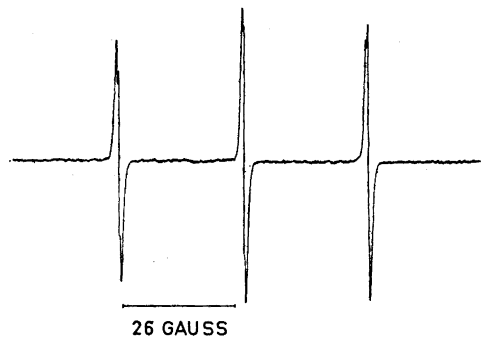

Fig. 1. ESR-spectrum of the light-induced free radicals in a solution of benzoylacetone (1 M) and TNM (1 M) in chloroform. Light source: Blue.

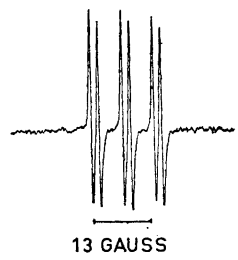

Fig. 2. In mesityl oxide + TNM. Light source: Blue.

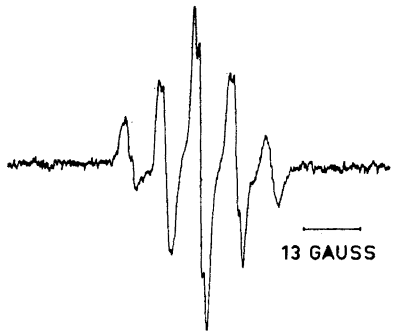

Fig. 3. In cyclohexene + TNM. Light source: Blue.

Included into group II were the following substances:

(*a*) *α,β*-unsaturated esters: methyl methacrylate, methyl acrylate and ethyl crotonate (reaction mixtures: colourless); (*b*) mesityl oxide (Fig. 2); (*c*) elaidic acid; (*d*) cyclic ketones, see I (*d*).

III. The ESR-spectra of this group exhibited a more or less symmetrical five-line structure. The following substances were found to belong to this group:

(*a*) cyclohexene. The five-line structure exhibited a partially resolved secondary splitting into three lines (Fig. 3); (*b*) methyl oleate and Δ^{10}-undecylenic acid.

IV. In this group are included substances which give rise to rather complicated spectra such as styrene (Fig. 4) and limonene. When irradiated by light no radicals could be detected in the highly coloured reaction mixtures of benzene, hexamethyl benzene and dimethyl sulphide.

In some of the systems investigated the wavelength of the exciting light (source Blue) is outside the region of absorption of both TNM and the substances but inside the absorption of the reaction mixtures.

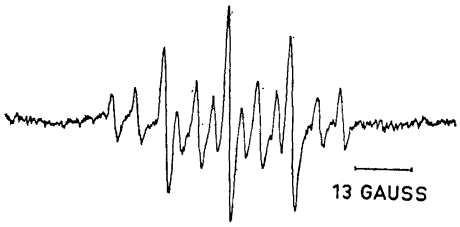

Fig. 4. In styrene + TNM. Light source: Blue.

The excitation of these systems leading to an unpairing of electrons seems to be connected with the absorption of radiant energy by a coloured EDA-complex. In other systems, including several coloured ones, light of a higher energy (source UV) had to be used in order to produce radicals. At present it does not seem possible to decide whether the excitation of the last-mentioned systems depends on the presence of a preformed non-excited complex, or whether the reaction mechanism involves an individual excitation of the donor molecules and/or TNM.

The common feature of the substances which give a positive radical reaction with TNM, is the presence of an olefinic double bond. The *β*-oxo compound and the ketones very probably react in their enol forms. The superposition spectra obtained with the cyclic ketones do not seem to depend on the presence of impurities but are believed to be due to photo-sensitized secondary reactions.

The triplet structure of groups I and II is very probably caused by the interaction of the unpaired electron with one nitrogen nucleus of TNM. The secondary splittings of the nitrogen levels seem to be due to the interaction with protons of the donor molecules. These findings would indicate that the radicals really are composed of parts both from the presumed donors and TNM. There seems to be a reciprocal relation between the magnitude of the nitrogen couplings and the presence and the magnitude of the proton splittings. The larger the nitrogen couplings, the smaller are the proton splittings and *vice versa*. This observation would indicate that the unpaired electrons of the radicals belonging to group I spend most of their time in the acceptor part of the complex. The sharing of the odd electron between the donor and the acceptor parts would be more pronounced in the radicals of group II.

The origin of the five-line structure of the spectra obtained in group III can be interpreted as due to an interaction of the odd electron with one nitrogen nucleus of TNM and with two equivalent protons of the donor assuming the coupling constants of the nitrogen and the protons to be equal. This interpretation should correspond to an intensity ratio of 1:3:4:3:1. Alternatively, the interaction of two equivalent nitrogen nuclei gives rise to a five-line spectrum with an intensity ratio of 1:2:3:2:1. The difference between the intensity ratios of these two alternatives is too

small to permit a definite decision by comparison with the experimentally obtained ratios.

The colour reaction of TNM with many unsaturated compounds is currently used for detecting the presence of double bonds. The value of the test is somewhat restricted as no colour is obtained with some unsaturated compounds such as α,β-unsaturated acids. Coloured products are also formed with non-olefinic substances such as benzene and alkyl sulphides. It is evident that the light-induced radical reaction here described is sometimes more specific for the presence of olefinic double bonds than are the absorption spectra in the visible and ultraviolet of the complexes formed with TNM.

1. Fieser, L. and Fieser, M. *Advanced Organic Chemistry*, New York 1961, p. 146.
2. Lagercrantz, C. and Yhland M. *Acta Chem. Scand.* **16** (1962) 1043.

Received August 7, 1962.

Di-(hydroxyalkyl) Diselenides

LARS-BÖRGE AGENÄS

Chemical Institute, University of Uppsala, Uppsala, Sweden

Di-(hydroxyalkyl) sulfides and disulfides have been known and studied over a long period. Thus di-(hydroxyethyl) disulfide was prepared as early as 1862 by F Guthrie [1], while the corresponding sulfide was prepared in 1886 by V Meyer [2]. Considerable attention has since been paid to these compounds and some of their higher homologues have been obtained. By comparison the corresponding selenium compounds have been given much less attention. Only di-(hydroxyethyl) selenide has been prepared by Smedslund [3,4] and while some ether derivatives of di-(hydroxyethyl) diselenide have been prepared [5] the diol itself has never been isolated.

As part of an investigation of di-(hydroxyalkyl) diselenides which is being undertaken in this Institute, the compounds I, II, and III have been prepared by reacting halohydrines with sodium diselenide solution. The reaction is almost immediate and only a slight evolution of heat has been observed.

The lowest reaction rate was found in the preparation of III; this is clearly a consequence of steric hindrance in the hydroxyneopentyl group. Thus the two compounds with a straight carbon chain were obtained after shaking the components for a few minutes, while the hydroxyneopentyl derivative was obtained only after heating the reaction mixture on a water bath for some hours.

The compounds were obtained as red-yellow oils which are almost insoluble in water but which dissolve easily in chloroform and in a proportionately large amount of ether. They have characteristic, more or less unpleasant odours. They tend to decompose when attempts are made to purify them by fractionation. As the substances are very high-boiling, the temperature necessary to distil the substances has obviously reached the temperature known to decompose diselenides. Decomposition can be avoided and thus the yield raised by distilling in high-vacuum.

The products obtained have been identified by selenium analyses and by infra-red spectroscopy. A comparison of the spectra of the starting materials and the products shows that in all three cases the bands in the 3 and 9.5 μ ranges of $-OH$ are unchanged by the reaction. The absorption peaks arising from the carbon chains are not altered to such a degree that rearrangement may be suspected. In the region investigated, the Se-Se bond shows no absorption and in the long-wave region where this bond is expected giving an absorption band, nobody has so far been able to identify it.

A more detailed report on further compounds of this type is planned.

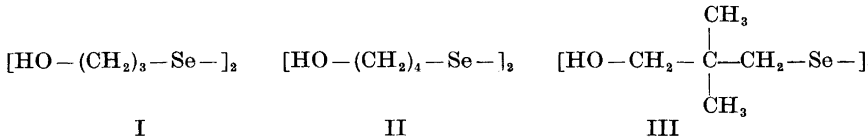

I II III

small to permit a definite decision by comparison with the experimentally obtained ratios.

The colour reaction of TNM with many unsaturated compounds is currently used for detecting the presence of double bonds. The value of the test is somewhat restricted as no colour is obtained with some unsaturated compounds such as α,β-unsaturated acids. Coloured products are also formed with non-olefinic substances such as benzene and alkyl sulphides. It is evident that the light-induced radical reaction here described is sometimes more specific for the presence of olefinic double bonds than are the absorption spectra in the visible and ultraviolet of the complexes formed with TNM.

1. Fieser, L. and Fieser, M. *Advanced Organic Chemistry*, New York 1961, p. 146.
2. Lagercrantz, C. and Yhland M. *Acta Chem. Scand.* **16** (1962) 1043.

Received August 7, 1962.

Di-(hydroxyalkyl) Diselenides

LARS-BÖRGE AGENÄS

Chemical Institute, University of Uppsala, Uppsala, Sweden

Di-(hydroxyalkyl) sulfides and disulfides have been known and studied over a long period. Thus di-(hydroxyethyl) disulfide was prepared as early as 1862 by F Guthrie [1], while the corresponding sulfide was prepared in 1886 by V Meyer [2]. Considerable attention has since been paid to these compounds and some of their higher homologues have been obtained. By comparison the corresponding selenium compounds have been given much less attention. Only di-(hydroxyethyl) selenide has been prepared by Smedslund [3,4] and while some ether derivatives of di-(hydroxyethyl) diselenide have been prepared [5] the diol itself has never been isolated.

As part of an investigation of di-(hydroxyalkyl) diselenides which is being undertaken in this Institute, the compounds I, II, and III have been prepared by reacting halohydrines with sodium diselenide solution. The reaction is almost immediate and only a slight evolution of heat has been observed.

The lowest reaction rate was found in the preparation of III; this is clearly a consequence of steric hindrance in the hydroxyneopentyl group. Thus the two compounds with a straight carbon chain were obtained after shaking the components for a few minutes, while the hydroxyneopentyl derivative was obtained only after heating the reaction mixture on a water bath for some hours.

The compounds were obtained as red-yellow oils which are almost insoluble in water but which dissolve easily in chloroform and in a proportionately large amount of ether. They have characteristic, more or less unpleasant odours. They tend to decompose when attempts are made to purify them by fractionation. As the substances are very high-boiling, the temperature necessary to distil the substances has obviously reached the temperature known to decompose diselenides. Decomposition can be avoided and thus the yield raised by distilling in high-vacuum.

The products obtained have been identified by selenium analyses and by infra-red spectroscopy. A comparison of the spectra of the starting materials and the products shows that in all three cases the bands in the 3 and 9.5 μ ranges of $-OH$ are unchanged by the reaction. The absorption peaks arising from the carbon chains are not altered to such a degree that rearrangement may be suspected. In the region investigated, the Se-Se bond shows no absorption and in the long-wave region where this bond is expected giving an absorption band, nobody has so far been able to identify it.

A more detailed report on further compounds of this type is planned.

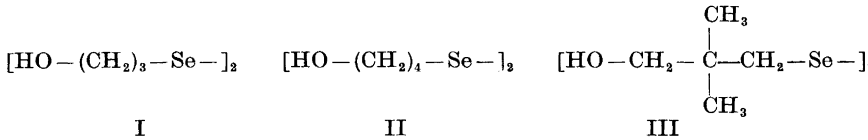

I II III

Experimental. Di-(3-hydroxypropyl) diselenide (I). A sodium diselenide solution was prepared by shaking 15.8 g (0.2 mole) of selenium, 8 g (0.2 mole) of sodium hydroxide, 15.4 g (0.1 mole) of sodium formaldehyde sulfoxylate, and 200 ml of water in a stoppered bottle for half an hour, and then adding 27.8 g (0.2 mole) of 3-bromopropanol-1. The bromohydrine reacted instantaneously and after shaking for a few minutes the water phase was colourless and a red-yellow oil had separated. The mixture was extracted with ether and the ether extract dried over sodium sulfate. After evaporating the ether, the residue was fractionated. During the distillation some decomposition was observed. The fraction boiling at 168–182°/0.2 mm was collected and found to weigh 15.2 g (52.5 %). When redistilled the product boiled at 160–170°/0.2 mm. n_D^{20} 1.5970. The product shows infra-red absorption peaks at 3.05, 3.49, 7.05, 8.05, 8.44, 8.80 μ. Found: Se 56.99. Calc. for $C_6H_{14}O_2Se_2$: Se 57.20).

Di-(4-hydroxybutyl) diselenide (II). A sodium diselenide solution was prepared by shaking 15.7 g (0.2 mole) of selenium, 8 g (0.2 mole) of sodium hydroxide, 15.4 g (0.1 mole) of sodium formaldehyde sulfoxylate, and 200 ml of water in a stoppered bottle for half an hour; 21.6 g (0.2 mole) of 4-chlorobutanol-1[6] was then added and the mixture was shaken for half an hour. A slight rise of temperature was observed during the reaction. The water phase was then colourless and a red-yellow oil had separated. The reaction mixture was extracted with ether and the ether extract was dried over sodium sulfate. After evaporating the ether, the residue was fractionated. During the distillation some decomposition was observed. The main fraction boiled at 182–187°/0.1 mm and weighed 15.2 g (51 %). n_D^{20} 1.5500. The red-yellow, viscid oil had an extremely unpleasant odour. The product shows infra-red absorption peaks at 3.05, 3.46, 6.92, 7.75, 8.11, 8.45, 9.40, 9.67, 13.35, 13.85 μ. (Found: Se 52.27. Calc. for $C_8H_{18}O_2Se_2$: Se 51.92).

Di-(3-hydroxy-2,2-dimethylpropyl) diselenide (III). A sodium diselenide solution was prepared by shaking 7.9 g (0.1 mole) of selenium, 4 g (0.1 mole) of sodium hydroxide, 7.7 g (0.05 mole) of sodium formaldehyde sulfoxylate, and 100 ml of water in a stoppered bottle for half an hour. The solution was placed in a flask with a mechanical stirrer and a reflux condenser and 16.7 g (0.1 mole) of 3-bromo-2,2-dimethylpropanol-1[7] was added. The mixture was heated with stirring on a boiling water bath for 4 h. The water phase was then colourless and a red-yellow oil had separated. The reaction mixture was extracted with ether and the ether extract dried over sodium sulfate. After the ether was evaporated the residue was fractionated. The main fraction, which crystallized in the condenser, boiled at 170–180°/0.2–0.3 mm and weighed 9.8 g (59 %). The product, that was red-yellow, on recrystallization from cyclohexane yielded bright yellow crystals in featherlike aggregates, melting at 46–47.5°. The product shows infra-red absorption peaks at 2.95, 3.42, 6.81, 7.24, 7.34, 8.12, 8.70, 9.60, 9.90, 10.20, 11.19, 12.34 μ. (Found: Se 47.29. Calc. for $C_{10}H_{22}O_2Se_2$: Se 47.54).

The selenium analyses were carried out according to Fredga [8].

Acknowledgements. I wish to express my sincere gratitude to Professor Arne Fredga for many valuable discussions and much advice and for all the facilities he has put at my disposal. A grant from the *National Institutes of Health, Bethesda, Md., U.S.A.* is gratefully acknowledged. I also wish to thank Miss Birgitta Karlsson, who has performed the selenium analyses, and Dr. Allan Brown, who has corrected the language in the manuscript.

1. Guthrie, F. *Ann.* **121** (1862) 108.
2. Meyer, V. *Ber.* **19** (1886) 3259.
3. Smedslund, T. *Finska Kemistsamfundets Medd.* **41** (1932) 13.
4. Smedslund, T. *Undersökningar över dietylselenidderivat.* Diss. Helsingfors 1932, p. 59.
5. Ward, H. P. and O'Donnell, I. L. *J. Am. Chem. Soc.* **67** (1945) 883.
6. Starr, D. and Hixon, R. M. *Org. Syntheses Coll. Vol.* **II** (1946) 571.
7. Searles, jr, S. *et al. J. Org. Chem.* **24** (1959) 1839.
8. Fredga, A. *Studien über Selen-di-karbonsäuren und Diselen-di-karbonsäuren.* Diss., *Uppsala Universitets årsskrift* **1935:5**, p. 16.

Received August 9, 1962.

The Identification of Organic Compounds

II. S-Benzylthiuronium Derivatives of Maleic Acid and Fumaric Acid

JØRGEN BERGER and
INGER ULDALL

Royal Danish School of Pharmacy, Chemical Laboratory B, Copenhagen, Denmark

In a previous paper [1] it was shown that adipic acid forms a monosalt and a disalt with S-benzylthiuronium chloride. Maleic acid and fumaric acid have now been included in the work. Details about other dicarboxylic acids will be given in a subsequent paper.

Mono- and disalt of maleic acid. The *monosalt* of maleic acid was first prepared by Donleavy [2] with m.p. 163°C. Veibel and Lillelund [3] found 173—174°C and Chabrier [4] found 186°C. In the standard method proposed by Veibel [5,p.199] *methyl red* is used as an indicator during the neutralisation of the acid. In our hands this technique leads to a mixture probably consisting of the mono- and the disalt (m.p. *ca.* 125—135°C). If, however, at least 3—4 ml of 1 N hydrochloric acid is added to the reaction mixture an almost pure monosalt precipitates. It is highly recommended that the solution of the acid should be half-neutralised (± 5 %), if a pure monosalt is wanted.

Berger [1] has shown that the melting point of an S-benzylthiuronium salt is strongly dependent on the rate of heating. It is now found that the temperature at which the capillary tube is introduced into the bath also is of outmost importance. This, however, is not sufficient to account for the discordant values mentioned above. It has now been found that values ranging from 158°C to 185°C can be recorded by using different methods.

A *disalt* of maleic acid can be obtained by using phenolphthalein as an indicator in the procedure. The formation of the disalt has not previously been observed probably due to a very slow precipitation.

It is known that S-benzylthiuronium chloride itself exhibits polymorphism [3,6]. Morita and Miles [7] have tried to prepare stable polymorphic forms of S-benzylthiuronium salts but they were unsuccessful. However, we are now able to report the first example of polymorphism for an S-benzylthiuronium derivative. The disalt exists in two forms.

Mono- and disalt of fumaric acid. Fumaric acid forms a disalt and its melting point has been recorded as 178°C (Donleavy [2]), as 182—183°C (decomp.) (Veibel and Lillelund [3]) and as 195°C (Vogel [8,p.593]). Veibel and Lillelund [3] state that a monohydrate is formed and that the water of crystallisation cannot be removed by drying at elevated temperature. Donleavy [2] claims an anhydrous salt. We have now been able to prepare three different disalts: An anhydrous salt, a monohydrate and a dihydrate. The temperature during the precipitation is determining the amount of water of crystallisation.

If the salt is used for determination of the equivalent weight by titration with perchloric acid, the amount of water can be determined by a Karl Fischer-titration. It has been found that contrary to the previous findings [3] the anhydrous form can easily be obtained by drying the hydrates. The amount of water of crystallisation has no influence on the melting point. This can be recorded anywhere in the range from 170°C to 210°C, depending on the method used.

An attempt to prepare a pure monosalt of fumaric acid was unsuccessful. The precipitate was analysed as a mixture of the mono- and the disalt.

Stability of hydrates. The stability of di-S-benzylthiuronium fumarate (dihydrate), di-S-benzylthiuronium succinate (dihydrate) and of S-benzylthiuronium acetate (monohydrate) have been determined. The salts were stored in desiccators which maintained the following constant relative humidities: 32 %, 47 %, 58 %, 66 %, and 78 %. Vapour pressure buffers according to Lange [9]. They were all stable during a two months period. Stored over concentrated sulfuric acid the androus forms were obtained after 24 h (fumarate) or after 10 days (acetate and succinate). The fumarate and the succinate can also be dried at 100°C (1 h) whereas the acetate is decomposed at this temperature.

Experimental. The melting points (corrected) were determined in an electrically heated silicone bath [1].

S-Benzylthiuronium hydrogen maleate. Maleic acid (0.3 g) is dissolved in 5 ml of water and 5.0 ml of 0.5 N sodium hydroxide is added. By addition of S-benzylthiuronium chloride (0.5 g dissolved in 5 ml of water) a precipitate is immediately formed. Yield about 90 %; equivalent weight found by titration with 0.1 N perchloric acid [1]: 280.2 (Calc. for $C_{12}H_{14}N_2O_4S$: 282.3). Recrystallisation from 40 % ethanol. The m.p. is highly dependent on the temperature at which the capillary tube is introduced into the silicone bath, and on the rate of heating. Introduced at 145°C: m.p. 158°C (1°/min) and 166°C (4°/min). Introduced at 160°C: m.p. 165°C (1°/min) and 170°C (4°/min). On "Kofler Heizbank" the instantaneous melting point is 183–185°C. It gradually decreases and is about 170°C two minutes later. The melting is always followed by a decomposition.

Di-S-benzylthiuronium maleate. Maleic acid (0.3 g) is dissolved in 5 ml of water and is neutralised with 2 N sodium hydroxide (phenolphthalein). A few drops of 0.5 N hydrochloric acid is added to remove the red colour. S-Benzylthiuronium chloride (1.0 g) is dissolved in 5 ml of water by heating and after cooling the solutions are mixed. No precipitate is formed until after standing for some hours in a refrigerator. Yield about 60 % (Found: Equiv. wt. 223.6; C 53.36; H 5.44. Calc. for $C_{20}H_{24}N_4O_4S_2$: Equiv. wt. 224.3; C 53.55; H 5.39).

The salt exists in two forms: m.p. 122–123°C and 133–134°C. In determining the melting point the capillary tube is introduced into the bath at about 100°C and the rate of heating is 4°/min; a nearly clear melt is obtained at about 123°C and after 2–3 sec the melt solidifies and upon further heating it remelts completely at 133–134°C (decomp.). If the capillary tube is introduced at a temperature between 116°C and 133°C the substance melts immediately and does not solidify again.

It is very difficult to recrystallise the salt. Water and ethanol could not be used as the salt decomposed during the heating. The following procedure has been used: 0.5 g was dissolved in 50 ml acetone by heating on a water bath. A small residue was removed by filtration. 0.3 g pure salt was isolated from the solution after standing several hours in a refrigerator.

Di-S-benzylthiuronium fumarate dihydrate. The temperature during the precipitation of the fumarate must be below *ca.* 40°C in order to obtain a dihydrate. If the temperature is above *ca.* 60°C an anhydrous salt is formed. At about 50°C a salt containing approximately one molecule of water is precipitated. Preparation of the dihydrate: Fumaric acid (0.3 g) is treated as described above (di-S-benzylthiuronium maleate). A precipitate is formed immediately. Yield about 90 % (Found: Equiv. wt. 242.7; H_2O (Karl Fischer-titration) 7.48. Calc. for $C_{20}H_{24}N_4O_4S_2 + 2H_2O$: Equiv. wt. 242.3; H_2O 7.44). Recrystallisation from water taking care that the precipitation takes place below 40°C. Room temperature was preferred in our experiments.

The m.p. can be recorded anywhere in the range from 170°C to 210°C, *e.g.* 179–180°C (decomp.) (4°/min) if the capillary tube is introduced at 170°C. The instantaneous melting point ("Kofler-Heizbank") is about 210°C. It decreases gradually to about 190°C.

Di-S-benzylthiuronium fumarate (anhydrous form). The anhydrous form can be obtained by drying the dihydrate at 100°C for 1 h. It can also be prepared by following the procedure mentioned above for the preparation of the dihydrate except that the two solutions must be 70–80°C when they are mixed. The temperature of the reaction mixture is in this way kept above ca. 60°C during the precipitation. The crystals are isolated immediately after precipitation. Yield about 60 % (Found: Equiv. wt. 226.9. Calc. for $C_{20}H_{24}N_4O_4S_2$: Equiv. wt. 224.3). A Karl Fischer-titration confirmed that it was an anhydrous salt. The melting point was identical with the one found for the dihydrate. It can be recrystallised from water but the temperature during the precipitation has carefully to be kept above *ca.* 60°C.

A transformation of the dihydrate into the anhydrous form and *vice versa* was effected by allowing the precipitation to occur at the temperatures specified above.

The microanalyses have been performed by Mr. A. Bernhardt, Max-Planck-Institut, Mühlheim.

1. Berger, J. *Acta Chem. Scand.* **8** (1954) 427.
2. Donleavy, J. J. *J. Am. Chem. Soc.* **58** (1936) 1004.
3. Veibel, S. and Lillelund, H. *Bull. soc. chim. France.* **1938** 1153.
4. Chabrier, P. *Bull. soc. chim. France.* **1947** 797.
5. Veibel, S. *The Identification of Organic Compounds*, 5th Ed., G. E. C. Gad Publisher, Copenhagen 1961.
6. Bhargava, P. N. and Verma, S. M. *J. Indian Chem. Soc.* **32** (1955) 283.
7. Morita, H. and Miles, N. M. *Anal. Chem.* **28** (1956) 1081.
8. Vogel, A. I. *Elementary Practical Organic Chemistry*, Longmans, Green and Co., London 1957.

9. Lange, N. A. *Handbook of Chemistry*, Handbook Publishers, Inc., Sandusky, Ohio 1956, p. 1420.

Received August 15, 1962.

The Enzymic Hydrolysis of S-Phosphorylated Thiols by Bovine Brain

STIG ÅKERFELDT

Research Institute of National Defence, Dept. 1, Sundbyberg 4, Sweden

In a previous communication [1] it was shown that an enzyme hydrolyzing the S—P bond of cysteamine S-phosphate (S-(2-aminoethyl) phosphorothioate) is present in the human erythrocyte. Since a number of S-phosphorylated thiols are now available [2] it was of interest to study the relative rates of enzymic hydrolysis of the S—P bond for a variety of these compounds. Information regarding the effect of substituents on the rate of enzymic hydrolysis could thus be obtained. The effect of substituents on the nonenzymic rate of hydrolysis of the corresponding compounds has been determined earlier [3].

Bovine brain was chosen as an easily accessible source of relatively stable enzyme for these investigations. Brain was chosen as an enzyme source also because of its low blood content. Interference by erythrocyte phosphatases [1] could thus be easily eliminated.

For the preliminary investigations cysteamine S-phosphate was used as a substrate. Pilot experiments with whole brain homogenate showed a pH optimum for hydrolysis of cysteamine S-phosphate around pH 7. The products of hydrolysis were cysteamine and orthophosphate. Mg^{2+} ions were strongly stimulatory. Of various brain fractions tested, the insoluble part of brain homogenate was found to account for 93 % of the total cysteamine S-phosphate hydrolyzing activity present in the homogenate. The insoluble brain fraction was therefore used in all subsequent experiments.

The cysteamine S-phosphate hydrolyzing activity was heat sensitive. 5 min at 50° destroyed 34 % of the initial activity; 5 min at 100° destroyed 84 % and 10 min at 100° destroyed all the initial activity. The hydrolyzing activity thus appeared to be enzymic in nature.

Effect of pH. The effect of pH on the cysteamine S-phosphate hydrolyzing enzyme was determined in the presence of Mg^{2+} ions (5 mM). An optimum was found at pH 7.0. At pH 8.0 the rate of enzymic hydrolysis was 67 % and at pH 6.0 it was 78 % of the rate at pH 7.0.

The enzymic formation of cysteamine from cysteamine S-phosphate was linear with time for about 60 min in a system as described in the legend to Table 2.

Effect of metal ions. Of the metal ions tested Mg^{2+} ions were found to be the most efficient ones in stimulating the cysteamine S-phosphate hydrolyzing activity. The optimum Mg^{2+} ion concentration was 5 mM, which increased the original activity by 210 % at pH 7.0. Of other metal ions tested only Fe^{2+} had an effect comparable to that of Mg^{2+} (Table 1). In contrast to the other cations, nickel ions were found to catalyze the nonenzymic hydrolysis of cysteamine S-phosphate at an extremely high rate (Table 1).

When enzyme was added in the presence of Ni^{2+} ions the amount of cysteamine formed was actually less than in the blank containing no enzyme. A sorbtion of Ni^{2+} ions on the protein probably accounts for this phenomenon.

Table 1. Effect of metal ions on the cysteamine S-phosphate hydrolyzing activity. Test system: cysteamine S-phosphate 5.0 μmoles; metal chloride 5.0 μmoles; enzyme corresponding to 60 mg of fresh brain and tris buffer pH 7.0 90 μmoles in 1.0 ml of water. The enzyme was omitted from the blanks (nonenzymic hydrolysis). Incubation: 30 min at 35°.

Metal ion added	μmoles of cysteamine formed	
	enzymically	nonenzymically
0	0.41	0.00
Mg^{2+}	0.86	0.00
Ca^{2+}	0.30	0.00
Fe^{2+}	0.78	0.04
Co^{2+}	0.06	0.06
Ni^{2+}	—	3.02

9. Lange, N. A. *Handbook of Chemistry*, Handbook Publishers, Inc., Sandusky, Ohio 1956, p. 1420.

Received August 15, 1962.

The Enzymic Hydrolysis of S-Phosphorylated Thiols by Bovine Brain

STIG ÅKERFELDT

Research Institute of National Defence, Dept. 1, Sundbyberg 4, Sweden

In a previous communication [1] it was shown that an enzyme hydrolyzing the S—P bond of cysteamine S-phosphate (S-(2-aminoethyl) phosphorothioate) is present in the human erythrocyte. Since a number of S-phosphorylated thiols are now available [2] it was of interest to study the relative rates of enzymic hydrolysis of the S—P bond for a variety of these compounds. Information regarding the effect of substituents on the rate of enzymic hydrolysis could thus be obtained. The effect of substituents on the nonenzymic rate of hydrolysis of the corresponding compounds has been determined earlier [3].

Bovine brain was chosen as an easily accessible source of relatively stable enzyme for these investigations. Brain was chosen as an enzyme source also because of its low blood content. Interference by erythrocyte phosphatases [1] could thus be easily eliminated.

For the preliminary investigations cysteamine S-phosphate was used as a substrate. Pilot experiments with whole brain homogenate showed a pH optimum for hydrolysis of cysteamine S-phosphate around pH 7. The products of hydrolysis were cysteamine and orthophosphate. Mg^{2+} ions were strongly stimulatory. Of various brain fractions tested, the insoluble part of brain homogenate was found to account for 93 % of the total cysteamine S-phosphate hydrolyzing activity present in the homogenate. The insoluble brain fraction was therefore used in all subsequent experiments.

The cysteamine S-phosphate hydrolyzing activity was heat sensitive. 5 min at 50° destroyed 34 % of the initial activity; 5 min at 100° destroyed 84 % and 10 min at 100° destroyed all the initial activity. The hydrolyzing activity thus appeared to be enzymic in nature.

Effect of pH. The effect of pH on the cysteamine S-phosphate hydrolyzing enzyme was determined in the presence of Mg^{2+} ions (5 mM). An optimum was found at pH 7.0. At pH 8.0 the rate of enzymic hydrolysis was 67 % and at pH 6.0 it was 78 % of the rate at pH 7.0.

The enzymic formation of cysteamine from cysteamine S-phosphate was linear with time for about 60 min in a system as described in the legend to Table 2.

Effect of metal ions. Of the metal ions tested Mg^{2+} ions were found to be the most efficient ones in stimulating the cysteamine S-phosphate hydrolyzing activity. The optimum Mg^{2+} ion concentration was 5 mM, which increased the original activity by 210 % at pH 7.0. Of other metal ions tested only Fe^{2+} had an effect comparable to that of Mg^{2+} (Table 1). In contrast to the other cations, nickel ions were found to catalyze the nonenzymic hydrolysis of cysteamine S-phosphate at an extremely high rate (Table 1).

When enzyme was added in the presence of Ni^{2+} ions the amount of cysteamine formed was actually less than in the blank containing no enzyme. A sorbtion of Ni^{2+} ions on the protein probably accounts for this phenomenon.

Table 1. Effect of metal ions on the cysteamine S-phosphate hydrolyzing activity. Test system: cysteamine S-phosphate 5.0 μmoles; metal chloride 5.0 μmoles; enzyme corresponding to 60 mg of fresh brain and tris buffer pH 7.0 90 μmoles in 1.0 ml of water. The enzyme was omitted from the blanks (nonenzymic hydrolysis). Incubation: 30 min at 35°.

Metal ion added	μmoles of cysteamine formed	
	enzymically	nonenzymically
0	0.41	0.00
Mg^{2+}	0.86	0.00
Ca^{2+}	0.30	0.00
Fe^{2+}	0.78	0.04
Co^{2+}	0.06	0.06
Ni^{2+}	—	3.02

Table 2. Hydrolyzing activity of the enzyme on various S-phosphorylated thiols. Test system: S-phosphorylated thiol 10.0 μmoles; $MgCl_2$ 5.0 μmoles; enzyme corresponding to 60 mg of fresh brain and tris buffer pH 7.0 90 μmoles in 1.0 ml of water. Incubation: 30 min at 35°. The enzyme was omitted from blanks (nonenzymically formed thiol).

Compound $RSPO_3^{2-}$ (R listed)	Formed thiol, μmoles	
	enzymically	nonenzymically
$NH_2CH_2CH_2$	1.10	0.00
$CH_3NHCH_2CH_2$	0.57	0.00
$(CH_3)_2NCH_2CH_2$	0.56	0.00
+ $(CH_3)_3NCH_2CH_2$	1.19	0.03
$[(CH_3)_2CH]_2NCH_2CH_2$	0.71	0.00
$NH_2CH_2CH_2CH_2$	0.32	0.25
$(CH_3)_2NCH_2CH(CH_3)$	0.70	0.00
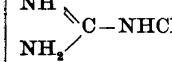	1.35	0.12
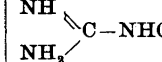	0.84	0.60
NH_2COCH_2	1.31	0.03
$HOCH_2CH_2$	0.77	0.64
$HOCH_2CH_2CH_2$	0.79	1.00

Effect of cystemaine S-phosphate concentration. The cysteamine S-phosphate concentration was varied from 0 to 15 mM. The hydrolyzing enzyme was saturated with substrate at about 10 mM of cysteamine S-phosphate.

Effect of the hydrolyzing enzyme on other S-phosphorylated thiols. In the presence of Mg^{2+} ions the protein fraction used in the study of the enzymic hydrolysis of cysteamine S-phosphate also catalyzed the hydrolysis of the S—P bond in a number of other S-phosphorylated thiols. A thiol and orthophosphate was formed. The results are presented in Table 2. (Only enzyme preparations with the same hydrolytic activity on cysteamine S-phosphate were used to obtain these values).

It is evident from Table 2 that all tested substances were hydrolyzed at a relatively slow rate. Individual variations in the rate of formation of thiol were not found to be very great. It can therefore be concluded that the enzyme(s) responsible for the observed reaction is a relatively non-specific one.

In Table 2 the formation of thiols from S-phosphorylated thiols at pH 7.0 in the presence of Mg^{2+} ions are also listed. No correlation is found between the nonenzymic and the enzymic hydrolysis.

In an earlier investigation on an enzyme from bovine brain, Feuer and Wollemann [4] demonstrated the enzymic hydrolysis of coenzyme A S-phosphate to coenzyme A and orthophosphate. The enzyme was active at pH 8 in the presence of Mg^{2+} ions.

Experimental. Preparation of enzyme. 20 ml of a 30 % homogenate of 0° (Potter-Elvehjelm homogenizer) of calves brain (the enzyme activity was found to be about the same in different parts of brain) was centrifuged for 5 min at 700 *g* at 0°. The supernatant was poured off. The precipitate was washed twice with 20 ml of ice cold distilled water followed each time by centrifuging for 5 min at 700 *g* at 0°. The supernatant precipitate was stirred up in ice cold water (final volume 20 ml) and was used within a few hours.

Determination of thiols in the presence of S-phosphorylated thiols. The described method is a modification of an earlier described procedure [1]. To 1.0 ml of incubated solution was added 1.0 ml of an ice cold 10 % solution of trichloroacetic acid in water. After rapid mixing, the precipitated protein was centrifuged down during 2 min at about 700 *g*. 1.0 ml of clear supernatant was immediately adjusted to about pH 7 by the addition of 0.8 ml of a 1 M phosphate buffer of pH 9.1. The hydrolysis of residual S-phosphorylated thiol during this procedure was less than 1 %.

The amount of thiol present was determined according to Grunert and Phillips [5]. The color yield of the various thiols had earlier been determined by hydrolysis of the corresponding pure S-phosphorylated thiols, prepared accord ing to Ref[2]. A correction was made for the small amount of thiol sometimes formed during storage of the S-phosphorylated thiols. In all experiments where the enzymic hydrolysis of S-phosphorylated thiols was determined a correction was made for the nonenzymic hydrolysis of the compounds under identical conditions.

The enzyme preparation used did not contain detectable amounts of nitroprussiate reactive substances.

The S-phosphorylated thiols used were prepared according to Ref[2]. The compounds that

were isolated as barium salts in Ref[2]. were converted to sodium salts before use by trituration with a slight excess of sodium sulfate (molar ratio 1:1.25).

1. Åkerfeldt, S. *Acta Chem. Scand.* **14** (1960) 1019.
2. Åkerfeldt, S. *Acta Chem. Scand.* **16** (1962) *In press.*
3. Åkerfeldt, S. *Acta Chem. Scand.* **17** (1963) *In press.*
4. Feuer, G. and Wollemann, M. *Acta Physiol. Acad. Sci. Hung.* **10** (1956) 1.
5. Grunert, R. R. and Phillips, P. H. *Arch. Biochem. Biophys.* **30** (1951) 217.

Received August 23, 1962.

Identification of An Impurity in Chlorine Gas from Mercury Cells

ROLF BRÄNNLAND

Mo och Domsjö AB, Örnsköldsvik, Sweden

When brine is electrolyzed in technical cells with mercury cathodes and graphite anodes chlorine gas is obtained which is saturated with water vapor at 60–70°C, and which also contains carbon dioxide, air, hydrogen, and traces of other impurities. The moist gas is first cooled, either directly with water or indirectly, then dried with sulfuric acid, and finally condensed after compression and cooling.

In the gas ducts leading to the drying equipment and in the drying equipment itself various kinds of impurities are deposited, thus interfering with the operation. Part of the impurities generally accompanies the chlorine to the condensation department, and then becomes dissolved or dispersed in the liquid phase, causing trouble in the customers' bleaching equipment, etc.

For these reasons it would be valuable to identify the compounds in order to, *e.g.*, find suitable methods for an easy removal of the deposits, but also to elucidate the mechanism of formation.

Earlier investigations. In some technical reports, solid impurities in chlorine gas are mentioned. Billiter[1] states, *e.g.*, that salt particles might be entrained in the gas stream at high loads. In some plants in USA glass fiber filters are employed in the chlorine pipes from the cells.

Wranglén[2] investigated corrosion products from hard rubber (ebonite) linings on cell covers and frames. In the deposits examined the chlorine content reached about 65 %. Age determination according to the ^{14}C method showed that up to 70 % of the impurities might originate from graphite, whereas only 30 % of the carbon was "fresh".

Penfield and Cushing[3] describe a fractionating column for removal of chlorinated organic compounds, the concentration of which is said to reach 0.2 % in liquid chlorine. The impurities had a "taffy-like" consistency and such a high vapor pressure that they sublimated at room temperature. About 1/3 was identified as chloroform and 1/6 as insoluble in chloroform, consisting mainly of hexachloroethane and hexachlorobenzene. By fractionating the chlorine in a column the impurity content decreased to less than 0.01 %.

Finally in a US patent[4] a method is described for purifying moist chlorine gas by injection of liquid chlorine. The hydrate thereby formed is said to bind such impurities as carbon tetrachloride, chloroform and hexachloroethane.

Chemical analysis of a sample. In connection with cleaning the drying towers in the Domsjö chlorine plant, which must be done at about 6 months' intervals, a sample of the deposits was taken. It had a fine crystalline structure, a pale yellow color, and a typical intense odor.

The crystals were only slightly soluble in ethanol and chloroform, but almost completely soluble in benzene. They sublimated upon slight heating. The melting point range of the sample was 220–260°C (the wide range indicates that the sample was impure).

The compound was purified by sublimation and chemically analyzed. The following result was obtained: C 27.8; H 0.5; O 10.5; Cl 59.6. (Sum 98.4 %). The corresponding molecular composition is represented by the formula $C_7H_{1.5}O_2Cl_5$. The high oxygen content is remarkable, since oxygen containing impurities have apparently not been reported in the literature earlier.

were isolated as barium salts in Ref[2]. were converted to sodium salts before use by trituration with a slight excess of sodium sulfate (molar ratio 1:1.25).

1. Åkerfeldt, S. *Acta Chem. Scand.* **14** (1960) 1019.
2. Åkerfeldt, S. *Acta Chem. Scand.* **16** (1962) *In press.*
3. Åkerfeldt, S. *Acta Chem. Scand.* **17** (1963) *In press.*
4. Feuer, G. and Wollemann, M. *Acta Physiol. Acad. Sci. Hung.* **10** (1956) 1.
5. Grunert, R. R. and Phillips, P. H. *Arch. Biochem. Biophys.* **30** (1951) 217.

Received August 23, 1962.

Identification of An Impurity in Chlorine Gas from Mercury Cells

ROLF BRÄNNLAND

Mo och Domsjö AB, Örnsköldsvik, Sweden

When brine is electrolyzed in technical cells with mercury cathodes and graphite anodes chlorine gas is obtained which is saturated with water vapor at 60–70°C, and which also contains carbon dioxide, air, hydrogen, and traces of other impurities. The moist gas is first cooled, either directly with water or indirectly, then dried with sulfuric acid, and finally condensed after compression and cooling.

In the gas ducts leading to the drying equipment and in the drying equipment itself various kinds of impurities are deposited, thus interfering with the operation. Part of the impurities generally accompanies the chlorine to the condensation department, and then becomes dissolved or dispersed in the liquid phase, causing trouble in the customers' bleaching equipment, etc.

For these reasons it would be valuable to identify the compounds in order to, *e.g.*, find suitable methods for an easy removal of the deposits, but also to elucidate the mechanism of formation.

Earlier investigations. In some technical reports, solid impurities in chlorine gas are mentioned. Billiter[1] states, *e.g.*, that salt particles might be entrained in the gas stream at high loads. In some plants in USA glass fiber filters are employed in the chlorine pipes from the cells.

Wranglén[2] investigated corrosion products from hard rubber (ebonite) linings on cell covers and frames. In the deposits examined the chlorine content reached about 65 %. Age determination according to the ^{14}C method showed that up to 70 % of the impurities might originate from graphite, whereas only 30 % of the carbon was "fresh".

Penfield and Cushing[3] describe a fractionating column for removal of chlorinated organic compounds, the concentration of which is said to reach 0.2 % in liquid chlorine. The impurities had a "taffy-like" consistency and such a high vapor pressure that they sublimated at room temperature. About 1/3 was identified as chloroform and 1/6 as insoluble in chloroform, consisting mainly of hexachloroethane and hexachlorobenzene. By fractionating the chlorine in a column the impurity content decreased to less than 0.01 %.

Finally in a US patent[4] a method is described for purifying moist chlorine gas by injection of liquid chlorine. The hydrate thereby formed is said to bind such impurities as carbon tetrachloride, chloroform and hexachloroethane.

Chemical analysis of a sample. In connection with cleaning the drying towers in the Domsjö chlorine plant, which must be done at about 6 months' intervals, a sample of the deposits was taken. It had a fine crystalline structure, a pale yellow color, and a typical intense odor.

The crystals were only slightly soluble in ethanol and chloroform, but almost completely soluble in benzene. They sublimated upon slight heating. The melting point range of the sample was 220–260°C (the wide range indicates that the sample was impure).

The compound was purified by sublimation and chemically analyzed. The following result was obtained: C 27.8; H 0.5; O 10.5; Cl 59.6. (Sum 98.4 %). The corresponding molecular composition is represented by the formula $C_7H_{1.5}O_2Cl_5$. The high oxygen content is remarkable, since oxygen containing impurities have apparently not been reported in the literature earlier.

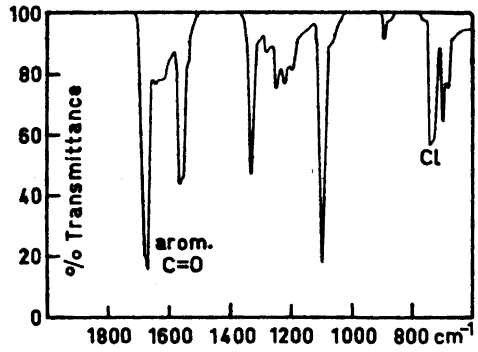

Fig. 1. Infrared absorption spectrum of the substance deposited in chlorine drying towers.

Infrared absorption spectrum of the compound. As a supplement to the chemical analysis the infrared absorption spectrum of the compound was recorded, *cf.* Fig. 1. For the analysis a pellet was prepared from 1 mg of the substance and 300 mg KBr. The minima at the wave numbers 700 – 750 and 1670 – 1680 cm^{-1} indicate that the substance is a chlorinated aromatic compound containing carbonyl groups.

An examination of oxygen containing chlorine compounds [5] with melting points above 220°C showed that the substance might be 2,3,5,6-tetrachlorobenzoquinone-1,4, *i.e.*, $C_6Cl_4O_2$ (chloranil). The infrared absorption spectrum shown in Fig. 1 also agrees well with a published spectrum for chloranil [6].

Discussion of the results. Melting point determination and chemical analysis indicate that the collected sample consists mainly of chloranil. The infrared absorption spectrum confirms this assumption.

The fact that the compound contains oxygen may indicate that it is formed at the electrolysis by oxidation of the anode graphite. If this is the case, it would be impossible, with the present cell construction, to avoid the formation of such compounds.

Since the deposition seems to be connected with local changes in gas velocity and temperature, it is difficult to estimate the total amount of chloranil formed, but the quantity deposited in the drying towers would be equivalent to 1 – 10 ppm in the cell gas. To this must be added impurities which are not deposited in this part of the equipment.

Choranil is very resistant to oxidation and is insoluble in many common solvents. However, the substance can be reduced with, *e.g.*, sulfite, to tetrachlorohydroquinone, which is easily soluble in alcohol, ether etc.

The author is indebted to many members of the technical staff of Mo och Domsjö AB for valuable assistance with sampling and analysis.

1. Billiter, J. *Die technische Elektrolyse der Nichtmetalle*, Springer, Wien 1954, p. 306.
2. Wranglén, G. *Svensk Kem. Tidskr.* **68** (1956) 396.
3. Penfield, W. and Cushing, R. E. *Ind. Eng. Chem.* **31** (1939) 377.
4. Redcay, A. K. Gulf Oil Corp, *US pat. No.* 2,785,055 (1957).
5. Huntress, E. H. *Organic Chlorine Compounds*, J. Wiley & Sons, New York 1948, p. 497.
6. Kainer, H. and Otting, W. *Chem. Ber.* **88** (1955) 1921.

Received August 29, 1962.

Structure Investigation of the Free Radical Tris-*p*-Nitrophenylmethyl

PER ANDERSEN and
BERNT KLEWE

Universitetets Kjemiske Institutt, Blindern-Oslo, Norway

The tris-*p*-nitrophenylmethyl radical was prepared using tris-*p*-nitrophenylmethyl bromide [1] and zinc in a Wurtz' synthesis. The advantage of this method is to overcome the difficulty of growing single crystals suitable for the X-ray method. A zinc rod was kept in a solution of tris-*p*-nitrophenylmethylbromide in a mixture of benzene and some acetone. Well developed single crystals of the radical grew out on the zinc rod. The presence of the radical was controlled using electron spin resonance.

The crystal is orthorhombic with a density 1.5 g/cm^3 and four molecules in the unit cell. The space group is $Pca2_1$. The cell dimensions are, a = 11.50 Å, b = 7.80 Å and c = 18.60 Å.

The [010] Patterson projection shown in Fig. 1 showed the threefold symmetry of the molecule and gave good indications as to the orientation of the molecules in the cell. A Fourier-projection along the b-axis was successfully refined using difference syntheses and the R value for this projection at the present stage of refinement is around 13 %. A uniform isotropic temperature factor of B = 5 has been used for all atoms.

A flat model with the distances 1.5 Å from the central carbon atom to the nearest ring carbon atoms has been assumed. The plane of the ring seems to be twisted about 30° out of the plane of the molecule with the nitro group in the plane of the ring. There are so far no indications of the molecule forming an unsymmetrical propeller.

The twisting of the benzene rings out of the plane does not necessarily have to be the same for all three rings as the threefold symmetry of the molecule is not required by the crystallographic symmetry in the solid state. A threedimensional model of the cell-content shows that the proposed

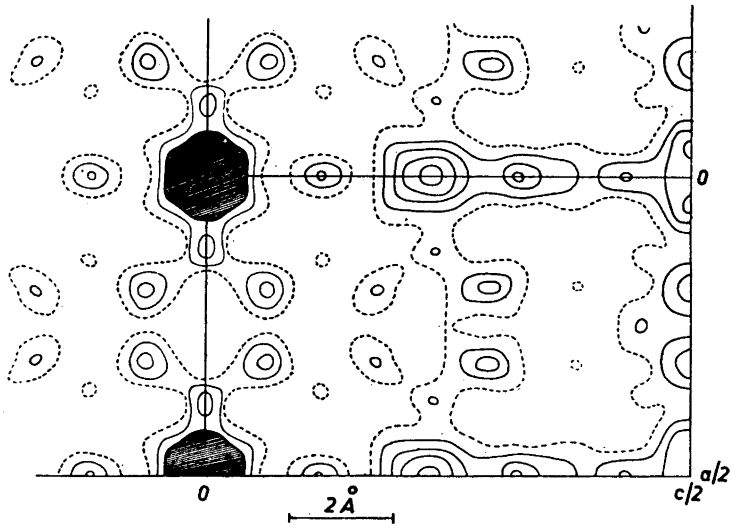

Fig. 1. The [010] Patterson projection of tris-*p*-nitrophenylmethyl.

structure is in harmony with space requirements.

A least squares refinement of the same projection resulted in an R value of around 10 %. However, because of the heavy damping the number of reflections is rather low considering the number of atomic parameters. Three-dimensional intensity data have been registered and a three-dimensional refinement of the structure is in progress.

1. Ziegler, K. and Boye, E. *Ann.* **458** (1927) 248.

Received July 3, 1962.

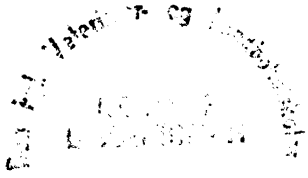

ACTA CHEMICA SCANDINAVICA 16 (1962) 1819–1830

Alkaloidal Glycosides from *Solanum dulcamara*

II *. Three New Alkaloidal Glycosides and a Reassessment of Soladulcamaridine

PER M. BOLL

Chemical Laboratory B, The Royal Danish School of Pharmacy, Copenhagen, Denmark

Three new alkaloidal glycosides, named α-, β- and γ-solamarine, are isolated from *Solanum dulcamara* L. The aglycone is Δ^5-tomatidenol-(3β) and the carbohydrate component of α-solamarine is formed from glucose (1 mole), galactose (1 mole) and rhamnose (1 mole), of β-solamarine from glucose (1 mole) and rhamnose (2 moles), and of γ-solamarine from glucose (1 mole) and rhamnose (1 mole). Furthermore, solasodine and yamogenin are isolated from the same plant.

The previously reported soladulcamaridine is found to be inhomogeneous, separable on thin-layer chromatography into Δ^5-tomatidenol-(3β) in addition to traces of $\Delta^{3,5}$-tomatidiene and solasodine. The name, hence, should be discontinued.

In a continuation of our investigation of the alkaloidal glycoside constituents of *Solanum dulcamara* L., three substances with $R_{\alpha\text{-solanine}}$-values 1.18, 2.65 and 3.80 have been detected paperchromatographically in plant material collected in July 1961 and August 1960. The plant material used earlier for the isolation of soladulcamarine [1] was collected in June 1957 and contained two substances with $R_{\alpha\text{-solanine}}$-values 0.80 and 1.18. The $R_{\alpha\text{-solanine}}$-value for soladulcamarine was 0.80. Now the alkaloids corresponding to $R_{\alpha\text{-solanine}}$ 1.18, 2.65 and 3.80 have been isolated and are given the names α-, β- and γ-solamarine (Table 1).

Upon acid hydrolysis the aglycone part from all three glycosides was shown by thin-layer chromatography in chloroform-methanol (19:1) to consist of three compounds with R_F-values 0.80, 0.51 and 0.34. The two components with the highest R_F-values represented the main constituents, whereas the one with R_F 0.34 is to be considered as a minor component.

Solasodine and tomatidine, chromatographed alone and in mixtures alongside the unknown aglycones, revealed that solasodine and tomatidine were

* Part I of this series: *Acta Chem. Scand.* **12** (1958) 802.

Table 1. Alkaloidal glycosides isolated from *Solanum dulcamara* L. (Lyngby Aamose).

Isolated glycoside	Formula	Aglycone	Carbohydrate components	$R_{\alpha\text{-solanine}}$
Soladulcamarine [1]	$C_{50}H_{81}NO_{18}$	Δ^5-tomatidenol-(3β)	1 mole glucose 2 moles rhamnose 1 mole arabinose	0.80
α-Solamarine	$C_{45}H_{73}NO_{16}$	Δ^5-tomatidenol-(3β)	1 mole galactose 1 mole glucose 1 mole rhamnose	1.18
β-Solamarine	$C_{45}H_{73}NO_{15}$	Δ^5-tomatidenol-(3β)	1 mole glucose 2 moles rhamnose	2.65
γ-Solamarine	$C_{39}H_{63}NO_{11}$	Δ^5-tomatidenol-(3β)	1 mole glucose 1 mole rhamnose	3.80

chromatographically undistinguishable from the two unknown aglycones with the lowest R_F-values. The third aglycone with the higher R_F-value could perhaps be a dehydrated aglycone. Furthermore, on chromatoplates sprayed with antimony trichloride all the unknown aglycones gave a reddish-violet colour similar to the colour produced by solasodine indicating unsaturated sapogenins. Saturated sapogenins, as tomatidine, give a greyish-violet colour with antimony trichloride.

By chromatography on alumina it was proved possible to isolate two of the aglycones. The first of these (R_F 0.80) was an anhydrogenin with the empirical formula $C_{27}H_{41}NO$, devoid of hydroxyl stretching vibration in the

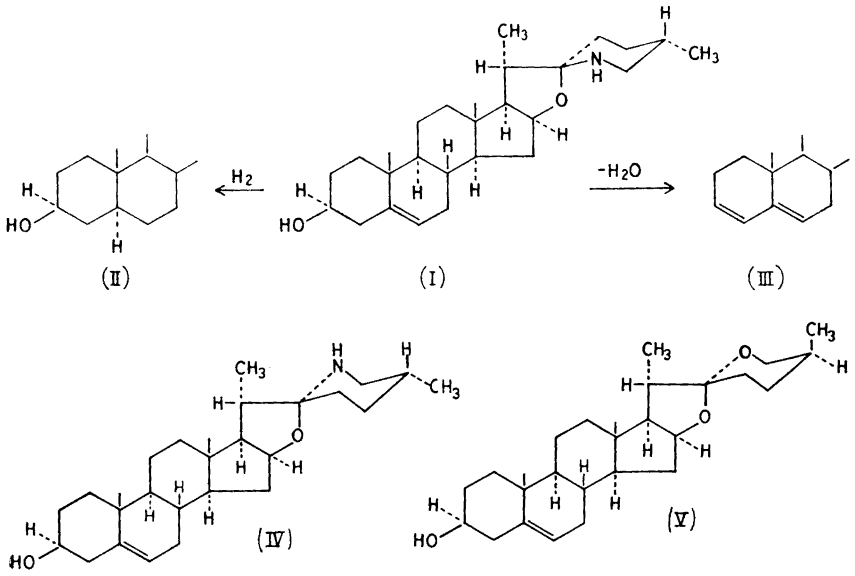

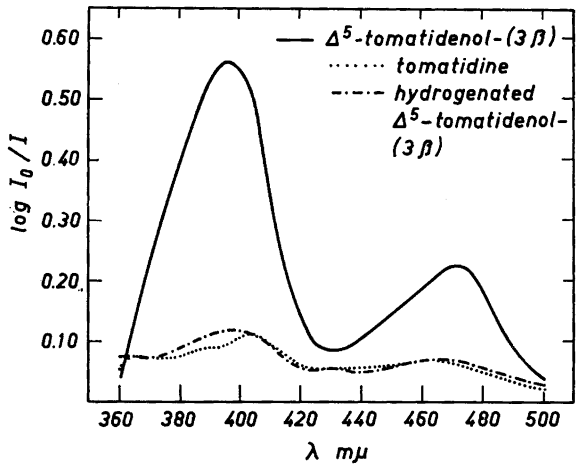

Fig. 1. Absorption spectra in ethanol-concentrated sulfuric acid [15].

IR-spectrum and exhibiting ultraviolet absorption maxima at 228 ,234 and 242 (shoulder) mμ, strongly indicating a heteroannular diene. The Rosenheim reaction for dienes was also positive.

The second compound (R_F 0.51), $C_{27}H_{43}NO_2$, isomeric with solasodine, could be converted into an O,N-diacetyl derivative. The digitonin precipitation assay suggested the presence of a 3β-hydroxyl grouping. One double bond was indicated through a yellow colour with tetranitromethane and the absorption of one mole of hydrogen in the presence of palladium on carbon. Furthermore, the colour reaction for 3β-hydroxy-Δ^5en-steroids according to Witter and Stone [2] was positive and the absorption spectrum in concentrated sulfuric acid-ethanol in accordance with a 3-hydroxy-Δ^5en-steroid (Fig. 1). Upon catalytic hydrogenation tomatidine (II) was obtained in good yield, identified on critical comparison with an authentic specimen of the latter. Hence, the second aglycone is considered to be Δ^5-tomatidenol-(3β) (I). On dehydration, the aforementioned anhydrogenin (R_F 0.81) is produced. Consequently, the latter may be an artefact, most likely $\Delta^{3,5}$-tomatidiene (III).

Table 2. Steroidal aglycones isolated from *Solanum dulcamara* L. (Lyngby Aamose).

Steroidal aglycone	Formula	M.p.	$[\alpha]_D^{20}$	R_F
$\Delta^{3,5}$-Tomatidiene	$C_{27}H_{41}NO$	136–138°	– 88.6°	0.80
Δ^5-Tomatidenol-(3β)	$C_{27}H_{43}NO_2$	238–240°	– 37.9°	0.51
Solasodine	$C_{27}H_{43}NO_2$	198–199°	– 91.8°	0.34
Yamogenin	$C_{27}H_{42}O_3$	189–191°	–121.3°	

The third aglycone isolated by fractional crystallization was found to be identical with solasodine (IV).

Schreiber and Rönsch [3] as well as Sander [4] recently reported the isolation of two aglycones from a geographical form of *S. dulcamara*. Both groups suggest that these are $^{3,5}\Delta$-tomatidiene and Δ^5-tomatidenol-(3β) *.

The isolation of Δ^5-tomatidenol-(3β) and small amounts of solasodine after hydrolysis of the three alkaloidal glycosides clearly indicated that the latter were not homogeneous. Attempts to find chromatographic solvent systems for separating them were unsuccessful, whereas fractional precipitation gave glycosides which on hydrolysis gave solely Δ^5-tomatidenol-(3β) and its dehydration product.

Upon complete hydrolysis with 1 N hydrochloric acid α-solamarine gave equimolecular amounts of glucose, galactose and rhamnose, in addition to the aglycone. β-Solamarine, on the other hand gave one mole of glucose and two moles of rhamnose, whereas γ-solamarine afforded one mole of glucose and 1 mole of rhamnose.

In addition, yamogenin (V) was isolated, a constituent previously reported by Schreiber and Rönsch [3].

Soladulcamaridine, the aglycone of soladulcamarine was tentatively assigned a solanidane structure [1]. This assignment was based only on its basicity, whereas its colour reactions were similar to those of solasodine. Soladulcamaridine has now been found to be inhomogeneous, separable on thin-layer chromatography into Δ^5-tomatidenol-(3β), in addition to traces of $^{3,5}\Delta$-tomatidiene and solasodine. The name soladulcamaridine, therefore, should be abandoned. The pK_B-value of pure Δ^5-tomatidenol-(3 β) has now been determined to 6.93, quite different from the value earlier presented [1].

DISCUSSION

Biochemically it is of interest that the carbohydrate components of α- and β-solamarine are the same as those found in leaves of the potato plant, *S. tuberosum*, as well as *S. chacoense* and *S. aviculare:*

Solanum tuberosum and *Solanum chacoense*
α-solanine: solanidine + galactose + glucose + rhamnose
α-chaconine: solanidine + glucose + rhamnose + rhamnose
Solanum aviculare
solasonine: solasodine + galactose + glucose + rhamnose
solamargine: solasodine + glucose + rhamnose + rhamnose
Solanum dulcamara
α-solamarine: Δ^5-tomatidenol-(3β) + galactose + glucose + rhamnose
β-solamarine: Δ^5-tomatidenol-(3β) + glucose + rhamnose + rhamnose.

Neither the four first mentioned alkaloidal glycosides, nor the plants containing these alkaloids have any effect on the potato beetle (*Leptinotarsa decemli-*

* According to a personal communication from Dr. K. Schreiber the structure of Δ^5-tomatidenol-(3β) has now been confirmed by synthesis.

neata) and its larvae. It is well-known that the carbohydrate moiety is responsible for the effect of some *Solanum* alkaloids on the potato beetle. Hence, it is not surprising if α- and β-solamarine would have no or only a very slight effect as "Frassgift", *i.e.* resistance factor, compared to the highly active tomatine and demissine both containing tetrasaccharide moieties. On the other hand, it is possible that soladulcamarine as a tetrasaccharide would exhibit some resistance towards attack of the potato beetle. In fact, the occurrence of this alkaloidal tetrasaccharide and its possible seasonal degradation to β-solamarine may be responsible for the fact that *S. dulcamara* often can be seen as a host plant for the potato beetle [5], although Schreiber [6] finds that some forms of the plant are not attacked by the beetle and that a crude glycoside mixture containing soladulcidine as aglycone is resistant towards attack.

In this connection it should be noticed that the $R_{\alpha\text{-solanine}}$-values for soladulcamarine and α-solamarine are not very different and that it is quite difficult to exclude that soladulcamarine is present in the plant material collected in July and August. On hydrolysis of the crude glycoside mixture from this plant material arabinose was chromatographically observed. The latter probably arises from soladulcamarine, although its formation as an artefact can hardly be excluded, since it has been pointed out by Harborne and Sherratt [7] that paper chromatography with solvents containing hydrochloric acid can produce arabinose as an artefact.

Schreiber and Rönsch [3] did not observe L-arabinose as part of alkaloidal glycosides on chromatography of several geographical forms of *S. dulcamara*, but favour the view that uronic acids take part in the biosynthesis of this type of glycosides and that L-arabinose may eventually arise from enzymic decarboxylation of D-galacturonic acid. Alkaloidal glycosides with uronic acid as part of the glycoside moiety will behave as zwitter ions. In this connection it is interesting that the yield of glycosides isolated from plant material collected in June is quite low (Table 3).

Soladulcamarine, solely formed in plant material collected in June, seems to be more rapidly converted than α-solamarine because plant material collected later in the year do not contain any soladulcamarine, but two new alkaloids, β- and γ-solamarine, differing from soladulcamarine only by being devoid of

Table 3. Yields of alkaloidal glycosides obtained from plant material collected at different dates.

Kg of fresh plant material	Data collected	G of crude precipitate	G ethanol soluble alkaloid	Yield in %
7.0	June 14, 1957	22.1	2.2	0.03
6.9	July 17, 1961	13.9	6.7	0.10
14.7	Aug. 7, 1960	49.7	37.7	0.26
1.0 (stems)	commercially available	0.8	0.002	0.00

arabinose and arabinose combined with rhamnose, respectively. α-Solamarine, on the other hand, appears to be present in all the plant materials investigated.

The presence of solasodine as aglycone together with Δ^5-tomatidenol-(3β) together with the fact that upon hydrolysis only the sugars characteristic for solasonine and solamargine are detected, strongly suggests the presence of the two latter glycosides in the glycoside mixture. Chromatographically solasonine and solamargine are difficult to differentiate from α- and β-solamarine, although one solvent system gave a clear indication of solasonine being present.

Schreiber and Rönsch [3] as well as Sander [4] have shown that *Solanum dulcamara* L., which with respect to morphology and anatomy is homogeneous, is quite heterogeneous in a phytochemical sense. Still, it is interesting that Δ^5-tomatidenol-(3β) and solasodine can be isolated, representing sapogenins of the 25L and 25D series, respectively, from the same plant material. The employed material was collected from an area of about 25 × 25 m, but even so it is difficult to ascertain that the plant material is homogeneous in genetic respect.

As to the stereochemistry of the sapogenins of the 25D and 25L series it is noteworthy that the alkaloidal sapogenins of the two series, *e.g.* solasodine and Δ^5-tomatidenol-(3β), can be separated by thin-layer chromatography, whereas the sapogenins of the spirostane type cannot [8]. This is in accordance with the earlier proposal [9,10] that alkaloidal sapogenins of the two series differ not only at C(25), but also at C(22) giving rise to compounds probably differing more with respect to chemical and physical properties than the ordinary neo- and iso-sapogenins which deviate only in the orientation of the methyl group at C(25).

EXPERIMENTAL

The melting points are uncorrected and have been determined with the Kofler hot stage microscope (manufacture C. Weygand).

Paper chromatography. Whatman's paper No. 1, equilibrated for 12 h, was used with the top phase of ethyl acetate-pyridine-water(3:1:3). In this solvent system, the following $R_{\alpha\text{-solanine}}$-values were recorded: solanine 1.00; solasonine 0.88; solamargine 2.92; tomatine 0.85; soladulcamarine 0.80; α-solamarine 1.18; β-solamarine 2.65; γ-solamarine 3.80.

A 25 % solution of antimony trichloride in chloroform was used as spray. When heated for 5 min at 110° the saturated compound tomatine gave a greyish-violet colour, whereas the other unsaturated compounds gave a reddish-violet colour.

In this system the compounds all give somewhat elongated spots. Therefore, mixtures of glycosides are difficult to differentiate.

The sugars from the hydrolysis were examined as previously described [1,11].

Thin-layer chromatography. The method described by Tschesche, Freytag and Snatzke[12] was used. Over 30 different solvent systems were tried on alkaloidal glycosides and it was found that the two systems given in Table 4 were far superior to the system described above as well as that utilized by Paseshnichenko and Guseva [13].

The alkaloidal sapogenins obtained by hydrolysis on Silica Gel G were examined by thin-layer chromatography in the system chloroform-methanol(19:1). The R_F-values as average of several chromatograms were: $\Delta^{3,5}$-tomatidiene 0.81; Δ^5-tomatidenol-(3β) 0.51; tomatidine 0.51; solasodine 0.36; 5α-solasodanol-(3β) 0.36; solanidine 0.32; 5α-solanidanol-(3β) 0.32.

Dragendorff's reagent and the above mentioned antimony trichloride reagent were used as sprays.

Table 4. R_F-values (average of several chromatograms) of alkaloidal glycosides using thin-layer chromatography on silicagel G.

Alkaloidal glycoside	Ethyl acetate 30 pyridine 10 (top layer) water 30		Chloroform 20 (bottom layer) ethanol 20 (bottom layer) 1 % NH_3-water 10	
	R_F	$R_{\alpha\text{-solanine}}$	R_F	$R_{\alpha\text{-solanine}}$
Solanine	0.22	1.00	0.26	1.00
α-Chaconine	0.35	1.59	0.36	1.38
Solasonine	0.24	1.09	0.33	1.27
Solamargine	0.45	2.06	0.55	2.12
Tomatine	0.29	1.32	0.29	1.12
Soladulcamarine	0.22	1.00	0.25	0.96
α-Solamarine	0.32	1.46	0.33	1.27
β-Solamarine	0.46	2.09	0.55	2.12
γ-Solamarine	0.60	2.73	0.78	3.00

Table 5. Fractionation of the glycoside mixture on neutral alumina.

Fraction	Alkaloidal glycoside (mg)	Colour	R_F (Chloroform-ethanol 1 % NH_3-water 2:2:1)
1 – 23	0		
24 – 59	283	brown oil	1.00
60 – 98	461	yellow colored	0.78
99 – 105	116	colorless	0.78 + 0.55
106 – 183	4981	–	0.55
184 – 201	433	–	0.55 + 0.33
202 – 238 + 2 liter	1945	–	0.33

α-Solanine ~ R_F 0.33; β-Solanine ~ R_F 0.55; γ-Solanine ~ R_F 0.78;
Δ^5-Tomatidenol-(3β) ~ R_F 1.00.

Isolation of the glycoside mixture. The plant material was collected at Lyngby Aamose near Copenhagen. The fresh tops (14.7 kg) were crushed in a mill and immediately extracted with 5 % acetic acid using the isolation procedure described by Kuhn and Löw [14]. The yield of crude ethanol-soluble alkaloidal glycoside was 37.7 g.

Fractionation of the glycoside mixture. Attempts to isolate the individual glycosides on columns of silica gel using the two solvent systems mentioned under thin-layer chromatography were not successful, just as precipitation of the glycoside mixture with cholesterol gave a gel unsuited for further fractionation. Therefore, it was attempted to use water-saturated 1-butanol on alumina, which has been successfully used by Kuhn and Löw [14], even when it was noted that only poor separation was achieved on thin-layer chromatography in this solvent system. Furthermore, the glycoside mixture tended to form a gel when dissolved in aqueous butanol.

1.5 kg of alumina (Woelm neutral, Act. I) was suspended in water-saturated 1-butanol and allowed to stand for 12 h before packing. To assure complete equilibration 1.5 l of the aqueous butanol was allowed to run through the column. The size of the column was 5.5 × 61 cm. The glycoside mixture (9.2 g) was dissolved in 200 ml of water-saturated 1-butanol by gentle heating and added warm to the column to avoid gel formation. 32-ml fractions were collected, individually examined by thin-layer chromatography and evaporated *in vacuo*. The results are presented in Table 5.

The component with R_F 1.00 was an oil which by thin-layer chromatography was shown to contain the aglycone, Δ^5-tomatidenol-(3β), described below. It was not possible to detect the dehydration product of the latter. γ-Solamarine was contaminated by a brown-coloured component which gave a positive Dragendorff reaction. It was possible partly to remove this impurity by extracting an ammoniacal solution of the glycoside with ethyl acetate. Upon acid hydrolysis all three glycosides on thin-layer chromatography indicated the presence of two aglycones and one anhydro-aglycone (R_F 0.34, 0.51, 0.80).

The glycosides were purified by fractional precipitation. Addition of acetone to concentrated methanolic solutions of the glycosides produced amorphous precipitates. Repeated fractionation gave colourless, semicrystalline glycosides, which after hydrolysis gave two spots on thin-layer chromatography, one representing an aglycone and one an anhydro-aglycone (R_F 0.51, 0.80).

α-Solamarine. M.p. 278–281° (decomp.), with sintering at 236°, $[\alpha]_D^{20}$ −45.0° (pyridine, *c* 0.65) (Found: C 57.34; H 8.41. Calc. for $C_{45}H_{73}NO_{16}$, 3 H_2O: 57.62; H 8.49. After drying to constant weight at elevated temperature: C 61.29; H 8.39. Calc. for $C_{45}H_{73}NO_{16}$: C 61.14; H 8.32). The equivalent weight was determined by titration (Found: 895, 909. Calc.: 884).

β-Solamarine. M.p. 275–277° (decomp.), with sintering at 270°, $[\alpha]_D^{20}$ −85.6° (pyridine, *c* 0.40) (Found: C 59.10; H 8.87. Calc. for $C_{45}H_{73}NO_{15}$, 3 H_2O: C 58.62; H 8.64. After drying to constant weight at elevated temperature: C 62.71; H 8.33. Calc. for $C_{45}H_{73}NO_{15}$: C 62.27; H 8.48). The equivalent weight was determined by titration (Found: 902, 873. Calc.: 877).

γ-Solamarine. M.p. 243–248° (decomp.), with sintering at 195°, $[\alpha]_D^{20}$ −86.1° (pyridine, *c* 0.36) (Found: after drying to constant weight at elevated temperature: C 64.77; H 8.83. Calc. for $C_{39}H_{63}NO_{11}$: C 64.88; H 8.80). The equivalent weight was determined by titration (Found: 756, 749. Calc.: 721).

Dihydro-β-solamarine. β-Solamarine (249 mg) was dissolved in 20 ml of a mixture of dioxan-glacial acetic acid-water (1:1:1) and hydrogenated at room temperature using palladium on carbon (10 %) as a catalyst. Uptake: 1.01 mole of hydrogen. The solution was filtered, evaporated *in vacuo*, dissolved in a small volume of 50 % methanol, and the glycoside was precipitated by adding concentrated ammonia. The glycoside would not crystallize, but was precipitated from a concentrated methanolic solution with acetone. M.p. 277–280° (decomp.), with sintering at 269°, $[\alpha]_D^{20}$ −74.8° (pyridine, *c* 1.03). For analysis the compound was dried *in vacuo* over P_2O_5. (Found: C 61.38; H 8.56. Calc. for $C_{45}H_{75}NO_{15}$, 1/2 H_2O: C 61.49; H 8.71).

Picrolonate of β-solamarine. The derivative was prepared in and recrystallized from 80 % ethanol. It formed yellow, rectangular plates, m.p. 193–195° (decomp.) (Found: C 56.91; H 7.26; H_2O 3.12. Calc. for $C_{45}H_{73}NO_{15}$, $C_{10}H_8N_4O_5$, 2 H_2O: C 56.54; H 7.33; H_2O 3.08).

Table 6. Fractionation of the aglycones on neutral alumina.

Fraction	Ml	Eluent	Aglycone (mg)	R_F
1	100	benzene	72	0.80
2	50	benzene-chloroform (9:1)	8	0.80
3	50	» » (7:3)	0	
4	50	» » (5:5)	23	0.51
5	50	chloroform	102	0.51

Hydrolysis. After refluxing 500 mg of pure β-solamarine with 20 ml of methanolic 1 N hydrochloric acid for 2 h, 241 mg (calc. 258 mg) of the aglycone-hydrochloride was obtained. The free base was liberated in 80 % methanol by adding concentrated ammonia. The aglycone was shown by thin-layer chromatography to consist of two substances, a major component with R_F 0.51 and a minor constituent with R_F 0.80. Subsequent to hydrolysis in aqueous solution, the two components were present in about equal amounts. α-Solamarine and γ-solamarine afforded the same products on hydrolysis. The above aglycone mixture (212 mg) was dissolved in 15 ml of benzene and chromatographed on 15 g of alumina (Woelm neutral, Act. III) (1.2 × 16 cm) as explained in Table 6.

$\Delta^{3,5}$-Tomatidiene (III). The residue obtained by evaporation of fraction 1 was recrystallized twice from methanol giving needles, m.p. 136–138°, $[\alpha]_D^{20}$ −88.6° (methanol, *c* 0.53). For analysis the compound was dried *in vacuo* over P_2O_5 (Found: C 81.92; H 10.20. Calc. for $C_{27}H_{41}NO$: C 81.99; H 10.44). The ultraviolet spectrum in methanol had λ_{max} 228 mμ (ε 21 100), λ_{max} 234 mμ (ε 22 500) and an inflection at 243 mμ (ε 13 900). The Rosenheim reaction for dienes was positive and no epimerization was possible: After treatment of a solution of the diene in chloroform with gaseous hydrogen chloride, thin-layer chromatography revealed only one spot, identical with the original material (R_F 0.80).

Δ^3-Tomatidenol-(3β) (I). Fractions 4 and 5 were evaporated and twice recrystallized from acetone to give needles, m.p. 238–240°, $[\alpha]_D^{20}$ −37.9° (methanol, *c* 0.37). (After drying *in vacuo* over P_2O_5: C 77.86; H 10.29. Calc. for $C_{27}H_{43}NO_2$: C 77.95; H 10.40). The equivalent weight 423 was determined by titration. After standing overnight an ethanolic solution of the aglycone and an 1 % solution of digitonin in 90 % ethanol had deposited a precipitate. The aglycone gave a positive pink colour in the Witter and Stone [2] reaction for 3β-hydroxy-Δ^5en-steroids and an absorption spectrum in ethanol-concentrated sulfuric acid characteristic for 3-hydroxy-Δ^5en-steroids (Fig. 1) [15].

Tomatidine (II). 1) Δ^5-Tomatidenol-(3β) (100 mg) dissolved in 10 ml of glacial acetic acid was hydrogenated at room temperature with palladium on carbon (10 %) as a catalyst. Uptake: 1.03 moles of hydrogen. The solution was filtered and evaporated *in vacuo* at 30°, concentrated ammonia was added and the aqueous phase was extracted with chloroform. The dried chloroform-solution was evaporated and the product recrystallized twice from acetone to give 39 mg of needles, m.p. 209–210°, alone or in admixture with authentic tomatidine, $[\alpha]_D^{20}$ + 5.6 (methanol, *c* 0.43), R_F 0.51.

2) Dihydro-β-solamarine (207 mg) was refluxed for 2 h in a mixture of 20 ml methanol and 2 ml concentrated hydrochloric acid. After concentration to 10 ml *in vacuo*, the aglycone was precipitated with concentrated ammonia. Yield 194 mg. On chromatography in benzene on 15 g of alumina (Woelm neutral, Act. III) no Δ^3-tomatidene was obtained. Elution with benzene-methanol (9:1) gave tomatidine, crystallizing from acetone in needles, m.p. and mixed m.p. 208–10°.

Table 7. Paper chromatography of the monosaccharides obtained by hydrolysis of the glycosides.

Compound	R_F-values in 1-butanol-ethanol-water (8:1:2)			R_{Glu}-values in ethyl acetate-pyridine-water (3.6:1:1.15)		
α-Solamarine	0.15	0.17	0.44	1.00	0.85	4.22
β-Solamarine	0.16		0.43	1.00		4.22
γ-Solamarine	0.17		0.46	1.01		4.23
D-Glucose	0.16			1.00		
D-Galactose		0.18			0.80	
L-Rhamnose			0.44			4.20

O,N-Diacetyl-tomatidine. 10 mg of the hydrogenated Δ^5-tomatidenol-(3β) was dissolved in 0.5 ml of pyridine and allowed to stand with 0.5 ml of acetic anhydride for 24 h. The solution was poured onto ice, the precipitate was collected and recrystallized from ethanol-water to give crystals, m.p. 193—195°, undepressed on admixture with authentic O,N-diacetyl-tomatidine.

O,N-Diacetyl-Δ^5-tomatidenol-(3β). Δ^5-Tomatidenol-(3β) (10 mg) was acetylated as described above. M.p. 160—2°, $[\alpha]_D^{20}$ —39.6° (methanol, *c* 0.36). (Found: C 74·73; H 9.50 Cal.c. for $C_{31}H_{47}NO_4$: C 74.81; H 9.52).

Dehydration of Δ^5-tomatidenol-(3β). Δ^5-Tomatidenol-(3β) (10 mg) was dissolved in 1 ml of methanol containing 20 % of dry hydrogen chloride (prepared by passing hydrogen chloride in methanol until the mixture had increased in weight by 20 %). When heated to 100° the solution became clear and needles of $\Delta^{3,5}$-tomatidiene hydrochloride started separating. This suspension was treated with hot dilute ammonia. In this way $\Delta^{3,5}$-tomatidiene was obtained. After crystallization from methanol the m.p. was 135—137°, alone and in admixture with the anhydro-aglycone obtained by hydrolysis of the glycosides. R_F 0.80.

Identification of the carbohydrates: The acidic mother-liquour from the hydrolysate of the three glycosides (described under "Hydrolysis") was treated with Amberlite IR-4B. Aliquots were chromatographed in 1-butanol-ethanol-water (8:1:2) and ethyl acetate-pyridine-water (3:6:1:1.15) [16]. Authentic D-glucose, D-galactose and L-rhamnose

Table 8. Quantitative determination of monosaccharides in 20 μl aliquots of α-, β- and γ-solamarine.

Compound	Glucose μg	Glucose mole × 10^8	Rhamnose μg	Rhamnose mole × 10^8	Galactose μg	Galactose mole × 10^8
α-Solamarine	24.5	13.6	21.4	13.0	21.0	11.7
β-Solamarine	20.5	11.4	37.6	23.0		
γ-Solamarine	26.6	14.8	22.1	13.5		

were chromatographed alongside the unknown monosaccharides. The results are given in Table 7 .

Quantitative determination of the carbohydrates. The amounts of individual monosaccharides were determined quantitatively utilizing the ability of the sugars to reduce 2,3,5-triphenyltetrazolium chloride to red formazan. 2.9, 2.5 and 2.6 mg of α-, β- and γ-solamarine, respectively, were refluxed in 0.5 ml N hydrochloric acid for 2 h (sealed tube). 20 μl aliquots of the three solutions were chromatographed and the amount of monosaccharide in each spot determined by the method of Fischer and Dörfel [17]. The results are given in Table 8.

Solasodine (IV). 2.00 g of the crude glycoside mixture was hydrolyzed in methanolic hydrochloric acid and worked up as described under "Hydrolysis". Thin-layer chromatography indicated the presence of three aglycones. Chromatography on alumina (Woelm neutral) separated the diene and gave 386 mg of a mixture of Δ^6-tomatidenol-(3β) and solasodine. Two crops of Δ^5-tomatidenol-(3β) were obtained by crystallization from acetone. The mother-liquor was evaporated and crystallization from methanol gave a mixture of the two components. The mother-liquor remaining from the last crystallization on standing deposited long needles of crude solasodine, m.p. 186—191°. Recrystallization from methanol gave a few mg of chromatographically pure solasodine, m.p. 198—199°, alone and in admixture with authentic solasodine.

Yamogenin (V). 10 l of the ammoniacal filtrate from the alkaloidal glycoside precipitation (*cf.* Ref.[14]) was concentrated to 500 ml and extracted three times with 250 ml of 1-butanol. The combined butanol extracts were mixed with an equal volume of water and the organic solvent largely removed by distillation. The water solution was made 1.5 N with respect to hydrochloric acid and refluxed for 5 h to effect hydrolysis. The crude precipitate was filtered off, washed with water and dried. Yield 360 mg. The precipitate was extracted with benzene in a Soxhlet extractor and chromatographed on alumina (Woelm neutral). Elution with benzene-chloroform (9:1) gave 57 mg of a compound which, recrystallized from methanol, melted at 189—191° (lit. value[18] 201°), $[\alpha]_D^{20}$ —121.3° (chloroform, c = 0.35). Acetylation at room temperature with acetic anhydride and pyridine and recrystallization from acetone gave the acetate, m.p. 181—182° (lit. value [18] 182°). The infrared spectrum showed the bands characteristic for a neo-sapogenin (a band at 920 cm^{-1} with about four times the intensity of the band at 897 cm^{-1}).

Part of this work was carried out during a stay at Organisch-Chemisches Institut der Universität Bonn. I am grateful to the head, Professor R. Tschesche, for his hospitality and encouragement, and to Dr. G. Legler and Dr. G. Snatzke for helpful advice on many points. Dr. H. Sander, Marburg, kindly provided me with a generous specimen of Δ^5-tomatidenol-(3β). I am also indebted to Professor S. Aa. Schou and Professor H. Kofod for supplying — through the state funds available for the School — a travel grant.

Microanalyses were performed by Dr. A. Schoeller, Kronach and Dr. A. Bernhardt, Mülheim.

REFERENCES

1. Baggesgaard Rasmussen, H. and Boll, P. M. *Acta Chem. Scand.* **12** (1958) 802.
2. Witter, R. F. and Stone, S. *Anal. Chem.* **29** (1957) 156.
3. Schreiber, K. and Rönsch, H. Vortrag, *2. Arbeitstagung Biochemie und Physiologie der Alkaloide*, Halle, May 1960.
4. Sander, H. *Arch. Pharm.* **295** (1962) 6.
5. Mühle, E. *Die Pharmazie* **2** (1947) 179.
6. Schreiber, K. *Der Züchter* **27** (1957) 289.
7. Harborne, J. B. and Sherratt, H. S. A. *Experientia* **13** (1957) 486.
8. Tschesche, R. and Wolf, G. *Personal communication.*
9. Schreiber, K. *Abhandl. Deutsch. Akad. Wiss. Berlin, Kl. Chem. Geol. u. Biol.* **1957**, 143.
10. Boll, P. M. *Acta Chem. Scand.* **14** (1960) 783.
11. Boll, P. M. *Acta Chem. Scand.* **12** (1958) 358.
12. Tschesche, R., Freytag, W. and Snatzke, G. *Ber.* **92** (1959) 3053.

13. Paseshnichenko, V. A. and Guseva, A. P. *Biokhimiya* **21** (1956) 585; *cf. Chem. Abstr.* **51** (1957) 5919f.
14. Kuhn, R. and Löw, I. *Ber.* **88** (1955) 289.
15. Oertel, G. W. and Eik-Nes, K. *Anal. Chem.* **31** (1959) 98.
16. Colombo, P., Corbetta, D., Pirotta, A., Ruffini, G. and Sartori, A. *J. Chromatography* **3** (1960) 343.
17. Fischer, F. G. and Dörfel, H. *Z. physiol. Chem. Hoppe-Seyler* **297** (1954) 164.
18. Marker, R. E., Wagner, R. B., Ulshafer, P. R., Wittbecker, E. L., Goldsmith, D. P. J. and Ruof, C. H. *J. Am. Chem. Soc.* **65** (1943) 1199.

Received April 16, 1962.

ACTA CHEMICA SCANDINAVICA 16 (1962) 1831–1836

Isomerisation of Penta-*O*-acetyl-β-D-glucopyranose with Hydrogen Fluoride

CHRISTIAN PEDERSEN

Department of Organic Chemistry, University of Technology, Copenhagen, Denmark

Prolonged treatment of penta-*O*-acetyl-β-D-glucopyranose with anhydrous hydrogen fluoride leads to the formation of derivatives of mannose and altrose identified through their conversion to methyl α-D-mannopyranoside and 1,6-anhydro-β-D-altropyranose, respectively. Addition of small amounts of acetic anhydride causes a higher yield of methyl α-D-mannopyranoside and a lower yield of 1,6-anhydro-β-D-altropyranose. Addition of larger amounts of acetic anhydride prevents rearrangement.

In 1926 Brauns [1] found that prolonged action of anhydrous hydrogen fluoride on cellobiose octaacetate led to the formation of 3,6-di-*O*-acetyl-4-*O*-(tetra-*O*-acetyl-β-D-glycopyranosyl)-α-D-mannopyranosyl fluoride in low yield. Recently Pedersen and Fletcher [2] obtained a 36 % yield of 3,4-di-*O*-benzoyl-β-L-ribopyranosyl fluoride from the reaction of β-L-arabinopyranose tetrabenzoate with liquid hydrogen fluoride. Thus, in both cases, the configuration at C_2 was inverted with simultaneous loss of an acyl grouping.

The objective of the present study was to reinvestigate the behavior of β-D-glucopyranose pentaacetate (I) towards liquid hydrogen fluoride. This reaction was first studied by Brauns [3] who showed that solution of the ester in hydrogen fluoride for 30 min at low temperature gave tetra-*O*-acetyl-α-D-glucopyranosyl fluoride (II) in *ca.* 40 % yield, similar to that obtained by the present author. Helferich and Böttger [4] found that solutions of β-D-glucopyranose pentaacetate (I) or tetra-*O*-acetyl-α-D-glucopyranosyl fluoride (II) in anhydrous hydrogen fluoride undergo considerable rotational changes during 10—20 h indicating that further reaction of the acetofluoroglucose is taking place. In accord herewith it has now been found that prolonged action of hydrogen fluoride on glucose pentaacetate gives a lower yield of acetofluoroglucose. Thus, after 20 h reaction at room temperature, followed by addition of methylene chloride and washing with water and sodium hydrogencarbonate to remove excess hydrogen fluoride, only traces of acetofluoroglucose was formed and no other crystalline material could be isolated from the syrupy product.

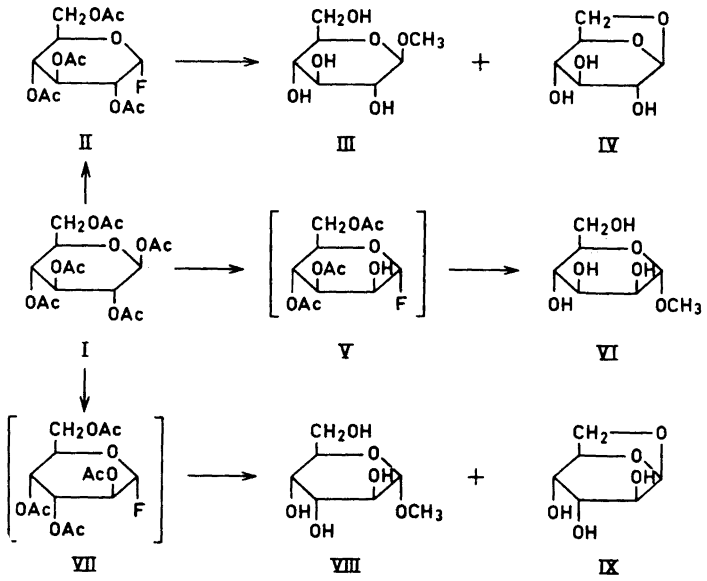

In order to obtain information about the nature of the product it was treated with sodium methoxide in methanol. Provided the product is a mixture of fully or partially acetylated glycosyl fluorides this treatment will, according to Micheel [5,6], give either 1,2-*trans* methyl glycosides or 1,6-anhydrides. Consequently, acetofluoroglucose (II) would give a mixture of methyl β-D-glucopyranoside (III) and 1,6-anhydro-β-D-glucopyranose (IV), acetofluoromannose methyl α-D-mannopyranoside (VI) [7], and, in general, a mixture of compounds may expected which can be separated on paper chromatography.

The sirupy product gave, when treated with methanolic sodium methoxide, a product from which was isolated a 16 % yield of methyl α-D-mannopyranoside (VI). Chromatography of the remaining product indicated that it was a mixture of methyl β-D-glucopyranoside (III), 1,6-anhydro-β-D-glucopyranose (IV), methyl α-D-altropyranoside (VIII), and 1,6-anhydro-β-D-altropyranose (IX).

The yield of crude acetofluoro compound was rather low in this experiment and, since it was suspected that losses occurred during washing the product with sodium hydrogencarbonate and water, another experiment was made in wich excess hydrogen fluoride was blown off with dry air. This again gave a syrup which was treated with methanolic sodium methoxide. After chromatography on a cellulose column this product afforded a 28 % yield of methyl α-D-mannopyranoside (VI) in addition to an 11 % yield of 1,6-anhydro-β-D-altropyranose (IX).

Two similar experiments were made in which β-D-glucopyranose pentaacetate was treated with hydrogen fluoride for 3 h only. In the case where the hydrogen fluoride was removed with aqueous sodium hydrogencarbonate a 21 % yield of methyl α-D-mannopyranoside (VI) was obtained. Besides, small

amounts of methyl β-D-glucopyranoside (III) and methyl α-D-altropyranoside (VIII) were isolated. When, however, excess hydrogen fluoride was removed with dry air a 25 % yield of methyl α-D-mannopyranoside was obtained; 1,6-anhydro-β-D-altropyranose (IX) could be detected by paper chromatography but it was not present in sufficient amounts to be isolated. Thus, shortening of the reaction time to 3 h does not have much influence on the amount of mannose derivative formed but it reduces the amount of altrose derivative.

A number of experiments have been made in which varying amounts of acetic anhydride was added to the hydrogen fluoride. It was found that addition of 10 % of acetic anhydride gave a higher yield of methyl α-D-mannopyranoside (VI), especially in the case where the hydrogen fluoride was removed by washing. The amount of 1,6-anhydro-β-D-altropyranose (IX) formed was, on the other hand, lower and in the case where the hydrogen fluoride was removed with dry air only a trace of 1,6-anhydro-β-D-altropyranose was isolated whereas an 11 % yield of this compound was obtained when no acetic anhydride was added. Addition of larger amounts of acetic anhydride suppressed the formation of mannose derivatives and when β-D-glucopyranose pentaacetate (I) was treated with a mixture of equal volumes of hydrogen fluoride and acetic anhydride for 20 h a 57 % yield of tetra-*O*-acetyl-α-D-glucopyranosyl fluoride (II) could be isolated together with a small amount of penta-*O*-acetyl-α-D-glucopyranose. Formation of the latter compound is in agreement with Helferich and Böttger [4] who suggested that this compound might be the first product formed in the reaction between β-D-glucopyranose pentaacetate and hydrogen fluoride.

It would, of course, be of interest to know the structure of the primary products formed in the rearrangement of β-D-glucopyranose pentaacetate and several attempts were made to obtain pure compounds by chromatographing the crude products on alumina. Fractions were obtained which had the composition of tetraacetyl- and triacetyl-glycopyranosyl fluorides indicating that acetyl groups are lost in the reaction with hydrogen fluoride. However, none of these fractions were homogeneous and it is therefore not clear whether loss of acetyl groups is associated with the rearrangement. On the basis of the results of Brauns [1] and Pedersen and Fletcher [2] it may be assumed that the mannose derivative formed is 3,4,6-tri-*O*-acetyl-α-D-mannopyranosyl fluoride (V). The structure of the altrose derivative formed is less certain since rearrangement induced by hydrogen fluoride at both C_2 and C_3 has not been previously observed.

Richtmyer and Hudson [8] found that lactose octaacetate, when treated with a mixture of aluminium chloride and phosphorus pentachloride, yielded 2,3,6-tri-*O*-acetyl-4-*O*-(tetra-*O*-acetyl-β-D-galactopyranosyl)-α-D-altropyranosyl chloride and by the same method cellobiose octaacetate was rearranged to 2,3,6-tri-*O*-acetyl-4-*O*-(tetra-*O*-acetyl-β-D-glucopyranosyl)-α-D-altropyranosyl chloride [9]. In both cases the configuration at C_2 and C_3 has been inverted without loss of acetyl groups. Similarly, Richtmyer [10] found that β-D-glucopyranose pentaacetate gave derivatives of mannose and altrose when treated with aluminium chloride and phosphorus pentachloride. A mixture of these two reagents thus seems to cause rearrangement similar to those produced by hydrogen fluoride.

EXPERIMENTAL

Melting points are uncorrected. The followings solvents were used for chromatography on paper (Whatman No. 1) or cellulose: (A) ethyl acetate:1-propanol:water (5:3:2); (B) butanol:pyridine:water (10:3:3); (C) butanone, saturated with water. Papers were sprayed with periodate-benzidine.

Excess hydrogen fluoride removed by washing

Reaction time 20 h. Penta-*O*-acetyl-β-D-glucopyranose (I, 5 g) was dissolved in liquid hydrogen fluoride (10 ml) in a polyethylene flask. The solution was kept at room temperature for 20 h. Methylene chloride (25 ml) was then added and the mixture was poured into ice-cold saturated sodium hydrogencarbonate (50 ml); the organic layer was separated and the aqueous phase was extracted with methylene chloride. The combined methylene chloride solutions were washed with saturated sodium hydrogencarbonate and water, and dried. Evaporation of the solvent left 2.1 g of a colourless syrup. The product was dissolved in methanol (50 ml) and 1 N sodium methoxide (20 ml) and boiled under reflux for 3 h. The solvent was removed *in vacuo*, the residue was dissolved in water and deionized by passage through Amberlite IR-400 and IR-50 C. Evaporation of the aqueous solution gave 1.35 g of a colourless syrup, crystallizing from ethanol (10 ml) to give 330 mg (13 %) of methyl α-D-mannopyranoside (VI), m.p. 188—191°, undepressed in admixture with an authentic sample.

The ethanolic mother liquor was put on a cellulose column (8 × 70 cm) and eluted with solvent A. The eluate was divided into two fractions. Fraction 1, on paper chromatography in solvent A, gave largely one spot corresponding to methyl α-D-mannopyranoside. On evaporation it gave 520 mg of a syrup from which 70 mg of methyl α-D-mannopyranoside crystallized, bringing the total yield of this compound to 16 %. Paper chromatography of the mother liquor material in solvent C gave several spots of which the largest two corresponded to methyl α-D-altropyranoside and 1,6-anhydro-β-D-glucopyranose. Fraction 2, on paper chromatography in solvent A, gave one spot with an R_F-value equal to that of 1,6-anhydro-β-D-altropyranose. Evaporation of this fraction gave 230 mg of a syrup from which no crystals could be obtained. Chromatography in solvents B and C gave 3 spots, the largest one corresponding to 1,6-anhydro-β-D-altropyranose.

In a similar experiment a 22 % yield of methyl α-D-mannopyranoside was obtained.

Reaction time 3 h. Penta-*O*-acetyl-β-D-glucopyranose (5 g) was kept in 10 ml of hydrogen fluoride for 3 h at room temperature. The mixture was then worked up as described above, giving 2.8 g of a colourless syrup. The product was boiled for 3 h with methanol (75 ml) and 1 N sodium methoxide (25 ml). Deionization and evaporation gave 1.75 g of syrup which from ethanol (10 ml) deposited 400 mg of methyl α-D-mannopyranoside, m.p. 187—190°. The mother liquor was fractionated on a cellulose column using solvent A as eluant. Fraction 1 gave 680 mg of syrupy material which from ethanol gave 120 mg of methyl α-D-mannopyranoside bringing the total yield of this compound to 21 %. The remaining part of fraction 1 was acetylated and from the product was isolated a small amount (20 mg) of methyl tetra-*O*-acetyl-α-D-altropyranoside, m.p. 87—89° either alone or in admixture with an authentic sample. Its infrared spectrum was identical with that of an authentic sample. Fraction 2 gave 200 mg of syrup from which was isolated 25 mg of impure methyl α-D-mannopyranoside. Finally, fraction 3 gave 290 mg of syrup which from ethanol deposited 150 mg of methyl β-D-glucopyranoside, m.p. 107—109° either alone or in admixture with an authentic sample.

Reaction time 20 h —10 % acetic anhydride. Penta-*O*-acetyl-β-D-glucopyranose (5 g) was added to a mixture of hydrogen fluoride (10 ml) and acetic anhydride (1 ml). The mixture was kept at room temperature for 20 h and then worked up as described above yielding 3.56 g of syrupy product. The product was boiled for 3 h with methanol (75 ml) and 1 N sodium methoxide (20 ml), then deionized and evaporated. Yield 2.1 g of a colourless syrup which from ethanol deposited 930 mg (37 %) of methyl α-D-mannopyranoside, m.p. 186—189°. The mother liquor, on paper chromatography in solvent C, gave spots corresponding to 1,6-anhydro-β-D-glucopyranose, methyl α-D-mannopyranoside, methyl α-D-altropyranoside, and 1,6-anhydro-β-D-altropyranose.

Reaction time 20 h — equal volume of acetic anhydride. Acetic anhydride (5 ml) was slowly added to 5 ml of hydrogen fluoride which was cooled in an ice-salt bath. To this mixture was added 5 g of β-D-glucopyranose pentaacetate and the solution was kept for 20 h at room temperature. Methylene chloride (30 ml) was added and the solution was washed with saturated sodium hydrogencarbonate and water and dried. Evaporation of the solvent left 4.9 g of a colourless syrup which from ether (20 ml) deposited 2.55 g (57 %) of tetra-*O*-acetyl-α-D-glucopyranosyl fluoride, m.p. 105—107°, $[\alpha]_D^{20}$ +91.3° ($CHCl_3$, *c* 1.1). Addition of pentane (25 ml) to the mother liquor gave an additional 1.05 g of crystalline material with m.p. 85—90°. This product was put on a column of alumina (35 g "Fluka" grade II, pH 6.0 ± 0.5). Elution with benzene (500 ml) gave 350 mg of tetra-*O*-acetyl-α-D-glucopyranosyl fluoride. Elution with benzene-ether (1:1, 200 ml) gave 70 mg of crystals which, after two recrystallizations from ether-pentane gave 50 mg of penta-*O*-acetyl-α-D-glucopyranose with m.p. 110—112°; the product was identified through analysis and mixed melting point with an authentic sample. Further elution of the column with ether gave syrupy products.

Excess hydrogen fluoride removed with dry air

Reaction time 20 h. Penta-*O*-acetyl-β-D-glucopyranose (5 g) was kept in 10 ml of hydrogen fluoride for 20 h at room temperature. Methylene chloride (20 ml) was added and the solution was evaporated in a stream of dry air. The residue was dissolved in methylene chloride and the last trace of hydrogen fluoride was removed by adding calcium carbonate. The mixture was filtered and the solvent was removed *in vacuo* leaving 4.3 g of a brown syrup which was boiled for 3 h with methanol (50 ml) and 1 N sodium methoxide (30 ml). The solution was then deionized and evaporated leaving 2.8 g of a brownish syrup. The product was put on a cellulose column and eluted with solvent A; the eluate was divided into 3 fractions according to paper chromatographic studies. Fraction 1 on evaporation gave 1.7 g of syrup which from ethanol (10 ml) deposited 700 mg (28 %) of methyl α-D-mannopyranoside, m.p. 188—190°. The mother liquor, when chromatographed in solvent C, gave 5—6 spots and was not studied further. Fraction 2 gave 420 mg of syrup which, from a few ml of ethanol, deposited 230 mg (11 %) of 1-6-anhydro-β-D-altropyranose, m.p. 120—130°. After two recrystallizations from ethanol the m.p. was 134—135° either alone or in admixture with an authentic sample, $[\alpha]_D^{20}$ −211° (methanol, *c* 0.62). The infrared spectrum was identical with that of an authentic sample. Fraction 3 gave 700 mg of syrup with very low R_F-value; it was not investigated further.

Reaction time 3 h. Penta-*O*-acetyl-β-D-glucopyranose (5 g) was kept for 3 h in 10 ml of hydrogen fluoride, then worked up as described above, yielding 4.5 g of a yellow syrup. Treatment with methanolic sodium methoxide gave 2.55 g of syrup which from ethanol deposited 180 mg of rather impure methyl α-D-mannopyranoside, m.p. 180—185°. The remaining product was fractionated on a cellulose column using solvent A. The eluate was divided into two fractions. Fraction 1 gave 1.3 g of syrup which from 10 ml of ethanol deposited 450 mg of methyl α-D-mannopyranoside with m.p. 187—190°, bringing the total yield of this compound to 25 %. The remaining part of fraction 1, on paper chromatography in solvent C, gave spots corresponding to methyl α-D-mannopyranoside and 1,6-anhydro-β-D-glucopyranose. Fraction 2 gave 450 mg of syrup which, on paper chromatography in solvent C, gave spots corresponding to methyl α-D-mannopyranoside, methyl β-D-glucopyranoside, and 1,6-anhydro-β-D-altropyranose. A few milligram of methyl β-D-glucopyranoside was isolated from this fraction.

Reaction time 20 h —10 % acetic anhydride. Penta-*O*-acetyl-β-D-glucopyranose (5 g) was dissolved in a mixture of hydrogen fluoride (10 ml) and acetic anhydride (1 ml). The solution was kept for 20 h and then worked up as described above, yielding 5.0 g of a dark syrup. Treatment with methanolic sodium methoxide gave 2.3 g of a brown syrup wich was fractionated on a cellulose column using solvent A as eluant. Fraction 1 (1.40 g) gave, from ethanol, 810 mg (32 %) of methyl α-D-mannopyranoside with m.p. 187—190°. Paper chromatography of the mother liquor in solvent C showed several components. Fraction 2 (200 mg) gave, from ethanol, 15 mg of impure 1,6-anhydro-β-D-altropyranose. Fraction 3 gave 1.6 g of material; it was not investigated further.

The author is indebted to Dr. H. G. Fletcher, Jr. and Dr. N. K. Richtmyer of The National Institutes of Health, U.S.A. for samples of 1,6-anhydro-β-D-altropyranose and methyl α-D-altropyranoside, and to cand. pharm. I. Krogh Andersen for the infrared spectra. This work is part of an investigation supported by *Kai Hansen's Fond.*

REFERENCES

1. Brauns, D. H. *J. Am. Chem. Soc.* **48** (1926) 2776.
2. Pedersen, C. and Fletcher, H. G., Jr. *J. Am. Chem. Soc.* **82** (1960) 945.
3. Brauns, D. H. *J. Am. Chem. Soc.* **45** (1923) 833.
4. Helferich, B. and Böttger, S. *Ann.* **476** (1929) 150.
5. Micheel, F. and Klemer, A. *Ber.* **91** (1958) 663.
6. Micheel, F. and Tork, L. *Ber.* **93** (1960) 1013.
7. Micheel, F. and Borrmann, D. *Ber.* **93** (1960) 1143.
8. Richtmyer, N. K. and Hudson, C. S. *J. Am. Chem. Soc.* **57** (1935) 1716.
9. Richtmyer, N. K. and Hudson, C. S. *J. Am. Chem. Soc.* **58** (1936) 2534.
10. Richtmyer, N. K. *Advances in Carbohydrate Chem.* **1** (1945) 37, p. 46.

Received February 24, 1962

ACTA CHEMICA SCANDINAVICA 16 (1962) 1837–1848

Studies on the Thiophene Analogues of Malachite Green. I. Protolytic Equilibria and Reaction Rate Constants of Thiophene Green in Aqueous Solutions

RUNE CIGÉN and GÖSTA BENGTSSON

Department of Inorganic and Physical Chemistry, Chemical Institute, University of Lund, Lund, Sweden

The protolytic equilibria and the rate constants of a Thiophene analogue of Malachite Green (MG), named Thiophene Green (TG), have been investigated spectrophotometrically in aqueous solutions with constant ionic strength 0.5 M at 20.0°C.

The results of the measurements have been compared with the results of the corresponding measurements of MG and the hydroxy- and methoxy-derivatives of MG. It was found that the hydration reactions of TG proceed more slowly and that the values of the hydration constants K_2 and $1/K_6$ are lower in TG than in MG. In this respect TG is similar to the *ortho*- and *para*-hydroxy and -methoxy derivatives of MG.

The reaction scheme used in previous investigations of MG and of derivatives of MG has been extended for the reactions in strongly acid solutions in order to explain some results of the kinetic measurements of TG.

The dyestuff Thiophene Green (TG) was first prepared by Levi [1]. Later Mason and Nord [2,3] have investigated Thiophene Green and some derivatives of it as regards their absorption curves, which were compared with the absorption curve of Malachite Green.

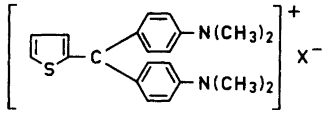

Thiophene Green

The present investigation is devoted to the protolytic and hydration reactions of TG in aqueous solutions, which have a constant ionic strength of 0.5 M.

The same reaction scheme that has been used in earlier studies on derivatives of Malachite Green [4–7] has been tried on Thiophene Green. It was found

that in its reactions TG is similar to Malachite Green. However, the substitution of a phenyl group for a thienyl group has a marked influence on the hydration equilibria and the rate constants. Furthermore, the kinetic measurements in HCl + KCl-buffers indicate a more complicated reaction scheme than that which was used for Malachite Green. In the discussion part of this paper the differences between Malachite Green and Thiophene Green will be further treated.

In neutral aqueous solutions Thiophene Green is really green in contrast to Malachite Green and many of its derivatives, which are blue or blue-green. If the solution of TG is made acid, pH $\approx$ 0, it turns red immediately and is then partially decolourized owing to hydration reactions. If the green solution of TG is made alkaline, it is completely decolourized at a rate that is directly proportional to [OH^-]. The above-mentioned reactions can be visualized with the following reaction scheme, which, however, does not consider the complications which arise in strongly acid solutions and which are discussed later in this paper. In the scheme is R = 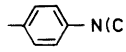

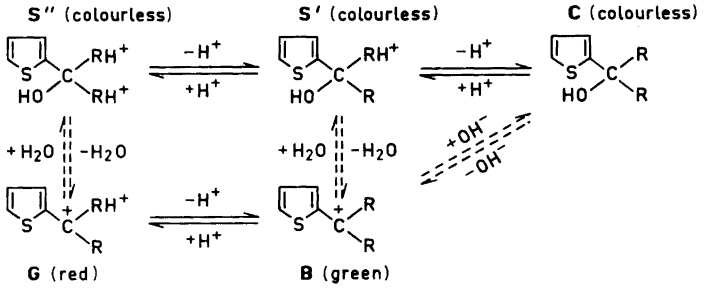

Full drawn arrows indicate that the reactions proceed at an immeasurable rate, *i.e.*, instantaneously, whereas dashed arrows indicate that the reactions take place at a measurable rate.

Definitions of constants and symbols

$$K_1 = \frac{[G]}{[B][H^+]}; \quad K_2 = \frac{[S'']_\infty}{[G]_\infty}; \quad K_3 = \frac{[S'][H^+]}{[S'']}; \quad K_4 = \frac{[C][H^+]}{[S']};$$

$$K_6 = \frac{[B]_\infty}{[S']_\infty}$$

h = $[H^+]$; oh = $[OH^-]$; $K_w = [H^+][OH^-]$.

k_1 = rate constant for the reaction G + H_2O → S''

k_2 = » » » » » S'' → G + H_2O

k_3 = » » » » » B + H_2O → S'

k_4 = » » » » » S' → B + H_2O

k_5 = » » » » » B + OH^- → C

k_6 = » » » » » C → B + OH^-

k = » » » » total reaction

ε_B, ε_G = the molar extinction coefficient of B and G

e_o, e_t, e_∞ = the absorbancy per cm of a solution at the times 0 and t and at equilibrium.
E_o, E_t, E_∞ = the total absorbancy.
e_B, e_G = the absorbancy per cm of a solution containing only B or G.
C_M = the total concentration of dyestuff.

The constants in the equilibrium scheme can be calculated, if the following quantities are determined for a large number of solutions with varying pH:

1. The absorbancy, e_o, at a moment immediately after the mixing of a dye stock solution with the appropriate buffers. The dye stock solution is (if possible) prepared in such a way that all of the dye is present as the coloured species B.
2. The absorbancy, e_∞, when equilibrium is reached.
3. The pH of the solutions.
4. The total rate constant, k, for the reactions that change the intensity of the colour of the solutions either by the hydration of the coloured species (B and G) to colourless species (C, S′, S″) or vice versa.

Equations

The following equations are used for the calculations of the constants in the reaction scheme

$$e_o = \frac{e_B + hK_1e_G}{1 + hK_1} \tag{1}$$

$$e_\infty = \frac{e_B + hK_1e_G}{1 + 1/K_6 + K_4/hK_6 + hK_1(1 + K_2)} \tag{2}$$

$$k = \frac{k_2h^2 + k_4hK_3 + k_6K_3K_4}{h^2 + hK_3 + K_3K_4} + \frac{k_1hK_1 + k_3 + k_5oh}{1 + hK_1} \tag{3}$$

Eqn. (1) is transformed to

$$\frac{h}{e_B - e_o} = \frac{h}{e_B - e_G} + \frac{1}{K_1(e_B - e_G)} \tag{4}$$

and K_1 is determined by a graphical method.

In acid solutions, pH ≤ 2, we can approximate eqn. (2) and write

$$K_2 = \frac{e_G}{e_\infty} + \frac{e_B - e_\infty(1 + hK_1 + 1/K_6)}{hK_1e_\infty} \tag{5}$$

In weakly alkaline solutions eqn. (2) is approximated and transformed to

$$\frac{h}{e_\infty} = h\frac{1 + K_6}{K_6e_B} + \frac{K_4}{K_6e_B} \tag{6}$$

According to eqn. (6), a straight line can be obtained, from which $(1 + K_6)/K_4$ is obtained.

EXPERIMENTAL

Chemicals and solutions. Thiophene Green. The leuco base was prepared according to Levi [1] by the condensation of N,N-dimethylaniline with 2-thiophenealdehyde. We used concentrated hydrochloric acid as a condensing agent, however, instead of zinc chloride. The leuco base was recrystallized from ethanol and obtained as light brown needles (m.p. 92–94°). The oxidation to dyestuff was performed with lead dioxide, added to a cooled solution of the leuco base dissolved in dilute hydrochloric acid. After the addition of sodium sulphate, lead sulphate and the remaining lead dioxide was filtered off.

The perchlorate of the dyestuff was precipitated with sodium perchlorate and was recrystallized twice from 3 % and 0.1 % acetic acid, respectively. The perchlorate was obtained as shining green needles with a violet lustre when viewed from certain angles. (Found: C 57.9; H 5.42; N 6.29; Cl 8.18; S 7.5. Calc. for $C_{21}H_{23}O_4N_2ClS$: C 58.0; H 5.33; N 6.44; Cl 8.15; S 7.37).

Stock solutions of the dye were prepared in the same manner as in Ref.[6] The chemicals used for the buffers and the apparatus used for the measurements were the same as in Ref.[6]

MEASUREMENTS AND RESULTS

In acetate buffer, pH = 4.8 Thiophene Green produces only one coloured species and more than 99 % of the dye is present as the coloured ion B. In Fig. 1 there can be seen the absorption curves for the green ion B in acetate buffer and for the red-yellow ion G in 0.2 M hydrochloric acid. The molecular extinction coefficients were calculated from the experimentally obtained absorption curves and eqn. (2) ($e_B = C_M\varepsilon_B$ and $e_G = C_M\varepsilon_G$). The following values were obtained: $\lambda_{B\,max} = 628$ mμ and 467 mμ; $\varepsilon_{B\,max} = 7.5 \times 10^4$ and 2.55×10^4 resp. $\lambda_{G\,max} = 505$ mμ; $\varepsilon_{G\,max} = 2.80 \times 10^4$.

An absorption curve of TG in 98 % acetic acid and 2 % acetone gave $\lambda_{B\,max} = 631$ mμ and 471 mμ; $\varepsilon_{B\,max} = 8.6 \times 10^4$ and 2.8×10^4, respectively.

Determination of K_1. The dye stock solution was mixed with an equivalent volume of suitable HCl + KCl-buffers and e_o was determined by extrapolation

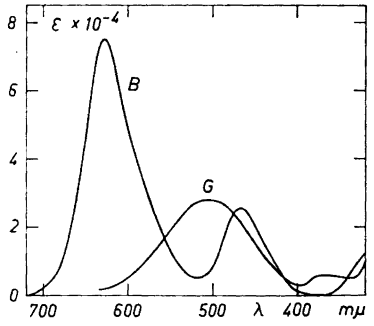

Fig. 1. Thiophene Green. Absorption curves. B is the curve for the green ion $[(Me_2NC_6H_4)_2CC_4H_3S]^+$ in acetate buffer, G is the curve for the yellow-red ion

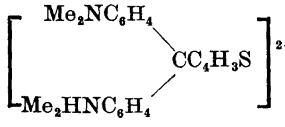

in dilute hydrochloric acid.

Table 1. Thiophene Green. e_o- and e_∞-values for the determination of K_1 and K_2. $\lambda = 630$ mμ, $C_M = 1 \times 10^{-5}$ M, $d = 1$ cm, $e_B = 0.720$, T = 20.0°C.

[H+] M	e_o	e_∞	K_2
0.010	0.562	0.302	3.99
0.020	0.464	0.192	3.97
0.030	0.398	0.142	3.92
0.040	0.342	0.112	3.93
0.050	0.304	0.092	3.99
0.060	0.275	0.078	4.01
0.070	0.247	0.069	3.95
0.080	0.228	0.0615	3.95
Mean value			3.96

Table 2. Thiophene Green. e_∞-values for the determination of $K_4/(K_6 + 1)$. $C_M = 1 \times 10^{-5}$ M, $d = 1$ cm, $\lambda = 630$ mμ, $T = 20.0°$.

[H+] × 10^7M	e_∞	[H+] × 10^7 M	e_∞
1.948	0.640	0.512	0.470
1.547	0.622	0.338	0.403
1.257	0.598	0.240	0.340
0.954	0.570	0.182	0.290
0.741	0.530	0.0911	0.174

of the absorbancies to $t = 0$. The measurements were carried out at the wavelength $\lambda = 630$ mμ. In Fig. 2 $[H^+]/(e_B - e_o)$ is plotted against $[H^+]$. A straight line is obtained. The slope l and the intercept y on the ordinate-axis of this line and eqn. (4) give ($e_B = 0.720$): $y = 0.0504$ M; $l = 1.405$; $\mathbf{K_1 = 27.9 \pm 0.5\ M^{-1}}$.

Determination of K_2. The dye stock solution was mixed with HCl + KCl-buffers and the equilibrium absorbancies, e_∞, were measured in 1 cm absorption cells. K_2 was calculated from eqn. (5), where $K_1 = 27.9$ is known and $1/K_6 \ll 1$. $e_B = 0.720$; $e_G = 0.008$ at the used wavelength, 630 mμ. The results are recorded in Table 1. From this table the mean value $\mathbf{K_2 = 3.96 \pm 0.10}$ is obtained.

Determination of $K_4/(K_6 + 1)$. A dye stock solution was mixed with appropriate phosphate buffers, pH = 6.7—8.0, and the equilibrium absorbancies, e_∞, where read after 30 h. $C_M = 1 \times 10^{-5}$, $d = 1$ cm, $\lambda = 630$ mμ. In Fig. 3 $[H^+]/e_\infty$ is plotted against $[H^+]$. A straight line is obtained, which gives $l = 1.367$; $y = 0.382 \times 10^{-7}$ M and from eqn. (6) $K_4/(K_6 + 1) = 2.79 \times 10^{-8}$ M is obtained.

Determination of K_3K_4. The following expression for the equilibrium absorbancy can be derived

$$e_\infty = \frac{e_B + K_1 h e_G}{1 + 1/K_6 + K_1 h + h/K_3K_6 + K_4/K_6 h} \qquad (7)$$

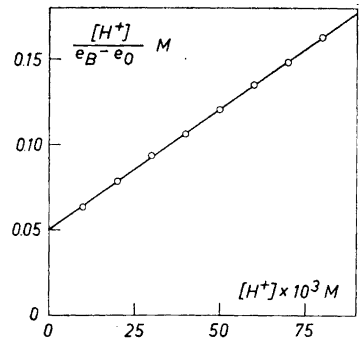

Fig. 2. $[H^+]/(e_B - e_0)$ plotted against $[H^+]$ for the determination of K_1.

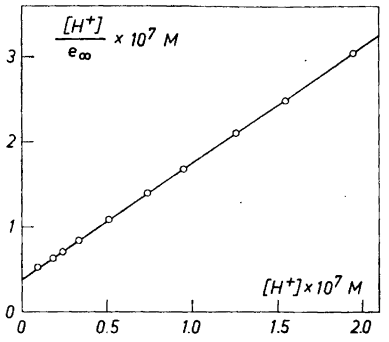

Fig. 3. $[H^+]/e_\infty$ plotted against $[H^+]$ for the determination of $K_4/(K_6 + 1)$.

In very weakly acid solutions, pH>3.5, K_1h can be neglected in the denominator and $K_1 h e_G$ in the numerator, if the measurements are carried out at a wavelength where $e_G \leq e_B$. After these approximations we can differentiate e_∞ in respect of $[H^+]$ and find that e_∞ has a maximum when $[H^+] = \sqrt{K_3K_4}$. Fig. 4 is obtained by plotting e_∞ against $[H^+]$. From the figure $pH_{e_\infty max} = 4.79 \pm 0.01$ is obtained, which gives $\sqrt{K_3K_4} = (1.62 \pm 0.04) \times 10^{-5}$ M. The accuracy of K_3K_4 is not very high, since the curve is rather flat in a large pH-range on both sides of the maximum.

There is, however, another, more accurate method of determining K_3K_4. We can write eqn. (3) as follows, since $hK_1 \ll 1$ in the actual pH-range,

$$\frac{k_1 h K_3}{h^2 + hK_3 + K_3K_4} + k_3 = k - \frac{k_2 h^2 + k_6 K_3 K_4}{h^2 + hK_3 + K_3K_4} - \frac{k_1 hK_1 + k_5 oh}{hK_1 + 1} = k - A \quad (8)$$

In eqn. (8) A is a correction term which amounts to 1—5 % of k in the pH-range 5.5—4.2. Therefore, it is not necessary to know the constants in the term A at any high degree of accuracy in the following treatment of eqn. (8). If eqn. (8) is differentiated with respect to $[H^+]$, it is found that $k-A$ has a maximum when $[H^+] = \sqrt{K_3K_4}$

$$(k-A)_{max} = \frac{k_4 K_3}{K_3 + 2\sqrt{K_3K_4}} + k_3 \quad (9)$$

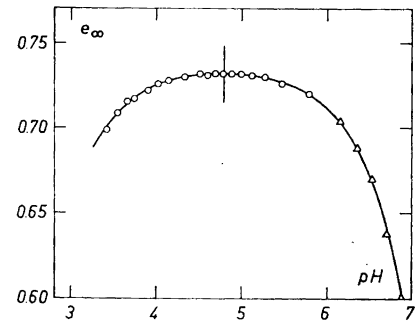

Fig. 4. e_∞ as a function of pH for the determination of K_3K_4.

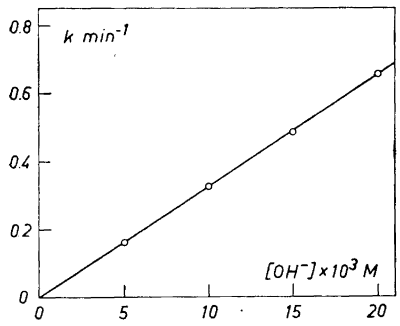

Fig. 5. k plotted against [OH^-] for the determination of k_5.

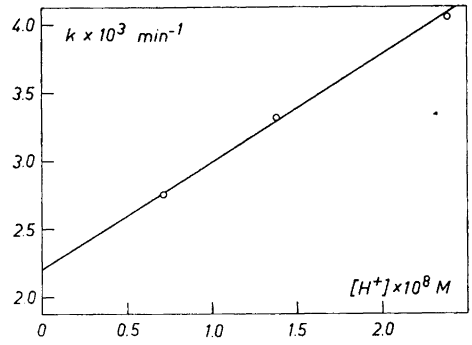

Fig. 6. k plotted against [H^+] for the determination of k_3.

Through kinetic measurements, which are reported below, $k-A$ was found to have a maximum when pH = 4.795 ± 0.005 giving $\sqrt{K_3K_4} = (1.60 \pm 0.02) \times 10^{-5}$ M; $k_{max} = 0.274$ min^{-1} and $(k-A)_{max} = 0.271$ min^{-1}. The value of $\sqrt{K_3K_4}$ obtained in this way agrees well with the value obtained from the equilibrium measurements.

Determination of k_5. For alkaline solutions eqn. (3) can be used in the following approximated form

$$k = k_3 + k_5\text{oh} + k_6 \tag{10}$$

The dye stock solution was mixed with NaOH + KCl-buffers and the fading rate was determined. In Fig. 5 the rate constant of the decolourization, k in eqn. (10), is plotted against [OH^-]. A straight line is obtained which passes almost through the origin. Consequently, $k_3 + k_6 \ll k_5\text{oh}$ in the pH-range used and only k_5 can be determined from Fig. 5, which gives $\mathbf{k_5 = 32.7 \pm 0.3\ M^{-1}\ min^{-1}}$.

Determination of k_3 *and* K_4/K_6. The rate constant k_3 was determined from kinetic measurements in phosphate buffers, pH 7—8. Eqn. (3) was approximated to

$$k = k_4\text{h}/K_4 + k_3 \tag{11}$$

since $k_3 \gg k_5\text{oh} + k_6$ in this pH-range. In Fig. 6 k is plotted as a function of [H^+]. The straight line obtained gives $\mathbf{k_3 = 0.00221 \pm 0.00003\ min^{-1}}$ and $k_4/K_4 = 7.85 \times 10^4$ min^{-1} M^{-1}. But since $k_4 = k_3K_6$, we get $K_4/K_6 = 2.82 \times 10^{-8}$ M in excellent agreement with the value of $K_4/(K_6 + 1) = 2.79 \times 10^{-8}$ M, since $K_6 \gg 1$, obtained by equilibrium measurements which have been reported above.

Determination of K_3, K_4, K_6, k_4, *and* k_6. A dye stock solution was partially decolourized by making it 0.02 M with respect to hydrochloric acid. The following reactions then occur in the forward direction (→): B + H^+ + H_2O ⇌ G + H_2O ⇌ S″ and B + H^+ + H_2O ⇌ S′ + H^+ ⇌ S″. This partially decolourized dye solution was then mixed with acetate buffers and the colour was more or

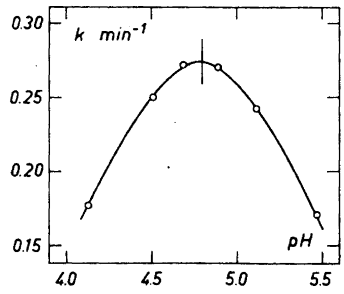

Fig. 7. The total rate constant k as a function of pH. The points represented by the symbols, O, are obtained experimentally. The curve is calculated from the non-approximated eqn. (3).

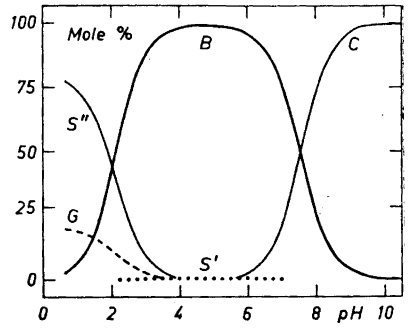

Fig. 8. The distribution of Thiophene Green between the different species as a function of pH.

less restored owing to the reactions above in the reverse direction. The rate constant for the restoring of the colour was determined at different pH-values.

In Fig. 7 k is plotted as a function of pH. Eqn. (9) can be written in the following form

$$(k-A)_{max} = \left(\frac{K_6}{K_4} \cdot \frac{K_3K_4}{K_3+2\sqrt{K_3K_4}} + 1\right) k_3 \qquad (12$$

since $k_4 = k_3K_6$. From Fig. 7 $k_{max} = 0.274$ min^{-1} is obtained and $(k-A)_{max} = 0.271$ min^{-1} using approximate values of the constants in the correction term A. In eqn. (12) $K_3K_4 = 2.57 \times 10^{-10}$ M^2 is known (*cf.* p. 1843) and so is k_3 and K_6/K_4. Consequently, K_3 can be calculated. The following results were obtained $\mathbf{K_3 = (4.38 \pm 0\ 08) \times 10^{-5}\ M}$, $\mathbf{K_4 = (5.87 \pm 0.10) \times 10^{-6}\ M}$, $\mathbf{K_6 = 209 \pm 4}$, $\mathbf{k_4 = 0.462 \pm 0.010\ min^{-1}}$. The rate constant $\mathbf{k_6 = (1.44 \pm 0.06) \times 10^{-5}\ min^{-1}}$ is obtained from $k_6 = k_5K_WK_6/K_4$, ($K_W = 1.24 \times 10^{-14}$ M^2).

The distribution of Thiophene Green between the different species at equilibrium is calculated for different pH-values and shown as a function of pH in Fig. 8.

Table 3. Thiophene Green. The total rate constant, k, from kinetic measurements in HCl + KCl-buffers and the rate constant k_1 calculated from eqn. (13). $C_M = 1 \times 10^{-5}$ M, $d = 1$ cm, $\lambda = 630$ and 500 mμ, $T = 20.0$°C.

[H+] M	k min^{-1}	k_1 min^{-1}	[H+] M	k min^{-1}	k_1 min^{-1}
0.010	0.0307	0.0569	0.100	0.0712	0.0712
0.020	0.0385	0.0590	0.120	0.0753	0.0730
0.040	0.0495	0.0615	0.160	0.0845	0.0775
0.060	0.0578	0.0645	0.200	0.0928	0.0838
0.080	0.0647	0.0675	0.250	0.1036	0.0914

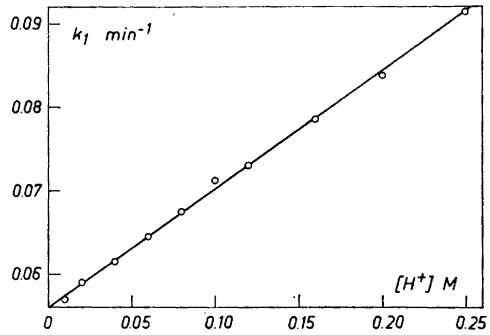

Fig. 9. The rate constant k_1 calculated from eqn. (13) plotted against [H$^+$].

Determination of k_1 and k_2. These rate constants were determined by kinetic measurements of the decolourization, which is caused by the reactions G + $H_2O \rightleftharpoons$ S″ and B + $H_2O \rightleftharpoons$ S′, when a dye stock solution is mixed with HCl + KCl-buffers. Eqn. (3) can be approximated and since $k_2 = k_1/K_2$, it is transformed to

$$k_1 = \frac{k - k_4K_3/h - k_3/(1 + K_1h)}{1/K_2 + K_1h/(1 + K_1h)} \qquad (13)$$

and k_1 can be calculated from eqn. (13) — K_1, K_2, k_3, and k_4 are known. Table 3 contains k-values experimentally found and values of k_1 calculated from eqn. (13). As can be seen from Table 3, k_1 is not constant but increases with [H$^+$]. In Fig. 9 the values of k_1 are plotted against [H$^+$]. A straight line is obtained and an extrapolation to [H$^+$] = 0 gives $\mathbf{k_1 = 0.056 \pm 0.0005\ min^{-1}}$; $\mathbf{k_2 = 0.0141 \pm 0.0004\ min^{-1}}$ since $k_2 = k_1/K_2$.

DISCUSSION

If the corresponding figures in Table 4 are compared, it is found that the reactions B + $H_2O \xrightarrow{k_3}$ S′ and G + $H_2O \xrightarrow{k_1}$ S″ are notably more slow in Thiophene Green than in Malachite Green. At the same time the values of the

Table 4. Comparison between corresponding constants of Malachite Green, *o*-hydroxy MG, *o*-methoxy MG, and Thiophene Green.

	$1/K_1$	$K_3 \times 10^5$	$K_4 \times 10^6$	K_2	$1/K_6$	k_1 min^{-1}	k_2 min^{-1}	k_3 min^{-1}	k_4 min^{-1}
Malachite Green	0.036	2.7	5.8	22	0.0147	0.168	0.0078	0.00647	0.44
o-Hydroxy MG	0.034	3.30	4.2	3.93	0.0038	0.045	0.0114	0.00129	0.34
o-Methoxy MG	0.033	2.83	3.7	4.65	0.0040	0.050	0.0107	0.00177	0.45
Thiophene Green	0.036	4.38	5.9	3.96	0.0048	0.056	0.0141	0.00221	0.46

hydration constants K_2 and $1/K_6$ are lowered — that is, the equilibria are more displaced towards the coloured species in Thiophene Green than in Malachite Green. This depends on the thiophene sulphur, which increases the electron density on the central methane carbon and makes the addition of a polarized water molecule more difficult.

The exchange of a phenyl-group in MG for a thienyl-group has about the same effect as the substitution of an *ortho*-hydrogen in the phenyl-group for a hydroxy- or methoxy-group. See Table 4.

Thiophene Green and the hydroxy- and methoxy-derivatives of Malachite Green are similar in another respect too. Previous investigations show that the rate constant k_1 of *p*-hydroxy, *p*-methoxy (Ref. [4]), *o*-methoxy (Ref.[7]), and *o*-hydroxy Malachite Green [8] increases somewhat with $[H^+]$, when k_1 is calculated from the reaction scheme on p. 1838. The value of k_1 of the *para*-derivatives increases with about 11 % in the range $[H^+] = 30-100$ mM, whereas the corresponding increase of the *ortho*-derivatives is about 6 % in the range $[H^+] = 10-100$ mM. In Thiophene Green k_1 increases with 60 % in the range $[H^+] = 10-250$ mM. This effect is not noticeable in the other investigated dyes.

The fact that k_1 increases linearly with $[H^+]$ in some dyes makes it reasonable to believe that the reaction scheme, which has been used, does not cover all the reactions which influence the results of the measurements.

In strongly acid solutions the dye can probably bond another proton according to the following scheme, which only shows the reactions in strongly acid solutions.

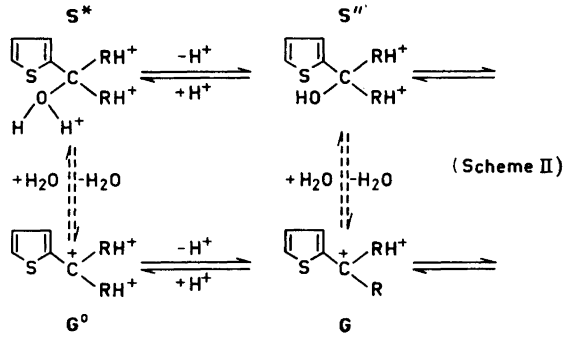

The following constants are defined

$$K_o = \frac{[G][H^+]}{[G^o]}\,;\quad K_o' = \frac{[S''][H^+]}{[S^*]}\,;\quad K = \frac{[S^*]_\infty}{[G^o]_\infty}$$

k_1' = rate constant for the reaction $G^o + H_2O \rightarrow S^*$
k_2' = » » » » » $S^* \rightarrow G^o + H_2O$

The fact that the determination of K_1 and K_2 is not obstructed by the presence of the species G^o and S^*, indicates that $[G^o]_o \ll [B]_o + [G]_o$ and $[S^*]_\infty \ll [B]_\infty + [G]_\infty + [S'']_\infty$ in the pH-range 1—2, where K_1 and K_2

are determined. However, the kinetics can be influenced by the presence of even very low concentrations of G° and S*, if k_1' and k_2' are large compared with k_1 and k_2.

The following equations for the kinetics in solutions with pH < 7 can be derived, if the reaction scheme on p. 1846 is assumed to be valid

$$k = \frac{h^2k_2' + hk_2K_o' + k_4K_o'K_3}{h^2 + hK_o' + K_o'K_3} + \frac{h^2k_1' + hk_1K_o + k_3K_oK_1}{h^2+hK_o+K_o/K_1} \qquad (14)$$

In the pH-range which has been used in Fig. 9, pH = 0.6—2, it holds that $h >> K_3$ and $K_o' >> h$, and eqn. (14) can, therefore, be approximated and at the same time rewritten as

$$k-k_4K_3/h-k_3/(1 + K_1h) = hk_2'/K_o' + k_2 + \frac{hk_1'/K_o + k_1}{1 + 1/K_1h} \qquad (15)$$

$$= \frac{hk_1'/K_o + k_1}{K_2} + \frac{hk_1' /K_o + k_1}{1 + 1/K_1h} \qquad (16)$$

since $k_1' = Kk_2'$, $k_1 = K_2k_2$, and $K_o'K = K_oK_2$. If we write $hk_1'/K_o + k_1 = k_1^o$ we finally get

$$k_1^o = \frac{k-k_4K_3/h-k_3/(1+K_1h)}{1/K_2 + K_1h/(1 + K_1h)} \qquad (17)$$

The right member of eqn. (17) is identical with the right member of eqn. (13) and k_1^o in eqn. (17) corresponds to k_1 in eqn. (13). If k_1^o is plotted against $[H^+]$, a straight line should be obtained. Fig. 9 gives such a line with the intercept on the ordinate-axis = k_1 and the slope = $k_1'/K_o = 0.142$ min^{-1} M^{-1}.

Thus, the kinetic measurements strongly support the expanded reaction scheme. The individual values of the constants K_o, K, K_o', k_1', and k_2' cannot, however, be determined.

An attempt was made to determine the absorption curve of G° but the result was somewhat confusing. The absorption curves of Thiophene Green in various, strongly acidic solutions were recorded in the range $\lambda = 320-600$ mμ. A dye solution, which is made 5 M, 2.5 M, and 1 M with respect to HCl, contains at equilibrium about 90 %, 50 %, and 30 %, respectively, of the dye in the form of coloured species. The dye is not quite resistent to conc. HCl. An absorption curve obtained with the dye dissolved in 4.5 M H_2SO_4 was found to agree with Curve G (Fig. 1) within such narrow limits that only one of the curves has been drawn in Fig. 1. Curve G is calculated from eqn. (2) using the e_∞-values obtained from a solution with $[H^+] = 0.2$ M.

There are two possible explanations of the agreement between Curve G (Fig. 1) and the curve obtained in 4.5 M H_2SO_4. First: The species G° and G may have similar absorption curves in the used wavelength range. If this is true, the equilibrium G° + H_2O ⇌ S* is strongly displaced towards the coloured G°. Second: The absorption curves of G° and G are not similar. If this is true, the ion G° does not reach measurable concentrations even in very strongly

acidic solutions. The marked increase of the colour of the dye, when the concentration of acid is raised, must then be explained as a very strong medium effect on the equilibrium $G + H_2O \rightleftharpoons S''$. We have found from other measurements of similar dyes that the equilibria "Coloured" $\rightleftharpoons$ "Colourless" are displaced towards the coloured species, if the dielectric constant of the solvent is decreased by the addition of organic substances such as ethanol, acetone and acetic acid, to an aqueous solution of the dye.

The reason for Thiophene Green, and probably *p*- and *o*-hydroxy and -methoxy Malachite Green too, reacting according to a more complicated scheme than that of MG and the rest of the investigated derivatives of MG, is the following: The thienyl-group as well as the hydroxy- and methoxy-substituted phenyl-group has a stronger electron donor character than the non-substituted phenyl-group. This is the reason why the reactions $S'' + H^+ \rightleftharpoons S^* \rightleftharpoons G^\circ + H_2O$ and $G + H^+ \rightleftharpoons G^\circ$ are so much facilitated that they manifest themselves in the kinetic measurements of Thiophene Green and the above-mentioned hydroxy- and methoxy-derivatives of MG. In Malachite Green and derivatives of MG with weakly electron-donating substituents these reactions may be possible, although they do not appreciably influence the kinetic measurements at pH $\approx$ 1.

Acknowledgements. The authors are indebted to the Analytical Department of the Chemical Institute, and its head prof. K.-J. Karrman, for the micro elementary analyses, and to prof. S. Fronæus, prof. I. Leden and Dr. J. Sandström for stimulating discussions and comments.

REFERENCES

1. Levi, L. *Ber.* **20** (1887) 513.
2. Mason, D. C. and Nord, F. F. *J. Org. Chem.* **16** (1951) 722.
3. Mason, D. C. and Nord, F. F. *J. Org. Chem.* **17** (1952) 778.
4. Cigén, R. *Protolysengleichgewichte und Reaktionsgeschwindigkeiten einiger basischer Triphenylmethanfarbstoffe* (Diss.), University, Lund 1956.
5. Cigén, R. *Acta Chem. Scand.* **14** (1960) 979.
6. Cigén, R. *Acta Chem. Scand.* **15** (1961) 1892.
7. Cigén, R. *Acta Chem. Scand.* **15** (1961) 1905.
8. Cigén, R. *Acta Chem. Scand.* **16** (1962) 192.

Received April 11, 1962

ACTA CHEMICA SCANDINAVICA 16 (1962) 1849–1857

Partial Acetylation Studies on Benzyl 4-*O*-Methyl-β-D-xylopyranoside

PER J. GAREGG

Träkemiska avdelningen, Svenska Träforskningsinstitutet, Stockholm Ö, Sweden

Partial acetylation studies on benzyl 4-*O*-methyl-β-D-xylopyranoside have shown that, with acetic anhydride and sodium acetate, the hydroxyl group on $C_{(2)}$ is the more reactive while the hydroxyl group on $C_{(3)}$ is the more reactive with acetic anhydride and perchloric acid. Other systems, such as acetic anhydride and pyridine, acetyl chloride and pyridine, and acetic anhydride and pyridine containing pyridine hydrochloride, give distributions of the acetyl groups showing lesser degrees of preferential reaction than these two extremes. The stability of the acetyl groups in benzyl 2-*O*-acetyl-4-*O*-methyl-β-D-xylopyranoside and benzyl 3-*O*-acetyl-4-*O*-methyl-β-D-xylopyranoside during methylation with methyl iodide and silver oxide in dimethylformamide, on treatment with silver oxide in dimethyl formamide, on carbamoylation with phenylisocyanate, and the stability concerning migration of the phenyl carbamoyl groups as well as the stability of the acetyl groups during treatment with monoethanolamine in ethanol, and during treatment with dimethyl sulphoxide have been examined. Previously reported work on the position of *O*-acetyl groups in birch xylan is discussed in the light of the results obtained.

So far, the isolation of two native acetylated polysaccharides from the cell wall of wood has been reported, an acetylated 4-*O*-methylglucuronoxylan from birch wood [1,2,3] and an acetylated glucomannan from pine [4,5] and spruce [6] wood. The problem of determining the exact position of attachment of the *O*-acetyl groups in native acetylated polysaccharides is complicated due to the alkali-lability of these groups and their ease of migration from one hydroxyl group to another given appropriate spatial arrangements. If an unequivocal method for the localisation of the *O*-acetyl groups can be found, the problem remains as to whether acetyl migration or selective removal of acetyl groups from some hydroxyl groups has occurred during the extraction and purification of the polysaccharide.

Various approaches to the determination of the position of the *O*-acetyl groups have been made. Periodate oxidations of the acetylated 4-*O*-methylglucuronoxylan [3] and of the glucomannan [4,5] have indicated that the *O*-acetyl

groups are located on the hydroxyl groups on $C_{(2)}$ and/or $C_{(3)}$ in the β-1,4-linked anhydroxylose residues and mainly on the hydroxyl groups on $C_{(2)}$ and/or $C_{(3)}$ in the β-1,4-linked anhydromannose residues respectively; the distribution of *O*-acetyl groups between these two positions could not be decided by this method. Methylation studies have been applied to the acetylated 4-*O*-methylglucuronoxylan [2,3], revealing that most of the *O*-acetyl groups in the acetylated, methylated xylan were attached to the hydroxyl group on $C_{(3)}$ and the remainder to the hydroxyl group on $C_{(2)}$. About 30 % of the *O*-acetyl groups were replaced by methoxyl groups during the methylations. A reasonably similar distribution was found by using phenylcarbamoyl groups as protective substituents [7], but rather more *O*-acetyl groups appeared to be attached to the hydroxyl groups on $C_{(2)}$ than found in the methylation study [2]. Less than 10 % of the *O*-acetyl groups were unaccounted for by this method.

Without attempting to elucidate the actual mechanism of biological acetylation in wood it was nevertheless of interest to acetylate under various conditions a model compound representative of the β-1,4-linked anhydroxyxylose units in the 4-*O*-methylglucuronoxylan to examine the relative reactivities towards acetylation of the hydroxyl groups on $C_{(2)}$ and $C_{(3)}$. As a suitable model compound benzyl 4-*O*-methyl-β-D-xylopyranoside was selected, the synthesis of this compound having been described earlier [8]. It was thought that after partial acetylation the benzyl group could be removed by catalytic hydrogenation [9] leaving the acetyl groups intact. In order to separate and identify the resulting partially substituted xylose derivatives it was desirable to have a method of performing paper electrophoresis in a buffer system which could form complexes with the substances in question at neutral pH where the acetyl groups are stable. Sulphonated phenylboronic acid was found to meet this requirement, as previously described [10].

The two monoacetates of benzyl 4-*O*-methyl-β-D-xylopyranoside, which were obtained pure as described below, were distinguished from one another and their structures assigned on the basis of their oxidation with lead tetraacetate [11] and their paper electrophoretic behaviour after hydrogenation. The hydrogenations were performed with palladium on carbon [12] in methanol or ether solution, and complete removal of benzyl groups with retention of virtually all the acetyl groups was achieved. 2-*O*-Acetyl-4-*O*-methyl-D-xylose consumed 0.08 mole lead tetraacetate and was immobile on paper electrophoresis in sulphonated phenylboronic acid at pH 7.4. 3-*O*-Acetyl-4-*O*-methyl-D-xylose consumed 0.95 mole lead tetraacetate and had a mobility similar to that of 3,4-dimethylxylose on paper electrophoresis in the same buffer. Under the conditions used for the oxidation 4-*O*-methylxylose consumed 2.2 mole lead tetraacetate and 2,3-di-*O*-acetyl-4-*O*-methyl-D-xylose prepared by hydrogenation of the corresponding benzyl β-D-xyloside did not consume any oxidant.

Benzyl 4-*O*-methyl-β-D-xylopyranoside was partially acetylated with acetic anhydride and sodium acetate, with acetic anhydride in pyridine, with acetyl chloride in pyridine, with acetic anhydride in pyridine containing 1.5 % by weight of hydrogen chloride combined as pyridine hydrochloride, and finally with acetic anhydride and perchloric acid. A chromatographic investigation

by thin layer chromatography [13] of the course of the reaction with acetic anhydride and sodium acetate indicated that the ratio of acetyl groups on the $C_{(2)}$ hydroxyl group to that on $C_{(3)}$ was of the order of 2:1 estimated by visual examination of the chromatograms. The acetylation mixtures from the partial acetylation with 1.1 mole acetic anhydride in pyridine and 1.1 mole acetyl chloride in pyridine were separated into the four components by chromatography on silicic acid columns and the ratio of the fractions determined by weighing. The molar ratio of benzyl 2,3-di-*O*-acetyl-4-*O*-methyl-β-D-xylopyranoside: benzyl 2-*O*-acetyl-4-*O*-methyl-β-D-xylopyranoside: benzyl 3-*O*-acetyl-4-*O*-methyl-β-D-xylopyranoside: benzyl 4-*O*-methyl-β-D-xylopyranoside was 2.5:4.0:2.3:1 with acetic anhydride as the acetylating agent and 2.0:1.1:1:1.4 with acetyl chloride. A visual examination of the thin layer chromatograms of the acetylation with 1.1 mole of acetic anhydride in pyridine containing 1.5 % by weight of hydrogen chloride indicated a ratio of about 1:1 of the two monoacetates, a semiquantitative estimation by thin layer chromatography by cutting out the appropriate areas from the plate, extracting and weighing gave a ratio of 1:1. The acetylations with acetic anhydride and perchloric acid were followed by thin layer chromatography. It was found that the hydroxyl on $C_{(3)}$ was by far the more reactive towards this type of acetylation. The ratio of the two monoacetates was in this case from 1:3 to 1:5, estimated by visual examination of the plates. Table 1 gives the ratio of the two monoacetates obtained in the various acetylations.

Jeanloz *et al.* in an investigation of the partial acylation of methyl 4,6-*O*-benzylidene-α-D-glucopyranoside [14] concluded that on acetylation of this compound with acetic anhydride in pyridine the acylation occurred preferentially at the $C_{(3)}$ hydroxyl. With other acylating agents such as acetyl chloride, benzoic anhydride, benzoyl chloride, methanesulphonic anhydride, methanesulphonyl chloride, *p*-toluenesulphonic anhydride and *p*-toluenesulphonyl chloride, all in pyridine solution, the preferential attack was at the $C_{(2)}$ hydroxyl. Acetic anhydride in pyridine containing a little pyridine hydrochloride gave the 2-*O*-acetyl derivative as the primary product. Bourne, Stacey *et al.* prepared the trifluoroacetyl derivative of methyl 4,6-*O*-benzylidene-α-D-glucopyranoside by controlled methanolysis of the bistrifluoroacetyl compound [15]. From the trifluoroacetyl derivative were prepared derivatives of methyl 4,6-*O*-benzylidene-α-D-glucopyranoside with substituents at either of the $C_{(2)}$ and $C_{(3)}$ hydroxyls depending on the reaction medium. The authors concluded that the remaining trifluoroacetyl group probably was on the $C_{(3)}$

Table 1. Ratios of benzyl 2-*O*-acetyl-4-*O*-methyl-β-D-xylopyranoside: benzyl 3-*O*-acetyl-4-*O*-methyl-β-D-xylopyranoside obtained in partial acetylations.

Reaction medium	Ratio 2-acetate : 3-acetate
Acetic anhydride, perchloric acid	approx. 1 : 3
Acetyl chloride, pyridine	1.1 : 1
Acetic anhydride, pyridine-pyridine hydrochloride	approx. 1 : 1
Acetic anhydride, pyridine	1.7 : 1
Acetic anhydride, sodium acetate	approx. 2 : 1

hydroxyl and that in pyridine media facile migration of the trifluoracetyl group occurred allowing the incoming group to take up its more favoured position, which was at the $C_{(2)}$ hydroxyl for the *p*-toluene sulphonyl group on acylation with the acid chloride in pyridine and at the $C_{(3)}$ hydroxyl for the acetyl group on acylation with the anhydride in pyridine.

That the configuration at the glycosidic carbon atom is of relatively little importance in determining the substitution pattern in partial acylations in this type of molecule is indicated by the work of Newth on the partial *p*-toluenesulphonation in pyridine solution of 1,5-anhydro-4,6-*O*-benzylidene-D-glucitol [16] where the $C_{(2)}$ hydroxyl again reacted preferentially and by the work reported by Jeanloz *et al.* on partial benzoylation and *p*-toluenesulphonation in pyridine of 1,6-anhydro-β-D-glucopyranose [17] where the $C_{(2)}$ hydroxyl again was more reactive than the $C_{(3)}$ hydroxyl. Substitution occurred preferentially at the $C_{(2)}$ and $C_{(4)}$ hydroxyl groups.

The results obtained for the partial acetylation of benzyl 4-*O*-methyl-β-D-xyloside indicating that the $C_{(2)}$ hydroxyl is the more readily acetylated in pyridine as well as with sodium acetate as catalyst and the $C_{(3)}$ hydroxyl with perchloric acid catalyst, therefore do not fall into the pattern described above for methyl 4,6-*O*-benzylidene-α-D-glucopyranoside, and it seems doubtful that the difference can be ascribed to the different confgiuration at the glycosidic carbon atom. The differences between the xyloside and the above compounds that govern its pattern of substitution on acetylation might be the conformational freedom of the xyloside as compared to the more rigid conformations in the other compounds.

The possibility of acetyl migration in the two monoacetates occurring in pyridine solution was checked by thin layer chromatography. Under the conditions used during the acetylations no migration was observed. The distribution of *O*-acetyl groups found in the partial acetylations in pyridine is therefore kinetically controlled.

The possibility of migration of the acetyl groups in the two monoacetates was also examined under the conditions pertinent to the previous studies on the position of the *O*-acetyl groups in birch xylan [2,3,7].

Methylation of each of the two monoacetates with methyl iodide and silver oxide in dimethyl formamide [2,3], removal of *O*-acetyl groups and hydrolysis led to a mixture of dimethylxylose and 2,3,4-tri-*O*-methylxylose. The composition of the dimethylxylose fraction which predominated was the same in each case and contained about 35 % 3,4-di-*O*-methylxylose and 65 % 2,4-di-*O*-methylxylose. This closely corresponds to the finding that 70 % of the *O*-acetyl groups in the previously reported methylated acetylated xylans were attached to the hydroxyl group on $C_{(3)}$ [2,3], which presumably represents a similar redistribution. A definite assignment of the position of the *O*-acetyl groups by this method is therefore improbable.

The *O*-acetyl groups also migrated in dimethyl formamide containing silver oxide albeit much more slowly than under the actual methylation conditions as indicated by thin layer chromatography [13]. Some deacetylation was observed in this case as well.

The *O*-acetyl groups did, however, appear quite stable towards treatment with hot dimethyl formamide under the conditions previously reported for

the carbanilation of the acetyl 4-*O*-methylglucuronoxylan [7]. Each of the two monoacetates was carbanilated with phenylisocyanate and the products were subjected to methanolysis to remove the *O*-acetyl groups, followed by methylation with methyl iodide and silver oxide in dimethyl formamide, removal of the phenylcarbamoyl groups by lithium aluminium hydride reduction and acid hydrolysis. Benzyl 2-*O*-acetyl-4-*O*-methyl-β-D-xylopyranoside on this treatment yielded essentially 2,4-di-*O*-methyl-xylose and benzyl 3-*O*-acetyl-4-*O*-methyl-β-D-xylopyranoside yielded essentially 3,4-di-*O*-methylxylose indicating that the phenylcarbamoyl groups were sufficiently stable towards the methylation conditions to be used in the assignment of the position of *O*-acetyl groups in compounds with the spatial arrangement of the hydroxyl groups on $C_{(2)}$ and $C_{(3)}$ in benzyl 4-*O*-methyl-β-D-xylopyranoside and hence probably in β-1,4-linked xylans.

Treatment of each of the two monoacetates in 3 % ethanolic monoethanolamine under the conditions used for the preparation of chlorine-monoethanolamine holocellulose [1-3] caused acetyl migration to near an equilibrium where the 3-*O*-acetyl isomer predominated somewhat over the 2-*O*-acetyl isomer as indicated by thin layer chromatography [13]. Some deacetylation also occurred. In the preparation of chlorine-monoethanolamine holocellulose the medium is heterogeneous, reservations for *O*-acetyl migration during the treatments with monoethanolamine must, however, be made. Bouveng [7] used delignification with chlorite and this is probably to be preferred to treatments with boiling monoethanolamine solutions.

No acetyl migration was observed on treating the 3-*O*-acetyl isomer with dimethyl sulphoxide under the conditions used for the extraction of acetyl 4-*O*-methyl-glucuronoxylans whereas with the 2-*O*-acetyl isomer a slight migration occurred. No deacetylation was observed. The extraction of native acetylated xylan with this solvent therefore should not give rise to any serious migration of *O*-acetyl groups.

EXPERIMENTAL

All melting points are corrected. Evaporations were carried out under reduced pressure at a bath temperature below 40°.

Chromatography. Paper chromatography: Papers: Whatman No. 1, water eluted Schleicher und Schüll 602 hP for preparative chromatography. Solvent: Butanol-ethanol-water 10:3:5. Thin layer chromatography [13]. Absorbent: Kieselgel G nach Stahl, E. Merck AG. Solvent: Ethyl ether.

Paper electrophoresis. Papers: Whatman No. 3 MM. Buffers: 0.1 M borate buffer at pH 10, 0.05 M sulphonated phenylboronic acid [10] at pH 7.4. Spray reagents: Anisidine hydrochloride for reducing sugars, potassium periodate-cuprate [18] for non-reducing, acetylated sugars. The spots on the thin layer chromatograms were located either with iodine vapour or with potassium periodate-cuprate.

Partial acetylation of benzyl 4-O-methyl-β-D-xylopyranoside with acetic anhydride in pyridine. The xyloside (1.333 g) was dissolved in anhydrous pyridine (2 ml), acetic anhydride (0.55 ml) was added and the solution was allowed to stand at room temperature for 3 days. The solution was poured into ice-water in a separating funnel and the mixture was extracted several times with chloroform. The combined chloroform extracts were successively washed four times with ice-cold 2 N sulphuric acid, three times with ice-cold saturated aqueous sodium bicarbonate and four times with water, dried over anhydrous sodium sulphate, filtered and concentrated to a syrup which was dried over phosphorus

pentoxide in a vacuum to yield 1.389 g syrup. Thin layer chromatography gave four spots, the slowest with a mobility corresponding to that of the starting material and the fastest to benzyl 2,3-di-*O*-acetyl-4-*O*-methyl-β-D-xylopyranoside. Of the two spots of intermediate mobility the slower, monoacetate B, predominated over the faster-moving monoacetate A. The mixture was added to the top of a silicic acid column (Mallinckrodt silicic acid, A.R., 100 mesh, activated by heating overnight at 180° and kept out of contact with moist air; 3.5 × 50 cm). The column was irrigated with mixtures of dry ethyl ether and benzene.

The eluate was divided into fractions of approximately 500 ml, the dry contents of which were weighed and examined by thin layer chromatography. Similar fractions were combined, concentrated to dryness and dried over phosphorus pentoxide in a vacuum. Benzene and ethyl ether, 9:1 (6700 ml), eluted benzyl 2,3-di-*O*-acetyl-4-*O*-methyl-β-D-xylopyranoside (381 mg) which crystallised on standing. Recrystallisation from isopropyl ether gave 304 mg crystals with m.p. 79.5—80°; $[\alpha]_D^{20}$ −104° (c = 1.0 in chloroform). (Found: C 60.1; H 6.56; O 33.2. Calc. for $C_{17}H_{22}O_7$: C 60.3; H 6.56; O 33.1). Benzene and ethyl ether, 4:1 (4500 ml), eluted monoacetate A (302 mg) which did not crystallise; $[\alpha]_D^{20}$ −84° (c = 1.0 in chloroform). Benzene and ethyl ether, 2:1 (6700 ml), eluted monoacetate B (528 mg) which did not crystallise; $[\alpha]_D^{20}$ −81° (c = 1.0 in chloroform). Benzene and ethyl ether; 2:1 (1700 ml), and finally ethyl ether eluted benzyl 4-*O*-methyl-β-D xylopyranoside (115 mg) which crystallised on standing. Two recrystallisations from isopropyl ether gave 68 mg with m.p. 73—76° undepressed on admixture with authentic material.

Partial acetylation of benzyl 4-O-methyl-β-D-xylopyranoside with acetyl chloride in pyridine. The xyloside (1.297 g) was dissolved in pyridine (2 ml) and cooled to −4°. Acetyl chloride (0.40 ml) at the same temperature was added with stirring. The mixture was allowed to stand for 24 h at −4° and was worked up as described above. Yield 1.260 g. Thin layer chromatography gave four spots, the slowest corresponding to the starting material. Of the two intermediate spots, the slower-moving, monoacetate B, predominated only slightly over the faster-moving, monoacetate A. Separation on a silicic acid column as described above yielded crystalline diacetate (525 mg) with m.p. 78—80° after recrystallisation from isopropyl ether, syrupy monoacetate A (234 mg), monoacetate B (262 mg), and crystalline starting material (278 mg) with m.p. and mixed m.p. 74—76.5° after recrystallisation from isopropyl ether.

Identification of the two monoacetates. Monoacetate A (54.8 mg) was hydrogenated at a pressure slightly over the atmospheric in abs. methanol (5 ml) with palladium on carbon (from 100 mg 5 % palladium chloride on carbon, prepared according to Mozingo [12], hydrogenated in methanol and washed free from hydrochloric acid on sintered glass [9]). The uptake was 4.5—5 ml in 2 h. The catalyst and carbon were filtered off on kiselguhr and washed with methanol. The filtrate was concentrated to dryness and dried over phosphorus pentoxide and silica gel in a vacuum. Yield 38.2 mg. Paper chromatography indicated complete removal of benzyl groups but retention of virtually all the acetyl-groups. The amount of reducing sugar was estimated by hypoiodite oxidation and found to be 34.9 mg. Oxidation with lead tetraacetate in abs. acetic acid according to Perlin [11] gave a net consumption of 0.95 mole oxidant per mole aldose. The aldose (14.3 mg) was dissolved in acetic acid (10 ml) and 10 ml of oxidant (1.0 g potassium acetate and 1.0 g lead tetraacetate in 50 ml acetic acid). Samples (5 ml) were withdrawn after 10, 30, 60 and 90 min, added to 10 ml "stopping solution" (20 g potassium iodide and 100 g sodium acetate in 200 ml water). The iodine formed was titrated with thiosulphate. The oxidation was complete in about 5 min. The carbon dioxide produced during the oxidation was measured in a Warburg apparatus and represented about 2—3 mole % of the oxidant used. Under the same conditions 4-*O*-methylxylose consumed 2.2 mole lead tetraacetate. 2,3-Di-*O*-acetyl-4-*O*-methylxylose, prepared by hydrogenating benzyl 2,3-di-*O*-acetyl-4-*O*-methyl-β-D-xylopyranoside as described above, but with dry ethyl ether as solvent during the hydrogenation of the xyloside, did not consume any lead tetraacetate under these conditions.

Paper electrophoresis of the hydrogenated monoacetate A run in sulphonated phenylboronic acid at pH 7.4 for 3 h at tap water temperature and about 20 V/cm gave a rate of migration similar to that of 3,4-dimethylxylose which had M_G 0.1.

Monoacetate B (37.8 mg) was hydrogenated as described above, but with dry ethyl ether as solvent during the hydrogenation of the xyloside. The yield of material dried over phosphorus pentoxide and silica gel in a vacuum was 21.0 mg. Paper chromatography indicated complete hydrogenation of benzyl groups and little (less than 5 %) deacetylation. Previous attempts to hydrogenate in methanolic solutions led to considerable deacetylation. The monoacetyl 4-*O*-methylxylose was oxidised with lead tetraacetate as described above. The net consumption of lead tetraacetate was 0.08 mole oxidant per mole aldose. The monoacetyl 4-*O*-methylxylose did not migrate on paper electrophoresis in sulphonate phenylboronic acid at pH 7.4 as described above.

These results prove that monoacetate A is benzyl 3-*O*-acetyl-4-*O*-methyl-β-D-xylopyranoside and monoacetate B is benzyl 2-*O*-acetyl-4-*O*-methyl-β-D-xylopyranoside.

Chromatographic investigations of acetylations of benzyl 4-O-methyl-β-D-xylopyranoside. (i) Acetic anhydride-sodium acetate. The xyloside (50 mg) was dissolved in acetic anhydride (0.25 ml) and anhydrous sodium acetate (25 mg) was added. The mixture was heated at 100°. The solution was spotted on to thin layer chromatograms at time intervals of 1 min. After 1 min both monoacetates were formed, after 3 min the diacetate appeared while starting material virtually disappeared. The proportion of diacetate increased rapidly and was the major component after 10 min. Throughout, the slower-moving monoacetate, monoacetate B, predominated over monoacetate A; the ratio was visually estimated as approx. 2:1 by comparison with a standard chromatogram containing known ratios of the two monoacetates.

(ii) Acetic anhydride-pyridine containing pyridine hydrochloride. Benzyl 4-*O*-methyl-β-D-xylopyranoside (120 mg) was dissolved in pyridine (0.2 ml) containing 1.5 % by weight of dry hydrogen chloride combined as pyridine hydrochloride. Acetic anhydride (0.05 ml) was added and the mixture allowed to stand overnight. Visual examination of thin layer chromatograms indicated a ratio of about 1:1 for the two monoacetates. The reaction mixture was streaked on to a thin layer plate which was run as described above. The streaks of the four components were located by brief exposure to iodine vapour, cut from the plate and the powder extracted with ethanol. The extracts were filtered, concentrated to dryness and the residues dried in a vacuum over phosphorus pentoxide and silica gel and weighed. The proportions found for diacetate, monoacetate A, monoacetate B, and starting material were 3:2:2:1. Thin layer chromatography of the four components showed each to be free from contamination by the others.

(iii) Acetic anhydride-perchloric acid. Benzyl 4-*O*-methyl-β-D-xylopyranoside (50 mg) was dissolved in acetic anhydride (0.25 ml) containing perchloric acid (0.3 %), and the solution was allowed to stand at room temperature. The solution was spotted on thin layer chromatograms at 1 min intervals. After 1 min the starting material had disappeared, both monoacetates as well as a small amount of diacetate were present. Monoacetate A predominated throughout and the ratio of the two monoacetates was visually estimated as described above to be about 3:1 at first, increasing to about 5:1 or more after about 10 min. The formation of diacetate was relatively slow and after 40 min an appreciable amount of monoacetate A was still left in the solution.

Treatment of the two monoacetates with pyridine. Each of the two monoacetates (5 mg) was dissolved in pyridine (0.1 ml) at room temperature and allowed to stand for 3 days at room temperature. Thin layer chromatography indicated that no acetyl migration had occurred.

Methylation studies on the monoacetates. Monoacetate A (116 mg) was treated for 20 h with silver oxide (1 g) and methyl iodide (2 ml) in dimethyl formamide (5 ml) [19] and worked up as previously described [20]. Yield 125 mg syrup. Deacetylation was performed by dissolving the syrup in 5 ml abs. methanol, adding 1 ml 10 % ammoniacal methanol, allowing the solution to stand overnight and concentrating to dryness. The resulting syrup was hydrolysed by heating with 8 % aqueous sulphuric acid at 100° for 2 h, neutralised with barium carbonate, filtered and concentrated to dryness to yield 66.2 mg material. Paper chromatography indicated about 70—80 % dimethylxylose, 20—30 % 2,3,4-tri-*O*-methylxylose and traces of 4-*O*-methylxylose to be present. The dimethylxylose fraction was separated from the other components by chromatography on thick paper, the yield being 31.5 mg. Paper electrophoresis in borate buffer indicated the presence of 2,4- and 3,4-di-*O*-methylxylose, the former predominating noticeably. Lead tetraacetate oxidation as described above gave a consumption of 0.37 mole oxidant per mole aldose, the quantity of aldose in the sample being previously determined by hypoiodite oxidation.

Monoacetate B (107 mg) was methylated, deacetylated and hydrolysed as described above to yield 61 mg syrup. Paper chromatography indicated a composition of methyl ethers very similar to that derived from monoacetate A, and the dimethylxylose fraction was obtained free from the other components by chromatography on thick paper; yield 36.6 mg. Lead tetraacetate oxidation of a sample gave a consumption of 0.33 mole oxidant per mole aldose.

The efficiency of the methylation treatments was checked by methylating benzyl 4-*O*-methyl-β-D-xyloside as described above. After hydrogenation with palladium on carbon in methanol solution as described above only traces of dimethylxylose were observed on paper chromatography, the practically pure 2,3,4-trimethyl-D-xylose crystallised, m.p. 88—91°, undepressed on admixture with an authentic specimen.

Treatment of the monoacetates with silver oxide in dimethyl formamide. Monoacetate A, homogeneous on thin layer chromatograms (10 mg) was dissolved in anhydrous dimethyl formamide (1 ml). Silver oxide (0.2 g) was added and the mixture shaken in a sealed ampoule for 18 h at room temperature. The silver oxide was removed by filtration on Kiselguhr, and washed with dimethyl formamide. The filtrate was poured into excess chloroform, and the chloroform solution was extracted ten times with water to remove the dimethylformamide. The chloroform layer was finally dried over sodium sulphate, filtered and concentrated to dryness. Thin layer chromatography revealed a slight degree of migration but no deacetylation. No spot corresponding to dimethyl formamide was observed.

Monoacetate B was treated in the same way. Again acetyl migration occurred to a slight extent.

On repeating this treatment of the two monoacetates for 72 h rather more migration was observed on thin layer chromatography (of the order of 10 %) and deacetylation also occurred. Monoacetate B (5 mg) was treated with dimethyl formamide (1 ml containing 1 % water) and silver oxide (0.2 g) for 20 h. Thin layer chromatography indicated that the rate of deacetylation had increased to some extent, but that the rate of acetyl migration was about the same as before.

Treatment of the monoacetates with hot dimethyl formamide. Each of the monoacetates as well as benzyl 2,3-di-*O*-acetyl-β-D-xylopyranoside (*ca.* 5 mg) were treated with dimethyl formamide (0.5 ml) in sealed ampoules at 100° for 3 h. The solutions were poured into excess chloroform, the chloroform was extracted ten times with water, dried over sodium sulphate, filtered and concentrated. Thin layer chromatography did not indicate any migration of the acetyl groups. No deacetylation was observed.

Carbanilation, hydrolysis, methylation, reduction, and hydrolysis of the two monoacetates. Monoacetate A (91 mg) in anhydrous dimethyl formamide (0.5 ml) was treated with phenylisocyanate (0.055 ml) in a sealed ampoule at 100° for 3 h [7]. The solution was concentrated to a syrup. Thin layer chromatography indicated complete reaction, only one spot with faster mobility than that of monoacetate A being observed. The syrup was dissolved in 2 % methanolic sulphuric acid (10 ml) and the solution boiled under reflux overnight to remove the acetyl groups. The solution was neutralised with 10 % methanolic ammonia [7], the salts were removed by filtration and the solution concentrated to a syrup which was dried over phosphorus pentoxide and silica gel in a vacuum. The syrup was methylated twice with methyl iodide (3 ml) and silver oxide (2 g) in dimethyl formamide (5 ml) as previously described [19,20]. The product was treated with an excess of lithium aluminium hydride in boiling dry tetrahydrofuran for 3 h. to remove the carbamoyl groups [7]. The excess lithium aluminium hydride was destroyed with ethanol and the alcoholates decomposed with water. After neutralisation with phosphoric acid [7] and filtration the solution was concentrated to dryness. The resulting syrup was hydrolysed with 0.5 N sulphuric acid (5 ml) at 100° overnight, neutralised with saturated aqueous barium hydroxide, filtered and concentrated to a syrup (17 mg). Paper chromatography and paper electrophoresis in borate indicated the presence of 3,4-di-*O*-methylxylose (M_G 0.33) with only traces of 4-*O*-methylxylose (M_G 0.19) and 2,4-di-*O*-methylxylose. (M_G 0.00). Monoacetate B (64 mg) was subjected to the same sequence of reactions as described above to yield 19 mg of a syrup. Paper chromatography and paper electrophoresis in borate indicated that 2,4-di-*O*-methylxylose was present along with only traces of 4-*O*-methylxylose and 3,4-di-*O*-methylxylose.

Treatment of the monoacetates with refluxing 3 % monoethanolamine in ethanol. Each of the two monoacetates (5 mg) was dissolved in 3 % monoethanolamine in 95.5 %

ethanol (0.5 ml), the solutions were sealed in ampoules and heated at 80° for 30 min. The solutions were poured into excess chloroform and the chloroform solutions extracted ten times with water, dried over sodium sulphate, filtered and concentrated. Thin layer chromatography indicated that acetyl migration reached a state of equilibrium. There was no difference between the mixtures obtained from the two monoacetates. Monoacetate A predominated over monoacetate B; the ratio was visually estimated to about 2:1. Considerable deacetylation (about 20–30 %) had occurred.

Treatment of the monoacetates with dimethyl sulphoxide at room temperature. Each of the monoacetates (*ca.* 5 mg) was dissolved in dimethyl sulphoxide (0.1 ml) and allowed to stand for 20 h in a sealed ampoule. The solutions were added to excess chloroform, the chloroform solutions were extracted ten times with water to remove the dimethyl sulphoxide. No spot corresponding to dimethylsulphoxide was observed on subsequent thin layer chromatograms. The chloroform solutions were dried over sodium sulphate, filtered and concentrated. Thin layer chromatograms indicated that no deacetylation of either of the two monoacetates had occurred. The acetyl groups in monoacetate A had not migrated; a slight migration of the acetyl groups had occurred in monoacetate B.

Acknowledgement. The author wishes to express his gratitude to Professor Bengt Lindberg for his interest and helpful advice.

REFERENCES

1. Hägglund, E., Lindberg, B. and McPherson, J. *Acta Chem. Scand.* **10** (1956) 1160.
2. Bouveng, H. O., Garegg, P. J. and Lindberg, B. *Acta Chem. Scand.* **14** (1960) 742.
3. Timell, T. E. *J. Am. Chem. Soc.* **82** (1960) 5211.
4. Koshijima, T. *J. Japan Wood Research Soc.* **6** (1960) 194.
5. Meier, H. *Acta Chem. Scand.* **15** (1961) 1381.
6. Annergren, G. E., Croon, I., and Enström, B. F. *Svensk Papperstidn.* **64** (1961) 386.
7. Bouveng, H. O. *Acta Chem. Scand.* **15** (1961) 96.
8. Garegg, P. J. *Acta Chem. Scand.* **14** (1960) 957.
9. Ballou, C. E., Roseman, S. and Link, K. P. *J. Am. Chem. Soc.* **73** (1951) 1140.
10. Garegg, P. J. and Lindberg, B. *Acta Chem. Scand.* **15** (1961) 1913.
11. Perlin, A. S. *J. Am. Chem. Soc.* **76** (1954) 5505.
12. Mozingo, R. *Org. Syntheses* **26** (1946) 77.
13. Stahl, E. *Pharmazeutische Rundschau* **1** No. 2 (1959) 1.
14. Jeanloz, R. W. and Jeanloz, D. A. *J. Am. Chem. Soc.* **79** (1957) 2579.
15. Bourne, E. J., Stacey, M., Tatlow, C. E. M. and Tatlow, J. C. *J. Chem. Soc.* **1951** 826.
16. Newth, F. H. *J. Chem. Soc.* **1959** 2717.
17. Jeanloz, R. W., Rapin, A. M. C. and Hakomori, S. *J. Org. Chem.* **26** (1961) 3939.
18. Bonner, T. G. *Chem. & Ind. London* **1960** 345.
19. Kuhn, R., Trischmann, H. and Löw, I. *Angew. Chem.* **67** (1955) 32.
20. Bouveng, H. O. *Acta Chem. Scand.* **12** (1958) 1977.

Received April 18, 1962.

ACTA CHEMICA SCANDINAVICA 16 (1962) 1858–1862

Some Products of the Metabolism of D-Xylose by *Pullularia pullulans*

HANS KIESSLING, BENGT LINDBERG and JAMES McKAY

Papperstekniska och träkemiska avdelningarna, Svenska Träforskningsinstitutet, Stockholm, Sweden

After the growth of *Pullularia pullulans* in nutrient media containing D-xylose as the sole carbon source, the following compounds were isolated from the cell- and polysaccharide-free culture solutions and characterised: D-xylulose, xylitol and D-xylonic acid. The presence of small amounts of glucose, gluconic and ribonic acids was detected, in addition, by paper chromatographic methods.

Moulds have the capacity to transform carbohydrate substrates into products, in many cases accumulating in large quantities in the culture media, which may reasonably be considered to be metabolic intermediates which, due to environmental conditions such as pH, or adverse competition from the original substrate, are only slowly transformed further or are not immediately required as sources of energy.

The metabolism of D-xylose by moulds has been studied but sparingly and relatively little is known of the mechanisms and pathways of its transformations to the small number of products which have so far been encountered. Two of the main types of end-product of the action of moulds on sugars are organic acids [1] and polysaccharides [1] and both types have been found to be formed from xylose. Although glucose is converted to gluconate by *Aspergillus* and *Penicillium*, as well as a few other species, including *Fusarium lini* and *Pullularia (Dematium) pullulans*, only the two latter have been observed to oxidise xylose to xylonate [1]. Xylose forms an excellent substrate for the formation of kojic acid by *Aspergillus flavus* [2] while it is converted to oxalic acid by *A. niger* [3]. This organism has also been found to incorporate ^{14}C from xylose into a mycelial glucan [4].

More recently, another sequence of transformations of xylose by *Penicillium chrysogenum* has been observed which may help to cast some light on the pathways to the other fermentation products. Chiang and Knight [5] have found that D-xylose is reduced by the organism to xylitol and that this is subsequently dehydrogenated to D-xylulose. This compound, on conversion to the 5-phosphate, can enter the pentose shunt and thereby the main paths of carbohydrate metabolism.

During studies concerned mainly with the polysaccharides produced by *P. pullulans* when grown in solutions of D-xylose, a brief investigation has been made of the products of low molecular weight appearing synchronously with polysaccharide in the culture media, and the findings are now presented. Concentration of the cell- and polysaccharide-free culture solution yielded a syrup which was shown by paper chromatography to contain a variety of components other than xylose. Fractionation of this syrup by cellulose column chromatography yielded D-xylulose, D-xylose, xylitol, glucose, and a mixture of inorganic and organic acid salts. D-Xylulose and xylitol were converted to crystalline derivatives identical to the authentic compounds.

After freeing the salt mixture from phosphate and cations, the organic acids were purified by adsorption on ion-exchange resin. Examination of the mixture by paper chromatography and paper electrophoresis showed the principal component to behave as xylonic acid and to form a lactone with the same chromatographic mobility as xylonolactone. Partial reduction of the lactone components with sodium borohydride yielded xylose, along with small amounts of ribose and glucose, as the only reducing sugars. Distillation of a small sample of the mixture under high vacuum afforded a small amount of a crystalline compound, mp. 90°, $[\alpha]_D^{23}$ + 95°, behaving as xylonolactone on paper chromatograms. A further sample of the acidic components was isolated by ion-exchange methods and from the crude mixture D-xylonic acid was isolated as its brucine salt and as its double salt with cadmium bromide, both identical to the authentic compounds.

From paper chromatograms it was clear that several other acids were present, other than xylonic, ribonic, and gluconic acids, some of which formed lactones distinct from the lactones of the acids named. The characteristic colour reaction given by kojic acid with ferric chloride was not obtained. Traces of organic phosphates and aminoacids could be detected but no evidence for the presence of ketoacids could be obtained.

P. pullulans would appear from these observations to have more than one route for the metabolism of D-xylose. One reaction sequence is obviously the transformation to D-xylulose *via* xylitol as observed in *P. chrysogenum* but there would seem in addition to be a route involving the oxidation of C1. A similar duality has been observed in *in vitro* experiments with the action of enzymes from rat lens on D-xylose [6]. It should be stated, however, that although D-xylulose and not the racemic mixture of D- and L- forms was identified, the presence of L-xylulose in the system in minor quantity cannot be excluded. No evidence was obtained for the formation of kojic acid or ketoacids. The fact that glucose and gluconic acid were detected cannot be considered significant as traces of glucose are to be found in commercially available xylose preparations.

EXPERIMENTAL

All evaporations were carried out under reduced pressure at temperatures not exceeding 50°C.

Paper chromatography was carried out on Whatman No. 1 paper with the following solvent systems:

(A) ethyl acetate, pyridine, water (8:2:1)
(B) ethyl acetate, acetic acid, water (3:1:3)
(C) water saturated methyl ethyl ketone

Paper electrophoresis was conducted on Whatman No. 3 paper in acetate buffer (pH 4) with 1 kV potential difference.

Components were detected on papers by the use of the following reagents:
(1) silver nitrate-sodium hydroxide for reducing sugars, aldonic acids, and alditols
(2) anisidine hydrochloride for reducing sugars
(3) resorcinol — hydrochloric acid for ketoses
(4) hydroxylamine—ferric chloride for lactones
(5) thymol blue indicator for acids
(6) dinitrophenyl hydrazine—hydrochloric acid for ketones
(7) ninhydrin for amino compounds and
(8) ammonium molybdate—hydrochloric acid for phosphates.

Culture of the mould. The general conditions of culture have been described previously [7]. The composition of the culture solution was 1.0 g KH_2PO_4, 0.2 g $CaCl_2 \cdot 6H_2O$, 0.3 g $MgSO_4 \cdot 7H_2O$, 0.1 g NaCl, 0.02 g $FeCl_3 \cdot 6H_2O$, 2.5 g $NaNO_3$ and 50 g D-xylose per litre. The xylose cultures were made in batches of 9 litres with continous aeration and stirring.

Isolation of the components of low molecular weight. The cells were removed from the cultures by super-centrifugation and the polysaccharides precipitated from the solutions by the addition of ethanol. The ethanolic supernatant solutions obtained after the centrifugation of the precipitated polysaccharides were evaporated to syrups. These syrups, on examination by paper chromatography in solvent (A), showed a mixture of components with R_{xylose} values 1.58, 1.50, 1.00, 0.71, 0.44 and 0.00.

Fractionation of the mixture. A portion of the syrup (4.4 g) was slurried with water and cellulose powder and the slurry was freeze-dried. The powder thus obtained was packed on the top of a cellulose column (45 × 4.5 cm) and elution was performed with solvent (A). The effluent was collected in 50 ml portions and the fractions obtained are listed below. The final fraction was obtained by elution with water.

Fraction	Tube Nos.	R_{xylose} of content	Weight, g
1	21— 23	1.58	0.028
2	34— 45	1.50	0.040
3	46— 50	1.50, 1.00	0.050
4	51— 60	1.00	0.542
5	61— 70	1.00, 0.71	0.369
6	71— 79	0.71, trace 1.00	0.514
7	80— 98	0.71	0.800
8	99—120	0.71, 0.44	0.162
9	121—150	0.44	0.124
10	164—174	0.00	1.820

All fractions, but especially the minor ones, were contaminated by non-volatile products which could not be removed completely by treatment with charcoal.

Examination of the fractions. Fraction 1. A very small amount of a substance with R_x 1.58 and reacting on paper chromatograms with reagents (1) and (2) was present. The fraction was not examined further.

Fraction 2. The syrup had R_x 1.50 and reacted with reagents (1)—(3), giving a grey colour with the latter. It was identical in colour reaction and chromatographic mobility to xylulose and had $[\alpha]_D^{25}$ −15° (*c*, 0.4 in water); D-xylulose has $[\alpha]_D$ −34° [8]. Reaction with phenylhydrazine gave a product which, after several recrystallisations from aqueous ethanol, melted at 162—163° and showed mutarotation in ethanol-pyridine solution (3:2) from $[\alpha]_D^{23}$ −14° to −31° (*c*, 0.8). The melting-point was unchanged by admixture with authentic D-xylosazone and the infra-red spectra of the two compounds were identical.

Fraction 4. This material was identical in chromatographic mobility, colour reaction, and optical rotation to D-xylose.

Fraction 7. The syrup reacted on paper chromatograms only with reagent (1) and showed identical chromatographic mobility to xylitol, but was distinct from ribitol and arabinitol in solvent (A). No optical activity could be detected. Reaction with formaldehyde and hydrochloric acid [9] yielded a compound which, after several recrystallisations from aqueous ethanol, had mp. 199—201°, undepressed on admixture with authentic 2,4:3,5-di-*O*-methylidene-DL-xylitol. The infra-red spectra of the two compounds were identical. Reaction with benzaldehyde [10] afforded a crystalline derivative mp. 184—186° (lit. 188°).

Fraction 9. This material was identical to glucose on chromatograms in both mobility and colour reaction.

Fraction 10. The syrup had $[\alpha]_D^{22}$ + 10° (*c*, 3.63 in water) and R_x 0.00 in solvent (A), 1.27 in solvent (B). Reaction was observed mainly with reagent (1) although the presence of phosphate and to a lesser extent aminoacid could be detected with reagents (7) and (8), respectively. Paper electrophoresis showed the main component detectable with reagent (1) to have the same mobility as xylonate. The mixture was dissolved in water, freed from cations by passage through Dowex 50 resin and the effluent neutralised with barium carbonate. The filtered solution was freed from barium ions by a repetition of the resin treatment. The acid, phosphate-free components were adsorbed on Dowex 2 (carbonate form). After washing away the neutral components with water, the acids were displaced with 10 % formic acid and the eluate concentrated to a syrup (520 mg). Chromatographic examination of the syrup revealed a mixture of acids and lactones with the principal components of the two groups being identical in chromatographic mobility to xylonic acid — solvent (B) — and xylonolactone — solvent (A) — respectively.

Distillation of a portion of the mixture (100 mg) under high vacuum allowed the isolation of a crystalline sublimate (19 mg) with the same chromatographic mobility in solvent (A) as xylonolactone, m.p. 90°, and $[\alpha]_D^{25}$ + 95° (*c*, 0.19 in water), *cf.* lit.[11] mp. 99—103°, $[\alpha]_D$ + 89.6°. Partial reduction with sodium borohydride in pyridine [12] of a portion of the mixture and paper chromatographic examination of the products in solvent (A) showed the presence of xylose and traces of ribose and glucose as the only reducing sugars. Unchanged lactone, free acid, and pentitol could be detected by reagent (1).

Further examination of the acidic components. By the use of ion-exchange resins as described above, an acid fraction (1.3 g) was obtained from a portion of the original syrup (*ca.* 13 g). Treatment of a portion of the mixture (1 g) with brucine afforded a brucine salt (1.3 g) which had mp. 152—154° after repeated recrystallisation from ethanol. The melting-point was undepressed by the admixture of authentic brucine D-xylonate and the two compounds gave identical infra-red spectra. The melting-points of both compounds were lower than the values given in the literature *viz.* 176° [11], 172—174° .[19]

A further portion (200 mg) was treated with cadmium carbonate and hydrobromic acid. From the reaction mixture a salt (90 mg) was obtained which on recrystallisation from aqueous ethanol gave $[\alpha]_D^{24}$ + 6° (*c*, 0.40 in water), *cf.* lit. + 8.8° [14], an infra-red spectrum and an X-ray interference pattern identical to those obtained from authentic cadmium bromide xylonate.

Examination of the acid fraction on paper chromatograms run in solvents (B) and (C) using reagents (4), (5) and (6) showed that several acids other than xylonic, ribonic and gluconic acids, and several lactones other than xylono-, ribono-, and glucono-lactones were present and that no keto-acid could be detected. The characteristic reaction of kojic acid with ferric chloride was not observed. The complex mixture was not examined further.

Equipment and laboratory facilities for the preparation of largescale cultures were generously supplied by the *Department of Applied Microbiology, The Royal Institute of Technology, Stockholm.* The authors are further indebted to Dr. S. T. Lundin for the determination of the X-ray interference pattern of cadmium bromide xylonate, and to *Cellulosaindustrins stiftelse för teknisk och skoglig forskning samt utbildning* for financial support.

REFERENCES

1. Foster, J. W. *Chemical Activities of Fungi*, Academic Press Inc., New York 1949.
2. Arnstein, H. R. V. and Bentley, R. *Biochem. J.* **62** (1956) 403.
3. Cleland, W. W. and Johnson, M. J. *J. Biol. Chem.* **220** (1956) 595.
4. Van Sumere, C. F. and Shu, P. *Can. J. Biochem. Physiol.* **35** (1957) 445.
5. Chiang, C. and Knight, S. G. *Biochim. et Biophys. Acta* **29** (1958) 664; **35** (1960) 454; *Biochem. Biophys. Research Communs.* **3** (1960) 554.
6. Van Heyningen, R. *Biochem. J.* **73** (1959) 197.
7. Bouveng, H. O., Kiessling, H., Lindberg, B. and McKay, J. *Acta Chem. Scand.* **16** (1962) 615.
8. Schmidt, O. T. and Treiber, R. *Ber.* **66** (1933) 1765.
9. Hann, R. M., Ness, A. T. and Hudson, C. S. *J. Am. Chem. Soc.* **66** (1944) 670.
10. Wolfrom, M. L. and Kohn, E. J. *J. Am. Chem. Soc.* **64** (1942) 1739.
11. Nef, J. U. *Ann.* **403** (1914) 220, 244, 291.
12. Isbell, H. S., Frush, H. L., Holt, N. B. and Moyer, J. D. *J. Research. Natl. Bur. Standards* **64A** (1950) 177; Wolfrom, M. L. and Wood, H. B. *J. Am. Chem. Soc.* **73** (1951) 2933; Wolfrom, M. L. and Anno, K. *Ibid* **74** (1952) 5563.
13. Neuburg, C. *Ber.* **35** (1902) 1473.
14. Hudson, C. S. and Isbell, H. S. *J. Am. Chem. Soc.* **51** (1929) 2227.

Received May 3, 1962.

ACTA CHEMICA SCANDINAVICA 16 (1962) 1863–1869

Heats of Combustion and Formation of the *n*-Alkane-α,ω-dithiols from Ethane through Pentane

M. MÅNSSON and S. SUNNER

*Thermochemistry Laboratory *, University of Lund, Sweden*

The heats of combustion of four *n*-alkane-α,ω-dithiols have been determined and therefrom values of the standard heats of formation, $\Delta H°$(liq), at 25°C, have been derived. From heat of vaporization measurements standard heat of formation values for the gaseous compounds, $\Delta H°_f$ (g), have been calculated. The obtained data are, for the liquid and gaseous states,

ethanedithiol-1,2: −12.91 and − 2.23;
propanedithiol-1,3: −18.90 and − 7.03;
butanedithiol-1,4: −25.20 and − 12.03;
pentanedithiol-1,5: −31.04 and − 16.87
kcal.mole^{-1}, respectively.

It is possible that in the near future agreement may be reached on the use of a slightly different value for the heat of formation of sulphuric acid, $\Delta H°_f$ (H_2SO_4, 115 H_2O) = a. In this case, the published values should be corrected by adding the quantity $2(a + 212.24)$ kcal. mole^{-1}.

In the experimental determination of the strain energy [1] of the dithiolane ring structure, by comparing the heat of oxidation of propanedithiol-1,3 with that of an alkane thiol to form dithiolane and an open dialkyl disulfide, respectively, it was assumed that the two thiol groups in the propanedithiol-1,3 behave energetically like thiol groups in separate molecules, *i.e.* intramolecular interactions between the thiol groups should be absent. In order to verify this, in itself very reasonable, assumption determinations of heats of combustion of a number of alkane-α,ω-dithiols were undertaken.

EXPERIMENTAL

Synthesis and purification of compounds

The dithiols were all synthesized by conversion of the corresponding dibromides to the bis-isothiouronium hydrobromides and subsequent hydrolysis using KOH [2,3].

* Sponsored by the *Swedish Natural Science Research Council* and the *Swedish Technical Research Council.*

The compounds were purified by repeated vacuum-distillation in a 50 cm column packed with glass helices at several pressures and in a nitrogen atmosphere. The purities of the fractions obtained were estimated by titration with iodine. Samples were sealed under nitrogen into small glass vials, which were broken under ethanol and titrated with 0.1 N iodine. The average deviation in a set of 4 titrations was found to correspond to an error in the purity of ± 0.1 %. From the results it is seen that only the titration on butanedithiol-1,4 indicated 100 % purity. Efforts to increase the purity of the other three dithiols as judged from iodine titrations were fruitless and it was concluded that the oxidation reaction in these cases was not quantitative. The same trend was observed by Grogan, Rice and Reid [4].

Ethanedithiol [2]. Distilled at 36 and 17 mm Hg, b.p. 61 and 45.8°C, respectively. Iodine titration 99.5 %.

Propanedithiol [3]. Distilled at 11 and 18 mm Hg, b.p. 51.8 and 67.0°C, respectively. Iodine titration 99.5 %.

Butanedithiol [3]. Distilled four times, the last two at 5 and 10 mm Hg, b.p. 61.6 and 71.7°C, respectively. Iodine titration 100. 1 %.

Pentanedithiol [3]. Distilled at 10 and 5.5 mm Hg, b.p. 89.0—89.2 and 81.7°C, respectively. Iodine titration 99.6 %.

The purities of the samples used for combustion studies were estimated from melting curves. These were determined using a simple "constant" heat input, thin layer method [8] using a calibrated platinum resistance thermometer *. The values obtained for the melting interval tend to be too high, particularly for low melting substances. Measurements on samples with known amounts of impurity added showed an increase in the melting interval of about 0.2°C per 0.1 mole % of impurity.

Table 1 gives estimated melting points for zero impurity and the purity of the samples as judged from the melting curves together with the results of density and refractive index measurements at 20 and 25°C.

Table 1.

Compound and reference	Density		Refractive index		M.p. °C	Estimated purity mole-%
	d_4^{20}	d_4^{25}	n_D^{20}	n_D^{25}		
Ethanedithiol-1,2.						
S. Mathias [5]	1.1243	1.1185	1.5590	—	—	
W.P. Hall and E.E. Reid [3]	—	1.1192	—	1.5558	—41.2	
S. Mathias [6]	—	1.11926	—	1.55632	—	
This work	1.1240_5	1.1189_4	1.5588_2	1.5562_8	—49.10	>99.8
Propanedithiol-1,3.						
S. Mathias [5]	1.0783	—	1.5406	—	—	
W.P. Hall and E.E. Reid [3]	—	1.0775	—	1.5371	—79	
Yu.K.Yur'ev and I.S.Levi [7]	1.0772	—	1.5392	—	—	
S. Mathias [6]	—	1.07338	—	1.53798	—	
This work	1.0779_6	1.0731_3	1.5406_2	1.5384_0	—90.65	>99.8
Butanedithiol-1,4.						
W.P. Hall and E.E. Reid [3]	—	1.0395	—	1.5265	—53.9	
S. Mathias [6]	—	1.03870	—	1.52724	—	
This work	1.0429_9	1.0385_2	1.5294_0	1.5273_8	—52.55	>99.8
Pentanedithiol-1,5.						
W.P. Hall and E.E. Reid [3]	—	1.0158	—	1.5194	—72.5	
S. Mathias [6]	—	1.01117	—	1.51799	—	
This work	1.0159_6	1.0115_8	1.5204_3	1.5183_9	—68.50	>99.9

* The 20 × 4 mm thermometer sealed in glass was not free from strain and showed a hysteresis effect. The absolute values of the given melting points therefore cannot be relied upon to better than ± 0.1°C.

Combustion calorimetry

Apparatus and procedure. The calorimetric system used was that described by Bjellerup [9]. The volatile liquid combustion samples were sealed in thin soft-glass ampoules. A platinum baffle was placed on top of the crucible to prevent splashing upon ignition. In combustion experiments with the dithiols the bomb was charged with 10 ml of water (in calibration experiments and paraffin oil combustions 0.79 ml). The amount of sulphur was limited to 5—7 m.atoms per experiment. All weighings have been reduced to mass and the molecular weights have been computed from the 1957 table of atomic weights [10].

The bomb liquid was analyzed for nitric and nitrous acids. The (HNO_3 + HNO_2)-content was determined by reduction with Devardas alloy [11]. Nitrous acid was measured colorimetrically according to a method by Griess [12(p. 38)]. The amount of nitric acid formed in benzoic acid and paraffin oil combustions was determined by potentiometric titration against 0.02 N NaOH.

Materials. The benzoic acid used in the calibration experiments was National Bureau of Standards standard sample 39h [13].

The paraffin oil used as auxiliary material was sample USBM-P3a, described in Ref.[9(p. 1531)].

The dithiol samples were dried over calcium sulphate and thereafter distilled at room temperature under reduced pressure into a receiver containing twelve glass ampoules. Dry nitrogen was introduced slowly, thereby forcing the liquid samples into the ampoules, and great care was taken to exclude air and moisture. The ampoules were sealed immediately, and in no case did more than four days pass between ampoule filling and combustion experiment.

Combustions in which the substance did not burn properly have all been rejected. The butanedithiol was particularly difficult to burn appropriately, which is apparent from the final over-all standard deviation figure.

RESULTS

Unit of energy. Auxiliary quantities. The results are expressed in terms of the defined thermochemical calorie equal to 4.1840 abs. joules. All symbols used are those introduced by Hubbard, Scott and Waddington [14]. The $(\partial E/\partial P)_T$ values were calculated from the corresponding density data using the approximate relation $(\partial E/\partial P)_T = -T(\partial V/\partial T)_P$. The $-\Delta E_c^\circ/M$ values refer to the reaction represented by eqn. 1, in which all reactants and products are in their thermodynamic standard states at the temperature t_h (25.0°C):

$$C_nH_{2n+2}S_2(\text{liq}) + (3n+7)/2\ O_2(\text{g}) + (231-n)\ H_2O(\text{liq}) \rightarrow \rightarrow n\ CO_2(\text{g}) + 2\ H_2SO_4,\ 115\ H_2O\ (\text{liq}) \quad (1)$$

In calibration experiments the certified value for the heat of combustion for the benzoic acid under certificate conditions $-\Delta E_c/M = 6317.88 \pm 0.72$ cal.g^{-1} was used. The standard heats of combustion were, for paraffin oil USBM-P3a $-\Delta E_c^\circ/M(\text{Oil}) = 10984.7 \pm 1.1$ cal.g^{-1}, and for the fuse $-\Delta E_c^\circ/M(\text{Fuse}) = 3971 \pm 4$ cal.g^{-1}.

Calculation of results. The results of the combustion experiments were calculated by use of the following main equations,

$$\varepsilon(\text{Calor}) = \varepsilon^\circ(\text{Calor}) - c_p(H_2O) \cdot m^i(\text{Cont.}) \quad (2)$$

$$-\Delta E_{\text{I.B.P}} = [\varepsilon(\text{Calor}) + \varepsilon^i(\text{Cont.})] \cdot \Delta t \quad (3)$$

$$-\Delta E_c^\circ/M(\text{Comp}) = \frac{1}{m'} \{-\Delta E_{\text{I.B.P.}} - [\Delta E^f_{\text{decomp.}}\ (HNO_3 + HNO_2) -$$

Table 2. Heat of combustion measurements.

t_h = 25.0°C V(Bomb) = 0.2628 liter m(Pt) = 18.579—18.587 g.
t_i = 24.1°C V^i(soln) = 0.01002 liter m(glass) = 0.055—0.085 g.
P^i(gas) = 30.0 atm. V^i(gas) = 0.2522 liter $m''' = 0.0045$—0.0056 g.

Compound	m' g	m'' g	Δt deg	$\Delta E^f_{dec.}(HNO_3 + HNO_2)$ cal	ΔE_{corr} cal	$-E^\circ_c/M$ cal.g^{-1}
Ethanedithiol-1,2	0.322188	0.248054	0.88098	5.80	1.32	7060.97
M = 94.202	0.319014	0.248649	0.87807	7.26	1.38	7061.10
m^i(Cont.) = 39.28 g	0.337311	0.237454	0.87930	6.93	1.09	7062.44
ε^i(Cont.) = 12.69 cal.deg^{-1}	0.295644	0.263450	0.87770	6.45	1.75	7063.97
ε°(Calor) = 5734.50 ± 0.18 cal.deg^{-1}	0.319137	0.248768	0.87860	6.18	1.38	7064.87
	0.338180	0.240850	0.88654	6.86	1.05	7063.37
				$-\Delta E^\circ_c/M$ = 7062.79 ± 0.64 *		cal.g^{-1}
Propanedithiol-1,3	0.301102	0.245206	0.87737	6.38	2.02	7590.29
M = 108.229	0.307973	0.240751	0.87789	7.41	2.02	7588.17
m^i(Cont.) = 39.28 g	0.316662	0.234803	0.87769	6.19	2.02	7589.23
ε^i(Cont.) = 12.68 cal.deg^{-1}	0.327658	0.227094	0.87748	6.27	1.84	7589.10
ε°(Calor) = 5733.17 ± 0.25 cal.deg^{-1}	0.313254	0.236435	0.87692	6.97	2.02	7591.99
	0.302096	0.245005	0.87817	6.27	2.03	7589.57
	0.297100	0.247847	0.87704	6.61	2.21	7588.39
				$-\Delta E^\circ_c/M$ = 7589.53 ± 0.49 *		cal.g^{-1}
Butanedithiol-1,4	0.366068	0.186837	0.87742	7.87	1.87	7990.21
M = 122.256	0.351432	0.197223	0.87719	7.61	2.03	7993.30
m^i(Cont.) = 39.28 g	0.372327	0.182754	0.87816	5.81	1.78	7996.55
ε^i(Cont.) = 12.65 cal.deg^{-1}	0.358977	0.192181	0.87750	7.96	1.95	7989.73
ε°(Calor) = 5734.50 ± 0.18 cal.deg^{-1}	0.357105	0.194532	0.88030	7.63	1.97	7999.27
	0.339743	0.206967	0.87955	7.12	2.15	7998.81
	0.347161	0.201679	0.87912	7.84	2.08	7989.00
	0.365220	0.191138	0.88404	5.99	1.89	7989.38
	0.351902	0.198965	0.88060	7.15	2.03	7990.46
				$-\Delta E^\circ_c/M$ = 7992.97 ± 1.39 *		cal.g^{-1}
Pentanedithiol-1,5	0.328171	0.211536	0.89037	7.18	2.71	8316.58
M = 136.283	0.347819	0.190724	0.87878	6.83	2.44	8317.08
m^i(Cont.) = 39.29 g	0.317980	0.212987	0.87825	6.66	2.74	8316.91
ε^i(Cont.) = 12.67 cal.deg^{-1}	0.332074	0.203277	0.88037	6.47	2.61	8315.41
ε°(Calor) = 5733.17 ± 0.25 cal.deg^{-1}	0.343615	0.193937	0.87942	7.12	2.50	8317.74
	0.330527	0.204358	0.88005	6.94	2.63	8316.54
				$-\Delta E^\circ_c/M$ = 8316.71 ± 0.32 *		cal.g^{-1}

* The given uncertainties are the standard deviations of mean.

Table 3. Derived data at 25°C.

Compound	ΔE_c° kcal.mole^{-1}	ΔH_c° kcal.mole^{-1}	ΔH_f°(liq) kcal.mole^{-1}	ΔH_v kcal.mole^{-1}	ΔH_f°(gas.) kcal.mole^{-1}
	a)	*a*)	*a*)	*b*)	*a*)
Ethanedithiol-1,2.	—665.33 ± 0.22	—668.00 ± 0.22	—12.91 ± 0.26	10.68 ± 0.03[20]	—2.23 ± 0.26
Propanedithiol-1,3.	—821.41 ± 0.26	—824.37 ± 0.26	—18.90 ± 0.28	11.87 ± 0.03[20]	—7.03 ± 0.28
Butanedithiol-1,4.	—977.19 ± 0.40	—980.45 ± 0.40	—25.20 ± 0.42	13.22 ± 0.09[20] 13.12 ± 0.06[19]	—12.03 ± 0.44
Pentanedithiol-1,5.	—1133.43 ± 0.28	—1136.98 ± 0.28	—31.04 ± 0.30	14.17 ± 0.10[19]	—16.87 ± 0.36

a) The uncertainties in this column are equal to twice the final over-all standard deviation.
b) The uncertainties in this column are the final over-all standard deviations.

$$- m'' \cdot \Delta E_c^\circ/M(\text{Oil}) - m''' \cdot \Delta E_c^\circ/M(\text{Fuse})] - \Delta E_{corr}\} \quad (4)$$

where ΔE_{corr} denotes the sum of items 81—85, 87—91 and 93—94 of the Washburn reduction as given in Ref.[14]

Experimental results. The results of the combustion experiments are summarized in Table 2. The uncertainties given in the table are the standard deviations of the mean. The final over-all precision of the $-\Delta E_c^\circ/M$ mean values was estimated by the method of Bjellerup [15(p. 132)] with one modification to make it applicable to organo-sulphur compounds. The quantity q_5 in these calculations stands for the heat of decomposition of nitric and nitrous acid in the final bomb solution. The ratio s_5/q_5 has been estimated at 0.01.

Derived data. Table 3 gives in the first two columns the values of the standard energies, ΔE_c°, and the standard enthalpies, ΔH_c°, at 25°C calculated according to eqn. 5.

$$\Delta H_c^\circ = \Delta E_c^\circ + \Delta nRT \quad (5)$$

All ΔE_c° and ΔH_c° data refer to the combustion reaction represented by eqn. 1 with all reactants and products in their thermodynamic standard states.

Standard heats of formation, ΔH_f°(liq), at 25°C referring to the reaction represented by eqn. 6

$$n\ \text{C (c, graphite)} + (n+1)\ \text{H}_2\text{(g)} + 2\ \text{S (c, rhombic)} \rightarrow \text{C}_n\text{H}_{2n+2}\text{S}_2\text{(liq)} \quad (6)$$

were calculated by combining the ΔH_c°(liq) values with the standard heats of formation of gaseous carbon dioxide [16], -94.0539 kcal.mole^{-1} *, liquid water [16], -68.3174 kcal.mole^{-1} and sulphuric acid [17] [H_2SO_4, 115 H_2O(liq)], -212.24 ± 0.06 kcal.mole^{-1}.

Heats of vaporization at 25°C have been measured in this laboratory, using two different methods, one applicable in the vapour pressure range 100—1 mm Hg [18], the second in the range $1-10^{-3}$ mm Hg [19]. The results have been included in Table 3 together with the calculated heat of formation data for the compounds in the gaseous state.

DISCUSSION

From the results it is seen that the CH_2-increment in the standard heat of formation values for the gaseous state between consecutive homologues in the series $HS(CH_2)_nSH$, $n = 2-5$, is constant within the limits of error of the measurements, or -4.80, -5.00 and -4.84 kcal.

Further, McCullough has estimated the heats of formation of the compounds from the collected work on thiols, as carried out at the Thermodynamics Laboratory, Bartlesville. A comparison between the experimental and the estimated values is found below. Our experimental values have been recalculated to S_2(g) [1/4 S_8(rhombic) → S_2(g) $\Delta H_{298.16}^\circ = +30.84$ kcal] [22] and a correction has been applied for the difference in heat of formation values for

* This value is corrected to the present atomic weight of 12.011 for carbon.

sulphuric acid between our laboratories; ΔH_f° (H_2SO_4, 115 H_2O) = −212.17 (Bartlesville) and −212.24 (Lund) kcal.mole^{-1}.

ΔH_f°(g)	$n = 2$	3	4	5
Calculated	−32.82	−37.75	−42.68	−47.61
Found	−32.93	−37.73	−42.73	−47.57

It is thus conclusively shown, that the propanedithiol-1,3 falls well within the homologous series and that the experimentally determined values of the strain energy in the dithiolane and dithiane ring systems are not affected by intramolecular interactions between the α and ω thiol groups.

Acknowledgement is made to the donors of *The Petroleum Research Fund*, administered by the American Chemical Society, for partial support of this research.

The cooperation of Dr. J. McCullough, Thermodynamic Laboratory, Bartlesville Petroleum Research Center, Bureau of Mines, Bartlesville, Oklahoma, is gratefully acknowledged.

REFERENCES

1. Sunner, S. *Nature* **176** (1955) 217.
2. *Org. Syntheses* **30** (1950) 35.
3. Hall, W. P. and Reid, E. E. *J. Am. Chem. Soc.* **65** (1943) 1466.
4. Grogan, C. H., Rice, L. M. and Reid, E. E. *J. Org. Chem.* **20** (1955) 50.
5. Mathias, S. *Bol fac. filosof., ciênc. e letras*, Univ. São Paulo **14**, Quim. No. 1 (1942) 75.
6. Mathias, S. Univ. São Paulo, Brazil. *Private communication.*
7. Yur'ev, Yu. K. and Levi, I. S. *Doklady Akad. Nauk SSSR* **73** (1950) 953; *Chem. abstr.* **45** (1951) 2934b.
8. Smit, W. M. *Rec. trav. chim.* **75** (1956) 1309.
9. Bjellerup, L. *Acta Chem. Scand.* **13** (1959) 1511.
10. Wichers, E. *J. Am. Chem. Soc.* **80** (1958) 4121.
11. Sunner, S. and Lundin, B. *Acta Chem. Scand.* **7** (1953) 1112.
12. Sunner, S. *Studies in Combustion Calorimetry Applied to Organo-Sulphur Compounds (Diss)*, Univ. Lund 1949.
13. *Certificate for Standard Sample 39h, Benzoic Acid*, National Bureau of Standards, Washington, D. C. 1958.
14. Hubbard, W. N., Scott, D. W. and Waddington, G. *Standard States and Corrections for Combustions in a Bomb at Constant Volume.* Chapter 5 of Rossini, F. D. (Ed.) *Experimental Thermochemistry*, Interscience, New York 1956.
15. Bjellerup, L. *Acta Chem. Scand.* **15** (1961) 121.
16. *Selected Values of Chemical Thermodynamic Properties.* Circular of Natl. Bur. Standards 500, Washington, D. C. 1952.
17. *Unpublished measurements, cf.* Good, W. D., Lacina, J. L. and McCullough, J. P. *J. Am. Chem. Soc.* **82** (1960) 5589.
18. Wadsö, I. *Acta Chem. Scand.* **14** (1960) 566.
19. Morawetz, E. and Sunner, S. *To be pubslished.*
20. Wadsö, A.-M. and Wadsö, I. *To be published.*
21. McCullough, J. P. *Private communication.*
22. Evans, W. H. and Wagman, D. D. *J. Research Natl. Bur. Standards* **49** (1952) 141.

Received April 14, 1962.

ACTA CHEMICA SCANDINAVICA 16 (1962) 1870–1876

Heats of Combustion and Formation of Thiolane and of the Thiolenes

JAMES V. DAVIES* and STIG SUNNER

Thermochemistry Laboratory **, *University of Lund, Lund, Sweden*

The following standard heat of formation values are reported for the compounds in the liquid and gaseous states, at 25°C:

2-thiolene	12.76 and 21.78
3-thiolene	11.31 and 20.86
thiolane	−17.40 and −8.02 kcal.mole^{-1}, respectively.

It is possible that in the near future agreement may be reached on the use of a slightly different value for the heat of formation of sulphuric acid, $\Delta H_f^\circ(H_2SO_4, 115\ H_2O) = a$. In this case, the published values should be corrected by adding the quantity $(a + 212.24)$ kcal. mole^{-1}.

This investigation was undertaken as a result of a discussion back in 1953 between one of the authors (S.S.) and the late Dr. S. F. Birch of the B. P. Research Centre, Sunbury-on-Thames, who had succeeded in separating and purifying the two dihydrothiophenes (thiolenes) two years earlier [1]. The question arose whether the high reactivity of the 2-thiolene over that of its 3-isomer could be traced back, at least in part, to an appreciable difference in strain energy, reflected in a higher heat of formation value for the former isomer.

At the same time it was felt to be within the scope of the investigation to redetermine the heat of combustion of tetrahydrothiophene (thiolane), for which values have been reported by Sunner [2] in 1949 and by Hubbard, Katz and Waddington [3] in 1954. These values are not in agreement and the results of the reinvestigation is, as expected, in close agreement with that of Hubbard *et al.**

Reported values of the heat of combustion of thiophene are in close agreement [4,5] and a redetermination was therefore not considered necessary.

* Now at Department of Chemistry, University of Manchester, Manchester, England.

** Sponsored by *The Swedish Natural Science Research Council* and *The Swedish Technical Research Council.*

*** The heat of combustion value in Ref.[2] was determined on a sample of only 2.4 g which obviously must have been contaminated somewhere during the last operations.

EXPERIMENTAL

Synthesis and purification of compounds

A 450 g sample of *thiolane* was prepared by reaction of sodium sulphide with 1,4-dichlorobutane according to the method of Lawson, Easley and Wagner [6]. The crude material obtained was first distilled fairly quickly through a 40 cm Vigreaux column. It was subsequently refluxed for 1 day over calcium hydride from which it was then fractionally distilled through a 150 cm column packed with glass rings having an efficiency of 25 theoretical plates. Ten equal fractions were collected and each was analysed by V.P.C. (Pye Argon Chromatograph, dioctylphthalate column). The six middle fractions (b.p. 121.11—121.12°C at 760 mm Hg) were judged to be of equally high purity and were combined and then further dried over silica gel and finally over calcium sulphate. The sample used for combustion studies was distilled *in vacuo* from calcium sulphate. Part of the combustion sample was contaminated with 0.05 mole % thiophene and V.P.C. analysis of this material gave a chromatogram with an easily detectable thiophene peak. Absence of any similar impurity peaks in the chromatogram of the combustion sample established the purity of this sample at > 99.95 mole %. The densities and refractive indices at 20 and 25°C and the melting point of the combustion sample were measured and these properties, together with the boiling point and estimated purity, are listed in Table 1.

Samples of *2-thiolene* and *3-thiolene* were supplied by the B.P. Research Centre, Sunbury-on-Thames, Middlesex, England. Further samples were prepared as described by Birch and McAllan [1] by the reduction of thiophene with sodium in a medium of liquid ammonia. Three syntheses yielded 110 g of 2-thiolene and 150 g of 3-thiolene in fairly high purity, as indicated by analysis with the Pye chromatograph (dioctylphthalate column). Care had to be taken in handling these compounds in view of their unstable nature. This was particularly so with the 2-isomer which polymerizes rapidly when brought into contact with air. Consequently, whenever possible, the compounds were handled in an atmosphere of dry nitrogen and stored in a refrigerator at −20°C.

After drying over calcium sulphate for 2 days the 2-thiolene was further purified by careful fractional distillation through the 150 cm column mentioned above in an

Table 1. Comparison with earlier data of the physical properties of the samples prepared in the present investigation.

Compound and reference	Density g/ml		Refractive index		Melting point for zero impurity (°C)	Boiling point (°C)	Estimated purity mole %
	20°C	25°C	n_D^{20}	n_D^{25}			
Thiolane							
A.P.I. Research Project 44	0.99869	0.99379	1.50483	1.50217	—96.16	121.12 (760 mm)	
This work	0.9988 ± 0.0002	0.9939 ± 0.0002	1.5049 ± 0.0002	1.5022 ± 0.0002	—96.8 ± 1.0	121.11—121.12 (760 mm)	>99.95
2-Thiolene							
Birch and McAllan [4]	1.0361		1.5311		—108.7	112.0 (760 mm)	97.5
This work	1.0391 ± 0.0002	1.0340 ± 0.0002	1.5301 ± 0.0002	1.5276 ± 0.0002	—109.6 ± 1.0	64.8—65.0 (160 mm)	99.86
3-Thiolene							
Birch and McAllan [4]	1.0591		1.5306		—49.3	122.3 (760 mm)	98.5
This work	1.0589 ± 0.0002	1.0536 ± 0.0002	1.5298 ± 0.0002	1.5274 ± 0.0002	—50.1 ± 1.0	76.2—76.3 (185 mm)	>99.88

atmosphere of dry nitrogen at 160 mm Hg. Four equal fractions were collected and chromatographed. Fractions II and III (b.p. 64.8 – 65.0°C at 160 mm Hg) were selected. After drying over calcium sulphate in a nitrogen atmosphere for 2 days this material was finally distilled *in vacuo* from calcium sulphate to provide the sample used for combustion studies. The physical properties of this sample are given in Table 1. Chromatographic analysis indicated the presence of a small amount of thiophene in the sample. This was estimated at 0.15 ± 0.07 mole % by contaminating part of the sample with a further 0.50 mole % thiophene and chromatographing this mixture and the purest sample under identical conditions. From the different areas under the thiophene peaks in the two chromatograms the percentage of thiophene in the purest sample was estimated. A repeat of this procedure checked the accuracy of the estimation. The chromatograms indicated the absence of any other impurity.

The 3-thiolene was further purified by careful fractionation through the 150 cm column in an atmosphere of dry nitrogen at 80 mm Hg. The purest fractions were selected by gas chromatographic analysis (dioctylphthalate column) and these were re-distilled twice in an atmosphere of dry nitrogen through a 75 cm column packed with glass helices. The purest fraction from the final distillation (b.p. 76.2 – 76.3°C at 185 mm Hg) was selected by V.P.C. analysis and this was then dried for 4 days in a nitrogen atmosphere over calcium sulphate from which it was then distilled *in vacuo*. Combustion studies and measurements of physical properties were made on this distillate. The physical properties are to be found in Table 1. Analysis with the Pye chromatograph, carried out in the manner described above, indicated the presence of 0.07 ± 0.04 mole% of thiophene in this sample. This analysis also indicated that the sample contained < 0.05 mole% 2-thiolene, which was the only other impurity.

Heat of combustion measurements

Apparatus and procedure. The rotating-bomb calorimeter system used was that of Bjellerup [7] and the combustion procedure of Sunner and Lundin [8] was followed. Concerning further details reference is made to the preceding paper [9].

Materials. The benzoic acid used in the calibration experiments was National Bureau of Standards standard sample 39h [10]. The paraffin oil used as auxiliary material was sample USBM-P3a, described in Ref.[7] (p. 1531).

The compounds were sealed in thin glass ampoules wich were filled by distilling the combustion sample *in vacuo* into a receiver containing the ampoules and then admitting a small pressure of dry nitrogen, so causing the ampoules to fill. With the 2-thiolene, even though the ampoules were dried in stream of dry nitrogen, they became coated with a film of polymeric material. This was removed by carefully cleaning the ampoules with concentrated nitric acid and then washing them with distilled water and acetone. No such difficulty was encountered with the other two compounds.

Some experiments were unsuccessful because of formation of sulphur dioxide which could often be smelt in the bomb gases after the combustion. Sulphur dioxide formation was also accompanied by the total absence of nitrous acid in the bomb solution and experiments in which no nitrous acid was formed were rejected.

Small corrections were made for the formation of significant quantities of carbon in experiments 2 and 3 on 2-thiolene. The measured heats of combustion of 2-thiolene and 3-thiolene were corrected for the presence of thiophene in the combustion samples using the value for the heat of combustion of thiophene $\Delta H_c^\circ = -675.88$ kcal/mole, reported by Sunner [4]. No correction was made for the 2-thiolene content (< 0.05 mole%) of the 3-thiolene sample.

Units. Auxiliary quantities. Calculation of results. Heats of combustion and formation are given in thermochemical calories, defined by 1 cal = 4.1840 abs. joules and refer to the isothermal process at 25°C and to the true mass. The molecular weights were computed from the 1957 table of atomic weights [11]. The $-\Delta E_c^\circ/M$ values refer to reaction (1) in which all reactants and products are in their thermodynamic standard states:

$$C_nH_mS(\text{liq}) + (n + \frac{m}{4} + \frac{3}{2})O_2(g) + (116 - \frac{m}{2})H_2O(\text{liq}) \rightarrow$$
$$\rightarrow n\,CO_2(g) + H_2SO_4, 115\,H_2O(\text{liq}) \qquad (1)$$

Table 2. Results of combustion experiments.

t_h = 25.0°C
t_i = 24.1°C
P^i(gas.) = 30.0 atm.
V(Bomb) = 0.2628 liter
V^i(soln.) = 0.01002 liter
V^i(gas.) = 0.2522 liter

ε°(Calor) = 5732.39 ± 0.42 cal deg^{-1}
ε^i(Cont.) = 12.61 − 12.62 cal deg^{-1}
m(Pt) = 18.585 − 18.621 g
m''' = 0.003548 − 0.004808 g
m(glass) = 0.0491 − 0.1061 g

m' g	m'' g	Δt deg	$\Delta E^f_{dec.}(HNO_3 + HNO_2)$ cal	$\Delta E_{corr.}$ cal	$-\Delta E^\circ_c/M$ cal g^{-1}
2-Thiolene					
0.456391	0.100425	0.88075	4.05	2.87	8542.92
0.431597	0.116093	0.87363	3.91	3.03	8540.63
0.432569	0.118540	0.88009	5.29	3.03	8541.62
0.476043	0.085173	0.88100	7.26	2.74	8541.43
0.438338	0.114194	0.88086	7.89	2.99	8545.12
				Mean	8542.34
			Standard deviation of mean		± 0.79
3-Thiolene					
0.480960	0.079493	0.87667	5.58	2.68	8528.69
0.475387	0.084467	0.87783	8.70	2.72	8524.95
0.457623	0.098802	0.87868	7.28	2.85	8527.28
0.476165	0.084004	0.87779	7.22	2.71	8527.86
0.483864	0.078562	0.87906	8.36	2.66	8527.60
0.460961	0.095843	0.87715	3.72	2.82	8523.45
0.476793	0.084023	0.87785	4.93	2.71	8523.89
0.468057	0.089835	0.87723	8.74	2.77	8526.91
0.477281	0.083287	0.87700	3.68	2.70	8522.34
				Mean	8525.89
			Standard deviation of mean		± 0.73
Thiolane					
0.452198	0.092219	0.87825	8.93	2.57	8775.85
0.425799	0.113271	0.87795	7.01	2.76	8778.74
0.455119	0.089705	0.87660	1.44	2.55	8775.99
0.467342	0.080231	0.87810	6.19	2.46	8779.39
0.433748	0.106491	0.87768	9.28	2.71	8777.08
				Mean	8777.41
			Standard deviation of mean		± 0.72

In calibration experiments the certified value for the heat of combustion of the benzoic acid under certificate conditions, $-\Delta E_c/M$ = 6317.88 ± 0.72 cal.g^{-1}, was used. The standard heats of combustion were, for paraffin oil USBM-P3a and for the fuse $-\Delta E^\circ_c/M$ = 10984.1 ± 1.8 and 3971 ± 4 cal.g^{-1}, respectively.

The results of the combustion experiments were calculated according to Hubbard, Scott and Waddington [12] and Bjellerup, *cf.* Ref.[9]

Experimental results. The results of the combustion experiments are summarized in Table 2. The symbols have the meanings given in Refs.[8,12] The uncertainties given are the standard deviations of the mean.

Derived data. Table 3 gives the values of the standard energies, ΔE°_c, and the standard enthalpies, ΔH°_c, at 25°C. All values refer to the combustion reaction represented by eqn. (1).

Table 3. Derived data at 25°C.[a]

Compound	ΔE_c° kcal·mole^{-1}	ΔH_c° kcal·mole^{-1}	ΔH_f°(liq) kcal·mole^{-1}	ΔH_v kcal·mole^{-1}	ΔH_f°(g) kcal·mole^{-1}
2-Thiolene	735.99 ± 0.25	737.85 ± 0.25[b]	12.76 ± 0.28	9.02 ± 0.10	21.78 ± 0.30
3-Thiolene	734.57 ± 0.25	736.40 ± 0.25[b]	11.31 ± 0.28	9.55 ± 0.06	20.86 ± 0.28
Thiolane	773.94 ± 0.25	776.01 ± 0.25	−17.40 ± 0.28[c]	9.38 ± 0.06[c]	−8.02 ± 0.28[c]

a) All uncertainties are twice the final over-all standard deviation.

b) After correction for thiophene content.

c) Ref.[3] gives the value = −17.31 ± 0.35 kcal.mole^{-1}, recalculated to the atomic weight of carbon 12.011 and the heat of formation value for sulfuric acid, H_2SO_4, 115 H_2O, ΔH_f° = −212.24 kcal.mole^{-1} used in this investigation, it becomes = −17.37 kcal.mole^{-1}. The heat of vaporization at 25°C given in Ref.[3] is 9.23 kcal.mole^{-1}, and thus ΔH_f°(g) becomes −8.14 ± 0.35 kcal.mole^{-1}.

The final over-all precision of the mean values was estimated by the method of Bjellerup [13]. They include allowances for the error in the measurements of the thiophene content of the samples. Standard heats of formation, ΔH_f°(liq), at 25°C were calculated using the standard heats of formation of gaseous carbon dioxide [14], liquid water [14] and sulphuric acid [15] [H_2SO_4, 115 H_2O] −94.0539, −68.3174 and −212.24 ± 0.06 kcal.mole^{-1}, respectively.

The heats of vaporization at 25°C were measured in this laboratory [16] using the apparatus described by Wadsö [17]. They have been included in Table 3 together with heat of formation data for the compounds in the gaseous state.

DISCUSSION

The heat of formation values for the two dithiolenes are only 0.9 kcal.mole^{-1} apart. The 2-isomer has the highest energy, although it should be stabilized due to conjugation between the C=C double bond and the sulphur atom. Unfortunately, no thermochemical data are available for the estimation of the resonance energy of the C=C—S moiety. However, vinyl ethyl ether

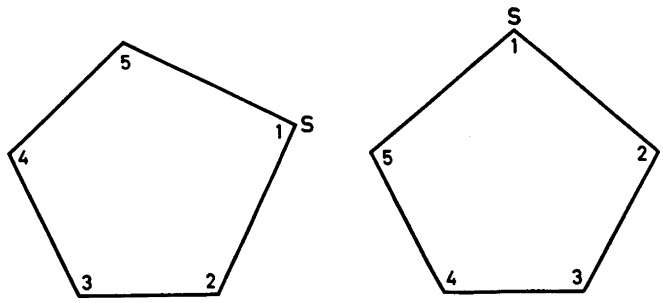

Fig. 1. The ring structure of

a) 2-thiolene (angle 1 equals 93°, 2 = 3 equal 115°, 4 = 5 equal 108—109°) and
b) 3-thiolene (angle 1 equals 98°, 2 = 5 equal 104°, 3 = 4 equal 117°).

and divinyl ether both show a resonance energy of *ca.* 3.5 kcal.mole^{-1} (Ref.[18, p. 85]) and the corresponding figure for the sulphur analogues should be less than that. Thus, the 2-thiolene seems to have a strain energy of about 3 to 4 kcal in excess of that of 3-thiolene.

The calculated heat of hydrogenation of 3-thiolene is $\Delta H_h = -28.9$ kcal·mole^{-1} which, within the limits of error, is the same as the heat of hydrogenation of *cis*-2-butene, -28.6 kcal.mole^{-1}. The strain energy of this isomer is therefore about the same as it is in thiolane. Using the revised value for the heat of formation of this compound its strain energy is estimated at 1.5—2 kcal.mole^{-1} according to the procedure described in Ref.[2] Thus, the strain energy of 3-thiolene is *ca.* 2 kcal.mole^{-1} whereas that of the 2-isomer *minus* its resonance energy is *ca.* 3 kcal.mole^{-1}.

A structural analysis is also in qualitative agreement with the above results. Taking reasonable values for the lengths of the various bonds in the two isomers [19] and assuming a coplanar ring structure, models of the two isomers can be constructed (Fig. 1) in which the angle strain is approximately minimized when compared with reasonable values of the bond angles in open chain molecules. Assuming normal bond angle values of 120° for C=C—X, 105° for C—S—C and 109.5° for C—C—X, X=C or S, it is seen that in order to obtain a ring the angles have to be compressed altogether by 24°. In 3-thiolene the distortions can be rather evenly distributed between the five ring angles, whereas in the 2-isomer the C=C—X and particularly the C—S—C angles have to take the whole angle compression. A more equal distribution leads to an expansion of the two C—C—X angles towards 109.5° and a considerable increase in the sum of the squares of the angle distortion, which is roughly proportional to the angle strain energy. The indication is that the angle strain in the 2-thiolene should be *ca.* 1.7 times that in the 3-isomer. In addition, the 2-isomer possesses two adjacent methylene groups in the eclipsed position which should increase its strain by at least 1 kcal.mole^{-1}.

It does not seem likely, that the rather small ring strain in 2-thiolene could bring about the high reactivity of this isomer. It is undoubtedly more easily explained as a result of the presence of the C=C—S vinyl system.

Acknowledgements. The authors thank Mr. Lennart Jönsson for assistance with the synthesis of the dihydrothiophenes and the B.P. Research Centre, Sunbury-on-Thames, Middlesex, England, for the gift of samples of the dihydrothiophenes. One of us (J.V.D.) thanks the University of Manchester and the Scandinavian Council for Applied Research through the Growing Points Programme, for financial support.

REFERENCES

1. Birch, S. F. and McAllan, D. T. *J. Chem. Soc.* **1951** 2256.
2. Sunner, S. *Studies in Combustion Calorimetry Applied to Organo-Sulphur Compounds* (Diss.), Univ. Lund 1949.
3. Hubbard, W. N., Katz, C. and Waddington, G. *J. Phys. Chem.* **58** (1954) 142.
4. Sunner, S. *Acta Chem. Scand.* **9** (1955) 847.
5. Hubbard, W. N., Scott, D. W., Frow, F. R. and Waddington, G. *J. Am. Chem. Soc.* **77** (1955) 5855.
6. Lawson, J. K., Easley, W. K. and Wagner, W. S. *Org. Syntheses* **36**, 89.
7. Bjellerup, L. *Acta Chem. Scand.* **13** (1959) 1511.

8. Sunner, S. and Lundin, B. *Acta Chem. Scand.* **7** (1953) 1112.
9. Månsson, M. and Sunner, S. *Acta Chem. Scand.* **16** (1962) 1863
10. *Certificate for Standard Sample 39h, Benzoic Acid*, National Bureau of Standards, Washington, D.C., 1958.
11. Wichers, E. *J. Am. Chem. Soc.* **80** (1958) 4121.
12. Hubbard, W. N., Scott, D. W. and Waddington, G. Chapter 5 of Rossini, F. D. (Ed.) *Experimental Thermochemistry*, Interscience, New York 1956.
13. Bjellerup, L. *Acta Chem. Scand.* **15** (1961) 121.
14. *Selected Values of Chemical Thermodynamic Properties.* Circular of Natl. Bur. Standards 500, Washington, D.C. 1952.
15. *Unpublished measurements.* Cf. Good, W. D., Lacina, J. L. and McCullough, J. P. *J. Am. Chem. Soc.* **82** (1960) 5589.
16. Wadsö, A. M. and Wadsö, I. *To be published.*
17. Wadsö, I. *Acta Chem. Scand.* **14** (1960) 566.
18. Wheland, G. W. *Resonance in Organic Chemistry*, Wiley & Sons, Inc., New York 1955.
19. *Tables of Interatomic Distances* . . . Spec. Publ. No. 11 The Chemical Society, London 1958.

Received April 14, 1962.

ACTA CHEMICA SCANDINAVICA 16 (1962) 1877–1881

The Conjugate Addition of *tert*-Butylmagnesium Chloride to 3,6-Disubstituted Pyridazines

INGOLF CROSSLAND

Organisk-kemisk Laboratorium, Polyteknisk Læreanstalt, Copenhagen, Denmark

The addition of *tert*-butylmagnesium chloride to 3,6-dichloropyridazine and 3,6-dimethoxypyridazine was shown to involve a 1,4-addition of the Grignard reagent to yield the corresponding 4-*tert*-butyl-3,6-disubstituted dihydropyridazine; apparently no dehydrogenated products were formed. The hydrolysis of the products was investigated.

In an attempt to synthesize alkylated pyridazine derivatives the reaction of 3,6-dichloro- and 3,6-dimethoxypyridazine with *tert*-butylmagnesium chloride was investigated.

The substitution of alkyl groups for halogens in the series of nitrogen heterocycles has been reported several times in the literature. The action of Grignard reagents on 2,3-dichloroquinoxaline [1], 1-chloro-4-phenylphthalazine and 1,4-dichlorophthalazine [2], cyanuric bromide [3] and 2-bromoquinoline [4] in all cases described leads to compounds in which the halogen is replaced by the alkyl group of the reagent. On the other hand, also conjugate addition has been encountered in many cases, for instance in the pyridine series [5,6]. The conjugate addition of butylmagnesium bromide to unsubstituted pyridazine has been reported [7], although in this case only the dehydrogenated 4-alkylated compound was obtained, *cf.* below.

RESULTS AND DISCUSSION

The reactions investigated are illustrated by the chart. The only compounds formed were those derived from 1,4-additions of the Grignard reagent to the C=C–C=N system (reaction I → III and II → IV).

The position of the *tert*-butyl group on the pyridazine nucleus follows from the products obtained by the hydrolysis of IV. The formation of *tert*-butylsuccinic acid indicates that the 4-position was the point of attack of the nucleophilic alkyl group of the Grignard reagent. Although the analytical data of the unstable compound III are rather erratic, its structure is evidenced by its facile transformation into IV.

Cautious hydrolysis of IV affords VI in good yield. The elementary analysis indicates the loss of one methoxy group, presumably the one which is not subject to steric hindrance by the *tert*-butyl group. The hydrolysis of III follows a similar reaction path. More energetic hydrolysis of the dimethoxy compound

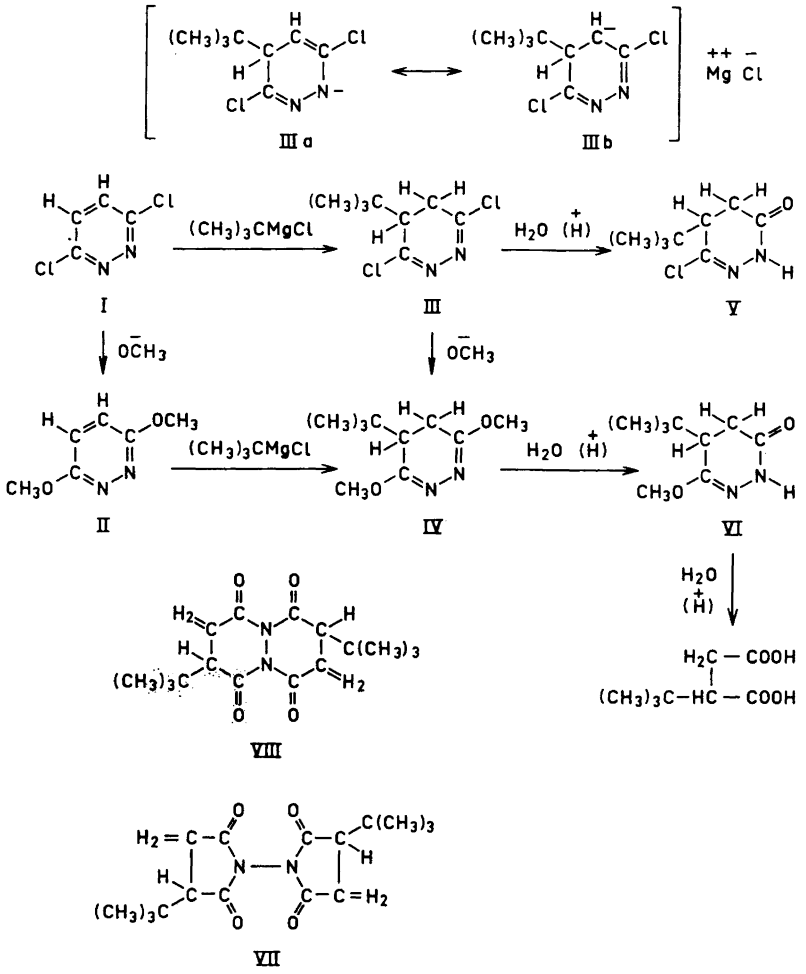

in some cases gives rise to the formation of a small amount of a compound, insoluble in both aqueous base and acid, besides the *tert*-butylsuccinic acid expected. On account of the empirical formula $(C_8H_{12}N_2O_2)_n$ the compound may be formulated as VII or VIII (including many isomers), *cf.* the corresponding compounds in the succinic acid series [8].

A characteristic and unexpected feature of the dihydro compounds III and IV is their resistance towards aromatization, which is in contrast to the readily occurring dehydrogenation encountered in, *e.g.*, the pyridine series. This may be illustrated by the oxidation of the compounds formed by the 1,4-addition of Grignard reagents to the corresponding pyridine derivatives [5] and by the catalytic dehydrogenation of 3,6-dimethyl-4,5-dihydropyridazine [9]. Whereas, in this laboratory, 3,6-dimethyl-4,5-dihydropyridazine has been readily dehydrogenated by the last mentioned method [9], 4-*tert*-butyl-3,6-dimethoxy-4,5-

dihydropyridazine (IV) failed to give the expected 4-*tert*-butyl-3,6-dimethoxypyridazine. Instead, IV was recovered unchanged. Preliminary investigations have shown that oxidizing agents such as bromine or acetyl peroxide did not bring about dehydrogenation of the dihydro compounds. The action of strong bases on any of the tautomeric forms of the dichloro compound III might be expected to afford dehydrohalogenated compounds. There is no supporting evidence that any reaction of this type has taken place. Even the Grignard reagent, present in excess during the synthesis of the dichloro compound III, does not effect elimination of hydrogen chloride. One could suggest that this fact is due to the partial negative charge of the magnesium chloride complex (IIIa ⟷ IIIb; also other structures may contribute to the resonance hybride) impeding the elimination of a proton. Apparently, this also applies to the reaction sequence III → IV, the action of methoxide ions resulting in substitution rather than elimination. The only evidence of the acidic properties of the dihydro compounds, as implicitely postulated by the formulation of the intermediate as IIIa and IIIb, is the heat of neutralization observed when the dichlorocompound III is added to a Grignard reagent. From this reaction mixture compound III may be regenerated in high yield by hydrolysis.

The reaction between the disubstituted pyridazines (I and III) and *tert*-butylmagnesium chloride is distinctly exothermic and takes place readily at the reflux temperature of ether. The exothermic nature of the reaction coupled with the characteristic resistance towards dehydrogenation is in accordance with the statement of Gilman [6] regarding the addition of allylmagnesium bromide to aza-aromatic heterocycles: "All the more reactive heterocycles gave the product in the dihydro form, whereas the less reactive heterocycles yielded the product in the oxidized form".

All attempts to prepare dihydro compounds corresponding to III from 3,6-dichloropyridazine and other Grignard reagents such as, *e.g.*, methylmagnesium iodide failed: When the ether extracts containing the reaction products were concentrated *in vacuo*, spontaneous decomposition took place with the evolution of hydrogen chloride.

The compounds formed by the reactions I → III and II → IV are suggested to be best formulated by the tautomers III and IV, respectively. Alder and Niklas [10] have investigated the analogous tautomers of the 3,6-diphenyldihydropyridazines, and suggested that in this case the 4,5-dihydro tautomer is the product obtained by saponification of the corresponding N,N′-di-(alkoxycarbonyl) compound.

Evidence as for the structure of compound IV may be gained from its NMR spectrum *. The spectrum of the pure liquid reveals two peaks (at δ 0.87 ppm and 3.70 ppm, attributed to the hydrogens of the *tert*-butyl group and of the two methoxy groups, respectively) and a complex group of peaks between δ 2.1 and 2.7 ppm, which may be attributed to the configuration CH—CH_2 of the ring; any formulation involving N—H bonds would not be expected to give peaks at the interval indicated.

* Spectra were taken in a Varian A-60 spectrometer at 60 Mc/sec. using tetramethylsilane as an internal zero of reference. The author wishes to thank professor Børge Bak for helping interpret the spectra.

When trifluoroacetic acid was used as a solvent the spectrum was changed only slightly with all the peaks shifted (0.2—0.5 ppm) towards lower fields. The methoxy peak appeared split into a doublet as to be expected if one proton is attached to IV in the acid medium.

The hydrogen ratio determined by the intergral curve is 9.0:6.2:2.9 as compared to the theoretical values 9:6:3.

EXPERIMENTAL

(All melting points are uncorrected).

4-tert-Butyl-3,6-dichloro-4,5-dihydropyridazine (III) (or tautomers). To a stirred solution of *tert*-butylmagnesium chloride, prepared from 12.5 g (0.51 mole) of magnesium and 50 g (0.54 mole) of *tert*-butyl chloride in 200 ml of ether (duration of addition, 2 h. *cf.* Organic Syntheses [11]), 50 g of 3,6-dichloropyridazine (I; prepared according to Mizzoni and Spoerri [12]) dissolved in 200 ml of ether was slowly added.

A considerable amount of heat was liberated during the reaction as indicated by the lively reflux of the ether. The solution aquired a deep, reddish brown colour. The addition of the 3,6-dichloropyridazine solution was discontinued when further addition did not result in any reflux of the ether, indicating that all the Grignard reagent had been consumed. This required 41.4 g (0.278 mole) of dichloropyridazine. After refluxing the solution for an additional 15 min, the pyridazine-magnesium chloride complex was decomposed by adding *ca.* 60 ml of a 20% aqueous ammonium chloride solution as fast as the reflux condenser would permit. Efficient stirring should be maintained, particularly during the addition of the last few ml of the ammonium chloride solution, since at this stage a slurry of salts precipitated. The addition of ammonium chloride solution was discontinued as soon as the ether solution became clear. The ether solution was separated by decantation. The salts were washed thoroughly with ether by decantation and the combined extracts immediately distilled, the bulk of the ether being removed at atmospheric pressure and the remaining ether at reduced pressure. The residue was distilled through a 20 cm Vigreux column 84—89°/1.5 mm. A small forerun contained some unreacted 3,6-dichloropyridazine. The yield of the colourless oil was 39 g (83 % based on 3,6-dichloropyridazine). A sample was redistilled for analysis, b.p. 80°/1.0 mm; (Found: C 47.40; H 6.16; Cl 31.50; N 13.62. Calc. for $C_8H_{12}Cl_2N_2$ (207): C 46.40; H 5.85; Cl 34.25; N 13.52). The discrepancy may partly be due to the instability of the compound, which was stored at −78° before analysis. It decomposed with the evolution of hydrogen chloride into a black tar after 24 h at room temperature. Decomposition also occurred at 0°, however, at a lower rate, presumably also because of the semi-crystalline character at the lower temperature. Repeated attempts to recrystallyze the compound were unsuccessful. The compound was soluble in petroleum ether and diethyl ether, but insoluble in water and hydrochloric acid. The crystals melted below 41°.

3,6-Dimethoxy-4-tert-butyl-4,5-dihydropyridazine (or tautomers) (IV). The preparation from dimethoxypyridazine (prepared according to Druey *et al.* [13]) was quite similar to that of the corresponding dichloro compound, only the low solubility of the 3,6-dimethoxypyridazine in ether rendered the addition of the compound in this solvent impractible; it was therefore simply added portionwise without solvent. From 7.5 g of magnesium, 30 g of *tert*-butyl chloride and 20 g of 3,6-dimethoxypyridazine, 24 g (85 %) of a colourless oil was obtained (b.p. 77°/0.5 mm, $n_D^{20} = 1.4792$). A sample was redistilled for analysis: (Found: C 60.30; H 9.20; N 16.33. Calc. for $C_{10}H_{18}N_2O_2$ (198) (IV): C 60.55; H 9.18; N 14.14) Repeated synthesis and fractionation gave a product showing the following values: C 60.55; H 9.07; N 16.24. Gas chromatographic analysis indicated the presence of a few percent of the dimethoxypyridazine, but this result cannot account for the high N-values.

The same compound (IV) may also be prepared as follows: To a solution of sodium methoxide prepared from 7.7 g (0.33 mole) of sodium and 150 ml of methanol was added slowly 25 g (0.121 mole) of 3,6-dichloro-4-*tert*-butyl-1,4-dihydropyridazine (III). The reaction was exothermic and sodium chloride precipitated. The solution was kept at 0° overnight, the sodium chloride (12.7 g 0.22 mole) filtered off and washed with methanol and the combined filtrates concentrated. Ether and water were added and the solution neu-

tralized with acetic acid. The ether was separated and the aqueous phase extracted with ether. The combined extracts were concentrated and the residue distilled to yield a slightly yellow oil, the infra-red spectrum of which was identical with that of IV as prepared above. Yield 15.9 g (66 %; b.p. *ca.* 70°/0.3 mm).

Products of hydrolysis. 5-tert-Butyl-6-chloro-2,3,4,5-tetrahydro-3-oxopyridazine (or isomer; V). 10 g of the dichloro compound (III) was added to a mixture of 25 ml of N hydrochloric acid, 25 ml of ethanol and 50 ml of water and heated to reflux, the yellow solution turning green. The solution was immediately cooled in ice and an oil separated which subsequently crystallized to yield 4.9 g of greenish crystals, m.p. 108—129°. Three crystallizations from ligroin (b.p. 80—110°) yielded colourless leaflets, m.p. 140°—141°. (Found: C 51.00; H 7.09; Cl 18.90; N 14.11. Calc. for $C_8H_{13}ClN_2O$ (188.5) (V): C 50.95; H 6.90; Cl 18.83; N 14.85).

5-tert-Butyl-6-methoxy-2,3,4,5-tetrahydro-3-oxopyridazine (or isomer; VI). 10 g of the dimethoxy compound (IV) were dissolved in 20 ml of 4 N hydrochloric acid at 0° and left at *ca.* 20° for four days. The white, crystalline mass was filtered, washed with water and dried to yield 7.95 g. One crystallization from ligroin (b.p. 110—140°) gave 6.7 g (72 %) of white crystals, m.p. 150—152°. A sample was crystallized twice from toluene, m.p. 151.5°—152.5°. Found: C 58.70; H 8.70; N 15.46. Calc. for $C_9H_{16}N_2O_2$ (184) (VI): C 58.63; H 8.82; N 15.20).

tert-*Butylsuccinic acid and anhydride.* 10 g of the dimethoxy compound (IV) dissolved in 150 ml of *ca.* 6 N hydrochloric acid were refluxed for 20 h, extracted 5 times with methylene chloride and the combined extracts concentrated *in vacuo* to yield 5.8 g of a viscous oil. Trituration with petroleum ether afforded 4.9 g of practically white crystals, m.p. 117—127°. A sample was crystallized three times from water and once from a mixture of toluene and ligroin (b.p. 110—140°) (6:4), m.p. 127—128.5°. (Authentic *tert*-butylsuccinic acid [14] was kindly supplied by Dr. Munch-Petersen; m.p. 128—130°, mixed m.p. 128—129.5°, *cf.* 132° (Wideqvist [15]).

tert-Butylsuccinic acid was refluxed for 10 h in excess of acetic anhydride, the acetic acid and reagent were removed *in vacuo* leaving an oil, which crystallized spontaneously. By three recrystallizations from ligroin, white crystals were obtained, m.p. 41.5—42°, (Found: C 61.40; H 7.56. Calc. for $C_8H_{12}O_3$: C 61.50; H 7.75).

Hydrolysis of the dimethoxy compound (IV) in concentrated hydrochloric acid. Compound IV (2 g) was dissolved in 4 ml of concentrated hydrochloric acid and kept at room temperature for 20 h, then at 60° for 4 h and finally refluxed for 4 h. A little water was added to ensure complete dissolution of the hydrazine hydrochloride formed. A white precipitate was filtered off and recrystallized from ethanol, the yield amounting to 115 mg of white crystals, m.p. 173—176°. An analytical specimen was recrystallized from ligroin-toluene (1:1), m.p. 176°—176.5°. (Found: C 62.60 and 62.30; H 7.95 and 7.71; N 9.20. Calc. for $C_{16}H_{24}N_2O_4$ (308) (*cf.* formula VII and VIII): C 62.31; H 7.86; N 9.08).

Analyses are by Mr. Preben Hansen, Microanalytical Division, The Chemical Laboratory, The University of Copenhagen.

REFERENCES

1. Ogg, R. A. and Bergstrom, F. W. *J. Am. Chem. Soc.* **53** (1931) 1846.
2. Mustafa, A., Harhash, A. H. and Saleh, A. A. S. *J. Am. Chem. Soc.* **82** (1960) 2735.
3. v. Meyer, E. and Näbe, F. *J. prakt. Chem.* [2] **82** (1910) 521.
4. Gilman, H., Eisch, J. and Soddy, T. S. *J. Am. Chem. Soc.* **81** (1959) 4000.
5. Lukes, R. and Kuthan, J. *Collection Czechoslov. Chem. Communs.* **26** (1961) 1422.
6. Gilman, H., Eisch, J. and Soddy, T. S. *J. Am. Chem. Soc.* **79** (1957) 1245.
7. Letsinger, R. L. and Lasco, R. *J. Org. Chem.* **21** (1956) 812.
8. Feuer, H., Bachman, G. B. and White, E. H. *J. Am. Chem. Soc.* **73** (1951) 4716.
9. Overberger, C. G., Byrd, N. R. and Mesbrobian, R. B. *J. Am. Chem. Soc.* **78** (1956) 1961.
10. Alder, K. and Niklas, H. *Ann.* **585** (1954) 81.
11. Puntambeker, S. V. and Zoellner, E. A. *Org. Syntheses*, Coll. vol. I, 2nd Ed. (1944) p. 524.
12. Mizzoni, R. H. and Spoerri, P. E. *J. Am. Chem. Soc.* **73** (1951) 1873.
13. Druey, J., Meier, K. and Eichenberger, K. *Helv. Chim. Acta* **37** (1954) 121.
14. Andersen, V. K. and Munch-Petersen, J. *Acta Chem. Scand.* **16** (1962) 947.
15. Wideqvist, S. *Arkiv Kemi* **2** (1950) 321.

Received April 23, 1962.

ACTA CHEMICA SCANDINAVICA 16 (1962) 1882–1889

The Crystal Structure of Benzenediazonium Tribromide

O. ANDRESEN and CHR. RØMMING

Universitetets Kjemiske Institutt, Blindern-Oslo, Norway

The crystal structure of benzenediazonium tribromide, $C_6H_5N_2Br_3$, has been determined by X-ray methods. The compound crystallizes in the monoclinic system with space group $C2/c$. The tribromide ions are situated in centers of symmetry and the benzenediazonium ions on two-fold axes. The Br—Br bond length is 2.543 Å; the N—N and N—C bond lengths in the diazonium ion are 1.11 and 1.41 Å, respectively.

Aryldiazonium trihalides were first prepared by Griess [1,2] who assumed their constitution to be analogous to that of tetraethylammonium periodide. Chattaway [3], on the other hand, preferred to formulate these compounds as $Ar{\cdot}NHal{\cdot}NHal_2$ since they may be prepared by letting halogen react directly with arylhydrazine. From the similarity between diazonium and alkali perhalides Hantzsch [4] and Forster [5] inferred, however, that the diazonium perhalides are true diazonium salts. Aroney and Le Fèvre [6] carried out an infrared spectroscopic investigation of several aryldiazonium tribromides, all of which gave a strong absorption band in the frequency range 2240—2250 cm^{-1}. An absorption band in this region is characteristic of the $Ar{\cdot}N_2^+$-group, and they therefore concluded that the compounds consist of aryldiazonium and tribromide ions. The structure of neither of these types of ions has been determined with great accuracy, and it was decided to investigate the structure of crystalline benzenediazonium tribromide by X-ray methods.

EXPERIMENTAL

To a freshly prepared aqueous solution of benzenediazonium chloride was added the solution of bromine in a potassium bromide solution under continuous stirring and ice cooling. The brown oil formed was separated and allowed to loose bromine in a dry air stream at room temperature, and after a few days single crystals of benzenediazonium tribromide in the form of orange-yellow plates had been formed.

The compound decomposes at 63—64°C, but is stable in dry air at room temperature. Because of their sensitiveness towards moisture the crystals were kept in capillary tubes during the X-ray exposure. The intensity data were obtained from integrated Weissenberg films taken at −20°C using filtered CuK-radiation (λ = 1.542 Å), the crystals used in the X-ray work had cross sections of 0.1 × 0.1 mm^2. The intensities were measured

photometrically except for the weakest reflections, the intensities of which were estimated visually. The numbers of non-equivalent reflections observed were 56 in the (*hk*0)-zone, 92 in the (0*kl*)-zone and 39 in the (*h*0*l*)-zone, the maximum numbers obtainable with Cu*Ka*-radiation are 65, 101 and 46, respectively. Most of the calculations carried out during the structure determination were performed on a Ferranti "Mercury" computer, the two dimensional least squares refinement program was that set up by Curtis [7]. Atomic form factors given as an analytical approximation by Forsyth and Wells [8] were used in these calculations.

CRYSTAL DATA

Oscillation and Weissenberg photographs show that the crystals are monoclinic with the cell constants:

$a = 6.73$ Å, $b = 14.10$ Å, $c = 11.00$ Å, $\beta = 106.8°$.

With *four* formula units per unit cell the calculated density is 2.31 g.cm^{-3}. Reflections are present only when $h + k = 2n$ and the condition for the presence of reflections in the (*h*0*l*)-zone is $l = 2n$. The space group is therefore either *Cc* or *C*2/*c*.

STRUCTURE DETERMINATION

The space group *Cc* contains no centres of symmetry and requires one molecular unit in each of the four-fold general positions. The space group *C*2/*c*, on the other hand, is centrosymmetric with eight-fold general positions and requires symmetry elements to be present both in the diazonium and in the tribromide ions. As a working hypothesis the latter space group was first assumed to be the correct one, and in the course of the structure determination the correctness of this assumption was actually confirmed. The positions of the bromine atoms could be derived from Patterson projections along *b* and *c*. Fourier maps based on the observed structure factors and with signs calculated from these bromine parameters were worked out, and from these maps approximate positions of the light atoms could be deduced. Successive Fourier refinements in the three projections were carried out in the usual way until no further changes of signs occurred. The coordinates were then submitted to further refinements using the method of least squares, alternatingly treating the three data sets so that at any time the best values of the parameters for the unresolved atoms could be used. The *R*-values thus finally arrived at were $R_{0kl} = 8.0$ %, $R_{hk0} = 7.3$ %, $R_{h0l} = 7.3$ %. The tribromide group was found to be centrosymmetric, the central bromine atom coinciding

Table 1. Atomic coordinates, fractions of cell edges.

	x	*y*	*z*
Br_1	0	0	0
Br_2	0.0049	0.1775	0.0418
N_1	0	0.762	0.250
N_2	0	0.683	0.250
C_1	0	0.583	0.250
C_2	0.106	0.543	0.174
C_3	0.104	0.440	0.175
C_4	0	0.395	0.250

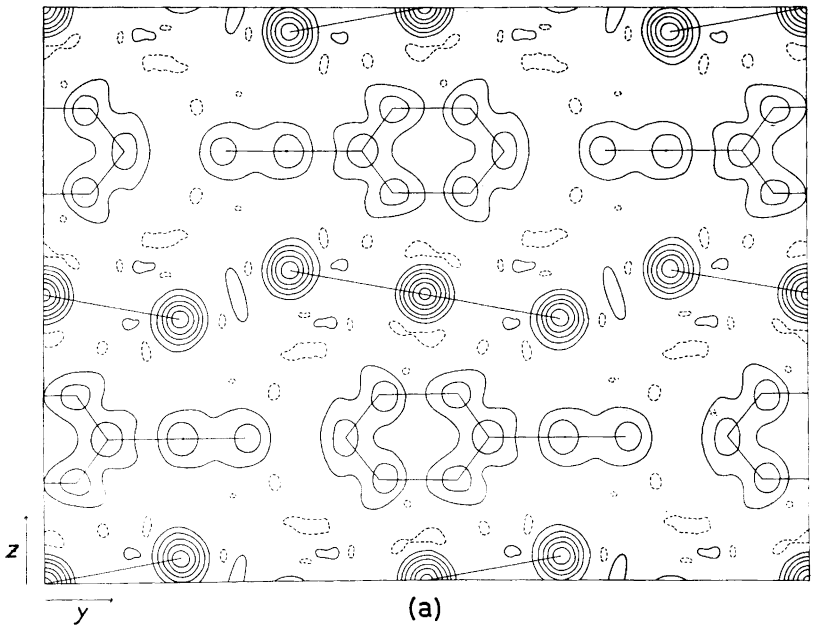

(a)

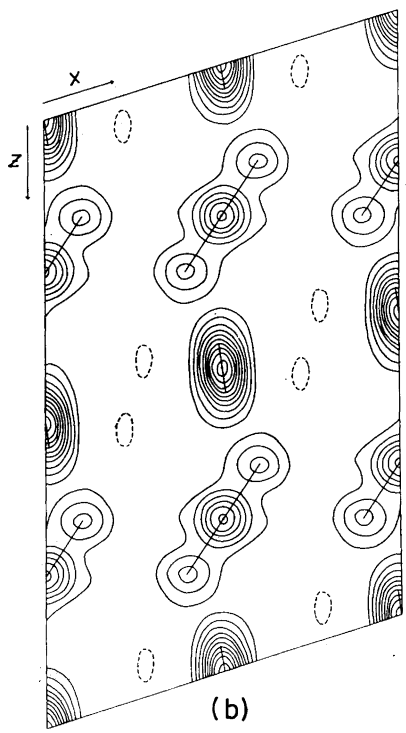

(b)

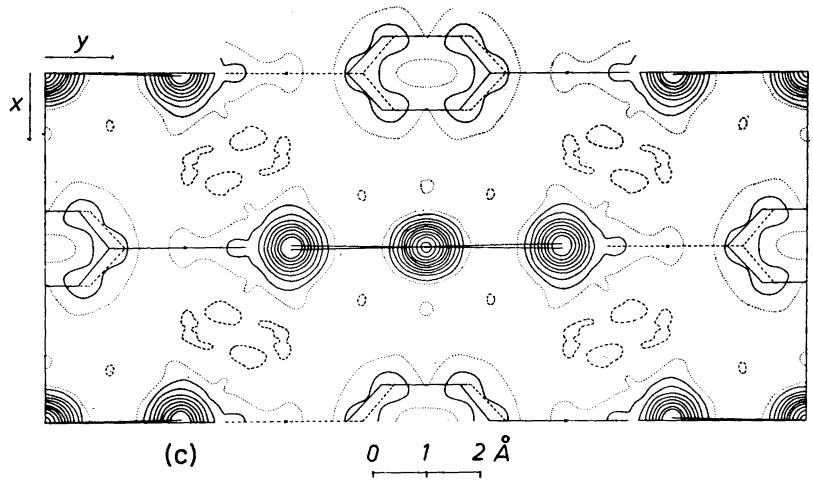

Fig. 1. Fourier projections of benzenediazonium tribromide, (a) along the *a* axis, (b) along the *b* axis and (c) along the *c* axis. Contour intervals 10 e Å^{-2} for bromine, 3 e Å^{-2} for carbon and nitrogen in (a) and 6 e Å^{-2} for carbon and nitrogen in (b) and (c).

with a centre of symmetry in the space group. The benzenediazonium ions are situated on two-fold axes running through the $N_2—N_1—C_1\cdots C_4$ atoms.

The atomic parameters judged to be the most accurate are listed in Table 1. The *y* and *z* parameters were determined from the 0*kl*-data, the *x* parameter of C_2 and C_3 from the Fourier projection along *b* assuming a planar benzene ring, and for the *x* parameter of the "outer" bromine atom the mean value of those found from the *hk*0 and *h*0*l* data has been listed. Fourier maps of the three projections are reproduced in Fig. 1. A comparison of the observed and calculated structure factors is given in Table 2.

DISCUSSION OF THE STRUCTURE

It follows from the present structure determination that benzenediazonium tribromide crystals have ionic character and consist of centrosymmetric tribromide ions and benzenediazonium ions with symmetry C_2. Since the N_2, N_1 and C_1 atoms are situated on a two-fold symmetry axis and no anisotropic thermal effects were indicated it may be stated that the N—N—C arrangement of the diazonium ion is linear. In Table 3 some interatomic distances and valence angles in the benzenediazonium ion are listed, the indexing of the atoms being that used in Fig. 2. The standard deviations indicated are estimated using the formula given by Cruickshank [9]. The C—C bond distances (mean value 1.40 Å) are, within the accuracy of the structure determination, identical with those found in the benzene molecule. However, the symmetry of the carbon ring is not hexagonal; the $C_6—C_1—C_2$ and $C_3—C_4—C_5$ angles are significantly larger than the other angles in the ring and therefore,

Table 2. Observed and calculated structure factors for benzenediazonium tribromide.

h	*k*	*l*	F_o	F_c	*h*	*k*	*l*	F_o	F_c	*h*	*k*	*l*	F_o	F_c
0	0	2	204	206			9	16	− 18	$\bar{4}$			160	156
		4	232	244			10	54	66	$\bar{6}$			104	108
		6	74	68			11	< 5	− 3	$\bar{8}$			44	56
		8	22	10			12	24	42	2	0	6	36	28
		10	24	− 36	0	10	0	66	62	4			< 7	15
		12	16	16			1	40	34	6			< 4	11
0	2	0	18	14			2	76	70	$\bar{2}$			68	68
		1	56	− 58			3	62	52	$\bar{4}$			40	36
		2	18	− 18			4	70	66	$\bar{6}$			32	24
		3	112	−112			5	100	94	$\bar{8}$			24	24
		4	16	10			6	28	24	2	0	8	20	16
		5	130	−134			7	42	44	4			20	24
		6	114	106			8	40	38	$\bar{2}$			56	48
		7	78	− 82			9	38	40	$\bar{6}$			68	56
		8	66	66			10	12	16	$\bar{6}$			40	36
		9	46	− 50			11	< 4	4	$\bar{8}$			9	12
		10	72	76	0	12	0	108	96	2	0	10	< 7	1
		11	6	− 8			1	30	− 24	4			< 3	3
		12	46	56			2	92	82	$\bar{2}$			32	− 32
		13	< 4	6			3	38	− 32	$\bar{4}$			16	− 20
0	4	0	66	68			4	72	70	$\bar{6}$			16	4
		1	64	66			5	44	− 42	2	0	12	< 3	6
		2	56	56			6	18	20	$\bar{2}$			24	16
		3	120	122			7	36	− 36	$\bar{4}$			12	4
		4	64	58			8	20	18	$\bar{6}$			< 4	2
		5	136	140			9	16	− 18	1	1	0	140	132
		6	86	76			10	4	− 2		3		124	−115
		7	94	98	0	14	0	32	− 24		5		240	246
		8	58	54			1	6	− 2		7		105	100
		9	46	52			2	16	− 10		9		22	− 10
		10	52	52			3	6	− 4		11		103	102
		11	12	12			4	< 7	4		13		17	18
		12	30	34			5	< 7	− 4		15		< 7	1
		13	< 4	− 3			6	26	26		17		28	31
0	6	0	208	218			7	4	− 4	2	0	0	373	399
		1	36	− 32			8	30	34		2		26	− 26
0	6	2	240	244	0	16	0	50	48		4		50	43
		3	34	− 34			1	6	6	2	6	0	173	175
		4	128	126			2	40	40		8		41	− 42
		5	52	− 50			3	32	26		10		53	53
		6	64	60			4	30	30		12		71	70
		7	32	− 34			5	20	20		14		21	− 20
		8	10	4			6	18	20		16		23	27
		7	46	52	0	18	0	24	28	3	1	0	138	137
		10	6	− 8			1	< 3	− 5		3		33	− 45
		11	< 6	− 2	2	0	2	148	140		5		148	159
		12	< 5	− 13	4			124	112		7		62	54
0	8	0	82	− 74	$\bar{6}$			64	72		9		23	− 24
		1	38	− 34	$\bar{2}$			260	264		11		63	65
		2	22	− 14	$\bar{4}$			184	176		13		8	10
		3	42	− 34	$\bar{6}$			84	84		15		< 6	2
		4	18	14	$\bar{8}$			28	32	4	0	0	158	172
		5	50	− 46	2	0	4	212	196		2		18	− 33
		6	42	38	4			112	108		4		26	19
		7	38	− 40	$\bar{6}$			40	44		6		106	113
		8	72	74	$\bar{2}$			192	196		8		< 7	− 11

Table 2 continued.

h k l	F_o	F_c	h k l	F_o	F_c	h k l	F_o	F_c
10	42	46	11	32	33	7 1 0	31	28
12	48	52	13	5	5	3	< 6	− 8
14	< 6	− 12	6 0 0	74	79	5	30	36
5 1 0	81	80	2	< 7	− 12	7	17	14
3	< 7	− 15	4	18	10	9	< 3	− 4
5	77	83	6	49	54	8 0 0	23	36
7	35	26	8	< 7	− 5	2	8	1
9	6	− 18	10	19	24	4	7	5
			12	20	26			

assuming a planar molecule, certainly larger than 120°. The C_1-C_4 distance is somewhat shorter than in benzene, an effect also observed in benzenediazonium chloride [10]. The C—N and N—N bond lengths are in full agreement with the corresponding distances observed in the chloride.

The tribromide ion is centrosymmetric, the two equivalent Br—Br bond distances are 2.543 (estimated standard deviation 0.004 Å) in accordance with the results obtained by Romers and Keulemans [11], 2.53 and 2.54 Å in the tribromide ion in trimethylammonium bromide tribromide.

Yamasaki and Cornwell [12,13] have discussed the results of molecular quadrupole coupling measurements in dichloroiodides and concluded that the *p*-bonded model suggested by Pimentel [14] and Hach and Rundle [15] represents a better description for the bonding than the sp^3d_{zz} hybridization model earlier regarded to be the correct one for trihalide ions. They estimated the electronic charge distribution on the three atoms of the dichloroiodide ion and found that each of the symmetrically arranged chlorine atoms carries a negative charge, the central iodine atom being neutral or possibly carrying a formal positive charge. Havinga and Wiebenga [16] performed approximate calculations along the lines suggested by Pimentel on several polyhalides and were thus able to explain the structural features in some detail. They showed the negative trihalide ions to have the lowest energy in the linear configuration and that the charge distributions are in agreement with the results obtained by Yamasaki and Cornwell for the dichloroiodide ion: roughly one half electron charge on each of the outer halogens in a symmetrical configuration. The present investigation provides an experimental support for the view that the negative charge is situated on the outer halogen atoms insofar as every N_2^+ group has *outer* (Br_3^-) bromine atoms as its nearest neighbours (*cf.* Fig. 2),

Table 3. Interatomic distances and valence angles in the benzenediazonium ion. Figures in brackets are estimated standard deviations.

N_1-N_2 : 1.11 Å (0.05 Å)	$<C_1-C_2-C_3$: 114° (3°)
C_1-N_1 : 1.41 Å (0.05 Å)	$<C_2-C_3-C_4$: 118° (3°)
C_1-C_2 : 1.37 Å (0.04 Å)	$<C_2-C_1-C_6$: 131° (4°)
C_2-C_3 : 1.45 Å (0.05 Å)	$<C_3-C_4-C_5$: 125° (4°)
C_3-C_4 : 1.38 Å (0.04 Å)	
C_1-C_4 : 2.65 Å (0.05 Å)	

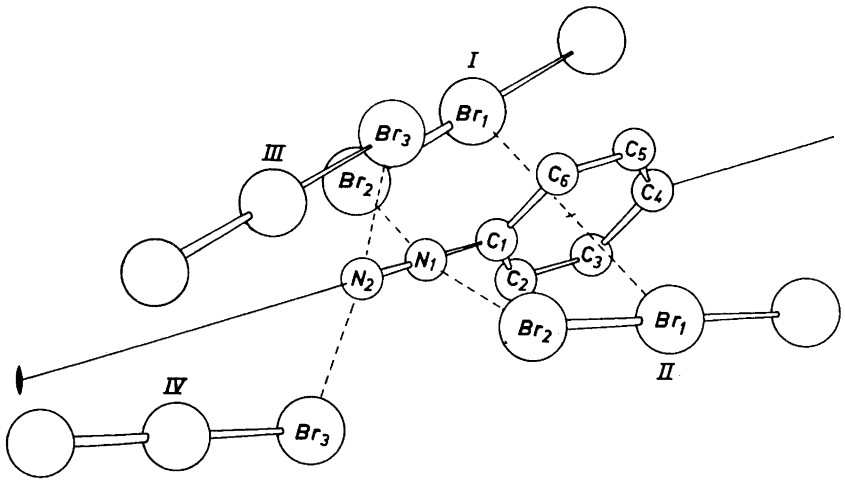

Fig. 2. Arrangement of tribromide ions about a benzenediazonium ion. The lines Br_1^I—Br_1^{II} and Br_3^{III}—Br_3^{IV} form angles of about 85° and 35° with the plane of the benzene ring, respectively.

while the central bromine atom is situated so close to the plane of a benzene ring that it is unlikely to carry a negative charge.

The spatial arrangement of tribromide ions about a diazonium ion is shown in Fig. 2. The tribromide ions I and III are related to II and IV by a two-fold axis of symmetry. The line Br_1^I—Br_1^{II} passes near the centre of the benzene ring and forms an angle of 85° with the ring plane. The bromine-benzene plane separation is 3.68 Å which is about 0.1 Å less than the sum of the van der Waals radius for bromine and the half-thickness of the benzene molecule. The shortest distance between a central bromine and a nitrogen atom is 4.34 Å.

The distances from the Br_2-atoms in the ions I and II to N_1 are 3.46 Å and from the Br_3-atoms in the ions III and IV to N_2 3.31 Å. It is remarkable that the shortest of the bromine to nitrogen distances is that to an outer nitrogen atom (N_2). According to classical valence concepts the N_1 atom is equivalent to an ammonium nitrogen atom and should therefore carry the positive charge. The short Br_3—N_2 distance would then indicate a van der Waals interaction and an electrostatic interaction exists only between the N_1 atom and the Br_2 atoms. However, the electron density of the triple bond may be displaced towards the N_1 atom (Sarkar [17]), in which case the positive charge is shared between the two nitrogen atoms. Electrostatic forces would then also be present between the Br_3 and N_2 atoms.

The Br_3—N_1 and the Br_2—N_2 distances are 3.76 and 3.65 Å, respectively.

REFERENCES

1. Griess, P. *Phil. Trans.* **157** (1864) 667; *Ann* **137** (1864) 50.
2. Griess, P. *J. Chem. Soc.* **20** (1867) 44.
3. Chattaway, F. D. *J. Chem. Soc.* **95** (1909) 862.
4. Hantzsch, A. *Ber.* **48** (1915) 1344.
5. Forster, M. O. *J. Chem. Soc.* **107** (1915) 260.
6. Aroney, M. and Le Fevre, R. J. W. *J. Chem. Soc.* **1955** 1630.
7. Curtis, A. R. *A.E.R.E. Mercury Autocode Program No. 29.*
8. Forsyth, J. B. and Wells, M. *Acta Cryst.* **12** (1959) 412.
9. Cruickshank, D. W. J. *Acta Cryst.* **2** (1949) 65.
10. Rømming, Chr. *Acta Chem. Scand.* **13** (1959) 1260.
11. Romers, C. and Keulemans, E. W. M. *Koninkl. Ned. Akad. Wetenschap. Proc. Ser. B.* **61** (1958) 345.
12. Yamasaki, R. S. and Cornwell, C. D. *J. Chem. Phys.* **30** (1959) 1265.
13. Cornwell, C. D. and Yamasaki, R. S. *J. Chem. Phys.* **27** (1957) 1060.
14. Pimentel, G. *J. Chem. Phys.* **19** (1951) 446.
15. Hach, R. J. and Rundle, R. E. *J. Am. Chem. Soc.* **73** (1951) 4321.
16. Havinga, E. E. and Wiebenga, E. H. *Rec. trav. chim.* **78** (1959) 724.
17. Sarkar, P. B. *J. Indian Chem. Soc.* **13** (1936) 19.

Received April 27, 1962.

ACTA CHEMICA SCANDINAVICA 16 (1962) 1890–1896

The Crystal Structure of $CsMnCl_3,2H_2O$

STIG JORGO JENSEN and PALLE ANDERSEN

Department of Technology, The Royal Dental College, Aarhus, Denmark, and

SVEND ERIK RASMUSSEN

Department of Inorganic Chemistry, University of Aarhus, Aarhus, Denmark

$CsMnCl_3$, $2H_2O$ is orthorhombic; the space-group is $Pcca-D^8_{2h}$ with $a = 9.060$ Å, $b = 7.285$ Å, $c = 11.455$ Å and four formula units per unit cell. The structure was determined by two-dimensional Patterson projections and was refined by Fourier difference synthesis. Each manganese atom is octahedrally coordinated to four chlorine atoms and two water molecules. The water molecules occupy *cis*-positions.

In connection with investigations of the structures of the double-salts of CsCl and anhydrous $MnCl_2$ of Andersen [1] we investigated some hydrates as well. We prepared $CsMnCl_3,2H_2O$ and $Cs_2MnCl_4,2H_2O$. The existence of the latter was reported by Vermande [2]. Of particular interest was the coordination around the manganous ion and the location of the water molecules. This paper presents the result of the crystal structure analysis of $CsMnCl_3,2H_2O$. The structure analysis of the other hydrate is in progress.

EXPERIMENTAL

$CsMnCl_3,2H_2O$ was prepared from an aqueous solution containing 0.01 mole CsCl and 0.01 mole $MnCl_2,4H_2O$ (Merck p.a.) and slow evaporation at 20°C. The crystals were rectangular or eight-sided pink prisms. Chemical analysis of the compound gave the following results: Mn 16.59; Cl 32.28; H_2O 10.92; Cs 40.21. Calc. for $CsMnCl_3,2H_2O$: Mn 16.63; Cl 32.22; H_2O 10.90; Cs 40.25. The Mn-content was determined by complexometric titration with EDTA, Cl by potentiometric titration using $AgNO_3$, and the water gravimetrically by heating the compound to 100°C. The crystals decompose at 58°C. Cs was calculated as the balance. The density was 2.84 g/cm³ (20°C) as measured by flotation in a mixture of carbon tetrachloride and acetylene tetrabromide.

The unit-cell dimensions were determined from a Guinier powder pattern using cesiumchloride as a reference. Fe$K\alpha$ radiation was employed. The lattice constant was found to be 4.122 Å (Fe$K\alpha$ = 1.93597 Å) from Bradley-Jay powder diagrams using a 19 cm camera. The Nelson, Riley [3] extrapolation procedure was used for this determination of a_{CsCl}.

For intensity measurements, a crystal of the dimensions 100 μ × 40 μ × 20 μ was mounted on a Weissenberg goniometer and oriented along the a-axis. The $h0l$ and $hk0$ reflexions were recorded with a Precession goniometer, the $0kl$ reflexions with an integrating Retigraph goniometer. Zr-filtered molybdenum radiation was used in all cases. The Precession-films were evaluated visually by means of a standard intensity-scale and the Retigraph-films with a densitometer. Corrections for Lorentz- and polarization factors were made using charts. No correction for absorption was made. The linear absorption coefficient is 76 cm^{-1}.

STRUCTURE DETERMINATION

The conditions limiting reflexions are the following:

hkl: no conditions; $0kl$: $l = 2n$; $h0l$: $l = 2n$; $hk0$: $h = 2n$. Consequently the space group is No. 54, $Pcca$—D_{2h}^{8}.

The unit cell contains four units of $CsMnCl_3,2H_2O$. The general position in $Pcca$ is eight-fold. Thus the Cs-atom, the Mn-atom and one of the Cl-atoms must occupy some of the special four-fold positions of the space group.

The parameters of the cesium and of the manganese atoms were obtained from 100 and 010 Patterson projections. The cesium atom was placed in the four-fold position 1/4, 0, z using the value 0.146 for z. The manganous ion was put into the other four-fold position 0,y,1/4 using for y 1/2. The positions of the symmetry-related manganous ions are thus: 0, 1/2, 1/4; 0, 1/2, 3/4; 1/2, 1/2, 3/4; 1/2, 1/2, 1/4. The positions of the chlorine ions were ambigous from the Patterson projections although their correct positions are clearly indicated on the Patterson maps.

Information on the positions of the lighter atoms was obtained from Fourier projections along the a- and b-axes. The signs of the structure factors $F(0kl)$ and $F(h0l)$ were calculated from the contributions of the Cs-atoms and the Mn-atoms. The positions of the chlorine atoms were clearly indicated on the Fourier maps. The positions of the oxygen atoms were, however, obscured by the chlorine atoms.

Difference Fourier projections were made incorporating the positions of the Cs, Mn and Cl atoms in the structure factor calculations. The difference projections were of the variety found rarely outside textbooks: The oxygen atoms appeared clearly, one set of chlorine atoms was seen on a gradient. The Mn-atoms which were assumed preliminary to overlap completely in the $0kl$ projection at $y = 1/2$ must obviously be moved to the positions $y = 1/2 + \delta$ and $y = 1/2 - \delta$.

Fig. 1 shows the first $0kl$ difference projection and Fig. 2 the first $h0l$ difference projection. The refinement was stopped after 3 cycles of difference Fourier projections on each of the $0kl$ and the $h0l$ projections.

The $hk0$ structure factors were not used for refinement. The agreement between observed and calculated structure factors is as good for this projections as for the other ones (Table 1).

Part of the computations were carried out by aid of a Fourier analogue computer of the Hägg-Laurent type built by Frank [4]. Most of the structure factor and Fourier-computations were carried out on the electronic digital computer DASK of Regnecentralen, Copenhagen.

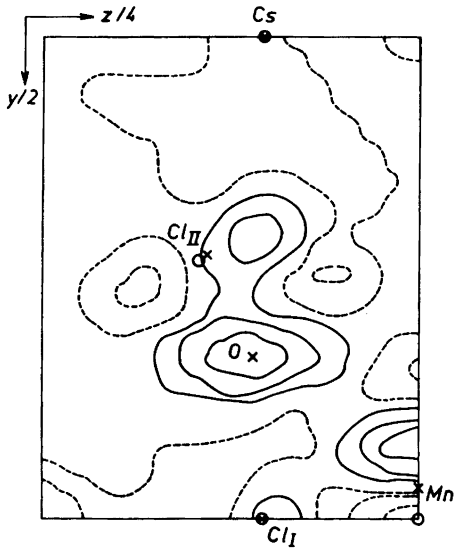

Fig. 1. First difference synthesis. Projection on (100). The contours are at arbitrary intervals. The broken lines represent zero and negative contours. The small circles show the atom locations derived from the Fourier projections and the small crosses show the final locations. The map shows the place of the oxygen atom, the errors in the locations of Cl_{II} and Mn and the too high temperature factor of the Cl_I-atom.

The following expression was used for calculating the atomic scattering factors:

$$f_n(\sin\Theta/\lambda) = A_n\exp[-a_n(\sin\Theta/\lambda)^2] + B_n\exp[-b_n(\sin\Theta/\lambda)^2] + C_n\exp[-c_n(\sin\Theta/\lambda)^2]$$

The following parameters which include isotropic temperature factors were used:

	A	B	C	a	b	c	Ref.
Cs	18.965	20.752	14.659	3.358	5.444	21.179	5
Mn	8.630	9.427	6.744	2.145	5.524	28.341	5
Cl_I	7.511	7.487	1.881	4.128	34.56	2.80	6
Cl_{II}	7.511	7.487	1.881	4.428	34.86	3.10	6
O	2.113	4.637	1.211	5.967	17.85	3.10	6

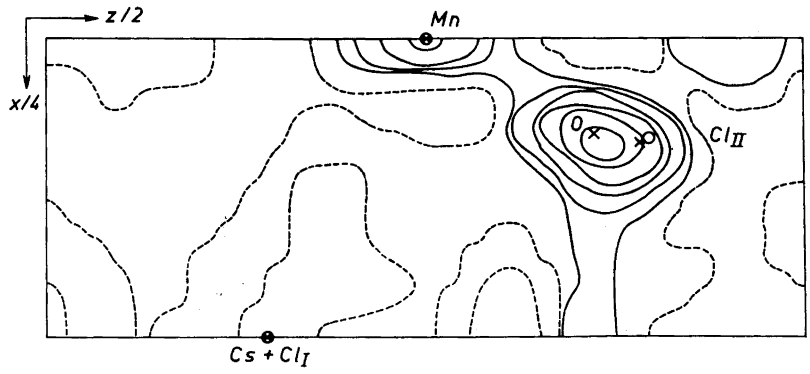

Fig. 2. First difference synthesis. Projection on (010). The map shows the place of the oxygen atom, the error in the location of Cl_{II} and the too high temperature factor of the Mn-atom.

The programmes were written according to descriptions of Westman, Blomqvist and Åsbrink [5] by Per Mondrup and Finn Larsen of Regnecentralen.

Crystal data

For convenience all pertinent crystal data are presented below:
Crystal system: orthorhombic

$$a = 9.060 \pm 0.005 \text{ Å}$$
$$b = 7.285 \pm 0.005 \text{ Å}$$
$$c = 11.455 \pm 0.005 \text{ Å}$$

Space group: No. 54, $Pcca-D_{2h}^{8}$
Density, calculated (four formula units in the elementary cell): 2.89 g/cm³.
Density, measured: 2.84 g/cm³
Absorption coefficient for Mo$K\alpha$ radiation: 76 cm^{-1}
$F(000) = 583$
Residual factor $R = \Sigma \| F_o| - |F_c \| / \Sigma | F_o |$; $R_{h0l} = 10.1$ %; $R_{hk0} = 9.5$ %; $R_{0kl} = 9.3$ %, including all reflexions with $\sin\Theta < 0.5$.
Non-observed reflexions are included with half the value of the smallest observed $F(hkl)$ value.
Atomic parameters and temperature factors:

Atom	x	y	z	B
Cs	0.250	0.000	0.146	3.15
Mn	0.000	0.467	0.250	1.80
Cl_I	0.250	0.500	0.146	2.80
Cl_{II}	0.085	0.228	0.391	3.10
O	0.080	0.669	0.361	3.10

Interatomic distances (in Å):

Within octahedrons:		Between neighbouring octahedrons:	
Mn $-Cl_I$	2.57	$Cl_I - Cl_{II}$	3.83
Mn $-Cl_{II}$	2.50	$Cl_{II} - Cl_{II}$	4.46
Mn $-$O	2.08	$Cl_{II} - Cl_{II}$	4.43
$Cl_I - Cl_{II}$	3.75	$Cl_{II} -$O	3.14
$Cl_I - Cl_{II}$	3.64	$Cl_{II} -$O	3.30
$Cl_{II} - Cl_{II}$	3.58	O $-$O	3.94
$Cl_{II} -$O	3.23	O $-$O	4.27
$Cl_I -$O	3.15		
$Cl_I -$O	3.24		
O $-$O	2.92		

From the cesium–atom:

Cs $-Cl_I$	3.64	Cs $-$O	3.78
Cs $-Cl_{II}$	3.59	Cs $-$O	3.84
Cs $-Cl_{II}$	3.67	Cs $-$O	4.33
Cs $-Cl_{II}$	3.48		

Table 1. Observed and calculated structure factors. For those reflexions too weak to be observed, F_o is listed as half the least observable value.

h k l	F_o	F_c	*h k l*	F_o	F_c
0 0 2	138	−147	7 0 4	62	− 53
0 0 4	235	−230	7 0 6	26	− 38
0 0 6	28	36	7 0 8	71	63
0 0 8	153	153	7 0 10	< 8	5
0 0 10	94	−102	7 0 12	43	− 40
0 0 12	< 8	16	8 0 0	103	101
0 0 14	< 8	8	8 0 2	60	− 58
0 0 16	< 8	1	8 0 4	15	− 16
1 0 2	156	−163	8 0 6	22	21
1 0 4	125	114	8 0 8	34	41
1 0 6	57	75	8 0 10	57	− 61
1 0 8	120	−115	8 0 12	15	19
1 0 10	< 8	− 9	9 0 2	111	− 99
1 0 12	68	70	9 0 4	15	24
1 0 14	< 8	− 13	9 0 6	65	59
1 0 16	22	− 26	9 0 8	15	− 28
2 0 0	70	− 81	9 0 10	15	− 17
2 0 2	< 8	− 16	10 0 0	< 8	− 15
2 0 4	183	184	10 0 2	< 8	− 8
2 0 6	174	−172	10 0 4	51	53
2 0 8	15	10	10 0 6	63	− 55
2 0 10	51	55	10 0 8	< 8	7
2 0 12	< 8	20	10 0 10	22	15
2 0 14	62	− 63	11 0 2	31	30
3 0 2	365	321	11 0 4	22	− 20
3 0 4	62	− 73	11 0 6	< 8	− 16
3 0 6	170	−161	11 0 8	22	24
3 0 8	62	73	12 0 0	72	65
3 0 10	40	43	12 0 2	22	− 23
3 0 12	22	− 41	12 0 4	26	− 22
3 0 14	< 8	6	0 1 0	45	42
4 0 0	202	198	0 1 2	62	57
4 0 2	131	−114	0 1 4	161	−168
4 0 4	26	− 36	0 1 6	107	114
4 0 6	60	51	0 1 8	<15	− 12
4 0 8	56	68	0 1 10	<15	− 6
4 0 10	113	−110	0 1 12	<15	− 25
4 0 12	26	29	0 1 14	33	37
4 0 14	22	21	0 1 16	<15	− 22
5 0 2	105	−103	0 2 0	180	189
5 0 4	76	71	0 2 2	153	−142
5 0 6	46	53	0 2 4	<15	− 17
5 0 8	82	− 81	0 2 6	90	78
5 0 10	< 8	− 7	0 2 8	42	59
5 0 12	46	50	0 2 10	131	−132
5 0 14	< 8	− 10	0 2 12	36	34
6 0 0	158	−150	0 2 14	33	32
6 0 2	22	− 21	0 3 0	61	68
6 0 4	217	194	0 3 2	<15	13
6 0 6	83	− 90	0 3 4	132	−136
6 0 8	37	− 32	0 3 6	111	117
6 0 10	< 8	16	0 3 8	<15	−3
6 0 12	22	27	0 3 10	30	− 33
6 0 14	15	− 34	0 3 12	<15	− 19
7 0 2	71	72	0 3 14	36	43

Table 1 continued.

h k l	F_o	F_c	h k l	F_o	F_c
0 4 0	253	233	8 1 0	< 8	17
0 4 2	78	− 65	10 1 0	43	− 54
0 4 4	122	−110	12 1 0	< 8	1
0 4 6	36	25	2 2 0	214	−196
0 4 8	87	82	4 2 0	279	258
0 4 10	60	− 61	6 2 0	16	− 24
0 4 12	<15	11	8 2 0	135	127
0 4 14	<15	7	10 2 0	51	− 42
0 5 0	82	70	12 2 0	34	32
0 5 2	<15	12	2 3 0	151	−156
0 5 4	102	− 93	4 3 0	50	45
0 5 6	45	41	6 3 0	84	− 96
0 5 8	<15	13	8 3 0	< 8	16
0 5 10	<15	− 3	10 3 0	50	− 47
0 5 12	<15	− 12	12 3 0	16	2
0 6 0	108	98	2 4 0	90	− 93
0 6 2	50	− 44	4 4 0	132	134
0 6 4	60	− 52	6 4 0	95	− 90
0 6 6	62	57	8 4 0	84	75
0 6 8	33	32	10 4 0	22	− 20
0 6 10	71	− 63	2 5 0	87	− 85
0 6 12	<15	7	4 5 0	16	29
0 7 0	<15	12	6 5 0	76	− 74
0 7 2	<15	− 11	8 5 0	16	15
0 7 4	<15	− 14	10 5 0	< 8	− 24
0 7 6	42	35	2 6 0	84	− 85
0 7 8	<15	− 2	4 6 0	98	96
0 7 10	<15	− 25	6 6 0	50	− 44
0 8 0	56	59	8 6 0	54	51
0 8 2	<15	− 9	10 6 0	37	− 26
0 8 4	45	− 49	2 7 0	54	− 58
0 8 6	<15	26	4 7 0	43	44
0 8 8	<15	18	6 7 0	< 8	− 12
0 9 0	45	48	8 7 0	22	23
0 9 2	<15	− 9	2 8 0	57	− 53
0 9 4	<15	− 28	4 8 0	43	41
0 9 6	<15	3	6 8 0	37	− 41
0 10 0	22	18	8 8 0	16	24
0 10 2	<15	0	2 9 0	< 8	− 7
2 1 0	236	−226	4 9 0	< 8	15
4 1 0	26	48	6 9 0	22	− 23
6 1 0	123	−121	2 10 0	26	− 36

DISCUSSION

The manganese atom lies near the centre of a distorted octahedron having four chlorine atoms and two oxygen atoms at the corners. Two chlorine atoms are placed on opposite sides of a trapezium consisting of two oxygen atoms and two chlorine atoms. These six atoms form a *cis*-octahedral coordination around the manganese atom. The octahedrons sharing corners are arrayed in zig-zag chains along the (100)-direction (Fig. 3). The octahedrons are connected through the cesium-atoms in such a way that each Cs-atom is surrounded by eight

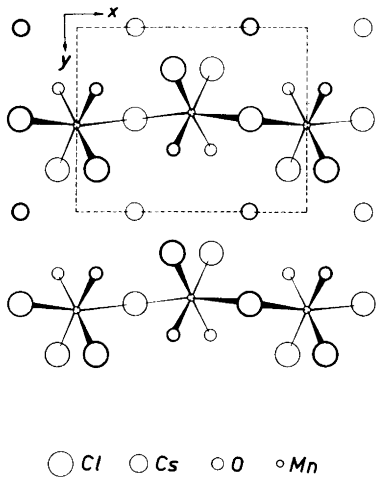

Fig. 3. Projection of the unit cell on (001).

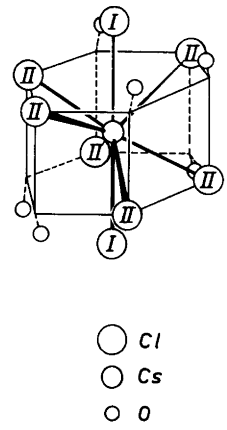

Fig. 4. The coordination around the cesium-atom.

chlorine atoms as nearest neighbours. Next-nearest neighbours are six oxygen atoms. These fourteen atoms form a coordination reminding of a distorted body-centered cubic packing (Fig. 4). The interatomic distances between Mn and Cl and between Mn and O are somewhat smaller than the corresponding distances in $MnCl_2,2H_2O$ found by Vajnstejn [7]. In $MnCl_2,2H_2O$, Mn—Cl is 2.57 Å and 2.60 Å and Mn—O is 2.19 Å and the coordination around Mn is *trans*-octahedral. In $K_2Mn(SO_4)_2,4H_2O$ analysed by Schneider [8] Mn is surrounded by six oxygen atoms in a distance varying from 2.08 Å to 2.17 Å.

Acknowledgement. The Danish State Science Foundation has covered the cost of the Hägg-Laurent computer and the programming and the computations on DASK. We express our thanks to the director of Regnecentralen, N. I. Bech for his active and willing cooperation in the solution of our computational problems, and to Mr. Finn Larsen for carrying out the electronic computations.

REFERENCES

1. Andersen, P. 9. Nordiske Kemikermøde, Århus 1956, p. 7.
2. Vermande, J. *Pharmaceutisch Weekblad* **33** (1918) 1131.
3. Nelson, J. B., Riley, D. P. *Proc. Phys. Soc.* **57** (1945) 160.
4. Frank, V. *J. Sci. Instr.* **34** (1957) 210.
5. Westman, S., Blomqvist, G. and Åsbrink, S. *Arkiv Kemi* **14** (1959) 535.
6. Forsyth, J. B. and Wells, M. *Acta Cryst.* **12** (1959) 412.
7. Vajnstejn, B. K. *Doklady Akad. Nauk. SSSR* **83** (1952) 227.
8. Schneider. W. *Acta Cryst.* **14** (1961) 784.

Received April 25, 1962.

ACTA CHEMICA SCANDINAVICA 16 (1962) 1897–1907

Further Studies on S-Substituted Phosphorothioic Acids

II *. Synthesis and Certain Properties of some Potential Antiradiation Drugs

STIG ÅKERFELDT

Research Institute of National Defence, Dept. 1, Sundbyberg 4, Sweden

1. 14 new compounds containing the $-SPO_3^{2-}$ group have been synthesized. The synthetic methods consisted of: (*a*) reaction of a substituted alkyl halide with the phosphorothioate ion; (*b*) reaction of an amino alkyl halide with the phosphorothioate ion followed by guanylation of the amino group by S-ethyl isothiouronium bromide; (*c*) reaction of dibromopropanols with the phosphorothioate ion. Reaction (*c*) gave compounds containing two phosphorylated thiol groups per molecule.

2. The reaction between cysteamine S-phosphate and bromine was investigated. The results favour the conception that the S–P bond is broken at an early stage of the oxidation, which most likely proceeds *via* sulfenylbromides.

3. Attempts to demonstrate intramolecular phosphate group transfer from S to O in some of the prepared compounds failed.

As a result of a search for new antiradiation drugs at this Institute it was recently reported by Hansen and Sörbo[1] that one of the S-substituted phosphorothioic acids earlier synthesized by Åkerfeldt, namely cysteamine S-phosphate, is a potent radioprotective agent when given to mice. This fact has stimulated the synthesis of a series of related compounds and their properties as antiradiation drugs are now beeing evaluated. The results of these studies will be reported elsewhere.

In this communication the synthesis and some properties of 12 new S-substituted phosphorothioic acids and of two S-phosphorylated dithiols is reported.

RESULTS AND DISCUSSION

Synthetic methods. In the method earlier developed by the author for the preparation of S-substituted phosphorothioic acids [2–5] a compound containing

* Part I: *Acta Chem. Scand.* **15** (1961) 575.

a reactive halogen is allowed to react at room temperature with trisodium phosphorothioate in aqueous medium with or without the use of DMF * as a catalyst. In all cases studied so far a quantitative reaction of the phosphorothioate ion has been obtained after a few hours of reaction.

It was earlier found advantageous to isolate the S-substituted phosphorothioic acids as mixed lithium sodium salts, since small amounts of orthophosphate formed could be conveniently removed as trilithium phosphate [5].

To simplify the analysis of the isolated products most of the compounds described in this paper were prepared from trilithium phosphorothioate. By the use of this compound only one metallic cation was (usually) present in the isolated products.

Trilithium phosphorothioate is easily obtained from $PSCl_3$ and lithium hydroxide. For its preparation a procedure similar to that worked out for the synthesis of trisodium phosphorothioate [4] was followed with the exception that water of crystallization was not removed by methanol. This step was omitted since trilithium phosphorothioate forms a gel-like suspension in this alcohol and isolation of the dehydrated product therefore becomes difficult.

The phosphorus content of trilithium phosphorothioate was determined by the bromine method [5]. The sulfur content can be determined by potentiometric iodine titration in aqueous medium as described by Yasuda and Lambert [6] for trisodium phosphorothioate. Visible detection of the endpoint is not feasible because of lack in sharpness. However, it was found during this investigation that it is possible to get a perfectly sharp endpoint for visible titration if the sample is dissolved in glacial acetic acid and titrated with iodine in methanol. This method also works well for trisodium phosphorothioate.

The S-substituted phosphorothioic acids described in this communication were prepared as follows:

(*a*) trilithium phosphorothioate (in a few cases Na_3SPO_3) was allowed to react with compounds containing one reactive halogen atom (usually bromine) in the presence of DMF:

$$RBr + SPO_3^{3-} \xrightarrow[H_2O]{DMF} RSPO_3^{2-} + Br^-$$

In this way 10 compounds were prepared. In a few cases it was found to be more convenient to isolate the substances as their barium salts and in one case the sodium salt was isolated.

(*b*) Trilithium phosphorothioate was first allowed to react with an aminoalkyl bromide as described under (*a*). The amino group was then guanylated by S-ethyl isothiouronium bromide in the presence of ammonia without isolation of the intermediary amino compound:

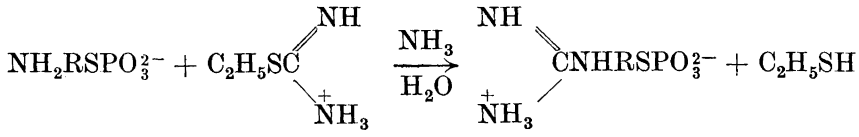

* Abbreviations: DMF = N,N-dimethyl formamide; EDTA = (ethylenedinitrilo) tetraacetic acid; CMNP = 2-chloromercuri-6-nitrophenol.

In this way two compounds were prepared, namely S-(2-guanidinoethyl) phosphorothioic acid and S-(3-guanidinopropyl) phosphorothioic acid.

Pant and Dubey [8] have recently shown that 2-aminoethanol O-phosphate can be N-guanylated by S-methyl isothiouronium bromide.

(*c*) Trilithium phosphorothioate was allowed to react with compounds containing two reactive bromine atoms in the presence of DMF. In this way the lithium salts of 1,3-dimercapto-2-propanol S_1,S_3-diphosphate (I) and 2,3-dimercapto-1-propanol S_2,S_3-diphosphate (II) were prepared.

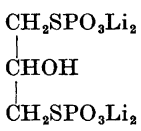

I

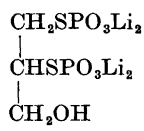

II

Compound I has the same spacing between the sulfur atoms as lipoic acid. It is of interest in this connection that Stadtman *et al.*[7] have shown 1,3-dimercapto-2-propanol to serve as a cofactor in the enzymic reduction of glycine in *E. sticklandii*. As an intermediate in this reaction an S-phosphorylated compound similar to I was suggested. Compound II is S-phosphorylated British Anti Lewisite (BAL). Compounds I and II represent a new class of compounds containing two phosphorylated thiol groups in the same molecule.

Structural investigations. As was pointed out in Part I of this series, and in earlier papers, there exists the theoretical possibility that the substituted alkyl halides used in the preparation of the S-substituted phosphorothioic acids by the outlined methods could also react with an oxygen atom of the phosphorothioate ion and thus form O-substituted phosphorothioic acids ($ROPSO_2^{2-}$) as contaminants of the major reaction products. In no case, however, could the presence of such contaminants be demonstrated in earlier synthesized compounds. All compounds described in this paper were tested for the presence of O-substituted phosphorothioic acids. It was not possible to demonstrate their presence in any isolated product.

The testing methods used included: (1) acid hydrolysis (5 min at 90—100° in 1 M HCl) of the compound and determination of liberated thiol (usually) by iodine titration. A subquantitative yield of thiol could indicate the presence of contaminants, but exact knowledge of the behavior of the corresponding O-substituted phosphorothioic acids towards oxidation by iodine is lacking. However, in no case tested was the amount of thiol released below the expected amount (within experimental error). The quantity of thiol obtained always corresponded very well with the phosphorus content of the compounds as determined by the bromine method [see (2)], a circumstance that would not be expected in the presence of O-substituted phosphorothioic acids. (S-Ethyl phosphorothioate could not be tested in this way because of liberation of volatile ethanethiol during hydrolysis). (2) Phosphate determination according to the bromine method [5]. Only the S—P bond would be expected to be broken by this mild method. The more stable O—P bond is usually not attacked at all by bromine treatment. A subquantitative yield of orthophosphate, as deter-

mined by the bromine method, would thus indicate the presence of contaminants. Within experimental error the phosphate recovery was quantitative for all compounds.

A possible decomposition of S-[2-(trimethylammonium)ethyl] phosphorothioate (thiocholine S-phosphate) was tested for by reacting the compound in alkaline solution with 2-chloromercuri-6-nitrophenol [17], CMNP. This treatment breaks down the S—P bond and MNP-thiols [17] are formed [2]. Paperchromatographic analysis of the resulting solutions according to Ref.[17] in the solvent systems 1, 2 and 3 gave only one thiol spot (R_F's 0.64, 0.76, and 0.70, respectively), much lower in position than the thiol spot obtained from, *e.g.*, S-(2-dimethylaminoethyl) phosphorothioate (R_F's 0.90 0.90, and 0.95, respectively). Acid hydrolysis of the compound followed by coupling to CMNP gave the same results. The compound thus appears to be homogeneous.

Guanylation of the two S-(aminoalkyl) phosphorothioates by S-ethyl isothiouronium bromide could possibly give contaminants that were guanylated on the phosphate residue. Acid hydrolysis of such contaminants should result in the formation of urea. Acid hydrolysates of S-(2-guanidinoethyl)- and of S-(3-guanidinopropyl) phosphorothioate were therefore subjected to paperchromatography in ethanol: pyridine: water, 2:1:1, in butanol:pyridine:water, 1:1:1 and in butanol: acetic acid:water, 4:1:1. After spraying with *p*-dimethylamino benzaldehyde urea could not be detected on the chromatograms.

A nonquantitative guanylation of the amino group would result in the presence of S-(aminoalkyl) phosphorothioates in the isolated products. Coupling to CMNP, as described above, followed by paper chromatographic analysis according to Ref.[17] showed the presence of only one thiol spot for each substance. No trace of MNP-2-aminoethanethiol or MNP-3-aminopropanethiol was detected in this way.

The analysis of 1,3-dimercapto-2-propanol S_1,S_3-diphosphate (I) and its isomer (II) presented certain difficulties. After acid hydrolysis sulfur in the liberated thiol could not be determined by iodine titration in the usual manner since the oxidation product is of unknown structure (see *e.g.* Ref.[27]). Instead a method depending on spectrophotometric measurements of the reduction of 2,6-dichlorophenol indophenol was used *. The S-substituted phosphorothioic acids themselves are not oxidized by this reagent. The developed procedure is a modification of the one described by Basford and Huennekens [9]. The method was standardized by the use of thiols obtained by acid hydrolysis of three of the prepared compounds with known composition (S-(carbamylmethyl-, S-[2-(trimethylammonium)ethyl]-, and S-(2-hydroxyethyl)-phosphorothioates). These three thiols gave the following absorbance values (per μmole in 3 ml of solution) at 600 mμ (1 cm light path): 3.73, 3.71, and 3.68, respectively. (Thiols containing reactive amino groups gave different values). An absorbance of 3.71 was considered representative. When the SH-content of the thiols obtained by hydrolysis at pH 4 for 5 min at 70° of compounds I and II was determined by this method a value of 2.04 $\pm$ 0.02 SH groups per

* The earlier developed thiol reagent, CMNP [17], was not useful for these SH determinations since the reaction products obtained with this reagent were soluble in toluene or in 1,2-dichloroethane. The nitroprussiate method [25] gave a very low color yield with the liberated dithiols.

molecule was obtained. Acid hydrolysis was thus considered to give a quantitative yield of thiol also in these two cases.

Paper chromatographic analysis according to Ref.[17] of the reaction product obtained from CMNP and the thiol released by acid hydrolysis of compound II gave identical results with commercial 2,3-dimercapto-1-propanol treated the same way.

Reaction with bromine. Phosphorus in the prepared compounds was determined as orthophosphate by the bromine method [5]. This method was preferred over the mercury method [2] since mercury (II) ions sometimes form insoluble mercaptides with the thiols released from S-substituted phosphorothioic acids. It was demonstrated in an earlier paper [5] that bromine liberates orthophosphate quantitatively from these compounds. No investigation, however, was performed at that time to establish what became of the thiol part of the compounds during this treatment. For an investigation of this problem cysteamine S-phosphate was chosen primarily because its oxidation products could be easily demonstrated by paperchromatographic analysis using ninhydrin as a spot detector *, secondly because oxidation products of cysteamine are easily available.

Saturated bromine water was added to cysteamine S-phosphate of pH $\leq$ 7 until the bromine color persisted. Paperchromatographic analysis was performed of the resulting solution after 24 h in butanol:pyridine:water, 1:1:1, in ethanol: water: pyridine, 2:1:1 (saturated with solid NaCl); and in butanol:acetic acid: water, 4:1:1. Subsequent development with ninhydrin gave only one spot in all three solvents identical in position and in ninhydrin color with 2-aminoethane sulfonic acid (taurin). However, if chromatograms were run immediately after bromine treatment of cysteamine S-phosphate three major spots were obtained. The spots were identical in position to taurin, 2-aminoethane sulfinic acid (hypotaurin) ** and 2,2′-dithiobisethylamine (cystamine) and gave identical ninhydrin colors to these. The spot corresponding to cystamine gave a positive cyanide-nitroprussiate reaction and reduced hexaiodoplatinate. The spot corresponding to hypotaurin gave a negative cyanide-nitroprussiate reaction but reduced hexaiodoplatinate. None of the ninhydrin positive spots gave orthophosphate on hydrolysis at 100° by acid molybdate spray. (In this way orthophosphate and a trace of unreacted cysteamine S-phosphate was found).

It was further noticed that bromine oxidation of cystamine gave exactly the same chromatograms as bromine oxidation of cysteamine S-phosphate. This fact and the actual demonstration of the presence of cystamine (the amount of cystamine in the cysteamine S-phosphate used was negligible) indicates that the oxidation of cysteamine S-phosphate to taurin by bromine at least partially proceeds *via* cystamine. This compound may be formed by a reaction similar to the one proposed for the reaction between cysteamine S-phosphate and iodine [4]. Other possible routes for the formation of interme-

* Preliminary chromatographic experiments had shown that the amino group of the molecule is little affected by bromine treatment. Any reaction taking place at this end of the molecule lay outside the scope of this investigation.

** 2-Aminoethyl 2-aminoethanethiol sulfonate could be separated from hypotaurin on the chromatograms. Small amounts of this substance were possibly present. It was prepared according to Field *et al.*[28]

diates *via* sulfenylhalides have been discussed by Stirling [10] for S-benzyl O,O-diethyl phosphorothioate.

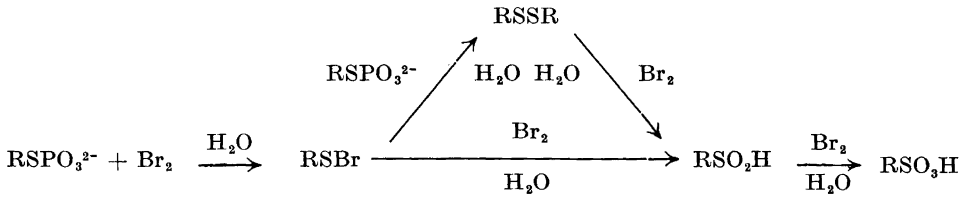

$R = \overset{+}{N}H_3CH_2CH_2-$

The present investigation does not give support to a scheme similar to the one suggested by Lordy and Epstein [11] for the oxidation of O,O,S-triethyl phosphorothioate by chlorine, where all the oxidation of sulfur to sulfonic acid should occur while sulfur was still bound to phosphorus. Obviously a disulfide would then not result, nor would a sulfinic acid be formed. One would then also expect to find traces of these phosphorus containing intermediates on the chromatograms.

Does intramolecular phosphate group migration occur in certain S-substituted phosphorothioic acids containing a hydroxyl group? Acetyl group migration from sulfur to oxygen in the same molecule has been demonstrated to occur under certain circumstances (*cf.*, *e.g.* Ref.[12]). The free energy of thiol ester hydrolysis is high [12] and so is the free energy of hydrolysis of the S—P bond in S-substituted phosphorothioic acids [13,14].

The question of intramolecular phosphate group migration from sulfur to oxygen was investigated for three compounds: S-(2-hydroxyethyl), S-(3-hydroxypropyl) phosphorothioate and 1,3-dimercapto-2-propanol S_1,S_3-diphosphate. A phosphate group migration taking place in the fashion mentioned would result in the formation of (*a*) free thiol groups, and (*b*) O—P bonds relatively resistent to hydrolysis. Since thiol groups are also beeing liberated by hydrolysis of the S—P bond the method chosen for the investigation was based on the formation of the relatively stable O—P bond. The bromine method for phosphate determination [5] was suitable since it would only be expected to break the S—P bond. The formation of O—P bonds would thus result in the disappearence of orthophosphate.

Samples of the three compounds were incubated at 35° in buffers of different pH for various lengths of time and orthophosphate was determined by the bromine method. Within experimental error no decrease of the orthophosphate amount was detected in any case. An intramolecular phosphate group transfer could thus not be demonstrated.

General remarks. The formulas as well as found and calculated analytical values for the 14 isolated compounds are tabulated in Table 1.

Some of the isolated compounds contained ethanol of crystallization (all compounds had been dried for at least 20 h at 8—10 mm Hg over fresh silica gel at + 4° before analysis was made). A strong affinity for methanol or ethanol was also earlier reported for several S-substituted phosphorothioic acids [5,15].

Table 1. Formulas, found and calculated analytical values of the isolated compounds.

Compound No.	Formula of isolated compound	Mol. weight	ANALYSIS										
			C		H		P		S		OTHER		
			calc.	found	calc.	found	calc.	found	calc.	found		calc.	found
1.	$C_2H_5SPO_3Li_2$	154.0	15.6	15.4	3.3	3.4	20.1	19.9	20.8	20.3[a]	—	—	—
2.	$HOCH_2CH_2SPO_3Li_2$	170.0	14.1	14.0	3.0	3.0	18.2	18.4	18.9	18.7	—	—	—
3.	$HOCH_2CH_2CH_2SPO_3Ba,2.5\,H_2O$	352.5	10.2	10.2	3.4	3.4	8.80	8.80	9.10	9.20	Ba	39.0	38.8
4.	$H_2NCOCH_2SPO_3Li_2$	183.0	13.1	13.2	2.2	2.0	16.9	16.9	17.5	17.6	N	7.7	7.7
5.	$H_3\overset{+}{N}CH_2CH_2CH_2SPO_3^-Li,0.5H_2O$	186.1	19.4	19.6	5.4	5.2	16.6	16.7	17.2	17.1	—	—	—
6.	$CH_3NHCH_2CH_2SPO_3Ba(C_2H_5OH)_{0.15}$ $1.5\,H_2O$	340.4	11.6	11.6	3.5	3.4	9.10	9.13	9.41	9.56	Ba C_2H_5OH/P	40.4 0.15	40.9 0.15
7.	$(CH_3)_2NCH_2CH_2SPO_3Ba,2H_2O$	356.6	13.5	13.6	3.9	4.1	8.70	8.68	8.99	8.90	Ba	38.6	38.4
8.	$(CH_3)_3\overset{+}{N}CH_2CH_2SPO_3^-Na,8H_2O$[d]	365.3	16.4	16.2	8.0	7.7	8.47	8.51	8.77	8.80	N	3.8	3.8
9.	$(i-C_3H_7)_2NCH_2CH_2SPO_3Ba,2.5H_2O$	421.7	22.8	22.5	5.5	5.4	7.34	7.45	7.6	7.2[c]	Ba	32.5	31.4
10.	$(CH_3)_2NCH_2CH(CH_3)SPO_3Li_2,2H_2O$	247.1	24.3	24.1	6.5	6.2	12.5	12.7	13.0	12.9	—	—	—
11.	$\begin{matrix} HN \\ \diagdown \\ C-NHCH_2CH_2SPO_3^-(NH_4)_{0.2}Li_{0.8},1.5 \\ \diagup \\ H_3N+ \end{matrix}$ H_2O	234.4	15.4	15.2	5.5	5.3	13.2	13.3	13.7	13.5	N Li/P	19.1 0.8	19.0 0.82
12.	$\begin{matrix} HN \\ \diagdown \\ C-NHCH_2CH_2CH_2SPO_3^-(NH_4)_{0.8}Li_{0.2}, \\ \diagup \\ H_3N+ \end{matrix}$ H_2O	246.0	19.5	19.2	6.6	6.9	12.6	12.5	13.0	13.0	N Li/P	21.6 0.2	21.4 0.18
13.	$Li_2PO_3SCH_2CH(OH)CH_2SPO_3Li_2,$ $(C_2H_5OH)_{0.9},3H_2O$[b]	403.4	14.3	14.4	4.3	4.3	15.4	15.5	15.9	16.3	C_2H_5OH/P	0.9	0.90
14.	$Li_2PO_3SCH_2CH(SPO_3Li_2)CH_2OH,$ $(C_2H_5OH)_{0.9},2H_2O$[b]	385.4	15.0	15.0	4.0	3.7	16.1	16.1	16.6	16.9	C_2H_5OH/P	0.9	0.85

[a]) Determined as sulfate after combustion of the substance.
[b]) Ethanol was not removed by further drying at 10 mm Hg.
[c]) Determined by 2,6-dichlorophenolindophenol reduction after acid hydrolysis of a 6 months old prepn. Iodine gives a colored adduct with the corresponding disulfide and iodine titration is therefore not suitable for S-detn.
[d]) The result of acid titration of the compound excluded the structure $(CH_3)_3N(OH)CH_2CH_2SPO_3^{2-}$.

Several of the compounds contained water of crystallization. No method was found that was entirely satisfactory for its quantitative determination. The amount of water of crystallization in the compounds was calculated from (*a*) the molecular weight as calculated from C, S, and P content; (*b*) from H determinations. For all compounds methods (*a*) and (*b*) were in close agreement.

Due to different reaction rates, different solubilities of the isolated salts and various experimental difficulties that arose during the preparation of the compounds it was found most suitable to present the synthesis of each individual compound *per se*.

DMF was found to catalyze the formation of cysteamine S-phosphate [2]. In other instances the reaction between the phosphorothioate ion and the substituted alkyl bromide proceeds at a convenient rate without the catalyst (*e.g.* in Ref.[5]). In the present investigation the reaction rate without DMF was not determined, but it was routinely added in all cases.

EXPERIMENTAL

General methods

Phosphate was determined colorimetrically by the bromine method [5]. Sulfur was determined as liberated thiol by iodine titration after hydrolysis at 90—100° of about 100 mg of substance in 25 ml of 1 M HCl for 5 min (unless otherwise stated). Ethanol was determined using the colorimetric method by Reid and Salmon [16] after passage of the sample through Dowex 50 W × 8 (H^+) and through Dowex 21 K (OH^-). Barium was determined by EDTA titration according to Anderegg *et al.*[23] Lithium was determined by the colorimetric method of Thomason [26] after passage of the sample through Dowex 21 K (OH^-).

Melting points were determined on the Kofler Heiz Bank.

Determination of thiols with 2,6-dichlorophenol indophenol. The following was added to a 4 ml cuvette (1 cm light path): 1.00 ml of a 1 M phosphate buffer pH 6.8; 0.10 ml of 2,6-dichlorophenol indophenol (50 mg in 250 ml of water) and 0.10 ml of thiol. The contents of the cuvette were mixed and allowed to react for 30 min at room temperature whereafter 1.80 ml of water were added. The absorbance was read at 600 mμ immediately. Water served as a blank. At the most individual readings of samples with the same composition varied 3—4 % of the mean, but were usually within 1—2 % of the mean.

Comments. To prevent a rapid autooxidation of reduced dye a pH slightly below 7 was chosen. To obtain a complete oxidation of the thiol by the dye an excess of dye must be present. The absorbance after completed reaction should therefore not be considerably below 0.200. Regardless of the nature of the thiol Beer's law was followed for the reduction of the dye up to absorbance differences well over 0.500 (provided an excess of dye was present). For the measurements a Beckman Model B Spectrophotometer was used.

Trilithium phosphorothioate

183 g (4.05 mole) of lithium hydroxide hydrate (containing 53 % LiOH, Merck and Co) were stirred up in 1000 ml of water and 70 ml (0.675 mole) of freshly distilled $PSCl_3$ were added. The temperature of the reaction mixture was kept at 80—85° under constant rapid stirring. After about 2 h all $PSCl_3$ had dissolved. The content of the reaction flask was cooled to room temperature under tap water and any precipitate was filtered off. 1500 ml of ethanol was added to the clear filtrate under rapid stirring and the precipitated trilithium phosphorothioate was filtered off and washed thoroughly with ethanol (500 ml). After drying first in the open air and then in vacuum about 136 g (88 %) of hydrated trilithium phosphorothioate was obtained. (Found: P [5] 13.5; S 13.7; H 5.0. Calc for Li_3SPO_3, 5.5 H_2O (231.0): P 13.4; S 13.9; H 4.8).

Determination of sulfur in trilithium phosphorothioate. About 200 mg of substance were dissolved in 30 ml of glacial acetic acid and titrated to persistent iodine color with iodine in methanol (50 mequiv/l). Anhydrous trisodium phosphorothioate [4] titrated in this fashion also gave the quantitative amount of iodine reduction (*i.e.* one equivalent of iodine reacts with one mole of phosphorothioate).

Synthesis of intermediates

The substituted alkyl halides used in this investigation were partly synthesized in this laboratory, partly commercial products.

2-Bromoethyl dimethylammonium bromide was prepared by a modified Leuckart methylation of 2-bromoethyl ammoniumbromide according to Bobranski *et al.*[18], m.p. 188–189° (ethanol). Ref.[18] gives m.p. 186–187°.

2-Bromoethyl trimethylammoniumbromide was prepared from trimethylamine and 1,2-dibromoethane according to Renshaw [19].

2-Bromoethyl methylammonium bromide was prepared from 2-methylaminoethanol and HBr according to Knorr and Meyer [20], m.p. 82° (ethanol).

1,3-Dibromo-2-propanol (Eastman Kodak Co) was redistilled and the fraction boiling at 103° at 16–17 mm Hg was used. $n_D^{25} = 1.5496$.

2,3-Dibromo-1-propanol was prepared by the addition of bromine to allyl alcohol [21], b.p. 102–105° at 11.5 mm Hg, $n_D^{25} = 1.5492$.

3-Bromopropylammonium bromide was prepared in principle according to Schöberl *et al.*[22] from 3-amino-1- propanol and HBr. Washing the product with ether and recrystallizing it from isopropanol gave a much more pure product than earlier described [22]. M.p. 171°. Yield: 67%. (Ref.[22] gives m.p. 162°). (Found: C 16.5; H 4.1. Calc for $Br^-NH^+{}_3CH_2CH_2CH_2Br$(218.9): C 16.4; H 4.2).

Synthesis of S-substituted phosphorothioic acids

Silver ion test for unreacted phosphorothioate. The test used to follow the rate of reaction between the alkyl halides and the phosphorothioate ion was the following. To two drops of test solution were added three drops of 5 M HNO_3 followed by five drops of 3 % $AgNO_3$. At the start of the reaction, when much unreacted phosphorothioate was still present, the Ag^+-test gave a black precipitate. It grew progressively lighter in color as the reaction proceeded. A light yellowish color of the precipitate indicated the endpoint of the reaction. In no case was the reaction stopped before all phosphorothioate had reacted as judged by this test.

Notes on the experimental technique. All substances prepared were precipitated by ethanol from aqueous solution, filtered and washed thoroughly with ethanol. They were dried in vacuum (about 8–10 mm Hg) at 2–4° in a refrigerator. *Due to the lability of the S–P bond all compounds were stored at –15° at all times when not in use.*

1. Dilithium S-(ethyl) phosphorothioate. 11.5 g of Li_3SPO_3,5.5 H_2O (50 mmole) were dissolved in 75 ml of water and 4.2 ml of bromoethane were added followed by 25 ml of DMF. The solution was stirred for 45 min after which time 1.0 ml of bromoethane (totally 69 mmole) was again added. After another hour of stirring the reaction product started to separate. Addition of 200 ml of ethanol precipitated most of the substance. Yield *: 6.7 g (87 %).

2. Dilithium S-(2-hydroxyethyl) phosphorothioate. 11.5 g of Li_3SPO_3, 5.5 H_2O (50 mmole) were dissolved in 100 ml of water. 8.75 g of 2-bromoethanol (70 mmole) and 25 ml of DMF were added. After stirring for 1.5 h the substance was precipitated by the addition of 250 ml of ethanol. Yield: 7.0 g (59 %).

3. Barium S-(3-hydroxypropyl) phosphorothioate. 9.0 g of Na_3SPO_3 (50 mmole) were dissolved in 125 ml of water (the reaction product is only sparingly soluble in water). 7.1 ml of 3-bromo-1-propanol (80 mmole) and 25 ml of DMF were added (the reaction is very slow with less bromopropanol). The solution was stirred for 1.5 h when 20.5 g of barium acetate monohydrate (75 mmole) dissolved in 50 ml of water were added under

* All yields are calculated on the amount of phosphorothioate used.

vigorous stirring. A microcrystalline precipitate was formed, which was completely precipitated by the addition of 100 ml of ethanol. The precipitate was stirred up in 300 ml of water for 20 min, filtered and pure material was precipitated from the clear filtrate by the addition of 200 ml of ethanol. Yield: 6.7 g (38 %).

4. Dilithium S-(carbamylmethyl) phosphorothioate. 11.5 g of Li_3SPO_3,5.5 H_2O (50 mmole) were dissolved in 100 ml of water. 5.2 g of chloroacetamide (55 mmole) and 25 ml of DMF were added. After 30 min of stirring 200 ml of ethanol were added. The crystalline precipitate was filtered off. Yield: 8.4 g (84 %).

5. Lithiumhydrogen S-(3-aminopropyl) phosphorothioate. This substance was prepared as No. *4* except that 12.0 g of 3-bromopropylammonium bromide (55 mmole) were added. Reaction time: 4.5 h. The addition of 300 ml of ethanol precipitated 6.7 g (72 %) of substance.

6. Barium S-[2-(methylamino)ethyl] phosphorothioate. 9.0 g of Na_3SPO_3 (50 mmole) were dissolved in 75 ml of water and 12.0 g of 2-bromoethylmethylammonium bromide (55 mmole) and 25 ml of DMF were added. The solution was stirred for 30 min. 20.5 g of barium acetate monohydrate (75 mmole) were added and a small precipitate was filtered off. 3.0 g of NaOH (75 mmole) in 25 ml of water were added followed by 400 ml of ethanol. Yield: 11.9 g (70 %).

7. Barium S-[2-(dimethylamino)ethyl] phosphorothioate. 9.0 g of Na_3SPO_3 (50 mmole) were dissolved in 75 ml of water and 12.8 g of 2-bromoethyldimethylammonium bromide (55 mmole) and 25 ml of DMF were added. After 30 min of stirring 20.5 g of barium acetate monohydrate (75 mmole) were added in 50 ml of water. A small precipitate was filtered off. 3.0 g of NaOH (75 mmole) in 25 ml of water were added followed by 200 ml of ethanol. Yield: 12.3 g (69 %).

8. Sodium S-[2-(trimethylammonium)ethyl] phosphorothioate. 9.0 g of Na_3SPO_3 (50 mmole) were dissolved in 175 ml of water. 13.6 g of 2-bromoethyltrimethylammonium bromide (55 mmole) and 30 ml of DMF were added. After 3 h of stirring the reaction mixture was slowly poored into 1500 ml of ethanol of 10° under rapid stirring. A microcrystalline precipitate was filtered off. Yield: 11.3 g (61 %). (Attempts to isolate the compound by precipitation of its barium or lithium salt from aqueous solution by ethanol failed).

9. Barium S-[2-(diisopropylamino)ethyl] phosphorothioate. 9.0 g of Na_3SPO_3 (50 mmole) were dissolved in 75 ml of water and 15.3 g of 2-bromoethyl-diisopropylammonium bromide (53 mmole) and 25 ml of DMF were added. The solution was stirred for 30 min. 12.2 g of barium chloride dihydrate (50 mmole) and 2.0 g of NaOH (50 mmole) were added dissolved in 75 ml of water under vigorous stirring. 200 ml of ethanol were then added under continous stirring and the microcrystalline precipitate was filtered off. 14.2 g (67 %) of dry substance were obtained.

10. Dilithium S-[(2-dimethylamino-1-methyl)ethyl] phosphorothioate. 11.5 g of Li_3SPO_3, 5.5 H_2O (50 mmole) were dissolved in 100 ml of water. 8.7 g of 2-chloropropyldimethylammonium chloride (55 mmole) and 25 ml of DMF were added. After stirring for 45 min 2.5 g of lithium hydroxide hydrate (containing 53 % LiOH, 55 mmole) were added in 30 ml of water. A small precipitate was filtered off and the substance was precipitated by the addition of 900 ml of ethanol. The fine precipitate was centrifuged down and stirred up in another 300 ml of ethanol. After renewed centrifugation the substance was dried in the open air and then in vacuum at 4°. Yield: 6.4 g (49 %).

11. Ammonium lithium S-(2-guanidinoethyl) phosphorothioate. 11.5 g of Li_3SPO_3, 5.5 H_2O (50 mmole) were dissolved in 100 ml of water. 10.9 g of 2-bromoethylammonium bromide (53 mmole) and 25 ml of DMF were added. The mixture was stirred for 1 h.The precipitated crystals were dissolved by the addition of 100 ml of ammonia (29 %) and 50 ml of water. 21.3 g of S-ethylisothiouronium bromide [24] (115 mmole) were added under stirring in small portions during 15 min. The reaction mixture was left at room temperature over night in a well ventilated hood (large amounts of ethanethiol are evolved). A small precipitate was filtered off and the reaction mixture was poured dropwise into 1000 ml of ethanol under rapid stirring. A crystalline precipitate containing a small amount of coprecipitated unreacted S-ethylisothiouroniumbromide was obtained. The substance was purified by dissolving it in 50 ml of water containing 2.3 g of lithium hydroxide hydrate (LiOH content 53 %, 50 mmole). 200 ml of ethanol were slowly added under rapid stirring. The precipitated crystals were filtered off. Yield: 6.5 g (56 %).

12. Ammonium lithium S-(3-guanidinopropyl) phosphorothioate. 11.5 g of Li_3SPO_3, 5.5 H_2O (50 mmole) were dissolved in 150 ml of water. 12.0 g of 3-bromopropylammonium bromide (55 mmole) and 25 ml of DMF were added. After stirring for 2.5 h 50 ml of ammonia (29 %) were added. The reaction mixture was then treated with 13.9 g of S-ethylisothiouroniumbromide (75 mmole) as described under No. *11.* The guanylated derivative was precipitated by the addition of 500 ml of ethanol. No further purification was needed in this case. Yield: 9.5 g (77 %).

13. Tetralithium 1,3-dimercapto-2-propanol S_1,S_3-diphosphate. 11.5 g of Li_3SPO_3,5.5 H_2O (50 mmole) were dissolved in 100 ml of water. 3.0 ml of 1,3-dibromo-2-propanol (28 mmole) and 25 ml of DMF were added. The solution was stirred for 1.5 h and a precipitate was filtered off and discarded (mostly consisting of Li_3PO_4). 400 ml of ethanol were added to the clear filtrate and the crystalline precipitate was filtered off and washed with ethanol. It was first dried in the open air and then in vacuum at 4° (repeated drying in vacuum did not remove the ethanol of crystallization). Yield: 6.3 g (31 %).

14. Tetralithium 2,3-dimercapto-1-propanol S_2,S_3-diphosphate. 11.5 g of Li_3SPO_3,5.5 H_2O (50 mmole) were dissolved in 100 ml of water. 2.95 ml of 2,3-dibromo-1-propanol (28 mmole) and 25 ml of DMF were added. The reaction mixture was set aside for 23 h at room temperature (this long reaction time was found necessary for quantitative reaction). A precipitate was filtered off and discarded. 400 ml of ethanol were added to the clear filtrate and the precipitated substance was filtered off. (Repeated drying in vacuum did not remove the ethanol of crystallization). Yield: 4.7 g (25 %).

The author wishes to thank ing. Sture Andersson for valuable technical assistance.

REFERENCES

1. Hansen, B. and Sörbo, B. *Acta Radiol.* **56** (1961) 141.
2. Åkerfeldt, S. *Acta Chem. Scand.* **13** (1959) 1479.
3. Åkerfeldt, S. *Acta Chem. Scand.* **13** (1959) 1897.
4. Åkerfeldt, S. *Acta Chem. Scand.* **14** (1960) 1980.
5. Åkerfeldt, S. *Acta Chem. Scand.* **15** (1961) 575.
6. Yasuda, S. K. and Lambert, J. L. *J. Am. Chem. Soc.* **76** (1954) 5356.
7. Stadtman, Th. C., Elliott, P. and Tiemann, L. *J. Biol. Chem.* **231** (1958) 961.
8. Pant, R. and Dubey, S. S. *Biochem. J.* **74** (1960) 491.
9. Basford, R. E. and Huennekens, F. M. *J. Am. Chem. Soc.* **77** (1955) 3873.
10. Stirling, C. J. M. *J. Chem. Soc.* **1957** 3597.
11. Lordy, N. G. and Epstein, J. *J. Am. Chem. Soc.* **80** (1958) 509.
12. Jencks, W. P., Cordes, S. and Carriuolo, J. *J. Biol. Chem.* **235** (1960) 3608.
13. Smith, R. A. *Univ. Microfilms* No. 25 286.
14. Feuer, G. and Wollemann, M. *Acta Phys. Acad. Sci. Hung.* **10** (1956) 1.
15. Wieland, T. and Lambert, R. *Chem. Ber.* **89** (1956) 2476.
16. Reid, V. W. and Salmon, D. G. *Analyst* **80** (1955) 704.
17. Åkerfeldt, S. *Acta Chem. Scand.* **13** (1959) 627.
18. Bobranski, B., Jakobiec, T. and Prelicz, D. *Roczniki Chem.* **30** (1956) 623.
19. Renshaw, R. R. *J. Am. Chem. Soc.* **34** (1912) 1615.
20. Knorr, L. and Meyer, G. *Ber.* **38** (1905) 3129.
21. Kohler, E. P. *Am. Chem. J.* **42** (1909) 375.
22. Schöberl, A., Kawohl, M. and Hansen, G. *Ann.* **614** (1958) 83.
23. Anderegg, G., Flaschka, H., Sallmann, R. and Schwarzenbach, G. *Helv. Chim. Acta* **37** (1954) 113.
24. *Organic Synthesis*, Coll. Vol. III, p. 440.
25. Grunert, R. R. and Phillips, P. H. *Arch. Biochem. Biophys.* **30** (1951) 217.
26. Thomason, P. F. *Anal. Chem.* **28** (1956) 1527.
27. Philipson, L. *Biochim. Biophys. Acta* **56** (1962) 375.
28. Field, L., Owen, T. C., Crenshaw, R. R. and Bryan, A. W. *J. Am. Chem. Soc.* **83** (1961) 4414.

Received April 17, 1962.

ACTA CHEMICA SCANDINAVICA 16 (1962) 1908–1918

Quantitative Determination of the Uronic Acid Composition of Alginates

ARNE HAUG and BJØRN LARSEN

Norwegian Institute of Seaweed Research, N.T.H., Trondheim, Norway

A method for quantitative determination of the uronic acid composition of alginates is described. The method is based on hydrolysis of the alginate with 80 % sulphuric acid at 20°C, followed by treatment with 2 N acid at 100°C, and separation of the uronic acids in the hydrolysate by chromatography on an anion exchange column. The amounts of the different uronic acids are determined by the orcinol reaction.

The loss of uronic acids in the different steps in the procedure has been investigated and a factor correcting for the different rate of breakdown of guluronic and mannuronic acid is introduced.

Until 1955 D-mannuronic acid was supposed to be the sole constituent of alginic acid. In that year, however, Fischer and Dörfel [1] discovered the presence of L-guluronic acid in hydrolysates of alginates. The presence of L-guluronic acid has later been confirmed by other authors [2,3].

Fischer and Dörfel described a method for quantitative determination of the uronic acid composition of alginates [1,4]. The method was based on hydrolysis with 80 % sulphuric acid at room temperature, followed by boiling in 2 N acid, separation of the uronic acids by paper chromatography and determination of the amounts by using the tetrazolium chloride reaction and extracting the coloured compounds from the paper. The uronic acid composition of a number of seaweed species was investigated.

Recent works have shown that there exists a close correlation between properties and composition of alginates [5–8], and that algae used as raw material for commercial alginate production may have very different uronic acid composition. It has therefore become of importance for the practical application of alginates to have a convenient routine method for the determination of the proportion of the two uronic acid residues in the alginates.

The method of Fischer and Dörfel has not proved satisfactory for routine determinations. The chromatographic separation requires very careful handling to give a separation good enough for quantitative work, and the colour reaction needs rigorously standardized conditions to give reproducible results.

The present communication describes a method suited for routine determination of the composition of alginate samples. All methods for chemical hydrolysis of polyuronides so far investigated lead to a considerable breakdown of uronic acids, and the rate of breakdown of guluronic and mannuronic acid has been shown to be different [2]. The loss of material during the procedure has therefore been investigated, and attempts have been made to correct the results for the different rate of breakdown of the two uronic acids.

EXPERIMENTAL

Standard procedure. The preparation of alginate from seaweed samples has been described earlier [9]. Sodium alginate (50 mg) is mixed with 0.5 ml of 80 % H_2SO_4 while the mixture is cooled in an ice bath. The mixture is left for 18 h in a thermostat at 20°C. The acid is diluted to obtain an acid strength of 2 N by adding 6.5 ml of water while the mixture is cooled in an ice bath. The mixture is then heated in a boiling water bath in sealed glass tubes for 5 h. Neutralization is carried out by adding a slight excess of $CaCO_3$ to the hydrolysate after cooling. The bulky precipitate is filtered off and washed with water until about twice the original volume of hydrolysate has passed through the filter. The column chromatography is carried out on Dowex 1 × 8 anion exchange resin (200—400 mesh). The resin was previously activated with 2 N NaOH and transformed to acetate form by washing with 2 N acetic acid and finally washed thoroughly with 0.5 N acetic acid. The column is 20 cm × 2 cm and is conveniently made of plexiglas tube, fitted with a screw cap bottom piece. A Teflon gasket is usually necessary. A 1.5 mm nylon tube is forced through a 1.0 mm hole in the bottom piece. Before the hydrolysate is applied to the column, all lactones are transformed to uronic acids by adding sufficient alkali to keep the solution at a pH of about 8 for half an hour. The elution of the column is carried out with acetic acid in a linear gradient from 0.5 N to 2 N. The flow rate is 0.3 ml per minute. Approximately 1 liter of acid is passed through the column in each run, and fractions of 10 ml are collected. The same column may be used for 10 to 20 runs.

Localization of the uronic acids is carried out by spotting a drop of each fraction on a filter paper strip. After drying, the filter paper strip is dipped in a solution containing 2.5 % aniline-trichloroacetate in glacial acetic acid, dried at room temperature and heated for 3 to 5 min at 100°C. The paper is examined in ultraviolet light. Apart from the first fractions which usually contain small amounts of neutral sugars, the fractions showing positive reaction with the staining reagent fall into two groups, the first containing guluronic and the second mannuronic acid [10]. The fractions in each group are combined and the volume determined. Care must be taken to include all fractions which contain uronic acids. The amount of uronic acid in each of the two groups is determined by the orcinol method [11].

Materials. Alginates prepared from four different seaweed samples were used in this investigation: *Ascophyllum nodosum*, Flak 6/8—58, *Laminaria hyperborea* stipes, Hustad 26/2—59, *Laminaria digitata*, Espevær 10/6—52 and 8/1—53. The uronic acid composition of the samples is given in Table 7. In addition the uronic acid composition of a few laboratory preparations and commercial samples has been investigated. Guluronic and mannuronic acid were prepared by chromatography of the lactones on cellulose columns as described by Fischer and Dörfel [4]. Attempts to crystallize guluronic acid and its lactone were unsuccessful, and the concentration of guluronic acid in the solutions used for standard curves was determined in the following way: The aqueous solution of guluronic acid was treated with alkali to transform any lactone present to salt, and the acid liberated by running the solution through a column of Dowex 50 W ion exchange resin. The solution was immediately titrated with 0.1 N sodium hydroxide.

Hydrolysis. Three methods of hydrolysis were investigated: (1) Sodium alginate (50 mg) was treated with 80 % sulphuric acid as in the standard procedure. After dilution to 2 N acid, more 2 N H_2SO_4 was added until a volume of 100 ml was obtained. The hydrolysis was carried out on a boiling water bath in a boiling flask fitted with a reflux condenser. (2) Sodium alginate (50 mg) was hydrolysed with 100 ml 1 N H_2SO_4 on the water bath

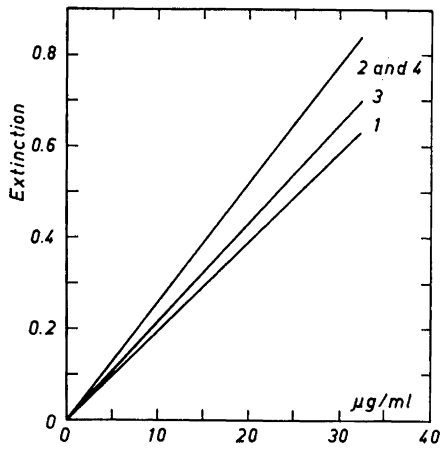

Fig. 1. The orcinol reaction. 1 = Guluronic acid. 2 = Mannuronic acid. 3 = Galacturonic acid. 4 = Glucuronic acid.

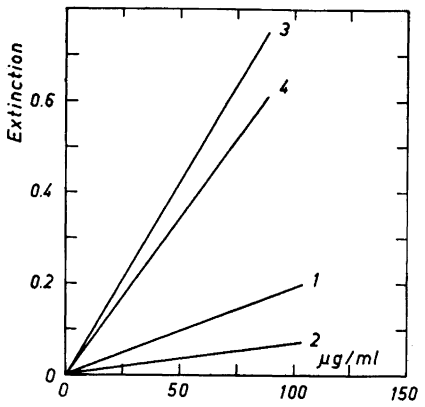

Fig. 2. The carbazole reaction. Symbols as in Fig. 1.

without pretreatment with concentrated acid. (3) Sodium alginate (50 mg) was hydrolysed with 100 ml 1 N oxalic acid on the water bath. In all cases, samples of 10 ml were taken out at fixed intervals for analysis.

Colour reactions. Apart from the orcinol reaction used in the standard procedure, the phenol sulphuric acid method [12] and the carbazole method [13] have been employed. In the phenol sulphuric acid reaction 0.5 ml of a 3 % solution of phenol was used. The colour was measured in a Beckman B spectrophotometer. In the orcinol reaction 1.5 ml samples were used, in the phenol-sulphuric acid reaction 2 ml and in the carbazole reaction 1 ml, according to the standard procedures.

Reducing power was determined by the method of Hagedorn and Jensen, modified to a semi-micro method by Fujita and Iwatake (described in Ref.[14]).

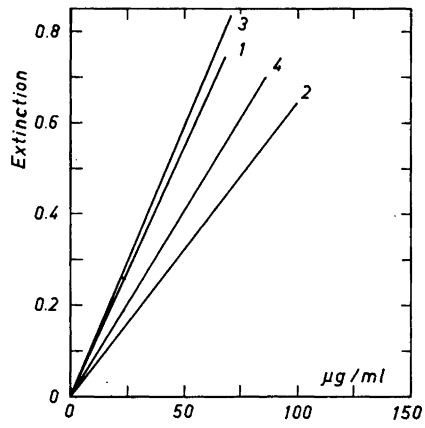

Fig. 3. The phenol-sulphuric acid reaction. Symbols as in Fig. 1.

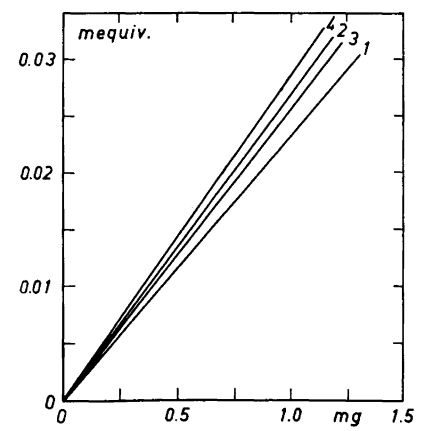

Fig. 4. Reducing power. Symbols as in Fig. 1.

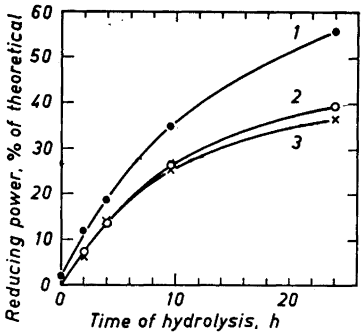

Fig. 5. Hydrolysis with 1 N oxalic acid. Alginate prepared from: 1 = *A. nodosum*, Flak, 6/8—58. 2 = *L. digitata*, Espevær, 10/6—52. 3 = *L. hyperborea* stipes, Hustad, 26/2—59.

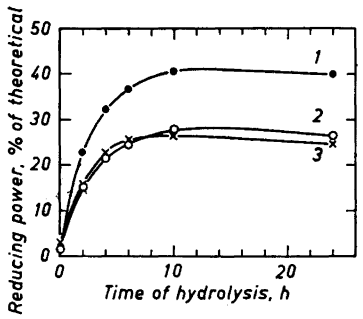

Fig. 6. Hydrolysis with 1 N sulphuric acid. Symbols as in Fig. 5.

RESULTS

Standard curves for the three colour reactions and the reducing power determination were determined for guluronic, mannuronic, galacturonic and glucuronic acid and the results are given in Figs. 1—4. The standard curves for the colour reactions refer to the concentration of uronic acids in the samples used in the reaction, given in μg per ml.

Three different methods of hydrolysis were investigated; (*a*) hydrolysis with 1.0 N oxalic acid, (*b*) with 1.0 N sulphuric acid and (*c*) with 2.0 N sulphuric acid after pretreatment with 80 % sulphuric acid at room temperature. The rate of hydrolysis has been investigated by measuring the reducing power of the hydrolysates, and the results are given in Figs. 5—7 for three

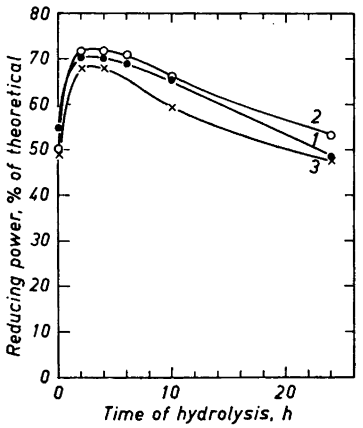

Fig. 7. Hydrolysis with 2 N H_2SO_4 after pretreatment with 80 % H_2SO_4 at 20°C. Symbols as in Fig. 5.

Table 1. Pretreatment with 80 % sulphuric acid at different temperatures. Reducing power and colour with phenolsulphuric acid as per cent of theoretical before and after hydrolysis with 2 N sulphuric acid for 5 h at 100°C.

Reducing power Pretreatment	*A. nodosum* 6/8		*L. digitata* 10/6		*L. hyperborea* stipes, 26/2	
at	Before	After	Before	After	Before	After
15°	41	66	42	61	36	55.5
20	50.5	66	53	65	45.5	56
25	60.5	65.5	61.5	64	54	61.5
30	62	59	63.5	64.5	58	62.5
35	66	56	68	60	65	58.5
Phenol-sulphuric acid						
15°	105	86	99	74	104	64
20	100	80	95	78	98	66
25	101	75	96	71	96	66
30	81	73	87.5	73	87	60
35	85	71	84.5	68	84	64

different alginate samples. The results are given as per cent of the theoretical value. The calculation of the theoretical value is based on the uronic acid composition of the hydrolysates, determined by the standard procedure. As shown by the figures, the highest reducing power was obtained by using pretreatment with strong sulphuric acid, followed by hydrolysis in dilute acid for a relatively short time.

The effect of different temperatures during the pretreatment with strong acid was investigated and the results obtained are shown in Table 1. Whilst high temperature during the pretreatment gives high values of the reducing power before hydrolysis with the dilute acid, the reducing power after 5 h hydrolysis with 2 N acid does not vary markedly with the temperature during the pretreatment, thus 20°C has been chosen for the standard procedure.

The loss of material which occurs throughout the procedure has been investigated by means of the phenol-sulphuric acid reaction, the orcinol reaction and reducing power determinations. The results are given in Table 2. It should be noted that the low value for unhydrolysed alginate by the orcinol reaction is not due to loss of material, but is caused by the fact that a complete reaction with orcinol is not obtained with the undegraded polymer.

Table 2. Recovery of material in the different stages of the standard procedure. Alginate from *L. digitata*, Espevær, 8/1—53. The results are given as per cent of the theoretical value for starting material.

	Phenol-sulphuric acid reaction	Orcinol	Reducing power
Before hydrolysis	102	54	0
After hydrolysis	84	63	73
After neutralization	75	56.5	64.5
Totale eluate from column	45.5	41.5	
Guluronic & mannuronic acid	40.0	39.5	40.5

Table 3. Loss of uronic acids in the neutralization with calcium carbonate. 100 mg alginate from *L. digitata* 8/1.

	Guluronic acid	Mannuronic acid	Total	M/G
Standard filtrate	12.9 mg	22.5 mg	35.4 mg	1.75
Second washing	0.86 »	1.8 »	2.66 »	2.09
Total	13.76 »	24.3 »	38.06 »	1.77

The loss in the different steps in the procedure has been investigated further, in order to establish if the loss of the two uronic acids is of the same magnitude, and, if that is not the case, to attempt to correct for the difference in recovery of the two components.

The loss occurring in the neutralization is due to incomplete removal of all uronic acids from the calcium sulphate precipitate. A sample of alginate from *L. digitata*, 8/1, was hydrolysed by the standard procedure and neutralized. After filtration and washing according to the standard procedure the uronic acid composition of the hydrolysate was determined. The residue on the filter was washed thoroughly with water and the washwater concentrated by evaporation and the uronic acid composition determined. The result is given in Table 3.

The loss occurring during hydrolysis was investigated by subjecting pure uronic acids to the same treatment as the alginate samples. After pretreatment with 80 % sulphuric acid at 20°C for 18 h, the uronic acids were heated in 2 N sulphuric acid on the water bath. The results are given in Figs. 8 and 9. As in the case of alginate hydrolysates (Table 2) the colour obtained with orcinol was considerably lower, compared to the theoretical value, than the reducing power and the colour with phenol-sulphuric acid. The results indicate

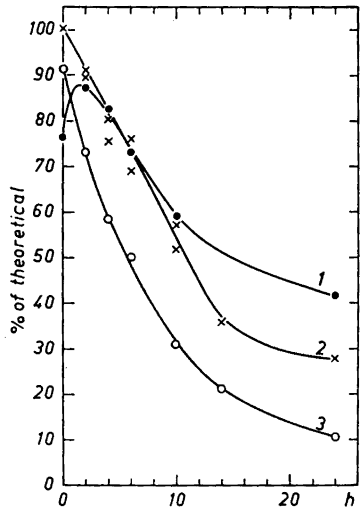

Fig. 8. Treatment of guluronic acid with 2 N H_2SO_4 at 100°C after pretreatment with 80 % H_2SO_4 at 20°C. 1 = Reducing power. 2 = Phenol-sulphuric acid reaction. 3 = Orcinol reaction.

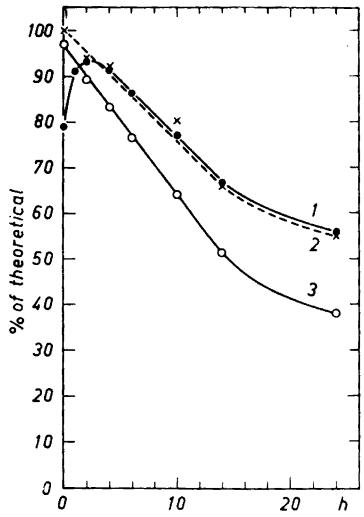

Fig. 9. Treatment of mannuronic acid with 2 N H_2SO_4 at 100°C after pretreatment with 80 % H_2SO_4 at 20°C. Symbols as in Fig. 8.

that the breakdown of uronic acids leads to formation of products which have reducing power and give colour formation with phenol-sulphuric acid but which give little or no colour with orcinol.

This point was further investigated by treating galacturonic and glucuronic acid with sulphuric acid as described above. After 24 h at 100°C the reducing power, orcinol colour and phenolsulphuric acid colour were determined and the solution passed through a column of anion exchange resin. The same quantities were determined in the eluate from the column. The results are given in Table 4 as a percentage of the theoretical value.

The separation of uronic acids on a column of anion exchange resin is described in an earlier work [10]. In order to study further the behaviour of an alginate hydrolysate on the column, the elution was followed by the orcinol and phenol-sulphuric acid reactions. A sample of alginate (50 mg) prepared from *L. digitata*, 8/1, was hydrolysed according to the standard procedure,

Table 4. Analysis of "hydrolysates" of uronic acid before and after treatment with anion exchange resin, given as per cent of theoretical value.

	Treatment with anion exchange resin	
	Before	After
Glucuronic acid		
Reducing power	57	39.9
Phenol-sulphuric acid	55	41.7
Orcinol	37.5	35.6
Galacturonic acid		
Reducing power	53	17.0
Phenol-sulphuric acid	35	21.8
Orcinol	18.5	18.5

Table 5. Chromatography of hydrolysate of alginate prepared from *L. digitata*, Espevær 8/1. Sample 50 mg.

Tube No.	Volume	Phenolsulphuric acid	Orcinol	Identity
1— 3	22	0.25 mg	0.08 mg	
4— 5	14.5	0.68 »	0.14 »	Neutral sugars
6— 82	430	0.63 »	0.18 »	
83—104	86	6.80 »	6.45 »	Guluronic acid
105—119	69.5	0.41 »	0.20 »	
120—131	96.5	11.00 »	10.80 »	Mannuronic acid
132—140	59.5	0.39 »	0.22 »	
141—164	150	0.35 »	0.27 »	
		20.51	18.44	

Table 6. Reproducibility of the determination and correction for different rate of breakdown in the hydrolysis. Alginate prepared from *L. digitata*, Espevær, 8/1. Proportion between mannuronic and guluronic acid (M/G).

	M/G	Average	Correction factor (Figs. 8 & 9)	Corrected result
Standard procedure	1.75			
(5 h, 100°, 2 N H_2SO_4)	1.67			
	1.74	1.75	53/80	1.16
	1.80			
	1.76			
10 h, 100°, 2 N H_2SO_4)	2.56			
	2.48	2.52	31/64	1.22
24 h, 100°, 2 N H_2SO_4)	4.20			
	4.77	4.48	10.5/37.5	1.25

Table 7. Uronic acid composition of some alginate samples, given as the proportion between mannuronic and guluronic acid residues (M/G).

Samples	M/G
A. nodosum, Flak, 6/8—58	1.82
L. hyperborea stipes, Hustad, 26/2—59	0.37
» » fronds, Reine, 30/1—57	1.28
L. digitata, Espevær, 8/1—53	1.16
» » , » , 10/6—52	1.58
Manucol SS/LD (*L. hyperborea* stipes)	0.46
» SA/LM (*A. nodosum*)	1.10
Protanal LF (*L. digitata*)	1.43
Kelco SS (*Macrocystis pyrifera*)	1.56

neutralized and added to the column. The results are given in Table 5 as mg substance in each fraction. For the fractions not identified as guluronic or mannuronic acid the calculation is based on an extinction corresponding to a mixture of guluronic and mannuronic acid in the same proportion as in the hydrolysate.

The reproducibility of the method was investigated by determining the uronic acid composition of five samples of the alginate prepared from *L. digitata*, 8/1, by the standard procedure. In addition two samples were hydrolysed for 10 h and two samples for 24 h and the results corrected for diffferent rate of breakdown of the two uronic acids during hydrolysis according to the curves for the orcinol reaction in Figs. 8 and 9. The results are given in Table 6.

The uronic acid composition of some laboratory preparations and commercial samples is given in Table 7, determined by the standard procedure. The results are corrected for the different rate of breakdown of the two uronic acids during hydrolysis by multiplying the proportion between the mannuronic and the guluronic acid in the hydrolysates with 0.66.

DISCUSSION

The different uronic acids give very different colour reaction with carbazole (Fig. 2) and our results are in agreement with earlier observations by Hoffman, Linker and Meyer [15]. The colour development in the phenol-sulphuric acid reaction is also different for the different uronic acids (Fig. 3) and significant differences are also found for the orcinol reaction (Fig. 1) [15]. The colour reaction may thus be used for a preliminary identification of the uronic acids.

As shown in Table 2, the phenol sulphuric acid reaction gives a colour corresponding to approximately 100 % of the theoretical value when carried out on an alginate solution not subjected to hydrolysis. On account of the marked difference in colour formation with this reagent for guluronic and mannuronic acid a rough estimation of the proportion between the two uronic acids may be obtained in this way. A more exact determination is not possible because of the small amounts of neutral sugars usually present in the alginate samples which interfere in the determination. The possibility of using the more specific carbazole reaction for this purpose is limited by the fact that small amounts of glucuronic acid is present in some alginate preparations, and that the sensitivity of the reaction is very much higher for this compound than for mannuronic and guluronic acid. It is also possible that a slight epimerization of mannuronic acid to glucuronic acid may occur in the acid medium in the reaction [16]. The orcinol reaction gives only a colour corresponding to approximately 50 % of the theoretical value when carried out on unhydrolysed alginate.

The results from the hydrolysis experiments (Figs. 5—7) indicate a considerable breakdown in the hydrolysis with sulphuric acid, while hydrolysis with oxalic acid does not give a sufficient yield in a reasonable time. While pretreatment with 80 % sulphuric acid gives the best results for our purpose, it should be pointed out that the experiments with pure uronic acids (curves 8 and 9) indicate a marked formation of reversion products in the strong acid treatment. This method should therefore be avoided if oligosaccharides produced by partial hydrolysis is to be studied for structural investigations.

The results in Table 2 show that loss of material occurs during the hydrolysis, in the neutralization and on the column, and that a small proportion of

the material eluted from the column is not guluronic or mannuronic acid. Considering the results from the orcinol reaction, the most important loss occurs in the hydrolysis (37 %) while 15 % is lost on the column. The results from the phenol-sulphuric acid reaction, however, indicate a loss of about 15 % in the hydrolysis and 30 % on the column. This is in agreement with the results from the experiments with pure uronic acids (Figs. 8 and 9 and Table 4) which clearly indicate that breakdown products are formed which give colour reaction with phenol-sulphuric acid but not with orcinol, and which are absorbed on the anion exchange resin. These products may be identical with the brown-coloured compounds which are irreversibly absorbed on the top of the anion exchange resin column. The results from Table 4 show that the compounds giving the orcinol reaction are quantitatively eluted from the column, thus indicating that these compounds are unchanged uronic acids. This has been confirmed by paper electrophoresis [17] and paper chromatography [4]. This suggests that the orcinol curves in Figs. 8 and 9 can be used for estimating the breakdown of uronic acids. According to these curves, between 20 and 50 % of the uronic acids are destroyed during the standard hydrolysis, depending on the proportion of the two uronic acids in the alginate.

For the alginate used in Table 2, this corresponds to a loss of about 35 % of the total amount of uronic acids, in good agreement with the loss during hydrolysis observed with the orcinol reaction.

While no significant loss of substance giving orcinol reaction could be observed by treating the "hydrolysates" of pure uronic acids with anion exchange resins (Table 4), about 15 % is lost when hydrolysates of alginates is chromatographed on anion exchange resin (Table 2). This loss may be due to unhydrolysed fragments of alginate or reversion products being absorbed on the column and not eluted with the acid strength used in our procedure.

Table 3 shows that no significant selective absorbtion of one of the uronic acids occurs on the calcium sulphate precipitate, and the loss of material during neutralization is thus of no importance for the determination of the proportion between the two uronic acids.

Analysis of the eluate from the column (Table 5) shows that 93.5 % of the substances eluted is mannuronic and guluronic acid if the calculation is based on the orcinol reaction and 87 % if based on the phenol-sulphuric acid reaction. This difference is probably due to small amounts of neutral sugars eluted in the first fractions giving a higher extinction in the phenol-sulphuric acid reaction than in the orcinol reaction.

According to Table 2, the recovery of uronic acids in the standard procedure is approximately 40 %. Of the 60 % lost in the procedure 43 to 44 % are due to loss during neutralization and breakdown in the hydrolysis. If the proportion between the two uronic acids in the 15 % of the material lost on the column is not very different from the proportion in the whole alginate, it should be possible to estimate the uronic acid composition of the alginate sample by correcting the results obtained by the standard procedure for the different rate of breakdown of guluronic and mannuronic acid. This correction by means of the orcinol curves in Figs. 8 and 9 has been tested by increasing the time of hydrolysis with 2 N acid to 10 and 24 hours. While the composition of the hydrolysates is very markedly altered by increasing the time of

hydrolysis, the corrected results show a satisfactory agreement. It seems safe to conclude that by using our standard procedure and multiplying the proportion between mannuronic and guluronic acid by 0.66 g good estimate of the uronic acid composition of the alginate sample is obtained.

REFERENCES

1. Fischer, F. G. and Dörfel, H. *Z. physiol. Chem., Hoppe-Seyler's* **302** (1955) 186.
2. Whistler, R. L. and Kirby, K. W. *Z. physiol. Chem., Hoppe-Seyler's* **314** (1959) 46.
3. Hirst, E. L. *Proc. Chem. Soc.* **1958** 177.
4. Fischer, F. G. and Dörfel, H. *Z. physiol. Chem., Hoppe-Seyler's* **301** (1955) 224.
5. Haug, A. *Acta Chem. Scand.* **13** (1959) 1250.
6. Haug, A. *Acta Chem. Scand.* **15** (1961) 950.
7. Haug, A. *Acta Chem. Scand.* **15** (1961) 1794.
8. Haug, A. and Larsen, B. *Proc. 4th Intern. Seaweed Symp.*, Biarritz 1962. *In press.*
9. Haug, A. *Acta Chem. Scand.* **13** (1959) 601.
10. Larsen, B. and Haug, A. *Acta Chem. Scand.* **15** (1961) 1397.
11. Brown, H. H. *Arch. Biochem.* **11** (1946) 269.
12. Dubois, M., Gilles, K. A., Hamilton, J. K., Ribers, P. A. and Smith, F. *Anal. Chem.* **28** (1956) 350.
13. Dische, Z. in Glick, D. *Methods of Biochemical Analysis* **2** (1954).
14. Bamann, R. and Myrbäck, K. *Die Methoden der Fermentforschung*, I. 1074, Leipzig 1941.
15. Hoffmann, Ph., Linker, A. and Meyer, K. *Science* **124** (1956) 1552.
16. Berner, E. and Sandlie, S. *Chem. & Ind. (London)* **1952** 1221.
17. Haug, A. and Larsen, B. *Acta Chem. Scand.* **15** (1961) 1395.

Received April 16, 1962.

ACTA CHEMICA SCANDINAVICA 16 (1962) 1919–1926

Studies on Cobaltammines

V. Anion-Exchange Investigations of the Outer-Sphere Complexity of the Cobalthexammine(III) Ion

RAGNAR LARSSON and INGA TOBIASON

Department of Inorganic and Physical Chemistry, Chemical Institute, University of Lund, Lund, Sweden

The distribution of the $Co(NH_3)_6^{3+}$ ion between an anion exchanger and water has been determined for varying concentrations in the aqueous phase of sulphate, thiosulphate, fluoride, chloride, bromide and acetate ions. From the distribution curves obtained the existence of the third sulphate and thiosulphate complexes is deduced as well as the fourth chloride and bromide complexes.

The tendency towards the formation of anionic complexes follows the order $S_2O_3^{2-} > SO_4^{2-}$ and $Br^- > Cl^- > F^-$. These results seem to support the concept of a second coordination sphere of the $Co(NH_3)_6^{3+}$ ion, which is closely analogous with the inner coordination sphere.

In recent years many reports have appeared concerning the association between various anions and complex ions, such as $Co(NH_3)_6^{3+}$ and $Cr(NH_3)_6^{3+}$. The association products have sometimes been described as "ion-pairs", sometimes as "outer-sphere complexes". The first term was introduced by Bjerrum [1] and formally describes the effect of the long-range electrostatic forces around such highly charged ions. These effects, however, can also be treated in other ways (Gronwall *et al.*[2], Mayer [3], Guggenheim [4]).

On the other hand, if the concept of "outer-sphere complexes" shall be used sensibly, we cannot confine ourselves to the mere existence of such association products, as they can be described as indicated above. The term "sphere" is intimately related to the coordination theory of Werner [5], and if the term "outer-sphere complexes" should have any pragmatic sense, we must demand that the same criteria shall apply to the *outer sphere of coordination* as to the *inner* one. That is, the ligands must be assumed to occupy a limited number of so-called coordination sites, and moreover, these should be spatially well defined. Such a situation obviously arises if some kind or kinds of specific interaction is at hand.

As in the case of coordination in the inner sphere, it is not necessary to specify the "forces" of interaction.

It seems to the present authors that an indication of the usefulness of the concept of outer-sphere coordination would be the detection of association products that cannot be explained in terms of "ion-pairing". Such association products would be anionic complexes, *e.g.* $[Co(NH_3)_6Cl_4]^-$ or $[Co(NH_3)_6(SO_4)_3]^{3-}$, *i.e.* of a composition that corresponds to an association between negatively charged ligands and uncharged or negatively charged central groups.

A method for the detection of anionic complexes has been devised by Fronæus [6]. This method has been used in this investigation to study the association between the cobalthexammine(III) ion and fluoride, chloride, bromide, acetate, sulphate and thiosulphate ions, respectively.

THEORY

The distribution of the hexammine cobalt complex, here denoted MA_6, between the anion exchange resin, saturated with the ligand B, and the aqueous solution with the total concentration of ligand C_B, is designated as:

$$\varphi = C_{(MA_6)R}/C_{MA_6} \tag{1}$$

The subscript R indicates the resin phase.

It can be shown [6] that

$$\varphi = K \cdot \frac{X([B]_R)}{[B]_R^\nu} \cdot \frac{[B]^\nu}{X([B])} \tag{2}$$

Here

$$X = 1 + \sum_{n=1}^{N} \beta_n [B]^n \tag{3}$$

K is the constant of the Donnan equation, and ν is the quotient between the absolute values of the ionic charge of the central group and that of the ligand.

Further-more it has been shown [6] that φ has a maximum value for such a [B] that the mean ligand number $\bar{n} = \nu$. This holds true whether ν is a whole number or not.

It can be seen from eqn. (2) that for two systems, for which K can be regarded as approximately equal, φ will be greatest — at corresponding values of [B], *e.g.* at the maximum — for the system that exhibits the greatest anion complexity in the resin phase (*cf.* Ref.[6], p. 3).

Thus there are two possible indications of the formation of the anionic complexes alluded to in the introduction: the appearance of a maximum, which indicates the formation of anionic complexes in the aqueous phase, and the magnitude of that maximum, which is a measure of the degree of formation of anionic complexes at the very high ligand concentrations that exist in the resin phase.

Furthermore, if we assume that $[B]_R$ is constant, it is easily deduced (Ref.[7], p. 1449) that

$$\mathrm{d\ ln}\ \varphi/\mathrm{d\ ln}\ [B] = \nu - \bar{n} \tag{4}$$

from which relation $\bar{n}$ may be estimated also beyond the value of ν.

MEASUREMENTS

Experimental technique. In 50 ml glass bottles with well ground stoppers a weighed amount (w g) of resin was added to 15 ml of a solution with a ligand concentration C'_B and a concentration C'_{MA_6} of $Co(NH_3)_6(ClO_4)_3$. w was always 1.00 g. The bottles were carefully closed and put into brass cylinders, which were kept rotating in a water thermostat (20°C) for 30 h at least.

The brass cylinders had the twofold purpose of preventing the bottles from breaking and of protecting the solutions from light, that might have produced decomposition of the cobalt complex [8].

After the indicated time, the solution was separated as completely as possible from the resin phase by backway filtration using a large-porous filterstick. The cobalt concentration was determined for both phases. As the φ values were in all cases $< 10^{-2}$ l/g, the cobalt charge of the resin phase could be quantitatively extracted by shaking with a certain volume v_1 (15 ml) of water. The cobalt used contained an amount of ^{60}Co (Harwell) and the determinations of the cobalt concentrations could thus be easily performed radiometrically.

Measurement of radioactivity. The detector and the scaler were the same as before [9]. In addition, auxiliary equipment, constructed in this laboratory, was used, which, together with a Tracergraph Printing Timer, allowed automatic registration of a series of samples. The reproducibility was 1 %.

Chemicals used. Sodium (in one case litium) salts of *pro analysi* quality were used. Stock solutions were made by dissolution of weighed amounts in distilled water. The concentrations were checked for the NaCl and NaBr solutions with argentometric titration, for Na_2SO_4 solution with alkalimetric titration after cation exchange and for the $Na_2S_2O_3$ solution with iodometric titration.

The anion exchange resin was Dowex 1 × 4, 50—100 mesh. It was converted to the proper ionic form and air-dried.

Calculation of [B]. The swelling factor of the resin, $\delta = C'_B/C_B$, was determined by a titration of the liquid phase for the chloride, bromide and thiosulphate systems (Fig. 1). For the sulphate system the values for the thiosulphate system were used. From these curves C_B could be calculated for any C'_B (the concentration of ligand before equilibrization). As C'_M was kept very low (0.2 mM), [B] was put equal to C_B in all cases but those of very low sulphate and thiosulphate concentrations, where $[B] = (C_B + 3\ C'_M)\ \delta^{-1}$ (*cf.* Ref.[6], p. 5).

Calculation of φ. To calculate C_{MR} we use the relation $C_{(MA_6)R} = v_1 \cdot C''_{MA_6} \cdot w^{-1}$ where C''_{MA_6} is the cobalt concentration of the washing-solution.

Thus

$$\varphi = C_{(MA_6)R}/C_{MA_6} = v_1\ C''_{MA_6}\ w^{-1}/C_{MA_6} \qquad (5)$$

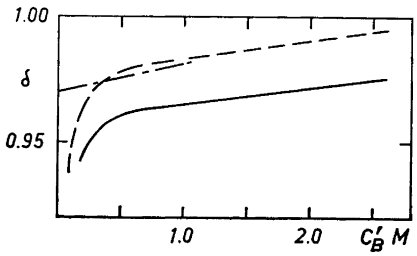

Fig. 1. Swelling factor $\delta = C'_B/C_B$ of the resin: chloride (——), bromide (— — —) and thiosulphate (— · — · —) solutions.

As $C''_{MA_6} = \text{Const} \cdot I_2$ and $C_{MA_6} = \text{Const} \cdot I_1$ where I_1 and I_2 are the γ-intensities of 10 ml of the first filtrate and the washing-solution, respectively, we then obtain

$$\varphi = v_1 I_2 w^{-1} / I_1 \text{ l/g} \quad (6)$$

A reproducibility of 5 % or better was obtained. As the resin particles could not be completely freed from adherent solution, there is a certain contribution, φ_a, in the thus calculated φ values. (*cf.* Sonesson, Ref.[7], p. 1448). In order to obtain the real φ we must make an estimate of φ_a. Sonesson [7] used the value 0.5 ml/g, a value obtained from his measurements of the gadolinium acetate system. This choice was based on the assumption that the tendency to form anionic complexes was very small within this system so that the φ obtained could be regarded as almost a pure φ_a-contribution. In the present investigation the estimate of φ_a is based upon the measurements of the fluoride and acetate systems, where very low and rather constant φ values are found (Table 3). As φ_a must be equal to or less than the smallest φ found, we make the estimate $\varphi_a = 0.45$ ml/g. This is in good agreement with the value used by Sonesson [7], as it should be for the same type of resin. Some difference must be expected caused by variations in particle size and separation effectivity.

Another correction, φ_s, that must be made, arises from the adsorption on the surface of the resin (Ref.[6], p. 4). This effect is more difficult to determine, as it must be expected that several factors are at hand. First, the most strongly adsorbed ionic species is of course, the tervalent uncomplexed MA_6, and so φ_s will decrease more rapidly the stronger the complexity of the system is. On the other hand, the adsorption must depend on the nature of the surface and thus on the ionic form of the resin. For this reason different correction terms have been used for φ_s in this paper. For the sulphate and thiosulphate systems the correction used by Sonesson [7] has been used, only slightly modified. This

Table 1. The distribution quotients for the sulphate and thiosulphate systems. ($C'_M = 0.2$ mM).

a. The sulphate system				b. The thiosulphate system			
[B] M	φ ml . g^{-1}	$(\varphi_a + \varphi_s)$ ml . g^{-1}	φ_{corr} ml . g^{-1}	[B] M	φ ml . g^{-1}	$\varphi_a + \varphi_s$ ml . g^{-1}	φ_{corr} ml . g^{-1}
1.6	1.32	1.3	—	1.6	3.30	1.3	2.0
18.4	2.73	1.63	1.10	11.0	5.20	1.65	3.55
34.9	2.48	1.16	1.32	17.9	5.36	1.62	3.74
51.8	2.37	0.82	1.55	35.2	4.94	1.16	3.78
103	2.13	0.54	1.59	52.5	4.52	0.82	3.70
273	1.60	0.45	1.15	104	3.62	0.54	3.08
340	1.35	0.45	0.90	276	2.25	0.45	1.80
543	1.14	0.45	0.69	345	1.94	0.45	1.49
678	0.95	0.45	0.50	550	1.51	0.45	1.06
945	0.82	0.45	0.37	686	1.30	0.45	0.85
				1020	1.13	0.45	0.68
				1620	0.96	0.45	0.51
				2015	0.90	0.45	0.45

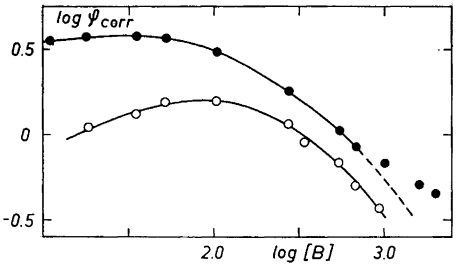

Fig. 2. The logarithms of the corrected distribution quotients of the sulphate (O) and thiosulphate (●) systems plotted against log[B].

correction was made, as it has been found to work properly for the system (gadolinium glycolate) studied by Sonesson [7], a system, which seems to be of about the same complexity as those two mentioned above (*vide infra*). For the chloride and bromide systems of a much weaker complexity the excessive value of φ for small C_B is much less, that is, φ_s does not contribute to any greater extent. Any correction in these cases is very much a question of choice, and the reported values (Fig. 3) have not been corrected for the adsorption effect.

RESULTS

The measurements of the sulphate and thiosulphate systems are given in Table 1. It can clearly be seen that both these systems exhibit a maximum of φ. In Fig. 2 log φ_{corr} is plotted against log[B]. The maximum of the thiosulphate system is greater and appears at a lower value of [B] than the one of the sulphate system.

From Fig. 2 one can obtain d log φ_{corr}/d log[B] and thus from eqn. (4) one can calculate $\bar{n}$. Such a calculation is very uncertain because of the many corrections made and also because of the unvalidity of the assumption of a constant $[B]_R$ at higher C_B values *. Nevertheless it has been attempted and can be found in Table 2. As the $\bar{n}$ values for large [B] are greater than 2, we must also assume the presence of the third complex.

It must be pointed out that the calculation of $\bar{n}$ for values of [B] $>$ 0.1 M is independent of the correction φ_s, as this function decreases rapidly for

Table 2. The sulphate and thiosulphate systems. $\bar{n}$ calculated from eqn. (4).

	a. The sulphate system			b. The thiosulphate system		
[B] M	0.2	0.5	0.9	0.14	0.2	0.5
$\bar{n}$	2.0	2.4	2.7	2.0	2.1	2.4 **

* Furthermore, the β_n values for the aqueous phase probably vary somewhat, as the ionic strength is not kept constant.

** This value is probably too low because of a beginning variation of $[B]_R$, which causes the experimental points to lie above the expected curve for greater C_B values (Fig. 2).

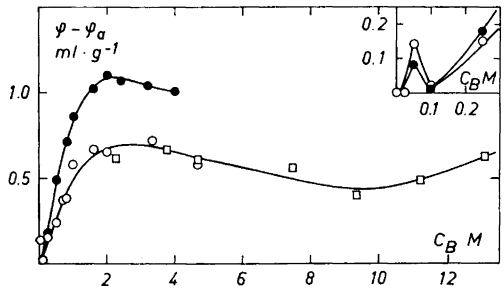

Fig. 3. The chloride and bromide systems. The distribution quotients corrected for the φ_a-contribution NaCl: ○, LiCl: □, NaBr: ●. (In the bromide case, precipitation occurred for $C_B > 4$ M.)

[B] < 0.1 M and is almost negligible for [B] > 0.1 M. The choice of the value of the correction φ_a is more critical. However, even if such a low value as 0.3×10^{-3} l/g is used, we obtain, *e.g.*, $\bar{n} = 2.35$ for $[SO_4^{2-}] = 0.7$ M. Thus the conclusion regarding the existence of the third complex is still valid.

The results of the measurements of the chloride and bromide systems are given graphically in Fig. 3. In both cases a slight maximum is observed, followed by an increase of φ at very high C_B values in the chloride case.

The maxima indicate the presence of anionic complexes. The subsequent increase of φ must be attributed to an complete invalidity of the assumption of the constancy of $[B]_R$. It is interesting to note the greater value of the maximum for the bromide system. This indicates a greater tendency towards formation of anionic complexes in the resin phase for this system as compared to the chloride system.

The measurements of the fluoride and acetate systems are given in Table 3. As it has been mentioned before, the estimate of φ_a is based upon these results. The low values of φ makes it probable that the tendency to formation of anionic complexes is negligible.

Table 3. The distribution quotients of the fluoride and acetate systems. ($C'_M = 0.2$ mM).

a. The fluoride system		b. The acetate system	
C'_B mM	φ ml · g^{-1}	C'_B mM	φ ml · g^{-1}
16	0.53	42	0.49
32	0.57	83	0.43
48	0.49	170	0.43
95	0.53	330	0.52
260	0.48	670	0.50
320	0.46	1330	0.59
510	0.53	1870	0.65
640	0.54		

DISCUSSION

From the existence of not only the second but also the third complex of the sulphate and thiosulphate systems, it follows that the criterion of outer-sphere coordination that was suggested in the introduction, is actually fulfilled. Also the existence of the fourth chloride and bromide complexes gives weight to the use of the concept of "outer-sphere coordination".

It is interesting to note that the order of increasing strength of the anionic complexity is $Br^- > Cl^- > F^-$ and $S_2O_3^{2-} > SO_4^{2-}$. The last sequence at least, is based both on the complexity in the aqueous phase (the position of the maximum) and in the resin phase (the magnitude of the maximum). This order is reverse to that reported by Evans and Nancollas [10] for the first complexity constant, $Cl^- > Br^- > I^-$. This fact may seem astonishing at first, but an inspection of the data of Evans and Nancollas [10] shows that this order of the free energy change, $Cl^- < Br^- < I^-$, is a consequence of very large positive entropy terms. The enthalpies of reaction were [10] all positive and followed the sequence $Cl^- > Br^- > I^-$. If we use this order of the enthalpies also for the formation of the higher complexes and use a rather small positive entropy term, we may wery well obtain an order of the free energy changes $Cl^- > Br^- > I^-$ which is in accordance with the sequence of anionic complexity that has been found here.

In this connection some words can be said in favour of the measurements of Evans and Nancollas [10]. These authors have used a method which is known to yield reliable results (Olerup [11], p. 63) and their result for the iodide system ($\beta_1 = 17$ M^{-1}, $I = 0.054$ M) agrees well with that, which was reported independently by Kubota [12], ($\beta_1 = 16$ M^{-1}, $I = 0.03-0.1$ M). Recently this work has been critized by other authors [13]. They, however, use a method, which is also known to yield very uncertain information in the case of weak complexity, (Olerup [11], p. 58). We therefore chose to base our discussion on the work of Evans and Nancollas [10].

The observed trend for the complexity is contrary to the one that was expected for pure electrostatic attraction. The degree of complex formation rather follows the same order as the polarizabilities of the ligands do: $Br^- > Cl^- > F^-$; $S_2O_3^{2-} > SO_4^{2-}$. This may be taken as an indication of a partial charge transfer from the ligands towards the cobalt centre. This is in agreement with the absorption spectra in the ultraviolet region [14], typical of "charge transfer complexes".

Thus, in conclusion, we may state that the studied association products have so many features in common with ordinary coordination complexes that the use of the concept of the second coordination sphere is well justified.

This work has been financially supported by the *Swedish Natural Science Research Council*, a fact which is gratefully acknowledged.

REFERENCES

1. Bjerrum, N. *Kgl. Danske Videnskab. Selskab, Mat.-fys. Medd.* **7** (1926) No. 9.
2. Gronwall, T. H., LaMer, V. K. and Sandved, K. *Physik. Z.* **29** (1928) 358.
3. Meyer, J. E. *J. Chem. Physics* **18** (1950) 1426.

4. Guggenheim, E. A. *Trans. Faraday Soc.* **56** (1960) 1152.
5. Werner, A. *Z. anorg. Chem.* **3** (1893) 267.
6. Fronæus, S. *Svensk Kem. Tidskr.* **65** (1953) 1.
7. Sonesson, A. *Acta Chem. Scand.* **13** (1959) 1437.
8. Adamson, A. W. and Sporer, H. H. *J. Am. Chem. Soc.* **80** (1958) 3685.
9. Larsson, R. *Acta Chem. Scand.* **11** (1957) 1405.
10. Evans, M. G. and Nancollas, G. H. *Trans. Faraday Soc.* **49** (1953) 363.
11. Olerup, H. *Järnkloridernas komplexitet*, (Diss.) Lund 1944.
12. Kubota, T. *J. Chem. Soc. Japan* **75** (1954) 552.
13. King, E. L., Espenson, J. H. and Visco, R. E. *J. Phys. Chem.* **63** (1959) 755.
14. Yoneda, H. *Bull. Chem. Soc. Japan* **28** (1955) 125.

Received May 12, 1962.

ACTA CHEMICA SCANDINAVICA 16 (1962) 1927–1935

Kinetics of the Alkaline Hydrolysis of Aminoalkyl Esters of Carboxylic Acids

BERTIL HANSEN

Research Institute of National Defence, Department 1, Sundbyberg 4, Sweden

The rates of the alkaline hydrolysis of the acetate esters of 3-dimethylamino-1-propanol (IV), 2-dimethylamino- (I), 2-diethylamino- (II), and 2-diisopropylaminoethanol (III) have been measured in 0.07 M $KClO_4$ at 25°. The rates of the reactions between hydroxyl ions and the amino forms of the esters are of the same magnitude as for ethyl acetate (for I, $\log k = -1.0$, and for IV, -0.85; k in $l\,mole^{-1}sec^{-1}$). Hydroxyl ions react more rapidly with the ammonium forms of the esters than with acetyl choline ($\log k$ for I, 1.63; II, 1.56; III, 1.47 and IV, 0.77). This can be explained in terms of catalysis by an intramolecular hydrogen bond. The pK_a'-values are for I, 8.45; II, 9.09; III, 9.40 and IV, 9.27.

In a previous paper[1] a method for the determination of the dissociation constant, K_a', and the two rate constants, k_1 and k_2 as defined below, of the alkaline hydrolysis of compounds containing an ionizable group was described. The method was based on rate measurements at constant pH at a number of pH-values. It was tested with 2-dimethylaminoethyl thiolopropionate for which values of K_a' and k_2 but not for k_1 could be determined. The value of k_2 was interesting because it was found to be 240 times greater than the second order rate constant of the reaction between the 2-trimethylammoniumethyl thiolopropionate (propionyl thiocholine) and hydroxyl ions[2].

$$R_2NCH_2CH_2YCOR' + OH^- \xrightarrow{k_1} R_2NCH_2CH_2YH + R'COO^- \quad (1)$$

$$R_2N^+HCH_2CH_2YCOR' + OH^- \xrightarrow{k_2} R_2N^+HCH_2CH_2YH + R'COO^- \quad (2)$$

$$R_2N^+HCH_2CH_2YCOR' \overset{K_a'}{\rightleftharpoons} R_2NCH_2CH_2YCOR' + H^+ \quad (3)$$

$Y = O$ or S

In a recent paper[3] Ågren *et al.* reported the same phenomenon for some aromatic esters of 2-diethylaminoethanol. As an explanation of these rate differences several authors[3–6] have proposed that an intramolecular hydrogen

bond of the type shown below is possible in the 2-dimethylammoniumethyl ester but not in the 2-trimethylammoniumethyl ester. Such a hydrogen bond is expected to increase the positive charge of the carbonyl carbon atom which is thus more easily attacked by a hydroxyl ion in an S_N2 reaction. Also the

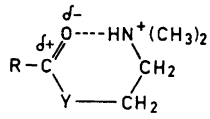

neutral hydrolysis of an ester is catalyzed by a dimethylammonium group in the alcohol part as shown by Shafer and Morawetz [7] for 2-dimethylaminoethyl hydrogen phthalate.

The work now presented is an investigation of how the rates of hydrolysis of tertiary aminoalkyl acetates in alkaline water solution are influenced by the N-alkyl groups and by the distance between the amino and the ester groups. Based on these measurements the above and other reaction mechanisms are discussed.

THEORY

The hydrolysis of aminoalkyl esters may be the result of several reactions. Reactions with hydroxyl ions, (1) and (2), have been mentioned above, and mechanisms in which the first step is an intramolecular reaction of the amine form of the ester are outlined in formulas (4) and (5). Uncatalyzed direct reactions between water and the ester are also possible, but as such reactions as a rule are much slower than reactions with hydroxyl ions in the pH-range now investigated (8.2—10.9) they will not be considered.

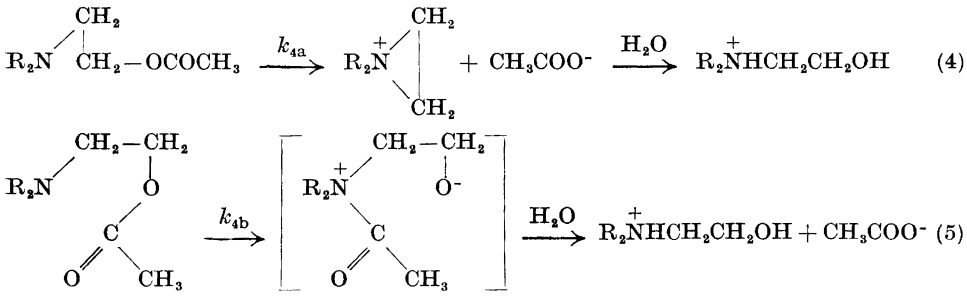

$$k_4 = k_{4a} + k_{4b} \qquad (6)$$

Reactions of type (4) are common for 2-aminoethyl halides [8], and the transacylation step in reaction (5) can be achieved for instance with 2-aminoethyl benzoate [9] and acetate [10]. In all the reactions (1), (2), (4), and (5) the concentrations of the reactants depend on pH. Therefore, to describe the rate of disappearance of the total amount of ester EHE (ammonium form EH^+ and amine form E) the complicated differential eqn. (7) is necessary.

$$\mathrm{d[EHE]} = -(k_2[\mathrm{EH^+}][\mathrm{OH^-}] + k_1[\mathrm{E}][\mathrm{OH^-}] + k_4[\mathrm{E}])\mathrm{d}t =$$
$$= -\left(k_2[\mathrm{OH^-}]\frac{h}{h + K_a'} + k_1[\mathrm{OH^-}]\frac{K_a'}{h + K_a'} + k_4\frac{K_a'}{h + K_a'}\right)[\mathrm{EHE}]\mathrm{d}t \qquad (7)$$

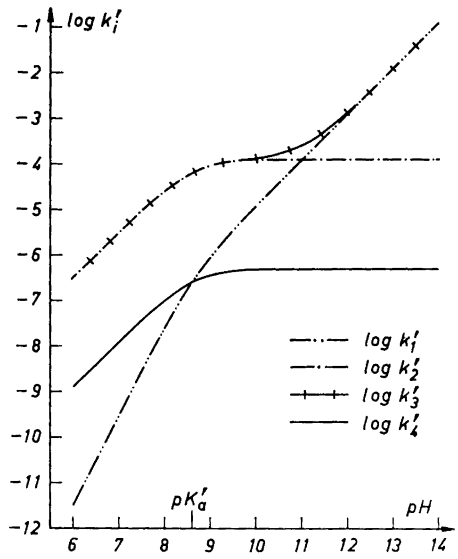

Fig. 1. The theoretical pH-dependence of the total rate, log k_3', and of the individual rates log k_1', log k_2', and log k_4' of the reactions (1), (2) and (4) + (5). Arbitrarily chosen values, $pK_a' = 8.60$, $k_1 = 10^{-0.9}$ l mole^{-1} sec^{-1}, $k_2 = 10^{1.5}$ l mole^{-1} sec^{-1} and $k_4 = 10^{-6.3}$ sec^{-1}.

h = hydrogen ion activity, [] = concentration, and $K_a' = h[E]/[EH^+]$. However, if the rate of hydrolysis is measured at constant pH, a much simpler expression (8) is obtained.

$$\frac{d[EHE]}{[EHE]} = -(k_4' + k_2' + k'_3)\,dt = -k'_3 dt \qquad (8)$$

$$k_1' = k_1[OH^-]\frac{K_a'}{h + K_a'}\,(9);\quad k_2' = k_2[OH^-]\frac{h}{h + K_a'}\,(10);\quad k_4' = k_4\frac{K_a'}{h + K_a'}\,(11)$$

The hydrolysis at constant pH may be treated as a sum of three first order reactions, for as shown by eqns. (9), (10), and (11), each of the values of k_1', k_2' and k_4' do not change during the duration of the reactions. But k_1', k_2' and k_4' are functions of the hydrogen ion concentration, and their contributions to to k_3' depend on pH. This is illustrated in Fig. 1 with arbitrarily chosen values of k_1, k_2 and k_4. With the values used in Fig. 1 k_3' at low pH-values is dominated by k_2' and at high pH-values by k_1' while k_4' is without influence. Fig. 1 also shows that the log k_2'/pH-curve and the log k_4'/pH-curve have the same form. That means that there are values of k_2 and k_4 (in this case $k_2 = 10^{-0.9}$ l mole^{-1} sec^{-1} and $k_4 = 10^{-3.9}$ sec^{-1}) such that log k_4' and log k_2' can change places in Fig. 1. If k_1 is given the same value as before, the resulting k_3' will also be the same as before but now dominated by k_4' at low pH-values while k_2' has no influence.

Inversely, if the experimental determination of the rate of hydrolysis of an aminoalkyl ester gives a log k_3'/pH-curve of the type occuring in Fig .1, the conclusion can be drawn, that at high pH-values the reaction (1) is the most important. At low pH-values the main reaction is either (2) or an intramolecular reaction of the amine form of the ester, *e.g.* (4) and (5), or all three types

at the same time. Accordingly, for a separation of the reactions (2), (4), and (5) other methods must be used, for instance, as in this report, comparisons of some homologous compounds.

In an earlier paper[1] a graphic method for the calculation of K_a', k_1 and k_2 from k_3' was described. The possibility of intramolecular reactions was then not recognized. But as there is a simple relation (12) between k_2 and k_4, obtained by putting $k_2' = k_4'$, the graphic method may be used also for the calculation of k_4

$$\log k_4 = \log k_2 + pK_a' - \log f_{OH^-} - pK_W \qquad (12)$$

where f_{OH^-} = activity factor and $K_W = h[OH^-]/f_{OH^-}$.

EXPERIMENTAL

Materials. One mole of dialkylaminoalcohol and 1.1 mole of acetic anhydride were mixed. When the exothermic reaction had ceased, the reaction mixture was dissolved in 10—15 parts of dry ether, and dry hydrogen chloride was led over the surface of the solution. The precipitated dialkylaminoalkyl acetate hydrochloride was recrystallized from acetone or from an ethanol/acetone mixture. The analyses are given in Table 1.

The quaternary salts were obtained by treating a solution of the ester in ether or acetone with alkyl iodide instead of hydrogen chloride. The compounds were recrystallized from ethanol/ether.

Kinetic measurements. The rate of hydrogen ion formation was measured with a recording pH-stat [13]. The compounds were dissolved in 30 ml of 0.07 M potassium perchlorate solution and automatically titrated at 25.0 ± 0.05° with sodium hydroxide from a 0.5 ml syringe.

The tertiary aminoalkyl ester hydrochlorides were titrated at 5—10 pH-values with 0.02, 0.05 or 0.1 M sodium hydroxide. The reactions were followed until they were 60—80 % complete. The rate constant k_3' was calculated according to Guggenheim's method.

The pK_a'-values were determined as follows. Less than one equivalent of sodium hydroxide was added to a solution (< 0.01 M) of the ester hydrochloride. The change of pH was

Table 1. Melting points and analyses

Compound	Mol. wt.	M.p. Found	M.p. Lit.	Analyses C Calc.	C Found	H Calc.	H Found
$[(CH_3)_2\overset{+}{N}HCH_2CH_2OCOCH_3]Cl^-$	167.6	133°	130—131°[11]	43.0	43.0	8.4	8.4
$[(CH_3CH_2)_2\overset{+}{N}HCH_2CH_2OCOCH_3]Cl^-$	195.7	116°	113—114°[11]	49.2	49.4	9.3	9.4
$[((CH_3)_2CH)_2\overset{+}{N}HCH_2CH_2OCOCH_3]Cl^-$	223.7	145°		53.8	53.5	9.9	9.9
$[(CH_3)_2\overset{+}{N}HCH_2CH_2CH_2OCOCH_3]Cl^-$	181.7	120°	118- 119°[11]	46.2	46.3	8.8	9.0
				I			
$[(CH_3CH_2)_3\overset{+}{N}CH_2CH_2OCOCH_3]I^-$	315.2	122°		40.3	40.0		
$[(CH_3)_3\overset{+}{N}CH_2CH_2CH_2OCOCH_3]I^-$	287.1	95°	80°[12]	44.2	44.0		

followed for a few minutes. A pH-value of the time of mixing was determined and used for the calculation of pK_a'. The pK_a'- and k_3'-values were then used for the determination of k_1 and k_2 (Table 2) by a curve fitting method described in an earlier paper [1]. The rate constants k_4 were calculated from k_2 using eqn. (12).

The rate constants, k_3, for the quaternary ammonium compounds were calculated from the initial rate of consumption of 0.02 M sodium hydroxide at pH 8.9. The recorded time/sodium hydroxide consumption curves were perfectly straight lines during the hydrolysis of the first two per cent of 0.4 mmole of the ester.

Infrared spectra of 0.05—0.1 M solutions of the hydrochlorides of the esters in dry chloroform were recorded at room temperature with a Perkin-Elmer spectrophotometer model 21. Some of the absorption frequencies are given in Table 3.

RESULTS

The experimental pH/log k_3' curves showed that the main reaction in the investigated pH-region is either a reaction between hydroxyl ions and the ester in ammonium form (2) or an intramolecular reaction of the amine form (4) and (5). Rate constants k_2 and k_4 for these alternatives are given in Table 2. In some cases the velocity constant, k_1, of the reaction between the amine form and hydroxyl ions (2) could also be determined.

Hall [17] has demonstrated that the Taft equation $\log k/k_o = \sigma^*\varrho^*$ can be applied on the relationship between substituents and pK_a of amines. Using Hall's equation for tertiary amines, $pK_a = -3.30\Sigma\sigma^* + 9.61$, and the pK_a-values for I and II, $\sigma^* = 0.38$ and 0.39 were calculated for $CH_3COOCH_2CH_2-$. When $\sigma^* = 0.39$ was used in the equation [17] $pK_a = -3.14\Sigma\sigma^* + 13.23$, a value $pK_a = 8.91$ was found for 2-aminoethyl acetate. This value is in good agreement with $pK_a = 8.84$ being the experimentally found value [10].

Table 2. Rates of hydrolysis of some aminoalkyl esters in 0.07 M $KClO_4$ solution at 25°. Unit of k_1 and k_2 l mole^{-1} sec^{-1}. Unit of k_4 sec^{-1}. The values found in the literature have been corrected [14] for the ionic strength and are valid for 0.07 M $KClO_4$. $pK_a = pK_a' - 0.10$.

Compound	pK_a'	log k_1	log k_2	log k_4	Measurements in pH-range
I $(CH_3)_2NCH_2CH_2OCOCH_3$	8.45 ± 0.02*	−1.0 ± 0.1	1.63 ± 0.02	−3.82	8.2—10.9
II $(CH_3CH_2)_2NCH_2CH_2OCOCH_3$	9.09 ± 0.02		1.56 ± 0.02	−3.25	8.5—10.9
III $((CH_3)_2CH)_2NCH_2CH_2OCOCH_3$	9.40 ± 0.02		1.47 ± 0.03	−3.02	8.2—10.0
IV $(CH_3)_2\overset{+}{N}CH_2CH_2CH_2OCOCH_3$	9.27 ± 0.01	−0.85 ± 0.05	0.77 ± 0.03	−3.86	8.8—10.9
V $(CH_3)_3\overset{+}{N}CH_2CH_2OCOCH_3$			0.17 [14]		
			0.17		
VI $(CH_3CH_2)_3\overset{+}{N}CH_2CH_2OCOCH_3$			0.12		
VII $(CH_3)_3\overset{+}{N}CH_2CH_2CH_2OCOCH_3$			−0.39 [12]		
			−0.34		
VIII $CH_3CH_2OCOCH_3$		−0.96 [16]			

* Tammelin [15] found $pK_a = 8.35$.

However, when, pK_a for III is calculated, a value, $pK_a = 9.58$ is obtained which exceeds the actually found one by 0.28. This indicates that in the compound III there is a steric hindrance for the formation of the ammonium ion which does not normally exist for tertiary amines [17], and consequently $\Sigma\sigma$ for $N(CH(CH_3)_2)_2$ shall be -0.30 instead of $2 \times (-0.19)$.

All the esters with ammonium groups have higher infrared C=O absorption frequencies than ethyl acetate (Table 3). The C=O frequency for ethyl acetate is not affected by the presence of 0.05 M triethylamine hydrochloride or trimethylamine hydrobromide. In the region 2000—2800 cm^{-1} all the compounds having $\overset{+}{N}H$ bonds exhibit one absorption band between 2400 and 2465 cm^{-1} and another between 2500 and 2580 cm^{-1}. The dimethylammoniumalkyl and diethylammoniumalkyl esters absorb also at about 2300 cm^{-1}. The spectrum of trimethylammonium bromide did not change between 2000 and 2800 cm^{-1} when 1—10 % (V/V) ethyl acetate was added to the solution.

DISCUSSION

Of the different proposed reaction mechanisms (1), (2), (4) and (5) for the hydrolysis of dialkylaminoethyl acetate the reaction (1) between hydroxyl ions and the ester in amine form will first be discussed. In this form the ester molecule has no electric change and no hydrogen atoms at the nitrogen atom which can give a hydrogen bond to the carboxylic group. It may therefore be expected that the molecule will behave like the ester that is obtained if the nitrogen atom is substituted for a CH group, *i.e.* like an acetate of a branched aliphatic alcohol.

Table 3. Infrared absorption frequencies in cm^{-1} of chloroform solutions.

	$\overset{+}{N}H$					C = O	O−C(=O)	C−O(−C=O)
	Band 1	Band 2	Band 3	$\varepsilon_1 : \varepsilon_2$	$\varepsilon_1 : \varepsilon_3$			
$(CH_3)_2\overset{+}{N}HCH_2CH_2OCOCH_3Cl]^-$	2400	2560	2300	1.25	1.00	1751	1235	1050
$(CH_3CH_2)_2\overset{+}{N}HCH_2CH_2OCOCH]_3Cl^-$	2400	2550	2310	1.21	1.04	1745	1233	1048
$(CH_3)_2CH)_2\overset{+}{N}HCH_2CH_2OCOCH_3]Cl^-$	2420	2520	—	1.19		1744	1233	1049
$(CH_3)_2\overset{+}{N}HCH_2CH_2CH_2OCOCH_3]Cl^-$	2400	2550	2300	1.23	1.01	1740	1239	1051
$(CH_3)_3\overset{+}{N}CH_2CH_2OCOCH_3]Cl^-$	—	—	—			1748	1230	1053
$H_3CH_2OCOCH_3$	—	—	—			1732	1250	1049
$(CH_3)_3\overset{+}{N}H]Br^-$	2440	2575	—	1.07				
$(CH_3CH_2)_3\overset{+}{N}H]Cl^-$	2425	2560	—	1.22				
$(CH_3)_2\overset{+}{N}HCH_2CH_2OH]Cl^-$	2465	2580	—	1.03				
$(CH_3)_2\overset{+}{N}HCH_2CH_2Br]Br^-$	2425	2500	—	1.05				

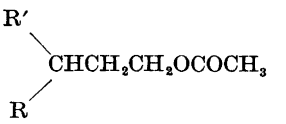

In those two cases when it was possible to determine values of k_1 (Table 2) these values were found to deviate less than 30 % from the value of the rate constant of the reaction between ethyl acetate and hydroxyl ions. This result strongly supports the above assumption that the amine form of a tertiary aminoalkyl acetate is very like an unsubstituted alkyl acetate. The primary 2-aminoethyl acetate does, however, not follow this rule as the acetyl group migrates to the nitrogen atom [9,10].

As mentioned in the theory it is not possible to distinguish between the reactions (1), (4), and (5) only by looking at the pH-dependence of the measured rate of hydrolysis, k_3'. For that reason values of both log k_2 and log k_4 are given in Table 2. In the following discussion it is assumed that only one of the reactions (1), (4), and (5) occurs. If we first look at the reaction (5) we will see that it gives a ring intermediate containing 5 atoms, *i.e.* a ring with normal bond angles. The reaction is an intramolecular nucleophilic substitution by an amino group, and it seems reasonable to assume a mechanism of S_N2 type. All S_N2 substitutions by amines giving strainless products are known to be slowed down if the N-alkyl group or groups are branched near the nitrogen atom [18]. This is true also for the aminolysis of an ester [19]. But the values of k_4 increase for the compounds, I, II, and III with increasing size of the N-alkyl groups. For that reason reaction (5) may be excluded.

In reaction (4) ethylenimonium ions are formed. These ions contain strained rings, and the influence of the N-alkyl groups on the rate of their formation is not easy to predict. However, such compounds are easily obtained from 2-dialkylaminoethyl bromides. The rates of their cyclization were measured, and in another paper [8] it is reported that log k at 25° for the cyclization of 2-dimethylaminoethyl bromide is −2.0, for the 2-diethylamino compound −0.4, and for the 2-diisopropyl compound + 1.4. It may be assumed that the difference between the log k values for the formation of two homologous ethylenimonium ions is of the same order irrespective of whether the leaving group is a bromide or an acetate ion. The differences between the log k_4-values for the aminoethyl bromides above have the same sign but are much greater than the differences between the log k_4 values for the corresponding aminoalkyl acetates I, II, and III. Accordingly, also reaction (4) can be excluded for the hydrolysis of 2-aminoethyl acetates.

The remaining alternative, besides of reaction (1), is a reaction (2) between hydroxyl ions and the ammonium form of the aminoalkyl ester. This reaction is for the aminoethyl esters 25—30 times faster than for the corresponding quaternary ammonium compounds and about 400 times faster than for ethyl acetate. This increase of k_2 by 400 times may be the result of several effects.

(*A*) Inductive effect through the carbon atom chain by the positively charged nitrogen atom.

(*B*) Electrostatic effect outside the chain by the positive charge.

(*C*) Hydrogen bonding.

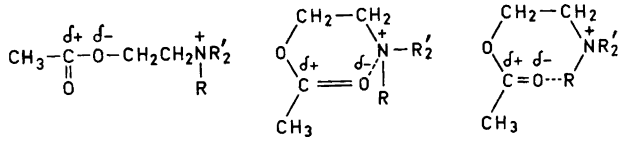

A B C

(*A*) From experiments by Holland *et al.*[20] the inductive effect through the chain can be estimated to increase k_2 by 4—5 times when the positive charge and the ester group are separated by two carbon atoms. The correctness of this value is supported by the fact that for several types of quaternary ammonium alkyl ester having two and three CH_2-groups between the nitrogen atom and the ester group the relative values of k_2 are 3.0 ± 0.2 and 1.0, respectively (V and VII in Table 2, the corresponding thiolo esters[2] and $CH_3P(O)(F)(O(CH_2)_n\overset{+}{N}(CH_3)_3$[4]). The main part of this difference can be explained as a difference in the inductive effect, because the steric conditions for the structure B are not changed very much.

(B) Esters of choline are hydrolyzed about 15 times faster than the corresponding ethyl esters (V and VIII in Table 2, and $CH_3P(O)(F)(OR)$[4]). As the increase under (A) is 4—5 times, the electrostatic effect outside the chain gives an increase of k_2 by about 3 times. If the N-methyl groups of a choline ester are substituted for ethyl groups the rate of hydrolysis goes down by 10 %. This is probably due to an increase of the distance between the nitrogen atom and the carbonyl oxygen atom, as the positive charge and the effect (*A*) may be regarded unchanged.

(*C*) In the ammonium form of the tertiary amino ester I the distance between the nitrogen atom and the oxygen atom is a little shorter than in the choline ester, V. This increases the electrostatic effect but not enough to explain more than a small part of the observed 25—30 fold increase of k_2. The rest of the increase may be explained as the result of a catalytic effect by an intramolecular hydrogen bonding. In monoesters of 1,2- and 1,3-diols it has been observed that the alkaline hydrolysis is 10—15 times faster when the steric conditions are such that an intramolecular hydrogen bonding is possible than when it is impossible[21]. If such a hydrogen-bonded hydroxy group is substituted by a methoxy group the rate goes down to a seventh[22]. The infra-red spectra of I, II, and IV also support the hydrogen bond theory. As shown in Table 3 these compounds absorb in the $\overset{+}{N}-H$ stretching region at 2300 cm^{-1} where no other tertiary ammonium compounds were found to have any absorption peak. The absorption cannot be caused by the solvent, chloroform, because ethyl acetate in chloroform has no absorption in this region. The spectra do not tell anything about which of the oxygen atoms that is hydrogen bonded, but the structure given above is favoured because a hydrogen bond to the ether oxygen atom results in a five-membered ring which can be regarded as less likely than a seven-membered hydrogen-bonded ring[23]. Also IV which has three CH_2-groups between the nitrogen and the oxygen

atoms, is rapidly hydrolyzed. The k_2-value is about 12 times that of the quarternary compound, VII, and the infra-red spectrum indicates a hydrogen bonded $\overset{+}{\text{N}}\text{H}$. In this case the ether oxygen atom is possible as acceptor of the hydrogen bond.

From the discussion it can be concluded that the mechanism of the hydrolysis of tertiary aminoalkyl esters in alkaline solution is better explained in terms of an intramolecular hydorgen bonding than by any other mechanism. In order to confirm this result it would be interesting to study some compounds in which the hydrogen bond for steric reasons is very unlikely.

REFERENCES

1. Hansen, B. *Acta Chem. Scand.* **12** (1958) 324.
2. Heilbronn, E. *Acta Chem. Scand.* **12** (1958) 1492, and *Personal communication.*
3. Ågren, A., Hedsten, U. and Jonsson, B. *Acta Chem. Scand.* **15** (1961) 1532.
4. Larsson, L. *Svensk Kem. Tidskr.* **70** (1958) 405, p. 423 and p. 412.
5. Schätzle, E., Rottenberg, M. and Thürkauf, M. *Helv. Chim. Acta* **42** (1959) 1708.
6. Bender, M. L. *Chem. Revs.* **60** (1960) 53, p. 71 and p. 90.
7. Shafer, J. A. and Morawetz, H. *Personal communication.*
8. Hansen, B. *Acta Chem. Scand.* **16** (1962) 1945.
9. Phillips, R. P. and Baltzly, R. *J. Am. Chem. Soc.* **69** (1947) 200.
10. Hansen, B. *To be published*
11. Campbell, K. N., O'Boyle, C. J. and Campbell, B. K. *Proc. Indiana Acad. Sci.* **58** (1949) 120.
12. Aksnes, G. and Prue, J. E. *J. Chem. Soc.* **1959** 103.
13. Larsson, L. and Hansen, B. *Svensk Kem. Tidskr.* **68** (1956) 521.
14. Olered, R. *Svensk Kem. Tidskr.* **68** (1956) 90.
15. Tammelin, L.-E. *Acta Chem. Scand.* **11** (1957) 487.
16. Salmi, E. J. and Korte, R. *Ann. Acad. Sci. Fennicae A* **54** (1940) No. 12.
17. Hall, Jr., H. K. *J. Am. Chem. Soc.* **79** (1957) 5441.
18. Hansson, J. *A Kinetic Study of the Addition of Amines to Propylene Oxide.* Lindstedts, Lund 1955, p. 22.
19. Arnett, E. McC., Miller, J. G. and Day, A. R. *J. Am. Chem. Soc.* **72** (1950) 5635.
20. Holland, G. F., Durant, R. C., Friess, S. L. and Witkop, B. *J. Am. Chem. Soc.* **80** (1958) 6031.
21. Henbest, H. B. and Lovell, B. J. *J. Chem. Soc.* **1957** 1965.
22. Bruice, T. C. and Fife, T. H. *Tetrahedron Letters* **8** (1961) 263.
23. Pimentel, G. C. and McClellan, A. L. *The Hydrogen Bond*, W. H. Freeman & Co., San Francisco 1960, p. 175.

Received April 6, 1962.

ACTA CHEMICA SCANDINAVICA 16 (1962) 1936–1944

A Method of Studying Metal Complex Formation in an Anion Exchanger Phase

STURE FRONÆUS, IRENE LUNDQVIST and ARTUR SONESSON

Department of Inorganic and Physical Chemistry, Chemical Institute, University of Lund, Lund, Sweden

A method is developed for studying the step-wise complex formation within an anion exchanger phase at increasing concentrations of an anionic ligand. The method presupposes the use of a salt medium in the outer solution and a knowledge of the complexity in this phase.

To test the method it is applied to the cadmium bromide system at 20°C and with sodium perchlorate as supporting electrolyte. The ligand number $\bar{n}_R$ in the resin phase is found to attain a limiting value of 4 at increasing ligand concentrations. The stability constants obtained are much higher than the corresponding ones in the outer solution.

In a previous paper (Fronæus [1]) a method was developed for studying the formation of anionic complexes in water solutions and in absence of a neutral salt medium. It was based upon the use of an anion exchanger saturated with the ligand. When this method was applied to copper(II) complex systems with glycolate and tartrate ions as ligands, it was found in preliminary measurements that the sorption of copper by the ion exchanger was of a much lower order of magnitude than the sorption of cadmium in the cadmium bromide system though the former systems have a stronger tendency to anionic complex formation in water solutions (*cf.* Ref.[2]).

In order to explain these differences it is necessary to know how the step-wise complex formation proceeds within the anion exchanger at an increasing ligand concentration. In the present paper a method is developed for the calculation of the complexity constants valid in the anion exchanger phase. The method presupposes the use of a salt medium in the outer solution and a knowledge of the complexity constants in this phase. To test the method it is applied to the cadmium bromide system, because its complexity in water solutions is well known at different ionic strengths.

THEORY OF THE METHOD

The notation used is the same as in previous papers (Fronæus [1,3]). The central ion is called M and the ligand A without any marking of the ionic charges. An index R indicates the resin phase.

The distribution of the free central ion between the anion exchanger and the water phase is given by the Donnan equation

$$[\mathrm{M}]_\mathrm{R} \cdot [\mathrm{A}]_\mathrm{R}^\nu = K[\mathrm{M}] \cdot [\mathrm{A}]^\nu \tag{1}$$

where ν is the ratio between the absolute values of the ionic charges of the central ion and the ligand. If the ionic strength can be kept constant in the outer solution as well as in the anion exchanger, we can presume that the factor K and the complexity constants in both the phases will be approximately constant when the concentration of A is varied within limited ranges. Generally the total concentrations C_M and C_MR of the central ion can be kept so low that variations in these quantities should not influence the constancy of the activity coefficients.

If we presuppose that only mononuclear complexes are formed, we have the following relations

$$C_\mathrm{M} = [\mathrm{M}](1 + \sum_{j=1}^{\mathrm{N}} \beta_j [\mathrm{A}]^j) \tag{2}$$

$$C_\mathrm{MR} = [\mathrm{M}]_\mathrm{R}(1 + \sum_{j=1}^{\mathrm{N}} \beta_{j\mathrm{R}} [\mathrm{A}]_\mathrm{R}^j) \tag{3}$$

or

$$C_\mathrm{M} = [\mathrm{M}] \cdot \mathrm{X} \tag{4}$$

$$C_\mathrm{MR} = [\mathrm{M}]_\mathrm{R} \cdot \mathrm{X}_\mathrm{R} \tag{5}$$

Combination of eqns. (1), (4) and (5) yields the following expression for the ratio φ between the equilibrium values of C_MR and C_M.

$$\varphi = K \cdot \frac{\mathrm{X}_\mathrm{R}}{[\mathrm{A}]_\mathrm{R}^\nu} \cdot \frac{[\mathrm{A}]^\nu}{\mathrm{X}} \tag{6}$$

Since the value of ν is not restricted to whole numbers it is evident that the deduction of eqn. (6) is *general* and does not presuppose the existence of a neutral complex. (The contrary has been asserted by Kraus and Nelson [4]).

However, in the case that ν is a whole number and if the uncharged complex MA_ν really exists the following relation holds [1]

$$K = l_\nu \cdot \beta_\nu \cdot \beta_{\nu\mathrm{R}}^{-1} \tag{7}$$

where l_ν is the Nernst distribution coefficient for this complex.

Calculation of $\bar{n}_\mathrm{R}$. It is possible to determine $\bar{n}_\mathrm{R} = (C_\mathrm{AR} - [\mathrm{A}]_\mathrm{R})/C_\mathrm{MR}$, *i.e.*, the ligand number in the resin phase, from eqn. (6). Derivation of $\ln\varphi$ with respect to $\ln[\mathrm{A}]_\mathrm{R}$ yields, if K is constant

$$\frac{\mathrm{d}\ln\varphi}{\mathrm{d}\ln[\mathrm{A}]_\mathrm{R}} = \frac{\mathrm{d}\ln\mathrm{X}_\mathrm{R}}{\mathrm{d}\ln[\mathrm{A}]_\mathrm{R}} - \nu + \left(\nu - \frac{\mathrm{d}\ln\mathrm{X}}{\mathrm{d}\ln[\mathrm{A}]}\right) \frac{\mathrm{d}\ln[\mathrm{A}]}{\mathrm{d}\ln[\mathrm{A}]_\mathrm{R}} \tag{8}$$

The definitions of the ligand numbers $\bar{n}$ and $\bar{n}_\mathrm{R}$ give the relations $\mathrm{d}\ln\mathrm{X}/\mathrm{d}\ln[\mathrm{A}] = \bar{n}$ and $\mathrm{d}\ln\mathrm{X}_\mathrm{R}/\mathrm{d}\ln[\mathrm{A}]_\mathrm{R} = \bar{n}_\mathrm{R}$. Hence

$$\bar{n}_\mathrm{R} = \nu + \frac{\mathrm{d}\ln\varphi}{\mathrm{d}\ln[\mathrm{A}]_\mathrm{R}} + (\bar{n} - \nu) \frac{\mathrm{d}\ln[\mathrm{A}]}{\mathrm{d}\ln[\mathrm{A}]_\mathrm{R}} \tag{9}$$

φ, $[A]_R$ and [A] are determined experimentally and then from plots of $\ln\varphi$ and $\ln[A]$ against $\ln[A]_R$ the derivatives in eqn. (9) can be obtained. $\bar{n}$ is in this case computed from the known complexity constants in the water phase.

Calculation of the complexity constants β_{jR}. From eqn. (6) the function $K \cdot X_R$ can be calculated for varying ligand concentrations $[A]_R$. Then the constants K and $K\beta_{jR}$ can be obtained, *e.g.* by extrapolations to $[A]_R = 0$ of this function and of the quantities KX_{jR} defined by the relation

$$KX_{jR} = \frac{KX_{j-1,R} - K\beta_{j-1,R}}{[A]_R} \qquad (10)$$

$$(X_R = X_{0R},\ \beta_{0R} = 1)$$

In general it is very difficult to determine φ experimentally with sufficient accuracy at so low values of $[A]_R$ that a safe K-value can be obtained by extrapolation. Consequently, in such cases the complexity constants determined are also rather uncertain. However, the stability constants $b_{jR} = \beta_{jR}/\beta_{j-1,R}$ can be calculated for $j > 1$ even if K is unknown.

Furthermore, in those cases where an uncharged complex MA_ν is formed, the distribution coefficient l_ν can be calculated from eqn. (7) when β_ν and $K\beta_{\nu R}$ are known.

Calculation of $\bar{n}$ *and* β_j. Under certain conditions it should be possible to use the anion exchange method for an independent determination of the complexity constants in the water phase.

If the ligand is sorbed much more easily than the perchlorate ion the anion exchanger will be almost saturated with respect to A, and thus $[A]_R$ will be approximately constant for varying but not too low values of [A]. Then eqn. (9) yields

$$\bar{n} \approx \nu - \frac{d\ln\varphi}{d\ln[A]} \qquad (11)$$

and the complexity constants β_j can be computed from the function $[A]^\nu/\varphi$, which in this case is proportional to X according to eqn. (6).

If the complexity is fairly strong and $[A]_R \gg [A]$ it can be expected that $\bar{n}_R$ is approximately equal to the coordination number N for not too low ligand concentrations. Thus, if $\bar{n}_R$ is calculated by the method developed above and is found to be constant and equal to an integer when [A] is varied, it is very probable that the values of $\bar{n}$ used in eqn. (9) are correct, and a confirmation of the complexity constants β_j, taken from another investigation, is obtained.

MEASUREMENTS AND CALCULATIONS

Chemicals used. A known amount of cadmium, containing some ^{115}Cd (from A.E.R.E., Harwell, England), was dissolved in nitric acid and the nitrate was converted into perchlorate by evaporation several times with perchloric acid. The concentration of the stock solution of radioactive cadmium perchlorate was calculated from the weighed amount of cadmium.

Sodium perchlorate was prepared by neutralizing perchloric acid with sodium carbonate. The crystals formed between 80°C and 135°C, in which region the perchlorate crystallizes without water of crystallization, were separated and dried at 110°C. A stock

solution was prepared, the concentration of which was checked by means of a cation-exchanger column in the hydrogen form.

Sodium bromide was of analytical grade, and the concentration of the stock solution was determined by titration according to Mohr.

The anion-exchanger was Dowex 2 × 8, containing fixed quaternary ammonium groups. It was converted to the bromide or perchlorate form and air-dried.

Method of investigation. The complex solutions had the initial composition

$$C'_M \text{ mM } Cd(ClO_4)_2 + C'_A \text{ mM NaBr} + (750 - C'_A - 3\,C'_M) \text{ mM } NaClO_4.$$

C'_M was kept constant in the measurement series. v litres of the complex solution were shaken for 20 h in a thermostat at 20.0°C with m grams of the air-dried exchanger. The value of vm^{-1} was always 0.015 lg^{-1}.

When a distribution equilibrium had been attained, the resin phase was separated from the solution. The remaining cadmium concentration C_M of the outer solution was determined by measurement of the gamma activity on 10 ml of the solution. For these determinations a scintillation detector (type P-20 from Tracerlab) was used. A glass cup containing 10 ml of the solution to be measured was placed in a fixed position in the lead shielding, in the centre of which the scintillation detector was immersed to a fixed depth. A satisfactory reproducibility of geometry was assured. In order to get a relation between counts per minute and cadmium concentration, the gamma activity of some reference solutions with known concentrations was determined. A rectilinear relation between activity and concentration was obtained, and this relation was not perceptibly affected by the presence of varying amounts of sodium bromide and perchlorate.

The load C_{MR} on the exchanger was calculated according to the relation $C_{MR} = vm^{-1}\,(C'_M - C_M\,\delta)$.

The equilibrium concentration C_A of the outer solution was determined by titration according to Mohr.

The load C_{AR} was determined by eluting the resin, which had been carefully separated from the solution, with v_1 litres of 2 M $NaClO_4$ in small portions. The bromide concentration C''_A of this solution was determined by titration, and C_{AR} was calculated from the relation $C_{AR} = v_1 m^{-1} C''_A$. The value of $v_1 m^{-1}$ was here 0.060 lg^{-1}. However, a certain amount of outer solution adhered to the particles of the separated resin, which could not be washed before the elution. But the ratio of surface area and mass of the resin was the same in all the measurements. Then, as the experiments were performed in quite the same manner, we have $C^a_{AR} = kC_A$, where k is a constant and C^a_{AR} is the contribution from the outer solution adherent to the resin particles. The correction term C^a_{AR} is, however, of rather little magnitude in comparison to C_{AR} and may be neglected.

An approximate value of the swelling factor δ was determined by shaking solutions of the composition

$$C'_A \text{ mM NaBr} + (750 - C'_A) \text{ mM } NaClO_4$$

with a known amount of the resin until equilibrium was reached. The value

of vm^{-1} was here as before 0.015 lg^{-1}. Then the value of δ was given by the ratio between the initial and the equilibrium sodium ion concentrations, which were determined by titrations with sodium hydroxide after percolating samples through a cation-exchanger column in the hydrogen form.

According to the description above, we will have the concentrations in the resin phase, C_{MR} and C_{AR}, expressed in mmoles per gram of the air-dried resin. In order to express the concentrations in moles per litre, it is necessary to know the water content of the resin in the swelled state. It is composed of two contributions: the water content of the air-dried resin and the water

Table 1. Anion exchange measurements on the cadmium bromide system. The anion exchanger initially in the bromide form. $C'_M = 2.987$ mM.

C_M mM	δ	$C_{MR} \times 10^2$ mmole·g^{-1}	C_{MR} mM	C_A M	C_{AR} mmole·g^{-1}	C_{AR} M	φ
1.7110	0.986	1.95	71.35	0.180	0.063	0.230	42
0.4780	0.986	3.77	135.0	0.320	0.185	0.665	285
0.3705	0.986	3.93	140.0	0.350	0.225	0.795	380
0.2940	0.986	4.05	144.0	0.390	0.245	0.875	490
0.2625	0.985	4.09	144.5	0.425	0.275	0.975	550
0.1585	0.985	4.25	147.5	0.475	0.350	1.20	930
0.1010	0.985	4.33	148.0	0.570	0.460	1.55	1 450
0.0465	0.984	4.41	145.5	0.655	0.685	2.25	3 100
0.0225	0.983	4.45	142.0	0.695	0.965	3.10	6 350
0.0115	0.982	4.46	135.5	0.725	1.45	4.45	12 000
0.0069	0.981	4.47	130.0	0.740	2.00	5.90	19 000
0.0032	0.981	4.48	127.5	0.745	2.55	7.25	39 500

Table 2. Anion exchange measurements on the cadmium bromide system. The anion exchanger initially in the perchlorate form. $C'_M = 1.513$ mM.

C_M mM	δ	$C_{MR} \times 10^2$ mmole·g^{-1}	C_{MR} mM	C_A M	C_{AR} mmole.g^{-1}	C_{AR} M	φ
1.5315	0.985	0.0074	0.29	0.007	0.0013	0.005	0.2
1.5215	0.985	0.022	0.87	0.015	0.0035	0.014	0.6
1.5010	0.985	0.052	2.04	0.029	0.0074	0.029	1.4
1.4805	0.985	0.083	3.25	0.042	0.010	0.040	2.2
1.4545	0.985	0.120	4.70	0.054	0.013	0.052	3.2
1.3670	0.984	0.250	9.77	0.081	0.022	0.085	7.1
1.2460	0.984	0.430	16.50	0.105	0.031	0.120	13
0.9620	0.984	0.850	32.00	0.160	0.053	0.200	33
0.6745	0.983	1.28	46.70	0.210	0.083	0.305	69
0.4590	0.983	1.59	57.10	0.265	0.115	0.405	125
0.3075	0.982	1.82	62.60	0.315	0.175	0.595	205
0.1690	0.982	2.02	68.30	0.420	0.225	0.755	405
0.0715	0.981	2.17	69.60	0.515	0.400	1.30	975
0.0240	0.980	2.24	69.30	0.610	0.690	2.15	2 900
0.0065	0.979	2.26	66.65	0.690	1.43	4.20	10 500

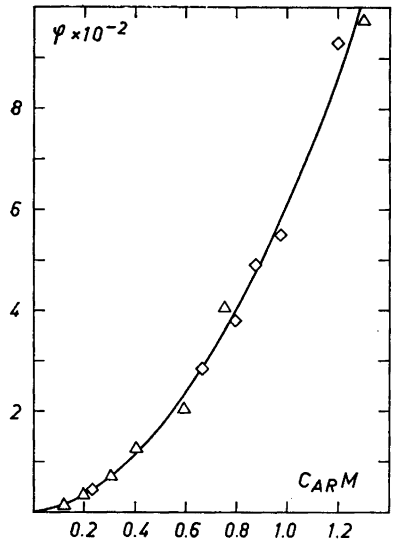

Fig. 1. The distribution φ of the cadmium bromide system as a function of the bromide concentration in the resin phase, C_{AR}. The anion-exchanger was initially either in the bromide form (symbol ◇) or in the perchlorate form (symbol △).

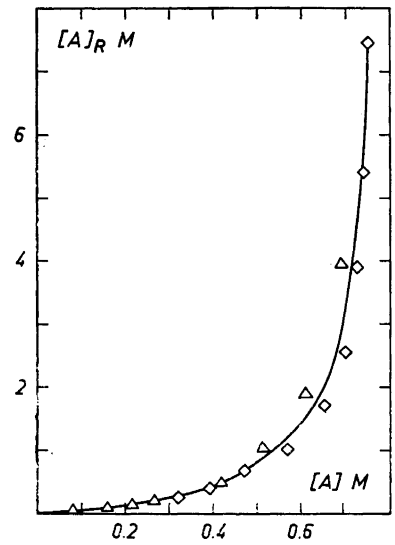

Fig. 2. The bromide ion concentration in the resin phase, $[A]_R$, as a function of the bromide ion concentration in the outer solution, [A]. The meaning of the symbols ◇ and △ is the same as in Fig. 1.

taken up by the air-dried resin during the swelling procedure. The first quantity can be determined from the loss of weight of the air-dried exchanger, when it is dried further (at about 80°C), until a constant weight is attained. The second quantity can be calculated by means of the swelling factor δ. If v represents the volume of the solution before the resin is added and $v\delta$ the volume of the outer solution at equilibrium, the volume of water taken up by the air-dried resin is $v(1-\delta)$.

The data from the measurements on the cadmium bromide system are collected in Tables 1 and 2. In Table 1 the bromide form of the anion exchanger was used, in Table 2 the anion exchanger was initially in the perchlorate form. The water content of the two forms in the air-dried state was for the first one 0.064 and for the second 0.024 grams water per gram of the air-dried exchanger.

Fig. 1 shows the distribution φ as a function of the ligand concentration C_{AR} for the two series. As seen in the figure, φ is a monotonously and rapidly rising function of C_{AR}.

The ligand numbers in the resin phase, $\bar{n}_R$, were calculated from eqn. (9). In this case $\nu = 2$. The terms $d\ln\varphi/d\ln[A]_R$ and $d\ln[A]/d\ln[A]_R$ were obtained by graphic methods, and $\bar{n}$ was computed from the relation $\bar{n} = \frac{C_A - [A]}{C_M} = \frac{X' \cdot [A]}{X}$. We mean by X the function $1 + \sum_{j=1}^{N} \beta_j [A]^j$ (*cf.* eqns. (2) and (4)) and by X′ the derivative of X with respect to [A].

Table 3. Computation of $\bar{n}_R$ for the cadmium bromide system. The anion exchanger initially in the bromide form.

φ	[A] M	$[A]_R$ M	$\frac{d\ln\varphi}{d\ln[A]_R}$	$\frac{d\ln[A]}{d\ln[A]_R}$	$\bar{n}$	$\bar{n}_R$
42	0.180				1.44	
285	0.320	0.25	1.10	0.55	1.94	3.1
380	0.350	0.35	1.20	0.55	2.04	3.2
490	0.390	0.40	1.20	0.52	2.14	3.3
550	0.425	0.48	1.30	0.48	2.24	3.4
930	0.475	0.67	1.40	0.42	2.36	3.6
1 450	0.570	1.00	1.60	0.36	2.58	3.8
3 100	0.655	1.70	1.70	0.23	2.80	3.9
6 350	0.695	2.55	1.75	0.15	2.90	3.9
12 000	0.725	3.90	1.80	0.09	2.94	3.9
19 000	0.740	5.40	1.90	0.06	2.98	4.0
39 500	0.745	6.75	2.00	0.04	3.00	4.0

Table 4. Computation of $\bar{n}_R$ for the cadmium bromide system. The anion exchanger initially in the perchlorate form.

φ	[A] M	$[A]_R$ M	$\frac{d\ln\varphi}{d\ln[A]_R}$	$\frac{d\ln[A]}{d\ln[A]_R}$	$\bar{n}$	$\bar{n}_R$
0.2	0.007	0.0048	0.80	1.20	0.21	0.7
0.6	0.014	0.013	1.20	1.20	0.38	1.3
1.4	0.028	0.026	1.36	1.18	0.59	1.7
2.2	0.041	0.033	1.50	1.17	0.73	2.0
3.2	0.053	0.042	1.60	1.16	0.83	2.2
7.1	0.080	0.060	1.70	1.14	1.00	2.6
13	0.105	0.074	1.70	1.10	1.14	2.8
33	0.160	0.100	1.70	0.95	1.37	3.1
69	0.210	0.145	1.70	0.75	1.57	3.4
125	0.265	0.205	1.70	0.70	1.76	3.5
205	0.315	0.365	1.70	0.56	1.93	3.7
405	0.420	0.495	1.70	0.40	2.25	3.8
975	0.515	1.05	1.75	0.30	2.49	3.9
2 900	0.610	1.90	1.80	0.20	2.69	3.9
10 500	0.690	3.95	1.87	0.13	2.83	4.0

At the calculation of the X- and X′-functions, the following values of the complexity constants were used for the outer solution, the ionic strength of which was 0.75 M (*cf.* Ref.[2], Kivalo and Ekari):

$$\beta_1 = 36\ M^{-1}, \quad \beta_2 = 125\ M^{-2}, \quad \beta_3 = 145\ M^{-3}, \quad \beta_4 = 340\ M^{-4}$$

The results are shown in Tables 3 and 4. In the calculation of $\bar{n}_R$ according to eqn. (9) at first an approximate value of $\bar{n}_R$ has been determined by using C_{AR} and C_A instead of $[A]_R$ and [A], respectively. Then $[A]_R$ and [A] have been computed from the relations

$$[A]_R = C_{AR} - \bar{n}_R \cdot C_{MR} \quad \text{and} \quad [A] = C_A - \bar{n} \cdot C_M$$

Table 5. Calculation of the stability constants of the cadmium bromide system in the resin phase.

$[A]_R$ M	KX_R	KX_{1R} M^{-1}	$KX_{2R}10^{-3}$ M^{-2}	$KX_{3R}10^{-4}$ M^{-3}	$KX_{4R}10^{-5}$ M^{-4}
0	*<0.1*	*25*	*2.0*	*10*	*3.0*
0.0048	0.118				
0.013	0.790	55	2.3		
0.026	2.55	95	2.7		
0.033	3.85	115	2.7		
0.042	6.60	155	3.1		
0.060	19.1	320	4.9		
0.074	41.0	550	7.1		
0.100	139	1400	14.0	12	
0.145	530	3700	26	17	
0.205	1770	8600	42	20	
0.365	89×10^2	245×10^2	67	18	
0.495	33×10^3	67×10^3	140	28	3.5
1.05	39×10^4	37×10^4	350	35	2.5
1.90	42×10^5	22×10^5	1200	65	3.0
3.95	72×10^6	18×10^6	4600	120	3.0

The difference between the approximate and the corrected values of $\bar{n}_R$ is rather slight. In the first series, starting with an anion exchanger in the bromide form, the $\bar{n}_R$-values are almost constant (≈ 4) throughout the greater part of the measurement series, that is the fourth complex is entirely dominating in the resin phase. This is also to be expected at the high ligand concentrations, which are attained in this experiment. The ionic strength of the inner solution is not quite constant through the series. It varies from about 9.5 to 7.4 M, the ionic strength thus decreasing somewhat at increasing C_{AR}, owing to the decreasing δ-values. As the fourth complex is dominating here in the series, it is, of course, impossible to compute any complexity constants from this material.

In the second series, where the anion-exchanger is initially in the perchlorate form, it is possible to reach down to lower C_{AR} values and consequently obtain a variation in the $\bar{n}_R$ values (Table 4). Here the ionic strength of the inner solution varies between 10.4 and 7.7 M (as before the lowest ionic strength is to be found in solutions with the highest C_{AR}-values).

Attempts have also been made to calculate approximate values of the complexity constants in the resin phase for the cadmium bromide system on the basis of these measurements. By successive extrapolations to $[A]_R = 0$ of the functions KX_{jR} the following values of $K\beta_{jR}$ are obtained (Table 5). $K < 0.1$,

$$K\beta_{1R} = 25 \pm 5 \text{ M}^{-1}, \qquad K\beta_{2R} = (2.0 \pm 0.5)10^3 \text{ M}^{-2},$$

$$K\beta_{3R} = (1.0 \pm 0.3)10^5 \text{ M}^{-3}, \qquad K\beta_{4R} = (3 \pm 1)10^5 \text{ M}^{-4}$$

Owing to the uncertainty in the determination of φ at low $[A]_R$-values and the rapid decrease of the KX_R-function at decreasing $[A]_R$, only an upper limit of K can be obtained. Thus, only lower limits of the complexity constants

$\beta_{j\mathrm{R}}$ can be determined. However, in spite of the lacking knowledge of the exact value of K, the stability constants of the system, $b_{j\mathrm{R}} = \beta_{j\mathrm{R}}/\beta_{j-1,\mathrm{R}}$, can be calculated for $j > 1$. The following values are obtained:

$$b_{1\mathrm{R}} > 200\ \mathrm{M}^{-1},\ b_{2\mathrm{R}} = 80 \pm 30\ \mathrm{M}^{-1},\ b_{3\mathrm{R}} = 50 \pm 25\ \mathrm{M}^{-1},\ b_{4\mathrm{R}} = 3.0 \pm 1.5\ \mathrm{M}^{-1}$$

In the case of the cadmium bromide system ν is a whole number, and the uncharged complex $CdBr_2$ is formed. The Nernst distribution coefficient l_2 of this complex can be calculated from eqn. (7) when β_2 and $K\beta_{2\mathrm{R}}$ are known. Inserting the values of these constants we get $l_2 = 16 \pm 4$.

DISCUSSION

The stability constants valid in the resin phase cannot be determined with any higher degree of accuracy. Especially the ratio $b_{3\mathrm{R}}/b_{4\mathrm{R}}$ is probably influenced by the fact mentioned above, that the ionic strength of the inner solution decreases somewhat at the higher ligand concentrations. Nevertheless, the values obtained are of great interest in so far as they can give the following information about the complexity of the cadmium bromide system within the anion exchanger phase.

(*a*) The ligand number $\bar{n}_{\mathrm{R}}$ attains the limiting value 4, and thus there is no steric hindrance to the formation of the higher complexes within the resin phase.

(*b*) The stability constants $b_{1\mathrm{R}}$, $b_{2\mathrm{R}}$, and $b_{3\mathrm{R}}$ are much higher than the corresponding ones in the outer solution, while $b_{4\mathrm{R}}$ and b_4 are of the same order of magnitude. This fact is probably connected with the very high ionic strength of the resin phase. Thus, according to an investigation by Kivalo and Ekari (*cf.* Ref.[2]) on the cadmium bromide system in water solutions the constants b_1, b_2, and b_3 increase monotonously, when the ionic strength of the solutions is increased from 1 to 3 M by addition of sodium perchlorate. b_4, on the other hand, does not increase.

The high values of the constants $b_{3\mathrm{R}}$ and $b_{3\mathrm{R}}b_{4\mathrm{R}}$ and of the distribution coefficient l_2 are obviously responsible for the fairly high sorption of cadmium by an anion exchanger saturated with bromide ions.

REFERENCES

1. Fronæus, S. *Svensk Kem. Tidskr.* **65** (1953) 1.
2. *Stability Constants of Metal-ion Complexes*, The Chemical Society, London, Part I, 1957; Part II, 1958.
3. Fronæus, S. *Svensk Kem. Tidskr.* **64** (1952) 317.
4. Kraus, K. A. and Nelson, F. In Hamer, W. J. (Ed.) *The Structure of Electrolytic Solutions*, John Wiley & Sons, New York 1959, p. 340.

Received May 5, 1962.

ACTA CHEMICA SCANDINAVICA 16 (1962) 1945–1955

Kinetics of Formation and Reactions of Quaternary Ethylenimonium Compounds

BERTIL HANSEN

Research Institute of National Defence, Department 1, Sundbyberg 4, Sweden

The rates of formation of ethylenimonium compounds from $(CH_3)_2NCH_2CHBrCH_3$ and from $RR'NCH_2CH_2X$, where R = R′ = H, R = R′ = CH_3, R = R′ = CH_3CH_2, R = R′ = $(CH_3)_2CH$, or R = CH_3, R′ = $(CH_3)_2CH$ and X = Br or Cl, have been measured at 25° and μ = 0.07 in aqueous solution. The rate constants increase strongly with the size of R and R′ from 5.6×10^{-4} sec^{-1} for R = R′ = H, X = Br to about 25 sec^{-1} for R = R′ = $(CH_3)_2CH$, X = Br. To explain these results it is proposed that the rate depends to some extent on the electron density at the nitrogen atom but mainly on the amount of energy necessary to change the bond angles at the nitrogen atom. These angles are different in the amine and in the ethylenimonium ion. The influence of R and R′ on the rates of the opening of the ethylenimonium rings by thiosulphate ions was found to be small. The smallest value at 25° and μ = 0.07 was 2.38×10^{-2} for R = R′ = H and the greatest 1.89×10^{-1} l $mole^{-1}$ sec^{-1} for R = R′ = $(CH_3)_2CH$. The rate measurements were made with a recording pH-stat.

One conceivable mechanism for the decomposition of 2-dialkylaminoethyl acetates in alkaline water solution is the formation of N,N-dialkylethylenimonium acetates [1]. For that reason it was necessary to study the influence of the N-alkyl groups on the rates of reactions at which N,N-dialkylethylenimonium compounds are known to be formed. As starting materials for such studies 2-dialkylaminoethyl halides are useful.

The rates of cyclization of primary ω-haloalkylamines as 2-bromoethylamine were measured by Freundlich and co-workers [2] in the period 1911–1933. A theoretical treatment of their work has been done by Salomon [3–5]. The decomposition of "nitrogen mustards", *i.e.* tertiary amines containing two 2-chloroethyl groups, has been thoroughly investigated by several authors [6–12]. Simonetta *et al.*[13] describe the kinetics of the cyclization of 2-dimethylaminoethyl chloride.

It is well known that ethylenimines and -imonium compounds easily react with nucleophilic reagents such as water, amines, hydroxyl and thiosulphate ions. Extensive studies in this field have been carried out by Clapp and his collaborators [14] and also by other investigators [6–9, 11, 12].

In this paper the rates of the cyclization of 2-aminoethyl bromide and of six 2-dialkylaminoethyl halides in aqueous solution are reported. Furthermore, as the rates were found to be unexpectedly strongly influenced by the N-alkyl groups, it was of interest to measure the rates of the reactions between the ethylenimonium compounds formed and thiosulphate ions. Special methods for the rate measurements with the use of a pH-stat have been worked out.

THEORY OF THE RATE MEASUREMENTS

For the determinations of the reaction rates indirect methods were used. They were based on the fact that hydrogen ions were formed during the formation of ethylenimonium ions and consumed in the reaction between these and thiosulphate ions. The amounts of alkali or acid necessary to keep the pH of the reaction mixture constant by automatic titrations were recorded[15]. The records were used for calculations of the velocity constants.

Cyclization of 2-dialkylaminoethyl halides

The method of the determination of the rate of the formation of ethylenimonium ions is similar to the method used for the determination of the rates of alkaline hydrolysis of aminoalkyl esters[16].

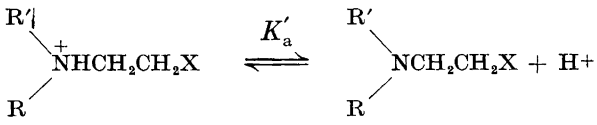

(1)

I II

$$\frac{c_{II} a_{H^+}}{c_I} = K'_a \qquad (2)$$

c = concentration, a = activity

In water solution there is an equilibrium (1) between the acid form, I, and the basic form, II, of the aminoethyl halide. Only II is able to form an ethylenimonium ion. This reaction (3) is first order and has the rate constant k_1.

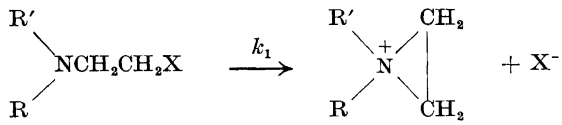

(3)

When the reaction (3) is running the equilibrium (1) is disturbed. But it is immediately corrected by the dissociation of I which results in the formation of hydrogen ions. These must be titrated with alkali to keep the pH constant. In order to obtain a practically measurable alkali consumption the amount of I must not be too small, that is the pH-value must be smaller or only slightly greater than the pK'_a-value. It can be shown (*cf.* Ref.[1], eqn. (11)) that the

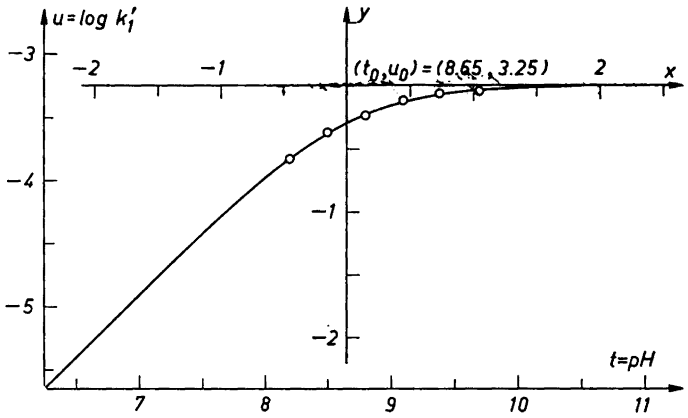

Fig. 1. Plot of the rate of cyclization of 2-bromoethylamine as function of pH, fitting the standard curve given by eqn. (5).

rate of alkali consumption, k_1', calculated from titration records, is first order and related to k_1 according to eqn. (4)

$$\log k_1' - \log k_1 = \log[1/(1 + 10^{-(\mathrm{pH}-\mathrm{p}K'_a)})] = -\log(1 + a_{H+}/K_a') \quad (4)$$

Eqn. (4) shows that knowledge of the value of K_a' is necessary for the calculation of k_1 from k_1'. As K_a' was unknown for all the amines the following method was used.

Values of k_1' were measured at a number of pH-values. When $u = \log k_1'$ was plotted against $t = \mathrm{pH}$ (Fig. 1) two types of diagrams were obtained: (A) containing a curved line as in Fig. 1, or (B) containing a straight line with the slope $+45°$.

(A) Curved lines are obtained if in the last term of (4) neither 1 nor a_{H+}/K_a' may be neglected, *i.e.* when the measurements are carried out in a pH-region around $\mathrm{p}K_a'$. The experimental curve drawn on a transparent paper is moved to fit, with parallel axis (Fig. 1), as well as possible a standard curve

$$y = \log[1/(1 + 10^{-x})] \quad (5)$$

The origin ($x = 0$, $y = 0$) of the coordinate system of the standard curve is marked on the experimental diagram and its coordinates (t_o, u_o) are read off (Fig. 1). It is easy to show that $t_o = \mathrm{p}K_a'$ und $u_o = \log k_1$.

(B) A straight line with a slope of $+45°$ is the result of the plot if the value of k_1 is so great that it is necessary to determine k_1' at pH-values at which the concentration of free amine is only a very small fraction of the total amine concentration, *i.e.* when $a_{H+}/K_a' \gg 1$ or $\mathrm{pH} \ll \mathrm{p}K_a'$. In this case eqn. (4) may be simplified to

$$\log k_1' - \log k_1 = \mathrm{pH} - \mathrm{p}K_a' \quad (6)$$

which is the equation of a straight line with a slope of +45° (the left part of the curve in Fig. 1). No determination of K_a' or k_1 is possible by any method. But if K_a' can be estimated, eqn. (6) can be used for an estimation of k_1.

Reactions between N,N-dialkylethylenimonium and thiosulphate ions

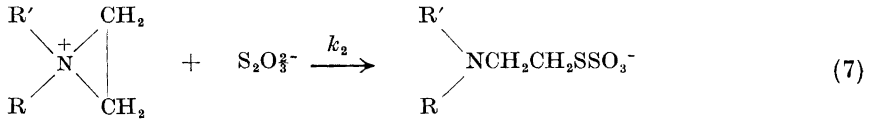

(7)

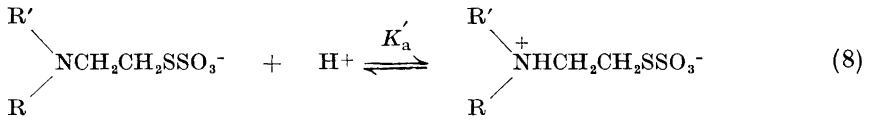

(8)

The opening of the ethylenimonium ring is in principle the reverse of the ring formation. This fact is recognized if the formulas (7) and (8) are compared with (3) and (1). That means that if the pH-value of the reaction mixture is smaller than or near the value of pK_a' of the amine formed, the ring opening is accompanied by a measurable consumption of hydrogen ions. The rate of this consumption, k_2', can be calculated from automatic, recorded titrations at constant pH. The rate of reaction (7) is in the pH-range around 7 independent of pH as both of the reactants are only involved in dissociation equilibria to a negligible extent. It is then easy to calculate k_2 from k_2' and the concentration of thiosulphate ions. This concentration can be kept constant by automatic addition of sodium thiosulphate.

$$k_2 = k_2'/c_{S_2O_3^{2-}} \tag{9}$$

EXPERIMENTAL

Materials

N,N-Dialkyl-2-bromoethylammonium bromides. The compounds were obtained from the corresponding aminoethanols and 50 % excess of hydrobromic acid. The reaction mixture was heated in an oilbath, and water was slowly distilled off through a 25 cm Widmer column. When the boiling point of the distillate had reached 125°, the residue was evaporated under reduced pressure to dryness. The crude products were recrystallized from acetone or absolute ethanol until the analyses in Table 1 were obtained.

N,N-Diethyl-2-chloroethylammonium chloride was obtained from 2-diethylaminoethanol and thionyl chloride [18] and recrystallized from absolute ethanol. For analyses see Table 1.

Kinetic measurements

The kinetic measurements were carried out as titrations at constant pH using an automatic recording titrator [15]. This gave records of the amount of titrant used as a function of time. From the records pseudo-first-order rate constants were calculated.

Table 1. Analyses and melting points of some 2-haloethylammonium halides. The melting points have been determined on a Kofler heating table.

Formula	Mol. wt.	M.p.		Analyses			
		Found	Lit.	C		H	
				Found	Calc.	Found	Calc.
$[H_3\overset{+}{N}CH_2CH_2Br]Br^-$	204.9	174°	172.5–173.5°[19]	11.7	11.7	3.6	3.62
$[(CH_3)_2\overset{+}{N}HCH_2CH_2Br]Br^-$	233.0	194°	188.5–188.9°[20]	20.6	20.6	4.6	4.76
$[(CH_3CH_2)_2\overset{+}{N}HCH_2CH_2Br]Br^-$	261.0	217°	208.1–208.4°[20]	27.8	27.6	5.7	5.80
$[((CH_3)_2CH)_2\overset{+}{N}HCH_2CH_2Br]Br^-$	289.1	141°	–	33.2	33.2	6.5	6.63
$[(CH_3)_2CH\overset{+}{N}H(CH_3)CH_2CH_2Br]Br^-$	261.0	122°	–	27.3	27.6	5.6	5.79
$[(CH_3)_2\overset{+}{N}HCH_2CHBrCH_3]Br^-$	247.0	199°	–	24.4	24.3	5.1	5.31
$[(CH_3CH_2)_2\overset{+}{N}HCH_2CH_2Cl]Cl^-$	172.1	216°	210 –211°[10]	41.7	41.9	8.8	8.77

The reactions took place under nitrogen atmosphere in a thermostated glass vessel at 25.00 ± 0.05°. The electrodes used, a Radiometer glass electrode type G 202 A (for 2-bromoethylamine type G 202 B), and a Radiometer saturated calomel electrode typ K 401, were standardized against 0.05 M potassium hydrogen phthalate, pH 4.01. In order to reduce the pH-fluctuations, which were less than ± 0.01 pH-unit, the buffer capacity of the reaction mixture was increased to about 9×10^{-5} equiv.l.$^{-1}$ (pH-unit)$^{-1}$ by adding small amounts of acetic acid or potassium dihydrogen phosphate solutions in the pH-region 4.6 – 9.4. No influence on the rates by these additions could be observed.

Cyclization of 2-aminoethyl halides. In each experiment $(1.3-1.6) \times 10^{-5}$ mole of 2-haloethylammonium halide was dissolved in 30 ml of 0.07 M potassium perchlorate solution and 0.1 – 1 ml of 0.05 M acetic acid or 0.05 M potassium dihydrogen phosphate solution and titrated at desired pH with 0.020 M sodium hydroxide solution from a 0.5 ml syringe. More concentrated solutions than 0.07 M potassium perchlorate were found to disturb the constancy of the e.m.f. of the calomel electrode. Potassium perchlorate was chosen instead of potassium chloride to give a constant ionic strength of the solution because perchlorate ions are known to react slower than chloride ions with ethylenimonium ions [14]. Rate determinations were carried out at least at 4 pH-values for each compound. Table 2 contains the results.

Reactions with thiosulphate ions. $(1.2-1.3) \times 10^{-5}$ mole of 2-haloethylammonium halide was dissolved in enough water and 0.07 M potassium perchlorate solution so that the ionic strength, $\mu = \frac{1}{2}\Sigma c_i z_i^2$, of the reaction mixture later after addition of sodium thiosulphate solution became 0.07. The mixture was titrated with 0.1 M sodium hydroxide solution at a pH such that at least 99.8 % of the amine had formed ethylenimonium ions in about 20 min. An exception was the formation of ethylenimine from 2-bromoethylamine which required 3 h at pH 9.0. After addition of 0.10 ml of 0.05 M potassium dihydrogen phosphate solution and adjustment of the pH to about 6.8 (for ethylenimine [14], $pK_a' = 8.0$, to 5.2) 1.50 or 3.00 ml of 0.101 M sodium thiosulphate solution was added. The total volume was now 30 ml. The ring opening reaction was followed by titration with 0.5 ml of 0.020 M hydrochloric acid solution. In order to keep the thiosulphate ion concentration constant in the reaction mixture 0.020 M sodium thiosulphate solution was added at the same rate as the hydrochloric acid solution [17]. Table 3 contains the results.

Table 2. pK_a' of and rate constants of the cyclization of some 2-haloethylamines. Temperature 25°. $\mu = 0.07$. Unit of k_1 and k_1', sec^{-1}. $pK_a = pK_a' - 0.10$

Compound	pK_a'			pH at which $\log k_1' = -3.5$	$\log k_1$			Measurements in pH-range
	found	estimated	lit.		found	estimated ± 0.2	lit.	
$NH_2CH_2CH_2Br$	8.65 ± 0.02		8.49/24° [21]	8.80 ± 0.01	−3.25 ± 0.01		−3.22 [22]	8.20–9.70
$(CH_3)_2NCH_2CH_2Br$		8.0		6.51 ± 0.01		−2.0		6.10–7.15
$(CH_3CH_2)_2NCH_2CH_2Br$		8.7		5.60 ± 0.01		−0.4		5.20–6.25
$((CH_3)_2CH)_2NCH_2CH_2Br$		9.0		4.06 ± 0.01		+1.4		3.70–4.45
$(CH_3)_2CHN(CH_3)CH_2CH_2Br$		8.7		5.54 ± 0.01		−0.4		5.20–6.10
$(CH_3CH_2)_2NCH_2CH_2Cl$	8.80 ± 0.04		8.6 [10]	7.35 ± 0.01	−2.03 ± 0.05		−2.02 [10]	7.00–8.05
$(CH_3)_2NCH_2CHBrCH_3$		8.0		5.86 ± 0.01		−1.1		5.50–6.40
$(CH_3)_2NCH_2CH_2Cl$							−3.54 [13]	

Table 3. Rate of the reactions between ethylenimonium and $S_2O_3^{2-}$-ions. Temperature 25°. μ = 0.07.

Compound	$c_{S_2O_3^{2-}}$ mmole l^{-1}	$10^2 \times k_2$ l mole^{-1} sec^{-1}	
		found ± 3 %	lit.
$H_2\overset{+}{N}CH_2CH_2$	10.1	2.38	0.536 [14]
$(CH_3)_2\overset{+}{N}CH_2CH_2$	10.1	8.65	
$(CH_3CH_2)_2\overset{+}{N}CH_2CH_2$	10.1	5.66	
	5.05	5.74	
$((CH_3)_2CH)_2\overset{+}{N}CH_2CH_2$	5.05	18.9	
$(CH_3)_2CH\overset{+}{N}(CH_3)CH_2CH_2$	5.05	4.71	
$(CH_3)_2\overset{+}{N}CH_2CHCH_3$	10.1	3.00	

RESULTS

The rates of cyclization of 2-haloethylamines to ethylenimines (Table 2) were slow enough only in the case of 2-bromoethylamine and 2-diethylaminoethyl chloride to make it possible to determine the true rate constant, k_1, and the pK_a' of the amine. The errors of k_1 and pK_a' were estimated from the largest deviations that could be made without getting an unacceptable fit between the experimental and the standard curve. The literature values for 2-diethylaminoethyl chloride are extrapolated from values determined at 0° and 15°.

For the other compounds the plot of log k_1' against pH gave straight lines with the expected angle coefficient = 1, except for 2-diisopropylaminoethyl bromide. In this case the slope of the straight line was 1.16, *i.e.* a tenfold increase of the hydrogen ion concentration decreased the k_1'-value 14.5 times. No explanation of this phenomenon has been found yet, and it was not taken into consideration at the estimation of k_1.

The pK_a'-values of those compounds for which no pK_a' could be determined were calculated according to Hall [23]. From the equation $pK_a = 13.23 - 3.14\ \Sigma\sigma^*$, the observed value $pK_a = 8.55$ for 2-bromoethylamine and $\sigma^* = 0.49$ for NH, the value $\sigma^* = 0.51$ was calculated for NCH_2CH_2Br. This value, combined with $\sigma^* = 0.00$ for NCH_3, -0.10 for NCH_2CH_3, -0.19 for $NCH(CH_3)_2$ and -0.30 for $N(CH(CH_3)_2)_2$ [1] and the equation $pK_a = 9.61 - 3.30\ \Sigma\sigma^*$, then gives the estimated pK_a'-values of Table 2. From these pK_a'-values and the

pH-values at which log $k_1' = -3.5$ the estimated log k_1-values were obtained when eqn. (6) was used.

The k_1-values (Table 2) of the cyclization reaction (1) are in good agreement with those found in the literature. The influence of the ionic strength seems to be small as Freundlich's and Kroepelin's k_1-value of 2-bromoethylamine [22] has been measured in a solution with $\mu = 0.15$ and the k_1-value of 2-diethylaminoethyl chloride obtained by Cohen *et al.*[10] refers to a solution with $\mu = 0.0025$. Nor is a great influence expected as the reacting molecule is uncharged and the reaction is intramolecular.

The deviations of the pK_a'-values now obtained from those found in other papers may be due to two facts. Firstly, the later values were determined in solutions with $\mu = 0.0025-0.01$ which gives smaller pK_a'-values than if $\mu = 0.07$. Secondly, these values were determined from pH-measurements of solutions of the haloethylammonium salts partly titrated with sodium hydroxide solution, which because of the cyclization must give somewhat unreliable values.

When the values of the rates of the reactions between the ethylenimonium and the thiosulphate ions (log k_2 in Table 3) were calculated, reactions of the ethylenimonium ions with other species, *i.e.* perchlorate ions and water, were not considered. The rates of these side reactions are unknown but must be so small that they may be neglected in comparison with the first mentioned reaction [14]. A proof for this assumption is an experiment in which 1.00 equivalent of diisopropylaminoethyl bromide hydrobromide was found to liberate 1.00 equivalent of hydrogen ions during the cyclization and after one hour at pH 6.0 and 25° consume 1.00 equivalent of hydrogen ions during the reaction with thiosulphate ions. No hydrolysis of the formed thiosulphate esters could be detected even if pH was as high as 10.

The large deviation of the literature value of log k_2 of the N-unsubstituted ethylenimonium ion refers to measurements in a solution with $\mu = 1.0$. The difference may to a great extent be due to difference of the ionic strengths as the rate of reactions between ions of opposite charges normally increases when the ionic strength is decreased [24].

DISCUSSION

For a great number of bimolecular reactions of tertiary amines the general rule is that increased branching at the 1-carbon atom reduces the reaction rate [25]. However, in the cyclization of 2-haloethylamines the effect of such branching is opposite (Table 2).

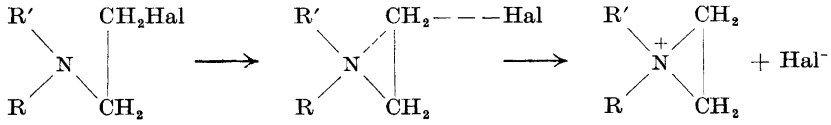

The cyclization may be regarded as an intramolecular nucleophilic substitution reaction. The alkyl groups at the 1-carbon atoms of R and R′ may effect the reaction velocity in two ways, partly, by influencing the steric conditions

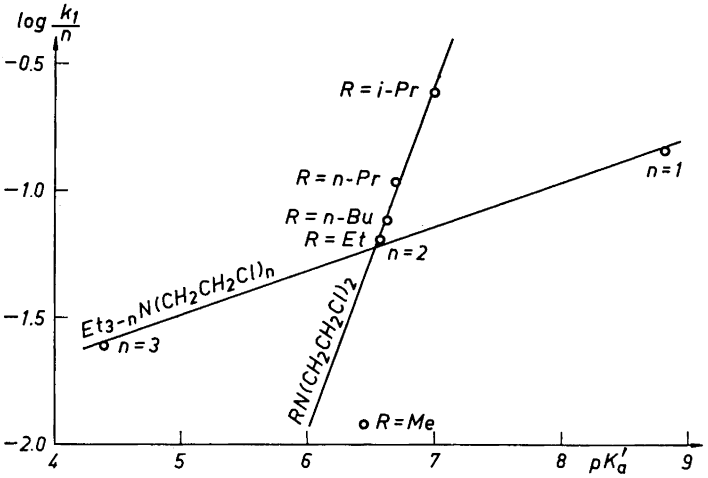

Fig. 2. Plot[10] of $\log(k_1/n)$ *versus* pK'_a for some 2-chloroethylamines, $R_{3-n}N(CH_2CH_2Cl)_n$, at 15°.

and, partly, by influencing the electron density at the nitrogen atom and by that its nucleophilic property.

Table 2 shows that each methyl group on the 1-carbon atoms increases the value of log k_1 by 0.8—1.0 units and also increases pK'_a [23]. Similar values were obtained by Cohen *et al.*[10] in their studies of the formation of ethylenimonium compounds from N-alkyl-bis(2-chloroethyl)amines with the N-alkyl groups methyl, isopropyl, ethyl, propyl and butyl. They also found, that pK'_a and log k_1 of the last three compounds were constant within $\pm$ 0.1 units, showing that the influence on log k_1 and pK'_a of the alkyl groups at the 2-carbon atoms is much smaller than of such groups at the 1-carbon atoms.

The existence of a linear relationship between pK'_a, which may be regarded as a measure of the electron density at the nitrogen atom, and log k_1 was shown by Cohen *et al.*[10] If in their series the N-methyl compound was excepted, a plot of log k_1 *versus* pK'_a (Fig. 2) gave a straight line with a slope of + 1.4 (log k_1)-units/pK'_a-unit.

If we assume that there are no steric effects in the cyclization, the same slope will be obtained when for the three compounds

$$(CH_3CH_2)_{3-n}N(CH_2CH_2Cl)_n,\ n = 1,\ 2\ ,\text{or } 3,$$

$\log(k_1/n)$ is plotted against pK'_a. The plot gives a straight line (Fig. 2) but the slope is much smaller, namely + 0.18 (log k_1)-units/pK'_a-unit. The choice of log (k_1/n) as a coordinate is due to the fact that the probability for cyclization may roughly be considered to be proportional to the number of $ClCH_2CH_2$-groups.

On the other hand, assume that only the steric conditions affect the reaction rate. If this is correct $\log(k_1/n)$ will have the same value $\pm$ 0.1 unit for all the compounds $(CH_3CH_2)_{3-n}N(CH_2CH_2Cl)_n$ as the chlorine atoms are

substituents on the 2-carbon atoms. But in fact $\log(k_1/n)$ decreases by about 0.4 units for each chlorine atom.

From what is said above the conclusion may be drawn that the rate of cyclization of tertiary 2-haloethylamines depends for a given halogen atom mainly on the number of alkyl groups on the 1-carbon atoms and to some extent on the electron density at the nitrogen atom.

The departing halide ion does not seem to have any influence on the relative rate of cyclization of two homologous 2-haloethylamines. A proof of this statement is that the difference between the log k_1 values for the dimethylamino- and the diethylaminoethylhalides is the same regardless of whether the halide is chloride or bromide.

The material now available is too small for an explanation of the reaction mechanism, but the following theory is proposed. In the N,N-dialkyl-ethylenimonium ion the angle ω between the ring bonds is about 60°. Thus the other bond angles, φ and Θ at the nitrogen atom must be somewhat greater than

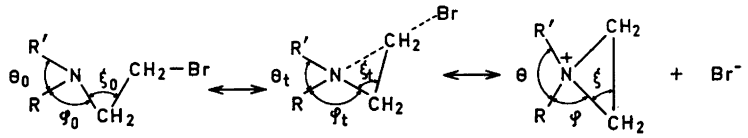

at a tertiary or quaternary nitrogen atom of an acyclic compound. Accordingly, for the formation of the transition state a part of the activation energy must be used to change the bond angles Θ_o, φ_o, and ξ_o. If R and R' are bulky groups, it can be assumed that Θ_o and φ_o have values closer to Θ_t and φ_t than if R and R' are small. This means that the formation of a transition state should be fascilitated and the reaction rate higher when R and R' are big, for the energy released during the completion of the ring closure should be rather independent of R and R'.

For similar reasons one may expect that the N,N-dialkylethylenimonium ring will be stabilized by bulky alkyl groups. In order to determine if this would hold true the rates of the reactions of these compounds with thiosulphate ions were measured (Table 3). But no simple relation was found between the size of the substituents at the nitrogen atom and the second order rate constants k_2. If the N-alkyl groups have only an inductive effect, k_2 for the di-isopropyl compound would have the smallest value, but it has the largest. There must accordingly be other effects, for instance steric ones, that are of greater importance for the reactions.

REFERENCES

1. Hansen, B. *Acta Chem. Scand.* **16** (1962) 1927.
2. Last paper: Freundlich, H. and Salomon, G. *Z. physik. Chem.* **166** A (1933) 161.
3. Salomon, G. *Helv. Chim. Acta* **16** (1933) 1361.
4. Salomon, G. *Helv. Chim. Acta* **17** (1934) 851.
5. Salomon, G. *Trans. Faraday Soc.* **32** (1936) 153.
6. Hanby, W. E., Hartley, G. S., Powell, E. O. and Rydon, H. N. *J. Chem. Soc.* **1947** 519.
7. Bartlett, P. D., Ross, S. D. and Swain, C. G. *J. Am. Chem. Soc.* **69** (1947) 2971.

8. Bartlett, P. D., Davis, J. W., Ross, S. D. and Swain, C. G. *J. Am. Chem. Soc.* **69** (1947) 2977.
9. Bartlett, P. D., Ross, S. D. and Swain, C. G. *J. Am. Chem. Soc.* **71** (1949) 1415.
10. Cohen, B., Artsdalen, E. R. Van and Harris, J. *J. Am. Chem. Soc.* **70** (1948) 281, correction p. 4275.
11. Cohen, B., Artsdalen, E. R. Van and Harris, J. *J. Am. Chem. Soc.* **74** (1952) 1875.
12. Cohen, B., Artsdalen, E. R. Van and Harris, J. *J. Am. Chem. Soc.* **74** (1952) 1878.
13. Simonetta, M., Modrone, N. V. Di and Favini, G. *Gazz. chim. ital.* **80** (1949) 129.
14. Last paper: Earley, J. E., O'Rourke, C. E., Clapp, L. B., Edwards, J. O. and Lawes, B. C. *J. Am. Chem. Soc.* **80** (1958) 3458.
15. Larsson, L. and Hansen, B. *Svensk Kem. Tidskr.* **68** (1956) 521.
16. Hansen, B. *Acta Chem. Scand.* **12** (1958) 324.
17. Larsson, L. *Svensk Kem. Tidskr.* **70** (1958) 405, 410.
18. *Organic Syntheses* Vol. **31** (1951) 37.
19. Gabriel, S. *Ber.* **50** (1917) 826.
20. Amundsen, L. H. and Krantz, K. W. *J. Am. Chem. Soc.* **63** (1941) 605.
21. Girault, G. and Rumpf, P. *Compt. rend.* **243** (1956) 663.
22. Freundlich, H. and Kroepelin, H. *Z. physik. Chem.* **122** (1926) 39.
23. Hall, Jr., H. K. *J. Am. Chem. Soc.* **79** (1957) 5441.
24. Moelwyn-Hughes, E. A. *The Kinetics of Reactions in Solution*, 2nd ed., reprinted by Oxford University Press London 1950, p. 97.
25. Hansson, J. *A Kinetic Study of the Addition of Amines to Propylene Oxide*, Lindstedts, Lund, Sweden, 1955, p. 22.

Received April 9, 1962.

ACTA CHEMICA SCANDINAVICA 16 (1962) 1956–1966

Studies on Aminonitrophenols

I. The Determination of the Protolytic Constants of 4-Amino-2-nitrophenol and 4-Amino-3-nitrophenol

HANS GUSTAF HANSSON

Department of Inorganic and Physical Chemistry, Chemical Institute, University of Lund, Sweden

The two substances mentioned above have the formula $C_6H_3(NH_2)(NO_2)(OH)$. In acid aqueous solutions they form the ion $C_6H_3(NH_3^+)(NO_2)(OH)$ and in alkaline aqueous solutions the ion $C_6H_3(NH_2)(NO_2)O^-$. The protolytic reactions are accompanied by colour changes of indicator character, which means that the forms $C_6H_3(NH_3^+)(NO_2)(OH)$, $C_6H_3(NH_2)(NO_2)(OH) \rightleftharpoons C_6H_3(NH_3^+)(NO_2)O^-$ and $C_6H_3(NH_2)(NO_2)O^-$ have different, well separated light absorption bands in the visible part of the spectrum.

By measuring the light absorption at suitable wave lengths and in proper buffer solutions it has been possible to determine the constants of the protolytic reactions for the two substances investigated. The constants determined are concentration constants referred to the temperature 25°C, the ionic strength 0.50 M (obtained by the addition of NaCl) and a solvent with the composition 99 % water + 1 % ethanol.

The structure of the compounds is discussed and it is shown that the aminonitrophenol molecules have practically no zwitter ion character.

Earlier investigations of the various monoaminomononitrophenols mainly concern the preparation of the substances and their reactions with organic chemicals. But up to now no accurate determination of the protolytic constants of the aminonitrophenols has been performed. Such a determination is of great interest, however, as it may be assumed that the differences between the constants of the various isomers could give important information about the molecular structure of the compounds. In this paper are presented the results of the determination of the protolytic constants of 4-amino-2-nitrophenol and 4-amino-3-nitrophenol. For both substances investigated the ion $C_6H_3(NH_3^+)(NO_2)(OH)$, the molecule $C_6H_3(NH_2)(NO_2)(OH)$ in equilibrium with the zwitter ion $C_6H_3(NH_3^+)(NO_2)O^-$ and the ion $C_6H_3(NH_2)(NO_2)O^-$, representing the

stages in the protolytic reactions, have different, well separated light absorption bands in the visible part of the spectrum.

The determination of the protolytic constants was performed by measuring the light extinction of the aminonitrophenols in a series of solutions with suitable $[H^+]$-values. The constants were calculated from coherent values of $[H^+]$ and the light extinction E. The way in which the investigation was carried out is thus a modification of the method previously used by the author, among others, in his investigation of some benzaurin derivatives [1–5]. The solutions used for the measurements were prepared by mixing 49 ml of the proper aqueous buffer with 1 ml of a stock solution of the aminonitrophenol in 50 % ethanol (+ a small amount of HCl). The results are thus throughout referred to a solvent with the composition 99 % water + 1 % ethanol. By the addition of NaCl to the buffer solutions, the ionic strength of the measurement solutions was kept constant at 0.50 M. The measurements were performed at the temperature 25°C.

THE PROBLEM

The protolytic scheme of an aminonitrophenol can be written as follows *:

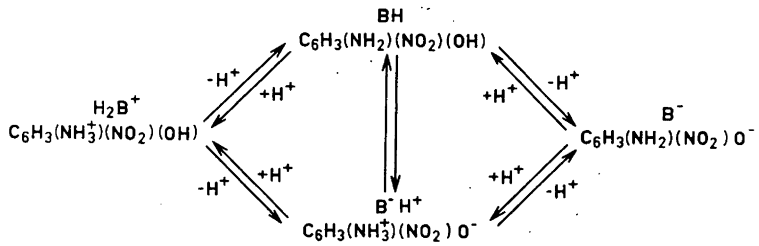

The equilibria above depend on the pH of the solution. This dependence appears as a shift of the colour of the solution. As is well-known the following constants can be defined for an ampholyte.

$$K_1' = \frac{[H^+] \cdot [BH]}{[H_2B^+]} \; ; \; K_2' = \frac{[H^+] \cdot [B^-]}{[BH]} \; ; K_a = \frac{[B^-H^+]}{[BH]}$$

$$K_1'' = \frac{[H^+] \cdot [B^-H^+]}{[H_2B^+]} \; ; \; K_2'' = \frac{[H^+] \cdot [B^-]}{[B^-H^+]}$$

As expected, equilibrium is reached instantaneously when the pH is changed. This means that separate determinations of [BH] and $[B^-H^+]$, which are always in equilibrium, are impossible. Only the sum [BH] + $[B^-H^+]$ can be determined. Thus it is convenient to define

$$K_1 = K_1' + K_1'' \; ; \; K_1 = \frac{[H^+] \cdot [HB]}{[H_2B^+]} \qquad (1)$$

* H_2B^+, BH, B^-H^+ and B^- are abbreviated formulas, used from now on.

$$\frac{1}{K_2} = \frac{1}{K_2'} + \frac{1}{K_2''}\,;\; K_2 = \frac{[H^+]\cdot[B^-]}{[HB]} \qquad (2)$$

where $[HB] = [BH] + [B^-H^+] = [BH]\cdot(1 + K_a)$

It follows that

$$K_1 = K_1'\cdot(1 + K_a) \text{ and } K_2 = \frac{K_2'}{1 + K_a}$$

The task is now to determine K_1 and K_2.

FORMULAS

If C is the total concentration of the aminonitrophenol,

$$C = [H_2B^+] + [HB] + [B^-] \qquad (3)$$

E = the light extinction of the solution at the pathlength d cm, and
E_{H,B^+} (E_{HB}, E_{B^-}) = the specific light extinction at unaltered pathlength of a solution in which $[H_2B^+]$ ($[HB]$, $[B^-]$) = C,
we can write

$$E = E_{H,B^+}\cdot\frac{[H_2B^+]}{C} + E_{HB}\cdot\frac{[HB]}{C} + E_{B^-}\cdot\frac{[B^-]}{C} \qquad (4)$$

From eqns. 1—4 we have the following general formula

$$E = \frac{E_{H,B^+}\cdot[H^+]^2 + E_{HB}\cdot K_1\cdot[H^+] + E_{B^-}\cdot K_1\cdot K_2}{[H^+]^2 + K_1\cdot[H^+] + K_1\cdot K_2} \qquad (5)$$

When the two equilibria concerned are well separated, *i.e.* when $K_1 \gg K_2$, it is possible to simplify formula (5) when used for the determination of K_1 and K_2.

A. If $[H^+] \gg K_2$ the terms $E_{B^-}\cdot K_1\cdot K_2$ and $K_1\cdot K_2$ may be neglected and formula (5) is transformed into

$$E = \frac{E_{H,B^+}\cdot[H^+] + E_{HB}\cdot K_1}{[H^+] + K_1} \qquad (6)$$

Eqn. (6) can be transformed into two different expressions, the left members of which are linear functions of $[H^+]$, suitable for a graphic representation of the measured quantities.

$$\frac{1}{E_{H,B^+} - E} = \frac{1}{E_{H,B^+} - E_{HB}} + \frac{[H^+]}{K_1\cdot(E_{H,B^+} - E_{HB})} \qquad (7)$$

$$\frac{[H^+]}{E - E_{HB}} = \frac{K_1}{E_{H,B^+} - E_{HB}} + \frac{[H^+]}{E_{H,B^+} - E_{HB}} \qquad (8)$$

B. If $[H^+] \ll K_1$ the terms $E_{H,B^+}\cdot[H^+]^2$ and $[H^+]^2$ may be neglected and formula (5) is transformed into

$$E = \frac{E_{HB} \cdot [H^+] + E_{B^-} \cdot K_2}{[H^+] + K_2} \quad (9)$$

Eqn. (9) can also be transformed into two different expressions, the left members of which are linear functions of $[H^+]$, suitable for a graphic representation of the measured quantities.

$$\frac{1}{E - E_{HB}} = \frac{1}{E_{B^-} - E_{HB}} + \frac{[H^+]}{K_2 \cdot (E_{B^-} - E_{HB})} \quad (10)$$

$$\frac{[H^+]}{E - E_{B^-}} = \frac{K_2}{E_{HB} - E_{B^-}} + \frac{[H^+]}{E_{HB} - E_{B^-}} \quad (11)$$

EXPERIMENTAL

The measurements of the light extinctions were performed with a Beckman Quarz Spectrophotometer, Model DU, at 25°C. Before the measurements were made the solutions were kept in a thermostat at this temperature.

The measurements of $[H^+]$ were performed with quinhydrone and a platinum-plate electrode or with hydrogen gas and a platinum-plate electrode covered with platinum-black. The reference solution had the composition 0.02 M HCl + 0.48 M NaCl. In some cases $[H^+]$ was calculated from the amount of HCl added.

In alkaline solutions there were difficulties in obtaining stable and reproducible values of E. This is probably due to an oxidation of the aminonitrophenol catalyzed by the small amounts of metal ions present in the solutions. The stability is thus considerably improved by the addition of small amounts of KCN or EDTA to the solutions. Consequently EDTA was added to all alkaline solutions used for the measurements; $[EDTA] = 4 \times 10^{-4}$ M. These solutions had reproducible light extinctions that kept stable for at least 1—2 h. The addition of EDTA (or KCN) has no undesired effects (except a slight poisoning of the Pt-electrode by CN^--ions).

The stock solutions of the aminonitrophenols were prepared by dissolving a weighed amount of the substance in 0.01 M HCl in 50 % ethanol. The concentration of the aminonitrophenol in the stock solutions was 5×10^{-3} M. The solutions used for the measurements were prepared by mixing 49.00 ml of a buffer solution with 1.058 ml of a stock solution of the aminonitrophenol. This was added to the buffer from a hypodermic syringe, the volume of which (1.058 ml) had been determined by weighing. Owing to a special stopping equipment of the hypodermic syringe the volume given from this is in fact reproducible within ± 0.1 %. The concentration of the aminonitrophenol in the solutions used for the measurements was thus of the order 1×10^{-4} M and reproducible within the limits mentioned above. The validity of Beer's law was verified in separate measurements not accounted for.

A short description of the syntheses of the substances investigated is given below. Other chemicals used were of the best qualities obtainable from Baker, Merck etc.

4-Amino-2-nitrophenol

The substance was prepared from *m*-nitroaniline according to the following reactions [6,7,10].

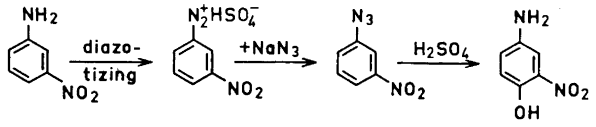

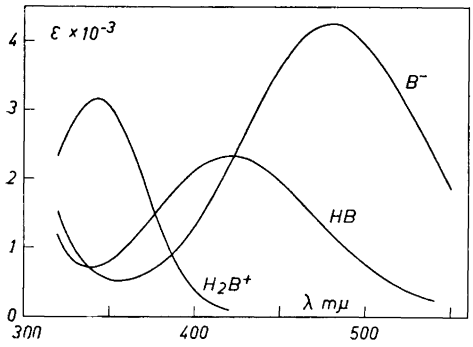

Fig. 1. 4-Amino-2-nitrophenol. Light extinction curves. The molecular extinction coefficient, ε, as a function of the wave length, λ, in mμ.

Before performing the last step the azide $C_6H_4(NO_2)N_3$ was recrystallised from diluted ethanol. After distillation with water vapour it formed white needles with the melting point 53 – 54°C. The final product of the aminonitrophenol was recrystallised from ethanol to a constant light absorption. The substance so obtained had m.p. 128 – 129°C. (Found: C 47.35; H 4.14; N 17.74. Calc. for $C_6H_6O_3N_2$: C 46.76; H 3.92; N 18.18).

Light extinction curves. In Fig. 1 are shown the curves for the different forms of the substance, *i.e.* for the red ion B^-, the yellow "molecule" HB and the pale yellow ion H_2B^+.

The diagram shows the molecular extinction coefficient, ε, as a function of the wave length, λ, in mμ. ε was calculated from the equation $E = \varepsilon \cdot C \cdot d$, and E, the light extinction, was measured at $d = 2$ cm for solutions with $C = 1.067 \times 10^{-4}$ M. The curve of H_2B^+ was taken up in an HCl-solution with $[H^+] = 0.500$ M (where $E \approx E_{H_2B^+}$), the curve of HB in a NaH_2PO_4-Na_2HPO_4-buffer with $[H^+] = 1.51 \times 10^{-6}$ M * and the curve of B^- in a NaOH—NaCl-solution with $[OH^-] = 0.00979$ M (where $E \approx E_{B^-}$). It was found that

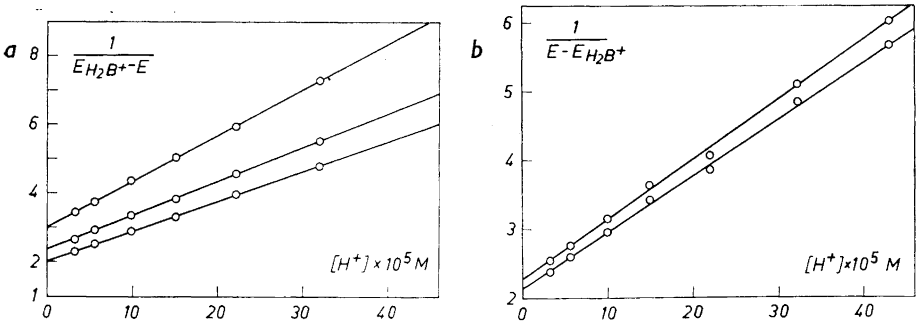

Figs. 2 a and b. 4-Amino-2-nitrophenol. $\pm 1/(E_{H_2B^+} - E)$, respectively, as a function of $[H^+]$ for the determination of K_1. The wave lengths are from above *in 2 a:* 360 mμ, 330 mμ, and 345 mμ and *in 2 b:* 410 mμ and 420 mμ. (The line for 430 mμ, not drawn, almost coincides with that for 420 mμ.)

* At this value of $[H^+]$ the contribution to E from the forms H_2B^+ and B^- cannot be neglected at all wave lengths. Therefore, when calculating ε, E_{HB}, obtained from formula (5), is substituted for E, the measured extinction.

$(\varepsilon_{H_2B^+})_{max} = 3.1(5) \times 10^3$ at $\lambda \approx 343$ mμ
$(\varepsilon_{HB})_{max} = 2.3(3) \times 10^3$ at $\lambda \approx 422$ mμ
$(\varepsilon_{B^-})_{max} = 4.2(6) \times 10^3$ at $\lambda \approx 481$ mμ

Determination of K_1. From the curves in Fig. 1 it is obvious that the measurements should be performed at $\lambda \approx 345$ mμ and $\lambda \approx 420$ mμ where the difference in E (ε) between H_2B^+ and HB is greatest. Two series of measurements were performed, one at the wave lengths 330, 345, and 360 mμ and the other at 410, 420, and 430 mμ. The solutions used for the measurements were made up from acetate buffers and a stock solution of the aminonitrophenol in the way described above. $[H^+]$ was determined (see above) and E was measured at $C = 1.067 \times 10^{-4}$ and with $d = 2$ cm. The measured quantities E and $[H^+]$ are represented graphically according to formula (7) where $E_{H_2B^+}$ is known from direct measurements. A straight line is obtained from which K_1 and E_{HB} are calculated; *cf.* Figs. 2 a and 2 b. The calculated value of E_{HB} is compared with the value found by measurement.

Results:		(calc.)	(found)
$\lambda = 330$ mμ	$K_1 = 2.40 \times 10^{-4}$	$E_{HB} = 0.19$	0.17
$\lambda = 345$ mμ	$K_1 = 2.34 \times 10^{-4}$	$E_{HB} = 0.18$	0.16
$\lambda = 360$ mμ	$K_1 = 2.27 \times 10^{-4}$	$E_{HB} = 0.228$	0.220
$\lambda = 410$ mμ	$K_1 = 2.62 \times 10^{-4}$	$E_{HB} = 0.472$	0.484
$\lambda = 420$ mμ	$K_1 = 2.60 \times 10^{-4}$	$E_{HB} = 0.484$	0.495
$\lambda = 430$ mμ	$K_1 = 2.52 \times 10^{-4}$	$E_{HB} = 0.477$	0.488

Average value $K_1 = (2.46 \pm 0.15) \times 10^{-4}$

The agreement between calculated and found values of E_{HB} is satisfying. In the first series ($\lambda = 330$—360 mμ) E_{HB} (calc.) is obtained as the difference

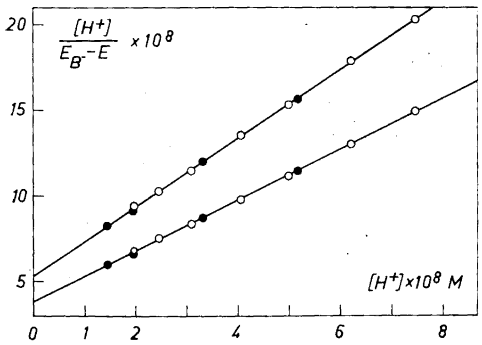

Fig. 3. 4-Amino-2-nitrophenol. $[H^+]/(E_{B^-} - E)$ as a function of $[H^+]$ for the determination of K_2. The wave lengths are from above 460 mμ and 480 mμ. (The line for 500 mμ, not drawn, almost coincides with that for 480 mμ.) The points ○ are for NaH_2PO_4—Na_2HPO_4 buffers and the points ● for H_3BO_3—NaOH buffers.

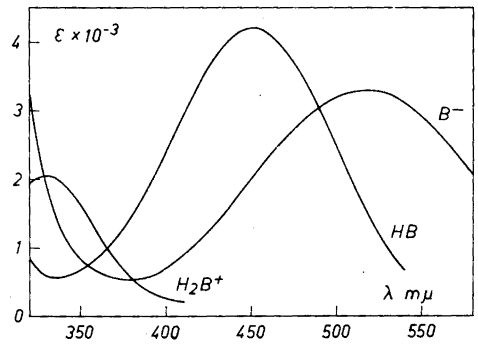

Fig. 4. 4-Amino-3-nitrophenol. Light extinction curves. The molecular extinction coefficient, ε, as a function of the wave length, λ, in mμ.

between two larger quantities (0.4—0.6), which explains the deviations between calculated and found values.

Determination of K_2. From Fig. 1 it is evident that a wave length suitable for the measurements is $\lambda \approx 480$ mμ. A series of measurements was performed at the wave lengths 460, 480, and 500 mμ. The solutions used for the measurements were made up from a stock solution of the aminonitrophenol and buffers containing the same small amount of EDTA (see above). The buffers used were NaH_2PO_4—Na_2HPO_4-buffers at $7.1 \leq pH \leq 7.7$ and H_3BO_3—NaOH-buffers (H_3BO_3—NaH_2BO_3) at $7.3 \leq pH \leq 7.8$. $[H^+]$ was determined and E was measured at $C = 1.067 \times 10^{-4}$ M and with $d = 2$ cm. The values of E and $[H^+]$ are represented graphically according to formula (11) where E_{B^-} is known from direct measurements. A straight line is obtained from which K_2 and E_{HB} are calculated; *cf.* Fig. 3. The calculated value of E_{HB} is compared with the value found by measurement.

Results:		(calc.)	(found)
$\lambda = 460$ mμ	$K_2 = 2.66 \times 10^{-8}$	$E_{HB} = 0.35$	0.36
$\lambda = 480$ mμ	$K_2 = 2.56 \times 10^{-8}$	$E_{HB} = 0.24$	0.26
$\lambda = 500$ mμ	$K_2 = 2.59 \times 10^{-8}$	$E_{HB} = 0.14$	0.16

Average value $K_2 = (2.6 \pm 0.1) \times 10^{-8}$

Here too, E_{HB}(calc.) is obtained as the difference between two larger quantities, which explains the deviations between calculated and found values of E_{HB}.

4-Amino-3-nitrophenol

The substance was prepared from *o*-nitroaniline in an analogous manner [6-9].

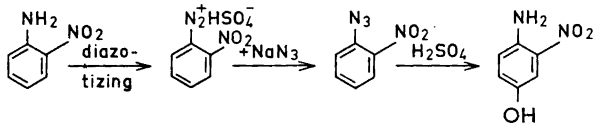

The final product of the aminonitrophenol, recrystallised from benzene to a constant light absorption, had the melting point 149—150°C. (Found: C 47.42; H 4.29; N 18.07. Calc. for $C_6H_6O_3N_2$: C 46.76; H 3.92; N 18.18).

Light extinction curves. Fig. 4 shows the curves (the molecular extinction coefficient ε as a function of the wave length λ in mμ) for the red-violet ion B^-, the yellow "molecule" HB and the almost colourless ion H_2B^+. As before, ε was calculated from the equation $E = \varepsilon \cdot C \cdot d$. E was measured at $d = 2$ cm for solutions with $C = 1.061 \times 10^{-4}$ M.

The curve of B^- was taken up in a NaOH—NaCl-solution with $[OH^-] = 0.0979$ M (where $E \approx E_{B^-}$) and the curve of HB in an acetate buffer with $[H^+] = 3.30 \times 10^{-5}$ M (where $E \approx E_{HB}$). The curve of H_2B^+ can be taken up but indirectly because of the relatively great value of K_1 (6×10^{-2}). From the measured E-values in an HCl-solution with $[H^+] = 0.500$ M the corresponding $E_{H_2B^+}$-values were calculated from formula (6) and from these $E_{H_2B^+}$-values ε was calculated.

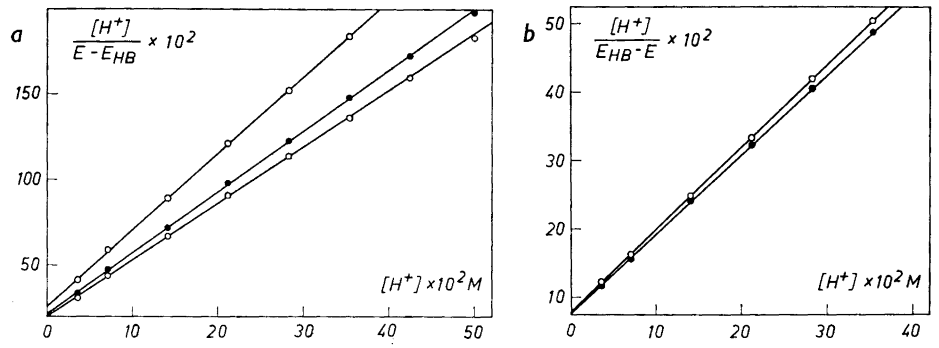

Figs. 5 a and b. 4-Amino-3-nitrophenol. $\pm[H^+]/(E-E_{HB})$, respectively, as a function of $[H^+]$ for the determination of K_1. The wave lengths are from above *in 5 a:* 320 mμ (O-points), 340 mμ (●-points) and 330 mμ (O-points) and *in 5 b:* 440 mμ (O-points) and 450 mμ (●-points). (The line for 460 mμ, not drawn, falls between the two in the figure).

It was found that

$(\varepsilon_{H_2B^+})_{max} = 2.0(5) \times 10^3$ at $\lambda \approx 330$ mμ
$(\varepsilon_{HB})_{max} = 4.2(1) \times 10^3$ at $\lambda \approx 452$ mμ
$(\varepsilon_{B^-})_{max} = 3.3(0) \times 10^3$ at $\lambda \approx 420$ mμ

Determination of K_1. From Fig. 4 it is obvious that the measurements should be performed at $\lambda \approx 330$ mμ and $\lambda \approx 450$ mμ, where the curves of H_2B^+ and HB differ considerably. The solutions used for the measurements were made up from a stock solution of the aminonitrophenol and a series of seven HCl—NaCl-solutions with proper accurately known $[H^+]$-values. ($[H^+]$ is known from the amount of HCl added). E was measured at $d = 2$ cm and with $C = 1.061 \times 10^{-4}$ M. The values of E and $[H^+]$ are represented graphically according to formula (8), where E_{HB} is known from direct measurement. A straight line is obtained from which K_1 (and $E_{H_2B^+}$) * can be calculated. See Figs. 5a and 5b.

Results:

$\lambda = 320$ mμ	$K_1 = 5.84 \times 10^{-2}$
$\lambda = 330$ mμ	$K_1 = 6.03 \times 10^{-2}$
$\lambda = 340$ mμ	$K_1 = 6.05 \times 10^{-2}$
$\lambda = 440$ mμ	$K_1 = 6.64 \times 10^{-2}$
$\lambda = 450$ mμ	$K_1 = 6.54 \times 10^{-2}$
$\lambda = 460$ mμ	$K_1 = 6.63 \times 10^{-2}$

Average value $K_1 = (6.3 \pm 0.3) \times 10^{-2}$

Determination of K_2. To judge from Fig. 4 it seems appropriate to perform the measurements at $\lambda \approx 450$ mμ and $\lambda \approx 520$ mμ where the difference between the curves of B^- and HB is relatively great **. The solutions used for the meas-

* The values of $E_{H_2B^+}$, calculated here, agree with those obtained above. But as these, too, were obtained indirectly, the agreement means no real check.

** An attempt was made to perform measurements at $\lambda \approx 320$ mμ too. The reproducibility of the E-values obtained was not good, however. This is probably due to the great slope of the B^--curve at this wave length. Nevertheless, the value of K_2 obtained (8.1×10^{-10}) is in relatively good agreement with the values obtained from the other measurements.

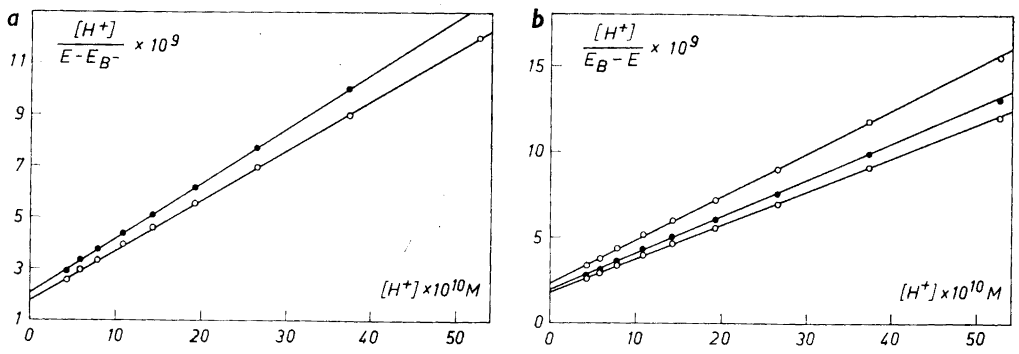

Figs. 6 a and b. 4-Amino-3-nitrophenol. $\pm[H^+]/(E-E_{B^-})$, respectively, as a function of $[H^+]$ for the determination of K_2. The wave lengths are from above *in 6 a:* 450 mμ (●-points) and 430 mμ (O-points) and *in 6 b:* 520 mμ (O-points), 530 mμ (●-points) and 540 mμ (O-points). (The line for 440 mμ, not drawn, falls between the two lines in 6 a).

urements were made up from a stock solution of the aminonitrophenol and a series of nine H_3BO_3—NaOH-buffers (H_3BO_3—NaH_2BO_3) containing the same small amount of EDTA (see above). $[H^+]$ was determined and E was measured at $C = 1.061 \times 10^{-4}$ M and with $d = 2$ cm. The values of E and $[H^+]$ were represented graphically according to formula (11); E_{B^-} is known from direct measurement. A straight line is obtained, from which K_2 and E_{HB} are calculated; *cf.* Figs. 6a and 6b. The E_{HB}-values calculated are compared with those obtained from direct measurements (see above). The agreement is strikingly good.

Results:

λ mμ	$K_2 \times 10^{10}$	E_{HB} calc.	E_{HB} found
430	9.30	0.809	0.808
440	9.20	0.861	0.868
450	9.56	0.893	0.894
520	8.99	0.308	0.303
530	9.01	0.220	0.214
540	9.15	0.149	0.143

Average value $K_2 = (9.2 \pm 0.2) \times 10^{-10}$

Summary

4-amino-2-nitrophenol
(the positive ion of)

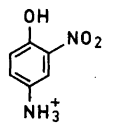

4-amino-3-nitrophenol
(the positive ion of)

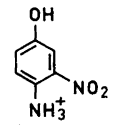

Protolytic constants:

$K_1 = 2.5 \times 10^{-4}$
$K_2 = 2.6 \times 10^{-8}$

$K_1 = 6.3 \times 10^{-2}$
$K_2 = 9.2 \times 10^{-10}$

DISCUSSION

It is well known that the presence of the electronattracting NO_2-groupin the benzene nucleus increases the acidity of protolytic substituents in the nucleus, and that this increasing effect is far more pronounced in the *ortho* (and *para*) than in the *meta* position.

Further it can be assumed that the mutual effects between the OH- and NH_2-groups do not essentially disturb the effect of the NO_2-group. Thus the constants determined could be compared with those of the corresponding nitroanilines and nitrophenols. As will be seen below such a comparison offers a possibility of determining the molecular structure of the aminonitrophenols.

The basicity constants of aniline, *o*-nitroaniline and *m*-nitroaniline are 3.8×10^{-10}, 1×10^{-14}, and 4×10^{-12}, respectively *. The acidity constants of the corresponding positive ions are thus 2.6×10^{-5}, 1, and 2.5×10^{-3}. The strong acidity-increasing effect of the NO_2-group is due to the fact that the inductive effect and the resonance effect operate in the same direction (see the formulas). Both effects are far more pronounced in the *ortho* than in the *meta* position. The same is true about the phenols. The acidity constants are 1.3×10^{-10}, 6.8×10^{-8} and 5.3×10^{-9} for phenol, *o*-nitrophenol, and *m*-nitrophenol, respectively *.

Thus by removing the NO_2-group from the *ortho* to the *meta* position in relation to the NH_3^+-group the acidity constant of the nitroanilinium ion is decreased by the factor 4×10^2 and in agreement with this K_1 is decreased from 6.3×10^{-2} to 2.5×10^{-4} *i.e.* by a factor of the same magnitude, 2.5×10^2.

Correspondingly, when the NO_2-group is removed from the *ortho* to the *meta* position in relation to the OH-group, the acidity constant of the nitrophenol is decreased by the factor 13 and K_2 by the factor 28 (from 2.6×10^{-8} to 9.2×10^{-10}).

It is obvious that the values of the constants determined, together with their relationship to other corresponding constants make it probable that the first proton given off from the positive ion of the aminonitrophenol is that of the NH_3^+-group and the second that of the OH-group. This means that the aminonitrophenol molecule has practically no zwitter ion character contrary to the aliphatic amino carboxylic acids. The structure is principally that of BH and the constant K_a is very small. This conclusion is in accordance with the view earlier developed by N. Bjerrum [11].** The plain light extinction curves of the HB-forms (Figs. 1 and 4) also indicate that *one* of the forms BH or B^-H^+ is quite predominating (> 95 %). If not, the curves would presumably have a more complicated course.

---

* The values are from C. Noller, *Chemistry of Organic Compounds*. Second Edition, 1957. W. B. Saunders Company, Philadelphia.

** Bjerrum's paper mainly concerns aliphatic amino carboxylic acids and the interpretation of their protolysis as acids and bases, respectively. But in addition he briefly noted the structures to be expected for some aromatic ampholytes.

A closer examination and discussion of the constants must be postponed until further results are available, which will presumably permit more and wider conclusions.

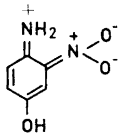

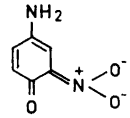

Resonance structures

4-amino-3-nitrophenol.

Resonance mainly between the NO_2- and NH_2-groups. The inductive effect of the NO_2-group is electron attracting.

4-amino-2-nitrophenol.
(negative ion B^-)

Resonance mainly between the NO_2- and O^--groups. The inductive effect of the NO_2-group is electron attracting.

The author's thanks are due to Dr. Stig Sunner, Head of the Thermochemistry Laboratory, University of Lund, for his kind interest in this work. Some of the syntheses were performed by Mrs. Brita Linderot, Lund. The author is indebted to Dr. Börje Holmberg, Malmö, for a careful revision of the English.

REFERENCES

1. Hansson, H. G. *Svensk Kem. Tidskr.* **73** (1961) 131.
2. Hansson, H. G. *Acta Chem. Scand.* **13** (1959) 1309.
3. Hansson, H. G. *Acta Chem. Scand.* **14** (1960) 407.
4. Hansson, H. G. *Acta Chem. Scand.* **14** (1960) 2021.
5. Hansson, H. G. *Acta Chem. Scand.* **15** (1961) 69.
6. Noelting, E., Grandmougin, E. and Michel, O. *Ber.* **25** (1892) 3328, p. 3338.
7. Frieländer, P. and Zeitlin, M. *Ber.* **27** (1894) 192.
8. Kehrmann, F. and Gauhe, E. *Ber.* **30** (1897) 2130.
9. Kehrmann, F. and Gauhe, E. *Ber.* **31** (1898) 2403.
10. Kehrmann, F. and Idskowska, M. *Ber.* **32** (1899) 1065.
11. Bjerrum, N. *Z. physik. Chem.* **104** (1923) 147.

Received March 20, 1962.

ACTA CHEMICA SCANDINAVICA 16 (1962) 1967–1975

The Electrostatic Effects in the Ionization of Weak Acids in Water and Water-Dioxane Mixtures

GUNNAR AKSNES

Chemical Institute, University of Bergen, Bergen, Norway

The equation for the ionization of weak acids: $-RT\ln(K/C) = A_{non} + A_{el}$, proposed by Gurney is discussed. It is shown that when A_{el} is expressed by Ne^2/r^*D according to Born, the plot of ΔF against $1/D$ is nearly linear. The r^*-values thus obtained for various acids differ from values found earlier by Baughan. The temperatures at which the ionization constants of various acids have their maximum values are in agreement with the temperatures evaluated from the Gurney equation. The empirical equation of Harned and Embree for the temperature dependence of the ionization constants around the maximum results from the equation of Gurney as a good approximation.

The ionization of weak acids in water-dioxane is discussed.

Gurney [1], twentyfour years ago, proposed that the free energy of ionization of acids in solution at infinite dilution of acid might be expressed as the sum of a non-electrostatic term A_{non} and an electrostatic term, A_{el}:

$$-RT\ln(K/C) = A_{non} + A_{el} \tag{1}$$

where C is a statistical factor. If the electrostatic term is expressed by Born's[2] formula, eqn. (1) takes the form:

$$\Delta F = -RT\ln K = \Delta F_{D=\infty} + Ne^2/r^*D \tag{2}$$

where r^* is defined as: $\frac{1}{r^*} = \frac{1}{2}\left(\frac{1}{r_+} + \frac{1}{r_-}\right)$; r_+ and r_- are the radii of the two ions. $\Delta F_{D=\infty}$ is the free energy of ionization at the hypothetical dielectric constant $D = \infty$. The factor C has been set equal to 1.

Baughan [3] and later LaMer and Brescia [4] and Magee *et al.* [5] have discussed the equation of Gurney and tested its applicability to the ionization of weak acids in water. Upon differentiation of eqn. (2) Baughan [3] derived the following expression for the enthalphy function:

$$\Delta H = \Delta H_{D=\infty} + \frac{Ne^2}{r^*}\left[\frac{1}{D}\left(1 + \frac{T}{D}\frac{dD}{dT}\right)\right] \tag{3}$$

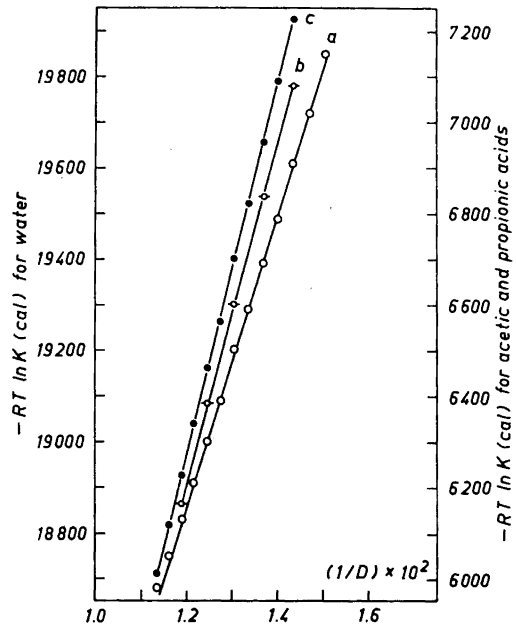

Fig. 1. Plots of $-RT\ln K$ against $1/D$ for the ionization of weak acids; a) water, b) acetic acid, c) propionic acid.

where $\Delta H_{D=\infty}$ is the enthalphy change at the hypothetical dielectric constant $D = \infty$. In Table 1 are recorded the values of r^* obtained by Baughan for several weak acids. Harned and Owen [6] have pointed out that the plot of ΔH against $\frac{1}{D}\left(1 + \frac{T}{D}\frac{\mathrm{d}D}{\mathrm{d}T}\right)$ shows distinct curvature, *i.e.*, eqn. (3) seems therefore not to be strictly valid.

An examination of the available data for ionization constants at various temperatures shows that the free energy of ionization of the acids is almost linearly dependent on $1/D$. Plots of $-RT\ln K$ against $1/D$ for water and for acetic and propionic acid are shown in Fig. 1. The plot for the ionization of water shows greatest deviation from linearity; however, when a straight line is drawn through the points in the middle of the temperature interval the observed ΔF-values at 0° and 60° are only approximately 30 cal higher than the values corresponding to the linear plot. If ΔF for the ionization of acids was exactly linearly dependent on $1/D$ then ΔF extrapolated to $D = \infty$ would be temperature independent, *i.e.*, $\Delta F_{D=\infty} = \Delta H_{D=\infty}$ and $\Delta S_{D=\infty} = 0$. The assumption of Gurney [1] that the free energy of ionization can be divided into two parts — a non-electrostatic part insensitive to the environment and independent of temperature, and an electrostatic part sensitive to the environment — seems therefore to be nearly fulfilled.

Table 1 also records the values of r^* for 31 weak acids calculated from the slope of the straight line plot of $-RT\ln K$ against $1/D$. The most remarkable

Table 1. Thermodynamic functions for ionization of weak acids *.

Acid	Mean radii r^* from Baughan [3]	Mean radii r^* This paper	T_{max} exp.	T_{max} from eqn. (8b)	T_{max} from eqn. (8c)	Ref.
Water	0.68	1.04	—	—		9
Acetic	0.85	0.89	298	295	291	9
Formic	0.68	1.14	297	298	293	9
Propionic	0.78	0.87	293	295	291	9
Butyric	0.65	0.81	283	273	279	9
Oxalic(2)	—	0.80	—	—	—	9
Sulphuric(2)	—	0.75	—	—	—	9
Phosphoric(1)	—	1.27	—	—	—	9
Phosphoric(2)	0.74	0.65	—	—	—	9
Glycine(A)	—	2.90	—	—	—	9
Glycine(B)	—	1.95	—	—	—	9
Alanine(A)	—	2.30	—	—	—	9
Alanine(B)	—	1.81	—	—	—	9
Boric	0.66	0.63	—	—	—	9
Lactic	0.63	1.14	~300	306	296	9
Glycolic	0.71	1.18	~300	314	300	9
Malonic(2)	—	0.66	—			9
Iodoacetic	—	1.05	—	—	—	15
Bromoacetic	—	1.15	—	—	—	15
Chloroacetic	0.76	1.19	—	—	—	15
Fluoroacetic	—	1.22	—	—	—	15
Benzoic	—	1.00	293	294	290	16
m-Cyanobenzoic	—	1.23	303	309	298	16
m-Chlorobenzoic	—	1.19	303	317	302	16
m-Bromobenzoic	—	1.13	298	300	294	16
p-Chlorobenzoic	—	1.15	308	319	303	16
p-Nitrobenzoic	—	1.25	303	301	294	16
p-Bromobenzoic	—	1.13	310	316	301	16
p-Cyanobenzoic	—	1.23	298	305	296	16
p-Hydroxybenzoic	—	1.01	306	322	304	16
Cyanoacetic	—	1.37	—	—	—	17

* The numerical value of Ne^2/r^*D is calculated with [14] $N = 6.0247 \times 10^{23}$, $e = 4.8029 \times 10^{-10}$ esu and 1 erg $= 2.3901 \times 10^{-8}$ cal.

feature is that the calculated r^*-values except for boric acid and dihydrogen phosphate are much larger than the values calculated by Baughan [3] from the ΔH function (eqn. 3). However, the new r^*-values are of the order of magnitude to be expected from theoretical considerations. The r^*-value calculated for the ionization of water is found to be 1.04 Å. The radius of the hydroxyl ion is probably very near 1 Å; that of the hydronium ion is perhaps somewhat greater than 1 Å. We find therefore that the calculated r^*-value for the ionization of water, 1.04 Å, is close to the value expected from the ionic radii. The second step in the dissociation of sulphuric, phosphoric, malonic and oxalic acids gives very small r^*-values which is in accordance with stronger electrostatic forces during the separation of the doubly negatively charged anion and the proton. The zwitterions alanine and glycine give very large r^*-values which are in agreement with the charge neutralization effect of the dipole. In series of substituted acids, for example halogen-substituted acetic acids and various substituted benzoic acids, the r^*-values increase with increasing capacity of the substituents to withdraw electrons from the dissociating hydroxyl group. The negative charge in the anion will thus be spread more evenly throughout the ion resulting in a decreasing electrostatic interaction between the proton and the anion during the separation process.

Eqn. (2) can also be used to calculate the temperature at which the ionization constant has its maximum value. Differentiation of eqn. (2) with respect to temperature gives:

$$-R\ln K - RT\frac{\mathrm{d}\ln K}{\mathrm{d}T} = \frac{Ne^2}{r^*}\frac{\mathrm{d}(1/D)}{\mathrm{d}T} \tag{4}$$

Thus, when K has its maximum value:

$$-R\ln K_{\max} = \frac{Ne^2}{r^*}\cdot\frac{\mathrm{d}(1/D)}{\mathrm{d}T} \tag{5}$$

The experimental values [7] for the dielectric constant, D, in the interval 0—60°C can be expressed as an inverse function of T^2 or T^3 with an accurancy better than $\pm$ 0.5 %:

$$D = \frac{1.013 \times 10^7}{T^2 + 4.0256 \times 10^4}\text{, or} \tag{6}$$

$$D = \frac{4.385 \times 10^9}{T^3 + 2.928 \times 10^7} \tag{7}$$

Substitution of eqn. (6) in eqn. (5) gives:

$$-R\ln K_{\max} = \frac{2Ne^2 \cdot T_{\max}}{r^* \times 1.013 \times 10^7} \tag{8a}$$

or

$$-\log K_{\max} = \frac{1.432 \times 10^{-2}}{r^*}\cdot T_{\max} \tag{8b}$$

When the same substitution is made with D according to eqn. (7) the following expression results:

$$-\log K_{max} = \frac{5.0 \times 10^{-5}}{r^*} \cdot T_{max}^2 \tag{8c}$$

The values of T_{max} calculated from the experimental values of K_{max} using the r^* values from column 3 in Table 1 are recorded in columns 5 and 6 of the same table. It is seen that the T_{max}-values of different acids calculated with the expression of D according to eqn. (6) and (7) show approximately the same conformity with the experimental T_{max}-values.

According to Harned and Embree [8] the ionization constants of various acids can approximately be expressed by the general equation:

$$\log K - \log K_{max} = -p(T-\Theta)^2 \tag{9}$$

Here, Θ is the temperature at which the ionization constant has its maximum value and p is a general constant which has the value of approximately 5.0×10^{-5} degree^{-2}. This experimental value of p can be derived on the basis of the above equations, as follows.

Substitution of expression (7) for the dielectric constant into eqn. (4), introduction of the numerical values of N and e, and subtraction of eqn. (8c), gives:

$$\log K - \log K_{max} = \frac{5.0 \times 10^{-5}}{r^*} (\Theta^2 - T^2) - T \frac{\mathrm{d} \log K}{\mathrm{d}T} \tag{10}$$

where T_{max} has been put equal to Θ. The last term is, from eqn. (9), equal to:

$$\mathrm{d} \log K/\mathrm{d}T = 2\,p\,(\Theta - T) \tag{11}$$

so that eqn. (10) becomes:

$$\log K - \log K_{max} = \frac{5.0 \times 10^{-5}}{r^*} (\Theta^2 - T^2) - 2p\,(\Theta T - T^2) \tag{12}$$

Equating the right sides of eqns. (9) and (12) now gives:

$$p = \frac{5.0 \times 10^{-5}}{r^*} \approx 5.0 \times 10^{-5} \tag{13}$$

since the values of r^* for the various acids for which eqn. (9) has been experimentally verified, according to Table 1 are of the order of 1 Å.

It might be argued that for example glycine and alanine which have r^*-values in the neighbourhood of 2 Å should not give so good agreement with the empirical eqn. (9) of Harned and Embree [8]. However, the T_{max} values for glycine and alanine used to fit eqn. (9) are very uncertain since they are derived from measurements below T_{max} only.

THE IONIZATION OF WEAK ACIDS IN WATER-DIOXANE MIXTURES

The ionization constants of weak acids become markedly smaller when dioxane is added to the water. Thus, K for acetic acid in pure water is 1.754×10^{-5} at 25°C as compared with 4.75×10^{-9} in 70 % dioxane-water mixture [9] (by weight). However, according to the experimental values of K at various temperatures [9] the temperature at which the ionization constant has its maximum value is very little different from that in pure water. If the ionization constant of weak acids in dioxane-water mixtures is expressed by eqn. (2) using the macroscopic dielectric constant of the mixture, the calculated values of r^* increase rapidly with the dioxane content. The same is true for the A_{non} term. Since the A_{non} term is the non-electrostatic contribution to the free energy of ionization one would expect this term to be relatively independent on whether the transfer of the proton from the acid to a neighbouring water molecule takes place in pure water, or in water-dioxane mixtures. Gurney [10] expresses the temperature at which the ionization constant has its maximum value as follows:

$$T_{max} = \vartheta(1 + A_{non}/A_{el}) \tag{14}$$

where ϑ is an empirical constant for expressing the temperature variation of the dielectric constant: $D = D_o \exp(-T/\vartheta)$. Since ϑ shows only a small decrease from water to dioxane-water mixtures (approximately 15 % decrease from pure water to 70 % dioxane-water mixtures) the decrease in T_{max} which is of the same magnitude as for ϑ can be explained if the ratio A_{non}/A_{el} has approximately the same value in water as in water-dioxane mixtures. If we assume that A_{non} is relatively independent of the dioxane content, as suggested above, it follows that also the electrostatic term, A_{el}, must be independent of the amount of dioxane present. We therefore tentatively conclude that A_{el} is dependent on the dielectric constant of the *water only* in the mixture. Consequently, eqn. (2) must be written:

$$-RT\ln K_c = \Delta F_{D=\infty} + Ne^2/r^*D_w \tag{15}$$

where D_w refers to the dielectric constant of the water in the mixtures.

The smaller ionization constants of weak acids in water-dioxane mixture thereby becomes a statistical effect. A statistical factor C is included in eqn. (1). Gurney [11] explains C as due to the difference between the number of solute molecules in reactants and products. For the ionization of water the reactant (the water) is not regarded as a solute but 2 solute species are formed, the hydronium ion and the hydroxyl ion, and Gurney, therefore, considers the difference as 2 and the statistical factor as 55.5 [2]. Since the ions formed in every ionization process strongly immobilize a certain number of water molecules in their hydration sphere we assume that these immobilized water molecules should be included in the reaction products; therefore, the statistical factor must also account for the disappearance of the free water molecules which are held in the hydration shell. The ionization of water should accordingly be formulated:

$$n\mathrm{H_2O} \rightleftharpoons \overset{+}{\mathrm{H}}_3\mathrm{O} \cdot x\mathrm{H_2O} + \overline{\mathrm{OH}} \cdot y\mathrm{H_2O} \tag{16}$$

where $n-2$ is the number of water molecules immobilized by the ions ($x + y = n-2$).

If the hydrated ions are regarded as separate units, then according to Gurney's view the difference between the solute particles in reactants and products is still 2. However, a statistical factor of 55.5^2 is much too small to account for the large decrease in the ionization constant of water in dioxane-water mixtures. A different approach to the problem seems possible from a reaction kinetic point of view. Suppose that a fixed relative orientation of a certain number of water molecules is necessary for the proton transfer to take place, not only of the two water molecules between which the proton is jumping but also of the water molecules which are necessary for the hydration of the proton and the hydroxyl ion formed. It seems reasonable to expect that for an exchange of the non-electrostatic energy (chiefly vibration) between the two water molecules and the two ions formed to occur, a spontaneous solvation of the ions in order to average out the energy with its environment is necessary. Since the frequency of vibration in water molecules is of the order of 10^{14} and the mean life time of hydrogen bonds [12] is of the order of 10^{-11} sec, the required configuration with closed hydrogen bonds between a certain number of water molecules should be able to exist over time intervals corresponding to a large number of vibrations. This necessary configuration may be regarded as a transition state and the number n of water molecules which is required in order to form the transition state will have to be included in the equilibrium equation:

$$n\mathrm{H_2O} \rightleftharpoons \left[\begin{matrix}\text{transition}\\ \text{state}\end{matrix}\right] \rightleftharpoons \overset{+}{\mathrm{H_3O}} \cdot x\mathrm{H_2O} + \overline{\mathrm{OH}} \cdot y\mathrm{H_2O}$$

and

$$K_c = \frac{\left[\overset{+}{\mathrm{H_3O}} \cdot x\mathrm{H_2O}\right] \cdot \left[\overline{\mathrm{OH}} \cdot y\mathrm{H_2O}\right]}{[\mathrm{H_2O}]^n} \tag{17}$$

where K_c means the ionization constant on the concentration scale.

If the dielectric constant of water and its temperature variation were exactly the same in dioxane-water mixtures as in pure water, it would follow that:

$$\log K_{c(\text{water})} - \log K_{c(\text{mixture})} = n(\log 55.5 - \log M) \tag{18}$$

where M is the number of moles of water per liter of the mixture.

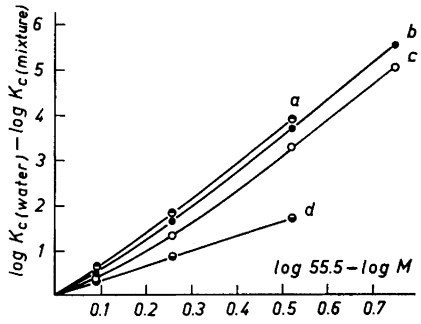

Fig. 2. Plots of [log K_c(water) − log K_c(mixture)] against [log 55.5 − log M] for different acids, a) water, b) acetic and propionic acids, c) formic acid, d) glycine.

Table 2. ΔH and ΔS for the ionization of weak acids in water and water-dioxane mixtures [13]. Temp. 25°C.

Acid	Water		Formic		Acetic		Propionic		Glycine, K_A	
Weight per-cent dioxane in water	ΔH kcal	ΔS e.u.	ΔH kcal	ΔS e.u.	ΔH kcal	ΔS e.u.	ΔH kcal	ΔS e.u.	ΔH kcal	ΔS e.u.
0	13.52	−18.7	−0.02	−17.6	0.09	−22.1	−0.16	−22.8	1.16	−6.9
20	13.52	−21.5	−0.36	−17.9	−0.05	−24.4	−0.05	−25.5	1.18	−8.1
45	13.19	−28.8	−1.07	−19.7	−0.44	−30.3	−0.21	−30.7	0.99	−10.9
70	12.66	−39.2	−1.47	−27.1	−0.61	−40.1	−0.20	−40.1	0.83	−15.4
82	—	—	−2.51	−31.8	−1.34	−50.8	−1.06	−51.2	—	—

Plots according to eqn. (18) are shown in Fig. 2. The curvature of the lines may indicate that D of water and its variation with temperature is not quite equal in pure water and in water-dioxane mixtures. It may also be due to an immobilization effect of the dioxane molecules upon the water in the mixture; this is easily seen to give deviation in the direction shown in Fig. 2. However, the n-values of about 5 to 7 which are calculated from the slopes of Fig. 2 for neutral acids are of the order of magnitude to be expected. Also, water has a n-value slightly higher than the fatty acids, which is in agreement with the ionization of water requiring one extra water molecule as compared with fatty acids. The average n-value for formic acid is somewhat smaller than the values for other fatty acids. This may be caused by greater conjugation in the formate ion as compared with the anions of other fatty acids; such an effect would be expected to reduce the average number of strongly immobilized water molecules. The n-value of glycine is approximately 3. Since glycine has a positively charged nitrogen atom and a zwitter ion is formed during the ionization process it is reasonable to expect that the difference between the number of strongly bonded water molecules in reactants and products will be greatly reduced as compared with neutral acids.

The experimentally evaluated ΔH- and ΔS-values for the ionization of weak acids in water-dioxane mixtures [9] (Table 2) show that the large decrease of the ionization constant is chiefly due to a much larger negative value of the entropy of ionization. These facts are thus in accordance with the assumption that the decrease of the ionization constant in dioxane-water mixtures is chiefly due to a statistical effect.

REFERENCES

1. Gurney, R. W. *J. Chem. Phys.* **6** (1938) 499.
2. Born, M. *Z. Physik* **1** (1920) 45.
3. Baughan, E. C. *J. Chem. Phys.* **7** (1939) 951.
4. LaMer, V. K. and Brescia, F. *J. Am. Chem. Soc.* **62** (1940) 617.

5. Magee, J. L., Ri, T. and Eyring, H. *J. Chem. Phys.* **9** (1941) 419.
6. Harned, H. S. and Owen, B. B. *The Physical Chemistry of Electrolytic Solutions*, Reinhold Publishing Corp., New York 1942, p. 531.
7. Collie, C. H., Hasted, J. B. and Ritson, D. M. *Proc. Phys. Soc. (London)* **60** (1948) 145.
8. Harned, H. S. and Embree, N. D. *J. Am. Chem. Soc.* **56** (1934) 1050.
9. Ref.[6], p. 581.
10. Gurney, R. W. *Ionic Processes in Solution*, McGraw-Hill Book Co., New York 1953, p. 128.
11. Ref.[10], p. 105.
12. Hall, L. *Phys. Rev.* **73** (1948) 775.
13. Ref.[6], p. 514.
14. Moore, W. J. *Physical Chemistry*, Longmans, Grenn and Co. New York 1957, p. 441.
15. Ives, J. G. and Pryor, J. H. *J. Chem. Soc.* **1955** 2104.
16. Briegleb, G. and Bieber, A. *Z. Electrochem.* **55** (1951) 250.
17. Feates, F. S. and Ives, J. G. *J. Chem. Soc.* **1956** 2798.

Received April 25, 1962.

ACTA CHEMICA SCANDINAVICA 16 (1962) 1976–1988

Zur Spaltung von β-Hydroxy-alkyl-aryläthern durch Alkali

II *. Der stereochemische Verlauf

JOSEF GIERER und ISA NORÉN

Die Holzchemische Abteilung des Schwedischen Holzforschungsinstituts, Stockholm, Schweden

The stereochemical aspects of the alkaline splitting of β-hydroxy-alkyl-aryl ethers (type I) were studied by investigating the configurations of the β-guaiacyl ethers IV and VI, as well as of the resulting glycols VIII and X, respectively. The configurations of VI, VIII and X could be determined using paper electrophoretic methods, the configuration of IV by converting the two steric forms of VI into the corresponding forms of IV *via* the tosyl esters and the iodine compounds.

The steric relationships between the β-guaiacyl ethers (IV and VI) and the resulting glycols (VIII and X) are in accordance with the view that the alkaline cleavage of the β-hydroxy-alkyl-aryl ether bonds mainly proceeds *via* an α,β-epoxide by a twofold inversion of the configuration.

The steric configurations of the phenolic substances VII, IX and XI were determined as well and their steric relationships to VI, VIII and X, respectively, were established by converting VII into VI, IX into VIII and XI into X by methylation with diazomethane.

In vorangegangenen Untersuchungen [1,2] wurde gezeigt, dass β-Hydroxy-alkyl-aryläther (I) durch Alkali über die Zwischenstufe der entsprechenden Epoxyde (II) zu 1,2-Glykolen (III) gespaltet werden:

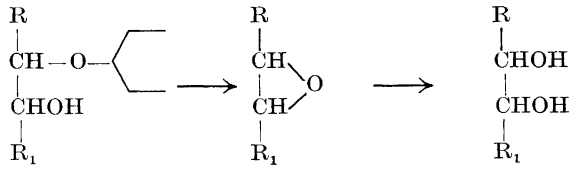

I II III

Die vorliegende Arbeit behandelt den stereochemischen Verlauf dieser Reaktion bei Verbindungen vom Typus I, in denen sowohl R, als auch R_1 ungleich H ist, die demnach in zwei stereoisomeren Racemformen vorliegen können. Da so-

* Teil I, siehe Ref.[1]

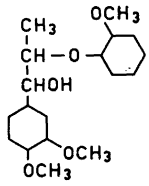
IV

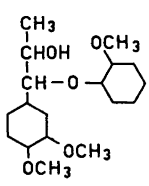
V

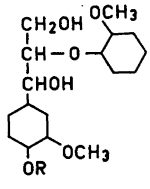
VI R=CH_3
VII R=H

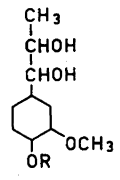
VIII R=CH_3
IX R=H

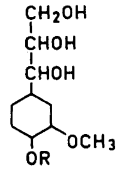
X R=CH_3
XI R=H

wohl Schliessung, als auch Öffnung des Epoxydringes im allgemeinen unter Inversion der Konfiguration erfolgt [3,4], ist zu erwarten, dass die alkalische Spaltung der β-Hydroxy-alkyl-aryläther über die Epoxyde entgegengesetzter Konfiguration zu den 1,2-Glykolen gleicher Konfiguration (wie die Ausgangssubstanzen) verläuft. Eine derartige zweifache Walden'sche Umkehrung wurde vor kurzem bei der unter schonenden Bedingungen durchgeführten Umwandlung von Ephedrinen über die 1-Phenyl-2-methyl-äthylenoxyde in die entsprechenden 1,2-Dihydroxy-phenylpropane durch Isolierung der Zwischen- und Endprodukte eindeutig nachgewiesen [5].

Die alkalische Spaltung von β-Hydroxy-alkyl-aryläthern (I) erfordert jedoch so drastische Reaktionsbedingungen, dass eine Isolierung der reaktionsfähigen Epoxydzwischenstufen (II) unmöglich ist. Der angenommene Verlauf kann jedoch auch ohne eine solche Isolierung durch Bestimmung der Konfigurationen der Ausgangs- (I) und der Endprodukte (III), sowie durch Untersuchung der sterischen Zusammenhänge überprüft werden. Im Folgenden wird dies am Beispiel der beiden Guajacyläther IV und VI und der daraus entstehenden Glykole VIII bzw. X zu zeigen versucht. Ausserdem werden die Konfigurationen der verschiedenen Formen der phenolischen Verbindungen VII, IX und XI bestimmt.

Bei der Ermittlung dieser bisher unbekannten Konfigurationen * kann mit Vorteil die Tatsache ausgenützt werden, dass die genannten Verbindungen als 1,2-Diole (VIII und IX), als 1,3-Diole (VI und VII), bzw. als 1,2,3-Triole (X und XI) mit Borat Komplexe bilden, deren Stabilität stark von der räumlichen Anordnung der Substituenten abhängig ist. Im Hochspannungsfeld wandern die Boratkomplexe der beiden sterischen Formen dieser Di- und

* Die Konfigurationen der beiden Formen von VIII ("α- und β-Form", siehe unten), der bei 83—84° schmelzenden Form von XI, sowie der bei 109.5—110° schmelzenden Form von X wurden vor kurzem auch auf andere Weise [6] festgelegt (siehe Ref.[7], Fussnote auf Seite 360). Die Ergebnisse stimmen mit unseren auf papierelektrophoretischem Weg gewonnenen Resultaten überein.

Triole mit deutlich verschiedener Geschwindigheit und können daher durch Papierelektrophorese bequem voneinander getrennt werden [8]. Die Konfiguration der beiden Formen der Verbindung IV wurde indirekt durch Überführung der Erythro- und der Threoform von VI in die entsprechenden Formen von IV bestimmt (siehe S. 1981).

1,2-Diole (III) bilden mit Borat einen (ebenen) 5-Ring. Der Komplex der Erythroform enthält die beiden Substituenten R und R_1 auf der gleichen

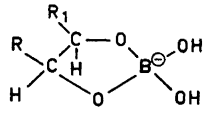

Seite der Ringebene in unmittelbarer Nachbarschaft zueinander und ist daher weniger stabil als der Komplex der Threoform [9]. Papierelektrophoretische Untersuchungen mit stereoisomeren 1,2-Diolen [10,8] ergaben in Übereinstimmung hiermit, dass die Erythroformen langsamer wandern als die entsprechenden Threoformen, sofern andere auf die Komplexbildung einwirkende Faktoren ausgeschlossen werden können. Die Substituenten R und R_1 beeinflussen zwar die Wanderungsgeschwindigkeit derartiger Boratkomplexe, kehren jedoch in keinem der bisher untersuchten Fälle diese Reihenfolge um (siehe Tabelle 2).

Noch deutlicher zeigt sich das unterschiedliche Verhalten der Komplexe der Erythro- und Threoformen von 1,2-Diolen im Hochspannungsfeld, wenn auf pH 6.5 neutralisierte, sulfonierte Phenylborsäure anstelle von Borat als Komplexbildner verwendet wird [11]. Unter diesen Bedingungen (siehe exp. Teil) wandern lediglich die Komplexe der Threoformen, während die der Erythroformen keine merkbare Mobilität zeigen. Die Zuordnung der verschiedenen Formen der 1,2-Diole VIII und IX und der 1,2,3-Triole X und XI zur Erythro- oder zur Threo-Konfiguration liess sich durch Anwendung dieser Variante der elektrophoretischen Methode bekräftigen (siehe die Tabellen 2 und 3).

1,3-Diole (z. B. VI und VII), hingegen, geben mit Borat einen 6-Ring und die sterischen Verhältnisse sind den bei Cyklohexanderivaten beobachteten analog. Der Komplex der Erythroform kann beide Substituenten (R und R_1)

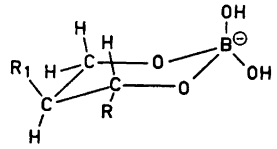

in ungehinderter äquatorieller Position enthalten und stellt daher die energetisch begünstigte Form dar. In der Threoform, hingegen, muss einer der Substituenten achseal sein und damit ganz in der Nähe eines achsealen Wasserstoffatoms und einer Hydroxylgruppe zu liegen kommen. Bei den 1,3-Diolen (z. B. VI und VII) sind daher die Boratkomplexe der Erythroformen stabiler [9] und im Hochspannungsfeld beweglicher als die der Threoformen.

Bei den 1,2,3-Triolen X und XI ist Komplexbildung zwischen dem α- und β-, dem β- und γ- und schliesslich auch zwischen dem α- und γ-Kohlenstoffatom der Glycerinseitenkette möglich. Ein Vergleich der Mobilitäten der verschiedenen Formen der 1,2,3-Triole X und XI (siehe Tabelle 3) mit denen der verschiedenen Formen der beiden 1,2-Diole VIII und IX (siehe Tabelle 2) zeigt grosse Unterschiede bei den Erythroformen, während die Threoformen von VIII und X mit fast gleicher und die von IX und XI mit nicht allzu verschiedener Geschwindigkeit wandern. Die mehr als doppelt so grossen Wanderungsgeschwindigkeiten der Erythro-1,2,3-Triole X und XI im Vergleich zu den entsprechenden Erythro-1,2-Diolen VIII und IX sind vermutlich auf die Bildung stabiler 1,3- (= α,γ-) Komplexe der Triole mit Borat zurückzuführen, die, wie oben gezeigt, aus sterischen Gründen energetisch begünstigt sind.

Wendet man nun diese papierelektrophoretische Methode zur Bestimmung der Konfiguration der 1,2-Diole VIII und IX, der 1,2,3-Triole X und XI, sowie der 1,3-Diole VI und VII an, ergibt sich folgendes:

1. Konfiguration der Ausgangssubstanzen der alkalischen Spaltung (β-Hydroxy-alkyl-aryläther)

Von den drei untersuchten β-Hydroxy-alkyl-aryläthern IV—VI [2,12] konnten die Konfigurationen der beiden Formen der Verbindung VI aufgrund ihrer 1,3-Diolnatur direkt papierelektrophoretisch bestimmt werden. Die kristallisierte Form (Schmp. 97,5—98,5°, Diacetat: Schmp. 59,5—60,5°, siehe experimenteller Teil) erwies sich als die Erythroform, die aus der Mutterlauge der kristallisierten Form von VI isolierte und über ihr kristallisiertes Diacetat (Schmp. 96—97°, siehe experimenteller Teil) gereinigte, ölige Form von VI als die Threoform (siehe Tabelle 1).

Tabelle 1. 1,3-Diole.

Substanz	R_m-Werte [a] in Borat pH 10,8	
Glycerin-β-guajacyläther	0,20	
α-(3,4-Dimethoxyphenyl)-glycerin-β-guajacyläther (VI), Schmp. 97,5—98,5°	0,30	
α-(3,4-Dimethoxyphenyl)-glycerin-β-guajacyläther (VI), Öl, über das Diacetat (Schmp. 96—97°) gereinigt	0,17	
α-(3,4-Dimethoxyphenyl)-glycerin-β-guajacyläther (VI), aus dem α-(3-Methoxy-4-hydroxyphenyl)-glycerin-β-guajacyläther (VII) durch Methylierung mit Diazomethan hergestellt; Gemisch beider stereoisomeren Formen	0,17	0,29
α-(3-Methoxy-4-hydroxyphenyl)-glycerin-β-guajacyläther (VII); Gemisch beider stereoisomeren Formen	0,21	(Hauptmenge) 0,41 (Hauptmenge)

[a] Siehe Fussnote S 1985.

Tabelle 2. 1,2-Diole.

Substanz	R_m-Werte in Borat pH 10,0		R_m-Werte in sulfonierter Phenylborsäure pH 6,5	
erythro-Butan-2,3-diol	0,14		0,0	
threo-Butan-2,3-diol	0,58		0,26	
Erythrit	0,83		0,12	
Threit	0,83		0,31	
Methyl-isoeugenolglykol (VIII), "α-Form"	0,17		0,0	
Methyl-isoeugenolglykol (VIII), "β-Form"	0,58		0,14	
Methyl-isoeugenolglykol (VIII), hergestellt aus Veratroyl-acetyl durch Reduktion mit Natrium-borhydrid, Gemisch beider stereoisomeren Formen	0,16 (4/5) [a]	0,58 (1/5)	0,0	0,14
Methyl-isoeugenolglykol (VIII), hergestellt aus Methyl-isoeugenolglykol-β-guajacyläther (IV, Schmp. 60—65°) durch Spaltung mit Alkali	0,15 (7/8)	0,58 (1/8)	0,0	0,13
Methyl-isoeugenolglykol (VIII), hergestellt durch alkalische Spaltung von Methyl-isoeugenolglykol-β-guajacyläther (IV), der aus α-(3,4-Dimethoxyphenyl)-glycerin-β-guajacyl-äther (VI, Schmp. 97,5—98,5°) gewonnen worden war	0,16	0,58 (Spuren)	0,0	0,14
Methyl-isoeugenolglykol (VIII), hergestellt aus Methyl-isoeugenolglykol-β-guajacyläther (IV, Öl nach Entfernung des krist. Anteiles) durch Spaltung mit Alkali	0,16 (1/4)	0,57 (3/4)	0,0	0,13
Methyl-isoeugenolglykol (VIII), hergestellt durch alkalische Spaltung von Methyl-isoeugenolglykol-β-guajacyläther (IV), der aus öligem α-(3,4-Di-methoxyphenyl)-glycerin-β-guajacyläther (VI) gewonnen worden war	0,58		0,14	
Methyl-isoeugenolglykol (VIII), hergestellt aus Methyl-isoeugenolglykol-α-guajacyläther (V, Schmp. 105—106°) durch Spaltung mit Alkali	0,16	0,58 (Spuren)	0,0	0,13
Methyl-isoeugenolglykol (VIII), hergestellt aus Methyl-isoeugenolglykol-α-guajacyläther (V, Öl nach Entfernung des krist. Anteiles) durch Spaltung mit Alkali	0,16 (2/3)	0,57 (1/3)	0,0	0,14
Glycerin-α-guajacyläther	0,33			

[a] in Klammern abgeschätztes Mengenverhältnis.

α-(3,4-Dimethoxyphenyl)-glycerin-α-methyläther aus α-(3,4-Dimethoxyphenyl)-glycerin durch Methylierung mit methanolischer Salzsäure	0,34			
α-(3,4-Dimethoxyphenyl)-glycerin-α-methyläther aus α-(3,4-Dimethoxyphenyl)-glycerin-α-methyläther-β-guajacyläther durch Spaltung mit Alkali	0,33			
Isoeugenolglykol (IX), Gemisch beider stereoisomeren Formen	0,31 (1/2)	0,65 (1/2)	0,0	0,10

Die kristallisierte (= Erythro-) Form der Verbindung VI konnte durch selektive Veresterung der primären Hydroxylgruppe mit *p*-Toluolsulfonsäurechlorid — Pyridin, Austausch der Tosyloxygruppe gegen Jod und des Jods gegen Wasserstoff in die Erythroform der Verbindung IV übergeführt werden. Aus der öligen (= Threo-) Form der Verbindung VI wurde auf gleichem Weg die Threoform der Verbindung IV erhalten. Die beiden auf diese Weise hergestellten, sterisch reinen Formen der Verbindung IV wurden direkt der alkalischen Spaltung unterworfen (siehe unten).

Die Konfigurationen der beiden Formen der Verbindung V[2] konnten auf diese Weise nicht bestimmt werden. Das der Verbindung IV ähnliche Verhalten bei der alkalischen Spaltung (siehe unten) deutet darauf hin, dass die kristallisierte Form (Schmp. 105—106° [2]) die Erythro- und die ölige Form die Threokonfiguration besitzt.

Das bei der Synthese der phenolischen Verbindung VII [13,14] anfallende Öl erwies sich als ein Gemisch aus beiden stereoisomeren Formen, in dem die Erythroform überwiegt. Durch Diazomethan-Methylierung wurde dieses Öl in ein Gemisch der beiden Formen von VI übergeführt, in dem, wie im Ausgangsgemisch, die Erythroform vorherrscht (siehe Tabelle 1).

2. Konfiguration der Produkte der alkalischen Spaltung (Diole und Triole)

Unterwirft man die kristallisierte Form der Verbindung IV, die zwischen 60 und 65° unscharf schmilzt, den Bedingungen einer Alkalikochung (2-stündiges Erhitzen in 2 N Natronlauge auf 170°C), bildet sich durch Spaltung der β-Arylätherbindung neben Guajakol vorwiegend die Erythroform des Methyl-isoeugenolglykols (VIII). Sie erwies sich sowohl aufgrund ihres Schmelzpunktes (124—126°, Mischprobe), als auch aufgrund ihrer Wanderungsgeschwindigkeit bei der Papierelektrophorese (siehe Tabelle 2) als ident mit der "α-Form" des Methyl-isoeugenolglykols [15], die, wie die "β-Form" [15], auch durch Reduktion von Veratroyl-acetyl mit Natriumborhydrid leicht zugänglich war [16]. Die gleiche sterische Form des Methyl-isoeugenolglykols (Erythroform) wurde isoliert und durch Schmelzpunkt (Mischprobe) identifiziert, wenn die aus der kristallisierten (= Erythro-) Form der Verbindung VI dargestellte Erythroform der Verbindung IV (siehe oben) alkalisch gespaltet wurde. Die papierelektrophoretische Untersuchung des Rohproduktes (vor der Kristallisation) zeigte neben der Erythroform des Methyl-isoeugenolgly-

kols nur Spuren der Threoform (siehe Tabelle 2). Die kristallisierte Form der Verbindung V (Schmp. 105—106°) gab bei der alkalischen Spaltung ebenfalls das *erythro*-Methyl-isoeugenolglykol vom Schmelzpunkt 124—126°.

Behandelt man hingegen die nach der Entfernung der kristallisierenden Anteile der Verbindungen IV und V zurückbleibenden Öle unter den gleichen Bedingungen mit Alkali, werden Gemische aus der Erythro- und aus der Threoform des Methyl-isoeugenolglykols (VIII) erhalten (siehe Tabelle 2). Die Threoform wurde ident mit der "β-Form" [15] vom Schmelzpunkt 80—80,5° befunden, die auch bei der Reduktion von Veratroyl-acetyl mit Natriumborhydrid (neben der Erythroform, siehe oben) erhalten wurde. Geht man von der reinen Threoform der Verbindung IV aus, welche aus der Threoform der Verbindung VI auf oben angegebenem Weg zugänglich ist, kann aus dem Reaktionsgemisch elektrophoretisch reines *threo*-Methyl-isoeugenolglykol isoliert werden.

Die bevorzugte (—wenn nicht ausschliessliche—) Bildung einer bestimmten sterischen Form des Methyl-isoeugenolglykols (VIII) aus der sterisch entsprechenden Form seines β-Guajacyläthers (IV) steht demnach in Übereinstimmung mit der eingangs erwähnten Annahme, wonach die alkalische Spaltung von Arylätherbindungen mit einer benachbarten alkoholischen Hydroxylgruppe (Typus I) unter zweifacher Inversion der Konfiguration über die Zwischenstufe der entsprechenden Epoxyde verläuft. Schema 1 zeigt den stereochemischen Verlauf der alkalischen Spaltung für die Erythroform der Verbindung IV:

Schema 1.

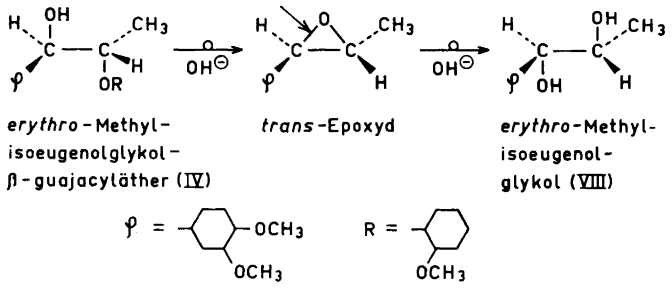

Das bei der Herstellung der phenolischen Verbindung IX [16] erhaltene Öl erwies sich als ein Gemisch beider Stereoisomerer, in dem die Erythroform überwiegt. Durch Diazomethan-Methylierung wird dieses Öl in ein Gemisch der beiden Formen der Verbindung X übergeführt, in dem, wie im Ausgangsgemisch, die Erythroform dominiert (siehe Tab. 1).

Etwas weniger übersichtlich wird der stereochemische Verlauf der alkalischen Spaltung von Aryl-alkylätherbindungen, wenn an beide der Arylätherbindung benachbarte Kohlenstoffatome des Alkylrestes je eine Hydroxylgruppe gebunden ist (XII). Wenn R verschieden von R_1 ist, muss mit der Bildung zweier strukturisomerer Epoxyde (XIIIa und XIIIb) gerechnet werden, die, je nach der Konfiguration des Ausgangsmaterials, entweder die *cis*-, oder die *trans*-Konfiguration besitzen und im weiteren Verlauf der alkalischen Spaltung die verschiedenen sterischen Formen des Triols XIV liefern:

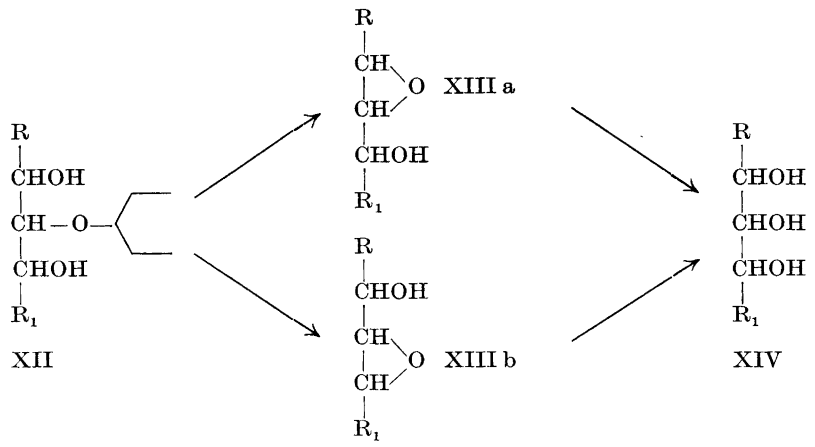

Im Falle der Substanz VI kommt zur Epoxydbildung zwischen dem α- und dem β-Kohlenstoffatom (siehe Schema 1, CH_3 ist durch CH_2OH zu ersetzen) auch noch die Möglichkeit der Epoxydbildung zwischen dem β- und dem γ-Kohlenstoffatom der Seitenkette. Da in Bezug auf die Konfigurationen an den beiden asymmetrischen Kohlenstoffatomen in α- und β-Stellung wohl die Schliessung des β,γ-Epoxydringes, nicht aber dessen alkalische Aufspaltung am terminalen Kohlenstoffatom [4,17] eine Inversion zur Folge hat, ist bei ausschliesslicher Annahme dieses Reaktionsverlaufes aus einer bestimmten sterischen Form der Verbindung VI ein α-(3,4-Dimethoxyphenyl)-glycerin (X) zu erwarten, das die dem Ausgangsmaterial (VI) entgegengesetzte Konfiguration besitzt (siehe Schema 2).

Schema 2.

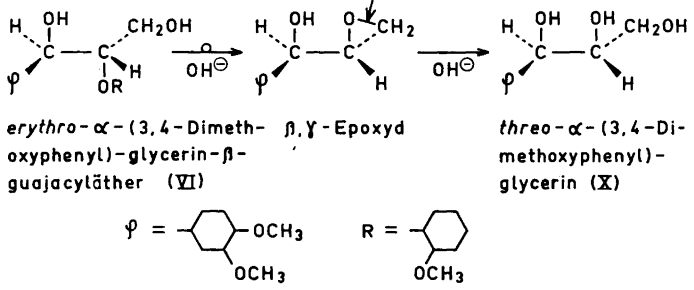

Die intermediäre Bildung eines β,γ-Epoxyds ist bei der alkalischen Spaltung eines Derivates der Verbindung VI anzunehmen, in dem die Epoxydbildung zwischen dem α- und dem β-Kohlenstoffatom durch selektive Methylierung der Hydroxylgruppe in α-Stellung blockiert ist. Das hierbei gebildete Glykol zeigt bei der Papierelektrophorese die gleiche Mobilität wie der α-Methyläther des α-(3,4-Dimethoxyphenyl)-glycerins (siehe Tabelle 2). Der α,γ-Dimethyläther der Verbindung VI, bei dem beide Möglichkeiten der Epoxydbildung aufgehoben sind, ist hingegen, wie gezeigt werden konnte [2], weitgehend alkalistabil.

Tabelle 3. 1,2,3-Triole.

Substanz	R_m-Werte in Borat pH 10,0	R_m-Werte in sulfonierter Phenylborsäure pH 6,5
Glycerin	0,60	0,0
α-(3,4-Dimethoxyphenyl)-glycerin (X, Schmp. 91—92°), hergestellt aus α-(3-Methoxy-4-hydroxyphenyl)-glycerin (XI, Schmp. 83—84°) durch Methylierung mit Diazomethan	0,48	0,0
α-(3,4-Dimethoxyphenyl)-glycerin (X, Schmp. 109.5—110°)	0,61	0,19
α-(3,4-Dimethoxyphenyl)-glycerin (X), hergestellt aus α-(3,4-Dimethoxyphenyl)-glycerin-β-guajacyläther (VI, Schmp. 97,5—98,5°) durch Spaltung mit Alkali	0,48 0,60 (Spuren)	0,0 0,19
α-(3,4-Dimethoxyphenyl)-glycerin (X), hergestellt aus α-(3,4-Dimethoxyphenyl)-glycerin-β-guajacyläther (VI, Öl, über Diacetat gereinigt) durch Spaltung mit Alkali	0,48 (1/4) 0,61 (3/4)	0,0 0,18
α-(3,4-Dimethoxyphenyl)-glycerin (X, Schmp. 110—111°), hergestellt aus α-(3,4-Dimethoxyphenyl)-glycerin-β-guajacyläther (VI, Öl, über Diacetat gereinigt) durch Spaltung mit Alkali	0,61	0,18
α-(3-Methoxy-4-hydroxyphenyl)-glycerin (XI, Schmp. 83—84°)	0,71	0,0
α-(3-Methoxy-4-hydroxyphenyl)-glycerin (XI, aus der Mutterlauge der Kristalle vom Schmp. 83—84°)	0,71 0,83 (Hauptm.)	0,0 0,11

Die kristallisierte (= Erythro-) Form der Verbindung VI gibt bei der alkalischen Spaltung fast ausschliesslich die Erythroform des α-(3,4-Dimethoxyphenyl)-glycerins (X); nur Spuren der Threoform von X können papierelektrophoretisch im Reaktionsgemisch nachgewiesen werden. Durch Diazomethan-Methylierung der kristallisierten Form des α-(3-Methoxy-4-hydroxyphenyl)-glycerins (XI, Schmp. 83—84° [13]) wurde kristallisiertes *erythro*-α-(3,4-Dimethoxyphenyl)-glycerin vom Schmelzpunkt 91—92° erhalten.

Die ölige (= Threo-) Form der Verbindung VI liefert bei der Behandlung mit Alkali ein Gemisch, das zu ungefähr 3/4 aus der Threo- und 1/4 aus der Erythroform der Verbindung X besteht. Das *threo*-α-(3,4-Dimethoxyphenyl)-glycerin konnte aus dem Reaktionsgemisch in kristallisierter Form isoliert und durch Schmelzpunktsbestimmung (109,5—110°, Mischprobe), sowie Papierelektrophorese (siehe Tabelle 2) mit der synthetisch dargestellten [18], kristallisierten Verbindung X identifiziert werden [2].

Der Umstand, dass eine bestimmte sterische Form des β-Aryläthers VI bei der alkalischen Spaltung der β-Arylätherbindung vorwiegend die gleiche

sterische Form des zugrundeliegenden Glycerinderivates X ergibt, lässt darauf schliessen, dass die Reaktion auch in diesem Falle vorzugsweise über das α,β-Epoxyd (1-(3,4-Dimethoxyphenyl)-2-methylol-äthylenoxyd) unter zweifacher Walden'scher Umkehrung verläuft (siehe Schema 1, CH_2OH anstatt CH_3).

Die kristallisierte Form des α-(3-Methoxy-4-hydroxyphenyl)-glycerins (XI, Schmp. 83—84° [13] erwies sich bei der Papierelektrophorese als die Erythroform und gab, wie bereits erwähnt, bei der Methylierung mit Diazomethan die Erythroform des α-(3,4-Dimethoxyphenyl)-glycerins (X, Schmp. 91—92°). Aus den Mutterlaugen der kristallisierten Verbindung XI wurde ein Öl isoliert, das vorwiegend die Threoform der Verbindung XI enthielt.

Die R_M-Werte * der erwähnten 1,3- und 1,2-Diole, sowie der 1,2,3-Triole sind in den Tabellen 1—3 zusammengestellt.

EXPERIMENTELLER TEIL

Substanzen

Bei der Darstellung der Substanzen IV—VI nach Ref.[2] bzw. Ref.[12] wurden zunächst farblose, bzw. schwach gelbliche Öle erhalten, die jedoch beim Umlösen aus Äthanol-Wasser (IV), bzw. beim Digerieren in Äther (V und VI) teilweise kristallisierten. Die kristallisierten Anteile wurden abgetrennt, sorgfältig gewaschen und aus Äthanol-Wasser (IV) [2], Äthanol (V) [2], bzw. aus Benzol (VI) umkristallisiert. Die kristallisierten Formen von IV und V wurden bereits näher beschrieben [2]. Acetylierung mit Essigsäureanhydrid-Pyridin gab nicht kristallisierende Monoacetate. Kristallisierter *α-(3,4-Dimethoxyphenyl)-glycerin-β-guajacyläther (VI)* schmolz bei 97,5—98,5°. (Gef. C 64,68; H 6,62; O 28,83; OCH_3 27,56. Ber. $C_{18}H_{22}O_6$ (334.2): C 64,69; H 6,58; O 28,72; OCH_3 27,84). Acetylierung mit Essigsäureanhydrid-Pyridin lieferte ein kristallisiertes *Diacetat* mit einem Schmp. von 59,5—60,5°. (Gef. C 63,35; H 6,20; O 30,60; OCH_3 22,00; CH_3CO 20,26. Ber. $C_{22}H_{26}O_8$ (418,3): C 63,18; H 6,22; O 30,60; OCH_3 22,05; CH_3CO 20,57).

Die in den Mutterlaugen und Waschflüssigkeiten der kristallisierten Verbindungen IV—VI enthaltenen Öle stellen Gemische der beiden stereoisomeren Formen von IV—VI dar. Das nach Entfernung der kristallisierten Form der Verbindung VI zurückbleibende Öl gab bei der Acetylierung mit Essigsäureanhydrid-Pyridin ein kristallisiertes *Diacetat*, das, nach zweimaligem Umkristallisieren aus Äthanol bei 96—97° schmolz. Die Mischung mit dem Diacetat aus der kristallisierten Form von VI (Schmp. 59,5—60,5°, siehe oben) schmolz unscharf zwischen 54 und 80°. Das kristallisierte Diacetat aus der öligen Form der Verbindung VI gab folgende Analysenwerte: Gef. C 63,16; H 6,24; O 30,48; OCH_3 22,17; CH_3CO 20,31. Ber. $C_{22}H_{26}O_8$ (418,3): C 63,18; H 6,22; O 30,60; OCH_3 22,05; CH_3CO 20,57. Für die unten beschriebene alkalische Spaltung wurde der ölige *α-(3,4-Dimethoxyphenyl)-glycerin-β-guajacyläther (VI)* über dieses kristallisierte Diacetat gereinigt. Er zeigte nach dieser Reinigung folgende Analysenwerte: Gef. C 64,70; H 6,80; O 28,95; OCH_3 27,45. Ber. $C_{18}H_{22}O_6$ (334,2): C 64,69; H 6,58; O 28,72; OCH_3 27,84.

Bezüglich der Darstellung der Verbindungen VII—XI siehe Ref.[13-16], sowie Ref.[18]. Die Verbindung VIII wurde ausserdem durch Reduktion von Veratroyl-acetyl mit Natriumborhydrid gewonnen [16].

Überführung der Verbindung VI in die Verbindung IV

α-(3,4-Dimethoxyphenyl)-glycerin-β-guajacyläther-γ-p-toluolsulfonsäureester. 2,0 g (= 6,0 Mmole) kristallisierter α-(3,4-Dimethoxyphenyl)-glycerin-β-guajacyläther (VI, Schmp. 97,5—98,5°) wurden in 6 ml wasserfreiem Pyridin gelöst, die Lösung mit einer

* $R_M = \frac{\text{tatsächliche Wanderungsstrecke der betreffenden Substanz}}{\text{tatsächliche Wanderungsstrecke von Mannit}}$

Eis-Kochsalzmischung gekühlt und mit 1,20 g (= 6,3 Mmolen) reinem *p*-Toluolsulfonsäurechlorid versetzt. Hierauf wurde eine Stunde unter Kühlung geschüttelt, wobei alles Toluolsulfonsäurechlorid in Lösung ging, und weitere 20 Stunden bei −4° aufbewahrt. Nach Abfiltrieren der abgeschiedenen Kristalle (Pyridiniumchlorid) wurde das Filtrat in vorgekühlte 0,5 N Schwefelsäure eingetragen, wobei der Ester als farbloses Öl ausfiel. Das Ganze wurde einigemale gründlich mit Chloroform ausgezogen und der Chloroformextrakt zuerst mit 0,5 %iger Natronlauge und hierauf mit Wasser ausgeschüttelt. Nach Trocknen der Lösung und Abdampfen des Lösungsmittels blieb ein farbloses, blasenziehendes Öl zurück, das ohne Reinigung weiterverarbeitet wurde. Ausbeute: 2,82 g (= 96 % d. Th.).

1-(3,4-Dimethoxyphenyl)-1-hydroxy-2-guajakoxy-3-jod-propan. Die gesamte Ausbeute an Toluolsulfonsäureester (2,82 g, siehe oben) wurde in 30 ml abs. Aceton gelöst, 1,86 g (= 12,4 Mmole) Natriumjodid zugesetzt und unter Rückfluss erhitzt. Schon nach kurzer Zeit begann ein weisser Niederschlag auszufallen, der nach weiterer 2-tägiger Rückflusskochung abfiltriert und zweimal mit abs. Aceton gewaschen wurde. Ausbeute an *p*-Toluolsulfonsaurem Natrium: 0,66 g (= 82 % d. Th.). Das Filtrat wurde zusammen mit der Waschflüssigkeit zur Trockne eingedampft, das zurückbleibende, gelbe Öl in Chloroform gelöst und die Lösung einmal mit 0,1 N Natriumthiosulfatlösung (Farbumschlag von Orange nach Grünlichgelb), sowie einmal mit Wasser ausgeschüttelt. Nach Trocknung der Lösung und Abdestillieren des Lösungsmittels blieb ein schwach gelbliches Öl zurück, das direkt weiterverarbeitet wurde. Ausbeute: 1,67 g (= 92 % d. Th.).

Methyl-isoeugenolglykol-β-guajacyläther (IV). 0,444 g (= 1 Mmol) der obigen Jodverbindung wurden in 70 ml 90%igem Methanol gelöst und der Lösung 1 ml 2 N Natronlauge zugesetzt. Die hydrierende Abspaltung des Jods wurde bei Normaldruck mit Pd auf Tierkohle als Katalysator durchgeführt [19]. Der Verbrauch an Wasserstoff, umgerechnet auf Normalbedingungen, betrug nach 70 Minuten 22,0 ml (= 98 % d. Th.). Nach Abfiltrieren des Katalysators und Nachwaschen mit Methanol wurde auf kleines Volumen eingeengt, mit Wasser verdünnt und einige Male mit Chloroform ausgeschüttelt. Nach Abdestillieren des Lösungsmittels blieb ein gelbliches Öl zurück, das nach dem Ergebnis der Dünnschichtschromatographie (Trennschicht: Kieselgel, Elutionsmittel: Chloroform oder Äthylacetat, Entwicklung durch Joddämpfe) fast reine Verbindung IV darstellte. Ausbeute: 0,25 g (= 78 % d. Th.).

Die Rohausbeute wurde ohne Reinigung der alkalischen Spaltung (siehe unten) unterworfen. Im Spaltungsansatz konnten papierelektrophoretisch neben *erythro*-Methyl-isoeugenolglykol nur Spuren der Threoform nachgewiesen werden. Die Erythroform (Schmp. 124—126°) liess sich, wie unten beschrieben, in einer Ausbeute von 55 % d. Th. isolieren (siehe Tabelle 2).

Auf analoge Weise wurde — ausgehend von der öligen, über das kristallisierte Diacetat (Schmp. 96—97°) gereinigten Form der Verbindung VI (siehe oben) — *via* den entsprechenden *p*-Toluolsulfonsäureester und die entsprechende Jodverbindung die andere sterische Form der Verbindung IV (Threoform) erhalten, die bei der alkalischen Spaltung elektrophoretisch reines *threo*-Methyl-isoeugenolglykol lieferte (siehe Tabelle 2).

Diazomethan-Methylierung der Verbindungen VII, IX und XI

Die phenolischen Verbindungen VII, IX und XI wurden in einer Mischung von abs. Dioxan (5 Teile) und abs. Methanol (1 Teil) gelöst. In die mit Eis gekühlten Lösungen wurde ein Überschuss an Diazomethan eingeleitet. Nach 2-tägigem Stehen im Kühlraum bei −4° wurden die Lösungsmittel und überschüssiges Diazomethan im Vakuum entfernt und die Reinheit der resultierenden Methyläther VI, VIII bzw. X sowohl durch Methoxylbestimmung, als auch durch Dünnschichtschromatographie (Trennschicht: Kieselgel, Elutionsmittel: Chloroform, Entwicklung durch Joddämpfe), überprüft. Die öligen, aus den beiden stereoisomeren Formen bestehenden Verbindungen VII und IX gaben ein Gemisch der beiden stereoisomeren Formen von VI (siehe Tabelle 1) bzw. VIII, die kristallisierte (= Erythro-) Form der Verbindung XI lieferte eine kristallisierte Form der Verbindung X (Schmp. 91—92°), die ebenfalls die Erythroform darstellt (siehe Tabelle 3).

Spaltungen der Substanzen IV—VI mit Alkali

Die Spaltungen der verschiedenen Formen der Verbindungen IV—VI mit Alkali und die Aufarbeitung der Reaktionsgemische wurden einheitlich durchgeführt. Sie seien am Beispiel der Spaltung der kristallisierten und der öligen Form der Verbindung VI näher beschrieben.

Spaltung von kristallisiertem und öligem α(3,4-Dimethoxyphenyl)-glycerin-β-guajacyläther (VI) mit Alkali. 4 g kristallisierte Verbindung VI (siehe oben) wurden in einem Autoklaven aus rostfreiem Stahl mit 120 ml 2 N Natronlauge versetzt und nach Verdrängen der Luft durch Stickstoff 2 Stunden unter Rotation auf 170° gehalten (Aufheizdauer: 1,5-Stunden). Nach vorsichtigem, schwachem Ansäuern des Reaktionsansatzes mit verd. Salzsäure wurde das abgespaltete Guajakol mit Äther ausgeschüttelt und hierauf den vereinigten Ätherextrakten durch Ausschütteln mit 2 N Natronlauge entzogen. Dieser alkalische Auszug wurde angesäuert, das Guajakol erneut mit Äther ausgeschüttelt und zur weiteren Reinigung mit Wasserdampf destilliert. Aus dem Destillat wurde das Guajakol durch Ausschütteln mit Äther und Verjagen des Äthers im Vakuum in chromatographisch (Dünnschichtschromatographie) reiner Form isoliert. Ausbeute: 1,085 g (= 74 % d. Th.).

Die schwach salzsaure, wässrige Lösung (nach Entzug des Guajakols) wurde neutralisiert, im Vakuum zur Trockne eingeengt und der Rückstand mit Chloroform erschöpfend ausgezogen. Der Chloroformauszug wurde auf kleines Volumen eingeengt und einige Male gründlich mit Wasser ausgeschüttelt. Das in der wässrigen Phase enthaltene Reaktionsprodukt wurde durch Ausschütteln mit wenig Chloroform gereinigt und nach Einengen der Lösung im Vakuum als fast farbloses Öl erhalten. Ausbeute: 1,77 g (= 65 % d. Th.). Die papierelektrophoretische Untersuchung dieses Öles zeigte, dass es neben der Erythro- nur Spuren der Threoform des α-(3,4-Dimethoxyphenyl)-glycerins (X) enthielt (siehe Tabelle 3). Impfung mit kristallisiertem *erythro-α*-(3,4-Dimethoxyphenyl)-glycerin, dargestellt durch Diazomethan-Methylierung aus kristallisiertem *erythro-α*-(3-Methoxy-4-hydroxyphenyl)-glycerin (siehe oben), führte nicht zur Kristallisation des Öles.

4 g ölige, über das kristallisierte Diacetat (Schmp. 96—97°) gereinigte Verbindung VI ergaben, auf gleiche Weise behandelt und aufgearbeitet, 1,03 g (= 69,5 % d. Th.) chromatographisch reines Guajakol und 1,41 g (= 51,5 % d. Th.) farbloses Öl, das nach dem Ergebnis der Papierelektrophorese zu ungefähr 3/4 aus der Threo- und zu ungefähr 1/4 aus der Erythroform des α-(3,4-Dimethoxyphenyl)-glycerins (X) bestand (siehe Tabelle 3). Nach längerem Stehen kristallisierte das Produkt teilweise. Nach Digerieren in etwas Chloroform wurden die Kristalle abfiltriert, mit wenig Chloroform nachgewaschen und — verlustreich — aus wenig Chloroform einmal umkristallisiert. Sie hatten dann einen Schmp. von 109.5—110° und gaben keine Schmp.-Depression mit synthetisch hergestelltem [18] α-(3,4-Dimethoxyphenyl)-glycerin (Schmp. 109—110°). Ausbeute an umkristallisiertem, elektrophoretisch reinem *threo-α*-(3,4-Dimethoxyphenyl)-glycerin: 0,28 g.

Aus den kristallisierten Formen des α- und des β-Guajacyläthers des Methyl-isoeugenolglykols (V bzw. IV) wurde unter Einhaltung der gleichen Arbeitsweise kristallisiertes Methyl-isoeugenolglykol (VIII) vom Schmp. 124—126° in Ausbeuten von 71 % bzw. 65 % d. Th. erhalten. Die öligen Formen von IV und V, hingegen, gaben Öle in Ausbeuten von 44 % bzw. 65 % d. Th., die sich als Gemische der beiden stereoisomeren Formen des Methyl-isoeugenolglykols erwiesen (siehe Tabelle 2).

Papierelektrophorese

Es wurde ein ähnlicher Apparat, wie von Kunkel und Tiselius [20] beschrieben, verwendet und die von Foster [8] angegebene Arbeitsweise eingehalten. Die Substanzen wurden auf Whatman Nr. 1 Filtrierpapier (57 × 20 cm) 20 cm vom Kathodenrand des Papiers in Abständen von mindestens 2 cm (die äussersten 3 cm vom Papierrand) aufgetragen. Hydroxymethyl-furfurol diente zur Festlegung der Startlinie unter Berücksichtigung der Elektroendosmose und Mannit als Bezugssubstanz zur Bestimmung der Wanderungsgeschwindigkeiten.

Bei den 1,2-Diolen und 1,2,3-Triolen wurde sowohl eine 0,1 M Lösung von Natriumborat vom pH 10 [8], als auch eine 0,05 M Lösung von sulfonierter Phenylborsäure, die mit

Natronlauge auf pH 6,5 eingestellt worden war [11], als Komplexbildner verwendet. Bei Verwendung von Natriumboratlösung betrug die angelegte Spannung 750 V, die Laufzeit 6 Stunden. Die Metallplatte wurde durch fliessendes Leitungswasser gekühlt. Bei Anwendung von sulfonierter, auf pH 6,5 eingestellter Phenylborsäure als Komplexbildner wurde eine Spannung von 500 V, eine Laufzeit von ebenfalls 6 Stunden und eine Temperatur der Metallplatte von 40° (zirkulierendes, thermostatiertes Wasser) gewählt. In diesem Falle wurde die Papierelektrophorese nach 3 Stunden unterbrochen, Kathoden- und Anodenflüssigkeit gemischt und wieder auf die beiden Elektrolytgefässe aufgeteilt, um die pH-Veränderungen während der Trennung möglichst klein zu halten [11].

Die 1,3-Diole wurden unter Verwendung einer 0,1 M Natriumboratlösung vom pH 10,8 bei einer Laufzeit von 8 Stunden und einer angelegten Spannung von 750 V untersucht.

Das Entwickeln der an der Luft getrockneten Elektropherogramme erfolgte bei den 1,2-Diolen und bei den 1,2,3-Triolen durch Besprühen mit Perjodat-Benzidin [21]. Phenolische Verbindungen (IX und XI) gaben hierbei orangefarbene, die entsprechenden Methyläther (VIII bzw. X) hellgelbe Flecke auf blauem Untergrund. Die 1,3-Diole VI und VII wurden durch Besprühen mit Eisessig und hierauf mit einer 0,5 %igen Lösung von 2,4,7-Trinitro-fluorenon in Benzol [22] als hellgelbe Flecke auf schwach rosa gefärbtem Untergrund sichtbar gemacht.

Die erhaltenen R_M-Werte waren bei strikter Einhaltung der gleichen Arbeitsweise sehr gut reproduzierbar.

Wir danken Herrn Professor B. Lindberg, Stockholm, für sein reges Interesse an dieser Arbeit. *Cellulosaindustrins Stiftelse för Teknisk och Skoglig Forskning samt Utbildning* sei für die Gewährung eines Forschungsbeitrages bestens gedankt.

LITERATUR

1. Gierer, J. und Kunze, I. *Acta Chem. Scand.* **15** (1961) 803.
2. Gierer, J. und Norén, I. *Acta Chem. Scand.* **16** (1962) 1713.
3. Winstein, S. und Lucas, H. J. *J. Am. Chem. Soc.* **61** (1939) 1576, Lucas, H. J., Schlatter, M. J. und Jones, R. C. *J. Am. Chem. Soc.* **63** (1941) 22, Lucas, H. J. und Gould, C. W. *J. Am. Chem. Soc.* **63** (1941) 2541.
4. Swern, D. *J. Am. Chem. Soc.* **70** (1948) 1235, Swern, D. *Org. Reactions* Bd. VII, S. 378.
5. Fischer, F. *Chem. Ber.* **89** (1956) 2438; **90** (1957) 357; **94** (1961) 897; Fischer, F. und Rönsch, H. *Chem. Ber.* **94** (1961) 901.
6. Adler, E. *Persönliche Mitteilung.*
7. Adler, E. und Marton, J. *Acta Chem. Scand.* **15** (1961) 357.
8. Foster, A. B. *Advances in Carbohydrate Chem.* **12** (1957) 81.
9. Dale, J. *J. Chem. Soc.* **1961** 910.
10. Frahn, J. L. und Mills, J. A. *Chem. & Ind. London* **1956** 578.
11. Garegg, P. J. und Lindberg, B. *Acta Chem. Scand.* **15** (1961) 1913.
12. Adler, E., Lindgren, B. O. und Saedén, U. *Svensk Papperstidn.* **55** (1952) 245.
13. Adler, E. und Eriksoo, E. *Acta Chem. Scand.* **9** (1955) 341.
14. Kratzl, K., Kisser, W., Gratzl, J. und Silbernagel, H. *Monatsh.* **90** (1959) 771.
15. Kolokolow, M. *J. Russ. Phys. Chem. Soc.* **29** (1897) 23; *Chem. Zentr.* **1897**, I, 915.
16. Gierer, J. und Norén, I. *Unveröffentlicht.*
17. Abderhalden, E. und Eichwald, E. *Ber.* **48** (1915) 1847, Sowden, J. C. und Fischer, H. O. L. *J. Am. Chem. Soc.* **64** (1942) 1291.
18. Adler, E. und Björkqvist, K. J. *Acta Chem. Scand.* **5** (1951) 241.
19. Rosenmund, K. W. und Zetzsche, F. *Ber.* **51** (1918) 578.
20. Kunkel, H. G. und Tiselius, A. *J. Gen. Physiol.* **35** (1951) 89.
21. Cifonelli, J. A. und Smith, F. *Anal. Chem.* **26** (1954) 1132.
22. Gordon, H. T. und Huraux, M. J. *Anal. Chem.* **31** (1959) 302.

Eingegangen am 4. Mai 1962.

ACTA CHEMICA SCANDINAVICA 16 (1962) 1989–1998

The Effect of Gamma Radiation on a Number of Water Soluble Vitamins

MONICA SJÖSTEDT and L.-E. ERICSON

Division of Food Chemistry, Royal Institute of Technology, Stockholm 70, Sweden

Solutions of thiamin hydrochloride, riboflavin, niacinamide, biotin, pteroylglutamic acid and N_5-formyltetrahydropteroylglutamic acid have been irradiated with γ-rays from a ^{60}Co-source. Residual activity as well as the formation of biologically active breakdown products was studied using microbiological test systems. No microbial growth factors other than the vitamins themselves were detected in irradiated solutions of thiamin, riboflavin and niacinamide. Biotin-L-sulphoxide was formed on irradiation of biotin and pteroic acid on irradiation of pteroylglutamic acid. A great number of biologically active breakdown fragments were observed in irradiated solutions of N_5-formyltetrahydropteroylglutamic acid, amongst them pteroylglutamic acid, N_{10}-formylpteroic acid, pteroic acid and N_{10}-formylpteroylglutamic acid as well as three chemically unidentified growth factors.

It was noted that the degree of destruction as determined spectrophotometrically appeared to be considerably lower than found on microbiological estimation.

For the study of the use of irradiation for food preservation, it is of interest to know the effect of ionizing radiation on the nutritive constituents of food. The problem has been examined from different points of view. For example, the stability of vitamins in their natural state has been studied (*cf.* Refs.[1–4]). Model vitamin systems have been investigated with reference to both the physical and chemical effects of ionizing radiation (*cf.* Refs.[5–12]). No efforts have however been made in order to find if biologically active fragments of the vitamins are formed during irradiation. In the experiments described here, the effect of γ-rays on some B-vitamins — thiamin-hydrochloride, riboflavin, niacinamide, biotin, pteroylglutamic acid and N_5-formyltetrahydropteroylglutamic acid — have been studied from this point of view. The pure vitamins were irradiated in buffer solutions. The biological activity after irradiation has been examined microbiologically using cup plate assays and in some cases tube assays. The production of biologically active fragments of some of the vitamins has, moreover, been observed bioautographically.

EXPERIMENTAL

Vitamin solutions. Thiamin-hydrochloride, riboflavin and biotin (all three from F. Hoffmann La Roche & Co, Ltd., Basel, Switzerland) were irradiated at a concentration of 100 μg/ml in 0.01 M acetate buffer having a pH of 5.0. Niacinamide (F. Hoffmann La Roche & Co, Ltd., Basel, Switzerland) was studied under the same conditions but in phosphate buffer instead of acetate. Pteroylglutamic acid (California Foundation for Biochemical Research, Los Angeles, Cal., USA), 100 μg/ml, was dissolved in 0.01 M phosphate buffers of pH 6.0, 6.5 and 7.5 while N_5-formyltetrahydropteroylglutamic acid ("Leucovorin" Lederle Laboratories Division, American Cyanamid Company, New York, USA), 100 μg/ml, was dissolved in pure water and in 0.01 M phosphate buffer of pH 5.0.

Irradiation. The irradiations were performed using a gamma source ("Hot Pot" with about 3000 Curie ^{60}Co) at the University of Stockholm. The dose rate was about 0.5 rad/h. The solutions of thiamin-hydrochloride, riboflavin, biotin and niacinamide were given doses of 10 000, 100 000 and 1 000 000 rad. Pteroylglutamic acid was irradiated with various doses from 5000 to 500 000 rad while N_5-formyltetrahydropteroylglutamic acid was subjected to doses from 5000 to 1 000 000 rad.

Microbiological test systems. The microbiological activity of the various solutions was determined by cup plate and tube assays. The following test organisms were used: For thiamin-hydrochloride and biotin *Lactobacillus fermenti* ATCC 9338, for riboflavin *Lactobacillus casei* ATCC 7469, for niacinamide *Streptococcus faecalis* ATCC 8043, and for folic and folinic acids *Streptococcus faecalis* ATCC 8043 and *Pediococcus cerevisiae* (*Leuconostoc citrovorum*) ATCC 8081.

In the cup plate assays, the plates were prepared as described by Bolinder and Larsen [13] of this laboratory. For the determination of thiamin, the Bacto Thiamin Assay Medium (Difco) was first tried but did not give satisfactory results. In later assays a basal acetate medium developed by Bolinder [13] was used. For the cup plate assays of riboflavin, the Bacto Riboflavin Assay Medium (Difco) was used. For the biotin determination the Difco's Bacto Biotin Assay Medium was not satisfactory for the cup plate technique. A modification of the acetate medium gave well-defined growth zones. The alteration consisted of an addition to the medium of 0.3 ml Tween 80 diluted 200 times. Furthermore, an increment in the turbidity of the bacteria suspension was made from 50 to 25 % transmittance adjusted with a blank of distilled water in a Coleman Model 11 Universal spectrophotometer.

The citrate medium described by Bolinder and Larsen [13] was used for the niacinamide assay. For the plates with *S. faecalis* for the determination of folic and folinic acids, this citrate medium supplemented with niacin and with folic acid excluded was employed. The basal acetate medium with niacin and ascorbic acid added was used for the plates containing *Pediococcus cerevisiae.*

Suitable ranges of concentration for the standard solutions used in the different cup plate assays were: For thiamin 0.5—10 μg/ml, for riboflavin 0.1—10 μg/ml and for biotin 0.001—0.1 μg/ml.

Tube assays were performed on folic and folinic acids in conformity with the method described by Bolinder and Larsen [13]. The same media were used as for the plate assays. The standard solutions pteroylglutamic acid and N_5-formyltetrahydropteroylglutamic acid were used in a concentration range of 0.02—2.0 μg/ml. The growth was determined by turbidimetric measurements at 640 mμ after an incubation period of 24 h at 37°C.

Bioautography. The different breakdown fragments formed upon irradiation were separated by paper chromatography on Whatman No. 1 filter paper using the descending technique. The thiamin chromatograms were run in a solvent system of *sec.* butanol:water:acetic acid (75:28:1 v/v) for 18 h and with unirradiated thiamin-hydrochloride as a standard spot. The same solvent system was used for riboflavin and biotin. The riboflavin chromatogram was run for 18 h and had riboflavin as standard. Biotin was chromatographed for 5 1/2 h and biotin and biotin-L-sulphoxide were used as reference substances. For the chromatography of niacinamide, isopropanol:water (77:23 v/v) was used and, as standard spots, niacin and niacinamide were employed. The chromatogram was run for 16 h. The solvent system for folic and folinic acids was *sec.* butanol:water:acetic acid (75:24:1 v/v). The papers were run for 18 h. Pteroylglutamic acid, N_5-formyltetrahyd-

ropteroylglutamic acid, pteroic acid, N_{10}-formylpteroic acid and N_{10}-formylpteroylglutamic acid were used as standards.

The chromatograms were dried at room temperature and then placed on agar plates containing the appropriate test medium and test organism. The test organisms used for seeding the plates were grown overnight in the Bacto Micro Inoculum Broth (Difco) supplemented as described by Bolinder and Larsen [13]. The cells were harvested by centrifugation, washed twice and suspended in saline to give a suitable transmittance reading. This was for the thiamin, riboflavin and niacinamide plates 50 %, for the biotin 25 %, for the folic and folinic acids *S. faecalis* plates 50 % and for the *P. cerevisiae* plates 70 %. Of such a suspension, 5 ml was taken for 150 ml agar medium.

Synthesis of biotin-L-sulphoxide. The biotin-L-sulphoxide, used as a standard on the biotin chromatograms, was synthesized according to Melville [14].

Spectra. The absorption spectra of unirradiated and irradiated pteroylglutamic and N_5-formyltetrahydropteroylglutamic acids were measured in a Beckman Model DU spectrophotometer. The concentration of the standard solutions was 10 μg/ml. The irradiated solutions were diluted ten times before measurement.

RESULTS AND DISCUSSION

The sensitivity of thiamin hydrochloride to ionizing radiation has been confirmed by several investigators [1,3,5]. In our tests thiamin hydrochloride was partly destroyed by doses of 10 000 and 100 000 rad as shown by the cup plate assay results presented in Table 1. In the bioautography test, the two solutions brought about the growth of the bacteria in zones having the same R_F value as standard thiamin hydrochloride. No biologically active fragments formed by the γ-rays were therefore indicated in this test. The solution irradiated with 1 Mrad did not give any growth in the cup plate assay. Nor did it stimulate the growth of the bacteria in the bioautography when 10 μl of the solution was applied to the chromatogram. The mechanism for the destruction of thiamin hydrochloride exposed to ionizing radiation is not known. Gregorlin *et al.*[15] have shown that, when diphosphothiamin was irradiated with γ-rays, thiochrome and oxythiamin were found among the breakdown products. These substances might have been formed also in our experiments but would not have been detected by our test methods.

The cup plate assay of irradiated riboflavin showed, as would be expected, that the extent of the destruction increased with increasing doses of radiation. The results are presented in Table 1. In the bioautography test, all

Table 1. Effect of γ-rays on thiamin, riboflavin and biotin.

Vitamin	Residual microbiological activity in % at the doses		
	10 000 rad	100 000 rad	1 000 000 rad
Thiamin	98	65	0
Riboflavin	98	58	2
Biotin	96	33	0.2

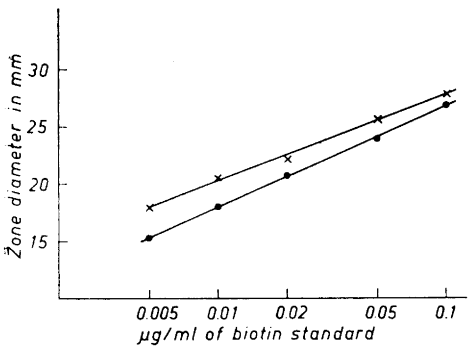

Fig. 1. Growth response of *L. fermenti* in the cup plate assay to various concentrations of non-irradiated biotin (×) and to dilutions of biotin irradiated with 1 Mrad (●). The highest concentration used of the irradiated solution was obtained by diluting the original solution containing 100 µg biotin/ml 1:3.3.

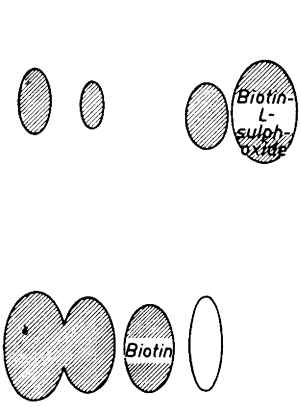

Fig. 2. Bioautography with *L. fermenti* of the following solutions:
1. 1 µl of a biotin solution (100 µg/ml) irradiated with 10 000 rad, diluted 1:100.
2. 1 µl of the biotin solution irradiated with 100 000 rad, diluted 1:50.
3. 1 µl of a standard solution containing 0.5 µg/ml of biotin.
4. 3 µl of the biotin solution irradiated with 1 Mrad, undiluted.
5. Biotin-L-sulphoxide.

three irradiated solutions gave growth only in zones corresponding to standard riboflavin. The chemical effects of the ionizing radiation on riboflavin are not quite unravelled. According to Goldblith *et al.*[8], lumichrome may be formed. Guldener [12] has found that the ionizing radiation leads to the formation of isoalloxazin. Neither of these substances has a growth promoting effect on *L. casei* and they have therefore not been observed in our experiments.

In the bioautography test on irradiated niacinamide, only growth zones with the same R_F value as the niacinamide standard were indicated. Neither niacin nor other biologically active fragments were formed during the irradiation. This shows that the $CO—NH_2$ bond in the niacinamide is relatively stable towards ionizing radiation.

The cup plate assays of irradiated biotin solutions showed that the effect of γ-rays on biotin was in accordance with the effect on the vitamins described

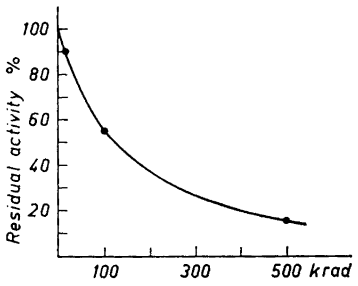

Fig. 3. Residual microbiological activity in solutions of pteroylglutamic acid (100 μg/ml) irradiated in phosphate buffer of pH 7.5. The values are calculated from a tube assay with *S. faecalis*.

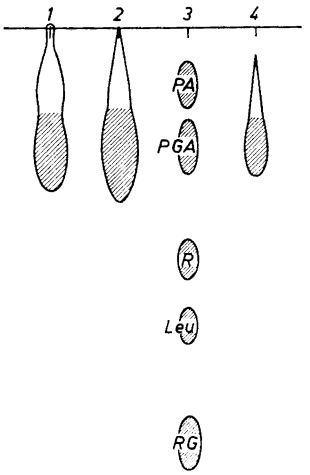

Fig. 4. Bioautography with *S. faecalis* of pteroylglutamic acid irradiated in phosphate buffer of pH 6.5:

1. 1 μl of a solution (100 μg/ml) irradiated with 10 000 rad, diluted 1:10.
2. 1 μl of the solution irradiated with 100 000 rad, diluted 1:10.
3. 1 μl of the following standard solutions: Pteroic acid (PA) 1 μg/ml, pteroylglutamic acid (PGA) 0.2 μg/ml, N_{10}-formylpteroic acid (R) 0.2 μg/ml, N_5-formyltetrahydropteroylglutamic acid (Leu) 0.2 μg/ml and N_{10}-formylpteroylglutamic acid (RG) 0.2 μg/ml.
4. 1 μl of the solution irradiated with 500 000 rad, diluted 1:10.

earlier. The microbiological activity of the solutions decreased the higher the doses which the solutions were subjected to. This is shown in Table 1. As can be seen in Fig. 1, the slope of the line representing growth diameter versus concentration was different for the biotin solution irradiated with 1 Mrad as compared to that for the non-irradiated biotin. This suggested that there might have been microbiologically active fragment(s) formed during the irradiation. The bioautography test verified this assumption because two different growth zones were obtained on the agar plate. This is shown in Fig. 2. One of the growth zones had an R_F value corresponding to biotin. The other growth factor was compared with earlier known biotin-active factors for *L. fermenti*. Biotin-L-sulphoxide was the most probable of these since its R_F value was the same as that of our unknown substance. We therefore synthesized biotin-L-sulphoxide and compared its chromatographic and microbiological properties with those of the unknown factor which confirmed

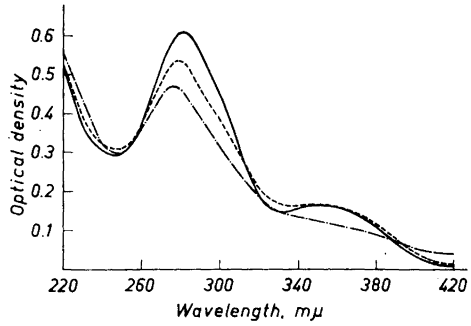

Fig. 5. Light absorption spectra for a solution of non-irradiated pteroylglutamic acid 10 μg/ml (———) and for pteroylglutamic acid solutions (100 μg/ml) irradiated with 100 000 rad (— — —) and 500 000 rad (—·—·—). The pteroylglutamic acid was dissolved in phosphate buffer of pH 7.5. The irradiated solutions were diluted ten times before measurement.

our presumptions, as can be seen in Fig. 2. As far as the authors know, this is the first published report on the effect of γ-rays on biotin and it is therefore not possible to compare our results with those of other research workers.

The loss of pteroylglutamic acid was determined by a tube assay with *S. faecalis*. Residual microbiological activity as a function of radiation dose is shown in Fig. 3. Dilutions of the irradiated pteroylglutamic acid solutions gave curves which closely followed the standard curve and thus did not suggest the presence of any biologically active factor in the irradiated solutions other than pteroylglutamic acid. However the bioautography test with *S. faecalis* indicated that at least one microbiologically active fragment was formed when the solution was subjected to γ-rays, especially at the lower dose levels. This can be seen in Fig. 4 where a growth zone with the same R_F value as pteroic acid appears. An identical chromatogram was also placed on an agar plate containing *P. cerevisiae*. No growth factor for this microorganism could be detected in γ-irradiated solutions of pteroylglutamic acid. The light absorption spectra, Fig. 5, showed that the irradiation caused a moderate decrease in the pteroylglutamic acid peak at 282 mμ. A tendency for the absorption peak to move towards shorter wavelengths was also noticed. The solution given a dose of 500 000 rad gave furthermore a somewhat lower curve between the wavelengths 330 and 390 mμ. Since this absorption maximum is considered to be caused by the pteridin part of the molecule, this observation is in accordance with the fact that the proportion of pteroic acid seemed to decrease in the irradiated solutions at higher doses (Fig. 4). However,

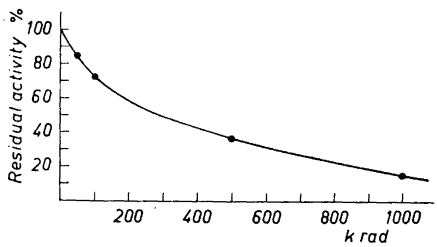

Fig. 6. Residual microbiological activity in solutions of Leucovorin (100 μg/ml) irradiated in phosphate buffer of pH 5.0. The values are calculated from a tube assay with *S. faecalis*.

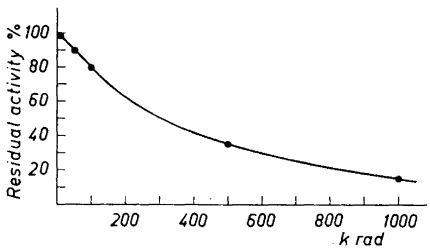

Fig. 7. Residual microbiological activity in solutions of Leucovorin (100 μg/ml) irradiated in phosphate buffer of pH 5.0. The values are calculated from a tube assay with *P. cerevisiae*.

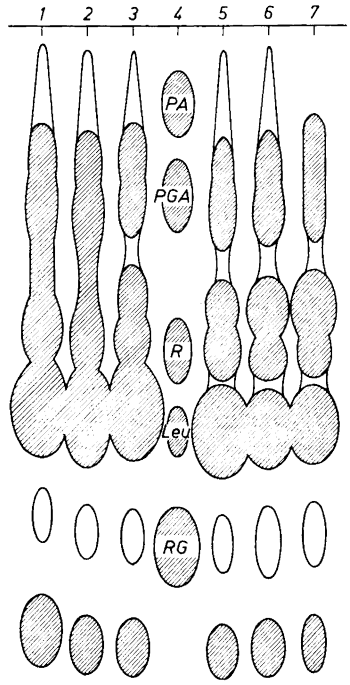

Fig. 8. Bioautography with *S. faecalis* of Leucovorin irradiated in phosphate buffer of pH 5.0. The solutions tested were:

1. 1 μl of a solution (100 μg/ml) irradiated with 5000 rad, diluted 1:5.
2. 1 μl of the solution irradiated with 10 000 rad, diluted 1:5.
3. 1 μl of the solution irradiated with 50 000 rad, diluted 1:5.
4. 1 μl of the following standard solutions: Pteroic acid (PA) 1 μg/ml, pteroylglutamic acid (PGA) 0.2 μg/ml, N_{10}-formylpteroic acid (R) 0.2 μg/ml, N_5-formyltetrahydroglutamic acid (Leu) 0.2 μg/ml and N_{10}-formylpteroylglutamic acid (RG) 0.2 μg/ml.
5. 1 μl of the solution irradiated with 100 000 rad, diluted 1:5.
6. 1 μl of the solution irradiated with 500 000 rad, diluted 1:3.3.
7. 1 μl of the solution irradiated with 1 Mrad, diluted 1:2.5.

Okada *et al.*[10] did not observe any destruction of pteridines in corresponding experiments.

No effects due to the pH variations in the buffer solution used could be observed either in spectrophotometrical or microbiological tests. In a separate

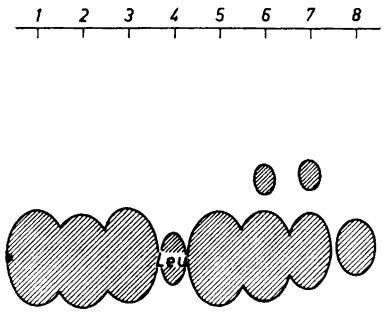

Fig. 9. Bioautography with *P. cerevisiae* of Leucovorin irradiated in phosphate buffer of pH 5.0. The solutions tested were:
1. 1 µl of a solution (100 µg/ml) irradiated with 5000 rad, diluted 1:10.
2. 1 µl of the solution irradiated with 10 000 rad, diluted 1:10.
3. 1 µl of the solution irradiated with 50 000 rad, diluted 1:10.
4. 1 µl of the following standard solutions: Pteroic acid 1 µg/ml, pteroylglutamic acid 0.2 µg/ml, N_{10}-formylpteroic acid 0.2 µg/ml, N_5-formyltetrahydropteroylglutamic acid (Leu) 0.2 µg/ml and N_{10}-formylpteroylglutamic acid 0.2 µg/ml.
5. 1 µl of the solution irradiated with 100 000 rad, diluted 1:10.
6. 1 µl of the solution irradiated with 500 000 rad, diluted 1:10.
7. 1 µl of the solution irradiated with 1 Mrad, diluted 1:10.
8. 1 µl of unirradiated Leucovorin 1 µg/ml.

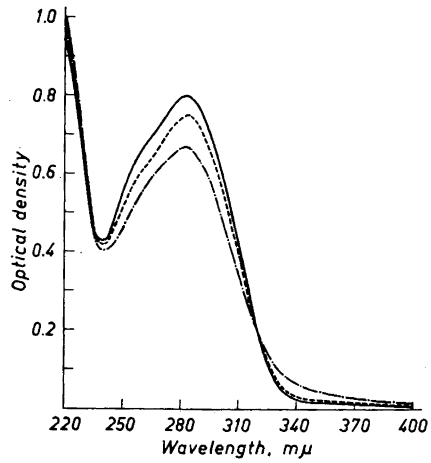

Fig. 10. Light absorption spectra for a solution of non-irradiated Leucovorin 10 µg/ml (———) and for Leucovorin solutions (100 µg/ml) irradiated in phosphate buffer of pH 5.0 with 100 000 rad (- - - -) and 500 000 rad (— · — · —). The irradiated solutions were diluted 1:10 before measurement.

experiment the pteroylglutamic acid solution was deaerated and 10 mg ascorbic acid/ml was added just before irradiation with 100 000 rad. The pteroylglutamic acid was then totally protected.

It might be supposed that the decrease in the pteroylglutamic acid peak at 282 mµ in the spectra should be a direct measure of the decrease in the amount of pteroylglutamic acid. That this is not the case is evident from the microbiological tests. These have given much lower values in spite of the fact that the solutions contain, besides pteroylglutamic acid, at least one other microbiologically active fragment. Okada *et al.*[10] have used the results from a polarographic test to calculate the amount of pteroylglutamic acid remaining after irradiation. The values obtained were also much higher than our micro-

biological data. It therefore seems to be inadequate to use physico-chemical measurements in order to obtain correct values for the vitamin destruction due to ionizing radiation. Probably there are substances formed during the irradiation which are chemically closely related to pteroylglutamic acid and are thus sensitive to this type of analysis but which lack biological activity. Since the main interest in the study of the effects of ionizing radiation on vitamins consists of the biological aspects, it is clear that biological tests should be performed.

The irradiated solutions of Leucovorin were tested by tube assays both with *S. faecalis* and *P. cerevisiae*. From these tests, residual microbiological activity relative to dose level was calculated. The results are presented in Figs. 6 and 7. Dilutions of the irradiated Leucovorin solutions gave curves that closely followed the standard curve. Therefore the tube assays did not suggest that any new microbiologically active fragments were formed during the irradiations. However, the bioautography test, especially with *S. faecalis*, clearly demonstrated that a number of new growth factors was formed. Fig. 8 gives a picture of such a bioautogram. It can be seen that the following degradation products could be identified: pteroylglutamic acid, N_{10}-formylpteroic acid, pteroic acid and N_{10}-formylpteroylglutamic acid. Only small quantities of the last two compounds were formed. Some unknown factors can also be observed. One of these is situated quite near pteroylglutamic acid, another just above N_{10}-formylpteroic acid. The growth zone at the very bottom might be caused by a factor identical to Factor I described by Ericson[16].

In Fig. 9, a *P. cerevisiae* plate is reproduced. Besides N_5-formyltetrahydropteroylglutamic acid, there is a new growth promoting factor, probably the same as that which appeared on the *S. faecalis* plate just above N_{10}-formylpteroic acid. After keeping the solutions at $-20°C$ for two months, they were then re-chromatographed. A new growth zone with an R_F-value lower than pteroic acid was found on both *S. faecalis* and *P. cerevisiae* plates. No differences could be noticed between Leucovorin solutions irradiated in water and in phosphate buffer.

The light absorption spectra for unirradiated and irradiated Leucovorin are shown in Fig. 10. The irradiated solutions have lower peaks, at the wavelength 282 mμ, than N_5-formyltetrahydropteroylglutamic acid and a somewhat greater absorption between 320 and 400 mμ. As could be noticed for pteroylglutamic acid, the decrease in the peak at 282 mμ is no measure of the destruction of the vitamin. The results from the Leucovorin experiments thus confirm the view that biological tests must be performed when the decrease in vitamin activity after irradiation is to be investigated.

The authors would like to acknowledge research grants from the *Swedish Technical Research Council* and the *Swedish Natural Science Research Council*.

REFERENCES

1. Alexander, H. D., Day, E. J., Sauberlich, H. E. and Salmon, W. D. *Federation Proc.* **15** (1956) 921.
2. Day, E. J., Alexander, H. D., Sauberlich, H. E. and Salmon, W. D. *J. Nutrition* **62** (1957) 27.

3. Day, E. J., Sauberlich, H. E., Alexander, H. D. and Salmon, W. D. *J. Nutrition* **62** (1957) 107.
4. Ziporin, Z. Z., Kraybill, H. F. and Thach, H. J. *J. Nutrition* **63** (1957) 201.
5. Dunlap, C. E. and Robbins, F. C. *Am. J. Roentgenol. Radium Therapy* **50** (1943) 641.
6. Proctor, B. E. and Goldblith, S. A. *Nucleonics* **3** (1948) 32.
7. Goldblith, S. A., Proctor, B. E., Hogness, J. R. and Langham, W. H. *J. Biol. Chem.* **179** (1949) 1163.
8. Goldblith, S. A. and Proctor, B. E. *Nucleonics* **5** (1949) 50.
9. Proctor, B. E. and Goldblith, S. A. *Nucleonics* **5** (1949) 56.
10. Okada, I., Hirano, T., Kikuchi, T. and Doguchi, M. *J. Tokyo Univ. Fisheries* **44** (1958) 39.
11. Ueno, Y. *Radioisotopes (Tokyo)* **8** (1959) 253.
12. Guldener, P. *Die Wirkung ionisierender Strahlungen auf Riboflavin* (Diss.) Bern 1960.
13. Bolinder, A. E. and Larsen, B. *Acta Chem. Scand.* **15** (1961) 823.
14. Melville, D. B. *J. Biol. Chem.* **208** (1954) 495.
15. Gregolin, C., Rossi, C. S. and Siliprandi, N. *Radiation Research* **13** (1960) 185.
16. Ericson, L.-E. *Arkiv Kemi* **6** (1953) 503.

Received May 10, 1962.

ACTA CHEMICA SCANDINAVICA 16 (1962) 1999–2004

The Effect of Gamma Radiation on Cyanocobalamin

MONICA SJÖSTEDT and L.-E. ERICSON

Division of Food Chemistry, Royal Institute of Technology, Stockholm 70, Sweden

Solutions of cyanocobalamin have been irradiated with various doses of γ-rays from a ^{60}Co-source. A number of breakdown fragments that could replace the vitamin as growth factor for *E. coli* 113—3 were detected. Some of these fragments seem to possess activity also towards *Ochromonas malhamensis*. The types of biologically active breakdown products formed and the degree of loss of microbiological activity of irradiated solutions were found to depend on a number of conditions, *e.g.* the dose given, the ionic strength, pH, presence of reducing substances and so forth. In a 0.1 M phosphate buffer of pH 5.0 containing 5 mg cyanocobalamin per ml and given a dose of 2 Mrad at least five compounds are formed that are growth factors for *E. coli* 113—3.

The radiosensitivity of cyanocobalamin in distilled water and raw milk was first established by Markakis *et al.* [1] in 1951. After several years of study, Lester Smith published in 1959 a paper [2] on the instability of vitamin B_{12} containing radioactive cobalt isotopes. This self-degradation has later been confirmed by other authors [3–5]. Burtseva *et al.* [4] have shown that labelled crystalline vitamin B_{12} prepared by neutron radiation disintegrates, when dissolved in water, giving three different coloured zones on a chromatogram. The work presented here has been mainly directed to a search for microbiologically active fragments formed on exposure of the vitamin to γ-rays. Fragments with such properties have been described in preliminary communications from this laboratory [6,7] and have also been observed by Barlow and Sanderson [3]. The latter investigators have found in self-degradated ^{60}Co-vitamin B_{12} a monocarboxylic acid derivate which was about one third as active in a microbiological test system as cyanocobalamin.

In this paper we will present a more detailed description of our experiments. Only model systems with pure cyanocobalamin in buffer solutions have so far been studied.

EXPERIMENTAL

Vitamin solutions. The vitamin cyanocobalamin (Merck, Sharp & Dohme, Haarlem, Netherland N.V.) was irradiated in buffer solutions. In most cases, 5 mg/ml was dissolved in 0.1 M phosphate buffer of pH 5.0. When other buffers and concentrations were used, this will be pointed out when the results are described.

Irradiation. The irradiations were performed in ^{60}Co gamma sources at Conservatom, Lyon, France, at the Danish Atomic Energy Commission, Risö, Roskilde, Denmark, at the University of Stockholm, and at the Swedish Institute for Food Preservation Research, Gothenburg. The vitamin solutions were subjected to various doses. These will be specified in the part of the paper in which the results of the separate experiments are presented. The effect of doses ranging from 0.01—15 Mrad was investigated but in most cases a dose of about 2 Mrad was employed.

Microbiological test systems. In order to determine the residual microbiological activity of the irradiated solutions of cyanocobalamin, tube assays with *Escherichia coli 113—3* ATCC 11105 and *Ochromonas malhamensis* ATCC 11532 were performed.

In a preliminary tube assay with *E. coli* 113—3, a simple medium — a modification of that of Diding [8] — was compared with a more complicated one used by Burkholder [9]. As the two media gave identical result, the simpler one was chosen for all subsequent tube assays. It had the following composition: Glucose 10 g, sodium-citrate·$2H_2O$ 0.5 g, KH_2PO_4 3 g, K_2HPO_4 7 g, $MgSO_4 \cdot 7H_2O$ 0.1 g, $(NH_4)_2SO_4$ 1 g, thiomalic acid 100 mg, KCN 1 mg, H_2O up to 600 ml, pH 6.8. To each test tube were added 5 ml medium and 5 ml test solution. The tubes were autoclaved for 5 min at 115°C, cooled and inoculated with two drops of a bacteria suspension. This was obtained by growing the bacteria overnight in a Bacto Micro Inoculum Broth (Difco), harvesting the cells by centrifugation, washing them twice with sterile saline, suspending them in saline to a transmittance reading of 70 % and diluting this suspension 1:50 with saline. The tubes were incubated at 37°C and the growth after 20 h was determined by turbidimetric measurements at 640 mμ in a Coleman Model 11 Universal spectrophotometer. A standard curve was obtained by means of a suitable series of dilutions of cyanocobalamin. The test solutions from irradiated vitamin B_{12} were diluted to give a growth falling within the range of the standard curve.

The *O. malhamensis* tests were in the main performed by means of Ford's method [10]. To each tube were added 5 ml test solution and 5 ml single strength medium prepared according to Ford [11]. The tubes were autoclaved for 10 min at 115°C, cooled and inoculated with 1 drop of an undiluted 4 day culture maintained as described in reference [11]. The tubes were shaken in darkness at 29°C and the growth was measured turbidimetrically at 24 h intervals from the second to the seventh day after the inoculation.

Separation methods. Paper chromatography of the irradiated vitamin B_{12} solutions was initially carried out in a solvent system consisting of *sec.* butanol:H_2O:HAc (75:24:1) supplemented with 1 ml of a 0.01 % KCN solution. Since no good separation could be attained even when the chromatograms were run for 48 h we were forced to try modified solvent systems. Friedrich *et al.*[12] have found that some salts (called "chromatotropic salts"), when added to the developer, had a positive effect on the separation of vitamins of the B_{12} group. We tried some of these and got the best separation in the shortest time with the following developer: *sec.* butanol:H_2O:KCN (0.01 % solution) (71:28:1) + 200 mg sodium tetraphenylboron. Whatman No. 4 filter paper and the descending technique were used. The papers were run for about 17 h at 21°C and dried at room temperature.

Electrophoresis of the irradiated vitamin B_{12} solutions was performed with an LKB paper electrophoresis apparatus. In most cases a buffer of 0.2 M HAc, pH 2.8, current of 0.2 mA, tension of 350 V and electrophoresis time of 16—17 h were used. The apparatus was operated in a room with a temperature of 2°C. The papers were dried at room temperature.

Location of spots. When large quantities of the irradiated solutions were applied to the chromatography and electrophoresis papers, different coloured spots could be observed after the separation. Since our main interest was to look for biologically active fragments, we applied however microbiological methods in order to reveal the positions of the substances. The papers were placed on agar plates seeded with *E. coli* 113—3. The plates were prepared as described by Bolinder and Larsen [13] of this laboratory and contained (per 150 ml medium) 5 ml of a bacteria suspension having a transmittance reading of 35—40 %. The same medium as that for the tube assay with *E. coli* was used. After incubation of the plates overnight at 37°C, the papers were removed and the growth zones recorded.

RESULTS AND DISCUSSION

The destructive effect of γ-rays on cyanocobalamin was first established in solutions containing 100 μg cyanocobalamin per ml of a 0.1 M phosphate buffer of pH 5.0 which had been given doses from 0.01 to 1.0 Mrad. A number of breakdown products were detected. Since it was desirable for the subsequent tests to obtain large amounts of irradiated material, the vitamin concentration of the solution was increased to 5 mg/ml. Consequently the doses were also increased so that comparable effects could be obtained. In Fig. 1, residual microbiological activity relative to radiation dose is recorded. The microbiological activity was calculated from a tube assay with *E. coli* 113—3. These activity values are not direct measures of residual cyanocobalamin because a number of new factors with growth-promoting effects on *E. coli* 113—3 are

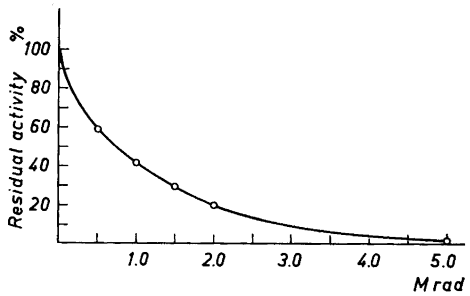

Fig. 1. Residual microbiological activity in solutions of cyanocobalamin (5 mg/ml) irradiated in 0.1 M phosphate buffer of pH 5.0. The values have been calculated from a tube assay with *E. coli* 113—3.

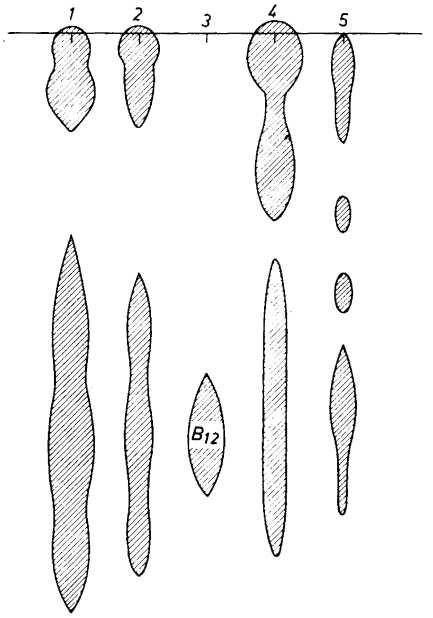

Fig. 2. Bioautography with *E. coli* 113—3 of cyanocobalamin irradiated in 0.1 M phosphate buffer of pH 5.0.

1. 1 μl of a cyanocobalamin solution (5 mg/ml) irradiated with 2 Mrad, diluted 1:100.
2. 1 μl of the same solution irradiated with 7 Mrad, diluted 1:20.
3. 1 μl of a standard solution containing 1 μg/ml cyanocobalamin.
4. 1 μl of the cyanocobalamin solution irradiated with 10 Mrad, undiluted.
5. 10 μl of the cyanocobalamin solution irradiated with 15 Mrad, undiluted.



Fig. 3. Bioautography with *E. coli* 113—3 of 1 μl of a cyanocobalamin solution, 5 mg/ml in 0.1 M phosphate buffer of pH 5.0, irradiated with 2 Mrad, diluted 1:250. Growth zone No. 5 from the top corresponds to cyanocobalamin.

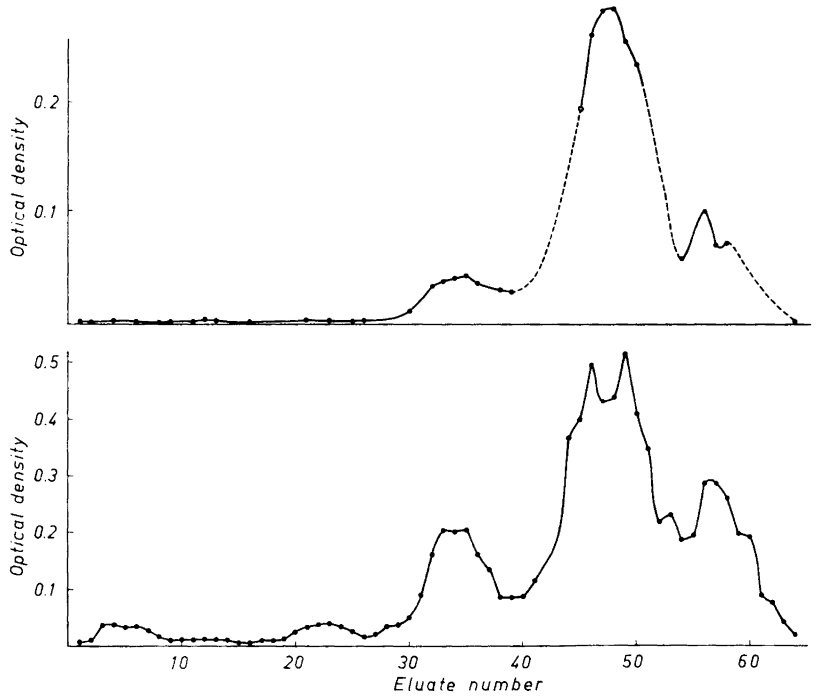

Fig. 4. Growth response to eluates from a paper chromatogram of cyanocobalamin, 5 mg/ml in 0.1 M phosphate buffer of pH 5.0, irradiated with 2 Mrad.
Upper curve: *O. malhamensis.*
Lower curve: *E. coli* 113—3.
The *O. malhamensis* curve is extrapolated in the parts marked with small dashes.

formed during the irradiation. This is shown in Fig. 2 which illustrates a bioautogram of cyanocobalamin solutions irradiated with doses from 2 to 15 Mrad. As can be noticed, the type of factors formed depends to some extent on the dose. Fig. 3 shows another bioautogram of the solution subjected to 2 Mrad. In this case, the chromatogram has been run for a longer time so that the separation is more complete. Six different growth zones can be clearly distinguished. A chromatogram identical to this was run with large quantities (applied as a band across the paper) of the same solution of cyanocobalamin irradiated with 2 Mrad. After drying, the chromatogram was cut in 5 mm broad strips parallel to the line of application. These strips were eluted with water. The eluates were tested by tube assays both with *E. coli* 113—3 and *O. malhamensis*. Optical density, as a measure of the growth in the tubes, is plotted for each eluate in two curves, one for *E. coli* 113—3 and one for *O. malhamensis* (Fig. 4). The growth in eluates 40—54 is probably caused by unchanged cyanocobalamin. It is seen that at least two breakdown fragments — in eluates 28—39 and 54—64 — have growth promoting effects on both the organisms. As is well known, *O. malhamensis* is considered to have a B_{12} requirement similar to that of higher animals.

Besides the paper chromatographic separations, paper electrophoresis in combination with bioautography was performed on the cyanocobalamin solution irradiated with 2 Mrad. In this test, at least four *E. coli* 113—3 active substances could be observed. Both positively and negatively charged compounds were formed.

In order to make it possible to examine the isolated breakdown fragments, we have tried using preparative separation methods on solutions irradiated with 2 Mrad. For instance, the application of column electrophoresis (apparatus of type LKB 3340) in a sucrose density gradient was investigated. In spite of the fact that visual inspection indicated a fairly complete separation — five distinct, coloured zones could be seen — none of the zones contained a single, isolated breakdown fragment. Cellulose ion exchangers have been used with good results by Pawelkiewicz *et al.* [14] and Menke [15] for the separation of cobalamins but application of this technique to our irradiated solutions has not yet given entirely satisfactory results. However, with some further modifications of, for example column length, eluate solvent etc., it might be possible to isolate at least some of the biologically active fragments. Work is being continued to this purpose. Preliminary separation attempts using an LKB 3500 ChroMax pressurized paper chromatography column have also given relatively promising results.

Since none of the microbiologically active fragments has been obtained in the pure state, it has not yet been possible to examine the chemical changes in the cyanocobalamin molecule caused by the γ-rays. One of the fragments might be the monocarboxylic acid derivate found in self-degradated ^{60}Co-cyanocobalamin by Barlow and Sanderson [3].

Some separate experiments with different buffers, buffer strengths and additions of sulphite and ascorbic acid were performed besides the above related studies in which cyanocobalamin was irradiated in a 0.1 M phosphate buffer of pH 5.0. Residual microbiological activity, determined with *E. coli* in a tube assay, was found to depend on the pH of the buffer, *e.g.* for 3 Mrad

it was 20 % for cyanocobalamin (5 mg/ml) irradiated in a 0.05 M acetate buffer of pH 3.0, 10 % in a 0.05 M phosphate buffer of pH 5.0 and 5 % in a 0.05 M phosphate buffer of pH 7.0. A lowering of the buffer strength had, as well as a decreased destruction effect, a tendency to change the proportions between the breakdown products formed. Ascorbic acid and sulphite, when added to the buffer before the irradiation, had a definite protective effect on the cyanocobalamin. Thus, when a solution containing 5 mg/ml of cyanocobalamin was irradiated in 0.05 M phosphate buffer of pH 5.0 with 3 Mrad, the residual *E. coli* activity was 25 % when the solution contained 50 mg ascorbic acid/ml (as compared with 10 % in the absence of vitamin C). In a 0.05 M sulphite buffer of pH 5.0, the residual activity was 33 %. In the cyanocobalamin solutions to which ascorbic acid or sulphite were added, breakdown products different from those discussed above were noticed.

We have also noticed that the polypeptide-cyanocobalamin complex isolated by Hedbom [16] is considerably more resistant to the destructive effect of γ-rays than the free vitamin.

The implication of the observations reported here and in the previous paper with regard to the wholesomeness of irradiated food is as yet unknown and must await studies on the effect of the breakdown fragments on higher animals. Furthermore, it remains to be demonstrated that biologically active destruction products are formed from the various vitamins when these are irradiated in food-stuffs.

The authors gratefully acknowledge the receipt of research grants from the *Swedish Technical Research Council* and the *Swedish Natural Science Research Council.*

REFERENCES

1. Markakis, P. C., Goldblith, S. A. and Proctor, B. E. *Nucleonics* **9** (1951) 71.
2. Smith, E. Lester *Lancet* **21** (1959) 387.
3. Barlow, G. H. and Sanderson, N. D. *Biochim. Biophys. Acta* **41** (1960) 146.
4. Burtseva, L. N. and Vasileiskii, S. S. *Metody Polucheniya i Izmeren. Radioaktiv. Preparatov, Sbornik Statei* **1960** 192.
5. Nabet, P. and Wolff, R. *Compt. rend. soc. biol.* **155** (1961) 381.
6. Sjöstedt, M. and Ericson, L.-E. *Acta Chem. Scand.* **13** (1959) 1711.
7. Ericson, L.-E. and Sjöstedt, M. *Risö Report* **16** (1960) 50.
8. Diding, N. Å. *Scand. J. Clin. & Lab. Invest.* **3** (1951) 215.
9. Burkholder, P. R. *Science* **114** (1951) 459.
10. Ford, J. E. *Brit. J. Nutrition* **7** (1953) 299.
11. Ford, J. E. *J. gen. Microbiol.* **19** (1958) 161.
12. Friedrich, W., Gross, G. and Bernhauer, K. *Mikrochim. Acta* **1—6** (1956) 134.
13. Bolinder, A. E. and Larsen, B. *Acta Chem. Scand.* **15** (1961) 823.
14. Pawelkiewicz, J., Walerych, W., Friedrich, W. and Bernhauer, K. *J. Chromatography* **3** (1960) 359.
15. Menke, K. H. *J. Chromatography* **7** (1962) 86.
16. Hedbom, A. *Biochem. J.* **74** (1960) 307.

Received May 10, 1962.

ACTA CHEMICA SCANDINAVICA 16 (1962) 2005–2009

Partial Methylation Studies on Methyl β-D-Glucopyranoside and some Derivatives

A. N. DE BELDER, BENGT LINDBERG and OLOF THEANDER

Träkemiska Avdelningen, Svenska Träforskningsinstitutet, Stockholm Ö, Sweden

The partial methylation of methyl β-D-glucopyranoside, unsubstituted and substituted in the 4-*O*-position with benzyl or tetrahydropyranyl (two stereoisomers) has been studied. The results are discussed in connection with the similar partial methylation of cellulose.

In previous communications from this Department, summarised in Ref. [1], studies on the distribution of substituents in some partially etherified celluloses have been reported. The differences in reactivity observed at the various positions (2, 3, 6) of a glucose residue in a cellulose molecule could be due to electronic and steric effects, the latter either from substituents in the same glucose residue or from adjacent glucose residues. Effects from other cellulose chains in heterogeneous reactions seem to be negligible, as the observed relative reactivities at the various positions were about the same in homogeneous and heterogeneous reactions [2]. In order to throw some light upon these questions the partial methylations of cellulose, [2] amylose, [3] xylan, [4] methyl 4,6-*O*-benzylidene-β-D-glucoside [3] and methyl 4,6-*O*-ethylidene-β-D-glucoside [3] were studied (Table 1).

The suggestion that the low reactivity at the 3-position in cellulose [5] was due to steric hindrance from the $-CH_2OH$ group at C-5 was ruled out when it was observed that esparto xylan also showed this low reactivity at C-3. It has been proposed [6] also that a strong hydrogen bond between the C-3

Table 1. Relative reactivities, at C-2, C-3 and C-6, of cellulose and some model substances towards methylation with methyl sulphate and sodium hydroxide.

	k_2	k_3	k_6	Ref.
Cellulose	3.5	1	2	2
Amylose	6	1	7	3
Xylan	2.5	1	—	4
Methyl 4,6-*O*-benzylidene-β-D-glucoside	1.3	1	—	3
Methyl 4,6-*O*-ethylidene-β-D-glucoside	1	1	—	3

hydroxyl and the ring oxygen in the contiguous glucose residue could contribute to this effect. This could be studied by the methylation of suitable model substances — the two acetals in Table 1 are probably not good models for the glucose residues in cellulose.

In the present communication, the synthesis of methyl 4-*O*-benzyl-β-D-glucoside and the partial methylation of this substance and of methyl 4-*O*-(2-tetrahydropyranyl)-β-D-glucoside (two stereoisomers) [7] and methyl β-D-glucopyranoside with dimethyl sulphate in sodium hydroxide is reported.

The benzyl derivative was prepared by benzylation of methyl 2,3,6-tri-*O*-acetyl-β-D-glucopyranoside, using the method described by Croon and Lindberg [8]. The product was then deacetylated and fractionated on a cellulose column. In this substance, as in the tetrahydropyranyl derivatives, the sub-

Table 2. Composition of the hydrolysate of partially methylated methyl 4-*O*-benzyl-β-D-glucoside (k_2:k_3:k_6 = 1.9:1:2.8).

Substance*	D.S. 0.72			D.S. 0.81		
	Exptl.	Calc.I	Calc.II**	Exptl.	Calc.I	Calc.II**
S_0	44.3	44.9	44.9	40.2	40.3	40.3
S_2	14.9	13.1	13.9	13.4	12.7	14.1
S_3	5.5	6.9	6.9	6.0	7.0	7.0
S_6	20.7	21.4	21.4	22.0	22.9	22.9
S_{23}	3.1	3.0	2.1	4.7	3.9	2.5
S_{26}	7.1	6.3	6.7	7.3	7.2	8.0
S_{36}	2.8	3.2	3.2	4.3	4.0	4.0
S_{236}	1.6	1.4	1.0	2.2	2.2	1.4

* S_0 = glucose; S_2 = 2-*O*-methyl-glucose, *etc.*
** Calc.II without allowing for adjacent group effects at C-2 and C-3.

Table 3. Composition of the hydrolysates of the partially methylated isomers of methyl 4-*O*-(2-tetrahydropyranyl)-β-D-glucoside.

Substance	(+)-isomer(k_2:k_3:k_6 = 3.3:1:3.9)						(−)-isomer(k_2:k_3:k_6 = 3.1:1:3.7)		
	D.S. 0.62			D.S. 0.98			D.S. 1.15		
	Exptl.	Calc.I	Calc.II*	Exptl.	Calc.I	Calc.II*	Exptl.	Calc.I	Calc.II*
S_0	48.1	47.7	47.7	31.2	31.6	31.6	22.7	22.8	22.8
S_2	18.6	16.1	16.7	17.2	17.2	18.5	17.6	16.6	18.3
S_3	1.9	4.5	4.5	2.9	4.8	4.8	3.2	4.7	4.8
S_6	21.9	20.0	20.0	23.4	23.2	23.2	24.3	23.1	23.1
S_{23}	2.3	2.2	1.6	5.6	4.0	2.8	4.0	5.6	3.8
S_{26}	4.6	6.7	7.0	10.8	12.6	13.6	17.0	16.8	18.5
S_{36}	1.8	1.9	1.9	4.9	3.5	3.5	5.7	4.8	4.8
S_{236}	0.8	0.9	0.7	4.1	3.0	2.1	5.7	5.6	3.9

* Calc.II without allowing for adjacent group effects at C-2 and C-3.

stituent in 4-position is easily removed under mild conditions by catalytic hydrogenation and acid hydrolysis, respectively. Partial methylation, removal of the 4-*O*-substituent and acid hydrolysis produces the same mixture of glucose and methyl ethers as was obtained from methyl cellulose. The method used by Croon and Lindberg [9] for the fractionation of this mixture was slightly modified, the mono-*O*-methyl glucoses being separated by electrophoresis in germanate buffer [10].

The methylations were performed with methyl sulphate in 18.9 % sodium hydroxide. The recovery of glucose and methylated glucoses was not quantitative, the average losses being 20—30 %. A careful check of each of the stages in the procedure showed that no one of the individual stages involved significant losses but that an accumulation of losses in the complete working-up operation resulted in this somewhat low recovery. There is no indication, however, that one or some of the components should be selectively removed during this procedure but rather that their relative proportions were uneffected.

The distributions of substituents calculated assuming the relative rate constants which gave the best agreement with the observed values, together with the experimental distributions, are given in Tables 2 and 3. The calculations were performed with and without the special assumption that the rate constant for substitution at C-3 is doubled when the position at C-2 is substituted. The agreement is better with this assumption, as was previously observed also for cellulose and other substances [1].

The complete analyses of partially methylated methyl β-D-glucopyranoside should involve the separation and determination of 16 components. Conditions were therefore chosen whereby the proportion of di- tri- and tetra-*O*-methyl glucoses were low. The monomethyl ether fraction was isolated by chromatography on thick filter paper and was quantitatively separated by paper electrophoreses in germanate buffer [10]. The relative rates at the various positions were then estimated from the proportions of these isomers. The results from the methylations of the model substances are summarised in Table 4.

As was observed for cellulose, all substances have lower reactivities in the 3- than in the 2- or 6-position. It therefore seems unnecessary to ascribe the difference in the case of cellulose to any special effect as, for example, hydrogen bonding between the C-3 hydroxyl and the ring oxygen in the adjacent glucose residue. It is more probable that the higher reactivities in the 2- and 6-positions are due to the greater acidity of the C-2 hydroxyl [11] and the lower steric requirements of the primary C-6 hydroxyl, respectively. The rates,

Table 4. Relative rates for the methylation of methyl β-D-glucopyranoside, some 4-*O*-substituted derivatives of it and cellulose with dimethyl sulphate in 18.9 % sodium hydroxide.

Substance	k_2	k_3	k_4	k_6
Methyl β-D-glucopyranoside	4	1	0.5	4
Methyl 4-*O*-benzyl-β-D-glucopyranoside	2	1	—	3
Methyl 4-*O*-(2-tetrahydropyranyl)-β-D-glucopyranoside (+ and −)	3	1	—	4
Cellulose	3.5	1	—	2

given in Table 4, are relative and not absolute, and it can not therefore be decided whether the differences between the substances are due to activations of some positions or to deactivation of others. It seems possible, however, that the lower reactivity of the 6-position of cellulose, as compared with the model substances, may be due to some steric hindrance at this position in the cellulose molecule.

The differences observed between the two 4-*O*-(2-tetrahydropyranyl)-derivatives are within the experimental errors but the differences between the other model substances are probably significant. Considering the complexity of the systems involved an attempt to interpret these rather small differences would hardly be justified.

EXPERIMENTAL

Methyl 4-O-benzyl-β-D-glucoside. Methyl 2,3,6-tri-*O*-acetyl-β-D-glucopyranoside [12] (6 g) was dissolved in dimethylformamide (60 ml) and benzyl bromide (24 ml), the solvents being dried and distilled before use. Silver oxide (24 g) was added over 1 h with stirring and the reaction left stirring overnight at room temperature. The product was worked up as described previously [8] – the dried chloroform extract was concentrated and high boiling liquids removed at 80° and reduced pressure (1 mm Hg). The residue was deacetylated with sodium methoxide in methanol and the products separated between hexane and water. The aqueous phase was deionised and concentrated, then fractionated on a cellulose column using water-saturated butanol as the eluant. The first optically active fractions contained the glucoside in about 15 % yield. Crystallisation from ethanol-hexane yielded the pure, hygroscopic substance, m.p. 58–68°, $[\alpha]_D^{25}$ −14° (water, *c* 1.0). (Found: C 58.9; H 7.29. $C_{14}H_{20}O_6$ requires C 59.1; H 7.09). The product had an R_F-value of 0.83 in butan-1-ol-ethanol-water (10:3:5) and could be detected with the periodate-benzidine spray reagent.

Acetylation in acetic anhydride and pyridine yielded methyl 2,3,6-tri-*O*-acetyl-4-*O*-benzyl-β-D-glucoside, m.p. 86.5–87.5°, $[\alpha]_D^{25}$ −25° (chloroform, *c* 2.0) after crystallisation from aqueous ethanol. (Found: C 58.8; H 6.43; O 34.8. $C_{20}H_{26}O_9$ requires C 58.5; H 6.39; O 35.1).

Methylations. A sample of a glucoside (0.5–1.5 g) was dissolved in 18.9 % aqueous sodium hydroxide (80–100 ml). Dimethyl sulphate (2–10 ml) was added over 45 min with stirring under an atmosphere of nitrogen. The stirring was continued for 4 h. The reaction mixture was then neutralised with 6 N sulphuric acid, the sodium sulphate precipitated with ethanol (400 ml) and the solution concentrated.

Removal of 4-O-substituent and hydrolysis. The methylated methyl 4-*O*-benzyl-β-glucoside was dissolved in methanol (20 ml), palladium on carbon catalyst (20 mg) was added and the mixture kept under hydrogen with shaking until the hydrogen uptake was constant. After filtration and concentration, the product was treated as below.

The methylated glucoside was dissolved in 1.8 N sulphuric acid (50–100 ml) and kept at 95° for 4 h. Most of the sulphate ions were removed by treatment with barium carbonate, remaining salts were removed by ion exchange and the solutions were concentrated.

Analytical procedure. The hydrolysis products were fractionated on a carbon-Celite column as described by Croon and Lindberg [9]. The monomethyl ethers, which are not separated well, were taken together and separated by paper electrophoresis in germanate buffer [10] (pH 10, 1000 V, 40°, 3 h). They were then estimated quantitatively by elution and hypoiodite titration [13].

The latter procedure was checked with standard samples, and although the absolute values were up to 10 % low, the relative analyses were within 5 %.

The procedure for the product obtained from partially methylated methyl β-D-glucopyranoside was somewhat different. The mixture was fractionated by chromatography on thick filter paper (butan-1-ol–ethanol–water, 10:3:5) giving glucose (79 %), mono-*O*-methylglucoses (16 %), di-*O*-methylglucoses (4 %) and higher ethers (approx. 1 %).

The proportions of the mono-*O*-methyl glucoses was determined by electrophoresis in germanate buffer as described above and found to be 43:11:5:41 for 2-, 3-, 4- and 6-*O*-methyl-D-glucose, respectively. The figures represent average values from 3 determinations.

REFERENCES

1. Croon, I. *Svensk Papperstidn.* **63** (1960) 247.
2. Croon, I. and Lindberg, B. *Svensk Papperstidn.* **60** (1957) 843.
3. Croon, I. *Acta Chem. Scand.* **13** (1959) 1235.
4. Croon, I. and Timell, T. E. *J. Am. Chem. Soc.* **82** (1960) 82.
5. Lemieux, R. V. *Paper presented at the 135th meeting of the American Chemical Society*, Boston, Mass., USA, April 1959.
6. Liang, C. Y. and Marchessault, R. H. *J. Polymer Sci.* **37** (1959) 385.
7. de Belder, A. N., Garegg, P. J., Lindberg, B., Petropavlovskij, G. and Theander, O. *Acta Chem. Scand.* **16** (1962) 623.
8. Croon, I. and Lindberg, B. *Acta Chem. Scand.* **13** (1959) 593.
9. Croon, I. and Lindberg, B. *Svensk Papperstidn.* **60** (1957) 843.
10. Lindberg, B. and Swan, B. *Acta Chem. Scand.* **14** (1960) 1043.
11. Sarkanen, K. and Larsen, K. *Paper presented at the 135th meeting of the American Chemical Society*, Boston, Mass., USA, April 1959.
12. Levene, P. A. and Raymond, A. L. *J. Biol. Chem.* **97** (1932) 763.
13. Hirst, E. L., Hough, L. and Jones, J. K. N. *J. Chem. Soc.* **1949** 57.

Received May 15, 1962.

ACTA CHEMICA SCANDINAVICA 16 (1962) 2010–2016

Cleavage of Some Derivatives of 2-Mercaptobenzothiazole *

BENGT WEIBULL and LEIF THORSELL

Research Laboratory, Mo och Domsjö AB, Örnsköldsvik, Sweden

In the presence of alkali 2-hydroxyethylthiobenzothiazole is cleaved with the formation of 2-hydroxybenzothiazole and ethylene sulphide polymer. 2-Ethylthiobenzothiazole and 2-carboxymethylthiobenzothiazole are cleaved analogously, but the reactions are much slower. With ammonia 2-hydroxyethylthiobenzothiazole also yields 2-hydroxybenzothiazole, but the reaction is very slow. With hydrazine hydrate all three sulphides yield 2-hydrazinobenzothiazole and the corresponding thiols. The reaction is slowest with the ethyl compound, fastest with the carboxymethyl compound, but also in this case much slower than the alkaline cleavage of 2-hydroxyethylthiobenzothiazole. In acid solution the ethyl compound is stable, but the other two compounds are slowly cleaved to 2-hydroxybenzothiazole and the corresponding thiols.

The exceptional behaviour of 2-hydroxyethylthiobenzothiazole in alkali seems to be due to the intermediate formation of an 1,3-oxathiolane. The reaction thus is analogous to the formation of ethylene sulphide from ethylene oxide and thiocyanate.

In connection with work on corrosion inhibitors derived from 2-mercaptobenzothiazole (I) it was observed that 2-(2-hydroxyethylthio)benzothiazole (II) was cleaved by aqueous alkali with the formation of 2-hydroxybenzothiazole (III) and ethylene sulphide polymer:



(1)

II III

The stability of 2-alkylthio derivatives of benzothiazole towards alkaline reagents or acids has not been reported, so it seemed worth while to investigate, if this type of cleavage is common to various types of such compounds. Sexton [1] observed that on heating above 125°C compound II decomposed according to a similar route giving III and possibly dithian.

* Part of this paper was presented at the "Tionde Nordiska Kemistmötet", Stockholm, August 17–22, 1959.

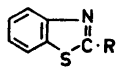

I: R = SH IV: R = SC_2H_5
II: R = SCH_2CH_2OH V: R = SCH_2COOH
III: R = OH VI: R = $NHNH_2$

As representatives of this class of compounds the following substances were chosen: 2-ethylthiobenzothiazole (IV), 2-(2-hydroxyethylthio)benzothiazole (II), and 2-carboxymethylthiobenzothiazole (V). The stability towards alkali, ammonia, and hydrazine was studied and, for comparison, also the behaviour in acid solution.

Reaction with alkali. As a working hypothesis the primary reaction was assumed to follow the scheme (Bt = 2-benzothiazolyl):

$$\underset{\text{II, IV or V}}{Bt{\cdot}SR} + 2\ OH^- \rightarrow \underset{\text{III}}{Bt{\cdot}O^-} + RS^- + H_2O \qquad (2)$$

Hydroxyl ion is consumed during the reaction with the formation of weaker bases, so an attempt was made to follow the progress of the reaction by means of potentiometric titrations of drawn samples. However, hydroxybenzothiazole (III) is not stable towards alkali, but slowly consumes hydroxyl ion with the formation of *o*-aminothiophenol and carbonate [2], so this method was not applicable:

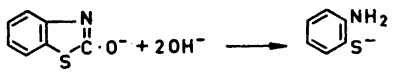 (3)

Also, in the presence of many bases of partly unknown strength it was difficult to determine the hydroxyl ion with any precision.

Another method is iodimetric titration of the thiol formed. In view of reaction (3) this could only give an upper estimate of the progress of reaction (2). This method was, however, used in the experiments with the ethyl and carboxymethyl compounds (IV and V). In the case of hydroxyethylthiobenzothiazole (II), it is doubtful whether the free thiol is ever formed. The corresponding solid polymer separates from the reaction mixture and was determined gravimetrically, giving a lower estimate of the progress of reaction (2).

All three sulphides were soluble in aqueous ethanol, so comparative experiments were carried out in that solvent at room temperature. Under these circumstances the ethyl and carboxymethyl compounds (IV and V) were practically stable, whereas the hydroxyethyl compound (II) was half decomposed in two hours, Fig. 1.

At higher temperatures, 70—100°, the former compounds were, however, slowly decomposed according to reaction (2). Hydroxybenzothiazole (III) was isolated in poor yield. The ethyl compound (IV) gave ethanethiol, recognised by its odour, and also a small amount of sodium carbonate according to reaction (3). The carboxymethyl compound (V) gave mercaptoacetic acid, identified as its mercaptal with benzaldehyde:

$$C_6H_5CHO + 2\ HSCH_2COOH \rightarrow C_6H_5CH(SCH_2COOH)_2 + H_2O \qquad (4)$$

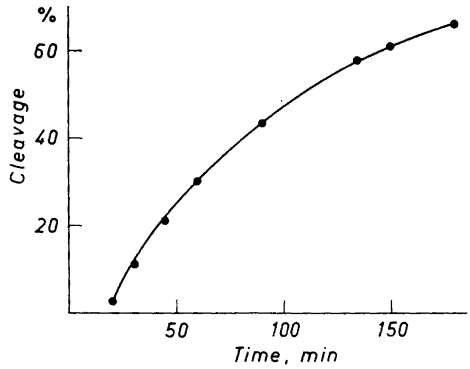

Fig. 1. Cleavage of 2-hydroxyethylthiobenzothiazole (II) by alkali at room temperature. For details see Experimental.

Reaction with ammonia. Experiments were made only with the hydroxyethyl compound (II). At room temperature no reaction was noticeable within a month. At 100° decomposition was observed with the formation of hydroxybenzothiazole (III).

Reaction with hydrazine. All three sulphides reacted analogously with the formation of 2-hydrazinobenzothiazole (VI) and the corresponding thiol:

$$\text{Bt·SR} + \text{H}_2\text{NNH}_2 \rightarrow \text{Bt·NHNH}_2 + \text{RSH} \qquad (5)$$

Comparative experiments showed, that the carboxymethyl compound (V) was cleaved most rapidly, followed by the hydroxyethyl compound (II). Table 1 presents the results of these experiments. The thiols were determined iodimetrically but not otherwise isolated or characterised. In this reaction no insoluble ethylene sulphide polymer was formed.

Reaction with acid. Hydrochloric acid was used in aqueous ethanol. Ethylthiobenzothiazole (IV) was not attacked at room temperature or at 65° whereas the other two sulphides were slowly hydrolised at 65° to hydroxybenzothiazole (III) and the corresponding thiol:

$$\underset{\text{II, V}}{\text{Bt·SR}} + \text{H}_2\text{O} \xrightarrow{\text{H}^+} \underset{\text{III}}{\text{Bt·OH}} + \text{RSH} \qquad (6)$$

Table 1. Hydrazinolysis of 2-benzothiazolyl sulphides.

Substance	Yield in %		M.p. of 2-hydrazinobenzothiazole
	2-hydrazinobenzothiazole	Thiol	
2-Ethylthiobenzothiazole (IV)	11	11	189 – 193°
2-Hydroxyethylthiobenzothiazole (II)	15	29	191 – 195°
2-Carboxymethylthiobenzothiazole (V)	26	31	190 – 192°

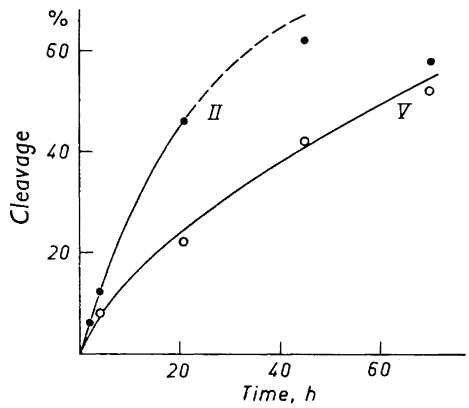

Fig. 2. Cleavage of 2-hydroxyethylthiobenzothiazole (II) and 2-carboxymethylthiobenzothiazole (V) by acid at 65°. For details see Experimental

Fig. 2 shows the iodimetrically estimated progress of the reactions. It is likely that the values for the cleavage of 2-hydroxyethylthiobenzothiazole (II) during the later part of the reaction are too small. The mercaptoethanol primarily formed condenses in the acid solution decreasing the amount of titratable mercapto groups.

DISCUSSION

Aliphatic and aromatic sulphides are generally stable towards the rather weak reaction conditions used in this study. The results obtained thus give rise to two questions: (1) Why are 2-alkylthiobenzothiazoles hydrolysed and hydrazinolysed and (2) Why is the hydrolysis of 2-hydroxyethylthiobenzothiazole by alkali, and only by alkali, much faster than the corresponding reactions with 2-ethylthio- and 2-carboxymethylthiobenzothiazole?

The answer to the first question seems to be that the thiazolylthio group contains a disguised dithiocarbimide group, $-N=C(S-)_2$. Very few simple dithiocarbimides have been described, but the dimethyl and diethyl esters are hydrolysed by alkali [3] just as related derivatives of carbonic acid. The relative stability of the benzothiazolyl sulphides is understandable since the dithiocarbimide group forms part of an aromatic ring system.

The answer to the second question may be found in the rather close analogy of the reaction described with the formation of ethylene sulphide from ethylene oxide and thiocyanate and various other substances containing sulphur. For this reaction the following mechanism seems well founded [4-9]:

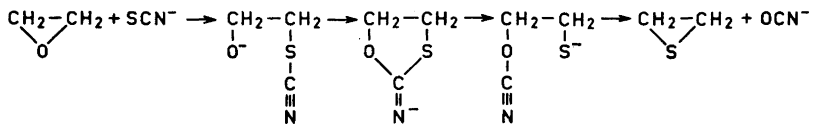

(7)

The analogous scheme is:

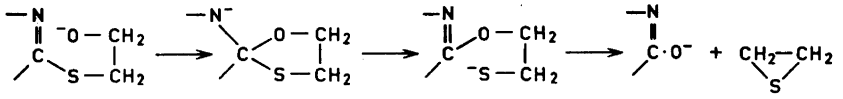

(8)

In the alkaline solution the ethylene sulphide is rapidly polymerised. This conclusion is supported by the fact that 2,4-dinitrothioethanol gives an exactly analogous reaction, where the cyclic intermediate is supposed to be [7]:

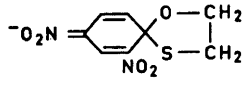

The rapid cleavage of 2-hydroxyethylthiobensothiazole by alkali is thus conditioned by the formation of an intermediate 1,3-oxathiolane. Ring closure is not possible in the alkaline cleavage of the other two sulphides or in the reactions of all three sulphides with hydrazine or acid and accordingly these reactions are much slower.

EXPERIMENTAL

Melting points are determined with a hot stage microscope and corrected.

2-Hydroxyethylthiobenzothiazole (II). Sexton [1] prepared the compound by alkylating the sodium salt of mercaptobenzothiazole (I) with ethylene chlorohydrin. It was found more convenient to use ethylene oxide. I (66.8 g, 0.4 mole) and sodium hydroxide (20 g, 0.5 mole) were dissolved in 250 ml of water. At 5° ethylene oxide (17.6 g, 0.4 mole) was added and the temperature kept below 25°. The solution rapidly turned turbid and an oil separated. After 30 min the upper, aqueous layer was decanted off and the lower layer was repeatedly washed with water. During this operation the oil solidified. It was crushed, washed on a filter and dried. The raw product (70 g, 83 %) melted at 48—53°. After recrystallisation from benzene-ligroin the m.p. rose to 58—59°. Sexton reports m.p. 56—58°.

2-Ethylthiobenzothiazole (IV). This compound was prepared according to Kendall and Suggate [10]. The yield of product, recrystallised from light petroleum, was 54 %. M.p. 26°. Kendall and Suggate report 26°.

2-Carboxymethylthiobenzothiazol (V). The procedure of Kucherov [11] was closely followed. I (50.1 g, 0.3 mole) was dissolved with sodium hydroxide (24 g, 0.6 mole) in 700 ml of water. Monochloroacetic acid (28.5 g, 0.3 mole) was added in portions. After two days at room temperature the solution was acidified yielding 64.5 g (95 %) of crystalline product, equiv. wt. (titration) 227.3, calc. 225.3, m.p. 154—157°. Kucherov reports 153.5—154°.

Alkaline cleavage of 2-hydroxyethylthiobenzothiazole (II). A preparative experiment was made in the manner described above from 33.4 g of I. However, the raw II was not separated, but the mixture was kept at 100° for 5 h yielding a yellow liquid with a grey-white precipitate. This was filtered off, yield 12.5 g, m.p. 161—164° (Found: S 48.7; OH 1.34. Calc. for C_2H_4S: S 53.34; the sulphur in the precipitate corresponds to 95 % of the mercapto group). Similar properties were reported for ethylene sulphide polymer obtained in other ways [12].

The filtrate on acidification yielded 22.7 g of pale-yellow crystals, recrystallised from benzene, m.p. 136.5—137.5. Hunter [13] for III reports m.p. 138°. (Found: equiv. wt. (titr.) 149.6; N 9.13; S 22.0. Calc. for C_7H_5NOS: equiv. wt. 151.2; N 9.27; S 21.2.)

In a crude *kinetic experiment* a solution 0.5 M with regard to II and 1.5 M with regard to sodium hydroxide was prepared from 5.28 g of II, 15 ml of 5 N NaOH, 5 ml of water and ethanol to a total of 50 ml. The solution was immediately parted in portions of 5 ml, which were left at room temperature. After appropriate times the polymer formed was

filtered off, washed with 80 % aqueous ethanol, dried at room temperature, and weighed. One portion was left for 19 h and yielded 166.6 mg of polymer. For a polymer containing 48.7 % sulphur the theoretical amount is 164.6 mg, so the reaction was considered complete after this time and the conversion calculated on this basis. Fig. 1 gives the results.

Alkaline cleavage of 2-ethylthiobenzothiazole (IV). Crude *kinetic experiments* were made corresponding to those mentioned previously. At room temperature no iodine was consumed by the solution after 68 h and potentiometric titration with hydrochloric acid revealed no formation of weak bases.

When a solution of the same composition was heated in a sealed glass ampoule at 100° the originally homogeneous solution parted in two liquid phases within a few hours. A small amount of crystalline material separated and was identified as sodium carbonate. Ethanethiol was formed, recognised by its odour and its reaction with iodine. Acidification of the reaction mixture yielded a small amount of crystalline material, identified as 2-hydroxybenzothiazole (III), m.p. 136—139°.

Alkaline cleavage of 2-carboxymethylthiobenzothiazole (V). In crude *kinetic experiments*, corresponding to those mentioned previously, practically no iodine was consumed by the solution after 48 h at room temperature.

A *preparative experiment* was carried out at 100°. A solution was made from 17 g (0.075 mole) of V, 60 ml of 5 N NaOH, and water to a total of 100 ml. After 23 h at 100° the solution was acidified, yielding crystals, identified as 2-hydroxybenzothiazole (III), m.p. 136—139°. Extraction of the mother liquor with ether, evaporation, and vacuum distillation of the residue yielded 2.5 g of distillate, b.p.$_{5\cdot5}$ 91—96°. The equiv. wt. on titration with alkali was 98.7, with iodine, 104, calc. for mercaptoacetic acid 92.1. A sample was mixed with an appropriate amount of benzaldehyde and a trace of conc. hydrochloric acid. A crystalline mass resulted, m.p. after recrystallisation from benzene 124—125.5°, equiv. wt. (titration) 136.7, for the mercaptal of mercaptoacetic acid with benzaldehyde calc. 136.1. The m.p. reported [14] is 126—127°.

Reaction of ammonia with 2-hydroxyethylthiobenzothiazole (II). Solutions were made from 2.11 g of II in 8 ml of conc. ammonia and 12 ml of ethanol. After a month at room temperature no change was observed. After 17 h at 100° 0.2 g of precipitate separated on cooling. On acidification the mother liquor yielded 1.2 g of crude 2-hydroxybenzothiazole (III), m.p. after recrystallisation from benzene 134—138°.

Reaction of hydrazine with 2-hydroxyethylthiobenzothiazole (II). A solutions was made from 2.11 g of II in 8 ml of hydrazine hydrate and 12 ml of ethanol. The solution was left 1 month at room temperature. The iodine consumption then corresponded to 52 % reaction. After 16 days crystals began to separate. The final yield of crystals was 0.5 g, m.p. 198—200°, efter two recrystallisations from water. Boggust and Cocker [15] report for 2-hydrazinobenzothiazole m.p. 199.5°. Titration with perchloric acid in glacial acetic acid gave the equiv. wt. 166.8, calc. 165.2.

A similar experiment carried out at 65° for 4 days yielded 0.5 g of the hydrazino compound. The iodine consumption of the mother liquor corresponded to 80 % cleavage.

Comparative experiments with hydrazine. Solutions were made with 10 mmoles of either II, IV or V in 8 ml of hydrazine hydrate and 12 ml of ethanol. After 5 h at 65° each solution was treated as follows. A sample of 1 ml was diluted with ethanol and titrated with 0.1 N iodine. The residue was diluted to 200 ml with water and acidified with 15 ml of conc. hydrochloric acid and cooled with ice water. The precipitated unchanged starting material was filtered off and the filtrate basified with 8 g of sodium hydroxide. Precipitated 2-hydrazinobenzothiazol was recovered and weighed and its m.p. determined. Results are given in Table 1.

Reactions in acid solution. In each experiment 25 mmoles of sulphide, 15 ml of 5 N HCl, 5 ml of water, and ethanol to 100 ml were mixed. The solutions were halfed, one half being kept at room temperature, the other at 65°. Samples were withdrawn at appropriate times and titrated with 0.1 N iodine. The former solutions did not consume any iodine within 8 days and the starting material was recovered unchanged. This was also observed with the solution containing the ethylthio compound (IV) at 65°. In the other two cases the consumption of iodine rose with time, as can be seen in Fig. 2. From the solutions hydroxybenzothiazole was isolated, m.p. and mixed m.p. 136—140°.

REFERENCES

1. Sexton, W. A. *J. Chem. Soc.* **1939** 470.
2. Sprague, M. J. and Land, A. H. in Elderfield, R. C. *Heterocyclic Compounds*, Vol. 5, Wiley, New York 1957, p. 553.
3. Delépine, M. *Bull. soc. chim. France.* [3] **29** (1903) 55.
4. Ettlinger, M. G. *J. Am. Chem. Soc.* **72** (1950) 4792.
5. van Tamelen, E. E. *J. Am. Chem. Soc.* **73** (1951) 3444.
6. Harding, J. S., Miles, L. W. C. and Owen, L. N. *Chem. & Ind. London* **1951** 887.
7. Culvenor, C. C., Davies, W. and Savige, W. E. *J. Chem. Soc.* **1952** 4480.
8. Price, C. C. and Kirk, P. F. *J. Am. Chem. Soc.* **75** (1953) 2396.
9. Bordwell, F. G. and Andersen, H. M. *J. Am. Chem. Soc.* **75** (1953) 4959.
10. Kendall, J. D. and Suggate, H. G. *J. Chem. Soc.* **1949** 1503.
11. Kucherov, V. F. *Zhur. Obshcheĭ Khim.* **19** (1949) 752.
12. Nylén, P. and Olsen, A. *Svensk Kem. Tidskr.* **53** (1941) 274.
13. Hunter, R. F. *J. Chem. Soc.* **1930** 125.
14. Holmberg, B. and Mattisson, K. *Ann.* **353** (1907) 125.
15. Boggust, W. A. and Cocker, W. *J. Chem. Soc.* **1949** 355.

Received May 8, 1962.

ACTA CHEMICA SCANDINAVICA 16 (1962) 2017–2024

Absorption Spectra of Cobalt(II) and Cobalt(III) Diethyldithiophosphates

CHR. KLIXBÜLL JØRGENSEN

Cyanamid European Research Institute, Cologny (Geneva), Switzerland

Whereas Co dtp_2($dtp^- = (C_2H_5O)_2PS_2^-$) occurs as a tetrahedral non-solvated form in carbon tetrachloride, an indigo-blue solvate of different symmetry is formed in ethanol. Application of the method of continuous variations demonstrates the presence of a 2 dtp^-: 1 Co complex, among others, in ethanolic solutions. The nearly regularly octahedral Co dtp_3 can be formed by oxidation of such solutions with hydrogen peroxide and the absorption spectrum is compared with those of Rh dtp_3 and Ir dtp_3 and discussed in terms of the spectrochemical and nephelauxetic series and the variation of optical electronegativities derived from electron transfer bands.

The absorption spectra of inner-complexes of the ligand $dtp^- = (C_2H_5O)_2PS_2^-$ forming M dtp_3 and M dtp_2 have been studied [1] of a variety of central ions M. The M.O. treatment of the trigonally distorted, octahedral $M(S_2P)_3$ was given in a paper [2] on the similar selenium-containing complexes $M(Se_2P(OC_2H_5)_2)_3$. In most cases, these inner-complexes form readily and in great yield, and in a way comparable to the preparation of the acetylacetonates.

However, in a few cases, the chemistry is considerably more complicated. Malatesta and Pizzotti [3] prepared a dark blue solution of Co dtp_2 by extraction from an aqueous solution containing $Co(H_2O)_6^{2+}$ and dtp^- into an organic solvent. These authors reported the preparation of diamagnetic Co dtp_3 in small quantities by oxidation of such a solution. In a recent description [4] of Cr dtp_3, it is shortly reported that Co dtp_3 has been prepared from cobalt(III) fluoride. This does not leave the impression that Co dtp_3 is a very accessible material. Actually, it can easily be made in large quantities, as we shall see.

An aqueous solution of 0.3 M cobalt(II) nitrate or perchlorate and 0.6 M ammonium diethyldithiophosphate has nearly the same spectrum as when no dtp^- is present. This is analogous to the behaviour of aqueous solutions containing $Ni(H_2O)_6^{2+}$ and dtp^- in large concentrations. However, in the latter case [1], purple crystals of Ni dtp_2 may precipitate. Such crystallization has not been observed of the cobalt(II) solutions, and they show hardly any tendency to oxidation in the air.

In the presence of an immiscible organic solvent, this oxidation is catalyzed strongly. The mechanism is that sky-blue Co dtp_2 is extracted into the solvent and then, in the course of some hours, oxidized by oxygen entering at the phase separation. The colour changes to green and finally to brown. By dilution, a clear yellow colour is observed.

As we shall see below, this corresponds to the compound Co dtp_3. In mixtures of a little water and much ethanol, cobalt(II) nitrate or perchlorate produce an indigoblue colour with dtp^- comparable to that of cobalt(II) chloride alone in the same solvent. The indigo-blue solutions are rather resistant to air oxidation and turn green or brown only in the course of several days.

The simplest way to produce Co dtp_3, however, is to prepare the indigoblue solution in 80 or 90 % ethanol and oxidize under rapid stirring with the stoichiometric amount of aqueous 30 % hydrogen peroxide. A dark brown powder separates. This can be recrystallized from ethanol and it is completely soluble in chloroform or dichloroethane. It can be syncrystallized with the colourless [1] In dtp_3.

In the following, we shall discuss the absorption spectra of the tetrahedral Co dtp_2, the one or more species occurring in the indigoblue ethanol solutions, and the octahedral Co dtp_3.

Co dtp_2 in carbon tetrachloride solutions. CCl_4 was chosen as solvent because it does not contain hydrogen atoms with subsequent high vibrational frequencies. On the Cary 14 recording spectrophotometer, it is actually possible to compare two 2 cm cells with CCl_4 readily out to 2200 mμ, whereas the slit-

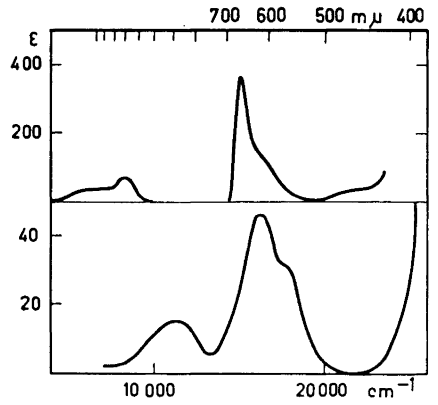

Fig. 1. Absorption spectra of tetrahedral Co dtp_2 in CCl_4 (upper half) and of the indigoblue form in ethanol (presumably containing Co dtp_2 $(C_2H_5OH)_2$) (in the lower part).

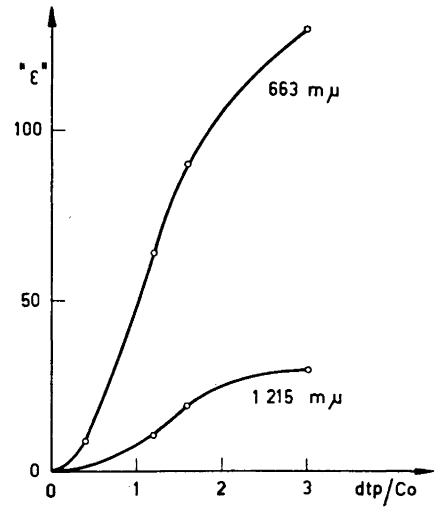

Fig. 2. Effective molar extinction coefficient "ε" by extraction experiments of aqueous solutions containing various ratios of total dtp^-/Co^{2+} concentrations into CCl_4 (where Co dtp_2 alone is extracted) as discussed p. 2019.

Table 1. Absorption bands of the tetrahedral form Co dtp_2 in carbon tetrachloride, the indigo-blue form in alcohol (presumably Co dtp_2 $(C_2H_5OH)_2$) and of Co dtp_3. Wavelengths λ in mμ, wavenumbers σ in cm^{-1} and molar extinction coefficients ε are given of maxima, and of shoulders in parentheses. The half-widths $\delta(-)$ towards smaller and $\delta(+)$ towards larger wavenumbers are indicated.

	λ	σ	ε	$\delta(-)$	$\delta(+)$
Co dtp_2	~1 600	6 700	~ 40	—	—
	1 215	8 200	~ 60	—	900
	663	15 100	~ 360	350	600
	(590)	(16 900)	~ 80	—	800
Co $dtp_2(C_2H_5OH)_2$(?)	870	11 500	15	2 200	1 400
	616	16 200	46	1 100	—
	(565)	(17 700)	32	—	—
Co dtp_3	(738)	13 550	450	1 200	1 400
	(526)	(19 000)	480	1 600	—
	406	24 600	6 500	2 200	--
	335	29 900	18 000	2 600	2 600
	233	43 000	9 500	3 900	—

width increases irregularly at longer wavelengths and makes the comparison slightly irreproducible. Small quantities of hydrogen-containing molecules such as ethanol produce very strong lines at 1400, 1690, 1730 and 2095 mμ and cut off longer wavelengths.

In each experiment, 0.5 ml of an aqueous solution (0.2 M $Co(ClO_4)_2$, and with the ratios NH_4 dtp/Co 0.4, 1.2, 1.6, or 3, respectively) was shaken with 10 ml CCl_4. When the phases were satisfactorily separated, the spectra were measured within a few minutes, avoiding the effects of air oxidation. In all cases, the spectra had the same form, as given in Fig. 1 and Table 1. The most characteristic feature is the narrow band at 663 mμ, having the half-width towards smaller wavenumbers $\delta(-) = 350$ cm^{-1}. This remarkably low figure suggests very strongly a tetrahedral micro-symmetry of $Co(S_2P(OC_2H_5)_2)_2$. The stoichiometric composition of this compound is also supported by the relative height of the 663 mμ peak as given in Fig. 2. At low values of dtp/Co in the aqueous phase, the intensity of the sky-blue colour in the CCl_4 phase increases more rapidly with this ratio than the first power. If only one dtp group were present in the complex extracted, the intensity would necessarily increase less than the first power if the mass-action law in concentration units is approximately valid in the aqueous phase and for the extraction

Table 2. Values of the sub-shell energy difference $-\Delta$ and Racah's parameter of interelectronic repulsion B in various tetrahedral cobalt(II) complexes.

	$-\Delta$	B
$CoCl_4^{2-}$ (Ref.[5])	3000 cm^{-1}	730 cm^{-1}
CoI_4^{2-} (Ref.[5])	2690	640
Co(II)in ZnS (Ref.[6])	3750	610
Co(II)in CdS (Ref.[6])	3300	610
» (Ref.[7])	3160	665
$Co(S_2P(OC_2H_5)_2)_2$	4000	665

coefficient. Furthermore, well known arguments lead to the conclusion that entities such as Co dtp$(H_2O)_2^+$ or Co dtp$(H_2O)(ClO_4)$ would not be extracted in carbon tetrachloride.

In the near infra-red spectrum of Co dtp_2, a band at 1215 mμ and a broad plateau 1500—1700 mμ are observed. This is closely analogous to the spectra of other regularly tetrahedral cobalt(II) complexes [5]. If the centre of gravity of the near infra-red band is fixed to 1450 mμ, that is 6900 cm^{-1}, and if the excited level is *a* $^4\Gamma_4$ whereas the band at 15 100 cm^{-1} has *b* $^4\Gamma_4$, the secular determinants for d^7 in T_d are satisfied by the parameters $\Delta = -4000$ cm^{-1} and $B = 665$ cm^{-1}. As discussed by Cotton, Goodgame and Goodgame [5], this choice of parameters is necessarily somewhat uncertain. Qualitatively, the values are very satisfactory when compared to the parameters compiled in Table 2. The spectrochemical position of dtp^- corresponds to more negative value of Δ than of Cl^-, whereas the nephelauxetic effect of dtp^- is more pronounced and corresponds to a value intermediate between Br^- and I^-.

The intensity is remarkably low. The extinction coefficients of the maxima (360 at 663 mμ and 60 at 1215) might be somewhat overestimated due to the indirect determination (based on the amount of cobalt *not* extracted in the organic solvent) but it is beyond all doubt that they are lower than in the corresponding tetrahalides [5]. This is in striking contrast to the octahedral complexes, where the tris (diethyldithiophosphates) have absorption bands some twenty times stronger than the corresponding hexahalides [1].

The indigo-blue solutions in ethanol. The effect of distortions of the tetrahedral symmetry to C_{3v} in CoX_3Y and to C_{2v} in CoX_2Y_2 have been studied by Cotton, Goodgame, Goodgame, and Sacco [8]. The extensive studies by Buffagni and Dunn [9] of $CoCl_2$ and $CoCl_4^{2-}$ in various organic solvents have

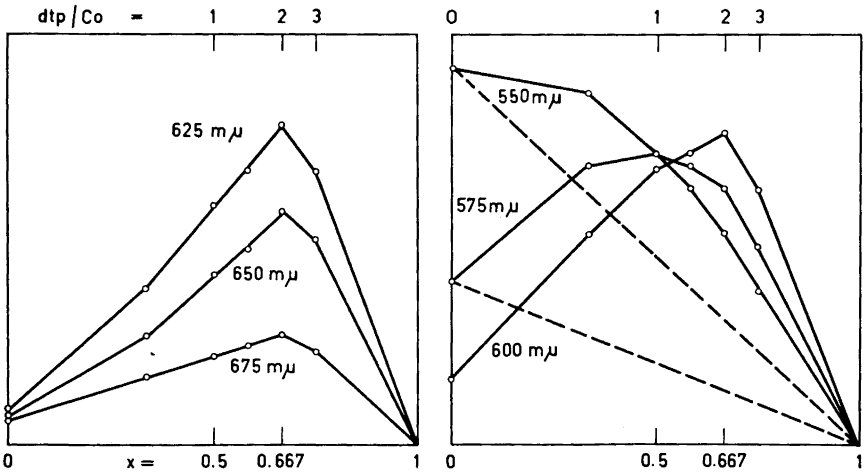

Fig. 3. Continous variation studies of the indigo-blue complex in ethanol $0.03(1-x)$ M $Co(NO_3)_2$ and $0.03x$ M NH_4dtp having optical densities measured at various wavelengths.

demonstrated the occurrence not only of a common $CoCl_4^{2-}$ without other ligands in the first coordination sphere, but also $CoCl_3X^-$ where X can be nitromethane or dimethyl formamide, and even the distorted $CoCl_2(CH_3NO_2)_2$. Hence, the indigo-blue solutions of Co(II) and dtp^- in ethanol might possibly contain many different species. The comparatively low intensity of the bands at 565 and 616 mμ and the occurrence of a new band at 850—870 mμ might suggest that the main species are not at all tetrahedral but rather distorted octahedral such as Co $dtp_2(C_2H_5OH)_2$ or Co $dtp(C_2H_5OH)^+$ would be.

It is well-known [10,11] that the method of continuous variations (Job's principle) is open to severe criticism if more than one definite complex is formed in solution. However, in our particular case, it is nevertheless one of the best ways available for determining the composition of the species occurring if the necessary circumspection is exercized by the interpretation of the results.

Solutions containing $Co(NO_3)_2$ and NH_4dtp at a total concentration of 0.03 M in ethanol (and a water concentration of 0.2 M) were studied, as shown on Fig. 3. At this water concentration, cobalt(II) alone is present mainly as a nitrato complex $Co(NO_3)(C_2H_5OH)_5^+$, and there are good reasons to believe that co-ordination of water will only play a minor role in the complex equilibria [12]. Fig. 3 shows that at some wavelengths (675, 650, 625 and 600 mμ), the formation of a complex containing two dtp^- per Co can be clearly demonstrated. The sharply triangular shape of the curves indicate that this bis-complex does not dissociate very much, *i.e.* it has a formation constant higher than the reciprocal cobalt concentration used here [13]. Actually, this is confirmed by the approximate validity of Beer's law in the concentration range 0.005 to 0.02 M Co(II) containing a slight excess above 2 dtp^-/Co. It cannot be excluded that small amounts of a tris-complex Co dtp_3^- are formed. In 0.1 M NH_4dtp in ethanol, the two first bands shift to 875 and 622 mμ. However, no conclusion will be drawn here.

On the other hand, it is completely certain that a mono-complex, perhaps Co $dtp(C_2H_5OH)_4^+$, is formed to some extent. This can be seen from the right-hand part of Fig. 3 where the curves for 575 and 550 mμ have a broad bell-shape. According to the method of continuous variations, it is actually the deviations from a linear variation (the dashed lines) as function of x which should be considered. If only these curves were known, the conclusion would be a rather ambiguous indication of a mixture of 1:1 and 2:1 among other possible complexes. Though the spectra of the 2:1 complex $\varepsilon_2(\lambda)$ and the dtp^- free solution $\varepsilon_0(\lambda)$ are known, it is not very easy to determine the spectrum of the 1:1 complex $\varepsilon_1(\lambda)$ from the data available. What would be experimentally accessible is the deviation of the intermediate spectra at a given dtp^-:Co ratio n:1 from the average spectrum of the two known complexes $(\varepsilon_0 + \varepsilon_2)/2$. Unfortunately, it is not possible in general, without further information, to estimate the relative proportion of the complexes even under the assumption that only three coloured sepcies are present. Hence, we will here refrain from attempts to estimate ε_1 and only note that such a complex has been detected.

The strong difference in spectral characteristics of the tetrahedral Co dtp_2 in inert solvents and the bis-complex in ethanol can only be rationalized by

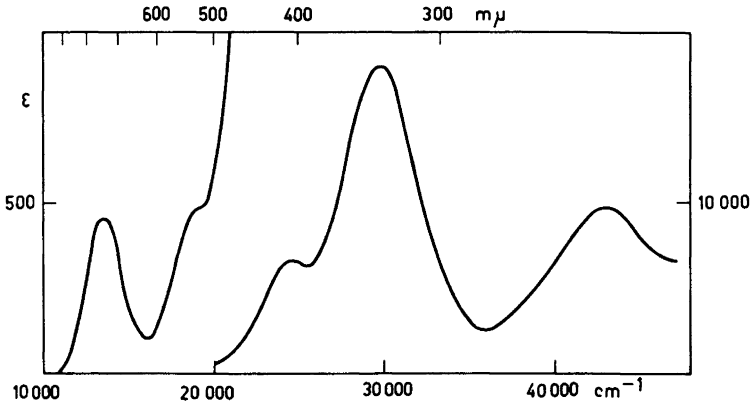

Fig. 4. Absorption spectrum of Co dtp_3 in ethanol.

solvation, forming, *e.g.*, Co $dtp_2(C_2H_5OH)_2$ of distorted octahedral symmetry (conceivably either low-spin or high-spin). Solutions of Co dtp_2 in CCl_4 or in dichloroethane change conspicuously (the 663 mμ peak decrease ε to the value 215 with 1.8 % ethanol, and disappears entirely at higher ethanol concentrations) with small amounts of ethanol. It is quite unexpected in this context that an aquated Co $dtp_2(H_2O)_2$ is not extracted from aqueous solutions in the inert solvents. Actually, one explanation of the relatively low intensity of the tetrahedral Co dtp_2 might involve the presence of such an aquated species in equilibrium. However, this is less probable when the absence of a band at 860 mμ is taken into account.

Approximately octahedral Co dtp_3. After the necessary recrystallization from ethanol, the oxidation product of the indigo-blue solution with H_2O_2 has the spectrum expected of $Co(S_2P(OC_2H_5)_2)_3$ given in Table 1 and Fig. 4. This inner-complex has also been studied by Schäffer [14]. Table 3 illustrates the close analogy between this lowspin $3d^6$ system and the analogous complexes [1] of the 4d-and the 5d-groups Rh dtp_3 and Ir dtp_3.

The spectrochemical development is quite ordinary [13,15] in the series Co(III), Rh(III) and Ir(III). The nephelauxetic effect is very pronounced in

Table 3. Wavenumbers in cm^{-1} and identification of absorption bands of cobalt(III), rhodium(III) and iridium(III) diethyldithiophosphates. Further on, parameters characterizing the transitions in the partly filled shell.

Assignment	Co dtp_3	Rh dtp_3	Ir dtp_3
$^1\Gamma_1 \rightarrow {}^1\Gamma_4$	13 550	21 300	26 200
$\rightarrow {}^1\Gamma_5$	19 000	24 400	28 600
$\pi_1 \rightarrow \gamma_3$	24 600	31 200	37 400
$\pi_2 \rightarrow \gamma_3$	29 900	38 800	45 700
M.O. energy difference Δ	14 200	21 900	26 700
Racah's parameter B	400	210	160
Nephelauxetic ratio β_{35}	0.36	0.29	(0.24)

all sulphur-containing complexes [14], and the nephelauxetic ratio β_{35} (between B derived from eqn. (1) below and the value in the corresponding gaseous ion) has the smallest values known of any complex of these central ions, except $Ir(Se_2P(OC_2H_5)_2)_3$ having a slightly smaller nephelauxetic ratio [2]. The quantities given in Table 3 are derived from Tanabe and Sugano's secular determinants with various assumptions [16], leading to the energy of the three lowest energy levels with zero total spin S:

$$\begin{aligned} {}^1\Gamma_1 &\quad -120\ B^2/\Delta \\ {}^1\Gamma_4\ \Delta &- \ 4\ B - 34\ B^2/\Delta \\ {}^1\Gamma_5\ \Delta &+ 12\ B - 118\ B^2/\Delta \end{aligned} \qquad (1)$$

where Δ is the M.O. energy difference between the sub-shells γ_5 and γ_3.

It is remarkable that the intensity of the $\gamma_5 \rightarrow \gamma_3$ transitions between the levels given in eqn. (1) is less than half as large in Co dtp_3 as in [1] Rh dtp_3 and Ir dtp_3.

The electron transfer spectra were discussed in general for this type of complexes [1,2]. It is seen from Table 3 that the optical electronegativity [17] x_{opt} of the γ_3-sub-shell is 1.8 of Co dtp_3, 1.6 of Rh dtp_3, and 1.4 of Ir dtp_3, if $x_{opt} = 2.7$ of the ligand dtp^-. When corrected for the highly varying values of Δ, the values of the optical electronegativity of the filled γ_5-sub-shell are seen to be about the same, 2.3 in all three complexes. The values of x_{opt} extrapolated from the behaviour of hexahalide complexes are 2.3 of Rh(III) and 2.2 of Ir(III). When a lower number of electrons are present in the γ_5-sub-shell, it is elsewise a general rule that the 4d-ions have x_{opt} 0.2 units higher than the corresponding 5d-ion.

EXPERIMENTAL

Stock solutions in water and in ethanol were made of AnalaR $Co(NO_3)_2,6H_2O$, of aqueous $Co(ClO_4)_2$ made from B.D.H. $CoCO_3$, and of NH_4dtp from American Cyanamid Laboratories, Stamford, Conn. The carbon tetrachloride used for the extraction experiments was p.a. Merck.

The absorption spectra were measured on a Cary 14 recording spectrophotometer.

The preparation of Co dtp_3 is discussed in the text above. The analysis. Found: C 23.42; H 4.93; P 15.98; S 33.99. Calc. for $C_{12}H_{30}O_6P_3S_6Co$: C 24.45; H 4.92; P 15.12; S 31.30.

Acknowledgment. I am very grateful to Professor W. Conrad Fernelius who first attracted my attention on dtp^- as ligand, and to Dr. Claus Schäffer for continued discussion and valuable advice and information on this type of complexes.

LITERATURE

1. Jørgensen, C. K. *J. Inorg. Nucl. Chem. In press.*
2. Jørgensen, C. K. *Molecular Phys.* **5** (1962) 485.
3. Malatesta, L. and Pizzotti, R. *Chimica e industria* **27** (1945) 6.
4. Coldbery, D. E., Fernelius, W. C. and Shamma, M. *Inorganic Syntheses* **6** (1960) 142.
5. Cotton, F. A., Goodgame, D. M. L. and Goodgame, M. *J. Am. Chem. Soc.* **83** (1961) 4690.
6. Weakliem, H. A. *J. Chem. Phys.* **36** (1962) 2117.
7. Pappalardo, R. and Dietz, R. E. *Phys. Rev.* **123** (1961) 1188.

8. Cotton, F. A., Goodgame, D. M. L., Goodgame, M. and Sacco, A. *J. Am. Chem. Soc.* **83** (1961) 4157.
9. Buffagni, S. and Dunn, T. M. *J. Chem. Soc.* **1961** 5105.
10. Woldbye, F. *Acta Chem. Scand.* **9** (1955) 299.
11. Schläfer, H. L. *Komplexbildung in Lösung*, in the series *Molekülverbindungen und Koordinationsverbindungen in Einzeldarstellungen*. Springer-Verlag, Berlin 1961.
12. Jørgensen, C. K. and Bjerrum, J. *Nature* **175** (1955) 426.
13. Jørgensen, C. K. *Absorption Spectra and Chemical Bonding in Complexes*. Pergamon Press, Oxford 1962.
14. Schäffer, C. E. *140th Meeting Am. Chem. Soc. 1961*, Abstr. of papers p. 24N.
15. Schäffer, C. E. and Jørgensen, C. K. *J. Inorg. & Nuclear Chem.* **8** (1958) 143.
16. Jørgensen, C. K. *Progress Inorg. Chem.* **4** (1962).
17. Jørgensen, C. K. *Solid State Physics* **13** (1962) 375.

Received May 2, 1962.

ACTA CHEMICA SCANDINAVICA 16 (1962) 2025–2040

Studies on the Coagulation of Chicken Blood

VIII. Use of Alumina, Ferric Oxide, Bismuth Sulfide, Magnesium Borate, and Zinc Tungstate for Differentiation and Assay of Strontium Carbonate Non-adsorbable Labile Factors

ØYVIND SØRBYE* and INGER KRUSE

Department of Biochemistry and Nutrition, Polytechnic Institute, Copenhagen, Denmark

Partial adsorption of the labile factor activity of strontium carbonate preadsorbed oxalated chicken plasma was obtained by use of different adsorbents. Six different categories of such adsorbents were recognized, permitting selective adsorption of six different labile coagulation factors. Provisional names for these factors are suggested: α (alpha)-factor, selectively adsorbed by Mg-borate; ϑ (theta)-factor, selectively adsorbed by Zn-tungstate; ξ (xi)-factor, selectively adsorbed by Fe-oxide; ω (omega)-factor, selectively adsorbed by Bi-sulfide; η (eta)-factor, selectively adsorbed by hydrochloric acid treated Merck 1095 Al-oxide; and ς (zeta)-factor, selectively adsorbed by Hopkin & Williams 1284 Al-oxide.

These six factors are different from the eight labile factors described in preceding papers. With a few exceptions the specific activity of each of these fourteen factors is influenced in a characteristic manner by the concentrations of the other thirteen. The ξ-, ω-, η-, and ς-factors are common components of the labile factor activities measured with thromboplastin and Russell's viper venom, with or without added cephalin, whereas the α- and ϑ-factors are thromboplastin specific labile coagulation factors.

In two preceding papers [1,2] the effects of crystalline adsorbents on the labile factor activity of strontium carbonate preadsorbed oxalated chicken plasma were investigated. Only a part of the total activity was adsorbed. These observations indicated that the labile factor activity was of complex nature, and suggested the use of such adsorbents for differentiation of the activity and characterization of the individual components. The results obtained with seventy-seven adsorbents were explained as selective adsorption of eight different labile factors (measured by thromboplastin), by eight different categories of adsorbents. Of these factors only two were parts of the labile factor activity measured by RVV **-cephalin, and only one was active

* Fellow of the Royal Norwegian Council for Scientific and Industrial Research.
** Russell's viper venom.

with RVV alone. The greater part of the labile factor activity measured by the two latter agents, was thus due to labile factors not adsorbed by any of the adsorbents tested. A few preliminary experiments also showed that the combined activities of the eight factors described did not account for more than 40—50 % of the total activity measured by thromboplastin.

A search for compounds with selective adsorption capacities for factors not adsorbed by the adsorbents described in preceding papers [1,2], led to a reexamination of the adsorption properties of a sample of alumina which previously had been tested only briefly [3].

It will be shown in this paper that (1) the effect of this alumina is due to adsorption of six discrete labile factors which differ from those already described [1,2], (2) the six factors can be adsorbed separately by other adsorbents, including special brands of alumina, and (3) four of these six factors are common components of the labile factor activities measured by thromboplastin, RVV-cephalin and RVV, whereas the remaining two factors are inactive in the two latter systems and must be regarded as thromboplastin specific labile coagulation factors.

MATERIALS AND METHODS

Except for the adsorbents the methods and materials used in this study were as described previously [1,2,4,5].

Adsorbents

The following adsorbents were prepared in this laboratory from high purity chemicals by adaption of methods described in Gmelin-Kraut's Handbuch der Anorganischen Chemie (*cf.* preceding papers [1,2]).

Borate of Mg was prepared from the oxide as described for Co-borate [1].

Tungstates of Mg and Zn were prepared from the chlorides as described for Ca-tungstate [1].

Aluminates of Mg and Zn were prepared from the sulfate and the chloride, respectively, as described for Co-aluminate [1].

Silicates of Mg and Zn were prepared from the sulfate and the chloride, respectively, as described for Co-silicate [1].

Oxides of Fe and Mn were prepared from the carbonate and the di-oxide, respectively, as described for Ce-oxide [2].

Sulfides of Bi and Hg were prepared by precipitation with hydrogen sulfide gas, Bi-sulfide from the nitrate (dissolved in dilute hydrochloric acid) and Hg-sulfide from the acetate (dissolved in dilute acetic acid). The precipitates were thoroughly washed and dried, then heated for 3—4 days at 280°C (Bi) or 240°C (Hg) in sealed evacuated ampullae.

Ba-metaborate was kindly supplied by the Department of Inorganic Chemistry of this Institute.

The following brands of *alumina* were obtained commercially:

Al-oxide I: Alumina, Type H, Grade 100—200, for Chromatographic Analysis, Peter Spence & Sons.

Al-oxide II: Aluminium oxide activated, for adsorption purposes, and for chromatographic analysis, 1284, Hopkin & Williams.

Al-oxide III: Aluminium oxydatum anhydricum puriss., 1095, Merck (non-uniform particle size).

Al-oxide IV: Aluminium oxydatum anhydricum puriss., 1095, Merck (uniform particle size).

Al-oxide VI: Aluminium oxide, suitable for analysis, A 17/18/66, May & Baker.

Al-oxide VII: Aluminiumoxyd "Woelm", sauer (anionotrop), Akt.-Stufe I, zur Chromatographie.

Al-oxide VIII: Aluminiumoxyd "Woelm", alkalifrei (annährend neutral), Akt.-Stufe I, zur Chromatographie.

Attempts were made to modify the adsorption properties of the Al-oxides I, III and IV, by stirring 50 g of the oxide with 500 ml of dilute acids at different temperatures. The details of this procedure for the modifications used in the present study were as follows:

b_1: treatment with 1 M hydrochloric acid at room temperature for 48 h.
b_2: treatment with 1 M hydrochloric acid on a steam bath for 24 h.
b_6: treatment with 6 M hydrochloric acid on a steam bath for 3 h.
d_0: a suspension of the Al-oxide in water was heated on a steam bath for 24 h and pH maintained at pH 3—3.5 by addition of nitric acid.
d_2: treatment with 1 M nitric acid on a steam bath for 24 h.
d_3: treatment with 4 M nitric acid at room temperature for 48 h.

All the above modifications of Al-oxide I were prepared. Of the Al-oxides III and IV the modifications b_2 and b_6 were prepared as for I.

Before use all adsorbents, including the various preparations of Al-oxide, were washed with hot distilled water, treated with 96 % ethanol and dried, as described previously [2].

EXPERIMENTS AND RESULTS

Adsorption of strontium carbonate non-adsorbable labile factors. The adsorbents were tested for adsorption of the labile factor activity of fresh, strontium carbonate preadsorbed, oxalated chicken plasma (strontium carbonate plasma) as described in preceding papers [1,2,4]. No inhibitory effects were detected in the adsorbed plasmas, and pH was not changed after adsorption, except with Ba-metaborate and some brands of Al-oxide which increased pH to 7.5—7.7. These pH changes did not interfere with the determination of labile factor activity, but made the activity of the plasmas less stable. However, with most adsorbents the non-adsorbed activity was stable for one hour or more when stored at 0°C. Most readsorption experiments were done with such plasmas. When less stable, adsorbed plasmas were used for readsorption experiments, the results were corrected for possible minor changes in activity occurring in control samples during the readsorption operations.

Adsorption by Al-oxide I. The labile factor activity of plasma aliquots was determined after adsorption by graded amounts of Al-oxide I. Fig. 1A shows a characteristic experiment where the labile factor activity was measured with thromboplastin as well as with RVV-cephalin [4,5]. Al-oxide I caused only partial adsorption of the activity and could therefore be regarded as a selective adsorbent. However, the curves for adsorption of the activity were more complex than those given by the selective adsorbents tested in previous papers [1,2]. Thus, the curve obtained with thromboplastin appeared to be composed of three rectilinear sections. The curve obtained with RVV-cephalin had only two such sections, the end points of which corresponded to the end points of sections two and three of the thromboplastin curve. In agreement with the interpretation of the two-, three- and four-sectioned curves obtained for adsorption of φ-factor activity by a variety of adsorbents [6], the present curves were interpreted as independent adsorption of three different (groups of) labile factors, one of which must be specific for the thromboplastin assay system. The three-sectioned adsorption curve is thus regarded as the result of a superposition of three single-sectioned rectilinear adsorption curves, each

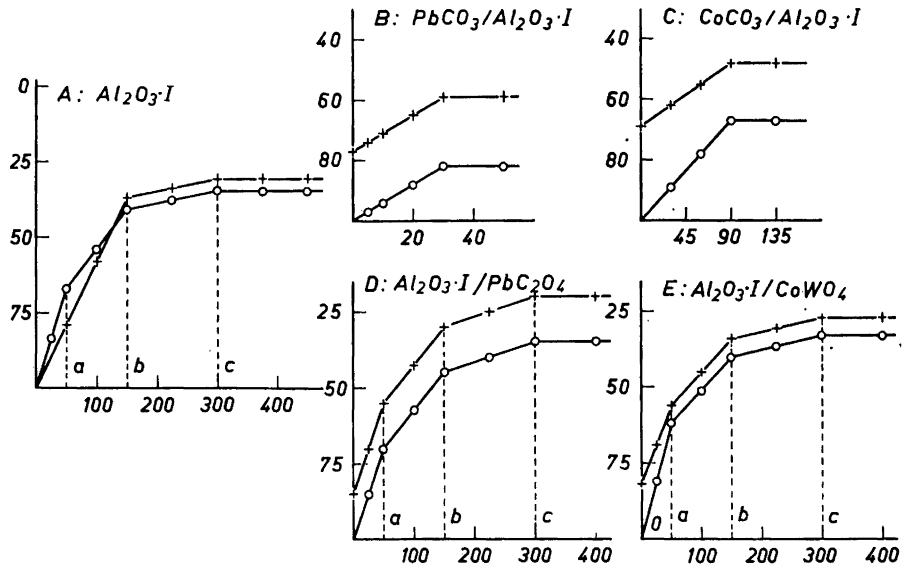

Figs. 1-10. All figures: Ordinates: labile factor activity in % of strontium carbonate plasma. Abscissæ: adsorbent in mg/ml.

Fig. 1. Effects of adsorption by Al-oxide I.

A: labile factor activity adsorption by Al-oxide I, measured by thromboplastin (O) and by RVV-cephalin (+)
B—E: Untreated strontium carbonate plasma : O
preadsorbed » » » +
B: Pb-carbonate adsorption, preadsorption by Al-oxide I (60 mg/ml)
C: Co-carbonate adsorption, preadsorption by Al-oxide I (50 mg/ml)
D: Al-oxide I adsorption, preadsorption by Pb-oxalate (20 mg/ml)
E: Al-oxide I adsorption, preadsorption by Co-tungstate (60 mg/ml)

representing adsorption of one (group of) labile factor(s), the adsorption of which is complete at *a*, *b* and *c*, respectively.

The new possibilities for differentiation of the labile factor activity of strontium carbonate plasma offered by Al-oxide I, were investigated. The relation between the factors adsorbed by this agent and those adsorbed by the selective adsorbents described previously [1,2], was studied in a series of matching experiments. Adsorption of labile factor activity by lead carbonate (adsorbing π-factor) before and after partial adsorption by Al-oxide I, is shown in Fig. 1B, and adsorption by Al-oxide I before and after preadsorption of the π-factor (by lead oxalate), in Fig. 1D. In both experiments the curves were parallel indicating that the factors adsorbed by Al-oxide I are different from π-factor and their activities independent of the concentration of the latter (*cf.* preceding papers [1,2]). Parallel curves were also obtained in the corresponding matching experiments with Al-oxide I and selective adsorbents for the ϱ-, ν-, μ-, γ-, β- and ε-factor activities [1,2]. The factors adsorbed by Al-oxide I were thus different from each of these seven factors and the activities of the

Table 1. Effect of adsorbents on the labile factor activity of strontium carbonate plasma.

Plasma no.	Adsorbent	mg/ml	Labile factor activity of adsorbed plasma in % of strontium carbonate plasma	Labile factor(s) adsorbed *
3592	Ba-metaborate	40	73	
		70	73	
615	Mg-borate	20	85	
		50	85	
3550	Mg-tungstate	30	90	a
		100	90	
5220	Mg-aluminate	30	89	
		50	89	
5220	Mg-silicate	30	89	
		50	89	
3551	Zn-tungstate	10	88	
		40	88	
4097	Zn-silicate	10	85	ϑ
		20	85	
5223	Zn-aluminate	1	88	
		10	88	
5622	Fe-sesquioxide	20	83	
		50	83	
5887	Mn-oxide (-ous, -ic)	20	86	ξ
		40	86	
5906	Al-oxide VI	50	82	
		100	82	
5611	Bi-sulfide	50	80	
		80	80	
5874	Hg-sulfide (ic)	10	91	ω
		40	91	
5623	Al-oxide Id_3	120	78	
		150	78	
4653	Al-oxide II	80	60	
		120	60	
5877	Al-oxide VIII	200	64	ς
		300	64	
3859	Al-oxide $IIIb_2$	80	78	
		180	78	
8703	Al-oxide $IIIb_6$	100	74	
		200	74	
3859	Al-oxide IVb_2	80	78	η
		180	78	
3861	Al-oxide IVb_6	100	72	
		250	72	
5568	Al-oxide Ib_1	100	81	
		250	81	
5570	Al-oxide Ib_2	100	79	$a + \vartheta$
		250	79	
3858	Al-oxide b_6	100	89	
		250	89	
5621	Al-oxide Id_6	150	68	
		300	68	
5573	Al-oxide Id_2	100	80	$\xi + \omega$
		150	80	
5875	Al-oxide VII	100	84	
		200	84	

* as determined by matching experiments (pp. 2031—2033.).

former independent of the concentrations of the latter. In contrast, adsorption of λ-factor (by Co-carbonate) before and after partial adsorption by Al-oxide I, gave converging curves (Fig. 1C). Adsorption by Al-oxide I before and after preadsorption of λ-factor (by Co-tungstate) gave the curves shown in Fig. 1E, of which sections one (0—*a*) are converging whereas the following sections (*a*—*b* and *b*—*c*) are parallel. The factors adsorbed by Al-oxide I are therefore also different from λ-factor, and their activities independent of the concentration of the latter, except for a factor completely adsorbed by Al-oxide I at *a*. This factor appears to act as a synergist for λ-factor, and *vice versa*.

Thus, the three (groups of) labile factors adsorbed more or less simultaneously by Al-oxide I, appeared to be different from the factors adsorbed by the selective adsorbents tested previously.

Adsorption by more selective adsorbents. For the purpose of separate adsorption of the factors adsorbed by Al-oxide I, a number of other adsorbents were tested. A summary of the results of a preliminary testing of these adsorbents is presented in Table 1. The selective properties of the adsorbents was demonstrated by the partial adsorption obtained.

More detailed studies revealed that with most adsorbents labile factor activity was adsorbed proportionally to the amounts of adsorbent added, up to a certain concentration of adsorbent beyond which no further adsorption of activity was obtained. As in previous studies with selective adsorbents [1,2,4], the labile factor activity of plasmas adsorbed once by adequate amounts of an adsorbent, could not be reduced further by renewed treatment with the same adsorbent. Adsorption curves obtained with five different adsorbents are shown in Figs. 2 (A—E). Similar curves were obtained with all the other adsor-

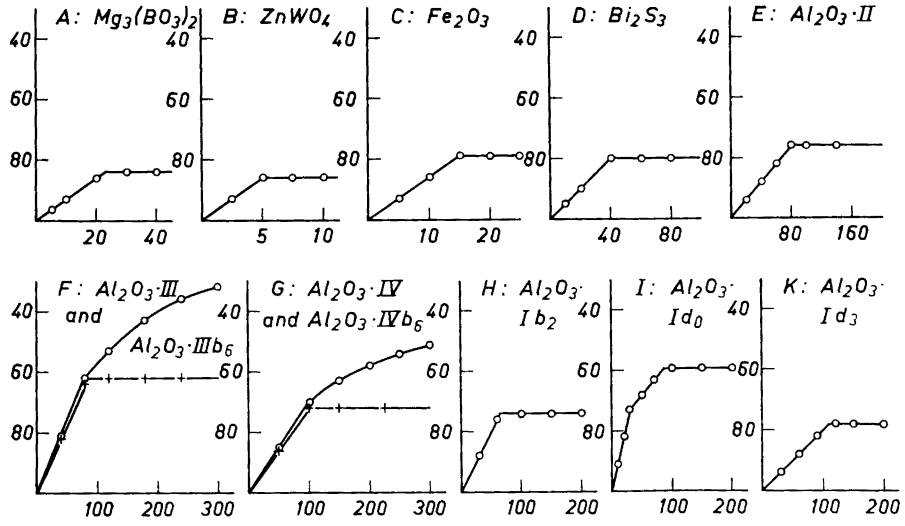

Fig. 2. Adsorption of labile factor activity by A: Mg-borate, B: Zn-tungstate, C: Fe-oxide, D: Bi-sulfide, E: Al-oxide II, F: Al-oxides III (O) and IIIb$_6$ (+), G: Al-oxide IV (O) and IVb$_6$ (+), H: Al-oxide Ib$_2$, I: Al-oxide Id$_0$, and K: Al-oxide Id$_3$.

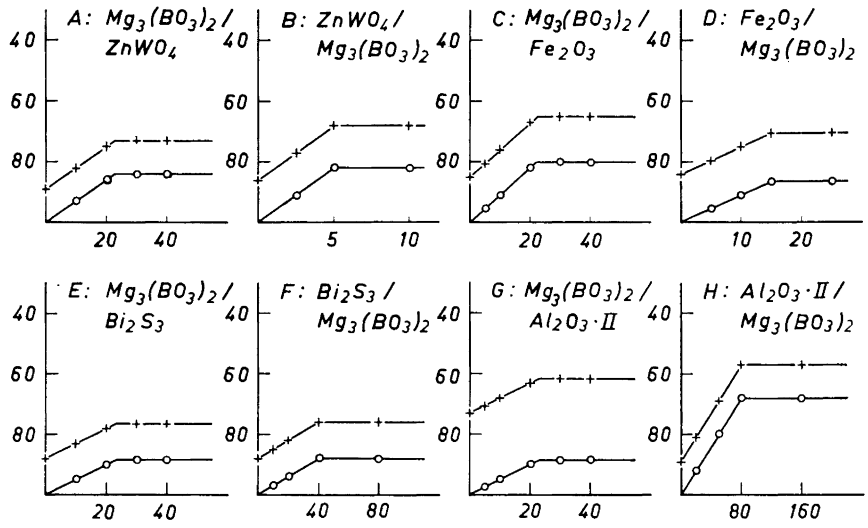

Fig. 3. Adsorption of labile factor activity from untreated (O) and preadsorbed (+) strontium carbonate plasmas.

A: Mg-borate adsorption, preadsorption by Zn-tungstate (20 mg/ml)
B: Zn-tungstate adsorption, preadsorption by Mg-borate (30 mg/ml)
C: Mg-borate adsorption, preadsorption by Fe-oxide (20 mg/ml)
D: Fe-oxide adsorption, preadsorption by Mg-borate (25 mg/ml)
E: Mg-borate adsorption, preadsorption by Bi-sulfide (30 mg/ml)
F: Bi-sulfide adsorption, preadsorption by Mg-borate (25 mg/ml)
G: Mg-borate adsorption, preadsorption by Al-oxide II (60 mg/ml)
H: Al-oxide II adsorption, preadsorption by Mg-borate (25 mg/ml)

bents tested, except the Al-oxides III and IV, and the d_0 and d_2 modifications of Al-oxide I. Hydrochloric acid treatment of the Al-oxides III and IV changed these preparations into selective adsorbents (Figs. 2F and 2G). Acid treatment of Al-oxide I also resulted in preparations with adsorption properties markedly different from the properties of the original material. Single-sectioned rectilinear adsorption curves were obtained with the b_1, b_2 (Fig. 2H), b_6 and d_3 (Fig. 2K) modifications of Al-oxide I, whereas the d_0 and d_2 modifications of this Al-oxide gave adsorption curves composed of two rectilinear sections as shown in Fig. 2I.

The adsorption properties of the adsorbents of Table 1 were compared in matching experiments. Representative experiments with eight adsorbents are shown in Figs. 3—6 (A—H). In agreement with our interpretations of similar previous experiments (p. 2028 and Refs.[1,2,4]) parallel curves (Figs. 3—5 (A—H) and 6 (A—D)) were interpreted as the results of matching experiments with compounds adsorbing different labile factors, the activities of which are mutually independent. Converging curves (Figs. 6E and 6F) were interpreted as the results of experiments with compounds adsorbing different labile factors, the specific activity of each of which is increased in the presence of the other (synergism). Two adsorbents giving the same maximal reduction of labile

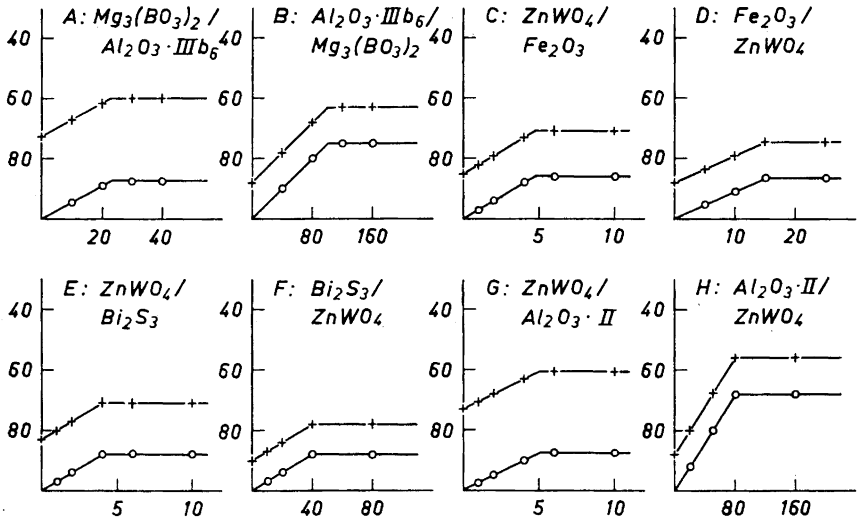

Fig. 4. Adsorption of labile factor activity from untreated (O) and preadsorbed (+) strontium carbonate plasmas.

A: Mg-borate adsorption, preadsorption by Al-oxide $IIIb_6$ (80 mg/ml).
B: Al-oxide $IIIb_6$ adsorption, preadsorption by Mg-borate (30 mg/ml).
C: Zn-tungstate adsorption, preadsorption by Fe-oxide (20 mg/ml).
D: Fe-oxide adsorption, preadsorption by Zn-tungstate (7.5 mg/ml).
E: Zn-tungstate adsorption, preadsorption by Bi-sulfide (30 mg/ml).
F: Bi-sulfide adsorption, preadsorption by Zn-tungstate (7.5 mg/ml).
G: Zn-tungstate adsorption, preadsorption by Al-oxide II (60 mg/ml).
H: Al-oxide II adsorption, preadsorption by Zn-tungstate (7.5 mg/ml).

factor activity, were considered to adsorb the same factor when readsorption by one of the adsorbents had no effect on the activity of plasma adsorbed by adequate amounts of the other (Figs. 6G and 6H).

It could thus be concluded that the labile factor adsorbed by Bi-sulfide was identical with the factor adsorbed by Al-oxide Id_3, and that the activity adsorbed by Ba-metaborate was due to a factor also adsorbable by Mg-borate. On the other hand, the labile factor activities adsorbed by Mg-borate (or Ba-metaborate), Zn-tungstate, Fe-oxide, Bi-sulfide (or Al-oxide Id_3), Al-oxide II and Al-oxide $IIIb_6$ were due to different labile factors. The activities of these factors proved to be mutually independent (parallel curves), the only exception being the factors adsorbed by the Al-oxides II and $IIIb_6$ which had synergistic effects (converging curves). For these factors we have adopted the following terms: α (alpha)-factor, selectively adsorbed by Mg-borate (or Ba-metaborate); ϑ(theta)-factor, selectively adsorbed by Zn-tungstate; ξ(xi)-factor, selectively adsorbed by Fe-oxide; ω(omega)-factor, selectively adsorbed by Bi-sulfide (or Al-oxide Id_3); ζ(zeta)-factor, selectively adsorbed by Al-oxide II and η(eta)-factor, selectively adsorbed by Al-oxide $IIIb_6$.

In similar experiments, the effect of the other adsorbents were compared to that of the adsorbents mentioned above. Figs. 7A and 7B show that the

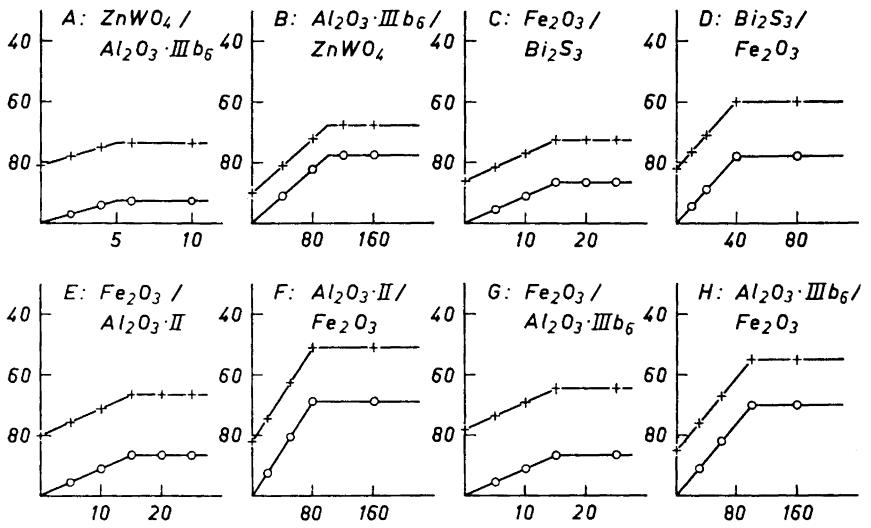

Fig. 5. Adsorption of labile factor activity from untreated (O) and preadsorbed (+) strontium carbonate plasmas.

A: Zn-tungstate adsorption, preadsorption by Al-oxide $IIIb_6$ (80 mg/ml).
B: Al-oxide $IIIb_6$ adsorption, preadsorption by Zn-tungstate (10 mg/ml).
C: Fe-oxide adsorption, preadsorption by Bi-sulfide (30 mg/ml).
D: Bi-sulfide adsorption, preadsorption by Fe-oxide (20 mg/ml).
E: Fe-oxide adsorption, preadsorption by Al-oxide II (60 mg/ml).
F: Al-oxide II adsorption, preadsorption by Fe-oxide (20 mg/ml).
G: Fe-oxide adsorption, preadsorption by Al-oxide $IIIb_6$ (80 mg/ml).
H: Al-oxide $IIIb_6$ adsorption, preadsorption by Fe-oxide (20 mg/ml).

factor completely adsorbed by Al-oxide Id_0 at *a*, was identical with ω-factor, whereas the factor completely adsorbed at *b* was identical with ξ-factor. The effect of Al-oxide Id_0 is thus explained as independent adsorption of the ω- and ξ-factors. Figs. 7C and 7D (simultaneous experiments with the same plasma) demonstrate that the activity adsorbed by Al-oxide Ib_2 was equal to the combined activities of the factors adsorbed by Mg-borate and Zn-tungstate, and that the same adsorbents had no effect on the labile factor activity of Al-oxide Ib_2 preadsorbed plasma. It was concluded that the effect of Al-oxide Ib_2 was due to adsorption of the α- and ϑ-factors. In similar experiments (Figs. 7E and 7F) it was shown that Al-oxide VII adsorbed the ω- and ξ-factors simultaneously. Al-oxide VIII adsorbed a factor acting as a synergist for η-factor (Fig. 7G). This factor proved to be ζ-factor (Fig. 7H). By the same technique the labile factors adsorbed by the remaining adsorbents of Table 1 were identified. The final results of the matching experiments are shown in the last column of this table.

As in previous experiments with selective adsorbents [1,2,4], the relative activity of an adsorbable factor varied in different experiments with the same adsorbents or with compounds shown to adsorb the same labile factor. Differences in the sensitivity of the substrate plasmas to adsorbable and non-adsor-

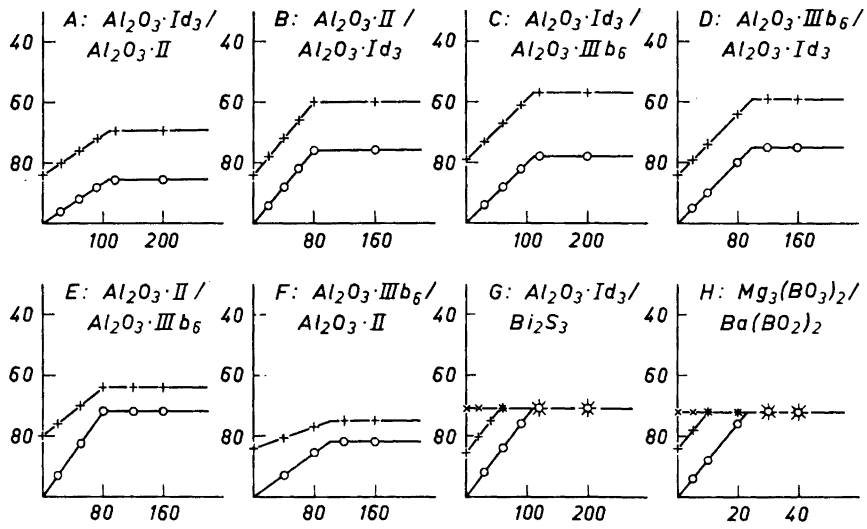

Fig. 6. Adsorption of labile factor activity from untreated (O) and preadsorbed (+ and ×) strontium carbonate plasmas.

A: Al-oxide Id_3 adsorption, preadsorption by Al-oxide II (60 mg/ml).
B: Al-oxide II adsorption, preadsorption by Al-oxide Id_3 (70 mg/ml).
C: Al-oxide Id_3 adsorption, preadsorption by Al-oxide $IIIb_6$ (70 mg/ml).
D: Al-oxide $IIIb_6$ adsorption, preadsorption by Al-oxide Id_3 (80 mg/ml).
E: Al-oxide II adsorption, preadsorption by Al-oxide $IIIb_6$ (50 mg/ml).
F: Al-oxide $IIIb_6$ adsorption, preadsorption by Al-oxide II (60 mg/ml).
G: Al-oxide Id_3 adsorption, preadsorptions by Bi-sulfide (20 mg/ml: +, and 50 mg/ml: ×).
H: Mg-borate adsorption, preadsorptions by Ba-metaborate (20 mg/ml: +, and 40 mg/ml: ×).

bed factors, and possible differences in the relative concentrations of these factors in the fresh plasmas employed, were regarded as the causes of such variations.

Identification of the factors adsorbed by Al-oxide I. Adsorption by the selective adsorbents described above was compared with adsorption by Al-oxide I for an identification of the factors adsorbed by the latter. Figs. 8A and 8B show that the α- and ϑ-factors were no longer present in plasmas preadsorbed by 55 mg/ml of Al-oxide I. The reverse experiments: adsorption by Al-oxide I of labile factor activity from untreated plasmas and plasmas preadsorbed by Mg-borate or Zn-tungstate, are seen in Figs. 8D and 8E. The amounts of Al-oxide I required for complete adsorption of the first of the three (groups of) factors, discernible by this adsorbent, were reduced after preadsorption by Mg-borate and Zn-tungstate (from a to a', a reduction of about 50 % in each case). The amounts of Al-oxide I required for complete adsorption of the two other (groups of) factors were not affected by these preadsorptions.

Figs. 8C, 9A and 9B demonstrate that preadsorption by Al-oxide I (50, 60 and 60 mg/ml, respectively) reduced the amounts of Fe-oxide, Bi-sulfide and Al-oxide $IIIb_6$ required for complete adsorption of the ξ-, ω-, and η-factors, respectively (by 33, 40 and 40 %, respectively). In the reverse experiments

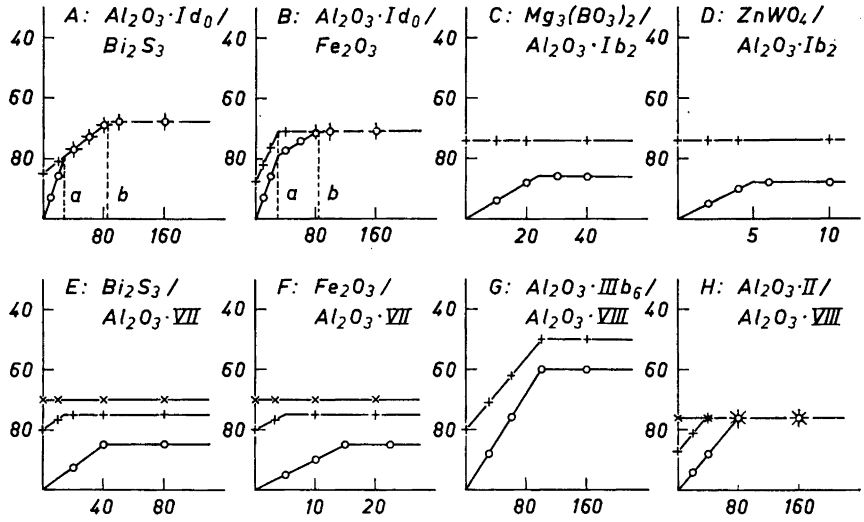

Fig. 7. Adsorption of labile factor activity from untreated (O) and preadsorbed (+ and ×) strontium carbonate plasmas.

A: Al-oxide Id_0 adsorption, preadsorption by Bi-sulfide (45 mg/ml).
B: Al-oxide Id_0 adsorption, preadsorption by Fe-oxide (18 mg/ml).
C: Mg-borate adsorption, preadsorption by Al-oxide Ib_2 (80 mg/ml).
D: Zn-tungstate adsorption, preadsorption by Al-oxide Ib_2 (80 mg/ml).
E: Bi-sulfide adsorption, preadsorptions by Al-oxide VII (50 mg/ml: +, and 100 mg/ml: ×).
F: Fe-oxide adsorption, preadsorptions by Al-oxide VII (50 mg/ml: +, and 100 mg/ml: ×).
G: Al-oxide $IIIb_6$ adsorption, preadsorption by Al-oxide VIII (80 mg/ml).
H: Al-oxide II adsorption, preadsorptions by Al-oxide VIII (80 mg/ml:, + and 160 mg/ml: ×).

(Figs. 8F, 9D and 9E), preadsorptions by the same three adsorbents reduced only the amounts of Al-oxide I required for complete adsorption of the second of the three adsorbable (groups of) factors (from *b* to *b'*, reductions of 29, 29 and 42 %, respectively).

Preadsorption by Al-oxide I (75 mg/ml) also reduced (by 25 %) the amounts of Al-oxide II required for complete adsorption of ζ-factor (Fig. 9C), and the factor completely adsorbed by Al-oxide I at the end of the third section (at *c*) of the curve for untreated plasma, was no longer present after preadsorption by Al-oxide II (Fig. 9F).

In confirmation of the above results, Fig. 10A shows that the factors completely adsorbed by Al-oxide I at the end of the first section (at *a*) of the curve for untreated plasma, were absent after preadsorption of the α- and ϑ-factors by Al-oxide Ib_6. Finally, preadsorption of the ξ-, ω-, and η-factors by a mixture of Al-oxide Id_0 and Al-oxide $IIIb_6$ removed the factors which were completely adsorbed by Al-oxide I at the end of the second section (at *b*) of the curve for untreated plasma (Fig. 10B).

It was therefore concluded that the effect of Al-oxide I on the labile factor activity of strontium carbonate plasma is fully explained and due to adsorp-

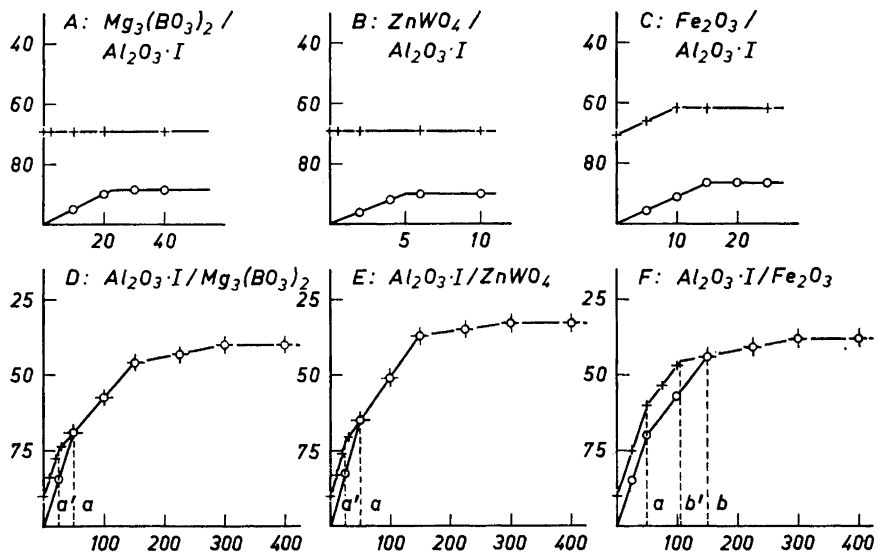

Fig. 8. Adsorption of labile factor activity from untreated (O) and preadsorbed (+) strontium carbonate plasmas.

A: Mg-borate adsorption, preadsorption by Al-oxide I (55 mg/ml).
B: Zn-tungstate adsorption, preadsorption by Al-oxide I (55 mg/ml).
C: Fe-oxide adsorption, preadsorption by Al-oxide I (50 mg/ml).
D: Al-oxide I adsorption, preadsorption by Mg-borate (30 mg/ml).
E: Al-oxide I adsorption, preadsorption by Zn-tungstate (7.5 mg/ml).
F: Al-oxide I adsorption, preadsorption by Fe-oxide (18 mg/ml).

tion of the six labile factors adsorbed separately by Mg-borate, Zn-tungstate, Fe-oxide, Bi-sulfide, Al-oxide $IIIb_6$ and Al-oxide II.

Additional matching experiments. The non-identity of the factors adsorbed by Al-oxide I and the factors adsorbed by the selective adsorbents used in the preceding papers was disclosed by the experiments cited on p. 2028 (Figs. 1 B—E). In confirmation of these results and for an identification of the factor acting as a synergist for λ-factor, the selective ϱ-, ν-, μ-, π-, γ-, β-, ε-, and λ-factor adsorbents were compared with the adsorbents for separate adsorption of the α-, ϑ-, ξ-, ω-, η-, and ζ-factors, in a series of additional matching experiments. Of the ninety-six different experiments carried out with adsorbent pairs from these two groups of adsorbents, only four are shown here because of space limitations. Parallel curves, similar to those shown in Figs. 10C and 10D, were obtained in ninety-four of these experiments. Selective adsorbents for the α-factor and for the λ-factor activities were the only adsorbent pairs giving converging curves (Figs. 10E and 10F). These experiments permitted identification of α-factor with the Al-oxide I adsorbable factor acting as a synergist for λ-factor.

The labile factor activities measured by RVV-cephalin and RVV. The effects of the adsorbents described in this paper were also studied in test systems

Table 2. Labile factors measured by RVV-cephalin or RVV.

Treatment of strontium carbonate plasma		Labile factor adsorbed	Labile factor activity in % of strontium carbonate plasma			
Adsorbent	mg/ml		Tpl.		RVV-ceph.	RVV
Untreated			100 [a]	100 [b]	100 [a]	100 [b]
Mg-borate	10	α	91.5	93	100	100
	20		83	86	—	—
	30		80.5	84	—	—
	40		80.5	84	100	100
Untreated			100 [a]	100 [b]	100 [a]	100 [b]
Zn-tungstate	2	ϑ	95	94	100	100
	4		90	88	—	—
	6		87.5	85	—	—
	10		87.5	85	100	100
Untreated			100 [c]		100 [c]	100 [c]
Fe-sesquioxide	5	ξ	94		95	96
	10		88		90	92
	15		82		85	88
	20		82		85	88
	30		82		85	88
Untreated			100 [d]		100 [d]	100 [d]
Bi-sulfide	10	ω	96		96.5	97
	20		92		93	94
	30		88		89.5	91
	40		84		86	88
	60		84		86	88
Untreated			100 [e]		100 [e]	100 [e]
Al-oxide II	20	ς	92		90	89.5
	40		84		80	79
	60		76		70	68.5
	80		68		60	58
	120		68		60	58
Untreated			100 [f]		100 [f]	100 [f]
Al-oxide $IIIb_6$	25	η	89		88.5	87.5
	50		78		77	75
	75		67		65.5	62.5
	100		56		54	50
	140		56		54	50

[a]: plasma No. 5050, [b]: plasma No. 3591, [c]: plasma No. 3862
[d]: plasma No. 3860, [e]: plasma No. 3856, [f]: plasma No. 3857

where thromboplastin was replaced by RVV, with or without added cephalin [1,2,4].

Representative experiments are summarized in Table 2. Adsorption of α-factor (by Mg-borate) or ϑ-factor (by Zn-tungstate) had no effect on the labile factor activities measured by RVV-cephalin or RVV alone. In contrast, adsorption of ξ-factor (by Fe-oxide), of ω-factor (by Bi-sulfide), of η-factor (by

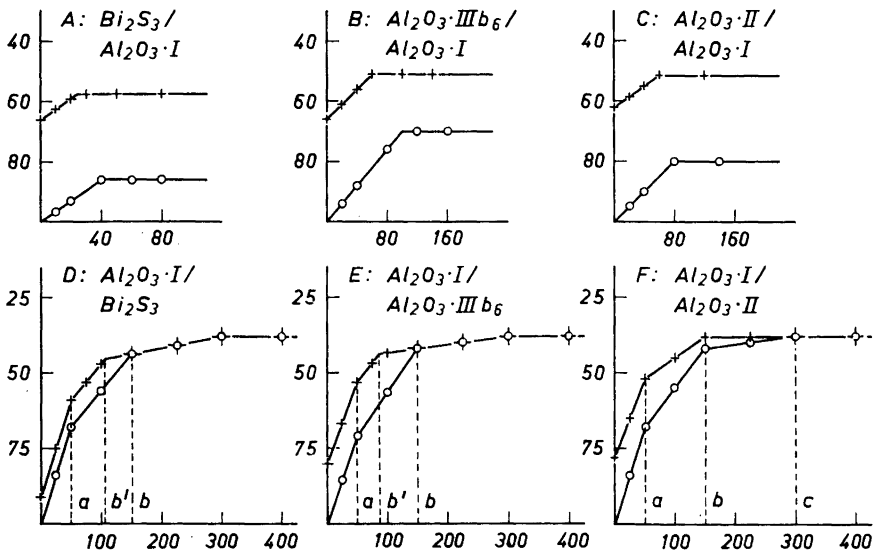

Fig. 9. Adsorption of labile factor activity from untreated (O) and preadsorbed (+) strontium carbonate plasmas.

A: Bi-sulfide adsorption, preadsorption by Al-oxide I (60 mg/ml).
B: Al-oxide $IIIb_6$ adsorption, preadsorption by Al-oxide I (60 mg/ml).
C: Al-oxide II adsorption, preadsorption by Al-oxide I (75 mg/ml).
D: Al-oxide I adsorption, preadsorption by Bi-sulfide (45 mg/ml).
E: Al-oxide I adsorption, preadsorption by Al-oxide $IIIb_6$ (100 mg/ml).
F: Al-oxide I adsorption, preadsorption by Al-oxide II (90 mg/ml).

Al-oxide $IIIb_6$), and of ζ-factor (by Al-oxide II) reduced the labile factor activity measured by all three coagulation accelerators, maximal reduction of activity being obtained at the same concentration of adsorbent. The ξ-, ω-, η-, and ζ-factors are therefore regarded as common components of the labile factor activities measured in the three different assay systems, whereas the α- and ϑ-factors must be thromboplastin specific labile coagulation factors.

DISCUSSION

The purpose of the experiments reported here was to find adsorbents which would permit characterization, by selective adsorption, of labile coagulation factors not adsorbed by the selective adsorbents tested previously [1,2]. The adsorption studies presented in the first part of this work indicated that this could be attained by use of Al-oxide I. However, Al-oxide I was not ideally suited for the purpose. The three-sectioned adsorption curve obtained with this adsorbent, pointed to the presence of three different "types" of adsorption sites in Al-oxide I, each causing selective adsorption of one or a few labile factors. A more satisfactory solution was reached only after tedious studies with other adsorbents which finally led to the recognition of no less than six different categories of selective adsorbents, each adsorbing only part of the Al-oxide I adsorbable activity. By means of these selective adsorbents

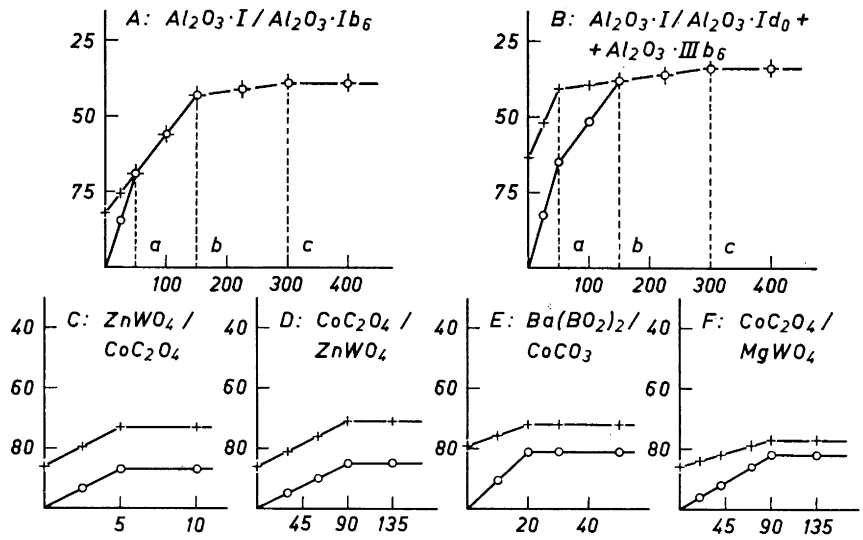

Fig. 10. Adsorption of labile factor activity from untreated (O) and preadsorbed (+) strontium carbonate plasmas.

A: Al-oxide I adsorption, preadsorption by Al-oxide Ib_6 (90 mg/ml).
B: Al-oxide I adsorption, preadsorption by Al-oxide Id_0 (95 mg/ml) and Al-oxide $IIIb_6$ (105 mg/ml).
C: Zn-tungstate adsorption, preadsorption by Co-oxalate (100 mg/ml).
D: Co-oxalate adsorption preadsorption by Zn-tungstate (10 mg/ml).
E: Ba-metaborate adsorption, preadsorption by Co-carbonate (100 mg/ml).
F: Co-oxalate adsorption, preadsorption by Mg-tungstate (30 mg/ml).

recognition and characterization of six different Al-oxide I adsorbable labile factors was achieved. The three-sectioned adsorption curve obtained with Al-oxide I, could then be explained as the results of: (1) competitive adsorption of the α- and ϑ-factors by one of the three different "types" of adsorption sites on Al-oxide I, (2) competitive adsorption of the ξ-, ω-, and η-factors by a second "type", and (3) selective adsorption of ζ-factor by a third "type" of adsorption sites. Moreover, the six categories of selective adsorbents permitted studies on the interrelationships between each of these six labile factors and the factors adsorbed by representatives of the eight categories of selective adsorbents described previously [1,2]. The conclusions reached by corresponding matching experiments with Al-oxide I, concerning the non-identity and activity interrelationships of the two groups of factors were confirmed. Furthermore, the final series of matching experiments permitted identification of α-factor with the Al-oxide I adsorbable synergist for λ-factor.

The observed differences in the adsorption properties of different brands of alumina may possibly be due to differences in the surface structure of Al-oxide particles prepared by different procedures. The effects of acid treatment on the adsorption properties of the Al-oxides I, III and IV are less readily deciphered. Thus, nitric acid treatment (d_0 and d_2) of Al-oxide I led to preparations which gave *independent adsorption* of the ξ-, and ω-factors,

but *no adsorption* of the α-, ϑ-, η-, and ζ-factors, while *only the* α-, *and* ϑ-*factor adsorption capacity* was retained after similar treatment of Al-oxide I with hydrochloric acid. On the other hand, η-*factor was the only factor* adsorbed by the hydrochloric acid treated Al-oxides $IIIb_{2(6)}$ and $IVb_{2(6)}$. No explanation of these phenomena can be suggested by the authors at present.

However, the selective adsorbents described in this paper offered an opportunity for differentiation and characterization of the individual factors which are adsorbed by Al-oxide I. This differentiation, as well as the differentiation of these six factors from the eight factors described previously [1,2], is thus based on differences in the physico-chemical properties of the factors. However, important differences in the functional properties of the factors, so defined, were also apparent. The specific activities of the ξ-, ω-, η-, ζ-, and ϑ-factors were independent of the concentrations of each of the eight factors studied previously [1,2]. In this respect, all members of the former group of factors differed functionally from the members of the latter (*cf.* preceding paper [1]). α-Factor differed functionally from each member of both of these two groups of factors by acting as a synergist for λ-factor, but not for any of the other factors. As for the remaining five factors, ξ-factor, ω-factor and ϑ-factor differed from η-factor and from ζ-factor by being independent of the concentrations of ζ-factor and η-factor, respectively. The synergistic relationship between η-factor and ζ-factor reflects the unique functional properties of each of these two factors.

Finally, differences between ϑ-factor and the ξ- and ω-factors were revealed by substituting RVV-cephalin for thromboplastin. Only ξ-factor and ω-factor were active in the RVV-cephalin assay system. These factors are accordingly the only strontium carbonate non-adsorbable labile coagulation factors for which no differences in function have been detected so far.

Methods for quantitative estimation of the α-, ϑ-, ξ-, ω-, η-, and ζ-factor concentrations in fresh plasma are suggested by the observed proportionality between adsorbed activity and concentration of the selective adsorbent employed. The minimum concentration of a selective adsorbent required for maximal adsorption of activity may be proportional to the concentration of the adsorbable factor and represent an absolute value for the plasma concentration of this factor. As with similar methods, suggested for quantitative estimation of the labile factors described previously [1,2,4], the values obtained will be independent of the plasma concentrations of non-adsorbed factors. However, due attention should be paid to the possibility that variations in the concentrations of inert plasma factors, adsorbed in competition with the adsorbable labile factor, may be the cause of possible variations in the results obtained by this procedure. These problems will receive further attention in future publications.

REFERENCES

1. Sørbye, Ø. and Kruse, I. *Acta Chem. Scand.* **16** (1962) 1468.
2. Sørbye, Ø. and Kruse, I. *Acta Chem. Scand.* **16** (1962) 1662.
3. Sørbye, Ø., Kruse, I. and Dam, H. *Acta Chem. Scand.* **5** (1951) 487.
4. Sørbye, Ø. and Kruse, I. *Acta Chem. Scand.* **16** (1962) 1221.
5. Sørbye, Ø. and Kruse, I. *Acta Chem. Scand.* **14** (1960) 2177.
6. Sørbye, Ø. *Acta Chem. Scand.* **16** (1962) 903.

Received May 9, 1962.

ACTA CHEMICA SCANDINAVICA 16 (1962) 2041–2049

Physical-Chemical Properties of N-Substituted Thioureas *

ANDERS KJÆR

Department of Organic Chemistry, Royal Veterinary and Agricultural College, Copenhagen, Denmark

RUDOLF ZAHRADNÍK**

Institute of Industrial Hygiene and Occupational Medicine, Prague, Czechoslovakia

KAREL DUŠEK and JIŘÍ KLABAN

Research Institute for Synthetic Resins and Lacquers, Pardubice, Czechoslovakia

The ultraviolet and infrared spectra, as well as the basicity and polarographic properties of fifty-three N-substituted thioureas are studied. Monosubstituted N-alkyl and N-alkenyl derivatives exhibit an intense absorption band (log $\varepsilon \sim 4$) at 237 $\pm$ 1 mμ (2 % ethanol in water). The pK_a-values fall within the range -1.17 ± 0.15, and the half-wave potentials of the anodic waves are found to be -0.30 ± 0.02 V (*vs.* NCE; 0.08 M NaOH). Infrared spectra are determined in the wave-length region 400–1700 cm^{-1} in KBr-discs and, in addition, in chloroform solution and liquid paraffin in the range 1480–1700 cm^{-1}. Special attention is given to bands in the regions 1490–1550 and 1600–1610 cm^{-1} (in $CHCl_3$), and 1445–1475 and 1500–1650 cm^{-1} (in KBr).

The object of the present investigation was to study the influence of various substituents attached to the nitrogen atom of thiourea on the position of the intense ultraviolet absorption maximum around 237 mμ, as well as on basicity, polarographic halfwave potentials, deformation vibrations of the NH_2-grouping, and infrared absorption bands in the ranges 1445–1475 and 1490–1550 cm^{-1}.

* Part VIII of the series: Reaction Kinetics and Properties of Compounds Belonging to Non-aromatic Homologous Series. Part VII: *Arch. intern. pharmacodynamie* 135 (1962) 330.

** Present address: Institute of Physical Chemistry, Czechoslovak Academy of Science, Máchova 7, Praha 2.

Table 1. Relative values of absorption maxima ($\Delta\lambda$) in the ultra-violet region, basicities (ΔpK) and polarographic half-wave potentials ($\Delta E_{1/2}$) (for the definition, *cf.* p. 2045) and wave numbers of infra-red bands of substituted thioureas.

No.	Thiourea	$\Delta\lambda$	ΔpK	$\Delta E_{1/2}$	IR-data, bands in the region (cm^{-1})			
					1445—1475 in KBr	1488—1554 in $CHCl_3$	1598—1608 in $CHCl_3$	1500—1650 in KBr
1	Non-subst.	—1	—0.17 ± 0.03	0.02	1469	—	1607	1590; 1616
2	Methyl	—1	—0.10 ± 0.03	0.00	1458	1531	1606	1558; 1632
3	Ethyl	0[a]	0.00[b]	0.00[c]	1449 1472	1524	1607	1546; 1565 1624; 1638
4	Isopropyl	1.5	0.12 ± 0.03	0.00	1449 1461	1516	1607	1566; 1624
5	*tert.*Butyl	4	0.34 ± 0.03	—0.02	1445 1461	—	1605	1566; 1623
6	Propyl	0.5	0.01 ± 0.03	—0.01	1464	1523	1606	1574; 1622
7	Isobutyl	1	0.02 ± 0.03	—0.01	1464 1468(sh.)	1524	1606	1562; 1597 1630
8	*sec.*Butyl	1.5	—	—0.02	1463	1516	1606	1564; 1619
9	Butyl	1	0.03 ± 0.03	0.00	1464	1522	1607	1565; 1622
10	Isoamyl	1	0.03 ± 0.03	—0.01	1457 1474	1523	1606	1557; 1626
11	Amyl	1	0.01 ± 0.03	0.00	1464	1526	1607	1563; 1598 1630
12	Hexyl	1	0.03 ± 0.03	0.00	1453 1466	1525	1607	1568; 1622
13	Cyclohexyl	2	0.10 ± 0.03	—0.03	1458 1465	1516	1606	1564; 1623
14	Allyl	2	—0.35 ± 0.03	—0.01	1463[f]	1521	1608	1541; 1630 1645(sh.)
15	α-Methallyl	2	—0.14 ± 0.02	0.00	1465	1505	1606	1564; 1616 1646(w.)
16	β-Methallyl	1.5	—0.30 ± 0.02	—0.01	1451	1518	1608	1537; 1555 1627
17	*trans*-Crotyl	1.5	—0.25 ± 0.04	0.00	1448 1468	1519	1607	1505; 1549 1631; 1641
18	3-Butenyl	1.5	—0.13 ± 0.02 —0.20 ± 0.02	—0.01	1447 1462	1519	1606	1557; 1620 1635
19	Benzyl	3	—0.44 ± 0.03	—0.03	1455	1518	1607	1554; 1630
20	β-Phenylethyl	2	—0.14 ± 0.03	—0.03	1456	1522	1606	1560; 1616(sh.) 1624

Table 1 continued.

No.	Thiourea	$\Delta\lambda$	ΔpK	$\Delta E_{1/2}$	IR-data, bands in the region (cm^{-1})			
					1445—1475 in KBr	1488—1554 in $CHCl_3$	1598—1608 in $CHCl_3$	1500—1650 in KBr
21	γ-Phenylpropyl	1	—0.13 ± 0.03	—0.03	1446 1453 1466	1523	1606	1523; 1564 1625
22	3-Methylthiopropyl	1.5	—0.20 ± 0.03	—0.04	1456(sh.)[g] 1474(vw)	1525	1607	1566; 1617
23	4-Methylthiobutyl	1	—0.03 ± 0.02[c]	—0.04	1454 1462(sh.) 1471	1521	1605	1544; 1576 1616; 1628
24	5-Methylthiopentyl	1	0.08 ± 0.04[c]	—0.05	1447 1460	1530 1550	1606	1566; 1616
25	6-Methylthiohexyl	1	0.09 ± 0.04[c]	—0.03	1470	1520	1606	1564; 1622
26	7-Methylthioheptyl	0.5	—0.09 ± 0.02[c]	—0.04	1465	1519	1607	1567; 1618
27	8-Methylthiooctyl	0.5	0.01 ± 0.02[c]	—0.05	1457 1471	1523	1606	1569; 1618
28	3-Methylsulphonyl-propyl	1.5	—0.47 ± 0.03	—0.02	1449 1462	1525	1605	1539; 1641
29	4-Methylsulphonyl-butyl	1	—0.17 ± 0.02	—0.01	1449 1459	—	1606	1550; 1595(w) 1640
30	(—)-N-5-Methylsul-phinylpentyl	1	—0.03 ± 0.03[c]	—0.03	1471	1524	1606	1551; 1640
31	(—)-N-10-Methyl-sulphinyldecyl	1	0.12 ± 0.05	—0.04	1471	1522	1606	1572; 1623
32	Acetyl	31	~—2.0	0.04				
33	1,1-Dimethyl	0	—0.04 ± 0.02	0.05	1458 1464	1534	1600	1541; 1619
34	1,1-Cyclopenta-methylen	4	—0.02 ± 0.05	0.01	1445 1469	1511	1600	1513; 1632
35	1,3-Dimethyl	—3	—0.32 ± 0.04	0.08	1447(?)	1506 1552	—	1566
36	1-Butyl-3-methyl	—2	—0.41 ± 0.07[c]	0.03	1471	1503 1554	—	1560
37	1,3-di-Butyl	—1	—0.40 ± 0.08[c]	0.01	1456 1473	1497 1539 1548	—	1523; 1557 1568

No.	Thiourea	$\Delta\lambda$	ΔpK	$\Delta E_{1/2}$	IR-data, bands in the region (cm^{-1})			
					1445—1475 in KBr	1488—1554 in $CHCl_3$	1598—1608 in $CHCl_3$	1500—1650 in KBr
38	1-Butyl-3-phenyl	11		—0.18	1452 1465			1523; 1543 1551; 1597
39	Diacetyl	37	<—3.0	0.02				
40	1,1,3-Trimethyl	—6	—	—	1447 1470	1538 1549	—	1543
41	1-Methyl-3,3-cyclo-tetramethylen	<—16	—	—	1447(sh.) 1457 1468	1532(sh.) 1544	—	1531; 1553
42	1-Methyl-3,3-cyclo-pentamethylen	<—16 1	—	—	h	1536	—	1549
43	1,1,3,3-Tetramethyl	9	—	—	1464(sh.) 1471	1512	—	1514
44	Phenyl	16	—1.2[d]	—0.15	1448 1463	1501 1526	1602	1519; 1533 1550(sh.); 1592 1614
45	1-(*o*-Tolyl)	7	—0.83 ± 0.05[d]	—0.16	1456 1471	1495	1599	1579(w.); 1622
46	1-(*m*-Tolyl)	12	—0.76 ± 0.17[d]	—0.15	1466	1494 1506(sh.)	1599	1516, 1539 1611, 1619
47	1-(*p*-Tolyl)	11	—1.01 ± 0.09[d]	—0.16	1449 1467	1488 1521	1598	1506, 1538 1586, 1616
48	1-(*p*-Bromophenyl)	21	—1.17 ± 0.12[d]	—0.16	1455	1499	1602	1508, 1577 1621
49	1-(*p*-Iodophenyl)	22	—1.47 ± 0.12[d]	—0.19	1467	1490	1606	1528, 1576 1621
50	*o*-Methoxybenzyl	2	—0.46 ± 0.04	—0.05	1451(sh.) 1465	1497 1522	1607	1557, 1591 1605, 1624, 1635
51	*m*-Methoxybenzyl	2	—0.46 ± 0.04	—0.05	1454(sh.) 1465	1494 1518	1607	1516, 1600 1606, 1633
52	*p*-Methoxybenzyl	2	—0.52 ± 0.06	—0.05	1460	1517	1608	1514, 1529 1591, 1616(sh.) 1629
53	1,3-bis-(Methoxy-methyl)			0.00				

[a] $\lambda_{max,Et}$ = 236 mμ (2 % ethanol in water); [b] pK_{Et} − 1.10; [c] With increasing value of $-H_0$ the pK value increases somewhat; the last place may be neglected; [d] Similar process as in *c* takes place. In these compounds the effect is probably caused by the nature of the aromatic substituent; [e] $E_{1/2}$ (ethyl) is —0.27_7 V (NCE, 0.08 N NaOH); [f] Very weak band; the nearest intense band at 1437 cm^{-1}; [g] The nearest intense band at 1444 cm^{-1}; [h] The nearest intense bands at 1436 and 1493 cm^{-1}.

Apart from infrared spectra, the same properties were formerly studied on fourteen analogous substances [1]. In order to obtain more detailed information regarding the influence of the structure of substituent on properties, some phenylthioureas were included in the present investigation, supplementary to an additional series of aliphatic substitutes. A broader knowledge of the physical-chemical properties of N-substituted thioureas was desirable also in connexion with current studies of naturally derived isothiocyanates (*cf.e.g.* Refs. [2,3]).

EXPERIMENTAL

Reagents and apparatus. Most of the substituted thioureas (Table 1) were synthesized in connexion with current investigations of isothiocyanates of natural derivation [2,3] (for substance 53, *cf.* Ref.[4], and for the substances 32 and 39, *cf.* Ref.[1]). The employed reagents were those specified in a previous communication [1].

In the range below 220 mμ, absorption curves were recorded in a nitrogen atmosphere on a CF4 spectrometer (Optica Milano, Italy). Other measurements were performed under the conditions and with the equipment specified in the previous paper [1].

Polarographic measurements were carried out on an LP55 polarograph (Laboratorní potřeby, Prague) with a galvanometer sensitivity of 2.46×10^{-9} A/mm. The capillary employed had a length of 11 cm; with no potential applied and a mercury head of 50 cm, the drop time was 2.86 sec. and the drop mass was 3.29 mg/sec.

Infrared spectra were recorded on a double beam UR-10 spectrometer (Zeiss, Jena). A KBr prism was employed in the range 400 – 700 cm^{-1}, whereas the region 700 – 1700 cm^{-1} was covered by a NaCl prism. The apparatus was calibrated with NH_3, CO_2 and polystyrene foil.

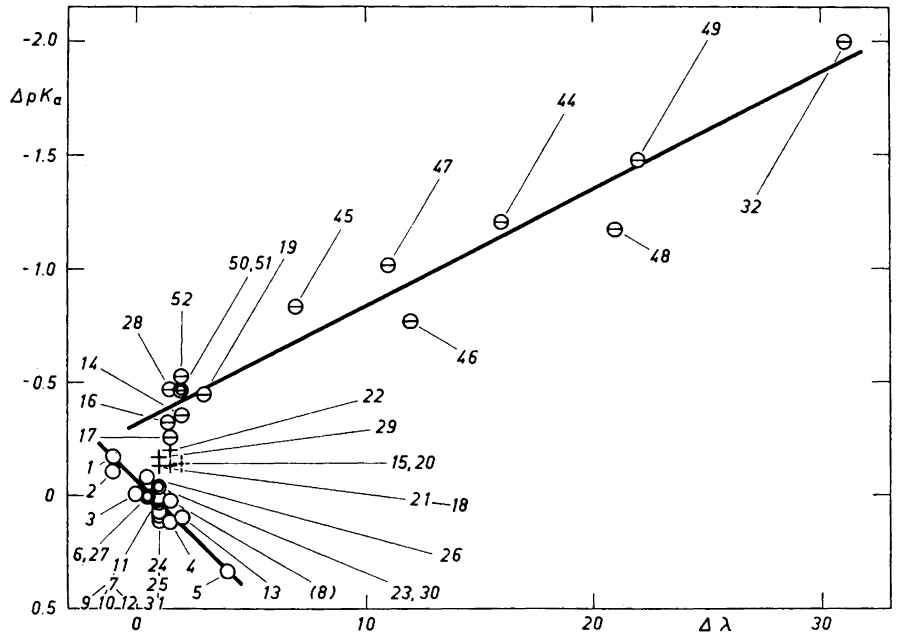

Fig. 1. ΔpK_a values plotted against $\Delta\lambda$ for N-monosubstituted thioureas: alkyls and substituted alkyls (○), transient substituents (+), alkenyls and aryls (⊖).

Methods. The absorption curves in the UV-region, the basicities and the half-wave potentials were measured as earlier described.[1]

Infrared spectra of the thioureas were recorded in KBr-discs, in suspensions of paraffin oil (Nujol), and in chloroform solution. The pellets were prepared at 10 t/cm² (for 6 min) from homogeneous mixtures of 2.3—3.5 mg of substance in 1.00 g of KBr. Due to the limited solubility of thioureas in chloroform, saturated solutions were utilized in most cases in cells of 0.25 mm path length.

RESULTS AND DISCUSSION

The results obtained are summarized in Table 1. The dependence of relative pK-values * on the relative position of the absorption maximum is shown in Fig. 1, from which it appears that the data corresponding to monosubstituted thioureas fall into two distinct and one transient group. The first of these, comprising 23 substances, include alkyl and substituted alkyl groups with low inductive effects. This category of compounds is represented by the following equation for the straight regression line (correlation coefficient, $r = 0.95$):

$$\Delta pK_I = 0.1002\ \Delta\lambda_I - 0.0637$$

The second group, comprising 15 compounds, fits the straight line expression:

$$\Delta pK_{II} = -0.0508\ \Delta\lambda_{II} - 0.3136\ (r = 0.97)$$

The latter includes substituents displaying conjugation (*e.g.* phenyl) or hyperconjugation effects (*e.g.* allyl), whereas the transient group embraces such substituents as: 3-butenyl (18), α-methallyl (15), β-phenylethyl (20), γ-phenylpropyl (21), 3-methylthiopropyl (22), and 4-methylsulphonylbutyl (29). The substances (15), (18), (20), and (21) contain a double bond or aromatic ring. Analogously, non-bonded interaction between the π-molecular orbitals of the functional group

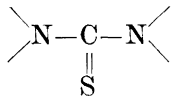

and a free-electron pair of the hetero atom of the substituent can be visualized in the compounds (22) and (29).

Table 2. Absorption maxima of thiourea in the UV-region.

Medium	mμ	kcm^{-1}	log ε	Design.
Water	194[a]	51.5	4.24	*1*
Water	235[b]	42.5	4.05	*2*
Ethyl alcohol	278 (sh)	36.0	~2	*3*

[a]Ref.[8]: 195 mμ (4.11). [b]Ref.[5]: 235 mμ (4.05).

* The relative value X is given by the relation $\Delta X = X_i - X_{Et}$, where X_i indicates the position of the maximum of UV-absorption λ, the pK_a-value, or the half-wave potential $E_{1/2}$; X_{Et} is the corresponding value for N-ethylthiourea.

In the range 190—380 mμ, the spectrum of thiourea is characterized by two absorption maxima and one shoulder (Table 2). As apparent from the intensity, the shoulder *3* (278 mμ) corresponds to a forbidden transition, whereas the two maxima can be attributed to allowed transitions. Since the shoulder is bathochromically displaced when ethyl alcohol is replaced by water, apparent from its mergence with the intense maximum *2*, this maximum may represent the $n \rightarrow \pi^*$ transition. Maximum *2* presumably corresponds to the $N \rightarrow V_1$ transition although it is slightly dislocated to shorter wave lengths when ethyl alcohol is replaced by water *. This interpretation of the origin of the maximum *2* and the shoulder *3* agree with the results of Janssen [5,6], based on calculations which suggest that the energy of the nearly *non*-bonding level is only slightly higher than that of the highest π-molecular orbital.

Further analyses were abandoned since electronic spectra of thiourea have recently been dealt with elsewhere [6,8] (*cf.* Ref. [5]). The work by Janssen [6] on a series of thione compounds indicates a need for theoretically better founded computations of the electronic spectra of thiourea. In fact, such calculations were recently presented by Hosoya *et al* [8]. who assigned the band at 195 mμ, unidentified in our work, to the internal charge-transfer process.

The ΔpK values (Table 1) fit the Taft equation with a ϱ^*-value of −1.3**.

The shifts in half-wave potentials are less marked than those of the UV-absorption maxima. It is evident, however, that negative values of $\Delta E_{1/2}$ in most cases correspond to positive values of $\Delta\lambda$. This means that easier formation of a salt with mercury, *i.e.* a shift to negative potential (at anodic waves), parallels a bathochromic shift of the absorption maximum. The relatively strong hypsochromic shift of the absorption maximum of trisubstituted thioureas is reflected by the disappearance of their polarographic waves. Expected shifts to positive values of half-wave potentials correspond to smaller hypsochromic shifts of three of the 1,3-disubstitutes. The position of the absorption maximum of substance (38) is obviously influenced by the combined hypsochromic effect of the 1,3-substitution and the bathochromic action of the phenyl group. The shift of the half-wave potential by 0.01—0.02 V to negative values corresponds to a bathochromic shift of 1—2 mμ for N-alkylthioureas. In the series of ω-methylthioalkyl derivatives, an even larger change of the half-wave potential (0.03—0.05 V) gives rise to a shift of only about 1 mμ. The extensive conjugation in N-arylthioureas is reflected by a notable shift (7—22 mμ) in the spectrum and also in the polarographic behaviour (0.15—0.19 V).

The position of infrared absorption bands, observed in chloroform solution in the ranges 1488—1554 and 1500—1650 cm^{-1}, and in KBr-discs in the regions 1445—1475 and 1500—1650 cm^{-1}, are presented in Table 1***.

---

* In the case of α-thiothiapyrone, a hypsochromic shift of three absorption maxima (log $\varepsilon \lesssim 4$) was previously observed on passing from less to more polar solvents [7]. At least two of these maxima correspond to N → V transitions.

** In our previous paper [1], Fig. 3 is incorrect. In fact, the experimental data should be expressed by a single, straight line. The splitting of data into two groups only applies to the ultraviolet data.

*** Infrared spectra will be sent on request.

The intense band in the region 1598—1608 cm^{-1} ($CHCl_3$) can safely be assigned to the deformation vibration of the $-NH_2$ grouping [9-11]. In this region, compounds 19—21, 38, 44—52 as expected give rise to the relatively less intense phenyl C=C in plane skeletal vibrations, evidently overlapped, however, by the more intense band from the $-NH_2$ grouping. The shift of this band by approximately 20 cm^{-1} towards higher wave numbers in going from solution to the solid phase is in agreement with reported data[11]. The correctness of the present assignment is supported by the absence of this band in the case of 1,3- and higher substituted thioureas. For substance 38, an intense band was observed in this region, probably attributable to the phenyl C=C in plane skeletal vibration. In chloroform solution, the frequency of this vibration is nearly constant for monosubstituted, non-aromatic derivatives, *viz.* 1606 $\pm$ 2 cm^{-1}. Correspondingly, the band appears at 1600 $\pm$ 2 cm^{-1} for aromatic derivatives (with exception of (49)). In the solid state, however, the band position is more variable ($\pm$ 10 cm^{-1}), probably due to special forces operating in the solid. In agreement herewith, the symmetric and asymmetric stretching modes of the $-NH_2$-grouping of thiourea (1), phenylthiourea (44) and 1,3-diphenylthiourea were found to be constant [10].

Assignment of the band in the range 1488—1554 cm^{-1} is more difficult. Supposedly, it represents the amide-II band, attributable to the stretching mode of the C=N linkage contributing to the total structure [11]. This idea is supported by the work of Mann [12] and Chatt *et al.* [13] who assigned a band in the 1480—1542 cm^{-1}-range in dithiocarbamates to the stretching mode of the C=N bond. It is remarkable that monosubstituted, aliphatic thioureas, with exception of (24), display only one band whereas most other compounds exhibit two bands within this range. On passing from solution to the solid state, the band is shifted about 38 cm^{-1} towards higher frequencies.

Chibisov and Pentin [10] recently reported that thiourea, 1-phenyl-, 1,3-diphenyl and 1,1-diphenylthiourea exhibit bands at 1473, 1468, 1460 and 1485 cm^{-1}, attributed to the thiourea grouping of the above-mentioned compounds. When analyzing our spectra we found that bands in fact occur in this region but we were unable to decide which type of vibration is involved. Moreover, this range is of limited analytical interest because several other bands may appear, belonging to deformation, scissoring vibrations of the CH_2 group, antisymmetric deformation vibrations of the CH_3 group and, finally, even stretching skeletal vibrations of the phenyl group. Furthermore, the deformation vibrations of CH_2 and CH_3 groups attached to nitrogen appear at approximately 1470 cm^{-1}.

From a comparison of the spectra measured in Nujol and in KBr it appears that frequencies of the main bands are constant within the experimental error ($\pm$ 2 cm^{-1}). Larger deviations were noticed for the substances (1), (36), and (43), in the first case probably due to complex formation with KBr [9].

The authors wish to thank Dr. M. Horák for valuable discussions and suggestions concerning the infrared spectra and Ing. J. Jonáš for carrying out the ultraviolet measurements below 220 mμ.

Added in proof: Janssen (private communication) has found the pK_a-values -1.19, -1.12, -1.08, and -1.32 for the compounds nos. 1, 2, 33, and 35, respectively.

REFERENCES

1. Zahradník, R. *Collection Czechoslov. Chem. Communs.* **24** (1959) 3678.
2. Kjær, A. *Fortschr. Chem. org. Naturstoffe* **18** (1960) 122.
3. Kjær, A. In N. Kharasch (Edit.) *Organic Sulphur Compounds*, Pergamon Press, Oxford-London-New York-Paris 1961, Vol. I, p. 409.
4. Dušek, K. *Collection Czechoslov. Chem. Communs.* **22** (1957) 732.
5. Janssen, M. J. *The Electronic Structure of Organic Thione Compounds*, Dissertation, Utrecht 1959.
6. Janssen, M. J. *Rec. trav. chim.* **79** (1960) 1066.
7. Zahradník, R., Párkányi, C. and Koutecký, J. *Collection Czechoslov. Chem. Communs.* **27** (1962) 1242.
8. Hosoya, H., Tanaka, J. and Nagakura, S. *Bull. Chem. Soc. Japan* **33** (1960) 850.
9. Stewart, J. E. *J. Chem. Phys.* **26** (1957) 248.
10. Chibisov, A. K. and Pentin, Yu. A. *Zhur. Obshcheĭ Khim.* **31** (1961) 11.
11. Bellamy, L. J. *The Infra-red Spectra of Complex Molecules*, Methuen, London; Wiley, New York 1959.
12. Mann, J. *Trans. Inst. Rubber Ind.* **27** (1951) 232.
13. Chatt, J., Duncanson, L. A. and Venanzi, L. M. *Suomen Kemistilehti* **29B** (1956) 75.

Received April 23, 1962.

ACTA CHEMICA SCANDINAVICA 16 (1962) 2050–2068

Short Communications

On the Tendency of the Tetracyano Nickelate(II) Ion to Form Complexes

MIHÁLY T. BECK* and JANNIK BJERRUM

Chemistry Department I. Inorganic Chemistry. The H. C. Ørsted Institute, University of Copenhagen, Copenhagen, Denmark

It is well known that in the presence of excess cyanide the colour of tetracyano nickelate(II) solutions becomes more intense. The reason for this change is evidently the formation of higher cyanide complex(es) [1]. There is disagreement about the composition and stability of the complex formed.

According to McCullough, Jones and Penneman [2] the tetracyano nickel(II) complex takes up only one further cyanide forming a pentacyano complex, the absorbancy of which in the visible, especially between 500 – 375 mμ, is much greater than that of the tetracyano complex. The stability constant was found to be about 0.2. The infrared study [2] of the same system gave the same results.

Almost simultaneously Blackie and Gold [3] published the results of a magnetic study of the same system. According to their proton magnetic resonance experiments, the tetracyano nickel(II) complex stoichiometrically reacts with two further cyanide ions. From their results it can be estimated that the stability constant of the hexacyano complex (K_5K_6) is at least $10^5 - 10^6$. The authors cited Kisova and Čuprova's spectrophotometric study [4] in support of their result. They did, however, not know the original paper by Kisova and Čuprova, but only the abstract of it. The results given by the Czechoslovak authors do not support the formation of a *stable* hexacyano complex, but in our opinion rather the formation of an unstable pentacyano complex.

The only difference between the cited spectrophotometric [2] and the magnetic study is that in the case of the latter experiments the authors worked with ammoniacal solutions, the concentration of which was not specified. Therefore we repeated the spectrophotometric study using ammoniacal solutions. However, instead of an increase of stability – which would possibly be expected considering the results of Blackie and Gold's study – a decreasing extent of formation of pentacyano complex with increasing ammonia concentration, or more correctly a fading of colour of solutions on the effect of ammonia, was observed (see Fig. 1a). It was further observed (see Fig. 1b) that a similar fading effect in approximately 1 M cyanide solution was caused by ethylenediamine, pyridine, butylamine, ethanol, methanol, dioxane, etc. Relatively small concentrations of these substances result in great change of absorbancy of solutions, so it is very probable that the reason of this peculiar behaviour is not a change in the spectra properties of species, but rather a change in the concentration of the high absorbing pentacyano nickel(II) complex.

A change of concentration of the pentacyano complex could be independently explained by

(a) a competition between the cyanide ion and the organic substance for a fifth coordination site of the tetracyano complex, assuming that the mixed complex has nearly the same absorbancy as the aquotetracyano nickel(II) complex;

(b) the activity coefficient corresponding to the mass action expression

$$F = f_{Ni(CN)_4^{2-}} f_{CN^-} / f_{Ni(CN)_5^{3-}}$$

* Permanent address: Institute of Inorganic and Analytical Chemistry, University of Szeged, Szeged, Hungary.

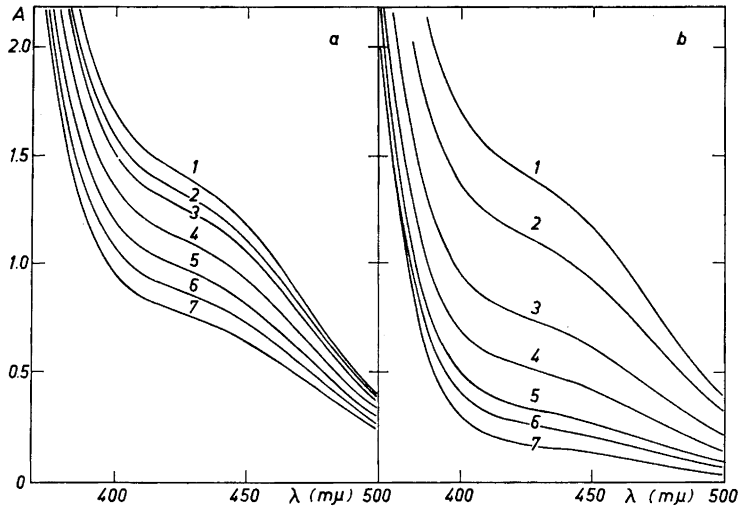

Fig. 1. The effect of ammonia (*a*), and pyridine (*b*) on the directly measured absorbancy A in 2 cm cells of solutions of the composition: $Ni(CN)_4^{2-}$ 0.04 M, CN^- 0.98 M

ammine conc. (curve nos.)

a: 0 (1), 0.454 M (2), 0.908 M (3), 1.82 M (4), 2.72 M (5), 3.63 M (6), 4.31 M (7).

b: 0 (1), 0.246 M (2), 0.738 M (3), 1.23 M (4), 1.97 M (5), 2.46 M (6), 3.7 M (7).

is supposed to decrease strongly on the effect on the added nonelectrolytes.

It is possible to explain the effect observed on the basis of either assumptions. The fact that molecules the coordination tendency of which is evidently extremely small (*e.g.* alcohols) result in the same effect as the ammines, however, supports the latter explanation. The decrease of the dielectric constant of the medium, which is an important factor in determining the activity coefficients, is practically the same with the different amines and alcohols [5]. It must be mentioned, however, that the dimethylformamide -- the dielectric constant of which is even greater than that of the water — has the same fading effect.

To elucidate the phenomenon observed, the effect of different salts on the absorbancy of the tetracyano nickel(II) complex and the system $Ni(CN)_4^{2-}$—CN^- was studied. Added salts cause in all cases an increase of absorbancy and mainly in the visible part of the spectrum. Table 1 shows

Table 1.

$K_2Ni(CN)_4$ 0.01 M

Salt	KCN	KSCN	KI	KBr	KCl	KF	KNO_3
Molarity	0.8	1.94	1.6	1.6	1.8	2	1.8
Δ %/M	747	290	196	26	7.2	7	15.5

$K_2Ni(CN)_4$ 0.01 M, KCN 0.8 M

Salt		KSCN	KI	KBr	KCl	KF	KNO_3
Molarity		1.94	1.6	1.6	1.8	2	1.8
Δ' %/M		26.5	60	45	45	65	20
Δ' %/Δ %		0.09	0.3	1.7	6.3	9.3	1.3

the increase of absorbancy at 400 mμ in per cent per mole/liter of salt.

The great effect of KCN, KSCN, KI and — to a much lesser extent — KBr on the absorbancy of the tetracyano complex can ba interpreted as a consequence of formation of pentacoordinated species. The effect of KCl, KF and KNO_3 seems to be a normal salt effect, however that of the KNO_3 is surprisingly high. The system $Ni(CN)_4^{2-}$ + CN^- is more complicated, and the interpretation in this case is not simple. Evidently the effect observed is the resultant of different factors: the salt effect on the two different absorbing species, and the competition between the cyanide and other anions for the fifth coordination place. The last line of Table 1 is informative and suggests a specific salt effect of KCl and even more of KF on the pentacyano species. In this connection it must be mentioned that Herrington and Kingsbury [6] suggested that the fluoride ion exerts a specific effect on the $Ti(IV)-H_2O_2$ complex. Their conclusion, however, is evidently wrong because the limiting value of absorbancy is reached already at 0.1 M fluoride concentration. The decrease of absorbancy and the shift of the band can be simply explained by the formation of a mixed complex: $Ti(IV)-H_2O_2-F^-$.

For comparison the effect of different salts on the spectrum of a coordinatively saturated cyano complex was also studied. Potassium hexacyanoferrate(II) was measured in the wavelength range 440—380 mμ, and Table 2 summarizes the increase of absorbancy at 380 mμ in per cent per mole/liter of salt.

Table 2.

$K_4Fe(CN)_6$ 0.01 M, λ = 380 mμ

Salt	KCN	KI	KBr	KCl	KF	KNO_3
Molarity	1.6	1.6	1.6	1.8	2	1.8
Δ %/M	15	10	9	7	11	13

In comparing the data it can be seen that the salt effect as a whole is very small. Therefore, on the basis of these studies the existence of the mixed complexes $Ni(CN)_4SCN^{3-}$, $Ni(CN)_4I^{3-}$ and $Ni(CN)_4Br^{3-}$ as well as that of the pentacyano-Ni(II) complex seems to be well established. The stability order is

$$Ni(CN)_5^{3-} > Ni(CN)_4SCN^{3-} > Ni(CN)_4I^{3-} > Ni(CN)_4Br^{3-}$$

These complexes are very weak ones and therefore it is impossible to give reliable numerical data for their dissociation. Although the paper by McCullough, Jones and Penneman appears correct as a whole, according to our experience the error of K_5 given by the authors seems to be too optimistic.

The results of the present study do not solve the discrepancy between the spectrophotometric and magnetic studies mentioned, but the interpretation of the proton magnetic resonance measurements seems to be incorrect.

Infrared absorption experiments may decide whether the effect of fluoride on the system $Ni(CN)_4^{2-}-CN^-$ is exerted on the activity coefficient expression, or on the pentacyano complex itself. In the latter case there may be a shift of the peak.

Experimental. The spectrophotometric measurements were made with a Cary 11MS-50 recording spectrophotometer and with a Beckman DU instrument. $K_2Ni(CN)_4 \cdot H_2O$ was prepared according to Fernelius and Burbage [7]. All the reagents used were c.p. quality.

Acknowledgment. One of the authors (M.T.B.) wishes to express his gratitude to the *Rask-Ørsted Foundation* and to the *Hungarian Academy of Sciences* for their support, and also to Professor N. Hofman-Bang giving working facilities in his Laboratory.

1. Job, A. and Samuel, A. *C. R. Acad. Sci. Paris* **177** (1923) 188.
2. McCullough, R. I., Jones, L. H. and Penneman, R. A. *J. Inorg. Nuclear Chem.* **13** (1960) 286.
3. Blackie, M. S. and Gold, V. *J. Chem. Soc.* **1919** 4033.
4. Kisova, V. and Čuprova, L. *Collection Czechoslov. Chem. Communs* **24** (1959) 862.
5. Haggis, G. H., Hasted, J. B. and Buchanan, T. J. *J. Chem. Phys.* **20** (1952) 1453.
6. Herrington, J. and Kingsbury, D. E. *J. Am. Chem. Soc.* **79** (1957) 5893.
7. Fernelius, W. C. and Burbage, J. J. *Inorganic Syntheses*, Vol. II (1946) 227.

Received September 10, 1962.

A Rapid Method for the Detection of H, Cl, Br, I, S and N in Organic Compounds

BENGT SMITH and ULF PERSMARK

Institutionen för Organisk kemi, Chalmers Tekniska Högskola, Göteborg, Sweden

Recently a method for the detection of oxygen in organic compounds utilizing a cracking technique has been described by one of the present authors [1]. The substance is pyrolyzed in an atmosphere of helium and the carbon oxide formed identified. In this paper the application of pyrolysis to the qualitative determination of several other elements will be described. It was found that, when organic substances were pyrolyzed over a glowing platinum wire in an atmosphere of hydrogen, there were formed hydrogen halides from halogen-containing compounds, hydrogen sulphide from sulphur-containing compounds and hydrogen cyanide from nitrogen-containing compounds. To analyze for hydrogen the substance was pyrolyzed in the presence of sulphur in an atmosphere of nitrogen — when the substance contained hydrogen, hydrogen sulphide resulted (*cf.* Ref. [2]). The inorganic compounds formed were identified by wet chemical methods.

The time of pyrolysis had to be adjusted to the aggregation state of the substance as well as to the element that was to be determined. Thus, a longer pyrolysis time was necessary for solid compounds than for liquids and, to get an adequate amount of hydrocyanic acid from a nitrogen compound, a longer pyrolysis time was necessary than for transferring the halogen and sulphur bound in organic compounds into their corresponding hydrogen compounds (*cf.* below). The present method has been applied to a substantial number of organic compounds of various types including aliphatic and aromatic halogen compounds, nitro compounds, amides, nitriles, amines, nitrogen-containing heterocyclic compounds, nitrogen-containing plastics, mercaptans, thioketones, sulphonic acids, and sulphur-containing heterocyclic compounds. Since the test was positive in every case, it seems that the method possesses a fairly general application for the determination of the elements specified in the heading. We believe that the method has some advantages over the sodium fusion method of Lassaigne because of its immediate availability and the rapidity with which an analysis can be performed.

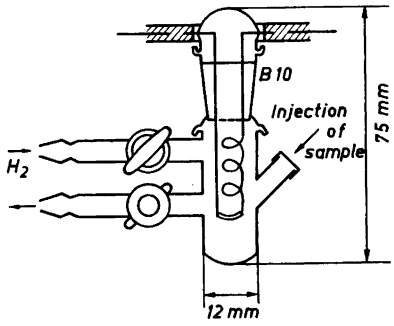

Fig. 1. Pyrolysis apparatus used for the elementary analysis.

The apparatus used for the analysis is shown in Fig. 1. It represents a development of the apparatus previously used in this laboratory for the determination of oxygen [1]. This apparatus was redesigned partly to allow an easier cleaning of the equipment and partly to make the connection of the contact wires to the apparatus more durable. The apparatus consisted of a pyrex glass tube with inlet and outlet tubes for the gas and a tube covered by a serum cap for the injection of liquid samples. The pyrex tube had a ground glass joint (B 10) at its upper end. A platinum glowing wire (0.5 mm diam.) was fastened in a stopcock, fitting the ground glass joint. The glowing wire was melted into tin in the inner parts of the side tubes connected to the stopcock and the outer copper contact wires were also fastened in the same way. This construction was more durable than the earlier one and it was also easier to replace a broken contact wire. At the lower end of the platinum spiral a small platinum bowl was welded to the platinum wire. Solid samples were placed in this bowl or liquid samples were injected into it through the side tube.

An analysis for C, Cl, Br, I, S, or N was performed in the following way. If the sample was a solid or a not too fugitive liquid, 3—5 mg of it was placed in the platinum bowl and the apparatus assembled. The inlet tube was connected to a hydrogen container and a stream of hydrogen passed through for some minutes. The

stopcock on the outlet tube was closed and thereafter the stopcock on the inlet tube. In this way, a slight hydrogen over-pressure was built up in the reactor tube. In the case of low-boiling liquids, 4—6 μl were injected at this stage through the serum cap into the platinum bowl. A voltage of 5 V was then applied to the platinum wire, causing it to glow.

As mentioned above, the time of pyrolysis had to be adjusted to the aggregation state of the sample as well as to the element which was to be determined. For the determination of halogen and sulphur in liquid organic compounds, a pyrolysis time of 10—15 sec was enough while for solid substances 20—30 sec were necessary. To determine nitrogen in liquids, a pyrolysis time of 50—60 sec was required and in solids 100—110 sec. This means that, whenever a full analysis is wanted, the long pyrolysis times have to be applied. After the completion of the pyrolysis, a test tube with 0.5 ml 10 % sodium hydroxide was connected to the outlet tube of the reactor and the pyrolysis products swept through the alkaline solution by a stream of hydrogen. The solution was analyzed for sodium halides, sodium sulphide and sodium cyanide using mainly the procedure described by Widmark [3].

When analyzing for H, 10—15 mg of sulphur was placed in the platinum bowl and, in the case of solid samples or not too fugitive liquids, mixed with about 5 mg of the substance. Low-boiling liquids (about 5 μl) were injected into the bowl after flushing the reactor with nitrogen. A pyrolysis time of 20—30 sec was found to be adequate and the pyrolysis products were absorbed, as before, in a 10 % solution of sodium hydroxide and the solution analyzed for sodium sulphide.

1. Smith, B. and Ohlson, R. *Acta Chem. Scand.* **14** (1960) 2245.
2. Feigl, F. and Jungreis, E. *Microchim. Acta* **1958** 812.
3. Widmark, G. *Acta Chem. Scand.* **7** (1953) 1395.

Received September 10, 1962.

Ozonolysis of Naphthoquinones

III. 1,2-Naphthoquinone

ERLING BERNATEK and
ARNE NICOLAI SOTELAND

Universitetets Kjemiske Institutt, Blindern-Oslo, Norway

In our previous papers in this series [1,2] we have confined ourselves to the discussion of the ozonolysis of some 1,4-naphthoquinones. We wish now to report on certain aspects of the behaviour of 1,2-naphthoquinone under ozonolytic cleavage.

The quinone, in chloroform, absorbed ozone readily though not quantitatively and the ozonisation was terminated when 3 moles of the gas had been applied. At this point the dark colour of the solution had changed to a light yellowish green. If the initial quinone solution was saturated or if carbon tetrachloride was added, a faintly yellow substance separated during ozonisation. It contained active oxygen but decomposed explosively in a few seconds if isolated and dried. This product may be a true ozonide, but a closer examination of it was difficult due to its labile character. Immediately after the ozonisation the solution contained about 1.2 g atoms of active oxygen per mole of starting material.

Table 1 gives the identified reaction products together with the results from the quantitative determinations.

Table 1.

Product	% recovered carbon	moles/mole reacted quinone
Carbon monoxide	0.80	0.08
Carbon dioxide	11.50	1.14
Formaldehyde	0.75	0.075
Formic acid	7.30	0.73
Phthaladehydic acid	61.50	0.77
Phthalic anhydride	15.50	0.19

The carbon oxides were evolved during ozonolysis as well as during hydrolysis of the reaction mixture, the phthalic anhydride was then usually recovered as phthalic acid. It will be noticed that more than 97 %

stopcock on the outlet tube was closed and thereafter the stopcock on the inlet tube. In this way, a slight hydrogen over-pressure was built up in the reactor tube. In the case of low-boiling liquids, 4—6 μl were injected at this stage through the serum cap into the platinum bowl. A voltage of 5 V was then applied to the platinum wire, causing it to glow.

As mentioned above, the time of pyrolysis had to be adjusted to the aggregation state of the sample as well as to the element which was to be determined. For the determination of halogen and sulphur in liquid organic compounds, a pyrolysis time of 10—15 sec was enough while for solid substances 20—30 sec were necessary. To determine nitrogen in liquids, a pyrolysis time of 50—60 sec was required and in solids 100—110 sec. This means that, whenever a full analysis is wanted, the long pyrolysis times have to be applied. After the completion of the pyrolysis, a test tube with 0.5 ml 10 % sodium hydroxide was connected to the outlet tube of the reactor and the pyrolysis products swept through the alkaline solution by a stream of hydrogen. The solution was analyzed for sodium halides, sodium sulphide and sodium cyanide using mainly the procedure described by Widmark [3].

When analyzing for H, 10—15 mg of sulphur was placed in the platinum bowl and, in the case of solid samples or not too fugitive liquids, mixed with about 5 mg of the substance. Low-boiling liquids (about 5 μl) were injected into the bowl after flushing the reactor with nitrogen. A pyrolysis time of 20—30 sec was found to be adequate and the pyrolysis products were absorbed, as before, in a 10 % solution of sodium hydroxide and the solution analyzed for sodium sulphide.

1. Smith, B. and Ohlson, R. *Acta Chem. Scand.* **14** (1960) 2245.
2. Feigl, F. and Jungreis, E. *Microchim. Acta* **1958** 812.
3. Widmark, G. *Acta Chem. Scand.* **7** (1953) 1395.

Received September 10, 1962.

Ozonolysis of Naphthoquinones

III. 1,2-Naphthoquinone

ERLING BERNATEK and
ARNE NICOLAI SOTELAND

Universitetets Kjemiske Institutt, Blindern-Oslo, Norway

In our previous papers in this series [1,2] we have confined ourselves to the discussion of the ozonolysis of some 1,4-naphthoquinones. We wish now to report on certain aspects of the behaviour of 1,2-naphthoquinone under ozonolytic cleavage.

The quinone, in chloroform, absorbed ozone readily though not quantitatively and the ozonisation was terminated when 3 moles of the gas had been applied. At this point the dark colour of the solution had changed to a light yellowish green. If the initial quinone solution was saturated or if carbon tetrachloride was added, a faintly yellow substance separated during ozonisation. It contained active oxygen but decomposed explosively in a few seconds if isolated and dried. This product may be a true ozonide, but a closer examination of it was difficult due to its labile character. Immediately after the ozonisation the solution contained about 1.2 g atoms of active oxygen per mole of starting material.

Table 1 gives the identified reaction products together with the results from the quantitative determinations.

Table 1.

Product	% recovered carbon	moles/mole reacted quinone
Carbon monoxide	0.80	0.08
Carbon dioxide	11.50	1.14
Formaldehyde	0.75	0.075
Formic acid	7.30	0.73
Phthaladehydic acid	61.50	0.77
Phthalic anhydride	15.50	0.19

The carbon oxides were evolved during ozonolysis as well as during hydrolysis of the reaction mixture, the phthalic anhydride was then usually recovered as phthalic acid. It will be noticed that more than 97 %

of the initial carbon is recovered in the products and that the aromatic balance (*i.e.* recovery of benzene nucleus) is about 96 % indicating an almost exclusive attack on the quinone ring.

A conspicuous feature of the results is that both aromatic products have lost two carbon atoms, but on the other hand no C_2-fragments could be found. This is not wholly unexpected, however, since the application of as much as three moles of ozone was needed to degrade the quinone quantitatively.

Formation of phthalaldehydic acid can simply be explained as an abnormal ozonolysis as indicated in (I) (or, in view of the content of active oxygen in the reaction mixture, as a rearrangement of an ozonide in the same direction) with the simultaneous formation of glyoxylic acid.

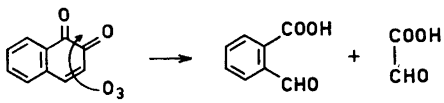

I

Glyoxylic acid is then probably oxidised by the prolonged action of ozone to carbon dioxide and formic acid. An abnormal ozonolysis with the expulsion of only a C_1-fragment followed by oxidation of the side-chain in the aromatic product is also theoretically possible. This reaction, however, produces the intermediate (II), which is a mixed anhydride of formic acid and will split off carbon monoxide. If this reaction path was dominant, far larger amounts than those found of this oxide would have been formed.

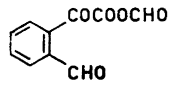

II

The really interesting result of this investigation is the formation of phthalic anhydride. It is fairly certain that the anhydride is a primary product and not the result of an anhydridisation of phthalic acid. If the free acid was formed initially it should have separated from the chloroform solution, where it is very slightly soluble. Further, some anhydride could be isolated in the chloroform phase even after addition of water to the reaction mixture.

Mechanistically the reaction can be explained in more than one way but the simplest one is to assume the initial formation of the zwitterion (III), which undergoes a ring-closure to the sterically more probable of three possible ozonides (IV).

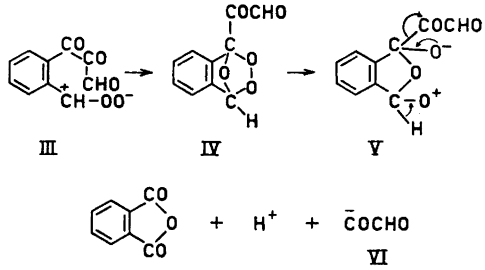

III IV V

VI

A heterolysis of the O—O bond takes us to the transitory entity (V), which by the indicated electronic shifts eliminates a proton and the carbanion (VI) thereby forming phthalic anhydride. The proton and (VI) combine, perhaps synchronously with the elimination, to glyoxal. Also this C_2-fragment is then oxidised by excess ozone to formic acid and carbon dioxide.

Formaldehyde, which is found in very small amounts only, is probably formed by hydrolytic cleavage of a carbonyl intermediate in a way similar to that discussed in connection with the ozonolysis of *p*-benzoquinone [3].

Experimental. Ozonolysis. The ozonisation technique and the decomposition with water were performed as decribed for 1,4-naphthoquinone [1,2].

Ozone absorption was measured by leading the effluent gases into aqueous potassium iodide, which was changed at intervals and the liberated iodine titrated. Active oxygen was also determined iodometrically by running aliquots of the reaction mixture into sodium iodide in glacial acetic acid.

Determination of products. Carbon monoxide and formic acid were determined as previously described [1,2]. Carbon dioxide was determined as accounted for in the ozonolysis of phenol [4]. Formaldehyde was identified through its dimedone derivative (m.p. and mixed m.p. 187°C) and determined spectroscopically through its colour reaction with chromotropic acid.

Phthalaldehydic acid was found in the aqueous decomposition solution as well as in the chloroform phase. It was identified through its 2,4-dinitrophenylhydrazone, m.p. 250.5°C. (Found: C 51.2; H 3.3; N 16.5. Calc. for

$C_{14}H_{10}N_4O_6$: C 50.9; H 3.3; N 17.0) and through its *p*-nitrophenylhydrazone, m.p. 206.5°C. (Found: C 58.5; H 3.9; N 15.1. Calc. for $C_{14}H_{11}N_3O_4$: C 58.9; H 3.9; N 14.8). For the quantitative determination the precipitation with dinitrophenylhydrazine was utilised after a small correction for the solubility of the derivative had been applied.

Phthalic anhydride was found as such in the chloroform phase, especially if the hydrolysis had been of short duration. By thermal decomposition of the ozonisation solution or by reduction with sodium iodide the formed phthalic anhydride can be isolated almost quantitatively while the content of phthalic acid is practically nil. M.p. and mixed m.p. 130°C (Found: C 64.3; H 2.9. Calc. for $C_8H_4O_3$: C 64,7; H 2.7). Quantitatively the anhydride was determined by two methods:

(*a*) After the hydrolysis the chloroform is evaporated from the heterogeneous mixture whereby the anhydride dissolves in the water as phthalic acid. The water is removed at room temperature and the residue (A) is extracted repeatedly with chloroform leaving almost pure phthalic acid which is then weighed. This method gives probably somewhat low results.

(*b*) The residue (A) is dissolved in water again and titrated with standard sodium hydroxide (indicator: phenolphthalein). From the titration values is then deducted the amount due to phthalaldehydic acid.

In all quantitative work the ozonisation batches consisted of 1.00 g of 1,2-naphthoquinone in 100 ml of chloroform.

Results:

Carbon monoxide during ozonisation 8.1, 8.6, 9.6 mg. Mean 8.8 mg. During hydrolysis 6.2, 6.8, 5.6 mg. Mean 6.2 mg.

Carbon dioxide during ozonisation 102, 86, 78, 94 mg. Mean 90 mg. During hydrolysis 302, 276, 307, 283 mg. Mean 290 mg.

Formaldehyde 14.2, 14.6 mg. Mean 14.4 mg.

Formic acid 182, 224, 215, 232 mg. Mean 213 mg.

Phthalaldehydic acid 733, 745, 711 mg. Mean 730 mg.

Phthalic anhydride. Method (*a*) 173, 161, 182 mg. Mean 172 mg.

Method (*b*) 191, 194, 200 mg. Mean 195 mg. Mean for both methods 183 mg.

One of the authors (E.B.) wants to express his thanks to *Fridtjof Nansens Fond* for a grant.

1. Bernatek, E. *Tetrahedron* **4** (1958) 213.
2. Bernatek, E. *Ozonolyses in the Naphthoquinone and Benzofuran Series. Thesis*, Oslo University Press 1960.
3. Bernatek, E. and Straumsgård, K. A. *Acta Chem. Scand.* **13** (1959) 178.
4. Bernatek, E. and Frengen, C. *Acta Chem. Scand.* **15** (1961) 471.

Received August 13, 1962.

Partition Chromatography on Ion Exchange Resins.

Separation of Sugars

OLOF SAMUELSON and BIRGIT SWENSON

Department of Engineering Chemistry, Chalmers Tekniska Högskola, Göteborg, Sweden

In earlier papers it has been demonstrated that strongly polar non-electrolytes such as sugars can be taken up effectively from ethanol-water mixtures by means of ion exchange resins. Only a few chromatographic separations have been carried out based upon this sorption mechanism [1,2]. In separations of monosaccharides overlapping curves are obtained in many systems. A systematic study of the factors which govern this sorption has shown that the ethanol concentration, and the rate of diffusion inside the resin particles are critical factors [3,4]. For this reason it is necessary to use an appropriate ethanol concentration, a small resin particle size, and a low flow rate in order to achieve satisfactory separations. In the present work some results are given demonstrating applications of this method to sugar separations.

Experimental. The resin (Dowex 1 X-8) was classified hydraulically to obtain the fraction 45 – 75 μ and transformed into its sulfate form. The column was prepared and operated in the normal way, and precautions were taken to avoid gas bubbles in the column [5]. The dimensions of the resin bed were 10 × 840 mm. The sample solutions which had a volume of 5 ml contained 75 % ethanol (by weight). The eluant was fed on to the column with a pump at a constant flow rate (0.8 ml $cm^{-2}min^{-1}$). The temperature was kept constant at 28°C.

The eluate was collected in a fraction collector and analyzed using the Technicon Auto-Analyzer [6].

$C_{14}H_{10}N_4O_6$: C 50.9; H 3.3; N 17.0) and through its *p*-nitrophenylhydrazone, m.p. 206.5°C. (Found: C 58.5; H 3.9; N 15.1. Calc. for $C_{14}H_{11}N_3O_4$: C 58.9; H 3.9; N 14.8). For the quantitative determination the precipitation with dinitrophenylhydrazine was utilised after a small correction for the solubility of the derivative had been applied.

Phthalic anhydride was found as such in the chloroform phase, especially if the hydrolysis had been of short duration. By thermal decomposition of the ozonisation solution or by reduction with sodium iodide the formed phthalic anhydride can be isolated almost quantitatively while the content of phthalic acid is practically nil. M.p. and mixed m.p. 130°C (Found: C 64.3; H 2.9. Calc. for $C_8H_4O_3$: C 64,7; H 2.7). Quantitatively the anhydride was determined by two methods:

(*a*) After the hydrolysis the chloroform is evaporated from the heterogeneous mixture whereby the anhydride dissolves in the water as phthalic acid. The water is removed at room temperature and the residue (A) is extracted repeatedly with chloroform leaving almost pure phthalic acid which is then weighed. This method gives probably somewhat low results.

(*b*) The residue (A) is dissolved in water again and titrated with standard sodium hydroxide (indicator: phenolphthalein). From the titration values is then deducted the amount due to phthalaldehydic acid.

In all quantitative work the ozonisation batches consisted of 1.00 g of 1,2-naphthoquinone in 100 ml of chloroform.

Results:

Carbon monoxide during ozonisation 8.1, 8.6, 9.6 mg. Mean 8.8 mg. During hydrolysis 6.2, 6.8, 5.6 mg. Mean 6.2 mg.

Carbon dioxide during ozonisation 102, 86, 78, 94 mg. Mean 90 mg. During hydrolysis 302, 276, 307, 283 mg. Mean 290 mg.

Formaldehyde 14.2, 14.6 mg. Mean 14.4 mg.

Formic acid 182, 224, 215, 232 mg. Mean 213 mg.

Phthalaldehydic acid 733, 745, 711 mg. Mean 730 mg.

Phthalic anhydride. Method (*a*) 173, 161, 182 mg. Mean 172 mg.

Method (*b*) 191, 194, 200 mg. Mean 195 mg. Mean for both methods 183 mg.

One of the authors (E.B.) wants to express his thanks to *Fridtjof Nansens Fond* for a grant.

1. Bernatek, E. *Tetrahedron* **4** (1958) 213.
2. Bernatek, E. *Ozonolyses in the Naphthoquinone and Benzofuran Series. Thesis*, Oslo University Press 1960.
3. Bernatek, E. and Straumsgård, K. A. *Acta Chem. Scand.* **13** (1959) 178.
4. Bernatek, E. and Frengen, C. *Acta Chem. Scand.* **15** (1961) 471.

Received August 13, 1962.

Partition Chromatography on Ion Exchange Resins.

Separation of Sugars

OLOF SAMUELSON and BIRGIT SWENSON

Department of Engineering Chemistry, Chalmers Tekniska Högskola, Göteborg, Sweden

In earlier papers it has been demonstrated that strongly polar non-electrolytes such as sugars can be taken up effectively from ethanol-water mixtures by means of ion exchange resins. Only a few chromatographic separations have been carried out based upon this sorption mechanism [1,2]. In separations of monosaccharides overlapping curves are obtained in many systems. A systematic study of the factors which govern this sorption has shown that the ethanol concentration, and the rate of diffusion inside the resin particles are critical factors [3,4]. For this reason it is necessary to use an appropriate ethanol concentration, a small resin particle size, and a low flow rate in order to achieve satisfactory separations. In the present work some results are given demonstrating applications of this method to sugar separations.

Experimental. The resin (Dowex 1 X-8) was classified hydraulically to obtain the fraction 45 – 75 μ and transformed into its sulfate form. The column was prepared and operated in the normal way, and precautions were taken to avoid gas bubbles in the column [5]. The dimensions of the resin bed were 10 × 840 mm. The sample solutions which had a volume of 5 ml contained 75 % ethanol (by weight). The eluant was fed on to the column with a pump at a constant flow rate (0.8 ml $cm^{-2}min^{-1}$). The temperature was kept constant at 28°C.

The eluate was collected in a fraction collector and analyzed using the Technicon Auto-Analyzer [6].

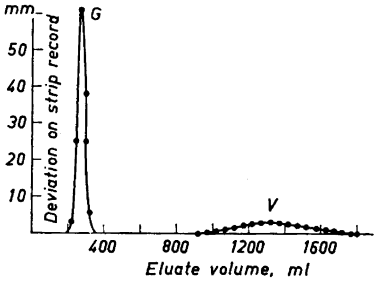

Fig. 1. Separation of 10 mg glucose (G) and 20 mg verbascose (V). Eluant: 65 % ethanol.

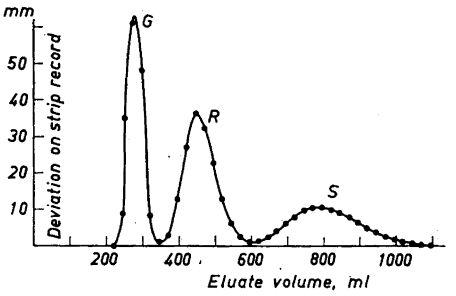

Fig. 3. Separation of 10 mg glucose (G), 20 mg raffinose (R), and 20 mg stachyose (S). Eluant: 65 % ethanol.

Results and discussion. A low ethanol concentration facilitates the diffusion inside the resin and is, therefore, desirable. The results given in Figs. 1 and 2 show that glucose is separated quantitatively from the pentasaccharide verbascose and from the tetrasaccharide stachyose in 65 % ethanol. An almost complete separation from raffinose in also achieved in this medium. As shown in Fig. 3, the separation of a mixture containing glucose, raffinose, and stachyose is almost complete under the same conditions.

An increased ethanol concentration results in increased distribution coefficients, *i.e.*, in increased peak elution volumes. The results given in Fig. 4 show that an increased separation factor is obtained. In agreement with theory (*cf.* Ref.[5]) a broadening of the elution bands occurs. An ethanol concentration of 72—74 % is suitable for the separation of monosaccharides from various disaccharides such as maltose (Fig. 5), cellobiose, sucrose, and

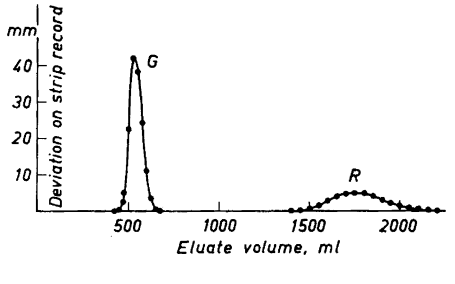

Fig. 4. Separation of 10 mg glucose (G) and 10 mg raffinose (R). Eluant: 74 % ethanol.

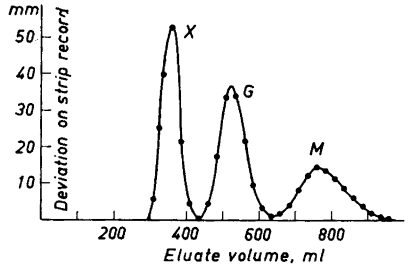

Fig. 5. Separation of 10 mg xylose (X), 10 mg glucose (G), and 20 mg maltose (M). Eluant: 74 % ethanol.

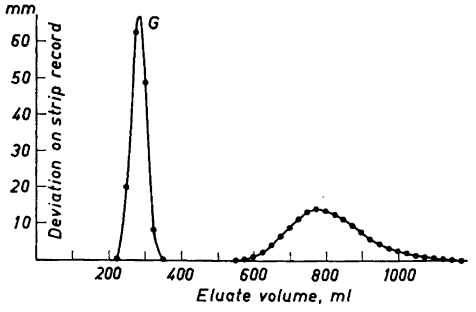

Fig. 2. Separation of 10 mg glucose (G) and 20 mg stachyose (S). Eluant: 65 % ethanol.

lactose. Among the sugars hitherto studied, all monosaccharides appear ahead of the polysaccharides, whereas the lower polysaccharides appear before those of a higher molecular weight. With complicated mix-

tures it is advantageous to use stepwise elution or gradient elution with eluants containing lower ethanol concentration in order to avoid an excessive broadening of the bands corresponding to higher saccharides. As an example it can be mentioned that a satisfactory separation of a mixture containing glucose, sucrose, raffinose, stachyose, and verbascose can be obtained by eluting the first two components with 74 % ethanol and then decreasing the ethanol concentration to 65 %.

A separation of monosaccharides from each other is also possible. The separation of xylose from glucose is demonstrated in Fig. 5. Similarly, it is possible to obtain a quantitative separation of mannose from glucose, whereas no satisfactory separation of galactose from glucose has been obtained under the experimental conditions chosen in the present work.

The financial support of the *Swedish Technical Research Council* is gratefully acknowledged.

1. Samuelson, O. and Sjöström, E. *Svensk Kem. Tidskr.* **64** (1952) 305.
2. Samuelson, O. Nordiske Kemikermöde, Aarhus 1956.
3. Rückert, H. and Samuelson, O. *Svensk Kem. Tidskr.* **66** (1954) 337; *Acta Chem. Scand.* **11** (1957) 303, 315.
4. Mattisson, M. and Samuelson, O. *Acta Chem. Scand.* **12** (1958) 1395.
5. Samuelson, O. *Ion Exchange Separations in Analytical Chemistry*, Almqvist & Wiksell, Stockholm, John Wiley & Sons, New York 1962.
6. Samuelson, O. and Swenson, B. *To be published.*

Received September 13, 1962.

Correction to "Conversion of Δ^5-Cholestene-3α-12α-diol to Cholic Acid in the Rabbit" *

HENRY DANIELSSON

In the title above *for* Δ^5-cholestene-3α-12α-diol *read* Δ^5-cholestene-3β-12α-diol.

* *Acta Chem. Scand.* **16** (1962) 1534.

Occurrence of Methyl Esters in Lymph

G. A. DHOPESHWARKAR and ROLF BLOMSTRAND

Department of Clinical Chemistry, Karolinska Institutet, Serafimerlasarettet, Stockholm, Sweden

Absorption of dietary triglycerides from intestines in a partially hydrolysed form has been established. Intestinal absorption of oleic acid 1—^{14}C has been studied by Bergström *et al.* [1] with cannulated thoracic duct in rats. They reported that oleic acid was transported *via* the lymph and incorporated into triglycerides and phospholipids whether fed as oleic acid or triolein. Blomstrand and Rumpf [2] have reported that when cetyl alcohol 1—^{14}C was fed to rats with thoracic duct fistula about 15 % of it was present as unchanged alcohol in the lymph. Borgström [4] fed ethyl esters of fatty acids but found only traces of unhydrolysed esters in the lymph. Blomstrand[5] noticed that chimyl alcohol could be absorbed unchanged but was extensively metabolised already in the mucosa cells. Dhopeshwarkar and Mead[6] have shown evidence for occurrence of methyl esters in body and blood lipids. In another study[7] they also showed that when methyl elaidate was fed to fat deficient animals a part of it was found unhydrolysed in body lipids. The purpose of this short study was to determine whether methyl esters were present in rat lymph and to find out if methyl oleate could be absorbed without undergoing complete hydrolysis.

Experimental. Cannulation of lymph duct was performed as described before [1] on two male albino rats maintained on a regular chow diet. Lymph was collected in suitable containers under ethyl alcohol, before and after feeding methyl oleate. Methyl oleate was purified by vacuum distillation and was found to contain 85 % oleate, 15 % palmitate and a small amount of palmitoleate. No attempt was made to remove these impurities. The total lipids were extracted as usual from lymph using ethanol-ether (3:1) and subjected to silicic acid chromatography. The fraction that was eluted with 2 % ether in petroleum ether

tures it is advantageous to use stepwise elution or gradient elution with eluants containing lower ethanol concentration in order to avoid an excessive broadening of the bands corresponding to higher saccharides. As an example it can be mentioned that a satisfactory separation of a mixture containing glucose, sucrose, raffinose, stachyose, and verbascose can be obtained by eluting the first two components with 74 % ethanol and then decreasing the ethanol concentration to 65 %.

A separation of monosaccharides from each other is also possible. The separation of xylose from glucose is demonstrated in Fig. 5. Similarly, it is possible to obtain a quantitative separation of mannose from glucose, whereas no satisfactory separation of galactose from glucose has been obtained under the experimental conditions chosen in the present work.

The financial support of the *Swedish Technical Research Council* is gratefully acknowledged.

1. Samuelson, O. and Sjöström, E. *Svensk Kem. Tidskr.* **64** (1952) 305.
2. Samuelson, O. Nordiske Kemikermöde, Aarhus 1956.
3. Rückert, H. and Samuelson, O. *Svensk Kem. Tidskr.* **66** (1954) 337; *Acta Chem. Scand.* **11** (1957) 303, 315.
4. Mattisson, M. and Samuelson, O. *Acta Chem. Scand.* **12** (1958) 1395.
5. Samuelson, O. *Ion Exchange Separations in Analytical Chemistry*, Almqvist & Wiksell, Stockholm, John Wiley & Sons, New York 1962.
6. Samuelson, O. and Swenson, B. *To be published.*

Received September 13, 1962.

Correction to "Conversion of Δ^5-Cholestene-3α-12α-diol to Cholic Acid in the Rabbit" *

HENRY DANIELSSON

In the title above *for* Δ^5-cholestene-3α-12α-diol *read* Δ^5-cholestene-3β-12α-diol.

* *Acta Chem. Scand.* **16** (1962) 1534.

Occurrence of Methyl Esters in Lymph

G. A. DHOPESHWARKAR and ROLF BLOMSTRAND

Department of Clinical Chemistry, Karolinska Institutet, Serafimerlasarettet, Stockholm, Sweden

Absorption of dietary triglycerides from intestines in a partially hydrolysed form has been established. Intestinal absorption of oleic acid 1—^{14}C has been studied by Bergström *et al.* [1] with cannulated thoracic duct in rats. They reported that oleic acid was transported *via* the lymph and incorporated into triglycerides and phospholipids whether fed as oleic acid or triolein. Blomstrand and Rumpf [2] have reported that when cetyl alcohol 1—^{14}C was fed to rats with thoracic duct fistula about 15 % of it was present as unchanged alcohol in the lymph. Borgström [4] fed ethyl esters of fatty acids but found only traces of unhydrolysed esters in the lymph. Blomstrand[5] noticed that chimyl alcohol could be absorbed unchanged but was extensively metabolised already in the mucosa cells. Dhopeshwarkar and Mead[6] have shown evidence for occurrence of methyl esters in body and blood lipids. In another study[7] they also showed that when methyl elaidate was fed to fat deficient animals a part of it was found unhydrolysed in body lipids. The purpose of this short study was to determine whether methyl esters were present in rat lymph and to find out if methyl oleate could be absorbed without undergoing complete hydrolysis.

Experimental. Cannulation of lymph duct was performed as described before [1] on two male albino rats maintained on a regular chow diet. Lymph was collected in suitable containers under ethyl alcohol, before and after feeding methyl oleate. Methyl oleate was purified by vacuum distillation and was found to contain 85 % oleate, 15 % palmitate and a small amount of palmitoleate. No attempt was made to remove these impurities. The total lipids were extracted as usual from lymph using ethanol-ether (3:1) and subjected to silicic acid chromatography. The fraction that was eluted with 2 % ether in petroleum ether

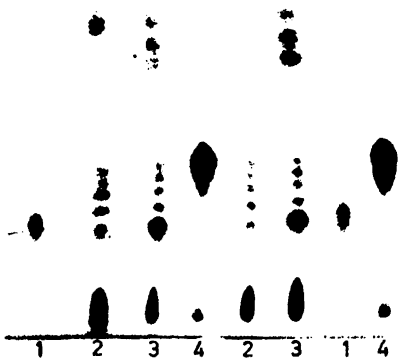

Fig. 1. Thin layer chromatogram. Developing solvent: 1.5 % Ethyl ether in normal hexane. Spraying solution: Saturated solution of phosphomolybdic acid in ethanol. Spot 1: Methyl oleate. 2: Lymph lipids before feeding methyl oleate. 3: Lymph lipids after feeding methyl oleate. 4: Cholesterol stearate.

was further subjected to thin layer chromatography as described previously [6]. The thin layer plates were sprayed with a saturated solution of phosphomolybdic acid in ethanol and heated at 100°C for a few minutes to bring about the color of the spots (Fig. 1). As this procedure cannot be used when recovery of the material is desired it was substituted by short exposure to iodine vapour to mark the spots, scraping off the silicic acid and extracting with ether. Experiments showed that this procedure did not alter the original compounds and so the ether extract was directly used for gas liquid chromatography (Fig. 2).

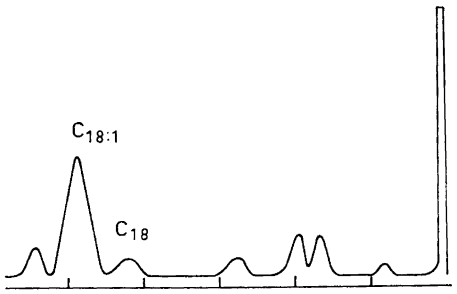

Fig. 2. Gas liquid chromatogram of methyl esters recovered from thin layer plate after feeding methyl oleate. Column: Polar polyester (LHC–R–296), 6 ft. Temp. 195°C.

Comments. It can be seen from Fig. 1 that the lymph lipids contained methyl esters even when no methyl esters were fed to the animals (Column 2). However, after feeding methyl oleate the same two spots were much more prominent (Column 3). Thus it was assumed that methyl oleate could be absorbed without complete hydrolysis. If this assumption was correct one would expect a pronounced peak of methyl oleate in the lymph lipid methyl esters after feeding methyl oleate. Examination by gas liquid chromatography (Fig. 2) showed that this was indeed the case. As a further confirmation the sample of methyl esters was hydrogenated using platinum oxide as catalyst and analysed by gas liquid chromatography. As predicted the original methyl oleate peak now merged into the stearic acid peak when retention times of known standard substances, analysed under similar conditions, were compared.

Thus it was concluded that rat lymph contained methyl esters and that at least a portion of the fed methyl oleate could be absorbed without complete hydrolysis. This observation is in accordance with the data on triglycerides and cetyl and chimyl alcohol reported earlier. Further work on the quantitative aspect is being undertaken.

This work is part of investigations supported by the *Swedish Medical Research Council*, and by grant HE–07663–01 of the *U.S. Public Health Service*.

1. Bergström, S., Blomstrand, R. and Borgström, B. *Biochem. J.* **58** (1954) 600.
2. Blomstrand, R. and Rumpf, J. A. *Acta Physiol. Scand.* **32** (1954) 374.
3. Blomstrand, R., Tryding, N. and Westöö, G. *Acta Physiol. Scand.* **37** (1956) 91.
4. Borgström, B. *Acta Physiol. Scand.* **25** (1952) 322.
5. Blomstrand, R. *Proc. Soc. Exptl. Biol. Med.* **102** (1959) 662.
6. Dhopeshwarkar, G. A. and Mead, J. F. *Proc. Soc. Exptl. Biol. Med.* **109** (1962) 425.
7. Dhopeshwarkar, G. A. and Mead, J. F. *J. Lipid Research* **3** (1962) 238.

Received October 8, 1962.

tures it is advantageous to use stepwise elution or gradient elution with eluants containing lower ethanol concentration in order to avoid an excessive broadening of the bands corresponding to higher saccharides. As an example it can be mentioned that a satisfactory separation of a mixture containing glucose, sucrose, raffinose, stachyose, and verbascose can be obtained by eluting the first two components with 74 % ethanol and then decreasing the ethanol concentration to 65 %.

A separation of monosaccharides from each other is also possible. The separation of xylose from glucose is demonstrated in Fig. 5. Similarly, it is possible to obtain a quantitative separation of mannose from glucose, whereas no satisfactory separation of galactose from glucose has been obtained under the experimental conditions chosen in the present work.

The financial support of the *Swedish Technical Research Council* is gratefully acknowledged.

1. Samuelson, O. and Sjöström, E. *Svensk Kem. Tidskr.* **64** (1952) 305.
2. Samuelson, O. Nordiske Kemikermöde, Aarhus 1956.
3. Rückert, H. and Samuelson, O. *Svensk Kem. Tidskr.* **66** (1954) 337; *Acta Chem. Scand.* **11** (1957) 303, 315.
4. Mattisson, M. and Samuelson, O. *Acta Chem. Scand.* **12** (1958) 1395.
5. Samuelson, O. *Ion Exchange Separations in Analytical Chemistry*, Almqvist & Wiksell, Stockholm, John Wiley & Sons, New York 1962.
6. Samuelson, O. and Swenson, B. *To be published.*

Received September 13, 1962.

Correction to "Conversion of Δ^5-Cholestene-3α-12α-diol to Cholic Acid in the Rabbit" *

HENRY DANIELSSON

In the title above *for* Δ^5-cholestene-3α-12α-diol *read* Δ^5-cholestene-3β-12α-diol.

* *Acta Chem. Scand.* **16** (1962) 1534.

Occurrence of Methyl Esters in Lymph

G. A. DHOPESHWARKAR and ROLF BLOMSTRAND

Department of Clinical Chemistry, Karolinska Institutet, Serafimerlasarettet, Stockholm, Sweden

Absorption of dietary triglycerides from intestines in a partially hydrolysed form has been established. Intestinal absorption of oleic acid 1—^{14}C has been studied by Bergström *et al.* [1] with cannulated thoracic duct in rats. They reported that oleic acid was transported *via* the lymph and incorporated into triglycerides and phospholipids whether fed as oleic acid or triolein. Blomstrand and Rumpf [2] have reported that when cetyl alcohol 1—^{14}C was fed to rats with thoracic duct fistula about 15 % of it was present as unchanged alcohol in the lymph. Borgström [4] fed ethyl esters of fatty acids but found only traces of unhydrolysed esters in the lymph. Blomstrand[5] noticed that chimyl alcohol could be absorbed unchanged but was extensively metabolised already in the mucosa cells. Dhopeshwarkar and Mead[6] have shown evidence for occurrence of methyl esters in body and blood lipids. In another study[7] they also showed that when methyl elaidate was fed to fat deficient animals a part of it was found unhydrolysed in body lipids. The purpose of this short study was to determine whether methyl esters were present in rat lymph and to find out if methyl oleate could be absorbed without undergoing complete hydrolysis.

Experimental. Cannulation of lymph duct was performed as described before [1] on two male albino rats maintained on a regular chow diet. Lymph was collected in suitable containers under ethyl alcohol, before and after feeding methyl oleate. Methyl oleate was purified by vacuum distillation and was found to contain 85 % oleate, 15 % palmitate and a small amount of palmitoleate. No attempt was made to remove these impurities. The total lipids were extracted as usual from lymph using ethanol-ether (3:1) and subjected to silicic acid chromatography. The fraction that was eluted with 2 % ether in petroleum ether

The Structure of Dibromodiethyl Ketone

CHRISTOFFER RAPPE and LENNART SCHOTTE

Institute of Chemistry, University of Uppsala, Uppsala, Sweden

When studying the products of the bromination of laevulic acid [1] one of us (C.R.) became interested in why some ketones give only the symmetrically substituted dibromoketone on bromination, for instance laevulic acid [1] and cyclohexanone [2], while others give only the unsymmetrically substituted dibromoketone, for example methyl ethyl ketone [3] and diethyl ketone [4]. In some cases both the symmetric and unsymmetric dibromo compound are obtained, for instance with acetone [5] and methyl propyl ketone [6].

Dibromodiethyl ketone was first prepared by Pauly [7], who assigned it a symmetric structure, but without any structural evidence. Later, one of us (L.S.) [4] proposed the unsymmetric structure on the basis of its hydrolysis reactions. Unfortunately, this method is not quite unambiguous as a rearrangement may take place during the hydrolysis *cf.* Reid, Gompf and Atwater [6] the possible effect of which was discussed in Ref. [4]. This uncertainty has prompted a reinvestigation of the structure using modern techniques.

The structure may be determined by means of nuclear magnetic resonance spectroscopy. The NMR-spectrum of dibromodiethyl ketone has been recorded and is given in Fig. 1. The spectrum shows two peaks at $\tau = 4.96$ ppm and $\tau = 8.20$ ppm with the relative intensities of 1:3. The methyl resonance is a doublet and the hydrogen band a quartet with the intensity ratio 1:3:3:1. The symmetry of the spectrum, the chemical shifts and the multiplicities are in accordance with the expected spectrum of the symmetric dibromoketone; thus its real structure is 2,4-dibromopentanone-3.

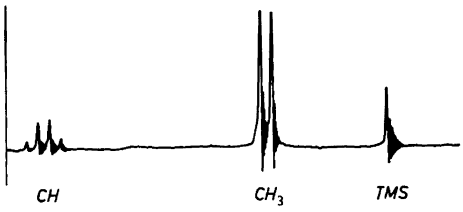

Fig. 1. The NMR-spectrum of dibromodiethyl ketone.

The compound can be obtained in good yields by both bromination in the presence of phosphorus [4] and by acid catalyzed bromination. No traces of the unsymmetric dibromoketone could be detected by means of NMR-spectroscopy in the twice distilled product, indicating that the amount of this isomer (if any) is less than a few percent. This unsymmetric ketone would have a CH_2-band with a τ-value similar to that of diethyl ketone ($\tau = 7.76$) and monobromodiethyl ketone ($\tau = 7.18$), and two different methyl resonances.

Experimental. The NMR-spectra were recorded on a Varian Associates Model A 40 spectrometer.

2,4-Dibromopentanone-3. I. Diethyl ketone was brominated as described by Schotte [4]. The boiling point 67–69°/9 mm was obtained. Schotte gave 75–77°/10 mm. $n_D^{25} = 1.5050$.

II. 320 g of bromine were added dropwise to 86 g of diethyl ketone mixed with 100 ml of hydrobromic acid (48 %) and chilled in an ice bath. The product was washed with water, sodium carbonate, and sodium bisulfite solutions and distilled. A fraction, b.p. 65–70°/8 mm, was collected, 182.5 g (75 %). On redistillation the b.p. 67–68°/8 mm and $n_D^{25} = 1.5042$ were obtained.

2-Bromopentanone-3 was prepared according to Pauly [7].

Acknowledgements. The authors wish to express their thanks to Professor Arne Fredga for his interest in this work and for all facilities put at their disposal. The NMR-spectra were recorded by Dr. Ragnar A. Hoffman.

1. Rappe, C. *Arkiv Kemi* **13** (1959) 425.
2. Metze, R. and Schreiber, P. *Chem. Ber.* **89** (1956) 2470.
3. Faworsky, A. and Issatschenko, B. *J. prakt. Chem.* (2) **88** (1913) 657.
4. Schotte, L. *Acta Chem. Scand.* **5** (1951) 969.
5. Weygand, F. and Schmied-Kowarzik, V. *Chem. Ber.* **82** (1949) 333.
6. Reid, E., Gompf, T. and Atwater, N. *J. Org. Chem.* **16** (1951) 1566.
7. Pauly, H. *Ber.* **34** (1901) 1771.

Received September 14, 1962.

Qualitative Observations on Cyanoplatinate(II)-Compounds

PAUL BERGSØE

Kofoedsminde, Nærum, Denmark

It is the purpose of the present note to point out that simple, qualitative experiments indicate the existence of a number of hitherto unreported cyanoplatinate(II) compounds, and that the methods implied most likely would be of help in a more systematic search for new materials of this type. The technique makes use of the fluorescence excited in the crystals by ultraviolet radiation, through the fact that the color of the fluorescence usually is characteristic of the species under study.

The formation of salt hydrates of a single cyanoplatinate(II) salt can be observed in the following way. A dilute solution of the salt is placed in a thin layer on the surface of a porous porcelain plate. After a gentle drying the centre of the plate is heated with a micro-burner. Under an ultraviolet lamp the colors corresponding to different salt hydrates can now be observed as rings going out from the centre. The color changes can be reversed when water vapor is admitted to the plate. It is in this way seen that the cyanoplatinate(II) salts in general form several salt hydrates. Only in very few cases are detailed investigations [1] available for comparison.

Evidence for the formation of double salts comes from small scale crystallization experiments. Solutions of two salts are mixed on a watch glass and allowed to crystallize. Double salt formation can now be deduced from the appearance of fluorescence colors not belonging to the constituents. Many such cases were observed.

A search for new cyanoplatinate(II) materials should be of special interest since it has recently been shown [2], in a study involving 11 salts, that a number of these show promise for scintillation counting. Thus, $Cs_2Pt(CN)_4 \cdot H_2O$ has a light yield of 70 % relative to NaI(Tl) and a decay time of 0.47 μsec, and must be regarded as having certain advantages in experimental nuclear physics and other fields where radiation detection is involved. It would indeed be very valuable if a reinvestigation of the cyanoplatinate(II) salts should result in a scintillator providing better energy resolution than NaI(Tl). However, even without the stimulus of practical and experimental applications a study of the chemistry and luminescence properties might well be rewarding.

The author is indebted to his former company "Paul Bergsøe og Søn" for placing the laboratory facility at his disposal. Stimulating discussions with Dr. C. F. Jacobsen and Mr. P. G. Hansen of the Chemistry Department, Research Establishment Risø, are gratefully acknowledged.

1. *Gmelin's Handbuch der anorganischen Chemie*, "Platin, Teil C". Very little has been added to the chemistry of the cyanoplatinate(II) salts since this volume was completed in 1940.
2. Bergsøe, P., Hansen, P. G. and Jacobsen, C. F. *Nuclear Instruments and Methods, In press.*

Received September 15, 1962.

On the Labelling of Sulphur-contaning Amino Acids and γ-Glutamylpeptides after Injection of Labelled Sulphate into Onion (*Allium cepa*)

TERTTU ETTALA and ARTTURI I. VIRTANEN

Laboratory of the Foundation for Chemical Research, Biochemical Institute, Helsinki, Finland

In order to establish the utilization of sulphate in the biosynthesis of the numerous sulphur-containing amino acids and peptides in the onion, sulphate labelled with ^{35}S was injected into onions in dilute NaCl solution. 0.2 ml of a solution containing 0.5 mC of ^{35}S was injected into the onion in five different places. The onion sets were placed for six days in moist sand before the injection. Subsequently, the enzymic reactions were inhibited by placing the onions in ethanol after certain intervals: the first onion 7 days after the injection, the second after 24 days, the third after 46 days, when some roots had been formed, and the last after 85 days, when the onion had green leaves. The experiment was started in September 1961, onions harvested in August being used as onion sets. Growth was extremely slow, as is revealed by the fact

Table 1. The radioactivities of the different fractions of onion injected with $^{35}SO_4^{2-}$. The onions were planted on September 9, 1961, $^{35}SO_4^{2-}$ was injected on September 15, 1961.

Dry weight of the onion g	Reaction time of $^{35}SO_4^{2-}$ days	Radioactivity of the amino acid fraction c/min *	Radioactivity of the water fraction c/min *
77	7	14 636 000	26 071 000
100	24	21 713 000	15 375 000
72	46	17 100 000	19 728 000
7 green leaves	85	759 000	1 367 000
95 bulb		10 400 000	16 550 000

* Countings uncorr.

that the first roots only began to appear after a month, and the green leaves only after two months.

The onions were chilled with solid carbon dioxide in ethanol, and then homogenized in cold ethanol. The ethanol content was

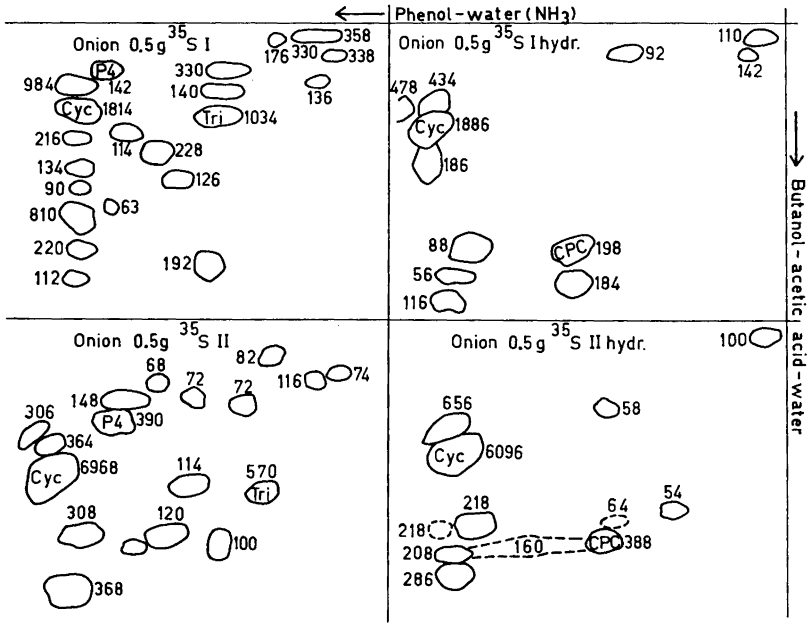

Fig. 1. Two-dimensional chromatograms of ^{35}S-containing amino acids and γ-glutamyl peptides in onion. Onions were placed for 6 days in moist sand and then injected with labelled sulphate. The upper chromatograms were developed 7, and the lower ones 46 days after the injection of labelled sulphate. The chromatograms to the left were developed before, and those to the right after hydrolysis. The spots were drawn on the basis of radiation measurements, and the numbers give the counts/min. Cyc = cycloalliin, P 4 = γ-L-glutamyl-(+)-S-(prop-1-enyl)-L-cysteine, Tri = γ-L-glutamyl-S-(β-carboxy-propyl)-L-cysteinyl-glycine, CPC = (−)-S-(β-carboxy-propyl)-L-cysteine.

70 % (= ethanol + the water which the onions contained). The homogenate was allowed to stand for 24 h, after which it was filtered and the precipitate washed with 70 % ethanol. The filtrates were combined, and the amino acids and acidic peptides (γ-glutamyl peptides) separated on an Amberlite IR-120 (H-form) column. 20 ml of resin and 300 ml of water were used for the separation, and 200 ml of 1 N ammonia for the elution of the amino acids and peptides.

In order to determine the radioactivity, the following samples were taken: (1) of the ethanol extract, (2) of the aqueous solution which had passed through the resin, (3) of the amino acid fraction eluted from the resin with ammonia. The radioactivity of the whole onion was calculated from that of the samples. A two-dimensional chromatogram (BuOH-AcOH-H_2O; 630—100—270; water-saturated phenol-NH_3) was prepared from the amino acid fraction. Radioautograms were made from the chromatograms obtained for the location of the active spots. The intensity of the radiation was then measured on the paper, and the paper chromatograms were sprayed with 0.25 % ninhydrin. The spots could partly be identified by comparison with chromatograms run on known amino acids and γ-glutamyl peptides.

Table 1 shows the radioactivity (c/min) of the amino acid fraction and the water fraction of the whole onion at different stages of growth.

The first radioautogram, made from the paper chromatogram of the amino acid fraction isolated, was prepared 7 days after the injection and showed 21 spots labelled with ^{35}S. When the amino acid fraction was hydrolyzed with 1 N HCl for 3 h at 100°C, only 12 radioactive spots could be seen on the paper chromatogram [1] (Fig. 1).

The decrease in the number of spots is partly due to the hydrolysis of γ-glutamyl peptides, partly to the decomposition of sulphur-containing amino acids (*e.g.* S-(prop-1-enyl)-cysteine sulpoxide). Some spots present on the chromatogram 7 days after the injection could not be seen on the paper chromatograms prepared from onions 46 days after the injection. On the other hand, new spots had now appeared (Fig. 1).

Among the spots occurring on the radioautograms cycloalliin [2] and γ-glutamyl-S-(β-carboxy-propyl)-L-cysteinyl-glycine [3] could be identified by comparison with the amino acids and γ-glutamyl peptides previously isolated in this laboratory, and after hydrolysis the corresponding S-(β-carboxy-propyl)-L-cysteine [3]. Methionine, glutathione and γ-glutamyl-S-(prop-1-enyl)-cysteine sulphoxide [4] probably also occurred on the chromatograms. The highest labelling was found in cycloalliin, which is the most abundant amino acid in the onion. The labelling of cycloalliin increased throughout the growing season (Table 2).

Table 2. The radioactivity of the cycloalliin spot on the paper chromatogram in different periods after the injection of $^{35}SO_4^{2-}$.

7	days	1814 c/min/0.5 g *	
24	,,	6064 ,,	
46	,,	6968 ,,	
85	,,	3540 ,,	green leaves
		4172	bulb

* Countings uncorr.

The spot (192 c/min) seen on the upper chromatogram (Fig. 1), which travels rapidly in butanol-acetic acid-water and with average speed in phenol-water, and which does not disappear on hydrolysis (184 c/min), is obviously a hitherto unknown S-containing amino acid.

Suzuki and his collaborators [5] have recently started to study the peptides in garlic, using sulphate labelled with ^{35}S during cultivation. After 24 h feeding, some of the γ-glutamylpeptides isolated in this laboratory from onion and chemically characterized, were labelled.

This research has been financed in part by a grant made by the *United States Department of Agriculture, Agricultural Research Service.*

1. Virtanen, A. I. *Ann. Rep. Foundation for Chemical Research* **1961** 8.
2. Virtanen, A. I. and Matikkala, E. J. *Suomen Kemistilehti* **B 31** (1958) 191; *Acta Chem. Scand.* **13** (1959) 623.
3. Virtanen, A. I. and Matikkala, E. J. *Suomen Kemistilehti* **B 33** (1960) 83; *Z. physiol. Chem.* **322** (1960) 8.
4. Virtanen, A. I. and Matikkala, E. J. *Suomen Kemistilehti* **B 34** (1961) 84, 114.
5. Suzuki, T., Sugii, M. and Kakimoto, T. *Chem. Pharm. Bull. Tokyo* **9** (1961) 78.

Received September 28, 1962.

Qualitative Observations on Cyanoplatinate(II)-Compounds

PAUL BERGSØE

Kofoedsminde, Nærum, Denmark

It is the purpose of the present note to point out that simple, qualitative experiments indicate the existence of a number of hitherto unreported cyanoplatinate(II) compounds, and that the methods implied most likely would be of help in a more systematic search for new materials of this type. The technique makes use of the fluorescence excited in the crystals by ultraviolet radiation, through the fact that the color of the fluorescence usually is characteristic of the species under study.

The formation of salt hydrates of a single cyanoplatinate(II) salt can be observed in the following way. A dilute solution of the salt is placed in a thin layer on the surface of a porous porcelain plate. After a gentle drying the centre of the plate is heated with a micro-burner. Under an ultraviolet lamp the colors corresponding to different salt hydrates can now be observed as rings going out from the centre. The color changes can be reversed when water vapor is admitted to the plate. It is in this way seen that the cyanoplatinate(II) salts in general form several salt hydrates. Only in very few cases are detailed investigations [1] available for comparison.

Evidence for the formation of double salts comes from small scale crystallization experiments. Solutions of two salts are mixed on a watch glass and allowed to crystallize. Double salt formation can now be deduced from the appearance of fluorescence colors not belonging to the constituents. Many such cases were observed.

A search for new cyanoplatinate(II) materials should be of special interest since it has recently been shown [2], in a study involving 11 salts, that a number of these show promise for scintillation counting. Thus, $Cs_2Pt(CN)_4 \cdot H_2O$ has a light yield of 70 % relative to NaI(Tl) and a decay time of 0.47 μsec, and must be regarded as having certain advantages in experimental nuclear physics and other fields where radiation detection is involved. It would indeed be very valuable if a reinvestigation of the cyanoplatinate(II) salts should result in a scintillator providing better energy resolution than NaI(Tl). However, even without the stimulus of practical and experimental applications a study of the chemistry and luminescence properties might well be rewarding.

The author is indebted to his former company "Paul Bergsøe og Søn" for placing the laboratory facility at his disposal. Stimulating discussions with Dr. C. F. Jacobsen and Mr. P. G. Hansen of the Chemistry Department, Research Establishment Risø, are gratefully acknowledged.

1. *Gmelin's Handbuch der anorganischen Chemie*, "Platin, Teil C". Very little has been added to the chemistry of the cyanoplatinate(II) salts since this volume was completed in 1940.
2. Bergsøe, P., Hansen, P. G. and Jacobsen, C. F. *Nuclear Instruments and Methods, In press.*

Received September 15, 1962.

On the Labelling of Sulphur-contaning Amino Acids and γ-Glutamylpeptides after Injection of Labelled Sulphate into Onion (*Allium cepa*)

TERTTU ETTALA and ARTTURI I. VIRTANEN

Laboratory of the Foundation for Chemical Research, Biochemical Institute, Helsinki, Finland

In order to establish the utilization of sulphate in the biosynthesis of the numerous sulphur-containing amino acids and peptides in the onion, sulphate labelled with ^{35}S was injected into onions in dilute NaCl solution. 0.2 ml of a solution containing 0.5 mC of ^{35}S was injected into the onion in five different places. The onion sets were placed for six days in moist sand before the injection. Subsequently, the enzymic reactions were inhibited by placing the onions in ethanol after certain intervals: the first onion 7 days after the injection, the second after 24 days, the third after 46 days, when some roots had been formed, and the last after 85 days, when the onion had green leaves. The experiment was started in September 1961, onions harvested in August being used as onion sets. Growth was extremely slow, as is revealed by the fact

A Rapid Method for the Quantitative Estimation of Urinary Oestrogens in the Pregnant Mare *

TORLEIV LUNAAS

Department of Reproductive Physiology and Pathology, Veterinary College of Norway, Oslo, Norway

During an attempt to develop an easily practicable pregnancy test in the mare based on the presence of urinary oestrogens it was found that the procedure arrived at apparently allowed crude quantitative estimations of the oestrogens when specific photometric measurements were included. In this communication the applicability of the method for this purpose is evaluated.

The material consisted of urine samples collected from 60 mares during the months 5 and 6 after breeding. Of the urine 1 ml was pipetted into a thinwalled 100 ml flask and diluted with 10 ml water of room temperature. Care was taken to select uniform glassware. To the diluted urine 15 ml of conc. H_2SO_4 were slowly added during swirling of the flask, and the reaction mixture (temperature *ca.* 110°C) was left warm for 5 min after which time it was diluted with 35 ml of water. Of this final dilution an aliquot of 15 ml was thoroughly cooled under the tap, and extracted with 5 ml of methylene chloride containing 2 % (w/v) *p*-nitrophenol [1] which was then centrifuged and submitted to colorimetry. For fluorimetry an aliquot of 1 ml (corre-

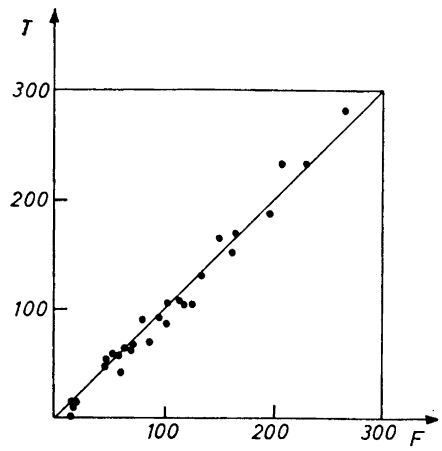

Fig. 1. Urinary oestrogen concentrations in mares calculated as μg oestrone per ml. Means of duplicate estimates obtained by colorimetry, T, and fluorimetry, F.

* A preliminary report on the application of the method as a pregnancy test has been presented at the 9. *Nordiske Veterinærmöde* (Section E-5), Copenhagen 1962.

Table 1. Precision of fluorimetric estimation of urinary oestrogens (calculated as oestrone) in the mare.

Range, μg/ml	Number, *n*, of duplicates	Standard deviation, *s*, of single estimates from their means, %	Fiducal range, *f*, of the mean, *M*, of two estimates ($P = 0.05$), %
0–2	22	47.9	$M \pm 70.0$
2–6	11	43.3	$M \pm 67.5$
6–10	lacking	—	—
10–20	4	16.8	$M \pm 33.0$
20–40	lacking	—	—
40–100	11	8.6	$M \pm 13.4$
100 (standards)	18	11.9	$M \pm 17.6$
100–300	13	11.5	$M \pm 17.5$

$s = \sqrt{\Sigma d^2/2n}$, d = difference between duplicates as per cent of the mean.
$f = ts/\sqrt{2}$

sponding to about 1/60 ml of urine) was similarly treated.

As standards 100 μg of oestrone were taken through the procedure in the presence of 1 ml of urine from a non-pregnant mare. All urine samples and standards were developed in duplicate.

The optical densities were read at the wavelength of maximal absorption of oestrone, 533 mμ, and also 33 mμ to both sides. The corrected optical densities calculated as $E_c = 2E_{533} - (E_{500} + E_{566})$ were assumed to be linearly related to the oestrogen concentration.

Fluorimetry of the methylene chloride extracts was performed with a Beckman model DU monochromator supplied with an attachment made in the laboratory (to be published) and a photomultiplier combination. As incident light an unfiltered beam of a wolfram continuum was used. The light emitted at a right angle of the incident beam was recorded at 550 mμ (maximal emission of oestrone) and at 520 mμ. The slit of the monochromator was kept at 0.1 mm corresponding to a half intensity band width of about 2.5 mμ. The difference between the light intensities at the two wavelengths was assumed to be due to oestrogens.

The results of colorimetric and fluorimetric analyses are plotted against each others in Fig. 1. It may be seen that the values of the oestrogen concentration obtained with both photometric methods were in good agreement. Estimates of the precision [2] of the fluorimetric method in different ranges of urinary oestrogen concentration are given in Table 1. It is evident that oestrogen concentrations below 10—20 μg per ml could not be determined with any reasonable confidence. It is questionable to which degree positive values in this range represent oestrogens. At very low oestrogen concentrations the net fluorescence was always positive whereas the corrected optical densities were sometimes negative. Colorimetry at low concentrations tended to give erratic results apparently due to the relatively high unspecific (background) absorption and inadequacy of the correction formula applied.

During the months 5 and 6 after breeding the ratio between oestrone and equilin, which apparently are the major oestrogens excreted in the pregnant mare, seems to be high, but may decrease towards parturition [3]. The results of the method described for the estimation of total urinary oestrogens would be influenced by any variations in this ratio since the chromogenic (and fluorigenic) value of equilin was much lower than that of oestrone.

The results reported indicate that the amounts of oestrogens being excreted in the pregnant mare are subject of large variations. Due to its practicability the crude method described might be of some value for further studies of these variations and of the possible variations of the time after breeding at which an appreciably increased excretion of oestrogens is initiated.

1. Ittrich, G. *Z. physiol. Chem.* **312** (1958) 1.
2. Youden, W. J. *Statistical Methods for Chemists.* John Wiley & Sons, New York 1951.
3. Savard, K. *Endocrinology* **68** (1961) 411.

Received August 10, 1962.

Isothiocyanates XLVI *. Glucocappasalin, a New Naturally Occurring Thioglucoside

ANDERS KJÆR and HELENE THOMSEN

Department of Organic Chemistry, Royal Veterinary and Agricultural College, Copenhagen, Denmark

Capparis salicifolia Griseb. *(Capparidaceae)* is a tree indigenous to the Chaco region of the Argentine. Paper chromatography of an extract of its seeds** revealed the presence of two new thioglucosides with R_B-values [1] of 0.81 and 1.17 in butanol:ethanol:water (4:1:4). We here wish to report on the structure of the fastest migrating glucoside for which the name *glucocappasalin* is proposed.

After purification by ion exchange, counter-current separation of the two glucosides (380 transfers), and acetylation, *glucocappasalin tetraacetate* was obtained

* Part XLV: *Phytochemistry. In press.*

** The authors are much indebted to Dr. U. Weiss, N. I. H., Bethesda, Md. for drawing our attention to this plant, and to Professor V. Deulofeu, University of Buenos Aires, and Dr. N. Fock, The Ethnographic Division of the Danish National Museum, for their help in providing seed material for the present study.

sponding to about 1/60 ml of urine) was similarly treated.

As standards 100 μg of oestrone were taken through the procedure in the presence of 1 ml of urine from a non-pregnant mare. All urine samples and standards were developed in duplicate.

The optical densities were read at the wavelength of maximal absorption of oestrone, 533 mμ, and also 33 mμ to both sides. The corrected optical densities calculated as $E_c = 2E_{533} - (E_{500} + E_{566})$ were assumed to be linearly related to the oestrogen concentration.

Fluorimetry of the methylene chloride extracts was performed with a Beckman model DU monochromator supplied with an attachment made in the laboratory (to be published) and a photomultiplier combination. As incident light an unfiltered beam of a wolfram continuum was used. The light emitted at a right angle of the incident beam was recorded at 550 mμ (maximal emission of oestrone) and at 520 mμ. The slit of the monochromator was kept at 0.1 mm corresponding to a half intensity band width of about 2.5 mμ. The difference between the light intensities at the two wavelengths was assumed to be due to oestrogens.

The results of colorimetric and fluorimetric analyses are plotted against each others in Fig. 1. It may be seen that the values of the oestrogen concentration obtained with both photometric methods were in good agreement. Estimates of the precision [2] of the fluorimetric method in different ranges of urinary oestrogen concentration are given in Table 1. It is evident that oestrogen concentrations below 10—20 μg per ml could not be determined with any reasonable confidence. It is questionable to which degree positive values in this range represent oestrogens. At very low oestrogen concentrations the net fluorescence was always positive whereas the corrected optical densities were sometimes negative. Colorimetry at low concentrations tended to give erratic results apparently due to the relatively high unspecific (background) absorption and inadequacy of the correction formula applied.

During the months 5 and 6 after breeding the ratio between oestrone and equilin, which apparently are the major oestrogens excreted in the pregnant mare, seems to be high, but may decrease towards parturition [3]. The results of the method described for the estimation of total urinary oestrogens would be influenced by any variations in this ratio since the chromogenic (and fluorigenic) value of equilin was much lower than that of oestrone.

The results reported indicate that the amounts of oestrogens being excreted in the pregnant mare are subject of large variations. Due to its practicability the crude method described might be of some value for further studies of these variations and of the possible variations of the time after breeding at which an appreciably increased excretion of oestrogens is initiated.

1. Ittrich, G. *Z. physiol. Chem.* **312** (1958) 1.
2. Youden, W. J. *Statistical Methods for Chemists.* John Wiley & Sons, New York 1951.
3. Savard, K. *Endocrinology* **68** (1961) 411.

Received August 10, 1962.

Isothiocyanates XLVI *. Glucocappasalin, a New Naturally Occurring Thioglucoside

ANDERS KJÆR and HELENE THOMSEN

Department of Organic Chemistry, Royal Veterinary and Agricultural College, Copenhagen, Denmark

Capparis salicifolia Griseb. *(Capparidaceae)* is a tree indigenous to the Chaco region of the Argentine. Paper chromatography of an extract of its seeds** revealed the presence of two new thioglucosides with R_B-values [1] of 0.81 and 1.17 in butanol:ethanol:water (4:1:4). We here wish to report on the structure of the fastest migrating glucoside for which the name *glucocappasalin* is proposed.

After purification by ion exchange, counter-current separation of the two glucosides (380 transfers), and acetylation, *glucocappasalin tetraacetate* was obtained

* Part XLV: *Phytochemistry. In press.*

** The authors are much indebted to Dr. U. Weiss, N. I. H., Bethesda, Md. for drawing our attention to this plant, and to Professor V. Deulofeu, University of Buenos Aires, and Dr. N. Fock, The Ethnographic Division of the Danish National Museum, for their help in providing seed material for the present study.

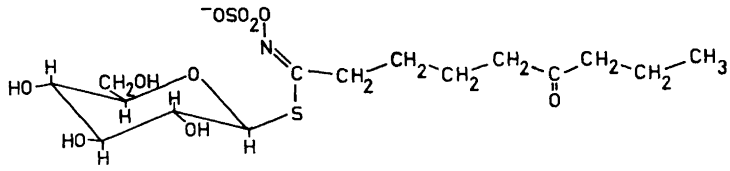

I

as a crystalline potassium salt, m.p.* 133–136° (decomp.), $[\alpha]_D^{22}$ −16.0° (*c* 1.0, H_2O). λ_{max}^{MeOH} 223 mμ (ε 6490) (shoulder at 210 mμ). IR-spectrum (KBr): very similar to that of glucocapangulin tetraacetate [2] with a sharp band at 1700 cm^{-1}, indicative of a keto-grouping. Analytical data** agreed with the composition $C_{23}H_{34}O_{14}NS_2K,0.5\ H_2O$ for the acetate. Assuming the general thioglucoside structure to be present, this formula leaves $(C_7H_{15})(CO)$ to be accomodated as the side-chain.

Ethanolysis, catalyzed by pyridinium ions[3], converted the acetate into *desulphoglucocappasalin tetraacetate*, $C_{23}H_{35}O_{11}NS$, m.p. 144°, $[\alpha]_D^{21}$ −16.1° (*c* 2.0, CH_3OH), λ_{max}^{MeOH} 213 mμ (ε 5100), IR_{KBr}:keto band at 1695 cm^{-1}. The NMR-spectrum*** (in $CDCl_3$) exhibited, besides the expected signals from a β-glucopyranoside tetraacetate moiety, a highly shielded (τ 9.12) triplet (J = 7 cps) corresponding in area to three protons and, hence, attributable to *one* CH_3-group located next to a CH_2-group and without double bond functions in β-position. The combined NMR-data clearly demonstrated the presence in glucocappasalin of an *unbranched* C_8-chain containing a C=O-grouping in γ, δ or ε-position relative to the terminal methyl group.

On acid hydrolysis glucocappasalin or its tetraacetate afforded, as expected [4], besides sugar, hydroxylamine and sulphate, an oxononanoic acid, characterized as the semicarbazone, m.p. 150°. On mass-spectroscopic analysis* the methyl ester of the oxo-acid could be unequivocally identified as 6-oxononanoic acid methyl ester (molecular ion peak at *m/e* 186, strong peaks at *m/e* 154, 155 (M−32, M−31), 143 (M−$CH_3(CH_2)_2$), 111 (143−32), 71 ($CH_3(CH_2)_2CO$)). On critical comparison with synthetic specimens of the semicarbazone of 6-oxononanoic acid, m.p. 150° (lit. values: 154−5° [5], 153° [6]), and the methyl ester[7] (identical IR and mass spectra), this identification was confirmed.

Hence, the glucocappasalin ion is represented by structure (I)**, which is a higher homologue of glucocapangulin previously encountered in *Capparis angulata* Ruiz et Pav. [2], a close botanical relative of *C. salicifolia* Griseb. The presence in (I) of an unbranched C_9-skeleton renders its biogenesis intriguing.

A full account of the present work will appear in a forthcoming paper.

1. Schultz, O.-E. and Wagner, W. *Z. Naturforsch.* **11b** (1956) 73.
2. Kjær, A., Thomsen, H. and (in part) Hansen, S. E. *Acta Chem. Scand.* **14** (1960) 1226.
3. Ettlinger, M. G. and Dateo, jr., G. P. *Studies of Mustard Oil Glucosides*, Final Report, Contract DA 19−129−QM−1059, Rice Institute, Houston, Texas (1961) 17.
4. Ettlinger, M. G. and Lundeen, A. J. *J. Am. Chem. Soc.* **78** (1956) 4172.
5. Plešek, J. *Chem. Listy* **49** (1955) 1840; *Chem. Abstr.* **50** (1956) 9294.
6. Lamant, M. *Compt. rend.* **246** (1958) 2380; *Chem. Abstr.* **52** (1958) 18249.
7. Brockman jr., J. A. and Fabio, P. F. *J. Am. Chem. Soc.* **79** (1957) 5027.

* Melting points are uncorrected. Heating rate: 1°/min.

** Satisfactory analyses and consistent infrared spectra have been obtained for the new compounds reported.

*** The authors are indebted to Dr. J. R. Andersen for measuring the NMR-spectrum on a Varian A-60 spectrometer.

* The authors are much indebted to Dr. R. Ryhage, Stockholm, for performing the mass spectra.

** In the semi-systematic naming of thioglucosides recently proposed [3], glucocappasalin would be: potassium 5-oxooctyl glucosinolate.

Received October 3, 1962.

Thin-layer Gel Filtration

BENGT G. JOHANSSON and LARS RYMO

Department of Medical Biochemistry
University of Göteborg, Sweden

The introduction by Porath and Flodin [1] of the gel filtration method, generally applied as a column chromatographic technique, permits a very convenient way of separating substances of different molecular size. In order to achieve a simple method to test the ability of separating substances of biological interest by gel filtration using very small amounts of material we have investigated the possibility of using a thin-layer chromatographic technique which we will present in this paper.

Methods and materials. In this study Sephadex G-25, fine (water regain 2.4), Sephadex G-75, fine (water regain 7.6) and Sephadex G-75, particle size < 400 mesh, were used. The thin-layer plates were made with the equipment delivered by C. Desaga GmbH, Heidelberg. The spreader was used with the slit width adjusted to 0.5 mm.

Procedure. For Sephadex G-25 gel filtration 10 g of the gel was stirred with 50 ml of 0.1 M sodium chloride or with an appropriate buffer solution for one hour. The slurry was then transferred to the spreader and immediately spread over either four glass plates of the dimensions of 8 × 20 cm or two plates of the dimensions of 20 × 20 cm. After 10 min the plates could be removed from the plastic support without disturbing the uniformity of the gel layer. The plates could be used at once or stored in a moist chamber for one or two days. Preparation of plates with Sephadex G-75, fine, and Sephadex G-75 (particle size < 400 mesh) was performed in a similar manner, but using 5 g of the gel, which was intermittently stirred for 5 h with 70 ml of a buffer solution, usually 0.02 M sodium phosphate buffer, pH 7.0, containing 0.2 M sodium chloride.

The samples were applied at a distance of 4 cm from the end of the plate as spots with a diameter of 3—5 mm, which was possible by using volumes of 1—5 µl. The plates were placed in a paper electrophoresis unit (LKB 3276 BN, Stockholm) with one of the electrode chambers 7—10 cm higher than the other. A piece of filter paper (Whatman No. 3 MM) ensured contact between the gel and the buffer reservoir, giving a liquid flow through the gel. With a plate of the dimensions of 20 × 20 cm the electrophoresis unit could not be used; instead the plates were placed in a moist chamber leaning against a buffer reservoir with a filter paper contact as described above. The flow rates varied somewhat, but this did not interfere with the reproducibility of the runs. A suitable coloured substance, usually 2,4-dinitrophenyl aspartic acid (DNP-aspartic acid), was always applied to the plate as a marker of filtration velocity. Running times of 5 h for Sephadex G-25 and 8 h for Sephadex G-75 generally gave good separations. This corresponded to a travelling distance of about 10—15 cm for substances, which by column gel filtration were found to have R_F-values close to 1.0. After complete filtration the plates were dried in an oven at 80°C, giving a thin opaque film of the gel on the glass plates, and then sprayed with 0.3 % ninhydrin in ethanol or dyed with amido black (Amidoschwarz 10 B, E. Merck AG, Darmstadt) according to the following procedure. The plates were placed in a saturated solution of the dye in methanol-acetic acid-water, 80:10:10 (v/v), and left for one hour. Excess dye was removed by repeated washings in methanol-acetic acid-water, 70:15:15 (v/v), leaving a faint blue background in the gel. The plates were then dried at room tem-

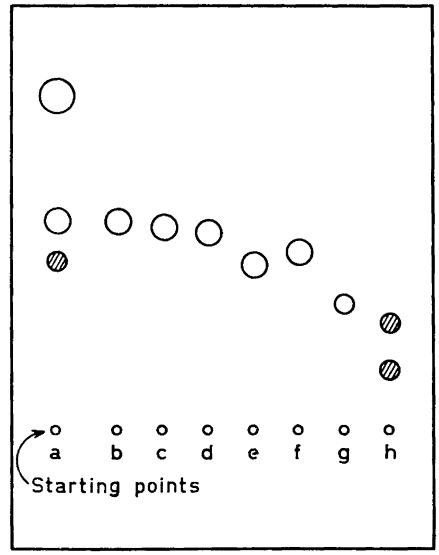

Fig. 1. Schematic representation of gel filtration on Sephadex G-25. a. Coeruleoplasmin and DNP-aspartic acid. b. Aspartic acid. c. Glycyl-glycine. d. Glycine. e. Phenylalanine. f. Tyrosine. g. Tryptophan. h. DNP-phenylalanine and DNP-tryptophan. Ninhydrin treatment of the plate.

perature. During the dyeing procedure a slight swelling of the gel was obtained, and it had a tendency to loosen from the plates. This, however, could be counteracted by careful handling.

Application of the method. Sephadex G-25 was used for the separation of a mixture of human coeruleoplasmin and DNP-aspartic acid as seen in Fig. 1. The separation was very sharp. Besides the yellow spot is seen a ninhydrin colouring substance coming from impurities in the DNP-amino acid preparation. Fig. 1 also shows the thin-layer filtration of some amino acids and amino acid derivatives. Glycyl-glycine moves with approximately the same rate as glycine. A slightly lower rate of movement is found for phenylalanine and tyrosine whereas tryptophan moves considerably slower than the other amino acids. The DNP-derivatives of phenylalanine and tryptophan are well separated and move slower than the corresponding amino acid. These results are in accordance with the fact that aromatic substances are retarded on the gel due to reversible adsorption [2].

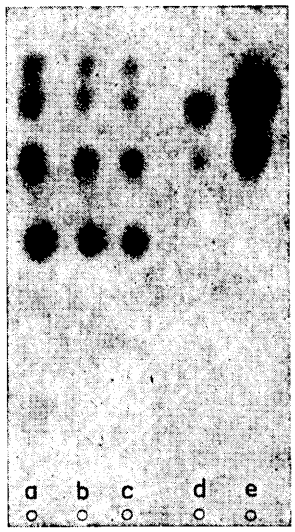

Fig. 2. Gel filtration on Sephadex G-75, fine. a—c. A mixture of bovine serum albumin β-lactoglobulin and α-lactalbumin. d, e. A sample of purified "Bence-Jones protein" from a pathological urine. Double amount of sample applied in e. The plate was dyed with amido black B.

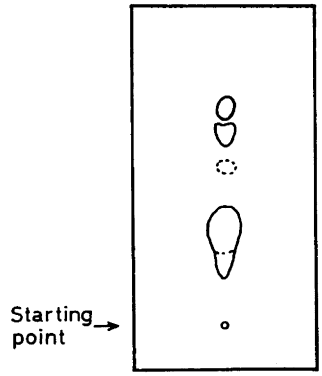

Fig. 3. Schematic representation of gel filtration of a tryptic hydrolysate of normal human γ-globulin on Sephadex G-75, fine. Ninhydrin colour.

An experiment using Sephadex G-75 is shown in Fig. 2. Artificial mixtures of bovine serum albumin, β-lactoglobulin and α-lactalbumin (molecular weights 69 000, 35 000 and 15 000) in equal parts are separated into four spots (Fig. 2a—c). In other experiments bovine serum albumin was found to give two spots. A sample of purified "Bence-Jones protein" gives two well separated spots (Fig. 2d, e). Filtration of a tryptic hydrolysate of human γ-globulin, finally, gives a separation in full accordance with the results obtained by column gel filtration [3] (Fig. 3).

The present method offers good possibilities of rapid comparative analyses by gel filtration and will be used in studies of human γ-globulin related proteins and their degradation products.

We are indebted to Miss Inger Karlsson for skilful technical assistance. The work was supported by a grant from the *Medical Faculty*, University of Göteborg.

A similar method for thin-layer gel filtration on Sephadex G-25 has quite recently been published by Determann[4].

1. Porath, J. and Flodin, P. *Nature* **183** (1959) 1657.
2. Porath, J. *Biochim. Biophys. Acta* **39** (1960) 193.
3. Hanson, L. Å. and Johansson, B. G. *Nature* **187** (1960) 599.
4. Determann, H. *Experientia* **18** (1962) 430.

Received October 8, 1962.

ACTA CHEMICA SCANDINAVICA 16 (1962) 2069–2086

Proton Magnetic Resonance Study of the Water Lattice Distortions in Aqueous Alkali Halide Solutions

M. S. BERGQVIST and E. FORSLIND

Division of Physical Chemistry, Royal Institute of Technology, Stockholm 70, Sweden

Dedicated to Professor *Ole Lamm* on his 60th birthday

The concentration dependence of PMR chemical shifts in aqueous solutions of all alkali halides, except the insoluble lithium fluoride, has been investigated at 40 Mc/sec, making use of an external reference substance and adding a macroscopic susceptibility correction.

An attempt has been made to resolve the molal shift into ionic contributions, assuming a law of approximate additivities shown to be successful, except in the cases of the lithium and the fluoride ions, which do not fit the simple linear relationship valid for the remaining alkali halides. The reasons for the deviation are discussed.

A comparison of PMR data with dielectric data of electrolytic solutions is made.

Already in 1954 Shoolery and Alder [1] investigated the influence of a dissolved diamagnetic salt on water using NMR techniques. By measuring the water proton resonance shifts in concentrated aqueous solutions of electrolytes, they were able to establish a relative scale of specific contributions made by ions to the total measured chemical shift, which, however, lacked corrections for magnetic susceptibility. The data of Shoolery and Alder have been included in Table 1 for a comparison with the results of the present investigation.

In the same year Gutowsky and Fujiwara [2] published a study of the PMR shifts in aqueous ammonium salt solutions.

A method for the interpretation of PMR shifts for acids and bases was first suggested by Gutowsky and Saika [3] who applied it to HNO_3, $HClO_4$, H_2SO_4 and NaOH in aqueous solution. Hood *et al.* [4–9] extended the method to the calculation of acid constants for $HClO_4$, HNO_3, H_2SO_4, HIO_3, CF_3COOH and C_3F_7COOH. Their procedure necessitated some assumptions concerning certain states of acid-water complexes which, however, seem to be supported by Raman spectroscopy investigations [10]. Happe *et al.* [11] made a study of the system HNO_3—H_2O.

A thorough study of the chemical shifts in diamagnetic salt solutions was published by Hertz and Spalthoff[12] in 1959. Concentration and temperature effects were investigated. Previously internal standards in water solutions had been avoided due to the influence of most solutes on water proton resonances. Hertz and Spalthoff showed the possibility of using *t*-butanol or, in a few cases, some tetraalkylammonium salts as internal standards and thus avoided the problem of susceptibility corrections. Hertz and Spalthoff maintained that the shift due to a constant concentration of the reference compound was constant in the whole electrolyte concentration range. This appeared to be a reasonable assumption in view of the fact that none of their results seemed to contradict it. A comparison between their values and the results of the present investigation is made in Table 1.

Recently Hindman[13] developed a model for correlating "effective hydration numbers" of 1—1-electrolytes with measured PMR shifts in water solutions. Hindman made use of *c*-pentane as an external reference.

In 1959 Axtmann[14] found a linear correlation between the molar proton chemical shifts for hydrated polyvalent cations and pK_a, where K_a is the first protolysis constant for the complex hydrate ion. Later, Axtmann *et al.*[15] found evidence for a strong coupling between aluminium ions and hydrate water in nitric acid solutions.

Connick and Poulson[16] measured the broadening of ^{17}O resonance signals in water caused by the paramagnetic ions Mn^{2+}, Cu^{2+}, Fe^{2+}, Co^{2+}, Cr^{3+} and Ni^{2+}.

Chemical shifts and relaxation effects in ^{17}O-resonances caused by gadolinium(III)-ions in aqueous solution were studied by Shulman and Wyluda[17].

Gutowsky and McGarvey[18] found large chemical shifts and concentration effects in a study of ^{205}Tl magnetic resonances in thallium(I) and thallium(III) solutions. To explain the shifts they assumed delayed collisions between positive and negative ions, *i.e.* a kind of ion pair formation which caused electronic excitation leading to a second order paramagnetic term (according to Ramsey[19]) and negative shifts *. Freeman *et al.*[20–22] observed a strong action of counter-ions upon the chemical shifts of thallium(I) in aqueous solutions.

Another type of presumed electronic process in water solution was studied by McConnell and Weaver[23]. By measuring the widths of the ^{63}Cu resonance line in acid solutions containing cuprous and cupric chloride they computed the bimolecular rate constant for the reaction $Cu^{2+} + Cu^{+} \rightarrow Cu^{+} + Cu^{2+}$.

^{35}Cl resonance was used by Wertz[24,25] and Chesnut[26] to study the exchange between water in bulk and hydrate water of some paramagnetic ions.

Wertz studied ^{24}Na magnetic resonance effects in water solutions of metabolites[27,28] and of inorganic and organic salts[29,30].

Connick and Poulsen[31] studied ^{27}Al and ^{19}F resonances in water solutions of NaF and $Al(NO_3)_3$ and could calculate the stability constants for AlF^{2+} and AlF^{+}. The same authors[32] also studied ion-pair effects in water solutions of NaF and KF. The sodium and potassium ions seemed to behave in entirely

* In this work a shift of a certain specimen is termed positive when the resonant field of the specimen is larger than that of a reference compound. This is also the case when reference is made to other authors who may have used the reverse definition in their original papers.

different manners when acting as counterions to the fluoride ion. The authors inferred that NaF formed ion pairs even at very low concentrations. For KF the phenomenon seemed to appear only at higher concentrations (>5 M).

Carrington *et al.*[33,34] performed ^{19}F magnetic resonance measurements for their study of ion-solvent and ion-ion interactions. They also measured the magnetic resonance of ^{133}Cs and could observe effects indicating ion pair formation.

The magnetic resonance of ^{127}I in aqueous solutions of alkali iodide was studied by Itoh and Yamagata [35].

^{79}Br, ^{81}Br and ^{127}I magnetic resonances were utilized by Hertz [36,37] in a study of concentration dependent line broadening effects in aqueous solutions of alkali and earth alkali halides.

Although the investigations quoted above shed some light on the various problems of electrolytic solutions, the situation is still far from clear. The aim of the present investigation is to contribute some additional information about the behaviour of the water proton in moderately concentrated aqueous solutions of alkali halides by means of PMR techniques.

In the experimental study, the water proton shifts have been measured using benzene as an external reference. The complex chemical situation introduced by an internal reference standard can be avoided by making use of the best available susceptibility [38,39] and density [40] data and applying susceptibility corrections according to the classical formula [41].

EXPERIMENTAL

The proton resonance measurements were made with a Varian Associates V-4300B spectrometer, operating at a fixed frequency of 40 Mc/sec. Field stability was achieved by a Varian V-K3506 Super Stabilizer. Precision coaxial glass tubing [42] was used with benzene reference in the annular space and electrolyte solution in the inner tube. The resonance line shifts were determined by means of conventional side-band techniques, using a Hewlett-Packard 200 CD Audio Oscillator. In order to attain an exact adjustment of the benzene side-band signal to the resonance line the oscillator frequency was varied around the coincidence positions during at least 50 or 100 sweep periods before the final reading was made. Three or four such readings were made for each specimen. An average was then taken over the obtained readings not exceeding the range 0.3 c/sec. Measurements which occasionally exceeded this range, due to accidental instability of the spectrograph or inhomogeneity of the magnet field, were discarded and repeated after the necessary adjustments were made. Room temperature was held at 22 $\pm$ 1°C. The purest chemicals available were used. Thus LiCl, LiBr, NaF, NaCl, NaBr, NaI, $KF.H_2O$, KCl, KBr, KI and CsCl were of reagent grade quality, while the salts $LiI{\cdot}2H_2O$, RbF, RbCl, RbBr, RbI, CsF, CsBr and CsI contained a few per cent impurities, these being other alkali halides. Emission spectroscopy was used to test the presence of iron group metals and showed no trace of paramagnetic ions. The preparation of solutions of different electrolyte concentrations were carried out by simple weighing and dilution procedures for the non-hygroscopic salts. The concentrations of the hygroscopic salts were determined by conventional chemical analysis.

In an investigation of this kind, requiring measurements of so small shifts as 0.1—10 c/sec, a very important point is the removal of irrelevant paramagnetic impurities. From that point of view dissolved paramagnetic oxygen called for a special investigation, because of the susceptibility effects on liquids due to dissolved oxygen found by Eggleston [43]. A comparison was therefore made between water specimens which had been (1) degassed by boiling in vacuum, (2) saturated with air, (3) degassed by bubbling through nitrogen and (4) degassed by Freon 12.

Ten frequency readings were made for each specimen. Statistical analysis of the results indicated that the averages drawn from the samples 2, 3 and 4 were identical with the average of specimen 1 — the level of significance being fixed at 99.5 %. It was accordingly concluded that ordinary distilled water could be used for the preparation of the solutions.

This result was expected, since a simple calculation leads to the conclusion that the susceptibility difference between chemically pure water and water saturated with oxygen would produce a proton resonance shift not exceeding 3×10^{-4} ppm.

The observation made by Solomon [44], that the spin-lattice relaxation time increased with the deoxygenation of water, is not at variance with the present conclusion, since the corresponding effects on the line width are unobservable.

For each salt, measurements of 8—16 solutions of different concentrations were made in the range 0—3 m (molal).

EXPERIMENTAL RESULTS

When evaluating the observed proton resonance shifts of the solutions, it is necessary to correct for certain macroscopic susceptibility effects when an external reference substance is used *. In the present case pure water was taken to relate the measurements performed on the various solutions.

The chemical shift Δ, corrected for the macroscopic susceptibility effect g, is defined by

$$\Delta = [(H - H_w)/H_w - g] \times 10^8 \quad (1)$$

where $g = (2\pi/3)\ (k - k_w) = (2\pi/3)\ [\varkappa_w\ (d - d_w) - (\varkappa_w - \varkappa_s) \cdot c \cdot M \times 10^{-3}]$ (2)

where H = water proton resonant field of the solution
k = volume susceptibility (c.g.s. units)
$\varkappa$ = specific » (c.g.s. units)
d = density g/ml
c = molarity
M = mole weight of salt.

The index w refers to pure water and s to the crystalline salt.

The molal shift δ for an 1—1 electrolyte, wholly dissociated, is defined as

$$\delta = m^{-1}\Delta \quad (3)$$

where m = molality.

A satisfactory approximation to the linearity assumed in eqn. (3) could actually be observed in the concentration range 0—2 m, permitting δ to be calculated from the Δ/m plot. The results of the measurements are summarized in Fig. 1.

The molal chemical shifts are given in Table 1. To illustrate the necessity for the susceptibility corrections (g) to the molal shifts they are included in Table 1, together with the estimated error of g evaluated from literature data.

This uncertainty, Δg, has been calculated according to the expression

$$\Delta g = (2\pi/3)\ [(\varkappa_w \Delta d)^2 + (c_1 \times 10^{-3}\ \Delta\chi_s)^2]^{1/2} \quad (4)$$

* A detailed investigation into the problem of the macroscopic susceptibility correction will be published elsewhere.

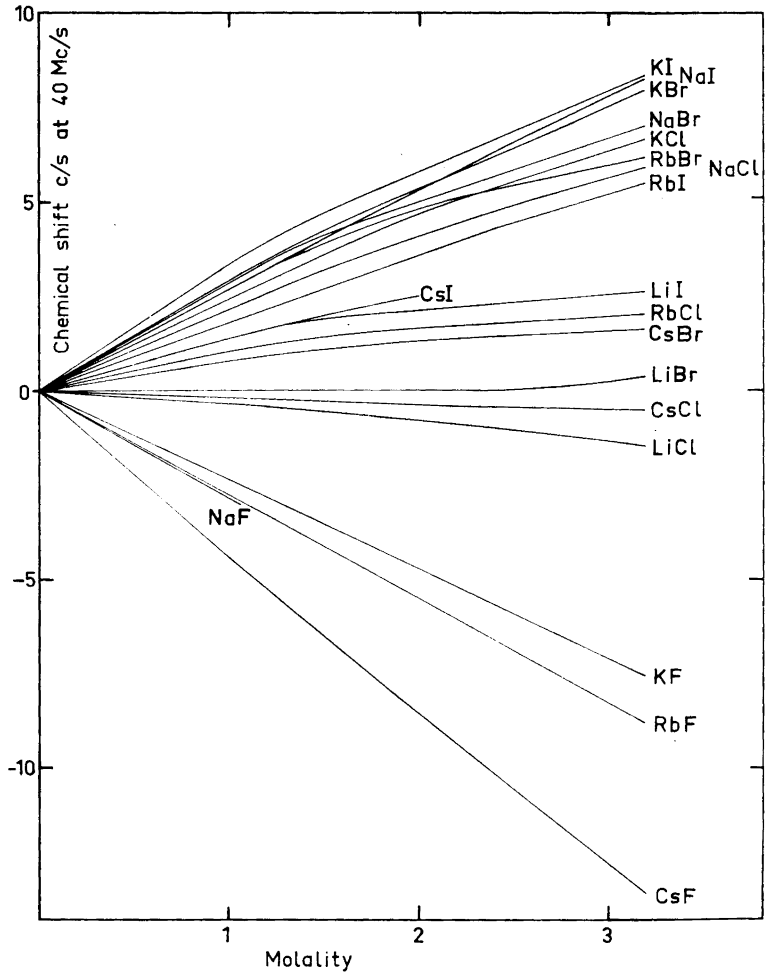

Fig. 1. The concentration dependence of the shift; no susceptibility correction is performed.

where Δd = uncertainty of the density of an 1-molal solution

$\Delta\chi_s$ = » » » molecular susceptibility of the salt, indicated in literature [38]

c_1 = molarity number, corresponding to molality m = 1.

ANALYSIS OF EXPERIMENTAL DATA

In the analysis of the properties of ions in aqueous solutions, the partitioning of a specific effect among the contributing types of ions presents a main problem. The question arises in studies of ionic entropies [45], dielectric data [46,47],

Table 1.

Salt	$(-g \pm \Delta g) \times 10^8$ [a]	$\delta \pm \varepsilon$ [b]		δ_{calc} [c]	$\delta_{H\ \&\ S}$ [d]	$\delta_{S\ \&\ A}$ [e]	δ_{Hn} [f]
LiCl	2.40 ± 0.06	1.7 ± 0.3			2.2 + 0.5	−0.8	1.0
LiBr	3.12 ± 0.05	3.1 ± 0.3				1.2	3.8
LiI	5.34 ± 0.18	8.8 ± 0.3					
NaF	3.48 ± 0.07	−3.6 ± 0.3			−2.5 ± 1		−1.8
NaCl	3.50 ± 0.05	8.6 ± 0.3		9.4	8.8 ± 0.5	5.8	7.3
NaBr	4.70 ± 0.06	11.9 ± 0.3		11.9	11.3 ± 0.5		10.0
NaI	6.41 ± 0.07	13.2 ± 0.3		14.4	15.0 ± 0.5	9.2	11.6
KF	3.58 ± 0.12	−2.2 ± 0.3			−2.5 ± 0.5	−4.9	−2.8
KCl	3.76 ± 0.06	9.9 ± 0.3		10.3	8.8 ± 0.5		7.1
KBr	4.93 ± 0.06	12.3 ± 0.3		11.4	11.3 ± 0.5		
KI	6.60 ± 0.17	15.0 ± 0.3		14.8	15.0 ± 0.5	10.6	
RbF	4.47 ± 0.14	−2.4 ± 0.3					
RbCl	4.80 ± 0.17	7.5 ± 0.3		8.2			6.1
RbBr	5.50 ± 0.18	12.3 ± 0.3		9.4			
RbI	7.02 ± 0.22	11.5 ± 0.3	(16.0) [g]	12.8	15.0 ± 0.5		
CsF	5.68 ± 0.16	−5.3 ± 0.3					
CsCl	6.38 ± 0.17	5.9 ± 0.3	(7.6) [g]	5.9			5.0
CsBr	6.60 ± 0.21	8.6 ± 0.3		7.0			
CsI	9.15 ± 0.25	9.5 ± 0.4	(14.9) [g]	10.4	14.6 ± 0.5		
$NaClO_4$	1.28 ± 0.11	13.2 ± 0.3					

a) Susceptibility correction and its uncertainty for 1-molal solutions.

b) ε is the estimated uncertainty in δ, $\varepsilon = [0.25^2 + (\Delta g)^2]^{1/2}$. The value 0.25 is the standard deviation of the shift due to errors in the frequency readings.

c) δ_{calc} is the molal shift calculated from estimated values of π and σ.

d) Molal shifts, determined by Hertz and Spalthoff [12], using internal standard.

e) Molar shifts, determined by Shoolery and Alder [1], without susc. correction.

f) Molal shifts, determined by Hindman [13], using external standard. A susceptibility correction has been included.

g) The values in parenthesis are molal shifts measured in this work with internal standard.

viscosity B-factors [48] etc. and plays a prominent role in the study of NMR molal shifts. Often rather arbitrary methods are chosen. In spite of the fact that Shoolery and Alder [1] neglected the susceptibility corrections, they were led to the assumption of an approximate additivity law for molal ionic shifts. This is perhaps not so surprising in view of the fact that molecular susceptibilities of salts are very nearly additive properties [49–52]. (Density effects, however, destroy the additivity of molal volume susceptibilities of electrolytic solutions to a certain degree, a fact, which can be seen in the calculations of g in Table 1).

In evaluating the experimental data, we have made use of the following conceptions regarding the structure and general behaviour of water and aqueous solutions.

Liquid water is treated as an essentially crystalline system, closely related to a slightly expanded, idealized ice lattice (Fig. 2), containing defects in thermal equilibrium with the lattice (theoretical papers [53–56], neutron diffraction studies [57–60], X-ray work [61], self-diffusion work with isotopic tracers [62].) The structure is very open and the interstitial space between the groups of molecules in tetrahedral coordination is sufficiently large to accomodate free, non-associated molecules without greatly disarranging the structural order.

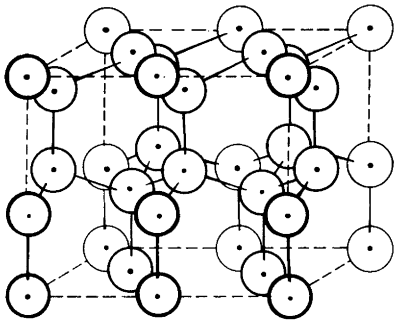

Fig. 2. Oxygen positions in the ideal ice lattice. Hydrogen bonds are indicated by full lines.

We may derive the properties of liquid water from the structure of the idealized ice lattice, if we remember that the molecules perform thermal vibrations around their positions of equilibrium, the intermolecular movements being both dilational and deformational. With rising temperature, the amplitudes of the deformational vibrations will gain in importance and eventually become large enough to break some hydrogen bonds, permitting the freed molecules to enter the interstitial spaces in the lattice. The arising lattice defects consist each of one vacant lattice point and one interstitial, non-associated molecule. This type of lattice imperfection is usually called a Frenkel defect. Each component of the defect is free to diffuse in the lattice, and some of the vacant lattice points may eventually reach a boundary of the molecular system, where they may be annihilated, causing a reduction of the total volume and leaving behind lone, interstitial molecules, so-called Schottky defects, which increase the density in bulk.

The density increase, associated with the appearance of Schottky defects at the ice/water transition will, in fact, continue until the thermal amplitudes have become sufficiently attenuated by the interstitial molecules to prevent the formation of new defects. At this stage, we say that the system has attained thermal equilibrium. Disregarding a slight thermal expansion of the lattice, the structure of the liquid phase is then essentially the same as that of the solid, the only difference being a higher bulk density due to the new Schottky defects, and an increased amount of complete Frenkel defects. Still, in liquid water at 0°C, only 9 % of the lattice points are vacant, while the number of interstitial molecules amounts to some 16 % of the total number of molecules in the system [55,56]. It is obvious that the rheological properties of the system will depend on the association of point defects to form dislocations which, under the influence of a shearing stress, will move against a rather small energy barrier to produce the relative lattice displacements constituting the flow process. Excess of interstitial matter will raise the barrier and counteract the flow.

Making use of the preceding conceptions, we may now visualize the internal boundary conditions of the water lattice to be affected by the introduction of foreign matter in the lattice interstices and vacancies in a similar manner, as occurs in solid solution.

Dissolved electrolytes are accordingly expected to produce lattice distortions due to steric effects, which depend on the size and shape of the ions. It is evident, that only those ions which possess a smallest radius larger than the radius of the interstitial space, are able to distort the lattice for purely geometrical reasons. Chemical bonding between the solute and the water lattice may, on the other hand, be expected to occur both in interstitial and lattice positions, giving rise to additional lattice distortions associated with the changes in the ionic and molecular charge distributions which are due to the bonding effects [63,64]. As may be inferred from the theoretical calculations for pure water, corroborated by experimental data [65,55] for water as well as for aqueous solutions, the number of free, *i.e.* interstitial water molecules is, in general, very small and, moreover, rather insensitive to changes in solute concentration. The implication of this observation is that nuclear spin relaxation mechanisms depending on the free rotation of water molecules or their translational motion in lattice interstitial channels, contribute very little indeed, to the total relaxation of the proton spin system.

In our model the reorientations of the overall molecular dipoles responsible for the high dielectric constant of water and ice, take place almost exclusively by way of simultaneous shifts of the proton positions as implied by Pauling's [54] structural model for ice. The individual proton shift occurs as a sort of chain reaction without disruption of hydrogen bonds. Increasing lattice distortion and coupling to solute molecules will, however, reduce the probability for unrestricted simultaneous proton displacements due to an increased number of barriers against the rehybridizations necessary for proton exchange between hydrogen bonded water molecules. The outcome is a reduction of the dielectric constant with increasing solute concentration. The effect may give the impression of being due to a restriction imposed on free molecular rotation. The free rotation, supposed to occur, is, however, expected to increase with weakening hydrogen bonds, which has sometimes given rise to an apparent contradiction. The simultaneous shortening of the dielectric and the proton magnetic relaxation times is, of course, due to the weakening of hydrogen bonds.

We moreover conclude from our model that the hydration process, *i.e.* the coupling between the solute and the solvent does not, as a rule, give rise to the formation of a distinct coordination sphere of water molecules surrounding an ion or an ionized atomic group, disrupted from the remainder of the lattice, and moving as an entity in the solvent. The dissolved ion or atom is instead regarded as integrated in the water lattice by ordinary chemical bonds of variable duration and strength, depending on the type of instantaneous coupling and the thermal excitation of the lattice. Under such conditions, it is obviously desirable to regard the relaxation processes as depending on the whole water lattice, the rotational energy of the observed nuclei being dissipated by a number of different, cooperating mechanisms, which for a proper treatment have to be described in terms of the lattice dynamics.

The present investigation is not concerned with this aspect of the problem, the solution of which, in our opinion, should only be attempted when more information about the structural properties of the water lattice has been obtained. In conformity with these ideas, we have, in the meantime, been looking for a correlation between the observed proton magnetic resonance shift of

aqueous solutions of the alkali salts and some ionic properties expected to influence the structural behaviour of the water.

Taking the proton resonance shift as a measure of the mean hydrogen bond energy changes, we have used the ionic volume and polarizability to characterize the solute. In order to find a quantitative expression for the relative polarizabilities of the ions and, at the same time, accounting for the characteristic ionic charge distributions, we have chosen to make a theoretical calculation of the atomic dipoles associated with a given ionic hybrid orbital state.

To this end we postulate that the molal shift δ, for an 1—1 electrolyte with the cation i and anion j, is composed according to the matrix equation

$$\begin{vmatrix} \sigma_{ii} & \sigma_{ij} & \pi_{ii} & \pi_{ij} \\ \sigma_{ji} & \sigma_{jj} & \pi_{ji} & \pi_{jj} \end{vmatrix} \begin{vmatrix} s_i \\ s_j \\ p_i \\ p_j \end{vmatrix} = \begin{vmatrix} \delta_{ij} \\ \delta_{ji} \end{vmatrix} \tag{5a}$$

$$\delta_{ij} + \delta_{ji} = \delta \tag{5b}$$

δ_{ij} is the water proton shift produced by the cation i when the anion j is present, δ_{ji} is the water proton shift produced by the anion j when the cation i is present. s and p stand for the hydrogen bond breaking (steric effect) and polarization effects respectively. σ and π are the proportionality factors. Then the sum of the terms containing ii and jj factors expresses the simple additivity law for ionic molal shifts, while the cross terms with ij or ji indices stand for ion-counterion effects, *i.e.* non-additivity and concentration dependence.

The parameter s. This parameter is chosen to represent the steric effect on the water lattice of the dissolved ions. It should accordingly be associated with the breaking of hydrogen bonds due to lattice distortion. The larger the volume of a dissolved ion, the stronger the steric disturbance on the water structure and the more extensive the zone around the ion in which hydrogen bonds are being disturbed or broken. Therefore the steric effect factor is put equal to the ionic volume, *i.e.*

$$s = (4\pi/3)r^3 \tag{6}$$

where r is expressed in Ångström units.

The choice of a suitable value for r can be discussed from many points of view [66]. The simplest way and the one chosen in this work is to make use of Pauling's [67] crystallographic radii. Objections can be raised to this choice since the difference between ionic environments in crystals and water solutions can be expected to influence the radii. Several authors have, however, shown that there is a simple relation between the crystallographic radii and the radii in aqueous solutions. U.V. absorption measurements of anions in solution led Stein and Treinin [68] to a calculated, constant ratio

$$f = r_{\text{soln.}}/r_{\text{cryst.}} = 1.30 \pm 0.03$$

for the halide ions. Mukerjee [69] in a study of partial molal volumes of ions in aqueous solutions recently redetermined this ratio obtaining the value $f = 1.21$.

Even if the correct ionic volumes are not expressed by the crystallographic radii, the deviation will be included in the nearly constant factor f. In the present case f enters the σ-factors.

The calculated s-values are shown in Table 2.

The polarization effect p. The electronic state of halides in solution and the ion/solvent coupling has long been studied by U.V. absorption methods [68,70–73].

Also in a recent investigation of aqueous alkali halide solutions, Walrafen [74] found peaks in Raman spectra which could be explained only by assuming hydrogen bonds of the type O—H. . .X⁻. It then seems natural to develop our model in the following way. When an ion is inserted into a water lattice it will leave its ground state $(ns)^2(np)^6$ due to the interaction with the surrounding water molecules. An atomic dipole μ, created by the orbital component np which is an unpaired electron left in the ground state, henceforth denoted by the index o, and the excited electron, henceforth denoted by the index m, can be written

$$\mu_{om} = e \cdot R_{om} \tag{7}$$

where e is the charge of the electron and R_{om} represents the radius vector to the centroid of the hybrid, according to

$$R_{om} = \int \bar{r}[\sqrt{\lambda_{om}}\varphi_o + \sqrt{1-\lambda_{om}}\varphi_m]^2 d\tau = 2\sqrt{\lambda_{om}(1-\lambda_{om})} \int \bar{r}\varphi_o\varphi_m d\tau \tag{8}$$

Here φ_o and φ_m are taken as normalized Slater-functions for the orbitals o and m. λ_{om} is the mixing coefficient expressing the fractional amount of o-character (ground state) in the normalized hybrid. $\bar{r}$ is the radius vector and $d\tau$ is the volume element.

Assuming preferential forms of hybridization and constant mixing coefficients for both cations and anions, we postulate the orbital m as the lowest available s-orbital above the np state, *i.e.* a (n + 1)s state. (The lithium ion having no p electrons constitutes an exception. In this case we have made use of a hybrid of the orbitals 2s and 2p).

We are accordingly allowed to write the atomic dipole moment for a cation i and an anion j as:

$$\mu_i = 2e\sqrt{\lambda_i(1-\lambda_i)} \cdot \int \bar{r}\varphi_i(np)\varphi_i((n+1)s)d\tau \tag{9a}$$

resp.

$$\mu_j = 2e\sqrt{\lambda_j(1-\lambda_j)} \cdot \int \bar{r}\varphi_j(np)\varphi_j((n+1)s)d\tau \tag{9b}$$

The moment integrals, given in Table 2, are now identified with p_i and p_j, *i.e.*

$$p_i = \int \bar{r}\varphi_i(np)\varphi_i((n+1)s)d\tau \tag{10a}$$

and

$$p_j = \int \bar{r}\varphi_j(np)\varphi_j((n+1)s)d\tau \tag{10b}$$

and the π-factors will include the mixing coefficient square root factors.

The complete assembly of nineteen salts gives 19 equations of the type (5) but involves in all 36 unknown σ- and π-factors. Thus, some simplifications

must be made, and this is possible in more than one way. A reasonable assumption seems to be

$$\pi_{ii} = \pi_+ = \pi \tag{11}$$

implying that the polarization proportionality factors are the same for all the cations. Similarly we may write

$$\pi_{jj} = \pi_- = \alpha\pi \tag{12}$$

implying a common polarization mechanism for the anions. In order to simplify the calculations the parameter α has been introduced, to express the ratio between π_- and π_+. Similar considerations of the steric effects lead to the assumption

$$\sigma_{ii} = \sigma_{jj} = \sigma \tag{13}$$

expressing a linear relationship between the disturbance and the ionic volumes, the proportionally factor σ being common for both cations and anions.

Further, neglecting the non-additive contributions to the shift, we obtain

$$\pi_{ij} = \pi_{ji} = 0 = \sigma_{ij} = \sigma_{ji} \tag{14}$$

Although the eqns. (11)—(14) are all rather crude approximations their justification may be inferred from the success of the procedure in its practical application.

Writing

$$p_i + \alpha p_j = P_{ij} \tag{15}$$

and

$$s_i + s_j = S_{ij} \tag{16}$$

we obtain for each salt, when omitting indices, the equation

$$\pi P + \sigma S = \delta \tag{17}$$

Writing this equation in the form

$$\pi(P/\delta) + \sigma(S/\delta) = 1 \tag{17a}$$

it is at once realized that if π and δ are real constants their values could be derived from the reciprocal axis intercepts of Fig. 3. In eqn. (17), however, another unknown constant is involved, namely $\alpha = \pi_-/\pi_+$, defined in eqns. (11) and (12). This constant may be chosen to optimize the adaptation to a linear relationship between P/δ and S/δ in eqn. (17a). This is achieved by letting α take the values 0, 0.1, 0.2. . . 1.0. The regression line parameters and the statistical correlation coefficient r for each α-value are then calculated. The latter, expressing the closeness of fit to a straight line, has its maximum for $\alpha = 0.2$ (see Fig. 4). Inserting this α-value in eqn. (17a) leads to the result shown in Fig. 3. All the points except those due to the lithium and fluoride salts lie close to the straight line which is the average of the two possible regression lines.

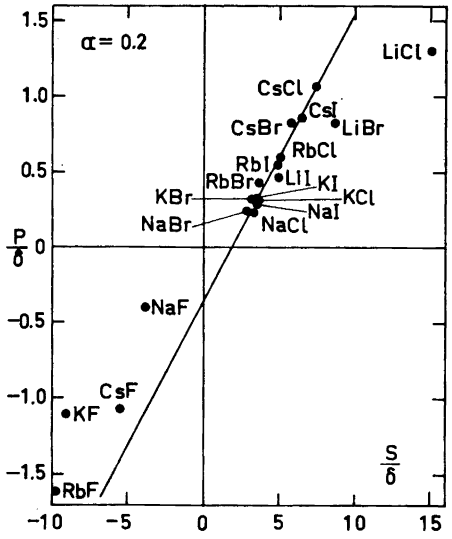

Fig. 3. The function $\pi(P/\delta) + \sigma(S/\delta) = 1$. The straight line is an average of the two regression lines, estimated from all the salts excepting the Li-salts and the fluorides.

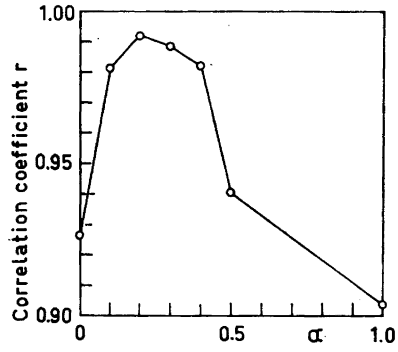

Fig. 4. Correlation coefficient as a function of the parameter α.

Hence the calculation of the constants α, π and σ does not include salts which contain lithium or fluorine. From Fig. 3 we obtain

$$\pi = -2.969 \text{ (a.u.)}^{-1}$$
$$\sigma = 0.5603 \text{ Å}^{-3}$$

The ionic molal shifts may now be computed from the equations

$$\delta_i = \pi p_i + \sigma s_i \tag{18}$$

$$\delta_j = \alpha\pi p_j + \sigma s_j \tag{19}$$

valid for cations and anions respectively. The molal shifts of Li^+ and F^-, however, have been computed according to the explanation given in Table 2. The results are summarized in Table 2 and shown in Fig. 5.

We find that for Cl^-, Br^- and I^- the shifts are essentially determined by the steric effects whereas the steric and polarization effects for Na^+ and K^+ almost cancel. The shifts of Rb^+ and Cs^+ indicate a stabilizing effect on the water lattice but are far from the extreme value of Li^+. The F^- shift value lies markedly lower than those of the other halides.

It appears that the coupling mechanisms for Li^+ and F^- deviate from those of the remaining salts. Since stable covalent bonds can, in general, only be formed when the main contribution to the bonding energy depends on stable electronic configurations, Li^+ obviously represents an exception with only

two 1s electrons in the ground state. Similarly, F^- is exceptional due to the extreme electronegativity of the fluorine atom and the correspondingly high polarizing ability in combination with an ionic volume/interstitial volume ratio close to unity. The assumption of an approximately constant ratio π_-/π_+ employed in the derivation of the eqn. (17a) obviously cannot be maintained in these two cases.

Table 2.

Ion	Dipole forming orbitals		p(a.u.)	s(Å^3)	σs	$-\pi_+ p$	$-\pi_- p$	$\delta_{\text{ion(calc)}}$
Li^+	2s	2p	1.090	0.94	—	—		— 7.8 [a]
Na^+	2p	3s	0.899	3.68	2.06	2.67		— 0.62
K^+	3p	4s	1.934	9.88	5.53	5.74		— 0.21
Rb^+	4p	5s	3.354	13.70	7.68	9.96		— 2.28
Cs^+	5p	6s	5.150	19.03	10.66	15.29		— 4.63
F^-	2p	3s	2.611	10.10	—		—	— 1.5 [a]
Cl^-	3p	4s	5.626	24.67	13.82		3.34	10.48
Br^-	4p	5s	9.742	31.09	17.42		5.78	11.64
I^-	5p	6s	14.96	42.69	23.92		8.88	15.04

a For Li^+ we estimate from LiCl $\delta_{Li^+} = 1.7 - 10.5 = -8.8$, from LiBr $\delta_{Li^+} = -8.5$ etc. The average value is −7.8. The corresponding calculation is made for F^-.

COMPARISON WITH OTHER INVESTIGATIONS

The agreement of our data with those of Hertz and Spalthoff [12] is rather satisfactory, except in one or two cases which are discussed below. The shift value of 1 m solutions generally coincide within the limits of error for the two methods. However, Hertz and Spalthoff find that the concentration dependence first deviates from the linear form in 3 m solutions, whereas we are able to prove the existence of non-linear forms of the chemical shift Δ (including the susceptibility correction) already in the concentration range 1—2 m. These findings cannot be ascribed to the use of susceptibility corrections since these are very linear up to high concentrations, a fact which has been shown previously [49–52] and also in control measurements initiated by us. To explain the difference we could assume that the error margins are larger than stated — which is not probable — or that the use of *t*-butanol or similar compounds as internal standards will complicate the chemical situation to produce anomalies due to some kind of "complexing". In the latter case the lines, which are in reality curved, appear straight owing to the presence of the large organic molecule.

In two special cases, namely RbI and CsI, a definite anomalous effect has been proved. We found a striking difference between our results and those of Hertz and Spalthoff, as can be seen from Table 1. To check the deviation we tested Hertz and Spalthoff's method using 0.3 m *t*-butanol as internal standard and found $\delta = 16.0$ and 14.9 for RbI and CsI, respectively. The correctness of Hertz and Spalthoff's values was thus confirmed but it is also clear that a fundamental difference exists between the two methods used in this case. To be still more certain, we compared results for CsCl (not measured by Hertz and Spalthoff) and found $\delta_{\text{int}} - \delta_{\text{ext}} = 7.5 - 5.9$. This result led us to

the conclusion that the combined action of the cations in question and *t*-butanol upon the water molecules give rise to upfield shifts which actually deviate from the law of additivity.

In order to investigate these observations in detail, it is desirable to perform measurements on solutions with constant electrolyte concentration but varying concentrations of the internal standard compound. Extrapolation of the shift may then be made to zero concentration of the reference compound.*

When Hertz and Spalthoff defined their reference point for the ionic chemical shifts, they refrained from a discussion of the detailed interactions between the ions and the solvent water owing to the complexity of the question. They preferred instead to make the molal shifts of the potassium and chloride ions equal, *i.e.* $\delta_{K^+} = \delta_{Cl^-} = 4.4$, a choice based upon the known similarities in the conductivities, transport numbers, hydration numbers and ionic sizes of the two species.

Recently Fabricand and Goldberg [75] published some PMR measurements for certain aqueous alkali halide solutions. Our experimental uncorrected values of molal shifts are in excellent agreement with theirs which were also obtained using an external reference method. There are, however, certain points in their treatment which we believe require some comments. (1) Instead of discussing their results on the basis of experimentally found susceptibilities, they have preferred the use of theoretically calculated ionic susceptibilities [76] which unfortunately show considerable deviations from the experimental values. (2) By an error of calculation they seem to have obtained corrections which are about two times too large. We regard our results as satisfactorily verified by their unambiguous agreement with those obtained by the independent method of Hertz and Spalthoff and also with those recently obtained by Hindman [13]. (3) After arbitrarily putting $\delta_{Cl^-} = 0$, to establish their shift scale, they stated that the shift difference between K^+ and F^-, $\delta_{F^-} - \delta_{K^+} = 2.8$, depends on the difference in the polarization contributions for these ions, the volumes being very nearly equal. Had they instead defined their zero point as $\delta_{Br^-} = 0$ the "difference in the polarization terms" would equal 4.0. Failure to introduce a physically or chemically satisfactory definition of the reference point make comparisons of this kind between positive and negative ions rather illusory. (4) Fabricand and Goldberg maintain that the ionic effects on the proton resonance shifts do not extend beyond the nearest-neighbour water molecules, a statement which they based upon certain breaks in the shift-concentration curves for six of the fourteen salts. Unfortunately the other eight salts did not show this behaviour.

The molal shifts of 1—1 electrolytes, measured by Hindman [13] do not differ appreciably from our results and those of Hertz and Spalthoff, though in general they tend to be slightly lower. Hindman also observed the anomalous behaviour of the lithium ion which he explained as a "structure-making effect". His point of reference was established by putting the molal shift of the ammonium ion equal to zero, justifying this choice by reference to the small effects produced on various properties of water by ammonium chloride in solution.

* Measurements performed after the completion of this investigation have confirmed the existence of a general internal standard effect on the water lattice and the proton resonance shift, elucidating the extrapolation conditions in the case of *t*-butanol.

COMPARISON BETWEEN THE EFFECTS OF ENHANCED TEMPERATURE AND DISSOLVED ELECTROLYTES ON THE HYDROGEN BOND STRENGTH IN WATER

Shoolery and Alder [1] made an early estimate of the steric effect on the total shift of an electrolyte. Making use of "the liquid association shift" determined by Schneider *et al.*[77] and applying the method of least squares we have tried to estimate the temperature dependence of "the liquid association shift", δ_{LAS}. This is the difference between the real shift of a certain compound in the liquid state and the shift value which is calculated for the liquid state. The latter shift value is derived from experimental data for the shift of the compound in the gaseous state and from the volume susceptibility of the liquid state, as expressed by the equation

$$\delta_{LAS} = \delta_{liq} - (\delta_{liq})_{calc} = \delta_{liq} - \delta_{gas} - (2\pi/3) \cdot k \times 10^8 \quad (20)$$

resulting in

$$\delta_{LAS} = 1.153\ t - 458 \quad (21)$$

for water, where t is °C. From eqn. (21) we obtain the value 115.3 for the shift between two water specimens at 100°C and 0°C, respectively.

From a knowledge of the difference in the number of broken hydrogen bonds for the two water specimens, the shifts per mole of broken hydrogen bonds in 1000 g water can be estimated. Several authors have computed the number of broken hydrogen bonds in water as a function of temperature. Thus Haggis *et al.*[65] found that the difference in the percentage of hydrogen bonds broken between 100°C and 0°C was 11.2. The corresponding number found by Forslind [55] was 8.6.

If an average of 10 % is assumed we obtain a "steric" shift of

$$\frac{115.3}{0.1} \cdot \frac{18}{1000} = 21$$

when two moles of hydrogen bonds are broken in 1000 g water. Assuming further that (*a*) one water of hydration molecule implies two broken hydrogen bonds and that (*b*) an arbitrary alkali halide has an apparent hydration number of 6 for the cation and anion together, then it should be possible to calculate the ionic sum of the polarization contributions, δ_{pol}, according to

$$\delta_{pol} = \delta_{salt} - 6 \times 21 \quad (21)$$

It is quite evident that this model leads to results which are difficult to accept since the probability that the two opposite effects (hydrogen bond stabilization resp. disrupture) should cancel for all the alkali halides is extremely small. This line of approach further gives rise to values of the steric effect which seem to be at variance with those of the present model. We therefore conclude that hydrogen bond rupture resulting from a rise of temperature bears very little resemblance to water lattice deformations caused by dissolved ions (*cf.* Kujumzelis [78]).

COMPARISON OF PMR DATA WITH DIELECTRIC DATA FOR ELECTROLYTIC SOLUTIONS

The dielectric methods for the study of ionic properties in electrolytic solutions were mainly developed by Hasted *et al.*[46,47,65] who interpreted the decrease of dielectric relaxation time ($\delta\lambda_s$) in increasingly concentrated solutions of strong, inorganic electrolytes as due to disrupture of hydrogen bonds. The dielectric constant depression ($\delta\varepsilon$) was regarded as being due to restriction of the water dipole rotation produced by the ions — the stronger the dipole coupling, the more effective the restriction of rotation (*cf.* the introductory notes on p. 2076). In this work we regard the PMR shift as resulting from both the effects of hydrogen bond rupture and polarization, also reflected in the two dielectric parameters. In Fig. 5 a remarkable parallelism is exhibited by (*a*) the molar dielectric relaxation depression $\delta\lambda_s$, (*b*) the molar dielectric constant depression $\delta\varepsilon$ and (*c*) the molal NMR shift δ of the alkali metal ions and halide ions. However, whilst we have an absolute scale for δ, according to the theoretical considerations used in this paper we have had to define arbitrary reference points for $\delta\lambda_s$ and $\delta\varepsilon$ by a procedure which is explained in Fig. 5. In all three diagrams of Fig. 5, the halide ions, without exception form a homologous series with the iodide ion exerting the largest effects and the fluoride ion the least. For the cations, the analogy is not quite so evident. Firstly, no dielectric studies known by us include measurements on cesium salts. Secondly, the uncertainty of $\delta\varepsilon$ does not allow any definite quantitative conclusions to be drawn concerning the ordering (analogous to the lyotropic series) of the cations. However, the anomalous behaviour of the lithium ion in the cation series is confirmed by the $\delta\lambda_s$ curve. Whilst Hasted correlated the dielectric constant decrease to "irrotationally bound water" and thus to

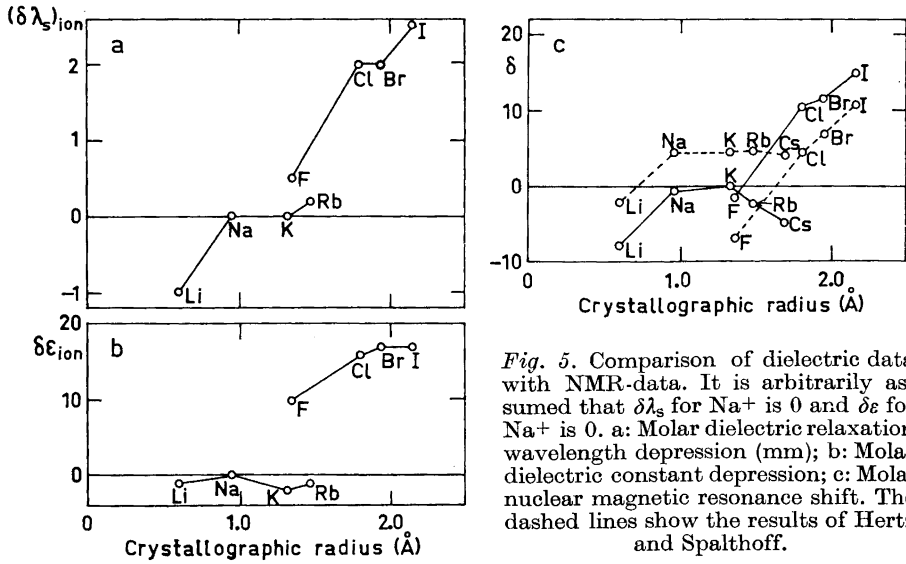

Fig. 5. Comparison of dielectric data with NMR-data. It is arbitrarily assumed that $\delta\lambda_s$ for Na^+ is 0 and $\delta\varepsilon$ for Na^+ is 0. a: Molar dielectric relaxation wavelength depression (mm); b: Molar dielectric constant depression; c: Molal nuclear magnetic resonance shift. The dashed lines show the results of Hertz and Spalthoff.

a hydration number, we think it wise to postpone such direct statements about δ. It should finally be remarked, that a similar sequence of the ions in question is found from Raman spectra [74,79].

Acknowledgements. We should like to thank Dr. A. Ehrenberg for his kindness in helping us with several measurements of susceptibilities. We are also greatly indebted to Dr. H. G. Hertz for his most valuable and helpful comments to a preprint of this paper. The NMR spectrograph has been made available to the research group by a generous grant from the *Knut and Alice Wallenberg's Foundation.*

REFERENCES

1. Shoolery, J. N. and Alder, B. J. *J. Chem. Phys.* **23** (1955) 805.
2. Gutowsky, H. S. and Fujiwara, S. *J. Chem. Phys.* **22** (1954) 1782.
3. Gutowsky, H. S. and Saika, A. *J. Chem. Phys.* **21** (1953) 1688.
4. Hood, G. C., Redlich, O. and Reilly, C. A. *J. Chem. Phys.* **22** (1954) 2067.
5. Hood, G. C., Redlich, O. and Reilly, C. A. *J. Chem. Phys.* **23** (1955) 2229.
6. Hood, G. C. and Reilly, C. A. *J. Chem. Phys.* **27** (1957) 1126.
7. Hood, G. C. and Reilly, C. A. *J. Chem. Phys.* **28** (1958) 329.
8. Hood, G. C., Jones, A. C. and Reilly, C. A. *J. Phys. Chem.* **63** (1959) 101.
9. Hood, G. C. and Reilly, C. A. *J. Chem. Phys.* **32** (1960) 127.
10. Hamer, W. J. *The structure of electrolytic solutions.* Wiley & Son, New York 1959, p. 35.
11. Happe, J. A. and Whittaker, A. G. *J. Chem. Phys.* **30** (1959) 417.
12. Hertz, H. G. and Spalthoff, W. *Z. Elektrochem.* **63** (1959) 1096.
13. Hindman, J. C. *J. Chem. Phys.* **36** (1962) 1000.
14. Axtmann, R. C. *J. Chem. Phys.* **30** (1959) 340.
15. Axtmann, R. C., Shuler, W. E. and Murray, B. B. *J. Phys. Chem.* **64** (1960) 57.
16. Connick, R. E. and Poulson, R. E. *J. Chem. Phys.* **30** (1959) 759.
17. Shulman, R. G. and Wyluda, B. J. *J. Chem. Phys.* **30** (1959) 335.
18. Gutowsky, H. S. and McGarvey, B. R. *Phys. Rev.* **91** (1953) 81.
19. Ramsey, N. F. *Phys. Rev.* **78** (1950) 699.
20. Freeman, R., Gasser, R. P. H., Richards, R. E. and Wheeler, D. H. *Mol Phys.* **2** (1959) 75.
21. Freeman, R., Gasser, R. P. H. and Richards, R. E. *Mol. Phys.* **2** (1959) 301.
22. Gasser, R. P. H. and Richards, R. E. *Mol. Phys.* **2** (1959) 357.
23. McConnell, H. M. and Weaver, H. E. *J. Chem. Phys.* **25** (1956) 307.
24. Wertz, J. E. *J. Chem. Phys.* **24** (1956) 484.
25. Wertz, J. E. *J. Phys. Chem.* **61** (1957) 51.
26. Chesnut, D. B. *J. Chem. Phys.* **33** (1960) 1234.
27. Jardetzky, O. and Wertz, J. E. *Am. J. Physiol.* **187** (1956) 608.
28. Wertz, J. E. *Arch. Biochem. Biophys.* **65** (1956) 569.
29. Wertz, J. E. and Jardetzky, O. *J. Chem. Phys.* **25** (1956) 357.
30. Jardetzky, O. and Wertz, J. E. *J. Am. Chem. Soc.* **82** (1960) 318.
31. Connick, R. E. and Poulsen, R. E. *J. Am. Chem. Soc.* **79** (1957) 5153.
32. Connick, R. E. and Poulsen, R. E. *J. Phys. Chem.* **62** (1958) 1002.
33. Carrington, A. and Hines, Th. *J. Chem. Phys.* **28** (1958) 727.
34. Carrington, A., Dravnicks, F. and Symons, M. C. R. *Mol. Phys.* **3** (1960) 174.
35. Itoh, J. and Yamagata, Y. *J. Phys. Soc. Japan* **13** (1958) 1182.
36. Hertz, H. G. *Z. Elektrochem.* **65** (1961) 20.
37. Hertz, H. G. *Z. Elektrochem.* **65** (1961) 36.
38. Foëx, G. *Constantes selectionnées. Diamagnetisme et paramagnetisme.* Masson et Cie. Paris 1957.
39. Myers, W. R. *Revs. of Modern Phys.* **24** (1952) 15.
40. Landolt-Börnstein, *Tabellen*, Erg. Band I—III, Tabelle 87.
41. Pople, J. A., Schneider, H. J. and Bernstein, W. G. *High-resolution Nuclear Magnetic Resonance*, McGraw-Hill, New York 1959, p. 81.
42. Manufactured by Wilmad Glass Co., Landisville, New Jersey.

43. Eggelston, B. C., Evans, D. F. and Richards, R. E. *J. Chem. Soc.* **1954** 941.
44. Solomon, I. *J. Phys. Rad.* **20** (1959) 768.
45. Latimer, W. M. *Chem. Rev.* **18** (1936) 349.
46. Hasted, J. B., Ritson, D. M. and Collie, C. H. *J. Chem. Phys.* **16** (1948) 1.
47. Hasted, J. B. and Roderick, G. W. *J. Chem. Phys.* **29** (1958) 17.
48. Cox, W. M. and Wolfenden, J. H. *Proc. Roy. Soc. (London) A* **154** (1934) 475.
49. Ikenmeyer, K. *Ann. Phys., 5 Folge* **1** (1929) 169.
50. Veiel, U. *Ann. Phys., 5 Folge* **24** (1935) 697.
51. Frivold, O. E. and Sögn, H. *Ann. Phys., 5 Folge* **23** (1935) 413.
52. Flordahl, M. and Frivold, O. E. *Ann. Phys., 5 Folge* **23** (1935) 425.
53. Bernal, J. D. and Fowler, R. H. *J. Chem. Phys.* **1** (1933) 515.
54. Pauling, L. *J. Am. Chem. Soc.* **57** (1935) 2680.
55. Forslind, E. *Proc. 2nd Intern. Congr. Rheology*, Oxford 1953, Butterworth's Sci. Publ., p. 50.
56. Forslind, E. *A theory of water, Acta Polytechnica* **155** (1952) No. 5.
57. Peterson, S. W. and Levy, H. A. *Acta Cryst.* **10** (1957) 70.
58. Singwi, K. S. and Sjölander, A. *Phys. Rev.* **119** (1960) 863.
59. Hughes, D. J., Palevsky, H., Kley, W. and Tunkelo, E. *Phys. Rev.* **119** (1960) 872.
60. Springer, T. *Nukleonik* **3** (1961) 110.
61. Brady, G. W. *J. Chem. Phys.* **33** (1960) 1079.
62. Wang, J. H., Robinson, C. V. and Edelman, I. S. *J. Am. Chem. Soc.* **75** (1953) 466.
63. Gurney, R. W. *Ions in Solution*, Cambridge 1936, p. 189.
64. Gurney, R. W. *J. Chem. Phys.* **6** (1938) 499.
65. Haggis, G. H., Hasted, J. B. and Buchanan, T. J. *J. Chem. Phys.* **20** (1952) 1452.
66. Stern, K. H. and Amis, E. S. *Chem. Revs.* **59** (1959) 1.
67. Pauling, L. *The Nature of the Chemical Bond.* 3rd Ed. Cornell University Press, Ithaca, N. Y. 1960, p. 526.
68. Stein, G. and Treinin, A. *Trans Faraday Soc.* **55** (1959) 1091.
69. Mukerjee, P. *J. Phys. Chem.* **65** (1961) 740.
70. Rabinowitch, E. *Revs. Modern Phys.* **14** (1942) 112.
71. Franck, J. and Scheibe, G. *Z. physik. Chem. A* **139** (1928) 22.
72. Platzman, R. and Franck, J. *Z. Physik* **138** (1954) 411.
73. Griffiths, T. R. and Symons, M. C. R. *Trans. Faraday Soc.* **56** (1960) 1125.
74. Walrafen, G. E. *J. Chem. Phys.* **36** (1962) 1035.
75. Fabricand, B. P. and Goldberg, S. *J. Chem. Phys.* **34** (1961) 1624.
76. Pauling, L. *Proc. Roy. Soc. (London) A* **114** (1927) 181.
77. Schneider, W. G., Bernstein, H. J. and Pople, J. A. *J. Chem. Phys.* **28** (1958) 601.
78. Kujumzelis, Th. G. *Z. Physik* **110** (1938) 742.
79. Schultz, J. W. and Hornig, D. F. *J. Phys. Chem.* **65** (1961) 2131.

Received May 2, 1962.

ACTA CHEMICA SCANDINAVICA 16 (1962) 2087–2099

The Effect of Polarization on the Retardation of Non-Relativistic Charged Particles

GUNNAR ANIANSSON

Division of Physical Chemistry, Royal Institute of Technology, Stockholm 70, Sweden

Dedicated to Professor *Ole Lamm* on his 60th birthday

The theory for the effect of dielectric polarization on the retardation of non-relativistic charged particles is re-examined. An expression for the effect is obtained in which the dominant term is similar to that obtained by Fermi [13]. It differs by a multiplicative factor and an additive term, both dependent on a parameter describing the form of the oscillator strength distribution.

The influence of the local field correction for the dielectric constant of the medium is also taken into account.

1. INTRODUCTION

The theory of the retardation of charged particles through loss of energy to the atoms or molecules of the medium traversed was first treated on the assumption that the interaction between the particle and each one of the atoms or molecules could be considered separately [1–10]. It was then remarked by Swann [11] that molecules, distant from the path of the particle, should be partly shielded from the particle by the dielectric polarization in the intervening molecules. A theory for this phenomenon was worked out by Fermi [12,13] using methods akin to those used by Frank and Tamm in the theory for the Cerenkov effect. A reduction in the energy loss was predicted which for particles with velocities smaller than the phase velocity of light in the medium was of the order of several percent. For higher velocities the effect eventually becomes dominant. In this theory it was assumed that the dielectric properties of the medium could be adequately described by a single dispersion frequency. This restriction has subsequently been removed and the theory developed for detailed application to particular cases [14–25]. In connection with its application to the retardation of α-particles in organic liquids, it was found to contain ambiguities affecting the order of magnitude of the predicted polarization effect [26]. A re-treatment of the theory was therefore undertaken with particular regard to its ultimate application to non-polar molecular liquids.

2. MICROSCOPIC AND MACROSCOPIC TREATMENT

In the full quantum-mechanical treatment of the interaction between a fast charged particle and a single molecule [8,9], the incoming particle is treated as a plane wave. The rate of change of the combined wave function for the particle and the molecule is then expanded into outgoing plane waves of the particle in different directions and with varying wave number combined with the different states of the molecule. The square of the coefficients of the expansion measures the probabilities of the changes of momentum and energy of the particle accompanied by changes in the state of the molecule. In order to obtain the mean retardation of the particle, a sum over the different probabilities has to be performed.

It was, however, proved by Mott [27] that when the change in momentum experienced by the particle is small its effect on the molecule is that of a classical point charge travelling with constant velocity in a straight line past (or through) the molecule. This situation obtains in particular for heavy particles, such as protons and α-particles, except for the rare, large angle deflections against the nuclei of the molecule.

When the velocity, v, of the particle is much larger than the average velocity v_0 of the electrons in the molecule, it is possible to divide the collisions into two groups [3,9] according to whether the perpendicular distance between the particle track and the center of the molecule is smaller or larger than a distance b such that

$$\bar{r} \ll b \ll \frac{v}{\omega_0} \tag{1}$$

where $\bar{r}$ is the average distance of the electrons from the center of the molecule $\hbar\omega_0$ is of the order of the electronic excitation energies. In the former case, *i.e.* close collisions, the electrons may be considered free since the major part of the disturbance caused by the particle is so rapid that the intra-molecular forces have no time to act. In the latter case the electric field from the particle is practically uniform over the whole molecule so that the treatment becomes a pure dispersion problem.

The energy transferred to the molecules of a gas from a traversing particle is now obtainable on the assumption that the disturbance caused in one molecule is not affected by the disturbances set up in the surrounding molecules. The rate of change of the energy E of the particle due to the molecules within the distance b from the particle track becomes [9]

$$\left(-\frac{\mathrm{d}E}{\mathrm{d}x}\right)_{<b} = \frac{4\pi q^2 e^4}{mv^2} NZ \ln \frac{2mvb}{\hbar k} \tag{2}$$

Here x is the distance along the particle track, $-e$ and m are the charge and mass of the electron, qe and v the charge and velocity of the particle, N the number of molecules per unit volume, Z the number of electrons per molecule, $2\pi\hbar$ Planck's constant and k a numerical constant = 1.123. Similarly for the molecules outside the distance b

$$\left(-\frac{dE}{dx}\right)_{>b} = \frac{4\pi q^2 e^4}{mv^2} NZ \sum_i f_i \ln \frac{kv}{\omega_i} \tag{3}$$

where $\hbar\cdot\omega_i$ is the energy difference between the i:th excited electronic state and the ground state of the molecules and f_i the corresponding oscillator strengths satisfying $\sum_i f_i = 1$.

The total rate of energy loss is then

$$-\frac{dE}{dx} = \frac{4\pi q^2 e^4}{mv^2} NZ \sum_i f_i \ln \frac{2m v^2}{\hbar\omega_i} \tag{4}$$

Due to the circumstance that the action of the particle on the molecules outside the radius b from the track is essentially a classical dispersion problem and because the radius b is larger than molecular dimensions, the macroscopic electrodynamic theory should be applicable to this part of the energy loss [12,13]. The description of the dielectric properties of the medium with a continuum theory automatically takes collective effects into account. For the close collisions on the other hand, collective effects should be relatively much smaller, thus allowing the results above for $(-dE/dx)_{<b}$ to be employed.

The rate of energy transferred to the medium outside the radius b around the track is determined by the total flux of the Poynting vector out of the cylinder with radius b. The energy loss per unit path is then $1/v$ of this rate:

$$\left(-\frac{dE}{dx}\right)_{b>} = \frac{c}{4\pi v} \int (\vec{E} \times \vec{H}) \cdot d\vec{s} \tag{5}$$

By Fourier expansion of the field vectors and introducing the complex dielectric constant $\varepsilon(\omega)$, Fermi obtained [13,14]

$$\left(-\frac{dE}{dx}\right)_{b>} = \frac{i\, b\, q^2 e^2}{\pi v^3} \int_0^\infty \frac{\omega^2}{\varepsilon \vartheta^2 \vartheta^*} K_0\left(\frac{\omega b}{\vartheta v}\right) K_0'\left(\frac{\omega b}{\vartheta^* v}\right) d\omega \tag{6}$$

$$+ \text{ complex conjugate,}$$

where $1/\vartheta^2 = 1-(v^2/c^2)\varepsilon$.

The Bessel function K_0 takes a simple form when $|\omega b/\vartheta v| \ll 1$. At the particle velocities considered, b may be chosen such that this restriction holds for the ω-values of importance. By further changing the path of integration from the positive real axis to the negative imaginary axis and back to $+\infty$ along an infinite radius, one obtains after adding $(-dE/dx_{<b})$:

$$-\frac{dE}{dx} = \frac{4\pi q^2 e^4}{mv^2} NZ\,[\ln 2mv^2 - \ln I] \tag{7}$$

In (7) $\ln I = \ln \hbar - J$ (8)

$$J = \lim_{R\to\infty} \left[\frac{m}{4\pi NZe^2} \int_0^R \left(1 - \frac{1}{\varepsilon(-ix)}\right) x\, dx - \ln R\right] \tag{9}$$

Eqns. (7) and (8) hold for $v < c/\sqrt{\varepsilon(0)}$, the phase velocity of low frequency light in the medium, except for a term $\{-\beta^2-\ln(1-\beta^2)\} \cong -\frac{1}{2}\beta^4$ which should be added to the bracket in (7) when $\beta \ll 1$. When relativistic velocities are taken into account, the same term enters (4) with equal contributions from (2) and (3).

For ε we should use the following form

$$\varepsilon = 1 + \frac{\dfrac{4\pi NZe^2}{m}\sum_i \dfrac{f_i}{\omega_i^2 - \omega^2 + i\omega g_i}}{1-(1-\gamma)\dfrac{4\pi NZe^2}{m}\sum_i \dfrac{f_i}{\omega_i^2 - \omega^2 + i\omega g_i}} \tag{10}$$

The Lorentz-Lorenz correction for the local field fixes γ to a value of 2/3. We shall, however, leave the particular values of γ open so that its influence on the polarization effect becomes clear.

Introducing (10) into (9) gives

$$J = \lim_{R\to\infty}\left[\int_0^R \frac{\sum_i \dfrac{f_i}{\omega_i^2 + x^2 + g_i x}}{1+\gamma\dfrac{4\pi NZe^2}{m}\sum_i \dfrac{f_i}{\omega_i^2 + x^2 + g_i x}} x\mathrm{d}x - \ln R\right] \tag{11}$$

In the limit of low densities (N small) we obtain

$$J = \lim_{R\to\infty}\left[\int_0^R \sum_i \frac{f_i}{\omega_i^2 + x^2 + g_i x} x\mathrm{d}x - \ln R\right] \tag{12}$$

Leaving out of consideration metals and strongly polar liquids, we may neglect the g_i:s in comparison with the ω_i:s and obtain from (12)

$$J = \sum_i f_i \ln\omega \tag{13}$$

At low densities then, (7) coincides with the Bethe formula (4) and the polarization effect is governed by the difference, p, between (11) and (12)

$$p = -\tfrac{1}{2}\lambda\int_0^\infty \frac{\varphi^2(z)}{1+\lambda\,\varphi(z)}\mathrm{d}z \tag{14}$$

$$\text{where } \lambda = \gamma\frac{4NZe^2}{m},\ n_i = \omega_i^2, \text{ and } \varphi(z) = \sum_i \frac{f_i}{n_i + z} \tag{15}$$

The total energy loss becomes

$$-\frac{\mathrm{d}E}{\mathrm{d}x} = \frac{4\pi q^2 e^4}{mv^2} NZ\left[\Sigma f_i \ln\frac{2mv^2}{\hbar\omega_i} + p\right] \tag{16}$$

Since p is negative the polarization effects a reduction in the energy loss which has also been found experimentally [28].

Before undertaking the evaluation of (14) we note that the f_i:s enter linearly into the sums. It is therefore free from the ambiguities referred to in the introduction.

3. EVALUATION of p

$\varphi(z)$ decreases monotonously with z so that the most important contribution to p comes from low z-values. A first approximation is therefore obtained by putting

$$\varphi(z) \cong \frac{1}{n_o + z} \tag{17}$$

where

$$\frac{1}{n_o} = \sum_i \frac{f_i}{n_i} \tag{18}$$

$\varphi(z)$ and $1/(n_o + z)$ are then equal for $z = 0$. Introducing (17) into (14) gives

$$p \cong -\tfrac{1}{2} \ln \frac{n_o + \lambda}{n_o} = -\tfrac{1}{2} \ln \frac{\varepsilon(0)}{\gamma + (1-\gamma)\,\varepsilon(0)} \tag{19}$$

If γ is put equal to 1, (19) agrees, as it should, with the expression obtained by Fermi [14] who neglected the local field correction.

In order to investigate under which conditions (19) is a good approximation, we put

$$\frac{1}{n_i} = \frac{1+\delta_i}{n_o} \tag{20}$$

From (20) and (18) follows

$$\sum_i f_i \delta_i = 0 \tag{21}$$

and

$$\varphi(z) = \frac{1}{n_o + z} + (\sum_i f_i \delta_i) \frac{n_o}{(n_o+z)^2} - (\sum_i f_i \delta_i^2) \frac{z n_o}{(n_o+z)^3} + \cdots\cdots \tag{22}$$

The second term on the right hand side of (22) is zero because of (21) and the validity of the approximation depends on whether the third and higher terms are small. If the oscillator strengths f_i were concentrated to $1/n_i$-values forming a region of small extent compared to $1/n_o$, $\Sigma f_i \delta_i^2$ etc. would be small and the approximation (17) justified. Since f_i decreases rapidly with increasing ω_i for transitions to the continuum, it might appear reasonable to assume that when there are "narrow gaps" between the first excited level and the ionization limit this requirement would be fulfilled [24]. It is therefore of primary interest to get an idea of the variations of f_i with $1/n_i$ in typical atomic and molecular systems. It will be seen that f_i as a function of $1/n_i$ is not confined to a small region around $1/n_o$. The situation is rather the opposite, thus invalidating the approximation (17).

3.1 Some oscillator strength distributions

The oscillator strength for a dipole transition from the ground state of an atom or molecule containing Z electrons is defined by

$$f_i = \frac{E_i - E_0}{3Z} \left| (0 \left| \sum_j \vec{r}_j \right| i) \right|^2 \tag{23}$$

E_0 and E_i are the energies of the ground and i:th excited state respectively, measured in rydbergs, $\vec{r}_j$ is the position vector of the j:th electron and

$$(0 \left| \sum_j \vec{r}_j \right| i) = \int \Psi_0^* (\sum_j \vec{r}_j) \Psi_i \, d\tau, \tag{24}$$

where Ψ_0 and Ψ_i are the ground and excited state wave functions. The unit of length is the Bohr radius, $\hbar^2/(m\,e^2)$

Eqn. (24) has been calculated exactly for all transitions of the hydrogen atom including the continuum [29,30]. For systems with more than one electron, the exact wave functions are not known and approximate ones have to be used. Since the matrix element (24) depends on the overlap between the ground and excited state wave functions, it is very sensitive to errors in these functions. The approximate wave functions are generally developed to give accurate expectation values of the energy. Since the latter is stationary with respect to variations of the wave function, large errors in the matrix elements (24) may result. Fairly accurate calculations exist, however, for the helium atom and the negative hydrogen ion based on Hylleraas wave functions for the ground state and suitable approximations for the excited state [31,32].

For other systems, values have been computed only for individual transitions from which it is difficult to obtain an overall picture.

Experimental determination of oscillator strengths is possible by several methods, *e.g.* light absorption measurements. A major part of these measurements has to be carried out in the vacuum ultraviolet region where large experimental difficulties appear [33]. Recently measurements have been reported for H_2 and C_6H_6 covering a large part of the continuum past the ionization limits [34].

3.11 *The hydrogen atom.* For the discrete spectrum we have [35]

$$E_n - E_0 = 1 - (1/n^2)$$

and

$$\left| (0 \left| x \right| n) \right|^2 = \frac{2^8}{3} n^7 \frac{(n-1)^{2n-5}}{(n+1)^{2n+5}}$$

where n is the principal quantum number. The n:th level is n^2 fold degenerate but the matrix elements of x are zero except for np_x states and similarly for y and z so that

$$\tfrac{1}{3} \left| (0 \left| \vec{r} \right| n) \right|^2 = \left| (0 \left| x \right| n) \right|^2$$

Thus

$$f_n = \frac{2^8}{3} n^5 \frac{(n-1)^{2n-4}}{(n+1)^{2n+4}} \tag{25}$$

In the continuum n is pure imaginary and may be written

$$n = 1/ik \tag{26}$$

where i is the imaginary unit and $2\pi/k$ is the wave length of the electron at an infinite distance from the nucleus. With the wave function for the excited state normalized with regard to k, *i.e.*

$$\int \Psi_{k'} \Psi_k \, \mathrm{d}\tau = \delta(k'-k), \tag{27}$$

the absolute square of the matrix element is [35]

$$\left|(0\,|\,x\,|\,n)\right|^2 = -\frac{2^8}{3} \frac{|n|^9}{1-\mathrm{e}^{-2\pi|n|}} \frac{(n-1)^{2n-5}}{(n+1)^{2n+5}} \tag{28}$$

and

$$f_n = \frac{2^8}{3} \cdot \frac{|n|^7}{1-\mathrm{e}^{-2\pi|n|}} \frac{(n-1)^{2n-4}}{(n+1)^{2n+4}} \tag{29}$$

As we wish to plot f as a function of $\eta = 1/\omega_i^2$, it must be normalized with respect to the same variable, *i.e.*

$$f(\eta)\,|\mathrm{d}n| = f_n\,|\mathrm{d}k| \tag{30}$$

Since

$$\eta = 1/[1-(1/n^2)]^2 \tag{31}$$

$$f(\eta) = \frac{2^6}{3} \cdot \frac{|n|^2}{1-\mathrm{e}^{-2\pi|n|}} \frac{(n-1)^{2n-1}}{(n+1)^{2n+1}} \tag{32}$$

or expressed in the real variable k

$$\eta = [k^2/(1+k^2)]^2 \tag{33}$$

and

$$f(\eta) = \frac{2^6}{3} \frac{\exp[-(4/k)\,\mathrm{arctg}k]}{(1+k^2)\,[1-\exp(-2/k)]} \tag{34}$$

$f(\eta)$ is shown diagramatically in Fig. 1a where the oscillator strengths for the discrete transitions have been spread out into block form. $f(\eta)$ is of a remarkably simple form extending with little change all the way down to zero abscissa. For the full curve drawn in this and some of the other figures, see section 3.2.

3.12 *Helium and the negative hydrogen ion.* Available theoretical values of the oscillator strengths of helium for both the discrete and continuous spectrum have been critically reviewed by Dalgarno and Lynn [31] and modified so as to agree with various experimental data. Their results are shown in Fig. 1b after suitable renormalization. It has the same general appearance as for the hydrogen atom but there is an even stronger accumulation towards low η-values.

For the continuum of the H^- ion, calculations have been reported by Chandrasekhar [32] who gives the photoelectric cross section $\varkappa_\nu$ from zero wave length to 16550 Å, the ionization limit. In the same units as above

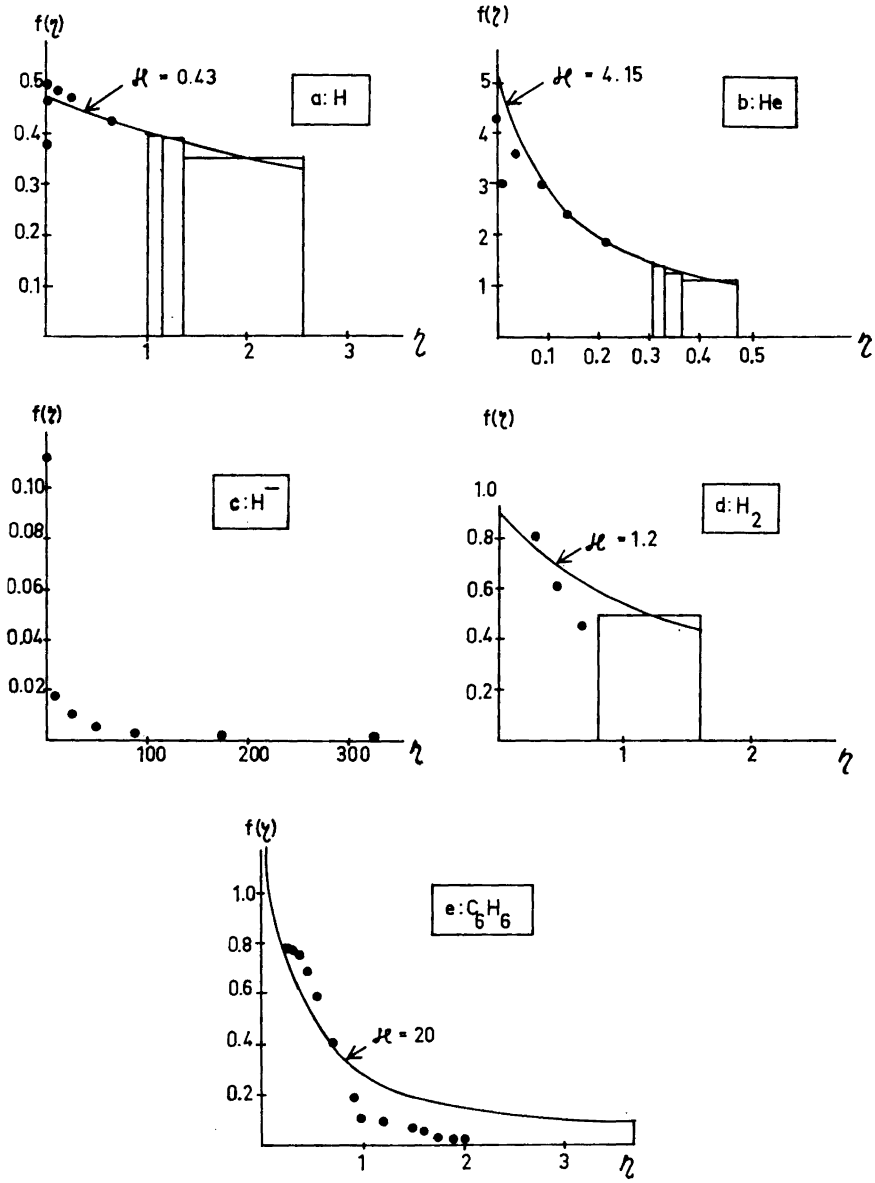

Fig. 1a—e. Oscillator strength distributions as functions of $\eta = 1/\omega^2_i$, the latter in units of the inverse square of the Rydberg frequency: $me^4/2\hbar^3$. Calculated or measured values are indicated by dots in the continuum and by blocks for "discrete" transitions. Figs. d and, in particular, e are incomplete. The full curves are approximations of the form given in equation (41).

$$f(\eta) = 23.5\, \varkappa_\nu/\lambda^3 \tag{35}$$

and

$$\eta = 1.21 \times 10^{10}\lambda^2 \tag{36}$$

where $\varkappa_\nu$ is given in cm^2 and λ in cm. The results are shown in Fig. 1c and are found to be drastically different from the previous ones. The oscillator strength tends to zero at the ionization limit, a behaviour entirely different from that of H and He. It is due to the circumstance that the excited electron in the H^- ion moves effectively in the field from an electrically neutral residue whereas for H and He this residue gives a coulomb field at large distances [36]. The tendency towards an accumulation of oscillator strength at low η-values is here extreme.

3.13 *Hydrogen and benzene.* From the absorption constant, μ, given by Bunch *et al.* [34], one obtains

$$f(\eta) = 1.75 \times 10^{12}\, \mu/\lambda^3 \tag{37}$$

with η given by (36). It is plotted in Figs. 1d and e. The oscillator strengths for the transitions to electronic levels below the ionization limits were not measured. For H_2 we have added a block of the content 0.42 being an estimate [35] of the sum of the oscillator strengths of all transitions below the ionization limit. At η-values somewhat smaller than the ionization limit, there should be contributions from doubly excited levels so that the overall shape becomes again similar to that of H and He.

For benzene the data are even more incomplete. No transitions to states below the ionization limits are included. Corresponding to the different ionization energies of the various π and σ electrons, there appear several steps. These will probably be largely filled out in a diagram containing all transitions. At $\eta \sim 0.002$, there will be a contribution from the K shell electrons of the carbon atoms. The important feature is again the monotonous decrease of f versus η.

3.2 A two-parameter description of $f(\eta)$

To take into account the features of $f(\eta)$ which were found above, we shall approximate $f(\eta)$ by means of the following continuous expression

$$f(\eta) = \frac{a}{b+\eta} \qquad 0 < \eta < \eta_m$$

$$f(\eta) = 0 \qquad \eta > \eta_m \tag{38}$$

The requirement that $\int f(\eta)\mathrm{d}\eta = 1$ reduces the number of independent parameters to two.

$$\int f(\eta)\mathrm{d}\eta = a \ln[1 + (\eta_m/b)] = 1 \tag{39}$$

Introducing

$$\eta_m/b = \varkappa \tag{40}$$

(38) reads

$$f(\eta) = \frac{1}{\ln(1+\varkappa)} \cdot \frac{1}{\mathrm{b}+\eta} \qquad 0 < \eta < \eta_m$$
$$f(\eta) = 0 \qquad \eta > \eta_m \tag{41}$$

$\varkappa$ determines the form, η_m the scale, of $f(\eta)$.

Inserting (41) into (15) we obtain the following expression for $\varphi(z)$:

$$\varphi(z) = \int_0^\infty \frac{f(\eta)}{(1/\eta)+z}\,\mathrm{d}\eta = \eta_m F(x) \tag{42}$$

where $x = \eta_m z$, $\beta = (1/\varkappa)\ln(1+\varkappa)$, and

$$F(x) = \frac{\beta x - \ln(1+x)}{\beta x\,(x-\varkappa)} \tag{43}$$

Changing to x as the integration variable we obtain the following expression for p:

$$p = -\frac{1}{2}\tau \int_0^\infty \frac{F^2(x)}{1+\tau F(x)}\,\mathrm{d}x; \quad \tau = \lambda\eta_m \tag{44}$$

An exact evaluation of (44) would probably yield a quite unwieldy expression. We shall develop two approximate expressions for p, viz.

$$p = -\frac{1}{2}\tau \int_0^\infty \frac{F_1^2(x)}{1+\tau F_1(x)}\,\mathrm{d}x \tag{45}$$

and

$$p = -\frac{1}{2}\tau \int_0^\infty F^2(x)\,\mathrm{d}x + \frac{1}{2}\tau^2 \int_0^\infty \frac{F_1^3(x)}{1+\tau F_1(x)}\,\mathrm{d}x \tag{46}$$

where

$$F_1(x) = \frac{F(0)}{1+\alpha x} \tag{47}$$

which coincides with $F(x)$ at $x = 0$. With F in place of F_1, (46) is identical to (44). Choosing α such that

$$F_1'(0) = F'(0) \tag{48}$$

we obtain an approximation which is accurate for small x-values, *i.e.* where F is large and gives the essential contribution to the integral in (45) and the last integral in (46).

Eqn. (46) will be a more accurate approximation than (45) since the main contribution from $F_1^3(x)$ is even more concentrated to low x-values than that from $F_1^2(x)$.

One finds

$$\alpha = \frac{1}{1-\beta}\left(\frac{1}{2} - \frac{1-\beta}{\varkappa}\right) \tag{49}$$

Eqns. (45) and (46) become

$$p = -\frac{1}{2}\frac{F(0)}{\alpha}\ln\left(1+\tau F(0)\right) \tag{45'}$$

and

$$p = -\frac{1}{2}\tau F(0)\cdot G(\varkappa)+\frac{1}{2}\frac{F(0)}{\alpha}\left[\tau F(0)-\ln(1+\tau F(0))\right] \tag{46'}$$

where *

$$G(\varkappa)=\frac{\beta\varkappa}{1-\beta}\left[-\frac{\ln(1+\varkappa)}{3\varkappa}-\frac{1}{\varkappa(1+\varkappa)}+\frac{4\zeta(2)}{\ln^2(1+\varkappa)}\left(\frac{1+(\varkappa/2)}{1+\varkappa}-\frac{\ln(1+\varkappa)}{\varkappa}\right)+\right.$$
$$\left.+2\frac{L_2(\varkappa/[1+\varkappa])}{\ln^2(1+\varkappa)}\left(\frac{1}{1+\varkappa}-\frac{\ln(1+\varkappa)}{\varkappa}+2\frac{L_3(\varkappa/[1+\varkappa])}{\varkappa\ln^2(1+\varkappa)}\right)\right] \tag{50}$$

a rather cumbersome expression. ζ is Riemann's zeta function [38], L_2 is Euler's dilogarithm [39,40] and

$$L_3(z)=\sum_{j=0}^{\infty}\frac{B_j}{j!}\frac{[-\ln(1-z)]^{j+2}}{j+2} \tag{51}$$

where B_j are the Bermoulli numbers. The difference between (46') and (45') is **

$$\frac{1}{2}\tau F(0)\left(\frac{F(0)}{\alpha}-G(\varkappa)\right) \tag{52}$$

From (10), (15), (42), and (44) we obtain

$$1+\tau F(0)=\frac{\varepsilon(0)}{1+(1-\gamma)(\varepsilon(0)-1)} \tag{53}$$

Finally

$$\frac{F(0)}{\alpha}=\frac{(1-\beta)^2}{\beta\varkappa\left(\frac{1}{2}-\frac{1-\beta}{\varkappa}\right)} \tag{54}$$

To calculate the polarization effect, we need $\varepsilon(0)$, γ, and $\varkappa$. $\varepsilon(0)$ is usually readily available and γ is equal to 2/3 when the Clausius-Mossotti formula holds. Otherwise one has to use the γ-value giving the best agreement between (10) and experimental dispersion relations. It therefore remains to determine $\varkappa$, the form factor of the oscillator strength distribution.

3.3 Determination of $\varkappa$

The two independent parameters in our description of $f(\eta)$ may be taken to be η_m and $\varkappa$. (53) gives one relation between these parameters since τ contains

* The author gratefully acknowledges the aid of Dr. B. Nagel in evaluating $\int_0^\infty F^2 dx$ in terms of known transcendental functions.

** A further improvement is probably obtained by choosing α such that (52) becomes zero.

η_m. A second relation is obtained from the mean excitation potential, I_o, obtainable from measurements on the substance in gaseous form:

$$\ln(I_o/\hbar)=\sum_i f_i \ln \omega_i$$

$$=-\frac{1}{2}\int f(\eta) \ln\eta \ \mathrm{d}\eta$$

$$=-\frac{1}{2}\ln\left(\frac{\eta_m}{1+\varkappa}\right)+\frac{1}{2}\frac{\mathrm{L}(_2\varkappa/[1+\varkappa])}{\ln(1+\varkappa)} \tag{55}$$

After elimination of η_m between (55) and (53), there results the following relation determining $\varkappa$:

$$H(\varkappa) = h[\varepsilon(0)] \cdot (I_o/\hbar)^2 \tag{56}$$

where

$$H(\varkappa)=\left(\frac{1}{\ln(1+\varkappa)}-\frac{1}{\varkappa}\right)(1+\varkappa)\ \exp\frac{\mathrm{L}_2(\varkappa/[1+\varkappa])}{\ln(1+\varkappa)} \tag{57}$$

and

$$h[\varepsilon(0)]=\frac{m}{4\pi\ NZ\ e^2}\cdot\frac{\varepsilon(0)-1}{1+(1-\gamma)(\varepsilon(0)-1)} \tag{58}$$

$h(\varepsilon(0))$ is proportional to the molecular polarizability.

4. CONCLUSIONS

The expressions for the polarization effect arrived at here are fairly similar to that deduced by Fermi [14] using a single frequency description of the dielectric constant:

$$p = -\frac{1}{2}\ln\varepsilon\,(0) \tag{59}$$

Our expression (45′) differs from Fermi's by the factor $F(0)/\alpha$ and the inclusion of the local field correction through γ. $F(0)/\alpha$ is a rather slowly varying function of $\varkappa$, being 0.750 for $\varkappa = 0$ and 0.565 for $\varkappa = 10$. This indicates that p is fairly insensitive to the finer details in the oscillator strength distribution. In the better approximation (46′), there enters moreover the additive term (52) which is negative, reducing the variation with $\varkappa$ still further.

To test the theory, measurements should be made on substances in gaseous and liquid form. The velocity of the particles, while fulfilling (1), should be as small as possible, in order that the relative effect of p in (16) should be as large as possible. For this purpose α-particles with an energy of about 5 MeV would be very suitable. Measurements of the energy loss of such particles in liquids may now be made with an accuracy of about 0.1 % [41]. A similar accuracy should be attainable in measurements on gases, thus allowing a detailed check to be made.

REFERENCES

1. Thomson, J. J. *Conduction of Electricity through Gases*. Cambridge 1906, pp. 370–389.
2. Darwin, C. G. *Phil. Mag.* **23** (1912) 907.
3. Bohr, N. *Phil. Mag.* **25** (1913) 10.
4. Bohr, N. *Phil. Mag.* **30** (1915) 581.
5. Henderson, G. H. *Phil. Mag.* **44** (1922) 680.
6. Fermi, E. *Z. Physik* **29** (1924) 315.
7. Bethe, H. A. *Ann. Physik* **5** (1930) 325.
8. Bethe, H. A. *Z. Physik* **76** (1932) 293.
9. Bloch, F. *Ann. Physik* **16** (1933) 285.
10. Bloch, F. *Z. Physik* **81** (1933) 363.
11. Swann, W. G. F. *J. Franklin Inst.* **226** (1938) 598.
12. Fermi, E. *Phys. Rev.* **56** (1939) 1242.
13. Fermi, E. *Phys. Rev.* **57** (1940) 485.
14. Halpern, O. and Hall, H. *Phys. Rev.* **57** (1940) 459.
15. Wick, G. C. *Nuovo cimento* **1** (1943) 302.
16. Halpern, O. and Hall, H. *Phys. Rev.* **73** (1948) 477.
17. Bohr, A. *Kgl. Danske Videnskab Selskab. Matem.-fys. Medd.* **24** (1948) No. 19.
18. Messel, H. and Ritson, D. *Phil. Mag.* **41** (1950) 1129.
19. Schoenberg, M. *Nuovo cimento* **8** (1951) 159.
20. Schoenberg, M. *Nuovo cimento* **9** (1952) 372.
21. Huybrechts, M. and Schoenberg, M. *Nuovo cimento* **9** (1952) 764.
22. Sternheimer, R. M. *Phys. Rev.* **88** (1952) 851.
23. Sternheimer, R. M. *Phys. Rev.* **93** (1954) 351.
24. Brandt, W. *Phys. Rev.* **104** (1956) 691.
25. Brandt, W. *Research report*, E. I. du Pont de Nemours & Co., 1957.
26. Aniansson, G. *Trans. Roy. Inst. Techn.* **1961** No. 178.
27. Mott, N. F. *Proc. Gambridge Phil. Soc.* **27** (1931) 553.
28. Aniansson, G. *Phys. Rev.* **98** (1955) 500.
29. Sugiura, Y. *Sci. Papers Inst. Phys. Chem. Res.* **11** (1929) 1.
30. Gordon, W. *Ann. Physik* **2** (1929) 1031.
31. Dalgarno, A. and Lynn, N. *Proc. Phys. Soc. A* **70** (1957) 802.
32. Chandrasekhar, S. and Elbert, D. D. *Astrophys. J.* **128** (1958) 633.
33. Price, W. C. *Advances in Spectroscopy* **1** (1959) 56.
34. Bunch, S. M., Cook, G. R., Ogawa, M. and Ehler, A. W. *J. Chem. Phys.* **28** (1958) 740.
35. Sommerfeld, A. *Wellenmechanik*, Braunschweig 1939.
36. Bethe, H. A. and Salpeter, E. E. *Encyclopedia of Physics*, Vol. 35, p. 402. Berlin 1957.
37. Mulliken, R. S. and Rieke, C. A. *Repts. Progr. Phys.* **8** (1941) 231.
38. Jahnke, E. and Emck, F. *Tables of Functions*, Leipzig 1933, p. 319.
39. Mitchell, K. *Phil. Mag.* **40** (1949) 351.
40. Erdélyi, A. *et al. Higher Transcendental Functions*, Vol. I, p. 31, New York 1953.
41. Aniansson, G. *Trans. Roy. Inst. Techn.* **1961** No. 177.

Received April 14, 1962.

ACTA CHEMICA SCANDINAVICA 16 (1962) 2100–2112

Determination of the Cross Section for the Reactions $^{42}Ca(n, p)^{42}K$ and $^{43}Ca(n, p)^{43}K$ and Methods for Production of Carrier-Free Potassium Isotopes

SEVALD FORBERG

Division of Nuclear Chemistry, The Royal Institute of Technology, Stockholm 70, Sweden

Dedicated to Professor *Ole Lamm* on his 60th birthday

The cross sections for the (n, p) reactions of ^{42}Ca and ^{43}Ca have been determined by reactor irradiation of $CaCO_3$, carrier-free separation of potassium and comparison of the ^{42}K and ^{43}K activities with the activity of ^{24}Na obtained in a monitor of pure aluminium.

The measured cross sections were 2.1 ± 0.4 and 1.5 ± 0.3 mb for ^{42}Ca and ^{43}Ca respectively, the theoretically predicted ones, 1.3 and 4.5 mb.

The carrier-free separation method utilized included the following steps, (*a*) dissolution of the irradiated calcium carbonate in hydrochloric acid, (*b*) sorption of the calcium on Dowex A 1 chelating resin, (*c*) selective displacement of the potassium by means of ammonium chloride, (*d*) substitution of the chloride with hydroxide, on an anion exchanger, and (*e*) evaporation of the ammoniacal solution.

This separation method should also be suitable for the production of carrier-free ^{42}K or ^{43}K activities from enriched ^{42}Ca and ^{43}Ca, and make possible the recovery, with a high yield, of the expensive, enriched calcium isotopes. A fission neutron flux of 5×10^{14} s^{-1} cm^{-2} should yield after one day's irradiation of 10 mg ^{43}Ca, about one mC of ^{43}K. Some advantages of carrier-free ^{43}K as compared with ordinary activated potassium are pointed out.

The neutron reaction denoted by (n, p) constitutes the standard method for the production of carrier-free activities of some important nuclides, *e.g.* ^{14}C, ^{32}P and ^{35}S. The cross sections for the reactions (n, p), (n, α) and also for (n, 2n) have been investigated for many nuclides for fission-spectrum neutrons, and in some cases several workers have studied the same cross section and arrived at more or less different results [1].

The theory presented by Hughes [2] made it possible to predict the cross section for a threshold reaction by simple calculations. Such calculations are

further simplified by a graphical method [3], and at present a table of Q-values for (n, p) and (n, α) reactions for many nuclides throughout the periodic system is available, including also many experimental cross sections [4]. For nuclides of low atomic numbers, the Q-values for some other reactions (*e.g.* (n,^{3}He); (n, d); (n, t)) have also been published [5].

In many cases the experimental cross section agrees fairly well with the predicted one, but in other cases, *e.g.* some titanium isotopes, the measured cross sections are one or two powers of ten lower than the theoretically calculated ones [6].

The calculations mentioned are based on an analytical expression for the fission neutron spectrum, on the theoretical probability for a proton or alpha particle to penetrate the coulomb barrier around a nucleus, and on the "geometric" dimensions of the nucleus. The cross section is given as the mean cross section, calculated for the entire fission neutron spectrum.

In more elaborate calculations of cross sections it is necessary to take into account other factors, for instance competing reactions, energy level schemes of the reaction product nuclides and neutron penetrabilities. Nevertheless, experimental determination of cross sections will always be of value. From a nuclear science point of view, it would be more interesting to study the cross sections for discrete neutron energies, and this has been done especially for 14 MeV neutrons from accelerator sources, see for instance [7] and [8].

In the case of very small cross sections and long half-lives, however, it is often more convenient to determine the mean cross sections for fission neutron spectra by means of irradiation in a nuclear reactor, and the values thus obtained are also more relevant for the planning of reactor production or, for instance, when judging eventual interferences in activation analysis performed by reactor irradiation.

In the case of calcium, the (n, p) reactions of ^{40}Ca have been the subject of extensive calculations, partly based on theories and partly on experimental data [9]; the (n, p) reaction of ^{44}Ca has been recognized, studied and utilized to obtain ^{44}K activities for decay scheme studies [10,11,12]; the corresponding reaction of ^{43}Ca is also mentioned [13] and the one of ^{42}Ca has been studied [14]. However, no attempts seem to have been made to determine the experimental mean cross sections for (n, p) reactions of calcium isotopes, induced by fission spectrum neutrons. It seemed interesting, therefore, to make an effort to do so. This first experiment was planned to give, from the same irradiation and the same separation, the cross sections for the (n, p) reaction of both ^{42}Ca and ^{43}Ca, because the induced activities, ^{42}K and ^{43}K, have similar half-lives, 12.5 h and 22.4 h, respectively. Other potassium isotopes produced from calcium should not interfere in this case, because their half-lives are much longer (^{40}K, half-life 10^9 years) or much shorter (^{44}K, 22 m). There are natural calcium isotopes also available for the production of ^{46}K and ^{48}K, which are both unknown so far, but it can be inferred from beta decay systematics that their half-lives ought to be negligibly small.

THEORETICAL INTERPRETATIONS. CHOICE OF EXPERIMENTAL CONDITIONS

1. *Nuclear considerations.* From the total disintegration energies of the β-decaying nuclides ^{42}K and ^{43}K and from the mass difference between the neutron and the proton, the Q-values of the reactions ^{42}Ca (n, p) ^{42}K and ^{43}Ca, (n, p) ^{43}K were calculated. After correction for the kinetic energy transmitted to the compound nucleus by the impact with the neutron, the neutron threshold energies, E_t, were calculated. The effective threshold energies, E_{eff}, according to Hughes were derived from the graph in his book [2] and the mean cross sections, $\bar{\sigma}_{theor.}$, for fission neutron spectrum were obtained from Inthoffs graph [3]. All these values are tabulated in Table 1, together with the natural abundances for the target nuclides. In the same table are also included E_{eff}

Table 1. Threshold energies and theoretical cross sections for the (n, p) reaction of ^{42}Ca and ^{43}Ca, with calculated cross sections or Q-values for some other reactions of calcium isotopes, competing either with respect to the cross sections or with respect to the production of ^{42}K and ^{43}K.

Target nuclide	^{42}Ca	^{43}Ca	^{44}Ca
Abundance of target isotope	0.64 %	0.145 %	2.06 %
Product nuclide from (n,p)	^{42}K	^{43}K	^{44}K
Half-life of product nuclide	12.5 h	22.4 h	22 m
E_t, threshold energy for (n,p)	2.8 MeV	1.1 MeV	
E_{eff}, for (n,p) [2]	6.4 MeV	4.7 MeV	
$\bar{\sigma}_{theor.}$ for (n,p)	*1.3 mb*	*4.5 mb*	
Q-value for (n,2n)	−11.4 MeV	− 8.05 MeV	
E_{eff}, for (n,α)	9.7 MeV	10.2 MeV	
$\bar{\sigma}_{theor.}$ for (n,α)	0.22 mb	0.13 mb	
Q-value for (n,d) [5]		− 8.5 MeV	− 9.9 MeV
Q-value for (n,t) [5]			−13.3 MeV

and $\bar{\sigma}_{theor.}$ for (n, α) reactions, calculated in the same way as above except for the Q-values, which were obtained from the mass differences between reacting and resulting nuclides and particles. Also included are the Q-values for the (n, 2n) reactions, calculated in the same way as for the (n, α) reactions together with Q-values for (n, d) and (n, t) taken from Ref.[5], in order to facilitate a judgement of the competition of these reactions with the (n, p) reactions.

Data for the calculations mentioned were taken from standard compilations [15,16].

From a nuclear spectroscopic point of view, the decay schemes of ^{42}K and ^{43}K are very well known [17,18] and the possibility of detection, identification and quantitative estimation of each of ^{42}K and ^{43}K in the presence of rather large activities of the other by means of gamma spectrometry is obvious with the exception that too high ^{42}K activities might mask the ^{43}K spectrum by the Compton, backscatter and Bremsstrahlung distributions.

2. *Chemical considerations.* When the cross section for a nuclear reaction is to be deduced from the induced activity, it is necessary to avoid, or take into account, the presence of nuclides which may, through other reactions, contribute to the same activity. In addition, although modern gamma spectro-

meter equipment often permits exclusive measurement of a given gamma energy in presence of others, foreign activities are likely to diminish the significance levels both in the qualitative identification and in the quantitative estimation. Hence, the growth of undesirable activities must be suppressed and a chemically pure target must be utilized. However, the purity of practically obtainable chemicals is limited, and very low contents of impurities with high activation cross sections might yield significant activities besides the interesting ones, because these are produced by low cross sections from isotopes of low abundances. Moreover, activities produced from other isotopes in the natural target element must be taken into account, *e.g.* ^{47}Ca and its daughter nuclide ^{47}Sc. Therefore it was decided to separate the alkali ions as one group from all other elements in the irradiated matter. With a successful separation method, the demand for ultimate purity of the target should then mainly be restricted to the alkalis and the actual target material was specifically processed for this purpose.

By removing the alkalis, the risk for irrelevant ^{42}K activities produced by neutron capture in ^{41}K is suppressed correspondingly. Other chemical sources for ^{42}K and ^{43}K activities will be mentioned under "discussion".

As for the chemical form of the target, it ought to be easily dissolvable and its anion should not give rise to activities contributing significantly to the dose rate level during the separation process after the irradiation. Further, the anion should not complicate the separation steps.

EXPERIMENTAL

1. *Preparation of the target substance.* The target substance was prepared from an analytical grade of calcium nitrate (Merck). An attempt was made to remove or diminish the alkali element impurities from the calcium by dissolving the salt in water, sorbing the calcium ions in a Dowex A 1 chelating resin and displacing the alkalis selectively by means of an alkali-free ammonium chloride solution.

The exchanging groups of the Dowex A 1 resin are nitrilodiacetate groups on a conventional divinylbenzene-styrene copolymer matrix [19]. By chelating effects this resin takes up bi- and polyvalent cations very selectively in presence of alkali ions, and therefore any of the alkalis can be selectively displaced by means of another monovalent cation [20], in the present case by ammonium. Also, the differences in stability constants for different chelated cations can be utilized for their separation [21].

The Dowex A 1 available to the author at the time of this experiment was a 50 – 100 mesh technical grade, containing many "dirty" particles with different appearences. It was therefore purified by back washing the fines, and the dirty-looking particles were removed fraction after fraction by suspending the exchanger in a mixture of trichloroethylene and ethyl alcohol and adjusting the mixture to a density slightly larger or smaller than the density of the main exchanger grains in that solvent, and leaving it overnight to separate. This was done with the exchanger firstly in the shrunk hydrogen form, secondly in the swollen ammonium form, and thirdly in the shrunk copper form. In each case a certain fraction of dark or oily particles together with some ordinary-looking exchanger separated from the bulk of the material. After this treatment the remaining exchanger looked and behaved very homogeneously.

The purified exchanger was packed in a polymethylmethacrylate column after displacing the other solvents by water. The copper was displaced by one-molar hydrogen chloride, and the resin was then saturated with ammonium from an ammonia solution.

Because a faint blue, copper chelate colour seemed to remain in the exchanger when the hydrogen and ammonia steps were performed at rates normal for cation exchangers

of the sulphonate types, these two cycles were repeated, this completely removed all visible copper colour. The kinetics of ion exchange in Dowex A 1 are known from other studies to be slow [22]. Because of the swelling properties of the Dowex A 1 resin, the ammonia saturations were performed by upwards flow.

The ammonium ions in the exchanger column were now substituted with calcium ions from an aqueous solution of calcium nitrate, and any alkali metals in the resin were displaced by a slightly ammonical, half-molar solution of ammonium chloride. Because the alkali content of this solution would set a theoretical limit for the resulting alkali level in the exchanger, it was prepared by passing distilled water through a mixed-resin bed and dissolving gaseous hydrogen chloride and gaseous ammonia in it. All operations were performed in polyethylene equipment. In order to test the purity of the deionized water, it was passed through an electrical conductivity cell, directly from the exchanger column so that atmospheric carbon dioxide should not contribute to the results. The measured conductivity was 130 % higher than that calculated for pure water from the dissociation constant and equivalent conductance of hydrogen and hydroxide ions at the experimental temperature, 19.1°C. No attempts were made to obtain water of higher resistance.

The amounts of ammonium chloride passed through the chelating exchanger column corresponded to four times the total exchange capacity.

The column was then rinsed with two bed volumes of demineralized water, and the calcium was displaced by means of half-molar hydrogen chloride in demineralized water. The displacement from the two feet high column was performed in a couple of hours, and the first and last quarters of the calcium chloride in the effluent were rejected because impurities might have been enriched at either end.

The middle fraction was collected in a polyethylene beaker, and ammonia gas was absorbed to a concentration slightly higher than that of the chloride.

Finally, gaseous carbon dioxide was absorbed until neutralization against thymol blue. The precipitated calcium carbonate was filtered on a sintered glass filter, washed once with demineralized water and dried to constant weight at 110°C.

The yield was almost eight grams of calcium carbonate. Two polyethylene tubes were filled with this substance, slightly more than 2 grams in each, for irradiation.

2. *Irradiation.* One sample of calcium carbonate was wrapped in a 0.3 mm thich cadmium foil together with 0.5 g of spectrographically standardized aluminium (Johnson, Matthey & Co., Ltd., London), 0.5 g of magnesium sulphate, 10 mg of sodium acetate and 10 mg of potassium acetate. The three last-mentioned substances were of analytical grade and all were contained in their own polyethylene tubes. The magnesium and sodium contents of the aluminium were estimated to 10 and 2 ppm by the purchaser. All samples were placed close to the calcium carbonate, and the sodium acetate specially close to the aluminium sample. The assemblage was irradiated for 21.5 h in a central position in the Swedish reactor R 1, the nominal thermal neutron flux being 12×10^{11} s^{-1} cm^{-2} and the expected flux of fast neutrons being almost one decade lower. The sodium salt was intended as a standard for the estimation of the impurity level of sodium in the calcium carbonate and also in the aluminium monitor, and the potassium salt served as a standard for the estimation of the potassium in the calcium carbonate. The sulphate was intended as a second neutron flux monitor.

In order to distinguish between the alkali activities induced by fast neutron activation of aluminium and calcium and the corresponding activities induced by neutron capture in the alkali impurities of the monitor and the target, a similar irradiation unit including calcium carbonate, aluminium, sodium and potassium acetates and without the cadmium shielding was irradiated during the last 16 3/4 hours of the irradiation time for the cadmium container and about 10 cm distant from it. Special care was taken in the packaging of the assemblage without cadmium to avoid too large errors from the thermal neutron flux gradient.

3. *Chemical separations of the irradiated targets.* The irradiated calcium carbonate samples were each dissolved in a small excess of hydrochloric acid. The solutions were neutralized to pH = 5 with ammonia and then passed into a Dowex A 1 column of 50 % higher capacity than the calcium amount. The exchanger was in the ammonium form, the interstitial solution pure water.

The activity of the effluent was monitored by means of a thin-window (1.4 mg/cm² mica) GM tube coupled to a counting ratemeter equipped with a recorder. The effluent

was passed through a flow cell, covered with a 0.6 mg/cm² film of chlorinated rubber and designed to make possible the detection of ^{45}Ca with a high efficiency yield.

The alkalis in the exchanger were now displaced with a half-molar ammonium chloride solution. An inspection by means of a GM tube of the longitudinal distribution of the beta activities in the column showed a peak below the calcium saturated region, which moved with the ammonium chloride solution in accordance with the expected behaviour of alkalis. The activity in the flow cell ascended to hundred times the background count rate when this peak passed, remained almost constant in an effluent volum corresponding to the excess capacity in the exchanger and descended steadily to the true background count rate (± 20 %). The volume containing this activity was collected as the fraction of interest.

After collection of the alkali activities, the calcium was displaced from the column with 0.2 M hydrochloric acid. Gamma spectrometry of all fractions of the effluent showed that no significant amounts of ^{42}K and ^{24}Na had been lost from the alkali fraction. The only additional gamma activity observed in these pure ^{47}Ca spectra was disregarding the growing ^{47}Sc peak, a small peak with an energy slightly below 0.4 MeV and a few hours half-life, probably due to strontium-87 m.

The ammonium chloride solution containing the potassium activities was passed through a column of Dowex 2 in the hydroxide form, with sufficient capacity to convert all the chloride to hydroxide. The ammonia effluent was evaporated under suction in a rotating evaporator to a volume of a couple of milliliters. The last evaporation, to dryness, was performed in a small beaker on a water bath. The total residue was estimated visually to be far less than one mg.

The residue was dissolved in a few drops of water and about half the solution was transferred with a micro pipet to a sulphonated spot on a polystyrene film [23], intended for 4π beta counting. The polystyrene film (1.0 mg/cm²) was sulphonated by placing one drop of concentrated sulphuric acid on it for a short time. The sulphonated area was a little more than one cm in diameter, and was left in the hydrogen form after it had been rinsed with distilled water. The activity of the transferred sample was totally absorbed by ion exchange and was not removed when the spot was rinsed with water.

The exact fraction of the total potassium activity transferred to the polystyrene film was determined by gamma spectrometry. That no potassium activities were lost during the evaporation or other steps, was confirmed by careful monitoring of all the equipment.

In order to decrease the content of ^{24}Na in the sample for gamma spectrometry, the sample was diluted to 20 ml, potassium and some sodium carrier were added and the potassium was precipitated as tetraphenylboron [24] and taken on a filter paper. More potassium carrier was added to the filtrate, a new precipitation was performed in the same beaker and the slurry filtered on a new paper. The ^{42}K activity of the last precipitate was shown by gamma spectrometry to be only 5 % of the first. In view of the fact that the first precipitate was not quantitatively transferred to the filter paper, this should prove that all the potassium activity was retained in the filter cakes, the precipitation conditions being the same in both cases.

4. *Radioactivity measurements.* All gamma spectra except four were obtained by means of a 3″ × 3″ NaI (Tl) crystal and a multichannel analyzer of the Hutchinson-Scarrott type, used in a 78 channel mode. All samples were placed on the central axis of the detector, at measured distances from its face. The distances were referred to the geometrical centra of the active bodies. An 8 mm aluminium absorber was utilized for all measurements.

The irradiated standard alkali acetates were dissolved in 50 ml volumes of carrier solutions, and small measured volumes were transferred to matched polyethylene tubes and diluted to a certain mark on the tube. The potassium tetraphenylboron precipitates together with the filter papers were compressed to the same volume in a similar tube. The aluminium monitors were divided into smaller pieces and that one with the most suitable activity level was utilized for comparisons with the potassium activities. The fractions of the ^{24}Na activities utilized were determined by weighing, assuming that the self-shielding against fast neutrons and the gradients in the fast neutron flux were both negligible within 0.5 g of aluminium.

Besides the more familiar comparisons of the intensities of the same gamma energy from different samples, the purpose of the measurements was to compare the ^{24}Na activity in the aluminium sample with the ^{43}K and ^{42}K activities from the irradiated calcium.

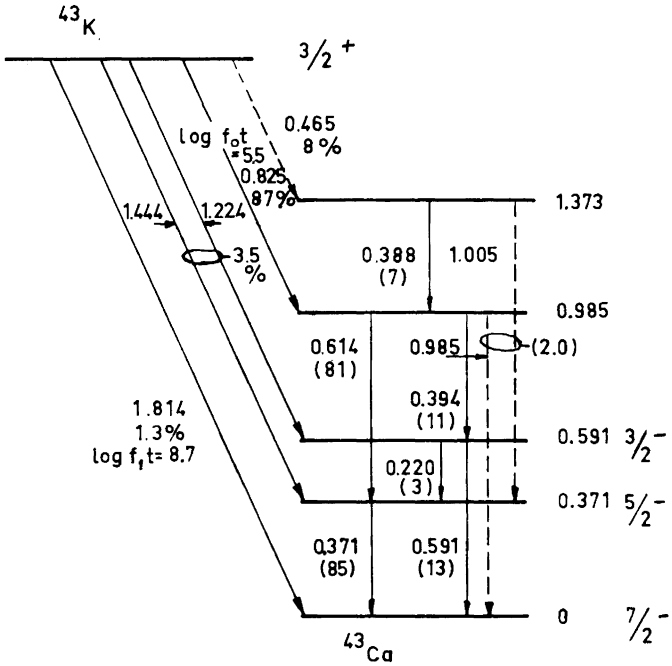

Fig. 1. The decay scheme of ^{43}K according to Benczer-Koller *et al.*[17]

The total disintegration rate of ^{42}K was calculated from the pulse rate under the 1.52 MeV photopeak, corrected for time resolution losses, for the total detection efficiency for this energy at the actual distance, 6.5 cm, for the peak to total ratio [25], and from the fact that the intensity of this transition is only 18 %.

The disintegration rate of ^{24}Na was determined in the same manner from the 1.37 MeV peak taking into account the losses from this peak due to coincidence with pulses from the coincident ($T_{½} = 2.5 \times 10^{-11}$ s) 2.75 MeV transition.

The decay scheme of ^{43}K (Fig. 1) is more complicated than those of ^{42}K and ^{24}Na and special care is necessary when its disintegration rate is determined. In Table 2 the different gamma energies from ^{43}K are tabulated together with their intensities [17].

Table 2. Gamma transitions in the ^{43}K decay scheme according to Ref.[17]

Gamma transitions			Compound peaks	
Number	Energy MeV	Intensity (Emitted quanta per 100 disintegrating nuclei)	Approximate energy, MeV	Intensity
γ_1	0.220	3 ± 1		
γ_2	0.371	85 ± 8		
γ_3	0.388	7 ± 1	0.38	103 %
γ_4	0.394	11 ± 1		
γ_5	0.591	13 ± 1	0.61	94 %
γ_6	0.614	81 ± 8		
γ_7	1.005	2 ± 0.2		

A conventional gamma spectrometer with its limited energy resolution will see the gamma energies γ_2, γ_3 and γ_4 as a somewhat broad, compound peak and γ_5 and γ_6 as another compound peak.

When the crystal is irradiated at a small solid angle from a ^{43}K source, the component intensities within each compound peak are additive, with 94 % as the resulting intensity at 0.61 MeV.

At the actual source-crystal distance, 6.5 cm, there are some coincidence gains and losses to account for. From Ref.[17] it seems likely that all successive internal transitions have short enough half-lives to be coincident when measured with a NaI (Tl) crystal. The assumption is made that no successive gamma emissions are angularly correlated to any significant extent.

The fractional loss of counts from a certain gamma *peak* caused by another, coincident gamma emission is equal to the total detection efficiency for this other gamma energy, multiplied by the ratio between the rate of coincident emission and the rate of emission of the gamma energy being studied. The contribution to a peak from two coincident gamma emissions with a suitable energy sum is calculated in the same way as the count losses, except that also the peak-to-total ratio must be taken into account.

In Table 3 are given the peak efficiencies for the actual energies calculated from the total detection efficiencies and peak-to-total ratios as interpolated from the graphs given in reference [25].

Table 4 shows the calculated losses and gains to and from other parts of the ^{43}K spectrum for the 0.61 MeV compound peak. Second-order terms were not taken into account. The resulting value was used to calculate the disintegration rate of ^{43}K in the source.

When the ^{43}K activity had decayed to an inconveniently low level for external measurements, its spectrum was recorded by means of 256 channel Nuclear Data Analyzer and a 3″ × 3″ NaI (Tl) well crystal. The counting time was 60 min., and four spectra were taken at one-day intervals.

The decay of the activities on the polystyrene film was followed by means of a Baird Atomic 4 π porportional counter, and a fraction of the ^{32}P activity separated from the irradiated magnesium sulphate was mounted on a similar (1 mg/cm^2) film and measured in the same counter.

Table 3. γ-Detection efficiencies at 6.5 cm distance from a 3″ × 3″ NaI (Tl) crystal [25].

γ-Energy	Nuclide	Total efficiency	Peak/Total	Peak efficiency
1.52	^{42}K	0.0297	0.313	0.0093
1.37	^{24}Na	0.0306	0.335	0.0102
0.61	^{43}K	0.039	0.57	0.0222
0.38	^{43}K	0.046	0.755	0.035
0.22	^{43}K	0.055	0.910	0.050

Table 4. Detection efficiency for the 0.61 MeV compound peak of ^{43}K at 6.5 cm distance from a 3″ × 3″ Na I (Tl) crystal, with corrections for coincidence gains and losses:

"Main" γ	Coinc. γ	Probable number of coincident emissions per 100 "main" gammas	Contributions to the 0.61 MeV peak efficiency, pulses per 100 decaying nuclei
γ_6			0.180
γ_6	γ_3	7.5	−0.0006
γ_6	γ_2	100	−0.008
γ_5			0.029
γ_5	γ_3	6.3	−0.0001
γ_5	γ_4	85	−0.0011
γ_1	γ_2	90	0.0047
γ_1	γ_3	6.3	0.0003
γ_1	γ_4	85	0.0044
			Total 0.209

RESULTS

Gamma spectra were first taken of the irradiated but unseparated samples, and the following results for ^{24}Na were obtained from the 2.75 MeV peak of these spectra.

The ^{24}Na activity calculated for 1 g of the cadmium shielded aluminium, equaled the activity from 77 μg of sodium from the acete standard. According to the spectrographically estimated sodium content in the aluminium, 2 ppm, 97 % of the ^{24}Na activity in aluminium originated from the (n, α) process.

The count rate per gram of the unshielded aluminium, for the peak at 2.75 MeV, was 1.7 $\pm$ 0.9 % higher than the corresponding value for the shielded material. The uncertainty given being the standard deviation from the counting statistics only.

The sodium content of the calcium carbonate was calculated to be 3.0 ppm from the cadmium shielded sample and 2.5 ppm from the unshielded one. The first value is assumed to be the most reliable one because the sodium standards were assymetrically located with respect to the carbonates and the gradient of the thermal neutron flux was unknown.

Fig. 2 shows a spectrum of the potassium tetraphenylboron precipitate 33 h after the irradiation. Also shown, is a part of another spectrum obtained under equal conditions of the same activity, but prior to the precipitation. The inserted spectrum was normalized to fit the ^{42}K peak.

Three gamma spectra of the potassium activities separated from the unshielded target were obtained on the first, second and third days after irradiation. The conditions of measurement were the same as for the spectrum in Fig. 2 and the spectral shape the same except for the 1.37 MeV peak from ^{24}Na which revealed a few tenths higher intensity than the peak inserted on Fig. 2. The small effect on the activation of sodium from the cadmium shield is consistent with the large resonance cross section for neutrons of 2.85 keV energy [26].

The ^{24}Na peak was quantitatively identified by its half-life and by comparison with the peak at 2.75 MeV (from another spectrum) and the spectrum of the standard sodium salt.

The ^{42}K peak was identified by its energy (within $\pm$ 2 % from the peak of the standard potassium salt) and its half-life [27].

The energies of the peaks I and II in Fig. 2 were found to be 0.39 $\pm$ 0.02 MeV and 0.61 $\pm$ 0.03 MeV, by interpolation between peaks from ^{57}Co and ^{22}Na. Both peaks decayed with a half-life of 22 $\pm$ 2 days.

The potassium tetraphenylboron precipitate was analyzed in the well type crystal on the third day after irradiation and on the three succeeding days. The first of these spectra is shown in Fig. 3. The peak numbered III is the sum peak of components from the ^{43}K compound peaks I and II. The half-life of each of these three peaks was calculated to be 23.3 $\pm$ 1.2; 22.7 $\pm$ 1.2 and 23.2 $\pm$ 1.5 days, respectively.

The profile of the valley between peak II and peak III maintained its form during the decay and is assumed to origin from secondary effects (compton or backscatter) from ^{43}K activity. The peak at 1.3 MeV and the one at 0.16 MeV decayed with half-lives of a few days, high error and unknown

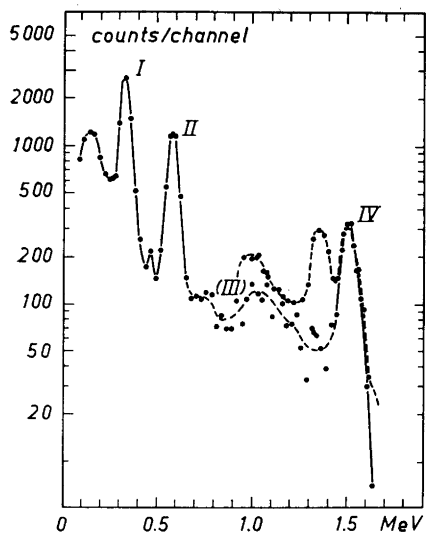

Fig. 2. Spectrum of the precipitated potassium activities obtained 33 h after irradiation at 6.5 cm distance from a 3″ × 3″ NaI (Tl) scintillation detector with an 8 mm Al absorber. I and II are the ^{43}K compound peaks at 0.38 and 0.61 MeV, IV is the 1.52 MeV peak from ^{44}K. The inserted part indicates the ^{24}Na activity of the sample before precipitation.

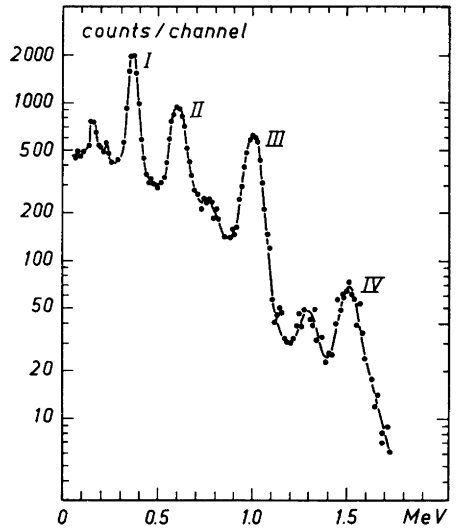

Fig. 3. Spectrum of the same sample as in Fig. 2, obtained by a 3″ × 3″ well type crystal. Peak numbers are the same as in Fig. 2, III is the sum peak of components from peak I and II.

background level prohibiting exact half-life determinations. From nucleogenetic points of view, ^{47}Ca and its daughter nuclide ^{47}Sc are assumed to be responsible for those peaks.

The ratio between the count rates for peak IV and II (see Fig. 2) for the potassium from the shielded target agreed, within the error limits, with the same ratio for the unshielded target, when corrected for the difference in irradiation times. Because the fission neutron flux was the same in both cases, the potassium content of the target substance was too low to be detected.

The ^{42}K activity per gram of the shielded calcium carbonate matched the activity from 8.5 μg of potassium in the standard. The limit for the potassium impurity deduced from these results is 0.5 ppm.

Finally, the cross sections for the (n, p) reactions of ^{42}Ca and ^{43}Ca were calculated from the count rates under the gamma peaks at 0.61 (^{43}K), 1.37 (^{24}Na) and 1.52 MeV (^{42}K), assuming a value of 0.56 mb for the reaction ^{27}Al (n, α) ^{24}Na [28].

For the calculation of the cross sections, the following factors were taken into account for each of the nuclides: amount of target nuclide irradiated, build up during irradiation and decay after it, decay scheme, detection effi-

ciency, absorption and dead time losses and the fraction of the total activity being analyzed.

The resulting cross sections for a fission neutron spectrum were for ^{42}Ca (n, p) ^{42}K: *2.1 ± 0.4 mb* and for ^{43}Ca (n, p) ^{43}K: *1.5 ± 0.3 mb*.

The ^{42}K (and ^{24}Na) activity in the β-source prohibited the isolation of the 22.4 h activity before it had decayed to a very low level. The cross sections calculated from a comparison with the count rate for the ^{32}P activity, assuming a cross sections of 60 mb [28] for the reactions ^{32}S (n, p) ^{32}P, agreed well with the cross sections obtained by means of gamma spectrometry. However, an uncertainty factor of two must be ascribed to this determination, and this uncertainty is based on the assumptions of the author rather than on a mathematical analysis.

DISCUSSION

The experimental cross sections for neutron threshold reactions found in the literature often deviate appreciably from one determination to another, for instance the values for ^{32}S (n, p) ^{32}P range from 154 to 21 mb [4]. When a threshold reaction is used to monitor the flux of fast neutrons, the result is obviously dependant on the reliability of the cross section of the monitor. In this case the value suggested by Mellish [28], 0.56 mb for ^{28}Al (n, α) ^{24}Na, was assumed as the reference.

A source of error in such determinations is the deviation from a true fission spectrum at the irradiation position [29]. Errors of this sort should be at a minimum, however, when the effective threshold energies, E_{eff}, for the monitor and the studied reaction match each other, as is nearly the case here.

Errors from flux fluctuations are negligible if the irradiation time is short in comparison with the half-lives or else when the activities from the target and the monitor have nearly the same half-life, as do ^{42}K and ^{24}Na. Errors of this type are likely to be negligible also in the case of ^{43}K.

The errors in gamma detection efficiencies have not been critically studied by the author, but they are assumed to cancel, especially in the case of energies of the same magnitude (^{42}K and ^{24}Na).

The small abundances of the target isotopes and the small cross sections studied make it necessary to discuss other possible nuclear reactions which might also result in the activities being studied. The case of ^{41}K(n, γ) ^{42}K has been mentioned under "results". ^{45}Sc might by an (n, α) reaction give ^{42}K. The cross section for this reaction is less than 5 mb [4], the content of scandium should according to the analysis of the calcium nitrate be *less* than 0.001 % and the scandium might have been depleted but not enriched during the chemical preparations of the target. The product (< 5) mb times (< 0.006) % has thus to be compared with 2 mb times 0.6 %, and a contribution to the ^{42}K activity from scandium can thus be disregarded. It seems justified to neglect, in the same way, the ^{45}Sc(n, ^{3}He)^{43}K reaction, because the Q-value of this reaction is -1.7 MeV against -0.4 MeV for ^{45}Sc(n, α)^{42}K [5].

^{44}Ca has higher abundance than ^{43}Ca, and could give ^{43}K by a (n, d) reaction. However, the Q-value of this and other (n, d) and (n, t) reactions presented in Table 1 indicate that their contribution to the ^{42}K and ^{43}K activities should be negligible.

Other types of error are mentioned under "results". The errors given for the final cross section values are not strictly mathematically deduced, as allowance was made for some systematic errors within the limits. The author is convinced that the errors should match a confidence level of at least 90 %, if the utilized values for the monitor cross section and the gamma intensities from ^{43}K are correct.

It is obvious that practically, carrier-free activities of ^{42}K and ^{43}K can be produced by the methods utilized in the present study. The ^{24}Na activity present could be diminished either by preparation of a purer target, by a sodium shield around the target (for absorption of neutrons of the resonance energy for ^{23}Na) or by separation of the sodium and potassium activities, for instance by means of a crystal ion exchanger [30]. In the last case, contamination of for instance ^{47}Ca and the grown in ^{47}Sc could also be more quantitatively eliminated. The availability of potassium isotopes of higher specific activities than those obtainable through (n, γ) activation of natural potassium is likely to be of value, for instance, for labelling of red corpuscules [31,32] or for studies of ion transport in heart muscles [33].

However, when corrections for decay or absorption must be applied, it is much more convenient to have a radiochemically pure activity.

^{43}K has for most purposes many advantages in comparison with ^{42}K, *e.g.*, longer half-life, much lower mean β energy, lower γ energies (higher detection efficiency) and much higher γ intensities. These circumstances make it preferable for autoradiographic purposes and for in vivo experiments where the dose rates are critical. ^{43}K has been suggested by Ullberg [34] for studies of differences in the distribution of cesium and potassium in animals by means of double-tracer autoradiography.

^{43}K has earlier been detected as a spallation product [35] and it has been produced from argon: ^{40}Ar (α, p) ^{43}K [36,17,37,38].

In order to obtain a radiochemically pure ^{43}K activity in a nuclear reactor, enriched ^{43}Ca targets must be utilized. With a cross section of 1.5 mb it should be possible to obtain after irradiation of 10 mg of ^{43}Ca for one day in a fission neutron flux of 5×10^{14} s^{-1} cm^{-2}, one millicurie of carrier-free ^{43}K.

By slight modifications of the method utilized here for the purification of the calcium target, it should be possible to recover, with a high yield, the expensive, enriched calcium isotope.

Acknowledgements. The author is indebted to the Head of this Division, Dr. T. Westermark, for stimulating discussions and his never-failing encouragement and to the Head of the Division of Physical Chemistry, Prof. O. Lamm, for the disposition of laboratory facilities. He also thanks Mr. K. Svärdström for very skilful technical assistance.

The financial support came mainly from the *Swedish Atomic Research Council.*

REFERENCES

1. Rochlin, R. S. *Nucleonics* **17** No. 1 (1959) 54.
2. Hughes, D. J. *Pile Neutron Research*, Addison-Wesley Publishing Co., Cambridge 42, Mass. 1953.
3. Inthoff, W. *Nucleonics* **13** No. 11 (1955) 67.
4. Konijn, J. *Q-values for (n, p) and (n, α) reactions*, Aktiebolaget Atomenergi, Stockholm, Sweden, 1961.

5. Endt, P. M. and van der Leun, C. *Nuclear Physics* **34** (1962) 1.
6. Mellish, C. E., Payne, J. A. and Otlet, R. L. *Radioisotopes in Scientific Research* (Proc, 1st UNESCO Intern. Conf., Paris 1957), Pergamon Press, London 1958, Vol. 1, p. 35.
7. *Table of Cross Sections for Fast Neutron Reactions*, Texas Nuclear Corporation, Austin 17, Texas 1960.
8. Koch, R. C. *Activation Analysis Handbook*, Chemistry Department, Nuclear Science and Engineering Corporation, Pittsburg 36, Pennsylvania.
9. Troubetzkoy, E. S., Kalos, M. H., Lustig, H., Ray, J. H. and Trupin, B. H. *Fast neutron cross sections of manganese, calcium, sulfur and sodium*, Nuclear Defense Laboratory, Army Chemical Center, Maryland, 1961 (NDL—TR-5).
10. Walke, H. *Phys. Rev.* **52** (1937) 663.
11. Cohen, B. L. *Phys. Rev.* **94** (1954) 117.
12. Sugiyama, K., Tohei, T., Sugawara, M., Dazai, T. and Kanda, Y. *J. Phys. Soc. Japan* **15** (1960) 1909.
13. Boyd and Simon PPR Mon N 370, 87 Sep. 1947.
14. Levkovskii, V. N. *Eksp. Teor. Fiz.* **33** (1957) 1520, *JETP* **6** (1958) 1174.
15. Sullivan, W. H. *Trilinear Chart of Nuclides*, USAEC Jan. 1957.
16. Dzhelepov, B.S. and Peker, L.K. *Decay Schemes of Radioactive Nuclei* (English translation), Pergamon Press, Oxford 1961.
17. Benczer-Koller, N., Schwarzschild, A. and Wu, C. S. *Phys. Rev.* **115** (1959) 108.
18. McCullen, J. D. and Krauschaar, J. J. *Phys. Rev.* **122** (1961) 555.
19. "*Dowex Chelating Resin A-1*", Dow Chemical Co., Technical Service and Development, Midland, Mich., Jan. 1959.
20. Forberg, S. and Lundgren, S. *Anal. Chem.* **32** (1960) 1202.
21. Christell, R., Forberg, S. and Westermark, T. *J. Inorg. & Nuclear Chem.* **19** (1961) 187.
22. Turse, R. and Rieman III, Vm. *J. Phys. Chem.* **65** (1961) 1821.
23. Westermark, T. *Acta Chem. Scand.* **6** (1952) 1194.
24. Sporek, K. and Williams, A. F. *Analyst* **80** (1955) 347.
25. Heath, R. L. *Scintillation Spectrometry*, Phillips Petroleum Co., Atomic Energy Division, Idaho Falls, Idaho 1957 (IDO-16408).
26. Hughes, D. J. and Schwartz, R. B. *Neutron Cross Sections*, Brookhaven National Laboratory, Upton, New York, July 1, 1958 (BNL 325).
27. Westermark, T. and Sjöstrand, B. *Intern. J. Appl. Radiation and Isotopes* **9** (1960) 63.
28. Mellish, C. E. *Nucleonics* **19** No. 3 (1961) 114.
29. Krumbein, A. D. *NDA-92-2 (Rev.)* 1957.
30. Amphlett, C. B., McDonald, L. A., Burgess, J S. and Maynard, J. C. *J. Inorg & Nuclear Chem.* **10** (1959) 69.
31. Hevesy, G. *Adventures in Radioisotope Research*, Pergamon Press, New York 1962, Vol. 2, p. 531.
32. Ljunggren, K. Isotope Technics Laboratory, Stockholm, Sweden, *Personal Communication.*
33. Öbrink, K. J. Department of Physiology, University of Uppsala, Uppsala, Sweden, *Personal Communications.*
34. Ullberg, S. Department of Pharmacology, The Royal Veterinary College, Stockholm, *Personal Communications.*
35. Friedlander, G., Miller, J. M., Wolfgang, R., Hudis, J. and Baker, E. *Phys. Rev.* **94** (1954) 727.
36. Folden, M. F. *UCRL-139* June 1948.
37. Petersen, F. R. *UCRL-9480* Nov. 1960.
38. Allen, R.A., Smith, D.B. and Hiscott, J.E. *Radioisotope Data, AERE-R 2938*, Isotope Research Div., Wantage Research Laboratory, Wantage, Berkshire, England.

Received April 16, 1962.

ACTA CHEMICA SCANDINAVICA 16 (1962) 2113–2116

Quenching Effect of Oxygen on the Light Emission Produced by Dissolution of Irradiated Sodium Chloride in Water

L. E. GÖRAN ERIKSSON

Divisions of Nuclear Chemistry and Physical Chemistry, The Royal Institute of Technology, Stockholm 70, Sweden *

Dedicated to Professor *Ole Lamm* on his 60th birthday

Light is emitted when irradiated sodium chloride is dissolved in water. It was shown that oxygen was a quencher. Some ideas were put forward about the mechanism by which the stored energy, represented by the structural defects, is released.

It has been shown that, when solids which have been treated with ionizing radiation are dissolved in liquids, chemical reactions typical for radiation chemistry, *e.g.* the oxidation of Fe^{2+} and I^- (Refs.[1–3]) apparently occur. Aqueous solutions of dissolved sodium chloride originally containing colour centers have been found to be slightly alkaline [4–6]. Hydrogen is evolved on dissolution [3]. Light emission is produced when irradiated solids, organic as well as inorganic, are dissolved in certain solvents with or without added solute [1,8–10]. With water, a small but readily observed light pulse was obtained when irradiated (some Mrads) NaCl was used [9].

The influence of dissolved gases on the light emission has not been investigated, and the water used in the experiments hitherto has not been air-free. The mechanism by which the stored energy, formally represented by the structural defects at the F- and V-centers, is released upon dissolving, for example, NaCl in water is unknown. If we assume that the released energy acts radiomimetrically the presence of oxygen in the water may be supposed to interfere in some way. Oxygen, having a biradical character, exhibits well established effects in radiation and photochemistry. An examination of the effects of dissolved gases on the light emission produced upon dissolution of irradiated NaCl in water has therefore been carried out.

* Present address: Division of Physical Chemistry, The Royal Institute of Technology, Stockholm 70, Sweden.

EXPERIMENTAL

From the laboratory supply of distilled water, an alkaline potassium permanganate solution was made and distilled. An acidic potassium bichromate solution produced using the water thus obtained was distilled in a carbon dioxide-free atmosphere. The distillation product obtained was distilled once more and finally in a two-step bidistillation quartz apparatus (Heraeus Quarzschmelze G.m.b.H., Hanau, Model Bi 3) where it was de-aerated to a considerable extent. The water was collected in a flask and saturated with nitrogen.

The fine-grained NaCl used had been given a dose of 5 Mrads by ^{60}Co γ-rays at room temperature and then stored dry and dark in a refrigerator ($-25°C$). The gases examined (oxygen, nitrogen and hydrogen) were of technical quality. The nitrogen was freed from oxygen by passing the gas through two copper columns kept at about 170°C. The packing material was prepared from sintered copper oxide reduced by flushing with hydrogen to a red colour. The gases were freed from carbon dioxide by means of an Ascarite filter.

The emission of light was observed with the photomultiplier arrangement described in Ref.[9] The integrated area of the light pulse gives an estimate of the stored energy transformed into light. (Due regard of course has to be taken to the spectral response of the photocathode.)

The irradiated NaCl (10 mg, 5 Mrads) was poured into the water (5 ml) which was contained in a quartz glass vessel placed at the top of the photomultiplier tube. The gas atmosphere in the space above the tube was varied. To make sure that the water was of the same quality in all measurements, nitrogen-saturated water was first used. The nitrogen was then replaced by air, freed from CO_2, by bubbling the gas directly through the water. Finally measurements were carried out with the water saturated with oxygen.

RESULTS AND DISCUSSION

Although the reproducibility of the light pulse areas was not good, it was evident that the presence of oxygen in the water reduced the light emission considerably. Thus water saturated with nitrogen gave light pulses with areas 10—15 times larger than those for oxygen-saturated water. The luminescence from more or less degassed water as well as from hydrogen-saturated water was of the same magnitude as that from the nitrogen-saturated water. Saturation with air reduced the light emission to about 1/4 of that of the nitrogen-saturated water. When NaCl of the same quality but unirradiated was tested, no light emission at all could be detected.

The existence of hydroperoxide in solutions saturated with NaCl which had been previously dosed with 50 Mrads has been investigated but with negative results. Spectrometry in the visible (titanium reagent) and ultra-violet regions has been carried out. The dissolution of NaCl in the presence of benzene in order to get phenol has also been examined. No phenol was found with the ultraviolet spectrometer (Beckman Model DK-2). The concentration of H_2O_2 and phenol may, however, have been to small to be detected under the conditions used.

The presence of "free sodium" [5,6] and "chlorine" [7] in NaCl containing colour centers has been pointed out. However, the chemical reactions produced when the NaCl crystal dissolves might more appropriately be termed consequences of reactions of electrons and holes rather than of free atoms in the crystal [11]. The minimum energy necessary to produce colour centers by light in NaCl is about 6 eV (from the absorption spectrum of pure NaCl). This is also stated to be the energy produced by a direct recombination of a free hole

with an electron in an F-center. Thermoluminescence, however, indicates that the energies of the emitted light are about 2.5—3.5 eV [12]. These recombination energies may be assumed to be the maximum available for the chemical reactions and the light emission when dissolving the salt. The emission of light probably takes place somewhere in a chain of energy transfer processes and oxygen has a quenching effect. It has been shown that reactions of free radicals produced electrolytically are accompanied by luminescence [13]. An increase in the luminescence was obtained when the water was oxygen-free.

The lowest excited level of water has a broad continuum centered at about 7.4 eV [14]. This is a repulsive level and thus there is no, or only very faint, luminescence due to excitation in this band [15]. The following reaction takes place:

$$H_2O\ *\ (\sim 7.4\ eV) \rightarrow OH\ (^2\Pi) + H\ (^2S) + 2\ eV\ \text{kinetic energy}$$

This reaction will, however, not account for the fates of the electrons and the holes when the crystal dissolves. The largest conceivable recombination energy is not sufficient to promote the reaction. Due to the low energy of the electron it will soon become thermal and most probably be captured by a water molecule according to:

$$H_2O + e^- \rightarrow H_2O^-$$

This entity (in solvated form) will then decompose

$$H_2O^- \rightarrow H + OH^-$$

Another and perhaps more likely explanation might be the formation of a self-trapped electron ("polaron") [16].

The presence of oxygen will give rise to other reaction mechanisms. Thus it is likely that available H atoms will react with oxygen to form hydroperoxy radicals:

$$H + O_2 \rightarrow HO_2$$

Oxygen has a high electron affinity and it may also react in other ways:

$$O_2 + e^- \rightarrow O_2^-$$
$$H_2O^- + O_2 \rightarrow H_2O + O_2^-$$
$$H_2O + O_2^- \rightarrow HO_2 + OH^-$$

The reactions stated do not give an explicit explanation of the light emission phenomenon but give some indications of how oxygen can play a role. In the competition between light emission and chemical reactions oxygen may act as a quencher. It would therefore be of interest to examine the effect of oxygen on the chemical dosimeter yield when dissolving irradiated NaCl and on the light yield when using fluorescent solutions. Further information about the nature of the light emitted may be obtained by investigating the spectral distribution of light.

The efficiency for the production of doubly ionized halogens and the conditions for the existence of such entities have been discussed [17,18]. It was postulated that Cl^+ ions with a high energy content were present. If this is true there is enough energy available to bring about reactions similar to the radiation chemistry of water.

Acknowledgements. The author is indebted to Dr. T. Westermark for helpful discussions and valuable criticism and to Prof. O. Lamm for the laboratory facilities. This work was supported by grants from *Statens Naturvetenskapliga Forskningsråd.*

REFERENCES

1. Westermark, T. *Risö Report* **16** (1960) 28.
2. Westermark, T., Biesèrt, N. and Grapengiesser, B. *Arkiv Kemi* **17** (1961) 151.
3. Burns, W. G. and Williams, T. F. *Nature* **175** (1955) 1043.
4. Kleinschrod, F. G. *Ann. Physik* **27** (1936) 97.
5. Hacskaylo, M. and Groetzinger, G. *Phys. Rev.* **87** (1952) 789.
6. Hacskaylo, M. and Otterson, D. *J. Chem. Phys.* **21** (1953) 552.
7. Hacskaylo, M., Otterson, D. and Schwed, P. *J. Chem. Phys.* **21** (1953) 1434.
8. Ahnström, G. and v. Ehrenstein, G. *Acta Chem. Scand.* **13** (1959) 855.
9. Westermark, T. and Grapengiesser, B. *Nature* **188** (1960) 395.
10. Westermark, T. and Grapengiesser, B. *Arkiv Kemi* **17** (1961) 139.
11. Heal, H. G. *Atomics* **6** (1955) 205, 241.
12. Halperin, A., Kristianpoller, N. and Ben-Zvi, A. *Phys. Rev.* **116** (1959) 1081.
13. Ahnström, G. *Acta Chem. Scand.* **15** (1961) 463.
14. Hochanadel, C. J. *Radiation Chemistry of Water.* Chapter 8 in *Comparative Effects of Radiation* (Editors: Burton, M., Kirby-Smith, J. S. and Magee, J. L.), J. Wiley & Sons Inc., London 1960.
15. Brown, L. O. and Miller, N. *Trans. Faraday Soc.* **51** (1955) 1623.
16. Weiss, J. *Nature* **186** (1960) 751.
17. Howard, R. E. and Smoluchowski, R. *Phys. Rev.* **116** (1959) 314.
18. Howard, R. E., Vosko, S. and Smoluchowski, R. *Phys. Rev.* **122** (1961) 1406.

Received April 18, 1962.

ACTA CHEMICA SCANDINAVICA 16 (1962) 2117–2122

Isotopic Effects in Systems Containing an Amine and Carbon Dioxide

KARL ERIK HOLMBERG

Section for Nuclear Chemistry, AB Atomenergi, Studsvik, Tystberga, Sweden

Dedicated to Professor *Ole Lamm* on his 60th birthday

On distillation of compounds of lower amines with carbon dioxide, which compounds are dissociated in the gas phase, there is an enrichment of several isotopes generally with the following elementary factors: $\alpha(^{14}N/^{15}N) = 1.013$, $\alpha(^{18}O/^{16}O) = 1.006-1.010$ and $\alpha(^{12}C/^{13}C) = 1.0025$. The isotope mentioned first enriches in the vapour during distillation. The vapour pressure of a secondary amine, deuterated at the nitrogen, by distillation with carbon dioxide becomes 7–9 % higher than that of the undeuterated compound at the temperature corresponding to the normal boiling point of the latter.

Carbon dioxide forms, with sufficiently low-boiling primary and secondary amines, distillable compounds, or azeotropes with a maximum boiling point. Melting and boiling points of such compounds, according to approximate determinations, are given in Table 1, which also includes some ternary azeotropes, containing ethanol or water as the third component. In this table, as in the following Me, Et, Pr and Bu represents methyl, ethyl, propyl and butyl groups, respectively.

When these compounds are distilled, there is a dissociation in the gas phase, and there is an isotopic effect for all elements whose binding conditions are changed by this dissociation. These elements are: carbon and oxygen of the carbon dioxide, and nitrogen and nitrogen-bonded hydrogen of the amine. The structure of these compounds is not known, but it is evident that these elements are involved.

Isotopic effects for carbon, oxygen and nitrogen in some of these systems have been determined by Rayleigh distillation. A similar determination of the hydrogen isotopic effects would probably meet considerable analytical difficulties. Instead, compounds deuterated at the nitrogen were prepared, and their boiling points were compared with those of the non-deuterated compounds. At the same time, other physical properties of the deuterated and non-deuterated compounds were compared.

Table 1. Melting and boiling points of compounds and azeotropes containing carbon dioxide and an amine.

	Melting point °C	Boiling point °C	B.p. of the amine °C
$MeNH_2 + CO_2$	109	83	−6.5
$EtNH_2 + CO_2$	116	81	16.6
$PrNH_2 + CO_2$	74	84	48.7
sec-$PrNH_2 + CO_2$	99	72	34
$BuNH_2 + CO_2$	75	93	78
iso-$BuNH_2 + CO_2$	77	86	68
sec-$BuNH_2 + CO_2$	44	77	63
$Me_2NH + CO_2$	35	61	7.4
$MeEtNH + CO_2$	−17	61	35
$Et_2NH + CO_2$	28	62	55.5
$MePrNH + CO_2$	< 0	72	63

	Complete solution °C	Boiling point °C
$MeNH_2 + CO_2 + EtOH$	—	72
$EtNH_2 + CO_2 + EtOH$	~36	74
$PrNH_2 + CO_2 + EtOH$	<10	77
$BuNH_2 + CO_2 + H_2O$	~−20	91

Table 2. Composition and properties of compounds between carbon dioxide and secondary amines.

Formula	Me_2NH 0.528 CO_2	Me_2ND 0.503 CO_2	MeEtNH 0.487 CO_2	MeEtND 0.498 CO_2	Et_2NH 0.353 CO_2	Et_2ND 0.356 CO_2
Weight % amine	66.0	67.55	73.4	73.25	82.5	82.45
Boiling point at 760 mm Hg, °C	60.2	58.5	61.12	59.51	62.03	60.62
Boiling point difference, °C	1.73		1.61		1.41	
$(dp/dt)_{760}$ mm Hg/°C	41.2		40.1		38.6	
Melting point, °C	34.5	36.2	−17	−13	28.3	29.9
d_4^{25}, g/ml	1.02299	1.04187	0.96429	0.97373	0.87654	0.88218
η_{25}, centipoise	64.9	78.2	45.9		4.45	4.12
n_D^{25}	1.4520	1.4521		1.4479	1.4333	1.4350

Table 3. Vapour pressure ratios of H and D forms of amine-CO_2 compounds and separation factors for other isotopes on distillation. The errors refer to the mass spectrometric measurements.

	$Me_2NH + CO_2$ at 60°C	MeEtNH + CO_2 at 61°C	$Et_2NH + CO_2$ at 62°C
$p(D)/p(H)$	1.094	1.085	1.072
$\frac{(^{14}N/^{15}N)_{vpp}}{(^{14}N/^{15}N)_{liq}}$	1.0137 ± 0.0012	—	1.0080 ± 0.0012
$\frac{(^{12}C/^{13}C)_{vap}}{(^{12}C/^{13}C)_{liq}}$	1.0021 ± 0.0006	—	1.0023 ± 0.0006
$\frac{(^{18}O/^{16}O)_{vap}}{(^{18}O/^{16}O)_{liq}}$	1.0065 ± 0.0009	—	1.0081 ± 0.0009

The following systems have been investigated in detail: $Me_2NH + CO_2$, MeEtNH + CO_2, $Et_2NH + CO_2$ and the ternary azeotropes $EtNH_2$ + + CO_2 + EtOH and $BuNH_2 + CO_2 + H_2O$. The results are presented in a number of tables. For example, Table 2 gives the physical properties of the compounds of ordinary and deuterated secondary amines. The deuterium content of the deuterated compounds is estimated to be 95 %. No correction has been made for this approximation. The data presented in the table are those actually measured.

It is evident that the compounds contain two moles of amine for one mole of carbon dioxide, except for diethyl amine, in which system there is an excess of amine.

From the boiling point differences, and the rate of change of vapour pressure with temperature, one may calculate the ratio of vapour pressures of deuterated and non-deuterated compounds at a common temperature, *e.g.* the boiling point of the former. These data and the separation factors for the carbon, oxygen and nitrogen isotopes, determined by Rayleigh distillation, are given in Table 3.

Table 4. Distillation of $Me_2NH + CO_2$ with a 4 m column.

	% ^{15}N	% ^{18}O	% ^{13}C
Top	0.169	0.296	0.966
Still pot	0.439	0.174	1.158
	$^{14}N/^{15}N$	$^{18}O/^{16}O$	$^{12}C/^{13}C$
$Q_{top/pot}$	2.60	1.70	1.198
α	1.0137	1.0065	1.0021
n theoretical plates	70	84	86

Table 5. Viscosities of amine + CO_2 compounds and ternary azeotropes at several temperatures, and extrapolated to the boiling point. Unit: centipoise.

$Me_2NH + CO_2$		$Et_2NH + CO_2$		$EtNH_2 + CO_2 + EtOH$		$BuNH_2 + CO_2 + H_2O$	
t°C	η	t°C	η	t°C	η	t°C	η
25.00	64.9	25.00	4.45	25.00	4.71	25.00	18.0
40.5	28.2			45	2.93	40.1	10.4
50.8	18.3			60	2.11	60.0	5.8
56	14.8			70	1.71	79.8	3.65
b.p. 60	11	b.p. 62	1.4	b.p. 74	1.6	b.p. 91	2.9

Table 6. Data for the ternary azeotropes $EtNH_2 + CO_2 + EtOH$ and $BuNH_2 + CO_2 + H_2O$.

Suggested composition	$EtNH_2 + 0.5\,CO_2 + 1.89\,EtOH$	$BuNH_2 + 0.5\,CO_2 + 2.51\,H_2O$
Weight % amine	29.2	57.35
Boiling point, °C	74.1	90.6
$(dp/dt)_{760}$, mm Hg/°C	36.6	31.8
Point of complete melting, °C	~36	~−20
d_4^{25}, g/ml	0.86694	0.96443
η_{25}, centipoise	4.71	18.0
n_D^{25}	1.3978	1.4282

Table 7. Separation factors on distillation of ternary azeotropes containing an anime and carbon dioxide.

	$EtNH_2 + CO_2 + EtOH$ at 74°C	$BuNH_2 + CO_2 + H_2O$ at 91°C
$\frac{(^{14}N/^{15}N)_{vap}}{(^{14}N/^{15}N)_{liq}}$	1.0144 ± 0.0012	1.0129 ± 0.0012
$\frac{(^{18}O/^{16}O)_{vap}}{(^{18}O/^{16}O)_{liq}}$	1.0104 ± 0.0009	1.0002 ± 0.0009
$\frac{(^{12}C/^{13}C)_{vap}}{(^{12}C/^{13}C)_{liq}}$	1.0000 ± 0.0006	1.0006 ± 0.0006

Some column distillations have been performed. Thus $Me_2NH + CO_2$ was distilled in a column of 4 m length and 13 mm inner diameter, packed with 2.7 × 2.4 × 2 mm glass helices. When approximate equilibrium had been attained, samples were taken from top and still pot. Data are given in Table 4. The small disagreement in calculated numbers of theoretical plates may derive from errors in the α values.

In another experiment, a column of 50 cm length and 6 mm i.d., packed with the same type of glass helices, was used to distil $Me_2ND + CO_2$ with 74 % D at the nitrogen position. From the boiling point, the D content at the

top was estimated to be 83 ± 3 % corresponding to separation by a factor 1.7. In this case the isotopic separation factor is probably different from the vapour pressure ratio given in Table 3, and therefore the number of theoretical plates cannot be stated. A direct determination of the isotopic factor has not been undertaken because of anticipated analytical difficulties.

In a third case a 2 m column of 30 mm internal diameter was used, packed with stainless steel Heli-Pak (1.3 × 2.5 × 2.5 mm). The still pot contained water with D_2O, the column proper $Et_2NH + CO_2$, and at the top there was an excess of pure Et_2NH. At equilibrium, the diethyl amine at the top contained 85 % Et_2ND determined from its density, and the water in the pot was calculated to contain 42 % D_2O. This is a total separation by the factor 7.75. The better performance in this case as compared to the next one may be due to the packing but more probably to the lower viscosity of $Et_2NH + CO_2$ (*cf.* Table 5).

The ternary azeotropes $EtNH_2 + CO_2 +$ EtOH and $BuNH_2 + CO_2 + H_2O$ were investigated with respect to boiling point and other properties, but no corresponding deuterated systems were investigated (Table 6). These azeotropes are of a type that may be represented by a saddle surface, and they are perhaps not quite stable upon distillation. For that reason, the composition of the samples investigated may depart somewhat from the correct values. By means of Rayleigh distillation, the separation factors for carbon, oxygen and nitrogen isotopes given in Table 7 were obtained.

The low values of the carbon isotope separation factors in Table 7 are probably due to errors. There is no reason to believe that carbon will behave differently in these systems compared to the simple amine—CO_2 systems and in fact from a column distillation of $BuNH_2 + CO_2 + H_2O$ there was obtained the single stage separation factor 1.0022 for the carbon isotopes.

After this investigation, somewhat similar work was reported by Brown [1] and by Yeatts, Jr.[2] It was found that Pr_2NH (b.p. 110.7°C) with carbon dioxide gives a compound which dissociates to CO_2 and liquid amine on heating. Upon exchange between gas and liquid the separation factor $\alpha(^{12}C/^{13}C)$ varied from 1.0059 to 1.0028 and $\alpha(^{18}O/^{16}O)$ from 1.0081 to 1.0096 when temperature varied from 25 to 60°C. On distillation of a number of compounds from among those given in Table 1, separation factors for oxygen between 1.0040 and 1.0105 were obtained. The agreement with the present work is satisfactory.

EXPERIMENTAL

Preparation of amine + CO_2 compound. This was generally done by saturating the amine with CO_2 and distilling with a column repeatedly until a product with a narrow boiling point range (about 0.1°C) was obtained.

A 25 % solution of Me_2NH in water was saturated with CO_2 and $Me_2NH + CO_2$ was distilled off and refractionated.

A 70 % solution of $EtNH_2$ in water was saturated with CO_2, ethanol was added and the ternary azeotrope was distilled off and redistilled to a constant boiling point.

Butyl amine mixed with water was saturated with CO_2 and distilled to give a ternary azeotrope.

Deuterated compounds were prepared correspondingly by saturating MeEtND and Et_2ND with CO_2 and distilling.

$Me_2ND + CO_2$ was obtained by mixing $Me_2NH + CO_2$ with D_2O, distilling off $Me_2ND + CO_2$, mixing it with a new amount of D_2O, and distilling off again. This operation was repeated until the exchange was sufficiently complete.

The deuterated amines were prepared similarly from ordinary amines and D_2O. The vapour pressure ratios of some such amines at the boiling point of one of them may be interesting and they are therefore given here:
pMeEtNH/pMeEtND = 1.0092, pEt$_2$NH/pEt$_2$ND = 1.0071 and pPrNH$_2$/pPrND$_2$ = 1.0125.

Physical properties were determined and *Rayleigh distillations* were performed as described earlier [3].

Preparation for isotopic analysis. CO_2 was liberated with anhydrous acetic acid and isolated by freezing out with liquid air. The nitrogen of the amines was transformed to NH_3 and H_4NCl by Kjeldahl digestion.

Errors. The only errors given are those derived from the mass spectrometric measurement. It has been observed earlier [3] that the Rayleigh distillation as performed here has a tendency to give too low separation, perhaps by 10—15 %. No corrections for this have been applied here.

Acknowledgements. Thanks are due to Mr. R. Cedenholt for assistance with the experimental work. The isotope abundance measurements were performed by the Mass Spectrometer Laboratory, Karolinska Institutet, Stockholm.

REFERENCES

1. Brown, L. L. ORNL-2983, Chemistry Division. Annual Progress Report for Period Ending June 20, 1960, p. 19.
2. Yeatts, Jr., L. B. *Ibid.*, p. 19.
3. Holmberg, K. E. *Acta Chem. Scand.* **13** (1959) 717.

Received May 2, 1962.

ACTA CHEMICA SCANDINAVICA 16 (1962) 2123–2130

A Simplified Method for the Determination of Arsenic by Means of Activation Analysis

ROLAND CHRISTELL* and BERNT SJÖSTRAND

Division of Nuclear Chemistry, Royal Institute of Technology, Stockholm 70, Sweden

Dedicated to Professor *Ole Lamm* on his 60th birthday

A simple and rapid method for determination of arsenic in virtually all sorts of biological materials and also in other cases by means of activation analysis has been developed and evaluated. Arsenic is separated radiochemically by distillation and precipitation and the radioactivity of ^{76}As measured by γ-spectrometry or β^--counting. The sensitivity is $10^{-8}-10^{-9}$ g, depending on the measurement technique, when irradiation is performed at a flux of the order of 10^{12} neutrons cm^{-2} sec^{-1}. The procedure has been applied to the determination of the arsenic content of the remains of the 16th century King Erik XIV of Sweden and of other materials.

In this laboratory, methods of activation analysis have been studied for some seven years. The general method of activation analysis is to irradiate the sample (usually with reactor neutrons) and then measure the induced radioactivity either directly or after some sort of chemical separation of the desired element. Measurements of γ-activities can be made energy-selective using a scintillation detector and a pulse-height analyzer. Thus one often distinguishes between "spectrometric activation analysis" and "chemical activation analysis". For more detailed information on activation analysis the reader is referred to review articles by Westermark *et al.*[1] and by Atkins and Smales [2].

Since γ-spectrometric activation analysis is rapid and non-destructive it is naturally preferred when possible. However, disturbing γ-radiations from other nuclides present often make chemical separation necessary. It was found very convenient to make some simple and rapid separations, *e.g.* group separation, followed by γ-spectrometry. This combined method is fairly rapid, gives a good sensitivity in most cases and simultaneously yields an accurate identification of the nuclide in question.

* Isotope Techniques Laboratory, Drottning Kristinas väg 45, Stockholm Ö, Sweden.

Earlier attempts by Westermark *et al.*[4,21] to determine arsenic in biological material by spectrometric activation analysis, showed that, due to disturbing γ-activities present, only an upper limit for the arsenic content of the sample can be given. Now a method of the "combined" type has been worked out.

Nuclear data of arsenic. The only naturally occurring isotope of As is stable ^{75}As, which when irradiated with thermal neutrons forms radioactive ^{76}As. According to Allen *et al.*[5] the activation cross section of the element for ^{76}As production is 4.2 barns. ^{76}As decays with a half-life of 26.5 h to stable ^{76}Se by the emission of β^-- and γ-radiation. The predominant maximum β^--energies are 2.97 (56 %) and 2.41 MeV (31 %) and the energy of the most abundant γ-ray is 0.56 MeV (45 %). In addition there are low intensity γ-rays such as 0.66 (6.3 %) and 1.21 MeV (5.3 %). The disintegration scheme can be found, *e.g.*, in a book by Dzhelepov and Peker [6]. The scheme indicates that some γ-rays are emitted in cascade and this fact might be used for selective measurements with a coincidence γ-ray spectrometer according to Ljunggren[7]. The intensities of the cascade emitted γ-rays are, however, weak ($\sim$8 %).

Neutron induced ^{76}As-activity can be formed by the following reactions:

$$^{75}\mathrm{As(n,\gamma)}^{76}\mathrm{As} \qquad \sigma = 4.2 \text{ b} \tag{1}$$

$$^{76}\mathrm{Se(n,p)}^{76}\mathrm{As} \qquad \sigma \approx 0.8 \text{ mb} \tag{2}$$

$$^{79}\mathrm{Br(n,\alpha)}^{76}\mathrm{As} \qquad \sigma = 10 \text{ mb} \tag{3}$$

$$\left.\begin{matrix} ^{74}\mathrm{Ge(n,\gamma)}^{75}\mathrm{Ge} \\ ^{75}\mathrm{As(n,\gamma)}^{76}\mathrm{As} \end{matrix}\right\} \xrightarrow[T_{1/2} = 82 \text{ min}]{\beta^-} {}^{75}\mathrm{As} \tag{4}$$

Reaction 1 predominates when arsenic is irradiated with thermal neutrons, while reactions 2 and 3 occur with fast neutrons. The activation cross section for reaction 2 is calculated from Inthoff [8] and for reaction 3 given by Blosser *et al.*[9] In the determination of arsenic in germanium reaction 4 can be a cause of error: Smales and Pate [10] have found an error corresponding to 0.08 ppm of arsenic for a 75 h irradiation of pure germanium dioxide at 2×10^{12} neutrons cm^{-2} sec^{-1}.

When arsenic is irradiated with fast neutrons reaction 5 occurs:

$$^{75}\mathrm{As(n,2n)}\ ^{74}\mathrm{As} \quad \sigma \approx \begin{cases} 50 \text{ mb}\ [11] \\ 545 \text{ mb}\ [27] \end{cases} \tag{5}$$

^{74}As decays with a half-life of 18 days emitting β^+-, β^-- and γ-radiation. The energy of the most abundant γ-ray is 0.596 MeV (62 %) [5]. In addition, the emitted positrons give rise to 0.51 MeV annihilation γ-rays.

In the determination of arsenic by activation analysis the reaction ^{75}As(n,γ) ^{76}As is the preferred one. The procedure is to irradiate the sample together with an arsenic standard in the thermal neutron flux of a reactor for about one half-life (26.5 h) and then separate the arsenic activity which is measured. Comparison of the activities of sample and standard gives the amount of arsenic present in the sample.

Radiochemical separation of arsenic. Activation analysis for arsenic has been reported by Smales and Pate [10], Lenihan and Smith [12], Lenihan [13] and Smith [14]. A compilation of the radiochemistry of arsenic is given by Beard [15].

In addition references to arsenic determinations can be found in bibliographies on activation analysis by Gibbons *et al.*[16],[17] and Bock-Werthmann and Schulze[18].

The radiochemical procedures described in these earlier arsenic determinations seem to involve too many steps. We have therefore developed a simplified method with only three steps preceding γ-spectrometry:

1. Dissolution with $HNO_3-H_2SO_4$
2. Distillation, as $AsCl_3$ and $AsBr_3$, with HCl—HBr
3. Precipitation, as the element, with $NH_4H_2PO_2$.

EXPERIMENTAL

Preparation of sample and standard. The sample, weighing 0.1—0.5 g, was sealed in a quartz ampoule. (Sealing technique see Westermark and Sjöstrand [3].) The sample (s) was then irradiated for about 20—30 h together with a suitable arsenic standard at a flux of $1-2 \times 10^{12}$ neutrons cm^{-2} sec^{-1} in the Swedish reactor R 1. The standard was prepared by sealing a known volume (0.1 ml) of a water solution of As_2O_3 in a quartz ampoule to give a known amount of 1—2 μg arsenic. After irradiation, the ampoules were left for a few hours to let shortlived activities decay.

Separation of arsenic. After careful cleaning, the ampoule was crushed in a plastic tube and transferred to a flask for decomposition of the organic material in 10 ml of a

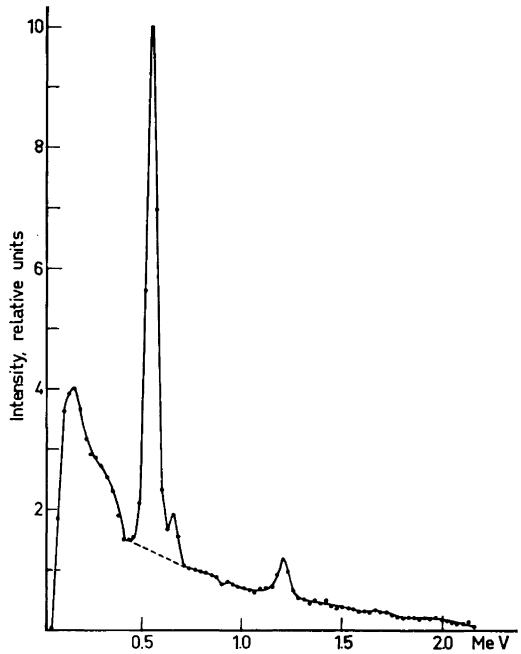

Fig. 1. ^{76}As γ-spectrum obtained from one of the samples (black smooth velvet from the 16th to the 17th century). Relative intensity is plotted against energy in MeV. The area enclosed by the curve at about 0.6 MeV and the dotted "back-ground" line was taken as a measure of the arsenic content of the sample. The γ-peaks at 0.66 MeV and 1.21 MeV are clearly visible in addition to the main peak at 0.56 MeV.

mixture of 3:1 fuming nitric acid and concentrated sulfuric acid. A known amount of about 25 mg As_2O_3 was added as a carrier. The flask was heated until no more nitrous gases or excess nitric acid were evolved; otherwise the hydrobromic acid added subsequently would be oxidized to free bromine. The flask was left to cool, then 15 ml hydrochloric acid was added dropwise. The sample was then transferred to the distillation flask and 10 ml 48 % hydrobromic acid was added. The flask was connected to the distillation apparatus and the distillation was continued until the volume in the distillation flask had been reduced by about one half. The temperature of the fumes was allowed to rise to 120—125°C. A stream of nitrogen was used as a carrier for the arsenic halides.

The condensate was collected in 10 ml water in an ice-cooled receiver flask and hydrochloric acid was added to it until the solution contained about 8 N HCl. Arsenic was then precipitated as the element by adding about 2 g of ammonium hypophosphite. After the ammonium hypophosphite had dissolved completely the solution was heated on a water-bath for 45 min. The precipitate formed was collected on a fine pore porcelain filter.

Recovery determination. The recovery of arsenic was determined by drying and weighing the porcelain filter before and after the filtration. The filters were dried to constant weight at 105°C. Comparison with the added amount of arsenic carrier gave the chemical yield which was regularly 80—100 %.

Standard treatment. Since the quartz in the ampoules contains small amounts of arsenic it seemed necessary to remove the standard solution from the ampoule before measuring its activity. It is also possible to correct for the As-content in the quartz by irradiating an empty ampoule (of the same quartz) together with the samples. In this case the standard activity should be measured by γ-spectrometry without breaking the ampoule.

In our procedure we have chosen to break the ampoule and let the standard undergo exactly the same procedures as the sample.

ACTIVITY MEASUREMENTS

After radiochemical separation of the arsenic the γ-spectra of samples and standards were measured using a 3″ × 3″ NaI(Tl)-scintillation detector coupled to either a multi-channel pulse height analyzer, of the Hutchinson-Scarrott type, or a single-channel analyzer. The latter is quite adequate when the radioactivity is not too weak. In Fig. 1 the γ-spectrum obtained from one of the samples is shown up to 2 MeV. The shape of the spectra from this and all other samples were identical with those obtained from the arsenic standards and the energy of the observed photo-peaks matched the γ-energies of ^{76}As within $\pm$ 15 keV. Half-life measurements yielded values between 25.0 and 27.5 h, which is in good agreement with the value 26.5 h given by Allen *et al.*[5]

Inspection of the $T_{1/2}$-E_γ-chart for radionuclides formed by neutron capture, published by Westermark and Sjöstrand [4], shows ^{76}As to be the only possible nuclide with the observed values of γ-energies and half-life.

As can be seen from Fig. 1 the emitted γ-rays of 0.56 MeV energy give rise to the largest peak and the area of this peak, plus that of the small 0.66 MeV peak, was used to determine the arsenic content of the samples.

Parallel to the spectrometric measurements, the β^--activity of the samples and standards was measured by counting with a G—M tube coupled to a scaler. These determinations gave half-lives of 25.5 to 26.5 h and values of arsenic content which were in excellent agreement with those obtained by γ-spectrometry, as can be seen in Table 1.

Table 1. Amount of arsenic in μg found by using different methods for measuring the ^{76}As-activity.

Sample	γ-spectrometry with single-channel analyzer 3″ × 3″ solid crystal	γ-spectrometry with multi-channel analyzer 3″ × 3″ solid crystal	Measurement of total γ-radiation 3″ × 3″ solid crystal	Measurement of total β^--radiation G—M tube	Average	Standard deviation in %
A	2.88	2.84	2.84	2.86	2.86	± 1
B	0.315	0.298	0.305	0.318	0.309	± 3
C	0.145	0.130	0.132	0.138	0.136	± 6
D	1.08	1.03	1.02	1.08	1.05	± 3

Table 2. Sensitivity limits of As-determination for different methods of activity measurement after irradiation in a flux of $\sim 10^{12}$ neutrons · cm^{-2} sec^{-1}.

Measurement method	γ-spectrometry			Total activity measurement		
	Multi-channel 3″ × 3″ crystal	Single-channel 3″ × 3″ crystal	Multi-channel well-crystal 1¾″ to 3″ diam.	3″ × 3″ crystal	well-crystal 1¾″ to 3″ diam.	G—M tube
Sensitivity limit in grams	10^{-8}	$\sim 10^{-7}$	$1-2 \times 10^{-9}$	5×10^{-9}	$5-10 \times 10^{-10}$	$5-10 \times 10^{-10}$

ARSENIC DETERMINATIONS

The method described has been applied to the determination of the arsenic content of the remains of the late King Erik XIV of Sweden. It has for a long time been a controversial problem in Swedish history whether King Erik was poisoned to death in 1577 by his brother King Johan III or not. Determination of the arsenic in King Erik's remains was of interest for this reason.

The samples were provided by Professor C. H. Hjortsjö at the University of Lund. Table 3 shows the arsenic concentrations in parts per million found in samples from the remains of King Erik and some samples used for comparison. The samples were taken for analysis as they were without previous drying or ashing.

The arsenic concentrations found in King Erik's remains are high compared with normal values for tissue given by Monier-Williams [19], Underwood [20] and Lenihan [12,13]. However, the high arsenic concentration in the remains of King Erik does not alone answer the poisoning question. A book with an account of all investigations, including activation analysis for arsenic and mercury and a discussion on the poisoning evidence (carried out after the opening of King Erik's tomb in 1958) is to be published in the autumn 1962 [21].

Table 3. Arsenic content of analyzed samples, in parts per million of As.

Sample	Character of sample	Arsenic content, ppm. (Standard deviation $\leq \pm$ 6 %)
1	Soft part from loin region	21.9
11	"Embalming paste"	1.1
12	Probably left lung	93.4
18 A	Scalp and hair	9.0
19	Possibly dry organ parts from the coffin-bottom under the stomach	8.4
22	Throat muscles	6.1
24	Possibly dry organ part from the coffin-bottom	4.2
32	Wood from the old coffin (two different samples)	9.7 12.9
Not numbered	Wood from the bottom of the new coffin	0.15
33	Part of rib-cartilage	7.3
38	Part of the seventh rib	2.6
Nail I	Root of nail	~18
Nail II	Center of nail	17.2
Nail III	Top of nail	18.8
Not numbered	Root of head hair	8.3
»	Top of head hair	2.6
»	Velvet from King Erik XIV's dress	33.8
»	Velvet from King Gustav Vasa's grave-clothes	2.8
»	Velvet lining from King Johan III's cap	5.7
»	Black smooth velvet from the 16th to the 17th century	8.2

In addition a work by Forshufvud *et al.*[22] might be mentioned here, namely determination of the arsenic content of a sample of hair stated to be probably taken from Napoleon I.

EVALUATION OF THE METHOD

A weak point in the analytical procedure is the decomposition and dissolution of the sample, a weakness which is shared with all other analytical procedures involving chemical operations. Investigations of trace element losses have been reported by Pijck *et al.*[23] and Gorsuch [24,25] and according to them losses of arsenic during wet oxidation is not serious. Wet oxidation has been found sufficient unless arsenic is present in samples with heterocyclic compounds as in, *e.g.*, tobacco leaves.

The chemical yield of the procedure is as high as 80 to 100 %, provided that the distillation is not stopped too early.

The sensitivity of the method is in the order of 10^{-8} g when irradiation in a flux of $\sim 10^{12}$ neutrons cm^{-2} sec^{-1} and γ-spectrometry with a solid 3″ × 3″ NaI(Tl)-crystal, 5 cm from the sample is performed. With β^--counting, using, *e.g.*, a G—M tube, the sensitivity can be increased by a factor of 10—15, depending on the counting geometry. When using β^--counting, accurate decay measurements are, of course, important.

Total γ-activity measurements with a $3'' \times 3''$ solid NaI(Tl)-crystal should increase the sensitivity by a factor of ~ 2 compared to spectrometric measurements.

By the use of a well-type NaI(Tl)-scintillation crystal and γ-spectrometry the sensitivity will be increased by a factor of 5—10, depending on the size of the crystal, compared to the sensitivity obtained with the use of a solid $3'' \times 3''$-crystal at a distance of 5 cm from the sample. The estimated sensitivities for the different methods of measurement are summarized in Table 2.

The sensitivity limit for the determination of arsenic by activation analysis is, according to Leddicotte *et al.*[26], 10^{-3} ppm at a flux of 5×10^{11} neutrons cm^{-2} sec^{-1}.

Production of ^{76}As from the reactions $^{76}Se(n, p)^{76}As$ and $^{79}Br(n,\alpha)^{76}As$ has been considered. For activation in the Swedish reactor R 1, which has a flux of fast neutrons approximately one tenth of the thermal flux, the ratio of ^{76}As formed from selenium, to ^{76}As formed from arsenic has been calculated to be about 2×10^{-6}. The analogous ratio for the ^{79}Br-reaction is about 10^{-4}.

The bromine concentration of biological matter, including human and animal tissue, is according to Underwood[20], of the order of 1—10 ppm. Thus the ^{79}Br-reaction must be considered when determining arsenic concentrations of 10^{-2}—10^{-3} ppm or lower.

Errors due to neutron flux depression in samples and standards are small when no material with exceedingly high neutron cross section is present in quantity. In our case all these errors were negligible. The standard deviation of the determined arsenic concentrations did not exceed $\pm$ 6 %. Some similar samples have been analysed for arsenic by both chemical and activation analysis[21] and the agreement was fairly good.

Acknowledgements. The authors are indebted to Professors T. Westermark and C. H. Hjortsjö for suggesting the arsenic determinations and also for valuable discussions. They also thank Mr. J. Hansén for the maintenance of the multi-channel analyzer. The authors are again indebted to Professor O. Lamm for providing laboratory space at the Institution of Physical Chemistry. *The Swedish Technical* and *Atomic Research Councils* have provided means for the instruments and other facilities. The English manuscript has been linguistically revised by Dr. Derek Lewis.

REFERENCES

1. Westermark, T., Ljunggren, K., Fineman, I. and Erwall, L.-G. *Svensk Kem. Tidskr.* **70** (1958) 211. (Four articles, in Swedish).
2. Atkins, D. H. F. and Smales, A. A. *Advances in Inorganic Chemistry and Radiochemistry* **1** (1959) 315.
3. Westermark, T. and Sjöstrand, B. *Intern. J. Appl. Rad. Isotopes* **9** (1960) 1.
4. Westermark, T. and Sjöstrand, B. *Intern. J. Appl. Rad. Isotopes* **9** (1960) 63.
5. Allen, R. A., Smith, D. B. and Hiscott, J. E. *Radioisotope Data* AERE—R 2938, 2nd ed., Wantage 1961.
6. Dzhelepov, B. S. and Peker, L. K. *Decay Schemes of Radioactive Nuclei*, Pergamon Press, 1961, p. 181.
7. Ljunggren, K. *Proc. Radioisotopes in the physical sciences and industry*, Vienna 1962, p. 199.
8. Inthoff, W. *Nucleonics* **13** (1955) No. 11, p. 67.
9. Blosser, H. G., Goodman, C. D. and Handley, T. H. *Phys. Rev.* **110** (1958) 531.
10. Smales, A. A. and Pate, B. D. *Anal. Chem.* **24** (1952) 717.
11. Cohen, B. L. *Phys. Rev.* **81** (1951) 184.

12. Lenihan, J. M. A. and Smith, H. *Proc. 2nd UN Intern. Conf. PUAE* **26** (1958) 238.
13. Lenihan, J. M. A. *Proc. Radioactivation Analysis Symposium*, London 1960, p. 85.
14. Smith, H. *Anal. Chem.* **31** (1959) 1361.
15. Beard, H. C. *The Radiochemistry of Arsenic*, National Academy of Sciences, NAS-NS 3002, Washington D.C. 1960.
16. Gibbons, D., Loveridge, B. A. and Millett, R. J. *Radioactivation Analysis* A.E.R.E. – I/R 2208, Harwell 1957.
17. Gibbons, D., Mapper, D., Millett, R. J. and Simpson, H. *Radioactivation Analysis* A.E.R.E. – I/R 2208 (Supplement 1) Harwell 1960.
18. Bock-Werthmann, W. and Schulze, W. *Aktivierungsanalyse* AED-C-14-1, Berlin-Wannsee 1961.
19. Monier-Williams, G. W. *Trace Elements in Food*, London 1949, p. 162.
20. Underwood, E. J. *Trace Elements in Human and Animal Nutrition*, New York 1956.
21. Hjortsjö, C. H. (ed.) *Erik XIV, Gravöppningen 1958 i Västerås Domkyrka*, Stockholm 1962.
22. Forshufvud, S., Smith, H. and Wassén, A. *Nature* **192** (1961) 103.
23. Pijck, J., Hoste, J. and Gillis, J. *Proc. Intern. Symposium on Microchemistry 1958*, Pergamon Press, p. 48.
24. Gorsuch, T. T. *Analyst* **84** (1959) 135.
25. Gorsuch, T. T. *Analyst* **87** (1962) 112.
26. Leddicotte, G. W., Mullins, W. T., Bate, L. C., Emery, J. F., Druschel, R. E. and Brooksbank, Jr., W. A. *Proc. 2nd UN Intern. Conf. PUAE* **28** (1958) 478.
27. Paul, E. B. and Clarke, R. L. *Can. J. Phys.* **31** (1953) 267.

Received May 2, 1962.

ACTA CHEMICA SCANDINAVICA 16 (1962) 2131–2144

Eine genaue und vielseitig anwendbare Vorrichtung zur Erzeugung von Flüssigkeitsgradienten

HARRY SVENSSON und ALFRED FORCHHEIMER

Abteilung für physikalische Chemie, Jubileumslaboratorium der Wallenberg-Stiftung, Karolinska Institutet, Stockholm, Schweden

Herrn Professor Dr. *Ole Lamm* zum 60. Geburtstag gewidmet

Es wird eine Mischvorrichtung zur Erzeugung von Gradienten in Flüssigkeiten beschrieben. Sie besteht aus mehreren geschlossenen, luftfreien, in Serie geschalteten, kapillar verbundenen und mit Rührkörpern versehenen Kammern, alle mit demselben freien Volumen. Das ganze Kammersystem ist in durchbohrten Kugelschliffen gelagert und wird mittels eines Motors in Rotation gesetzt, während die Rührkörper auf den zylindrischen Kammerwänden frei rollen. Durch Wahl verschieden grosser Rührkörper kann das Gesamtvolumen des Kammersystemes leicht verändert werden. Die Volumengleichheit der Kammern macht die mathematische Berechnung der Ausflusskonzentration besonders einfach und die allgemeine Lösung der Differentialgleichung eines Systemes mit beliebiger Anzahl von Kammern wird gegeben. Obgleich die Lösung eine Exponentialfunktion ist, wird gezeigt und durch Versuche bestätigt, dass sehr genau lineare Ausflussfunktionen (konstante Gradienten) erhalten werden können, falls die Ausgangskonzentrationen passend gewählt werden. Die luftfreie Füllung des Kammersystemes gewährt eine ausserordentlich gute Reproduzierbarkeit, und eine vollkommene Übereinstimmung der Ausflussfunktionen mit der Theorie wird ebenfalls bestätigt.

Physikalisch-chemische Prozesse mit Anwendung veränderlicher Flüssigkeitseigenschaften, z. B. mit Hinsicht auf Polarität, Dichte, pH, Leitfähigkeit u. s. w., gewinnen mehr und mehr an Bedeutung. Als Folge davon steigen die Anforderungen an Mischvorrichtungen ständig. Viele solche Vorrichtungen sind bereits beschrieben worden. Die meisten davon haben jedoch eine schlechte Reproduzierbarkeit oder ein allzu begrenztes Anwendungsgebiet. In der Absicht, eine Mischvorrichtung zu konstruieren, welche so vielen experimentell bedingten Anforderungen wie möglich genügt, haben die Verfasser die wünschenswerten Eigenschaften einer solchen Vorrichtung in folgenden acht Punkten zusammengefasst.

1) Die Vorrichtung soll eine vielseitige Gestaltung der Funktion $P(v)$ zulassen, wobei v das von der Vorrichtung vom Startaugenblick an abgegebene Flüssigkeitsvolumen und P die stetig veränderliche Eigenschaft darstellen. Die Möglichkeit, eine lineare Funktion $P(v)$, d. h. einen konstanten Gradienten $P'(v)$ zu erzeugen, wird als besonders wichtig betrachtet.

2) Die Vorrichtung soll eine bequeme Variation des Gesamtvolumens zulassen, innerhalb dessen sich die Eigenschaft P verändert.

3) Die Funktion $P(v)$, welche von der Vorrichtung geliefert wird, soll von allen anderen Eigenschaften der Flüssigkeitskomponenten unabhängig sein. So soll beispielweise ein Polaritätsgradient von der Dichte der Flüssigkeitskomponenten, und ein Dichtegradient von einer eventuellen Verschiedenheit der Viskosität unabhängig sein.

4) Es soll möglich sein, den Verlauf der Funktion $P(v)$ mit Hilfe der Ausgangsbedingungen zu berechnen und umgekehrt, geeignete Ausgangsverhältnisse aus einer bestimmten gewünschten Form der Funktion $P(v)$ zu ermitteln.

5) Die Vorrichtung soll genau und reproduzierbar arbeiten, d. h. bei wiederholten Versuchen unter denselben Ausgangsbedingungen genau dieselbe Funktion $P(v)$ liefern. Diese Funktion soll ausserdem auch von der Ausflussgeschwindigkeit aus der Vorrichtung unabhängig sein.

6) Die Vorrichtung soll für chromatographische Elution hinreichend langsam und zur Bereitung von stabilisierenden Dichtegradienten genügend schnell arbeiten können.

7) Die Bedienung der Vorrichtung soll bequem und die Instandhaltung leicht sein.

8) Die Vorrichtung soll, sei es dass sie kommerziell oder in der Laborwerkstatt hergestellt werde, zu einem Preis erhältlich sein, welcher zu dem Anwendungsgebiet und einem gewöhnlichen Laboratorienbudget in angemessenem Verhältnis steht.

Ein Studium der meist angewendeten Mischvorrichtungen zeigt deutlich, wie schwer es ist, alle diese Anforderungen gleichzeitig zu erfüllen. So ergibt beispielweise die Zusammenschaltung einer geschlossenen Mischkammer mit einem offenen Behälter nur eine einzige (exponentielle) Form der Funktion $P(v)$, und das anwendbare Flüssigkeitsvolumen ist durch den Rauminhalt der Mischkammer bestimmt. Andererseits genügt eine solche Vorrichtung den Anforderungen in den Punkten 3) bis 8). Eine Vorrichtung mit zwei parallelgeschalteten Kammern, die eine mit nach oben zunehmendem und die andere mit abnehmendem Querschnitt, ist für spezielle Zwecke anwendbar, genügt aber nicht den Anforderungen in den Punkten 1), 3) und 5). Eine Anordnung mit zwei in Serie geschalteten offenen Zylindern, von denen der eine mit Rührwerk versehen ist, wird häufig angewendet und genügt den Anforderungen 1), 2), 4), 6), 7) und 8). Der resultierende Gradient ist jedoch von Unterschieden mit Hinsicht auf Dichte und Viskosität abhängig und ändert sich ausserdem mit der Ausflussgeschwindigkeit. Peterson und Sober's [1] Apparat "Varigrad" * arbeitet nach diesem Prinzip, doch mit neun in Serie geschalteten, mit Rührwerk versehenen zylindrischen Gefässen. Die grosse Anzahl der Gefässe lässt eine praktisch genommen unbegrenzte Formbarkeit

* Hersteller: Buchler Instruments Inc., 514 West 147th Street, New York, N. Y.

der Funktion $P(v)$ zu; die Abhängigkeit von Dichte, Viskosität und Ausflussgeschwindigkeit bleibt jedoch bestehen. Bisher beschriebene Methoden zur Bereitung von Flüssigkeitsgradienten wurden von Peterson und Sober [1] sowie von Svensson [2] zusammengestellt.

Sämtliche Mischvorrichtungen mit offenen Behältern weisen Abhängigkeit von Dichte- und Viskositätsunterschieden auf. Um die wichtige Anforderung 5) zu erfüllen, haben die Verfasser deshalb eine Ausführung mit geschlossenen und mit Rührkörpern versehenen Kammern gewählt, wobei die Luft völlig aus dem Kammersystem ausgeschlossen ist. Die Wahl eines Systemes mit mehreren Kammern ist notwendig, um der Anforderung 1) zu genügen, weil eine einzige Kammer nur eine unveränderliche Exponentialfunktion liefert. Weiterhin wurde für sämtliche Kammern das gleiche freie Flüssigkeitsvolumen gewählt, da dies die mathematischen Berechnungen in Zusammenhang mit den Anforderungen in Punkt 4) bedeutend erleichtert. Mit Hinsicht auf Punkt 2) wurde eine Konstruktion gewählt, in welcher austauschbare Rührkörper es möglich machen, das freie Flüssigkeitsvolumen zu verändern. Wie die übrigen hier aufgestellten Anforderungen erfüllt werden geht aus der Beschreibung der Apparatur hervor.

THEORETISCHE GRUNDLAGEN VON MISCHVORRICHTUNGEN, BESTEHEND AUS EINER BELIEBIGEN ANZAHL IN SERIE GESCHALTETER, MIT RÜHRKÖRPERN VERSEHENER MISCHKAMMERN GLEICHEN RAUMINTHALTES

Der Verlauf der Konzentration des Ausflusses aus einer Mischvorrichtung mit einer einzigen, geschlossenen und mit Rührkörper versehenen Kammer wird durch die wohlbekannte Gleichung:

$$c_1(x) = c_0 + (c_1 - c_0)\ \mathrm{e}^{-x} \tag{1}$$

dargestellt, wobei x das Verhältnis zwischen dem abgegebenen Flüssigkeitsvolumen v und dem freien Kammervolumen V darstellt, das heisst:

$$x = v/V \tag{2}$$

c_0 ist die der Mischvorrichtung zugeführte konstante Konzentration der einen Komponente, und c_1 ist die Ausgangskonzentration derselben Komponente in der Kammer.

Zwei geschlossene Kammern des gleichen freien Rauminhaltes V, mit Umrührern versehen, in Serie geschaltet und kapillar verbunden, ergeben folgenden Konzentrationsverlauf des Ausflusses:

$$c_2(x) = c_0 + (c_2 - c_0)\ \mathrm{e}^{-x} + (c_1 - c_0)\ x\ \mathrm{e}^{-x} \tag{3}$$

wobei c_2 die Ausgangskonzentration in der zweiten Kammer bedeutet. Diese Gleichung wurde zuerst von Drake [3] aufgestellt und deren Herleitung kann in ihren Einzelheiten aus seiner Schrift oder aus einer späteren Veröffentlichung von Svensson[4], entnommen werden.

Die gleiche Methodik des Berechnungsganges, auf eine dritte Mischkammer angewendet, liefert die Gleichung:

$$c_3(x) = c_0 + (c_3 - c_0)\ e^{-x} + (c_2 - c_0)\ x\ \mathrm{e}^{-x} + (c_1 - c_0)\ (x^2/2)\ \mathrm{e}^{-x} \tag{4}$$

Dies lässt vermuten, dass die Konzentration des Ausflusses aus der n:ten Mischkammer von der Gleichung

$$c_n(x) = c_0 + e^{-x} \sum_{i=1}^{i=n} (c_i - c_0) \frac{x^{n-i}}{(n-i)!} \tag{5}$$

wiedergegeben werden kann. Die Richtigkeit ist leicht mit Hilfe des mathematischen Induktionsbeweises nachweisbar. Die Differentialgleichung der Kammer Nummer $(n + 1)$ lautet:

$$c_n(x)\ dx - c_{n+1}(x)\ dx = d(c_{n+1}\ (x)) \tag{6}$$

und hat die allgemeine Lösung:

$$c_{n+1}(x) = e^{-x} \int c_n(x)\ e^x\ dx \tag{7}$$

welche eine Rekursionsformel darstellt. Setzt man $c_n(x)$ aus Gleichung (5) ein, so erhält man dieselbe Gleichung mit $n + 1$ statt n. Die Gleichung (5) liefert differenziiert folgenden Ausdruck für den Ausflussgradienten:

$$c_n'(x) = e^{-x} \sum_{i=1}^{i=n} (c_{i-1} - c_i) \frac{x^{n-i}}{(n-i)!} \tag{8}$$

Die Herstellung eines konstanten Gradienten. Gewisse einfache Mischvorrichtungen mit mangelnder Reproduzierbarkeit sind imstande, im Wesentlichen lineare Funktionen $P(v)$ über das ganze zugängliche Konzentrationsintervall zu liefern. Mit geschlossenen, seriengeschalteten Kammern ist eine komplette Linearität nicht zu erhalten, was aus der Gleichung (5) hervorgeht. Unabhängig von der Natur der Polynome von x, nähert sich die Funktion asymptotisch dem Wert c_0, was in diesem Bereich einen konstanten, nicht verschwindenden Gradienten ausschliesst. Dass wir trotzdem geschlossene Kammern gewählt haben, beruht darauf, dass wir gute Reproduzierbarkeit und hohe Genauigkeit höher schätzen als die Fähigkeit, eine vollständige Linearität zu geben. Es wird jedoch im Folgenden gezeigt, dass praktisch genommen konstante Gradienten über mehr als 70 % des zur Verfügung stehenden Konzentrationsunterschiedes erreicht werden können, wenn die Anzahl der Kammern 5 oder mehr ausmacht und die Ausgangskonzentrationen sorgfältig gewählt werden. Nachdem konstante Gradienten für viele Anwendungen ausserordentlich wünschenswert sind, lohnt es sich, die Annäherungsmöglichkeiten für Anordnungen nach den hier beschriebenen Prinzipien näher zu untersuchen.

Man versteht unmittelbar, dass Ausgangskonzentrationen, welche eine aritmetische Reihe bilden, im ersten Teil des Ausflusses einen annähernd konstanten Gradienten geben müssen. In diesem Falle ist der Konzentrationsunterschied zwischen den Kammern:

$$\Delta c_i = c_{i-1} - c_i \tag{9}$$

durch das ganze System konstant, und man erhält für den Gradienten die Gleichung:

$$c_n'(x) = \Delta c\ e^{-x} \sum_{i=0}^{n-1} \frac{x^i}{i!} \tag{10}$$

die bereits im Jahre 1960 von einem der Verfasser [2] aufgestellt wurde. Da das Polynom in dieser Gleichung die Potenzreihe von e^x, am n:ten Glied unterbrochen, darstellt, wird der Gradient mit wachsender Anzahl Kammern mehr und mehr konstant und nähert sich dem Wert Δc.

Die Konzentrationen und Konzentrationsgradienten, welche man erhält, wenn man Ausgangskonzentrationen in aritmetischer Reihe anwendet, sind in Abb. 1 bis zu sechs Kammern graphisch dargestellt.

Im Folgenden wird das Ergebnis von Versuchen, mit einer Vorrichtung beschriebener Art einen konstanten Gradienten zu erreichen, quantitativ durch den Teil des zur Verfügung stehenden Konzentrationsunterschiedes ausgedrückt, innerhalb dessen der Gradient weniger als $\pm$ 10 % von einem Mittelwert abweicht. Im vorliegenden Diagramm wurden diese Bruchteile erhalten, indem man von einer Waagrechten $c'(x) = 9/11$ ausging und von deren Schnittpunkten mit den Gradientkurven lotrechte Linien bis zum Schnitt mit den entsprechenden Integralkurven zog. Die Konzentrationsintervalle zwichen Null und diesen Punkten stellen die Gebiete dar, in welchen die Konzentration, gemäss oben gegebener Definition, hinreichend linear verläuft. Dieses Gebiet wächst mit zunehmender Anzahl von Kammern erst stark und dann immer langsamer an. Für eine Ein-Kammer-Mischvorrichtung werden die Linearitätsabweichungen schon bei $0{,}18\, c_0$ grösser als $\pm$ 10%, während ein Sechs-Kammer-System ein bis auf $\pm$ 10 % lineares Gebiet von 0,60 c_0 aufweist.

Es ist faktisch möglich, die Linearität der Konzentrationsfunktion noch zu verbessern, wenn man von dem Prinzip der Anwendung von Ausgangskonzentrationen in aritmetischer Reihe absteht. Die Gleichung:

$$e^x c_n''(x) = \Delta c_1 \frac{x^{n-1}}{(n-1)!} + \sum_{i=1}^{n-1} (\Delta c_{i+1} - \Delta c_i) \frac{x^{n-i-1}}{(n-i-1)!} = 0 \qquad (11)$$

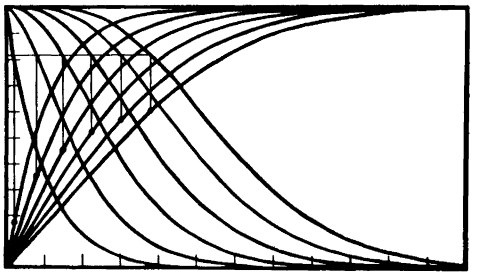

Abb. 1. Ausflusskonzentrationen (steigende Kurven) und deren Gradienten (fallende Kurven) von einem Kammersystem mit einer bis sechs Kammern als Funktion des gelieferten Volumens in Einheiten des Kammervolumens, für den Fall, dass die Ausgangskonzentrationen eine aritmetische Reihe bilden.

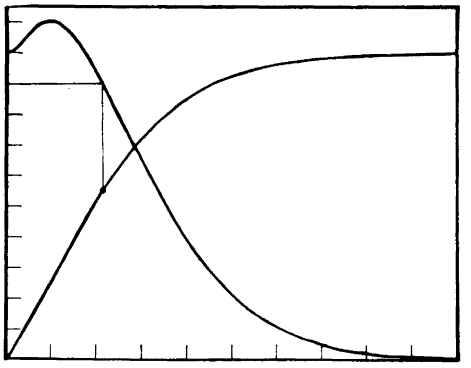

Abb. 2. Ausflusskonzentration (steigende Kurve) und deren Gradient von einem Kammersystem mit drei Kammern als Funktion des gelieferten Volumens, für den Fall, dass die vier Ausgangskonzentrationen den Zahlen 4, 2, 1 und 0 proportional sind. (Vgl. die Gleichungen 12 bis 16.)

gibt die x-Werte für welche der Konzentrationsverlauf Inflexionspunkte aufweist. Die Gleichung ist $(n-1)$:ten Grades mit Koeffizienten, welche von den Unterschieden der Ausgangskonzentrationen gebildet werden. Es ist offenbar möglich, die Anfangskonzentrationen so zu wählen, dass die Gleichung (11) $n-1$ reelle Wurzeln für vorherbestimmte x-Werte hat. Wählt man diese Punkte sorgfältig, kann eine Konzentrationskurve erreicht werden, welche mit derartig kleinen Amplituden um eine gerade Linie spielt, dass sie kaum von einer solchen unterschieden werden kann. Dieses Verfahren wird hier durch einige Beispiele erläutert.

Für drei Kammern in Serie nimmt die Gleichung (11) folgende Form an:

$$\Delta c_1(x^2/2) + (\Delta c_2 - \Delta c_1)x + (\Delta c_3 - \Delta c_2) = 0 \tag{12}$$

Werden Inflexionspunkte bei $x = 0$ und $x = 1$ gewählt, muss diese Gleichung mit $x(x-1) = 0$ identisch sein. Hieraus erhält man die Beziehungen:

$$\Delta c_3 = \Delta c_2 \quad \text{und} \quad \Delta c_1 = 2\Delta c_2 \tag{13}$$

Für die Ausgangskonzentrationen in beliebigen Einheiten sind dann die Zahlenfolgen

$$4,\ 2,\ 1,\ 0 \quad \text{und} \quad 0,\ 2,\ 3,\ 4 \tag{14}$$

möglich, wobei sich die eine Zahlenfolge auf einen positiven und die andere auf einen negativen Gradienten beziehen. Werden diese Ziffern in die Gleichungen (5) und (8) eingesetzt, erhält man folgenden Konzentrationsverlauf:

$$c_3(x) = (c_0/4)\,(x^2 + 3x + 4)\ \mathrm{e}^{-x} \tag{15}$$

und den Gradienten:

$$c_3'(x) = (c_0/4)\,(x^2 + x + 1)\ \mathrm{e}^{-x} \tag{16}$$

Diese Kurven zeigt Abbildung 2 mit den Konstruktionslinien zum Auffinden des Konzentrationsintervalles mit Linearitätsabweichungen innerhalb der zugelassenen Grenzen. Dieses Intervall erstreckt sich über 56 % von c_0 und ist mit dem aus Abbildung 1 für ein Drei-Kammer-System entnommenen Wert 46 % zu vergleichen.

Mit vier Mischkammern in Serie erhält man gemäss Gleichung (11):

$$\Delta c_1\ (x^3/6) + (\Delta c_2 - \Delta c_1)\ (x^2/2) + (\Delta c_3 - \Delta c_2)\ x + (\Delta c_4 - \Delta c_3) = 0 \tag{17}$$

Diese Gleichung ist für gewünschte Inflexionspunkte bei $x = 0$, 1 und 2 mit $x(x-1)\ (x-2) = 0$ zu identifizieren. Dies führt zu den Beziehungen:

$$\Delta c_4 = \Delta c_3 \qquad \Delta c_2 = 0 \qquad \Delta c_1 = 3\Delta c_4 \tag{18}$$

und zu den folgenden möglichen Konzentrationsreihen:

$$5,\ 2,\ 2,\ 1,\ 0 \qquad \text{und} \qquad 0,\ 3,\ 3,\ 4,\ 5 \tag{19}$$

Die entsprechenden Gleichungen für die Konzentration und deren Gradienten sind (für den positiven Gradienten):

$$c_4(x) = c_0 - 0{,}1\ c_0\ (x^3 + 3x^2 + 8x + 10)\ \mathrm{e}^{-x} \tag{20}$$

$$c_4'(x) = 0{,}1\ c_0\ (x^3 + 2x + 2)\ \mathrm{e}^{-x} \tag{21}$$

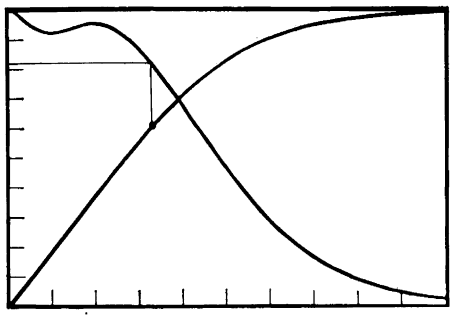

Abb. 3. Ausflusskonzentration (steigende Kurve) und deren Gradient von einem Kammersystem mit vier Kammern als Funktion des gelieferten Volumens, für den Fall, dass die fünf Ausgangskonzentrationen den Zahlen 5, 2, 2, 1 und 0 proportional sind. (Vgl. die Gleichungen 17 bis 21.)

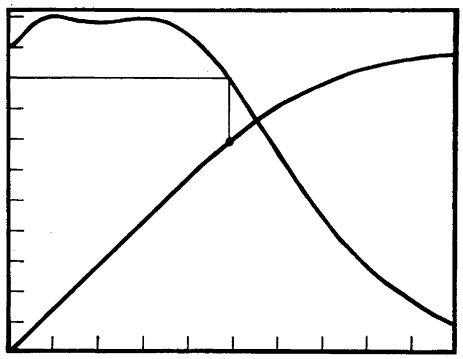

Abb. 4. Ausflusskonzentration (steigende Kurve) und deren Gradient von einem Kammersystem mit fünf Kammern als Funktion des gelieferten Volumens, für den Fall, dass die sechs Ausgangskonzentrationen den Zahlen 15, 3, 9, 4, 2 und 0 proportional sind. (Vgl. die Gleichungen 22—23).

Diese Funktionen werden in Abb. 3 graphisch dargestellt. Man sieht, dass man eine genügende Linearität bis zu 0,62 c_0 erhält, im Vergleich zu 0.525 c_0 für Ausgangskonzentrationen in aritmetischer Reihe.

Berechnungen gleicher Art für fünf Kammern und mit Inflexionspunkten bei $x = 0, 1, 2$ und 3 ergeben die Konzentrationsfolgen:

15, 3, 9, 4, 2, 0 und 0, 12, 6, 11, 13, 15

Die erste Folge (steigende Konzentration) entspricht den Funktionen:

$$c_5(x) = c_0 - (c_0/30)\,(x^4 + 2x^3 + 11x^2 + 26x + 30)\,\mathrm{e}^{-x} \qquad (22)$$

$$c_5'(x) = (c_0/30)\,(x^4 - 2x^3 + 5x^2 + 4x + 4)\,e^{-x} \qquad (23)$$

Diese Kurven werden in Abb. 4 gezeigt. Der den Anforderungen genügende Linearitätsumfang ist jetzt auf 0,695 c_0 angewachsen, verglichen mit dem Wert 0,57 c_0 bei Abwesenheit von Inflexionspunkten (Abb. 1).

Bei einem Sechs-Kammer-System können die Inflexionspunkte auf die Werte $x = 0, 1, 2, 3$ und 4 verlegt werden, woraus die Konzentrationsfolgen:

$$60, 0, 60, 15, 20, 13, 6 \quad \text{und} \quad 0, 60, 0, 45, 40, 47, 54 \qquad (24)$$

errechnet werden. In diesem Falle umfasst der Gradient 54 Konzentrationseinheiten, während 60 Einheiten zu dessen Aufbau notwendig sind. Die Konzentration:

$$c_6\,(x) = c_0 - (c_0/120)\,(x^5 + 15x^3 + 40x^2 + 94x + 108)\,\mathrm{e}^{-x} \qquad (25)$$

und ihr Gradient

$$c_6'(x) = (c_0/120)\,(x^5 - 5x^4 + 15x^3 - 5x^2 + 14x + 14)\,e^{-x} \qquad (26)$$

sind graphisch in Abb. 5a dargestellt. Wie man aus dieser Abbildung entnehmen kann, ist der Gradient über etwa 4 Kammervolumina bis auf $\pm$ 1 %

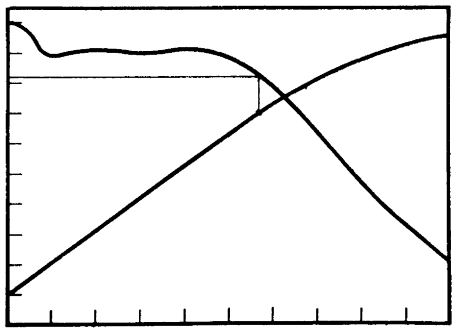

Abb. 5a. Ausflusskonzentration (steigende Kurve) und deren Gradient von einem Kammersystem mit sechs Kammern als Funktion des gelieferten Volumens, für den Fall, dass die sieben Ausgangskonzentrationen den Zahlen 60, 0, 60, 15, 20, 13 und 6 proportional sind. (Vgl. die Gleichungen 25–26.)

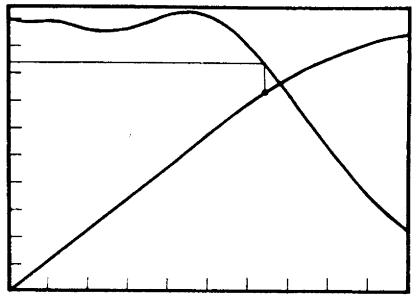

Abb. 5b. Ausflusskonzentration (steigende Kurve) und deren Gradient von einem Kammersystem mit sechs Kammern als Funktion des gelieferten Volumens, für den Fall, dass die sieben Ausgangskonzentrationen den Zahlen 984, 24, 696, 300, 230, 115 und 0 proportional sind. (Vgl. die Gleichungen 27–28.)

konstant. Die Grenze für eine $\pm$ 10 %-ige Abweichung ist aber nur 0,70 c_0, also nicht besser als für das Fünf-Kammer-System. Ohne Inflexionspunkte (Abb. 1) erreicht man 0,60 c_0.

Versucht man, um den Linearitätsbereich noch zu erweitern, die Inflexionspunkte auf zu hohe x-Werte zu legen, so ergeben die Identitäten manchmal negative Konzentrationen. Es ist aber durchaus möglich, den Linearitätsbereich durch Verlegung gewisser Inflexionspunkte zwischen ganzzahlige x-Werte zu verbessern. Falls man z. B. in einem Sechs-Kammer-System die Inflexionspunkte an $x = 0$, 1/2, 1, 5/2 und 9/2 verlegt, so bekommt man für eine wachsende Ausflusskonzentration die folgenden Ausgangskonzentrationen:

984, 24, 696, 300, 230, 115, 0

welche der Ausflusskonzentration:

$$c_6(x) = c_0-(c_0/984)\ (8x^5 + 12x^4 + 114x^3 + 377x^2 + 869x + 984)\ e^{-x} \quad (27)$$

und dem Ausflussgradienten:

$$c_6'(x) = (c_0/115)\ (8x^5-28x^4 + 66x^3 + 35x^2 + 115x + 115)\ e^{-x} \quad (28)$$

entsprechen. Diese Kurven werden in Abb. 5b gezeigt. Man sieht dort, dass der Gradient bis zu 0,735 c_0 eine $\pm$ 10 %-ige Konstanz besitzt.

BESCHREIBUNG DER APPARATUR

Konstruktive Gesichtspunkte. Wesentlich für die Reproduzierbarkeit und gute Übereinstimmung der Ausflusskonzentrationen mit der Theorie sind hauptsächlich Volumengleicheit der Kammern und eine wirksame Durchmischung des Kammerinhaltes.

Die erstgennante Forderung ist durch Einhalten enger Toleranzen bei Herstellung und Bearbeitung der Kammerbestandteile weitgehendst erfüllbar. Der Durchmischungsgrad des Kammerinhaltes ist von einer Reihe verschiedener Faktoren abhängig. Abgesehen von Viskositäts- und Hafteigenschaften der Flüssigkeit sind einige dieser Faktoren für die Gestaltung und Dimensionierung der Apparatur von Bedeutung. Insbesondere gilt dies die Form der Rührkörper und deren relative Bewegung zu den Kammerwänden.

Die Aneinanderschaltung kapillar verbundener und mit Rührwerk versehener Kammern kan konstruktiv verschieden durchgeführt werden. Mit Hinsicht auf die erwähnte relative Bewegung zwischen Rührkörpern und Kammerwandung kann man zwei Prinzipien unterscheiden. Einerseits ein stillstehendes Kammersystem mit einer durch sämtliche Kammern geführten Achse, an welcher die Rührkörper beispielweise ausschwenkbar befestigt sind, oder ein um seine eigene Achse rotierendes Kammersystem, wobei die Kammern mit freiliegenden, rollenden Rührkörpern, wie Kugeln, Zylindern, oder dergleichen versehen sind. Im ersteren Falle ist die Ab- und Zuführung der Flüssigkeit leicht durch festen Anschluss an die Endkammern zu bewerkstelligen. Schwieriger gestaltet sich die Konstruktion des Rührwerkes und dessen Lagerung. Bei rotierenden Kammern dagegen ist die Ab- und Zuführung der Flüssigkeit schwieriger.

Ein Aufbau des Kammersystemes aus einfachen Komponenten, wie plattenförmigen Trennungswänden zwichen rohrförmigen Kammerelementen gestattet zum Zwecke der Reinigung ein leichtes Auseinandernehmen und Zusammensetzen. Eine weitere wertfolle Folge einer solchen Konstruktion liegt darin, dass Rührkörper verschiedener Grösse angewendet werden können. Diese erhalten hierdurch eine doppelte Aufgabe, teils die der Durchmischung und teils die der Änderung des freien Kammervolumens. In gewissen Grenzen kann also mit demselben Apparat durch Wahl verschieden grosser Rührkörper der Gradient über ein gewünschtes Flüssigkeitsvolumen verteilt werden.

Ausführung. Wir haben die Konstruktionsalternative der rotierenden Kammern gewählt und die Frage des Ab- und Zuflusses so gelöst, dass wir als Lagerung des Kammersystemes gewöhnliche Kugelschliffe mit kapillarem Durchfluss anwenden. Die Abbildungen 6—9 zeigen Gesamtansicht der betriebsfertigen Apparatur, Gesamtansicht der Apparatur mit zur Füllung aufgestelltem Kammersystem, Teilansicht des Kammersystemes mit Hinsicht auf den Kammeraufbau, und Teilansicht je einer Zwischen- und Endkammerplatte. Die konstruktiven Einzelheiten sind aus den Figurtexten zu entnehmen.

Die Kugelpfannen (9, s) sind in die Aussenwände der Endkammern (6, f, q) versenkt, während die Kugeln mit ihren Stutzen (6, a, v), durch Gummihülsen geschützt, in Lagerböcken (7, b, u) festgeschraubt sind. Der eine dieser Lagerböcke (7, b) ist auf der Grundplatte (7, y) in einer Führung (7, z) verschiebbar ausgeführt. Der Lager- und Abflusstutzen (7, a) ist gegen den Lagerbock (7, b) federnd gelagert. Die Verschiebbarkeit des Lagerbockes (7, b) gewährt ein leichtes Einsetzen und Herausnehmen des Kammersystems, sowie die Möglichkeit, die Anzahl der Kammern zu variieren. Die Federung (7, c) garantiert einen gleichartigen Lagerdruck. Mit einer dünnen Schicht hochwertigen Fettes in den Schliffen haben wir selbst bei mehrtägigem dauerndem Gang des Apparates keinen Flüssigkeitsaustritt an den Lagerstellen beobachten können. Auch

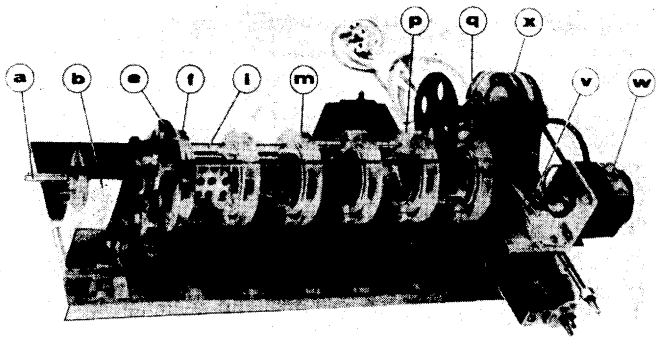

Abb. 6.

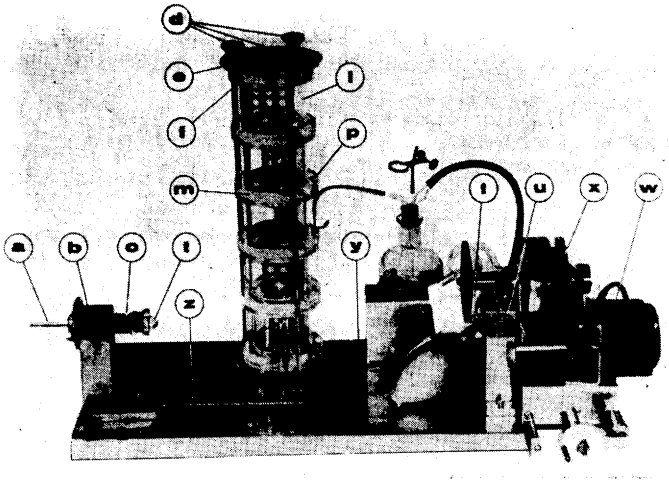

Abb. 7.

der befürchtete Verschleiss der Schliffe ist trotz der jetzt schon mehrjährigen Anwendung nicht feststellbar.

Die Kammern bestehen aus losen Rohrstücken (8, i), Platten (9), und Rührkörpern (8, h). Jede Platte, mit Ausnahme der beiden Endplatten (6, f, q), bildet Scheidewand zwischen zwei Kammern und ist in der Mitte kapillar durchbohrt (9, n). Die beiden Endplatten (6 f, q) tragen, wie oben erwähnt, die Pfannen der Lagerkugelschliffe. Dichten und Zentrieren der Kammern gegeneinander geschieht selbsttätig durch ringförmige Nuten (9, k) in den Plattenseiten. Diese Nuten sind dimensionsmässig an die Enden der rohrförmigen Kammerelemente angepasst. Das Füllen der Kammern geschieht durch kapillare Bohrungen (9, o) durch die Platten von aussen (7). Diese Kanäle

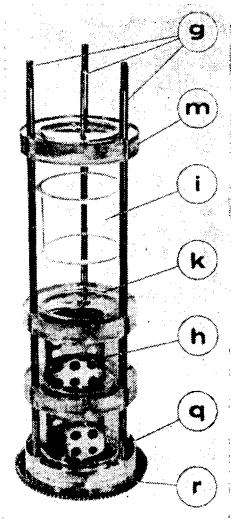

Abb. 8.

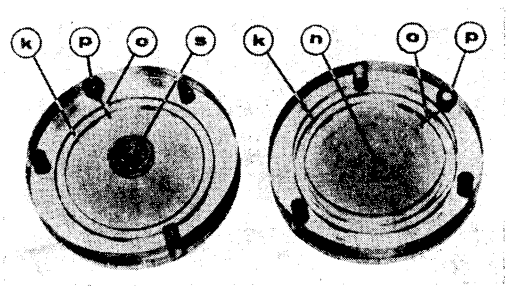

Abb. 9.

Abb. 6. Gesamtansicht der betriebsfertigen Apparatur.

Abb. 7. Gesamtansicht der Apparatur mit zur Füllung aufgestelltem Kammersystem.

Abb. 8. Teilansicht des Kammersystemes mit Hinsicht auf den Kammeraufbau.

Abb. 9. Teilansicht je einer Zwischen- und Endkammerplatte.

Die Buchstaben in der Abbildungen 6—9 bezeichnen: a) Abflusstutzen mit Lagerkugelschliff. b) Verschiebbarer Lagerbock. c) Feder zur Einstellung des Lagerdruckes. d) Gerändelte Spannmuttern. e) Metallspannplatte. f) Endplatte gegen Abflusseite. g) Spannstangen. h) Rührkörper. i) Rohrförmiges Kammerelement. k) Ringförmige Steuernuten. m) Plattenförmige Kammerzwischenwand. n) Kapillare Durchflussbohrung in der Kammermitte. o) Verchliessbare Einfüllöffnung. p) Konischer Verschlusstopfen. q) Endplatte gegen Antriebseite. r) Als Zahnrad ausgeformte Metallspannplatte. s) Pfannenteil der Kugelschlifflagerung. t) Kugelteil der Kugelschlifflagerung. u) Fester Lagerbock. v) Zuflusstutzen mit Lagerkugelschliff. w) Motor. x) Getriebe. y) Grundplatte. z) Führungsnute für verschiebbaren Lagerbock.

werden nach erfolgter Füllung durch Drehung eines durchbohrten Stopfens (9, p), der wie ein Hahnküken wirkt, verschlossen. Eine solche Verschlusskonstruktion führt keine Druckänderung oder sonstige Einflüsse auf den Kammerinhalt mit sich.

Wir haben erst mit sechs und später mit fünf Kammern gearbeitet, da sich eine solche Beschränkung der Kammeranzahl für uns als vollauf genügend erwies, um in den aufgestellten Grenzen einen konstanten Gradienten zu erreichen. Jede Kammer hat einen grössten freien Rauminhalt von 100 cm^3. Der hierbei angewendete Rührkörper besteht aus zwei Ringen, welche mittels einer vielfach durchbohrten rechteckigen Platte zentrisch so verbunden sind, dass sie miteinander parallel und winkelrecht zur Verbindungsplatte stehen.

Diese auf den Ringen rollenden Rührkörper (8, h) sind aus Messing gefertigt und nachträglich hartvergoldet. Die grössten Rührkörper sind im Wesentlichen zylindrisch. Zum Ausschluss von Luftblasen bei Füllung der Kammern wurden die Plattenseiten konisch ausgearbeitet und die Füllanschlüsse so plaziert, dass das Kammersystem während der Füllung vertikal steht.

Der Dichtungsdruck der Kammern gegeneinander wird durch Spannstangen (8, g) gewährleistet, welche mit Metallendplatten (7, e; 8, r) zusammenwirken und mit Hilfe von gerändelten Muttern (7, d) angezogen werden. Die eine der Metallendplatten (8, r) ist als Zahnrad zum Antrieb des Systemes mittels Motor (6, w) und Getriebe (6, x) ausgeformt. Aus Gründen der Zeitersparnis und für einen schnellen Nachweis der Übereinstimmung mit der Theorie wurde die hier beschriebene Apparatur aus Plexiglas hergestellt. Es ist jedoch eine Glaskonstruktion auf demselben Prinzip unter Arbeit.

Handhabung. Die Zusammensetzung des Kammersystemes geschieht durch abwechselndes Aneinanderreihen von platten- und rohrförmigen Kammerelementen. Man beginnt den Aufbau mit der Zahnradspannplatte (8, r) und den von dieser getragenen Spannstangen (8, g). Die eine Endplatte (8, q) wird, von den Spannstangen geführt, so angesetzt, dass die Kugelpfanne gegen das Zahnrad gewendet ist. Hierauf wird eines der rohrförmigen Kammerelemente (8, i) mit einem der offenen Enden in die Zentriernute (9, k) der Endplatte (8, q) gepresst. Zum Zwecke der sicheren Abdichtung kann man vor der Zusammensetzung des Kammersystems sämtliche Zentriernuten in den Plattenelementen mit dünnen Dichtungsringen aus einem passenden Material, wie Polyaethylen, Polytetrafluoraethylen o. dgl. versehen. Nach Ansatz des Rohrelementes wird ein Rührkörper eingelegt und hierauf eine der Zwischenplatten (8, m), von den Spannstangen geführt, so aufgesetzt, dass die untere Zentriernute der Platte das darunterliegende offene Rohrende erfasst, steuert und abdichtet. Hierbei ist darauf zu achten, dass die Einfüllanordnung mit dem konischen Stopfen (7, p) so gerichtet ist, dass in jede auf beschriebene Weise entstehende Kammer eine Einfüllöffnung mündet.

Da die Zwischenplatten (8, m) auf beiden Seiten mit Zentrier- und Dichtungsnuten (9, k) versehen sind, kann der Aufbau der übrigen Kammern auf analoge Weise fortgesetzt werden, bis schliesslich die letzte Kammer mit der Endplatte (7, f) abgeschlossen wird. Die Kugelschlifflagerpfanne dieser Endplatte ist dabei nach aussen zu wenden, wobei die Zentriernute das letzte offene Rohrende abdichtet. Das ganze Kammersystem wird dann mit der Metallspannplatte (7, e) abgeschlossen, und die gerändelten Spannmuttern (7, d) werden aufgesetzt und angezogen. Es ist vorteilhaft, diesen Aufbau vertikal durchzuführen, insbesondere da das System in dieser Stellung gefüllt wird. Vor der Füllung ist die kapillare Öffnung der in der vertikalen Stellung unteren Kugelpfanne mit einem kleinen Stopfen, z. B. einer Zahnstocherspitze, zu verschliessen, um das Austreten der Flüssigkeit während der Füllung zu verhindern. Die vorbereiteten Lösungen der gewählten Konzentrationsreihe werden, von der untersten Kammer angefangen, in ihre Kammern eingefüllt, wobei man sich entweder des Überdruckes der Flüssigkeit in einem Einfüllröhrchen mit Trichter bedient oder, wie aus Abb. 7 hervorgeht, eines erzeugten Luftüberdruckes. Sobald die Flüssigkeit beginnt, die obere Abschlussfläche einer Kammer zu benetzen, wird die Zuflussgeschwindigkeit soweit herabgesetzt, dass man imstande ist, den Zufluss augenblicklich zu unterbrechen. Dies geschieht, wenn die Flüssigkeit die kapillare Bohrung zur darüberliegenden leeren Kammer gerade füllt, ohne in diese Kammer einzutreten. Der Ausschluss von Luftblasen und die Beobachtung des Flüssigkeitsspiegels bei Eintritt in die obere kapillare Bohrung einer Kammer wird wesentlich von der konischen Ausführung der Plattenseiten begünstigt. Nach erfolgter Füllung des ganzen Kammersystemes wird der Lager- und Zuflusstutzen (6, v) mit der Vorratsflüssigkeit gefüllt und luftfrei mit dem Vorratsgefäss oder dem Pumpensystem der Vorratslösung verbunden. Dies ist notwendig, um das Eindringen von Luft in das Kammersystem zu verhindern. Der verschiebbare Lagerbock (7, b) wird in die äusserste Lage geführt, worauf, nach Abdichtung der oberen Kugelpfanne, der Verschlusstopfen der unteren Kugelpfanne entfernt werden kann. Jetzt kann das Kammersystem an den festen Lagerbock (7, u) angesetzt und in die Horizontallage überführt werden. Nach

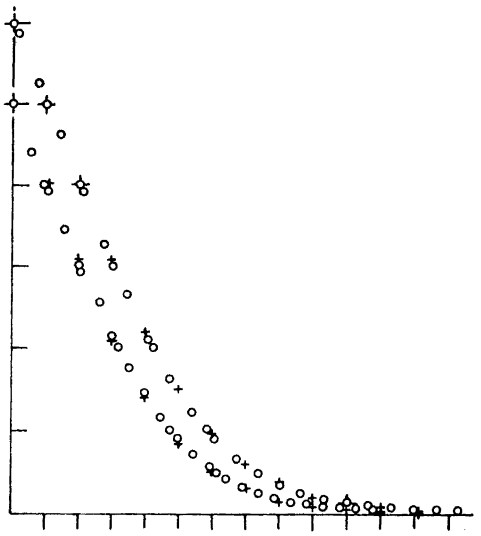

Abb. 10. Vergleich der Ausflusskonzentrationen mit den theoretisch berechneten Werten. Gemessene Konzentrationen: O. Berechnete Konzentrationen: +. Die obere Kurve wurde mit einem Sechs-Kammer-System erhalten, in welchem die Ausgangskonzentrationen 0 (Vorratslösung), 1, 2, 3, 4, 5 und 6 Millimol Natriumbenzoat per Liter waren. Die untere Kurve rührt von einem Fünf-Kammer-System her mit den Ausgangskonzentrationen 0, 1, 2, 3, 4 und 5 Millimol per Liter.

Entfernung der Abdichtung der Kugelpfanne kann der verschiebbare Lagerbock (7, b) mit dem federnd gelagerten Abflusschliff (7, a) zugeschoben und verriegelt werden. Der Lagerdruck wird von der Feder (7, c) bestimmt und ist durch kleine Verschiebungen des Lagerbockes (7, b) leicht zu regulieren. Der Abflusstutzen (7, a) wird an die Kolonne, in welcher der Gradient angewendet werden soll, angeschlossen, und der Motor (6, w) in Betrieb gesetzt. Je nach Art der Flüssigkeit und Rührkörper kann mit Hilfe des Getriebes (6, x) eine optimale Durchmischung erreicht werden.

Erst wenn das Kammersystem rotiert, wird die Zuleitung der Vorratslösung geöffnet. Der notwendige Druck kann von einem höherliegenden Vorratsgefäss oder von einer Pumpe vermittelt werden.

Nach erfolgter Überführung der gewünschten Flüssigkeitsmenge zur Kolonne wird zuerst der Zufluss zum Kammersystem gesperrt und der Motor (6, w) abgeschaltet. Darauf erst wird die Zuleitung zur Kolonne gesperrt. Jetzt kann das Kammersystem auseinandergenommen werden. Dies geschieht am besten in umgekehrter Reihenfolge zum Aufbau. Unter Verschiebung des Lagerbockes (7, b) wird das Kammersystem gegen den festen Lagerbock (7, u) gepresst und die freie Kugelpfanne abgedichtet. Hierauf kann auch die andere Kugelpfanne abgedichtet und das System in aufrechte Stellung gebracht werden. Die Spannmuttern (7, d), die Metallspannplatte (7, e), der Verschluss der oberen Kugelpfanne und die Kammerendplatte (7, f) werden in genannter Reihenfolge entfernt. Die obere Kammer liegt jetzt offen und kann mit einer Pipette oder Absaugvorrichtung entleert werden. Hierauf wird das rohrförmige Element und der Rührkörper der obersten Kammer abgenommen und der Abbau der übrigen Kammern analog durchgeführt.

Bei dem beschriebenen Auseinandernehmen des Kammersystemes in aufrechter Stellung hat sich das Eigengewicht der Kammern als genügend erwiesen, um den notwendigen Dichtungsdruck nach Entfernung der Spannmuttern zu liefern, sodass kein unkontrollierter Flüssigkeitsaustritt stattfand. Um ganz sicher zu sein kann man jedoch während des Abbaus den jeweils unter der Abbauebene liegenden Teil der Kammersäule mit einer Hand gegen die Unterlage gedrückt halten, da das Auseinandernehmen schnell und leicht mit der anderen Hand durchgeführt werden kann.

EXPERIMENTELLES

Oben beschriebene Mischvorrichtung ist die zweite Ausführungsform gemäss den dargelegten Prinzipien. Die erste Konstruktion wurde im Frühjahr 1960 fertiggestellt, während diese Zweite seit dem Sommer 1961 zur Verfügung stand und häufig in unserem Laboratorium angewendet wurde. Ausserdem haben wir das Instrument mit Hinsicht auf Reproduzierbarkeit und Übereinstimmung der Ausflusskonzentration mit der Theorie kritisch geprüft. Dabei haben wir eine ausserordentlich gute Reproduzierbarkeit gefunden; die Abweichungen liegen unter dem mit gewöhnlichen Methoden Messbaren. Die Experimente zur Prüfung der Übereinstimmung mit der Theorie werden hier näher beschrieben.

In einigen Versuchen wurden die Kammern mit Wasserlösungen von Natriumbenzoat mit Konzentrationen in aritmetischer Reihe gefüllt. Der Ausfluss wurde durch die Küvette des registrierenden UV-Absorptiometers "Uvicord" * geleitet. Für die genannten Lösungen wies die Eichung des Instrumentes strenge Gültigkeit des Lambert-Beer'schen Extinktionsgesetzes in weiten Konzentrationsgrenzen aus. Nichtsdestoweniger wurden die Kurven so aufgenommen, dass vor Beginn und nach Abschluss des Versuches je eine von Anfang separierte Menge Flüssigkeit jeder Ausgangskonzentration registriert wurde. Auf diese Weise konnte eine sich über die ganze Ausflussperiode erstreckende Eichkurve aufgenommen und damit eventuelle systematische Streuungen der registrierenden Apparatur während dieser Periode kompensiert werden. Das Resultat zweier Versuche wird in Abb. 10 gezeigt. Man sieht dort, dass die Übereinstimmung mit der Theorie sehr gut ist. Andere Versuche, die auch Ausgangskonzentrationen zur Erzeugung von Ausflussfunktionen mit Inflexionspunkten umfassten, haben dieses Ergebnis durchaus bestätigt.

Dank. Die Theorie dieser Mischvorrichtung wurde vor einigen Jahren ausgearbeitet. Die Herstellung des Instrumentes und dessen Ausprüfung wurde durch die Einrichtung eines neuen Laboratoriums ermöglicht. Die Verfasser danken dafür der *Wallenberg-Stiftung*, der *Wenner-Green Gesellschaft* und *Magnus Bergvalls Stiftung*. Die experimentelle Arbeit wurde weiter von den *medizinischen*, *naturwissenschaftlichen* und *technischen Forschungsräten* unterstützt. Für das sorgfältige Berechnen und Zeichnen der Kurven in den Abb. 1–5 danken wir Frl. Kerstin Svensson.

SCHRIFTTUM

1. Peterson, E. A. und Sober, H. A. *Anal. Chem.* **31** (1959) 857; "*A Laboratory Manual of Analytical Methods of Protein Chemistry, Including Polypeptides*", Vol. **1**, Eds. P. Alexander and R. J. Block, Pergamon Press, London 1960, p. 88.
2. Svensson, H. "*A Laboratory Manual of Analytical Methods in Protein Chemistry, Including Polypeptides*" Vol. **1**, Eds. P. Alexander and R. J. Block, Pergamon Press, London 1960, p. 195.
3. Drake, B. *Arkiv Kemi* **8** (1955) 1.
4. Svensson, H. *Science Tools* **5** (1958) 37.

Eingegangen am 18. April 1962.

* Hersteller: LKB-Produkter, Box 12220, Stockholm 12.

ACTA CHEMICA SCANDINAVICA 16 (1962) 2145–2148

Preparation of Cyclohexane-d_{12} by Deuteration of Benzene-d_6

A. RUPPRECHT and M. S. BERGQVIST*

Research Group for NMR, Division of Physical Chemistry, The Royal Institute of Technology, Stockholm 70, Sweden

Dedicated to Professor *Ole Lamm* on his 60th birthday

A method for the preparation of cyclohexane-d_{12} is described, which utilizes the deuteration of benzene-d_6 in a heterogeneous catalytic process. A mixture of benzene-d_6 damp and excess electrolytically generated deuterium gas is supplied to a furnace containing cobalt on pumice as a catalyst, and the cyclohexane-d_{12} formed is collected in a cold trap. The excess of deuterium is recycled continuously which gives a nearly stoichiometric yield.

Several methods concerning the introduction of deuterium into cyclohexane have been published in the literature. Most of the exchange reactions, as a rule in the liquid state, have given rather low yields. Thus, several attempts to let D_2SO_4 exchange hydrogens with ordinary cyclohexane, were discouraging [1,2]. Experiments performed in a ND_3-milieu and with KND_2 present as a catalyst gave negative results [3,4], as did an investigation using a platinum catalyst in an acetic acid medium [5].

Methods utilizing gaseous reactants and some kind of metal catalyst have in some cases given good results of exchange [6], but evidently the choice of the catalyst and its treatment have been rather critical.

Hydrogenation reactions readily converting benzene to cyclohexane are reported in literature and should be more suitable to produce a highly deuterated cyclohexane. Hall and Emmet [7] obtained a nearly complete conversion of benzene to cyclohexane at 162°C over certain copper-nickel alloys. However, the preparation of the catalyst required very highly purified materials and extreme care with the treatment. These disadvantages did not pertain to a method worked out by Lihl *et al.*[8,9] They prepared a cobalt catalyst which was not easily poisoned, but instead apparently improved with time. Furthermore, the temperature ranges for the catalyst formation and the hydrogenation itself were generously wide.

* Present address: Sandvikens Jernverk, Sandviken, Sweden.

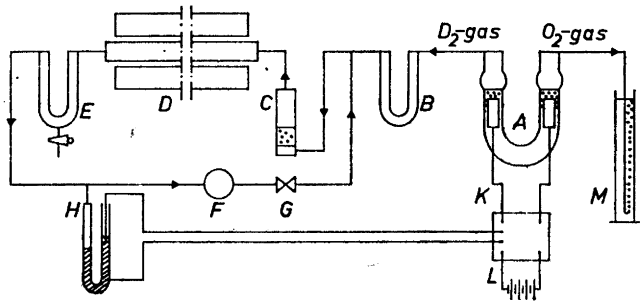

Fig. 1. Apparatus for the deuteration of benzene-d_6 to cyclohexane-d_{12}. A, electrolyzer; B, cold trap; C, bubble flask containing benzene-d_6; D, tube-type furnace; E, cold trap; F, pump; G, valve; H , mercury manometer with a contact point; K, d.c. relay; L, voltage source; M, level regulator.

Accordingly, by letting deuterium gas react with benzene-d_6 on such a catalyst, a deuterated cyclohexane should result. Such experiments are described in this report.

APPARATUS

A schematic diagram of the apparatus is shown in Fig. 1. Deuterium gas prepared in the heavy water electrolyzer (A) is brought through a cold trap (B), for trapping heavy water damp, into a small bubble flask (C) containing benzene-d_6. The gas mixture formed is then supplied to a tube-type furnace (D) containing the catalyst. The reaction product is collected in another cold trap (E), while the excess deuterium is forced back into the system with a pump (F). When the increasing excess of deuterium gas creates a certain over-pressure, contact will be established between the mercury column (H) and the contact point, and the d.c. relay (K) switches off the electrolyzing current supplied by the voltage source (L). The levels of the electrolyte in the two half-cells of the electrolyzer can easily be adjusted by the level regulator (M).

The *electrolyte*, a 4 M solution of KOD, is prepared in a nitrogen box by letting potassium metal react with heavy water which contains 99.80 % D_2O, by weight.

The *electrodes* are made of rolled platinum foils, giving a very large surface area.

The *production capacity* of the electrolyzer, working continuously, is a deuterium gas flux corresponding to 20 ml cyclohexane-d_6 per 24 h.

The *benzene-d_6* used is a product of a method described by Rupprecht [10], and has a deuterium content of 99.50 atom %. In order to obtain a wanted molar ratio of D_2:C_6D_6 of 5:1 in the gas mixture formed, the temperature of the benzene bubble flask is controlled at 32.5°C.

The temperature of the electrically heated *tube-type furnace* is measured by a copper-constantan thermocouple.

The preparation of the *catalyst* follows quite nearly the description given by Lihl [8,9]. 170 g pumice is supplied to a slurry of 60 g $CoCO_3$ in water, 75 ml

formic acid (70 %) is added, and cobaltous formiate is formed with the development of carbon dioxide. After the reaction is finished, the water and excess acid are evaporated by a heat lamp. The cobalt formiate and its carrier are supplied to the furnace (D) and a hydrogen gas flux of 40 l/h is introduced. Reduction at 400°C is continued for a 6-h period and then the temperature is lowered to 180°C, which is the temperature chosen for hydrogenation/deuteration. When the apparatus is not in use, nitrogen gas is blown through in order to impede entrance of air oxygen into the system.

The working point of the *mercury manometer-d.c.-relay circuit* is chosen at about 5 mm Hg above the air pressure. Thus no eventual leakages of the system allow air to enter and spoil the catalyst.

The *pump* used is of a membrane type and in combination with the valve it nicely maintains the deuterium flux adjusted.

EXPERIMENTS

In order to test the effectiveness of the catalyst, ordinary benzene and water were used as starting materials. In a 48-h run, 11.75 g H_2O and 16.97 g benzene were consumed; this corresponds to a molar ratio of $H_2O:C_6H_6 = 3.002$, while the theoretical value is 3. The refractive index of the product was $n_D^{20} = 1.4258$ while a reference specimen of cyclohexane showed a value $n_D^{20} = 1.4256$. However, the weight of the product was only 16.59 g, a yield of 90.8 %. Since the cold trap could be expected to trap 100 % of the product, the loss was ascribed to material still adsorbed on the catalyst.

After this successful test, two runs were made with heavy water and benzene-d_6 (about 5 g in each run) as starting materials. In the first of these runs, newly reduced catalyst was used, while in the other run the catalyst after reduction was swept through with nitrogen for 48 h to remove the light hydrogen adsorbed. The light hydrogen content of the starting materials and of the product was measured with a proton magnetic resonance method [11] and with a refractive index measurement. The latter, when compared with literature data [12], showed the same degree of conversion as in the light hydrogen run. The results from the PMR analysis are shown in Table 1.

Table 1. Analytical data from proton magnetic resonance measurements.

	Atom percentage of deuterium		
Run	C_6D_6	D_2O	C_6D_{12}
1	99.50	99.78	95.37
2	99.50	99.78	97.51

DISCUSSION

The expected atom percentage of deuterium in cyclohexane-d_{12} should be the arithmetical average of the values of benzene-d_6 and heavy water, *i.e.* 99.64 %. This value was not reached in either of the two runs; the second run was the better of the two. The only explanation for this is that rather large amounts of light hydrogen remain strongly adsorbed at the surface of the reduced catalyst and the intended elimination of this light hydrogen by blowing through nitrogen gas was not completely effective. Successive runs with the same catalyst (without further reduction with light hydrogen), however, should render the maximum deuterium content. If only a high deuterium

content product is desired, recirculation of deuterium through the catalyst at 400°C before its use is a more economical way to get rid of the light hydrogen adsorbed.

Acknowledgements. The authors wish to express their gratitude to Professor Ole Lamm, Head of this Division, for excellent working facilities, and to Dr. E. Forslind, Head of the Research Group for NMR, for several interesting discussions.

REFERENCES

1. Setkina, V. N., Kursanov, D. N., Sterlingov, O. D. and Liberman, A. L. *Doklady Akad. Nauk S.S.S.R.* **85** (1952) 1045.
2. Stevenson, D. P., Wagner, C. D., Beech, O. and Otvos, J. W. *J. Am. Chem. Soc.* **74** (1952) 69.
3. Shatenstein, A. I., Dykhno, N. M., Izrailvich, E. A., Vasileva, L. N. and Faivuch, M. *Doklady Akad. Nauk S.S.S.R.* **79** (1951) 479.
4. Shatenstein, A. I., Vasileva, L. N., Dykhno, N. M. and Izrailvich, E. A. *Doklady Akad. Nauk S.S.S.R.* **85** (1952) 381.
5. Bell, J. and Thompson, S. J. *J. Chem. Soc.* **1952** 572.
6. Anderson, J. R. and Kemball, C. *Proc. Roy. Soc. (London)* **A 226** (1954) 472.
7. Hall, W. K. and Emmett, P. H. *J. Phys. Chem.* **62** (1958) 816.
8. Lihl, F., Wagner, H. and Zemsch, P. *Z. Elektrochem.* **56** (1952) 613.
9. Lihl, F. and Zemsch, P. *Z. Elektrochem.* **56** (1952) 979.
10. Rupprecht, A. *Acta Chem. Scand.* **16** (1962) 2189.
11. The NMR–EPR Staff of Varian Associates, *NMR and EPR Spectroscopy*, Pergamon Press, Oxford 1960, p. 112.
12. Dixon, J. A. and Schneider, R. W. *J. Am. Chem. Soc.* **76** (1954) 2197.

Received April 16, 1962.

ACTA CHEMICA SCANDINAVICA 16 (1962) 2149–2161

Analysis of Nuclear Magnetic Resonance Wide Line Spectra

S. E. SVANSON and E. FORSLIND

Research Group for NMR, Division of Physical Chemistry, Royal Institute of Technology, Stockholm 70, Sweden

Dedicated to Professor *Ole Lamm* on his 60th birthday

It is attempted, by the use of a formal mathematical analysis of NMR wide line spectra, to throw some light on the well-known difficulties associated with the experimental and theoretical determination of line moments.

The analysis is based on the observation that the squared fundamental eigenfunction of the harmonic oscillator represents a Gaussian distribution, a correction to which may be obtained by the addition of the subsequent squared eigenfunctions in a series expansion of expected rapid convergence. This expectation is confirmed by the present investigation and it is shown that, in general, a spectral line may be optimally approximated with a maximum of 5 terms in the expansion. It is further shown that the method may be successfully applied to the analysis of complex spectra when the overlap between the spectral components satisfies certain conditions and that the accuracy of the analysis is satisfactory. Several applications and conclusions are treated in the text.

The theoretical treatment of NMR wide line spectra for crystalline systems represents, at the present stage of development, a formidable mathematical task, permitting only rough approximations to the solution of the problem. These difficulties have led to certain limitations in the practical application of the nuclear magnetic methods to the study of solid systems. On the other hand, the magnetic resonance methods are in several respects indispensable for the detailed study of coupling mechanisms and molecular motions in hydrogels and hydrogen bonded high polymers and other solids which makes it very desirable to improve and extend the now available methods for the analysis of wide line spectra [1].

The above-mentioned mathematical difficulties derive from the coupling effects between the individual nuclear moments which occur in crystalline spin systems. While an ensemble of uncoupled spins may be described by means of a statistical operator matrix of the order $(2I + 1)\ (2I + 1)$ where I is the

spin quantum number, the coupled spin system compels one to treat the whole observed system of N nuclear spins as *one* element in a statistical ensemble, the description of which leads to an operator of the order $(2I + 1)^N (2I + 1)^N$. The coupling between the nuclei occurs in several ways; one dominant term in the spin energy function may be described as a classical dipole-dipole coupling between the magnetic moments of the nuclei, and is assumed in the following discussion to elucidate the analytical problem.

The dipole coupling may be regarded as a perturbation of the Zeeman effect and the individual contribution to the coupling energy from two interacting nuclei may be split in six components characterised by their varying influence on the magnetic quantum number of the energy function.

If we confine the calculation to first order perturbations, only two components are of interest, namely those which lead to unchanged total magnetic quantum number. One of these terms represents simultaneous re-orientations of anti-parallel spins. It is accordingly only operative when the interacting spins have commensurable frequencies of rotation, which usually implies like spins in fields of comparable magnitude. A strong quadruple coupling in a distorted lattice, leads for instance to the inhibition of this contribution to the dipole coupling, due to the relative changes in rotational frequency of the nuclei affected by the quadrupole fields. The remaining terms of the dipole coupling operator lead, in addition, to secondary and tertiary resonances which, as a rule, are associated with intensities too low to permit direct observation, but which may contribute significantly to the integrated intensity if included in the energy operator. We shall presently return to this question.

The coupling between the nuclei leads to an energy exchange and a relaxation mechanism the time dependence of which may be described by a function $G(t)$. The normalized Fourier transform

$$f(\omega) = \varkappa \int_0^\infty G(t) \cos\omega t \, dt$$

characterizes the shape of the absorption band as a function of the angular velocity $\omega = 2\pi\nu$ of the radio-frequency field. The shape of the absorption band may, on the other hand, be connected with the nth moment, M_n, defined by the equation

$$M_n = \int_{-\infty}^{+\infty} f(\omega)(\omega - \omega_0)^n d\omega$$

where M_0 represents the area, A, under the absorption curve proportional to the number of nuclei which contribute to the resonance, M_1 the static moment of the area, with respect to the reference point ω_0 etc. If $f(\omega)$ is symmetrical with respect to ω_0 all odd moments disappear.

The moments M_n may, as has been shown by Van Vleck [2], be calculated from primary data without a knowledge of the eigenvalues of the energy operator by means of the expansion of $G(t)/\cos\omega_0 t$ in a power series of t. The coefficients of the series may indeed be determined independently of the choice of base functions in the matrix elements of the corresponding operators. If,

accordingly, a representation is chosen in which the individual spin quantum numbers of the nuclei characterize the operators for the coupling energy and the resonance magnetisation, it is possible to circumvent the at present insoluble problem of finding the eigenfunctions and eigenvalues for the energy operator of the coupled spin system.

One of the weaknesses of the method depends on the circumstance that all coupling effects which commute with the transversal angular momentum may modify the shape of the absorption band without influencing the second moment which, accordingly, cannot be uniquely correlated with the coupling and relaxation mechanisms. In order to evaluate the deviation from the signal amplitude distribution, supposed Gaussian, of the uncoupled system, it is desirable to calculate the fourth moment and the ratio M_4/M_2^2 which takes the value 3 for a pure Gaussian distribution. This, however, emphasizes a fundamental difficulty associated with the experimental determination of moments, namely, that the essential contributions to the higher moments derive from the wings of the absorption band which usually are unobservable due to the general background of noise. The effect is obviously of extreme importance in the practical application of the method of moments to the study of molecular re-orientations and chain motion in solids where, as a rule, the observable part of the second moment varies, while the total second moment remains invariant with respect to the lattice motions.

For a comparison between the theoretical calculated moments and the experimental ones, it is desirable to find a satisfactory method for the indirect determination of the unobservable wings of the spectral band, while leaving out the terms in the energy operator which are responsible for the satellites in the theoretical calculation of moments.

We believe that it is possible to throw some light on these problems by the expansion of the experimental resonance line in a rapidly converging series of suitable functions for the description of the line shape and of the deviation from the Gaussian distribution. The adaptation to the experimental spectral band is performed in the frequency range where the signal to noise ratio is favourable and the moments of the spectral line are then calculated by the integration of the analytical expression so obtained. In the present paper our investigation is confined to the methodological aspect of the problem and no attempt has been made to connect the results with the current theories of the line width. The possibility to characterize the line shape with the aid of the expansion parameters as a function of the composition and the physical state of the system under investigation, is of great practical use in wide line spectrography.

As suitable functions for the series expansion, we have chosen the eigenfunctions of the harmonic oscillator, the squared fundamental of which represents a Gaussian distribution. The following expansions then have been used for the description of a single absorption band:

$$\varphi = \sum_k a_k \Phi_k^2 \text{ and } \varphi = \Sigma a_k \Phi_k$$

where

$$\Phi_k = H_k(\sqrt{\alpha}x)\ \exp(-\tfrac{1}{2}\alpha x^2)$$

$H_k(\sqrt{\alpha}x)$ are Hermite polynomials, x representing the magnetic field intensity or the corresponding frequency. The function Φ_k is an even function for even k, and odd for odd k. The first series can therefore be applied to even functions only, whereas the second one can be used for asymmetrical functions. Although the electronic computer programme has been worked out for both cases, the application of the method will be illuminated by a few examples of even functions only.

Proton resonance spectra of an organic solid containing water, as a rule, consist of a broad band superimposed by a narrow band. The derivatives of both bands are centrosymmetrical with respect to a common centre of inversion. The broad band usually derives from:

(*a*) hydrogens attached to a carbon chain and which only slowly take part in exchange processes,

(*b*) hydrogens attached to nitrogen or oxygen included as heteroatoms in the carbon chain and which can be exchanged with relative ease for deuterium *via* an adjacent liquid or gaseous phase,

(*c*) hydrogen atoms attached to oxygen belonging to water, which is either included in the crystalline lattice or, otherwise, appears as an adsorbed phase.

The narrow band usually derives from hydrogen in water with approximately normal coordination and proton exchange frequency, so-called "free" water, although the line width may display great variations with the degree of freedom. In reality, the width of the narrow band is determined by so many boundary conditions that the term "free water" is rather inadequate.

A partial exchange of hydrogen against deuterium modifies the shape of the bands and their intensities and the detailed study of these changes makes possible, in principle, an identification of the contributions from the different proton containing groups. In all the cases where the individual line shapes are unknown, spectra of this kind, therefore, have to be expanded as the superposition of two distinct series. The expansion takes, in this case, the following form:

$$\varphi = \sum_k a_{k1}\Phi_{k1}^2 + \sum_k a_{k2}\Phi_{k2}^2$$

$$\Phi_{k1} = H_k(\sqrt{\alpha_1}x)\ \exp(-\tfrac{1}{2}\alpha_1 x^2)$$

$$\Phi_{k2} = H_k(\sqrt{\alpha_2}x)\ \exp(-\tfrac{1}{2}\alpha_2 x^2)$$

Both α_1 and α_2 are estimated from experimental data and chosen for the best fit, each series representing a complete description of an even function. When the difference in width between the two bands is great, the calculation can easily be carried out with a finite number of terms in each band, the two series being fitted to each part of the experimental band, one in comparative independence of the other. When, on the other hand, the overlap between the two bands becomes great, the conditions for the unique determination of the two series are insufficient, especially in the case when a greater number of terms are involved. With increasing overlap between the two bands, the calculation must accordingly be carried out with a decreasing number of coefficients. The applicability of the method has been tested in some simple cases corresponding to these conditions.

DESCRIPTION OF THE PROGRAMME

The programme has been worked out for the Swedish electronic computer Facit at the Swedish Board for Computing Machinery (MNA) in Stockholm, where it is available under designation 41095.

Taking the inversion centre of the symmetric absorption line derivative as origin, a sufficient number of equidistant amplitudes are measured and tabulated. The two branches of the curve are treated in the same way, and for both of them abscisses (x_i), as well as ordinates (y_i) are expressed as positive numbers

$$x_i = hi \qquad \text{for } i = 0,\ 1,\ 2, \ldots\ldots,\ q$$
$$x_i = hq + hp(i-q) \qquad \text{for } i = q+1,\ q+2, \ldots\ldots,\ n$$

where h is the step length and q denotes the point from which the step length is increased to ph, p being an integer.

From the observed derivative (x_i,y_i) the absorption band, $F(x)$ is computed by numerical integration.

Putting $x = hj$ we have

$$F(hj) = h\int_0^\infty y\mathrm{d}j - h\int_0^j y\mathrm{d}j$$

and $$\int_0^j y\mathrm{d}j = z_i = y_1 + y_2 + \ldots + y_{i-1} + \tfrac{1}{2}\, y_i = z_{i-1} + \tfrac{1}{2}\,(y_{i-1} + y_i)$$
$$\text{for } i = 1,\ 2,\ 3,\ \ldots,\ q$$

and $$z_i = y_1 + y_2 \ldots + y_{q-1} + \tfrac{1}{2}\, y_q + \tfrac{1}{2} p y_q + p y_{q+1} + \ldots + p y_{i-1} + \tfrac{1}{2}\, p y_i =$$
$$= z_{i-1} + \tfrac{1}{2}\ p\ (y_{i-1} + y_i) \qquad \text{for } i = q+1,\ q+2, \ldots,\ n.$$

When both parts of the curve are registered, a zero-line correction can be applied. In making this correction, a quantity ε is subtracted from the y_i-values of the first branch of the curve and added to the y_i-values of the second branch. The z-values are, in other words, substituted by G-values defined as follows for the branch I

$$G_i = z_i - \varepsilon i \qquad \text{for } i = 0,\ 1,\ 2,\ \ldots,\ q.$$
$$G_i = z_i - \varepsilon\{q + p\,(i-q)\} \qquad \text{for } i = q+1,\ q+2, \ldots, n$$

and for branch II
$$G_i' = z_i' + \varepsilon i \qquad \text{for } i = 0,\ 1,\ 2, \ldots, q.$$
$$G_i' = z_i' + \varepsilon\{q + p(i-q)\} \qquad \text{for } i = q+1,\ q+2, \ldots, n.$$

ε is determined by the conditions $G_n = G_n'$ and

$$\varepsilon = \frac{z_n - z_n'}{2\{q + p(n-q)\}}$$

The integral $\int_0^\infty y\mathrm{d}j$ is approximated by z_n or G_n, respectively, and the

absorption line is approximated by

$$\varphi_i = \frac{G_n - G_i}{G_n}$$

where $F(hj) = hG_n\varphi_i$.

The area under the φ-function is computed by numerical integration

$$\int_0^\infty \varphi_i \mathrm{d}j = B_0 = \tfrac{1}{2}\varphi_0 + \varphi_1 + \varphi_2 + \ldots + \varphi_{q-1} + \tfrac{1}{2}\varphi_q + \tfrac{1}{2}p\varphi_q + p\varphi_{q+1} + \ldots + p\varphi_n$$

In the following, this sum is abbreviated as

$$B_0 = \sum_{i=0}^{n}{}' t_i\varphi_i$$

the prime indicating the preceding convention to be observed.

The area under the absorption line, computed by direct numerical integration will then be

$$A_0 = h^2G_nB_0$$

The serial expansion takes the form

$$\varphi_i = \sum_{kl} a_{kl}\Phi_{kl}^2$$

where $\Phi_{kl} = H_k\ (\sqrt{\alpha_l}x)\ \exp(-\tfrac{1}{2}\alpha_l x^2)$

and $H_k(\sqrt{\alpha_l}x)$ are the Hermite polynomials.

The programme allows computation of one-, two- or three-component lines (summation over l from 1 to max. 3). The number of terms in each component can be chosen from 1 to max. 7 (summation over k for 0 to max. 6).

For ease of calculation the parameter α_l is transformed to a shape parameter m_l

$$\alpha_l = 1/2h^2m_l^2$$
$$\alpha_l x^2 = j^2/2m_l^2$$

When the absorption line is dominated by the Gaussian, the absciss of the maximum point of the registered derivative is $x_m = hm_l$. In the spectra considered here, the values of m_l have been roughly estimated from the abscisses of the derivative maxima.

The overdetermined equation system takes the form

$$\varphi_i = \sum_{\nu=1}^{\nu_m} x_\nu f_\nu(i) \qquad \text{where } i = 0, 1, 2, \ldots, n \text{ and } n < \nu_m$$

Introducing

$$\begin{aligned} \nu &= k + 1 && \text{for } l = 1 \\ \nu &= k_m + 1 + k + 1 && \text{for } l = 2 \\ \nu &= 2(k_m + 1) + k + 1 && \text{for } l = 3 \end{aligned}$$

where $k_m + 1$ is the number of expansion coefficients in each component line, we can write $a_{kl} = x_\nu \quad \Phi_{kl}^2 = f_\nu$

This system is solved to make the total square deviation attain a minimum and to obtain a uniform adaptation over the whole range of the line.

$$M = \tfrac{1}{2}(\varphi_0 - \varphi_0^b)^2 + (\varphi_1 - \varphi_1^b)^2 + \ldots + (\varphi_{q-1} - \varphi_{q-1}^b)^2 + \tfrac{1}{2}(\varphi_q - \varphi_q^b)^2 + \tfrac{1}{2} r(\varphi_q - \varphi_q^b)^2 +$$

$$+ r(\varphi_{q+1} - \varphi_{q+1}^b)^2 + \ldots + r(\varphi_n - \varphi_n^b)^2 = \sum_{i=0}^{n}{}' t_i \{\varphi_i - \sum_\nu x_\nu f_\nu(i)\}^2$$

where φ_i^b is computed from $f_\nu(i)$ and the resolved values of x_ν.

The condition of minimum

$$\frac{\partial M}{\partial x_\eta} = -2 \sum_{i=0}^{n}{}' t_i \{\varphi_i - \sum x_\nu f_\nu(i)\} f_\eta(i) = 0$$

gives the equation system

$$\sum_\nu x_\nu \sum_{i=0}^{n}{}' t_i f_\nu(i) f_\eta(i) = \sum_{i=0}^{n}{}' t_i \varphi_i f_\eta(i)$$

from which the values of x_ν are determined.

Putting $r = p$ the sums $\sum_{i=0}^{n}{}' t_i f_\nu(i) f_\eta(i)$ and $\sum_{i=0}^{n}{}' t_i \varphi_i f_\eta(i)$ approximate to the integrals $\int_0^\infty f_\nu f_\eta \mathrm{d}j$ and $\int_0^\infty \varphi_i f_\eta \mathrm{d}j$.

φ_i^b and $\varphi_i - \varphi_i^b$ are computed and, if desired, printed.

The integral $\int_0^\infty f_\nu f_\eta \mathrm{d}j$ may, in the case of $r = p$, be calculated analytically, leading to a considerable reduction of the machine time required for the computation.

Finally, the standard deviation is computed

$$s = \sqrt{\frac{M}{q + r(n-q)}}$$

assuming the number of coefficients to be small compared to n.

The coefficients a_{kl} are transformed to a series

$$b_{kl} = a_{kl} \frac{\int_0^\infty \Phi_{kl}^2 \mathrm{d}j}{B_l} \qquad \text{where} \qquad B_l = \sum_k a_{kl} \int_0^\infty \Phi_{kl}^2 \mathrm{d}j$$

$$\text{and} \quad \int_0^\infty \varphi_i \mathrm{d}j = B = \sum_l B_l \sum_k b_{kl}$$

$$\sum_k b_{kl} = 1; \qquad \sum_l B_l = B$$

Table 1. Expansion parameters for the ^1H-resonance in aqueous solutions of $MnSO_4$.

(1)	(2) b_0	b_1	b_2	b_3	b_4	b_5	b_6	(3)	(4)	(5)
0.01	0.900	−0.040	0.092	0.020	0.023	0.000	0.005	20.18	20.02	1.9
0.1	0.810	−0.025	0.133	0.022	0.045	0.000	0.015	20.90	20.88	4.2
0.5	0.830	−0.010	0.120	0.015	0.035	0.000	0.008	20.68	20.56	14.5
2.0	0.820	−0.010	0.125	0.020	0.035	0.000	0.010	20.44	20.37	51.0

(1) Molarity for the aqueous solutions of $MnSO_4$
(2) Expansion coefficients.
(3) The area under the absorption line (A)
(4) The area under the absorption line computed by direct numerical integration (A_0)
(5) Line width parameter m giving the best degree of adaptation.

The area under the absorption line computed from the analytical expression is

$$A = h^2 \, G_n \, B$$

The quantities G_n, B_0, B, B_l/B, b_{kl} and s are given as the result of the evaluation. B_l/B denotes the fraction of the contribution from line number l to the area under the absorption line, and b_{kl} denotes the fraction of the contribution from function number k to the area under the absorption line of line number l.

APPLICATIONS TO EXPERIMENTAL DATA

The ^1H resonance of aqueous solutions of $MnSO_4$ in the concentration range 0.01 to 2.0 M has been evaluated, and the results used to demonstrate the general properties of the series expansion. The line width of these solutions is determined by the presence of the paramagnetic manganese ions.

The coefficients of the expansion, the standard deviation and the area under the absorption line are shown in Fig. 1 as functions of the line width parameter m for the aqueous solution of 0.5 M $MnSO_4$. The remaining results, under conditions of closest fit, are summarized in Table 1. The coefficients turn out to be well reproducible for the two branches of the spectra and in the comparison between spectra recorded on different occasions.

The coefficients of the Gaussian dominate and the magnitude of the coefficients decreases rapidly with rising order. The degree of approximation to the experimental curve is characterized by the standard deviations. Plotted as a function of the line width parameter m, s generally shows a marked minimum. The minimum, however, is, as a rule, sufficiently flat to make the determination of m uncertain to about $\pm$ 2 to $\pm$ 5 %. The magnitude of the standard deviation, as well as the location of its minimum point, show a somewhat diminished reproducibility as compared to that of the coefficients.

When the expansion is extended to seven terms the two last terms are in all cases negligible at closest fit. An expansion to five terms accordingly gives

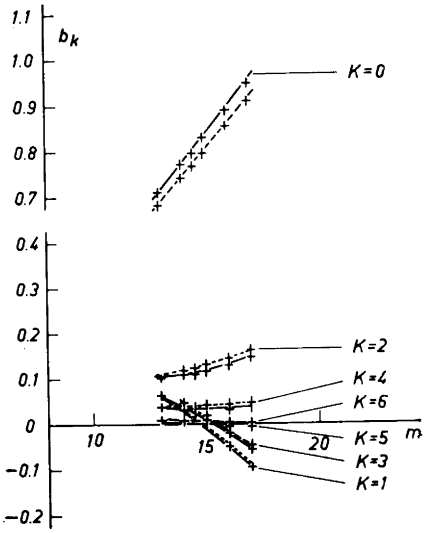

Fig. 1 a. The coefficients (b_k) of the ^{1}H-resonance of aqueous solution of 0.5 M $MnSO_4$.
Part I of the curve ————
Part II of the curve - - - - - -

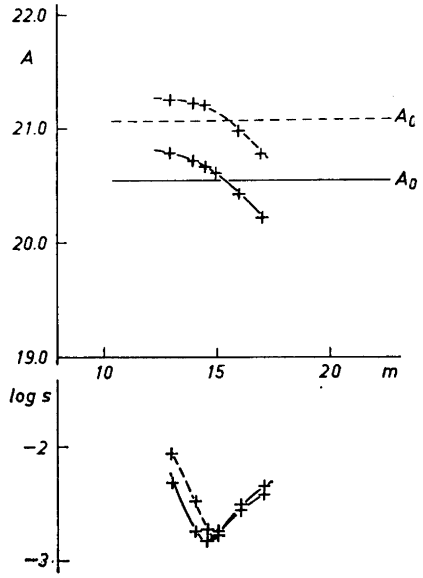

Fig. 1 b. The area under the absorption line (A) and the standard deviation (s) of the ^{1}H-resonance of aqueous solution of 0.5 M $MnSO_4$.
Part I of the curve ————
Part II of the curve - - - - - - -

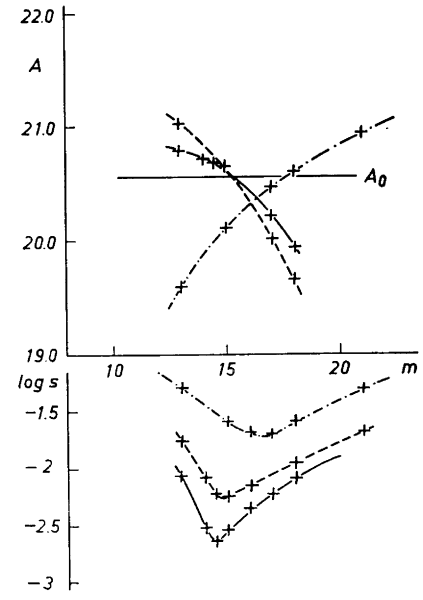

Fig. 1 c. The area under the absorption line (A) and the standard deviation (s) of the ^{1}H-resonance of aqueous solution of 0.5 M $MnSO_4$. Part I of the curve
Evaluation using 7 coefficients ————
Evaluation using 5 coefficients - - - - - - -
Evaluation using 3 coefficients —·—·—

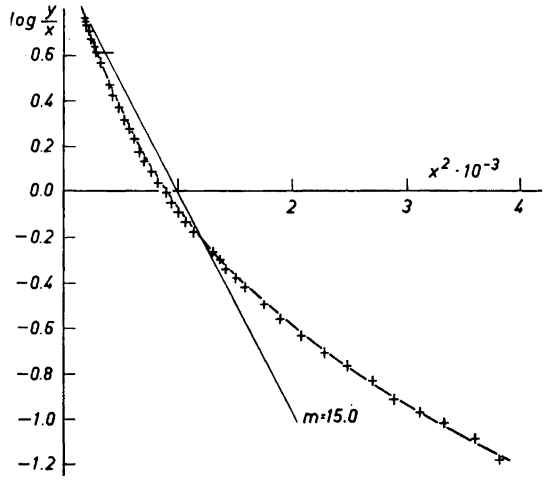

Fig. 2 a. The ^{1}H-resonance of aqueous solution of 0.5 M $MnSO_4$.

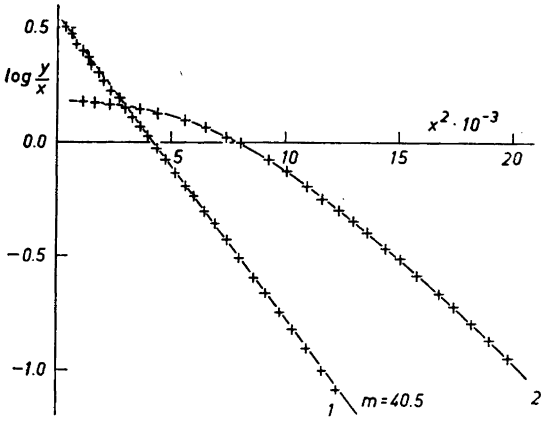

Fig. 2 b. 1) The ^{1}H-resonance of $(NH_4)_2SO_4$ powder. 2) The ^{1}H-resonance of NH_4Cl powder. In this diagram the Gaussian gives a straight line.

a satisfactory result and stationary values of the coefficients. The minima of the standard deviations coincide in the two cases. Using only three terms, the values of the expansion coefficients show considerable variation while the minimum of the root mean square deviation is displaced towards a somewhat higher m value.

The area A of the absorption band computed from the analytical functions is influenced by the number of terms in the expansion. As shown in Fig. 1c, the area becomes less dependent on m with an increasing number of terms. The uncertainty in the determination of the best fit thus introduces an error

less than $\pm$ 1 % of the A value at 5 or 7 terms. The area A_0 of the absorption band has also been determined by direct numerical integration. Fig. 1b shows that the difference between the two determinations of the A values is indeed small. The A values computed from the analytical functions at closest fit, usually exceed the corresponding A_0 values by 1 to 2 %, which shows that for spectra of this type the area can be computed through direct numerical integration without serious disturbance from cut off effects. A values calculated for the different $MnSO_4$ solutions and corrected for the varying ^1H concentration, show a scattering of $\pm$ 3 %.The A values computed from the analytical functions at closest fit show the same relative scattering as the A_0 values.

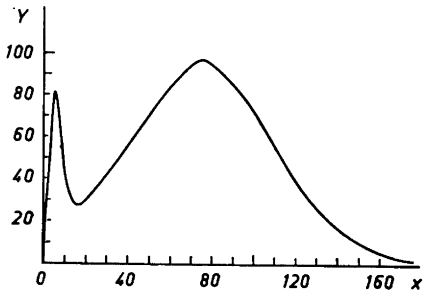

Fig. 3 a. Spectral line composed of the ^1H-resonances of an aqueous solution of 0.04 M $MnSO_4$ and an NH_4Cl powder.

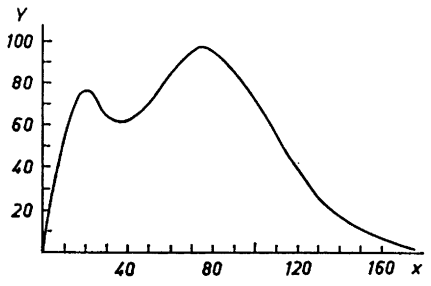

Fig. 3 b. Spectral line composed of the ^1H-resonances of an aqueous solution of 0.5 M $MnSO_4$ and an NH_4Cl powder.

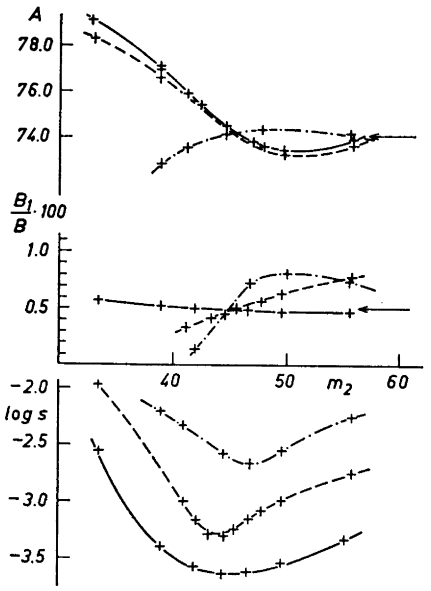

Fig. 4. The area under the absorption line (A), the fraction of the contribution from the narrow line to the area under the absorption line (B_1/B) and the standard deviation (s) for the spectrum in Fig. 3 a. Evaluation using 7 coefficients ———— Evaluation using 5 coefficients - - - - - - - Evaluation using 3 coefficients —·—·— The correct values are shown by the arrows.

In spite of the dominance of the Gaussian, the deviation from the Gaussian distribution is quite pronounced in these spectra. In Fig. 2 log y/x is plotted as a function of x^2 for a spectrum of 0.5 M $MnSO_4$ solution. In such a diagram a Gaussian is represented by a straight line. In the actual case the line is curved making it impossible to determine the m value from the inclination of the line. The adaptation to a Lorentz curve would, in this case, be considerably better but, even so, the approximation to a simple line shape is poor.

Spectra of some other substances have also been evaluated. Thus the absorption line of ^{19}F in teflon and of ^1H in the polysaccharide gum-arabic shows expansion coefficients which agree rather well with those for the spectra of $MnSO_4$ in aqueous solution. On the other hand, the spectra of NH_4Cl and $(NH_4)_2SO_4$ give rise to quite different expansion coefficients. In the spectrum of NH_4Cl, the Gaussian dominates together with the first harmonic, while for the spectrum of $(NH_4)_2SO_4$ the agreement with the Gaussian alone seems to be complete. These observations are detailed in Fig. 2b. The spectrum of NH_4Cl gives rise to a non-linear relationship, while the curve characteristic of $(NH_4)_2SO_4$ very accurately reproduces a straight line.

Some spectra artificially composed by the addition of two known components, consisting of two separately registered spectral bands, have been similarly studied to test the resolving power of the numerical analysis. The ^1H line of NH_4Cl has been used, while the ^1H lines of several aqueous solutions of $MnSO_4$ have been taken to represent the various narrow components. Figs. 3a and 3b show two such artificial spectra which have been subjected to a detailed analysis. The narrow bands of these spectra are somewhat overmodulated.

The results of these calculations are summarized in Fig. 4. In the part of the spectrum where the narrow band is dominating, the adaptation of the analytical form to the experimental curve is essentially determined by the value of m_1, while in the part of the spectrum where the broad band dominates, the form of the analytical expression is principally determined by m_2. The standard deviations for these two parts of the spectrum coincide rather well with the deviations of the spectral lines determined separately, and the m_1 and m_2 values corresponding to the closest fit can be accurately determined from the complex spectrum. When the m values are known, the remaining parameters determining the shape of the spectrum are easily found.

The use of 5 or 7 terms in the expansion for each band produces a good agreement with the results from the spectral bands registered separately. On the other hand, the use of 3 terms only, gives rise to considerable deviations, especially with regard to the ratio B_1/B leading, in this case, to an error of about 15 %. Similar difficulties are, however, also encountered in the analysis of the spectrum shown in Fig. 3b, where the overlap between the bands is considerable. Expansion to 7 terms in each band leads, as expected, to erroneous results, while an expansion to 5 or 3 terms, on the other hand, permits a separation of the band components at a corresponding loss of accuracy which is especially significant in the determination of B_1/B.

The calculations carried out show that the method can be safely applied when $m_2 > 8\, m_1$. As a rule, this condition is fulfilled in a great many practical cases. It is, however, a matter of importance to be able to extend the use of

the method to spectra with large overlap, and some simple modifications of the method of calculation seem to make such an extension possible.

Acknowledgements. Thanks are due to Mrs. M. Andersson of the Swedish Board for Computing Machinery, who coded the programme. The free machine time granted by the *Swedish Board for Computing Machinery* and the financial support provided by the *Swedish Natural Science Research Council* and the *State Council of Technical Research* is gratefully acknowledged. The cost of the NMR spectrograph has been defrayed by a generous grant from the *Knut and Alice Wallenberg Foundation.*

REFERENCES

1. Abragam, A. *The Principles of Nuclear Magnetism*, Oxford 1961.
2. Van Vleck, I. H. *The Theory of Electric and Magnetic Susceptibilities*, Oxford 1932.

Received May 2, 1962.

ACTA CHEMICA SCANDINAVICA 16 (1962) 2162–2176

Neuartige Berechnungsmethoden und Forderungen an scherinterferometrische Präzisionsbestimmungen von Diffusionskoeffizienten

OLOF BRYNGDAHL und STIG LJUNGGREN

Institute für optische Forschung und physikalische Chemie der Kgl. Technischen Hochschule, Stockholm 70, Schweden

Herrn Professor Dr. *Ole Lamm* zum 60. Geburtstag gewidmet

Im Anschluss an die Scherinterferometermethode wird ein neues Evaluierungsverfahren zur Bestimmung des Diffusionskoeffizienten entwickelt. Im Rahmen eines Überblickes über die verschiedenen Möglichkeiten zur Bestimmung des konzentrationsabhängigen Diffusionskoeffizienten und der Polydispersität werden neue Berechnungsmethoden ausführlich diskutiert. Es wird eine Evaluierungsart der Streifenmuster, die bei der Scherinterferometer- und Schlierenmethode entstehen, beschrieben, die es ermöglicht den ganzen Konzentrationsgradienten zu erfassen. Für Präzisionsbestimmungen werden Vorschläge und Forderungen an die experimentellen Anordnungen gegeben.

In den letzten Jahren haben optische Methoden auf dem Gebiete der Diffusionsmessungen immer grösser werdendes Interesse auf sich gelenkt. Bedeutende Beiträge für die Weiterentwicklung mit Hilfe optischer Methoden gab Lamm [1] durch seine jetzt klassisch gewordenen Skalen- und Schlierenmethoden. Diese haben sowohl Impulse als auch Inspiration für neue Methodenvorschläge auf diesem Gebiete gegeben. So hat sich z.B. eine neue Interferometermethode für Präzisionsbestimmungen der Diffusionskoeffizienten herauskristallisiert [2–4]. Diese Arbeit geht darauf hinaus, Klarheit in Bezug auf experimentelle Unvollkommenheiten zu schaffen und die früheren Evaluierungsverfahren zu vervollständigen, ebenso Berechnungen der konzentrationsabhängigen Diffusionskoeffizienten zu empfehlen.

I. OPTISCHE METHODE *

Die Scherinterferometermethode beruht auf der Anwendung von Doppelbrechungsinterferenzen; sie ist für geringe Konzentrationsdifferenzen sehr empfindlich und gibt eine Abbildung von der gesamten Diffusionssäule. Der optische Aufbau ist bereits in früheren Artikeln [2-6] beschrieben worden.

Durch das Einfügen einer doppelbrechenden Doppelkristallplatte (Savartsche Platte) in das parallele Licht nach der Küvette bei der optischen Anordnung erscheint eine Verdopplung der Wellenfront. Wenn gekreuzte Polarisatoren, deren Polarisationsrichtung unter 45° im Verhältnisse zu der Hauptebene der Kristallplatte steht, zu beiden Seiten der Savartschen Platte eingesetzt werden, werden Lichtintensitätsminima in den Ortspunkten, wo die optische Wegdifferenz zwischen den beiden Wellenfronten eine gerade Ganzzahl von Wellenlängen ist, hervorgerufen. Die Interferenzstreifen drücken bestimmte Werte der Ableitung $\partial n/\partial x$ aus. Eigentlich stellen die Messungen den Differenzenquotienten $\Delta n/\Delta x$ dar. Die Korrektionen der Ableitung kann man leicht beim Übergange vom Differenzenquotienten zum Differentialquotienten berechnen, wie es im Nachfolgenden gezeigt wird.

II. REGISTRIERUNG UND BERECHNUNG DES DIFFUSIONSKOEFFIZIENTEN

Um den Diffusionskoeffizienten bestimmen zu können, wird eine Anzahl photographischer Aufnahmen des Interferenzmusters zu bestimmten Zeitpunkten während des Diffusionsverlaufes vorgenommen. Man verfolgt ein bestimmtes Interferenzstreifenpaar, welches einen konstanten Wert des Ausdruckes $\Delta n/\Delta x$ in Bezug auf die Zeit darstellt. Aus diesen Messungen kann man bei symmetrischen Diffusionskurven ein Diagramm über $(2x)^2$ als Funktion von t erhalten [4]; $2x$ stellt den Abstand zwischen den Interferenzstreifen und t die dazugehörende Zeit dar. Den Diffusionskoeffizienten erhält man nun durch

* Hinweis: Kürzlich ist ein Artikel "Scherinterferometrische Präzisionsmethoden — für Gradientenuntersuchungen besonders geeignet" in *Monatsh. Chem.* **93** (1962) 984 von O. Bryngdahl herausgegeben worden, der die vielseitige Möglichkeit der Methodenanwendung auf dem Gebiete der Diffusion, Elektrophorese, Sedimentation, Wärmeleitung und Wärmeströmung behandelt.

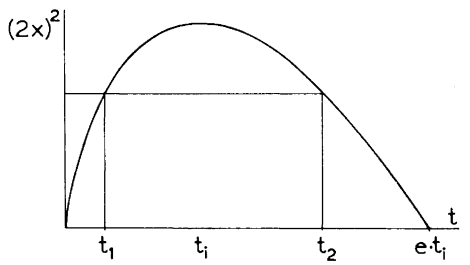

Fig. 1. Quadrat des Streifenabstandes als Funktion der Zeit.

die von Lamm vorgeschlagene Art von Berechnung, indem ein Wert von $(2x)^2$ und die dazugehörenden Zeitpunkte t_1 und t_2 in nachfolgende Gleichung

$$D = \frac{(2x)^2(1/t_1 - 1/t_2)}{8 \ln t_2/t_1} \tag{1}$$

eingesetzt werden.

III. NEUES EVALUIERUNGSVERFAHREN FÜR EXPERIMENTE NACH DER SCHERINTERFEROMETER- UND SCHLIERENMETHODE

Nachstehend wird ein Evaluierungsverfahren schematisiert, welches zu einem linearen Zusammenhange führt, wobei der Diffusionskoeffizient aus einem Neigungskoeffizienten erhalten wird.

Die Gleichung für eindimensionale Diffusion lautet:

$$\frac{\partial c}{\partial t} = \frac{\partial}{\partial x}\left(D \frac{\partial c}{\partial x}\right) \tag{2}$$

wobei c die Konzentration der Flüssigkeit bezeichnet. Wenn der Diffusionskoeffizient D konzentrationsunabhängig ist, kann man die Lösung der Diffusionsgleichung (2) in folgender Form zum Ausdruck bringen:

$$\frac{\partial n}{\partial x} = \frac{\Delta n^\circ}{2\sqrt{\pi D t'}} \exp(-x^2/4Dt') \tag{3}$$

n ist hier der Brechungsindex der Flüssigkeit, Δn° ist der Brechzahlunterschied zwischen den Ausgangskonzentrationen, d.h. zwischen unterer und oberer Lösungsschicht in der Diffusionszelle.

Bei differentiellen Diffusionsexperimenten kann man allgemein ohne Einschränkung Formel (3) benutzen. Man sollte allerdings für t' in Formel (3) folgende Berücksichtigung treffen — für t' setzt man $t + \Delta t$ ein; dabei ist t die gemessene Zeit und Δt stellt die Nullzeitkorrektion dar. So erhält man:

$$\frac{\partial n}{\partial x} = \frac{\Delta n^\circ}{2\sqrt{\pi D(t + \Delta t)}} \exp(-x^2/4D(t + \Delta t)) \tag{4}$$

Nach Kapitel II entspricht ein gewisses Interferenzstreifenpaar einem bestimmten konstanten Werte von $\Delta n/\Delta x$:

$$\Delta n/\Delta x = a \tag{5}$$

$\Delta x = b$, gleichbedeutend der Scherstrecke.

Es muss uns nun die Beziehung zwischen $\Delta n/\Delta x$ und $\partial n/\partial x$ bekannt sein; diese wird durch die Taylorsche Reihenformel am einfachsten erhalten:

$$\left(\frac{\Delta n}{\Delta x}\right)_{\Delta x = b} = \frac{\partial n}{\partial x}\left\{1 + \frac{1}{2^2 \cdot 3!} \cdot \frac{b^2}{2Dt} \cdot \frac{x^2 - 2Dt}{2Dt} + \frac{1}{2^4 \cdot 5!} \cdot \frac{b^4}{4D^2t^2} \cdot \frac{x^4 - 12x^2Dt + 12D^2t^2}{4D^2t^2} + \ldots\right\} \tag{6}$$

Setzen wir nun Gleichung (4) und (6) in Formel (5) ein, so erhalten wir in der Approximation erster Ordnung:

$$a \approx \frac{\Delta n^\circ}{2\sqrt{\pi D(t+\Delta t)}} \cdot \left(1 + \frac{b^2}{48Dt} \cdot \frac{x^2-2Dt}{2Dt}\right) \cdot \exp(-x^2/4D(t+\Delta t)) \quad (7)$$

oder

$$\exp(x^2/4D(t+\Delta t)) = \frac{\Delta n^\circ}{2a\sqrt{\pi D(t+\Delta t)}} \left(1 + \frac{b^2}{48Dt} \frac{x^2-2Dt}{2Dt}\right) \quad (8)$$

Die Logarithmierung beider Gleichungsseiten in (8) ergibt:

$$\frac{(2x)^2}{t+\Delta t} = C - 8D \ln \frac{t+\Delta t}{t_o} + \frac{b^2}{3t} \cdot \frac{x^2-2Dt}{2Dt} \quad (9)$$

C ist dabei eine Konstante ($C = 8D(\ln t_i/t_o) + 1$); t_i ist der Zeitpunkt des Durchganges der Inflexionspunkte und t_o eine angenommene Zeiteinheit). In diesem Fall ist $\ln(1+\alpha) \approx \alpha$ für kleine α-Werte ausgenützt worden.

Für kleine Δt-Werte kann die Formel (9) weiterhin umgeschrieben werden:

$$\frac{(2x)^2}{t}\left(1 - \frac{\Delta t}{t}\right) = C - 8D \ln \frac{t}{t_o} - 8D \frac{\Delta t}{t} + \frac{b^2}{3t} \frac{x^2-2Dt}{2Dt} \quad (10)$$

Nach Vereinfachung ergibt sich:

$$\frac{(2x)^2}{t} = C - 8D \ln \frac{t}{t_o} + \frac{1}{t}\left(\frac{(2x)^2}{t} - 8D\right)\left(\frac{b^2}{24D} + \Delta t\right) \quad (11)$$

Führt man nun die Bezeichnungen

$$\eta = (2x)^2/t \text{ und } \tau = \ln (t/t_o)$$

ein, so sieht Gleichung (11) folgendermassen aus:

$$\eta = C - 8D\tau + \frac{\eta - 8D}{t}\left(\frac{b^2}{24D} + \Delta t\right) \quad (12)$$

wobei b die Scherstrecke ist. Wir sehen, dass die Abweichung infolge der Registrierung $\Delta n/\Delta x$ in der ersten Approximation wie ein konstanter Beitrag zur Nullzeitkorrektion erscheint:

$$\Delta t_e = \Delta t_w + \frac{b^2}{24D} \quad (13)$$

(e = erscheinend; w = wirklich).

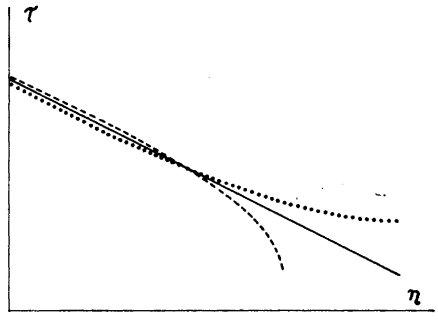

Fig. 2. Diagramm über τ als Funktion von η. $\Delta t_e > 0$ wird punktiert, $\Delta t_e = 0$ durchgezogen und $\Delta t_e < 0$ gestrichelt dargestellt. $\Delta t_e < 0$ trifft nur für die bis lang angewandten Küvetten bei fehlerhaften Zeitbestimmungen oder inkorrekt ausgeführten Versuchen zu.

Am einfachsten geschieht nun die Evaluierung durch die Aufzeichnung von τ als Funktion von η in einem logarithmischen Diagramm (vgl. Fig. 2). Die Nullzeitkorrektion Δt_e wird gemäss Gl. (12) berechnet. Wenn die Nullzeitkorrektion eingeführt wird, geht die Kurve in eine gerade Linie mit der Gleichung

$$\eta = C - 8D\tau \tag{14}$$

über. Der Diffusionskoeffizient D lässt sich nun ganz einfach aus der Neigung der Linie berechnen.

IV. EVALUIERUNG EINES KONZENTRATIONSABHÄNGIGEN DIFFUSIONSKOEFFIZIENTEN

Auch für den Fall, dass der Diffusionskoffizient D konzentrationsabhängig ist, kann die vorher beschriebene Evaluierungsart angewandt werden. Wir behandeln in diesem Abschnitt den Fall, wo D eine exponentielle Konzentrationsabhängigkeit hat, d.h.

$$D(c) = D_0 \exp(\alpha c) \tag{15}$$

Für kleine Konzentrationsunterschiede gilt in diesem Falle für Gleichung (2) folgende approximative Lösung [7]:

$$\left(\frac{\partial c}{\partial x}\right)_{\Delta c \text{ klein}} \approx \frac{\Delta c}{2\sqrt{\pi D_0 t}} \exp\left(-x^2/4D_0 t\right) \left\{1 - \alpha\bar{c}\left(\frac{1}{2} - \frac{x^2}{4D_0 t}\right) + \right.$$
$$\left. + \frac{\alpha^2\bar{c}^2}{8}\left[7 - 8\,\frac{x^2}{4D_0 t} + 4\left(\frac{x^2}{4D_0 t}\right)^2\right]\right\} \tag{16}$$

$c = (c_I + c_{II})/2$ stellt die mittlere Konzentration dar.

Damit erhält Gleichung (8) folgendes Aussehen:

$$\exp(x^2/4D_0(t + \Delta t)) = \frac{\Delta n^o}{2a\sqrt{\pi D_0(t + \Delta t)}}\left(1 + \frac{b^2}{48D_0 t} \cdot \frac{x^2 - 2D_0 t}{2D_0 t}\right) \times$$
$$\times \left\{1 - \alpha\bar{c}\left(\frac{1}{2} - \frac{x^2}{4D_0 t}\right) + \frac{\alpha^2\bar{c}^2}{8}\left[7 - 8\,\frac{x^2}{4D_0 t} + 4\left(\frac{x^2}{4D_0 t}\right)^2\right]\right\} \tag{17}$$

Nach Logarithmierung ergibt sich:

$$\frac{(2x)^2}{t + \Delta t} = C - 8D_0 \ln\frac{t + \Delta t}{t_0} + \frac{b^2}{3t} \cdot \frac{x^2 - 2D_0 t}{2D_0 t} - 16D_0\alpha\bar{c}\left(\frac{1}{2} - \frac{x^2}{4D_0 t}\right) +$$
$$+ 2D_0\alpha^2\bar{c}^2\left[7 - 8\,\frac{x^2}{4D_0 t} + 4\left(\frac{x^2}{4D_0 t}\right)^2\right] \tag{18}$$

Nach Einführung von τ und η in Übereinstimmung mit Kapitel III erhält man in der ersten Approximation

$$\eta \approx C - 8D_0\tau + \frac{\eta - 8D_0}{t}\left(\frac{b^2}{24D_0} + \Delta t\right) + \alpha\bar{c}(\eta - 8D_0) \tag{19}$$

Dies kann man auch auf nachstehende Art schreiben:

$$\eta \approx C' - 8D'\tau + \frac{\eta - 8D_o}{t}\left(\frac{b^2}{24D_o} + \Delta t\right)(1 + \alpha\bar{c}) \qquad (20)$$

Dieses Resultat zeigt, dass die gemessene Diffusionskonstante $D' = D_o(1 + \alpha\bar{c})$ für Werte der mittleren Konzentration gilt.

Dadurch dass $\partial c/\partial x$ nach Gleichung (16) eine gerade Funktion von x ist, kann man im Ausdruck (20) wie auch in (12) $2x$ durch den Abstand zwischen zwei symmetrisch liegenden Interferenzstreifen ersetzen.

V. WIENERSCHE SCHIEFENEINWIRKUNG AUF DIE EVALUIERUNG

Die Aberrationen, die die Wienersche Schiefe [8] bedingen, verschwinden nach Berechnung von Svensson [9], wenn man auf 1/3 der Zelldicke von der vorderen Küvettenwand betrachtet fokussiert. Wenn man dagegen die Fokussierung auf die Zellmitte vornimmt, werden die Interferenzstreifen um ein Stück

$$\Delta x = \frac{d^2}{6m} \cdot \frac{\partial n}{\partial x}$$

seitlich verschoben. d ist die Zelldicke und m ist der Brechungsindex der Zellflüssigkeit bei der Fokussierung. Bei dieser Evaluierungsmethode ist $\partial n/\partial x =$ konstant und die seitliche Verschiebung der Interferenzstreifen übt keinerlei Einfluss auf den η-Wert in Figur 2 aus.

Daraus geht hervor, dass diese Aberrationsart die Methodenanwendung nicht beeinflusst.

VI. POLYDISPERSITÄTSUNTERSUCHUNGEN MIT HILFE DER SCHERINTERFEROMETERMETHODE

Wir betrachten hier die Verteilungsfunktion $f(D)$ bezüglich des Diffusionskoeffizienten D. Um die Verteilung $f(D)$ in einer polydispersen Lösung zu erhalten, übertragen wir eine Methode nach Freund und Daune [10] in die bei dieser Scherinterferometermethode erhaltene experimentelle Kurve. Durch eine doppelte Fouriersche Transformation wird die Funktion $f(D)$ erhalten wie folgt:

(*a*) Bei gewöhnlichen Diffusionsversuchen ist

$$\frac{\partial n}{\partial x} = \int_0^\infty \frac{\exp(-x^2/4Dt)}{2\sqrt{\pi Dt}} f(D)\, \mathrm{d}D \qquad (21)$$

$f(D)$ ist eine Verteilungsfunktion solcher Art, dass $f(D)\mathrm{d}D$ als der Beitrag zum Brechungsindex von Molekülen, deren Diffusionskoeffizienten zwischen D und $D + \mathrm{d}D$ liegen, aufgefasst werden kann.

Durch folgende Variablensubstitution

$\xi = \ln(x^2/4t) = 2 \ln \zeta$ (ermöglicht dadurch, dass der Integrand in (21) eine gerade Funktion von x ist),

$\vartheta = \ln D$

erhält Gleichung (21) folgendes Aussehen:

$$\frac{\partial n}{\partial x} = \int_{-\infty}^{+\infty} \frac{\exp\{-\exp(\xi-\vartheta)\}}{2\sqrt{\pi t}\,\exp(\vartheta/2)} \cdot \exp(\vartheta) \cdot f\{\exp(\vartheta)\}\,\mathrm{d}\vartheta =$$

$$= \frac{1}{2\sqrt{\pi t}} \int_{-\infty}^{+\infty} \exp\{-\exp(\xi-\vartheta)\} \cdot \exp(\vartheta/2) \cdot f\{\exp(\vartheta)\}\,\mathrm{d}\vartheta \qquad (22)$$

(*b*) Bei Bodenschichtdiffusion [11] geht Gleichung (21) über in

$$\frac{\partial n}{\partial x} = -\int_{0}^{\infty} \frac{x \cdot \exp(-x^2/4Dt)}{2Dt\sqrt{\pi Dt}}\, f(D)\,\mathrm{d}D \qquad (23)$$

Lässt man gleiche Variablensubstitution wie oben gelten, so erhält man:

$$\frac{\partial n}{\partial x} = -\frac{\exp(\xi/2)}{t\sqrt{\pi}} \int_{-\infty}^{+\infty} \exp\{-\exp(\xi-\vartheta)\} \cdot \exp(-\vartheta/2) \cdot f\{\exp(\vartheta)\}\,\mathrm{d}\vartheta \qquad (24)$$

Wir wollen nun zeigen wie die Scherinterferometermethode in diesem Zusammenhange angewandt werden kann und wählen hier Fall (*a*) aus.

Nach Gleichung (22) ist

$$\frac{\partial n}{\partial x} \cdot 2\sqrt{\pi t} = \int_{-\infty}^{+\infty} \varphi(\xi-\vartheta) \cdot g(\vartheta)\,\mathrm{d}\vartheta \qquad (25)$$

dabei ist $g(\vartheta) = \exp(\vartheta/2) \cdot f\{\exp(\vartheta)\}$

und $\varphi(\xi-\vartheta) = \exp\{-\exp(\xi-\vartheta)\}$

Die linke Seite der Formel (25) ist eine Funktion von ξ, somit können wir

$$\psi(\xi) = \frac{\partial n}{\partial x}\, 2\sqrt{\pi t}$$

einführen, sodass (25) in

$$\psi(\xi) = \int_{-\infty}^{+\infty} \varphi(\xi-\vartheta) \cdot g(\vartheta)\,\mathrm{d}\vartheta = \varphi * g \qquad (26)$$

übergeht, d.h. also ein Faltungsprodukt. Da nun bei der Scherinterferometermethode für jedes Streifenpaar $\partial n/\partial x$ = konstant ist, gilt

$$\psi(\xi) = A\sqrt{t}$$

wobei A eine Konstante ist.

Wenn die Fouriersche Transformation mit F ($F(f) = \int_{-\infty}^{+\infty} f(\xi) \exp(2\pi i x\xi)\,\mathrm{d}\xi$) bezeichnet wird, so ergibt sich aus Formel (26) mit Hilfe des Faltungssatzes

$$F(\psi) = F(\varphi) \cdot F(g)$$

oder

$$F(g) = F(\psi)/F(\varphi) \qquad (27)$$

$F(\psi)$ kann graphisch oder numerisch aus einem Diagramm über $\sqrt{t}\,(=\psi(\xi)/A)$ als Funktion von $\xi(=\ln(x^2/4t)=\ln(\eta/16))$ erhalten werden. Nach Division mit $F(\varphi)$ kennen wir nun $F(g)$. Durch inverse Fouriersche Transformation von $F(g)$ erhält man $f(g)$ und danach lässt sich $f(D)$ durch die Relation im Anschluss an Gleichung (25) entwickeln.

Eine andere Möglichkeit $f(D)$ zu bestimmen ist durch die Entwicklung der Momente gegeben. Die Momente von f kann man nämlich aus den Momenten von $\partial n/\partial x$ (M_r) erhalten wie folgt:

$$M_r = \int_{-\infty}^{+\infty} x^r \frac{\partial n}{\partial x}\,\mathrm{d}x \tag{28}$$

Nach Gleichung (21) ist nun

$$M_r = \int_{-\infty}^{+\infty} x^r\,dx \int_0^{\infty} \frac{\exp(-x^2/4Dt)}{2\sqrt{\pi Dt}}\, f(D)\,\mathrm{d}D \tag{29}$$

Durch die Substitution

$$\chi = x/2\sqrt{Dt}$$

kann der Ausdruck (29) in nachstehende Form transformiert werden:

$$M^r = \frac{2^r t^{r/2}}{\sqrt{\pi}} \int_0^{\infty} f(D)\; D^{r/2}\,\mathrm{d}D \int_{-\infty}^{+\infty} \chi^r \exp(-\chi^2)\,\mathrm{d}\chi \tag{30}$$

Indem wir nun

$$\mu_{r/2} = \int_0^{\infty} f(D)\; D^{r/2}\,\mathrm{d}D \tag{31}$$

oder

$$\mu_r = \int_0^{\infty} f(D)\; D^r\,\mathrm{d}D \tag{32}$$

einführen, erhalten wir

$$M_r = \frac{2^r t^{r/2}}{\sqrt{\pi}}\,\Gamma\left(\frac{r+1}{2}\right)\cdot \mu_{r/2} \tag{33}$$

wenn r eine gerade Ganzzahl > 0 ist,
oder

$$M_{2r} = \frac{2^{2r} t^r}{\sqrt{\pi}}\,\Gamma\left(r+\frac{1}{2}\right)\cdot \mu_r = 2t^r\,\frac{\Gamma(2r)}{\Gamma(r)}\cdot \mu_r \tag{34}$$

wo r jetzt eine beliebige Ganzzahl > 0 ist.

Da ein einfacher Zusammenhang zwischen μ_r und dem Moment M_{2r} besteht (vgl. Abschnitt VII), kann $f(D)$ aus der Kurve über $\partial n/\partial x$ als Funktion von x erhalten werden.

VII. AUSDRUCK DER MOMENTE BEI DER ANWENDUNG DER SCHERINTERFEROMETERMETHODE

Die Gleichung (2) ist für den Fall des beiderseitigen unendlichen Halbraumes von Boltzmann behandelt worden [12]. Unter der Voraussetzung, dass der Diffusionskoeffizient entweder konzentrationsunabhängig ist, oder nur von der Konzentration abhängt, lässt sich die Konzentration c mit Hilfe einer einzigen Variablen

$$\zeta = x/2\sqrt{t}$$

ausdrücken; $c = c(\zeta)$ — daraus folgt auch für den polydispersen Fall, da wie bekannt eine Summe von Funktionen von ζ auch eine Funktion von ζ sein muss, dass $n = n(\zeta)$ ist.

Wir suchen nun die Relation zwischen den Momenten von $\mathrm{d}n/\mathrm{d}\zeta$ ($\mathcal{M}_r$) und den von $\partial n/\partial x$ (M_r). Führen wir $\zeta = x/2\sqrt{t}$ in die Gleichung (28) ein, so erhalten wir:

$$M_r = 2^r t^{r/2} \int_{-\infty}^{+\infty} \zeta^r \frac{\mathrm{d}n}{\mathrm{d}\zeta}\,\mathrm{d}\zeta = 2^r t^{r/2}\,\mathcal{M}_r \tag{35}$$

Überträgt man dies auf die Gleichung (34) in dem vorangegangenen Abschnitt (VI), so ergibt sich:

$$\mu_r = 2^{2r-1}\frac{\Gamma(r)}{\Gamma(2r)}\,\mathcal{M}_{2r} \tag{36}$$

Folglich kann auch $f(D)$ als eine Funktion von $\mathcal{M}_{2r}$ geschrieben werden. Nach Zernike [13] ist

$$f(D) = \frac{\exp(-D^2/2\sigma^2)}{\sigma\sqrt{2\pi}}\left\{1 + \sum_{i=3}^{\infty}\frac{k_i}{i!}\,H_i\,(D/\sigma)\right\} \tag{37}$$

wobei H_i das i-te Hermitesche Polynom, $\sigma^2 = \mu_2 - 2\mu_1^2 = \frac{4}{3}\,\mathcal{M}_4 - 8\,\mathcal{M}_2^2$ ist und k_i in den Momenten wie folgt ausgedrückt werden kann:

$$k_3 = \frac{2^5\Gamma(3)}{\sigma^3\Gamma(6)}\,\mathcal{M}_6$$

$$k_4 = \frac{2^7\Gamma(4)}{\sigma^4\Gamma(8)}\,\mathcal{M}_8 - 3$$

$$k_5 = \frac{2^9\Gamma(5)}{\sigma^5\Gamma(10)}\,\mathcal{M}_{10} - 10\,\frac{2^5\Gamma(3)}{\sigma^3\Gamma(6)}\,\mathcal{M}_6$$

$$k_6 = \frac{2^{11}\Gamma(6)}{\sigma^6\Gamma(12)}\,\mathcal{M}_{12} - 15\,\frac{2^7\Gamma(4)}{\sigma^4\Gamma(8)}\,\mathcal{M}_8 + 30$$

usw.

Wegen der hohen Ordnung der einbegriffenen Momente ist dieser Ausdruck hauptsächlich von theoretischem Interesse.

VIII. VERSUCHE MIT KONZENTRATIONSABHÄNGIGEM DIFFUSIONSKOEFFIZIENTEN IM ALLGEMEINEN FALLE MIT DEM SCHERINTERFEROMETER

Durch Einführen der neuen Variablen $\zeta = x/2\sqrt{t}$ kann man Gleichung (2) in eine gewöhnliche Differentialgleichung umformen, da nach Boltzmann [12] $c = c(\zeta)$ ist, kann auch D als eine Funktion von ζ betrachtet werden und die Differentialgleichung kann in der folgenden Weise geschrieben werden:

$$-2\zeta \frac{dc}{d\zeta} = \frac{d}{d\zeta}\left\{ D(\zeta) \frac{dc}{d\zeta} \right\} \tag{38}$$

Wir wollen nun D bestimmen, deshalb integrieren wir (38) von $-\infty$ bis ζ so erhalten wir

$$D(\zeta') \frac{dc}{d\zeta} \int_{-\infty}^{\zeta} = -2 \int_{-\infty}^{\zeta} \zeta' \, c_\zeta(\zeta') \, d\zeta' \tag{39}$$

wobei wir $dc/d\zeta = c_\zeta$ abgekürzt haben.

Da $D(\zeta) \cdot c_\zeta$ für $\zeta = -\infty$ verschwindet, ergibt sich:

$$D(\zeta) = -\frac{2}{c_\zeta(\zeta)} \int_{-\infty}^{\zeta} \zeta' \, c_\zeta(\zeta') \, d\zeta' \tag{40}$$

Nach Zernike [13,14] kann nun $dc/d\zeta$ durch

$$\frac{dc}{d\zeta} = \frac{\exp(-\zeta^2/D_o)}{\sqrt{\pi D_o}} \{1 + \sum_{i=3}^{\infty} \frac{k_i}{i!} H_i(\zeta/\sqrt{D_o/2})\} \tag{41}$$

wobei D_o eine Konstante ist, ausgedrückt werden; H_i ist das i-te Hermitesche Polynom und k_i kann in den Momenten entwickelt werden (vgl. Formel (37)). Diese Entwicklung ist aber infolge ihrer langsamen Konvergenz in der Praxis undurchführbar. Um die Momente für eine Lösung anwenden zu können, muss man nach einer einfacheren Entwicklung (mit schnellerer Konvergenz) streben.

Wir wollen nun zeigen wie die Evaluierungen praktisch auf eine einfache Art bei der Scherinterferometermethode durchgeführt werden.

Die Skalenmethode und ähnliche geben primär $\partial c/\partial x$ als Funktion von x. Die Scherinterferometer- und Schlierenmethode liefern dagegen nur den x-Wert für $\partial c/\partial x = a$ (die Interferenzstreifen stellen die x-Werte dar, wo $\partial c/\partial x$ approximativ gleich einem bestimmten konstanten a-Wert ist). Dies wirkt zunächst wie eine Einschränkung der Anwendung der Scherinterferometermethode, wir wollen aber im Nachfolgenden beweisen, dass dies in keiner Weise der Fall ist.

Wir haben

$$\frac{\partial c}{\partial x} = \frac{dc}{d\zeta} \cdot \frac{\partial \zeta}{\partial x} = \frac{1}{2\sqrt{t}} \cdot \frac{dc}{d\zeta} \tag{42}$$

dabei ist $\zeta = x/2\sqrt{t}$, oder übertragen auf die Scherinterferometermethode, wo $\partial c/\partial x = a$ ist, erhalten wir:

$$\frac{dc}{d\zeta} = 2\sqrt{t} \cdot \frac{\partial c}{\partial x} = 2a\sqrt{t} \tag{43}$$

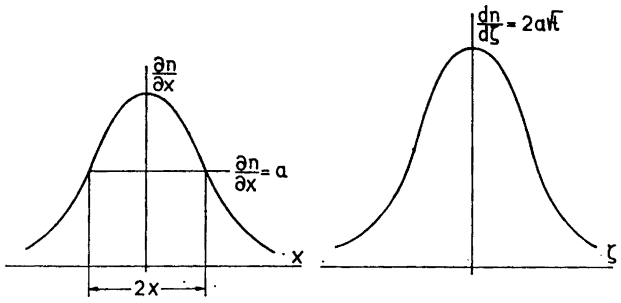

Fig. 3. Veranschaulichung der ganzen Gradientenkurve durch die Registrierungen der Interferenzstreifenlage. Links wird gezeigt, wie ein bestimmtes Streifenpaar den Abstand zwischen den Punkten, wo der Gradient $\partial n/\partial x = a$ ist, darstellt. Rechts ist $dn/d\zeta$ als Funktion von ζ aufgezeichnet ($\zeta = x/2\sqrt{t}$). Die Kurve wird erhalten, wenn $2a\sqrt{t}$ gegen ζ gesetzt wird.

Dies gilt auch für Versuche mit konzentrationsabhängigen Diffusionskoeffizienten, wenn nur, wie nach Boltzmann [12], $c = c(\zeta)$ ist.

Aus diesem geht hervor, dass, wenn $2a\sqrt{t}$ in einem Diagramm gegen ζ gesetzt wird, $dc/d\zeta$ demnach als eine Funktion von ζ hervortreten muss.

Bei einem konstanten t-Wert gilt andererseits, dass $\zeta(= x/2\sqrt{t}) = x \cdot$ Konstante und $dc/d\zeta$ $[= (1/2\sqrt{t})(\partial c/\partial x)] = (\partial c/\partial x) \cdot$ Konstante ist. Zeichnet man nun $\sqrt{t}$ als Funktion von ζ in ein Diagramm, stellt diese Kurve bei einem gewissen bekannten Masstabe $\partial c/\partial x$ als Funktion von x dar, wenn nur $c = c(\zeta)$ ist (vgl. Figur 3). Dies ist ja bei beiden, dem konzentrationsabhängigen Diffusionskoeffizienten und bei Polydispersität der Fall, und sogar bei gleichzeitigem Auftreten beider.

Dies hier vorgelegte einfache Evaluierungsverfahren bei Anwendung der Scherinterferometer- oder Schlierenmethode ist hervorragend, denn es ist den Registrierungen von $\partial c/\partial x$ zu allen Zeitpunkten völlig gleichwertig.

Gl. (40) lässt sich jetzt bei Anwendung von Gl. (43) in folgender Weise schreiben:

$$D(\zeta) = -\frac{2}{\sqrt{t(\zeta)}} \int_{-\infty}^{\zeta} \zeta' \sqrt{t(\zeta')}\, d\zeta' \tag{44}$$

dabei ist selbstverständlich

$$c(\zeta) = c(-\infty) + \int_{-\infty}^{\zeta} c_\zeta(\zeta')\, d\zeta' = c(-\infty) + \frac{2a}{dn/dc} \int_{-\infty}^{\zeta} \sqrt{t(\zeta')}\, d\zeta' \tag{45}$$

Wenn man einen analytischen Ausdruck für $D(\zeta)$ aus der experimentellen Kurve erhalten kann, so kann man folgendes für die Kontrolle der Gl. (40) anwenden. Man kann aus Gleichung (38) die Konzentration $c(\zeta)$ bestimmen, wenn $D(\zeta)$ bekannt ist. Somit kann der Ausdruck (38) wie nachstehend geschrieben werden:

$$\frac{d^2c}{d\zeta^2} = -\frac{2\zeta + D'(\zeta)}{D(\zeta)} \frac{dc}{d\zeta} \tag{46}$$

Setzt man nun

$$u = \mathrm{d}c/\mathrm{d}\zeta$$

ein, geht die Formel (46) in

$$\frac{\mathrm{d}u}{\mathrm{d}\zeta} = -\frac{2\zeta + D'(\zeta)}{D(\zeta)} \tag{47}$$

über. Die Lösung dieser Gleichung ist:

$$u = u_o \exp\{-\int_{\zeta_0}^{\zeta} \frac{2\zeta' + D'(\zeta')}{D(\zeta')}\,\mathrm{d}\zeta'\} \tag{48}$$

daraus entwickelt sich

$$c(\zeta) = u_o \int_{\zeta_0}^{\zeta} \exp\{-\int_{\zeta'_0}^{\zeta'} \frac{2\zeta'' + D'(\zeta'')}{D(\zeta'')}\,\mathrm{d}\zeta''\}\mathrm{d}\zeta' \tag{49}$$

Den Nullpunkt der Kurve (hierbei gleichbedeutend mit der Lage $\zeta = 0$) über $\partial c/\partial\zeta$ als Funktion von ζ erhält man einfach aus $\mathcal{M}_1 = 0$, denn

$$\mathcal{M}_1 = \int_{-\infty}^{+\infty} \zeta \frac{\mathrm{d}c}{\mathrm{d}\zeta}\,\mathrm{d}\zeta = -\frac{1}{2}\int_{-\infty}^{+\infty} \frac{\mathrm{d}}{\mathrm{d}\zeta}\left\{D(\zeta)\,\frac{\mathrm{d}c}{\mathrm{d}\zeta}\right\}\mathrm{d}\zeta =$$

$$= -\frac{1}{2}\,D(\zeta)\,\frac{\mathrm{d}c}{\mathrm{d}\zeta}\Bigg|_{-\infty}^{+\infty} = 0$$

hierbei ist Gleichung (38) zur Anwendung gekommen.

Bei den Versuchen benutzt man als provisorische Referenz die Einritzung eines Striches in das Zellfenster und im Verhältnis zu diesem wird die Lage der Interferenzstreifen gemessen (Beachte: die Interferenzstreifen liegen im allgemeinen nicht symmetrisch).

IX. BEDEUTUNG DES BEGRIFFES "REDUZIERTES MOMENT"

Bei den Methoden, deren Experimente $\partial c/\partial x$ als Funktion von x geben, pflegt man bisweilen bei der Berechnung des Diffusionskoeffizienten das reduzierte Moment anzuwenden. Folgende Definition wird hier für das reduzierte Moment aufgestellt:

$$\mathcal{D}_p^p = \frac{\Gamma(p)}{t^p\Gamma(2p)} \cdot \frac{M_{2p}}{M_o} \tag{50}$$

In dem idealen Falle, d.h. mit nur einem diffundierenden Stoff und konzentrationsunabhängigen Diffusionskoeffizienten $\bar{D}$, tritt mit dieser Definition folgender Zusammenhang auf:

$$\mathcal{D}_p = \bar{D} \tag{51}$$

der für $p = 1, 2, 3, \ldots$ gilt.

Bei Polydispersität folgt aus Gleichung (34), dass

$$\mathcal{D}_p = (\mu_p/\mu_o)^{1/p} \tag{52}$$

Dabei ist

$$\mu_p = \int_0^\infty f(D)\ D^p\ \mathrm{d}D$$

d.h.

$$\mathscr{D}_p^p = \frac{\int_0^\infty f(D)\ D^p\ \mathrm{d}D}{\int_0^\infty f(D)\ \mathrm{d}D} \tag{53}$$

Wir sehen nun, dass, wenn $f(D) = \text{Konst.} \cdot \delta(D-\bar{D})$ ist (δ repräsentiert eine Deltafunktion), sich die Gleichung (51) bildet.

Bei konzentrationsabhängigem Diffusionskoeffizienten ergibt sich:

$$\mathscr{D}_1 = \frac{1}{c_2-c_1} \int_{c_1}^{c_2} D(c)\ \mathrm{d}c$$

und

$$\mathscr{D}_{\frac{1}{2}} = 0$$

Die anderen (höheren) $\mathscr{D}_p$-Werte erhalten in diesem Falle einen komplizierteren Ausdruck.

Auf Grund der in Abschnitt VIII beschriebenen praktischen Evaluierungsmöglichkeiten kann die in diesem Teil beschriebene Berechnungsart ebenso bei der Scherinterferometermethode wie eine Alternative zu dem Lammschen- oder dem logarithmischen Evaluierungsverfahren angewandt werden.

X. BEHANDLUNG DER SYSTEME MIT NICHT VERNACHLÄSSIGBAREM VOLUMENEFFEKT BEI DIFFUSION

Für Fälle, wo sich die Volumeneffekte bei Mischungen geltend machen, gilt folgende Gleichung: [15]

$$\frac{\partial c}{\partial t} = \frac{\partial}{\partial x}\left\{ D_v \frac{\partial c}{\partial x} + c \int_{-\infty}^{x} \left(\frac{\partial \bar{v}}{\partial c}\right) \frac{D_v}{1-\bar{v}c} \left(\frac{\partial c}{\partial x}\right)^2 \mathrm{d}x \right\} \tag{54}$$

D_v ist der Diffusionskoeffizient und $\bar{v}$ ist der Lösung partielles spezifisches Volumen. Wenn $\bar{v}$ konstant ist, geht die Formel (54) in die gewöhnliche Diffusionsgleichung über.

Wie Fujita [16] betont hat, ist $c = c(\zeta)$ und die Transformation $\zeta = x/2\sqrt{t}$ kann eingeführt werden. Die Formel (54) erhält dann in Folge das Aussehen

$$-2\zeta \frac{\mathrm{d}c}{\mathrm{d}\zeta} = \frac{\mathrm{d}}{\mathrm{d}\zeta}\left\{ D_v(c) \frac{\mathrm{d}c}{\mathrm{d}\zeta} + c \int_{-\infty}^{\zeta} \left(\frac{\partial \bar{v}}{\partial c}\right) \frac{D_v(c)}{1-\bar{v}c} \left(\frac{\mathrm{d}c}{\mathrm{d}\zeta}\right)^2 \mathrm{d}\zeta \right\} \tag{55}$$

Da die Scherinterferometermethode $\mathrm{d}c/\mathrm{d}\zeta = 2a\sqrt{t}$ als Funktion von ζ liefert, kann man die Scherinterferometermethode demnach auch für den Fall, wo Gleichung (54) gilt, anwenden.

XI. OPTIMALES VERHALTEN BEI DIFFUSIONSVERSUCHEN, WENN INNERHALB DER ZELLWÄNDE FEHLER VORHANDEN SIND

Auf Grund der hohen Empfindlichkeit der Scherinterferometermethode hat es sich in der Praxis erwiesen, dass grosse Anforderungen an die Oberflächenebenheit der Zellwände gestellt werden, wenn Präzisionsmessungen vorgenommen werden sollen. Folgend wollen wir einige praktische Ratschläge betreffend Versuchsaufbau bei diesen Messungen unterbreiten.

Bei nicht vollkommenen Küvetten wird eine integrierende Methode vorgeschlagen. Wenn dagegen die Scherinterferometermethode (Differentierungsmethode) trotzdem benutzt wird, wirkt der Fehler der Zelle, wie später berichtet wird, am wenigsten auf die Interferenzstreifen, die auf der Höhe der Inflexionspunkte liegen.

Nimmt man an, dass der Fehler im Glasmaterial als ein Gradient der optischen Weglänge W beschrieben wird, die zu der richtigen Weglänge $d \cdot \partial n/\partial x$ (d = Zelldicke) hinzugefügt werden kann, so wird der Fehler der Interferenzstreifenlage

$$\frac{1}{d} \cdot \frac{\partial W}{\partial x} \Big/ \frac{\partial^2 n}{\partial x^2}$$

Vergleiche hierzu Figur 4. Der relative Fehler der Streifenlage (F_{rel}) ergibt diesen oben angeführten Wert dividiert durch den Streifenabtsand $2x$;

$$F_{rel} = \frac{(1/d)(\partial W/\partial x)}{(\partial^2 n/\partial x^2)\ 2x} = \frac{\partial W}{\partial x} \cdot \frac{2Dt\sqrt{\pi Dt}\ \exp(x^2/4Dt)}{d \cdot x^2 \Delta n^\circ} \tag{56}$$

$\exp(x^2/4Dt) = \exp[\frac{1}{2}(1 + \ln\ (t_i/t)] = \sqrt{et_i/t}$ (vgl. Ref. 4) und somit gilt nachstehende Proportionalität

$$F_{rel} \sim (\Delta n^\circ)^{-1}\ \frac{t}{x^2} \sqrt{t_i} \tag{57}$$

Führt man nun die Bezeichnung $\eta = (2x)^2/t$ ein, so erhält man

$$F_{rel} \sim \sqrt{t_i}/(\Delta n^\circ \cdot \eta)$$

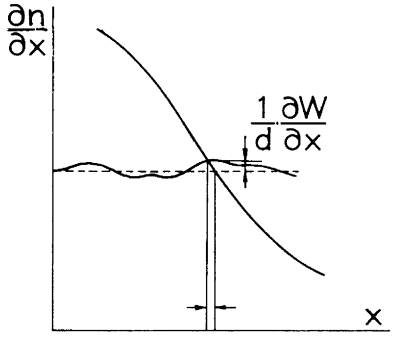

Fig. 4. Veranschaulichung der Interferenzstreifenlagenfehler, bedingt durch das Vorhandensein eines geringen Gradienten (Küvettenfensterfehler).

Wir haben aber [4]

$$\sqrt{t_i} = \frac{\Delta n^\circ}{2\sqrt{\pi D d}\ kv}$$

$$(t_i \sim (\Delta n^\circ/v)^2)$$

wobei k eine Konstante ist und v ist die Ordnungsnummer der Streifenpaare.

Daraus ergibt sich:

$$F_{\text{rel}} \sim 1/v\eta \tag{58}$$

Bei der Schlierenmethode gilt $F_{\text{rel}} \sim 1/u_o\eta$, da u_o gleich der Spaltverschiebung ist, während $t_i \sim (\Delta n^\circ/u_o)^2$ ist.

In der Praxis bleibt das η-Gebiet bei allen Versuchen ungefähr das gleiche, da man ja beiderseits von t_i liegen will (in Nähe der Inflexionspunkte).

Man soll also v und u_o so gross wie nur möglich im Hinblick auf das praktische Verhältnis wählen. Danach justiert man Δn_o in der Art, dass t_i genügend gross wird, ca. 2 Stunden.

LITERATUR

1. Lamm, O. *Nova Acta Regiae Soc. Sci. Upsaliensis* **10** (1937) No. 6.
2. Ingelstam, E. *Arkiv Fysik* **9** (1955) 197.
3. Ingelstam, E. *J. Opt. Soc. Am.* **47** (1957) 536.
4. Bryngdahl, O. *Acta Chem. Scand.* **11** (1957) 1017.
5. Bryngdahl, O. *Acta Chem. Scand.* **12** (1958) 684.
6. Bryngdahl, O. *Arkiv Fysik* **21** (1962) 289.
7. Clarke, D. M. *J. Chem. Phys.* **27** (1957) 29.
8. Wiener, O. *Ann. Phys. Chem.* N.F. **49** (1893) 105.
9. Svensson, H. *Optica Acta* **1** (1954) 25.
10. Freund, L. und Daune, M. *J. Polymer Sci.* **29** (1958) 161.
11. Ljunggren, S. und Lamm, O. *Acta Chem. Scand.* **11** (1957) 340.
12. Boltzmann, L. *Wied. Ann.* **53** (1894) 959.
13. Zernike, F. *Handbuch der Physik*, Springer, Berlin 1928, Vol. III, S. 448.
14. Margenau, H. und Murphy, G. M. *The Mathematics of Physics and Chemistry*, Nostrand, New York 1943, S. 421.
15. Kirkwood, J. G., Baldwin, R. L., Dunlop, P. J., Gosting, L. J. und Kegeles, G. *J. Chem. Phys.* **33** (1960) 1505.
16. Fujita, H. *J. Am. Chem. Soc.* **83** (1961) 2862.

Eingegangen am 26. April 1962.

ACTA CHEMICA SCANDINAVICA 16 (1962) 2177–2188

Measurements of the Self-diffusion of Water in Pure Water, H_2O-D_2O Mixtures and Solutions of Electrolytes

LENNART DEVELL*

Division of Physical Chemistry, The Royal Institute of Technology, Stockholm 70, Sweden

Dedicated to Professor *Ole Lamm* on his 60th birthday

The self-diffusion of water was measured at 25.0°C in pure water, H_2O-D_2O mixtures and solutions of NaCl, LiBr and $MgSO_4$. The diffusion cells used were of the shearing boundary type and are described. Deuterium and tritium were used as tracers. Analysis of deuterium was performed by means of a mass spectrometer. Tritium has been detected by means of liquid scintillation technique, or by an improved version of the bremsstrahlung method. Comparative measurements in pure water at 25.0°C with deuterium and tritium as tracers gave identical results $(2.25 \pm 0.02) \times 10^{-5}$ cm²/sec, in good agreement with Longsworth's extrapolated value (2.27) obtained from measurements on H_2O-D_2O mixtures using a precision optical method. The result thus indicates that the isotope effect is within experimental error. The self-diffusion of water in H_2O-D_2O mixtures, having tritium as tracer, seems to decrease linearly with the increase in deuterium content. The self-diffusion coefficient in dilute salt solutions was very moderately affected. In concentrated solutions decreasing effects were most pronounced in solutions of $MgSO_4$. A comparison of the inverse viscosity *versus* solute concentration with the self-diffusion shows a similar course for the two functions. The results in the case of salt solutions is discussed briefly in terms of the theory of Wang. Data of others are included for comparison.

The purpose of the present investigation was to study the self-diffusion of water and especially the influence of electrolytes. Previous measurements with different tracers and methods have resulted in different diffusion coefficients for the self-diffusion of pure water. Contradictory data obtained from measurements with ^{18}O and D have been interpreted even as an indication of different mechanisms for the transfer of oxygen and hydrogen [1]. In the present work with HDO and HTO as tracers similar experimental techniques have been used for the two isotopes in order to reduce systematic errors.

* Present address: AB Atomenergi, Studsvik, Tystberga, Sweden.

By measuring the self-diffusion with D and T as tracers it was intended to make a rough extrapolation to the true self-diffusion coefficient of water. The present result, however, indicate that the isotope effect from measurements with D and T is within experimental error. Measurements using spin echo techniques have been rather inaccurate so far and cannot yet serve as a measure of the isotope effect.

EXPERIMENTAL

In the diffusion experiments the principle of restricted diffusion was used. The diffusion cells were of sheared boundary type.

Apparatus. The two cells, which were of the type developed by Undeman, consisted of cylinders made of stainless steel and divided into four segments. In each segment circular holes (three in one cell, six in the other) were drilled, which could be separated or made to overlap by turning a screw. Thus one experiment could give three or six values of the diffusion coefficient. In Fig. 1 one of the cells is sketched. The centre parts were of equal height (3.998 ± 0.001 cm). The normal procedure for a diffusion experiment was as follows. The cell was placed upside down and the bottom part filled with the thermostated (± 0.2) sample, by means of a syringe, the cell was then turned over and the upper part filled. The cell was placed vertically in a thermostat bath and when temperature equilibrium was reached the experiment was started (by means of turning the two centre segments). The correct position was indicated by a conical bolt which locked the segments in place. The diffusion experiment was stopped when the average concentration difference was about half of the original value. It takes from one to three days for these conditions to be reached. Disturbances from vibrations were eliminated by means of a firm cell holder, which was fixed on a steady pillar in the building. The stirrer in the bath was not allowed to have any mechanical contact with the cell. Variations from the vertical position were investigated in some experiments and values of about 0.5° were found. This gives an estimated error in the diffusion coefficient of less than 0.3 %. Convection during the shearing procedure was determined in some experiments, with very short diffusion times, and was found to contribute 0 – 2 % to the randomised errors in the diffusion coefficient.

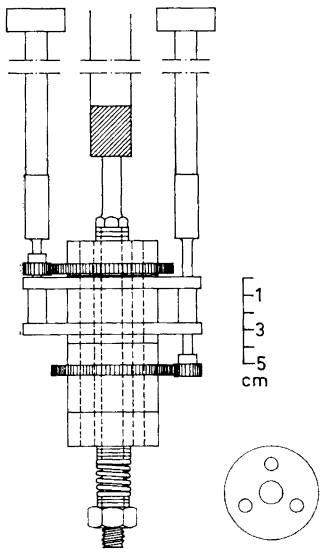

Fig. 1. Diffusion cell (for explanation see text).

On completing the diffusion process the liquid in the two parts of the chamber were well mixed and samples withdrawn by means of a syringe. The samples were then analysed for deuterium and tritium content.

Material. The deuterium oxide (about 99.8 %) was obtained from Norsk Hydro, Rjukan, Norway, and the tritiated water (about 5 C/ml) from the Radiochemical Centre, Amersham. In preparing the salt solutions ordinary distilled or redistilled water was used and the salts were of analytical grade. In order to assure that no convection should arise in the cell in the case of diminutive density gradient in the cell, the same sort of water was used from a stock. This procedure also made it possible to eliminate the need for accurate knowledge of the deuterium content in the water.

Thermostating. In order to reduce the heat convection in the diffusion cell a thermostat bath has been developed, which maintained the temperature constant to within ± 0.0002°C. For the purpose, an isolated bath (45 l) was used and placed in a thermostated room (25 ± 0.2°C). To achieve such a constant temperature in the bath, the main principle was to supply and carry off as small amounts of heat as possible. By this means excellent stability was reached and the control instruments closely followed the slowly changes in temperature. In practice it was arranged so that the cooler and heater were adjusted on low and approximately equal values, thus given a cooling and heating effect to the bath of normally 0.002°C/min in the steady state. The heater was a commercial water bath heater (60 W) connected to a power supply transformer. The cooling effect was obtained by the evaporation of the bath water, this was compensated for with a continual and automatic supply of water. A mercury contact thermo-regulator was used as the adjusting instrument. The mercury stem expansion was about 2 cm/°C. With the control instrument, a Beckmann-thermometer, temperature differences of 0.0002°C could be detected with the aid of a cathetometer. Temperature gradients in the bath were eliminated by means of a propeller (70 rpm). Tests at several points in the bath showed no temperature variation ($\Delta T < 0.0002$°C). The absolute temperature was measured with a calibrated (0.01°C) mercury thermometer.

Method of calculating the diffusion coefficient. Under favourable conditions, with practically no concentration gradients and no volume changes, Fick's second law is fulfilled. With the initial condition ($t = 0$)

$$\begin{aligned} c &= 0 \quad \text{for} \quad 0 < x < h \\ c &= c_0 \quad \text{for} \quad -h < x < 0 \end{aligned}$$

and the condition

$$\frac{\partial c}{\partial h} = 0 \quad \text{for} \quad \begin{cases} x = h \\ x = -h \end{cases}$$

where x = distance from the shearing boundary
h = half the height of the diffusion cell

the solution of the differential diffusion equation can be written:

$$\frac{c_{av}}{c_0} = \frac{1}{2} - \frac{4}{\pi^2} \sum_{n=1}^{\infty} \frac{1}{(2n-1)^2} \exp\left\{ - \frac{(2n-1)^2 \pi^2}{4h^2} Dt \right\} \tag{1}$$

or

$$\frac{c_{av}}{c_0} = \frac{\sqrt{Dt}}{h} \left\{ \frac{1}{\sqrt{\pi}} + \sum_{n=1}^{\infty} (-1)^n 2 \ \text{ierfc} \ \frac{nh}{\sqrt{Dt}} \right\} \tag{2}$$

where c_{av} = average concentration in the upper part of the cell. The function

ierfc $x \equiv \int_x^\infty (1-\text{erf}\ \eta)\ d\eta \equiv \frac{1}{\sqrt{\pi}} \exp(-x^2) - x\ \text{erfc}\ x$ has been calculated by means of tables of the error function [2]. If the concentration of the tracer in the upper part differs from zero at $t = 0$ and has the value c_B the definition of c_{av} and c_0 is changed to:

$$c_{av} = c_B' - c_B \tag{3}$$

$$c_0 = c_A' - c_B \tag{4}$$

where c_B' and c_A' are the absolute concentrations of the tracer in the upper and lower parts of the cell. Eqns. (3) and (4) have been used in the analytical procedure concerning deuterium with the advantage that it was necessary to determine only the ratio of two concentrations above the natural deuterium content of water. In order to correlate the signal from the mass spectrometer with this ratio, standard solutions were made up with the known ratio c_{av}/c_0 from D_2O and the stock water. The same procedure is possible when ^{18}O is used as tracer thus eliminating most of the systematic errors in the analytical procedure. A valuable control of the analyses is the relationship

$$\frac{c_{av}}{c_0} + \frac{c_{av}'}{c_0} = 1 \tag{5}$$

where c_{av}' = the average conc. in the lower part of the cell.

Isotope analyses. At first deuterium was determined by a modified version of the gradient tube method [3,4], but this was considered to be too time consuming to give the necessary accuracy. Most of the deuterium analyses were performed instead by the mass

Table 1. The effect on the stability of the output signal (n) from the liquid scintillation unit, caused by small changes of certain variables, compared with error due to the vial position and the statistical disintigration rate (Typical values).

Amount of water (x_1 ml)		Amount of ethanol (x_2 ml)		Amount of scintillator (x_3 ml)		Temperature changes (t°C)		Number of measurements * a		Statistical dis. rate	
x_1	$\lvert\frac{\partial n}{n}/\frac{\partial x_1}{x_1}\rvert$	x_2	$\lvert\frac{\partial n}{n}/\frac{\partial x_2}{x_2}\rvert$	x_3	$\lvert\frac{\partial n}{n}/\frac{\partial x_3}{x_3}\rvert$	t	$\lvert\frac{\partial n}{n}/\frac{\partial t}{t}\rvert$	a	$\frac{\Delta n}{n}$ **	*** μC/ml	$\frac{\Delta n}{n}$
0.4	<0.1	6	0.3	9.5	< 3	−17	0.3	1	0.01 −0.04	0.12	0.004
0.5	<0.1	8	0.3	10	< 3	−20	0.06	2	0.007−0.03	0.6	0.002
0.7	0.6	10	0.3	10.5	< 3	−22	0.02	4	0.005−0.02		

* in different vial positions.
** n = standard deviation of the average.
*** quoted figures indicate the conc. interval normally used.

spectrometer technique. In the region of low deuterium content (< 1 % D) the spectrometer measurements were reproducible to within 0.5 %.

Tritium analyses were performed with the aid of the bremsstrahlung method [5] or by the liquid scintillation technique. The latter method required removal of the water from the salt solutions by distillation before measurements were made. The distillations were carried out to completion to avoid isotope effects. In the bremsstrahlung method the high tritium content required (> 1 mC/ml), caused heat to be generated in the cell, and thus, at least from a theoretical point of view, convection could occur. It was therefore worthwhile to compare the results from the two independent analytical methods. By a systematic search for different sources of inaccuracies in the liquid scintillation method the standard deviation of single analyses could be reduced to about 0.6 %. No standard solution was needed either in the liquid scintillation method or in the bremsstrahlung method, as the net pulses were shown by experimental tests to be proportional to the tritium content.

An Ekco liquid scintillation unit (model N-612) with single photomultiplier working at −22°C was used normally. Another instrument, the Packard Tri-Carb spectrometer (model 314-X), was tested in order to obtain increased reproducibility, but no improvement was attained. The liquid scintillation system was a conventional one: 0.2 − 0.5 g water, 10 ml scintillator (6 g PPO/l toluene) and 8 ml ethanol. Some of the effects influencing the stability of the output signal such as amount of sample, quenching effects of the components, temperature, stability of the instrument, vial placing, randomized disintegration rate, are quoted in Table 1. Every sample was counted 4 − 5 times with different vial positions in order to reduce the random variation due to vial location and each sample was counted 3 − 5 times in 100 sec in a single vial position. The whole instrument was kept in a dark room which had only a red light, and the vials were kept in the refrigerator for at least 20 min before counting.

The bremsstrahlung method [5] has been improved now by including two GM-tubes with mica windows (Philips PW 1962) and a more suitable cell (Fig. 2). The bremsstrahlung method was developed originally to give a good reproducibility. The reproducibility was of the same order as the deviations due to the randomized disintegration rate. The amount of sample necessary for counting was about 1.2 ml with a tritium content of normally 10 − 50 mc/ml given 1000 − 5000 cpm. The background was 100 cpm and the counting time 20 − 60 min. The background was measured before and after each c_{av} and c_0, to ensure that instability or increased background would not influence the net counting rate. In order to avoid contamination and health hazards, precautions must be taken when working with tritiated water having a high T-content. Special care should be taken to avoid skin permeation and lung absorption. Some urine analyses, however, indicated no body burden of tritium.

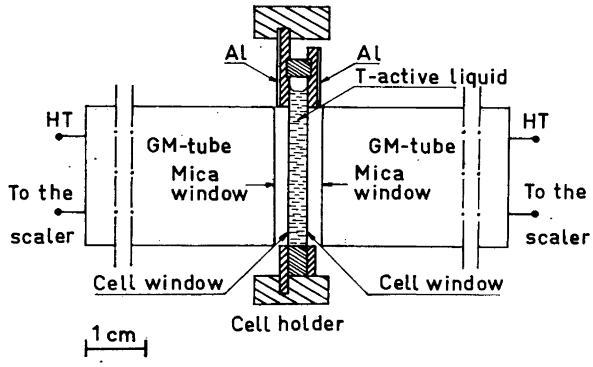

Fig. 2. Scheme of T-measurement on active liquids by bremsstrahlung.

RESULTS

Natural water. The self-diffusion of water was determined at 25.0 ± 0.05°C with deuterium at the average concentrations (N) 0.025, 0.135 and 2.0 molar percent. The results, averages of n single determinations, are given in Table 2. The initial concentration difference in the diffusion cell is quoted (ΔN). Analyses at the two lower concentrations were performed with a mass spectrometer, while the 2 % solution was analysed by means of the gradient tube method. Because of the larger standard deviation of the latter method these results are not included in the total average. The measure of accuracy is given both as the standard deviation of the mean (σ) and the deviation of the mean at the 90 % confidence limit (σ_{90}).

Table 2. The self-diffusion coefficient of water at 25.0°C. Deuterium as tracer.
N = av. deuterium conc. (molar fraction), ΔN = initial conc. difference
n = number of measurements
σ = standard deviation in the mean
σ_{90} = deviation at 90 % confidence limit

$N \times 10^2$	$\Delta N \times 10^2$	n	$D \times 10^5$ cm²/sec	σ	σ_{90}	Method of analysis *
0.025	0.065	4	2.24	0.02	0.05	M
0.135	0.29	5	2.27	0.02	0.04	M
2.0	4.0	(7)	(2.37)	(0.09)	(0.18)	G
	average	9	2.25	0.01	0.02	

* M = mass spectrometer, B = bremsstrahlung method, L = liquid scintillation technique G = gradient tube method.

Table 3. The self-diffusion coefficient of water at 25.0°C. Tritium as tracer.

$N \times 10^2$	$\Delta N \times 10^2$	n	$D \times 10^5$ cm²/sec	σ	σ_{90}	Method of analysis
0	0	5	2.29	0.03	0.06	B
0.5—2	1—4	6	2.23	0.01	0.02	B
0.5—2	1—4	6*	2.22	0.02	0.03	B
0.5	1	(9)	(2.26)	(0.06)	(0.11)	L
	average	17	2.25	0.01	0.02	

* these measurements at pH = 4.9.

Table 4. The self-diffusion of water at 25.0°C. Comparison of literature data. ΔD = reported accuracy.

Tracer or method	D	ΔD	Authors	Ref.	Remarks
NMR	2.13	7 %(a), 3 %(b)	Simpson and Carr (1958)	16	
	~2.33	—	Douglass and McCall (1959)	17	25.5°C; from diagram
^{18}O	2.66	± 0.12(c)	Wang *et al.* (1953)	11	
	2.57	± 0.02(c)	Wang (1954)	14	
	~2.57	± 2 %(e)	Adamson and Irani (1957)	1	from diagram
D	2.34	± 0.08(c)	Wang *et al.* (1953)	11	
	2.26	± 0.001(c)	Longsworth (1954)	13	extrapol.value
	2.25	± 0.01(d)	Undeman (1955)	15	
	2.38	± 4 %(e)	Adamson and Irani (1957)	1	extrapol.value
	2.27	± 0.001(c,g)	Longsworth (1960)	18	extrapol.value
	2.25	± 0.02(f)	This work	Table 2	
T	2.44	± 0.06(c)	Wang *et al.* (1953)	11	
	2.64	5 %(e)	Cuddeback *et al.* (1953)	12	
	2.25	± 0.02(f)	This work	Table 3	

(a) estimation of the max.deviation
(b) » of max. systematic error
(c) standard deviation
(d) » » in the mean
(e) reproducibility
(f) deviation in the mean at 90 % confidence limit
(g) this value replaces 2.26 in Ref.[13]

Table 5. The self-diffusion of water in H_2O-D_2O mixtures at 25.0°C. Tritium as tracer.

$N \times 10^2$	$\Delta N \times 10^2$	n	$D \times 10^5$ cm²/sec	σ	σ_{90}	Method of analysis
0—2	0—4	Table 3	2.25	0.01	0.02	B
50	4	6	2.11	0.01	0.02	B
98	1.5	6	1.90	0.02	0.04	B

Results with tritium as tracer are given in Table 3. The total average value for tritium does not include the results from the liquid scintillation method due to the increased standard deviation. To obtain a positive density gradient in the diffusion cell, 1 % D_2O was usually added to the solution in the lower part of the diffusion cell. This amount of deuterium causes only a very slight change in the diffusion coefficient as can be seen from Fig. 3. A moderate decrease of pH to 4.9 had no influence on the diffusion coefficient (Table 3).

Comparison between the results in Tables 2 and 3 shows that the isotope effect seems to be within the experimental error. Data on the self-diffusion

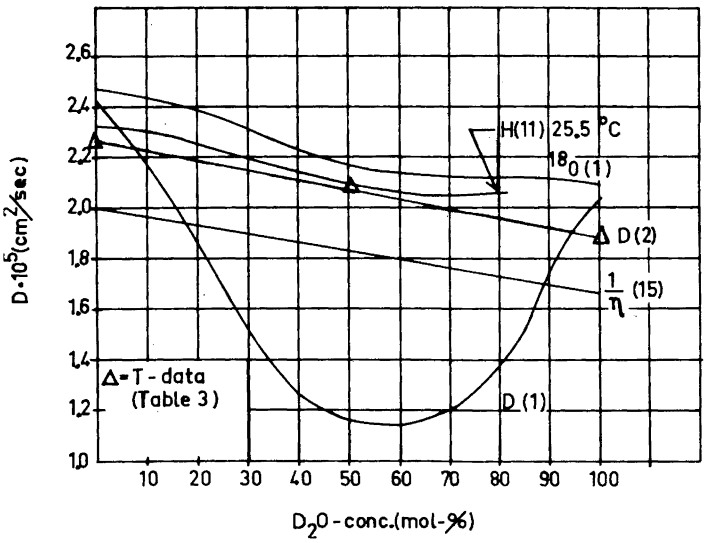

Fig. 3. Comparison of literature data concerning the self-diffusion coefficient of water at 25.0°C in H_2O-D_2O mixtures. Figures within brackets indicate reference numbers. Viscosity data are normalized to 2.0 for pure H_2O.

coefficient of water obtained from measurements with different tracers and methods may be inaccurate and could contain systematic errors, thus making it impossible to estimate the isotope effect from literature data. Results of known data measured at 25°C and obtained with different techniques [1,11–18] are given in Table 4. Measurements of Orr and Thomson [6], Temkin [7], Orr and Butler [8], Lamm [9] and Rögener [10] are not included. It is intended to do further investigations using ^{18}O and the present method in order to verify if the isotope effect is insignificant in that case too.

Table 6. The self-diffusion of water in electrolytic solutions at 25.0°C. Tritium as tracer. c = solute conc. (molarity).

	c	n	$D \times 10^5$ cm²/sec	σ	σ_{90}
NaCl	0.17	3	2.30	0.02	0.06
	0.99	6	2.15	0.01	0.02
	1.96	9	1.99	0.05	0.09
	4.05	8	1.64	0.03	0.06
LiBr	0.012	2	2.30	0.01	0.06
	0.12	8	2.26	0.02	0.04
	0.52	3	2.26	0.04	0.12
	3.27	5	1.70	0.02	0.04
$MgSO_4$	0.078	3	2.29	0.01	0.03
	0.36	6	1.96	0.03	0.06
	0.72	5	1.68	0.01	0.02

H_2O—D_2O mixtures. To justify the addition of 1 % D_2O to the solutions in the lower part of the cell the diffusion coefficient of HTO in 50 % and 100 % D_2O was differentially measured at 25°C. The results are given in Table 5. These measurements together with those of other workers are plotted in Fig. 3. As can be seen from Fig. 3 the self-diffusion coefficient and the inverse viscosity follow the same course when increasing the deuterium content, and the product ηD_0 is almost constant within the whole concentration interval.

Salt solutions. The results from measurements in dilute and moderately concentrated solutions of NaCl, LiBr and $MgSO_4$ at 25.0°C are given in Table 6 and normalized in Fig. 4. This figure also includes measurements of Wang [14] and unpublished data of Undeman [15]. The inverse viscosity obtained from literature data is given as a comparison. The absolute values of Wang's data obtained with ^{18}O as tracer differ from the present data, but on normalizing at $c = 0$ the agreement is excellent as can be seen from the NaCl data.

Estimation of errors. With the present technique efforts were made to minimize the systematic errors. The only data necessary to calculate D, apart from c_{av}/c_0, are the diffusion time and the length of the cell. The values of the analyses of the D and T content in both compartments of the cell were tested by inserting them in eqn. (5) thus reducing the possibility of inaccuracy.

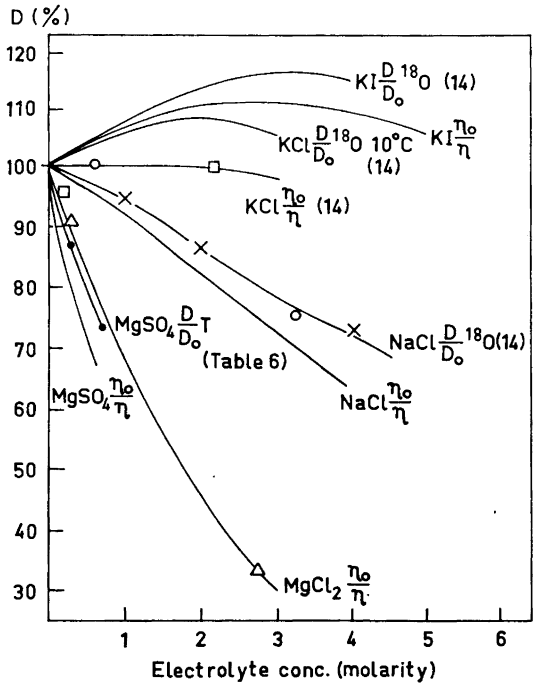

Fig. 4. Normalized self-diffusion coefficient of water at 25.0°C in salt solutions. Comparison of data of Wang, Undeman and the present work.
□ = KCl$(D/D_0)D^{15}$; △ = $MgCl_2(D/D_0)D^{15}$; × = NaCl$(D/_0D)T$, (Table 6);
○ = LiBr$(D/D_0)T$, (Table 6).

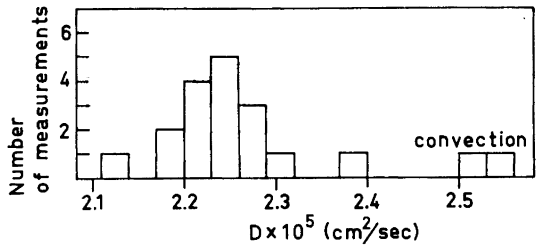

Fig. 5. Frequency distribution of the data on the self-diffusion coefficient in pure water. Tritium used as tracer. Analyses performed with the bremsstrahlung method.

Systematic errors may result *a priori* from convection in the diffusion cell; this has been observed in about 10 % of the experiments. Convection results in a cast Gaussian distribution of the self-diffusion coefficient. This distribution becomes extended at higher values of the coefficient as no compensating lowering effect exists. In Fig. 5 the distribution of the data from measurements on pure water demonstrates this phenomenon. Diffusion data appreciably higher than the average have therefore been excluded. This procedure is justified mathematically if one can make the assumption that the probability of a certain convection effect decreases when the effect increases. Though convection did occur it was possible to make accurate measurements at initial density differences as low as 10^{-5} g/cm^3.

DISCUSSION

According to Lamm's [19,20] theory concerning the relationship between mutual diffusion and self-diffusion, the latter can be written in the case of a two component system as:

$$D_0 = \frac{RT}{\Phi_{12} + \Phi_{0(3)}} \tag{6}$$

where the components 0 and 3 may be water and a salt respectively. Component 0 is composed of the two isotopic components 1 and 2 (*e.g.* H_2O and HTO). This formula thus takes into account the existence of different friction properties between the two components ($\Phi_{0(3)}$) compared with the friction between molecules of the same species (Φ_{12}). Even if there is no exact relationship between the mutual diffusion coefficient (D_{03}) and the self-diffusion coefficient (D_0) Lamm [20] has proposed the approximate relation

$$D_0 \approx \frac{D_0^0 D_{03}}{D_{03}\ n_0 v_0^0 + B_{03}\ N_3 D_0^0} \tag{7}$$

where n_0 = concentration of comp. 0
v_0^0 = molar volume of pure 0
N_3 = molar fraction of comp. 3
D_0^0 = self-diffusion coefficient of pure 0
B_{03} = thermodynamic factor

Johnson and Babb [21] found that for the ideal organic system benzene-carbon tetrachloride the eqn. (7) holds to within 10 % and even in the non-ideal systems benzene-methanol and benzene-ethanol to within 15 %. As pointed out by Lamm [20] the approximate relationship expressed by eqn. (7) is not valid however if component 3 changes the specific friction properties of component 0. In the case of dilute and moderately concentrated salt solutions, where the solute does affect the water structure, the use of eqn. (7) would result in too small an effect on the self-diffusion coefficient.

The experimental results on the self-diffusion of water in salt solutions may hypothetically be interpreted in a qualitative manner according to Wang [14,22]: There are two lowering factors, the obstruction and the direct hydration effects. The obstruction effects is due to the diffusion species having to diffuse by a longer path round the ions or hydrated ions, which are more immobile than the water molecules. The obstruction effect for a practically immobile solute can be written [22]:

$$D_0 = D_0^0 \ (1-\alpha x) \tag{8}$$

where α = factor depending on the shape of the obstructing molecules ($\alpha = 1.5$ for spherical molecules).

x = volume fraction of the hydrated obstructing molecules.

In the case of hydrated ions of strong electrolytes, where the mobility is not appreciably lower than that of water, it is expected that the obstruction effect is weak.

The hydration effect arises when solvent molecules are attached to the solute and the rate of exchange between free and bound water is slow compared with the diffusion displacement. With a modification of the formula of Douglas *et al.*[23] the direct hydration effect concerning an immobile solute can be written:

$$D_0 = D_0^0 \left[1-f\left(1-\frac{v_b}{v_0}\right)\right] \tag{9}$$

Where v_b and v_0 are the frequencies of the diffusion displacement of the hydrated water and free water, respectively. f is the fraction of water molecules attached to the solute. In the case of slow interaction between bound and free water eqn. (9) is simplified to

$$D_0 = D_0^0 \ (1-f) \tag{10}$$

In salt solutions the distortion effect increases the self-diffusion and is due to the breaking down of the water structure outside the hydrated complex and thus decreases the local viscosity. Our results and those of Undeman agree with the concept of Wang. Mg^{2+} is more strongly hydrated than Na^+, and $MgCl_2$ therefore has an enhanced obstruction and direct hydration effect compared with Na^+. The distortion effect of Mg^{2+} is weaker than that of Na^+ and weaker still for K^+. The net result expected is a decrease in the self-diffusion coefficient of water in Mg^{2+}-salts compared with the data valid for Na^+. The hydration and obstruction effect of Li^+ is stronger and the distortion effect is weaker than that for Na^+. On the other hand Br^- is thought to have more radical structure-breaking properties than Cl^-. Thus the self-diffusion of water in solutions of LiBr is expected to be approximately the

same as in NaCl solutions. This agrees with the experimental results. If the above theory of Wang is correct the results from measurements on $MgSO_4$ indicate that, in the case of SO_4^{2-}, the obstruction and hydration effect dominate over the distortion effect. The maxima found by Wang in measurements on KCl and KI solutions at about 2 and 3 mole/l respectively and the decrease in the self-diffusion at higher concentrations (see Fig. 4) may be due to the fact that in these concentrated solutions most of the water molecules are bound and thus any further solute molecules added have no water structure to distort.

Acknowledgements. The author is grateful to Professor Ole Lamm for his valuable advice and interest in the present work. Valuable suggestions regarding the detecting methods were kindly offered by Dr. T. Westermark. Mrs. M. Wellmar has assisted with most of the experimental work and she is gratefully acknowledged.

Thanks are also due to Dr. R. Ryhage and Mr. Lerjestad at the Mass-Spectrometer Laboratory for the mass spectrometer analyses and to be Isotope Techniques Laboratory for the use of the liquid scintillation apparatus. Economical support was given by *Statens Naturvetenskapliga Forskningsråd*. The author thanks Dr. I. Wellings for correcting the English in the manuscript.

REFERENCES

1. Adamson, A. W. and Irani, R. R. *J. Am. Chem. Soc.* **79** (1957) 2967.
2. Natl. Bureau of Standard *Tables of the Error Function and its Derivatives*, Washington 1954.
3. Linderstrøm-Lang, K. and Lanz, Jr., H. *Compt. rend. trav. lab. Carlsberg, Ser. chim.* **21** (1938) 315.
4. Linderstrøm-Lang, K., Jacobsen, O. and Johansen, G. *Compt. rend. trav. lab. Carlsberg, Ser. chim.* **23** (1938) 17.
5. Westermark, T., Devell, L. and Ghanem, N. *Nuclear Instr. and Methods* **9** (1960) 141.
6. Orr, W. J. C. and Thomson, D. W. *Nature* **134** (1934) 776.
7. Temkin, M. *Nature* **136** (1935) 552.
8. Orr, W. J. C. and Butler, J. A. V. *J. Chem. Soc.* **1935** 1273.
9. Lamm, O. *Nova Acta Regia Soc. Sci. Upsaliensis Ser IV* **10** (1937) No. 6.
10. Rögener, H. *Z. Elektrochem.* **47** (1941) 164.
11. Wang, J. H., Robinson, C. V. and Edelman, I. S. *J. Am. Chem. Soc.* **75** (1953) 466.
12. Cuddeback, R. B., Koeller, R. C. and Drickamer, H. G. *J. Chem. Phys.* **21** (1953) 589.
13. Longsworth, L. G. *J. Phys. Chem.* **58** (1954) 770.
14. Wang, J. H. *J. Phys. Chem.* **58** (1954) 686.
15. Undeman, C. L. *Unpublished.*
16. Simpson, J. H. and Carr, H. Y. *Phys. Rev.* **111** (1958) 1201.
17. Douglass, D. C. and McCall, D. W. *J. Chem. Phys.* **31** (1959) 569.
18. Longsworth, L. C. *J. Phys. Chem.* **64** (1960) 1914.
19. Lamm, O. *Acta Chem. Scand.* **6** (1952) 1331.
20. Lamm, O. *Acta Chem. Scand.* **8** (1954) 1120.
21. Johnsson, P. A. and Babb, A. L. *J. Phys. Chem.* **60** (1956) 14.
22. Wang, J. H. *J. Am. Chem. Soc.* **76** (1954) 4755.
23. Douglass, D. C., Frisch, H. L. and Anderson, E. W. *Biochim. et Biophys. Acta* **44** (1960) 401.

Received May 14, 1962.

ACTA CHEMICA SCANDINAVICA 16 (1962) 2189–2194

Preparation of Benzene-d_6 by Polymerization of Acetylene-d_2

A. RUPPRECHT

Research Group for NMR, Division of Physical Chemistry, The Royal Institute of Technology, Stockholm 70, Sweden

Dedicated to Professor *Ole Lamm* on his 60th birthday

A water-cooled reaction tube with a centered heating rod electrically heated to about 700°C has been used for the preparation of benzene-d_6 by polymerization of acetylene-d_2. A specially constructed generator is charged with calcium carbide and heavy water is supplied dropwise at a rate corresponding to an acetylene-d_2 production of about 6 l per hour. After some purification, the acetylene-d_2 is fed to the reaction tube and the reaction products formed condense on the cold walls and are collected in a small tube below and parallel to the reaction tube. One third by weight of the raw product is benzene-d_6. After the reaction is completed, the generator is heated to about 600°C which decomposes the calcium hydroxide-d_2 so that the excess water is completely recovered. The yield of benzene-d_6 calculated from the heavy water consumed is about 20 %. The deuterium content of the product lies near that of the heavy water used. The apparatus has also been used for preparation of benzene containing tritium.

Several methods concerning the preparation of benzene-d_6 have been described. They are based on catalyzed hydrogen-deuterium exchange in benzene [1–4] or on polymerization of acetylene-d_2 [4–6]. Only some of these are suitable for preparation on a larger scale, *e.g.*, the method of Brüllman, Gerber and Meier [3] where the deuterium exchange between deuterium chloride and benzene is utilized.

The preparation of benzene-d_6 by polymerization of acetylene-d_2 can be performed by heating acetylene-d_2 to about 600°C in a tube [5]. One difficulty is that the reaction heat liberated by the polymerization creates local hot areas with the resulting formation of higher polymers and coal-like substances. In addition, the conditions for formation of benzene-d_6 are unfavourable from a thermodynamical point of view; naphthalene-d_{10}, for instance, is more likely to be formed [7]. However, by using a reaction vessel with a high temperature gradient, it is possible to reduce these problems. In such a reaction vessel, the "lighter" products formed rapidly diffuse from the hot to the cold zone

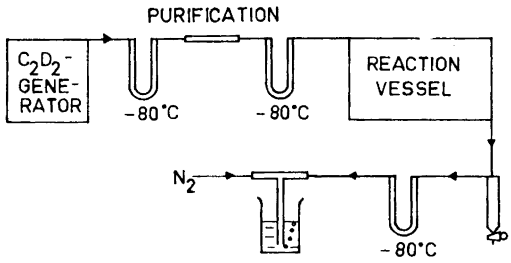

Fig. 1. Flow scheme.

and are thus protected from further reaction. This principle has been utilized for the preparation of benzene by polymerization of acetylene [8], and for the preparation of naphthalene-d_{10} by polymerization of acetylene-d_2[7]. The present method utilizes the principle for the preparation of benzene-d_6.

APPARATUS

The flow scheme shown in Fig. 1 has been used. The specially constructed generator is charged with calcium carbide, and heavy water is supplied dropwise at a rate corresponding to an acetylene-d_2 production of about 6 l per hour. After passing a cold trap, a purification tube [7] containing a mixture of 46 % copper oxide, 46 % manganese dioxide and 8 % silver oxide *, and a second cold trap, the acetylene-d_2 is fed to a slightly inclined reaction vessel consisting of a water-cooled reaction tube with a centered heating rod electrically heated to about 700°C. The reaction proceeds quite calmly and continuously. The reaction products condense on the cold wall of the reaction tube and flow down into a thinner tube parallel to and below the reaction tube. From the reaction vessel, the dark-red liquid flows into a collecting flask from which it can be withdrawn through a stopcock. Gases which do not condense in the cold trap placed after the collecting flask leave the system through a water lock consisting of a T-tube, one arm of which dips down 3—4 cm in water. A slow stream of nitrogen is supplied to the third arm of the T-tube, which maintains a slight over-pressure in the apparatus.

The generator

Acetylene-d_2 has been prepared by many investigators [4–7,9] from calcium carbide and heavy water. In order to get a high yield one utilizes the fact that calcium hydroxide-d_2 gives off water upon heating to about 600°C. From a practical point of view there are some difficulties with the methods generally employed. The moist calcium hydroxide-d_2 formed has a tendency to enclose carbide particles which prevents complete reaction in a reasonable time. By heating this mixture to 600°C, heavy water is liberated and reacts with the carbide particles giving acetylene-d_2. The acetylene-d_2, however, decomposes

* Caution: use of a high concentration of silver oxide can result in explosion.

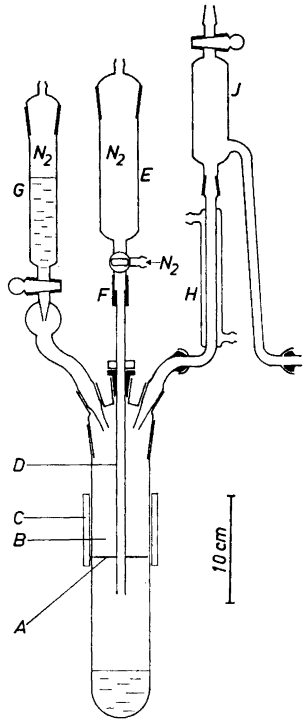

Fig. 2. Acetylene-d_2 generator. A, stainless steel plate; B, carbide; C, electrical element; D, stainless steel tube; E, G, container for heavy water; F, three-way stopcock; H, cooler; J, container which together with H can be bent down at the ball-joints.

in the mixture with mainly coal and deuterium as a result. This problem is eliminated with the generator shown in Fig. 2. As is seen, the generator is supplied with an extra bottom (A) on which lies the carbide (B) heated to about 100°C with an electrical element (C) outside the generator tube. This bottom, which consists of a round stainless steel plate perforated with holes of 3 mm diameter, is attached to a stainless steel tube (D) which fits through a gas-tight Teflon plug at the top of the generator. On the real bottom of the quartz generator tube lies heavy water supplied from the container (E) through the three-way stopcock (F) and the tube (D). The heavy water is allowed to flow into the generator only after all the air in the apparatus has been swept out by nitrogen, also supplied through the stopcock (F). By dropping heavy water from the container (G), acetylene-d_2 and calcium hydroxide-d_2 are formed. The acetylene-d_2 escapes through the cooler (H) where most of the heavy water which follows it condenses and drops back down onto the carbide. The calcium hydroxide-d_2, which exists as a dry white powder as a result of the heating, passes the carbide bed and falls together with small carbide particles down into the heavy water in excess on the real bottom of the generator where the carbide particles react completely. To get a continuous transport through the carbide bed and thus continuous acetylene-d_2 production, one can use a vibrator or some device on the outside attached to the stainless steel tube (D) to periodically swing the tube (D) and the upper bottom through a small

angle. It is also advisable to cool the outside of the real generator bottom with ice water to prevent the reaction heat liberated there from volatilizing the heavy water. When all the carbide has been transformed into calcium hydroxide-d_2 on the real bottom of the generator, this bottom is heated to about 600°C. The heavy water liberated condenses in the cooler (H) which is now bent down at the ball joint and the heavy water is finally collected in the container (J). A practically complete yield is achieved.

The reaction vessel

The reaction vessel used is shown in Fig. 3. A water cooler (K) made of Pyrex glass cools the reaction tube (L) and a small collecting tube (M) connected to the latter by several equidistant short cross-tubes. This unit, which is made of Vycor glass, is tightly held in place by rubber plugs (N) at the ends of the cooler. (It is advisable to use some rubber glue to achieve complete tightness and rigidity). At the center of the reaction tube sits a heating rod (O) made of a quartz tube with an inner heating spiral in a nitrogen atmosphere which heats the rod to about 700°C. The quartz tube is held in place at the ends of the reaction tube by gas-tight Teflon plugs (P). The left plug also holds the inlet (Q) for acetylene-d_2.

The collecting tube contains a device consisting of a movable stainless steel rod (S) with a knob (R) and with Teflon membranes attached at the same intervals as the cross-tubes mentioned above. (Every membrane is held in place between two small nuts on the screwed rod). The membranes, when in a position away from the openings of the cross-tubes, fit tightly to the walls of the collecting tube thus preventing gases, mainly acetylene-d_2, from escaping the reaction tube. The main reaction occurs at the left end of the reaction tube where the acetylene-d_2 is supplied. This is concluded from the fact that the heating rod is hotter (is more light-red) in this area because of the heat liberated by the reaction. Also at this end, the fumes and gases can be seen to circulate between the reaction tube and the collecting tube. This occurs because of the inclination of the tube (about 1:10) and the influence of the temperature gradient. The reaction products condense on the walls of the reaction and the collecting tubes and are finally automatically collected in the latter as a dark-

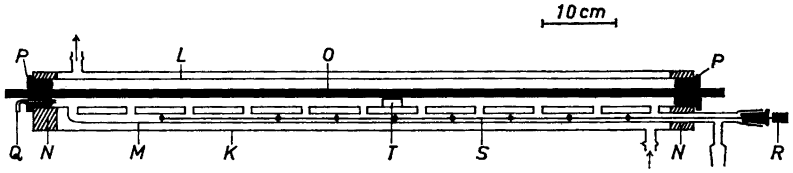

Fig. 3. Reaction vessel for polymerization of acetylene-d_2 to benzene-d_6. K, water cooler made of Pyrex glass; L, reaction tube connected to the collecting tube M by equidistant cross-tubes, the unit is made of Vycor glass; N, rubber plug; O, heating rod; P, gas-tight Teflon plug; Q, inlet for acetylene-d_2; R, knob for displacing the insert S; T, quartz support for O.
The reaction vessel is slightly inclined to the right.

red, clear liquid. By displacing the insert (S) in the collecting tube so that the Teflon membranes come just in front of the crosstubes, the product is allowed to flow out into the collecting flask described earlier.

EXPERIMENTAL

For an 8 h experiment the generator is charged with 80 g of calcium carbide previously heated to about 600°C to decompose the calcium hydroxide on the surface of the carbide pieces. The container (G) (Fig. 2) is supplied with 25 g of heavy water, the container (E) with 25—50 g. The three-way stopcock (F) is then opened for nitrogen for about 20 min so that all the air in the apparatus is swept out. Then the stopcock is turned so that all the heavy water in the container (E) is transferred to the bottom of the generator. Now heavy water is supplied dropwise from the container (G) at a rate corresponding to an acetylene-d_2 production of about 6 l per hour. In the reaction tube, the heating rod, if new, will be covered with a thin layer of coal when acetylene-d_2 first is introduced. This coal layer seems to have a catalyzing effect. If the supply of acetylene-d_2 is irregular or too high, the acetylene-d_2 concentration near the heating rod will be so high that a direct decomposition into coal and deuterium will occur [7,10]. This appears as a flame wandering some centimeters along the heating rod giving rolling veils of coal attached to the heating rod. The phenomenon slightly diminishes the yield, but on the other hand because of the catalyzing effect of the veils, it increases the capacity of the reaction tube. When the preparation is completed, after about 4 h, the excess heavy water in the generator is driven off by heating to about 600°C as described above. The heavy water thus recovered is used for filling the container (E) of the generator in the next run and so on. The raw product is distilled for benzene-d_6.

Table 1 shows the yields of four successive runs, each starting from 80 g of pre-heated technical calcium carbide. This amount of carbide theoretically should consume 25.4 g of heavy water corresponding to 35.5 g of benzene-d_6.

The fresh heavy water used contained 99.78 atom % deuterium in the hydrogen. The deuterium content measurements were made with a proton magnetic resonance method [11].

Table 1. Results from four successive runs.

Run	D_2O-consumed (g)	Generator-yield (%)	Amount rawproduct (g)	Amount C_6D_6 received (g)	Yield of C_6D_6 (%)	Deuterium-content of the product (atom %)
1	25.4	100.0	21.8	~7	~20	99.50
2	25.0	98.4	21.5	~7	~20	—
3	25.5	100.3	Break because of mishap		—	—
4	24.9	98.0	21.7	~7	~20	99.40

The deuterium content of the heavy water recovered after the forth run had decreased to 99.60 atom %.

DISCUSSION

As described above, one third by weight of the raw product is benzene-d_6 corresponding to a yield of about 20 %. The residue has not been thoroughly investigated but it contains toluene-d_8, naphthalene-d_{10} and many other aromatic substances which can be of interest in themselves. However, by burning this residue in oxygen to heavy water, it should be possible to increase the net yield of benzene-d_6 to about 50 %.

As is shown in Table 1 the deuterium content of the product is about 0.3 atom % lower than that of the heavy water used. This is mainly due to the method used here in charging the generator with carbide. The previously dehydrated carbide was poured from its container into the generator and could react with moisture in the air during this procedure. The thin but invisible layer of calcium hydroxide thus formed contributes in later reactions to the light hydrogen content of the product and of the heavy water recovered. This contamination can be avoided if the carbide is pre-heated to 600°C *inside* the generator under slow passage of nitrogen to withdraw the light water liberated. Thereafter, generation of acetylene-d_2 will give the maximum deuterium content [6]. The net yield of benzene-d_2 increases with the purity of the acetylene-d_2 because of a decreased tendency to side reactions. Especially pure carbide has thus been used by some workers [4]. On the other hand, the purification described above seems to be effective, and further purification has failed to increase the yield.

Starting from acetylene containing other isotopes of hydrogen and/or carbon it is possible to use the apparatus for the preparation of products containing these isotopes. Thus the apparatus has been utilized for preparing benzene containing tritium starting from calcium carbide and water containing tritium.

Acknowledgements. The author wishes to express his gratitude to Professor Ole Lamm, Head of this Division, for excellent working facilities, and to Dr. E. Forslind, Head of the Research Group for NMR, for interesting discussions.

REFERENCES

1. Ingold, C. K., Raisin, C. G. and Wilson, C. L. *J. Chem. Soc.* **1936** 915.
2. Leitch, L. C. *Can. J. Chem.* **32** (1954) 813.
3. Brüllmann, M., Gerber, H. J. and Meier, D. *Helv. Chim. Acta* **41** (1958) 1831.
4. Murray, A. and Williams, D. L. *Organic syntheses with Isotopes* II, New York 1958, with further references.
5. Clemo, G. R. and McQuillen, A. *J. Chem. Soc.* **1935** 851.
6. Shapiro, I. *J. Am. Chem. Soc.* **79** (1957) 3294.
7. Goubeau, J., Luther, H., Feldmann, K. and Brandes, G. *Ber.* **86** (1953) 214.
8. South-Manchurian Railroad Co. **Japan 163, 150,** Mar. 23, 1944. (Patent).
9. Breuer, F. W. *J. Am. Chem. Soc.* **58** (1936) 1289.
10. Robertson, W. W., Magee, E. M., Fain, J. and Matsen, F. A. *Fifth Intern. Symposium of Combustion*, Pittsburg 1954, publ. 1955, p. 628.
11. The NMR–EPR Staff of Varian Associates, *NMR and EPR Spectroscopy*, Pergamon Press, Oxford 1960, p. 112.

Received April 16, 1962.

ACTA CHEMICA SCANDINAVICA 16 (1962) 2195–2198

Some Observations on Protein Biosynthesis

OLLE SNELLMAN

The Cancer Research Division of Radiumhemmet, Karolinska Institute, Stockholm 60, Sweden

Dedicated to Professor *Ole Lamm* on his 60th birthday

It has been pointed out that the high entropy change in protein biosynthesis necessitates another synthesis mechanism than that for the synthesis of the usual di- or tripeptides, where the entropy effect is not so large. The possibility of an upper limit for one step formation of a peptide chain is discussed. In consequence of this, longer peptide chains, as in collagen, must be built in two steps.

Proteins are polymers of amino acids, but they are polymers which are closely defined as to structure and molecular weight. Studies of the amino acid sequences of proteins indicate a remarkable specificity in the sequences, indicating a well organized biosynthesis machinery. During recent years the biosynthesis of proteins has been a main interest in biochemistry since ways have been found to elucidate some features of the process.

The biosynthesis can be divided into three different main steps. The first stage consists in the sending out of information from the nuclear part of the cell to the synthesis mechanism as to how the protein should be built up. The second part is the synthesis of the peptide chain or chains which build the protein, and the last step is the formation of the protein from the chains. The discussion here concerns mainly the second stage, *i.e.* the biosynthesis of the peptide chain.

Studies of Hoagland [1] and others show that the first step in the route of amino acid incorporation is that the acids are esterified to ATP * by special enzymes. There are as many different enzymes performing this esterification as there are amino acids. When studying the incorporation of labelled amino acids Hoagland *et al.* [2,3] found that the amino acids were then transferred to a ribonucleic acid from the soluble fraction (s-RNA). Even here there is one kind of specific acceptor for each amino acid (Leahy *et al.*[4]). The amino acid is bound terminally to s-RNA by an ester linkage (Zachau *et al.*[5]). From the work

* Abbreviations: ATP, adenosine triphosphate; GTP, guanosine triphosphate; s-RNA, soluble ribonucleic acid.

of Zamecnik *et al.*[6] it is known that the microsome particles (called ribosomes) are involved in the last step where the peptide synthesis occurs. The ribosomes contain on the surface nucleic acid, which, together with the s-RNA, might give the right sequence. Not much is known about the condensation mechanism which is independent of the sequence giving factor. It has been shown that GTP takes part in the condensation (Keller and Zamecnik[7]) but the extent to which it has broken down is unknown as specific systems have not been used. A transferring enzyme, having an SH-group, is known to exist. The author has shown that vitamin C cooperates with it [8].

It seems that a distinction should be made between protein synthesis and polypeptide synthesis when investigating *in vitro*. Protein synthesis will be defined as a synthesis performed in such a way that every amino acid occurs in its right place in the sequence as determined by the information given for the protein. Polypeptide synthesis will be an incorporation of amino acids more randomly. This distinction means that it is not always enough to show that a tracer amino acid has been incorporated with peptide bonds in a chain. It ought also to be shown that it is in its right site in the sequence.

Lipmann [9] has shown that labelled leucine esterified to s-RNA of bacterial origin, together with ribosomes from liver, shows an incorporation of the labelled leucine in peptide bonds on the ribosome. He remarks on the low specificity of the bacterial s-RNA in synthesis reactions. However it seems that in this case one is dealing with a polypeptide synthesis and that this can explain the low specificity of the bacterial s-RNA. The peptide bond synthesis is independent of the ordering factor and it is possible to perform the peptide bond synthesis with any amino acyl residue. It may thus happen now and then that an amino acyl ester will come in such a position that a peptide bond synthesis can occur without any ordering factor taking part in the process. The rate of synthesis *in vitro* is very low, being about 0.001 of that *in vivo*, and in many cases where the ratio between s-RNA amino acids and ribosomes is unfavorable only polypeptide synthesis is obtained. It is certain that *in vivo* factors will be found regulating the ratio between s-RNA and ribosomes so that the order will not be disturbed.

As can be seen, protein synthesis requires a large amount of energy. The energy for inserting each amino acid in the peptide bond chain is taken from ATP and GTP. The peptide bond in a chain has, however, a low value of free energy (Borsook [10]). This very great discrepancy depends of course on the very high change in entropy occurring when a system with a high degree of order is obtained. The consequence of this is that the enzymatic processes as they usually occur cannot be used here. Often only one choice of combination is used and the entropy change is not of this magnitude.

It is therefore not possible to study the synthesis of peptide bonds using only one choice, as in hippuric acid and glutathione, and expect to obtain any information of great value about protein synthesis. In such cases the synthesis mechanism is quite different and it would be a waste of energy to use there the process of protein synthesis. In the case of the former synthesis the principle of active surfaces can be used to lower the energy of activation of the reaction. In the ordinary reactions the enzyme thus tunnels under the energy pass between the reactants and the results of the reaction.

The energy of activation is, according to Eyring [11], a function of the entropy, and if the change is large the energy of activation cannot be lowered appreciably. It is then quite understandable that the energy providing reaction in protein synthesis must be quite unspecific as concerning amino acids. The different amino acids have nothing in common except the two groups taking part in the reaction. The usual principle of active surfaces for the enzyme cannot be used between the amino acids and the enzyme cannot directly take part in the coupling process. It can only release and transport energy for the process. It takes part in an activation process of the α-amino group. In this process the enzyme cooperates with dehydroascorbic acid forming a complex which is the active enzyme. The α-amino group is phosphorylated to a high energy compound by transfer of pyrophosphate from guanosine triphosphate [12]. Both amino and imino groups can be phosphorylated while both amino and imino acids are incorporated in peptide chain. It is shown by the synthesis of poly-α-amino acids from their methyl esters that the reaction is unspecific as far as the type of esterbonds is concerned [13].

The phosphorylation can only be done if the amino group is unionized. Thus the start of the synthesis is a problem, because at the pH where the reaction occurs the amino acids and most dipeptides have their amino groups ionized and only longer peptides have sufficiently low pK values of their α-amino groups. The hormone thyroxine, however, is an exception in a low enough pK value of its α-amino group to react [14]. In a reaction mixture with tyrosine methylester as a substrate no polyamino acid is synthesized unless thyroxine is added as an initiator of the synthesis [13].

Thus, in the synthesis of the peptide chain both vitamin C and the hormone thyroxine take part.

Concerning the biosynthesis of proteins the following question will at last be discussed: How large is the largest peptide that can be synthesized in one step of the synthesizing machinery?

The biosynthesis occurs on the surface of the ribosomes. If it is now supposed that every ribosome is an independent synthesizing site some very rough estimate can be made. The ribosomes have, during recent years, been studied quite a lot with different physicochemical methods. They seem to be built up of smaller units which are cemented together by magnesium ions. The largest particles have a diameter of about 150 Å and it is such particles which will be found on the microsomes. The synthesis takes place on the surface of these larger ribosome particles. If the whole surface were covered with amino acids, each taking up a space of 34 Å^2, a peptide chain of a molecular weight of 450 000 could be synthesized. Now only a small part of the surface can be free for the peptide chain, because ribonucleic acid takes up most of it and even other substances adhere. A very rough estimate shows that less than one tenth can be occupied by the chain. Thus the upper limit of the molecular weight is 45 000.

Without laying any greater weight on the value it can be supposed that a comparatively low value can be estimated as the upper limit for the synthesis of a peptide chain in one step. This can give some conclusion about the structure of proteins.

It is to be expected that many of the proteins with higher molecular weights are built up of smaller peptides. Such an example is the tobacco mosaic virus which is built up of 2 400 peptides with the molecular weight of 17 500. An other example is haemoglobin having a molecular weight of 66 000 and composed of four peptide chains. Many other examples can be given. It seems that an optimal molecular weight for the peptide chains formed could be anywhere in the vicinity of 17 000—20 000. It is quite possible, in spite of all criticism, that there is a kernel of truth in the old theory of Svedberg [15] that all larger proteins were built up from a subunit of molecular weight 17 500.

There must be many exceptions to this rule. In every case where an exception is suspected the structure must first be investigated so that it is really certain that only one long peptide chain occurs. It can then be expected that the chain has been built up in at least two steps. In the second step the smaller peptides are synthesized together to longer peptides.

The investigations of the author [16] on the biosynthesis of collagen show that this really occurs. The collagen molecule is built up of three chains, every one having a molecular weight of about 120 000. They are thus much longer than could be expected from what has been said above. However, in this case smaller nucleotide peptides of collagen are first synthesized and are then synthesized together to form the peptide chains in another step outside the cell. This necessity for a two step synthesis will support the presumption of an upper limit for the peptide synthesis on the ribosomes. If the structure of the molecule alone was known one would have imagined that an upper limit did not exist.

Acknowledgements. The author is indebted to the chief of the laboratory Dr. B. Sylvén for his kind interest. The investigations are supported by grants from the *Swedish Natural Science Research Council*, the *Swedish Cancer Society*, the *Swedish Medical Research Council, King Gustaf V's Jubilee Fund, King Gustaf V's 80th Anniversary Fund.*

REFERENCES

1. Hoagland, M. B. *Biochim. et Biophys. Acta* **16** (1955) 228.
2. Hoagland, M. B., Zamecnik, P. C. and Stephenson, M. L. *Biochim. et Biophys. Acta* **24** (1957) 215.
3. Hoagland, M. B., Stephenson, M. L., Scott, J. F., Hecht, L. Z. and Zamecnik, P. C. *J. Biol. Chem.* **231** (1958) 241.
4. Leahy, L., Allen, E. and Schweet, R. *Federation Proc.* **18** (1959) 270.
5. Zachau, H. G., Acs, G. and Lipmann, F. *Proc. Natl. Acad. Sci. U.S.* **44** (1958) 885.
6. Littlefield, J. W., Keller, E. B., Gross, J. and Zamecnik, P. C. *J. Biol. Chem.* **217** (1955) 111.
7. Keller, E. B. and Zamecnik, P. C. *J. Biol. Chem.* **221** (1956) 45.
8. Snellman, O. *To be published.*
9. Nathans, D. and Lipmann, F. *Biochim. et Biophys. Acta* **43** (1960) 126.
10. Borsook, H. *Advances in Protein Chem.* **8** (1953) 127.
11. Glasstone, S., Laidler, K. and Eyring, H. *The Theory of Rate Processes*, Mc Graw-Hill, New York 1941.
12. Snellman, O. *To be published.*
13. Snellman, O. *To be published.*
14. Snellman, O. *To be published.*
15. Svedberg, T. *Proc. Roy. Soc. (London)* **B 127** (1939) 1.
16. Snellman, O. *J. Biophys. Biochim. Cytol. In press.*

Received April 13, 1962.

ACTA CHEMICA SCANDINAVICA 16 (1962) 2199–2211

On the Thermodynamic Theory for the Effect of Pressure on Surface Tension

JAN CHRISTER ERIKSSON

Division of Physical Chemistry, Royal Institute of Technology, Stockholm 70, Sweden

Dedicated to Professor *Ole Lamm* on his 60th birthday

Using the thermodynamic methods for treating planar surface systems which have previously been discussed by the author, equations are derived stating the effect of pressure upon the surface tension of binary liquid-gas systems. By applying these equations to experimental data it is shown that the pressure dependence of the surface tension can be predicted with satisfactory accuracy for pressures up to several hundred atm. The calculated molecular surface areas for the gaseous components are in reasonable agreement with the corresponding surface areas which are commonly employed in the BET surface area method.

It has long been recognized that the surface tension derivative with respect to pressure fulfills the relationship

$$\left(\frac{\partial \gamma}{\partial p}\right)_{T,A} = \left(\frac{\partial V}{\partial A}\right)_{T,p} \tag{1}$$

where V is the total volume and A the surface area of the system. Lewis and Randall [1] pointed out that this equation should be valid for *all* closed equilibrium systems, regardless of the number of constituents present and of possible dissolution and adsorption equilibria. This statement is apparently correct, since for a closed equilibrium surface system the Gibbs free energy differential is

$$\mathrm{d}G = -S\mathrm{d}T + V\mathrm{d}p + \gamma\mathrm{d}A \tag{2}$$

G being defined as $G = U - TS + pV$. It thus appears that the condition for the validity of eqn. (1) is that G is a state function, *i.e.* that $\mathrm{d}G$ is a total differential. Rice [2] deduced that the volume change, caused by an increase in the surface area of a liquid-gas system at constant T and p, is mainly made up of two counteracting contributions *viz.* (*a*) an intrinsic volume increase due to the decreased density of the surface phase, (*b*) a decrease of the gas phase volume

caused by adsorption at the liquid-gas interface. He also concluded that the first-mentioned effect might be predominating only when using an inert gas like helium which is weakly adsorbed. In such a case it could therefore be expected, according to eqn. (1), that the surface tension increases when applying a higher pressure. This prediction was later confirmed experimentally by Slowinski, Jr. *et al.*[3] for water-helium and by Gielessen and Schmatz [4] for hexane-helium and nonane-helium. For all other liquid-gas systems so far investigated the converse behaviour has been found [3-5]. Although Gibbs' adsorption formula has been applied to cases of surface tension lowering [6], evidently no detailed theory based on Gibbs' thermodynamics for surface systems has yet been developed which may account quantitatively for all the experimental finding, including the behaviour of the liquid-helium systems and the course of γ-p curves at higher pressures. The present author therefore judged that it might be worth while to apply the theoretical methods described in an other paper [7] to these questions.

THEORY

It has been shown (*cf.* Ref.[7]) that for a planar equilibrium system the chemical potential μ_i^s of a substance in a surface phase is related to μ_i^b, the chemical potential in a bulk phase, by

$$\mu_i^s = \mu_i^b + A_i\gamma \tag{3}$$

where γ is the surface tension and A_i the partial molar surface area defined as $A_i = v_i^s/\tau$ where v_i^s denotes the partial molar volume in the surface phase and τ the thickness of the surface phase, *i.e.* the depth of the region near the surface with properties differing from the bulk phase properties. μ_i^s as well as v_i^s should be regarded as mean values of the local properties within this surface layer. It is evident that A_i corresponds to the projected area of a molecular volume only in the case of a monolayer. In this connection we may conveniently regard A_i as independent of pressure (but not of composition), thus postponing the most general treatment.

If it were possible to subject a two-component liquid-gas system to pressure at constant temperature without the appearance of adsorption and dissolution reactions of the gaseous component, we would expect that the surface tension would increase. This is because on differentiating eqn. (3), applied to the liquid component B_1, with respect to pressure and taking into account that for 1 mole of a pure substance (* denoting the pure state)

$$\left(\frac{\partial\mu_i^{s*}}{\partial p}\right)_T = v_i^{s*} \qquad \left(\frac{\partial\mu_i^{b*}}{\partial p}\right)_T = v_i^{b*} \tag{4 a, b}$$

the eqn.

$$\left(\frac{\partial\gamma_1^*}{\partial p}\right)_T = (v_1^{s*} - v_1^{b*})/A_1^* \tag{5}$$

is obtained, where $v_1^{s*} - v_1^{b*} > 0$ for most liquids[8]. Actually, these circumstances are never encountered; it is instead necessary to regard both the liquid bulk phase (b′) and the surface phase (s) as mixtures consisting of two components.

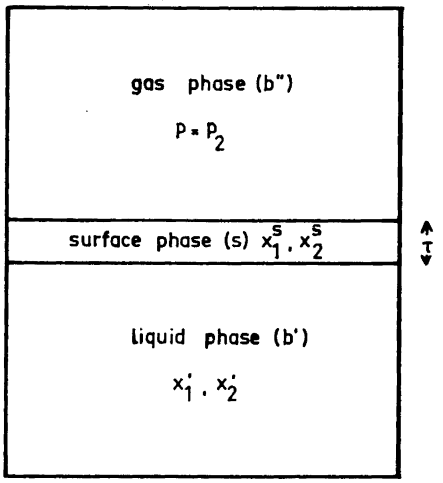

Fig. 1. Sketch of the system studied.

However, since the vapour pressure of the liquid component is often comparatively small, the gas phase (b″) may be considered as containing only the gaseous component B_2, implying that the total pressure p can be equalled to the pressure p_2. Only binary systems of the above category will be dealt with here (*cf.* Fig. 1). Thus we have to investigate the consequences of the following equilibrium conditions

$$\mu_1^s = \mu_1' + A_1\gamma \tag{6}$$

$$\mu_2^s = \mu_2' + A_2\gamma \tag{7}$$

$$\mu_2' = \mu_2'' \tag{8}$$

where *indices* ′ and ″ refer to the two bulk phases b′ and b″ and all μ:s should be regarded as functions of composition and pressure. By introducing Lewis' activity definition and taking the pure substances at the temperature T and the varying pressure p as the *reference states* [9], eqns. (6) and (7) can be written

$$x_1^s/x_1' = F_1 \exp[(A_1\gamma - A_1^*\gamma_1^*)/RT] \tag{9}$$

$$x_2^s/x_2' = F_2 \exp[(A_2\gamma - A_2^*\gamma_2^*)/RT] \tag{10}$$

F_i denoting a ratio of activity factors *viz.*, f_i'/f_i^s. It is, however, easily derived on integrating eqn. (5) and the corresponding eqn. for pure B_2 and inserting $A_i^* = A_i^\circ$ that at constant T

$$A_i^*\gamma_i^* = A_i^\circ\gamma_i^\circ + \int_1^p (v_i^{s*} - v_i'^*)\, dp \tag{11}$$

where *index* ° refers to a *standard state* defined as the pure substance at the temperature T and a pressure of 1 atm. Since the pressure dependence of F_i is given by

$$\left(\frac{\partial \ln F_i}{\partial p}\right)_{T,x} = \frac{(v_i' - v_i'^*) - (v_i^s - v_i^{s*})}{RT} \tag{12}$$

it may thus be derived from eqns. (9) and (10) that

$$x_1^s/x_1' = F_1^o \, \Gamma_1 \, \exp \, [(A_1\gamma - A_1^o\gamma_1^o)/RT] \tag{13}$$

$$x_2^s/x_2' = F_2^o \, \Gamma_2 \, \exp \, [(A_2\gamma - A_2^o\gamma_2^o)/RT] \tag{14}$$

where F_i^o is the activity factor ratio referred to 1 atm pressure and Γ_i is defined by

$$\Gamma_i = \exp \left[- \int_1^p \frac{v_i^s - v_i'}{RT} \, dp \right] \tag{15}$$

As the compressibility of a liquid is usually very small and as the volume change due to mixing is often of neglible magnitude it might be postulated that at the temperature T the relationships

$$v_i^s = v_i^{s*} = v_i^{so} \; , \; v_i' = v_i'^* = v_i'^o, \quad A_i = A_i^* = A_i^o \tag{16, a, b, c}$$

are approximately fulfilled for many solutions. Eqn. (16 c) also presupposes that no molecules show a concentration dependent orientation at the interface. In the case of liquid-gas solutions, the application of (16) implies that the dissolved gas is supposed to behave as a *liquid* component. A satisfactory approximation for eqn. (15) may thus be

$$\Gamma_i = \exp \, [-(v_i^{so} - v_i'^o)(p-1)/RT] \tag{17}$$

The standard state of B_2 used here, *i.e.* the liquid state of pure B_2 at the (room) temperature T and pressure 1 atm, comprises a *hypothetical* standard state which is characterized by the surface tension γ_2^o, the molar surface area A_2^o and the molar volumes v_2^{so} and $v_2'^o$. Such a liquid state of B_2 could only be forced to exist if it were possible to increase the *internal* pressure by supplying stronger intermolecular attraction forces opposing the effect of thermal motion. We may therefore conclude that γ_2^o often attains a *negative* value for this unrealizable state, at least for gases with low critical temperatures. One may also discuss this standard state from a formal point of view, regarding its properties as calculation constants which *in principle* can be obtained through extrapolation of the corresponding properties of the existing solutions. However, it also seems plausible to introduce an assumption of equality between the molar valumes of the dissolved and the condensed gas. Such a hypothesis would make it possible to calculate the properties of the standard state of B_2 from the properties of the condensed gas. This procedure will subsequently be shown to be rather successful. Concerning the activity factors f_1^s and f_2^s appearing in eqns. (9) and (10), it has previously been emphasized that they may contain a structure-dependent factor which equals unity only for a homogeneous surface phase or for a monolayer (*cf.* Ref.[7]).

Proceeding in a similar way from eqn. (8), eqn. (18) may be derived, if the standard states are chosen as the ideal gas at 1 atm and the hypothetical liquid state of pure B_2,

$$x_2'/p = F_H^o \, \Gamma_H \, K_H = H \tag{18}$$

Here K_H denotes the gas solubility at 1 atm, *i.e.* approximately the inverse Henry law constant, and F_H° is an activity factor expression referred to 1 atm *viz.*,

$$F_H^\circ = (f_2')_{K_H}^\circ / (f_2')_{x_2'}^\circ \tag{19}$$

whereas Γ_H is defined by

$$\Gamma_H = \exp\left[\int_1^p (\alpha/p - v_2'/RT)\,dp\right] \tag{20}$$

supposing that the compressibility factor of the gas may be written

$$pV/RT = 1 + \alpha \tag{21}$$

$\alpha = \alpha(p)$ standing for the virial expansion expressed in powers of the pressure. It appears that K_H in the ideal case, when $F_H^\circ = 1$, $\alpha = 0$ and $v_2' = v_2'^\circ$, is

$$K_H^{id} = (1/\bar{p}_2)\ \exp\ [(\bar{p}_2 - 1)\ v_2'^\circ/RT] \tag{22}$$

$\bar{p}_2$ symbolizing the hypothetical vapour pressure of pure liquid B_2. Thus the ideal solubility of the gas is established as

$$(x_2')^{id} = (p/\bar{p}_2)\ \exp[(\bar{p}_2 - p)\ v_2'^\circ/RT] \tag{23}$$

Obviously, this equation is a generalized form of Raoult's law. However, in this connection non-ideal behaviour should be assumed for the solutions under study. From eqns. (18), (19) and (20) we then get

$$(f_2')_{K_H}^\circ = \frac{1}{\bar{p}_2 K_H} \exp\left[\int_1^{\bar{p}_2} \left(\frac{v_2'}{RT} - \frac{\alpha}{p}\right) dp\right] \tag{24}$$

On combining eqns. (13) and (14) it can be shown that

$$x_1' F_1^\circ \Gamma_1\ e^{\Delta g_1} + x_2' F_2^\circ \Gamma_2 e^{\Delta g_2} = 1 \tag{25}$$

where for convenience the abbreviated notation

$$\Delta g_i = (A_i\gamma - A_i^\circ \gamma_i^\circ)/RT \tag{26}$$

has been introduced. Since x_2' is determined by eqn. (18) it follows that

$$(1-Hp)\ F_1^\circ \Gamma_1 e^{\Delta g_1} + Hp\ F_2^\circ \Gamma_2 e^{\Delta g_2} = 1 \tag{27}$$

This equation states in an implicit form the dependence between the variables γ and p for the systems studied, and it constitutes therefore the main equation of the present paper. The pressure derivative of γ can be calculated from eqn. (27) and for subsequent use it is written here in two different forms, *viz.*

$$A_1 \left(\frac{\partial \gamma}{\partial p}\right)_T = \frac{v_1^s - v_1' - HRT(K_L - 1)(1 + \alpha) - Hp(v_2' + v_1^s - v_1' - K_L v_2^s)}{1 + Hp(rK_L - 1)} \tag{28}$$

$$\left(\frac{\partial \gamma}{\partial p}\right)_T = \frac{x_1^s(v_1^s - v_1') + x_2^s[v_2^s - K_L^{-1} v_2' - (1 - K_L^{-1})v_2'']}{x_1^s A_1 + x_2^s A_2} \tag{29}$$

where K_L denotes the expression

$$K_L = \frac{F_2^\circ \Gamma_2}{F_1^\circ \Gamma_1} \exp\ (\Delta g_2 - \Delta g_1) = (x_2^s/x_2')(x_1'/x_1^s) \tag{30}$$

and r is the ratio A_2/A_1. It may readily be demonstrated that the assumptions K_L = constant and x_2', $K_H \ll 1$ lead to the Langmuir adsorption law because then eqn. (30) can be approximated to

$$x_2^s = \frac{K_L K_H p}{1 + K_L K_H p} \tag{31}$$

When $A_1 = A_2$ this expression represents a good approximation because in that case K_L remains almost a constant, but for the general case this condition is not fulfilled. When x_2' and p approach zero K_L attains the value

$$K_L = F_2^\circ \exp[A_2^\circ(\gamma_1^\circ - \gamma_2^\circ)/RT] = F_2^\circ K_e^\circ \tag{32}$$

if the very small influence of the Γ-factors is neglected and if it is supposed that γ_1^* (0 atm) $\approx \gamma_1^\circ$ and $A_i = A_i^\circ$. The index e in K_e° symbolizes that K_e° is the equilibrium constant referred to 1 atm for the *exchange* (adsorption) reaction (*cf.* Ref.[7])

$$rB_1^s + B_2' \rightarrow rB_1' + B_2^s \tag{33}$$

occurring at the actual temperature T and pressure p. For small pressures eqn. (28) thus reduces to

$$A_1\left(\frac{\partial \gamma}{\partial p}\right)_T = v_1^s - v_1' - K_H RT\,(K_c^\circ F_2^\circ - 1) \tag{34}$$

There are other ways of deducing an expression for $(\partial\gamma/\partial p)_T$ $(=(\partial\gamma/\partial p)_{T,A}$ since γ is independent of A for the systems studied) which will also be described. According to eqn. (1) the desired relationship could be obtained by analyzing the derivative $(\partial V/\partial A)_{T,p}$. The physical meaning of this derivative is obviously the volume change per unit area at a reversible increase of the system's surface area carried out at constant p and T and constant *total* amounts of the components. Since a reversible increase of the surface area must be considered to imply a reversible transport of molecules from the bulk phases to the surface phase, we may conveniently introduce a *transport reaction*

$$\nu_1' B_1' + \nu_2' B_2' + \nu_2'' B_2'' \rightarrow \nu_1^s B_1^s + \nu_2^s B_2^s \tag{35}$$

Here ν_1' symbolizes the stoichiometric coefficient associated with the transport of B_1 from the b′-phase, *etc.* Evidently, because the system is closed, the following relationships must be satisfied

$$\nu_1' = \nu_1^s \tag{36}$$

$$\nu_2' + \nu_2'' = \nu_2^s \tag{37}$$

In order to calculate ΔV for the transport reaction we thus have to know the ratio of ν_2' and ν_2''. Since it is necessary for the reaction (35) to proceed at constant p and T it is realized that x_2' must be maintained constant (*cf.* eqn. (18)). We may therefore write

$$\nu_1'/\nu_2' = \nu_1^s/\nu_2' = x_1'/x_2' \tag{38}$$

and since ν_1^s and ν_2^s state the equilibrium composition of the surface phase we have

$$\nu_1^s/\nu_2^s = x_1^s/x_2^s \tag{39}$$

On combining these eqns. it is found that

$$\nu_2' = K_L^{-1}\nu_2^s \tag{40}$$

$$\nu_2'' = (1-K_L^{-1})\nu_2^s \tag{41}$$

The volume change per Donder of the transport reaction is consequently

$$\Delta V = \nu_1^s\,(v_1^s - v_1') + \nu_2^s\,[v_2^s - K_L^{-1}v_2' - (1-K_L^{-1})v_2''] \tag{42}$$

As the corresponding increase of the surface area is given by

$$\Delta A = \nu_1^s A_1 + \nu_2^s A_2 \tag{43}$$

and since all of V and A are extensive properties it may be concluded that

$$\left(\frac{\partial\gamma}{\partial p}\right)_T = \left(\frac{\partial V}{\partial A}\right)_{T,p} = \frac{x_1^s(v_1^s - v_1') + x_2^s[v_2^s - K_L^{-1}v_2' - (1-K_L^{-1})v_2'']}{x_1^s A_1 + x_2^s A_2} \tag{44}$$

i.e. the same expression as was derived above (eqn. (29)) using other methods. On the other hand it is not possible to obtain eqn. (28) along these lines without making use of eqns. (13) and (14). It appears clearly that the concept of a physical surface phase which is characterized by a certain composition, volume $V^s = \Sigma n_i^s v_i^s$ and surface area $A = \Sigma n_i^s A_i$ and which contains only the region influenced by surface forces is essential for the present deduction. Actually, this concept also constitutes the basis of eqn. (3) which was the starting point of the first deduction. In Gibbs' theory of capillarity [10] a surface phase with the volume V^G is considered instead which must be chosen in such a way as to contain also parts of the bulk phases. At constant T, Gibbs adsorption formula *viz.*,

$$-A\ \mathrm{d}\gamma = n_1^E\ \mathrm{d}\mu_1^b + n_2^E\ \mathrm{d}\mu_2^b \ldots . \tag{45}$$

always holds for a planar equilibrium surface system, n_i^E denoting the surface excess $n_i^G - n_i' - n_i''$ where n_i' and n_i'' are the mole numbers we would have within V^G if the bulk phases extended to the Gibbs dividing surface. For the bulk phases, however, the Gibbs-Duhem equation should be applicable, implying for the system under consideration that

$$n_1'\ \mathrm{d}\mu_1^b + n_2'\ \mathrm{d}\mu_2^b = V'\ \mathrm{d}p \tag{46}$$

$$n_2''\ \mathrm{d}\mu_2^b = V''\ \mathrm{d}p \tag{47}$$

and since $V' + V'' = V^G$, it is found that

$$-A\ \mathrm{d}\gamma = n_1^G\ \mathrm{d}\mu_1^b + n_2^G\ \mathrm{d}\mu_2^b - V^G\ \mathrm{d}p \tag{48}$$

If now the Gibbs surface phase is divided into three sub-phases

$$V^G = V^s + V^{G'} + V^{G''} \tag{49}$$

V^s representing as before the physical surface phase and $V^{G'}$ and $V^{G''}$ the parts with bulk phase properties, it becomes evident that eqn. (48) may be reduced to

$$-A\ \mathrm{d}\gamma = n_1^s\ \mathrm{d}\mu_1^b + n_2^s\ \mathrm{d}\mu_2^b - V^s\ \mathrm{d}p \tag{50}$$

since again the Gibbs-Duhem equation should hold for the bulk phase regions. This equation can also be transformed into eqn. (29) by taking into account eqns. (46) and (47) and provided that the assumptions $V^s = \Sigma n_i^s v_i^s$ and $A = \Sigma n_i^s A_i$ are introduced. In Gibbs' theory no such assumptions are included, thus securing perfect universality, since the actual surface phase properties are not *a priori* well-defined due to the presumed non-homogeneity. However, precise definitions can be established (*cf.* Ref.[7]). Obviously, if the physical surface phase concept is consistently introduced much more detailed predictions about surface systems can be made. The applicability of the equations derivable from eqn. (3) to experimental data comprises the crucial test of this approach.

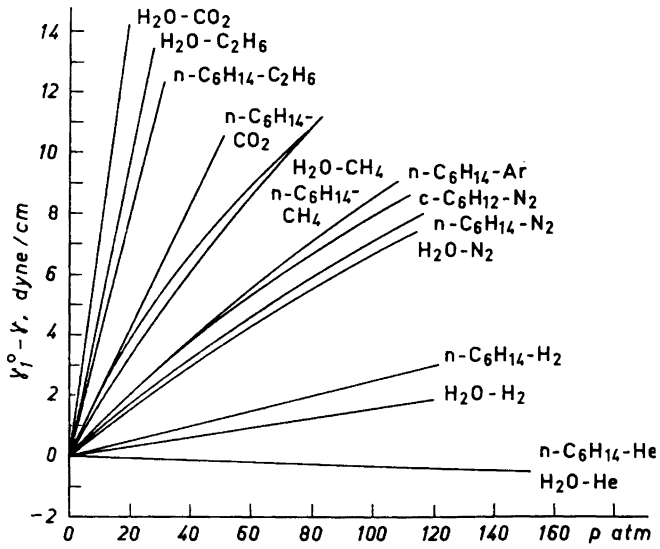

Fig. 2. Experimental γ-p curves at room temperature according to Refs.[3,4]

CALCULATIONS

By means of eqns. (27) and (34) we have carried out tentative calculations on the experimental γ-p curves given by Slowinski *et al.*[3] and Gielessen and Schmatz [4] (*cf.* Fig. 2) assuming the restrictions (16) to be fulfilled for the solutions studied. The gas solubilities at 1 atm, K_H, were taken or, in some cases, estimated from the critical review of solubility experiments given by Jolley and Hildebrand[11] and from the compilation in *Handbook of Chemistry and Physics*[12]. The molecular surface areas A_1° for the solvents water, hexane and cyclohexane were chosen as 17 [7], 51 [13], and 51 Å [2], respectively. The activity factor expressions could be estimated in the following way. For a regular mixture as defined by Hildebrand[14] the relationships

$$\ln\ (f_1')^\circ = (W/RT)(x_2')^2$$
$$\ln\ (f_2')^\circ = (W/RT)(x_1')^2 \qquad (51\ a, b)$$

hold true, W denoting a characteristic constant which can be evaluated from heat of mixing data. For a monolayer, it is reasonable, according to the discussion given by Hoar and Melford[15], to put

$$\ln\ (f_1^s)^\circ = l'(W/RT)(x_2^s)^2$$
$$\ln\ (f_2^s)^\circ = l'(W/RT)(x_1^s)^2 \qquad (52, a, b)$$

where l' is a fractional factor, the numerical value of which lies within the range 0.5—0.75. Choosing $l' = 2/3$ we obtain

$$\ln\ F_1^\circ = (W/RT)\ [(x_2')^2 - 2/3(x_2^s)^2]$$
$$\ln\ F_2^\circ = (W/RT)\ [(x_1')^2 - 2/3(x_1^s)^2] \qquad (53\ a, b, c)$$
$$\ln\ F_H^\circ = (W/RT)\ [(1-K_H)^2 - (x_1')^2]$$

For small p, F_1° and F_H° may consequently be put equal to unity because generally $K_H \ll 1$ whereas

$$\ln\ F_2^\circ = (1/3)(W/RT) \approx \tfrac{1}{3}\ \ln\ (f_2')_{K_H}^\circ \qquad (54)$$

However, using eqn. (24), $(f_2')_{K_H}^\circ$ can be evaluated if $\bar{p}_2$, $v_2'^\circ$ and α are known thus enabling the determination of W/RT. It should be mentioned here that the activity factor expressions (51) and (52) are based upon the assumption of equal molecular volumes of the two components. Hence eqns. (53) are to be regarded only as rather rough estimations of the activity factor ratios. We have supposed that the properties of the dissolved gas are related to the properties of the condensed gas. Thus the $\bar{p}_2$-values were estimated from the vapour pressure equations for the gaseous components[16] (*cf.* Saylor and Battino[17]) and the molar volume of the dissolved gas was calculated from the density of the condensate at the boiling point. The surface tension γ_2°, ascribed to the standard state of B_2, could be evaluated through extrapolation of the surface tension of the real liquid at low temperatures[18]. This extrapolation of γ_2^* *vs.* temperature should be performed linearly since from eqn. (3) on assuming A_2^* to be temperature independent

Table 1. Calculations on experimental data using eqn. (34).

System liquid-gas	t°C	$\left(\frac{d\gamma}{dp}\right) \times 10^3$ erg cm^{-2} atm^{-2}	$A_1^\circ \left(\frac{d\gamma}{dp}\right)_{p=0}$ ml mole^{-1}	$K_H \times 10^5$ atm^{-1}	γ_2° dyn cm^{-1}	$\bar{p}_2$ atm	$(f_2')^\circ K_H$	$v_2'^\circ$ ml mole^{-1}	K_e°	A_2°calcd) Å^2 molecule^{-1}	A_2°(BET) Å^2 molecule^{-1}
H_2O-He	25	0.3	3.0	0.691	−33.7	66.3	2245	32	12.1	9.8	15.4
n-$C_6H_{14}-He$	22	0.3	9.1	26.0	−33.4	66.2	59.7	32	3.11	8.9	15.4
H_2O-H_2	25	− 1.6	− 16.2	1.42	−45.3	758	141	29	25.7	11.4	14.2
n-$C_6H_{14}-H_2$	25	− 2.5	− 75.8	63.0	−45.3	758	3.16	29	7.60	15.8	14.2
H_2O-N_2	25	− 7.7	− 77.8	1.22	−39.2	2791	82.1	35	74.6	16.0	16.2
n-$C_6H_{14}-N_2$	22	− 8.8	− 267	140	−38.5	2671	0.74	35	12.4	17.9	16.2
c-$C_6H_{12}-N_2$	22	−10.0	− 303	75.5	−38.5	2671	1.225	35	20.4	19.4	16.2
H_2O-CH_4	25	−21.6	− 218	2.42	−20.9	383	296	39	63.0	18.4	18.1
n-$C_6H_{14}-CH_4$	25	−16.2	− 491	468	−20.9	383	1.53	39	5.19	17.4	18.1
$H_2O-C_2H_6$	25	−49.9	− 504	3.30	0.1	41.6	1159	46	58.2	23.2	22.2
n-$C_6H_{14}-C_2H_6$	25	−38.0	−1152	3770	0.1	41.6	1.01	46	2.33	19.1	22.2
H_2O-CO_2	25	−79.3	− 801	60.8	− 0.7	63.5	89.4	62	12.8	14.4	17.0
n-$C_6H_{14}-CO_2$	25	−21.1	− 640	1240	− 0.7	63.5	4.38	62	2.06	15.8	17.0
n-$C_6H_{14}-Ar$	22	−10.1	− 306	253	−42.7	1026	0.95	24	7.37	13.3	14.4

$$\left(\frac{\partial \gamma_2^*}{\partial T}\right)_p = -(s_2^{s*} - s_2^{b*})/A_2^* \tag{55}$$

and according to Eötvös' rule [19], $s_2^{s*} - s_2^{b*}$ has a constant value approximately equal to 4.2 cal mole^{-1} deg^{-1} for many liquids. The temperature variation of A_2^* within the range of the surface tension measurements is certainly small, and since the desired γ_2°-value should correspond to a density typical for the liquid state, γ_2^* had to be extrapolated linearly. Actually, the γ_2^*-T relationships for the considered condensates were linear to a good degree of accuracy. It may also be deduced from eqn. (5) that $(\partial \gamma_2^*/\partial p)_T$ has the order of magnitude 10^{-2} erg cm^{-2} atm^{-1} for the liquids involved. Hence no large errors were introduced in the calculations when surface tension values, measured for the liquid under its own vapour pressure ranging from 0—5 atm, were ascribed to the pressure of 1 atm, *i.e.* to the pressure of the standard state. The described procedure for evaluating γ_2° implies that the surface enthalpy, $h_2^{s*} - h_2^{b*}$, is considered as temperature independent, a consequence which is consistent with the assumption of constant molar volumes for the pure condensed state.The value of α at different pressures was obtained from pVT-data [20,21] for the corresponding gas. Rice [22] estimated the volume difference $v_i^{so} - v_i'^{o}$ to be of the same order of magnitude as $v_i'^{o}$ itself. The most consistent results were obtained with the present calculations if $v_1^{so} - v_1'^{o}$ for water, hexane and cyclohexane were given the values 30, 80, resp. 80 ml mole^{-1}. In Table 1 the results of the calculations based upon eqn. (34) are summarized. In view of the approximations involved the calculated molecular surface areas for the gaseous components seem rather conclusive. The corresponding BET molecular surface areas were calculated from the formula [23]

$$A_2^\circ \text{ (BET)} = 1.091 \ (v_2'^{o}/N)^{2/3} \text{ Å}^2 \tag{56}$$

This expression is exact for a monolayer surface consisting of closepacked equal-sized, spherical molecules. Since the BET surface areas substantially agree with the calculated surface areas except for helium for which eqn. (56)

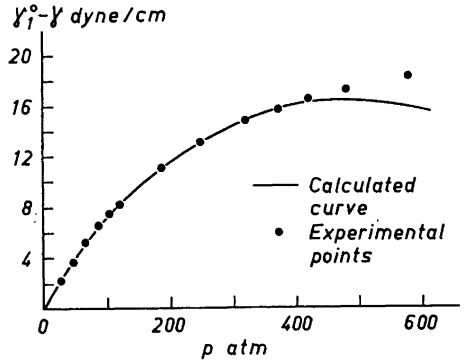

Fig. 3. The interfacial tension of n-C_6H_{14}—N_2 *versus* pressure at 22°C.

is known from specific surface area measurements to yield too large a value, we may conclude that the monolayer description is adequate and that the presumed relationships between the properties of the dissolved and the condensed states are reasonable for the systems treated.

The validity of eqn. (27) was investigated for hexane-nitrogen. For this system γ has been measured over a wide pressure range (*cf.* Ref.[4]). The previously calculated A_2°-value was inserted and $v_2^{so}-v_2^{'o}$ was put equal to 30 ml mole^{-1}. As is seen from Fig. 3 the agreement with experiment is satisfactory up to 400 atm corresponding to $x_2^{'} = 0.30$ and $x_2^{s} = 0.96$. It is of course unlikely that eqns. (16) would be fulfilled at high concentrations of B_2. Moreover, since the Γ-factors become very important at high pressures, errors in the values for $v_1^{so}-v_1^{'o}$, $v_2^{so}-v_2^{'o}$, $v_2^{'o}$ may also seriously affect the result.

DISCUSSION

A characteristic feature of the experimental γ-p curves is (*cf.* Fig. 2) that the derivatives $(\partial\gamma/\partial p)_T$ for $p \approx 0$ for systems with different liquid components but with the same gaseous component have the same order of magnitude. An explanation of this fact may be attempted along the following lines. For small p, $K_H RTK_c^\circ F_2^\circ$ is the predominant term of eqn. (34) for most of the systems. According to an empirical relationship pointed out by Uhlig [24], a low solubility of a certain gas is connected with a high surface tension γ_1° of the solvent and *vice versa*, *i.e.* the magnitudes of K_H and K_c° are changed in opposite directions when passing between liquid components with different γ_1°-values (*cf.* eqn. (32) and Table 1). Thus the variation of $(\partial\gamma/\partial p)_T$ for $p \approx 0$ should be limited for this category of systems if the A_1°-values are not widely different. This conclusion is not affected by the approximate relationship $F_2^\circ = (\bar{p}_2\ \bar{\Gamma}_H K_H)^{-1/3}$ which can be derived from eqns. (24) and (54). The converse behaviour could be expected for systems with the same liquid component but different gaseous components that have approximately equal γ_2°-values, because a large molar surface area A_2° (*i.e.* a large K_c°) should be associated with a large polarizability and thus also a high solubility of the gaseous component.

It is interesting to note that the performed calculations indicate that τ, the thickness of the surface monolayer, for the water and hexane solutions would be 4—5 Å and 6—7 Å, respectively. The fact that the A_2°-values are not much affected by changing the substrate and that the BET-formula (eqn. (56)), based upon the molar volume $v_2^{'o}$, is applicable suggests that molecules in a surface phase are characterized by an increased amplitude of thermal motion mainly in the direction perpendicular to the surface. This observation is in good agreement with the molecular theory of surface tension based on the cell theory for liquids. Accordingly, a molecule at a surface has a larger *free volume* than a molecule in a bulk phase since the former is surrounded by fewer molecules than the latter [25]. However, this difference of the free volumes cannot account for all the entropy difference so it is also necessary to assume that more holes are present in the surface phase [26].

The present investigation lends strong support to the validity and applicability of the thermodynamic method for treating surface systems founded on the physical surface phase concept which has been discussed elsewhere by the author. Actually, the monolayer model is adequate for the systems dealt with in this paper. However, it would also be of value to test the derived formulae on systems with a more complicated surface phase structure. Likewise, the interfacial tensions of liquid-liquid systems could be studied using analogous methods.

Acknowledgement. The author wishes to thank the Head of the Division, Professor Ole Lamm for many valuable and stimulating discussions.

REFERENCES

1. Lewis, G. N. and Randall, M. *Thermodynamics*, McGraw-Hill Book Co. New York 1923, p. 248.
2. Rice, O. K. *J. Chem. Phys.* **15** (1947) 333.
3. Slowinski, Jr., E. J., Gates, E. E. and Waring, C. E. *J. Phys. Chem.* **61** (1957) 808.
4. Gielessen, J. and Schmatz, W. Z. *Z. physik. Chem. N.F.* **27** (1961) 157.
5. Kundt, A. *Ann. physik. Chem.* **12** (1881) 538.
6. Defay, R. and Prigogine, I. *Tension superficielle et adsorption*, Edition Désoer, Liège 1951, p. 73.
7. Eriksson, J. C. *Advances in Chem. Phys.* **6** (1963). *In press.*
8. Adamson, A. W. *Physical Chemistry of Surfaces*, Interscience, New York, London 1960, p. 54.
9. Lewis, G. N., Randall, M., Pitzer, K. S. and Brewer, L. *Thermodynamics*, 2nd Ed., McGraw-Hill Book Co., New York, Toronto, London 1961, p. 249.
10. Gibbs, J. W. *The Collected Works of Josiah Willard Gibbs*, Longmans Green & Co., London 1928, Vol. I, p. 219.
11. Jolley, J. E. and Hildebrand, J. H. *J. Am. Chem. Soc.* **80** (1958) 1050.
12. *Handbook of Chemistry and Physics*, 40th Ed., Chemical Rubber Publishing Co., Cleveland 1958.
13. Isirikyan, A. A. and Kiselev, A. V. *J. Phys. Chem.* **65** (1961) 601.
14. *cf.* Ref.[9], p. 282.
15. Hoar, T. P. and Melford, D. A. *Trans. Faraday Soc.* **53** (1957) 315.
16. *Int. Crit. Tables, Vol. III*, p. 202.
17. Saylor, J. H. and Battino, R. *J. Phys. Chem.* **62** (1958) 1334.
18. *Int. Crit. Tables, Vol. IV*, p. 441.
19. Eötvös, R. V. *Wied. Ann.* **27** (1886) 456.
20. Daniels, F. and Alberty, R. A. *Physical Chemistry*, 2nd Ed. John Wiley & Sons, New York, London 1961.
21. Hirschfelder, J. O., Curtiss, C. F. and Bird, R. B. *Molecular Theory of Gases and Liquids*, John Wiley & Sons, New York, London 1954.
22. Rice, O. K. *J. Chem. Phys.* **15** (1947) 314.
23. Emmet, P. H. and Brauner, S. *J. Am. Chem. Soc.* **59** (1937) 1553.
24. Uhlig, H. H. *J. Phys. Chem.* **41** (1937) 1215.
25. Lennard-Jones, J. and Corner, J. *Trans. Faraday Soc.* **36** (1940) 1156.
26. Harasima, A. *Advances in Chem. Phys.* **1** (1958) 203.

Received May 2, 1962.

ACTA CHEMICA SCANDINAVICA 16 (1962) 2212–2220

Analysis of NMR Wide Line Shapes Generated by Two Broadening Mechanisms

S. E. SVANSON

Research Group for NMR, Division of Physical Chemistry, The Royal Institute of Technology, Stockholm 70, Sweden

Dedicated to Professor *Ole Lamm* on his 60th birthday

The use of Fourier transforms for the analysis of NMR wide line spectra generated by two broadening mechanisms is discussed. Some examples are given of analysis performed for spectra perturbed by quadrupole interaction and also of spectra of crystalline solids containing groups of interacting nuclei.

The line-shape of NMR wide line spectra is, in many cases, determined by two or more broadening mechanisms. The most important factors responsible for the line-shape of this type of spectra are the nuclear dipole-dipole interaction and the magnetic and electric nuclear-electronic interactions. The dipole-dipole interaction is always of importance in non-rotating specimens[1] and must be taken into account in all cases where any other broadening mechanism is present.

As an example of a spectral type generated by two broadening mechanisms, the NMR spectra perturbed by quadrupole couplings in polycrystalline samples, may be studied. The following functional assignments are assumed for the generation of the modified line-shape. Let $Q(\xi)$ denote the line-shape yielded by the quadrupole coupling. The fraction of nuclei $Q(\xi)\xi$ with a displacement in the interval ξ to $\xi + \mathrm{d}\xi$ is assumed to be distributed over the function $K(x,\xi)$ due to the dipole-dipole interaction. K is, moreover, subjected to the condition

$$\int_{-\infty}^{+\infty} K(x,\xi)\mathrm{d}x, = 1$$

The absorption line may be written

$$f(x) = \int_{\xi_1}^{\xi_2} K(x,\xi)Q(\xi)\mathrm{d}\xi \qquad (1)$$

where the function $Q(\xi)$ is defined in the interval ξ_1 to ξ_2. If the two broadening mechanisms are mutually independent, the function due to the dipole-dipole interaction can be written as $P(x-\xi)$, and the absorption line takes the form

$$f(x) = \int_{\xi_1}^{\xi_2} P(x-\xi)Q(\xi)\mathrm{d}\xi \tag{2}$$

This equation is given earlier, for example by Hughes and Mac Donald [2]. In mathematical texts $f(x)$ in eqn. (2) is called the convolution of P and Q. The theory of the dipole-dipole interaction shows that the P-function is symmetric, which is utilized in the following to simplify the analysis. It should be remembered however that individual dipole-broadened component lines in a spectrum are not always symmetric as has been shown by Itoh *et al.*[3] and Silver *et al.*[4], and in such cases the following deductions are not applicable.

With these assumptions, the nth moment of $f(x)$ is easily calculated. In particular

$$M_0 = \int_{-\infty}^{+\infty} f(x)\,\mathrm{d}x = \int_{-\infty}^{+\infty}\int_{\xi_1}^{\xi_2} P(x-\xi)Q(\xi)\mathrm{d}\xi\mathrm{d}x = \int_{\xi_1}^{\xi_2} Q(\xi)\{\int_{-\infty}^{+\infty} P(x-\xi)\mathrm{d}x\}\,\mathrm{d}\xi$$

$$= \int_{\xi_1}^{\xi_2} Q(\xi)\{\int_{-\infty}^{+\infty} P(\zeta)\mathrm{d}\zeta\}\,\mathrm{d}\xi = \int_{\xi_1}^{\xi_2} Q(\xi)\mathrm{d}\xi$$

$$M_1 = \int_{-\infty}^{+\infty} x\cdot f(x)\mathrm{d}x = \int_{\xi_1}^{\xi_2} Q(\xi)\{\int_{-\infty}^{+\infty} xP(x-\xi)\mathrm{d}x)\}\,\mathrm{d}\xi =$$

$$= \int_{\xi_1}^{\xi_2} Q(\xi)\{\int_{-\infty}^{+\infty} (\zeta+\xi)\ P(\zeta)\mathrm{d}\zeta\}\,\mathrm{d}\xi = \int_{\xi_1}^{\xi_2} \xi Q(\xi)\mathrm{d}\xi$$

as $\int_{-\infty}^{+\infty} \zeta\cdot P(\zeta)\mathrm{d}\zeta = 0$ for even functions $P(\zeta)$.

M_0 and M_1 are thus independent of P. This well-known fact has, for example, been used by Otsuka and Kawamura [5] in a study of dislocation effects on the iodine-resonance in some crystalline alkali iodides. All higher moments depend on P. So is for example

$$M_2 = \int_{\xi_1}^{\xi_2} \xi^2\cdot Q(\xi)\mathrm{d}\xi + \int_{-\infty}^{+\infty} \zeta^2\cdot P(\zeta)\mathrm{d}\zeta\cdot\int_{\xi_1}^{\xi_2} Q(\xi)\mathrm{d}\xi$$

The simple analytical form of M_1 is due to the assumed symmetry of the function $P(\zeta)$. Similarly, the sine and cosine transforms of $f(x)$ lead to very simple analytical expressions if $P(\zeta)$ is assumed to be even, since in this case the integral

$$\int_{-\infty}^{+\infty} P(\zeta)\cdot\sin(u\zeta)\mathrm{d}\zeta$$

disappears, and

$$F(u) = \int_{-\infty}^{+\infty} f(x) \cdot \cos(ux)\mathrm{d}x = \int_{-\infty}^{+\infty} \int_{\xi_1}^{\xi_2} P(\zeta) \cdot \cos u(\zeta + \xi)\mathrm{d}\zeta \cdot Q(\xi)\mathrm{d}\xi =$$

$$= \int_{-\infty}^{+\infty} P(\zeta) \cdot \cos(u\zeta)\mathrm{d}\zeta \cdot \int_{\xi_1}^{\xi_2} Q(\xi) \cdot \cos(u\xi)\mathrm{d}\xi \tag{3}$$

$$G(u) = \int_{-\infty}^{+\infty} f(x) \cdot \sin(ux)\mathrm{d}x = \int_{-\infty}^{+\infty} \int_{\xi_1}^{\xi_2} P(\zeta) \cdot \sin u(\zeta + \xi)\mathrm{d}\zeta \cdot Q(\xi)\mathrm{d}\xi =$$

$$= \int_{-\infty}^{+\infty} P(\zeta) \cdot \cos(u\zeta)\mathrm{d}\zeta \cdot \int_{\xi_1}^{\xi_2} Q(\xi) \cdot \sin(u\xi)\mathrm{d}\xi \tag{4}$$

Relations of this kind are well-known from the theory of the convolution. From eqns. (3) and (4) we have

$$\frac{F(u)}{G(u)} = \frac{\int_{\xi_1}^{\xi_2} Q(\xi) \cdot \cos(u\xi)\mathrm{d}\xi}{\int_{\xi_1}^{\xi_2} Q(\xi) \cdot \sin(u\xi)\mathrm{d}\xi} \tag{5}$$

With this expression it is possible to make an assumed analytical form of $Q(\xi)$ with unknown parameters to coincide with experimental data, without making any other assumptions than those stated above about the function $P(\zeta)$. The development can be made in a large interval of u-values.

The method can be simplified for practical use by calculating the Fourier-transforms of the function $f'(x)$, measured in the wide line technique.

Here is

$$f'(x) = \int_{\xi_1}^{\xi_2} P'(x-\xi)\, Q(\xi)\mathrm{d}\xi \tag{6}$$

and we compute

$$F_1(u) = \int_{-\infty}^{+\infty} f'(x) \cdot \cos(ux)\mathrm{d}x = -\int_{-\infty}^{+\infty} P'(\zeta) \cdot \sin(u\zeta)\mathrm{d}\zeta \cdot \int_{\xi_1}^{\xi_2} Q(\xi) \cdot \sin(u\xi)\mathrm{d}\xi \tag{7}$$

$$G_1(u) = \int_{-\infty}^{+\infty} f'(x) \cdot \sin(ux)\mathrm{d}x = \int_{-\infty}^{+\infty} P'(\zeta) \cdot \sin(u\zeta)\mathrm{d}\zeta \cdot \int_{\xi_1}^{\xi_2} Q(\xi) \cdot \cos(u\xi)\mathrm{d}\xi \tag{8}$$

as $\int_{-\infty}^{+\infty} P'(\zeta)\cos(u\zeta)\mathrm{d}\zeta = 0$ for odd functions $P'(\zeta)$.

The integral

$$\int_{-\infty}^{+\infty} P'(\zeta) \cdot \sin(u\zeta)\mathrm{d}\zeta = \int_{-\infty}^{+\infty} P(\zeta) \cdot \sin(u\zeta) - u \int_{-\infty}^{+\infty} P(\zeta) \cdot \cos(u\zeta)\mathrm{d}\zeta =$$

$$= -u \int_{-\infty}^{+\infty} P(\zeta) \cdot \cos(u\zeta)\mathrm{d}\zeta$$

as $P(\zeta)$ goes towards zero in both limits.

Thus eqn. (3) can be substituted by

$$\frac{F_1(u)}{u} = \int_{-\infty}^{+\infty} P(\zeta) \cdot \cos(u\zeta)\mathrm{d}\zeta \cdot \int_{\xi_1}^{\xi_2} Q(\xi) \cdot \sin(u\xi)\mathrm{d}\xi \tag{9}$$

and eqn. (4) by

$$-\frac{G_1(u)}{u} = \int_{-\infty}^{+\infty} P(\zeta) \cdot \cos(u\zeta)\mathrm{d}\zeta \cdot \int_{\xi_1}^{\xi_2} Q(\xi) \cdot \cos(u\xi)\mathrm{d}\xi \tag{10}$$

Finally eqn. (5) can be replaced by

$$-\frac{G_1(u)}{F_1(u)} = \frac{\int_{\xi_1}^{\xi_2} Q(\xi) \cdot \cos(u\xi)\mathrm{d}\xi}{\int_{\xi_1}^{\xi_2} Q(\xi) \cdot \sin(u\xi)\mathrm{d}\xi} \tag{11}$$

In the following eqns. (3), (4), and (5) have been used but it is assumed, however, that $F(u)$, $G(u)$ and $F(u)/G(u)$ are replaced by $-G_1(u)/u$, $F_1(u)/u$ and $-G_1(u)/F_1(u)$, respectively, for reasons of convenience.

This transformation is of great practical importance in the numerical calculations since the integrals $F_1(u)$ and $G_1(u)$ converge faster than $F(u)$ and $G(u)$. For small values of u the convergence is the same as for $\int_{-\infty}^{+\infty} f'(x)\mathrm{d}x$, and for large values of u the convergence is still faster due to the alternating signs of the successive contributions in both limits.

When the constant u is large, the evaluation of the integrals becomes difficult because of the violent oscillation of the trigonometric functions. A method for the evaluation of the integrals in this case is given by Kopal [6] yielding correct results and error estimates for a limited number of measured points on the curve.

Also, if the function $Q(\xi)$ is symmetric, the eqn. (4) disappears. The use of eqn. (5) is consequently limited to unsymmetrical functions $Q(\xi)$. Such functions appear in the case of polycrystalline samples subjected to second-order quadrupole interaction or anisotropic Knight shift.

The displacement due to the quadrupole interaction, first- or second-order, depends on the orientation of the external magnetic field in relation to the principal axes of the electric field gradient tensor. The condition of mutual independence of the distributions $P(\zeta)$ and $Q(\xi)$ will thus in this case require that the function $P(\zeta)$ describing the dipolar broadening is independent of the orientation of the external magnetic field in the crystal lattice. This

requirement of isotropy of $P(\zeta)$ is indispensable for a detailed analysis of all spectra of polycrystalline samples, and it seems hardly possible ever to resolve spectra of this kind, unless this condition is fulfilled.

The aforementioned investigation by Otsuka and Kawamura provides an example of a single crystal giving rise to an unsymmetric function $Q(\xi)$ of interest for the future study of this problem and the applicability of eqn. (5).

Many examples of symmetric functions $Q(\xi)$ exist. Valuable information can in this case be obtained from eqn. (3) if the integral $\int_{\xi_1}^{\xi_2} Q(\xi) \cdot \cos(u\xi)\mathrm{d}\xi$ has zeros that can be distinguished from the zeros of $\int_{-\infty}^{+\infty} P(\zeta)\cdot\cos(u\zeta)\mathrm{d}\zeta$.

Assuming $P(\zeta)$ to be Gaussian, $P(\zeta) = \mathrm{e}^{-a\zeta^2}$, the cosine transform is $\int_{-\infty}^{+\infty} P(\zeta)\cdot\cos(u\zeta)\mathrm{d}\zeta = \sqrt{\frac{\pi}{a}} \cdot \mathrm{e}^{-u^2/4a}$. A narrow function $P(\zeta)$ thus has a broad transform and *vice versa*.

The experimental $P(\zeta)$ curves of pure dipole-broadened functions give transforms which, for small u, coincide rather well with the Gaussian and go towards zero as u goes towards infinity. For large u, however, the transforms usually have a sequence of zeros, and the narrower the dipole-broadened function the higher the u-values for the zeros.

When $P(\zeta)$ is narrow enough in comparison with the $Q(\xi)$-function, the zeros in the transform of $Q(\xi)$ will occur for smaller u-values than the zeros in the transform of $P(\zeta)$. In this case, the zeros are easily distinguished.

Polycrystalline samples perturbed by first-order quadrupole interaction, in all cases lead to symmetric functions $Q(\xi)$.

Spectra of polycrystalline solids where the nuclei occur in groups give spectra of rather similar form. The spectra of hydrated crystals provide an example.

The two protons in the water molecule here constitute a pair of nuclear magnets, which are nearest neighbours. The dipole-dipole interaction formally can be divided into two parts one from the interaction between the protons in the water molecule giving a shape function $Q(\xi)$, and one from the interaction with the other neighbours giving a dipole-broadened function $P(\zeta)$.

$Q(\xi)$ for a diamagnetic polycrystalline hydrate is, for example given by Andrew [7] as

$$Q(\xi) = Q_1(\xi) + Q_2(\xi)$$

$$Q_1(\xi) = \frac{1}{4\sqrt{3}\cdot b} \cdot \frac{1}{\sqrt{1+(\xi/b)}} \quad \text{for } -b < \xi < 2b \tag{12}$$

$$Q_2(\xi) = \frac{1}{4\sqrt{3}\cdot b} \cdot \frac{1}{\sqrt{1-(\xi/b)}} \quad \text{for } -2b < \xi < b$$

where $b = (3/2) \times (\mu/r^3)$ is the proton moment and r is the distance between the nuclei.

Here is

$$\int_{-\infty}^{+\infty} Q(\xi)\cos u\xi \mathrm{d}\xi = \frac{1}{4\sqrt{3}\cdot b}\cdot\int_{-b}^{2b}\frac{\cos u\ \xi\ \mathrm{d}\xi}{\sqrt{1+(\xi/b)}} + \frac{1}{4\sqrt{3}\cdot b}\cdot\int_{-2b}^{b}\frac{\cos u\ \xi\ \mathrm{d}\xi}{\sqrt{1-(\xi/b)}} \quad (13)$$

With the substitution $Z = \sqrt{(2ub/\pi)[1 + (\xi/b)]}$ in the first integral and the substitution $Z = \sqrt{(2ub/\pi)[1-(\xi/b)]}$ in the second integral eqn. (13) is transformed to

$$\int_{-\infty}^{+\infty} Q(\xi)\cos\ u\xi\mathrm{d}\xi = \sqrt{\pi/6ub}\cdot\cos(ub)\int_{0}^{\sqrt{6ub/\pi}}\cos\frac{\pi}{2}Z^2\mathrm{d}Z +$$

$$+\sqrt{\pi/6ub}\ \sin\ (ub)\int_{0}^{\sqrt{6ub/\pi}}\sin\frac{\pi}{2}Z^2\mathrm{d}Z \quad (14)$$

The zeros of the transform of $Q(\xi)$ is shown in Fig. 1. For the calculation of the transform the values of the Fresnel integrals

$$C(\sqrt{6ub/\pi}) = \int_{0}^{\sqrt{6ub/\pi}}\cos\frac{\pi}{2}Z^2\mathrm{d}Z \text{ and } S(\sqrt{6ub/\pi}) = \int_{0}^{\sqrt{6ub/\pi}}\sin\frac{\pi}{2}Z^2\mathrm{d}Z$$

have been taken from a table given by van Wijngaarden and Scheen [8].

The first three zeros occur for $u_1b = 2.16$, $u_2b = 5.63$ and $u_3b = 8.53$ from which b and r can be determined. From the values of the quotients u_2/u_1 and u_3/u_1 it can be tested whether the conditions necessary for a good adaptation are fulfilled.

Spectra composed by separate lines can also be evaluated by means of Fourier transforms.

An absorption line composed by n lines can be written as

$$f(x) = \sum_{\nu=1}^{n} P_\nu(x-\xi_\nu) \quad (15)$$

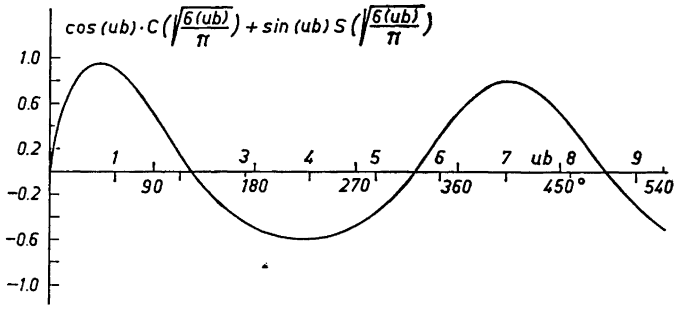

Fig. 1. The function $\cos(ub)\cdot\int_{0}^{\sqrt{6ub/\pi}}\cos\frac{\pi}{2}Z^2\mathrm{d}Z + \sin(ub)\cdot\int_{0}^{\sqrt{6ub/\pi}}\sin\frac{\pi}{2}Z^2\mathrm{d}Z$.

The function P_ν is the dipole-function of line number ν, which is symmetric with its symmetry point for $x = \xi_\nu$.

A spectrum composed by two separate lines can be studied as a simple example.

$$f(x) = P_1(x-\xi_1) + P_2(x-\xi_2) \tag{16}$$

When the lines overlap, it is of importance to determine the value of the displacement $(\xi_2-\xi_1)$ and the line-shapes for the two components.

In this case ξ_1 and ξ_2 are unknown, and it is convenient to calculate the transforms $F(u,a)$ and $G(u,a)$ for an arbitrary origin.

$$F(u,a) = \int_{-\infty}^{+\infty} f(x)\cdot\cos u(x-a)\mathrm{d}x = S_1(u)\cdot\cos u(\xi_1-a) + S_2(u).\cos u(\xi_2-a) \tag{17}$$

$$G(u,a) = \int_{0}^{+\infty} f(x)\cdot\sin u(x-a)\mathrm{d}x = S_1(u)\cdot\sin u(\xi_1-a) + S_2(u)\cdot\sin u(\xi_2-a) \tag{18}$$

Where

$$S_1(u) = \int_{-\infty}^{+\infty} P_1(\zeta)\cdot\cos u\zeta\,\mathrm{d}\zeta, \quad S_2(u) = \int_{-\infty}^{+\infty} P_2(\zeta)\cdot\cos u\zeta\,\mathrm{d}\zeta.$$

If $a = \frac{1}{2}\cdot(\xi_1+\xi_2)$ we get

$$F(u,a) = \{S_1(u) + S_2(u)\}\cdot\cos\frac{1}{2}\cdot u(\xi_2-\xi_1) \tag{19}$$

$$G(u,a) = \{S_1(u)-S_2(u)\}\cdot\sin\frac{1}{2}\cdot u(\xi_2-\xi_1) \tag{20}$$

The zeros of $F(u,a)$ and $G(u,a)$ are studied as functions of u for different a-values. By means of iterational calculations that a-value is determined for which the zeros of $\cos\frac{1}{2}u(\xi_2-\xi_1)$ and $\sin\frac{1}{2}u(\xi_2-\xi_1)$ can be identified among the zeros of $F(u,a)$ and $G(u,a)$, respectively.

The displacement $(\xi_2-\xi_1)$ is determined from the u-values for the zeros of these two series. $S_1(u)$ and $S_2(u)$ are then easily obtained from eqns. (19) and (20).

In application, the transforms have only to be calculated for a value of a, for instance $a = 0$, since

$$F(u,a) = F(u,0)\cdot\cos(ua) + G(u,0)\cdot\sin(ua)$$
$$G(u,a) = G(u,0)\cdot\cos(ua) - F(u,0)\cdot\sin(ua)$$

A few spectra of this kind have been evaluated. Spectra with a known value of the chemical shift $(\xi_2-\xi_1)$ have been gained through numerical addition of single spectral lines. The ^{1}H-resonance of water solutions of $MnSO_4$ have been used. The results show that the method is applicable when $(\xi_2-\xi_1)$

is in the interval 0.5 m to 3.0 m, where m is the linewidth parameter (for the definition of m, *cf.* Ref.[9]). In this interval $(\xi_2-\xi_1)$ has been determined with an error ranging from $\pm$ 6 % to $\pm$ 2 % for spectra with good signal/noise-ratio. When $(\xi_2-\xi_1)$ is smaller than 0.5 m, the series of zeros in the trigonometric functions cannot be distinguished from those in $\{S_1(u) + S_2(u)\}$ and $\{S_1(u)-S_2(u)\}$. When $(\xi_2-\xi_1)$ is larger than 3.0 m, the displacement can be determined directly from the spectrum.

The ^{1}H-resonance of hydrated crystals constitutes a special case of the above mentioned spectral type. A single crystal, where the water molecule has one crystallographic orientation, gives a symmetric spectrum

$$f(x) = P(x-\xi) + P(x + \xi) \tag{21}$$

where $$\xi = \frac{3}{2}\,\mu\, r^{-3} \cdot (3\cos^2\Theta - 1)$$

μ is the proton moment. r is the distance between the nuclei and Θ is the angle between the magnetic field and the proton-proton vector.

The line-width is rather large compared to the maximum separation between the lines $3\,\mu\, r^{-3}$. Therefore, in a large interval, ξ cannot be directly determined from the spectrum.

With the origin in the symmetry-point of the spectrum we get

$$F(u) = 2 \cdot S(u) \cdot \cos(u\xi), \text{ where } S(u) = \int_{-\infty}^{+\infty} P(\zeta) \cdot \cos(u\zeta)\mathrm{d}\zeta$$

assuming P to be symmetric.

A series of zeros in $F(u)$ thus occur for $u \cdot \xi = \frac{\pi}{2} + n\pi \quad n = 0, 1, 2, \ldots$, from which ξ can be determined. The symmetry properties of P may be ascertained from the values of the quotients of the zeros.

Spectra from single crystals affected by first-order quadrupole interaction are also composed by separate lines. For spin I such a spectrum can be written

$$f(x) = \sum_{n=k}^{-k} P_n(x-n \cdot \xi) \tag{22}$$

where $k = I - \frac{1}{2}$ and $\xi = \nu_Q f_o$; *cf.* Cohen and Reif [10].

The position of the resonance of the unaffected signal can, in these cases, be determined experimentally, and the transforms can be computed with this point as the origin.

For $I = 1$ is

$$f(x) = P_{1/2}(x-\frac{\xi}{2}) + P_{-1/2}(x + \frac{\xi}{2}) \text{ and}$$

$$F(u) = \{S_{1/2}(u) + S_{-1/2}(u)\} \cdot \cos(u\,\frac{\xi}{2})$$

$$G(u) = \{S_{1/2}(u)-S_{-1/2}(u)\} \cdot \sin(u\,\frac{\xi}{2})$$

and ξ can be determined from the zeros of $F(u)$ and $G(u)$. If $P_{-½}$ and $P_{+½}$ are identcial, the spectrum will be symmetric and can be treated in the same way as the spectrum of single hydrated crystals, described above.

For $I = \frac{3}{2}$ is

$$f(x) = P_1(x-\xi) + P_0(x) + P_{-1}(x+\xi)$$
$$F(u) = \{S_1(u) + S_{-1}(u)\} \cdot \cos(u\xi) + S_0(u)$$
$$G(u) = \{S_1(u) - S_{-1}(u)\} \cdot \sin(u\xi)$$

and ξ can here be determined from the zeros of $G(u)$. If the line-shapes of the three lines are identical, the spectrum will be symmetric. The relative intensities of the lines are determined by the quadrupole interaction and in this case is

$$S_0(u) = \frac{4}{10} \cdot \{S_1(u) + S_0(u) + S_{-1}(u)\}$$

$$S_1(u) = S_{-1}(u) = \frac{3}{10} \cdot \{S_1(u) + S_0(u) + S_{-1}(u)\}$$

Thus $$F(u) = \{\frac{6}{10} \cdot \cos(u\xi) + \frac{4}{10}\} \cdot \{S_1(u) + S_0(u) + S_{-1}(u)\}$$

and ξ can be determined from the series of zeros in $\cos(u\xi) = -\frac{2}{3}$ occurring in $F(u)$.

For $I > \frac{3}{2}$ a similar method may be used if the line-shapes of the different lines are identical.

It seems probable that the evaluation of many spectra can be facilitated by the use of Fourier transforms. No attempt, however, has been made to go into the mathematical side of the problem. The cases, as described above, only serve to examplify some simple practical applications of the method.

Acknowledgements. The author would like to thank the Head of the NMR group Dr. E. Forslind and Dr. U. Hellsten, for their kind interest in this work. The financial support provided by the *Swedish Natural Science Research Council* and the *State Council of Technical Research* is gratefully acknowledged.

REFERENCES

1. Andrew, E. R., Bradbury, A. and Eades, R. G. *Nature* **183** (1959) 1802.
2. Hughes, D. G. and Mac Donald, D. K. C. *Proc. Phys. Soc.* **78** (1961) 75.
3. Itoh, J., Kusaka, R., Yamagata, Y., Kiriyama, R. and Ibamoto, H. *J. Phys. Soc. Japan* **8** (1953) 293.
4. Silver, A. H., Kushida, T. and Lambe, J. *Phys. Rev.* **124** (1962) 1147.
5. Otsuka, E. and Kawamura, H. *J. Phys. Soc. Japan* **12** (1957) 1071.
6. Kopal, Z. *Numerical Analysis*, Chapman Hall Ltd. London 1955, p. 408.
7. Andrew, E. R. *Nuclear Magnetic Resonance*, Cambridge, University Press 1956, p. 155.
8. van Wijngaarden, A. and Scheen, W. L. *Nederl. Akad. v. Wetenschappen* **19**, Amsterdam 1949.
9. Svanson, S. E. and Forslind, E. *Acta Chem. Scand.* **16** (1962) 2149.
10. Cohen, M. H. and Reif, F. *Solide State Phys.* **5** (1957) 321.

Received May 2, 1962.

ACTA CHEMICA SCANDINAVICA 16 (1962) 2221–2239

Studies on the Hydrolysis of Metal Ions

Part 41. The Hydrolysis of the Cadmium Ion, Cd^{2+}

GEORGE BIEDERMANN and LIBERATO CIAVATTA

Department of Inorganic Chemistry, Royal Institute of Technology, Stockholm 70, Sweden

The hydrolysis equilibria of the Cd(II) ion have been studied at 25°C by measuring the hydrogen ion concentration of a series of cadmium perchlorate solutions, using a glass or a quinhydrone half-cell. The $[Cd(II)]_{tot}$ has ranged from 0.1 to 1.45 M. For each $[Cd(II)]_{tot}$ the $[H^+]$ was increased from a value corresponding to a solution saturated with $Cd(OH)_2$, until the hydrolysis became negligible. All solutions studied were made to contain 3 M ClO_4^- by adding $LiClO_4$.

The emf data, which show that only a small part of the Cd^{2+} ions can be transformed to hydrolysis products without precipitation, may be explained by assuming the equilibria

$$Cd^{2+} + H_2O \rightleftharpoons CdOH^+ + H^+ \qquad \log\beta_{1,1} = -10.2 \pm 0.1 \quad (1)$$

$$2\,Cd^{2+} + H_2O \rightleftharpoons Cd_2OH^{3+} + H^+ \qquad \log\beta_{1,2} = -9.10 \pm 0.05 \quad (2)$$

$$4\,Cd^{2+} + 4H_2O \rightleftharpoons Cd_4(OH)_4^{4+} + 4\,H^+ \qquad \log\beta_{4,4} = -31.8 \pm 0.1 \quad (3)$$

It may be deduced on the basis of the equilibrium constants (1), (2) and (3) that for $[Cd(II)]_{tot} \geq 0.1$ M the principal product of hydrolysis is the species Cd_2OH^{3+}.

Symbols often used in the text

- h = equilibrium concentration of hydrogen ions
- H = analytical excess of hydrogen ions = $[ClO_4^-] - 2[Cd(II)] - [Li^+]$
- b = concentration of Cd^{2+}
- B = total concentration of cadmium
- Z = $(h-H)B^{-1}$ = average number of hydrogen ions set free per cadmium atom
- K_p = formation constant for all species containing p OH groups
- $\beta_{p,q}$ = formation constant of the species $Cd_q(OH)_p$
- p = number of OH groups bound to the hydrolysis products
- q = number of cadmium atoms present in the hydrolysis products

A number of methods have been used to study the reactions between the Cd^{2+} ion and water. In 1904 Kullgren [1], the pioneer investigator in this field,

determined the hydrogen ion concentration at 100°C of several carefully purified cadmium chloride solutions containing sucrose by measuring the rate of inversion. Kullgren explained his data by assuming the equilibrium

$$Cd^{2+} + H_2O \rightleftharpoons CdOH^+ + H^+;\ \beta_{1,1} = [CdOH^+]h\,b^{-1} \qquad (1)$$

with $\log \beta_{1,1} = -9.5$.

In 1919 Löfman [2] studied the hydrolysis of Cd(II) by Vesterberg's method [3]. Löfman equilibrated cadmium acetate solutions at 20°C with ether, and measured the acetic acid concentration of the ether phase. On the basis of the distribution and dimerization constants of acetic acid Löfman was able to calculate for each $[Cd(II)]_{tot}$ the ratio $[HAc]_{aq}[Cd(II)]_{tot}^{-1}$, which under his experimental conditions is very nearly equal to the average number of OH groups bound per cadmium ion. By taking the value 2×10^{-5} for the dissociation constant of acetic acid and by neglecting complex formation between Cd^{2+} and acetate, we have calculated from Löfman's data $\log \beta_{1,1} = -9.2$.

In 1957 Marcus [4] titrated a series of cadmium perchlorate solutions at 25°C with NaOH, using a glass electrode. The $[Cd(II)]_{tot}$ ranged from 0.011 to 0.910 M and all the solutions were made to contain 3 M ClO_4^- by adding $NaClO_4$. Marcus interpreted the potentiometric data by assuming equilibrium (1) with $\log \beta_{1,1} = -9.2 \pm 0.2$. He encountered difficulties in obtaining accurate experimental results. The considerable scatter of the Z $(\log h)_B$ data (see Fig. 1 of Ref.[4]) was ascribed by Marcus to the presence of a weak protolyte in the NaOH solutions used, and further, to the slow establishment of the hydrolysis equilibria. We believe that the latter complication was due to the transient precipitation of $Cd(OH)_2$ caused by a local excess of OH^-. This is hard to avoid when a strong base is added to a poorly buffered cadmium solution.

The solubility of $Cd(OH)_2$ in dilute $HClO_4$ and NaOH solutions at 25°C was studied by Gayer and Woontner [5] in 1957. These investigators explained the variation of the $[Cd(II)]_{tot}$ in the saturated solutions, in the $\log h$ region -7 to -9.4, by postulating the equilibrium

$$Cd(OH)_2(s) + H^+ \rightleftharpoons CdOH^+ + H_2O \qquad K = [CdOH^+]h^{-1} \qquad (2)$$

with $\log K = 4.51$ *. This implies that in the $\log h$ range studied, the dissolved cadmium would exist predominantly as $CdOH^+$. However, the results of other investigations [1,2,4] including the present work, indicate that for $\log h = -9.4$ the ratio $[CdOH^+][Cd^{2+}]^{-1}$ is at most equal to 0.5 and that it is reduced below 0.01 when $\log h$ tends to -7. Gayer and Woontner's data, which were obtained in solutions with small buffer capacity, may have been influenced by minute amounts of impurities, such as substances dissolved from glass (*cf.* Ref.[6]).

* Marcus [4] considered that Gayer and Woontner [5] calculated from their solubility measurements $\log \beta_{1,1} = -9.3$. He probably derived this result by combining K of (2) with Feitknecht and Reinmann's value [7] for the solubility product of $Cd(OH)_2$, $pK_s = 14.21$, which is based on the assumption that in the saturated solution $[Cd^{2+}] = [Cd(II)]_{tot}$.

METHOD OF INVESTIGATION

In the present work the hydrolysis equilibria have been studied by measuring the hydrogen ion concentration of a series of cadmium perchlorate solutions at 25°C, using a glass or a quinhydrone electrode. The value of B ranged from 0.1 to 1.45 M, and the test solutions were made to contain 3 M ClO_4^- by adding $LiClO_4$. Some arguments have been given earlier [8] for preferring $LiClO_4$ to $NaClO_4$, and a quantitative study [9] now being made in this laboratory has yielded further evidence in support of this preference of $LiClO_4$.

The cadmium amalgam electrode was not used in this study, because it could be inferred from the h measurements that, at most, only 2 % of B may be transformed to the hydrolysis products before a precipitate forms. A decrease of the $[Cd^{2+}]$ by 2 % corresponds to a change of 0.25 mV in the potential of the cadmium half-cell; we have never been able, however, to measure the emf of cells containing liquid junctions with an uncertainty lower than $\pm$ 0.02 mV.

Preparation of the test solutions. Since the solubility product of $Cd(OH)_2$ has a low value ($pK_s \sim 14$) and the Cd(II) ion proved to be a rather weak acid clear, precipitate-free, cadmium solutions containing an appreciable amount of hydrolysis products are very poorly buffered. The preparation and preservation of such solutions represented the most serious problem in this investigation.

We were confronted with a similar situation when the hydrolysis of Ag^+ and of La^{3+} were studied in this laboratory [8,10]. The experience gained in connection with the studies of these ions was of great value to adopt a suitable method of preparation for cadmium solutions.

As the starting material 2 M cadmium perchlorate stock solutions, containing 0.001 M hydrogen ions, have been employed. At such a high acidity (where the hydrolysis is quite negligible) CO_2 can be easily expelled with N_2, and no reaction with pyrex glass could be detected. By diluting a weighed amount of the stock solution with 4 M $LiClO_4$, and NH_3- and CO_2-free water, solutions with the composition B' M Cd(II), H_0' M H^+, $(3.000 - 2B' - H_0')$ M Li^+, 3.000 M ClO_4^- = solution S_0' were prepared. B' had values ranging from 0.1 to 1.45 M, and H_0' varied from 10^{-4} to 10^{-3} M, depending on B'. In order to saturate S_0' with $Cd(OH)_2$, and thus to attain the maximum Z, a small excess of freshly ignited CdO was added to S_0' and the mixture was stirred for 12 to 16 h. The dark brown CdO preparation used was, within a couple of hours, transformed completely into white $Cd(OH)_2$ which is the stable phase at 25°C [11]. The excess of $Cd(OH)_2$ was removed by filtration and the resulting clear, saturated solution was sucked into a stoppered burette in which it was preserved. All these manipulations were carried out under an atmosphere of purified nitrogen in the apparatus shown in Fig. 1, the operation of which will be described in the section "Materials and Analysis".

A part of the saturated solution, S_0, was used to determine the $[Cd(II)]_{tot} = B$, which was found to exceed B' by 0.5 to 2 %, depending on B'. Since the solubility of $Cd(OH)_2$ in solutions S_0' proved to be low, the volume changes

caused by its dissolution may be neglected. The saturated solutions thus had the general composition

B M Cd(II), H_0 M H^+, (3.000 − $2B'$ − H_0') M Li^+, 3.000 M ClO_4^- = solution S_0

where $H_0 = H_0' - 2(B-B')$ denotes the analytical excess of hydrogen ions. Because B has always been very near to B', and H_0' has been known with an uncertainty of a few percent, an accurate value for H_0 had to be determined by emf measurements (see below). H_0 proved to be negative for each value of B studied.

In the course of the emf measurements, which were carried out as potentiometric titrations, the hydrogen ion concentration of the test solutions was varied by starting with V_0 ml of S_0 and adding to it successively increasing volumes, V_T ml, of another solution, T, which had the composition B M Cd(II), H_T M H^+, (3.000 − $2B$ − H_T) M Li^+, 3.000 M ClO_4^- = solution T. A high value was chosen for H_T, such that the hydrolysis in T could be neglected ($H_T = h > -H_0$). Thus all the solutions studied by emf measurements had the general composition

B M Cd(II), H_S M H^+, (3.000 − $2B$ − H_S) M Li^+, 3.000 M ClO_4^- = solution S

where

$$H_S = (H_0V_0 + H_TV_T)(V_0 + V_T)^{-1} \quad (3)$$

It is important to note that with this technique, a fresh saturated solution was prepared for each series of measurements. Thus, the reproducibility of the $\bar{Z}(\log h)_B$ data gives some idea of the effectiveness of our efforts to prevent contamination. The three sets of acceptably agreeing data obtained for solutions with B = 0.1 M, which have the lowest buffer capacity, seem to show (see Fig. 2) that the amount of protolysing impurities could be kept at so low a value that they had no appreciable influence on emf data of the present accuracy.

Determination of h by emf measurements. The hydrogen ion concentration of solution S was determined by measuring the emf of the cell

$$-\ \text{GE/solution S/SE}\ + \quad (A)$$

where GE denotes a glass electrode and SE represents the reference half-cell

/3.000 M $LiClO_4$/0.010 M Ag^+, 2.990 M Li^+, 3.000 M ClO_4^-/AgCl, Ag

The emf of cell (A) at 25°C may be written

$$E = E'_0 - 59.15 \log h - 59.15 \log f(H^+) + E_j(h,B) \quad (4)$$

In (4), E'_0 is a constant, $f(H^+)$ denotes the activity factor of hydrogen ions and $E_j(h,B)$ represents the liquid junction potential of the junction solution S/3 M $LiClO_4$. The standard state is defined so that the activity factors of all reacting species tend to unity as the composition of the solution approaches 3 M $LiClO_4$.

In each series of measurements B was kept constant while $\log h$ was successively increased from about −7.5 to −2.3. Since Z never exceeded 0.02, the composition of solution S changed only slightly in the course of acidifica-

tion. Consequently, we may regard it as a good approximation to assume that for B = constant, $f(H^+)$ = constant. Thus (4) may be simplified to

$$E = E_0 - 59.15 \log h + E_j(h,B) \quad (5)$$

where E_0 is a function of B.

The liquid junction potential of the junction h M H^+, (3—h) M Li^+, 3 M ClO_4^-/3 M $LiClO_4$ was found in a previous work [8] to be closely approximated for $h \leq 0.1$ M by the equation $E_j(h,0) = -15.8\ h$ mV. $E_j(h, 1.45)$ has been determined by measuring the emf of the cell

$$-\mathrm{SE}/h\ \mathrm{M}\ H^+,\ 1.450\ \mathrm{M}\ Cd^{2+},\ (0.100-h)\ \mathrm{M}\ Li^+,\ 3\ \mathrm{M}\ ClO_4^-/\overset{\mathrm{GE}}{\mathrm{quinhydrone(s)}},\mathrm{Pt}\ +$$

as a function of h in the region 0.01 to 0.1 M. The data could be well described with the linear formula $E_j(h, 1.45) = -22.4\ h$ mV. Since 0.005 M was the highest hydrogen ion concentration measured with cell (A), we could use in the whole B range the $E_j(h,0)$ function to calculate h from (5). The maximum error introduced by this approximation is much below the uncertainty of the E measurements, $\pm$ 0.1 mV.

In order to calculate h and Z from the E data the constants E_0 and H_0 need to be known. These were ascertained by determining at the end of each series of measurements a sequence of E values in the h range 0.5 to 5×10^{-3} M, where the hydrolysis is negligible. H_0 was computed from the E data obtained at these high acidities by constructing a Gran [12] plot. E_0 was then calculated for each point employed to find H_0. In all cases E_0 proved to be constant within $\pm$ 0.1 mV.

The main part of each series of experiments was devoted to the study of solutions in which log $h < -5$, where the hydrolysis becomes appreciable. With the known E_0 and H_0 values, and using (5) and (3), h and Z could be calculated for each point of the extensive series of E data obtained in the low acidity range. The family of functions $Z(\log h)_B$ serves as the basis for the calculations presented in later sections.

Comparison of the glass and the quinhydrone half-cells. In order to check the glass electrode, a few series of measurements have been made with the cell

$$-\ \mathrm{Pt},\ \mathrm{quinhydrone(s)/solution\ S/GE}\ + \quad (Q)$$

In the log h range -2 to -6.5, the emf of cell (Q) was found to be constant within $\pm$ 0.2 mV for each value of B studied. This result demonstrates the important point that the dependence on h of the emf of cell (A) is accurately described by eqn. (5).

Decomposition of quinhydrone and its dissociation products prevented us from extending the measurements with cell (Q) to lower acidities. It is worthwhile to note that, although air was carefully excluded from the cell, the decomposition could not be entirely inhibited.

Supplementary emf measurements. To enable us to estimate the influence of impurities introduced with the solvent salt, $LiClO_4$, a series of measurements was carried out in 0.21 M $(Li^+)ClO_4^-$ solutions. B was kept constant at 0.1 M, while log h was increased stepwise from -7.3 (= the acidity of the saturated solution) to -3. The $Z(\log h)_B$ data obtained in the medium 0.21 M $(Li^+)ClO_4^-$

could be satisfactorily interpreted in terms of hydrolysis products containing the same number of OH groups as those found to be present in solutions in which $[ClO_4^-] = 3$ M and $B = 0.1$ M. Moreover, the logarithms of the monoligandic equilibrium constant, log K_1, determined in 0.21 M and 3M media differ only by 0.1 unit (see Table 2). We may thus conclude that the amount of impurities in our $LiClO_4$ preparations do not appreciably affect the results derived from the emf data.

All emf measurements considered hitherto were performed by increasing gradually the acidity of the test solutions. Doubts may therefore arise whether the true equilibria could be attained in this way. To furnish some light on this essential question a series of measurements was made, employing the glass electrode, by starting with a partially hydrolyzed solution in which $B = 0.7$ M and log $h = -7.1$, and adding to it increasing volumes of another solution containing 3 M $LiClO_4$ and 0.736 mM $HClO_4$. At the end of the series B had decreased to 0.2 M and log h to -7.4. The set of Z(log h, B) data calculated from these measurements could be accurately described with the same equilibrium constants as were used to explain the data found for acidified solutions, see Fig. 2. This fact affords evidence that the real equilibria were closely approached when the hydrolysis was successively suppressed, *i.e.* using the technique outlined in the preceding sections.

MATERIALS AND ANALYSIS

Cadmium perchlorate stock solutions were prepared by dissolving CdO in a small excess of dilute $HClO_4$. CdO was made by igniting $Cd(NO_3)_2(H_2O)_4$. This salt was chosen because it can be easily purified by recrystallization, and because it decomposes to CdO at around 400°C. Pure $Cd(NO_3)_2(H_2O)_4$ was prepared in two ways: (*a*) $Cd(NO_3)_2(H_2O)_4$ (Baker, p.a.) was twice recrystallized from 0.01 M HNO_3, (*b*) Cadmium rods, Baker p.a., that had been first etched with 8 M HNO_3, were dissolved in an excess of 16 M HNO_3. The resulting solution was slowly evaporated and the cadmium nitrate crystals, which formed, were separated by filtration. This product was further purified by two recrystallizations from water. No Fe^{3+}, Pb^{2+}, Cl^- or SO_4^{2-} ions could be detected in either type of preparation. The $Z(\log h)_B$ data obtained in solutions originating from cadmium nitrate of type (*a*) and (*b*) have always agreed within the experimental uncertainty ($\pm$ 0.003 log h units).

The cadmium nitrate must be heated gradually to 400°C, and it must be stirred continuously. If these precautions are not taken, a sintered product is formed, and moreover, the melt or the boiling solution is likely to froth over at the transition temperatures of cadmium nitrate. The melt was kept at 400°C, while being stirred, until no more nitrogen oxide fumes could be detected. Finally, the CdO thus formed was ignited overnight at 800°C to expel the last traces of nitrogen oxides. The resulting powder-like CdO was completely transformed into $Cd(OH)_2$ within a couple of hours after it was brought into contact with our solutions at 25°C.

The cadmium concentrations of the stock and of the test solutions were determined gravimetrically by precipitating $CdNH_4PO_4H_2O$. The analyses were carried out following closely Winkler's prescriptions [13], in this way an accuracy of 0.1 % could be attained.

The hydrogen ion concentration ($\sim$ 0.001 M) of the stock solutions was estimated by adding a measured volume of standardized $HClO_4$ to a weighed amount of the stock solution and titrating this mixture with NaOH using methyl-red as indicator. The uncertainty of the results did not exceed 2 %.

$LiClO_4$, $AgClO_4$ and $HClO_4$ solutions were prepared and analyzed as described in an earlier publication [8].

The saturated solutions, S_0, were prepared using the apparatus shown in Fig. 1. Nitrogen was supplied through the tubes a_1 and a_2. The gas, which was taken from a cylinder, was purified and presaturated by passing it through 0.5 M NaOH, then water and finally solution S_0'. The stoppers R_1, R_2 and R_3 were made from rubber, this material was chosen to attain some flexibility. The stoppers were cleaned by soaking them in boiling 1 M NaOH and then in water. A thin layer of filter paper pulp was placed on the filter surface of the sintered glass filter funnel, g, to retain the smallest $Cd(OH)_2$ particles. One quarter of a "Whatman ashless tablet" was used for each filtration. No acid or alkaline impurities, Cl^-, SO_4^{2-} or heavy metal ions could be detected in the tablets, which were tested as given earlier [8].

The apparatus was operated as follows. First the three-way stopcock C_1 was turned to the right and C_3 was opened. Then 70 ml of S_0' was placed in the vessel A_1 and nitrogen was passed through the solution for two hours. R_1 was then lifted for a moment and freshly ignited CdO (taken from a N_2-filled desiccator) was dropped into S_0'. This solution was saturated by stirring it, using a teflon covered magnet bar, with the CdO for a night, while a vigorous stream of N_2 was maintained. Next morning the flask A_2 was flushed with N_2 entering at a_2 and leaving at C_4, this gas current was continued throughout the filtration. A portion of the saturated solution was pressed into the funnel g by turning C_1 to the vertical, then C_1 was returned to the right and thereby N_2 passed through the solution while it was trickling through the filter. Successive portions of S_0 were transferred to g until about 60 ml filtrate was obtained. C_4 was now closed and the burette was flushed with N_2 by turning C_2 to the vertical. Finally the filtrate was drawn up into the burette by connecting it to a water-jet pump. The saturated solution was preserved in the burette under N_2 at atmospheric pressure.

In each case the filtrate was carefully examined for turbidity, but no suspended $Cd(OH)_2$ particles could be detected. No indication of slow precipitation was found in filtrates which were tested for turbidity regularly during a week.

Experimental details of the emf measurements. All emf measurements were carried out at 25°C. The cell arrangement, which was kept in a paraffin oil thermostat, was similar to that described by Forsling, Hietanen and Sillén [14]. Air had been displaced with N_2 in the titration vessel before the test solution was introduced and a N_2 stream was maintained throughout the series of measurements. Nitrogen, which was taken from a cylinder, was passed through successively 0.5 M NaOH, H_2O and 3 M $LiClO_4$ for purification and presaturation.

A number of glass electrodes of the type Beckman No 40498 were employed. Ten minutes after each addition of solution T the emf of cell (A) showed a value which remained constant within ± 0.1 mV for many hours. $E-E_0$ values obtained with different glass electrodes agreed always within 0.2 mV. E was measured with a valve potentiometer

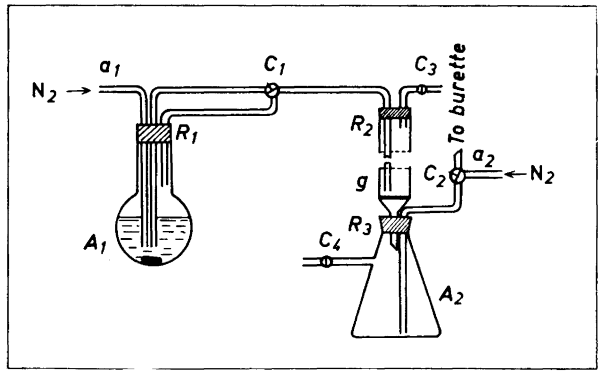

Fig. 1. Apparatus used to prepare saturated solutions.

Table 1. Survey of measurements.

B = 1.450 M
$Z \times 10^3$, $-\log h$. Series a. 20.6_8, 7.128; 19.7_8, 7.116; 18.9_3, 7.104; 18.0_6, 7.089; 17.2_3 7.074; 15.6_0, 7.040; 14.0_3, 7.006; 12.5_2, 6.969; 11.0_7, 6.925; 9.6_7, 6.874; 8.31, 6.818; 7.00, 6.747; 5.73, 6.665; 4.51, 6.565; 3.33, 6.433; 2.18, 6.259; 1.07, 5.953; 0.52, 5.813.
Series b. 20.6_4, 7.121; 19.4_0, 7.106; 18.3_7, 7.092; 17.0_2, 7.069; 15.7_3, 7.043; 14.3_0, 7.011; 13.0_8, 6.982; 11.7_6, 6.950; 10.3_2, 6.903; 8.94, 6.849; 7.61, 6.786.

B = 1.000 M
$Z \times 10^3$, $-\log h$. Series a. 17.3_2, 7.221; 16.1_6, 7.200; 15.2_5, 7.185; 13.9_0, 7.155; 12.8_1, 7.128; 11.7_3, 7.102; 10.4_7, 7.065; 9.64, 7.031; 8.43, 6.986; 7.44, 6.937; 6.65, 6.894; 5.88, 6.844; 5.125, 6.785; 4.38, 6.715; 3.82, 6.663; 3.17, 6.599; 2.73, 6.519; 2.19, 6.426; 1.66, 6.310; 1.14, 6.146; 0.62, 5.874.
Series b. 16.0_4, 7.188; 13.7_6, 7.141; 11.5_8, 7.097; 9.47, 7.036; 7.44, 6.952; 6.46, 6.896.

B = 0.700 M
$Z \times 10^3$, $-\log h$. Series a. 13.4_2, 7.283; 12.6_6, 7.268; 11.9_0, 7.249; 10.9_1, 7.220; 9.70, 7.178; 8.51, 7.136; 7.34, 7.080; 6.19, 7.014; 5.06, 6.935; 3.96, 6.831; 3.09, 6.725; 2.44, 6.622; 1.81, 6.498; 1.18, 6.319; 0.76, 6.138; 0.35, 5.821.
Series b. 13.7_8, 7.302; 12.5_1, 7.276; 11.2_7, 7.243; 10.0_5, 7.205; 8.86, 7.160; 7.92, 7.118; 6.99, 7.072; 6.08, 7.014; 5.18, 6.952; 4.51, 6.889; 3.86, 6.820; 3.21, 6.742; 2.57, 6.649; 2.14, 6.568; 1.72, 6.475; 1.30, 6.350; 0.88, 6.179; 0.68, 6.054; 0.47, 5.882.

B = 0.500 M
$Z \times 10^3$, $-\log h$. Series a. 11.28, 7.342; 10.1_8, 7.309; 9.10, 7.273; 8.04, 7.229; 7.00, 7.175; 6.39, 7.140; 5.58, 7.087; 4.59, 7.004; 3.61, 6.903; 2.66, 6.769; 1.90, 6.629; 1.16, 6.416; 0.61, 6.136; 0.25, 5.726.
Series b. 11.4_6, 7.344; 10.8_0, 7.319; 9.93, 7.297; 9.06, 7.266; 8.01, 7.222; 6.97, 7.170; 6.16, 7.123; 5.55, 7.080; 4.96, 7.031; 4.37, 6.977; 3.79, 6.915; 3.21, 6.847; 2.64, 6.764; 2.26, 6.698; 1.70, 6.577; 1.33, 6.472; 0.96, 6.333; 0.60, 6.122; 0.24, 5.699.

B = 0.250 M
$Z \times 10^3$, $-\log h$. Series a. 8.16, 7.493; 7.29, 7.452; 6.43, 7.407; 5.59, 7.347; 5.10, 7.309; 4.44, 7.248; 3.96, 7.200; 3.33, 7.123; 2.70, 7.030; 2.24, 6.945; 1.78, 6.845; 1.33, 6.715; 1.03, 6.594; 0.73, 6.431; 0.44, 6.157.
Series b. 8.38, 7.500; 7.86, 7.476; 6.99, 7.435; 6.14, 7.386; 5.48, 7.337; 4.82, 7.285; 4.34, 7.243; 3.70, 7.173; 3.07, 7.094; 2.60, 7.020; 2.14, 6.933; 1.69, 6.830; 1.38, 6.746; 1.09, 6.639; 0.79, 6.492; 0.35, 6.092.

B = 0.100 M
$Z \times 10^3$, $-\log h$. Series a. 5.62, 7.593; 5.20, 7.559; 4.53, 7.505; 3.95, 7.439; 3.55, 7.400; 2.94, 7.309, 2.55, 7.238; 1.94, 7.118; 1.55, 7.003; 1.16, 6.851; 0.97, 6.759; 0.78, 6.641; 0.58, 6.487; 0.40, 6.257.
Series b. 6.80, 7.653; 6.16, 7.608; 5.53, 7.560; 4.91, 7.506; 4.29, 7.440; 3.89, 7.388; 3,49, 7.336; 3.29, 7.305; 2.89, 7.239; 2.50, 7.168; 2.10, 7.084; 1.71, 7.003; 1.33, 6.864; 0.95, 6.676; 0.56, 6.303.
Series c. 7.10, 7.664; 6.46, 7.623; 5.83, 7.579; 5.21, 7.530; 4.59, 7.467; 3.98, 7.401; 3.38, 7.322; 2.98, 7.261; 2.59, 7.190; 2.19, 7.106; 1.81, 7.018; 1.42, 6.884; 1.04, 6.698; 0.56, 6.367.

B = 0.100 M, $[ClO_4^-] = 0.21$ *M*
$Z \times 10^3$, $-\log h$. 2.46, 7.297; 1.85, 7.173; 1.65, 7.121; 1.25, 6.994; 1.05, 6.906; 0.85, 6.837; 0.65, 6.710; 0.45, 6.541; 0.25, 6.283.

Special series of measurements where B was varied
$Z \times 10^3$, *B*, $-\log h$. 8.05, 0.700, 7.116; 7.97, 0.651, 7.143; 7.85, 0.588, 7.182; 7.65, 0.507, 7.229; 7.45, 0.446, 7.266; 7.25, 0.398, 7.298; 6.85, 0.327, 7.342; 6.45, 0.278, 7.358; 5.65, 0.213, 7.405.

Radiometer PHM4, Copenhagen, this instrument was frequently calibrated against a Leeds & Northrup potentiometer of type K3. Ag—AgCl electrodes were prepared according to Brown [15].

The potential of the quinhydrone half-cell was measured by immersing into solution S two platinum foil electrodes. These always agreed within 0.1 mV. The quinhydrone, Merck p.a., had been recrystallized from water, and had been kept for a week in a desiccator over H_2SO_4. No protolyzing impurities or Fe(III) and Cl^- ions could be detected in the recrystallized product.

ASCERTAINMENT OF THE COMPOSITION OF THE HYDROLYSIS PRODUCTS

The sets of $Z(\log h)_B$ data, which are summarized in Table 1 and are graphically represented in Fig. 2, form the basis of the following calculations.

The method to be employed for finding the composition of the hydrolyzed species and the corresponding equilibrium constants is mainly determined by the range of B studied. In the present work B values ranging from 0.1 to 1.45 M could be investigated. With more dilute solutions (*e.g.* for $B = 0.05$ M) we have not been able to obtain reliable results, thus, when a series of measurements was repeated, the deviations of the corresponding Z values considerably exceeded one percent, which we set as the highest limit of acceptable uncertainty. This failure can be explained by the slight buffer capacity of dilute cadmium solutions. The buffer capacity is proportional to BZ, and Fig. 2 shows that the accessible range of BZ narrows rapidly as B is decreased. In forthcoming publications, dealing with investigations where hydrolyzed solutions were prepared by electrolysis (using a coulometer), some arguments will

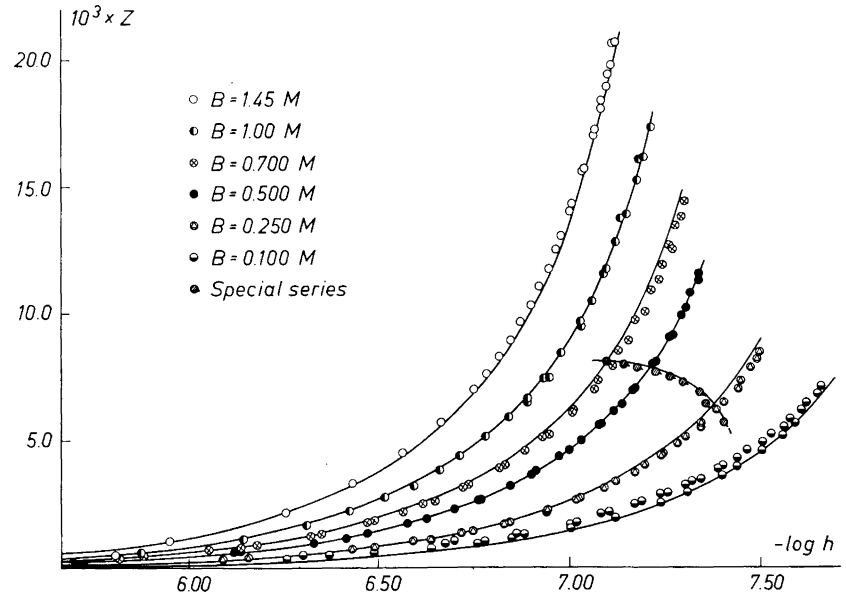

Fig. 2. Z = the average number of hydrogen ions set free per cadmium atom as a function of $-\log h$. The curves were calculated with the $\beta_{p,q}$ values proposed in Table 3.

be presented which make it seem probable that the difficulties arising for $B < 0.1$ M are mainly caused by nephelometrically undetectable amounts ($\sim$1—2 micromoles/liter of filtrate) of $Cd(OH)_2$ particles passing through the filter.

The variations of the activity factors of the reacting species, due to the replacement of 2 Li^+ by Cd^{2+}, are certainly not negligible in our test solutions containing such high concentrations of cadmium. Consequently, our data cannot be treated by methods worked out for an inert medium. On the other hand the self-medium method proposed by Hietanen and Sillén [16] proved to be of great value (section I). The main idea of this method is that data obtained at each value of B are considered separately. Since only low Z values were accessible and since Cd^{2+} was found to be a weak acid, the changes in composition are small when B is kept constant while the hydrolysis is suppressed by adding dilute $HClO_4$ to a solution saturated with $Cd(OH)_2$. Thus the assumption that for B = constant the activity factors are constants may be regarded as a close approximation. Evidently, by the separate analysis of each set of $Z(\log h)_B$ data only the number of OH groups bound to the hydrolysis products, p, and the corresponding homoligandic equilibrium constants, K_p, can be evaluated, whereas this treatment cannot give any information on the number of cadmium atoms, q, present in the complexes, because B is always very close to b.

A plausible estimate of the probable values of q may be obtained by examining the functions $K_p(B)$. When we disregard the variation of the activity factors K_p represents a power series of the single variable B. If the series contains only one or two terms, reasonable values for the exponents of B, the q's, can be derived easily (section II). Clearly, this treatment is approximate and the conclusions involve the uncertainty due to the unknown variation of activity factors. Nevertheless some evidence will be given [17] in a work concerned with the hydrolysis of Y(III), covering the yttrium concentration range 0.01 to 1 M, that the values of q and $\beta_{p,q}$ deduced by the method of section II are not likely to be seriously in error.

In sections I and II a number of approximations were introduced and the several groups of data were discussed separately, it was therefore desirable to compare the complete set of data with normalized model functions based on the exact equations. This forms the subject of section III, which moreover contains a treatment according to the generalised least squares method, proposed by Sillén [20], to provide an additional check on the consistency of the results of our calculations.

I. Determination of p by the self-medium method

In this section each set of $Z(\log h)_B$ data will be dicussed separately.

In a series of solutions, where B is kept constant while Z is varied, the molar concentration of OH groups bound per cadmium, $h-H$, can be expressed by the equation

$$h-H = BZ = \sum_p \sum_q p[Cd_q(OH)_p] = \sum_p \sum_q p\beta_{p,q} b^q h^{-p} \qquad (6)$$

In (6) the variables p and q may assume a series of integral values, and $\beta_{p,q}$ designates the formation constant of the hydrolysis product $Cd_q(OH)_p^{(2q-p)+}$

$$\beta_{p,q} = [Cd_q(OH)_p]h^p b^{-q} \tag{7}$$

To find the number of OH groups bound to the hydrolysed species the $Z(\log h)_B$ data will be compared with functions representing different hypotheses concerning the prevailing values of p. For the calculation of these model functions on the basis of (6) some assumptions must be made also about the dependence of b upon h. Since the maximum Z has never exceeded 0.021, b must be always very close to B. Consequently, we have to estimate only an upper and a lower limit for b and then we have to examine how much the deduced values of p are influenced when b varies from maximum to minimum.

The inequality $b < B$ yields B as the upper limit, to estimate the lower one we have postulated that hydrolysis products with $q/p > 2$ do not occur in appreciable concentrations. This postulate is based on the consideration that the formation of species with $q/p > 2$ would involve an accumulation of positive charges which is improbable because of the electrostatic repulsion.

The results of section II strongly support the validity of this postulate. Were complexes with $q/p > 2$ formed in significant amounts, their presence would certainly have been detected by the treatment described in section II.

We may therefore regard the inequality

$$B > b \geq B(1-2\ Z) \qquad (q \leq 2\ p) \tag{8}$$

to provide reasonable limits for b.

On the basis of (6) and (8) two types of model functions, F and Φ, have been constructed to approximate the experimental BZ values:

$$F(h) = \sum_p \sum_q p\, B^q \beta_{p,q} h^{-p} = \sum_p p K_p h^{-p} \quad (> BZ) \tag{9}$$

and

$$\Phi(w) = \sum_p \sum_q p B^q \beta_{p,q} w^p = \sum_p p K_p w^p \quad (\leq BZ) \tag{10}$$

where K_p , the homoligandic equilibrium constant, is equal to

$$K_p = \sum_q B^q \beta_{p,q} \tag{11}$$

and

$$w = (1-2Z)^2 h^{-1} \tag{12}$$

When a particular hypothesis concerning the p values was tested, both the F and the Φ functions were compared with the data. It should be pointed out immediately that identical numbers were obtained for the most probable values of p when either approximation (9) or (10) was used. Moreover, the log K_p values calculated with F and Φ never differed more than 0.01 units. These results indicate that the conclusions derived by the self-medium method are not appreciably influenced by the fact that the b values are not known exactly. In the following discussion only the F functions will be given explicitly, the calculations involving Φ were analogous except that w was used instead of h^{-1} as the independent variable.

In the first instance we have attempted to explain the data in the simplest way by assuming that all the hydrolysis products are homoligandic. The F

function corresponding to the hypothesis, that a single value of $p = P$ occurs, F_P, can be brought to the following normalized form

$$F_P = P\ K_P\ h^{-P} = P\ x^P = F_P(\log x),\ \log x = P^{-1} \log K_P - \log h \qquad (13)$$

A group of F_P functions covering the range of P from 1 to 6 was plotted, and each of them was superimposed on the $BZ(\log h)_B$ data. The complete set of $BZ(\log h)_{0.1}$ data was found to be satisfactorily described by $F_1(\log x)$. No member of the F_P group could, however, be fitted throughout the experimentally accessible $\log h$ range to any set of data obtained in more concentrated cadmium solutions. On the other hand, at each value of $B \geq 0.25$ M the experimental points seemed to approach F_1 as Z decreased, and moreover, the lower the value of B considered the greater was the part of the total range of Z which appeared to agree with F_1.

We may thus conclude that in solutions where BZ is low the main products of hydrolysis are monoligandic, while species containing several OH groups are formed in increasing amount as BZ tends to the maximum value attainable 0.03. On the basis of the F_P functions no certain information could be gained concerning the composition of the multiligandic species.

The predominance of monoligandic species in the region where $BZ \leq 0.003$ can be clearly demonstrated by calculating the average number of OH groups bound to the hydrolysis products, $\bar{p}$, as a function of $\log h$. Using approximation (9) $\bar{p}$ is obtained by the equation [8]

$$\bar{p} = \frac{\Sigma p[\mathrm{Cd}_q(\mathrm{OH})_p]}{\Sigma\ [\mathrm{Cd}_q(\mathrm{OH})_p]} = BZ\ (2.303 \int_{\log h}^{\infty} BZ\ \mathrm{dlog}\ h)^{-1} \qquad (14)$$

When BZ is approximated with Φ the integral in (14) is to be replaced by $\int_0^{\log w} BZ\ \mathrm{dlog}\ w$. The $\bar{p}$ values calculated with the F and Φ functions were found in each case to coincide within the limits of experimental uncertainty.

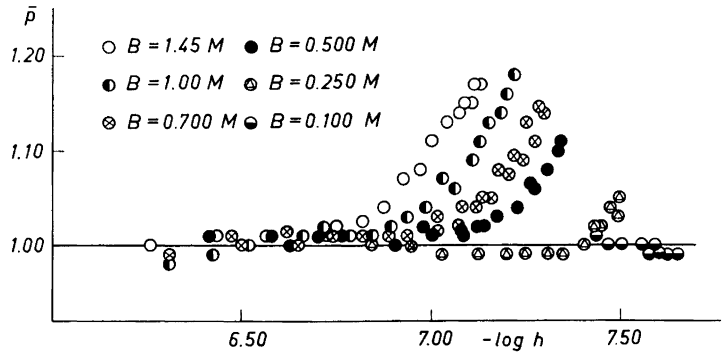

Fig. 3. $\bar{p}$ = average number of OH groups bound to the hydrolysis products as a function of $-\log h$.

The integration was performed using the trapezoidal rule. In order to avoid the arbitrariness associated with smoothed curves the experimental points were taken directly, thus unequal integration intervals were chosen. The magnitudes of the residual integrals $\int_{-6.5}^{\infty} BZ \, d\log h$ and $\int_{0}^{-6.5} BZ \, d\log w$ were estimated graphically using the extrapolation method described earlier [8]. For $Z > 0.003$, where the uncertainty arising from the extrapolation becomes negligible, the calculated $\bar{p}$ values may be considered to be reliable within $\pm$ 2 %.

The $\bar{p}(\log h)_B$ plots, shown in Fig. 3, indicate that at each value of B a log h region can be found where $\bar{p}$ remains constant within 1.00 ± 0.02. For each experimental point falling in this region, which is seen in Fig. 3 to be narrowed as B increases, $\log K_1 = \log (BZh)$ was calculated, these have shown no appreciable trend with h. The most probable values of $\log K_1(B)$ are summarized in Table 2, the uncertainty of the constants was assumed to be equal to the maximum deviation from the mean value.

In order to explain the data from measurements made in solutions where $BZ > 0.003$ it was assumed that besides Cd_qOH another species containing p' OH groups, $Cd_{q'}(OH)_{p'}$, is also formed. It is recalled that in these formulas q and q' denote unknowns which can take several integral values, whereas p' is a constant.

To test the validity of this assumption which may be expressed by the equation

$$BZ = F_{1,p'} = K_1 \, h^{-1} + p' \, K_{p'} \, h^{-p'} \tag{15}$$

the data were recalculated to the form $\log (BZh)$ *versus* $(\log h)_B$, and a plot of them was constructed. The plot was compared with the following normalized function derived from (15)

$$W_{p'} = \log F_{1,p'} - \log K_1 + \log h = \log (1 + p' u^{(p'-1)}) = W_{p'} (\log u) \tag{16}$$

$$\log u = (p'-1)^{-1} \log (K_{p'}/K_1) - \log h \tag{17}$$

The advantage of using (16) is that it makes possible to evaluate both $\log K_1$ and $\log K_{p'}$. A group of $W_{p'}$ functions covering the p' range 2 to 8 was calculated and a plot of each was superimposed on the data. All the available sets of log (BZh) data could be fitted to W_4, whereas systematic deviations were found

Table 2. Survey of the homoligandic equilibrium constants.

B M	$-\log K_1$ eqns. (14) and (16)	$-\log K_4$ eqn. (16)	p' $b = B$	p' $b = (1-2Z) B$
0.100	10.81 ± 0.02	—	—	—
0.250	10.19 ± 0.01	—	—	—
0.500	9.65 ± 0.01	33.10 ± 0.01	4.5 ± 0.5	4.1 ± 0.5
0.700	9.39 ± 0.01	32.57 ± 0.01	4.1 ± 0.5	3.9 ± 0.5
1.000	9.08 ± 0.01	31.96 ± 0.01	3.8 ± 0.5	3.6 ± 0.5
1.450	8.74 ± 0.01	31.30 ± 0.01	4.0 ± 0.5	3.8 ± 0.5
0.100 *	10.89 ± 0.01	—	—	—

* $[ClO_4^-] = 0.21$ M.

in some part of the studied log h range with any other member of the $W_{p'}$ group. This result indicates that the data of present accuracy can be satisfactorily explained by assuming the formation of Cd_qOH and $Cd_{q'}(OH)_4$ but no other mechanism involving only two p values is acceptable.

The probable values of the constants log K_1 and log K_4 were obtained by reading off in the position of best fit the difference W_4 —log (BZh) and log u — (—log h). The fit was always found to be satisfactory. The log K_1 values calculated in this way practically coincided with those in Table 2 which were derived on the basis of the $\bar{p}(\log h)_B$ plots. The log K_4 values obtained with (16) are also inserted in this table.

Additional evidence can be afforded for the conclusions reached with the curve-fitting by a numerical treatment which enables one to examine systematically how the experimental error and the underlying assumptions affect the estimation of p'. Eqn. (15) may be rearranged to the form

$$\log (BZ - K_1 h^{-1}) = \log p' + \log K_{p'} - p' \log h \qquad (18)$$

Thus, provided the hypothesis that only species with $p = 1$ and $p = p'$ are formed is valid, log $(BZ - K_1 h^{-1})$ should be a linear function of log h having the slope $-p'$. For each experimental point corresponding to $BZ \geq 0.003$ three values of log $(BZ - K_1 h^{-1})$ have been calculated by inserting the most probable value of log K_1, and as well as its lower and higher limit, as given in Table 2. In this connection there was no need to take into account the uncertainty of BZ, since it is much lower than that of K_1. For a particular set of data the most probable value of p' was computed with the formula

$$p' = \frac{\sum_{1}^{n} y_i - \sum_{n+1}^{2n} y_i}{\sum_{1}^{n} x_i - \sum_{n+1}^{2n} x_i}$$

where y_i and x_i designate a pair of values of log $(BZ - K_1 h^{-1})$ and log h. In order to gain an idea on the influence of random experimental error the number of points $(2n)$ considered for a particular value of K_1 was varied from 4 to 12. In the final step all the calculations were repeated with approximation (10), in this case instead of (18) the equation

$$\log (BZ - K_1 w) = \log p' + \log K_{p'} + p' \log w \qquad (18a)$$

was used.

The results are presented in Table 2, the limits indicate the maximum deviation from the mean of all the p' values obtained by varying K_1 and n. The reasonable constancy of the p' values appears to justify the conclusions deduced graphically. Thus the experiments have been of sufficient accuracy to exclude the hypothesis that besides Cd_qOH and $Cd_{q'}(OH)_4$ other hydrolysis products may be present in appreciable concentration.

II. Estimation of the probable values of q and q'

If we introduce the approximation that in our solutions of $[ClO_4^-] = 3$ M the activity factor ratios occuring in the exact expressions for the formation constants

$$\beta'_{p,q} = \beta_{p,q} f(p,q) f^p(H^+) f^{-q}(Cd^{2+}) \qquad (19)$$

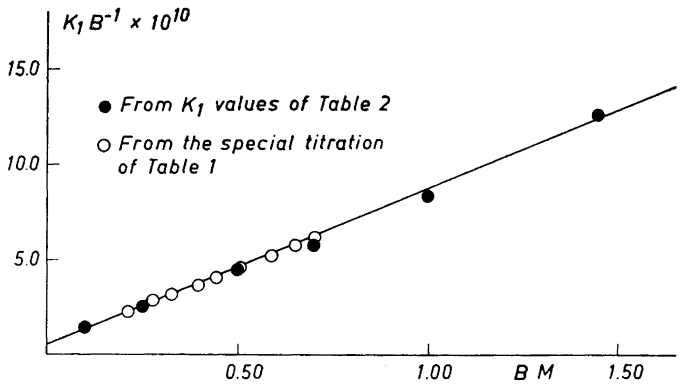

Fig. 4. $K\ B^{-1}$ (eqn. (20)) as a function of B. The line represents the equation: $K_1 B^{-1} = 5 \times 10^{-11} + 8.2 \times 10^{-10}\ B$.

vary to a negligible extent, the number of cadmium atoms present in the species Cd_qOH and $Cd_{q'}(OH)_4$ can be evaluated by analysing the functions $K_1(B)$ and $K_4(B)$.

According to (11) K_1 is equal to

$$K_1 = B\ \beta_{1,1} + B^2\beta_{1,2} + \ldots \qquad (20)$$

A plot of K_1B^{-1} *versus* B is shown in Fig. 4. This plot was calculated from the K_1 values of Table 2 (full circles), and as well as from the series of measurements performed by adding 3 M $LiClO_4$ to a partially hydrolyzed solution of $B = 0.7$ M (circles). It can be inferred from the $\bar{p}$ $(\log h)_B$ functions in Fig. 3 that each point of this series of measurements (recorded in Table 1) falls in the region where the monoligandic species predominate.

All the points of Fig. 4 are seen to fit a straight line within the limits of experimental uncertainty, consequently the data can be explained by assuming the formation of $CdOH^+$ and Cd_2OH^{3+} only. The most probable values of of $\beta_{1,1}$ and $\beta_{1,2}$ were estimated using the method of least squares. This yielded the results

$$\log\ \beta_{1,1} = \log\ ([CdOH^+]\ h\ [Cd^{2+}]^{-1}) = -10.3 \pm 0.2$$

and

$$\log\ \beta_{1,2} = \log\ ([Cd_2OH^{3+}]\ h\ [Cd^{2+}]^{-2}) = -9.10 \pm 0.05$$

In order to find the prevailing values of q' a plot of $\log K_4 = \log\ (\Sigma B^{q'}\ \beta_{4,q'})$ against $\log B$ was constructed. The points, taken from Table 2, seemed to fit a line of slope 4, indicating the formation of the single species $Cd_4(OH)_4^{4+}$. The correctness of this hypothesis is illustrated in Fig. 5 where $\log K_4 - q' \log B$ is plotted as a function of B for the q' values 3,4 and 5. It is seen from this figure that $\log K_4 - 4 \log B$ shows no appreciable trend with B, while large systematic deviations occur for $q' = 3$ and $q' = 5$. Moreover, the deviations

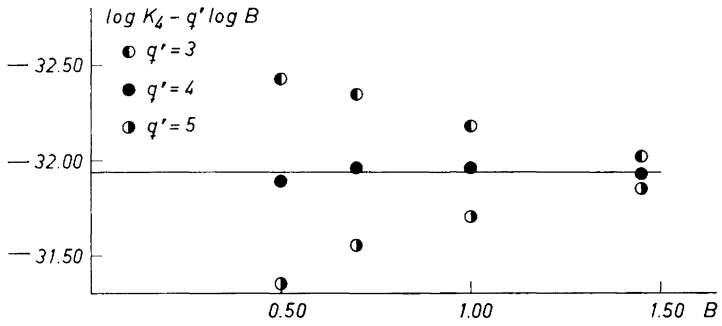

Fig. 5. log $K_4 - q'$log B (eqn. (11)) as a function of B for q' values 3, 4 and 5. For the sake of clarity the points for $q' = 3$ have been shifted vertically by -0.25 units and those for $q' = 5$ by $+ 0.25$ units.

change sign as q' passes through 4. Thus the data are only compatible with the assumption that $Cd_4(OH)_4^{4+}$ is formed. Taking the average value of log $K_4 -$ 4 log B we can write

$$\log \beta_{4,4} = \log ([Cd_4(OH)_4^{4+}]\ h^4[Cd^{2+}]^{-4}) = -31.8 \pm 0.1$$

III. Comparison of the complete set of data with normalized model functions

The calculations presented in section II have furnished evidence for the formation of the monoligandic species $CdOH^+$ and Cd_2OH^{3+}, and for the presence of a single tetraligandic hydrolysis product $Cd_4(OH)_4^{4+}$. The numerical values given in section II for the formation constants should be regarded, however, as first approximations and should be refined by direct comparison with the $BZ(\log h)_B$ data.

In order to obtain more trustworthy values of $\beta_{p,q}$ the totality of the experimental data was compared with normalized projection maps. This method, which has been developed by Sillén [18], has proved to be of great value for the investigation of complicated ionic equilibria. It has the essential advantage over many other approaches that the same set of experimental data can be compared with model functions representing different hypotheses, and moreover the method yields a reliable estimate for the uncertainty in the magnitudes of the formation constants. Since the projection maps are calculated with exact equations the results derived on the basis of them provide a check on the magnitude of the errors caused by approximations (9) and (10).

The computation procedure described in a previous publication [19] was closely followed. First the $Z(\log h)_B$ data were recalculated to the form log $B(3 \log B - 4 \log h)_Z$ by graphical interpolation. This did not involve any significant loss of accuracy because the curves fitted to the $Z(\log h)_B$ points had a rather low slope. A plot of the log $B(3 \log B - 4 \log h)_Z$ data, covering

the Z range 0.002 to 0.015, has been compared with a group of normalized functions

$$\log B^*(X)_{Z,\gamma} \tag{21}$$

where $\log B^* = \log B + 1/3 \log \beta_{4,4} - 4/3 \log \beta_{1,1}$ (22)

$$X = 3 \log B - 4 \log h + \log \beta_{4,4} \tag{23}$$

and

$$\log \gamma = \log \beta_{1,2} + \tfrac{1}{3}(\log\beta_{1,1} - \log \beta_{4,4}) \tag{24}$$

The $\log B^*(X)_{Z,\gamma}$ functions are based on the fundamental equations

$$B = b(1 + \beta_{1,1}h^{-1} + 2\ \beta_{1,2}\ b\ h^{-1} + 4\ \beta_{4,4}b^3\ h^{-4}) \tag{25}$$

and

$$Z = (\beta_{1,1}h^{-1} + \beta_{1,2}b\ h^{-1} + 4\beta_{4,4}b^3 h^{-4})(1 + \beta_{1,1}h^{-1} + 2\,\beta_{1,2}b\,h^{-1} + 4\,\beta_{4,4}b^3h^{-4})^{-1} \tag{26}$$

Introducing the new variables

$$\alpha = \beta_{1,1}h^{-1} \text{ and } u = \beta_{4,4}^{1/3}\ \beta_{1,1}^{-1/3}\ h^{-1}b \tag{27}$$

two of the three constants can be eliminated from (25) and (26) which then will take the form

$$B^* = u\ \alpha^{-1}(1 + \alpha + 2\gamma u + 4\ u^3\alpha) \tag{28}$$

$$Z = (\alpha + \gamma u + 4\alpha u^3)(1 + \alpha + 2\gamma u + 4\alpha u^3)^{-1} \tag{29}$$

Eqns. (28) and (29) show that when Z and γ are kept constant α becomes a function of u only, consequently $\log B^*(X)_{Z,\gamma} = \log B^*(3 \log B^* + 4 \log \alpha)_{Z,\gamma}$

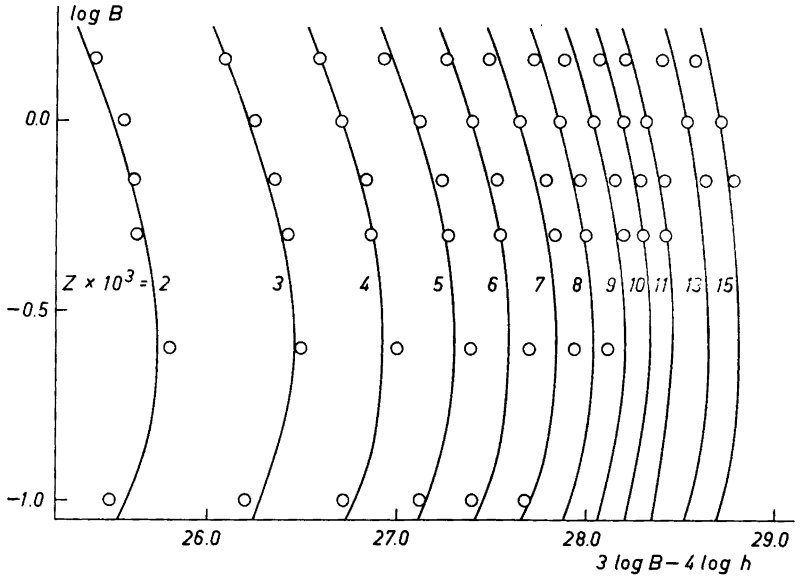

Fig. 6. log B as a function of 3 log B − 4 log h in the Z range 0.002 to 0.015. The circles represent the experimental data and the curves were calculated with the formation constants given in the third row of Table 3.

Table 3. Survey of the formation constants estimated using different approaches.

Method	log $\beta_{1,1}$	log $\beta_{1,2}$	log $\beta_{4,4}$
Eqn. (11)	-10.3 ± 0.1	-9.10 ± 0.05	-31.8 ± 0.1
Projection maps	-10.2 ± 0.1	-9.10 ± 0.05	-31.8 ± 0.2
LETAGROP	$-10.2_6 \pm 0.06$	-9.10 ± 0.01	-31.82 ± 0.03
proposed value	-10.2 ± 0.1	-9.10 ± 0.05	-31.8 ± 0.1

can be evaluated by ascribing a series of values to u. The actual calculations were carried out with a Ferranti-Mercury high speed computer employing the "PROKAIS" program of Ingri and Sillén [21]. Log γ was varied from -1.75 to -2.75, and for each value of γ a family of log $B^*(X)_{Z,\gamma}$ functions, where Z ranged from 0.002 to 0.015, was calculated. Each family of plots representing a particular γ value was superimposed on the experimental points. The best agreement was found with log $\gamma = -1.90$, but the fit was acceptable throughout the log γ interval -1.85 to -1.95. By reading off the differences log B^* — log B and X — (3 log B — 4 log h) in the position of best agreement we have calculated, using (22), (23) and (24), the constants given in Table 3. The fit obtained with these $\beta_{p,q}$ values is illustrated in Fig. 6.

The magnitudes of the formation constants estimated using the projection maps are seen from Table 3 to agree satisfactorily with those derived in section II. Thus the approximate method employed there yielded reliable conclusions in our case.

Finally the data have been treated by the generalized least square method, "LETAGROP", recently proposed by Sillén [20]. 120 experimental points were chosen and the set of $\beta_{1,1}$, $\beta_{1,2}$ and $\beta_{4,4}$ values making the error square sum = $\Sigma(Z-Z_k)^2$ a minimum were calculated as outlined in Ingri and Sillén's publication [21]. Z_k in the error square sum expression denotes the value of the function (26) for a particular triplet of the constants. The values of log $\beta_{1,1}$, log $\beta_{1,2}$ and log $\beta_{4,4}$ leading to the minimum error square sum are recorded in Table 3, the results are seen to agree well with those deduced by other approaches. The uncertainties given for the constants calculated with "LETAGROP" represent three times the "standard deviations" as defined by the D boundary [20], these are of course lower than the maximum errors estimated on the basis of the graphical methods.

As the most important test for the correctness of our calculations let us consider Fig. 2. This shows that the data of present accuracy can be satisfactorily described with the proposed values of the constants given in Table 3. From the $(Z-Z_k)$ values computed with the LETAGROP a quantitative measure of the agreement may be gained. From a total 120 points 69 have shown positive deviations whereas 51 negative ones. The average of the positive deviations $(1-Z_k\ Z^{-1})$ amounts to 4 % and the average of the negative deviations $(Z_k Z^{1-} - 1)$ equals 2.5 %. The magnitude and the sign of the deviations did not exhibit any appreciable trend either with B or log h.

It may inferred from the values of the formation constants that in the range of B studied the main product of hydrolysis is Cd_2OH^{3+}. The predominance of this highly charged species seems to suggest that short range forces, which can counteract a considerable electrostatic repulsion, are mainly responsible for the formation of the polynuclear cadmium species.

Acknowledgements. We would like to thank Professor Lars Gunnar Sillén for his great interest and for his valuable criticism. We are indebted to Dr. Clara Berecki-Biedermann for many helpful suggestions, to Mr. John Crabtree, Oxford, England, for his cooperation in the initial stage of this work and to Dr. Derek C. Lewis for revising the English text. We would like to thank Mr. Frans Ericson for constructing and repairing many parts of our apparatus.

This investigation was financially supported by *Statens Naturvetenskapliga Forskningsråd (Swedish Natural Science Research Council)* and the *Air Force Office of Scientific Research of the ARDC, USAF*, through its European Office, on contract No AF 61(052)—162.

REFERENCES

1. Kullgren, C. *Thesis* (1904) Uppsala. A summary in German was given in *Z. physik. Chem.* **85** (1913) 466.
2. Löfman, N. *Z. anorg. Chem.* **107** (1919) 241.
3. Vesterberg, K. A. *Z. anorg. Chem.* **94** (1916) 371.
4. Marcus, Y. *Acta Chem. Scand.* **11** (1957) 690.
5. Gayer, K. H. and Woontner, L. *J. Phys. Chem.* **61** (1957) 364.
6. Biedermann, G. and Sillén, L. G. *Acta Chem. Scand.* **14** (1960) 717.
7. Feitknecht, W. and Reinmann, R. *Helv. Chim. Acta* **34** (1951) 2255.
8. Biedermann, G. and Ciavatta, L. *Acta Chem. Scand.* **15** (1961) 1347.
9. Ciavatta, L. *Arkiv Kemi. In press.*
10. Biedermann, G. and Hietanen, S. *Acta Chem. Scand.* **14** (1960) 711.
11. Feitknecht, W. *Löslichkeiten von Hydroxyden*, Preliminary report to the Analytical Section of IUPAC, July 1953 (mimeographed).
12. Gran, G. *Analyst* **77** (1952) 661.
13. Winkler, L. W. *Ausgewählte Untersuchungsverfahren für das chemische Laboratorium*, Enke Verlag, Stuttgart 1936.
14. Forsling, W., Hietanen, S. and Sillén, L. G. *Acta Chem. Scand.* **6** (1952) 901.
15. Brown, A. S. *J. Am. Chem. Soc.* **56** (1934) 646.
16. Hietanen, S. and Sillén, L. G. *Acta Chem. Scand.* **13** (1959) 533.
17. Biedermann, G. and Ciavatta, L. *To be published.*
18. Sillén, L. G. *Acta Chem. Scand.* **10** (1956) 803.
19. Biedermann, G. and Sillén, L. G. *Acta Chem. Scand.* **10** (1956) 1011.
20. Sillén, L. G. *Acta Chem. Scand.* **16** (1962) 159.
21. Ingri, N. and Sillén, L. G. *Acta Chem. Scand.* **16** (1962) 173.

Received May 9, 1962.

ACTA CHEMICA SCANDINAVICA 16 (1962) 2240–2244

Studies on the Chemistry of Lichens

17 *. The Structure of Umbilicin

BENGT LINDBERG and BÖRJE WICKBERG

Organisk-kemiska Institutionen och Träkemiska Institutionen, Kungl. Tekniska Högskolan, Stockholm, Sweden

A kinetic study of the lead tetraacetate oxidation of the D-arabinitol-β-*D*-galactofuranoside, umbilicin, and some model substances, and of their tritylation products, showed that the arabinitol residue was substituted in the 2- or 4-position. A choice between these alternatives could be made by comparing the electrophoretic mobilities of umbilicin and suitable model substances in germanate buffer and sulphonated phenyl boronic acid buffer; this showed that umbilicin is 2-*O*-β-D-galactofuranosyl-D-arabinitol.

An arabinitol galactoside, umbilicin, was isolated from the lichen *Umbilicaria pustulata* [1] and was shown to occur in several other lichens of the order Gymnocarpene [2]. It was shown to be a D-arabinitol-β-D-galactofuranoside [3], the position of substitution in the D-arabinitol residue being undetermined. In the present paper studies directed at the determination of the full structure are reported.

When umbilicin is treated either with periodate or lead tetraacetate, a considerable "overoxidation" is observed, due to the intermediate formation of a malonaldehyde structure. The same effect is observed when ethyl-β-D-galactofuranoside is oxidised with these agents [3,4]. This "overoxidation" was also severe when these furanosides were oxidised with lead tetraacetate in the presence of potassium acetate [5], and neither in the consumption of oxidant nor the formation of formaldehyde *versus* time curves could any marked discontinuities be observed. However, when the oxidation was performed in chloroform—acetic acid—pyridine, umbilicin and ethyl-β-D-galactofuranoside rapidly consumed about 5 and 2 moles of oxidant, respectively, and subsequently suffered a slower "overoxidation" (Fig. 1). Formic acid, under the same conditions, rapidly consumed one mole of oxidant. The very rapid glycol cleavage and the enhancement of the formic acid oxidation in the presence of pyridine have been observed previously (*cf.* Ref.[6]).

* Part 16. *Acta Chem. Scand.* **16** (1962) 599.

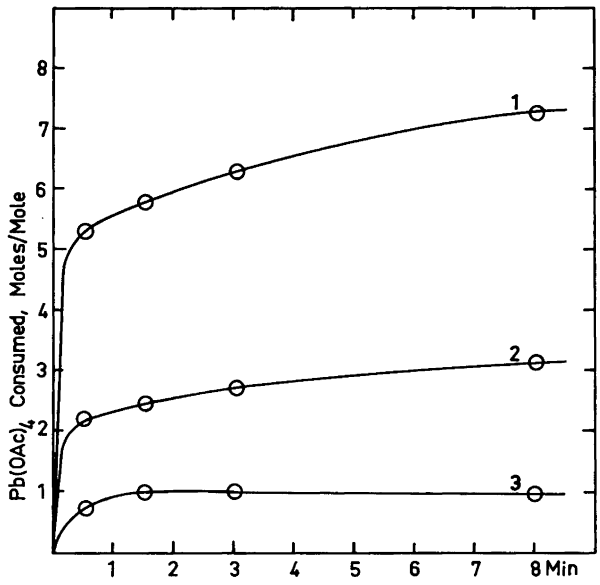

Fig. 1. Rates of consumption of lead tetraacetate by umbilicin (1), ethyl-β-D-galactofuranoside (2) and formic acid (3).

Assuming that 5 moles of oxidant were used up for normal glycol cleavage of umbilicin and for oxidation of the formic acid formed, 2 of these should have been used up by the galactofuranose residue, leaving 3 moles for the oxidation of the arabinitol residue. This indicates a substitution of position 2 or 4 in the latter, with 2 moles of the oxidising agent being consumed by glycol cleavage and one by the formic acid formed. An arabinitol residue substituted in the 1- or 5-position would consume 5 moles of lead tetraacetate and an arabinitol residue substituted in the 3-position would consume only 2 moles.

Further support for this structure was obtained when D-arabinitol, umbilicin and ethyl-β-D-galactofuranoside were treated with trityl chloride in pyridine and the reaction mixtures subjected to lead tetraacetate oxidation (Fig. 2). For arabinitol the consumption of oxidant rapidly approached the value of 3 moles, in agreement with the assumption that tritylation was restricted to the primary groups and was complete for these and that the ether groups were not hydrolysed during the oxidation. For the two galactofuranosides more than the theoretical amounts of oxidant was consumed but the curves showed marked discontinuities at about one mole for the ethyl-β-D-galactofuranoside and 2 moles for umbilicin. Further, during the first 60 min. umbilicin consumed about one mole more lead tetraacetate than ethyl-β-D-galactofuranoside. This difference is also in agreement with a substitution in position 2 or 4 in the arabinitol residue in umbilicin, since a substitution in position 1 or 5 would require a difference of 3 moles and, in position 3, no difference.

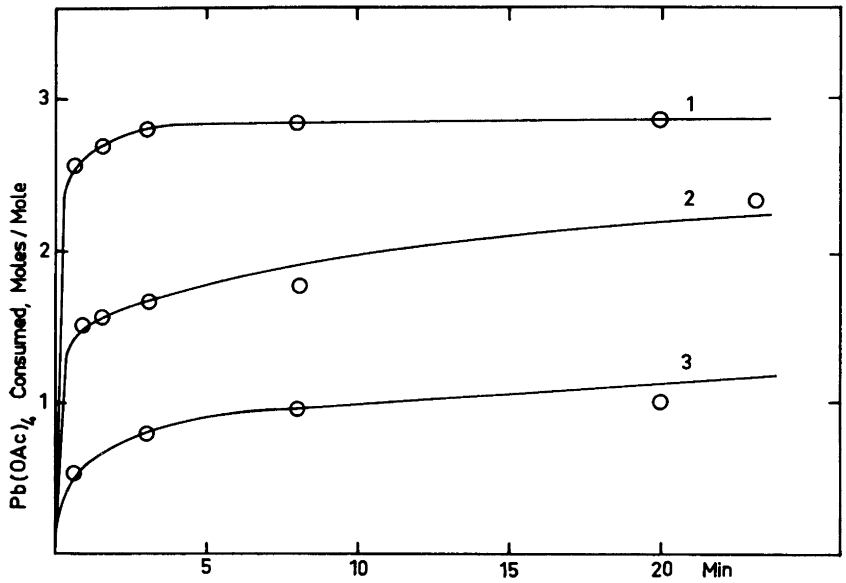

Fig. 2. Rates of consumption of lead tetraacetate by tritylated D-arabinitol (1), umbilicin (2) and ethyl-β-D-galactofuranoside (3).

These results thus clearly indicate that umbilicin is either 2- or 4-*O*-β-D-galactofuranosyl-D-arabinitol (I or II) but do not distinguish between these alternatives. One of these (I) contains a *cis*-α-diol (*erythro*-configuration),

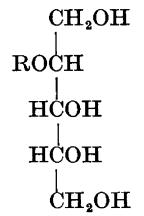

I R = β-D-galactofuranosyl
III R = CH_3

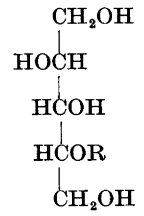

II R = β-D-galactofuranosyl
IV R = CH_3

the other (II) a *trans*-α-diol grouping (*threo*-configuration). It is known that the latter has a much greater tendency than the former to form 5-membered rings, *e.g.* cyclic acetals and ketals [7] or borate complexes [8]. The contribution from non-cyclic α-*trans*-diol structures to the electrophoretic mobility of carbohydrates is especially pronounced in germanate buffer at pH 10 [9] and sulphonated phenyl boronic acid at pH 6.5 [10]. The paper electrophoretic mobilities of umbilicin and some model substances in these buffers were therefore deter-

Table 1. M_A-values * of umbilicin and some model substances.

Substance	M_A	
	In germanate buffer	In sulphonated phenyl-boronic acid buffer
Umbilicin	0.3	0.2
Ethyl-β-D-galactofuranoside	0.1	0.1
D-Arabinitol	1	1
2-*O*-Methyl-D-arabinitol	0.2	0.1
4-*O*-Methyl-D-arabinitol	0.8	0.8

* M_A = electrophoretic mobility, relative to that of arabinitol.

mined (Table 1). Ethyl-β-D-galactofuranoside and 2-*O*-methyl-D-arabinitol * (III) have low mobilities, but 4-*O*-methyl-D-arabinitol * (IV) has a high mobility, close to that of D-arabinitol. Umbilicin has a low mobility, in agreement with the expected mobility of 2-*O*-β-D-galactofuranosyl-D-arabinitol (I) but not with that of the 4-*O*-substituted isomer (II).

EXPERIMENTAL

Oxidation experiments. The oxidations were carried out at 0°. A 0.1 M solution (4 ml) of lead tetraacetate in chloroform containing 10 % v/v of acetic acid was added with stirring to a solution of the substance (0.025 mmole) in pyridine (1 ml). At intervals samples (0.5 ml) were withdrawn and immediately transferred to a flask containing sodium iodide (0.15 g) in acetic acid (1 ml) and saturated aqueous sodium acetate (2 ml). Liberated iodine was titrated with sodium thiosulphate (0.05 N) using starch indicator.

The trityl compounds were prepared by adding anhydrous calcium sulphate (50 mg) and trityl chloride (0.2 mmole) to a solution of the sample (0.05 mmole of D-arabinitol or ethyl-β-D-galactofuranoside, 0.025 mmole of umbilicin) in pyridine (1 ml). After standing at 60° for 12 h and then being cooled to 0°, the reaction mixtures were oxidised as described above. Blanks were run parallel to these experiments and were found not to change significantly within 20 min. oxidation time.

Paper electrophoresis was performed in 0.05 M germanate buffer [9] at pH 10 and 40° and in 0.05 M sulphonated phenyl boronic acid buffer [10] at pH 6.5 and 40°. The spots were developed with the periodate-benzidine [13] reagent.

2-O-Methyl-D-arabinitol. 3-*O*-Methyl-D-glucose was oxidised with lead tetraacetate, the reaction mixture worked up as described by Charlson and Perlin [11] and the syrupy 2-*O*-methyl-D-arabinose reduced with Raney-nickel [12] in boiling 80 % aqueous ethanol. The resulting 2-*O*-methyl-D-arabinitol contained traces of impurities, as demonstrated by paper chromatography and paper electrophoreses, but was not further characterised.

4-O-Methyl-D-arabinitol was prepared in the same manner from 3-*O*-methyl-D-galactose. It also contained traces of impurities and was characterised by paper chromatography and paper electrophoresis only.

The authors are indebted to Mr. Lars Nordén for his skilful assistance.

* These previously unknown compounds were prepared by lead tetraacetate oxidation of 3-*O*-methyl-D-glucose and 3-*O*-methyl-D-galactose, respectively, according to Charlson and Perlin [11], followed by reduction of the resulting 2-*O*-methyl-D-arabinose and 2-*O*-methyl-D-lyxose with Raney-nickel [12].

REFERENCES

1. Lindberg, B., Wachtmeister, C. A. and Wickberg, B. *Acta Chem. Scand.* **6** (1952) 1052.
2. Lindberg, B., Misiorny, A. and Wachtmeister, C. A. *Acta Chem. Scand.* **7** (1953) 591.
3. Lindberg, B. and Wickberg, B. *Acta Chem. Scand.* **8** (1954) 821.
4. Hocket, R. C., Nickerson, M. H. and Reeder, W. H., III. *J. Am. Chem. Soc.* **66** (1944) 472.
5. Perlin, A. S. *J. Am. Chem. Soc.* **76** (1954) 5505.
6. Perlin, A. S. *Advances in Carbohydrate Chem.* **14** (1959) 9.
7. Barker, S. A. and Bourne, E. J. *Advances in Carbohydrate Chem.* **7** (1952) 138.
8. Frahn, J. L. and Mills, J. A. *Austral. J. Chem.* **12** (1959) 65.
9. Lindberg, B. and Swan, B. *Acta Chem. Scand.* **14** (1960) 1043.
10. Garegg, P. and Lindberg, B. *Acta Chem. Scand.* **15** (1961) 1913.
11. Charlson, A. J. and Perlin, A. S. *Can. J. Chem.* **34** (1956) 1200.
12. Karabinos, J. V. and Ballun, A. T. *J. Am. Chem. Soc.* **75** (1953) 450.
13. Cifonelli, J. A. and Smith, F. *Anal. Chem.* **26** (1954) 1132.

Received May 30, 1962.

ACTA CHEMICA SCANDINAVICA 16 (1962) 2245–2250

Studies on Succinic Acids

VI *. On the Hydrolysis of Monomethyl Esters of Tetraethyl- and *Rac.*-2,3-Di-(*tert.*-butyl)-Succinic Acid

LENNART EBERSON

Department of Organic Chemistry, University of Lund, Lund, Sweden

The possibility of intramolecular *carboxyl* group catalysis in the hydrolysis of monomethyl esters of dicarboxylic acids exhibiting anomalously high K_1/K_2-ratios is discussed on the basis of the behaviour of monomethyl tetraethyl- and *rac.*-2,3-di-(*tert.*-butyl)-succinate upon attempted hydrolysis at different hydrogen ion concentrations.

It is well established that intramolecular carboxylate ion catalysis plays an important role in the hydrolysis of monoaryl esters of substituted succinic and glutaric acids [1–3]. By detailed kinetic analysis and tracer experiments it has been shown that these rapid hydrolyses proceed through a cyclic anhydride intermediate formed by the attack of a neighbouring carboxylate ion on the ester moiety, followed by solvolysis of the anhydride (1).

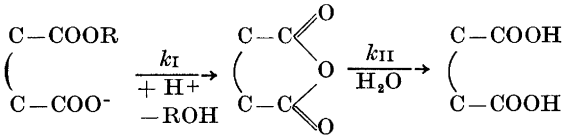

(1)

Originally it was thought that the group displaced from the ester group had to consist of a stabilized ion of some sort, *e.g.*, a phenoxide ion, but later on evidence was presented that the *n*-alkyl ester, methyl hydrogen phthalate, is also hydrolyzed according to the mechanism (1) [4]. Only in the case of *p*-methoxyphenyl 3,6-endoxo-Δ^4-tetrahydrophthalate could the anhydride be directly observed by determining the rate of base addition necessary to maintain a constant pH during the solvolysis of the intermediate [1]. This rate was identical at pH 5.5 and pH 6.5 with that observed in the solvolysis of authentic *exo*-3,6-endoxo-Δ^4-tetrahydrophthalic anhydride.

* Part. V: *Acta Chem. Scand.* **14** (1960) 641.

In the hydrolysis of alkyl-substituted monoaryl succinates and glutarates the rate of ester hydrolysis increased with increasing degree of alkyl substitution in the carbon chain as would be predicted by consideration of the "geminal dimethyl effect" normally operating in ring closure reactions [1]. It was concluded that the increase in rate accompanying alkyl substitution was due to a decrease in the probability of unprofitable rotamer distributions in which the reacting groups were directed away from each other. When the carbophenoxy and carbonyl groups were rigidly held in an eclipsed conformation, as in the monoesters of maleic and 3,6-endoxo-Δ^4-tetrahydrophthalic acids, a pronounced rate enhancement on anhydride formation was observed.

These data strongly support the conclusion that the distribution of conformations in the monoesters of dicarboxylic acids is influenced by alkyl substitution in much the same way as in the corresponding diacids. An anomalously high K_1/K_2-ratio of a dicarboxylic acid implies that the favoured conformation has the carboxyl groups close to each other making strong electrostatic interaction and intramolecular hydrogen bonding possible [5,6]. In Fig. 1 it is shown that there is a rough linear correlation between the logarithm of the relative rate of monoester solvolysis and the ΔpK of the corresponding diacid.

The kinetic data were taken from the work of Bruice and Pandit [1] and the ΔpK values were obtained from various sources [7-9]. If the data obtained by Gaetjens and Morawetz [3] for the hydrolysis of mono-*p*-acetamidophenyl esters of the diastereoisomers of 2,3-dimethyl- and 2,3-diisopropylsuccinic acid are treated in the same way, it is found that the meso-diisopropyl compound falls completely out of the scheme. However, since the stereochemical homogeneity of this compound was not rigorously proved, it is possible that partial epimerization had occurred during the preparation of the intermediate anhydride. This has been observed under similar conditions in a number of cases [10-12].

Thus, it may be safely concluded that a high K_1/K_2-ratio of a diacid is accompanied by a high rate of intramolecular carboxylate ion attack in its monoester and that this effect is mainly steric in origin. From this point of view studies on the hydrolysis of monomethyl tetraethyl- and *rac.* 2,3-di-(*tert.*-butyl)-succinate [5] have been initiated, as the corresponding acids exhibit very high K_1/K_2-ratios in water (ΔpK 4.58 and 8.0, respectively) [13] and in 50 % by weight ethanol (ΔpK 6.6 and 9.5, respectively) [5]. The methyl esters were chosen since only one case of intramolecular catalysis in *n*-alkyl esters has been studied previously [4] and it could also be expected that the rate constants for the hydrolysis of the aryl esters would be too high to be measurable [3]. This paper is a report of the preparative part of the study, which allows some preliminary conclusions to be drawn regarding the hydrolysis mechanism.

RESULTS AND DISCUSSION

When monomethyl *rac.*-2,3-di-(*tert.*-butyl)-succinate (I) was refluxed for 15 h in 5 % aqueous sodium carbonate solution, where it exists only in its ionized form, no hydrolysis took place and the ester was almost quantitatively recovered. Under the same conditions, *rac.*-2,3-di-(*tert.*-butyl)-succinic anhydride (II) was completely hydrolyzed within 4 h. Boiling I at pH 7 in 50 % by volume dioxane-water, where about 50 % of the ester exists in the ionized

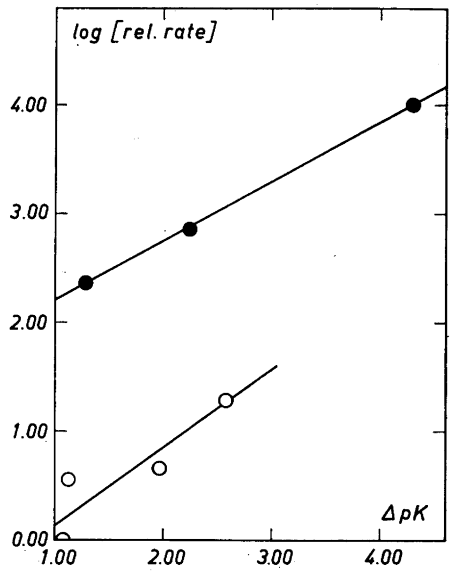

Fig. 1. Plots of log $(k_I/k_{I\ glutarate})$ [1] *versus* ΔpK [7-9] ● Monoesters of diacids with 1,2-carboxyl groups (succinic [7], 2,2-dimethylsuccinic [9], maleic acid [7]). ○ Monoesters of diacids with 1,3-carboxyl groups (glutaric [7], 2,2-dimethylglutaric [8], 3-methylglutaric [7], 3,3-dimethylglutaric acid [7]).

state, gave the anhydride in almost quantitative yield. Under the same conditions II was not affected. Finally, boiling I in 50 % dioxane-water at pH 1.5 for 15 h gave the anhydride, and likewise II alone was not affected by this treatment.

These results differ from those obtained previously for monoaryl esters [1-3] in the following ways: Firstly, under the conditions most favourable for intramolecular carboxylate ion attack, no hydrolysis took place although any anhydride formed would have been hydrolyzed. Secondly, at a hydrogen ion concentration (pH 7) where the unionized form exists in appreciable quantity, the anhydride was formed but not hydrolyzed, presumably due to steric hindrance to the approach of lyate species to the anhydride carbonyl group [1]. Thirdly, at pH 1.5, where only the unionized form can exist, the anhydride was formed but not hydrolyzed. This is a special case, since at this pH the equilibrium (2) is completely on the side of the anhydride under the reaction conditions employed.

$$\text{Diacid} \rightleftharpoons \text{anhydride} + H_2O \qquad (2)$$

Only at pH values where the diacid is appreciably neutralized is (2) displaced to the left.

Evidently we cannot consider this reaction as an example of intramolecularly catalyzed hydrolysis, as actually no hydrolysis occurs. However, if we picture the reaction as an example of intramolecular carboxyl group catalysis according to the mechanism (3)

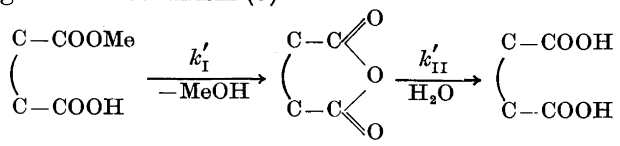

(3)

we may consider I as an extreme case with $k'_{I} >> k'_{II}$. Intramolecular carboxyl group catalysis has been observed in the hydrolysis of the amide acid, phthalamic acid [14], and cannot be excluded in the case of methyl hydrogen phthalate, for which intramolecular carboxylate ion catalysis has been postulated [4]. A weakly active carboxyl group catalysis might be masked by intramolecular hydrogen ion catalysis and would not be easily detected. Pekkarinen's [15] work on the hydrolysis of monoethyl maleate and citraconate is also worth mentioning in this connection. In aqueous solution the hydrolysis rate of these esters was found to be proportional to the concentration of the undissociated ester acid and at least approximately independent of the hydrogen ion concentration in the range where ionization was totally suppressed. This effect was attributed to internal hydrogen bond formation in the ester acid.

Monomethyl tetraethylsuccinate (III) turned out to be a less extreme case than I. When III was boiled in 50 % dioxane-water at pH 7, where about 50 % of the ester acid exists in the carboxylate ion form, tetraethylsuccinic anhydride (IV) and tetraethylsuccinic acid could be isolated in approximately equimolecular amounts from the reaction mixture. The same treatment at pH 1.5 yielded the anhydride exclusively, whereas boiling for 15 h in 5 % aqueous sodium carbonate solution produced an almost quantitative yield of the diacid. Under the same conditions, IV was recovered unchanged at pH 1.5, solvolyzed to an extent of 60 % at pH 7, and completely hydrolyzed in sodium carbonate solution.

These results clearly indicate that mechanism (3) is feasible also for III and in such case the rate constants for anhydride formation and hydrolysis at pH 7 (k'_{I} and k'_{II}) are of the same order of magnitude. At pH 1.5 equilibrium (2) is on the side of the anhydride and no hydrolysis will occur. In sodium bicarbonate solution complete hydrolysis occurred, which may be due to intramolecular carboxylate group catalysis or intermolecular hydroxide ion catalysis. Evidently mechanism (1) cannot be exluded in this case.

Summarizing, the monoesters I and III differ from previously studied compounds of this type in the following respects:

1. Due to steric hindrance to hydrolysis the intermediate anhydrides can be isolated and identified.

2. At hydrogen ion concentrations where the corresponding diacid exists in the unionized form the anhydride (II or IV) is the thermodynamically stable form even in aqueous solvents [16]. This behaviour is well known from the series of alkyl-substituted maleic acids [17,18] and there is also kinetic evidence that "normal" dicarboxylic acids, *e.g.*, succinic acid [19], can exist in equilibrium with its anhydride in water at elevated temperatures, although the concentration of anhydride at equilibrium is very low. Tetramethylsuccinic acid appears to be an intermediate case between these two extremes, the equilibrium in aqueous solution at room temperature being essentially on the side of the acid and at 70° displaced about 25 % towards the side of the anhydride [16].

3. Mechanism (1) is of no or very little importance in the hydrolysis of I but is possible for III. Mechanism (3) involving intramolecular carboxyl group catalysis is possible in the hydrolysis of III.

As evidence or mechanism (3) the cases described in this work must be considered as extreme ($k'_I \geqq k'_{II}$). More suitable cases would involve monomethyl esters of diacids with high K_1/K_2-ratios, where the hydrolysis of the corresponding anhydrides is not subjected to steric hindrance from bulky alkyl groups in the carbon chain. Such acids include maleic and alkyl-substituted maleic acids [1,15,17,20], tri- and tetramethylsuccinic acid [1,21], *cis*-diacids in the bicycloheptane series, and *cis*-caronic acid. Kinetic studies on the hydrolysis of methyl esters of some of these acids as well as I and III are under way.

EXPERIMENTAL

Materials. The monoesters I and III were prepared as described previously [5].

Hydrolysis experiments. 1 A. Monoester I in 5 % aqueous sodium carbonate (pH 11). I(1.0 g) was boiled for 15 h with 30 ml of 5 % aqueous sodium bicarbonate (pH about 11). Cooling and acidification precipitated the unchanged monoester in almost quantitative yield.

1 B. Monoester I in 50 % dioxane-water of pH 7. I (1.0 g) was dissolved in 30 ml of 50 % by volume dioxane-water and the pH was adjusted to 7.0 (as measured by the glass electrode) by addition of 10 % aqueous sodium hydroxide. The solution was refluxed for 15 h and then cooled in an ice-bath. Ice-cold 1 % aqueous sodium carbonate (70 ml) was added in order to prceipitate the anhydride and to keep any unreacted ester in solution. After half an hour the solid (0.80 g, 87 %) was filtered, m.p. 112—115° *, mixed m.p. with authentic anhydride (II) 113—115°. Minute amounts of the monoester were obtained from the mother liquor upon acidification.

1 C. Monoester I in 50 % dioxane-water of pH 1.5. I (1.0 g) was dissolved in 30 ml of 50 % aqueous dioxane-water and the pH was adjusted to 1.5 by the addition of 10 % aqueous hydrochloric acid. The solution was refluxed for 15 h, cooled in an ice-bath and diluted with 70 ml of ice-cold 1 % aqueous sodium carbonate. Filtration gave the anhydride (II) in 90 % yield. Minute amounts of the monoester were recovered from the mother liquor upon acidification.

2. Anhydride II. When II was treated as under 1 A, B, and C, complete hydrolysis occurred at pH 11. (In a separate experiment it was found that hydrolysis was complete after 4 h). At pH 1.5 and pH 7 the anhydride was recovered unchanged (pH 7 was maintained by means of a phosphate buffer).

3 A. Monoester III in 5 % aqueous sodium carbonate. III (1.0 g) was boiled under reflux for 15 h with 30 ml of 5 % aqueous sodium carbonate. Cooling and acidification gave a 90 % yield of tetraethylsuccinic acid, m.p. 135—143° (decomp.), mixed m.p. with the authentic acid, 137—45° (decomp.).

3 B. Monoester III in 50 % dioxane-water of pH 7. III (1.0 g) was treated as under 1 B, yielding 45 % of the anhydride IV, m.p. 81—83°, mixed m.p. with authentic tetraethylsuccinic anhydride 80—83°. Acidification of the mother liquor gave 40 % of the diacid, m.p. 130—44° (decomp.).

3 C. Monoester III in 50 % dioxane-water of pH 1.5. III (1.0 g) was treated as under 1 C, which gave anhydride IV in 85 % yield, m.p. 80—82°.

4. Anhydride IV. Treating IV under the conditions given under 1 A, B, and C resulted in complete hydrolysis at pH 11, 60 % hydrolysis at pH 7 (phosphate buffer), and no hydrolysis at pH 1.5.

REFERENCES

1. Bruice, T. C. and Pandit, U. K. *J. Am. Chem. Soc.* **82** (1960) 5858.
2. Bender, M. L. *Chem. Revs.* **60** (1960) 53.
3. Gaetjens, E. and Morawetz, H. *J. Am. Chem. Soc.* **83** (1961) 1738.

* All melting points were determined by a melting point microscope.

4. Bender, M. L., Chloupek, F. and Neveu, M. C. *J. Am. Chem. Soc.* **80** (1958) 5384.
5. Eberson, L. *Acta Chem. Scand.* **13** (1959) 211.
6. Eberson, L. *Svensk Kem. Tidskr.* **71** (1959) 153, and references cited therein.
7. Brown, H. C., McDaniel, D H. and Häfliger, O. in Braude, E. A. and Nachod, F. C. *Determination of Organic Structures by Physical Methods*, Academic Press, New York 1955, p. 624.
8. Simon, W., Menche, D. and Heilbronner, E. *Helv. Chim. Acta* **39** (1956) 290.
9. Le Moal, H. *Bull. soc. chim. France* **1956** 418.
10. Bone, W. A. and Sprankling, C. G. H. *J. Chem. Soc.* **77** (1900) 654.
11. Linstead, R. P. and Whalley, M. *J. Chem. Soc.* **1954** 3722.
12. Golden, J. H. and Linstead, R. P. *J. Chem. Soc.* **1958** 1733.
13. Eberson, L. and Glasoe, P. *To be published.*
14. Bender, M. L., Chow, Y.-L. and Chloupek, F. *J. Am. Chem. Soc.* **80** (1958) 5380.
15. Pekkarinen, L. *Ann. Acad. Sci. Fennicae*, Ser. A II, No **62** (1954) 77.
16. Eberson, L. *Unpublished results.*
17. Koskikallio, J. *Acta Chem. Scand.* **10** (1956) 822.
18. Koskikallio, J. *Suomen Kemistilehti B* **29** (1956) 5.
19. Eberson, L., Higuchi, T., McRae, J., Ockerlander, H., and Windheuser, J. *To be published. Cf.* also Higuchi, T. and Miki, T. *J. Am. Chem. Soc.* **83** (1961) 3899.
20. Wheeler, O. H. and Granell, E. E. *J. Org. Chem.* **26** (1961) 4763.
21. Verkade, P. E. *Rec. Trav. Chim.* **40** (1921) 199.

Received May 18, 1962.

ACTA CHEMICA SCANDINAVICA 16 (1962) 2251–2262

Studies on the Pyridine Analogues of Malachite Green. I. Protolytic Equilibria and Reaction Rate Constants of 4-Pyridine Green in Aqueous Solutions

RUNE CIGÉN and GÖSTA BENGTSSON

Department of Inorganic and Physical Chemistry, Chemical Institute, University of Lund, Lund, Sweden

The protolytic and hydration reactions of 4,4′-bis(dimethylaminophenyl)-4″-pyridylmethanol, named 4-Pyridine Green (4-PG), have been investigated spectrophotometrically in aqueous solutions with a constant ionic strength 0.5 M at 20.0°C.

The reaction scheme proposed for Crystal Violet has been found valid also for 4-Pyridine Green, which gives seven species, three coloured (B, G, and Y) and four colourless (C, S_1, S_2 and S_3), between which the following reversible reactions take place:
$B + 2\ H^+ \rightleftharpoons G + H^+ \rightleftharpoons Y$; $C + 3\ H^+ \rightleftharpoons S_1 + 2\ H^+ \rightleftharpoons S_2 + H^+ \rightleftharpoons S_3$; $Y + H_2O \rightleftharpoons S_3$; $G + H_2O \rightleftharpoons S_2$; $B + H_2O \rightleftharpoons S_1$; $B + OH^- \rightleftharpoons C$. The equilibria between B, G, and Y and between C, S_1, S_2, and S_3 are reached instantaneously, whereas the other reactions are slow. Five protolytic, three hydration and eight rate constants of the reactions indicated above have been determined, and the results were compared with the results from the corresponding investigation of Crystal Violet.

The existence of pyridine analogues of Malachite Green has been known since the beginning of this century. Harries and Lénart made a report of the preparation of 2-Pyridine Green in 1915 [1] and compared the absorption curve of this dye with the absorption curve of Malachite Green, but since then no further attention seems to have been paid to the pyridine analogues of Malachite Green.

As a part of the investigations of triarylmethane dyes in this laboratory[2–7], all three pyridine analogues of Malachite Green have been prepared. In the present investigation protolytic and hydration equilibria and reaction rates of the hydration reactions of 4-Pyridine Green have been studied spectrophotometrically in aqueous solutions with a constant ionic strength 0.49 M at 20.0°C.

The dyestuff 4-Pyridine Green can be represented by the schematic structural formula

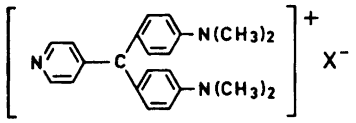

Preliminary semiquantitative experiments indicated a reaction scheme very similar to that found by Cigén [3] for Crystal Violet. This scheme includes three coloured species in instantaneously reached proton-equilibrium with each other and four colourless species, which also are in momentaneously reached proton-equilibrium with each other. Transition between coloured and colourless species occurs through reversible hydration reactions which proceed at a measurable rate.

The reaction scheme used (which is fully supported by the measurements) is the following:

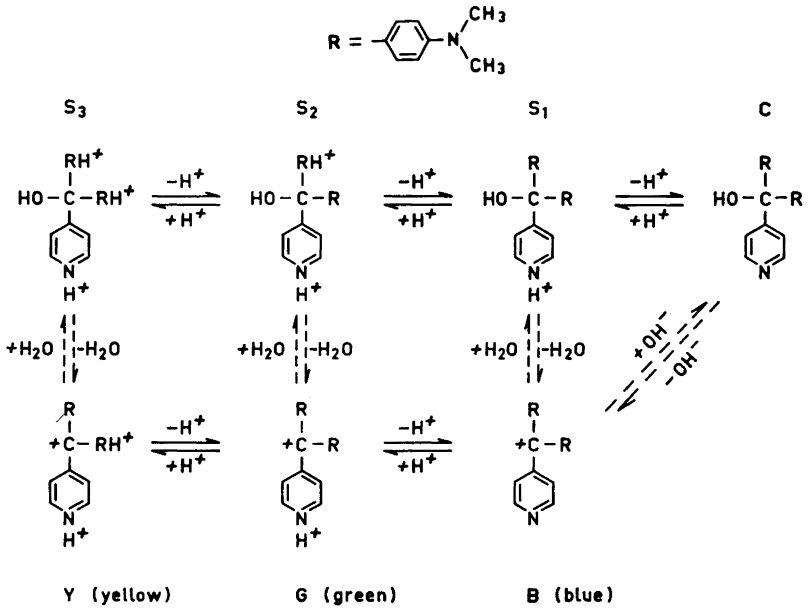

Full drawn arrows indicate that the reactions proceed at an immeasurable rate — that is, instantaneously — whereas dashed arrows indicate that the reactions take place at a measurable rate.

The following definitions and symbols are used

(*a*) *Dissociation constants:* $K_1 = [G][H^+]/[Y]$; $K_2 = [B][H^+]/[G]$; $K_1' = [S_2][H^+]/[S_3]$; $K_2' = [S_1][H^+]/[S_2]$; $K_3' = [C][H^+]/[S_1]$.

(*b*) *Hydration constants:* $K_4 = [S_3]_\infty/[Y]_\infty$; $K_5 = [S_2]_\infty/[G]_\infty$; $K_6 = [S_1]_\infty/[B]_\infty$.

(*c*) *Rate constants*

k_1 and k_2 = rate constants for the reactions $Y + H_2O \underset{k_2}{\overset{k_1}{\rightleftharpoons}} S_3$

k_3 and k_4 = » » » » » $G + H_2O \underset{k_4}{\overset{k_3}{\rightleftharpoons}} S_2$

k_5 and k_6 = » » » » » $B + H_2O \underset{k_6}{\overset{k_5}{\rightleftharpoons}} S_1$

k_7 and k_8 = » » » » » $B + OH^- \underset{k_8}{\overset{k_7}{\rightleftharpoons}} C$

k = rate constant for the total reaction

(*d*) ε_B, ε_G, ε_Y = molar absorbancy coefficients of B, G, and Y.

e_o, e_t, e_∞ = absorbancy per cm of a solution at the times 0 and t and at equilibrium.

E_o, E_t, E_∞ = total absorbancies.

e_B, e_G, e_Y = absorbancy of a solution containing only B, G or Y.

C_M = total concentration of dyestuff.

$h = [H^+]$; $oh = [OH^-]$; $K_w = [H^+][OH^-]$.

The changes in colour nuances and colour intensities that take place, when the pH of an aqueous solution of 4-Pyridine Green is changed, depend on the reactions visualized in the reaction-equilibrium scheme. The values of the constants in the equilibrium scheme can be calculated, if the following quantities are determined for a large number of solutions with varying pH:

1. The absorbancy, e_o, at a moment immediately after the mixing of a stock solution with the appropriate buffer. The dye stock solution is (if possible) prepared in such a way that all of the dye is present as the coloured species B.
2. The absorbancy, e_∞, when equilibrium is reached.
3. The pH of the solutions.
4. The rate constant, k, of the total reaction that changes the intensity of the colour of the solutions either by the hydration of the coloured species (B, G, and Y) to colourless species (C, S_1, S_2, and S_3) or *vice versa*.

EQUATIONS

The following expressions for the initial absorbancy, e_o, the equilibrium absorbancy, e_∞, and the rate constant of the total reaction, k, as functions of the hydrogen ion concentration can be derived (*cf.* Ref.[3])

$$e_o = \frac{K_1K_2e_B + hK_1e_G + h^2e_Y}{K_1K_2 + hK_1 + h^2} \quad (1)$$

$$e_\infty = \frac{K_1K_2e_B + hK_1e_G + h^2e_Y}{K_1K_2(1 + K_6 + K_6K_3'/h) + hK_1(1 + K_5) + h^2(1 + K_4)} \quad (2)$$

$$k = \frac{1}{t} \ln \frac{e_o - e_\infty}{e_t - e_\infty} = \frac{h^3 k_2 + h^2 k_4 K_1' + h k_6 K_1' K_2' + k_8 K_1' K_2' K_3'}{h^3 + h^2 K_1' + h K_1' K_2' + K_1' K_2' K_3'} + \\ + \frac{h^2 k_1 + h k_3 K_1 + k_5 K_1 K_2 + k_7 oh K_1 K_2}{h^2 + h K_1 + K_1 K_2} \quad (3)$$

The eqns. (1—3) can be approximated, since certain species and reaction steps can be neglected in some pH-ranges. These approximations will be further considered in connection with the determination of the individual constants.

EXPERIMENTAL

Preparation of the dyestuff. The leuco base was prepared by the standard procedure of condensing dimethylaniline (0.3 mole) with 4-pyridinealdehyde (0.1 mole) (from L. Light & Co., Colnbrook, England) in a nitrogen atmosphere. Concentrated hydrochloric acid (0.3 mole) was used as a condensing agent. Recrystallization from a mixture of 75 % ethanol-25 % water gave a white powder, m.p. 123—125°C. The leuco base was dissolved in dilute hydrochloric acid and oxidized to dyestuff with lead dioxide.

A perchlorate of the dye was precipitated with sodium perchlorate and recrystallized from 0.2 M acetic acid. Since there are no data available about this dyestuff, its identity is established from: (1) The identity of the initial substances used in the preparation and the method of preparation. (2) The absorption curves of the dye which have the forms that should be expected from a substance of this type. (3) The other two pyridine analogues of Malachite Green, 2- and 3-Pyridine Green, have also been prepared and found to have properties very similar to, but yet in some respects strikingly different from, the present preparation. Furthermore, the leuco base of 2-Pyridine Green was found to have m.p. 110°C, which is exactly the value found by Harries and Lénart. (4) The elementary analyses which are consistent with the mono-perchlorate. (Found: C 61.4; H 5.68; O 14.8; N 9.75; Cl 8.16. Calc. for $C_{22}H_{24}O_4N_3Cl$: C 61.46; H 5.63; O 14.89; N 9.77; Cl 8.25).

A stock solution of the dye was prepared by weighing and dissolving the perchlorate in acetone. A solution was prepared for measurement in the following way. 1 ml of the acetone dye stock solution was added to 49 ml of an appropriate buffer solution, which was well thermostated, and the rate of the change of the colour intensity was measured and the initial and equilibrium absorbancies were determined. The measurements were carried out at the wavelength 639 mμ; the ionic strength was 0.49 M and the temperature 20.0°C.

The chemicals used for the buffer solutions and the apparatus used for the measurements were the same as in Ref.[3] In this paper pH means $-\log[H^+]$ and not $-\log a_{H^+}$.

The dyestuff, in aqueous solutions, is adsorbed on the walls of the vessels and absorption cells used for the measurements. The adsorption phenomena were not, however, so troublesome as in the case of Crystal Violet (Ref.[3]).

MEASUREMENTS AND RESULTS

Absorption curves. Fig. 1 shows the absorption curves of the three coloured species B, G, and Y. The curve of B was obtained in a phosphate buffer, pH = 6.36, where B proved to be the only coloured species; [Y] $\ll$ [G] $\ll$ [B]. $\varepsilon_B = e_B/C_M$ was determined by measuring the fading of the colour in phosphate buffers and extrapolating the absorbancy back to $t = 0$. As can be seen from eqn. (1), we have $e_B \approx e_o$ in solutions with $[H^+] \ll K_2$, since $K_2 \ll K_1$ and $e_Y \ll e_G \ll e_B$ at the used wavelength, $\lambda = 639$ mμ.

There is no pH-range, where G is the only coloured species. Therefore, the curve of G was calculated from an absorption curve obtained from the equi-

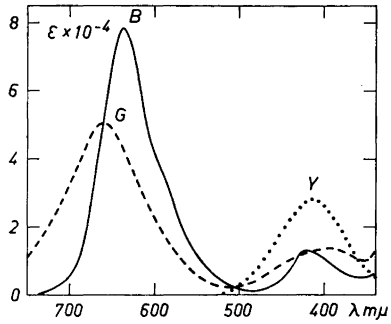

Fig. 1. Absorption curves of 4-Pyridine Green in aqueous solutions. The Curves B, G, and Y are the curves of the blue species B, the green species G, and the yellow species Y, respectively.

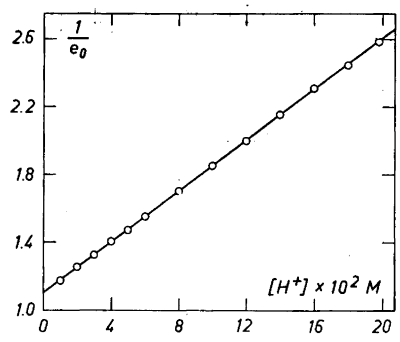

Fig. 2. $1/e_o$ plotted against $[H^+]$ for the determination of K_1 and e_G. $C_M = 2 \times 10^{-5}$ M, $d = 1$ cm.

librium absorbancies in an acetate buffer, pH = 3,25, and eqn. (2). At pH = 3.25, B and G are the only coloured species, *i.e.* $[Y] \ll [G] \approx [B]$.

The absorption curve of Y was calculated from eqn. (1) and a number of e_o-values, measured at different wavelengths, in 0.5 M hydrochloric acid.

The obtained values of λ_{max} and ε_{max} were

$\lambda_{B\ max} = 636$ and 420 mμ; $\varepsilon_{B\ max} = 7.9 \times 10^4$ and 1.3×10^4 respectively
$\lambda_{G\ max} = 660$ » 395 mμ; $\varepsilon_{G\ max} = 5.1 \times 10^4$ » 1.4×10^4 »
$\lambda_{Y\ max} = 413$ mμ; $\varepsilon_{Y\ max} = 2.8 \times 10^4$

Determination of K_1 *and* e_G. In HCl + KCl-buffers $[B] \ll [G] + [Y]$ and eqn. (1) can be approximated and written as

$$\frac{1}{e_o} = \frac{1}{e_G} + \frac{h}{K_1 e_G} \tag{4}$$

if the measurements are carried out at a wavelength where $e_Y \ll e_G$. The acetone dye stock solution, in which the dye is present as the coloured species B, was mixed with suitable buffers.

The equilibria $B + 2\ H^+ \rightleftharpoons G + H^+ \rightleftharpoons Y$ are then reached instantaneously, whereupon the solutions are decolourized owing to the hydration reactions $G + H_2O \rightleftharpoons S_2$ and $Y + H_2O \rightleftharpoons S_3$. The initial absorbancy, e_o, was determined by following the fading of the colour and extrapolating the absorbancy to $t = 0$. In Fig. 2 $1/e_o$ is plotted *versus* $[H^+]$, and a straight line is obtained which gives $e_G = 0.907$ and $K_1 = 0.146$ M ($C_M = 2 \times 10^{-5}$ M, $d = 1$ cm).

Determination of K_2. For acetate buffers, pH = 3.2—4, eqn. (1) can be used in the following approximated form

$$\frac{h}{e_B - e_o} = \frac{K_2}{e_B - e_G} + \frac{h}{e_B - e_G} \tag{5}$$

Table 1. e_o, and k-values for the determination of K_1, k_1, and e_G. $\lambda = 639$ mμ, $C_M = 2 \times 10^{-5}$ M, $d = 1$ cm, $T = 20.0$°C.

[H+] M	e_o	k min^{-1}	[H+] M	e_o	k min^{-1}
0.005		0.00573	0.080	0.587	0.0226
0.010	0.852	0.00735	0.100	0.539	0.0255
0.020	0.798	0.01034	0.120	0.500	0.0279
0.030	0.754	0.01297	0.140	0.464	0.0294
0.040	0.711	0.0154	0.160	0.433	0.0309
0.050	0.679	0.0175	0.180	0.409	0.0326
0.060	0.644	0.0193	0.196	0.387	0.0339

Table 2. e_o-Values for the determination of K_2 and e_G in acetate buffers. $\lambda = 639$ mμ, $C_M = 1 \times 10^{-5}$ M, $d = 1$ cm, $e_B = 0.775$, $T = 20.0$°C.

[H+] $\times 10^7$ M	e_o	[H+] $\times 10^4$ M	e_o
0.955	0.651	2.23	0.585
1.274	0.628	2.82	0.569
1.50	0.614	3.86	0.546
1.81	0.598	5.69	0.525

The intial absorbancy, e_o, was determined through the extrapolation procedure described above, and $e_B = 0.775$ was determined in a similar way from kinetic measurements in phosphate buffers where [Y] $\ll$ [G] $\ll$ [B] and, therefore, $e_o \approx e_B$. In Fig. 3 $[H^+]/(e_B - e_o)$ is plotted *versus* $[H^+]$. ($C_M = 1 \times 10^{-5}$ M, $d = 1$ cm, $\lambda = 639$ mμ). From the obtained straight line we get the intercept $y = K_2/(e_B - e_G) = 4.62 \times 10^{-4}$ M and the slope $l = 1/(e_B - e_G) = 3.17$. Consequently $K_2 = 1.46 \times 10^{-4}$ M and $e_G = 0.459$ are obtained.

Determination of K_6 and K_3'. In phosphate buffers with pH ≥ 6.3 the only species of the dye to be considered are B, S_1, and C. Eqn. (2) can be approximated to

$$\frac{h}{e_\infty} = \frac{K_3' K_6}{e_B} + \frac{h(1 + K_6)}{e_B} \qquad (6)$$

Table 3. E_∞-Values for the determination of K_6 and K_3' in phosphate buffers. $\lambda = 639$ mμ, $C_M = 1 \times 10^{-5}$ M, $d = 5$ cm, $e_B = 0.775$, $T = 20.0$°C. $E_{\infty\ \mathrm{corr.}} = E_\infty - 0.007$.

[H+] $\times 10^7$ M	$E_{\infty\ \mathrm{corr.}}$	[H+] $\times 10^7$ M	$E_{\infty\ \mathrm{corr.}}$
1.55	0.250	3.56	0.476
1.94	0.298	4.40	0.552
2.37	0.351	5.43	0.637
2.92	0.410		

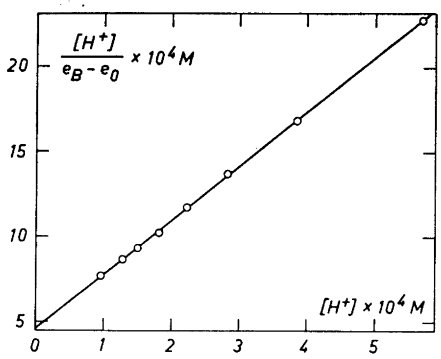

Fig. 3. [H+]/($e_B - e_0$) plotted against [H+] for the determination of K_2. $C_M = 1 \times 10^{-5}$ M, $d = 1$ cm.

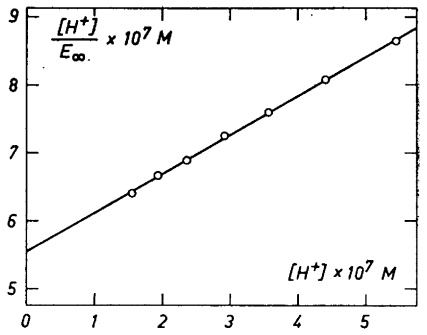

Fig. 4. [H+]/$E_{\infty\ \text{corr.}}$ plotted against [H+] for the determination of K_6 and K_3'. $C_M = 1 \times 10^{-5}$ M, $d = 5$ cm.

The equilibrium absorbancies, E_∞, were measured 26 h after the mixing of the dye stock solution with appropriate phosphate buffers. No straight line was, however, obtained, when [H+]/E_∞ was plotted against [H+]. The line was curved and the curvature became more pronounced the lower the absorbancies were. The reason for this was the fact that in alkaline solutions, where the dyestuff was assumed to be completely decolourized, a small remaining absorbancy persisted ($E_\infty = 0.007$ when $C_M = 1 \times 10^{-5}$ M and $d = 5$ cm). This remaining absorbancy had to be especially considered. If the corrected E_∞-values are used, a plotting of [H+]/$E_{\infty\ \text{corr.}}$ against [H+] gives a straight line, Fig. 4. The intercept of this line on the ordinate-axis, y, and the slope, l, are: $y = 5.56 \times 10^{-7}$ M, $l = 0.568$. Since $E_B = 5\ e_B = 5 \times 0.775$ we obtain, according to eqn. (6), $K_6 = 1.20$ and $K_3' = 1.79 \times 10^{-6}$ M.

Determination of K_4 and K_5. In the pH-range 3—4 eqn. (2) can be approximated and written as

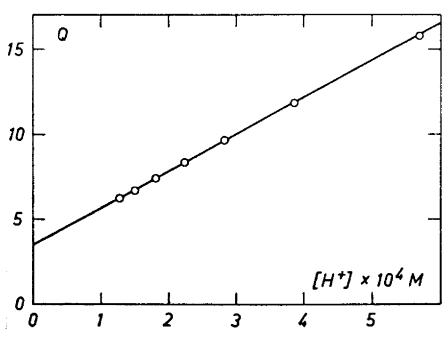

Fig. 5. The right member of eqn. (7), Q, plotted against [H+] for the determination of K_5 and K_4/K_1. $C_M = 2 \times 10^{-5}$ M, $d = 1$ cm.

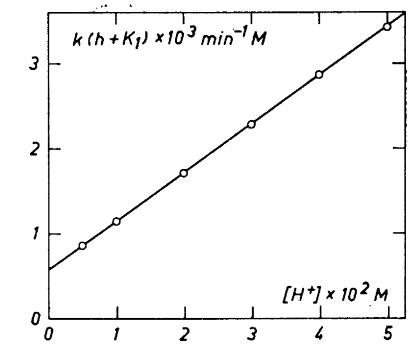

Fig. 6. $k(h + K_1)$ as a function of [H+] for the determination of k_3. [H+] = 5—50 mM.

Table 4. E_∞-Values for the determination of K_4 and K_5 from equilibrium measurements in HCl + KCl-buffers and acetate buffers. $\lambda = 639$ mμ, $C_M = 2 \times 10^{-5}$ M, $d = 1$ and 5 cm, $e_B = 1.474$, $e_G = 0.874$.

HCl + KCl-buffers, $d = 5$ cm			Acetate buffers, $d = 1$ cm			
$[H^+] \times 10^3$ M	$E_\infty = 5\,e_\infty$	$K_4 \times 10^3$	$[H^+] \times 10^4$ M	e_∞	$[H^+] \times 10^4$ M	e_∞
2.00	0.096	3.37	1.274	0.263	2.82	0.139
3.00	0.066	3.25	1.500	0.233	3.86	0.105
4.00	0.051	3.16	1.81	0.202	5.69	0.0724
5.00	0.041	3.13	2.23	0.170		
	Mean value	3.23			$K_{4\text{graph.}} = 3.12 \times 10^3$	
					$K_{5\text{graph.}} = 3.52$	

$$K_5 + \frac{hK_4}{K_1} = \frac{e_G}{e_\infty} + \frac{K_2 e_B}{he_\infty} - \frac{K_2(1 + K_6)}{h} - 1 \qquad (7)$$

since $K_3' \ll h$ in the actual pH-range and $h^2 e_Y$ in the numerator of eqn. (2) can be neglected at the used wavelength, $\lambda = 639$ mμ, where $e_Y \ll e_G < e_B$. The equilibrium absorbancies were measured in acetate buffers ($C_M = 2 \times 10^{-5}$ M, $d = 1$ cm). The right member of eqn. (7) was calculated, using the already determined values of e_B, e_G, K_2, and K_6, and plotted against $[H^+]$. Fig. 5. A straight line was obtained; $y = 3.52$, $l = 2.14 \times 10^4$. From the values of y and l we get, according to eqn. (7), $K_5 = 3.52$ and $K_4 = 3.12 \times 10^3$, since $K_1 = 0.146$.

The hydration constant K_4 can also be calculated from e_∞-values obtained in HCl + KCl-buffers, pH 2.3—2.7. In this pH-range eqn. (2) is approximated to

$$K_4 = \frac{K_1 K_2 e_B + hK_1 e_G}{he_\infty} - \frac{K_1 K_2(1 + K_6)}{h^2} - \frac{K_1(K_1 + h) + K_1 K_5}{h} \qquad (8)$$

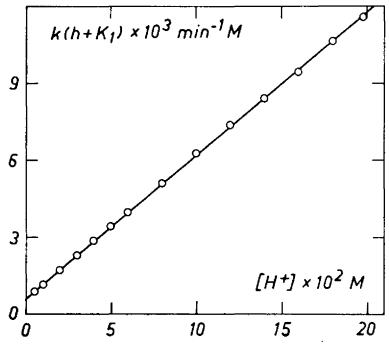

Fig. 7. $k(h + K_1)$ as a function of $[H^+]$ for the determination of k_1. $[H^+] = 5-200$ mM.

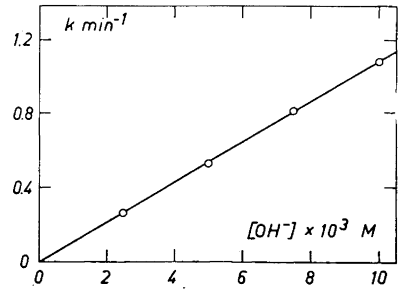

Fig. 8. The rate constant k as a function of $[OH^-]$ for the determination of k_7.

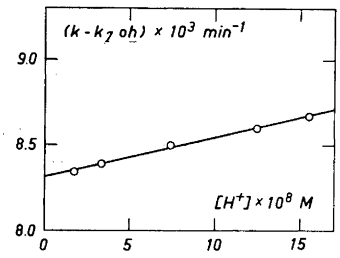

Fig. 9. ($k - k_7$oh) plotted against [H$^+$] in the pH-range 6.8—7.8 for the determination of k_5.

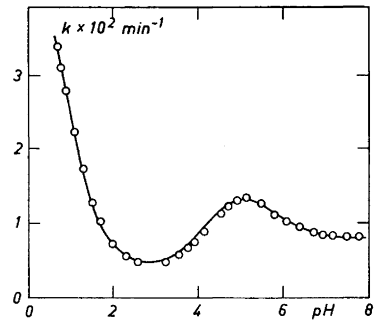

Fig. 10. The rate constant k as a function of pH in the pH-range 0.7—8. The points represented by the symbol O are experimentally obtained. The full-drawn curve is calculated from the non-approximated eqn. (3).

Even a roughly estimated value of K_5 can be used in the calculation of K_4 since the last two terms of eqn. (8) have the character of correction terms, amounting to 1—2 % of K_4. The calculated values of K_4 are recorded in Table 2 from which the mean value $K_4 = 3.23 \times 10^3$ is obtained. This value of K_4 is not, however, very reliable because of the low absorbancies.

Calculation of K_1' and K_2'. By definitions are

$$K_1' = K_1K_5/K_4 \tag{9}$$

and

$$K_2' = K_2K_6/K_5 \tag{10}$$

From the values of K_1, K_2, K_4, K_5, and K_6, reported above we thus obtain $K_1' = 1.65 \times 10^{-4}$ M and $K_2' = 4.98 \times 10^{-5}$ M.

Determination of k_1, k_2, k_3, and k_4. For kinetic measurements in HCl + KCl-buffers, pH = 0.7—2.3, eqn. (3) can be approximated to

$$k(K_1 + \mathrm{h}) = k_3K_1 + k_1\mathrm{h} \tag{11}$$

$k(K_1 + \mathrm{h})$ is plotted as a function of [H$^+$] in Figs. 6 and 7. Fig. 6, which is an enlargement of the lower, left part of Fig. 7, has the intercept on the ordinate-axis $y = 5.76 \times 10^{-4}$ min^{-1} M and consequently we get $k_3 = 3.94 \times 10^{-3}$ min^{-1}, since $K_1 = 0.146$ M. The value of the rate constant $k_4 = 1.12 \times 10^{-3}$ min^{-1} is obtained from $k_4 = k_3/K_5$. The slope of the straight line in Fig. 7 gives $k_1 = 5.57 \times 10^{-2}$ min^{-1}, and $k_2 = 1.79 \times 10^{-5}$ is then calculated from $k_2 = k_1/K_4$.

Determination of k_7 and k_8. For strongly alkaline solutions eqn. (3) is approximated to

$$k = k_5 + k_7\mathrm{oh} + k_8 \tag{12}$$

The rate of the decolourization is, however, directly proportional to [OH$^-$] as can be seen in Fig. 8, where k is plotted *versus* [OH$^-$]. In the pH-range used

Table 5. 4-Pyridine Green. A summary of the obtained values of the constants.

Protolytic constants				
K_1 M	$K_2 \times 10^4$ M	$K_1' \times 10^4$ M	$K_2' \times 10^5$ M	$K_3' \times 10^6$ M
0.146 ± 0.05	1.46 ± 0.05	1.65 ± 0.15	5.0 ± 0.5	1.8 ± 0.1

Hydration constants		
$K_4 \times 10^{-3}$	K_5	K_6
3.12 ± 0.12	3.5 ± 0.2	1.2 ± 0.1

Rate constants			
$k_1 \times 10^2$ min^{-1}	$k_3 \times 10^3$ min^{-1}	$k_5 \times 10^3$ min^{-1}	k_7 M^{-1} min^{-1}
5.6 ± 0.1	3.9 ± 0.1	8.3 ± 0.1	107 ± 1
$k_2 \times 10^5$ min^{-1}	$k_4 \times 10^3$ min^{-1}	$k_6 \times 10^3$ min^{-1}	$k_8 \times 10^5$ min^{-1}
1.8 ± 0.6	1.1 ± 0.1	6.9 ± 0.4	6.1 ± 0.4

in Fig. 8, pH = 11.3—11.9, is thus $k_7\text{oh} \gg k_5 + k_8$ and only k_7 can be obtained from the figure; $k_7 = 107$ min^{-1} M^{-1}. The rate constant k_8 can be calculated from the expression $k_8 = k_7 K_w / K_3' K_6$, which can be obtained from the definitions of the constants; $k_8 = 6.15 \times 10^{-7}$ min^{-1}. ($K_w = 1.24 \times 10^{-14}$ M^2).

Determination of k_5 and k_6. In neutral and very weakly alkaline solutions eqn. (3) can be approximated to

$$k - k_7\text{oh} = k_5 + \frac{\text{h}k_6 + k_8 K_3'}{\text{h} + K_3'} \qquad (13)$$

In Fig. 9 $k - k_7$oh is plotted as a function of [H$^+$]. $k_7$oh is, compared with k in the pH-range used in Fig. 9, pH = 6.8—7.8, a correction term which only amounts to 0.01—0.9 % of k. Extrapolation of the almost straight line to [H$^+$] = 0 gives an intercept $y = k_5 + k_8 = 8.32 \times 10^{-3}$ min^{-1} but $k_8 \ll k_5$ and therefore we obtain $k_5 = 8.32 \times 10^{-3}$ min^{-1}. The expression $k_6 = k_5 / K_6$ then gives $k_6 = 6.93 \times 10^{-3}$ min^{-1}.

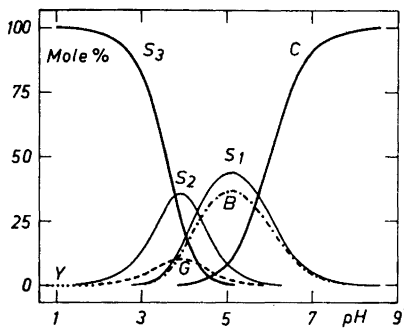

Fig. 11. The distribution of 4-Pyridine Green between the different species as a function of pH. The notations are the same as in the text.

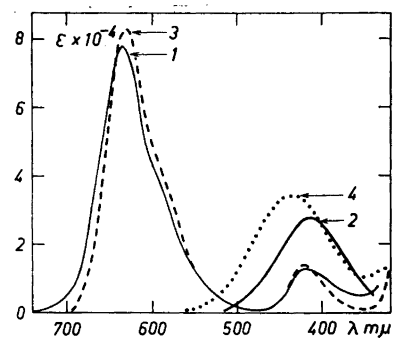

Fig. 12. Absorption curves of 4-Pyridine Green and Crystal Violet. The Curves 1 and 2 are the absorption curves of the blue species B and the yellow species Y, respectively, of 4-Pyridine Green. The Curves 3 and 4 are the absorption curves of the ions $[(Me_2NC_6H_4)_2CC_6H_4NHMe_2]^{2+}$ and $[Me_2NC_6H_4C(C_6H_4NHMe_2)_2]^{3+}$, respectively, of Crystal Violet.

The determined values of the constants are summarized in Table 5. It is hardly possible to perform an objective estimation of the errors of the values of the constants in such a complicated reaction scheme as the present one and, therefore, the errors given are subjective ones, based on the reproducibility of the measurements and the experience of the reliability of the used method and apparatus.

Fig. 10 shows the rate constant k as a function of pH. The solid curve has been calculated from eqn. (3) using the constants in Table 5. The circles are experimentally found k-values. The agreement between the calculated curve and the experimental points is fairly good, but the curve cannot be used as a control of the obtained values of the constants, since the curve is rather insensitive to variations in these (especially to variations in K_1', K_2', and K_3').

Fig. 11 shows the distribution at equilibrium, of the seven species of the dye as a function of pH. The curve of Y is, however, so low that it cannot be drawn apart from the 0 % line.

DISCUSSION

A comparison between the corresponding absorption curves and values of the constants of 4-Pyridine Green and Crystal Violet, $[(Me_2NC_6H_4)_3C^+]\ X^-$ is interesting. The substitution of a $Me_2NC_6H_4$-group of Crystal Violet for a NC_5H_4-group has a very marked influence on the hydration reactions and some of the protolytic reactions. The equilibria "Coloured" $\rightleftharpoons$ "Colourless" are strongly displaced towards "Colourless" when we go from Crystal Violet (CV) to 4-Pyridine Green. Compare $K_{4(CV)} = 74$ with $K_{4(4\text{-}PG)} = 3120$,

$K_{5(CV)} = 0.0319$ with $K_{5(4\text{-}PG)} = 3.5$, and $K_{6(CV)} = 0.00014$ with $K_{6(4\text{-}PG)} = 1.2$. There is also a marked difference between $K_{2(CV)} = 0.00406$ and $K_{2(4\text{-}PG)} = 0.000146$, whereas the values of the remaining protolytic constants of 4-Pyridine Green are of the same order of magnitude as corresponding values of Crystal Violet.

The great difference between $K_{2(CV)}$ and $K_{2(4\text{-}PG)}$ indicates that, as regards the species G, the proton from the reaction $B + H^+ \rightleftharpoons G$ is attached to the pyridine nitrogen as it is shown in the reaction scheme on p. 2252. A further support for this suggestion is given by the absorption curves. Fig. 12. The absorption curve of the species B is very similar to the absorption curve of the ion $[(Me_2NC_6H_4)_2CC_6H_4NHMe_2]^{2+}$ of Crystal Violet. This ion of Crystal Violet has two proton-free amino nitrogens like the species B. The absorption curve of the species Y is very similar to the absorption curve of the ion $[Me_2NC_6H_4C(C_6H_4NHMe_2)_2]^{3+}$ of Crystal Violet and this ion of Crystal Violet has one proton-free amino nitrogen like the species Y. The species G has an absorption curve which is different from the absorption curves of Malachite Green and derivatives of Malachite Green and, therefore, it is assumed that the protolytic reactions of 4-Pyridine Green proceed according to the reaction scheme. The species B and Y have absorption curves which are of the same type as the absorption curves of Malachite Green and its derivatives. However, it is difficult to decide whether the proton from the reaction $C + H^+ \rightleftharpoons S_1$ is mainly attached to the pyridine nitrogen or to an amino nitrogen.

REFERENCES

1. Harries, C. and Lénart, G. H. *Ann.* **410** (1915) 111.
2. Cigén, R. *Protolysengleichgewichte und Reaktionsgeschwindigkeiten einiger basischer Triphenylmethanfarbstoffe* (Diss.), University, Lund 1956.
3. Cigén, R. *Acta Chem. Scand.* **12** (1958) 1456.
4. Cigén, R. *Acta Chem. Scand.* **14** (1960) 979.
5. Cigén, R. *Acta Chem. Scand.* **15** (1961) 1892.
6. Cigen, R. *Acta Chem. Scand.* **15** (1961) 1905.
7. Cigén, R. and Bengtsson, G. *Acta Chem. Scand.* **16** (1962) 1837.

Received May 24, 1962.

ACTA CHEMICA SCANDINAVICA 16 (1962) 2263–2266

The Crystal Structure of Calcium Cyanamide

NILS-GÖSTA VANNERBERG

Department of Inorganic Chemistry, Chalmers University of Technology, Göteborg, Sweden

The crystal structure of calcium cyanamide has been reinvestigated using threedimensional X-ray data. The bond length C—N was found to be 1.22 ± 0.02 Å.

To be able to study the solubility of calcium cyanamide in calcium carbide it is necessary to know the dimensions of the cyanamide ion accurately. The crystal structure of calcium cyanamide was first investigated by X-ray methods by Dehlinger [1]. He found that the compound had rhombohedral symmetry with $a = 5.11$ Å and $\alpha = 43°50'$. The C—N bond distance was found to be about 1.6 Å, an improbable large distance. Bredig [2] some years later confirmed the rhombohedral symmetry but found the unit cell edge to be 5.40 Å, while the interaxial angle was 39°55′. Moreover, the C—N distance was determined to 1.16 ± 0.08 Å, in agreement with the known bond lengths in isoelectronic groups, for instance in N_3^-, NCO^- or CO_2 (Ref.[3]). The figure is very little accurate, as the author also observes. The investigation was based on a sample which contained only 70 % calcium cyanamide. Only 13 powder diffraction lines were registered. A refinement of the structure of calcium cyanamide seemed consequently to be desirable.

PREPARATION OF THE COMPOUND

Calcium cyanamide was prepared from calcium carbonate and hydrogen cyanide [4]. A mixture of nitrogen and hydrogen cyanide vapor was led over pure calcium carbonate at a temperature of about 800°C.

$CaCO_3(s) + 2HCN(g) \rightleftharpoons CaCN_2(s) + CO(g) + H_2(g) + CO_2(g)$ The sample which contained 96 % calcium cyanamide and had very small crystallite size, was then heated to 1300°C in a nitrogen atmosphere. The preparation did not lose any nitrogen under this treatment. It melted or at least sintered and the product contained well developed crystals suited for single crystal work.

The nitrogen content was in all cases determined by the Kjeldahl method.

DETERMINATION OF THE CRYSTAL STRUCTURE

The elementary cell dimensions were determined with the aid of X-ray powder photographs using the Guinier technique; NaCl was used as internal

Table 1. Powder diffraction data for $CaCN_2$. $a = 5.347 \pm 0.004$ Å $\alpha = 40°26' \pm 10'$.

hkl	$10^4\sin^2\Theta_{obs}$	$10^4\sin^2\Theta_{calc}$	I_{obs}
111	248	247	w
110	688	690	vs
211	1018	1020	m
221	1262	1267	s
$1\bar{1}0$	1740	1740	s
322	1926	1926	m
210	1982	1988	m
332	2338	2338	w
200	2426	2430	m
321	2725	2729	w
220	2753	2756	w
433	3328	3327	w
331	3658	3666	w
444	3960	3955	w
432		3965	
$2\bar{1}1$	4169	4171	w
320	4753	4748	vw

Table 2. Parameter values for $CaCN_2$. Space group $R\bar{3}m$.

Atom	Position	Number	*x*	*y*	*c*
Ca	*a*	1	0	0	0
C	*b*	1	½	½	½
N	*c*	2	0.4168	0.4168	0.4168

standard. A comparison of calculated and determined $\sin^2\Theta$ values can be found in Table 1.

The unit cell was found to be rhombohedral

$$a = 5.347 \pm 0.004 \text{ Å}$$
$$\alpha = 40°26' \pm 10'$$

The structural investigation was based on single crystal methods. The single crystals were mounted inside capillary tubes in order to prevent atmospheric attack. Filtered Mo$K\alpha$ radiation was used. The crystals were rotated about $[1\bar{1}0]$ and all zones detectable with Mo radiation were registered using an integrating Weissenberg camera and a multiple film technique. The intensities were estimated by visual comparison with known scales, and corrected by Lorentz and polarization factors. The absorption could be neglected as the crystals were very small, about 0.1 mm, while the radiation was hard.

No systematic extinctions were found. The space group was assumed to be $R\bar{3}m$. The atomic parameters, Table 2, were calculated from a threedimensional Fourier synthesis using a Besk electronic computer [5,6]. The observed and calculated structure factors can be found in Table 3. The errors in the atomic parameters were calculated by Cruichkshank's method.

Table 3. Observed and calculated structure factors for $CaCN_2$.

hkl	F_o	F_c	*hkl*	F_o	F_c
200	32.3	31.4	$32\bar{1}$	13.0	11.1
300	9.0	11.1	$42\bar{1}$	11.9	10.3
400	9.1	9.7	222	14.7	17.1
500	9.1	8.3	322	30.2	29.4
101	46.7	48.1	422	15.2	15.6
201	18.9	17.7	522	8.0	9.4
301	14.0	15.0	622	9.8	12.1
401	13.0	13.0	323	19.9	20.1
$10\bar{1}$	49.3	43.2	423	14.4	13.5
$20\bar{1}$	6.4	6.1	523	16.7	17.6
$30\bar{1}$	13.8	16.5	723	11.9	11.1
202	18.7	18.7	424	19.3	21.0
302	16.9	18.3	524	8.7	4.8
402	10.2	8.6	624	13.5	15.4
502	10.6	10.1	$22\bar{4}$	9.8	8.7
$20\bar{2}$	19.3	20.3	525	13.8	17.0
303	9.5	9.6	725	9.8	9.8
403	11.3	12.5	626	9.7	10.5
503	8.8	8.1	$23\bar{1}$	13.0	11.4
$30\bar{3}$	10.5	11.4	$33\bar{1}$	9.2	11.4
505	9.4	8.9	$33\bar{2}$	9.0	7.1
211	29.3	26.1	333	15.5	17.2
311	21.3	23.6	433	24.9	26.7
411	8.1	9.6	434	6.7	6.2
511	8.7	11.1	534	22.3	22.8
$11\bar{1}$	4.9	6.6	734	10.8	11.5
$21\bar{1}$	26.0	23.7	635	12.8	14.6
$31\bar{1}$	9.7	9.7	735	11.3	6.3
$41\bar{1}$	9.0	8.8	636	8.3	7.1
212	35.1	34.3	$44\bar{1}$	9.2	8.1
312	13.4	13.6	444	25.5	28.6
412	15.8	17.0	544	6.2	5.5
512	10.6	10.1	644	13.4	16.5
$11\bar{2}$	22.6	24.2	744	8.2	7.1
$21\bar{2}$	8.2	4.6	844	12.0	6.7
$31\bar{2}$	12.5	13.0	545	15.7	19.4
313	20.4	21.4	645	9.3	9.0
413	12.5	13.0	745	9.1	9.0
513	9.9	8.3	646	10.8	10.1
613	11.8	11.2	746	10.9	10.1
$11\bar{3}$	7.6	4.1	555	9.4	10.4
414	8.4	9.3	655	9.5	11.4
514	14.2	13.8	755	9.6	11.2
714	10.9	9.5	656	10.8	12.8
116	9.3	6.6	756	9.4	7.1
316	11.8	12.9			
417	10.9	9.7			

Table 3. cont.

hkl	F_o	F_c	*hkl*	F_o	F_c
856	9.7	9.2	867	10.3	6.3
757	9.6	10.0	868	10.6	10.0
857	10.7	7.1	877	11.6	11.0
666	8.2	8.0	888	19.1	11.5
766	11.3	11.4			
767	8.9	8.7			

DISCUSSION

The structure is built up by calcium and cyanamide CN_2^{2-} ions. Each calcium ion is octahedrally surrounded by six nitrogen atoms belonging to six different cyanamide ions, and each cyanamide ion is octahedrally surrounded by six calcium ions. The distance between the nitrogen atom and a calcium ion is 2.461 ± 0.016 Å. The cyanamide ion is linear as are all the isoelectronic species, for instance the carbon dioxide molecule and the azide ion. The cyanamide ion has a somewhat lower nuclear charge so its interatomic distances are somewhat longer than in the mentioned species. This distance between the nitrogen and carbon atom is 1.224 ± 0.016 Å. It is worth while to compare the bond distances in the three isoelectronic species N_2, CN^- and C_2^{2-} with the corresponding distances in N_3^-, CN_2^{2-} and C_3^{4-}.

Species	Electronic structure	Bond distances
N_2	:N:::N:	1.095 Å
CN^-	:C:::$\bar{N}$:	1.168 Å
C_2^{2-}	:$\bar{C}$:::$\bar{C}$:	1.20 Å
N_3^-	$^{-}$:$\ddot{N}$::$^{+}$N::$\ddot{N}$:$^{-}$	1.17 Å
CN_2^{2-}	$^{-}$:$\ddot{N}$::C::$\ddot{N}$:$^{-}$	1.224 Å
C_3^{4-}	:$\bar{\bar{C}}$::C::$\bar{\bar{C}}$:	1.309 Å

The values for the bond lengths were taken from Ref.[3] In some cases the bond lengths for the corresponding hydrides were used.

Acknowledgement. The author's thanks are due to the *Swedish Natural Science Research Council* for financial support of this investigation.

REFERENCES

1. Dehlinger, U. *Z. Krist.* **65** (1927) 286.
2. Bredig, M. A. *J. Am. Chem. Soc.* **64** (1942) 1730.
3. *Tables of interatomic distances and configurations in molecules and ions.* London, The Chemical Society 1958.
4. Franck, H. H. and Heimann, H. *Angew. Chem.* **44** (1931) 372; Brauer, G. *Handbuch der präparative anorganischen Chemie*, Ferdinand Enke Verlag, Stuttgart 1960, Vol. 1, p. 836.
5. Westman, S., Blomqvist, G. and Åsbrink, S. *Arkiv Kemi* **14** (1959) 535.
6. Åsbrink, S., Blomqvist, G. and Westman, S. *Arkiv Kemi* **14** (1959) 545.

Received May 25, 1962.

ACTA CHEMICA SCANDINAVICA 16 (1962) 2267–2274

Studies on Cobaltammines

VI. A Polarimetric Investigation of Some Outer-sphere Complexes of the *d*-Trisethylenediaminecobalt(III) Ion

RAGNAR LARSSON

Department of Inorganic and Physical Chemistry, Chemical Institute, University of Lund, Lund, Sweden

The optical rotation of the *d*-$[Coen_3]^{3+}$ ion has been measured in aqueous solutions of increasing concentrations of sulphate, thiosulphate, fluoride, chloride and perchlorate ions. In the first two cases a minimum of the rotatory power was obtained. This result indicates the existence of the first two outer-sphere complexes in these systems. For the thiosulphate system there are also some indications of the third outer-sphere complex as well as of a slight tendency to the formation of polynuclear complexes.

The other three systems showed a monotonous change of the rotatory power, the chloride system towards greater values, the fluoride and the perchlorate systems towards smaller values than that of the free *d*-$[Coen_3]^{3+}$ ion.

The relation between the changes observed and the polarizabilities of the ions is discussed.

It is a well known fact [1,2] that changes in the composition of the second coordination sphere of transition metal complexes do not cause great changes in the visible spectrum of the complex. However, it was demonstrated already by Werner [3] that the optical rotation of a complex ion in solution is strongly dependent upon the nature of the counter-ion. Following the work of Werner, Jaeger [4] measured the rotation dispersion of a series of complexes and found considerable differences for different counter-ions. To the best of the author's knowledge, it was not until the repetition and extension of these investigations by Kirschner and coworkers [5], that this effect was used for the investigation of outer-sphere complexity.

However, the above-mentioned authors [5] seem to have been measuring the optical rotation at only one concentration of the counter-ions, *viz.* that determined by the concentration of the complex ion and the stoechiometry of the salt in question. The rotations obtained by this method must depend on the degree of the outer-sphere affinity of the different counter-ions and on the molar rotations of the outer-sphere complexes. Thus they cannot be used directly as a measure of the complexity.

A better approach would be to measure the optical rotation of the complex central ion, as the concentration of the ligand is gradually changed. Then one may obtain evidence of a consecutive outer-sphere complex formation. The situation must be especially favorable, if the molar rotations of the consecutive complexes differ very much.

Such measurements have been performed in this paper. The rotatory power of the *d*-$[Coen_3]^{3+}$ ion has been determined for solutions holding varying amounts of sulphate, thiosulphate, fluoride, chloride and perchlorate ions, respectively.

METHOD AND FORMULAE

During the measurements no attempt was made to maintain a constant ionic strength. Thus the stability constants β_n used below are not to be regarded as true constants. Nevertheless, valuable information may be obtained from a quantitative formulation of the dependence of the rotatory power on the ligand concentration.

Let ϑ be the observed rotation, when the cobalt complex concentration is C_{Men_3}, when the total ligand concentration is C_B and the cell length is d dm. Then we define

$$\psi = \frac{\vartheta - \vartheta_o}{d \cdot C_{Men_3}} \tag{1}$$

where ϑ_o is ϑ for $C_B = 0$.

If we assume that only mononuclear complexes exist, it is easily deduced that

$$\psi = \frac{\sum_{n=0}^{N} \delta_n \beta_n [B]^n}{\sum_{n=0}^{N} \beta_n [B]^n} - \delta_o \tag{2}$$

and

$$\frac{d\psi}{d\ \ln[B]} = \sum_{n=0}^{N} (n - \bar{n})(\delta_n - \delta_n)\alpha_n \tag{3}$$

Here δ_n denotes the molar rotation of the complex $[(Coen_3)B_n]$ and β_n is the stability constant of that complex. $\bar{n}$ is the mean ligand number and α_n is the fraction of the cobalt existing as the n:th outer-sphere complex at the concentration [B] of free ligand.

Eqn. (3) is derived under the assumption of constant β_n and is thus valid only within a limited concentration range. It is obvious that if $\delta_1 < \delta_o$ and $\delta_2 > \delta_o$, γ will exhibit a minimum value. The position of this minimum can be estimated from eqn. (3). If only the first two terms in the right member of this equation are taken into account, we get:

$$\frac{d\psi}{d\ \ln[B]} = (1 - \bar{n})(\delta_1 - \delta_o)\alpha_1 + (2 - \bar{n})(\delta_2 - \delta_o)\alpha_2 \tag{4}$$

The first term of the right side changes sign, when $\bar{n} = 1$. The second term is positive, when $\bar{n} < 2$, but as α_2 is rather small when $\bar{n} \approx 1$, this term does

contribute only little to the value of $d\psi/d \ln[B]$. We may then conclude that, when $\bar{n}$ is only slightly less than one, $d\psi/d \ln[B]$ changes sign. This relation will be exemplified below.

EXPERIMENTAL

Chemicals used. *d*-[$Coen_3$]Cl *d*-tartrate was prepared as described by Werner [1]. This salt was dissolved and the perchlorate was precipitated with concentrated perchloric acid, washed with alcohol and ether and air-dried. Other chemicals were of *pro analysi* quality.

The polarimeter was a Hilger M 323, three-field Lippich-type for visual observation. The light source was a conventional sodium lamp and the instrument was equipped with a bichromate filter. The readings could be reproduced within 0.01°. Every reading was repeated 3—4 times to minimize random errors. The polarimeter tubes were kept at a constant temperature (20°C) by passing thermostated water through jackets on the tubes. The length of the tube was 4 dm in all cases but for the measurements at $C_M = 32$ mM, when a 2 dm tube was used.

RESULTS

The measurements of the sulphate and thiosulphate systems are reported in Tables 1 and 2. A graphical comparison between the two systems is given in Fig. 1. It can immediately be seen that whereas the minimum values are of the same order of magnitude, the subsequent increase of ψ is much more pronounced in the thiosulphate system. The minimum occurs at a lower value of C_B for the thiosulphate system than for the sulphate one. As the measurements reported in Fig. 1 were made at the same C_{Men_3} and as the minima are expected to occur at approximately the same value of $\bar{n}$, this means that the minimum also occurs at a smaller value of [B] for the thiosulphate system. This result indicates that the complexity is stronger in the system first men-

Table 1. Determination of ψ for the sulphate and thiosulphate systems. $C_{Men_3} = 16.00$ mM. $d = 4$ dm. $\delta_0 = 52.7$ degr. dm^{-1} M^{-1}.

The sulphate system			The thiosulphate system		
C_B mM	ϑ degr.	ψ degr.dm^{-1} M^{-1}	C_B mM	ϑ degr.	ψ degr.dm^{-1} M^{-1}
0	3.37_4	0	0	3.37_4	0
15.7	3.22_5	-2.3_3	14.0	3.25_0	-1.9_4
31.4	3.16_0	-3.3_4	31.4	3.17_5	-3.1_1
59	3.09_6	-4.3_4	58	3.12_0	-3.9_7
87	3.08_6	-4.5_0	87	3.15_9	-3.3_6
126	3.09_1	-4.4_2	157	3.31_1	-0.9_8
157	3.10_2	-4.2_5	330	3.65_1	$+4.3_3$
222	3.13_6	-3.7_2	595	4.11_8	+11.6
331	3.19_3	-2.8_3	900	4.59_8	+19.1
440	3.24_3	-2.0_5	1440	5.23_5	+29.1
595	3.33_0	-0.6_9	1800	5.57_8	+34.4
790	3.40_6	$+0.5_0$	2400	6.10_0	+42.6
990	3.47_8	$+1.6_3$	3000	6.42_8	+47.7

Table 2. Determination of ψ for the thiosulphate system. (Continued)

C_{Men_3} = 8.00 mM, d = 4 dm			C_{Men_3} = 32.0 mM, d = 2 dm		
C_B mM	ϑ degr.	ψ degr.dm^{-1} M^{-1}	C_B mM	ϑ degr.	ψ degr.dm^{-1} M^{-1}
15.7	1.58_3	$-\ 3.2_5$	47.7	3.21_4	$-\ 2.5_0$
47.2	1.52_6	$-\ 5.0_3$	72	3.19_2	$-\ 2.8_4$
79	1.56_3	$-\ 3.8_8$	358	3.69_7	$+\ 5.0_5$
450	1.95_2	$+\ 8.2_8$	596	4.10_5	+ 11.4
900	2.28_5	+ 18.7	1125	4.85_3	+ 23.1
1200	2.45_5	+ 24.0	1800	5.54_9	+ 34.0

tioned. This is in agreement with the results of ion-exchange measurements of the analogous $Co(NH_3)_6^{3+}$ systems [6].

In Fig. 2 the results for different C_{Men_3} in the thiosulphate case are given. It can be seen that the minimum of ψ is not independent of C_{Men_3}. This means that the assumptions made at the deduction of eqn. (2) are not fulfilled. The

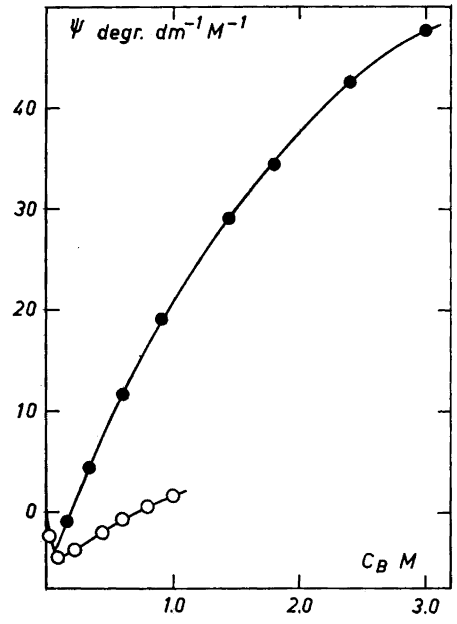

Fig. 1. ψ for the sulphate (○) and the thiosulphate (●) systems. C_{Men_3} = 16.00 mM.

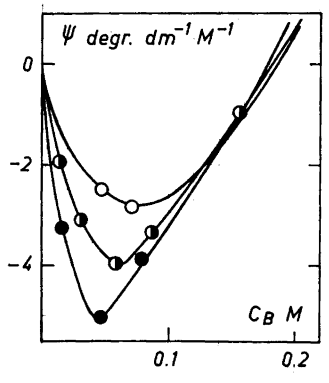

Fig. 2. The thiosulphate system. C_{Men_3} = 32.0 mM (○); C_{Men_3} = 16.00 mM (◑) and C_{Men_3} = 8.00 mM (●).

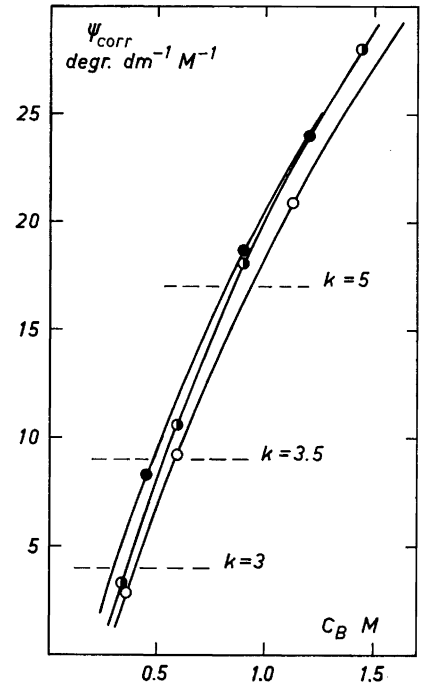

Fig. 3. The thiosulphate system. The ψ-curves after the correction mentioned in the text. The k-values are the means of the readings for (C''_{Men_3} = 32 mM, C'_{Men_3} = 8 mM) and (C''_{Men_3} = 32 mM, C'_{M} = 16 mM). C_{Men_3} = 32 mM (○); C_{Men_3} = 16 mM (◑); C_{Men_3} = 8 mM (●).

author therefore proposes that there is some tendency towards formations of polynuclear complexes within the studied system. This proposal is supported by the observation that the ψ values at high C_B and C_{Men_3} = 8 and 32 mM (Table 2) do not lie in a proper position in relation to the line drawn in Fig. 1. In a situation similar to this one, Fronæus (Ref.[7], p. 129) has used an approximative correction, implying the adjustment of the ψ values with a certain constant value, so that the extreme values of the curves coincide. The present author is well aware of the arbitrariness of this correction if the difference between the minimum values is not very small, and especially at ψ values far from the extreme point. Nevertheless, such a correction has been attempted, by reducing the ψ values for C_{Men_3} = 16 mM and C_{Men_3} = 32 mM with 1.05 and 2.20 degrees dm^{-1} M^{-1}, respectively. This operation makes the minima of the three curves (Fig. 2) to coincide. The resulting ψ values are given in Fig. 3. The sequence of the curves is now the one expected if no polynuclear complexes are formed. Then for a constant value of ψ, corresponding to a constant value of [B], we form the quotient $k = (C''_B - C'_B)/(C''_{Men_3} - C'_{Men_3})$ for two points (C'_{Men_3}, C'_B) and (C''_{Men_3}, C''_B) of the selected ψ. Some k-values

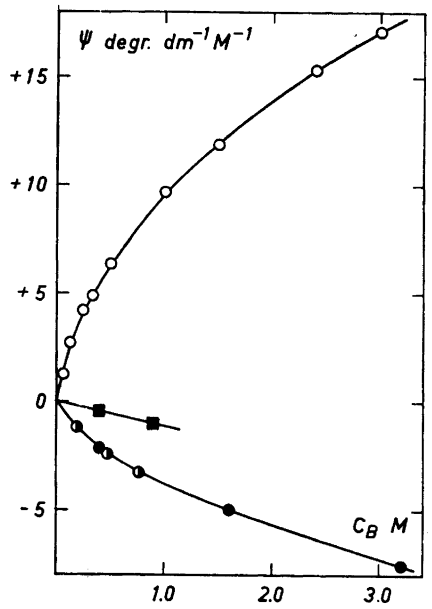

Fig. 4. ψ for the chloride (O) fluoride (◑: NaF; ●:KF) systems, $C_{Men_3} = 16.00$ mM, $d = 4$ dm; and for the perchlorate system (■), $C_{Men_3} = 8.00$ mM, $d = 4$ dm.

obtained in this way are indicated in Fig. 3. In the ideal case k should be equal to $\bar{n}$. The results are certainly too high. This is obviously due to an overcorrection and the correct $\bar{n}$ should be somewhat lower, as the degree of formation of polynuclear complexes is probably lower at these high values of C_B, compared to what was the case in the vicinity of the minimum.

The most important point of the argumentation is that the result of the correction makes it probable that the difference in magnitude of the minima for different C_{Men_3} (Fig. 2) is due to the existence of polynuclear complexes. An equally likely explanation is, however, that the difference in ionic strength in the three cases, which is noticeable in the low C_B-range, may have caused the difference in the magnitude of the minimum. It is improbable, however, that such an effect should persist up to the high C_B-range, where the *relative* difference in ionic strengths is small, and thus the result of the correction would be the same.

In the series of measurements with $C_{Men_3} = 32$ mM, precipitation occurred for $C_B = 100$ mM. Analysis of the precipitate showed that its composition was $[Coen_3]_2\ (S_2O_3)_3$. No precipitation was encountered for the other C_B-values. This obviously means that there is a minimum of solubility somewhere in the range 70 mM $< C_B <$ 350 mM. This fact, implies that $\bar{n} = 1.5$ somewhere in this concentration range.

The results of the measurements of the fluoride, chloride and perchlorate systems are reported graphically in Fig. 4. For these systems ψ varies monoto-

nously with ligand concentration. In order to reach high fluoride concentrations, potassium fluoride was used. It can be seen from Fig. 4 that ψ is apparently not influenced by a change from a sodium salt medium to a potassium one.

It is a matter of choice if the slight decrease of ψ found in the measurements of the perchlorate solutions should be ascribed to complex formation or to the variation of δ_0 with the ionic strength.

DISCUSSION

From the submitted results it follows that the existence of at least the first two sulphato- and thiosulphato complexes has been proved. The very steep rise of ψ for the thiosulphato system makes it probable that also a third complex exists. Indeed, even at as high a ligand concentration as 3 M the curve is still rising, indicating the fact that the complex formation has not yet come to a stop. It is difficult to see how this continued rise can be compatible with values of $\bar{n} = 1$ at so small a ligand concentration as [B] $\approx$ 0.05 M and $n = 1.5$ at [B] $\approx$ 0.2 M, without assuming the existence of a third complex. In connection with this it should be observed that anion-exchange measurements [6] of the similar system $Co(NH_3)_6^{3+}-S_2O_3^{2-}$ gave positive evidence of the existence of a third complex.

In an effort to obtain a more definite indication of the third complex the following approximate calculations were performed: From the values ($\bar{n} = 1$; [B] = 0.05 M) and ($\bar{n} = 1.5$; [B] = 0.2 M) the stability constants were obtained; $\beta_1 = 65$ M^{-1}, $\beta_2 = 400$ M^{-2}. Furthermore d ψ/d ln [B] was estimated from Figs. 2 and 1 at [B] $\approx$ 0.01 M and 0.2 M, respectively. Using the values of β_1 and β_2 given above, α_1, α_2 and $\bar{n}$ were calculated at the [B] values given. (Table 3.) Hence, $\delta_1-\delta_0$ and $\delta_2-\delta_0$ could be obtained from eqn. (4). Then d ψ/d ln [B] was calculated at [B] = 2.8 M, assuming that eqn. (4) is still valid, *i.e.* that only the first two complexes exist at this concentration. One then obtained d ψ/d ln [B] = 1.1 degr. dm^{-1} M^{-1} (Table 3). An estimation from Fig. 1 gave d ψ/d ln [B] = 24 degr. dm^{-1} M^{-1} at this value of [B].

The discrepancy is of such a magnitude that we must conclude that the assumptions made are not correct, *i.e.*, more than two complexes must exist at large ligand concentrations.

The most striking result of the present investigation is the large effect of the outer-sphere ligands on the rotatory power of the complex. *E.g.*, at the

Table 3. Calculation of d ψ/d ln [B] at [B] = 2.8 M from $\beta_1 = 65$ M^{-1} and $\beta_2 = 400$ M^{-2} (*cf.* the text).

[B] M	α_1	α_2	$\bar{n}$	d ψ/d ln [B] degr. dm^{-1} M^{-1}	
0.01	0.39	0.02	0.43	−1.3 (obs.)	$\delta_1-\delta_0 = -5.8$
0.2	0.43	0.53	1.5	5.9 (obs.)	$\delta_2-\delta_0 = 17.3$
2.8	0.05	0.95	1.95	1.1 (calc.)	

largest thiosulphate concentrations the rotatory power of the present species is almost twice that of the free d-$[Coen_3]^{3+}$ ion.

As it has not been possible to resolve the data into stability constants (β_n) and molar rotation coefficients (δ_n) we cannot make any quantitative comparisons between the different systems.

There is one puzzling problem, however, which presents itself readily. For the sulphate and thiosulphate systems $\delta_1 < \delta_o$ and $\delta_2 > \delta_o$, and for the fluoride system all δ_n (if there is more than one complex) are less than δ_o. On the other hand $\delta_n > \delta_o$ in the chloride system for all complexes that may exist.

It may be reasonable that the change of the rotatory power of the d-$[Coen_3]^{3+}$ ion is dependent on the position of the ligand in relation to the reference frame of the inner-sphere ligand. Especially the variation of the directions of greatest and smallest polarization in relation to this reference frame seems to be important [8]. It is thus possible to understand that $S_2O_3^{2-}$ exerts a greater effect than SO_4^{2-} does, as SO_4^{2-} has a lower polarizability. It also seems plausible that the highly polarizable chloride ion changes the rotation towards higher values, whereas the less polarizable fluoride ion changes it towards lower values in comparison with the free $[Coen_3]^{3+}$ ion.

But it is strange that the first thiosulphate complex has $\delta_1 > \delta_o$, *i.e.* follows the same trend as the first fluoride complex with its much less polarizable ligand. Perhaps at least two important factors must be considered: the charge of the ligand and its polarizability. These two factors seem to exert opposite effects resulting in the above-mentioned observations. Another factor of importance may be any kind of specific preference of the various ligands for different coordination sites, *e.g.* caused by different affinity towards hydrogen bond formation.

Although the interpretation given above is very vague, it seems to the present author, that, if a complete theory of the phenomenon of optical rotation of transition metal complexes were at hand (there have been interesting discussions recently [8,9]), it should be possible to make assignments of the coordination sites, occupied by the ligands in association complexes such as those investigated here. Then the concept of the second coordination sphere can be promoted from the twilight of a disputed possibility into the daylight of established reality.

The author is indebted to Professor S. Fronæus for valuable advice.

REFERENCES

1. Yoneda, H. *Bull. Chem. Soc. Japan* **28** (1955) 125.
2. Bjerrum, J., Adamson, A. W. and Bostrup, O. *Acta Chem. Scand.* **10** (1956) 329.
3. Werner, A. *Ber.* **45** (1912) 121.
4. Jaeger, F. M. *Z. Krist.* **55** (1915) 209.
5. Albinak, M. J., Bhatnagar, D. C., Kirschner, S. and Sonnessa, A. J. *Proc. 6th Intern. Conf. Coord. Chem.* (Ed. S. Kirschner) New York 1961, p. 154.
6. Larsson, R. and Tobiasson, I. *Acta Chem. Scand.* **16** (1962) 1919.
7. Fronæus, S. *Komplexsystem hos koppar*, (Diss.) Lund 1948.
8. Jones, L. L. and Eyring, H. *J. Chem. Ed.* **38** (1961) 601.
9. Sugano, S. *J. Chem. Phys.* **33** (1960) 1883.

Received June 4, 1962.

ACTA CHEMICA SCANDINAVICA 16 (1962) 2275–2283

Studies on a Galactan from Tension Wood of Beech (*Fagus silvatica* L.)

HANS MEIER*

Träkemiska avdelningen, Svenska Träforskningsinstitutet, Stockholm, Sweden

Chlorite holocellulose has been prepared from beech tension wood and has been extracted with dimethylsulphoxide, hot water and sodium hydroxide. The hemicellulose mixture extracted with the latter was fractionated with Fehling's solution and with cetyl-trimethylammonium hydroxide and a galactan was isolated with $\overline{DP}_n$ 380 and a uronic acid content of 28 %. On hydrolysis it yielded D-galactose, 69.3 %, L-arabinose, 6 %, D-xylose 4.2 % and L-rhamnose 20.5 %. From a partial hydrolysate of the galactan there were isolated — by carbon column chromatography and by chromatography on thick filter paper — the following neutral oligosaccharides: 6-*O*-β-D-galactopyranosyl-D-galactose, 4-*O*-β-D-galactopyranosyl-D-galactose, 6-*O*-β-D-galactopyranosyl-6-*O*-β-D-galactopyranosyl-D-galactose, 6-*O*-β-D-galactopyranosyl-4-*O*-β-D-galactopyranosyl-D-galactose, 6-*O*-β-D-galactopyranosyl-6-*O*-β-D-galactopyranosyl-6-*O*-β-D-galactopyranosyl-D-galactose, and the following acidic sugars: D-galacturonic acid, 4-*O*-methyl-D-glucuronic acid, 2-*O*-α-D-galacturonopyranosyl-L-rhamnose, 6-*O*-(4-*O*-methyl-β-D-glucuronopyranosyl)-D-galactose as well as a few others which were identified tentatively.

The galactan thus obviously contains both β-1,4- as well as β-1,6-linked galactose units, a combination which has not previously been demonstrated to occur in a natural polysaccharide.

Tension wood of several hardwood species has been shown to contain a higher percentage of galactose residues than normal wood [1,2]. In the present investigation the parent galactan was isolated from beech tension wood (*Fagus silvatica L.*) and characterised.

ISOLATION OF THE GALACTAN

The beech stem from which the galactan was isolated contained some 30 % typical tension wood which, in the fresh state in transverse sections through the stem, could be distinguished macroscopically from the normal wood by its light appearance. Microscopically it was found that the light area contained

* Present address: Botanisches Institut, Universität Fribourg, Fribourg, Switzerland.

Table 1. Carbohydrate analyses of polysaccharide fractions from beech tension wood.

	Yield g	Galactose %	Glucose %	Mannose %	Arabinose %	Xylose %
A: Beech tension wood, extracted with acetone (Klason lignin: 18.1 %)	961.7	4.9	73.3	trace	2.0	18.8
(Normal beech wood		1.3	57.6	4.3	1.0	35.8)
B: Polysaccharides from the delignification liquor						
B_1: Precipitated with 80 % ethanol	22.5	trace	31.8	4.6	21.8	41.8
B_2: Precipitated with 90 % ethanol	6.0	17.5	2.4	8.7	21.1	50.4
C: Holocellulose	833.5	4.6	75.8	trace	1.2	18.4
D: Polysaccharides from DMSO-extract	5.7	3.4	14.0	3.4	1.0	78.3
E: Polysaccharides from hot water extract	4.0	40.5	—	trace	11.9	47.7
F: Polysaccharides from 8 % sodium hydroxide extract	139.0	14.8	—	trace	6.5	78.7
G: Residual pulp	570.0	2.5	91.8	—	1.1	4.5

80 to 90 % tension wood fibres. The sugar analysis of a hydrolysate of the tension wood area showed only traces of mannose, a low xylose and a high glucose and galactose content (*A*, Table 1), which can be considered typical for tension wood. An analysis for normal beech wood is also given in Table 1.

Acetone-extracted, milled tension wood was delignified by the chlorite method and two fractions (B_1 and B_2, Table 1) were recovered from the delignification liquor. Both contained large amounts of materials other than polysaccharides. Only relatively small amounts of hemicelluloses had been dissolved during the chlorite treatment of the wood. The extraction of the holocellulose with DMSO (dimethylsulphoxide) and the subsequent extraction with hot water yielded two small fractions, *D* and *E*, respectively, of which the former was essentially a xylan and the latter a mixture of a xylan and a galactan. Large amounts of hemicellulose were then extracted with 8 % sodium hydroxide. This fraction, *F*, yielded on hydrolysis 14.8 % galactose which corresponded to about half of the galactose content of the wood. *F* was therefore subfractionated to separate the galactan from the large amounts of xylan also present in this fraction. Part of the xylan could be precipitated by adding Fehling's solution to an aqueous solution of *F*. The precipitate (F_1, Table 2) contained only a small amount of galactose residues. The polysaccharides (F_2)

Table 2. Carbohydrate analyses of the subfractions of *F*.

Fraction	Galactose %	Arabinose %	Xylose %	Rhamnose %
F_1	2.2	—	97.8	—
F_2	47.6	5.5	34.7	12.2
F_3	trace	—	100.0	—
F_4	69.3	6.0	4.2	20.5
F_5	16.5	2.5	81.0	trace

recovered from the soluble fraction contained 47.6 % galactose and 34.7 % xylose residues. When a sample of F_2 was redissolved in a small volume of water, no more xylan could be precipitated either by addition of Fehling's solution or of barium hydroxide. F_2 was then further fractionated with cetyltrimethyl ammonium hydroxide (CTA-OH).[3,4] CTA-OH was added to an aqueous solution of F_2 until precipitation was complete. The soluble fraction (F_3) was a pure xylan. The precipitate, which still was a mixture of a galactan and a xylan, was dispersed in water and sodium chloride solution was added until the precipitate was redissolved. On addition of water a new partial precipitation occurred. This new precipitate (F_4) was a galactan almost free from xylose residues whereas the soluble fraction (F_5) was essentially a xylan.

CHARACTERISATION OF THE GALACTAN (F_4)

Electrophoresis of F_4 on glass fibre sheets gave an elongated spot but no distinct components could be detected. F_4 contained 28 % uronic acids and had, in the acid form, $[\alpha]_D^{25}$ +11°. Its degree of polymerisation ($\overline{DP}_n$) was 380, determined osmometrically on the sodium salt in 0.1 M sodium chloride solution. The relative amounts of neutral sugars obtained by hydrolysis of F_4 (4 % sulphuric acid at 120° for 1 h) are given in Table 2. The xylose residues are most likely no integral part of the galactan but belong to a contaminating xylan.

Table 3. Carbon column fractionation of the neutral compounds from the partially hydrolysed galactan.

Fraction	Yield mg	Compound[a]		M_G[b]	R_{aG}[c]
25–49	620		galactose, arabinose, xylose rhamnose		
50–75	87	*a*	Gap $\xrightarrow[\beta]{1\ 6}$ Ga, monosaccharides	0.84	0.39
76–86	74	*b*	Gap $\xrightarrow[\beta]{1\ 4}$ Ga	0.45	0.59
		c	Gap $\xrightarrow[\beta]{1\ 6}$ Gap $\xrightarrow[\beta]{1\ 6}$ Ga	0.78	0.18
87–103	40	*d*	Gap $\xrightarrow[\beta]{1\ 6}$ Gap $\xrightarrow[\beta]{1\ 4}$ Ga	0.49	0.24
		e	Gap $\xrightarrow[\beta]{1\ 6}$ Gap $\xrightarrow[\beta]{1\ 6}$ Gap $\xrightarrow[\beta]{1\ 6}$ Ga	0.69	0.08
104–160 and 50 % ethanol eluate	180		higher oligosaccharides		

[a] Ga: D-galactose; *p*: pyranose form
[b] Paper electrophoretic mobility in 0.1 M borate buffer, pH 10.0 relative to glucose.
[c] Paper chromatographic mobility relative to galactose in solvent (i).

From a hydrolysate of F_4, after the acidic components had been removed by ion exchange, galactose crystallised directly. The mother liquor was fractionated by chromatography on thick filter paper, from which arabinose and rhamnose were recovered by elution with water. They were also obtained in the crystalline state and after recrystallisation of the three sugars their melting points and optical rotations were identical with those of D-galactose, L-arabinose and L-rhamnose, respectively.

A sample of F_4 was subjected to partial hydrolysis, the yield of lower oligosaccharides being improved by separation and further hydrolysis of the higher oligosaccharides. The hydrolysate was then separated into a neutral fraction (*I*) and an acidic fraction (*J*). *I* was fractionated by carbon column chromatography and by paper chromatography on thick filter paper. Table 3 gives the order in which the different compounds were eluted from the carbon column. All the oligosaccharides, on total hydrolysis, yielded galactose only. The two disaccharides (*a* and *b*) and the two trisaccharides (*c* and *d*) were obtained in the crystalline state. The structures of the disaccharides were determined by comparing them with authentic samples. The structures of the trisaccharides and of the tetrasaccharide (*e*) were elucidated by partial hydrolysis and chromatographic and electrophoretic identification of the products obtained. Substance *d*, a trisaccharide, previously unknown, was also reduced

Table 4. Carbon column fractionation of the acid compounds from the partially hydrolysed galactan.

Fraction	Yield mg	Compound[a]		R_{Gaa}[b]	M_{Gla}[c]	M_G[d]
17–35	130	*f*	Gaa	1.00	0.92	1.18
		g	MGla ca.	3.0	1.00	0.89
91–103	93	*h*	Gaa*p* $\xrightarrow[\alpha]{1\,2}$ Rh, minor amounts of *i*	0.74	0.65	0.67
104–131	116	*i*	MGla*p* $\xrightarrow[\beta]{1\,6}$ Ga, minor amounts of *j*	0.54	0.69	1.06
132–165	94	*j*	Gla*p* $\xrightarrow[\beta]{1\,6}$ Ga (?)	0.44	0.68	1.08
		k	MGla*p* $\xrightarrow[\beta]{1\,6}$ Ga*p* $\xrightarrow[\beta]{1\,6}$ (?)	0.38	0.54	0.92
166–209	156	*l*	MGla*p* $\xrightarrow[\beta]{1\,6}$ Ga*p* $\xrightarrow[\beta]{1\,6}$ Ga*p* $\xrightarrow[\beta]{1\,6}$ Ga (?)	0.19	0.46	0.88
		m	MGla*p* $\xrightarrow[\beta]{1\,6}$ Ga*p* $\xrightarrow[\beta]{1\,6}$ Ga*p* $\xrightarrow[\beta]{1\,4}$ Ga (?)	0.25	0.46	0.61
			Several other higher aldouronic acids			

[a] Gaa: D-galacturonic acid; MGla: 4-*O*-methyl-D-glucuronic acid; Gla: D-glucuronic acid; Rh: L-rhamnose; Ga: D-galactose; *p*: pyranose form.

[b] Paper chromatographic mobility relative to galacturonic acid in solvent *ii*.

[c] Paper electrophoretic mobility in 0.1 M acetate buffer, pH 4, relative to glucuronic acid.

[d] Paper electrophoretic mobility in 0.1 M borate buffer, pH 10, relative to glucose.

with sodium borohydride before it was subjected to partial hydrolysis, and yielded then *a* as the only reducing disaccharide.

The acidic fraction *J* from the partially hydrolysed galactan contained only small amounts of aldobiuronic acids but large amounts of higher aldouronic acids. It was therefore hydrolysed further and after the neutral sugars had been removed the acids were fractionated as the barium salts by carbon column chromatography. The fractions were then further fractionated by chromatography on thick filter paper. The compounds obtained are listed in Table 4. They were identified as described in the experimental part.

The uronic acids, the aldobi-, aldotri- and aldotetrauronic acids could easily be distinguished from each other by electrophoresis in acetate buffer (Table 4). Only two uronic acids, *i.e.* D-galacturonic acid (*f*) and 4-*O*-methyl-D-glucuronic acid (*g*) were detected, although a third, *viz.* glucuronic acid, was found in small amounts as a component of an aldobiuronic acid (*j*). Two aldobiuronic acids, *h* and *i* were found in relatively large amounts. An aldotriuronic acid, *k*, and two aldotetrauronic acids, *l* and *m*, all appeared to be derived from substance *i* which they yielded on hydrolysis together with galactose and 4-*O*-methyl-D-glucuronic acid.

DISCUSSION

That the galactan, F_4, is a homogeneous polysaccharide cannot be decided from the present study. F_4 could possibly consist of two acidic polysaccharides which are not separated by the fractionation technique used. The oligosaccharides obtained from the partial hydrolysate show, that both β-1,4- and β-1,6-galactopyranosidic linkages are present in the same molecular species which also contains 4-*O*-methyl-D-glucuronic acid residues. No aldotri- or aldotetrauronic acids were found containing 2-*O*-α-D-galacturonopyranosyl-β-rhamnose as a component. This can most probably be explained by the fact that rhamnosidic linkages are hydrolysed much faster than *e.g.* galactosidic linkages. No conclusions can be drawn from the present study as to whether the galacturonosyl-rhamnose is an integral part of the galactan or not. The same is true for the arabinose residues found in the hydrolysate of F_4. Since no oligosaccharides containing arabinose residues were found the latter are most likely to be present in the furanoside form as non-reducing end groups in the polysaccharide. The rhamnose residues in F_4 seem to a large extent to be present in aldobiuronic acid residues. However, relatively mild hydrolysis of the polysaccharide under conditions where aldobiuronic acids are not split also yielded rhamnose.

The 2-*O*-α-D-galacturonopyranosyl-L-rhamnose which in the present study was found to be a component of tension wood galactan has previously been found in a hydrolysate of pine wood by Roudier and Eberhard [5], but it has never been reported from a hardwood. The same authors have also isolated 6-*O*-β-D-glucuronopyranosyl-D-galactose from pine. The 6-*O*-(4-*O*-methyl-β-D-glucuronopyranosyl)-D-galactose units found in tension wood galactan represent a new aldobiuronic acid for wood and a polysaccharide containing both β-1,6-linked and β-1,4-linked galactose residues has not previously been demonstrated in nature. Gillham and Timell [6] have isolated from a hydrolysate

of white birch β-1,4-linked galactobiose which might have originated from a galactan similar in structure to tension wood galactan.

The galactan isolated from tension wood of beech differs markedly from compression wood galactan [7] but has a strong similarity to many gums. Both gum myrrh as well as mesquite gum [8] contain galactose, arabinose and 4-*O*-methyl-D-glucuronic acid as component sugars. In the former the uronic acid residues are partly linked to C_4 and partly to C_6 of galactose residues, which themselves are both β-1,3- and β-1,6-linked. 2-*O*-α-D-galacturonopyranosyl-β-rhamnose has been found in many different gums [8]. *Khaya grandifolia* gum [8,9] contains galactose, rhamnose, a trace of arabinose, galacturonic acid and 4-*O*-methyl-D-glucuronic acid, the same sugars which have been found in the tension wood galactan. Two aldobiuronic acids have been isolated from *Khaya grandifolia* gum, *viz.* 4-*O*-(4-*O*-methyl-D-glucuronopyranosyl)-D-galactose and 2-*O*-D-galactopyranosyl-L-rhamnose.

EXPERIMENTAL

Melting points are corrected. Concentration of solutions was effected under reduced pressure at a bath temperature of 40°.

Paper chromatography and paper electrophoresis. Whatman No. 1 and No. 3 MM papers were used. The chromatograms were run in the solvent systems (v/v):

(i) ethyl acetate-pyridine-water, 2:1:2 (upper layer).
(ii) ethyl acetate-acetic acid-formic acid-water, 19:3:1:4.
(iii) ethyl acetate-acetic acid-pyridine-water, 5:1:5:3.

The method of Saeman *et al.* [10] was used for quantitative determinations of monosaccharides. Paper electrophoreses were run in 0.1 M borate buffer of pH 10, in 0.1 M acetate buffer of pH 4, in germanate buffer [11] of pH 10.7 or in sulphonated phenylboronic acid buffer [12] of pH 7.

$\overline{DP}_n$-determination of F_4. The $\overline{DP}_n$ was determined osmometrically as described earlier for an arabinoglucuronoxylan [13]. For the calculation of the $\overline{DP}_n$ from the molecular weight of the polymer a molecular weight of 160 was assumed for the monomer units.

Isolation and fractionation of the polysaccharides. Tension wood areas from a 65 year old bent beech (*Fagus silvatica* L.) were cut out and wood meal was prepared in a Whiley mill. The fraction between 1 and 2 mm was extracted with acetone and chlorite holocellulose was prepared. The spent chlorite solution was dialysed against tap water for 8 days and concentrated to 3 l. After acidification with acetic acid hemicellulose fraction B_1 was precipitated with ethanol (12 l), centrifuged off, washed with ethanol and acetone, and dried. Further amounts of ethanol (15 l) were added to the centrifugate and the new precipitate (B_2) was centrifuged off and recovered in the usual way. The holocellulose (C) was extracted successively with dimethylsulphoxide, hot water and 8 % sodium hydroxide, the latter extraction being made under a nitrogen atmosphere. The polysaccharides from the different extracts were recovered by precipitation with ethanol (fractions D, E and F, respectively). A sample of F (87 g) was dissolved in water (2.5 l). Fehling's solution (1.5 l) was added, the precipitate was centrifuged, washed with dilute Fehling's solution and dissolved in 20 % acetic acid (2 l). The polysaccharides were then precipitated with ethanol (8 l) and washed free from copper with ethanol-water (4:1) containing small amounts of hydrochloric acid. Finally the precipitate was washed with ethanol and acetone and dried (F_1, yield 50 g). The centrifugate from the precipitation with Fehling's solution was treated with cation exchange resin (Dowex 50) and the hemicelluloses (F_2) were precipitated by the addition of ethanol and recovered in the usual way (yield 15.3 g).

A sample of F_2 (15 g) was dissolved in water (0.5 l) and neutralised with sodium hydroxide. A small insoluble fraction was discarded and a 5 % aqueous solution (150 ml) of cetyl-trimethylammonium hydroxide (CTA-OH) was added until precipitation was complete. The precipitate was centrifuged off and the centrifugate was treated with cation exchange resin (Dowex 50). By addition of ethanol a precipitate (F_3) was obtained

and recovered. The precipitate which had been obtained with CTA-OH was washed once with water by centrifugation and then dispersed in water (200 ml). On the addition of 10 % sodium chloride solution (50 ml) the precipitate dissolved. Water (1 l) was slowly added with stirring and the precipitate formed (F_4) was centrifuged off, dissolved in dilute acetic acid and recovered by precipitation with ethanol. The centrifugate from F_4 was neutralised with acetic acid, concentrated and the polysaccharides (F_5) were recovered by precipitation with ethanol. F_4, $[\alpha]_D^2$ +11.5° (*c* 2.0, H_2O) yielded sulphate ash, 2.4 %, and contained uronic acid, 28.2 %, calculated as galacturonic acid. Electrophoresis of F_4 in acetate buffer gave an elongated spot with $M_{\text{glucuronic acid}}$ *ca.* 0.3.

Identification of neutral monosaccharides from a hydrolysate of F_4. A sample of F_4 (1 g) was hydrolysed by heating for 1 h at 120° with 4 % sulphuric acid (200 ml). After neutralisation with barium hydroxide and centrifugation of the barium sulphate, the acidic sugars were removed by ion exchange using Dowex 1 resin in the acetate form. The solution containing the neutral sugars was concentrated to dryness and on trituration with moist methanol galactose crystallised. After two recrystallisations it had m.p. 162—165°, undepressed on admixture of D-galactose and $[\alpha]_D^{25}$ +79°(*c* 2.0, H_2O). The mother liquor was applied to thick filter paper which was irrigated with solvent (i) and rhamnose and arabinose were eluted from the paper. The rhamnose crystallised as the monohydrate and had m.p. 75° and 95° for hydrated and anhydrous forms, respectively. undepressed on admixture of L-rhamnose, and $[\alpha]_D^{25}$ +7.3° (*c* 1.0, H_2O). The arabinose also crystallised and had m.p. 150—154°, undepressed on admixture of L-arabinose, and $[\alpha]_D^{25}$ 103° (*c* 3.0, H_2O).

Partial hydrolysis of F_4 *and identification of the compounds obtained.* A sample of F_4 (3.9 g) dissolved in N sulphuric acid (400 ml) was heated on the steam bath for 30 min and then was cooled and neutralised with barium hydroxide. Barium sulphate was removed by centrifuging and washed twice with 25 % ethanol. Since the recovery of material was very incomplete, the barium sulphate precipitate was washed with dilute acetic acid whereby further material was obtained. Centrifugate and washings were combined and concentrated to 30 ml. By addition of ethanol (60 ml) the more highly polymeric material was precipitated and again partially hydrolysed as before. The whole procedure was repeated twice. All the low polymer fractions were combined (2.5 g) and the neutral sugars (*I*) were separated from the acidic (*J*) by adsorption of the latter on anion exchange resin (Dowex 1, acetate form), from which they then were eluted with 3 N acetic acid.

The neutral sugars (*I*) (1.2 g) were applied to a carbon/Celite column (4 × 40 cm). Gradient elution with aqueous ethanol (5 l, 0—25 %) effected a partial separation of the components (Table 3). All the fractions were fractionated further by chromatography on thick filter paper. All the oligosaccharides obtained yielded on hydrolysis galactose only. Partial hydrolysis of *c*, *d* and *e* was carried out on 3 mg samples in N sulphuric acid (0.5 ml) for 20 min at 100°.

a (22 mg), 6-*O*-β-D-galactopyranosyl-D-galactose crystallised from methanol with methanol as solvent of crystallisation, m.p. 97—100°, $[\alpha]_D^{25}$ +26° (c 2.5, H_2O)[14] and was chromatographically (solvent (i)) and electrophoretically (borate buffer) indistinguishable from an authentic sample.

b (39 mg), 4-*O*-β-D-galactopyranosyl-D-galactose crystallised from methanol and had m.p. 209—213°, undepressed on admixture of an authentic sample, $[\alpha]_D^{25}$ +67° (*c* 1.8, H_2O)[8,9] and was chromatographically (solvent (i)) and electrophoretically (borate buffer) indistinguishable from an authentic sample.

c (22 mg), 6-*O*-β-D-galactopyranosyl-6-*O*-β-D-galactopyranosyl-D-galactose crystallised from methanol and had m.p. 148—150° and $[\alpha]_D^{25}$ +5° (*c* 1.0, H_2O). A somewhat higher m.p. 157—160° and optical rotation $[\alpha]_D^{25}$ +16° have been reported by Aspinall *et al.*[15] Partial hydrolysis of *c* yielded substance *a* as the only disaccharide. On paper electrophoresis in sulphonated phenyl boronic acid *c* showed an M_G -value similar to that of substance *a*.

d (19 mg), 6-*O*-β-D-galactopyranosyl-4-*O*-β-D-galactopyranosyl-D-galactose crystallised from methanol and had m.p. 132—140° (explosive swelling) and 176—178° (melting) and

$[\alpha]_D^{25}$ +37° (*c* 2.3, H_2O). On partial hydrolysis *d* yielded the two disaccharides *a* and *b*. After reduction with sodium borohydride and partial hydrolysis *a* was obtained as the only reducing disaccharide. On paper electrophoresis in sulphonated phenyl boronic acid *d* showed an M_G-value similar to that of substance *b*.

e (6 mg), 6-*O*-β-D-galactopyranosyl-6-*O*-β-D-galactopyranosyl-6-*O*-β-D-galactopyranosyl-D-galactose yielded on partial hydrolysis galactose, *a* and *c*.

The acidic sugars (*J*, 1.3 g) from the partial hydrolysate of F_4 were further hydrolysed with 4 % sulfuric acid at 120° for 30 min and the neutral sugars were again separated as above from the acidic ones. The acidic sugars (0.7 g) were then applied as their barium salts to a carbon-Celite column (4 × 45 cm) which first was irrigated with water (2 l) and then with aqueous ethanol (5 l, 0—20 %). 30 ml fractions were collected and similar fractions were combined (Table 4). The main fractions were then further fractionated by chromatography on thick filter paper (solvent (ii)).

f (48 mg), D-galacturonic acid, was heated over night in an ampoule in 2 % methanolic hydrogen chloride in a boiling methanol bath. After neutralisation with silver carbonate the solution was centrifuged and concentrated. The methyl-(methyl-α-D-galactopyranosyl)-uronate crystallised from methanol-butanol and had m.p. 146—150°, undepressed on admixture with an authentic sample, and $[\alpha]_D^{55}$ +125°(*c* 1.0, H_2O).

g (38 mg), 4-*O*-methyl-D-glucuronic acid. From a sample of *g* (5 mg) the methyl ester methyl glucuronoside was prepared as decribed for substance *f*. The compound was dissolved in water (0.5 ml) and reduced by addition of sodium borohydride (20 mg). After 1 h the solution was neutralised with dilute acetic acid and deionised with a mixture of IR 4B and Dowex 50 resins. The sample was then hydrolysed with N sulphuric acid and neutralised. On paper electrophoresis in germanate buffer which separates the different monomethyl ethers of glucose very well, a strong spot with the same M_G-value as 4-*O*-methyl-D-glucose was obtained. Demethylation of the sample with boron trichloride [16] yielded glucose.

h (76 mg), 2-*O*-α-D-galacturonopyranosyl-L-rhamnose, had +76° (*c* 2.0, H_2O, Ba-salt) [7]. On hydrolysis with 8 % sulphuric acid (1 h at 120°) rhamnose and galacturonic acid were obtained. The paper chromatographic (solvents (ii) and (iii)) mobility of *h* was identical with that of an authentic sample of 2-*O*-α-D-galacturonpyranosyl-L-rhamnose (kindly supplied by Dr. A. Roudier) and when the chromatograms were developed with triphenyl tetrazolium chloride [7,17] *h* showed a negative formazan reaction.

i (117 mg), 6-*O*-(4-*O*-methyl-β-D-glucuronopyranosyl)-D-galactose, $[\alpha]_D^{25}$ +8° (*c* 1,1, H_2O, Ba-salt) [18] yielded on hydrolysis with 8 % sulphuric acid (1 h at 120°) 4-*O*-methyl glucuronic acid and galactose. The methyl glucuronoside was prepared from *i* (10 mg) and reduced with sodium borohydride as described above for *g*. The reduced compound was subjected to total hydrolysis and neutralised, and paper electrophoresis (germanate buffer) and paper chromatography (solvent (*i*)) indicated the presence of 4-*O*-methyl-glucose and galactose. The former, on demethylation with boron trichloride [16], yielded glucose. Partial hydrolysis of the reduced methyl ester methyl glucuronoside gave on paper electrophoresis (borate buffer, electrogram developed with anisidine hydrochloride) two spots with the same M_G-values as 4-*O*-methyl-glucose and galactose, respectively, and a third with M_G somewhat lower than that of 6-*O*-methyl-galactose but much higher than that of 4-*O*-methyl-galactose, indicating the presence of 6-*O*-(4-*O*-methyl-glucopyranosyl)-D-galactose. *i* showed a positive formazan reaction. A sample of *i* (26 mg) was converted into the methyl ester methyl glucuronoside and then fully methylated by the procedure of Kuhn *et al.* [19] The methylated product was dissolved in methanol and reduced by addition of sodium borohydride. The substance was recovered in the usual way and hydrolysed with N sulphuric acid. Chromatography of the reaction mixture on dimethylsulfoxide impregnated paper [20] with ethyl ether as irrigant and with the following reference substances: 2,3,4-tri-*O*-methyl-D-glucose, 2,3,4-, 2,4,6- and 2,3,6-tri-*O*-methyl-D-galactose, revealed the presence of 2,3,4-tri-*O*-methyl-glucose and of 2,3,4-tri-*O*-methyl-galactose, giving further evidence for the structure proposed for *i*.

j (11 mg), yielded on hydrolysis galactose and an uronic acid together with its lactone which on paper chromatography in two solvents, (ii) and (iii), had the same R_F-values as glucuronic acid and its lactone, respectively. Although *j* could be easily distinguished chromatographically from substance *i* it had almost the same M_G-value as the latter on

paper electrophoresis in borate buffer, thus probably being 6-*O*-β-D-glucuronopyranosyl-D-galactose.

k (51 mg), *l* (7 mg) and *m* (11 mg) on hydrolysis all yielded, amongst other compounds, substance *i* and galactose. A comparison of the M_G-values of *k*, *l* and *m* (Table 4) with those of *a*, *c* and *d* (Table 3), respectively, gives some evidence for the structures proposed for *k*, *l*, and *m* in Table 4. Further evidence for the structures of *l* and *m* was obtained by partial hydrolysis, *l* yielding galactose, *i*, *k* and *a*, and *m* yielding galactose, *i*, *k* and *b* together with the unchanged compounds.

Acknowledgement. The author is much indebted to Professor Bengt Lindberg for his interest in this work and to Miss Anita Stridsberg and Mr. Nils-Håkan Wallin for skilful assistance.

REFERENCES

1. Gustafsson, C., Ollinmaa, P. J. and Saarnio, J. *Acta Chem. Scand.* **6** (1952) 1299.
2. Schwerin, G. *Holzforschung* **12** (1958) 43.
3. Scott, J. E. *Methods of Biochemical Analysis* **8** (1960) 145.
4. Bouveng, H. O. and Lindberg, B. *Acta Chem. Scand.* **12** (1958) 1977.
5. Roudier, A. J. and Eberhard, L. *Bull. soc. chim. France* **1960** 2074.
6. Gillham, J. K. and Timell, T. E. *Svensk Papperstidning* **61** (1958) 540.
7. Bouveng, H. O. and Meier, H. *Acta Chem. Scand.* **13** (1959) 1884.
8. Smith, F. and Montgomery, R. *The Chemistry of Plant Gums and Mucilages*, New York 1959.
9. Aspinall, G. O., Hirst, E. L. and Matheson, N. K. *J. Chem. Soc.* **1956** 989.
10. Saeman, J. F., Moore, W. E., Mitchell, R. L. and Millet, M. A. *Tappi* **38** (1954) 336.
11. Lindberg, B. and Swan, B. *Acta Chem. Scand.* **14** (1960) 1043.
12. Garegg, P. J. and Lindberg, B. *Acta Chem. Scand.* **15** (1961) 1913.
13. Meier, H. *Acta Chem. Scand.* **12** (1958) 1911.
14. Haq, S. and Adams, G. A. *Can. J. Chem.* **39** (1961) 1563.
15. Aspinall, G. O., Hirst, E. L. and Ramsted, E. *J. Chem. Soc.* **1958** 593.
16. Bonner, T. G., Bourne, E. J. and McNally, S. *J. Chem. Soc.* **1960** 2929.
17. Wallenfels, K. *Naturwiss.* **37** (1950) 491.
18. Jones, J. K. N. and Nunn, J. R. *J. Chem. Soc.* **1955** 3001.
19. Kuhn, R., Trischmann, H. and Löw, I. *Angew. Chem.* **67** (1955) 32.
20. Wickberg, B. *Acta Chem. Scand.* **12** (1958) 615.

Received May 25, 1962.

ACTA CHEMICA SCANDINAVICA 16 (1962) 2284–2292

Electronic Absorption Spectra of Unconjugated Alkyl Thials and Thiones

KJ. ROSENGREN*

*Thermochemistry Laboratory **, University of Lund, Lund, Sweden*

The electronic spectra of a number of simple aliphatic thials and thiones have been evaluated. The C=S compounds were obtained together with the corresponding thiols by photolysis of disulfides in hydrocarbon glasses at 77°K. Besides the previously known absorption in the visible region ($n \rightarrow \pi^*$ transition), two peaks were recorded in the far ultraviolet, one of which was seen only at room temperature. By comparison with analogous oxygen compounds the two peaks were attributed to $n \rightarrow \sigma^*$ and $\pi \rightarrow \pi^*$ transitions, respectively, the latter, disappearing at 77°K, occurring from a vibrationally excited level.

When the solutions were stored at room temperature the intensity of the thiocarbonyl absorption gradually disappeared. For one compound, ethanethial, the disappearance was shown to correspond to a simultaneous formation of the trimer, 2,4,6-trimethyl trithiane.

Much work has been devoted to the study of the spectral behaviour of simple alkyl compounds containing a chromophor with a multiply bonded basic group such as >C=O, $-NO_2$, −N=O, −N=N−. The thiocarbonyl group belongs to this cathegory; however, very little is known about the light absorption of pure aliphatic thials or thiones without a second heteroatom. Some alicyclic thiones, including cyclopentane- and cyclohexane-thione, have been reported by Sen [1] to show a red color when freshly distilled. In a second paper [2] the author gives more precise data for the light absorption of benzene solutions of thiocamphor, thiofenchone and bisthiocamphor, all of which show an absorption band between 527 and 453 mμ with a peak at 495 mμ. Janssen [3] has recorded the spectrum of cyclohexanethione and reports λ_{max} at 495 and 504 mμ in ethanol and cyclohexane, respectively: ε_{max} lies between 1 and 10.

Our lack of knowledge concerning the simple aliphatic thiocarbonyl compounds can be ascribed to their instability. According to the literature most attempts to synthesize them yield the trimer or some other polymer as a pro-

* Research Fellow at The Swedish Technical Research Council.

** Sponsored by The Swedish Natural Science Research Council and by The Swedish Technical Research Council.

duct. Comprehensive reviews summarizing the various methods of preparation have been published by Campaigne [4] and by Reid [5].

It has previously been reported that in photolysis experiments [6] with dialkyl disulfides aiming at the production and trapping of thiyl radicals at liquid nitrogen temperature, the instantaneous stoichiometrically simple over-all reaction was found to be:

$$R_1R_2CHSSCHR_1R_2 \rightarrow R_1R_2C{=}S + HSCHR_1R_2$$

R = H or Alk.

The absence of disturbing side reactions together with the fact that the amount of conversion could easily be determined allowed an evaluation of the UV-spectrum of the thiocarbonyl compounds formed *. The analogous disproportionation reaction has been reported to occur when alicyclic disulfides are pyrolysed; for instance, bornyldisulfide is reported to yield thiocamphor and thioborneol (Ref.[4], pp. 32, 33).

EXPERIMENTAL TECHNIQUE AND MATERIALS

The spectra were taken using a Unicam Model SP 700 recording double-beam spectrophotometer. A specially designed unit allowing two identical quartz cells (diam. 19 mm, path length 17 mm) to be kept at liquid-nitrogen temperature was substituted for the standard cell-compartment. The wavenumber scale was calibrated using spectral lamps (Zn and Hg, low pressure) and the error in transmission values introduced by stray-light was found to be negligible in any case up to 50 kc.cm^{-1}.

The photolysis set-up consisted of two super high-pressure mercury lamps (900 W each), together with appropriate cooling and filter devices. The disulfides were irridiated in hydrocarbon mixtures that formed fully transparent glasses at 77°K. Most experiments were performed with isopentane/3-methyl pentane (6:1).

Further details are given elsewhere concerning the low-temperature cell compartment [7], the general experimental procedure [8] as well as the methods for preparation and purification of the disulfides [6] and the purification of the hydrocarbons [9].

RESULTS

The disulfides were all photolysed in 0.05 and 0.4 mM solutions. For the lowest concentration the most striking spectral change, besides the disappearance of the disulfide peak, was the appearance of a strong absorption peak at about 45 kc.cm^{-1} (stable at 77°K). The rate of increase in intensity of this peak corresponds to its formation from a first-order decay of the disulfide. This fact allowed an evaluation of the shape of the peak after all of the disulfide had been photolyzed. From the kinetic plot the fraction of the disulfide that had been decomposed at the end of photolysis could be determined; this fraction was always kept at 70—90 %. The extrapolated peak was attributed to the presence of both the thiocarbonyl compound and the mercaptan. By subtracting the calculated absorbance of the known amount of mercaptan the UV-absorption of the thiocarbonyl compound at 77°K was obtained.

The experimental conditions allowed a spectrum to be recorded 4—5 min after the irridiated cell had been brought to room temperature. From this

* However, during photolysis of 0.25 mM dimethyl disulfide a side-reaction was found to occur to some extent (*cf.* Ref.[6]).

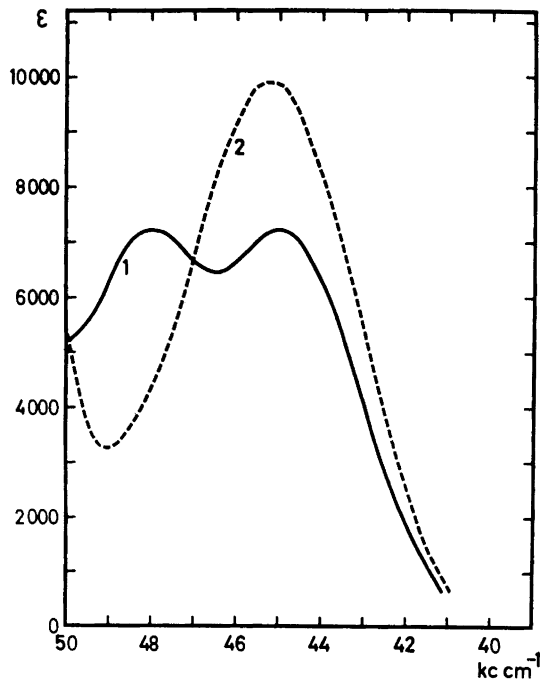

Fig. 1. Ultraviolet spectrum of butanethial at room temperature (1) and at 77°K (2).

measurement the spectrum of the thiocarbonyl compound could be evaluated by subtracting the absorbance of the mercaptan and the remaining disulfide. Figs. 1—3 show the evaluated spectra obtained in typical runs with three disulfides. The spectral characteristics at 77 and 298°K are summarized in Table 1 for all disulfides investigated. When the irradiated solutions were stored at room temperature the transmission at the thiocarbonyl peak slowly increased. (*cf.* Fig. 9 in Ref.[6]) However, when a 0.4 mM disulfide solution was photolyzed the rate of the spectral change of the thiocarbonyl compounds, after warm-up, was much faster. Fig. 4 gives the spectra recorded at various times for an ethanethial solution, showing a well-defined isosbestic point at 40.4 kc.cm^{-1}. The decrease in absorption is caused by the formation of the trimer, which is a 1,3,5-trithiacyclohexane derivate. This is illustrated in Fig. 5, which gives the absorption spectra of ethanethial and one third of that of its trimer, corresponding to the conversion of 1 mole of monomer to 1/3 mole of trimer.

A photolysis experiment with diethyl disulfide was also carried out at 2 mM concentration. The rate of photolysis could be followed by observing the decrease in the disulfide absorption at 35—36 kc.cm^{-1}. After 80 min of irradiation 74 % of the disulfide had been converted to mercaptan and thial. The sample now had a pale red color and after warm-up a very weak absorption

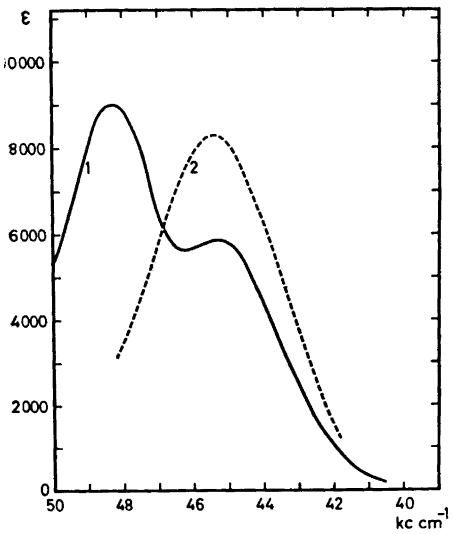

Fig. 2. Ultraviolet spectrum of ethanethial at room temperature (1) and at 77°K (2).

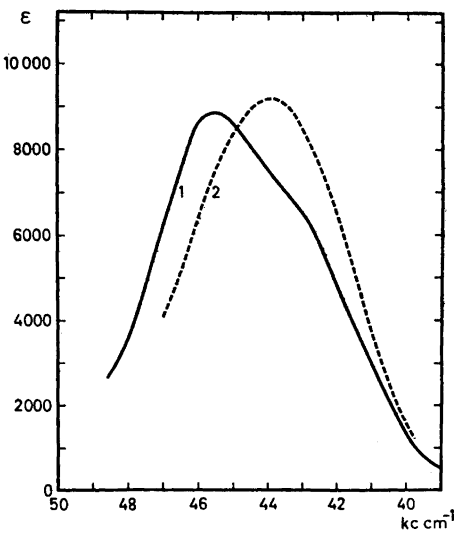

Fig. 3. Ultraviolet spectrum of 2-propanethione at room temperature (1) and at 77°K (2).

Table 1. Ultraviolet spectrophotometric characteristics at 77 and 298°K for various alkyl thiocarbonyl compounds. Figures in parentheses indicate the number of experiments. The uncertainties are expressed as mean deviations.

	At 77°K		At 298°K	
	Wavenumber of peak kc.cm^{-1}	log ε_{max}	Wavenumber of peak(s)[a] kc.cm^{-1}	log ε_{max}
Methanethial	48.07 (1)	(3.8) (1)	[b]	[b]
Ethanethial	45.50 ± 0.05 (5)	3.90 ± 0.03 (3)	48.2 (3)	3.89 ± 0.07 (3)
			45.3 (3)	3.72 ± 0.07 (3)
Propanethial	45.27 ± 0.05 (2)	4.0 ± 0.1 (1)	48.0 (2)	3.90 ± 0.09 (2)
			45.3 (2)	3.79 ± 0.06 (2)
Butanethial	45.21 ± 0.03 (7)	3.93 ± 0.03 (6)	47.9 (4)	3.85 ± 0.02 (4)
			45.0 (5)	3.83 ± 0.05 (5)
2-Methylpropanethial	45.06 ± 0.02 (2)	3.90 ± 0.07 (2)	47.9 (2)	3.77 ± 0.04 (2)
			45.2 (2)	3.80 ± 0.05 (2)
2,2-Dimethylpropanethial	44.97 ± 0.02 (2)	4 (2)	47.7 (2)	3.90 ± 0.03 (2)
			45.0 (2)	3.85 ± 0.02 (2)
2-Propanethione	44.00 ± 0.03 (2)	3.95 ± 0.02 (2)	45.5 (2)	3.96 ± 0.02 (2)
			S 43 (2)[c]	3.83 ± 0.02 (2)
2-Butanethione	44.03 ± 0.04 (3)	3.93 ± 0.02 (2)	45.4 (2)	3.87 ± 0.02 (2)
			S 43.5 (2)	3.83 ± 0.02 (2)
Cyclohexanethione	44.60 ± 0.03 (2)	3.90 ± 0.04 (2)	44.8 (2)	3.76 ± 0.02 (2)

[a] The uncertainty of all values in this column is ± 0.1 kc.cm^{-1}.

[b] At room temperature the methanethial solution only shows a steadily increasing absorption towards the vacuum ultraviolet.

[c] S = shoulder.

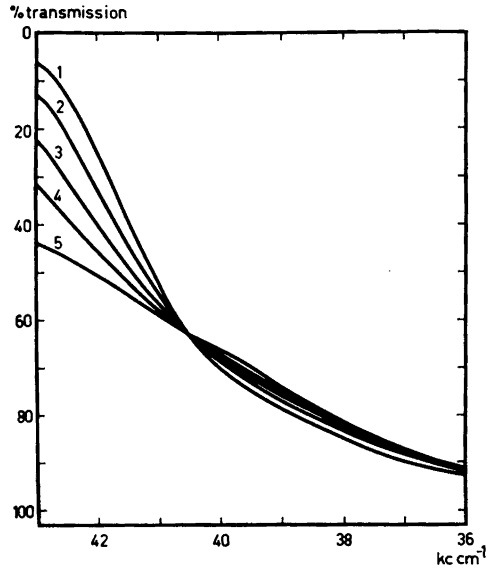

Fig. 4. Ultraviolet spectra of 0.4 mM ethanethial 5 min (1), 15 min (2), 30 min (3), 1 h (4) and 3.5 h (5) after warm-up.

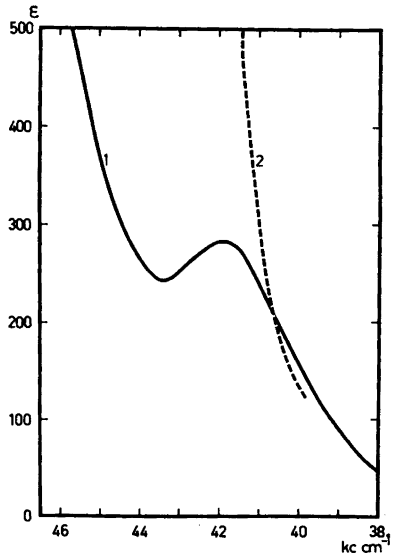

Fig. 5. Ultraviolet spectra of 2,4,6-trimethyl trithiane (1) and ethanethial (2). One third of the molar extinction for the trimer has been plotted.

peak was recorded between 17—23 kc.cm^{-1}; the transmission at the maximum at 19 kc.cm^{-1} was reduced by 4 %. These observations gave a calculated ε_{max} of 6 $\pm$ 2 for the thiocarbonyl absorption in the visible. When photolyzed in 5 mM solutions ethyl, butyl and cyclohexyl disulfide all showed a red color and an absorption band between 17 and 24 kc.cm^{-1}, with a peak at about 19—20 kc.cm^{-1}. At this concentration the mercaptan formed during the primary photolysis process is photolyzed to a significant extent and the high UV-absorption of the secondary photolysis products [10] interferes with the disulfide and thiocarbonyl absorption, preventing an evaluation of ε_{max} for the thiocarbonyl band.

The spectrum of cyclohexanethione has been reported by Janssen [3] to have no strong absorption band (log $\varepsilon > 3.5$) at wavenumbers below 45.5 kc.cm^{-1}. As previously reported [6] a dilute solution of freshly distilled cyclohexanethione showed a broad band around 45 kc.cm^{-1} both at 77 and 298°K.

DISCUSSION

A. Classification of bands

With respect to their intensity, wavenumber region and different behaviour at 77°K and room temperature the absorption bands of the thiocarbonyl compounds can be divided into three types:

1. An absorption in the visible region of low molar extinction. For ethanethial, butanethial and cyclohexanethione the absorption band ranged from 17 to 23 kc.cm^{-1} with a peak at 19 – 20 kc.cm^{-1}. This band will be classed as a Type I band.

2. At 77°K all compounds listed in Table 1 showed a characteristic absorption band in the far ultraviolet. The peak wavenumber of this band, which will be classified as a Type II band, seemed to be slightly dependent on the molecular structure. At 77°K it was found between 45.5 and 45.2 kc.cm^{-1} for the straight-chain alkane thials investigated, for branched chain thials the absorption was slightly displaced towards lower wavenumbers. The thione peak was found at 44.0 kc.cm^{-1} for alkane thiones and at 44.6 kc.cm^{-1} for cyclohexanethione. The molar extinction at 77°K was about the same for both thiones and thials (log ε_{max} 3.9 – 4.0).

The position of the absorption peaks changed only slightly when the solutions were brought to room temperature. However for thiones, the Type II peak became distinguishable only as shoulder, owing to the appearance of a second band (see below). For menthanethial the peak was not discernable at all at room temperature; the spectrum only showed a monotonously increasing absorption towards the vacuum-ultraviolet. This absorption, however, decreased at a normal rate when the methanethial was left at room temperature for a longer period of time (see above).

3. When the irridiated solution was brought to room temperature, a second band (Type III) was found in the far ultraviolet for all thiocarbonyl compounds investigated except methanethial and cyclohexanethione. The position of the peak, at 47.9 – 48.0 kc.cm^{-1} for straight-chained thials and at 45.5 kc.cm^{-1} for thiones, indicates a stronger influence of molecular structure upon the peak position than was found for the Type II band. The Type III band invariably disappeared upon cooling to 77°K and reappeared upon warm-up *.

B. Preliminary assignment of the bands

A low-intensity band has been reported for a number of thiones, mainly conjugated with a second heteroatom like N, S, or O. It was early postulated [11] that this absorption is due to a $n \rightarrow \pi^*$ transition according to the terminology suggested by Kasha [12]. Janssen [13] has shown a rectilinear relation between the transition energies calculated by a LCAO—MO treatment of the various thioketones and the peak wavenumber of the Type I band. His investigation included the unconjugated thiocarbonyl group for which the calculated energy value for the $n \rightarrow \pi^*$ transition corresponds to an absorption maximum at

* The possibility that the protomeric enethiol-form is responsible for the Type III peak and that the disappearance of this peak upon cooling to 77°K corresponds to a change in equilibrium towards the thial- or thione-forms can be ruled out for the following reasons. In the first place, the protomerization should be too slow in the non-polar solvent to allow the required very rapid conversion when the solution is brought from room temperature down to 77°K within 5 min. Secondly, this suggestion seems to be excluded owing to the fact that 2,2-dimethylpropanethial (from neopentyl disulfide) did show a normal behaviour – that is, the Type III peak existed at room temperature and vanished upon cooling. This compound does not have an α-hydrogen atom and therefore cannot exist in the enethiol-form.

20 kc.cm^{-1}. This is in good agreement with the value reported for cyclohexanethione [3] and the values for ethanethial, butanethial and cyclohexanethione from this investigation.

Although a definite assignment of the Type II and III bands is not possible with the experimental evidence available, their molar extinction values strongly indicate that they are connected with symmetry-allowed transitions. Some preliminary information about their origin can be gained from a comparison between the thiocarbonyl compounds and their oxygen analogues, aldehydes and ketones. For formaldehyde, acetaldehyde and acetone two absorption bands have been reported in the vaccuum ultraviolet, one around 55 and the other around 60 kc.cm^{-1}; Ref.[14], p. 306. The transitions involved are $n \rightarrow \sigma^*$ and $\pi \rightarrow \pi^*$, respectively, both being allowed by local symmetry in the CO and CS groups [15]. From experimental evidence, summarized in the following three points, it can be shown that it is plausible to find these two transitions displaced towards lower wavenumbers in alkylthiocarbonyl compounds:

1. In thiocarbonates and thiocarboxyl acid derivatives the $\pi \rightarrow \pi^*$ band is found at lower wavenumbers than in the carbonates and carboxylic esters. This indicates a smaller energy separation for the π- and the π^*-orbitals in the thiocarbonyl than in the carbonyl group; Ref.[14], p. 314.

2. Measurements of the ionization potential results in a lower value for the sulfur lone-pair electrons than for the corresponding oxygen electrons [16]. Thus in the thiocarbonyl group the n-level is of higher energy than in the carbonyl group.

3. The C—S bond dissociation energy is lower than that of the C—O bond [17] and it is plausible to assume the same statement to be true for the σ^* antibonding states.

Janssen has shown that a linear relationship exists between calculated transition energy values and the wavenumbers for the $\pi \rightarrow \pi^*$ bands for conjugated molecules of the type A.CS.B [13]. He has also calculated the transition energy value for the unconjugated C=S group to 1.812 β. This should correspond to an absorption of about 46 kc.cm^{-1} as judged from a rather remote extrapolation of the straight line given by Janssen.

In a study of the relation between spectra and electronic orbitals, Walsh [18] has pointed out that for molecules of the type H_2AB the binding energy of the upper repulsive state of that orbital which is formed from $2p_{x(A)}$ and $2p_{x(B)}$ increases with increasing non-planarity of the molecule. Formaldehyde and — by analogy — thioformaldehyde have planar ground states with no electron in the orbital referred to (a π^*-orbital in the planar configuration); instead all occupied orbitals are at the lowest energy levels in the planar state. If, however, an electron is promoted from one of these orbitals to an orbital striving towards non-planarity of the molecule the result may be a structure which is pyramidal at equilibrium in the excited state. An example of this is the $n \rightarrow \pi^*$ transition, where in fact for formaldehyde in the upper state an angle greater than 25° is found between the plane of the methylene group and the carbonyl axis [19] and progressions of the out-of-plane bending vibrations (ν_6) appear in the fluorescence spectrum. Besides this angle deformation, formaldehyde also shows a considerably increased carbonyl bond length in the excited state, 1.32 Å as compared with 1.22 in the ground state.

Compared with the situation for the $n \rightarrow \pi^*$ transition an even greater out-of-plane angle can be expected for the state reached by a $\pi \rightarrow \pi^*$ transition, as in this case the promoted electron is taken from an orbital where its presence contributes more to stabilize the planar structure than a non-bonding electron does. The transformation of a bonding electron to a non-bonding electron would also cause a further increase of the A—B bond length than that found for the $n \rightarrow \pi^*$ transition. Considering these large structural changes of the molecule accompanying a $\pi \rightarrow \pi^*$ transition, the energy required must be considerably lower if the transition takes place from a vibrationally excited state than from the ground state, provided the excited vibration includes the molecular changes involved. A non-planar structure for the excited state involving a π^*-orbital can also be expected for compounds where alkyl groups have been substituted for one or both hydrogen atoms -- that is, for aldehydes, ketones, thials and thiones.

In contrast to the π-orbital the antibonding state of the carbonyl σ-orbital has a lowest energy level corresponding to a planar structure [18]. However, an increased carbonyl bond length is expected also in this case.

Taking the above arguments into consideration it seems reasonable to make the following assignments:

Type II: a $n \rightarrow \sigma^*$ band, corresponding to transitions from the vibrational ground state.

Type III: a $\pi \rightarrow \pi^*$ band corresponding to transitions from a vibrationally excited level. At 77°K the population of this level is decreased and the band disappears.

The intensity of the Type III band corresponds to a population of the excited vibrational state of not less than 10 % at room temperature and a ratio between the population at room temperature and that at 77°K of at least 10. These two requirements fix the wavenumber of the vibration involved to lie between 165 and 480 cm^{-1}. These figures sound reasonable for an out-of-plane bending vibration of the molecule. If the force constant for this vibration is put equal to 1/2 the value reported for formaldehyde [20] (a relationship applicable to phosgen thiophosgen [20,21]) an estimated wavenumber of 770 cm^{-1} is found for methanethial and 290 cm^{-1} for propanethione. The high value calculated for methanethial corresponds to only 2.5 % of the molecules in the first excited level at room temperature and is in agreement with the fact that a significant Type III band is absent in the thioformaldehyd spectrum. For cyclohexanethione the ring structure is expected to render the out-of-plane bending vibration more difficult, which may be the reason why the Type III band is not found in this compound.*

The assignment of the Type III band to a $\pi \rightarrow \pi^*$ transition also agrees with the expected influence from molecular structure [15]. On the contrary the $n \rightarrow \sigma^*$ transition is less sensitive to conjugation and ought to be found in the same wavenumber region also for simple conjugated molecules. In fact, Sandström

* *Added in proof:* Dr. B. Bak, Copenhagen, has pointed out that ring vibrations < 480 cm^{-1} should be present in cyclohexanethione, facilitating the discussed out-of-plane bending vibration. However, the band may be too weak to be observed.

recently reported[22] a band at 43 kc.cm^{-1} for thioacetamide in addition to the already known $n \rightarrow \pi^*$ and $\pi \rightarrow \pi^*$ bands[23,24]. This band may well be the $n \rightarrow \sigma^*$ band since it shows the expected solvent dependence.

Acknowledgements. The author wishes to thank Mr. Bengt Nelander for valuable discussions.

This investigation has been supported in part by *Air Force Office of Scientific Research*, OAR, through the European Office, Aerospace Research, United States Air Force, and by the *Swedish Technical Research Council.*

REFERENCES

1. Sen, D. C. *J. Indian Chem. Soc.* **13** (1936) 268.
2. Sen, D. C. *J. Indian Chem. Soc.* **14** (1937) 214.
3. Janssen, M. J. *Rec. trav. chim.* **79** (1960) 464.
4. Campaigne, E. E. *Chem. Rev.* **39** (1946) 1.
5. Reid, E. E. *Organic Chemistry of Bivalent Sulfur*. Chemical Publishing Co., New York 1960. Volume III, p. 148.
6. Rosengren, Kj. *Acta Chem. Scand.* **16** (1962) 1401.
7. Rosengren, Kj., Sunner, S. and Timm, D. *Acta Chem. Scand.* **16** (1962) 467.
8. Rosengren, Kj., Sunner, S. and Timm, D. *Acta Chem. Scand.* **16** (1962) 495.
9. Rosengren, Kj. *Acta Chem. Scand.* **16** (1962) 1421.
10. Rosengren, Kj. *Acta Chem. Scand.* **16** (1962) 1418.
11. McMurry, H. L. *J. Chem. Phys.* **9** (1941) 231.
12. Kasha, M. *Discussions Faraday Soc.* **9** (1950) 14.
13. Janssen, M. J. *Rec. trav. chim.* **79** (1960) 1066.
14. Mason, S. F. *Quart. Rev.* **15** (1961) 287.
15. Sidman, J. W. *Chem. Rev.* **58** (1958) 689.
16. Watanabe, T. *J. Chem. Phys.* **26** (1957) 542.
17. Cottrell, T. L. *The Strengths of the Chemical Bonds*. 2nd Ed. Butterworths, London 1958.
18. Walsh, A. D. *J. Chem. Soc.* (1953) 2306.
19. Brand, J. C. D. *J. Chem. Soc.* (1956) 858.
20. Overend, J. and Evans, J. C. *Trans. Faraday Soc.* **55** (1959) 1817.
21. Duchesne, J. *J. Phys. Rad.* **15** (1954) 211.
22. Sandström, J. *Acta Chem. Scand.* **16** (1962) 1616.
23. Hantzsch, A. *Ber.* **64** (1931) 561.
24. Janssen, M. J. *Rec. trav. chim.* **79** (1960) 454.

Received May 25, 1962.

ACTA CHEMICA SCANDINAVICA 16 (1962) 2293–2310

Short Communications

On the Biological Methylation of Histamine. 5. Inhibition by Histamine Analogues

K. M. LINDAHL-KIESSLING

Institute of Zoophysiology and Institute of Medical Genetics, University of Uppsala, Sweden

Histamine is attacked mainly by two enzymes, one being diamineoxidase, which is fairly well known. This enzyme can be inhibited effectively by aminoguanidine. When diamine oxidase is thus inhibited *in vivo* by injection of aminoguanidine, the other histamine-metabolizing enzyme, S-adenosylmethionine — histamine methyltransferase continues histamine inactivation to completion [1].

It is evident that a potent inhibitor of the histamine methyltransferase could help in clarifying the physiology of histamine. So far only nonspecific inhibitors have been reported [2-4]. Therefore some histamine analogues were examined for possible inhibition of histamine methyltransferase.

The method for the assay of the enzyme has been described recently [4]. A new method for purification of the enzyme using TEAE-cellulose chromatography and Sephadex-filtration has since been used and will be described in detail elsewhere. The histamine analogues were obtained through the courtesy of Drs Kahlson and White at the Physiological Institute, University of Lund, Sweden.

Table 1. The effect of some histamine analogues on histamine methyltransferase. The roman figures refer to Lee and Jones [5].

Compound	Inhibition in % at different inhibitor concentrations			
	2.5×10^{-3} M	1×10^{-3} M	1×10^{-4} M	1×10^{-5} M
V 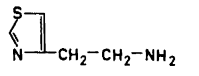	30	17	5	0
VIII 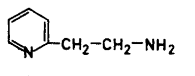	42	8	0	0
IX 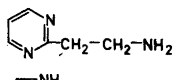	80	18	24	13
XIII 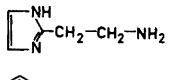	65	37	4	3
XXIV 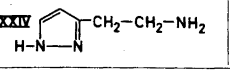	75	51	19	12

The compounds tested are listed in Table 1, which shows their inhibitory effect on histamine methyltransferase. The roman figures refer to the investigation by Lee and Jones [5], in which they examined the effect of the same compounds on isolated guinea pig ileum and on the blood pressure of the anesthetized cat. Compounds Nos. V, VIII, and IX had some activity, but XIII and XXIV were devoid of histamine-like activity. Evidently there is no correlation between the biological activity and the enzyme inhibition.

Table 2. Inhibitory effect of 3-β-aminoethylpyrazole (XXIV) on histamine methyltransferase at different histamine concentrations. The inhibitor concentration was 2.5×10^{-3} M.

Histamine concentration, mM	Inhibition, %
0.034	79
0.067	72
0.168	41
0.337	1

In Table 2 it is shown that the inhibition by compound XXIV is of competitive nature. This finding makes it doubtful if the compound can be used with any success as an inhibitor *in vivo*, although its lack of biological activity would permit rather high doses.

A full report of these experiments will be published.

1. Lindell, S. E., Nilsson, K., Roos, B.-E. and Westling, H. *Brit. J. Pharmacol.* **15** (1960) 351.
2. Lindahl, K. M. *Acta Chem. Scand.* **13** (1959) 1476.
3. Brown, D. D., Tomchick, R. and Axelrod, J. *J. Biol. Chem.* **234** (1959) 2948.
4. Lindahl, K. M. *Acta Physiol. Scand.* **49** (1960) 114.
5. Lee, H. M. and Jones, R. G. J. *Pharmacol. Exptl. Therap.* **95** (1949) 71.

Received September 12, 1962.

The Structures of Three Mesomorphous Phases in the Sodium Caprylate-Decanol-Water System

KRISTER FONTELL, PER EKWALL, LEO MANDELL and INGVAR DANIELSSON

Institute of Physical Chemistry, Åbo Akademi, Åbo, Finland

Of the liquid-crystalline phases that under certain conditions separate from concentrated aqueous association colloid systems, the so-called middle soap phase has a two-dimensional hexagonal structure. This was proposed already by McBain and Marsden [1] in the cases of dodecylsulphonic acid and triethanolamine laurate. These authors concluded that the phase in question consists of long fibres, rods or ribbons that are arranged in a hexagonal network with water occluded between the fibres. Luzzati and co-workers [2] have recently established that association colloids of different types including the salts of higher fatty acids (C_{12}—C_{18}) form middle soaps with a two-dimensional hexagonal structure and were able to present detailed information about the inner structure and unit dimensions of the phases.

We have studied the middle soap formation by a fatty acid soap with a shorter chain, sodium caprylate (C_8) [3-4]. A liquid-crystalline phase separates at 20°C from aqueous solutions of this soap when the concentration exceeds 40.5 %. Between 46.0 and 51.5 % sodium caprylate this mesomorphous phase is homogeneous. The phase is both macroscopically (it is a transparent, rigid "gel") and microscopically (it has a fanlike and angular texture: 222.5 and 226.1 in Rosevear's system [5]) similar to the middle soaps of some higher fatty acid soaps and its X-ray diffraction pattern reveals a hexagonal structure. We therefore felt justified in drawing the conclusion that the middle soap of sodium caprylate has a inner structure resembling the structure of the middle soaps of the higher soaps. Subsequent X-ray studies have confirmed this conclusion. We have recorded for the middle soap of sodium caprylate, besides a weak diffuse reflection at the position $s = 1/4.5$ Å^{-1} ($s = 2 \sin \Theta/\lambda$), as many as three sharp reflections with Bragg spacings of 25.9, 15.0, and 13.0 Å in the central part of the X-ray diffraction pattern. The positions of these lines do not vary over

The compounds tested are listed in Table 1, which shows their inhibitory effect on histamine methyltransferase. The roman figures refer to the investigation by Lee and Jones [5], in which they examined the effect of the same compounds on isolated guinea pig ileum and on the blood pressure of the anesthetized cat. Compounds Nos. V, VIII, and IX had some activity, but XIII and XXIV were devoid of histamine-like activity. Evidently there is no correlation between the biological activity and the enzyme inhibition.

Table 2. Inhibitory effect of 3-β-aminoethylpyrazole (XXIV) on histamine methyltransferase at different histamine concentrations. The inhibitor concentration was 2.5×10^{-3} M.

Histamine concentration, mM	Inhibition, %
0.034	79
0.067	72
0.168	41
0.337	1

In Table 2 it is shown that the inhibition by compound XXIV is of competitive nature. This finding makes it doubtful if the compound can be used with any success as an inhibitor *in vivo*, although its lack of biological activity would permit rather high doses.

A full report of these experiments will be published.

1. Lindell, S. E., Nilsson, K., Roos, B.-E. and Westling, H. *Brit. J. Pharmacol.* **15** (1960) 351.
2. Lindahl, K. M. *Acta Chem. Scand.* **13** (1959) 1476.
3. Brown, D. D., Tomchick, R. and Axelrod, J. *J. Biol. Chem.* **234** (1959) 2948.
4. Lindahl, K. M. *Acta Physiol. Scand.* **49** (1960) 114.
5. Lee, H. M. and Jones, R. G. J. *Pharmacol. Exptl. Therap.* **95** (1949) 71.

Received September 12, 1962.

The Structures of Three Mesomorphous Phases in the Sodium Caprylate-Decanol-Water System

KRISTER FONTELL, PER EKWALL, LEO MANDELL and INGVAR DANIELSSON

Institute of Physical Chemistry, Åbo Akademi, Åbo, Finland

Of the liquid-crystalline phases that under certain conditions separate from concentrated aqueous association colloid systems, the so-called middle soap phase has a two-dimensional hexagonal structure. This was proposed already by McBain and Marsden [1] in the cases of dodecylsulphonic acid and triethanolamine laurate. These authors concluded that the phase in question consists of long fibres, rods or ribbons that are arranged in a hexagonal network with water occluded between the fibres. Luzzati and co-workers [2] have recently established that association colloids of different types including the salts of higher fatty acids (C_{12}—C_{18}) form middle soaps with a two-dimensional hexagonal structure and were able to present detailed information about the inner structure and unit dimensions of the phases.

We have studied the middle soap formation by a fatty acid soap with a shorter chain, sodium caprylate (C_8) [3-4]. A liquid-crystalline phase separates at 20°C from aqueous solutions of this soap when the concentration exceeds 40.5 %. Between 46.0 and 51.5 % sodium caprylate this mesomorphous phase is homogeneous. The phase is both macroscopically (it is a transparent, rigid "gel") and microscopically (it has a fanlike and angular texture: 222.5 and 226.1 in Rosevear's system [5]) similar to the middle soaps of some higher fatty acid soaps and its X-ray diffraction pattern reveals a hexagonal structure. We therefore felt justified in drawing the conclusion that the middle soap of sodium caprylate has a inner structure resembling the structure of the middle soaps of the higher soaps. Subsequent X-ray studies have confirmed this conclusion. We have recorded for the middle soap of sodium caprylate, besides a weak diffuse reflection at the position $s = 1/4.5$ Å^{-1} ($s = 2 \sin \Theta/\lambda$), as many as three sharp reflections with Bragg spacings of 25.9, 15.0, and 13.0 Å in the central part of the X-ray diffraction pattern. The positions of these lines do not vary over

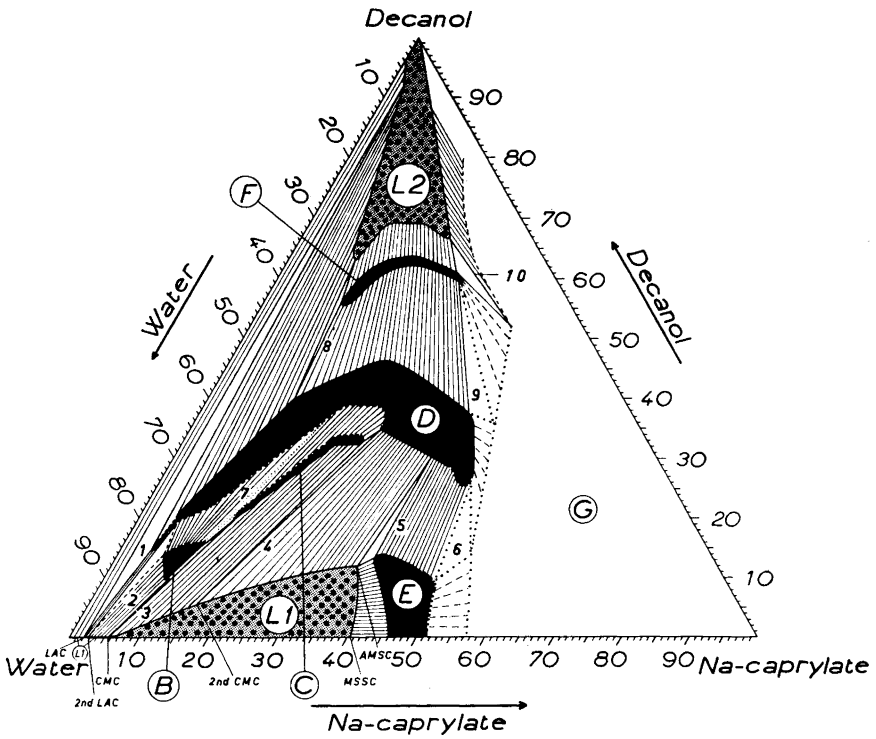

Fig. 1. Phase diagram for the three-component system sodium caprylate-decanol-water at 20°C.(Ekwall, Danielsson and Mandell). L 1 isotropic aqueous solutions, L 2 isotropic decanol solutions, B—F homogeneous mesomorphous phases, 1—10 three-phase triangles, G systems with a fiber structure, not included in this study.

the homogeneous middle soap region. The ratios of the Bragg spacings are $1:1/\sqrt{3}:1/\sqrt{4}$, which is the condition for a two-dimensional hexagonal arrangement of particles. If the planes are given the indices $10\bar{1}0$, $11\bar{2}0$ and $20\bar{2}0$, this means that the unit cell dimension of the two-dimensional hexagonal cell is about 30 Å. X-Ray diffraction photographs which exhibit a hexagonal symmetry of the type seen in Fig. 5 in Ref.[3] are sometimes obtained. The observations thus lead to the conclusion that the middle soap of sodium caprylate has the same structure as that of the higher soaps with parallel hexagonally oriented cylindrical aggregates which in turn are composed of radially oriented caprylate ions with the hydrocarbon chains pointing inwards and the carboxyl groups outwards into the water that separates the cylinders. The conditions within the cylindrical aggregates formed by the paraffin chains are, as Luzzati has shown, similar to those in liquid hydrocarbons, whereas the aggregates themselves are ordered to such an extent that they give rise to "crystalline" X-ray reflections.

Our previous studies did not, however, relate only to the two-component system sodium caprylate-water, but also and primarily to the three-component system sodium caprylate-decanol-water, which has served as a model for a large group of three-component systems composed of an association colloid, an amphiphilic compound with dominating lipophilic character, and water. The triangular diagram in Fig. 1 shows the phase equilibria of the

Table 1. Bragg spacing values for the three innermost "crystalline" lines of the phases E, D and F.

	NaCy %	Decanol %	H_2O %	d_1 Å	d_2 Å	d_3 Å
Phase E	46	—	54	25.9	15.1	13.0
	47	—	53	25.9	15.0	13.0
	49	—	51	26.0	14.9	12.9
	50	—	50	25.9	14.9	—
	43.9	4.3	51.8	27.6	15.9	13.7
	41.0	7.7	51.3	30.1	17.4	15.1
	39.8	9.1	51.1	31.1	18.0	15.4
	38.2	13.8	48.0	31.3	18.4	15.9
	37.9	14.1	48.0	32.3	18.7	15.9
	47.0	4.0	49.0	27.8	15.9	14.2
	45.9	6.1	48.0	28.8	16.7	14.7
Phase D	40.2	34.7	25.1	30.4	14.9	9.9
	31.9	41.8	26.3	31.2	15.5	10.3
	33.9	38.0	28.1	30.4	15.1	—
	19.6	45.2	35.2	35.6	17.7	—
	19.0	43.8	37.2	36.4	18.2	—
	16.9	39.7	43.4	40.3	19.8	—
	16.5	37.6	45.9	41.7	20.6	—
	12.0	32.9	55.1	52.0	25.9	—
	7.0	20.0	73.0	84.9	42.2	—
Phase F	11.3	55.7	33.0	40.3	23.3	19.8
	11.4	57.2	31.4	39.6	22.9	19.8
	13.0	57.0	30.0	37.3	21.4	18.7
	12.8	60.1	27.1	35.3	20.1	17.7
	15.2	62.5	22.3	31.4	18.0	15.5
	16.0	63.4	20.6	31.4	17.9	15.5
	16.5	61.4	22.1	31.0	18.1	15.4

system mentioned at 20°C. That reversible thermodynamic equilibria are actually involved is shown by, among other things, the fact that a certain mixture of sodium caprylate, decanol and water gives rise to the same phases with identical properties and compositions irrespective of the mode of preparation and previous history of the mixture. The diagram reveals the existence of a number of homogeneous phases separated by two- and three-phase regions, including two regions L 1 and L 2 of isotropic solutions and several regions (B—F) where a homogeneous mesomorphous phase exists.

The above-mentioned middle soap region of the caprylate-water system lies in the diagram on the base line of the triangle between the caprylate concentrations 46.0 and 51.5 %. On adding decanol this middle soap region expands so that it covers the whole of the region marked by E. In this region the mesomorphous substance has an unchanged macro- and microscopic character and gives X-ray diffraction pictures of similar appearance. The wiew we have presented previously that the mesomorphous substance existing in the region E has the same structure as the decanol-free caprylate-water middle soap has been confirmed by continued X-ray studies; over the whole of the region E X-ray diffraction lines are obtained whose Bragg spacings satisfy the two-dimensional hexagonal ratio (Table 1). The unit cell dimension of the two-dimensional cell increases more or less linearly with the decanol content. The experimental data are consistent with the assumption that the decanol molecules are incorporated within the caprylate cylinders of the

middle soap, the hydrocarbon chains pointing inwards and the hydroxyl groups outwards into the water.

In the upper part of the triangular diagram there is a long and narrow horizontal homogeneous single-phase region where a mesomorphous phase designated F exists. Already previously we have pointed out the close resemblance both in the macro- and microscopic respect between phases F and E (transparent, rigid "gel" with a fanlike and angular texture, 222.5 and 222.6 in Rosevear's system) and in the appearance of their X-ray diffraction pictures. Also in this case we have obtained X-ray diffraction photographs exhibiting hexagonal symmetry. We have found that also the phase F gives rise to a diffuse reflection at $s = 1/4.5$ Å^{-1} and, in the central part of the X-ray diffraction picture, to sharp reflections whose Bragg spacings are in the ratio $1:1/\sqrt{3}:1/\sqrt{4}$ (Table 1). The unit cell dimension of the two-dimensional hexagonal cell in this case increases linearly with the mole ratio of water to sodium caprylate, but is relatively independent of the decanol content. The experimental data are in agreement with a structure consisting of parallel, hexagonally oriented, densely packed aggregates of cylinders with a water-filled core surrounded by radially arranged caprylate ions and decanol molecules, the carboxyl and hydroxyl groups of the latter pointing inwards into the water and the hydrocarbon chains outwards. The diffuse reflection at $s = 1/4.5$ Å^{-1} shows that the hydrocarbon regions surrounding the water cylinders are liquid-like.

In the middle of the triangular diagram between E and F there is a relatively wide region designated D consisting of a homogeneous mesomorphous phase that differs completely from the two phases E and F in its macro- and microscopic properties. This phase is more mucous than the other two phases and exhibits a mosaic and planar texture as well as spherical positive units (122.1, 122.3, 121.1 and 113.1 in Rosevear's system). Also its X-ray diffraction picture differs clearly from the pictures of the phases E and F. There is the diffuse reflection at 1/4.5 Å^{-1} as well as a strong and two weaker reflections in the central part of the diffraction picture whose interplanar spacings are in the ratio 1:2:3 (Table 1). In many cases an orientation perpendicular to the axis of the capillary tube containing the sample was observed. As long as the mole ratio of decanol to caprylate does not exceed a value of about two, the water content of the phase is relatively low (does not exceed about 40 %) and the values of the interplanar spacings remain relatively unaltered. At higher mole ratios, however, the water content may increase greatly (up to 75–80 %) without any marked change in the nature of the phase. The value of the interplanar spacing then increases linearly with the mole ratio of water to the sum of sodium caprylate and decanol (Table 1). This phase hence exhibits a layer structure consisting of double layers of caprylate ions and decanol molecules separated by water layers into which the hydrophilic groups project. The hydrocarbon region of the double layer is also in this case "liquid"; the thickness of the double layer varies only slightly, but the thickness of the water layer varies greatly in samples in which the mole ratio of decanol to caprylate is higher than two.

Hence in the three-component system investigated there exist two different regions of hexagonal mesomorphous phases, E and F, separated from each other by a region where there exists a mesomorphous phase D with a layer structure. It is of interest that the regions of existence for the hexagonal phases under the conditions studied are limited to certain mole ratios of decanol to caprylate. Thus we have not found that the phase E contains more than one mole of decanol to about three moles of caprylate at 20°. Neither have we found the phase F to contain less decanol than two moles of decanol to about one mole of caprylate. At least when the former ratio is exceeded (phase E) or the decanol content decreases below the latter ratio (phase F), a two-phase region exists, within which the system is divided into two separate phases, one of which is the hexagonal phase, the other the phase D with its layer structure. These two-phase regions between E and D and between F and D are quite wide as seen in Fig. 1. The tie lines in them show the distribution of the phases. The composition of phase D varies between much wider limits than the compositions of the other two phases; if, however, we consider only those parts of the system where phase D is in equilibrium with both hexagonal phases we have a variation of the mole ratio of decanol to caprylate from 10:3 (max.) to 6:10 (min.). It may be appropriate to stress further the fact that the two hexagonal phases are never in direct equilibrium with each other, but only with the intermediate layer phase.

Our investigation has revealed that the hydrocarbon regions in all three mesomorphous phases are "liquid". Therefore it is probably not the exchange of the paraffin hydrocarbon chain of the caprylate for that of the decanol that causes the hexagonal structure of phase E to be replaced by the layer structure of phase D and that this again is replaced by

the hexagonal structure of phase F, when, with the pure caprylate middle soap as a starting point, the decanol content of the system is increased at the expense of its caprylate and water concentration. It is more likely that the reason is a change in the layer of hydrophilic groups at the interfaces between the hydrocarbon and water regions. Whereas the negative carboxyl groups of the caprylate ions repel each other, hydrogen bonds are formed between the hydroxyl groups of the decanol molecules and the oxygen atoms of the carboxyl groups. The incorporation of hydroxyl groups of decanol molecules between the ionized carboxyl groups of caprylate may thus lead to a denser packing in the layer of hydrophilic groups. Calculations reveal that this is actually the case but that in the region of a homogeneous mesomorphous phase the density of the packing varies between rather narrow limits. The differences in the packing between the different phases are, however, quite large. The area per polar group is much smaller in phase D than in phase E and again much smaller in phase F than in phase D. The existence of the various mesomorphous phases hence seems to be determined by the density of the packing of the end groups which in each case cannot deviate greatly from a certain characteristic value.

Acknowledgements. One of the authors, K.F., is indebted to Prof. Rolf Hosemann and Dr Richard Bonart, Fritz Haber-Institut der Max Planck Gesellschaft, Berlin, for valuable discussions.

1. Marsden, S. S., Jr. and McBain, J. W. *J. Am. Chem. Soc.* **70** (1948) 1973.
2. Luzzati, V., Mustacchi, H. and Skoulios, A. *Nature* **180** (1957) 600; Discussions Faraday Soc. **25** (1958) 43; Luzzati, V., Mustacchi, H., Skoulios, A. and Husson, F. *Acta Cryst.* **13** (1960) 660; Husson, F., Mustacchi, H. and Luzzati, V. *Acta Cryst.* **13** (1960) 668.
3. Ekwall, P., Danielsson, I. and Mandell, L. *Kolloid-Z.* **169** (1960) 113.
4. Ekwall, P., Danielsson, I. and Mandell, L. *3rd Intern. Conf. Surface Activity*, Vol. I, Section A, pp. 189 and 193, Cologne 1960; Ekwall, P., Danielsson, I., Fontell, K. and Mandell, L. *Finska Kemistsamfundets Medd.* **70** (1961) 51.
5. Rosevear, F. B. *J. Am. Oil Chemist's Soc.* **12** (1954) 628.

Received September 29, 1962.

The Biosynthesis of Gentisic Acid

S. GATENBECK and I. LÖNNROTH

Institute of Biochemistry, University of Lund, Lund, Sweden

In the series of reactions leading to the formation of the antibiotic patulin in *Penicillium urticae*, 6-methylsalicylic acid occupies a key position. Some other products synthesized by the same organism are gentisalcohol, gentisaldehyde and gentisic acid [1]. The acetate origins of 6-methylsalicylic acid [2] and patulin [3] are well established, and furthermore, good evidence has been obtained for the biological transformation of 6-methylsalicylic acid to patulin [4]. These results are consistent with Birkinshaws' suggestion [5] that patulin is formed by a ring-opening process of gentisaldehyde. However, the acetate origin of gentisaldehyde or gentisic acid has never been confirmed. On the contrary, indications have been obtained that gentisic acid is formed along other pathways, presumably *via* shikimic acid.

In this communication results will be presented which clearly show that gentisic acid is derived from acetate in *P. urticae*. In a preliminary experiment acetate-2-^{14}C was given to a growing culture and 6-methylsalicylic acid and gentisic acid were isolated from the culture medium. The specific radioactivity of 6-methylsalicylic acid was found to be six times that of gentisic acid which could be explained by a larger nonlabelled pool of gentisic acid at the moment the labelled substrate was added. Decarboxylation of gentisic acid showed that the carboxyl group contained 25 % of the total radioactivity, indicating the acetate origin of gentisic acid and supporting the hypothesis that it is formed by oxidation and decarboxylation of 6-methylsalicylic acid. This hypothesis if further emphasized by time aspect studies of the production of the two substances as the amount of 6-methylsalicylic acid is reaching a maximum before that of gentisic acid.

A more extensive degradation of gentisic acid labelled from acetate-1-^{14}C was performed to confirm the alternate labelling of the ring. After tosylating the gentisic acid in 5-position, the toluenesulphonic acid group was removed by refluxing with Raney nickel in alcohol according to the method of Kenner and Murray [6]. Nitration of the formed salicylic acid yielded picric acid which was further degraded with ba-

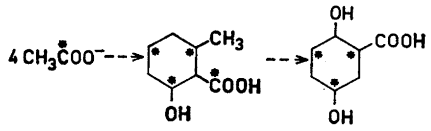

Fig. 1.

rium hypobromite to bromopicrin and carbon dioxide. Of the total radioactivity of gentisic acid 93.5 % were found in the bromopicrin and 2.8 % in the carbon dioxide (Table 1). These values show that the labelled positions in gentisic acid are those expected when formed from 6-methylsalicylic acid (Fig. 1).

The production of gentisic acid in nature is not restricted to *P. urticae* but has been found in many other organisms as well, e.g. *Polyporus tumulosus* [7]. This organism produces along with gentisic acid *p*-hydroxyphenylacetic acid, 3,4-dihydroxyphenylacetic acid, 2,5-dihydroxyphenylglyoxylic acid and some other acids. As these types of aromatic acids are known to be derived from shikimic acid *via* phenylpyruvic acid, it is possible that gentisic acid in *P. tumulosus* is not formed from acetate but, e.g., by an oxidative decarboxylation of 2,5-dihydroxyphenylglyoxylic acid.

Table 1.

Substance	Cpm/mmole
Gentisic acid	13.85×10^3
Bromopicrin (C1, C3, C4 in gentisic acid)	12.92×10^3
Carbon dioxide (C2, C4, C6 in gentisic acid)	0.39×10^3

Experimental

Culture conditions. Penicillium urticae Bainier was incubated as shake culture at 27°C in Czapek Dox medium. When the production of the phenolic substances had started labelled tracer substrates (0.5 mC acetate-2-^{14}C and 0.5 mC acetate-1-^{14}C) were added to separate cultures in 500 ml Erlenmeyer flasks containing 150 ml of medium, and the cultures were harvested after another two days incubation.

Isolation of gentisic acid and 6-methylsalicylic acid. The culture filtrates were acidified and extracted with ether. The residues of the ether extracts were separated on paper chromatograms (Whatman 3 MM) with ethylmethylketone-water-diethylamine (921:77:2) as the solvent and gentisic acid (R_F 0.36) and 6-methylsalicylic acid (R_F 0.62) eluted from the paper with acetone. After sublimation of the two substances their specific radioactivities were determined in a liquid scintillation counter using internal standard.

Degradation of gentisic acid. The radioactive gentisic acid was recrystallized with nonlabelled carrier from acetone-ligroin to constant specific radioactivity. A part of the sample derived from acetate-2-^{14}C was oxidized to carbon dioxide by wet combustion and the remaining portion decarboxylated by refluxing with aqueous ferri chloride. 105 mg of the labelled gentisic acid obtained from acetate-1-^{14}C was treated with an equivalent amount of *p*-toluenesulphonyl chloride in 3 ml of 1 N sodium hydroxide at room temperature until a clear solution was obtained. Acidification with concentrated hydrochloric acid gave a precipitate that was filtered off, washed with water and recrystallized from benzene. Yield 88.5 mg, m.p. 169°C. The formed tosylderivative was refluxed for 3 h in an alcoholic solution with a large excess of Raney nickel. The reaction mixture was made acidic and the catalyst sucked off and thoroughly washed with ethanol. Evaporation of the filtrate to dryness and subsequent sublimation of the residue yielded a substance that proved to be identic with salicylic acid (18.5 mg, m.p. 159°C). The radioactive salicylic acid was recrystallized from water with 150 mg of nonlabelled carrier and 130 mg of the dry substance heated with 0.5 ml of nitric acid (*d* 1.52) to dryness on the steam bath. The procedure was repeated with the same amount of nitric acid. Extraction of the dry residue with benzene and evaporation of the solvent gave picric acid which was recrystallized from water (130 mg, m.p. 122°C). The degradation of picric acid with barium hypobromite to bromopicrin and carbon dioxide and the subsequent combustion of the bromopicrin has been described elsewhere [8].

Measurements of radioactivity. All measurements of the radioactivities in the degradation series were performed in a liquid scintillation counter with the samples as barium carbonate suspended in a gel of Aerosil in a toluene solution of 2,5-diphenyloxazol.

1. Ehrensvärd, G. *Exptl. Cell Research Suppl.* **3** (1955) 102.
2. Birch, A. J., Massey-Westropp, R. A. and Moye, C. J. *Australian J. Chem.* **8** (1955) 539.
3. Bu'Lock, J. D. and Ryan, A. J. *Proc. Chem. Soc.* **1958** 222.
4. Bassett, E. W. and Tanenbaum, S. W. *Biochim. Biophys. Acta* **40** (1960) 535.
5. Birkinshaw, J. H. *Ann. Rev. Biochem.* **22** (1953) 371.
6. Kenner, G. W. and Murray, M. A. *J. Chem. Soc. Suppl.* **1949** 178.
7. Crowden, R. K. and Ralph, B. J. *Australian J. Chem.* **14** (1961) 475.
8. Gatenbeck, S. *Acta Chem. Scand.* **12** (1958) 1985.

Received October 29, 1962.

Chloride Complexes of Tervalent Americium

INGMAR GRENTHE

Department of Inorganic and Physical Chemistry, Chemical Institute, University of Lund, Lund, Sweden

The behaviour of various actinides in hydrochloric acid solution has been the subject of several investigations *e.g.* [1-4]. In this study the stability constants of the americium(III) complexes present in a perchloric-hydrochloric acid medium with an acidity and ionic strength of 4 M were determined. The complexes were studied by the cation exchange method developed by Fronæus [5] with the ion exchanger (Dowex 50 W × 8, 50–100 mesh) in the hydrogen form. The experimental procedure was as follows:

0.100 ml of an americium(III)-stock solution was added to 5.00 ml of solutions of the composition:

$$C_{HCl} = a \text{ M}$$
$$C_{HClO_4} = 4.00 - a \text{ M}$$

The solution was then equilibrated with 250 mg ion exchanger in a thermostat at a temperature of 20°C. The americium concentration was determined radiometrically before and after equilibrium and from these data the distribution coefficient φ was computed. At each ligand concentration the distribution coefficient was determined at different values of the total americium concentration. In no case did the distribution coefficient vary with the americium concentration; the ion exchanger is thus monofunctional in the concentration range used here. The reproducibility of the measurements was within ± 2 %.

The φ-values and the functions necessary for the computation of the stability constants are given in Table 1. The notation and the method of calculation is described in an earlier communication [6]. From the experimental data given in the table it is possible to determine the stability constants of two complexes $AmCl^{2+}$ and $AmCl_2^+$. The following values were obtained:

$$\beta_1 = 0.69 \pm 0.03 \text{ M}^{-1}$$
$$\beta_2 = 0.18 \pm 0.04 \text{ M}^{-2}$$

The value of β_1 is in good agreement with previously determined values (*e.g.* Ref.[3]). No value of β_2 has so far appeared in the literature.

Table 1. Corresponding values of $[Cl^-]$, φ, φ_1, f and β_1 for the americium chloride system.

$[Cl^-]$ mM	$\varphi \times 10^3$ l. g^{-1}	φ_1 M^{-1}	f M^{-2}	β_1 M^{-1}
0	42.5	*0.66*	*0.275*	
100	39.6	0.73		
300	35.0	0.71	0.289	
500	31.0	0.74	0.324	
750	27.0	0.77	0.364	
1000	23.5	0.81	0.385	0.73
1250	20.6	0.85	0.409	0.71
1750	16.1	0.94	0.460	0.66
2000	14.3	0.99	0.488	0.65
2500	11.8	1.04	0.534	0.68
3000	10.0	1.08	0.574	0.71
3500	8.1	1.21	0.642	0.67

1. Street, Jr., K. and Seaborg, G. T. *J. Am. Chem. Soc.* **72** (1950) 2790.
2. Diamond, R. M., Street, Jr., K. and Seaborg, G. T. *Ibid.* **76** (1954) 1461.
3. Ward, M. and Welch, G. A. *J. Inorg. Nucl. Chem.* **2** (1956) 295.
4. Choppin, G. R. and Chatham-Strode, A. *Ibid.* **15** (1960) 377.
5. Fronæus, S. *Svensk Kem. Tidskr.* **65** (1953) 19.
6. Grenthe, I. *Acta Chem. Scand.* **16** (1962) 1695.

Received October 15, 1962.

Organic Syntheses with Heavy Isotopes

Attempted Synthesis of Perdeuterio-Behenic Acid

NGUYÊN DINH-NGUYÊN

Institute of Medical Biochemistry, University of Göteborg, Sweden

With the intention to compare the phase transitions in monomolecular films of behenic acid [1] with those of its heavy isotopic analogue, a synthesis of perdeuterio-behenic acid has been attempted. It was performed with only classical chemical reactions. The main difficulty has been to avoid loss of deuterium in the various steps of the synthesis. It is quite evident that work of this type cannot be undertaken without mass spectrometric analysis of all intermediate products. The final product consists of a mixture of deuterio-behenic acids from $C_{22}H_{18}D_{26}O_2$ to $C_{22}H_1D_{43}O_2$, with $C_{22}H_7D_{37}O_2$ as the most abundant component. The end product together with the principal intermediate compounds and the mode of preparation are given in Chart 1.

Preparation of tetradeuterio-succinic acid (III) and some of its derivatives (II, IV) was executed according to the procedure of McLean and Adams [2]. Dideuterio-malonic acid-d_2 (XII) and trideuterio-acetic acid-d (XIII) were prepared according to the technique reported by Halford and Anderson [3].

Catalytic hydrogenation of dimethyl acetylene dicarboxylate (I) with pure deuterium using deuterium-reduced Adams' catalyst in dry ethyl acetate gave dimethyl deuterio-succinate (II). This was converted into deuterio-succinic acid (III) by hydrolysis with water containing a small amount of nitric acid. The acid was transformed to deuterio-succinic anhydride (IV) by means of acetic anhydride. Methyl hydrogen deuterio-succinate (V) was obtained by refluxing the anhydride with absolute methanol.

Kolbe's anodic condensation [4] has been a valuable method for the preparation of dimethyl deuterio-adipate (VI), dimethyl deuterio-sebacate (VIII), dimethyl deuterio-octadecane-1,18-dioate (X), methyl deuterio-caproate (XIV) and methyl deuterio-behenate (XVI). In electrolyses the monocarboxylic acids (XIII, XV) and/or half-esters of dicarboxylic acids (V, VII, IX, etc.) were previously totally neutralized with sodium methoxide, and the reaction conducted in methanolic solutions. For preparation of dimethyl deuterio-adipate (VI), the reaction may be carried out [5] with equivalent amounts of deuterio-succinic anhydride (IV) and sodium in methanol. The electrolyses were performed by using a cell previously described by the author [6], where mercury is employed as the cathode and a rotating platinum sheet as the anode. During the reaction the temperature was not allowed to exceed 50°.

In the alkaline hydrolysis, the temperature was rigorously controlled. It was observed that when dimethyl deuterio-adipate (VI) was submitted to a partial hydrolysis with $NaOCH_3$ at 80°, a half-ester was obtained which had a density lower than that of a specimen obtained from hydrolysis with KOH at 40°. Infrared and mass spectrometric analyses showed that these half-esters differed in deuterium content. In the hydrolysis at 80° a partial replacement of deuterium by hydrogen evidently took place.

The melting points, densities and refractive indices of the deuterium-containing compounds were determined and compared with those of their light hydrogen analogues. With the exception of the anhydride, it was noted that under the same conditions the deuterium-containing compounds

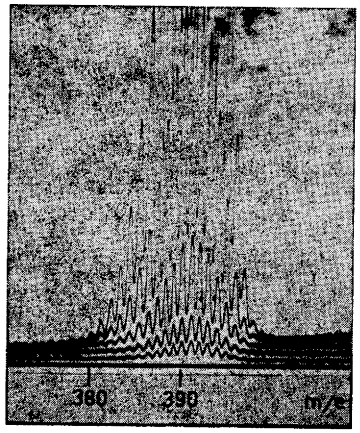

Fig. 1. The high-mass end of mass spectrum of methyl deuterio-behenate.

Chart 1.

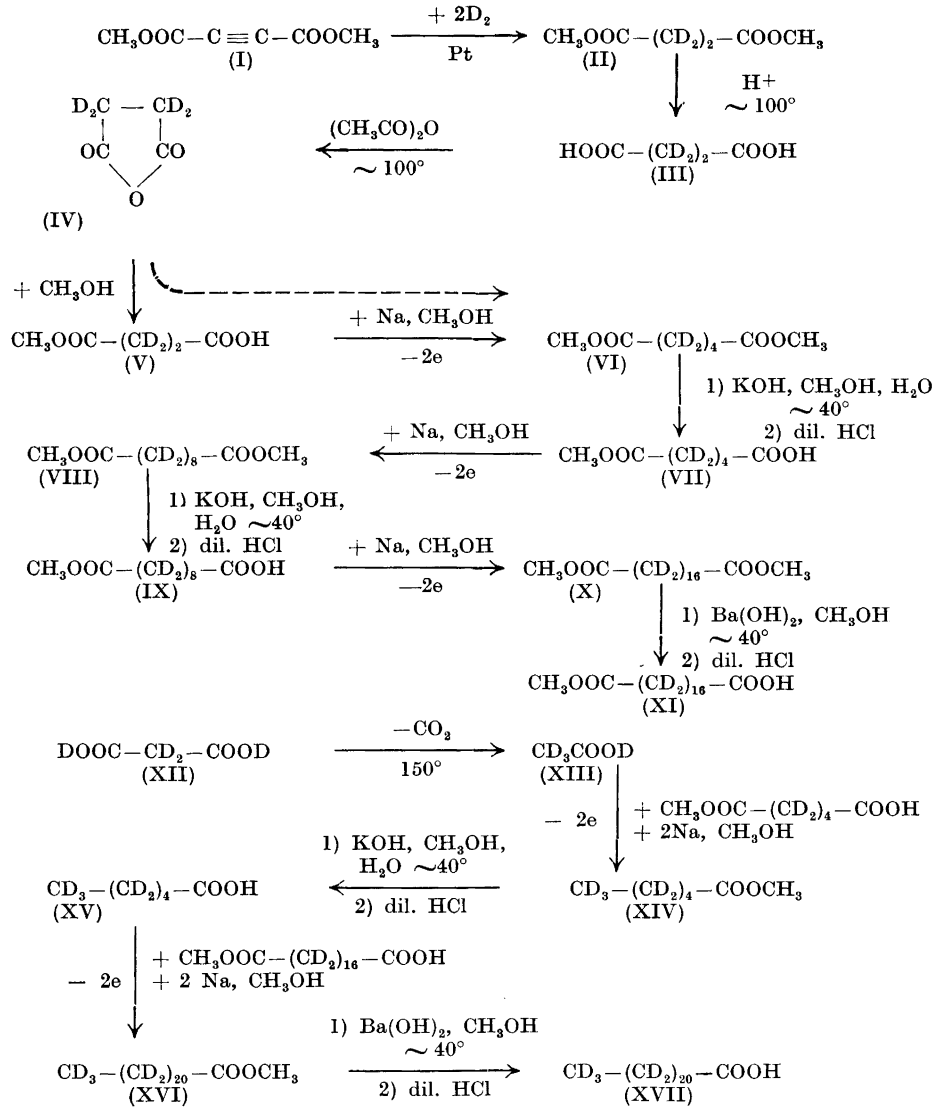

generally have lower melting points [2,3,7] and lower refractive indices than the light hydrogen analogues, but the latter have lower densities [2].

Infrared spectrometric analyses of these deuterium compounds have been performed and the results will be the subject of a separate communication.

With the exception of the dideuteriomalonic acid-d_2 (XII), all deuterium compounds were submitted to mass spectrometric analysis. Spectra of these products were compared with those of the light hydrogen analogues, which have been published by Ryhage and Stenhagen [8], and from that comparison the deuterium content of each product has been qualitatively determined. The high-mass end of the mass spectrum of the methyl deuterio-behenate reproduced in Fig. 1 shows a series of molecule-ion peaks from *m/e* 380 to *m/e* 397, corresponding to a series of esters of varying deuterium content from $C_{23}H_{20}D_{26}O_2$ to $C_{23}H_3D_{43}O_2$. The prominent peak at *m/e* 391 corresponds to the highest concentration of methyl heptatriadeuteriobehenate ($C_{23}H_9D_{37}O_2$) in the synthesized product. It is evident from Fig. 1 that molecules of mass 397, corresponding to the methyl perdeuterio-behenate (XVI), have been present, because the peak at *m/e* 397 is higher than that expected for the ^{13}C isotope peak of *m/e* 396.

Full details will be published later.

This work has been carried out with the aid of grants from *The Swedish Natural Science Research Council* to Dr. Stina Ställberg-Stenhagen. Thanks are due to Prof. Einar Stenhagen for his kind suggestions and for the time he has given to discussion. The author is indebted to Dr. Ragnar Ryhage for the mass spectrometric analysis.

1. Ställberg-Stenhagen, S. and Stenhagen, E. *Nature* **156** (1945) 239; **159** (1947) 814.
2. McLean, A. and Adams, R. *J. Am. Chem. Soc.* **58** (1936) 804.
3. Halford, J. O. and Anderson, L. *J. Am. Chem. Soc.* **58** (1936) 736.
4. See reviews: (*a*) Weedon, B. C. L. in *Advan. Org. Chem.* **1** (1960) 1; *Quart. Rev. London* **6** (1952) 380. (*b*) Svadkovskaya, G. E. and Voitkevich, S. A. *Russ. Chem. Rev.* **29** (1960) 161.
5. Bouveault, L. *Bull. soc. chim. France* **29** (1903) 1038.
6. Dinh-Nguyên, Ng. *Acta Chem. Scand.* **12** (1958) 585.
7. Wilson, C. L. *J. Chem. Soc.* **1935** 492.
8. Ryhage, R. and Stenhagen, E. *Arkiv Kemi* **13** (1959) 523; **14** (1959) 497.

Received October 16, 1962.

Isolation of 3-Hydroxy-1-(4-hydroxy-3-methoxyphenyl)-2-propanone from Lignin

KNUT LUNDQUIST

Institutionen för organisk kemi, Chalmers Tekniska Högskola, Göteborg, Sweden

According to the work of Hibbert [1], a series of guaiacylpropanones (III a–d) is formed from softwood lignin on heating with ethanolic hydrochloric acid for 48 h ("ethanolysis"). It was suggested [1] that these products originated from a structure of type II (3-hydroxy-1-(4-hydroxy-3-methoxyphenyl)-2-propanone) or its enol form ("β-oxyconiferyl alcohol") assumed to be part of the lignin molecule. Later, it was proposed [2,3] that the ketones III originate from arylglycerol-β-aryl ether structures (I), the ketol II being an intermediate in the ethanolysis process rather than a genuine structural element of lignin. This view was supported by the finding that ethanolysis of model compounds of type I yielded "Hibbert ketones" (III a, c, d); similarly, ketones III c, d and e were obtained on "acidolysis" (heating with 0.2 N HCl in dioxane-water (9:1)) of lignin as well as of the model compounds of type I [3].

In order to obtain further evidence for the presence of structure I in lignin and of

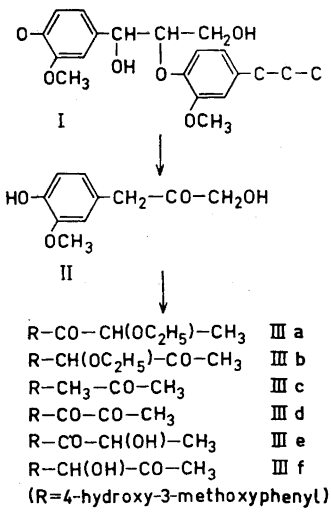

With the exception of the dideuteriomalonic acid-d_2 (XII), all deuterium compounds were submitted to mass spectrometric analysis. Spectra of these products were compared with those of the light hydrogen analogues, which have been published by Ryhage and Stenhagen [8], and from that comparison the deuterium content of each product has been qualitatively determined. The high-mass end of the mass spectrum of the methyl deuterio-behenate reproduced in Fig. 1 shows a series of molecule-ion peaks from *m/e* 380 to *m/e* 397, corresponding to a series of esters of varying deuterium content from $C_{23}H_{20}D_{26}O_2$ to $C_{23}H_3D_{43}O_2$. The prominent peak at *m/e* 391 corresponds to the highest concentration of methyl heptatriadeuteriobehenate ($C_{23}H_9D_{37}O_2$) in the synthesized product. It is evident from Fig. 1 that molecules of mass 397, corresponding to the methyl perdeuterio-behenate (XVI), have been present, because the peak at *m/e* 397 is higher than that expected for the ^{13}C isotope peak of *m/e* 396.

Full details will be published later.

This work has been carried out with the aid of grants from *The Swedish Natural Science Research Council* to Dr. Stina Ställberg-Stenhagen. Thanks are due to Prof. Einar Stenhagen for his kind suggestions and for the time he has given to discussion. The author is indebted to Dr. Ragnar Ryhage for the mass spectrometric analysis.

1. Ställberg-Stenhagen, S. and Stenhagen, E. *Nature* **156** (1945) 239; **159** (1947) 814.
2. McLean, A. and Adams, R. *J. Am. Chem. Soc.* **58** (1936) 804.
3. Halford, J. O. and Anderson, L. *J. Am. Chem. Soc.* **58** (1936) 736.
4. See reviews: (*a*) Weedon, B. C. L. in *Advan. Org. Chem.* **1** (1960) 1; *Quart. Rev. London* **6** (1952) 380. (*b*) Svadkovskaya, G. E. and Voitkevich, S. A. *Russ. Chem. Rev.* **29** (1960) 161.
5. Bouveault, L. *Bull. soc. chim. France* **29** (1903) 1038.
6. Dinh-Nguyên, Ng. *Acta Chem. Scand.* **12** (1958) 585.
7. Wilson, C. L. *J. Chem. Soc.* **1935** 492.
8. Ryhage, R. and Stenhagen, E. *Arkiv Kemi* **13** (1959) 523; **14** (1959) 497.

Received October 16, 1962.

Isolation of 3-Hydroxy-1-(4-hydroxy-3-methoxyphenyl)-2-propanone from Lignin

KNUT LUNDQUIST

Institutionen för organisk kemi, Chalmers Tekniska Högskola, Göteborg, Sweden

According to the work of Hibbert [1], a series of guaiacylpropanones (III a–d) is formed from softwood lignin on heating with ethanolic hydrochloric acid for 48 h ("ethanolysis"). It was suggested [1] that these products originated from a structure of type II (3-hydroxy-1-(4-hydroxy-3-methoxyphenyl)-2-propanone) or its enol form ("β-oxyconiferyl alcohol") assumed to be part of the lignin molecule. Later, it was proposed [2,3] that the ketones III originate from arylglycerol-β-aryl ether structures (I), the ketol II being an intermediate in the ethanolysis process rather than a genuine structural element of lignin. This view was supported by the finding that ethanolysis of model compounds of type I yielded "Hibbert ketones" (III a, c, d); similarly, ketones III c, d and e were obtained on "acidolysis" (heating with 0.2 N HCl in dioxane-water (9:1)) of lignin as well as of the model compounds of type I [3].

In order to obtain further evidence for the presence of structure I in lignin and of

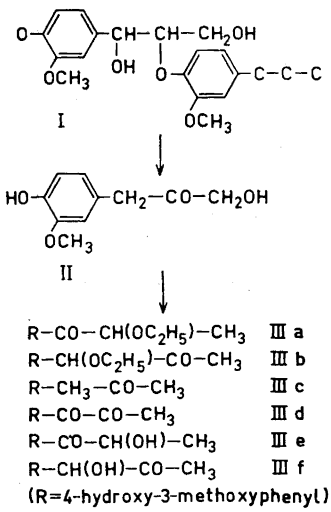

its role as a precursor of the Hibbert ketones, it was desirable to isolate the predicted intermediate II. Its formation as an intermediate in the acidolysis of model substances for structure I, *viz.*, guaiacyl glycerol and its β-guaiacyl ether, has recently been demonstrated in this laboratory [4].

It has now been possible to isolate II from the ether-soluble fraction (A) of the reaction products obtained on similar "acidolysis" (4 h) of spruce Björkman lignin. The presence of II in fraction A was demonstrated by paper chromatography (upper layer of a ligroin-water-chloroform-methanol 7:5:2:1 mixture [5], red-violet spot with diazotized sulfanilic acid, R_F 0.04) and by thin-layer chromatography on silica gel (benzene-acetone 4:1, spot with iodine vapour, R_F 0.16). The isolation of II was accomplished by chromatography on a silica gel column, benzene-acetone 9:1 being used as an eluent. The effluent fractions, which on examination by thin layer chromatography gave only one spot with R_F 0.16, were collected and yielded an oil (yield, 7 % of the lignin used). The infra-red spectrum of the oil was identical with that of synthetic II [6]. After distillation the product crystallized, m.p. 81—82°(lit.[6] 81—82°), no depression on admixture with authentic II.

Paper chromatography of the effluent fractions not containing II revealed the presence of vanillin, coniferyl aldehyde, α-hydroxypropioguaiacone (III e) and other unidentified constituents. In addition, small amounts of a phenolic ketone were isolated, which gave a blue colour reaction with 2,6-dibromo-N-chloroquinonimine (characteristic of *p*-hydroxybenzyl alcohols [7]), and an orange colour with diazotized sulfanilic acid. Its infra-red spectrum was very similar to that of guaiacylacetone (III c) between 1000—5000 cm^{-1} but showed an additional band at 1080 cm^{-1} (sec. alcohol). The substance was presumed to be 1-hydroxy-1-(4-hydroxy-3-methoxyphenyl)-2-propanone (III f). While experiments regarding the structure of this acidolysis product were in progress, Gardner [8] published the synthesis of III f. The colour reactions and infra-red data reported for the synthetic sample are consistent with those of our product. Further work on the identification of the latter will be published later.

The results reported above constitute further experimental evidence for the presence of structural elements of type I in lignin [2,3,9,10] and for the mechanism of their acidolytic degradation proposed earlier [3,4a].

Acknowledgement. The author is very indebted to professor E. Adler for his kind interest in this work.

1. *Cf.* Brauns, F. E. *The Chemistry of Lignin*, Academic Press, New York 1952, p. 465—482.
2. Adler, E. and Lindgren, B. O. *Svensk Papperstidn.* **55** (1952) 563.
3. Adler, E., Pepper, J. M. and Eriksoo, E. *Ind. Eng. Chem.* **49** (1957) 1391.
4. (*a*) Adler, E. *Paper and Timber (Finland)* **43** (1961) 634. (*b*) Lundgren, R. *Ibid.*, *p.* 670.
5. Kratzl, K. and Schweers, W. *Monatsh.* **85** (1954) 1046.
6. Fisher, H. E. and Hibbert, H. *J. Am. Chem. Soc.* **69** (1947) 1208.
7. Ziegler, E. and Gartler, K. *Monatsh.* **80** (1949) 759; Gierer, J. *Acta Chem. Scand.* **8** (1954) 1319; *Chem. Ber.* **80** (1956) 257.
8. Gardner, J. A. F., Henderson, D. W. and MacLean, H. *Can. J. Chem.* **40** (1962) 1672.
9. Freudenberg, K., Schlüter, H. and Eisenhut. W. *Naturwiss.* **41** (1954) 576; Freudenberg, K. *Paper and Timber (Finland)* **43** (1961) 630.
10. Kratzl, K., Kisser, W., Gratzl, J. and Silbernagel, H. *Monatsh.* **90** (1959) 771.

Received October 16, 1962.

Studies on Cobaltammines
VII. An Investigation of the Coordination Number of Outer-sphere Complexes

RAGNAR LARSSON

Department of Inorganic and Physical Chemistry, Chemical Institute, University of Lund, Lund, Sweden

The estimation of the number of coordination sites available for ligands, coordinated in the outer sphere of cobaltammines, is a difficult task. Most complex systems of this kind are so weak that it is not possible to reach the saturated complex in aqueous solution. In order to escape this difficulty an extraction technique has been employed.

The cobalthexammine(III) ion is easily extracted into cyclohexanone from aqueous solutions of sodium salicylate. This probably corresponds to the following reaction

$$MA_{6\,aq} + 3B_{aq} + nK_{aq} \rightleftharpoons [MA_6B_3K_n]_{org} \quad (1)$$

where $MA_6 = Co(NH_3)_6^{3+}$

B = salicylate ion
K = cyclohexanone

In order to determine n it is necessary to vary the concentration of K in the organic phase. As a diluent 2-octanol has been used. This solvent is a rather poor extracting agent in this case. The cobalt concentration in the two phases was determined radiometrically [1]. The organic solvents were the same as before [2] and the sodium salicylate was recrystallized from ethanol.

If $[MA_6B_3]_{org}$ is the concentration of the salicylato complex in the organic phase that does not contain any ketone (but probably water and octanol), we define the complexity constants of the ketone complexes in the organic phase as

$$\beta_{n\,org} = \frac{[MA_6B_3K_n]_{org}}{[MA_6B_3]_{org}\,[K]^n_{org}} \quad (2)$$

$$\text{Furthermore } D = \frac{[MA_6B_3]_{org}}{[MA_6B_3]_{aq}} \quad (3)$$

and $\varphi = C_{M\,org}/C_{M\,aq}$

We then have

$$\varphi = D \cdot \alpha_{3\,aq} \cdot (1 + \Sigma\beta_{n\,org}\,[K]^n_{org}) \quad (4)$$

where α_3 is the portion of the cobalt in the aqueous phase which exists as the third salicylato complex.

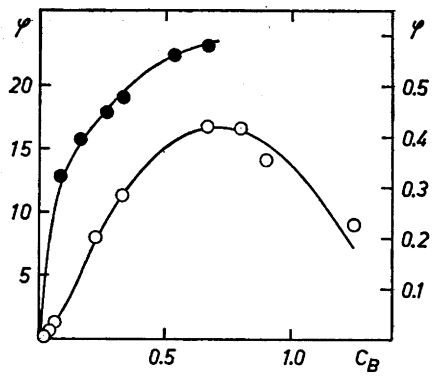

Fig. 1. The partition quotient φ as a function of the salicylate concentration in the aqueous phase.

○: $Co(NH_3)_6^{3+}$; C_K = 1.9 M; left ordinate scale.
●: $Co\,en_2(NCS)_2^+$; C_K = 1.0 M; right ordinate scale.

For constant $[B]_{aq}$, we obtain

$$\varphi = \varphi_o(1 + \Sigma\beta_{n\,org}\,[K]^n_{org} \quad (5)$$

From this equation $\beta_{n\,org}$ can be determined.

In order to determine a suitable [B], φ was determined at $[K]_{org}$ = 1.93 M (Fig. 1). (In all cases [B] and [K] were taken to be the respective total concentrations.) Obviously, the measurements should be performed at a value of [B] near the position of the maximum in Fig. 1, as φ is then not very dependent on [B]. In Fig. 2 measurements of φ are given for C_B = 0.67 M and 0.80 M. The linear rise of φ indicates the presence of only one ketonic complex; eqn. 5 gives $\beta_{1\,org} = 0.9 \pm 0.1\ M^{-1}$. φ deviates strongly from linearity at high values of $[K]_{org}$. This, as well as the drastic drop of φ in Fig. 1, may be caused by changes in activity coefficients as some cyclohexanone dissolves in the aqueous phase. A still more likely explanation, however, is to assume the existence of an anionic complex MA_6B_4 in the aqueous phase. This explains at once the decrease of φ in Fig. 1. Regarding the deviation from linearity in Fig. 2, it is illuminating that we obtain a greater deviation for a greater C_B. This must mean that the tendency towards the formation of an anionic complex is increased

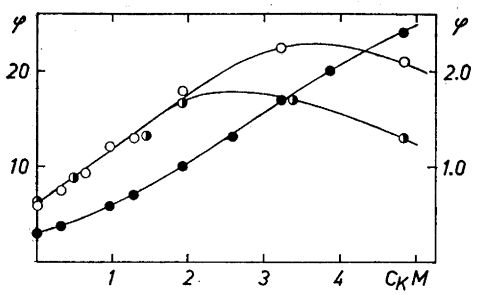

Fig. 2. The partition quotient φ as a function of the ketone concentration in the organic phase.

○: $Co(NH_3)_6^{3+}$; C_B = 0.67 M; left ordinate scale.
◐: $Co(NH_3)_6^{3+}$; C_B = 0.80 M; left ordinate scale.
●: Co $en_2(NCS)_2^+$; C_B = 0.67 M; right ordinate scale.

as some cyclohexanone dissolves in the aqueous phase (*cf.* Ref.[2], p. 709).

Analogous measurements were also performed by using the *trans*-Co $en_2(NCS)_2^+$ ion as the inert cobalt complex ion. Then the extracted species contains probably only one salicylate ion and more space should be available for the ketonic ligands. The cobalt concentration in the two phases was determined colorimetrically. The results are given in Figs. 1 and 2. C_B = 0.67 M was used for the measurements of Fig. 2. It is easily deduced that eqn. 5 should also apply here. In Fig. 3 $(\varphi/\varphi_o - 1)\,[K]^{-1}_{org}$ is plotted against $[K]_{org}$. The linearity indicates the presence of two complexes. $\beta_{1\,org}$ = (0.76 ± 0.05) M^{-1} and $\beta_{2\,org}$ = (0.24 ± 0.05) M^{-2}. Also here deviation from linearity occurs at high $[K]_{org}$.

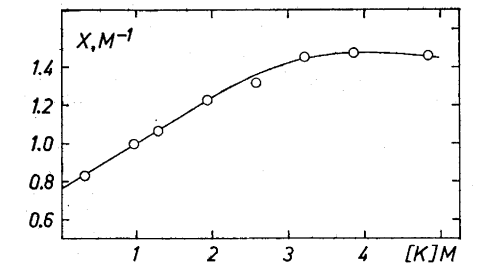

Fig. 3. $X_1 = (\varphi/\varphi_o - 1)\,[K]^{-1}_{org}$ plotted against $[K]_{org}$.

If we assume that each salicylate ion uses two coordination sites, which is likely but not quite certain, at least seven coordination sites are filled in the outer sphere of the $Co(NH_3)_6^{3+}$ ion and four sites in that of the Co $en_2(NCS)_2^+$ ion.

It is interesting to note that the coordination number found in this case, for the cobalthexammine ion is very near the number eight expected from geometrical considerations. In the anionic complex discussed above, we should indeed have an example of outer-sphere coordination number eight. It is also interesting to note the similar magnitude of $\beta_{1\,org}$ for the two central groups studied. The possibility of an association of ketones with cobaltammines has been suggested earlier [3] from other measurements.

I would like to express my gratitude to Miss Inga Tobiason, Fil.mag., for valuable technical assistance, and to the *Swedish Natural Research Council* for financial support.

1. Larsson, R. *Acta Chem. Scand.* **11** (1957) 1405.
2. Larsson, R. *Acta Chem. Scand.* **14** (1960) 697.
3. Larsson, R. *Acta Chem. Scand.* **12** (1958) 708.

Received October 24, 1962.

Pteroylglutamic Acid as a Growth Factor for a Strain of *Rhodotorula*

BRITA NYMAN and NILS FRIES

Institute of Physiological Botany, University of Uppsala, Uppsala, Sweden

In a study of fungi occurring on slime-flux of tree stumps, a strain of *Rhodotorula*, called 18 b, was isolated. This appeared to require *p*-aminobenzoic acid (PAB) as an essential factor for growth [1]. Since such a requirement is extremely rare among fungi, the nutrition of strain No. 18 b was more closely studied. This strain does not belong to *Rhodotorula aurantiaca*, the PAB-requirement of which has been investigated by Robbins and Ma [2], nor does it seem to be identical with any other earlier described species of the genus *Rhodotorula*.

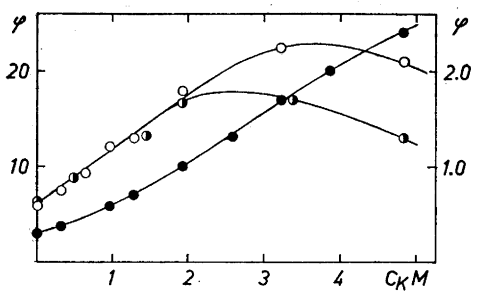

Fig. 2. The partition quotient φ as a function of the ketone concentration in the organic phase.

○: $Co(NH_3)_6^{3+}$; C_B = 0.67 M; left ordinate scale.
◐: $Co(NH_3)_6^{3+}$; C_B = 0.80 M; left ordinate scale.
●: Co $en_2(NCS)_2^+$; C_B = 0.67 M; right ordinate scale.

as some cyclohexanone dissolves in the aqueous phase (*cf.* Ref.[2], p. 709).

Analogous measurements were also performed by using the *trans*-Co $en_2(NCS)_2^+$ ion as the inert cobalt complex ion. Then the extracted species contains probably only one salicylate ion and more space should be available for the ketonic ligands. The cobalt concentration in the two phases was determined colorimetrically. The results are given in Figs. 1 and 2. C_B = 0.67 M was used for the measurements of Fig. 2. It is easily deduced that eqn. 5 should also apply here. In Fig. 3 $(\varphi/\varphi_o - 1)\,[K]^{-1}_{org}$ is plotted against $[K]_{org}$. The linearity indicates the presence of two complexes. $\beta_{1\,org}$ = (0.76 ± 0.05) M^{-1} and $\beta_{2\,org}$ = (0.24 ± 0.05) M^{-2}. Also here deviation from linearity occurs at high $[K]_{org}$.

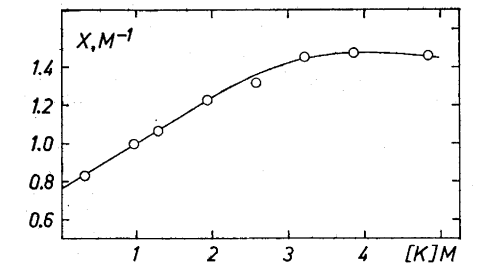

Fig. 3. $X_1 = (\varphi/\varphi_o - 1)\,[K]^{-1}_{org}$ plotted against $[K]_{org}$.

If we assume that each salicylate ion uses two coordination sites, which is likely but not quite certain, at least seven coordination sites are filled in the outer sphere of the $Co(NH_3)_6^{3+}$ ion and four sites in that of the Co $en_2(NCS)_2^+$ ion.

It is interesting to note that the coordination number found in this case, for the cobalthexammine ion is very near the number eight expected from geometrical considerations. In the anionic complex discussed above, we should indeed have an example of outer-sphere coordination number eight. It is also interesting to note the similar magnitude of $\beta_{1\,org}$ for the two central groups studied. The possibility of an association of ketones with cobaltammines has been suggested earlier [3] from other measurements.

I would like to express my gratitude to Miss Inga Tobiason, Fil.mag., for valuable technical assistance, and to the *Swedish Natural Research Council* for financial support.

1. Larsson, R. *Acta Chem. Scand.* **11** (1957) 1405.
2. Larsson, R. *Acta Chem. Scand.* **14** (1960) 697.
3. Larsson, R. *Acta Chem. Scand.* **12** (1958) 708.

Received October 24, 1962.

Pteroylglutamic Acid as a Growth Factor for a Strain of *Rhodotorula*

BRITA NYMAN and NILS FRIES

Institute of Physiological Botany, University of Uppsala, Uppsala, Sweden

In a study of fungi occurring on slime-flux of tree stumps, a strain of *Rhodotorula*, called 18 b, was isolated. This appeared to require *p*-aminobenzoic acid (PAB) as an essential factor for growth [1]. Since such a requirement is extremely rare among fungi, the nutrition of strain No. 18 b was more closely studied. This strain does not belong to *Rhodotorula aurantiaca*, the PAB-requirement of which has been investigated by Robbins and Ma [2], nor does it seem to be identical with any other earlier described species of the genus *Rhodotorula*.

The fungus was cultivated in continuously shaken test tubes with 10 ml of a synthetic liquid medium, A 2 + B, containing glucose, ammonium phosphate, and mineral salts[3]. For growth in this medium the fungus also required, apart from PAB, an addition of thiamine (100 μg/l). The growth was estimated photometrically at 610 mμ with an Engel colorimeter (Kipp, Delft). Extinction values were expressed according to the formula, $Z = (e_n - e_o) \times 10^3$, where e_o represents the original extinction value of the culture after inoculation and e_n the value obtained after an incubation period of n hours. Each extinction value represents an average of determinations for three tubes. The incubation temperature was 25°C and the initial pH was 6.4.

Experiments with different concentrations of PAB showed that the strain responded to a 10^{-9} M solution of PAB, *i.e.* 0.0014 μg per 10 ml nutrient medium, a sensitivity which is about the same as that of previously studied PAB-heterotrophic organisms. However, an unexpectedly high concentration ($\sim$ 0.75 μg per 10 ml) was necessary for a maximum rate of growth, a fact which might indicate a partial deficiency for other growth factors (Table 1).

In contrast to, *e.g.*, certain strains of *Saccharomyces cerevisiae* [4] our PAB-requiring strain of *Rhodotorula* is able to utilize pteroyl glutamic acid (PtG) instead of PAB (Table 1). Ten to fifty times as much PtG as PAB (in terms of moles) is necessary in order to produce the same growth response. In this respect *Rhodotorula* 18 b is like *Lactobacillus arabinosus*, *L. plantarum*[5] and *Clostridium acetobutylicum*[6].

Table 1. Response of *Rhodotorula* 18 b to *p*-aminobenzoic acid (PAB) and pteroylglutamic acid (PtG). 3.2 μg of PtG is equivalent to 1 μg of PAB

Expt. No.	PAB μg/l	PtG μg/l	Growth expressed as extinction values, Z, obtained after 75 h	140 h	168 h
10	0	0	40	—	70
	0.1	0	110	—	280
	1	0	190	—	510
	10	0	240	—	840
	50	0	310	—	1340
	100	0	360	—	1280
	200	0	330	—	1220
11	0	0	30	50	—
	100	0	480	1180	—
	0	320	180	340	—
	0	16 000	500	1160	—
	0	32 000	480	1160	—

Table 2. The inhibiting effect of sulphadiazin on *Rhodotorula* 18 b grown with PAB or PtG. Incubation time 96 h.

Addition to the medium			Extinction value, Z, of the culture
PAB μg/l	PtG μg/l	Sulphadiazin mg/l	
0	—	0	70
100	—	0	850
100	—	1	710
100	—	10	430
100	—	30	170
100	—	100	10
1000	—	0	740
1000	—	10	480
1000	—	100	10
—	16 000	0	730
—	16 000	10	330
—	16 000	100	10

The possibility that the effect of PtG was due to contamination by PAB was tested. A chromatographical analysis, with butanol saturated with 1.5 N NH_4OH as the solvent [7] and with methyl red as the colour reagent, showed that the preparation of PtG used contained less than 0.6 % PAB. Thus, *Rhodotorula* 18 b was able to utilize PtG as such.

In the great majority of cases, so far known, where PtG can be used as well as PAB, the growth-inhibiting effect of sulphadiazin disappears when PAB is replaced by PtG (or its derivative leucovorin). *Rhodotorula* 18 b, however, is also inhibited by sulphadiazin when grown with PtG (Table 2). This may indicate that PtG is not directly incorporated, but that it is first broken down, and only the PAB part is utilized.

Finally, the possibility was investigated that PAB could be entirely or partially substituted by a mixture of amino acids and purines. This had been demonstrated in some earlier investigated cases (by, e.g., Cutts and Rainbow [8], and Aaronson and

Table 3. The sparing effect of some nucleic acid components and amino acids on the requirement for PAB in *Rhodotorula* 18 b. AN-mixture: L-methionine 10 mg/l, DL-histidine 20 mg/l, L-leucine 10 mg/l, L-serine 10 mg/l, and thymine 30 mg/l.

Additions to the medium			Extinction value, *Z*, of the culture after	
PAB µg/l	AN-mixture + adenosine, 20 mg/l	AN-mixture + inosinic acid, 29 mg/l	104 h	144 h
0	–	–	250	350
1	–	–	290	400
10	–	–	450	660
50	–	–	710	1070
100	–	–	870	1260
0	+	–	300	370
1	+	–	520	680
10	+	–	700	970
50	+	–	870	1300
100	+	–	840	1290
0	–	+	330	450
1	–	+	480	690
10	–	+	570	880
50	–	+	880	1380
100	–	+	820	1320

Rodriguez [9]). Preliminary tests with thymine, amino acids and various purines, alone and combined, showed that a mixture of adenosine, thymine and four amino acids gave the highest rate of growth in the presence of PAB (Table 3). This mixture was not a substitute for PAB, but exerted a sparing action, so that half maximum growth rate was attained with approximately 1 µg instead of 10 µg of PAB per liter. Adenosine could be exchanged for inosinic acid with no appreciable loss of activity of the mixture.

1. Nyman, B. *Svensk Bot. Tidskr.* **55** (1961) 129.
2. Robbins, W. J. and Ma, R. *Science* **100** (1944) 85.
3. Fries, L. *Svensk Bot. Tidskr.* **49** (1955) 475.
4. Woods, D. D. *Ciba Foundation Symp. on Chemistry and Biology of Pteridines.* (Ed. Wolstenholme, G. E. W. and Cameron, M. P.) London 1954, p. 220.
5. Lampen, J. O. and Jones, M. J. *J. Biol. Chem.* **170** (1947) 133.
6. Nimmo-Smith, R. H. and Woods, D. D. *J. Gen. Microbiol.* **2** (1948) X.
7. Lederer, E. and Lederer, M. *Chromatography, a Review of Principles and Applications.* Amsterdam 1957.
8. Cutts, N. S. and Rainbow, C. *J. Gen. Microbiol.* **4** (1950) 150.
9. Aaronson, S. and Rodriguez, E. *J. Bacteriol.* **75** (1958) 660.

Received October 25, 1962.

Observation of Proton Magnetic Resonance Shifts in H_2O-D_2O Mixtures

MATS S. BERGQVIST* and L. E. GÖRAN ERIKSSON

Division of Physical Chemistry, The Royal Institute of Technology, Stockholm 70, Sweden

Isotope effects on nuclear magnetic resonance have been reported for specific groups in organic compounds. Carbon and hydrogen isotope effects have been observed in fluorine and proton magnetic resonance (PMR). In all the investigations the resonance of observed nuclei in a group containing a heavy isotope of the same or another element was displaced upfield relative to the resonance in a group with a light isotope. The present note reports a PMR study of H_2O-D_2O mixtures. PMR shifts were determined at 60 Mc/sec both by internal and external reference methods. Recently the PMR spectrum of the HDO and H_2O species in an acetone solution was reported [1]; the HDO resonance signal, a triplet due to the H–D spin-spin coupling, was observed at a slightly higher field than the singlet line of H_2O.

Experimental. The PMR spectra were recorded with a Varian Associates A-60 spectrometer, operating at the fixed frequency of 60 Mc/sec. The resonance line shifts were determined by means of side band technique using a Hewlett Packard Model 202 A audio oscillator. The determination of the frequency was carried out by means of a Model 5512 A electronic

* Present address: Sandvikens Jernverks AB, Sandviken, Sweden.

Table 3. The sparing effect of some nucleic acid components and amino acids on the requirement for PAB in *Rhodotorula* 18 b. AN-mixture: L-methionine 10 mg/l, DL-histidine 20 mg/l, L-leucine 10 mg/l, L-serine 10 mg/l, and thymine 30 mg/l.

Additions to the medium			Extinction value, *Z*, of the culture after	
PAB µg/l	AN-mixture + adenosine, 20 mg/l	AN-mixture + inosinic acid, 29 mg/l	104 h	144 h
0	–	–	250	350
1	–	–	290	400
10	–	–	450	660
50	–	–	710	1070
100	–	–	870	1260
0	+	–	300	370
1	+	–	520	680
10	+	–	700	970
50	+	–	870	1300
100	+	–	840	1290
0	–	+	330	450
1	–	+	480	690
10	–	+	570	880
50	–	+	880	1380
100	–	+	820	1320

Rodriguez [9]). Preliminary tests with thymine, amino acids and various purines, alone and combined, showed that a mixture of adenosine, thymine and four amino acids gave the highest rate of growth in the presence of PAB (Table 3). This mixture was not a substitute for PAB, but exerted a sparing action, so that half maximum growth rate was attained with approximately 1 µg instead of 10 µg of PAB per liter. Adenosine could be exchanged for inosinic acid with no appreciable loss of activity of the mixture.

1. Nyman, B. *Svensk Bot. Tidskr.* **55** (1961) 129.
2. Robbins, W. J. and Ma, R. *Science* **100** (1944) 85.
3. Fries, L. *Svensk Bot. Tidskr.* **49** (1955) 475.
4. Woods, D. D. *Ciba Foundation Symp. on Chemistry and Biology of Pteridines.* (Ed. Wolstenholme, G. E. W. and Cameron, M. P.) London 1954, p. 220.
5. Lampen, J. O. and Jones, M. J. *J. Biol. Chem.* **170** (1947) 133.
6. Nimmo-Smith, R. H. and Woods, D. D. *J. Gen. Microbiol.* **2** (1948) X.
7. Lederer, E. and Lederer, M. *Chromatography, a Review of Principles and Applications.* Amsterdam 1957.
8. Cutts, N. S. and Rainbow, C. *J. Gen. Microbiol.* **4** (1950) 150.
9. Aaronson, S. and Rodriguez, E. *J. Bacteriol.* **75** (1958) 660.

Received October 25, 1962.

Observation of Proton Magnetic Resonance Shifts in H_2O-D_2O Mixtures

MATS S. BERGQVIST* and L. E. GÖRAN ERIKSSON

Division of Physical Chemistry, The Royal Institute of Technology, Stockholm 70, Sweden

Isotope effects on nuclear magnetic resonance have been reported for specific groups in organic compounds. Carbon and hydrogen isotope effects have been observed in fluorine and proton magnetic resonance (PMR). In all the investigations the resonance of observed nuclei in a group containing a heavy isotope of the same or another element was displaced upfield relative to the resonance in a group with a light isotope. The present note reports a PMR study of H_2O-D_2O mixtures. PMR shifts were determined at 60 Mc/sec both by internal and external reference methods. Recently the PMR spectrum of the HDO and H_2O species in an acetone solution was reported [1]; the HDO resonance signal, a triplet due to the H–D spin-spin coupling, was observed at a slightly higher field than the singlet line of H_2O.

Experimental. The PMR spectra were recorded with a Varian Associates A-60 spectrometer, operating at the fixed frequency of 60 Mc/sec. The resonance line shifts were determined by means of side band technique using a Hewlett Packard Model 202 A audio oscillator. The determination of the frequency was carried out by means of a Model 5512 A electronic

* Present address: Sandvikens Jernverks AB, Sandviken, Sweden.

counter of the same manufacture. The oscillator frequency was observed as the sweep passed the first side band signal. The value given by the frequency counter is the mean oscillator frequency. The procedure was repeated several times and the shifts obtained were averaged.

The deuterium oxide was 99.8 % (d_4^{20} = = 1.10518) from Norsk Hydro, Norway. Ordinary water was distilled in a quartz apparatus. No precautions to keep the water deaerated were taken since dissolved oxygen has no observable influence on the resonance shifts [2]. The mixtures were prepared by weighing. 0.3 *m* *t*-butanol was used as internal standard which is convenient in aqueous solution [3]. As external reference, benzene was placed in the annular space between precision bore coaxial glass tubings. The temperature in the probe was 32.0 ± 0.1°C. The spinning samples were kept in the probe long enough to obtain that temperature. The influence of a small temperature drift was taken into consideration by measuring the samples in a random order. As there is an enrichment of ^{18}O in deuterium oxide the shift in water enriched in ^{18}O from Fluka A. G. was also measured.

Results. The experimental resonance shifts, all upfield relative to H_2O, in mixtures of different mole fractions of D_2O are plotted in Fig. 1. The proton resonance in pure H_2O has been taken as zero. Values obtained with external reference have been corrected for the macroscopic magnetic susceptibility shifts, the susceptibility being a strictly additive function of the concentration [4]. The correction at 60 Mc/sec for a cylindrical specimen is [5]

$$60 \times 10^6 \times (2\pi/3)\{d[y\varkappa_D + (1-y)\varkappa_H] - \varkappa_H d_H\} \text{ c/sec}$$

where y is the weight fraction of D_2O, $\varkappa_D$ and $\varkappa_H$ are the specific susceptibilities of D_2O and H_2O, respectively. The values -0.6467×10^{-6} and -0.7200×10^{-6} at 20°C were chosen as the most accurate available [4], and the temperature dependence of the specific susceptibilities may be neglected. In this formula d is the density of the mixture calculated under the assumption of additive molar volumes [4]. The density of H_2O is denoted by d_H. The maximum calculated susceptibility correction, *viz.* that of D_2O, was −0.40 c/sec at 60 Mc/sec.

In Fig. 1 straight lines have been fitted to the measured points according to the method of least squares. When the temperature was carefully adjusted (by means of the spinner turbine air stream) it was possible to reproduce the straight lines within the standard deviation of the first experimental series. The inclination of the line of the internal reference method was 1.00 c/sec/mole fraction D_2O, as compared to 1.38 c/sec/mole fraction D_2O of the external reference method. Standard errors in both cases were ± 0.04 c/sec/mole fraction D_2O. The value of the inclination is identical with the PMR shift between D_2O and H_2O. In a water specimen enriched to 5 % in ^{18}O a small, not significant, upfield PMR shift relative to ordinary water was observed. Since this enrichment is several times larger than that expected in concentrated D_2O no corrections due to the ^{18}O content were needed. The effect of an enrichment in ^{17}O (spin 5/2) has not been studied.

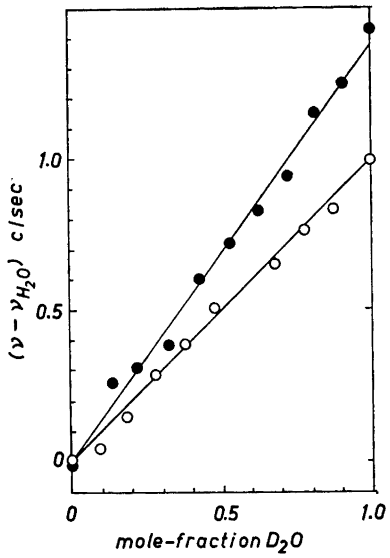

Fig. 1. PMR shift in H_2O-D_2O mixtures *vs.* concentration of D_2O at 32°C. ○ Internal reference; ● external reference.

Discussion. The PMR shift in H_2O-D_2O mixtures appears to be a linear function of the deuterium concentration. The results obtained by the internal and external reference methods do not coincide. The following reasons for the deviation may be stated: (*a*) erroneous susceptibility corrections, (*b*) temperature instability effects, (*c*) internal standard effects and (*d*) nuclear relaxation effects. The corrections for the macroscopic susceptibility may be incor-

rect either because the applied theoretical formula is too approximate or due to errors in densities or specific susceptibilities. The shifts are very sensitive to temperature instability and in a separate investigation with a Varian Associates V-4300 B spectrometer, operating at 40 Mc/sec, a temperature dependence was observed in the range 0—70°C. It was found that the shift between a water specimen and external benzene reference satisfied the equation

$$(H_{H_2O} - H_{C_6H_6})/H_{C_6H_6} = 8.828 \times 10^{-3}\ t + 1.527 \text{ ppm}$$

where H is the resonant field and t is the temperature in °C. The method of least squares was applied to obtain the constants of the equation. Accordingly, the temperature coefficient for the shift between water and external benzene is 0.53 c/sec, °C at 60 Mc/sec. It was, however, possible to reproduce the lines from time to time and thus temperature instability as a reason for the deviation may be discounted. Due to anomalies expected at low internal standard concentrations it is not possible to eliminate the effect of the standard by extrapolating to zero concentration. The alcohol will take part in the hydrogen transfer and also break hydrogen bonds in the water lattice. In H_2O and D_2O these interferences may be of different magnitude. It is not likely that the effects will influence the chemical shift of the reference methyl protons very much. The connection between different relaxation mechanisms and observed shifts are far from clear. Without further experimental information it seems, however, difficult to settle the question of the observed discrepancy between the internal and external reference methods.

The heavier deutron isotope slows down the rapid hydrogen transfer in D_2O as compared to H_2O. Accordingly, the mean life time of a preferred hydrogen position in the neighbourhood of the one oxygen of the two in a hydrogen bond will increase, anp then upfield shifts ("increased shieldings") are originated. Moreover, the difference in the strength of the deuterium and protium hydrogen bond must be noticed. A linear decrease of the self-diffusion coefficient with increasing deuterium concentration was found in H_2O-D_2O mixtures [6]. This is in agreement with our result on the PMR dependence. In a diluted acetone solution the HDO triplet was centered at 0.03 ppm toward higher field relative to the H_2O line [1]. The temperature was not reported. Our results indicate a PMR shift for a proton in D_2O relative to that in H_2O of about 0.02 ppm (average between internal and external reference methods). The lower value is probably due to the rapid hydrogen transfer in absence of organic solvent, resulting in a decreased resonant field for the proton.

Acknowledgements. We would like to thank Dr. E. Forslind for many valuable discussions.

A grant from the *Knut and Alice Wallenberg's Foundation*, which made the NMR equipment available, is gratefully acknowledged.

1. Holmes, J. R., Kivelson, D. and Drinkard, W. C. *J. Chem. Phys.* **37** (1962) 150.
2. Bergqvist, M. S. and Forslind, E. *Acta Chem. Scand.* **16** (1962) 2069.
3. Hertz, H. G. and Spalthoff, W. *Z. Elektrochem.* **63** (1959) 1096.
4. Kirshenbaum, I. *Physical properties and analysis of heavy water*, McGraw-Hill, New York 1951.
5. Pople, J. A., Schneider, W. G. and Bernstein, H. J. *High-resolution Nuclear Magnetic Resonance*, McGraw-Hill, New York 1959, p. 81.
6. Devell, L. *Acta Chem. Scand.* **16** (1962) 2177.

Received October 29, 1962.

ACTA CHEMICA SCANDINAVICA 16 (1962) 2311–2317

Crystal Structures of Oxalyl Bromide and Oxalyl Chloride

P. GROTH and O. HASSEL

Universitetets Kjemiske institutt, Blindern, Oslo, Norway

Details are presented of crystal structure determinations of oxalyl bromide and oxalyl chloride. The crystals are not isomorphous and their structures quite different. In the oxalyl bromide structure weak charge transfer bonds connect every molecule with its four nearest neighbours, the O...Br separation (3.27 Å) being only slightly shorter than the expected van der Waals separation. The C—Br...O angle is found equal to 169°.

In the oxalyl chloride structure charge transfer bonds between oxygen and chlorine are not indicated.

In order to collect empirical facts regarding the atomic arrangement in solids containing charge transfer bonds the crystal structure of a considerable number of addition compounds formed by typical donor molecules and halogen molecules have been determined and general principles formulated [1]. As had already been suggested [2] the bonds mainly responsible for the formation of the 1:3 addition compounds between iodoform and quinoline or sulphur (S_8) and the corresponding sulphur compound of antimony triiodide are in fact iodine-nitrogen resp. iodine-sulphur bonds. This has been proved by crystal structure determinations carried out in our laboratory during the last few years [3]. Moreover, the arrangement carbon-iodine-donor atom (resp. antimony-iodine-sulphur) is very nearly *linear* in all cases and corresponds to the arrangement halogen-halogen-donor atom observed in all true addition compounds in which a halogen molecule is the acceptor. In the 1:1 addition compound 1,4-dithiane-iodoform the same type of iodine-sulphur bonds have also been observed [4]. Similar but obviously much weaker bonds have been found in two 1:1 addition compounds formed by 1,4-dioxan and oxalyl halides [5].

The question now arose if intermolecular charge transfer bonds might not be expected even in crystals containing a single molecular species when the molecule in question contains both electron donor and electron acceptor atoms. In the crystalline cyanogen halides infinite linear chains of molecules have been observed which indicate the presence of comparatively strong bonds connecting nitrogen belonging to one molecule and halogen belonging to the neighbour molecule. In the trimeric forms — the cyanuric halides — analogous bonds might be expected to occur between tertiary nitrogen atoms and halogen

Table 1. Lattice parameters, space groups for oxalyl bromide (A) and oxalyl chloride (B).

	A	B
a	6.18 Å	6.44 Å
b	5.46 Å	6.08 Å
c	7.80 Å	11.93 Å
β	112.4°	
Space group	$P2_1/c$	*Pbca*
Z	2	4

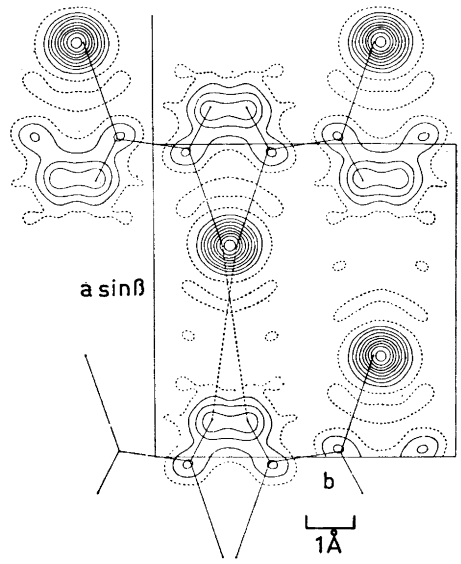

Fig. 1 a. Fourier projection of oxalyl bromide along [001]. Contour lines at intervals of 3 e.Å^{-2} for C and O, 12 e.Å^{-2} for Br. Dotted line corresponds to 3 e.Å^{-2}.

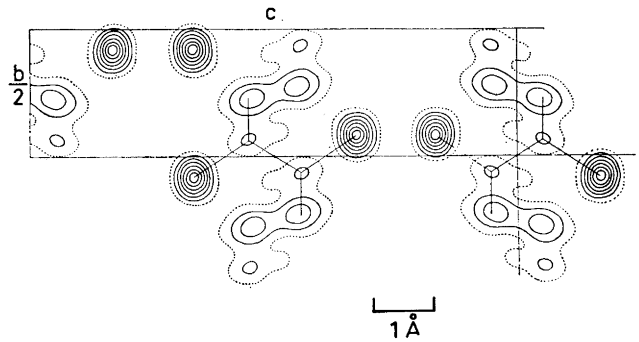

Fig. 1 b. Fourier projection of oxalyl chloride along [100]. Contour lines at intervals of 3 e.Å^{-2}. Dotted line corresponds to 3 e.Å^{-2}.

atoms, leading to infinite planar nets. The results of a preliminary X-ray investigation appeared to confirm this suggestion [6] although the authors seem to have overlooked the possibility of the bonds just mentioned.

In crystals of certain carboxylic acid halides the possibility of charge transfer bonds between halogen and oxygen appeared to be possible. As a consequence of the observations made in the case of the crystalline addition compounds formed by oxalyl chloride and oxalyl bromide with dioxan we started X-ray work on the oxalyl halides themselves. These two substances are not isomorphous as might perhaps have been expected, had the melting point of the chloride not been higher than that of the bromide (−12°C and −19.5°C, respectively). However, the space group symmetry and the number of molecules in the unit cells (*cf.* Table 1) require the molecules to be crystallographically equivalent and centrosymmetrical in both cases. The crystallographic findings therefore indicate that if charge transfer bonds exist at all, every molecule must take part in the formation of *four* such bonds.

The X-ray analysis of the two substances, which are both liquid at room temperature, had to be carried out at a lower temperature and the single crystals were grown in capillary tubes. Prolonged trials revealed that it is indeed possible to obtain crystals in which one of the crystallographic directions is approximately parallel to the axis of the capillary tube, and it was found that this direction is not necessarily always the same. Weissenberg single crystal technique could therefore conveniently be employed both for the chloride and the bromide and two-dimensional Patterson and Fourier syntheses worked out. The atomic coordinates thus arrived at were then refined using least squares computations. The axes of rotation were [010], [100] and [110] in the case of the chloride, [010], [001] and [011] in the case of the bromide. Final atomic parameters are listed in Table 2. Structure factors (F_c) computed from these coordinates together with the observed values (F_o) may be found in Table 3. In Figs. 1a and b one electron density map is reproduced for each of the two substances. For the bromine compound a second Fourier map has previously been published [7].

The results obtained for the bromide confirm the suggestion that charge transfer bonds are present between neighbouring molecules. The oxalyl bromide structure may indeed be described as being built up of (non-planar) sheets within which every molecule is linked to four neighbours by O...Br bonds of length 3.27 Å a value only slightly smaller than that expected for a van der Waals contact. The angle C—Br..O is 169°. Moreover, it follows from the atomic coordinates given in Table 2 that the oxalyl bromide molecules are at least very nearly planar with bond distances and angles listed in Table 4. Within the sheet an intermolecular O—Br separation of 3.63 Å is also observed;

Table 2. Final atomic coordinates for oxalyl bromide (A) and oxalyl chloride (B).

	A				B		
	x	*y*	*z*		*x*	*y*	*z*
Br	0.321	0.228	0.162	Cl	−0.084	−0.083	0.167
O	0.883	0.191	0.377	O	0.118	0.230	0.050
C	0.020	0.119	0.906	C	−0.006	0.062	0.053

Table 3.

a. Observed calculated structure factors for oxalyl bromide.

*hk*0-projection

h	*k*	F_o	F_c	*h*	*k*	F_o	F_c	*h*	*k*	F_o	F_c
0	1	11	− 13	2	2	50	49	4	4	10	− 9
0	2	49	− 49	2	3	59	− 55	4	5	19	− 20
0	3	73	76	2	4	17	16	4	6	10	13
0	4	17	− 15	2	5	32	33	5	1	28	− 28
0	5	35	− 36	2	6	22	− 23	5	2	20	21
0	6	28	29	3	1	60	55	5	3	5	5
1	1	85	− 90	3	2	55	− 51	5	4	19	− 19
1	2	90	91	3	3	17	− 15	5	5	9	10
1	3	29	26	3	4	35	36	6	0	19	− 18
1	4	55	− 55	3	5	20	− 18	6	1	9	9
1	5	22	21	3	6	10	− 10	6	2	10	10
1	6	9	10	4	0	40	42	6	3	15	− 16
1	7	19	− 24	4	1	25	− 24	7	1	8	11
2	0	115	−112	4	2	32	− 31				
2	1	30	29	4	3	31	30	R = 5.1 %			

*h*0*l*-projection

h	*l*	F_o	F_c	*h*	*l*	F_o	F_c	*h*	*l*	F_o	F_c
0	1	31	28	2	0	23	− 24	4	$\bar{2}$	11	− 10
0	2	17	− 15	2	1	13	12	5	$\bar{4}$	9	12
0	3	28	− 21	2	2	36	30	5	$\bar{3}$	9	10
0	$\bar{4}$	12	− 10	2	3	12	10	5	$\bar{1}$	17	− 21
1	$\bar{4}$	11	− 9	2	$\bar{4}$	2	− 2	5	0	17	− 18
1	$\bar{3}$	19	15	3	$\bar{4}$	8	− 7	5	1	6	4
1	$\bar{2}$	40	36	3	$\bar{3}$	24	− 25	5	$\bar{2}$	9	10
1	$\bar{1}$	38	36	3	$\bar{2}$	22	− 27	6	$\bar{3}$	12	− 16
1	0	5	− 7	3	$\bar{1}$	18	22	6	$\bar{2}$	11	− 13
1	1	61	− 52	3	0	34	38	6	0	13	13
1	2	17	− 14	3	1	25	23	6	1	11	11
1	3	9	7	3	$\bar{3}$	18	− 12	7	$\bar{2}$	8	11
1	$\bar{4}$	10	10	4	$\bar{4}$	10	− 9	7	$\bar{1}$	7	9
2	$\bar{4}$	14	14	4	$\bar{2}$	18	24				
2	$\bar{3}$	18	15	4	$\bar{1}$	21	27				
2	$\bar{2}$	23	− 23	4	0	8	− 8				
2	$\bar{1}$	39	− 41	4	1	20	− 18	R = 14.1 %			

Projection along [011]. $h' = h$; $k' = k-l$; $l' = l = 0$.

h	*k'*	F_o	F_c	*h*	*k'*	F_o	F_c	*h*	*k'*	F_o	F_c
0	1	20	− 27	2	$\bar{2}$	67	76	4	$\bar{2}$	36	− 41
0	2	32	− 38	2	$\bar{1}$	20	− 13	4	0	20	− 16
0	3	9	− 11	2	0	50	− 48	4	2	39	39
0	$\bar{4}$	23	− 19	2	1	7	− 3	4	$\bar{4}$	10	− 17
1	$\bar{4}$	39	− 41	2	2	15	− 12	5	$\bar{2}$	44	− 43
1	$\bar{3}$	9	− 5	2	3	11	12	5	0	38	36
1	$\bar{2}$	40	45	2	$\bar{4}$	26	27	5	1	9	7
1	$\bar{1}$	31	26	3	$\bar{4}$	23	23	5	$\bar{3}$	8	− 8
1	0	12	13	3	$\bar{2}$	27	28	6	$\bar{4}$	13	− 18
1	1	8	2	3	$\bar{1}$	17	14	6	0	31	31
1	2	81	− 89	3	0	76	− 77	6	$\bar{2}$	18	− 20
1	$\bar{4}$	25	27	3	2	42	34	7	$\bar{2}$	15	17
2	$\bar{4}$	18	− 19	3	$\bar{4}$	7	6				
2	$\bar{3}$	10	− 10	4	$\bar{4}$	30	33	R = 12.3 %			

b. observed and calculated structure factors for oxalyl chloride.

h0l-projection

h	*l*	F_o	F_c	*h*	*l*	F_o	F_c	*h*	*l*	F_o	F_c
0	1	8	− 9	2	4	7	− 6	5	1	7	7
0	2	12	− 11	2	5	3	4	5	2	4	3
0	3	24	− 23	2	6	4	3	5	3	3	1
0	4	17	− 17	2	7	1	1	5	4	3	− 3
0	5	9	10	3	1	20	20	5	5	2	− 2
0	6	8	6	3	2	28	27	5	6	1	0
0	7	3	3	3	3	3	− 4	6	0	9	− 9
1	1	13	14	3	4	10	− 10	6	1	5	− 5
1	2	28	28	3	5	7	− 8	6	2	3	4
1	3	6	− 7	3	6	1	0	6	3	6	7
1	4	7	− 5	3	7	2	3	6	4	1	2
1	5	4	− 6	4	0	16	− 15	6	5	1	− 2
1	7	2	2	4	2	4	3	7	1	2	− 2
2	0	36	37	4	3	5	7				
2	1	3	0	4	4	2	4				
2	2	5	− 5	4	5	2	− 2				
2	3	11	− 9	4	6	2	− 2	R = 10.2 %			

0*kl*:projection

k	*l*	F_o	F_c	*k*	*l*	F_o	F_c	*k*	*l*	F_o	F_c
0	2	10	8	1	7	17	14	2	7	10	11
0	4	14	− 12	1	8	5	− 3	2	8	2	2
0	6	27	24	1	9	2	− 2	2	11	4	− 5
0	8	19	− 21	1	10	2	− 1	2	12	3	− 3
0	10	11	− 11	1	11	7	− 7	2	13	4	3
0	12	9	8	1	12	5	5	3	0	11	− 12
0	14	3	− 4	1	13	7	6	3	3	5	− 1
1	0	9	12	1	14	2	− 2	3	5	3	− 1
1	1	24	29	2	0	4	− 6	3	6	7	− 7
1	2	18	− 18	2	1	16	17	3	8	4	4
1	3	8	− 10	2	2	10	10				
1	4	9	− 10	2	4	6	6				
1	5	28	− 28	2	5	12	− 13				
1	6	16	15	2	6	9	− 9	R = 12.6 %			

Projection along [100]. $h' = h-k$; $k' = h + k = 0$; $l' = l$.

h′	*l*	F_o	F_c	*k*	*l*	F_o	F_c	*k*	*l*	F_o	F_o
0	2	17	16	1	13	3	3	3	7	5	− 4
0	4	24	− 23	1	14	5	− 5	3	8	4	2
0	6	48	46	1	15	3	− 6	3	10	2	0
0	8	34	− 37	2	0	31	32	3	12	3	− 1
0	10	19	− 21	2	1	29	− 25	4	0	3	3
0	12	17	15	2	3	5	2	4	1	14	10
0	14	5	− 7	2	5	20	20	4	2	7	− 5
1	1	67	72	2	6	6	10	4	3	9	3
1	2	17	− 15	2	7	15	− 14	4	4	6	− 3
1	3	49	− 47	2	8	8	− 7	4	6	4	5
1	4	53	55	2	10	4	− 3	4	7	7	7
1	5	29	26	2	11	4	8	5	1	3	5
1	6	14	14	2	13	6	− 4	5	2	4	4
1	7	11	12	3	1	10	8	5	3	5	− 9
1	8	13	− 11	3	2	10	7	5	4	4	− 4
1	9	26	− 25	3	3	7	6	5	5	4	4
1	10	8	11	3	4	12	10	5	7	2	3
1	11	9	8	3	5	4	− 1				
1	12	3	− 2	3	6	6	6	R = 14.1 %			

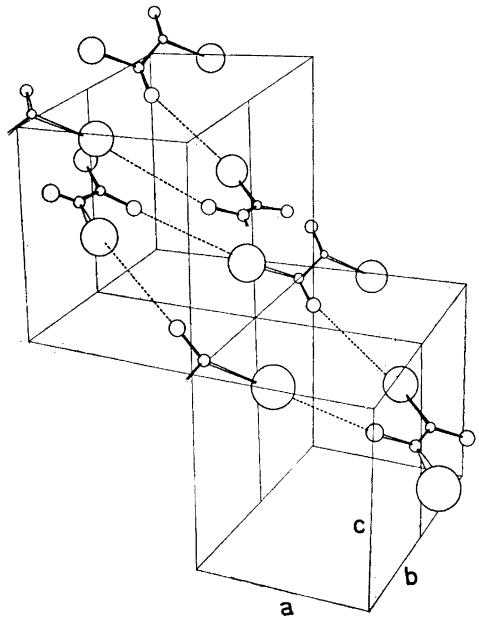

Fig. 2 a. Drawing of the oxalyl bromide structure.

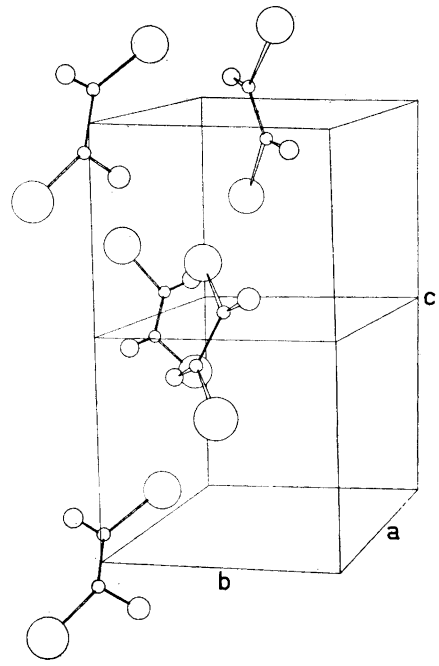

Fig. 2 b. Drawing of the oxalyl chloride structure.

the nearest approach between O and Br atoms belonging to neighbouring sheets is still larger, *viz.* 3.90 Å. Fig. 2a visualizes both the arrangement within the sheets and the mutual arrangement of neighbouring sheets.

The structure of oxalyl chloride differs very much from that of the bromide, although the molecules are situated in centres of symmetry even in this case. The shortest O—Cl separation is found equal to 3.50 Å and the angle C—O...Cl is very far from approaching 180°. It must therefore be admitted that in the oxalyl chloride structure no indications of bonds connecting chlorine and oxygen atoms can be traced. The oxalyl chloride structure is reproduced schematically in Fig. 2b. Unlike the oxalyl bromide molecules the molecules of oxalyl chloride do not appear to be strictly planar. The aim of the present investigation was not, however, to arrive at a very accurate determination of the parameters of the latter molecule. The computed values for the oxalyl chloride molecule probably being less reliable than those listed for the bromide molecule — the former are not included in Table 4.

Table 4. Bond distances and bond angles within the oxalyl bromide molecule.

Distance		Angle	
O—Br	1.84 Å	O—C—Br	128.3°
C=O	1.17 Å	Br—O—C	108.8°
C—C	1.56 Å	O—C—C	122.3°

It would appear interesting to investigate crystal structures of substances containing electron donors like, *e.g.*, oxygen and as acceptors halogen atoms directly linked not to carbon but rather to atoms known to be more strongly electronegative, for example nitrogen. In such crystals one might expect the formation of somewhat stronger bonds between halogen and the donor atom. One structure of this kind has accidentally been investigated, namely that of N-chlorosuccinimide [8]. Here, the arrangement N—Cl...O is nearly linear (the N—Cl—O— angle being approximately 170°) and the Cl—O distance (2.88 Å) is significantly shorter than the van der Waals radius sum. Addition compounds might be expected to exist between N-halogenosuccinimide and a number of molecules containing donor atoms. So far, we have not been able to prepare crystals of such compounds, however, probably because of the high chemical reactivity of the halogen atom in N-halogenosuccinimides.

This investigation has in part been sponsored by the *United States Air Force Development Command* under the contract AF 61 (052)—71.

REFERENCES

1. Hassel, O. *Proc. Chem. Soc.* **1957** 250; *Mol. Phys.* **1** (1958) 241; Hassel, O. and Römming, Chr. *Quart. Revs. (London)* **16** (1962) 1.
2. Hassel, O. *Proc. Chem. Soc.* **1957** 250.
3. Bjorvatten, T. and Hassel, O. *Acta Chem. Scand.* **13** (1959) 1261; Bjorvatten, T. *Acta Chem. Scand.* **16** (1962) 249.
4. Bjorvatten, T. and Hassel, O. *Acta Chem. Scand.* **15** (1961) 429.
5. Bjorvatten, T., Hassel, O. and Römming, Chr. *Nature* **189** (1961) 137; Hassel, O. *Tidsskr. Kjemi Bergvesen Met.* **3** (1961) 60.
6. Hoppe, W., Lenné, H. U. and Morandi, G. *Z. Krist.* **108** (1957) 32.
7. Groth, P. and Hassel, O. *Proc. Chem. Soc.* **1961** 343.
8. Brown, R. N. *Acta Cryst.* **14** (1961) 711.

Received June 21, 1962.

ACTA CHEMICA SCANDINAVICA 16 (1962) 2318–2320

Preparation of 1-^{13}C Enriched Benzonitrile, *Mono*-^{13}C Enriched Benzene, and a Mixture of *Mono*-^{13}C Enriched Benzonitriles

BØRGE BAK, JØRN JOHS. CHRISTIANSEN, LEIF LIPSCHITZ and JØRGEN TORMOD NIELSEN

Chemistry Department, University of Copenhagen, Copenhagen, Denmark

Preparations of 55 % ^{13}C-enriched $CH_3{}^{13}COONa$ (yield 87 %), $CH_3{}^{13}COOC_2H_5$ (85 %), 1-methyl-[1-^{13}C]cyclohexanol-1 (76 %), 1-methyl-[1-^{13}C]benzene (85 %), [1-^{13}C]benzoic acid (76 %), [1-^{13}C]benzonitrile (62 %), *mono*-^{13}C benzene (95 %), and a mixture of *mono*-^{13}C enriched benzonitriles (38 %) are described. The purity has been checked gaschromatographically (where ever feasible) and spectroscopically.

The present work was undertaken in order to make available 1-^{13}C enriched benzonitrile (I), *mono*-^{13}C enriched benzene (II), and a mixture of mono-^{13}C enriched benzonitriles (III), all for use in spectroscopic investigations and for later use in further preparative work.

The route followed was:

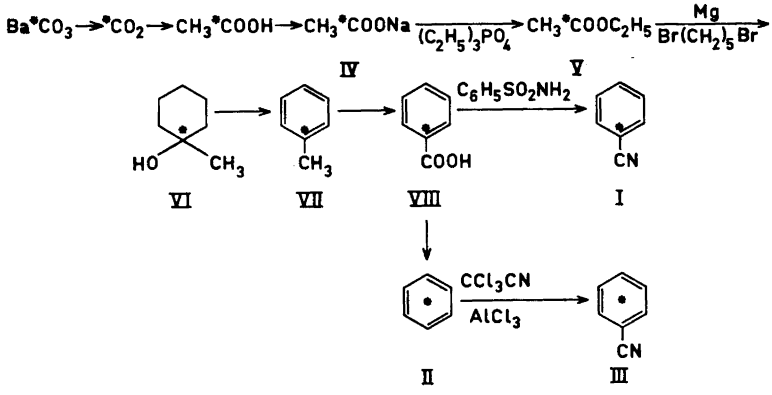

EXPERIMENTAL

*CH_3*COONa (IV).* A Grignard solution was prepared from 240 mmole of CH_3I in 300 ml ether and an excess of magnesium. After dilution of the reaction mixture with 300 ml ether, 145 mmole of *CO_2 (from 29.55 g (150 mmole) Ba*CO_3 (55 % enriched) and conc. H_2SO_4) was introduced under cooling. After hydrolysis (200 ml H_2O), addition of 48 g (154 mmole) of Ag_2SO_4, cooling to 0°C, and addition of 50 ml half-concentrated H_2SO_4, steam-distillation of the product produced an aqueous solution of about 3 l, containing the available CH_3*COOH. After neutralization by 1 N NaOH, water was evaporated at 100°C, leaving (IV), which was finally dried on the vacuumline to constant weight, 10.75 g (130 mmole).

*CH_3*$COOC_2H_5$ (V).* Slow distillation of 130 mmole of (IV) with 30 ml of triethylphosphate from a flask, immersed in an oil-bath (170°—210°C) produced a mixture of (V) and triethylphosphate. By distillation *in vacuo* at 0°C under stirring, fractions of (V) were collected until the vapor-pressure had decreased to 7 mm of mercury. Yield 9.71 g (110 mmole). The infrared spectrum (650—4000 cm^{-1}) showed that this sample was more than 99 % pure. Also, the proton magnetic resonance (PMR) spectrum at 60 Mc/s showed the presence of ^{13}C (spin 1/2) in the *carbonyl* group with characteristic coupling to the CH_2 protons of the C_2H_5-group (3.1—3.2 c/s), no coupling to the CH_3 protons of the C_2H_5 group, but with a coupling of 6.9 c/s to the protons of the second, adjacent CH_3 group. From the PMR spectrum, the percentage of $CH_3{}^{13}COOC_2H_5$ was seen to be 52. Within the experimental error this is consistent with the assumed percentage of 55 of the commercial Ba*CO_3 applied.

1-Methyl-[1-^{13}C]cyclohexanol-1 (VI) was prepared as indicated in Ref.[1] 9.20 g (104 mmole) of (V) was converted to 8.95 g (79 mmole) of (VI). The final purification was carried out by means of a "preparative" gaschromatograph of conventional design (Perkin-Elmer 116E, column "C", length 2.7 m), treating 1 g at a time. A gaschromatogram of an analytical quantity (5 mg) showed the presence of an (unidentified) impurity of *ca.* 2 %.

1-Methyl-[1-^{13}C] benzene (VII). In an evacuated system, 8.49 g (74 mmole) of (VI) was distilled into a perpendicular column containing a platinum catalyst (10 g H_2PtCl_6 (40 % Pt) reduced on 50 g of granulated coal). The column was electrically heated to 310°C. The totally dehydrated, but only partly dehydrogenated product was collected in a trap over 2—3 h. Weight 7.99 g. It consisted of an aqueous and an "organic" liquid phase. Gaschromatographic analysis (column "A", length 2 m) of the latter showed the presence of rapidly passing, unidentified components (0.4 %), cyclohexane (0.3 %), benzene (1.2 %), methylcyclohexane (9.1 %, (VII) in a yield of 88 %, and 0.6 % of slowly passing, unidentified components. The high yield makes it improbable that isomerization, spreading the ^{13}C over the positions of the ring, has occurred. PMR-analysis confirmed this. If, namely, the CH_3-group had migrated during the formation of (VII), lines originating from ^{13}C—H coupling would be observable. Such lines would be displaced 50—110 c/s with respect to the "ordinary" aromatic toluene protons. No such lines were observed. Instead, the expected coupling between 1-^{13}C and the protons of the adjacent CH_3 group of (VII) showed up with a coupling constant of 5.9—6.0 c/s. From the intensity of the displaced CH_3-group lines the enrichment of (VII) was estimated to 55 %. The estimated quantity of (VII) in the mixture mentioned above was 5.8 g (63 mmole). For the present purpose (*vide infra*), separation from the impurities was unnecessary and not carried out.

[1-^{13}C]benzoic acid (VIII). The above-mentioned sample of crude (VII) was heated under stirring and reflux on a steam-bath with a solution of 22 g $KMnO_4$ in 270 ml H_2O until the $KMnO_4$-colour disappeared (5 h). After acidification with conc. HCl and reduction of MnO_2 by gaseous SO_2 at room temperature the reaction mixture was cooled to 0°C which caused the main quantity of (VIII) to crystallize. After filtering, the mother-liquid was extracted 3 times by 50 ml of ether. The combined ethereal extracts were treated by 50 ml 2 N NaOH. Acidification of the separated aqueous layer and cooling, produced an additional amount of (VIII). After drying *in vacuo*, the total yield was 6.09 g, m.p. 122°—123°C (lit. 123°C). Combustion analyses showed the presence of about 3 % ashes, the yield of (VIII) is, therefore, 5.90 g (48 mmole). A KBr-disc spectrum of 1 mg in 30 mg KBr confirmed that the purity is > 95 %.

* The asterisk indicates the position enriched by ^{13}C.

[1-^{13}C]benzonitrile (I). 1.10 g of crude (VIII), containing 8.7 mmole of acid, was intimately mixed with 2.52 g benzenesulfonamide (16 mmole) [3] and placed in a 50 ml cylindrical vessel, which was closed to the atmosphere by a $CaCl_2$-tube. The vessel, which was kept cold at the top by a stream of air, was immersed in a heated Wood's metal bath (220–225°C). Immediately after the melting of the reaction mixture magnetic stirring was started. After 2 h of heating at 220°C the temperature was increased to 300°C in the course of 15 min. After further 30 min of heating at 300°C, the reaction mixture was allowed to cool to room temperature. The cylindrical vessel was connected to a vacuum line and evacuated at −190°C. Then the temperature was raised to 0°C. A vapor-pressure of 25 mm of mercury (from benzene) was observed, internal magnetic stirring being applied. Fractions of these vapors were collected until the equilibrium vapor-pressure had dropped to 5–6 mm. Then the temperature of the vessel was raised to 25°C (vapor-pressure 25 mm). Fractions were again removed over a 36 h period until the pressure had fallen to 0.8 mm, the vapor-pressure of (I). (I) was distilled-off *in vacuo*. Yield 560 mg (5.4 mmole). The gaschromatogram showed the presence of only 0.3 % benzene. No infrared spectrum was taken, but the infrared spectrum of a sample, prepared in a test experiment using non-enriched material, was quite satisfactory. In a subsequent microwave investigation of the enriched sample (I) only lines from benzonitrile were observable. The relative intensity of the two microwave spectra corresponded to an approximate 1:1 ratio of the two components.

Mono-^{13}C benzene (II). 1.83 g of crude (VIII), corresponding to 14.5 mmole of pure (VIII), was mixed with 0.3 g CuO and added to 10 ml quinoline. Decarboxylation was affected following Ref.[4] The trap, in which the yield was collected, was connected to a vacuum line and evacuated at −80°C. After subsequent heating to room temperature benzene was distilled-off into a second trap, containing 2–3 g P_2O_5 which removed H_2O and a trace of quinoline. After 1 h, (II) was distilled-off. Weight 1.08 g (13.8 mmole). Judging from a gas chromatogram of (II), (column "A", length 2 m), purity was higher than 99.9 %.

Mixture of mono-^{13}C enriched benzonitriles (III). Using a modification of Houben and Fischer's method [5] 1.07 g of (II) (13.6 mmole) was mixed with 2.44 g (17 mmole) CCl_3CN, 5.5 g anhydrous $AlCl_3$, and 5.5 ml chlorobenzene in a 25 ml flask. Dry HCl was passed through, until all atmospheric air had been replaced after which a constant pressure of HCl from a bomb was maintained for 2 days, during which the reaction vessel was continuously shaken. After disruption of the bomb connection, the shaking was continued for 5 days. Following the instructions of Ref.[5] very closely, we ended up by 9–10 g of a mixture of (III), chlorobenzene, ether etc. The vessel, containing the mixture, was connected to a vacuum line, cooled in liquid air, evacuated, and heated to 0°C. At this temperature a fraction (2.37 g) was removed, mainly consisting of ether and about 5 % chlorobenzene. After initial elevation of the temperature to 25°C and afterwards to 80°C, a second fraction (F) was collected, consisting of ether and the two aromatic components (5.30 g). A resinous remanence (about 1 g) was left. (F) was separated on a "preparative" gas chromatograph (column "C", length 2.7 m and use of O-rings covered with teflon to prevent diffusion). The yield of (III) was 600 mg. The purity of this sample was 98 % according to gas chromatographic analysis (column "A", length 2 m). The contaminations were H_2O and unidentified, volatile products from the reaction mixture and from decomposition from the stationary liquid phase of the gas chromatograph. A single distillation on the vacuum line under pressure control removed most of these impurities so that the purity of the final product was 99 % (gas chromatogram). Weight 540 mg (5.2 mmole). At a subsequent microwave examination the impression of high purity was confirmed.

REFERENCES

1. Fields, M., Leaffer, M. A., Rotschild, S. and Rohan, J. *J. Am. Chem. Soc.* **74** (1952) 5498.
2. Pachendorf, K. and Leder-Pachendorf, L. *Ber.* **67** (1934) 1388.
3. Oxley, P., Partridge, M. W., Robson, T. D. and Short, W. F. *J. Chem. Soc.* **1946** 763.
4. Calvin, M. *et al. Isotopic Carbon*, John Wiley (1949), p. 230.
5. Houben, J. and Fischer, W. *Ber.* **66** (1933) 339.

Received June 22, 1962.

ACTA CHEMICA SCANDINAVICA 16 (1962) 2321–2324

Calculation of Urey-Bradley Potential Constants

II. Planar XY_2Z Molecules

E. MEISINGSETH

Institutt for teoretisk kjemi, Norges tekniske høgskole, Trondheim, Norway

The Urey-Bradley force constants were calculated for $^{11}BY_2Z$ (Y,Z = F, Cl, Br). The BY stretching constants (K_{XY}) showed a systematic variation with the Pauling electronegativity of the Z-atoms. The calculated vibrational frequencies of $^{10}BY_2Z$ are in good agreement with those reported in the literature.

In the previous article [1] the Urey-Bradley force constants of boron trihalides have been reported. It seems now reasonable to calculate the force constants for mixed boron trihalides.

For small displacements from the equilibrium distances (see Fig. 1) the Urey-Bradley potential function is given by

$$\begin{aligned} V = & \sum_i [K'_i r_i \Delta r_i + 1/2\, K_i (\Delta r_i)^2] \\ & + \sum_{i<j} [H'_{ij} r_{ij}^2 \Delta\alpha_{ij} + 1/2\, H_{ij} (r_{ij} \Delta\alpha_{ij})^2] \\ & + \sum_{i<j} [F'_{ij} d_{ij} \Delta d_{ij} + 1/2\, F_{ij} (\Delta d_{ij})^2] \end{aligned} \qquad (1)$$

Here K', K, H', H, F', and F denote the force constants. r and α represent the bond lengths and inter-bond angles, respectively, d is used to identify the distances between non-bonded atoms, and $r_{ij} = (r_i r_j)^{\frac{1}{2}}$.

APPLICATION TO THE PLANAR XY_2Z MODEL

In eqns. (1) the Δd's may be eliminated to express the potential function in terms of the valence coordinates (r, α).

Using the redundant condition ($\Delta\alpha_{12} + \Delta\alpha_{13} + \Delta\alpha_{23} = 0$) and following the same procedure as previously outlined [1], the potential function can be transformed to a quadratic form. The appropriate expression is given in Ref. [1] and need not be reported here. Wilson's secular equation [2]

$$|GF - \lambda E = 0|$$

has been utilized in the calculations.

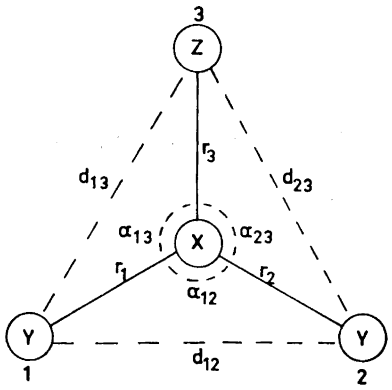

Fig. 1.

The considered planar XY_2Z molecules belong to the C_{2v} symmetry. Hence the following set of symmetry coordinates may be constructed.

Symmetry species A_1: $S_1 = (1/\sqrt{2})\,(\Delta r_1 + \Delta r_2)$
$S_2 = R\Delta\alpha_{12}$
$S_3 = \Delta r_3$
» » B_1: $S_4 = (1/\sqrt{2})\,(\Delta r_1 + \Delta r_2)$
$S^5 = (R/\sqrt{2})\,(\Delta\alpha_{13} + \Delta\alpha_{23})$

The meanings of r and α is the same as in eqns. (1). R designates the X—Y equilibrium distance.

For the presently chosen set of symmetry coordinates the elements of the F and G matrices read:

Species A_1: $F_{11} = K_{XY} + t_{YZ}^2 F'_{YZ} + 2s_{YY}^2 F_{YY} + s_{YZ}^2 F_{YZ}$
$F_{22} = H_\beta - s_{YY}^2 F'_{YY} + t_{YY}^2 F_{YY}$
$F_{33} = K_{XZ} + 2t_{YZ}^2 F_{YZ} + 2s_{YZ}^2 F_{YZ}$
$F_{12} = \sqrt{2}\, t_{YY} s_{YY} (F'_{YY} + F_{YY})$
$F_{23} = 0$
$F_{13} = -\sqrt{2}\, t_{YZ} t_{ZY} F'_{YZ} + \sqrt{2}\, s_{YZ} s_{ZY} F_{YZ}$
Species B_1: $F_{44} = K_{XY} + 2t_{YY}^2 F'_{YY} + t_{YZ}^2 F'_{YZ} + s_{YZ}^2 F_{YZ}$
$F_{55} = H_\alpha - s_{YZ} s_{ZY} F'_{YZ} + t_{YZ} t_{ZY} F_{YZ}$
$F_{45} = -t_{YZ} s_{ZY} F'_{YZ} - t_{ZY} s_{YZ} F_{YZ}$

Here $s_{ij} = (r_i - r_j \cos\alpha_{ij})/d_{ij}$, $s_{ji} = (r_j - r_i \cos\alpha_{ji})/d_{ij}$,
$t_{ij} = r_j \sin\alpha_{ij}/d_{ij}$ and $t_{ii} = r_j \sin\alpha_{ij}/d_{ij}$.

Species A_1: $G_{11} = 2\mu_x \cos^2 A + \mu_y$
$G_{22} = 4\mu_x \sin^2 A + 2\mu_y$
$G_{33} = \mu_x + \mu_y$
$G_{12} = 2\sqrt{2}\, \mu_x \cos A \sin A$
$G_{23} = 2\mu_x \sin A$
$G_{13} = \sqrt{2}\, \mu_x \cos A$
Species B_1: $G_{44} = 2\mu_x \sin^2 A + \mu_y$

$$G_{55} = 2\mu_x\left(\frac{R}{L}-\cos A\right)^2 + \mu_y + 2\left(\frac{R}{L}\right)^2\mu_z$$

$$G_{45} = 2\mu_x\left(\frac{R}{L}-\cos A\right)\sin A$$

Here μ represent the inverse atomic masses. R and L are the X—Y and X—Z equilibrium distances, respectively. A is used to designate the equilibrium YXZ angle.

NUMERICAL RESULTS

For the molecule model here considered one has eight UB force constants, but only five frequencies. To solve the secular equation, the number of independent force constants have to be reduced. Here the usual assumption of $F' = -1/10\ F$ was made. Furthermore, F_{YY}/K_{XY} values were transferred

Table 1. Calculated force constants mdyne/Å units

	BF_3	BF_2Cl	BF_2Br	BCl_3	BBr_2Cl	BBr_3
F_{YY}	(0.9263)	0.8813	0.8734	(0.5370)	0.4982	(0.4459)
K_{XY}	(6.0446)	5.7550	5.7036	(3.0212)	2.5708	(2.2997)
K_{XZ}		2.9374	2.6328		2.7328	
$H\alpha$		0.3737	0.5718		0.0665	
$H\beta$	(0.2125)	0.5916	0.5267	(0.0549)	0.1208	(0.0880)

$H\alpha$ and $H\beta$ represent the force constants for the YXZ and YXY angle bending, respectively. The values in parentheses are taken from Ref. [1]

Table 2. Calculated and observed frequencies for $^{10}BY_2Z$. * (cm^{-1} units.)

		$\nu_{obs.}$	$\nu_{calc.}$	% dev.
$^{10}BF_2Cl$	ν_1	1268	1283	0.2
	ν_2	701	725	3.4
	ν_3		399	
	ν_4	1470	1473	0.2
	ν_5	366	368	0.5
$^{10}BF_2Br$	ν_1	1247	1250	0.2
	ν_2	637	650	2.0
	ν_3		312	
	ν_4	1468	1470	0.2
	ν_5		347	
$^{10}BBr_2Cl$	ν_1	954	957	0.3
	ν_2		351	
	ν_3		153	
	ν_4	864	891	2.9
	ν_5		211	

* The data are taken from Ref[3].

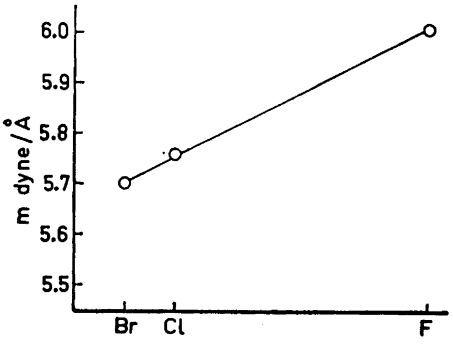

Fig. 2. K_{XY} plotted against the Pauling electronegativity of the Z-atom.

from the calculations on boron trihalides [1]. The numerical calculations were carried out using $a = A = 120°$ and based upon experimental frequencies from Ref. [3] The resulting force constants for the three molecules here considered are given in Table 1, and are compared to those for the boron trihalides.

The vibrational frequencies for $^{10}BY_2Z$ were computed from the presently calculated UB force constants. The results are given in Table 2 and show good agreement with the observed frequencies.

CORRELATION WITH ELECTRONEGATIVITY

Except for K_{XZ} in BF_2Cl, the values of the stretching force constants (K) showed to vary systematically with the electronegativity of the halogens.

In Fig. 2 the values of K_{XY} in BF_3, BF_2Cl and BF_2Br are plotted against the Pauling electronegativity [4] of the Z-atoms. The diagram shows that the stretching force constants for the B—Y bond increase with increasing electronegativity of the Z-atom. As halogens are more electronegative than boron, a substitution of the Z-atom with a more electronegative one will increase the positive charge on the boron atom. The negative charge displacement from the Y-atom to the boron atom is a second-order effect. In consequent, the resulting effect of the substitution will be a stronger B—Y bond.

REFERENCES

1. Meisingseth, E. *Acta Chem. Scand.* **16** (1962) 1601
2. Wilson, E. B., Jr., Decius, J. C. and Cross, P. C. *Molecular Vibrations*, McGraw-Hill Book Co., New York 1955.
3. Lindemann, L. P. and Wilson, M. K. *J. Chem. Phys.* **24** (1956) 242.
4. Pauling, L. *The Nature of the Chemical Bond*, Cornell Univ. Press, New York 1960.

Received May 22, 1962.

ACTA CHEMICA SCANDINAVICA 16 (1962) 2325–2336

The Structure of Nickel(II) Dithiosemicarbazide Sulphate Trihydrate

RITA GRØNBÆK and SVEND ERIK RASMUSSEN

Department of Inorganic Chemistry, University of Aarhus, Aarhus, Denmark

Nickel(II) dithiosemicarbazide sulphate can be obtained in different forms. The crystal structure of one of these, a trihydrate, has been solved by X-ray analysis using two dimensional Fourier methods. The complex nickel ion has a *trans*-planar structure. One of the hydrazine nitrogens and the sulphur atom coordinate to the nickel ion. Water molecules do not coordinate to the nickel ion. Atomic coordinates, standard deviations and temperature factors are reported.

A previous note [1] communicated preliminary results from an X-ray investigation of the two forms of nickel(II) dithiosemicarbazide sulphate. These compounds were prepared originally by K. A. Jensen [2] and considered *cis-trans* isomers.

Stereoisomerism of nickel complexes is not established definitely in the literature. The object of this X-ray investigation was the complete structure analysis of the so called α-isomer.

EXPERIMENTAL

Chemistry. α-Nickel(II) dithiosemicarbazide sulphate crystallized as a trihydrate by mixing a 0.1 M solution of $NiSO_4$ with a 0.2 M solution of thiosemicarbazide. Nickel was determined by precipitation with dimethylglyoxime after destruction of the thiosemicarbazide with 30 % H_2O_2. Calc. 15.01, found 15.35.

The crystals exhibit dichroism when viewed in the polarizing microscope. The powdered product looks green.

Water was removed at room temperature by P_2O_5 or by heating to 105°C. The dehydrated products regained water by exposure to atmospheric humidity.

X-Ray powder patterns proved that the anhydrous products obtained in these two ways were identical. The trihydrate was recovered by sorption of water as proved by powder diagrams.

The so called β-isomer precipitated by mixing boiling aqueous solutions of nickel sulphate and of thiosemicarbazide. This product contained no water of crystallization and absorbed no detectable amount of atmospheric humidity.

The X-ray powder pattern of the β-form was different from that of any of the α-compounds, hydrates or anhydrates.

The α-compound may be converted into the β-compound when heated in the presence of its saturated solution as described by Jensen [2]. Conversion in the solid state takes place less easily.

A sample of α-compound which had been heated to 150°C for four days yielded an X-ray powder pattern showing the lines of both the α-compound and the β-compound.

The colour of the sample changed gradually during the four days from green into greyish pink. The proper colour of the pure β-compound was not obtained.

A thermogravimetric analysis of the α-compound yielded the following results: Water was removed between 100 and 140°C. The anhydride was stable between 140°C and 260°C. At 260°C a rather vigourous reaction took place. The loss of weight corresponded to no simple reaction product. Possibly a mixture of NiO and $NiSO_4$ was formed. At 700°C the product was converted to NiO.

X-Ray techniques. Powder patterns were obtained with a 19 cm Bradley-Jay camera using filtered Cr-radiation. The camera was evacuated to a pressure of about 1 mm Hg during the exposure.

The dehydrated products of the α-compounds were placed in sealed Lindemann-glass tubes during the exposure.

A Guinier-de Wolff powder pattern was taken of the trihydrate and of highly purified sodium chloride, the latter being used as a reference for lattice constants measurements.

Integrated and non integrated Weissenberg data were obtained using filtered Cu-radiation. The axis of rotation was *c*. The crystal was about 0.15 × 0.15 × 0.5 mm.

30° Precession photographs were taken using filtered Mo-radiation. The precession axis was *a*.

The intensities of the integrated Weissenberg reflexions were measured photometrically. All other intensities were measured visually. Reflexions from the crystal being investigated were used for the preparation of calibrated intensity scales for the Weissenberg and the precession exposures.

Intensities were corrected for polarization and Lorentz factors using Cochran's chart for Weissenberg data and Waser's chart for precession data. Two sets of relative F^2 values were obtained: $F^2(hk0)$ and $F^2(0kl)$. No absorption correction was applied.

During the refinement of the structure it became evident, that the 100 reflexion was heavily affected by extinction. Therefore the crystal used was dipped in liquid nitrogen and a new set of intensities was collected. The intensity of the 100 reflexion increased by 50 %. All other intensities were constant within the accuracy of measurement.

Some of the Fourier summations were performed on a Hägg-Laurent computer built by Frank [3].

The major part of structure factor and fourier computation was carried out on the electronic digital computer DASK of Regnecentralen, Copenhagen.

DETERMINATION OF THE STRUCTURE

The α-$Ni(CH_5N_3S)_2SO_4,3H_2O$ is monoclinic. The unit cell has the following dimensions:

$$a = 6.98 \text{ Å}$$
$$b = 16.43 \text{ Å}$$
$$c = 6.35 \text{ Å}$$
$$\beta = 99.2°$$

The density is 1.84 g/cm³. Consequently there are two units of $Ni(CH_5N_3S)_2\ SO_4,\ 3H_2O$ per unit cell.

The only systematic extinctions are $0k0$ when k is odd. The possible space groups are $P2_1$ and $P2_1/m$. No piezoelectric effect was detected according to a private communication from professor V. Frank.

In the preliminary publication the space group $P2_1$ was favoured. The structure analysis proved, however, that the proper space group is $P2_1/m$,

which implies that several atoms are placed in special positions. Patterson projections $P(u, v, o)$ and $P(o, v, w)$ were calculated. An interpretation of the $P(u, v, o)$ projection was unsuccesful when based upon the assumption that the space group were $P2_1$.

Then the nickel atom was placed at the origin and the sulphur positions were found at once and it became evident that the correct space group is $P2_1/m$.

The nickel atom and the three sulphur atoms were used as searcher atoms in the interpretation of the Patterson projections. Graphical superposition methods were used to obtain a quick survey of the possible positions of the light atoms and analytical methods were used to obtain more accurate positions. The procedure was equivalent to the use of the Buerger minimum function [4,5] using an M_8 function. The trial structure obtained in this way was essentially correct.

The structure was refined by aid of successive difference fourier projections along the a- and the c-axes.

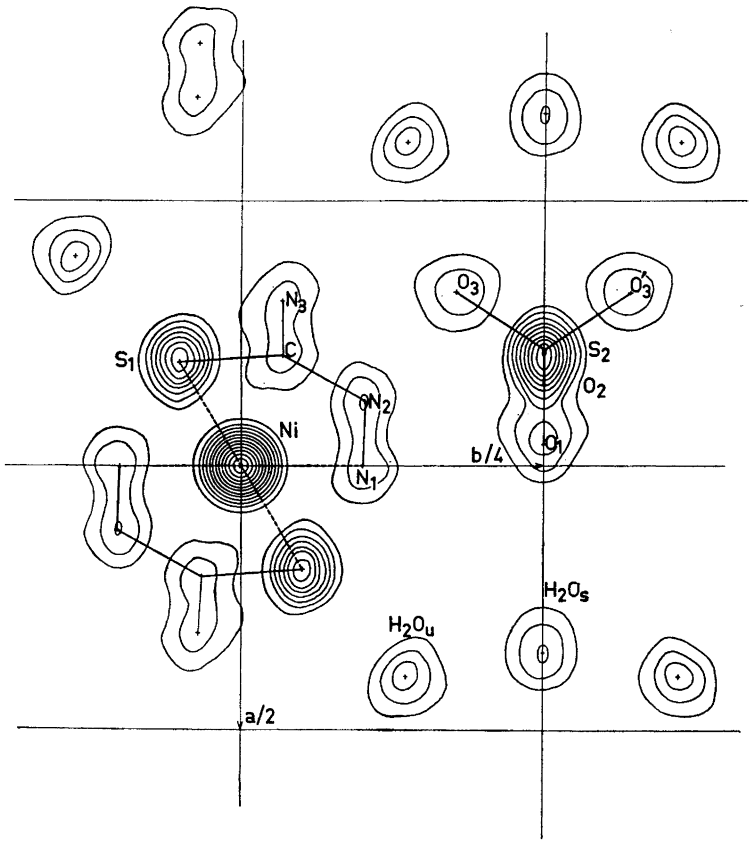

Fig. 1. Fourier projection x,y. Contour lines with equal but arbitrary intervals.

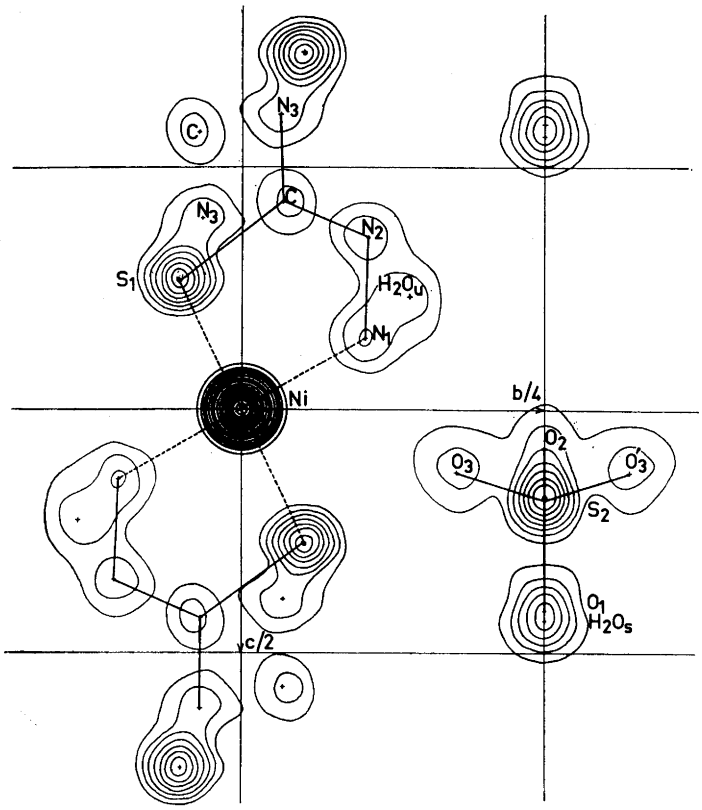

Fig. 2. Fourier projection y,z. Contour lines with equal but arbitrary intervals.

The R-values $\Sigma||F_o|-|F_c||/\Sigma|F_o|$ were reduced from $R(hk0) = 42$ %, $R(0kl) = 26$ % to $R(hk0) = 10.7$ % and $R(0kl) = 10.9$ % through seven successive refinements. Individual isotropic temperature factors were used. The B-factors were refined too from the difference maps using the procedure suggested by Cochran [6].

We now began looking for hydrogen atoms in the difference maps. We actually did find small peaks in positions which could be attributed to the hydrogens of the thiosemicarbazide group assuming the hydrogens to be located according to the usual stereochemical rules. Inclusion of the supposed locations of these hydrogens in the structure factor calculations caused a small decrease in the R-values. We therefore looked for the hydrogen atoms of the water molecules as well and we believe that we have found reasonable positions of these hydrogens too. After two more cycles of refinement we have stopped at the following R-values:

$$R(hk0) = 10.7\ \% \qquad R(0kl) = 10.2\ \%$$

excluding hydrogen atoms and

$$R(hk0) = 9.1\ \% \qquad R(0kl) = 9.3\ \%$$

including hydrogen atoms.

Not observed reflexions are omitted if F_c is well below the lowest observed F-value, else they are included in the R-values and the difference-fourier syntheses with the value $F_{o\ min}/2$.

The two final Fourier projections are shown in Figs. 1 and 2. The following expression [7,8] was used for calculating the atomic scattering factors:

$$f_n(\sin\Theta/\lambda) = A_n\exp[-a_n(\sin\Theta/\lambda)^2] + B_n\exp[-b_n(\sin\Theta/\lambda)^2] + C_n\exp[-c_r(\sin\Theta/\lambda)^2]$$

The parameters used are given in Table 1.

CRYSTAL DATA

All pertinent crystal data are presented below:
Crystal system: Monoclinic.
Unit cell: Mean values from precession, Weissenberg and Guinier diagrams:

$a = 6.98 \pm 0.01$ Å $\quad b = 16.43 \pm 0.01$ Å $\quad c = 6.35 \pm 0.01$ Å
$\beta = 99.2° \pm 0.1°$

Space group: $P2_1/m$, No. 11 (C_{2h}^2); unique axis b.

The coordinates found, their standard deviations and the temperature factors used for $hk0$ (Cu-radiation) and $0kl$ (Mo-radiation), respectively: Table 2.

As no correction for absorption was applied the temperature factors probably include absorption effects. This is a probable explanation of the difference between the two sets of B-factors.

For the standard deviations were used the formulae given by Cruickshank [9] with the second derivative $\partial^2\varrho/\partial r^2$ found by the procedure used by Cochran [10].

The interatomic distances and standard deviations found are given in Table 3. The bond angles found are given in Table 4. The shortest Van der Waals distances are given in Table 5.

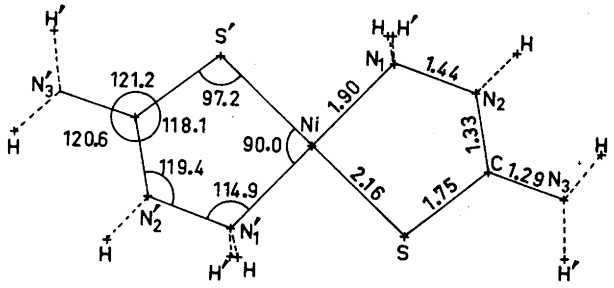

Fig. 3. Bond lengths and bond angles of the nickel(II)dithiosemicarbazide ion.

Table 1.

	A	*B*	*C*	*a*	*b*	*c*	Ref.
Ni_{Cu}	12.76	8.638	2.550	2.637	19.88	0	7
Ni_{Mo}	12.76	8.638	5.650	2.637	19.88	0	
S	7.603	6.354	1.924	1.637	39.98	0	7
C	1.771	1.424	2.779	0.473	9.499	28.008	8
N	1.788	2.606	2.693	0.344	8.670	23.826	8
O	2.113	4.637	1.211	2.867	14.75	0	7
H	0.3882	0.6011	0.0076	7.151	30.18	0	7

Table 2.

Atom	*x/a*	*y/b*	*z/c*	σx Å	σy Å	σz Å	*B*(Cu-radiation) Å²	*B*(Mo-radiation) Å²
Ni	0	0	0	0.004	0.002	0.003	1.4	1.7
S_1	0.1915	0.0515	0.2685	0.006	0.003	0.005	2.0	2.35
N_1	0.001	−0.1005	0.147	0.02	0.015	0.015	2.1	2.4
N_2	0.123	−0.1025	0.352	0.03	0.01	0.015	2.2	2.5
N_3	0.311	−0.034	0.619	0.045	0.02	0.02	2.5	2.8
C	0.208	−0.0345	0.432	0.05	0.015	0.02	2.2	2.5
S_2	−0.215	0.250	0.187	0.008	0.004	0.007	1.85	2.2
O_1	−0.041	0.250	0.086	0.025	0.015	0.05	2.7	3.0
O_2	−0.155	0.250	0.417	0.05	0.01	0.02	2.7	3.0
O_3	−0.324	0.1785	0.127	0.02	0.025	0.035	2.95	3.25
O_5	0.342	0.250	0.438	0.02	0.015	0.02	2.8	3.1
O_4	0.396	0.136	0.773	0.015	0.015	0.02	2.8	3.1
H'_{N_1}	0.048	−0.145	0.060				3.7	4.0
H''_{N_1}	−0.130	−0.117	0.175				3.7	4.0
H_{N_2}	0.125	−0.150	0.445				3.7	4.0
H'_{N_3}	0.375	−0.080	0.706				3.7	4.0
H''_{N_3}	0.344	0.013	0.719				3.7	4.0
$H'_{H_2O_5}$	0.210	0.250	0.362				3.7	4.0
$H''_{H_2O_5}$	0.415	0.250	0.322				3.7	4.0
$H'_{H_2O_4}$	0.500	0.150	0.885				3.7	4.0
$H''_{H_2O_4}$	0.380	0.172	0.655				3.7	4.0

Table 3. Interatomic distances and standard deviations (in Å).

$Ni-S_1$	2.16 ± 0.01
$Ni-N_1$	1.90 ± 0.02
N_1-N_2	1.44 ± 0.04
N_2-C	1.33 ± 0.05
$C-N_3$	1.29 ± 0.05
S_1-C	1.75 ± 0.03
S_2-O_1	1.46 ± 0.05
S_2-O_2	1.45 ± 0.03
S_2-O_3	1.42 ± 0.04
O_1-O_2	2.36
O_1-O_3	2.35
O_2-O_3	2.34
O_3-O_4	2.35

The hydrogen atoms have been placed so that distances N—H are 1.00 Å and O—H 0.96 Å, and so that the valency angles are close to commonly accepted values.

Table 4. The bond angles found are:

S_1-Ni-N_1:	89.97°
$Ni-S_1-C$:	97.23°
$Ni-N_1-N_2$:	114.88°
N_1-N_2-C:	119.42°
N_2-C-N_3:	120.56°
N_2-C-S:	118.07°
N_3-C-S:	121.18°
$O_1-S_2-O_2$:	108.35°
$O_1-S_2-O_3$:	109.26°
$O_2-S_2-O_3$:	109.02°
$O_3'-S_2-O_3$:	111.85°

Table 5. The shortest Van der Waals distances are (in Å):

$H_2O_u-N_1$:	2.95
$H_2O_u-N_3$:	2.99
$H_2O_u-O_3$:	2.82
$H_2O_u-H_2O_s$:	2.82
$H_2O_s-O_1$:	3.20
$H_2O_s-O_2$:	3.45—3.53
$H_2O_s-O_3$:	3.49
N_1-O_1:	2.90
N_2-O_2:	2.82
N_3-O_3:	2.86

DISCUSSION

The nickel(II) dithiosemicarbazide ion has the *trans* configuration and is nearly planar. The deviations from planarity are within the standard deviations.

In this structure the water of crystallization is not coordinated to the nickel atom, the shortest nickel-water distance being 3.98 Å. The bonding $Ni-H_2O$ distance is generally close to 2.0 Å.

Asmussen [11] reported diamagnetism for the anhydrous compound and paramagnetism of $Ni(CH_5N_3S)_2,(NO_3)_2,2H_2O$.

Hare [12] reported that the trihydrate of nickel thiosemicarbazide sulphate is diamagnetic whereas an aqueous solution of the composition:

$C(Ni(NO_3)_2) = 0.1$ m, $C(CH_5N_3S) = 0.2$ m is paramagnetic.

To our knowledge the α-$Ni(CH_5N_3S)_2SO_4$, $3H_2O$ is the only diamagnetic nickel compound containing water.

There is practically no tendency to octahedral coordination around the nickel atom. The N_3-atoms of neighbouring molecules are the next nearest neighbours of the nickel-atom. The $Ni-N_3$ distance is 3.55 Å which is far from bonding distance and is large even for a van der Waals distance.

Fig. 3 shows the bond lengths and bond angles of the complex ion. The Ni—N distance is significantly shorter than the corresponding distance in paramagnetic Ni-complexes (2.0—2.2 Å). It is comparable to the Ni—N distances in other diamagnetic complexes:

1.84 Å in bis-salicylaldiminato-Ni(II), Stewart and Lingafelter [13]

1.86 Å in bis-salicylaldoximato-Ni (II), Merritt *et al.*[14]

Table 6. Calculated and observed structure factors.

h k l	F_c	F_o	*h k l*	F_c	F_o
0 2 0	51.6	46.6	3 9 0	−21.8	−24.3
0 4 0	69.8	61.9	3 10 0	46.6	47.6
0 6 0	−19.3	−21.8	3 12 0	28.4	29.4
0 8 0	51.6	51.4	3 13 0	− 7.3	− 9.4
0 10 0	−33.0	−32.4	3 14 0	15.0	−19.5
0 12 0	20.1	20.8	3 15 0	− 2.7	− 3.4
0 14 0	−29.9	−28.6	3 16 0	2.8	3.2
0 16 0	28.0	26.2	3 17 0	−12.5	−13.5
0 18 0	6.2	10.0	3 19 0	5.4	2.7
0 20 0	30.9	32.7	4 0 0	18.8	21.9
1 0 0	86.3	94.3	4 1 0	12.7	10.8
1 1 0	42.0	39.4	4 2 0	30.8	31.5
1 2 0	57.6	52.5	4 3 0	40.4	40.4
1 3 0	−38.4	−40.7	4 4 0	41.4	41.3
1 4 0	46.0	46.1	4 5 0	3.6	6.7
1 5 0	9.9	9.7	4 6 0	10.9	14.9
1 6 0	−23.6	−23.5	4 7 0	39.3	36.4
1 7 0	−10.3	−18.2	4 8 0	15.7	19.7
1 8 0	35.3	36.9	4 9 0	− 4.9	− 6.0
1 9 0	7.3	10.3	4 10 0	12.3	12.1
1 10 0	26.8	27.7	4 11 0	1.2	5.4
1 11 0	7.2	5.4	4 12 0	17.4	18.6
1 12 0	24.9	27.3	4 13 0	−20.8	−20.4
1 13 0	47.5	46.8	4 14 0	5.0	2.0
1 16 0	12.1	13.2	4 15 0	−10.1	− 9.6
1 17 0	10.7	13.5	4 16 0	9.6	8.0
1 18 0	17.1	18.1	4 17 0	−12.5	−15.1
1 19 0	− 8.0	− 8.1	4 18 0	7.1	6.0
1 20 0	21.7	21.9	5 0 0	59.1	57.4
2 0 0	−27.3	−30.5	5 1 0	4.4	8.8
2 1 0	42.9	40.6	5 2 0	28.7	28.5
2 2 0	17.4	17.5	5 3 0	− 7.2	− 8.2
2 3 0	−30.1	−31.9	5 4 0	28.5	31.6
2 4 0	−26.7	−25.6	5 5 0	16.4	13.7
2 5 0	− 9.4	−13.9	5 6 0	− 5.2	− 5.3
2 6 0	30.8	31.7	5 7 0	− 5.3	− 6.2
2 7 0	−71.1	−71.9	5 8 0	18.1	19.3
2 8 0	48.1	44.3	5 9 0	12.6	11.5
2 9 0	27.0	27.0	5 10 0	−14.9	−12.5
2 10 0	64.1	66.0	5 11 0	− 9.5	−11.6
2 11 0	− 3.9	− 2.0	5 12 0	4.8	6.1
2 12 0	26.3	25.3	5 13 0	− 3.1	− 4.9
2 13 0	18.7	21.9	5 14 0	5.7	2.0
2 14 0	34.2	34.5	5 15 0	− 5.3	− 3.4
2 15 0	5.7	5.9	5 16 0	18.3	18.1
2 17 0	14.0	14.5	6 0 0	41.7	37.0
2 18 0	11.0	11.9	6 1 0	− 2.7	− 2.0
2 19 0	− 8.6	− 9.2	6 2 0	24.0	25.5
3 0 0	31.4	32.2	6 3 0	−29.5	−28.5
3 1 0	−13.5	−16.0	6 4 0	22.0	19.3
3 2 0	7.2	10.5	6 6 0	7.7	8.1
3 3 0	14.5	15.6	6 7 0	−15.9	−15.0
3 4 0	8.8	9.0	6 9 0	6.1	6.2
3 5 0	9.9	10.3	6 10 0	5.8	7.0
3 6 0	51.6	52.1	6 11 0	− 4.8	− 4.9
3 8 0	31.7	34.5	6 12 0	8.3	9.4

Table 6, contd.

h k l	F_c	F_o	*h k l*	F_c	F_o
6 13 0	14.0	10.6	0 9 2	9.1	5.6
7 1 0	3.7	5.4	0 10 2	48.1	43.3
7 2 0	14.6	13.5	0 11 2	6.3	6.1
7 3 0	−11.4	− 9.2	0 12 2	36.0	35.3
7 4 0	− 6.0	− 8.8	0 13 2	−15.3	−12.7
7 5 0	−13.3	−11.9	0 14 2	19.0	20.7
7 6 0	16.2	14.7	0 0 3	15.4	18.8
7 8 0	12.3	13.0	0 1 3	−21.2	−20.7
7 9 0	4.4	6.3	0 2 3	74.4	74.8
7 10 0	28.0	24.6	0 3 3	45.6	45.9
7 11 0	2.9	2.0	0 4 3	30.7	33.1
7 12 0	8.2	9.8	0 5 3	27.3	33.3
8 0 0	− 3.5	− 2.0	0 6 3	33.0	37.4
8 1 0	− 5.2	− 7.5	0 7 3	19.7	19.3
8 3 0	1.4	3.4	0 8 3	7.5	8.1
8 4 0	− 5.0	− 6.1	0 9 3	−10.1	− 6.3
8 5 0	1.7	5.8	0 10 3	16.8	27.6
8 6 0	7.4	8.5	0 13 3	−14.4	−12.5
8 8 0	20.4	17.8	0 14 3	24.3	25.6
			0 15 3	− 9.4	−10.4
0 2 0	58.6	48.1	0 16 3	6.2	7.4
0 4 0	76.7	74.6	0 17 3	−15.7	−13.1
0 6 0	−13.5	−19.1	0 18 3	21.0	19.8
0 8 0	57.2	60.6	0 0 4	17.2	17.2
0 10 0	−27.1	−28.5	0 1 4	9.7	13.2
0 12 0	24.6	26.3	0 2 4	45.1	43.7
0 14 0	−24.1	−24.3	0 3 4	−35.1	−40.3
0 16 0	30.5	33.0	0 4 4	27.6	32.6
0 18 0	9.4	10.1	0 5 4	5.3	8.7
0 20 0	31.2	37.4	0 6 4	23.9	26.5
0 0 1	26.9	27.6	0 7 4	−25.5	−29.6
0 1 1	−34.1	−35.7	0 8 4	9.9	12.7
0 2 1	3.3	6.3	0 9 4	4.6	7.2
0 3 1	52.8	50.9	0 11 4	−10.8	−11.3
0 4 1	10.2	11.4	0 13 4	17.3	17.7
0 5 1	−100.4	−96.5	0 14 4	29.7	27.2
0 6 1	50.2	48.7	0 16 4	21.1	21.1
0 7 1	−41.1	−46.2	0 17 4	9.7	10.1
0 8 1	30.7	32.8	0 18 4	16.4	14.0
0 9 1	−22.0	−28.1	0 0 5	28.6	34.8
0 10 1	39.7	38.5	0 1 5	− 5.1	− 7.2
0 11 1	38.2	37.4	0 2 5	10.4	8.8
0 12 1	37.9	36.1	0 3 5	−17.7	−19.3
0 14 1	24.3	23.6	0 4 5	30.0	35.6
0 15 1	32.9	29.2			
0 16 1	24.4	22.2	0 5 5	−18.7	−17.8
0 18 1	14.5	15.3	0 6 5	13.4	13.1
0 20 1	10.9	11.3	0 7 5	8.9	8.3
0 0 2	−19.7	−25.0	0 8 5	40.0	40.1
0 1 2	−15.0	−11.3	0 9 5	7.4	7.2
0 2 2	13.7	12.5	0 10 5	11.1	11.3
0 3 2	28.3	31.4	0 11 5	3.2	7.2
0 4 2	63.0	59.0	0 12 5	19.6	19.6
0 5 2	15.0	17.1	0 15 5	8.1	7.2
0 6 2	47.2	53.4	0 16 5	10.0	9.4
0 8 2	41.0	40.3	0 0 6	4.0	10.1

Table 6, contd.

h k l	F_c	F_o
0 3 6	9.7	11.3
0 4 6	7.6	8.8
0 6 6	13.0	11.6
0 7 6	8.2	7.2
0 8 6	23.6	26.2
0 9 6	− 5.0	− 6.7
0 10 6	29.6	29.0
0 12 6	22.1	21.4
0 13 6	− 9.2	− 9.4
0 14 6	8.4	7.9
0 0 7	22.8	24.4
0 2 7	21.5	23.4
0 3 7	13.4	14.9
0 4 7	17.1	18.6
0 5 7	5.9	6.1
0 6 7	10.8	8.3
0 7 7	13.4	14.0
0 0 8	13.3	13.7
0 2 8	20.0	26.0
0 3 8	− 6.7	− 6.3

Not observed reflexions:

h k l	F_c
0 17 1	− 2.4
0 19 1	4.9
0 7 2	− 1.9
0 15 2	6.0
0 16 2	4.2
0 17 2	− 5.9
0 18 2	4.5
0 20 2	− 1.6
0 11 3	1.4
0 12 3	1.7
0 19 3	− 0.8
0 10 4	− 4.3
0 15 4	− 3.3
0 13 5	3.7
0 14 5	7.1
0 1 6	5.0
0 2 6	5.5
0 5 6	− 4.6
0 11 6	− 3.3
0 9 7	− 2.9
0 10 7	5.3
0 1 8	− 4.0
1 15 0	0.9
2 16 0	0.8
3 11 0	0.8
3 18 0	1.4
6 5 0	0.9
6 8 0	1.2
6 14 0	− 1.8
7 7 0	− 1.8
8 2 0	1.0
8 7 0	1.0

The Ni—S distance is comparable to the corresponding distance in nickel diethyldithiocarbamate as determined by Shugam and Levina [15]. These Ni—S distances are remarkably short compared to the sum of the radii of the nickel ion and the sulphur atom: 2.4—2.5 Å.

The N_1—N_2 distance is close to the N—N distances of several hydrazine compounds.

The carbon atom may be described as trigonally hybridized. The two C—N and the C—S distances correspond to a bond order of 1.3.

The N_2 atom also seems to be trigonally hybridized. The difference maps indicate the presence of a hydrogen atom in the plane of the complex. Similar considerations may be applied to the N_3 atom, whereas the N_1 atom is probably sp^3 hybridized.

Our bond lengths of the thiosemicarbazide molecule agree with those reported by Cavalca, Nardelli and Branchi [14] for $Zn(CH_5N_3S)Cl_2$. Our Ni—N and Ni—S distances are significantly shorter, by 0.21 Å and 0.13 Å, respectively, than the Zn—N and the Zn—S distances. The difference in ionic radius between Zn^{2+} and Ni^{2+} is 0.10 Å.

Probably the N_3-atom cannot coordinate to the Ni^{2+} ion because bonding orbitals are unavailable in the sp^2 state. The hybridization of sulphur is still

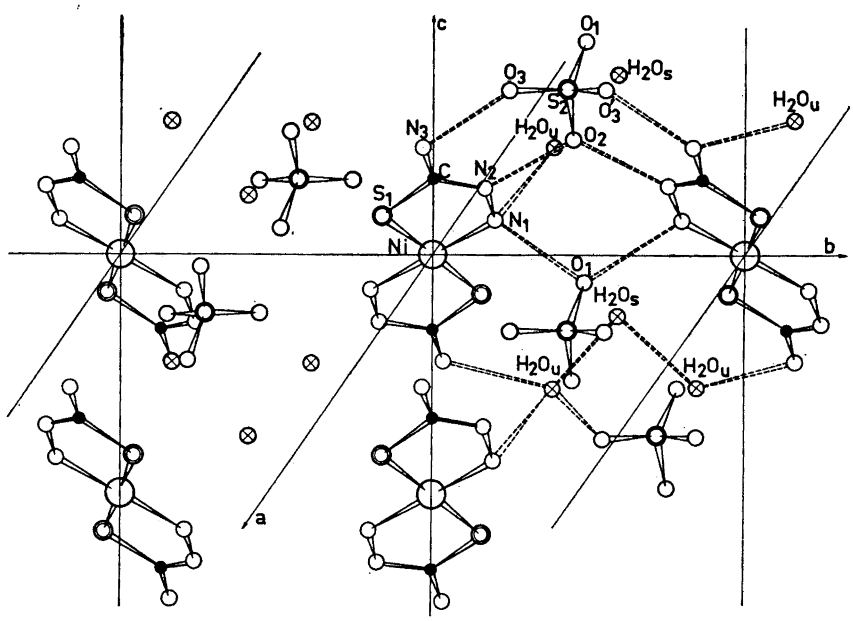

Fig. 4. Parallel projection of selected parts of the structure showing the hydrogen bonding scheme.

undetermined. The bonding between Ni^{2+} and sulphur is rather strong as indicated by the relatively short Ni—S distance.

Bond lengths and bond angles of the sulphate group agree well with accepted values.

The water molecules fit into holes between the complex ions and the sulphate groups. Some of the distances between the water molecules, the sulphate oxygen atoms and the nitrogen atoms indicate weak hydrogen bonding. The interatomic distances in question are 2.8—2.9 Å.

A reasonable hydrogen bonding scheme is shown in Fig. 4 which is a parallel projection of the structure. Some atoms have been omitted to give a clearer picture of details pertinent to the discussion.

One hydrogen of N_1 points towards an oxygen atom of the sulphate group, the other hydrogen towards the oxygen of the H_2O_u molecule. Similar considerations apply to the N_3 atom. The H-atom of the N_2 atom points towards a sulphate oxygen. One hydrogen atom of the H_2O_u molecule points towards a water molecule in the symmetry plane, the other one towards a sulphate oxygen. The hydrogen bonding around the H_2O_u molecule is approximately tetrahedral.

The H-bonding scheme around the water of the symmetry plane is somewhat different. One hydrogen atom is located on the line from the water-oxygen perpendicular to the connecting line between two oxygens of the sulphate group $O_1—O_2$, the other hydrogen approximately points towards the

middle of the line between the other sulphate oxygens $O_3—O_3'$ of the next group in the direction of the x-axis but with some deviation in the direction of a third oxygen (O_2—3.53 Å away).

No hydrogen atoms appear to be located on any of the lines connecting two hydrogen bonded atoms.

Acknowledgements. We thank the following persons and institutions for helping us in various stages of this work: Professors J. Bjerrum, N. Hofman-Bang, and V. Frank and Dr. C. Hare.

Carlsbergfonden, Videnskabsfonden and Statens teknisk videnskabelige fond have given financial support.

Regnecentralen cooperated efficiently in the solution of our computational problems.

REFERENCES

1. Grønbæk, R. and Rasmussen, S. E. *Acta Chem. Scand.* **14** (1960) 782.
2. Jensen, K. A. and Rancke Madsen, E. *Z. anorg. Chem.* **219** (1934) 243; **221** (1934) 11; **229** (1936) 277.
3. Frank, V. *J. Sci. Instr.* **34** (1957) 210.
4. Buerger, M. J. *Acta Cryst.* **4** (1951) 531.
5. Rasmussen, S. E. *Acta Chem. Scand.* **13** (1959) 2009.
6. Cochran, W. *Acta Cryst.* **4** (1951) 408.
7. Forsyth, J. B. and Wells, M. *Acta Cryst.* **12** (1959) 412.
8. Åsbrink, S., Blomqvist, G. and Westman, S. *Arkiv Kemi* **14** (1959) 545.
9. Cruickshank, D. W. J. *Acta Cryst.* **2** (1949) 154.
10. Cochran, W. *Acta Cryst.* **4** (1951) 81.
11. Asmussen, R. W. *Magnetokemiske undersøgelser* (1944).
12. Hare, C. *Private communication.*
13. Stewart, J. M. and Lingafelter, E. C. *Acta Cryst.* **12** (1959) 842.
14. Merritt, L. L., Guare, C. and Lessor, A. E. *Acta Cryst.* **9** (1956) 253.
15. Shugam, E. A. and Levina, V. M. *Kristallografiya* **5** (1960) 257; Transl. (1960) 239.

Received June 20, 1962.

ACTA CHEMICA SCANDINAVICA 16 (1962) 2337–2340

An Electron Diffraction Analysis of the Conformational Ratio in Monofluorocyclohexane

PER ANDERSEN

Universitetets Kjemiske Institutt, Blindern-Oslo, Norway

Monofluorocyclohexane has been investigated using electron diffraction methods in the gas phase in order to determine the ratio between the axial and equatorial conformations. The best agreement with the experimental distribution curve is obtained when the theoretical curve contains 57 % of the conformation with fluorine in the equatorial position corresponding to an energy difference between the two conformations of approximately 170 cal/mole.

During the last five years attempts have been made using spectroscopic methods, NMR and electron diffraction to determine the ratio of the two conformations in halogenated cyclohexanes. Klæboe, Lothe and Lunde [1,2] investigated the vibrational spectra of the monohalogenated cyclohexanes in the liquid and solid state and concluded that the *e*-conformation dominates in monochloro- and monobromocyclohexane in the liquid state with 78 % and 85 %, respectively. In the case of monofluorocyclohexane identical spectra were obtained for the liquid, the cubic and the anisotropic solid states. The spectra were investigated down to −150°C and the transition from the cubic to the anisotropic modification was studied in polarized light. It was concluded that one conformation only is present in the liquid state, and it was suggested that an intramolecular hydrogen bond C-H---F might stabilize one of the conformations. Reeves and Strömme [3] made an investigation using NMR on monochloro- and monobromocyclohexane and found that the *e*-conformation dominates in both cases with 77 % and 81 %, respectively, in good agreement with the infrared work mentioned above. However, an electron diffraction investigation of monochlorocyclohexane by Atkinson [4] shows that 55 % of the *e*-conformation is present in the gaseous state. Moreover, an electron diffraction analysis of 1,4-dichloro- and 1,4-dibromocyclohexane by Atkinson and Hassel [5] led to the conclusion that the *e* and *a* positions are equally populated in both the chloro- and bromo compound. In these substances one should expect to find approximately the same interaction between halogen and the nearest neighbouring carbon and hydrogen atoms as in the monoderivative.

Unless the presence of an intramolecular hydrogen bond should favour one of the conformations of the monofluorocyclohexane molecule there appears to be no reasons for believing that a steric interaction may result in a difference in energy large enough to make one conformation dominate completely. It might be expected that an electron diffraction investigation of the vapour should make it possible to decide at least qualitatively if both axial and equatorial forms are present. An interpretation of the infrared investigation according to which the solid compound contains both forms is not to be excluded but does not appear very satisfactory in view of previously established facts regarding cyclohexane derivatives.

The sample used in the present investigation was kindly placed at the author's disposal by K. Lunde. The diffraction pictures were taken with a distance of 19 resp. 48 cm between the photographic plate and the point of scattering; the intensity curve extended from $s = 1.25$ to $s = 49.5$ ($s = 4\pi \sin \vartheta/\lambda$). The intensity curve was treated as described elsewhere [6] and employing three different values of the constant k in the damping expression, *viz.* 0.009, 0.0015 and 0.0036. The radial distribution curve obtained with $k = 0.0036$ is shown in Fig. 1.

THE RADIAL DISTRIBUTION CURVE

An analysis of the radial distribution curves (Fig. 1) shows that both conformations must be present in the gaseous state. In order to determine the distances associated with the fluorine atom alone it was assumed that the sixmembered ring was undistorted and had the same angles and bond lengths as in cyclohexane itself. The following unpublished cyclohexane values determined in this institute were used; C—C = 1.53 Å, the C—C—C angle 111.5°. A theoretical radial distribution curve built up from Gaussian curves for all the carbon-carbon and carbon-hydrogen distances was subtracted from the experimental $\sigma(r)/r$ curve. The experimental distribution curve and the difference curve containing only the F—C distances are shown in Fig. 1. A theoretical intensity curve was calculated on the basis of all distances and assuming both the *e* and the *a* conformation to be present each with 50 %

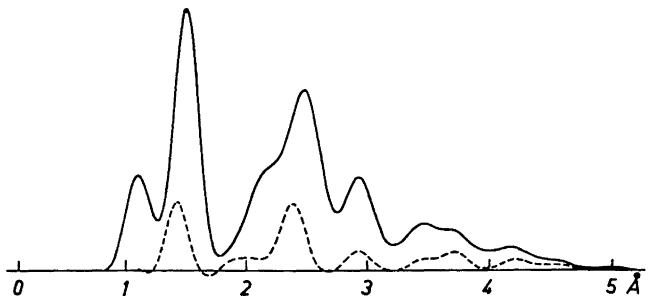

Fig. 1. Radial distribution curve of monofluorocyclohexane (full line) and the distribution curve after subtraction of the contribution from the cyclohexane ring (broken line).

contribution. The experimental intensity curve was extended from $s = 1.25$ to $s = 0$ by adding the theoretical curve and the envelope of the distribution curve was corrected according to the intensity curve.

The radial distribution curve after subtraction of the contribution from the cyclohexane ring itself reproduced in Fig. 1 clearly indicates the presence of all distances both in the equatorial and in the axial conformation. The F—C(1) bond distance at about 1.4 Å and the F—C(2) distance around 2.4 Å should be nearly the same in both conformations, although F_e—C(2) and F_a—C(2) could differ slightly if the C—C—F angle is distorted. The peak at 2.43 Å corresponds to a F_a—C(3) distance and the one around 4.2 Å to the F_e—C(4) distances. The maximum between 3.3 and 3.9 Å contains distances F_a—C(4) around 3.5 Å and F_e—C(3) at about 3.75 Å. The position of the fluorine in the two conformations relative to the cyclohexane ring were determined from these six peaks. Here, an undistorted six-membered ring (C—C: 1.53 Å and C—C—C angle 111.5°) has been assumed. The following distances were determined: F—C: 1.41 Å; F—C(2): 2.35 Å; F_e—C(3): 3.74 Å; F_e—C(4): 4.22 Å; F_a—C(3): 2.93 Å and F_a—C(4): 3.50 Å.

Using these distances theoretical radial distribution curves were constructed from Gaussian curves for both conformations and are reproduced in Fig. 2a.

A least squares procedure on the part of the curve $r > 2.6$ Å was employed in order to determine the ratio of the two conformations from the experimental radial distribution curve. The best agreement with the experimental curve was obtained when the theoretical curve contained 57 % of the *e* form and 43 % of the *a* form leading to a standard deviation ± 2 %. This corresponds to an energy difference of approximately 170 cal/mole between the two conformations. The calcultions of the two theoretical radial distribution curves (Fig. 2a) were carried out assuming a cyclohexane ring having the symmetry

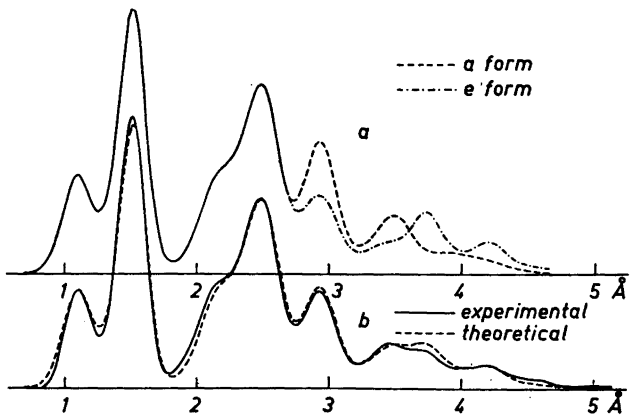

Fig. 2. a: Theoretical radial distribution curves of monofluorocyclohexane for the *e*- and *a*-conformation.
b: Experimental and theoretical radial distribution curves. The theoretical curve containing 57 % of the *e*-conformation.

D_{3d} and this makes it difficult to estimate the accuracy of the determined ratio between the two conformations.

The distances determined show that the C—F bond direction is probably not strictly parallel to the chief axis of the ring when fluorine is in the axial position. The tilting is calculated to be 2° away from the axis and could indicate that a slight steric hindrance is present in the axial position. If the hydrogen atoms are assumed to occupy the same positions as in cyclohexane itself the $F_a—H_a(3)$ and $F_e—H_a(2)$ distances will be 2.59 Å and 2.58 Å, respectively, and the fluorine is thus surrounded by hydrogen in the same way in the equatorial and axial positions. There can be no doubt, however, that monofluorocyclohexane is present in both conformations in the gaseous state and the two forms in approximately equal amounts. So far no cases are known where more than one conformation of a cyclohexane derivative has been found in the crystalline state. If the difference in energy of the two conformations is very small, however, one might hope to find cases of polymorphism depending on a transition between different conformations. Transition phenomena in crystals which may be of this kind are now being investigated in this institute.

Acknowledgement. The author wishes to thank Cand.real. Arne Almenningen for taking the electron diffraction pictures and Siv.ing. Liv Fernholt for her assistance with the numerical calculations.

REFERENCES

1. Klæboe, P., Lothe, F. J. and Lunde, K. *Acta Chem. Scand.* **10** (1956) 1465.
2. Klæboe, P., Lothe, F. J. and Lunde, K. *Acta Chem. Scand.* **11** (1957) 1677.
3. Reeves, L. W. and Strömme, K. O. *Can. J. Chem.* **38** (1960) 1241.
4. Atkinson, V. A. *Acta Chem. Scand.* **15** (1961) 599.
5. Atkinson, V. A. and Hassel, O. *Acta Chem. Scand.* **13** (1959) 1737.
6. Bastiansen, O. and Skancke, P. N. *Advan. Chem. Phys.* **3** (1961) 323.

Received June 30, 1962.

ACTA CHEMICA SCANDINAVICA 16 (1962) 2341–2349

A Recalculation of Experiments on Mutarotation of D-Glucose and D-Mannose with an Interpretation of its Results

J. A. CHRISTIANSEN

Sundvænget 9, Hellerup, Denmark

A programme is described for calculating the equilibrium optical rotation of a solution from non-equilibrium data, referring to cases where only one reactant and one resultant are present. The calculations yield furthermore a well defined value for the equilibrium-fraction ω, (number of resultant moles)/(total number of moles).

The programme is applied to measurements (Isbell and Pigman, Levene) on the reaction β-anomer $\rightleftharpoons$ α-anomer for D-glucose and D-mannose. The result is that ω is very nearly 4/11 for glucose and 2/3 for mannose. The former fraction is independent of temperature and the same is probably true of the latter.

It is attempted to interpret the empirical results by means of mechanical and statistical-thermodynamical considerations of molecular models. The result is that the empirical values of the two fractions can and can only be interpreted in a natural way if it be assumed that the configurations of the two sugars at C_5, C_4, C_3, and C_2 are the current ones (Haworth, Hassel, Reeves) but that the HO-groups at C_1 are equatorial in the α-anomers and axial in the β-anomers (Blom).

We shall consider the case in which only the α- and β-anomeric pyranose forms of D-glucose and of D-mannose exist in measurable amounts in their aqueous solutions at equilibrium and during their transformation into each other; *cf.* Blom and Christiansen [8].

Let us assume that we have at our disposal two series, α and β, of observations performed at the same temperature and with the same concentrations, beginning with pure α-anomer and pure β-anomer, respectively.

Let the stoichiometric equation be written

$$\beta = \alpha \tag{1}$$

The velocity of (1) then is

$$v = k_+ C_\beta - k_- C_\alpha \tag{2}$$

while the equilibrium constant K becomes

$$K = k_+/k_- = (C_\alpha/C_\beta)_{eq} \tag{3}$$

Theory then yields

$$r_\alpha = C + A \exp(-kt_\alpha)$$
$$r_\beta = C - B \exp(-kt_\beta) \qquad k \equiv k_+ + k_- \tag{4}$$

where r_α and r_β are rotations observed at times t_α and t_β respectively. If both series contain a sufficient number of observations it is always possible by interpolation to get sets of values for r_α and r_β at times $t_\alpha = t_\beta = t$. It is also possible to extrapolate to time $t_\alpha = t_\beta =$ zero with reasonable although not quite so good accuracy.

Evidently C means the equilibrium rotation which is a constant common to the two series. Omitting the subscripts at t in (4) we get by subtraction

$$r_\alpha - r_\beta = (A + B)\exp(-kt) \tag{5}$$

and by combination with the second (4)

$$C = r_\beta + \omega(r_\alpha - r_\beta);\ \omega = B/(A + B) \tag{6}$$

where according to the theory

$$B/A = k_+/k_- = K = \omega/(1-\omega) \tag{7}$$

Eqn. (6) shows that it is possible from the pairs of observations to determine a value of ω which causes C to be independent of time. The advantage of this method is, that it yields for each pair of observations one value of C and for the whole series a single value of ω, which must be so chosen, that any perceptible trend in the C-values disappears. The calculations will show that the determination of ω becomes rather accurate, the accuracy evidently depending on the accuracy of the experiments. The single C-values will scatter around some mean value which can easily be found, the same weight being ascribed to the different values.

From the existing measurements the author has primarily chosen those by Isbell and Pigman [1], because their experimental material seems to be homogeneous and their experiments very carefully performed.

D-*Glucose*. The author has found it convenient to assume ω to equal $(1 + x)/3$ for glucose and $2(1 + y)/3$ for mannose, where x and y are small fractions, the latter being probably zero inside the accuracy of the experiments. Table 1 shows the complete course of the calculation, starting from the interpolated values.

From Table 2 one may read the values of ω, the rotation $(r_\alpha)_0$ of the pure β-anomer, the rotation $(r_\beta)_0$ of the pure β-anomer and the equilibrium rotation C_{av}, where it must be remembered that $(r_\alpha)_0$ and $(r_\beta)_0$ are obtained by *extra*polation. Of course the same quantities can be calculated from Isbell and Pigman's [1] formulae of the form (4). However, so far as ω is concerned, this procedure is ambiguous owing to the circumstance that the values chosen by I. and P. for the constant k differ a little at the same temperature. The same is true for the equilibrium rotation C. It is therefore not certain, that it has a meaning to take the mean of I. and P.'s values for C, but nevertheless we shall do so, adding these mean values in parentheses in Table 2. Concerning the initial values of r_α and r_β they must always be determined by some sort of extrapolation and it is difficult to tell, whether the simple linear extrapola-

Table 1. D-Glucose. Measurements by Isbell and Pigman [1] interpolated by J. A. Chr. Temp. 0.2°C. Concentration 3.9 g/100 ml, 4 dm tube. Rotations in saccharimeter degrees, °S. Time t in min. $\omega = 1.086/3 = 0.362$. C rotation in °S at equilibrium.

t	r_α	r_β	$r_\alpha - r_\beta$	$\omega(r_\alpha - r_\beta)$	C
0	50.79	8.37	42.42	15.36	23.73
5	50.54	8.49	42.05	15.23	23.72
10	50.34	8.68	41.66	15.09	23.77
20	49.83	8.87	40.96	14.83	23.70
40	48.96	9.39	39.57	14.33	23.72
60	48.14	9.85	38.29	13.86	23.71
90	46.96	10.56	36.40	13.17	23.73
120	45.85	11.19	34.66	12.55	23.74
180	43.72	12.41	31.31	11.34	23.75
240	41.83	13.49	28.34	10.27	23.76
300	40.07	14.52	25.55	9.25	23.77
400	37.56	15.93	21.63	7.83	23.76
550	34.46	17.65	16.81	6.08	23.73
1350	Interpolation uncertain				
				$C_{av} =$	23.74

Table 2. D-glucose. Concentration 3.9 g/100 ml, 4 dm tube. Temperatures in °C. Rotations in saccharimeter degrees, °S. The values in parentheses are taken from Isbell and Pigman [1].

Temp.	ω	$(r_\alpha)_0$	$(r_\beta)_0$	C
0.2	0.3620	50.79	8.37	23.74
0.2		(50.79)	(8.37)	(23.70)
20	0.3620	50.91	8.56	23.89
20		(50.95)	(8.54)	(23.96)

tion used in the present recalculation is better or worse than that implied in I. and P.'s tables. Here again the results of the latter authors have been included in Table 2 in parentheses.

To save space complete tables corresponding to Table 1 for glucose at 20°C and the corresponding tables for mannose have been omitted.

From Table 2 it appears, that ω is independent of temperature. This is corroborated by the findings of Nelson and Beegle [2] who extended their measurements from zero to 37°C. The same authors refer through secondary sources, unavailable to the present author, to a statement, probably about 100 years old, by Dubrunfaut and Mataqozeh to the effect, that the independency of temperature of the equilibrium ratio between the two forms of glucose extends to about 100°C. We shall therefore assume in the following that for D-glucose $K = \omega/(1-\omega)$ is to all intents and purposes independent of temperature.

It may be added, that the slight increase of ω from 0.3620 to 0.3636 would remove the last trace of a trend in the C values. This can be estimated from Table 1, and it is also true of the series of observations at 20°C. A similar further increase would reintroduce a trend but in the opposite direction, the first values becoming too high in relation to the last ones. We shall later see that it seems possible to give a reasonable interpretation of the value $4/11 = 0.3636$ for ω.

D-*Mannose*. Also in the case of mannose the measurements by Isbell and Pigman [1] seem to be among the most accurate ones. They are, however,

Table 3. D-Mannose. Concentration 4.0 g/100 ml, 4 dm tube. Temperature in °C. Rotations in saccharimeter degrees, °S. The values in parentheses are taken from Isbell and Pigman [1].

Temp.	w	$(r_\alpha)_0$	$(r_\beta)_0$	C
0.3	2(1.026)/3	13.12	−7.60	6.55
0.3		(13.10)	(−7.62)	(6.65) [a]
20.1	2/3	13.70	−7.54 [b]	6.59
20.1		(13.70)	(−7.63)	(6.51) [c]

[a] Mean of 6.63 and 6.66.
[b] Possibly low because of uncertainty in extrapolation.
[c] Mean of 6.63 and 6.38

peculiar in some respects. First of all the α-series have been obtained at 0.1°C and 20.0°C while the temperatures for the β-series were, respectively, 0.3 and 20.1°C.

The author has therefore referred the α-series to the latter two temperatures by the following procedure: From the values for the velocity-constant k given by Isbell and Pigman at the two temperatures it was calculated, that an increase in temperature of 0.2°C would increase the constant by 2.08 % and by the half of that value for an increase of 0.1°C. Therefore the times in the tables were reduced by these amounts, the rotations being left unchanged. After that the α,β tables at the two temperatures are comparable and were treated by interpolation as described under glucose.

The results of the recalculation are in Table 3.

Table 3 shows two peculiarities. In the first place ω is essentially larger at about 0°C than at 20°C at which temperature it is exactly (inside the accuracy of the experiments) 2/3. The value 2/3 at 20°C was also obtained by the extremely careful measurements by Riiber and Minsaas [3] which furthermore were discussed by N. A. Sørensen on pages 104 to 106 in his important book [4] on the kinetics of mutarotation. Now, even if ω were dependent on temperature it might happen that it became at 20°C exactly 2/3, but this would be a rather improbable incident. In the second place the rotation of the α-anomer at 0°C is essentially lower than that at 20°C. According to remarks by Nelson and Beegle [2] and by comparison with the data for glucose and for the β-anomer of mannose in this paper, this seems an improbable result. As we shall show, both peculiarities disappear if it be assumed that the α-specimen used by Isbell and Pigman for their experiment at 0°C has contained 2.5 % of the β-form.

In this connection a few words on the preparation of mannose may be of interest. According to Nelson and Sawyer [5] β-mannose can be prepared in good yield from finely ground "ivory nuts", seeds from the tagua palm (*Phytelephas macrocarpa*) by hydrolysis with 75 % sulfuric acid. The α-anomer was first prepared by Levene [6], who in a later paper [7] revised and improved his method and his mutarotation experiments. It is thus evident that it is much easier to get the β-form free from the α-form than *vice versa*.

Note added in proof. Riiber and Minsaas [3] recommend a different procedure. They show that, if a laboratory has become contaminated by crystal nuclei of either of the two forms, the preparation must be performed under "aseptic" conditions to get pure products.

Now if we start an α,β-pair of experiments with the pure β-form but with an α-specimen containing the fraction β of the β-anomer it can be shown that, by the method described above, we shall arrive at an apparent value of ω, $\omega_{app} = \omega/(1-\beta)$. Now from $1/0.975 = 1.0256$ we conclude that the α-specimen at 0.3°C may have contained very nearly 2.5 % of the β-form. Furthermore, if we calculate $(r_a)_o = x$ from C at 0.3°C (which of course is independent of the fraction β) under the assumption that $\omega = 2/3$, we get from Table 3

$$2x/3 - 7.60/3 = 6.55$$

or at 0.3°C $(r_a)_o = 13.63$°S which is not more different from the value 13.70 at 20°C than could be expected.

Recalculation of the apparent rotation of the α-form then yields $(r_a)_{app} = 13.10$°S, which is not significantly different from the 13.12°S at 0.3°C in Table 3.

However, although the results of Isbell and Pigman may be consistent with the assumption, that $\omega = 2/3$ independently of temperature, more direct evidence would seem to be needed. To this end the author has recalculated the experiments by Levene in his second paper [1], where he has taken the utmost care to get a pure α-specimen. The results are in Table 4.

Although Levene's data are, relatively, a little less accurate than Isbell and Pigman's, it appears from Table 4 that 2/3 is a better choice for ω than $0.684 = 2(1.026)/3$. For lack of further information we therefore adopt the value 2/3 for ω at all temperatures.

The result of the recalculation is then that for D-glucose the fraction ω, that fraction which is present at equilibrium in aqueous solution as α-glucose, is very nearly 4/11 at all available temperatures and that the corresponding β-fraction therefore is 7/11.

For D-mannose the α-fraction is 2/3 at 20°C. It seems probable, experimentally, that the same is true at 0°C, but a strict experimental proof would require further experiments. Evidently then the equilibrium fraction of β-mannose is 1/3.

INTERPRETATION OF THE RESULTS FOR D-GLUCOSE AND D-MANNOSE

We shall treat the equilibrium between E- and A-molecules of the two sugars. For both the E-form is the one in which the HO at C_1 is located equatorially and the A-form the one in which it is located axially (and "southwards") [8]. We assume the solution to behave ideally, that is, we assume that interactions between solute molecules can be neglected. The solvent is supposed to be water, which by exchange with the solutes cannot produce perceptible changes. We write the reaction as

$$A = E \qquad (8)$$

Table 4. Experiments by P. A. Levene [7]. Temperature 1°C. Concentration 10 %, 2 dm tube. Rotations in angular degrees. Time in min.

Time	0	19	40	60	90
$C(\omega = 0.684)$	2.92	2.92	2.89	2.85	2.87
$C(\omega = 2/3)$	2.77	2.78	2.77	2.75	2.79
$C_{av}(\omega = 2/3)$	2.77				

Therefore the equilibrium constant K becomes

$$K = (C_E/C_A)_{eq} \tag{9}$$

Glucose. It was shown by Blom and the author [8] that for glucose K must approximate 1/2. In the following we shall therefore consider $2K$ instead of K.

From thermodynamics it is known that

$$RT \ln(2K) = \mu_A - \mu_E \tag{10}$$

where the μ's are chemical potentials of the pure substances at unit (or equal) concentrations. The difference can be written

$$\mu_A - \mu_E = H_A - H_E + T(S_E - S_A) \tag{11}$$

If the temperature interval is not too large the differences in the right side of (11) can be considered as being constants, representing the two differences at some standard temperature T_o chosen inside the temperature-interval covered by the measurements. This is so because of the fact that at the temperature $T = T_o$ both the function O and its first differential quotient dO/dT disappear, O being defined as

$$O \equiv \int_{To}^{T} C_p dT - T \int_{To}^{T} (C_p/T)\ dT \tag{12}$$

The experiments show that K is independent of temperature, which means that $H_A = H_E$. The dimensionless difference $(S_E - S_A)/R$ is then also a constant which we denote by $\ln \sigma$. Assuming as we did, that the numerical value of ω is 4/11 we get

$$2K = 8/7 = \sigma \tag{13}$$

The question then is, how are we to interpret this empirical result? To answer the question we use statistical thermodynamics although with some simplifications.

It is known [9] that an assembly of molecules of the same kind at unit concentration has a chemical potential μ given by

$$-\mu/RT = -H/RT + \Sigma \ln({}^iQ) \tag{14}$$

where ${}^iQ$ is the partition function (german:Zustandssumme) relating to the i'th type of motion of the molecule. (14) implies that the different types of motion (*e.g.* translations, rotations, vibrations) can, with sufficient approximation, be considered as non-interfering with each other. H and only this is in principle independent of temperature. Applying (14) to (10) we get

$$\ln(2K) = (H_A - H_E)/RT + \Sigma \ln({}^iQ_E/{}^iQ_A) \tag{15}$$

The constants H include in the first place the potential energy of the molecule. The E- and A-molecules being alike except for the configuration at C_1 we need only consider the "bond energies" of H and OH at this carbon atom. The bond energies are defined as the work necessary to remove the atom or the group from its equilibrium place in the molecule into infinity. It is natural to assume that these bond energies are very nearly independent of the locations (*e*- or *a*-) of the atom or the group in question, provided that only forces

between them and C_1 come into play. If for example there were an OH at C_3 located axially southwards it might interact strongly with an OH at C_1 also located axially southwards. In such a case we may expect the bond energy of the OH at C_1 to be significantly larger in the A-form of the molecule than in the E-form. Such cases will be treated by J. Blom, who has drawn the authors attention to this possibility. However, neither in D-glucose nor in D-mannose can a complication of this kind arise. The constants H_E and H_A may beside the bond energy also contain contributions of vibrational origin, namely socalled zero-point energies. These arise from the circumstance that, according to quantum-mechanics, a harmonic vibrator is never at rest not even at 0°K. It has at least the energy $h\nu/2$ where ν is the frequency of the vibrator calculated according to classical mechanics. These vibrations must be considered as vibrations of different characteristic frequencies of vibration of the entire molecule superimposed on each other and cannot therefore, strictly speaking, be ascribed to single bonds. But some of them may approximately be ascribed to vibrations at bonds which are either unique or are repeated in several places in the molecule. An example of the unique kind is the bond between C_5 and C_6. This bond may give rise both to longitudinal and to transversal vibrations, these expressions being understood as relating to the direction of the "valency" between the two carbon atoms. The restoring forces necessary to produce such vibrations must arise mainly from the electron-cloud surrounding the bond in question and must therefore be nearly equal for the E- and the A-form of the molecule. Thus the corresponding energies cancel in the difference $H_A - H_E$. An example of the "repeated" kind are the bonds H—C_5, H—C_4, H—C_3 and H—C_2. These are common to the E- and A-form and their energy will cancel in the difference above. Assuming as we did before, that the restoring forces at a bond are mainly determined by the electron-cloud surrounding the bond in question we may with some confidence assume that the frequencies (longitudinal and transversal) of the C_1—H bond as well are the same in the E- and the A-form. The situation is similar so far as longitudinal vibrations of the four bonds HO—C_4, HO—C_3, HO—C_2 and HO—C_1 are concerned. The question of transversal vibrations at the same four bonds will be treated below, but it may be stated at once that the empirically found equality between H_A and H_E shows that the energy of the collective transversal vibrations of the mentioned four vectors HO—C actually is the same for the two isomers.

Next we discuss the partition-functions Q. The first one may be taken as the one belonging to the translational movements of the molecule as a whole, ${}^{tr}Q$. We get one such Q for each of the three directions in space. Each of them is given by the familiar expression

$$ {}^{tr}Q = \int_{-\infty}^{+\infty} \exp(-p^2/2mkT)\, dp = \sqrt{2\pi mkT} \qquad (16) $$

The three ${}^{tr}Q$'s are therefore equal for the two forms and their ratio disappears from eqn. (15). It is much more complicated to calculate the three possible ${}^{rot}Q$'s corresponding to the three possible rotations of the entire molecule, but owing to the fact that the three fundamental moments of inertia of the

molecule are large, it can be estimated, that also the three ${}^{rot}Q$'s must be equal for the two isomers (E and A). Therefore also the corresponding ratios disappear from (15). What remains on the right side of (15) are then different vibrational partition functions ${}^{vib}Q$'s each depending on its own characteristic frequency, ν. It is known from textbooks that, omitting the superscript

$$Q(\nu) = (2\sinh(x/2))^{-1};\ x = Lh\nu/RT \tag{17}$$

where L is Avogadro's number.

There are two limiting cases to consider.

$$(a)\ Lh\nu \gg RT:\quad 2Q(\nu) = \exp(-x/2) \tag{18}$$

$$(b)\ Lh\nu < RT:\quad 2Q(\nu) = (x/2)^{-1} = 2RT/Lh\nu \tag{19}$$

For most of the vibrators considered conditions (a) will obtain because the restoring forces are large. This is probably true for all longitudinal vibrations and also for transversal vibrations of H-atoms. It may not be true for transversal vibrations of the vector $C_5—C_6$ but this is common to the two isomers and the corresponding Q-ratio therefore disappears from (15). In cases where (a) obtains the corresponding ln Q's evidently appear as contributions to H, the case we have already discussed.

Concerning (b) we note, that even if $Lh\nu = RT$ the approximation (19) is not a bad one, it being only about 4 % larger than the true one. What remains to discuss are the Q's corresponding to transversal vibrations of the four HO—C vectors. So far as restoring forces due to the electron-cloud around the vector in question are concerned, these are expected to be nearly equal for the two isomers and the corresponding Q-ratios will therefore disappear from (15). But apart from this kind of vibrations there must be one, in which the restoring force is due to interaction between neighbouring equatorial HO-groups. These restoring forces must be rather weak so that we expect condition (b) to obtain. Of neighbouring equatorial HO-groups there are four in the E-anomer (of glucose). In the A-anomer there are only three equatorial C—OH vectors and one whose "valency" is parallel to the axis of the molecule. In both cases they will be strongly coupled to each other and form a collectively vibrating system with one characteristic frequency for each anomer, denoted by ν_E and ν_A, respectively. In this case there must be phase relations between the vibrations of the single vectors, most probably so that two neighbouring ones are always in counter phase.

The approximation (19) then yields, for this Q-pair

$$Q_E/Q_A = \nu_A/\nu_E \tag{20}$$

The energies U_A and U_E of the two collectives must be equal (U) because of the independence of $\ln(2K)$ of temperature, but the energy of each vibrator in the collective and therefore the frequency of vibration of the collective may be different for the two anomers. For the E-anomer U will be divided equally between the four equally situated C—OH vibrators. According to classical mechanics the vibrational energy of a harmonic vibrator is on the average half potential and half kinetical, corresponding to the two square terms in its energy expression, its Hamiltonian. Thus on each square term we shall have the energy $U/8$ and for one vibrator $2U/8$. Therefore $\nu_E = 2U/8h$.

In the A-anomer the situation is different so far as the $HO-C_1$ vector is concerned. The transversal restoring force of the kind considered can only come from the triplet of vectors at C_4, C_3 and C_2. The restoring force on $HO-C_1$ from this triplet must be parallel to the axis of the molecule and to the axial vector at C_1. It has therefore no component transversal to the $HO-C_1$ vector. The corresponding square term in the Hamiltonian will thus be missing, and only its kinetical square term will remain. The energy on each square term will therefore in the A-case be $U/7$ which yields $\nu_A = 2U/7h$. As all other Q-ratios equal unity we get from (15) and (20)

$$2K = 8/7 \tag{21}$$

which is the result found empirically for glucose, where $(C_\alpha/C_\beta)_{eq} = K = 4/7$.

D-*Mannose*. In mannose we have at C_4, C_3 a doublet of equatorial C—OH vectors and at C_2 a singlet pointing axially northwards. In the A-anomer the singlet at C_1 points axially southwards. Using the same argument as we did in the case of A-glucose we see that two square terms are missing, one from each of the vectors at C_2 and C_1. In A-mannose we therefore have only $2 \times 2 + 2 = 6$ square terms in the Hamiltonian. In E-mannose the singlet at C_1 is equatorial but rather distant from the C_4,C_3 doublet, the angular distance between the middle of the latter and the singlet at C_1 being 150°. As now the two vectors in the doublet most probably vibrate in counter-phase the resulting transversal effect on the equatorial C_1-singlet will disappear and the restoring force on this vector becomes zero also in E-mannose. Thus we get again 6 square terms in the Hamiltonian and consequently

$$Q_E/Q_A = \nu_A/\nu_E = 1 \tag{22}$$

Remembering that the statistical factor for mannose is 2 and reasoning as we did in the case of glucose we find

$$K/2 = 1 \tag{23}$$

which is the result found empirically for the equilibrium

$$\beta\text{-mannose} \rightleftharpoons \alpha\text{-mannose}.$$

The empirical results for glucose and mannose can thus be interpreted in a manner which seems natural, but only if the current assignment of E- and A-forms to the α- and β-anomers be reversed.

REFERENCES

1. Isbell, H. S. and Pigman, W. W. *J. Research, Natl. Bur. Stand.* **18** (1939) 141, tables p. 179, 180.
2. Nelson, J. M. and Beegle, F. M. *J. Am. Chem. Soc.* **41** (1919) 559.
3. Riiber, C. N. and Minsaas, J. *Ber* **60** (1927) 2402.
4. Sørensen, N. A. *Kgl. Norske Videnskab. Selskab. Skrifter*, Trondheim (1937) Nr. 2.
5. Hudson, C. S. and Sawyer, H. L. *J. Am. Chem. Soc.* **39** (1917) 470.
6. Levene, P. A. *J. Biol. Chem.* **57** (1923) 329.
7. Levene, P. A. *J. Biol. Chem.* **59** (1924) 129.
8. Blom, J. and Christiansen, J. A. *Acta Chem. Scand.* **16** (1962) 1519.
9. As examples of text-books the following may be mentioned: Fowler, R. H. *Statistical Mechanics*, Cambridge University Press 1929; Fowler, R. H. and Guggenheim, E. A. *Statistical Thermodynamics*, Cambridge University Press 1939; Guggenheim, E. A. *Thermodynamics*, North Holland Publishing Company, Amsterdam 1949 and later editions.

Received June 25, 1962.

ACTA CHEMICA SCANDINAVICA 16 (1962) 2350–2356

Studies on the Hydrolysis of Metal Ions

42. A Thermochemical Study of Hydrolysed $Pb(ClO_4)_2$ Solutions

BIRGITTA CARELL and ÅKE OLIN

Department of Inorganic Chemistry, Royal Institute of Technology, Stockholm 70, Sweden

The enthalpy and entropy changes of the main hydrolysis reactions of Pb^{2+} have been determined by enthalpy titrations with hydrolysed $Pb(ClO_4)_2$ solutions in 3 M $(Na)ClO_4$ at 25°C. The results obtained were:

$4Pb^{2+} + 4H_2O \rightleftharpoons Pb_4(OH)_4^{4+} + 4H^+$; $\Delta H = 20.07 \pm 0.12$ kcal/mole; $\Delta S = -20.8 \pm 0.8$ e.u.

$3Pb^{2+} + 4H_2O \rightleftharpoons Pb_3(OH)_4^{2+} + 4H^+$; $\Delta H = 26.5 \pm 0.8$ kcal/mole; $\Delta S = -15.8 \pm 3.8$ e.u.

$6Pb^{2+} + 8H_2O \rightleftharpoons Pb_6(OH)_8^{4+} + 8H^+$; $\Delta H = 49.44 \pm 0.8$ kcal/mole; $\Delta S = -27.0 \pm 3.1$ e.u.

The hydrolysis reactions of the Pb^{2+} ion have been studied with emf methods by one of the present authors [1,2]. The following species were identified and the numerical values of the corresponding formation constants in 3 M $NaClO_4$ medium were determined.

$$Pb^{2+} + H_2O \rightleftharpoons PbOH^+ + H^+ \qquad \log \beta_{1,1} = -7.9 \pm 0.1$$
$$2Pb^{2+} + H_2O \rightleftharpoons Pb_2OH^{3+} + H^+ \qquad \log \beta_{1,2} = -6.4 \pm 0.1$$
$$3Pb^{2+} + 4H_2O \rightleftharpoons Pb_3(OH)_4^{2+} + 4H^+ \qquad \log \beta_{4,3} = -22.87 \pm 0.1$$
$$4Pb^{2+} + 4H_2O \rightleftharpoons Pb_4(OH)_4^{4+} + 4H^+ \qquad \log \beta_{4,4} = -19.25 \pm 0.1$$
$$6Pb^{2+} + 8H_2O \rightleftharpoons Pb_6(OH)_8^{4+} + 8H^+ \qquad \log \beta_{8,6} = -42.12 \pm 0.1$$

No thermochemical data are available for these reactions and the present investigation was undertaken in order to obtain such information.

EXPERIMENTAL

The experiments were carried out in a calorimeter constructed by Dr. K. Schlyter. The calorimeter design and the experimental technique used with this calorimeter have been described in great detail by him[3]. In brief, a titration technique is used. The calorimeter vessel is charged with one of the reactants and the other reactant is added gradually from a thermostated buret. The change in temperature of the calorimeter contents is

determined after each addition from the buret and the temperature in the calorimeter is brought back to its initial value by a cooling device before a new addition is made.

The performance of the calorimeter was occasionally checked by test titrations with HCl. The heats of dilution of HCl found in these tests generally agreed to within 1 % with those calculated from the data given by Sturtevant [4]. This was considered sufficient for the present purpose.

The hydrolysed lead perchlorate solution was prepared by mixing calculated volumes of carefully analysed stock solutions of $Pb(ClO_4)_2$, NaOH and $NaClO_4$, in a volumetric flask in an atmosphere of nitrogen. Such solutions react with CO_2 and form lead hydroxide carbonates and must therefore be prepared and handled in an inert atmosphere. The hydrolysed solution was transferred with a calibrated pipet of ca 225 ml volume to the calorimeter vessel, which had been filled with N_2 beforehand. The stirrer in the vessel was provided with an air-tight seal, which prevented the contents of the calorimeter vessel from coming into contact with the CO_2 of the air.

The titrant was also mixed from stock solutions. The compositions of the solutions were chosen so that the total concentration $[Pb(II)] = B$, and $[ClO_4^-] = 3$ M were kept constant in each experiment. The addition of acid from the buret was continued till the heat evolved per addition was zero. This occurred when the hydrolysed lead species had been converted to Pb^{2+} and H_2O.

The values of B used were 0.08, 0.04, 0.02 and 0.01 M. For each value of B two titrations were made. Table 1 gives the analytical hydrogen ion excess of the starting solution in the calorimeter vessel, H_S, and of the titrating solution in the buret, H_T. The value of the analytical hydrogen ion excess, which usually is a negative number, in each point of a titration can be calculated from eqn. (1).

Table 1. Survey of titrations.

	B = 0.08 M	B = 0.04 M	B = 0.02 M	B = 0.01 M
H_S, M	−0.07096	−0.05297	−0.02592	−0.01299
H_T, M	0.8767	0.5971	0.3185	0.2844

Table 2. Data from titrations with B = 0.02 M.

v ml	Q cal	Q_{calc} cal	$Q-Q_{calc}$ cal
1	2.82	2.90	−0.08
3	5.60	5.54	0.06
5	4.85	4.89	−0.04
7	3.98	3.97	0.01
9	3.47	3.47	0.00
11	3.32	3.31	0.01
13	3.24	3.26	−0.02
15	3.26	3.23	0.03
17	3.30	3.22	0.08
2	5.72	5.72	0.00
4	5.32	5.27	0.05
6	4.35	4.43	−0.08
8	3.70	3.67	0.03
10	3.36	3.38	−0.02
12	3.30	3.27	0.03
14	3.26	3.24	0.02
16	3.26	3.22	0.04
18	3.29	3.22	0.07

$$H = (vH_T + V_oH_S)/(V_o + v) \quad (1)$$

V_o = initial volume of the solution in the calorimeter vessel (always 224.08 ml) and v = the volume of solution added from the buret.

The titrations with $B = 0.02$ M are given in Table 2 as an example of the experimental results obtained.

RESULTS AND CALCULATIONS

Two ml of acid were added each time from the buret. The heat evolved per addition, which was primarily registered as a deflection of a galvanometer light spot, was calculated as described by Schlyter [3].

If heats of dilution are neglected the heat evolved per addition, Q, is given by

$$Q = \sum_{p,q} \delta n_{pq} l_{pq} \quad (2)$$

δn_{pq} = the change of the number of moles of the species $Pb_q(OH)_p^{(2q-p)+}$ per addition of acid and l_{pq} = the enthalpy change (ΔH) of the reaction $q\ Pb^{2+} + p\ H_2O \rightleftharpoons Pb_q(OH)_p^{(2q-p)+} + p\ H^+$. In eqn. (2) the Q are known from the calorimeter experiments. The δn_{pq} have been calculated from the known analytical compositions of the solutions and the equilibrium constants which were taken from the emf work [1,2]. We are thus presented with a set of linear equations in the unknowns, l_{pq}. The l_{pq} have been found by solving eqn. (2) by the method of least squares. The calculations were performed with an electronic computer (Ferranti-Mercury). The first step was the calculation of δn_{pq}. This was accomplished by a modified version of the program HALTA described by Ingri and Sillén [5]. The input information used with the program was B, H_T, H_S, v and V_o and the equilibrium constants. The computer then calculates the equilibrium concentrations of the various species for each point in a titration and the δn_{pq}. The δn_{pq} and the Q are then used with a "least squares program".

The first attempt to solve eqn. (2) for all the l_{pq} failed and indicated that with the present experimental accuracy l_{11} and l_{12} cannot be found. This situation is caused by the smallness of δn_{11} and δn_{12} which at most are 1 % of $\Sigma \delta n_{pq}$. The following approximation was therefore resorted to: l_{11} and l_{12} were set equal and were assumed to have the values 5 kcal/mole or 10 kcal/mole. Corrected values of Q were next calculated.

$$Q(\text{corrected}) = -Q - (\delta n_{11} + \delta n_{12})\ (5 \text{ or } 10) \quad (3)$$

The use of $\Delta H = 5$ and 10 kcal/mole was chosen from results with other systems studied by Schlyter. These studies have shown that the heat evolved per mole of OH^- lies in the range 5—10 kcal. This is also true for the present system as will be seen later. It should also be noted that these corrections are at most 2 % of Q.

With the corrected Q the following values of l_{pq} were found.
($l_{11} = l_{12} = 5$ kcal/mole)
$l_{44} = 20.07$ kcal/mole; $l_{43} = 26.53$ kcal/mole; $l_{86} = 49.44$ kcal/mole.
($l_{11} = l_{12} = 10$ kcal/mole)
$l_{44} = 20.13$ kcal/mole; $l_{43} = 26.03$ kcal/mole; $l_{86} = 49.85$ kcal/mole.

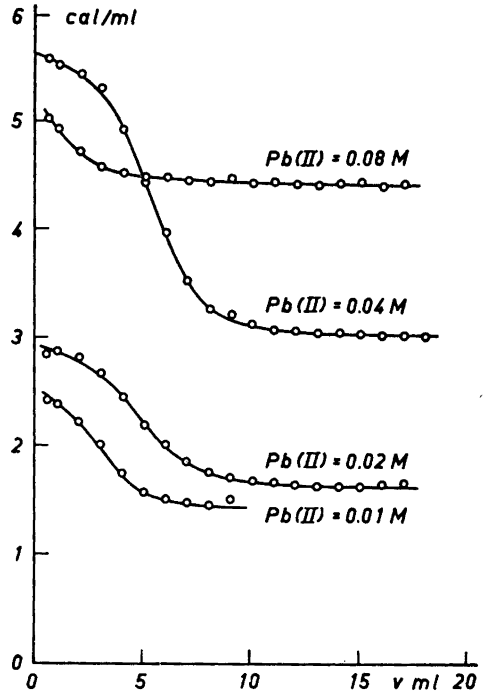

Fig. 1. Q and Q_{calc} (in cal per ml of acid added) as a function of v. The full lines represent Q_{calc} and the symbols represent Q.

$\Sigma(Q-Q_{calc})^2$ is smaller for the first set of l_{pq} and these will therefore be accepted as the best values. Justification for this choice also comes from the fact that the average value of the heat evolved per mole of OH^- is closer to 5 than to 10 kcal.

With the above values of l_{pq}, calculated values of the heat evolution per addition, Q_{calc}, have been obtained. These are given in the second column in Table 2. The difference between Q and Q_{calc} is given in the third column of the same table. The results are presented graphically in Fig. 1. From the figure it is seen that systematic deviations between Q and Q_{calc} are absent. The estimated standard deviation in Q, (Ref.[6]).

$$S = \pm \sqrt{\Sigma(Q-Q_{calc})^2/\nu} \qquad (4)$$

where ν is the number of degrees of freedom, is found to be $\pm$ 0.05 cal. This may be compared with a value of $\pm$ 0.04 cal calculated (at the 95 % confidence level) from the calorimetry measurement uncertainties (Ref.[3]).

The standard deviations in the l_{pq} given by the least squares treatment are smaller than the uncertainties arising from the choice of the value for l_{11} and l_{12}. We shall therefore assign an uncertainty in l_{pq} of twice the difference in l_{pq} between the two choices and obtain

$$l_{44} = 20.07 \pm 0.12 \text{ kcal/mole}$$
$$l_{43} = 26.5 \pm 1 \text{ kcal/mole}$$
$$l_{86} = 49.44 \pm 0.8 \text{ kcal/mole}$$

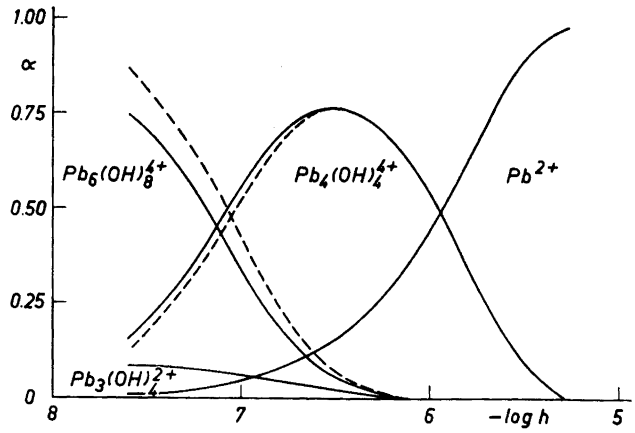

Fig. 2. The relative amounts (α) of the hydrolysis products of Pb(II), at $B = 0.04$ M, expressed as percentages of the total lead. The amounts of $PbOH^+$ and Pb_2OH^{3+} are so small as not to appear in the figure. The full lines represent the distribution on the assumption that $Pb_3(OH)_4^{2+}$ is present, whereas the broken lines represent the distribution on the assumption that $Pb_3(OH)_4^{2+}$ is absent.

The interpretation of the emf measurements given in Ref.[1] leads to a distribution of the various lead species according to Fig. 2. $Pb_4(OH)_4^{4+}$ and $Pb_6(OH)_8^{4+}$ are the main hydrolysis products whereas the amount of $Pb_3(OH)_4^{2+}$ is relatively small. Since $[Pb_3(OH)_4^{2+}]$ is small, calculations, on the heat data have also been made on the assumption that this complex is not present. In order to find δn_{pq} the equilibrium constants found from the emf measure-

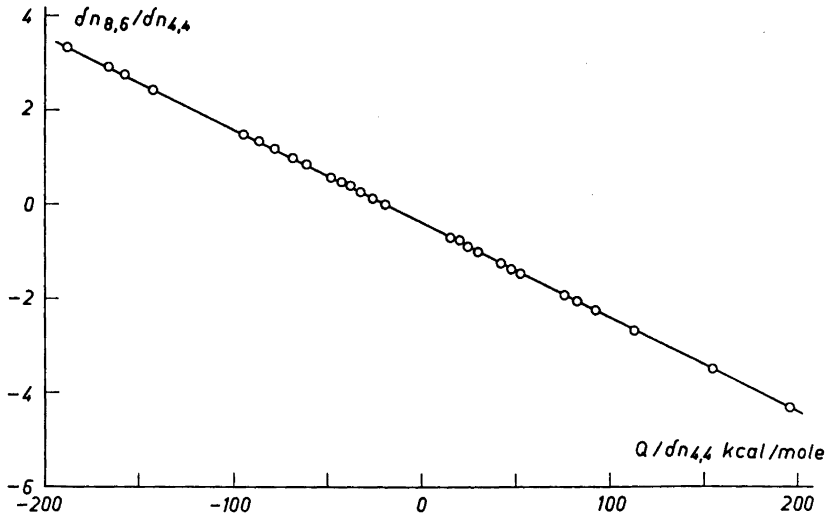

Fig. 3. Graphical determination of l_{44} and l_{86} according to eqn. (5a).

ments on this assumption were used, namely log $\beta_{4,4} = -19.25$ and log $\beta_{8,6} = -42.0$. In addition calculations were made where these constants were allowed to change by $\pm$ 0.2 log units. We have

$$Q = \delta n_{44}\ l_{44} + \delta n_{86}\ l_{86} \tag{5}$$

or

$$Q/\delta n_{44} = l_{44} + (\delta n_{86}/\delta n_{44})\ l_{86} \tag{5a}$$

The plots of eqn. (5a) were linear, Fig. 3, and for log $\beta_{4,4} = -19.25$ and log $\beta_{8,6} = -42.0$ the enthalpy changes were found to be

$$l_{44} = 20.08 \pm 0.15 \text{ kcal/mole}$$
$$l_{86} = 49.8 \pm 0.8 \text{ kcal/mole}$$

which are thus very close to the values found with the previous treatment. For the other pairs of log $\beta_{4,4}$ and log $\beta_{8,6}$ used the ΔH were the same within the limits of error given.

We find that enthalpy titrations of the present precision cannot be used to distinguish whether $Pb_3(OH)_4^{2+}$ is present or not. The reason for this is seen from the distribution curves in Fig. 2. The removal of $Pb_3(OH)_4^{2+}$ and the subsequent change of log $\beta_{8,6}$ has the effect that Pb(II) present as $Pb_3(OH)_4^{2+}$ will be reckoned as $Pb_6(OH)_8^{4+}$. The distribution curves for Pb^{2+} and $Pb_4(OH)_4^{4+}$ are changed but little. Very accurate heat data will be needed in order to distinguish whether $Pb_3(OH)_4^{2+}$ is negligible or whether $l_{86} \approx 2\ l_{43}$ unless external considerations indicate that $l_{86} \approx 2\ l_{43}$ is unreasonable.

The heat data cannot be used to confirm the presence of $Pb_4(OH)_4^{4+}$, although the horizontal parts of the curves in Fig. 1 strongly indicate the presence of only one complex. This situation arises from the fact that the heat data cannot be used to calculate (indirectly) the hydrogen ion concentration in the equilibrium solutions when the hydrolysis occurs in neutral or weakly acidic medium. For those metal ions which are strong acids, *e.g.* Bi^{3+}, and hydrolyse in strongly acidic solution the situation is different. In this case the heat data can be used to give information on the hydrolysis mechanism as will be shown in a later communication.

SUMMARY OF THE HEAT DATA

We have accepted the hydrolysis mechanism suggested by the emf measurements and find

$$4Pb^{2+} + 4H_2O \rightleftharpoons Pb_4(OH)_4^{4+} + 4H^+$$
$\Delta G = 26.26 \pm 0.13$ kcal/mole; $\Delta H = 20.07 \pm 0.12$ kcal/mole
$\Delta S = -20.8 \pm 0.8$ e.u.

$$3Pb^{2+} + 4H_2O \rightleftharpoons Pb_3(OH)_4^{2+} + 4H^+$$
$\Delta G = 31.2 \pm 0.13$ kcal/mole; $\Delta H = 26.5 \pm 1$ kcal/mole
$\Delta S = -15.8 \pm 3.8$ e.u.

$$6Pb^{2+} + 8H_2O \rightleftharpoons Pb_6(OH)_8^{4+} + 8H^+$$
$\Delta G = 57.49 \pm 0.13$ kcal/mole; $\Delta H = 49.44 \pm 0.8$ kcal/mole
$\Delta S = -27.0 \pm 3.1$ e.u.

Acknowledgements. This work has been financially supported by *Statens tekniska forskningsråd (Swedish Technical Research Council)* and *Statens naturvetenskapliga forskningsråd (Swedish Natural Science Research Council).*

REFERENCES

1. Olin, Å. *Acta Chem. Scand.* **14** (1960) 126.
2. Olin, Å. *Acta Chem. Scand.* **14** (1960) 814.
3. Schlyter, K. *Trans. Royal Inst. Tech. Stockholm*, No. **132** (1959).
4. Sturtevant, J. M. *J. Am. Chem. Soc.* **62** (1940) 584.
5. Ingri, N. and Sillén, L. G. *Acta Chem. Scand.* **16** (1962) 173.
6. Guest, P. G. *Numerical methods of curve fitting.* Cambridge University Press 1961.

Received May 28, 1962.

ACTA CHEMICA SCANDINAVICA 16 (1962) 2357–2362

Studies on the Hydrolysis of Metal Ions

43. A Thermochemical Study of Hydrolysed $Be(ClO_4)_2$ Solutions

BIRGITTA CARELL and ÅKE OLIN

Department of Inorganic Chemistry, Royal Institute of Technology, Stockholm 70, Sweden

Enthalpy titrations have been performed with hydrolysed $Be(ClO_4)_2$ solutions (25°C, 3 M $(Na)ClO_4$). The hydrolysis mechanism proposed by Kakihana and Sillén [1], *viz.*

$$2Be^{2+} + H_2O \rightleftharpoons Be_2OH^{3+} + H^+ \quad (1)$$

$$3Be^{2+} + 3H_2O \rightleftharpoons Be_3(OH)_3^{3+} + 3H^+ \quad (2)$$

has been used as the basis for the interpretation of the heat data. These gave for reaction (1)

$\Delta H = 4.43 \pm 0.10$ kcal/mole; $\Delta S = 0.2 \pm 0.6$ e.u.

and for reaction (2)

$\Delta H = 15.18 \pm 0.05$ kcal/mole; $\Delta S = 11.3 \pm 0.3$ e.u.

No thermochemical data are available for hydrolysed beryllium salt solutions. This paper reports enthalpy titrations with hydrolysed $Be(ClO_4)_2$ solutions containing 3 M $(Na)ClO_4$ as supporting electrolyte. The interpretation of the experimental data in terms of ΔH values of the hydrolysis reactions has been based on the mechanism proposed by Kakihana and Sillén [1] from emf measurements, namely

$$2Be^{2+} + H_2O \rightleftharpoons Be_2OH^{3+} + H^+ \quad (1)$$

$$3Be^{2+} + 3H_2O \rightleftharpoons Be_3(OH)_3^{3+} + 3H^+ \quad (2)$$

$$Be^{2+} + 2H_2O \rightleftharpoons Be(OH)_2 + 2H^+ \quad (3)$$

This mechanism has been confirmed by Carell and Olin [2] using a technique similar to that of Kakihana and Sillén, but with emphasis on concentrated $Be(ClO_4)_2$ solutions. The presence of Be^{2+} mainly as $Be_3(OH)_3^{3+}$ in dilute solution is also supported by solubility measurements of α-$Be(OH)_2$ in acids [3,4].

EXPERIMENTAL

The calorimeter constructed and described by Schlyter [5] has been used. The performance of the apparatus was tested by a determination of the heat of dilution of HCl. The results were compared with the values calculated from Sturtevant's data [6] and were found to agree to within 1 %.

The calorimeter was charged with a hydrolysed solution of $Be(ClO_4)_2$ and this solution was titrated with $HClO_4$ from a thermostated buret. The compositions of the two solutions were so chosen that in each experiment $[Be(II)]_{tot} = B$ and $[ClO_4^-] = 3$ M were constant. The additions of acid were continued till the heat evolved per addition had dropped practically to zero, *i.e.* when all the hydrolysed Be(II) had been converted to Be^{2+}aq.

The hydrolysed beryllium solutions were prepared by mixing stock solutions of $Be(ClO_4)_2$, $NaHCO_3$ and $NaClO_4$. The CO_2 formed was expelled by bubbling N_2 through the solutions for 2 h. The titrant was also made up from stock solutions. Kakihana and Sillén had observed that in solutions with a ratio OH^-/Be^{2+} ($= Z$) greater than 0.8 the attainment of equilibrium was somewhat slow. Since slow reactions cannot be studied with the calorimeter we chose an initial value of $Z \simeq 0.6$ in our solutions. The values of B and the analytical hydrogen ion excess, H, in the various solutions used in the titrations are given in Table 1. The value of H, which is usually a negative number, at each point of a titration can be calculated from

$$H = (vH_T + V_oH_S)/(V_o + v) \quad (4)$$

where $H_T = H$ of the buret solution; H_S = initial value of H in the calorimeter solution; V_o = initial volume of the solution in the calorimeter vessel (always 224.08 ml); v = volume of buret solution added.

As an example of the experimental results obtained the titration with $B = 0.04$ M is given in Table 2.

Table 1. Survey of titrations.

	$B = 0.32$ M	$B = 0.08$ M	$B = 0.04$ M	$B = 0.02$ M	$B = 0.01$ M
H_S, M	−0.0960	−0.0480	−0.0240	−0.0120	−0.00700
H_T, M	1.372	0.9037	0.4117	0.2740	0.1580

RESULTS AND CALCULATIONS

The heat evolved per addition of acid from the buret, Q, was calculated from the equations given by Schlyter [5].

If the heats of dilution are neglected Q is related to the enthalpy changes of the reactions

$$2Be^{2+} + H_2O \rightleftharpoons Be_2OH^{3+} + H^+ \qquad \Delta H = l_{12} \quad (1a)$$

$$3Be^{2+} + 3H_2O \rightleftharpoons Be_3(OH)_3^{3+} + 3H^+; \qquad \Delta H = l_{33} \quad (2a)$$

and the change in the number of moles of Be_2OH^{3+} and $Be_3(OH)_3^{3+}$ per addition of acid from the buret, δn_{12} and δn_{33}, by

$$Q = \delta n_{12} l_{12} + \delta n_{33} l_{33} \quad (5)$$

The concentration of $Be(OH)_2$ in the solutions studied is very small and has been neglected. The concentration changes have been calculated from the

Table 2. Data from titrations with $B = 0.04$ M.

v ml	Q cal	Q_{calc} cal	$Q-Q_{calc}$ cal	v ml	Q cal	Q_{calc} cal	$Q-Q_{calc}$ cal
1	2.100	2.083	0.017	2	4.103	4.177	−0.074
3	4.201	4.172	0.029	4	4.143	4.154	−0.011
5	4.151	4.141	0.010	6	4.140	4.130	0.010
7	4.166	4.118	0.048	8	4.085	4.097	−0.012
9	4.119	4.071	0.048	10	4.059	4.029	0.030
11	3.999	3.956	0.043	12	3.824	3.807	0.017
13	3.403	3.381	0.022	14	2.230	2.271	−0.041
15	0.976	0.963	0.013	16	0.401	0.310	0.091
17	0.162	0.133	0.029	18	0.075	0.073	0.002
19	0.065	0.046	0.019	20	0.043	0.032	0.011
21	0.025	0.023	0.002	22	0.031	0.017	0.014
23	0.004	0.014	−0.010	24	0.004	0.013	−0.009

analytical composition of the solutions and the equilibrium constants obtained from the emf work [2]. These calculations have been made with an electronic computer (Ferranti Mercury) and using a computer program whose essential part is the program HALTA described by Ingri and Sillén [7]. The computations were made on data with $B = 0.08$, 0.04, 0.02 and 0.01 M and with $\log \beta_{1,2} = -3.21$ and $\log \beta_{3,3} = -8.66$. Eqn. (5) was then solved for l_{12} and l_{33} according to the method of least squares.

The values of l_{12} and l_{33} thus found were

$$l_{12} = 4.43 \pm 0.10 \text{ kcal/mole}$$
$$l_{33} = 15.18 \pm 0.05 \text{ kcal/mole}$$

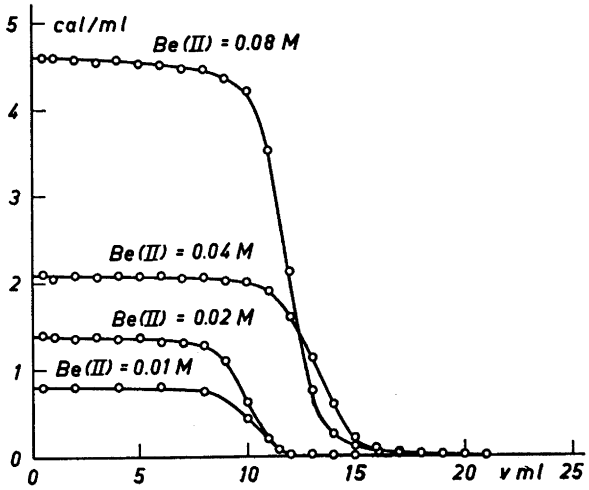

Fig. 1. Experimental Q and Q_{calc} (in cal per ml of acid added) as a function of v. The smooth curves have been drawn through the points for Q_{calc}, and the symbols represent Q for $B = 0.08$, 0.04, 0.02, 0.01 M.

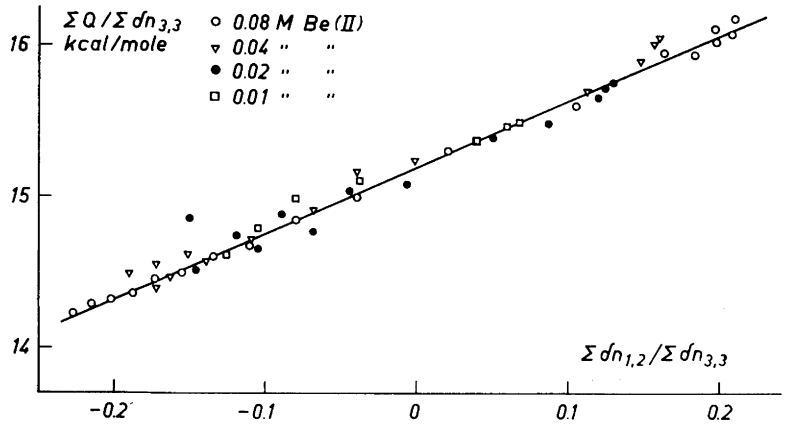

Fig. 2. Graphical determination of l_{12} and l_{33} according to eqn. (5a).

with these values of l_{12} and l_{33} the "expected" heat evolution per addition, Q_{calc}, has been calculated from eqn. (5) and is given in the second column of Table 2. In the third column of the same table the difference between Q and Q_{calc} can be found.

From Fig. 1, which is a graphical representation of Q and Q_{calc} for the various B values, it is seen that systematic deviations are absent. The estimated standard deviation in Q (for $Q > 0.5$ cal),

$$S = \pm \sqrt{\Sigma(Q-Q_{calc})^2/\nu} \qquad (6)$$

where ν is the number of degrees of freedom, is found to be $\pm$ 0.034 cal. This is comparable with a value of $\pm$ 0.03 cal calculated (at the 95 % confidence level) from the calorimetric measurement uncertainties (Ref.[5]).

The values of l_{12} and l_{33} can also be found graphically. For that purpose eqn. (5) is written

$$\Sigma Q/\Sigma\delta n_{33} = l_{33} + (\Sigma\delta n_{12}/\Sigma\delta n_{33})l_{12} \qquad (5a)$$

i.e. accumulated values of Q, δn_{12} and δn_{33} have been used. The plot of eqn. (5a) is shown in Fig. 2 together with the best straight line obtained from the least squares treatment above.

The results from the enthalpy titrations substantiate the hydrolysis mechanism suggested for Be^{2+} in so far as a reasonable interpretation of the heat data is obtained with this mechanism. At low values of B, however, the main part of the hydrolysed Be^{2+} is present as $Be_3(OH)_3^{3+}$ whereas $[Be_2OH^{3+}]$ is relatively small. It was therefore considered worthwhile to study a higher value of B also, since the proportion of Be_2OH^{3+} increases with B.

$B = 0.32$ M was chosen for this purpose and this concentration was studied in the range $0 < Z < 0.3$. These data were treated in the way described above. When the results were plotted as done in Fig. 1 small, systematic deviations

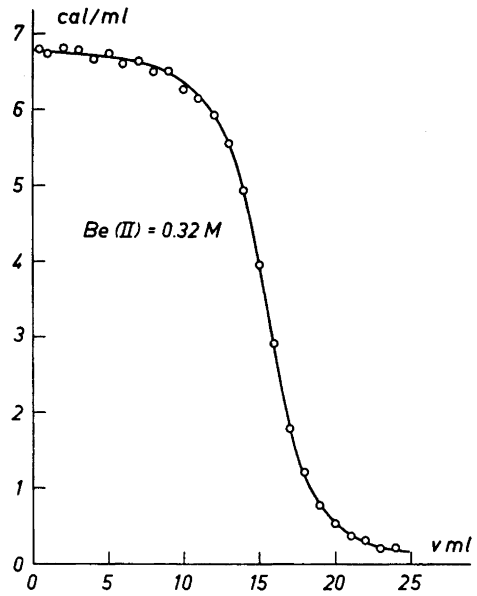

Fig. 3. Q and Q_{calc} (in cal per ml of acid added) as a function of v. The smooth curve has been drawn through the calculated points Q_{calc} and the symbols represent Q for $B = 0.32$ M.

were found. These deviations could be almost removed by an adjustment of the equilibrium constants. Values of β were sought which made the error square sum, $U = (Q-Q_{calc})^2$, a minimum. It was found that that variations in $\log \beta_{3,3}$ of the order of 0.1 logarithmic units did not appreciably change U whereas $\log \beta_{1,2} = -3.14$ gave U a pronounced minimum. This value of $\log \beta_{1,2}$ thus differs from the value -3.21 found from the emf measurements by 0.07 logarithmic units. This is slightly larger than the estimated uncertainty of 0.05 in the latter value of $\log \beta_{1,2}$. The values of the enthalpy changes found were

$$l_{12} = 4.68 \pm 0.10 \text{ kcal/mole}$$
$$l_{33} = 14.95 \pm 0.05 \text{ kcal/mole}$$

They differ somewhat from the values obtained with $B \leq 0.08$ M. No calculations on the data with $B \leq 0.08$ M were done with $\log \beta_{1,2} = -3.14$, since it is believed that $\log \beta_{1,2} = -3.21$, found by emf methods (Ref.[1,2]), is a better value of $\log \beta_{1,2}$ for these values of B. Future experience with other systems will show if the significant difference of 1 % between the two values of l_{33} is reasonable or not. The results of the treatment of the data for $B = 0.32$ M is shown in Fig. 3 and we might conclude that these titrations again support the hydrolysis mechanism identified by emf methods.

Summary of the thermochemical data for $B \leq 0.8$ M

$$2Be^{2+} + H_2O \rightleftharpoons Be_2OH^{3+} + H^+$$

$\Delta G = 4.379 \pm 0.07$ kcal/mole; $\Delta H = 4.43 \pm 0.1$ kcal/mole; $\Delta S = 0.2 \pm 0.6$ e.u.

$$3Be^{2+} + 3H_2O \rightleftharpoons Be_3(OH)_3^{3+} + 3H^+$$

$\Delta G = 11.815 \pm 0.04$ kcal/mole; $\Delta H = 15.18 \pm 0.05$ kcal/mole; $\Delta S = 11.3 \pm 0.3$ e.u.

This work has been financially supported by *Statens tekniska forskningsråd (Swedish Technical Research Council)* and *Statens naturvetenskapliga forskningsråd (Swedish Natural Science Research Council)*.

REFERENCES

1. Kakihana, H. and Sillén, L. G. *Acta Chem. Scand.* **10** (1956) 985.
2. Carell, B. and Olin, Å. *Acta Chem. Scand.* **15** (1961) 1875.
3. Gilbert, R. A. and Garrett, A. B. *J. Am. Chem. Soc.* **78** (1956) 5501.
4. Schindler, P. and Garrett, A. B. *Helv. Chim. Acta* **43** (1960) 2176.
5. Schlyter, K. *Trans. Royal Inst. Tech. Stockholm*, No. **132** (1959).
6. Sturtevant, J. M. *J. Am. Chem. Soc.* **62** (1940) 584.
7. Ingri, N. and Sillén, L. G. *Acta Chem. Scand.* **16** (1962) 195.

Received May 28, 1962.

ACTA CHEMICA SCANDINAVICA 16 (1962) 2363–2367

Determination of Distribution Constants by Potentiometric Titration

J. A. CHRISTENSEN

A/S FERROSAN, Copenhagen, Denmark

By potentiometric titration of a substance with acid-base properties in a medium consisting of an emulsion of two equally large immiscible liquid-phases a titration curve is obtained of normal appearance, but shifted log $(1 + K_D)$ units along the pH axis, where K_D is the distribution constant for the substance between the two phases. This titration curve can in many instances afford an estimation of the distribution of the substance between the aqueous phase and the lipid phase in a biological system. A method is here suggested to determine the pH required in a counter-current distribution.

Verification of theories on the mechanisms of action of pharmacons will often require knowledge of the distribution constants of a number of substances between an aqueous and a lipid phase with reasonable though not very great accuracy.

In the course of time a number of substances have been used as lipid-phase models, *e.g.* olive oil [1,2], chloroform, benzene, heptane [3], and oleyl alcohol [4]. In this laboratory decanol is generally employed, *inter alia* because it is a well-defined and easily accessible compound.

Titration of a substance with acid-base properties in aqueous solution will give

$$\mathrm{pH} = \mathrm{p}K_a + \log\frac{[A^-]}{[A]}$$

During titration in a two-phase system where the acidic form is so distributed between the two phases that the same species of molecule is found in both phases, the distribution law

$$\frac{[A_o]}{[A_{aq}]} = K_D$$

will apply.

pH in the aqueous phase is determined by

$$\mathrm{pH} = \mathrm{p}K_a + \log\frac{[A^-]}{[A_{aq}]}$$

Assuming that A^- does not occur in the organic phase, the amount of A will be

A = vol. water ($[A_{aq}] + [A^-]$) + vol. organic phase $[A_o]$

The computations below will consider only the case where the two phases are of equal volume, *i.e.*

A = phase vol. ($[A_{aq}] + [A_o] + [A^-]$)
= phase vol ($[A] + [A^-]$)

where

$[A] = [A_{aq}] + [A_o] = [A_{aq}](1 + K_D)$

Hence, with pH in terms of a function of $[A^-]$:

$$pH = pK_a + \log\frac{[A^-]}{[A]} + \log\ (1 + K_D)$$

Titration in a two-phase system will thus cause the titration curve to be shifted log $(1 + K_D)$ units to the basic side, and no other changes.

If the substance is of such a nature that the basic form is distributed between the two phases and the acidic form is found only in the aqueous phase, *e.g.* hydrochlorides of amines, the formula will be the same, but with opposite sign for the term log $(1 + K_D)$, *i.e.* the titration curve is shifted to the acidic side.

Where the assumption of the same species of molecule in the two phases is untenable, *e.g.* in the case of carboxylic acids in the water/toluene system where the carboxylic acid occurs mostly as double molecules in the toluene phase, K_D, as defined by the ratio of concentration in the two phases, will not be constant, but depend upon the concentration.

The ratio

$$K_{D2} = \frac{[A_2]\ (\text{toluene})}{[A]^2\ (\text{aq})}$$

is constant, the process being:

$$2\ A\ (\text{water}) \rightleftharpoons A_2\ (\text{toluene})$$

The total concentration of non-ionized A is now:

$$[A] = [A_{aq}] + [A_o] = [A_{aq}] + K_{D2}\ [A_{aq}]^2$$

hence:

$$[A_{aq}] = \frac{\sqrt{1 + 4\ K_{D2}\ [A]} - 1}{2\ K_{D2}}$$

which does not lead to any convenient expression.

From the qualitative point of view, however, a high total concentration means comparatively much material in the organic phase whereas a low total concentration means comparatively little, *i.e.* the shifting of the titration curve is most pronounced while there is but little of the ionized form present. The content of substance in either phase at any pH-value is, moreover, computable from an experimental curve, and the applicability of this distribution law will thus be verifiable.

For the titrations were used Radiometer's titrator TTT1 and titrigraph SBR2/SBU1. Without discussing how the instrument functions we shall merely state that a curve is obtained which presents pH as a function of an added amount of base. Satisfactory working of the instrument requires continuous equilibrium in the system, but even the most effective mechanical stirring fails to maintain sufficient equilibrium in the mixture of water and decanol, and the curves obtained are entirely unsatisfactory. It appears that introduction of an emulsifier to the system improves the curve's appearance, presumably because of the minute droplets then obtained.

1 % Tween 80 * proved very suitable for oil-phases like benzene, toluene, and decanol, but not, however, for chloroform. The application of several other emulsifiers (Tween 20, Span 20, 60 and 80) has been attempted for the water/chloroform system, but without success. It is characteristic of this system that the pH-meter is unsteady and erratic, possibly owing to formation of an emulsion of the water-in-chloroform type, which impairs the conductivity in the emulsion.

In order to enhance the method's applicability, the medium's own protolytic reaction is compensated for by subtracting a blind curve of the medium from the experimental curve so that the amounts of base consumed at the same pH are subtracted as suggested by Grove-Rasmussen [5], *cf.* [6].

For the purpose of estimating the accuracy of the method, the distribution constants of some substances in the water/decanol system have been determined, in part by distribution without emulsifier and subsequent determination of concentrations in the two phases by titration, in part by recording titration curves in water and in water/decanol emulsion (Table 1).

Table 1.

	$C_{decanol}$ mole/l	C_{water} mole/l	K_D	shifting of the titration curve	K_D acc. to this method
Acetic acid	0.0115	0.0323	0.35	0.13	0.35
Propionic acid	0.0190	0.0141	1.35	0.36	1.30
Butyric acid	0.135	0.0275	4.9	0.78	5.0
4-Aminobenzoic acid	0.044	0.013	3.4	0.73	4.3
Aniline	0.083	0.0125	6.6	0.83	5.8

The criterion for the method's applicability is that the quantities relating to the solubility, the acidity constant and the distribution constant of the substance are such as to permit the determination of a titration curve in the emulsion of the two phases.

If, for instance, 0.2 mmole of substance can be dissolved in 10 ml emulsion and titrated with 1 N acid or base, the apparent pK_a-value of the substance

* Tween 80 = polyoxyethylene sorbitan monooleate.

in the emulsion can be determined, provided the latter is located between 3 and 11, *i.e.* for an acid:

$$3 < pK_a + \log (1 + K_D) < 11$$

If $\log (1 + K_D)$ is small, K_D will not be very well determined since the method applied will determine $\log (1 + K_D)$ with an accuracy of 0.1 approx., which means that the method in inapplicable where $K_D < 0.5-1$, all according to the accuracy required.

In many cases the pK_a of the substance cannot be determined by potentiometric titration because of its slight solubility, but the choice of method is inessential.

If $K_D > 10$, the substance is found essentially as A_o and A^-, *i.e.* the titration curve will indicate the concentration in water-phase and oil-phase, respectively, as a function of pH, a function that is often of some importance for the discussion of biological problems.

The titration curve of a substance dissolved in emulsion will likewise prove useful in planning a counter-current distribution for the purpose of determining the pH-value which a water-phase is to have in order to make the distribution of a substance between the water-phase and an organic phase equal to 1.

In the titration curve of the substance in an emulsion the distance from the pH-axis to a point on the curve represents the amount of A^-, and the distance from the point to the equivalence line $A_{aq} + A_o$.

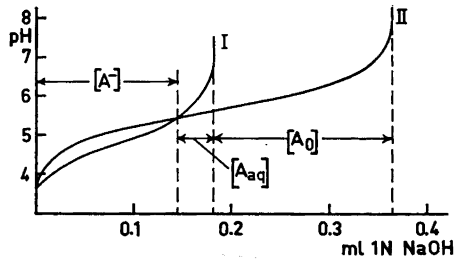

Fig. 1. I: Titration curve of 25 mg of 4-aminobenzoic acid in 10 ml of water.

II: Titration curve of 50 mg of 4-aminobenzoic acid in a mixture of 5 ml of water, 5 ml of decanol and 100 mg of Tween 80.
$[A^-]$: Concentration of ionized 4-aminobenzoic acid in the water phase.
$[A_{aq}]$: Concentration of non-ionized 4-aminobenzoic acid in the water phase.
$[A_o]$: Concentration of 4-aminobenzoic acid in the decanol phase.

What is required is that $[A_o] = [A_{aq}] + [A^-] = \frac{1}{2}[A_{total}]$. The pH-value is found as the point of intersection of this titration curve and a titration curve of half the amount of substance in water.

Acknowledgement. The author wishes to thank civilingeniør O. Rosenlund Hansen for valuable discussions and Mr. Peer Everland for technical assistance.

REFERENCES

1. Meyer, H. *Arch. Exptl. Pathol. Pharmakol.* **42** (1899) 109.
2. Overton, E. *Studien über die Narkose*, G. Fischer, Jena 1901.
3. Mayer, S., Maickel, R. P. and Brodie, B. B. *J. Pharmacol. Exptl. Therap.* **127** (1957) 205.
4. Albert, A. and Hampton, A. *J. Chem. Soc.* **1954** 505.
5. Grove-Rasmussen, K. V. *Kem. Månedsblad* **27** (1946) 161.
6. Tanford, C. and Wawzonek, S. in Weissberger, A. (Ed.) *Physical Methods of Organic Chemistry*, Vol. 1, part IV, Interscience Publishers, New York 1960, p. 2956.

Received June 8, 1962.

ACTA CHEMICA SCANDINAVICA 16 (1962) 2368–2372

Studies of Hydrogen Bonding

Part VI *. A Comparison between the Ability of the ≡P=O and the ≡P=S Groups to Form Addition Compounds with Iodine and to Take Part in Hydrogen Bonding

THOR GRAMSTAD and WILLY JOHANNES FUGLEVIK

Norwegian Defence Research Establishment, Division for Toxicology, Kjeller, Norway

It has been found that $(C_2H_5O)_3PO$ takes part in hydrogen bonding more readily than $(C_2H_5O)_3PS$ but that the reverse is the case for complex formation with iodine. These, and earlier results, are discussed in terms of the mechanism of association of proton donors and iodine with compounds containing oxygen, sulphur, and nitrogen.

In a previous publication [1], the ability of organophosphorus compounds containing the ≡P=O group to form hydrogen bonds was compared with their ability to take part in complex formation with iodine. It was found that the ≡P=O group forms hydrogen bonds readily, whereas its ability to form addition compounds with iodine is considerably smaller. It was therefore of interest to extend these measurements to compounds containing the ≡P=S group.

RESULTS AND DISCUSSION

In a recent paper Zingaro and Hedges [5] describe a spectrophotometric study of the interaction of the halogens and interhalogens with organophosphorus compounds containing the ≡P=O or ≡P=S group. They found that the infrared frequency shifts upon complex formation, $\Delta\nu_{P=O}$ and $\Delta\nu_{P=S}$, are related to the polarity of acceptor molecule according to the sequence $ICl > IBr > I_2 > Br_2$. The frequency shift for a ≡P=S compound is smaller than that observed for the ≡P=O compound. The factors which affect the ≡P=O and ≡P=S frequency shifts were discussed, and it was pointed out that special importance must be attached to π bonding between the p and d orbitals of the oxygen or sulphur and the phosphorus, and back-bonding

* Part V. *Acta Chem. Scand.* 16 (1962) 1369.

from the p orbitals of the halogens to the d orbitals of the sulphur atom. This latter effect is impossible in the phosphoryl complexes owing to the lack of a suitable d orbital on the oxygen.

As has been shown previously [1,2,8], the K_{ass} values for the association of organophosphorus compounds with hydroxy compounds and iodine depend upon the electron density on the phosphoryl oxygen atom which in turn is controlled by the inductive and mesomeric effects of the substituents attached to the phosphorus atom. K_{ass} is largest for the most polarised $\equiv P=O$ group. Furthermore, it has been shown [1] that the $\equiv P=O$ frequency shift, $\Delta\nu_{P=O}$, is much larger upon complexation with iodine than upon formation of a hydrogen bond, *i.e.*, that $\Delta\nu_{P=O}$ depends both on the substituents on the phosphorus atom and those on the complexing agent. Some examples are given below:

	$K_{ass}^{20°}$ l/mole	$\Delta\nu_{PO}$ cm^{-1}	Ref.
$(C_2H_5)_3PO-HOC_6H_5$	2522.0	23	2
$(C_2H_5)_3PO-I_2$	83.2	46	1
$(C_2H_5O)_3PO-HOC_6H_5$	350.5	30	2
$(C_2H_5O)_3PO-I_2$	6.2	36	1

The sequence of decreasing $\equiv P=O$ frequency shift upon complex formation is, iodine monochloride > iodine monobromide > iodine > bromine [5] > pentachlorophenol > α-naphthol and phenol > methanol, although the enthalpies of formation ($-\Delta H$) of the hydrogen bonds are larger than those of the analogous iodine complexes (Table 1 and Ref.[1]). The observations on the $\equiv P=O$ frequency shifts in iodine complexes may be interpreted as indicating that the structure $\equiv P=\overset{\delta+}{O}\ldots I-\overset{\delta-}{I}$ (or perhaps $\equiv P=\overset{+}{O}I\ldots\overset{-}{I}$) is of major importance, whereas in the hydrogen bond complexes the structure $\equiv P=\overset{\delta-}{O}\ldots\overset{\delta+}{H}-OR$ makes the largest contribution. In Table 1 results are tabulated which show that triethyl phosphorothionate forms more stable iodine complexes than hydrogen bond complexes, these observations being the reverse of those found for phosphoryl derivatives. The values of K_{ass} and $-\Delta H$ are larger for the system $(C_2H_5O)_3P=S-I_2$ than for $(C_2H_5O)_3P=O-I_2$, being 10.0 and 6.2 l/mole, 5.9 and 3.2 kcal/mole, respectively. Similar results have been reported by Tsubomura and Lang [6] for $(C_2H_5)_2S-I_2$ and $(C_2H_5)_2O-I_2$ (see Table 2). Spectrophotometric measurements on the $\equiv P=S$ and $\equiv P=O$ complexes thus show that the sulphur compound is more strongly complexed to iodine than is the $\equiv P=O$ compound; the relative stability of these complexes is related to the shift in the iodine peak (72 and 77 mμ, respectively, for the $(C_2H_5O)_3P=O$ and $(C_2H_5O)_3P=S$ complexes, see Table 1). In contrast, the $\equiv P=O$ stretching frequency shift, $\Delta\nu_{P=O}$ in the infrared is larger than the $\equiv P=S$ frequency shift, $\Delta\nu_{P=S}$ on complexing with iodine, in spite of the fact that a larger enthalpy ($-\Delta H$) value is found for the phosphorothionate complex (Table 1). Following Zingaro and Hedges [5], this discrepancy may be due to greater S → P π bonding in the phosphorothionate complex than O → P π bonding

Table 1. A comparison of the abilities of triethyl phosphate and triethyl phosphorothionate to form hydrogen bonds and to form addition compounds with iodine.

Electron donor / Electron acceptor	$(C_2H_5O)_3P=O$[a]							$(C_2H_5O)_3P=S$							
	$\Delta\nu_{O-H}$ cm^{-1}	$K_{ass}^{20°}$ l/mole	$K_{ass}^{50°}$ l/mole	ΔH kcal/mole	ΔF kcal/mole	ΔS e.u.	$\Delta\nu_{P-O}$ cm^{-1}	$\Delta\nu_{O-H}$ cm^{-1}	$K_{ass}^{20°}$ l/mole	$K_{ass}^{50°}$ l/mole	ΔH kcal/mole	ΔF kcal/mole	ΔS e.u.	$\Delta\nu_{P-S}$ cm^{-1}	Solvent
Phenol	345	350.5	121.1	−6.7	−3.4	−11.1	30	157	5.5	4.0[c]	−2.9	−1.0	−9.7	16	CS_2
								172	4.5	2.7	−3.2	−0.9	−8.4		CCl_4
Pentachloro-phenol	481	153.1	67.1	−5.2	−2.9	−7.7	33	181	2.3	1.7[c]	−2.8	−0.5	−8.3	27	CS_2
								202	2.9	1.7	−3.3	−0.6	−9.9		CCl_4
Iodine	72[b]	6.2	3.7	−3.2	−1.1	−7.9	36	77[b]	4.0	2.1[c]	−5.9	−0.8	−18.7	22	CS_2
								77[b]	10.0	3.9	−5.9	−1.3	−16.7		CCl_4

[a] Corrected data from Part II, Ref.[2]
[b] Means shifted iodine visible band (mμ), see Part IV, Ref.[1]
[c] Measured at 40°C.

Table 2. A comparison of thermodynamic data for hydrogen bonds and iodine complexes for various oxygen, nitrogen and sulphur compounds. Solvents were carbon tetrachloride and n-heptane respectively for hydrogen bonded complexes and iodine complexes.

Electron acceptor / Electron donor	Iodine [6]			Phenol		
	$\Delta\lambda_{I-I}$ mμ	$K_{ass}^{20°}$ l/mole	ΔH kcal/mole	$\Delta\nu_{O-H}$ cm^{-1}	$K_{ass}^{20°}$ l/mole	ΔH kcal/mole
$(C_2H_5)_2S$	87	210	− 7.82	165	4.7	−3.4
$(C_2H_5)_2O$	60	1.16	− 4.2	270 [a]	9.6	−4.6
CH:CHCH:CHCH:N	100	269	− 7.8	492 [b]	59.8	−7.0
$(C_2H_5)_3N$	108	6460	−12.0	380 [b]	90.9	−7.8

[a] see Ref. [9] [b] see Ref. [3]

in the phosphate complex, which will give greater stability to the former. The frequency shift $\Delta\nu_{P=O}$ is also larger than $\Delta\nu_{P=S}$ on hydrogen bonding, but here as distinct from complexation with iodine, the enthalpy ($-\Delta H$) of complex formation is largest for the phosphate-phenol complex (Table 1). We consider, however, that the lower K_{ass} value for the system $\equiv P=S-HOR$ as compared with $\equiv P=O-HOR$ is due to a lower electron density around the sulphur than around the oxygen atom consistent with their relative electronegativities (2.5 and 3.5, respectively). The smaller frequency shift, $\Delta\nu_{O-H}$, for the association of phenol with triethyl phosphorothionate as compared with triethyl phosphate (172 and 345 cm^{-1}, respectively, Table 1) is also consistent with the lower electronegativity of sulphur. If we compare $(C_2H_5O)_3PO$ and $(C_2H_5)_2O$ with $(C_2H_5O)_3PS$ and $(C_2H_5)_2S$ with respect to their ability to form a complex with iodine, we see that while the ability of $(C_2H_5O)_3PS$ is smaller than that of $(C_2H_5)_2S$ the reverse is the case for the oxygen analogues (Tables 1 and 2). However, $(C_2H_5)_2S$ has no back-bonding from the sulphur and hence has a higher electron density on the sulphur than has $\equiv P=S$. The most probable contributing structures are thus $(C_2H_5)_2\overset{+}{S}I\ldots\overset{-}{I}$ and $(C_2H_5)_2\overset{\delta+}{S}\ldots I-\overset{\delta-}{I}$. These structures are favoured by the strong $+I$ effect of the ethyl groups. Further, as shown earlier [1], iodine forms more stable addition compounds with nitrogen bases than with oxygen bases, whereas the reverse is the case with hydrogen bonding. It seems therefore, that the nitrogen bases resemble the sulphur bases when abilities to form hydrogen bonds and addition compounds with iodine are compared. The unshared electron pair on nitrogen has a greater tendency to form a covalent bond with the acceptor and hence $\equiv\overset{+}{N}-I\ldots\overset{-}{I}$ should predominate [1,3]. This is in accordance with the X-ray

work of Hassel *et al.*[7] whose observed N—I distance in the triethylamine and pyridine addition compounds with iodine indicates that the N—I bond is more covalent than electrostatic in nature. Thermodynamic data for some typical systems are given in Table 2.

Solvent interaction. As shown earlier [2,3] the thermodynamic properties of hydrogen bonds are greatly affected by solvent interaction. The lower association constants found for the systems OPC-pentachlorophenol and amides-pentachlorophenol [9] compared with those for OPC-phenol and amides-phenol was suggested as being due, at least partly, to hydrogen bond formation between the proton donor and the solvent. When carbon tetrachloride was replaced by carbon disulphide as the solvent a marked increase in the association constant was observed for most systems. With regard to complex formation with iodine, however, the effect of these solvents on complexing ability appears to be reversed. As can be seen in Table 1, a decrease in the association constant for triethyl phosphorothionate and iodine was found when carbon tetrachloride was replaced by carbon disulphide. An explanation for this reversal in the effect of these two solvents may be that iodine interacts more strongly with CS_2 (to form S=C=S. . .I—I) than it does with CCl_4.

EXPERIMENTAL

The instruments, the instrumental conditions, the methods of determining the spectra, the method of calculation of the association constants, and the solvents used were the same as described elsewhere [9]. Triethyl phosphorothionate was purchased from Aldrich Chemical Co., Inc.

REFERENCES

1. Gramstad, T. and Snaprud, S. I. *Acta Chem. Scand.* **16** (1962) 999.
2. Gramstad, T. *Acta Chem. Scand.* **15** (1961) 1337.
3. Gramstad, T. *Acta Chem. Scand.* **16** (1962) 807.
4. Nagakura, S. *J. Am. Chem. Soc.* **80** (1958) 520.
5. Zingaro, R. A. and Hedges, R. M. *J. Phys. Chem.* **65** (1961) 1132.
6. Tsubomura, H. and Lang, R. P. *J. Am. Chem. Soc.* **83** (1961) 2085.
7. Hassel, O. and Hvoslef, J. *Acta Chem. Scand.* **8** (1954) 873; **10** (1956) 138; Hassel, O. and Römming, C. *Acta Chem. Scand.* **10** (1956) 696; **11** (1957) 195; Hassel, O. *Proc. Chem. Soc.* **1957** 250; Hassel, O. and Strömme, K. O. *Acta Chem. Scand.* **13** (1959) 275; Hassel, O. and Hope, H. *Acta Chem. Scand.* **14** (1960) 391.
8. Aksnes, G. and Gramstad, T. *Acta Chem. Scand.* **14** (1960) 1485.
9. Gramstad, T. *To be published.*

Received March 22, 1962.

ACTA CHEMICA SCANDINAVICA 16 (1962) 2373–2383

The Crystal Structure of the Calcium and Strontium Salts of Arabonic Acid

SVEN FURBERG and STEN HELLAND

Institute of Chemistry, Blindern-Oslo, Norway

The crystal structures of the calcium and strontium salts of arabonic acid have been determined by X-ray crystallographic methods, using the isomorphous replacement technique. The carbon atoms of the arabonate anion form a nearly planar zig-zag chain. The bond C_2-O_2 is approximately coplanar with the carboxyl group. The cations are surrounded by eight oxygen atoms which lie in the corners of a distorted Archimedean antiprism. The structures of the two isomorphous compounds are compared.

As part of a program of investigations of the conformations of simple sugars, we have determined the crystal structure of arabonic acid, $CH_2OH(CHOH)_3COOH$, in the form of its calcium and strontium salts. Amongst earlier crystal structure analysis related to the structure of this compound should be mentioned those of β-arabinose [2] and potassium gluconate [1]. A comparison of the open-chain structure of arabonic acid with the ring structure of the parent sugar would appear to be of interest.

EXPERIMENTAL. CRYSTAL DATA

A sample of the Ca-D-arabonate, $Ca(C_5O_6H_9)_2.5H_2O$, was supplied by Fluka AG. In order to prepare the strontium salt, the calcium ions were first removed as oxalate. Subsequent addition of $SrCO_3$ and alcohol yielded big, well-developed crystals. The crystals had the same habit for the two salts, being elongated along the b axis and bounded by {100}, {101} and {001}.

Oscillation and Weissenberg photographs were taken about the b and c axes using filtered copper radiation ($\lambda = 1.542$ Å). They showed the crystals to be monoclinic, with unit cell dimensions $a = 14.74$ Å, $b = 5.82$ Å, $c = 11.40$ Å, $\beta = 99°$ for the Ca salt and $a = 14.79$, $b = 5.83$, $c = 11.78$ Å, $\beta = 99°$ for the Sr salt (all $\pm$ 0.5 %). The compounds are thus isomorphous. Reflections are absent for odd values of $h + k$, and the lattice is therefore C-centered. As the compounds are optically active, the space group must be $C2$. By flotation in mixtures of CCl_4 and $CHBr_3$ the density was found to be 1.59 g/cm³ for the Ca salt and 1.69 g/cm³ for the Sr salt, which gives two (calc. 2.01 for both salts) molecules $Ca(Sr)(C_5O_6H_9)_2.5H_2O$ in the unit cell.

The intensities were measured on integrated Weissenberg diagrams by means of a Hilger Watts photometer and corrected for Lorentz-polarization effects. Small crystals of crossection about 0.1 × 0.1 mm were used and no correction for absorption applied.

For the calcium salt 163 reflections were observed in the *b* projection and 53 in the *c* projection, the numbers obtainable by copper radiation being 210 and 60, respectively. In the two corresponding projections of the strontium salt only six reflections were not observed with measurable intensity.

DETERMINATION OF THE STRUCTURE OF CALCIUM ARABONATE

The data given above show that the calcium ion, as well as one molecule of water, must lie on two-fold axes. The position of the ion was chosen as origin and the structure solved by the isomorphous replacement method.

The b projection. This projection is centrosymmetric, and the difference between the structure factors for the two salts should be given simply by the difference in the scattering power of the calcium and strontium ions corrected for thermal vibrations. This was borne out by the experimental values after their reduction to absolute scale, and the signs of the structure factors were directly deduced. In general, the signs were positive, as was to be expected, but surprisingly, the sign of the very strongest reflection, $60\bar{1}$, was found to be negative. Because of this our first attempts to solve the structure by the heavy atom method were unsuccessful. The corresponding Fourier map showed clearly the positions of the carbon and oxygen atoms, and the calculated structure factors agreed well with the observed ones, the value of the reliability

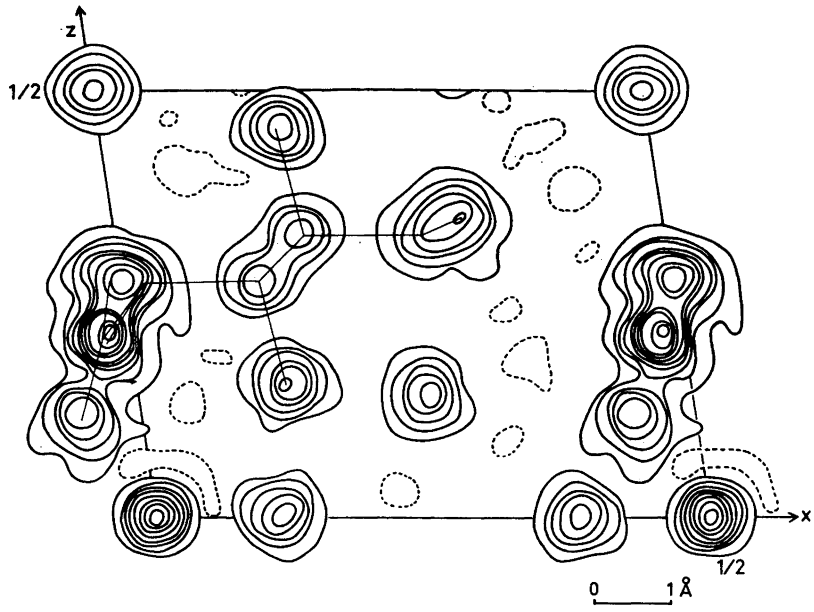

Fig. 1. Electron density projection in direction of *b* axis. Contours at 0, 2, 4, ... e.Å^{-2}, the zero line being dotted. For the calcium ion every second contour is omitted.

Table 1. Atomic coordinates of Ca-arabonate as fractions of the corresponding cell edge.

Atom	x	y	z	B_{hol}
Ca	0.0000	0.000	0.0000	1.1
C_1	−0.0248	−0.322	0.218	2.5
C_2	0.0195	−0.094	0.2741	2.0
C_3	0.1249	−0.110	0.2765	2.0
C_4	0.1718	0.111	0.3335	2.0
C_5	0.2763	0.120	0.3261	2.5
O_0	−0.0550	−0.321	0.1117	2.2
O_1	−0.0096	−0.506	0.2825	2.0
O_2	−0.0170	0.091	0.2051	2.2
O_3	0.1355	−0.110	0.1536	2.0
O_4	0.1620	0.132	0.4552	2.2
O_5	0.3169	0.338	0.3495	2.8
O_6	0.1145	0.303	0.0012	3.0
O_7	0.2618	−0.427	0.1414	2.6
O_8	0.0000	−0.333	0.5000	2.5
H_1	0.010	−0.05	0.362	3.0
H_2	0.138	−0.25	0.293	—
H_3	0.158	0.27	0.317	—
H_4	0.303	0.02	0.387	—
H_5	0.285	0.02	0.235	—
H_6	0.495	−0.40	0.415	—
H_7	0.483	0.22	0.234	—
H_8	0.405	0.45	0.035	—
H_9	0.163	0.40	0.047	—
H_{10}	0.278	0.43	0.208	—
H_{11}	0.300	−0.38	0.095	—
H_{12}	0.175	−0.22	0.150	—
H_{13}	0.330	0.43	0.480	—
H_{14}	0.378	0.28	0.400	—

index, $R = \Sigma||F_c|-|F_o||/\Sigma|F_o|$, being 0.21. The structure was further refined by least squares calculations and difference syntheses. The final value of R for all reflections obtainable by copper radiation is 0.09. In the calculation of R non-observed reflections are only taken into account when F_c exceeds the observable limit of intensity. The atoms C_1 and O_2 overlap and their coordinates are less certain than those of the other atoms. The positions of the hydrogen atoms were derived partly from the difference maps, partly by stereochemical considerations. The atomic scattering curve of Forsyth and Wells [4] was used for the Ca ion, and those of Berghuis *et al.*[5] for the other atoms. In the temperature factor, $\exp(-B\sin^2\Theta/\lambda^2)$, B is 1.1 for the Ca ion and 2.0—3.0 for the other atoms. The final difference map, from which the atomic coordinates given in Table 1 are derived, indicates clearly that the vibrations of a number of atoms are anisotropic, but this has not been taken into account in the structure factor calculations. Fig. 1 shows the electron density map and in Table 3 observed and calculated values of the structure factors are compared.

The c projection. This non-symmetrical projection was solved by applying the isomorphous replacement procedure described by Bokhoven *et al.*[3], the resulting double Fourier synthesis being interpreted by means of the known b projection of the structure. For the two water molecules several positions

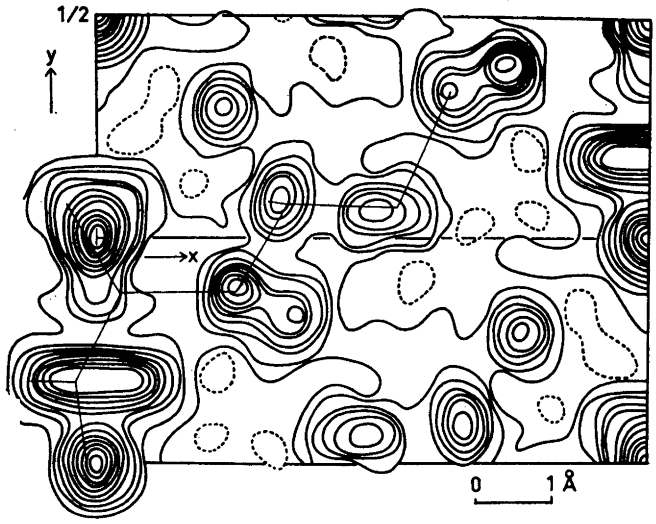

Fig. 2. Electron density projection in direction of *c* axis. Contours as in Fig. 1.

were suggested by the maps. The correct ones were deduced by comparing observed and calculated structure factors. The y coordinates were then refined by least squares calculations, maintaining the x coordinates derived from the b projection unchanged. The resolution is very poor in this projection and no really efficient refinement could be carried out. The final value of R is 0.09. The electron density map is shown in Fig. 2.

DESCRIPTION AND DISCUSSION OF THE STRUCTURE OF CALCIUM ARABONATE

The bond lengths and bond angles calculated from the coordinates in Table 1 are given in Table 2 and Fig. 3. The Cruickshank formulae [6] give the following values for the standard deviations of the atomic coordinates: $\sigma(x) = \sigma(z) = 0.008$ Å, $\sigma(y) = 0.012$ Å for the carbon atoms, and $\sigma(x) = \sigma(z) = 0.006$ Å, $\sigma(y) = 0.009$ Å for the oxygen atoms. The corresponding standard deviation in the bond lengths lie in the range 0.011—0.015 Å for the C—C bonds and 0.009—0.013 Å for C—O bonds. However, lack of resolution makes the uncertainty considerably greater for most bonds and we do not consider deviations less than 0.05 Å significant. The limit of error in the bond angles is estimated to be about 3° for most angles.

The arabonate ion. The carbon atoms form an extended, nearly planar zigzag chain with the oxygen atoms lying above and below this plane (Fig. 3), as was found in the gluconate ion [1]. Certain chemical properties of sugars have also been explained by this arrangement [8] and it appears reasonable to assume that it is the preferred conformation of all open-chain sugars. One might

Table 2. Bond lengths (in Å units) and bond angles in Ca-arabonate. Primes indicate atoms in neighbouring molecules.

C_1-C_2	1.57	$C_1-C_2-C_3$	108°
C_2-C_3	1.55	$C_2-C_3-C_4$	110°
C_3-C_4	1.55	$C_3-C_4-C_5$	113°
C_4-C_5	1.56	$O_0-C_1-O_1$	125°
C_1-O_0	1.29	$O_0-C_1-C_2$	118°
C_1-O_1	1.23	$O_1-C_1-C_2$	117°
C_2-O_2	1.39	$C_1-C_2-O_2$	108°
C_3-O_3	1.43	$C_3-C_2-O_2$	111°
C_4-O_4	1.42	$C_2-C_3-O_3$	104°
C_5-O_5	1.41	$C_4-C_3-O_3$	107°
$Ca-O_0$	2.47	$C_3-C_4-O_4$	112°
$Ca-O_2$	2.45	$C_5-C_4-O_4$	108°
$Ca-O_3$	2.52	$C_4-C_5-O_5$	114°
$Ca-O_6$	2.44	$C_3-O_3-O_6$	124°
O_3-O_6	2.95	$C_3-O_3-O_7$	104°
O_7-O_6'	2.95	$C_5-O_5-O_7$	103°
O_6-O_0'	2.62	$C_4-O_4-O_5'$	135°
O_3-O_7	2.64	$O_5-O_7-O_3$	115°
O_4-O_5'	2.79	$O_7-O_6-O_0$	107°
O_5-O_7	2.75	$C_5-O_5-O_8$	97°
O_1-O_8	2.66	$O_3-O_7-O_6$	86°
O_2-O_1'	2.50	$C_2-O_2-O_1'$	122°
O_6-O_7	2.94		
O_5-O_8	3.13		

expect non-planar carbon chains for sugars in which a planar chain gives unfavourable O—O distances. Glucose is such a sugar, but in spite of this the chain is planar, favourable O—O contacts being obtained by widening some of the angles at the carbon atoms. From the data given on the gluconate ion the O_2-O_4 distance is calculated to be 2.97 Å, whereas a structure based on tetrahedral angles gives 2.52 Å.

The plane of the carboxyl ion is roughly co-planar with the plane $C_1C_2O_2$ containing the α-hydroxyl oxygen O_2, the angle between the planes being about 20°. The distance O_0-O_2 is somewhat smaller (2.64 Å) than normal van der Waals approach and could be extended by rotation about the C_1-C_2

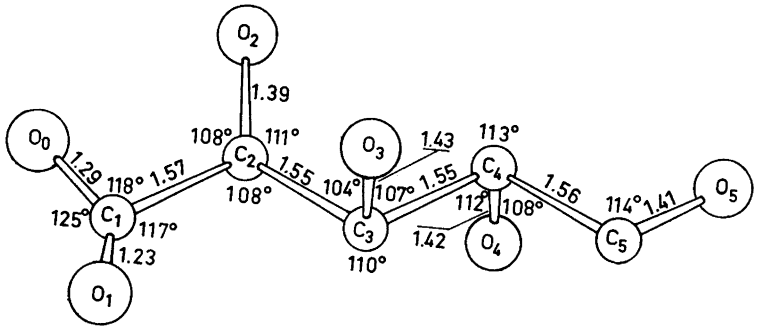

Fig. 3. The structure of the arabonate ion.

bond. This structural feature appears to be common to all compounds containing the groups C(OH)COOH and $C(OH)COO^-$ and has been discussed by Jeffrey and Parry [7].

The two C—O bonds in the carboxyl group are found to have lengths 1.23 Å and 1.29 Å, respectively. A symmetrical structure is to be expected [9]. The difference is probably mainly due to inaccuracy in the structure analysis, as the atom C_1 is unresolved in both projections. Part of it may, however, be caused by crystal forces, the external bonding being different for the two oxygen atoms.

The C—C and C—O bond lengths do not deviate significantly from the normal values of about 1.53 Å and 1.43 Å, respectively. The mean C—C—C angle is 110° and the mean C—C—OH angle 109°.

The open-chain structure derived in the present work can be transformed into the pyranose form of arabinose by a rotation of 120° around the bonds $C_2—C_3$, $C_3—C_4$ and $C_4—C_5$. This places O_5 near O_1 (or O_0) and the structure corresponds to one of the two chair conformations characteristic of arabopyranose (2e3e4a ⇌ 2a3a4e), dependent on the direction of rotation.

The ionic environment. Each calcium ion is surrounded by eight oxygen atoms related in pairs by the operation of the two-fold axis on which the ion is situated. They lie in the corners of a distorted square Archimedean antiprism.

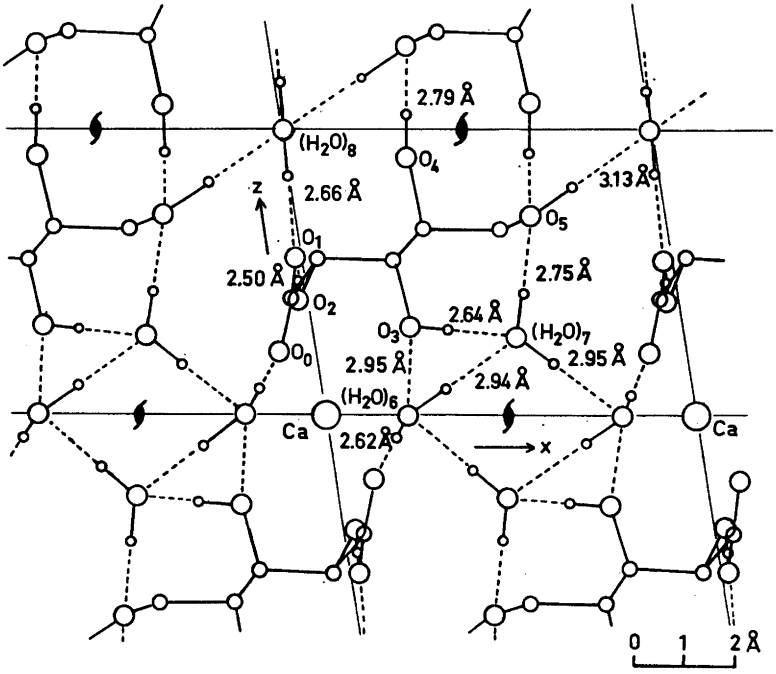

Fig. 4. The *b*-projection of the structure. Short contacts are shown by broken lines. The smallest circles indicate the proposed positions of the oxygen-bonded hydrogen atoms.

Table 3. Observed (F_o) and calculated (F_c) structure factors for Ca arabonate.

$h\,k\,l$	F_o	F_c	$h\,k\,l$	F_o	F_c
0 0 1	41	43	4 0 0	77	75
0 0 2	51	− 54	4 0 1	38	36
0 0 3	31	31	4 0 2	5	− 1
0 0 4	42	41	4 0 3	12	11
0 0 5	14	− 10	4 0 4	5	4
0 0 6	74	71	4 0 5	22	21
0 0 7	52	48	4 0 6	13	− 10
0 0 8	38	33	4 0 7	6	− 1
0 0 9	35	33	4 0 8	6	3
0 0 10	14	14	4 0 9	6	4
0 0 11	24	22	4 0 10	35	33
0 0 12	6	6	4 0 11	< 8	11
0 0 13	< 6	5	4 0 12	< 6	2
0 0 14	24	24	4 0 13	< 6	− 0
2 0 $\bar{14}$	24	23	6 0 $\bar{14}$	17	19
2 0 $\bar{13}$	< 6	− 0	6 0 $\bar{13}$	12	10
2 0 $\bar{12}$	< 6	− 4	6 0 $\bar{12}$	< 6	5
2 0 $\bar{11}$	13	15	6 0 $\bar{11}$	18	20
2 0 $\bar{10}$	36	39	6 0 $\bar{10}$	< 8	4
2 0 $\bar{9}$	13	11	6 0 $\bar{9}$	7	8
2 0 $\bar{8}$	50	46	6 0 $\bar{8}$	< 6	6
2 0 $\bar{7}$	40	33	6 0 $\bar{7}$	< 6	− 4
2 0 $\bar{6}$	49	− 51	6 0 $\bar{6}$	39	39
2 0 $\bar{5}$	45	46	6 0 $\bar{5}$	38	38
2 0 $\bar{4}$	88	89	6 0 $\bar{4}$	63	69
2 0 $\bar{3}$	8	− 8	6 0 $\bar{3}$	29	30
2 0 $\bar{2}$	17	− 18	6 0 $\bar{2}$	38	− 35
2 0 $\bar{1}$	73	80	6 0 $\bar{1}$	126	−129
2 0 0	75	70	6 0 0	106	110
2 0 1	42	37	6 0 1	54	45
2 0 2	6	− 1	6 0 2	19	17
2 0 3	8	6	6 0 3	30	26
2 0 4	121	120	6 0 4	45	46
2 0 5	9	16	6 0 5	6	− 3
2 0 6	22	17	6 0 6	13	12
2 0 7	10	5	6 0 7	6	5
2 0 8	8	6	6 0 8	< 8	− 0
2 0 9	9	− 3	6 0 9	14	14
2 0 10	60	58	6 0 10	12	16
2 0 11	31	31	6 0 11	23	24
2 0 12	< 6	1	6 0 12	6	6
2 0 13	< 6	0	8 0 $\bar{13}$	20	22
4 0 $\bar{14}$	14	15	8 0 $\bar{12}$	< 6	5
4 0 $\bar{13}$	< 6	− 1	8 0 $\bar{11}$	< 6	− 2
4 0 $\bar{12}$	< 6	− 0	8 0 $\bar{10}$	18	21
4 0 $\bar{11}$	10	− 11	8 0 $\bar{9}$	< 8	2
4 0 $\bar{10}$	26	24	8 0 $\bar{8}$	32	31
4 0 $\bar{9}$	17	18	8 0 $\bar{7}$	63	67
4 0 $\bar{8}$	29	29	8 0 $\bar{6}$	< 6	− 1
4 0 $\bar{7}$	11	− 4	8 0 $\bar{5}$	14	17
4 0 $\bar{6}$	27	27	8 0 $\bar{4}$	68	68
4 0 $\bar{5}$	15	− 17	8 0 $\bar{3}$	25	21
4 0 $\bar{4}$	58	61	8 0 $\bar{2}$	21	− 21
4 0 $\bar{3}$	18	− 21	8 0 $\bar{1}$	54	51
4 0 $\bar{2}$	85	− 92	8 0 0	71	71
4 0 $\bar{1}$	12	− 10	8 0 1	34	36

$h\,k\,l$	F_o	F_c	$h\,k\,l$	F_o	F_c
8 0 2	14	16	14 0 $\bar{10}$	9	12
8 0 3	15	− 12	14 0 $\bar{9}$	< 6	3
8 0 4	49	47	14 0 $\bar{8}$	< 6	− 2
8 0 5	33	30	14 0 $\bar{7}$	12	13
8 0 6	49	46	14 0 $\bar{6}$	< 7	1
8 0 7	27	27	14 0 $\bar{5}$	7	7
8 0 8	15	14	14 0 $\bar{4}$	20	20
8 0 9	22	− 18	14 0 $\bar{3}$	19	19
8 0 10	21	19	14 0 $\bar{2}$	< 7	0
8 0 11	23	24	14 0 $\bar{1}$	< 7	0
8 0 12	12	11	14 0 0	< 7	10
10 0 $\bar{13}$	< 5	6	14 0 1	24	23
10 0 $\bar{12}$	23	23	14 0 2	17	19
10 0 $\bar{11}$	8	12	14 0 3	12	− 12
10 0 $\bar{10}$	6	9	14 0 4	< 7	8
10 0 $\bar{9}$	16	15	14 0 5	< 6	0
10 0 $\bar{8}$	35	36	14 0 6	12	13
10 0 $\bar{7}$	15	− 13	14 0 7	15	16
10 0 $\bar{6}$	7	10	16 0 $\bar{9}$	8	10
10 0 $\bar{5}$	19	19	16 0 $\bar{8}$	32	29
10 0 $\bar{4}$	61	63	16 0 $\bar{7}$	12	10
10 0 $\bar{3}$	49	53	16 0 $\bar{6}$	< 6	5
10 0 $\bar{2}$	8	11	16 0 $\bar{5}$	< 6	− 7
10 0 $\bar{1}$	9	− 4	16 0 $\bar{4}$	10	9
10 0 0	21	19	16 0 $\bar{3}$	17	21
10 0 1	20	16	16 0 $\bar{2}$	16	19
10 0 2	10	5	16 0 $\bar{1}$	15	16
10 0 3	38	35	16 0 0	17	20
10 0 4	29	29	16 0 1	13	15
10 0 5	25	23	16 0 2	< 6	1
10 0 6	24	23	16 0 3	< 5	5
10 0 7	21	19	16 0 4	< 5	55
10 0 8	8	− 4	16 0 5	11	11
10 0 9	6	− 3	18 0 $\bar{5}$	< 5	3
10 0 10	34	32	18 0 $\bar{4}$	16	16
10 0 11	14	17	18 0 $\bar{3}$	15	15
12 0 $\bar{12}$	6	7	18 0 2	13	17
12 0 $\bar{11}$	6	7	18 0 1	< 6	1
12 0 $\bar{10}$	6	10	18 0 0	13	15
12 0 $\bar{9}$	16	16	1 1 0	82	74
12 0 $\bar{8}$	13	11	3 1 0	49	52
12 0 $\bar{7}$	< 7	5	5 1 0	43	44
12 0 $\bar{6}$	< 7	0	7 1 0	52	57
12 0 $\bar{5}$	< 7	1	9 1 0	13	7
12 0 $\bar{4}$	31	34	11 1 0	19	16
12 0 $\bar{3}$	21	21	13 1 0	13	15
12 0 $\bar{2}$	19	21	15 1 0	15	15
12 0 $\bar{1}$	14	− 17	17 1 0	12	12
12 0 0	23	22	0 2 0	53	58
12 0 1	< 7	1	2 2 0	34	28
12 0 2	14	14	4 2 0	106	103
12 0 3	7	2	6 2 0	35	33
12 0 4	< 8	1	8 2 0	51	47
12 0 5	< 7	10	10 2 0	31	26
12 0 6	29	28	12 2 0	30	37
12 0 7	10	11	14 2 0	20	21
12 0 8	7	2	16 2 0	20	17
12 0 9	< 5	9	1 3 0	30	24

$h\,k\,l$	F_o	F_c	$h\,k\,l$	F_o	F_c
3 3 0	65	60	3 5 0	<10	10
5 3 0	31	30	5 5 0	<10	13
7 3 0	13	10	7 5 0	16	15
9 3 0	39	34	9 5 0	< 9	10
11 3 0	13	13	11 5 0	15	15
13 3 0	15	14	13 5 0	12	11
15 3 0	18	16	0 6 0	10	17
0 4 0	35	40	2 6 0	25	23
2 4 0	46	47	4 6 0	19	13
4 4 0	32	29	6 6 0	14	18
6 4 0	< 9	9	8 6 0	< 7	3
8 4 0	15	14	10 6 0	13	16
10 4 0	20	25	1 7 0	9	8
12 4 0	16	14	3 7 0	10	8
14 4 0	16	16	5 7 0	13	12
1 5 0	42	39			

In any one molecule, the carboxyl oxygen (O_0) and the hydroxyl oxygens O_2 and O_3 are coordinated to the same calcium ion. A water molecule completes the scheme. Each cation is thus coordinated to only two anions. The four Ca—O distances are nearly equal, lying in the range 2.44—2.52 Å, in agreement with the values found in other structures containing eight-coordinated calcium ions.

The hydrogen bonds. In the structure there are ten different intermolecular O—O distances shorter than 3.2 Å. The number of oxygen-bonded hydrogen atoms is nine. It appears reasonable to assume that these all are involved in hydrogen bond formation, although the refinement is not so complete that the hydrogen atoms appear clearly on the difference map. The one short contact which is not a hydrogen bond, might be $O_5—O_8$ as this distance is considerably longer (3.13 Å) than the other O—O distances (Table 2). However, in the isomorphous strontium compound all short O—O contacts are unchanged to

Table 4. Atomic coordinates of Sr arabonate as fractions of the corresponding cell edge.

Atom	x	y	z
Sr	0.000	0.000	0.000
C_1	−0.023	−0.315	0.219
C_2	0.018	−0.090	0.280
C_3	0.124	−0.119	0.283
C_4	0.170	0.094	0.333
C_5	0.277	0.108	0.331
O_0	−0.059	−0.323	0.121
O_1	−0.009	−0.499	0.287
O_2	−0.019	0.082	0.210
O_3	0.139	−0.120	0.163
O_4	0.160	0.128	0.456
O_5	0.315	0.337	0.352
O_6	0.122	0.313	−0.006
O_7	0.260	−0.429	0.147
O_8	0.000	−0.344	0.500

Table 5. Bond lengths (in Å units) and bond angles in Sr arabonate.

C_1-C_2	1.58	$C_1-C_2-C_3$	103°
C_2-C_3	1.57	$C_2-C_3-C_4$	108°
C_3-C_4	1.49	$C_3-C_4-C_5$	115°
C_4-C_5	1.59	$O_0-C_1-O_1$	124°
C_1-O_0	1.34	$O_0-C_1-C_2$	124°
C_1-O_1	1.19	$O_1-C_1-C_2$	113°
C_2-O_2	1.35	$C_1-C_2-O_2$	106°
C_3-O_3	1.46	$C_3-C_2-O_2$	115°
C_4-O_4	1.49	$C_2-C_3-O_3$	106°
C_5-O_5	1.45	$C_4-C_3-O_3$	105°
$Sr-O_0$	2.59	$C_3-C_4-O_4$	113°
$Sr-O_0$	2.60	$C_5-C_4-O_4$	105°
$Sr-O_3$	2.68	$C_4-C_5-O_5$	114°
$Sr-O_6$	2.58	$C_3-O_3-O_6$	126°
O_3-O_6	3.20	$C_3-O_3-O_7$	107°
O_7-O_6'	3.04	$C_4-O_4-O_5'$	133°
O_6-O_0	2.68	$O_5-O_7-O_3$	113°
O_3-O_7	2.57	$O_7-O_6'-O_0$	103°
O_4-O_5'	2.81		
O_5-O_7	2.78		
O_1-O_8	2.65		
O_2-O_1'	2.55		
O_6-O_7	2.86		
O_5-O_8	3.12		

within 0.10 Å except O_3-O_6, which is increased from 2.95 Å to 3.20 Å. We therefore prefer to consider O_3-O_6 to be the one contact which is not a hydrogen bond. The appearance of the difference map lends some support to this view. However, other distributions of the hydrogen atoms cannot be ruled out, and it is also possible that the hydrogen bond system is different in the two compounds. The proposed positions of the hydrogen atoms is shown in Fig. 4 and in Table 1. The hydrogen bonds conform well to the general stereochemistry of the molecules and link them together in a three-dimensional network. Three short hydrogen bonds of lengths 2.50, 2.62, and 2.66 Å are associated with the carboxyl oxygens. The water molecule $(H_2O)_7$ is linked to the hydroxyl oxygens O_3 and O_5 in different molecules by bonds of lengths 2.64 and 2.75 Å, and appears also to be connected with two different $(H_2O)_6$ molecules by weaker bonds of lengths 2.95 and 2.94 Å. These four bonds are roughly tetrahedrally distributed, whereas the arrangements around $(H_2O)_6$ and $(H_2O)_8$ are rather irregular.

THE STRUCTURE OF STRONTIUM ARABONATE

Refinements were carried out in two projections also on this compound, mainly by least squares calculations. The final value obtained for R was 0.10 for both projections. The atomic coordinates are given in Table 4, and the corresponding interatomic distances and bond angles in Table 5. The accuracy of the data is lower than for the calcium compound and we do not consider the differences in molecular dimensions significant although the deviation

from a symmetrical carboxyl ion is surprisingly large. The four Sr—O distances vary between 2.58 and 2.68 Å corresponding to a difference of 0.14 Å in the ionic radii of eight-coordinated strontium and calcium ions.

A comparison of the atomic coordinates (Tables 1 and 4) shows what happens when the calcium ion is substituted by the larger strontium ion. The x and y coordinates of the arabonate ion are nearly unchanged, but all the atoms have moved 0.12—0.18 Å in direction of the positive z axis (mean value 0.16 Å). The water molecules $(H_2O)_7$ and $(H_2O)_8$ follow the movement of the arabonate ion. On the other hand, $(H_2O)_6$, which is linked to the cation, moves away from the cation principally in the direction of x (by 0.12 Å), but also considerably (0.08 Å) in direction of the negative z axis. This latter movement is evidently due to the strong hydrogen bond (2.62 Å) between $(H_2O)_6$ and O_0. Consequently, the distance $O_3—O_6$ is much longer (by 0.25 Å) in the strontium compound (see Fig. 4), as mentioned above. It is notable that the hydrogen bonds are changed only to a small extent by the expansion of the structure, the largest difference being 0.09 Å. The mean length of the hydrogen bonds in the calcium compound is 2.78 Å, in the strontium compound 2.79 Å.

One of us (S.F.) wishes to acknowledge a grant from *Norsk Hydros fond.*

REFERENCES

1. Littleton, C. O. *Acta Cryst.* **6** (1953) 775.
2. Hordvik, A. *Acta Chem. Scand.* **15** (1961) 16.
3. Bokhoven, C., Schoone, J. C. and Bijvoet, J. M. *Acta Cryst.* **4** (1951) 275.
4. Forsyth, F. J. and Wells, M. *Acta Cryst.* **12** (1959) 412.
5. Berghuis, J. *et al. Acta Cryst.* **8** (1955) 478.
6. Cruickshank, D. W. J. *Acta Cryst.* **2** (1959) 65.
7. Jeffrey, G. A. and Parry, G. S. *Nature* **169** (1952) 1105.
8. Barker, S. A., Bourne, E. J. and Whiffen, D. H. *J. Chem. Soc.* **1952** 3865.
9. Hahn, I. *Z. Krist.* **109** (1957) 438.

Received June 18, 1962.

ACTA CHEMICA SCANDINAVICA 16 (1962) 2384–2388

Stability of the Mixed Copper Complex of 1,2-Diaminopropane and 5-Sulphosalicylic Acid in Aqueous Sodium Perchlorate Solutions

REINO NÄSÄNEN, PAAVO MERILÄINEN and SAKARI LUKKARI

Department of Chemistry, University of Helsinki, Helsinki, Finland

The stability constant of the mixed copper complex ($CuXY^-$) of 1,2-diaminopropane (Y) and 5-sulphosalicylic acid (H_3X) was determined by the potentiometric pH method. The measurements were carried out at seven different ionic strengths adjusted with sodium perchlorate. As expected, the stability of the mixed complex was highly dependent on ionic strength. The gross stability constant of the mixed complex at 25°C is $10^{20.39}$, $10^{19.09}$, $10^{18.49}$ and $10^{18.74}$ at ionic strengths 0, 0.1, 1, and 2, respectively. At the same ionic strengths and temperature the equilibrium constant of the disproportionation $2\,MXY^- \rightleftharpoons MX_2^{4-} + MY_2^{2+}$ was found to be $10^{-3.94}$, $10^{-1.83}$, $10^{-0.09}$ and $10^{+0.25}$, respectively.

In a recent study [1] the formation of mixed copper complexes of 1,2-diaminopropane and 5-sulphosalicylic acid was dealt with. It was shown that one mixed complex was formed. These measurements were made without any additional neutral salt present. This investigation has since been continued by paying attention especially to the effect of sodium perchlorate.

The method used consisted of a potentiometric pH titration of a mixed solution of copper perchlorate, sulphosalicylic acid (H_3X) and diprotonated 1,2-diaminopropane added as its perchlorate ($H_2Y(ClO_4)_2$) with sodium hydroxide solution. The experimental details have been described recently [1,2].

It is possible to calculate the concentration of the mixed complex MXY^- at each point of the titration curve since the stability constants of all the other complexes are known [2]. The following equations can be written:

$$c_x = [H_2X] + [HX] + [MX] + 2\,[MX_2] + [MXY] \quad (1)$$

$$c_y = [H_2Y] + [HY] + [MY] + 2\,[MY_2] + [MXY] \quad (2)$$

$$c_M = [M] + [MX] + [MX_2] + [MY] + [MY_2] + [MXY] \quad (3)$$

$$3c_x + 2c_y + c_A - c_B = [H] + [HX] + 2\,[H_2X] + [HY] + 2\,[H_2Y] \quad (4)$$

where c_x, c_y, c_A, c_M, and c_B are the respective total concentrations of H_3X, $H_2Y(ClO_4)_2$, free perchloric acid, copper ion, and sodium hydroxide. In addition, the following equilibrium constants are known:

$$[H]\,[HX]/[H_2X] = K_2^{(x)};\ [H]\,[HY]/[H_2Y] = K_1^{(y)} \quad (5)$$

$$[MX]\,[H]/[M]\,[HX] = K_I^{(x)};\ [MX_2]\,[H]/[MX]\,[HX] = K_{II}^{(x)} \quad (6)$$

$$[MY]\,[H]^2/[M]\,[H_2Y] = K_I^{(y)};\ [MY_2]\,[H]^2/[MY]\,[H_2Y] = K_{II}^{(y)} \quad (7)$$

Combination of eqns. (4) and (5) gives

$$[HX] = a - b\,[H_2Y] \quad (8)$$

where

$$a = \frac{3c_x + 2c_y + c_A - c_B - [H]}{1 + 2[H]/K_2^{(x)}};\quad b = \frac{2 + K_1^{(y)}/[H]}{1 + 2[H]/K_2^{(x)}} \quad (9)$$

All measurements were made with $c_M = c_y$. On this condition eqns. (1)—(8) give

$$A_1[H_2Y]^3 + A_2[H_2Y]^2 + A_3[H_2Y] + A_4 = 0 \quad (10)$$

The coefficients A_1, A_2, A_3, and A_4 can be calculated from

$$A_1 = b^2hm - hk + bdk - b^3dm \quad (11)$$

$$A_2 = -2\,abhm + b^2cm + b^2dl + 3\,ab^2dm - hn - ck - adk \quad (12)$$

$$A_3 = a^2hm - bcl - 2\,abcm - bd - 2\,abdl - 3\,a^2bdm - h \quad (13)$$

$$A_4 = c + acl + acm + ad + a^2dl + a^3dm \quad (14)$$

where

$$\begin{aligned} c &= c_y - c_x; & d &= 1 + [H]/K_2^{(x)} \\ h &= 1 + K_1^{(y)}[H]; & k &= K_I^{(y)}\,K_{II}^{(y)}[H]^4 \\ l &= K_I^{(x)}/[H]; & m &= K_I^{(x)}\,K_{II}^{(x)}/[H]^2 \\ n &= K_I^{(y)}/[H]^2 \end{aligned} \quad (15)$$

The calculation of $[H_2Y]$ was carried out with an IBM 1620 computer by Dr. Heikki Varho in the Computing Centre of the University of Helsinki.

After $[H_2Y]$ had been obtained, [HX] was calculated from eqn. (8) and the concentration of copper ion from

$$[M] = (c + d[HX])/(1 - m[HX]^2 + n[H_2Y] + k[H_2Y]^2) \quad (16)$$

The concentrations of all the other species except the mixed complex could then be calculated from eqns. (6) and (7) and the concentration of the mixed complex from one of eqns. (1)—(3).

The equilibrium constants defined by eqns. (5), (6) and (7) have been determined earlier in our laboratory [2]. The results for sodium perchlorate solutions are

$$pK_2^{(x)} = 2.84 - \frac{2.04\sqrt{I}}{1 + 2.1\sqrt{I}} + 0.17\,I \quad (17)$$

$$pK_I^{(x)} = 1.77 + \frac{3.054\sqrt{I}}{1+3.3\sqrt{I}} + 0.013\ I \quad (18)$$

$$pK_{II}^{(x)} = 6.09 - \frac{6.11\sqrt{I}}{1+2.4\sqrt{I}} + 0.064\ I \quad (19)$$

$$pK_1^{(y)} = 6.607 + \frac{1.018\sqrt{I}}{1+1.42\sqrt{I}} + 0.180\ I \quad (20)$$

$$pK_2^{(y)} = 9.817 - \frac{0.509\sqrt{I}}{1+2.2\sqrt{I}} + \frac{0.509\sqrt{I}}{1+\sqrt{I}} + 0.214\ I \quad (21)$$

$$\log\beta_1^{(y)} = 10.56 + 0.89\ I - 0.52\ I^{3/2} + 0.13\ I^2 \quad (22)$$

$$\log\beta_2^{(y)} = 19.64 + 2.11\ I - 1.24\ I^{3/2} + 0.28\ I^2 \quad (23)$$

$$pK_I^{(y)} = pK_1^{(y)} + pK_2^{(y)} - \log\beta_1^{(y)} \quad (24)$$

$$pK_{II}^{(y)} = pK_I^{(y)} + 2\log\beta_1^{(y)} - \log\beta_2^{(y)} \quad (25)$$

Titrations were carried out at seven different ionic strengths. The ionic strengths were calculated from $I = \frac{1}{2}\ \Sigma\ c_i z_i^2$. Data from a typical titration are

Table 1. The calculation of the concentration of the mixed complex from the data of a titration of an aqueous solution of copper ion, 5-sulphosalicylic acid and diprotonated 1,2-diaminopropane with sodium hydroxide. Ionic strength adjusted by addition of sodium perchlorate to the value one. $c_M = c_y$. 25°C.

$c_x \times 10^3$	$c_y \times 10^3$	$c_A \times 10^3$	$c_B \times 10^3$	$[H] \times 10^6$	$[H_2Y] \times 10^3$	$[HX] \times 10^3$	$[MXY] \times 10^3$	$K_A \times 10^3$
23.619	5.905	0.655	61.106	5.00	0.722	20.712	0.612	0.080
23.529	5.882	0.652	61.254	4.25	0.590	20.518	0.728	0.088
23.440	5.860	0.650	61.401	3.52	0.466	20.313	0.836	0.093
23.351	5.838	0.647	61.547	2.87	0.358	20.077	0.963	0.098
23.264	5.816	0.645	61.692	2.30	0.268	19.812	1.110	0.104
23.176	5.794	0.642	61.836	1.75	0.187	19.523	1.222	0.103
23.090	5.772	0.640	61.978	1.31	0.1286	19.200	1.205	0.087
23.004	5.751	0.638	62.120	0.921	0.0816	18.855	1.457	0.100
22.918	5.730	0.635	62.261	0.596	0.0473	18.483	1.453	0.086
							Mean	0.093

recorded in Table 1. In this table the values of the equilibrium constant K_A of the reaction

$$MY^{2+} + HX^{2-} \rightleftharpoons MXY^- + H^+ \quad (26)$$

are given as calculated from different points on the titration curve. This reaction was chosen for scrutiny since the species MY^{2+}, HX^{2-}, and MXY^- predominate in the experimental conditions in question and the hydrogen ion concentration could be directly determined. The results are summarised in Table 2. The respective values of the equilibrium constant K_B of the reaction

$$MX^- + Y \rightleftharpoons MXY^- \quad (27)$$

Table 2. Effect of ionic strength on the stability of the mixed copper complex of 1,2-diaminopropane and 5-sulphosalicylic acid at 25°C. No sodium perchlorate was added in the three first experiments.

I	pK_A	$\log K_B$	pK_D
0	2.70	—	3.94
0.017	3.07	9.55	2.87
0.045	3.20	9.54	2.44
0.100	3.41	9.46	1.83
0.550	3.87	9.44	0.57
1.000	4.03	9.51	0.09
2.000	4.19	9.76	−0.25

calculated from

$$\log K_B = \log\beta_1^{(y)} + pK_I^{(x)} - pK_A \tag{28}$$

are also given in Table 2. The exceptional variation of constant K_B at low ionic strengths may be due to systematic errors. In fact, this constant is presented by the equation

$$\log K_B = 9.48 + 0.109\ I \tag{29}$$

with an average deviation of $\pm$ 0.07. Also the values of the constant K_D of the disproportionation

$$2\ MXY^- \rightleftharpoons MX_2^{4-} + MY_2^{2+} \tag{30}$$

calculated from

$$pK_D = pK_{II}^{(x)} - pK_I^{(x)} - \log\beta_2^{(y)} + 2\log K_B \tag{31}$$

are given in Table 2. As expected, the variation of this constant with ionic strength is very great.

The constant K_A can be presented by the equation

$$pK_A = 2.70 + \frac{3.054\sqrt{I}}{1+1.25\sqrt{I}} - 0.035\ I \tag{32}$$

within $\pm$ 0.02. Using eqns. (32) and (17)—(25), it is possible to calculate the values of all the equilibrium constants at an arbitrary ionic strength.

The values of the gross stability constants $\beta_2^{(x)}$, $\beta_2^{(y)}$, and $\beta_2^{(xy)}$, the last defined by

$$[MXY]/[M]\,[X]\,[Y] = \beta_2^{(xy)} \tag{33}$$

Table 3. Stability constant $\beta_2^{(xy)}$ of the mixed complex and the constants $\beta_2^{(x)}$ and $\beta_2^{(y)}$ in sodium perchlorate solutions at 25°C.

I	$\log\beta_2^{(x)}$	$\log\beta_2^{(y)}$	$\log\beta_2^{(xy)}$
0	17.20	19.64	20.39
0.017	16.85	19.67	19.70
0.045	16.70	19.72	19.43
0.100	16.50	19.82	19.09
0.550	16.14	20.37	18.54
1.000	16.10	20.79	18.49
2.000	16.27	21.47	18.74

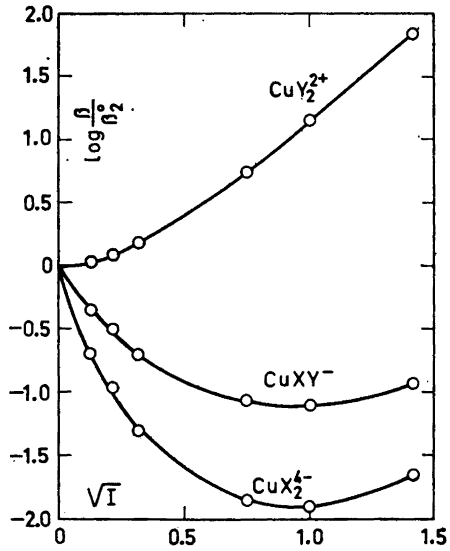

Fig. 1. The gross stability constants of CuX_2^{4-}, $CuXY^-$ and CuY_2^{2+} as functions of ionic strength in sodium perchlorate solutions at 25°C.

at the above ionic strengths are shown in Table 3. The stability constant of the mixed complex was calculated from

$$\log\beta_2^{(xy)} = pK_3^{(x)} + \log\beta_1^{(y)} - pK_A \qquad (34)$$

and that of MX_2^{4-} from

$$\log\beta_2^{(x)} = 2\,pK_3^{(x)} - pK_I^{(x)} - pK_{II}^{(x)}. \qquad (35)$$

In the calculation of $\beta_2^{(x)}$ and $\beta_2^{(xy)}$ also the values of the third acid dissociation constant of 5-sulphosalicylic acid were needed. The result of Näsänen and Paakkola [3]

$$pK_3^{(x)} = 12.53 - \frac{3.054\sqrt{I}}{1+1.31\sqrt{I}} + 0.262\,I \qquad (36)$$

referring to sodium perchlorate solutions was used. The variation of the gross stability constants $\beta_2^{(x)}$, $\beta_2^{(y)}$ and $\beta_2^{(xy)}$ of complexes MX_2^{4-}, MY_2^{2+}, and MXY^- with ionic strength is seen in Fig. 1. The marked dependence of the stability of the mixed complex on ionic strength appears from this figures as well as from the values of the disproportionation constant K_D given in Table 2.

REFERENCES

1. Näsänen, R. and Meriläinen, P. *Suomen Kemistilehti* **B 34** (1961) 75.
2. Näsänen, R. and Meriläinen, P. *Suomen Kemistilehti* **B 34** (1961) 47; Näsänen, R., Meriläinen, P. and Heinänen, E. *Ibid.* **B 35** (1962) 15; Näsänen, R. and Meriläinen, P. *Ibid.* **B 35** (1962) 79.
3. Näsänen, R. and Paakkola, K. *Suomen Kemistilehti* **B 34** (1961) 19.

Received June 21, 1962.

ACTA CHEMICA SCANDINAVICA 16 (1962) 2389–2394

Pyridazine Studies

II. 3-Chloro-6-hydrazino-4- and 5-methyl-pyridazine and Some Tetrazolo[1,5-b]- and *s*-Triazolo[4,3-b]pyridazines

SØREN LINHOLTER and REGITZE ROSENØRN

Department of Organic Chemistry, The Royal Technical University, Copenhagen, Denmark

The structures of the two isomeric products 3-chloro-6-hydrazino-4- and 5-methyl-pyridazine (I and II) from the reaction of 3,6-dichloro-4-methyl-pyridazine with hydrazine were established by reduction with Raney nickel to the amino derivatives and by oxidation with hypochlorite to the corresponding 3-chloro-4- and 5-methyl-1,6-dihydro-6-oxo-pyridazines. The structures found are not in agreement with Takahayashi's results [1]. The hydrazino compounds (I and II) were converted into 6-chloro-7- and 8-methyl-tetrazolo[1,5-b]pyridazine (III and IV) and 6-chloro-7- and 8-methyl-*s*-triazolo[4,3-b]pyridazine (V and VI). V and VI were hydrolysed to 7- and 8-methyl-5,6-dihydro-6-oxo-*s*-triazolo[4,3-b]pyridazine, and through comparison of the infra-red spectra it was shown that the product from the reaction between acetoacetic ester and 4-amino-1,2,4-triazole is 6-methyl-8-hydroxy-*s*-triazolo[4,3-b]pyridazine as postulated by Bülow[2] and not 8-methyl-5,6-dihydro-6-oxo-*s*-triazolo[4,3-b]pyridazine as suggested by Kost and Gents [3].

As part of our investigations on 3- and/or 6-substituted 4-methyl-pyridazines [4], 3-chloro-6-hydrazino-4- and 5-methyl-pyridazine were prepared from 3,6-dichloro-4-methyl-pyridazine and 50 % aqueous hydrazine. Separation of the two isomeric compounds was achieved by several recrystallisations from water or aqueous ethanol. The melting points of the two components I and II were 158° and 199°, I being the more soluble isomer. The purity of the compounds was demonstrated through their infra-red and NMR spectra.

In order to establish the structures of the hydrazino derivatives, they were hydrogenated in methanolic potassium hydroxide solution at atmospheric pressure using Raney nickel as a catalyst. Cleavage of the hydrazino group and removal of the chlorine atom was expected, and from II (m.p. 199°) a compound $C_5H_7N_3$ with m.p. 193.5° was obtained. 6-Amino-4- and 5-methyl-pyridazine were previously unknown, but an NMR spectrum of the hydrogenation product showed the presence of two adjacent aromatic hydrogen atoms (H_3: $\tau = 1.85$ ppm, H_4: $\tau = 3.62$ ppm, $J = 4.5$ cps in aqueous solution with TMS as external reference) indicating the structure 6-amino-5-methyl-pyridazine.

Hydrogenation of I (m.p. 158°) gave a mixture of products from which 3-chloro-6-amino-4-methyl-pyridazine [1,4], m.p. 187°, was isolated. This compound was identified through mixed melting point with an authentic sample, through its infra-red spectrum and its acetyl derivative [4]. It was later shown that hydrogenation of 3-chloro-6-amino-4-methyl-pyridazine under the conditions described above proceeded extremely slowly.

Consequently, I (m.p. 158°) must have the structure 3-chloro-6-hydrazino-4-methyl-pyridazine and II (m.p. 199°) the structure 3-chloro-6-hydrazino-5-methyl-pyridazine.

Takahayashi [1] reported the preparation of these hydrazino derivatives and assigned the structures as follows: 3-chloro-6-hydrazino-4-methyl-pyridazine, m.p. 193°, and 3-chloro-6-hydrazino-5-methyl-pyridazine, m.p. 149°. The structures were established by "heating strongly for 8 hrs. with conc. HCl to form the corresponding hydroxy derivatives in poor yields" [1]. Thus the hydrazino compound with m.p. 193° gave 3-chloro-6-hydroxy-4-methyl-pyridazine (3-chloro-4-methyl-1,6-dihydro-6-oxo-pyridazine) m.p. 227°, and the hydrazino compound with m.p. 149° gave 3-chloro-6-hydroxy-5-methyl-pyridazine (3-chloro-5-methyl-1,6-dihydro-6-oxo-pyridazine) m.p. 148°. This hydrolysis could not be reproduced in our laboratory and was contrary to our results.

Conversion of the hydrazino derivatives into the pyridazones could be performed by oxidation with hypochlorite or hypobromite in 5 N sulfuric acid solution. From I (m.p. 158°) we obtained 3-chloro-4-methyl-1,6-dihydro-6-oxo-pyridazine (XIII), m.p. 224° subl., thus establishing the structure of I as chloro-6-hydrazino-4-methyl-pyridazine. Likewise, II (m.p. 199°) yielded 3-chloro-5-methyl-1,6-dihydro-6-oxo-pyridazine (XIV), m.p. 170° subl. The identity of the oxidation products was proven trough their infra-red spectra and mixed melting points with authentic samples [4].

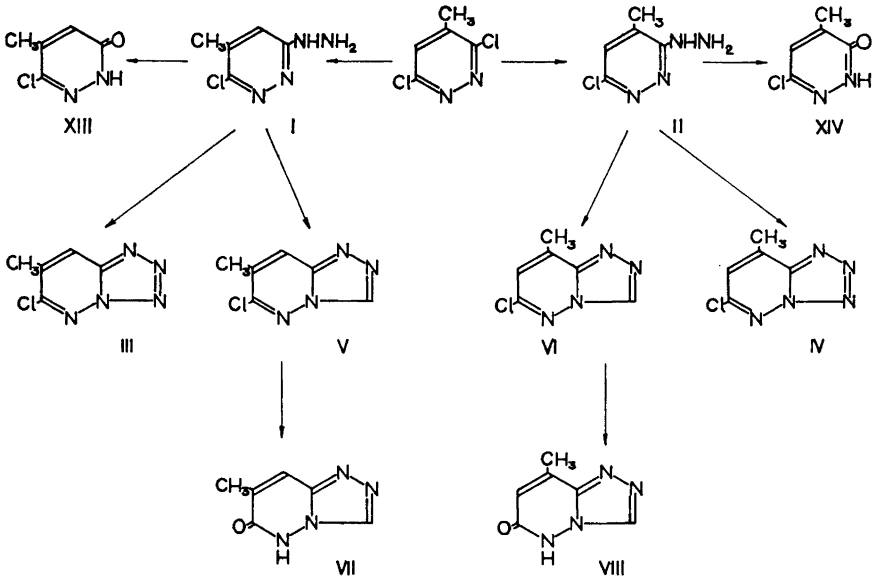

The application of this oxidation procedure to the preparation of hydroxy-, chloro- and bromo-substituted N-hetero-aromatics will be described in detail in a later publication.

Treatment of 3-chloro-6-hydrazino-4- and 5-methyl-pyridazine (I and II) with sodium nitrite in acetic acid solution yielded 6-chloro-7- and 8-methyl-tetrazolo[1,5-b] pyridazine (III and IV). That ring closure had occurred was seen from the infra-red spectra, which showed no azide absorption band in the region 2160—2120 cm^{-1}. The melting points were 140.5° and 107.0°, respectively. The latter (IV) has previously been reported (m.p. 97°) by Takahayashi [5].

Without isolation of the intermediately formed β-formylhydrazino-derivatives 6-chloro-7- and 8-methyl-*s*-triazolo[4,3-b]pyridazine (V and VI, m.p.'s 157.5—158.0° and 134.0—134.5°) were obtained when the hydrazino compounds were heated under reflux with 80 or 100 % formic acid. For these compounds Takahayashi [1] reported the melting points 158° and 107°. Hydrolysis of V and VI in potassium hydroxide solution yielded 7- and 8-methyl-5,6-dihydro-6-oxo-*s*-triazolo[4,3-b]pyridazine (VII and VIII), melting points above 265°.

In 1909 Bülow [2] allowed various β-keto-esters to react with 4-amino-1,2,4-triazole. He formulated the reaction products as derivatives of 8-hydroxy-*s*-triazolo[4,3-b]pyridazine without any proof of structures. Thus acetoacetic ester gave 8-hydroxy-6-methyl-*s*-triazolo[4,3-b]pyridazine (IX).

In 1959 Steck and Brundage [5] reported the preparation of some 8-substituted 6-methyl-*s*-triazolo[4,3-b]pyridazines based on acetoacetic ester and 4-amino-1,2,4-triazole, yet without any proof of structures.

In 1958 Kost and Gents [3] reported the preparation of a series of 7- and/or 8-substituted 5,6-dihydro-6-oxo-*s*-triazolo[4,3-b]pyridazines from β-keto-esters and 4-amino-1,2,4-triazole considering these alternative structures of the reaction products more probable than the ones postulated by Bülow [2].

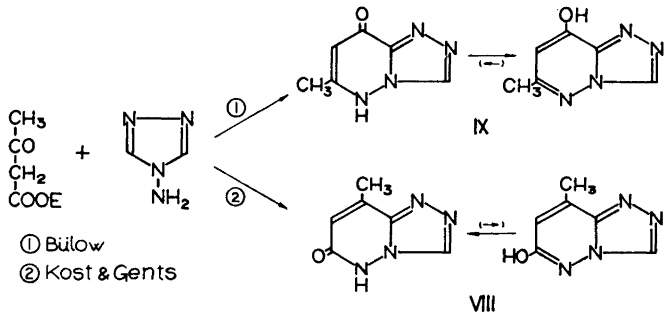

If the reaction between acetoacetic ester and 4-amino-1,2,4-triazole followed the route proposed by Kost and Gents, the product should be identical with VIII, 8-methyl-5,6-dihydro-6-oxo-*s*-triazolo[4,3-b]pyridazine. The melting points of these substances are far too high to allow any comparison by mixed melting points, but the infra-red spectra clearly showed that the reaction product IX was different from VIII. The spectra of VII and VIII (in KBr discs) contained carbonyl absorption bands at 1634 and 1624 cm^{-1}, respectively, whereas the spectrum of IX only showed an extremely weak band in

this region. This indicated that IX in the solid state exists as 8-hydroxy-6-methyl-*s*-triazolo[4,3-b]pyridazine and not in the tautomeric vinylog lactam form 6-methyl-5,8-dihydro-8-oxo-*s*-triazolo[4,3-b]pyridazine. The infra-red spectra were consistent with the fact, that only IX gave a positive, intense red colour reaction with ferric chloride solution. The spectra of all three compounds contained two broad bands between 2600 and 1700 cm^{-1}, showing the presence of strong hydrogen bonding. This may in the case of VII and VIII explain why the intensity of the carbonyl bands is less than usual for this kind of lactams.

As a further control the reaction product was treated with phosphoryl chloride as described by Steck and Brundage [5], and this reaction yielded 8-chloro-6-methyl-*s*-triazolo[4,3-b]pyridazine [5,6], which was not identical with VI, the product from the reaction between 3-chloro-6-hydrazino-5-methyl-pyridazine and formic acid. Thus, Bülow's original formula for the product formed from acetoacetic ester and 4-amino-1,2,4-triazole is correct.

Treatment of 6-chloro-7-methyl-*s*-triazolo[4,3-b]pyridazine with hydrazine gave as described by Takahayashi [1] the corresponding 6-hydrazino derivative. When this compound was treated with formic acid under conditions similar to those applied for the preparation of the triazolo-pyridazines, only the 6-formyl-hydrazino derivative was obtained. Ring closure to a bis-*s*-triazolo [4,3-b:3′,4′-f] pyridazine could not be performed.

EXPERIMENTAL

All melting points are uncorrected. The infra-red spectra were recorded on a Perkin-Elmer Model 21 Spectrometer in KBr discs. The microanalyses were carried out by P. Hansen, The Chemical Laboratory of the University of Copenhagen.

3-Chloro-6-hydrazino-4- and 5-methyl-pyridazine (I and II). 3,6-Dichloro-4-methyl-pyridazine (81.0 g, 0.5 mole) was heated with 250 ml of a 50 % aqueous solution of hydrazine hydrate. As the reaction mixture was heated above the melting point of 3,6-dichloro-4-methyl-pyridazine (87°) a vigorous reaction started with the separation of the hydrazino derivatives. The suspension was boiled under reflux for ½ h to complete the reaction, and 250 ml of water were added. The reflux was continued for further 20 min and insoluble material was removed from the hot suspension by filtration. Recrystallisation of the collected material from 400 ml of water gave 12.7 g of 3-chloro-6-hydrazino-5-methyl-pyridazine (II), m.p. 199–200°.

From the filtrate was isolated 3.0 g of II and 34.0 g of the more soluble component 3-chloro-6-hydrazino-4-methyl-pyridazine (I), m.p. 158° after numerous recrystallisations from water or ethanol-water. The yield of I was significantly lower than the amount of I formed due to heavy losses during the separation procedure. (Found for I: C 37.70; H 4.54; N 35.36; Cl 22.27. Found for II: C 37.55; H 4.46; N 34.81; Cl 22.20. Calc. for $C_5H_7N_4Cl$: C 37.87; H 4.45; N 35.34; Cl 22.36).

Characteristic infra-red absorption bands:

	I	II
NH_2 deformation	1610 *	1627
Ring stretching	1610 *, 1495	1598, 1560, 1495
C–CH_3 deformation	1382	1378
γCH (out-of-plane) deformation	898	880, 917
βCH (in-plane) deformation, ring breathing, etc.	1225, 1145, 1066, 985, 763	1314, 1129, 1086, 1002, 974, 797

* Absorption considered to be the superimposition of two peaks.

Hydrogenation of 3-chloro-6-hydrazino-4-methyl-pyridazine. To a solution of 6.3 g (0.04 mole) of 3-chloro-6-hydrazino-4-methyl-pyridazine (I) in 200 ml of methanol were added 8 g of Raney nickel. Addition of hydrogen was carried out at atmospheric pressure, but no hydrogen was absorbed. 2.2 g of potassium hydroxide were added and absorption of hydrogen proceeded slowly. After 36 h 0.04 mole of hydrogen was absorbed, and the Raney nickel was filtered off. The alkaline, black filtrate was acidified with acetic acid and evaporated to dryness *in vacuo*. The residue was dissolved in 25 ml of water and after filtration a dark coloured material crystallised on cooling, m.p. 186—187°. It was purified by recrystallisation from water and charcoal. A mixed melting point with an authentic sample [4] and an infra-red spectrum established the structure as 3-chloro-6-amino-4-methyl-pyridazine. Yield: 0.9 g (16 %).

Concentration of the filtrate and crystallisation yielded 0.5 g of dark coloured material with m.p. 140—150° (decomp.), which was considered to be a mixture of various hydrogenation products.

The isolated amino-chloro compound (0.2 g) was heated to boiling with a few milliliters of acetic anhydride and the acetyl derivative crystallised on cooling, m.p. 216°. Mixed melting point with an authentic sample [4] showed no depression.

Hydrogenation of 3-chloro-6-hydrazino-5-methyl-pyridazine. 6-Amino-5-methyl-pyridazine. To a solution of 3.2 g (0.02 mole) of 3-chloro-6-hydrazino-5-methyl-pyridazine (II) in 60 ml of methanol were added 5 g of Raney nickel and 40 ml of a 1 N methanolic solution of potassium hydroxide (0.04 mole). Hydrogenation was carried out at atmospheric pressure, and the theoretical amount of hydrogen was absorbed within 24 h. The Raney nickel was filtered off and the methanol evaporated off *in vacuo*. The residue was dissolved in boiling water, and the solution was filtered and cooled to 0°. Yellowish crystals (needles, 1.2 g) could be isolated, m.p. 192—193°. Concentration of the filtrate yielded another 0.4 g, m.p. 190—192°. Recrystallisation from water raised the m.p. to 193.5°. The Beilstein test for halogen was negative. The analysis showed the empirical formula $C_5H_7N_3$, $\frac{1}{2}H_2O$. Recrystallisation from chloroform gave 1.4 g (64 %) of anhydrous 5-methyl-6-amino-pyridazine, m.p. 193.5°. (Found: C 54.80; H 6.28; N 38.42. Calc. for $C_5H_7N_3$: C 55.03; H 6.47; N 38.51).

Oxidation of I and II with sodium hydrochlorite or sodium hypobromite. 3-Chloro-4- and 5-methyl-1,6-dihydro-6-oxo-pyridazine (XIII and XIV). A 3 M sodium hypochlorite solution was prepared from 70 ml of water, 20 g of sodium hydroxide, and 21 g (0.3 mole) of chlorine. The solution was chilled in ice during the addition of chlorine. Finally the solution was diluted to 100 ml with water.

0.79 g (0.005 mole) of 3-chloro-6-hydrazino-4-methyl-pyridazine (I) were dissolved in 10 ml of 5 N sulfuric acid, the solution was cooled to 0°, and 3.5 ml 3 M sodium hypochlorite solution (slight excess) were added from a dropping funnel. Evolution of nitrogen started with the immediate separation of a white precipitate. After the addition of hypochlorite solution the precipitate was filtered off and recrystallised from water. Yield: 0.39 g (54 %) of 3-chloro-4-methyl-1,6-dihydro-6-oxo-pyridazine (XIII), m.p. 224° subl., identified through mixed melting point with an authentic sample [4] and infra-red spectra.

Oxidation of 3-chloro-6-hydrazino-5-methyl-pyridazine (II) with sodium hypochlorite was carried out analogously. The greater solubility of the product, 3-chloro-5-methyl-1,6-dihydro-6-pyridazine (XIV) necessitated the extraction with chloroform after the filtration of separated material, thus yielding 0.26 g (37 %) of XIV, m.p. 169—170° after recrystallisation from water. The product was identified through mixed melting point with an authentic sample [4] and infra-red spectra.

The same compounds, XIII and XIV, were obtained when a 2 M solution of sodium hypobromite was used as oxidative agent.

6-Chloro-7- and 8-methyl-tetrazolo[1,5-b]pyridazine (III and IV). To a well-stirred and ice cooled solution of 7.9 g (0.05 mole) of 3-chloro-6-hydrazino-4-methyl-pyridazine (I) in 200 ml 15 % acetic acid were added 25 ml of a 3 M sodium nitrite solution (0.05 mole) from a dropping funnel. At the end of the addition the separation of a white solid started and the reaction mixture was left with stirring for ½ h. The precipitate was filtered off and recrystallised from water. Yield: 6.1 g (72 %) of 6-chloro-7-methyl-tetrazolo[1,5-b] pyridazine (III), m.p. 140.5°. (Found: C 35.05; H 2.55; N 41.15; Cl 20.83. Calc. for $C_5H_4N_5Cl$ C 35.43; H 2.38; N 41.30; Cl 20.90).

By a similar procedure was obtained a 79 % yield of 6-chloro-8-methyl-tetrazolo[1,5-b] pyridazine (IV), m.p. 107.0°, from 3-chloro-6-hydrazino-5-methyl-pyridazine (II). (Found: C 35.35; H 2.55; N 41.30; Cl 20.65. Calc. for $C_5H_4N_5Cl$: C 35.43; H 2.38; N 41.30; Cl 20.90).

6-Chloro-7- and 8-methyl-s-triazolo[4,3-b]pyridazine (V and VI). 3-Chloro-6-hydrazino-4-methyl-pyridazine (I, 7.9 g, 0.05 mole) was boiled under reflux for 2 h with 80 ml 80 % (or 100 %) formic acid. The solvent was evaporated off *in vacuo* and the residue distilled at 1 mm. The distillate could be recrystallised from either petrol or water. Yield: 7.6 g (91 %) of 6-chloro-7-methyl-*s*-triazolo 4,3-b pyridazine (V), m.p. 157.5–158.0°. (Found: C 42.63; H 3.13; N 33.07; Cl 21.18. Calc. for $C_6H_5N_4Cl$: C 42.75; H 3.01; N 33.25; Cl 21.02).

6-Chloro-8-methyl-*s*-triazolo[4,3-b]pyridazine (VI), m.p. 134.0–134.5°, was prepared in a 89 % yield from 3-chloro-6-hydrazino-5-methyl-pyridazine (II) by a similar procedure. (Found: C 42.45; H 3.16; N 33.00; Cl 20.86. Calc. for $C_6H_5N_4Cl$: C 42.75; H 3.01; N 33.25; Cl 21.02).

7-and 8-Methyl-5,6-dihydro-6-oxo-s-triazolo[4,3-b]pyridazine (VII and VIII). The chloro derivatives V and VI (1.7 g, 0.01 mole) were boiled under reflux for 1 h with a solution of 1.1 g of potassium hydroxide in 25 ml of water. On acidification with acetic acid a white solid precipitated, which was recrystallised from water acidified with a minute amount of acetic acid. Yield of 7- and 8-methyl-5,6-dihydro-6-oxo-*s*-triazolo[4,3-b] pyridazine 1.25 g (83 %) and 1.15 g (77 %), respectively. Melting points above 265°. (Found for VII: C 47.85; H 4.20; N 37.52. Found for VIII: 47.90; H 4.06; N 37.50. Calc. for $C_6H_6N_4O$: C 48.00; H 4.03; N 37.32).

6-Hydrazino-7-methyl-s-triazolo[4,3-b]pyridazine (XI). 6-Chloro-7-methyl-*s*-triazolo-[4,3-b]pyridazine (V, 1.7 g, 0.01 mole) was dissolved in 10 ml of 80 % aqueous hydrazine hydrate by gentle heating. After 1–2 min the separation of a white solid started and after boiling for 10 min the mixture was cooled and filtered. The isolated material was recrystallised from water. Yield of 6-hydrazino-7-methyl-*s*-triazolo[4,3-b]pyridazine 1.3 g (80 %), m.p. above 265°. (Found: C 43.80; H 4.86; N 51.38. Calc. for $C_6H_8N_6$: C 43.89; H 4.91; N 51.20).

6-(β-Formylhydrazino)-7-methyl-s-triazolo[4,3-b]pyridazine (XII). A solution of 1.0 g (0.006 mole) of 6-hydrazino-7-methyl-*s*-triazolo[4,3-b]pyridazine (XI) in 10 ml of formic acid (100 %) was heated under reflux for 2 h. The formic acid was evaporated off *in vacuo*, and the residue was recrystallised from water, giving a quantitative yield (1.15 g) of 6-(β-formylhydrazino)-7-methyl-*s*-triazolo[4,3-b]pyridazine, m.p. above 265°. (Found: C 43.65; H 4.25; N 43.58. Calc. for $C_7H_8N_6O$: C 43.75; H 4.20; N 43.73).

Acknowledgement. The authors are grateful to professor Børge Bak, The Chemical Laboratory of the University of Copenhagen, for the determination of the infra-red and NMR spectra.

REFERENCES

1. Takahayashi, N. *Pharm. Bull. Japan* **5** (1957) 229.
2. Bülow, C. *Ber.* **42** (1909) 2594.
3. Kost, A. N. and Gents, F. *J. Gen. Chem. U.S.S.R.* **26** (1958) 2796.
4. Linholter, S., Kristensen, Aa. B., Rosenørn, R., Nielsen, S. E. and Kaaber, H. *Acta Chem. Scand.* **15** (1961) 1660.
5. Steck, E. A. and Brundage, R. P. *J. Am. Chem. Soc.* **81** (1959) 6289.
6. Bülow, C. and Haas, K. *Ber.* **43** (1910) 1975.

Received May 28, 1962.

ACTA CHEMICA SCANDINAVICA 16 (1962) 2395–2405

The Reaction between Thiohydrazides and Ethyl Benzoylchloroacetate

Part I. Formation of Ethyl 5-Phenylpyrazole-4-carboxylates

JAN SANDSTRÖM

Department of Organic Chemistry, University of Lund, Lund, Sweden

The reaction between thiohydrazides and ethyl benzoylchloroacetate in the presence of slightly less than one equivalent of sodium ethoxide leads to the formation of ethyl 5-phenylpyrazole-4-carboxylates. Thiohydrazides with free or benzyl substituted amino groups give hydroxy-dihydro-thiadiazines as unstable intermediates, whereas the 1-phenylthiohydrazides give more stable, ring-open intermediates. Both products are dehydrated by acids to red, unstable intermediates, probably thiadiazines which rapidly eliminate sulphur and give the pyrazole esters, usually in good yields. These esters, particularly the N-unsubstituted ones, are remarkably resistant to nucleophilic reagents. This has been explained by the electron donating effect of the pyrazole ring, which is most pronounced after ionization. This interpretation has been supported by a LCAO—MO calculation of the π electron distribution in a pyrazole-4-carboxylic ester and its anion. The acid dissociation constants are given for some N-unsubstituted pyrazole esters.

In previous investigations by the present author [1,2] and by Beyer and collaborators [3–5] it has been shown that thiohydrazides react with a variety of α-halogen carbonyl compounds to give labile 1,3,4-thiadiazines, which undergo ring-contraction with extrusion of sulphur to form pyrazoles. The reactions between thiohydrazides with free amino groups and α-chlorodesoxybenzoin has been shown to proceed *via* two intermediates that can be isolated, *viz.* a hydroxydihydro-thiadiazine and a thiadiazine [2]. The thiadiazine was comparatively stable, which was ascribed to conjugation with the phenyl group in the position 5. Previously [1,3] it had been found that electron attracting groups in the position 6 facilitated the ring contraction. The present investigation was undertaken in order to study the combined effect of a phenyl group in the position 5 and a carbethoxy group in the position 6. Each of the five thiohydrazides (I a—e) was dissolved in one equivalent of N sodium ethoxide and was made to react with one equivalent of ethyl benzoylchloroacetate. It was

observed that when a small excess of sodium ethoxide was employed, the reaction took an unexpected course with formation of benzoylhydrazones of ethoxycarbonylmethyl thiolcarboxylates, as will be described in Part II of this series. Only the 1-phenyl substituted thiohydrazides reacted according to expectation in the presence of an excess of base. When excess base was avoided, and the reaction was performed at room temperature, no intermediates could be isolated, and it could be shown by paper chromatography that pyrazoles appeared in the reaction mixtures already after a few minutes. However, if the reactants in absolute ethanol solution were mixed at −30°, crystalline products were obtained. The analytical results were in agreement with the expected hydroxy-dihydrothiadiazine structure (II), but infrared spectra (Fig. 1) showed that only the products from the thiohydrazides (I a—c) had this structure. In the spectra of the derivatives of the phenyl substituted thiohydrazides (I d) and (I e) two carbonyl bands appeared, one at 1730 cm^{-1}, originating from the ester carbonyl group, and one at 1680 cm^{-1} from a C-benzoyl group. Therefore, these intermediates must still be open, and have the general structure (III). A strong band at 1600 cm^{-1} may be due to a conjugated carbon-nitrogen double bond stretching mode. The compounds (II a—c) show only the ester carbonyl band near 1730 cm^{-1} in this region.

The intermediates (II) are rapidly decomposed at room temperature in an exothermic reaction, but they can be stored for some time at −30°. The intermediates (III) show a normal stability.

Attempts to isolate the intermediate thiadiazines (IV) have hitherto been in vain. Previously [2] the transformation of hydroxydihydrothiadiazines to thiadiazines could be effected by careful heating or by treatment with acetic

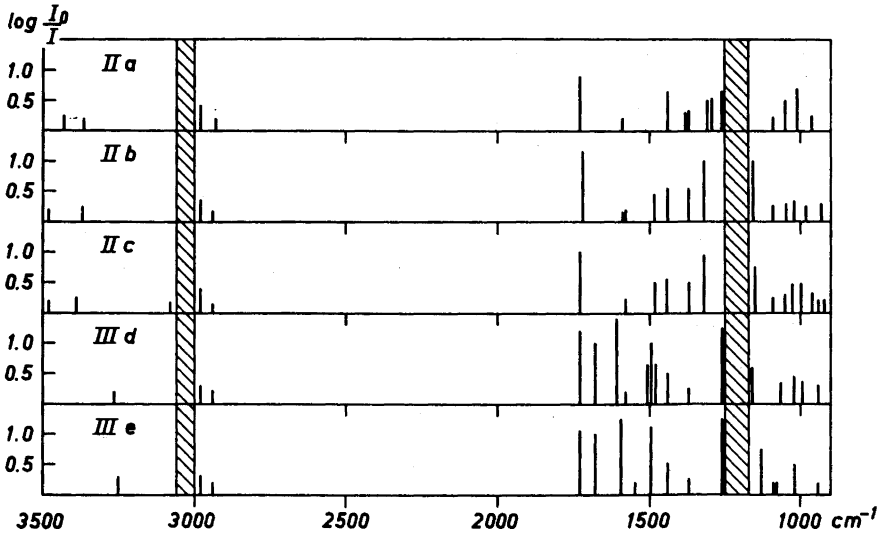

Fig. 1. Infrared spectra of the intermediates (II) and (III) in chloroform. The shaded areas indicate regions of high solvent absorption. $c = 0.15$.

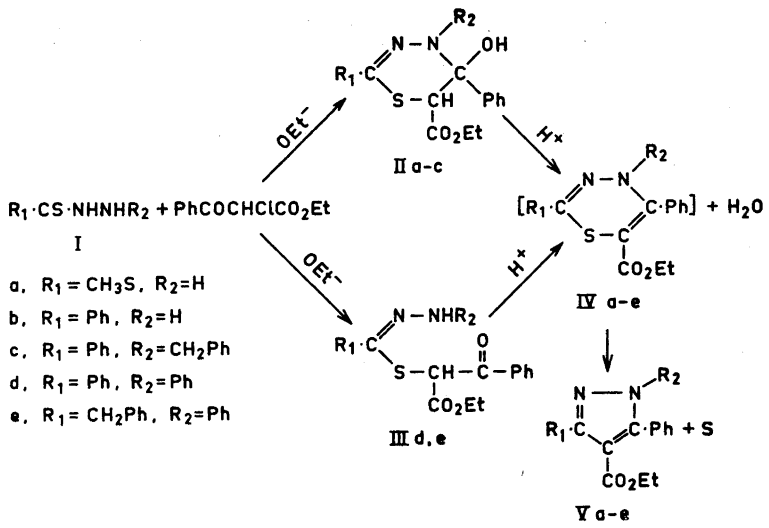

anhydride or acids. However, the compounds described here were always directly transformed to pyrazoles and sulphur, no matter how carefully the solutions were heated up. On treatment with acetic anhydride or very dilute hydrochloric acid a red to reddish-yellow colour appeared, which soon faded under simultaneous precipitation of sulphur. The colour is probably due to the thiadiazines, since Beyer *et al.*[5] have found that the ethyl 2-methylthio-5-methyl-1,3,4-thiadiazine-6-carboxylate is red. The change could be followed spectrophotometrically. All compounds with the structures (II) and (III) in slightly acid medium developed absorption bands in the region 4000—4500 Å with an apparent extinction coefficient of about 1000 to 1700. The bands appeared very rapidly and reached the maximum absorption before any readings could be made. Thereafter they disappeared gradually in a rate, which increased with the concentration of acid. When attempts were made to repeat the experiments on a preparative scale, red, non-crystalline products were obtained. However, the colour of these substances faded in the course of the purification procedures, even during paper chromatography, and finally only pyrazoles and sulphur were obtained.

The thiadiazines derived from thiohydrazides with a free amino group can have either of the structures (IV) and (VI).

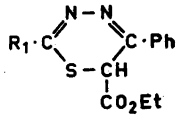

VI

The appearance of the very similar absorption maxima between 4000 and 4500 Å indicates that the red colour in all cases is due to the structure (IV), which is the only possible one for the thiadiazines from (II c), (III d), and (III e). Bulka *et al.*[6] have concluded, from the result of a reaction with *p*-nitrobenzaldehyde, that the structure corresponding to (VI) is the best representation of the thiadiazines. However, the two forms may well exist in equilibrium.

Thus, the results of this part of the investigation show, according to expectation, that the intermediate thiadiazines are considerably destabilised by the 6-carbethoxy group.

This reaction may be a convenient tool for the preparation of N-substituted pyrazoles with known constitution. The scope of the reaction has been considerably widened by the recent very extensive work of Jensen *et al.*[7–9], by which a wide variety of new thiohydrazides has become available.

As has been noticed previously [1], the pyrazole-4-carboxylic esters are remarkably stable to hydrolysis. This applies in particular to the esters with a free NH group. Thus ethyl 3,5-diphenylpyrazole-4-carboxylate (Vb) is not detectably hydrolysed after two hours reflux in two equivalents of 0.5 N ethanolic potassium hydroxide. Under the same conditions the 1-methyl analogue is hydrolysed to 51 % and the 1-phenyl analogue to 73 %. The slow hydrolysis of the pyrazole esters has been explained by the electron donating effect of the pyrazole ring [10] (VII), which increases the electron density around the carbonyl carbon atom and thereby impedes attacks by nucleophilic reagents. The greater reactivity of the 1-phenyl derivative was explained by a competing migration of electrons into the benzene ring. However, this effect can only explain the difference between the 1-phenyl and 1-methyl esters, but not the much greater difference between the 1-methyl and the 1-unsubstituted ones. It was observed during this investigation that the latter esters are

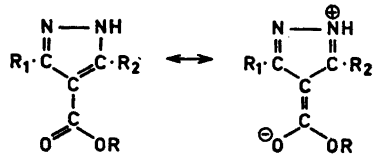

VII

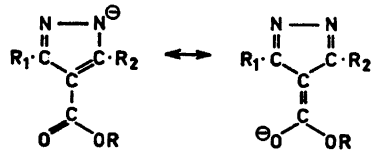

VIII

considerably more acidic than the unsubstituted pyrazole (Table 1). Therefore, the esters are probably completely ionised under the conditions of hydrolysis. Qualitatively it is easily understood that the migration of π electrons from the ring to the carbethoxy group is facilitated by ionisation, since then it can take place without separation of charges (VIII). This effect has also been demonstrated in a more quantitative way by a LCAO-MO calculation of the π electron distribution in a simple pyrazole ester and its anion. The method of calculation employed is the interative procedure devised by Janssen [12]. Two sets of Coulomb and resonance integrals are used (Table 2) in order to show that the result is not too dependent on the choice of parameters. The β_{CN} and β_{NN} values of set II and the β_{CO} values are derived from the overlap integrals

Table 1.

pK_a values for 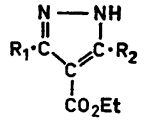 at 20°C.

R_1	R_2	pK_a
C_2H_5O	CH_3[a]	11.8
C_2H_5S	CH_3[a]	11.4
CH_3S	C_6H_5	10.5
C_6H_5	C_6H_5	11.1
Pyrazole		14 [b]

[a] Ref.[1] [b] Ref.[11]

Table 2. Coulomb and resonance integrals for pyrazole-4-carboxylate and its anion.

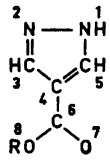

	Acid		Anion	
	I	II	I	II
α_1	$\alpha + 1.5\beta$	$\alpha + 1.5\beta$	$\alpha + 0.5\beta$	$\alpha + 0.5\beta$
α_2	$\alpha + 0.5\beta$	$\alpha + 0.5\beta$	$\alpha + 0.5\beta$	$\alpha + 0.5\beta$
α_3	α	α	α	α
α_4	α	α	α	α
α_5	α	α	α	α
α_6	α	α	α	α
α_7	$\alpha + \beta$	$\alpha + \beta$	$\alpha + \beta$	$\alpha + \beta$
α_8	$\alpha + 2\beta$	$\alpha + 2\beta$	$\alpha + 2\beta$	$\alpha + 2\beta$
β_{12}	β	0.65β	β	0.65β
β_{23}	β	0.85β	β	0.90β
β_{34}	β	β	β	β
β_{45}	β	β	β	β
β_{15}	β	0.92β	β	0.90β
β_{46}	β	β	β	β
β_{67}	0.85β	0.85β	0.85β	0.85β
β_{68}	0.70β	0.70β	0.70β	0.70β

taken from the tables of Mulliken *et al.*[13] and under the assumption that the resonance integral of a bond is proportional to its overlap integral[14]. The carbon-nitrogen and nitrogen-nitrogen bond lengths in pyrazole are taken from the work of Ehrlich[15].

The carbon-oxygen bond lengths, 1.22 and 1.36 Å, are taken from methyl acetate[16]. In the anion both β_{CN} values are put equal to 0.90 β, and the π electron density of each nitrogen atom is given as 1.5 electrons at the start of the calculation, in order to do justice to the symmetry of the anion. The Coulomb integral for the nitrogen atom 2 is chosen as $\alpha + 0.5\ \beta$[17]. Since atom 1 gives up one electron more to the delocalised bond, the method of calculation requires that its Coulomb integral shall be $\alpha + 1.5\ \beta$. The value for the carbonyl oxygen atom is derived from the electronegativity differences[18], and the value for the alkoxy oxygen atom must be one unit of β higher.

The results of the calculation are given in Table 3. For comparison the calculated π electron distribution in a simple aliphatic ester is also given. The numbering of the atoms is according to Table 2. As could be expected, set I gives the greater separation of charges, but the differences for the carbethoxy group are insignificant. As was predicted by qualitative considerations, the π electron density is higher at the carbonyl carbon atom (atom 6) in a pyrazole-4-carboxylic ester than in a simple aliphatic ester, and this density is further increased on ionisation.

Table 3. π Electron distribution.

Atom No.	Acid		Anion		Simple ester
	I	II	I	II	
1	1.621	1.690	1.321	1.371	
2	1.152	1.187	1.321	1.371	
3	1.039	0.994	1.036	0.987	
4	1.095	1.081	1.122	1.114	
5	0.958	0.917	1.036	0.987	
6	0.825	0.825	0.832	0.836	0.784
7	1.384	1.380	1.405	1.407	1.303
8	1.926	1.926	1.928	1.929	1.912

Longuet-Higgins[19] has shown how differences in π electronic charge can be related to differences in acidity constants for the conjugate acids of aza-aromatic compounds. The same treatment can be applied to pyrazole and 4-carbethoxypyrazole. Assuming the same entropy of ionization for the two systems we obtain $2.3\ RT\ (pK_{a_1} - pK_{a_2}) = -\Delta q_N \cdot \Delta\alpha_N$, where Δq_N is the difference between the π electron densities of the imino nitrogen atoms of pyrazole and its ester, and $\Delta\alpha_N$ is the difference in Coulomb integral between $=N-H$ and $=N^{\ominus}$. In the present approximation $\Delta\alpha_N$ is one unit of β, and Δq_N is 0.22 and 0.25 with the parameter set I and II, respectively. We use 0.24 as a mean value for Δq_N. An estimation of $pK_{a_1} - pK_{a_2}$ requires the evaluation

of β in common energy units. If we use the old and much criticized [20] value of -20 kcal/mole, we obtain $pK_{a_1} - pK_{a_2} = 3.6$. The agreement must be regarded as fortuitous considering the uncertainty in the β value and the effect of the substituents in the pyrazole esters, but it is gratifying that the direction and order of magnitude of the effect of the 4-carbethoxy group are correctly reproduced.

The 1-unsubstituted esters were hydrolysed by dissolving in concentrated sulphuric acid at 110°. On dilution with water the acids were obtained in fair yields. Hydrazinolysis is very slow, and the 1-unsubstituted esters were recovered unchanged after two days in a great excess of boiling anhydrous hydrazine. The 1-substituted esters also react slowly, but from them hydrazides have been obtained.

The pyrazole-4-carboxylic acids were decarboxylated at their melting points to the corresponding 4-unsubstituted pyrazoles.

EXPERIMENTAL

Ethyl 2-methylthio-5-hydroxy-5-phenyl-Δ^2-dihydro-1,3,4-thiadiazine-6-carboxylate (IIa). Methyl dithiocarbazate [21] (I a, 2.6 g) in N sodium ethoxide (20 ml) and ethyl benzoylchloroacetate [22] (4.5 g) in absolute ethanol (10 ml) were mixed at $-30°$. Crystallization started at once, and on the following day colourless rods (3.9 g, 63 % yield) were collected and washed with water to remove the sodium chloride. By addition of water (20 ml) a further amount of the product (1.2 g, 20 % yield) was precipitated. The combined products crystallised from chloroform-light petroleum (b.p. 40–60°) as colourless rods, m.p. 80–85°. Drying, recrystallization and storing were performed at $-30°$. (Found: C 49.9; H 5.06; N 8.93; S 20.5. $C_{13}H_{16}N_2O_3S_2$ (312.40) requires C 50.0; H 5.16; N 8.97; S 20.5). Even at $-30°$ the product turns first reddish-yellow and then pale yellow due to decomposition. At room temperature the reaction can be vigorous with a considerable raise in temperature.

λ_{max}: 3130 Å with ε: 10 500, and 2060 Å with ε: 15 300, in absolute ethanol. When 1.0 ml of 10^{-2} N HCl in absolute ethanol was added to 9.0 ml of a 10^{-3} M solution of (II a) in absolute ethanol, an absorption maximum appeared at 4160 Å with a maximum apparent ε value of about 1000, which then fell to half of this value in about four minutes.

Ethyl 3-methylthio-5-phenyl-pyrazole-4-carboxylate (V a). The hydroxy-dihydrothiadiazine (II a, 3.1 g) was dissolved in ethanol (20 ml), and 2 N HCl in ethanol (10 ml) was added. The mixture turned deep red, but the colour soon faded, and a precipitate of pure sulphur was formed (0.27 g, 84 % yield). Water (50 ml) was added to the filtered solution, and colourless rods were precipitated (2.5 g, 96 % yield), m.p. 131–132° after recrystallization from toluene-heptane. (Found: C 59.5; H 5.34; N 10.6; S 12.1. $C_{13}H_{14}N_2O_2S$ (262.32) requires C 59.5; H 5.38; N 10.7; S 12.2).

In general the preparation of the pyrazole esters is most conveniently performed *via* the isolation of the intermediates (II) or (III). If the reaction is performed at room temperature, the isolation of the pyrazoles is rendered more difficult due to the formation of by-products.

3-Methylthio-5-phenyl-pyrazole-4-carboxylic acid. The ester (V a, 5.2 g) was dissolved in concentrated sulphuric acid (15 ml). The solution was kept at 110° for 20 min, and then it was poured into water (100 ml). A colourless solid separated, which was extracted with N sodium bicarbonate solution (40 ml) and gave a residue of unreacted ester (0.27 g, 5 %). On acidification, the sodium bicarbonate solution deposited a colourless powder (4.0 g, 87 % yield), which crystallised from ethanol as colourless, irregular prisms, m.p. 289–290° (decomp.). (Found: C 56.2; H 4.37; N 11.9; S 13.6; equiv.wt. 230. $C_{11}H_{10}N_2O_2S$ (234.27) requires C 56.4; H 4.30; N 12.0; S 13.7; equiv.wt. 234).

3-Methylthio-5-phenyl-pyrazole hydrochloride. The acid (0.46 g) was kept at 300° until the evolution of gas had ceased. The residue was dissolved in absolute ether (5 ml), and 4 N HCl in absolute ether (5 ml) was added. Colourless crystals separated at once (0.40 g, 89 % yield), m.p. 165–167°, consisting of the hydrochloride of the desired

pyrazole. (Found: C 52.8; H 5.00; Cl 15.8; N 12.4. $C_{10}H_{11}ClN_2S$ (226.73) requires C 53.0; H 4.89; Cl 15.6; N 12.4). When the hydrochloride was decomposed with water, a colourless oil was formed, which crystallised when cooled to −10° but melted again at room temperature.

Ethyl 2,5-diphenyl-5-hydroxy-Δ²-dihydro-1,3,4-thiadiazine-6-carboxylate (II b). Thiobenzhydrazide [23] (I b) in 0.95 equiv. of N sodium ethoxide was made to react with 1 equiv. of ethylbenzoylchloroacetate at −30° as in the preparation of (II a) and gave a total yield of 84 % of (II b), colourless rods from chloroform-light petroleum, m.p. 91−93°. (Found: C 62.8; H 5.38; N 8.17; S 9.20. $C_{18}H_{18}N_2O_3S$ (342.40) requires C 63.1; H 5.30; N 8.18; S 9.36). This compound is less labile than (II a), but it is completely transformed into pyrazole and sulphur after a few days at room temperature.

λ_{max}: 2940 Å with ε: 10 000, and 2070 Å with ε: 29 500, in absolute ethanol. In acid solution a transient absorption band appears at 4440 Å with a maximal apparent ε value of about 1000.

Ethyl 3,5-diphenyl-pyrazole-4-carboxylate (V b). This pyrazole was prepared like (V a) in 90 % yield and crystallised from toluene-heptane as colourless prisms, m.p. 141−142°. (Found: C 73.8; H 5.47; N 9.51. $C_{18}H_{16}N_2O_2$ (292.33) requires C 74.0; H 5.52; N 9.59).

3,5-Diphenyl-pyrazole-4-carboxylic acid. The ester (V b) was hydrolysed in sulphuric acid like (V a) and gave 12 % of unchanged ester and 82 % of crude acid, which crystallised from ethanol-dimethyl sulphoxide as colourless, rhombic plates, m.p. 289−290° (decomp.). (Found: C 72.6; H 4.77; N 10.6; equiv.wt. 268. $C_{16}H_{12}N_2O_2$ (264.28) requires C 72.7; H 4.58; N 10.6; equiv.wt. 264).

3,5-Diphenylpyrazole. Diphenylpyrazole-4-carboxylic acid (0.5 g) was kept at 300° until the evolution of gas had ceased. The residue was recrystallised from 50 % aqueous ethanol (10 ml) and gave colourless, irregular prisms (0.23 g, 54 % yield), m.p. 199−200°. (Found: C 81.6; H 5.67. $C_{15}H_{12}N_2$ (220.27) requires C 81.8; H 5.49). This compound has been described by several authors, and the reported data are in good agreement with those obtained in the present work.

Ethyl 2,5-diphenyl-4-benzyl-5-hydroxy-Δ²-dihydro-1,3,4-thiadiazine-6-carboxylate (II c). This compound was prepared as (II a) and (II b) from 1-benzylthiobenzhydrazide [24] (I c) and ethyl benzoylchloroacetate in 85 % yield, colourless rods from chloroform-light petroleum, m.p. 90−91°. (Found: C 69.2; H 5.44; N 6.45; S 7.40. $C_{25}H_{24}N_2O_3S$ (432.52) requires C 69.4; H 5.59; N 6.48; S 7.41).

λ_{max}: 3055 Å with ε: 10 000, and 2085 Å with ε: 33 500. In acid solution the transient absorption band appears at 4300 Å with a maximal apparent ε value of about 1000.

Ethyl 1-benzyl-3,5-diphenyl-pyrazole-4-carboxylate (V c). This pyrazole was prepared as (V a) and (V b) in 92 % yield. It crystallised from methanol as colourless rods, m.p. 86−87°. (Found: C 78.6; H 5.80; N 7.44. $C_{25}H_{22}N_2O_2$ (382.44) requires C 78.5; H 5.80; N 7.33).

(V c) was also prepared by benzylation of (V b). This compound (2.9 g) was dissolved in N NaOH (15 ml) and ethanol (30 ml). Benzyl chloride (1.3 ml) was added, and within a few minutes a colourless oil started to separate. It solidified on scratching (3.8 g, quantitative yield) and crystallised from methanol as colourless rods, m.p. 86−87°, undepressed on admixture with the product described above.

1-Benzyl-3,5-diphenyl-pyrazole-4-carboxylic acid. The pyrazole ester (V c, 3.8 g) was refluxed for 4 h in N ethanolic potassium hydroxide (20 ml). On acidification with N HCl (20 ml), a colourless solid separated (2.8 g, 79 % yield), which crystallised from ethanol as colourless rods, m.p. 207−208° (decomp.). (Found: C 77.7; H 5.23; N 7.93; equiv.wt. 354. $C_{23}H_{18}N_2O_2$ (354.39) requires C 77.9; H 5.12; N 7.91; equiv.wt. 354).

1-Benzyl-3,5-diphenylpyrazole. The carboxylic acid just described (0.5 g) was kept at 220° until the evolution of gas had ceased. The semisolid residue was dissolved in ethanol (5 ml). The solution was cooled to −20° and deposited colourless, irregular prisms, m.p. 91−92° (0.27 g, 60 % yield). (Found: C 84.8; H 5.78; N 9.00. $C_{22}H_{18}N_2$ (310.38) requires C 85.1; H 5.84; N 9.03).

Ethyl 1-methyl-3,5-diphenyl-pyrazole-4-carboxylate. The pyrazole (V b, 5.8 g) was dissolved in N NaOH (25 ml) and ethanol (50 ml), and methyl iodide (4.5 g) was added. The resulting clear solution soon turned cloudy, and on the following day a solid precipitate had formed (6.05 g, 99 % yield), which crystallised from heptane as colourless needles, m.p. 98−99°. (Found: C 74.3; H 5.83; N 9.18. $C_{19}H_{18}N_2O_2$ (306.35) requires C 74.5; H 5.92; N 9.15).

1-Methyl-3,5-diphenyl-pyrazole-4-carboxhydrazide. The pyrazole ester (6.1 g) was refluxed with absolute ethanol (10 ml) and anhydrous hydrazine (10 ml) for 96 h. Then the reaction mixture was poured into water (200 ml). A semisolid, colourless mass separated, which could not be induced to crystallise. It was then dissolved in chloroform (50 ml) and extracted with three successive portions of N HCl (50 ml each). The combined acid extracts were brought to pH 5 by the addition of solid sodium acetate, and a precipitate was formed (2.6 g, 45 % yield), which crystallised from 25 % aqueous ethanol as colourless rods, m.p. 181—182°. (Found: C 69.4; H 5.54; N 19.2. $C_{17}H_{16}N_4O$ (292.33) requires C 69.8; H 5.52; N 19.2). Evaporation of the chloroform solution gave unchanged starting material (3.1 g, 50 %).

S-[Benzoyl-ethoxycarbonyl-methyl]-1-phenyl-isothiobenzhydrazide (III d). 1-Phenylthiobenzhydrazide [25] (I d) and ethyl benzoylchloroacetate reacted in the usual way to give a reddish-yellow solid in 98 % yield, which crystallised from chloroform-light petroleum as pale yellow, rhombic prisms, m.p. 55—56°. (Found: C 68.8; H 5.27; N 6.60; S 7.64. $C_{24}H_{22}N_2O_3S$ (418.50) requires C 68.9; H 5.30; N 6.70; S 7.66).

λ_{max}: 3525 Å with ε: 16 000, 2920 Å with ε: 10 500, 2450 Å with ε: 25 100, and 2070 Å with ε: 29 000 in absolute ethanol. In acid solution a transient absorption maximum appeared at 4280 Å with a maximal apparent ε value of about 1700.

Ethyl 1,3,5-triphenyl-pyrazole-4-carboxylate (V d). The phenylhydrazone (III d, 4.2 g) was dissolved in absolute ethanol (30 ml), and 2 N HCl in absolute ethanol (5 ml) was added. The solution turned deep red, but the colour soon faded, and a precipitate of pyrazole and sulphur was formed. Purification was effected by successive recrystallizations from acetic acid (50 ml) and butanol (25 ml) and gave pale yellow rods (3.0 g, 82 % yield), m.p. 146—147°. (Found: C 77.9; H 5.29; N 7.68. $C_{24}H_{20}N_2O_2$ (368.42) requires C 78.2; H 5.47; N 7.61).

This ester has previously been described by Minunni and D'Urso [26], who report m.p. 145—146.5°.

1,3,5-Triphenylpyrazole-4-carboxylic acid. The pyrazole (V d, 3.7 g) was refluxed for 4 h with N ethanolic potassium hydroxide (20 ml). Acidification with N HCl (20 ml) gave a microcrystalline powder (2.4 g, 70 % yield), which crystallised from ethanol as colourless rods, m.p. 243—243.5° (decomp.). (Found: Equiv.wt. 342. $C_{22}H_{16}N_2O_2$ requires equiv.wt. 340). This acid has also been described by Minunni and D'Urso [26], who report m.p. 237—238°.

1,3,5-Triphenyl-pyrazole-4-carboxhydrazide. The pyrazole ester (V d, 3.7 g) was refluxed for 48 h with anhydrous hydrazine (25 ml) and absolute ethanol (25 ml). Then the mixture was poured into water (250 ml), and a colourless solid separated (3.1 g, 78 % yield), which crystallised from 70 % aqueous ethanol as colourless rods, m.p. 166—167°. (Found: C 74.2; H 5.24; N 15.6. $C_{22}H_{18}N_4O$ (354.39) requires C 74.6; H 5.12; N 15.8).

This hydrazide (0.7 g) and benzaldehyde (0.3 g) reacted in 70 % aqueous ethanol (10 ml) to give a colourless product (0.68 g, 78 % yield), which crystallised from butanol as colourless, long plates, m.p. 185—186°. (Found: C 78.4; H 5.30; N 12.6. $C_{29}H_{22}N_4O$ (442.50) requires C 78.7; H 5.01; N 12.7).

1,3,5-Triphenylpyrazole. Triphenylpyrazole-4-carboxylic acid (0.68 g) was kept at 250° until the evolution of gas had ceased. The liquid residue was dissolved in ethanol (5 ml), and N NaOH (2 ml) was added. A solid product separated (0.44 g, 74 % yield), which crystallised from butanol as colourless rods, m.p. 138—139°. (Found: C 84.9; H 5.60. $C_{21}H_{16}N_2$ (296.36) requires C 85.1; H 5.44).

Wislicenus [27] reports m.p. 136.5—137.5 for this pyrazole.

S-[Benzoyl-ethoxycarbonyl-methyl]-1-phenyl-isothiophenylacethydrazide (III e). 1-Phenylthiophenylacethydrazide [9] (I e) and ethyl benzoylchloroacetate reacted in the usual way to give 81 % of (III e), which crystallised from chloroform-light petroleum as pale yellow rods, m.p. 111—112°. (Found: C 69.6; H 5.59; N 6.36; S 7.37. $C_{25}H_{24}N_2O_3S$ (432.52) requires C 69.4; H 5.59; N 6.48; S 7.41).

λ_{max}: 2875 Å with ε: 17 500, 2480 Å with ε: 17 500, and 2075 Å with ε: 34 500 in absolute ethanol. In acid solution a transient absorption maximum appeared at 3990 Å with an apparent ε value of about 1500.

Ethyl 1,5-diphenyl-3-benzyl-pyrazole-4-carboxylate (V e). The phenylhydrazone (III e, 4.3 g) was dissolved in ethanol (40 ml), and 2 N HCl in ethanol (10 ml) was added. The mixture first turned red and then pale yellow and deposited a small amount of sticky material. Addition of water (200 ml) to the filtered solution precipitated a semisolid mass,

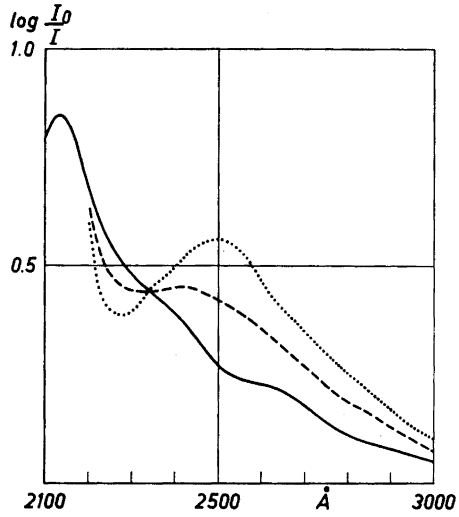

Fig. 2. Ultraviolet spectra of ethyl 3-ethylthio-5-methylpyrazole-4-carboxylate in water at pH 6 (———), pH 11.5 (– – –), and pH 13.7 (· · · · ·). $c = 5 \times 10^{-5}$.

which was dissolved in benzene (5 ml) and subjected to chromatography on alumina. Light petroleum eluted sulphur (0.16 g, 50 % yield), and benzene gave a colourless solid (1.6 g, 42 % yield), which crystallised from heptane as colourless rods, m.p. 111—112°. (Found: C 78.5; H 5.70; N 7.38. $C_{25}H_{22}N_2O_2$ (382.44) requires C 78.5; H 5.80; N 7.33).

Acid dissociation constants (Table 1). These were determined by standard spectrophotometric technique in 5×10^{-5} M solutions in water with 0.5 % of ethanol. All spectra showed a bathochromic displacement on ionisation (Fig. 2). The spectra of the anions were recorded in 0.5 N NaOH, in which solution even the weakest of the acids is ionised to more than 98 %. As a consequence of the solvent effect on the spectra, the K_a values calculated at different wavelengths differed with up to 5 %, but the values of K_a calculated from measurements at five different pH values around the pK_a value showed good agreement for each wavelength, and the average pK_a values are considered to be reliable up to 0.1 unit.

The ultraviolet spectra were recorded with a Beckman DU spectrophotometer with photomultiplier attachment except for the spectra of the compounds (II a—c) and (III d, e) in acid solution, which were recorded with a Perkin-Elmer Model 137 recording spectrophotometer.

The infrared spectra were recorded with a Perkin-Elmer Model 221 prism-grating instrument.

The LCAO-MO calculations were performed on the electronic digital computor "SMIL" at the Department of Numerical Analysis of the University of Lund.

Acknowledgements. The author is indebted to the *Swedish Natural Science Research Council* for financial support, to Miss Ingeborg Leutiger and Fil.kand. Kristina Arvidsson for skilful experimental assistance, and to Mrs Kerstin Kulle-Pettersson for recording the infrared spectra. The LCAO-MO calculations were programmed by Fil.kand. Leif Robertsson, and Laborator Carl-Erik Fröberg and Ingenjör Kjell Jönsson gave valuable advice concerning the use of the computor.

REFERENCES

1. Sandström, J. *Arkiv Kemi* **8** (1955) 523.
2. Sandström, J. *Arkiv Kemi* **15** (1960) 195.
3. Beyer, H. and Wolter, G. *Chem. Ber.* **89** (1956) 1652.
4. Beyer, H., Wolter, G. and Lemke, H. *Chem. Ber.* **89** (1956) 2550.
5. Beyer, H., Bulka, E. and Beckhaus, F. W. *Chem. Ber.* **92** (1959) 2593.
6. Bulka, E., Ahlers, K.-D. and Beyer, H. *Chem. Ber.* **94** (1961) 1122.
7. Jensen, K. A. *Acta Chem. Scand.* **15** (1961) 1067.
8. Jensen, K. A. and Pedersen, Chr. *Acta Chem. Scand.* **15** (1961) 1097.
9. Jensen, K. A., Baccaro, H. R., Buchardt, O., Olsen, G. E., Pedersen, Chr. and Toft, J. *Acta Chem. Scand.* **15** (1961) 1109.
10. Sandström, J. *Svensk Kem. Tidskr.* **68** (1956) 143.
11. Mason, S. F., cited in Albert, A. *Heterocyclic Chemistry*. Essential Books, Fair Lawn 1959, p. 143.
12. Janssen, M. J. *Rec. trav. chim.* **79** (1960) 1066.
13. Mulliken, R. S., Rieke, C. A., Orloff, D. and Orloff, H. *J. Chem. Phys.* **17** (1949) 1248.
14. Mulliken, R. S. *J. Chim. Phys.* **46** (1949) 712.
15. Ehrlich, H. W. W. *Acta Cryst.* **13** (1960) 946.
16. O'Gorman, J. M., Shand, Jr., W. and Shomaker, V. *J. Am. Chem. Soc.* **61** (1950) 4222.
17. Gerson, F. and Heilbronner, E. *Helv. Chim. Acta* **41** (1958) 2332.
18. Daudel, R., Lefebvre, R. and Moser, C. *Quantum Chemistry, Methods and Applications*. Interscience Publishers, New York 1959, p. 76.
19. Longuet-Higgins, H. C. *J. Chem. Phys.* **18** (1950) 275.
20. Streitwieser, A., Jr. *Molecular Orbital Theory for Organic Chemists*. John Wiley and Sons, New York 1961, p. 241.
21. Busch, M. and Starke, M. *J. prakt. Chem.* [2] **93** (1916) 59.
22. Peratoner, A. *Gazz. chim. ital.* **22 II** (1892) 41.
23. Holmberg, B. *Arkiv Kemi, Mineral. Geol.* **17 A** (1944) N:o 23, p. 7.
24. Forsgren, B. and Sandström, J. *Acta Chem. Scand.* **14** (1960) 789.
25. Holmberg, B. *Arkiv Kemi* **7** (1954) 517.
26. Minunni, G. and D'Urso, S. *Gazz. chim. ital.* **58** (1928) 691.
27. Wislicenus, J. *Ann.* **308** (1899) 253.

Received June 7, 1962.

ACTA CHEMICA SCANDINAVICA 16 (1962) 2406–2410

New Theory for the Electron Transfer Spectra of Acetylacetonate Complexes

CHR. KLIXBÜLL JØRGENSEN

Cyanamid European Research Institute, Cologny (Geneva), Switzerland

The strong dependence of electron transfer wavenumbers in halide complexes on the number q of electrons in the partly filled shell suggests that recent interpretations of the strong absorption bands of acetylacetonates M aca_3 may have to be changed. Good agreement with observed band positions is obtained by the same theory as used for other transition group complexes, assuming that all possible transitions between π, the sub-shells γ_5 and γ_3, and the empty π^* orbitals occur. The optical electronegativity of the π orbitals of aca^- is found to be roughly 2.7. The band at 26 kK of Cu aca_2 is presumably $\pi \rightarrow (x^2-y^2)$. It is suggested to revise several accepted ideas of $\gamma_5 \rightarrow \gamma_3$ transitions in Ti aca_3 and Mn aca_3.

Recently, Barnum [1] used M. O. Theory for the description of the absorption spectra of neutral tris-acetylacetonates M aca_3 with the central ion containing q (= 0, 1, 2, 3, 4, 5, 6) electrons in a partly filled d shell. Though Barnum's treatment undoubtedly presents a large part of the truth, it is surprising to see that the M. O. energy differences vary very little with q. The present writer has introduced the concept of optical electronegativities [2–4] and has recently related the behaviour of 3d complexes [5] with the previously known regularities in the 4d and 5d group. Usually, the partly filled shell becomes more stable, by an amount $(E-A)$, for each unit increase of q. In most cases, $(E-A)$ is about 6 kK (1 kK = 1000 cm^{-1}). In tetrahedral 3d complexes, it seems to be smaller. It is necessary to correct this linear dependence with the spin-pairing energy dependence [3] on the total spin S of the central ion*

$$D[\langle S(S+1)\rangle - S(S+1)] \qquad (1)$$

where D is roughly $7B$ for d-electrons. Furthermore, we may sometimes consider the higher, σ-anti-bonding sub-shell γ_3 at an energy Δ higher than

* This concept is used in the description of electron transfer spectra in the same way as Hund used the idea of weakly coupled configurations in atomic spectroscopy. Though in quantum mechanics, S is only defined for the whole system, the energy levels of a hole in the widely extended, normally filled, M.O. combined with the partly filled shell are distributed to the first approximation as if the partly filled shell had an individual value of S to be inserted in eqn. (1).

Table 1. Parameters describing the electron transfer wavenumbers as function of the number of electrons q in the partly filled d shell. The coefficient to D is determined from eqn. (1). V_1 and V_2 determine the points of reference for the variation of the wavenumbers (the two partly filled sub-shells being stabilized $q(E-A)$) and are hence, for our purpose, entirely empirical parameters used as starting-point for our comparison.

q =	I. $\pi \rightarrow \gamma_5$	II. $\pi \rightarrow \gamma_3$	III. $\gamma_5 \rightarrow \pi^*$	IV. $\gamma_3 \rightarrow \pi^*$
0	V_1	$V_1 + \Delta$	–	–
1	$V_1 - (E-A) - 2/3D$	$V_1 + \Delta - (E-A) - 2/3D$	V_2	–
2	$V_1 - 2(E-A) - 4/3D$	$V_1 + \Delta - 2(E-A) - 4/3D$	$V_2 + (E-A) + 2/3D$	–
3	$V_1 - 3(E-A) + 2D$	$V_1 + \Delta - 3(E-A) - 2D$	$V_2 + 2(E-A) + 4/3D$	–
4 high-spin	$V_1 - 4(E-A) + 7/3D$	$V_1 + \Delta - (E-A) - 8/3D$	$V_2 + 3(E-A) + 2D$	$V_2 - \Delta + 3(E-A) + 2D$
4 low-spin	$V_1 - 4(E-A) + 4/3D$	$V_1 + \Delta - 4(E-A) - 5/3D$	$V_2 + 3(E-A) - 2D$	–
5 high-spin	$V_1 - 5(E-A) + 8/3D$	$V_1 + \Delta - 5(E-A) + 8/3D$	$V_2 + 4(E-A) + 8/3D$	$V_2 - \Delta + 4(E-A) + 8/3D$
5 low-spin	$V_1 - 5(E-A) + 2/3D$	$V_1 + \Delta - 5(E-A) - 4/3D$	$V_2 + 4(E-A) - 4/3D$	–
6 low-spin	–	$V_1 + \Delta - 6(E-A) - D$	$V_2 + 5(E-A) - 2/3D$	–

the lower, triply degenerate set γ_5 of M.O. We are here approximating M aca_3 by octahedral symmetry which seems to be a very good approximation, the dichroitic effects on wavenumbers being comparatively small [6].

The difference between the optical electronegativities of the loosest bound orbitals of the ligands and of the appropriate sub-shell of the central atom is defined [2–5] as the wavenumber of the corresponding electron transfer band (corrected by use of eqn. (1)) divided by 30 kK. The halogens have characteristic optical electronegativities which can be fixed at the values F (3.9), Cl (3.0), Br (2.8), and I (2.5).

It is suggested that the complicated aspects of the absorption spectra in the near ultraviolet are caused by the simultaneous presence of four different types of electron transfer spectra, *viz.*

$$\text{I. } \pi \rightarrow \gamma_5 \qquad \text{II. } \pi \rightarrow \gamma_3 \qquad \text{III. } \gamma_5 \rightarrow \pi^* \qquad \text{IV. } \gamma_3 \rightarrow \pi^* \tag{2}$$

besides the internal transitions in the ligands which may be classified as (V· $\pi \rightarrow \pi^*$) and produce characteristic bands at somewhat higher wavenumbers [7,8]. It is emphasized that this is a rather unusual complication though similar phenomena occur by comparison of Fe(II) and Fe(III) complexes of aromatic diimines [9].

Table 1 gives the dependence on the parameters V_1, V_2, $(E-A)$ and D of the transitions in eqn. (2) as function of q. In the case of $q = 4$ (Mn aca_3) and $q = 5$ (Fe aca_3), high-spin behaviour is realized, whereas $q = 6$ (Co aca_3) is low-spin. For comparison, low spin $q = 4$ and 5 are also considered in Table 1.

We derive the numerical value of V_1 from experiment, noting that the strong band of Fe aca_3 at 23.2 kK must belong [9] to class I. D is known from internal transitions in the partly filled d shell of similar complexes to be roughly 4.5 kK. Table 2 gives the result of the final assumption of $V_1 = 31$ kK and $(E-A) = 4$ kK (a rather small value, but much larger than suggested by Barnum's choice of parameters).

We will make the rather unorthodox proposal that the broad band with conspicuous vibrational structure of Ti aca_3 centered around 17 kK is not an internal $\gamma_5 \rightarrow \gamma_3$ transition intensified by the absence of a centre of inversion, but is an electron transfer band of class III, comparable to the iridium-pyridine bands [10,11]. It is instructive to see in Table 2 that such a band soon will increase

Table 2. Numerical values obtained from Table 1 with the choice of parameters (in kK): $V_1 = 31$, $V_2 = 17$, $(E-A) = 4$, $D = 4.5$, $\Delta = 18$ (except 20 for $q = 6$). Experimental wavenumbers from Barnum. Tentative assignments in parentheses.

	I. $\pi - \gamma_5$		II. $\pi - \gamma_3$		III. $\gamma_5 - \pi^*$		IV. $\gamma_3 - \pi^*$	
$q =$	calc.	obs.	calc.	obs.	calc.	obs.	calc.	obs.
0 Sc(III)	31	—	49	—	—	—	—	—
1 Ti(III)	24	25.7	42	—	17	17	—	—
2 V(III)	17	(21.7)	35	29.2	24	25.6	—	—
3 Cr(III)	28	26.0	28	26.0	31	30.2	—	—
4 Mn(III)	25.5	(25.0)	21	(22.5)	38	—	20	(18)
5 Fe(III)	23	23.2	41	—	45	—	27	28.5
6 Co(III)	—	—	22.5	(25)	34	(31)	—	—

to high wavenumbers as function of increasing q. On the other hand, even in the rather oxidizing Mn(III) and Fe(III) complexes, the presence of γ_3 electrons will bring the class IV transition down to rather low wavenumbers. Δ is assumed to be 18 kK, except in the case of Co aca_3 where it is fixed to 20 kK. Without the introduction of multiple π or π^* orbitals (which it would be quite legitimate to expect [1]), Table 2 exhausts essentially all the bands observed below the ligand $\pi \rightarrow \pi^*$ transitions. Table 2 represents several new features. Suspicion is thrown upon the identification of visible bands of V aca_3 and Mn aca_3 as $\gamma_5 \rightarrow \gamma_3$ transitions in the partly filled shell. The pronounced vibrational structure around 26 kK of Cr aca_3 has always been suspected [12] for not simply being the second spin-allowed, Laporte-forbidden transition to $^4\Gamma_4$ predominantly belonging to the sub-shell configuration $\gamma_5^2\gamma_3$. The moderately strong band [1,6] of Mn aca_3 at 8.9 kK, on the other hand, is presumably such an internal, spin-allowed transition. This classification necessitates the hypothesis of relatively strong deviations from octahedral symmetry, perhaps in the form of a dynamic Jahn-Teller effect [13,14]. (Similar conclusions were drawn quite recently by Dingle [24]).

The distortion may either be along a trigonal axis, splitting the excited term $^5\Gamma_5$ into two components, or along a tetragonal axis, removing also the orbital degeneracy of the cubic ground-term $^5\Gamma_3$. A comparable transition has been observed in manganese(III) tris(diethyldithiocarbamate) extracted into CCl_4 (avoiding infra-red lines due to vibration of hydrogen atoms in the solvent). This compound shows a broad band at 1750 mμ (5.7 kK) with the half-widths $\delta(-) = 1.8$ and $\delta(+) = 2.3$ kK.

It is a quite intricate problem whether acetylacetonates in general always have weak bands in the near ultraviolet close to 26 kK. Piper and Linn Belford [15] presented convincing evidence that such a band of Cu aca_2 in various solvents, which had been ascribed to an internal 3d transition by several authors, does not have this origin, and that presumably all the internal transitions in the partly filled shell occur between 14 and 18 kK. It is not very probable that the 26 kK band should be a spin-forbidden transition in the ligand aca^- intensified by intermediate coupling effects in the central atom. Actually, In aca_3 does not present such a weak band in the near ultraviolet though the relativistic effects were expected to be much stronger.

It is quite plausible that the band is caused by electron transfer of class II type. This would correspond to a difference between the optical electronegativities x_{opt} of aca^- and Cu(II) about 0.4 units, and since the lowest d-like orbitals of Cu(II)[5] have $x_{opt} = 2.3$, this would give aca^- a reducing character somewhere between bromide and iodide. Unfortunately, a clear-cut value of x_{opt} for Fe(III) cannot easily be given [5]. Considering the octahedral nature of Fe aca_3 we may adopt 2.3. The value of $V_1 = 31$ kK and $(E-A) = 4$kK in Table 2 then corresponds to 2.7 for the highest, filled π orbitals of aca^-. Due to the charge separation effects, there is no simple relation [16] between the expression $V_2 + V_1 - (E-A) = 44$ kK and the wavenumbers of the $\pi \rightarrow \pi^*$ transitions in the ligand.

It has become increasingly clear in the recent years that the absorption spectra of acetylacetonates indicate that the nature of the chemical bonding in these inner-complexes is not so incomprehensible as once many authors

believed. For instance, the octahedral micro-symmetry of MO_6 clusters postulated [12] from spectra of the nickel(II) complex has now been verified by crystallography [17,18] the high-spin species being a trimer Ni_3 aca_6, and also the spectra of Jahn-Teller stable M aca_3 do not encourage the assumption of strong, unusual deviations from octahedral symmetry. Regarding the question of possible strong π- (and not only σ-) bonding in these complexes, the observation in Cr aca_3 of luminescence spectra [19] of the excited term $^2\Gamma_3$ of γ_5^3 suggesting rather small values of the nephelauxetic [20] ratio β_{55} is very important. Actually, these measurements suggest a stronger delocalization of the π^* bonding subshell than in the comparable compounds [21,22] $Cr(S_2P(OC_2H_5)_2)_3$ and $Cr(Se_2P(OC_2H_5)_2)_3$.

The extended understanding of electron transfer spectra of acetylacetonates gives some hope that a rational classification of energy levels according to M.O. configurations can be obtained in a few years of transition group complexes of fairly complicated oxygen- and nitrogen-containing organic ligands about which a rich experimental material is available [7,23].

Acknowledgments. I am grateful to Dr. D. W. Barnum, Dr. R. L. Carlin, and Dr. R. Linn Belford for valuable discussions about the complex spectra of acetylacetonates.

REFERENCES

1. Barnum, D. W. *J. Inorg. & Nuclear Chem.* **21** (1961) 221; **22** (1961) 183.
2. Jørgensen, C. K. *Orbitals in Atoms and Molecules.* Academic Press, London 1962.
3. Jørgensen, C. K. *Solid State Physics* **13** (1962) 375.
4. Jørgensen, C. K. *Molecular Physics* **5** (1962) 271.
5. Jørgensen, C. K. *Molecular Physics* **6** (1963). *In press.*
6. Carlin, R. L. and Piper, T. S. *J. Chem. Phys. In press.*
7. Sone, K. *J. Am. Chem. Soc.* **75** (1953) 5207.
8. Holm, R. H. and Cotton, F. A. *J. Am. Chem. Soc.* **80** (1958) 5658.
9. Williams, R. J. P. *J. Chem. Soc.* **1955** 137.
10. Jørgensen, C. K. *Acta Chem. Scand.* **11** (1957) 166.
11. König, E. and Schläfer, H. L. *Z. physik. Chem.* **26** (1960) 371.
12. Jørgensen, C. K. *Acta Chem. Scand.* **9** (1955) 1362.
13. Forman, A. and Orgel, L. E. *Molecular Physics* **2** (1959) 362.
14. Cotton, F. A. and Meyers, M. D. *J. Am. Chem. Soc.* **82** (1960) 5023.
15. Piper, T. S. and Linn Belford, R. *Molecular Physics* **5** (1962) 169.
16. Jørgensen, C. K. *Absorption Spectra and Chemical Bonding in Complexes.* Pergamon Press, Oxford 1962.
17. Bullen, G. J., Mason, R. and Pauling, P. *Nature* **189** (1961) 291.
18. Cotton, F. A. and Fackler, J. P. *J. Am. Chem. Soc.* **83** (1961) 2818 and 3775.
19. Forster, L. S. and Armond, K., de, *Proc.* **7**. *ICCC*, Stockholm 1962, paper 1 B3, p. 20.
20. Jørgensen, C. K. *Progr. Inorg. Chem.* **5** (1962). *In press.*
21. Jørgensen, C. K. *J. Inorg. & Nuclear Chem. In press.*
22. Jørgensen, C. K. *Molecular Physics.* **5** (1962) 485.
23. Kiss, A. and Szabo, R. *Z. anorg. Chem.* **252** (1943) 172.
24. Dingle, R. *J. Mol. Spectr.* **9** (1962) 426.

Received July 5, 9162.

ACTA CHEMICA SCANDINAVICA 16 (1962) 2411–2420

Studies on the Coagulation of Chicken Blood

IX. Labile Factor Activity of Fresh Oxalated Plasma: the Combined Activity of Sixteen Discrete Labile Coagulation Factors

ØYVIND SØRBYE*

Department of Biochemistry and Nutrition, Polytechnic Institute, Copenhagen, Denmark

The labile factor activity of fresh oxalated chicken plasma is fully accounted for by the combined activity of sixteen discrete labile coagulation factors which are active with chicken brain thromboplastin. With Russell's viper venom (RVV)-cephalin only eight of these factors are active, and the combined activity of the eight factors accounts for all labile factor activity measured by this agent. The labile factor activity measured with RVV, unsupplemented by cephalin, can be accounted for by the combined activity of seven of the eight factors measured by RVV-cephalin. The eight factors specific for the thromboplastin assay system, may be regarded as co-factors for generation of hypothetical intermediate activation products of thromboplastin. The remaining eight factors are probably involved in the transformation of thromboplastin activation products and of RVV-cephalin into prothrombin converting principles. It is suggested that the various labile factors of chicken plasma may be involved in alternative mechanisms for formation of such principles.

The idea that the labile factor activity of fresh oxalated chicken plasma is of complex nature and due to the combined activity of discrete labile coagulation factors, originated in the observations that only part of the total activity was adsorbed by treatment of the plasma with crystalline adsorbents [1–5]. The selective adsorption thus obtained, was interpreted as adsorption of one (or a few) labile coagulation factor(s) which, in this respect, differed from the factors responsible for the non-adsorbable part of the activity. As a result of continued testing of insoluble crystalline compounds, more than one hundred adsorbents with selective properties are known at present [2–5]. The effects obtained by use of different adsorbents were compared by matching experiments. Thus, all selective adsorbents were in turn classified according to the identity or non-identity of the activities adsorbed. These experiments gradually led to the recognition of sixteen different categories of selective

* Fellow of the Royal Norwegian Council for Scientific and Industrial Research.

adsorbents and accordingly to the existence of sixteen discernible labile coagulation factors in fresh, oxalated chicken plasma [2-5].

The present experiments were carried out to examine to what extent the labile factor activity of fresh oxalated chicken plasma could be accounted for by the combined activity of these sixteen factors.

MATERIALS AND METHODS

The materials and methods used in this study were as described previously [2-5]. Labile factor activity [2] was determined using stored, oxalated normal chicken plasma as substrate and the assay accelerators chicken brain thromboplastin, Russell's viper venom (RVV)-cephalin, and RVV alone. The coagulation time of the substrates was usually 3 – 6 times the value for fresh normal plasmas. Substrates with longer coagulation times were generally adjusted to coagulation times of 4 – 5 times the value for normal plasma by addition of traces of fresh plasma.

In this work the quantities of the adsorbents used for preparation of the adsorbed plasma samples were always adequate for *complete* adsorption of the adsorbable factor(s).

EXPERIMENTS AND RESULTS

Strontium carbonate adsorbable labile factor activity. It has been shown already [2] that barium oxalate and calcium carbonate adsorb two different parts (σ-factor and ψ-factor) of the labile factor activity adsorbed by strontium carbonate, and that the combined activity of these two factors is equal to the activity adsorbed by strontium carbonate. Some additional experiments are shown in Table 1, confirming that the activity adsorbed by strontium carbonate is fully accounted for by the combined activity of the σ- and ψ-factors, regardless of large variations in the relative activities of the two factors in different experiments.

Strontium carbonate non-adsorbable labile factor activity. By means of the fourteen different categories of selective adsorbents described in three preceding papers [3-5], fourteen different components of the labile factor activity of fresh, oxalated, strontium carbonate preadsorbed plasma could be distin-

Table 1. Combined activity of the ψ- and σ-factors.

Adsorbent in mg/ml	Activity of adsorbed factor(s) in % of total activity of plasmas Nos.:										Labile factor(s) adsorbed
	5053	3441		4397	4413	4418	4681	5052*	5230	5348	
Ca-carbonate 5	10	15	12.5	3.5	14	16	5	4	11	4	ψ
Ba-oxalate 5	12	12	11	12.5	15	5	4	4	11	4	σ
Sr-carbonate 25	22	27	23.5	16	29	21	9	8	22	8	$\psi + \sigma$
Assay accelerator **:	V	Vc	Chicken brain thromboplastin								

* Coumachlor plasma, thromboplastin coagulation time > 20 min.

** V: Russell's viper venom; Vc: Russell's viper venom-cephalin.

Table 2. Effect of adsorption of single factors on the specific activity of the others. 0 indicates no change, *i.e.* the factors act independently (additively); + indicates reduced specific activity, *i.e.* the factors have synergistic effects.

Adsorption of factor	Effect on the specific activity of factors													
	ϱ	ν	μ	π	γ	β	ε	λ	α	η	ζ	ϑ	ξ	ω
ϱ		+	0	0	0	0	0	0	0	0	0	0	0	0
ν	+		+	0	0	0	0	0	0	0	0	0	0	0
μ	0	+		+	0	0	0	0	0	0	0	0	0	0
π	0	0	+		+	0	0	0	0	0	0	0	0	0
γ	0	0	0	+		+	0	0	0	0	0	0	0	0
β	0	0	0	0	+		+	0	0	0	0	0	0	0
ε	0	0	0	0	0	+		+	0	0	0	0	0	0
λ	0	0	0	0	0	0	+		+	0	0	0	0	0
α	0	0	0	0	0	0	0	+		0	0	0	0	0
η	0	0	0	0	0	0	0	0	0		+	0	0	0
ζ	0	0	0	0	0	0	0	0	0	+		0	0	0
ϑ	0	0	0	0	0	0	0	0	0	0	0		0	0
ξ	0	0	0	0	0	0	0	0	0	0	0	0		0
ω	0	0	0	0	0	0	0	0	0	0	0	0	0	

guished. Of these factors, only six were components of the labile factor activity measured by RVV-cephalin. The activity of one of the latter six factors was shown to depend on the presence of added cephalin in the test mixture.

For the development of a satisfactory procedure for determination of the combined activity of the fourteen labile factors active with thromboplastin, the following facts had to be considered: With the exception of three factors the specific activity of each of the fourteen factors depends on the concentrations of the others in a complex and characteristic manner [3–5]. In Table 2 is presented a summary of previous experiments showing how the specific activity of each of the fourteen factors is related to the concentration of the other thirteen. Nine of the factors are interlinked synergistically (ϱ—ν—μ—π—γ—β—ε—λ—α), whereas the specific activity of each of these factors is independent of the concentrations of the ϑ-, ξ-, ω-, η-, and ζ-factors, and *vice versa*. Of the latter five factors, only the η- and ζ-factors are interdependent. The ϑ-, ξ-, and ω-factors are thus the only labile factors, the specific activity of each of which is independent of the concentrations of all the others. The combined activity of these three factors could consequently be determined as the sum of activities adsorbed by the three corresponding selective adsorbents in parallel experiments. The η- and ξ-factors are synergists, but the specific activity of each of these two factors is independent of the concentrations of the other twelve. The combined activity of the η- and ζ-factors would thus be equal to the activity of η-factor, determined in the presence of ζ-factor, plus the activity of ζ-factor, determined in the absence of η-factor, or *vice versa*. A two-step adsorption procedure with the respective selective adsorbents would then be required for determination of the combined activity of the η- and ζ-factors.

Table 3. Adsorption of labile factors by mixtures of selective adsorbents (thromboplastin assay).

Chick No.	Pretreatment(s) of plasma	Adsorbent(s) in mg/ml	Activity of adsorbed factor(s) in % of $SrCO_3$ plasma	Labile factor(s) adsorbed
2885	$SrCO_3$, 25 mg/ml (A)	Bi-phosphate 15 (B)	11	ϱ
		Bi-oxalate 15 (C)	11	μ
		Mixture of (B) and (C)	22	$\varrho + \mu$
2887	(A)	Pb-carbonate 35 (D)	9	π
		Pb-phosphate 70 (E)	7	β
		Mixture of (D) and (E)	16	$\pi + \beta$
		Ni-oxalate 15 (F)	6	ε
		Mg-borate 30 (G)	7	α
		Mixture of (F) and (G)	13	$\varepsilon + \alpha$
2896	(A)	Cd-phosphate 70 (H)	11	ν
	(A) followed by (H)	Bi-phosphate 15 (B)	3	ϱ
		Bi-oxalate 15 (C)	3	μ
		Mixture of (B) and (C)	6	$\varrho + \mu$
	(A)	Mixture of (B), (H) and (C)	17	$\varrho + \nu + \mu$
2896	(A)	Ba-phosphate 80 (I)	6.5	γ
	(A) followed by (I)	Pb-carbonate 35 (D)	5.5	π
		Pb-phosphate 70 (E)	5.5	β
		Mixture of (D) and (E)	11	$\pi + \beta$
	(A)	Mixture of (D), (I) and (E)	17.5	$\pi + \gamma + \beta$
2885	(A)	Co-carbonate 120 (K)	18	λ
	(A) followed by (K)	Ni-oxalate 15 (F)	3	ε
		Mg-borate 30 (G)	3	α
		Mixture of (F) and (G)	6	$\varepsilon + \alpha$
	(A)	Mixture of (F), (K) and (G)	24	$\varepsilon + \lambda + \alpha$
3858	(A)	Al-oxide $IIIb_6$ 110 (L)	20	η
	(A) followed by (L)	Al-oxide II 90 (M)	8	ζ
	(A)	Mixture of (L) and (M)	28	$\eta + \zeta$

The synergistic interrelationships between the nine remaining factors (ϱ—ν—μ—π—γ—β—ε—λ—α) indicate that the sum of activities adsorbed from strontium carbonate plasma by the respective selective adsorbents, would give erroneously high results for the combined activity of these nine factors. A correct estimate of this activity would require a nine-step adsorption procedure, starting with selective adsorption of ϱ-factor, followed by successive adsorption of the ν-, μ-, π-, γ-, β-, ε-, λ-, and α-factors, or by successive adsorption of these factors in the reverse order. The number of adsorption steps could be reduced to five, starting with selective adsorption of γ-factor, followed by successive adsorption of the π-, μ-, ν-, and ϱ-factors and of the β-, ε-, λ-, and α-factors in two parallel series of adsorption experiments. However, the limited stability of the labile factor activity of adsorbed plasmas [5] did not leave sufficient time for such multi-step adsorption procedures.

Another approach to this problem was suggested by the observation that adsorption of a labile factor by a selective adsorbent was unaffected by a

Table 4. Combined activity of the strontium carbonate non-adsorbable, labile factors; thromboplastin assay.

Adsorbent(s) in mg/ml *		Activity of adsorbed factor(s) in % of strontium carbonate adsorbed plasmas, Nos.:										Labile factor(s) adsorbed
		5898	5895	6190	6201	6324	6321	6329	6208[a]	6316[b]	3856	4155	
Mixture of (B), (H) and (C)		5	6	12.5	11	7	7	5	10	5	—	—	ϱ, ν, μ
Mixture of (D), (I) and (E)		28	18	14	13.5	20	14	17	15	19	—	—	π, γ, β
Mixture of (F), (K) and (G)		6	13	11.5	11.5	7	7	7	12	8	—	—	ε, λ, α
Mixture of (L) and (M)		38	37	35.5	36	45	43	41	34	51	40	31	η, ζ
Zn-tungstate	10	5	10	11.5	11	6	7	10	10	5	6.5	8	ϑ
Fe-oxide	20	12	12	11.5	11	6	14	11	12	6	6.5	8	ξ
Bi-sulfide	50	12	12	12.5	15	15	14	16	15	13	6.5	8	ω
Mg-borate	30	—	—	—	—	—	—	—	—	—	6.5	8	α
	Sum:	106	108	109	109	106	106	107	108	107	66	63	
	Max. expected [c]	104	106	108	108	105	105	104	107	104			
Al-oxide I	350	—	—	—	—	—	—	—	—	—	65.5	63	α,ϑ,ξ,ω,η,ζ

* Symbols (B)–(M) as in Table 3.
[a] Coumachlor plasma, thromboplastin coagulation time 175 min/100 (normal plasma 24–26).
[b] Vitamin K-deficient plasma, thromboplastin coagulation time > 10 min.
[c] 100 + 1/3 of the activities adsorbed by the [(B), (H), (C)] and [(F), (K), (G)] mixtures.

simultaneous adsorption of one or two other labile factors by selective adsorbents of other categories. Table 3 shows that the activity adsorbed by certain mixtures of selective adsorbents was equivalent to the sum of activities adsorbed in parallel or successive adsorptions using the individual components of these mixtures. The combined activity of the η- and ζ-factors could thus be determined by a one-step adsorption using a mixture of the respective selective adsorbents (see Table 3). Similarly, the activities of the ($\varrho-\nu-\mu$), ($\pi-\gamma-\beta$), and ($\varepsilon-\lambda-\alpha$) groups of factors could be determined separately by parallel one-step adsorptions using three adsorbent mixtures, each composed of selective adsorbents from three different categories of such compounds. The sum of the activities adsorbed by the latter three adsorbent mixtures will, however, not represent the correct value for the combined activity of the nine factors, since the synergistic effects of the μ- and π-factors and of ε- and β-factors are counted twice. Correct values might be obtained by successive adsorption of the three groups of factors, or by simultaneous adsorption of all nine factors by use of a single mixture containing all the corresponding nine selective adsorbents. However, neither of these two alternative procedures has been tried out experimentally. For routine work parallel adsorptions were preferred to more time-consuming procedures involving two or three successive adsorptions; and the chances of undesirable interactions between the adsorbents is presumably reduced by use of three mixtures of three adsorbents each, instead of the complex and rather voluminous mixture of nine adsorbents. The activities of the ($\varrho-\nu-\mu$) ($\pi-\gamma-\beta$), and ($\varepsilon-\lambda-\alpha$) groups of factors were consequently determined separately in parallel experiments. The combined activity

Table 5. Combined activity of the strontium carbonate non-adsorbable labile factors; Russell's viper venom (RVV)-cephalin assay.

Adsorbent(s) in mg/ml*		Activity of adsorbed factor(s) in % of strontium carbonate adsorbed plasmas, Nos.:										Active labile factor(s) adsorbed
		5906	5925	6183	6187	6201	6322	6330	6204[a]	4156	4155	
Pb-phosphate	70	9	9	8	20	15	12	10	11	7	7	β
Co-oxalate	100	20	18	11.5	10	15	12	10	12.5	37	31	λ
Mixture of (L) and (M)		29	38	50	52	42	44	54	39	32	32	η, ζ
Fe-oxide	20	21	19	11.5	10	10	10	8	14	11	15	ξ
Bi-sulfide	50	22	17	20	8	18	22	19	24	13	15	ω
	Sum:	101	101	101	100	100	100	101	100.5	100	100	
Al-oxide I	350	—	—	—	—	—	—	—	—	56	62	ξ, ω, η, ζ

* Symbols (L) and (M) as in Table 3.
[a] Vitamin K-deficient plasma, RVV-cephalin coagulation time 90 min/100 (normal plasma: 19—21).

of the η- and ζ-factors, and the activity of each of the ϑ-, ξ-, and ω-factors were determined as outlined above by simultaneous adsorption of four additional aliquots of the plasma. The sum of the adsorbed activities determined by this procedure will then exceed the correct values by the synergistic effects of the μ- and ε-factors on the π- and β-factor activities, respectively. This "excess activity" will be somewhat less than the combined activity of the μ- and ε-factors and, therefore, probably no more than one third of the combined activity of the $(\varrho-\nu-\mu)$ and $(\varepsilon-\lambda-\alpha)$ groups of factors.

Table 4 is a summary of representative experiments using chicken brain thromboplastin as assay accelerator and plasmas from chickens fed on a vitamin K-deficient diet or on various normal diets [6,7]. The experiments showed that the combined activity of the fourteen factors added up to 106—109 %. The results were thus slightly (1—3 %) above the expected maximum values, which in these experiments were estimated to be in the range of 104—108 %.

It is concluded, therefore, that the labile factor activity of strontium carbonate plasmas is adequately accounted for by the combined activity of the fourteen labile factors reported in previous papers. Table 4 also shows that the activity adsorbed by Al-oxide I is equivalent to the combined activity of the α-, ϑ-, ξ-, ω-, η-, and ζ-factors, in agreement with previous experiments [5].

Table 5 is a summary of experiments with RVV-cephalin as assay accelerator. The ϱ-, ν-, μ-, π-, γ-, ε-, α-, and ϑ-factors are inactive in this assay system [3-5], and the combined activity of the β-, λ-, η-, ζ-, ξ-, and ω-factors accounts for all labile factor activity of strontium carbonate plasmas. The activity adsorbed by Al-oxide I is equivalent to the combined activity of the ξ-, ω-, η-, and ζ-factors, as predicted by previous experiments [5].

Table 6. Combined activity of the strontium carbonate non-adsorbable labile factors; Russell's viper venom (RVV) assay.

Adsorbent(s) in mg/ml*		Activity of adsorbed factor(s) in % of strontium carbonate adsorbed plasmas, Nos.:										Active labile factor(s) adsorbed
		5927	6183	6190	6321	6329	6187	5895	6202[a]	3856	4152	
Co-oxalate	100	12	9	14	14	17	17	18	15	29	26	λ
Mixture of (L) and (M)		62	58	62	50	62	50	42	52	55	52	η, ζ
Fe-oxide	20	14	14	9	14	9	17	22	15	6	11	ξ
Bi-sulfide	50	12	19	15	22	13	17	18	18	10	11	ω
	Sum:	100	100	100	100	101	101	100	100	100	100	
Al-oxide I	350	—	—	—	—	—	—	—	—	71	74	ξ, ω, η, ζ

* Symbols (L) and (M) as in Table 3.

[a] Vitamin K-deficient plasma, RVV-buffer coagulation time 155 min/100 (normal plasma: 35—40).

Table 6 shows the results obtained with RVV, unsupplemented by cephalin. In the absence of added cephalin β-factor is inactive [3], and the combined activity of the λ-, ξ-, ω-, η-, and ζ-factors accounts for all labile factor activity of strontium carbonate plasmas *. The activity adsorbed by Al-oxide was equivalent to the combined activity of the ξ-, ω-, η-, and ζ-factors (*cf.* Ref.[5]).

DISCUSSION

The results presented here indicate that the labile factor activity of fresh oxalated chicken plasma is adequately accounted for by the combined activity of sixteen discrete labile factors, measured by chicken brain thromboplastin. Similarly, the labile factor activities measured with RVV-cephalin and RVV as assay accelerators, are accounted for by the combined activity of eight and of seven, respectively, of these sixteen factors. The experimental possibilities of a differentiation of the labile factor activity of chicken plasma by adsorption with selective adsorbents [2–5], thus seem to be exhausted.

Labile factor or proaccelerin activity of plasmas is generally recognized as the activity of a single entity: the labile factor or proaccelerin. The very complex nature of the labile factor activity of chicken plasma detected by adsorption analysis, may therefore appear surprising. However, chicken plasma differs from a number of mammalian plasmas in certain respects, *e.g.* by the absence of "contact activation" [10], and by low yield and slow formation of intrinsic plasma thromboplastin [11], due to deficiencies in prothromboplastic factors [10,11] (Hageman factor, PTA, and PTC). It is conceivable, therefore, that the hemostatic mechanism of chickens may depend on plasmatic coagulation factors (possibly labile) which are not present in mammalian plasma. They very rapid deterioration of chicken labile factor actitity (and of hemophilic factor A) during storage [2,11] indicate the further possibility that some of the factors which are labile in chicken plasma may correspond to factors which are stable in mammalian plasma, or at least not reduced below optimal levels during storage or incubation. A relation between mammalian labile factor activity and the chicken labile factors may probably be established through studies on the adsorption of mammalian labile factor activity by the selective adsorbents used for characterization of the chicken labile factors.

The individual labile factors in chicken plasma do not appear to be functionally identical, as judged by their complex interrelationships. These facts indicate that none of the labile factors can be replaced completely by any of the others. We are thus presented with the problem of assigning a specific function to each of sixteen labile coagulation factors. A possible clue to a future solution of this problem is suggested by the observed inactivity of the ϱ-, ν-, μ-, π-, γ-, ε-, α-, and ϑ-factors in the RVV-cephalin assay system [3–5]. These eight factors are accordingly thromboplastin specific and may be considered as cofactors for generation of possible intermediate activation products of thrombo-

* When the RVV assay is used, attention should be paid to the fact that the RVV coagulation time is sensitive to variations in the plasma levels of certain lipids [8,9]. Therefore, occasional failures to reach 100 % by the combined activity of the five labile factors, do not necessarily prove the existence of additional labile factors. Such results may be due to a very low concentration of active lipids in the stored plasma substrate compared to that of the fresh plasma employed.

plastin, one or more of which may have coagulant properties qualitatively similar to that of RVV-cephalin. The thromboplastin specific φ-factors [12] are probably also involved in these reactions, which may be analogous with the formation of convertin from proconvertin and thromboplastin in humans [13,14]. The λ-, ξ-, ω-, η-, ζ-, ν-, ψ- and σ-factors could then be regarded as co-factors for formation of prothrombin converting principle(s) (prothrombinase(s) [14]) from RVV-cephalin and from the above hypothetical intermediate activation product(s) of thromboplastin. Some of the latter group of factors might also be considered as possible accelerators of the fibrinogen-fibrin conversion. The inactivity of the β-factor in the RVV assay system [3] indicates that this factor is involved in reactions which only operate in the presence of added cephalin (as such, or in the form of thromboplastin).

The sixteen labile factors may not all be regarded as coagulation factors in the sense that a deficiency in one factor will cause a hemorrhagic diathesis or grossly abnormal plasma coagulation times. Reduction (by adsorption) of the ψ- and σ-factor levels of plasma to about 15 % of normal values had no effect on the thromboplastin coagulation time [2]. Complete adsorption of either of the two factors was associated with a minor prolongation of the thromboplastin coagulation time only. It appears unlikely, therefore, that the thromboplastin specific factors should all be essential for generation of RVV-cephalin equivalent activation products of thromboplastin, or that the β-, λ-, ξ-, ω-, η-, ζ-, ψ-, and σ-factors should all be indispensable for the transformation of these agents into prothrombin converting principles. It seems more likely that the formation of activation products of thromboplastin and of RVV may occur by more than one mechanism in chicken plasma. The labile factors could then be considered as parts of *alternative mechanisms* for formation of such activation products. Some of these mechanisms may not be expected to contribute significantly to observed coagulation rates of plasmas except under special experimental conditions. The accelerating effect of, *e.g.* β-factor is thus manifest only in plasma coagulation systems containing added cephalin.

So far no systematic approach has been made to the problem of elution of the adsorbed factors from the respective selective adsorbents, but unpublished data indicate that elution may be accomplished by use of phosphate buffers. However, the yields were low, presumably due to the labile nature of the factors, stressing the importance of using plasmas with high levels of labile factors for such studies. Great variations in the relative activities of the various factors were observed in different experiments [2–5]. These results diverted our immediate attention away from the elution problems and towards development of methods for quantitative determination of each of the sixteen labile factors, with the purpose of studying the causes of such variations. A series of forthcoming papers will be devoted to this subject.

REFERENCES

1. Sørbye, Ø., Kruse, I. and Dam, H. *Acta Chem. Scand.* **5** (1951) 487.
2. Sørbye, Ø. and Kruse, I. *Acta Chem. Scand.* **16** (1962) 1221.
3. Sørbye, Ø. and Kruse, I. *Acta Chem. Scand.* **16** (1962) 1468.
4. Sørbye, Ø. and Kruse, I. *Acta Chem. Scand.* **16** (1962) 1662.

5. Sørbye, Ø. and Kruse, I. *Acta Chem. Scand.* **16** (1962) 2025.
6. Sørbye, Ø. and Kruse, I. *Acta Chem. Scand.* **14** (1960) 2177.
7. Sørbye, Ø. and Kruse, I. *Acta Chem. Scand.* **15** (1961) 1517.
8. Macfarlane, R. G., Trevan, J. W. and Attwood, A. M. P. *J. Physiol.* **99** (1941) 7P.
9. Poole, J. C. F. *Brit. J. Exptl. Pathol.* **36** (1955) 248.
10. Didisheim, P., Hattori, K. and Lewis, J. H. *J. Lab. Clin. Med.* **53** (1959) 866.
11. Wartelle, O. *Rev. d'Hematol.* **12** (1957) 351.
12. Sørbye, Ø. *Acta Chem. Scand.* **16** (1962) 903.
13. Aas, K. *Prokonvertin og konvertin.* Thesis, Oslo 1952.
14. Hjort, P. F. *Scand. J. Clin. Lab. Invest.* **9** (1957) Suppl. 27 (Thesis).

Received July 5, 1962.

ACTA CHEMICA SCANDINAVICA 16 (1962) 2421–2428

Ozonolysis of Phenols

III. 1- and 2-Naphthol

ERLING BERNATEK and CARLY FRENGEN

Universitetets Kjemiske Institutt, Blindern-Oslo, Norway

1- and 2-naphthol have been ozonised in ethyl acetate at 3–4°. The ozonolysis fragments, carbon dioxide, formic, oxalic, *o*-carboxylcinnamic, *o*-formylcinnamic, phthalic, and phthalaldehydic acids as well as phthalaldehyde have been determined quantitatively. Combinations of common ozonolysis reactions types are proposed to explain qualitative and quantitatives results.

In our previous papers [1,2] in this series we have discussed the fate of some simple phenols when exposed to the action of ozone. It was found that the degradation products for the greater part consisted of rather small molecules such as carbon monoxide and dioxide, formic and oxalic acids, and some glyoxal. In the case of the dihydric phenols, catechol, resorcinol and quinol, there was a certain amount of products which remained unidentified, mainly because of their labile and untractable character. By introducing a relatively inert aromatic nucleus, as in 1- and 2-naphthol, it was hoped to obtain degradation products, which more easily could be isolated and identified. As will be seen from the present paper these expectations have been fulfilled and, especially in the case of 2-naphthol, the distribution of the carbon from the starting material can be accounted for in detail.

Dissolved in ethyl acetate both phenols absorbed ozone readily. The two first moles were consumed quantitatively, but after that point ozone escaped in increasing amounts. The total ozone consumption would probably have been large, leading to the complete destruction of the compounds under investigation. The experiments recorded here, however, are only concerned with the reactions which take place when one or two moles of ozone are applied.

After the ozonisation the solutions contained active oxygen and for both phenols in amounts corresponding roughly to half the absorbed ozone. The nature of the peroxidic compounds has not been investigated closely, but the existence of an ozonide cannot be excluded since hydrogen peroxide was formed by hydrolysis. On the other hand, the active product is remarkably stable only losing a few per cent of the activity in twenty-four hours. During this time traces of carbon monoxide were evolved. Small amounts of carbon dioxide were formed during the ozonisation.

Table 1. Reaction products from ozonolysis of 1- and 2-naphthol with 2 moles of ozone.

Reaction product	1-Naphthol moles/mole	1-Naphthol % recovered C	2-Naphthol moles/mole	2-Naphthol % recovered C
CO_2 (ozonolysis)	0.09	2.6	0.09	10.8
CO_2 (hydrolysis)	0.17		0.99	
Formic acid	1.80	17.8	0.92	9.2
Oxalic acid	—	—	0.04	0.9
o-Carboxylcinnamic acid	—	—	0.23	22.6
o-Formylcinnamic acid	—	—	0.15	15.2
Phthalaldehydic acid	(0.40)	(32)	—	—
Phthalic acid	0.59	46.6	0.15	11.9
Phthalaldehyde	—	—	0.34	27.1

The ozonisation mixture was treated with water at room temperature until the active oxygen had disappeared from the ethyl acetate layer. The aqueous layer gave initially a yellow coloration with titanium reagent, indicative of hydrogen peroxide. Further amounts of carbon dioxide were evolved during hydrolysis. From the aqueous layers were isolated formic and oxalic acids, while the ethyl acetate layer afforded *o*-carboxylcinnamic, *o*-formylcinnamic, phthalaldehydic and phthalic acids beside phthalaldehyde. The results from the quantitative determinations of these compounds are summarised in Table 1.

The values for phthalaldehydic acid are only tentative as this compound could not be determined directly. The mixture of non-volatile ozonolysis products from 1-naphthol were analysed for carbon and 78.9 % of the original carbon were found here. Together with the carbon recovered in the volatile compounds carbon dioxide and formic acid, this adds up to a carbon balance of 99.3 %. Phthalaldehydic acid is thus regarded as the difference between the total nonvolatile matter and phthalic acid. Probably this difference also encompasses minor amounts of unidentified products. Summation of the recovered carbon from 2-naphthol gives a carbon balance of 97.7 %. A determination of carbon content in the dry matter from this phenol amounts to 78.3 %, which together with the carbon from volatile products gives a carbon balance of 98.3 %.

From Table 1 it will be seen that the aromatic ozonolysis products from 1-naphthol evidently are the result of a reaction with two molecules of ozone since only two carbon atoms are left of the phenolic ring. Further the "aromatic balance" (*i.e.* the percentage of recovered aromatic ring per mole of naphthol) is excellent: 99 %. This is indicative of an exclusive attack on the hydroxylated ring leaving the unsubstituted ring intact. 1-Naphthol can of course be split up by ozone in a number of ways. If we take into account the three usual modes of ozonolysis, anomalous ozonolysis, acid-rearrangement and hydrolysis of an ozonide, at least 19 reaction combinations are theoretically possible. Only three of these are necessary, however, to explain our qualitative and quantitative results in a satisfactory way. If we use our customary shorthand for the reaction types:



anomalous ozonolysis acid-rearrangement hydrolysis of ozonide

we can represent the pertinent reaction combinations in the following way:

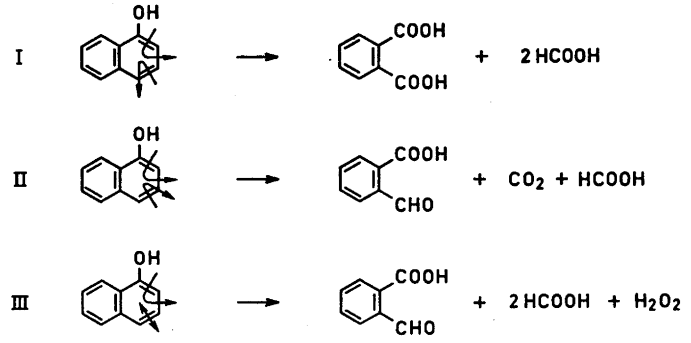

The bond adjacent to the hydroxyl group is probably attacked first and we have here in all three reaction schemes the same type of anomalous ozonolysis. This is to be expected in a bond of this type. At the other bond in question the attack evidently takes another course: acid-rearrangement which can take either course as in I and II or the formation of an ozonide with subsequent hydrolysis. Assuming that 59 % of the 1-naphthol follows scheme I, 26 % follows II and 15 % III, one gets the following quantitative distribution of reaction products in moles per mole of naphthol: Phthalic acid 0.59, phthalaldehydic acid 0.41, carbon dioxide 0.26, formic acid 1.74, hydrogen peroxide 0.15, in good agreement with the results in Table 1. It is noteworthy that no phenolic compound can have been formed in any appreciable amount as would have been the case if anomalous ozonolysis had taken either or both courses in scheme IV.

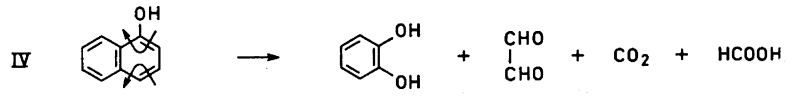

Finally we shall briefly discuss the oxygen balance. The number of oxygen atoms in the reaction products per mole of starting material is 7.98 (if we take into account the assumed 0.15 moles of hydrogen peroxide). On the side of reactants we have one atom of oxygen in the naphthol, six in the applied ozone and 1.15 in the water necessary for hydrolysis of the primary ozonisation products, which is 8.15 atoms in all and in fair agreement with the experimental results.

2-Naphthol gives relatively large amounts of the mono-ozonolysis products *o*-formylcinnamic acid *o*-carboxylcinnamic acids, which can be caused by a more tardy reaction of these compounds with ozone or by the consumption of ozone in side-reactions not leaving enough for complete cleavage of the phenolic ring. The aromatic balance points in this latter direction as it amounts only to 87 % indicative of a certain degradation of the entire naphthalene

ring system. Theoretically 2-naphthol can be split up by one molecule of ozone in nine different ways and by two molecules in nineteen ways (attack on the phenolic ring only), but only a limited number are necessary to explain the experimental results. Mono-ozonolysis seems exclusively to have taken place at the bond adjacent to the hydroxyl group, which is to be expected since this bond as in the case of 1-naphthol probably is attacked first. The only likely formation of the cinnamic acid derivatives is through a hydrolysis of ozonide and acid-rearrangement as in V and VI, respectively.

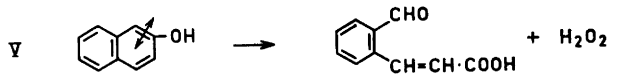



Phthalic acid can simply be formed through a double acid-rearrangement:



This leaves us with one molecule of glyoxylic acid, a substance which has not been detected among the reaction products. Glyoxylic acid, however, would react readily with hydrogen peroxide present in the hydrolysis mixture and become oxidised to carbon dioxide and formic acid.

Phthalaldehyde can theoretically be formed in five different ways two of which give identical products. As the main reaction we regard the following cleavage:

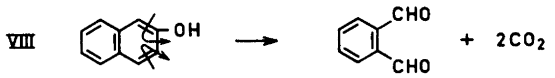

Through the mentioned four reaction schemes the experimental results can be explained qualitatively but still not quantitatively. The low value for the aromatic balance implies a reaction of the following type:

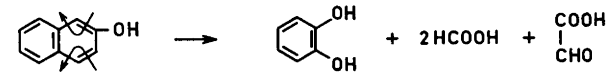

Catechol is readily attacked by ozone, the ozonolysis having been investigated by one of the present authors [2]. It was found that the dihydric phenol mainly was split up into formic acid and carbon dioxide while oxalic acid and glyoxal occurred in lesser amounts.

Assuming that 15 % of 2-naphthol is ozonolysed according to V, 23 % according to VI, 15 % according to VII, 34 % according to VIII and 13 % according to IX (with subsequent cleavage of catechol as previously described [2]), we arrive at the following distribution of reaction products in moles per mole of naphthol: Carbon dioxide 1.15, formic acid 0.79, *o*-formylcinnamic

acid 0.15, *o*-carboxylcinnamic acid 0.23, phthalic acid 0.15 and phthalaldehyde 0.34. Due to the chosen percentages of the different reactions the amounts of aromatics of course fit the experimental data exactly. On the other hand the value for carbon dioxide is too high and that for formic acid too low. Participation to a small extent of reaction X where less carbon dioxide is produced than in VIII and in addition one molecule of formic acid is formed, could give a very close agreement with the experiments.

X 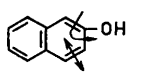 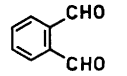 + CO_2 + HCOOH + H_2O_2

Oxalic acid is assumed to result from the degradation of catechol only, which gives an amount of about 0.025 moles as compared with the value in Table 1 of 0.04 moles.

Ozone consumption also need some comment since appreciable amounts mono-ozonolysis products are found. These products correspond to 38 % of the starting material, which could mean that 0.38 moles of the applied ozone have not reacted. If catechol is formed in an amount of 0.13 moles this will consume three molecules of ozone per molecule, *i.e.* in all 0.39 moles, which fits in nicely with the above mentioned value.

In checking the oxygen balance we find that ozonolysis products contain 6.8 atoms of oxygen per mole of starting material. The phenol contains one oxygen atom and the applied ozone six, in all seven atoms. Our chosen reaction paths require that some water enter into this balance. VIII will lead to the formation of one molecule of water, *i.e.* totally 0.34 moles. IX would need two moles of water for hydrolysis of primary products, in our case 0.26 moles. The further degradation of catechol requires one molecule, *i.e.* 0.13 moles. This is a negative balance of 0.05 moles, which does not materially affect our previous value. The water needed for formation of hydrogen peroxide in V and X do not enter the account as the peroxide is consumed in the oxidation of glyoxylic acid.

Ozonolysis with one mole of ozone led to the identification of no new compounds, but the relative amounts of the products were quite different

Table 2. Reaction products from ozonolysis of 1- and 2-naphthol with 1 mole of ozone.

Reaction product	1-Naphthol moles/mole	1-Naphthol % recovered C	2-Naphthol moles/mole	2-Naphthol % recovered C
CO_2 (ozonolysis)	—	—	—	—
CO_2 (hydrolysis)	0.05	0.5	0.16	1.5
Formic acid	0.85	8.5	0.53	5.2
Oxalic acid	—	—	—	—
o-Carboxylcinnamic acid	0.14	11.5	0.27	27.0
o-Formylcinnamic acid	—	—	0.52	51.8
Phthalaldehydic acid	+	+	—	—
Phthalic acid	—	—	—	—
Phthalaldehyde	—	—	0.03	2.4
Naphthol	+	+		17.5

from the previous results. Only for 2-naphthol a quantitative analysis has been carried out and even here the carbon balance is only 90 % due to the occurrence of some tarry matter. The analysis for carbon in the total non-volatile matter indicates that the percentage of recovered carbon actually is about 97. The same procedure gave for 1-naphthol a carbon balance of about 93 %. As expected certain amounts of unreacted naphthols also were found.

The values for 2-naphthol are calculated in relation to the amount of reacted material (82.5 %). This is not possible in the case of 1-naphthol since unreacted material has not been determined; the values refer to the initial amount of naphthol and are consequently too low.

A conspicuous feature in the mono-ozonolysis of 2-naphthol is the formation of rather large amounts of *o*-formylcinnamic acid and small amounts of phthalaldehyde as compared with the results in Table 1. It seems that *o*-formylcinnamic acid is a precursor for phthalaldehyde, which is compatible with the reaction schemes already proposed. If, as in V, an ozonide is formed at the 1,2-bond this can rearrange in the direction of the 2,3-bond and the reaction thus becomes indistinquishable from the anomalous ozonolysis indicated in VIII or X. The 3,4-bond can then be attacked with subsequent acid-rearrangement or formation of ozonide. A certain amount of rearrangement of ozonide is indeed to be reckoned with as the content of active oxygen after the ozonolysis is much greater than is inherent in the different reaction schemes presented in this paper. The absence of phthalic acid is countered by the increased amount of *o*-carboxylcinnamic acid even if the increase is not so great as could be expected. Reaction scheme VI explains this as it in the initial stage is a precursor for reaction VII.

The carbon balance for mono-ozonolysis of 2-naphthol is not too good, only about 88 %, while elemental analysis for carbon in the sum of non-volatile products leads to a total carbon balance of 97 %.

A new feature in Table 2 is the formation of *o*-carboxylcinnamic acid from 1-naphthol in quite considerable amounts. It can be a precursor for phthalic as well as phthalaldehydic acid.

Wiley and Hobson [3] prepared in 1949 *o*-formylcinnamic acid by a Perkin condensation of phthalaldehyde and malonic acid in the presence of pyridine. Their product had m.p. 163—164°C, while the substance we have designated *o*-formylcinnamic acid has m.p. 124—125°C. The formation of the latter compound from a cyclic compound with a mild reagent like ozone followed by a cautious working-up procedure strongly suggest that it is the *cis*-compound, *o*-formyl-*allo*-cinnamic acid. On the other hand the acid from the Perkin reaction must be the *trans*-compound. The difference in melting points can well be explained by this assumption. As mentioned in the experimental part, the infra-red spectrum shows a carbonyl absorption at 1700 cm^{-1}. This is indicative of a lactol carbonyl in a strain-free ring. A lactol form of the acid as XI is therefore very probable and confirmed by the hydroxyl absorption at 3200 cm^{-1}. Only the *cis*-form can possibly form such a lactol.

XI 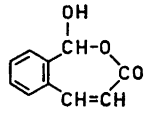

EXPERIMENTAL

Ozonolysis. The ozonisation technique and the decomposition with water are described in a preceding communication [1].

Ozone absorption was measured by leading the effluent gases into aqueous potassium iodide, which was changed every third minute and the liberated iodine titrated. Until about 1.8 moles of ozone per mole of naphthol had been applied, virtually no ozone escaped and when 2.17 moles had been applied 2.12 moles had been absorbed in the case of both naphthols. Of 2.79 moles 2.58 moles were absorbed by 1-naphthol and 2.63 moles by 2-naphthol.

Active oxygen was determined by pipetting aliquots of the ozonised solution into sodium iodide in glacial acetic acid and titrating liberated iodine. 1-Naphthol gave 0.63 and 2-naphthol 0.52 g atoms active oxygen per mole of starting material. After standing for 24 h both solutions contained 0.48 g atoms of active oxygen.

Determination of products. The determinations of carbon dioxide during ozonisation and decomposition, formic and oxalic acids were performed as before [1]. Volatile products were determined from ozonolysis of 1 g of naphthol and non-volatile products from 10 g.

A. 1-Naphthol

(*a*) With 1 O_3: Carbon dioxide during ozonisation nil, during hydrolysis 14, 15, 17, and 12 mg. Formic acid 259, 291, 276, and 257 mg. Oxalic acid nil.

(*b*) With 2 O_3: Carbon dioxide during ozonisation 29, 30, 28, and 29, during hydrolysis 54, 55, 46, and 48 mg. Formic acid 706, 553, 552, and 467 mg. Oxalic acid nil.

B. 2-Naphthol

(*a*) With 1 O_3: Carbon dioxide during ozonisation nil, during hydrolysis 42 41, 40, and 41 mg. Formic acid 106, 157, 157, and 135 mg. Oxalic acid nil.

(*b*) With 2 O_3: Carbon dioxide during ozonisation 40, 21, 24, 33, 28, and 33 mg, during hydrolysis 275, 328, 279, 314, 299, 311, and 277 mg. Formic acid 329, 230, 302, and 319 mg. Oxalic acid 266, 288, and 286 mg.

o-*Carboxylcinnamic acid.* This acid was found in the ethyl acetate layer after hydrolysis of the ozonisation mixture. The ester phase was extracted with aqueous sodium bicarbonate and the extract acidified with concentrated hydrochloric acid to pH *ca.* 1. In some cases a small precipitate was formed at this point. The acidified solution was extracted with ethyl acetate and the extract dried and evaporated. The residue was extracted with boiling water and the undissolved part was combined with the material immediately separating from the aqueous extract. Recrystallisation first from acetone-carbon tetrachloride and thereafter from large amounts of water (charcoal) gave a white, crystalline substance with m.p. 192°C. (Found: C 62.4; H 4.1; *E* 96. Calc. for $C_{10}H_8O_4$: C 62.5; H 4.2; E_{dibasic} 96.) The precipitates from the acidified bicarbonate extracts contained mainly this substance. $C_{10}H_8O_4$ decolorised permanganate instantaneously. The infra-red spectrum (Nujol) showed the following absorption bands: Carboxyl group 3300—2200, 1690, 1280, and 920 cm^{-1}. C—C double bond in conjugation with the aromatic nucleus 1631 cm^{-1}. Aromatic absorption 1601, 1576, and 1487 cm^{-1}. *Ortho*-disubstitution 758 cm^{-1}.

Yields: 1-Naphthol (1 O_3) gave 1.84 g. 2-Naphthol (1 O_3) gave 2.96 g, (2 O_3) 3.07 and 3.01 g.

o-*Formylcinnamic acid.* The aqueous extract from the above experiment was, after separation of *o*-carboxylcinnamic acid, extracted with ethyl acetate. This extract was in turn extracted with a small amount of concentrated aqueous sodium bicarbonate, which upon acidifying with 6 N hydrochloric acid to pH ca. 4 gave a white precipitate. Recrystallised from water (charcoal), m.p. 124—125°C. Long white needles. (Found: C 67.9; H 4.7; *E* 177. Calc. for $C_{10}H_8O_3$: C 68.2; H 4.5; *E* 176). The substance gave a 2.4-dinitrophenylhydrazone, which recrystallised from alcohol had m.p. 214°C (decomp.) (Found: C 54.2; H 3.4; N 15.7. Calc. for $C_{16}H_{12}N_4O_6$: C 53.9; H 3.4; N 15.7). Some $C_{10}H_8O_3$ was

contained in the precipitates from the acidified bicarbonate solution mentioned in the foregoing experiments. The infra-red spectrum (KBr-pellet) showed the following absorption bands: Hydroxyl 3200 cm^{-1}. Conjugated lactone (lactol) carbonyl in strain-free ring 1700 cm^{-1}. Conjugated double bond and α,β-unsaturated ester 1642 and 821 cm^{-1}, respectively. Aromatic absorption 1600 and 1570 cm^{-1}. *Ortho*-disubstitution 745 cm^{-1}. Yields: 2-Naphthol (1 O_3) gave 5.22 g, (2 O_3) 1.86 g.

Phthalaldehyde. The ethyl acetate layer, which after the hydrolysis had been exhaustively extracted with saturated aqueous sodium bicarbonate, was dried and evaporated. Light yellow oil, which for the greater part crystallised and consisted of fairly pure phthalaldehyde. A sample was sublimated at 50 – 60°C and 10 mm Hg. Light yellow needles, m.p. 54 – 56°C, which gave a precipitate with 2,4-dinitrophenylhydrazine, reduced Tollens' and Schiff's reagents and gave a characteristic green coloration of the skin. (Found: C 71.6; H 4.6. Calc. for $C_8H_6O_2$: C 71.6; H 4.5). The substance was readily oxidised to phthalic acid by Beckmann's reagent. Further amounts of phthalaldehyde were found in the aqueous decomposition solution and isolated by extraction with ether. This fraction contained traces of *o*-carboxylcinnamic and oxalic acids. Yields: 2-Naphthol (1 O_3) gave 0.23 g, (2 O_3) from ethyl acetate 1.77, 1.57, 1.86, and 1.83 g, from water 1.42 and 1.36 g.

Phthalaldehydic acid. After the hydrolysis the ethyl acetate layer was evaporated to dryness and the residue extracted with chloroform. The extract left upon evaporation a crystalline substance which was sublimated *in vacuo*. Small white crystals, m.p. 88°C. (Found: C 63.4; H 4.1. Calc. for $C_8H_6O_3$: C 64.0; H 4.0). The sublimate evidently consisted of somewhat impure phthalaldehydic acid. It easily formed an oxime with m.p. 120°C, undepressed on admixture with an authentic sample. 2,4-Dinitrophenylhydrazone, m.p. 255°C. (Found: C 50.8; H 3.3; N 16.2. Calc. for $C_{14}H_{10}N_4O_6$: C 50.9; H 3.3; N 17.0). The sample with m.p. 88°C was subjected to repeated sublimations *in vacuo* and thereafter identified as phthalaldehydic acid by its infra-red spectrum. In substance phthalaldehydic acid was isolated only from the ethyl acetate after ozonolysis of 1-naphthol with two moles of ozone while it was identified through its oxime in the aqueous layer. Likewise after ozonolysis of 1-naphthol with one mole of ozone, the acid was identified through the oxime.

Phthalic acid. The acid filtrate from the isolation of *o*-formylcinnamic acid was exhaustively extracted with ether and the collected extracts dried and evaporated. A crystalline mass resulted, which was triturated with chloroform leaving a greyish crystalline substance. Recrystallised from acetone-carbon tetrachloride and water. White crystals. M.p. 192°C alone and in admixture with an authentic sample of phthalic acid. The identity of the substance was confirmed by its infra-red spectrum. (Found: *E* 84. Calc. for $C_8H_6O_4$: 83). Yields: 1-Naphthol (2 O_3) gave 6.71 g and 2-naphthol (2 O_3) 1.83, 1.60 g.

Unreacted naphthols. (*a*) 1-Naphthol. The ethyl acetate after treatment with water and extraction with aqueous sodium bicarbonate was evaporated. The resulting syrupy mass was dissolved in sodium hydroxide (2 N), diluted with water and acidified with hydrochloric acid. The violet precipitate was recrystallised from dilute alcohol and sublimated *in vacuo*. Long colourless crystals. M.p. 88 – 90°C alone and mixed with an authentic specimen of 1-naphthol.

(*b*) 2-Naphthol. After evaporation of the ethyl acetate as in the above experiment the resulting mass was sublimated *in vacuo* (1 mm Hg) at 100 – 110°C and afforded a white crystalline substance. Recrystallised from water. M.p. 121°C alone and in mixture with an authentic specimen of 2-naphthol. The picrate had m.p. 155°C, undepressed in mixture with 2-naphthol picrate. Yields: 1.76, 1.72, and 1.75 g.

The authors' thanks are due to Mag. sc. Else Augdahl for the determination of infra-red spectra.

REFERENCES

1. Bernatek, E. and Frengen, C. *Acta Chem. Scand.* **15** (1961) 471.
2. Bernatek, E., Møskeland, J. and Valen, K. *Acta Chem. Scand.* **15** (1961) 1454.
3. Wiley, R. H. and Hobson, P. H. *J. Am. Chem. Soc.* **71** (1949) 2429.

Received June 6, 1962.

ACTA CHEMICA SCANDINAVICA 16 (1962) 2429–2433

Chloride-Bromide Exchange Equilibria in Binary Molten Salts

The Experimental Method. The System LiCl, LiBr, HCl, HBr

T. FØRLAND, B. SAETHER, O. FYKSE, A. BLOCK-BOLTEN, J. M. TOGURI and H. FLOOD

Royal Norwegian Council for Scientific and Industrial Research, Institute for Silicate Science, The Technical University of Norway, Trondheim, Norway

The equilibrium LiBr(l) + HCl(g) = LiCl(l) + HBr(g) has been studied at 800°C and at various ratios of p_{HBr}/p_{HCl}. The equilibrium constant was found to vary with the composition of the salt melt. The ideal equilibrium constant was found to be $\ln K_{800°C} = +0.35$.

The variation of $\ln K$ with composition corresponds to a positive deviation from ideality in the binary system LiCl-LiBr.

The development of the theory of molten salt mixtures and a critical evaluation of existing theories have been limited by the lack of experimental data. For example, the exploration of the effect of such factors as charge, radius, and polarizability of ions on the deviation from ideality in fused salt systems are still in the embryonic stage. It was anticipated that from a study of anion exchange equilibria, some new information might be obtained about these effects.

The experimental work was started by B. Saether and the techniques were subsequently improved during the time that O. Fykse, A. Block-Bolten and J. Toguri worked on the project. The data to be presented here originate from the last period only.

From an investigation of the equilibrium reaction of the type

$$MeBr(l) + HCl(g) = MeCl(l) + HBr(g)$$

one can determine the values of $p_{HBr}.N_{MCl}/p_{HCl}.N_{MBr}$ as a function of the composition of the fused salt mixture. (N = molefraction, p = partial pressure.) Assuming the (Br-Cl) mixture to form regular solutions, the energy of mixing of pure MeCl and MeBr may be estimated where Me might be either a single cation or a mixture of several cations. Further the validity of the regular solution equation may be checked by such measurements.

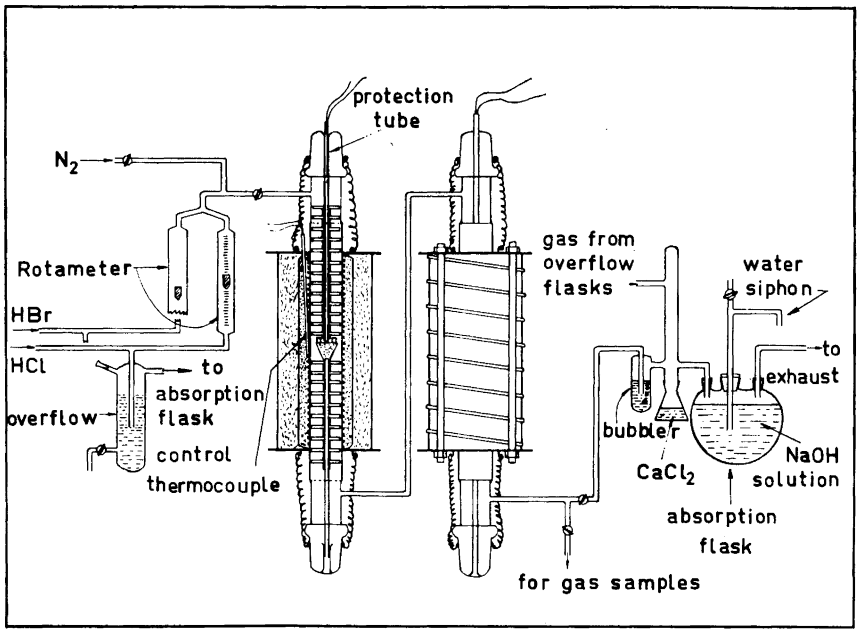

Fig. 1. Apparatus.

In the present paper a detailed account of the experimental procedure is given together with results for the system LiCl-LiBr. Results for the other alkali and alkaline earth systems will be presented in a following communication.

EXPERIMENTAL

The experimental procedure which seemed to be most suitable for the equilibrium studies, was the flow method. The components HCl and HBr were taken from cylinders at a constant flow rate, mixed and passed over the liquid salt mixtures, which were maintained at a constant temperature, until equilibrium was established.

A diagram of the apparatus is shown in Fig. 1. Two ordinary resistance furnaces were utilized (see Fig. 1). With these furnaces a constant temperature zone ($\pm$ 1°C) of 6 cm was readily obtained. A control thermocouple, placed between the windings of the furnace and insulation, was connected to a Kent two point controller which regulated the temperature. The actual temperature was determined by a chromel-alumel thermocouple protected by an alumina sheath, and placed into the sample holder as shown in the diagram. Baffles made from dense porcelain were used to minimize heat losses as well as to insure mixing of the gases utilized.

The system is essentially an all glass construction. A ceramic to glass seal connects the Haldenwanger High Temperature Porcelain furnace tube to the apparatus. Minimum number of stopcocks were utilized, and where required, stopcocks with teflon were used. All joints were lubricated with Florube grease. This grease was not attacked by the HCl and HBr gases.

The flow of HCl and HBr was controlled by means of rotameter tubes with tantalum floats obtained from Rotameter Manufacturing Co. Ltd. The pressure was regulated by means of a sealed overflow tube containing Shell Risella oil 27 which was found to be chemically inert.

A line supplying purified nitrogen was added to the system to permit flushing of the system.

The samples were contained in platinum cups 1 cm in diameter by 1 cm in height. Platinum lids with holes were used to cover the sample in order to minimize possible transfer of salts from one crucible to another crucible *via* the gas phase.

A flask containing NaOH solution served to absorb the HCl and HBr. To prevent moisture from entering into the system, a $CaCl_2$ trap was placed between the absorption flask and bubbler with Shell Risella oil 27. The latter also served this function.

The cylinders of anhydrous HBr and HCl gases were obtained from Matheson Co. Inc., East Rutherford N. J., U.S.A. The analysis of these gases are as follows.

HBr – 99.9 %, contains no free bromine or moisture, the principle impurity being nitrogen.

HCl – 99.3 %, inerts 0.2 %, CO_2 0.5 %.

The LiCl used throughout this investigation was Fisher certified Reagent grade.

All experiments reported in this communication were carried out at 800 ± 2°C, which corresponds to an error of ± 0.02 in ln K_K. The course of a typical experiment was as follows: Samples of approximately 0.5 g of pure LiCl were placed into platinum crucibles. The crucibles with their lids were then placed into the furnace and the system flushed with N_2 gas for approximately 4 h. During this period the furnace temperature was raised to 800°C. At this point the N_2 flow was stopped and the HCl and HBr gas flow of desired HBr/HCl ratio was started. The total flow rate used throughout the present study was of the order of 100–200 ml/min, a rate sufficient to prevent thermal diffusion errors. The experiments were then allowed to continue for 5–6 h, a period of time found to be sufficient for establishing equilibrium. Although rotameters were used, the actual ratio of HBr/HCl was determined for each experiment by sampling the gas after it has passed through the reaction zone. A number of gas samples were taken at various periods during the experiment. After the equilibration period, the HBr and HCl gas mixture was exchanged with nitrogen and the system flushed. Then the furnace temperature was decreased.

The ratio of Br/Cl in the salt mixtures was determined by chemical analysis. This was accomplished by titrating potentiometrically with $AgNO_3$. The equivalent point was determined according to a method worked out by Lydersen (to be published).

Table 1. Summary of results.

Gas phase		Salt mixture				
% Br	p_{HBr}/p_{HCl}	% Br	N_{Cl}/N_{Br}	K'	ln K'	$N_{Cl}-N_{Br}$
69.85	2.317	77.30	0.294	0.680	−0.385	−0.546
63.07	1.708	71.34	0.402	0.686	−0.377	−0.427
60.43	1.527	68.92	0.451	0.689	−0.373	−0.378
59.91	1.494	68.48	0.460	0.688	−0.374	−0.370
52.08	1.087	60.96	0.640	0.696	−0.362	−0.219
50.10	1.004	59.03	0.694	0.697	−0.361	−0.181
41.19	0.700	49.71	1.012	0.709	−0.344	+ 0.006
40.68	0.686	49.26	1.030	0.706	−0.348	+ 0.015
37.98	0.612	46.37	1.157	0.708	−0.345	+ 0.073
33.07	0.494	40.80	1.451	0.717	−0.333	+ 0.184
31.56	0.461	39.20	1.551	0.715	−0.335	+ 0.216
30.29	0.434	37.78	1.647	0.716	−0.335	+ 0.244

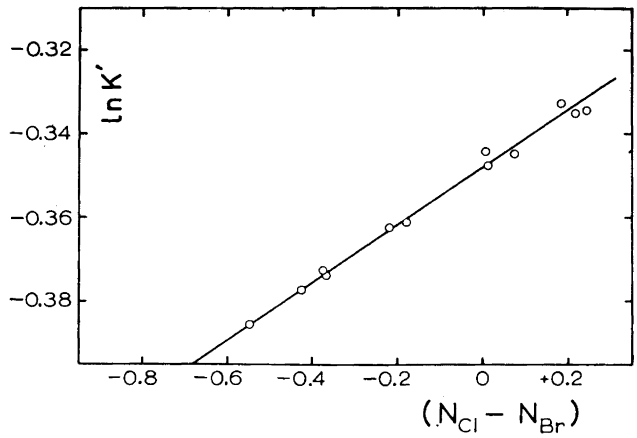

Fig. 2. $\ln K' = \ln N_{Cl}p_{HCl}/N_{Br}p_{HBr}$ in dependence of $(N_{Cl}-N_{Br})$.

RESULTS

The experiments were conducted at 800°C over a p_{HBr}/p_{HCl} range of approximately 0.43—2.32. The results are tabulated in Table 1.

The equilibrium concerned in this study is

$$LiBr(l) + HCl(g) = LiCl(l) + HBr(g) \quad (1)$$

for which the equilibrium constant is

$$K_a = (p_{HBr}/p_{HCl}) \times (a_{LiCl}/a_{LiBr}) = \underbrace{(p_{HBr}/p_{HCl}) \times (N_{Cl}/N_{Br})}_{K'} \times (\gamma_{LiCl}/\gamma_{LiBr}) \quad (2)$$

where N_{Br} and N_{Cl} are ionic fractions of the respective Br^- and Cl^- ions in the melt, and γ is the activity coefficient.

On the assumption of regular solution, and symmetrical activity functions of composition, the acitivity coefficients can be replaced by expression of the following type.

$$RT \ln \gamma_{LiBr} = b_{Li}N_{Cl}^2 \quad (3)$$

where b_{Li} is a constant.

Hence

$$\ln K' = \ln \frac{p_{HBr}}{p_{HCl}} \cdot \frac{N_{Cl}}{N_{Br}} = \frac{b_{Li}}{RT}(N_{Cl} - N_{Br}) + \ln K_a \quad (4)$$

In eqn. (4) the ratio p_{HBr}/p_{HCl} and all the concentration terms are known experimentally. Thus by plotting $\ln [p_{HBr}/p_{HCl} \times N_{Cl}/N_{Br}]$ against $(N_{Cl}-N_{Br})$ a straight line with slope equal to b/RT should be obtainable. $\ln K'$, the ideal equilibrium constant, should then correspond to the intercept of the experimental line at $(N_{Cl}-N_{Br}) = 0$.

The present results are plotted in this manner, as shown in Fig. 2 and in Table 1. From a least square analysis, the following values are obtained for the equilibrium constant

$$\ln K_a = 0.348 \pm 0.005$$

From this the value $b_{\mathrm{Li}} = 150 \pm 25$ kcal/mole is obtained.

The positive value of b_{Li} corresponds to an endothermic heat of mixing for pure liquid LiCl with pure liquid LiBr.

However, the significance of this data will be discussed in a following communication which will also report the results for other alkali bromide-chloride systems.

Acknowledgement. One of the authors (J.M.T.) is grateful to the *Royal Norwegian Council for Scientific and Industrial Research* for a Post Doctorate Fellowship.

We are also grateful to *Borgestad legat* for financial support of the analytical work.

Received May 28, 1962.

ACTA CHEMICA SCANDINAVICA 16 (1962) 2434–2451

Calcium, Magnesium, and Manganese(II) Complexes of Some O-Phosphorylated Peptides *

RAGNAR ÖSTERBERG

Department of Medical Biochemistry, University of Göteborg, Sweden

Complex formation between calcium, magnesium, and manganese(II) ions and O-phosphorylated ethanolamine, seryllysine, serylglycine, glycylserine, glycylserylglycine and serylglutamic acid has been measured by pH titration at 25° in an ionic medium, whose anion concentration, [Cl^-], was kept constant by potassium chloride, and whose initial ionic strength was 0.15 M. The experimental data could be explained by assuming that complexes of the type M_pH_qA are formed, where $(p;q)$ = (1;1), (1;0) for the first two ligands, $(p;q)$ = (1;1) (1;0), (2;0) for the next three ligands ($(p;q)$ = (2;0) was not measurable, when M = Ca^{2+}), and $(p;q)$ = (1;2), (1;1), (1;0), (2;1), (2;0) for the last ligand. The stability constants of the complexes have been computed, and the coordination sites are discussed.

The observed differences in complexity between the calcium and magnesium ions support Williams' conclusion [1] that their complexing ability can be correlated to ionic size. The definitely greater tendency of magnesium and manganese(II) to dinuclear complex formation as compared to calcium is discussed in relation to the specificity of enzymes for these metal ions.

Most enzyme reactions, which involve phosphorylated substrates, have an absolute requirement for divalent metal ions, in general, magnesium, calcium or manganese (see Refs.[1–3], for review). In some such systems the metal ion is assumed to activate by forming a ternary complex, coordinating both the substrate phosphoryl and some enzyme protein groups [1]. The relative catalytic activity of these metal ions varies, however, from enzyme to enzyme, and in some cases one of them can even completely inhibit the action of one other [1–3]. In respect to magnesium and calcium this contrary action does not agree with their similarity in chemical reactions and electron configuration of the outer shell.

Williams recently explained the enzymic calcium/magnesium specificity on the basis of ionic size [1]. He suggested that the larger calcium ion forms com-

* Presented in part at the Vth International Congress of Biochemistry, Moscow, August 10–16, 1961.

Table 1. Ligands.

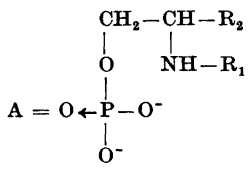

Ligand	Abbreviation	R_1	R_2
O-Phosphorylethanolamine	P-ethanolamine	$-H$	$-H$
O-Phosphoryl-D,L-serylglycine	SerP-Gly	$-H$	$-CO-NH-CH_2-COO^-$
O-Phosphoryl-L-seryl-L-glutamic acid	SerP-Glu	$-H$	$-CO-NH-CH(CH_2-CH_2-COO^-)-COO^-$
O-Phosphoryl-L-seryl-L-lysine	SerP-Lys	$-H$	$-CO-NH-CH((CH_2)_4-NH_3^+)-COO^-$
Glycyl-O-phosphoryl-D,L--serylglycine	Gly-SerP-Gly	$-CO-CH_2-NH_2$	$-CO-NH-CH_2-COO^-$
Glycyl-O-phosphoryl-D,L-serine	Gly-SerP	$-CO-CH_2-NH_2$	$-COO^-$

plexes different from those of the magnesium ion by the coordination of more dentate groups. On the other hand, no systematic study appears to have been undertaken on the complex formation between these metal ions or between Mn(II) and such phosphorylated ligands that include different types of metal binding groups present in proteins. Therefore, calcium, magnesium, and manganese(II) complexes of some O-phosphorylated peptides have been investigated and the results interpreted quantitatively in the form of stability constants. The ligands studied are shown in Table 1.

SYMBOLS *

A	ligand, see Table 1
a	molar concentration of free A
h	molar concentration of free hydrogen ions
M	complex forming metal ion: Ca^{2+}, Mg^{2+} or Mn^{2+}
m	molar concentration of free M
p,q	number of metal and hydrogen ions bound in M_pH_qA
Q,S,T	maximum number of q in H_qA, MH_qA and M_2H_qA, see eqn. 1
r	number of hydrogen ions bound in M_pH_rA; $p \neq 0$
C_A	total molar concentration of ligand $= \sum_{p=0} \sum_{q=0} [MpHqA]$
C_M	total molar concentration of metal ions $= m + \sum_{p=1} \sum_{q=0} p[M_pH_qA] + [MOH]$

* All charges are omitted for the sake of convenience.

C_S total molar concentration of bound hydrogen ions =
$= \sum_{p=0} \sum_{q=1} q[M_pH_qA] - [MOH] = jC_A - [KOH] - h + [OH]$
where j is the number of dissociable hydrogen ions bound to the ligand A form in solide state, and [KOH] the molar concentration of KOH added.

Z ligand number $= \sum_{p=1} \sum_{q=0} [M_pH_qA](m + \sum_{p=1} \sum_{q=0} p[M_pH_qA] + [MOH])^{-1}$, see eqn. 6

$b_{M_pH_qA}$ stoichiometric stability constant of the complex
$M_pH_qA = [M_pH_qA]m^{-1}([M_{p-1}H_qA])^{-1} = \varkappa_{pq_1}(\varkappa_{(p-1)q_1})^{-1}$; $p \neq 0$

$K_{M_pH_qA}$ stoichiometric acid ionization constant of M_pH_qA
$= h[M_pH_{q-1}A]([M_pH_qA])^{-1} = \varkappa_{p(q-1)_1}(\varkappa_{pq_1})^{-1}$; $q \neq 0$

$*K_1$ stoichiometric hydrolysis constant $= [MOH]hm^{-1}$

$*K_{MA}$ stoichiometric hydrolysis constant $= [MAOH]h([MA])^{-1}$

$pK_{M_pH_qA}$ $= -\log K_{M_pH_qA}$

$\varkappa_{pq_1}$ stoichiometric equilibrium constant, defined by eqn. 3, $\varkappa_{100} = \varkappa_{010} = \varkappa_{001} = 1$

φ_r defined by eqn. 4a

METHOD

pH titrations [4] were carried out for the values of C_A and C_M, as shown in Table 2. In each titration these quantities were held practically constant, and h and C_S were varied by additions of potassium hydroxide. Activity coefficients were assumed to be constant by keeping the concentration of the negatively charged counter-ion (Cl^-) constant [5] with potassium chloride at a value, which corresponded to 0.15 M initial ionic strength.

If mononuclear and dinuclear complexes only are formed, the following equilibria (*cf.* discussion on pp. 2445–2449) may be successively present during the titration process:

$$\left\{H_QA\right\} \rightleftharpoons \ldots \rightleftharpoons \left\{\begin{matrix} H_SA \\ MH_SA \end{matrix}\right\} \rightleftharpoons \ldots \rightleftharpoons \left\{\begin{matrix} H_TA \\ MH_TA \\ M_2H_TA \end{matrix}\right\} \rightleftharpoons \ldots \rightleftharpoons \left\{\begin{matrix} A \\ MA \\ M_2A \end{matrix}\right\} \quad (1)$$

where $Q > S > T$. The complex formation is summarized by

$$pM + qH + A \rightleftharpoons M_pH_qA \quad (2)$$

and is defined by the equilibrium constants

$$\varkappa_{pq_1} = \frac{[M_pH_qA]}{m^p h^q a} \quad (3)$$

p and q may attain values, which conform to eqn. 1, *i.e.* ($p = 0$; $q = 0, 1, \ldots, Q$), ($p = 1$; $q = 0, 1, \ldots, S$), ($p = 2$; $q = 0, 1, \ldots, T$).

In accord with eqn. 1, pH regions are selected, where M_pH_rA ($r = S, S-1, \ldots, 0$) species successively dominate and metal complexes with $q < r$ can be neglected [6]. In each region $\varkappa_{1r1}$ and $\varkappa_{2r1}$ are solved by (*cf.* eqn. 7a in Ref.[6])

$$\frac{Z(1 + *K_1h^{-1})}{(1-Z)ah^r} - \sum_{q=r+1}^{S} \varkappa_{1q_1}h^{q-r} - \sum_{q=r+1}^{T} \frac{(1-2Z)}{(1-Z)} \varkappa_{2q_1}mh^{q-r} = \frac{m(1-2Z)}{(1-Z)} \varkappa_{2r1} + \varkappa_{1r1} \quad (4)\ *$$

using data of two or more C_M. In general $\varkappa_{1r1}$ is first computed from measurements with $C_M \sim C_A$, and then $\varkappa_{2r1}$ from titrations with $C_M \geq 5C_A$, where $m \approx C_M$. Alternatively,

* In the following all equations assume occurrence of MOH species, and that $*K_1$ is known from the literature.

$\varkappa_{1r1}$ and $\varkappa_{2r1}$ are obtained from two series of measurements with $C_M \geqslant 5C_A$. The left hand side is easily determined, as a and Z can be computed from known, (C_A, C_M, $\varkappa_{pq1}$; $q > r$, if $p \neq 0$), and measured, (h, C_S), quantities.

When $C_M \geqslant 5C_A$, the following equations are used [6]

$$a = \frac{C_S - rC_A + {}^*K_1 mh^{-1}}{\sum_{p=0} \sum_{q=0} (q-r)\varkappa_{pq1} m^p h^q} \quad (q > r, \text{ when } p = 1,2) \tag{5}$$

$$Z = \frac{C_A - a \sum_{q=0} \varkappa_{0q1} h^q}{C_M} \tag{6}$$

The $\varkappa_{0q1}$ are obtained from pK values, computed from a titration in the absence of complex forming metal ions. $\varkappa_{pq1}$ ($q > r$) are known from calculations performed on data in lower pH regions. The quantity $m \approx C_M$ may be better approximated by the relation

$$m = C_M - Z'C_M - am^2 \sum_{q=r} \varkappa_{2q1} h^q - {}^*K_1 mh^{-1} \tag{7}$$

where Z' is an approximate value of Z. The m value obtained is refined by successive approximation *.

When $C_M \sim C_A$, dinuclear species may be neglected. For $r < S$, a and Z are solved for each measuring point from the intersection of the $Z(a)_{C_S,h}$ curves of eqn. 6 and the following equation [6]:

$$Z = 1 - \frac{\left[C_S - rC_A - a \sum_{q=0}^{Q} (q-r)\varkappa_{0q1} h^q\right]\left[1 + {}^*K_1 h^{-1}\right]}{C_M\left[a \sum_{q=r+1}^{S} (q-r)\varkappa_{1q1} h^q - {}^*K_1 h^{-1}\right]} \tag{8}$$ **

For $r = S$ eqns. 5 and 6 are used.

EXPERIMENTAL

Material. The phosphorylated compounds were those synthesized by Fölsch [7-10]. Analytical data for O-phosphorylated glycylserine and glycylserylglycine have been given in Ref.[7], and for O-phosphorylated ethanolamine in Ref.[9] O-Phosphorylated serylglutamic acid and seryllysine were freed from minor impurities before titration and converted to free and hydrochloride forms, respectively, by means of cation exchange chromatography [10]; analytical data were reported in Ref.[10]

A new preparation of O-phosphorylserylglycine, which had been run through a cation exchange column (Dowex 50-X2, H^+-form, 1.6 × 40 cm, eluted with water) moved as one spot (0.5 mg applied) at paper chromatography, exactly as a sample of a previous preparation [7], in the solvents: phenol/water, 4:1 (v/v), R_F 0.10, and butanol:acetic acid: water, 4:1:5 (v/v/v), upper phase), R_F 0.10, as developed by ninhydrin and phosphate (ammonium molybdate) reagents. (Found: N 11.5; P 12.6. Calc. for $C_5H_{11}O_7N_2P$ (242.1): N 11.6; P 12.8). Acid-base titration gave pK values: 3.13, 5.41, and 8.00, which agree with those reported [9]: 3.13, 5.41 and 8.01.

Aqueous stock solutions of all phosphoryl compounds in free form and in one case, O-phosphorylseryllysine, in the dihydrochloride form, were standardized by potentiometric titration. When not used, the solutions were kept in a refrigerator at −20°. Aqueous stock solutions of complex forming metal ions were prepared from Merck's *p. a.* $CaCl_2 \cdot 6H_2O$, $MgCl_2 \cdot 6H_2O$ and $MnCl_2 \cdot 4H_2O$. For standardization, samples of these

* The first approximation does not consider the last two terms. A roughly estimated value of $\varkappa_{2r1}$ was used, as the figure corresponding to $q = r$ in the sum was usually less than 1 % of m.

** The equation is identical with eqn. 9 of Ref.[6], when used for MA ($r = 0$) in the presence of MHA.

Table 2. Stability constants * (in M^{-1}) of the metal complexes.

Ligand	Metal ion	$C_M^o \times 10^3$	$C_A^o \times 10^3$	b_{MHA}	b_{MA}	b_{M_2A}
P-ethanolamine	Ca	5.19	4.97	14 ± 2	37 ± 1	—
P-ethanolamine	Ca	19.9	2.32	12 ± 2	36 ± 3	—**
P-ethanolamine	Mg	4.99	4.97	18 ± 2	50 ± 3	—
P-ethanolamine	Mg	9.80	1.90	16 ± 2	49 ± 4	—**
P-ethanolamine	Mg	19.8	1.90	17 ± 2	53 ± 5	—**
P-ethanolamine	Mn	4.99	4.97	53 ± 2	359 ± 24	—
P-ethanolamine	Mn	20.0	2.32	53 ± 2	354 ± 41	—**
SerP-Lys	Ca	19.9	1.86	14 ± 1	34 ± 5	
SerP-Lys	Mg	9.90	1.86	16 ± 1	43 ± 7	—**
SerP-Lys	Mg	19.9	1.86	18 ± 1	43 ± 5	—**
SerP-Lys	Mn	19.9	1.86	60 ± 2	212 ± 20	
Gly-SerP-Gly	Ca	19.9	2.00	28 ± 2	65 ± 3	
Gly-SerP-Gly	Mg	9.80	1.74	29 ± 3	61 ± 3	9 ± 6
Gly-SerP-Gly	Mg	19.8	1.74	30 ± 2		
Gly-SerP-Gly	Mn	20.0	2.00	119 ± 2		
Gly-SerP	Ca	19.9	1.48	30 ± 2	59 ± 2	
Gly-SerP	Mg	9.80	2.33	45 ± 2	72 ± 3	24 ± 8
Gly-SerP	Mg	19.8	2.33	43 ± 2		

Ligand	Metal ion	$C_M^o \times 10^3$	$C_A^o \times 10^3$	b_{MH_2A}	b_{MHA}	b_{M_2HA}	b_{MA}	b_{M_2A}
SerP-Gly	Ca	5.19	5.21		21 ± 1		71 ± 3	—
SerP-Gly	Ca	19.9	2.00		19 ± 1		71 ± 1	—**
SerP-Gly	Mg	4.99	5.21		28 ± 2		87 ± 5	—
SerP-Gly	Mg	9.81	2.03		23 ± 3		***	17 ± 3
SerP-Gly	Mg	14.8	2.03		23 ± 3		86 ± 2	18 ± 4
SerP-Gly	Mg	19.8	2.03		28 ± 3			18 ± 2
SerP-Gly	Mn	4.99	5.21		75 ± 3		422 ± 11	—
SerP-Gly	Mn	20.0	2.00		80 ± 2		—	35 ± 4
SerP-Glu	Ca	5.19	4.74	12 ± 1	44 ± 2	—	138 ± 3	—
SerP-Glu	Ca	19.9	1.98	12 ± 2	—	11 ± 3	—	29 ± 2
SerP-Glu	Mg	4.99	4.74	10 ± 2	43 ± 2	—	122 ± 3	—
SerP-Glu	Mg	9.91	1.98	10 ± 2	—	36 ± 5	—	66 ± 4
SerP-Glu	Mg	19.9	1.98	11 ± 1	—	28 ± 4	—	62 ± 4
SerP-Glu	Mn	4.99	4.74	26 ± 3	173 ± 4	—	962 ± 4	—
SerP-Glu	Mn	19.9	1.98	27 ± 4	—	21 ± 3	—	89 ± 3

* Uncertainties given refer to greatest deviation from the mean observed for individual calculations.

** No true evidence for existence of M_2A species, see the text.

*** Value obtained by extrapolation of the line: $(\varphi_0)_{h/K_{HA}=0} = \frac{(1-2Z)m}{(1-Z)} b_{MA}b_{M_2A} + b_{MA}$; to $\frac{(1-2Z)m}{(1-Z)} = 0$ for these three C_{Mg}; the slope $b_{MA}b_{M_2A}$ gave $b_{M_2A} = 19$; ordinates were obtained by extrapolation of eqn. 4a ($r = 0$) to $h/K_{HA} = 0$ (Fig. 3).

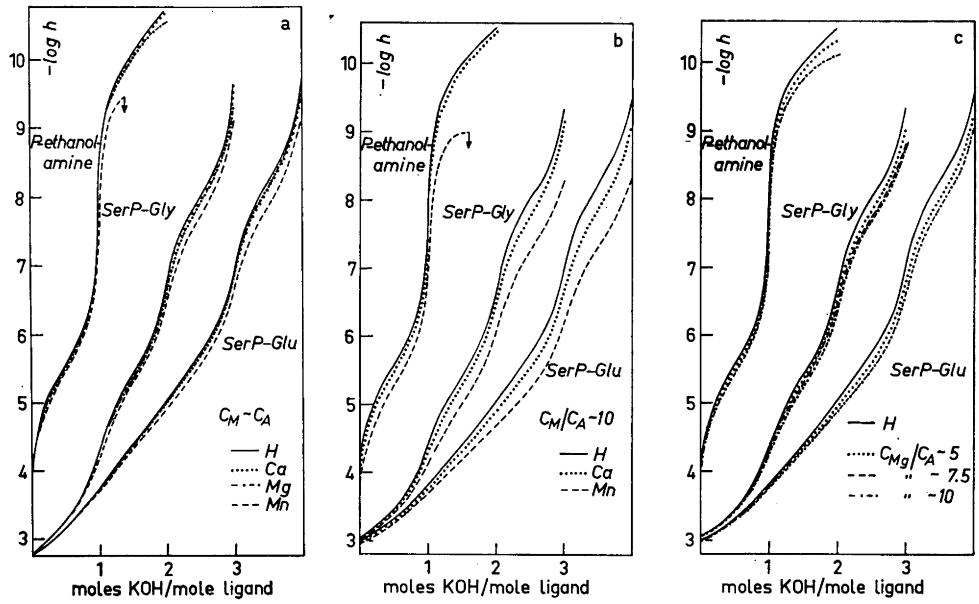

Fig. 1. Titration curves of O-phosphorylated ethanolamine, serylglycine and serylglutamic acid in the absence of complex forming metal ions, H, and in the presence of Ca^{2+}, Mg^{2+}, and Mn^{2+}.

a. $C_M \sim C_A \sim 0.005$. Apparent confluence of Ca and Mg curves is shown as Mg curve. The H curves gave pK_{H_4A}; pK_{H_3A}; pK_{H_2A}; pK_{HA} (P-ethanolamine): —; —; 5.57; 10.16; (SerP-Gly): —; 3.13; 5.41_5; 8.02; (SerP-Glu): 3.02_5; 4.38_5; 5.68; 8.25.

b. $C_A \sim 0.002$. The H curves gave pK_{H_4A}; pK_{H_3A}; pK_{H_2A}; pK_{HA} (P-ethanolamine): —; —; 5.57; 10.12; (SerP-Gly): —; 3.13_5; 5.41_5; 8.00; (SerP-Glu): 3.02_5; 4.38_5; 5.69; 8.25.

c. $C_A \sim 0.002$. The H curves gave pK_{H_3A}; pK_{H_2A}; pK_{HA}; (P-ethanolamine): —; 5.57; 10.12_5; (SerP-Gly): 3.13_5; 5.41_5; 8.00; (SerP-Glu): see *a*.

solutions were passed through a hydrogen ion saturated cation exchanger, and then titrated with standard potassium hydroxide. The manganese solutions were never used later than 6 h after preparation.

Carbonate-free 0.2979 M KOH, containing 0.15 M KCl, was prepared according to Powell and Hiller [11], and standardized against potassium hydrogen phthalate. Merck's *p.a.* bromide-free KCl was used as supporting electrolyte, without further purification. All stock solutions were prepared from freshly triply quartz-distilled water.

Measurements. Titration solutions were prepared by mixing stock solutions of phosphate ester, complex forming metal(II) chloride, and potassium chloride to obtain the concentrations, C_A^o, C_M^o (Table 2), the volume, 10 ml, and the ionic strength, 0.15 M, originally present. pH was measured with a Radiometer glass electrode (G202B), in combination with a saturated calomel electrode (K100), connected *via* a saturated KCl bridge. Standardization of the pH meter (Radiometer PHM 4) and routine calibration of the measuring system (reproducibility: 0.01 pH unit) were performed as described [9]. The readings were converted to values of $-\log h$ by a calculated apparent activity coefficient [9] of 0.79 ± 0.02. The titration equipment was that previously described [9]. All titrations were carried out at 25.00 ± 0.03° in a thermostatically controlled water bath in a room temperature of 23 ± 1°. Nitrogen, which had previously bubbled through 10 % H_2SO_4, 10 % NaOH and 0.15 M KCl, was bubbled through the solution. After

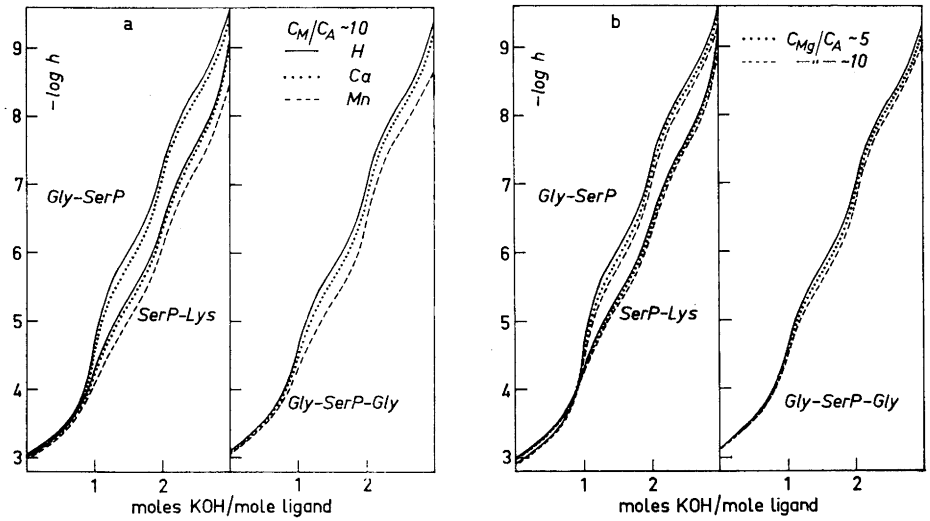

Fig. 2. Titration curves of O-phosphorylated glycylserine, seryllysine and glycylserylglycine in the absence of complex forming metal ions, H, and in the presence of Ca^{2+}, Mn^{2+} and Mg^{2+}. At zero abscissa one equivalent of phosphorylseryllysine dihydrochloride has been titrated.

a. $C_A \sim 0.002$. The H curves gave pK_{H_3A}; pK_{H_2A}; pK_{HA}(Gly-SerP): 2.91_5; 6.03_5; 8.42; (SerP-Lys): 2.98_5; 5.33_5; 7.58_5; (Gly-SerP-Gly): 3.29_5; 5.77_5; 8.21_5.
b. $C_A \sim 0.002$. The H curves gave pK_{H_3A}; pK_{H_2A}; pK_{HA} (Gly-SerP): 2.89_5; 6.03_5; 8.41_5; (SerP-Lys): see *a.*; (Gly-SerP-Gly): 3.29; 5.77_5; 8.21_5.

titration, peptide solutions with $C_M \sim 10C_A$ were subjected to paper chromatography in the aforementioned solvents (p. 2437). Each sample produced a single ninhydrin- and phosphate-positive spot within an R_F-region as expected.

The results, represented as titration curves, are shown in Figs. 1 and 2. These curves are based on mean values of data recorded from two or more identical experiments and measured at an interval of about 0.1 pH unit. The reproducibility was within 0.01 pH unit (0.005 pH for $C_A \sim 0.005$) in the pH ranges used for calculations of the constants. These calculations utilized the mean values.

Titrations for each ligand stock solution were performed in the absence of complex forming metal ions (Figs. 1 and 2). Then pK values could be computed, which conformed as exactly as possible to the experimental conditions. The results (see the legends of Figs. 1 and 2) agree, within the limits of experimental uncertainty, with those previously reported [9,10].

EVALUATION OF CONSTANTS

The ionization steps, shown in Figs. 1 and 2, apparently involve the successive ionization of the second phosphate and amino groups of phosphorylethanolamine (Fig. 1); the α-carboxyl, second phosphate, and α-amino groups of phosphorylserylglycine, phosphorylseryllysine, glycylphosphorylserylglycine,

Table 3. Computation of $b_{M_pH_qA}$ (in M^{-1}) of the O-phosphorylserylglutamic acid-calcium(II) system *. The numbers within parentheses refer to equation numbers **.

$C_A^o = 4.74 \times 10^{-3}$; $C_M^o = 5.19 \times 10^{-3}$; $[Cl^-] = 0.145$					$C_A^o = 1.98 \times 10^{-3}$; $C_M^o = 19.9 \times 10^{-3}$; $[Cl^-] = 0.130$					
V	$-\log h$	$a \times 10^{10}$ (5)		b_{MH_2A} (9)	V	$-\log h$	$a \times 10^{10}$ (5)			b_{MH_2A} (9)
0.1620	3.764	3.049		13.0	0.0740	3.878	2.573			14.0
0.1760	3.875	6.406		12.3	0.0820	4.012	6.071			13.0
0.1900	3.987	13.27		11.4	0.0900	4.146	13.86			12.5
0.2040	4.097	26.56		11.2	0.0980	4.280	30.51			12.3
0.2180	4.205	51.34	$b_{MH_2A} =$	11.7	0.1040	4.382	54.35	$b_{MH_2A} =$		12.3
0.2320	4.313	97.30	$= 12 \pm 1$	11.3				$= 12 \pm 2$		
V	$-\log h$	$a \times 10^7$ (6,8)	Z (6,8)	b_{MHA} (4)	V	$-\log h$	$a \times 10^7$ (5)	Z (6)	X_1*** (4)	b_{M_2HA} (4)
0.3120	4.948	2.716	0.0552	42.2	0.1280	4.802	0.4809	0.0191	51.1	8.4
0.3240	5.048	4.303	0.0606	42.4	0.1330	4.895	0.7431	0.0208	51.0	8.4
0.3360	5.148	6.692	0.0670	43.8	0.1380	4.987	1.124	0.0228	51.8	9.4
0.3480	5.249	10.28	0.0734	44.3	0.1430	5.079	1.662	0.0250	54.2	12.4
0.3600	5.350	15.51	0.0802	44.9	0.14805	5.173	2.458	0.0271	54.7	13.0
0.3720	5.453	23.22	0.0864	44.7	0.1530	5.267	3.589	0.0289	53.9	12.1
0.3840	5.558	34.41	0.0920	43.9	0.1580	5.364	5.184	0.0313	55.2	13.8
0.3960	5.666	50.74	0.0952	41.6	0.1630	5.464	7.478	0.0335	55.2	13.9
		$b_{MHA} = 44 \pm 2$					$b_{M_2HA} = 11 \pm 3$			
V	$-\log h$	$a \times 10^4$ (6,8)	Z (6,8)	b_{MA} (4)	V	$-\log h$	$a \times 10^4$ (5)	Z (6)	X_0*** (4)	b_{M_2A} (4)
0.4920	7.242	3.247	0.161	137.0	0.2100	7.176	6.764	0.0537	212.9	31.0
0.4960	7.323	3.835	0.164	135.0	0.2130	7.293	8.467	0.0550	212.0	31.0
0.5020	7.436	4.810	0.170	135.9	0.2160	7.396	10.20	0.0563	208.5	29.7
0.5080	7.534	5.800	0.177	139.5	0.2190	7.492	12.03	0.0577	209.7	30.3
0.5140	7.624	6.835	0.182	138.7	0.2220	7.581	13.89	0.0588	206.5	29.1
0.5220	7.731	8.220	0.190	138.5	0.2250	7.663	15.70	0.0601	206.2	29.1
0.5320	7.855	10.03	0.199	138.0	0.2290	7.770	18.21	0.0618	204.4	28.5
0.5420	7.969	11.84	0.211	140.8	0.2330	7.873	20.68	0.0636	204.3	28.6
0.5520	8.079	13.70	0.220	140.0	0.2370	7.976	23.13	0.0653	204.1	28.7
		$b_{MA} = 138 \pm 3$			0.2410	8.081	25.50	0.0671	205.6	29.6
							$b_{M_2A} = 29 \pm 2$			

* pK values of Fig. 1a and 1b were used.
** V = ml 0.2979 M KOH added; $C_A = C_A^o\ (1 + 0.1\ V)^{-1}$; $C_M = C_M^o\ (1 + 0.1\ V)^{-1}$.
*** $X_1 K_{HA}$ and X_0 are equal to the left hand side of eqn. 4 for $r = 1$ and $r = 0$, respectively.

glycylphosphorylserine (Figs. 1 and 2); and the α-carboxyl, γ-carboxyl, second phosphate, and amino groups of phosphorylserylglutamic acid (Fig. 1) *.

* The first phosphate group in all ligands and the ε-amino group of the lysine peptide were not titrated. The ionization of these groups did not require any consideration, as the pH values used in the calculations were more than 3 pH units away from their pK values [9,10].

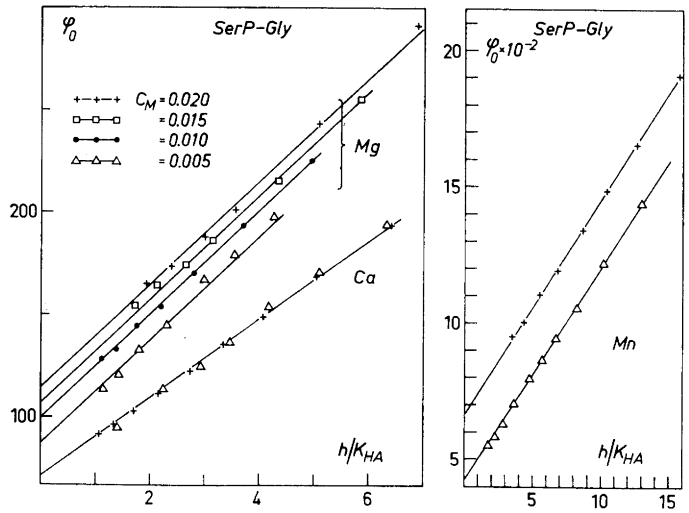

Fig. 3. Survey of the computation of b_{MHA}, b_{MA} and b_{M_2A} in the O-phosphorylseryl-glycine systems, *cf.* the text. Experimental data plotted by eqn. 4a for $r = 0$, assuming $S = 1$ and $T = 0$. The curves are calculated from the constants of Table 4 and those of the legend of Fig. 1, using eqn. 4a.

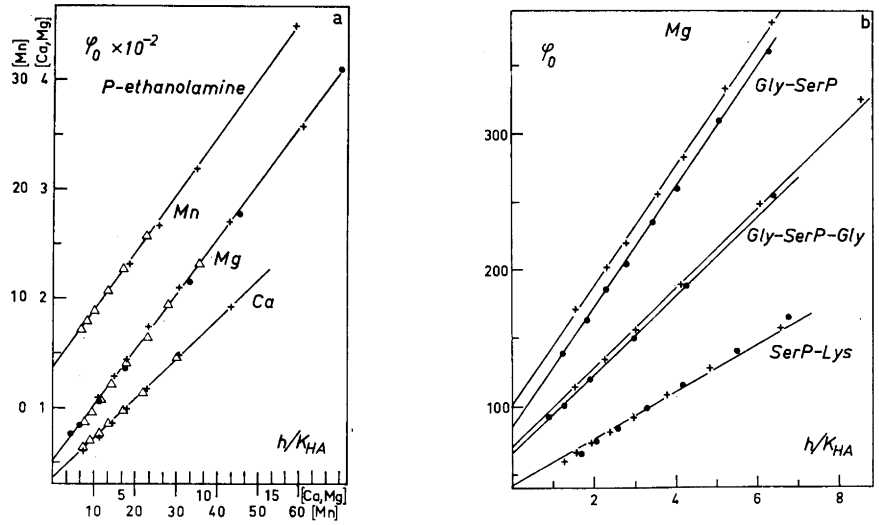

Fig. 4. Survey of the computation of b_{MHA}, b_{MA} in the systems of O-phosphorylated ethanolamine (*a.*) and seryllysine (*b.*), and b_{MHA}, b_{MA}, b_{M_2A} in those of O-phosphorylated glycylserine and glycylserylglycine (*b.*). Experimental data plotted by eqn. 4a for $r = 0$, assuming $S = 1$ and $T = 0$ and using the symbols of Fig. 3. The curves are calculated from the constants of Table 4 and those of the legends of Figs. 1 and 2, as well as b_{MHA}; b_{MA}; b_{M_2A} (Gly-SerP): **44**; 72; 24; (Gly-SerP-Gly): 29; 61; 9 M^{-1}, using eqn. 4a.

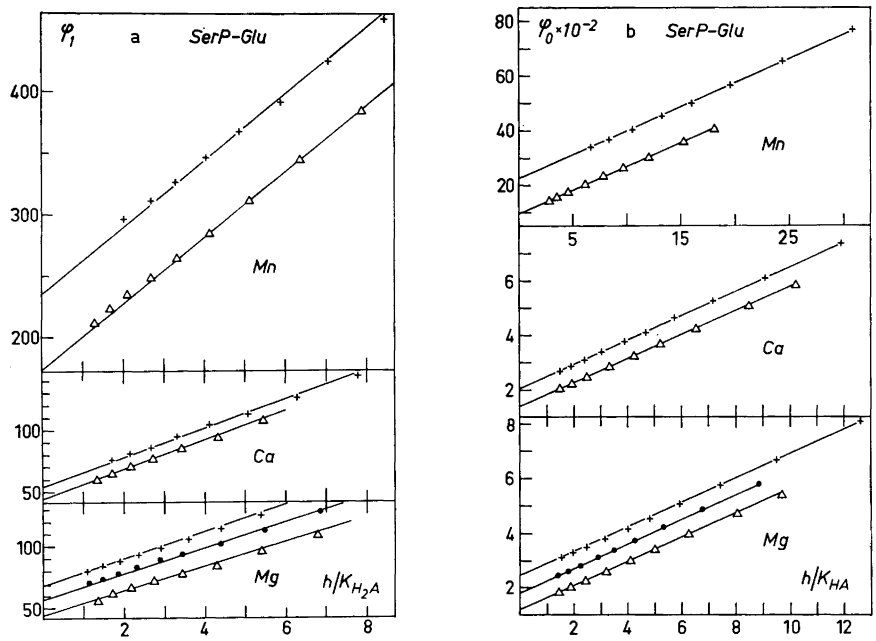

Fig. 5. Survey of the computation of b_{MH_2A}, b_{MHA}, b_{M_2HA} (*a.*) and b_{MHA}, b_{MA}, b_{M_2A} (*b.*) in the O-phosphorylserylglutamic acid systems. Experimental data plotted by eqn. 4a for $r = 1$ (*a.*) and $r = 0$ (*b.*), assuming $S = 2$ and $T = 1$ and using the symbols of Fig. 3. The curves are calculated from the constants of Table 2 and those of the legend of Fig. 1, using eqn. 4a.

Figs. 1 and 2 also indicate that the complex formation begins in the buffer region of the second phosphate group, however, for phosphorylserylglutamic acid systems in that of the γ-carboxyl group. Then complexes corresponding to $S = T = 2$ (phosphorylserylglutamic acid systems) and $S = T = 1$ (other systems) had to be considered at the computation of the $\varkappa_{pq1}$ constants. An example of the computations comprises Table 3, where the Ca(II)-phosphorylserylglutamic acid system is presented. The $\varkappa_{pq1}$ constants have been converted to $b_{M_pH_qA}$.

The computation of $\varkappa_{121}$ could not entirely neglect MHA + M_2HA species. Expressions for $q = 1$ ($p = 1, 2$) were therefore introduced in eqn. 5, using approximate values for $\varkappa_{111}$ and $\varkappa_{211}$ *. The constant was obtained from

$$\varkappa_{121} = \frac{C_S - C_A - a \sum_{q=0}^{q=4} (q-1)\varkappa_{0q1}h^q}{h^2a\left[C_M - C_A + a \sum_{q=0}^{q=4} \varkappa_{0q1}h^q\right]} \qquad (9)$$

and the value obtained was refined by successive approximation.

* The contributions of $-\varkappa_{111}\, mh$, ($C_A \sim C_M$), and $-mh(\varkappa_{111} + m\varkappa_{211})$, ($C_M \sim 10C_A$), to the denominator of eqn. 5 were 0.05–1 % and 0.4–5 %, respectively, in the calculations compiled in Table 3.

Species of the type MOH were considered in all of the Mn(II) systems and in the Mg(II)-phosphorylethanolamine system (for $r = 0$); $*K_1 = 10^{-10.7}$ and 10^{-12} were used [12].

The S values assumed gave approximately constant values for $\varkappa_{121}$ (phosphorylserylglutamic acid systems, $r = 2$) and the left hand side of eqn. 4 (other systems, $r = 1$) in the selected parts of the titration curves (*cf.* Table 3). Other S values (1 and 0, respectively) gave a definitely trend in the left hand side of eqn. 4 ($r = 1$ and $r = 0$) with pH.

In the former calculations $\varkappa_{121}$ and the left hand side of eqn. 4 were also almost constant for different C_M, and consequently the species were mononuclear [13]. For $r = 1$, 0 in the phosphorylserylglutamic acid systems and $r = 0$ in some of the other systems, the computations indicated dinuclear complex formation. T will then be 1 and 0, respectively, which is apparent from Figs. 3—5. Individual calculations of systems studied at different C_M are surveyed graphically [6] for these r values by the plot φ_r against $h(K_{H_{r+1}A})^{-1}$, where

$$\varphi_r = \frac{Z(1 + *K_1 h^{-1})}{(1-Z)\varkappa_{0r1} a h^r} - \sum_{q=r+2}^{S} \varkappa_{1q1}\varkappa_{0r1}^{-1} h^{q-r} - \sum_{q=r+1}^{T} \frac{1-2Z}{1-Z} \varkappa_{2q1}\varkappa_{0r1}^{-1} h^{q-r} m =$$

$$= h b_{MH_{r+1}A}(K_{H_{r+1}A})^{-1} + b_{MH_rA} + \frac{(1-2Z)}{(1-Z)} b_{MH_rA} b_{M_2H_rA} m \qquad (4a)$$

Due to the last expression in the right hand side, the presence of dinuclear species will increase φ_r with C_M (Figs. 3, 4b, 5). When the equilibria are mononuclear, this expression cancels, and the plotted data are independant of C_M (Figs. 3 and 4).

Phosphorylated seryllysine, glycylserine * and glycylserylglycine were titrated at one (Ca^{2+} and Mn^{2+}) and two (Mg^{2+}) C_M only (Table 2), due to a lack of material. All of these Ca^{2+} systems as well as the Mn^{2+}system of phosphorylseryllysine were assumed to be mononuclear; *cf.* the plots of the Ca(II)-phosphorylserylglycine and Mg(II)-phosphorylseryllysine systems in Figs. 3 and 4b. With regard to other glycine peptides (Figs. 3 and 4b) glycylphosphorylserylglycine was assumed to form Mg_2A species, though there is only weak experimental evidence (Fig. 4b). As this ligand might also form Mn_2A complexes, no calculations were carried out for $r = 0$ in its Mn(II) system.

Values computed for $\varkappa_{pq1}$ were converted to corresponding stability constants, $b_{M_pH_qA}$ which are found in Table 2.

DISCUSSION

Data of the phosphorylserylglycine systems indicate the presence of dinuclear magnesium and manganese(II) complexes, while the existence of such a calcium complex could not be demonstrated (Fig. 3). The same type of complex formation seems to be valid for the other glycine peptide systems. This follows from Fig. 4b and from their "b_{CaA}", which are smaller than the b_{CaA} of the phosphorylserylglycine system (Table 2). Occurrence of a greater amount

* No Mn^{2+} titration could therefore be carried out with this ligand.

of Ca_2A should have appreciably increased the size of these "b_{CaA}" (in this case taken as equal to the left hand side of eqn. 4 at $r = 0$), as $C_M \sim 10C_A$.

The increase in φ_r (eqn. 4a) with C_M is used to show the presence of dinuclear species (Figs. 3, 4b, 5). As this increase is not generally observed (in all systems at all r; *cf.* Figs. 3 and 4 and the previous section), it cannot be due to systematic errors, arising from the variations in C_M. Such errors would be, *e.g.*, changed activity factors and liquid junction potentials, caused by the increasing contribution of complex forming metal ions to the ionic strength.

At the present C_A, weak MH_3A (phosphorylserylglutamic acid systems) and MH_2A (other systems) complexes (stability constant < 3 M^{-1}) cannot be detected. Existence of such species would, however, neither invalidate those reported, or appreciably change the relations between their constants. There is no support for the occurrence of complexes with two or more ligands per central metal ion, as no upward trend in φ_r is seen for decreasing h (Figs. 3—5). We can also eliminate complexes of the type MA(OH), which most probably should be formed in the phosphorylethanolamine-Mn(II) system. If we assume $*K_{MA}$ to be equal to $*K_1$ ($= 10^{-10.7}$, Ref.[12]) in this system, [MA(OH)] will constitute 2 % of [MA] and b_{MA} will be changed from 342 to 332 M^{-1} at the most alkaline point of calculation (0.1000 ml 0.2979 M KOH; $-\log h = 8.850$) at $C_M \sim 10C_A$ *. Phosphorylethanolamine-Mn(II) was the only system, where MOH species had a marked influence on b_{MA}. Neglecting these species, "b_{MA}" will be 460 ± 20 ($C_M \sim C_A$) and 690 ± 40 M^{-1} ($C_M \sim 10C_A$).

Previous works on complexes of related phosphate esters. At 0.1—0.2 M ionic strength and 20—25° stability constants of the following 1:1 complexes have been reported: **

HPO_4^{2-}—Ca^{2+}; —Mg^{2+}; —Mn^{2+} (Ref.[12]): 32; —; —; (Ref.[14]): 50; 76; 382; AMP^{2-}—Ca^{2+}; —Mg^{2+}; —Mn^{2+} (Ref.[14]): 27; 49; 156; (Refs.[15,16]): 26; 49; —; (Ref.[17]): 58; 89; 204; (Ref.[18]): —; 100; —; CrP^{3-}—Ca^{2+}; —Mg^{2+}; —Mn^{2+} (Ref.[14]): 14; 20; 110; $FructoseP^{2-}$—Ca^{2+}; —Mg^{2+} (Ref.[19]): 30; 39; $GlycerolP^{2-}$—Ca^{2+}; —Mg^{2+} (Ref.[19]): 46; 63; $GA2P^{3-}$ —Mg^{2+}; —Mn^{2+} (Ref.[20]): 280; 1225; PAP^{3-} —Mg^{2+}; —Mn^{2+} (Ref.[20]): 180; 560; $SerP^{2-}$ —Ca^{2+}; —Mg^{2+}; —Mn^{2+} (Ref.[6]): 27; 40; 81; $SerP^{3-}$ —Ca^{2+}; —Mg^{2+}; —Mn^{2+} (Ref.[6]):138; 245; 6600 M^{-1}.

In all ligands the phosphate group has the charge —2. With the exception of the $GA2P^{3-}$, PAP^{3-}, and $SerP^{3-}$ constants, all corresponding constants, including the present (Table 2), are similar in magnitude. The phosphate group may therefore be the main dentate group in these systems [19].

The $GA2P^{3-}$ and PAP^{3-} constants can be explained by the presence of the carboxyl group; therefore these ligands may also require consideration of M_2A species for accurate interpretation of data $C_M > C_A$. Wold *et al.*[20] apparently used such concentrations (no C_M is given), though they did not consider any dinuclear species. The aforementioned $SerP^{3-}$ constants [6] have

* As $r = 0$, the expressions $-b_{MA}*K_{MA}h^{-1}$ and $-b_{MA}*K_{MA}h^{-1}m$ related to [MA(OH)] were introduced in eqn. 4 (left hand side) and eqn. 5 (denominator), respectively, using $b_{MA} = 356$ M^{-1}.

** The abbreviations signify: AMP: adenosine-5′-monophosphate, CrP^{3-}: creatinephosphate; $FructoseP^{2-}$: fructose monophosphate; $GlycerolP^{2-}$: glycerol monophosphate; $GA2P^{3-}$: glyceric acid 2-phosphate; PAP^{3-}: enolpuruvic acid phosphate; SerP: O-phosphorylserine.

Table 4. Effect of different substituents, R, on the complex formation of compounds indicated.

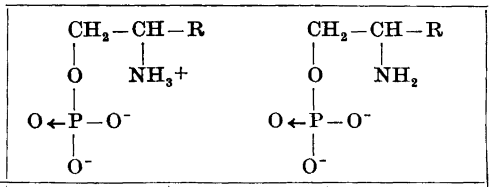

Compound	R	b_{MHA}			b_{MA}			b_{M_2A}		
		Ca	Mg	Mn	Ca	Mg	Mn	Ca	Mg	Mn
P-ethanolamine	$-H$	13	17	53	36	50	356	—*	—*	—*
SerP **	$-COO^-$	27	40	81	138	245	6600	—*	14	17
SerP-Gly	$-CO-NH-CH_2-COO^-$	20	25	78	71	86	422	—*	18	35
SerP-Glu	$-CO-NH-CH(-(CH_2)_2-COO^-)-COO^-$	44	43	173	138	122	962	29	64	89
SerP-Lys	$-CO-NH-CH(-(CH_2)_4-NH_3^+)-COO^-$	14	17	60	34	43	212	—*	—*	—*

* No true evidence for existence of M_2A species, see the text.
** Ref.[6]

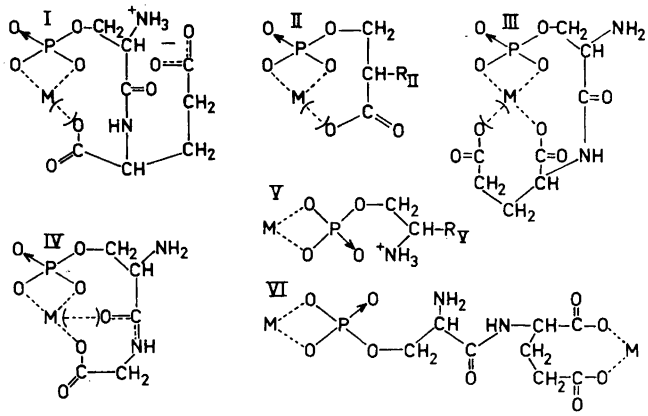

Fig. 6. Schematic structures of metal complexes. Coordination positions of the metal ions may be filled by water molecules.
I, III, VI: MHA, MA and M_2A complexes of phosphorylserylglutamic acid.
II: MHA complex; phosphorylserine: $R_{II} = -NH_3^+$; glycylphosphorylserine: $R_{II} = -NH-CO-CH_2-NH_3^+$.
IV: MA complex of phosphorylserylglycine.
V: MHA complex; phosphorylethanolamine: $R_V = -H$; phosphorylseryllysine: $R_V = -CO-NH-CH(-(CH_2)_4-NH_3^+)-COO^-$.

been computed from data $C_M \sim C_A/2$. A reconsideration of the findings of that work [6], when compared with the present results, suggests that magnesium and manganese(II) may form M_2A complexes, whereas calcium might not (Figs. 4b, c in Ref.[6], where $Z/(1-Z)A$ equals φ_0 of eqn. 4a).

Coordination sites. Table 4 shows influence of substituents (R) on the coordination of compounds with phosphorylethanolamine structure. The carboxyl group substituents increase the complex forming tendency; the phosphorylserine complexes are more stable than those of phosphorylethanolamine and the glutamic acid peptide complexes are more stable than those of the glycine peptide.

The α-carboxyl group may, thus, partially contribute to the MHA stability of phosphorylserylglutamic acid and probably to that of phosphorylated serine, glycylserine, and glycylserylglycine (*cf.* Table 2). This is shown by I and II in Fig. 6. The γ-carboxyl group of phosphorylserylglutamic acid may be intramolecularly neutralized by the amino group (I). Such "neutralization" may occur also in the MHA species of phosphorylated serylglycine (amino and carboxyl groups) and seryllysine [10] (ε-amino and carboxyl groups).

Decharging of the amino groups of the glutamic acid and glycine peptides may liberate the carboxyl groups mentioned, which are then free to interact with the central metal ions (III and IV in Fig. 6). These groups rather than the amino groups may engage the metal ions, as the present metal ions bind to oxygen in preference to nitrogen [21-24]. Contribution through the peptide bond oxygen [25], favoured due to resonance, is possible in the phosphorylserylglycine MA complexes, IV in Fig. 6 (more unlikely due to steric reasons in the reversed dipeptide and the tripeptide complexes, as judged from Stuart-Briegleb molecular models). The relatively high b_{MA} of the phosphorylserine complexes (Table 4) may be explained by the capacity of this ligand to bind both through the phosphate group and a five-membered chelate ring, formed by the amino and carboxyl groups *.

The MHA complex formation of phosphorylated ethanolamine and seryllysine may be influenced by the α-amino groups (V in Fig. 6); *cf.* the low b_{MHA} in Table 4. These groups may also be involved in the MA complex formations (Mn^{2+} complexes, specially [21,22]), but they are then deprotonized and increase the stability. — The general weak complexity of phosphorylseryllysine and inability to form M_2A species (Table 4) indicate some impairment of its donor groups; probably due to interaction of the charged ε-amino group [10].

Complex formation of dinuclear type may straighten the ligands, and one metal ion may be bound at each end. Phosphate and carboxyl groups may be the main dentate groups (*cf.* VI in Fig. 6). Apart from the carboxyl group the peptide bond carbonyl group [25] may contribute in the glycine peptide complexes and the amino group in the phosphorylserine complexes. Their b_{M_2A} (Table 2) compare better with b_{MA} (Ref.[4]) of glycollate, lactate ($-Mg^{2+}$: 8—23), glycylglycine ($-Mg^{2+}$: 11), succinate ($-Mg^{2+}$: 16), and glutarate ($-Mg^{2+}$: 12) complexes than b_{MA} (Ref.[4]) of acetate, propionate, and butyrate

* Dividing the b_{MA} (Table 4) with approximate b_{MA} of the corresponding complexes of an esterbound phosphate group (see compilation on page 2445 and Table 2), (Ca^{2+}): 25; (Mg^{2+}): 35; (Mn^{2+}): 100, results in: 6; 7; 66, which may be compared to b_{MA} of alanine complexes [26] (multiplied with an activity factor [27], 0.56, and a statistical factor [28], 0.17): 2; 8; 97 M^{-1}.

(—Mg^{2+}: ~3) complexes [23]. The lower stability of the dinuclear tripeptide complex relative to those of the other glycine peptides (Table 2) may be attributed to an error in b_{M_2A}, accumulated from errors in $\varkappa_{0q1}$ and $\varkappa_{1q1}$, or to the more rigid nature of the tripeptide.

The b_{M_2A} of the Ca and Mg(II) complexes of phosphorylserylglutamic acid (Table 4) are very similar to b_{CaA} and b_{MgA} reported for glutamic acid complexes [29]: 27 and 79 M^{-1} in 0.1 M KCl at 25°. A structure (VI, Fig. 6) involving the two carboxyl groups as dentate sites thus seems reasonable [30].

Conclusions. pK values of the acid complexes (Table 5) indicate that all present complexes, except the MH_2A of the phosphorylserylglutamic acid systems and the MA of those of phosphorylethanolamine, exist in the physiological pH range (pH 6—8). The pK_{MHA} values are appreciably lower than their corresponding pK_{HA} (the legends of Figs. 1 and 2). The amino groups will, thus, become more acidic, when the ligands are complexed. These groups will also increase the complex stability 2—4 times by their deprotonizing processes (*cf.* b_{MHA} and b_{MA} in Tables 2 and 4), though the may not act as donor groups themselves (Fig. 6).

Table 2 shows that the stability order $Ca^{2+} < Mg^{2+} < Mn^{2+}$ in general is valid. An increasing number of dentate groups, however, will successively increase the calcium complex stability relative that of magnesium [1] (Table 4). As a consequence the larger calcium ion forms mononuclear phosphorylserylglutamic acid complexes with equal or greater strength as compared to magnesium. The smaller magnesium ion may then fail to engage as many donor atoms as the calcium ion [1,23].

A further consequence of ionic size may be that magnesium and manganese ions form dinuclear complexes more easily than calcium ions (Tables 2 and 4). The dinuclear species may have a conformation other than the mononuclear species (*cf.* Fig. 6 and p. 2447), and Mg^{2+} or Mn^{2+} may induce a stretched conformation, when Ca^{2+} induces a compact conformation. The findings therefore offer a possibility beside that proposed by Williams [1] to explain the action of Mg^{2+} (Mn^{2+}) as opposed to Ca^{2+} in certain enzyme systems. The enzymic meaning may be that the activating ions by complex formation give the enzyme active site (alternatively the substrate or both the enzyme

Table 5. pK values of acid complexes.

Ligand	Constant	Ca	Mg	Mn
P-ethanolamine	pK_{MHA}	9.70	9.65	9.29
SerP-Gly		7.45	7.46	7.27
SerP-Lys		7.18	7.18	7.04
Gly-SerP-Gly		7.85	7.89	—
Gly-SerP		8.12	8.19	—
		7.76	7.80	7.50
SerP-Glu	pK_{MH_2A}	5.12	5.05	4.87
	pK_{M_2HA}	7.34	7.47	6.88

active site and the substrate) a suitable conformation for catalysis. When an extended shape is catalytically favoured, magnesium (manganese) ions may activate and calcium ions inhibit, while these effects may be reversed, if a compact form is preferred.

APPENDIX

The results obtained for titrations with $C_M \sim C_A$ rest on the assumption that the species formed are mononuclear in M and A. We therefore tried to check some of these results by calculations performed by another procedure. Values of a were found directly by integration of a $\bar{q}$ (log h) curve, where $\bar{q} = C_S/C_A$. The equation used was derived in analogy with the principles given by Sillén [31], and we will only give the main result.

We define the function

$$S = \sum_p \sum_q \sum_v [M_pH_qA_v] = \sum_p \sum_q \sum_v m^p h^q a^v \varkappa_{pqv} \quad \begin{matrix}(p,q,v = 0, 1, 2, \ldots; \\ v \neq 0, \text{ if } (p+q) > 1)\end{matrix} \qquad (10)\ *$$

and write the differential of this function $S(m,h,a)$

$$dS = (C_A - a)\ d\ \ln\ a + C_S\ d \ln h + (C_M - m)\ d \ln m \qquad (11)$$

By introducing $\bar{q}C_A = C_S$ and then transform to

$$d(C_A \ln\ a + C_M \ln\ m - S - a - m) = \ln\ a\ dC_A - \bar{q}C_A\ d\ \ln\ h + \ln\ m\ dC_M \qquad (12)$$

we get

$$\left(\frac{\partial \ln a}{\partial \ln h}\right)_{C_A,C_M} = -\left(\frac{\partial \bar{q}C_A}{\partial C_A}\right)_{h,C_M} = -\left[q + \left(\frac{\partial \bar{q}}{\partial \ln C_A}\right)_{h,C_M}\right] \qquad (13)$$

We solve this equation for log a in the range log h_o to log h and add $-\log C_A$ to both sides

$$\log\ a/C_A = \log\ a_0/C_A - \left[\int_{\log h_o}^{\log h} \left[\bar{q} + \log e \left(\frac{\partial \bar{q}}{\partial \log C_A}\right)_{h,C_M}\right] d\ \log h\right]_{C_A,C_M} \qquad (14)$$

For $p = 0,1$ we can write the differential of the function C_M (m,h,a)

$$dC_M = C_M\ d\ \ln\ m + (C_A - a\sum_{q=0} h^q \varkappa_{0q1}) d\ \ln\ a + (C_S - a\sum_{q=1} q h^q \varkappa_{0q1}) d\ \ln\ h = \\ = C_M\ d\ \ln\ m \qquad (15)$$

Transformation and substitution, $(\bar{q}C_A = C_S)$, gives

$$d(C_A \ln\ a - a\sum_{q=0} h^q \varkappa_{0q1}) = \ln\ a\ dC_A - \bar{q}C_A\ d\ \ln\ h \qquad (16)$$

whence we obtain eqns. 13 and 14, which are independent of constancy in C_M. For $v = 0, 1$ the partial derivative $(\partial \bar{q}/\partial\ \log\ C_A)_{h,C_M}$ in eqn. 14 becomes zero. Consequently, the condition $p,v = 0, 1$ will reduce eqn. 14 to

* We thus first assume that v may attain higher values than 0 and 1, and that species corresponding to these v are included in C_A, C_M and C_S (*cf.* eqns. 2, 3 and the symbol section).

Table 6. Comparison of a,Z values for the Ca(II)—O-phosphorylserylglutamic acid system ($C_M \sim C_A$, for details see Table 3), as computed by eqns. 5, 6, 8, and eqns. 14a *, 17, 18*.

** $-\log h$	$a \times 10^{10}$ (14a)	$a \times 10^{10}$ (5)	** $-\log h$	$a \times 10^{7}$ (14a)	$a \times 10^{7}$ (6,8)	** Z (17,18)	Z (6,8)	** $-\log h$	$a \times 10^{4}$ (14a)	$a \times 10^{4}$ (6,8)
			4.948	2.716	2.716	0.0547	0.0552	7.242	3.251	3.247
3.764	3.051	3.049	5.048	4.303	4.303	0.0607	0.0606	7.323	3.842	3.835
3.875	6.406	6.406	5.148	6.690	6.692	0.0666	0.0670	7.436	4.811	4.810
3.987	13.26	13.27	5.249	10.28	10.28	0.0729	0.0734	7.534	5.796	5.800
4.097	26.54	26.56	5.350	15.52	15.51	0.0794	0.0802	7.624	6.827	6.835
4.205	51.32	51.34	5.453	23.20	23.22	0.0860	0.0864	7.731	8.200	8.220
4.313	97.23	97.30	5.558	34.32	34.41	0.0936	0.0920	7.855	9.975	10.03
			5.666	50.40	50.74	0.1011	0.0952	7.969	11.75	11.84
								8.079	13.55	13.70

* The trapezoid formula was used in the plot $\bar{q}$ or $\bar{q}_h$ *versus* log h. Smoth curves were drawn through the experimental points, and the integration was done with intervals of 0.05 log h units.

** $\log h_0 = -3.750$, where $\log a_0/C_{A_0} \approx \log [(\bar{q}-2)/\sum_{q=0}^{q=4} (q-2)h^q \varkappa_{0q_1}]$ and $\log C_{A_h}/C_{A_0} =$ $= \log \left(a_0 C_{A_0}^{-1} \sum_{q=0}^{q=4} h^q \varkappa_{0q_1}\right)$; the $\varkappa_{0q_1}$ were obtained from the pK of the legend of Fig. 1a.

$$\log a/C_A = \log a_0/C_{A_0} - \int_{\log h_0}^{\log h} \bar{q} \, \mathrm{d} \log h \qquad (14a)$$

Table 6 shows values of a computed by eqn. 14a for the Ca(II)-O-phosphorylserylglutamic acid system ($C_M \sim C_A$), as compared to those computed by eqns. 5, 6, and 8 (*cf.* Table 3).

In the pH region, where the acid ionizations of this ligand overlap, some Z values were checked by

$$Z = \frac{1 - C_{A_h}/C_A}{C_M/C_A} \qquad (17)$$

Here C_{A_h} equals $a \sum_{q=0}^{q=4} h^q \varkappa_{0q_1}$ and C_{A_h}/C_A was obtained from (*cf.* eqn. 25 in Ref.[31])

$$\log C_{A_h}/C_A = \log C_{A_h}/C_{A_0} + \int_{\log h_0}^{\log h} \bar{q}_h \, \mathrm{d} \log h - \int_{\log h_0}^{\log h} \bar{q} \, \mathrm{d} \log h \qquad (18)$$

where

$$\bar{q}_h = \left(a \sum_{q=1}^{q=4} q h^q \varkappa_{0q_1}\right) C_{A_h}^{-1} \qquad (19)$$

The first integral in eqn. 18 was determined by a $\bar{q}_h(\log h)$ curve, based on an acid-base titration of the ligand (H in Fig. 1a). The Z values calculated are listed in Table 6, and for comparison those calculated previously (Table 3) by eqns. 6, 8, are included.

The stability constants ($b_{MH_2A} = 12 \pm 1$; $b_{MHA} = 44 \pm 2$; $b_{MA} = 140 \pm 9$), which finally were computed, agree with those of Table 3 within the uncertainties given.

Acknowledgements. I wish to express my sincere gratitude to Dr. G. Fölsch for the gift of the phosphorylated compounds, to Laborator Ido Leden for valuable comments on the manuscript, to Drs. S. Aleby and K. Larsson for valuable discussion, and to Mrs. Clara Wadsworth for correcting the English. The investigation was aided by grants from the *Medical Faculty, University of Göteborg* and from *Lennanders' fund.*

REFERENCES

1. Williams, R. J. P. in Boyer, P. D., Lardy, H. and Myrbäck, K. *The Enzymes*, 2nd ed., Academic Press, New York **1** (1959) 391.
2. Koshland, D. E., Jr. *Ibid.* **1** (1959) 305.
3. Vallee, B. L. *Ibid.* **3** (1960) 225.
4. Bjerrum, J., Schwarzenbach, G. and Sillén, L. G. *Stability Constants, Part I: Organic Ligands*, The Chemical Society Spec. Publ. No. 6, London 1957.
5. Biedermann, G. and Sillén, L. G. *Arkiv Kemi* **5** (1953) 425.
6. Österberg, R. *Arkiv Kemi* **13** (1959) 393.
7. Fölsch, G. *Acta Chem. Scand.* **12** (1958) 561.
8. Fölsch, G. *Acta Chem. Scand.* **13** (1959) 1407.
9. Fölsch, G. and Österberg, R. *J. Biol. Chem.* **234** (1959) 2298.
10. Fölsch, G. and Österberg, R. *Acta Chem. Scand.* **15** (1961) 1963.
11. Powell, J. E. and Hiller, M. A. *J. Chem. Educ.* **34** (1957) 330.
12. Bjerrum, J., Schwarzenbach, G. and Sillén, L. G. *Stability Constants, Part II: Inorganic Ligands*, The Chemical Society Spec. Publ. No. 7, London 1958.
13. Leden, I. *Dissertation*, Lund 1943, pp. 22–23.
14. Smith, R. M. and Alberty, R. A. *J. Am. Chem. Soc.* **78** (1956) 2376.
15. Martell, A. E. and Schwarzenbach, G. *Helv. Chim. Acta* **39** (1956) 653.
16. Schwarzenbach, G. and Martell, A. E. *J. Phys. Chem.* **62** (1958) 886.
17. Walaas, E. *Acta Chem. Scand.* **12** (1958) 528.
18. Nanninga, L. B. *J. Phys. Chem.* **61** (1957) 1144.
19. Schwarzenbach, G. and Anderegg, G. *Helv. Chim. Acta* **40** (1957) 1229.
20. Wold, F. and Ballou, C. E. *J. Biol. Chem.* **227** (1957) 301.
21. Irving, H. and Williams, R. J. P. *J. Chem. Soc.* **1953** 3192.
22. Schwarzenbach, G. *Anal. Chem.* **32** (1960) 6.
23. Williams, R. J. P. *J. Chem. Soc.* **1952** 3770.
24. Basolo, F. and Pearson, R. G. *Mechanisms of Inorganic Reactions*, John Wiley & Sons, London 1958, pp. 60–61.
25. Rabin, B. R. *Trans. Faraday Soc.* **52** (1956) 1130.
26. Monk, C. B. *Trans. Faraday Soc.* **47** (1951) 297.
27. Davies, C. W. *J. Chem. Soc.* **1938** 2093.
28. Bjerrum, J. *Dissertation*, Copenhagen 1941 p. 40.
29. Lumb, R. F. and Martell, A. E. *J. Phys. Chem.* **57** (1953) 690.
30. Schubert, J. *J. Am. Chem. Soc.* **76** (1954) 3442.
31. Sillén. L. G. *Acta Chem. Scand.* **15** (1961) 1981.

Received May 22, 1962.

ACTA CHEMICA SCANDINAVICA 16 (1962) 2452–2472

Short Communications

Mean Amplitudes of Vibration and Bastiansen-Morino Shrinkage Effects in Some Octahedral XY_6 Molecules

E. MEISINGSETH and S. J. CYVIN

Institutt for teoretisk kjemi, Norges tekniske høgskole Trondheim, Norway

Spectroscopic calculations of mean amplitudes of vibration [1] and shrinkage effects [2] are of great interest in modern electron-diffraction studies on gas molecules. The recent communications on sulphur hexafluoride [3] contain some aspects of the theory. The same procedure was used in the present calculations on six octahedral hexafluorides.

Vibrational frequencies of the presently considered molecules have been collected by Pistorius [4]. They were used for a recalculation of force constants, following the same principles as described exhaustively in the mentioned paper [4]. To obtain the shrinkage effects, some estimates of equilibrium distances are needed. In the present work the following values were used.

SF_6:	S–F = 1.58	Å [5]
SeF_6:	Se–F = 1.70	Å [5]
TeF_6:	Te–F = 1.84	Å [5]
MoF_6:	Mo–F = 1.830	Å [6]
WF_6:	W–F = 1.89	Å [7]
UF_6:	U–F = 1.994	Å [6]

The final results for mean amplitudes of vibration (Table 1) and shrinkage effects (Table 2) contain the recalculated values

Table 1. Mean amplitudes of vibration for six octahedral hexafluorides (Å units).

Atom pair (Distance)	SF_6	SeF_6	TeF_6	MoF_6	WF_6	UF_6
XF (Bonded)	0.04103 [a]	0.03881	0.03782	0.04104	0.03723	0.04000
	0.04190 [b]	*0.04005*	*0.03916*	*0.04482*	*0.03853*	*0.04236*
FF(X, F...F)	0.05557	0.05795	0.06712	0.06442	0.06898	0.08126
	0.06041	*0.07092*	*0.07793*	*0.07891*	*0.08185*	*0.10512*
FF (F–X–F)	0.05100	0.05119	0.05109	0.05140	0.05031	0.05571
	0.05301	*0.05319*	*0.05304*	*0.05349*	*0.05209*	*0.05952*

[a] Absolute zero.
[b] Absolute temperature of 298°K.

Table 2. Bastiansen-Morino shrinkage effects for six octahedral hexafluorides (Å units).

Molecule	Nonlinear FF $\begin{pmatrix} & X & \\ & \diagup\ \diagdown & \\ F & \cdots & F \end{pmatrix}$	Linear FF (F—X—F)
SF_6	0.000644 [a]	0.002071
	0.000677 [b]	*0.002520*
SeF_6	0.000560	0.002132
	0.000721	*0.005431*
TeF_6	0.000601	0.002385
	0.001056	*0.003305*
MoF_6	0.001100	0.002666
	0.001843	*0.004897*
WF_6	0.000591	0.002327
	0.001213	*0.003412*
UF_6	0.000812	0.003122
	0.000868	*0.006977*

[a,b] See footnote to Table 1.

for sulphur hexafluoride along with the values for the five additional hexafluorides here considered.

1. Cyvin, S. J. *Kgl. Norske Videnskab. Selskabs Skrifter* **1959** No. 2.
2. Bastiansen, O. and Trætteberg, M. *Acta Cryst.* **13** (1960) 1108; Morino, Y. *Acta Cryst.* **13** (1960) 1107; Morino, Y., Cyvin, S. J., Kuchitsu, K. and Iijima, T. *J. Chem. Phys.* **36** (1962) 1109; Cyvin, S. J. *Tidsskr. Kjemi Bergvesen Met.* **22** (1962) 44, 73.
3. Bye, B. H. and Cyvin, S. J.; Cyvin, S. J. and Meisingseth, E. *To be published.*
4. Pistorius, C. W. F. T. *J. Chem. Phys.* **29** (1958) 1328.
5. Gaunt, J. *Trans. Faraday Soc.* **49** (1955) 1122.
6. Claassen, H. H. *J. Chem. Phys.* **30** (1959) 968.
7. Gaunt, J. *Trans. Faraday Soc.* **50** (1954) 546.

Received October 22, 1962.

Coriolis C Matrix and the Mean-Square Amplitude Σ Matrix in the Problem of Rotation-Vibration Interaction

S. J. CYVIN and L. KRISTIANSEN

Institutt for teoretisk kjemi, Norges tekniske høgskole, Trondheim, Norway

The "Coriolis" C matrix method developed by Meal and Polo [1] will probably become the standard method for studying Coriolis interaction in rotating-vibrating molecules. The method has been applied to specific molecular models by several authors [2], and has also been considered in general by Mills [3].

The Coriolis interaction is closely connected with the force constants of a molecule. In fact the Coriolis coefficients (ζ-values) may be calculated through the L matrix (S = LQ), which is obtainable from the force constants. One has

$$\zeta^{\alpha} = \mathrm{L}^{-1}\ \mathrm{C}^{\alpha}\ \widetilde{\mathrm{L}^{-1}} \qquad (1)$$

using the conventional symbols [1]. Here the C^{α} matrix may be defined by

$$\mathrm{C}^{\alpha} = \mathrm{B}\ \mathbf{M}^{\alpha}\ \widetilde{\mathrm{B}} \qquad (2)$$

We prefer to think of the B matrix as associated with the usual cartesian displacements (S = BX) rather than the mass-weighed coordinates $q_i = m_i^{1/2}\ x_i$. Then the $\mathbf{M}^{\alpha}$ matrix must be defined in the following way. It consists of the blocks $\mathbf{M}_1^{\alpha}, \mathbf{M}_2^{\alpha}, \ldots, \mathbf{M}_N^{\alpha}$ (N = number of atoms) along the main diagonal, which are defined for $\alpha = x,y,z$ by

$$\mathbf{M}_i^{x} = \begin{bmatrix} 0 & 0 & 0 \\ 0 & 0 & \mu_i \\ 0 & -\mu_i & 0 \end{bmatrix}$$

$$\mathbf{M}_i^{y} = \begin{bmatrix} 0 & 0 & -\mu_i \\ 0 & 0 & 0 \\ \mu_i & 0 & 0 \end{bmatrix}$$

$$\mathbf{M}_i^{z} = \begin{bmatrix} 0 & \mu_i & 0 \\ -\mu_i & 0 & 0 \\ 0 & 0 & 0 \end{bmatrix}$$

μ_i denotes as usual the inverse mass of the i-th atom. Our eqn. (2) appears to be a slight modification of eqn. (II—3) from the ingenious work of Meal and Polo [1]. Our equation shows more closely the analogy with the definition of the G matrix, which usually is written in the form

Table 2. Bastiansen-Morino shrinkage effects for six octahedral hexafluorides (Å units).

Molecule	Nonlinear FF $\begin{pmatrix} & X & \\ & \diagup\ \diagdown & \\ F & \cdots & F \end{pmatrix}$	Linear FF (F—X—F)
SF_6	0.000644 [a]	0.002071
	0.000677 [b]	*0.002520*
SeF_6	0.000560	0.002132
	0.000721	*0.005431*
TeF_6	0.000601	0.002385
	0.001056	*0.003305*
MoF_6	0.001100	0.002666
	0.001843	*0.004897*
WF_6	0.000591	0.002327
	0.001213	*0.003412*
UF_6	0.000812	0.003122
	0.000868	*0.006977*

[a,b] See footnote to Table 1.

for sulphur hexafluoride along with the values for the five additional hexafluorides here considered.

1. Cyvin, S. J. *Kgl. Norske Videnskab. Selskabs Skrifter* **1959** No. 2.
2. Bastiansen, O. and Trætteberg, M. *Acta Cryst.* **13** (1960) 1108; Morino, Y. *Acta Cryst.* **13** (1960) 1107; Morino, Y., Cyvin, S. J., Kuchitsu, K. and Iijima, T. *J. Chem. Phys.* **36** (1962) 1109; Cyvin, S. J. *Tidsskr. Kjemi Bergvesen Met.* **22** (1962) 44, 73.
3. Bye, B. H. and Cyvin, S. J.; Cyvin, S. J. and Meisingseth, E. *To be published.*
4. Pistorius, C. W. F. T. *J. Chem. Phys.* **29** (1958) 1328.
5. Gaunt, J. *Trans. Faraday Soc.* **49** (1955) 1122.
6. Claassen, H. H. *J. Chem. Phys.* **30** (1959) 968.
7. Gaunt, J. *Trans. Faraday Soc.* **50** (1954) 546.

Received October 22, 1962.

Coriolis C Matrix and the Mean-Square Amplitude Σ Matrix in the Problem of Rotation-Vibration Interaction

S. J. CYVIN and L. KRISTIANSEN

Institutt for teoretisk kjemi, Norges tekniske høgskole, Trondheim, Norway

The "Coriolis" C matrix method developed by Meal and Polo [1] will probably become the standard method for studying Coriolis interaction in rotating-vibrating molecules. The method has been applied to specific molecular models by several authors [2], and has also been considered in general by Mills [3].

The Coriolis interaction is closely connected with the force constants of a molecule. In fact the Coriolis coefficients (ζ-values) may be calculated through the L matrix (S = LQ), which is obtainable from the force constants. One has

$$\zeta^{\alpha} = \mathrm{L}^{-1}\ \mathrm{C}^{\alpha}\ \widetilde{\mathrm{L}^{-1}} \qquad (1)$$

using the conventional symbols [1]. Here the C^{α} matrix may be defined by

$$\mathrm{C}^{\alpha} = \mathrm{B}\ \mathbf{M}^{\alpha}\ \widetilde{\mathrm{B}} \qquad (2)$$

We prefer to think of the B matrix as associated with the usual cartesian displacements (S = BX) rather than the mass-weighed coordinates $q_i = m_i^{1/2}\ x_i$. Then the $\mathbf{M}^{\alpha}$ matrix must be defined in the following way. It consists of the blocks $\mathbf{M}_1^{\alpha}, \mathbf{M}_2^{\alpha}, \ldots, \mathbf{M}_N^{\alpha}$ (N = number of atoms) along the main diagonal, which are defined for $\alpha = x,y,z$ by

$$\mathbf{M}_i^{x} = \begin{bmatrix} 0 & 0 & 0 \\ 0 & 0 & \mu_i \\ 0 & -\mu_i & 0 \end{bmatrix}$$

$$\mathbf{M}_i^{y} = \begin{bmatrix} 0 & 0 & -\mu_i \\ 0 & 0 & 0 \\ \mu_i & 0 & 0 \end{bmatrix}$$

$$\mathbf{M}_i^{z} = \begin{bmatrix} 0 & \mu_i & 0 \\ -\mu_i & 0 & 0 \\ 0 & 0 & 0 \end{bmatrix}$$

μ_i denotes as usual the inverse mass of the i-th atom. Our eqn. (2) appears to be a slight modification of eqn. (II—3) from the ingenious work of Meal and Polo [1]. Our equation shows more closely the analogy with the definition of the G matrix, which usually is written in the form

Appendix: Summary of relations containing eqns. (4)–(11) along with several alternative forms.

(1)	$\zeta^{\alpha} = \widetilde{L}\, G^{-1} C^{\alpha} \widetilde{L^{-1}}$	$\lvert G^{-1}C^{\alpha} - \sigma E \rvert \equiv \lvert \zeta^{\alpha} - \sigma E \rvert = 0$
(2)	$\Lambda\zeta^{\alpha} = \widetilde{L}\, F\, C^{\alpha} \widetilde{L^{-1}}$	$\lvert FC^{\alpha} - \gamma E \rvert \equiv \lvert \Lambda\zeta^{\alpha} - \gamma E \rvert = 0$
(3)	$\Delta^{-1}\zeta^{\alpha} = \widetilde{L}\Sigma^{-1}C^{\alpha}\widetilde{L^{-1}}$	No practical importance (?)
(1′)	$\zeta^{\alpha} = L^{-1}C^{\alpha}G^{-1}$	$\lvert C^{\alpha}G^{-1} - \sigma' E \rvert \equiv \lvert \zeta^{\alpha} - \sigma' E \rvert = 0$
(2′)	$\zeta^{\alpha}\Lambda = L^{-1}C''\, F\, L$	$\lvert C^{\alpha}F - \gamma' E \rvert \equiv \lvert \zeta^{\alpha}\Lambda - \gamma' E \rvert = 0$
(3′)	$\zeta^{\alpha}\Delta^{-1} = L^{-1}C^{\alpha}\,\Sigma^{-1}L$	No practical importance (?)
(1″)	$\zeta^{\alpha} = L^{-1}C^{\alpha}G^{-1}L$	Identical with (1′)
(2″)	$\Lambda^{-1}\zeta^{\alpha} = L^{-1}F^{-1}G^{-1}C^{\alpha}G^{-1}L$	$\lvert F^{-1}G^{-1}C^{\alpha}G^{-1} - \gamma'' E \rvert \equiv \lvert \Lambda^{-1}\zeta^{\alpha} - \gamma'' E \rvert = 0$
(3″)	$\Delta\,\zeta^{\alpha} = L^{-1}\,\Sigma\,G^{-1}\,C^{\alpha}\,G^{-1}\,L$	$\lvert \Sigma G^{-1}C^{\alpha}G^{-1} - \varkappa E \rvert \equiv \lvert \Delta\zeta^{\alpha} - \varkappa E \rvert = 0$
(1‴)	$\zeta^{\alpha} = L^{-1}C^{\alpha}G^{-1}L$	Identical with (1′)
(2‴)	$\zeta^{\alpha}\Lambda^{-1} = L^{-1}C^{\alpha}G^{-1}F^{-1}G^{-1}L$	$\lvert C^{\alpha}G^{-1}F^{-1}G^{-1} - \gamma''' E \rvert \equiv \lvert \zeta^{\alpha}\Lambda^{-1} - \gamma''' E \rvert = 0$
(3‴)	$\zeta^{\alpha}\Delta = L^{1-}C^{\alpha}G^{-1}\Sigma G^{-1}$	$\lvert C^{\alpha}G^{-1}\,\Sigma G^{-1} - \varkappa' E \rvert \equiv \lvert \zeta^{\alpha}\Delta - \varkappa' E \rvert = 0$

$$G = B\ \mu\ \widetilde{B} \qquad (3)$$

Here the μ matrix may be defined in terms of the diagonal blocks $\underline{\mu}_1, \underline{\mu}_2, \ldots, \underline{\mu}_N$, where

$$\underline{\mu}_i = \begin{bmatrix} \mu_i & 0 & 0 \\ 0 & \mu_i & 0 \\ 0 & 0 & \mu_i \end{bmatrix}$$

Cyvin [4] has introduced the Σ matrix (mean-square amplitude matrix), and proved it to be equivalent with the force constant matrix. Thus the L matrix may be obtained from the complete Σ matrix, as well as the force constant matrix. It seems, therefore, very reasonable to seek for some relations between ζ-values and the Σ-matrix elements, similar to the existing relations between ζ-values and the force constants. Such relations have been evaluated in this work.

By combining eqn. (1) with $E = \widetilde{L}\, G^{-1}\, L$ and $\Lambda = \widetilde{L}\, F\, L$, respectively, one obtains the relations of Meal and Polo [1], *viz.*

$$\zeta^{\alpha} = \widetilde{L}\ G^{-1}\ C^{\alpha}\ \widetilde{L^{-1}} \qquad (4)$$

$$\Lambda\zeta^{\alpha} = \widetilde{L}\ F\ C^{\alpha}\ \widetilde{L^{-1}} \qquad (5)$$

from which the following characteristic equations have been deduced [1]

$$\lvert G^{-1}\, C^{\alpha} - \sigma E \rvert \equiv \lvert \zeta^{\alpha} - \sigma E \rvert = 0 \qquad (6)$$

$$\lvert F\, C^{\alpha} - \gamma E \rvert \equiv \lvert \Lambda\zeta^{\alpha} - \gamma E \rvert = 0 \qquad (7)$$

It is true that an analogous relation may be obtained from $\Lambda^{-1} = \widetilde{L}\ \Sigma^{-1}L$ combined with (1). This relation would contain Σ^{-1} and is assumed not to have practical importance, at least before any clear physical significance is found for the inverse Σ matrix. Hence we proceeded in an other way, combining $\Lambda = L^{-1}\Sigma\ \widetilde{L^{-1}}$ with (1). In addition we utilized the well-known relation $G^{-1} = \widetilde{L^{-1}}\ L^{-1}$ and obtained the result

$$\Delta\zeta^{\alpha} = L^{-1}\ \Sigma G^{-1}\ C^{\alpha}\ G^{-1}\ L \qquad (8)$$

This is a similarity transformation. Hence the $\Delta\zeta^{\alpha}$ and $\Sigma G^{-1}\ C^{\alpha}\ G^{-1}$ matrices have identical characteristic values, and consequently

$$\lvert \Sigma G^{-1}\ C^{\alpha}\ G^{-1} - \varkappa E \rvert \equiv \lvert \Delta\zeta^{\alpha} - \varkappa E \rvert = 0 \qquad (9)$$

The relation has been applied to the case of planar symmetrical XY_3 molecules, and has proved its usefulness [5].

We also wish to point out that a relation of the form (9) exists for the *inverse* F matrix. One has

$$\Lambda^{-1}\zeta^{\alpha} = L^{-1}\ F^{-1}\ G^{-1}\ C^{\alpha}\ G^{-1}\ L \qquad (10)$$

and consequently

$$\lvert F^{-1}\ G^{-1}\ C^{\alpha}\ G^{-1} - \gamma'' E \rvert \equiv \lvert \Lambda^{-1}\zeta^{\alpha} - \gamma'' E \rvert = 0 \qquad (11)$$

1. Meal, J. H. and Polo, S. R. *J. Chem. Phys.* **24** (1956) 1119, 1126.
2. Günthard, H. H., Lord, R. C. and McCubbin, T. K., Jr. *J. Chem. Phys.* **25** (1956) 768; Nakagawa, I. and Shimanouchi, T. *Spectrochim. Acta* **18** (1962) 513.

3. Mills I. M. *Spectrochim. Acta* **16** (1960) 35; *J. Mol. Spectr.* **5** (1960) 334.
4. Cyvin, S. J. *Acta Chem. Scand.* **13** (1959) 2135; *Spectrochim. Acta* **15** (1959) 828.
5. Kristiansen, L. and Cyvin, S. J. *To be published.*

Received October 22, 1962.

On the Mechanism of Rhodanese Inhibition by Sulfite and Cyanide

BO SÖRBO

Nobel Medical Institute, Biochemical Department, Stockholm, Sweden

The inhibition of rhodanese by cyanide [1] or sulfite [2] has been interpreted as being due to a reaction of the inhibitor with a disulfide bond in the enzyme [3,4]. However, Green and Westley [5] have recently observed that the inhibition of rhodanese by cyanide was more rapid in dilute than in concentrated enzyme solutions, which would not be expected if the inhibition was due to a direct reaction of the inhibitor with the enzyme. Furthermore they found that crystalline rhodanese contained labile sulfur, which could be exchanged with the outer sulfur atom of thiosulfate or removed from the enzyme by incubation with cyanide or sulfite. The sulfur-rhodanese complex was formed when the free enzyme reacted with a sulfur donor, *e.g.* thiosulfate, and thus represents an intermediate in the rhodanese reaction. Since thiosulfate is present in some of the purification steps used for the preparation of crystalline rhodanese [6,7], the latter is obtained in the form of this sulfur complex. Green and Westley suggested that either cyanide or sulfite inactivates rhodanese by removing the labile sulfur from the enzyme; this treatment yields the free enzyme, which was supposed to be very unstable and rapidly denatured. However, one objection against this mechanism is the fact that sulfite is a more potent inhibitor than cyanide [3], although it is a less active sulfur acceptor in rhodanese catalyzed reactions [8].

It has now been observed that the inhibition of rhodanese with sulfite or cyanide required the presence of oxygen (Table 1) and that rhodanese, inhibited by sulfite or cyanide, could be reactivated by treatment with sulfhydryl compounds such as cysteamine, mercaptoethanol, or thioglycolate. Dialysis against phosphate buffer or sodium acetate gave no reactivation. If the enzyme was denatured by incubation with 8 M urea, neither dialysis against buffer nor treatment with sulfhydryl compounds had any reactivating effect. Thus the sulfhydryl compounds could not reactivate urea-denatured rhodanese, and their reactivating effect on sulfite- or cyanide-inhibited rhodanese must apparently be explained by another mechanism. Experiments with ^{35}S-labelled sulfite and crystalline rhodanese (Table 2) furthermore showed that the inhibitor became bound to the enzyme during the inhibition and was liberated again from the inhibited enzyme when the latter was reactivated by cysteamine. The rhodanese preparation used in these experiments was 3 times crystallized (specific activity 252 RU/mg) and contained 1.3 atoms of labile sulfur per molecule enzyme. The labile sulfur was determined by treating the enzyme with an excess of cyanide and colorimetric determination [9] of the thiocyanate formed after the remaining cyanide had been removed by aeration from the acidified sample. The number of labile sulfur atoms per molecule rhodanese found for this preparation agreed with the number of sulfite molecules bound to one molecule of rhodanese during inhibition (Table 2). However, Westley and coworkers [5,10] reported 1.5—1.9 atoms per molecule. When crystalline rhodanese was oxidized with performic acid [11] and cysteic acid determined with an automatic amino

Table 1. Effect of oxygen on sulfite and cyanide inhibition of rhodanese. Rhodanese (partially purified) was incubated with the inhibitor in Warburg flasks containing air or purified nitrogen as indicated. Inhibitor concentration was 0.01 M in all experiments, pH was 7.0 in case of sulfite and 7.4 in case of cyanide, time of incubation was 10 min in case of sulfite and 30 min in case of cyanide. Controls were run in nitrogen with omission of the inhibitor. Rhodanese activity was determined as in Ref. [6].

Inhibitor	*Gas phase*	*Activity* % of control
Sulfite	Air	0.5
,,	Nitrogen	100
Cyanide	Air	4.3
,,	Nitrogen	88.7

3. Mills I. M. *Spectrochim. Acta* **16** (1960) 35; *J. Mol. Spectr.* **5** (1960) 334.
4. Cyvin, S. J. *Acta Chem. Scand.* **13** (1959) 2135; *Spectrochim. Acta* **15** (1959) 828.
5. Kristiansen, L. and Cyvin, S. J. *To be published.*

Received October 22, 1962.

On the Mechanism of Rhodanese Inhibition by Sulfite and Cyanide

BO SÖRBO

Nobel Medical Institute, Biochemical Department, Stockholm, Sweden

The inhibition of rhodanese by cyanide [1] or sulfite [2] has been interpreted as being due to a reaction of the inhibitor with a disulfide bond in the enzyme [3,4]. However, Green and Westley [5] have recently observed that the inhibition of rhodanese by cyanide was more rapid in dilute than in concentrated enzyme solutions, which would not be expected if the inhibition was due to a direct reaction of the inhibitor with the enzyme. Furthermore they found that crystalline rhodanese contained labile sulfur, which could be exchanged with the outer sulfur atom of thiosulfate or removed from the enzyme by incubation with cyanide or sulfite. The sulfur-rhodanese complex was formed when the free enzyme reacted with a sulfur donor, *e.g.* thiosulfate, and thus represents an intermediate in the rhodanese reaction. Since thiosulfate is present in some of the purification steps used for the preparation of crystalline rhodanese [6,7], the latter is obtained in the form of this sulfur complex. Green and Westley suggested that either cyanide or sulfite inactivates rhodanese by removing the labile sulfur from the enzyme; this treatment yields the free enzyme, which was supposed to be very unstable and rapidly denatured. However, one objection against this mechanism is the fact that sulfite is a more potent inhibitor than cyanide [3], although it is a less active sulfur acceptor in rhodanese catalyzed reactions [8].

It has now been observed that the inhibition of rhodanese with sulfite or cyanide required the presence of oxygen (Table 1) and that rhodanese, inhibited by sulfite or cyanide, could be reactivated by treatment with sulfhydryl compounds such as cysteamine, mercaptoethanol, or thioglycolate. Dialysis against phosphate buffer or sodium acetate gave no reactivation. If the enzyme was denatured by incubation with 8 M urea, neither dialysis against buffer nor treatment with sulfhydryl compounds had any reactivating effect. Thus the sulfhydryl compounds could not reactivate urea-denatured rhodanese, and their reactivating effect on sulfite- or cyanide-inhibited rhodanese must apparently be explained by another mechanism. Experiments with ^{35}S-labelled sulfite and crystalline rhodanese (Table 2) furthermore showed that the inhibitor became bound to the enzyme during the inhibition and was liberated again from the inhibited enzyme when the latter was reactivated by cysteamine. The rhodanese preparation used in these experiments was 3 times crystallized (specific activity 252 RU/mg) and contained 1.3 atoms of labile sulfur per molecule enzyme. The labile sulfur was determined by treating the enzyme with an excess of cyanide and colorimetric determination [9] of the thiocyanate formed after the remaining cyanide had been removed by aeration from the acidified sample. The number of labile sulfur atoms per molecule rhodanese found for this preparation agreed with the number of sulfite molecules bound to one molecule of rhodanese during inhibition (Table 2). However, Westley and coworkers [5,10] reported 1.5—1.9 atoms per molecule. When crystalline rhodanese was oxidized with performic acid [11] and cysteic acid determined with an automatic amino

Table 1. Effect of oxygen on sulfite and cyanide inhibition of rhodanese. Rhodanese (partially purified) was incubated with the inhibitor in Warburg flasks containing air or purified nitrogen as indicated. Inhibitor concentration was 0.01 M in all experiments, pH was 7.0 in case of sulfite and 7.4 in case of cyanide, time of incubation was 10 min in case of sulfite and 30 min in case of cyanide. Controls were run in nitrogen with omission of the inhibitor. Rhodanese activity was determined as in Ref. [6].

Inhibitor	*Gas phase*	*Activity* % of control
Sulfite	Air	0.5
,,	Nitrogen	100
Cyanide	Air	4.3
,,	Nitrogen	88.7

Table 2. Inhibition of rhodanese with ^{35}S-labelled sulfite. A sample of 0.1 μmole crystalline rhodanese was incubated with 100 μmoles $Na_2{}^{35}SO_3$ (sp.a. about 0.02 mC/mmole) in air at pH 7.0 and the excess sulfite removed by dialysis against 0.01 M sodium acetate or 0.1 M cysteamine + 0.01 M phosphate buffer pH 7.4. The rhodanese activity was compared with that of the non-treated enzyme.

Treatment	*Activity* %	^{35}S-*incorporated* μmole/μmole enzyme
Sulfite	0.4	1.31
Sulfite + cysteamine	81	0.137

acid analyzer [12] after hydrolysis of the protein, 3.85 moles of cysteic acid per mole of enzyme were obtained. This indicated that rhodanese contained 4 cysteine or half-cystine residues per molecule. The enzyme was then assayed for SH-groups by amperometric titration with silver ions [13] and it was found that the native enzyme reacted with silver ions to a very slight extent without giving an endpoint. However, in the presence of a detergent (5 % dodecyl sulfate) a value of 4.35 SH/mole enzyme was obtained. These results indicated that rhodanese contains 4 cysteine and no cystine residues. When sulfite-inhibited rhodanese was titrated in the presence of detergent only 3.16 SH/mole enzyme was found; thus one SH-group had reacted during the inhibition.

The results now obtained suggest that rhodanese contains an active sulfhydryl group (the free enzyme is represented by ESH in the reactions below) and the enzyme-sulfur complex a persulfide group (ESSH). The otherwise rather unstable persulfide group is probably stabilized by bonding to another site in the enzyme, as the labile sulfur is released when the enzyme-sulfur complex is denatured [5,10]. The inhibition mechanism in case of sulfite would be

$$ESH + O + SO_3^{2-} = ESSO_3^- + OH^-$$

and the reactivation by a sulfhydryl compound (RSH)

$$ESSO_3^- + RSH = ESSR + HSO_3^-$$

followed by

$$ESSR + RSH = ESH + (RS)_2.$$

Similar reactions can be written for the cyanide inhibition except that a thiocyanate ester (ESCN) is formed instead of a thiosulfate ester ($ESSO_3^-$). The possibility that rhodanese contains an active sulfhydryl group has in fact been previously suggested [2,14] from inhibition experiments with sulfhydryl reagents, but it was pointed out [2] that these compounds had a rather weak inhibitory effect on the enzyme. This may be due to the fact that in these experiments the enzyme was present as the rhodanese-sulfur complex which may be less reactive in the presence of inhibitors than the free enzyme.

A full report of the present findings, including the complete amino acid analysis of rhodanese, will be published in this journal.

Acknowledgements. This work has been supported by a grant from the *Swedish Medical Research Council*. Able technical assistance was given by Mr. U. Andersson, Miss A. M. Fridén and Mr. I. Hedenborg.

1. Lang, K. *Z. Vitamin. Hormon. Fermentforsch.* **2** (1949) 288.
2. Sörbo, B. *Acta Chem. Scand.* **5** (1951) 724.
3. Sörbo, B. *Acta Chem. Scand.* **5** (1951) 1218.
4. Sörbo, B. *Acta Chem. Scand.* **7** (1953) 1137.
5. Green, J. R. and Westley, J. *J. Biol. Chem.* **236** (1961) 3047.
6. Sörbo, B. *Acta Chem. Scand.* **7** (1953) 1128.
7. Westley, J. and Green, J. R. *J. Biol. Chem.* **234** (1959) 2325.
8. Sörbo, B. *Acta Chem. Scand.* **11** (1957) 628.
9. Nyström, C. and Sörbo, B. *Scand. J. Clin. & Lab. Invest.* **9** (1957) 223.
10. Westley, J. and Nakamoto, T. *J. Biol. Chem.* **237** (1962) 547.
11. Pierce, J. G. *J. Am. Chem. Soc.* **77** (1955) 184.
12. Spackman, D. H., Stein, W. H. and Moore, S. *Anal. Chem.* **30** (1958) 1190.
13. Benesch, R. E., Lardy, H. A. and Benesch, R. *J. Biol. Chem.* **216** (1955) 663.
14. Saunders, J. P. and Himwich, W. A. *Am. J. Physiol.* **163** (1950) 404.

Received November 21, 1962.

Molecular Conformation of 4- and 5-Hydroxypipecolic Acids

JAMES N. SHOOLERY

Varian Associates, Palo Alto, California

and ARTTURI I. VIRTANEN

Laboratory of the Foundation for Chemical Research, Biochemical Institute, Helsinki, Finland

Two hydroxypipecolic acids were isolated from *Rhapis*, *Acacia*, and *Albizzia* species, as well as from some other plants, and characterized chemically by Virtanen and Kari as 5- and 4-hydroxypipecolic acids [1,2]. The position of the hydroxy group was estimated by oxidation with potassium permanganate whereby mainly, or only, glutamic acid was formed from the 5-hydroxy acid and aspartic acid beside other products, but no glutamic acid was formed from the 4-hydroxy acid.

Since doubts had been expressed regarding the position of the hydroxy group in the compound characterized as 4-hydroxypipecolic acid [3], the acid was reinvestigated thoroughly. The position of the hydroxy group was confirmed to be consistent with our previous result [4].

The NMR spectra of 4- and 5-hydroxypipecolic acids were obtained in the Varian Laboratories from preparations sent by one of us as early as in 1959. The molecular conformation of these acids was hereby established. The estimation was repeated this year using an HR-100 High Resolution NMR Spectrometer operating at 100 mc/sec. The samples were dissolved in D_2O which resulted in a strong HDO peak in the spectrum due to exchange of the labile hydrogens. This peak was arbitrarily labelled zero and an audio-frequency sideband was introduced 350 cps upfield to serve as a calibration.

Fig. 1 shows the spectrum of 4-hydroxypipecolic acid. The quintet at 52 cps must arise from H_1 since only this proton has four neighbors. Since all four are equally spin coupled to H_1, H_1 must be equatorial. The pair of doublets at 83 cps is assigned to H_2 since only this proton has just two neighbors. The large coupling, characteristic of axial-axial neighbors, shows that H_2 is axial. The pattern centered at 145 cps is assigned to H_3 and H_4 while the complex group of lines at higher field strengths are due to the remaining four protons. The structure and conformation shown in Fig. 3a is consistent with the NMR data.

Fig. 2 shows the spectrum of 5-hydroxypipecolic acid. The resonance from H_1 at 102 cps is now a septet which must arise from coupling to two neighbors with a small coupling constant and coupling to two other neighbors with a coupling constant twice as large. The large coupling shows that H_1 is now axial. H_2 is also axial since it is strongly coupled according to the assignments of Fig. 2. Thus, the conforma-

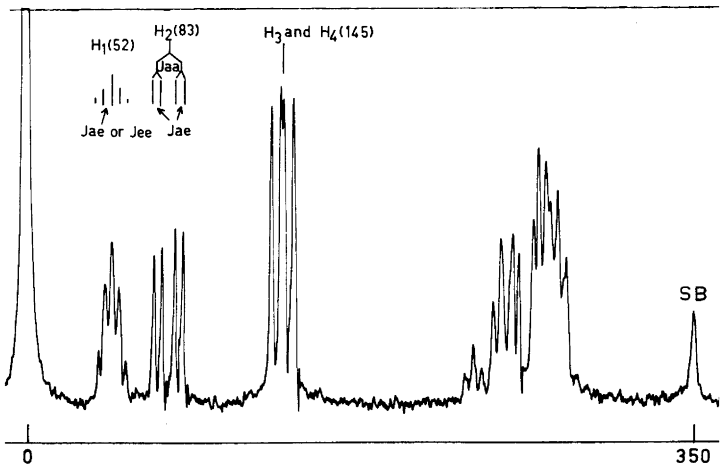

Fig. 1. The NMR-spectrum of 4-hydroxypipecolic acid.

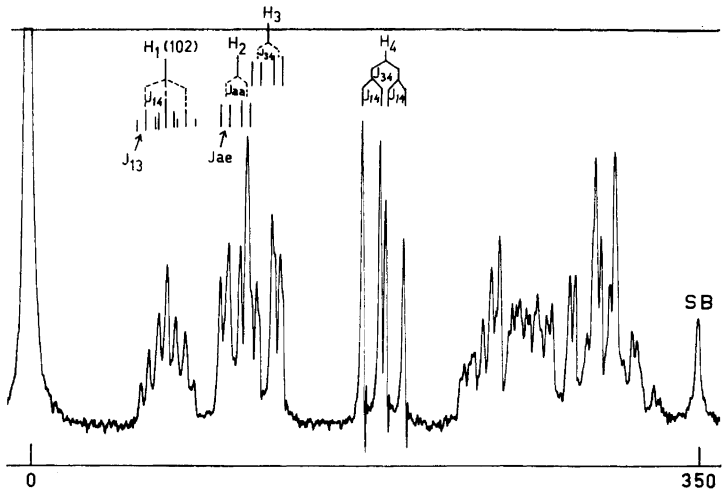

Fig. 2. The NMR-spectrum of 5-hydroxypipecolic acid.

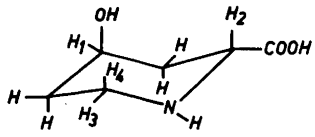

a

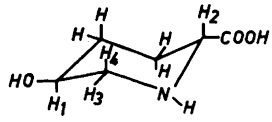

b

Fig. 3. Molecular conformation of 4-hydroxypipecolic acid (a) and 5-hydroxypipecolic acid (b).

tion of Fig. 3b is consistent with the NMR data for 5-hydroxypipecolic acid.

Witkop and Foltz[5] estimated the configuration of 5-hydroxypipecolic acid, and Clark-Lewis and Mortimer[6] that of 4-hydroxypipecolic acid using a chemical method. Their result is in agreement with ours.

1. Virtanen, A. I. and Kari, S. *Acta Chem. Scand.* **8** (1954) 1290.
2. Virtanen, A. I. and Kari, S. *Ibid.* **9** (1955) 170.
3. Fowden, L. *Biochem. J.* **70** (1958) 629.
4. Virtanen, A. I. and Gmelin, R. *Acta Chem. Scand.* **13** (1959) 1244.
5. Witkop, B. and Foltz, C. M. *J. Am. Chem. Soc.* **79** (1957) 192.
6. Clark-Lewis, J. W. and Mortimer, P. I. *J. Chem. Soc.* **1961** 189.

Received November 9, 1962.

On the Existence of the Suboxides Cr_3O and Mo_3O

LARS KIHLBORG

Institute of Chemistry, University of Uppsala, Uppsala, Sweden

In two papers published in 1954 Schönberg reported the preparation of two new oxides of chromium and molybdenum with the probable formulas Cr_3O [1] and Mo_3O [2]. Neither was obtained as a single phase.

Cr_3O was said to be formed by three different methods, namely (*a*) when Cr_2O_3 was reduced with titanium, vanadium or zirconium at about 1500°C, (*b*) when chromium metal was oxidized by steam in a large excess of hydrogen at 600°C, and (*c*) in trace amounts when chromium metal

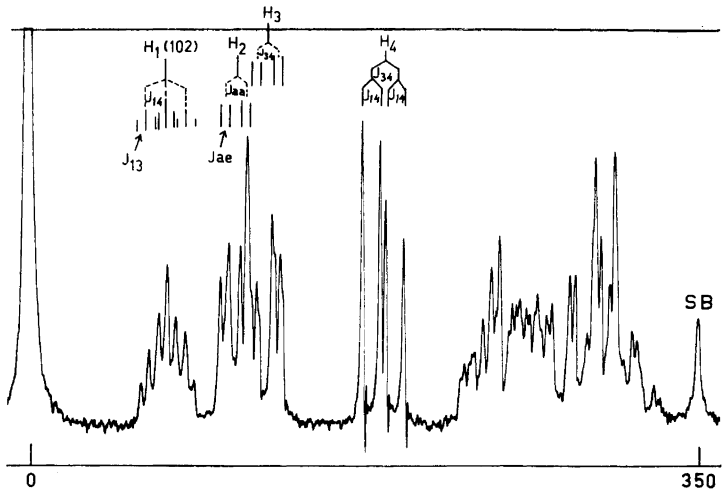

Fig. 2. The NMR-spectrum of 5-hydroxypipecolic acid.

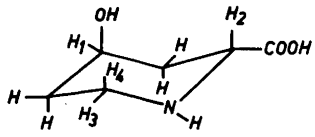

a

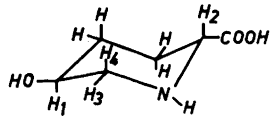

b

Fig. 3. Molecular conformation of 4-hydroxypipecolic acid (a) and 5-hydroxypipecolic acid (b).

tion of Fig. 3b is consistent with the NMR data for 5-hydroxypipecolic acid.

Witkop and Foltz[5] estimated the configuration of 5-hydroxypipecolic acid, and Clark-Lewis and Mortimer[6] that of 4-hydroxypipecolic acid using a chemical method. Their result is in agreement with ours.

1. Virtanen, A. I. and Kari, S. *Acta Chem. Scand.* **8** (1954) 1290.
2. Virtanen, A. I. and Kari, S. *Ibid.* **9** (1955) 170.
3. Fowden, L. *Biochem. J.* **70** (1958) 629.
4. Virtanen, A. I. and Gmelin, R. *Acta Chem. Scand.* **13** (1959) 1244.
5. Witkop, B. and Foltz, C. M. *J. Am. Chem. Soc.* **79** (1957) 192.
6. Clark-Lewis, J. W. and Mortimer, P. I. *J. Chem. Soc.* **1961** 189.

Received November 9, 1962.

On the Existence of the Suboxides Cr_3O and Mo_3O

LARS KIHLBORG

Institute of Chemistry, University of Uppsala, Uppsala, Sweden

In two papers published in 1954 Schönberg reported the preparation of two new oxides of chromium and molybdenum with the probable formulas Cr_3O [1] and Mo_3O [2]. Neither was obtained as a single phase.

Cr_3O was said to be formed by three different methods, namely (*a*) when Cr_2O_3 was reduced with titanium, vanadium or zirconium at about 1500°C, (*b*) when chromium metal was oxidized by steam in a large excess of hydrogen at 600°C, and (*c*) in trace amounts when chromium metal

and Cr_2O_3 were heated in an induction furnace. The oxide was reported to be isomorphous with Cr_3Si (β—W structure type) and to have the same cubic cell dimension as this phase.

Mo_3O was obtained by heating mixtures of Mo and MoO_2 at 1000°C and then lowering the temperature to 400°C at a constant rate of 10° per day. A defect version of the *anti*-BiF_3 type structure was proposed for this phase.

No papers confirming the existence of these suboxides have appeared since 1954 and for several reasons a repetition of some of these experiments under more carefully controlled conditions was thought desirable.

Cr_3O. The formation of the phase described as Cr_3O by method (*b*) above was used by Schönberg as evidence that this product was in fact a binary oxide. Thus method (*a*) involved reactions in a ternary system, one component of which was a metal noted for its reactivity towards most crucible materials, while the traces of "Cr_3O" detected in the powder patterns of samples prepared by method (*c*) could easily have been Cr_3Si. For this reason method (*b*) was chosen in the attempts described below to repeat the preparation of Cr_3O.

Hydrogen gas was passed through a tube containing platinized asbestos heated to about 600°C to combine the free oxygen, dried in conc. H_2SO_4 and passed through a tube containing activated carbon at liquid nitrogen temperatures. A given percentage of H_2O was then added by passing the gas through water maintained at 25°C or 0°C after which it was led into a tube of supremax glass and so over an alumina boat containing the chromium to be oxidized. The metal was in the form of a powder crushed to more than 150 mesh. The temperature of the reaction tube was maintained at 600°C during the 24 h period of each experiment. The products were analyzed by means of X-ray powder diffraction patterns recorded in a Guinier focusing camera using Cr$K\alpha$ radiation.

When high grade chromium ("*Ges.f. Elektrometallurgie m.b.H. Werk Nürnberg*", 99.96 % Cr) was used no lines other than those due to Cr and Cr_2O_3 could be observed in the powder patterns of the reaction products, even when long exposure times were used to record the X-ray photographs. Experiments were also made with chromium of the same origin as that used by Schönberg ("*AB Ferrolegeringar*, Stockholm, 99.4 %"). Contamination of this material was demonstrated by the presence in its powder pattern of several additional faint lines. In this case also, however, the only detectable change in the powder patterns after the reaction was the appearance of Cr_2O_3 lines. It is possible that Schönberg attributed some of these impurity lines to "Cr_3O".

The intensity data published for "Cr_3O" [1] are confusing. Since no information is given about the type (or types) of camera used values of I_{calc} cannot be recalculated. On the basis of the proposed structure $p.F^2_{calc}$-values have been recomputed by the present author, but the ratio between these and the published values of I_{calc} varies in a way which can hardly be accounted for by any probable instrumental ϑ-function (or functions).

Mo_3O. Efforts were made to prepare Mo_3O according to the method given by Schönberg [2]. The starting materials were molybdenum powder ("*Kahlbaum*" or "*Kebo*") and MoO_2 which had been prepared by reducing MoO_3 with hydrogen. These were intimately mixed in the proportions required to give the composition Mo_3O and put into high grade alumina tubes which were sealed inside silica tubes under vacuum. The tubes were heated to 1040°C after which the temperature was reduced to 400°C at a rate of 10° per day by means of a programmed regulator.

The Guinier powder patterns (Cu$K\alpha$ radiation) of the products following this heat treatment did not give even the faintest indication of lines additional to those of the starting materials. The same result was obtained with a sample which had been pressed to a pellet and also with samples heated at 1200°C for one day.

The conclusion that can be drawn from the negative results obtained by these experiments is that the oxides Cr_3O and Mo_3O cannot be reproducibly obtained by the methods reported and at present there seems to be no definite proof of their existence.

Acknowledgements. I wish to thank Professor G. Hägg for suggesting this reinvestigation and Dr. S. Rundqvist for stimulating discussions.

1. Schönberg, N. *Acta Chem. Scand.* **8** (1954) 221.
2. Schönberg, N. *Acta Chem. Scand.* **8** (1954) 617.

Received November 22, 1962.

Studies on Cobaltammines

VIII. The Infrared Spectrum of the Cobalthexammine(III) Ion in Aqueous Solutions of some Electrolytes

RAGNAR LARSSON

Infrared Laboratory, Chemical Institute, University of Lund, Lund, Sweden

In previous works in this series it has been shown that the cobalthexammine(III) ion can bind various ligands in its second sphere of coordination. The question then arises: what kind are the bonding forces in these outer-sphere complexes? There are — in addition to mere electrostatic attraction — two possibilities: hydrogen bonding *via* the ammonia groups and an electron transfer bonding. The latter effect can be detected [1] by ultraviolet spectroscopy, whereas infrared spectroscopy may be a useful tool for the detection of hydrogen bonding.

Hydrogen bonding should shift the N—H stretching vibration towards lower frequencies. In order to investigate this effect $Co(NH_3)_6Cl_3$ has been dissolved in heavy water or in heavy water containing Na_2SO_4 or KF. Heavy water must be used, as ordinary water absorbs light too strongly in the actual frequency region (3500—2800 cm^{-1}). The chloride must be used to achieve sufficently high concentrations of the complex. The experimental conditions were the same as before [2], but for the use of 34 μ platinum spacers and the fact that the instrument was run with "routine" settings. In order to suppress the isotope exchange, a small quantity of conc. perchloric acid was added to the heavy water (pH $\approx$ 2). In the case of the fluoride solutions pH was then by necessity higher (pH $\approx$ 7). One should therefore expect a rapid isotope exchange [3,4]. However, only a slow fading of the intensity of the N—H absorption was observed (also at 2950 cm^{-1}). One possible explanation of this phenomenon may be that the fluoride ions block the positions where hydroxide ions can coordinate and thus the reaction path proposed by Block and Gold [4] would be obstructed.

Some representative results are given in Fig. 1. The most striking feature is the position of the main peak at 3400 cm^{-1}. This is decidedly higher than any position

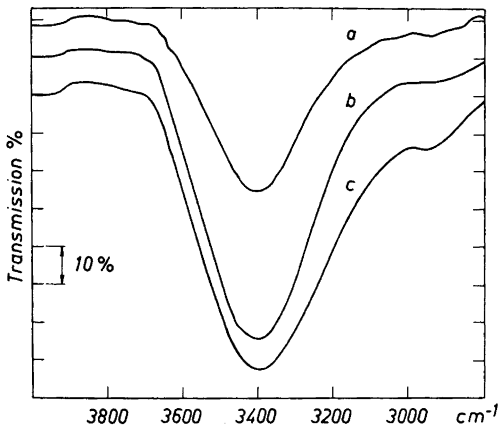

Fig. 1. Curve a: 0.06 m $Co(NH_3)_6Cl_3$ dissolved in 1.0 m Na_2SO_4. Curve b: 0.19 m $Co(NH_3)_6Cl_3$. Curve c: 0.19 m $Co(NH_3)_6Cl_3$ dissolved in 4.0 m KF. The curves are displaced with 10 % intervals along the ordinate scale to increase the readability.

of N—H stretching vibrations reported for solid cobalthexammine(III) salts (*e.g.* Ref. [5]). It rather corresponds to the position reported (Ref. [6], p. 259) for "free" $R—NH_3^+$ ions in solution. A small peak is apparent at $\sim$ 2950 cm^{-1} for all solutions studied. It is most clearly resolved for the fluoride solutions for which a broadening of the 3400 cm^{-1}-peak is observed. This peak at $\sim$2950 cm^{-1} probably corresponds to hydrogen-bonded species. However, as the extinction coefficient of this peak should be expected to be greater than that of the non-hydrogen-bonded one (Ref. [7], p. 101), we are forced to conclude that neither water nor the dissolved anions coordinate *via* hydrogen bonds to any greater extent. This conclusion is obviously in accordance with the one that can be reached from the position of the main peak.

This somewhat astonishing result is probably related to the nonlinearity of the Co—N—H bonds. If a strong hydrogen bond is to be formed, the N—H— —B bond should be linear (Ref. [7], p. 101 and Ref. [8]). Then the atom B will not be in a position as close as possible to the cobalt atom. If the attraction from the cobalt centre supersedes the attraction of the N—H proton, a bent N—H bond will result,

which may not change the N—H vibration frequency much.

I want to thank Mrs Kerstin Pettersson for her splendid technical assistance in recording the spectra. The heavy water was obtained through the courtesy of the A. B. Atomenergi.

1. Yoneda, H. *Bull. Chem. Soc. Japan* **28** (1955) 125.
2. Fronæus, S. and Larsson, R. *Acta Chem. Scand.* **16** (1962) 1433.
3. Anderson, J. S., Briscoe, H. V. A. and Spoor, N. L. *J. Chem. Soc.* **1943** 361.
4. Block, H. and Gold, V. *J. Chem. Soc.* **1959** 966.
5. Hill, D. H. and Rosenberg, A. F. *J. Chem. Phys.* **24** (1956) 1219.
6. Bellamy, L. J. *The Infrared Spectra of Complex Molecules*, Meuthen & Co, Ltd, London 1958.
7. Pimentel, G. C. and McClellan, A. L. *The Hydrogen Bond*, W. H. Freeman and Co., San Fransisco and London 1960.
8. Cannon, C. G. *Spectrochim. Acta* **10** (1958) 341.

Received November 23, 1962.

A New γ-Glutamylpeptide, γ-L-Glutamyl-S-(prop-1-enyl)-L-cysteine, in the Seeds of Chives (*Allium schoenoprasum*)

E. J. MATIKKALA and A. I. VIRTANEN

Laboratory of the Foundation for Chemical Research, Biochemical Institute, Helsinki, Finland

The precursor of the lachrymatory factor was isolated in this laboratory two years ago from onion bulbs (*Allium cepa*) and was characterized chemically as (+)-S-(prop-1-enyl)-L-cysteine sulphoxide [1]. In larger amounts this sulphoxide is present in onion bound with the γ-carboxyl group of L-glutamic acid [2] (γ-L-glutamyl-S-(prop-1-enyl)-L-cysteine sulphoxide). We have now isolated the corresponding peptide with a reduced S-atom from the seeds of chives. The isolation of the pure peptide met with difficulties because of its instability. The isolation was finally performed as follows.

1 kg of ground seeds were thoroughly extracted with 70 % ethanol, the amino acids and peptides were separated on an Amberlite IR-120 column, and 0.5 N acetic acid was added to the evaporated ammonia eluate. 200 mg of Johns-Manville filter gel was added to the turbid solution, and the mixture filtered. The fractionation of the solution was performed using a 4.9 × 59 cm column filled with Dowex 1 × 8 resin in acetate form. The eluant was at first 0.5 N acetic acid, after 170 fractions 1 N acetic acid, after 516 fractions 2 N acetic acid, and after 801 fractions 1 N HCl. 1025 fractions of 20.3 ml each were taken in all. Several unknown spots occurred on the paper chromatograms in the fractions separated.

Peptide 12 (the peptide in question) emerged from the column in fractions 594—633. The fractions were evaporated to dryness by lyophilization. The residue was dissolved in 70 % v/v isopropanol and was fractionated with this solvent on a 6.4 × 36.5 cm cellulose powder column. Peptide 12 emerged from the column in fractions 59—81, the volume of the fractions being 18.4 ml. The fractions were evaporated to dryness *in vacuo*, and the peptide was crystallized from an acetone-water mixture. The yield was 1.02 g of white needle-shaped crystals. Since the peptide is to some degree unstable, losses were probably considerable. Several faint spots which travelled slower than the peptide occurred on the paper chromatogram developed with butanol-acetic acid-water as solvent. When the peptide was separated by cutting off the corresponding zone and running a new chromatogram with the same solvent system, the same faint spots appeared again. The peptide accordingly decomposed to some extent during the preparation of the chromatogram.

Structure elucidation of peptide 12. The γ-glutamyl bond in the peptide was established by determining the free α-amino and carboxyl groups according to Linko [3]. 79.8 % of ammonia and 96.3 % of carbon dioxide were split off by the effect of ninhydrin. According to the method of Buchanan [4], 90 % of the theoretical amount of NH_3 was split off.

An enzyme preparation of calf kidney hydrolyzed the peptide in a phosphate buffer at pH 7.4. Glutamic acid and a sulphur-containing amino acid which travelled at much the same speed as S-propyl-cysteines were established by paper chro-

which may not change the N—H vibration frequency much.

I want to thank Mrs Kerstin Pettersson for her splendid technical assistance in recording the spectra. The heavy water was obtained through the courtesy of the A. B. Atomenergi.

1. Yoneda, H. *Bull. Chem. Soc. Japan* **28** (1955) 125.
2. Fronæus, S. and Larsson, R. *Acta Chem. Scand.* **16** (1962) 1433.
3. Anderson, J. S., Briscoe, H. V. A. and Spoor, N. L. *J. Chem. Soc.* **1943** 361.
4. Block, H. and Gold, V. *J. Chem. Soc.* **1959** 966.
5. Hill, D. H. and Rosenberg, A. F. *J. Chem. Phys.* **24** (1956) 1219.
6. Bellamy, L. J. *The Infrared Spectra of Complex Molecules*, Meuthen & Co, Ltd, London 1958.
7. Pimentel, G. C. and McClellan, A. L. *The Hydrogen Bond*, W. H. Freeman and Co., San Fransisco and London 1960.
8. Cannon, C. G. *Spectrochim. Acta* **10** (1958) 341.

Received November 23, 1962.

A New γ-Glutamylpeptide, γ-L-Glutamyl-S-(prop-1-enyl)-L-cysteine, in the Seeds of Chives (*Allium schoenoprasum*)

E. J. MATIKKALA and A. I. VIRTANEN

Laboratory of the Foundation for Chemical Research, Biochemical Institute, Helsinki, Finland

The precursor of the lachrymatory factor was isolated in this laboratory two years ago from onion bulbs (*Allium cepa*) and was characterized chemically as (+)-S-(prop-1-enyl)-L-cysteine sulphoxide [1]. In larger amounts this sulphoxide is present in onion bound with the γ-carboxyl group of L-glutamic acid [2] (γ-L-glutamyl-S-(prop-1-enyl)-L-cysteine sulphoxide). We have now isolated the corresponding peptide with a reduced S-atom from the seeds of chives. The isolation of the pure peptide met with difficulties because of its instability. The isolation was finally performed as follows.

1 kg of ground seeds were thoroughly extracted with 70 % ethanol, the amino acids and peptides were separated on an Amberlite IR-120 column, and 0.5 N acetic acid was added to the evaporated ammonia eluate. 200 mg of Johns-Manville filter gel was added to the turbid solution, and the mixture filtered. The fractionation of the solution was performed using a 4.9 × 59 cm column filled with Dowex 1 × 8 resin in acetate form. The eluant was at first 0.5 N acetic acid, after 170 fractions 1 N acetic acid, after 516 fractions 2 N acetic acid, and after 801 fractions 1 N HCl. 1025 fractions of 20.3 ml each were taken in all. Several unknown spots occurred on the paper chromatograms in the fractions separated.

Peptide 12 (the peptide in question) emerged from the column in fractions 594—633. The fractions were evaporated to dryness by lyophilization. The residue was dissolved in 70 % v/v isopropanol and was fractionated with this solvent on a 6.4 × 36.5 cm cellulose powder column. Peptide 12 emerged from the column in fractions 59—81, the volume of the fractions being 18.4 ml. The fractions were evaporated to dryness *in vacuo*, and the peptide was crystallized from an acetone-water mixture. The yield was 1.02 g of white needle-shaped crystals. Since the peptide is to some degree unstable, losses were probably considerable. Several faint spots which travelled slower than the peptide occurred on the paper chromatogram developed with butanol-acetic acid-water as solvent. When the peptide was separated by cutting off the corresponding zone and running a new chromatogram with the same solvent system, the same faint spots appeared again. The peptide accordingly decomposed to some extent during the preparation of the chromatogram.

Structure elucidation of peptide 12. The γ-glutamyl bond in the peptide was established by determining the free α-amino and carboxyl groups according to Linko [3]. 79.8 % of ammonia and 96.3 % of carbon dioxide were split off by the effect of ninhydrin. According to the method of Buchanan [4], 90 % of the theoretical amount of NH_3 was split off.

An enzyme preparation of calf kidney hydrolyzed the peptide in a phosphate buffer at pH 7.4. Glutamic acid and a sulphur-containing amino acid which travelled at much the same speed as S-propyl-cysteines were established by paper chro-

matography as hydrolysis products. The sulphur-containing amino acid was isolated in crystalline form by fractionation on a cellulosepowder column using butanol-acetic acid-water as solvent. It travelled as S-isopropyl-cysteine on the paper chromatogram (butanol-acetic acid-water) but the colour formed with ninhydrin distinguished it from this cysteine derivative. S-propyl-cysteine travelled somewhat faster, and S-allyl-cysteine somewhat slower than the S-containing amino acid of peptide 12.

When the precursor of the lachrymatory substance was reduced with sodium bisulfite [5], a crystalline substance was obtained. On the basis of both paper chromatography and the IR spectrum it was identical with the sulphur-containing amino acid formed from peptide 12 on enzymic hydrolysis. The unknown sulphur-containing amino acid was thus S-(prop-1-enyl)-cysteine, and hence peptide 12 was γ-glutamyl-S-(prop-1-enyl)-cysteine. In order still to corroborate the result, peptide 12 was oxidized with hydrogen peroxide in glacial acetic acid. It was then established by paper chromatography that peptide 4, γ-glutamyl-S-(prop-1-enyl)-cysteine sulphoxide, isolated from onion, was formed. Both peptides were hydrolyzed by the kidney preparation, and an enzyme preparation of onion was added to the phosphate buffer solutions of the evaporated hydrolysates. An easily recognized lachrymatory substance was then formed from both.

The configuration of the glutamic acid and the cysteine contained in peptide 12 was determined by hydrolyzing 300 mg of the peptide by adding 3 g of dry Amberlite IR-120 resin in H^+-form, and 10 ml of 70 % ethanol. The mixture was placed in a test tube from which air was removed by nitrogen gas, and the sealed tube was kept for 4 h in a water bath. The amino acids were separated in the usual way and fractionated on a Dowex 1 × 8 column. Glutamic acid, cystine, and in addition an unknown compound and very small amounts of unknown decomposition products were formed on hydrolysis. It is interesting to note that by this method of hydrolysis S-(prop-1-enyl)-cysteine remains largely undecomposed although it decomposes completely on ordinary acid hydrolysis.

The optical rotation of the glutamic acid isolated: $[\alpha]_D^{23} = +35.2$ in 6 N HCl, and of the cystine separated on a cellulose powder column: $[\alpha]_D^{23} = -179$ in 1 N HCl were found.

Both glutamic acid and cysteine are thus L-forms, and the new peptide 12 is accordingly γ-L-glutamyl-(prop-1-enyl)-L-cysteine.

The R_F-values for peptide 12 and different alkyl and alkylene cysteines are given in Table 1.

This research has been financed in part by a grant from the *United States Department of Agriculture, Agricultural Research Service.*

Table 1.

Compounds	Solvents	
	butanol-acetic acid-water (63:10:27)	phenol-water (NH_3)
Alanine	0.21	0.57
γ-L-Glutamyl-S-(prop-1-enyl)-L-cysteine	0.42	0.21
S-(Prop-1-enyl)-cysteine	0.55	0.81
S-Propyl-cysteine	0.58	0.81
S-Allyl-cysteine	0.50	0.81
S-Isopropyl-cysteine	0.56	0.83

1. Virtanen, A. I. and Spåre, C.-G. *Suomen Kemistilehti B* **34** (1961) 72; Spåre, C.-G. and Virtanen, A. I. *Acta Chem. Scand.* **17** (1963) *In press.*
2. Virtanen, A. I. and Matikkala, E. J. *Suomen Kemistilehti B* **34** (1961) 84; 114.
3. Linko, P. *Suomen Kemistilehti B* **28** (1955) 96.
4. Buchanan, D. L., Haley, E. E. and Markiw, R. T. *Biochemistry* **1** (1962) 612.
5. Micheel, F. and Schmitz, H. *Ber.* **72** (1939) 992.

Received November 26, 1962.

Biosynthesis of Spermine and Spermidine in the Developing Chick Embryo

AARNE RAINA

Department of Medical Chemistry, University of Helsinki, Helsinki, Finland

Although the occurrence of spermine and spermidine in the animal organism has been known for a long time, very little has been reported about the biosynthesis of these amines until recently. In the last few years much work has been done to elucidate their biosynthesis in micro-organisms. Studies with labelled putrescine have indicated that putrescine is incorporated as a unit into polyamines in growing cultures of *Escherichia coli* and *Aspergillus nidulans* [1]. Greene [2,3] demonstrated that in cultures of *Neurospora crassa* 2-^{14}C-DL-methionine added to the growth medium is incorporated into spermidine, being the source of the three-carbon chain of spermidine. Subsequent experiments [4-7] with whole cells and with cell-free preparations and purified enzyme systems of *E. coli* have confirmed that putrescine, and in one report [5] ornithine, is the source of the four-carbon chain of spermine and spermidine. Similarly, the important role of methionine in the biosynthesis of spermidine has been proved.

The studies cited above still leave open the question of whether the mechanism is the same in animal tissues, except for the preliminary note by Tabor *et al.* [1], which indicates a small incorporation of labelled putrescine into the polyamine fraction in minced rat prostate.

In the present work, incorporation studies have been carried out with developing chick embryos, because the synthesis of spermine and spermidine seems to be very rapid in growing organisms. With the method [8] used in this study the polyamines from the embryos could already be determined on the 3rd day of development, whereas none could be detected in unincubated eggs or their hydrolysates.

Methods. Of the radioactive material (putrescine-1,4-^{14}C dihydrochloride, specific activity 4.17 mC/mM, NEC—150; DL-ornithine-2-^{14}C hydrochloride, specific activity 1.0 mC/mM, California Corporation, Los Angeles; DL-methionine-2-^{14}C, specific activity 1.27 mC/mM, Volk Radiochemical Company, Illinois), 1—10 μC was injected onto the chorioallantoic membrane of developing chick embryos on the 9th day of development. The embryos were killed 5, 15, 30 or 60 h after administration. The radioactivity of the spermine and spermidine was determined in an Ecko type 664 A liquid scintillation counter directly from paper [9], after partial purification by extraction into butanol and paper electrophoretic separation of the amines [8].

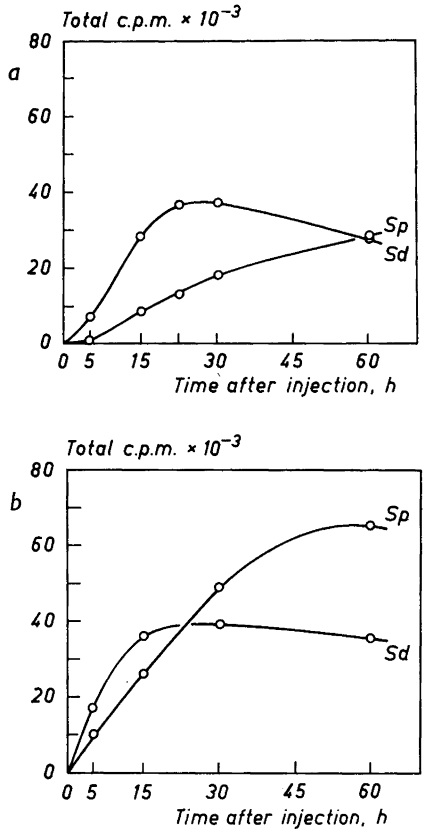

Fig. 1. Incorporation of radioactivity into spermine and spermidine in the developing chick embryo after injection of 5 μC of 1,4-^{14}C-putrescine (1a) or 5 μC of 2-^{14}C-DL-methionine (1b) onto the chorioallantoic membrane (total counts per minute per embryo). Sp = spermine, Sd = spermidine.

Results. The incorporation of labelled putrescine into these polyamines is seen in Fig. 1a. The total activity in the sper-

midine fraction reached its maximum about 20 h after administration of 5 μC of putrescine. Incorporation into spermine was slower. After a lag period, the total activity seemed to increase up to at least 60 h. Of the total radioactivity injected into the egg, about 1 % could be detected in the polyamines 60 h after treatment.

Studies with labelled ornithine showed a similar incorporation. It was interesting to note that after paper electrophoretic separation radioactivity was also found in the "putrescine area". In control experiments it was demonstrated that this unknown compound (putrescine?) was not produced during the isolation procedure.

Incorporation of 2-^{14}C-methionine into spermidine was quite similar to that of putrescine (Fig. 1b). After administration of 5 μC of methionine the maximum of total counts was about 40 000 c.p.m. in spermidine at 30 h after injection. The incorporation of methionine into spermine was more rapid than that of putrescine. 60 h after injection, about 65 000 c.p.m. could be detected in spermine and 35 000 c.p.m. in the spermidine fraction. Of the total radioactivity injected into the egg about 2.8 % was recovered in the polyamines 60 h after administration.

The results described here demonstrate that putrescine, ornithine and methionine can act as precursors in the biosynthesis of spermine and spermidine in the chick embryo. In addition, spermidine seems to be a precursor of spermine.

A more detailed report of the methods and results described here will be published in the near future.

1. Tabor, H., Rosenthal, S. M. and Tabor, C. W. *Federation Proc.* **15** (1956) 367.
2. Greene, R. C. *Federation Proc.* **16** (1957) 189.
3. Greene, R. C. *J. Am. Chem. Soc.* **79** (1957) 3929.
4. Tabor, H., Rosenthal, S. M. and Tabor, C. W. *J. Am. Chem. Soc.* **79** (1957) 2978.
5. Tabor, H., Rosenthal, S. M. and Tabor, C. W. *J. Biol. Chem.* **233** (1958) 907.
6. Tabor, H. and Tabor, C. W. *Federation Proc.* **19** (1960) 6.
7. Tabor, C. W. in Colowick, S. P. and Kaplan, N. O. *Methods in Enzymology*, Vol. V. Acad. Press, New York 1962, p. 756.
8. Raina, A. *Scand. J. Clin. Lab. Invest.* **14** (1962) 318.
9. Bosquet, W. F. and Christian, J. F. *Anal. Chem.* **32** (1960) 722.

Received November 26, 1962.

On the Tautomerism of 5(7)H-1-Pyrindine

GÖRAN BERGSON
and ANNE-MARIE WEIDLER

Chemical Institute, University of Uppsala, Sweden

In 1923, Ingold and Piggott [1] investigated the tautomerism of the three-carbon system of the methoxy-indenes Ia and Ib.

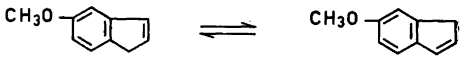

Ia *Ib*

These two forms could not be separated, different synthetic methods only yielding identical samples. The single substance thus isolated gave, however, by oxidation a mixture of two methoxy-homophthalic acids, and on blocking the tautomeric system by condensation with piperonal, a mixture of two, separable, derivatives was obtained.

Robison [2] synthesized and investigated 5(7)H-1-pyrindine (II) in which the same kind of tautomerism is possible (IIa and IIb) as in the methoxyindenes. A third tautomeric form (IIc) with the proton attached to nitrogen is, however, also possible, and Anderson *et al.* [3] have suggested that this form is responsible for the

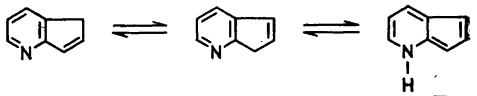

IIa *IIb* *IIc*

orange color of II as observed by Robison. Quite recently Reese [4] has confirmed this hypothesis in a very beautiful way, by synthesizing 1-methyl-1-pyrindine, discussed long ago by Armit and Robinson [5], and comparing its UV-spectrum with that of Robison's substance. The outcome of this investigation was that II contains 1.1 parts per 1000 of the coloured pseudoazulene IIc.

We have for some time been interested in the tautomerism of three-carbon systems, and in particular the tautomerism of 5(7)H-1-pyrindine and related compounds. Due to the current interest in this substance we wish to report the results

midine fraction reached its maximum about 20 h after administration of 5 μC of putrescine. Incorporation into spermine was slower. After a lag period, the total activity seemed to increase up to at least 60 h. Of the total radioactivity injected into the egg, about 1 % could be detected in the polyamines 60 h after treatment.

Studies with labelled ornithine showed a similar incorporation. It was interesting to note that after paper electrophoretic separation radioactivity was also found in the "putrescine area". In control experiments it was demonstrated that this unknown compound (putrescine?) was not produced during the isolation procedure.

Incorporation of 2-^{14}C-methionine into spermidine was quite similar to that of putrescine (Fig. 1b). After administration of 5 μC of methionine the maximum of total counts was about 40 000 c.p.m. in spermidine at 30 h after injection. The incorporation of methionine into spermine was more rapid than that of putrescine. 60 h after injection, about 65 000 c.p.m. could be detected in spermine and 35 000 c.p.m. in the spermidine fraction. Of the total radioactivity injected into the egg about 2.8 % was recovered in the polyamines 60 h after administration.

The results described here demonstrate that putrescine, ornithine and methionine can act as precursors in the biosynthesis of spermine and spermidine in the chick embryo. In addition, spermidine seems to be a precursor of spermine.

A more detailed report of the methods and results described here will be published in the near future.

1. Tabor, H., Rosenthal, S. M. and Tabor, C. W. *Federation Proc.* **15** (1956) 367.
2. Greene, R. C. *Federation Proc.* **16** (1957) 189.
3. Greene, R. C. *J. Am. Chem. Soc.* **79** (1957) 3929.
4. Tabor, H., Rosenthal, S. M. and Tabor, C. W. *J. Am. Chem. Soc.* **79** (1957) 2978.
5. Tabor, H., Rosenthal, S. M. and Tabor, C. W. *J. Biol. Chem.* **233** (1958) 907.
6. Tabor, H. and Tabor, C. W. *Federation Proc.* **19** (1960) 6.
7. Tabor, C. W. in Colowick, S. P. and Kaplan, N. O. *Methods in Enzymology*, Vol. V. Acad. Press, New York 1962, p. 756.
8. Raina, A. *Scand. J. Clin. Lab. Invest.* **14** (1962) 318.
9. Bosquet, W. F. and Christian, J. F. *Anal. Chem.* **32** (1960) 722.

Received November 26, 1962.

On the Tautomerism of 5(7)H-1-Pyrindine

GÖRAN BERGSON
and ANNE-MARIE WEIDLER

Chemical Institute, University of Uppsala, Sweden

In 1923, Ingold and Piggott [1] investigated the tautomerism of the three-carbon system of the methoxy-indenes Ia and Ib.

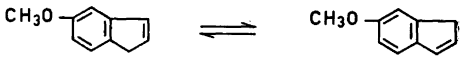

Ia *Ib*

These two forms could not be separated, different synthetic methods only yielding identical samples. The single substance thus isolated gave, however, by oxidation a mixture of two methoxy-homophthalic acids, and on blocking the tautomeric system by condensation with piperonal, a mixture of two, separable, derivatives was obtained.

Robison [2] synthesized and investigated 5(7)H-1-pyrindine (II) in which the same kind of tautomerism is possible (IIa and IIb) as in the methoxyindenes. A third tautomeric form (IIc) with the proton attached to nitrogen is, however, also possible, and Anderson *et al.* [3] have suggested that this form is responsible for the

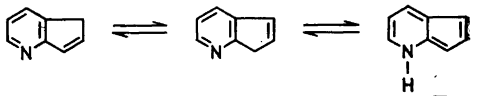

IIa *IIb* *IIc*

orange color of II as observed by Robison. Quite recently Reese [4] has confirmed this hypothesis in a very beautiful way, by synthesizing 1-methyl-1-pyrindine, discussed long ago by Armit and Robinson [5], and comparing its UV-spectrum with that of Robison's substance. The outcome of this investigation was that II contains 1.1 parts per 1000 of the coloured pseudoazulene IIc.

We have for some time been interested in the tautomerism of three-carbon systems, and in particular the tautomerism of 5(7)H-1-pyrindine and related compounds. Due to the current interest in this substance we wish to report the results

Talbe 1. Calculated and observed excitation energies.

Molecule	ΔE calc. (β_0)		ΔE calc. (kcal/mole)		ΔE obs. (kcal/mole)	
	ΔE_1	ΔE_2	ΔE_1	ΔE_2	ΔE_1	ΔE_2
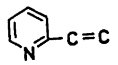	−1.308	−1.608	101.9	125.3	102.1	121.7
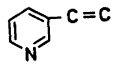	−1.320	−1.566	—	122.0	102.88	120.2
	−0.987	−1.317	76.9	102.6	61.0	—
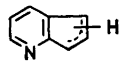					101.1	115.8

of a preliminary theoretical investigation of this problem. The molecules IIa and IIb are interesting since their σ-bond skeletons are equivalent and any difference in their properties should thus be due to differences in π-electron structure and energy. Furthermore, if hyperconjugation is neglected, the π-electron systems of IIa and IIb are the same as in 2- and 3-vinylpyridine, respectively, at least within the Hückel approximation. We have calculated the electronic excitation energies and the total π-electron energies of 2- and 3-vinylpyridine and 1H-1-pyrindine (IIc) by the standard Hückel-method neglecting overlap and with the parameters recommended by Pullman and Pullman [6].

The calculated and observed excitation energies are given in Table 1. The parameter β_0, occurring in the Hückel theory, was determined empirically from the first transition of 3-vinylpyridine, and the value thus obtained was used in the prediction of the other excitation energies. The first thing to be noticed is the prediction of a much lower excitation energy for IIc as compared to 2- or 3-vinylpyridine. The numerical discrepancy between the calculated value and that observed by Reese is not surprising in view of the approximations involved in the theoretical method. In general, a good prediction is possible only within a series of related iso-π-electronic molecules. Furthermore, the agreement between the three other calculated and observed excitation energies is surprisingly good, and the difficulty of deciding between the two tautomers IIa and IIb from UV-spectra [2,4] is further substantiated by this theoretical result.

It is also interesting to note that the total π-electron energies of 2- and 3-vinylpyridine are identical (10.865 β_0) despite the small but significant differences in charge distribution and bond-orders. When IIa or IIb is exposed to conditions catalyzing a tautomeric rearrangement, one would therefore expect to obtain a mixture, and Robison's [2] remark: "it is likely that the material is a mixture of labile tautomeric forms", is certainly appropriate. The close energetic similarity between IIa and IIb is not unexpected if one remembers that both forms are derived from the same alternating hydrocarbon (indene), and this

point is the subject of our further investigations.

1. Ingold, C. K. and Piggott, H. A. *J. Chem. Soc.* **123** (1923) 1469. *Cf.* however Koelsch, C.F. and Scheiderbauer, R.A. *J. Am. Chem. Soc.* **65** (1943) 2311.
2. Robison, M. M. *J. Am. Chem. Soc.* **80** (1958) 6254.
3. Anderson, A. G., Jr., Harrison, W. F., Anderson, R. G. and Osborne, A. G. *Ibid.* **81** (1959) 1255.
4. Reese, C. B. *Ibid.* **84** (1962) 3979.
5. Armit, J. W. and Robinson, R. *J. Chem. Soc.* **121** 827. (1922)
6. Pullman, B. and Pullman, A. *Rev. Modern Phys.* **32** (1960) 436.

Received December 3, 1962.

The Absolute Configuration of 2-Hydroxy-2-Methylbutyric Acid

BO W. CHRISTENSEN and ANDERS KJÆR

Organic Chemistry Department, Royal Veterinary and Agricultural College, Copenhagen, Denmark

The absolute configuration is unknown of the simplest, asymmetric, tertiary α-hydroxy-acid, 2-hydroxy-2-methylbutyric acid (2-ethyl-lactic acid), occurring in ester linkage in the *Veratrum* alkaloids protoveratrine A [1,2] (protoveratrine [3,4]), deacetylprotoveratrine A [5] (deacetylprotoveratrine [6]), germerine [7,8] and germitrine [8], as well as in the bitter principle glaucarubin [9]. We now report that the naturally derived *dextro*rotatory acid possesses the (*S*)-configuration (I).

Upon reaction with diazomethane, (+)-*threo*-2,3-dihydroxy-2-methylbutyric acid, to which we recently assigned the (2*R*,3*S*)-configuration (II,R=H) [10], afforded the corresponding methyl ester (II, R=CH_3)*, b.p. 45°/0.1 mm, n_D^{25} 1.4428, $d_4^{21.5}$ 1.141, $[\alpha]_D^{22}$ −2.5° (neat), which was further converted into the *p*-toluenesulphonate (III, R=*p*-$CH_3C_6H_4SO_2O$), m.p. 66−67°, $[\alpha]_D^{23}$ −6.0° ((*c* 11.5, $CHCl_3$). Treatment of the latter with sodium methoxide in methanol yielded a glycidic ester, b.p. 54°/11 mm, n_D^{25} 1.4160, $d_4^{21.5}$ 1.042, $[\alpha]_D^{22}$ + 21.1° (neat), possessing the configuration (IV) on basis of the well-established inversion accompanying ring-closure reactions of the present type, induced through nucleophilic displacement. Nucleophilic attack on (IV) with methyl mercaptide, again accompanied by inversion at C-3, afforded the sulphide (III, R=CH_3S), b.p. 100°/10 mm, n_D^{25} 1.4737, d_4^{22} 1.107, $[\alpha]_D^{25}$ −6.7° (neat). Raney nickel hydrogenolysis converted this sulphide into the methyl ester (III, R=H), b.p. 153°, n_D^{25} 1.4137, d_4^{21} 1.002, $[\alpha]_D^{25}$ −6.45° (neat). Lastly, alkaline hydrolysis of the ester yielded (*R*)-2-hydroxy-2-methylbutyric acid, m.p. 73.5−74.5°, $[\alpha]_D^{25}$ −1.5° ± 0.1° (*c* 1.7, H_2O); −6.9° (*c* 1.5, 0.2 N NaOH); −8,5° (*c* 3.0, $CHCl_3$), *p*-phenylphenacyl ester, m.p. 122°, $[\alpha]_D^{22}$ −2.1° (*c* 3.0, $CHCl_3$). The melting points agree with literature values [2,6-9] whilst the optical rotations of the acid are equal in magnitude * but *opposite in sign* to those reported for the *dextro*rotatory acid of natural

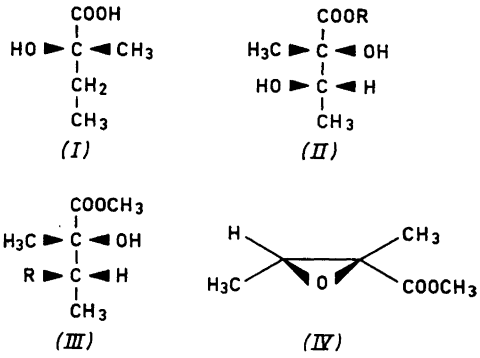

* Satisfactory analyses and consistent infrared and NMR-spectra have been obtained for all new compounds reported.

* Except for one set of rotation values [8] ($[\alpha]_D^{24}$ + 4.4° (*c* 1.6, H_2O); + 12° (*c* 1.28, 0.2 N NaOH)) which we consider to be somewhat too high. (The original preparation has deteriorated and redeterminations of the reported rotations hence are excluded. Slightly too high polarimeter readings seem to be the only possible source of error (Dr. O. Wintersteiner, private communication)).

point is the subject of our further investigations.

1. Ingold, C. K. and Piggott, H. A. *J. Chem. Soc.* **123** (1923) 1469. *Cf.* however Koelsch, C.F. and Scheiderbauer, R.A. *J. Am. Chem. Soc.* **65** (1943) 2311.
2. Robison, M. M. *J. Am. Chem. Soc.* **80** (1958) 6254.
3. Anderson, A. G., Jr., Harrison, W. F., Anderson, R. G. and Osborne, A. G. *Ibid.* **81** (1959) 1255.
4. Reese, C. B. *Ibid.* **84** (1962) 3979.
5. Armit, J. W. and Robinson, R. *J. Chem. Soc.* **121** 827. (1922)
6. Pullman, B. and Pullman, A. *Rev. Modern Phys.* **32** (1960) 436.

Received December 3, 1962.

The Absolute Configuration of 2-Hydroxy-2-Methylbutyric Acid

BO W. CHRISTENSEN and ANDERS KJÆR

Organic Chemistry Department, Royal Veterinary and Agricultural College, Copenhagen, Denmark

The absolute configuration is unknown of the simplest, asymmetric, tertiary α-hydroxy-acid, 2-hydroxy-2-methylbutyric acid (2-ethyl-lactic acid), occurring in ester linkage in the *Veratrum* alkaloids protoveratrine A [1,2] (protoveratrine [3,4]), deacetylprotoveratrine A [5] (deacetylprotoveratrine [6]), germerine [7,8] and germitrine [8], as well as in the bitter principle glaucarubin [9]. We now report that the naturally derived *dextro*rotatory acid possesses the (*S*)-configuration (I).

Upon reaction with diazomethane, (+)-*threo*-2,3-dihydroxy-2-methylbutyric acid, to which we recently assigned the (2*R*,3*S*)-configuration (II,R=H) [10], afforded the corresponding methyl ester (II, R=CH_3)*, b.p. 45°/0.1 mm, n_D^{25} 1.4428, $d_4^{21.5}$ 1.141, $[\alpha]_D^{22}$ −2.5° (neat), which was further converted into the *p*-toluenesulphonate (III, R=*p*-$CH_3C_6H_4SO_2O$), m.p. 66−67°, $[\alpha]_D^{23}$ −6.0° ((*c* 11.5, $CHCl_3$). Treatment of the latter with sodium methoxide in methanol yielded a glycidic ester, b.p. 54°/11 mm, n_D^{25} 1.4160, $d_4^{21.5}$ 1.042, $[\alpha]_D^{22}$ + 21.1° (neat), possessing the configuration (IV) on basis of the well-established inversion accompanying ring-closure reactions of the present type, induced through nucleophilic displacement. Nucleophilic attack on (IV) with methyl mercaptide, again accompanied by inversion at C-3, afforded the sulphide (III, R=CH_3S), b.p. 100°/10 mm, n_D^{25} 1.4737, d_4^{22} 1.107, $[\alpha]_D^{25}$ −6.7° (neat). Raney nickel hydrogenolysis converted this sulphide into the methyl ester (III, R=H), b.p. 153°, n_D^{25} 1.4137, d_4^{21} 1.002, $[\alpha]_D^{25}$ −6.45° (neat). Lastly, alkaline hydrolysis of the ester yielded (*R*)-2-hydroxy-2-methylbutyric acid, m.p. 73.5−74.5°, $[\alpha]_D^{25}$ −1.5° ± 0.1° (*c* 1.7, H_2O); −6.9° (*c* 1.5, 0.2 N NaOH); −8,5° (*c* 3.0, $CHCl_3$), *p*-phenylphenacyl ester, m.p. 122°, $[\alpha]_D^{22}$ −2.1° (*c* 3.0, $CHCl_3$). The melting points agree with literature values [2,6-9] whilst the optical rotations of the acid are equal in magnitude * but *opposite in sign* to those reported for the *dextro*rotatory acid of natural

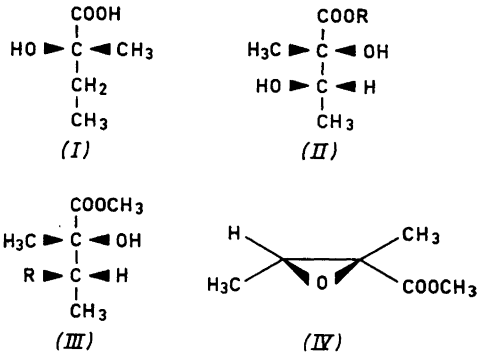

* Satisfactory analyses and consistent infrared and NMR-spectra have been obtained for all new compounds reported.

* Except for one set of rotation values [8] ($[\alpha]_D^{24}$ + 4.4° (*c* 1.6, H_2O); + 12° (*c* 1.28, 0.2 N NaOH)) which we consider to be somewhat too high. (The original preparation has deteriorated and redeterminations of the reported rotations hence are excluded. Slightly too high polarimeter readings seem to be the only possible source of error (Dr. O. Wintersteiner, private communication)).

derivation [2,6,7,9]. Hence, the latter possesses the (*S*)-configuration (I).

The present correlation supports the configurational assignment arrived at by application of Prelog's rule [11] to the reported preferential synthesis of *dextro* rotatory barium 2-hydroxy-2-methyl-butyrate from (−)-menthyl pyruvate and ethylmagnesium bromide [12].

1. Nash, H. A. and Brooker, R. M. *J. Am. Chem. Soc.* **75** (1953) 1942.
2. Stoll, A. and Seebeck, E. *Helv. Chim. Acta* **36** (1953) 718.
3. Glen, W. L., Myers, G. S., Barber, R., Morozovitch, P. and Grant, G. A. *Nature* **170** (1952) 932.
4. Klohs, M. W., Arons, R., Draper, M. D., Keller, F., Koster, S., Malesh, W. and Petracek, F. J. *J. Am. Chem. Soc.* **74** (1952) 5107.
5. Kupchan, S. M., Ayres, C. I. and Hensler, R. H. *J. Am. Chem. Soc.* **82** (1960) 2616.
6. Myers, G. S., Glen, W. L., Morozovitch, P., Barber, R., Papineau-Couture, G. and Grant, G. A. *J. Am. Chem. Soc.* **78** (1956) 1621.
7. Poethke, W. *Arch. Pharm.* **275** (1937) 571.
8. Fried, J., White, H. L. and Wintersteiner, O. *J. Am. Chem. Soc.* **72** (1950) 4621.
9. Ham, E. H., Schafer, H. M., Denkewalter, R. G. and Brink, N. G. *J. Am. Chem. Soc.* **76** (1954) 6066.
10. Christensen, B. W. and Kjær, A. *Proc. Chem. Soc.* **1962** 307.
11. Prelog, V. *Helv. Chim. Acta* **36** (1953) 308.
12. McKenzie, A. *J. Chem. Soc.* **89** (1906) 365.

Received November 24, 1962.

The Structures of some Polybromo Substituted Simple Ketones

CHRISTOFFER RAPPE

Institute of Chemistry, University of Uppsala, Uppsala, Sweden

In a recent paper it was shown by Rappe and Schotte [1] using NMR-techniques that the two bromo atoms in dibromodiethyl ketone are symmetrically substituted on both sides of the keto group and not unsymmetrically as earlier proposed by Schotte [2]. Among the di-, tri- and tetrabromo compounds of the lower aliphatic ketones several are described in the literature as having unsymmetric structures. As the methods used previously for structure determinations are rather ambiguous owing to possible rearrangements during the procedure [3] it is of interest to make a new determination of the structures of these bromo ketones by means of NMR-spectroscopy.

The direct treatment of aliphatic ketones with bromine is reported to give impure products since the liberated hydrogen bromide tends to promote the formation of condensation products [4]. Although several other methods are available, the author made the bromo ketones by an acid catalyzed bromination of ketones dissolved in hydrobromic acid. The ketones used are acetone, methyl ethyl ketone, methyl propyl ketone and diethyl ketone. By using two, three or four equivalents of bromine, the di-, tri- or tetrabromo compound of the corresponding ketone could be obtained. In Table 1 the results of these syntheses are collected, and new structures (based on NMR-spectra) for most of the bromoketones are proposed. In some cases the yield of pure bromo ketone was better than the yield previously reported employing bromination with other methods.

It appears to be a common feature that the two and four bromo atoms in di- and tetrabromo ketones are symmetrically placed one or two on each side of the keto group. The tribromo compounds of symmetrical ketones have two of the bromo atoms on one side and the third on the other. The unsymmetrical ketones give mixtures of the two possible α-substituted tribromo isomers.

A more detailed account of these works is to be published in *Arkiv för Kemi*.

derivation [2,6,7,9]. Hence, the latter possesses the (*S*)-configuration (I).

The present correlation supports the configurational assignment arrived at by application of Prelog's rule [11] to the reported preferential synthesis of *dextro* rotatory barium 2-hydroxy-2-methyl-butyrate from (−)-menthyl pyruvate and ethylmagnesium bromide [12].

1. Nash, H. A. and Brooker, R. M. *J. Am. Chem. Soc.* **75** (1953) 1942.
2. Stoll, A. and Seebeck, E. *Helv. Chim. Acta* **36** (1953) 718.
3. Glen, W. L., Myers, G. S., Barber, R., Morozovitch, P. and Grant, G. A. *Nature* **170** (1952) 932.
4. Klohs, M. W., Arons, R., Draper, M. D., Keller, F., Koster, S., Malesh, W. and Petracek, F. J. *J. Am. Chem. Soc.* **74** (1952) 5107.
5. Kupchan, S. M., Ayres, C. I. and Hensler, R. H. *J. Am. Chem. Soc.* **82** (1960) 2616.
6. Myers, G. S., Glen, W. L., Morozovitch, P., Barber, R., Papineau-Couture, G. and Grant, G. A. *J. Am. Chem. Soc.* **78** (1956) 1621.
7. Poethke, W. *Arch. Pharm.* **275** (1937) 571.
8. Fried, J., White, H. L. and Wintersteiner, O. *J. Am. Chem. Soc.* **72** (1950) 4621.
9. Ham, E. H., Schafer, H. M., Denkewalter, R. G. and Brink, N. G. *J. Am. Chem. Soc.* **76** (1954) 6066.
10. Christensen, B. W. and Kjær, A. *Proc. Chem. Soc.* **1962** 307.
11. Prelog, V. *Helv. Chim. Acta* **36** (1953) 308.
12. McKenzie, A. *J. Chem. Soc.* **89** (1906) 365.

Received November 24, 1962.

The Structures of some Polybromo Substituted Simple Ketones

CHRISTOFFER RAPPE

Institute of Chemistry, University of Uppsala, Uppsala, Sweden

In a recent paper it was shown by Rappe and Schotte [1] using NMR-techniques that the two bromo atoms in dibromodiethyl ketone are symmetrically substituted on both sides of the keto group and not unsymmetrically as earlier proposed by Schotte [2]. Among the di-, tri- and tetrabromo compounds of the lower aliphatic ketones several are described in the literature as having unsymmetric structures. As the methods used previously for structure determinations are rather ambiguous owing to possible rearrangements during the procedure [3] it is of interest to make a new determination of the structures of these bromo ketones by means of NMR-spectroscopy.

The direct treatment of aliphatic ketones with bromine is reported to give impure products since the liberated hydrogen bromide tends to promote the formation of condensation products [4]. Although several other methods are available, the author made the bromo ketones by an acid catalyzed bromination of ketones dissolved in hydrobromic acid. The ketones used are acetone, methyl ethyl ketone, methyl propyl ketone and diethyl ketone. By using two, three or four equivalents of bromine, the di-, tri- or tetrabromo compound of the corresponding ketone could be obtained. In Table 1 the results of these syntheses are collected, and new structures (based on NMR-spectra) for most of the bromoketones are proposed. In some cases the yield of pure bromo ketone was better than the yield previously reported employing bromination with other methods.

It appears to be a common feature that the two and four bromo atoms in di- and tetrabromo ketones are symmetrically placed one or two on each side of the keto group. The tribromo compounds of symmetrical ketones have two of the bromo atoms on one side and the third on the other. The unsymmetrical ketones give mixtures of the two possible α-substituted tribromo isomers.

A more detailed account of these works is to be published in *Arkiv för Kemi*.

Table 1.

Starting material	Formula	Analyses			Calculated		
		C	H	Br	C	H	Br
Acetone	$C_3H_4Br_2O$	16.70	1.87	74.14	16.69	1.87	74.03
»	$C_3H_3Br_3O$	12.34	1.07	81.01	12.22	1.03	81.32
»	$C_3H_2Br_4O$[a]	9.60	0.56	85.48	9.64	0.54	85.54
Methyl ethyl ketone	$C_4H_6Br_2O$[a]	20.70	2.65	69.50	20.90	2.63	69.52
» » »	$C_4H_5Br_3O$[a]	15.43	1.62	77.63	15.56	1.63	77.63
» » »	$C_4H_4Br_4O$[a]	12.42	1.10	82.42	12.39	1.04	82.44
Diethyl ketone	$C_5H_8Br_2O$[a]	24.68	3.35	65.34	24.62	3.31	65.52
» »	$C_5H_7Br_3O$[a]	18.59	2.22	74.22	18.60	2.19	74.26
Methyl propyl ketone	$C_5H_8Br_2O$	24.36	3.28	65.55	24.62	3.31	65.52
» » »	$C_5H_7Br_3O$[a]	18.64	2.21	74.08	18.60	2.19	74.26
» » »	$C_5H_6Br_4O$[a]	14.74	1.55	79.41	14.95	1.51	79.56

[a] new structure.
[b] product from the oxidation of the carbinol.

Experimental. General procedure. The ketone was mixed with 48 % hydrobromic acid (100 ml/mole ketone) and chilled with ice-water. The bromine was added dropwise. After addition of water (200 ml/mole bromine), the heavier organic layer separated and was washed with sodium bicarbonate and sodium bisulphite solutions and dried with calcium chloride. The crude product was fractionated under reduced pressure.

Acknowledgements. The author wishes to express his thanks to Professor Arne Fredga for his interest in this work and for all facilities put at his disposal. For the micro analyses I am indebted to Dr. Arthur Bengtsson of the Department of Analytical Chemistry, University of Uppsala. A grant from the *Faculty of Mathematics and Natural Sciences*, University of Uppsala, is gratefully acknowledged.

1. Rappe, C. and Schotte, L. *Acta Chem. Scand.* **16** (1962) 2060.
2. Schotte, L. *Acta Chem. Scand.* **5** (1951) 969.
3. Reid, E., Gompf, T. and Atwater, N. *J. Org. Chem.* **16** (1951) 1566.
4. Catch, J. R., Elliott, D. F., Hey, D. H. and Jones, E. R. H. *J. Chem. Soc.* **1948** 272.
5. Weygand, F. and Schmied-Kowarzik, V. *Chem. Ber.* **82** (1949) 33.
6. Faworsky, A. and Issatschenko, B. *J. prakt. Chem.* [2] **88** (1913) 655.
7. Petrov, A. A. *J. Gen. Chem. USSR* **11** (1941) 713. *Chem. Abstr.* **36** (1942) 404 [5].
8. Pastureau, M. *Compt. Rend.* **143** (1906) 967.
9. Shah, S. V. and Pishawikar, G. *Current Sci. (India)* **7** (1938) 182, *Chem. Abstr.* **33** (1939) 1660[8].
10. Pastureau, M. *Bull. Soc. Chim. France* [4] **5** (1909) 226.

Received December 4, 1962.

B·p. °C/mm Hg	M.p. °C	Structure	Previously given structure
79.5– 80.5/9	25.5–27.0	$CH_2BrCOCH_2Br$	$CH_2BrCOCH_2Br$ [5]
107–107.5/9	30.0–30.5	$CHBr_2COCH_2Br$	$CHBr_2COCH_2Br$ [5]
129–130/7	37 –38	$CHBr_2COCHBr_2$	CBr_3COCH_2Br [5]
79– 80/8	–	$CH_3CHBrCOCH_2Br$	$CH_3CBr_2COCH_3$ [6] $CH_3CHBrCOCH_2Br$ [7b]
100–102.5/9	–	$CH_3CBr_2COCH_2Br$ + $CH_3CHBrCOCHBr_2$	xxx-Tribromo [6]
–	52.5–53.5	$CH_3CBr_2COCHBr_2$	$CBr_3CH_2COCH_2Br$ [8] xxxx-Tetrabromo [9]
67–68/8	–	$CH_3CHBrCOCHBrCH_3$	$CH_3CBr_2COCH_2CH$ [2] $CH_3CHBrCOCHBrCH_3$ [1]
95–95.5/7	–	$CH_3CHBrCOCBr_2CH_3$	$CH_3CHBrCOCHBrCH_2Br$ [10]
88–89/10	–	$CH_3CH_2CHBrCOCH_2Br$	$CH_3CH_2CHBrCOCH_2Br$ [3]
119–119.5/10	–	$CH_3CH_2CBr_2COCH_2Br$ + $CH_3CH_2CHBrCOCHBr_2$	–
–	58–59.5	$CH_3CH_2CBr_2COCHBr_2$	$CH_3CHBrCH_2COCBr_3$ [10]

Mutual Arrangement of the Iodo-Cyano-Acetylene Molecules in the Solid

B. BORGEN, O. HASSEL and CHR. RÖMMING

Universitetets Kjemiske Institutt, Blindern-Oslo, Norway

In solid cyanogen iodide [1] and bromide [2] bonds are present between nitrogen and halogen atoms of neighbouring molecules and infinite linear chains of atoms result. All the chains are parallel and the packing of the chains is at least approximately that to be expected if the chains may be regarded as cylinders of infinite length. The structure of iodo-cyano-acetylene might be expected to be of a similar kind. As this substance had so far not been described in the literature we suggested to Dr. Else Kloster-Jensen to try to synthesize it. When the synthesis had been sucessfully carried out [3] we prepared rotation X-ray diagrams of crystals obtained by sublimation of the substance at temperatures well below 0°C. The crystals, fibre-like and poorly developed, turned out to have an identity period along their fibre axis of 8.60 Å, a value which corresponds to that estimated for chains of the kind we had expected. The mutual arrangement of the

Table 1.

Atomic coordinates

	x	*y*	*z*
I	0.0569	0.25	0.3255
C	0.864	0.25	0.112
C	0.702	0.25	0.969
C	0.546	0.25	0.805
N	0.400	0.25	0.667

Interatomic distances in the chain

N---I	2.93 Å	C–C	1.39 Å
I–C	1.79 Å	C≡N	1.20 Å
C≡C	1.27 Å		

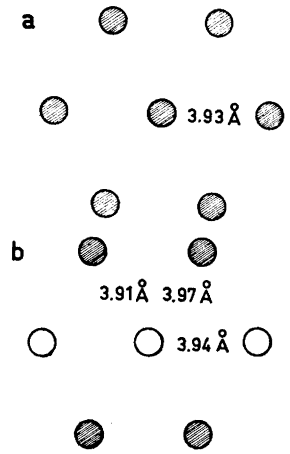

Fig. 1. Arrangement of chains in a) the low temperature form, b) the monoclinic form.

B·p. °C/mm Hg	M.p. °C	Structure	Previously given structure
79.5– 80.5/9	25.5–27.0	$CH_2BrCOCH_2Br$	$CH_2BrCOCH_2Br$ [5]
107–107.5/9	30.0–30.5	$CHBr_2COCH_2Br$	$CHBr_2COCH_2Br$ [5]
129–130/7	37 –38	$CHBr_2COCHBr_2$	CBr_3COCH_2Br [5]
79– 80/8	–	$CH_3CHBrCOCH_2Br$	$CH_3CBr_2COCH_3$ [6] $CH_3CHBrCOCH_2Br$ [7b]
100–102.5/9	–	$CH_3CBr_2COCH_2Br$ + $CH_3CHBrCOCHBr_2$	xxx-Tribromo [6]
–	52.5–53.5	$CH_3CBr_2COCHBr_2$	$CBr_3CH_2COCH_2Br$ [8] xxxx-Tetrabromo [9]
67–68/8	–	$CH_3CHBrCOCHBrCH_3$	$CH_3CBr_2COCH_2CH$ [2] $CH_3CHBrCOCHBrCH_3$ [1]
95–95.5/7	–	$CH_3CHBrCOCBr_2CH_3$	$CH_3CHBrCOCHBrCH_2Br$ [10]
88–89/10	–	$CH_3CH_2CHBrCOCH_2Br$	$CH_3CH_2CHBrCOCH_2Br$ [3]
119–119.5/10	–	$CH_3CH_2CBr_2COCH_2Br$ + $CH_3CH_2CHBrCOCHBr_2$	–
–	58–59.5	$CH_3CH_2CBr_2COCHBr_2$	$CH_3CHBrCH_2COCBr_3$ [10]

Mutual Arrangement of the Iodo-Cyano-Acetylene Molecules in the Solid

B. BORGEN, O. HASSEL and CHR. RÖMMING

Universitetets Kjemiske Institutt, Blindern-Oslo, Norway

In solid cyanogen iodide [1] and bromide [2] bonds are present between nitrogen and halogen atoms of neighbouring molecules and infinite linear chains of atoms result. All the chains are parallel and the packing of the chains is at least approximately that to be expected if the chains may be regarded as cylinders of infinite length. The structure of iodo-cyano-acetylene might be expected to be of a similar kind. As this substance had so far not been described in the literature we suggested to Dr. Else Kloster-Jensen to try to synthesize it. When the synthesis had been sucessfully carried out [3] we prepared rotation X-ray diagrams of crystals obtained by sublimation of the substance at temperatures well below 0°C. The crystals, fibre-like and poorly developed, turned out to have an identity period along their fibre axis of 8.60 Å, a value which corresponds to that estimated for chains of the kind we had expected. The mutual arrangement of the

Table 1.

Atomic coordinates

	x	*y*	*z*
I	0.0569	0.25	0.3255
C	0.864	0.25	0.112
C	0.702	0.25	0.969
C	0.546	0.25	0.805
N	0.400	0.25	0.667

Interatomic distances in the chain

N---I	2.93 Å	C–C	1.39 Å
I–C	1.79 Å	C≡N	1.20 Å
C≡C	1.27 Å		

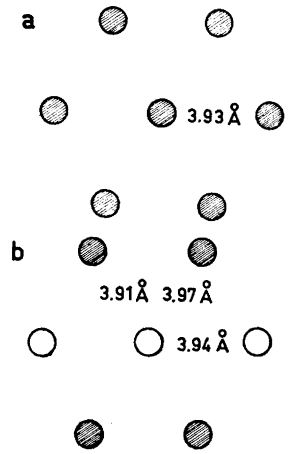

Fig. 1. Arrangement of chains in a) the low temperature form, b) the monoclinic form.

chains also appeared to conform to our expectations.

At room temperature the stable form of the crystals turned out to be monoclinic (space group P^2_1m) with two molecules in the unit cell. The parameters are:

$a = 4.43$ Å; $b = 6.72$ Å; $c = 7.65$ Å; $\beta = 93.9°$

It appeared probable that the chains in this modification would turn out to run parallel to the [101] direction, the period of which is 8.58 Å. The correctness of this assumption has been verified by the crystal structure determination which followed. From intensity data based on zero layer Weissenberg diagrams with rotation about [010], [100], and [001], Patterson and Fourier maps were computed followed by least squares refinements. The atomic parameters listed in Table 1 were obtained. This table also contains the interatomic distances within the chains.

The final R values were: $R_{h0l} = 0.05$; $R_{hk0} = 0.05$; $R_{0kl} = 0.08$. The B values arrived at show that the vibration amplitudes of iodine are larger perpendicular to the chains than along the chains.

In the low temperature form the distance between neighbouring chains (which are all running in the same direction) is 3.93 Å. In the monoclinic form stable at room temperature the chains are situated in the planes $y = \frac{1}{4}$ and $y = \frac{3}{4}$, the chain direction being the same within a particular layer but changing 180° from layer to layer. The situation is visualized schematically in Fig. 1 a (low temperature form) and 1 b (monoclinic form). It is worth mentioning that the distances between neighbouring chains in the monoclinic form, 3.91, 3.94, and 3.97 Å has a mean value 3.94 closely corresponding to that observed in the low temperature modification (3.93 Å) and that the packing is very much the same in both cases. Corresponding observations have been made in the case of the cyanogen halides [2]. In the orthorhombic cyanogen bromide, however, the two different values found for the distances between neighbouring chains differ more than in the monoclinic iodo-cyano-acetylene.

1. Ketelaar, J. A. A. and Zwartzenberg, J. W. *Rec. Trav. Chim.* **58** (1939) 448.
2. Geller, S. and Schawlow, A. L. *J. Chem. Phys.* **23** (1955) 779.
3. Kloster-Jensen, E. *Chem. & Ind. (London)* **1962** 658.

Received December 5, 1962.

Note on Ascorbigen as a Source of Vitamin C

Ž. PROCHÁZKA and W. FELDHEIM

Institute of Organic Chemistry and Biochemistry, Czechoslovak Academy of Science, Prague, Czechoslovakia, and Institute of Nutritional Science, Justus-Liebig-University, Giessen, Germany

Recently Kiesvaara and Virtanen (K. and V.) published a paper in this journal [1] (see also Ref.[2]), in which they state, in accordance with older work by Sumtsov [3], that ascorbigen possesses "vitamin C effect". We have also studied the question of the antiscorbutic activity of ascorbigen but arrived at essentially the opposite conclusions [4,5].

K. and V. found [2] that a 15 mg dose of ascorbic acid per guinea pig of 250–300 g body weight per day had the same effect on the weight increase of animals fed on a scorbutogenic diet as 26 mg of their preparation of synthetic ascorbigen.

On the other hand we have found [5] that a 10 mg dose of ascorbigen per guinea pig of 120–150 g body weight per day (corresponding to 20 mg of ascorbigen for older guinea pigs as used by K. and V.) did not show any curative effect on animals kept on a scorbutogenic diet, whereas even 0.5 mg of ascorbic acid had a full curative effect. The same effect was obtained by a 1 mg dose of hydrolysed ascorbigen [4]. Scurvy was diagnosed in our experiments on younger animals, which are more sensitive to vitamin C, not only by the weight decrease of the animals or their external appearance, but also by the more sensitive and reliable odontoblast test [6].

The following facts emerge in a comparison of the two sets of results: The curative dose of ascorbic acid per animal (250–300 g) per day is 1 mg. However, in their control experiment K. and V. administered 15 times this amount to scorbutic animals, thus invalidating their results for quantitative purposes. Only a qualitative conclusion can be drawn from their experiments, *i.e.* that a very high dose of their preparation can, under their experimental conditions, prevent the experimentally induced scurvy. However, even the results of Feldheim [4] (which are

chains also appeared to conform to our expectations.

At room temperature the stable form of the crystals turned out to be monoclinic (space group P^2_1m) with two molecules in the unit cell. The parameters are:

$a = 4.43$ Å; $b = 6.72$ Å; $c = 7.65$ Å; $\beta = 93.9°$

It appeared probable that the chains in this modification would turn out to run parallel to the [101] direction, the period of which is 8.58 Å. The correctness of this assumption has been verified by the crystal structure determination which followed. From intensity data based on zero layer Weissenberg diagrams with rotation about [010], [100], and [001], Patterson and Fourier maps were computed followed by least squares refinements. The atomic parameters listed in Table 1 were obtained. This table also contains the interatomic distances within the chains.

The final R values were: $R_{h0l} = 0.05$; $R_{hk0} = 0.05$; $R_{0kl} = 0.08$. The B values arrived at show that the vibration amplitudes of iodine are larger perpendicular to the chains than along the chains.

In the low temperature form the distance between neighbouring chains (which are all running in the same direction) is 3.93 Å. In the monoclinic form stable at room temperature the chains are situated in the planes $y = \frac{1}{4}$ and $y = \frac{3}{4}$, the chain direction being the same within a particular layer but changing 180° from layer to layer. The situation is visualized schematically in Fig. 1 a (low temperature form) and 1 b (monoclinic form). It is worth mentioning that the distances between neighbouring chains in the monoclinic form, 3.91, 3.94, and 3.97 Å has a mean value 3.94 closely corresponding to that observed in the low temperature modification (3.93 Å) and that the packing is very much the same in both cases. Corresponding observations have been made in the case of the cyanogen halides [2]. In the orthorhombic cyanogen bromide, however, the two different values found for the distances between neighbouring chains differ more than in the monoclinic iodo-cyano-acetylene.

1. Ketelaar, J. A. A. and Zwartzenberg, J. W. *Rec. Trav. Chim.* **58** (1939) 448.
2. Geller, S. and Schawlow, A. L. *J. Chem. Phys.* **23** (1955) 779.
3. Kloster-Jensen, E. *Chem. & Ind. (London)* **1962** 658.

Received December 5, 1962.

Note on Ascorbigen as a Source of Vitamin C

Ž. PROCHÁZKA and W. FELDHEIM

Institute of Organic Chemistry and Biochemistry, Czechoslovak Academy of Science, Prague, Czechoslovakia, and Institute of Nutritional Science, Justus-Liebig-University, Giessen, Germany

Recently Kiesvaara and Virtanen (K. and V.) published a paper in this journal [1] (see also Ref.[2]), in which they state, in accordance with older work by Sumtsov [3], that ascorbigen possesses "vitamin C effect". We have also studied the question of the antiscorbutic activity of ascorbigen but arrived at essentially the opposite conclusions [4,5].

K. and V. found [2] that a 15 mg dose of ascorbic acid per guinea pig of 250–300 g body weight per day had the same effect on the weight increase of animals fed on a scorbutogenic diet as 26 mg of their preparation of synthetic ascorbigen.

On the other hand we have found [5] that a 10 mg dose of ascorbigen per guinea pig of 120–150 g body weight per day (corresponding to 20 mg of ascorbigen for older guinea pigs as used by K. and V.) did not show any curative effect on animals kept on a scorbutogenic diet, whereas even 0.5 mg of ascorbic acid had a full curative effect. The same effect was obtained by a 1 mg dose of hydrolysed ascorbigen [4]. Scurvy was diagnosed in our experiments on younger animals, which are more sensitive to vitamin C, not only by the weight decrease of the animals or their external appearance, but also by the more sensitive and reliable odontoblast test [6].

The following facts emerge in a comparison of the two sets of results: The curative dose of ascorbic acid per animal (250–300 g) per day is 1 mg. However, in their control experiment K. and V. administered 15 times this amount to scorbutic animals, thus invalidating their results for quantitative purposes. Only a qualitative conclusion can be drawn from their experiments, *i.e.* that a very high dose of their preparation can, under their experimental conditions, prevent the experimentally induced scurvy. However, even the results of Feldheim [4] (which are

unfortunately not quoted by K. and V.) give a clearer picture in spite of the fact that owing to lack of ascorbigen he could compare only the minimum curative dose of ascorbic acid (0.5 mg per animal of 125—130 g daily) with the same amount of bound ascorbic acid, *i.e.* with 1 mg of ascorbigen. This shows that at this critical dose ascorbigen is completely inactive, or, in other words, that its activity must be less than half that of L-ascorbic acid. We therefore fed our animals with large doses of ascorbigen [5] in order to establish, perhaps even quantitatively, the activity of ascorbigen relative to L-ascorbic acid. However, this problem was only partially solved. We concluded from our experiments that free ascorbic acid is over 20 times more active than ascorbigen. We have therefore critically reexamined both sets of experimental conditions [1,5] and have arrived at the following conclusions.

In their diet, as described by K. and V., older, less sensitive guinea pigs were given daily 0.3 mg of ascorbic acid contained in the dried grass, and another 0.13 mg contained in their preparation of ascorbigen. This is a total of 0.43 mg, which represents almost one-half (43 %) of the minimum curative dose. From the description of the preparation of ascorbigen by the Finnish authors it follows that the reaction mixture (10 g of indole, 30 g of ascorbic acid, 5.2 g of formaldehyde in 400 ml of a 0.05 M citrate buffer were mixed and heated at 54° for 7—8 h) was merely filtered and the filtrate, which necessarily contained large amounts of ascorbic acid, and possibly some dehydroascorbic acid, was worked up in such a way that appreciable amounts of these must have been extracted, as we have demonstrated in our own experiments [5]. The ascorbic acid and other impurities were removed from our extracts by chromatography on a polyamide column and by fractional precipitation. K. and V., on the other hand, only concentrated and dried their extract. They state, that their material "according to paper chromatograms and the UV-spectrum was pure ascorbigen". According to our experiences neither paper chromatography nor UV-spectrophotometry are sufficiently reliable criteria for the purity of ascorbigen. The ascorbigen of K. and V. must have contained, as was already pointed out, a certain amount of ascorbic acid that passed from the aqueous phase into the ethyl acetate layer during the extraction. In order to verify this possibility we repeated their experiments. We reproduced their method of ascorbigen synthesis [1] (see above) on one-tenth of their scale, and obtained one-third of the yield, quoted by them. The UV-spectra and paper chromatograms clearly showed the presence of ascorbic acid in the preparation. According to 2,6-dichlorophenol indophenol titration the ascorbigen sample thus obtained [1] contained approximately 5 % of free ascorbic acid, *i.e.* 10 times the amount quoted by the Finnish authors. If an aqueous solution of this sample was left to stand the ascorbic acid content increased and was doubled after 3 h. This rapid increase of ascorbic acid cannot be explained by the hydrolysis of ascorbigen since this is extremely slow; in neutral medium according to Ettlinger [7] it occurs to the extent of 1 % per hour at most, and according to Prochàzka and Jindra [8] hardly at all. Hence the concentrate must have contained ascorbic acid combined in a form more labile than ascorbigen. It is known [9] that the reducing power of ascorbic acid is rapidly diminished at certain pH values in the presence of formaldehyde. We therefore carried out a control experiment, again using the above mentioned procedure of the Finnish authors, but leaving out the indole from the reaction mixture. The resulting product, whose weight was only one-half of that obtained in the presence of indole, and which could not contain any ascorbigen, contained approximately 2.3 % of free ascorbic acid and no dehydroascorbic acid. When an aqueous solution of this extract was left to stand, the titre of ascorbic acid increased steadily until it reached a value eight times that of the original solution, *i.e.* the ascorbic acid content (free + combined with formaldehyde) was 18.4 %. In a subsequent experiment we showed that under the conditions used (3 g of ascorbic acid, 0.52 g of formaldehyde, in 40 ml of 0.05 M citrate buffer) ascorbic acid reacts very rapidly in the cold (80 % after 1.5 h), and that the complex can be extracted with ethyl acetate, although much less readily than ascorbigen. Experiments with the extracted complex showed that it is more stable in 1 % sulphuric acid than in distilled water. It is quite stable in organic solvents.

Thus it is probable that the preparation of K. and V. contained ascorbic acid, both free and combined with formaldehyde, in sufficient amount to produce a curative effect on experimental scurvy when a 26 mg dose per animal and per day was

administered. Such a dose of a preparation made by us according to their prescription contained 1.3 mg of free ascorbic acid and 1.3 mg combined with formaldehyde. Under the conditions and diet used by K. and V. 0.7 mg or less of ascorbic acid would have sufficed to cure the scurvy.

The possibility that the dose tested by K. and V. represents the threshold dose under their experimental conditions should be verified, as should the possibility that their animals were more sensitive, or able to hydrolyze ascorbigen *in vivo*.

Our theory regarding the inactivity, or rather the very low activity of ascorbigen is also supported by our findings that ascorbigen is not hydrolysed in the stomach and that it rapidly passes into the blood stream, where, as a result of a relatively low hydrogen ion concentration (pH 7.4), it is quickly converted into a material (substance C^{10}) which does not liberate ascorbic acid any more, and that most of it is excreted in the urine either unchanged or in the form of substance C.

1. Kiesvaara, M. and Virtanen, A. I. *Acta Chem. Scand.* **16** (1962) 510.
2. Virtanen, A. I. and Kiesvaara, M. *Suomen Kemistilehti B* **35** (1962) 24.
3. Sumtsov, B. M. *Biokhimiya* **12** (1947) 539.
4. Feldheim, W. *Intern. Z. Vitaminforschung* **31** (1961) 297.
5. Feldheim, W. and Procházka, Ž. *Intern. Z. Vitaminforschung* **32** (1962) 251.
6. Crampton, E. W., Collier, B. C., Wollsey, L. D. and Framer, F. A. *Science* **100** (1944) 599.
7. Ettlinger, M. *Personal communication.*
8. Procházka, V. and Jindra, A., *Česk. Farm.* **5** (1956) 328.
9. Krishnamurthy, P. V. *J. Indian Chem. Soc.* **18** (1941) 383.
10. Šanda, V., Constantzas, N. and Procházka, Ž. *Collection Czechoslov. Chem. Communs.* **27** (1962) 554.

Received October 22, 1962.